The Human Nervous System

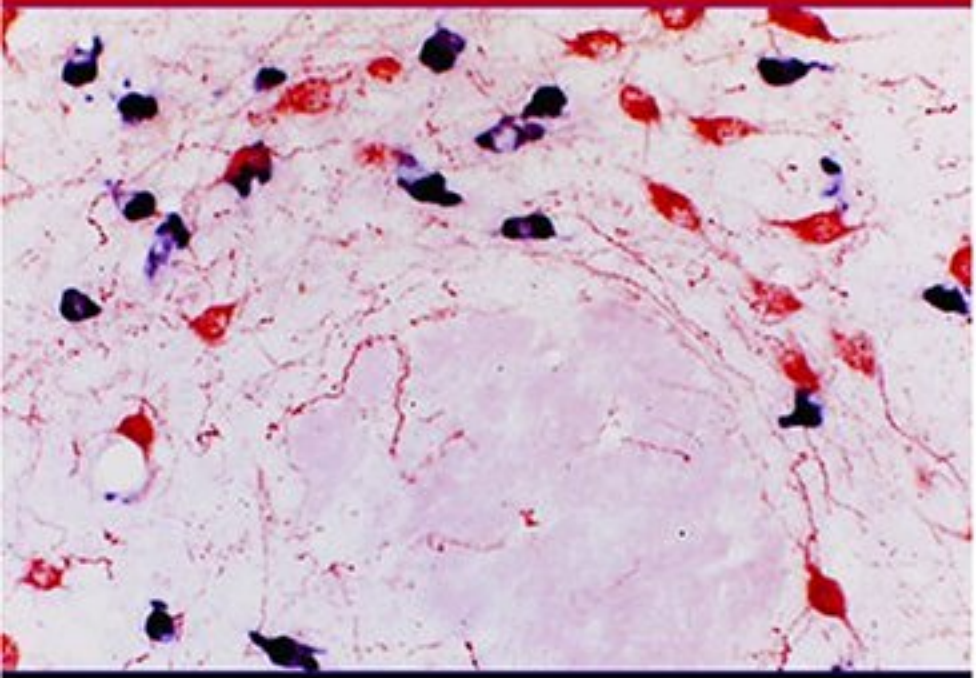

SECOND EDITION

Edited by

GEORGE PAXINOS • JÜRGEN K. MAI

Elsevier Academic Press
525 B Street, Suite 1900, San Diego, California 92101-4495, USA
84 Theobald's Road, London WC1X 8RR, UK

This book is printed on acid-free paper. ♾

Cover image: Figure 17.12, Panel A: illustrates the mixing of neurons that stain with antiserum against ORX (brown) and with a digoxygenin-labeled probe for MCH mRNA (blue) in the perifornical region of a rat. Although the two types of neurons cluster closely with one another around the edge of the fornix, there is virtually no colocalization within individual neurons. Modified from Elias, C.F., Saper, C.B., Maratos-Flier, E., Tritos, N.A., Lee, C., Kelly, J., Tatro, J.B., Hoffman, G.E., Ollmann, M.M., Barsh, G.S., Sakurai, T., Yanagisawa, M., and Elmquist, J.K. (1998b). Chemically defined projections linking the mediobasal hypothalamus and the lateral hypothalamic area. *J. Comp. Neurol.* **402,** 442–459.

Library of Congress Catalog Card Number: 2003107471

International Standard Book Number: 0-12-547626-4

For information on all Academic Press publications
visit our website at www.academicpress.com

Printed in Chile
03 04 05 06 07 08 9 8 7 6 5 4 3 2 1

Contents

Contributors

Numbers in parentheses indicate the pages on which the authors' contributions begin.

David G. Amaral, (871), Center for Neuroscience, University of California, Davis, California, USA

Ken W. S. Ashwell, (49, 95, 1093), Department of Anatomy, School of Medical Sciences, The University of New South Wales, Sydney, Australia

William W. Blessing, (464), Departments of Physiology and Medicine, Centre for Neuroscience, Flinders University, Adelaide, Australia

Jean A. Büttner-Ennever, (479, 1212), Institute of Anatomy, Ludwig-Maximilian University Munich, Munich, Germany

David Burke, (113), College of Health Sciences, The University of Sydney, Sydney, Australia

Thomas Carlstedt, (250), PNI-Unit, The Royal National Orthopaedic Hospital, Stanmore, United Kingdom, and Karolinska Institutet, Stockholm, Sweden

Pascal Carrive, (393), Department of Anatomy, School of Medical Sciences, The University of New South Wales, Sydney, Australia

Iain J. Clarke, (562), Prince Henry's Institute of Medical Research, Melbourne, Australia

Staffan Cullheim, (250), Department of Neuroscience, Karolinska Institutet, Stockholm, Sweden

Jose DeOlmos, (739), Instituo de Investigacion Medica "Mercedes y Martin Ferreyra", Cordoba, Argentina

Richard L. M. Faull, (190), Department of Anatomy with Radiology, Faculty of Medical and Health Sciences, The University of Auckland, Auckland, New Zealand

Simon C. Gandevia, (113), Prince of Wales Medical Research Institute, The University of New South Wales, Sydney, Australia

Martha Johnson Gdowski, (676), Department of Neurobiology and Anatomy, University of Rochester School of Medicine, Rochester, New York, USA

Nicolaas M. Gerrits, (1212, 1306), Department of Anatomy, Erasmus University, Rotterdam, The Netherlands

Stefan Geyer, (973), C. and O. Vogt-Brain Research Institute, Heinrich Heine University of Düsseldorf, Düsseldorf, Germany

Ian Gibbins, (134), Department of Anatomy and Histology, Flinders University, Adelaide, Australia

Rainer Goebel, (1280), Department of Neurocognition, Faculty of Psychology, Universiteit Maastricht, Maastricht, The Netherlands

Gunnar Grant, (233), Department of Neuroscience, Karolinska Institutet, Stockholm, Sweden

Suzanne N. Haber, (676), Department of Pharmacology and Physiology, University of Rochester School of Medicine, Rochester, New York, USA

Glenda Halliday, (267, 449), Prince of Wales Medical Research Institute, The University of New South Wales, Sydney, Australia

Patrick R. Hof, (915), Fishberg Research Center for Neurobiology, Department of Geriatrics and Adult Development, Mount Sinai School of Medicine, New York, USA

Gert G. Holstege, (1306), Department of Anatomy and Embryology, Faculty of Medical Sciences, University of Groningen, Groningen, The Netherlands

Anja K. E. Horn, (479), Institute of Anatomy, Ludwig-Maximilian University Munich, Munich, Germany

Jean-Pierre Hornung, (424), Institut de Biologie Cellulaire et de Morphologie, University of Lausanne, Lausanne, Switzerland

Eva Horvath, (551), Department of Laboratory Medicine and Pathobiology, St. Michael's Hospital, University of Toronto, Toronto, Ontario, Canada

Xu-Feng Huang, (267), Department of Biomedical Sciences, University of Wollongong, Wollongong, Australia

Ricardo Insausti, (871), Department of Health Sciences, School of Medicine, University of Castilla-La Mancha, Albacete, Spain

Jon H. Kaas, (1059), Department of Psychology, Vanderbilt University, Nashville, Tennessee, USA

Dae-Shik Kim, (1280), Center for Magnetic Resonance Research, University of Minnesota, Minneapolis, MN, USA

George Kontogeorgos, (551), Department of Pathology, General Hospital of Athens, Athens, Greece

Yuri Koutcherov, (267), Prince of Wales Medical Research Institute, The University of New South Wales, Sydney, Australia

Kalman Kovacs, (551), Department of Laboratory Medicine and Pathobiology, St. Michael's Hospital, University of Toronto, Toronto, Ontario, Canada

Fred H. Linthicum, Jr., (1241), Department of Histopathology, House Ear Institute, Los Angeles, California, USA

Giuseppe Luppino, (973), Dipartimento di Neuroscienze, Sezione di Fisiologia, Università Di Parma, Parma, Italy

Jürgen K. Mai, (49), Institute of Neuroanatomy, Heinrich-Heine University of Düsseldorf, Düsseldorf, Germany

Massimo Matelli, (973), Dipartimento di Neuroscienze, Sezione di Fisiologia, Università Di Parma, Parma, Italy

Michael J. McKinley, (562), Howard Florey Institute of Experimental Physiology and Medicine, University of Melbourne, Victoria, Australia

Jean K. Moore, (1241), Department of Neuroanatomy, House Ear Institute, Los Angeles, California, USA

Michael M. Morgan, (393), Department of Psychology, Washington State University, Vancouver, Washington, USA

Leonora J. Mouton, (1306), Department of Anatomy and Embryology, Faculty of Medical Sciences, University of Groningen, Groningen, The Netherlands

Lars Muckli, (1280), Department of Neurophysiology, Max-Planck Institute of Brain Research, Frankfurt, Germany

Fabiola Müller, (22), University of California School of Medicine, Davis, California, USA

Ralph E. Norgren, (1171), Department of Neural and Behavioral Sciences, Hershey Medical Center, Pennsylvania State University College of Medicine, Hershey, Pennsylvania, USA

Brian J. Oldfield, (562), Howard Florey Institute of Experimental Physiology and Medicine, University of Melbourne, Victoria, Australia

Ronan O'Rahilly, (22), University of California School of Medicine, Davis, California, USA

Deepak Pandya, (950), Departments of Anatomy and Neurobiology, Boston University School of Medicine, Boston, Massachusetts, USA, and Havard Neurological Unit, Beth Israel Hospital, Boston, Massachusetts, USA

George Paxinos, (267), Prince of Wales Medical Research Institute, The University of New South Wales, Sydney, Australia

Gerard Percheron, (592), Institut National de la Santé et de la Recherche Medicale, Paris, France

Michael Petrides, (950), Montreal Neurological Institute, and Department of Psychology, McGill University, Montreal, Quebec, Canada

Joseph L. Price, (1197) Department of Anatomy and Neurobiology, Washington University School of Medicine, St. Louis, Missouri, USA

Thomas C. Pritchard, (1171), Department of Neural and Behavioral Sciences, Hershey Medical Center, Pennsylvania State University College of Medicine, Hershey, Pennsylvania, USA

Mårten Risling, (250) Department of Neuroscience, Karolinska Institutet, Stockholm, Sweden, and Department of Defence Medicine, Swedish Defence Research Agency (FOI), Stockholm, Sweden

Clifford B. Saper, (513), Harvard Medical School, Department of Neurology, Beth Israel Deaconess Medical Center, Boston, Massachusetts, USA

Jean Schoenen, (190, 233), Department of Neuroanatomy and Neurology, University of Liège, Liège, Belgium

Oscar U. Scremin, (1325), Department of Veterans Affairs, Greater Los Angeles Healthcare System, Los Angeles, California, USA

Lucia Stefaneanu, (551), Department of Laboratory Medicine and Pathobiology, St. Michael's Hospital, University of Toronto, Toronto, Ontario, Canada

Georg F. Striedter, (3), Department of Neurobiology and Behavior, University of California at Irvine, Irvine, California, USA

Brent A. Vogt, (915), Cingulum NeuroSciences Institute, Manlius, New York, USA, and Department of Neuroscience and Physiology, State University of New York Upstate Medical University, Syracuse, New York, USA

Lesley J. Vogt, (915), Cingulum NeuroSciences Institute, Manlius, New York, USA, and Department of Neuroscience and Physiology, State University of New York Upstate Medical University, Syracuse, New York, USA

Jan Voogd, (321), Department of Neuroscience, Erasmus University Rotterdam, Rotterdam, The Netherlands

Phil M. E. Waite, (95, 1093), Department of Anatomy, School of Medical Science, The University of New South Wales, Sydney, Australia

Karin N. Westlund, (1125), Department of Anatomy and Neurosciences, University of Texas Medical Branch, Galveston, Texas, USA

William D. Willis, Jr., (1125), Department of Anatomy and Neurosciences, The University of Texas Medical Branch, Galveston, Texas, USA

Karl Zilles, (973, 997), Institute of Medicine, Research Center Jülich, and C. & O. Vogt-Institute of Brain Research, University of Düsseldorf, Düsseldorf, Germany

Preface

Neuroscience comprises increasingly diverse fields ranging from molecular genetics to neurophilosophy. The common thread between all these fields is the structure of the human nervous system. Knowledge on the structure, connections and function of the brain of experimental animals is readily available. On the other hand the structure of the human brain was studied by the classical anatomists and their work is difficult to retrieve. With the current intense interest in the structure of the human brain engendered particularly by imaging studies, groups of scientists familiar with the classical works, but who are also versed in modern neuroscience technologies, have commenced human brain studies.

The present book gives an authoritative account of the structure of the human brain tempered by functional considerations. The task of describing all parts of the nervous system in the context of modern hypotheses of structural and functional organization would be overwhelming for a single individual. We have, therefore, asked scientists with knowledge and affection for their research areas to contribute to this edited volume. We trust that the combined effort of contributors to The Human Nervous System 2e will do justice to the data and concepts available in our field while stimulating the readers' brains, arousing curiosity and providing a framework for thinking.

George Paxinos and Jürgen K Mai
Sydney and Düsseldorf

CHAPTER

1

Brain Evolution

GEORG F. STRIEDTER
Department of Neurobiology and Behavior
University of California at Irvine
Irvine, California, USA

"The route to an understanding of humans leads just as surely through an understanding of animals, as the evolutionary pathway of humans has led through animal precursors."—*Konrad Lorenz*, "The Russian Manuscript," p. xxvii

The question of how the brain of *Homo sapiens* differs from that of chimpanzees, gorillas, and other animals was intensely debated by Richard Owen and T. H. Huxley around the time that Darwin published his *Origin of Species*. Owen had been Britain's most prominent comparative anatomist and he vigorously opposed the very idea of biological evolution. Regarding the possibility that humans might have evolved from apes, Owen argued that the overall pattern of morphological development differs so dramatically between apes and humans that it is difficult to see how one could have been transformed into the other. Owen also noted that human brains are significantly larger than chimpanzee or gorilla brains, both absolutely and relative to body size, and that this size difference arises because human brains continue to grow for a much longer postnatal period (Owen, 1859). Moreover, Owen described three anatomical features that supposedly distinguish human brains from those of apes, namely, a posterior cerebral lobe, a posterior horn of the lateral ventricle, and the hippocampus minor, a ridge in the floor of the posterior horn of the lateral ventricle (Owen, 1857). Owen later conceded that these three structures might not be strictly unique to humans, but he continued to insist that these three human brain structures differ markedly from their homologues in apes (Owen, 1859). In Owen's view, these neuroanatomical differences were important because they could, in large measure, account for the enormous mental and behavioral differences between humans and apes. In fact, Owen argued that the neuroanatomical differences between apes and humans were so great that they warranted the placement of humans into their own taxonomic subclass, the Archencephala or "ruling brains" (Owen, 1857).

T. H. Huxley, in contrast, argued that humans differ anatomically from apes no more than apes differ from one another and that man must, therefore, "take his place in the same order with them" (Huxley, 1863, p. 86). In a very famous and rather vicious attack, Huxley assailed Owen's 1857 claim that the posterior lobe, posterior horn, and hippocampus minor are unique to humans (Huxley, 1863; Cosans, 1994; Desmond, 1994).[1] Specifically, Huxley argued that many well-respected neuroanatomists had already observed homologues of these three structures in chimpanzees and other apes and that Owen, who must have known about these

[1]It is worth noting that Huxley's attack on Owen was not quite fair, since Huxley (1863) never bothered to rebut Owen's 1859 argument that human brains differ from those of apes primarily in how they have modified homologous brain structures. Instead, Huxley continued to attack Owen's 1857 statement that humans possess some brain structures that have no homologues in apes (Cosans, 1994).

prior findings, was severely biased, if not dishonest, in his analysis. Huxley conceded that "there is a very striking difference in absolute mass and weight between the lowest human brain and that of the highest ape," but he claimed that "the difference in weight of brain between the highest and the lowest men is far greater, absolutely and relatively, than that between the lowest man and the highest ape" (Huxley, 1863, pp. 120–122). Therefore, Huxley contended, the brains of humans and other apes are really quite similar in terms of anatomical detail and overall size. This conclusion, in turn, led Huxley to suggest that the "vast intellectual chasm" between humans and other apes is due primarily to nonneural differences, specifically to the possession of articulate speech, which he considered to be "the grand distinctive character of man (whether it be absolutely peculiar to him or not)" (p. 122). Ironically, then, Huxley's attack on Owen's position narrowed the "zoological gulf" between man and ape but failed to provide a biological explanation of the "intellectual chasm" between them. Therefore, it is not surprising to discover that Huxley was a great admirer of Descartes, did not believe in physiological explanations of human intelligence, and ultimately abandoned faith not only in God (he coined the word *agnostic*) but also in the possibility of obtaining a scientific account of human consciousness (Cosans, 1994; Desmond, 1994).

My rationale for beginning this essay on brain evolution with a recounting of the old Owen–Huxley debate is that many of the issues raised in their quarrel remain of interest even today. For instance, how significant is the difference in overall brain size between humans and other primates, and what is its relationship to the differences in their mental abilities? Do human brains possess any truly unique features or brain areas? What is the relationship of language to the human brain and does human language have homologues in other species? And how can our ideas about God and consciousness be reconciled with Darwin's ideas about evolution and, more generally, with the search for biological explanations of the human mind? These are tough questions and, despite considerable effort, they remain largely unresolved (Preuss, 1995; Deacon, 1997; Miller, 1999). Nor do I pretend to have definitive answers. I will, however, attempt here to show that evolutionary neurobiology has progressed considerably since Darwin's days, that many of the old ideas about brain evolution have been replaced by better theories (Striedter, 1998a), and that it is time to reapproach some of the questions that intrigued Owen and Huxley.

Specifically, I review below what we now know about the historical pattern of vertebrate brain evolution. Next, I discuss the relationship between brain development and evolution, emphasizing how phylogenetic transformations may be explained in terms of changing developmental mechanisms. In the final section, I take up the questions of how the human brain differs from that of other primates and how a knowledge of these neuroanatomical differences might help us to understand exactly what it is that sets humans apart from other animals. My general thesis is that the insights gained during the last century, particularly during the last 20 years, by evolutionary neurobiologists studying nonhuman brains can now be used to remove at least some of the mystery, and often outright confusion, that has traditionally surrounded the problem of human brain evolution. It is in this sense that I agree with Lorenz, quoted above, that a full understanding of human nature requires insights gained from the study of animals (Lorenz, 1996).

HISTORICAL PATTERN OF VERTEBRATE BRAIN EVOLUTION

The most insidious idea in the study of brain evolution is the very old notion that biological evolution proceeded in a linear and progressive manner, from lower to higher forms of organization and with *Homo sapiens* at the very top of the so-called phylogenetic scale. The belief that all living creatures can be arranged in a linear sequence had its origin in the theological and decidedly nonevolutionary concept of a *scala naturae*, with archangels at the top and sponges near the bottom, but continued to thrive in the minds of most post-Darwinian thinkers (Hodos and Campbell, 1969; Bowler, 1988). For example, Huxley himself wrote, in what might well be the first explicit account of brain evolution:

> The brain of a fish is very small,… In Reptiles, the mass of the brain, relatively to the spinal cord, increases and the cerebral hemispheres begin to dominate over the older parts; while in Birds this predominance is still more marked. The brain of the lowest Mammals, such as the duck-billed Platypus and the Opossums and Kangaroos, exhibits a still more definite advance in the same direction. The cerebral hemispheres have now so much increased in size as, more or less, to hide the representatives of the optic lobes, which remain comparatively small.… A step higher in the scale, among the placental Mammals, the structure of the brain acquires a vast modification.…
> The appearance of the "corpus callosum" in the

> placental mammals is the greatest and most sudden modification exhibited by the brain in the whole series of vertebrated animals.… In the lower and smaller forms of placental Mammals the surface of the cerebral hemispheres is either smooth or evenly rounded, or exhibits a very few grooves.… But in the higher orders, the grooves, or sulci, become extremely numerous, and the intermediate convolutions proportionately more complicated in their meanderings, until, in the Elephant, the Porpoise, the higher Apes, and Man, the cerebral surface appears a perfect labyrinth of tortuous foldings. (Huxley, 1863, pp. 112–114).

This linear and progressive view of brain evolution dominated evolutionary neurobiology throughout the 19th and most of the 20th century (Edinger, 1908; Kappers *et al.*, 1936; Herrick, 1948). Over the years, several specific hypotheses were proposed to explain how brains became more complex as they "ascended" the phylogenetic scale, e.g., by the addition of phylogenetically new brain parts to older brains or by an increase in the histological differentiation of ancestral brain regions (e.g., MacLean, 1990; Ebbesson, 1984). These theories were well publicized and influential within the neuroscience community, where terms such as "subhuman primates" and "lower vertebrates" are still commonly used. However, most evolutionary neurobiologists now consider these theories to be patently false or, at least, distressingly incomplete. Because the *scala naturae* way of thinking is so well entrenched among medically oriented neuroscientists, psychologists, and anthropologists (Cartmill, 1990; Campbell and Hodos, 1991), I will expend some effort here to review why the strictly linear view of brain evolution is untenable and what alternative view has taken its place.

Perhaps the most obvious difficulty with the *scala naturae* view of evolution is that different authors generally have different ideas about how to rank different species along the phylogenetic scale. Dolphins and other toothed whales, for example, are sometimes considered high on the phylogenetic scale because they are capable of complex vocal behaviors, have remarkably large brains for their body size, and display highly convoluted cerebral and cerebellar cortices (Fig. 1.1); (Ridgway, 1986; McCowan and Reiss, 1997; Marino, 1998; Janik, 2000). However, other authors have deemed dolphin brains to be quite primitive because their cerebral cortex is relatively thin, represents a relatively small fraction of total brain volume, exhibits little areal differentiation, and is poorly laminated (Fig. 1.1); (Glezer *et al.*, 1988; see Deacon, 1990a). The perceived position of dolphins on the phylogenetic scale therefore

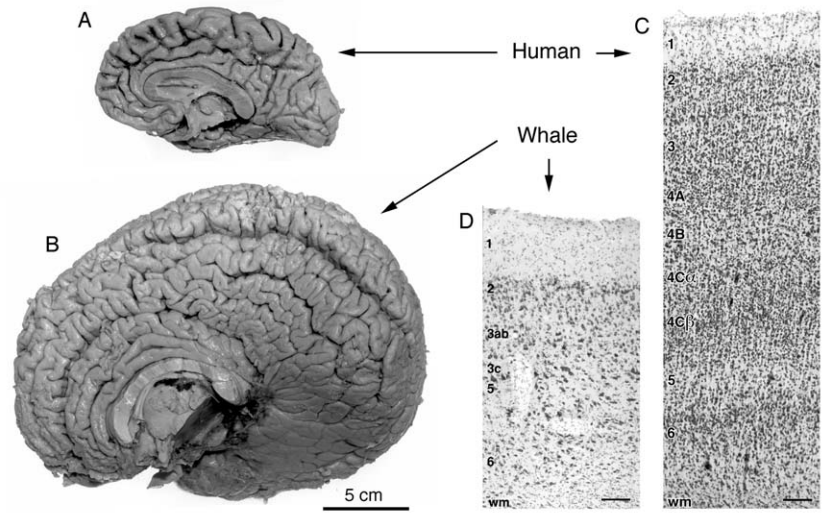

FIGURE 1.1 The brain of a human **(A)** is smaller and less convoluted than that of a killer whale **(B),** but the neocortex is thicker and more highly laminated in a human **(C)** than in a pygmy sperm whale **(D);** shown here are sections through primary visual cortex. In addition, one can note that the corpus callosum is proportionately smaller in the whale than in the human brain. Both brains are shown at the same scale and from a medial view. The scale bars for the neocortical sections both equal 150 μm. Abbreviations: 1, 2, 3, 4A, 4B, 4C, 5, and 6, neocortical layers; wm, white matter. Panels A and B are reproduced from Ridgway (1986) with permission of Sam Ridgway and Lawrence Erlbaum Associates. The photographs of the neocortical sections are reproduced from Preuss (2001) with the permission of Todd Preuss, Patrick Hof, and Cambridge University Press.

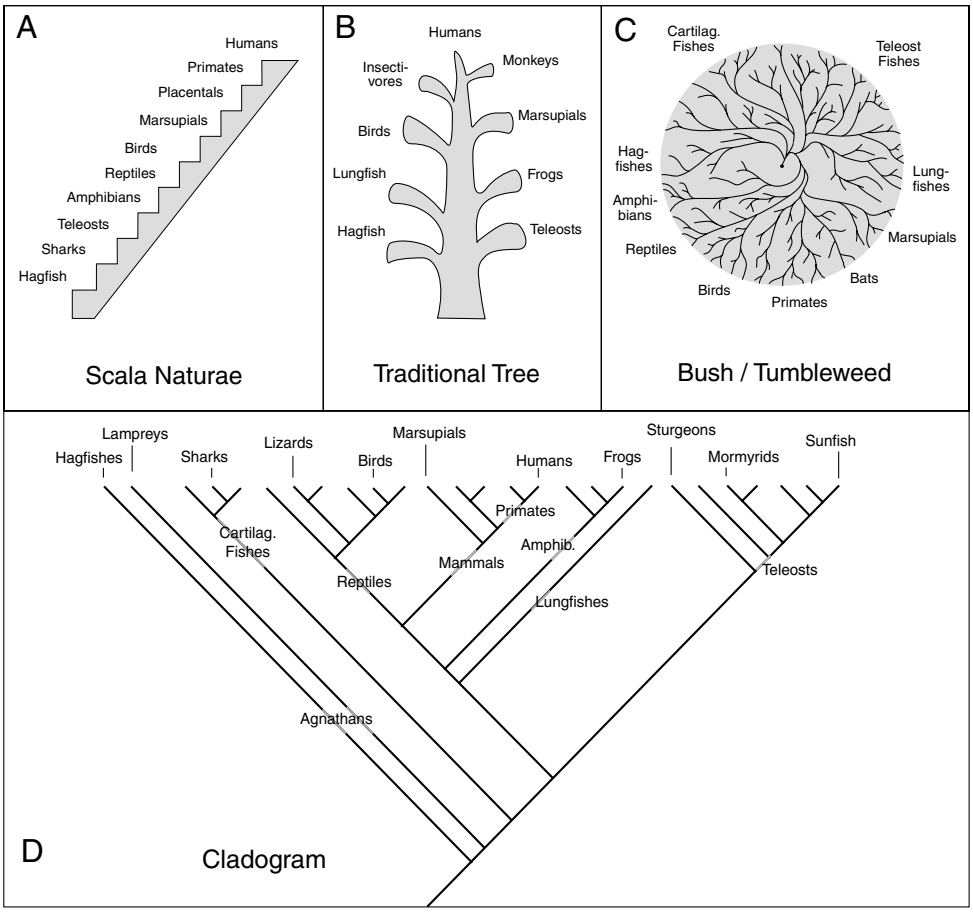

FIGURE 1.2 Vertebrate phylogeny has been depicted in a variety of ways. According to the deeply entrenched *scala naturae* view of evolution, vertebrates can be arranged along a linear phylogenetic scale **(A).** Phylogenetic trees, in contrast, have a branched topology. Traditionally, most phylogenetic trees place humans at the top and represent other taxa as side branches off the main trunk **(B).** More accurately, however, vertebrate phylogeny would be represented as a severely pruned bush, or tumbleweed, with extant taxa occupying only the tips of the outermost branches **(C).** In practice, most evolutionary biologists work with dichotomously branching "cladograms" **(D),** which represent both extant and extinct species along the top of the diagram.

depends on which characters are being considered. Nor are dolphins the only thorn in the side of the phylogenetic scale. Monotremes, for example, are often considered to be quite primitive in the sense that they are the oldest surviving order of mammals, but echidnas (spiny anteaters) actually have quite large and convoluted brains (Rowe, 1990). Similarly, birds and bony fishes are often judged to be "lower vertebrates," but parrots are capable of cognitive feats that put many mammals to shame (Pepperberg, 1990; Hile *et al.*, 2000), and mormyrid electric fish have exceptionally large brains that consume an astonishing 60% of the body's oxygen, compared to about 20% in humans and 2% to 8% in most other vertebrates (Nilsson, 1996). Even the "lowly" hagfish, one of the jawless vertebrates, does not contain the simple nervous system one might have expected, but instead displays a bulky and highly differentiated brain that includes a five-layered telencephalic region (Wicht and Northcutt, 1992; Wicht and Nieuwenhuys, 1998).

Instead of a linear phylogenetic scale, then, vertebrate species form a phylogenetic tree, bush, or tumbleweed that has been severely pruned by extinction events (Fig. 1.2). Nonhuman lineages do not represent "blind alleys" explored by evolution in its quest for *Homo sapiens* (Huxley, 1942); (Fig. 1.2B) but rather the outcome of divergent and opportunistic descent with modification (Darwin, 1859). Moreover, the currently living species represent only the outermost terminal branchlets of the phylogenetic tumbleweed, which means that they are unlikely to represent the transitional forms or "missing links" of evolutionary lore. There are,

of course, some "living fossils" that have changed very little over many millions of years, but even these often exhibit unique specializations that disqualify them as strictly transitional forms. For example, the coelacanth *Latimeria chalumnae,* is probably a representative of the extinct rhipidistians that gave rise to tetrapods, but it also exhibits several peculiar nonancestral (i.e., derived) features, including ovoviviparity, a huge and mysterious "rostral organ" that is probably used to detect electrical signals emitted by prey, and an odd telencephalon with "rostral bodies" that are not found in any other vertebrates (Nieuwenhuys, 1998a). Even with bona fide (i.e., dead) fossils it is generally difficult, and some would argue impossible, to determine whether a specimen is "the" sought-after ancestor or merely an independent offshoot from the lineage of interest (Eldredge and Cracraft, 1980; Wolpoff, 1999). Regardless of one's position on this point, the controversy is largely moot for evolutionary neurobiologists since brains generally do not fossilize and skull endocasts provide minimal information about the structural organization of extinct brains (Rogers, 1998). In sum, the brains available for comparative study are scattered across the outer surface of the phylogenetic tumbleweed, and each is likely to be a mosaic of both primitive and uniquely derived features. If this is so, then how can evolutionary neurobiologists hope to reconstruct the course of brain evolution?

For most contemporary evolutionary neurobiologists the answer to this question is "cladistics," a formal and widely applicable method for taxonomic classification and phylogenetic reconstruction (Hennig, 1966; Kirsch and Johnson, 1983; Northcutt, 1985a; Northcutt and Wullimann, 1988; Nieuwenhuys, 1994). Cladistics (also termed phylogenetic systematics) was created primarily to aid in the classification of organisms; however, once a classification has been established, the method can also be used to distinguish between homologous[2] and homoplasous (i.e., independently evolved) features and to reconstruct when in phylogeny a particular feature evolved (Eldredge and Cracraft, 1980; Ridley, 1986). Consider, for example, the corpus callosum. This great commissure, coursing between the cerebral hemispheres of all placental mammals, is not found in any marsupials or monotremes, and is likewise lacking in all nonmammalian vertebrates (Owen, 1857; Elliot Smith, 1910). This phylogenetic distribution strongly suggests that the corpus callosum evolved with the origin of placental mammals because all alternative scenarios would be significantly less parsimonious, involving multiple phylogenetic losses and/or gains. Consider further the observation that the corpus callosum is significantly smaller (relative to total brain weight) in toothed whales than in other large-brained placental mammals (Fig. 1.1); (Rilling and Insel, 1999a). This phylogenetic distribution makes it most parsimonious to conclude that the corpus callosum shrank in size, relative to the rest of the brain, with the origin of toothed whales (also known as the Odontoceti). Interestingly, the phylogenetic shrinkage of the corpus callosum in toothed whales was apparently accompanied by a phylogenetic decrease in the relative thickness and volume of the neocortex (Ridgway and Wood, 1988).[3] Cladistics is, of course, more complicated than is apparent from these examples, and its practical and logical limitations are severe when one attempts to analyze characters that evolve readily, and hence repeatedly, in different lineages. Nonetheless, cladistics is the best available method for reconstructing the phylogeny of neural characters, and it has met with considerable success in that capacity (e.g., Northcutt, 1985a, b, 1995; Butler and Hodos, 1996; Nieuwenhuys *et al.,* 1998).

Perhaps the most important finding to have emerged from the modern cladistic analyses of brain evolution is that relative brain size increased independently in most major vertebrate lineages (Northcutt, 1981, 1985a). Manta rays, for example, have brains that are almost 40 times larger than the brains of other cartilaginous fishes with similar body weights (R. G. Northcutt, personal communication). Among bony fishes, relative brain size increased significantly in the lineage leading to teleosts, the most speciose class of vertebrates (Lauder and Liem, 1983), and within teleosts brain size increased again several times, most notably in the above-mentioned mormyrids (Nilsson, 1996) and in some coral reef and pelagic fishes (Bauchot *et al.,* 1989). In sauropsids (i.e., reptiles and birds), relative brain size increased significantly in the lineage leading to modern birds and, within birds, in parrots, corvids (e.g., ravens), and owls (Stingelin, 1958; Portmann and Stingelin, 1961). Among mammals, relatively large brains evolved in primates, toothed whales, and elephants.

[2]Many different definitions of homology have been proposed over the years (see Hall, 1994). In my view, it is best to say simply that features in two or more different species (or larger taxonomic groups) are homologous if, and only if, (1) they are similar enough to be identified as "the same character" and (2) they originated just once, in a common ancestor of the taxa being considered, and were then retained with a continuous history in the descendent lineages under consideration (see Striedter and Northcutt, 1991; Striedter, 1998b, 1999).

[3]It may also account for the unusual ability of dolphins to sleep with one cerebral hemisphere at a time (Ridgway, 1986).

One frequently neglected aspect of these phylogenetic increases in brain size is that they are accompanied by major changes in brain organization. Simply put, the phylogenetically enlarged brains are not isometrically scaled-up versions of their smaller cousins, for different brain regions generally increase at different rates (i.e., allometrically) as overall brain size increases (Deacon, 1990a; Finlay and Darlington, 1995). Largely because of this allometric scaling, the neocortex, for example, occupies a far greater percentage of the whole brain in large mammals than in small ones. Moreover, larger brains generally exhibit a greater degree of cytoarchitectural complexity (i.e., a greater number of distinct, nonidentical cellular aggregates) than do smaller brains. Consistent with this general principle are the findings that (1) mormyrids have one of the most complex telencephalons among teleost fishes (Nieuwenhuys and Meek, 1990), (2) the forebrain of birds is more complex than that of reptiles (Nieuwenhuys *et al.*, 1998), and (3) primates have a greater number of distinct neocortical areas than do other mammals (Brodmann, 1909; Kaas, 1987). Thus, both brain size and brain complexity have increased several times independently in diverse branches of the phylogenetic tumbleweed.

Although brain size and complexity have tended to increase, rather than decrease, during vertebrate evolution, there are several lineages in which relative brain size and complexity have been reduced. Specifically, some lungfishes (i.e., the South American and African genera) and the urodele amphibians (i.e., salamanders) have unexpectedly small and simple brains, with extremely small cerebella and few distinct cell groups (Northcutt, 1986; Roth *et al.*, 1997; Nieuwenhuys, 1998b). Although these lungfishes and salamanders have manifestly similar brains, they do not constitute adjacent branches of the phylogenetic tree and are separated, phylogenetically speaking, by several taxa with larger and more complicated brains (e.g., the Australian lungfishes and anuran amphibians). Therefore, it is most parsimonious to conclude that small and simple brains evolved independently in these two lineages, probably as a result of pedomorphosis—the general retention of juvenile characteristics (Gould, 1977; Bemis, 1984). If this is true, then it is misguided to assume that the brain of a modern salamander can, on account of its general simplicity, be a good model for "the" primitive vertebrate brain (Herrick, 1948). Instead, the features of the most ancestral vertebrate brain must be discovered by a complex phylogenetic analysis to determine, character by character, which neural features are primitive and which derived. To the inevitable frustration of those in search of truly primitive brains, this collection of primitive features, i.e., the vertebrate morphotype, is unlikely to exist in any species living today (Northcutt, 1985b, 1995; Wicht and Nieuwenhuys, 1998). An analogous dilemma exists for those interested in "the" primitive mammalian brain. Hedgehogs, tenrecs, and other "basal insectivores" (Stephan, 1967), for example, have relatively simple brains with very little neocortex, but they are a rather heterogeneous assemblage of taxa (Eisenberg, 1981), and their simplicity may be derived rather than primitive (Kirsch *et al.*, 1983). Even monotremes and marsupials, the two earliest branches of the mammalian radiation, are quite diverse in brain structure and far from uniformly primitive (Rowe, 1990). Therefore, those who seek to establish the ancestral pattern of mammalian brain organization must sample broadly and proceed cautiously.

The traditional explanation of how brains increased (or decreased) in complexity during the course of evolution is that brain regions were successively added to (or lost from) ancestral brains (Edinger, 1908; MacLean, 1990). According to this view, brains evolve in a manner analogous to the transformation of a medieval fortress into a king's palace by the successive addition of new structures (think, for example, of the Louvre in Paris). This additive view of brain evolution was enormously influential, as evidenced by the prevalence of the prefixes "neo," "archi," and "paleo" in the neuroanatomical nomenclature. It is unlikely to be correct, however, at least as a general theory, because most of the supposedly "added" brain divisions have now been identified, albeit in modified form, also in those taxa that were supposedly lacking them (Karten, 1969; Northcutt, 1981; Reiner *et al.*, 1984; Butler and Hodos, 1996). A homologue of mammalian neocortex, for example, has been identified in virtually all nonmammalian vertebrates (although its extent and composition is still debated; Northcutt, 1995; Striedter, 1997; Puelles *et al.*, 2000). Therefore, it appears that most major brain divisions are conserved across vertebrates and that phylogenetic differences in complexity arise because these conserved brain regions diverge in their embryonic development in such a way that they become subdivided to varying degrees and/or, occasionally, in fundamentally different ways (Striedter, 1999). Phylogenetically new structures therefore can and do arise in brain evolution, but they cannot be thought of as simple additions to adult ancestral brains. Returning to the architectural analogy, it is better to compare brain evolution to the history of ancient Troy, which was destroyed and rebuilt many times, doubtlessly retaining some major features across each iteration but also varying in countless details (Schliemann, 1875). Viewed from this perspective, one must marvel at the fact that brains are "rebuilt" so faithfully across each

generation and that a considerable number of features are conserved across millions of years (Striedter, 1998b). One may also begin to wonder what role the mechanisms and rules of neural development have in guiding the course of brain evolution, and whether it might not be possible to understand the process of brain evolution in terms of the developmental transformations which it depends.

DEVELOPMENTAL MECHANISMS UNDERLYING BRAIN EVOLUTION

The relationship between development and evolution has long held great fascination for comparative biologists. According to Haeckel's famous biogenetic law, phylogenetic change causes additional stages to be appended to an organism's ontogeny, which therefore comes to "recapitulate" the organism's phylogenetic history. In Haeckel's view, then, phylogeny is the mechanism that underlies ontogenetic change (Haeckel, 1889). This idea was turned on its head by Garstang and others who argued instead that ontogenetic changes are the driving force behind phylogenetic change and that ontogenies may change in a variety of different ways, including nonterminal addition of stages, deletion of stages, and divergence of ontogenetic trajectories (Garstang, 1922; de Beer, 1958; Alberch, 1980). Garstang's anti-Haeckelian view of development and evolution has now become widely accepted, partly because it fits better with the comparative embryological data (von Baer, 1828), but also because the *scala naturae* view of evolution, which is complexly intertwined with Haeckel's ideas on recapitulation, has generally fallen out of favor (Gould, 1977). In addition, Garstang's approach allows comparative embryologists to go beyond the reconstruction of phylogenetic history and to create developmental explanations for why particular phylogenetic changes have occurred (or did not occur). The phylogenetic loss of lateral line organs in direct-developing frogs, for example, can be explained by a loss of ectodermal competence for lateral line placode induction (Schlosser *et al.*, 1999). Such mechanistic explanations for phylogenetic change are more difficult to attain when it comes to brain evolution, but there are several areas of developmental neurobiology that can already be discussed with this goal in mind. Below, I briefly review (1) the implication of finding highly conserved embryonic regions in vertebrate brains, (2) the correlation between when a brain region is "born" and how much its size tends to change during phylogeny, and (3) the data on how changes in one brain region affect the development of other brain regions.

Shortly after neurulation, when vertebrate embryos reach the so-called phylotypic stage of development (Richardson *et al.*, 1997), the brain is quite similar (though not identical) across the major vertebrate taxa (Bergquist and Källén, 1954). Most conserved across species is the embryonic hindbrain which is, at that age, divided into a series of segments, or neuromeres (Fig. 1.3), each of which constitutes a lineage restriction domain and expresses a unique combination of transcription factors (Fraser *et al.*, 1990; Gilland and Baker, 1993; Lumsden and Krumlauf, 1996). The discovery of these highly conserved hindbrain neuromeres has revitalized the field of comparative neuroembryology and stimulated many investigators to look for conserved neuromeres also at more rostral levels of the neuraxis. This search has yielded a great deal of data but little consensus, particularly about whether the forebrain is segmentally organized (Figdor and Stern, 1993; Puelles and Rubenstein, 1993; Alvarez-Bolado *et al.*, 1995; Guthrie, 1995; Shimamura *et al.*, 1997; Smith Fernandez *et al.*, 1998; Nieuwenhuys, 1998c; Striedter *et al.*, 1998; Striedter and Keefer, 2000; Puelles *et al.*, 2000). At this point, it seems most prudent to conclude simply that there are at least some lineage restriction compartments in the embryonic forebrain and that some of these coincide with spatially restricted patterns of gene expression. More detailed studies will be needed to determine the exact number of these compartments, their orientation with respect to the brain's long axis (Puelles *et al.*, 1987), and the details of how gene expression is related to lineage restriction. It also remains to be seen exactly how well conserved the forebrain's compartmental organization is between taxa (Wullimann and Puelles, 1999). Nonetheless, the modern cellular and molecular studies have confirmed that vertebrate brains are far more similar to one another at embryonic stages than later on (Bergquist and Källén, 1954).

Less certain is how the phylogenetic conservation of embryonic brain regions is reflected in the organization of adult brains. For example, the hindbrain neuromeres are somewhat ephemeral structures, bearing little obvious relation to adult morphology or function. Recent fate-mapping studies have shown that some embryonic neuromere boundaries later become coincident with the rostrocaudal boundaries of adult cell groups (Marín and Puelles, 1995; Díaz *et al.*, 1998), but it remains difficult, if not impossible, to identify any adult structural or functional features that are uniquely shared by the adult derivatives of a particular neuromere (Bass and Baker, 1997). This suggests that the hindbrain neuromeres are conserved not for their

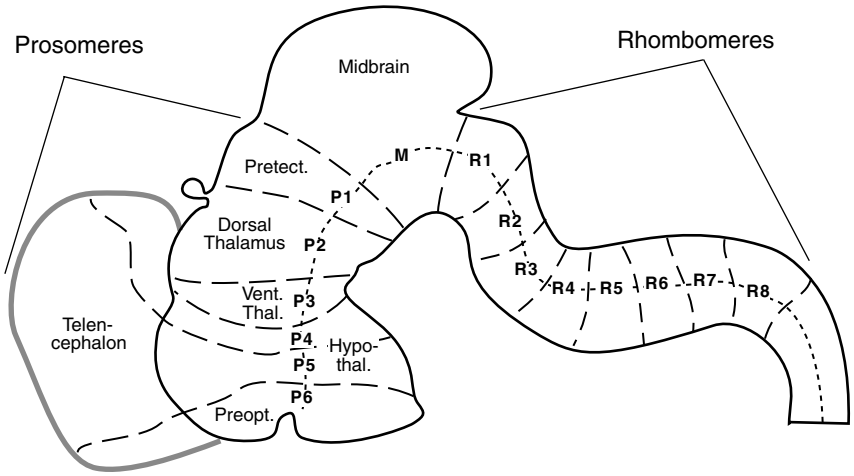

FIGURE 1.3 Schematic diagram of the neuromeric model of embryonic vertebrate brain organization (see Rubenstein *et al.*, 1994). Each neuromere can be thought of as a doughnut-shaped ring around the brain's longitudinal axis *(fine dotted line)*. The borders between adjacent neuromeres *(heavy dotted lines)* are thought to be sites of cell lineage restriction and correspond to the boundaries of some regulatory gene expression domains. The neuromeric model of brain organization conflicts with other models of brain organization (such as Herrick's four-tiered model of diencephalic organization), but several classically recognized brain divisions, such as the dorsal and ventral thalami, correspond quite well to the dorsal or ventral portions of one or more neuromeres. Hypothal, hypothalamus; M, mesomeres; P1 to P6, prosomeres; Preopt., preoptic area; Pretect., pretectum; R1 to R8, rhombomeres; Vent. Thal., ventral thalamus.

adult function but because they play an important role in hindbrain morphogenesis, possibly setting the stage for the later formation of other developmental compartments (see Davenne *et al.*, 1999). Indeed, a steadily growing amount of information indicate that brain compartmentalization is an ongoing process, generating successively smaller compartments and ultimately leading to the formation of functionally coherent adult cell groups (Redies and Takeichi, 1996; Redies, 2000). If this is correct, then a phylogenetic change in the development of early embryonic brain compartments may divert the course of subsequent morphogenesis in such a way that it leads to the phylogenetic repatterning of a major brain region in the adult. Such early developmental changes may, for example, underlie the radically divergent nature of telencephalic organization in teleost fishes, where the telencephalon everts rather than evaginates (Nieuwenhuys and Meek, 1990), and in sauropsids, where telencephalic development is dominated by the formation of several intraventricular ridges (Striedter, 1997). Moreover, whenever development diverges so dramatically, it may well be impossible to homologize the individual adult cell groups across the divergent taxa (Striedter, 1999). Finally, to the extent that early embryonic brain regions impart on their adult derivatives some shared adult features, one may be able to homologize higher level adult brain regions, e.g., the mammalian neocortex, even when it is not possible to homologize many of the constituent lower level characters, e.g., the individual neocortical areas (Northcutt and Kaas, 1995).

A second major approach to the study of brain development and evolution consists of trying to explain phylogenetic changes in the size of the adult brain, or of specific adult brain areas, in terms of phylogenetic changes in the dynamics of cell proliferation and neurogenesis. It is likely, for example, that phylogenetic differences in the onset and duration of neurogenesis (and hence in the amount of time during which neuronal precursors multiply exponentially; Caviness *et al.*, 1995; Takahashi *et al.*, 1997; Kornack and Rakic, 1998) can, in large measure, account for the enormous differences in adult brain size between small and large mammals (Stephan *et al.*, 1981). Moreover, the time of peak neurogenesis for any particular brain area is remarkably well correlated with the degree to which that brain area enlarges phylogenetically as overall brain size increases (Finlay and Darlington, 1995). This finding has led to the hypothesis that, as brain development is prolonged and overall brain size enlarged, the brain regions with relatively late neuronal "birthdates" (and hence relatively protracted periods of precursor proliferation) are constrained to enlarge much more than brain regions with relatively early neuronal birthdates (Finlay and Darlington, 1995). For example, since the most anterior and dorsal portions

of the embryonic brain are "born" after most of the other brain areas, the brain regions derived from these anterior dorsal portions of the neural tube should exhibit the proportionately greatest enlargement as overall brain size increases. Consistent with this hypothesis, mammalian neocortex derives from the most anterior and dorsal region of the embryonic brain, exhibits a relatively late and prolonged period of neurogenesis, and is enlarged disproportionately as overall brain size increases phylogenetically (Hofman, 1989; Finlay and Darlington, 1995; Finlay *et al.*, 1998). Finlay and Darlington's general theory is thus consistent with an impressive amount of correlative data, but many questions remain about the cellular mechanisms that control overall brain size and regional variations in the timing of neurogenesis.

The finding that brain areas enlarge in a rather predictable manner as overall brain size increases (Fig. 1.4) may mean that brain evolution is governed by developmental constraints that prevent brain regions from varying in size independently of one another (Finlay and Darlington, 1995). This "developmental constraint" hypothesis receives some support from the finding that, across 22 species of mammals, the area of neocortex devoted to corticospinal projections correlates more strongly with total neocortical area than with a variety of behavioral and ecological measures, including digital dexterity and hand–eye coordination (Nudo and Masterton, 1990a). On the other hand, the same data also reveal several important, and allometrically poorly predicted, species differences in areal distribution, density, and size of the corticospinal neurons (Nudo and Masterton, 1990a, b; Nudo *et al.*, 1995). Moreover, even in the dataset used by Finlay and Darlington, the sizes of the olfactory bulb and olfactory cortex are poorly correlated with overall brain size (Sacher, 1970; Gould, 1975; Stephan *et al.*, 1981). In fact, the developmental constraint hypothesis predicts the size of individual brain regions at best to within a factor of 2.5, which still leaves room for impressive regional differences in size.[4] Thus, the finding that the cerebellum is 45% larger than expected in apes than in monkeys (Rilling and Insel, 1998b) is consistent with the developmental constraint hypothesis, but it nonetheless suggests that the cerebellum develops and evolves somewhat independently of other brain regions. Finally, it remains unclear how well the developmental constraint hypothesis applies to nonmammals. For

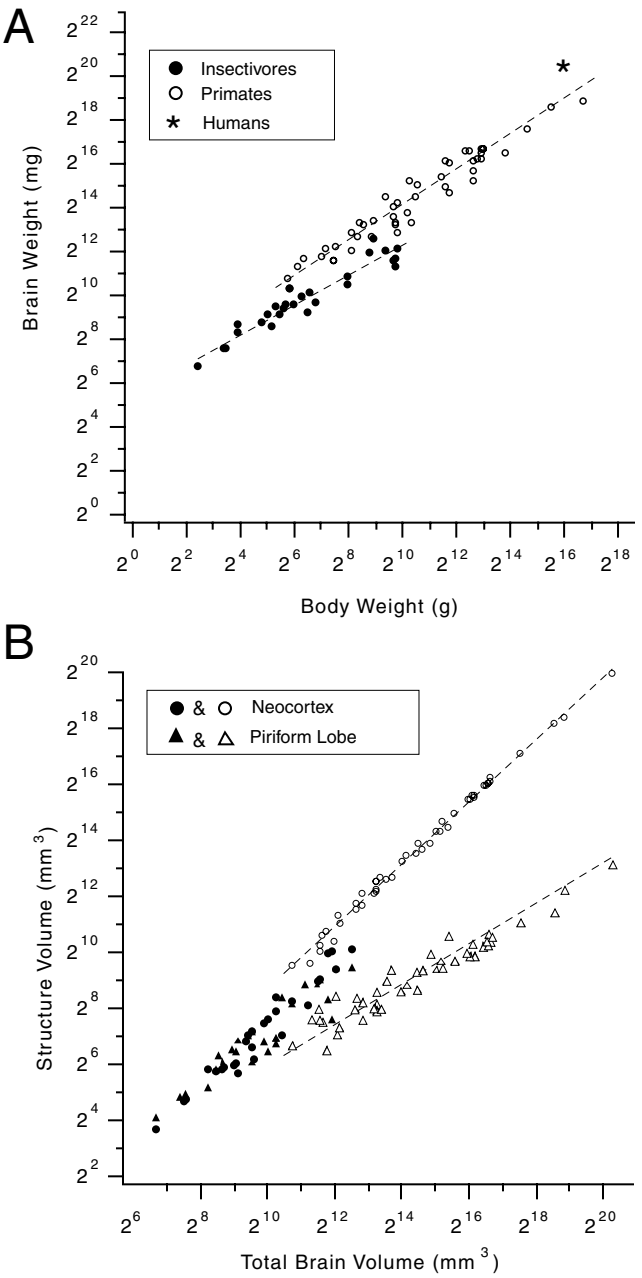

FIGURE 1.4 **(A)** Brain and body weight plotted for 27 insectivores and 47 primates on a log-log plot. The slopes of the regression lines are slightly less than 1, which means that relative brain weight decreases as body weight increases (i.e., negative allometry). It is interesting to note that primate brains are approximately twice as large as insectivore brains of equal body size and that human brains are approximately three times as large as would be expected for a typical primate of the same body size. **(B)** A log-log plot showing that the neocortex expands more quickly than the piriform lobe as total brain size increases, which means that large brains have proportionately more neocortex. As in (A), the solid symbols refer to data from insectivores while the open symbols are primate data points. The data used to generate both graphs were taken from Stephan *et al.* (1981).

[4]This expected range of size differences is based on Finlay and Darlington's two-factor model, considering both overall brain size and the size of the main olfactory bulb. The range would be even larger if overall brain size is used as the only factor in predicting the size of a specific brain region.

example, the cerebellar valvula in mormyrid teleosts is clearly expanded beyond any allometric expectations (Nieuwenhuys and Nicholson, 1969). In summary, then, developmental constraints can account reasonably well for phylogenetic changes in the relative size of many brain regions, particularly for mammals of vastly different body sizes, but they leave plenty of room for mosaic brain evolution, i.e., for changes in the size of individual brain regions that are relatively independent of changes in overall brain size.

A third major area of research into brain evolution and development consists of attempts to explain the evolution of neuronal circuits in terms of changes in axonal development and axon-mediated developmental interactions. It has been proposed, for example, that some phylogenetically new connections in adult animals (e.g., the postmammillary fornix projections in adult cats, rabbits, and, probably, elephants) may have evolved because axon collaterals that were developmentally transient in the ancestral condition became permanent during the course of evolution (Stanfield *et al.*, 1987). In addition, species differences in the adult size of some cell groups may be due to phylogenetic changes in the amount of naturally occurring developmental cell death, which in turn may be regulated by axon-mediated trophic interactions with other brain areas (Katz, 1982). Phylogenetic increases in the size of a particular muscle, for example, are likely to cause a phylogenetic increase in the size of the motor neuron population innervating that muscle by reducing the amount of naturally occurring, trophic factor–dependent cell death among those motor neurons (Holliday and Hamburger, 1976). Such trophic interactions might cascade throughout large portions of the nervous system (Wilczynski, 1984) but are likely to be buffered out quickly whenever neurons can derive trophic support from multiple sources, i.e., whenever neural connections diverge or converge (Finlay *et al.*, 1987). Finally, it is important to note that trophic cascades are affected by the phenomenon of compensatory innervation, in which a reduction in the size of one afferent projection causes a compensatory (and probably trophic factor–mediated) increase in the size of another projection or, in some cases, the sprouting of previously nonexistent projections (Katz *et al.*, 1981). Large neonatal midbrain lesions in hamsters or ferrets, for example, cause the sprouting of compensatory projections from the retina to auditory or somatosensory thalamic nuclei that were partially denervated by the lesions (Schneider, 1973; Frost, 1981; Sur *et al.*, 1988). This rerouting of visual information to normally nonvisual thalamic nuclei, in turn, leads to developmental changes in some (but not all) thalamocortical and intracortical connections (Pallas *et al.*, 1990; Gao and Pallas, 1999).

Most of what we know about how changes in development can alter adult brain organization comes from experimental lesion or transplantation studies, but there is some evidence that similar phenomena also occur naturally. The dorsal lateral geniculate nucleus of congenitally eyeless mice, for example, receives ascending somatosensory projections (Asanuma and Stanfield, 1990) and contains some types of synapses (Katz *et al.*, 1981) that are not usually found in normal mice, strongly suggesting that some kind of compensatory innervation has take place. Similar compensatory changes may have taken place also in blind mole rats (Heil *et al.*, 1991), but this remains controversial. According to the best available evidence, it appears that the enormous decrease in the size of the retina in blind mole rats is associated with a dramatic reduction in the size of the lateral geniculate nucleus, an elimination of the typically precise topography of the thalamocortical visual projection, and an expansion of the normal auditory and/or somatosensory thalamocortical systems (Necker *et al.*, 1992; Cooper *et al.*, 1993a; Rehkämper *et al.*, 1994). These differences in adult organization might have been predicted from what we know about trophic interactions between interconnected cell groups (Oppenheim, 1981), the activity-dependent fine tuning of topographical projections (Meyer, 1983), and cross-modal competitive interactions and compensation (Rauschecker *et al.*, 1992). Unexpectedly, however, the suprachiasmatic nucleus, which receives retinal input and controls the timing of circadian rhythms in most mammals, has remained relatively large in blind mole rats (Cooper *et al.*, 1993b). This fact is only surprising, however, if one assumes (1) that blind mole rats are truly blind, which is not true since they have rudimentary retinas that are required for the photic entrainment of their circadian rhythms (Pevet *et al.*, 1984), and (2) that the suprachiasmatic nucleus depends on its retinal input for trophic support, which is also likely to be incorrect because transplanted suprachiasmatic nucleus cells can survive even if they do not receive retinal afferents (Lehman *et al.*, 1995). Thus, the available data suggest that many of the neural features that distinguish blind mole rats from other, sighted rodents can be explained as secondary developmental consequences of an early embryonic reduction in retinal size.

Although a full synthesis of the developmental and phylogenetic data on brain organization has not yet been achieved, the examples reviewed above demonstrate that it is already possible to sketch out some mechanistic developmental explanations for at least some phylogenetic changes in brain organization. In addition, one can begin to discern a few fairly general rules about how brain development and evolution

relate to one another. For example, neuronal cell groups that receive trophic support via a limited set of axonal connections should be more phylogenetically labile than those that either do not depend on other cell groups for trophic support or have a large number of different inputs and outputs (Finlay *et al.*, 1987; Striedter, 1990a, b). Furthermore, as brain size increases phylogenetically, the proportions of the various brain regions to one another should change dramatically (largely in accordance with allometric predictions) and this, in turn, should alter the outcome of at least some competitive interactions during axonal development, thereby leading to potentially major phylogenetic changes in neural circuitry (Deacon, 1990a). More generally, this realization implies that neural connections should be more phylogenetically labile than the cell groups they interconnect (Striedter, 1992) and that superficially similar brains, which appear in Nissl stains to differ only in the relative size of homologous cell groups, may nonetheless differ significantly in terms of neural circuitry and functional organization. Armed with these insights, and with the tools of modern evolutionary neurobiology for reconstructing phylogenetic change, one can again approach the question originally posed by Owen and Huxley: how did human brains change during the course of hominid evolution?

EVOLUTION OF UNIQUELY HUMAN BRAINS

Comparisons between humans and other animals always involve both similarities and differences. Among evolutionary biologists interested in behavior, there is a long tradition of highlighting the similarities between human and animal behavior (Romanes, 1881; Wilson, 1975), but many differences also stand out. Clearly, only humans sit around the fire (or dinner table) to tell each other jokes and stories about past glories or future plans, and only a human would eagerly read what Owen wrote about primate brains 140 years ago. Moreover, only humans use general engineering skills to overcome environmental challenges that other animals can solve solely through evolution by natural selection. These are, of course, merely some of the major differences between human and animal behavior, but they suffice to pique one's interest in the general question of how human brains differ from those of other animals and how these neuroanatomical differences might relate to the known differences in behavior. In the following paragraphs I will review some of what we know about (1) phylogenetic size increases in human brains, (2) the existence of uniquely human neuroanatomical features, (3) phylogenetic changes in the relative proportions of various brain areas in primates, and (4) the possibility of major connectional and functional changes in human brain evolution. Given the limitations of space and my own expertise, I offer not a complete review of the relevant literature but merely an outline of how one might begin to untangle the mysteries of human brain evolution. I have also omitted from this discussion any speculations about the selective pressures or chance events that might explain *why* human brains evolved their particular anatomical or behavioral features (Gould and Lewontin, 1979; Lauder, 1996).

Although it is generally accepted that humans have the largest brains among vertebrates, absolute brain size is actually much greater in elephants and many whales than it is in humans (5–10 kg for whales and elephants, 1.4 kg on average for humans; van Dongen, 1998). Even relative to overall body size, human brains do not come out at the "top of the scale" because the brain comprises only about 2% of the body's weight in adult modern humans, but more than 3% in mormyrid teleosts and nearly 10% in adult mice (Stephan *et al.*, 1981; Nilsson, 1996). Indeed, the only way to become convinced that humans have uniquely enlarged brains is to plot brain size versus body size for a large number of species, to realize that relative brain size decreases predictably as body size increases, and then to note that the relative brain size of humans significantly exceeds the value predicted from that negative allometric relationship (Fig. 1.5A). Using this kind of allometric analysis, it becomes apparent that the brain is approximately twice as large in primates as in other mammals of similar body size and that the brain of modern humans is roughly three times larger than expected from an analysis of other primates (Passingham, 1982). Human brains should really be housed in bodies the size of King Kong (Deacon, 1990a). Analysis of the hominid fossil record indicates that relative brain size increased rather late in hominid evolution (approximately 2–3 million years ago) and that this increase was not due to a phylogenetic reduction of body size, which actually increased considerably during hominid evolution (Tobias, 1973; Hofman, 1983; Wolpoff, 1999). In developmental terms, the phylogenetic increase in human brain size is due primarily to the fact that in humans the brain grows at the high (primate typical) fetal growth rate for a much longer time than it does in other primates (Fig. 1.5B; Count, 1947; Passingham, 1985; Deacon, 1990c). Thus, Owen's original hypothesis that human brains are larger than those of apes because they grow for a longer period (Owen, 1859) has been substantiated by modern research. It is likely, however, that additional mechanisms also contribute to the

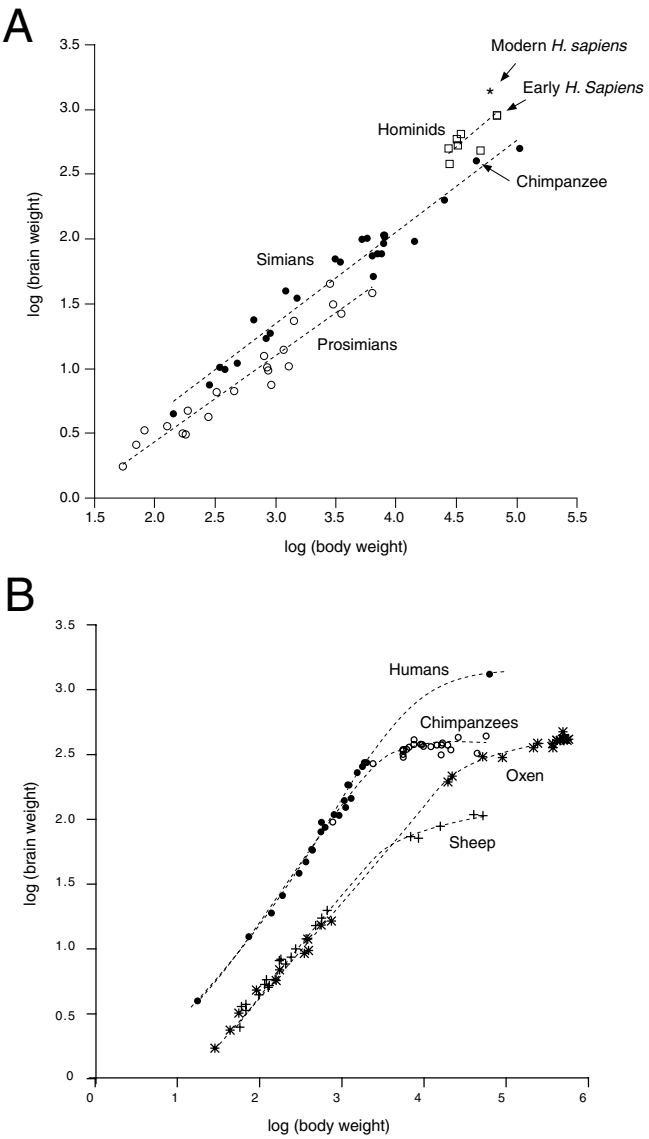

FIGURE 1.5 **(A)** Log-log plot of brain versus body weight for various primates, showing that simians (monkeys and apes) tend to have larger brains than prosimians of similar body weight, that hominids tend to have larger brains than simians, and that relative brain size has increased again in modern *Homo sapiens*. The data used to generate this plot were taken from Stephan et al. (1981) and Wolpoff (1999). **(B)** An analysis of brain development reveals that human brains grow at the nearly exponential rate typical of fetal brain growth for a longer period of time than do chimpanzee brains. The data also show that primate brains are already significantly larger than sheep or ox brains at very early stages of embryonic development. These data are from Count (1947).

phylogenetic increase in human brain size, for brain cell density appears to be higher in humans than in macaques at early embryonic stages (Widdowson, 1981).

Given that human brains have increased in terms of both absolute and relative size, many investigators have wondered whether human brains possess some regions or features that are not found in smaller brains. The classic comparative cytoarchitectonic studies of Brodmann and others (e.g., Brodmann, 1909; see Chapter 27) already suggested that primates have a greater number of distinct neocortical areas than most nonprimates, and this has been confirmed in modern studies. Specifically, it appears that the principal sensory and motor areas are highly conserved across mammals, but that many higher order cortical areas are more difficult to homologize between primates and other mammals (Kaas, 1987). The developmental mechanisms underlying this phylogenetic increase in the number of cortical areas remain controversial, but probably involve interactions between dorsal thalamic afferents, intracortical axons, and enlarged cortical precursor regions that cause embryonic regions to differentiate into a greater number of adult cortical areas than were present in the ancestral condition (Kaas, 1989; Killackey, 1990; Krubitzer, 1995; Striedter, 1998b). Whatever the mechanistic details, it is clear that many neocortical areas cannot be homologized in a one-for-one manner between primates and other mammals (Kaas, 1983), particularly when one compares primates and cats, which have independently evolved elaborate visual systems with many neocortical areas (Sereno and Allman, 1991). Turning to comparisons between humans and other primates, Brodmann and others identified several cortical areas in the human frontal, temporal, and parietal lobes, including the famous "language areas" of Broca and Wernicke, that did not appear to have homologues in nonhuman primates (Brodmann, 1909). However, these claims were gradually eroded by later investigators who showed that homologues of the human language areas probably do exist in at least some nonhuman primates (Deacon, 1992; Aboitiz and Garciá, 1997) and, more generally, that human and anthropoid monkey cortices are remarkably similar to one another in terms of cytoarchitectural organization (Galaburda and Pandya, 1983; Petrides and Pandya, 1999; to see how similar prefrontal cortex is between rhesus monkeys and humans, refer to Chapter 25). The currently available data therefore suggest that the phylogenetic increase in overall brain size during hominid evolution was not associated with a dramatic increase in the number of distinct brain regions.

Although humans probably evolved very few truly "new" brain areas (or neuronal cell types, but see Nimchinsky *et al.*, 1999; Preuss *et al.*, 1999), several regions in the human brain clearly differ from their ape homologues in terms of relative size. Most strikingly, human brains contain 15–24% more neocortical gray matter (and 22% more neocortical white matter) than would be expected for nonhuman primate brains of

equal size (Rilling and Insel, 1999b). Interestingly, this phylogenetic size increase affects some neocortical regions more than others. For example, primary visual cortex, constitutes an unexpectedly small percentage of the human neocortex (although it is roughly as large as would be expected given human body and retinal size; Passingham, 1973; Holloway, 1979). Prefrontal cortex, on the other hand, is enlarged significantly in human brains. This finding has been challenged repeatedly (Uylings and van Eden, 1990; Semendeferi et al., 1997), but a careful application of allometric techniques and cytoarchitectonic criteria suggests that, indeed, prefrontal cortex is approximately twice as large in humans as would be expected for nonhuman primates with a neocortex of equal size (Passingham, 1973; Deacon, 1997). This interpretation is further supported by the finding that human prefrontal cortex is significantly more complexly folded than would be expected from the study of nonhuman primates (Zilles *et al.*, 1989; Rilling and Insel, 1999b). In addition, it is likely that some portions of the parietal and temporal lobes, several dorsal thalamic nuclei, the cerebellar hemispheres, and several brain regions directly connected to the cerebellum are also unexpectedly large in humans (Holloway, 1972; Passingham, 1973; Armstrong, 1982; Rilling and Insel, 1998b). Many of these conclusions remain debatable, however, due to a dearth of quantitative data and/or difficulties associated with the allometric analyses (Deacon, 1990b, c). Finally, it may be noted that one supposed hallmark of human brain organization, namely, the bilateral asymmetry in the size of the language-related planum temporale, has now been observed also in the brains of chimpanzees and other great apes (Gannon *et al.*, 1998; Hopkins *et al.*, 1998).

The observed changes in the relative sizes of homologous brain areas between humans and other primates may seem to be of minor importance, given that new brain areas have evolved repeatedly during vertebrate evolution, but they are likely to be associated with functionally significant changes in neuronal connectivity. It has been argued, for example, that the phylogenetic expansion of neocortex inevitably leads to a reduction in the degree of neocortical interconnectedness (Frahm *et al.*, 1982; Stevens, 1989; Deacon, 1990a; Ringo, 1991), a hypothesis that is supported by the finding that during primate evolution increases in neocortical white matter outpace increases in gray matter much less than would be expected if interconnectedness remained constant (Frahm *et al.*, 1982; Rilling and Insel, 1999a, b). In addition, changes in the relative size of brain areas are likely to be associated with changes in the size of the related afferent and efferent pathways, and changes in the relative sizes of these pathways are likely to (1) alter the balance of functional interactions between adult brain areas, leading to changes in the relative importance of particular brain areas for some behaviors, and (2) bias the outcome of competitive interactions during axonal development in such a way that some connections are completely lost while others appear *de novo* (Deacon, 1990a). These hypotheses are supported by the observation that the enlarged prefrontal cortex in humans probably has connections that are not present in other primates, including important connections to the midbrain and medullary vocal control areas (Deacon, 1989, 1992). Just as the prefrontal cortex thus appears to have become "co-opted" into the machinery for vocal communication in humans, so other neocortical areas in humans may have become necessary for the performance of behaviors that are less dependent on the neocortex in other mammals. However, such apparent shifts in neural function toward the neocortex, sometimes referred to as "neocorticalization," remain poorly understood. Perhaps the best studied case of neocorticalization involves the corticospinal tract, which projects more strongly to spinal motor neurons in primates than in other mammals (Heffner and Masterton, 1975) and is both larger and functionally more important in humans than in other primates (Lawrence and Kuypers, 1968; Heffner and Masterton, 1983). Interestingly, this increase in the functional importance of the corticospinal tract in humans appears to be accompanied by the phylogenetic elimination of the rubrospinal tract, which is prominent and important for motor control in most other mammals (Voogd *et al.*, 1990, and Voogd, Chapter 11).

The behavioral correlates of the neuroanatomical differences between humans and apes are difficult to assess with rigor. The phylogenetic enlargement of the human brain has frequently been interpreted as an indication of increased intelligence (Jerison, 1973), but this hypothesis has been difficult to confirm in detail (Holloway, 1974), largely because it is so difficult (if not impossible) to define "general intelligence" (Macphail, 1982). Overall brain size has also been linked to life span (Sacher, 1973; Allman *et al.*, 1993), metabolic rate (Armstrong, 1985), social complexity (Byrne and Whiten, 1988), diet and home range (Clutton-Brock and Harvey, 1980). Unfortunately, all of these interpretations involve at least some questionable assumptions and are difficult to separate (van Dongen, 1998). Some of these difficulties may be avoided by searching for more specific correlations between structure and function. It is likely, for example, that the fine digital dexterity and power grip of humans are due to specific phylogenetic changes in the human corticospinal tract (Heffner and Masterton, 1983). Similarly, the phylogenetic co-option

of prefrontal cortex into the vocal control system probably facilitated the emergence of symbolic language during hominid evolution (Deacon, 1997). More generally, it seems reasonable to speculate that the phylogenetic enlargement of the prefrontal cortex in modern humans has enhanced their ability to inhibit automatic responses, form symbolic representations of external objects, monitor the contents of working memory, and plan future courses of action (see Owen *et al.*, 1996, 1999; Deacon, 1997). Clearly, however, even these conjectures will have to be made more specific in terms of both anatomical and behavioral differences or similarities. To this end, it will be important to perform comparable functional imaging studies in both humans and apes and to develop ever better methods for tracing neuronal pathways in human brains (e.g., Conturo *et al.*, 1999).

CONCLUSIONS

Students of brain evolution have traditionally emphasized either the discontinuity between brains of different species or their fundamental similarities in structural organization. Thus, the early, pseudo-Darwinian view that brain evolution proceeds linearly along a phylogenetic scale (Bowler ,1988), driven by the steady accretion of novel parts, gradually gave way to the view that all vertebrate brains are constructed according to a common plan, implying that vertebrate brains consist mostly of homologous parts (Kuhlenbeck, 1967–77; Northcutt, 1981; Butler and Hodos, 1996; Nieuwenhuys *et al.*, 1998). Faith in the conservative nature of brain evolution should not be carried too far, however, because many adult brain structures cannot be homologized across all vertebrates and telencephalic organization, in particular, differs dramatically between major taxa (Northcutt, 1981; Striedter, 1997, 1999). In mammals, the neocortex does exhibit some highly conserved anatomical features (Rockel *et al.*, 1980; but see Skoglund *et al.*, 1996). However, new neocortical areas and features have evolved in several mammalian lineages, and it is probably wishful thinking to argue that rat neocortex is a good model for most aspects of human neocortical structure or function (Kolb and Tees, 1990; see Preuss, 1995). In contrast, the brains of apes, seem remarkably similar to human brains in terms of gross structure and cytoarchitectural organization. For example, the rhesus monkey atlas of Paxinos *et al.* (2000) displays the same prefrontal cortical areas as can be found in human brain maps. Yet it is important to remember that we still know relatively little about the details of human (or, for that matter, ape) neuroanatomy (see Preuss, 1995, in press) and that some of the relative size differences between human and ape brains are probably associated with significant, and as yet unknown, phylogenetic changes in neuronal connections and functional organization.

In summary, it seems fair to say that the goal of explaining human uniqueness in terms of species differences in brain development and adult structure appears increasingly attainable, particularly as new data emerge on human and primate brain organization (e.g., Rilling and Insel, 1999a, b). It is appropriate, therefore, to close this chapter with a quote from the much maligned, yet rarely read, Owen, who clearly shared this ambition when he wrote:

> The long-continued growth and superior size of the human brain, more especially the superior relative size of the cerebral hemispheres and their numerous deep and complex convolutions, are associated with psychical powers, compensating for and permitting the absence of natural weapons of offence and defence; they are corelated with those modifications of the lower limbs which free the upper ones from any call to serve the body in the way of moving and supporting it, and leave them at the command of the intellect, for such purposes, in the fabrication of clothing, weapons, etc., as it may energize upon according to its measure of activity in the individual.
> (Owen, 1859, p. 270).

References

Aboitiz, F., and Garciá, R. (1997). The evolutionary origin of the language areas in the human brain. A neuroanatomical perspective. *Brain Res. Rev.* **25,** 381–396.

Alberch, P. (1980). Ontogenies and morphological diversification. *Amer. Zool.* **20,** 653–667.

Allman, J., McLaughlin, T., and Hakeem, A. (1993). Brain weight and life-span in primate species. *Proc. Natl. Acad. Sci.* **90,** 118–122.

Alvarez-Bolado, G., Rosenfeld, M. G., and Swanson, L. W. (1995). Model of forebrain regionalization based on spatiotemporal patterns of POU-III homeobox gene expression, birthdates, and morphological features. *J. Comp. Neurol.* **355,** 237–295.

Armstrong, E. (1982). Mosaic evolution in the primate brain: differences and similarities in the hominoid thalamus. *In* "Primate brain evolution" (E. Armstrong and D. Falk, Eds.), pp. 131–161, Plenum, New York.

Armstrong, E. (1985). Relative brain size in monkeys and prosimians. *Am. J. Phys. Anthropol.* **66,** 263–273.

Asanuma, C., and Stanfield, B. B. (1990). Induction of somatic-sensory inputs to the lateral geniculate nucleus in congenitally blind mice and in phenotypically normal mice. *Neurosci.* **39,** 533–545.

Bass, A. H., and Baker, R. (1997). Phenotypic specification of hindbrain rhombomeres and the origins of rhythmic circuits in vertebrates. *Brain Behav. Evol.* **50** (suppl 1), 3–16.

Bauchot, R., Randall, J. E., Ridet, J.-M., and Bauchot, M.-L. (1989). Encephalization in tropical teleost fishes and comparison with their mode of life. *J. Hirnforsch.* **30,** 645–669.

Bemis, W. E. (1984). Paedomorphosis and the evolution of the Dipnoi. *Paleobiol.* **10,** 293–307.
Bergquist, H., and Källén, B. (1954). Notes on the early histogenesis and morphogenesis of the central nervous system in vertebrates. *J. Comp. Neurol.* **100,** 627–659.
Bowler, J. P. (1988). "The non-Darwinian revolution: reinterpreting a historical myth." Johns Hopkins University Press, Baltimore.
Brodmann, K. (1909). "Vergleichende Lokalisationslehre der Grosshirnrinde in ihren Prinzipien dargestellt auf Grund des Zellenbaues." Barth, Leipzig.
Butler, A. B., and Hodos, W. (1996). "Comparative vertebrate neuroanatomy." Wiley-Liss, New York.
Byrne, R. W., and Whiten, A., Eds. (1988). "Machiavellian intelligence: social expertise and the evolution of intellect in monkeys, apes and humans." Oxford University Press, Oxford.
Campbell, C. B. G., and Hodos, W. (1991). The *scala naturae* revisited: evolutionary scales and anagenesis in comparative psychology. *J. Comp. Psych.* **105,** 211–221.
Cartmill, M. (1990). Human uniqueness and theoretical content in paleoanthropology. *Int. J. Primatol.* **11,** 173–192.
Caviness, V. S. J., Takahashi, T., and Nowakowski, R. S. (1995). Numbers, time and neocortical neuronogenesis: a general developmental and evolutionary model. *Trends Neurosci.* **18,** 379–383.
Clutton-Brock, T. H., and Harvey, P. H. (1980). Primates, brains and ecology. *J. Zool. Lond.* **190,** 309–323.
Conturo, T. E., Lori, N. F., Cull T. S., Akbudak, E., Snyder A. Z., Shimony, J. S., McKinstry, R. C., Burton, H., and Raichle, M. E. (1999). Tracking neuronal fiber pathways in the living human brain. *Proc. Natl. Acad. Sci. USA* **96,** 10422–10427.
Cooper, H. M., Herbin, M., and Nevo, E. (1993a). Visual system of a naturally micropthalmic mammal: the blind mole rat, *Spalax ehrenbergi*. *J. Comp. Neurol.* **328,** 313–350.
Cooper, H. M., Herbin, M., and Nevo, E. (1993b). Ocular regression conceals adaptive progression of the visual system in a blind subterranean mammal. *Nature* **361,** 156–159.
Cosans, C. (1994). Anatomy, metaphysics, and values: the ape brain debate reconsidered. *Biology and Philosophy* **9,** 129–165.
Count, E. W. (1947). Brain and body weight in man: their antecedents in growth and evolution. *Ann. N.Y. Acad. Sci.* **46,** 993–1122.
Darwin, C. R. (1859). "On the origin of species by means of natural selection." Murray, London.
Davenne, M., Maconochie, M. K., Neun, R., Pattyn, A., Chambon, P., Krumlauf, R., Rijli, F. M. (1999). *Hoxa*2 and *Hoxb*2 control dorsoventral patterns of neuronal development in the rostral hindbrain. *Neuron* **22,** 677–691.
Deacon, T. W. (1989). The neural circuitry underlying primate calls and human language. *Human Evol.* **4,** 367–401.
Deacon, T. W. (1990a). Rethinking mammalian brain evolution. *Amer. Zool.* **30,** 629–705.
Deacon, T. W. (1990b). Fallacies of progression in theories of brain-size evolution. *Int. J. Primatol.* **11,** 193–236.
Deacon, T. W. (1990c). Problems of ontogeny and phylogeny in brain size evolution. *Int. J. Primatol.* **11,** 237–282.
Deacon, T. W. (1992). Cortical connections of the inferior arcuate sulcus cortex in the macaque brain. *Brain Res.* **573,** 8–26.
Deacon, T. W. (1997). "The symbolic species: the coevolution of language and the brain." Norton, New York.
de Beer, G. (1958). "Embryos and Ancestors." Oxford University Press, London.
Desmond, A. (1994). "Huxley: from Devil's disciple to evolution's high priest." Addison-Wesley, Reading, Mass.
Díaz, C., Puelles, L., Marín, F., and Glover, J.C. (1998). The relationship between rhombomeres and vestibular neuron populations as assessed in quail-chicken chimeras. *Dev. Biology* **202,** 14–28.
Ebbesson, S. O. E. (1984). Evolution and ontogeny of neural circuits. *Behav. Brain Sci.* **7,** 321–366.
Edinger, L. (1908). "Vorlesungen über den Bau der Nervösen Zentralorgane des Menschen und der Tiere - für Ärzte und Studierende." Vogel Verlag, Leipzig.
Eisenberg, J. F. (1981). "The Mammalian Radiations." Chicago, University of Chicago Press.
Eldredge, N., and Cracraft, J. (1980). "Phylogenetic patterns and the evolutionary process." Columbia University Press, New York,.
Elliot Smith, G. (1910). Some problems relating to the evolution of the brain. *The Lancet* **88,** 1–6.
Figdor, M. C., and Stern, C. D. (1993). Segmental organization of embryonic diencephalon. *Nature* **363,** 630–634.
Finlay, B. L., and Darlington, R. B. (1995). Linked regularities in the development and evolution of mammalian brains. *Science* **268,** 1577–1584.
Finlay, B. L., Hersman, M. N., and Darlington, R. B. (1998). Patterns of vertebrate neurogenesis and the paths of vertebrate evolution. *Brain Behav. Evol.* **52,** 232–242.
Finlay, B. L., Wikler, K. C., and Sengelaub, D. R. (1987). Regressive events in brain development and scenarios for vertebrate evolution. *Brain Behav. Evol.* **30,** 102–117.
Frahm, H. D., Stephan, H., and Stephan, M. (1982). Comparison of brain structure volumes in insectivora and primates. I. Neocortex. *J. Hirnforsch.* **23,** 375–389.
Fraser, S., Keynes, R., and Lumsden , A. (1990). Segmentation in the chick embryo hindbrain is defined by cell lineage restrictions. *Nature* **344,** 431–435.
Frost, D. O. (1981). Orderly anomalous retinal projections to the medial geniculate, ventrobasal and lateral posterior nuclei of the hamster. *J. Comp. Neurol.* **203,** 227–256.
Galaburda, A. M., and Pandya, D. N. (1983). The intrinsic, architectonic and connectional organization of the superior temporal region of the rhesus monkey. *J. Comp. Neurol.* **221,** 169–184.
Gannon, P. J., Holloway, R. L., Broadfield, D. C., and Braun, A. R. (1998). Asymmetry of chimpanzee planum temporale: humanlike pattern of Wernicke's brain language area homologue. *Science* **279,** 220–222.
Gao, W.-J., and Pallas, S. L. (1999). Cross-modal reorganization of horizontal connectivity in auditory cortex without altering thalamocortical projections. *J. Neurosci.* **19,** 7940–7950.
Garstang, W. (1922). The theory of recapitulation: a critical restatement of the biogenetic law. *Zool. J. Linn. Soc. London* **35,** 81–101.
Gilland, E., and Baker, R. (1993). Conservation of neuroepithelial and mesodermal segments in the embryonic vertebrate head. *Acta Anat.* **148,** 110–123.
Glezer, I. I., Jacobs, M. S., and Morgane, P. J. (1988). Implications of the "initial" brain concept for brain evolution in cetacea. *Behav. Brain. Sci.* **11,** 75–116.
Gould, S. J. (1975). Allometry in primates, with emphasis on scaling and evolution of the brain. *Contrib. Primat.* **5,** 244–292.
Gould, S. J. (1977). "Ontogeny and phylogeny." Harvard University Press, Cambridge.
Gould, S. J., and Lewontin, R. C. (1979). The spandrels of San Marco and the Panglossian paradigm: a critique of the adaptationist programme. *Proc. Roy. Soc. Lond. Ser. B* **205,** 581–598.
Guthrie, S. (1995). The status of the neural segment. *Trends Neurosci.* **18:** 74–79.
Haeckel, E. (1889). "Natürliche Schöpfungsgeschichte." Georg Reimer, Berlin.
Hall, B. K. (1994) "Homology: the hierarchical basis of comparative biology." Academic Press, San Diego.
Heffner, R., and Masterton, B. (1975). Variation in form of the pyramidal tract and its relationship to digital dexterity. *Brain Behav. Evol.* **12,** 161–200.
Heffner, R. S., and Masterton, R. B. (1983). The role of the corticospinal

tract in the evolution of human digital dexterity. *Brain Behav. Evol.* **23,** 165–183.
Heil, P., Bronchti, G., Wollberg, Z., and Scheich, H. (1991). Invasion of visual cortex by the auditory system in the naturally blind mole rat. *NeuroReport* **2,** 735–738.
Hennig, W. (1966). "Phylogenetic systematics." University of Illinois Press, Urbana.
Herrick, C. J. (1948). "The brain of the tiger salamander." University of Chicago Press, Chicago.
Hile, A. G., Plummer, T. K., and Striedter, G. F. (2000) Male vocal imitation produces call convergence during pair-bonding in budgerigars *(Melopsittacus undulatus). Anim. Behav.* **59,** 1209–1218.
Hodos, W., and Campbell, C. B. G. (1969). *Scala naturae:* why there is no theory in comparative psychology. *Psychol. Review* **76,** 337–350.
Hofman, M. A. (1983). Encephalization in hominids: evidence for the model of punctuationalism. *Brain Behav. Evol.* **22,** 102–117.
Hofman, M. A. (1989). On the evolution and geometry of the brain in mammals. *Prog. Neurobiol.* **32,** 137–158.
Holliday, M., and Hamburger, V. (1976). Reduction of naturally occurring motoneuron loss by enlargement of the periphery. *J. Comp. Neurol.* **170,** 311–320.
Holloway, R. L. (1972). Australopithecine endocasts, brain evolution in the hominoidea, and a model of hominid evolution. *In* "The functional and evolutionary biology of primates" (R. Tuttle, Ed.), pp. 185–203, Aldine-Atherton, Chicago.
Holloway, R. L. (1974). On the meaning of brain size. *Science* **184,** 677–679.
Holloway, R. L. (1979). Brain size, allometry, and reorganization: toward a synthesis. *In* "Development and evolution of brain size" (M. E. Hahn, C. Jensen, and B. C. Dudek, Eds.), pp. 59–88, Academic Press, New York.
Hopkins, W. D., Marino, L., Rilling, J. K., and MacGregor, L. A. (1998) Planum temporale asymmetries in great apes as revealed by magnetic resonance imaging (MRI). *NeuroReport* **9,** 2913–2918.
Huxley, J. S. (1942). "Evolution: the modern synthesis." Harper, New York.
Huxley, T. H. (1863). "Man's place in nature." University of Michigan Press, Ann Arbor.
Janik, V. M. (2000) Whistle matching in wild bottlenose dolphins *(Tursiops truncatus). Science* **289,** 1355–1357.
Jerison, H. J. (1973). "Evolution of the brain and intelligence." Academic Press, New York.
Kaas, J. H. (1983). What, if anything, is S1? Organization of first somatosensory area of cortex. *Physiol. Re.v* **63,** 206–231.
Kaas, J. H. (1987). The organization of neocortex in mammals: implications for theories of brain function. *Ann. Rev. Psychol.* **38,** 129–151.
Kaas, J. H. (1989). The evolution of complex sensory systems in mammals. *J. Exp. Biol.* **146,** 165–176.
Kappers, C. U. A., Huber, C. G., and Crosby, E. C. (1936). "Comparative anatomy of the nervous system of vertebrates, including man." Macmillan, New York.
Karten, H. J. (1969). The organization of the avian telencephalon and some speculations on the phylogeny of the amniote telencephalon. *Ann. N.Y.Acad. Sci.* **167:** 164–179.
Katz, M. J. (1982). Ontogenetic mechanisms: the middle ground of evolution. *In* "Evolution and Development" (J. T. Bonner, Ed.), pp. 207–212, Springer Verlag, Berlin.
Katz, M. J., Lasek, R. J., and Kaiserman-Abramof, I. R. (1981). Ontophyletics of the nervous system: eyeless mutants illustrate how ontogenetic buffer mechanisms channel evolution. *Proc. Natl. Acad. Sci. USA* **78,** 397–401.
Killackey, H. P. (1990). Neocortical expansion: an attempt toward relating phylogeny and ontogeny. *J. Cog. Neurosci.* **2,** 1–17.
Kirsch, J. A. W., and Johnson , J. I. (1983). Phylogeny through brain traits: trees generated by neural characters. *Brain Behav. Evol.* **22,** 60–69.
Kirsch, J. A. W., Johnson, J. I., and Switzer, R.C. (1983). Phylogeny through brain traits: the mammalian family tree. *Brain Behav. Evol.* **22,** 70–74.
Kolb, B., and Tees, R. C. (1990). The rat as a model of cortical function. *In* "The cerebral cortex of the rat" (B. Kolb and R. C. Tees, Eds.), pp. 3–17, MIT Press, Cambridge, Mass.
Kornack, D. R. and P. Rakic (1998). Changes in cell-cycle kinetics during the development and evolution of primate neocortex. *Proc. Natl. Acad. Sci. (USA)* **95,** 1242–1246.
Krubitzer, L. (1995). The organization of neocortex in mammals: are species differences really so different? *Trends Neurosci.* **18,** 408–417.
Kuhlenbeck, H. (1967–77). "The Central Nervous System of Vertebrates." Karger A.G. and Academic Press, Basel and New York.
Lauder, G. V. (1996). The argument from design. *In* "Adaptation" (G. V. Lauder and M. R. Rose, Eds.), pp. 55–91, Academic Press, San Diego.
Lauder, G. V., and Liem, K. F. (1983). The evolution and interrelationships of the actinopterygian fishes. Bull. Mus. Comp. Zool., **150,** 95–197.
Lawrence, D. G., and Kuypers, H. G. J. M. (1968). Functional organization of the motor system in the monkey. II. The effect of bilateral pyramidal lesions. *Brain* **91,** 1–14.
Lehman, M. N., Lesauter, J., Kim, C., Berriman, S. J. , Tresco, P. A., and Silver, R. (1995). How do fetal grafts of the suprachiasmatic nucleus communicate with the host brains? *Cell Transplantation* **4,** 75–81.
Lorenz, K. (1996). "The natural science of the human species: an introduction to comparative behavioral research; the "Russian Manuscript" (1944–1948)." The MIT Press, Cambridge.
Lumsden, A., and Krumlauf, R. (1996). Patterning the vertebrate neuraxis. *Science* **274,** 1109–1114.
MacLean, P. D. (1990). "The triune brain in evolution: role in paleocerebral functions." Plenum Press, New York.
Macphail, E. M. (1982). "Brain and intelligence in vertebrates." Clarendon Press, Oxford.
Marín, F., and Puelles, L. (1995). Morphological fate of rhombomeres in quail/chick chimeras: a segmental analysis of hindbrain nuclei. *Europ. J. Neurosci.* **7,** 1714–1738.
Marino, L. (1998) A comparison of encephalization between odontocete cetaceans and anthropoid primates. *Brain, Behav. Evol.* **51,** 230–238 [erratum: *Brain, Behav. Evol.* **52,** 22].
McCowan, B., and Reiss, D. (1997). Vocal learning in captive bottlenose dolphins: a comparison with humans and non-human animals. *In* "Social influences on vocal development" (C. T. Snowdon and M. Hausberger, Eds.), pp. 178–207, Cambridge Univ. Press, Cambridge.
Meyer, R. L. (1983). Tetrodotoxin inhibits the formation of refined retinotopography in goldfish. *Dev. Brain Res.* **6,** 293–298.
Miller K. (1999) "Finding Darwin's God: a scientist's search for common ground between God and evolution." Cliff Street Books, New York.
Necker, R., Rehkämper, G., and Nevo, E. (1992). Electrophysiological mapping of body representation in the cortex of the blind mole rat. *NeuroReport* **3,** 505–508.
Nieuwenhuys, R. (1994). Comparative neuroanatomy: place, principles, practice and programme. *Europ. J. Morphol.* **32,** 142–155.
Nieuwenhuys, R., ten Donkelaar, H. J., and Nicholson, C. (1998). "The central nervous system of vertebrates." Springer Verlag, Berlin.
Nieuwenhuys, R. (1998a). The coelacanth *Latimeria chalumnae. In* "The central nervous system of vertebrates." (R. Nieuwenhuys,

H. J. ten Donkelaar, and C. Nicholson, Eds.), pp. 1007–1043, Springer Verlag, Berlin.

Nieuwenhuys, R. (1998b). Lungfishes. *In* "The central nervous system of vertebrates" (R. Nieuwenhuys, H. J. ten Donkelaar, and C. Nicholson, Eds.), pp. 939–1006, Springer Verlag, Berlin.

Nieuwenhuys, R. (1998c). Morphogenesis and general structure. *In* "The central nervous system of vertebrates" (R. Nieuwenhuys, H. J. ten Donkelaar, and C. Nicholson, Eds.), pp. 159–229, Springer Verlag, Berlin.

Nieuwenhuys, R., and Meek, J. (1990). The telencephalon of actinopterygian fishes. *In* "Cerebral cortex" (E. G. Jones and A. Peters, Eds.), Vol. 8A, pp. 31–73, Plenum Press, New York.

Nieuwenhuys, R., and Nicholson, C. (1969). A survey of the general morphology, the fiber connections, and the possible functional significance of the gigantocerebellum of mormyrid fishes. *In* "Neurobiology of cerebellar evolution and development" (R. Llinas, Ed.), pp. 107–134, Am. Med. Assoc. Educ. Res. Found., Chicago.

Nilsson, G. E. (1996). Brain and body oxygen requirements of *Gnathonemus petersii,* a fish with an exceptionally large brain. *J. Exp. Biol.* **199,** 603–607.

Nimchinsky, E. A., Gilissen, E., Allman, J.M., Perl, D.P., Erwin, J.M., and Hof, P.R. (1999). A neuronal morphologic type unique to humans and great apes. *Proc. Natl. Acad. Sci. USA* **96,** 5268–5273.

Northcutt, R. G. (1981). Evolution of the telencephalon in non-mammals. *Ann. Rev. Neurosci.* **4,** 301–350.

Northcutt, R. G. (1985a). Brain phylogeny: speculations on pattern and cause. *In* "Comparative neurobiology" (M. J. Cohen and F. Strumwasser, Eds.), pp. 351–378, Wiley, New York.

Northcutt, R. G. (1985b). The brain and sense organs of the earliest vertebrates: reconstruction of a morphotype. *In* "Evolutionary biology of primitive fishes" (R. E. Foreman, A. Gorbman, J. M. Dodd, and R. Olsson, Eds.), pp. 81–112, Plenum, New York.

Northcutt, R. G. (1986). Lungfish neural characters and their bearing on sarcopterygian phylogeny. *J. Morphol. Suppl.* **1,** 277–297.

Northcutt, R. G. (1995). The forebrain of gnathostomes: in search of a morphotype. *Brain Behav. Evol.* **46,** 275–318.

Northcutt, R. G., and Kaas, J. H. (1995). The emergence and evolution of mammalian neocortex. *Trends Neurosci.* **18,** 373–379.

Northcutt, R. G., and Wullimann, M. F. (1988). The visual system in teleost fishes: morphological patterns and trends. *In* "Sensory Biology of Aquatic Animals" (J. Atema, R. R. Fay, A. N. Popper, and W. N. Popper, Eds.), pp. 515–552, Springer Verlag, New York.

Nudo, R. J., and Masterton, R. B. (1990a). Descending pathways to the spinal cord. IV: some factors related to the amount of cortex devoted to the corticospinal tract. *J. Comp. Neurol.* **296,** 584–597.

Nudo, R. J. and Masterton, R. B. (1990b). Descending pathways to the spinal cord, III: sites of origin of the corticospinal tract. *J. Comp. Neurol.* **296,** 559–583.

Nudo, R. J., Sutherland, D. P., and Masterton, R. B. (1995). Variation and evolution of mammalian corticospinal somata with special reference to primates. *J. Comp. Neurol.* **358,** 181–205.

Oppenheim, R. W. (1981). Neuronal cell death and some related regressive phenomena during neurogenesis: a selective historical review and progress report. *In* "Studies in Developmental Neurobiology: Essays in Honor of Victor Hamburger" (W. M. Cowan, Ed.), pp. 74–133, Oxford University Press, New York.

Owen, A. M., Doyon, J., Petrides, M., and Evans, A. C. (1996). Planning and spatial working memory: a positron emission tomography study in humans. *Europ. J. Neurosci.* **8,** 353–364.

Owen, A. M., Herrod, N. J., Menon, D. K., Clark, J. C. , Downey, S. P. M. J., Carpenter, T. A., Minhas, P.S., Turkheimer, F.E., Williams, E. J., Robbins, T. W., Sahakian, B. J., Petrides, M., Pickard, J. D. (1999). Redefining the functional organization of working memory processes within the human lateral prefrontal cortex. *Europ. J. Neurosci.* **11,** 567–574.

Owen, R. (1857). On the characters, principles of division, and primary groups of the class MAMMALIA. *J. Proc. Linn. Soc.* **2,** 1–37.

Owen, R. (1859). Contributions to the natural history of the anthropoid apes. No. VIII. On the external characters of the Gorilla *(Trogloodytes Gorilla, Sav.). Transact. Zool. Soc.* **5,** 243–283.

Pallas, S. L., Roe, A. W., and Sur, M. (1990). Visual projections induced into the auditory pathway of ferrets. I. Novel inputs to primary auditory cortex (AI) from the LP/Pulvinar complex and the topography of the MGN-AI projection. *J. Comp. Neurol.* **298,** 50–68.

Passingham, R. E. (1973). Anatomical differences between the neocortex of man and other primates. *Brain Behav. Evol.* **7,** 337–359.

Passingham, R. E. (1982). "The Human Primate." Freeman, Oxford.

Passingham, R. E. (1985). Rates of brain development in mammals including man. *Brain Behav. Evol.* **26,** 167–175.

Paxinos, G., Huang, S.F., Toga, A.W. (2000) The rhesus monkey brain in stereotaxic coordinates. Academic Press, San Diego.

Pepperberg, I. M. (1990). Some cognitive abilities of an African grey parrot *(Psittacus erithacus).* In "Advances in the study of behavior" (P. J. B. Slater, J. S. Rosenblatt, C. Beer, and M. Milinski, Eds.), pp. 357–409, Academic Press, New York.

Petrides, M., and Pandya, D. N. (1999). Dorsolateral prefrontal cortex: comparative cytoarchitectonic analysis in the human and the macaque brain and corticocortical connection patterns. *Europ. J Neurosci.* **11,** 1011–1036.

Pevet, P., Heth, G., Hiam, A., and Nevo, E. (1984). Photoperiod perception in the blind mole rat (*Spalax ehrenbergi,* Nehring): involvement of the Harderian gland, atrophied eyes, and melatonin. *J. Exp. Zool.* **232,** 41–50.

Portmann, A., and Stingelin, W. (1961). The central nervous system. *In* "Biology and Comparative Physiology of Birds" (J. Marshall, Ed.), Vol. 2 A, pp. 1–36, Academic Press, New York.

Preuss, T. M. (1995). The argument from animals to humans in cognitive neuroscience. In "The Cognitive Neurosciences" (M. S. Gazzaniga, Ed.), pp. 1227–1241, MIT Press, Cambridge.

Preuss, T.M. (2001) The discovery of cerebral diversity: an unwelcome scientific revolution. *In* "Evolutionary Anatomy of the Primate Cerebral Cortex" (D. Falk and K. Gibson, Eds.), Cambridge University Press, Cambridge.

Preuss, T. M., Qi, H., and Kaas, J. H. (1999) Distinctive compartmental organization of human primary visual cortex. *Proc. Natl. Acad. Sci. USA* **96,** 11601–11606.

Puelles, L., and Rubenstein, J. L. R. (1993). Expression patterns of homeobox and other putative regulatory genes in the embryonic mouse forebrain suggest a neuromeric organization. *Trends Neurosci.* **16,** 472–479.

Puelles, L., Domenech-Ratto, G., and Martinez-de-la-Torre, M. (1987). Location of the rostral end of the longitudinal brain axis: review of an old topic in light of marking experiments on the closing rostral neuropore. *J. Morphol.* **194,** 163–171.

Puelles, L., Kuwana, E., Puelles, E., Bulfone, A., Shimamura, K., Keleher, J., Smiga, S., and Rubenstein, J. L. R. (2000) Pallial and subpallial derivatives in the embryonic chick and mouse telencephalon, traced by the expression of the genes *Dlx-2, Emx-1, Nkx-2.1, Pax-6* and *Tbr-1. J. Comp. Neurol.* **424,** 409–438.

Rauschecker, J. P., Tian, B., Korte, M., and Egert, U. (1992). Cross-modal changes in the somatosensory vibrissa/barrel system of visually deprived animals. *Proc. Natl. Acad. Sci. USA* **89,** 5063–5067.

Redies, C. (2000) Cadherins in the central nervous system. *Prog. Neurobiol.* **61,** 611–648.

Redies, C., and Takeichi, M. (1996). Cadherins in the developing

central nervous system: an adhesive code for segmental and functional subdivisions. *Dev. Biol.* **180,** 413–423.

Rehkämper, G., Necker, R., and Nevo, E. (1994). Functional anatomy of the thalamus in the blind mole rat *Spalax ehrenbergi:* an architectonic and electrophysiologically controlled tracing study. *J. Comp. Neurol.* **347,** 570–584.

Reiner, A., Brauth, S. E., and Karten, H. J. (1984). Evolution of the amniote basal ganglia. *Trends Neurosci.* **7,** 320–325.

Richardson, M. K., Hanken, J., Gooneratne, M. L., Pieau, C., Raynaud, A., Selwood, L., and Wright, G. M. (1997). There is no highly conserved embryonic stage in vertebrates: implications for current theories of evolution and development. *Anat. Embryol.* **196:** 91–106.

Ridgway, S. H. (1986). Physiological observations on dolphin brains. *In* "Dolphin cognition and behavior: a comparative approach" (R. J. Schusterman, J. A. Thomas, and F. G. Wood , Eds.), pp. 31–59, Lawrence Erlbaum Assoc., Hillsdale.

Ridgway, S. H., and Wood, F. G. (1988). Cetacean brain evolution. *Brain Behav. Sci.* **11,** 99.

Ridley, M. (1986). "Evolution and classification: the reformation of cladism." Longman Group, Essex.

Rilling, J. K., and Insel, T. R. (1998). Evolution of the cerebellum in primates: differences in relative volume among monkeys, apes and humans. *Brain Behav. Evol.* **52,** 308–314.

Rilling, J. K., and Insel, T. R .(1999a) Differential expansion of neural projection systems in primate brain evolution. *NeuroReport* **10,** 1453–1459.

Rilling, J. K., and Insel, T. R. (1999b). The primate neocortex in comparative perspective using magnetic resonance imaging. *J. Human Evol.* **37,** 191–223.

Ringo, J. L. (1991). Neuronal interconnection as a function of brain size. *Brain Behav. Evol.* **38,** 1–6.

Rockel, A. J., Hiorns, R. W., and Powell, T. P. S. (1980). The basic uniformity in structure of the neocortex. *Brain* **103,** 221–244.

Rogers, S. W. (1998). Exploring dinosaur neuropaleobiology: computed tomography scanning and analysis of an *Allosaurus fragilis* endocast. *Neuron* **21,** 673–679.

Roth, G., Nishikawa, K. C., and Wake, D. B. (1997). Genome size, secondary simplification, and the evolution of the brain in salamanders. *Brain Behav. Evol.* **50,** 50–59.

Romanes, G. (1881). "Animal Intelligence." Kegan Paul & Trench, London.

Rowe, M. (1990). Organization of the cerebral cortex in monotremes and marsupials. *In* "Cerebral Cortex" (E. G. Jones and A. Peters, Eds.), Vol. 8 B, pp. 263–334, Plenum Press, New York.

Rubenstein, J. L. R., Martinez, S., Shimamura, K., and Puelles, L. (1994). The embryonic vertebrate forebrain: the prosomeric model. *Science* **266,** 578–580.

Sacher, G. A. (1970). Allometric and factorial analysis of brain structure in insectivores and primates. In "The Primate Brain" (C. R. Noback and W. Montagna, Eds.), pp. 245–287, Appleton-Century-Crofts, New York.

Sacher, G. A. (1973). Maturation and longevity in relation to cranial capacity in hominid evolution. In "Primate functional morphology and evolution" (R. H. Tuttle, Ed.), pp. 417–441, Mouton, Paris.

Schliemann, H. (1875). "Troy and its remains: a narrative of researches and discoveries made on the site of Ilium and in the Trojan plain." Murray, London.

Schlosser, G., Kintner, C., and Northcutt, R. G. (1999). Loss of ectodermal competence for lateral line placode formation in the direct developing frog *Eleutherodactylus coqui. Dev. Biol.* **213,** 354–369.

Schneider, G. E. (1973). Early lesions of superior colliculus: factors affecting the formation of abnormal retinal connections. *Brain Behav. Evol.* **8,** 73–109.

Semendeferi, K., Damasio, H., Frank, R., and van Hoesen, G. V. (1997). The evolution of the frontal lobes: a volumetric analysis based on three-dimensional reconstructions of magnetic resonance scans of human and ape brains. *J. Hum. Evol.* **32,** 375–388.

Sereno, M. I., and Allman, J. M. (1991). Cortical visual areas in mammals. *In* "The neural basis of visual function" (A. G. Leventhal, Ed.), pp. 160–172, MacMillan, London.

Shimamura, K., Martinez, S., Puelles, L., and Rubenstein, J. L. R. (1997). Patterns of gene expression in the neural plate and neural tube subdivide the embryonic forebrain into transverse and longitudinal domains. *Dev. Neurosci.* **19,** 88–96.

Skoglund, T. S., Pascher, R., and Bethold, C. H. (1996) Heterogeneity in the columnar number of neurons in different neocortical areas in the rat. *Neurosci. Lett.* **208,** 97–100.

Smith Fernandez, A., Pieau, C., Repérant, J., Boncinelli, E., and Wassef, M. (1998). Expression of the *Emx-1* and *Dlx-1* homeobox genes define three molecularly distinct domains in the telencephalon of mouse, chick, turtle and frog embryos: implications for the evolution of telencephalic subdivisions in amniotes. *Development* **125,** 2099–2111.

Stanfield, B. B., Nahin, B. R., and O'Leary, D. D. M. (1987). A transient postmamillary component of the rat fornix during development: implications for interspecific differences in mature axonal projections. *J. Neurosci.* **7,** 3350–3361.

Stephan, H. (1967). Zur Entwicklungshöhe der Insektivoren nach merkmalen des Gehirns und die definition der 'basalen Insektivoren'. *Zool. Anz.* **179,** 177–199.

Stephan, H., Frahm, H., and Baron, G. (1981). New and revised data on volumes of brain structures in insectivores and primates. *Folia Primatol.* **35,** 1–29.

Stevens, C. F. (1989) How cortical interconnectedness varies with network size. *Neural Comp.* **1,** 473–479.

Stingelin, W. (1958). "Vergleichend Morphologische Untersuchungen am Vorderhirn der Vøgel ouf Cytologischer und Cytoarchitektonischer Grundlage." Helbing & Lichtenhahn, Basel.

Striedter, G. F. (1990a). The diencephalon of the channel catfish, *Ictalurus punctatus.* II. Retinal, tectal, cerebellar and telencephalic connections. *Brain Behav. Evol.* **36,** 355–377.

Striedter, G. F. (1990b). The diencephalon of the channel catfish, *Ictalurus punctatus.* I. Nuclear organization. *Brain Behav. Evol.* **36,** 329–354.

Striedter, G. F. (1992). Phylogenetic changes in the connections of the lateral preglomerular nucleus in ostariophysan teleosts: a pluralistic view of brain evolution. *Brain Behav. Evol.* **39,** 329–357.

Striedter, G. F. (1997). The telencephalon of tetrapods in evolution. *Brain Behav. Evol.* **49,** 179–213.

Striedter, G. F. (1998a). Progress in the study of brain evolution: from speculative theories to testable hypotheses. *Anat. Rec. (New Anat.)* **253,** 105–112.

Striedter, G. F. (1998b). Stepping into the same river twice: homologues as recurring attractors in epigenetic landscapes. *Brain Behav. Evol.* **52:** 218–231.

Striedter, G. F. (1999). Homology in the nervous system: of characters, embryology and levels of analysis. *In* "Homology ." Novartis Foundation Symposium # 222, pp. 158–172, Wiley & Sons, Chichester.

Striedter, G.F., Keefer, B.P. (2000) Cell migration and aggregation in the developing telencephalon: pulse-labeling chick embryos with BrdU. *J. Neurosci.* **20,** 8021–8030.

Striedter, G. F., Marchant, T. A., and Beydler, S. (1998). The "neostriatum" develops as part of the lateral pallium in birds. *J. Neurosci.* **18,** 5839–5849.

Sur, M., Garraghty, P. E., and Roe, A. W. (1988). Experimentally

induced visual projections into auditory thalamus and cortex. *Science* **242,** 1437–1441.

Takahashi, T., Nowakowski, R. S., and Caviness, V. S. Jr. (1997). The mathematics of neocortical neuronogenesis. *Dev Neurosci.* **19,** 17–22.

Tobias, P. V. (1973). Brain evolution in the hominoidea. *In* "Primate functional morphology and evolution" (R. H. Tuttle, Ed.), pp. 353–392, Mouton , Paris.

Uylings, H. B. M., and van Eden, C. G. (1990). Qualitative and quantitative comparison of the prefrontal cortex in rat and in primates, including humans. *Progr. Brain Res.* **85,** 31–62.

van Dongen, B. A. M. (1998). Brain size in vertebrates. *In* "The central nervous system of vertebrates" (R. Nieuwenhuys, H. J. ten Donkelaar, and C. Nicholson, Eds.), pp. 2099–2134, Springer Verlag, Berlin.

von Baer, K. E. (1828). "Über Entwicklungsgeschichte der Thiere: Beobachtung und Reflexion." Bornträger, Königsberg.

Voogd, J., Feirabend, H. K. P., and Schoen, J. H. R. (1990). Cerebellum and precerebellar nuclei. *In* "The human nervous system" (G. Paxinos, Ed.), pp. 321–386, Academic Press, San Diego.

Wicht, H., and Nieuwenhuys, R. (1998). Hagfishes (Myxinoidea). *In* "The central nervous system of vertebrates" (R. Nieuwenhuys, H. J. ten Donkelaar, and C. Nicholson, Eds.), pp. 497–549, Springer Verlag, Berlin.

Wicht, H., and R. G. Northcutt (1992). The forebrain of the pacific hagfish: a cladistic reconstruction of the ancestral craniate forebrain. *Brain Behav. Evol.* **40,** 25–64.

Widdowson, E. M. (1981). Growth of creatures great and small. *Symp. Zool. Soc. Lond.* **46,** 5–17.

Wilczynski, W. (1984). Central neural systems subserving a homoplasous periphery. *Amer. Zool.* **24,** 755–763.

Wilson, E. O. (1975). "Sociobiology: the new synthesis." Harvard University Press, Cambridge.

Wolpoff, M. H. (1999). "Paleoanthropology." McGraw-Hill, Boston.

Wullimann, M. F., and Puelles, L. (1999). Postembryonic neural proliferation in the zebrafish forebrain and its relationship to prosomeric domains. *Anat. Embryol.* **329,** 329–348.

Zilles, K., Armstrong, E., Moser, K. H., Schleicher, A., and Stephan, H. (1989). Gyrification in the cerebral cortex of primates. *Brain Behav. Evol.* **34,** 143–150.

CHAPTER

2

Embryonic Development of the Central Nervous System

FABIOLA MÜLLER and RONAN O'RAHILLY
University of California School of Medicine
Davis, California, USA

This account of the development of the human nervous system during the embryonic period is based largely on the authors' investigations, particularly on a series of 14 articles (O'Rahilly and Müller, 1981, 1990; Müller and O'Rahilly, 1983–1990c) and on a book, "The Embryonic Human Brain" (O'Rahilly and Müller, 1999a), in which many additional details and an extensive bibliography can be found. The references provided in this chapter relate to mammals and are mostly concerned with humans unless otherwise indicated. All 16 tables are based on the authors' research.

The following points emphasize the importance of studying the development of the nervous system, in particular the embryonic human brain.

1. The embryonic period has particular importance in that during its course most major malformations appear, and their origin and timing are related to very early developmental processes.
2. The positions of areas and nuclei in the embryonic brain are frequently quite different from those in the adult, so that their identification depends more on their fiber connections than on their topography.
3. The development of the brain in rodents and even more so in the chick and quail differs appreciably from that in primates, including humans. Indeed, development in primates differs in many respects from the common mammalian pattern.
4. The timing of the appearance of areas and nuclei in the brain bears a relationship to functional considerations and its investigation is necessary for an understanding of early gene expression. Nevertheless, straightforward extrapolation from the chain of events

characteristic of murine ontogeny to that of the human is not permissible (Gérard *et al.*, 1995). Moreover, despite the high degree of sequence conservation of certain genes (Vieille-Grosjean *et al.*, 1997), appreciable differences are being found between the possible effects of human and mouse genomes, so that the mouse may not be a satisfactory model for many aspects of early human development.

5. Studies of the human embryo with the aid of recent methods confirm and further clarify many morphological findings, such as the formation of the neocortical layers published by Müller and O'Rahilly in 1990(a, b). The validity of such comparisons depends on studies being made of the one species, in this instance human, and with the aid of precise staging.

DEVELOPMENTAL STAGES AND AGES

Prenatal life is conveniently divided into the embryonic period, comprising the first eight postfertilizational weeks, and the fetal period, extending thereafter to birth. Within the embryonic period, staging (O'Rahilly and Müller, 1987) is essential for serious work in human embryology. However, it is unfortunate that in the vast majority of studies of other species such as mouse and rat, morphological staging is rarely used, although staging systems are available and have been collected conveniently in an atlas by Butler and Juurlink (1987).

Approximate ages in postfertilizational (or postovulatory) weeks have been assigned to these morphological stages, as listed in Table 2.1. These ages are revised from time to time as new information, e.g., from ultrasonography *in vivo*, becomes available. Although the use of postmenstrual weeks and days is perfectly legitimate in obstetrics, these are not age and should not be so designated. The highly ambiguous term, "gestational weeks" or "gestational age" should be discarded (O'Rahilly and Müller, 2000a).

TABLE 2.1 Initial Appearance of Various Features of the Nervous System

Features	Stage	Weeks[a]
Neural folds and groove	8	
Mesencephalic flexure; primary neuromeres; Rh., M, Pros.	9	
Neural tube begins; Tel. medium and Di.	10	4
Rostral neuropore closes	11	
Caudal neuropore closes; secondary neurulation begins	12	4½
Closed neural tube; cerebellar primordium; isthmus	13	
Pontine flexure; medial ventricular eminence; future cerebral hemispheres; all 16 neuromeres present	14	
Myelencephalon, metencephalon; hippocampal thickening; lateral ventricular eminence	15	5
Epiphysial evagination	15, 16	
Thalamus; all cranial nerves present	16	
Internal and external cerebellar swellings; neurohypophysial evagination; synapses in primordial plexiform layer	17	6
Future corpus striatum; defined interventricular foramina; choroid fissure; dentate nucleus; inferior cerebellar peduncles	18	
Olfactory bulb; insula; choroid plexus of fourth ventricle	19	
Choroid plexus of lateral ventricles	20	7
Cortical plate; anterior and inferior horns of lateral ventricle; circulus arteriosus complete	21	
Internal and external capsules; claustrum	22	
Caudate nucleus and putamen; anterior commissure begins; external germinal layer in cerebellum	23	8

[a]The weeks given are postfertilizational.

AREAS WITH SPECIAL INDUCTIVE INFLUENCE

The prechordal plate (Fig. 2.1A, stippled in the inset) is a multilayered accumulation (up to eight rows) of spherical cells in the human. They resemble endothelial elements but are larger and contain numerous granules (Müller and O'Rahilly, 2003). The dorsal surface of the plate is in close contact with the medial part of the future forebrain, i.e., with the neural groove. The prechordal plate provides a primary signal *(sonic hedgehog, shh)* for the suppression of the medial part of the originally unseparated optic fields, thereby inducing two separate primordia for the future retinae. Lack of this suppression would result in cyclopia.

Later (clearly in stage 10) the areas of the neural plate dorsal to the prechordal plate are the diencephalic region D1 and the future rostral parencephalon with the neurohypophysis. The caudal (epinotochordal) part of the neural plate will develop a floor plate.

The primitive streak (Fig. 2.1B) is the caudal axial structure of the early embryo. It lacks a basement membrane, allowing the emigration of cells, and a high percentage of its cells contribute to the neural plate. Its rostral part contains a proliferative population

that forms the primitive node. The primitive streak gives rise to axial mesoderm, the notochordal process, and foregut endoderm (by way of the notochordal process).

The notochordal process, which becomes the notochordal plate and later the notochord, ends at the oropharyngeal membrane (near the adenohypophysial pouch). It is caudal to the prechordal plate (Fig. 2.1, inset). The notochordal process and the notochord induce the floor plate by means of diffusible factors. The floor plate is a specialized group of median neuroepithelial cells that appear to regulate differentiation of motor neurons and axonal growth, and that also synthesize shh, as does the notochord.

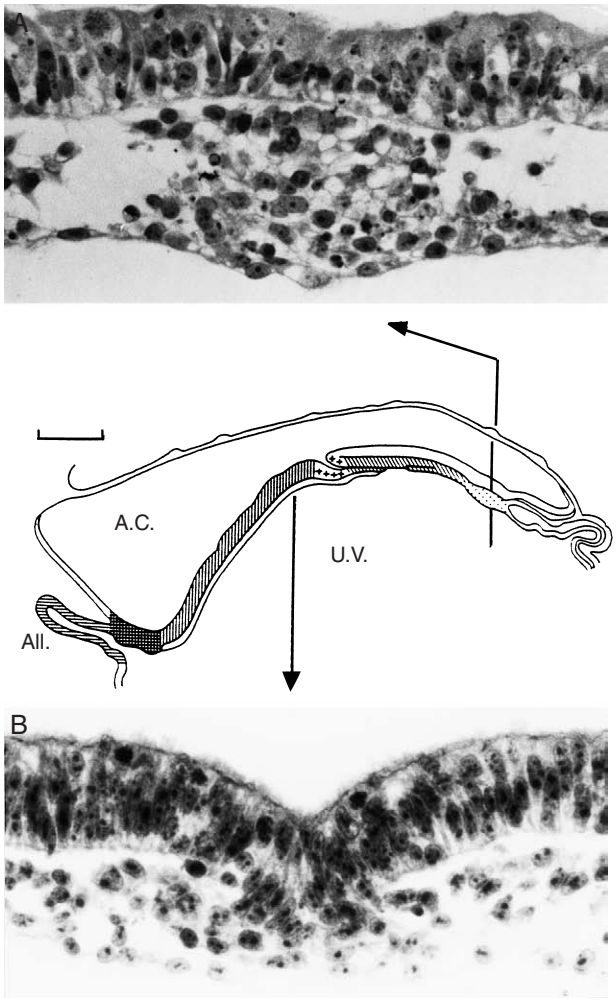

FIGURE 2.1 Areas with special inductive functions. **(A)** Cross-section of the prechordal plate (stage 8a), separated by a basement membrane from the neural ectoderm, which possesses two to three rows of cells. Above the neural ectoderm is the amniotic cavity; below the prechordal plate is the umbilical vesicle. Loose mesenchyme is visible on both sides of the prechordal plate. **(B)** Cross-section of the primitive streak, from which cells can move readily ventrally and ventrolaterally in the absence of a basement membrane. The key is a median reconstruction (stage 8b) showing the levels of sections A and B, as well as the primitive node and neurenteric canal. The notochordal process is shown in oblique hatching and the prechordal plate is stippled. A.C., amniotic cavity; All., allantoic diverticulum; U.V., umbilical vesicle. The bar represents 0.23 mm. A is from R. O'Rahilly and F. Müller, "The Embryonic Human Brain," 2nd Ed. Copyright ©, 1999, Wiley-Liss. B is from R. O'Rahilly and F. Müller, "Human Embryology and Teratology," 3rd Ed. Copyright ©, 2000, Wiley-Liss. Reprinted by permission of John Wiley and Sons, Inc.

NEURULATION

Although it is generally maintained that neural induction requires a positive signal from the "organizer," an alternative view is that "neuralization" of the epiblast occurs when the cells do not receive signals that induce them to form epidermis, mesoderm, or endoderm (Hemmati-Brivanlou and Melton, 1997, in a study of amphibia).

Neurulation is the formation of the neural tube and it involves two different processes, termed primary and secondary.

Primary Neurulation

This process extends from the appearance of the neural plate and neural groove to the formation of the neural tube (Fig. 2.2). The closure of the neural folds to constitute the neural tube involves fusion of neural

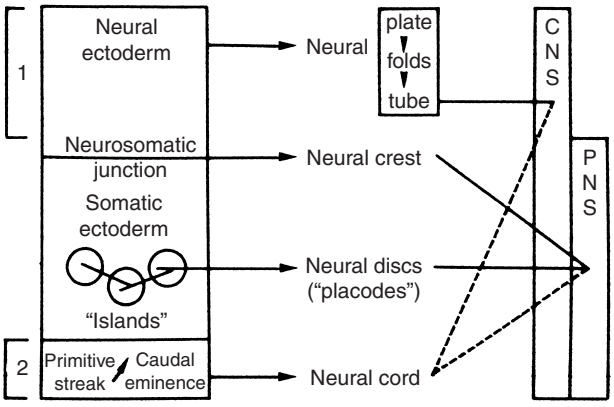

FIGURE 2.2 The origin of the nervous system. (1) Primary neurulation involves the neural ectoderm. (2) Secondary neurulation occurs by way of the caudal eminence and the neural cord. Additional contributions to the nervous system are made by the neural crest, which arises at the neurosomatic junction (i.e., at the junction of neural ectoderm and somatic ectoderm), and by neural discs (so-called placodes), which were regarded by Streeter as "islands" of neural ectoderm situated in the "ocean" of somatic ectoderm. After table 19-1 from R. O'Rahilly and F. Müller, "Human Embryology and Teratology," 3rd ed. Copyright ©, 2000, Wiley-Liss. Reprinted by permission of John Wiley and Sons, Inc.

ectoderm, fusion of surface ectoderm, and finally interposition of mesenchyme. Failure of fusion of the neural folds leads to anencephaly and/or spina bifida, whereas a defect in the formation of mesenchyme results in reopening of an already formed neural tube and/or favors the development of an encephalocele.

The neural ectoderm is at first (stage 8) a pseudostratified epithelium. Mitotic figures are present and are superficial (Fig. 2.1).

The neuropores are the openings that are left before final fusion of the neural folds (Figs. 2.3B, C, and 2.4A, B). The rostral neuropore appears and closes first (during stage 11), followed by the caudal neuropore (during stage 12). It must be emphasized that a specific pattern of multiple sites of fusion such as has been described in the mouse is not found in the human (O'Rahilly and Müller, 2002). However, additional small loci, variable in position, may be encountered at stage 10 (Müller and O'Rahilly, 1985, figure 2; Nakatsu *et al.*, 2000, figure 2).

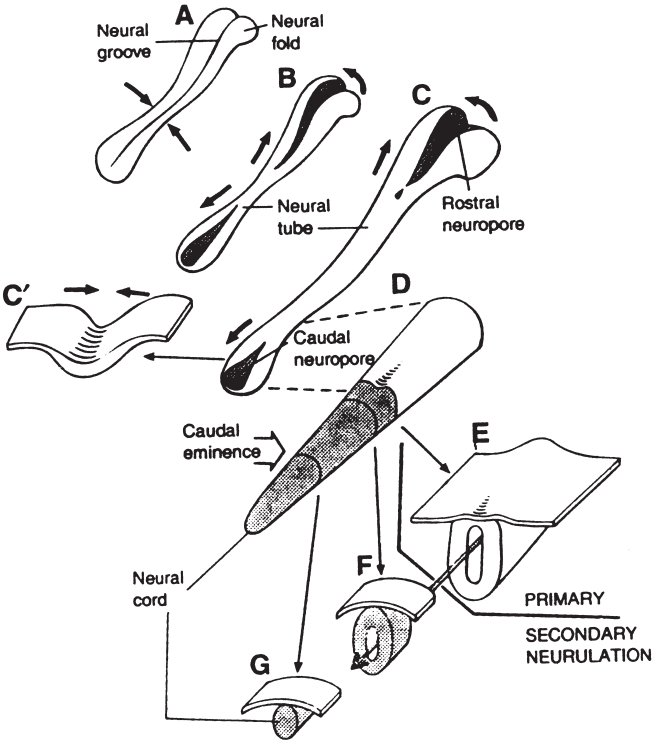

FIGURE 2.3 Primary and secondary neurulation. **(A)** The neural folds and neural groove. **(B)** The folds begin to fuse (stage 10). **(C)** Continuation of the fusion rostrally and caudally leaves two neuropores, which soon close (stages 11 and 12). **(C′)** The arrows indicate the fusion of the left and right neural folds. **(D)** A slight pit indicates the site of the former caudal neuropore, beyond which the neural tube is formed by secondary neurulation. In **E** to **G** the surface ectoderm has been added. The long arrow is placed in the lumen of the neural tube, which develops by both primary and secondary neurulation (**E** and **F**). The cavity formed by secondary neurulation **(F)** appears in the solid neural cord **(G).** From R. O'Rahilly and F. Müller, "Human Embryology and Teratology," 3rd Ed. Copyright ©, 2000b, Wiley-Liss. Reprinted by permission of John Wiley and Sons, Inc.

Secondary Neurulation

This is the continuing formation of spinal cord without direct involvement of the surface ectoderm, i.e., without the intermediate phase of a neural plate (Fig. 2.3D–G). It begins once the caudal neuropore has closed (during stage 12). The caudal eminence, which is already recognizable very early (stages 9 and 10) and slowly replaces the primitive streak, is an ectoderm-covered mass of pluripotent mesenchymal tissue. It provides structures comparable to those formed more rostrally from the three germ layers. Its derivatives include the caudal portions of the digestive tube, caudal blood vessels, notochord, somites, and spinal cord. The caudal eminence (stage 12) gives rise to a solid cellular mass known as the neural cord, which forms the nervous system of the caudal part of the body. The central canal of the more rostrally situated spinal cord extends into the neural cord. The caudal eminence gives rise to at least somitic pair 32 and those following. The mesenchyme for pairs 30–34 is the material for sacral vertebrae 1–5.

The impact of a disturbance of secondary neurulation is difficult to evaluate, and even in animals there is no experimental evidence "that an open spina bifida can result solely from defective secondary neurulation" (Copp and Brooks, 1989).

Neural Crest

Neural crest cells, mostly pluripotent, are given off dorsolaterally from the neural folds at the neurosomatic junction (Fig. 2.4A). They can be distinguished very early in the mesencephalic region (stage 9, Müller and O'Rahilly, 1983), which is earlier than previously indicated. The formation of neural crest cells in the head takes place mainly during primary neurulation, that of the spinal cord chiefly during secondary neurulation. The neural crest cells lose cadherins when they become migratory, but they reexpress them during formation of the peripheral ganglia. The migration of neural crest cells depends on the extracellular matrix through which they travel. Fibronectin and laminin in the matrix facilitate migration, whereas chondroitin sulfate proteoglycans inhibit it. The induction of neural crest is probably caused by local interactions between neural and nonneural ectoderm (induced by a particular range of BMP-4 activity); signals from the mesoderm are also important, and fibroblast growth

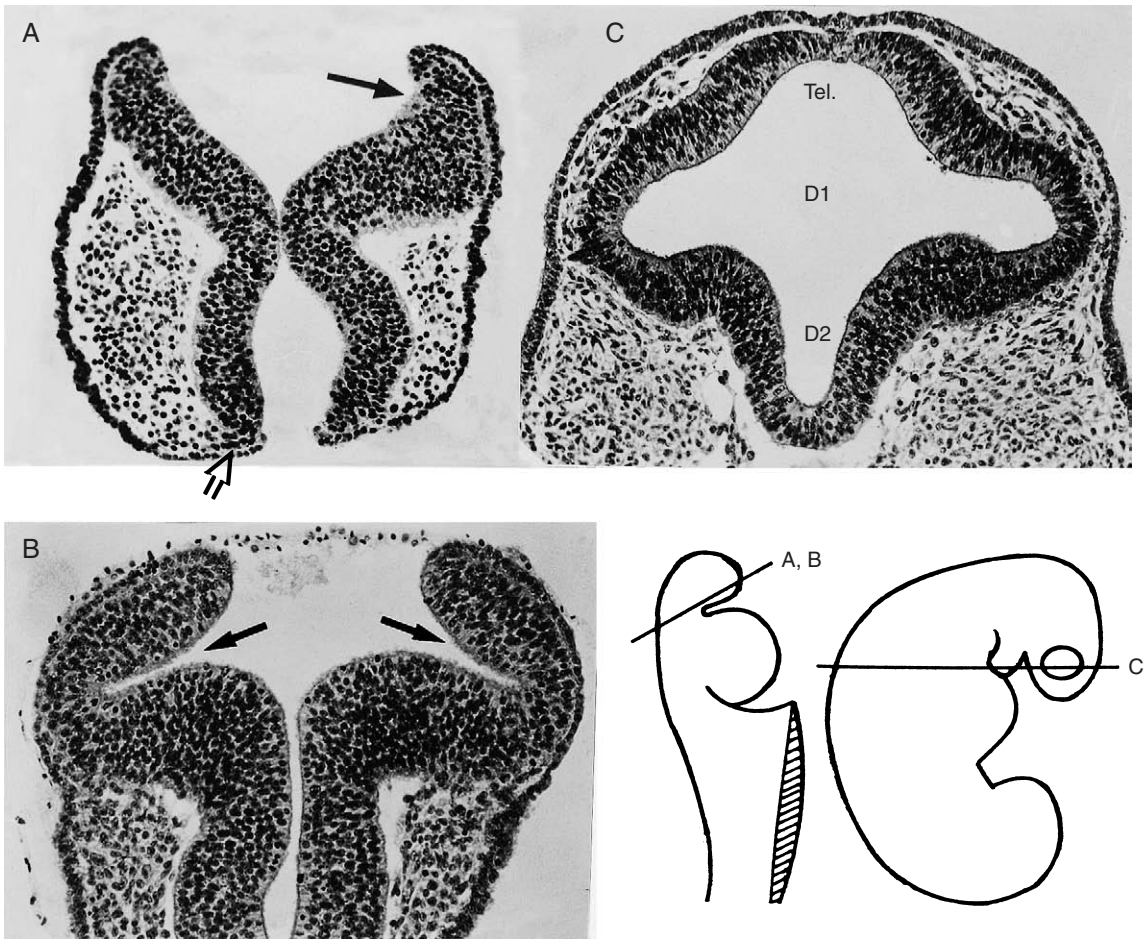

FIGURE 2.4 Sections showing rostral neuropore, optic sulci, and the location of mitotic figures in the early development of the prosencephalon. Rostral is uppermost. **(A)** A widely open rostral neuropore (stage 11). The optic sulcus of the right side is marked by a *black arrow.* Although the telencephalon has already begun its appearance (stage 10), it is not visible in this section. The narrow part of the neural groove leads to the mesencephalon, which gives off neural crest cells *(white arrow)* that are important for the future development of the head. **(B)** In a more advanced embryo (stage 11), the optic sulci *(large arrows)* have become deeper and the optic vesicles are well defined. The rostral neuropore is still open. **(C)** Here (stage 12) the rostral neuropore is closed by fusion of surface ectoderm and neural ectoderm, which over a certain distance are sealed together. The telencephalon medium (Tel.) and its ventricle are visible rostral to the optic vesicles of D1. The unpaired caudal segment represents D2. Levels of sections A and B are indicated on left side of inset, C on right. B is from R. O'Rahilly and F. Müller, "The Embryonic Human Brain," 2nd Ed. Copyright ©, 1999, Wiley-Liss. Reprinted by permission of John Wiley and Sons, Inc.

factors seem necessary (at least in birds). Neural crest in the hindbrain is restricted to Rh. 2, 3, and 5–8. It is maintained that crest cells are killed by the secretion of BMP-4 in the even-numbered rhombomere 4. Neural crest cells develop into a variety of cells and tissues. Their specification into neurons is believed to depend on a concerted action of neurotrophins and other growth factors.

NEUROCYTOGENESIS

The cells of the nervous system arise from the neural folds and tube at two main sites: (1) the ventricular layer and (2) the neural crest. It should be noted that the term *spongioblast* has long since been abandoned and that the term *neuroblast* (for immature neurons) is incorrect.

Because the neural plate is exposed to the amniotic fluid (Figs. 2.1A, 2.4A, B), the mitotic figures of this germinal layer are in a superficial location. They become separated from the amniotic cavity when the neuropores close and cell division is characterized by interkinetic nuclear migration. As the neural tube develops, the mitotic figures are adjacent to the future ventricular cavity (Fig. 2.4C). This layer of cells is termed the ventricular layer or zone. Marginal and intermediate layers soon develop. The marginal layer, at first almost acellular, later contains the processes of postmitotic cells. In the neopallium, Cajal–Retzius cells and afferent fibers constitute the primordial plexiform layer. The intermediate layer is characterized by larger, more rounded cells with more widely spaced nuclei belonging mostly to postmitotic cells. The subventricular layer, which appears in the neopallium only after the establishment of the cortical plate (stage 21), is formed by cells at the interface between the ventricular and intermediate layers. These cells continue to divide without interkinetic nuclear migration and may be a source for therapeutic cellular replacement. Further details of the neopallial layers are given later.

Morphogenesis of the brain is dependent not only on cell production but also on apoptosis (Linden, 1997), which is believed to affect half of the neurons formed. Its function seems to be the removal of an excess of neurons and the establishment of appropriate synaptic connections. The process occurs in the brain in such regions as the cortical subplate, the granular cells of the cerebellum, and the pyramidal cells of the hippocampus. It takes place in the olfactory epithelium throughout life. The apoptotic zones of the embryonic human nervous system have been studied and tabulated by Iliés (1969). Reduction of cell death can cause severe malformations, e.g., failure of closure of the neural tube (Kuan *et al.*, 2000).

Neural Stem Cells

Neuronal stem cells persist in the adult mammalian central nervous system (e.g., in the ependyma; Rao, 1999) and participate in plasticity and regeneration, but they have the immunocytochemical markers of glia (Fields and Stevens-Graham, 2002). The only site in the adult peripheral nervous system where production of neural stem cells is documented is the olfactory neuroepithelium (Alvarez-Buyilla *et al.*, 2001, cited in Geuna *et al.*, 2001). A pool of progenitor cells within the human dentate gyrus continues to produce new granule cells throughout life.

Cloned human neural stem cells implanted into the lateral ventricles of monkeys of 12–13 weeks became distributed into two subpopulations (Ourednik *et al.*, 2001): one contributed to corticogenesis by migration along radial glia to the cortical plate and differentiated into neurons and glia; the other remained undifferentiated and contributed to the subventricular zone.

Special Neurons and Their Connections

Genes specific for the central nervous system "are expressed only in the nervous system and repressed in other tissues" (Lunyak *et al.*, 2002).

Catecholaminergic cell groups have been detected very early (stages 13 and 14) in the human rhombencephalon and mesencephalon, and similar groups are soon found in the hypothalamus (stages 15 and 16). A band of densely packed cells corresponding to the primordia of the dopaminergic substantia nigra and ventral tegmental area has been recorded (at approximately stage 20; Verney *et al.*, 1991).

Moreover, it is now believed that catecholaminergic neurons in the human embryo arise along the entire cerebral axis rather than from a few localized sources.

Cajal–Retzius cells are among the first-formed neurons and their early presence is proven by *reeler* immunoreactivity (Zecevic *et al.*, 1999). The population of Cajal–Retzius cells in the future molecular layer matures late in trimester 2 (Verney and Derer, 1995) and is most striking near the middle of prenatal life (Tsuru *et al.*, 1996). These cells are thought to be fully mature when they express neurofilament proteins strongly and when the pyramidal neurons are already generated. *Reelin* produced by the Cajal–Retzius cells is responsible for the normal migration of the neurons from the ventricular layer to the periphery of the wall of the brain.

A distinction has been made between Cajal and Retzius cells (Meyer *et al.*, 1999). Cajal cells lie closer to the pia, are smaller, and are frequently triangular or piriform. They appear when the Retzius cells have already largely disappeared.

Bergmann cells are modified radial glial cells of the cerebellum that develop early in the fetal period (Choi and Lapham, 1980).They are essential for the migration of the Purkinje cells, which will be present at the end of trimester 1 (Rakic and Sidman, 1970).

Purkinje (piriform) cells are established early (stage 21). They form "multiple populations of chemically distinct cells that migrate in a coordinated fashion" to form sagittal bands of cells (Hawkes and Mascher, 1994). Their characteristic shape is acquired by the middle of prenatal life, although migration, as well as changes in shape and size, continues postnatally (for about 18 months?).

DEVELOPMENT OF THE NEURAL PLATE AND GROOVE

The primordium of the central nervous system appears (at stage 8; Fig. 2.1A) before the heart or other organs become evident, at a time when very few morphological features are present. At that time, the embryo is a slightly vaulted disc that possesses a longitudinal axis. The axis is indicated by (1) the primitive streak and groove, which begin at the primitive node and proceed caudally; and (2) the notochordal process (Fig. 2.1, inset) and the neural groove. Retinoic acid is implicated in the pattering of the rostrocaudal axis of the brain and the induction of *HOX* gene expression in the mouse and rat (Morriss-Kay, 1993; Ruberte *et al.*, 1991).

The neural groove is seen only in the largest embryos of the group (stage 8b; Fig. 2.1A). The neural ectoderm of the groove and of the bilateral vaulted areas isthe first visible sign of the future nervous system. The neurenteric canal (Fig. 2.2, inset) may be important in the formation of a split notochord (diastematomyelia), and its persistence may lead to a dorsal enteric cyst.

When one to three pairs of somites have appeared (stage 9), the neural groove is considerably deeper and the three major divisions of the brain (prosencephalon, mesencephalon, and rhombencephalon) can be identified in the unfused neural folds. They are distinguishable by their position in relation to the mesencephalic flexure and not as so-called vesicles, as so commonly stated. The rhombencephalon is the longest portion of the brain at this time.

Neuromeres

Neuromeres are morphologically identifiable transverse subdivisions perpendicular to the longitudinal axis of the embryonic brain and extending onto both sides of the brain. They appear early (stage 9) and subdivisions are soon visible (stage 11). In the hindbrain they are termed rhombomeres (Rhs.).

Four primary rhombomeres (A, B, C, D) and the otic disc can be discerned in the open neural folds (stage 9) before the neural tube has begun to form. Rh. A lies between the mesencephalic flexure and the otic disc, Rh. B is adjacent to the otic disc, Rh. C is at the base of the mesencephalic flexure, and Rh. D is adjacent to the occipital somites. Eight secondary rhombomeres (Table 2.2) develop from them. Rh. A divides into Rh. 1, 2, 3; Rh. B becomes Rh. 4; Rh. C. divides into Rh. 5, 6, 7; and Rh. D becomes Rh. 8. The development of the neuromeres in the human embryo has been described in detail elsewhere (Müller and O'Rahilly, 1997) and the arrangement at 5 weeks (stage 14) is summarized in Table 2.2. Other schemes, including six prosomeres described in the mouse, are not supported for the human (Müller and O'Rahilly, 1997). Later (stage 15) a longitudinal organization begins to be superimposed on the neuromeres (Fig. 2.5).

TABLE 2.2 The 16 Secondary Neuromeres of the Human Embryo and Their Stage of Appearance

No.	Neuromere	Abbreviation	Stage
1	Telencephalon medium	T	10
2	Diencephalon 1	D1	10
3–5	Diencephalon 2	D2	10
	3 Parencephalon rostralis	Par.r.	14
	4 Parencephalon caudalis	Par.c.	14
	5 Synencephalon	Syn.	13
6	Mesencephalon 1	M1	12
7	Mesencephalon 2	M2	12
8	Isthmus rhombencephali	Isth.	13
9–16	Rhombomeres 1–8	Rh.	11

Domains of gene expression coincide more or less with the neuromeres in some instances, but in others they may cross interneuromeric boundaries.

Early Gene Expression

Because chromosomal anomalies are present in patients with holoprosencephaly at the level of p21, p24-7, and 18p, those chromosomes are clearly important in the normal development of the brain. Furthermore, within the 7q36 band are more genes that are necessary (Gillessen-Kaesbach, 1996; Gurrieri and Muenke, 1996).

Preliminary studies have been undertaken on the role of *Pax* genes in the early development of the human embryo (Gérard *et al.*, 1995). *Pax 3* is expressed in the neural groove and closed neural tube, and later in the mesencephalon, rhombencephalon, and spinal cord. *Pax 5* expression is restricted to the mes-rhombencephalic boundary and the spinal cord. *Pax 6* is expressed in the optic neuromere (D1) of the neural tube and later in the rhombencephalon, spinal cord, and somites, but not at the level of the mesencephalon. Mesencephalon and cerebellum both require the *Wnt-1* gene for development; it is expressed in a restricted area of the neural plate. Furthermore, *En* and *Wnt* genes are involved in the patterning of the mesencephalon and metencephalon in human and mouse embryos (Song *et al.*, 1996). Regionalization in the neural tube is regulated by genes that display temporally and spatially restricted expressions.

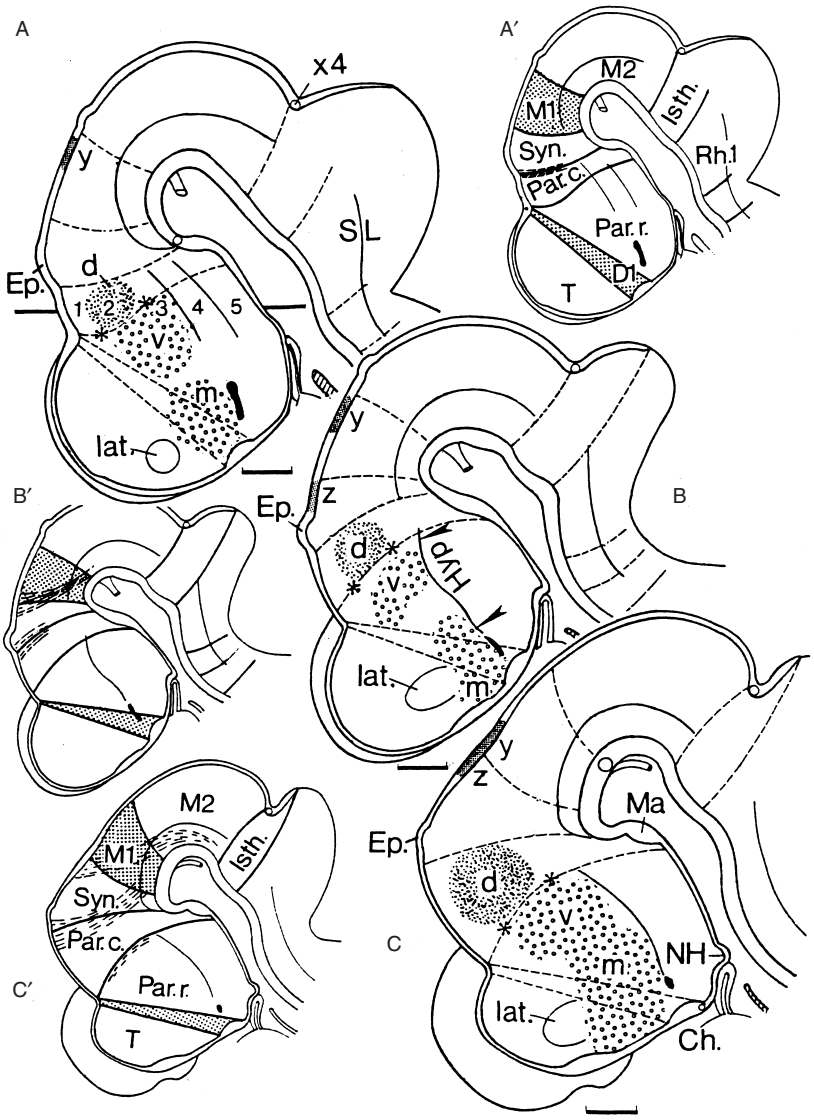

FIGURE 2.5 Median reconstructions at **A** stage 15, **B** stage 16, and **C** stage 17. The opening to the optic ventricle, now small, is shaded black. The horizontal line in **A** indicates a section that would include all five longitudinal zones of D2. The asterisks in **A, B,** and **C** mark the sulcus medius. **A′, B′,** and **C′** are key drawings to show the limits of the neuromeres, and D1 and M1 are stippled. In **A′** the habenulointerpeduncular tract is shown by interrupted lines. In **B′** the tract of the posterior commissure has been added higher up (more caudally). In **C′** the three tracts shown are, from above down (caudorostrally), the tract of the posterior commissure, the habenulointerpeduncular, and the tract of the zona limitans intrathalamica. Ch., optic chiasma; D, dorsal thalamus; Ep., epiphysis cerebri; m, medial ventricular eminence; Ma, mamillary region; NH, neurohypophysial recess; SL, sulcus limitans; v, ventral thalamus; X4, trochlear decussation; y, commissure of superior colliculi; z, posterior commissure; Bar in A = 0.2 mm; in B = 0.22 mm; in C = 0.4 mm. From F. Müller and R. O'Rahilly, Acta Anatomica, 1997. Copyright ©, 1997, S. Karger AG. Reprinted by permission of S. Karger AG.

A high degree of conservation of the pharyngeal *Hox* code has been found in a study of various groups of *Hox* genes that have been shown to be expressed in the human rhombomeres and pharyngeal arches (Vieille-Grosjean *et al.*, 1997).

THE BRAIN FROM 4 TO 6 POSTFERTILIZATIONAL WEEKS

The external development of the brain from 4½ to 7 weeks (stages 12–18) is represented in Fig. 2.6. The optic and otic primordia are shown.

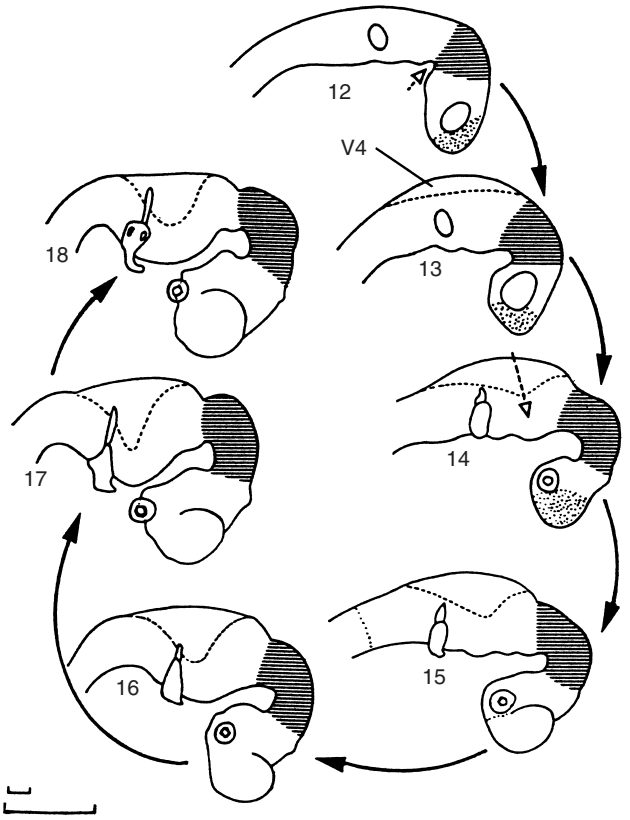

FIGURE 2.6 External form of the brain from about 4–6 weeks (stages 12–18), based on graphic reconstructions by the authors. The mesencephalon is hatched. The stippling at stages 12–14 shows the extent of the telencephalon. The arrows at stages 12 and 14 indicate the mesencephalic and pontine flexures, respectively. The magnification has been decreased progressively from stage 12 (large bar, 1 mm) to stage 18 (small bar, 1 mm). V.4, fourth ventricle.

The two components of the forebrain, the diencephalon and the telencephalon, can be detected extremely early (stage 10), as first shown by the present authors (Müller and O'Rahilly, 1985, 1987), i.e., at or before 4 weeks. The end component is the telencephalon medium or impar (stage 11), a week before the future cerebral hemispheres begin to evaginate. The widely open forebrain (Figs. 2.4A, B) presents two diencephalic neuromeres: D1, the optic part, characterized by the optic sulci; and D2, the thalamic part. Neuromere D1 is related to the chiasmatic plate and is characterized by evagination of the optic vesicles. Neuromere D2 is in line with the hypophysial primordium, which can be recognized because the neurohypophysial region of D2 is adjacent to the adenohypophysial epithelium, which, in turn, is immediately rostral to the oropharyngeal membrane.

The neural folds grow mediad (stage 11) and fuse to form the rostral wall of the telencephalon medium, which then (stage 12) expands as a neuromere (Fig. 2.4C, stippled in Fig. 2.6). A new subdivision, the synencephalon, is recognizable (stage 13) as a dorsolateral outpocketing in the caudal portion of D2, and later it gives rise to the pretectum and prerubrum. The pontine flexure becomes identifiable (stage 14) and the cerebral hemispheres evaginate from the telencephalon medium (stage 15). As the pontine flexure deepens, the brain changes from its tubular appearance to a more compact form (stages 16–18).

In contrast, the endlessly repeated scheme of three "vesicles" being transformed into five gives a totally inadequate, indeed erroneous, idea of the development of the human brain (O'Rahilly and Müller, 1999b).

SOME INDIVIDUAL REGIONS OF THE BRAIN

Tables 2.3–2.14 summarize the timing and sequence of events as determined by the authors.

Telencephalon: Formation of the Neocortex (Table 2.3)

Ventricular Zone

The layer adjacent to the ventricular cavity is where the primary proliferative phase takes place (Fig. 2.7A). Most of the mitotic divisions that generate neurons and radial glia are localized here and are characterized by interkinetic nuclear migration. Subsequently, the ventricular zone develops into the ependymal zone.

Neurons and glia are derived from the same progenitors (Fields and Stevens-Graham, 2002). More

TABLE 2.3 Development of the Neocortex

Features	Stage
Neocortical areas distinguishable from other cortical areas	16
Primordial plexiform layer with one row of horizontal cells	17
First synapses in primordial plexiform layer	17
Ventricular layer diminishing to 75–80%	18–20
Primordial plexiform layer with several rows of cells; choroid plexus; Cajal-Retzius and subplate cells	19
Neopallial fibers; thalamocortical earlier than corticothalamic[a]	20, 21
Cortical plate; formation of subplate and layer 1	21
Claustrum	22
Internal capsule	22, 23
External capsule	23

[a]This is not so in rodents, in which corticothalamic fibers appear earlier than thalamocortical fibers.

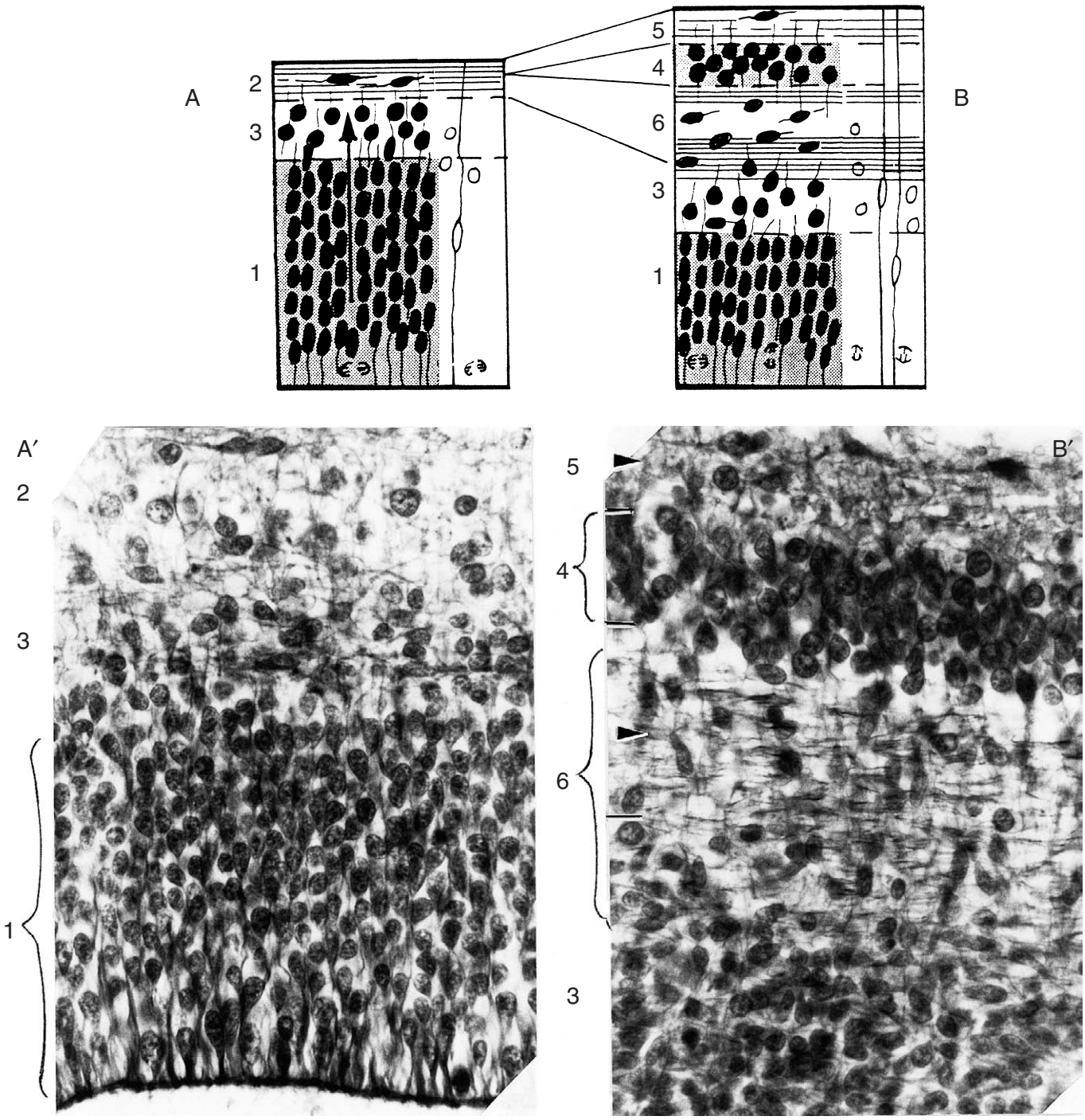

FIGURE 2.7 Formation of the neopallium by production of neurons, glial cells, and fibers. The layers are numbered here according to their order of appearance. **(A)** The intermediate layer (3) is between the ventricular (1) and primordial plexiform (2) layers (stage 18). The cells in layer 2 are Cajal–Retzius, the spherical cells in layer 3 are the precursors of subplate neurons. **(B)** The cortical plate (4) represents future layers 2–6 of the cerebral cortex (stage 21). Future layer 1 (marked 5 here) is superficial; the subplate (6) is deeper. Reelin-positive cells are found in 5. The fibers at the interface between 6 and 3 are dopaminergic. Some radial glial cells are shown at the right-hand side, where the neurons have been omitted for clarity. **(A′)** Section of a frontal region without a cortical plate (at stage 23) corresponding to A, showing radial fibers in the ventricular, and tangential fibers in the intermediate layer. **(B′)** Section (at stage 23) corresponding to B. Tangential fibers have appeared in the subplate. From R. O'Rahilly and F. Müller, "The Embryonic Human Brain," 2nd Ed. Copyright ©, 1999, Wiley-Liss. Reprinted by permission of John Wiley and Sons, Inc.

neurons than glial cells are produced early in development, whereas later (probably at the time of formation of the cortical plate) the percentage of glial cells versus neurons increases. Two proliferative phases are described and both extend well into the fetal period. The account below is based largely on studies in the mouse.

During proliferative phase 1, neurons and radial glial cells develop. Stem cells divide asymmetrically; one daughter cell usually remains in the proliferative unit, whereas the other leaves the ventricular layer (Rakic, 1991, 1996). The first neurons in the neopallial wall migrate into the marginal layer as future Cajal–Retzius cells. Together with afferent nerve fibers, they form the primordial plexiform layer (Fig. 2.6), in which the cells of the future cortical layer 1 and of the subplate mature first. Here is where the first synapses develop (Molliver *et al.*, 1973; Larroche, 1981; Choi, 1988). The postmitotic cells that will become the neurons of layers 2–6 migrate from the ventricular to the intermediate zone and later (stage 21) into the cortical plate.

During proliferative phase 2, most of the glial cells are produced in the subventricular and intermediate zones. The precursor cells arise in the ventricular layer but move into the subventricular and the intermediate zones when the cortical plate begins to form at 7 weeks (stage 21). In these two strata, interkinetic nuclear migration does not occur and almost no neurons are produced (except in the olfactory bulb). Formation of glial cells, which was minimal during phase 1, increases greatly at 8 weeks (probably at about stage 23). Radial glia can generate neurons by asymmetrical cell division (Noctor *et al.*, 2001, in Fields and Stevens-Graham, 2002). Phase 2 continues throughout the fetal period, and the production of both glial and neural cells is believed to end together. A secondary proliferative population is lacking in the subiculum, hippocampus, and dentate gyrus.

During and after migration, the young neurons that arise in the ventricular layer differentiate. The progression from a neuroepithelial cell to a specific neuron is programmed by specific genes, and different types of receptors of a neuron respond to different transmitters. Thyroid hormone receptors are particularly important for normal development of the brain.

Five categories of neuronal migration are described:

1. *Nonradial migration*. If neurons do not use radial glia as a migratory substrate, they have to glide across one glial fiber to another (O'Rourke *et al.*, 1995).
2. *Radial migration* of neurons from the ventricular to the subventricular layer and beyond is most likely mediated by radial glial cells. Radial migration is prominent in the development of the telencephalic cortex (Sidman and Rakic, 1973).
3. *Tangential migration*, which may be more prevalent than previously suspected, concerns mostly young neurons parallel to the pia (O'Rourke *et al.*, 1995,). It occurs in the cerebral cortex (Zecevic and Milosevic, 1997; Marin *et al.*, 2001; Ulfig *et al.*, 2001) and in the rhombencephalon (Fig. 2.10A3).
4. *Combined radial and tangential migration.* In the cerebral cortex γ-aminobutyric acid (GABA)–positive cells use both directions for dispersing from the ventricular zone: radial migration toward the pia, tangential migration parallel to the pia. In the cerebellum radial migration is from the ventricular zone, tangential from the rhombic lip (p. 40 and Fig. 2.10B).
5. *Chain migration provides* "a steady supply of new GABAergic neurons destined for the olfactory bulb" and originating in the subventricular layer of the cortex (Verney *et al.*, 2002). The cells migrate as a "chain of neurons ensheathed by a protective layer of glial cells" (Wolf *et al.*, in Hatten, 2002; Lois, 1996).

Intermediate Zone

This layer is characterized by larger, more rounded, and more widely spaced nuclei belonging mostly to postmitotic cells (Fig. 2.7A).

Marginal Zone

This is considered to be an axon-free and a cell-free layer, which, after its initial development, is present only in the hippocampal primordium. In all other telencephalic parts an initial marginal zone is replaced by a primordial plexiform layer as soon as corticipetal fibers arrive (Fig. 2.7A). It is now believed by some that a primordial plexiform layer is present not only in the neopallium but in all parts of the brain (Zecevic *et al.*, 1999), as was already suspected earlier for the diencephalon by the present authors (Müller and O'Rahilly, 1989a).

Development of Fibers

The development of fibers is associated with the change of the marginal into the primordial plexiform layer. The development of axons depends on adhesion, guidance, migration, and growth to reach appropriate targets. Three phases have been distinguished: (1) initial elongation, (2) collateral sprouting, and (3) pruning of extraneous connections.

The earliest afferent (probably catecholamine) fibers in the human embryo can be detected in the primordial plexiform layer of the future temporal cortex at

6 weeks (stage 17). This is the neopallial wall overlying the primordium of the amygdaloid region. Such fibers can easily be identified in silver-impregnated sections (Fig. 2.7A). Catecholamine fibers may perhaps participate in early synaptogenesis within the subplate in the human embryo (Larroche, 1981). The following is the usual pattern later in development. As the cortical plate forms the primordial plexiform layer, the latter is separated by the cortical plate into two parts: future layer 1 and the subplate (Fig. 2.7B). Accordingly, the fibers are also separated into two sets: a group remains in future layer 1 and another group now constitutes axons of the subplate. The initial subpial plexiform layer contains fibers that express neurofilament proteins, and phosphorylated fibers are found later (Zecevic *et al.*, 1999). Thalamocortical fibers were found by the authors in embryos of stages 20 and 21 (Table 2.3). Thalamocortical input seems to have little influence on the initial organization of the cortex of the mouse (Rakic, 2001). In the subplate a few dopaminergic fibers are present at 7–8 weeks (stages 21–23) (Zecevic and Verney, 1995). At the time (stage 21), "when the first cortical plate neurons are present," catecholamine fibers "penetrate the lateral cerebral wall." They become located mainly in the subplate, only sparsely in the subependymal layer (Verney *et al.*, 2002). A few dopaminergic fibers are also present in the subplate at 7–8 weeks (stages 21–23) (Zecevic and Verney, 1995; Verney *et al.*, 2002). At 8 weeks (corresponding to stage 23), two types of fibers were observed in the "cortical anlage": the serotoninergic fibers from the raphe and another kind that does not resemble the classical CA fibers (Verney *et al.*, 2002). In the human, penetratio of monoamine fibers of the cortical plate occurs at the end of trimester 1, and the highest density is found in the deep part of the human cortical plate and in the subplate (Verney *et al.*, 1993).

Primordial Plexiform Layer

This layer, also known as the preplate (Fig. 2.6A), has a significant role in the structural organization of the neocortex (Marín-Padilla, 1992). It consists of fibers and early neurons, and its composition is far more complex than hitherto believed (Zecevic *et al.*, 1999; Meyer *et al.*, 2000). Among the fibers are (1) corticipetal fibers, as mentioned above; (2) horizontal fibers from Cajal–Retzius cells; and (3) apical dendrites from radially migrating neurons during the formation of the cortical plate. The first neopallial synapses are detected in the primordial plexiform layer of embryos of 6 weeks (approximately stage 17: Choi, 1988; Zecevic and Milosevic, 1997). The neurotrypsin gene, which is expressed in the developing human brain from about $6\frac{1}{2}$ to 15 weeks, is a regulator of synaptic development. Mutation of the gene is associated with nonsyndromic mental retardation (i.e., with apparently normally developing brain and no other clinical features) (Molinari *et al.*, 2002).

Certain portions of the primordial plexiform layer are considered to be functionally active quite early (at stage 20) in the human embryo (Marín-Padilla and Marín-Padilla, 1982), and this stratum assumes an important role in the functional organization of the adult cerebral cortex. It represents the barrier at which newly arrived neurons normally stop their migration and become detached from their substrate of glial fibers. Preplate cells are responsible for the formation of a localized extracellular matrix. The *reeler* gene product is an ECM-like protein that is expressed by its cells and indicates a critical role for ECM in cortical lamination.

During migration the apical dendrites of all neurons reach layer 1 (Marín-Padilla, 1992). However, only pyramidal neurons are retained and expand their original connections with that layer; other types of neurons lose their connections. The structural and functional contacts with the elements of layer 1, their orderly placement in the cortical plate, and their preservation as early differentiated neurons until ready to begin their specific phenotypic differentiation and maturation are considered to be dependent on layer 1.

In the *reeler* anomaly in the mouse the primordial plexiform layer remains undivided and the cortical cells accumulate below it. In addition, the cortical position of neurons is inverted: the earliest formed lie most superficially, whereas the later formed stop their migration at successively deeper cortical levels.

Cortical Plate

This important stratum develops within the primordial plexiform layer (stage 21), mainly in the area of the future insula, and it expands over the whole neopallial area (stage 23; Fig. 2.6B, B′). The plate represents the future layers 2–6 of the cerebral cortex. Future layer 1 (part of the primordial plexiform layer) is superficial and subpial, whereas the subplate is deep to the cortical plate. During the development of the cortical plate (stage 21), basal forebrain fibers grow tangentially through the subplate. In the primordial plexiform layer the earliest generated neurons are the most peripheral. In the plate, however, the oldest neurons are in the depths, whereas the earliest are superficial ("inside out" placement).

Various types of abnormality of the cortical plate are known, e.g., nodular, vertical neuronal stripes with polymicrogyria, a four-layered cortex probably of

vascular origin, and lissencephaly caused by defective neuronal migration traced to the *LIS 1* gene on chromosome 17.

Subplate

This stratum appears in stage 21, much earlier than hitherto believed (Müller and O'Rahilly, 1990b and Table 2.3). Neurons in the subplate throughout the neocortex are believed to be required for "cortical target selection" and for the ingrowth of thalamic axons. At $6\frac{1}{2}$ weeks both dopaminergic and noradrenergic fibers have been recorded. At about 7 weeks, catecholamine axons enter the telencephalic wall and occupy the subplate and, more sparsely, the marginal layer (Verney *et al.*, 2002). It is possible, therefore, that the initial contact between catecholaminergic fibers and GABA-positive neurons is established at this early time (Zecevic and Milosevic, 1997; Verney *et al.*, 2002). However, several classes of afferent fibers wait for weeks before penetrating the cortical plate and the role they play in the transitory synaptic organization of the subplate is still unclear.

Subventricular Zone

This layer appears only after the establishment of the cortical plate (stage 21). It is formed by cells at the interface between the ventricular and intermediate zones. The cells divide without interkinetic nuclear migration and form a distinct population in the mouse. They may possibly have different functions in different areas. The cells may also be a source for therapeutic replacement. In the mouse the subventricular layer of the neopallium remains active into adulthood. The production of cells in the subventricular zone is considered to be the secondary proliferative phase. Most glial cells are produced here and in the intermediate layer. A few dopaminergic fibers are visible at 7–8 weeks (Zecevic *et al.*, 1999, probably stages 21–23).

Subpial Granular Layer

This layer, associated with the name Bruns, is present before the middle of prenatal life (Choi, 1988; Marín-Padilla, 1995). It is fully developed by the end of trimester 2, when regression begins, and it disappears during trimester 3 (Spreafico *et al.*, 1999). The cells are located above those of Cajal–Retzius (Verney and Derer, 1995). Mitotic figures are not found, and the layer is formed by a tangential "chain migration" from the subventricular layer of the olfactory bulb, whence cells are given off shortly after the appearance of the neocortical plate. The layer is composed of both differentiated and undifferentiated cells, and it contains glial precursors that become transformed into astrocytes and later migrate into the gray matter (Marín-Padilla, 1995). Most, if not all, cells are neurons (Meyer *et al.*, 1999). They produce *reelin* early in the fetal period (Meyer and Wahle, 1999) and represent a precursor pool of neurons that complement earlier generated cells during the critical period of cortical migration.

The following developmental events have been studied by immunohistochemistry (Meyer *et al.*, 2000): (1) appearance of *reelin*-expressing neurons along the outer aspect of the neuroepithelium and establishment of a cell-sparse marginal zone (stages 16–18); (2) formation of a monolayer of horizontal, calretinin-positive and/or GAD (glutamic acid decarboxylase)–positive neurons, concurrent with the segregation of a *reelin*-positive subpial cell compartment; (3) condensation of a "pioneer plate" populated by calretinin-positive, GAD-negative pioneer cells (stage 21); and (4) appearance of the cortical plate proper within the framework of the pioneer plate (stages 21–22).

The Corpus Striatum and Other Basal Nuclei
(Table 2.4)

Both the diencephalon and the telencephalon contribute to the complicated formation of the corpus striatum. The diencephalon, which gives rise to the medial ventricular eminence, has a relatively short proliferative phase, and this seems to extend postnatally (Brana *et al.*, 1995) in contrast to the long phase of the telencephalon, from which the lateral ventricular eminence originates. These eminences, named by the present authors, were formerly known incorrectly as "ganglionic" *(Ganglienhügel).*

The medial ventricular eminence appears early. It arises as a thickening rostral to the optic stalk (Fig. 2.8A) and represents the ventral part of the torus

TABLE 2.4 Development of the Corpus Striatum

Features	Stage
Amygdaloid body:	
Medial ventricular eminence	14
Cortical and anterior amygdaloid nuclei	17
Medial and basolateral amygdaloid nuclei	18
Striatum:	
Lateral ventricular eminence	15
Subthalamic nucleus	16, 17
Red nucleus	17
Rostral part of caudate nucleus	18
Substantia nigra	18, 19
Pallidum:	
Globus pallidus	
Globus pallidus externus	18, 19
Globus pallidua internus	21

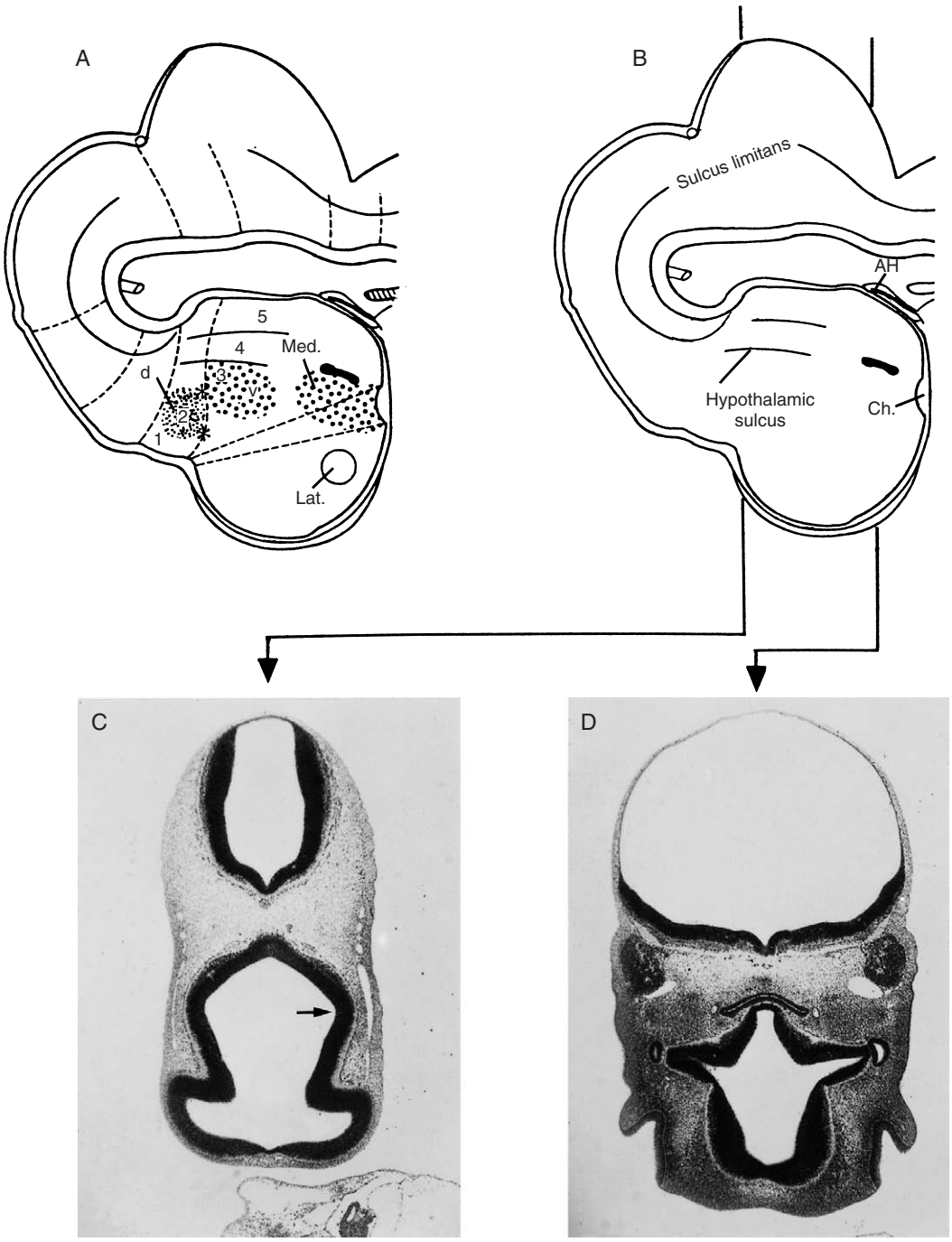

FIGURE 2.8 **A** and **B** are graphic reconstructions of the brain (at stage 15) by the authors. **(A)** A scheme of the transverse (neuromeric) and the longitudinal subdivisions of the diencephalon. In **A** the longitudinal parts are indicated by numbers: 1, epithalamus, 2, dorsal thalamus; 3, ventral thalamus; 4, subthalamus; 5, hypothalamus (with early evagination of the neurohypophysis). The asterisks are at the ends of the sulcus medius, which is the site of the future tract of the zona limitans intrathalamica; the tract is shown in Fig. 2.5C′. **(B)** The planes of section of the two photomicrographs. **(C)** Section at the level of the evaginating cerebral hemispheres *(below)*, showing the very thin lamina terminalis. The hypothalamic sulcus is indicated by an arrow. The rhombencephalon visible here is the rostral area of Rh.1. **(D)** Section at the level of the adenohypophysis. The optic stalks are still in open communication with the third ventricle. The thickening rostral to the optic stalks is the torus hemisphericus, which represents the medial ventricular eminence. The very wide caudal area of Rh.2 with the trigeminal ganglion is evident in the upper part of the photomicrograph. AH, adenohypophysial primordium; Ch, chiasmatic plate; d, dorsal thalamus; Lat, lateral ventricular eminence; Med., medial ventricular eminence; v, ventral thalamus.

hemisphericus, which separates the developing telencephalic hemispheres from the diencephalon. Later, because of growth gradients, the medial eminence becomes displaced rostrally into telencephalic territory.

The lateral ventricular eminence is purely telencephalic and neostriatal, and appears as a discrete internal swelling in the neopallial wall (circle in Fig. 2.8A). Cell production occurs in the ventricular and later also in the subventricular zone, although an intermediate layer seems to be lacking. Migration from the matrix begins at about 5 weeks (Kahle, 1969).

The eminences are characterized by their large size and by the exceptional persistence of their subventricular layer. At the end of the embryonic period, both eminences lie along the floor of the lateral ventricle, separated from each other by a faint "intereminential sulcus" (a term introduced by the present authors). Exhaustion of the matrix, which proceeds caudorostrally, does not begin until trimester 2 (Sidman and Rakic, 1982). The medial eminence is probably more closely related to the (diencephalic) globus pallidus than to the (telencephalic) lateral eminence, and seems to be related also to the nucleus accumbens, the tail of the caudate nucleus, and the caudal part of the putamen (Hewitt, 1958). The claustrum arises (at stage 21) shortly before the internal capsule enters the telencephalon and before the fibers of the external capsule are present.

The Olfactory Region (Table 2.5)

Neurons that produce luteinizing hormone–releasing hormone (LHRH; Schwanzel-Fukuda *et al.*, 1996; Verney *et al.*, 2002) develop from the medial parts of the nasal pits (stage 16; Fig. 2.9D) and probably earlier from the nasal discs (stage 13). These cells are transported (stage 19) by fibers of the vomeronasal nerve and the nervus terminalis to the olfactory bulbs and to the forebrain septum. These gonadotropin-producing cells are accompanied by TH-positive neurons (Verney *et al.*, 2002). Cells in the ventricular layer of the olfactory ventricle destined for the subpial granular layer are given off shortly after the appearance of the cortical plate. The vomeronasal organ in the human contains no recognizable neuroepithelium (Smith *et al.*, 2002) and its function is still unclear.

TABLE 2.5 Development of the Olfactory Region

Features	Stage
Nasal discs	11
Terminal–vomeronasal neural crest	13
Olfactory eminence (thickened telencephalic wall opposite nasal disc)	14
Nasal pit	15
Olfactory field of brain with intermediate layer; neurons with luteinizing hormone–releasing-hormone develop; first olfactory nerve fibers; islands in olfactory tubercle	16
Fibers from olfactory tubercle to medial forebrain bundle; fibers of terminal and vomeronasal nerves; fibers from olfactory tubercle to amygdaloid region; olfactory fibers enter olfactory bulb	17
Anterior olfactory nucleus ?; vomeronasal ganglion; fibers from olfactory bulb to olfactory tubercle	18
Ganglion of N. terminalis	19

The Forebrain Septum (Table 2.6)

The basal part of the medial telencephalic wall (septum verum) forms as the cerebral hemispheres expand beyond the lamina terminalis, and it extends between the olfactory bulb and the commissural plate (Fig. 2.9, inset). The earliest part of the septum is the olfactory tubercle (stage 16), which contains cellular clusters and receives the nervus terminalis (stage 17) (Humphrey, 1967; O'Rahilly *et al.*, 1988; Müller and O'Rahilly, 1990a). Connections to the olfactory bulb and the amygdaloid nuclei develop. The septal nuclei are cellular agglomerations at the periphery of the intermediate layer. The first septal nucleus develops caudomedial to the olfactory tubercle and is probably the diagonal nucleus. The identification of the nucleus of the diagonal band is based on the observation of fiber projections to the hippocampus (stage 20). Some cells of the nuclei basales (of Meynert) may begin to differentiate caudally toward the end of the embryonic period.

The Amygdaloid Region (Table 2.7)

The future amygdaloid body appears as four nuclei consisting of postmitotic cells located in the intermediate layer. These arise from rapid cell production

TABLE 2.6 Development of the Forebrain Septum

Features	Stage
Forebrain septum (verum)[a] present; first septal nuclei	17
Medial nucleus and nucleus diagonalis	18–20
Fibers between diagonal nucleus and hippocampus; connection between medial nucleus and hippocampus	20

[a]Basal part of the medial telencephalic wall (between olfactory bulb and commissural plate) and hence forming at the time that the hemispheres expand beyond the lamina terminalis.

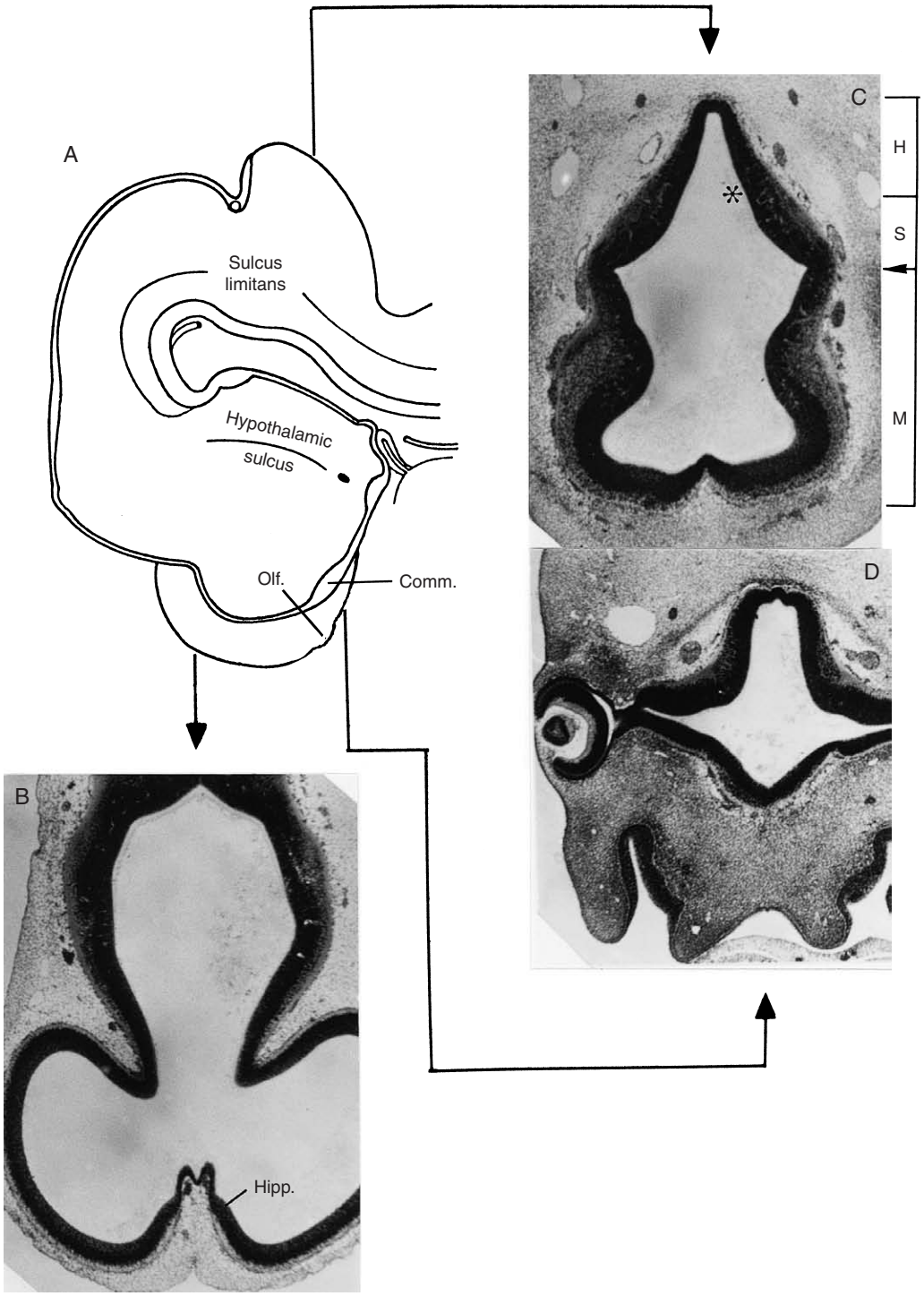

FIGURE 2.9 Transverse sections of the brain (at stage 17). **(A)** The planes of section of the three photomicrographs, shown in a graphic reconstruction by the authors of a brain at this stage. **(B)** The cerebral hemispheres, in which the hippocampal thickening, interventricular foramina, and diencephalon are recognizable. **(C)** Section through the basal part of the cerebral hemispheres. An asterisk is placed next to a very slight indentation between the hypothalamus *(above)* and the subthalamus *(below)*. An arrow points to the hypothalamic sulcus. The area peripheral to the medial ventricular eminence represents the future temporal cortex, with a well-developed primordial plexiform layer. **(D)** From rostral *(below)* to caudal *(above)* the nasal epithelium and its neural crest, the entry to the optic stalks, and the subthalamic and hypothalamic regions are visible. Comm., commissural plate; H, hypothalamus; Hipp., hippocampal primordium; M, medial ventricular eminence; Olf., olfactory bulb; S, subthalamus.

TABLE 2.7 Development of the Amygdaloid Region and Nuclei

Features	Stage
Medial ventricular eminence for most of the future amygdaloid nuclei; superficial neurons with fibers	14
Fibers begin to form medial forebrain bundle	15
1–2 amygdaloid nuclei: cortical and anterior	17
Mediolateral and basolateral nuclei	18
Amygdalohabenular fibers[a]	19
Fibers to stria medullaris thalami; fibers between amygdaloid nuclei and hippocampus	21–23

[a] A direct connection between the amygdaloid and habenular nuclei has been shown in the rat and is also present in the human.

almost exclusively in the ventricular zone of the medial ventricular eminence (stages 17 and 18), which is diencephalic. However, the overlying cortex belongs to the future temporal pole and acquires a primordial plexiform layer early. Ascending fibers of the future medial forebrain bundle have been recognized by immunological methods at about 7 weeks (Zecevic and Verney, 1995), and they reach this region rapidly. It seems possible that those monoamine fibers influence the rapid formation of the amygdaloid nuclei. Elongated (probably Cajal–Retzius) cells are found, and connections of the amygdaloid nuclei with the stria medullaris thalami develop (stage 18).

The Hippocampal Formation (Table 2.8)

The hippocampal formation is a convenient term used for the dentate gyrus, the hippocampus, the subiculum, and the parahippocampal gyrus. It can be discerned early but it develops slowly. The first sign is a marginal layer situated dorsomedially in the telencephalic roof at about 5 weeks (stages 14 and 15). Soon this area extends as far rostrobasally as the olfactory bulb (stage 16) and shows a discrete thickening near the ventricle (Fig. 2.9A). The dentate area then becomes visible (stage 17). The hippocampus *sensu stricto* can be recognized (stages 18–23) by (1) its projection into the ventricle, (2) its broad marginal and intermediate layers, and (3) its narrow ventricular layer. A C-shaped form is present at $6\frac{1}{2}$ weeks (stage 18). The embryonic development is characterized mainly by cellular production and migration. Whether the cells in the various components of the hippocampal formation appear simultaneously or develop successively (dentate area, hippocampus, presubiculum) seems to depend on the species. The rostral, middle, and occipital regions are alike in the embryo; the successive curved, S-shaped, and infolded organizations develop during the fetal period (O'Rahilly and Müller, 1999a, Figure 25-5). An intermediate form of cortex develops in the hippocampal formation, where a condensation of postmitotic cells forms a plate during the fetal period, i.e., after that in the neocortex.

TABLE 2.8 Development of the Hippocampal Formation

Features	Stage
Marginal layer in future hippocampal region	14, 15
Area epithelialis and future area dentata	17
C-shaped hippocampal thickening reaches olfactory tubercle	18
Fiber connection with forebrain septum	20

The Diencephalon (Table 2.9)

At 5 weeks a longitudinal subdivision (stage 15; Müller and O'Rahilly, 1988c, 1997) is superimposed on the transverse organization provided earlier by the neuromeres (stages 9–14) (Fig. 2.5). The sulcus limitans extends from the spinal cord into the hindbrain and midbrain, but it ends at the supramamillary recess (authors' reconstructions). (The correct spelling is *mamillary*, derived from the Latin *mamilla*.) Other interpretations have been discussed elsewhere (O'Rahilly and Müller, 1999a).

In the human embryo, the hypothalamic sulcus, together with the marginal ridge, contributes to the establishment of five longitudinal zones. These are, from the roof to the floor: epithalamus, dorsal and ventral thalamus, subthalamus, and hypothalamus (Figs. 2.5, 2.7A). The hypothalamic cell cord, in which the preopticohypothalamic tract develops, is well advanced at this time. It blends with the interstitial nucleus in the prerubral area, where the medial longitudinal fasciculus arises. The habenular nuclei are evident in the epithalamus, in which fibers of the fasciculus retroflexus develop. Two commissures become visible (stage 15): the posterior commissure at the transition to the mesencephalon, and the supramamillary commissure.

Dopaminergic cells extend from the mamillary area to the infundibulum, and catecholaminergic fibers of the fasciculus retroflexus enter the habenular region (stages 15 and 16; Verney *et al.*, 1991). It is likely that radial glial cells aid in subdividing the wall of the prosencephalon.

All embryos are exposed to maternal estrogen, and male fetuses additionally to their own testosterone; the hypothalamus is especially involved. Later, these

TABLE 2.9 Development of the Diencephalon

Features	Stage
Optic sulcus in D1	10
Optic vesicle	11
Optic neural crest	11, 12
Adenohypophysial pocket	12
Optic cup and lens disc; interstitial nucleus; hypothalamic cell cord	13
Evagination of synencephalon	13, 14
Preopticohypothalamic tract; medial ventricular eminence (amygdaloid area), part of torus hemisphericus; lens vesicle	14
Fibers in amygdaloid area; hypothalamic sulcus; mamillotegmental tract; epiphysis cerebri; intermediate layer in medial ventricular eminence and in ventral thalamus and subthalamus; subthalamic nucleus begins; supramamillary commissure; zona limitans intrathalamica and sulcus medius; lateral mamillary nucleus; lateral habenular nucleus	15
Posterior commissure and tract	15, 16
Fibers in lateral habenular nucleus; marginal ridge; habenulointerpeduncular tract	16
Evagination of neurohypophysis; medial ventricular eminence protrudes towards telencephalon	16, 17
Intermediate layer in dorsal thalamus; follicles in epiphysis	17
Stria medullaris thalami; paraphysis; supraoptic commissure	18
Globus pallidus externus	18, 19
Fibers in optic commissure	19
Lateral geniculate body; optic tract; entopeduncular nucleus	21

TABLE 2.10 Development of the Mesencephalon

Features	Stage
One mesencephalic neuromere	9–11
Two neuromeres: M1 and M2	12
Nucleus of oculomotor N.; interstitial nucleus	13
Commissure of superior colliculi	14
Morphological differences between M1 and M2; nucleus of trigeminal mesencephalic tract; nucleus of medial tectobulbar tract	15
Ventral proliferative area giving rise to interpeduncular nucleus	16
Red nucleus	17
Substantia nigra	18, 19
Ventral tegmental area	20

hormones play a "housekeeping" role in the growth and maintenance of cells of the brain in both sexes. A shortage of estrogen is believed to affect memory and thought processes.

The Mesencephalon (Table 2.10)

The midbrain (Fig. 2.6) can be recognized very early (stage 9) by the mesencephalic flexure, and soon (stage 12) it consists of two neuromeres, M1 and M2. The oculomotor nucleus appears in M2 (stage 14), although the trochlear nucleus lies in the isthmus rather than strictly in the midbrain. The tegmental region begins to develop early (stage 13), and marginal and intermediate zones become visible (stage 14). The commissure of the future superior colliculi arises at 5 weeks (during stage 15). The ventral proliferative area (stage 15) develops several rows of cells that represent the primordium of the interpeduncular nucleus. These cellular groups become traversed (stage 20) by fibers that probably belong to the rubrocerebellar tract (superior cerebellar peduncle). The interpeduncular nucleus, which is situated immediately dorsal to the interpeduncular fossa, is an important dopamine-producing area, as are also the ventral tegmental area (dorsal to it) and the substantia nigra. The connection with the habenular nuclei by the fasciculus retroflexus (habenulointerpeduncular tract; Fig. 2.5) is completed by about 7 weeks (stage 21). The dopamine-producing areas in the human have been illustrated elsewhere (O'Rahilly and Müller, 1999a, figures 20-5 to 20-9).

The ventricular zone and the ventral tegmental region, including the substantia nigra, have been shown at 5 weeks by immunological methods (Puelles and Verney, 1998). They are the first areas to display TH-immune reactivity in human embryos of about 6½ or 7 weeks (Freeman *et al.*, 1991). Nigrostriatal fibers develop at about the same time (Puelles and Verney, 1998), which agrees well with the survival of human dopamine suspension grafts (Freeman *et al.*, 1995b). Such fibers extend initially into the subventricular zone of the lateral ventricular eminence (Freeman *et al.*, 1995a). Dopamine-producing cells from the ventral part of the midbrain are best developed near the end of the embryonic period (Brundin *et al.*, 1989).

The Cerebellum (Table 2.11)

The paired cerebellar primordia can be distinguished early (stage 13) but develop rather slowly during the embryonic period. The cerebellar cells are derived mainly from the alar plates of the isthmus and from Rh. 1. A very limited contribution from Rh. 2 is also probable.

TABLE 2.11 Development of the Cerebellum and Isthmus Rhombencephali

Features	Stage
Isthmus present; nucleus of N.4	13
Cerebellar primordium is widest part of brain	14
Decussation of N.4; isthmic nucleus; extramural fibers in N.4; future superior medullary velum; intermediate zone; vestibulocerebellar fibers enter marginal layer of cerebellum; fibers between marginal and intermediate zones (trigeminocerebellar?)	15
Intra- and extraventricular thickenings; rhombic lip with mitotic activity	17
Cell production in dentate nucleus; dentatorubral fibers	18
Inferior cerebellar peduncle	21
External germinal layer	23

Two main components, which differ with regard to timing, source, and future localization, are characteristic of the cerebellum (Fig. 2.10B).

1. The ventricular and subventricular zones give origin to the piriform (Purkinje) cells and to the deep cerebellar nuclei. These early-forming precursor cells migrate peripherally. The piriform cells begin to appear at 7 weeks (stage 21; Müller and O'Rahilly, 1990b) rather than at 9 weeks (Sidman and Rakic, 1973). Fibers that are mostly trigeminal develop between the ventricular and intermediate zones (stage 15), and vestibulocerebellar fibers enter the marginal zone (stages 15–17; Müller and O'Rahilly, 1989a, b).

2. The rhombic lip, which is only the most lateral part of the alar plate and is continuous with the roof plate (Ellenberger *et al.*, 1969), corresponds to the subventricular zone. The lip begins its mitotic activity (approximately at stage 16) after that in the ventricular zone and its cells contribute mainly to the external germinal layer, although they may be involved also in the development of the dentate nucleus. The cells of the rhombic lip migrate tangentially and centrally. The external germinal (or granular) layer has been observed by the present authors to begin at 8 weeks (stage 23), which is 2–3 weeks earlier than reported by other workers (Sidman and Rakic, 1973; Zecevic and Rakic, 1976). The cells divide *in situ* and their proliferation lasts much longer than that in the ventricular zone, perhaps continuing for several months after birth (Friede, 1989). The granule cells are formed later from cells of the external germinal layer that migrate centrally.

Inferior and superior cerebellar peduncles begin their development during the embryonic period.

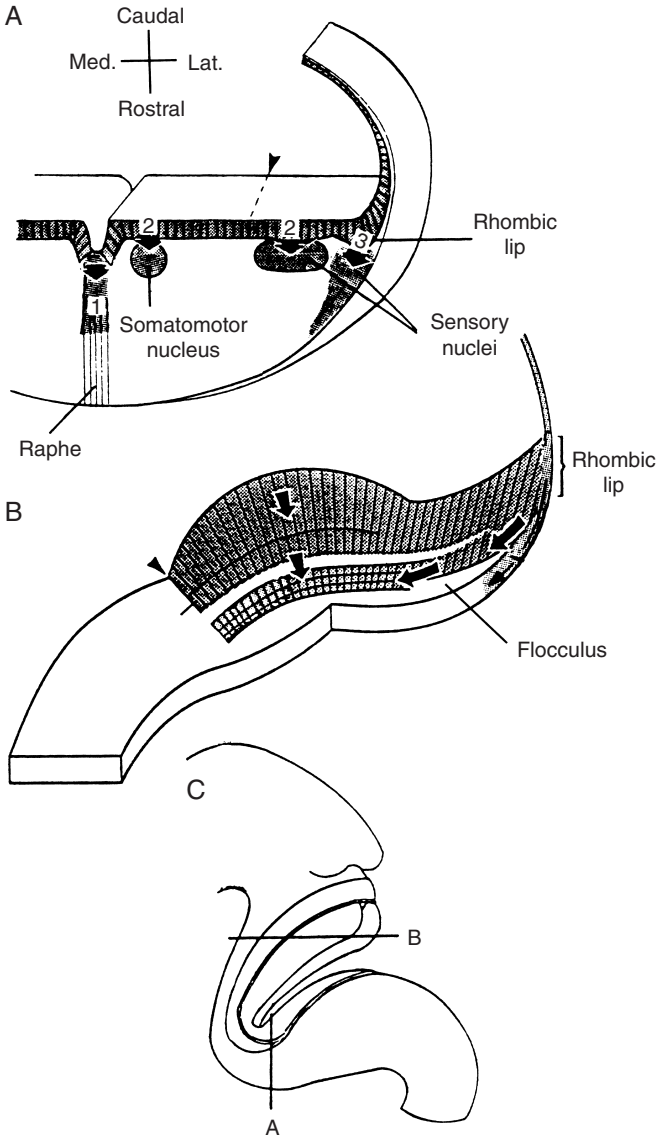

FIGURE 2.10 Cerebellum and cranial nerves. **(A)** Schematic representation of the rhombencephalon with early migrating cells (1) from the floor plate to the raphe, (2) from the ventricular layer for motor and sensory nuclei, and (3) from the rhombic lip for the cochlear nuclei **(B)** At the level of rhombomere 1 the primordium of the cerebellum shows an intraventricular thickening towards the fourth ventricle (future corpus cerebelli) and an extraventricular thickening (area of future flocculus). The vertical arrows indicate the radial route of the neurons that originate in the ventricular layer. The horizontal arrows show the tangential and superficial migration of neurons from the rhombic lip. The sulcus limitans is indicated by arrowheads in A and B. **(C)** Left lateral view of the hindbrain showing the planes of section of A and B. From R. O'Rahilly and F. Müller, "The Embryonic Human Brain," 2nd Ed. Copyright ©, 1999, Wiley-Liss. Reprinted by permission of John Wiley and Sons, Inc.

Remainder of the Rhombencephalon and Related Cranial Nerves (Tables 2.12 and 2.13)

The development of the rhombencephalon, its neuromeres, neural crest, cranial nerves, and their nuclei and ganglia (Tables 2.12 and 2.13) as well as tracts, has been studied in detail by the authors, and an account of the rhombencephalon at the end of the embryonic period is available (Müller and O'Rahilly, 1990c).

The hypoglossal nerve is the first to appear in Rh. 8. Its original four roots are segmentally arranged and innervate the four occipital somites. Although neural crest is present, no ganglia are formed, and that of Froriep (Froriep and Beck, 1895) is not present in human embryos.

The ganglia of the cranial nerves are derived from two sources: (1) their proximal parts from neural crest cells and (2) their distal portions from epipharyngeal

TABLE 2.12 Development of Motor and Sensory Rhombencephalic Nuclei

Motor Nuclei and Tracts	Stage
Hypoglossal nucleus; lateral longitudinal fasciculus	12
Thin rhombencephalic roof	12, 13
Common afferent tract[a]; lateral longitudinal fasciculus[b]; ventral longitudinal fasciculus	13
Medial longitudinal fasciculus	13, 14
Trigeminal spinal tract	14
Mesencephalic trigeminal nucleus	15
Septum medullae (raphe)	15, 16
Mesencephalic root of N.5	16
Dorsal efferent nucleus of vagus	20

[a]Containing fibres of the future tractus solitarius.
[b]Pathway concerned with the transportation of monoamines. The earliest projections to the spinal cord pass via this fascicle.

Sensory Nuclei and Ganglia	Stage
Trigeminal, facial, and glossopharyngeal/vagal superior ganglia	12
Vestibular ganglion[a]; glossopharyngeal/vagal inferior ganglia	12, 13
Cochlear ganglion	15
Superior and inferior salivary nuclei	15, 16
Main sensory trigeminal nucleus	18
Plexus folds and areae membranaceae	18, 19
Nuclei ambiguus and solitarius	19?
Accessory olivary nucleus; ventral and dorsal cochlear nuclei	19
Lateral vestibular nucleus	21
Superior vestibular nucleus	22
Nuclei gracilis and cuneatus	Before 23
Principal nucleus of inferior olive	23

[a]The central processes are probably the first axons to enter the cerebellar primordium.

TABLE 2.13 Development of the Motor Components of the Cranial Nerves

Nerves and nuclei	Original site		Cells migrate	Peripheral fibers appear	Final site
	Ventrolateral (SE) cell column	Ventromedial (VE) cell column			
Rhombencephalon					
Abducent	13, 14				
Trigeminal		13	14	14	17
Facial		13	13 to fetal	14, 15	23 and later
Superior salivary nucleus		13	13–17	N.intermedius, 16	15, 17
Glossopharyngeal		13	13–17	14, 15	16, 17
Inferior salivary nucleus		13	13–17		15, 17
Vagal		13	13–17	14, 15	16, 17
Accessory		13	13–17	14, 15	16, 17
Hypoglossal	12			12, 13	
Isthmus					
Trochlear	13			16	
Mesencephalon					
Oculomotor	13			15	

discs (Fig. 2.1). Accumulation of neural crest cells at their future loci can be seen early (stage 10), and a little later (stage 11) they are more compact. Participation of the epithelium of the pharyngeal arches (there are no branchial structures in mammals) can next be observed (stage 12), when the ganglia of the cranial nerves form a complete series. It has been shown in other species that the rhombencephalic floor plate is induced by the notochord and that it controls the pattern of cellular types that appear along the dorsoventral axis. By releasing chemoattractants the floor plate acts as an intrinsic organizer of axons in the developing brain and spinal cord. Throughout the rhombencephalon, cells are produced in the ventricular zone and in the rhombic lip (Fig. 2.10A). Cells that migrate from the ventricular layer settle in the intermediate zone and form the nuclei of the cranial nerves (Table 2.12), as well as groups of catecholaminergic neurons.

The subventricular zone of the rhombic lip gives rise to postmitotic cells that migrate tangentially along the external surface of the brain stem, where they form the transient corpus pontobulbare, which has been reconstructed and described elsewhere (Müller and O'Rahilly, 1990c). Two streams of cells migrate from the lip (stages 20–23). A site of origin of the rhombic lip that has been largely ignored in the literature is in the region of the vestibulocochlear nerve (Shaner, 1934); it is represented schematically here (Fig. 2.10A).

Motor Nuclei of the Cranial Nerves (Table 2.12)

The motor nuclei are organized segmentally. To reach their targets, motor axons follow highly stereotyped pathways leaving the hindbrain only via exit points in the even-numbered rhombomeres. The cells of the trigeminal motor nucleus are located in Rh. 2 , Rh. 3, and a few in Rh. 1. Their fibers exit from Rh. 2. The cells of the nucleus of the facial nerve arise in Rh. 4 and 5, their fibers leave in Rh. 4; the localization of the glossopharyngeal nuclei is in Rh. 6 and 7, and the fibers exit in Rh. 6.

In most published diagrams the visceromotor material is shown already located laterally in relation to the somatic motor nuclei during development, although that is imprecise. At first (stages 12 and 13) the cells of each group are congregated in an uninterrupted cell column: a medioventral column of visceromotor and a ventrolateral column of somatomotor cells (Table 2.13). The visceromotor cells begin to migrate toward the sulcus limitans (stage 13; figures 8 and 10 in Müller and O'Rahilly, 1988a, b). The relocation of those cells and their organization into definitive nuclei are almost finished by 6 weeks (stage 18), except for the facial nucleus, which occupies its final position early in the fetal period (Table 2.13 and O'Rahilly *et al.*, 1984; Müller and O'Rahilly, 1990c). The movement of the visceromotor cells is frequently cited as an example of neurobiotaxis (Ariëns Kappers, 1932), whereby functionally active fiber tracts would attract nerve cells and direct the migration of entire groups toward them.

Sensory Nuclei (Table 2.12)

The pontine nucleus of the trigeminal nerve is visible at about 6 weeks (stage 18), as is also the medial accessory olivary nucleus (stage 19). Early in the fetal period, the complete olivary nucleus is present and five subdivisions have been distinguished (Müller and O'Rahilly, 1990c). Cochlear and vestibular nuclei are recognizable at 8 weeks (stage 23), more by their topography and their relationship to fibers than by the characteristics of their cells.

Serotonin-Producing Nuclei

The raphe nuclei, which are related to the locus ceruleus, the substantia nigra, and the red nucleus, are essential for the development of the brain because of their neurotransmitters. The locus ceruleus is recognizable early at its rhombencephalic level (stage 14). The septum medullae (Fig. 2.9A), which is penetrated by fibers from nuclei of the cranial nerves, soon becomes evident (at stages 15 and 16), and its tall cells spread out from the rhombencephalic floor plate (stage 16). Connections of the raphe nuclei with the forebrain develop at 7–8 weeks (stages 21–23), probably via the central tegmental tract, and the nuclei come to be situated within the septum medullae (stage 23). Two distinct raphe nuclei at 8 weeks (stage 23) have been reconstructed (O'Rahilly and Müller, 1999a, figures 23–27).

The rhombencephalon is one of the most rapidly developing parts of the embryonic brain. At the end of the embryonic period (stage 23), its organization is so complex that functional activity should be assumed.

With regard to fibers and tracts in the rhombencephalon, the lateral longitudinal fasciculus begins to form early (stage 12), adjacent to the sulcus limitans, and later it extends from the hindbrain to the isthmus rhombencephali. The ventral longitudinal fasciculus begins to appear a few days later than the lateral, as does also the common afferent tract, which consists of afferent vestibulospinal fibers and fibers of the tractus solitarius (stage 17). The numerous rhombencephalic tracts present at the end of the embryonic period closely resemble those found in the newborn (Müller and O'Rahilly, 1990c).

VENTRICLES, CHOROID PLEXUSES, AND CIRCUMVENTRICULAR ORGANS

The Ventricles

The embryonic ventricular system (O'Rahilly and Müller, 1990) begins its definitive development with the closure of the caudal neuropore (during stage 12). Because the walls of the brain are of uniform thickness at this time (up to stages 13 and 14), the ventricles follow closely the shape of the brain. Future changes are caused mainly by alterations in the thickness of the walls (e.g., by the thinning of the roof of the fourth ventricle and the formation of the ventricular eminences) and by evaginations.

The first cavity of the telencephalon to appear is that of the telencephalon medium, which is visible very early (stages 12 and 13, Fig. 2.4C). At 5–6 weeks (stages 15 and 16) the lateral ventricles are distinguishable, and soon the medial and lateral ventricular eminences of the forebrain produce indentations, as does the cerebellar plate in the lateral wall of the fourth ventricle. Growth of the ventricular eminences transforms the formerly even outline of the lateral ventricle into a C-shaped cavity, and a first indication of anterior and inferior horns can be seen at 7 weeks (stage 21). The interventricular foramen can soon be recognized (at about stage 17; Fig. 2.9) as a wide opening, and by 8 weeks (stage 23) it is considerably reduced.

The fourth ventricle becomes evident at about 5 weeks (stages 13 and 14; Fig. 2.6). The isthmic part of it is compressed by the growing cerebellum. The lateral recesses of the fourth ventricle are long, lateral expansions at 8 weeks (stage 23).

Three different liquids are in contact successively with the developing brain: (1) the amniotic fluid until closure of the neuropores, (2) the ependymal fluid after closure, and (3) the cerebrospinal fluid after the formation of the choroid plexuses. The term "ependymal fluid" is used here for the fluid believed to be produced by the lining cells that will later develop into ependymal and choroid plexus cells.

The Choroid Plexuses

The ventricular cells that do not form neurons or glioblasts constitute lining cells known as ependymoblasts, which give rise to ependymal cells and choroid plexus cells. The plexus fold of the lateral ventricles at 7 weeks (stages 18 and 19) consists of three to four rows of cells. Choroid villi, which are absent at first, soon develop stumpy projections in the plexus fold (stage 20), although the villi become more slender (stage 21) when the epithelium is composed of about two rows of cells. The choroid plexuses are voluminous at the end of the embryonic period (stage 23) and their epithelial layer consists of a single row of cells.

In the bilaminar roof of the third ventricle, folds are seen at 8 weeks (stage 23), and they are the first indication of the choroid villi that develop during the fetal period.

The roof of the fourth ventricle is characterized by folded and unfolded epithelia. Choroid villi and bilateral choroid folds appear at 6–7 weeks (stages 18 and 19). The choroid primordium is slightly ahead of that in the telencephalon. Two membranous areas develop in the rhombencephalic roof. The area membranacea rostralis is rostral in relation to the plexus folds and appears first (stage 18). The area membranacea caudalis is more caudal and is present a little later (stages 19 and 20). The caudal area corresponds to the central bulge of Brocklehurst (1969) and to the saccular ventricular diverticulum of Wilson (1937). The formation of the median aperture was believed by Brocklehurst to be related to this area, although no openings in the roof of the embryonic fourth ventricle were observed by the present authors. Both areae mebranaceae have been discussed in relation to the formation of the subarachnoid space (Weed, 1916, 1917). Intraventricular fluid would leave the fourth ventricle and enlarge the mesenchymal meshes at the surface of the medulla oblongata. Illustrations and further details are given in a detailed article by O'Rahilly and Müller (1990).

The Circumventricular Organs

The circumventricular organs consist of "modified ependymal elements, which despite their modification, still retain their epithelial lining character" (Kuhlenbeck, 1970). They begin their development only late during the embryonic period, and the few present at that time lack the characteristics of the definitive arrangement, such as a highly specialized vascularization.

A median evagination of the mesencephalon is the first of these to appear (stage 15). It is found for at least another couple of weeks (stage 19), and it was observed by Hochstetter (1929). It consists of elongated cells with a basal nucleus and a long cytoplasmic apex. A dense capillary network develops at its extrapial surface.

The neurohypophysis appears as an evagination of the diencephalon (stage 16), although its area is clearly defined much earlier (stage 10) by its relationship to the adenohypophysial primordium. Folding of the wall and lengthening of the stalk are observed at 6 weeks (stages 17 and 18). Production of mesenchyme between

adeno- and neurohypophysis begins at the same time. However, even at the end of the embryonic period (stage 23), the median eminence is not yet evident. The hypothalamohypophysial system is functional by the end of trimester 1 (Mai *et al.*, 1997).

The epiphysis cerebri is visible as an evagination at 5–6 weeks (stage 16) and it forms a rostrally directed protrusion containing follicles. Some nerve fibers from the habenular area soon (stage 19) enter the primordium.

The subcommissural organ, which is ventral to the posterior commissure and adjacent to the cavity of the third ventricle, contains elongated cells with their apices toward the ventricular cavity (stages 19–21; O'Rahilly and Müller, 1990, figure 5G, H).

The paraphysis, which is at the di-telencephalic border and belongs to the telencephalon medium, possesses one or more evaginations formed by a single layer of cylindrical, ciliated cells. It is at the height of its development at the end of the embryonic period.

The area postrema, which in the newborn lies dorsal to the nucleus of the tractus solitarius, contains "a few neurons, and many nerve fibers of undetermined origin" (Netsky and Suangshoti, 1975). Its presence is indicated by penetrating nerve fibers from the tractus solitarius, as seen by the present authors. This innervation accords well with the claim, based on clinical evidence, that vagal fibers are functionally involved in the area postrema.

THE CEREBRAL ARTERIES
(Table 2.14)

The brain is supplied by two pairs of vessels, namely, the internal carotid and the vertebral arteries. At about 4 weeks (stage 10) the internal carotid possesses two divisions (stage 13). The caudal division becomes the posterior communicating artery (stage 14), which gives rise to the posterior cerebral artery. The posterior communicating is a relatively large vessel prenatally and in the newborn. At about 6 weeks the cranial division of the internal carotid gives origin to the anterior choroidal (stage 16) and the middle and anterior cerebral (stage 17). Also by this time, two longitudinal vessels (stage 13) fuse to become the basilar artery (stage 16), and anastomoses of cervical segmental vessels on each side have formed the vertebral arteries (stage 16). When the two anterior cerebral vessels become united by the anterior communicating artery at 7 weeks, the circulus arteriosus is complete (stages 20 and 21). Caroticobasilar anastomoses (stage 13) formed by the trigeminal, otic, and hypoglossal arteries normally disappear, but any one of them may persist. The stapedial artery (stage 17), which traverses the primordium of the stapes, is a temporary channel that contributes to the formation of other vessels, particularly the middle meningeal artery. Detailed information can be found in Padget (1948), from whose valuable illustrations simplified drawings have been constructed and additional stages added (O'Rahilly and Müller, 1999a).

TABLE 2.14 Development of the Main Arteries

Vessels	Stage
Internal carotid begins	12
Trigeminal, otic, hypoglossal	13
Posterior communicating	14
Basilar and vertebral	15, 16
Anterior choroid, ophthalmic	16
External carotid, hyaloid; posterior choroid; posterior cerebral	17
Labyrinthine	19
Anterior communicating	20
Circulus arteriosus	20, 21

MEASUREMENTS
(Tables 2.15 and 2.16)

Mean measurements were calculated in 60 embryos from $2\frac{1}{2}$ to $3\frac{1}{2}$ weeks (stages 6a–9; Table 2.15). It was found that (1) embryos with a neural groove (stage 8b) tend to be longer than those (stage 8a) without; (2) the neural groove (stage 8b) suddenly becomes much longer (stage 9); (3) embryos with a neural groove (stage 8b) have a long primitive streak; (4) the primitive streak increases in length (stage 8) but soon becomes reduced (stage 9); and (5) although embryonic length increases throughout, embryonic width decreases (from stage 8b to stage 9) in association with the altered shape of the embryo.

TABLE 2.15 Mean Measurements (mm) in 60 Embryos of Stages 6a–9

Stage	6a	6b	7	8a	8b	9
Embryonic length	0.23	0.31	0.59	0.90	1.30	1.44
Embryonic width			0.44	0.68	0.81	0.68
Length of primitive streak		0.08	0.23	0.28	0.43	0.27
Length of neural groove					0.31	0.97
n	18	13	13	7	4	5

TABLE 2.16a Length of the Brain and Its Parts (mm) in 25 Embryos of Stages 9–16

Stage	Length of brain	T	Di	P	M	Rh.	n
9	1.16			0.27	0.15	0.74	3
10	1.55			0.42	0.15	0.98	1
11	1.72	0.05	0.27	0.32	0.15	1.25	4
12	2.39	0.16	0.34	0.50	0.32	1.57	3
13	3.88	0.32	0.41	0.73	0.65	2.5	4
14	5.3	0.4	0.9	1.3	0.8	3.2	5
15	7.27	0.77	1.09	1.86	1.61	3.8	2
16	7.55	0.85	1.49	2.34	1.58	3.63	3

TABLE 2.16b Percentages of the Parts of the Brain in Relation to the Total Length of the Brain in 91 Embryos of Stages 9–16

Stage	T	D1[a]	D2[a]	P	M1	M2	M	Rh.	*n*
9				23			12.5	64.5	3
10	1	10	16	27			10	63	13
11	2	7	10	19			10	71	12
12	5	8	7.5	20.5	8	6.5	14.5	65	15
13	6.8	5.8	5.7	18.3	7.2	8.1	15.3	66.4	13
14	11.9	4	3.8	19.7	7.8	6.5	14.3	66.4	4
15	12.6	3.1	3.9	19.6	10.4	10.5	20.9	59.5	13
16	14.6	3.4	4.7	22.7	10.4	11.2	21.6	55.7	18

[a]D1 and D2 relate to stages 9–12. D2 becomes subdivided in stage 13 into three parts: parencephalon rostralis, parencephlon caudalis, and synencephalon.

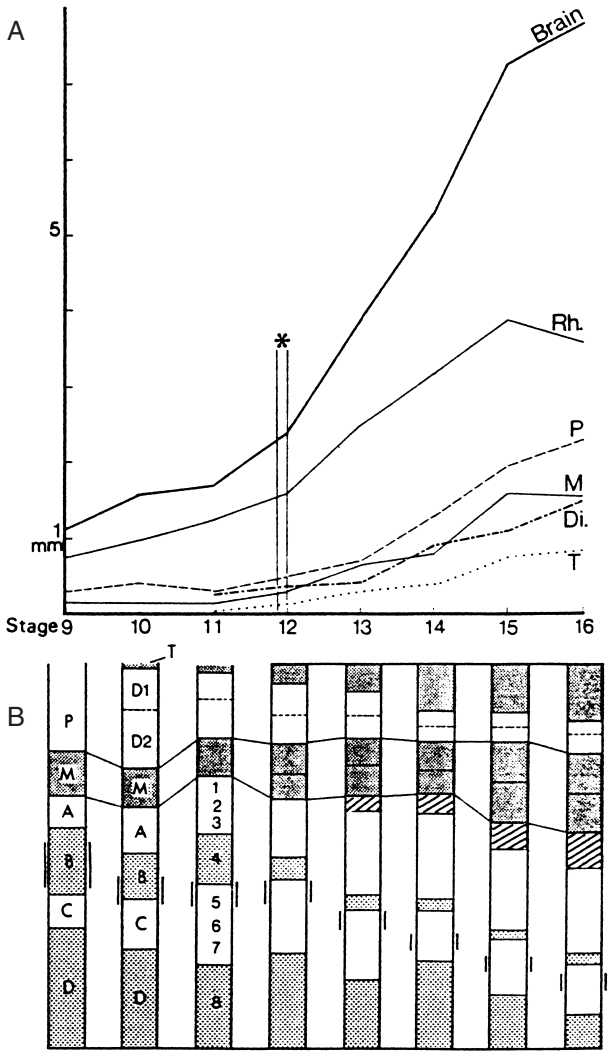

FIGURE 2.11 **(A)** Lengthening of the brain and its subdivisions in millimeters; from about 3½ to 5½ weeks (stages 9 to 16) based on the author's data. The asterisk indicates the transition from an open neural tube to a closed system. See also Table 2.16a. **(B)** Changes in length of the parts of the brain indicated as percentages of the total length. Vertical lines outside the rhombencephalic part of the columns indicate the site of the otic primordia. See also Table 2.2. A, B, C, D, early (primary) rhombomeres; Di., diencephalon; D1, diencephalon 1; D2, diencephalon 2; M, mesencephalon; P, prosencephalon; Rh., Rhombencephalon; 1–8, rhombomeres; T, telencephalon. The isthmus rhombencephali is shown by diagonal hatching.

Further measurements (Fig. 2.11 and Table 2.16a, b) show that the prosencephalon occupies nearly one-fourth of the total length of the brain, both early (stages 9 and 10) and again about 2 weeks later (stage 16). The telencephalon medium continues to increase and is accompanied by a relative reduction in the diencephalon. The rhombencephalon occupies more than half of the total length of the brain. The isthmus and Rh. 1–3 show a threefold increase in length (stage 16) compared to the earlier Rh. A (stage 9). The otic primordium, which is at first opposite Rh. B, descends progressively to Rh. 5 (stages 14–16) and hence it is not a reliable indicator of rhombomeric level. Rh. D and its successor, Rh.8, decrease from a maximum (stage 9) to a minimum (stage 16).

The absolute longitudinal growth of the brain and its parts were measured (stages 9–16) and found to be uniform, except for the midbrain, the length of which doubles (between stages 14 and 15; Fig. 2.11 and Table 2.16a). The closure of the rostral neuropore (near the end of stage 11; asterisk in Fig. 2.11A) is neither accompanied nor immediately followed by any significant change in growth.

SUMMARY

The brain begins to develop very early in the embryonic period (stage 8). At 8 postfertilizational

weeks (stage 23) it is quite complex and the rhombencephalon closely resembles that of the newborn. In the mesencephalon, dopamine-producing areas are believed to be functional. The most advanced regions of the prosencephalon are the forebrain septum, amygdaloid body, habenular nuclei, and subthalamic and hypothalamic nuclei.

Investigations of the timing and sequence of the development of the brain, like that of other organs, require the use of morphological stages. It is frequently not appreciated that a considerable body of precisely staged information concerning the human embryo is now available. Studies of the developing brain in species other than Homo sapiens continue to yield valuable information, but great caution is needed in efforts to extrapolate the results to human beings.

References

Ariëns Kappers, C.U. (1932). Principles of development of the nervous system (neurobiotaxis). *In* "Cytolology and Cellular Pathology of the Nervous System" (W. Penfield, Ed.). Hoeber, New York.

Brana, C., Charron, G., Aubert, I., *et al.* (1995). Ontogeny of the striatal neurons expressing neuropeptide genes in the human fetus and neonate. *J. Comp. Neurol.* **360,** 488–505.

Brocklehurst, G. (1969). The development of the human cerebrospinal fluid pathway with particular reference to the roof of the fourth ventricle. *J. Anat.* **105,** 467–475.

Brundin, P., Widner, H., Nilsson, O. G., *et al.* (1989). Intracerebral xenografts of dopamine neurons: the role of immunosupression and the blood–brain barrier. *Exp. Brain Res.* **75,** 195–207.

Butler, H., and Juurlink, B.H.J. (1987). "An Atlas for Staging Mammalian and Chick Embryos" CRC Press, Boca Raton, Florida.

Choi, B.H., (1988). Developmental events during the early stages of cerebral cortical neurogenesis in man. *Acta Neuropathol.* **75,** 441–447.

Choi, B.H., and Lapham, W. (1980). Evolution of Bergmann glia in developing human fetal cerebellum: a Golgi electron microscopic and immuno-fluorescent study. *Brain Res.* **190,** 369–383.

Copp, A.J., F.A. Brook (1989). Does lumbosacral spina bifida arise by failure of neural folding or by defective canalisation? *J. Med. Genet.* **26,** 160–166.

Ellenberger, C., Hanaway, J., and Netsky, M. G. (1969). Embryogenesis of the inferior olivary nucleus in the rat: A radioautographic study and a re-evaluation of the rhombic lip. *J. Comp. Neurol.* **137,** 71–77.

Fields, R.D., and Stevens-Graham, B. (2002). New insights into neuron-glia communication. *Science* **298,** 536–562.

Freeman, T. B., Spence, M. S., Boss, B. D., *et al.* (1991). Development of dopaminergic neurons in the human substantia nigra. *Exp. Neurol.* **113,** 344–353.

Freeman, T. B., Sanberg, P. R., and Isacson, O. (1995a). Development of the human striatum: implications for fetal striatal transplantation in the treatment of Huntington's disease. *Cell Transplantation* **4,** 539–545.

Freeman, T. B., Sanberg, P. R., Nauert, G. M., *et al.* (1995b). The influence of donor age and the survival of solid and suspension intraparenchymal human embryonic nigral grafts. *Cell Transplantation* **4,** 141–154.

Friede, R.L. (1989). "Developmental Neuropathology," 2nd Ed. Springer-Verlag; Berlin.

Froriep, A., Beck, W. (1895), Über das Vorkommen dorsaler Hypoglossuswurzeln mit Ganglion in der Reihe der Säugetiere. *Anat.Anz.* **10,** 688–96.

Gérard, M., Abitbol, A.-L. Delezoide, J.L, *et al.* (1995). PAX-genes expression during human embryonic development, a preliminary report. *S.C.Acad.Sci.* **318,** 57–66.

Geuna, S., Fornaro, M. Giacobini-Robecchi, M.G. (2001). Adult stem cells and neurogenesis: historical roots and state of the art. *Anat. Rec,* **265,** 132–141.

Gillessen-Kaesbach, G. (1996). Familial holoprosencephaly: further example of autosomal recessive inheritance. *Birth Defects: Orig. Art. Ser.* **30,** 251–259.

Gurrieri, F., and Muenke, M. (1996). The search for genes that cause holoprosencephaly: possible approaches. *Birth Defects: Orig. Art. Ser.* **30,** 247–250.

Hatten, M.E. (2002). New directions in neuronal migration. *Science* **297,** 1660–1663.

Hawkes, R., Mascher, C. (1994). The development of molecular compartmentation in the cerebellar cortex. *Acta Anat.* **151,** 139–149.

Hemmati-Brivanlou, A., and Melton, D. (1997). Vertebrate embryonic cells will become nerve cells unless told otherwise. *Cell* **88,** 13–17.

Hewitt (1958). The development of the human caudate and amygdaloid nuclei. *J. Anat.* **92,** 377–382.

Hochstetter, F. (l929). "Beiträge zur Entwicklungsgeschichte des menschlichen Gehirns. II.Teil, 3.Lieferung. Die Entwicklung des Mittel- und Rautenhirns." Deuticke, Vienna.

Humphrey, T. (1967). The development of the human tuberculum olfactorium during the first three months of embryonic life. *J. Hirnforsch.* **9,** 437–469.

Iliés, A. (1969). La topographie et la dynamique des zones nécrotiques normales chez l'embryon humain de 11–30 mm. II. Système nerveux central et périphérique. Etude histologique et histochimique. *Rev.Roum.Embryol.Cytol., Sér.Embryol.* **6,** 31–44.

Kahle, W. (1969). Die Entwicklung der menschlichen Grosshirnhemisphäre. *Schriftenreihe Neurologie* **1,** 1–116.

Kuan, Ch.-Y., Roth, K.A., Flavell, A., *et al.* (2000). Mechanisms of programmed cell death in the developing brain. *Trends Neurosc.* **23,** 291–297.

Kuhlenbeck, H. (1970). Structural Elements. Biology of Nervous Tissue. *In* "The Central Nervous System of Vertebrates," Vol. 3/1. Karger, Basel.

Larroche, J-C. (1981). The marginal layer in the neocortex of a 7-week-old human embryo. *Anat. Embryol.* **162,** 301–312.

Linden, R. (1997). Neuron death: a developmental perspective. *In* "Principles of Neural Aging." Dani, Hori, and Walter (Eds.) Elsevier, New York, pp. 229–246.

Lois, C., Garcia-Verdugo J., Alvarez-Buyilla, A. (1996). Chain migration of neuronal precursors. *Science* **271,** 978–981.

Lunyak, V.V., Burgess, R., Prefontaine, G.G., *et al.* (2002). Corepressor-dependent silencing of chromosomal regions encoding neuronal genes. *Science* **298,** 1747–1752.

Mai, J.K., Lensing-Höhn, S., Ende, A.E., *et al.* (1997). Developmental organization of neurophysin neurons in the human brain. *J. Comp. Neurol.* **385,** 477–489.

Marin, O., Yaron, A., Bagri, A., *et al.* (2001). Sorting of striatal and cortical interneurons regulated by semaphorin-neuropilin interactions. *Science* **293,** 872–875.

Marín-Padilla, M. (1992). Ontogenesis of the pyramidal cell of the mammalian neocortex and developmental cytoarchitectonics: a unifying theory. *J. Comp. Neurol.* **321,** 223–240.

Marín-Padilla, M. (1995). Prenatal development of fibrous (white matter), protoplasmic (gray matter), and layer 1 astrocytes in

the human cerebral cortex: a Golgi study. *J. Comp. Neurol.* **357,** 554–572.

Marín-Padilla, M., and Marín-Padilla, M. T. (1982). Origin, prenatal development and structural organization of layer I of the human cerebral (motor) cortex). A Golgi study. *Anat. Embryol.* **164,** 161–206.

Meyer , G., Goffinet, A.M., and Fairén A. (1999). What is a Cajal-Retzius cell? A reassessment of a classical cell type based on recent observations in the developing neocortex. *Cerebral Cortex* **9,** 765–775.

Meyer, G. and Wahle, P. (1999). The paleocortical ventricle is the origin of reelin-expressing neurons in the marginal zone of the fetal human neocortex. *Eur. J. Neurosci.* **11,** 3937–3944.

Meyer, G., Schaaps, J.P, Moreau, L., *et al.* (2000). Embryonic and early fetal development of the human neocortex. *J. Neurosci.* **20,** 1858–1868.

Molinari, F., Rio, M. Meskenaite, *et al.* (2002). Truncating neurotrypsin mutation in autosomal recessive nonsyndromic mental retardation. *Science* **298,** 1779–1781.

Molliver, M.E., Kostovic, I., and van der Loos, H. (1973). The development of synapses in cerebral cortex of the human fetus. *Brain Res.* **50,** 403–407.

Morriss-Kay, G. (1993). Retinoic acid and craniofacial development: molecules and morphogenesis. *BioEssays* **15,** 9–15

Müller, F., and O'Rahilly, R. (1983). The first appearance of the major divisions of the human brain at stage 9. *Anat. Embryol.* **168,** 419–432.

Müller, F., and O'Rahilly, R. (1985). The first appearance of the neural tube and optic primordium in the human embryo at stage 10. *Anat. Embryol.* **172,** 157–169.

Müller, F., and O'Rahilly, R. (1986). The development of the human brain and the closure of the rostral neuropore at stage 11. *Anat. Embryol.* **175,** 205–222.

Müller, F., and O'Rahilly, R. (1987). The development of the human brain, the closure of the caudal neuropore, and the beginning of secondary neurulation at stage 12. *Anat Embryol.* **176,** 413–430.

Müller, F., and O'Rahilly, R. (1988a). The development of the human brain from a closed neural tube at stage 13. *Anat. Embryol.* **177,** 203–224.

Müller, F., and O'Rahilly, R. (1988b). The first appearance of the future cerebral hemispheres in the human embryo at stage 14. *Anat. Embryol.* **177,** 495–511.

Müller F, O'Rahilly, R (1988c). The development of the human brain, including the longitudinal zoning in the diencephalon at stage 15. *Anat. Embryol.* **179,** 55–71

Müller, F., and O'Rahilly, R. (1989a). The human brain at stage 16, including the initial evagination of the neurohypophysis. *Anat. Embryol.* **179,** 551–569.

Müller, F., and O'Rahilly, R. (1989b). The human brain at stage 17, including the appearance of the future olfactory bulb and the first amygdaloid nuclei. *Anat. Embryol.* **180,** 353–369.

Müller, F., and O'Rahilly, R. (1990a). The human brain at stages 18-20, including the choroid plexuses and the amygdaloid and septal nuclei. *Anat. Embryol.* **182,** 285–306.

Müller, F., and O'Rahilly, R. (1990b). The human brain at stages 21-23, with particular reference to the cerebral cortical plate and to the development of the cerebellum. *Anat. Embryol.* **182,** 375–400.

Müller, F., and., and O'Rahilly, R. (1990c). The human rhombencephalon at the end of the embryonic period proper. *Am. J. Anat.* **189,** 127–145.

Müller, F., and O'Rahilly, R. (1997). The timing and sequence of appearance of neuromeres and their derivatives in staged human embryos. *Acta Anat.* **158,** 83–99.

Müller, F., and O'Rahilly, R. (2003). The prechordal plate, the rostral end of the notochord, and nearby median features in staged human embryos. *Cells Tissues Organs* **173,** 1–20.

Nakatsu, T., Uwabe, C., and Shiota, K. (2000). Neural tube closure in humans. *Anat. Embryol.* **201,** 455–466.

Netski, M.G., and Shuangshoti I. (1975). Origin of choroid plexus and ependyma. *In* "The Choroid Plexus in Health and Disease" (M.G. Netsky and I. Shuangshoti, Eds.). Wright, Bristol.

O'Rahilly R, and Müller, F. (1981). The first appearance of the human nervous system at stage 8. *Anat. Embryol* **163,** 1–13.

O'Rahilly, R., and Müller, F. (1987). "Developmental Stages in Human Embryos Including a Revision of Streeter's Horizons and a Survey of the Carnegie Collection." Publication No. 637, Carnegie Institution of Washington, Washington, D.C.

O'Rahilly, R., and Müller, F. (1990). Ventricular system and choroid plexuses of the human brain during the embryonic period proper. *Am. J. Anat.* **189,** 285–302.

O'Rahilly, R., and Müller, F. (1999a). "The Embryonic Human Brain. An Atlas of Developmental Stages," 2nd Ed. Wiley-Liss, New York.

O'Rahilly, R., and Müller, F. (1999b). Summary of the initial development of the human nervous system. *Teratology* **60,** 39–41.

O'Rahilly R, and Müller, F. (2000a). Prenatal ages and stages: measures and errors. *Teratology* **61,** 382–384.

O'Rahilly, R., and Müller, F. (2000b). "Human Embryology and Teratology," 3rd Ed. Wiley-Liss, New York.

O'Rahilly, R. and Müller, F. (2002). The two sites of fusion of the neural folds and the two neuropores in the human embryo. *Teratology* **65,** 162–170.

O'Rahilly, R., Müller, F., Hutchins, G. M., *et al.* (1984). Computer ranking of the sequence of appearance of 100 features of the brain and related structures in staged human embryos during the first 5 weeks of development. *Am. J. Anat.* **171,** 243–257.

O'Rahilly, R., Müller, F., Hutchins, G. M., *et al.* (1988). Computer ranking of the sequence of appearance of 40 features of the brain and related structures in staged human embryos during the seventh week of development. *Am. J. Anat.* **182,** 295–317.

O'Rourke, N.A., Sullivan, D.P., Kaznowski, C.E., *et al.* (1995). Tangential migration of neurons in the developing cerebral cortex. *Development* **121,** 2165–2176.

Ourednik, V., Ourednik, J, Flax, J.D., *et al.* (2001). Segregation of human neural stem cells in the developing primate forebrain. *Science* **293,** 1820–1823.

Padget, D.H. (1948). The development of the cranial arteries in the human embryo. *Contr.Embryol.Carnegie Instn* **22,** 205–261. Carnegie Institution of Washington, Washington, D.C.

Puelles, L., and Verney, C. (1998). Early neuromeric distribution of tyrosine-hydroxylase-immunoreactive neurons in human embryos. *J. Comp. Neurol.* **394,** 283–308.

Rakic, P. (1991). Development of the primate cerebral cortex. *In* "Child and Adolescent Psychiatry" (M. Lewis, Ed.). Williams & Wilkins, Baltimore.

Rakic, P. (1996). Development of the cerebral cortex in human and nonhuman primates. *In* "Child and Adolescent Psychiatry" (M. Lewis, Ed.). Williams & Wilkins, Baltimore.

Rakic, P. (2001). Neurocreationism-making new cortical maps. *Science* **294,** 1011–1012.

Rakic, P. and Sidman, R.L. (1970). Histogenesis of cortical layers in human cerebellum, particularly the lamina dissecans. *J. Comp. Neurol.* **139,** 473–500.

Rao, M.S. (1999). Multipotent and restricted precursors in the central nervous system. *Anat.Rec.* **257,** 137–148.

Richter, E. (1965). Die Entwicklung des Globus pallidus und des Corpus subthalamicum. *Monographien aus dem Gesamtgebiete der Neurologie und Psychiatrie* **108,** 1–131.

Ruberte,E., Dolle, P., Chambon P., *et al*. (1991). Retinoic acid receptors and cellular retinoid binding proteins. *Development* **111,** 45–60.

Schwanzel-Fukuda, M., Crossin, K.L., Pfaff, D.W., *et al*. (1966). Migration of Luteinizing hormone-releasing hormone (LHRH) neurons in early human embryos. *J.Comp.Neurol*. **366,** 547–557.

Shaner, R. F. (1934). The development of the nuclei and tracts related to the acoustic nerve in the pig. *J. Comp. Neurol*. **60,** 5–14.

Sidman, R. L., and Rakic, P. (1973). Neuronal migration, with special reference to developing human brain: a review. *Brain Res*. **62,** 1–35.

Sidman, R. L., and Rakic, P. (1982). Development of the human central nervous sytem. *In* "Histology and Histopathology of the Nervous System" (W. Haymaker and R.D. Adams, Eds.). Thomas, Springfield, Illinois.

Smith, T.D., Phatnagar, K.P. Shimp, K.L., *et al*. (2002). Histological definition of the vomeronasal organ in humans and chimpanzees, with a comparison to other primates. *Anat.Rec*. **267,** 166–176.

Song, D.-L., Chalepakis, G., Gruss, P., *et al*. (1996). Two PAX-binding sites are required for early embryonic brain expression of an Engrailed-2 transgene. *Development* **122,** 627–635.

Spreafico, R., Arcelli, P. Frassoni, C., *et al*. (1999). Development of layer I of the human cerebral cortex after midgestation: architectonic findings, immunocytochemical identification of neurons and glia, and in situ labeling of apoptotic cells. *J. Comp. Neurol*. **410,** 126–142.

Tsuru, A., Mizuguchi, M. Uyemura, K., *et al*. (1996). Immunohistochemical expression of cell adhesion molecule L1 during development of the human brain. *Early Hum. Dev.* **45,** 93–101.

Ulfig, N., Neudörfer, F., Feldhaus, C., *et al*. (2001). Neue Perspektiven zur entwicklungsgeschichtlichen Bedeutung des humanen Ganglienhügels. *Verh. Anat.Ges*. **96,** 99.

Verney, C. and Derer, P. (1995). Cajal-Retzius neurons in human cerebral cortex at midgestation show immunoreactivity for neurofilament and calciumbinding proteins. *J. Comp. Neurol*. **359,** 144–153.

Verney, C., Zecevic, N., Nikolic, B., *et al*. (1991). Early evidence of catecholaminergic cell groups in 5- and 6-week-old human embryos using tyrosine hydroxilase and dopamine-3-hydroxylase immunocytochemistry. *Neurosci. Lett*. **131,** 121–124.

Verney, C., Milosevic, A., Alvarez, C., *et al*. (1993). Immunocytochemical evidence of well-developed dopaminergic and noradrenergic innervations in the frontal cerebral cortex of human fetuses at midgestation. *J. Comp. Neurol*. **336,** 331–344.

Verney, C., Lebrand, C., and Gaspar, P. (2002). Changing distribution of monoaminergic markers in the developing human cerebral cortex with special emphasis on the serotonin transporter. *Anat. Rec*. **267:** 87–93.

Vieille-Grosjean, I., Hunt, P., Gulisano, M., *et al*. (1997) Branchial HOX gene expression and human craniofacial development. *Dev. Biol*. **183,** 49–60.

Weed, L.H. (1916). The formation of the cranial subarachnoid spaces. *Anat. Rec*. **10,** 475–481.

Weed, L.H. (1917). The development of the cerebro-spinal spaces in pig and in man. *Contr. Embryol.Carnegie Instn* **5,** 5–110. Carnegie Institution of Washington, Washington, D.C.

Wilson, J.T. (1937). On the nature and mode of origin of the foramen of Magendie. *J. Anat*. **71,** 423–436.

Zecevic, N. (1998). Synaptogenesis in layer I of the human cerebral cortex in the first half of gestation. *Cerebral Cortex* **8,** 245–-252.

Zecevic, N., and Milosevic, A. (1997). Initial development of γ-aminobutyric acid immunoreactivity in the human cerebral cortex. *J. Comp. Neurol*. **380,** 495–506.

Zecevic, N., and Rakic, P. (1976). Differentiation of Purkinje cells and their relationship to other components of developing cerebellar cortex in man. *J. Comp. Neurol*. **167,** 27–48.

Zecevic, N., and Verney, C.(1995). Development of the catecholamine neurons in human embryo and fetuses with special emphasis on the innervation of the cerebral cortex. *J. Comp. Neurol.* **351,** 509–535.

Zecevic, N., Milosevic, A., Rakic, S., *et al*. (1999). Early development and composition of the human primordial plexiform layer: an immunohistochemical study. *J. Comp. Neurol*. **412,** 241–254.

CHAPTER

3

Fetal Development of the Central Nervous System

JÜRGEN K. MAI
Institute of Neuroanatomy
Heinrich-Heine University of Düsseldorf
Düsseldorf, Germany

KEN W. S. ASHWELL
Department of Anatomy, School of Medical Sciences
University of New South Wales
Sydney, Australia

CEREBRAL CORTEX (Fig. 3.1)

Neocortex

The general aspects of neocortical development will be dealt with before discussing development of individual regions (visual, auditory, somatosensory and frontal regions and callosal neurons), glial and vascular differentiation, and development of gyrification, structural asymmetry, and gender differences.

General Features of Neocortical Development

From the fourth to the fifth week[1] of development, the developing isocortex is about 140 µm wide and consists of two layers: the ventricular and marginal zones (Zecevic, 1993). Electron microscopy and Golgi

[1]week: weeks after fertilization; w.g. weeks of gestational age

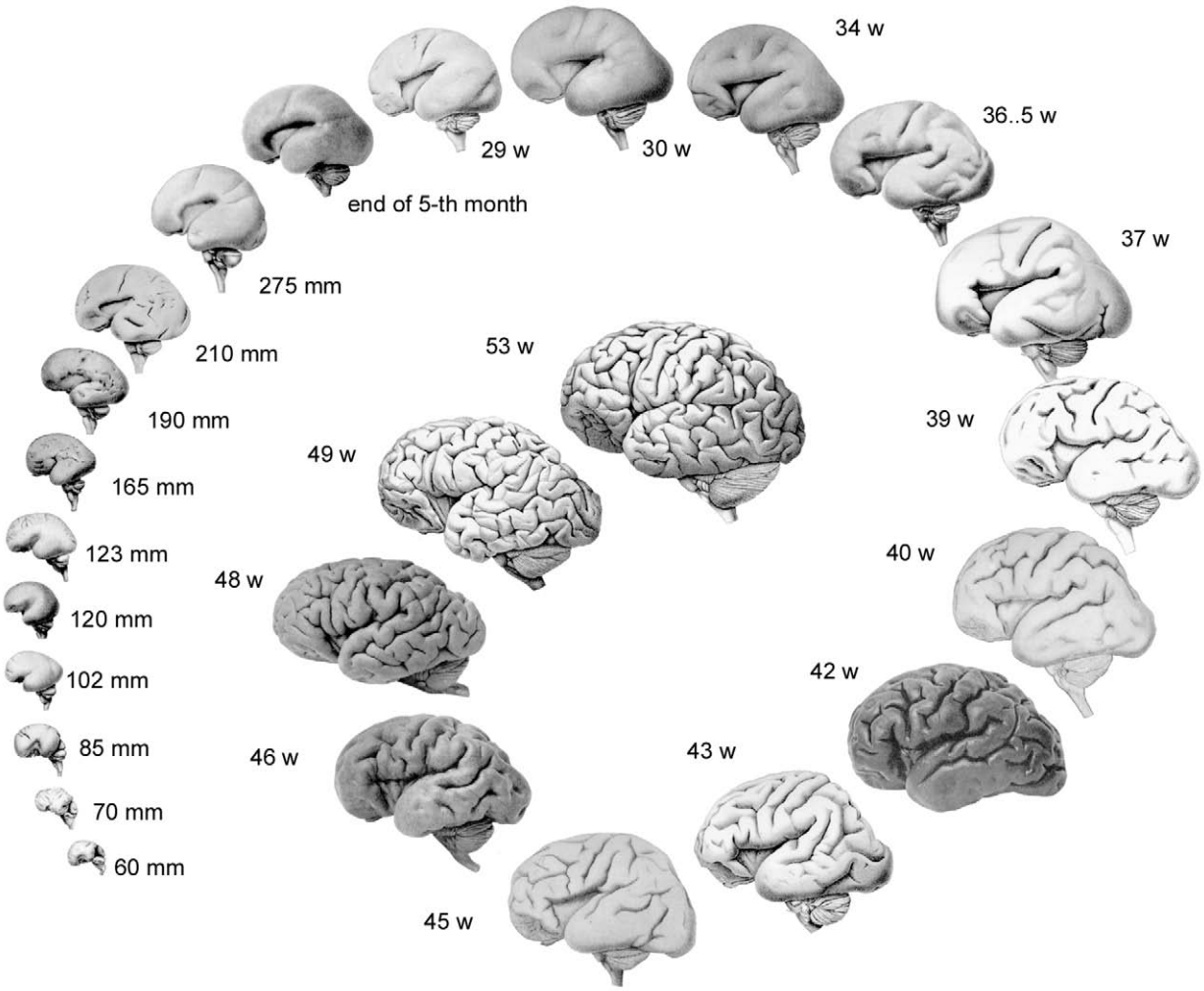

FIGURE 3.1 External morphology of brains showing the growth of the hemispheres and the development of the sulcal pattern during the period covered in this text. Modified from Retzius (1896).

impregnation studies have shown that the cortical wall is made up exclusively of bipolar ventricular cells and their pial-directed processes. Within a week (6 weeks), the intermediate zone appears between the ventricular and marginal zones and the total cortical thickness reaches 220 μm. The radial glial scaffolding that will guide subsequent migration of young neurons (Rakic, 1972; see Hatten 1999 for detailed review) begins to be established between 5 and 7 w.g. (Choi, 1988). At this time, detached cells (mainly simple or branched bipolar neurons with occasional horizontal cells) begin to appear in the ventricular zone and incipient intermediate zone. Horizontal cells at the intermediate/ventricular boundary may represent early Cajal–Retzius cells. The precocious development of these cells has been shown with a wide variety of cellular markers (Meyer and Gonzalez-Hernandez, 1993; Zecevic *et al.*, 1999). Synapses in the future layer of the cortex begin to appear at 6–7 w.g. (Zecevic, 1998).

The cortical plate begins to appear at about the seventh week of development in the ventrolateral part of the telencephalic wall. At about this time the intermediate zone can be divided into a superficial part, which will be known as the presubplate layer, and a deeper part, which will become the future white matter. Development of the cortical plate coincides with rapid increase in the density of synapses in the future layer I (Zecevic, 1998).

By about 8 w.g. a subventricular zone appears between the ventricular and intermediate layers. Both the ventricular and subventricular zones are sites of intense proliferation during the first half of the second trimester (Simonati *et al.*, 1999) producing large and small neurons and some glial cells. Proliferating cells are also found in the internal capsule and cerebral cortex white matter from 15 w.g. (Kendler and Golden, 1996). The number of proliferative cells in the internal capsule decreases by the end of the second trimester,

whereas mitosis continues in the cerebral cortex white matter well into the last trimester, probably responsible for the production of glial cells of the deep white matter.

Recent studies of defective cortical lamination in the reeler mutant mouse have led to the identification of reelin, a secreted extracellular matrix glycoprotein that is believed to have an important role in the normal development of cortical lamination. Immunoreactivity for reelin is initially found at 11 w.g. in mono- or bipolar Cajal–Retzius cells of the marginal layer (future layer I) (Meyer and Goffinet, 1998) and is subsequently found in different cell types of the superficial cortex.

The neurotrophin superfamily of proteins includes brain-derived neurotrophic factor (BDNF), nerve growth factor, neurotrophins-3, 4/5, and 6. All these neurotrophins share structural similarities, have overlapping functional effects, and recognize two classes of cell surface receptors: low and high affinity. The low-affinity receptor is known as the p75 neurotrophin receptor (Bothwell, 1991), whereas the high-affinity receptors are the trk subfamily of tyrosine protein kinases (trkA, trkB, trkC) (Bothwell, 1991). Somata immunoreactive for trk appear in the cortical subplate at 15 w.g. (Chen *et al.*, 1996), and the number of these subplate neurons peaks by 24 w.g. Cells immunoreactive for trk are never seen in the cortical plate, marginal zone, or ventricular zone, although trk-immunoreactive fibers appear in the marginal zone at 14 w.g. and this neuropil staining extends into the cortical plate by 16 w.g. (Chen *et al.*, 1996). Neurons immunoreactive for p75 are first seen in the subplate at 15 w.g., immunoreactivity increases to peak at 20 w.g., declines from 22 w.g., and completely disappears by 34 w.g.

Apoptosis in many regions of the cerebral cortex (frontal, motor, somatosensory, and visual) appears to occur mainly at the end of gestation, as indicated both by estimations of neuronal numbers (Rabinowicz *et al.*, 1996) and TUNEL labeling of fragmented DNA (Chan and Yew, 1998). The increase in apoptotic index with gestational age is inversely proportional to the decline in immunoreactivity to Bcl-2, the oncoprotein with a protective function against apoptosis (Chan and Yew, 1998).

Development of Visual Cortex

Cytoarchitectural and Ultrastructural Development In the fetal human visual cortex, a presubplate zone can be distinguished below the cortical plate as early as 13 w.g. (Kostovic and Rakic, 1990). In the visual cortex the presubplate zone is extremely narrow but sharply delineated from the underlying intermediate zone, and in Golgi preparations at this age the presubplate can be seen to contain a population of large neurons with no clear orientation. By this stage, the cortical plate neurons have begun to develop apical and basal dendrites, and the latter extend to the presubplate zone. Transformation of the deep cortical plate into subplate zone occurs later in the visual area (13 w.g.) than in the somatosensory cortex (12 w.g.), and the change begins earlier in the lateral occipital lobe than in the medial occipital lobe. At this age, Cajal–Retzius cells are the principal neuronal elements in the marginal zone (developing layer I; Zheng *et al.*, 1989). Axosomatic and axodendritic contacts are also visible in immature layer II at this age.

During the period from 16 to 18 w.g., the visual region subplate increases dramatically in thickness, in line with the ingrowth of axonal plexuses and growth cones, and enlargement of extracellular spaces. At 17 w.g., degenerating apical dendrites are occasionally seen in developing layer I (Zheng *et al.*, 1989).

Between 18 and 30 w.g., the visual cortical plate begins to show lamination. Synapses at this age are present in the subplate zone, in the deep half of the cortical plate, and in the marginal zone (Kostovic and Rakic, 1990). Postsynaptic structures in the subplate at this time include large proximal dendrites, randomly oriented small dendritic branches, and growth cone–like swellings. Toward 30 w.g., synapses spread into the superficial part of the cortical plate. From 30 w.g., the visual cortical subplate begins to dissipate and has disappeared by 1 month after birth (Kostovic and Rakic, 1990), although those authors suggest that some large multipolar neurons with ultrastructural features similar to subplate neurons survive into the adult cerebral hemisphere.

The adult level of neuronal density is reached in the striate cortex at about 16 weeks after birth (Zilles *et al.*, 1986). Dendritic development of cortical neurons plateaus at about 11 weeks after birth in the case of layer V pyramids and 15 weeks after birth for layer III pyramidal neurons (Becker *et al.*, 1984).

Development of Connections The development of intracortical connections in the visual cortex has been studied using carbocyanine dye tracing techniques (Burkhalter *et al.*, 1993). Vertical (intracolumnar) connections between layers II/III and V, linking neurons within the same cortical column and serving the same point in visual space, develop at 26–29 w.g. On the other hand, connections between columns develop later, at about 37 w.g. with layers IVB and V. The fiber density of connections increases rapidly after birth and shows a uniform plexus at about 7 weeks after birth. The adult-like patchiness of the intracortical connections develops at more than 8 weeks of gestation. Long-range horizontal connections within layers II/III

begin to develop at 16 weeks after birth, well after horizontal connections between layers IVB/V, and reach mature form before 15 months after birth. An interesting difference between the pattern of development of long-range projections formed between layers II/III on the one hand and layers IVB/V on the other is that the lower layer horizontal projections develop by collateral elimination (i.e., loss of inappropriate connections), whereas upper layer horizontal connections develop by precise targeting of appropriate destination regions.

Development of thalamocortical projections to the prestriate cortex (Brodmann's areas 18, 19, 20 and 21) have been followed during prenatal development using the transient acetylcholinesterase (AChE) activity of the pulvinar to prestriate cortex projection (Kostovic and Rakic, 1984). Thalamocortical projections from the pulvinar reach the subplate zone of prestriate cortex between 17 and 20 w.g. From 21 w.g., AChE positive fibers accumulate in the subplate and from 26 w.g. these thalamocortical fibers begin to invade the prestriate cortex. After 35 w.g., AChE activity in the pulvinar decreases and pulvinar thalamocortical fibers cannot be identified.

Development of Chemically Identified Neuronal Classes Distribution of γ-aminobutyric acid (GABA), calbindin D28k, and nitric oxide synthase (NOS) immunoreactivity and reactivity for NADPH-diaphorase has been followed in the developing human visual cortex (Yan *et al.*, 1992, 1997; Judas *et al.*, 1999). Calbindin D28k and NOS studies have both found transient patterns of immuno- and histochemical reactivity.

Calbindin-immunoreactive neurons are present in the visual cortex by 15 w.g. (Yan *et al.*, 1997), when they are found scattered in the ventricular, intermediate, and marginal zones. By 20 w.g., calbindin-immunoreactive neurons are still in the marginal and intermediate zones, although immunoreactivity has begun to appear in layers V and VI, the only two layers that have differentiated from the cortical plate by this age. Calbindin-positive bipolar and multipolar neurons can be seen in the cortical plate at 26 w.g., and by 34 w.g. a periodic pattern of neuropil immunoreactivity can be seen in layers III and IV. Transient calbindin immunoreactivity is seen in Cajal–Retzius cells in the marginal zone, migrating neurons in the intermediate and ventricular zones, and tangential fibers in the intermediate zone.

NADPH-diaphorase-reactive and NOS-immunoreactive cells appear transiently in the subplate of the human fetal cerebral cortex (15 w.g.; Judas *et al.*, 1999) and in some cortical regions, including the striate cortex, are transiently expressed in somata and proximal dendrites of pyramidal neurons themselves. The transient overexpression of NOS in both neuropil and specific neuronal populations may indicate that NO plays a significant part in development of fetal cortex.

Development of Auditory Cortex

By 11 w.g., the auditory cortex consists of marginal zone, cortical plate, intermediate, subventricular, and ventricular zones (Krmpotic-Nemanic *et al.*, 1979). At this age, immature multipolar neurons can be seen in Golgi impregnations in the marginal and superficial intermediate zones. Apical processes of cortical plate neurons branch in the marginal zone, whereas the basal processes of cortical plate neurons arborize within the superficial intermediate zone. Also at this age, AChE-reactive Cajal–Retzius cells can be identified in the marginal zone (Krmpotic-Nemanic *et al.*, 1987). During the 13th w.g., the deepest part of the cortical plate becomes less dense. In Golgi impregnations, the number of multipolar neurons increases in the superficial part of the intermediate zone and the deeper layers of the cortical plate. At the same time, the superficial part of the intermediate zone becomes well defined and the incipient subplate begins to appear as large, round nuclei. By 14 w.g., the subplate is characterized by large cell bodies with round, pale nuclei. In Golgi impregnations subplate neurons appear as polymorphous neurons with no particular orientation, in contrast to the radial orientation of cortical plate pyramidal neurons.

Developing auditory thalamocortical fibers can be readily identified by their AChE. These fibers penetrate the auditory cortex subplate at 16–18 w.g. and grow into the auditory cortical plate at 22–28 w.g. (Krmpotic-Nemanic *et al.*, 1983). The intensity of approaching auditory thalamocortical afferents is so great at 22 w.g. that the edge of the band of AChE reactivity precisely defines the boundary between auditory and adjacent nonauditory temporal cortex (Krmpotic-Nemanic *et al.*, 1980). By 24–26 w.g., AChE reactivity in ingrowing afferents appears in the middle of the cortical plate and the subplate region begins to reduce in intensity. A columnar arrangement of AChE activity in the middle third of the cortical plate appears by 28 w.g., with alternating zones 140–200 μm wide separated by narrow interspaces of lower staining intensity, appearing at this stage (Krmpotic-Nemanic *et al.*, 1980). The development of this complex pattern of AChE activity in the auditory cortex coincides with the onset of auditory cortical evoked potentials at 30 w.g. (Vaughan, 1975).

Analysis of cellular column development in the fetal human auditory cortex indicates that there is a

progressive increase in linear orientation of cells in the upper cortical layers during fetal life (Buxhoeveden *et al.*, 1996).

Development of Somatosensory Cortex

The overall sequence of development of the somatosensory cortex is similar to that seen in the visual cortex, but each step occurs at a slightly earlier stage (Kostovic and Rakic, 1990). The presubplate stage occurs just before 12 w.g. when dendritic and axonal processes as well as large cell bodies with pale nuclei begin to accumulate below the cortical plate. Electron microscopy at this stage reveals that the cortical plate is made up of geometrically regular processes and vertically oriented cells, while the presubplate consists of a loose arrangement of neuronal processes of variable orientation. Even at this early age a few asymmetric synapses on the large proximal dendrites located within the presubplate sone and the most superficial part of the intermediate zone. However, the cortical plate itself is free of synapses at this age.

The subplate proper forms at about 12–13 w.g. (Kostovic and Rakic, 1990). A broad but poorly delineated tissue band develops between the subplate proper and the cortical plate. By about 14 w.g., the cortical plate of the somatosensory cortex is about 250 μm thick and the subplate zone is clearly divided into an upper transitional ("loose") zone and a cell-poor lower subplate zone. Asymmetric synapses are present in both upper and lower parts of the subplate zone and in the marginal zone.

Between 15 and 18 w.g., the cortex increases rapidly in thickness as many afferents invade the region. The region of the subplate invaded by axons from the ventral posterior lateral thalamus is marked by transient AChE activity as seen for the pulvinar and medial geniculate projections discussed above for other cortical regions. Cortical lamination begins to appear in the somatosensory cortical plate at 20 w.g. as a pale band at the border between the superficial two-thirds and the deep one-third of the cortical plate. Synapses begin to appear in the cortical plate, with most being concentrated in the lower layers (Kostovic and Rakic, 1990). By 22 w.g. the subplate is up to 5 mm thick, making it the thickest layer of the cerebral wall, and a variety of neuronal morphologies appear in the subplate from this age.

After 35 w.g. a six-layered laminar pattern becomes visible in the developing somatosensory cortex, although the borders of individual layers are poorly defined. The subplate is progressively reduced in size toward birth and disappears at about 1 month postnatal, although some remnants of it may be seen up until 6 months after birth. The loss of subplate neurons may be due to both apoptosis and incorporation into the developing cortex.

Development of Frontal Cortex

Cytoarchitectural and Ultrastructural Development

The cortical plate is formed in the frontal region between 7 and 9 w.g. (Mrzljak *et al.*, 1990) and by 10–12 w.g., the frontal cortical anlage consists of a marginal zone, cortical plate, primordial subplate, intermediate zone, subventricular zone, and ventricular zone. At this early stage, neurons in the cortical plate have a simple bipolar morphology and the subplate contains inverted pyramidal neurons, numerous immature neurons with small cell bodies and horizontal or oblique dendrites, radial glial fibers, and immature dendrites.

Between 26 and 29 w.g., differentiation of the cortical plate begins to reveal the cortical layers, with lower cortical layers appearing from the cortical plate before upper layers. The subplate of the frontal lobe reaches its maximum width at around 28–30 w.g., and between 32 and 36 w.g. the subplate begins to show regional variation, with thinning of the subplate at the bottom of sulci. Golgi impregnations at this age (25–36 w.g.) show several types of Cajal–Retzius neurons in the marginal zone (future layer I) and these are immunoreactive for calretinin (Spreafico *et al.*, 1999). Deeper in the cortex, the late fetal period sees rapid differentiation of layer III and V pyramidal neurons and nonpyramidal neurons. The total lengths of basal dendritic trees of both lower layer III and layer V pyramidal neurons show rapid increases from 26 w.g. (Mrzljak *et al.*, 1990). By contrast, pyramidal neurons in the superficial part of layer III still display less developed basal and apical dendritic trees. The first dendritic spines are seen on the apical and basal dendrites of layer V pyramidal neurons at 26–29 w.g., and fusiform neurons begin to be discernible in the lower cortical layers at this time. At about 26–27 w.g. a very specialized type of nonpyramidal neuron, the "double bouquet" neuron, appears in the frontal cortex, but the first immature basket neurons are not seen in layer V until after 30 w.g. During the last half of gestation, the subplate neurons can be seen to form projections both into the developing cortex and down to subcortical targets, suggesting that there are two distinct populations of neurons in the subplate: projection neurons and cortical plate interneurons.

From birth onward, the frontal cortex shows large increases in size of the dendritic trees and spine growth of pyramidal neurons. There is a decrease in cell packing density as neuropil increases and the mature appearance of the six-layered cortex begins to develop. Several types of interneuron (multipolar and bitufted nonpyramidal neurons, chandelier and neurogliaform

cells) do not appear until after birth. Unlike in other (primary sensory and motor) cortical regions, the subplate layer of the prefrontal cortex contains neurons well into postnatal life (Kostovic *et al.*, 1989).

Development of Connections Thalamocortical fibers grow into the frontal lobe cortical plate between 26 and 24 w.g. (Kostovic and Goldman-Rakic, 1983), and this is correlated with both rapid growth of dendritic length of pyramidal neurons and the period of initial synaptogenesis (Molliver *et al.*, 1973). During the latter half of gestation, ingrowing thalamocortical fibers in the cortical plate are distributed in a more diffuse pattern (Kostovic and Goldman-Rakic, 1983) than in the adult primate prefrontal cortex (Giguere and Goldman-Rakic, 1989). Afferents from the basal forebrain are believed to enter the prefrontal cortex at about 30–34 w.g. (Kostovic, 1990). The growth of commissural and associative pathways is believed to occur mainly during the perinatal and infant period, when there is a further differentiation and growth spurt of pyramidal and nonpyramidal neurons in layer III (Mrzljak *et al.*, 1988, 1990).

Development of Chemically Identified Neuronal Classes and Afferents The development of dopaminergic and noradrenergic innervation of the frontal cortex at midgestation (20–24 w.g.) has been studied by Verney and coworkers (1993). Even though the cortex is still immature at this age, the widespread catecholaminergic innervation of the different areas and layers of the fetal cortex is comparable to that seen in the adult, indicating early differentiation of these afferents. Nevertheless, there is strong innervation of the subplate at this age, and somata of tyrosine hydroxylase–immunoreactive neurons are visible in the subplate, so that some reorganization of catecholaminergic innervation of the cortex is likely during late prenatal and early postnatal life.

Neurons immunoreactive for neuropeptide Y (NPY) are first seen in the frontal cortex at 14 w.g. (Delalle *et al.*, 1997; Uylings and Delalle, 1997) when they are found mainly in the lower subplate. NPY-immunoreactive neurons begin to appear in the cortical plate at 15 w.g., and the number of NPY-immunoreactive neurons in both cortical plate and subplate increases from 23 to 28 w.g. After about 28 w.g. the cortical plate and marginal zone are transformed into the six cortical layers of postnatal life. The number of NPY-immunoreactive neurons in the subplate begins to decline and the proportion of all NPY-immunoreactive cells found in the cortex increases. The laminar distribution of NPY-immunoreactive neurons becomes homogeneous over the first 2–4 years of postnatal life.

NADPH-diaphorase-reactive and NOS-immunoreactive neurons appear in the frontal lobe as early as 15 w.g. (Yan *et al.*, 1996) and are mainly found in the subplate at these early ages (Ohyu and Takashima, 1998; Downen *et al.*, 1999). An adult-like distribution of large heavily stained, nonpyramidal, sparsely spiny type I cells in the cortex appears very early (by 32 w.g.) although most heavily stained cells are located within the white matter during prenatal life. Smaller lightly stained type II cells appear later (from 32 w.g.), especially in layers II–IV of the developing cortex and increase in number up until term (Yan *et al.*, 1996).

Somatostatinergic neurons undergo a similar pattern of development to that seen for NOS-immunoreactive neurons. The earliest somatostatinergic neurons appear in the subplate of the fetal frontal cortex at about 22 w.g. (Kostovic *et al.*, 1991). Around 32 w.g., there is an increase in somatostatinergic neurons at the boundary between the subplate and cortical plate. Around the time of birth there is reorganization of somatostatinergic neurons in the cortex as peptidergic neurons increase in the upper layers and decrease in the lower layers and subplate.

Development of Callosal Neurons

Very few data are available concerning the development of callosal neurons in the human fetal cortex. The cingulate cortex is known to contain callosally projecting neurons as early as 25 w.g. (DeAzevedo *et al.*, 1997), in both the cortical plate and subplate. Callosal neurons in the cortical plate at 26–32 w.g. are mainly spiny pyramidal cells with somata distributed throughout the depths of the plate. At this stage they have well-differentiated apical and basal dendrites. Subplate callosal neurons are relatively smooth cells with many different morphologies (radially oriented, horizontally oriented, multipolar, and inverted pyramidal) and distributed throughout the subplate thickness.

Development of Cortical Glia and Vasculature

The time of development of glial cell types in the human cerebral cortex has been followed through Golgi impregnation, immuno- and lectin and enzyme histochemical markers (Stagaard and Møllgard, 1989; Fujimoto *et al.*, 1989; Wilkinson *et al.*, 1990; Marín-Padilla, 1995; Wierzba-Bobrowicz *et al.*, 1998; Pal *et al.*, 1999).

In very young embryos (about 4–6 w.g.) vimentin immunoreactivity is found throughout the cells of the neuroepithelium (Stagaard and Møllgard, 1989). By 9 w.g., radial glia are clearly distinguishable by their vimentin immunoreactivity (Wilkinson *et al.*, 1990) and they will retain that immunoreactivity until late fetal life. Cells showing immunoreactivity for S-100 and

with the morphology of astrocytes appear by 9 w.g. (Wilkinson *et al.*, 1990), but glial fibrillary acidic protein–immunoreactive astrocytes cannot be clearly distinguished until 14 w.g. according to those authors. Biochemical assays of fetal brain also indicate production of glial fibrillary acid protein (GFAP) from about 17 w.g. (Pal *et al.*, 1999). Maturation of oligodendrocytes in the fetal cerebrum begins from about the end of the first trimester, with the first appearance of carbonic anhydrase II–positive oligodendrocytes from 17 w.g. (Wilkinson *et al.*, 1990).

The differentiation of astrocytes in the cerebral cortex has been followed in detail by Marin-Padilla (1995). Marin-Padilla proposes that, at the beginning of cortical development, there are three glial precursors in the developing neocortex: (1) radial neuroctodermal cells with nuclei above the primordial plexiform layer, which lose their ependymal attachments to become early astrocytes of layer I; (2) neuroectodermal cells with nuclei below the primordial plexiform layer, which retain their pial and ependymal attachment to become type I radial glia and serve to guide neurons during later fetal development (see section on general cortical development); and (3) neuroectodermal cells, which lose their pial attachment, are transformed into type II radial glia, and eventually become fibrous astrocytes of the subplate and developing white matter. Protoplasmic astrocytes of the gray matter appear from 15 w.g., by migration from layer I and appear coincidentally with vascularization of the cortex. The transformation of layer I glial cells into astrocytes and their incorporation into the cortical plate is supported by the findings of Spreafico and coworkers (1999).

Microglial cells in the cerebral cortex can be identified as early as 5–6 w.g. (Fujimoto *et al.*, 1989), when round nucleoside diphosphatase (ameboid) cells appear in the cortical wall. By 7 w.g., ramifying cells can be seen mainly in the marginal layer (developing layer I). Density of ramified microglia increase progressively from 13 w.g. (Woerzba-Bobrowicz *et al.*, 1998), so that by 22 w.g. numerous poor and highly ramified microglial cells are present throughout all layers of the cortex. At least some of the highly ramified cells are derived from the ameboid microglia, and the invasion of the cortex by ramified microglia coincides with vascularization of the differentiating cortex (Rezaie *et al.*, 1997).

At 15 w.g., the only vessels coursing through the developing cortex are radially oriented vessels (presumably arteries) arising from leptomeningeal arteries (Norman *et al.*, 1986). These early vessels course through without branching, to supply the subcortical tissue. From about 20 w.g., horizontal vessels arise from the radial vessels, particularly in the lower levels of the differentiating cortex. As horizontal branches in the lower half of the cortex increase through 20–27 w.g., these branches also begin to appear in the upper cortex. Shorter radial vessels appear from 27 w.g., and just before and after birth a fine network of capillaries proliferates, particularly in layers IV and V (Norman *et al.*, 1986; Mito *et al.*, 1991; Miyawaki *et al.*, 1998).

Development of Gyrification, Structural Asymmetry and Gender Differences

Developmental changes in gyrification of the human brain have been studied using unbiased stereological techniques (Mayhew *et al.*, 1996). Those authors found that there are transient increases in gyrification between 85 and 129 mm crown–rump length (approximately 12–17 w.g.) and toward the end of the fetal period. This is in agreement with findings that the proportion of intrasulcal cortex rises from about 22% at 17–18 w.g. to 66% in the newborn and adult (Henery and Mayhew, 1989). These findings indicate that the transition from fetal to adult gyrification values occurs at about the time of birth.

Left/right asymmetries in the temporal speech areas of the human fetal brain have been studied by Chi *et al.* (1977). They reported that asymmetries of the transverse temporal gyri and planum temporale associated with left hemispheric speech and language dominance become recognizable by 31 w.g. and that these asymmetries appear as soon as the relevant gyri become clearly recognizable. In other regions, fetal cerebral asymmetry has been found in the prefrontal cortex and striate/extrastriate cortex (de Lacoste *et al.*, 1991). Striate/extrastriate cortex is far more asymmetric in male fetuses than females. In terms of total cerebral volume, male brains tend to have a larger right hemisphere, whereas female brains tend to have two hemispheres of the same size or a left hemisphere slightly larger than the right. These gender-based differences may arise from the early action of testosterone on fetal cerebral cortical growth.

Neurochemical analysis of cortical development also indicates the early onset of cerebral asymmetry. Bracco *et al.* (1984) have found that there is asymmetric development of choline acetyltransferase (ChAT) in the brains of fetuses aged 26 to 40 w.g. Values of ChAT are much higher in the right first temporal gyrus (Brodmann's area 22) than in the left, even though there is no asymmetry in levels of ChAT at this age in the precentral gyrus (Brodmann's area 4). The level of ChAT in the right area 22 is comparable to that in the adult brain, suggesting that there is precocious development of ChAT in the temporal lobe during fetal life, which could also account for the early asymmetry.

Hippocampal Formation and Connections with Entorhinal Cortex

The archicortical plate begins to show evidence of morphological differentiation at about 10 w.g., and its major subdivisions can be distinguished on cytoarchitectural criteria from about 11 to 15 w.g. (Kostovic *et al.*, 1989, 1993). Synapses have been identified in the hippocampal formation as early as midgestation (Kostovic *et al.*, 1989) and dendritic spine development is evident at 26 w.g. on pyramidal neurons of cornu Ammonis, relatively advanced compared to visual cortex (Purpura, 1982).

Analysis of entorhinal cortex development using Golgi and Nissl staining techniques has been undertaken by Kostovic and coworkers (1993). Those authors found that the first signs of cytoarchitectural differentiation of the entorhinal cortex are at 10–10.5 w.g., when multilayered spreading of the deeper part of the cortical plate appears, along with the appearance of a monolayer of large neurons at the superficial part of the cortical plate, adjacent to the marginal zone. Golgi impregnation at the same age shows that large neurons with widely bifurcating apical dendrites occupy the cortical plate–marginal zone interface. The authors called these early differentiating cells "promoters" because the cells develop area-specific morphology before the appearance of the full set of cytoarchitectonic features of the entorhinal cortex. By 13 w.g., the entorhinal cortex shows the first appearance of its major characteristic cytoarchitectonic feature—the lamina dissecans, separating two principal layers of the cortex. At this stage the authors were also able to distinguish five cytoarchitectonic subdivisions, indicating the early areal differentiation of the entorhinal cortex. Golgi preparations at 13 w.g. show significantly advanced neuronal differentiation compared to 10.5 w.g. with differentiation of the other cortical plate neurons already well developed.

Hevner and Kinney (1996) have used carbocyanine dye tracing techniques to identify connections of the hippocampal formation during fetal life. They found that robust connections between the entorhinal cortex, hippocampus, and subiculum are present at 19 w.g. (the earliest age they studied) and that these connections are essentially the same anatomically as those seen in adult primates. Projections to the hippocampus and subiculum originated from neurons in layers II and III of the entorhinal cortex, whereas projections to the entorhinal cortex originated from pyramidal neurons in CA1 and subiculum. On the other hand, projections from the entorhinal cortex to the dentate gyrus and connections with adjacent neocortex are only rudimentary at 22 w.g. (the last age they studied), suggesting that hippocampal pathways develop before isocortical pathways.

The development of NO-synthesizing cells in the prenatal human hippocampus has been studied by Yan and Ribak (1997) using NADPH-diaphorase histochemistry. Strongly reactive nonpyramidal neurons appear in the hippocampal subplate at 15 w.g. and increase rapidly in both this region and the overlying cortical plate between 17 and 24 w.g. The distribution pattern of NADPH-diaphorase-positive cells stabilized at about 28 w.g., when reactive cells are mainly distributed at the border between the cortex and subcortical white matter in the case of the entorhinal cortex and subiculum, and between the cortex and alveus in the case of the hippocampus. Moderately stained nonpyramidal neurons appear in the dentate gyrus at 17 w.g. and increase in this region up to 28 w.g. A third type of nonpyramidal neuron, small and lightly stained, can be first seen at 32 w.g. and increases in number by term. In addition, hippocampal pyramidal and granule neurons transiently show NADPH-diaphorase activity, mainly between 15 and 24 w.g.

Interest in the possible involvement of disordered hippocampal development in the etiology of schizophrenia has prompted several studies of receptor development and binding in the prenatal human hippocampus. Gurevich *et al.* (1997) have found that dopamine D2 receptor mRNA is expressed very early during development in both subiculum and cornu Ammonis. D2 mRNA–positive neurons appear in both the subiculum and cornu Ammonis as early as 13 w.g. Even at this early stage, some of the D2 mRNA–positive cells in CA1 have clearly pyramidal morphology, while the most densely stained have the appearance of immature, newly migrated neurons. The proportion of D2 mRNA–positive cells decreases during development (from 13 to 25 w.g.) to about 20–26%. By the 34th week only mature pyramidal neurons in the deeper layers express D2 mRNA. Since dopamine may play a direct role in normal cellular differentiation of cortical neurons, it is possible that the presence of the D2 dopamine receptor in the hippocampus may have a special morphogenetic role in the maturation of neurons in specific fields of the hippocampus.

Serotonin receptors in the developing hippocampus appear to be well developed by the end of fetal life, with strong signals for 5-HT_{1A} mRNA being found in cornu Ammonis stratum pyramidale and the granule cell layer of the dentate gyrus by 35 w.g. (del Olmo *et al.*, 1998). Muscarinic cholinergic receptor binding is also well developed by midgestation (21 w.g.; Egozi *et al.*, 1986; Gremo *et al.*, 1987), with early evidence of receptor heterogeneity and an age-related decline during prenatal life.

Several genes are known to regulate apoptosis in various tissues. One of them is *bcl-2*, which encodes for the protein Bcl-2, which is expressed in many neurons during development. Chan and Yew (1998) have examined apoptosis and Bcl-2 expression in the developing hippocampus. Apoptosis in the polymorphic and molecular layers of the human fetal hippocampus becomes more prominent as fetal age progresses, but the apoptotic index in the pyramidal layer remains low and variable throughout prenatal life. On the other hand, Bcl-2 expression is strong in the pyramidal neurons during early gestation (14–27 w.g.) and declines to negativity during late fetal life (32 w.g.).

The expression of neurotrophin receptors in the developing human hippocampus has been investigated by Chen *et al.* (1996). Trk-immunoreactive neurons are first seen in the hippocampus at 16 w.g. At this early stage and up to about 19 w.g., most hippocampal trk-immunoreactive neurons are scattered within the stratum oriens and stratum pyramidale of the cornu Ammonis and show multipolar or fusiform morphology with a short dendritic branching pattern (Chen *et al.*, 1996). After 20 w.g., there is a progressive increase in the number of trk-immunoreactive neurons in the cornu Ammonis. Those authors also reported that trk-immunoreactive neurons are present within the hilar region of the dentate gyrus between 16 and 34 w.g. In contrast, only a small population of transiently p75-immunoreactive neurons are seen within the hippocampal formation during fetal life. These are found in the hilar region of the dentate gyrus between 16 and 24 w.g. (Chen *et al.*, 1996). Chen and coworkers have pointed out that the distribution of trk-immunoreactive neurons in the developing human hippocampus parallels the expression of BDNF and NT-3 in this region. In particular, BDNF is highly expressed in pyramidal neurons in the CA3 and CA2 subfields, with lower levels in CA1 and the granule cells of the dentate gyrus. NT-3 is also expressed in neurons of the medial part of CA1 and CA2 and in the granule cell layer of the dentate gyrus. Nevertheless, the precise role of trk and p75 during development of the hippocampus, and the way in which these two neurotrophin receptors interact, remains to be elucidated.

DEEP TELENCEPHALIC NUCLEI

Forebrain Segmentation by Radial Glia

At 9 weeks, radial glial cells (RGCs) can be demonstrated throughout the ventricular zone by the intermediate filament protein vimentin (VIM, see "Development of Chemically Identified Neuronal Classes and Afferents"). In the forebrain, their evenly spaced, radially aligned processes can be traced to the cortical plate. Only in the prospective fimbrial glioepithelium (Altman and Bayer, 1990), IR is intense and reaches the pial surface. In subcortical areas VIM-positive radial glial processes are much less dense than in the pallial region and their course and destination can therefore be more easily assessed (Fig. 3.2). In some regions, VIM-immunoreactive processes are condensed and form boundaries, as in the external capsule, the internal lamellae of the thalamus, or the ventral thalamus (Fig. 3.2). Another marker for the demonstration of RGC is CD15 (see Mai, 2002). Antibodies against this epitope reveal a subpopulation of the VIM-positive RGC. The CD15 cells appear later in the prosencephalon, around 12–13 weeks, are much less abundant and less uniform. Initially they are concentrated in a small area at the lateral ventricular (ganglionic) eminence (LVE) close to the corticostriatal sulcus (Mai *et al.*, 2003). Their number and density reach a maximum around 24 weeks (Fig. 3.3a–c). Due to their nonuniform and highly restricted manner they outline distinct domains, like those that have been described in the mouse and wallaby brain (Mai *et al.*, 1998a; Cheng *et al.*, 2002) (Fig. 3.4a). Registration of the CD15+ processes in the mouse prosencephalon in all planes of orientation has resulted in a spatial map (Fig. 3.4b) that generally fits to the so-called prosomeric organization as characterized in the rodent brain by structural and biochemical features like expression of regulatory genes (see Keyser, 1972; Rubenstein *et al.*, 1994; Martínez and Puelles, 2000) (Fig. 3.4c).

From the location of the CD15 RGC and the orientation of their processes it is clear that the CD15 segments are not complete on the transverse axis: they align between pretectal, dorsal thalamic, and ventral thalamic domains in the alar plate but are absent from the equivalent regions of the basal plate (Fig. 3.4a, c). This incomplete dorsoventral extent might be important with respect to the continuation of the alar-basal boundary (sulcus limitans). Using the highest density and the orientation of CD15-immunoreactive processes as parameters, evidence suggests that the alar–basal boundary continues along the ventral thalamus to the choroidal roof of the forebrain at the level of the interventricular foramen. Here the radial glial cells come in contact with the intense labeling by CD15 of the commissural plate at the anterior wall of the forebrain (Fig. 3.4d) (see Rakic and Yakovlev, 1968). This site is related to the lateral plexus evagination at the border between the di- and telencephalon (Bailey, 1916). If the condensation of CD15+ RGC corresponds to the sulcus

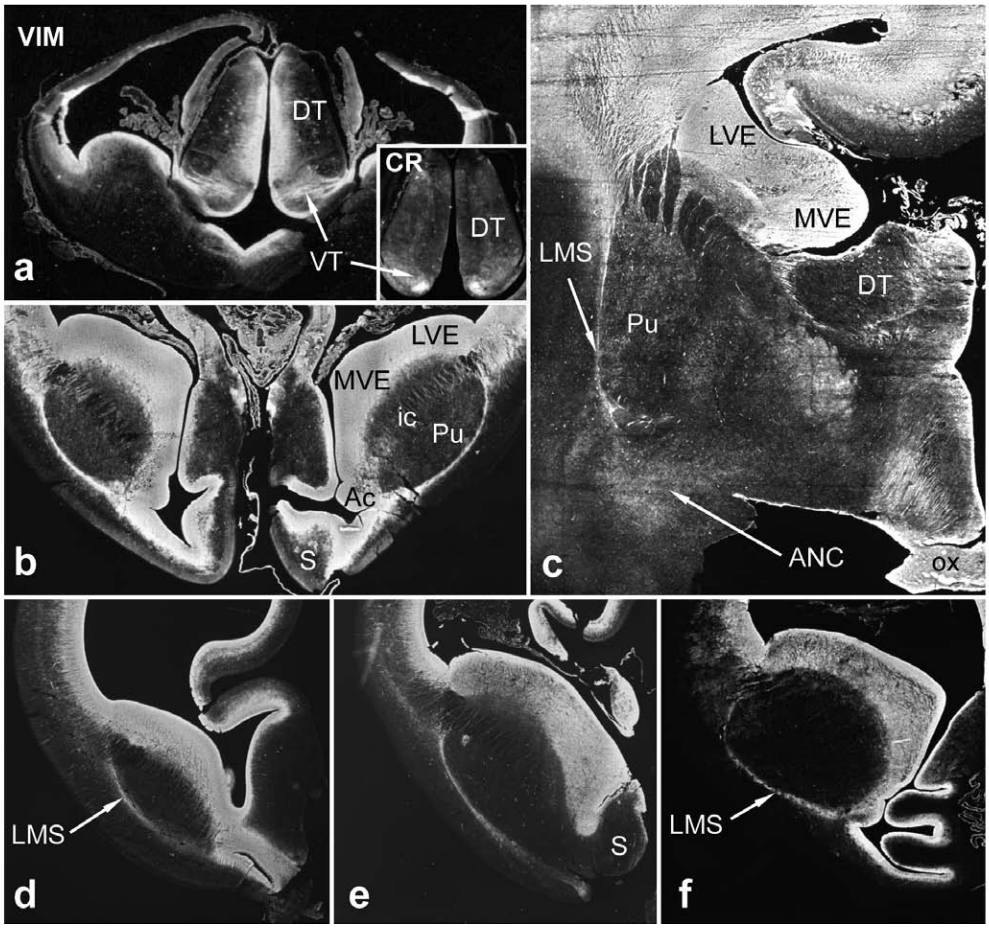

FIGURE 3.2 Coronal sections reacted for the demonstration of vimentin (VIM). **a.** Cross-section through the anterior thalamus at 10 weeks. Dense VIM immunoneactivity (IR) is seen in the dorsal thalamus (DT). The border between DT and the ventral thalamus (VT) is indicated by the shallow sulcus medialis and the unlabeled medial part of the tract of the zona limitans intrathalamica. Strands of VIM processes are typical for the VT; these converge at the stem of the tenia. *Inset:* **a.** Calretinin IR (CR) marks an area of reduced VIM IR. **b.** VIM IR at the level of the precommissural hippocampus from a 14-week fetus. The ventricular eminences (LVE and MVE) are completely filled with immunoreactive processes without distinction between both divisions. A bulge indicates the part of the VE from which the accumbens nucleus (Ac) is derived. **c.** Coronal section at 21 weeks. **A.** VIM-positive processes outline the external capsule. **d–f.** VIM IR in different section levels of the basal forebrain of a 14-week fetus. The lateral migratory stream (LMS) surrounds the lateral aspect of the putamen. ANC; amygdaloid nuclear complex; ic, internal capsule; ox, optic chiasma; Pu, putamen; S, septum.

limitans as shown in the mouse brain stem and spinal cord (Ashwell and Mai, 1997a, b), then it is unlikely that the sulcus ends at the supramamillary recess as described by O'Rahilly and Mueller (Chapter 2 of this volume), or at the chiasmatic plate as proposed by the prosomeric model (Puelles and Rubenstein, 1993); (Fig. 3.4b). The course of the sulcus limitans as suggested by our observations would correspond to the interpretation by Spatz (1921), Kahle (1956), and Richter (1965) and would fit well with the drawings from Hines (1922, e.g., her figures 18–20). However, since the sulcus limitans widens at the border between the syn- and diencephalon, a true continuation or junction of any of the diencephalic sulci is not seen (Keyser, 1972), and other parameters have to be applied before conclusive evidence is achieved. Confirmation awaits the definition of the contents of the CD15 divisions by the delimitation of regulatory gene expression patterns within these boundaries.

The same morphological features as described in the developing mouse brain also become visible in the developing human forebrain (Fig. 3.4d). CD15-positive RGC and their processes in the human forebrain outline areas that appear homologous to those in the

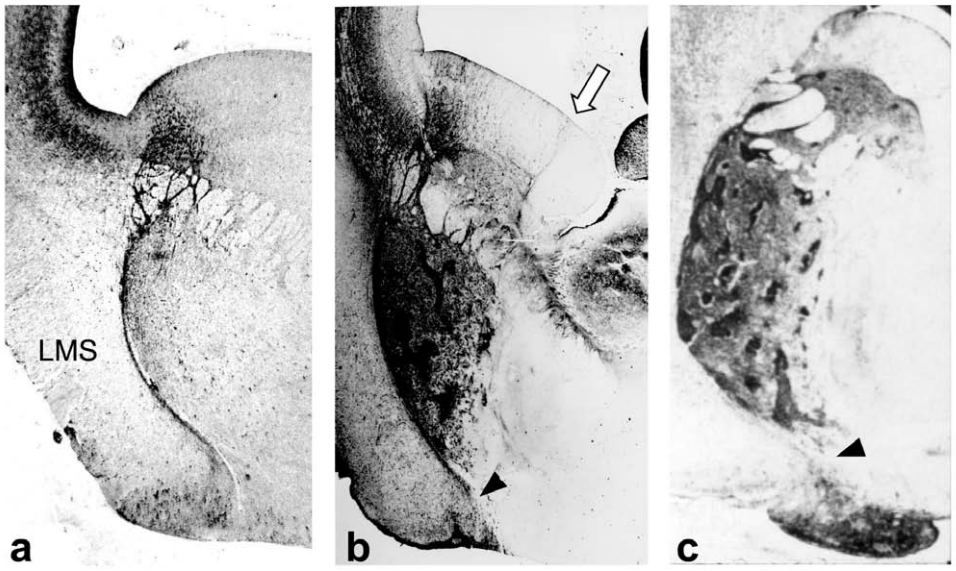

FIGURE 3.3 Frontal sections cut at the level of the ventricular eminence and striatum. **a.** At 13 weeks CD15 immunoreactivity *(black)* is very pronounced along the lateral portion of the striatum, outlining the lateral migratory stream (LMS) in the external capsule. A set of immunoreactive processes separates from the perimeter of the putamen to continue toward the pial surface *(arrowhead)*. **b.** At 17 weeks CD15 IR becomes more intense and involves the dorsal striatum, where the differentiation between patch and matrix compartments is advanced. Processes in the LMS separate at the border between the dorsal and ventral striatum (at the level of the intersection with the anterior commissure) and proceed between the olfactory tubercle and accumbens nucleus medially and the piriform cortex laterally. **c.** At 25 weeks CD15 IR is present in the dorsal striatum. *Arrows* point to the border between the piriform cortex and the olfactory tubercle; the *open arrow* in **b** points to the interstriatal glial sling, separating the LVZ and MVZ.

mice, providing evidence that the same boundaries exist in the human (Fig. 3.4e).

The intense labeling of the individual processes of RGC allows them to be traced from the ventricular epithelium through the brain substance. During early CNS development RG processes are radially oriented from the ventricular to the pial surfaces, and this spatial registry between both extremes appears to be maintained during the subsequent developmental steps; therefore, the orientation of RG processes at later (fetal) time still indicates the registration between corresponding ventricular and pial locations. Tracing of CD15-positive RG processes, which is easier because it labels only a subgroup of RGC, has allowed selective visualization of a wide-ranging and precisely organized system that has several interconnected components (Fig. 3.5). These can be arbitrarily separated into a lateral stream that connects the lateral ventricular zone with the basal forebrain, an intereminential sling, and a portion associated with the stem of the choroid plexus.

Lateral Stream

The lateral stream is composed of processes of the VIM and CD15-immunoreactive RGC cells that are located in the lateral ventricular eminence close to the corticostriatal sulcus. They cross through the internal capsule (or stem bundle, respectively) and pass to the external capsule. As a thin but extensive sheet, these processes outline the lateral perimeter of the putamen (Figs. 3.2a, 3.3). Several major relations can be distinguished in CD15-stained sections (Figs. 3.5 and 3.6): first, with CD15-immunoreactive patches in the dorsal striatum that stand in continuity with the CD15-positive processes along the lateral caudate nucleus and putamen (Fig. 3.3b, c); (Mai *et al.*, 1999a; see below); second, with the lateral portion of the olfactory recess of the lateral ventricle (Fig. 3.2); third, with the pial surface of the piriform cortex (Fig. 3.3) and finally, with the amygdaloid nuclear complex. The processes that pass to the piriform cortex separate from the external capsule at the level of the border between the dorsal and ventral putamen and pass between the olfactory tubercle and accumbens nucleus medially and the piriform cortex laterally, thus defining the border of the isocortical plate (Mantelkante of His) (Figs. 3.3 and 3.5). The processes that proceed to the amygdaloid nuclear complex mark the superficial nuclei (supraamygdaloid area of Brockhaus, 1940) which thus stand out against the unstained deep amygdaloid nuclei, indicating a border between both divisions (Figs. 3.5 and 3.6; compare to Fig. 3.11).

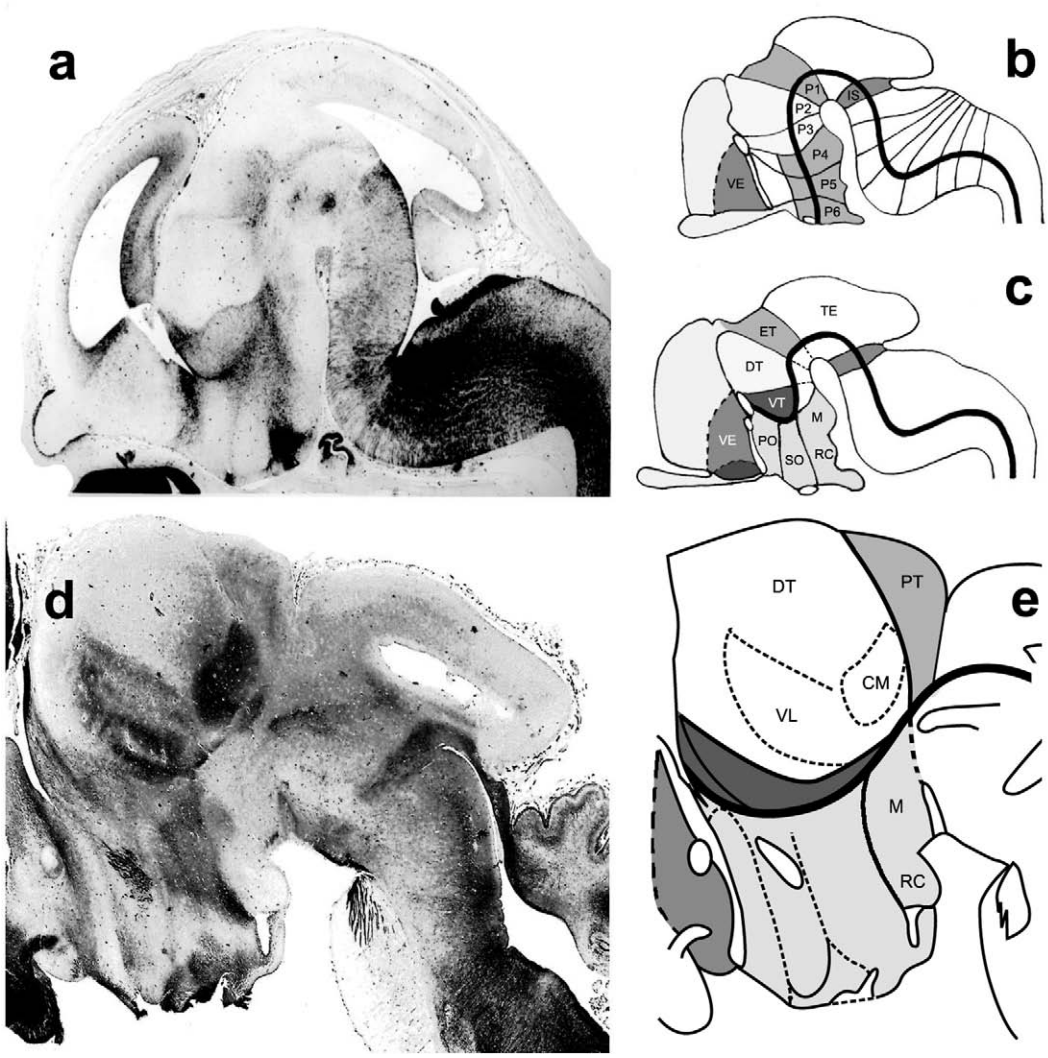

FIGURE 3.4 Comparison of the CD15 immunoreactivity (IR) between the mouse and human brain. **a.** Sagittal section close to the midline through a mouse brain at the embryonic age of 12.5 days. **b.** Modified drawing of the prosomeric boundaries as interpreted from the expression of transcription markers. According to this model, the alar–basal boundary (sulcus limitans) ends at the optic recess. **c.** Schematic drawing representing the major divisions as evidenced by CD15 and vimentin IR. The sulcus limitans in this schema continues along the ventral thalamus to the anterior choroidal roof at the level of the anterior interventricular foramen. **d.** Parasagittal section through a human fetal brain at the age of 15 weeks. **e.** Outlines of segments distinguished in the human brain by CD15 IR as interpreted from the distribution pattern of CD15 IR.

The location and arrangement of the CD15-immunoreactive processes from the proliferative neuroepithelium to the external capsule and further to the above described destinations corresponds to that of the lateral (cortical) migratory stream (LMS) as described in the brains of various nonhuman species (Brunjes *et al.*, 1998; Stoykova, *et al.*, 1996, 1997). Since radial glial processes act as a guidance structure for migrating postmitotic neurons, those disclosed in the human brain might likewise provide a substrate for the migration of a comparable population of cells. In analogy to findings in nonhuman brains, it appears that the correspondence between the starting and end points of the radial glial connection allows the correlation between matrix (proliferation) and homing (settling) areas of cells. Knowledge about that correlation may aid the neuropathological evaluation of abnormal migration patterns as a consequence of restricted vascular lesions into the VE (Solcher, 1968; Ulfig, 2002).

Besides forming a scaffold responsible for the migrational restriction of cells from the lateral ventricular eminence, the CD15 processes might also help to establish a boundary between striatum and pallium

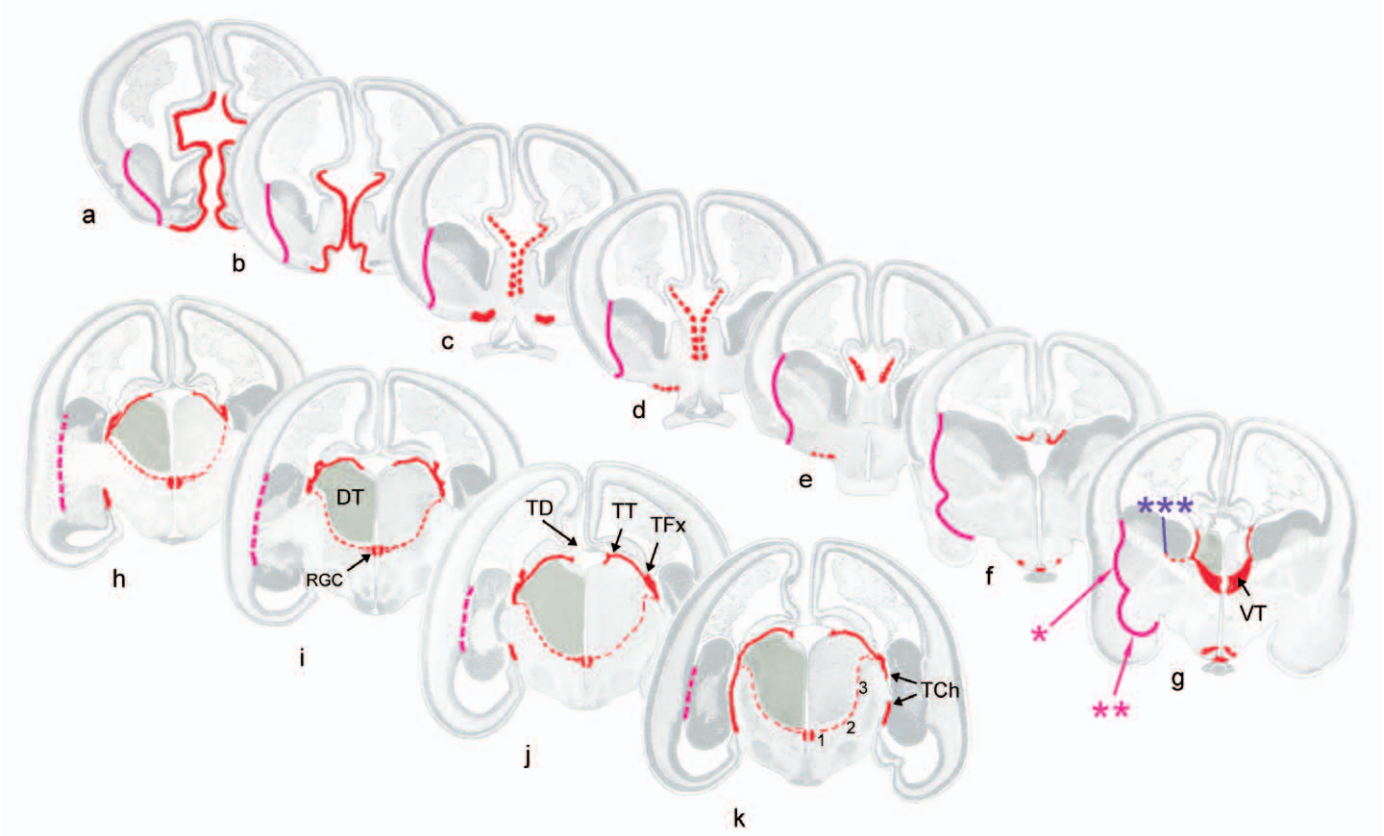

FIGURE 3.5 Series of coronal sections of a human fetus of approximately 14 weeks. The arrangement and extent of the CD15-immunoreactive processes are schematically indicated from rostral **(a)** to caudal section levels **(k).** In each section the cross-sectional area of the dorsal thalamus has been darkened on the left side. In **g,** the processes in the external capsule, corresponding to the lateral migratory stream, are indicated by an asterisk. The continuation of the CD15 processes into the amygdaloid nuclear complex are indicated by two asterisks. Three asterisks point to the intereminential CD15 glial sling. At the level of the interventricular foramen **(g).** a dense stream of radial glia processes passes from the ventricular epithelium through the ventral thalamus (VT) toward the choroid tenia (Ch). Posteriorly **(h–k)** small stripes of radial glial cells (RGCs) are still found at the ventricular border of the ventral thalamus, but only few radial glia processes can be traced along the perimeter of the dorsal thalamus *(broken lines)*. TCh, choroid tenia; TFx, fornical tenia; TT, thalamic tenia. Reproduced from Retzius, 1896.

during forebrain development (Götz *et al.*, 1996). Its location and orientation fits well to the striatopallial boundary, which becomes disclosed by virtue of the expression of transcription factors and of adhesion molecules such as R-cadherin (Matsunami and Takeichi, 1995; Stoykova *et al.*, 1996, 1997; Chapouton *et al.*, 1999; see also Puelles, 2001). In the Pax 6 mutant mouse, the boundary is no longer existent and restriction of cell migration is lost (Chapouton, 1999). Finally, this boundary might be a locus of increased vulnerability with respect to vascular accidents (Solcher, 1968).

Intereminential Area

CD15 IR demarcates the LVE from the MVE (Figs. 3.3b and 3.5g). This demarcation appears at 16 weeks but becomes pronounced in the following weeks by the steady increase in the number of RGCs and their processes in the LVE, whereas the MVE remains largely free of IR (Figs. 3.3b and 3.9a). Even more, at the interganglionic boundary an intense CD15 sling is formed. This boundary extends from the ventricular surface (sulcus interstriatus of Brockhaus, or the intereminential sulcus of O'Rahilly and Müller, Chapter 2 of this volume) perpendicularly through the VE to an area of focal increase of CD15 IR at the exact location where the ventral margin of the caudate nucleus and the internal capsule meet (Fig. 3.3b). This point, which remains visible until the consumption of the matrix cells in the GE around the time of birth, is connected with other CD15 processes (see below).

Albeit not yet described in nonhuman brains, there exists indirect evidence that this glial sling is important

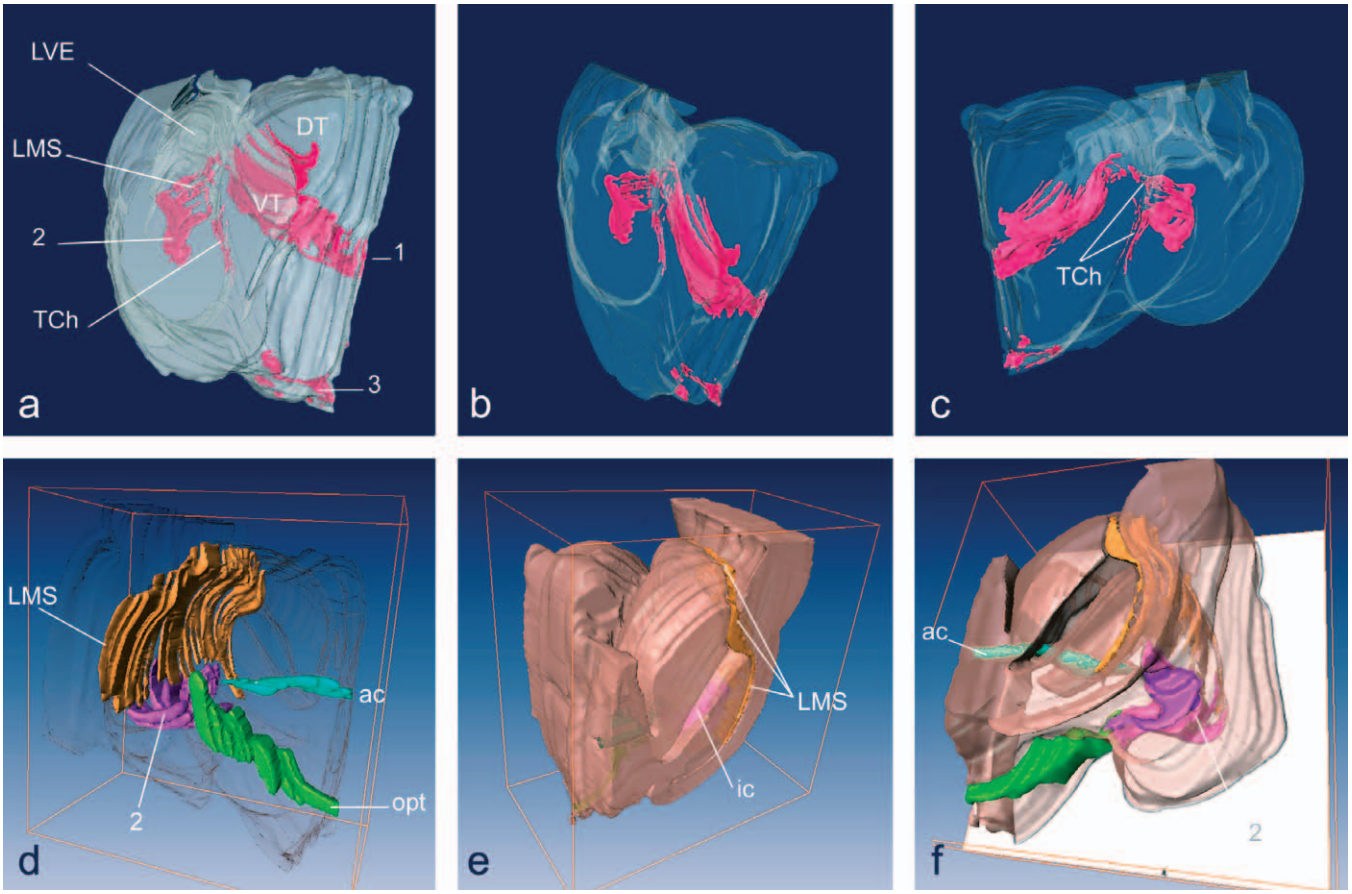

FIGURE 3.6 Computer reconstructions of the CD15-immunoreactive strands of processes in the prosencephalon of a human fetus at age 15 weeks **(a–c)** and 17 weeks **(d–f).** 1, Indicates the radial glial cells and processes in the ventral thalamus (VT) which converge at the stem of the choroid tenia (TCh). 2, Set of processes between the external capsule and the amygdaloid nuclear complex. 3: Set of radial glial cells in the hypothalamus. Other abbreviations: ac, anterior commissure; DT, dorsal thalamus; ic, internal capsule; LMS, lateral migratory stream; LVE, lateral ventricular eminence; opt, optic tract.

for axonal navigation of thalamocortical and corticothalamic axons (Metin and Godement, 1996; Molnar *et al.*, 1998, Auladell *et al.*, 2000). These axons pass through diverse territories, like the ventral thalamus, telencephalic stalk, and basal ganglia, before they finally reach the presumptive targets in the neocortex and thalamus, respectively. On this route through the diverse territories the thalamic and cortical axons are dependent on several path-finding steps. One important location that the thalamic and cortical axons must meet for correct routing in the subcortical telencephalon could well match by topography to the glial sling of the intereminential border (reaching from the ventricular surface to the internal capsule) (Metin and Godement, 1996; Tuttle *et al.*, 1999; Molnar *et al.*, 1998). CD15 might provide a guidance cue as has been suggested for optic and olfactory axons (Marcus *et al.*, 1999; Plank and Mai, 1992; see Mai, 2002).

Linkage of the Ventricular Zone of the Ventral Thalamus to the Root of the Tenia

The ventral thalamus constitutes another region where the registration between ventricular and pial surfaces is obvious (Forutan *et al.*, 2001). Here CD15 characterizes a subpopulation of radial glial cells located in the ventricular surface along the entire extent of the ventral thalamus (Figs. 3.5g and 3.6a). Processes of these cells can be followed distally where they converge at the stem or root of the choroid tenia (10–15 weeks). Because the RG processes converge at the root of the tenia, this structure becomes particularly well visible in CD15 stained sections as a thin, continuous line at the dorsolateral surface of the thalamus, thereby attaining different topographic relations with the plexus (choroid tenia, fornical tenia, thalamic tenia; Fig. 3.5h–k). At the anterior midline the tenia forms part of the choroidal roof of the forebrain and is here contiguous with the

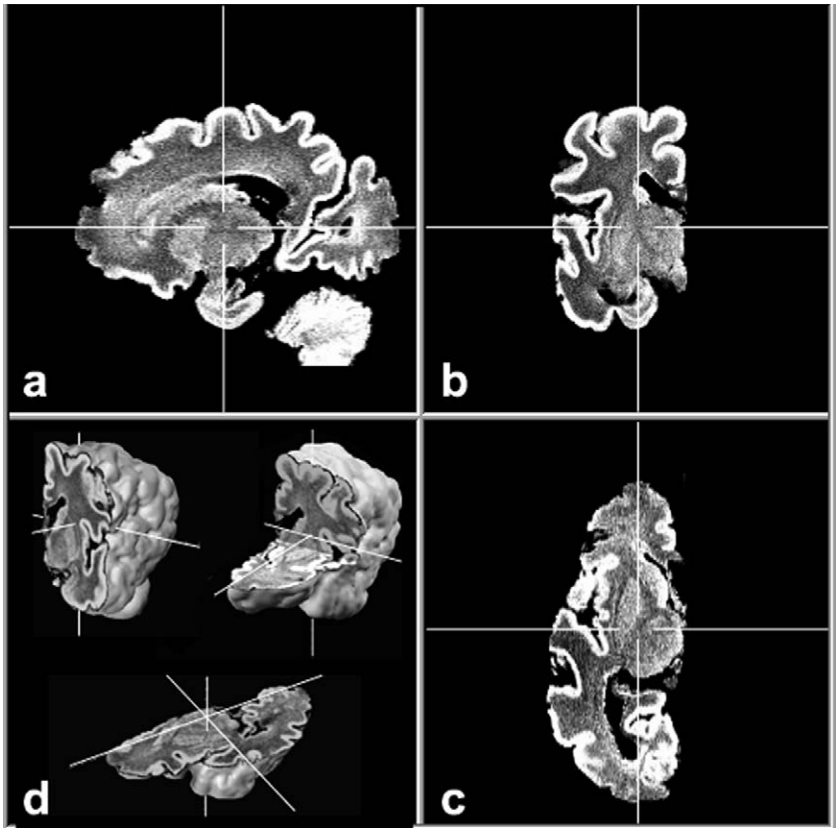

FIGURE 3.7 Magnetic resonance (MR) images of an autopsy brain of 36 weeks showing the high contrast and resolution obtained. From an MR image series the brain volume was calculated such that the brain can be virtually sliced in any orthogonal plane. The centers of the crosses in **a–c** indicate the voxel which is common for all sections. In **d,** the location of the sections in the reconstructed brain is visualized. Three-dimensional navigation is possible as is the matching between the MR images with the sections after histological or histochemical treatment.

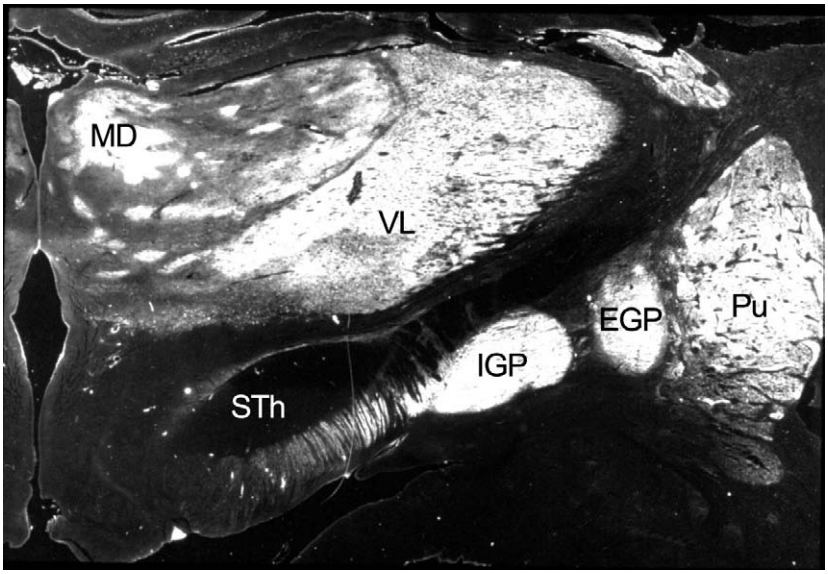

FIGURE 3.8 Lumogram (immunoreaction product appearing in white) showing CD15 IR in the thalamus and basal ganglia at age 27 weeks. EGP, IGP, external and internal globus pallidus; Pu, putamen; STh, subthalamic nucleus; VL, ventrolateral thalamus.

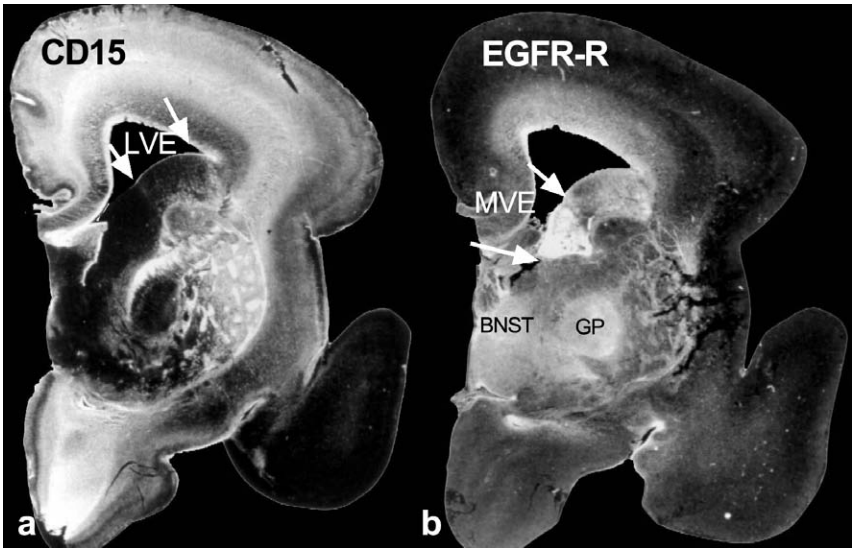

FIGURE 3.9 Distribution of CD15 and epidermal growth factor receptor (EGFR) in the forebrain of a transverse section through the 22-week fetal forebrain. In the deep-forebrain structures CD15 is concentrated in the lateral ventricular eminence (LVE) and dorsal striatum; EGFR is enriched in the medial ventricular eminence (MVE), globus pallidus (GP), and bed nucleus of the stria terminalis (BNST).

likewise highly CD15-positive commissural plate and lamina terminalis (Fig. 3.4e, compare with Fig. 3.13). The three-dimensional orientation of the CD15-positive stem of the choroid corresponds to the choroid fissure and the hem of the hemispheres; its curvature directly reflects the changes in shape which the prosencephalon has undergone. In a caudal direction the CD15 IR of the stem of the tenia is continuous along the infra-choroidal tenial leaf with the sulcus terminalis; thereby outlining the junction between the cerebral hemisphere and diencephalon. From the depths of the sulcus terminalis IR is continuous with the patch of IR at the base of the intereminential border (thereby forming a boundary between the medial ventricular eminence and the stria terminalis on one side, and the thalamus on the other) (Fig. 3.6b, c). This stretch, located between the ventricular eminence and the pulvinar; possibly corresponds to the corpus gangliothalamicum, a passageway for the stream of migrating cells in transit from the LVE to the posterior thalamus (Rakic and Sidman, 1969).

Summary

Shortly after the beginning of the fetal period a three-dimensional scaffold appears, which by its topography fits well to the organization described in the mouse brain. This, in turn, matches the topological data obtained from expression patterns of regulatory genes and guidance factors. Radial glial cells of this system apparently provide a substrate for neuronal or glial cell migration, as suggested by its high, transient expression in areas of described migration, as in LMS or the corpus gangliothalamicum. In addition, the units specified by CD15-positive RGC and processes might provide the boundaries for regional domains in which specific nuclei with characteristic neuronal types appear and differentiate, or they might impose barriers to deter the growth of axonal pathways (see Silver *et al.*, 1993). The further development of many areas in the forebrain, particularly the basal ganglia, amygdaloid complex, and thalamus, supports this view (see below).

All relations described above apparently represent not separate entities but form a three-dimensional interrelated scaffold (Fig. 3.6). At this early fetal period it appears to be rather complicated; however, since its origin is in the direct correspondence between the ventricle and pial surface (at an earlier developmental stage) its registration is an important step for the description of fundamental subdivisions of the brain architecture and for the future modeling of the formal development of the human brain.

Corpus Striatum and Other Basal Nuclei

The development of the deep telencephalic nuclei is closely related to the lateral and medial eminences which make different contributions to the individual nuclei (see O'Rahilly and Mueller, Chapter 2 of this volume). Both structures show molecular and clonal

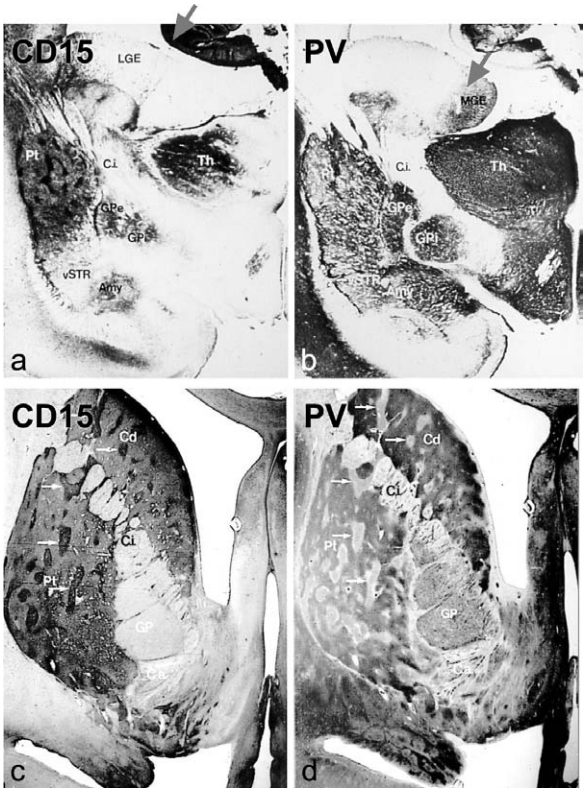

FIGURE 3.10 Distribution of CD15 **(a, c)** and parvalbumin **(b, d)** in the forebrain of transverse sections through the fetal forebrain at the age of 18 weeks **(a, b)** and of 3 weeks postnatal **(c, d).**

differences (Halliday and Cepko, 1992; Acklin and van der Kooy, 1993; Olsson *et al.*, 1995, 1997; Rubenstein *et al.*, 1997). In the fetal human brain molecularly distinct subsets of radial glial cells can be discriminated by CD15 (Mai *et al.*, 2003), epidermal growth factor receptor (EGFR) (Mai *et al.*, 1995), antibodies against S1515 and parvalbumin (Figs. 3.9 and 3.10). Some distribution patterns show differing localization with only partial overlap in their distribution. CD15 IR marks the LVE (see above); EGFR IR becomes present (predominantly) in the medial part of the VE at 15 weeks in radial glial cells, and their processes are often directed ventrally. The separation between the two neurochemically distinct compartments of the VE is maintained throughout the rostrocaudal extent of the VE.

Figure 3.9 demonstrates the principally dichotomous character of the labeling in the deep telencephalic nuclei in relation to the labeling of either the LVE or the MVE. Such results lead to suggest that distinct sets of radial glial cells contribute differently to the chemical organization of the deep forebrain structures; in other words, it is probable that structures like the basal ganglia, the amygdaloid nuclear complex, and the bed nucleus of the stria terminalis are populated by neurons that have different birthplaces and specific molecular tags as established in the mouse. In the human forebrain there is presently only minimal information concerning the location of the respective progenitor cells, the derivation of neurons which settle in different parts of a given structure, the migratory pathways, and the settling areas (see Hamasaki *et al.*, 2003) despite several detailed descriptions of the morphological development of the normal basal forebrain (Richter, 1965; Kahle, 1956; Lemire *et al.*, 1975; Kostovic, 1990; Ulfig, 2002). Such information is indispensable before an understanding of the architecture of the forebrain region, where many distinct developing cell pools that are closely associated can be derived.

Basal Ganglia: Dorsal Striatopallidal System (Dorsal Striatum and Dorsal Pallidum)

The dorsal striatum (caudate-putamen) and the globus pallidus are clearly identified at the ninth week. Around 15 weeks, the dorsal striatum attains an inhomogeneous organization due to the formation of cytoarchitectonic and histochemical compartments, termed *patch* and *matrix*, that together contribute to a mosaic organization (Kostovic, 1990). Even before, from 13 weeks, the first patches of tyrosine hydroxylase IR (Zecevic and Verney, 1995) and CD15 IR appear in the putamen (Mai *et al.*, 1999a) (Fig. 3.3). CD15 patches in the caudate nucleus appear 4 weeks later. The discrete nature and the precise margination at this time make it probable that the dopaminergic fibers and CD15 interact in an unknown way. The ventral striatum does not become immunoreactive for CD15 until the last few weeks before birth (see below) and therefore the border between the dorsal and ventral striatum is easily recognized throughout the fetal period.

Sections stained for parvalbumin and the S1515 antigen disclose IR in the MVE and during the last trimester an inverse pattern in the striatum if compared with CD15 IR (Fig. 3.10). It is therefore very probable that the patch/matrix components of the human striatum receive different contributions from molecularly distinct divisions of the VE. The CD15 IR in the matrix compartment progressively increases during further development; therefore, the contrast with patches disappears around birth.

The vast majority (90%) of the neuronal population of the striatum are projection neurons, with connections to the globus pallidus and substantia nigra. Applying a retrograde tracing technique, efferent fibers were observed at 10 w.g. (Sailaja and Gopinath, 1994). In CD15-stained sections delicate fiber bundles are noted by 17 weeks which pass to the external pallidal lamina and the globus pallidus (and later to the substantia

nigra) (Mai *et al.*, 1999a). The appearance of fibers in the pallidum at 17 weeks is coupled with transient IR in this structure which peaks at 22 weeks (Fig. 3.8) and disappears at birth. It appears that the occurrence of CD15 striatopallidal fibers and the emerging IR at their target site in the pallidum are coupled events, so that ingrown CD15-positive axons establish functional interactions and provoke CD15 expression. The differentiation of the large cholinergic interneurons occurs after the 16th week (Kostovic, 1990).

The two pallidal segments and the subthalamic nucleus have their origin in a primordium directly under the surface of the ventrolateral diencephalon. Between the third and the fifth month the three nuclei become displaced in a rostral direction. Thereby the globus pallidus attains first a characteristic location below the hemispheric stalk and then—after rotation in rostrolateral direction, correlated with the expansion of the hemispheres in caudal direction—next to the putamen (intussusception of Spatz). The subthalamic nucleus is pushed anteriorly by the unfolding fibers of the cerebral peduncle. At about 5 months the three nuclei, which are initially arranged in a longitudinal sequence, are seen in one frontal section (Kahle, 1956; Richter, 1965; Lemire *et al.*, 1975). In accordance with the early exhaustion of the matrix zone of the area from which all three nuclei originate, the differentiation occurs synchronically and early (before the third month), and myelinated fibers appear before birth.

Basal Forebrain Area

Basal forebrain area (BFA) is a broad topographic term describing a heterogeneous set of structures on the medial and ventral cerebral hemisphere. The BFA comprises various cellular structures, the ventral striatopallidal system (VSPS), the septal nuclei, the olfactory tubercle, the magnocellular basal forebrain system (DB,NBM), the bed nucleus of the stria terminalis (BST), extended amygdala, and dispersed cell populations such as the neurophysin-immunoreactive neurons (Mai *et al.*, 1993). These diverse constituents form an intricate complex to which the various traversing fibers, like the medial forebrain bundle, ventral amygdaloid fibers, inferior thalamic peduncle, and neurotransmitter bundles, contribute. Nevertheless, all of them can be identified and defined by means of their chemical properties; therefore, the term "substantia innominata" has become superfluous (Alheid and Heimer, 1988; DeOlmos and Heimer, 1999).

The Ventral Striatopallidal System (Ventral Sriatum or Accumbens Nucleus, Part of Olfactory Tubercle and Ventral Pallidum) The ventral striatum shows marked differences compared with its dorsal counterpart. Neurons in the dorsal striatum are homogeneously distributed and the organization into patch and matrix compartments is obvious. The ventral striatum contains smaller neurons, which are more densely packed and more irregularly distributed, often forming strings or islands of cells. These cells are embedded in a more strongly stained ground substance and the processes are thinner with less myelin (Brockhaus, 1942). Patch-matrix compartments are not characteristic; instead the ventral striatum is "invaded" by nonautochthonous elements and the relationship between the distribution pattern of D1 and D2 receptors and AChE activity are different in the ventral and dorsal striatum (Berendse and Richfield, 1993). Such differences are underlined by different input and output relations (see Haber and Gdowski, Chapter 21 of this volume) and the chemical characteristics of constituent neurons. The various components of the BFA are much easier to separate in adulthood because the differentiation of this region is very heterochronous and the appearance and peak production of neuroactive substances occurs at different times. In spite of this, a detailed ontogenetic analysis is still missing.

In the nonhuman brain, the ventral striatum is often divided into core and shell regions on the basis of chemoarchitecture and fiber connections (Groenewegen *et al.*, 1999, Haber and Gdowski, Chapter 21 of this volume). As distinguishing feature between both divisions, the abundance of calbindin-28 in the core region as compared with its absence in the shell region has been described. In addition, a medial segment of the core region has been discriminated on the basis of the presence of AChE activity, substance P, neurotensin, serotonin, and μ-opiatereceptor (Haber and MacFarland, 1999). It appears, however, that it might be misleading to adopt the well-established shell-core organization found in rodents for the more complex three-dimensional organization in the human.

On the other hand, it has been already stressed by Brockhaus (1942) and Namba (1957) that the organization of the striatum follows a ventral-to-dorsal gradient that leads to the distinction of a ventral perimeter (fundus subventricularis), an intermediate fundus striati, and the dorsal striatum. This organization, also adopted in a recent human brain Atlas (Mai *et al.*, 1997), is supported from developmental findings. The fundus subventricularis was subdivided by Brockhaus (1942) into a medial and lateral part. This separation is supported by the transient appearance of a distinguished (sub-)ventricular zone that overlies the medial fundus subventricularis (medial accumbens nucleus) (Fig. 3.3b). From this portion of the VE the cells of the medial part of the accumbens nucleus appear to be derived.

Important for the interpretation of the ventral striatum are islands of cells that appear as distinct units (Brockhaus, 1942; Sanides, 1957; see also Nauta and Haymaker, 1969, their figure 4-15). In single sections these islands appear randomly located. However, their reconstruction in the adult brain revealed a very characteristic spatial and topographic arrangement where all islands are shown to be connected with the subependymal region of the caudate nucleus, the remnant of the VE (Hartz-Schütt and Mai, 1992). This organization, elaborated in the adult human brain on the basis of the determination of AChE activity, exists in a strikingly similar way also in the fetal brain and thus appears as a principal feature of the human basal forebrain organization. The strands described in the external capsule correspond to the lateral ventricular stream (described above) and their continuation in the adult amygdaloid nuclear complex (ANC) corresponds to the portion of the LMS that is depicted in Fig. 3.11. Strands that pass medial to the caudate and putamen correspond to a stream of immunoreactive glial fibers that probably have their origin in the MVE. The orientation of the radial glial processes from the MVE corresponds to this stream in the adult involving the bed nucleus of the stria terminalis and olfactory tubercle. By this indirect evidence it is suggested that the latter

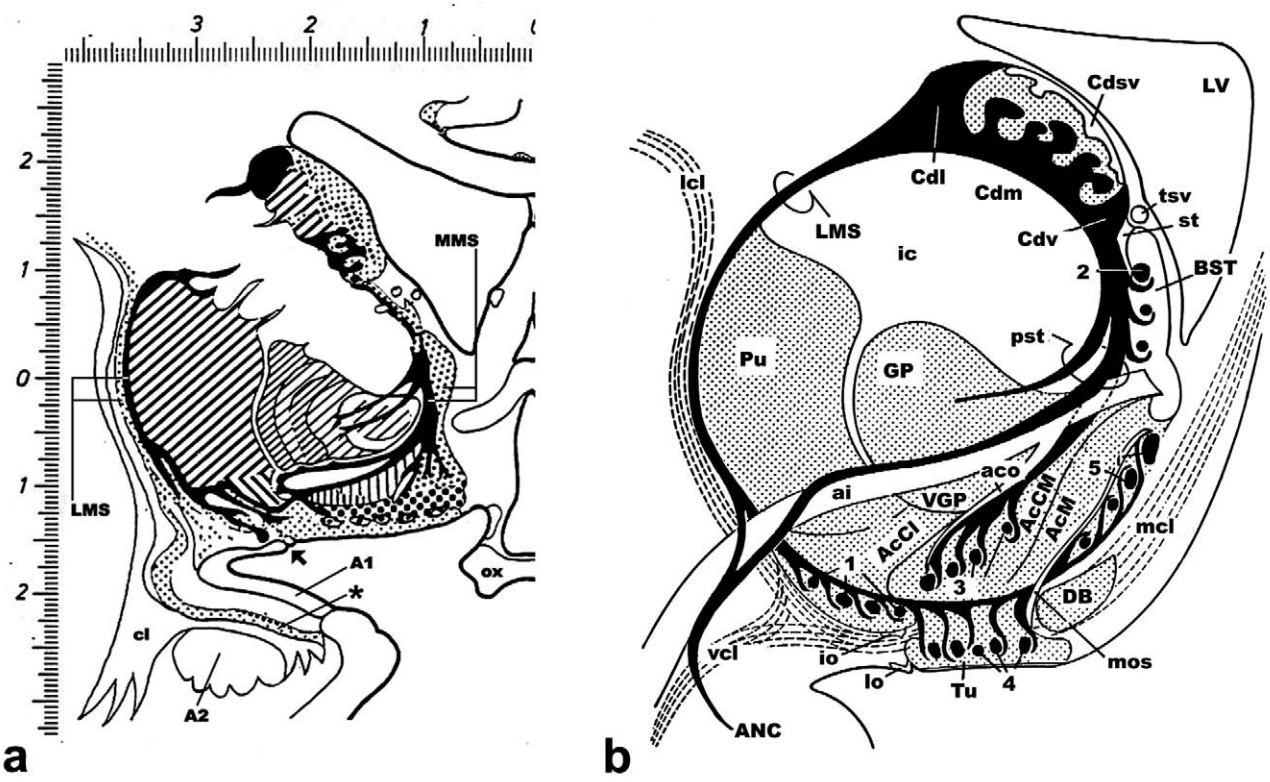

FIGURE 3.11 Distribution of acetylcholinesterase (AChE) activity in the adult human brain. **a.** Schematic representation of the distribution at the level of the anterior commissure and optic chiasma. **b.** Summary diagram of the organization of cholinergic structures in the forebrain, which is based on a serial reconstruction of sections. Strands of AChE emerge from the subependymal region of the caudate nucleus and reach five areas that are characterized by their globular character, called "terminal" islands (labeled here 1–5). The AChE strands in the external capsule correspond in their location to the lateral ventricular stream and then to the portion of the LMS that separates the superficial and deep parts of the ANC (A1 and A2, respectively; compare to Figs. 3.6 and 3.7). Strands that pass medial to the caudate and putamen and cross the internal capsule as parastriate fibers (pst) correspond to a stream of immunoreactive glial fibers that during development link the medial ventricular eminence (MVE) with the bed nucleus of the stria terminalis (BST), the great terminal island (Calleja), and the olfactory tubercle (Tu). 1–5, Different clusters of teminal islands; ai, anterior commissure; A1, superficial amygdaloid region; A2, deep amygdaloid region; AcCL, accumbens nucleus, centrolateral part; AcCM, accumbens nucleus, centromedial part; AcM, accumbens nucleus, medial part; aco, anterior commissure, olfactory limb; ANC, amygdaloid nuclear complex; BST, bed nucleus of the stria terminalis; Cdm, caudate nucleus, medial part; Cdl, caudate nucleus, lateral part; DB, diagonal nucleus; io, intermediate olfactory stria; lcl, lateral corticolenticular fibers; LMS, lateral migratory stream; lo, lateral olfactory stria; LV, lateral ventricle; mcl, medial corticolenticular fibers; MMS, medial migratory stream; mo, medial olfactory stria; pst, parastriate bridges; Pu, putamen; PuV, ventral putamen; st, stria terminalis; tsv, thalamostriate vein; Tu, olfactory tubercle, vcl, ventrolateral corticolenticular fibers; VGP, ventral pallidum.

structures are supplied with cells from the MVE that migrate through a corridor, named, the medial migratory stream.

The Olfactory Tubercle The olfactory tubercle is characterized as a territory that becomes invaded by terminal islands (Fig. 3.11b) (Hartz-Schütt and Mai, 1992) as already indicated in the foregoing text. The constituent cells of these islands most probably derive from the LVE (and MVE) and pass through the LMS and MMS, respectively. The continuity with striatal tissue is supported by the high cholinesterase (ChE) content (Kostovic, 1986) and by the direct continuation (between 3 and 4 months) of the CA–fiber system from the rostral neostriatum to the olfactory tubercle; these fibers were reported to aggregate into fluorescent islands (Nobin and Björklund, 1973).

In light of the described organization, it appears questionable to distinguish in the human brain between shell and core regions and to disregard the two most important features of the ventral striatum: the gradient character and the patterning by the terminal islands.

The Magnocellular Basal Forebrain System The magnocellular basal forebrain system consists of the medial and lateral parts of the nucleus basalis of Meynert (NBM), the nucleus of the diagonal band of Broca (NDB), and the medial septal nucleus (Mufson *et al.*, 2003; Morres and Mai, 1992). The precursor neurons of the basal nucleus of Meynert derive from the VE (Ulfig, 2002). The earliest signs of ChE activity appear as early as 9 w.g. in the area where the prospective basal nucleus develops. The first ChE-reactive bundles (among them a well-developed fiber stratum passing through the lateral pallium) form between this age and 10.5 w.g. The first ChE-reactive cells appear at 15 w.g. and the basal nucleus can be segregated into several strongly reactive subdivisions. Innervation of the developing cortex and subcortical areas by ChE-reactive fibers occurs between 16 and 28 w.g. Well before birth, an overall high degree of structural and chemical complexity is achieved (Kostovic, 1986).

While many studies have been aimed at assessing the cytology and chemistry of neurons of the cholinergic cells, the role of glial cells has received less attention. Interestingly, a high density of CD15-positive astrocytes with the complementary absence of GFAP-immunoreactive astrocytes has been stressed (Morres *et al.*, 1992). This CD15 IR becomes obvious around 35 w.g.

Amygdaloid Nuclear Complex

The terminology and topological interpretation of the amygdaloid nuclear complex (ANC) is still inconsistent. Brockhaus (1938), who provided a very extensive description of the structural organization of the human ANC, distinguished a superficial and a deep region, the latter comprising the lateral, basolateral or basal (intermediate), accessory basal (medial), and paralaminar (ventral) nuclei, respectively (see Gloor, 1997, pp. 596–600). This separation between superficial and deep regions in the human, on the basis of cell and fiber stains, appears relevant because it concurs with the division that was later stressed as important in the interpretation of the rodent ANC (Swanson and Petrovich, 1998; Swanson, 2003). The organization of radial glial fibers during the middle fetal period also speaks for this separation (see above, Fig. 3.5).

The view that the ANC is a derivative of the MVA as proposed by Mueller and O'Rahilly (1990), and; O'Rahilly and Mueller (1999, p.144; also this volume) is in accordance with the high expression of EGFR in both the MVE and the ANC. Cells of the amygdala are considered to represent the earliest postmitotic neurons in the telencephalon, and therefore the major sub-

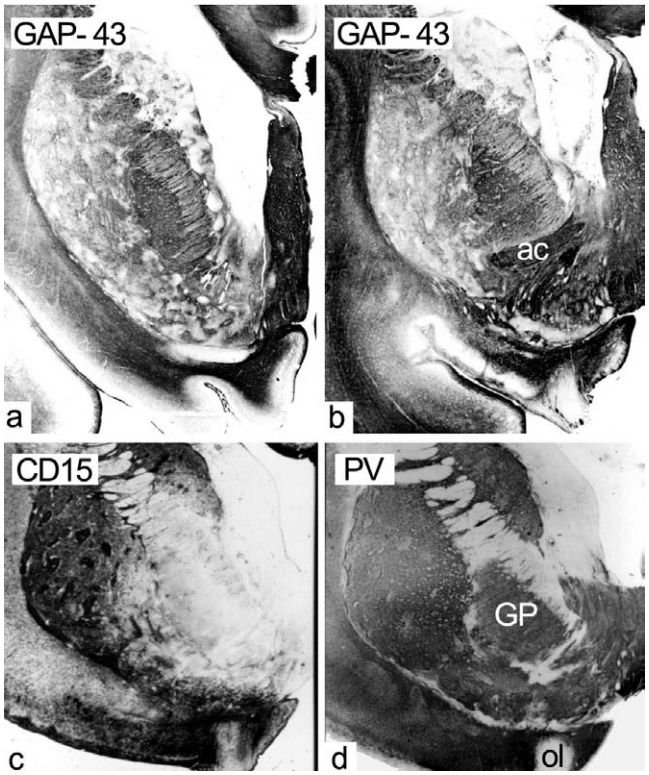

FIGURE 3.12 Distribution of GAP-43, CD15, and parvalbumin (PV) in cross-sections though the basal forebrain. **a, b.** GAP-43 shows a variegated pattern in the ventral striatum as compared to the dorsal part (18 weeks). **c.** In the CD15 (24 weeks) section the IR is continuous with the retrobulbar region. **d.** Parvalbumin shows a distinct border between the deep nuclei and paleocortex (24 weeks).

divisions and nuclei of the ANC are already discerniable (between 8 and 9 weeks) (Macchi, 1951; Lemire *et al.*, 1975; Mueller and O'Rahilly, 1990; also O'Rahilly and Mueller, Chapter 2 of this volume). By the eighth week (approximately stage 21–23), all nuclei are identifiable and differentiation takes place between the superficial and deep nuclei. After 13 weeks the ANC undergoes a rotation that is directed medially (Kostovic, 1992).

Around 14 weeks, the continuation of the CD15-positive LMS (as described above) by VIM and CD15 IR marks the territory of the superficial ANC. From 16 weeks, moderate CD15 IR is found for the first time within the deep nuclei. Initially IR is restricted to the dorsal knoblike portion of the basal nucleus (Ap.im), which protrudes into the superficial region. During cell differentiation, IR progresses in a graded fashion from dorsal to ventral. The accessory basal nucleus (Ap.i) shows the most intense labeling. Many other substances display differential distributions within the human ANC, such as GAP-43 (Ulfig *et al.*, 1999) and calcium-binding proteins (Setzer and Ulfig, 1999) (Fig. 3.12). In spite of the heterogeneous distribution, these substances have not yet provided clues for a systematic parcellation of the ANC.

DIENCEPHALON

The embryonic development of the diencephalon is described in the foregoing chapter by O'Rahilly and Mueller. By the end of the embryonic period all of the ventricular sulci in the prosencephalon are present (Figs. 3.13 and 3.14). The dorsal, medial, and ventral sulci then characterize four divisions of the diencephalon: epithalamus (ET), dorsal thalamus (DT), ventral thalamus (VT), and hypothalamus (HT). Within the hypothalamic division; Kahle (1956) and O'Rahilly and Mueller (Chapter 2 of this volume) distinguished an additional subthalamic division. ET, VT, and HT differentiate first but already between stages 20 and 21 (18–24 CRL) the DT begins burgeoning growth (Lemire *et al.*, 1975). As a consequence, the increasing size of the DT leads to a shift of the ET caudally and displacement of the VT laterally.

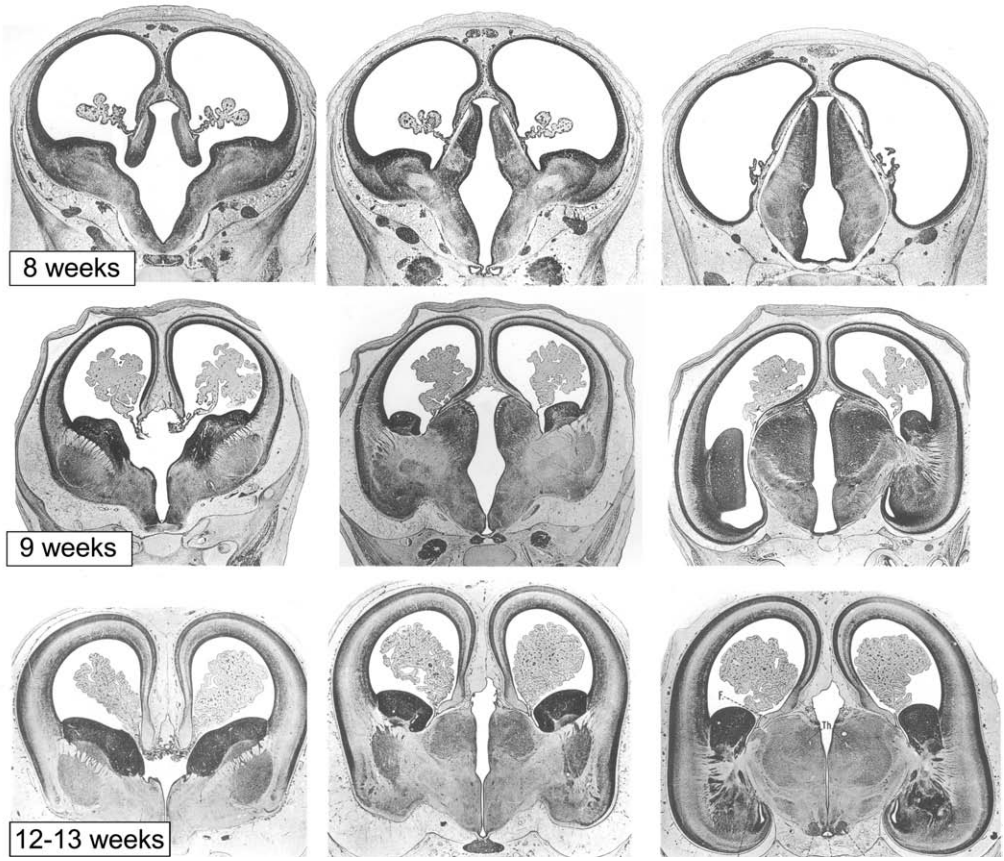

FIGURE 3.13 Transverse sections through the forebrain at 8, 9, and about 12–13 weeks. Modified from Hochstetter (1919).

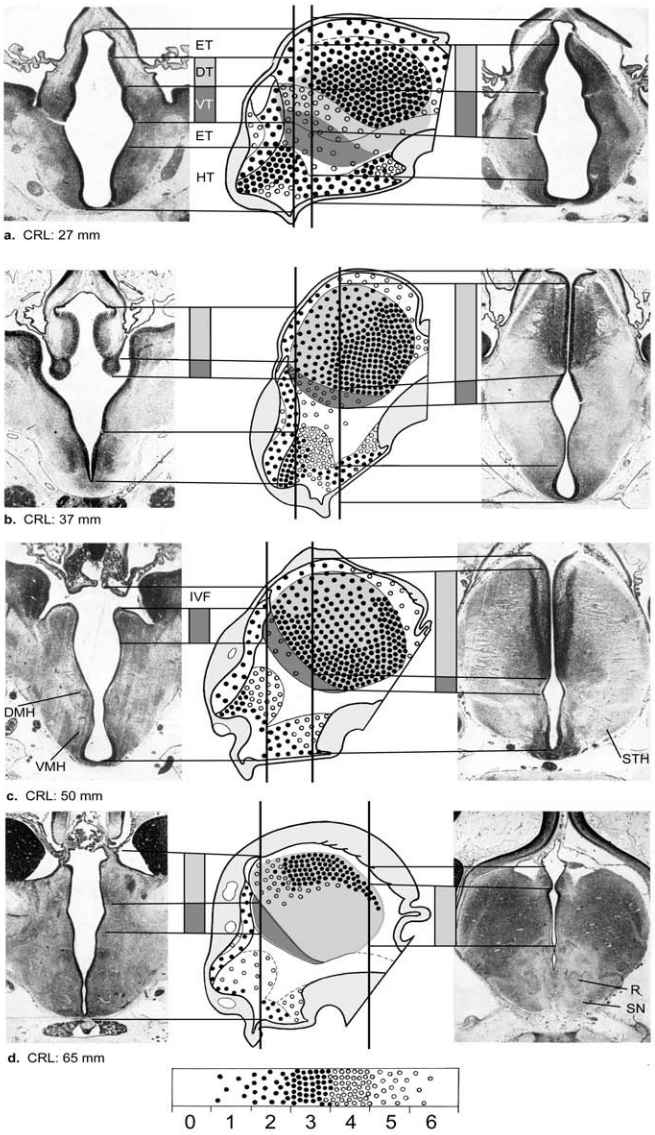

FIGURE 3.14 Characteristics of the matrix layer of the wall of the third ventricle of human embryos at the approximate ages of 8 weeks (27 CRL), 9–10 weeks (37 CRL), 11 weeks (50 CRL), and 12 weeks (65 CRL). The location of the photographs on the left and right sides is indicated in the diagrams by perpendicular lines, and correspondence with the matrix zones shown in the photographs is provided by the horizontal lines. The progression from proliferation of cells within the matrix, migration of cells out of the matrix into the mantle layer (differentiation zone), and exhaustion of the matrix layer is subdivided into different phases (0–6, *bottom line*) advancing from the situation before migration (0) to beginning (1), advanced (2), and full (3) migration and the phases of beginning (4), advanced (5), and complete (6) exhaustion of the matrix. Comparison of the various ages represented shows that the matrix zones show considerable variation, indicating that migration phases show different time profiles. Local differences in the course of the matrix phases are primarily arranged in longitudinal zones. Theses zones are separated by horizontal lines and are indicated as ET (epithalamus), DT (dorsal thalamus), VT (ventral thalamus), ST (subthalamic longitudinal zone), and HT (hypothalamus). Modified from Kahle (1956).

These divisions represent basic elements that are founded on the histogenetic proliferative properties of the germinal (matrix) zone, constitute the material for nuclear differentiation, and represent true genetic entities. Antibodies against several epitopes have disclosed a zonal pattern with borders corresponding to the described divisions. This pattern or its constituents may persist even when the development has proceeded and the structural organization becomes more complicated.

Kahle (1951, 1956) analyzed the dynamics and progression of the proliferation and migration of cells in the diencephalon. Both events are reflected in distinct morphological changes: during the phase of migration the germinal epithelium (matrix) broadens and becomes progressively less marginated against the mantle layer. At the peak of migration an obvious borderline disappears. During the phase of "beginning exhaustion" the decreasing width of the matrix is accompanied by a restored margination. Finally, in the phase of "complete exhaustion" the matrix becomes extremely narrow and transformed into the ependymal lining. He mapped the heterochronous development of the matrix in different regions of the diencephalon for the definition of morphological entities. The corresponding changes are seen in Figs. 3.13 and 3.14, which show transverse sections through the forebrain from the time of transition from embryonic to fetal life until about 13 weeks (65 CRL). Comparison of the various ages represented demonstrates considerable variation in the matrix zones, indicating different time profiles for migration phases.

Dorsal and Ventral Thalamus

Cooper (1950) and Kahle (1956) described in detail the great changes in the position and the cytological appearance of the thalamic structures. Figures 3.13 and 3.14 show the associated changes on transverse sections through the diencephalon that are representative of the time between the end of the embryonic period (stage 23 or approximately 57 days) until 13 weeks. Figure 3.14 demonstrates how the cytological changes are correlated with the appearance of the germinal layer of the third ventricle. The fast growth of the dorsal thalamus, which occurs between 7 and 11 weeks, gradually decreases the earlier predominance of the ventral thalamus and likewise displaces the ventral thalamus ventrally and laterally. At 8 weeks, the dorsal thalamus, which has already reached about the same size as the ventral thalamus, is separated from the epithalamus by the deep sulcus dorsalis. The zona limitans intrathalamica, which passes laterally from the sulcus medialis and which is regarded to correspond

to the future external medullary lamina (Miura, 1933), divides the dorsal and ventral thalamus. Within the dorsal thalamus a lateral and medial territory are recognizable at the beginning of the fetal period (Fig. 3.2a). In the medial part, differentiation is retarded; in the lateral part, the ventral lateral geniculate body can be recognized at 10 weeks (Gilbert, 1935). Between 10 and 14 weeks, segregation of neurons into different thalamic nuclei begins, whereby first the lateral geniculate nucleus, then the centrum medianum and the mediodorsal nucleus (Lemire *et al.*, 1975) are distinguished (Grünthal, 1934; Cooper, 1950; Yamadori, 1965; Yakovlev, 1969; Rakic and Sidman, 1969; Rakic, 1974; Kostovic and Goldman-Rakic, 1983; Mojsilovic and Zecevic, 1991). After 14 weeks all major thalamic nuclei can be recognized. At this time the ventricular zone is already reduced to ependyma and no mitotic figures were detected in Nissl-stained specimens (Mojsilovic and Zecevic, 1991). Differentiation still shows a gradient from lateral to medial, but a caudal-to-rostral gradient of maturation is obvious only for the ventral nuclei. The definitive cytological organization is reached between 16 and 18 weeks in most parts of the thalamus (Cooper, 1950; Kahle, 1956), except in the pulvinar which is then only poorly developed. Cells for the pulvinar appear to proliferate in the lateral ventricular eminence from which they enter the thalamus by a transient cell layer termed the corpus gangliothalamicum. This structure is located under the external surface of the developing pulvinar of fetuses from the 18th to the 34th week (Rakic and Sidman, 1969).

Neurochemical differentiation of the dorsal and ventral thalamus is observed from the earliest phase of fetal development. As noted above, intensely stained vimentin-immunoreactive processes are denser at the borders between epithalamus, dorsal, and ventral thalamus. In the same locations, parvalbumin is present by 10 weeks (Fig. 3.15). Cholinesterase activity was observed at 10.5 w.g. in the prospective mediodorsal nucleus (MD) (Kostovic and Goldman-Rakic, 1983). This activity increases strikingly after 16 w.g. until a peak activity is reached between 20 and 28 w.g., which correlates with the period when outgrowth and establishment of thalamocortical axons occurs. Afterward the cholinesterase activity is gradually reduced and becomes virtually undetectable in the MD by 6 months of age. Calretinin appears at 14 weeks in the ventral thalamus. It has been described that the derivatives of the ventral thalamus retain the calretinin IR after migration to their homing sites, thus facilitating identification of such cell clusters during later development (Forutan *et al.*, 2001). In the dorsal thalamus, calretinin-immunoreactive structures include the intralaminar nuclei (labeled from 16 weeks), the anteroventral and limitans nuclei (from 18 weeks), and the mediodorsal nucleus (from 22 weeks). Calbindin IR is very helpful for the discrimination of thalamic cell groups. It is a reliable marker from 14 weeks for the ventrolateral parts of the ventroanterior and ventrolateral nuclei, and also in the ventromedial nucleus. The SMI-32 antibody stains neurons in the ventroposterior lateral nucleus (VPL) from 21 weeks, in the magnocellular part of the ventroanterior nucleus between 23 and 39 weeks, and in the anterior part of the ventrolateral nucleus (VLA) and ventromedial nucleus (VM, lateral leaf) between 23 and 27 weeks. SMI-32 IR thus enables one to distinguish VPLs from those adjacent nuclei that are positive for calbindin. SMI-32 IR is also found in the centrum medianum and parafascicular nucleus (CM/PF) complex.

FIGURE 3.15 Distribution of parvalbumin (PV), calretinin (CR), and GAP-43 in neighboring transverse sections of the forebrain at age 10 weeks. In the diencephalon, parvalbumin and calretinin are concentrated in the ventral thalamus, thereby marking the border with the dorsal thalamus. This border is indicated medially by a shallow furrow, medial hypothalamic sulcus. A transversely oriented parvalbumin-immunoreactive band is seen demarcating the habenula from the dorsal thalamus. Parvalbumin IR is also found at the meningeal blade facing the thalamic surface. GAP-43 IR outlines thalamo- and corticofugal fibers.

In contrast to the early and intense labeling of VIM- positive radial glial cells (RGCs) in the dorsal thalamus stands the absence of CD15, which is confined to the ventral thalamus. When CD15 labeling appears in the dorsal thalamus at 14 weeks, it is not associated with RG processes but with the neuropil in differentiating prospective nuclei (Figs. 3.8 and 3.16). The occurrence of this granular CD15 labeling is very precise in time and specific for each nucleus (Forutan *et al.*, 2001). It progresses from the centrum medianum and the ventral nuclear group to the lateral and medial geniculate nuclei (16 weeks), the medial division of the ventroposterior nucleus (VPM), and the limitans nucleus (Mai and Schönlau, 1992; Mai *et al.*, 1999b). VPL and VPM are recognized by the high CD15 IR and the sharply demarcated borders between both nuclei. The pulvinar becomes progressively labeled after 20 weeks. At this time only the subventricular region

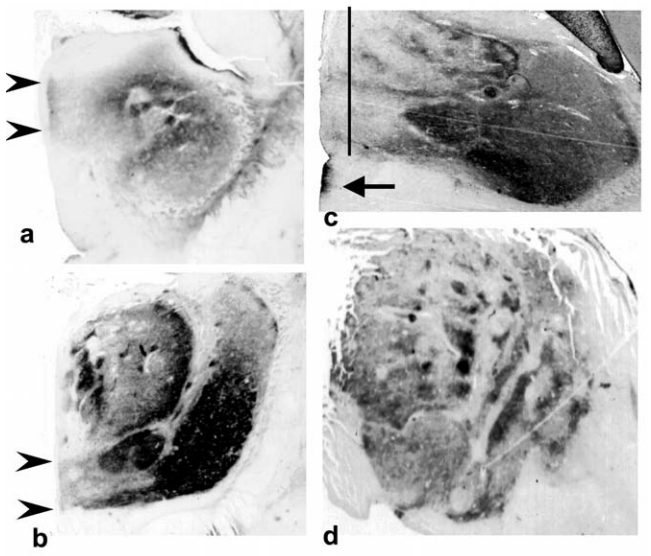

FIGURE 3.16 CD15 IR discloses a relationship between the (sub-)ependymal zone and differentiating nuclei (**a:** 17 weeks; **b:** 16 weeks). **c, d:** Variegated or tubular pattern in MD (**c:** 19 weeks; **d:** 23 weeks). The perpendicular line in **c** indicates the orientation of the section shown in **d.** *Arrow:* stretch of CD15 radial glial cells in the ventral thalamus.

remains unlabeled. A thin but well-delimited CD15-positive leaflet extends from the ventrolateral and VPL nuclei to the ventricle. It represents the ventral margin of the thalamus, which is thus well delimited against its surroundings.

The distinction between the individual nuclei of the ventral nuclear group is facilitated by comparison with sections stained for calbindin and SMI-32 (see above). Within the ventral nuclei, calbindin IR is present in the ventrolateral fields of VA (VAL), in the anterior part of the ventrolateral nucleus (VLA), and in the VM. SMI-32 is concentrated, from 17 w.g., in VLA and VPL; CD15 and SMI-32 mark the same overlapping field in the VPL (Forutan *et al.*, 2001).

CD15 expression in the mediodorsal nucleus shows a variegated pattern, which differs from the rather uniform pattern found in the other thalamic nuclei. The intensely labeled patches reveal a tubular organization that is reminiscent of the modular organisation of the patch and matrix compartments of the striatum (Fig. 3.16c, d).

CD15 appears in the dorsal thalamus (at 14 weeks) when the proliferative activity ends (Kahle, 1956) and the thalamic nuclei are already becoming discernable by cytoarchitectonic criteria (Rakic and Sidman, 1969; Rakic, 1974; Mojsilovic and Zecevic, 1991). This speaks against a direct correlation with the process of migration and the in- or outgrowth of thalamocortical and corticothalamic axons (Dekaban, 1954; Kostovic and Goldman-Rakic, 1983). Instead, it coincides with the period of outgrowth of local processes and the targeting of presynaptic terminals. This interpretation is supported by the intranuclear gradients for CD15 expression that run in parallel with morphogenetic gradients of cellular differentiation as described in the developing rat brain (Altman and Bayer, 1989).

A comparison between the chronology of CD15 expression in the lateral geniculate nucleus and parameters of maturation of the visual system has revealed congruent temporal profile patterns with respect to morphological signs of early maturation (Mai and Schönlau, 1992). The rapid transformation from a very-high-intensity labeling to an almost complete loss of IR was coincident with visual experience and the period of synaptic stabilization at the end of the critical period. This result suggests that high CD15 expression is linked to aspects related to initial synaptic events after stabilization of synaptic contacts (Mai and Schönlau, 1992).

The way that CD15 is expressed in the intralaminar nuclei supports the view that they are composed of two separate groups of nuclei: the (CM/PF) complex and the central nuclei (central medial, central lateral nuclei, and paracentral nuclei) (see Percheron, Chapter 20 of this volume). CM/PF are among the first thalamic nuclei to become CD15 positive and are filled with intense homogeneously distributed CD15 IR, which is clearly marginated. By contrast, calbindin IR is extremely low and calretinin IR entirely absent. On the other hand, the central nuclei appear later in development, contain irregular CD15 material with many patches, are poorly marginated, and show areas with intense calretinin IR. Finally, the medial subventricular division appears also distinct, and may be regarded as part of the periventricular gray matter. The inverse labeling of CM/PF by CD15 and calbindin is interesting in light of the recent description of the involvement of this structure in Parkinson's disease and in supranuclear palsy (Henderson *et al.*, 2000) since a reciprocal staining pattern for CD15 and calbindin has been also found in the adult human substantia nigra (Oeder, 1998).

CD15 staining also reveals a possible relationship between circumscribed ventricular areas and differentiating nuclei. As a transient phenomenon, fine punctiform and homogeneously distributed CD15 material has been described that stretches from the ventricular zone to some differentiating nuclei, like the ventral nuclear group, the CM/PF complex, and the anteroventral nucleus. This has been interpreted to reflect the derivation of the constituent cells of these nuclei from the corresponding parts of the ventricular neuroepithelium (Forutan *et al.*, 2001). If correct, CD15

IR would disclose the correspondence between the location of immature but committed cells in circumscribed patches of the neuroepithelium and their target structure. This interpretation not only implies that subdivisions of the thalamus arise from histogenetic primordia with discrete progenitor domains in the neuroepithelium but also that their spatial relationship is preserved until differentiation.

Hypothalamus

The ontogenesis of individual hypothalamic cell groups and nuclei in humans has been the issue of many classical reports (reviewed in Diepen, 1962) and recent accounts (O'Rahilly and Mueller, Chapter 2 of this volume; Koutcherov *et al.*, 2002). As stressed by O'Rahilly and Mueller, no staging system exists for the fetal period exists; thus, it is not surprising that the data provided for important developmental events can vary considerably. Those regarding the beginning of migration in the hypothalamus range from 6 weeks (CRL 9–11) to 10 weeks (LeGros Clark, 1938; Kahle, 1956; Diepen, 1962). This may be due to the very heterogeneous matrix morphology at the beginning of the fetal period. Some areas are passing through advanced stages of migration while others show early signs of exhaustion.

Neurogenesis and migration in the human hypothalamus occurs, as in the rodent brain, in three waves (Koutcherov *et al.*, 2002; Altman and Bayer, 1986). The first generated neurons migrate into the future lateral longitudinal zone of the hypothalamus where they give rise to the lateral hypothalamic area, posterior hypothalamus, lateral tuberal nucleus, and perifornical nucleus. These structures are generally associated with arousal and autonomic responses in feeding and reproduction, whereas their connections are dominated by the medial forebrain bundle and the fornix (Koutcherov *et al.*, 2002). The second wave of postmitotic neurons settles in the prospective intermediate longitudinal zone or hypothalamic core. These neurons form more conspicuous cell groups that include the medial preoptic nucleus, anterior hypothalamic nucleus, ventromedial nucleus, dorsomedial nucleus, and mamillary body. These cell groups are thought to mediate autonomic responses in the regulation of homeostasis. Limbic afferents from the hippocampal formation, amygdala and septum, and major intrahypothalamic connections are characteristic pathways for this region. The last neurons to be generated are those which differentiate in direct proximity to the ventricular wall, or periventricular zone. Nuclei in this zone are the suprachiasmatic nucleus, the arcuate nucleus, the paraventricular nucleus, and the supraoptic nucleus. They are considered critical for the regulation of biological rhythms, neuroendocrine output, and integrated autonomic responses and are directly connected with the retina, pituitary, and autonomic centers in the brain stem and spinal cord (Fig. 3.17). In humans, all the nuclei are apparent by 13 w.g. (see Gluckman and Bassett, 1988).

The sites of settlement and differentiation thus already reflect the advanced regionalization of the adult human hypothalamus with three longitudinal subdivisions, the *periventricular* or *midline* zone, the *intermediate* zone or *core*, and the *lateral* zone (Crosby and Woodburne, 1940). This arrangement, which is typical throughout phylogeny (see Nauta and Haymaker, 1969), is confirmed in the neurogenetic pattern of the developing hypothalamic nuclei (Altman and Bayer, 1986) and validated by chemoarchitectonic (Koutcherov *et al.*, 2003) and functional evidence (Swanson, 1991).

At the beginning of the fetal period the three longitudinal zones are already discriminable. The *intermediate* zone of the hypothalamus is generally characterized by a lower cell density than the *lateral* zone, with the exception of distinct cell clusters of potential nuclei. The *periventricular* or *midline* zone at this age is a layer of tightly packed cells in the proliferative neuroepithelium. The fetal development of the human hypothalamus has been described on the basis of chemoarchitectonic criteria in much detail by Koutcherov (Koutcherov *et al.*, 2002), and therefore most of the following data derive from their report (Fig. 3.17).

Lateral Longitudinal Hypothalamic Zone

As in the other regions of the human brain, strong transient expression of parvalbumin heralds structural differentiation of the hypothalamus and is observed by the early fetal period. GAP-43 IR, which is present at around 10 weeks, suggests that axonal end-arbors and provisional synaptic contacts are formed. The fornix appears at 12 weeks, and IR for GAP-43 and synaptophysin in its fibers is found after 15 weeks. From 17 weeks, cells of the prospective perifornical nucleus are ensheathing the fornix.

The lateral tuberal nucleus develops at 16–19 weeks as a tightly packed group of small neurons in the ventrolateral margin of the lateral hypothalamic area. The nucleus is outstanding by its marked GAP-43 negativity within the otherwise GAP-43-positive area. Another distinguishing feature is the densely packed small calbindin-immunoreactive cells and the absence of the large calretinin neurons that are characteristic of the neighboring lateral hypothalamic area. Late in the development, shortly before birth, a very dense

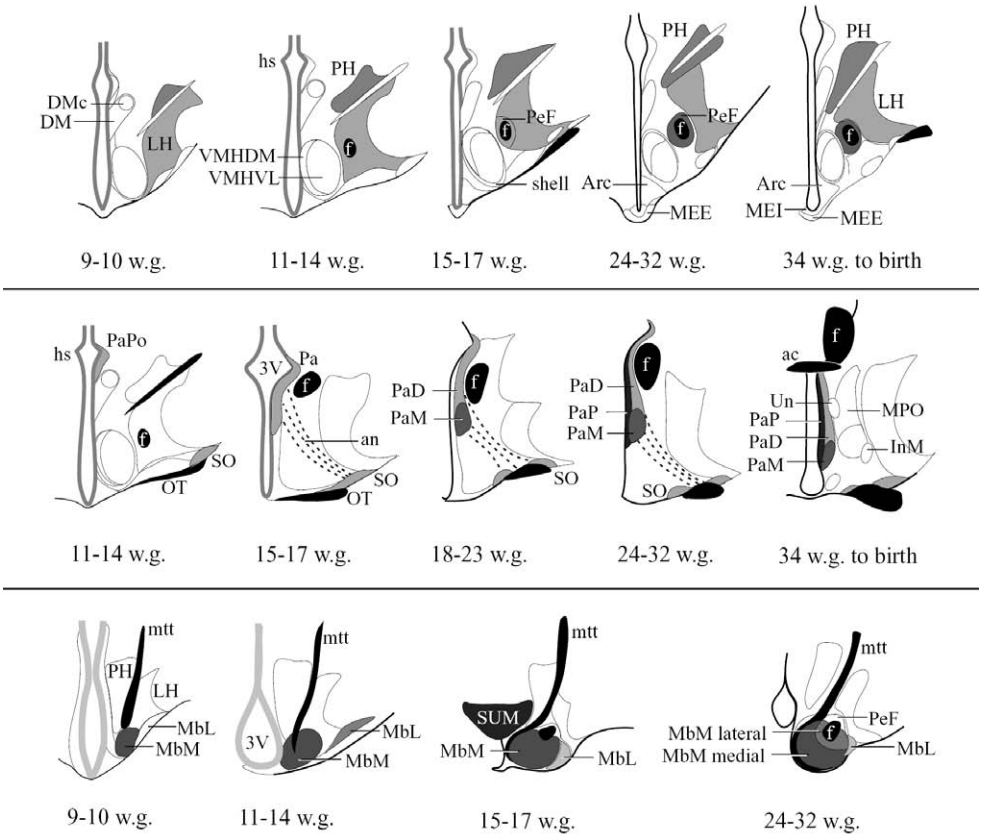

FIGURE 3.17 The organization of major cell groups in the developing human hypothalamus shown at landmark stages of fetal differentiation. The hypothalamus is depicted at three rostrocaudal levels *(upper, middle, and lower line)* for each developmental stage. Please note that these diagrams are not drawn to scale. 3V, third ventricle; AN, accessory neurons; Arc, arcuate nucleus; DM, dorsomedial nucleus of the hypothalamus; DMc, caudal portion of the DM; f, fornix; hs, hypothalamic sulcus; InM, intermediate nucleus; LH, lateral hypothalamic area; MbL, lateral mamillary body; MbM, medial mamillary body; MEE: median eminence, external part; MEI, median eminence, internal part; MPO, medial preoptic nucleus; mtt, mamillothalamic tract; ot, optic tract; Pa, paraventricular nucleus (PaD, PaM, PaP, PaPo: dorsal, medial, parvocellular, posterior parts); PeF, perifornical nucleus, PH: posterior hypothalamus; SUM, supramamillary nucleus; SO, supraoptic nucleus; Un, uncinate nucleus; VMHDM, ventromedial hypothalamic nucleus, dorsomedial part; VMHVL, ventromedial hypothalamic nucleus, ventrolateral part. From Koutcherov *et al.*, 2003.

labeling by synaptophysin clearly differentiates this nucleus from the surrounding ventral tuberomamillary nucleus (Koutcherov *et al.*, 2003).

The very heterogeneous matrix morphology is reflected in the already differentiated organization of the human lateral hypothalamic zone into various subcompartments and great chemoarchitectonic differences between its constituent structures. For example, cells in the posterior but not the lateral hypothalamic area show distinct CD15 IR from 19 weeks until birth. Furthermore, the lateral hypothalamic area contains calretinin- and calbindin-positive neurons and GAP-43 IR early in fetal gestation, unlike the adjacent tuberomamillary nucleus, which acquires calbindin-positive neurons only late in gestation. Finally, Koutcherov *et al.* (2000b) showed abundant NK-3 IR in neurons of the perifornical nucleus, thus distinguishing this structure from its NK-3-negative surrounding.

Intermediate Zone of the Hypothalamus

The next significant event in the development of the human hypothalamus is differentiation of the intermediate hypothalamic zone, which occurs between 16 and 34 weeks (Koutcherov *et al.*, 2003).

The medial preoptic nucleus, located rostrally in the hypothalamus at the level of the optic chiasm, can be identified at 10 weeks as a condensed cluster of cells with strong transient expression of parvalbumin. However, its differentiation is protracted and continues after birth (Swaab and Hofman, 1988). A clear distinction into several subnuclei and their homologues to the nuclei of rodent hypothalami cannot be made (Koutcherov *et al.*, 2003; Lu *et al.*, 2000).

The ventromedial hypothalamic nucleus and the dorsomedial hypothalamic nucleus are already recognized between 10 and 12 weeks (Gilbert, 1935). Both nuclei develop in a field of vimentin- and CD15-

immunoreactive radial glial fibers that arch from the middle of the subsulcal ventricular wall and which become more prominent after 14 weeks (Fig. 3.2a). This ontotopographic feature has led some authors to suggest that both nuclei in the human also derive from the same anlage, with comparable connectivity and similar functional associations (Koutcherov *et al.*, 2003) as in the rat (Altman and Bayer, 1986).

In the ventromedial hypothalamic nucleus a distinction between a well-differentiated and more compact dorsomedial part and a bigger, more dispersed, ventrolateral part can be made after 13 weeks on the basis of a complimentary distribution of calbindin- and calretinin-positive cells. After 17 weeks, a third principal part with GAP-43-immunoreactive positive fibers forms a shell around both the other parts (core region). This is reminiscent of the situation seen in the adult rat, where the cell-poor shell is a prominent target for the amygdalohypothalamic fibers carried via the stria terminalis (Krettek and Price, 1978; Post and Mai, 1980). The dorsomedial hypothalamic nucleus appears ventral to the hypothalamic sulcus and close to the ventricular zone after 10 weeks. At 12 weeks it has a well-defined oval structure where compact and diffuse parts can be distinguished by Nissl staining. This differentiated organization persists until 24 weeks, but afterward the compact and diffuse compartments become progressively less defined.

The mamillary body differs from the rest of the hypothalamic nuclei because of the absence of a regular mantle layer (Kahle, 1956). It can be identified for the first time between 9 and 11 weeks, and from the beginning of differentiation a larger, spherical, medial part and a smaller, droplet-shaped lateral mamillary subnucleus can be distinguished. From 14 weeks the medial part becomes wrapped dorsomedially by the mamillothalamic tract, and 2 weeks later the fornix reaches its lateral boundary. A supramamillary nucleus (SUM) was recognized by Koutcherov *et al.* as a transient structure between 15 and 17 weeks, but not later in gestation.

Periventricular or Midline Zone of the Hypothalamus

The midline hypothalamus is composed of structures differentiating in direct proximity to the ventricular lining. During early stages of fetal development (i.e., 9–10 weeks) the primordia of the midline structures are concealed because of the cell-dense periventricular neuroepithelium.

The neurons for the paraventricular (Pa) and supraoptic (SO) nuclei and the accessory cell groups derive from a common neurogenetic primordium at the hypothalamic sulcus (Mai *et al.*, 1997). This location corresponds to the homologous source of cells in rodents (Altman and Bayer, 1986; van Eerdenburg and Rakic, 1993). From here, neurons migrate laterally and ventrally to their homing sites, possibly along radial glial processes shown in Fig. 3.2a. The onset of differentiation at 11 weeks coincides with the expression of vasopressin and neurophysin (Fellmann *et al.*, 1979; Burford and Robinson, 1982; Mai *et al.*, 1997; Goodyer, 1988). Oxytocin cells are found later, between 14 and 15 weeks. By 19 weeks the posterior and dorsal parts of the Pa attain their postnatal morphology and topography. At 20 weeks the densely packed, magnocellular neurons of the medial Pa begin to form and reach their postnatal morphological appearance by 24 weeks. From 24 weeks small calbindin-positive neurons are found throughout the Pa.

By 27 weeks the adult-like subnuclear cytological and chemical organization of Pa can be demonstrated (Koutcherov *et al.*, 2000a, 2002) and the number of neurons in the adult human Pa is reached (Gouldsmit *et al.*, 1992). At this time, small calbindin-stained cells are present throughout the Pa, with the exception of the parvocellular portion. The population of cells that express vasopressin, however, still increases until birth to remain constant only thereafter (Murayama *et al.*, 1993). Interestingly, a subpopulation of the Pa and SO neurons features coexpression of neurophysin (NPH) with CD15 (Mai *et al.*, 1994). This population also labels the hypothalamohypophyseal fiber bundle arching from the medial Pa toward SO and further ventromedially to the external component of the median eminence. The number of NPH+/CD15+ neurons peaks around birth when up to about 60% of the NPH-immunoreactive neurons are also positively labeled for CD15. Afterward, the number of CD15 neurons declines and colocalization of the two peptides becomes gradually lost (Mai *et al.*, 1994).

The initial stages of the generation of the arcuate nucleus cannot be assessed by simple morphological examination because it is concealed by the funnel of tightly packed periventricular cells. From 19 weeks until the perinatal period the nucleus harbors a prominent calbindin-immunoreactive fiber bundle that extends from the ventricular to the ventral pial surface of the hypothalamus. At 22 weeks, the earliest neuropeptide-Y-immunoreactive neurons appear. Their axons are located in the internal component of the median eminence, segregated from the NPH-positive neurohemal pathway arising from the SO and Pa and running in the external segment. The arcuate nucleus is rich in many other neuroactive substances, including neurokinin B, somatostatin, neurotensin, luteinizing hormone-releasing hormone (LHRH), and catecholamines (Spencer *et al.*, 1985; Schwanzel-Fukuda *et al.*,

1989; Swaab, 1997; Chawla *et al.*, 1997). Absence of LHRH neurons in the arcuate nucleus, which is due to failure to migrate from the olfactory placode into the brain, appears to be the basis of Kallman's syndrome (Schwanzel-Fukuda *et al.*, 1989; Swaab, 1997).

The cells of the suprachiasmatic nucleus originate from the neuroepithelium of the midline recess of the floor of the optic evagination of the third ventricle. From the beginning of differentiation, at 19 weeks, a central part, specified by vasoactive intestinal polypeptide (VIP), and a dorsally located part with neurophysin/vasopressin cells, can be distinguished. These latter cells are developmentally distinct from those of the SO and Pa. At 23 weeks a GAP-43-positive fiber bundle, presumably the retinohypothalamic tract, connects the optic tract with the suprachiasmatic nucleus, forming a dense and well-marginated plexus (Koutcherov *et al.*, 2002). At 35 weeks calbindin-positive cells appear in the central part, completing the characteristic chemoarchitectonic adult feature of the nucleus (Mai *et al.*, 1991). Differentiation of the suprachiasmatic nucleus is relatively late consistent with reports that the SCh is still immature at term since it then contains only 13% of the adult number of vasopressin neurons. However, oscillations by a fetal biological clock occur, and these oscillations may be entrained by the mother already before birth, probably as early as at 30 weeks (Reppert, 1992; Mirmiran *et al.*, 1992).

Besides the lateral-to-medial gradients of hypothalamic differentiation, a caudorostral gradient also exists (Kostovic, 1990). Morphological evidence suggests that this gradient develops in correspondence with the hypothalamic segments mentioned in "Forebrain Separation by Radial Glia," Fig. 3.4d and e).

In many of the studies mentioned, the nuclear organization of the human hypothalamus has been reported to show a close correspondence with that of rodents. However, the elaboration of a growing list of similarities between the human and rodent hypothalamus does not exclude relevant differences in the nuclear organization. LeGros Clark (1936) already stressed a number of features that distinguish the human hypothalamus, like the extensive distribution of large cells, the differentiation of the tuberal nuclei, the relative size and differentiation of the posterior hypothalamic nuclei and of the medial mamillary nucleus, and the reduced size of the lateral mamillary nucleus.

Fiber Systems

At the beginning of the fetal period, many hypothalamic fiber systems have already developed (see O'Rahilly and Mueller, Chapter 2 of this volume). At 11 weeks, fornix fibers reach the mamillary nucleus. Continuous maturation of the fornix is marked by the appearance of CD15 IR which transiently becomes very strong between 25 and 34 weeks. The mamillothalamic tract has been described at 14 weeks (Yamadori, 1965). The final stage of neuronal differentiation is heralded by the onset of myelination, which occurs mostly after birth (Vogt and Vogt, 1902; Krieg, 1960; Diepen, 1962; Yakovlev and Lecours, 1967.

The human fetal hypothalamus is supplied by rich neurotransmitter and neuropeptide systems. Probably most of them are operative in the human hypothalamus prior to the onset of synaptogenesis. Monoaminergic fibers in the medial forebrain bundle appear at 7 weeks (Zecevic and Verney, 1995). Catecholamine fibers in several hypothalamic nuclei are present in 3- to 4-month-old fetuses (Nobin and Björklund, 1973). At the same time, hypothalamic nuclei become supplied by cholinergic fibers. All neuropeptide systems under study could be demonstrated in the hypothalamus and median eminence between 10 and 20 weeks (Gluckman and Bassett, 1988; Goodyer, 1988; Bugnon *et al.*, 1987). Neuroactive substances may be detected much earlier by immunoassay in whole-brain homogenates (Gluckman and Bassett, 1988).

The early appearance of neurotransmitter and neuropeptide systems indicates that they have other functions during development. They might influence ontogenetic events, such as neurogenesis and morphogenesis, postnatal neuro- and gliogenesis, and axonal growth and synaptogenesis; they might also regulate energy expenditure and fetal metabolism or have impact on sex hormones in the developing brain.

Functional Differentiation

It has long been known that the multitude of vital bodily processes mediated by the hypothalamus (including cardiovascular regulation, sleep, metabolism, stress, thermoregulation, water and electrolyte balance, appetite regulation, sexual behavior, and immune responses) necessitates an intricate interaction among the nuclei. Yet, relatively little information is available in the human about the differentiation patterns of cell groups that are required for the establishment of a functional network (see Swaab *et al.*, 1993, 1997; Saper, Chapter 17 of this volume). The knowledge of the organization and functioning of neurotransmitter and neuropeptide systems is important because of the ability of pharmacological agents to interact with these compounds and to cause defects of the brain.

MIDBRAIN

The midbrain contains several regions with major clinical significance, which have attracted developmental studies.

Substantia Nigra

The development of the human fetal substantia nigra is considered to be important because of the potential use of its immature neurons in therapy for Parkinson's disease. Between 8 and 10 w.g., the region of the developing substantia nigra is occupied by small round cells (Sailaja and Gopinath, 1994). Between 10 and 13 w.g., cells become more loosely packed, and by 14 w.g. pars compacta and reticulata can be clearly distinguished. The cellular density of the pars reticulata decreases from 14 to 20 w.g., so that the adult pattern of reticulata can be recognized by 22 w.g. and neurons of the pars compacta assume adult morphological characteristics in Golgi and Nissl-stained material by about 20–22 w.g. (Sailaja and Gopinath, 1994). The nearby crus cerebri begins to develop at 14 w.g. as descending projection fibers pass through this region.

Immunoreactivity for tyrosine hydroxylase (TH) can first be seen in a few cells in the ventral mesencephalon as early as 5.5 w.g. (Silani *et al.*, 1994). Immunoreactive cells accumulate in the developing substantia nigra over the next few weeks, so that from about 8 w.g., TH immunoreactivity is localized in the perikarya and proximal dendrites of neurons of the substantia nigra, ventral tegmental area, and ventrolateral regions of the periaqueductal region (Pearson *et al.*, 1980; Sailaja and Gopinath, 1994). Immunoreactive cells seen to be lying ventrolateral to the cerebral aqueduct at 8–14 w.g. are aligned with the cell body directed ventrally, giving the impression that the cells are migrating from periaqueductal proliferative regions. From 19 w.g., groups of dopaminergic cells can be divided into the substantia nigra pars compacta, ventral tegmental area, and retrorubral area (Aubert *et al.*, 1997). When human ventral mesencephalic cells are maintained in culture, the addition of basic fibroblast growth factor stimulates increased TH activity, maintains neuronal survival and has proliferative effects on glial cells of the region (Silani *et al.*, 1994).

Substantia nigra neurons can be retrogradely labeled from the caudate at 10 w.g. after insertion of carbocyanine dyes into the caudate, indicating that at least some of the nigrostriatal pathway is established by this early age (Sailaja and Gopinath, 1994).

From about 12 w.g., substantia nigra pars compacta neurons begin to exhibit markers of dopamine transmission (Aubert *et al.*, 1997). D2 dopamine receptor (D2R) mRNA, D2R binding sites, dopamine membrane transporter mRNA, D1 receptor (D1R) protein, and D1R binding sites are all expressed from 12 w.g. This has been taken to indicate that the striatonigral neurons, which are known to express the D1R gene, have developed pathways connecting with the substantia nigra by 12 w.g. (Aubert *et al.*, 1997).

Periaqueductal Gray Matter

The periaqueductal gray is believed to have a central role in the integration and control of responses to stressful or threatening situations. Developmental changes in binding of neurotransmitters in this region have been studied by Reddy and coworkers (1996). Although binding to all types of receptors under study (nicotinic, muscarinic, serotonergic, opioid, and kainate) could be demonstrated by mid-gestation (i.e. 22 w.g.), subsequent changes in binding were different for each type of receptor. Binding of serotonin receptors decreases markedly between fetal and neonatal ages as well as between neonatal and adult ages. Binding of nicotinic receptors also decreases between fetal and neonatal ages, but remains stable from birth to adult life. Opioid receptor binding (^{3}H-naloxone) remains relatively constant from fetal to neonatal life, but increases slightly to adult life, whereas muscarinic cholinergic receptor binding remains constant from fetal to adult life. Finally, kainate binding tends to decrease with advancing age, but the differences were found not to be statistically significant. Overall, the most significant differences between fetal and neonatal ages were found to be in the serotonergic and nicotinic cholinergic receptor binding.

Interpeduncular Nucleus

The interpeduncular nucleus is an important component of the limbic midbrain circuitry and has been implicated in a wide variety of functions, including sleep regulation (Haun *et al.*, 1992) and pain sensitivity (Meszaros *et al.*, 1985). The human interpeduncular nucleus is cytoarchitecturally simple but chemically complex, with a lateral subdivision showing high muscarinic and serotonergic binding in the dorsal subdivision of the nucleus and high opioid binding in the medial subdivision. This chemoarchitectural subdivision is apparent at all ages of development from midgestation (19–26 w.g.) through infancy (38–74 weeks postconception) to childhood (4 years). The levels of muscarinic, nicotinic, and, to some extent, serotonergic receptor binding decline through development, but opioid and kainate remain relatively constant from midgestation to maturity.

Development of Glia in the Mesencephalon

The human fetal mesencephalon has been used as a study area to examine the development of microglia and astrocytes (Wierzba-Bobrowicz *et al.*, 1997). Ameboid microglia are already present in the fetal human mesencephalon at 8 w.g., and the number of these cells peaks at about 12 w.g. Ameboid microglia

are progressively replaced by ramified microglia from 11 w.g., and astrocytes also appear at about 11 w.g. Similar changes in the numbers of ramified microglia and astrocytes may be seen in human fetal mesencephalon, suggesting that there may be interactions between these two types of glia during development.

CEREBELLUM AND PRECEREBELLAR NUCLEI

Introduction

At the end of the embryonic period (stage 23 or approximately 57 days gestation), the developing cerebellum has a layered structure, with two germinal zones and the beginnings of some of the major neuronal populations already present (Müller and O'Rahilly, 1990). Adjacent to the fourth ventricle lies the ventricular germinal layer. A broad intermediate layer intervenes between the ventricular layer and the internal fiber layer. The intermediate layer contains cells that correspond to the future Purkinje cells. Further still from the ventricular surface lies the developing deep cerebellar nuclei. Finally, the external surface of the developing cerebellum is covered by an external germinal layer.

Two genes, *En-1* and *En-2*, which appear to specify the cerebellar domain, have been identified in mice (Davis and Joyner, 1988). Animals with targeted disruption of *En-1* show cerebellar and collicular agenesis (Wurst *et al.*, 1994), whereas *En-2* knockout results in subtle defects in cerebellar foliation (Millen *et al.*, 1994). In the developing human fetus (18–21 w.g.), the RNA signal for both EN1 and EN2 is strongest in the cerebellar granular layers, white matter of the vermis and flocculus, inferior olive, arcuate nucleus, and premigrational neurons of the corpus pontobulbare (Zec *et al.*, 1997).

The gross development of the human fetal cerebellum has been followed by magnetic resonance imaging (Press *et al.*, 1989; Hansen *et al.*, 1993). Fusion of the cerebellar vermis begins in the eighth to ninth week of gestation. By the third month, the midportion of the vermis and the cerebellar hemispheres begin to proliferate more rapidly than the rest of the cerebellum and the shape begins to swell centrally. The horizontal fissure appears by the end of the fourth month, and soon thereafter the cerebellar hemisphere growth overtakes that of the vermis so that the inferior vermal groove develops. The semilunar lobule and gracile lobe of the cerebellum expand to displace the flocculonodular lobes and cerebellar tonsils inferiorly. The nodule is progressively pushed anteriorly to indent the roof of the fourth ventricle (Press *et al.*, 1989; Hansen *et al.*, 1993). Peak growth of the rhombencephalon and cerebellum occurs after birth (Koop *et al.*, 1986), at about 400–500 days after conception, and is probably mainly accounted for by the development of the cerebellar cortex (see below).

Development of Cerebellar Cortex

Purkinje Cells

Differentiation of Purkinje cells in the human cerebellum has been followed by Zecevic and Rakic (1976). Those authors divided Purkinje cell differentiation into three stages. The first stage occupies the fourth fetal month (12–16 w.g.), and during this time Purkinje cells are bipolar in shape and are distributed several cells deep. Their somatas are relatively smooth during this early stage, with only a few processes at their apical and basal cell poles. At this early stage, some immunoreactivity for plasma proteins may be detected (Jacobsen and Møllgard, 1983). The second stage runs from 16 to 28 w.g., and during this stage the Purkinje cells become organized into a single layer. The somata of Purkinje cells begin to develop additional randomly directed processes and numerous somatic spines. This period of dendritic and other process outgrowth is accompanied by transient Purkinje neuron immunoreactivity for microtubule-associated protein 5 (MAP5; Ohyu *et al.*, 1997). At the beginning of the second stage, the first synapses begin to appear on the somatic spines of the immature Purkinje cells and on their immature dendritic spines, and these increase in number during the second stage. Toward the end of the second stage (23–24 w.g.), Purkinje cells can be labeled by immunoreactivity for the GM3 ganglioside (Heffer-Lauc *et al.*, 1996) and begin to show strong immunoreactivity for EAAT4, a glutamate receptor subtype (Itoh *et al.*, 1997). The third stage of Purkinje cell development extends through the remainder of prenatal life (28–40 w.g.), the first year of postnatal life, and even continues after 1 year of age. During the third stage, the dendritic arbor takes on its characteristic flattening in the plane perpendicular to the axis of the folium. Somatic spines disappear and spines begin to develop on the secondary and tertiary branches of the expanding dendritic tree. Elongation of Purkinje cell dendrites is accompanied by the development from about 35 to 36 w.g. of the glycolytic enzyme aldolase C, which is a selective marker for Purkinje cells in the adult cerebellum (Royds *et al.*, 1987). Maturation of the Purkinje cells in humans appears to occupy a much greater period of time after birth than is the case in nonhuman primates.

Milutinovic *et al.* (1992) reported that Purkinje cells in both the cerebellar hemispheres and vermis undergo substantial reduction in numbers between 12 w.g. and 25 w.g., with approximately 90% of the loss occurring between 12 and 20 w.g. This period of neuronal loss would coincide with migration of immature granule cells past the Purkinje cell layer, the formation of Purkinje cells into a single layer, and the formation of the first synapses on somatic spines of Purkinje cells. Immunoreactivity for the apoptosis promoter protein Bak has been shown to be weak in Purkinje cells under 17 w.g. but is strongly present from 19 to 34 w.g. (Obonai *et al.*, 1998). Expression of the apoptosis inhibitor protein Bcl-x is also intense during the period from 24 to 38 w.g. (Sohma *et al.*, 1996). These results indicate that control of Purkinje cell numbers arises from complex interaction between apoptosis promoter and inhibitor factors during fetal development. After birth, Bcl-x protein is expressed in Purkinje cells at low levels until adulthood (Sohma *et al.*, 1996). Immunoreactivity for Bak remains low throughout early adult life, but increases again in elderly subjects (Obonai *et al.*, 1998).

The hypothesis that Ca signaling has an important role in developmental processes of the cerebellum has prompted several recent studies of the development of intracellular Ca-signaling molecules and calcium-binding proteins (inositol 1,4,5-triphosphate receptor type 1, IP3R1; ryanodine receptor, RyR; calbindin D-28k, CB; and parvalbumin, PV) in the prenatal human cerebellum. Immunoreactivity to IP3R1 appears in the nascent Purkinje cell layer as early as 13 w.g. (Milosevic and Zecevic, 1998; Miyata *et al.*, 1999; Zecevic *et al.*, 1999). This immunoreactivity to IP3R1 increases by the 17- to 24-w.g. period, but the labeling is curiously patchy, with regions of strong immunoreactivity interspersed with immunonegative zones. Immunoreactivity for IP3R1 increases in the dendrites and spiny branchlets as these develop, progressing rapidly during the 6 months after birth (Miyata *et al.*, 1999). Immunoreactivity for RyR is expressed for the first time at 18 w.g. in the cell bodies and proximal dendrites of Purkinje cells. The patchiness of Purkinje cell layer labeling observed with immunoreactivity to IP3R1 can also be seen with RyR immunoreactivity, although the RyR-immunoreactive patches are smaller that those seen with IP3R1 (Milosevic and Zecevic, 1998).

Immunoreactivity for CB can be seen as early as 4–5 w.g. in bipolar migrating neurons (Milosevic and Zecevic, 1998), and by 10–13 w.g. labeled Purkinje cells and axons of the inferior cerebellar peduncle can be seen. Immunoreactivity for PV can be seen for the first time at 11 w.g. labeling cells in the rostral part of the external germinal layer. By 13 w.g., a bundle of PV-immunoreactive fibers arising from the pontine nuclei can be observed in the cerebellar intermediate zone. At this time, alternating CB- and PV-immunoreactive fiber bundles can be seen on frontal sections throughout the intermediate zone of the cerebellum. By 18 w.g., uneven patches of CB immunoreactivity can be seen in the Purkinje cell layer, which correspond to those observed with IP3R1 immunoreactivity. Immunoreactivity to PV labels Purkinje cells by 18 w.g. (Yew *et al.*, 1997) and at this age also showed discontinuities in labeling (Milosevic and Zecevic, 1998) as seen with immunoreactivity for intracellular Ca^{2+} receptors. The discontinuities in immunoreactivity noted with these four markers as well as immunoreactivity to phosphorylated and nonphosphorylated neurofilament (Milosevic and Zecevic, 1998) continue to be visible until the end of prenatal life. Although the precise role of the intracellular calcium-signaling and calcium-binding system during cerebellar development remains obscure, the discontinuous pattern of immunoreactivity to these markers suggests a possible role in the developmental patterning of the cerebellum and may help define functional regions during development (Milosevic and Zecevic, 1998).

Granule Cells

As in all mammals, granule cells of the developing human cerebellum are generated in the external germinal layer and migrate to the cerebellar primordium, past the Purkinje cells, to come to rest in the (internal) granular layer. In the human, the external germinal layer can be identified by about stage 21 (51 days gestation; Müller and O'Rahilly, 1990) and can still be identified after birth. The external germinal layer can be divided into a superficial proliferative layer and a deeper premigratory layer, both of which show strong immunoreactivity for neuronal nuclear antigen during fetal life (Sarnat *et al.*, 1998) and express developmental stage-specific antigens (Moss *et al.*, 1988). The external germinal (also sometimes called granular) layer was traditionally believed to give rise to granule cells, basket cells, stellate cells, and Golgi cells (Rakic and Sidman, 1982), but recent studies suggest that only granule cells are derived from this layer (Zsang and Goldman, 1996). Migration of immature granule cells past the Purkinje cells begins at about the end of the first trimester, so that the internal granular layer begins to appear from 15 w.g. (Gudovic *et al.*, 1998) and most of the cells of the internal granular layer appear between 20 and 30 w.g. Nevertheless, it is likely that migration and differentiation of some granule cells continues (albeit at a low pace) through the first postnatal year (Gudovic *et al.*, 1998). The period of major increase in number of granule cells (20–30 w.g.)

corresponds to the arrival of mossy fibers in the internal granular layer and the appearance of the lamina dissecans (Rakic and Sidman, 1970).

The internal granular layer shows moderate immunoreactivity for MAP5 from its first appearance (15 w.g.) and throughout the rest of fetal life (Ohya *et al.*, 1997). Moderate to strong immunoreactivity for MAP5 also appears in the outer and inner halves of the molecular layer during the period from 24 w.g. to about 8 months after birth, corresponding to growth of parallel and climbing fibers into the zone beyond the Purkinje cell layer. The period of parallel fiber elongation is also characterized by positive immunoreactivity for the CD15 epitope (3-fucosyl-*N*-acetyllactosamine), which is presumably correlated with synaptogenesis (Gocht *et al.*, 1992). Interestingly, cells of the granule cell lineage, which express neuronal nuclear antigen during proliferation and premigratory stages in the external germinal layer, lose that antigen during settling in the internal granular layer. They do not express the antigen again until the period of outgrowth of parallel fibers to the developing molecular layer (from 24 w.g.; Sarnat *et al.*, 1998). Granule cells can also be identified during migration and after settling in the granule cell layer by immunoreactivity against the neuronal class III β-tubulin isotype, which also defines parallel fibers, stellate and basket neurons (Katsetos *et al.*, 1993).

Granule cells also exhibit intense immunoreactivity for the apoptosis inhibitior protein, Bcl-x, during the period from 13 to 22 w.g. (Sohma *et al.*, 1996), corresponding to the period of migration and settling of granule cells in the internal granular layer followed by the initial outgrowth of parallel fibers into the developing molecular layer.

Development of Deep Cerebellar Nuclei

At the beginning of the fetal period (8–10 w.g.), the dentate nucleus consists of only a diffusely arranged population of cells, with no differentiation of neuronal types. The dentate nucleus emerges as a distinct nuclear entity at around 16 w.g. (Mihajlovic and Zecevic, 1986), when it appears from the cerebellar white matter. It initially has the form of a thick band of cells that gradually attenuates and begins to fold from about 24 w.g., and gyri can be seen over the entire surface by about 28–29 w.g. Subdivision of the human dentate nucleus into a smaller microgyric rostral part and the larger macrogyric caudal part is achieved by 35 w.g. (Yamaguchi and Goto, 1997).

Differentiation into small and large neuron types can be first identified at 16 w.g. (Mihajlovic and Zecevic, 1986), with large neurons approximately 20 μm in their largest diameter and small neurons approximately 7–10 μm in the largest diameter. In Golgi-impregnated preparations, two principal types of large neurons can be identified in the 16- to 22-w.g. period. Fusiform neurons can be found scattered throughout the dentate nucleus at this stage and have three to four primary dendrites emerging from the apex of the cell body. Dendrites of fusiform neurons are completely devoid of spines or other appendages. Multipolar neurons at 16–22 w.g. can be further divided into three groups: border cells, central neurons and asymmetric neurons. Border neurons are concentrated at the inner and outer borders of the nuclear lamina and possess four to five primary dendrites, all of which extend into the nuclear lamina. Central neurons lie in the deeper parts of the nuclear lamina and possess three to four dendrites extending in all directions. Asymmetric multipolar neurons are evenly distributed throughout the nuclear lamina and have five to six primary dendrites, one of which is substantially longer than the rest, giving an asymmetric appearance to the dendritic field. Small neurons can be divided into two types: bipolar and small multipolar neurons.

Multipolar neurons begin to develop typical dendritic spines from about 18–20 w.g. By about 24 w.g., small neurons begin to develop spines, and by 27 w.g., small neurons begin to attain the size and shape of postnatal nerve cells. Mihajlovic and Zecevic (1986) also commented that large neurons of the dentate nucleus appeared to be more morphologically mature than Purkinje cells at the same age. The period of extension of dentate neuronal dendrites (16–26 w.g.) corresponds to mild transient expression of MAP5 (Ohyu *et al.*, 1997).

Studies of chemical differentiation of deep cerebellar nuclei neurons have shown that GABA and parvalbumin immunoreactivity appear in both neurons and fibers of the deep nuclei as early as 16 w.g. (Yu *et al.*, 1996; Gudovic *et al.*, 1987; Hayaran *et al.*, 1992).

Development of Neurotransmitter Receptor Binding in the Cerebellum

Neurotransmitter binding appears to be higher in the fetal cerebellum than in early postnatal or adult humans. Court *et al.* (1995) have found that nicotine and muscarine binding in fetuses (23–29 w.g.) exceeds binding in young adults by factors of 6 and 2, respectively, in the dentate nucleus and by a factor of 3 in the white matter. The binding of these were also higher in the external germinal layer than in the internal granule layer of the adult, indicating that immature granule cells of the external germinal layer bind nicotine and muscarine more avidly than the mature neurons. Binding of α-bungarotoxin is also raised in the dentate

gyrus compared to the adult. The M_2 subtype appears to be the predominant muscarinic receptor in the human cerebellum, but this receptor type accounts for a lower proportion of muscarinic binding in the fetus than it does in the adult. The developmental significance of these changes remains unknown.

There also appear to be significant differences in the densities of 5-HT_{1A} receptors in fetal human cerebellum compared to the adult (del Olmo *et al.*, 1994). Those authors found high densities of 5-HT_{1A} receptors over the cerebellar cortex during fetal and neonatal stages, whereas the adult cerebellum is nearly devoid of this type of binding. This transient presence of receptors may reflect a developmental role for serotonin in dendritic growth or axonal branching, but this remains to be definitively proven.

Development of Inferior Olivary Nuclei

The human inferior olivary nuclear complex is composed of three subdivisions: medial accessory olivary nucleus (MAO), dorsal accessory olivary nucleus (DAO), and principal nucleus (PIO). Analysis of human pathology suggests that the MAO and DAO project to the rostral lobules of the cerebellar hemispheres; the caudal ventral lamella of the PIO projects to the caudal cerebellar hemispheres and the dorsal lamella and rostral pole of the PIO project to the rostral lobules of the cerebellar hemispheres.

Inferior olivary nucleus neurons are generated from the germinal matrix of the corpus pontobulbare component of the rhombic lip between about 5 and 7 w.g., and neurons migrate to their final resting site in the medulla during the period from 5 and 18 w.g. At midgestation (about 20 w.g.) axons from the inferior olive extend into the cerebellar white matter (Hayaran and Bijlani, 1992). At 28 w.g., these axons make synapses with immature Purkinje cells. From 34 w.g. the climbing fibers begin to climb the Purkinje cell dendrites and this process continues into postnatal life. Pruning of the number of climbing fibers occurs postnatally (Marin-Padilla, 1985), although Gudovic and Milutinovic (1996) have claimed that the number of inferior olivary nucleus neurons declines mainly in the period from 12.5 w.g. to 25 w.g., in parallel with loss of Purkinje cells from the cerebellar cortex.

Neurochemical studies (Armstrong *et al.*, 1999) have compared neurotransmitter binding in fetal, neonatal, and adult inferior olivary nuclei. These patterns of change in receptor binding are different for each of the subdivisions of the inferior olivary complex. For the principal nucleus between midgestational fetal and neonatal (1–6 months) stages: opioid binding decreases, kainate increases, while muscarinic cholinergic, nicotinic cholinergic, and α-$_2$ adrenergic binding remain stable. For the DAO over the same period: nicotinic, muscarinic, α-$_2$, and opioid binding decreases, whereas kainate binding increases.

Development of Pontine Nuclei

Neurons of the basilar pontine nuclei are derived from the corpus pontobulbare portion of the rhombic lip and migrate around the circumference of the ventral surface of the brain stem. They contribute mossy fibers to the developing cerebellar cortex from 20 w.g. onward. The period of maturation of pontine neurons corresponds to the development of neuronal nuclear antigen, which begins to appear in pontine neurons at 14 w.g. and is strongly developed by 20 w.g. (Sarnat *et al.*, 1998).

PONS AND MEDULLA

Within the developing human rhombencephalon, selected pathways and nuclei have received attention according to their perceived clinical significance. Those systems that have been best studied are the auditory pathway, cranial nerve nuclei, and selected reticular formation nuclei, particularly those involved in respiratory and cardiovascular control.

Auditory Pathway

Auditory function develops well before birth, and assessment of auditory function is useful in assessing the developmental state of preterm infants.

The cochlear nuclei in humans consist of a larger ventral nucleus lying rostrally and a smaller dorsal nucleus lying more caudally and extending into the lateral recess of the fourth ventricle. At 12 w.g., neurons of the ventral cochlear nucleus cannot be distinguished from glia, but differentiation of neurons begins to be noticeable from 16 w.g. The number of identifiable neurons increases to about 40,000 by 21 w.g. and appears to remain stable throughout fetal and postnatal life. Cytoarchitectural features of the main ventral cochlear neuron types (large round and small spindle shaped) gradually develop after 21 w.g. (Nara *et al.*, 1993). Cytoarchitectural features of the inferior colliculus begin to appear after 12 w.g. (Nara *et al.*, 1996), and after 16 w.g. neurons of the inferior colliculus begin to differentiate into two distinct morphological classes (large and small) on the basis of appearance in Nissl-stained material.

The human olivocochlear system can be identified using immunoreactivity to choline acetyltransferase

(ChAT) and calcitonin gene–related peptide (CGRP), both of which label those central neurons of the superior olivary complex that contribute to the olivocochlear bundle. Both ChAT and CGRP immunoreactivity is visible by 21 w.g. in neurons of the dorsal and ventral periolivary region, although neurons of the medial and lateral superior olivary nuclei are still of immature appearance in Nissl stains made at this age. Neurons immunoreactive for ChAT become more dispersed as prenatal development proceeds (Moore *et al.*, 1999). Neurofilament immunohistochemistry indicates that olivocochlear fibers grow out between 22 and 29 w.g. (Moore *et al.*, 1997). This is consistent with reports of the first appearance of efferent nerves and terminals in the cochlea at 20–22 w.g. (Igarashi and Ishii, 1980) and the first appearance of mature synapses onto outer hair cells between 24 and 28 w.g. (Lecanuet and Schaal, 1996).

The development of ascending, commissural, and descending pathways associated with the auditory system have been studied with neurofilament immunohistochemistry. The first fibers of the cochlear nerve invade the ventral cochlear nucleus at about 16 w.g. (Moore *et al.*, 1997). At about the same time, several trapezoid body–lateral lemniscus axons reach the superior olivary nucleus and inferior colliculus. The ascending auditory pathway undergoes a marked expansion between 16 and 26 w.g., with collateralization of ascending axons by 26 w.g. and formation of terminal plexuses in target nuclei from 26 to 29 w.g. (Moore *et al.*, 1997). Commissural pathways (dorsal commissure of the lateral lemniscus, commissure of the inferior colliculus) develop from 22 w.g.

Myelination of auditory pathways begins at about 26 w.g. (Moore et al., 1995). At that stage linear arrays of oligodendrocytes are located alongside axons in all segments of the auditory pathway. At 29 w.g., the cochlear nerve contains lightly myelinated axons and the primary axons can be seen to bifurcate and radiate in the ventral cochlear nucleus. Further up the auditory pathways at this stage, myelination is also present in the lateral lemniscus and trapezoid body by 26 w.g., and myelination in the inferior brachium develops from about 29 w.g. Myelination continues into the first postnatal year and at 1 year of age auditory pathway myelination appears comparable to that in the mature brain.

Functional development of the auditory system parallels the morphological development outlined above. Studies of the development of the auditory blink–startle response in fetuses (Birnholtz and Benecarraf, 1983; Kuhlman *et al.*, 1988) indicate that the first short-latency responses to sound may be obtained at 25–26 w.g. This response is seen in virtually all fetuses by 28 w.g., closely paralleling the development of myelination in the auditory pathways, as outlined above.

Cranial Nerve Nuclei

Motor Nuclei

Detailed information concerning the development of motor nuclei in the human brain stem is not available, with only a few studies focusing on these structures.

Most of the major motor nuclei (motor trigeminal, abducens, ambiguus, spinal accessory) attain their final positions in the brain stem by the end of the embryonic period (8 w.g.) (Jacobs, 1970). Only the facial nucleus and accessory facial nucleus (which supplies the posterior belly of digastric and stapedius muscles) have failed to reach their final resting places by 10 w.g. The trigeminal nucleus, which consists of dorsal, intermediate, and ventral subdivisons, begins to show further differentiation into separate compartments at 10 w.g.

Cytoarchitectural development of the hypoglossal nucleus has been followed by Nara *et al.* (1989). Their data indicate that the number of neurons in the hypoglossal nucleus does not show any consistent change in the period from 16 w.g. to late adult life. This stands in contrast to their report that degenerating neurons are found between 21 and 33 w.g. (Nara *et al.*, 1989).

Human cranial nerve motor nuclei show strong activity for succinic dehydrogenase and AChE by 12 w.g. (Wolf *et al.*, 1975). Several cranial nerve motor nuclei (facial, hypoglossal, and ambiguus) show transient activity for NADPH-diaphorase between 19 and 21 w.g. (Gonzalez-Hernandez *et al.*, 1994). These nuclei are negative by 23 w.g., indicating a very short period of activity. This transient activity may indicate that NO is involved in early regulatory processes during motor nuclei development, but this requires further investigation.

Autonomic Effector Nuclei

The dorsal motor nucleus of the vagus (10) is the only autonomic effector nucleus which has been studied in detail during fetal life (Nara *et al.*, 1991). The dorsal motor nucleus of the vagus can be seen to be divided into three main subdivision (caudal, dorsal, and ventral) by 16 w.g. The dorsal subdivision is described as containing polygonal or spindle-shaped neurons, while the ventral subdivision has round or oval neurons. The caudal subdivision was described as containing more rounded neurons that the dorsal. Various anatomical parameters show gradual increase

throughout the fetal period indicating moderate development across this interval.

Detailed analysis of dendritic development of neurons in the vagal sensorimotor complex is not available. Nevertheless, a study of dendritic spine development in the dorsal medullary reticular formation indicates that dendritic spines density increases steadily from 20 w.g. to term, before declining during early postnatal life (Becker and Zhang, 1996).

One study has examined the development of substance P–immunoreactive fibers in the dorsal motor nucleus of the vagus nerve. Wang *et al.* (1993) found that substance P–immunoreactive fibers are first distributed to this nucleus at 16 w.g. By 23 w.g., these fibers were of low-to-moderate density and continued to increase in staining intensity until birth. By the last age examined the substance P–immunoreactive fibers had become coarser and with more varicosities than previously.

Sensory Nuclei

Development of the trigeminal sensory nuclei will be dealt with in Chapter 29 on the human trigeminal system.

The human nucleus of the solitary tract can be distinguished in the brain stem at about 16 w.g. and individual subnuclei can be discerned over the following weeks (Wang *et al.*, 1993). Substance P immunoreactivity can be seen for the first time at 16 w.g., at which stage it is present in fibers distributed mainly over the dorsal and dorsolateral parts of the nucleus. At this early stage the fibers are thin, smooth, with few varicosities and some terminal boutons. As for the developing nucleus of the solitary tract, the density of substance P–immunoreactive fibers increases steadily in the nucleus of the solitary tract over the fetal period until the last age examined (40 w.g.). Binding of opiates to the fetal nucleus of the solitary tract as well as the trigeminal sensory nuclei is similar to the adult by midgestation indicating possible early maturation of opioid systems (Kinney *et al.*, 1990).

Respiratory and Cardiovascular Areas

Only a few studies to date have examined the development of respiratory and cardiovascular centers in the developing human brain stem. Consequently, only an incomplete picture of maturation of these important regions is available at present.

Although the arcuate nucleus has classically been regarded as a precerebellar nucleus, its has also been implicated in central control of respiratory and vasomotor responses (Filiano *et al.*, 1990). In fact, those authors have pointed out the cytoarchitectural similarity between the human arcuate nucleus neurons and neurons in the chemosensitive S area of the ventral medullary surface in the cat. Zec *et al.* (1997) have examined the connections between the human fetal arcuate nucleus and identified cardiorespiratory regions at 19–22 w.g., using carbocyanine dye (DiI) diffusion techniques. They identified labeled fibers arising from the arcuate nucleus and reaching the medial reticular formation (nucleus paragigantocellularis), medullary raphe, as well as fibers coincident with the external arcuate fibers. None of the fibers labeled by DiI insertion into the arcuate nucleus were seen to enter the inferior cerebellar peduncle, but this may reflect a technical problem with the carbocyanine dye diffusion because of the great distance involved.

Prenatal development of substance P immunoreactivity in two regions associated with control of respiratory and cardiovascular function (parabrachial nuclei, Kolliker–Fuse nucleus, and nucleus of the solitary tract) has been studied by Wang and coworkers (1992, 1993). The nucleus of the solitary tract has been discussed above (see cranial nerve sensory nuclei) but, in brief, shows steady increase in substance P immunoreactivity throughout fetal life (Wang *et al.*, 1993). In the case of the parabrachial and Kolliker–Fuse nuclei (Wang *et al.*, 1992), low densities of substance P–immunoreactive fibers and terminals can be seen as early as 16 w.g. By 23 w.g. there is clear differentiation of staining intensity in this region, with the strongest immunoreactivity being over the lateral parabrachial nucleus. This differential staining continues until the end of fetal life, as staining intensity of the whole region continues to increase progressively throughout prenatal life (Wang *et al.*, 1992).

Somatostatinergic systems are believed to be involved in the maturation of respiratory control, and the development of somatostatin binding in 16 respiratory nuclei of the human brain stem has been analyzed by Carpentier *et al.* (1997). Somatostatin binding is particularly strong during fetal life in the nucleus of the solitary tract and dorsal cochlear nucleus, whereas moderate activity is present in other sensory cranial nerve nuclei (Carpentier *et al.*, 1996). In all respiratory regions, somatostatin binding is particularly strong in early to midgestational stages (about 20 w.g.) and declines during fetal life. In most respiratory centers, somatostatin binding declines gradually either throughout the developmental period or mainly during fetal life. On the other hand, in two nuclei (lateral parabrachial and locus coeruleus) there is an abrupt decrease in the density of somatostatin binding sites at the time of birth.

One major stimulus for studies of the maturation of cardiorespiratory regions in the fetal human brain stem

is the goal of understanding the effects of maternal smoking on the maturation of the fetal brain stem and postnatal cardiorespiratory function. Kinney *et al.* (1993) have studied nicotine binding in the developing human brain stem. They have shown that nicotine binding is heavy in midgestational fetuses in those brain stem tegmental regions serving cardiorespiratory function, arousal, attention, rapid eye movement (REM) sleep, and somatic motor control. Nicotine binding decreases sharply during the last half of prenatal life in these region, whereas binding over cerebellar relay nuclei (inferior olivary nuclei and pontine nuclei) does not change greatly. This suggests that there is an opportunity during midgestation for the development of cardiorespiratory centers to be modified by maternal smoking.

Monoaminergic Pathways

Detectable levels of noradrenaline (NA) and serotonin (5-HT) appear in the pons, medulla oblongata, and spinal cord from 5 to 6 w.g. (Sundström *et al.*, 1993). For the rest of the first trimester, levels of NA and 5-HT increase consistently, but there is a noticeable increase in interindividual variability of levels with advancing age. Immunocytochemistry of first trimester brain stem shows that immature neurons immunoreactive for TH are present by 4 weeks postconception (Sundström *et al.*, 1993), and several TH and 5-HT nerve cell groups can be found in the pons and medulla from 5 weeks. TH-immunoreactive cells matured from round uni-/bipolar cells at 5 w.g. to multipolar neurons with extensive neurite outgrowth at 8 w.g. After this stage there are only minor additional increases in somata size, but the innervation of the surrounding neuropil increases. Similarly, 5-HT-immunoreactive neurons in the human brain stem differentiate from unipolar cells at 5 weeks to large, multipolar neurons by 11 w.g., although some brain stems showed poorer differentiation of these cells by the end of the first trimester. By about the 15th week, all the major NA and 5-HT cell groups can be identified by fluorescence techniques (Olson *et al.*, 1973).

Other Reticular Formation Nuclei

The cytoarchitectural development of the gigantocellular reticular nucleus has been examined by Yamaguchi *et al.* (1994). The nucleus appears as early as 16–18 w.g., but most neurons are still immature at this age. Typical large multipolar neurons appear at 21 w.g. and myelination has been noted as early as 22–23 w.g. (Yamaguchi *et al.*, 1994). Neuronal numerical density of the giganticellular reticular nucleus declines between 16 w.g. and birth. Those authors suggested that differentiation and maturation of gigantocellular neurons progresses gradually and monotonically during fetal life.

Development of Fiber Tracts in the Pons and Medulla

Growth-associated protein 43 (GAP-43) serves as a substrate for protein kinase C and is thought to have a critical role in axonal growth (Meiri *et al.*, 1986; Skene *et al.*, 1986). GAP-43 is enriched in growth cones (DeGraan *et al.*, 1985; Meiri *et al.*, 1986) and present in high levels during the period of axonal elongation (Jacobson *et al.*, 1986; Karns *et al.*, 1987). At midgestation (19–22 w.g.), GAP-43 immunoreactivity is moderate in intensity in many brain stem nuclei, but is already absent or low in the hypoglossal nucleus, facial motor nucleus, superior olivary nucleus, and nucleus of the inferior colliculus (Kinney *et al.*, 1993). The corticospinal tract shows strong immunoreactivity in the fetal medulla and pons. This pattern was also seen at 26 w.g., whereas at 38 w.g. staining was completely absent from the facial motor nucleus. At infancy strong GAP-43 immunoreactivity remains visible in the intermediate reticular zone and begins to decline in the pyramidal tract. The pontine tegmentum remains strongly reactive, but many other brain stem tracts such as the solitary tract, medial and lateral lemnisci, amiculum and hilum of the inferior olive, transverse pontocerebellar fibers, and cerebellar peduncles are poorly immunoreactive by infancy. Since GAP-43 appears to be associated with fiber tract development and plasticity, these findings suggest that most of the major fiber tracts are well developed by the time of birth, with the exception of the pyramidal tract. This is in agreement with studies of myelination in the human fetal brain stem (Tanaka *et al.*, 1995), which found that the corticospinal tract is slow to complete myelination, whereas the medial longitudinal fasciculus, cuneate fasciculus, and solitary tract complete myelination earlier. Synapses have been observed in the human pyramidal tract as early as 23 w.g. (Bruska and Wozniak, 1994) and may represent the early formation of collateral axon synapses with brain stem regions.

SPINAL CORD

General Features of Neuronal Differentiation

In the developing brain, neuron-specific enolase (NSE), a neuronal form of the glycolytic enzyme enolase, is not expressed in germ cells or immature

neurons, and so can be taken as an indicator of the onset of neuronal differentiation. In the ventral horn of the spinal cord, NSE begins to appear at about 7–8 w.g. and is definitely present by 10 w.g. (Kato *et al.,* 1994). In the dorsal horn, NSE develops slightly later—beginning to appear at 7–8 w.g. and definitely present by 22 w.g. Marti *et al.* (1987) showed that immunoreactivity for neurofilament triplet proteins develops in the major neuronal types of the spinal cord (both ventral and dorsal gray) as early as 6 w.g.

Development of the intermediolateral cell column appears to be slightly delayed relative to both the dorsal and ventral horns. Immunoreactivity for neurofilament triplet proteins appears in cells and fibers of the lateral horn at about 35 w.g., almost 30 weeks after neurofilament immunoreactivity appears in neurons of the ventral and dorsal horns (Marti *et al.,* 1987).

Morphological differentiation of ventral horn spinal cord neurons occurs in parallel with the appearance of NSE and neurofilament protein immunoreactivity. In Golgi preparations (Choi, 1981), ventral horn cells are well differentated by 7.5 w.g. with smooth thin dendrites extending at least as far as the boundary between mantle and marginal layers, while at this stage neurons in the intermediate zone are smaller, more slender, and frequently bipolar in shape.

Glial Differentiation in the Spinal Cord

Using electron microscopy, radial glial cells can be identified in the developing human spinal cord as early as 6 w.g. (Choi, 1981), although characteristic radial glia are difficult to identify by Golgi impregnation techniques at this early stage. By 7.5 w.g., radial glia can be clearly identified in Golgi preparations and distinguished from developing nerve cells. At that stage, many radial glial cells extend their processes across the entire distance from the central canal to the pial surface. The contour of these radial glia is irregular with many laterally projecting lamellar processes. Also at this stage the radial glia in the ventral and dorsal fissures show smoother outlines than cells in other regions and have an uninterrupted extension from the central canal to the pial surface. Immunoreactivity for GFAP can be detected in radial glial cells of the human spinal cord as early as 9 w.g. (Choi, 1981).

At 16 w.g., the central canal of the spinal cord becomes much narrower than at previous ages and is lined by a single layer of cuboidal or columnar cells with short processes (Choi, 1981). At this stage, not all the processes of radially oriented cells reach the pial surface. Scattered cells with much shorter bushy projections, showing features of stellate astroglial cells, begin to appear at this stage. Oligodendroglial cells are also seen at 16 w.g. in association with myelinated axons (see "Development of Long Tracts and White Matter").

Development of Identified Cellular Populations

The most detailed study of identified neuronal populations in the human fetal spinal cord has been undertaken by Marti *et al.* (1987) who found that immunoreactivity for identified neurotransmitters appeared earlier in the ventral horn than in the dorsal horn or dorsal root ganglion cells. Immunoreactivity for CGRP and galanin appears as early as 6 w.g. in cells and fibers of the ventral horn but does not appear until 10 and 20 w.g., respectively, in fibers of the dorsal horn. Similarly, neuronal immunoreactivity for somatostatin appears in the ventral horn by 8 w.g., but somatotstatin immunoreactivity in the somata of dorsal root ganglia does not appear until 10 w.g. (Charnay *et al.,* 1987). Substance P immunoreactivity of fibers in the ventral horn appears at 6 w.g., while those fibers appear at 11 w.g. in the dorsal horn. By contrast, immunoreactivity for fibers with neuropeptide Y (appearing at 10 w.g.), enkephalin (appearing at 10 w.g.), and vasoactive intestinal polypeptide (appearing at 20 w.g.) occurs simultaneously in ventral and dorsal horns (Marti *et al.,* 1987; Shen et al., 1994).

Just as neurofilament development in the intermediolateral cell column is delayed relative to the ventral and dorsal horn, neurotransmitter development also occurs later in fetal life (Marti *et al.,* 1987). Immunoreactivity for somatostatin in cells and fibers of the lateral horn appears at about 20 w.g., 10–12 weeks after the development of somatostatin immunoreactivity in neurons of the ventral and dorsal horns. Similarly, fiber immunoreactivity for enkephalin develops at 20 w.g., substance P develops at 24 w.g., NPY develops at 24 w.g, and CGRP develops at 24 w.g., 10–18 weeks after these immunoreactive fibers can be found in the ventral horn.

Development of Long Tracts and White Matter

Immunoreactivity for the phosphorylated variant of high molecular weight neurofilament protein is present in the longitudinal processes of the marginal zone (developing white matter) and the mantle layer of the spinal cord from the embryonic to the fetal period (8–30 w.g.; Lukas *et al.,* 1993).

Immunoroeactivity for the low-affinity receptor of nerve growth factor has been studied in fetal human spinal cord (Suburo *et al.,* 1992). Positive fibers may be found in regions of the spinal cord containing primary sensory afferents (e.g., dorsal root, dorsal and dorsolateral funiculi, and restricted regions of the dorsal

horn) but are not found in the ventrolateral funiculus. Immunoreactive fibers are initially found in the periphery of the thoracic-level dorsal funiculus as early as 7 w.g. and spread into other regions in older fetuses. In the upper spinal cord, immunoreactive fibers were seen in the gracile and cuneate fasciculi, extending to the dorsal column nuclei of the medulla (11 w.g.). Labeling of the dorsal funiculus is transient and has disappeared by 20 w.g., although labeling in both thoracic and lumbar levels of the dorsolateral funiculus continues to be present until adult life. Immunoreactivity for *trk* receptors, which have essential roles in signal transduction mediated by nerve growth factor and related neurotrophins, has been shown to appear in the dorsal columns from 23 to 39 w.g. (Muragaki *et al.,* 1995).

The calmodulin-binding phosphoprotein GAP-43, which also serves as a substrate for protein kinase C, is thought to have a critical role in axonal growth (Meiri *et al.,* 1986; Skene *et al.,* 1986). GAP-43 is enriched in growth cones (DeGraan *et al.,* 1985; Meiri *et al.,* 1986) and present in high levels within developing nerves during the period of axonal elongation (Jacobson *et al.,* 1986; Karns *et al.,* 1987). An *in situ* hybridization study with antisense GAP-43 riboprobe has revealed high signal in the developing spinal cord as early as 6 w.g. (Kanazir *et al.,* 1996), with levels sustained into fetal life.

Synaptophysin is an integral membrane protein of vesicles and appears at an early stage of neuronal differentiation. Despite the relatively mature cytoarchitectural appearance of ventral horn motoneurons in the human fetal spinal cord achieved at 10 w.g. (see above), synaptophysin immunoreactivity does not develop until 12–14 w.g. (Sarnat and Born, 1999). At this stage, synaptophysin immunoreactivity is found around neuronal somata as coarsely granular reactivity and as beaded axon-like structures in the neuropil between neurons.

Detailed information about the development of individual tracts in the human fetal spinal cord is rare. One study of 5-HT- and catecholamine-containing neuron systems in the fetal brain stem (Olson *et al.,* 1973) noted in passing the presence of axons showing fluorescence consistent with serotonergic and catecholaminergic function in the spinal cord as early as 9.8 mm crown–rump length (about 12 w.g.). Sundström *et al.* (1993) have reported that fibers immunoreactive for NA and 5-HT begin to appear in the cervical cord as early as 5 w.g., in the entire spinal cord from 6 w.g., and in the gray matter of the spinal cord at 9 w.g.

The development of myelination in the developing human spinal cord has been followed using myelin stains such as Luxol fast blue (LFB) and immunoreactivity for myelin basic protein (MBP)(Gilles, 1976; Tanaka *et al.,* 1995). Myelin sheaths stain earlier and more strongly with MBP immunohistochemistry, so that the subsequent discussion will concentrate on development times as revealed by MBP immunoreactivity. The medial longitudinal fasciculus is the earliest site of myelination as assessed by both myelin staining and MBP immunohistochemistry. The medial longitudinal fasciculus first shows myelination at about 20 w.g., and myelination appears to be complete by 34 w.g. (Tanaka *et al.,* 1995). Major ascending sensory pathways, such as the cuneate and gracile fasciculi, begin to myelinate slightly later. *In situ* hybridization shows MBP mRNAs *(MBP X5b-11)* in the gracile fasciculus, and periphery of the ventral and lateral funiculi as early as 20 w.g. (Pribyl *et al.,* 1996). Based on MBP immunoreactivity, the cuneate fasciculus begins to undergo myelination at 23 w.g. and completes myelination at about 36 w.g. (Tanaka *et al.,* 1995). Descending motor tracts begin myelination somewhat later than sensory pathways (Gilles, 1976; Tanaka *et al.,* 1995). The corticospinal tracts begin myelination at about 28–30 w.g., and myelination is not complete to an extent seen elsewhere in the CNS until after birth. In contrast to this relative delay in myelination of descending motor tracts, ventral roots appear to complete myelination at about the same time (35 w.g.) as dorsal roots (36 w.g.).

In general, myelination of sensory pathways starts in the peripheral nerves, dorsal spinal nerve roots, and posterior columns of the spinal cord in the second trimester and progresses after birth in the direction of ascending transmission of sensory information, i.e., medial lemniscus, posterior internal capsule, and central corona radiata (Yakovlev and Lecours, 1967). In contrast, in motor systems, myelination first appears in peripheral nerves and ventral spinal roots. Myelination of central motor pathways begins in the corticospinal tracts in the pons and progresses both rostrally and caudally from there (Yakovlev and Lecours, 1967).

Acknowledgment

We thank Drs. Y. Koutcherov, Ch. Andressen, D. Nohr, and Dipl. Biol. Th. Voss for their efficient help and invaluable assistance for this work, and Profs. Dr. W. Wechsler and Dr. J. Bohl for providing autopsy material.

References

Acklin, S.E., and van der Kooy, D. (1993). Clonal heterogeneity in the germinal zone of the developing rat telencephalon. *Development* **18,** 175–92.

Alheid, G.F., and Heimer, L. (1988). New perspectives in basal forebrain organization of special relevance for neuropsychiatric disorders: the striatopallidal, amygdaloid, and corticopetal components of substantia innominata. *Neuroscience* **27,** 1–39.

Altman, J., and Bayer, S.A. (1986). The development of the rat hypothalamus. *Adv. Anat. Embryol. Cell Biol.* **100,** 1–178.

Altman, J., and Bayer, S.A. (1989). Development of the rat thalamus: IV. The intermediate lobule of the thalamic neuroepithelium, and the time and site of origin and settling pattern of neurons of the ventral nuclear complex. *J. Comp. Neurol.* **284,** 534–566.

Armstrong, D.D., Assman, S., and Kinney, H.C. (1999). Early developmental changes in the chemoarchitectures of the human inferior olive: a review. *J. Neuropathol. Expl. Neurol.* **58,** 1–11.

Ashwell, K.W.S., and Mai, J.K. (1997a). Developmental expression of the CD15-epitope in the hippocampus of the mouse. *Cell Tiss. Res.* **289,** 17–23.

Ashwell, K.W.S., and Mai, J.K. (1997b). Developmental expression of the CD15-epitope in the brainstem and spinal cord of the mouse. *Anat. Embryol.* **196,** 13–25.

Aubert, I., Brana, C., Pellevoisin, C., Giros, B., Caille, I., Carles, D., Vital, C., and Bloch, B. (1997). Molecular anatomy of the development of the human substantia nigra. *J. Comp. Neurol.* **379,** 72–87.

Auladell, C., Perez-Sust, P., Super, H., and Soriano, E. (2000). The early development of thalamocortical and corticothalamic projections in the mouse. *Anat. Embryol.* **201,** 169–179.

Bailey, P. (1916). Morphology of the roof-plate of the forebrain and the lateral choroid plexus in the human embryo. *J. Comp. Neurol.* **26,** 79–120.

Becker, L.E., Armstrong, D.L., Chan, F., and Wood, M.M. (1984). Dendritic development in human occipital cortical neurons. *Dev. Brain Res.* **13,** 117–124.

Becker, L.E., and Zhang, W. (1996). Vagal nerve complex in normal development and sudden infant death syndrome. *Can. J. Neurol. Sci.* **23,** 24–33.

Berendse, H.W., and Richfield, E.K. (1993). Heterogeneous distribution of dopamine D1 and D2 receptors in the human ventral striatum. *Neurosci Lett.* **150,** 75–79.

Birnholz, J.C., and Benacerraf, B.R. (1983). The development of fetal hearing. *Science* **222,** 516–518.

Bothwell, M. (1991). Keeping track of neurotrophin receptors. *Cell* **65,** 915–918.

Bracco, L., Tiezzi, A., Ginanneschi, A., Campanella, C., and Amaducci, L. (1984). Lateralization of choline acetyltransferase (ChAT) activity in fetus and adult human brain. *Neurosci. Lett.* **50,** 301–305.

Brana, C., Charron, G., Aubert, I., Carles, D., Martin-Negrier, M.L., Trouette, H., Fourmier, M.C., Vital, C., and Bloch, B. (1995). Ontogeny of the striatal neurons expressing neuropeptide genes in the human fetus and neonate. *J. Comp. Neurol.* **360,** 488–505.

Brockhaus, H. (1938). Zur normalen und pathologischen Anatomie des Mandelkerngebietes. *J. Psychol. Neurol.* **49,** 1–136.

Brockhaus, H. (1940). Beitrag zur normalen Anatomie des Hypothalamus und der Zona incerta beim Menschen. *J. Psychol. Neurol.* **51,** 96–195.

Brockhaus, H. (1942). Zur feinen Anatomie des Septum und des Striatum. *J. Psychol. Neurol.* **51,** 1–56. Translated in: "Human Brain Dissection." Pope A., ed. (1983). U.S. Government Printing Office Publ. **381–132,** 3096.

Brunjes, P.C., Fisher, M., and Grainger, R. (1998). The small-eye mutation results in abnormalities in the lateral cortical migratory stream. *Dev. Brain Res.* **110,** 121–125.

Bugnon, C., Fellmann, D., Bloch, B., Bresson, J.L., Gouget, A., Lenys, D., and Clavequin, M.C. (1987). Contribution of immunocytochemistry to the study of the development of neuroglandular peptidergic systems in the human fetal hypothalamus. *Ann. Endocrinol. (Paris).* **48,** 343–351.

Burford, G.D., and Robinson, C.A.F. (1982). Oxytocin, vasopressin and neurophysins in the hypothalamo-neurohypophyseal system of the human fetus. *J. Endocrinol.* **95,** 403–408.

Burkhalter, A., Bernando, K.L., and Charles, V. (1993). Development of local circuits in human visual cortex. *J. Neurosci.* **13,** 1916–1931.

Buxhoeveden, D., Lefkowitz, W., Loats, P., and Armstrong, E. (1996). The linear organization of cell columns in human and nonhuman anthropoid Tpt cortex. *Anat. Embryol.* **194,** 23–36.

Carlsen, J. (1989). New perspectives on the functional anatomical organization of the basolateral amygdala. *Acta Neurol. Scand. Suppl.* **122,** 1–27.

Carpentier, V., Vaudry, H., Mallet, E., Laquerriere, A., Tayot, J., and Leroux, P. (1996). Anatomical distribution of somatostatin receptors in the brainstem of the human fetus. *Neuroscience* **73,** 865–879.

Carpentier, V., Vaudry, H., Mallet, E., Tayot, J., Laquerriere, A., and Leroux, P. (1997). Ontogeny of somatostatin binding sites in respiratory nuclei of the human brainstem. *J. Comp. Neurol.* **381,** 461–472.

Chan, W.Y., and Yew, D.T. (1998). Apoptosis and Bcl-2 oncoprotein expression in the human fetal central nervous system. *Anat. Rec.* **252,** 165–175.

Chapouton, P., Gartner, A., and Gotz M. (1999). The role of Pax6 in restricting cell migration between developing cortex and basal ganglia. *Development* **126,** 5569–5579.

Charnay, Y., Chayvialle, J.-A., Pradayrol, L., Bouvier, R., Paulin, C., and Dubois, P.M. (1987). Ontogeny of somatostatin-like immunoreactivity in the human fetus and infant spinal cord. *Dev. Brain Res.* **36,** 63–73.

Chawla, M.K., Gutierrez, G.M., Young, W.S. 3rd, McMullen, N.T., and Rance, N.E. (1997). Localization of neurons expressing substance P and neurokinin B gene transcripts in the human hypothalamus and basal forebrain. *J. Comp. Neurol.* **384,** 429–442.

Chen, E-Y., Mufson, E.J., and Kordower, J.H. (1996). TRK and p75 neurotrophin receptor systems in the developing human brain. *J. Comp. Neurol.* **369,** 591–618.

Cheng, G. Marotte, LR, Mai, J.K, and Ashwell, K.W.S. (2002). Early development of the hypothalamus of a wallaby *(Macropus eugenii). J. Comp. Neurol.* **453,** 199–215.

Chi, J.G., Dooling, E.C., and Gilles, F.H. (1977). Left-right asymmetries of the temporal speech areas of the human fetus. *Arch. Neurol.* **34,** 346–348.

Choi, B.H. (1981). Radial glia of developing human fetal spinal cord: Golgi, immunohistochemical and electron microscopic study. *Dev. Brain Res.* **1,** 249–267.

Choi, B.H. (1988). Developmental events during early stages of cerebral cortical neurogenesis in man. A correlative light, electron microscopic, immunohistochemical and Golgi study. *Acta Neuropathol.* **75,** 441–447.

Cooper, E.R.A. (1950). The development of the thalamus. *Acta Anat.* **9,** 14–226.

Cooper, E.R.A. (1954). The development of the human lateral geniculate body. *Brain* **68,** 222–239.

Court, J.A., Perry, E.K., Spurden, D., Griffiths, M., Kerwin, J.M., Morris, C.M., Johnson, M., Oakley, A.E., Birdsall, N.J.M., Clementi, F., and Perry, R.H. (1995). The role of the cholinergic system in the development of the human cerebellum. *Dev. Brain Res.* **90,** 159–167.

Crosby, E.C, and Woodburne, R.T. (1940). The comparative anatomy of the preoptic area and the hypothalamus. *Proc. Assoc. Res. Nervous. Mental Dis.* **20,** 52–169.

Davis, C.A., and Joyner, A.L. (1988). Expression patterns of the homeobox containing genes *En-1* and *En-2* and the proto-oncogene *Int-1* diverge during mouse development. *Genes Dev.* **2,** 1736–1744.

DeAzevedo, L.C., Hedin-Perreira, C., and Lent, R. (1999). callosal neurons in the cingulate cortical plate and subplate of human fetuses. *J. Comp. Neurol.* **386,** 60–70.

DeGraan, P.N.E., Van Hooff, C.O.M. Tilly B.C., Oestreicher A.B., Schotman P., and Gispen W.H. (1985). Phosphoprotein B-50 in nerve growth cones from fetal rat brain. *Neurosci. Lett,* **61,** 235–241.

Dekaban, A. (1954). Human thalamus. Development of the human thalamic nuclei. *J. comp. Neurol.* **100,** 63.

De Lacoste, M-C., Horvath, D.S., and Woodward, D.J. (1991). Possible sex differences in the developing human brain. *J. Clin. Exp. Neuropsychol.* **13,** 831–846.

de Olmos, J.S., and Heimer, L. (1999). The concepts of the ventral striatopallidal system and extended amygdala. *Ann. N. Y. Acad. Sci.* **877,** 1–32.

Delalle, I., Evers, P., Kostovic, I., and Uylings, H.B.M. (1997). Laminar distribution of neuropeptide Y-immunoreactive neurons in human prefrontal cortex during development. *J. Comp. Neurol.* **379,** 515–522.

Del Olmo, E., Diaz, A., Guirao-Pineyro, M., del Arco, C., Pascual, J., and Pazos, A. (1994). Transient localization of 5HT1A receptors in human cerebellum during development. *Neurosci Lett.* **166,** 149–152.

Del Olmo, E., López-Gimenez, J.F., Vilaró, M.T., Mengod, G., Palacios, J.M., and Pazos, A. (1998). Early localization of mRNA for 5HT1A receptors in human brain during development. *Mol. Brain Res.* **60,** 123–126.

Diepen, R. (1962). Der Hypothalamus. *In* "Handbuch der Mikroskopischen Anatomie des Menschen," Vol IV/7, W.v. Möllendorff and W. Bergmann (Eds.), Springer-Verlag, Berlin, pp. 1–525.

Downen, M, Zhao, M.L., Lee, P., Weidenheim, K.M., Dickson, D.W., and Lee, S.C. (1999) Neuronal nitric oxide synthase expression in developing and adult human CNS. *J. Neuropathol. Expl. Neurol.* **58,** 12–21.

Egozi, Y., Sokolovsky, M., Schejter, E., Blatt, I., Zakut, H., Matzkel, A., and Soreq, H. (1986). Divergent regulation of muscarinic binding sites and acteylcholinesterase in discrete regions of the developing human fetal brain. *Cell. Mol. Neurobiol.* **6,** 55–70.

Fellmann, D., Bloch, B., Bugnon, C., and Lenys, D. (1979). Etude immunocytologique de la maturation des axes neuroglandulaires hypothalamo-neurohypophysaires chez le foetus humain. *J. Physiol. (Paris)* **75,** 37–43.

Feremutsch, K. (1955). "Strukturanalyse des menschlichen Hypothalamus." Karger, Basel.

Filiano, J.J., Choi, J.C., and Kinney, H.C. (1990). Candidate cell populations for respiratory chemosensitive fields in the human infant medulla. *J. Comp. Neurol.* **293,** 448–465.

Forutan, F., Mai, J.K., Ashwell, K.W.S., Lensing-Höhn, S., Nohr, D., Voss, T., Bohl, J., and Andressen Ch. (2001). Organisation and maturation of the human thalamus revealed by CD15. *J. Comp. Neurol.* **437,** 476–495.

Fujimoto, E., Miki, A., and Mizoguti, H. (1989). Histochemical study of the differentiation of microglial cells in the developing human cerebral hemispheres. *J. Anat.* **166,** 253–264.

Giguere, M., and Goldman-Rakic, P.S. (1988). Mediodorsal nucleus: areal, laminar and tangential distribution of afferents and efferents in the frontal lobe of rhesus monkeys. *J. Comp. Neurol.* **277,** 195–213.

Gilbert, M. (1935). The early development of the human diencephalon, *J. Comp. Neurol.* **62,** 81–116.

Gilles, F.H. (1976). Myelination in the neonatal brain. *Hum. Pathol.* **7,** 244–248.

Gloor, P. (1997). "The Temporal Lobe and Limbic System." Oxford University Press, New York.

Gluckman, P.D., and Bassett, N.S. (1988). Development of hypothalamic function in the perinatal period. In CRC Handbook of Human Growth and Developmental Biology, Vol. 2, Part A (E. Meisami, and P.S. Timiras, eds.), pp. 3–20. CRC Press, Boca Raton.

Gocht, A., Zeunert, G., Laas, R., and Löhler, J. (1992). The carbohydrate epitope 3-fucosyl-*N*-acetyllactosamine is developmentally regulated in the human cerebellum. *Anat. Embryol.* **186,** 543–556.

Goetz, M., Wizenmann, A., Reinhardt, S., Lumsden, A., and Price, J. (1996). Selective adhesion of cells from different telencephalic regions. *Neuron.* **16,** 551–564.

González-Hernández, T., González-González, B., Mantolán-Sarmiento, B., Méndez-medina, R., Ferres-Torres, R., and Meyer, G. (1994). transient NADPH-diaphorase activity in motor nuclei of the foetal human brain stem. *Neuroreport* **5,** 758–760.

Goodyer, C.G. (1988). Development of the anterior pituitary. *In* "CRC Handbook of Human Growth and Developmental Biology," Vol. 2, Part A (E. Meisami, and P.S. Timiras, eds.), pp. 21–48. CRC Press, Boca Raton.

Gouldsmit, E., Neijmeijer-Leloux A., and Swaab, D.F. (1992). The human hypothalamo-neurohypophyseal system in relation to development, aging and Alzheimer's desease. *In* "Progress in Brain Research," Vol. 93 (D.F. Swaab, M.A. Hofman, M. Mirmiran, R. Ravid, and F.W. van Leeuwen, Eds.), pp. 237–248. Elsevier, Amsterdam.

Gremo, F., Palomba, M., Marchisio, A.M., Marcello, C., Mulas, M.L., and Torelli, S. (1987). Heterogeneity of muscarinic cholinergic receptors in the developing human fetal brain: regional distribution and characterization. *Early Hum. Dev.* **15,** 165–177.

Groenewegen, H.J., Wright, C.I., Beijer, A.V., and Voorn, P. (1999). Convergence and segregation of ventral striatal inputs and outputs. *Ann. N. Y. Acad. Sci.* **877,** 49–63.

Grünthal, E. (1934). Der Zellaufbau im Thalamus der Säuger und des Menschen. *J. Psychol. Neurol.* **46,** 41.

Grünthal, E. (1952). Untersuchungen zur Ontogenese und über den Bauplan des Gehirns. *In* "Beiträge zur Entwicklungsgeschichte und normalen Anatomie des Gehirns." (K. Feremutch and E. Grünthal, eds), pp. 5–35. Bibl. Psychiatr. Neurol., Basel.

Gudovic, R., Marinkovic, R., and Aleksiv, S. (1987). The development of the dentate nucleus in man, *Anat. Anz.* **163,** 233–238.

Gudovic, R., and Milutinovic, B. (1996). Regression changes in inferior olivary nucleus compared to changes of Purkinje cells during development in humans. *J. Brain Res.* **37,** 67–72.

Gudovic, R., Milutinovic, B., and Ristanovic, D. (1998). Dynamics of granule cells migration into the internal granular layer in developing human cerebellum. *J. Brain Res.* **39,** 223–229.

Gurevich, E.V., Kordower, J., and Joyce, J.N. (1997). Dopamine D2 receptor mRNA is expressed in maturing neurons of human hippocampal and subicular fields. *Neuroreport* **8,** 3605–3610.

Halliday, A.L. and Cepko, C.L. (1992). Generation and migration of cells in the developing striatum.

Hamasaki, T., Goto, S., Nishikawa, S., and Ushio, Y. (2003). Neuronal cell migration for the developmental formation of the mammalian striatum. *Brain Res. Rev.* **41,** 1–12.

Hansen, P.E., Ballesteros, M.C., Soila, K., Garcia, L., and Howard, J.M. (1983). MR Imaging of the developing human brain. *Radiographics* **13,** 21–36.

Hartz-Schütt, Ch., and Mai J.K. (1992). Atlas der Cholinesterase-Aktivität im menschlichen Striatum unter besonderer Berücksichtigung der Insulae terminales. *J. Hirnforsch.* **32,** 317–342.

Hatten, M.E. Central nervous system neuronal migration. *Annu. Rev. Neurosci.* **22,** 511–539.

Haun, F., Eckenrode, T.C., and Murray, M. (1992). Habenula and thalamus cell transplants restore normal sleep behaviours disrupted by denervation of the interpeduncular nucleus. *J. Neurosci.* **12,** 3282–3290.

Hayaran, A., and Bijlani, V. (1992). Polyacrylamide as an infiltrating and embedding medium for vibratome sectioning of human fetal cerebellum containing DiI-filled axons. *J. Neurosci. Meth.* **42,** 65–68.

Heffer-lauc, M., Cacic, M., Judas, M., and Müthing, J. (1996). Anti-G_{M3} (II^3Neu5Ac-lactosylceramide) ganglioside antibody labels human fetal Purkinje neurons during the critical stage of cerebellar development. *Neurosci. Lett.* **213,** 91–94.

Henery, C.C., and Mayhew, T.M. (1989). The cerebrum and cerebellum of the fixed human brain: efficient and unbiased estimates of volumes and cortical surface areas. *J. Anat.* **167,** 167–180.

Hevner, R.F., and Kinney, H.C. (1996). Reciprocal entorhinal-hippocampal connections established by human fetal midgestation. *J. Comp. Neurol.* **372,** 384–394.

Hines, M. (1922). Studies on the growth and differentiation of the telencephalon in man. The fissura hippocampi. *J. Comp. Neurol.* **34,** 73–171.

Hochstetter, F. (1919). "Beiträge zur Entwicklungsgeschichte des menschlichen Gehirns I." Deuticke, Wien.

Igarashi, Y., and Ishii, T. (1980). Embryonic development of the human organ of Corti: electron microscopic study. *Int. J. Paediatr. Otorhinolaryngol* **2,** 51–62.

Itoh, M., Watanabe, Y., Watanabe, M., Tanaka, K., Wada, K., and Takashima, S. (1997). Expression of a glutamate transporter subtype, EAAT4, in the developing human cerebellum. *Brain Res.* **767,** 265–271.

Jacobs, M.J. (1970). The development of the human motor trigeminal complex and accessory facial nucleus and their topographic relations with the facial and abducens nuclei. *J. Comp. Neurol.* **138,** 161–194.

Jacobsen, M., and Møllgard, K. (1983). Intracellular localization of some plasma proteins in human embryonic and fetal brain with special reference to the developing cerebellum. *Ann. NY Acad. Sci.* **417,** 330–343.

Jacobson, R.D., Virag, I., and Skene, J.H.P. (1986). A protein associated with axon growth, GAP-43, is widely distributed and developmentally regulated in rat CNS. *J. Neurosci.* **6,** 1843–1855.

Judas, M., Sestan, N., and Kostovic, I. (1999). Nitrinergic neurons in the developing and adult human telencephalon: transient and permanent patterns of expression in comparison to other mammals. *Microsc. Res. Tech.* **45,** 401–419.

Kahle, W. (1951). Studien über die Matrixphasen und die örtlichen Reifungsunterschiede im embryonalen menschlichen Gehirn. *Deutsche. Z. Nervenheilkunde* **166,** 273.

Kahle, W. (1956). Zur Entwicklung des menschlichen Zwischenhirnes. Studien über die Matrixphasen und die örtlichen. Reifungsunterschiede im embryonalen menschlichen Gehirn. II. Mitteilung. *Dtsch Z Nervenheilk.* **175,** 259–318.

Kanazir, S., Ruzdijic, S., Vukosavic, S., Ivkovic, S., Milosevic, A., Zecevic, N., and Rakic, L. (1996). GAP-43 mRNA expression in early development of human nervous system. *Mol. Brain Res.* **38,** 145–155.

Karns, L.R., S.-C. Ng, J.A. Freeman, and M.C. Fishman (1987). Cloning of complementary DNA for GAP-43, a neuronal growth related protein. *Science* **236,** 597–600.

Kato, M., and Takashima, S. (1994). Immunohistochemical and morphometrical development of the dorsal root ganglion as a neural crest derivative: comparison with the fetal CNS. *Early Human Dev.* **38,** 81–90.

Katsetos, C.D., Frankfurter, A., Christakos, S., Mancall, E.L., Vlachos, I.N., and Urich, H. (1993). Differential localization of class III β-tubulin isotype and calbindin-D28k defines distinct neuronal types in the developing human cerebellar cortex. *J. Neuropathol. Expl. Neurol.* **52,** 655–666.

Kendler, A., and Golden, J.A. (1996). Progenitor cell proliferation outside the ventricular and subventricular zones during human brain development. *J. Neuropathol. Expl. Neurol.* **55,** 1253–1258.

Keyser, A. (1972). The development of the diencephalon of the Chinese hamster. An investigation of the validity of the criteria of subdivision of the brain. *Acta Anat. Suppl. (Basel).* **59,** 1–178.

Kinney, H.C., O'Donnell, T.J., Kriger, P., and White, W.F. (1993). Early developmental changes in [^{3}H] nicotine binding in the human brainstem. **55,** 1127–1138.

Kinney, H.C., Ottoson, C.K., and White, W.F. (1990). Three-dimensional distribution of 3H-naloxone binding to opiate receptors in the human fetal and infant brainstem. *J. Comp. Neurol.* **291,** 55–78.

Kinney, H.C., Rava, L.A., and Benowitz, L.I. (1993). Anatomic distribution of the growth-associated protein GAP-43 in the developing human brainstem. *J. Neuropathol. Expl. Neurol.* **52,** 39–54.

Koop, M., Rilling, G., Herrmann, A., and Kretschmann, H.-J. (1986). Volumetric development of the fetal telencephalon, cerebral cortex, diencephalon, and rhombencephalon including the cerebellum in man. *Bibliotheca anat. 28,* 53–78.

Kostovic, I. (1986). Prenatal development of nucleus basalis complex and related fiber systems in man: a histochemical study. *Neuroscience* **17,** 1047–1077.

Kostovic, I. (1990a). Structural and histochemical reorganization of the human prefrontal cortex during perinatal and postnatal life. *In* "Progress in Brain Research," Vol. 85 (H.B.M. Uylings, C.G. Van Eden, M.A. De Bruin, M.A. Corner, M.G.P. Feenstra, eds.) pp. 223–240. Elsevier, Amsterdam.

Kostovic, I. (1990b). Zentralnervensystem. *In* "Humanembryologie" (K.V. Hinrichsen, ed.). Springer-Verlag, Berlin.

Kostovic, I., and Goldman-Rakic, P.S. (1983). Transient cholinesterase staining in the mediodorsal nucleus of the thalamus and its connections in the developing human and monkey brain. *J. Comp. Neurol.* **219,** 431–447.

Kostovic, I., and Rakic, P. (1984). Development of prestriate visual projections in the monkey and human fetal cerebrum revealed by transient cholinesterase staining. *J. Neurosci.* **4,** 25–42.

Kostovic, I., and Rakic, P. (1990). Developmental history of the transient subplate zone in the visual and somatosensory cortex of the macaque monkey and human brain. *J. Comp. Neurol.* **297,** 441–470.

Kostovic, I., Lukinovic, N., Judas, M., Bogdanovic, N., Mrzljak, L., Zecevic, N., and Kubat, M. (1989). Structural basis of the developmental plasticity in the human cerebral cortex: the role of the transient subplate zone. *Metab. Brain Dis.* **4,** 17–23.

Kostovic, I., Seress, L., Mrzljak, and Judas, M. (1989). Early onset of synapse formation in the human hippocampus: a correlation of Nissl–Golgi architectonics in 15- and 16.5 week fetuses. *Neuroscience* **30,** 105–116.

Kostovic, I., Stefulj-Fucic, A., Mrzljak, L., Jukic, S., and Delalle, I. (1991). Prenatal and perinatal development of the somatostatin-immunoreactive neurons in the human prefrontal cortex. *Neurosci. Lett.* **124,** 153–156.

Kostovic, I., Petanjek, Z., and Judas, M. (1993). Early areal differentiation of the human cerebral cortex: entorhinal area. *Hippocampus* **3,** 447–458.

Koutcherov, Y., Ashwell, K.W.A., Mai, J.K., and Paxinos G. (2000a). Organisation of the human paraventricular hypothalamic nucleus. *J. Comp. Neurol.* **423,** 299–318.

Koutcherov, Y., Ashwell, K.W.S., and Paxinos, G. (2000b). The distribution of the neurokinin B receptor in the human and rat hypothalamus. *Neuroreport* **11,** 3127–31.

Koutcherov, Y., Mai, J.K., Ashwell, K.W.S., and Paxinos, G. (2002). Organization of human hypothalamus in fetal development. *J. Comp. Neurol.* **446,** 301–324.

Krettek, J.E., and Price, J.L. (1978). Amygdaloid projections to subcortical structures within the basal forebrain and brainstem in the rat and cat. *J. Comp. Neurol.* **178,** 225–254.

Krieg, W.E. (1960). "Atlas of Sections of the Infant Brain illustrating Krieg's Architectonics of Human Cerebral Fiber Systems." Brain Books, Box Nine, Evanston, IL.

Krmpotic-Nemanic, J., Kostovic, I., Nemanic, D., and Kelovic, Z. (1979). The laminar organization of the prospective auditory cortex in the human fetus (11–13.5 weeks of gestation). *Acta Otolaryngol.* **87,** 241–246.

Krmpotic-Nemanic, J., Kostovic, I., Kelovic, Z., and Nemanic, D. (1980). Development of actelycholinesterase (AChE) staining in human fetal auditory cortex. *Acta Otolaryngol.* **89,** 388–392.

Krmpotic-Nemanic, J., Kostovic, I., Kelovic, Z., Nemanic, D., and Mrzljak, L. (1983). Development of the human fetal auditory cortex: growth of afferent fibers. *Acta Anat.* **116,** 69–73.

Krmpotic-Nemanic, J., Kostovic, I., Vidic, Z., Nemanic, D., and Kostovic-Knezevic, L. (1987). Development of Cajal–Retzius cells in the human auditory cortex. *Acta Otolaryngol.* **103,** 477–480.

Kuhlman, K.A., Burns, K.A., Depp, R., and Sabbagha, R.E. (1988). Ultrasonic imaging of normal fetal response to external vibratory acoustic stimulation. *Am. J. Obstet. Gynecol.* **158,** 47–51.

Lecaneut, J-P., and Schaal, B. (1996). Fetal sensory competencies. *Eur. J. Obst. Gynecol.* **68,** 1–23.

LeGros Clark, W.E. (1936). The topography and homologies of the hypothalamic nuclei in man. *J. Anat.,* **70,** 203–214.

Lemire, R.L., Loeser, J.D., Leech, R.W., and Alvord E.C. (1975). "Normal and Abnormal Development of the Human Nervous System." Harper and Row, Hagerstown, PA.

Lu J, Greco, M.A., Shiromani, P., and Saper, C.B. (2000). Effect of lesions of the ventrolateral preoptic nucleus on NREM and REM sleep. *J. Neurosci.* **20,** 3830–3842.

Lukas, Z., Draber, P., Bucek, J., Dráberová, E., Viklicky, V., and Dolezel, S. (1993). Expression of phosphorylated high molecular weight neurofilament protein (NF-1) and vimentin in human developing dorsal root ganglia and spinal cord. *Histochemistry* **100,** 495–502.

Macchi, G. (1951). The ontogenetic debelopment of the olfactory telencephalon in man. *J. Comp. Neurol.* **95,** 245–305.

Mai, J.K. (2002) CD15. *In* "Encyclopedia of Molecular Medicine" (T.E. Creighton, ed.), pp. 555–558. John Wiley and Sons, New York.

Mai, J.K., and Schönlau, Ch. (1992). Age-related Expression Patterns of the CD15 Epitope in the human lateral geniculate nucleus (LGN) *Histochem. J.* **24,** 878–889.

Mai, J.K., Kedziora, O., Teckhaus, L., and Sofroniew M.V. (1991). Evidence for subdivisions in the human suprachiasmatic nucleus. *J. Comp. Neurol.* **305,** 508–525.

Mai, J.K., Berger, K., and Sofroniew, M. V. (1993). Morphometric evaluation of neurophysin-immunoreactivity in the human brain: pronounced inter-individual variability and evidence for altered staining patterns in schizophrenia. *J. Hirnforsch.* **34,** 133–154.

Mai, J.K., Lensing-Höhn, S., and Düllberg, S. (1994). Colocalization of the CD15 epitope with neurophysin positive neurons. 17th Annual Meeting ENA, Wien.

Mai, J.K., Lensing-Höhn, S., Ende, A.A., and Sofroniew, M.V. (1997). Developmental organisation of neurophysin neurons in the human brain. *J. Comp. Neurol.* **385,** 477–489.

Mai, J.K., Assheuer, J., and Paxinos, G. (1997). "Atlas of the Human Brain." Academic Press, San Diego.

Mai, J.K., Andressen C, and Ashwell KWS. (1998). Demarcation of prosencephalic regions by CD15-positive radial glia. *Eur. J. Neurosci.* **10,** 746–751.

Mai, J.K., Krajewski S, Reifenberger, G, Genderski, B., Lensing-Höhn, S., and Ashwell, K.W.S. (1999a). Spatiotemporal expression gradients of an adhesion molecule epitope (CD15) during development of the human basal ganglia. *Neuroscience* **88,** 847–858.

Mai, J.K., Winking, R. and Ashwell, K.W.S. (1999b). Transient CD15 expression reflects stages of differentiation and maturation in the human subcortical central auditory pathway. *J. Comp. Neurol.* **404,** 197–211.

Mai, J.K., Krajewski, S., Ashwell, K.W.S., and Andressen C. (in press). CD15 immunoreactive subpopulation of radial glial cells in the developing human lateral ganglionic eminence.

Marcus, R.C., Shimamura, K., Sretavan, D., Lai, E., Rubenstein, J.L., and Mason, C.A. (1999). Domains of regulatory gene expression and the developing optic chiasm: correspondence with retinal axon paths and candidate signaling cells. *J. Comp. Neurol.* **403,** 346–358.

Marin-Padilla, M. (1985). Neurogenesis of the climbing fibers in the human cerebellum: a Golgi study. *J. Comp. Neurol.* **235,** 82–96.

Marin-Padilla, M. (1995). Prenatal development of fibrous (white matter), protoplasmic (grey matter), and layer I astrocytes in the human cerebral cortex: a Golgi study. *J. Comp. Neurol.* **357,** 554–572.

Marti, E., Gibson, S.J., Polak, J.M., Facer, P., Springall, D.R., van Aswegen, G., Aitchison, M., and Koltzenburg, M. (1987). Ontogeny of peptide- and amine-containing neurones in motor, sensory, and autonomic regions of rat and human spinal cord, dorsal root ganglia, and rat skin. *J. Comp. Neurol.* **266,** 332–359.

Martinez, S., and Puelles, L. (2000). Neurogenetic compartment of the mouse diencephalon and some characteristic gene expression patterns. *In* "Mouse Brain Development" (AM Goffinet and P. Rakic, eds.), pp. 91–106. Springer-Verlag, Berlin.

Matsunami, H., and Takeichi, M. (1995). Fetal brain subdivisions defined by R- and E-cadherin expressions: evidence for the role of cadherin activity in region-specific, cell-cell adhesion. *Dev. Biol.* **172,** 466–478.

Mayhew, T.M., Mwamengele, G.L.M., Dantzer, V., and Williams, S. (1996). The gyrification of mammalian cerebral cortex: quantitative evidence of anisomorphic surface expansion during phylogenetic and ontogenetic development. *J. Anat.* **188,** 53–58.

Meiri, K.F., Pfenninger, K.H., and Willard, M.B. (1986). Growth associated protein, GAP-43, a polypeptide that is induced when neurons extend axons, is a component of growth cones and corresponds to pp46, a major polypeptide of a subcellular fraction enriched in growth cones. *Proc. Natl. Acad. Sci. U.S.A.* **83,** 3537–3541.

Meszaros, I., Gajewska, S., and Tarchalska-Krynska-Krynska (1985). Habenulo-interpeduncular lesions: The effects on pain sensitivity, morphine analgesia and open-field behaviour in rats. *J. Pharmacol. Pharm.* **37,** 469–477.

Metin, C., and Godement, P. (1996). The ganglionic eminence may be an intermediate target for corticofugal and thalamocortical axons. *J. Neurosci.* **16,** 3219–3235.

Meyer, G., and Goffinet, A,M, (1998). Prenatal development of reelin-immunoreactive neurons in the human neocortex. *J. Comp. Neurol.* **397,** 29–40.

Meyer, G., and González-Hernández, T. (1993). Developmental changes in layer I of the human neocortex during prenatal life: A DiI-tracing and AChE and NADPH-d histochemistry study. *J. Comp. Neurol.* **338,** 317–336.

Mihajlovic, P., and Zecevic, N. (1986). Development of the human dentate nucleus. *Hum. Neurobiol.* **5,** 189–197.

Millen, K.J., Wurst, W., Herrup, K., and Joyner, A.L. (1994). Abnormal embryonic development and patterning of postnatal foliation in two mouse Engrailed-2 mutants. *Development* **120,** 695–706.

Milosevic, A., and Zecevic, N. (1998). Developmental changes in human cerebellum: expression of intracellular calcium receptors, calcium binding proteins and phosphorylated and non-phosphorylated neurofilament protein. *J. Comp. Neurol.* **396,** 442–460.

Milutinovic, B., Gudovic, R., and Malesevic, J. (1992). Regressional changes of human cerebellar cortex and hypoglossal nucleus during development. *J. Hirnforsch.* **33,** 357–360.

Mirmiran, M., Kok, J.H., Boer, K., and Wolf, H. (1992). Perinatal development of human circadian rhythms: role of the foetal biological clock. *Neurosci. Biobehav. Rev.* **16,** 371–378.

Mito, T., Konomi, H., Houdou, S., and Takashima, S. (1991). Immunohistochemical study of the vasculature in the developing brain. *Ped. Neurol.* **7,** 18–22.

Miura, R. (1933). Über die Differenzierung der Grundbestandteile im Zwischenhirn des Kaninchens. *Anat. Anz.* **77,** 1.

Miyata, M., Miyata, H., Mikoshiba, K., and Ohama, E. (1999). Development of Purkinje cells in humans: an immunohistochemical study using a monoclonal antibody against the inositol 1,4,5-triphosphate type 1 receptor (IP3R1). *Acta Neuropathol.* **98,** 226–232.

Miyawaki, T., Matsui, K., and Takashima, S. (1998). Developmental characteristics of vessel density in human fetal and infant brains. *Early Hum. Dev.* **53,** 65–72.

Mojsilovic, J., and Zecevic, N. (1991). Early development of the human thalamus: Golgi and Nissl study. *Early Hum. Dev.* **27,** 44–119.

Molliver, M.E., Kostovic, I., and Van der Loos, H. (1973). The development of synapses in the human fetus. *Brain Res.* **50,** 403–407.

Molnar Z., Adams R., and Blakemore C. (1998). Mechanisms underlying the early establishment of thalamocortical connections in the rat. *J. Neurosci.* **18,** 5723–5745.

Moore, J.K., Perazzo, L.M., and Braun, A. (1995). Time course of axonal myelination in the human brainstem auditory pathway. *Hearing Res.* **87,** 21–31.

Moore, J.K., Guan, Y.-L., and Shi, S.-R. (1997). Axogenesis in the human fetal auditory system, demonstrated by neurofilament immunohistochemistry. *Anat. Embryol.* **195,** 15–30.

Moore, J.K., Simmons, D.D., and Guan, Y-L. (1999). The human olivocochlear system: organization and development. *Audiol. Neurootol.* **4,** 311–325.

Morres, S. A., Mai, J. K., and Teckhaus, L. (1992). Expression of the CD15 epitope in the human magnocellular basal forebrain system. *Histochem. J.* **24,** 902–910.

Moss, T.J., Rosenblatt, H.M., and Seeger, R.C. (1988). Expression of a developmental stage-specific antigen by neuronal precursor cells of human fetal cerebellum. *J. Neuroimmunol.* **20,** 3–14.

Mrzljak, L., Uylings, H.B.M., Kostovic, I., and van Eden, C.G. (1988). Prenatal development of neurons in the human prefrontal cortex: I. A qualitative Golgi study. *J. Comp. Neurol.* **271,** 355–386.

Mrzljak, L., Uylings, H.B.M., Van Eden, C.G., and Judas, M. (1990). Neuronal development in human prefrontal cortex in prenatal and postnatal stages. In "Progress in Brain Research," Vol. 85 (H.B.M. Uylings, C.G. Van Eden, J.P.C. De Bruin, M.A. Corner, and M.G.P. Feenstra, eds.), pp. 185–222. Elsevier, Amsterdam.

Mufson, E.J., Ginsberg, S.D., Ikonomovic, M.D., and DeKosky, S.T. (2003). Human cholinergic basal forebrain: chemoanatomy and neurologic dysfunction. *J. Chem. Neuroanat.* (in press).

Mueller, F., and O'Rahilly, R. (1990). The human brain at stages 21–23, with particular reference to the cerebral cortical plate and to the development of the cerebellum. *Anat. Embryol.* **182,** 375–400.

Muragaki, Y., Timothy, N., Leight, S., Hempstead, B.L., Chao, M.V., Trojanowski, J.Q., and Lee, V.M-Y. (1995). Expression of trk receptors in the developing and adult human central and peripheral nervous system. *J. Comp. Neurol.* **356,** 387–397.

Murayama, K., Meeker, R.B., Murayama, S., and Greenwood, R.S. (1993). Developmental expression of vasopressin in the human hypothalamus: double-labeling with in situ hybridisation and immunocytochemistry. *Pediat Res.* **33,** 152–158.

Namba, M. (1957). Cytoarchitektonische Untersuchung am Striatum. *J. Hirnforsch.* **3,** 24–48.

Nara, T., Goto, N., and Yamaguchi, K. (1989). Development of the human hypoglossal nucleus: a morphometric study. *Dev. Neurosci.* **11,** 212–220.

Nara, T., Goto, N., and Hamano, S-I. (1991). Development of the human dorsal nucleus of vagus nerve: A morphometric study. *J. Auton. Nerv. System* **33,** 267–276.

Nara, T., Goto, N., Hamano, S-I., and Okada, A. (1996). Morphometric development of the human fetal auditory system: inferior collicular nucleus. *Brain Dev.* **18,** 35–39.

Nara, T., Goto, N., Nakae, Y., and Okada, A. (1993). Morphometric development of the human auditory system: ventral cochlear nucleus. *Early Hum. Dev.* **32,** 93–102.

Nobin, A., and Björklund, A. (1973). Topography of the monoamine neuron systems in the human brain as revealed in fetuses. *Acta Physiol. Scand. Suppl.* **388,** 1–40.

Norman, M.G., and O'Kusky, J.R. (1986). The growth and development of microvasculature in human cerebral cortex. *J. Neuropathol. Expl. Neurol.* 45, 222–232.

Obonai, T., Mizuguchi, M., and Takashima, S. (1998). Developmental and aging changes of Bak expression in the human brain. *Brain Res.* **783,** 167–170.

Oeder, J. (1998). CD15 Immunreaktivität in der Substantia nigra unter Berücksichtigung der Zyto-, Myelo-, und Chemoarchitektur. Thesis. Medical Faculty, University of Duesseldorf.

Ohyu, J., andTakashima, S. (1998). Developmental characteristics of neuronal nitric oxide synthase (nNOS) immunoreactive neurons in fetal to adolescent human brains. *Dev. Brain Res.* **110,** 193–202.

Ohyu, J., Yamanouchi, H., and Takashima, S. (1997). Immunohistochemical study of microtubule-associated protein 5 (MAP5) expression in the developing human brain. *Brain & Dev.* **19,** 541–546.

Olson, L., Boréus, L.O., and Seiger, A. (1973). Histochemical demonstration and mapping of 5-hydroxytryptamine- and catecholamine- containing neuron systems in the human fetal brain. *Z. Anat. Entwickl. Gesch.* **139,** 259–282.

Olsson, M (1997). Phenotypic specification of striatal progenitors. Thesis, Dept. Physiol. and Neurosci, University of Lund, Sweden.

Olsson, M., Björklund A., and Campbell, K. (1995). Projection neurons in fetal striatal transplants are predominantly derived from the lateral ganglonic eminence. *Neuroscience* **69,** 1169–1182.

O'Rahilly, R., and Müller, F. (1994). The embryonic human brain: an atlas of developmental stages. Willey-Liss, New York.

O'Rahilly, R., Mueller, F. (2000) Prenatal ages and stages: measures and errors. *Teratology* **61,** 382—384.

Pal, U., Chaudhury, S., and Sarkar, P.K. (1999). Tubulin and glial fibrillary acidic protein gene expression in developing fetal human brain at midgestation. *Neurochemical Res.* **24,** 637–641.

Panigrahy, A., Sleeper, L.A., Assmann, S., Rava, L.A., White, W.F., and Kinney, H.C. (1998). Developmental changes in heterogeneous patterns of neurotransmitter receptor binding in the human interpeduncular nucleus. *J. Comp. Neurol.* **390,** 322–332.

Pearson, J., Brandeis, L., and Goldstein, M. (1980). Appearance of tyrosine hydroxylase immunoreactivity in the human embryo. *Dev. Neurosci.* **3,** 140–150.

Plank, J., Mai, J.K. (1992). Developmental expression of the 3-fucosyl-N-acetyl-lactosamine (FAL) epitope by an olfactory receptor cell subpopulation in the olfactory bulb of the rat. *Dev. Brain Res.* **66,** 257–261.

Post, S., and Mai, J.K. (1980). Contribution to the amygdaloid projection field in the rat. A quantitative autoradiographic study. *J. Hirnforsch.* **21,** 199–225.

Press, G.A., Murakami, J., Courchesne, E., et al. (1989). The cerebellum in sagittal plane: anatomic-MR correlation. II. The cerebellar hemispheres. *Am. J. Neurosci. Res.* **10,** 667–676.

Pribyl, T.M., Campagnoni, C.W., Kampf, K., Ellison, J.A., Landry, C.F., Kashima, T., McMahon, J., and Campagnoni, A.T. (1996). Expression of the myelin basic protein gene locus in neurons and oligodendrocytes in the human fetal central nervous system. *J. Comp. Neurol.* **374,** 342–353.

Puelles, L., and Rubenstein, J.L. (1993). Expression patterns of homeobox and other putative regulatory genes in the embryonic mouse forebrain suggest a neuromeric organization. *TINS* **16,** 472–479.

Purpura, D. P. (1982). Normal and aberrant neuronal development in the cerebral cortex of human fetus and young infant, p 141–169.

Rabinowicz, T., De Courten-Myers, G.M., McDonald-Comber Petetot, J., Xi, G-H., and De Los Reyes, E. (1996). Human cortex development: Estimates of neuronal numbers indicate major loss late during gestation. *J. Neuropathol. Expl. Neurol.* **55,** 320–328.

Rakic, P. (1972). Mode of cell migration to the superficial layers of fetal monkey neocortex. *J. Comp. Neurol.* **145,** 61–84.

Rakic, P. (1974). Embryonic development of the pulvinar-LP complex in man. *In* "The Pulvinar–LP Complex" (I.S. Cooper, P. Rakic, and M. Riklan, eds.), pp. 3–35. Charles C Thomas, Springfield, IL.

Rakic, P., and Sidman RL. (1969). Telencephalic origin of pulvinar neurons in the fetal human brain. *Z. Anat. Entwicklungsgesch.* **129,** 53–82.

Rakic, P., and Sidman, R.L. (1970). Histogenesis of cortical layers in human cerebellum, particularly the lamina dissecans. *J. Comp. Neurol.* **139,** 437–500.

Reddy, S.C., Panigrahy, A., White, W.F., and Kinney, H.C. (1996). Developmental changes in neurotransmitter receptor binding in the human periaqueductal gray. *J. Neurpathol. Expl. Neurol.* **55,** 409–418.

Reppert, S.M. (1992). Pre-natal development of a hypothalamic biological clock. *Prog. Brain Res.* **93,** 119–31.

Rezaie, P., Cairns, N.J., and Male, D.K. (1997). Expression of adhesion molecules on human fetal cerebral vessels: Relationship to microglial colonisation during development. *Dev. Brain Res.* **104,** 175–189.

Richter, E. (1965). Die Entwicklung des Globus pallidus und des Corpus subthalamicum. *Monograph. Gesamtgeb. Neurol. Psychat.* **108,** 1–131.

Royds, J.A., Ironside, J.W., Warnaar, S.O., Taylor, C.B., and Timperley, W.R. (1987). Monoclonal antibody to aldolase C: A selective marker for Purkinje cells in the human cerebellum. *Neuropathol. Appl. Neurobiol.* **13,** 11–21.

Rubenstein, J.L., Martinez S., Shimamura K., and Puelles, L. (1994). The embryonic vertebrate forebrain: the prosomeric model. *Science* **266,** 578–580.

Sailaja, K., and Gopinath, G. (1994). Developing substantia nigra in human: a qualitative study. *Dev. Neurosci.* **16,** 44–52.

Sanides, F. (1957). Die Insulae terminales des Erwachsenengehirns des Menschen. *J. Hirnforsch.* **3,** 243

Sarnat, H.B., and Born, D.E. (1999). Synaptophysin immunocytochemistry with thermal intensification: A marker of terminal axonal maturation in the human fetal nervous system. *Brain Dev.* **21,** 41–50.

Sarnat, H.B., Nochlin, D., and Born, D.E. (1998). Neuronal nuclear antigen (NeuN): a marker of neuronal maturation in the early human fetal nervous system. *Brain Dev.* **20,** 88–94.

Schubert, F., George, J.M., and Rao, B. M. (1981). Vasopressin and oxytocin content of human fetal brain at different stages of gestation. *Brain Res.* **213,** 111–117.

Schwanzel-Fukuda, M., Bick, D., and Pfaff, D. (1989). Luiteinizing hormone-releasing hormone (LHRH)–expressing cells do not migrate normally in an inherited hypogonadal (Kallmann) syndrome. *Mol. Brain Res.* **6,** 311–326.

Setzer, M., and Ulfig, N. (1999). Differential expression of calbindin and calretinin in the human fetal amygdala. *Microsc. Res. Tech.* **46,** 1–17.

Shen, W.Z., Luo, C.B., Dong, L., Chan, W.Y., and Yew, D.T. (1994). Distribution of neuropeptide Y in the developing human spinal cord. *Neuroscience* **62,** 251–256.

Sidman, R.L., and P. Rakic (1982). Development of the human central nervous system. *In* "Histology and Histopathology of the Nervous System" (W. Haymaker and S. Adams, eds.), pp. 3–110. Charles C Thomas, Springfield, IL.

Silani, V., Mariani, D., Donato, F.M., Ghezzi, C., Mazzucchelli, F., Buscaglia, M., Pardi, G., and Scarlato, G. (1994). Development of dopaminergic neurons in the human mesencephalon and *in vitro* effects of basic fibroblast growth factor treatment. *Expl. Neurol.* **128,** 59–76.

Simonati, A., Tosati, C., Rosso, T., Piazzola, E., and Rizzuto, N. (1999). Cell proliferation and death: morphological evidence during corticogenesis in the developing human brain. *Microsc. Res. Tech.* **45,** 341–352.

Skene, J.H.P., Jacobson, R.D., Snipes, G. J., McGuitre, C.B., Norden, J.J., and Freeman, J.A. (1986). A protein induced during nerve growth (GAP-43) is a major component of growth cone membranes. *Science* **233,** 783–786.

Sohma, O., Mizuguchi, M., Takashima, S., Yamada, M., Ikeda, K., and Ohta, S. (1996). High expression of Bcl-x protein in the developing human cerebellar cortex. *J. Neurosci Res.* **43,** 175–182.

Solcher, H. (1968). Zur Neuroanatomie und Neuropathologie der Frühfetalzeit. Springer-Verlag, Berlin.

Spatz, H. (1921). Zur Anatomie der Zentren des Streifenhügels. *Münch. Med. Wschr.* 45, 1441.

Spencer, S., Saper, C.B., Joh, T., Reis, D.J., Goldstein, M., and Raese, J.D. (1985). Distribution of catecholamine-containing neurons in the normal human hypothalamus. *Brain Res.* **328,** 73–80.

Spreafico, R., Arcell, P., Frassoni, C., Canetti, P., Giaccone, G., Rizzutti, T., Mastrangelo, M., and Bentivoglio, M. (1999). Development of layer I of the human cerebral cortex after midgestation: architectonic findings, immunocytochemical identification of neurons and glia, and *in situ* labeling of apoptotic cells. *J. Comp. Neurol.* **410,** 126–142.

Stagaard, M., and Møllgard, K. (1989). The developing neuro-epithelium in human embryonic and fetal brain studied with vimentin-immunocytochemistry. *Anat. Embryol.* **180,** 17–28.

Stoykova, A., Fritsch, R., Walther, C., and Gruss, P. (1996). Forebrain patterning defects in small eye mutant mice. *Development* **122,** 3453–3465.

Stoykova, A., Goetz, M., Gruss, P., and Price, J. (1997). Pax6-dependent regulation of adhesive patterning, R-cadherin expression and boundary formation in developing forebrain. *Development* **124,** 3765–3777.

Suburo, A.M., Gu, X.-H., Moscoso, G., Ross, A., Terenghi, G., and Polak, J.M. (1992). Developmental pattern and distribution of nerve growth factor low-affinity receptor immunoreactivity in human spinal cord and dorsal root ganglia: comparison with synaptophysin, neurofilament and neuropeptide immunoreactivities. *Neuroscience* **50,** 467–482.

Sundström, E., Kölare, S., Souverbie, F., Samuelsson, E.-B., Pschera, H., Lunell, N.-O., and Seiger, A. (1993). Neurochemical differentiation of human bulbospinal monoaminergic neurons during the first trimester. *Dev. Brain Res.* **75,** 1–12.

Swaab, D.F. (1993). Neurohypophysial peptides in the human hypothalamus in relation to development, sexual differentiation, aging and disease. *Regul. Pept.* **45,** 143–147.

Swaab, D.F. (1997). Neurobiology and neuropathology of the human hypothalamus. *In* "Handbook of Chemical Neuroanatomy," Vol. 13: The Primate Nervous System, Part I. (F.E. Bloom, A. Björklund, and T. Hökfelt, eds.), Elsevier Science B.V., Amsterdam.

Swaab, D.F. and Hofman, M.A. (1988). Sexual differentiation of the human hypothalamus: ontogeny of the sexually dimorphic nucleus of the preoptic area. *Dev. Brain Res.* **44,** 314–318.

Swaab, D.F., Hofman, M.A. and Honnebier, M.B.O.M. (1990). Development of the vasopressin neurons in the human suprachiasmatic nucleus in relation to birth. *Dev. Brain Res.* **52,** 289–293.

Swanson, L.W. (1991). Biochemical switching in hypothalamic circuits mediating responses to stress. *Prog. Brain Res.* **87,** 181–200.

Swanson, L.W. (2003). The amygdala and its place in the cerebral hemisphere. *Ann. N. Y. Acad. Sci.* **985,** 174–184.

Swanson, L.W., and Petrovich G.D. (1998). What is the amygdala? *Trends Neurosci.* **21,** 323–331.

Tanaka, S., Mito, T., and Takashima, S. (1995). Progress of myelination in the human fetal spinal nerve roots, spinal cord and brainstem with myelin basic protein immunohistochemistry. *Early Hum. Dev.* **41,** 49–59.

Tuttle, R., Nakagawa, Y., Johnson, J.E., and O'Leary, D.D. (1999). Defects in thalamocortical axon pathfinding correlate with altered cell domains in Mash-1- deficient mice. *Development* **126,** 1903–1916.

Ulfig, N. (2002). Ganglionic eminence of the human fetal brain—new vistas. *Anat. Rec.* **267,** 191–195.

Ulfig, N., Setzer M., and Bohl J. (1999). Distribution of GAP-43 immunoreactive structures in the human fetal amygdala. *Eur. J. Histochem,* **43,** 19–27.

Ulfig, N., Setzer, M., Neudorfer, F., and Saretzki, U. (2000). Changing distribution patterns of synaptophysin-immunoreactive structures in the human dorsal striatum of the fetal brain. *Anat. Rec.* **258,** 198–209.

Ulfig, N., Setzer M., and Bohl J. (2003). Ontogeny of the human amygdala. *Ann. N. Y. Acad. Sci.* **985,** 22–33.

Uylings, H.B.M., and Delalle, I. (1997). Morphology of neuropeptide Y-immunoreactive neurons and fibers in human prefrontal cortex during prenatal and postnatal development. *J. Comp. Neurol.* **379,** 523–540.

Van Eerdenburg, F.J.C.M., and Rakic, P. (1993). Early neurogenesis in the anterior hypothalamus of the rhesus monkey. *Dev. Brain Res.* **79,** 290–296.

Vaughan, H.G. (1975). Electrophysiological analysis of regional cortical maturation. *Biol. Psychiatr.* **10,** 513–526.

Verney, C., Milosevic, A., Alvarez, C., and Berger, B. (1993). Immunocytochemical evidence of well-developed dopaminergic and noradrenergic innervations in the frontal cerebral cortex of human fetuses at midgestation. *J. Comp. Neurol.* **336,** 331–344.

Verney, C., Zecevic, N., and Puelles, L. (1997). Prenatal development of the central catecholaminergic neurons in human embryos and fetuses. *Pediatr. Pulmonol. Suppl.* **16,** 220–221.

Vogt, C., and Vogt, O. (1902). "Neurobiologische Arbeiten." Erste Serie; Beiträge zur Hirnfaserlehre. Gustav Fischer, Jena.

Wang, L.G., Rao, Z.R., and Li, J.S. (1992). Prenatal ontogeny of substance P-like immunoreactivity in the parabrachial nucleus of the human fetus—an immunocytochemical study. *Brain Res.* **590,** 316–320.

Wang, L.G., Rao, Z.R., Li, H.M., and Li, J.S. (1993). Prenatal ontogeny of substance P-like immunoreactivity in the nucleus tractus solitarii and dorsal motor nucleus of the vagus nerve of the human fetus: An immunocytochemical study. *Brain Res.* **605,** 9–17.

Wierzba-Bobrowicz, T., Kosno-Kruszewska, E., Gwiazda, E., and Lechowicz, W. (1998). The comparison of microglia maturation in different structures of the human nervous system. *Folia Neuropathol.* **36,** 152–160.

Wierzba-Bobrowicz, T., Lechowicz, W., and Kosno-Kruszewska, E. (1997). A morphometric evaluation of morphological types of microglia and astroglia in human fetal mesencephalon. *Folia Neuropathol.* **35,** 29–35.

Wilkinson, M., Hume, R., Strange, R., and Bell, J.E. (1990). Glial and neuronal differentiation in the human fetal brain at 9 – 23 weeks of gestation. *Neuropathol. Expl. Neurobiol.* **16,** 193–204.

Wolf, P., Hösli, E., Roches, J.C., Zumstein, H.R., Heitz, Ph., and Hösli, L. (1975). Histochemical investigations on the presence of acetylcholinesterase and succinic dehydrogenase in fetal human spinal cord and brain stem at different stages of development. *Eur. Neurol.* 1**3,** 31–46.

Wurst, W., Auerbach, A.B., and Joyner, A.L. (1994). Multiple developmental defects in Engrailed-1 mutant mice: An early mid-hindbrain deletion and patterning defects in forelimbs and sternum. *Development* **120,** 2065–2075.

Yakovlev, P.I. (1969). The development of the nuclei of the dorsal thalamus and of the cerebral cortex; morphogenetic and tectogenetic correlation. *In* "Modern Neurology" (S. Locke, ed.), pp. 15–53. Little Brown & Co., Boston.

Yakovlev, P.J., and Lecours, A.R. (1967). The myelogenetic cycles of regional maturation of the brain. *In* "Regional Development of the Brain in Early Life" (A. Minkowski, ed.), pp. 3–10. Oxford.

Yamadori, T. (1965). Die Entwicklung des Thalamuskerns mit ihren ersten Fasersystemen be menschlichen Embryonen. *J. Hirnforsch.* **7,** 393–413.

Yamaguchi, K., and Goto, N. (1997). Three-dimensional structure of the human cerebellar dentate nucleus: a computerized reconstruction study. *Anat. Embryol.* **196,** 343–348.

Yamaguchi, K., Goto, N., and Honma, K. (1994). Development of the human gigantocellular reticular nucleus: a morphometric study. *Acta Anat.* **150,** 191–197.

Yan, X-X., and Ribak, C.E. (1997). Prenatal development of nicotinamide adenine dinucleotide phosphate-diaphorase activity in the human hippocampal formation. *Hippocampus* **7,** 215–231.

Yan, X-X., Zheng, D.S., and Garey, L.J. (1992). Prenatal development of GABA-immunoreactive neurons in the human striate cortex. *Dev. Brain Res.* **65,**191–204.

Yan, X-X., Garey, L.J., and Jen, L.S. (1996). Prenatal development of NADPH-diaphorase-reactive neurons in human frontal cortex. *Cerebral Cortex* **6,** 737–745.

Yan, X-X., Cao, Q.L., Luo, X.G., and Garey, L.J. (1997). Prenatal development of calbindin D-28k in human visual cortex. *Cerebral Cortex* **7,** 57–62.

Yew, D.T., Luo, C.B., Heizmann, C.W., and Chan, W.Y. (1997). Differential expression of calretinin, calbindin D28k and parvalbumin in the developing human cerebellum. *Dev. Brain Res.* **103,** 37–45.

Yu, M.C., Cho, E., Luo, C.B., Li, W.W.Y, Shen, W.Z., and Yew, D.T. (1996). Immunohistochemical studies of GABA and parvalbumin in the developing human cerebellum. *Neuroscience* **70,** 267–276.

Zec, N., Filiano, J.J., and Kinney, H.C. (1997). Anatomic relationships of the human arcuate nucleus of the medulla: A DiI labeling study. *J. Neuropathol. Expl. Neurol.* **56,** 509–522.

Zec, N., Rowitch, D.H., Bitgood, M.J., and Kinney, H.C. (1997). Expression of the homeobox-containing genes EN1 and EN2 in human fetal midgestational medulla and cerebellum. *J. Neuropathol. Expl. Neurol.* **56,** 236–242.

Zecevic, N. (1993). Cellular composition of the telencephalic wall in human embryos. *Early Hum. Dev.* **32,** 131–149.

Zecevic, N. (1998). Synaptogenesis in layer I of the human cerebral cortex in the first half of gestation. *Cerebral Cortex* **8,** 245–252.

Zecevic, N., and Rakic, P. (1976). Differentiation of Purkinje cells and their relationship to other components in developing cerebellar cortex in man. *J. Comp. Neurol.* **167,** 27–47.

Zecevic, N., and Verney, C. (1995). Development of the catecholamine neurons in human embryos and fetuses, with special emphasis on the innervation of the cerebral cortex. *J. Comp. Neurol.* **351,** 509–535.

Zecevic, N., Milosevic, A., and Ehrlich, B. (1999). Calcium signaling molecules in human cerebellum at midgestation and in ataxia. *Early Hum. Dev.* **54,** 103–116.

Zecevic, N., Milosevic, A., Rakic, S., and Marín-Padilla, M. (1999). Early development and composition of the human primordial plexiform layer: an immunohistochemical study. *J. Comp. Neurol.* **412,** 241–254.

Zheng, D.R., Guan, Y.L., Luo, Z.B., and Yew, D.T. (1989). Scanning electron microscopy of the development of layer I of the human visual cortex (area 17). *Dev. Neurosci.* **11,** 1–10.

Zilles, K., Werners, R., Büsching, U., and Schleicher, A. (1986). Ontogenesis of the laminar structure in areas 17 and 18 of the human visual cortex. *Anat. Embryol.* **174,** 339–353.

Zsang, L., and Goldman, J.E. (1996). Generation of cerebellar interneurons from dividing progenitors in white matter. *Neuron* **16,** 47–54.

CHAPTER

4

Development of the Peripheral Nervous System

KEN W. S. ASHWELL and PHIL M. E. WAITE
Department of Anatomy, School of Medical Science
University of New South Wales
Sydney, Australia

CRANIAL NERVES

Olfactory Epithelium and Nerve

The olfactory epithelium is well delineated in human embryos by about day 37 postconception (pc) (Bossy, 1980), and axonal growth from olfactory receptor neurons through the olfactory epithelial basal lamina is evident a few days later, with olfactory glial cells accompanying the nascent olfactory rootlets (Pyatkina, 1982). By 11 weeks pc, there has been complete morphological differentiation of olfactory receptor neurons and Bowman's glands have formed in the olfactory epithelium (Pyatkina, 1982). By day 41, the olfactory nerve is seen to be divided into two plexus-like laminae (Fig. 4.1). The medial plexus receives the terminal nerve/vomeronasal organ strand of axons and these elements are directed to the caudal part of the olfactory bulb anlage (Bossy, 1980). The lateral plexus is initially smaller than the medial plexus, arises from the lateral olfactory epithelium, and is directed to the lateral portion of the olfactory bulb anlage. By day 57 pc, vomeronasal fibers are gathered into two posterior filaments, which arrive in the vomeronasal ganglion, located near the dorsomedial aspect of the olfactory bulb, and the fibers from the ganglion terminate in the developing accessory olfactory bulb (Bossy, 1980). The fibers of the terminal nerve are directed to the medial septal area. Teratological studies indicate that the initial development of the olfactory nerve fibers is independent of the presence or absence of the target structure, the olfactory bulb (Braddock *et al.*, 1995).

Later in development (11–18 weeks pc), the human vomeronasal organ has been shown to have what appear to be receptor cells (Ortmann, 1989). Ortmann reported that there appears to be a great deal of individual variation in differentiation and individual constituents of the organ. Gradual regression of the human terminal nerve system begins toward the end of the embryonic period. Nevertheless, there are still as

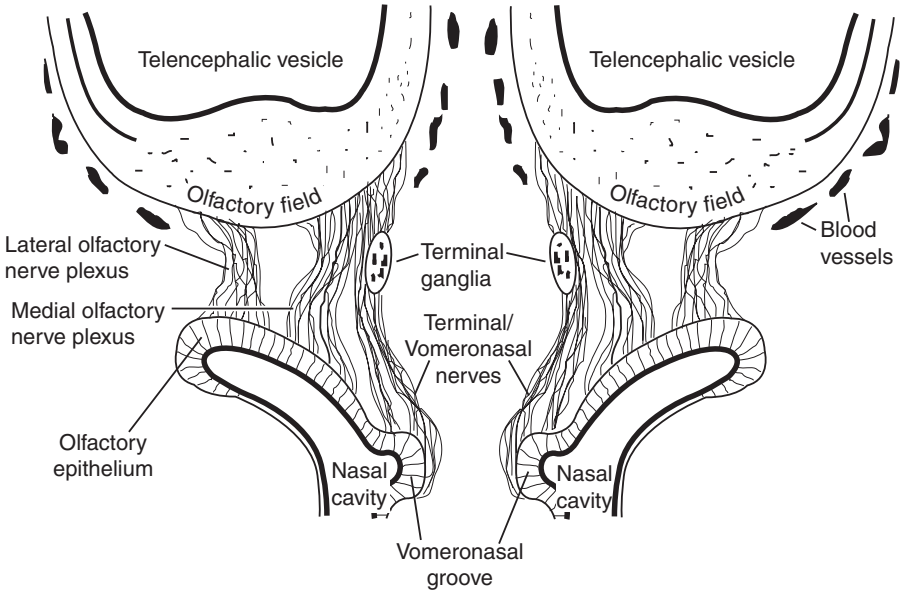

FIGURE 4.1 Diagrammatic oblique plane representation of the developing olfactory system at stage 18 (approximately 42 days postconception). Note the presence of medial and lateral olfactory plexuses and the close association of the vomeronasal organ efferents, terminal nerve, and terminal ganglion with the medial olfactory plexus.

many as 850 neurons present in the system by 4 months after birth (Oelschläger *et al.*, 1987). Termination sites of the terminal nerve system in blood vessel walls and nerve endings in the nasal epithelium indicate autonomic and sensory functions (Pearson, 1941, Oelschläger *et al.*, 1987). In rodent development, luteinizing hormone–releasing hormone (LHRH) immunoreactivity first appears in the ganglion cells of the terminal nerve system. In human embryos, LHRH can be detected in the olfactory epithelium as early as 5.5 weeks pc and migration of these cells along the developing vomeronasal/terminal nerve complex occurs shortly thereafter (Verney *et al.*, 1996). It has been proposed that the terminal nerve system and vomeronasal organ (Kjaer and Fischer Hansen, 1996) are both essential to the maturation and differentiation of the hypothalamus–pituitary–gonadal axis (Schwanzel-Fukuda *et al.*, 1985) because they provide the major source of LHRH–positive neurons for the developing hypothalamus. Failure of migration of LHRH neurons from the olfactory placode to the hypothalamus may result in Kallman syndrome, in which hypogonadotrophic hypogonadism is associated with reproductive dysfunction and, often, anosmia.

Development of the olfactory bulb occurs somewhat later than the olfactory epithelium. Lamination appears in the olfactory epithelium by about 13 weeks pc, with axodendritic synapses appearing in the presumptive glomerular layer at about 17 weeks pc (Chuah and Zheng, 1992). Although olfactory marker protein is first detected in olfactory receptor neurons at 24 weeks pc (Johnson *et al.*, 1995), it is not detectable in the bulb olfactory nerve layer and glomeruli until 32 weeks pc (Chuah and Zheng, 1987).

Mutations in the homeobox gene *Hesx1* have been shown to be associated with abnormal olfactory development in mice and humans, as well as defective development of the forebrain and Rathke pouch (Dattani *et al.*, 1998). Nevertheless, further work is necessary to identify genes specifically involved in olfactory development.

Behavioral studies of prenatal human olfactory function are few. Nevertheless, studies of the responsiveness of term infants to amniotic fluid suggest that human fetuses can detect and store chemosensory information about maternal amniotic fluid and show preferential turning towards familiar, as opposed to unfamiliar, amniotic fluid (Varendi *et al.*, 1996; Schaal *et al.*, 1998).

Retina and Optic Nerve

The retina is of course of central origin, but for the sake of a complete treatment of the cranial nerves it is useful to summarize here key stages in human retinal development. As in the developing cerebral cortex, proliferation to produce retinal neurons occurs at two different levels in the developing retina—the external

neuroblastic or ventricular layer adjacent to the optic cup lumen and the internal neuroblastic or subependymal layer (Robinson *et al.*, 1985). By the end of the embryonic period (about 8 weeks pc) the retina is composed of a pigment layer, future external limiting membrane, proliferative zone, external neuroblastic layer, transient fiber layer, internal neuroblastic layer, nerve-fiber layer, and internal limiting membrane (O'Rahilly and Gardner, 1975). By the middle of gestation all the layers of the adult retina are present. Throughout development the posterior pole or central part of the retina is always developmentally advanced compared to peripheral retina.

Some studies have examined the development of immunoreactivity for γ-aminobutyric acid (GABA) and the calcium-binding proteins (calbindin D-28k, parvalbumin) in fetal human retina. GABA expression has been seen as early as 12 weeks pc in the undifferentiated cells of the inner neuroblast layer. From 16 to about 25 weeks pc intense labeling may be found in amacrine, displaced amacrine, and some retinal ganglion cells, as well as horizontal cells in the process of migration and differentiation (Nag and Wadhwa, 1997). Parvalbumin immunoreactivity is already apparent at 13 weeks pc in the cells of the ganglion cell layer, spreading to the inner and outer borders of the inner nuclear layer by 15 weeks pc and staining horizontal cells from 20 weeks pc. By 32 weeks pc, the pattern of parvalbumin immunoreactivity has stabilized, with strong labeling of ganglion and horizontal cell somata as well as in their processes in the outer plexiform layer, nerve fiber layer, and two bands in the inner plexiform layer (Yan, 1997). Calbindin immunopositive cells are found in the ganglion cell layer and outer neuroblast layer by 13 weeks. Two weeks later, it is apparent that there are discrete populations of calbindin-positive horizontal and amacrine cells in the retina and by 24 weeks pc the laminar pattern of calbindin immunoreactivity is complete, with positive amacrine and horizontal cells and immunoreactivity in neuropil of the inner and outer plexiform layers (Yan, 1997).

Vascularization of the retina begins at about 15 weeks pc, as spindle cells appear in the vicinity of the hyaloid artery (Ashton, 1970). These spindle cells proliferate in the nerve head and subsequently invade the nerve fiber layer of the retina. These solid cords of cells become canalized to form capillaries, initially localized to the optic nerve head but progressively spreading into the retinal periphery as three fan-shaped vascular fronts (Ashton, 1970). Initially vessels are confined to the nerve fiber layer, but plexuses develop in the superficial and deep parts of the inner nuclear layer from 28 and 30 weeks pc, respectively (Gariano *et al.*, 1994). Human retinal vasculature does not undergo complete development until after birth.

Human retinal microglia have been reported to be derived from two distinct sources. Provis *et al.* (1996) have noted that microglia enter the retina from the ciliary margin prior to the onset of retinal vascularization, and from both the optic disc and ciliary margin after vascularization (14–15 weeks pc). They argue that macrophage–antigen–positive microglia become established in the retina as vessel-associated (peri- and paravascular) microglia, and that major histocompatibility complex (MHC)–positive and macrophage–antigen–negative microglia (retinal dendritic cells) become established as the parenchymal ramified microglia.

The human optic nerve has been the subject of many studies of glial and connective tissue development. Vascularization of the human fetal optic nerve mainly occurs between 12 and 14 weeks pc (Sturrock, 1975), although vessel density continues to rise until about 20 weeks pc. There is a close spatial correlation between the astrocyte population and vascularity, reflecting the close involvement of astrocytes in vascular development of neural tissue like the retina (Penfold *et al.*, 1990) and optic nerve. Microglial population size also rises in parallel with increasing vascularity, but this correlation is thought to be coincidental (Sturrock, 1984), reflecting greater ease of invasion by microglia as optic nerve vessels increase in number and size. In an immunohistochemical study of fascicle and collagen development, Jeffrey *et al.* (1995) showed that no connective tissue staining of collagen types I–VI is present at 26 weeks pc, but collagen immunoreactivity begins to appear by 34 weeks pc. Immunoreactivity for glial fibrillary acidic protein appears by 24 weeks pc, while myelin basic protein appears by 32 weeks pc (Takayama *et al.*, 1991). The meninges of the human optic nerve develop along a similar time course to the vascularization and astrocytic differentiation. A collagen-rich dural layer does not develop until about 15 weeks pc, but development is rapid thereafter, so that the optic nerve meninges are well differentiated by 18 weeks pc (Sturrock, 1987).

As in other developing mammalian motor and sensory systems, the fetal human optic nerve shows overproduction and subsequent elimination of retinal ganglion cell axons. Provis *et al.* (1985b) found that by about 10 weeks pc there are 1.9 million axons in the human optic nerve (Fig. 4.2). This peaks at 3.7 million axons at about 16 weeks pc and falls to 1.1 million axons at about 27 weeks pc. The number of substance P (SP) immunoreactive fibers in the human optic nerve and lateral geniculate nucleus also peaks at 16–17 weeks pc and declines thereafter (Wadhwa *et al.*, 1988).

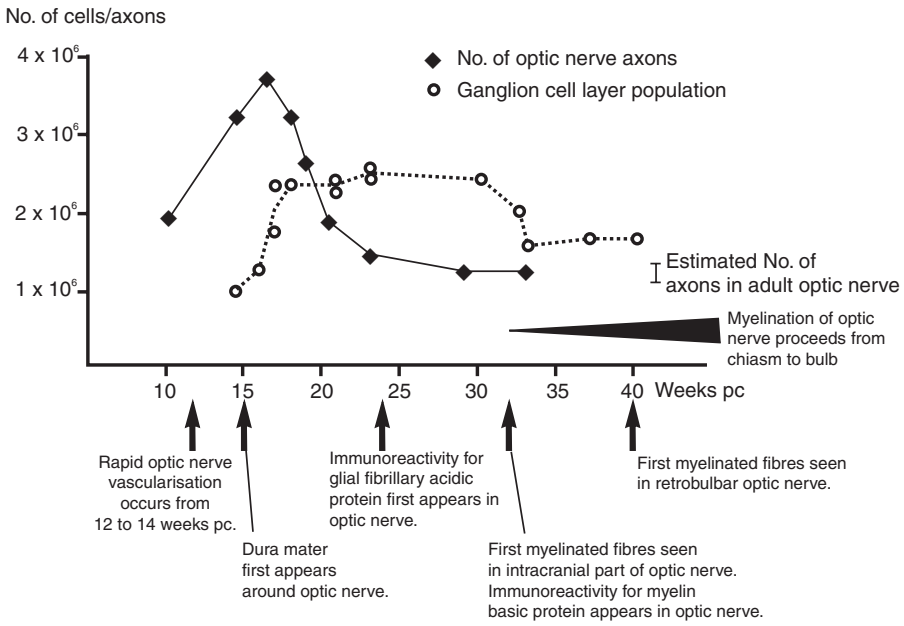

FIGURE 4.2 Major developmental events in the human optic nerve and retina. Figure representing changes in retinal ganglion cell population and optic nerve axons adapted from Provis *et al*. Human fetal optic nerve: overproduction and elimination of retinal axons during development. J. Comp. Neurol. 238, 429–451. © 1985. Reprinted by permission of Wiley-Liss, Inc., a subsidiary of John Wiley & Sons, Inc. Dates of significant events in development are also indicated, as cited in the text.

The period of loss of cells from the retinal ganglion cell layer occurs after 30 weeks pc (Provis *et al.*, 1985a), indicating that many cells in the fetal ganglion cell layer do not contribute axons to the optic nerve during the period from 20 to 30 weeks pc. Myelination of the optic nerve does not begin until after 32 weeks pc, and myelination is largely complete by 7 months after birth (Magoon and Robb, 1981).

Studies with carbocyanine dye tracing techniques indicate that there is some topographic organization of axons within the fetal optic nerve according to retinal quadrant but that there is mixing of peripheral and central axons within each quadrant (Fitzgibbon, 1997). This rough patterning appears to be a passive process in that it arises as a consequence of combining the fascicles of the retinal nerve fiber layer from each retinal quadrant into a matching optic nerve quadrant. There does not appear to be any active process during development, which reorders fibers in either the optic nerve or tract. Factors controlling the direction taken by optic nerve axons at the chiasm have been the subject of considerable research in experimental animals. Analysis of optic chiasm formation in mouse and zebra fish *Pax-2* mutants (Favor *et al.*, 1996) suggests that the *Pax-2* gene regulates the expression of surface molecules involved in contact attraction of retinal ganglion cell axons entering the chiasm (Alvarez-Bolado *et al.*, 1997). The ventral forebrain midline, where the optic chiasm will develop, is formed by neuroepithelial cells expressing *Sonic hedgehog (Shh)* and it has been suggested that both *Pax-2* and *Shh* have important roles in chiasm formation.

Extraocular Muscle Innervation and Oculomotor, Trochlear, and Abducens Nerves

The cells that form the Edinger–Westphal nucleus are derived from the dorsal portion of the mesencephalic basal plate and migrate along primitive blood vessels to the tegmentum (Hogg, 1966).

An electron microscopic study of the intracranial protion of the human fetal trochlear nerve found that at 10 weeks pc this nerve has approximately 4000 unmyelinated axons arranged in 18 bundles (Mustafa and Gamble, 1978), while a specimen at 13 weeks pc had approximately 6000 axons. No other age groups have been examined to date.

Trigeminal Nerve

The trigeminal nerve contains both motor and sensory divisions. The motor division supplies the muscles of the first pharyngeal arch, namely, the muscles of mastication and the mylohyoid, anterior

belly of digastric, tensor tympani, and tensor veli palatini. Early motor cells can be seen migrating from the germinal zone of the special visceral efferent (ventromedial) column by 28 days pc (Bruska, 1991a). Medial and lateral cell groups are initially present within the developing motor nucleus, but the medial group subsequently disappears, leaving the lateral as the definitive motor nucleus (Bruska, 1991b). Windle and Fitzgerald (1994) describe trigeminal motor fibers emerging in 4-mm embryos (stage 13, 28 days pc) and the nerve is clearly present at stage 14 (Yokoh, 1968; O'Rahilly *et al.*, 1984). As for many other nuclei, cell death of trigeminal motor neurons has been reported (Hamano *et al.*, 1988). Innervation of jaw muscles occurs during the second month pc, with reflex opening of the mouth seen by 9.5 weeks (Hooker, 1942).

The sensory trigeminal neurons develop from the neural crest and epidermal placode of the mandibular arch, as in other species. The trigeminal ganglion can be recognized in the human by 26 days (stage 12, O'Rahilly *et al.*, 1984; Müller and O'Rahilly, Chapter 2). By 32 days, Bruska and Wozniak (1989) described two divisions: a smaller ophthalmic part and a larger maxillomandibular region. This has also been noted in the chick (D'Amico-Martel and Noden, 1980), although in the rat (Altman and Bayer, 1982) the separation is into a large ophthalmic maxillary region and a smaller mandibular part.

Yokoh (1968) described three short branches emerging from the trigeminal ganglion in the 4.5-mm embryo (stage 14) (Fig. 4.3). By stage 15 (about 36 days pc) the trigeminal ganglion is the largest of the cranial ganglia (Bruska, 1987) and lies directly inferior and lateral to the pons. Three divisions are recognizable, i.e., ophthalmic, maxillary, and mandibular, with nerves arising from each. By 5 weeks pc, the maxillary nerve has grown into the maxillary process and the inferior alveolar nerve is within the mandible (Pearson, 1977). Central projections to the pons develop concurrently, i.e., axons are present in the trigeminal tract from about the same time (from stage 14, Müller and O'Rahilly, Chapter 2) and the mesencephalic root of the trigeminal nerve appears from stage 16 (Müller and O'Rahilly, Chapter 2). By 8–8.5 weeks pc, central projections of all three divisions extend as far as the C_2 spinal cord level, with the maxillary and mandibular inputs terminating about one segment more caudally (i.e., C_3–C_4) than the ophthalmic (Humphrey, 1952).

As in avian and rodent ganglia, the human trigeminal ganglion shows light cells and dark cells (Bruska, 1986; D'Amico-Martel and Nodem, 1980). Satellite cells are present around the developing neurons by 6 weeks pc (Bruska, 1990), with usually two satellite cells per neuroblast by 9 weeks pc (Bruska and Wozniak ,1991). Schwann cells are present around the axons by week 9, with the first signs of myelination at 12 weeks pc (Bruska and Wozniak, 1991). SP and calcitonin gene-related peptide (CGRP) are expressed in a proportion of the ganglion cells from at least 25 weeks pc (Quartu *et al.*, 1996). Moreover, many developing ganglion cells have been shown to express the neurotrophic receptors trkA, trkB, and trk C, although unlike the rat, not all cells have been found to be immunopositive (Quartu *et al.*, 1996).

Neurons responsible for proprioception from the facial region lie in the mesencephalic trigeminal nucleus within the midbrain and pons, not the trigeminal ganglion. The mesencephalic trigeminal tract can be distinguished at stage 15 (O'Rahilly *et al.*, 1984).

The role of early innervation in tooth formation has been the subject of considerable interest (Christensen *et al.*, 1993). Epithelial thickening to form the dental lamina starts at around 6 weeks pc, prior to innervation. As epithelial buds develop, nerve fibers grow toward them, with the dental follicle receiving its first nerve fibers at the cap stage. By 15 weeks pc, a dental nerve is associated with each developing tooth. Fibers are seen in the dental papilla by 22 weeks pc, after the onset of dentinogenesis (Christensen *et al.*, 1993).

Several studies have examined the development of innervation of the face and development of perioral reflexes. Facial skin regions are the first to become sensitive and give rise to reflexes in the embryo. The earliest responses, from perioral skin, occur at around 7.5 weeks pc (Hooker, 1942) and involve contralateral flexion of the neck and upper trunk. By 8.5 weeks pc, the reflex spreads caudally to involve lateral flexion of entire trunk combined with pelvic rotation. Local reflexes first appear at 9.5 weeks pc, with mouth opening in response to stimulation of the lips. By 10–10.5 weeks pc, perioral stimulation leads to swallowing whereas eyelid stimulation causes contraction of the orbicularis oris and oculi muscles. This is about the time that the skin on the hands becomes sensitive, with palmar stimulation resulting in finger flexion. Plantar flexion first occurs at 11–11.5 weeks (Humphrey and Hooker, 1959).

Facial Nerve

The facial nerve collects axons from motor nuclei lying in rhombomeres 4/5 of the embryonic brain and exit from rhombomere 4 to innervate the second pharyngeal arch derivatives (Lumsden and Keynes, 1989; Guthrie and Lumsden, 1992). Experiments with *Hoxa1* and *Hoxb1* null mutants indicate that both genes act synergistically to pattern the hindbrain facial nerve and second pharyngeal arch (Gavalas *et al.*, 1998). In humans, the facial nerve can be identified at 4 weeks

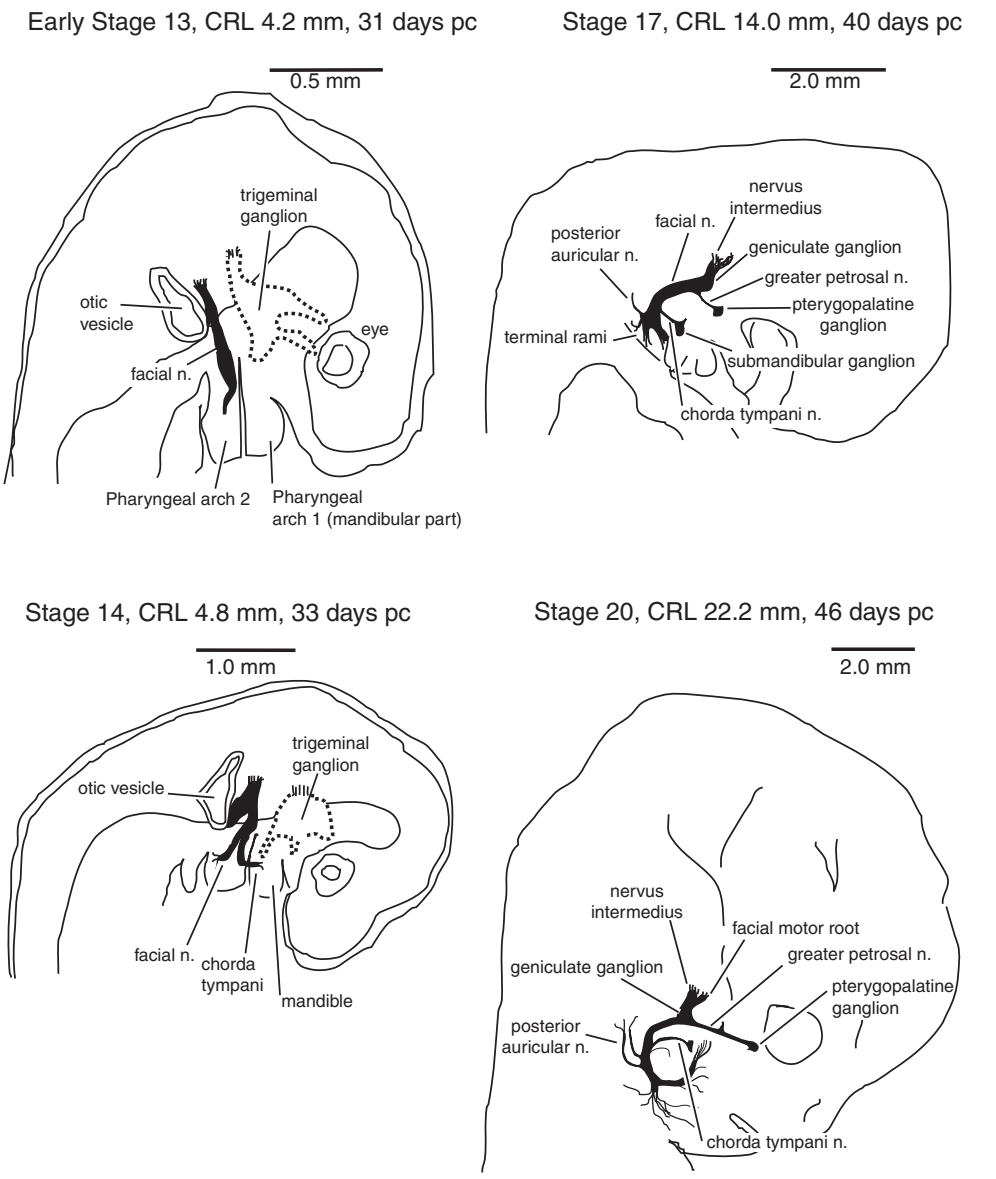

FIGURE 4.3 Development of the human facial nerve. This figure has been adapted from Gasser (1967) with permission of Annals, Inc. Note the early appearance of the chorda tympani (by 4.8 mm CRL) and the greater superficial petrosal nerve (by 14 mm CRL). Most significant rami have appeared by 46 days postconception.

pc (Gasser, 1967) as an unbranched bundle attached to the metencephalon immediately rostral to the otic vesicle (Fig. 4.3). Late in the fourth week, the facial nerve splits into two branches, with the chorda tympani coursing rostrally to enter the mandibular arch, and a caudal trunk merging into second arch mesenchyme. The geniculate ganglion and nervus intermedius appear during the fifth week pc, and the greater superficial petrosal nerve is also apparent for the first time. At about 6 weeks pc, the superficial layer of the second arch mesenchyme spreads to establish four laminae (occipital, cervical, mandibular, and temporal), which will give rise to the facial muscle groups (Sataloff, 1990). The pterygopalatine ganglion appears by about 6 weeks pc. Peripheral branches of the main trunk become apparent from 7 to 9 weeks pc, and anastomoses with branches of the trigeminal nerve develop and become extensive from 10 to 15 weeks pc. From about 9 to 14 weeks pc, the parotid gland progressively grows around the facial nerve, completely engulfing it (Espin-Ferra, 1991). The definitive communications of the facial nerve are established by 16 weeks pc.

Studies using mice with deletions of genes coding neurotrophin-4 (NT-4) and brain-derived neurotrophic factor (BDNF) have demonstrated that sensory nerve cells of the geniculate and nodose-petrosal ganglia are particularly sensitive to NT-4 deficiency, whereas facial motorneurons and superior cervical sympathetic ganglion cells are unaffected. Cells of the vestibular, geniculate, and nodose-petrosal ganglia are depleted in *bdnf*$^{-/-}$ homozygotes, whereas facial motorneurons are unaffected (Liu *et al.*, 1995).

Inner Ear and Vestibulocochlear Nerve

By day 32 of development, the otocyst lies alongside the fifth and sixth rhombomeres of the developing brain stem and the endolymphatic appendage is already set apart from the developing utricle by a fold (Bruska and Wozniak, 1994). Within a day or two, the otocyst can be seen to be divided into several pouches. A dorsal pouch represents the endolymphatic duct and site of development of the semicircular ducts, whereas a ventral pouch gives rise to the primitive cochlear duct. At about 32 days pc, the vestibulocochlear and geniculate ganglia form a common complex surrounded by a mesenchymal capsule, although three distinct ganglionic components are visible in this mass at this stage. Branches of the vestibular ganglion penetrate the otic epithelium at day 33 to form ampullary nerves, whereas the central axons of vestibular ganglion cells enter the brain stem at about the same time. The cochlear ganglion lies rostrally and medially to the vestibular ganglion and is slightly less advanced in development than the trigeminal, geniculate, and vestibular ganglia. It contributes centrally directed axons to enter the brain stem at about 37–40 days pc. The cochlea starts to curl by 6 weeks pc, reaching its full morphological development (3 mm diameter and 2.5 turns) by 10 weeks pc and its final adult size by 20 weeks pc (Lecanuet and Schaal, 1996). The organ of Corti develops in the cochlea from about 8 weeks pc, and both inner and outer hair cells can be seen by 11 weeks pc. Final cell positioning on the basilar membrane is reached by 14 weeks pc (Lecanuet and Schaal, 1996). Based on purely morphological criteria, the vestibular apparatus is considered mature by 14 weeks pc (Lecanuet and Schaal, 1996).

In the absence of tracing studies, the olivocochlear system in humans has been identified using immunoreactivity to choline acetyltransferase (ChAT) and CGRP, both of which label central neurons as well as efferents in the organ of Corti. By 21 and 22 weeks pc, ChAT immunoreactivity is visible in neurons of the dorsal and ventral periolivary region, although neurons of the medial and lateral superior olivary nuclei are still of immature appearance in Nissl stains made at this age. Neurons immunoreactive for ChAT become more dispersed as prenatal development proceeds. Neurons immunoreactive for CGRP are visible from 21 weeks pc and increase steadily from a population of about 300 at 21 weeks pc to a plateau population size of about 620 during the period from 24 weeks pc to 6 months after birth (Moore *et al.*, 1999).

Glossopharyngeal Nerve

Nerve branches from the inferior ganglion of the glossopharyngeal nerve to the aortic arches have been identified in 9- to 11-mm-long embryos (about 5 weeks pc; Golub *et al.*, 1979). The first glossopharyngeal nerve fibers growing into the third aortic arch (future carotid sinus) are also seen at this stage, and these fibers precede both vagal and sympathetic nerves in the innervation of the primitive vascular tree in this region.

The lingual branch of the glossopharyngeal nerve enters the tongue concurrently with the lingual and hypoglossal nerves and can be identified as early as 40 days (Vij and Kanagasuntheram, 1972). Glomus-like collections of cells resembling taste buds can be first observed at about 55–60 days pc and nerve fibers can first be demonstrated among these cells at this stage.

Vagus and Spinal Accessory Nerves

The developing nucleus ambiguus makes contributions to the developing glossopharyngeal and vagal nerves as early as 28–30 days pc (Brown, 1990). Functional development of visceral reflexes associated with the vagus have been correlated with maturation of nucleus ambiguus neurons. As noted above, the earliest overt evidence of swallowing in the human fetus has been reported in response to perioral stimulation at 10.5 weeks pc (Brown, 1990), whereas at 12.5 weeks pc swallowing is a consistent consequence of perioral stimulation (Humphrey, 1968). By 10.5 weeks pc, subnuclear groupings have begun to appear in the nucleus ambiguus, and these neurons are well differentiated by 12.5 weeks pc (Brown, 1990).

The ganglia of the vagus nerve are already delineated in human embryos of 4 mm length (approximately 30 days pc) and they form a common ganglionic mass up to 5 weeks pc (Streeter, 1905, 1908). By 6 weeks pc, vagal trunks have reached the walls of the stomach and a branch from the posterior trunk has reached the celiac plexus (Wozniak *et al.*, 1979). Ultrastructural studies of differentiation of fetal sensory nerve cells in the human inferior vagal ganglion have shown that there is a transition from the immature apolar and bipolar ganglion cells to unipolar type at about 8–10 weeks pc

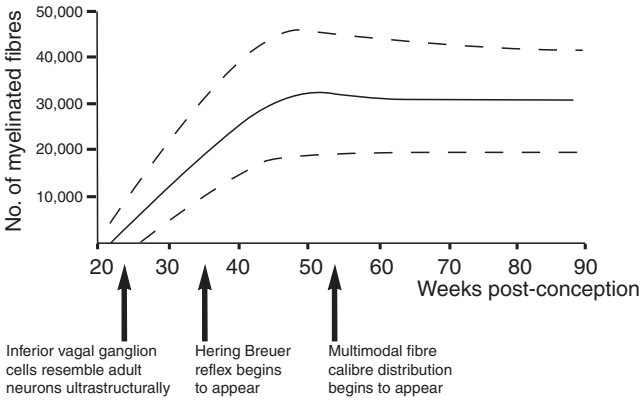

FIGURE 4.4 Significant events in the development of the human vagus nerve. Data for graph of number of myelinated vagal fibers against postconceptional age taken from Sachis *et al.* (1982). Note the large range in values for number of myelinated fibers indicating significant variation between individual fetuses and neonates.

(Bruska and Wozniak, 1980). Ultrastructurally, inferior vagal ganglion cells resemble adult cells by about 23 weeks pc.

The importance of the vagus in carrying information vital to pulmonary reflexes has prompted several studies of development of that nerve. Myelination of the human vagus nerve begins between 14 and 17 weeks pc (Wozniak and O'Rahilly, 1981). Total numbers of myelinated fibers in the vagus increase linearly from about 5000 at 26 weeks pc to as many as 40,000, the adult value, at 10 weeks after birth (Sachis *et al.*, 1982) (Fig. 4.4). Immaturity of the vagus may be responsible for the unstable breathing patterns in preterm infants. Indeed, the Hering–Breuer inspiration-inhibiting reflex, which is mediated by large myelinated vagus fibers, is reported to be weak in infants of 32 weeks pc but increases in strength until 38 weeks pc (Bodegard *et al.*, 1969). After birth, the number of myelinated axons in the vagus remains fairly constant (Sachis *et al.*, 1982), and a multimodal distribution of fiber size begins to appear at about 3 months after birth (Pereyra *et al.*, 1992). Delayed maturation of the vagus nerve has been claimed to be present in infants dying from sudden infant death syndrome, with affected infants having more small (<1.5 μm diameter) and fewer larger (>2.0 μm diameter) axons (Becker *et al.*, 1993).

Vagal innervation of human fetal viscera has received some attention, although a full dataset is not yet available. Palatine and pharyngeal muscles begin to appear at about 5–6 weeks pc and receive their innervation (from trigeminal, glossopharyngeal, and vagal nerves) from about 8 weeks pc (Doménech-Ratto, 1977). In the developing larynx (Müller *et al.*, 1981, 1985), the adult pattern of motor innervation is present from stage 23 (about 52 days pc) although sensory innervation is not complete at this stage. Leonard *et al.* (1983) have suggested that mechanical support from the left vagus and left recurrent laryngeal nerve during development ensures that the ductus arteriosus differentiates as a muscular artery, although this vessel will obliterate its lumen in early postnatal life. Inferior vagal ganglion cells can be retrogradely labeled by carbocyanine dye insertion into the pylorus from 12 weeks pc (Abel *et al.*, 1998), but see below for development of the gastric enteric plexus.

The spinal accessory nucleus is already present at about 30 days pc as a group of cells lying in the dorsolateral part of the ventral horn of the upper four to six cervical segments (Pearson, 1938; Skórzewska *et al.*, 1994a, b). At no stage during development does the spinal accessory nucleus show any continuity with the nucleus ambiguus. Several rootlets leave the nucleus, ascending on the dorsolateral surface of the spinal cord forming the spinal accessory nerve (Pearson, 1938), which ascends to join the vagus nerve at the level of the superior vagal ganglion. By 41 days pc, the external branch of accessory gives off secondary branches to supply the differentiating trapezius and sternomastoid muscles (Skórzewska *et al.*, 1994b).

Hypoglossal Nerve

The hypoglossal nucleus appears at approximately 26 days pc (O'Rahilly and Müller, 1984). Hypoglossal nerve roots emerge at about 28 days and form a hypoglossal nerve at about 32 days. The hypoglossal nerve reaches the tongue muscles by 37 days and the ansa cervicalis becomes apparent at 41 days. Further subdivisions of the hypoglossal nerve in the tongue are apparent by about 50 days, and at this time the fine terminations of the nerve approach close to the epithelium (Vij and Kanagasuntheram, 1972). No data are currently available concerning the later development of the hypoglossal nerve, although it is known that natural neuronal death in the hypoglossal nucleus occurs between about 15 and 25 weeks pc (Nara *et al.*, 1989; Milutinovic *et al.*, 1992).

SOMATIC PERIPHERAL NERVOUS SYSTEM

Dorsal Root Ganglia

Dorsal root ganglion cells develop in the human embryo at about 4 weeks pc and immediately begin to migrate ventrally, so that they come to lie within the intervertebral foramina during the seventh week and are surrounded by dural sleeves during the eighth week

of gestation (Sensenig, 1957). Ultrastructural studies of fetal human dorsal root ganglia have reported no significant morphological differences related to segmental level. In other words, the cellular types and sequence of differentiation are similar in cervical, thoracic, and lumbosacral segmental levels. In 6- to 7-week pc embryos, dorsal root ganglia are composed of loosely packed and randomly oriented cells with wide intercellular spaces and scattered processes (Olszewska *et al.*, 1979). Most cells at this stage are apolar, undifferentiated neuroblasts. Early bipolar neurons begin to appear during the seventh and eighth weeks pc. These cells are oval, with processes arising from each end. There has been an increase in cytoplasm and proliferation of organelles compared to the apolar type. Evidence of apoptosis in the form of oval cells with electron dense pyknotic nuclei is seen in dorsal root ganglia at about the eighth week. Intermediate bipolar neurons, with prominent development of rough endoplasmic reticulum, begin to appear at 9–10 weeks pc, while unipolar neurons, which have well-developed organelles and a single broad process arising form one pole, appear at about 11 weeks pc (Olszewska, 1979). The appearance of unipolar neurons correlates with the onset of reflex responsiveness from the skin of the upper limb (Hooker, 1942); signifying that both central and peripheral processes of a significant proportion of these cells have reached their appropriate target structures.

Studies of the development of proteins, growth factors, and biochemical markers within human dorsal root ganglion cells have shown that biochemical maturation coincides closely with the sequence of ultrastructural maturation summarized above. Both high molecular weight neurofilament protein and vimentin are present in dorsal root ganglion cells at 6 weeks pc (Lukás *et al.*, 1993; Almqvist *et al.*, 1994). Immunoreactivity for vimentin declines in ganglion cells but increases with age in differentiating satellite cells. Immunoreactivity for neuron-specific enolase, a neuron-specific enzyme that is useful as a marker of neuronal differentiation, develops in dorsal root ganglion cells at about the same time (7 weeks pc) as its appearance in the spinal cord (Kato and Takashima, 1994). Immunoreactivity for somatostatin begins to appear in a few dorsal root ganglion cells at 9 weeks pc (Charnay *et al.*, 1987; Marti *et al.*, 1987) and remains stable in terms of number of immunoreactive neurons throughout fetal life. Somatostatin-immunoreactive processes in the dorsal horn of the spinal cord appear at 9 weeks pc, increase in number and density during the period from 12 to 28 weeks pc, and remain stable from 36 weeks pc to 4 months after birth (Charnay *et al.*, 1987). Immunoreactivity for the low-affinity nerve growth factor receptor (NGFr) also appears at about 9 weeks pc in larger ganglion cells, and immunoreactive fibers appear in the medial dorsal horn between 12 and 20 weeks pc (Suburo *et al.*, 1992). Both of these immunoreactivities are absent in the adult. Immunoreactivity for NGFr in the lateral and superficial parts of the dorsal horn appears at 14 weeks pc and, unlike the immunoreactivity in the medial dorsal horn, remains present until adult life (Suburo *et al.*, 1992). Immunoreactivity for enkephalin and CGRP appears in dorsal root ganglia somata at 14 weeks pc, whereas galanin and SP immunoreactivity do not appear in dorsal root ganglia somata until 24 weeks pc (Marti *et al.*, 1987). There is a pronounced increase in the number and intensity of CGRP-, galanin-, somatostatin-, and SP-immunoreactive fibers in the dorsal horn around the time of birth. In rodents this has also been found to coincide with the earliest appearance of these markers in sensory fibers in the epidermis (Marti *et al.*, 1987), but this has not been investigated in human fetuses.

Development of Peripheral Somatic Nerves

The human upper limb bud appears at about 30 days pc and formation of the brachial plexus is evident from about 34–35 days (O'Rahilly and Gardner, 1975; Shinohara *et al.*, 1990; see Fig. 4.5). At between 38 and 40 days, the major branches of the brachial plexus are visible, and median, radial, and ulnar nerves enter the hand plate. By about 46–48 days all the upper limb nerves can be seen to have already adopted an orientation and arrangement similar to those seen in the adult. This is in agreement with findings that movements of the human upper limb can be observed at about 20–23 mm crown rump length (approximately 48–50 days postconception) (Windle and Fitzgerald, 1937; Fitzgerald and Windle, 1942).

Hindlimb bud development and innervation occur slightly later. Ultrastructural studies (Davison *et al.*, 1973; Fidzianska, 1976) of the sciatic nerve have shown that initially (9–11 weeks pc) the human fetal sciatic nerve is formed of fascicles of unmyelinated fibers surrounded by an epineurium of collagen and fibroblasts. At this stage some, but certainly not all, fascicles are surrounded by Schwann cell processes. Between 12 and 17 weeks pc, there is a marked increase in the number of Schwann cells, so that by the end of this period there are a few instances of one axon to one Schwann cell. The 18th week of gestation is marked by loose spiraling of the mesaxon around the axon within a Schwann cell (i.e., the beginnings of myelination), and by 23 weeks pc most Schwann cells are associated with only one axon (Davison *et al.*, 1973). The period from 17 to 20 weeks pc also sees the appearance of

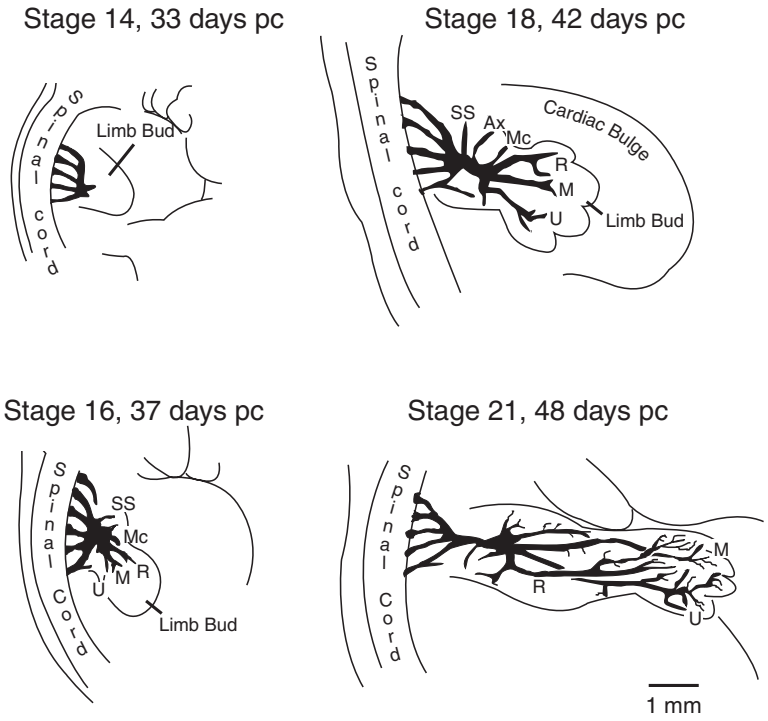

FIGURE 4.5 Development of the brachial plexus in human embryos. Note the early appearance of major nerve branches (by stage 16) and their substantial elaboration by stage 21. Ax, axillary nerve; M, median nerve; Mc, musculocutaneous nerve; R, radial nerve; SS, subscapular nerve; U, ulnar nerve. All figures have been drawn to the same scale.

lecithin, cerebrosides, sulfatides, and other lipids in the developing sciatic nerve (Davison *et al.*, 1973). As in other mammals, fetal human sciatic nerve axons show prominent beading or varicosities along their length, which may be partly artifactual, but may nevertheless reflect particular vulnerability of fetal nerve fibers (Tomé *et al.*, 1988). The fetal human sural nerve shows a similar time course of myelination to that seen in the sciatic nerve, with no myelinated fibers visible at 16 weeks pc but well-myelinated fibers plentiful by 21 weeks pc (Shield *et al.*, 1986).

The development of receptors for the somatosensory system appears to follow a rough rostrocaudal/distal-to-proximal pattern (Fig. 4.6). Free nerve endings can be found in the mouth and peribuccal region as early as 8–9 weeks pc (Lecanuet and Schaal, 1996), whereas Meissner and Pacinian corpuscles develop soon after. Tactile receptors may be seen in the face, palms, and soles of the feet by 11 weeks pc, and on the trunk and proximal zones of the arms and legs by 15 weeks. Their initial density, especially of the less differentiated free nerve ending type, is greater than in the adult, suggesting some early exuberance.

Electron microscopic studies of the human fetal phrenic nerve have shown that axons in this nerve begin to undergo myelination at about 15 weeks pc (Wozniak *et al.*, 1982) compared with 12 weeks pc for trigeminal nerve (Bruska and Wozniak, 1991). Compact myelin is apparent by 17 weeks pc, and although the phrenic nerve has a mature form by 23 weeks pc, many fibers are still in the process of myelinating at this age. Communications between the celiac plexus and the right phrenic nerve have also been seen in fetal material (Pearson and Sauter, 1971), and this may have considerable clinical significance for referred pain from foregut-derived structures.

Functional studies of peripheral nerves in very preterm infants indicate that motor nerve conduction velocity in both tibial and ulnar nerves increases steadily from about 10 m/s at 26 weeks pc to about 25 m/s at term (Smit *et al.*, 1999).

AUTONOMIC AND ENTERIC NERVOUS SYSTEM

Sympathetic Trunk and Sympathetic Outflow to Head and Limbs

The first visible anlage of the sympathetic trunk in the human fetus appears near the aorta in the thoracic and lower cervical region (late 4 weeks pc; Lutz, 1968).

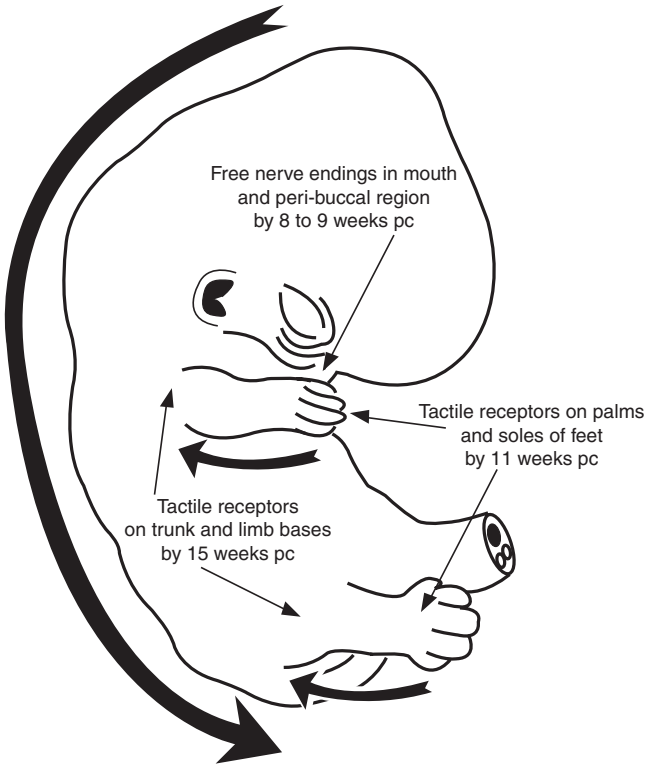

FIGURE 4.6 Schematic representation of development of tactile receptors in the human embryo and early fetus. Thick arrows indicate temporospatial gradients of receptor development. See text for citations.

Later in development (middle of fifth week pc), the sympathetic trunk extends to the base of the skull and segmentation appears in parallel with the longitudinal growth of the vertebral column.

Development of human sympathetic ganglion cells has been followed in a light and electron microscopic study of the human fetal superior cervical ganglion (Hervonen and Kanerva, 1972). Superior cervical ganglion neuroblasts already contain catecholamine at 12 weeks pc. Primitive sympathetic cells are characterized by their dark chromatin, in contrast to the larger and paler nuclei of more mature neuroblasts. At the electron microscope level, primitive sympathetic cells show a strong rim of condensed chromatin inside the nuclear membrane, do not have nucleoli, and possess scant cytoplasm.

Innervation of structures by branches of the cervical sympathetic trunk has been followed by some authors. Sympathetic nerve innervation of the area around the carotid sinus develops later than the glossopharyngeal and vagal innervation of this region. Thin fiber bundles from the anterior surface of the superior cervical ganglion reach the root of the internal carotid artery by 6 weeks pc (Golub *et al.*, 1979). Similarly, sympathetic innervation of the internal carotid plexus does not develop until late in the sixth week pc to early seventh week pc, although branches from cranial nerves are already present by early sixth week pc (Golub *et al.*, 1979).

At more caudal levels, sympathetic outflow from lumbosacral sympathetic trunk to the sciatic nerve first appears between 18 and 21 weeks pc (Koistinaho, 1991). These nerves are distributed from the outset to both epiperineurial blood vessels and to the endoneurium itself, not related to blood vessels.

Adrenal Medulla and Paraganglia

Formaldehyde-induced fluorescence of adrenal medullary cells can be demonstrated as early as 9 weeks pc (Hervonen, 1971). The number of medullary cells increases rapidly between 9 and 13 weeks pc, and fine nerve fibers are found adjacent to catecholamine-storing cells by 12 weeks pc. Ultrastructurally, the fetal adrenal medullary cells contain only the noradrenaline type of catecholamine granules until 16 weeks pc, but after that age adrenaline-type granules are also found. Synaptic contacts between preganglionic axons and catecholamine-storing cells are morphologically mature by 14 weeks pc.

Formaldehyde-induced fluorescence can be detected in paraganglia by about 8–9 weeks pc (Hervonen, 1971), but invasion of the paraganglia by nerve fibers from the sympathetic trunk does not occur until after 12 weeks pc.

Cardiac Innervation and Conducting System

Innervation of the coronary arteries begins before 8 weeks pc, by which stage both the aorta and pulmonary artery are surrounded by five or six small nerve fascicles (Smith, 1970). At about 8–9 weeks pc, an adventitial plexus of small nerve bundles is associated with both coronary arteries and their main branches. Myelination of the cardiac plexus and invasion of the adventitia by a fine plexus of nerves occurs by 120 mm crown–rump length.

Intrinsic cardiac autonomic ganglion cells are believed to migrate along the vagus nerve into the developing heart and appear as early as 6–7 weeks pc in the atrial wall (Smith, 1971a). Intrinsic ganglion cells showing mature morphological features are seen by about 16 weeks pc, although many presumably immature (binucleate) cells persist at this age. The number of binucleate cells declines between midgestation and term. By the time of birth, ganglia form an apron across the atrioventricular groove of the heart, extending onto the superior ventricular surface and up the pulmonary trunk and aorta (Smith, 1971b).

The conducting system of the fetal heart is present by 8 weeks pc (Gardner and O'Rahilly, 1976). Synaptogenesis of cardiac ganglion cells initially occurs at about the fifth week of gestation, although well-developed synapses with many synaptic vesicles cannot be seen until the eighth week of gestation (Shvalev and Sosunov, 1989; Shvalev *et al.*, 1992).

The development of peptidergic innervation of the human fetal heart has been investigated by Gordon *et al.* (1993). Those authors found that peptide-immunoreactive nerves cannot be identified in the heart until 10 weeks pc. The first identified and most prevalent nerves in the fetal heart were neuropeptide Y (NPY)–immunoreactive fibers. These fibers showed a descending atrial-to-ventricular density gradient. Somatostatin and vasoactive intestinal peptide (VIP) first appear at 10–12 weeks pc and are mainly distributed in the atria. Somatostatin immunoreactivity is found in cell bodies in the cardiac ganglia, whereas VIP- and NPY-immunoreactive fibers appear to be of extrinsic origin. Innervation by CGRP- and SP-immunoreactive fibers does not occur until late in gestation (18–24 weeks pc), suggesting that sensory innervation does not occur until at least 6 weeks after autonomic supply develops. Studies of the development of CGRP- and SP-immunoreactive fibers in autonomic regions of the spinal cord show that both of these immunoreactive sensory fibers appear at about 24 weeks pc (Marti *et al.*, 1987).

Early functional studies of the human fetal heart have used electrical stimulation to stimulate release of autonomic transmitters such as acetylcholine and noradrenaline (Walker, 1975). Electrical stimulation was found to have no effect on the human fetal heart prior to 13 weeks pc, suggesting that autonomic nerves are too immature to release neurotransmitter at this stage. After 13 weeks, responses to electrical stimulation are blocked by tetrodotoxin, indicating that the responses are indeed due to neurotransmitter release. Other studies have shown that fetal myocardium possesses intrinsic pacemaker activity not seen in adult myocardium (Coltart *et al.*, 1971). Human fetal myocardium also appears to be less sensitive to cholinergic and adrenergic agents than adult myocardium.

Later studies of isolated fetal hearts (reviewed in Papp, 1988) showed that muscarinic cholinergic responses to acetylcholine can be detected from 4 weeks pc, i.e., soon after the initiation of the first heartbeats. Similarly, β-adrenergic responsiveness to noradrenaline, adrenaline, and other adrenergic stimulants appears slightly later (at 5–8 weeks pc; Gennser and Nilsson, 1970). It appears that the parasympathetic–cholinergic control of the developing heart becomes functional (15–17 weeks pc) before the sympathetic–adrenergic neural control (23–28 weeks pc). At first, adrenergic regulation of the heart is achieved by action of paraaortic chromaffin tissues (at 9–11 weeks pc; Phillippe, 1983), prior to sympathetic neural control. Furthermore, the cooperative action of the adrenal medulla does not become effective until later in fetal life.

Studies of intact "whole body" cardiovascular function among human fetuses have been undertaken using ultrasound techniques (DiPietro *et al.*, 1996). Fetal heart rates slow with increasing gestation, going from an average of 146.8 beats/min at 20 weeks pc to 140.0 beats/min at term. With increased gestational age there is also increased heart rate variability, coalescence of heart rate and movement patterns into distinct behavioral states, and increased responsiveness of heart rate to sensory stimulation. Power spectral analysis of human fetal heart rate (see Segar, 1997 for detailed review) indicates an increase in parasympathetic contribution to the control of resting fetal heart rate with maturation.

Enteric Nervous System

There have only been a few studies of development of the human enteric nervous system. In a study of the development of innervation of the human stomach, Abel *et al.* (1998) found that expression of neurotransmitters in the pylorus progressed from the adventitia toward the mucosa. Nerve fibers immunoreactive for PGP 9.5, a neuronal protein and marker of fine axons, and SP were found in the adventitia from 8 weeks pc, whereas VIP and neuronal nitric oxide synthase (nNOS) were not expressed until 11 and 13 weeks pc, respectively. In the mucosa and submucosa, SP, VIP, and nNOS appear somewhat later, with SP first detected in the submucosa at 11 weeks pc and mucosa at 23 weeks pc, VIP first detected in the submucosa at 12 weeks pc, and nNOS first detected in the mucosa at 15 weeks pc (Abel *et al.*, 1998). Those authors also reported a craniocaudal pattern of expression in the muscular layer, with the highest concentrations of peptides and nerve protein markers found toward the duodenum. An adult-like profile of innervation and expression of these markers was not attained until 23 weeks pc.

Pelvic Viscera Innervation

The pelvic plexus is first seen at about the middle of the seventh gestational week (Slabikowski *et al.*, 1996) as a group of nerve fibers and cells surrounding the rectum and genitourinary sinus. Pelvic splanchnic nerves arising from the second to fourth sacral segments appear coincidentally with the pelvic plexus.

The pelvic plexus forms a large plate lying on the lateral side of the rectum and genitourinary sinus and behind the bladder. Secondary plexuses (uterovaginal in females and inferior vesical in males) develop over the next 2 weeks. Sacral splanchnic nerves arising from the sympathetic trunk contribute to the pelvic plexus as early as 41 days pc.

Studies of the innervation of abdominal and pelvic organs in human fetuses have shown that the peripheral autonomic plexuses are diffusely ganglionated and that distinct nerves directed to certain organs cannot be identified (Baljet and Drukker, 1981). The peripheral distribution of the autonomic nervous system appears to be organized according to regions rather than specific organs. This means that within a given region individual organs will share their supply from a diverse autonomic plexus.

Cholinergic receptors in the detrusor muscle of the human urinary bladder appear quite early in fetal life (about 13 weeks pc), and slightly later in the sphincter vesicae (17–18 weeks pc) (Mitolo-Chieppa *et al.*, 1983). Spontaneous motility of the urinary bladder is quite high between 14 and 18 weeks pc and is progressively reduced to negligible levels by the end of the second trimester. Nerves immunoreactive for NPY form a dense plexus throughout the detrusor muscle coat by 17 weeks pc (Jen *et al.*, 1995a). Tyrosine hydroxylase and dopamine β-hydroxylase–immunoreactive fibers, indicative of sympathetic innervation, are first seen in the intramural portions of the ureters at 30 weeks pc and the detrusor muscle at 35 weeks pc (Jen *et al.*, 1995a). Sensory fibers, as revealed by staining for PGP 9.5, are first seen beneath the urinary bladder epithelium at 23 weeks pc. Responsiveness of the detrusor muscle to noradrenaline does not appear until the end of the second trimester, at which time noradrenaline begins to have contractile effects on the sphincter vesicae. Presumptive noradrenergic nerves appear relatively late in prenatal life and mainly supply the intramural ureters and superficial trigone (35 weeks pc; Jen *et al.*, 1995a).

In the developing male reproductive organs (Jen *et al.*, 1995b; Dixon and Jen, 1995), NOS-immunoreactive nerve fibers could be found in the prostate as early as 13 weeks pc, but NOS-immunoreactive fibers cannot be detected in the muscle coat of the ductus deferens and seminal vesicle until 23 weeks pc. Even at 30 weeks pc, they still form only a small proportion of intramuscular fibers in the seminal vesicle and ductus deferens. On the other hand, NOS-immunoreactive fibers contribute to the submucosal plexus of the bladder from 23 weeks pc. Those authors concluded that although NO may have an increasingly important role in the autonomic control of the lower urinary tract during fetal development, its involvement in the functional control of the fetal ductus deferens and seminal vesicle is probably minor. Studies of immunoreactivity to tyrosine hydroxylase, NPY, and enkephalin have shown that most intramuscular fibers in the fetal seminal vesicle and ductus deferens are noradrenergic in type (Jen *et al.*, 1995b). A subepithelial plexus developing in the ductus and seminal vesicle around 20 weeks pc contains abundant NPY, but not VIP, unlike the adult arrangement.

References

Abel, R.M., Bishop, A.E., Moscoso, G., Spitz, L., and Polak, J,M, (1998). The ontogeny and innervation of the human pylorus. *J. Paediatr. Surg.* **33,** 613–618.

Almqvist, P., Pschera, H., Samuelsson, E-B., Lunell, N-O., and Seiger, A. (1994). Morphology and growth of embryonic human dorsal root ganglion explants in long-term culture: expression of cell type-specific markers during early differentiation. *Expl. Neurol.* **125,** 1–14.

Altman, J., and Bayer, S.A. (1982). Development of the cranial nerve ganglia and related nuclei in the rat. *Adv. Anat. Embryol. Cell Biol.* **74,** 1–90.

Alvarez-Bolado, G., Schwarz, M., and Gruss, P. (1997). *Pax-2* in the chiasm. *Cell Tissue Res.* **290,** 197–200.

Ashton, N. (1970). Retinal angiogenesis in the human embryo. *Br. Med. Bull.* **26,** 103-106.

Baljet, B., Drukker, J. (1981). Some aspects of the innervation of the abdominal and pelvic organs in the human female fetus. *Acta Anat.* **111,** 222–230.

Becker, L.E., Zhang, W., and Pereyra, P.M. (1993). Delayed maturation of the vagus nerve in sudden infant death syndrome. *Acta Neuropathol.* **86,** 617–622.

Bodegard, G., Schwieler, G.H., Skoglund, S., and Zetterstrom, R. (1969). Control of respiration in newborn babies. I. The development of the Hering–Breuer inflation reflex. *Acta Paediatr. Scand.* **58,** 567–571.

Bossy, J. (1980). Development of olfactory and related structures in staged human embryos. *Anat. Embryol.* **161,** 225-236.

Braddock, S.R., Grafe, M.R., and Jones, K.L. (1995). Development of the olfactory nerve: its relationship to the craniofacies. *Teratology* **51,** 252–256.

Brown, J.W. (1990). Prenatal development of the human nucleus ambiguus during the embryonic and early fetal periods. *Am. J. Anat.* **189,** 267–283.

Bruska, M. (1986). Light and dark cells in the human embryonic trigeminal ganglion. *Folia Morphology (Warsz.).* **45,** 307–315.

Bruska, M. (1987). The trigeminal ganglion in human embryos at stage 15 (5th week). *Folia Morphol. (Warsz.).* **46,** 141–146.

Bruska, M. (1990). Ultrastructure of satellite cells of the trigeminal ganglion in human embryos during 6th, 7th and 8th week of development. *Folia Morphol. (Warsz.).* **49,** 1–2, 83–96.

Bruska, M. (1991a). Migration zone during the development of the trigeminal motor nucleus. Part I. Embryos at developmental stages 13 to 17. *Folia Morphol. (Warsz.).* **50,** 1–2.

Bruska, M. (1991b). Migration zone during the development of the trigeminal motor nucleus. Part II. Embryos at developmental stages 18 to 23. F*olia Morphol. (Warsz).* **50,** 119–125.

Bruska, M. (1992). Fine structure of the glial cells in the inferior ganglion of the vagus nerve in human embryos and fetuses. *Folia Morphol.* **51,** 129–149.

Bruska, M., and Wozniak, W. (1980). Ultrastructural studies on differentiation of nerve cells in the human embryonic and fetal inferior vagal ganglion of the vagus. *Anat. Anz.* **148,** 30–41.

Bruska, M., and Wozniak, W. (1989). The trigeminal ganglion in human embryos of stage 14 (approximately 32 postovulatory days). *Folia Morphol (Warsz.).* **48,** 89–95.

Bruska, M., and Wozniak, W. (1991). Ultrastructure of glial cells in the human fetal trigeminal ganglion. *Folia Morphol. (Warsz.).* **50,** 1–2.

Bruska, M., and Wozniak, W. (1994) Relation of the vestibular ganglion to the otocyst and cochlear ganglion in human embryos during 5th and 6th week of development. *Folia Morphol. (Warsz.).* **53,** 85–93.

Charnay, Y., Chayvialle, J.-A., Pradayrol, L., Bouvier, R., Paulin, C., and Dubois, P.M. (1987). Ontogeny of somatostatin-like immunoreactivity in the human fetus and infant spinal cord. *Dev. Brain Res.* **36,** 63–73.

Christensen, L.R., Janas, M.S., Mollgard, K., and Kjaer, I. (1993). An immunocytochemical study of the innervation of developing human fetal teeth using protein gene product 9.5 (PGP 9.5). *Oral Biol.* **38,** 1113–1120.

Chuah, M.I., and Zheng, D.R. (1987). Olfactory marker protein is present in olfactory receptor cells of human fetuses. *Neuroscience* **23,** 363–370.

Chuah, M.I., and Zheng, D.R. (1992). The human primary olfactory pathway: fine structural and cytochemical aspects during development and in adults. *Microsc. Res. Techn.* **23,** 76–85.

Coltart, D.J., Spilker, B.A., and Meldrum, S.J. (1971). Development of autonomic neural responses in human heart. *Br. Heart J.* **33,** 612.

D'Amico-Martel, A., and Noden, D.M. (1980). An autoradiographic analysis of the development of the chick trigeminal ganglion. *J. Embryol. Exp. Morph.* **55,** 167–182.

Dattani, M.T., Martinez-Barbera, J-P., Thomas, P.Q., Brickman, J.H., Gupta, R., Martensson, I-L., Toresson, H., Fox, M., Wales, J.K.H., Hindmarsh, P.C., Krauss, S., Beddington, R.S.P, and Robinson, I.C.A.F. (1998). Mutations in the homeobox gene *HESX1/Hesx1* associated with septo-optic dysplasia in human and mouse. *Nat. Genet.* **19,** 125–133.

Davison, A.N., Duckett, S., and Oxberry, J.M. (1973). Correlative morphological and biochemical studies of the human fetal sciatic nerve. *Brain Res.* **58,** 327–342.

DiPietro, J.A., Hodgson, D.M., Costigan, D.M., Hilton, S.C., and Johnson, T.R.B. (1996). Fetal neurobehavioural development. *Child Devel.* **67,** 2553–2567.

Dixon, J.S., and Jen, P.Y.P. (1995). Development of nerves containing nitric oxide synthase in human male urogenital organs. *Br. J. Urol.* **76,** 719–725.

Doménech-Ratto, G. (1977). Development and peripheral innervation of the palatal muscles. *Acta Anat.* **97,** 4–14.

Espin-Ferra, J., Merida-Velasco, J.A., Garcia-Garcia, J.D., Sanchez-Montesinos, I., and Barranca-Zafra, R.J. (1991). Relationships between the parotid gland and the facial nerve during human development. *J. Dent. Res.* **70,** 1035–1040.

Favor, J., Sandulache, R., Neuhäuser-Klaus, A., Pretsch, W., Chatterjee, B., Senft, E., Wurst, W., Blanquet, V., Grimes, P., Spörle, R., and Schughart, K. (1996). The mouse *Pax2*^{1Neu} mutation is identical to a human *PAX2* mutation in a family with renal-coloboma syndrome and results in developmental defects of the brain, ear, eye and kidney. *Proc. Natl. Acad. Sci. U.S.A.* **93,** 13870–13875.

Fidzianska, A. (1976). Fine structure of human fetal nerve. *Polish Med. Sci. Hist. Bull.* **15,** 281–289.

Fitzgerald, J.E., and Windle, W.F. (1942). Some observations on early human fetal movements. *J. Comp. Neurol.* **76,** 159–167.

Fitzgibbon, T. (1997). The human fetal retinal nerve layer and optic nerve head: a DiI and DiA tracing study. *Vis. Neurosci.* **14,** 433–447.

Fritsch, H. (1989). Topography of the pelvic autonomic nerves in human fetuses between 21–29 weeks of gestation. *Anat. Embryol.* **180,** 57–64.

Gardner, E., and O'Rahilly, R. (1976). The nerve supply and conducting system of the human heart at the end of the embryonic period proper. *J. Anat.* **121,** 571–587.

Garriano, R.F., Iruela-Arispe, M.L., and Hendrickson, A.E. (1994). Vascular development in primate retina: comparison of laminar plexus formation in monkey and human. *Invest. Ophthalmol. Vis. Sci.* **35,** 3442–3455.

Gasser, R.F. (1967). The development of the facial nerve in man. *Ann. Otol. Rhinol. Laryngol.* **76,** 37–56.

Gavalas, A., Studer, M., Lumsden, A., Rijli, F.M., Krumlau, R., and Chambon, P. (1998). *Hoxa1* and *Hoxb1* synergize in patterning the hindbrain, cranial nerves and second pharyngeal arch. *Development* **125,** 1123–1136.

Gennser, G., and Nilsson, E. (1970). Response to adrenaline, acetylcholine, and change of contraction frequency in early human fetal hearts. *Experientia* **26,** 1105–1107.

Golub, D.M., Loyko, R.M., and Novikov, I.I. (1979). Development of reflexogenic zone innervation of the human cardiovascular system. *Anat. Anz.* **145,** 474–492.

Gordon, L., Polak, J.M., Moscoso, G.J., Smith, A., Kuhn, D.M., and Wharton, J. (1993). Development of the peptidergic innervation of human heart. *J. Anat.* **183,** 131–140.

Guthrie, S., and Lumsden, A. (1992). Motor neuron pathfinding following rhombomere reversals in the chick embryo hindbrain. *Development* **114,** 663–673.

Hamano, S., Goto, N., and Nara, T. (1988). Development of the human trigeminal nucleus. *Pediatr. Neurosci.* **14,** 230–235.

Hervonen, A. (1971). Development of catecholamine-storing cells in human fetal paraganglia and adrenal medulla. *Acta Physiol. Scand.* **S368,** 1–94.

Hervonen, A., and Kanerva, L. (1972). Cell types of human fetal superior cervical ganglion. *Z. Anat. Entwickl. Gesch.* **137.** 257–269.

Hogg, I.D. (1966) Observations of the development of the nucleus of Edinger–Westphal in man and albino rat. *J. Comp. Neurol.* **126,** 567–584.

Hooker, D. (1942). Fetal reflexes and instinctual processes. *Psychosom. Med.* **4,** 199–205.

Humphrey, T. (1952). The spinal tract of the trigeminal nerve in human embryos between 7.5 and 8.5 weeks of menstrual age and its relation to early fetal behaviour. *J. Comp. Neurol.* **97,** 143–210.

Humphrey, T., and Hooker, D. (1959). Double simultaneous stimulation of human fetuses and the anatomical patterns underlying the reflexes elicited. *J. Comp. Neurol.* **112,** 75–102.

Humphrey, T. (1968). The development of mouth opening and related reflexes involving the oral area of human fetuses. *Alabama J. Med. Sci.* **5,** 126–157.

Jeffrey, G., Evans, A., Albon, J., Duance, V., and Neal, J. (1995). The human optic nerve: fascicular organisation and connective tissue types along the extra-fascicular matrix. *Anat. Embryol.* **191,** 491–502.

Jen, P.Y.P., Dixon, J.S., and Gosling, J.A. (1995a). Immunohistochemical localization of neuromarkers and neuropeptides in human fetal and neonatal urinary bladder. *Br. J. Urol.* **75,** 230–235.

Jen, P.Y.P., Dixon, J.S., and Gosling, J.A. (1995b). Development of peptide-containing nerves in the human fetal vas deferens and seminal vesicle. *Br. J. Urol.* **75,** 378–385.

Johnson, E.W., Eller, P.M., and Jafek, B.W. (1995). Distribution of OMP-, PGP 9.5- and CaBP-like immunoreactive chemoreceptor

neurons in the developing human olfactory epithelium. *Anat. Embryol.* **191,** 311–317.
Kato, M., and Takashima, S. (1994). Immunohistochemical and morphometrical development of the dorsal root ganglion as a neural crest derivative: comparison with the fetal CNS. *Early Human Dev.* **38,** 81–90.
Kjaer, I., and Fischer Hansen, B. (1996). The human vomeronasal organ: prenatal developmental stages and distribution of luteinizing hormone-releasing hormone. *Eur. J. Oral Sci.* **104.** 34–40.
Koistinaho, J. (1991). Adrenergic nerve fibers in the human fetal sciatic nerve. *Acta Anat.* **140,** 369–372.
Lecanuet, J-P., and Schaal, B. (1996). Fetal sensory competencies. *Eur. J. Obst. Gynecol.* **68,** 1–23.
Leonard, M.E., Hutchins, G.M., and Moore G.W. (1983). Role of the vagus nerve and its recurrent laryngeal branch in the development of the human ductus arteriosus. *Am. J. Anat.* **167,** 313–327.
Liu, X., Ernfors, P., Wu, H., and Jaenisch, R. (1995). Sensory but not motor neuron deficits in mice lacking NT4 and BDNF. *Nature* **375,** 238–241.
Lukas, Z., Draber, P., Bucek, J., Dráberová, E., Viklicky, V., and Dolezel, S. (1993). Expression of phosphorylated high molecular weight neurofilament protein (NF-1) and vimentin in human developing dorsal root ganglia and spinal cord. *Histochemistry* **100,** 495–502.
Lumsden, A., and Keynes, R. (1989). Segmental patterns of neuronal development in the chick hindbrain. *Nature* **337,** 424–428.
Lutz, G. (1968). Die Entwicklung des Halssympathicus and des Nervus vertebralis. *Zeitschrift für Anatomie und Entwicklungsgeschichte* **127,** 187–200.
Magoon, E.H., and Robb, R.M. (1981). Development of myelin in human optic nerve and tract. A light and electron microscopic study. *Arch. Ophthalmol.* **99,** 655–670.
Marti, E., Gibson, S.J., Polak, J.M., Facer, P., Springall, D.R., van Aswegen, G., Aitchison, M., and Koltzenburg, M. (1987). Ontogeny of peptide- and amine-containing neurones in motor, sensory, and autonomic regions of rat and human spinal cord, dorsal root ganglia, and rat skin. *J. Comp. Neurol.* **266,** 332–359.
Milutinovic, B., Gudovic, R., and Malesevic, J. (1992). Regressional changes of human cerebellar cortex and hypoglossal nucleus during development. *J. Hirnforsch.* **33,** 357–360.
Mitolo-Chieppa, D., Schönauer, S., Grasso, G., Cicinelli, E., and Carratu, M.R. (1983). Ontogenesis of autonomic receptors in detrusor muscle and bladder sphincter of human fetus. *Invest. Urol.* **21,** 599–603.
Moore, J.K., Simmons, D.D., and Guan, Y-L. (1999). The human olivocochlear system: organization and development. *Audiol. Neurootol.* **4,** 311–325.
Müller, F., O'Rahilly, R., and Tucker, J.A. (1981). The human larynx at the end of the embryonic period proper. I. The laryngeal and infrahyoid muscles and their innervation. *Acta Otolaryngol.* **91,** 323–336.
Müller, F., O'Rahilly, R., and Tucker, J.A. (1985). The human larynx at the end of the embryonic period proper. 2. The laryngeal cavity and the innervation of its lining. *Ann. Otol. Rhinol. Laryngol.* **94,** 607–617.
Mustafa, G.Y., and Gamble, H.J. (1978). Observations on the development of the connective tissues of developing human nerve. *J. Anat.* **127,** 141–155.
Nag, T.C., and Wadhwa, S. (1997). Expression of GABA in the fetal, postnatal and adult human retinas. *Vis. Neurosci.* **14,** 425–432.
Nara, T., Goto, N., and Yamaguchi, K. (1989). Development of the human hypoglossal nucleus: a morphometric study. *Dev. Neurosci.* **11,** 212–220.
Oelschläger, H.A., Buhl, E.H., and Dann, J.F. (1987). Development of the nervus terminalis in mammals including toothed whales and humans. *Ann. New York Acad. Sci.* **519,** 447–464.
Olszewska, B., Wozniak, W., Gardner, E., and O'Rahilly, R. (1979). Types of neural cells in the spinal ganglia of human embryos and early fetuses. *Z. mikrosk. Anat. Forsch.* **93,** 1182–1199.
O'Rahilly, R., and Gardner, E. (1971). The timing and sequence of events in the development of the human nervous system during the embryonic period proper. *Z. Anat. Entwickl.-Gesch.* **134,** 1–12.
O'Rahilly, R. (1975). The prenatal development of the human eye. *Exp. Eye Res.* **21:** 93–112.
O'Rahilly, R., and Gardner, R., (1975). The timing and sequence of events in the development of the limbs in the human embryo. *Anat. Embryol.* **148,** 1–23.
O'Rahilly, R., and Müller, F. (1984). The early development of the hypoglossal nerve and occipital somites in staged human embryos. *Am. J. Anat.* **169,** 237–257.
O'Rahilly, R., Muller, F., Hutchins, G.M., and Moore, G.W. (1984). Computer ranking of the sequence of appearance of 100 features of the brain and related structures in staged human embryos during the first 5 weeks of development. *Am. J. Anat.* **171,** 243–257.
Ortmann, R. (1989). Über Sinneszellen am fetalen vomeronasalen Organ des Menschen. *HNO* **37,** 191–197.
Papp, J.G. (1988). Autonomic responses and neurohumoral control in the human antenatal heart. *Basic Res. Cardiol.* **83,** 2–9.
Pearson, A.A. (1938). The spinal accessory nerve in human embryos. *J. Comp. Neurol.* **68,** 243–266.
Pearson, A.A. (1941). The development of the nervus terminalis in man. *J. Comp. Neurol.* **75,** 39–66.
Pearson, A.A., and Sauter, R.W. (1971). Observations on the phrenic nerves and the ductus venosus in human embryos and fetuses. *Am. J. Obstet. Gynecol.* **110,** 560–565.
Pearson, A.P. (1977). The early innervation of the developing deciduous teeth. *J. Anat.* **123,** 563–577.
Penfold, P.L., Provis, J.M., Madigan, M.C., van Driel, D., and Billson, F.A. (1990). Angiogenesis in normal human retinal development: The involvement of astrocytes and macrophages. *Graefe Arch. Clin. Exp. Ophthalmol.* **228,** 255–263.
Pereyra, P.M., Zhang, W., Schmidt, M., and Becker, L.E. (1992). Development of myelinated and unmyelinated fibers of human vagus nerve during the first year of life. *J. Neurol. Sci.* **10,** 107–113.
Phillippe, M. (1983). Fetal catecholamines. *Am. J. Obstet. Gynecol.* **146,** 840–855.
Provis, J.M., van Driel, D, Billson, F.A., and Russell, P. (1985a). Development of the human retina: patterns and mechanisms of cell distribution and redistribution in the ganglion cell layer. *J. Comp. Neurol.* **233,** 429–451.
Provis, J.M., van Driel, D., Billson, F.A., and Russell, P. (1985b). Human fetal optic nerve: overproduction and elimination of retinal axons during development. *J. Comp. Neurol.* **238,** 92–100.
Provis, J.M., Diaz, C.M., and Penfold, P.L. (1996). Microglia in human retina: a heterogeneous population with distinct ontogenies. *Persp. Dev. Neurobiol.* **3,** 213–222.
Pyatkina, G.A. (1982). Development of the olfactory epithelium in man. *Z. Mikrosk. Anat. Forsch.* **96,** 361–372.
Quartu, M., Setzu, D., and Del Fiacco, M. (1996). Trk-like immunoreactivity in the human trigeminal ganglion and subnucleus caudalis. *Neuroreport,* **7,** 1013-–1019.
Robinson, S. R., Rapaport, D, H., and Stone J. (1985). Cell division in the developing cat retina occurs in two zones. *Brain Res.* **351,** 101–9.
Sachis, P.N., Armstrong, D.L., Becker, L.E., and Bryan, A.C. (1982). Myelination of the human vagus nerve from 24 weeks

postconceptional age to adolescence. *J. Neuropathol. Exp. Neurol.* **41,** 466–472.
Sataloff, R.T. (1990). Embryology of the facial nerve and its clinical applications. *Laryngoscope* **100,** 969–984.
Schaal, B., Marlier, L., and Soussignan, R. (1998). Olfactory function in the human fetus: evidence from selective neonatal responsiveness to the odor of amniotic fluid. *Behav. Neurosci.* **112,** 1438–1449.
Schwanzel-Fukuda, M., Morrell, J.I., and Pfaff, D.W. (1985). Ontogenesis of neurons producing luteinizing hormone-releasing hormone (LHRH) of the rat. *J. Comp. Neurol.* **238,** 348–364.
Segar, J.L. (1997). Ontogeny of the arterial and cardiopulmonary baroreflex during fetal and postnatal life. *Am. J. Physiol.* **273,** R457–R471.
Sensenig, E.C. (1957). The early development of the meninges of the spinal cord in human embryos. *Contr. Embryol. Carnegie Instn.* **34,** 145–157.
Shield, L.K., King, R.H.M., and Thomas, P.K. (1986). A morphometric study of human fetal sural nerve. *Acta Neuropathol.* **70,** 60–70.
Shinohara, H., Naora, H., Hashimoto, R., Hatta, H., and Tanaka, O. (1990). Development of the innervation pattern in the upper limb of staged human embryos. *Acta Anat.* **138,** 265–269.
Shvalev, V.N., and Sosunov, A.A. (1989). Electron microscopic study of cardiac ganglia in human fetuses. *J. Auton. Nerv. Syst.* **26,** 1–9.
Shvalev, V.N., Guski, H., Fernández-Britto, J.E., Sosunov, A.A., Pavlovich, E.R., Anikin, A.Yu., Zhuchova, N.I., and Kargina-Terentyeva, R.A. (1992). Neurohistochemical and electron microscopic investigations of pathological and age-related changes in the cardiovascular system. *Acta Histochem.* **42** Suppl., 345–352.
Skórzewska, A., Wozniak, W., and Bruska, M. (1994a). The development of the spinal accessory nerve in human embryos during the 5th week (stages 14 and 15). *Folia Morphol.* **53,** 177–184.
Skórzewska, A., Wozniak, W., and Bruska, M. (1994b). The spinal accessory nerve in human embryos at 6th week (stages 16 and 17). *Folia Morphol.* **53,** 239–248.
Slabikowski, A., Wozniak, W., and Bruska, M. (1996). Origin and topography of the pelvic nerves in human embryos and fetuses. *Folia Morphol.* **55,** 101–113.
Smit, B.J., Kok, J.H., de Vries, L.S., Dekker, F.W., and Ongerboer de Visser, B.W. (1999). Motor nerve conduction velocity in very preterm infants. *Muscle Nerve* **22,** 372–377.
Smith, R.B. (1970). Development of innervation of coronary arteries in human foetus up until 230 mm stage (mid-term). *Br. Heart J.* **32,** 108–113.
Smith, R.B. (1971a). The development of autonomic neurons in the human heart. *Anat. Anz.* **129,** 70–76.
Smith, R.B. (1971b). Observations on nerve cells in human, mammalian and avian cardiac ventricles. *Anat. Anz.* **129,** 436–444.
Streeter, G.L. (1905). The development of the cranial and spinal nerves in the occipital region of the human fetus. *Am. J. Anat.* **4,** 83–116.
Streeter, G.L. (1908). The peripheral nervous system in the human embryo at the end of the first month (10 mm). *Am. J. Anat.* **8,** 285–301.
Sturrock, R.R. (1975). A light and electron microscopic study of proliferation and maturation of fibrous astrocytes in the optic nerve of the human embryo. *J. Anat.* **119,** 223–234.
Sturrock, R.R. (1984). Microglia in the human embryonic optic nerve. *J. Anat.* **139,** 81–91.
Sturrock, R.R. (1987). Development of the meninges of the human embryonic optic nerve. *J. für Hirnforschung* **28,** 603–613.
Suburo, A.M., Gu, X.-H., Moscoso, G., Ross, A., Terenghi, G., and Polak, J.M. (1992). Developmental pattern and distribution of nerve growth factor low-affinity receptor immunoreactivity in human spinal cord and dorsal root ganglia: comparison with synaptophysin, neurofilament and neuropeptide immunoreactivities. *Neuroscience* **50,** 467–482.
Takayama, S., Yamamoto, M., Hashimoto, K., and Itoh, H. (1991). Immunohistochemical study on the developing optic nerves in human embryos and fetuses. *Brain Dev.* **13,** 307–312.
Tomé, F.M.S., Tegnér, R., and Chevallay, M. (1988). Varicosities in human fetal sciatic nerve fibers. N*europathol. Appl. Neurobiol.* **14,** 495–504.
Varendi, H., Porter, R.H., and Winberg, J. (1996). Attractiveness of amniotic fluid odor: evidence of prenatal olfactory learning? *Acta Paediatr.* **85,** 1223–1227.
Verney, C., El Amraoui, A., and Zecevic, N. (1996). Comigration of tyrosine hydroxylase- and gonadotrophin-releasing hormone-immunoreactive neurons in the nasal area of human embryos. *Dev. Brain Res.* **97,** 251–259.
Vij, S., and Kanagasuntheram, R. (1972). Development of the nerve supply to the human tongue. *Acta Anat.* **81,** 466–477.
Wadhwa, S., Rizvi, T.A., and Bijlani, V. (1988). Substance P-immunoreactivity in the developing human retinogeniculate pathway. *Neurosci. Lett.* **89,** 25–30.
Walker, D. (1975). Functional development of the autonomic innervation of the human fetal heart. *Biol. Neonate* **25,** 31–43.
Windle, W.F., and Fitzgerald, J.E. (1937). Development of the spinal reflex mechanism in human embryos. *J. Comp. Neurol.* **67,** 493–509.
Wozniak, W., Bruska, M., Olszewska-Jachimska, B., and Poroski, L. (1979). The development of the vagus nerve in human embryonic period proper. *Folia Morphol.* **28,** 141–156.
Wozniak, W., and O'Rahilly, R. (1981). Fine structure and myelination of the developing human vagus nerve. *Acta Anat.* **109,** 218–230.
Wozniak, W., O'Rahilly, R., and Bruska, M. (1982). Myelination of the human fetal phrenic nerve. *Acta Anat.* **112,** 281–296.
Yan, X-X. (1997). Prenatal development of calbindin D-28k and parvalbumin immunoreactivities in the human retina. *J. Comp. Neurol.* **377,** 565–576.
Yokoh, Y. (1968). The early development of the nervous system in man. *Acta Anat.,* **71,** 492–518.

CHAPTER

5

Peripheral Motor System

SIMON C. GANDEVIA and DAVID BURKE
Prince of Wales Medical Research Institute
University of New South Wales
and College of Health Sciences
The University of Sydney
Sydney, Australia

This chapter describes first the innervation of human muscle and then some features of muscle organization. Muscle is the largest sense organ in the body. It contains receptors responsive to mechanical deformation, to changes in temperature, to metabolites produced by muscle activity, and to injurious stimuli that evoke pain. In addition, the nerve to a muscle may carry the afferent innervation of the joints that the muscle crosses, of the underling bone and periosteum, and of any interosseous membrane. Of all the myelinated axons in a muscle nerve, less than 20% are motor axons from α motoneurons that innervate extrafusal muscle fibers and so produce muscle contraction (Barker, 1974; see also Shoenen and Faull, Chapter 7). Cutaneous receptors are not considered part of the motor system and therefore will not be discussed at length in this chapter, even though the feedback from cutaneous receptors may be as important as that from muscle receptors in the control of movement, particularly for the upper limb. A comprehensive description of cutaneous receptors and the central somatosensory system is given by Kaas (Chapter 28).

COMPOSITION OF MUSCLE NERVES

Lloyd and Chang (1948) classified the afferent fibers coming from feline muscles into four groups based on fiber size (Table 5.1): group I, large myelinated afferents, 12–20 μm in diameter (conduction velocity range 72–120 m/s); group II, medium-sized, 6–12 μm (36–72 m/s); group III, small 1–6 μm (6–36 m/s); and group IV, unmyelinated, approximately 1 μm (0.5–2 m/s). On the assumption of a linear relationship between size and conduction velocity for myelinated axons (constant: 6; Hursh, 1939), the conduction velocities given in parentheses above are widely used to identify the group to which a particular myelinated afferent belongs. However, many workers have questioned the generality of a single scaling factor, and Boyd and Kalu (1979) recommended 5.7 for group I afferents and 4.6 for groups II and III in the cat.

The situation is further complicated by the adoption of a different size-based nomenclature for cutaneous afferents, namely, Aβ and Aδ for myelinated afferents (from mainly tactile mechanoreceptors, and from cold receptors and nociceptors, respectively) and C for unmyelinated afferents (mainly from warmth receptors and nociceptors). In the cat, the largest cutaneous afferents have conduction velocities that overlap the group II muscle afferent range. Because the threshold for activation of an afferent by an external electrical

TABLE 5.1 Afferent Nerve Fiber: Function Correlations in the Cat

Afferent	Size (μm)	Conduction velocity (m/s)	Receptor
Ia Ib	12–20	72–120	Primary spindle endings; Golgi tendon organs
II	6–12	36–72	Secondary spindle endings; Pacinian/Paciniform corpuscles; free nerve endings
III	1–6	6–36	Pacinian/Paciniform corpuscles; free nerve endings
IV	1[a]	0.5–2	Free nerve endings

[a]Unmyelinated nerve fiber.

Note that conduction velocities for comparable afferent classes are slower in human than cat axons.

TABLE 5.2 Efferent Nerve Fiber: Function Correlations in the Cat

Efferent	Size (μm)	Conduction velocity (m/s)	Function
α	10–20	55–110	Skeletomotor
β	10–20	55–110	Skeletofusimotor
γ	2–8	<50	Fusimotor
Sympathetic	1[a]	0.5–2	Vasculature

[a]Unmyelinated nerve fiber.

Note that conduction velocities for α axons are slower in humans than in the cat.

stimulus depends on axonal diameter, it is possible in the cat to activate group I afferents selectively with weak stimuli delivered to a muscle nerve or to a mixed nerve that innervates skin and muscle.

There are limited data for human muscle afferents. However, certain cutaneous nerves can be biopsied in humans producing only minor and usually transient deficits; therefore, more data are available for human cutaneous afferents. In the radial nerve, histograms of the sizes of myelinated cutaneous afferents have clear peaks at 4–5 and 10.5–12 μm, with the largest fibers 14.0–16.0 μm in diameter (O'Sullivan and Swallow, 1968; Tackmann *et al.*, 1976). The ratio of conduction velocity to axonal diameter is 4.67 for the fastest axons (Tackmann *et al.*, 1976). A comparable bimodal distribution is seen in histograms of myelinated fiber size for cutaneous afferents in the sural nerve: peaks at 3.5–4.5 and 9.0–11.5 μm, with the largest fibers 12.5–15.0 μm in diameter (Swallow, 1966), and with a velocity: diameter ratio of 4.55 (Tackmann *et al.*, 1976).

In biopsied human spindle preparations, Swash and Fox (1972) reported group I and II muscle afferents to be of comparable diameter to those measured at equivalent sites in the cat, but Cooper and Daniel (1963) considered them to be slightly smaller. However, measurements made on major stem axons before they taper are necessary to determine axonal size. This issue is of some importance because human group I afferents have slower conduction velocities than those of the cat, and equality of size would imply a different velocity: diameter ratio. For example, in the human upper limb, the fastest muscle afferents, presumably group I, have the same conduction velocity as the fastest cutaneous afferents, i.e., up to about 70 m/s (Gandevia *et al.*, 1984). In the human lower limb, the group I muscle afferents differ little in conduction velocity from the fastest cutaneous afferents (Burke *et al.*, 1981; Gandevia *et al.*, 1983; Macefield *et al.*, 1989; Shefner and Logigian, 1994). There are no data on the range of conduction velocities for the three groups of myelinated fibers or on the degree of overlap between groups, but it has been estimated that the fastest group II muscle afferents have conduction velocities of 45–50 m/s (Simonetta-Moreau *et al.*, 1999).

Unmyelinated group IV muscle affarents probably have the same velocities as unmyelinated sympathetic efferents, namely, 0.5–2 m/s. Given the longer conduction pathways and the slower afferent conduction velocities of myelinated fibers in humans, the role of afferent feedback in modulating movement may differ in cats and humans.

The efferent fibers in muscle nerve are conventionally divided into three groups based on size and function (Table 5.2): large myelinated α efferents from the α motoneurons in the anterior horn of the spinal cord, innervating the contractile bulk of the muscle (hence "skeletomotor," motor to skeletal muscle); small myelinated γ efferents from γ motoneurons, innervating the modified muscle fibers inside the muscle spindle (hence "fusimotor," motor to the fusiform receptor); and unmyelinated sympathetic efferents innervating intramuscular blood vessels. For α efferents, axonal size and conduction velocity are correlated with motoneuron properties (size, input resistance, and recruitment threshold) and with motor unit/muscle fiber properties (twitch time and strength, fatigability and histochemical profile), as detailed in "Features of Muscle" and "Muscle Units and Motor Units." In limb nerves of the cat, α efferents have diameters of approximately 10–20 μm and conduction velocities of 55–110 m/s. Few human α efferents conduct faster than 50–60 m/s, the values for the upper limb, generally being about 10 m/s faster than those for the lower limb, much as for afferent axons. Based on indirect estimates,

the majority of human α efferents conduct at a rate of over 80–85% of the maximal conduction speed. The slowest fibers may have velocities down to 60–65% of the maximum (Thomas *et al.*, 1959). Small myelinated γ efferents have diameters of approximately 2–8 μm and conduction velocities of less than 50 m/s in the cat. In humans, γ efferents are likely to conduct at less than 25–30 m/s. There is a further group of efferents, called β efferents, that innervate both the main contractile muscle (as do α efferents) and the muscle spindle (as do γ efferents). The size and conduction velocities of these β axons fall within the α range and their function is termed "skeletofusimotor." In biopsied human spindles, both large and small myelinated efferent fibers, presumably β and α axons, respectively, have been demonstrated entering the spindle (Swash and Fox, 1972).

MUSCLE RECEPTORS

The literature on mammalian muscle receptors is derived mainly from the cat, though there are some data for the muscle spindle and the Golgi tendon organ from nonhuman primates and humans. The most common receptor in muscle is the free nerve ending (Abrahams, 1986; Stacey, 1969). The most studied are the muscle spindle and tendon organs, although their afferents comprise only about 20% of the afferents coming from muscle. A number of other receptors occur in association with ligaments, joint capsules, and extramuscular tissue. With the exception of pacinian and paciniform corpuscles, discussed in "Pacinian and Paciniform Corpuscles," these extramuscular receptors will not be considered in this chapter because their physiological roles are, at present, uncertain. The interested reader should consult Barker (1974). Figures 5.1 illustrates the muscle receptors considered in this chapter and their innervation in cat muscle.

Muscle Spindle

More work has been done on muscle spindles than on any other muscle receptor. There are enough data for human and monkey spindles, not only to confirm the essential features found in the cat (see Barker, 1974; Barker and Banks, 1986; Boyd and Gladden, 1985; Cheney and Preston, 1976; Matthews, 1972) but also to establish differences. The reported differences include:

- The ratio of spindle length to muscle length is higher in cat than human spindles.
- There are more connective tissue connections between extrafusal muscle and human spindles.
- There are more intrafusal fibers in human spindles.
- The primary ending terminals on human chain fibers are scanty.
- There is nonselective γ innervation of intrafusal fibers in humans and monkeys.
- The unmyelinated terminal segment of human and monkey γ efferents is longer than in the cat.
- Afferent and efferent axons may be of similar sizes, but conduction velocities are slower for human axons.

However, the structure and function of the spindle have been a subject of debate since spindles were first recognized over 100 years ago, and such is the changing state of knowledge (see Barker and Banks, 1986; Boyd and Gladden, 1985) that older texts may contain inaccuracies.

As in the cat (Fig. 5.1), the human muscle spindle is a fusiform structure of some 7–10 mm in length, significantly shorter than the ordinary muscle fibers (so-called 'extrafusal' muscle fibers because they are outside the fusiform receptor), with which they lie in parallel. Human spindles are slightly larger than cat spindles (Cooper and Daniel, 1963) but, given the much greater size of human muscles, the relative size of human spindles is quite small, and direct or indirect attachment to extrafusal muscle rather than tendon must be more common. Human muscle spindles contain 2–14 "intrafusal" muscle fibers (Cooper and Daniel, 1963; Kennedy, 1970; Kucera and Dorovini-Zis, 1979; Swash and Fox, 1972), which is, on average, slightly more than in the cat. In the longest, the nuclei are clustered together at the equatorial region of the fibers (hence, nuclear bag fibers); in the shortest, the nuclei form a single chain along the middle portion of the fibers (hence, nuclear chain fibers). A lamellated fibrous capsule encloses the middle third of the spindle and has its greatest diameter (some 200–300 μm) at the equatorial region, where the capsule dilates to enclose a fusiform fluid-filled space (Fig. 5.1). The nuclear bag fibers and the long-chain fibers (if present) project from the capsular investment at the spindle poles before inserting onto extrafusal connective tissue, the endomysium of extrafusal fibers, or tendon. There are more connective tissue interconnections between human spindles and adjacent extrafusal muscle fibers than in cats, and occasionally the human spindle capsule encloses neighboring extrafusal fibers (Cooper and Daniel, 1963; Kennedy, 1970; Kucera and Dorovini-Zis, 1979; Sahgal and Subramani, 1986), a finding that would allow extrafusal contraction to affect muscle spindle activity more frequently than in the cat, a view

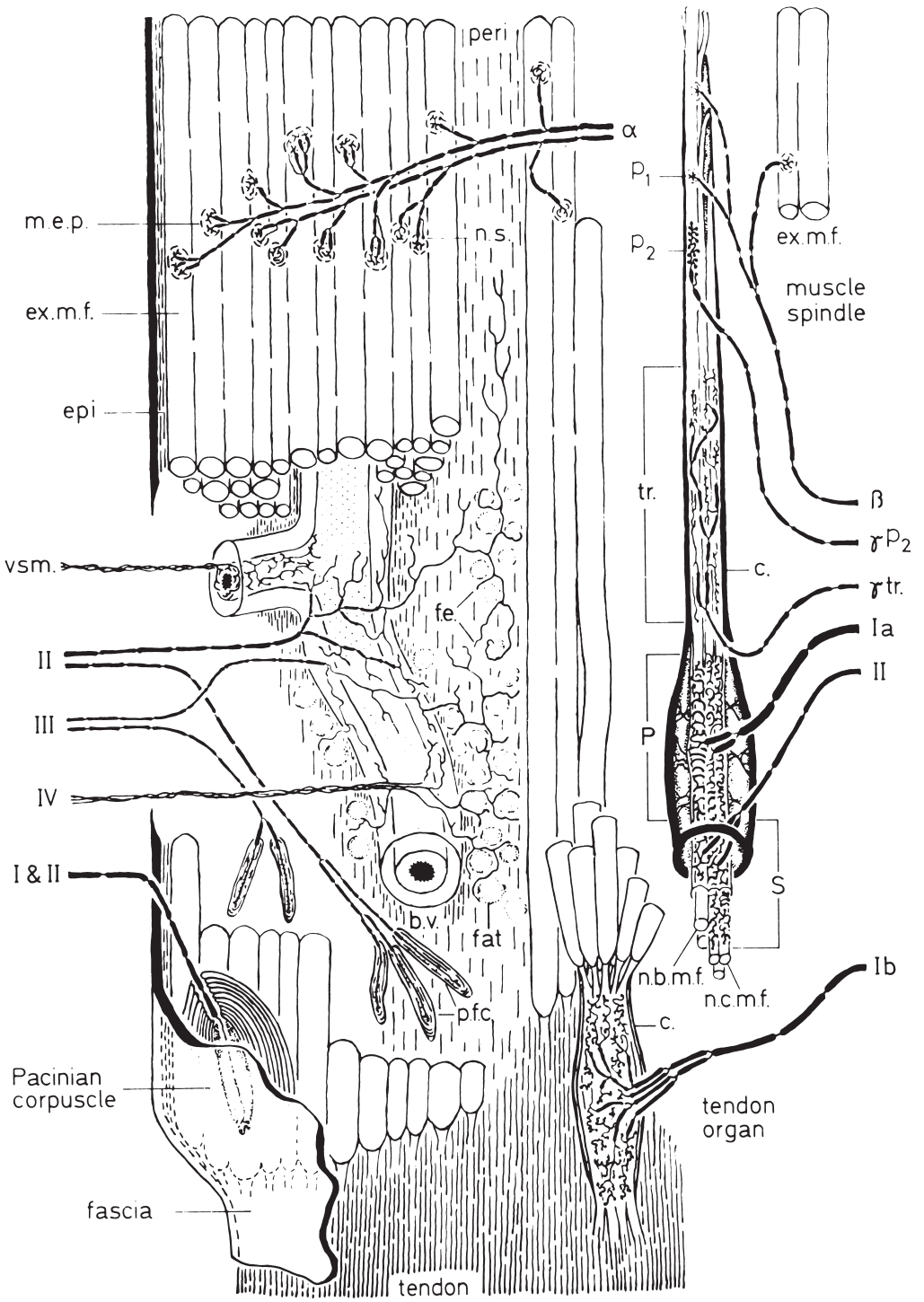

FIGURE 5.1 Innervation of mammalian skeletal muscle based on a study of cat hindlimb muscles. Those nerve fibers shown on the right of the diagram are exclusively concerned with muscle innervation; those on the left also take part in the innervation of other tissues. Roman numerals refer to the groups of myelinated (I, II, III) and nonmyelinated (IV) sensory fibers; Greek letters refer to motor fibers. The spindle pole is cut short to about half its length, and the extracapsular portion is omitted. B. v., Blood vessel; c., capsule; epi., epimysium; ex.m.f., extrafusal muscle fibers; f.e., free nerve endings; m.e.p., motor endplate; n.b.m.f., nuclear bag muscle fiber; n.c.m.f., nuclear chain muscle fiber; n.s., nodal sprout; p, primary ending; P_1, P_2, two types of intrafusal endplates; peri., perimysium; p.f.c., paciniform corpuscle; S, secondary ending; tr., trail ending; vsm., vasomotor fibers. Reproduced with permission from Barker (1974). See Barker and Banks (1986) for a detailed diagram of spindle structure.

for which there is physiological evidence (Burke *et al.*, 1987). In human muscles, it is common to find several spindles arranged in tandem, with nuclear bag fibers extending through both spindles, and there may be other complex forms such as two spindles sharing a common capsule (Cooper and Daniel, 1963; Kennedy, 1970; Swash and Fox, 1972).

Distribution

Virtually all human skeletal muscles contain spindles, except for facial muscles and the digastric, a jaw-opening muscle (Kubota and Masegi, 1977). Spindles are spread unevenly throughout both mono- and multiarticular muscles, following the distribution of the major intramuscular nerve branches (Barker and Chin, 1960; Swett and Eldred, 1960). In some cat muscles, more spindles are found along the line of pull of the tendon, in association with a greater concentration of slow-twitch motor units (Botterman *et al.*, 1978; see also Yellin, 1969). Small muscles tend to have shorter spindles; for example, 70% of spindles in the intrinsic muscles of the human hand (lumbricals) measure 1–3 mm (Voss, 1937). Because of their different anatomical locations, spindles in any one muscle are not subjected to an identical disturbance during active or passive movement, and each sends a slightly different message to the nervous system (Meyer-Lohman *et al.*, 1974; see also Binder and Stuart, 1980; Scott and Loeb, 1994). However, the summed activity of all spindles in a muscle reflects overall muscle length quite accurately, at least under passive conditions (Vallbo, 1974).

Spindle counts have been done for many human muscles (e.g., Voss, 1971). In absolute terms, counts range from less than 50 for some intrinsic muscles of the hand (Table 5.3) to 1350 for the quadriceps femoris. When muscle size is taken into account, spindle density is highest in the intrinsic muscles of the hand and muscles of the neck, and lowest in muscles of the thigh and shoulder. However, the functionally important expression of spindle numbers may be neither absolute count nor density. Larger muscles tend to have larger motor units. In view of suggestions that muscle spindles can act as monitors of the minute length changes produced by the activity of nearby motor units (for cats, Binder and Stuart, 1980; Windhorst, 1979; for humans, McKeon and Burke, 1983), a more appropriate scaling factor might be the number of motor units in the particular muscle. Table 5.3 shows that the number of muscle spindles per motor unit is not greater in the intrinsic muscles of the hand than in other limb muscles. This conclusion is consistent with the finding that kinesthetic acuity for passive movement detection (expressed in "muscle" terms) may be no greater for the distal joints of the hand than for the elbow joint (Hall and McCloskey, 1983; Refshauge *et al.*, 1995).

Intrafusal Muscle Fibers

Originally, only two types of intrafusal fiber (nuclear bag and nuclear chain) were recognized in cat and human spindles (cat, Barker, 1974; Matthews, 1972; human, Cooper and Daniel, 1963; Kennedy, 1970; Swash and Fox, 1972), but there is now anatomical and physiological evidence that there are two types of nuclear bag fiber in the cat (Baker and Banks, 1986; Boyd, 1986; Boyd and Gladden, 1985), and this has been confirmed anatomically for human spindles (Kucera and Dorovini-Zis, 1979). The bag_2 fiber tends to be thicker and longer, and to contain more nuclei than bag_1 fiber (Kucera and Dorovini-Zis, 1979). Other

TABLE 5.3 Counts for Human Muscles of Motor Units, Muscle Spindles, and Muscle Fibers[a]

Muscle	Motor units	Spindles	Spindles/motor unit	Muscle fiber/motor unit[b]
Biceps brachii	774	320	0.41	750 (209)
Brachioradialis	330	65	0.20	390
First dorsal interosseous	119	34	0.29	340
First lumbrical	98	53	0.54	110
Opponens pollicis	133	44	0.33	595
Masseter	1020	160	0.16	980
Temporalis	1150	217	0.19	1300
Medial gastrocnemius	580	80	0.14	1720
Tibialis anterior	445	284	0.64	610 (329)

[a]Data from Buchthal and Schmalbruch (1980) and Gath and Stålberg (1981).
[b]The values in parentheses for biceps brachii and tibialis anterior denote the estimated number of fibers per motor unit using direct electrophysiological (rather than anatomical) techniques.

ultrastructural features may help distinguish bag_1 and bag_2 fibers in cat (Gladden, 1976), monkey (Kucera, 1985a), and human spindles (Kucera and Dorovini-Zis, 1979), including the abundance of elastic fibers associated with bag_2 fibers and the scarcity with bag_1 fibers (Gladden, 1976). The three types of intrafusal fiber are also histochemically different and can be differentiated by the intensity of their staining for myosin ATPase, under acidic and alkaline conditions (Barker, 1974; Harriman *et al.*, 1974; Kucera and Dorovini-Zis, 1979; Ovalle and Smith, 1972).

Of the 2–14 intrafusal fibers in human muscle spindles, there are 1–4 nuclear bag fibers (always one or more bag fibers, usually one bag_1 fiber) of diameter 20–30 μm, and 3–10 nuclear chain fibers of diameter 9–12 μm. At the equator the diameter of intrafusal fibers decreases. The diameter of chain fibers becomes little more than that of a single nucleus and the myofibril content of the fibers is greatly reduced. the 50–100 nuclei in bag fibers extend over a length of 50–100 μm and, in human spindles, may be 5–6 abreast (Cooper and Daniel, 1963; Kennedy, 1970). The chain fibers contain a single strand of some 20–50 nuclei. For further morphological and for ultrastructural details the reader is referred to Kucera and Dorovini-Zis (1979) and Barker and Banks (1986). Physiological studies have shown that the dynamic response of deefferented spindle afferents comes from sensory endings on the bag_2 fiber and that static responses come from sensory endings on chain fibers (Boyd and Gladden, 1985; Proske *et al.*, 1991; Scott, 1991; see also Proske, 1997). However, the increase in the dynamic response to stretch produced by fusimotor action is mediated by activation of bag_1 fibers. The background firing rate of primary endings is controlled predominantly via the bag_2 fiber (Proske *et al.*, 1991).

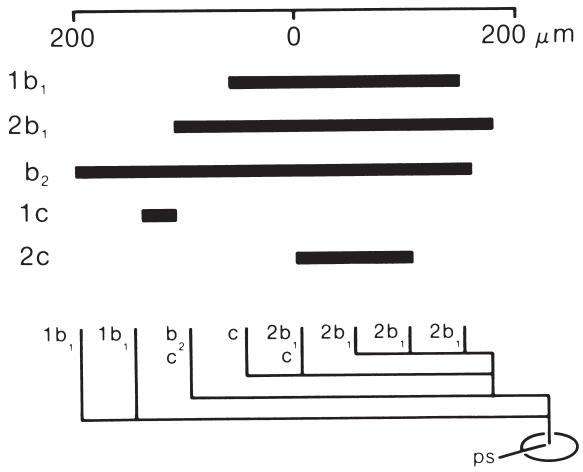

FIGURE 5.2 The extent of primary sensory contact areas *(solid horizontal bars)* for a human spindle containing two bag_1 (b_1), one bag_2 (b_2), and four chain (c) fibers. Distribution of the myelinated branches of a single Ia afferent fiber (ps) to the three types of intrafusal fiber is indicated. Reconstructed from serial, 1-μm-thick transverse sections stained with toluidine blue. Scale in micrometers, with the center of the equator at zero. Note that two of the four chain fibers received no primary ending terminals and that the contact area on bag fibers was much greater than for chain fibers. Reproduced with permission from Kucera (1986).

Sensory Innervation

Each muscle spindle receives one large myelinated (group Ia) afferent and 1–5 smaller myelinated (group II) afferents, forming a single nerve bundle that penetrates the capsule near the midequatorial region. The nerve bundle also contains some γ efferent axons which innervate the intrafusal muscle fibers. The group Ia afferent branches 2–4 times and becomes unmyelinated only 25–30 μm before its sensory terminals wrap around and indent the intrafusal fibers to form the primary ending (Kennedy *et al.*, 1975; Swash and Fox, 1972). In human but not in cat spindles, the primary ending formed by the Ia afferent is well developed only on nuclear bag fibers (Kucera, 1986; Swash and Fox, 1972). Figures 5.2 illustrates the extent of innervation by a group Ia afferent of a human muscle spindle containing seven intrafusal fibers (two bag_1, one bag_2, and four chain). The γ efferent innervation of this spindle is illustrated in Figure 5.3. Only two of the four chain fibers received Ia terminals, and the contact area between terminals and the chain fibers was much smaller than for the three bag fibers. In cat spindles, the primary ending formed by the Ia afferent classically resembles a tightly coiled spring with a number of spirals, but in human spindles there is only a single or double spiral (Swash and Fox, 1972), a number of loops instead of spirals (Kennedy, 1970), or an irregular coil with branches and varicose swellings (Cooper and Daniel, 1963; Kennedy *et al.*, 1975). The fine structure and microfilament content of the human primary ending have been described in detail by Kennedy and colleagues (1974, 1975). Local mechanical and electrical pacemaker interactions influence the output from primary spindle endings (e.g., Banks *et al.*, 1997).

Group II afferents innervate secondary endings located in the juxtaequatorial regions of predominantly the nuclear chain fibers, which are usually more extensively developed on one side of the equator. Spindles receive 1–5 group II afferents, although some human spindles appear to be devoid of secondary endings and group II innervation (Cooper and Daniel, 1963; Kucera, 1986; Swash and Fox, 1972). If there are two secondary endings on a chain fiber, they are usually

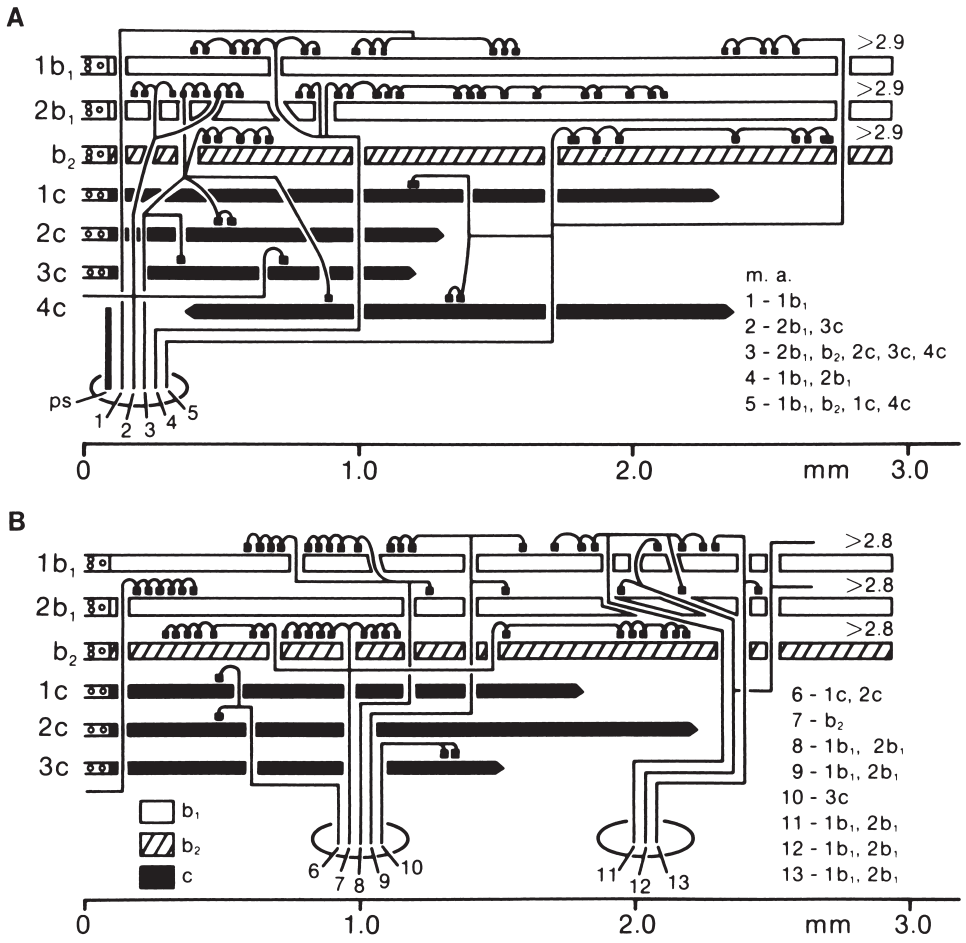

FIGURE 5.3 Representation of the nerve supply to the **(A)** proximal and **(B)** distal poles of the same human spindle as in Fig. 5.2. Equators of bag_1 (b_1), bag_2 (b_2), and chain (1*c*-4*c*) intrafusal fibers are shown on the left. Numbers at the ends of intrafusal fibers denote length of pole in millimeters. Thirteen motor axons (m. a.), all γ efferents, approached the spindle in three nerve bundles and branched to terminate in motor endings *(solid bars)* on the intrafusal fibers. The branching pattern of the single Ia afferent (ps) supplying the spindle is shown in Fig. 5.2. Reproduced with permission from Kucera (1986).

innervated by different group II afferents. Much as in the cat (Barker, 1974), secondary endings may be spiral, somewhat similar to the primary ending (Swash and fox, 1972), or have a classical "flower spray" appearance with interlacing varicose terminals (Kennedy, 1970; Swash and Fox, 1972).

Efferent Innervation

Much as in other mammals, human spindle endings are innervated by small thinly myelinated γ efferents, which enter the spindle in three discrete nerve bundles at the equatorial and midpolar positions (Kucera, 1986; Swash and Fox, 1972). There may be 8–15 γ efferents innervating any one spindle in the cat (Barker, 1974), monkey (Kucera, 1985a), or human subject (Kucera, 1986). The efferents typically lose their myelin sheath just prior to the motor ending in cat spindles, but at considerably greater distances, often several hundred micrometers, in human and monkey spindles (Kucera, 1985a, 1986). In addition, a thickly myelinated, presumably β-efferent axon may accompany the more profuse γ efferents (Swash and Fox, 1972). That γ efferents innervate only muscle spindles and are therefore exclusively fusimotor is well established. The full extent of β innervation of primate spindles has not yet been established. However, in the cat, physiological studies have demonstrated β innervation of 20–30% spindles (Emonet-Dénand *et al.*, 1980), with greater β innervation in small muscles where more than 50% of

spindles receive it (Jami *et al.*, 1982; McWilliam, 1975; Scott *et al.*, 1995).

There are no exclusively fusimotor efferents of α size (Ellaway *et al.*, 1972), suggesting that a large myelinated efferent entering a spindle is likely to be the fusimotor branch of a β (skeletofusimotor) efferent. In the monkey, Kucera (1985a) found that 4 whole spindles and 16 half-spindles (i.e., 24 spindle poles) from the lumbrical muscles were innervated by 37 γ axons and 18 β axons. It seems that whether a spindle receives β innervation depends on its location in the muscle: "the major determinant … may be proximity of the spindle to the innervation zone of extrafusal muscle fibers" (Kucera, 1985b), an association that is more likely to occur in small muscles.

In the cat, the fusimotor innervation of intrafusal muscle is reasonably selective. The γ efferents that innervate the bag_1 fiber rarely innervate bag_2 and chain fibers, and hence have a predominantly dynamic effect on the sensitivity of the primary ending (Boyd and Gladden, 1985). The γ efferents innervating bag_2 and chain fibers have a predominantly static γ action. Boyd (1986) suggested that there are two types of static axons, those innervating chain fibers and those innervating bag_2 fibers, each with a distinctly different effect on afferent discharge, and potentially different central control. The selectivity and subdivision of γ innervation of bag_2 and chain fibers in cat spindles is, however, debated by other authorities (Banks *et al.*, 1985) and may be largely random (Celichowski *et al.*, 1994). The β axons innervate either the bag_1 fiber, thereby having a dynamic action, or the long-chain fiber (should there be one in the spindle), thereby having a static action. The β axons that innervate the bag_1 fiber have conduction velocities in the slow α range, and innervate extrafusal muscle of the SO type (i.e., slow contracting, rich in oxidative enzymes; see Table 5.5 and "Classification and Properties of Motor Units"). The β axons innervating the long-chain fiber have faster conduction velocities and innervate extrafusal muscle of the FOG type (i.e., fast contracting, rich in oxidative and glycolytic enzymes) or, more rarely, the FG type (i.e., fast contracting, rich in glycolytic enzymes).

In monkey and possibly human spindles, the selectivity of γ-efferent innervation is less than in the cat (Kucera, 1985a, 1986), and individual axons may innervate bag_1, bag_2, and chain fibers or any combination thereof. For the human spindle illustrated in Figure 5.3, Kucera (1986) identified 13 γ efferents, of which 7 innervated only the 2 bag_1 fibers. Of 3 axons to the bag_2 fiber, 2 also innervated bag_1 and chain fibers. Of the 5 axons to chain fibers, 2 innervated only the chain fibers, the remaining 3 also each innervated a bag_1 fiber. The β innervation of monkey spindles has been demonstrated anatomically (Kucera, 1985b; Murthy *et al.*, 1982). There is suggestive anatomical (Kennedy, 1970; Kucera and Dorovini-Zis, 1979; Swash and Fox, 1972) and physiological (Aniss *et al.*, 1988; Rothwell *et al.*, 1990; Kakuda *et al.*, 1998) evidence for β innervation of human spindles. The anatomical evidence rests on the presence of a large myelinated axon entering the spindle in the polar bundle of nerve fibers and on the common finding of P_1 plate endings on intrafusal fibers. These latter are morphologically identical to endplates on extrafusal fibers and have been considered evidence of β innervation (Barker, 1974; however, see next paragraph). In the monkey the distribution of β axons is selective, with separate β axons innervating the bag_1, bag_2 and chain fibers (Kucera, 1985b). Selective β innervation also occurs in the cat, but it has no β innervation of bag_2 fibers. Hence, in primate spindles, selective innervation of intrafusal fibers may be a feature of the β innervation, but it is not a feature of the γ innervation.

The motor endplates on intrafusal muscle of cat, monkey and human spindles are morphologically of three different types, described as P_1 plates, P_2 plates, and trail endings (Barker, 1974; see also Kennedy, 1970; Kucera and Dorovini-zis, 1979; Swash and Fox, 1972). It has generally been considered that the morphology of the ending was evidence of innervation by a particular efferent (Barker, 1974). The P_1 plate, morphologically identical to endplates on extrafusal muscle fibers, was considered evidence of β innervation; the P_2 plate was considered the termination of dynamic γ axons on bag_1 fibers; and the trail ending the termination of static γ axons on bag_2 and chain fibers. Subsequent studies have both supported (Banks *et al.*, 1985) and challenged (Kucera and Walro, 1986) these concepts. However, both studies agree that factors other than the type of innervating efferent axon are important determinants of endplate morphology. These include the type of intrafusal fiber and the distance of the endplate from the spindle's equator (γ endplates are usually intracapsular, β endplates usually extracapsular). Predictions of motor axon type from endplate morphology are potentially erroneous (Kucera and Walro, 1986).

Golgi Tendon Organ

Golgi termed the receptor that now bears his name a musculotendinous end-organ (Golgi, 1880), a name that serves to emphasize that this receptor is not in the tendon proper. The majority of tendon organs line the aponeuroses of origin and insertion, where muscle fibers insert directly into the receptor capsule. They are also found at musculotendinous junctions and in

pennate muscles will therefore lie within the confines of the muscle itself. Less than 10% of tendon organs are found wholly within the tendon (Barker, 1974; Proske, 1981). Some tendon organs are found in association with joint capsules near tendon insertions (e.g. Backenkohler *et al.*, 1997). Tendon organ properties have been reviewed by Proske (1981) and Jami (1992).

The term "tendon spindle" has also been used for Golgi tendon organs, a name which emphasizes that this encapsulated receptor is not spherical but fusiform, much as is the muscle spindle (see Fig. 5.1). The tendon organ is much smaller than the muscle spindle: the mean length of 10 human tendon organs was 1.6 mm, mean width at the widest point 0.12 mm (Bridgman, 1970). The number of tendon organs in a muscle varies, as does the number of spindles, but there is no strict correlation and some muscles are devoid of either (Barker, 1974). In the monkey, the intrinsic muscles of the hand are rich in spindles but contain few tendon organs (Devanandan *et al.*, 1983). Spindles, judging by the numbers of their afferents in muscle nerves, are generally more plentiful than tendon organs, in a ratio of 1–2:1 (Barker, 1974).

The tendon organ has a thin capsule enveloping collagenous fascicles, which are continuous with the tendon. Extrafusal muscle fibers insert into the fascicles, so that contraction exerts a force directly onto the fascicle and its contents, the afferent terminals. In the cat, the mean number of muscle fibers inserting into a tendon organ is 10.5 (Barker, 1974). Bridgman (1970) reported that there were 10–20 muscle fibers inserted into each of 10 human tendon organs, sometimes terminating on the outer surface of the receptor capsule. As discussed in "Muscle Units and Motor Units," the fibers of different motor units intermingle and it is unusual to find more than two adjacent muscle fibers from the same motor unit. It is therefore likely that each tendon organ samples the activity of 10–20 motor units, one muscle fiber from each motor unit. In physiological studies this has proved to be the case (see Proske, 1981; Jami, 1992). The inserting muscle fibers come from motor units of different physiological type, so that if the receptor mechanism does not saturate, the afferent discharge of the tendon organ is proportional to contraction strength. Certainly, the ensemble discharge of tendon organs should follow muscle force.

Tendon organs are innervated by large myelinated afferent axons of group I size (Ib afferents) with one afferent per receptor in over 85% of cases. The Ib afferent divides into a few branches before penetrating the capsule of the receptor. Inside the capsule these branches subdivide, forming arborizations in the connective tissue fascicles of the end organ, terminating in a flower-spray appearance (Barker, 1974).

Tendon organs may be found in association with other muscle receptors, particularly the muscle spindle, the Paciniform corpuscle and free nerve endings, but the true functional significance of these associations has not been established. The association of spindle and tendon organ, to form a "dyad," may occur when the intrafusal muscle fibers of the relevant spindle insert into the musculotendinous junction alongside a tendon organ. Presumably this occurs more often in small but richly endowed muscles; perhaps that is why dyads are quite common in, for example, cat extensor digitorum brevis (Marchand *et al.*, 1971) and neck muscles (Richmond and Abrahams, 1975). Up to 10% of tendon organs have associated Paciniform corpuscles, orientated longitudinally outside or, more often, inside the capsule (Barker, 1974). There seem to be no specific features about free nerve endings innervating structures in and around the tendon organ. This may be a quite common association, at least in humans (Stilwell, 1957; Weddell and Harpman, 1940), though Stacey (1969) considers the relationship more casual than specific.

Because of the direct insertion of muscle fibers into the intracapsular fascicles containing the afferent terminals, tendon organs are exquisitely sensitive to muscle contraction, a single twitch of a single muscle fiber being sufficient to generate an afferent discharge. The tendon organ is "in series" anatomically and functionally with those motor units that have a muscle fiber inserting into it. It is anatomically "in parallel" with the remaining motor units, and it is possible for selective activation of them to unload a tendon organ and decrease its afferent discharge (Proske, 1981). However, during normal motor behavior this may not occur because each tendon organ sees a reasonable sample of different motor unit types, and because the sensitivity to contraction-induced forces is higher than to passive force applied less directly to the afferent terminals. In a similar way, passive stretch of non-contracting muscles produces forces that are poorly transmitted to afferent terminals, and the sensitivity of tendon organs to stretch is very much less than that to muscle contraction.

Pacinian and Paciniform Corpuscles

Pacinian corpuscles are rare in muscle, being associated with noncontractile tissue such as fascia, interosseous membranes, aponeuroses and tendons (Barker, 1974). Paciniform corpuscles are similar but much smaller structures, having an oval rather than round shape and a capsule with only 4–8 lamellae rather than 20–60 as in the pacinian corpuscle. There are only a few Paciniform corpuscles in muscle, occur-

ring mainly at musculotendinous junctions where they are commonly associated with Golgi tendon organs, even lying inside the capsule of that receptor (Barker, 1974; Stacey, 1969). Perhaps 1–5 Paciniform corpuscles may be associated with any one tendon organ. Elsewhere, Paciniform corpuscles are found in tendons, aponeuroses, and joint capsules. The afferent axons innervating Pacinian and Paciniform corpuscles traverse the appropriate muscle nerve and are generally of groups II and III size, i.e., 3–12 μm (corresponding to a conduction velocity range of approximately 18–72 m/s in the cat).

Free Nerve Endings

All tissue within muscle, apart from the capillary network, is richly innervated by free nerve endings derived from myelinated and unmyelinated parent axons (Abrahams, 1986; Stacey, 1969). These unmyelinated unencapsulated nerve terminals may be activated by muscle stretch, muscle contraction, nociceptive stimuli (such as trauma or the injection of algogenic agents), and changes in temperature, presumably because they are sensitive to mechanical deformation, changes in their chemical environment, and other stimuli (e.g., Abrahams, 1986; Kniffki *et al.*, 1978; Mense and Stahnke, 1983). These endings are believed to be responsible or muscle pain (Kniffki *et al.*, 1978; Mense and Stahnke, 1983), a view for which there is indirect (Kellegren, 1939) and direct evidence (Marchettini *et al.*, 1996). They also contribute to the cardiovascular and respiratory reflexes induced by exercise (Kniffki *et al.*, 1978; McCloskey and Mitchell, 1972). While free nerve endings are polymodal (i.e., they respond to a number of different stimuli), they do not form a homogeneous population. Individual afferents have marked differences in sensitivity to, for example, muscular exercise and nociceptive stimuli.

All group IV muscle afferents (i.e., unmyelinated afferents) terminate as free nerve endings, but so too do many small myelinated (group III) and some medium-sized myelinated (group II) afferents (Stacey, 1969). It is unusual for larger afferents (group I) to end as free nerve endings.

FEATURES OF MUSCLES

The development of active muscle force is the prime role of skeletal muscle. The development of force may result in muscle shortening (a "concentric" contraction) if contractile force is sufficient to overcome the load on the muscle or muscle lengthening (an "eccentric" contraction) if it is not. All muscles act against internal loads, imposed by the skeleton, as well as external loads such as objects lifted by the limbs. The contraction of one limb muscle alters the mechanical conditions required for action not only of its antagonist, but also for muscles acting on proximal and distal segments. Control of movement by the central neurons system (CNS) must take into account the mechanical interactions generated between various limb segments during movement and the gravitational force acting on the segments (Gandevia and Mahutte, 1982; Partridge and Benton, 1981). Conventional descriptions of the anatomy and physiology of muscle play down the global features of muscle control in favor of the more approachable fields, such as the description of the contractile mechanism of single muscle fibers and the various types of muscle fibers. A discussion of the molecular and mechanical events underlying muscle contraction is outside the scope of this chapter (for reviews, see Peachey, 1983; Weiss, 1996).

Peripheral Organization of Muscle

The number of muscles that act at a joint exceeds the number of degrees of freedom for motion at that joint. Theoretically, three muscles could achieve independent flexion and extension at the elbow, with or without supination or pronation of the forearm. The reason for the abundance of muscles in unclear. It does not allow a greater variety of movements, but it may reduce energy expenditure (Alexander, 1981). Human muscles have many forms; the representation of a muscle as fusiform in shape is rarely correct. A commonly used terminology refers to unipennate (or simply pennate), bipennate, and multipennate muscles. The degree of "pennation" depends on the number of visible sets of parallel muscle fascicles that insert at a particular angle into a common tendon. Other adjectives to describe muscle form include quadrilateral, triangular, circumpennate, spiral, radial, straplike, and straplike with tendinous intersections (e.g., Williams and Warwick, 1980). No uniform nomenclature is likely to describe fully the range of muscle morphology, particularly as the mechanical arrangement of muscle fascicles is even more complex at a microscopic level. Furthermore, the neural control of muscles of the same form is not necessarily the same. An example is the different central organization of splenius capitis and semitendinosis in the cat. These muscles in both humans and cats have tendinous inscriptions, so that the muscles contain end-to-end compartments rather than fascicles that run the full length of the muscle (Barrett, 1962; Bodine *et al.*, 1982; Richmond *et al.*, 1985; Trotter, 1990).

The contraction of muscle fibers ultimately acts to bring the ends of the muscle together. This is not achieved simply through independent, parallel contractile elements that span the connective tissue ends of the muscle. Each muscle fiber is enveloped outside its basement membrane by the endomysium, consisting of a network of collagen fibrils that take a mostly longitudinal path. Outside this envelope are thicker collagen strands commonly running in the direction of the tendon rather than the muscle fibers (i.e., perimysium). The endomysium contributes to the mechanical strength (or breaking strain) of the muscle and to the increase in tension when the muscle is stretched well beyond its resting length. These extracellular connective tissue elements distribute the contractile force across the muscle and tendon, and may help maintain the sarcomeres in register. Both the contractile material and the tendon have an important role in the storage of elastic energy. Individual muscle fibers taper close to their ends and separate into projections, which usually attach to the connective tissue of the tendon. It is becoming increasingly recognized that, in some fascicles in nonhuman muscles, individual fibers may not run the whole length of the muscle so that at one end they are bound to adjacent muscle fibers. At least in most mammals larger than the mouse, muscles longer than about 20 mm contain a significant component of serially arranged fibers (see Barrett, 1962; Paul, 2000; Richmond *et al.*, 1985; Trotter, 1990). This recognition will lead to questions as to how such muscle fibers develop in series and how they are controlled by the central nervous system. Already there is interest in the mechanical properties and reflex control of muscles with tendinous inscriptions (i.e., the extreme instance of fibers in series) and specific compartments (for review, see Stuart *et al.*, 1987). Most human muscles appear to be single fibered with a single zone of neuromuscular junctions, but a few (e.g., gracilis and sartorius) have multiple endplate zones and may have a significant number of in-series fibers (e.g., Paul, 2000).

Before the histochemical properties of individual muscle fibers are considered, two examples will be given to illustrate the relevance of intramuscular architecture for muscle performance. Additional details about the length and angulation of muscle fibers are reviewed by Gans and de Vree (1987).

1. Although the relationship between the length of an isolated muscle or its fibers and the contractile force is well known (e.g., Gordon *et al.*, 1966), the importance of the relationship cannot be assessed functionally unless the contractile force can be translated (according to joint and tendon mechanics) into force acting on the limb segments, and unless the muscle length can be translated into the angular position of the segment. The optimal position for force development by the dorsiflexors of the human ankle (10^8 plantar flexion) does not correspond with any of the "rest" positions adopted by the joint during sitting, standing and lying (Marsh *et al.*, 1981). Furthermore, muscle contraction significantly lengthens the intra- and extramuscular tendon and this is associated with increases in the muscle pennation angle (Herbert and Gandevia, 1995; Kawakami et al., 2000; Narici *et al.*, 1996). In addition, fascial layers surrounding single or groups of human muscles, especially in the lower limb, may directly influence the force exerted (Garfin *et al.*, 1981).

TABLE 5.4 Architectural Variables of the Average Medial and Lateral Head of the Human Gastrocnemius[a]

Variable	Medial gastrocnemius	Lateral gastrocnemius
Sarcomeres	17,614	21,371
Optimal length (mm)		
Fibers	52	63
Muscle	244	213
Index of architecture[b]	0.2	0.3
Fiber angle with respect to tendon plate (degrees)	18	9
Tendon plate length (mm)	192	154
Volume (cm^3)	160	90
Physiological cross-section (cm^2)	31.3	14.2

[a]Data from Huijing (1985).
[b]The index of architecture is defined as the ratio of the optimal fiber and muscle length.

2. The importance of the force–length relationship can be shown by considering the medial and lateral gastrocnemii, a synergistic "pair" of knee flexor and ankle extensor muscles. These muscles have significant differences in overall length, muscle fiber length, tendon length and cross-sectional area, as well as in the architecture of the fiber array (Table 5.4). Such factors will influence the angular range over which each muscle is effective. For example, the greater degree of pennation of the medial gastrocnemius reduces its working range (e.g., Woittiez *et al.*, 1983). The need for practical data about strength and the excursions of individual muscles and tendons has already prompted detailed descriptions of muscles in both human upper and lower limbs (Brand *et al.*, 1981; Silver *et al.*, 1985) and increased use of *in vivo* imaging methods such as ultrasonography. Presumably, incorporation of additional architectural features in these descriptions will enhance their usefulness in the surgical treatment

of paralyzed muscles. To understand a muscle's function requires knowledge of its unique physical and architectural features.

Muscle Fiber Types

Human muscle fibers, like those of other mammals, are not uniform in their properties. There are differences in the ultrastructure, in the biochemical and physiological properties of single muscle fibers, and in the fibers of individual motor units. In the 1870s, Ranvier correlated white and red muscles in the rabbit with rapid and slow contractions, respectively (see Dubowitz, 1985). Investigations followed of the correlation between anatomical, biochemical, and physiological properties of different muscle and, subsequently, of their constituent fibers. The following discussion concentrates on some of the histochemical classifications of human muscle fibers and the *in vivo* properties of the different fiber types.

Histochemical and Other Classifications

Many classifications have been used for the types of muscle fiber revealed by a particular (usually histochemical) technique, and some are detailed in Table 5.5. Human muscle fibers can be separated into two histochemical groups, one with high oxidative and low glycolytic activity (type I), and the other low oxidative and high glycolytic activity (type II) (Dubowitz and Pearse, 1960). This subdivision of fibers usually corresponds to groups of fibers with low and high myofibrillar adenosine triphosphatase (or mATPase) activity, respectively (Engel, 1962). The latter classification was subsequently expanded to four types because the type II fibers can be divided into three according to different susceptibility of the mATPase reaction to preincubation at various pH levels (Brooke and Kaiser, 1970). The specific levels vary but are usually about pH 9.4, 4.6, and 4.3. Most normal human limb muscles are composed almost entirely of type I, IIA, and IIB fibers with occasional type IIC, "intermediate" fiber. An early histochemical study of human muscles that employed a stain for the oxidative enzyme succinic dehydrogenase suggested a tripartite classification with low enzyme activity in large fibers, high activity in small fibers, and a group of intermediate fibers (Wachstein and Meisel, 1955). However, a study using morphological analysis of histochemically identified fibers has revived the debate about the subtypes of the type II fibers identified with the usual mATPase techniques. Type IIAB fibers were detected that had an intermediate staining reaction after preincubation at pH 4.6. The lipid and mitochondrial volumes for these fibers were below those for type IIA but above those for IIB fibers (Staron *et al.*, 1983; see also Injer, 1979). In addition, human type I fibers can also be divided into IA and IB based on a range of histochemical reactions (Askansas and Engel, 1975). Another classification concentrated on the metabolic capacity of muscle fibers. It divided fibers into three major types (Barnard *et al.*, 1971), which were subsequently named slow oxidative (SO) fibers, fast oxidative glycolytic (FOG) fibers, and fast glycolytic (FG) fibers (Peter *et al.*, 1972). Fibers that reacted strongly with ATPase (at pH 9.4, i.e., type II fibers) were associated with fast contraction times, whereas those with weak reactions were associated with slow contraction times. There is a strong correlation between the speed of muscle contraction and overall myosin ATPase activity (Barany, 1967), a correlation that holds

TABLE 5.5 Correlation of Fiber Types Based on Histochemical and Physiological Properties[a]

Property	Fiber type			
	I	IIA	IIB/IIX[b]	IIC
Histochemical fiber type				
Putative physiological type				
Peter et al. (1972)	SO (slow oxidative)	FOG (fast oxidative gycolytic)	FG (fast glycolytic)	
Burke et al. (1973)	S (slow)		FR (fast fatigue resistant)	FF (fast fatigable)
Properties of motor units				
Tension produced	Low	Intermediate	High	Intermediate
Contraction speed	Slow	Fast	Fast	Slow
"Fatigue" resistance	High	Intermediate/high	Low	High
Recruitment order	First	Second	Third	Unknown

[a]This table provides a simplified correlation between muscle fiber types and their physiological properties. Additional subtypes within the type II group have not been included. Data for IIC fibers are taken from Maxwell *et al.* (1983). It is likely that for many human muscles there is greater uniformity in the contractile and fatigue properties than predicted from data obtained in the cat.

[b]Type IIB fibers assessed with myosin ATPase histochemistry contain type IIX myosin (Ennion *et al.*, 1995).

among the fast myosin isoforms (Larsson and Moss, 1993).

Classifications are useful only if they allow further deductions about muscle pathology or performance. Recognition of the classifical type I/type II subdivision has been of practical and conceptual importance, as has the SO, FOG, FG division. For example, the presence of atrophic type I and type II fibers in a muscle biopsy suggests denervation, grouping of fibers of one type suggests reinnervation, and a predominance of type I fibers may indicate a selective atrophy of type II fibers. Furthermore, the division into type I, IIA, and IIB fibers separates the muscle into fibers with different function roles such that fiber-type composition can predict some physiological properties and vice versa (see below).

Classification of muscle fiber types has been dramatically helped by the introduction of molecular techniques, particularly those directed at the highly conserved and diverse myosin genes (e.g., Sellers, 2000). This has shown that the human IIB myosin is very similar to the IIX myosin in the rat, and thus IIB fibers should be more accurately classified as IIX fibers (Ennison *et al.,* 1995; see also Larsson *et al.,* 1991). It may represent the "default" muscle myosin gene (Goldspink *et al.,* 1991). Thus, the term IIX is rapidly replacing the term IIB. Furthermore, individual fibers may contain a mix of the various myosin isoforms such that the fiber's physiological performance will be determined by the predominant type. Myosin is the major structural protein of the thick filament and is more heterogeneous than revealed simply by the standard ATPase reaction. At least five different myosin isoforms are recognizable in human skeletal muscle by their eletrophoretic patterns (Fitzsimons and Hoh, 1981). Human type I and type II fibers also contain distinct classes of myosin light chains. The potential diversity within this major structural protein is great (for review, see Fitzsimons and Sewry, 1985; Schmalbruch, 1985; Weiss and Leinward, 1996). Recognition of the various myosin forms has become more important in assessment of pathological changes in muscle, as occurs for example in the muscular dystrophies, and for understanding the development and adaptability of human muscle.

Ultrastructural differences exist between the three common fiber types in humans. Although these differences are less than for other species, they have allowed reliable classification of fibers from human biopsy material prepared for electron microscopy (Sjöström *et al.,* 1982). The differences include variation in the apparent complexity of the M band and in the diameter of the Z discs. The latter was wider in type I (125 nm) than in either type IIA (101 nm) or IIB fibers (86 nm). The distribution of these diameters was such that accurate fiber typing was possible for 80–95% of fibers with this measurement alone and so detailed ultrastructral measurements (e.g., of mitochondria and their distribution) can be made for human muscle fibers of known type. In addition, type I fibers usually have greater numbers of mitochondria, but smaller areas of T tubules and sarcoplasmic reticulum (Dubowitz, 1985).

Another factor that varies according to fiber type is the distribution of muscle capillaries. Only about 1% of total muscle volume is occupied by capillaries, and a close correlation exists between the muscle capillarity and the maximal oxygen uptake by the muscle (for review, see Saltin and Gollnick, 1983). In human vastus lateralis there are an average of three capillaries in contact with each IIB fiber and four capillaries in contact with both type I and IIA fibers. Even when these estimates take account of differences in the size of muscle fibers (by expression of capillary counts relative to fiber area), the corrected capillary density is greater for type I fibers (Andersen and Henriksson, 1977). Many of the correlations between capillarity, fiber type and fiber diameter noted in animal studies have now been found for human muscle biopsies. An important relationship for oxygen delivery is that the number of capillaries per fiber increases as fiber diameter increases. This relationship was found in a large group of control subjects for samples taken from vastus lateralis, biceps femoris or deltoid (Carry *et al.,* 1986). Changes in muscle fiber diameter due to neuropathic or myopathic disease are usually associated with a parallel change in capillary numbers (Carry *et al.,* 1986).

Myoglobin concentration, which is related to the capcity for intracellular oxygen transport (and responsible for muscle's red color), does not vary as much between human type I and type II fibers as in other species (Németh and Lowry, 1984). The reason for this relative homogeneity is not resolved, but it is consistent with the finding that the activity of some oxidative enzymes may vary little between the two main fiber types and that the difference in the endurance properties of the main fiber types in various limb muscles is smaller in humans than in many laboratory animals and other species.

Fiber-Type Variations Between and Within Muscles

The proportions of type I, IIA and IIB fibers within an individual subject vary between muscles (e.g., Johnson *et al.,* 1973), within regions of a single muscle (Elder *et al.,* 1982), and even within a single muscle fascicle (Sjöström *et al.,* 1986). Given that muscle performance at a whole-muscle or single-fiber level is

influenced by fiber type (see below), it is perhaps surprising that there is still some controversy about the determinants of the main fiber type division (type I/II) and that factors affecting the distribution of fiber types within muscles have received so little attention.

Both genetic and environmental factors influence muscle fiber types; the former were generally believed to control the "boundaries" for the proportion of type I and type II fibers and the latter the proportion of subtypes within the type II group (e.g., Booth and Thomason, 1991). Studies of monozygotic and dizygotic twins have emphasized the role of heredity in fiber type determination (Komi *et al.,* 1977). Fiber type distributions in vastus lateralis are closer in pairs of monozygotic than dizygotic twins. In contrast, it is becoming increasingly clear that even the type I/type II distribution is mutable with prolonged changes in muscle use (Larsson and Ansved, 1985; cf. Harridge *et al.,* 1998).

In an autopsy study of 36 human muscles, the percentage of type I fibers varied within and between subjects (Johnson *et al.,* 1973). The highest percentages of type I fibers were in soleus (100% in one subject) and the lowest in orbicularies oculi. Studies of fewer muscles, often using newer methods, have confirmed these observations. Human matiscatory muscles do not fit easily into this scheme. In addition to the classical types of fiber based on ATPase staining, jaw-closing muscles contain fibers with intermediate staining properties in the ATPase reaction at pH 9.4 (Ringqvist, 1974), the pH used to distinguish type I form type II fibers. These data argue for the expression of a greater number of biochemically distinct fiber types than predicted by early classifications. There are a number of isoenzymes for fetal and adult human myosin, but a functional role for each distinct form is not yet known for adult muscle (Fitzsimons and Sewry, 1985). Individual muscle fibers may contain "hybrids" of the different isoforms (Gauthier *et al.,* 1979). Physiologically the myosin isoforms are the primary determinant of the fiber's speed of shortening (Lowey *et al.,* 1993).

Differences in the percentages of type I and type II fibers in different regions of one muscle have been reported for animal and human muscles. While these differences are usually thought to be comparatively small (only about 10%), the systematic variation across some muscles is more marked. For example, a peak in the distribution of type II fibers occurs over the anterior portion of human tibialis anterior with at least one other peak deep within the muscle (Henriksson-Larsen, 1985), and in the masseter the frequency of type IIB fibers is significantly higher in the superficial posterior part of the muscle (Ericksson, 1982). Variations in fiber type distributions according to muscle architecture have been documented in animal studies, and hypotheses have been developed to explain them (Ringqvist, 1974; for review, see Binder and Stuart, 1980; Botterman *et al.,* 1978). One hypothesis depended on the frequent association of high counts of muscle spindle endings and tendon organs in zones (usually in deep parts of the muscle) with a preponderance of type I fibers (Botterman *et al.,* 1978). The major implication of this hypothesis, namely, a close functional linkage between specialized muscle *receptors* and muscle *fibers* within an intramuscular region, has not been supported by physiological studies on human tibialis anterior (McKeon *et al.,* 1984), but it has received support from studies in some muscles in the cat (Stuart *et al.,* 1987). The variable distribution of muscle fiber types across a muscle and the possible association with the distribution of muscle receptors need further study.

There is some difficulty in estimating the different fiber types from conventional muscle biopsies. When between 13 and 17 sites within muscles were sampled (soleus, vastus lateralis, biceps brachii, and triceps brachii), the variability in fiber type distribution exceeded that of a muscle with a random distribution of fibers (Elder *et al.,* 1982). With the exception of triceps, significant within-site variability occurred. This may arise because there is significant difference in fiber type distributions at the edges of muscle fascicles with boundaries containing a higher percentage of type II fibers (Sjöström *et al.,* 1986). This factor must make an important contribution to the variation in fiber type distribution between nearby sections from the one site in the muscle. Whenever there are some muscle fibers in series, fiber type distribution may vary slightly for different cross-sections of the same muscle region. The role of local mechanical factors and possible neural influences on the fiber type distribution at the borders of whole muscle and individual fascicles is unknown.

The proportion of type II fibers in vastus lateralis of healthy sedentary individuals declines progressively with age between the fourth and ninth decade (Larsson, 1983). This change may simply represent a selective reduction in the number of motoneurons supplying type II muscle fibers.

MUSCLE UNITS AND MOTOR UNITS

The muscle fibers which have a common efferent innervation by a single anterior horn cell constitute the smallest "muscle units that can be controlled by the CNS." The term motor unit applies to both this muscle

unit and the motoneuron that supplies it. Each muscle fiber from a motor unit has the same physiological and biochemical properties. This is important for two reasons. First, it emphasizes the likely role of the motoneuron in determination of muscle unit properties (although it does not reveal how this determination is achieved). This view has been further supported by meticulous studies in which the enzyme activities for individual fibers from identified muscle units have been quantified. Uniformity among fibers from the same unit is striking compared with the variation between fibers of the same histochemical type. This enzymatic uniformity is evident despite variation in size of fibers from one motor unit (e.g. Németh *et al.*, 1986; *cf.* Larsson, 1992). Uniformity of muscle unit properties is likely to apply to human muscle (see below). Also, it defuses some of the criticism of those histochemical studies that fail to reveal separate nonoverlapping distributions of human muscle fibers (e.g., Reichmann and Pette, 1982) and that have emphasized the heterogeneity of metabolic profiles within a muscle.

The force produced by a motor unit is proportional to the number of fibers within it. The number of fibers per motor unit probably varies within a muscle and certainly varies between muscles. Anatomical techniques to determine this "innervation ratio" in humans have usually involved counts of the large-diameter axons in the motor nerve (more than 7–8 μm in diameter), estimation (from animal studies) of the percentage of the fibers that are efferent, and then measurement of the number of muscle fibers within a cross-section of muscle. The potential for errors in each of these measurements is not small. Estimates based on such indirect anatomical methods are shown in Table 5.3. An electrophysiological method using single-fiber electromyography estimates the innervation ratio for biceps brachii at about 210 fibers per motor unit, smaller than the figure obtained with anatomical methods (Table 5.3). There are insufficient data for human muscles to support uncritically the view derived from animal studies that the innervation ratio is highest for large muscles that produce large forces and lowest for small muscles (including extraocular muscles) that produce small forces.

The arrangement of muscle fibers innervated by a single α motoneuron has been investigated using an electrode inserted into the muscle so as to sample the electromyographic activity simultaneously at different depths within the muscle. The near-synchronous discharge of muscle fibers from a motor unit can be recorded from approximately circular cross-sectional regions of limb muscles with a diameter of 5–10 mm (Buchthal and Schmalbruch, 1980). Single-fiber electrodes that record from a semicircular area of 270 μm in diameter have revealed that such an area contains about 10 muscle fibers, usually derived from 6 or more motor units. These electrophysiological data show that fibers belonging to one muscle unit do not form discrete clusters but are spread across a specific subvolume of the muscle (Stålberg *et al.*, 1976) and that in normal human limb muscles the distribution of fibers across that volume is approximately uniform (Gath and Shenhav, 1985).

A combination of electrophysiological and histochemical methods has permitted visualization of the region of muscle that contains fibers innervated by a single motoneuron. Repetitive stimulation of a single motor axon *in vivo* produces selective depletion of glycogen stores within the innervated muscle fibers, as revealed by staining for glycogen. Application of this technique in the rat and cat has demonstrated that adjacent fibers rarely belong to the same motor unit (Burke and Tsairis, 1973; Edström and Kugelberg, 1968) and that there is extensive overlap of motor unit territories. There is support for a similar arrangement in humans from the biopsy findings. For example, in a patient with myokymia, a disorder associated with repeated contractions of several motor units, the contractions depleted glycogen in two regions of the biopsy, one containing IIA fibers and the other containing IIB fibers. Depleted fibers did not occur next to one another (Williamson and Brooke, 1972). This "mosaic" arrangement of fibers belonging to one unit ensures wide distribution of the contractile force into the tendon and minimization of local shearing force, and may tend to smooth the final force output. There is increased speculation about the physiological role of lateral connections between muscle fibers (e.g., Huijing, 1999; Young *et al.*, 2000).

Finally, some muscles can be subdivided into volumes according to the anatomical zones innervated by the primary branches of the nerve as it enters the muscle. Thus, although motor unit territories do not represent a discrete cross-sectional area of the muscle, there is a tendency (at least in some animal muscles) for compartments of muscle to contain unique sets of motor units (English and Weeks, 1984). If this form of "compartmentalization" is widespread among human muscles, then it represents a neural substrate for independent control by the CNS of specific regions of a muscle. Indeed, a "muscle" such as extensor digitorum communis contains anatomical compartments that insert into four separate tendons. It contains discrete zones of muscle that produce extension of each finger and that can be separately activated by the CNS. Such considerations blur the anatomical definition of what is the smallest volume that constitutes a "muscle," but emphasize the importance of the function of different

muscle "compartments," whether they are defined morphologically or according to primary motor nerve branches.

Classification and Properties of Motor Units

Classical studies by Burke and colleagues (1973) involved physiological characterization of a single motor unit in the cat and its stimulation to induce glycogen depletion with subsequent histochemical identification. The physiological assessment revealed three types of motor unit in cat gastrocnemius muscle that were termed type S (slow twitch), type FR (fast twitch, resistant to fatigue), and type FF (fast twitch, fatigable). This division, based on physiological criteria (primarily contraction speed and resistance to fatigue produced by repetitive stimulation), correlated well with the histochemical division into type SO, FOG, and FG fibers, respectively (Table 5.5). Subsequent physiological studies have revealed that in some cat muscles there are fast-twitch motor units of intermediate resistance to fatigue (F int, units) (for review, see Burke, 1981).

In an attempt to apply to humans the techniques used to classify animal motor units and their fibers, Garnett *et al.* (1978) stimulated single motor axons near the motor point of medial gastrocnemius and then biopsied the muscle. Twitch contraction times under isometric conditions ranged from 40 to 110 ms (mean 76 ms), with the suggestion of a bimodal distribution. Units with fast contraction times of less than 85 ms were designated type F and more than 99 ms type S. The division of human muscle contractile responses into slow and fast types had previously been suggested from studies of isolated bundles of fibers (e.g., Eberstein and Goodgold, 1968), and had been confirmed for single motor units in extensor digitorum brevis (e.g., Sica and McComas, 1971), but not for other muscles, including the intrinsic muscles of the hand (e.g., Burke *et al.*, 1974; Milner-Brown *et al.*, 1973; Thomas *et al.*, 1986, 1991). Separation of the responses according to contraction time also revealed characteristic differences in contractile force. In the study of Garnett *et al.*, presumed type S units produced relatively low tensions (mean 12 g) whereas presumed type F units produced a range of tensions from 5 to 204 g (mean 23 g). Type F units were conveniently separated into two groups (FR and FF) according to their resistance to fatigue. Figure 5.4 illustrates the interrelationships between three indices of mechanical performance as a three-dimensional plot (contraction time, twitch tension, and fatigue resistance). Thus three separate subpopulations of motor units emerge from the study of Garnett *et al.* These three types seem analogous to those described

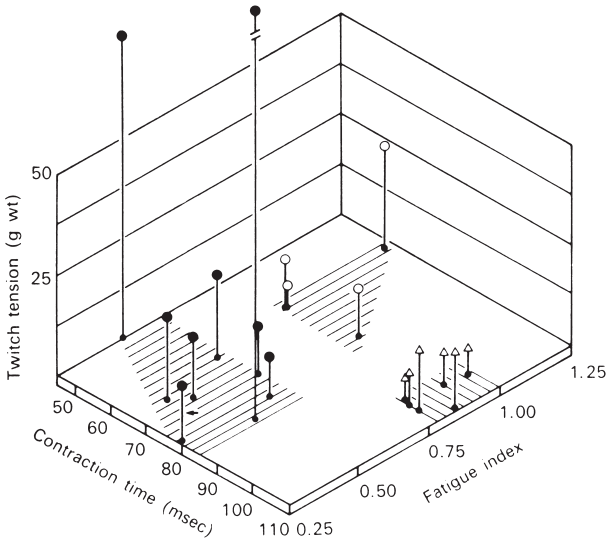

FIGURE 5.4 Three-dimensional graph to show a possible subdivision of motor units supplying human medial gastrocnemius. Data for 18 motor units isolated functionally by bipolar stimulation at the motor point. The "fatigue index" is expressed so that a value of one represents no decline in force after 3000 stimuli. The population divides into type S units (triangles: slow contraction time, high resistance to fatigue), type FR units (open circles: fast contraction time, high resistance to fatigue), and type FF units (filled circles: fast contraction time, low resistance to fatigue). The FF unit shown by an arrow had a fatigue index of zero. Reproduced with permission from Garnett *et al.* (1978). This subdivision shown here emphasizes the differences between motor units. Analysis of a larger sample of units would reveal more overlap among the groups of motor units (e.g. Thomas *et al.*, 1991).

in experimental animals. In five of six single motor units confirmation of the correlation between physiological and histochemical properties was obtained: three of four type S units contained type I fibers in the muscle biopsy, and one type FF unit contained type IIB fibers. This is the only study to attempt to correlate mechanical and histochemical properties of single human motor *units*. In contrast to these data for human gastrocnemius, data for human thenar muscles obtained with microneurographic techniques reveal a greater uniformity in contraction times, twitch forces, and fatigue properties (e.g., Thomas *et al.*, 1991). Unless large numbers of units are sampled, the full overlap of physiological properties among the various histochemical types may not be reliably determined.

Activation of Motor Units

The behavior of muscle units during voluntary contractions reveals a number of orderly features that have been documented for a variety of human skeletal muscles. First, muscle units with slow contractile speed and low-twitch tensions are activated initially,

followed by units of greater contractile speed and force. Second, the first activated units are resistant to the development of fatigue, whereas those activated during stronger contractions fatigue rapidly. Such a stereotyped recruitment of motor units (type S, then FR, then FF) or muscle fibers (type I, then IIA, then IIB) has both energetic and design advantages. For example, low forces can be achieved with finely graded force "steps," without development of fatigue while using oxidative metabolism. High forces can be achieved by full recruitment of all motor units within the muscle, although the maximal force produced can be sustained only briefly. This simplistic description of orderly motor unit activation may not occur under all circumstances. Thus, muscles that cross more than one joint or have complex actions may have slight variation in the recruitment pattern that is dependent on which muscle action is required (Thomas *et al.*, 1986; Van Zuylen *et al.*, 1988), and some peripheral feedback may favor activation of the fast-twitch (type II) muscle fibers (Garnett and Stephens, 1980). Histochemical techniques have been used to assess the recruitment of the different fiber types during prolonged bicycle exercise. Initially, glycogen depletion occurred only for type I and IIA fibers, but as exercise progressed the glycogen depletion was evident for type IIAB then type IIB fibers (Vøllestad *et al.*, 1984). This result confirms the probable physiological importance of the three subgroups of type II fibers. The pattern of motor unit recruitment in patients with upper motoneuron lesions may change during fatigue (Grimby *et al.*, 1974; for review, see Gandevia, 2001).

There is a relationship between anatomical and physiological properties of the motoneurons and the muscle units that they innervate. Small motoneurons with a low peripheral conduction velocity tend to innervate type S muscle units and large motoneurons with a high conduction relocity tend to innervate fast-twitch (type FR, FF) muscle units. Small motoneurons are usually recruited first in voluntary contractions. The "size principle" of motoneuron recruitment refers to the recruitment of motoneurons of increasing size (Henneman, 1957). The small motoneurons preferentially discharge at low rates. Thus, there is a "speed match" between the contractile properties of a muscle unit and the size and conduction velocity of its motoneuron. Furthermore, there is a "recruitment match" such that the susceptibility of a motoneuron to discharge decreases with the twitch tension of its muscle units (Burke, 1981; Henneman and Mendell, 1981; Kernell, 1986). The speed match is influenced by the total number of discharges of the relevant motoneurons such that mixed muscles that receive chronic stimulation change their properties toward those of a muscle with predominantly type S units. These changes result in a "slowing" of the myosin ATPase system, an increase in oxidative and a decrease in glycolytic enzymes. There is also a reduction in size of individual muscle fibers. Some of these changes have been documented for human muscles (e.g., Andersen *et al.*, 1999; Edwards *et al.*, 1982; Zhou *et al.*, 1985).

Finally, as suggested above, human muscle has significant plasticity, i.e., a capacity for adaptation to changes in pattern and condition of use (for review, see Edström and Grimby, 1986). In adult human muscles the compensatory changes following different exercise programs involve not only the sarcoplasmic reticulum, the contractile proteins and metabolic pathways, but also the size of individual muscle fibers and their associated capillarity. In addition to muscle fiber atrophy, which accompanies disuse, and hypertrophy, which may accompany strength training, the number of muscle fibers might change. There are limited, but controversial, data to suggest that following some training programs adult human muscle may show an increase in fiber numbers (i.e., hyperplasia), and there may be conversion between type I and type II fibers (e.g., Gonyea *et al.*, 1986; Jansson *et al.*, 1978; Larsson and Ansved, 1985; Larsson and Tesch, 1986; cf. Saltin and Gollnick, 1983), particularly from type I to IIA and type IIX to IIA.

Acknowledgement

This work was support by the National Health and Medical Research Council of Australia (#3806).

References

Abrahams, V. C. (1986). Group III and IV receptors of skeletal muscle. *Can J. Physiol. Pharmacol.* **64,** 504–514.

Alexander, R. M. (1981). Mechanics of skeleton and tendons. *In* "Handbook of Physiology" (V.B. Brooks, ed.), Sect. 1, Vol. II, pp. 17–42. Am. Physiol. Soc., Washington, D.C.

Andersen, J. L., Gruschy-Knudsen, T., Sandri, C., Larsson, L., and Schiaffino, S. (1999). Bed rest increases the amount of mismatched fibers in human skeletal muscle. *J. Appl. Physiol.* **86,** 455–460.

Andersen, P., and Henriksson, J. (1977). Capillary supply of the quadriceps femoris muscle of man: adaptive response to exercise. *J. Physiol. (London)* **270,** 677–690.

Aniss, A. M., Gandevia, S. C., and Burke, D. (1988). Reflex changes in muscle spindle discharge during a voluntary contraction. *J. Neurophysiol.* **59,** 908–921.

Arkansas, V., and Engel, W. K. (1975). Distinct subtypes of type I fibers of human skeletal muscle. *Neurology* **25,** 879–887.

Backenkohler, U., Strasmann, T. J. and Halata, Z. (1997). Topography of mechanoreceptors in the shoulder joint region—a computer-aided 3d reconstruction in the laboratory mouse. *Anat. Rec.* **248,** 433–441.

Banks, R. W., Barker, D., and Stacey M. J. (1985). Form and classification of motor endings in mammalian muscle spindles. *Proc. R. Soc. London B.* **225,** 195–212.

Banks, R. W., Hulliger, M., Scheepstra, K. A. and Otten, E. (1997). Pacemaker activity in a sensory ending with multiple encoding sites: the cat muscle spindle primary ending. *J. Physiol. (London)* **498,** 177–99.

Barany, M. (1967). ATPase activity of myosin correlated with speed of muscle shortening. *J. Gen. Physiol.* 50, Suppl. 6, Part 2, pp. 197–218.

Barker, D. (1974). The morphology of muscle receptors. *In* "Handbook of Sensory Physiology" (C. C. Hunt, Ed.), Vol. 3, Part 2, pp. 1–190. Springer-Verlag, Berlin.

Barker, D., and Banks, R.W. (1986). The muscle spindle. *In* "Myology" (A. G. Engel and B. Q. Banker, Eds.), Vol. 1, Part 1, pp. 309–341. McGraw-Hill, New York.

Barker, D., and Chin, N. K. (1960). The number and distribution of muscle-spindles in certain muscles of the cat. *J. Anat.* **94,** 473–486.

Barnard, R. J. Edgerton, V. R., Furukawa, T, and Peter, J. B. (1971). Histochemical, biochemical and contractile properties of red, white and intermediate fibers. *Am. J. Physiol.* **220,** 410–414.

Barrett, B. (1962). The length face mode of termination of individual muscle fibres in the human sartorius and posterior femoral muscles. *Acta Anat.* **48,** 242–257.

Binder, and Stuart, (1980). Motor unit-muscle receptors interactions: design features of the neuromuscular control system. *Prog. Clin. Neurophysiol.* **8,** 72–98.

Bodine, S. C., Roy, R. R., Meadows, D. A., Zernicke, R E., Sacks, R. D., Fournier, M., and Edgerton, V. R. (1982). Architectural, histochemical, and contractile characteristics of a unique biarticular muscle: the cat semitendinosus. *J. Neurophysiol.* **48,** 192–201.

Botterman, B. R., Binder, M. d., and Stuart, D. G. (1978). Functional anatomy of the association between motor units and muscle receptors. *Am Zool.* **18,** 135–152.

Boyd, I. A. (1986). Two types of static γ-axon in cat muscle spindles. *Q. J. Exp. Physiol. Cogn. Med Sci.* **71,** 307–327.

Boyd, I. A., and Gladden, M. H. (1985). "The Muscle Spindle." Macmillan, London.

Boyd, I. A., and Kalu, K. U. (1979). Scaling factor relating conduction velocity and diameter for myelinated afferent nerve fibres in the cat hind limb. *J. Physiol. (London)* **289,** 277–297.

Brand, P. W., Beach, R. B., and Thompson D. E. (1981). Relative tension and potential excursion of muscle in the forearm and hand. *J. Hand Surg.* **6,** 209–219.

Bridgman, C. E. (1970). Comparisons in structure of tendon organs in the rat, cat and man. *J. Comp. Neurol.* **138**, 369–372.

Brooke, M. H., and Kaiser, K. K. (1970). Muscle fiber types: how many and what kind? *Arch. Neurol. (Chicago)* **23,** 369–379.

Buchthal, E, and Schmalbruch, H. (1980). Motor unit of mammalian muscle. *Physiol. Rev.* **60,** 90–142.

Burke, D., Skuse, N. F., and Lethelan, A. K. (1974). Isometric contraction of the abductor digiti minimi muscle in man. *J. Neurol. Neurosurg. Psychiatry* **37,** 825–834.

Burke, D., Skuse, N. F., and Lethelan, A. K. (1981). Cutaneous and muscle afferent components of the cerebral potential evoked by electrical stimulation of human peripheral nerves. *Electroencephalogr. Clin. neurophysiol.* **51,** 579–588.

Burke, D., Aniss, A. M., and Gandevia, S. C. (1987). In-parallel and in-series behavior of human muscle spindle endings. *J. Neurophysiol.* **58,** 417–426.

Burke, R. E. (1981). Motor units: anatomy, physiology, and functional organization. In "Handbook of Physiology" (V. B. Brooks, Ed.), Sect. 1, Vol. II, pp. 351–364. Am. Physiol. Soc. Washington, D. C.

Burke, R. E., and Tsairis, P. (1973). Anatomy and innervation ratios in motor units of cat gastrocnemius. *J. Physiol. (London)* **234**, 749–765.

Burke, R. E., Levine, D. N., Tsairis, P., and Zajac, F. E., III (1973). Physiological types and histochemical profiles in motor units of the cat gastrocnemius. *J. Physiol. (London)* **234,** 723–748.

Carry, M. R., Ringel, S. P., and Starcevich, J. M. (1986). distribution of capillaries in normal and diseased human skeletal muscle. *Muscle Nerve* **9,** 445–454.

Celichowski, J., Emonet-Denand, F., Laporte, Y. and Petit, J. (1994). distribution of static gamma axons in cat peroneus tertius spindles determined by exclusively physiological criteria. *J. Neurophysiol.* **71,** 722–732.

Cheney, P. D., and Preston, J. B. (1976). Classification and response characteristics of muscle spindle afferents in the primate. *J. Neurophysiol.* **39,** 1–8.

Cooper, S., and Daniel, P. M. (1963). Muscle spindles in man: their morphology in the lumbricals and the deep muscles of the neck. *Brain* **86,** 563–586.

Devanandan, M. S., Ghosh, S., and John, K. T. (1983). A quantitative study of muscle spindles and tendon organs in some intrinsic muscles of the hand in the bonnet monkey (Macaca radiata). *Anat. Rec.* **207,** 263–266.

Dubowitz, V., ed. (1985). "Muscle Biopsy: A Practical Approach," 2nd Ed. Bailliére, London.

Dubowitz, V., and Pearse, A. G. E. (1961). Reciprocal relationship of phosphorylase and oxidative enzymes in skeletal muscle. *Nature (London)* **185,** 701.

Eberstein, A., and Goodgold, J. (1968). Slow and fast twitch fibers in human skeletal muscle. *Am. J. Physiol.* **215,** 535–541.

Edström, L., and Grimby, L. (1986). Effect of exercise on the motor unit. *Muscle Nerve* **9,** 104–126.

Edström, L., and Kugelberg, E. (1968). Histochemical composition, distribution of fibres and fatiguability of single motor units. Anterior tibial muscle of the rat. J. Neurol. *Neurosurg. Psychiatry* **31,** 424–433.

Edwards, R. H. T., Jones, D. A., and Newham, D. J. (1982). Low frequency stimulation and changes in human muscle contractile properties, *J. Physiol. (London)* **328,** 29.

Elder, g. C. B., Bradbury, K., and Roberts, R. (1982). Variability of fiber type distributions within human muscles. *J. Appl. Physiol.* **53,** 1473–1480.

Ellaway, P. H., Emonet-Dénand, E, Joffroy, M. and Laporte, Y. (1972). Lack of exclusively fusimotor α-axons in flexor and extensor leg muscles of the cat. *J. Neurophysiol.* **35,** 149–153.

Emonet-Dénand, E, Jami, L., and Laporte, Y. (1980). Histophysiological observations on the skeleto-fusimotor innervation of mammalian spindles. *Prog. Clin. Neurophysiol.* **8,** 1–11.

Engel, W. K. (1962). The essentiality of histo- and cytochemical studies of skeletal muscle in the investigation of neuromuscular disease. *Neurology* **12,** 778.

English, A. W., and Weeks, O. I. (1984). Compartmentalization of single muscle units in cat medial gastrocnemius. *Exp. Brain Res.* **56,** 361–368.

Ennion, S., Sant'ana Pereira, J., Sargeant, A. J., Young, A. and Goldspink, V. (1995). Characterization of human skeletal muscle fibres according to the myosin heavy chains they express. *J. Musc. Res. Cell Motil.* **16,** 35–43.

Eriksson, P. O. (1982). Muscle fibre composition of the human mandibular locomotor system. *Swed. Dent. J., Suppl.* **12,** 1–44.

Fitzsimons, R. B., and Hoh, J. E. Y. (1981). Isomyosins in type 1 and type 2 skeletal muscle fibres. *Biochem. J.* **193,** 229–233.

Fitzsimons, R. B., and Sewry, C. A. (1985). Immunocytochemistry. *In* "Muscle Biopsy: A Practical Approach" (V. Dubowitz, Ed.), 2nd ed., pp. 185–207. Baillière, London.

Gandevia, S. C. (2001) Spinal and supraspinal factors in human muscle fatigue. *Physiol. Rev.* **81,** 1725–1789.

Gandevia, S. C., and Mahutte, C. K. (1982). The effects of joint position on the interpretation of signals of intramuscular tension. *J. Theor. Biol.* **97,** 141–153.

Gandevia, S. C., Burke, D., and McKeon, B. B. (1983). The relationship between the size of a muscle afferent volley and the cerebral potential it produces. *J. Neurol. Neurosurg. Psychiatry* **45,** 705–710.

Gandevia, S. C., Burke, D., and McKeon, B. B. (1984). The projection of muscle afferents from the hand to cerebral cortex in man. *Brain* **107,** 1–13.

Gans, C., and de Vree, E (1987). Functional bases of fiber length and angulation in muscle. *J. Morphol.* **192,** 63–85.

Garfin, S. R., Tipton, C. M., Mubarek, S. J., Woo, S. L. -Y., Hargens, A. R., and Akeson, W. H. (1981). Role of fascia in maintenance of muscle tension and pressure. *J. Appl. Physiol.* **51,** 317–320.

Garnett, R.A. F, and Stephens, J. A. (1980). The reflex responses of single motor units in human first dorsal interosseous muscle following cutaneous afferent stimulation. *J. Physiol. (London)* **303,** 351–364.

Garnett, R. A. E., O'Donovan, M. J., Stephens, J. A., and Taylor, A. (1978). Motor unit organization of human medial gastrocnemius. *J. Physiol. (London)* **287,** 33–43.

Gath, I., and Shenhav, R. (1985). Probabilistic model of the spatial distribution of muscle fibres in human muscles. *Biol. Cybernet.* **53,** 773–382.

Gath, I., and Stålberg, E. (1981). In situ measurement of the innervation ratio of motor units in human muscles. *Exp. Brain Res.* **43,** 377–382.

Gauthier, G. F., and Lowey, S. (1979). Distribution of myosin isoenzymes among skeletal muscle fiber types. *J. Cell Biol.* **81,** 10–25.

Gladden, M. H. (1976). Structural features relative to the function of intrafusal muscle fibres in the cat. *Prog. Brain Res.* **44,** 51–59.

Goldspink, G., Scutt, A., Martindale, J., Jaenicke, T., Turay, L. and Gerlach, G. F. (1991). Stretch and force generation induce rapid hypertrophy and myosin isoform gene switching in adult skeletal muscle. *Biochem. Soc. Trans.* **19,** 368–73.

Golgi, C. (1880). Sui nervi dei tendini dell'uomo e di altri vertebrati e di un nuovo organo nervoso terminale musculo-tendrineo. *Mem. R. Accad. Sci. Torino* **32,** 359–385.

Gonyea, W. J., Sale, D. G., Gonyea, E B., and Mikesty, A. (1986). Exercise induced increases in muscle fiber number. *Eur. J. Appl. Physiol.* **55,** 137–141.

Gordon, A. M., Huxley, A. E., and Julian, F. J. (1966). The variation in isometric tension with sarcomere length in vertebrate muscle fibres. *J. Physiol (London)* **184,** 170–192.

Grimby, L., Hannerz, J., and Anlund, T. (1974). Disturbances in the voluntary recruitment order of anterior tibial motor units in spastic paraparesis upon fatigue. *J. Neurol. Neurosurg. Psychiatry* **37,** 40–46.

Hall, L. A., and McCloskey, D. I. (1983). Detections of movements imposed on finger, elbow and shoulder joints. *J. Physiol. (London)* **335,** 519–533.

Hariman, D. G. E., Parker, P. L., and Elliot, B. J. (1974). The histochemistry of human intrafusal muscle fibres. *J. Anat.* **119,** 205–206.

Henneman, E. (1957). Relation between size of neurons and their susceptibility to discharge. *Science* **126,** 1345–1347.

Henneman, E., and Mendell, L. M. (1981). Functional organization of motoneuron pool and its inputs. *In* "Handbook of Physiology" (V. B. Brooks, Ed.), Sect. 1, Vol. II, pp. 423–507. Am. Physiol. Soc., Washington, D. C.

Henriksson-Larsen, K. (1985). Distribution, number and size of different types of fibres in whole cross sections of female *M tibialis* anterior. An enzyme histochemical study. *Acta Physiol. Scand.* **123,** 229–235.

Herbert, R. D., and Gandevia, S. C. (1999). Changes in pennation with joint angle and muscle torque: in vivo measurements in human brachialis muscle. *J. Physiol. (London)* **484,** 523–32.

Huijing, P. A. (1985). Architecture of the human gastrocnemius muscle and some functional consequences. *Acta Anat.* **123,** 101–107.

Huijing, P. A. (1999). Muscle as a collagen fiber reinforced composite: a review of force transmission in muscle and whole limb. *J. Biomechan.* **32,** 329–45.

Hursh, J. B. (1939). Conduction velocity and diameter of nerve fibres. *Am. J. Physiol.* **127,** 131–139.

Injer, E. (1979). Effects of endurance training on muscle fibre ATP-ase activity, capillary supply and mitochondrial conent in man. *J. Physiol. (London)* **294,** 419–432.

Jami, L. (1992). Golgi tendon organs in mammalian skeletal muscle: funcitonal properties and central actions. *Physiol. Rev.* **72,** 623–666.

Jami, L., Murthy, K. S. K., and Petit, J. (1982). A quantitative study of skeletofusimotor innervation in the cat peroneus tertius muscle. *J. Physiol. (London)* **325,** 125–144.

Jansson, E., Sjödin, B., and Tesch, P. (1978). Changes in muscle fibre type distribution in man after physical training. *Acta Physiol. Scand.* **104,** 235–237.

Johnson, M. A., Polgar, J., Weightman, D., and Appleton, D. (1973). Data on the distribution of fibre types in thirty six human muscles. An autopsy study. *J. Neurol. Sci.* **18,** 111–129.

Kawakami, Y., Ichinose, Y., Kubo, K., Ito, M., Imai, M. and Fukunaga, T. (2000). Architecture of contracting human muscles and its functional significance. *J. Appl. Biomech.* **16,** 88–97.

Kellgren, J. H. (1938). Observations on referred pain arising from muscle. *Clin. Sci.* 3.

Kennedy, W. R. (1970). Innervation of normal human muscle spindles. *Neurology* **20,** 463–475.

Kennedy, W. R., Webster, H. deF, Yoon, K. S., and Jean, D. H. (1974). Human muscle spindles: microfilaments in the group IA sensory nerve endings. *Anat. Rec.* **180,** 521–532.

Kennedy, W. R., Webster, H. deF, and Yoon, K. S. (1975). Human muscle spindles: fine structure of the primary sensory ending. *J. Neurocytol.* **4,** 675–695.

Kernell, D. (1986). Organization and properties of spinal motoneurones and motor units. *Prog. Brain Res.* **64,** 21–30.

Kniffki, K. -D., Mense, S., and Schmidt, R. F. (1978). Responses of group IV afferent units from skeletal muscle to stretch, contraction and chemical stimulation. *Exp. Brain Res.* **31,** 511–522.

Komi, P. V., Viitasalo, J. H. T., Havu, M., Thorstensson, A., Sjödin, B., and Karlsson, T. (1977). Skeletal muscle fibres and muscle enzyme activities in monozygous and dizygous twins of both sexes. *Acta Physiol. Scand.* **100,** 385–392.

Kubota, K., and Masego, I. (1977). Muscle spindle supply to the human jaw muscle. *J. Dent. Res.* **56,** 901–909.

Kucera, J. (1985a). Characteristics of motor innervation of muscle spindles in the monkey. *Am. J. Anat.* **173,** 113–125.

Kucera, J. (1985b). Distribution of skeletofusimotor axons in lumbrical muscles of the monkey. *Anat. Embryol,* **173,** 95–104.

Kucera, J. (1986). Reconstruction of the nerve supply to a human muscle spindle. *Neurosci. Lett.* **63,** 180–184.

Kucera, J., and Dorovini-Zis, K. (1979). Types of human intrafusal muscle fibers. *Muscle Nerve* **2,** 437–451.

Kucera, J., and Walro, J. M. (1986). Factors that determine the form of neuromuscular junctions of intrafusal fibers in the cat. *Am. J. Anat.* **176,** 97–117.

Larsson, L. (1983). Histochemical characteristics of human skeletal muscle during aging. *Acta Physiol. Scand.* **117,** 469–471.

Larsson, L. (1992). Is the motor unit uniform? *Acta Physiol. Scand.* **144,** 143–54.

Larsson, L., and Ansved, T. (1985). Effects of long term training and detraining on enzyme histochemical and funtional skeletal muscle characteristics in man. *Muscle Nerve* **8,** *714–722.*

Larsson, L., Edström, L. Lindegren, B., Gorza, L. and Schiaffino, S. (1991). MHC composition and enzyme-histochemical and physiological properties of a novel fast-twitch motor unit type. *Am. J. Physiol.* **261,** C93–101.

Larsson, L., and Moss, R. L. (1993). Maximum velocity of shortening in relation to myosin isoform composition in single fibres from human skeletal muscles. *J. Physiol. (London)* **472,** 595–614.

Larsson, L., and Tesch, P. A. (1986). Motor unit fibre density in extremely hypertrophied skeletal muscles in man. Electrophysiological signs of muscle fibre hyperplasia. *Eur. J. Appl. Physiol.* **55,** 130–136.

Lloyd, D. P. C., and Chang, H. T. (1948). Afferent fibres in muscle nerves. *J. Neurophysiol.* **11,** 199–207.

Lowey, S., Waller, G. S. and Trybus, K. M. (1993). Function of skeletal muscle myosin heavy and light chain isoforms by an in vitro motility assay. *J. Biol. Chem.* **268,** 20414–20418.

Macefield, G., Gandevia, S. C., and Burke, D. (1989). Conduction velocities of muscle and cutaneous afferents in the upper and lower limbs of human subjects. *Brain* **112,** 1519–1532.

Marchand, R., Bridgman, C. E., Shumpert, E., and Eldred, E. (1971). Association of tendon organs with spindles in muscles of the cat's leg. *Anat. Rec.* **169,** 23–32.

Marchettini, P., Simone, D. A., Caputi, G. and Ochoa, J. L. (1996). Pain from excitation of identified muscle nociceptors in humans. *Brain Res.* **740:** 109–116.

Marsh, E., Sale, D. G., McComas, A. J., and Quinlan, J. (1981). Influence of joint position on ankle dorsiflexion in humans. *J. Appl. Physiol.* **51,** 160–167.

Matthews, P. B. C. (1972). "Mammalian Muscle Receptors and Their Central Actions." Arnold, London.

Maxwell, L. C., McCarter, R. J. M., Kuehl, T. J., and Robotham, J. L. (1983). Development of histochemical and functional properties of baboon respiratory muscles. *J. Appl. Physiol.* **54,** 551–561.

McCloskey, D. I., and Mitchell, J. H. (1972). Reflex cardiovascular and respiratory responses originating in exercising muscle. *J. Physiol. (London)* **224,** 173–186.

McKeon, B., and Burke, D. (1983). Muscle spindle discharge in response to contraction of single motor units. *J. Neurophysiol.* **49,** 291–302.

McKeon, B., Gandevia, S. C., and Burke, D. (1984). Absence of somatotopic projection of muscle afferents onto homonymous motoneurons in man. *J. Neurophysiol.* **51,** 185–194.

McWilliam, P. N. (1975). The incidence and properties of beta axons to muscle spindles in the cat hindlimb. *Q. J. Exp. Physiol. cogn. Med.* Sci. **60,** 25–36.

Mense, S., and Stahnke, M. (1983). Responses in muscle afferent fibres of slow conduction velocity to contractions and ischaemia in the cat. *J. Physiol. (London).* **342,** 383–397.

Meyer-Lohman, J., Riebold, W., and Robrecht, D. (1974). Mechanical influence of the extrafusal muscle on the static behaviour of deefferented primary muscle spindle endings in the cat. *Pflügers Arch.* **352,** 267–278.

Milner-Brown, H. S., Stein, R. B., and Yemm, R. (1973). The orderly recruitment of human motor units during voluntary isometric contractions. *J. Physiol. (London)* **230,** 359–370.

Murthy, K. S. K., Letbetter, W. D., Eidelberg, E., Cameron, W. E., and Petit, J. (1982). Histochemical evidence for the existence of skeletofusimotor (P) innervation in primate muscle. *Exp. Brain Res.* **52,** 6–8.

Narici, M. V., Binzoni, T., Hiltbrand, E., Fasel, J., Terrier, and Cerretelli, P. (1996). In vivo human gastrocnemius architecture with changing joint angle at rest and during graded isometric contraction. *J. Physiol. (London)* **496,** 287–297.

Németh, P. M., and Lowry, O. H. (1984). Myoglobin levels in individual human skeletal muscle fibers of different types. *J. Histochem. Cytochem.* **32,** 1211–1216.

Németh, P. M. Solanki, L., Gordon, D. A., Hamm, T. M., Reinking, R. M., and Stuart, D. G. (1986). Uniformity of metabolic enzymes within individual motor units. *J. Neurosci.* **6,** 892–898.

O'Sullivan, D. J., and Swallow, M. (1968). The fibre size and content of the radial and sural nerves. *J. Neurol. Neurosurg. Psychiatry* **31,** 464–470.

Ovalle, W. K., and Smith, R. S. (1972). Histochemical identification of three types of intrafusal muscle fibres in the cat and monkey based on the myosin ATPase reaction. *Can J. Physiol. Pharmacol.* **50,** 195–202.

Partridge, L. D., and Benton, L. A. (1981). Muscle, the motor. *In* "Handbook of Physiology (v. B. Brooks, Ed.), Sect. I, Vol. II, pp. 43–106. am Physiol. Sec., Washington, D. C.

Peachey, E. D., ed. (1983). "Handbook of Physiology," Sect. 10. Am. Physiol. Soc., Washington, D. C.

Peter, J. B., Barnard, R. J., Edgerton, v. R., Gillespie, C. A., and Stempel, K. E. (172). Metabolic profiles of three fiber types of skeletal muscles in guinea pigs and rabbits. *Biochemistry* **11,** 2627.

Proske, U. (1981). The Golgi tendon organ. Properties of the receptor and reflex action of impulses arising from tendon organs. *Int. Rev. Physiol.* **25,** 127–171.

Proske, U. (1997). The mammalian muscle spindle. *NIPS* **12,** 37–42.

Proske, U., Gregory, J. E. and Morgan, D. L. (1991). Where in the muscle spindle is the resting discharge generated? *Exp. Physiol.* **76,** 777–785.

Refshauge, K. M., Chan, R., Taylor, J. L. and McCloskey, D. I. (1995). Detection of movements imposed on human hip, knee, ankle and toe joints. *J. Physiol. (London)* **488,** 231–41.

Reichmann, W., and Pette, D. (1982). A comparative microphotometric study of succinate dehydrogenase activity levels in type I, IIA and IIB fibres of mammalian and human muscles. *Histochemistry* **74,** 27–41.

Richmond, F. J. R., and Abrahams, V. C. (1975). The morphology and distribution of muscle spindles in dorsal muscles of the cat neck. *J. Neurophysiol.* **38,** 1322–1339.

Richmond, F. J. R., MacGills, D. R. R., and Scott, D. A. (1985). Muscle-fiber compartmentalization in cat splenius muscles. *J. Neurophysiol.* **53,** 868–885.

Ringqvist, M. (1974). fiber types in human masticatory muscles. Relation to function. *Scand. J. Dent. Res.* **82,** 333–355.

Rothwell, J. C., Gandevia, S. C. and Burke, D. (1990). Activation of fusimotor neurones by motor cortical stimulation in human subjects. *J. Physiol. (London)* **431,** 743–756.

Sahgal, V., and Subramani, V. (1986). Attachments of human intrafusal fibers (ultrastructural study). *Muscle Nerve* 9, Suppl. **5S** 226.

Saltin, B., and Gollnick, P. D. (1983). Skeletal muscle adaptability: significance for metabolism and performance. *In* "Handbook of Physiology" (L. D. Peachey, Ed.), Sect. 10, pp. 555–631. Am. Physiol. Soc., Washington, D. C.

Schmalbruch, H. (1985). "Skeletal Muscle." Springer-Verlag, Berlin.

Scott, J. J. (1991). Responses of Ia afferent axons from muscle spindles lacking a bag_1 intrafusal muscle fibre. *Brain Res.* **543,** 97–101.

Scott, J. J., Kummel, H. and Illert, M. (1995). Skeletofusimotor (beta) innervation of proximal and distal forelimb muscles of the cat. *Neurosci. Lett.* **190,** 1–4.

Scott, S. H., and Loeb, G. E. (1994). The computation of position sense from spindles in mono- and multiarticular muscles. *J. Neurosci.* **14,** 7529–7540.

Sellers, J. R. (2000). Myosins: a diverse superfamily [Review]. *Biochim. Biophys. Acta Mol. Cell Res.* **1496,** 3–22.

Shefner, J. M., and Logigian, E. L. (1994). Conduction velocity in motor, cutaneous afferent, and muscle afferent fibers within the same mixed nerve. *Muscle Nerve* **17,** 773–778.

Sica, R. E. P., and McComas, A. J. (1971). Fast and slow twitch units in a human muscle. *J. Neurol. Neurosurg. Psychiatry* **34,** 113–120.

Silver, R. -L., de la Garza, J., and Rang, M. (1985). The myth of muscle balance. A study of relative strengths and excursions of normal muscles about the foot and ankle. *J. Bone Joint Surg.,* **67B,** 432–437.

Simonetta-Moreau, M., Marque, P., Marchand-Pauvert, V. and Pierrot-Deseilligny, E. (1999). The pattern of excitation of human lower limb motoneurones by probable group II muscle afferents. *J. Physiol. (London)* **527,** 287–300.

Sjöström, M. Bingquist, K.-E., Bylund, A.-C., Fridén, J., Gustavsson, L., and Schersten, T. (1982). Morphometric analyses of human muscle fiber types. *Muscle Nerve* **5,** 538–553.

Sjöström, M., Downham, D. Y., and Lexell, J. (1986). Distribution of different fiber types in human skeletal muscles: why is there a difference within a fascicle? *Muscle Nerve* **9,** 30–36.

Stacey, M. J. (1969). Free endings in skeletal muscle of the cat. *J. Anat.* **105,** 231–254.

Stålberg, E., Schwatz, M. S., Thiele, B., and Schiller, H. H. (1976). The normal motor unit in man. A single fibre EMG multielectrode investigation in man. *J. Neurol. Sci.* **27,** 291–301.

Staron, R. S., Hikida, R. S., and Hagerman, E. C. (1983). Reevaluation of human muscle fast-twitch subtypes: evidence for a continuum. *Histochemistry* **78,** 33–39.

Stilwell, D. L. (1957). The innervation of tendons and aponeuroses. *Am. J. Anat.* **100,** 289–317.

Stuart, D. G., Hamm, T. M., and Vanden Noven, S. (1987). Partitioning of monosynaptic Ia EPSP connections with motoneurons according to neuromuscular topography: generality and functional implications. *Prog. Neurobiol.* **30,** 437–447.

Swallow, M. (1966). Fibre size and content of the anterior tibial nerve of the foot. *J. Neurol. Neurosurg. Psychiatry* **29,** 205–213.

Swash, M. and Fox, K. P. (1972). Muscle spindle innervation in man. *J. Anat.* **112,** 61–80.

Swett, J. E., and Eldred, E. (1960). Distribution and numbers of stretch receptors in medial gastrocnemius and soleus muscles of the cat. *Anat. Rec.* **137,** 453–460.

Tackmann, W., Spalke, G., and Oginszus, H. J. (1976). Quantitative histometric studies of relation of number and diameter of myelinated fibres to electrophysiological parameters in normal sensory nerves of man. *J. Neurol.* **212,** 71–84.

Thomas, C. K., Johansson, R. S. and Bigland-Ritchie, B. (1991). Attempts to physiologically classify human thenar motor units. *J. Neurophysiol.* **65,** 1501–1508.

Thomas, C. K., Ross, B. H., and Stein, R. B. (1986). Motor-unit recruitment in human first doral interosseous muscle for static contractions in three different directions. *J. Neurophysiol.* **55,** 1017–1029.

Thomas, P. K., Sears, T. A., and Gilliatt, R. W. (1959). The range of conduction velocity in normal motor nerve fibres to the small muscles of the hand and foot. *J. Neurol. Neurosurg. Psychiatry* **22,** 175–181.

Trotter, J. A. (1990). Interfiber tension transmission in series-fibered muscles of the cat hindlimb. *J. Morphol.* **206,** 351–361.

Vallbo, Å. B. (1974). Afferent discharge from human muscle spindles in non-contracting muscle. Steady state impulse frequency as a function of joint angle. *Acta Physiol. Scand.* **90,** 303–318.

van Zuylen, E. J., Gielen, C. C. and Denier van der Gon, J. J. (1988). Coordination and inhomogeneous activation of human arm muscles during isometric torques. *J. Neurophysiol.* **60,** 1523–1548.

Vøllestad, N. K., Vange, O., and Hermansen, L. (1984). Muscle glycogen depletion patterns in type I and subgroups of type II fibres during prolonged severe exercise in man. *Acta Physiol. Scand.* **122,** 433–441.

Voss, V. H. (1937). Untersuchungen über Zahl, Anordnung und Lange der Muskelspindeln in den Lumbricalmuskeln des Menschen und einiger Tiere. *Z. Mikrosk.-Anat. Forsch.* **42,** 509–524.

Voss, V. H. (1971). Tabelle der absoluten und relativen Muskelspindelzahlen der menschlichen Skelettsmuskulatur. *Anat. Anz.* **129,** 562–572.

Wachstein, M., and Meisel, E. (1955). The distribution of demonstrable succinic dehydrogenase and mitochondria in tongue and skeletal muscle. *J. Biophys. Biochem. Cytol.* **1,** 483–488.

Weddell, G., and Harpman, J. A. (1940). The neurohistological basis for the sensation of pain provoked from deep fascia, tendon, and periosteium. *J. Neurol. Psychiatry* **3,** 319–328.

Weiss, A., and Leinwand, L. A. (1996). The mammalian myosin heavy chain gene family. *Annu. Rev. Cell Dev. Biol.* **12,** 417–439.

Williams, P. L., and Warwick, R. (1980). Myology. *In* "Gray's Anatomy," 36th Ed., pp. 506–529. Churchil Livingstone, Edinburgh.

Williamson, E., and Brooke, M. H. (1972). Myokymia and the motor unit. *Arch. Neurol. (Chicago)* **26,** 11–16.

Windhorst, U. (1979). A possible partitioning of segmental muscle stretch reflex into incompletely de-coupled parallel loops. *Biol. Cybernet.* **34,** 205–213.

Woittiez, R. O., Huijing, P. A., and Rozendal, R. W. (1983). Influence of muscle architecture on the length-force diagram of mammalian muscle. *Pflügers Arch.* **399,** 275–279.

Yellin, H. (1969). A histochemical study of muscle spindles and their relationship to extrafusal fibre types in the rat. *Am. J. Anat.* **125,** 31–46.

Young, M., Paul, A., Rodda, J., Duxson, M. and Sheard, P. (2000). Examination of intrafascicular muscle fiber terminations: implications for tension delivery in series-fibered muscles. *J. Morphol.* **245,** 130–45.

Zhou, M. Y., Klitgaard, H., Saltin, B., Roy, R. R., Edgerton, V. R. and Gollnick, P. D. (1995). Myosin heavy chain isoforms of human muscle after short-term space flight. *J. Appl. Physiol.* **78,** 1740–1744.

CHAPTER

6

Peripheral Autonomic Pathways

IAN GIBBINS
Department of Anatomy and Histology
Flinders University
Adelaide, Australia

GENERAL ORGANIZATION OF AUTONOMIC PATHWAYS

Together with the somatic motor pathways and neuroendocrine pathways, the autonomic pathways comprise the three motor outputs from the central nervous system (CNS). Functionally, the autonomic pathways provide motor control to a wide variety of visceral, vascular, and cutaneous effector tissues. These target tissues primarily consist of cardiac muscle, smooth muscle, or secretory epithelia, although autonomic nerve fibers also can be found in association with many other tissue types. Anatomically, autonomic pathways are characterized by the presence of final motor neurons lying completely outside the central nervous system. Usually, the final motor neurons and their associated supporting cells are aggregated into collections known as ganglia. This has led to the final motor neurons often being called "postganglionic neurons," although, strictly speaking, the term "postganglionic" refers only to the axons of these neurons.

Within the enteric plexuses of the gastrointestinal tract, the autonomic pathways contain well-defined sensory neurons and interneurons. However, there are probably no other autonomic sensory neurons outside the enteric plexuses. As discussed further below, the relations between spinal or cranial sensory pathways and autonomic motor pathways are complex and do not allow any simple and consistent classification that matches the various components of the autonomic motor pathways. Indeed, the final motor output of autonomic pathways is a coordinated series of specific patterns of activity generated in response to the full

range of sensory stimuli and central motor commands. This chapter will deal only with the peripheral components of the autonomic motor pathways. For discussion of various aspects of the organization of central pathways involved in autonomic motor function, see Chapters 8–10, 12, 13, 15, 17, 22, and 36. Unless stated otherwise, all of the information presented here pertains to humans.

Organization of Autonomic Ganglia

The final motor neurons in most autonomic pathways are aggregated into collections of cells called ganglia (from a Greek word meaning "knot"; singular: "ganglion"). The ganglia also contain satellite or glial cells (Schwann cells) that ensheath the neurons and their processes, and a varying amount of other tissues, such as blood vessels, connective tissue, cells of the immune system, and clusters of extraadrenal chromaffin cells. Depending on the pathway, a ganglion may contain from less than 10 to more than a million final motor neurons. Although there may be some variation from individual to individual, ganglia tend to have characteristic shapes and locations.

The final motor neurons in most autonomic pathways receive synaptic inputs from preganglionic neurons that have cell bodies located within the CNS. In most pathways, the preganglionic neurons provide the sole source of synaptic input to the final motor neurons. Two exceptions that will be discussed below include the prevertebral ganglia projecting to the gut, which receive additional inputs from neurons located in the enteric plexuses, and the final motor neurons within the enteric plexuses themselves, most of which do not receive any direct synaptic input from central neurons.

The axons of preganglionic neurons branch extensively within the ganglia and diverge to provide inputs for up to several hundred target neurons. In turn, each final motor neuron may receive convergent synaptic inputs from many preganglionic neurons. The divergence of preganglionic axons allows for a significant spatial amplification of the central command generated by a relatively small number of preganglionic neurons. By analogy with a somatic motor neuron and the muscle cells it innervates (a "motor unit"), a preganglionic neuron and the final autonomic motor neurons it innervates has been called a "neural unit" (Purves and Wigston, 1983). Almost certainly, the size of the neural units varies between different autonomic pathways. The convergence of several preganglionic inputs onto a single autonomic final motor neuron may allow the same neuron to be activated by different central pathways depending on the specific physiological or pathophysiological requirements at the time.

Microscopic Structure of Autonomic Final Motor Neurons

Studies in a variety of experimental animals have shown that final motor neurons in different pathways can show a wide range of morphological appearances (Gibbins, 1995). Generally, the neurons have a well-defined cell body (soma) and a variable number of dendrites, which may extend for several cell diameters, typically in the same plane as the major axis of the cell body. The dendrites usually show a relatively small degree of branching as they twist through the neuropil around other nearby neurons. Their terminal branches may be fine and varicose, although the functional significance of this morphology is unknown. Within the ganglia, the neuronal cell bodies tend to be closely packed. Most of the surface of the cell bodies and dendrites is covered with the processes of Schwann cells (satellite cells). Data from amphibians, mice, and guinea pigs indicate that synapses occur on only about 1–2% of the surface of the final motor neurons (Gibbins *et al.*, 1998).

Overall, the number of convergent preganglionic inputs to a final motor neuron seems to be positively correlated with the number of primary dendrites. Moreover, the total number of synapses formed on the cell body and dendrites of a final motor neuron also is proportional to its size (Gibbins, 1995; Gibbins *et al.*, 1998). Thus, in general, neurons with a relatively simple morphology receive a smaller number of convergent inputs and synapses than do neurons with more extensive dendritic fields. Although there have been no direct studies in humans, the relatively complex dendritic morphology of the final motor neurons in many human autonomic pathways suggests that a high degree of convergence of preganglionic inputs is likely to be common.

Autonomic Neuroeffector Junction

One characteristic feature of autonomic motor pathways is that the final motor neurons do not form neuroeffector junctions that are as well defined morphologically as the motor endplates found in the somatic motor pathways. The traditional view of the organization of the autonomic neuroeffector apparatus is that specialized neuroeffector junctions do not exist. According to this view, the terminal axons of the final motor neurons become varicose and ramify around or between the cells of the effector tissues, be they smooth muscle cells or secretory epithelia, without forming any special morphological relationship with them. When the neurons are stimulated, the transmitter diffuses relatively freely over a variable

distance (typically 50–1000 nm) from the release sites to activate receptors on the target cells.

During the last 10 years, extensive ultrastructural and functional studies in many different tissues from laboratory animals have revealed that this conventional view of the autonomic neuroeffector apparatus is likely to be wrong or, at best, too simplistic. Instead, it appears that specialized neuroeffector junctions are present in many tissues innervated by autonomic motor neurons (Bennett, 1996; Hirst *et al.*, 1996). Serial section electron microscopic analyses have shown clearly that many varicosities of the terminal axons of autonomic motor neurons form close associations with target effector cells. At these sites (autonomic neuroeffector junctions), varicosities, largely free of Schwann cell cover, come within 50–80 nm of the surface of the target cell. Within these closely contacting varicosities, small synaptic vesicles are clustered toward the prejunctional membrane adjacent to the effector cell. In some cases, these vesicles cluster toward a small prejunctional density similar to those seen in presynaptic membranes at motor endplates. Although there has been no morphological evidence to date for a corresponding postjunctional specialization, functional studies have demonstrated that the receptors mediating responses from neurally released transmitter are often different from those activated by exogenously applied agonists. The simplest interpretation of these data is that there are specialized postjunctional receptors that are activated by neurally released transmitter from close neuroeffector junctions, and that these receptors are different from extrajunctional receptors located more widely over the surface of the effector cells (Hirst *et al.*, 1996).

Recent experimental studies in laboratory mammals have shown that autonomic neuroeffector transmission to smooth muscle may occur via intermediary cell types, such as interstitial cells in the gastrointestinal tract (Burns *et al.*, 1996; Ward *et al.*, 1998, 2000) or endothelial cells in blood vessels (e.g., Häbler *et al.*, 1997). The organization and roles of these cells in autonomic pathways will be discussed in the appropriate sections below.

Autonomic Neurotransmitters

Historically, major advances in the understanding of chemical neurotransmission have come from studies of peripheral autonomic pathways, including the first demonstrations of chemical transmission itself. Compared with somatic motor neurons, the final motor neurons in autonomic pathways are now known to use a diverse array of chemical neurotransmitters. Unlike somatic motor neurons, which only have excitatory effects on their target muscle cells, autonomic transmitters may stimulate or inhibit the activity of the effector cells.

One of the most surprising discoveries of the last 25 years is that any single autonomic final motor neuron may contain five or more potential transmitters. Furthermore, the precise combination of transmitters expressed by the neurons generally varies from pathway to pathway. Typically, a particular functional class of autonomic final motor neurons utilizes a range of transmitters with different time courses of action on their effector cells (Morris and Gibbins, 1992). Rapid responses may be mediated by low molecular weight transmitters such as nitric oxide (NO) or adenosine 5′-triphosphate (ATP). Responses with somewhat longer time courses may be mediated by noradrenaline (NA) or acetylcholine (ACh), whereas the slowest responses are mediated by peptides such as neuropeptide Y (NPY) or vasoactive intestinal polypeptide (VIP). Many of these transmitters also may have prejunctional effects, which generally tend to inhibit further transmitter release. Indeed, some neuropeptides, such as opioid peptides or somatostatin, appear to have predominantly presynaptic inhibitory actions.

Not only is there considerable diversity of the combinations of transmitters used by autonomic final motor neurons, but there is a comparable diversity in the postjunctional receptors on the effector cells. Thus, transmitters such as NA, ACh, or VIP, may have excitatory or inhibitory actions depending on both the exact subclass of postjunctional receptor and the type of effector cell. For example, the action of NA on β-adrenoceptors may inhibit smooth muscle activity or stimulate cardiac muscle contractility. Similarly, VIP relaxes most smooth muscle cells but stimulates the secretory activity of many epithelia.

Regardless of the pathway within which they lie, preganglionic neurons utilize ACh as the primary transmitter mediating fast ganglionic transmission. However, many preganglionic neurons also contain neuropeptides, which tend to have one of two actions: some, such as VIP, substance P or calcitonin gene–related peptide (CGRP), enhance the excitability of the target neurons, whereas others, such as enkephalin, inhibit the release of ACh. More recently, NO has been identified as a potential transmitter in preganglionic neurons, but its contributions to ganglionic transmission are complex and not yet well characterized.

Functional Divisions of Autonomic Pathways

Peripheral autonomic pathways can be classified by a variety of criteria, such as their function (e.g., vasoconstrictor or vasodilator), their transmitter content

(e.g., NA or ACh), the location of their ganglia (e.g., cranial or pelvic, paravertebral or prevertebral), or the central origin of their preganglionic neurons (e.g., thoracic or sacral levels of the spinal cord). Many of these features tend to correlate to varying degrees, which has led to the most widely used scheme for classifying autonomic pathways into three main divisions, as originally proposed by Langley. In this scheme, the autonomic pathways are classified primarily by the sources of their preganglionic inputs. Accordingly:

Sympathetic pathways contain preganglionic inputs from neurons located in thoracic and upper lumbar spinal cord. The final motor neurons are found in ganglia associated anatomically with the spinal nerves (paravertebral or sympathetic chain ganglia), the ventral branches of the abdominal aorta (prevertebral ganglia), branches of the carotid artery (cervical ganglia), or the pelvic viscera (pelvic ganglia). Most sympathetic final motor neurons utilize NA as one of their transmitters, together with other transmitters such as ATP and peptides such as NPY and galanin. However, some sympathetic final motor neurons use ACh as their main nonpeptide transmitter and, in addition, may contain peptides such as VIP and CGRP.

Parasympathetic pathways, according to traditional classifications, contain preganglionic inputs from either of two disparate sets of central neurons. *Cranial* parasympathetic neurons receive preganglionic inputs from neurons located in the midbrain or brain stem (see Chapters 10 and 16). Their ganglia are associated with branches of the cranial nerves. Parasympathetic neurons located in ganglia associated with the *pelvic* viscera receive preganglionic inputs from neurons projecting from sacral segments of the spinal cord. The final motor neurons in parasympathetic pathways usually use ACh, NO, or both as their nonpeptide transmitters. A wide range of peptides occur in various populations of parasympathetic neurons, including VIP, CGRP, somatostatin, and opioid peptides. Under normal circumstances, no parasympathetic neurons use NA as a transmitter.

The third division of autonomic neurons is made up of the *enteric* plexuses. These neurons are aggregated into series of small ganglia located in the walls of the gastrointestinal tract. The enteric plexuses are unique among autonomic pathways for two main reasons: first, most of the enteric neurons lack direct inputs from central preganglionic neurons; second, in addition to motor neurons, the enteric plexuses contain interneurons and sensory neurons. As a consequence, much of the activity of the enteric plexuses can occur in the absence of direct central control. Nevertheless, central control of at least some enteric neurons can be achieved by the activity of vagal preganglionic inputs to the foregut, sacral preganglionic inputs to the hindgut, and prevertebral sympathetic neurons projecting to much of the gastrointestinal tract. Enteric neurons use a wide range of transmitters, including NO, ACh, ATP, and many neuropeptides. The precise combinations of transmitters vary with the projection and function of the neurons. Other potential transmitters, including serotonin (5-HT) and amino acids, such as γ-aminobutyric acid (GABA) and glutamate, also may be used by some enteric neurons. However, few if any enteric neurons synthesize catecholamine transmitters such as NA.

While the scheme summarized above is reasonably useful, it has two limitations. First, although the cranial and sacral parasympathetic pathways have some features in common, functionally they are not closely related. For example, there is no reason to link the cranial pathways involved in salivary secretion with the sacral pathways involved in micturition. Furthermore, regulation of the activity of many pelvic organs requires coordinated control via both sympathetic and sacral parasympathetic pathways, often in association with the relevant somatic motor pathways (e.g., during sexual behavior). Indeed, many of the ganglia in pelvic pathways contain mixtures of neurons, some of which receive preganglionic inputs from lumbar spinal levels (by definition, sympathetic) and others of which receive preganglionic input from sacral spinal levels (by definition, parasympathetic). Some individual neurons receive convergent inputs from both lumbar and sacral preganglionic neurons, and they may be considered to lie in both sympathetic *and* parasympathetic pathways. Consequently, I will deal with the cranial parasympathetic pathways separately from the sacral parasympathetic pathways. The latter will discussed together with the relevant sympathetic pathways as *pelvic* pathways.

The second problem with the traditional classification of the autonomic pathways is that it leads to their being considered as generic "systems" operating as blocks, usually in opposition to each other, as in the case of the sympathetic and parasympathetic divisions. However, a huge body of data from studies in animals and humans has demonstrated clearly that this idea is a gross and misleading oversimplification. It is abundantly clear from the following descriptions that neither the sympathetic "system" not the parasympathetic "system" is ever activated in its entirety. Rather, each major division of the autonomic motor outflow consists of a series of discrete functional pathways that may be activated independently or in various combinations as required by ongoing physiological or pathophysiological demands on the organism. More-

over, while many effector tissues are innervated by sympathetic and parasympathetic pathways with opposing actions, there are many situations where neurons in sympathetic and parasympathetic pathways may be coactivated. Finally, some target tissues may be innervated by multiple sympathetic or parasympathetic pathways, which may have opposing or complementary actions.

Are There "Autonomic Sensory" Neurons?

Autonomic pathways generally are defined as motor pathways. However, terms like "sympathetic afferents" are sometimes used to refer to sensory neurons with cell bodies in the dorsal root ganglia that innervate visceral targets such as the heart or gastrointestinal tract. The main argument for using this terminology is that these sensory fibers stimulate autonomic reflexes when activated. However, almost any sensory input can generate a response that contains autonomic components. For example, visual stimuli activate pupillomotor and accommodation responses, whereas olfactory and gustatory stimuli can generate salivatory and vasodilator responses. Conversely, visceral nociceptive afferents can produce responses involving somatic motor pathways, such as the contractions of abdominal muscles accompanying severe pain from the gastrointestinal tract or peritoneum. Even from these simple and obvious examples, it is clear that few if any cranial or spinal afferent pathways are associated exclusively with autonomic responses.

Although there are probably no autonomic spinal afferent neurons, within the enteric plexuses there are well-defined populations of neurons that have a primary sensory function (Furness *et al.*, 1998; Kunze and Furness, 1999). The projections of these neurons are restricted to the gut where they participate in local reflexes. They respond to distention of the gut wall or changes in its chemical environment and are essential for the generation of appropriate patterns of activity of enteric neurons regulating gastrointestinal motility, secretion, and blood flow. The intrinsic sensory neurons project either directly or via interneurons to another population of enteric neurons, which in turn project out from the gut (*intestinofugal* neurons) to prevertebral sympathetic ganglia where they can influence the excitability of neurons regulating gut activity (discussed further below).

Despite occasional reports to the contrary, there is little good evidence for genuine sensory neurons within autonomic ganglia lying in sympathetic, parasympathetic, or pelvic pathways. However, many autonomic ganglia contain axon collaterals of unmyelinated sensory neurons (Gibbins, 1995; Mawe, 1995) that may modify the excitability of the autonomic neurons under some circumstances.

Autonomic Pathways as Functional Entities

The following descriptions will focus on the microscopic, chemical, and functional neuroanatomy of the peripheral autonomic pathways of humans. Much of the microscopic anatomy is derived from old studies that have not been repeated or validated with modern techniques. Furthermore, much of the more recent chemical neuroanatomy has not taken into account the possibility that many of the markers that have been examined either may not be specific for the neuronal populations under investigation or may coexist with other markers and potential transmitters. All these problems are confounded by the difficulties in obtaining suitable human material for detailed study. Nevertheless, there are very many studies on the function of autonomic motor pathways in humans that, taken together, shed valuable light on the underlying organization of the pathways. The overwhelming message from these studies is that the autonomic motor pathways in humans, as in animals, are organized into a series of functional entities allowing the precise and graded regulation of the activity of specific effector tissues. It is in this context that the following descriptions of the peripheral autonomic pathways are presented.

CRANIAL AUTONOMIC PATHWAYS

The cranial autonomic pathways project to a wide variety of targets in the head, neck, thorax, and abdomen (Table 6.1). The pathways are associated functionally with four of the cranial nerves: the oculomotor (third cranial nerve; 3n), facial (seventh cranial nerve, 7n), glossopharyngeal (ninth cranial nerve, 9n) and the vagus (tenth cranial nerve, 10n). The last three of these pathways are associated with derivatives of the branchial arches and share many anatomical, neurochemical, and functional features. Most of the final motor neurons in each of these cranial autonomic pathways are in four pairs of major ganglia located bilaterally in the head: the ciliary (3n), pterygopalatine (7n), submandibular (7n), and otic (9n). The ciliary, pterygopalatine, and otic ganglia lie in close anatomical association with each of the main branches of the trigeminal nerve (fifth cranial nerve; the ophthalmic, maxillary, and mandibular branches, respectively; Fig. 6.1), although apparently none of them receives preganglionic inputs from this nerve (see Larsell and Fenton, 1928). Scattered throughout the cranial nerves,

TABLE 6.1 Sources of Parasympathetic Innervation to Cranial Targets

Target	Primary source	Secondary source	Potential transmitters	Function
Iris	Cil		ACh	Contract constrictor[a] Relax dilator[a] (constriction of pupil)
		PtPGn	ACh/NO/VIP	Dilation of pupil?
Ciliary muscles	Cil		ACh	Contract (accommodation)
Choriod vessels	Local neurons	PtPGn	ACh/NO/VIP	Vasodilation
Lacrimal gland	PtPGn	Cil, Otic	ACh/NO/VIP/PACAP	Secretion; vasodilation
Nasal mucosa	PtPGn		ACh/NO/VIP/PACAP	Secretion; vasodilation
Palatine mucosa	PtPGn		ACh/VIP	Secretion; vasodilation
Cerebral arteries	PtPGn	Otic	ACh/NO/VIP	Vasodilation
Superior tarsal muscle	PtPGn		ACh/VIP?	?
Tarsal (Meibomian) glands	PtPGn		ACh/VIP?	?
Hair follicles & glands	PtPGn		ACh/VIP	?
Submandibular gland	SMnGn	Local neurons	ACh/VIP ACh/NO/VIP	Secretion; vasdilation
Sublingual gland	SMnGn	Local neurons	ACh/VIP ACh/NO/VIP	Secretion; vasodilation
Parotid gland	Otic		ACh/VIP ACh/NO/VIP	Secretion; vasodilation
Facial blood vessels	Otic	PtPGn	ACh/NO/VIP	Vasodilation

[a]Pathways that are tonically active.

ACh, acetylcholine; Cil, ciliary ganglion; Otic, otic ganglion; NO, nitric oxide; PACAP, pituitary adenylate cylcase–activating peptide; PtPGn, pterygopalatine ganglion; SMnGn, submandibular ganglion; VIP, vasoactive intestinal polypeptide.

especially the intracranial ramifications of the facial and glossopharyngeal nerves, there are small aggregations of autonomic nerve cell bodies forming microganglia (Fig. 6.1). The final motor neurons of the vagal autonomic pathways (10n) probably lie entirely extracranially, mostly in microganglia associated with the target organs. As far as is known, all the preganglionic neurons in the cranial pathways are cholinergic, although at least some of these neurons also contain nitric oxide synthase (NOS; Gai and Blessing, 1996), the enzyme responsible for synthesis of NO.

Ciliary Ganglion and Oculomotor Pathways

The autonomic pathways of the oculomotor nerve (3n) are involved in the regulation of many important facets of ocular function, including the control of pupil diameter, focus (lens accommodation), and local blood flow. The final motor neurons are primarily located in the *ciliary ganglion*. Most of the preganglionic neurons project from the Edinger–Westphal nucleus via the oculomotor nerve, reaching the ciliary ganglion along the branch to the inferior oblique muscle (Grimes and von Sallman, 1960; Lang, 1981; Mitchell, 1953a; Warwick, 1954). Some preganglionic fibers probably also reach the ciliary ganglion via the long ciliary branch of the trigeminal nerve (Kuchiiwa *et al.* 1993; Zhang *et al.*, 1994).

The ciliary ganglion is a small ganglion, less than 2 mm long, which lies in fat-filled connective tissue in the posterior orbit, just anterior to the superior orbital fissure (Kuntz, 1945; Mitchell, 1953a). On average, the human ciliary ganglion contains about 3000 neurons (range 1000–6800 neurons; Pearson and Pytel, 1978b; Perez and Keyser, 1987), mostly 20–35 μm in diameter (Slavich, 1932). Most of the neurons are multipolar, bearing short branching dendrites (Kuntz, 1945; Slavich, 1932; Warwick, 1954). They are surrounded by dense pericellular networks of preganglionic terminals (Slavich, 1932). Ultrastructural studies in macaques show that many of the synapses from these terminals are made onto short spinelike processes from the cell body or dendrites of the target neurons (May and Warren, 1993; Zhang *et al.*, 1994). The final motor neurons project to the iris and ciliary muscles through postorbital fat via 12–20 short ciliary nerves that are grouped superior and inferior to the optic nerve (Grimes and von Sallman, 1960; Mitchell, 1953a). The ciliary nerves penetrate the sclera and run anteriorly in the perichoroid space to reach their targets.

A small accessory ciliary ganglion occurs in the long ciliary nerves arising from the ophthalmic nerve

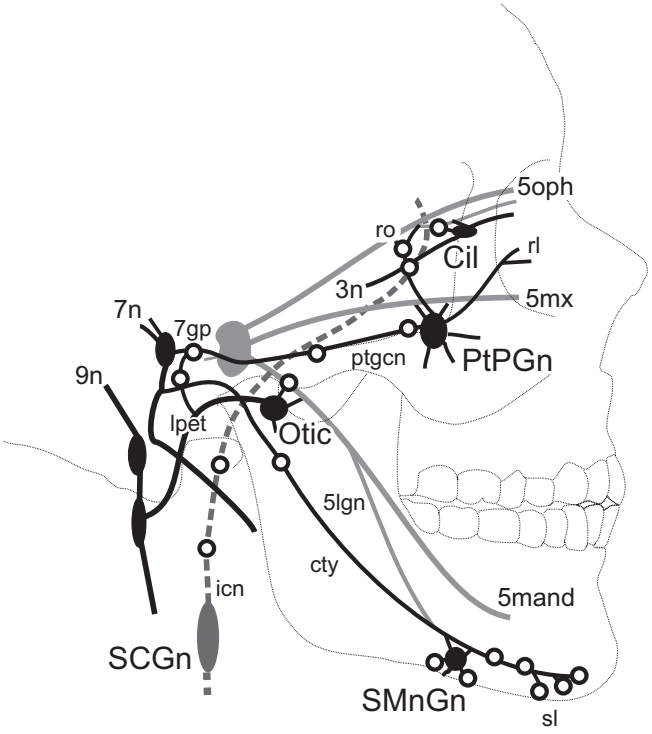

FIGURE 6.1 Distribution of major autonomic ganglia and microganglia *(open circles)* in the cranial nerves. Major branches of the trigeminal nerve are shown in gray (5oph, ophthalmic division; 5mx, maxillary division; 5mand, mandibular division). Other cranial nerves include the oculomotor nerve (3n); facial nerve (7n) and glossopharyngeal nerve (9n). The main path of the internal carotid nerve (icn) carrying sympathetic fibers along the internal carotid artery from the superior cervical ganglion (SCGn) is shown by the dashed gray line. Cil, ciliary ganglion; cty, chorda tympani; 7gp, greater superficial petrosal nerve; lpet, lesser petrosal nerve; 5lgn, lingual nerve; ptgcn, nerve of the pterygoid canal (Vidian nerve); Otic, otic ganglion; PtPGn, pterygopalatine ganglion; rl, lacrimal rami from pterygopalatine ganglion; ro, orbital rami from pterygopalatine ganglion; sl, nerves to sublingual gland; SMnGn, submandibular ganglion.

(Grimes and von Sallman, 1960; Kuchiiwa *et al.*, 1993). In addition, scattered nerve cell bodies also occur along the ciliary nerves, along the nasociliary nerve, and within the choroid (Bryson *et al.*, 1966; Flügel *et al.*, 1994; Givner, 1939; Grimes and von Sallman, 1960; Miller *et al.*, 1983; Sunderland and Hughes, 1946).

The ciliary ganglion neurons are functionally cholinergic. Although some of them contain immunoreactivity to tyrosine hydroxylase, they lack dopamine β-hydroxylase, so that none of them is likely to be noradrenergic (Kirch *et al.*, 1995). They primarily mediate pupilloconstriction and contraction of the ciliary muscles (Lograno and Reibaldi, 1986). These responses must be mediated by separate pathways and populations of final motor neurons, since pupilloconstriction and accommodation can occur independently of each other. Pupilloconstriction is likely to be achieved by the simultaneous contraction of the iris sphincter muscle and relaxation of the iris dilator muscle, both actions being mediated by muscarinic receptors (Ehinger *et al.*, 1968; Heller *et al.*, 1990; Narita and Watanabe, 1982; Suzuki *et al.*, 1983). Recent studies in monkeys indicate that some neurons in the ciliary ganglion also innervate the lacrimal gland (Van der Werf *et al.*, 1996), although their function is unknown.

The neurons located in the choroid contain NOS and VIP (Flügel *et al.*, 1994; Miller *et al.*, 1983) and almost certainly innervate the choroidal blood vessels (Flügel *et al.*, 1994; Miller *et al.*, 1983; Stone *et al.*, 1986; Uusitalo *et al.*, 1984), where they presumably cause vasodilation. These neurons also may innervate the ciliary muscles (Miller *et al.*, 1983; Stone *et al.*, 1986; Uusitalo *et al.*, 1984). However, all these targets also may be innervated neurons containing NOS and VIP that project from the pterygopalatine ganglion (Nilsson, 2000; Ruskell, 1985; see below).

Autonomic Pathways of the Facial and Glossopharyngeal Nerves

The autonomic pathways associated with the facial (7n) and glossopharyngeal (9n) nerves have several features in common: their main functions are secretomotor and vasodilator, their preganglionic neurons are closely associated in the superior and inferior salivatory nuclei, and there are direct anatomical connections between the intracranial pathways. These pathways include the pterygopalatine, submandibular, and otic ganglia, as well as numerous microganglia. Embryologically, the facial nerve is associated with the second branchial arch and its derivatives, whereas the glossopharyngeal nerve is associated with the third branchial arch and its derivatives. The preganglionic neurons in these pathways are organized according to the branchiomeric origins of the corresponding nerves. However, there is no simple relationship between the projections of the autonomic final motor neurons in these pathways and the branchial arch origins of their targets.

Pathways Through the Pterygopalatine Ganglion

The pterygopalatine ganglion (also known as the sphenopalatine ganglion or, more rarely these days, the nasal ganglion or Meckel's ganglion; Gloster, 1961; Larsell and Fenton, 1928) lies deep within the pterygoid fossa, rostral to the anterior opening of the pterygoid canal and inferior to the maxillary nerve (second division of the trigeminal nerve; Kuntz, 1945; Mitchell, 1953a). It can be considered the main parasympathetic ganglion of the upper jaw and related structures. The ganglion is about 3 mm long and contains about 56,500 closely packed nerve cell bodies

(Pearson and Pytel, 1978b). They tend to be ovoid, 20×30 μm in diameter, with thick branching dendrites that often bear knob-shaped endings (Pearson and Pytel, 1978b; Slavich, 1932; Wilson, 1984). In some cells, the dendrites are long, multibranched, and contribute to dense dendritic glomeruli (Slavich, 1932). Secretomotor neurons are larger on average than the vasomotor neurons (e.g., Kuchiiwa *et al.*, 2000; see Gibbins, 1995).

Preganglionic axons reach the pterygopalatine ganglion from the facial nerve via the greater superficial petrosal nerve and the nerve of the pterygoid canal (Vidian nerve). In addition, small groups of nerve cell bodies are found in the distal portion of the nerve of the pterygoid canal, proximal to its junction with the pterygopalatine ganglion (Nomura and Matsuura, 1972).

Final motor neurons in the pterygopalatine ganglion project to blood vessels and glands of the nasal cavity and palate via the nasal, palatine, and pharyngeal nerves (Table 6.1; Azuma *et al.*, 1982; Kuntz, 1945). Lacrimal rami carry postganglionic fibers, probably from separate populations of neurons, to the blood vessels and secretory acini of the lacrimal gland (Fig. 6.1; Ruskell, 1971; Van der Werf *et al.*, 1996). Ocular rami carry postganglionic vasodilator fibers projecting to blood vessels of the eye (Fig. 6.1; Ruskell, 1970a, b, 1985). In addition to these discrete pathways, many postganglionic axons leave the pterygopalatine ganglion and follow the periarterial plexuses to the vascular beds of the nose (Mitchell, 1954) and eye (Ruskell, 1970b). The pterygopalatine ganglion has been shown to innervate the cerebral circulation in laboratory mammals (Hara *et al.*, 1985; Keller *et al.*, 1985; Walters *et al.*, 1986). This arrangement is also likely to occur in humans, with the probable pathways following the ethmoidal arteries and nerves (Hara and Weir, 1988; Mitchell, 1954). There may be a parasympathetic innervation of hair follicles in the face and at least some of these fibers originate from the pterygopalatine ganglia (Gibbins, 1990; cf. Montagna *et al.*, 1964).

Most of the neurons in human pterygopalatine ganglia are functionally cholinergic. They stain strongly for acetylcholinesterase (AChE; Nomura and Matsuura, 1972) and contain VIP, its gene-related peptide, peptide histidine methionine (PHM), and other peptides from the same family including pituitary adenylate cyclase–activating peptide (PACAP; Lundberg *et al.*, 1984; Sibony *et al.*, 1988; Lacroix *et al.*, 1990; Uddman *et al.*, 1999) and helospectin (Hauser-Kronberger *et al.*, 1992b). Most of them (86%) also contain NOS (Gorelova *et al.*, 1996; Hanzawa *et al.*, 1997; Minami *et al.*, 1994; Tasman *et al.*, 1998; Toda *et al.*, 2000; Uddman *et al.*, 1999).

Final motor neurons in the pterygopalatine ganglion give rise to dense networks of non-noradrenergic axons found around the blood vessels (including veins to a lesser extent) and glands in the nasal mucosa (including the olfactory mucosa), oral mucosa, and lacrimal glands, where they mediate secretion and vasodilation (Chorobski and Penfield, 1932; Cauna and Cauna, 1975; Cauna *et al.*, 1972; Golding-Wood, 1961, 1973; Hanazawa *et al.*, 1997; Hauser-Kronberger *et al.*, 1992b; Higbee, 1949; Hilliges *et al.*, 1994; Konno and Togana, 1979; Kulkarni *et al.*, 1994; Lundberg *et al.*, 1984; Nomura and Matsuura, 1972; Riederer *et al.*, 1996, 1999; Rossoni *et al.*, 1979; Sibony *et al.*, 1988; Slade *et al.*, 1986; Tasman *et al.*, 1998; Uddman and Sundler, 1979; Uddman *et al.*, 1980b). Most of these neurons contain ACh, NO, VIP, and probably helospectin. However, animal studies indicate that separate populations of final motor neurons, distinguished by both morphology and transmitter content, innervate the blood vessels and secretory tissues within the cranial glands (Morris *et al.*, 1997; Yasui *et al.*, 1997; Kuchiiwa *et al.*, 2000). Some neurons in the pterygopalatine ganglion project to the smooth muscle part of the superior tarsal muscle (levator palpebrae superioris), tarsal (meibomian) glands, and other small glands in the upper eyelid (Van der Werf *et al.*, 1993; Seifert and Spitznas, 1999). However, in each case their function is unknown.

Specific populations of vasodilator neurons in the pterygopalatine ganglion, probably containing VIP, PACAP, and NOS, innervate the cerebral arteries (Edvinsson *et al.*, 1987; Suzuki *et al.*, 1984; Minimi *et al.*, 1994; Kimura *et al.*, 1997; Ignacio *et al.*, 1997; Toda *et al.*, 2000a, b). The cerebral vasodilator pathways may be tonically active to some degree (Toda *et al.*, 2000a). Neurons containing NOS and VIP also project from the pterygopalatine ganglion to the blood vessels of the eye (Miller *et al.*, 1983; Nilsson, 2000; Stone *et al.*, 1986; Uusitalo *et al.*, 1984), where they cause vasodilation and may mediate increases in intraocular pressure (Nilsson, 2000; Ruskell, 1970b, 1985).

Although secretory responses of the nasal mucosa or lacrimal glands to pterygopalatine nerve stimulation are atropine sensitive and, therefore, are mediated primarily by ACh, vasodilator responses in the cranial circulation, including the cerebral vessels, are largely unaffected by atropine treatment (e.g., Gloster, 1961; Ruskell, 1985; Toda, 1981). These responses are probably mediated by various combinations of NO, VIP, and PHM, coreleased with ACh (Barroso *et al.*, 1996; Ignacio *et al.*, 1997; Izumi, 1999; Kimura *et al.*, 1997; Lundberg, 1981; Minami *et al.*, 1994; Okita and Ichimura, 1998; Tasman *et al.*, 1998; Toda and Okamura, 1996; Toda *et al.*, 2000a, b) .

Pathways Through the Submandibular Ganglion

The submandibular ganglion is fusiform, 2–3 mm long, and is closely associated with the lingual nerve

as it crosses the superior part of the hyoglossus muscle. Preganglionic axons leave the facial nerve in the chorda tympani nerve and join the lingual nerve to reach the submandibular ganglion (Diamant and Wiberg, 1965; Mitchell, 1953a). There is also a possible preganglionic input from the glossopharyngeal nerve (Laage-Hellman and Stromblad, 1960; Reichert and Poth, 1933). Axons of the final motor neurons leave the ganglion to supply the submandibular salivary gland and, after reentering the lingual nerve, the major sublingual gland (Kuntz, 1945; Mitchell, 1953a). Additional final motor neurons in this pathway are embedded in the substance of the submandibular gland, especially around the point of entry of blood vessels and nerves (Kuntz and Richins, 1946; Magielski and Blatt, 1958; Uddman *et al.*, 1980a). A similar group of ganglion cells may occur in the sublingual gland (Chorobski and Penfield, 1932). Some axons in the sublingual and submaxillary glands may arise from final motor neurons located in the chorda tympani itself (Ekstrom *et al.*, 1984; Gibbins *et al.*, 1984).

The neurons provide a dense secretomotor and vasodilator innervation to the submandibular and sublingual glands (Diamant and Wiberg, 1965; Reichert and Poth, 1933). The axons are strongly AChE positive (Garret, 1967; Rossoni *et al.*, 1979), and at least some of them contain VIP and PHM (Hauser-Kronberger *et al.*, 1992a; Kusakabe *et al.*, 1997; Lundberg *et al.*, 1984; Uddman *et al.*, 1980a). Nevertheless, the density of innervation in humans seems to be less than that in the glands of small laboratory mammals (Garret, 1967; Lundberg *et al.*, 1984; Uddman *et al.*, 1980a). On average, the density of VIP fibers around mucous acini is greater than around serous acini (Kusakabe *et al.*, 1997).

It is likely that secretion is largely mediated by ACh but that vasodilation is largely mediated by NO, VIP, and PHM (Ekström,1999; Lundberg, 1981). However, NO, VIP, and PHM all may modify the composition of the saliva, including the content of proteins (e.g., amylase) and bicarbonate ions (Brown *et al.*, 1995; Ekström,1999; Garrett and Kidd, 1993; Larsson *et al.*, 1986) .

Pathways Through the Otic Ganglion

The otic ganglion is very small and may exist only as a group of small ganglia, medial to the mandibular nerve, just distal to its exit from the skull (Kuntz, 1945; Mitchell, 1953a). The preganglionic pathway is usually said to arise from the glossopharyngeal nerve (9n) via the tympanic plexus and the lesser petrosal nerve. However, lesioning studies strongly suggest that an additional preganglionic pathway to the otic ganglion runs via the chorda tympani nerve and that there is at least some preganglionic input from the facial nerve (Diamant and Wiberg, 1965; Kuchiiwa *et al.*, 1998; Kuntz, 1945; Mitchell, 1953a; Reichert and Poth, 1933). Postganglionic axons leave the ganglion mainly via the auriculotemporal nerve to reach the parotid gland (Kuntz and Richins, 1946). Some otic ganglion neurons may project directly to the vasculature of the jaws and the cerebral circulation (Kaji *et al.*, 1988; Segade *et al.*, 1987; Walters *et al.*, 1986), whereas others may provide weak innervation to sweat glands around the lips (List and Peet, 1938; Wilson, 1935). Studies in cats indicate that there also is a small projection from the otic ganglion to the lacrimal gland (Cheng *et al.*, 2000); this projection may correspond to one of the facial nerve pathways through the ganglion.

The neurons of the otic ganglion are morphologically similar to those of the pterygopalatine ganglion (Slavich, 1932). Most of the neurons contain VIP, PACAP, and NOS (Uddman *et al.*, 1999). They provide a moderately dense AChE-positive innervation of the parotid gland (Garret, 1967; Rossoni *et al.*, 1979). Earlier reports suggested that there apparently are relatively few VIP-containing axons in this gland (Uddman *et al.*, 1980a). However, more recent studies have revealed that there is a relatively dense innervation of the acini and blood vessels by fibers containing VIP (Hauser-Kronberger *et al.*, 1992a; Matsuda *et al.*, 1997). Otic ganglion neurons mediate a cholinergic secretion of the parotid gland and contribute to vasodilation responses in the gland and in the vasculature of the jaw (Izumi, 1999; Kaji *et al.*, 1988; Segade *et al.*, 1987). These vasodilations are likely to be mediated primarily by NO and VIP or related peptides (Nozaki *et al.*, 1993; Soinila *et al.*, 1996). Animal studies have shown consistently that some otic ganglion neurons project to the cerebral vasculature, where they probably cause vasodilation (eg. Kadota *et al.*, 1996; Suzuki *et al.*, 1988; Uemura *et al.*, 1988).

Microganglia

In addition to the microganglia already described in the distal nerve of the pterygoid canal and in association with the salivary glands, microganglia are found in several other branches of the facial and glossopharyngeal nerves (Fig. 6.1).

The largest collection of these ganglia is located in the cavernous plexus, lying intracranially but extradurally. The largest ganglion is about 1 mm in diameter and contains at least 500 neurons. It is consistently located between the internal carotid plexus, which follows the internal carotid artery, and the abducens nerve (6n; Gellert, 1934; Lang, 1981; Ruskell and Simons, 1987). In the same region are several smaller ganglia (Mitchell, 1953c), while another collection of microganglia lies between the abducens nerve and the ophthalmic nerve (Gellert, 1934). More rostrally, these

ganglia and their interconnections form the retroorbital plexus (Ruskell, 1970a; Ruskell and Simons, 1987), which communicates directly with the pterygopalatine ganglion via the orbital rami (Ruskell, 1970a).

The facial nerve communicates with the cavernous plexus via the greater superficial petrosal nerve (Chorobski and Penfield, 1932). The glossopharyngeal nerve communicates with the cavernous plexus via the lesser petrosal nerve and small filaments from the tympanic plexus located in the middle ear (Chu, 1968; Mitchell, 1954; Rosen, 1950). Groups of ganglion cells may occur along all these pathways (Chorobski and Penfield, 1932; Gibbins *et al.*, 1984; Hara and Kobayashi, 1987; Van Buskirk, 1945). In laboratory mammals, most of the neurons in the cavernous plexus contain VIP and are thought to contribute to the vasodilator innervation of the cerebral circulation (Gibbins *et al.*, 1984; Hara and Kobayashi, 1987; Walters *et al.*, 1986).

Another major aggregation of ganglion cells lies along the lingual nerve. Within the anterior two-thirds of the tongue are up to 1500 microganglia (Chu, 1968; Fitzgerald and Alexander, 1969; Gomez, 1961). They may receive preganglionic input from both the glossopharyngeal nerve (Fitzgerald and Alexander, 1969; Gomez, 1961) and the facial nerve, via the chorda tympani (Hellekant, 1972). These neurons are strongly AChE positive (Fitzgerald and Alexander, 1969) and probably contain VIP (Lundberg *et al.*, 1984) and NO. It is likely that they mediate vasodilation and mucous secretion from the lingual glands (Hellekant, 1972).

Vagal Pathways

The vagus nerve (10n) carries preganglionic fibers involved in the autonomic regulation of several organs, including the heart, the airways, pancreas, and at least the proximal part of the gastrointestinal tract (Table 6.2). Some of these neurons contain substance P (Halliday *et al.*, 1988). The vagus controls several different effectors in each organ. Furthermore, any particular target tissue may be controlled by two independent vagal pathways with opposite actions.

Most of the final motor neurons in the vagal pathways to these organs are located in ganglionated plexuses relatively close to their target tissues, although some nerve cell bodies are scattered along the vagal nerves (Botar *et al.*, 1950; Dolgo-Saburoff, 1936; Hoffman and Kuntz, 1957). The range of responses mediated by these neurons is diverse and it is not possible to generalize their function. Anatomical connections exist between the vagus and other cranial nerves, especially the glossopharyngeal nerve (Mitchell, 1953a, c, 1954), but there is little functional evidence for direct vagal control of any cranial structures.

Airways

Vagal preganglionic fibers travel to the airways in the pulmonary branches of the vagus, which arise from the vagi posterior to the root of the lung. Together with the vagal and spinal sensory fibers and sympathetic fibers, they form the pulmonary plexus. Microganglia are associated with the plexus and the peripheral ends of the vagal nerve branches in the larynx, epiglottis, trachea, and bronchi. The great majority of these ganglia are associated with the posterior wall of the trachea and bronchi, especially in the region of the bronchial bifurcation (Kuntz, 1945; Taylor and Smith, 1971). The ganglia are located both superficial and deep to the cartilages of the trachea and bronchi. Some ganglion cells are found in the submucosa, especially in the vicinity of the secretory glands (Fisher, 1964; Gaylor, 1934; Larsell and Dow, 1933; Partanen *et al.*, 1982; Spencer and Leof, 1964; Taylor and Smith, 1971). The ganglia of the extrachondrial plexus generally are larger, containing 10–20 neurons, whereas the ganglia of the subchondrial plexus contain only 4–8 cells (Fisher, 1964; Richardson and Ferguson, 1980). The extrachondrial ganglia tend to be arranged as a longitudinal chain, which originally develops as two distinct chains of ganglia on either side of the trachea (Fisher, 1964; Sparrow *et al.*, 1999; Taylor and Smith, 1971). There are extensive connections between the different layers of the tracheobronchial plexus, and small groups of ganglion cells occur at nodal points in the plexus. Ganglion cells also are located near branches of nearby blood vessels (Fisher, 1964; Gaylor, 1934; Larsell and Dow, 1933; Partanen *et al.*, 1982; Spencer and Leof, 1964; Taylor and Smith, 1971).

The nerve cell bodies within the microganglia of the tracheobronchial plexus are usually multipolar with long dendrites (Fisher, 1964; Gaylor, 1934; Larsell and Dow, 1933; Spencer and Leof, 1964). The ganglionic neuropil is complex (Larsell and Dow, 1933), and synapses between axon profiles and nerve cell bodies or their processes are common (Richardson and Ferguson, 1980). However, it is not known how many of these synapses represent vagal preganglionic inputs and how many may be derived from intrinsic neurons or collaterals of unmyelinated sensory neurons. Varicose VIP fibers which could be of either origin have been described in these ganglia (Laitinen *et al.*, 1985; Lundberg *et al.*, 1984). A high proportion of the ganglion cells are labeled for AChE (Partanen *et al.*, 1982; Taylor and Smith, 1971) and choline acetyltransferase (ChAT; Fischer *et al.*, 1996), the enzyme responsible for ACh synthesis, whereas only some of them contain detectable VIP (Dey *et al.*, 1981; Fisher *et al.*, 1996; Laitinen *et al.*, 1985; Lundberg *et al.*, 1984). Many of the neurons also contain NOS, with the

TABLE 6.2 Targets of Parasympathetic Neurons in Vagal Pathways

Target	Potential transmitters	Function
Airways		
Smooth muscle	NO/VIP	Airway dilation
	ACh	Airway constriction
Glands	ACh/NO/VIP	Secretion
Blood vessels	ACh/NO/VIP	Vasodilation
Heart		
Myocardium	ACh/±Som	Negative inotropism[a]
Sinoatrial node		Negative chronotropism[a]
Atrioventricular node		Negative dromotropism, antiarrhythmic
Valves	ACh/?	?
Endocardium	ACh/Som?/VIP?	?
Coronary vessels	ACh/NO?	Vasodilation?
Thyroid		
Follicular cells	ACh/VIP	Thyroid hormone secretion
Blood vessels	NO/VIP/?	Vasodilation
Parathyroid		
Chief cells	ACh/VIP/PACAP	Inhibition of PTH secretion?
Thymus	ACh/VIP	Mobilize lymphocytes?
Pancreas		
Acini	ACh/NO/VIP/Gal/GRP?	Enzyme secretion[a]; bicarbonate secretion[a]
Islets	ACh/NO/VIP/Gal/GRP?	Pancreatic polypeptide secretion; somatostatin secretion; insulin secretion; glucagon secretion
Blood vessels	ACh/NO/VIP	Vasodilation
Esophagus		
Smooth muscle	ACh/?	Contraction
	NO/VIP/NPY/Gal?	Relaxation
Stomach		
Smooth muscle	ACh/SP	Contraction[a]
	ATP/NO/VIP	Relaxation
Gastric mucosa	ACh/?	Acid secretion[a]; gastrin secretion; somatostatin secretion; bicarbonate secretion[a]; pepsinogen secretion;
Blood vessels	NO/VIP?	Vasodilation
Gall bladder		
Smooth muscle	ACh/?	Contraction[a]
	NO/(VIP)	Relaxation
Sphincter of Oddi	NO/VIP	Relaxation[a]
Mucosa	ACh?/NO/VIP	Secretion
Liver	ACh/?	Potentiate insulin response

[a]Pathways that probably are tonically active.

ACh, acetylcholine; ATP, adenosine 5′-triphosphate; Gal, galanin; GRP, gastrin-releasing peptide; NO, nitric oxide; NPY, neuropeptide Y; PACAP, pituitary adenylate cyclase–activating peptide; Som, somatostatin; VIP, vasoactive intestinal polypeptide.

proportion of NOS-positive neurons increasing in ganglia associated with the small bronchi (Fischer and Hoffmann, 1996). There are probably no catecholamine-containing ganglion cells in this area (Partanen *et al.*, 1982).

Axons of the vagal final motor neurons distribute through the tracheobronchial plexus to innervate mainly the submucosal glands and the smooth muscle. Within the muscle, fine varicose fibers run parallel to the smooth muscle cells (Gaylor, 1934; Partanen *et al.*, 1982). Compared with smaller laboratory mammals, the innervation of the tracheal and bronchial smooth muscle in humans is somewhat scanty (Dey *et al.*, 1981; Richardson and Ferguson, 1980). The density of innervation seems to decrease with the decreasing caliber of the airways (Belvisi *et al.*, 1995; Fischer and Hoffmann, 1996; Gaylor, 1934; Laitinen *et al.*, 1985; Richardson, 1983).

The smooth muscle of the trachea and bronchi is innervated by at least two populations of neurons: one population contains NOS and VIP; the other contains ChAT (Dey *et al.*, 1981; Fischer and Hoffmann, 1996; Fischer *et al.*, 1996; Laitinen *et al.*, 1985; Lundberg *et al.*, 1984; Uddman and Sundler, 1979). Some neurons also

contain heme oxygenase-2 (HOX-2), an enzyme responsible for the production of carbon monoxide (CO) for use as a neurotransmitter (Canning *et al.,* 1998). Neurons containing VIP also may contain other neuropeptides such as PACAP and galanin (Luts *et al.,* 1993). Most of the fibers innervating the airway smooth muscle are likely to originate from local ganglia. However, studies in animals have shown clearly that a population of neurons containing NOS and VIP project to the airways from microganglia associated with the esophageal plexus of the vagus (Fischer *et al.,* 1998).

Within the bronchial glands, axons are in close association with both the secretory cells and the myoepithelial cells (Meyrick and Reid, 1970). Many of the axons surrounding the submucosal glands contain both NOS and VIP; they probably also contain ChAT and presumably arise from cell bodies in nearby ganglia (Dey *et al.,* 1981; Fischer and Hoffmann, 1996; Fischer *et al.,* 1996; Laitinen *et al.,* 1985; Lundberg *et al.,* 1984; Uddman and Sundler, 1979). Fibers containing NOS, VIP, and probably ChAT, also likely to be of local origin, innervate pulmonary blood vessels (Dey *et al.,* 1981; Fischer and Hoffmann, 1996; Fischer *et al.,* 1996; Laitinen *et al.,* 1985; Lundberg *et al.,* 1984). Unmyelinated axon profiles have been described in the alveoli (Fox *et al.,* 1980; Hertweck and Hung, 1980), but it is not known if these endings are autonomic or sensory. However, they do not seem to contain NOS or VIP, so that an autonomic origin seems unlikely.

The vagal final motor neurons controlling airway diameter are of two functional types, mediating contraction and relaxation of tracheobronchial smooth muscle, respectively. The neurogenic constriction of the airways is mediated by cholinergic neurons acting on muscarinic receptors (Davis *et al.,* 1982; Richardson and Beland, 1976; Sheppard *et al.,* 1982; Taylor *et al.,* 1984). These neurons are probably tonically active under vagal drive, thereby contributing to resting tracheobronchial tone (De Troyer *et al.,* 1979; Nadel and Widdicombe, 1963; Severinghans and Stupfel, 1955; Sheppard *et al.,* 1982; van der Velden and Hulsmann, 1999; Vincent *et al.,* 1970). The reflex activity of the constrictor neurons can be decreased by deep inspiration (Vincent *et al.,* 1970) and can be increased by irritation of the airways (e.g., Kaufman and Wright, 1969; Nadel, 1980; Nadel and Widdicombe, 1963; Sheppard *et al.,* 1982; van der Velden and Hulsmann, 1999).

Electrical stimulation of nerves within isolated human airways smooth muscle has clearly demonstrated the presence of vagal neurons that relax both tracheal and bronchial smooth muscle. These neurons are the major source of inhibitory innervation of human airway muscle (Barnes, 1984; Richardson, 1983). The neurogenic relaxation is mediated by a transmitter that is neither ACh nor a catecholamine (Davis *et al.,* 1982; Richardson and Beland, 1976; Taylor *et al.,* 1984). Although both VIP and PHM relax preconstricted airway smooth muscle (Barnes and Dixon, 1984; Palmer *et al.,* 1986), almost the entire inhibitory response to vagal stimulation is abolished following the inhibition of NO synthesis, providing strong evidence that NO is the primary transmitter responsible for neurogenic dilation of the airways (Bai and Bramley, 1993; Belvisi *et al.,* 1992, 1995).

The neurons projecting to the submucosal glands of the airways are likely to be secretomotor. Most secretion is blocked by atropine, indicating predominantly cholinergic control. However, glandular secretion, especially from serous cells, may be enhanced by VIP (see Marin, 1986; Webber and Widdicombe, 1987), as in cat salivary glands (see Lundberg *et al.,* 1987). VIP is a potent vasodilator of human pulmonary arteries (Greenberg *et al.,* 1987) and, together with NO, may be a mediator of neurogenic vasodilation from vagal postganglionic neurons (Lundberg *et al.,* 1987; Martling *et al.,* 1985). There also is a neurogenic vasodilation of the pulmonary arteries mediated in part by NO (Scott *et al.,* 1996), but it is not known if the neurons generating this response lie within vagal pathways.

Heart

Vagal preganglionic fibers travel to the heart via (1) the superior cervical rami, originating just distal to the origin of the superior laryngeal nerve; (2) the inferior cervical ramus, arising from the recurrent laryngeal nerve; and (3) the thoracic rami from the thoracic vagal nerves (Kuntz, 1945). These nerves anastomose with the cardiac sympathetic nerves in the region of the ascending aorta and the aortic arch to form the cardiac plexus (Mitchell, 1953b). The dorsal parts of this plexus communicate with the tracheobronchial plexus in the region of the tracheal bifurcation. Small groups of ganglion cells may occur at any point along the nerves feeding into the plexus, but they become more common closer to the heart (Dogiel, 1877). The largest ganglion in the region is the "ganglion of Wrisberg," which lies inferior to the aortic arch between the tracheal bifurcation and the division of the pulmonary arterial trunk (Mitchell, 1953b) at the entry of the left superior sympathetic cardiac nerve to the cardiac plexus (Kuntz, 1945).

Ganglion cells are abundant in the extensions of the cardiac plexus associated with the heart itself (Fig. 6.2). These intrinsic cardiac ganglia mostly are found subepicardially. They are rare within the muscular tissue outside the interatrial septum and do not normally occur in the endocardium (Conti, 1948; Dogiel, 1877;

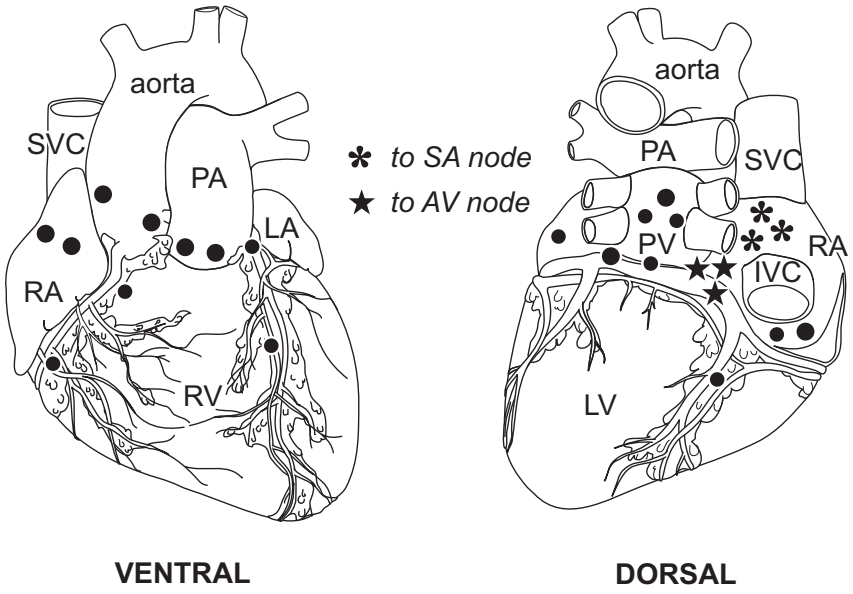

FIGURE 6.2 Distribution of microganglia of the surface of the heart. Microganglia containing final motor neurons to the sinoatrial (SA) node and atrioventricular (AV) node are indicated by different symbols. All of these ganglia are in vagal pathways. IVC, inferior vena cava; LA, left atrium; LV, left ventricle; PA, pulmonary artery; PV, pulmonary veins; RA, right atrium; RV, right ventricle; SVC, superior vena cava.

Francillon, 1928; Lissauer, 1909). The ganglia range in size from 5 to more than 400 neurons (Conti, 1948; King and Coakley, 1958; Pauza *et al.*, 2000; Van der Zypen *et al.*, 1974). The number of ganglia associated with the heart ranges from around 700 to 1500, containing a total of about 43,000 neurons (Pauza *et al.*, 2000). They are grouped together in five main locations together with other smaller groups of neurons (Fig. 6.2; Armour *et al.*, 1997; Conti, 1948; Dogiel, 1877; King and Coakley, 1958; Kuntz, 1945; Mitchell, 1953c; Pauza *et al.*, 2000; Perman, 1924; Smith, 1970, 1971; Van der Zypen *et al.*, 1974):

1. In the adventitia around the origins of the aorta and pulmonary trunk,
2. On the superior surface of the left atrium, extending to the area around the entry of the pulmonary veins,
3. On the superior and dorsal surface of the right atrium, extending to the dorsal interatrial groove and the entry of the superior and inferior caval veins. These neurons are particularly prominent in the area of the sinoatrial node,
4. In a circlet in the atrioventricular groove, with a large group of about 1700 neurons near the atrioventricular node,
5. Within the interatrial septum, especially in the superior ventral portion.

More than 50% of cardiac ganglia are located in the first two areas (Armour *et al.*, 1997; Pauza *et al.*, 2000). Additional isolated ganglion cells may follow the adventitial plexus of the coronary arteries to the ventricles, but they are rare (Conti, 1948; Davies *et al.*, 1952).

The neuronal cell bodies generally are multipolar, varying from 10 to 85 μm in diameter, (King and Coakley, 1958; Kuntz, 1945; Lasowsky, 1930; Pauza *et al.*, 2000; Smith, 1971), and occasionally are binucleate (Conti, 1948; Dogiel, 1877; Lissauer, 1909). The neurons may bear more than 15 dendrites, which may branch several times. Both the size of the neurons and their dendritic complexity increase with age from birth (Conti, 1948; Lasowsky, 1930). In some ganglia, dendrites from different cells may intermingle to form dendritic glomeruli (Kuntz, 1945). The neurons gathered near the atrioventricular node tend to be smaller and have fewer dendrites than those in other locations (Smith, 1971). The dendrites provide a major target for synapses from vagal preganglionic inputs (Ellison and Hibbs, 1976; Kuntz, 1945; Van der Zypen *et al.*, 1974). Studies on laboratory animals have provided evidence that some of the neurons in the cardiac ganglia probably function as interneurons (Horackova *et al.*, 1999; Randall *et al.*, 1998; Steele *et al.*, 1994, 1996) and perhaps as sensory neurons (Klemm *et al.*, 1997); it would be surprising if a similar diversity of neurons did not occur in the human cardiac plexuses.

The great majority of atrial ganglion cells are AChE positive (Van der Zypen *et al.*, 1974). Some of these

neurons also contain somatostatin, probably in its longer form, somatostatin-28 (Day *et al.*, 1985; Franco-Cereceda *et al.*, 1986; Gordon *et al.*, 1993). A separate population of cardiac neurons contains VIP (Lundberg *et al.*, 1984; Gordon *et al.*, 1993; Rechardt *et al.*, 1986). None of the intrinsic cardiac neurons normally contains histochemically detectable catecholamines (Kyösola *et al.*, 1976), although immunoreactivity to a variety of enzymes involved in monoamine synthesis has been reported in many cardiac neurons (Singh *et al.*, 1999). NOS has been detected in neurons both with and without AChE reactivity (Yoshida and Toda, 1996).

Although there is a rich innervation of the myocardial tissue, including the atrioventricular valves (Ferreira and Rossi, 1974; Marron *et al.*, 1995), in most parts of the heart only a relatively small proportion of these axons are non-noradrenergic and therefore likely to be of intrinsic origin (Chiba and Yamauchi, 1970; Kyösola *et al.*, 1976; Marron *et al.*, 1995; Rechardt *et al.*, 1986). The non-noradrenergic axons usually run in multiaxonal bundles with the noradrenergic axons. Nevertheless, there is a relatively dense innervation of the sinoatrial and atrioventricular nodes by final motor neurons in vagal pathways (Kent *et al.*, 1974; Crick *et al.*, 1994). The vagal innervation of the ventricles is less dense than that of the atria and is concentrated in the conducting tissue (Kent *et al.*, 1974; Crick *et al.*, 1994). At least some of the non-noradrenergic axons in the myocardium contain somatostatin-28 (Day *et al.*, 1985; Franco-Cereceda *et al.*, 1986; Wharton *et al.*, 1988). These fibers are most dense in the atrioventricular node and right atrium. VIP-containing axons occur in the atrial myocardium (Lundberg *et al.*, 1984; Rechardt *et al.*, 1986; Wharton *et al.*, 1988) and around coronary blood vessels (Lundberg *et al.*, 1984). Axons containing enkephalin have also been described in human myocardium (Rechardt *et al.*, 1986), but their origin is uncertain.

The major action of vagal stimulation is to reduce the rate of heart beat, mainly by the action of ACh on the sinus node (Higgins *et al.*, 1973; Levy, 1984; Levy *et al.*, 1981; Prystowsky *et al.*, 1981). Force of atrial contraction is also reduced by vagal stimulation, but effects on the ventricle are more subtle (Higgins *et al.*, 1973; Levy *et al.*, 1981). Atrioventricular conduction is reduced (Fee *et al.*, 1987; Higgins *et al.*, 1973; Kent *et al.*, 1974; Levy *et al.*, 1981; Prystowsky *et al.*, 1981) and the ventricular refractory period is increased (Prystowsky *et al.*, 1981).

From experiments in a range of species, including humans and nonhuman primates, it is likely that the various effects of vagal stimulation are mediated by different groups of ganglion cells (Fee *et al.*, 1987; Randall *et al.*,1998). Neurons located in the fat pad on the dorsal surface of the right atrium preferentially innervate the sinoatrial node and selectively decrease the rate of atrial beating without any significant effects on atrioventricular conduction (Billman *et al.*, 1989; Bluemel *et al.*, 1990; Carlson *et al.*, 1992; Nakano *et al.*, 1998; Quan *et al.*, 1999; Randall *et al.*, 1991). In contrast, neurons located in ganglia within epicardial fat pads between the inferior vena cava and the left atrium selectively innervate the atrioventricular node. These neurons decrease atrioventricular conduction with relatively few inotropic effects on the ventricles (Billman *et al.*, 1989; Gatti *et al.*, 1995; Wallick and Martin, 1990). Additional populations of neurons near the superior vena cava and aortic outlet regulate atrial force of beat (Tsuboi *et al.*, 2000) and another population at the cranial end of the medial borders of the ventricles seems to regulate ventricular force (Dickerson *et al.*, 1998; Gatti *et al.*, 1997). Furthermore, experimental evidence from animals strongly indicates that ACh released from vagal nerve endings interacts with a specific population of muscarinic receptors that are located within the neuroeffector junction and that these receptors exert their actions on cardiac contractility in a unique way (Campbell *et al.*, 1989).

The responses to vagal stimulation, especially in the ventricle, are particularly prominent in the presence of concurrent sympathetic stimulation of the heart. Under these conditions, there is likely to be vagally mediated presynaptic inhibition of sympathetic activity (Levy, 1984; Levy *et al.*, 1981; Priola *et al.*, 1998; Randall *et al.*, 1998). An important consequence of these diverse actions of the vagus on the heart is that ventricular fibrillation threshold is increased and the ventricle is protected against potentially catastrophic dysrhythmias (Eckberg, 1980; Kent *et al.*, 1974; Levy, 1984). It seems probable that a separate population of intrinsic vagal neurons is responsible for most of the inhibition of sympathetic activity (Furukawa *et al.*, 1996; Hoyano *et al.*, 1997).

Some of the effects of vagal stimulation in the human heart may be mediated by somatostatin in addition to ACh. Somatostatin decreases the duration of the cardiac action potential and decreases the force of atrial contraction. More importantly, somatostatin can suppress abnormal automaticity of cardiac muscle (e.g., in paroxysmal supraventricular tachycardia) and can restore sinus rhythm (Franco-Cereceda *et al.*, 1986, 1987; Greco *et al.*, 1984; Hou *et al.*, 1987).

Under normal resting conditions, the heart is influenced by a low tonic level of vagal activity, mediated by ACh acting on muscarinic receptors (Carlsten *et al.*, 1957). The level of tone tends to be higher in fit, well-trained athletes (Carlton *et al.*, 1965).

Vagal activity is rapidly reduced at the onset of exercise (Hollander and Bouman, 1975; Maciel *et al.*, 1987; Martin *et al.*, 1974; Pickering *et al.*, 1972) to a degree that is dependent on the magnitude of the exercise (Eckberg *et al.*, 1972; Robinson *et al.*, 1953). At the completion of exercise, vagal activity helps speed the return of heart rate to normal levels (Savin *et al.*, 1982).

In conditions when basal heart rate is very slow, such as during sleep, in highly trained athletes, and in patients with sinus bradycardia, vagal stimulation actually may result in a positive chronotopic response by shortening the time between atrial depolarizations (Yang *et al.*, 1985). While ACh contributes to this response, VIP, which has excitatory actions on the heart (De Neef *et al.*, 1984; Taton *et al.*, 1982), also may be involved. The normal effects of vagal stimulation on the coronary circulation of humans are still unclear (Young and Vatner, 1986; Feigl, 1998). ACh constricts isolated human coronary arteries in which the intima has been shown to be undamaged (Ginsburg *et al.*, 1984; Kalsner, 1985; Yasue *et al.*, 1986). Conversely, intracoronary infusion of muscarinic agonists causes epicardial coronary artery vasodilation in humans without any signs of atherosclerosis, although atherosclerotic vessels constrict both *in vivo* and *in vitro* (Feigl, 1998; Kalsner, 1985; Ludmer *et al.*, 1986; Yasue *et al.*, 1986). However, the application of exogenous ACh is not likely to mimic the responses of the vessels to stimulation of neurons that probably release some combination of ACh, NO, and VIP. On the basis of their transmitter complement, the most likely response to activation of the vagal pathways to the coronary circulation would be vasodilation.

Thyroid and Parathyroid Glands

Small groups of neurons, almost certainly lying within vagal pathways, are found associated with the thyroid gland. They project to the follicular cells and their blood vessels. Some neurons also may project to these targets from small ganglia near the larynx (Grunditz *et al.*, 1996; Ramaswamy *et al.*, 1994). These neurons are probably cholinergic and contain VIP and PHM (Ahren *et al.*, 1980; Grunditz *et al.*, 1986; Van Sande *et al.*, 1980). Both acetylcholine and a range of peptides, including VIP, PHM, and PACAP, stimulate thyroid hormone release from the follicular cells and probably also contribute to a neurogenic vasodilator response (Brandi *et al.*, 1987; Chen *et al.*, 1993; Grunditz *et al.*, 1986; Ishii *et al.*, 1968; Ito *et al.*, 1987; Siperstein *et al.*, 1988; Toccafondi *et al.*, 1984). However, some experiments in rats suggest that the involvement of VIP in responses of the thyroid to vagal stimulation *in vivo* may not be so clear-cut (Michalkiewicz *et al.*, 1994).

There is probably only sparse innervation of the parathyroid glands by vagal autonomic fibers (Luts *et al.*, 1995). The neurons are likely to be cholinergic and contain VIP and PACAP. It is difficult to predict the actions of these neurons on parathyroid hormone secretion because ACh inhibits secretion (Stern *et al.*, 1994; WIlliams *et al.*, 1985) and VIP stimulates it (Joborn *et al.*, 1991).

Thymus

Animal studies have demonstrated autonomic microganglia in the thymus that almost certainly lie in vagal parasympathetic pathways reaching the gland via branches of the recurrent laryngeal nerve (Al-Shawaf *et al.*, 1991; Bulloch and Pomerantz, 1984; Dovas *et al.*, 1998). These neurons are presumably cholinergic and contain VIP (Al-Shawaf *et al.*, 1991). They may influence the differentiation, migration, and release of lymphocytes or alter local blood flow (Antonica *et al.*, 1994; Bulloch and Pomerantz, 1984). The main effects on lymphocytes are likely to be mediated mostly via VIP, since receptors for VIP are widespread on both thymocytes and lymphocytes (Delgado *et al.*, 1999; Head *et al.*, 1998; Reubi *et al.*, 1998). The regulation of thymic activity by neurally released VIP is complicated by the presence of VIP in at least some lymphocytes (Delgado *et al.*, 1999; Leceta *et al.*, 1996).

Pancreas

Final motor neurons within vagal parasympathetic pathways are located in small microganglia scattered throughout the pancreas in interlobular septa, often in close association with the islets of Langerhans (Kroutikova, 1971; Simard, 1937; Singh and Webster, 1978; Van Campenhout, 1927). Studies in animals have shown that some of the pancreatic ganglia may receive synaptic inputs from neurons located in the gut as well as from vagal preganglionic neurons, suggesting that there may be peripheral modulation of vagal pathways to the pancreas (see Mawe, 1995).

At least some of pancreatic ganglion neurons are functionally cholinergic, and they probably provide the predominant autonomic secretomotor innervation of the exocrine and endocrine cells of the human pancreas (Forssmann and Greenberg, 1978; Singh and Webster, 1978). Most of the neurons contain VIP. Many also contain NOS and probably both galanin and gastrin-releasing peptide (GRP). They project to blood vessels, secretory acini and ducts, and the islets (Ahren *et al.*, 1991; Bishop *et al.*, 1980; De Giorgio *et al.*, 1994; Ekblad *et al.*, 1994; Marongiu *et al.*, 1993; Shimosegawa *et al.*, 1992, 1993; Sundler *et al.*, 1978; Verchere *et al.*, 1996). Presumably, as in the heart, there are micro-

anatomical, neurochemical, and functional differences between neurons projecting to specific intrapancreatic targets, but there are no studies to illuminate this point. Vagal preganglionic fibers reach the pancreas via the celiac and superior mesenteric plexuses and enter it with the pancreatic arteries (Singh and Webster, 1978; Woods and Porte, 1974). Some neurons in the vagal ganglia are surrounded by baskets of VIP-containing fibers (Marongiu *et al.,* 1993). It is not known if these fibers are of preganglionic origin or if they originate elsewhere, such as the intestinofugal neurons of the gut (see below).

Bicarbonate and enzyme secretion from the exocrine pancreas occurs at a basal rate that is then increased in two phases after a meal. Part of the basal secretion of bicarbonate and digestive enzymes from the exocrine pancreas is likely to be the result of resting vagal secretomotor activity (Anagostides *et al.,* 1984; Solomon, 1987). Increased vagal activity is responsible for the first phase of meal-induced secretion of pancreatic juice, bicarbonate, and especially enzymes (Huertas *et al.,* 1992). These effects are mediated mainly by cholinergic neurons (Anagostides *et al.,* 1984; Dreiling *et al.,* 1952; Singh and Webster, 1978; Solomon, 1987). Atropine-resistant components of the responses may be mediated by VIP, galanin or perhaps NO (Ahrén *et al.,* 1986; Barrett *et al.,* 1993; Ekblad *et al.,* 1994; Holst *et al.,* 1994; Kirschgessner *et al.,* 1994).

The secretion of bicarbonate and enzymes from the exocrine pancreas is further controlled by the vagus via its actions on the endocrine pancreas. Vagal stimulation results in increased secretion of somatostatin and pancreatic polypeptide from islet cells. These responses are reduced by atropine, indicating the involvement of cholinergic final motor neurons (Bysschaer *et al.,* 1985; Feldman *et al.,* 1979; Glaser *et al.,* 1981; Schwartz *et al.,* 1978; Walsh, 1987). Pancreatic polypeptide and somatostatin each inhibit enzyme secretion from the exocrine pancreas, but only pancreatic polypeptide inhibits bicarbonate secretion (Walsh, 1987). It seems likely that these peptides inhibit secretion by an action on the intrinsic pancreatic neurons (Holst *et al.,* 1990, 1993). The late phase of pancreatic secretion is stimulated primarily by local gastrointestinal hormones, especially secretin and cholecystokinin (CCK; De Fillipi *et al.,* 1982; Solomon, 1987; Walsh, 1987, 1988), neither of which is under direct vagal influence (Walsh, 1987).

Although there is good evidence for vagal stimulation of secretion of insulin and glucagon from the pancreatic islets of some species (Ahrén *et al.,* 1986; Havel and Valverde, 1996; Woods and Porte, 1974), the situation in humans is not at all clear (Brunicardi *et al.,* 1995; Havel and Taborsky, 1994; Taborsky *et al.,* 1998). Some reports have confirmed, and others have denied, that the vagus stimulates insulin and glucagon release in humans (e.g., Havel and Ahren, 1997; Hedo *et al.,* 1978; Kinami *et al.,* 1997; Palmer *et al.,* 1979; Russell *et al.,* 1974; Taylor and Feldman, 1982). These discrepancies may arise in part from the high level of inter and intraindividual variation in responses (Russell *et al.,* 1974; Sjöstrom *et al.,* 1980). Furthermore, vagal stimulation actually may indirectly inhibit insulin and glucagon secretion by releasing pancreatic somatostatin (Ahren, 2000; Walsh, 1987). When vagal stimulation of islet hormone secretion can be demonstrated, it is due mostly to the actions of ACh on muscarinic receptors, although peptides such as VIP, PACAP, and GRP also may be involved (Ahren, 2000). Another complicating factor is the potential involvement of NO, which may be synthesized and released from some of the islet cells in addition to being a cotransmitter with ACh and peptides from the vagal neurons (Ekblad *et al.,* 1994). NO probably potentiates both glucagon secretion and insulin secretion in response to vagal stimulation (Atiya *et al.,* 1996; Bilski *et al.,* 1995; Konturek *et al.,* 1997a). Overall, there is now a general consensus from both animal and human studies that the vagus is involved in the cephalic phase of regulation of peptide release from the pancreatic islets. The most likely role of these vagal motor pathways is to synchronize the activity of the various groups of islet cells (Taborsky *et al.,* 1998; Ahren, 2000).

Gastrointestinal Tract

The alimentary tract itself contains a highly developed system of intrinsic neurons that form the enteric division of the autonomic nervous system. Vagal input to this system occurs primarily in the esophagus and stomach, but may extend to the proximal small intestine and parts of the colon (see Christensen, 1987; Holst *et al.,* 1997; Kuntz, 1945; Roman and Gonella, 1987). The gallbladder also contains an intrinsic ganglionated plexus somewhat similar in structure to the enteric plexuses, and is under a degree of vagal control.

Distal to the roots of the lungs, the vagus nerves divide into a small number of branches that follow the distal esophagus and intermingle to form an open-meshed esophageal plexus. Immediately superior to the diaphragm, the esophageal plexus reforms into anterior and posterior vagal trunks which enter the abdomen to break up into several distinct branches supplying different areas of the stomach, biliary tract, and pancreas (Kuntz, 1945; Mitchell, 1953a; Schein, 1981; Skandalakis *et al.,* 1980). In the esophagus and stomach, most of the vagal plexus lies outside the muscle layers and communicates with the intrinsic

plexuses via fine connections (Rash and Thomas, 1962). There have been no detailed microscopic studies of the relationship between vagal preganglionic fibers and the intrinsic neurons of the digestive tract of humans, but animal studies suggest that vagal preganglionic endings ramify extensively through the ganglia of the myenteric plexus (Holst *et al.*, 1997).

Esophagus

The upper part of the esophagus contains striated muscle controlled by vagal motoneurons acting through motor end plates. In contrast, the lower part of the esophagus contains smooth muscle and is under autonomic control by intrinsic enteric neurons, by sympathetic pathways, and by the vagus (Dodds *et al.*, 1981; Phaosawasdi *et al.*, 1981). Vagal pathways provide both excitatory and inhibitory control of esophageal smooth muscle function via inputs to intrinsic neurons located mainly in the myenteric plexus. Lower esophageal sphincter tone is likely to be actively maintained by cholinergic excitatory neurons under direct vagal control (Dodds *et al.*, 1981; Holloway *et al.*, 1986; Roman and Gonella, 1987). However, following vagotomy, opening of the lower esophageal sphincter during swallowing is inhibited (Roman and Gonella, 1987), implying the presence of a vagal pathway that relaxes the muscle of the sphincter region (Goyal and Rattan, 1978; Meyer *et al.*, 1981). This response may be mediated in part by VIP, which is found together with NOS, NPY, and perhaps galanin in intrinsic neurons projecting to the muscle of the lower esophageal sphincter (Aggestrup *et al.*, 1985; Singaram *et al.*, 1994; Wattchow *et al.*, 1987b), and which relaxes the preconstricted sphincter (Domschke *et al.*, 1978). However, most of the inhibitory response is normally mediated by NO, which is probably released together with VIP from the same neurons (Guelrud *et al.*, 1992; McKirdy *et al.*, 1992; Preiksaitis *et al.*, 1994; Richards *et al.*, 1995; Singaram *et al.*, 1994; Tomita *et al.*, 1997). Inhibitory neurons also project to the circular muscle of the body of the esophagus, but it is not so clear that this pathway is under direct vagal control.

Stomach

In the stomach, the vagus influences both gastric motility and secretion (see Furness and Costa, 1987). When the stomach is being filled, vagal activation causes relaxation of gastric smooth muscle primarily in the proximal stomach, so that gastric distention can occur (Furness and Costa, 1987; Jahnberg, 1977; Meyer, 1987; Roman and Gonella, 1987; Staadas, 1975). This response occurs reflexively during swallowing ("receptive relaxation") or as a direct result of increased intragastric pressure ("accommodation"). The inhibitory transmitters involved are likely to be a some combination of ATP, NO, and VIP, which probably coexist in the same neurons (Belai *et al.*, 2000; Furness and Costa, 1987; Ekblad *et al.*, 1994; Tonini *et al.*, 2000), with much of the accommodation response likely to be mediated by NO (Tonini *et al.*, 2000). The circular muscle of the pylorus is densely innervated by neurons containing NOS and VIP, which presumably represent inhibitory inputs to the muscle (Domoto *et al.*, 1992; Wattchow *et al.*, 1987a). Indeed, functional experiments in animals have revealed a vagal inhibitory input to the pylorus (Malbert *et al.*, 1995; Paterson *et al.*, 2000), but once again, the transmitter mediating most of this response in humans is NO (Tomita *et al.*, 1999). The vagus also can stimulate increases in gastric motility, particularly in the distal stomach (Furness and Costa, 1987; Meyer, 1987), since gastric emptying is slowed significantly after vagotomy (Roman and Gabella, 1987; Staadas, 1975). The excitatory effects of vagal stimulation on gastric motility are probably mediated by intrinsic cholinergic neurons (Edin, 1980; Meyer, 1987; Tomita *et al.*, 1999).

The vagus exerts multiple controls over gastric acid secretion (Fig. 6.3). The details of this control are complex and seem to vary between species and experimental approach (Debas, 1987; Schiller *et al.*, 1980; Walsh, 1987, 1988). One pathway involves intrinsic cholinergic neurons that apparently project directly to acid-secreting parietal cells and that can stimulate acid secretion via muscarinic receptors (Debas, 1987; Feldman, 1985; Feldman *et al.*, 1979; Walsh, 1987). This pathway has a low level of tonic activity and works together with locally released histamine to produce a basal level of acid secretion (Debas, 1987). Alternatively, acid secretion can be stimulated by the release of gastrin from gastric mucosal G cells. Gastrin release is stimulated by vagal activation during eating (Debas, 1987; Walsh, 1987). In addition, there may be a low level of tonic vagal stimulation of gastrin release (Walsh, 1988). The vagal stimulation of gastrin secretion is probably mediated by intrinsic neurons utilizing GRP as a transmitter (Walsh, 1988), although immunohistochemical studies suggest that there is not a simple anatomical relationship between the projections of these neurons and the gastrin-releasing cells (Sjovall *et al.*, 1990).

The amount of gastrin released by vagal stimulation is increased by atropine, suggesting the presence of an inhibitory pathway that may be activated simultaneously with the excitatory pathway and that contains cholinergic neurons acting on muscarinic receptors (Debas, 1987; Feldman *et al.*, 1979; Feldman and Walsh, 1980; Schiller *et al.*, 1980; Walsh, 1987). The

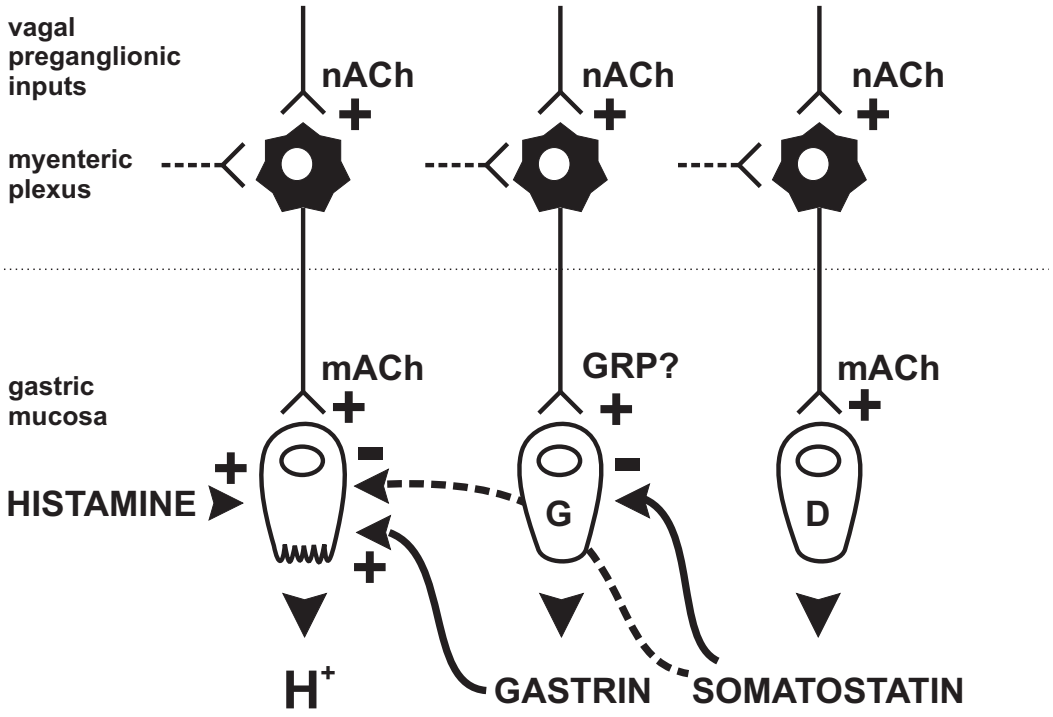

FIGURE 6.3 Simplified circuit diagram showing vagal inputs to the control of acid secretion from the stomach. Note that the acid-secreting parietal cells are in the mucosa of the proximal stomach, whereas the G cells secreting gastrin and the D cells secreting somatostatin are in the mucosa of the distal stomach. Gastrin probably reaches acid-secreting cells via the local circulation; somatostatin probably influences the gastrin cells in a paracrine manner. Many other factors also can influence acid secretion. GRP, gastrin-releasing peptide; mACh, excitatory effect of acetylcholine on muscarinic receptors; nACh, excitatory effect of acetylcholine on nicotinic receptors.

cholinergic neurons in this pathway stimulate the release of somatostatin from D cells in the gastric mucosa, which mediates the inhibition of gastrin release (see Furness and Costa, 1987; Walsh, 1988). Furthermore, somatostatin can inhibit acid secretion directly and also may be able to inhibit local histamine production (Sandvik and Waldum, 1991). Some vagal pathways may modulate somatostatin release indirectly via intrinsic VIP neurons (Holst *et al.*, 1992; Schubert, 1991). Finally, in at least some species the vagus may exert some level of inhibitory feedback control of somatostatin release (Debas and Carvajal, 1994; Holst *et al.*, 1992). However, the relative significance of this pathway in humans is not known.

Simultaneously with the secretion of acid from the stomach, vagal stimulation results in secretion of bicarbonate from nonparietal cells of the stomach, which presumably helps to buffer intragastric pH. The final motor neurons in this pathway probably are cholinergic, although other transmitters may be involved to a lesser extent (Fandriks and Jonson, 1990; Feldman, 1985; Flemstrom, 1987; Forssell and Olbe, 1987a, b; Konturek *et al.*, 1987). There is also likely to be an independent vagal pathway stimulating pepsinogen release from the gastric mucosa (Furness and Costa, 1987).

It is likely that at least some of the neurons within vagal pathways to effectors in the stomach release NO. However, the effects of NO on acid secretion are complex. Overall, experiments in animals suggest that NO will contribute to enhancing acid secretion, but the major effect of NO is to increase blood low to the gastric mucosa (Bilski *et al.*, 1994; Gustaw *et al.*, 1994; Pique *et al.*, 1992). Nevertheless, it is still unknown if this regulation is under direct vagal control.

Biliary Tree

Although much of the regulation of gallbladder activity is under the control of local hormones such as CCK, an intact vagus is required for the normal function of the gallbladder and biliary tract. Much of the innervation of the gallbladder arises from an extensive plexus of small ganglia lying between the serosal and muscularis layers. There also are small ganglia in the

connective tissue underlying the epithelium (De Giorgio *et al.*, 1994, 1995; Uemura *et al.*, 1997). Preganglionic fibers reach the plexuses of the gallbladder via the hepatic branches of the vagus (Hopton, 1973; Inberg and Vuorio, 1969; Parkin *et al.*, 1973; Schein, 1981). The organization of the ganglia within the gallbladder seems to be intermediate between that of the small vagal parasympathetic ganglia associated with organs such as the airways or heart and that of the enteric plexuses.

Immunohistochemical studies in humans and laboratory mammals have indicated that there are probably several functional classes of neurons within the ganglia of the gallbladder. Consequently, vagal activity may have excitatory or inhibitory effects on motility of smooth muscle in the biliary tree, as well as stimulating secretory activity (Mawe, 1995). Most of the neurons within the wall of the gallbladder are likely to be cholinergic (Talmage *et al.*, 1996). However, many of them contain VIP and some of them also contain NOS in addition to a range of coexisting peptides, including PACAP, somatostatin, NPY, and tachykinins (De Giorgio *et al.*, 1994, 1995; Sundler *et al.*, 1977; Uemura *et al.*, 1997).

Following vagotomy, the gallbladder may become distended and the flow of bile from the gallbladder to the duodenum via the sphincter of Oddi may decrease (Fisher *et al.*, 1985; Hopton, 1973; Inberg and Vuorio, 1969; Parkin *et al.*, 1973). Some of these effects are mimicked by atropine, suggesting that some vagal pathways may tonically activate cholinergic neurons that increase gallbladder contractile activity (Fisher *et al.*, 1985; Ryan, 1947; Schein, 1981).

The inhibition of gallbladder contractility and motility seen after vagal stimulation (Fisher *et al.*, 1985; Ryan, 1987) are probably mediated by the intrinsic neurons containing NOS and VIP (Bjorck *et al.*, 1986; De Giorgio *et al.*, 1994), although much of the inhibitory action on the smooth muscle is mediated by NO. Indeed, experimental studies indicate that a tonic relaxation of the sphincter of Oddi, presumably as a result of vagal ongoing activity, is likely to be mediated mostly by NO (Sand *et al.*, 1997; Thune *et al.*, 1995). In contrast, both NO and VIP contribute to secretory responses of the biliary tree (Feeley *et al.*, 1984; Greaves *et al.*, 1998; Konturek *et al.*, 1997b; Luiking *et al.*, 1998; McKirdy *et al.*, 1994; Nilsson *et al.*, 1994, 1996a, b; Sanger *et al.*, 1999; see Mawe, 1995).

Earlier authors have described the hepatic nerves carrying vagal fibers to the liver (e.g., Kuntz, 1945), but the direct effects of vagal stimulation on the liver of humans have been difficult to ascertain (Friedman, 1982; Lautt, 1980, 1983). Ultrastructural data suggest there is relatively little non-noradrenergic innervation of the human liver (Nobin *et al.*, 1978). However, immunohistochemical studies indicate that nerve fibers containing VIP and probably other peptides are associated with the blood vessels and interlobular connective tissue (Akiyoshi *et al.*, 1998; El-Salhy *et al.*, 1993). Moreover, recent functional studies in laboratory mammals suggest that cholinergic vagal neurons have an action that is synergistic with insulin on hepatic glucose metabolism (Moore and Cherrington, 1996; Sadri and Lautt, 2000; Xie and Lautt, 1995; Xue *et al.*, 2000). The locations of the vagal final motor neurons involved in these responses are unknown, but they are most likely to be found in the plexuses associated with the bile duct and gallbladder.

Summary

From the data presented above, some cautious generalizations can be made concerning vagal function. The vagus provides multiple excitatory and inhibitory inputs to its final effectors, including the heart. Many of the final motor neurons in these pathways are cholinergic, and in most tissues the pathways containing cholinergic motor neurons tend to be tonically active. The final motor neurons in noncholinergic vagal pathways probably utilize a range of cotransmitters, most commonly including NO and VIP (Table 6.2). These pathways may be activated reflexively under specific conditions where simple withdrawal of activity in the cholinergic pathway would be inadequate. Whereas some vagal pathways may be relatively simple, as in the inhibitory neurons to airway smooth muscle, others are complex and may involve multiple effectors with feedback via local hormones, as in the regulation of secretion of gastric acid from the stomach or peptides from the endocrine pancreas.

SYMPATHETIC PATHWAYS

The neurons of the sympathetic division of the autonomic nervous system are aggregated into two main collections of ganglia: the paravertebral ganglia, which form the sympathetic chain each side of the vertebral column, and the prevertebral ganglia, which are associated with the abdominal aorta and its major branches (Fig. 6.4). Sympathetic neurons project to most tissues of the body (Tables 6.3–6.5), commonly reaching them by following major nerves containing predominantly sensory and somatic motor nerve fibers. Within the sympathetic chain ganglia, there is little obvious topographic organization of neurons projecting to different targets, although cell bodies tend to be somewhat more clustered near the nerve trunks carrying their axons.

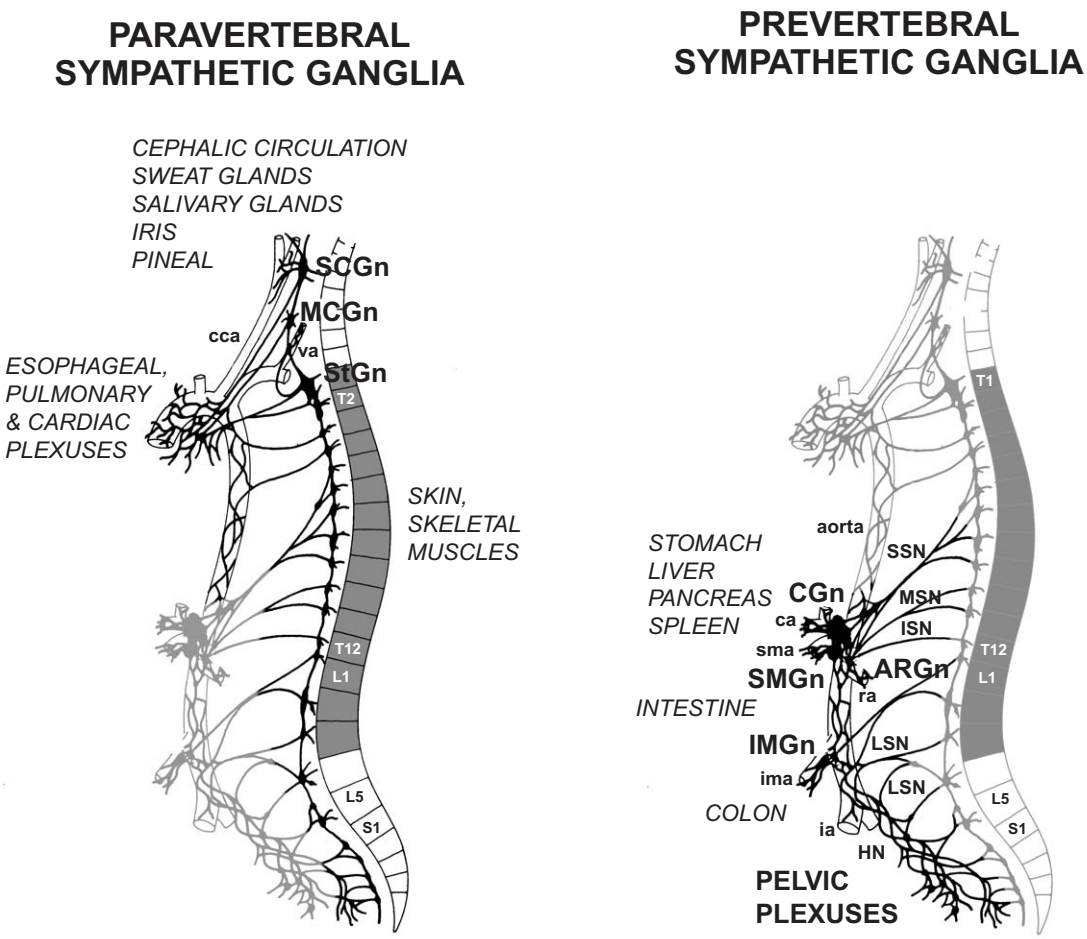

FIGURE 6.4 Anatomical arrangement of the paravertebral and prevertebral sympathetic ganglia, and their main connections. The preganglionic outflows arise from spinal segments T1 to about L3 *(shaded gray)*. ARGn, aorticorenal ganglia; ca, celiac artery; cca, common carotid artery; CGn, celiac ganglion; HN, hypogastric nerve; ia, iliac artery; ima, inferior mesenteric artery; IMGn, inferior mesenteric ganglion; ISN, inferior thoracic splanchnic nerve; LSN, lumbar splanchnic nerves; MCGn, middle cervical ganglion; MSN, middle thoracic splanchnic nerve; ra, renal artery; SCGn, superior cervical ganglion; SMGn, superior mesenteric ganglion; SSN, superior thoracic splanchnic nerve; StGn, stellate ganglion; va, vertebral artery.

TABLE 6.3 Targets of Sympathetic Neurons Projecting from Paravertebral Chain Ganglia

Target	Potential transmitters	Function
Cutaneous vasculature	ATP/NA/NPY	Vasoconstriction[a]
Cutaneous arteriovenous anastomoses	ATP/NA/NPY? ACh?/VIP	Vasoconstriction[a] Vasodilation
Skeletal muscle vasculature	ATP?/NA/NPY ACh/NO	Vasoconstriction[a] Vasodilation
Sweat glands	ACh/VIP/PHM/CGRP/Som	Sudomotor vasodilation
Piloerector muscles	NA	Piloerection ("goose bumps")
Periosteum/bone	ACh?/NO?/VIP	Osteoblast/osteoclast activity; vasodilation
Adipose tissue	NA/NPY?	Lipolysis
Various thoracic, abdominal and pelvic viscera	NA/NPY/±Gal	Various, tissue specific[b]

[a]Pathways that are tonically active.
[b]Visceral targets vary with spinal level. For details of different visceral targets, see text. Neurons projecting to visceral targets form a small proportion of paravertebral ganglion neurons.

ACh, acetylcholine; ATP, adenosine 5′-triphosphate; CGRP, calcitonin gene–related peptide; Gal, galanin; NA, noradrenaline; NO, nitric oxide; NPY, neuropeptide Y; PHM, peptide histidine methionine; Som, somatostatin; VIP, vasoactive intestinal polypeptide.

TABLE 6.4 Cranial Targets of Sympathetic Neurons Projecting from the Superior Cervical Ganglion

Target	Potential transmitters	Function
Cutaneous blood vessels	NA/NPY ACh/VIP/NO?	Vasoconstriction[a] Vasodilation
Facial vein	NA/NPY	Vasodilation
Cerebral arteries	NA/NPY	Vasoconstriction[a]
Sweat glands	ACh/VIP/PHM/CGRP/Som	Secretion; local vasodilation
Salivary glands	NA	Increase protein in saliva
Olfactory mucosa (Bowman's glands)	NA/NPY	Mucous secretion
Iris	NA/NPY	Pupillodilation
Superior tarsal muscle (levator palpebrae superiorus)	NA/NPY	Contract muscle (open eye)[a]
Cornea	NA/NPY?	?
Pineal gland	NA/NPY	Melatonin production

[a]Pathways that are tonically active.
ACh, acetylcholine; CGRP, calcitonin gene–related peptide; NA, noradrenaline; NO, nitric oxide; NPY, neuropeptide Y; PHM, peptide histidine methionine; Som, somatostatin; VIP, vasoactive intestinal polypeptide.

TABLE 6.5 Targets of Sympathetic Neurons Projecting from Prevertebral Ganglia

Target	Function
Mesenteric circulation	Vasoconstriction[a]
Myenteric plexus	Inhibit motor activity[a,b]
Submucous plexus	Inhibit secretomotor activity[a,b]
Sphincter smooth muscle	Contraction[a]
Liver	Promote gluconeogenesis, vasoconstriction[a]
Pancreas	Inhibit insulin secretion; promote glucagon secretion; promote pancreatic polypeptide secretion
Spleen	Contract splenic capsule; vasoconstriction
Kidneys	Vasoconstriction[a]; stimulate renin release; antidiuresis; antinatriuresis
Ovary	Promote ovulation
Testis	Vasoconstriction

[a]Pathways that are tonically active.
[b]These neurons receive peripheral inputs from intestinofugal neurons projecting from the myenteric plexus.

Pathways through the Paravertebral Ganglia

Arrangement of the Paravertebral Ganglia

The paravertebral ganglia are interconnected to make up the sympathetic chains extending from cervical to sacral levels (Fig. 6.4). Although they initially develop segmentally, there can be considerable fusion of adjacent ganglionic primordia, so that the total number of macroscopic ganglia is variable.

Within the cervical region, three or four major ganglia are present. The largest is the superior cervical ganglion, which is about 2.5–3.0 cm long (Fig. 6.4; Becker and Grunt, 1957; Mitchell, 1953a) and which usually contains more than 1 million neurons (Ebbesson, 1963; Pearson and Pytel, 1978a). The ganglion normally lies immediately dorsal to the origin of the internal carotid artery. It has anatomical connections with the cranial nerves (excluding the first, second, and eighth), either directly or via the internal carotid nerve and plexus, and with the first to fourth or fifth cervical spinal nerves (Hoffman, 1957; Mitchell, 1953a, c, 1954; Parkinson, 1988; Parkinson *et al.*, 1978; Pick and Sheehan, 1946). These pathways distribute the axons of the final motor neurons to most of their cephalic targets. Other targets may be reached by fibers following cephalic arteries (Mitchell, 1954). Along the proximal course of the internal carotid nerves there are small microganglia in addition to those described in the cavernous plexus (Mitchell, 1953c).

In about 60% of individuals, there is a middle cervical ganglion that is 0.7–0.8 cm long, located at about the level of the sixth cervical vertebra, just superior to the inferior thyroid artery (Fig. 6.4). It has anatomical connections with the fifth and sixth cervical spinal nerves and contributes to the esophageal, tracheal, and aortic plexuses. In some cases, the middle cervical ganglion fuses to the inferior pole of the superior cervical ganglion to create a combined "mediosuperior" cervical ganglion up to 4.5 cm long (Becker and Grunt, 1957; Hoffman, 1957; Mitchell, 1953a; Wrete, 1959).

Inferior to the middle cervical ganglion there is usually a small vertebral ganglion, lying immediately ventral to the vertebral artery. The vertebral nerves arise from this ganglion. It is sometimes fused with the middle cervical ganglion (Becker and Grunt, 1957; Mitchell, 1953a; Wrete, 1959).

The lowest ganglion of the neck is the inferior cervical ganglion, which usually fuses with the first thoracic ganglion to form the stellate ganglion (Fig. 6.4; Becker and Grunt, 1957; Harman, 1900; Hoffman, 1957; Mitchell, 1953a; Pick and Sheehan, 1946; Wrete, 1959). The combined ganglion may extend up to 2.8 cm. Sometimes it and all the thoracic ganglia down to the fourth segment are fused (Wrete, 1959).

The remaining thoracic sympathetic ganglia are usually associated with each spinal nerve, apart from the most inferior ganglia, which may fuse with adjacent lumbar ganglia (Pick and Sheehan, 1946; Wrete, 1959). The ganglia are relatively small, each containing about 90,000–100,000 nerve cell bodies.

The thoracic ganglia distribute fibers to corresponding or adjacent spinal nerves, and the more superior ganglia make direct contributions to the aortic, cardiac, pulmonary, and esophageal plexuses (Fig. 6.4). The stellate ganglion also supplies sympathetic fibers to the upper limb (Kuntz, 1945; Kuntz *et al.*, 1956; Mitchell, 1953a). The splanchnic nerves arise from the thoracic ganglia and provide sympathetic pathways to the abdominal viscera. The autonomic components of the nerves include not only axons of final motor neurons in the thoracic ganglia, but also preganglionic axons destined for the sympathetic neurons of the prevertebral ganglia. The superior thoracic (or greater) splanchnic nerve is the largest splanchnic nerve, and originates from the fifth or sixth to the ninth or tenth thoracic ganglia (Fig. 6.4; Pick and Sheehan, 1946). It has anatomical connections with the esophageal and aortic plexuses and connects distally to the celiac, superior mesenteric, and aorticorenal ganglia. Where the nerve crosses the aorta, there is usually a small ganglion (Kuntz, 1945; Mitchell, 1953a). The middle thoracic (or lesser) splanchnic nerve arises from the ninth and tenth or tenth and eleventh thoracic segments and communicates with the cardiac plexus and aorticorenal ganglia (see below). The inferior thoracic (or least) splanchnic nerve, when present, originates from the lowest thoracic ganglia and primarily feeds into the renal plexus and ganglia (Fig. 6.4).

The lumbar sympathetic ganglia are extraordinarily variable in their number and location along the lumbar sympathetic chains, and there is no constant pattern to their arrangement (Cowley and Yeager, 1949; Kuntz and Alexander, 1950; Mitchell, 1953a; Webber, 1955, 1958). On average, unfused lumbar ganglia contain from about 60,000 to 85,000 nerve cell bodies (Webber, 1958). The lumbar ganglia have variable anatomical connections with the lumbar spinal nerves and distribute fibers with the lumbar splanchnic nerves to the inferior mesenteric and hypogastric plexuses and the aortic plexus (Fig. 6.4). Many neurons in the lumbar ganglia project to targets in the lower limbs (Kuntz and Alexander, 1950; Kuntz *et al.*, 1956; Mitchell, 1953a; Pick and Sheehan, 1946; Webber, 1955, 1958). Occasionally, in the lumbar region there may be direct cross-connections between the two sympathetic chains, which is probably the only region where this occurs (Cowley and Yeager, 1949; Pick and Sheehan, 1946; Webber, 1955).

At sacral levels, the sympathetic ganglia are small and generally are regularly spaced. As many as six ganglia on each side may be present (Wrete, 1959). Both sympathetic chains meet and fuse at coccygeal levels, where there may be a single small ganglion ("ganglion impar"; Mitchell, 1953a; Pick and Sheehan, 1946). Neurons in these ganglia project via the sacral and coccygeal nerves to the pelvic plexus (Fig. 6.4) and, more distally, to large blood vessels in the pelvic region.

Associated with the sympathetic chain at all levels are large numbers of "accessory" microganglia. These ganglia are found in the ventral roots, especially at lumbar levels (Alexander *et al.*, 1949; Boyd, 1957), and in the sympathetic roots (gray communicating rami) of the spinal nerves (Boyd, 1957; Kuntz and Alexander, 1950; Kuntz *et al.*, 1956; Pick and Sheehan, 1946; Skoog, 1947; Webber, 1955). Microganglia are also found in the lumbar splanchnic nerves (Webber, 1955, 1958) and along the internal carotid nerve and vertebral nerves arising from the cervical ganglia (Becker and Grunt, 1957; Harman, 1900; Hoffman, 1957; Kuntz *et al.*, 1957; Mitchell, 1953c). The microganglia usually contain from a few hundred to a few thousand nerve cell bodies (Kuntz *et al.*, 1956, 1957; Webber, 1955, 1958), although some accessory ganglia may contain 10,000–20,000 neurons (Alexander *et al.*, 1949; Kuntz *et al.*, 1957; Webber, 1958).

Structure of Sympathetic Final Motor Neurons

The structure of the final motor neurons in human sympathetic ganglia has been observed mostly in silver-stained preparations, in which only a subset of neurons and their dendritic processes are fully stained (Fig. 6.5). The cell bodies of sympathetic neurons range from 15 to about 60 μm in diameter, with large cells (35–60 μm) being most common in the superior and middle cervical ganglia (De Castro, 1932). The cells are multipolar, bearing from 1 to 10 or 12 long dendrites. Some of these multipolar cells also have a large number of short dendrites that do not penetrate the satellite cell capsule. Other cells lack long dendrites and have only short intracapsular dendrites (De Castro, 1932; Kuntz, 1945; Ramón y Cajál, 1911). The number of dendrites and their degree of branching have been reported to increase with age (Botar, 1966; De Castro, 1932). The long dendrites may branch considerably and bear varicose terminations that form "dendritic nests" enclosing other ganglion cells. Commonly, the long branching dendrites from several nearby cells intermingle to form complex "dendritic glomeruli." The shorter dendrites usually end as fine tapering processes, but often they terminate with bulbous expansions (De Castro, 1932; Kuntz, 1945; Ramón y Cajál, 1911). Axons usually lack collaterals within the ganglia and arise from the proximal portion of a large dendrite (De Castro, 1932). In animals, there is good evidence that sympathetic neurons in different functional pathways can be distinguished by morphological features such as the size of the cell body and dendritic fields (see Gibbins, 1995). To date, there is no information available to address this issue directly in humans.

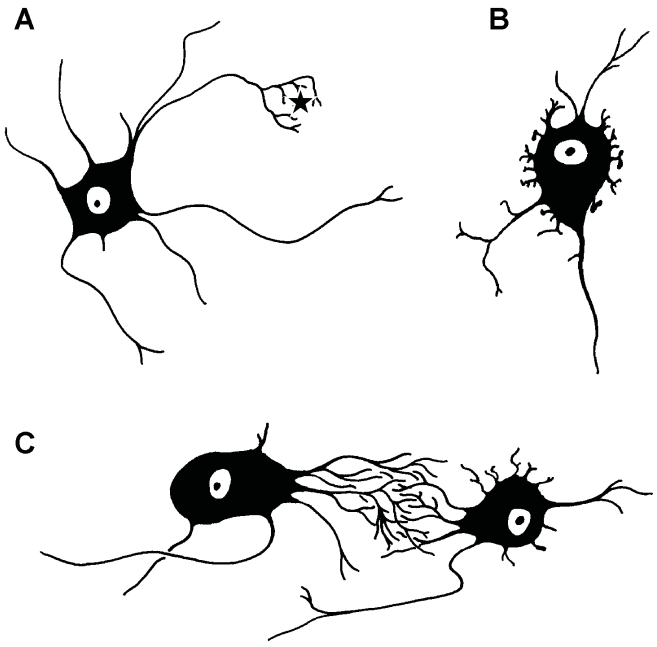

FIGURE 6.5 Shapes of sympathetic final motor neurons as seen in silver-stained preparations based on the descriptions of Ramon y Cajal (1911) and De Castro (1932). These preparations are unlikely to reveal the full extent of dendritic arborisation as would be seen by intracellular dye injections, but such data are not yet available for humans. In laboratory mammals, single neurons may bear more than 15 dendrites with a total dendritic tree length of several millimeters (Gibbins, 1995). **(A)** Neuron with long dendrites, some of which branch around another cell body *(star)*. It is not at all clear if this represents a specific functional relationship or is just a consequence of the packing of the dendrites in the neuropil surrounding the cell bodies. **(B)** This neuron shows many short intracapsular dendritic process in addition to some longer dendrites. The spaces between the short dendrites are likely to be filled by Schwann cells. **(C)** Two neurons with multibranched dendrites form a "dendritic glomerulus." Such arrangements are relatively common in sympathetic and parasympathetic ganglia. Once again, their functional significance, if any, is not known. The cell bodies are typically from 25–50 μm in diameter.

Preganglionic axons lose their myelin sheath before they reach the cell bodies of the final motor neurons within the ganglia (Pick *et al.*, 1964). They encircle the proximal axon and axon hillock region but generally end around the intracapsular dendrites, where they form synapses (De Castro, 1932; Hervonen *et al.*, 1980; Pick, 1970; Pick *et al.*, 1964; Ramón y Cajál, 1911). Preganglionic synapses also occur on the extracapsular dendrites, particularly where they form dendritic glomeruli (De Castro, 1932; Kuntz, 1945; Pick, 1970; Pick *et al.*, 1964). All preganglionic neurons in sympathetic pathways are functionally cholinergic. However, some contain neuropeptides, such as enkephalin (Helen *et al.*, 1984; Hervonen *et al.*, 1980; Przewlocki *et al.*, 1983), and many may contain NOS (Smithson and Benarroch, 1996).

Peptide Expression

As has been observed consistently in a wide range of vertebrate species (Gibbins, 1995), different functional populations of final motor neurons in sympathetic ganglia differentially express immunoreactivity to various neuropeptides (Tables 6.3 and 6.4). There also is selective expression of neuropeptides in different populations of preganglionic fibers projecting to neurons in the ganglia.

At least 80% of the neurons in the superior cervical ganglion are noradrenergic, whereas at lumbar levels, about 75% of neurons are noradrenergic. At all levels in the paravertebral chain, about 50% of the noradrenergic neurons contain NPY (Baffi *et al.*, 1992; Harkonen and Penttila, 1971; Hervonen *et al.*, 1978b; Lundberg *et al.*, 1982; Schmitt *et al.*, 1988; Tajti *et al.*, 1999). There is indirect evidence that galanin may occur in at least some populations of sympathetic

neurons. A small proportion of neurons, most of which are likely to be cholinergic, contain various combinations of VIP, somatostatin, or CGRP (Baffi *et al.*, 1992; Jarvi *et al.*, 1987; Schmitt *et al.*, 1988; Tajti *et al.*, 1999). The remaining neurons are probably non-noradrenergic and represent cholinergic sympathetic neurons (see below). They may comprise up to 20–25% of neurons in the lumbar ganglia. Most of the non-noradrenergic neurons are surrounded by the terminals of preganglionic neurons that contain enkephalin and related peptides (Helen *et al.*, 1984; Hervonen *et al.*, 1980; Przewlocki *et al.*, 1983).

Additional information on the patterns of peptide expression of the final motor neurons in the paravertebral ganglia comes from the analysis of their projections to peripheral targets.

Cutaneous Targets

The best understood paravertebral sympathetic neurons in humans are those projecting to targets in the skin. These pathways primarily are involved in thermoregulation and innervate the cutaneous vasculature, the sweat glands, and the piloerector muscles. Together these effectors make up most of the targets of the paravertebral sympathetic neurons (Table 6.3).

Humans are unique in having a dense innervation of cutaneous sweat glands throughout the skin. On average, an adult human has about 3 million sweat glands (Szabo, 1967). The size of the terminal field of individual sudomotor fibers ranges from about 25 mm^2 to more than 350 mm^2 depending on the exact location (Fig. 6.6; Riedl *et al.*, 1998; Schmelz *et al.*, 1998). In the hairy skin of the limbs, this would mean that each sudomotor neuron innervates about 100 sweat glands. However, each sweat gland is innervated by more than one sudomotor neuron (see Gibbins, 1997). The distribution of sudomotor fibers follows an irregular segmental pattern to the trunk and limbs that shows substantial variation between individuals and even between sides in the same individual (Fig. 6.6; Greenhalgh *et al.*, 1971; Randall *et al.*, 1955; Richter and Otenasek, 1946). The sudomotor fibers to the face are derived mostly from neurons in the superior cervical ganglion. Fibers reach the facial skin via the internal carotid nerve and then via branches of the trigeminal nerve (Guttman, 1940; List and Peet, 1938; Wilson, 1935). As there are 0.5–1.0 million sweat glands in the

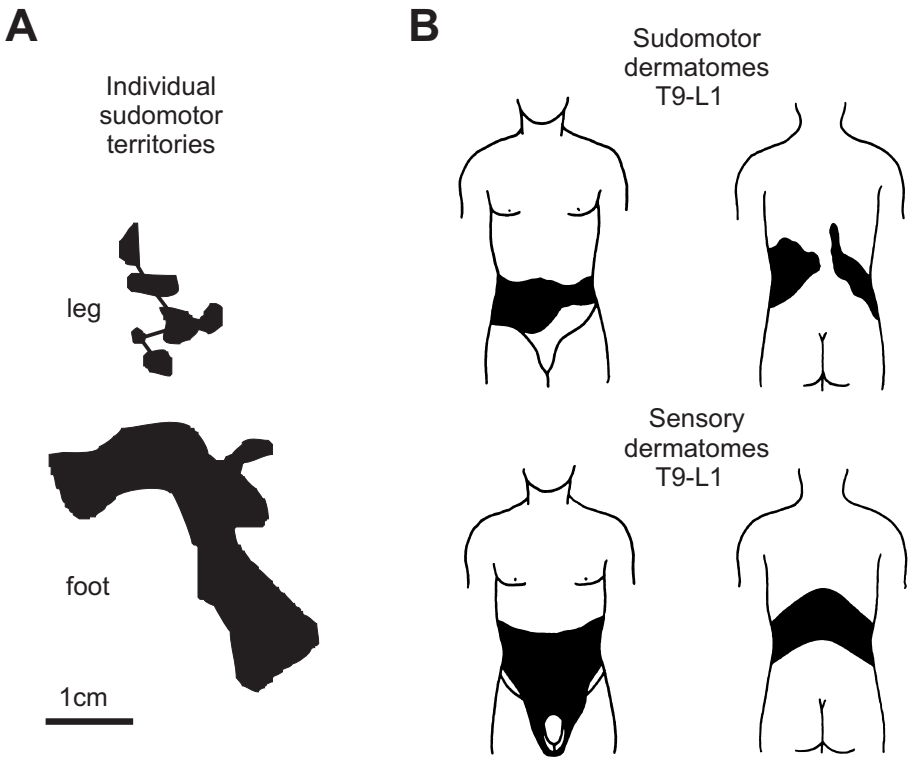

FIGURE 6.6 Organization of the peripheral projections of sudomotor neurons. **(A)** Examples of cutaneous territories of single sudomotor neurons (adapted from Schmelz *et al.*, 1998). **(B)** Distribution of sudomotor projections originating from spinal segments T9 to L1 compared with cutaneous sensory nerve originating from the same spinal levels (adapted from Richter and Otenasek, 1946). Scale bar applies to A only.

facial skin (Gibbins, 1997), sweat glands make up one of the largest targets of final motor neurons in the superior cervical ganglion.

The sudomotor neurons are functionally cholinergic (Foster and Weiner, 1970; Greenhalgh *et al.*, 1971; List and Peet, 1938; Wilson, 1935), but they also contain VIP and PHM as well as CGRP and somatostatin (Björklund *et al.*, 1986; Hartschuh *et al.*, 1984; Johansson, 1986; Schmitt *et al.*, 1988; Vaalasti *et al.*, 1985). The effect of the VIP and CGRP may be to enhance the secretomotor effects of cholinergic stimulation (Yamashita *et al.*, 1987) and to contribute to the noncholinergic vasodilator responses in hairy skin (Brengelmann *et al.*, 1981; Kaada *et al.*, 1984; Rowell, 1981). There may also be a minor noradrenergic innervation of the sweat glands (Tainio *et al.*, 1986; Uno, 1977).

Noradrenergic axons are prominent around cutaneous arteries and veins, where they generally mediate vasoconstriction (Arneklo-Nobin and Owman, 1985; Rothe, 1983; Rowell, 1977; Shepherd and Mancia, 1986). Most of the perivascular noradrenergic axons also contain NPY (Björklund *et al.*, 1986; Johansson, 1986; Lundberg *et al.*, 1983; Sugenoya *et al.*, 1998; Tainio *et al.*, 1986), which may contribute to the vasoconstrictor responses. Experiments in laboratory animals have established that blood flow through small cutaneous arteries and arteriovenous anastomoses is controlled selectively by specific populations of sympathetic vasoconstrictor neurons (Morris, 1997).

The blood vessels of the hairy skin and the skin of the face, but not of the glabrous skin of the hands and feet, are also under sympathetic vasodilator control, which is largely noncholinergic and dependent on the presence of a functional innervation of the sweat glands (Blumberg and Wallin, 1987; Fox and Edholm, 1963; Jänig *et al.*, 1983; Nordin, 1990; Rowell, 1981). Nevertheless, digital arteriovenous anastomoses are innervated by non-noradrenergic axons, at least some of which contain VIP (Hartschuh *et al.*, 1984; Hurley and Mescon, 1956); under some conditions, active sympathetic vasodilation in the skin can be seen in the absence of sweating (Bell and Robbins, 1997; Crandell *et al.*, 1995; Lundberg *et al.*, 1989). The facial vein, draining the skin of the face, is unusual in that it has a dense innervation by sympathetic noradrenergic fibers, which in this case cause vasodilation via the action of noradrenaline on β receptors (Mellander *et al.*, 1982).

Surprisingly, there is a dense noradrenergic innervation of piloerector muscles throughout the hairy skin of humans, except for most of the head (Breathnach, 1977; Orfanos and Mahrle, 1973; Uno, 1977). On average, more than 2 million hair follicles are present, each with a piloerector muscle (Szabo, 1967), forming a substantial peripheral target of the paravertebral neurons. The pilomotor neurons lack NPY, and on this basis it can be estimated that as many as 25% of neurons in the paravertebral ganglia are likely to lie in pilomotor pathways, as is the case in furry mammals such as guinea pigs and rats (see Gibbins, 1997). Pilomotor fibers generally run together with vasoconstrictor and sudomotor fibers in small fascicles to the skin. They have a similar distribution that does not closely follow the sensory dermatomes (Ray *et al.*, 1943; Wallin and Elam, 1997). Activation of the pilomotor pathway results in "goose-bumps" in a now futile attempt to trap an insulating layer of air between the hairs. These observations suggest that hairlessness has evolved only very recently in humans. All of the sympathetic neurons projecting to targets in the skin have a primary thermoregulatory function, although the sudomotor pathways to the palms of the hands, soles of the feet, and the face can be activated selectively by a variety of emotional stimuli (Gibbins, 1997). The activity of cutaneous vasoconstrictor neurons is coordinated with the activity of vasomotor neurons in other vascular beds to maintain cardiac output (Johnson, 1986), but they are relatively insensitive to changes in baroreceptor input (Wallin and Elam, 1997; Wallin and Fagius, 1988). Both lesioning and functional studies have indicated that each of these pathways can be controlled independently as components of a range of respiratory and cardiovascular reflexes in addition to their thermoregulatory roles (Bini *et al.*, 1980a, b; Jänig *et al.*, 1983; Johnson, 1986; Macefield and Wallin, 1996, 1999; Okamoto *et al.*, 1994; Randall *et al.*, 1955; Wallin and Elam, 1997; Wallin and Fagius, 1988).

Vascular Targets

The arteries in skeletal muscle vascular beds are innervated by noradrenergic vasoconstrictor neurons that contain NPY (Lundberg *et al.*, 1983). These pathways are tonically active and are under strong baroreceptor control. The skeletal muscle vasculature also is probably innervated to varying degrees by non-noradrenergic vasodilator neurons (Bell, 1996; Hjemdahl and Kahan, 1996; Jänig *et al.*, 1983; Roddie and Shepherd, 1963; Rowell, 1981), although the presence of this pathway has been disputed repeatedly (Reed *et al.*, 2000; see Joyner and Halliwell, 2000). When it can be observed, active sympathetic vasodilation of skeletal muscle vascular beds seems to be mediated by some combination of ACh and NO (Dietz *et al.*, 1997). The conditions under which sympathetic vasodilation of skeletal muscle vascular beds occurs naturally are not well known, but one possibility is during shivering, when blood flow to thermogenic

muscles needs to be increased in the absence of metabolic vasodilators.

The cell bodies of final motor neurons in both skeletal muscle vasoconstrictor and vasodilator pathways are in the paravertebral ganglia. Nevertheless, each of these pathways almost certainly is regulated independently of the other by the CNS. Furthermore, these pathways are anatomically and functionally distinct from those controlling the cutaneous vascular beds (Brengelmann, 1983; Christensen and Galbo, 1983; Gibbins, 1995; Jänig, 1988; Jänig *et al.*, 1983; Wallin and Fagius, 1988).

In addition to the cutaneous and skeletal muscle vascular beds, noradrenergic neurons, mostly containing NPY, innervate blood vessels throughout the body (Edvinsson *et al.*, 1987; Gu *et al.*, 1983a; Lundberg *et al.*, 1983; Wharton and Gulbenkian, 1987). These neurons generally are vasoconstrictors, and NPY is likely to contribute to these responses along with neuronally released noradrenaline (Franco-Cereceda and Lundberg, 1987; Kahan *et al.*, 1992; Lundberg *et al.*, 1985; Pernow and Lundberg, 1986; Racchi *et al.*, 1997; Schuerch *et al.*, 1998). Veins seem to be particularly sensitive to the constrictor actions of NPY (Linder *et al.*, 1996; Peduzzi *et al.*, 1995). The release of NPY with noradrenaline from some of these neurons has been demonstrated following their reflex activation, usually under conditions where there are high levels of sympathetic vasoconstrictor activity, such as during intense exercise, lower body negative pressure, or heart failure (e.g., Eckberg *et al.*, 1988; Hauser *et al.*, 1996; Kahan *et al.*, 1992; Morris *et al.*, 1986; Pernow *et al.*, 1986). In some vessels at least, ATP can act as a cotransmitter together with noradrenaline and NPY from sympathetic vasoconstrictor neurons (Racchi *et al.*, 1999; Rump *et al.*, 1994).

Cranial Targets

Neurons in the cervical ganglia innervate many nonvascular targets in the cranial region (Table 6.4). Within the eye, noradrenergic axons containing NPY are abundant in both the sphincter and dilator muscles of the iris (Ehinger, 1966; Nomura and Smelser, 1974; Stone, 1986). When light levels are very low the pupil is dilated by the β-adrenoceptor-mediated relaxation of the sphincter and α-adrenoceptor-mediated contraction of the dilator muscle. During normal daylight levels, these neurons are largely inactive (Sears, 1984). The smooth muscle of the levator palpebrae superioris muscle (superior tarsal muscle), which elevates the upper eyelid and keeps the eye open, is innervated by a small set of NPY-containing neurons in the superior cervical ganglion. These neurons are tonically active as long as we are awake. Sympathetic fibers also have been observed in the cornea, especially in the region of the corneoscleral limbus. Some of these fibers are associated with small blood vessels, where they presumably mediate vasoconstriction. The function of the sympathetic fibers in the cornea itself is not known (Marfurt and Ellis, 1993; Chen *et al.*, 1999).

Noradrenergic neurons in the cervical ganglia innervate the secretory cells of the parotid and submandibular salivary glands, but not the sublingual glands (Rossoni *et al.*, 1979). There is a dense sympathetic supply to the lacrimal gland (Ehinger, 1966). These neurons probably do *not* contain NPY (Lundberg *et al.*, 1983). They modulate secretion that is controlled primarily by cranial autonomic neurons. Based on animal studies, the neurons projecting to the salivary glands would be expected to have very large cell bodies (Gibbins, 1995), and they may correspond to the large cells observed in the superior cervical ganglion by De Castro (1932). Sympathetic fibers containing NPY are abundant in the nasal and olfactory mucosa. In the latter, they probably stimulate mucus secretion from the Bowman glands, which contribute to maintaining an appropriate environment for the olfactory receptors (Chen *et al.*, 1993).

The thyroid gland is innervated by noradrenergic neurons containing NPY, which originate in the middle cervical ganglion and which may stimulate hormone secretion (Grunditz *et al.*, 1984; Melander *et al.*, 1974; Romeo *et al.*, 1986). Sympathetic neurons containing NPY also project from the superior cervical ganglion to the pineal gland, where they stimulate melatonin production. They reach the pineal bilaterally via the internal carotid nerve and the "nervus conarius" that runs through the tentorium cerebelli (Korf, 1996).

Thoracic and Abdominal Targets

The sympathetic noradrenergic innervation of the heart is derived mainly from the cervical and upper thoracic ganglia (T1 to T4 or T5). These neurons exert positive inotropic and chronotropic effects on the heart. For example, they tend to be activated at the commencement of exercise, after withdrawal of vagal inhibitory tone (Eckberg *et al.*, 1972; Maciel *et al.*, 1987; Savin *et al.*, 1982). However, baroreflex-mediated tachycardia is likely to be a direct sympathetic excitation overriding the effects of vagal activity (Eckberg, 1980). The sympathetic neurons projecting to the heart contain NPY, which is released mostly under conditions of high levels of sympathetic activity to the heart, such as exercise or anoxia (Gu *et al.*, 1983a; Kaijser *et al.*, 1990, 1994; Lundberg *et al.*, 1983). A major action of this NPY is to inhibit the activity of vagal final motor neurons within the cardiac plexuses (Potter, 1985).

The cervical and upper thoracic ganglia also contain neurons that project out along the vagus to the foregut (Furness and Costa, 1987; see below). There is virtually no functional sympathetic innervation of the airway smooth muscle, despite abundant β-adrenoceptors in that tissue (Barnes, 1984; Goldie *et al.*, 1997; Partanen *et al.*, 1982; Richardson, 1983). Furthermore, there is little direct sympathetic innervation of the respiratory mucosae of the distal airways (Cauna *et al.*, 1972; Nomura and Matsuura, 1972).

A potentially enormous target of noradrenergic neurons in the paravertebral ganglia is adipose tissue. There is increasing evidence that sympathetic activity can increase lipolysis, perhaps stimulated by the central effects of leptin (Nonogaki, 2000). However, the direct innervation of adipocytes in white-fat tissue seems to be relatively sparse. The activity of any innervation of the adipose tissue is almost certainly coordinated with that of the sympathetic outflows to the endocrine pancreas and liver (Nonogaki, 2000).

In addition to sudomotor neurons and vasodilator neurons, there are probably other small populations of non-noradrenergic neurons in the paravertebral ganglia. For example, there is now good evidence that some VIP-containing paravertebral neurons innervate the periosteum (Hohmann *et al.*, 1986). These neurons may regulate the activity of osteoblasts and osteoclasts as well as influencing local blood flow to the bone (Togari *et al.*, 1997; Winding *et al.*, 1997).

Pathways through the Prevertebral Ganglia

The prevertebral ganglia lie in complex plexuses associated with the abdominal aorta and its major arterial branches (Fig. 6.4). The sympathetic final motor neurons in these ganglia regulate a wide range of effectors in the abdominal and pelvic regions (Table 6.5). The neurons contribute to the most complex peripheral autonomic circuits outside the enteric plexuses. The celiac plexus surrounds the proximal segment of the celiac artery and the root of the superior mesenteric artery. The celiac ganglion has two major poles, each about 20–25 mm by 10–15 mm, and about 3–5 mm thick, which lie either side of the celiac nerve trunk (Mitchell, 1953a). Together they contain about 1.8 million nerve cell bodies (Botar, 1966). The ganglia themselves are somewhat diffuse. Nevertheless, commonly a detached inferolateral portion on each side can be identified as the aorticorenal ganglion (interrenal ganglia). Sometimes, a distinct single superior mesenteric ganglion occurs on the aorta just superior or inferior to the origin of the superior mesenteric artery (Kuntz, 1945; Mitchell, 1953a). Preganglionic fibers reach the celiac ganglion via the superior splanchnic nerves, and the middle splanchnic nerves provide input to the aorticorenal ganglia. Most of the neurons in the ganglia are noradrenergic and innervate the gastrointestinal tract and its associated structures, including liver, gallbladder, and pancreas. The sympathetic innervation of the spleen probably originates from cell bodies in the celiac plexus (Felten *et al.*, 1987), while the innervation of the kidneys is derived largely from neurons in the aorticorenal ganglia (Ferguson and Bell, 1993; Mitchell, 1935). The aorticorenal ganglia also provide much of the innervation of the gonads (Dail, 1993; Stjernquist, 1996; Traurig and Papka, 1993).

The celiac plexus extends inferiorly toward the inferior mesenteric plexus as the intermesenteric plexus, within which small ganglia are usually found (Baljet and Drukker, 1981; Wozniak and Skowronska, 1967). The inferior mesenteric plexus surrounds the root of the inferior mesenteric artery and contains the inferior mesenteric ganglia. The main ganglion is at most 1–2 mm long and may consist only of a diffuse collection of microganglia (Kuntz, 1940; Southam, 1959; Trumble, 1933–1934). Preganglionic inputs run in the inferior splanchnic nerve and lumbar splanchnic nerves. Sympathetic final motor neurons in these ganglia project to the colon via the colonic nerves and inferiorly to the pelvic plexus via the superior hypogastric plexus (Baljet and Drukker, 1981; Mitchell, 1935; Trumble, 1933–1934).

The superior hypogastric plexus (also known as the hypogastric nerve or the presacral nerve) consists of several ganglionated nerve trunks extending from the inferior mesenteric plexus to the inferior hypogastric, or pelvic, plexus. These neurons mainly supply the pelvic viscera and will be discussed further in "Pelvic Autonomic Pathways."

The neurons of the celiac and inferior mesenteric plexuses have ranges of shapes and dendritic branching patterns similar to those of neurons in the paravertebral ganglia (Botar, 1966; Kuntz, 1938, 1940). Although the largest cell bodies in the prevertebral ganglion are not as big as those in the superior cervical ganglion, there are relatively few small cells. Most cells are between 35 and 45 μm in diameter (Botar, 1966; De Castro, 1932). In addition to their spinal preganglionic input from the splanchnic nerves, many of these neurons are unique among sympathetic pathways in that they receive excitatory inputs from peripheral enteric neurons, which are cholinergic and probably contain VIP (Furness and Costa, 1987; Gibbins, 1995; Quartu *et al.*, 1993). Thus, prevertebral sympathetic neurons can participate in peripheral reflexes that may be at least partially independent of

direct central control (Furness and Costa, 1987; Kuntz, 1938, 1940; Mawe, 1995; Szurzewski, 1981).

One population of prevertebral neurons provides vasoconstrictor innervation to the blood vessels of the mesenteries and gut. The neurons contain and release NPY in addition to noradrenaline (Ahlborg *et al.*, 1991). These pathways are under strong baroreceptor control; consequently, the level of vasoconstrictor activity in the splanchnic circulation can have a major impact on central blood pressure. Splanchnic blood flow also varies depending on the level of activity of the gut (Mathias *et al.*, 1996).

The sympathetic neurons projecting to the kidney cause vasoconstriction and have an important role in stimulating renin release. They also have complex effects on renal water and electrolyte balance, with a net result of reducing water and sodium excretion (Kopp and Di Bona, 1993). Although the renal nerves controlling different aspects of renal function may arise from distinct populations of final motor neurons, they probably all contain NPY (Ferguson and Bell, 1993). It is clear that the pathways causing renal vasoconstriction can be activated independently of vasoconstrictor pathways to other major vascular beds such as the mesentery or skeletal muscles (Jänig, 1988).

Most of the noradrenergic neurons with cell bodies in the celiac and inferior mesenteric plexuses regulate gastrointestinal motility and secretion (Fig. 6.7). One group of these neurons inhibits gastrointestinal motility mainly by inhibiting the activation of intrinsic cholinergic motor neurons with cell bodies in the myenteric plexus (Furness and Costa, 1987; Roman and Gonella, 1987). A second population of prevertebral neurons exerts a tonic inhibitory influence on the secretomotor neurons located in the submucous plexus of the intestines (Furness and Costa, 1987). In both locations, noradrenergic terminals ramify throughout the ganglia, often in close association with enteric ganglion cells (Llewellyn-Smith *et al.*, 1984). In contrast, there is a direct sympathetic innervation of the gastrointestinal sphincters that usually results in their contraction, further contributing to the sympathetic inhibition of the transit of contents along the digestive tract (Christensen, 1987; Furness and Costa, 1987; Roman and Gonella, 1987). All of these prevertebral sympathetic neurons can be activated reflexively by mechanical distention of the bowel or by chemical stimulation of the mucosa. Some of these reflexes are mediated in part by the enteric neurons projecting directly to neurons in the prevertebral

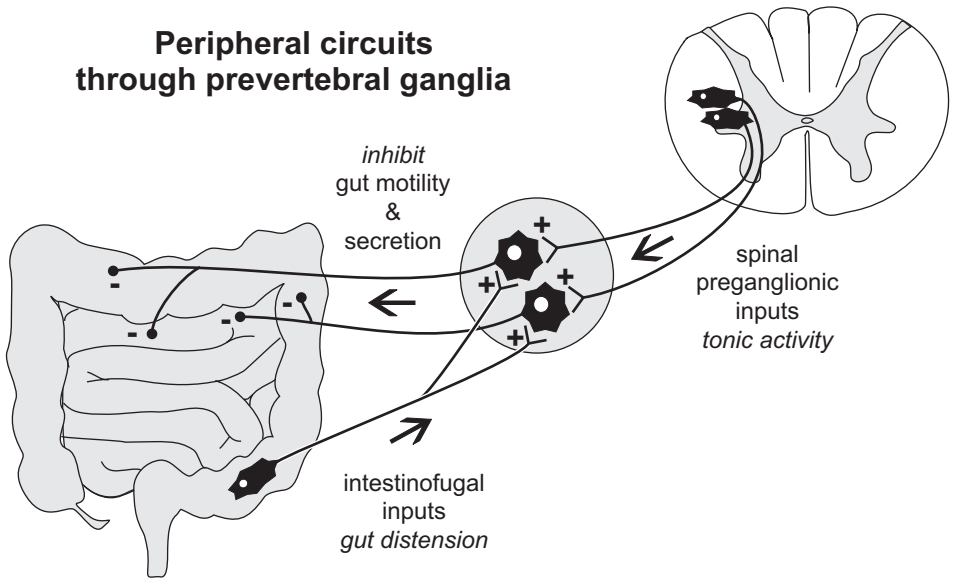

FIGURE 6.7 Diagram of the intestinofugal circuit through the prevertebral sympathetic ganglia. Sympathetic neurons in the ganglia receive inputs from both spinal preganglionic neurons and enteric intestinofugal neurons. All these inputs are excitatory and mediated by the actions of acetylcholine on nicotinic receptors. However, other substances, including nitric oxide and a range of peptides, may be released from these cholinergic terminals. The spinal inputs are tonically active, while the enteric inputs are activated in response to distention of the gut. Separate populations of sympathetic neurons project to the myenteric plexus to inhibit gut motility and to the submucous plexus to inhibit secretomotor activity. Some sympathetic neurons project back to the initial site of distension, but others project to more oral regions of the gut. Intestinofugal neurons occur throughout the small and large intestines. The arrows in the diagram refer to the direction of neural traffic.

ganglia (Fig. 6.7; Furness and Costa, 1987; Kuntz, 1938, 1940; Szurzewski, 1981). It can be argued that the primary function of the pathways through the prevertebral ganglia is to contribute to blood volume regulation by controlling fluid secretion and excretion from the gastrointestinal tract. This function is under central control via the spinal preganglionic inputs to the prevertebral ganglion cells. However, the inputs from peripheral enteric neurons that respond to gut distention allows the gut to take some level of priority in the control of the activity of the prevertebral neurons, presumably under conditions when its integrity may become compromised.

The abundant noradrenergic innervation of the parenchyma and vasculature of the liver arises from the celiac plexus (Nobin *et al.*, 1978). Sympathetic stimulation is involved in stimulating glucose output from the liver to the blood (Friedman, 1982; Lautt, 1980). Sympathetic neurons in the celiac plexus innervate the islets of the pancreas, where they have a complex variety of actions. Overall, insulin secretion is inhibited, whereas secretion of glucagon and pancreatic polypeptide is stimulated by sympathetic inputs. Most of these actions are mediated by noradrenaline, with the precise roles of peptides such as NPY and galanin being difficult to ascertain in humans (Ahren *et al.*, 1991; Ahren, 2000; Ahlborg *et al.*, 1992; Dunning and Taborski, 1988; Edwards and Bloom, 1996; Nonogaki, 2000; Verchere *et al.*, 1996; Yamaguchi, 1992). The combined effect of the activation of sympathetic pathways through the celiac plexus to the liver and pancreas is an increase in blood glucose concentration.

The functions of the sympathetic innervation of the gonads are still not well understood. There is relatively little direct innervation of the testes, with most sympathetic fibers innervating local blood vessels, where they presumably cause vasoconstriction. The smooth muscle of the epididymis is heavily innervated by sympathetic fibers, but it is likely that these fibers arise from neurons in the hypogastric plexus (Dail, 1993; Stjernquist, 1996). In contrast, the ovary is well supplied with sympathetic fibers, mostly originating from various levels of the prevertebral plexuses. The fibers are associated mainly with contractile cells around the follicles, and they probably facilitate ovulation (Stjernqusit, 1996; Traurig and Papka, 1993).

PELVIC AUTONOMIC PATHWAYS

The pelvic autonomic pathways provide sympathetic and parasympathetic innervation to a wide variety of pelvic viscera (Table 6.6). In most viscera, the primary target of the innervation is smooth muscle, although there is increasing evidence for innervation of secretory epithelia and mucosal glands. There also is some evidence that nonsympathetic innervation of the gonads may arise from parts of the pelvic plexus (Jorgensen *et al.*, 1996; Tainio, 1994). Perhaps more than any other set of autonomic pathways, the activity of the pelvic autonomic neurons must be coordinated with the activity of somatic motor pathways. This can be seen during sexual activity and the control of micturition, defecation, and continence.

The prevertebral sympathetic plexuses extend inferiorly into the pelvis as a continuous meshwork of ganglionated nerve trunks. This plexus has been divided into the superior and inferior hypogastric plexuses (e.g., Baljet and Drukker, 1981; Mitchell, 1935; Wozniak and Skowronska, 1967). The latter plexus lies on each side of the rectum and interconnects dorsal to the rectum. The plexus extends ventrally toward the bladder and internal genital organs (Baljet and Drukker, 1981; Curtis *et al.*, 1942; Mitchell, 1935, 1953a; Wozniak and Skowronska, 1967). Most earlier authors have used the term "pelvic plexus" only for the inferior hypogastric plexus (Curtis *et al.*, 1942; Davis, 1933; Mitchell, 1935; Trumble, 1933-1934; Wozniak and Skowronska, 1967). However, more recent experimental studies, mainly in nonhumans, indicate that all the neurons in the pelvic region, including the superior and inferior hypogastric plexuses, are best considered together as the "pelvic plexuses" (Costa and Furness, 1973; Keast, 1995, 1999; Owman *et al.*, 1983; Szurzewski, 1981).

The ganglia in the pelvic plexuses contain both noradrenergic and non-noradrenergic neurons (Keast, 1995; and references below). Immunohistochemical observations in humans and a range of other mammals indicate that there are many different subsets of pelvic neurons that can be distinguished by the combinations of potential transmitters they contain. The noradrenergic neurons probably mostly contain NPY, although some may contain somatostatin or galanin. It seems that most of the non-noradrenergic neurons are cholinergic and contain immunoreactivity for ChAT and the vesicular ACh transporter (VAChT), even though ACh itself may have only a minor role in neurotransmission to a specific target tissue. Many of these neurons also contain immunoreactivity to NOS, and there is now considerable evidence that NO itself is a major transmitter in most of these neurons. It seems that most of the cholinergic neurons contain NPY, and those that contain NOS also contain VIP and related peptides, such as PHM. A high proportion of the latter neurons also contain immunoreactivity for HOX-2, although the role of CO is unknown. Neurons

TABLE 6.6 Targets of Neurons Projecting from Pelvic Ganglia

Target	Potential transmitters	Function
Ureter	NO/VIP/NPY	Inhibit smooth muscle activity
	NO/VIP	Secretomotor, vasodilator
Detrusor	ATP/ACh/NPY/± NO	Contraction
	NO/VIP	Relaxation
Urethra	NA/NPY	Contraction
	ACh/NO/VIP	Relaxation
Vas deferens	ATP/NA/NPY/Gal	Contraction
	ACh/NO/VIP/NPY±Som	Relaxation? secretion?
Seminal vesicles	ATP/NA/NPY/Gal	Contraction
	ACh/NO/VIP/NPY±Som	Relaxation? secretion?
Prostate	ATP/NA/NPY/Gal	Contraction
	ACh/NO/VIP/NPY±Som	Relaxation? secretion?
Penile erectile tissue	ACh/NO/VIP/PHM	Vasodilation
	NA/±NPY	Vasoconstriction
Uterus	NA/NPY	Contraction (nonpregnant)
		Relaxation (pregnant)
	NO/VIP	Relaxation, vasodilation, secretion
Vagina	NA/NPY	Contraction
	NO/VIP	Relaxation, vasodilation, secretion
Colon/Rectum	NA/?	Inhibit activity
	ACh/?	Contraction
Internal anal sphincter	NA/?	Contraction
	NO/VIP	Relaxation

ACh, acetylcholine; ATP, adenosine 5′-triphosphate; Gal, galanin; NA, noradrenaline; NO, nitric oxide; NPY, neuropeptide Y; PHM, peptide histidine methionine; Som, somatostatin; VIP, vasoactive intestinal polypeptide.

containing NOS, VIP, NPY, and HOX-2 almost certainly relax smooth muscle but cause secretion from epithelia lining most of the pelvic viscera. A potentially confounding issue is the presence of neurons that contain immunoreactivity for tyrosine hydroxylase and NOS. Some of these neurons may use both noradrenaline and NO as transmitters, but it has not yet been established that all these neurons actually synthesize and release catecholamines.

Preganglionic inputs to the ganglion cells arise mainly from lumbar levels via the hypogastric nerves and the second to fourth sacral levels via the pelvic nerves. The lumbar inputs are directed primarily to noradrenergic neurons, and the sacral inputs generally supply non-noradrenergic neurons. However, some neurons may receive inputs from both lumbar and sacral levels (Keast, 1995, 1999; Szurzewski, 1981). Thus, some neurons may be activated by both sympathetic and parasympathetic central pathways (Keast, 1995, 1999; Mitchell, 1953a). Furthermore, sympathetic neurons with cell bodies in the sacral paravertebral ganglia contribute to the pelvic plexuses via the pelvic splanchnic nerves (Baljet and Drukker, 1981; Mitchell, 1953a; Owman *et al.*, 1983; Trumble, 1933–1934). At least some of these neurons end in the ganglia themselves where they can modify ganglionic transmission from the preganglionic inputs (De Groat and Booth, 1993; Keast, 1995). Finally, there is good experimental evidence from animals that intestinofugal neurons in the enteric plexus of the distal gastrointestinal tract project to neurons in the pelvic plexuses, raising the possibility that the activity of some final motor neurons in the pelvic plexuses can be influenced directly by peripheral enteric neurons (Luckensmeyer and Keast, 1996).

The details of the functional anatomy of the pelvic plexuses in humans are still incomplete and are best described in relation to the organs they innervate. The plexuses tend to be larger and contain more ganglia in males than in females. This simply reflects the greater variety of targets in the internal reproductive organs of males (Keast, 1995). For an excellent overview of these pathways in mammals, see Maggi (1993).

Ureter, Urinary Bladder, and Urethra

Ureter

Much of the motility of the ureter seems to be myogenic with a pacemaker located in the region of the renal pelvis (Amann, 1993). Surprisingly, there is

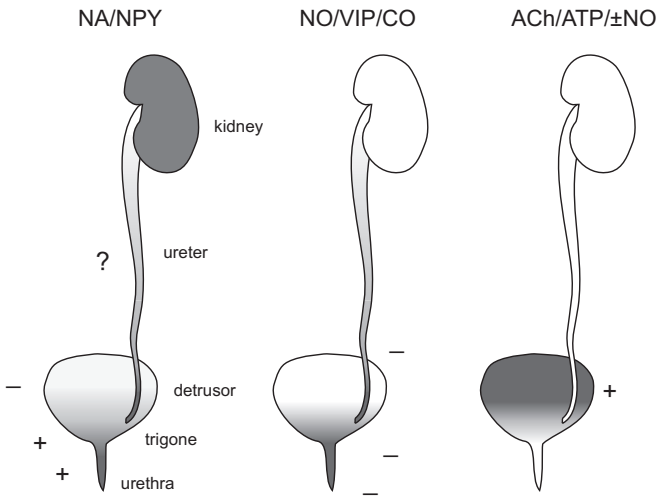

FIGURE 6.8 Diagrams summarizing the distribution of different neurochemical and functional classes of neurons projecting to the urinary tract. The density of shading represents the relative density of nerve fibers in the smooth muscle of each region of the tract. ACh/ATP?±NO, fibers releasing acetylcholine, adenosine 5′-triphosphate, and perhaps nitric oxide, which contract the detrusor. They arise from local intramural ganglia and nearby ganglia in the pelvic plexus; NA/NPY, fibers releasing noradrenaline and neuropeptide Y. They arise from the sympathetic chain, the prevertebral ganglia, and the pelvic plexus. Their function varies with location. NO/VIP/CO?, fibers releasing nitric oxide and vasoactive intestinal polypeptide. They also contain the enzyme for synthesizing carbon monoxide, whose function is unknown. These neurons inhibit smooth muscle activity and arise from intramural and nearby pelvic plexus ganglia.

little idea of how this motility is regulated by autonomic neurons (Amann, 1993; Brindley, 1988; Ferguson and Bell, 1993). The innervation of the smooth muscle of the ureters varies along their length, with the innervation density increasing distally (Fig. 6.8). Noradrenergic fibers, presumably in sympathetic pathways, contain NPY, whereas non-noradrenergic fibers, presumably in parasympathetic pathways, contain NOS, VIP, and NPY (Edyvane *et al.*, 1992, 1994; Jen *et al.*, 1996; Smet *et al.*, 1994). The neurons containing NOS, VIP, and NPY are particularly prominent at the ureterovesical junction (Goessl *et al.*, 1995; Grozdanovic and Baumgarten, 1996; Iselin *et al.*, 1997, 1998; Smet *et al.*, 1994), which they almost certainly relax, thereby facilitating urine flow into the bladder. Axons containing NOS and VIP, which probably have secretomotor and vasodilator functions, also occur beneath the mucosal epithelium of the ureter (Edyvane *et al.*, 1994; Goessl *et al.*, 1995; Smet *et al.*, 1994; Vaalasti *et al.*, 1986).

There are no intramural nerve cell bodies in the ureter (Duarte-Escalante *et al.*, 1969; Schulman, 1974), but clusters of microganglia occur around the lower segment of the ureter and in the region of the ureterovesical junction. Neurons in these ganglia contain NOS, VIP and NPY and almost certainly represent the source of the nonadrenergic axons within the lower ureter (Grozdanovic and Baumgarten, 1996; Jen *et al.*, 1996). Noradrenergic nerve terminals are prominent in the ureteric ganglia, and they form synapses onto some of these ganglion cells (Duarte-Escalante *et al.*, 1969; Schulman, 1974). The source of these fibers is unknown but they are likely to inhibit transmission from spinal preganglionic neurons through the ganglia, as occurs in the bladder ganglia (see below).

Urinary Bladder

Activation of the sacral parasympathetic pathways to the bladder is absolutely essential for micturition to occur. The smooth muscle of the body of the urinary bladder (the detrusor muscle) is densely innervated almost entirely by non-noradrenergic, presumably cholinergic, neurons (Fig. 6.8; Daniel *et al.*, 1983; Dixon *et al.*, 2000; Ek *et al.*, 1977; Kluck, 1980; Sundin *et al.*, 1977). Most of the neurons have their cell bodies in microganglia located extramurally around the base of the bladder and within the walls of the bladder itself (Dixon *et al.*, 1983; Kluck, 1980; Smet *et al.*, 1996a). These neurons contain a complex array of peptides in various combinations. Nearly all of them contain NPY, whereas less than half contain VIP. Somatostatin, galanin, CGRP, and substance P also may occur in some subsets of neurons. Furthermore, at least half of the neurons contain NOS (Dixon *et al.*, 1997, 2000; Jen *et al.*, 1996; Smet *et al.*, 1996a, b). Neurons containing VIP selectively project to the trigone region (Fig. 6.8), but apart from that, there is little information on the precise targets of the different neurochemical classes of neurons in the bladder ganglia.

The preganglionic input to neurons in bladder ganglia comes primarily from the third sacral segment, with smaller contributions from the adjacent segments. Stimulation of this pathway results in contraction of the detrusor muscle. In normal bladders, the response seems to be mediated almost entirely by ACh acting on muscarinic receptors (Hoyle and Burnstock, 1993; Husted *et al.*, 1983; Sibley, 1984; Sjögren *et al.*, 1982). However, a substantial atropine-resistant component of the response is seen in unstable or hypertrophied bladders (Husted *et al.*, 1983; Sjögren *et al.*, 1982). This part of the response may be mediated by ATP or a compound with similar pharmacological actions (Husted *et al.*, 1983; Hoyle and Burnstock, 1993). Neurons containing both NOS and VIP are likely to have an inhibitory effect on detrusor contractility (Gu *et al.*, 1983c; James *et al.*, 1993; Klarskov *et al.*, 1984; Vaalasti *et al.*, 1986). The function of NOS in cholinergic neurons providing excitatory innervation to most of the

bladder smooth muscle is not at all clear. One untested possibility is that a low level of ongoing nonsynaptic release of NO from cholinergic neurons may help to keep the detrusor relaxed when there is no overt activity of the pathway, as seen during bladder filling.

There are few noradrenergic axons in the body of the bladder, but they are more abundant in the trigone region, where most of them contain NPY (Fig. 6.8; Benson *et al.*, 1979; Daniel *et al.*, 1983; Dixon *et al.*, 1983; Ek *et al.*, 1977; Kluck, 1980; Sundin *et al.*, 1977). Here they cause sphincter-like contraction of the smooth muscle via α-adrenoceptors (Brindley, 1988; Caine *et al.*, 1975; Lincoln and Burnstock, 1993). The source of these fibers is not absolutely clear. On the basis of fluorescence histochemical localization of catecholamines, there appear to be no noradrenergic nerve cell bodies in the bladder ganglia themselves (Benson *et al.*, 1979; Dixon *et al.*, 1983; Ek *et al.*, 1977; Kluck, 1980; Sundin *et al.*, 1977). Most of the sympathetic fibers probably arise from neurons in lumbosacral chain ganglia or the pelvic plexus. However, a variable proportion of neurons within the bladder wall and vesical ganglia contain immunoreactivity to tyrosine hydroxylase. At least some of these neurons have been reported also to contain immunoreactivity to NOS and the vesicular ACh transporter, suggesting that they are functionally cholinergic (Dixon *et al.*, 1999; Jen *et al.*, 1996; Smet *et al.*, 1996a, b). These observations are difficult to interpret, but they raise the possibility that a population of neurons projecting to the bladder may have the potential to utilize a combination of catecholamines, ACh, and NO as cotransmitters (perhaps together with ATP) under certain circumstances.

Noradrenergic axons are prominent in the small ganglia lying on the outside of the bladder but are absent from the intramural microganglia (Dixon *et al.*, 1983; Kluck, 1980). These fibers probably arise from cell bodies in the lumbosacral sympathetic ganglia and reduce bladder contractile activity by inhibiting transmission through the extramural ganglia (see De Groat and Steers, 1988; De Groat and Booth, 1993a). The combined effects of noradrenergic stimulation on the trigone and the bladder ganglia are to promote continence (Lincoln and Burnstock, 1993).

The neurons in the bladder ganglia also are surrounded by fibers with various neuropeptides, including VIP, CGRP, NPY, and enkephalin (Jen *et al.*, 1996; Smet *et al.*, 1996a). These fibers could be axons of sympathetic final motor neurons, terminals of spinal preganglionic neurons, collaterals of unmyelinated sensory neurons, or projections from viscerofugal neurons located in the colon (Luckensmeyer and Keast, 1996; see below). However, in humans, the patterns of peptide expression have not been correlated with each functional population of fibers in the ganglia. Nevertheless, experiments in animals have indicated that there can be considerable modulation of synaptic transmission in the pelvic ganglia involved in regulating bladder function and that neuropeptides are likely to have an important role in this modulation (De Groat and Booth, 1993a; Keast, 1995, 1999)

Urethra

The autonomic innervation of the smooth muscle of the urethra operates in concert with that of the urinary bladder during continence and micturition. Autonomic activity also must be coordinated with somatic motor pathways projecting to the striated muscles of the lower urinary tract (see De Groat *et al.*, 1993). The smooth muscle of the urethra has a dense innervation by NPY-containing noradrenergic neurons, which, when stimulated via the hypogastric plexus, cause contraction of the muscle, particularly in males (Fig. 6.8; Andersson *et al.*, 1983; Brindley, 1988; Gosling *et al.*, 1977; Lincoln *et al.*, 1986; von Heyden *et al.*, 1998). There are also axons containing VIP and NOS in the urethral smooth muscle (Fig. 6.8; Crowe *et al.*, 1986; Ho *et al.*, 1999; Leone *et al.*, 1994; Smet *et al.*, 1996b; Tainio, 1993). In males, these neurons probably mediate noncholinergic neurogenic relaxation of the urethra distal to the openings of the vasa deferentia and the prostatic ducts during micturition and semen emission (Andersson *et al.*, 1983; Ehren *et al.*, 1994; Leone *et al.*, 1994). The coordinated activity of excitatory and inhibitory neurons to the urethra would facilitate the passage of semen along the urethra during emission while tending to prevent reflux into the bladder (Brindley, 1988).

Male Genital Tract

The autonomic innervation of the male genital tract is complex, and the way it functions is not fully understood (Brindley, 1988; Dail, 1993; De Groat and Booth, 1993b; Sjöstrand, 1981). Noradrenergic axons containing NPY and, in some cases, galanin predominate in the smooth muscle of the vas deferens, seminal vesicle, and prostate gland (Adrian *et al.*, 1981; Baumgarten *et al.*, 1971; Dail, 1993; Dixon *et al.*, 1998; Gu *et al.*, 1983b; Jen *et al.*, 1999; Vaalasti and Hervonen, 1980). When stimulated, they cause contraction of the smooth muscle, largely mediated by NA acting on α-adrenoceptors, although ATP and NPY also may be involved (Anton and McGrath, 1977; Caine *et al.*, 1975; Stjärne *et al.*, 1986). Most of the noradrenergic neurons receive preganglionic input via the hypogastric nerves and have cell bodies in ganglia located in the more superior parts of the pelvic plexuses (Bell, 1972;

Brindley, 1988; Owman *et al.*, 1983). However, some noradrenergic cell bodies have been localized in small ganglia near the prostate gland (Vaalasti and Hervonen, 1980).

The smooth muscle of the vas deferens, seminal vesicles, and prostate gland receives a sparse innervation by cholinergic neurons containing VIP and NOS. Some also contain NPY, and others may contain enkephalin or somatostatin (Alm, 1982; Del Fiacco, 1982; Dixon *et al.*, 1998, 2000; Gu *et al.*, 1983b; Jen *et al.*, 1997,1999; Vaalasti *et al.*, 1986). Axons containing NOS and VIP are more abundant in the epithelium of the vas deferens and around the secretory glands of the prostate, where they are likely to have a secretomotor function (Alm, 1982; Bloch *et al.*, 1997; Dixon *et al.*, 1998; 2000; Grozdanovic and Goessl, 1999; Gu *et al.*, 1983b; Hedlund *et al.*, 1997; Jen *et al.*, 1999; Vaalasti *et al.*, 1986). These axons are likely to originate from different populations of nerve cell bodies in local microganglia (Alm, 1982; Grozdanovic and Goessl, 1999; Gu *et al.*, 1983b).

The erectile tissues and blood vessels of the penis are innervated by noradrenergic neurons (Benson *et al.*, 1980; Gu *et al.*, 1983b) and cholinergic neurons, most of which contain NOS, VIP, and PHM (Burnett *et al.*, 1993; Ehmke *et al.*, 1995; Gu *et al.*, 1983b; Hedlund *et al.*, 2000; Polak *et al.*, 1981; Steers *et al.*, 1984; Tamura *et al.*, 1995; Willis *et al.*, 1983). The noradrenergic axons probably originate from nerve cell bodies in the superior pelvic plexus, and mostly receive preganglionic inputs via the hypogastric nerves (Bell, 1972; Brindley, 1988). The axons containing NOS and VIP in these tissues are likely to have their cell bodies in local ganglia (Gu *et al.*, 1983b; Polak *et al.*, 1981). They receive preganglionic input from the second and third sacral ventral roots via the pelvic nerves (Brindley, 1988; Weiss, 1972).

Erection requires vasodilation of the penile vessels and relaxation of the erectile tissue of the penis (the corpus cavernosum and corpus spongiosum) to allow its engorgement with blood. These responses normally are neurogenic and are mediated by the sacral parasympathetic pathways. Although VIP both relaxes smooth muscle from erectile tissues and dilates penile blood vessels (Adaikan *et al.*, 1986; Hedlund and Andersson, 1985; Kirkeby *et al.*, 1992; Steers *et al.*, 1984; Willis *et al.*, 1983), the transmitter primarily responsible for erection is not VIP but NO (Hedlund *et al.*, 2000; Leone *et al.*, 1994). These neurons probably also contain and release ACh, which by itself has little effect on erectile tissues (Benson *et al.*, 1980; Blanco *et al.*, 1988; Saenz de Tejada *et al.*, 1988). Erection is prevented by tonic activity of a noradrenergic sympathetic pathway running through the hypogastric nerves (Brindley, 1988) and part of the action of ACh seems to be to inhibit the effects of these neurons (Argiolas and Melis, 1995; Saenz de Tejada *et al.*, 1988; Sjöstrand, 1981).

There is an additional pathway running through the lumbar sympathetic ganglia that can cause erection, especially following psychogenic reflex stimulation (Brindley, 1988; Weiss, 1972; Whitelaw and Smithwick, 1951). The final transmitter in this sympathetic pathway is neither NA nor ACh (Brindley, 1988), but which of a diverse mix of potential transmitters is involved is still unknown.

Recently, HOX-2 has been found to coexist with NOS and VIP in most cholinergic neurons of the pelvic plexus, including those innervating the erectile tissues and the lower urinary tract (Grozdanovic and Goessl, 1999; Hedlund *et al.*, 2000; Ho *et al.*, 1999; Iselin *et al.*, 1997, 1998). It remains to be seen how CO may be involved in the autonomic regulation of the urogenital tract.

Female Genital Tract

The smooth muscle of the oviducts, uterus, and cervix is innervated by noradrenergic neurons containing NPY and non-noradrenergic neurons containing NOS and VIP. Much of this innervation is likely to arise from nerve cell bodies in the inferior parts of the pelvic plexuses, especially the paracervical ganglia. These ganglia lie in the broad ligament immediately dorsal to the origin of the uterine artery (Curtis *et al.*, 1942; Davis, 1933; Gemmell, 1926) and contain both noradrenergic and non-noradrenergic neurons (Alm *et al.*, 1980; Helm, 1981; Jorgensen *et al.*, 1989; Marshall, 1970; Owman *et al.*, 1967; Yoshida *et al.*, 1995). In addition, some of the noradrenergic postganglionic neurons may have cell bodies in the lumbar paravertebral ganglia or the superior hypogastric plexus (Bell, 1972; Marshall, 1970). There are no intramural ganglia in the uterus (Curtis *et al.*, 1942).

The noradrenergic innervation of the smooth muscle is generally abundant but is most dense in the isthmus of the oviduct and in the cervix (Helm, 1981; Owman *et al.*, 1967). Stimulation of these neurons causes contraction of the oviducts as well as the nonpregnant uterus, and this is mediated by α-adrenoceptors (Helm, 1981; Sporrong *et al.*, 1982). However, during pregnancy, β-adrenoceptors mediating myometrial relaxation tend to become more prominent, so that sympathetic nerve stimulation may then inhibit myometrial activity (Bell, 1972; Marshall, 1970).

Axons containing NOS and VIP are most common in the smooth muscle of the isthmus of the oviduct and in the cervix. In addition, they provide a prominent innervation to the glands in the endometrium and

cervical mucosa. They also innervate blood vessels of the cervix, vagina, and erectile tissue of the external genitalia (Alm *et al.*, 1980; Hoyle *et al.*, 1996; Lynch *et al.*, 1980; Ottesen, 1983; Ström *et al.*, 1981; Yoshida *et al.*, 1995). These neurons are likely to relax or inhibit spontaneous contractile activity of smooth muscle in the oviduct, nonpregnant myometrium, and cervix (Helm *et al.*, 1982; Ottesen *et al.*, 1982, 1983). However, they may be much less effective in inhibiting contractions of the pregnant myometrium (Ottesen *et al.*, 1982), when β-adrenoceptor-mediated relaxation is better developed. Neurons containing NOS and VIP also are likely to be responsible for dilating the vasculature of the vaginal circulation during sexual stimulation (Hoyle *et al.*, 1996; Wagner and Levin, 1980).

Colon

Preganglionic neurons in the sacral spinal cord also project through the pelvic plexus to neurons in and near the distal colon and rectum. Some preganglionic axons ascend for a large distance within the colon. The intramural neurons form part of the myenteric plexus, whereas the extramural neurons lie in small ganglia in the distal ends of the pelvic nerves running to the gut (Christensen, 1987; Keast, 1995, 1999; Mitchell, 1953a). The extramural neurons may project both to the smooth muscle of the hindgut directly and to intrinsic myenteric neurons (Roman and Gonella, 1987). Many neurons in the extramural colonic and rectal ganglia may actually project away from the gut back to the pelvic ganglia and spinal cord; such neurons probably receive inputs from distention sensitive myenteric neurons (Luckensmeyer and Keast, 1998).

Stimulation of the pelvic nerves results predominantly in contraction of the colon, mediated via cholinergic neurons, and relaxation of the internal anal sphincter via non-noradrenergic, noncholinergic neurons that probably act primarily via NO (O'Kelly *et al.*, 1993; Stebbing *et al.*, 1997). In addition, there may be a separate pelvic pathway resulting in inhibition of colonic activity and contraction of the sphincter muscle; these responses may be mediated by noradrenergic pelvic neurons (Christensen, 1987; Keast, 1995; Roman and Gonella, 1987).

Blood Vessels

As well as the vasodilator innervation of erectile tissue described above, the pelvic plexuses are likely to provide vasodilator innervation to much of the pelvic circulation (Mitchell, 1953a). Indeed, all reports on the distribution of neurons containing both VIP and NOS in the pelvic viscera cited above describe the presence of axons containing VIP and NOS around small and medium-sized arteries. These neurons almost certainly represent vasodilator neurons.

ENTERIC PLEXUSES

In Langley's original classification of the autonomic nervous system, the enteric neurons form the third major division. The cell bodies of enteric neurons are grouped into intramural ganglia that form a vast interconnected system extending the full length of the gastrointestinal tract. Enteric neurons outnumber by far all the rest of the autonomic neurons; there are in the order of 100 million neurons in the enteric nervous system of humans (Furness and Costa, 1987). Delineating the structure and function of the enteric nervous system results in a large and complex area of research. Much of the more recent work has been reviewed comprehensively in several major publications and reviews (Furness, 2000; Furness and Costa, 1987; Johnson, 1987; Kunze and Furness, 1999; Makhlouf and Schultz, 1989; Tache *et al.*, 1994; Wood and Schultz, 1989). The following description is restricted to a summary of some of the important features of the enteric nervous system of humans, with additional information from experimental studies of animals.

The intramural ganglia are grouped into two plexuses: the myenteric plexus, lying between the outer longitudinal and the inner circular muscle layers; and the submucous plexus, which lies in the connective tissue between the circular muscle and the muscularis mucosae. Although the myenteric plexus extends virtually the full length of the gastrointestinal tract, the submucous ganglia are rare or absent in the esophagus and stomach. In general, the neurons of the myenteric plexus are involved in the regulation of the activity of the smooth muscle, whereas neurons in the submucous plexus regulate mucosal secretion and blood flow.

Most enteric neurons are multipolar. Some have relatively short dendrites with irregular shapes and a prominent axon (type I of Dogiel). Others have several long processes that cannot be identified easily as axons or dendrites (type II of Dogiel). Most enteric neurons fall into one of these morphological classes, although many neurons have other shapes, some of which are intermediate between the main classes. Indeed, some classification schemes have recognized many more morphological classes. More importantly, experimental studies on laboratory mammals, especially guinea pigs, but also rats, pigs, dogs, cats, and mice, have clearly demonstrated that neurons with different morphologies

have characteristic projections, connections, transmitter profiles, and functions (Brookes, 2001; Furness, 2000).

The microanatomical and functional complexity of the enteric nervous system is second only to that of the CNS. Although the activity of enteric neurons can be modified by the CNS via inputs through the vagus, pelvic plexus, and prevertebral ganglia (see above), much control of gastrointestinal function can be achieved by the enteric nervous system independent of central influences. Intrinsic neuronal circuits regulate gastrointestinal motility, mucosal secretion and absorption, and local blood flow, largely as a result of activating intrinsic reflexes. Necessary components of these circuits include sensory neurons, associative neurons or interneurons, and final excitatory or inhibitory motor neurons. A great array of potential neurotransmitters has been localized in different classes of enteric neurons. Animal experiments have demonstrated unambiguously that these transmitters, which include ACh, NO, ATP, a wide range of neuropeptides, and probably 5-HT and GABA, are colocalized in combinations that are specific for particular populations of neurons with well-defined cell shapes, projections, and functions (Brookes, 2001; Furness, 2000; Furness and Costa, 1987). The following simplified description of the functional organization of the enteric plexuses applies most closely to the intestine, but the general pattern applies to varying degrees throughout the gut. It is based mostly on data summarized in the reviews already quoted. Specific references refer to details known to be applicable to humans.

Intrinsic Sensory Neurons Within the Enteric Plexuses

A characteristic feature of the enteric plexuses is that they contain neurons with a primary sensory function (for reviews, see Furness *et al.*, 1998; Kunze and Furness, 1999). Animal studies have shown that these neurons have cell bodies in both the myenteric and submucous plexuses, and have a characteristic morphology, with long dendritic processes that ramify extensively (Dogiel type II; Wattchow *et al.*, 1995). They can respond to chemical stimuli from the lumen of the gut and to mechanical stimuli, such as distention of the gut wall, although it is not yet clear whether different populations of sensory neurons are involved in these responses. The output of these neurons runs in both the oral and anal directions along the myenteric plexus, where they form synapses primarily with interneurons, motor neurons, and perhaps other sensory neurons. Indeed, one feature of these neurons that distinguishes them from sensory neurons located in the dorsal root ganglia is that they normally receive synaptic inputs. Synaptic transmission from the enteric neurons is likely to be mediated in part by ACh, but other noncholinergic transmitters also may be involved.

One class of myenteric neurons that receives input from the intrinsic sensory neurons is the intestinofugal neurons. These neurons occur in the small and large intestines and project out of the gut to neurons in the prevertebral and pelvic ganglia (Gibbins, 1995; Keast, 1995; Mawe, 1995). They are activated primarily by gut distention and participate in a peripheral reflex arc that leads to inhibition of gut activity, perhaps as part of a protective reflex (Fig. 6.7). In most species where they have been studied functionally, the intestinofugal neurons are cholinergic and generally contain a range of peptides, most notably VIP (Gibbins, 1995; Mawe, 1995; Quartu *et al.*, 1993). Some neurons in the distal colon and rectum may project directly to the spinal cord (Neuhuber *et al.*, 1993), but their function is unknown.

Myenteric Plexus and the Regulation of Motility

Most of the intrinsic enteric neurons regulating gastrointestinal motility have their cell bodies within the ganglia of the myenteric plexus (Fig. 6.9). Overall, there are two main functional classes of motor neurons innervating the gastrointestinal smooth muscle: excitatory motor neurons and inhibitory motor neurons. Generally, the excitatory motor neurons are cholinergic (Porter *et al.*, 1996, 1997) and may contain peptides, most commonly substance P (Wattchow *et al.*, 1988, 1997). The inhibitory motor neurons usually contain NOS and VIP (Porter *et al.*, 1997; Wattchow *et al.*, 1997). Both NO and VIP, perhaps together with ATP, contribute to inhibitory transmission to varying degrees in different regions of the gut (Brookes, 1993; Tonini *et al.*, 2000). However, there is some evidence that not all neurons projecting to the muscle that contain VIP necessarily contain NOS and vice versa (Gaumnitz *et al.*, 1995; Matini *et al.*, 1995; Porter *et al.*, 1997). In many regions of the gut, including the esophagus, colon, and appendix, presumed inhibitory motor neurons also contain NPY in addition to other potential transmitters (Ekblad *et al.*, 1989; Nichols *et al.*, 1994; Wattchow *et al.*, 1987b, 1996). A subset of neurons containing NOS and VIP projecting to circular muscle contain galanin, which tends to oppose or limit the inhibitory action of VIP (esophagus: Singaram *et al.*, 1994; colon: Burleigh and Furness, 1990; Gaumnitz *et al.*, 1995)

Whether they are excitatory or inhibitory, motor neurons have a similar morphology, with short

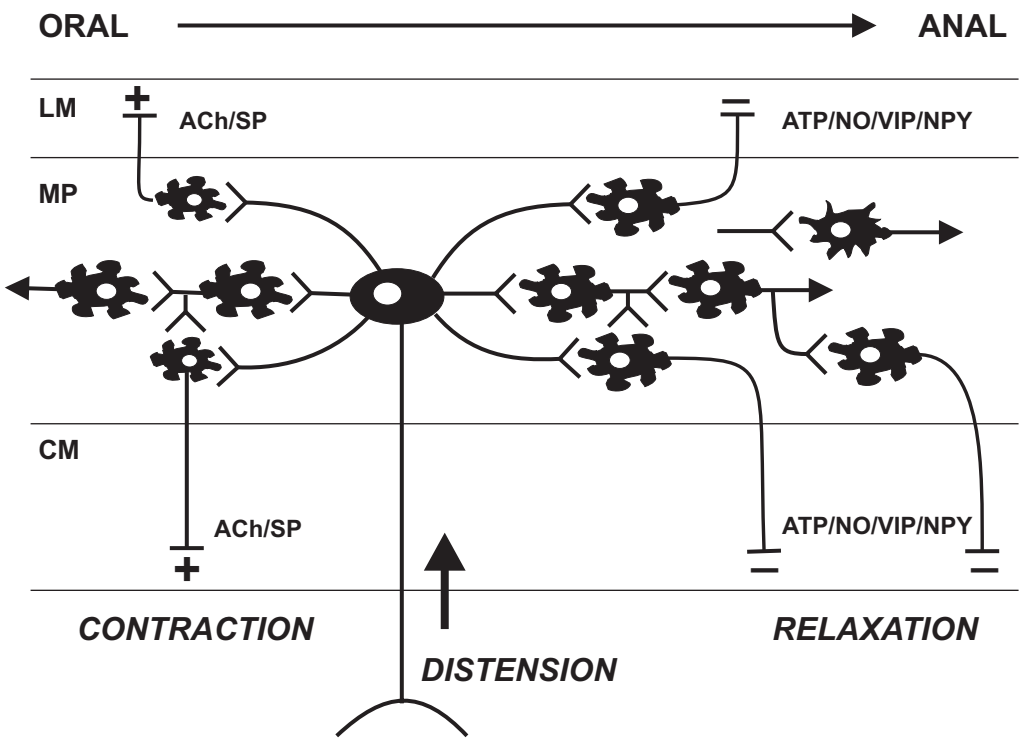

FIGURE 6.9 Simplified diagram of the generalized circuit within the myenteric plexus that underlies the propulsion of intestinal contents in an oral to anal direction. Distention activates intrinsic sensory neurons, either directly or indirectly, with cell bodies in the myenteric plexus (MP). The neurons project in both the oral and anal directions. Some projections in each direction form synapses with interneurons, while others form synapses with motor neurons. All the synapses work primarily via acetylcholine (ACh) acting on nicotinic receptors, although other transmitters are almost certainly involved in specific parts of these pathways. Different populations of motor neurons project to the longitudinal muscle (LM) and the circular muscle (CM). Excitatory motor neurons to the muscle contain ACh and substance P (SP). The inhibitory neurons act via a combination of adenosine 5′-phosphate (ATP), nitric oxide (NO), and vasoactive intestinal polypeptide (VIP); they also often contain neuropeptide Y (NPY). Note that the excitatory neurons project to muscle oral to the distention, while inhibitory neurons project to muscle anal to the distention. This arrangement establishes the polarity of a reflex that can propel gut contents in an oral-to-anal direction. The exact details of the connections and transmitter content of different classes of neurons varies with species and region of the gut. Adapted from Furness and Costa, 1987; Kunze and Furness, 1999.

branched dendrites or lamellar processes (Dogiel type I; Porter *et al.*, 1996; Wattchow *et al.*, 1995). Tracing studies have shown that different populations of motor neurons innervate the longitudinal and circular muscle layers. Some motor neurons project directly to the nearby muscle layers, but others may project for longer distances orally or anally along the myenteric plexus before innervating the muscle. Thus, each muscle layer may be innervated by different populations of excitatory or inhibitory motor neurons that have long or short projections within the myenteric plexuses.

In the esophagus and stomach, and probably the duodenum, some of the final motor neurons receive convergent synaptic inputs from vagal preganglionic neurons (see "Cranial Autonomic Pathways" above). Similarly, some motor neurons in the distal colon and rectum receive synaptic inputs from sacral preganglionic neurons. Most of these inputs are likely to occur onto neurons in the myenteric plexus rather than the submucous plexus (Holst *et al.*, 1997). However, throughout the myenteric plexus, the primary input to motor neurons is from intrinsic sensory neurons or interneurons that also are located in the myenteric plexus. The CNS can inhibit gastrointestinal motility by the activity of noradrenergic sympathetic neurons projecting from the prevertebral ganglia to the motor neurons of the myenteric plexus.

There seem to be several different functional classes of interneurons in the myenteric plexus, particularly those that project in an anal direction. Most interneurons are functionally cholinergic. Some ascending

interneurons contain tachykinins, such as substance P (Wattchow *et al.*, 1997), and some descending interneurons contain various combinations of 5-HT, NOS, GABA, and neuropeptides, including VIP (Gershon, 1999; Krantis *et al.*, 1998; Porter *et al.*, 1997; Wattchow *et al.*, 1997). Consequently, not all transmission between interneurons can be blocked with cholinergic antagonists. Potential transmitters include ATP, 5-HT, NO, and substance P (Galligan *et al.*, 2000; Gershon, 1999).

The basic circuit of the myenteric plexus of the intestine seems to be adapted to provide a mechanism for the propulsion of gut contents (Fig. 6.9; Furness and Costa, 1987). In its simplest version, distention of the intestine at a point results in stimulation of intrinsic sensory neurons that provide excitatory inputs onto interneurons that project orally or anally within the myenteric plexus. The orally projecting interneurons make excitatory synapses with cholinergic excitatory motor neurons, whereas anally projecting interneurons make excitatory synapses with inhibitory motor neurons acting via some combination of ATP, NO and VIP. The excitatory motor neurons themselves project up to 11 mm orally, whereas the inhibitory motor neurons project up to nearly 20 mm anally (colon: Porter *et al.*, 1997). Thus, the gut contracts above a site of distention and relaxes below it to propel the gut contents in an oral-to-anal direction.

Recent experiments in laboratory mammals have shown that the mechanism of motor innervation of the gastrointestinal smooth muscle is much more complex than originally thought. Throughout the myenteric plexus and the circular muscle layers, there are networks of cells known as the "interstitial cells of Cajal." It is now becoming increasingly clear that these cells function both as pacemakers for smooth muscle contractile activity (Huizinga *et al.*, 1997) and as intermediaries for at least some aspects both inhibitory and excitatory transmission to the muscle (Burns *et al.*, 1996; Ward *et al.*, 1998, 2000).

Submucous Plexus and the Control of Secretion

The neurons in the submucous plexus of the intestine tend to be smaller than those in the myenteric plexus and contain fewer functional cell types. Nevertheless, the anatomical arrangement of the plexus is complicated, and naming of its various possible subcomponents has been a source of argument for many years (see Furness and Costa, 1987; Wedel *et al.*, 1999). The ganglia include multiple populations of secretomotor neurons projecting to the gut mucosa, as well as vasodilator neurons innervating the local microcirculation (Vanner and Surprenant, 1996). The submucous ganglia probably also contain some intrinsic sensory neurons with receptive endings projecting to the mucosa and with outputs projecting to other submucous neurons or to the myenteric plexus. About two-thirds of submucosal neurons are likely to be cholinergic, whereas both secretomotor and vasodilator neurons are likely to contain some combination of VIP and NOS (Bosshard *et al.*, 1989; Crowe *et al.*, 1992; Porter *et al.*, 1996, 1999). Other submucous neurons contain 5-HT or substance P (Crowe *et al.*, 1992). At least in the colon, some neurons in the submucous plexus project to the deeper layers of the circular muscle. These neurons are located closer to the circular muscle layer; some of them contain NOS and VIP and may mediate relaxation of the muscle (Domoto *et al.*, 1990; Porter *et al.*, 1999); the possible functions of other submucosal neurons projecting to the muscle are unknown.

As in the myenteric plexus, activity of the motor neurons in the submucous plexus are tonically inhibited by sympathetic neurons projecting from the prevertebral ganglia. Experiments in guineapigs have shown clearly that the sympathetic neurons responsible for tonic inhibition of secretomotor neurons in the submucous plexus form a population that is separate from those responsible for a low level of tonic inhibition of myenteric motor neurons (Furness and Costa, 1987; Mawe, 1995).

ADRENAL MEDULLA AND PARAGANGLIA

The adrenal medullary cells are derived from the neural crest and are a major source of circulating catecholamines, particularly adrenaline. Adrenaline and noradrenaline are secreted from different populations of cells (Coupland and Fujita, 1976). Adrenal medullary cells receive cholinergic preganglionic inputs directly via the splanchnic nerves traveling through the celiac ganglion (Parker, 1996). In addition to catecholamines, some of the adrenal medullary cells contain proenkephalin-derived peptides and NPY, often coexisting (Linnoila and Diaugustine, 1980; Lundberg *et al.*, 1979; Osamura *et al.*, 1987). A small number of other cells contain VIP or somatostatin (see Kondo, 1985). These peptides may function locally within the adrenal gland to modulate secretion or local blood flow, or they may enter the circulation and have a hormonal role.

Small ganglia occur close to the adrenal medulla and they may be the source of VIP axons abundantly distributed through the adrenal medulla (Kondo, 1985;

Linnoila and Diaugustine, 1980). These neurons may influence secretion and blood flow in the adrenal gland.

An additional source of circulating catecholamines and peptides is likely to be the paraganglia, consisting of small groups of extraadrenal chromaffin cells. Paraganglia are associated mainly with the prevertebral and pelvic plexuses. They also occur along the vagal nerve and to a much lesser extent in the paravertebral ganglia (Hervonen *et al.*, 1976, 1978a). The cells are morphologically and neurochemically heterogeneous. In organs such as the carotid and aortic bodies, they are involved in arterial chemoreception, and this function may extend to chromaffin cells outside these areas (Kummer, 1996). Their functions in other locations are unknown but may involve local paracrine or endocrine roles (see Böck, 1982; Kummer, 1996).

CONCLUDING REMARKS

This chapter illustrates that peripheral autonomic neurons are organized into a complex system of pathways controlling a multitude of visceral functions. Most of these pathways can be activated independently of each other by their central inputs as part of a coordinated motor response along with appropriate somatic motor and neuroendocrine outputs. The net result is an integrated and coordinated regulation of effector tissues by autonomic pathways. Some of this coordination must take place in the ganglia themselves, primarily as a result of the arrangement and transmitter repertoire of the preganglionic inputs. Interneurons clearly exist in the enteric nervous system, and some sympathetic neurons innervate (and inhibit) other final motor neurons in the parasympathetic, pelvic, and enteric ganglia. Within the prevertebral and pelvic ganglia, final motor neurons receive and integrate inputs from both central preganglionic neurons and peripheral enteric neurons.

There are few general rules that distinguish the functions of sympathetic and parasympathetic pathways. Tonic activity can occur in both (e.g., parasympathetic innervation of the iris; sympathetic innervation of cutaneous blood vessels), and both can have excitatory and inhibitory neurons projecting to the same effector (e.g., vagal innervation of the airways; sympathetic innervation of skeletal muscle vasculature). Although in some effector tissues the sympathetic and parasympathetic neurons tend to oppose each other (e.g., heart, blood vessels), in others they cooperate (e.g., male genital tract).

Most tissues receiving autonomic innervation are also innervated by unmyelinated primary sensory neurons. Neuropeptides released from the peripheral terminals of these neurons by axon reflexes can modify the autonomic control of peripheral tissues either by exerting direct effects on the targets or by interacting with the autonomic neurons themselves. These effects have been ignored here, but they are almost certain to play a crucial role in the modulation of autonomic motor control in a wide range of pathophysiological conditions.

Most peripheral autonomic neurons contain several different potential transmitters. The exact combinations of transmitters in individual neurons are highly correlated with their projections (see Furness *et al.*, 1989; Gibbins, 1995). These results imply that there is scope for multiple levels of autonomic regulation of peripheral effector tissues with a degree of precision and specificity far greater than has been suspected until now (Morris and Gibbins, 1992). The details and functional consequences of neurotransmitter coexistence in human autonomic neurons remain to be determined in most cases. However, the scope for the development of new therapeutic interventions based on knowledge of these interactions is potentially enormous.

Acknowledgments

Work from this laboratory was supported by grants from the National Health and Medical Research Council of Australia, the National Heart Foundation of Australia, the Clive and Vera Ramaciotti Foundation, Flinders University Research Budget, and the Flinders Medical Centre Foundation. I would like to thank Associate Professor Judy Morris for helpful comments on the manuscript. Kiley MacDonald and Amanda Bettesworth provided excellent secretarial assistance.

References

Adaikan, P. G., Kottegoda, S. R., and Ratnam, S. S. (1986). Is vasoactive intestinal polypeptide the principal transmitter involved in human penile erection? *J. Urol.* **135,** 638–640.

Adrian, T. E., Gu, J., Allen, J. M., Tatemoto, K., Polak, J. M., and Bloom, S. R. (1981). Neuropeptide Y in the human male genital tract. *Life Sci.* **35,** 2643–2648.

Aggestrup, S., Uddman, R., Jensen, S. L., Sundler, F., Schaffalitzky de Muckadell, O., Holst, J. J., Håkanson, R., Ekman, R., and Sørensen, H. R. (1985). Regulatory peptides in the lower oesophageal sphincter of man. *Regul. Peptides* **10,** 167–178.

Ahlborg, G., and Lundberg, J. M. (1991). Splanchnic release of neuropeptide Y during prolonged exercise with and without beta-adrenoceptor blockade in healthy man. *Clin. Physiol.* **11,** 343–351.

Ahlborg, G., Weitzberg, E., Sollevi, A., and Lundberg, J. M. (1992). Splanchnic and renal vasoconstrictor and metabolic responses to neuropeptide Y in resting and exercising man. *Acta Physiol. Scand.* **145,** 139–149.

Ahren, B. (2000). Autonomic regulation of islet hormone secretion—implications for health and disease. *Diabetologia* **43,** 393–410.

Ahrén, B., Alumets, J., Ericsson, M., Fahrenkrug, J., Fahrenkrug, L., Hakanson, R., Hedner, P., Loren, l., Melander, A., Rerup, C., and Sundler, F. (1980). VIP occurs in intrathyroidal nerves and stimulates hormone secretion. *Nature* **287,** 343–345.

Ahrén, B., Taborsky, G. J., and Porte, D. (1986). Neuropeptidergic versus cholinergic and adrenergic regulation of islet hormone secretion. *Diabetologica* **29,** 827–836.

Ahren, B., Ar'Rajab, A., Bottcher, G., Sundler, F., and Dunning, B. E. (1991). Presence of galanin in human pancreatic nerves and inhibition of insulin secretion from isolated human islets. *Cell. Tissue Res.* **264,** 263–267.

Akiyoshi, H., Gonda, T., and Terada, T. (1998). A comparative histochemical and immunohistochemical study of aminergic, cholinergic and peptidergic innervation in rat, hamster, guinea pig, dog and human livers. *Liver* **18,** 352–359.

Alexander, W. P., Kuntz, A., Henderson, W. P., and Ehrlich. E. (1949). Sympathetic ganglion cells in ventral roots. Their relation to sympathectomy. *Science* **109,** 484.

Alm, P. (1982). On the autonomic innervation of the human vas deferens. *Brain Res. Bull.* **9,** 673–677.

Alm, P., Alumets, J., Håkanson, R., Helm, G., Owman, C., Sjöberg, N. O., and Sundler, F. (1980). Vasoactive intestinal polypeptide nerves in the human female genital tract. *Am. J. Obstet. Gynecol.* **136,** 349–351.

al-Shawaf, A. A., Kendall, M. D., and Cowen, T. (1991). Identification of neural profiles containing vasoactive intestinal polypeptide, acetylcholinesterase and catecholamines in the rat thymus. *J. Anat.* **174,** 131–143.

Amann, R. (1993). Neural regulation of ureteric motility. *In* "Nervous Control of the Urogenital System" (C. A. Maggi, ed.), pp. 209–226. Harwood Academic, Chur.

Anagostides, A., Chadwick, U. S., Selden, A. C., and Maton, P. N. (1984). Sham feeding and pancreatic secretion. Evidence for direct vagal stimulation of output. *Gastroenterology* **87,** 109–114.

Andersson, K. E., Matthiasson, A., and Sjögren, C. (1983). Electrically induced relaxation of the noradrenaline contracted isolated urethra from rabbit and man. *J. Urol.* **129,** 210–214.

Anton, P. G., and McGrath, J. C. (1977). Further evidence for adrenergic transmission in the human vas deferens. *J. Physiol. (Lond.)* **273,** 45–55.

Antonica, A., Magni, F., Mearini, L., and Paolocci, N. (1994). Vagal control of lymphocyte release from rat thymus. *J. Auton. Nerv. Syst.* **48,** 187–197.

Argiolas, A., and Melis, M. R. (1995). Neuromodulation of penile erection: An overview of the role of neurotransmitters and neuropeptides. *Prog. Neurobiol.* **47,** 235–255.

Armour, J. A., Murphy, D. A., Yuan, B. X., MacDonald, S., and Hopkins, D. A. (1997). Gross and microscopic anatomy of the human intrinsic cardiac nervous system. *Anat. Rec.* **247,** 289–298.

Arneklo-Nobin, B., and Owman, C. (1985). Adrenergic and serotonergic mechanisms in human hand arteries and veins studied by fluorescence histochemistry and in vitro pharmacology. *Blood Vessels* **22,** 1–12.

Atiya, A., Cohen, G., Ignarro, L., and Brunicardi, F. C. (1996). Nitric oxide regulates insulin secretion in the isolated perfused human pancreas via a cholinergic mechanism. *Surgery* **120,** 322–327.

Azuma, E., Askura, K., and Kataura, A. (1982). Histochemical demonstration of peripheral autonomic innervation in canine nasal mucosa by retrograde axonal transport of horseradish peroxidase. *Acta Otolaryngol.* **93,** 139–146.

Baffi, J., Gorcs, T., Slowik, F., Horvath, M., Lekka, N., Pasztor, E., and Palkovits, M. (1992). Neuropeptides in the human superior cervical ganglion. *Brain Res.* **570,** 272–278.

Bai, T. R., and Bramley, A. M. (1993). Effect of an inhibitor of nitric oxide synthase on neural relaxation of human bronchi. *Am. J. Physiol.* **264,** L425–L430.

Baljet, B., and Drukker, J. (1981). Some aspects of the innervation of the abdominal and pelvic organs in the human female fetus. *Acta Anat.* **111,** 222–230.

Barnes, P. J. (1984). The third nervous system in the lung: physiology and clinical perspectives. *Thorax* **39,** 561–567.

Barnes, P. J., and Dixon, C. M. S. (1984). The effect of inhaled vasoactive intestinal peptide on bronchial reactivity to histamine in humans. *Am. Rev. Respir. Dis.* **130,** 106–166.

Barrett, J., McDougall, J. J., and Morrison, J. D. (1993). Enhancement by atropine of the pancreatic exocrine secretions evoked by vagal stimulation in the pithed rat. *J Physiol* **469,** 443–457.

Barroso C. P., Edvinsson L., Zhang W., Sa M. C. E., Springall D. R., Polak J. M., and Gulbenkian S. (1996) Nitroxidergic innervation of guinea pig cerebral arteries. *J. Auton. Nerv. Syst.* **58,** 108–114.

Baumgarten, H. G., Holstein, A. F., and Rosengren, E. (1971). Arrangement, ultrastructure and adrenergic innervation of smooth musculature of the ductuli efferentes, ductus epididymidis and ductus deferens of man. *Z. Zellforsch. Mikrosk. Anat.* **120,** 37–79.

Becker, R. F., and Grunt, J. A. (1957). The cervical sympathetic ganglia. *Anat. Rec.* **127,** 1–14.

Belai, A., and Burnstock, G. (2000). Pattern of distribution and colocalization of NOS and ATP in the myenteric plexus of human fetal stomach and intestine. *Neuroreport* **11,** 5–8.

Bell, C. (1972). Autonomic nervous control of reproduction: Circulatory and other factors. *Pharmacol. Rev.* **24,** 657–736.

Bell, C. (1996). Cholinergic vasodilator mechanisms. *In* "Nervous Control of Blood Vessels" (T. Bennett and S.M. Gardiner, eds.), pp. 59–74. Harwood Academic, Amsterdam.

Bell, C., and Robbins, S. (1997). Autonomic vasodilation in the skin. *In* "Autonomic Innervation of the Skin" (J.L. Morris and I.L. Gibbins, eds.), pp. 87–110, Harwood Academic, Amsterdam.

Belvisi, M. G., Stretton, C. D., Miura, M., Verleden, G. M., Tadjkarimi, S., Yacoub, M. H., and Barnes, P. J. (1992). Inhibitory NANC nerves in human tracheal smooth muscle: a quest for the neurotransmitter. *J. Appl. Physiol.* **73,** 2505–2510.

Belvisi, M. G., Ward, J. K., Mitchell, J. A., and Barnes, P. J. (1995). Nitric oxide as a neurotransmitter in human airways. *Arch. Int. Pharmacodyn. Ther.* **329,** 97–110.

Bennett, M. R. (1996). Autonomic neuromuscular transmission at a varicosity. *Prog. Neurobiol.* **50,** 505–532.

Benson, G. S., McConnell, J. A., and Wood, J. G. (1979). Adrenergic innervation of the human bladder body. *J. Urol.* **122,** 189–191.

Benson, G. S., McConnell, J. A., Lipschultz, L. I., Corriere, J. R., and Wood, J. G. (1980). Neuromorphology and neuropharmacology of the human penis. *J Clin. Invest.* **65,** 506–513.

Billman, G. E., Hoskins, R. S., Randall, D. C., Randall, W. C., Hamlin, R. L., and Lin, Y. C. (1989). Selective vagal postganglionic innervation of the sinoatrial and atrioventricular nodes in the non-human primate. *J. Auton. Nerv. Syst.* **26,** 27–36.

Bilski, J., Konturek, P. C., Konturek, S. J., Cieszkowski, M., and Czarnobilski, K. (1994). Role of endogenous nitric oxide in the control of gastric acid secretion, blood flow and gastrin release in conscious dogs. *Regul. Peptides.* **53,** 175–184.

Bilski, J., Konturek, J. W., Konturek, S. J., and Domschke, W. (1995). The involvement of endogenous nitric oxide in vagal-cholinergic stimulation of exocrine and endocrine pancreas in dogs. *Int. J. Pancreatol.* **18,** 41–49.

Bini, G., Hagbarth, K. E., Hynninen, P., and Wallin. B. G. (1980a). Thermoregulatory and rhythm-generating mechanisms governing the sudomotor and vasoconstrictor outflow in human cutaneous nerves. *J. Physiol. (Lond.)* **306,** 537–552.

Bini, G., Hagbarth, K. E., Hynninen, P., and Wallin, B. G. (1980b). Regional similarities and differences in thermoregulatory vaso- and sudomotor tone. *J. Physiol. (Lond.)* **306,** 553–565.

Bishop, A. E., Polak, J. M., Green, I. C.. Bryant. M. G., and Bloom, S. R. (1980). The location of VIP in the pancreas of man and rat. *Diabetologica* **18,** 73–78.

Bjorck, S., Fahrenkrug, J., Jivegard, L., and Svanvik, J. (1986). Release of immunoreactive vasoactive intestinal peptide (VIP) from the gallbladder in response to vagal stimulation. *Acta Physiol. Scand.* **128,** 639–642.

Björklund, H., Dalsgaard, C.-J., Jonsson, C.-E., and Hermansson, A. (1986). Sensory and autonomic innervation of nonhairy and hairy human skin. An immunohistochemical study. *Cell Tissue Res.* **236,** 51–57.

Blanco, R., Saenz de Tejada, I., Goldstein, l., Krane, R. J., Wotiz, H. H., and Cohen, R. A. (1988). Cholinergic neurotransmission in human corpus cavernosum. II. Acetylcholine synthesis. *Am. J. Physiol.* **254,** H468–H472.

Bloch, W., Klotz, T., Loch, C., Schmidt, G., Engelmann, U., and Addicks, K. (1997). Distribution of nitric oxide synthase implies a regulation of circulation, smooth muscle tone, and secretory function in the human prostate by nitric oxide. *Prostate* **33,** 1–8.

Bluemel, K. M., Wurster, R. D., Randall, W. C., Duff, M. J., and O'Toole, M. F. (1990). Parasympathetic postganglionic pathways to the sinoatrial node. *Am. J. Physiol.* **259,** H1504–H1510.

Blumberg, H., and Wallin, B. G. (1987). Direct evidence of neurally mediated vasodilation in hairy skin of the human foot. *J. Physiol. (Lond.)* **382,** 105–121.

Böck, P. (1982). "The Paraganglia" Handbuch der Mikroskopischen Anatomie des Menschen, Vol. 6, Part 8. Springer-Verlag, Berlin.

Bosshard, A., Chery-Croze, S., Cuber, J. C., Dechelette, M. A., Berger, F., and Chayvialle, J. A. (1989). Immunocytochemical study of peptidergic structures in Brunner's glands. *Gastroenterology* **97,** 1382–1388.

Botar, J. (1966). "The Autonomic Nervous System." Akademia Kiadó, Budapest.

Botar, J., Afra, D., Moritz, P., Schiffman, J., and Scholz, M. (1950). Die Nervenzellen und Ganglien des *N. vagus*. *Acta Anat.* **10,** 284–314.

Boyd, J. D. (1957). Intermediate sympathetic ganglia. *Br. Med. Bull.* **13,** 207–212.

Brandi, M. L., Tanini, A., and Toccafondi, R. (1987). Interaction of VIPergic and cholinergic receptors in human thyroid cell. *Peptides* **8,** 893–897.

Breathnach, A. S. (1977). Electron microscopy of cutaneous nerves and receptors. *J. Invest. Dermatol.* **69,** 8–26.

Brengelmann, G. L. (1983). Circulatory adjustments to exercise and heat stress. *Annu. Rev. Physiol.* **45,** 191–212.

Brengelmann, G. L., Freund, P. R., Rowell, L. B., Oleurd. J. E., and Kraning, K. K. (1981). Absence of cutaneous vasodilation associated with congenital absence of sweat glands in man. *Am. J. Physiol.* **240,** H571–H575.

Brindley, G. S. (1988). Autonomic control of the pelvic organs. *In* "Autonomic Failure" (R. Bannister, ed.), 2nd Ed., pp. 223–237. Oxford University. Press, London.

Brookes, S. J. (1993). Neuronal nitric oxide in the gut. *J. Gastroenterol. Hepatol.* **8,** 590–603.

Brookes, S. J. (2001). Classes of enteric nerve cells in the guinea-pig small intestine. *Anat. Rec.* **262,** 58–70.

Brown, C. M., Snowdon, C. F., Slee, B., Sandle, L. N., and Rees, W. D. (1995). Neural influences on human esophageal and salivary alkali secretion. *Dig. Dis. Sci.* **40,** 1642–1650.

Brunicardi, F. C., Shavelle, D. M., and Andersen, D. K. (1995). Neural regulation of the endocrine pancreas. *Int. J. Pancreatol.* **18,** 177–195.

Bryson, J. M., Wolter, J. R., and O'Keefe, N. T. (1966). Ganglion cells in the human ciliary body. *Arch. Ophthalmol. (Chicago)* **75,** 57–60.

Bulloch, K., and Pomerantz, W. (1984). Autonomic nervous system innervation of thymic-related lymphoid tissue in wild type and nude mice. *J. Comp. Neurol.* **228,** 57–68.

Burleigh, D. E., and Furness, J. B. (1990). Distribution and actions of galanin and vasoactive intestinal peptide in the human colon. *Neuropeptides* **16,** 77–82.

Burnett, A. L., Tillman, S. L., Chang, T. S., Epstein, J. I., Lowenstein, C. J., Bredt, D. S., Snyder, S. H., and Walsh, P. C. (1993). Immunohistochemical localization of nitric oxide synthase in the autonomic innervation of the human penis. *J. Urol.* **150,** 73–76.

Burns, A. J., Lomax, A. E. J., Torihashi, S., Sanders, K. M., and Ward, S. M. (1996). Interstitial cells of Cajal mediate inhibitory neurotransmission in the stomach. *Proc. Natl. Acad. Sci. U.S.A.* **93,** 12008–12013.

Bysschaer, T. M., Donckier, J., Dive, A., Ketelslegers, J., and Lambert, A. (1985). Gastric acid and pancreatic polypeptide responses to sham feeding are impaired in diabetic subjects with autonomic neuropathy. *Diabetes* **34,** 1181–1185.

Caine, M., Raz, S., and Zeigler, M. (1975). Adrenergic and cholinergic receptors in the human prostate, prostatic capsule and bladder neck. *Br. J Urol.* **47,** 193–202.

Campbell, G. D., Edwards, F. R., Hirst, G. D., and O'Shea, J. E. (1989). Effects of vagal stimulation and applied acetylcholine on pacemaker potentials in the guinea-pig heart. *J. Physiol. (Lond)* **415,** 57–68.

Canning, B. J., and Fischer, A. (1998). Localization of heme oxygenase-2 immunoreactivity to parasympathetic ganglia of human and guinea-pig airways. *A. J. Resp. Cell . Mol. Biol.* **18,** 279–285.

Carlson, M. D., Geha, A. S., Hsu, J., Martin, P. J., Levy, M. N., Jacobs, G., and Waldo, A. L. (1992). Selective stimulation of parasympathetic nerve fibers to the human sinoatrial node. *Circulation* **85,** 1311–1317.

Carlsten, A., Folkow, B., and Hamberger, C. A. (1957). Cardiovascular effects of direct vagal stimulation in man. *Acta Physiol. Scand.* **41,** 68–76.

Carlton, R. A., Graettinger, T. S., and Bowyer, A. F. (1965). Parasympathetic influence on the atrial myocardium and atrioventricular node of man. *J. Lab. Clin. Med.* **66,** 413–422.

Cauna, N., and Cauna, D. (1975). The fine structure and innervation of the cushion veins of the human nasal respiratory mucosa. *Anat. Rec.* **181,** l–16.

Cauna, N., Cauna, D., and Hinderer, K. H. (1972). Innervation of human nasal glands. *J. Neurocytol.* **1,** 49–59.

Chen, W., Inui, T., Hachiya, T., Ochi, Y., Nakajima, Y., and Kajita, Y. (1993). Stimulatory action of pituitary adenylate cyclase–activating polypeptide (PACAP) on thyroid gland. *Biochem. Biophys. Res. Commun.* **194,** 923–929.

Chen, Y., Getchell, T. V., Sparks, D. L., and Getchell, M. L. (1993). Patterns of adrenergic and peptidergic innervation in human olfactory mucosa: age-related trends. *J. Comp. Neurol.* **334,** 104–116.

Chen, Z., Jia, W., Kaufman, P. L., and Cynader, M. (1999). Immunohistochemical localization of dopamine-beta-hydroxylase in human and monkey eyes. *Curr. Eye Res.* **18,** 39–48.

Cheng, S. B., Kuchiiwa, S., Kuchiiwa, T., and Nakagawa, S. (2000). Three novel neural pathways to the lacrimal glands of the cat: an investigation with cholera toxin B subunit as a retrograde tracer. *Brain Res.* **873,** 160–164.

Chiba, T., and Yamauchi, A. (1970). On the fine structure of the nerve terminals in the human myocardium. *Z. Zellforsch. Mikrosk. Anat.* **108,** 324–338.

Chorobski, J., and Penfield, W. (1932). Cerebral vasodilator nerves and their pathway from the medulla oblongata, with observations on the pial and intracerebral vascular plexus. *Arch. Neurol. Psychiatry* **28,** 1257–1289.

Christensen, J. (1987). Motility of the colon. *In* "Physiology of the Gastrointestinal Tract" (L. R. Johnson, ed.), 2nd Ed., pp. 665–693. Raven Press, New York.

Christensen, N. J., and Galbo, H. (1983). Sympathetic nervous activity during exercise. *Annu. Rev. Physiol.* **45,** 139–153.

Chu, C. H. U. (1968). Solitary neurons of the human tongue. *Anat. Rec.* **162,** 505–510.

Conti, G. (1948). Etudes sur la morphologie des cellules des ganglions sympathetiques intramuraux du coeur humain. *Acta Anat.* **5,** 255–290.

Costa, M. and Furness, J. B. (1973). Observations of the anatomy and amine histochemistry of the nerves and ganglia which supply the pelvic viscera and on associated chromaffin tissue in the guinea-pig. *Z. Anat. Entwicklungsgesch.* **140,** 85–108.

Coupland, R. E., and Fujita. T. (1976). "Chromaffin, Enterochromaffin and Related Cells." Elsevier, Amsterdam.

Cowley, R. A., and Yeager. G. H. (1949). Observations on the lumbar sympathetic nervous system. *Surgery (St. Louis)* **25,** 880–890.

Crandall, C. G., Musick, J., Hatch, J. P., Kellogg, D. L., and Johnson, J. M. (1995). Cutaneous vascular and sudomotor responses to isometric exercise in humans. *J. Appl. Physiol.* **79,** 1946–1950.

Crick, S. J., Wharton, J., Sheppard, M. N., Royston, D., Yacoub, M. H., Anderson, R. H., and Polak, J. M. (1994). Innervation of the human cardiac conduction system. A quantitative immunohistochemical and histochemical study. *Circulation* **89,** 1697–1708.

Crowe, R.. Light, K., Chilton, C. P., and Burnstock, G. (1986). Vasoactive intestinal polypeptide-, somatostatin-, and substance P-immunoreactive nerves in the smooth and striated muscle of the intrinsic external urethral sphincter of patients with spinal cord injury. *J. Urol.* **136,** 487–491.

Crowe, R., Kamm, M. A., Burnstock, G., and Lennard-Jones, J. E. (1992). Peptide-containing neurons in different regions of the submucous plexus of human sigmoid colon. *Gastroenterology* **102,** 461–467.

Curtis, A. H., Anson, B. J., Ashley, F. J., and Jones, T. (1942). The anatomy of the pelvic autonomic nerves in relation to gynaecology. *Surg. Gynecol. Obstet.* **75,** 743–750.

Dail, W. G. (1993). Autonomic innervation of male reproductive genitalia. *In* "Nervous Control of the Urogenital System" (C. A. Maggi, ed.). pp 69–101. Harwood Academic, Chur.

Daniel, E. E., Cowan, W., and Daniel, V. P. (1983). Structural bases for neural and myogenic control of human detrusor muscle. *Can. J. Physiol. Pharmacol.* **61,** 1247–1273.

Davies, F., Francis, E. T. B., and King, T. S. (1952). Neurological studies of the cardiac ventricles of mammals. *J. Anat.* **86,** 130–143.

Davis, A. A. (1933). The innervation of the uterus. *J. Obstet. Gynaecol. Br. Emp.* **40,** 481–507.

Davis, C., Kannan, M. S., Jones, T R., and Daniel, E. E. (1982). Control of human airway smooth muscle: in vitro studies. *J. Appl. Physiol.* **53,** 1080–1087.

Day, S., Gu, J., Polak, J., and Bloom, S. (1985). Somatostatin in the human heart and comparison with guinea-pig and rat heart. *Br. Heart J.* **53,** 153–157.

Debas, H. (1987). Peripheral regulation of gastric acid secretion. *In* "Physiology of the Gastrointestinal Tract" (L. R. Johnson, ed.), 2nd Ed., pp. 931–945. Raven Press, New York.

Debas, H. T., and Carvajal, S. H. (1994). Vagal regulation of acid secretion and gastrin release. *Yale J. Biol. Med.* **67,** 145–151.

De Castro, F. (1932). Sympathetic ganglia normal and pathological. *In* "Cytology and Cellular Pathology of the Nervous System" (W. Penfield, ed.), Vol. 1, pp. 319–379. Harper (Hoeber), New York.

De Fillipi, C., Solomon, T. E., and Valenzuela, J. E. (1982). Pancreatic secretory response to sham feeding in humans. *Digestion* **23,** 217–223.

De Giorgio, R., Parodi, J. E., Brecha, N. C., Brunicardi, F. C., Becker, J. M., Go, V. L., and Sternini, C. (1994). Nitric oxide producing neurons in the monkey and human digestive system. *J. Comp. Neurol.* **342,** 619–627.

De Giorgio, R., Zittel, T. T., Parodi, J. E., Becker, J. M., Brunicardi, F. C., Go, V. L., Brecha, N. C., and Sternini, C. (1995). Peptide immunoreactivities in the ganglionated plexuses and nerve fibers innervating the human gallbladder. *J. Auton. Nerv. Syst.* **51,** 37–47.

De Groat, W. C., and Steers, W. D. (1988). Neural control of the urinary bladder and sexual organs: experimental studies in animals. *In* "Autonomic Failure" (R. Bannister, ed.), 2nd Ed., pp. 196–222. Oxford University Press, London.

De Groat, W. C., and Booth, A. M. (1993a). Synaptic transmission in pelvic ganglia. *In* "Nervous Control of the Urogenital System" (C. A. Maggi, ed.), pp. 291–348. Harwood Academic, Chur.

De Groat, W. C., and Booth, A. M. (1993b). Neural control of penil erection. *In* "Nervous Control of the Urogenital System" (C. A. Maggi, ed.), pp. 467–524. Harwood Academic, Chur.

De Groat, W. C., Booth, A. M., and Yoshimura, N. (1993). Neurophysiology of micturition and its modification in animal models of human disease. *In* "Nervous Control of the Urogenital System" (C. A. Maggi, ed.), pp. 227–290. Harwood Academic, Chur.

Del Fiacco, M. (1982). Enkephalin-like immunoreactivity in the human male genital tract. *J. Anat.* **135,** 649–656.

Delgado, M., Martinez, C., Leceta, J., and Gomariz, R. P. (1999). Vasoactive intestinal peptide in thymus: synthesis, receptors and biological actions. *Neuroimmunomodulation* **6,** 97–107.

De Neef, P., Robberecht, P., Chatelain, P., Waelbroeck, M., and Christophe, J. (1984). The *in vitro* chronotropic and inotropic effects of vasoactive intestinal peptide (VIP) on the atria and ventricular papillary muscle from *Cynomolgus* monkey heart. *Regul. Peptides* **8,** 237–244.

De Troyer, A., Yernault, J. C. and Rodenstein, D. (1979). Effects of vagal blockade on lung mechanics in normal man. *J. Appl. Physiol.* **46,** 217–226.

Dey, R.D., Shannon, W.A., and Said, S.I. (1981). Localization of VIP-immunoreactive nerves in airways and pulmonary vessels of dogs, cats and human subjects. *Cell Tissue Res.* **220,** 231–238.

Diamant, H., and Wiberg, A. (1965). Does the chorda tympani in man contain secretory fibres for the parotid gland? *Acta Otolaryngol.* **60,** 255–264.

Dickerson, L. W., Rodak, D. J., Fleming, T. J., Gatti, P. J., Massari, V. J., McKenzie, J. C., and Gillis, R. A. (1998). Parasympathetic neurons in the cranial medial ventricular fat pad on the dog heart selectively decrease ventricular contractility. *J. Auton. Nerv. Syst.* **70,** 129–141.

Dietz, N. M., Engelke, K. A., Samuel, T. T., Fix, R. T., and Joyner, M. J. (1997).Evidence for nitric oxide–mediated sympathetic forearm vasodilatation in humans. *J. Physiol. (Lond.)* **498,** 531–540.

Dixon, J. S., Gilpin, S. A., Gilpin, C. J., and Gosling, J. A. (1983). Intramural ganglia of the human urinary bladder. *B. J. Urol.* **55,** 195–198.

Dixon, J. S., Jen, P. Y., and Gosling, J. A. (1997). A double-label immunohistochemical study of intramural ganglia from the human male urinary bladder neck. *J. Anat.* **190,** 125–134.

Dixon, J. S., Jen, P. Y., and Gosling, J. A. (1998). Structure and autonomic innervation of the human vas deferens: a review. *Microsc. Res. Tech.* **42,** 423–432.

Dixon, J. S., Jen, P. Y. P., and Gosling, J. A. (1999). Tyrosine hydroxylase and vesicular acetylcholine transporter are coexpressed in a high proportion of intramural neurons of the human neonatal and child urinary bladder. *Neurosci. Lett.* **277,** 157–160.

Dixon, J. S., Jen, P. Y., and Gosling, J. A. (2000). The distribution of vesicular acetylcholine transporter in the human male genitourinary organs and its co-localization with neuropeptide Y and nitric oxide synthase. *Neurourol. Urodyn.* **19,** 185–194.

Dodds, W J., Dent, J., Hogan, W. J., and Arndorfer, R. C. (1981). Effect of atropine on oesophageal motor function in humans. *Am. J. Physiol.* **240,** G290–G296.

Dogiel, J. (1877). Die Ganglienzellen des Herzens bei verschiedene Thieren und beim Menschen. *Arch. Mikrosk. Anat.* **14,** 470–480.

Dolgo-Saburoff, B. (1936). Zur Lehre von Aufbau des Vagus systems. I. Uber die Nervenzellen in den Stammen des *N. vagus*. *Z. Anat. Entwicklungsgesch.* **105,** 79–93.

Domoto, T., Bishop, A. E., Oki, M., and Polak, J. M. (1990). An in vitro study of the projections of enteric vasoactive intestinal polypeptide-immunoreactive neurons in the human colon. *Gastroenterology* **98,** 819–827.

Domoto, T., Oki, M., Kotoh, T., and Nakamura, T. (1992). Heterogenous distribution of peptide-containing nerve fibres within the circular muscle layer of the human pylorus. *Clin. Auton. Res.* **2,** 403–407.

Domschke, W., Lux, G., Domschke, S., Strunz, U., Bloom, S. R., and Wunsch, E. (1978). Effects of vasoactive intestinal peptide on resting and pentagastrin-stimulated lower esophageal sphincter pressure. *Gastroenterology* **75,** 9–12.

Dovas, A., Lucchi, M. L., Bortolami, R., Grandis, A., Palladino, A. R., Banelli, E., Carretta, M., Magni, F., and Paolocci, N. (1998). Collaterals of recurrent laryngeal nerve fibres innervate the thymus: a fluorescent tracer and HRP investigation of efferent vagal neurons in the rat brainstem. *Brain. Res.* **809,** 141–148.

Dreiling, D. S., Druckerman. L. J., and Hollander, F. (1952). The effect of complete vagisection and vagal stimulation on pancreatic secretion in man. *Gastroenterology* **20,** 578–586.

Duarte-Escalante, O., Labay, P., and Boyarsky, S. (1969). The neuro-histochemistry of mammalian ureter: a new combination of histochemical procedures to demonstrate adrenergic, cholinergic and chromaffin structures in ureter. *J. Urol.* **101,** 803–811.

Dunning, B. E., and Taborsky, G. J., Jr. (1988). Galanin—sympathetic neurotransmitter in endocrine pancreas? *Diabetes* **37,** 1157–1162.

Ebbesson, S. O. E. (1963). A quantitative study of human superior cervical sympathetic ganglia. *Anat. Rec.* **146,** 353–356.

Eckberg, D. L. (1980). Parasympathetic cardiovascular control in human disease: a critical review of methods and results. *Am. J. Physiol.* **239,** H581–H593.

Eckberg, D. L., Fletcher, G. F., and Braunfeld, E. (1972). Mechanism of prolongation of the R-R interval with electrical stimulation of the carotid sinus nerves in man. *Circ. Res.* **30,** 131–138.

Eckberg, D. L., Rea, R. F., Andersson, O. K., Hedner, T., Pernow, J., Lundberg, J. M., and Wallin, B. G. (1988). Baroreflex modulation of sympathetic activity and sypathetic neurotransmitters in humans. *Acta Physiol. Scand.* **133,** 221–231.

Edin, R. (1980). The vagal control of the pyloric motor function. A physiological and immunohistochemical study in cat and man. *Acta Physiol. Scand., **Suppl.*** **485,** 1-30.

Edwards, A. V., and Bloom, S. R. (1996). Innervation of the endocrine pancreas. *In* "Autonomic–Endocrine Interactions" (K. Unsicker, ed.), pp. 209–230. Harwood Academic, Amsterdam.

Edvinsson, L., Ekman, R., Jansen, I., Ottosson, A., and Uddman, R. (1987). Peptide-containing nerve fibres in human cerebral arteries: immunocytochemistry, radioimmunoassay and in vitro pharmacology. *Ann. Neurol.* **21,** 431–437.

Edyvane, K. A., Trussell, D. C., Jonavicius, J., Henwood, A., and Marshall, V. R. (1992). Presence and regional variation in peptide-containing nerves in the human ureter. *J. Auton. Nerv. Syst.* **39,** 127–137.

Edyvane, K. A., Smet, P. J., Trussell, D. C., Jonavicius, J., and Marshall, V. R. (1994). Patterns of neuronal colocalisation of tyrosine hydroxylase, neuropeptide Y, vasoactive intestinal polypeptide, calcitonin gene–related peptide and substance P in human ureter. *J. Auton. Nerv. Syst.* **48,** 241–255.

Ehinger, B. (1966). Adrenergic nerves to the eye and to related structures in man and in the cynomolgus monkey *(Macaca irus)*. *Invest. Ophthalmol.* **5,** 42–52.

Ehinger, B., Falck, B., and Persson, H. (1968). Function of cholinergic nerve fibres in the cat iris dilator. *Acta Physiol. Scand.* **72,** 139–147.

Ehmke, H., Junemann, K. P., Mayer, B., and Kummer, W. (1995). Nitric oxide synthase and vasoactive intestinal polypeptide colocalization in neurons innervating the human penile circulation. *Int. J. Impot. Res.* **7,** 147–156.

Ehren, I., Iversen, H., Jansson, O., Adolfsson, J., and Wiklund, N. P. (1994). Localization of nitric oxide synthase activity in the human lower urinary tract and its correlation with neuroeffector responses. *Urology* **44,** 683–687.

Ek, A., Alm, P., Andersson, K.-E., and Persson, C. G. A. (1977). Adrenergic and cholinergic nerves of the human urethra and urinary bladder. A histochemical study. *Acta Physiol. Scand.* **99,** 345–352.

Ekblad, E., Arnbjornsson, E., Ekman, R., Håkanson, R., and Sundler, F. (1989). Neuropeptides in the human appendix. Distribution and motor effects. *Dig. Dis. Sci.* **34,** 1217–1230.

Ekblad, E., Alm, P., and Sundler, F. (1994). Distribution, origin and projections of nitric oxide synthase-containing neurons in gut and pancreas. *Neuroscience* **63,** 233–248.

Ekström, J. (1999). Role of nonadrenergic, noncholinergic autonomic transmitters in salivary glandular activities in vivo. *In* "Neural Mechanisms of Salivary Gland Secretion; Frontiers in Oral Biology," Vol. 11 (J. R. Garrett, J. Ekström, L. C. Anderson, eds.), pp. 94–130. Karger, Basel.

Ekström, J., Brodin, E., Ekman, R., Håkanson, R., and Sundler, F. (1984). Vasoactive intestinal peptide and substance P in salivary glands of the rat following denervation or duct ligation. *Regul. Peptides* **10,** 1–10.

Ellison, J. P., and Hibbs, R. G. (1976). An ultrastructural study of mammalian cardiac ganglia. *J. Mol. Cell. Cardiol.* **8,** 89–101.

el-Salhy, M., Stenling, R., and Grimelius, L. (1993). Peptidergic innervation and endocrine cells in the human liver. *Scand. J. Gastroenterol.* **28,** 809–815.

Fandriks, L., and Jonson, C. (1990). Vagal and sympathetic control of gastric and duodenal bicarbonate secretion. *J. Intern. Med. Suppl.* **732,** 103–107.

Fee, J. D., Randall, W. C., Wurster, R. D., and Ardell, J. C. (1987). Selective ganglionic blockade of vagal inputs to sinoatrial and/or atrioventricular regions. *J. Pharmacol. Exp. Ther.* **242,** 1006–1012.

Feeley, T. M., Clanachan, A. S., and Scott, G. W. (1984). The effects of vasoactive intestinal polypeptide on the motility of human and guinea-pig gall bladder. *Can. J. Physiol. Pharmacol.* **62,** 356–359.

Feigl, E. O. (1998). Neural control of coronary blood flow. *J. Vasc. Res.* **35,** 85–92.

Feldman, M. (1985). Gastric H^+ and HCO_3^- secretion in response to sham feeding in humans. *Am. J. Physiol.* **248,** G188–G191.

Feldman, M., and Walsh, J. H. (1980). Acid inhibition of sham feeding-stimulated gastrin release and gastric acid secretion: effect of atropine. *Gastroenterology* **78,** 772–776.

Feldman, M., Richardson, C., Taylor, I., and Walsh, J. H. (1979). Effect of atropine on vagal release of gastrin and pancreatic polypeptide. *J. Clin. Invest.* **63,** 294–298.

Felten, D. L., Felten, S. Y., Bellinger, D. L., Carlsson, S. L., Ackerman, K. D., Madden, K. S., Olschowki, J. A., and Livnat, S. (1987).

Noradrenergic sympathetic neural interactions with the immune system: structure and function. *Immunol. Rev.* **100,** 225–260.
Ferguson, M., and Bell, C. (1993). Autonomic innervation of the kidney and ureter. *In* "Neural Control of the Urogenital System" (C. A. Maggi, ed.), pp. 1–32. Harwood Academic, Chur.
Ferreira, A. L., and Rossi, M. A. (1974). Innervation of human atrioventricular valves. *Acta Anat.* **87,** 57–65.
Fischer, A., and Hoffmann, B. (1996). Nitric oxide synthase in neurons and nerve fibers of lower airways and in vagal sensory ganglia of man: correlation with neuropeptides. *Am. J. Resp. Crit. Care Med.* **154,** 209–216.
Fischer, A., Canning, B. J., and Kummer, W. (1996). Correlation of vasoactive intestinal peptide and nitric oxide synthase with choline acetyltransferase in the airway innervation. *Ann. N. Y. Acad. Sci.* **805,** 717–722.
Fischer, A., Canning, B. J., Undem, B. J., and Kummer, W. (1998). Evidence for an esophageal origin of VIP-IR and NO synthase-IR nerves innervating the guinea pig trachealis: a retrograde neuronal tracing and immunohistochemical analysis. *J. Comp. Neurol.* **394,** 326–334.
Fisher, A. W. F. (1964). The intrinsic innervation of the trachea. *J. Anat.* **98,** 117–124.
Fisher, R. S., Rock, E., and Malmud, L. S. (1985). Cholinergic effects on gallbladder emptying in humans. *Gastroenterology* **89,** 716–722.
Fitzgerald, M. J. T., and Alexander, R. W. (1969). The intramuscular ganglia of the cat's tongue. *J. Anat.* **105,** 27–46.
Flemstrom, G. (1987). Gastric and duodenal mucosal bicarbonate secretion. *In* "Physiology of the Gastrointestinal Tract" (L. R. Johnson, ed.), 2nd Ed., pp. 1011–1029. Raven Press, New York.
Flügel, C., Tamm, E. R., Mayer, B., and Lütjen-Drecoll, E (1994). Species differences in choroidal vasodilative innervation: evidence for specific intrinsic nitrergic and VIP-positive neurons in the human eye. Invest. *Ophthalmol. Vis. Sci.* **35,** 592–599.
Forssell, H., and Olbe, L. (1987a). Effect of fundic distension on gastric bicarbonate secretion in man. *Scand. J. Gastroenterol.* **22,** 627–633.
Forssell, H., and Olbe, L. (1987b). Effect of proximal gastric vagotomy on basal and vagally stimulated gastric bicarbonate secretion in duodenal ulcer patients. *Scand. J. Gastroenterol.* **22,** 949–955.
Forssmann, W. G., and Greenberg, J. (1978). Innervation of the endocrine pancreas in primates. *In* "Peripheral Neuroendocrine interaction" (R. E. Coupland and W. G. Forssmann, eds.), pp. 124–133, Springer-Verlag, Berlin.
Foster, K. G., and Weiner, J. S. (1970). Effects of cholinergic and adrenergic agents on the activity of the eccrine sweat glands. *J. Physiol. (Lond.)* **210,** 883–895.
Fox, B., Bull, T. B., and Guz, A. (1980). Innervation of alveolar walls in the human lung: an electron microscopic study. *J. Anat.* **131,** 683–692.
Fox, R. H., and Edholm, O. G. (1963). Nervous control of the cutaneous circulation. *Br. Med. Bull.* **19,** 110–114.
Francillon, M. R. (1928). Zur Topographie der Ganglien des menschlichen Herzens. *Z. Anat. Entwicklungsgesch.* **85,** 131–165.
Franco-Cereceda, A., and Lundberg, J. M. (1987). Potent effects of neuropeptide Y and calcitonin gene–related peptide on human coronary vascular tone *in vitro*. *Acta Physiol. Scand.* **131,** 159–160.
Franco-Cereceda, A., Lundberg, J. M., and Hökfelt, T. (1986). Somatostatin: an inhibitory parasympathetic transmitter in the human heart? *Eur. J. Pharmacol.* **132,** 101–102.
Franco-Cereceda, A., Bengtsson, L., and Lundberg, J. M. (1987). Inotropic effects of calcitonin gene-related peptide, vasoactive intestinal polypeptide and somatostatin on the human right atrium in vitro. *Eur. J. Pharmacol.* **134,** 69–76.
Friedman, M. I. (1982). Hepatic nerve endings. *In* "The Liver: Biology and Pathobiology" (1. Arias, H. Popper, D. Schachter, and D. A. Shafritz, eds.), pp. 663–673. Raven Press, New York.
Furness, J. B. (2000). Types of neurons in the enteric nervous system. *J. Auton. Nerv. Syst.* **81,** 87–96.
Furness, J. B., and Costa, M. (1987). "The Enteric Nervous System." Churchill Livingstone, Edinburgh.
Furness, J. B., Morris, J. L., Gibbins, I. L., and Costa, M. (1989). Chemical coding of neurons and plurichemical transmission. *Annu. Rev. Pharmacol. Toxicol.* **29,** 289–306.
Furness, J. B., Kunze, W. A. A., Bertrand, P. P., Clerc, N., and Bornstein, J. C. (1998). Intrinsic primary afferent neurons of the intestine. *Progr. Neurobiol.* **54,** 1–18.
Furukawa, Y., Hoyano, Y., and Chiba, S. (1996). Parasympathetic inhibition of sympathetic effects on sinus rate in anesthetized dogs. *Am. J. Physiol.* **271,** H44–50.
Gabella, G. (1976). "Structure of the Autonomic Nervous System." Chapman and Hall, London.
Gai, W. P., and Blessing, W. W. (1996). Human brainstem preganglionic parasympathetic neurons localized by markers for nitric oxide synthesis. *Brain* **119,** 1145–1152.
Galligan, J. J., LePard, K. J., Schneider, D. A., and Zhou, X. (2000). Multiple mechanisms of fast excitatory synaptic transmission in the enteric nervous system. *J. Auton. Nerv. Syst.* **81,** 97–103.
Garret, J. R. (1967). The innervation of normal human submandibular and parotid salivary glands. *Arch. Oral Biol.* **12,** 1417–1436.
Garrett, J. R., and Kidd, A. (1993). The innervation of salivary glands as revealed by morphological methods. *Microsc. Res. Tech.* **26,** 75–91.
Gatti, P. J., Johnson, T. A., Phan, P., Jordan, I. K., 3rd, Coleman, W., and Massari, V. J. (1995). The physiological and anatomical demonstration of functionally selective parasympathetic ganglia located in discrete fat pads on the feline myocardium. *J. Auton. Nerv. Syst.* **51,** 255–259.
Gatti, P. J., Johnson, T. A., McKenzie, J., Lauenstein, J. M., Gray, A., and Massari, V. J. (1997). Vagal control of left ventricular contractility is selectively mediated by a cranioventricular intracardiac ganglion in the cat. *J. Auton. Nerv. Syst.* **66,** 138–144.
Gaumnitz, E., Sweet, M. A., Sengupta, A., and Singaram, C. (1995). Nitrinergic and peptidergic innervations and their interrelationships in human colon. *Neuropeptides* **29,** 1–9.
Gaylor, J. B. (1934). The intrinsic nervous mechanism of the human lung. *Brain* **57,** 143–160.
Gellert, A. (1934). Ganglia of the internal carotid plexus. *J. Anat.* **68,** 318–322.
Gemmell, A. A. (1926). A method of demonstrating the ganglia of the cervix uteri. *J. Obstet. Gynaecol. Br. Emp.* **33,** 259–261.
Gershon, M. D. (1999). Review article: roles played by 5-hydroxytryptamine in the physiology of the bowel. *Aliment. Pharmacol. Ther.* **13,** 15–30.
Gibbins, I. L. (1990). Target-related patterns of co-existence of neuropeptide Y, vasoactive intestinal peptide, enkephalin and substance P in cranial parasympathetic neurons innervating the facial skin and exocrine glands of guinea-pigs. *Neuroscience* **38,** 541–560.
Gibbins, I. L. (1995). Chemical neuroanatomy of sympathetic ganglia. *In* "Autonomic Ganglia" (E. M. McLachlan, ed), pp. 73–121. Harwood Academic, Luxembourg.
Gibbins, I. L. (1997). Autonomic pathways to cutaneous effectors. *In* "Autonomic Innervation of the Skin" (J. L. Morris and I.L. Gibbins, eds.), pp. 1–56, Harwood Academic, Amsterdam.
Gibbins, I. L., Brayden, J. E., and Bevan, J. A. (1984). Perivascular nerves with immunoreactivity to vasoactive intestinal

polypeptide in cephalic arteries of the cat: distribution, possible origins and functional implications. *Neuroscience* **13,** 1327–1346.
Gibbins, I. L., Rodgers, H. F., Matthew, S. E., and Murphy, S. M. (1998). Synaptic organisation of lumbar sympathetic ganglia of guinea pigs: serial section ultrastructural analysis of dye-filled sympathetic final motor neurons. *J. Comp. Neurol.* **402,** 285–302.
Ginsburg, R., Bristow, M. R., Davis, K., Dibiase, A., and Billingham, M. E. (1984). Quantitative pharmacologic responses of normal and atherosclerotic isolated human epicardial coronary arteries. *Circulation* **69,** 430–410.
Givner, I. (1939). Episcleral ganelion cells. *Arch. Ophthalmol. (Chicago)* **22,** 82–88.
Glaser, B., Vinik, A., Valysson, G., and Zoghlin, G. (1981). Truncal vagotomy abolishes the somatostatin response to insulininduced hypoglycemia in man. *J. Clin. Endocrinol. Metab.* **52,** 823–828.
Gloster, J. (1961). Influence of the facial nerve on intra-ocular pressure. *Br. J. Ophthalmol.* **45,** 259–278.
Goessl, C., Grozdanovic, Z., Knispel, H. H., Wegner, H. E., and Miller, K. (1995). Nitroxergic innervation of the human ureterovesical junction. *Urol. Res.* **23,** 189–192.
Goldie, R. G., Spina, D., and Lulich, K. M. (1997). Adrenergic nerves and receptors. *In* "Autonomic Control of the Respiratory System" (P. J. Barnes, ed.), pp. 119–138. Harwood Academic, Amsterdam.
Golding-Wood, P. H. (1961). Observations on petrosal and vidian neurectomy in chronic rhinitis. *J. Laryngol. Otol.* **75,** 232–247.
Golding-Wood, P. H. (1973). Vidian neurectomy: its results and complications. *Laryngoscope* **83,** 1673–1683.
Gomez, H. (1961). The innervation of the lingual salivary glands. *Anat. Rec.* **139,** 69–76.
Gordon, L., Polak, J. M., Moscoso, G. J., Smith, A., Kuhn, D. M., and Wharton, J. (1993). Development of the peptidergic innervation of human heart. *J. Anat.* **183,** 131–140.
Gorelova E., Loesch A., Bodin P., Chadwick L., Hamlyn P. J., and Burnstock G. (1996) Localisation of immunoreactive factor VIII, nitric oxide synthase, substance P, endothelin-1 and 5-hydroxytryptamine in human postmortem middle cerebral artery. *J. Anat.* **188,** 97–107.
Gosling, J. A., Dixon, J. S., and Lendon, R. G. (1977). The autonomic innervation of the human male and female bladder and proximal urethra. *J. Urol.* **118,** 302–305.
Goyal, R. K., and Rattan, S. (1978). Neurohumoral, hormonal and drug receptors for the lower esophageal sphincter. *Gastroenterology* **74,** 598–619.
Greaves, R., Miller, J., O'Donnell, L., McLean, A., and Farthing, M. J. (1998). Effect of the nitric oxide donor, glyceryl trinitrate, on human gall bladder motility. *Gut* **42,** 410–413.
Greco, A., Ghirlanda, G., Barone, C., Bertoli, A., Caputo, S., Uccioli, L., and Manna, R. (1984). Somatostatin in paroxysmal supraventricular and junctional tachycardia. *Br. J. Med.* **288,** 288.
Greenberg, B., Rhoden, K., and Barnes, P. J. (1987). Vasoactive intestinal peptide causes non-endothelial dependent relaxation in human and bovine pulmonary arteries. *Blood Vessels* **24,** 45–50.
Greenhalgh, R. M., Rosengarten, D. S., and Martin, P. (1971). Role of sympathectomy to hyperhydrosis. *Br. Med. J.* **1,** 332–334.
Grimes, P., and von Sallman, L. (1960). Comparative anatomy of the ciliary nerves. *Arch. Ophthalmol (Chicago)* **64,** 81–91.
Grozdanovic, Z., and Baumgarten, H. G. (1996). Colocalisation of NADPH-diaphorase with neuropeptides in the ureterovesical ganglia of humans. *Acta Histochem.* **98,** 245–253.
Grozdanovic, Z., and Goessl, C. (1999). Comparative localization of heme oxygenase-2 and nitric oxide synthase in the autonomic innervation to the human ductus deferens and seminal vesicle. *J. Urol.* **162,** 2156–2161.
Grunditz, T., Hakanson, R., Rerup, C., Sundler, F., and Uddman, R. (1984). Neuropeptide Y in the thyroid gland: Neuronal localization and enhancement of stimulated thyroid secretion. *Endocrinology* **115,** 1537–1542.
Grunditz, T., Hakanson, R., Hedge, G., Rerup, C., Sundler, F., and Uddman, R. (1986). Peptide histidine isoleucine amide stimulates thyroid hormone secretion and coexists with vasoactive intestinal polypeptide in intrathyroid nerve fibers from laryngeal ganglia. *Endocrinology* **118,** 783–790.
Grunditz, T., Luts, L., and Sundler, F. (1996). Innervation of the thyroid and parathyroid glands; emphasis on neuropeptides. *In* "Autonomic-Endocrine Interactions" (K. Unsicker, ed.), pp. 181–207. Harwood Academic, Amsterdam.
Gu, J., Adrian, T. E., Tatemoto, K., Polak, J. M., Allen, J. M., and Bloom, S. R. (1983a). Neuropeptide tyrosine (NPY)—a major cardiac neuropeptide. *Lancet* **1,** 1008–1010.
Gu, J., Polak, J. M., Probert, L., Islam, K. N., Marango, P. J., Mina, S., Adrian, T. E., McGregor, G. P., O'Shaughnessy, D. J., and Bloom, S. R. (1983b). Peptidergic innervation of the human male genital tract. *J. Urol.* **130,** 386–391.
Gu, J., Restorick, J. M., Blank, M. A., Huang, W. M., Bloom, S. R., and Mundy, A. R. (1983c). Vasoactive intestinal polypeptide in the normal and unstable bladder. *Br. J. Urol.* **55,** 645–647.
Guelrud, M., Rossiter, A., Souney, P. F., Rossiter, G., Fanikos, J., and Mujica, V. (1992). The effect of vasoactive intestinal polypeptide on the lower esophageal sphincter in achalasia. *Gastroenterology* **103,** 377–382.
Gustaw, P., Pawlik, W. W., Czarnobilski, K., Sendur, R., and Konturek, S. J. (1994). Nitric oxide is involved in the mediation of gastric blood flow and tissue oxygenation. *J. Physiol. Pharmacol.* **45,** 361–368.
Guttman, L. (1940). The distribution of disturbance of sweat secretion after extirpation of certain sympathetic cervical ganglia in man. *J. Anat.* **74,** 537–549.
Habler, H. J., Wasner, G., and Janig, W. (1997). Attenuation of neurogenic vasoconstriction by nitric oxide in hindlimb microvascular beds of the rat in vivo. *Hypertension* **30,** 957–961.
Halliday, G. M., Li, Y. W., Joh. T. H., Cotton, R. G. H., Howe, P. R. C., Geffen, L. B., and Blessing, W. W. (1988). Distribution of substance P-like immunoreactive neurons in the human medulla oblongata: colocalization with monoamine-synthesizing neurons. *Synapse* **2,** 353–370.
Hanazawa, T., Tanaka, K., Chiba, T., and Konno, A. (1997). Distribution and origin of nitric oxide synthase–containing nerve fibers in human nasal mucosa. *Acta Otolaryngol.* **117,** 735–737.
Hara, H., and Kobayashi, S. (1987). Vasoactive intestinal polypeptide (VlP)–like immunoreactive cells in the skull base of rats. *Histochemistry* **87,** 217–221.
Hara, H., and Weir, B. (1988). Pathway of nerves with vasoactive intestinal polypeptide–like immunoreactivity to the major cerebral arteries of the rat. *Cell Tissue Res.* **251,** 275–780.
Hara, H., Hamill, G. S., and Jacobowitz, D. M. (1985). Origin of cholinergic nerves to rat major cerebral arteries: coexistence with vasoactive intestinal polypeptide. *Brain Res. Bull.* **14,** 179–188.
Harkonen, M., and Penttila, A. (1971). Catecholamines, monoamine oxidase and cholinesterase in the human sympathetic ganglion. *Acta Physiol. Scand.* **82,** 310–321.
Harman, N. B. (1900). The anterior limit of the cervico-thoracic visceral efferent nerves in man. *J. Anat. Physiol.* **34**, 359–380.
Hartschuh, W., Reinecke, M., Weihe, E., and Yanaihara, N. (1984). VlP-immunoreactivity in the skin of various mammals: immunohistochemical, radioimmunological and experimental evidence for a dual localization in cutaneous nerves and Merkel cells. *Peptides* **5,** 239–245.

Hauser, G. J., Danchak, M. R., Colvin, M. P., Hopkins, R. A., Wocial, B., Myers, A. K., and Zukowska-Grojec, Z. (1996). Circulating neuropeptide Y in humans: relation to changes in catecholamine levels and changes in hemodynamics. *Neuropeptides* **30,** 159–165.

Hauser-Kronberger, C., Albegger, K., Saria, A., and Hacker, G. W. (1992a). Neuropeptides in human salivary (submandibular and parotid) glands. *Acta Otolaryngol.* **112,** 343–348.

Hauser-Kronberger, C. E., Hacker, G. W., Sundler, F., Thurner, J., and Albegger, K. (1992b). Distribution and co-localization of immunoreactive helospectin with vasoactive intestinal polypeptide and peptide histidine methionine in human nasal mucosa, soft palate and larynx. *Eur. Arch. Otorhinolaryngol.* **249,** 201–205.

Havel, P. J., and Ahren, B. (1997). Activation of autonomic nerves and the adrenal medulla contributes to increased glucagon secretion during moderate insulin-induced hypoglycemia in women. *Diabetes* **46,** 801–807.

Havel, P.J., and Taborsky, G.J. (1994). The contribution of the autonomic nervous system to increased glucagon secretion during hypoglycemic stress: update 1994. *Endocrine Rev.* **2,** 201–204.

Havel, P. J., and Valverde, C. (1996). Autonomic mediation of glucagon secretion during insulin-induced hypoglycemia in rhesus monkeys. *Diabetes* **45,** 960–966.

Head, G. M., Mentlein, R., von Patay, B., Downing, J. E., and Kendall, M. D. (1998). Neuropeptides exert direct effects on rat thymic epithelial cells in culture. *Dev. Immunol.* **6,** 95–104.

Hedlund, H., and Andersson, K.-E. (1985). Effects of some peptides on isolated human erectile tissue and cavernous artery. *Acta Physiol. Scand.* **124,** 413–419.

Hedlund, P., Ekstrom, P., Larsson, B., Alm, P., and Andersson, K. E. (1997). Heme oxygenase and NO-synthase in the human prostate—relation to adrenergic, cholinergic and peptide-containing nerves. *J. Autonom. Nerv. Syst.* **63,** 115–126.

Hedlund, P., Ny, L., Alm, P., and Andersson, K. E. (2000). Cholinergic nerves in human corpus cavernosum and spongiosum contain nitric oxide synthase and heme oxygenase. *J. Urol.* **164,** 868–875.

Hedo, J. A., Villanueva, M. L., and Marco, J. (1978). Stimulation of pancreatic polypeptide and glucagon secretion by 2-deoxy-D-glucose in man: evidence for cholinergic mediation. *J. Clin. Endocrinol. Metab.* **47,** 366–371.

Helén, P., Panula, P., Yang, H.-Y. T., Hervonen, A., and Rapoport, S. (1984). Location of substance P-, bombesin-, gastrinreleasing peptide-, [Met^5] enkephalin-, and [Met^5] enkephalinArg^6-Phe^7-like immunoreactivities in adult human sympathetic ganglia. *Neuroscience* **12,** 907–916.

Hellekant, G. (1972). Circulation of the tongue. *Wenner-Gren Cent. Int. Symp. Ser.* **20,** 127–136.

Heller, P. H., Perry, F., Jewett, D. L., and Levine, J. D. (1990). Autonomic components of the human pupillary light reflex. *Invest. Ophthalmol. Vis. Sci.* **31,** 156–162.

Helm, G. (1981). Adrenergic and peptidergic neuromuscular mechanisms in the human fallopian tube, with special regard to cyclic influences. *Acta Obstet. Gynecol. Scand.*, Suppl. **104,** 1–23.

Helm, G., Håkanson, R., Leander, S., Owman, C., Sjöberg, N.-O., and Sporrong, B. (1982). Neurogenic relaxation mediated by vasoactive intestinal polypeptide (VIP) in the isthmus of the human fallopian tube. *Regul. Peptides* **3,** 145–153.

Hertweck, M. S., and Hung, K.-S. (1980). Ultrastructural evidence for the innervation of human pulmonary alveoli. *Experientia* **36,** 112–113.

Hervonen, A., Vaalasti, A., Vaalasti, T., Partanen, M., and Kanerva, L. (1976). Paraganglia in the urinogenital tract of man. *Histochemistry* **48,** 307–313.

Hervonen, A., Partanen, S., Vaalasti, A., Partanen, M., Kanerva. L., and Alho, H. (1978a). The distribution and endocrine nature of the abdominal paraganglia of adult man. *Am. J. Anat.* **153,** 563–572.

Hervonen, A., Vaalasti, A., Partanen, M., Kanerva, L., and Hervonen, H. (1978b). Effects of ageing on the histochemically demonstrable catecholamines and acetylcholine of human sympathetic ganglia. *J. Neurocytol.* **7,** 11–23.

Hervonen, A., Pelto-Huikko, M., Helén, P., and Alho, H. (1980). Electron microscopic localization of enkephalin-like immunoreactivity in axon terminals of human sympathetic ganglia. *Histochemistry* **70,** 1–6.

Higbee, D. (1949). Functional and anatomic relation of sphenopalatine ganglion to the autonomic nervous system. *Arch. Otolaryngol.* **50,** 45–58.

Higgins, C. B., Vatner, S. F., and Braunwald, E. (1973). Parasympathetic control of the heart. *Pharmacol. Rev.* **25,** 119–155.

Hilliges, M., Hellman, M., Ahlström, U., and Johansson, O. (1994) Immunohistochemical studies of neurochemical markers in normal human buccal mucosa. *Histochem.* **101,** 235–244.

Hirst, G. D. S., Choate, J. K., Cousins, H. M., Edwards, F. R., and Klemm, M. F. (1996). Transmission by post-ganglionic axons of the autonomic nervous system: The importance of the specialized neuroeffector junction. *Neuroscience* **73,** 7–23.

Hjemdahl, P., and Kahan, T. (1996). Skeletal muscle circulation. *In* "Nervous Control of Blood Vessels" (T. Bennett and S.M. Gardiner, eds.), pp. 305–348. Harwood Academic, Amsterdam..

Ho, K. M., Ny, L., McMurray, G., Andersson, K. E., Brading, A. F., and Noble, J. G. (1999). Co-localization of carbon monoxide and nitric oxide synthesizing enzymes in the human urethral sphincter. *J. Urol.* **161,** 1968–1972.

Hoffman, H. H. (1957). An analysis of the sympathetic trunk and rami in the cervical and upper thoracic regions in man. *Ann. Surg.* **145,** 94–103.

Hoffman, H. H., and Kuntz, A. (1957). Vagus nerve components. *Anat. Rec.* **127,** 551–568.

Hohmann, E. L., Elde, R. P., Rysavy, J. A., Einzig, S., and Gebhard, R. L. (1986). Innervation of periosteum and bone by sympathetic vasoactive intestinal peptide–containing nerve fibres. *Science* **232,** 868–871.

Hollander, A. P., and Bouman, L. N. (1975). Cardiac acceleration in man elicited by a muscle–heart reflex. *J. Appl. Physiol.* **138,** 272–278.

Holloway, R. H., Dodds, W. J., Helm, J. F., Hogan, W. J., Dent, J., and Arndorfer, R. C. (1986). Integrity of cholinergic innervation to the lower esophageal sphincter in achalasia. *Gastroenterology* **90,** 924–929.

Holst, J. J., Schaffalitzky de Muckadell, O. B., and Fahrenkrug, J. (1990). Somatostatin inhibits neurally stimulated pancreatic secretion indirectly. *Pancreas* **5,** 611–614.

Holst, J. J., Skak-Nielsen, T., Orskov, C., and Seier-Poulsen, S. (1992). Vagal control of the release of somatostatin, vasoactive intestinal polypeptide, gastrin-releasing peptide, and HCl from porcine non-antral stomach. *Scand. J. Gastroenterol.* **27,** 677–685.

Holst, J. J., Rasmussen, T. N., Harling, H., and Schmidt, P. (1993). Effect of intestinal inhibitory peptides on vagally induced secretion from isolated perfused porcine pancreas. *Pancreas* **8,** 80–87.

Holst, J. J., Rasmussen, T. N., and Schmidt, P. (1994). Role of nitric oxide in neurally induced pancreatic exocrine secretion in pigs. *Am. J. Physiol.* **266,** G206–213.

Holst, M. C., Kelly, J. B., and Powley, T. L. (1997). Vagal preganglionic projections to the enteric nervous system characterized with *Phaseolus vulgaris* leucoagglutinin. *J. Comp. Neurol.* **381,** 81–100.

Hopton, D. S. (1973). The influence of the vagus nerves on the biliary system. *Br. J. Surg.* **60,** 216–218.

Horackova, M., Armour, J. A., and Byczko, Z. (1999). Distribution of intrinsic cardiac neurons in whole-mount guinea pig atria identified by multiple neurochemical coding: a confocal microscope study. *Cell Tiss. Res.* **297,** 409–421.

Hou, Z.-Y., Lin, C.-l., Chiu, T. H., Chiang, B. N., Cheng, K.-K., and Ho, G. T. (1987). Somatostatin effects in isolated human atrial fibres. *J. Mol. Cell. Cardiol.* **19,** 177–185.

Hoyano, Y., Furukawa, Y., Kasama, M., and Chiba, S. (1997). Parasympathetic inhibition of sympathetic effects on atrioventricular conduction in anesthetized dogs. *Am. J. Physiol.* **273,** H1800–H1806.

Hoyle, C. H. V., and Burnstock, G. (1993). Postganglionic efferent transmission in the bladder and urethra. *In* "Nervous Control of the Urogenital System" (C. A. Maggi, ed.), pp. 349–382. Harwood Academic, Chur.

Hoyle, C. H., Stones, R. W., Robson, T., Whitley, K., and Burnstock, G. (1996). Innervation of vasculature and microvasculature of the human vagina by NOS and neuropeptide-containing nerves. *J. Anat.* **188,** 633–644.

Huertas, J. R., Acebal, F., Ballesta, M. C., Martinez-Victoria, E., Manas, M., and Mataix, F. J. (1992). Late postprandial pancreatic secretion periods in conscious dogs. Effect of vagotomy. *Arch. Int. Physiol. Biochim. Biophys.* **100,** 191–195.

Huizinga, J. D., Thuneberg, L., Vanderwinden, J. M., and Rumessen, J. J. (1997). Interstitial cells of Cajal as targets for pharmacological intervention in gastrointestinal motor disorders. *Trends Pharmacol. Sci.* **18,** 393–403.

Hurley, H. J., and Mescon, H. (1956). Cholinergic innervation of the digital arteriovenous anastomoses of human skin. A histochemical localization of cholinesterase. *J. Appl. Physiol.* **9,** 82–84.

Husted, S., Sjögren, C., and Andersson, K. -E. (1983). Direct effects of adenosine and adenine nucleotides on isolated human urinary bladder and their influence on electrically inducedcontractions. *J. Urol.* **130,** 392–398.

Ignacio C. S., Curling P. E., Childres W. F., and Bryan R. M. (1997) Nitric oxide–synthesizing perivascular nerves in the rat middle cerebral artery. *Am. J. Physiol.* **42,** R661–R668.

Inberg, M., and Vuorio, M. (1969). Human gallbladder functions after selective gastric and total abdominal vagotomy. *Acta Chir. Scand.* **135,** 625–633.

Iselin, C. E., Alm, P., Schaad, N. C., Larsson, B., Graber, P., and Andersson, K. E. (1997). Localization of nitric oxide synthase and haemoxygenase, and functional effects of nitric oxide and carbon monoxide in the pig and human intravesical ureter. *Neurourol. Urodyn.* **16,** 209–227.

Iselin, C. E., Ny, L., Larsson, B., Schaad, N. C., Alm, P., Graber, P., Morel, D. R., and Andersson, K. E. (1998). The nitric oxide synthase/nitric oxide and heme oxygenase/carbon monoxide pathways in the human ureter. *Eur. Urol.* **33,** 214–221.

Ishii, J., Shizume, K., and Okinaka, S. (1968). Effect of stimulation of the vagus nerve on the thyroidal release of ^{131}I-labelled hormones. *Endocrinology (Balt)* **82,** 7–16.

Ito, H., Matsuda, K., Sato, A., and Tohgi, H. (1987). Cholinergic and VIP-ergic vasodilator actions of parasympathetic nerves on the thyroid blood flow in rats. *Jpn. J. Physiol.* **37,** 1005–1017.

Izumi, H. (1999). Nervous control of blood flow in the orofacial region. *Pharmacol. Ther.* **81,** 141–161.

Jahnberg, T. (1977). Gastric adaptive relaxation. Effects of vagal activation and vagotomy. An experimental study in dogs and in man. *Scand. J. Gastroenterol.* **12,** Suppl. 46, 5–32.

James, M. J., Birmingham, A. T., and Hill, S. J. (1993). Partial mediation by nitric oxide of the relaxation of human isolated detrusor strips in response to electrical field stimulation. *Br. J. Clin. Pharmacol.* **35,** 366–372.

Jänig, W. (1988). Pre- and postganglionic vasoconstrictor neurons: differentiation, types and discharge properties. *Annu. Rev. Physiol.* **50,** 525–540.

Jänig, W., Sundlof, G., and Wallin, B. G. (1983). Discharge patterns of sympathetic neurons supplying skeletal muscle and skin in man and cat. *J. Auton. Nerv. Syst.* **7,** 239–256.

Jarvi, R., Pelto-Huikko, M., Helen, P., and Hervonen, A. (1987). Somatostatin-like immunoreactivity in human sympathetic ganglia. *Cell Tissue Res.* **249,** 1–5.

Jen, P. Y., Dixon, J. S., and Gosling, J. A. (1996). Co-localisation of tyrosine hydroxylase, nitric oxide synthase and neuropeptides in neurons of the human postnatal male pelvic ganglia. *J. Auton. Nerv. Syst.* **59,** 41–50.

Jen, P. Y., Dixon, J. S., and Gosling, J. A. (1997). Co-localization of nitric oxide synthase, neuropeptides and tyrosine hydroxylase in nerves supplying the human post-natal vas deferens and seminal vesicle. *Br. J. Urol.* **80,** 291–299.

Jen, P. Y. P., Dixon, J. S., and Gosling, J. A. (1999). Colocalisation of neuropeptides, nitric oxide synthase and immunomarkers for catecholamines in nerve fibres of the adult human vas deferens. *J. Anat.* **195,** 481–489.

Joborn, H., Larsson, R., Rastad, J., Nygren, P., Akerstrom, G., and Ljunghall, S. (1991). Vasoactive intestinal polypeptide stimulates parathyroid hormone release by interaction with cyclic adenosine monophosphate production of bovine parathyroid cells. *Acta Endocrinol (Copenh)* **124,** 54–59.

Johansson, O. (1986). A detailed account of NPY-immunoreactive nerves and cells of the human skin. Comparison with VIP-, substance P- and PHI-containing structures. *Acta Physiol. Scand.* **128,** 147–153.

Johnson, J. M. (1986). Nonthermoregulatory control of human skin blood flow. *J. Appl. Physiol.* **61,** 1613–1622.

Johnson, L. R., ed. (1987). "Physiology of the Gastrointestinal Tract," 2nd ed. Raven Press, New York.

Jorgensen, J. C., Sheikh, S. P., Forman, A., Norgard, M., Schwartz, T. W., and Ottesen, B. (1989). Neuropeptide Y in the human female genital tract: localization and biological action. *Am. J. Physiol.* **257,** E220–E227.

Jorgensen, J. C., Giwercman, A., and Ottesen, B. (1996). Neuropeptide Y in the human prenatal and mature gonads. *Neuropeptides* **30,** 293–301.

Joyner, M. J., and Halliwill, J. R. (2000). Neurogenic vasodilation in human skeletal muscle: possible role in contraction-induced hyperaemia. *Acta Physiol. Scand.* **168,** 481–488.

Kaada, B., Olsen, E., and Eielsen, O. (1984). In search of mediators of skin vasodilation induced by transcutaneous nerve stimulation. III. Increase in plasma VIP in normal subjects and in Raynaud's disease. *Gen. Pharmacol.* **15,** 107–113.

Kadota, O., Matsuda, S., Ohta, S., Kumon, Y., Sakaki, S., and Sakanaka, M. (1996). Origins of nitric oxide synthase–containing nerve fibers in the rat basilar artery with reference to the fine structure of the nerve fibers. *Brain Res.* **706,** 129–136.

Kahan, T., Taddei, S., Pedrinelli, R., Hjemdahl, P., and Salvetti, A. (1992). Nonadrenergic sympathetic vascular control of the human forearm in hypertension: possible involvement of neuropeptide Y. *J. Cardiovasc. Pharmacol.* **19,** 587–592.

Kaijser, L., Pernow, J., Berglund, B., and Lundberg, J. M. (1990). Neuropeptide Y is released together with noradrenaline from the human heart during exercise and hypoxia. *Clin. Physiol.* **10,** 179–188.

Kaijser, L., Pernow, J., Berglund, B., Grubbstrom, J., and Lundberg, J. M. (1994). Neuropeptide Y release from human heart is enhanced during prolonged exercise in hypoxia. *J. Appl. Physiol.* **76,** 1346–1349.

Kaji, A., Shigematsu, H., Fujita, K., Maeda, T., and Watanabe, S. (1988). Parasympathetic innervation of cutaneous blood vessels

by vasoactive intestinal polypeptide-immunoreactive and acetylcholinesterase-positive nerves: histochemical and experimental study on rat lower lip. *Neuroscience* **25,** 353–362.

Kalsner, S. (1985). Cholinergic mechanisms in human coronary artery preparations: implications of species differences. *J. Physiol. (Lond.)* **358,** 509–526.

Kaufman, J., and Wright, G. W. (1969). The effect of nasal and nasopharyngeal irritation on airway resistance in man. *Annu Rev. Respir. Dis.* **100,** 626–630.

Keast, J. R. (1995). Pelvic ganglia. *In* "Autonomic Ganglia" (E. M. McLachlan, ed.), pp. 445–480. Harwood Academic, Luxembourg.

Keast, J. R. (1999). Unusual autonomic ganglia: connections, chemistry, and plasticity of pelvic ganglia. *Int. Rev. Cytol.* **193,** 1–69.

Keller, J. T., Beduk, A., and Saunders, M. C. (1985). Origin of fibres innervating the basilar artery of the cat. *Neurosci. Lett.* **58,** 263–268.

Kent, K. M., Epstein, S. E.. Cooper, T., and Jacobowitz, D. M. (1974). Cholinergic innervation of the canine and human ventricular conducting system. *Circulation* **50,** 948–955.

Kimura T., Yu J. G., Edvinsson L., and Lee T. J. F. (1997) Cholinergic, nitric oxidergic innervation in cerebral arteries of the cat. *Brain Res.* **773,** 117–124.

Kinami, S., Miwa, K., Sato, T., and Miyazaki, I. (1997). Section of the vagal celiac branch in man reduces glucagon-stimulated insulin release. *J. Auton. Nerv. Syst.* **64,** 44–48.

King, T. S., and Coakley, J. B. (1958). The intrinsic nerve cells of the cardiac atria of mammals and man. *J. Anat.* **92,** 353–376.

Kirch, W., Neuhuber, W., and Tamm, E. R. (1995). Immunohistochemical localization of neuropeptides in the human ciliary ganglion. *Brain Res.* **681,** 229–234.

Kirchgessner, A. L., Liu, M. T., and Gershon, M. D. (1994). NADPH diaphorase (nitric oxide synthase)–containing nerves in the enteropancreatic innervation: sources, co-stored neuropeptides, and pancreatic function. *J. Comp. Neurol. 342,* 115–130.

Kirkeby, H. J., Fahrenkrug, J., Holmquist, F., and Ottesen, B. (1992). Vasoactive intestinal polypeptide (VIP) and peptide histidine methionine (PHM) in human penile corpus cavernosum tissue and circumflex veins: localization and in vitro effects. *Eur. J. Clin. Invest.* **22,** 24–30.

Klarskov, P., Gerstenberg, T., and Hald, T. (1984). Vasoactive intestinal polypeptide influence in lower urinary tract smooth muscle from human and pig. *J. Urol.* **131,** 1000–1004.

Klemm, M. F., Wallace, D. J., and Hirst, G. D. S. (1997). Distribution of synaptic boutons around identified neurones lying in the cardiac plexus of the guinea-pig. *J. Autonom. Nerv. Syst.* **66,** 201–207.

Kluck, P. (1980). The autonomic innervation of the human urinary bladder, bladder neck and urethra: a histochemical study. *Anat. Rec.* **198,** 439–447.

Kondo, H. (1985). Immunohistochemical analysis of the localization of neuropeptides in the adrenal gland. *Arch. Histol. Jpn.* **48,** 453–481.

Konno, A., and Togana, K. (1979). Role of Vidian nerve in nasal allergy. *Ann. Oto-Laryngol.* **88,** 258–266.

Konturek, S. J., Kwiecien, N., Obtulowicz, W., Thor, P., Konturek, J. W., Popiela, T., and Oleksy, J. (1987). Vagal cholinergic control of gastric alkaline secretion in normal subjects and duodenal ulcer patients. *Gut* **28,** 739–744.

Konturek, J. W., Hengst, K., Kulesza, E., Gabryelewicz, A., Konturek, S. J., and Domschke, W. (1997a). Role of endogenous nitric oxide in the control of exocrine and endocrine pancreatic secretion in humans. *Gut* **40,** 86–91.

Konturek, J. W., Konturek, S. J., Pawlik, T., and Domschke, W. (1997b). Physiological role of nitric oxide in gallbladder emptying in men. *Digestion* **58,** 373–378.

Kopp, U. C., and Di Bona, G. F. (1993). The neural control of renal function. *In* "Nervous Control of the Urogenitial System" (C. A. Maggi, ed.), pp. 143–196. Harwood Academic, Chur.

Korf, H.-W. (1996). Innervation of the pineal gland. *In* "Autonomic-Endocrine Interactions" (K. Unsicker, ed.), pp.129–180. Harwood Academic, Amsterdam.

Krantis, A., Nichols, K., and Staines, W. (1998). Neurochemical characterization and distribution of enteric GABAergic neurons and nerve fibres in the human colon. *J. Auton. Nerv. Syst.* **68,** 33–42.

Kroutikova, 1. F. (1971). Details de la neuroarchitectonie du pancréas humain sous l'angle clinique. *Acta Anat.* **78,** 58–66.

Kuchiiwa, S., Kuchiiwa, T., Nakagawa, S., and Ushikawa, M. (1993). Oculomotor parasympathetic pathway to the accessory ciliary ganglion bypassing the main ciliary ganglion by way of the trigeminal nerve. *Neurosci. Res.* **18,** 79–82.

Kuchiiwa, S., Kuchiiwa, T., Nonaka, S., and Nakagawa, S. (1998). Facial nerve parasympathetic preganglionic afferents to the accessory otic ganglia by way of the chorda tympani nerve in the cat. *Anat. Embryol.* **197,** 377–382.

Kuchiiwa, S., Cheng, S. B., and Kuchiiwa, T. (2000). Morphological distinction between vasodilator and secretomotor neurons in the pterygopalatine ganglion of the cat. *Neurosci Lett.* **288,** 219–222.

Kulkarni, A. P., Getchell, T. V., and Getchell, M. L. (1994). Neuronal nitric oxide synthase is localized in extrinsic nerves regulating perireceptor processes in the chemosensory nasal mucosae of rats and humans. *J. Comp. Neurol.* **345,** 125–138.

Kummer, W. (1996). Innervation of paraganglia. *In* "Autonomic–Endocrine Interactions" (K. Unsicker, ed.), pp. 315–356. Harwood Academic, Amsterdam.

Kuntz, A. (1938). The structural organization of the celiac ganglia. *J. Comp. Neurol.* **69,** 1–12.

Kuntz, A. (1940). The structural organization of tlle inferior mesenteric ganglia. *J. Comp. Neurol.* **72,** 371–382.

Kuntz, A. (1945). "The Autonomic Nervous System," 3rd ed. Lea & Febiger, Philadelphia.

Kuntz, A., and Alexander, W. I. (1950). Surgical implications of lower thoracic and lumbar independent sympathetic pathways. *Arch. Surg. (Chicago)* **61,** 1007–1018.

Kuntz, A., and Richins, C. A. (1946). Components and distribution of the nerves of the parotid and submandibular glands. *J. Comp. Neurol.* **85,** 21–32.

Kuntz, A., Hoffman, H. H., and Jacobs, M. W. (1956). Nerve fiber components of communicating rami and sympathetic roots in man. *Anat. Rec.* **126,** 29–41.

Kuntz, A., Hoffman, H. H., and Napolitano, L. M. (1957). Cephalic sympathetic nerves. *Arch. Surg. (Chicago)* **75,** 108–115.

Kunze, W. A., and Furness, J. B. (1999). The enteric nervous system and regulation of intestinal motility. *Annu. Rev. Physiol.* **61,** 117–142.

Kusakabe, T., Matsuda, H., Kawakami, T., Syoui, N., Kurihara, K., Tsukuda, M., and Takenaka, T. (1997). Distribution of neuropeptide-containing nerve fibers in the human submandibular gland, with special reference to the difference between serous and mucous acini. *Cell Tissue Res.* **288,** 25–31.

Kyosola, K., Partenen, S., Kokkala, O., Merikallio, F., Pentilla, O., and Siltanen, P. (1976). Fluorescence histochemical and electron-microscopical observations on the innervation of the atrial myocardium of the adult human heart. *Virchow's Arch. A Pathol. Anat. Histol.* **371,** 101–119.

Laage-Hellman, J. E. and Stramblad, B. C. R. (1960). Secretion from human submaxillary gland after section of the chorda tympani. *J. Appl. Physiol.* **15,** 295–297.

Lacroix, J. S., Anggard, A., Hökfelt, T., O'Hare, M. M., Fahrenkrug, J., and Lundberg, J. M. (1990). Neuropeptide Y: presence in

sympathetic and parasympathetic innervation of the nasal mucosa. *Cell Tissue Res.* **259,** 119–128.
Laitinen, A., Partanen, M., Hervonen, A., Pelto-Huikko, M., and Laitinen, L. A. (1985). VIP-like immunoreactive nerves in human respiratory tract. Light and electron microscopic study. *Histochemistry* **82,** 313–320.
Lang, J. (1981). Topographical anatomy of the cranial nerves. *In* "The Cranial Nerves" (M. Samii and P. J. Jannetta, eds.), pp. 6–15. Springer-Verlag, Berlin.
Langley, J. N. (1921). "The Autonomic Nervous System," Part 1. Heffer, Cambridge.
Larsell, O., and Dow, S. (1933). The innervation of the human lung. *Am. J. Anat.* **52,** 125–146.
Larsell, O., and Fenton, R. (1928). The embryology and neurohistology of sphenopalatine ganglia connections: A contribution to the study of otalgia. *Laryngoscope* **38,** 371–389.
Larsson, O., Duner-Engstrom, M., Lundberg, J. M., Fredholm, B. B., and Anggard, A. (1986). Effects of VIP, PHM and substance P on blood vessels and secretory elements of the human submandibular gland. *Regul. Peptides* **13,** 319–326.
Lasowsky, J. M. (1930). Normale und pathologische histologie der Herzganglien des Menschen. *Virchow's Arch. A Pathol. Anat. Physiol.* **279,** 464–485.
Lautt, W. W. (1980). Hepatic nerves: a review of their functions and effects. *Can. J. Physiol. Pharmacol.* **58,** 105–123.
Lautt, W. W. (1983). Afferent and efferent neural roles in liver function. *Prog. Neurobiol.* **21,** 323–348.
Leceta, J., Martinez, C., Delgado, M., Garrido, E., and Gomariz, R. P. (1996). Expression of vasoactive intestinal peptide in lymphocytes: a possible endogenous role in the regulation of the immune system. *Adv. Neuroimmunol.* **6,** 29–36.
Leone, A. M., Wiklund, N. P., Hokfelt, T., Brundin, L., and Moncada, S. (1994). Release of nitric oxide by nerve stimulation in the human urogenital tract. *Neuroreport* **5,** 733–736.
Levy, M. N. (1984). Cardiac sympathetic—parasympathetic interactions. *Fed. Proc.* **43,** 2598–2602.
Levy, M. N., Martin, P. J., and Stuesse, S. L. (1981). Neural regulation of the heart beat. *Annu. Rev. Physiol.* **43,** 443–453.
Lincoln, J., and Burnstock, G. (1993). Autonomic innervation of the urinary bladder and urethra. *In* "Nervous Control of the Urogenital System" (C. A. Maggi, ed.), pp. 33–68. Harwood Academic, Chur.
Lincoln, J., Crowe, R., Bokor, J., Light, J. K., Chilton, C. P., and Burnstock, G. (1986). Adrenergic and cholinergic innervation of the smooth and striated muscle components of the urethra from patients with spinal cord injury. *J. Urol.* **135,** 402–408.
Linder, L., Lautenschlager, B. M., and Haefeli, W. E. (1996). Subconstrictor doses of neuropeptide Y potentiate alpha 1-adrenergic venoconstriction in vivo. *Hypertension* **28,** 483–487.
Linnoila, R. 1., and Diaugustine, R. P. (1980). Distribution of [Met^5]- and [Leu^5]-enkephalin-, vasoactive intestinal polypeptide- and substance P-like immunoreactivities in human adrenal glands. *Neuroscience* **5,** 2247–2259.
Lissauer, M. (1909). Uber die Lage der Ganglienzellen des menschlichen Herzens. *Arch. Mikrosk. Anat.* **74,** 217–222.
List, C. F., and Peet, M. M. (1938). Sweat secretion in man. IV. Sweat secretion of the face and its distribution. *Arch. Neurol. Psychol.* **40,** 443–470.
Llewellyn-Smith, I. J., Furness, J. B., O'Brien, P. E., and Costa, M. (1984). Noradrenergic nerves in human small intestine. Distribution and ultrastructure. *Gastroenterology* **87,** 513–529.
Lograno, M. D., and Reibaldi, A. (1986). Receptor responses in fresh human ciliary muscle. *Br. J. Pharmacol.* **87,** 379–385.
Luckensmeyer, G. B., and Keast, J. R. (1996). Immunohistochemical characterisation of viscerofugal neurons projecting to the inferior mesenteric and major pelvic ganglia in the male rat. *J. Auton. Nerv. Syst.* **61,** 6–16.
Luckensmeyer, G. B., and Keast, J. R. (1998). Characterisation of the adventitial rectal ganglia in the male rat by their immunohistochemical features and projections. *J. Comp. Neurol.* **396,** 429–441.
Ludmer, P. L., Selwyn, A. P., Shook, T. L., Wayne, R. R., Mudge, G. H., Alexander, R. W., and Ganz, P. (1986). Paradoxical vasoconstriction induced by acetylcholine in atherosclerotic coronary arteries. *N. Engl. J. Med.* **315,** 1046–1051.
Luiking, Y. C., Weusten, B. L., Portincasa, P., Van Der Meer, R., Smout, A. J., and Akkermans, L. M. (1998). Effects of long-term oral L-arginine on esophageal motility and gallbladder dynamics in healthy humans. *Am. J. Physiol.* **274,** G984–G991.
Lundberg, J., Norgren, L., Ribbe, E., Rosen, I., Steen, S., Thorne, J., and Wallin, B. G. (1989). Direct evidence of active sympathetic vasodilatation in the skin of the human foot. *J. Physiol. (Lond)* **417,** 437–446.
Lundberg, J. M. (1981). Evidence for coexistence of vasoactive intestinal polypeptide (VIP) and acetylcholine in neurons of cat exocrine glands. Morphological, biochemical and functional studies. *Acta Physiol. Scand.* **112,** Suppl. 496, 1–57.
Lundberg, J. M., Hamberger, B., Schultzberg, M., Hökfelt, T., Granberg, P.-O., Efendic, S., Terenius. L., Goldstein, M., and Luft, R. (1979). Enkephalin- and somatostatin-like immunoreactivities in human adrenal medulla and pheochromocytoma. *Proc. Natl. Acad. Aci. U.S.A.* **76,** 4079–4083.
Lundberg, J. M., Terenius, L., Hökfelt, T., Martling, C. R., Tatemoto, K., Mutt, V., Polak, J., Bloom. S., and Goldstein, M. (1982). Neuropeptide Y (NPY)–like immunoreactivity in peripheral noradrenergic neurons and effects of NPY on sympathetic function. *Acta Physiol. Scand.* **116,** 477–480.
Lundberg, J. M., Terenius, L., Hökfelt. T., and Goldstein, M. (1983). High levels of neuropeptide Y in peripheral noradrenergic neurons in various mammals including man. *Neurosci. Lett.* **42,** 167–172.
Lundberg, J. M., Fahrenkrug, J., Hökfelt. T., Martling, C.-R., Larsson, O., Tatemoto, K., and Änggård, A. (1984). Coexistence of peptide HI (PHI) and VIP in nerves regulating blood flow and bronchial smooth muscle tone in various mammals including man. *Peptides* **5,** 593–606.
Lundberg, J. M. . Torsell, L., Sollevi, A., Pernow, J., Theodorsson Norheim, E., Änggård, A., and Hamberger, B. (1985). Neuropeptide Y and sympathetic vascular control in man. *Regul. Peptides* **13,** 41–52.
Lundberg, J. M., Lundblad. L., Martling, C.-R., Saria, A., Stjärne, P., and Änggård, A. (1987). Coexistence of multiple peptides and classic transmitters in airway neurons: functional and pathophysiologic aspects. *Am. Rev. Respir. Dis.* **136,** S16–S22.
Luts, A., Uddman, R., Alm, P., Basterra, J., and Sundler, F. (1993). Peptide-containing nerve fibers in human airways: distribution and coexistence pattern. *Int. Arch. Allergy Immunol.* **101,** 52–60.
Luts, L., Bergenfelz, A., Alumets, J., and Sundler, F. (1995). Peptide-containing nerve fibres in normal human parathyroid glands and in human parathyroid adenomas. *Eur. J. Endocrinol.* **133,** 543–551.
Lynch, E. M., Wharton, J., Bryant, M. G., Bloom, S. R., Polak, J. M., and Elder, M. G. (1980). The differential distribution of vasoactive intestinal polypeptide in the normal human female genital tract. *Histochemistry* **67,** 169–177.
Macefield, V. G., and Wallin, B. G. (1996). The discharge behaviour of single sympathetic neurones supplying human sweat glands. *J. Autonom. Nerv. Syst.* **61,** 277–286.
Macefield, V. G., and Wallin, B. G. (1999). Respiratory and cardiac modulation of single sympathetic vasoconstrictor and sudomotor neurones to human skin. *J. Physiol. (Lond.)* **516,** 303–314.

Maciel, B. C., Gallo, L., Neto, J. A. and Martins, L. E. B. (1987). Autonomic nervous control of the heart rate during isometric exercise in normal man. *Pflueger's Arch.* **408,** 173–177.

Maggi, C. A., ed. (1993) "Nervous Control of the Urogenital System." Harwood Academic, Chur.

Magielski. J. E., and Blatt, I. M. (1958). Submaxillary salivary flow: a test of chorda tympani nerve function as an aid in diagnosis and prognosis of facial nerve paralysis . *Laryngoscope* **68,** 1770–1789.

Makhlouf, G. M., and Schultz, S. G., eds. (1989). "Handbook of Physiology, Section 6: The Gastrointestinal System; Vol. 2, Neural and Endocrine Biology." American Physiology Society, Bethesda.

Malbert, C. H., Mathis, C., and Laplace, J. P. (1995). Vagal control of pyloric resistance. *Am. J. Physiol.* **269,** G558–G569.

Marfurt, C. F., and Ellis, L. C. (1993). Immunohistochemical localization of tyrosine hydroxylase in corneal nerves. *J. Comp. Neurol.* **336,** 517–531.

Marin, M. G. (1986). Pharmacology of airway secretion. *Pharmacol. Rev.* **38,** 273–289.

Marongiu, L., Perra, M. T., Pinna, A. D., Sirigu, F., and Sirigu, P. (1993). Peptidergic (VIP) nerves in normal human pancreas and in pancreatitis: an immunohistochemical study. *Histol. Histopathol.* **8,** 127–132.

Marron, K., Wharton, J., Sheppard, M. N., Fagan, D., Royston, D., Kuhn, D. M., de Leval, M. R., Whitehead, B. F., Anderson, R. H., and Polak, J. M. (1995). Distribution, morphology, and neurochemistry of endocardial and epicardial nerve terminal arborizations in the human heart. *Circulation* **92,** 2343–2351.

Marshall, J. M. (1970). Adrenergic innervation of the female reproductive tract: anatomy, physiology and pharmacology. *Ergeb. Physiol. Biol. Chem. Exp. Pharmakol.* **62,** 6–67.

Martin, C. E., Shaver, J. A., Leon, D. F., Thompson, M. E., Reddy, P. S., and Leonard, J. J. (1974). Autonomic mechanisms in hemodynamic responses to isometric exercise. *J. Clin. Invest.* **54.** 104–115.

Martling, C. R., Änggård, A., and Lundberg, J. M. (1985). Non-cholinergic vasodilation in the tracheo-bronchial tree of the cat induced by vagal nerve stimulation. *Acta Physiol. Scand.* **125,** 343–346.

Mathias, C. J., Chaudhuri, K.R., and Thomaides, T. (1996). Neural control of the gastrointestinal circulation. *In* "Nervous Control of Blood Vessels" (T. Bennett and S. M. Gardiner, eds.), pp. 435–464. Harwood Academic, Amsterdam.

Matini, P., Faussone-Pellegrini, M. S., Cortesini, C., and Mayer, B. (1995). Vasoactive intestinal polypeptide and nitric oxide synthase distribution in the enteric plexuses of the human colon: an histochemical study and quantitative analysis. *Histochem. Cell. Biol.* **103,** 415–423.

Matsuda, H., Kusakabe, T., Kawakami, T., Nagahara, T., Takenaka, T., and Tsukuda, M. (1997). Neuropeptide-containing nerve fibres in the human parotid gland: a semiquantitative analysis using an antibody against protein gene product 9.5. *Histochem. J.* **29,** 539–544.

Mawe, G.M.. (1995). Prevertebral, pancreatic and gallbladder ganglia: non-enteric ganglia that are involved in gastrointestinal function. *In* "Autonomic Ganglia" (E. M. McLachlan, ed.), pp. 397–444, Harwood Academic, Luxembourg.

May, P. J., and Warren, S. (1993). Ultrastructure of the macaque ciliary ganglion. *J. Neurocytol.* **22,** 1073–1095.

McKirdy, H. C., McKirdy, M. L., Lewis, M. J., and Marshall, R. W. (1992). Evidence for involvement of nitric oxide in the non-adrenergic non-cholinergic (NANC) relaxation of human lower oesophageal sphincter muscle strips. *Exp. Physiol.* **77,** 509–511.

McKirdy, M. L., McKirdy, H. C., and Johnson, C. D. (1994). Non-adrenergic non-cholinergic inhibitory innervation shown by electrical field stimulation of isolated strips of human gall bladder muscle. *Gut* **35,** 412–416.

Melander, A., Ericson, L. E., Ljungeren, J.-G., Norbert, K.-A., Persson, B., Sundler, F., Tibbin, S., and Westgren, U. (1974). Sympathetic innervation of the normal human thyroid. *J. Clin. Endocrinol. Metab.* **39,** 713–718.

Mellander. S., Andersson, P.-O., Afzelius, L.-E., and Hellstrand, P. (1982). Neural beta-adrenergic dilatation of the facial vein in man. Possible mechanism in emotional blushing. *Acta Physiol. Scand.* **114,** 393–399.

Meyer, G. W, Gerhardt, D. C., and Castell, D. O. (1981). Human esophageal response to rapid swallowing: muscle refractory period of neural inhibition? *Am. J. Physiol.* **241,** G129–G136.

Meyer, J. H. (1987). Motility of the stomach and gastroduodenal junction. *In* "Physiology of the Gastrointestinal Tract" (L. R. Johnson, ed.), 2nd Ed., pp. 613–629. Raven Press, New York.

Meyrick, B., and Reid, L. (1970). Ultrastructure of cells in the human bronchial submucosal glands. *J. Anat.* **107,** 281–299.

Michalkiewicz, M., Huffman, L. J., Dey, M., and Hedge, G. A. (1994). Immunization against vasoactive intestinal peptide does not affect thyroid hormone secretion or thyroid blood flow. *Am. J. Physiol.* **266,** E905–E913.

Miller, A. S., Coster, D. J., Costa, M.. and Furness. J. B. (1983). Vasoactive intestinal polypeptide immunoreactive nerve fibres in the human eye. *Aust. J. Ophthalmol.* **11,** 185–193.

Minami Y., Kimura H., Aimi Y., and Vincent S. R. (1994). Projections of nitric oxide synthase-containing fibers from the sphenopalatine ganglion to cerebral arteries in the rat. *Neuroscience.* **60,** 745–759.

Mitchell, G. A. G. (1935). The innervation of the kidney, ureter, testicle and epididymis. *J. Anat.* **70,** 10–32.

Mitchell, G. A. G. (1953a). "Anatomy of the Autonomic Nervous System." Livingstone, Edinburgh.

Mitchell, G. A. G. (1953b). The innervation of the heart. *Br. Heart J.* **15,** 159–171.

Mitchell, G. A. G. (1953c). The cranial extremities of the svmpathetic trunks. *Acta Anat.* **18,** 195–201.

Mitchell, G. A. G. (1954). The autonomic nerve supply of the throat, nose and ear. *J. Laryngol.* **68,** 495–516.

Montagna, W., Yun, J., Ore, B., Formisano. V., and Ri, P. (1964). Histological cytochemistry of human skin. 30. Cholinesterase-containing nerves in the face. *J. Invest. Dermatol.* **90,** 526–529.

Moore, M. C., and Cherrington, A. D. (1996). Regulation of net hepatic glucose uptake: interaction of neural and pancreatic mechanisms. *Reprod. Nutr. Dev.* **36,** 399–406.

Morris, J. L. (1997). Autonomic vasoconstriction in the skin. *In* "Autonomic Innervation of the Skin," (J. L. Morris and I. L. Gibbins, eds.), pp. 57–86. Harwood Academic, Amsterdam.

Morris, J. L., and Gibbins, I. L. (1992). Co-transmission and neuromodulation. *In* "Autonomic Neuroeffector Mechanisms" (G. Burnstock and C. H. V. Hoyle, eds.), pp. 33–119. Harwood Academic, Chur.

Morris J. L., Kondo M., and Gibbins I. L. (1997) Selective innervation of different target tissues in guinea-pig cranial exocrine glands by sub-populations of parasympathetic and sympathetic neurons. *J. Auton. Nerv. Syst.* **66,** 75–86.

Morris, M. J., Elliott, J. M., Cain, M. D.. Kapoor, V., West, M. J., and Chalmers, J. P. (1986). Plasma neuropeptide Y levels rise in patients undergoing exercise tests for the investigation of chest pain. *Clin. Exp. Pharmacol. Physiol.* **13,** 437–440.

Nadel, J. A. (1980). Autonomic regulation of airway smooth muscle. *In* "Physiology and Pharmacology of the Airways" (J. A. Nadel, ed.), pp. 217–258. Marcel Dekker, New York.

Nadel, J. A., and Widdicombe, J. G. (1963). Reflex control of airway size. *Ann. N. Y. Acad. Sci.* **109,** 712–722.

Nakano, H., Furukawa, Y., Inoue, Y., Sawaki, S., Oguchi, T., and Chiba, S. (1998). Right ventricular responses to vagus stimulation

of fibers to discrete cardiac regions in dog hearts. *J. Auton. Nerv. Syst.* **74,** 179–188.

Narita, S., and Watanabe, M. (1982). Response of isolated rat iris dilator to adrenergic and cholinergic agents and electrical stimulation. *Life Sci.* **30,** 1211–1218.

Neuhuber, W. L., Appelt, M., Polak, J. M., Baier-Kustermann, W., Abelli, L., and Ferri, G. L. (1993). Rectospinal neurons: cell bodies, pathways, immunocytochemistry and ultrastructure. *Neuroscience* **56,** 367–378.

Nichols, K., Staines, W., and Krantis, A. (1994). Neural sites of the human colon colocalize nitric oxide synthase-related NADPH diaphorase activity and neuropeptide Y. *Gastroenterology* **107,** 968–975.

Nilsson, B., Theodorsson, E., Jivegard, L., Thune, A., Friman, S., and Svanvik, J. (1994). VIP-antiserum inhibits fluid secretion by the inflamed gallbladder mucosa. *Regul. Peptides* **49,** 179–184.

Nilsson, B., Delbro, D., Friman, S., Thune, A., and Svanvik, J. (1996a). Sympathetic and VIP-ergic control of calcium and bicarbonate transport in the feline gall bladder mucosa in vivo. *J. Auton. Nerv. Syst.* **60,** 49–55.

Nilsson, B., Delbro, D., Hedin, L., Conradi, N., Thune, A., Friman, S., Wennmalm, A., Yan, Z. Q., and Svanvik, J. (1996b). Role of nitric oxide in induction of inflammatory fluid secretion by the mucosa of the feline gallbladder. *Gastroenterology* **110,** 598–606.

Nilsson S. F. E. (2000). The significance of nitric oxide for parasympathetic vasodilation in the eye and other orbital tissues in the cat. *Exp. Eye Res.* **70,** 61–72.

Nobin, A., Baumgarten, H. G., Falck, B., Ingemansson, S., Moghimzadeh, E., and Rosengren, E. (1978). Organization of the sympathetic innervation in liver tissue from monkey and man. *Cell Tissue Res.* **195,** 371–380.

Nomura, Y., and Matsuura, T. (1972). Distribution and clinical significance of the autonomic nervous system in the human nasal mucosa. *Acta Oto-Laryngol.* **73,** 493–501.

Nomura, Y., and Smelser, G. K. (1974). The identification of adrenergic and cholinergic nerve endings in the trabecular meshwork. *Invest. Ophthalmol.* **13,** 525–532.

Nonogaki, K. (2000). New insights into sympathetic regulation of glucose and fat metabolism. *Diabetologia* **43,** 533–549.

Nordin, M. (1990). Sympathetic discharges in the human supraorbital nerve and their relation to sudo- and vasomotor responses. *J. Physiol. (Lond)* **423,** 241–255.

Nozaki, K., Moskowitz, M. A., Maynard, K. I., Koketsu, N., Dawson, T. M., Bredt, D. S., and Snyder, S. H. (1993). Possible origins and distribution of immunoreactive nitric oxide synthase–containing nerve fibers in cerebral arteries. *J Cereb. Blood Flow Metab.* **13,** 70–79.

Okamoto, T., Iwase, S., Sugenoya, J., Mano, T., Sugiyama, Y., and Yamamoto, K. (1994). Different thermal dependency of cutaneous sympathetic outflow to glabrous and hairy skin in humans [published erratum appears in Eur J Appl Physiol 1994;69(3):276]. *Eur. J. Appl. Physiol.* **68,** 460–464.

O'Kelly, T., Brading, A., and Mortensen, N. (1993). Nerve mediated relaxation of the human internal anal sphincter: the role of nitric oxide. *Gut* **34,** 689–693.

Okita, W., and Ichimura, K. (1998). Contribution of nitric oxide and sensory transmitters to non-adrenergic, non-cholinergic innervation of nasal blood vessels. *Acta Otolaryngol. Suppl* **539,** 76–78.

Orfanos, C. E., and Mahrle, G. (1973). Ultrastructure and cytochemistry of human cutaneous nerves. *J. Invest. Dermatol.* **61,** 108–120.

Osamura, R. Y., Tsutsumi, Y., Yanaihara, N., Imura, H., and Watanabe, K. (1987). Immunohistochemical studies for multiple peptide immunoreactivities and colocalization of met-enkephalin-Arg^{6}–Gly^{7}-Leu^{8}, neuropeptide Y and somatostatin in human adrenal medulla and pheochromocytomas. *Peptides (N. Y.)* **8,** 77–87.

Ottesen, B. (1983). Vasoactive intestinal polypeptide as a neurotransmitter in the female genital tract. *Am. J. Obstet. Cynecol.* **147,** 208–224.

Ottesen, B., Ulrichsen, H., Fahrenkrug, J., Larsen, J. J., Wagner, G., Schierup, L., and Söndergaard, F. (1982). Vasoactive intestinal polypeptide and the female genital tract-relationships to reproductive phase and delivery. *Am. J. Obstet. Gynecol.* **143,** 414–420.

Ottesen, B., Söndergaard, F., and Fahrenkrug, J. (1983). Neuropeptides in the regulation of female genital smooth muscle contractility. *Acta Obstet. Gynecol. Scand.* **62,** 591–592.

Owman, C., Roengren, E., and Sjöberg, N.-O. (1967). Adrenergic innervation of the human female reproductive organs: a histochemical and chemical investigation. *Obstet. Gynecol. (Amsterdam)* **30,** 763–773.

Owman, C., Alm, P., and Sjöberg, N.-O. (1983). Pelvic autonomic ganglia: structure, transmitters, function and steroid influence. *In* "Autonomic Ganglia" (L.-G. Elfvin, ed.), pp. 125–143. Wiley, Chichester.

Palmer, J. B. D., Cuss, F. M., and Barnes, P. J. (1986). VIP and PHM and their role in nonadrenergic inhibitory responses in isolated human airways. *J. Appl. Physiol.* **61,** 1322–1328.

Palmer, J. P., Werner, P. L., Hollander, P., and Ensink, J. W. (1979). Evaluation of the control of glucagon secretion by the parasympathetic nervous system in man. *Metab. Clin. Exp.* **28,** 549–552.

Parker, T. L. (1996). Innervation of the adrenal medulla. *In* "Autonomic–Endocrine Interactions" (K. Unsicker, ed.), pp. 289–314. Harwood Academic, Amsterdam.

Parkin, G. J. S., Smith, R. B., and Johnson, D. (1973). Gallbladder volume and contractility after truncal, selective and highly selective (parietal wall) vagotomy in man. *Ann. Surg.* **178,** 581–586.

Parkinson, D. (1988). Further observations on the sympathetic pathway to the pupil. *Anat. Rec.* **220,** 108–109.

Parkinson, D., Johnson, J. A., and Chaudhuri, A. (1978). Sympathetic connections of the fifth and sixth cranial nerves. *Anat. Rec.* **191,** 221–226.

Partanen, M., Laitinen, A., Hervonen, A., Toivanen, M., and Laitinen, L. A. (1982). Catecholamine- and acetylcholinesterase-containing nerves in human lower respiratory tract. *Histochemistry* **76,** 175–188.

Paterson, C. A., Anvari, M., Tougas, G., and Huizinga, J. D. (2000). Determinants of occurrence and volume of transpyloric flow during gastric emptying of liquids in dogs: importance of vagal input. *Dig. Dis. Sci.* **45,** 1509–1516.

Pauza, D. H., Skripka, V., Pauziene, N., and Stropus, R. (2000). Morphology, distribution, and variability of the epicardiac neural ganglionated subplexuses in the human heart. *Anat. Rec.* **259,** 353–382.

Pearson, J., and Pytel, B. (1978a). Quantitative studies of sympathetic ganglia and spinal cord intermedio-lateral gray columns in familial dysautonomia. *J. Neurol. Sci.* **39,** 47–59.

Pearson, J., and Pytel, B. (1978b). Quantitative studies of ciliary and sphenopalatine ganglia in familial dysautonomia. *J. Neurol. Sci.* **39,** 123–130.

Peduzzi, P., Simper, D., Linder, L., Strobel, W. M., and Haefeli, W. E. (1995). Neuropeptide Y in human hand veins: pharmacologic characterization and interaction with cyclic guanosine monophosphate-dependent venodilators in vivo. *Clin. Pharmacol. Therap.* **58,** 675–683.

Perez, G. M., and Keyser, R. B . (1987). Cell body counts in human ciliary ganglia. *Invest. Ophthalmol. Visual Sci.* **27,** 1428–1431.

Perman, E. (1924). Anatomische Untersuchungen über die Herzennerven bei den hoheren Saugetieren und beim Menschen *Z. Ges. Anat.* **71,** 382–457.

Pernow, J., and Lundberg, J. (1986). Neuropeptide Y constricts human skeletal muscle arteries via a nifedipine sensitive mechanism independent of extracellular calcium. *Acta Physiol. Scand.* **128,** 655–656.

Pernow, J., Lundberg, J. M., Kaijser, L., Hjemdahl, P., Theodorsson-Norheim, E., Martinsson, A., and Pernow, B. (1986). Plasma neuropeptide Y-like immunoreactivity and catecholamines during various degrees of sympathetic activation in man. *Clin. Physiol.* **6,** 561–578.

Phaosawasdi, K., Malmud, L. S., Tolin, R. D., Stelzer, F., Applegate, G., and Fisher, R. S. (1981). Cholinergic effects on esophageal transit and clearance. *Gastroenterology* **81,** 915–920.

Pick, J. (1970). "The Autonomic Nervous System: Morphological, Comparative, Clinical and Surgical Aspects." Lippincott, Philadelphia.

Pick, J., and Sheehan, D. (1946). Sympathetic rami in man. *J. Anat.* **80,** 12–20.

Pick, J., De Lemos, C., and Gerdin, C. (1964). The fine structure of sympathetic neurons in man. *J. Comp. Neurol.* **122,** 19–68.

Pickering, T. G., Gribbin, B., Petersen, E. S., Cunningham, D. J. C., and Sleight, P. (1972). Effect of autonomic blockade on the baroreflex in man at rest and during exercise. *Circ. Res.* **30,** 177–185.

Pique, J. M., Esplugues, J. V., and Whittle, B. J. (1992). Endogenous nitric oxide as a mediator of gastric mucosal vasodilatation during acid secretion. *Gastroenterology* **102,** 168–174.

Polak, J. M., Mina, S., Gu, J., and Bloom, S. R. (1981). VIPergic nerves in the penis. *Lancet* **2.** 217–219.

Porter, A. J., Wattchow, D. A., Brookes, S. J. H., Schemann, M., and Costa, M. (1996). Choline acetyltransferase immunoreactivity in the human small and large intestine. *Gastroenterology* **111,** 401–408.

Porter, A. J., Wattchow, D. A., Brookes, S. J., and Costa, M. (1997). The neurochemical coding and projections of circular muscle motor neurons in the human colon. *Gastroenterology* **113,** 1916–1923.

Porter, A. J., Wattchow, D. A., Brookes, S. J., and Costa, M. (1999). Projections of nitric oxide synthase and vasoactive intestinal polypeptide–reactive submucosal neurons in the human colon. *J. Gastroenterol. Hepatol.* **14,** 1180–1187.

Potter, E. K. (1985). Prolonged noradrenergic inhibition of cardiac vagal action following sympathetic stimulation: neuromodulation by neuropeptide Y? *Neurosci. Lett.* **54,** 117–121.

Preiksaitis, H. G., Tremblay, L., and Diamant, N. E. (1994). Nitric oxide mediates inhibitory nerve effects in human esophagus and lower esophageal sphincter. *Dig. Dis. Sci.* **39,** 770–775.

Priola, D. V., Cao, X. L., Anagnostelis, C., and Bassenge, E. (1998). Intrinsic neural regulation of the heart in the chronic, conscious dog. *Am. J. Physiol.* **43,** H2074–H2084.

Prystowsky, E. N., Jackman, W. M. Rinkenberger, R. L., Heger, J. J., and Zipes, D. P. (1981). Effect of autonomic blockade on ventricular refractoriness and atrioventricular nodal conduction in humans: evidence supporting a direct cholinergic action on ventricular muscle refractoriness. *Circ. Res.* **49,** 511–518.

Przewlocki, R., Gramsch, C., Pasi, A., and Herz, A. (1983). Characterization and localization of immunoreactive dynorphin, alpha-neo-endorphin, met-enkephalin and substance P in human spinal cord. *Brain Res.* **280,** 95–103.

Purves, D., and Wigston, D. J. (1983). Neural units in the superior cervical ganglion of the guinea-pig. *J. Physiol. (Lond.)* **334,** 169–178.

Quan, K. J., Lee, J. H., Geha, A. S., Biblo, L. A., Van Hare, G. F., Mackall, J. A., and Carlson, M. D. (1999). Characterization of sinoatrial parasympathetic innervation in humans. *J. Cardiovasc. Electrophysiol.* **10,** 1060–1065.

Quartu, M., Polak, J. M., and Del Fiacco, M. (1993). Neuropeptides in the human celiac/superior mesenteric ganglionic complex: an immunohistochemical study. *J. Chem. Neuroanat.* **6,** 79–99.

Racchi, H., Schliem, A. J., Donoso, M. V., Rahmer, A., Zuniga, A., Guzman, S., Rudolf, K., and Huidobro-Toro, J. P. (1997). Neuropeptide Y Y1 receptors are involved in the vasoconstriction caused by human sympathetic nerve stimulation. *Eur. J. Pharmacol.* **329,** 79–83.

Racchi, H., Irarrazabal, M. J., Howard, M., Moran, S., Zalaquett, R., and Huidobro-Toro, J. P. (1999). Adenosine 5′-triphosphate and neuropeptide Y are co-transmitters in conjunction with noradrenaline in the human saphenous vein. *Br. J. Pharmacol.* **126,** 1175–1185.

Ramaswamy, S., Shankar, S. K., Manjunath, K. Y., Devanathan, P. H., and Nityaseelan, N. (1994). Ultrastructure of the ganglion on human internal laryngeal nerve. *Neurosci. Res.* **18,** 283–290.

Ramón y Cajál, S. (1911). "Histologie du systeme nerveux de l'homme et des vertebres." Institute Ramón y Cajál, Madrid (2nd ed., 1972).

Randall, D. C., Brown, D. R., Li, S. G., Olmstead, M. E., Kilgore, J. M., Sprinkle, A. G., Randall, W. C., and Ardell, J. L. (1998). Ablation of posterior atrial ganglionated plexus potentiates sympathetic tachycardia to behavioral stress. *Am. J. Physiol.* **44,** R779–R787.

Randall, W. C., Wurster, R. D., Duff, M., O'Toole, M. F., and Wehrmacher, W. (1991). Surgical interruption of postganglionic innervation of the sinoatrial nodal region. *J. Thorac. Cardiovasc. Surg.* **101,** 66–74.

Randall, W. C., Cox, J. W., Alexander, W. F., and Coldwater, K. E. (1955). Direct examination of the sympathetic outflows in man. *J. Appl. Physiol.* **7,** 688–698.

Rash, R. M., and Thomas, M. D. (1962). The intrinsic innervation of the gastro-oesophageal and pyloro-duodenal junctions. *J. Anat.* **96,** 389–396.

Ray, B. S., Hinsey, J. C., and Geohegan, W. A. (1943). Observations on the distribution of the sympathetic nerves to the pupil and upper extremity as determined by stimulation of the anterior roots in man. *Ann. Surg.* **118,** 647–655.

Rechardt, L., Aalto-Setala, K., Purjeranta, M., Pelto-Huikko, M., and Kyosola, K. (1986). Peptidergic innervation of human atrial myocardium: an electron microscopical and immunocytochemical study. *J. Auton. Nerv. Syst.* **17,** 21–32.

Reed, A. S., Tschakovsky, M. E., Minson, C. T., Halliwill, J. R., Torp, K. D., Nauss, L. A., and Joyner, M. J. (2000). Skeletal muscle vasodilatation during sympathoexcitation is not neurally mediated in humans. *J. Physiol. (Lond.)* **525,** 253–262.

Reichert, F. L., and Poth, E. J. (1933). Pathways for the secretory fibres for the salivary glands in man. *Proc. Soc. Exp. Biol. Med.* **30,** 973–977.

Reubi, J. C., Horisberger, U., Kappeler, A., and Laissue, J. A. (1998). Localization of receptors for vasoactive intestinal peptide, somatostatin, and substance P in distinct compartments of human lymphoid organs. *Blood* **92,** 191–197.

Richards, W. G., Stamler, J. S., Kobzik, L., and Sugarbaker, D. J. (1995). Role of nitric oxide in human esophageal circular smooth muscle in vitro. *J. Thorac. Cardiovasc. Surg.* **110,** 157–164.

Richardson, J. B. (1983). Recent progress in pulmonary innervation. *Am. Rev. Respir. Dis.* **128,** Suppl. S65–S68.

Richardson, J. B., and Beland, J. (1976). Non-adrenergic inhibitory nerves in human airways. *J. Appl. Physiol.* **41,** 764–771.

Richardson, J. B., and Ferguson, C. C. (1980). Morphology of the airways. *In* "Physiology and Pharmacology of the Airways" (J. A. Nadel, ed.), pp. 1–30. Marcel Dekker, New York.

Richter, C. P., and Otenasek, F. J. (1946). Thoracolumbar sympathectomies examined with the electrical skin resistance method. *J. Neurosurg.* **3,** 120–134.

Riederer, A., Fischer, A., Knipping, S., Unger, J., Lange, W., and Kastenbauer, E. (1996). Basic innervation pattern and distribution of classic autonomic neurotransmitters in human nasal mucosal vasculature. *Laryngoscope* **106,** 286–291.

Riederer, A., Held, B., Mayer, B., and Worl, J. (1999). Histochemical and immunocytochemical study of nitrergic innervation in human nasal mucosa. *Ann. Otol. Rhinol. Laryngol.* **108,** 869–875.

Riedl, B., Nischik, M., Birklein, F., Neudorfer, B., and Handwerker, H. O. (1998). Spatial extension of sudomotor axon reflex sweating in human skin. *J. Autonom. Nerv. Syst.* **69,** 83–88.

Robinson, S., Perry, M., Bruekman, R. F., Nicholas, J. R., and Miller, D. I. (1953). Effects of atropine on heart rate and oxygen intake in working man. *J. Appl. Physiol.* **5,** 508–512.

Roddie, I. C., and Shepherd. J. T. (1963). Nervous control of the circulation in skeletal muscle. *Br. Med. Bull.* **19,** 115–119.

Roman, C., and Gonella, J. (1987). Extrinsic control of digestive tract motility. *In* "Physiology of the Gastrointestinal Tract" (L. R. Johnson, ed.), 2nd Ed., pp. 507–553. Raven Press, New York.

Romeo, H. E., Solveyra, C. G., Vacas, M. 1., Rosenstein, R. E., Barontini, M., and Cardinali. D. P. (1986). Origins of the sympathetic preojections to rat thyroid and parathyroid glands. *J. Auton. Nerv. Syst.* **17,** 63–70.

Rosen, S. (1950). The tympanic plexus. *Arch. Otolaryngol.* **52,** 15–18.

Rossoni, R. D., Machado, A. B., and Machado, C. R. S. (1979). A histochemical study of catecholamines and cholinesterases in the autonomic nerves of the human minor salivary glands. *Histochem. J.* **11,** 661–668.

Rothe, C. F. (1983). Reflex control of veins and vascular capacitance. *Physiol. Rev.* **63,** 1281–1342.

Rowell, L. B. (1977). Reflex control of cutaneous vasculature. *J. Invest. Dermatol.* **69,** 154–166.

Rowell, L. B. (1981). Active neurogenic vasodilatation in man. *In* "Vasodilatation" (P. M. Vanhoutte and I. Leussen, eds), pp. 1–17. Raven Press, New York.

Rump, L. C., and von Kugelgen, I. (1994). A study of ATP as a sympathetic cotransmitter in human saphenous vein. *Br. J. Pharmacol.* **111,** 65–72.

Ruskell, G. L. (1970a). The orbital branches of the pterygo-palatine ganglion and their relationship with internal carotid nerve branches in primates. *J. Anat.* **106,** 323–339.

Ruskell, G. L. (1970b). An ocular parasympathetic pathway of facial nerve origin and its influence on intraocular pressure. *Exp. Eye Res.* **10,** 319–330.

Ruskell, G. L. (1971). The distribution of autonomic post-ganglionic nerve fibres to the lacrimal gland in monkeys. *J. Anat.* **109,** 229–242.

Ruskell, G. L. (1985). Facial nerve distribution to the eye. *Am. J. Optom. Physiol. Opt.* **62,** 793–798.

Ruskell, G. L., and Simons. T. (1987). Trigeminal nerve pathways to the cerebral arteries in monkey. *J. Anat.* **155,** 23–37.

Russell, R. C. G., Thompson. J. P. S., and Bloom, S. R. (1974). The effect of truncal and selective vagotomy on the release of pancreatic glucagon, insulin and enteroglucagon. *Br. J. Surg.* **61,** 821–824.

Ryan, J. P. (1987). Motility of the gallbladder. *In* "Physiology of the Digestive Tract" (L. R. Johnson, ed.), 2nd Ed., pp. 695–721. Raven Press, New York.

Sadri, P., and Lautt, W. W. (2000). Glucose disposal by insulin, but not IGF-1, is dependent on the hepatic parasympathetic nerves. *Can. J. Physiol. Pharmacol.* **78,** 807–812.

Saenz de Tejada, I., Blanco. R., Goldstein, I., Azadzoi, K., De las Morenas, A., Krane, R. J., and Cohen, R. A. (1988). Cholinergic neurotransmission in human corpus cavernosum. I. Responses of isolated tissues. *Am. J. Physiol.* **254,** H459–H467.

Sand, J., Arvola, P., Jantti, V., Oja, S., Singaram, C., Baer, G., Pasricha, P. J., and Nordback, I. (1997). The inhibitory role of nitric oxide in the control of porcine and human sphincter of Oddi activity. *Gut* **41,** 375–380.

Sandvik, A. K., and Waldum, H. L. (1991). Aspects of the regulation of gastric histamine release. *Scand. J. Gastroenterol.* **Suppl. 180,** 108–112.

Sanger, P. R., Sommerfeldt, D. W., and Hanisch, E. W. (1999). Non-adrenergic, non-cholinergic regulation of stone-diseased and stone-free human gallbladders. *Eur. J. Gastroenterol. Hepatol.* **11,** 1085–1091.

Savin, W. M., Davidson, D. M., and Haskell, W. L. (1982). Autonomic contribution to heart rate recovery from exercise in humans. *J. Appl. Physiol.* **53,** 1572–1576.

Schein, C. J. (1981). A rationale for hepatic plexus vegotomy in certain biliary disorders. *J. Clin. Gastroenterol.* **3,** 89–91.

Schiller, L. R., Walsh, J. H., and Feldman, M. (1980). Distension-induced gastrin release. Effects of luminal acidification and intravenous atropine. *Gastroenterology* **78,** 912–917.

Schmelz, M., Schmidt, R., Bickel, A., Torebjork, H. E., and Handwerker, H. O. (1998). Innervation territories of single sympathetic C fibers in human skin. *J. Neurophysiol.* **79,** 1653–1660.

Schmitt, M., Kummer, W., and Heym, C. (1988). Calcitonin gene-related peptide (CGRP)–immunoreactive neurons in the human cervico-thoracic paravertebral ganglia. *J. Chem. Neuroanat.* **1,** 287–292.

Schubert, M. L. (1991). The effect of vasoactive intestinal polypeptide on gastric acid secretion is predominantly mediated by somatostatin. *Gastroenterology* **100,** 1195–1200.

Schuerch, L. V., Linder, L. M., Grouzmann, E., and Haefeli, W. E. (1998). Human neuropeptide Y potentiates alpha1-adrenergic blood pressure responses in vivo. *Am. J. Physiol.* **275,** H760–H766.

Schulman, C. L. (1974). Electron microscopy of the human uretric innervation. *Br. J. Urol.* **46,** 609–623.

Schwartz, T., Holst, J., Fahrenkrug, J., Lindkaer Jensen, S., Nielsen, O., and Rehfeld, J. (1978). Vagal, cholinergic regulation of pancreatic polypeptide secretion. *J. Clin. Invest.* **61,** 781–789.

Scott, J. A., Craig, I., and McCormack, D. G. (1996). Nonadrenergic noncholinergic relaxation of human pulmonary arteries is partially mediated by nitric oxide. *Am. J. Respir. Crit. Care Med.* **154,** 629–632.

Sears, M. L. (1984). Autonomic nervous system: adrenergic agonists. *Handb. Exp. Pharmacol.* **69,** 193–248.

Segade, L. A. G., Quintanilla, D. S., and Nunez, J. M. S. (1987). The postganglionic parasympathetic fibres originating in the otic ganglion are distributed in several branches of the trigeminal mandibular nerve: an HRP study in the guineapig. *Brain Res.* **411,** 386–390.

Seifert, P., and Spitznas, M. (1999). Vasoactive intestinal polypeptide (VIP) innervation of the human eyelid glands. *Exp Eye Res* **68,** 685–692.

Severinghaus, J. W., and Stupfel, M. (1955). Respiratory dead space increase following atropine in man, and atropine, vagal or ganglionic blockade and hypothermia in dogs. *J. Appl. Physiol.* 8, 81–87.

Shepherd, J. T., and Mancia, G. (1986). Reflex control of the human cardiovascular system. *Rev. Physiol. Biochem. Pharmacol.* **105,** 1–99.

Sheppard, D., Epstein, J., Holtzman, M. J., Nadel, J. A., and Boushey, H. A. (1982). Dose-dependent inhibition of cold airinduced bronchoconstriction by atropine. *J. Appl. Physiol.* **53,** 169–174.

Shimosegawa, T., Asakura, T., Kashimura, J., Yoshida, K., Meguro, T., Koizumi, M., Mochizuki, T., Yanaihara, N., and Toyota, T.

(1993). Neurons containing gastrin releasing peptide–like immunoreactivity in the human pancreas. *Pancreas* **8,** 403–412.

Shimosegawa, T., Moriizumi, S., Koizumi, M., Kashimura, J., Yanaihara, N., and Toyota, T. (1992). Immunohistochemical demonstration of galaninlike immunoreactive nerves in the human pancreas. *Gastroenterology* **102,** 263–271.

Sibley, C. N. A. (1984). A comparison of spontaneous and nerve-mediated activity in bladder muscle from man, pig and rabbit. *J. Physiol. (Lond.)* **354,** 431–443.

Sibony, P. A., Walcott, B., McKeon, C., and Jakobiec, F. A. (1988). Vasoactive intestinal polypeptide and the innervation of the human lacrimal gland. *Arch. Ophthalmol.* **106,** 1085–1088.

Simard, L. D. (1937). Les complexes neuro-insulaires de pancreas humain. *Arch. Anat. Microsc.* **33,** 49–65.

Singaram, C., Sengupta, A., Sweet, M. A., Sugarbaker, D. J., and Goyal, R. K. (1994). Nitrinergic and peptidergic innervation of the human oesophagus. *Gut* **35,** 1690–1696.

Singh, M., and Webster, P. D. (1978). Neurohormonal control of pancreatic secretion. *Gastroenterology* **74,** 294–309.

Singh, S., Johnson, P. I., Javed, A., Gray, T. S., Lonchyna, V. A., and Wurster, R. D. (1999). Monoamine- and histamine-synthesizing enzymes and neurotransmitters within neurons of adult human cardiac ganglia. *Circulation* **99,** 411–419.

Siperstein, A. E., Miller, R. A., and Clark, O. H. (1988). Stimulatory effect of vasoactive intestinal polypeptide on human normal and neoplastic thyroid tissue. *Surgery* **104,** 985–991.

Sjögren, C., Andersson, K.-E., Husted, S., Mattiasson, A., and Moller-Madsen, B. (1982). Atropine resistance of transmurally stimulated isolated human bladder muscle. *J. Urol.* **128,** 1368–1371.

Sjöstrand, N. O. (1981). Smooth muscles of vas deferens and other organs in the male reproductive tract. *In* "Smooth Muscle: An Assessment of Current Knowledge" (E. Bulbring, A. F. Brading, A. W. Jones, and T. Tomita, eds.), pp. 367–376. University of Texas Press, Austin.

Sjöstrom, L., Garellick, G., Krotklewski, M., and Luyckx, A. (1980). Peripheral insulin in response to sight and smell of food. *Metab. Clin. Exp.* **29,** 901–909.

Sjovall, M., Ekblad, E., Lundell, L., and Sundler, F. (1990). Gastrin-releasing peptide: neuronal distribution and spatial relation to endocrine cells in the human upper gut. *Regul. Peptides* **28,** 47–55.

Skandalakis, J. E., Gray, S. W., Soria, R. E., Sorg, J. L., and Rowe, J. S. (1980). Distribution of the vagus nerve to the stomach. *Am. Surg.* **46,** 130–139.

Skoog, T. (1947). Ganglia in the communicating rami of the cervical sympathetic trunk. *Lancet* **2,** 457–460.

Slade S. G., Linberg J. V., and Immediata A. R. (1986) Control of lacrimal secretion after sphenopalatine ganglion block. *Ophthalm. Plast. Reconstr. Surg.* **2,** 65–70.

Slavich, E. (1932). Confronti fra la morfologia di ganglia del para-simpatico encefalico del simpatico cervicale con speciale viguardo alla struttura del ganglio ciliare. *Z. Zellforsch. Mikrosk. Anat.* **15,** 688–730.

Smet, P. J., Edyvane, K. A., Jonavicius, J., and Marshall, V. R. (1994). Colocalization of nitric oxide synthase with vasoactive intestinal peptide, neuropeptide Y, and tyrosine hydroxylase in nerves supplying the human ureter. *J. Urol.* **152,** 1292–1296.

Smet, P. J., Edyvane, K. A., Jonavicius, J., and Marshall, V. R. (1996a). Neuropeptides and neurotransmitter-synthesizing enzymes in intrinsic neurons of the human urinary bladder. *J. Neurocytol.* **25,** 112–124.

Smet, P. J., Jonavicius, J., Marshall, V. R., and de Vente, J. (1996b). Distribution of nitric oxide synthase-immunoreactive nerves and identification of the cellular targets of nitric oxide in guinea-pig and human urinary bladder by cGMP immunohistochemistry. *Neuroscience* **71,** 337–348.

Smith, R. B. (1970). The development of the intrinsic innervation of the human heart between the 10 and 70 mm stages. *J. Anat.* **107,** 271–279.

Smith, R. B. (1971). The occurrence and location of intrinsic cardiac ganglia and nerve plexuses in the human neonate. *Anat. Rec.* **169,** 33–40.

Smithson, I. L., and Benarroch, E. E. (1996). Organization of NADPH-diaphorase-reactive neurons and catecholaminergic fibers in human intermediolateral cell column. *Brain Res.* **723,** 218–222.

Soinila, S., Vanhatalo, S., Lumme, A., Back, N., and Soinila, J. (1996). Nitric oxide synthase in the autonomic and sensory ganglia innervating the submandibular salivary gland. *Microsc. Res. Techn.* **35,** 32–43.

Solomon, T. E. (1987). Control of exocrine pancreatic secretion. *In* "Physiology of the Gastrointestinal Tract" (L. R. Johnson, ed.), 2nd Ed., pp. 1173–1207. Raven Press, New York.

Southam, J. A. (1959). The inferior mesenteric ganglion. *J. Anat.* **93,** 304-308.

Sparrow, M. P., Weichselbaum, M., and McCray, P. B. (1999). Development of the innervation and airway smooth muscle in human fetal lung. *Am. J. Resp. Cell Mol. Biol.* **20,** 550–560.

Spencer, H., and Leof, D. (1964). The innervation of the human lung. *J. Anat.* **98,** 599–609.

Sporrong, B., Helm, G., Owman, C., Sjöberg, N.-O., and Walles, B. (1982). Electron microscopic and pharmacologic evidence for a functional adrenergic innervation of the smooth musculature in the human fallopian tube. *Brain Res. Bull.* **9,** 695–699.

Staadas, J. O. (1975). Intragastric pressure/volume relationship before and after proximal gastric vagotomy. Scand. *J. Gastroenterol.* **10,** 129–134.

Stebbing, J. F., Brading, A. F., and Mortensen, N. J. (1997). Role of nitric oxide in relaxation of the longitudinal layer of rectal smooth muscle. *Dis. Colon Rectum* **40,** 706–710.

Steele, P. A., Gibbins, I. L., Morris, J. L., and Mayer, B. (1994). Multiple populations of neuropeptide-containing intrinsic neurons in the guinea-pig heart. *Neuroscience* **62,** 241–250.

Steele, P. A., Gibbins, I. L., and Morris, J. L. (1996). Projections of intrinsic cardiac neurons to different targets in the guinea-pig heart. *J. Autonom. Nerv. Syst.* **56,** 191–200.

Steers, W. D., McConnell, J., and Benson, G. S. (1984). Anatomical localization and some pharmacological effects of vasoactive intestinal polypeptide in human and monkey corpus cavernosum. *J. Urol.* **132,** 1048–1053.

Stern, J. E., Sarmiento, M. I., and Cardinali, D. P. (1994). Parasympathetic control of parathyroid hormone and calcitonin secretion in rats. *J. Auton. Nerv. Syst.* **48,** 45–53.

Stjärne, L., Lundberg, J., and Åstrand, P. (1986). Neuropeptide Y—a cotransmitter with noradrenaline and adenosine 5′-triphosphate in the sympathetic nerves of the mouse vas deferens? A biochemical, physiological and electropharmacological study. *Neuroscience* **18,** 151–166.

Stjernquist, M. (1996). Innervation of ovarian and testicular endocrine cells. *In* "Autonomic–Endocrine Interactions" (K. Unsicker, ed.), pp. 231–256. Harwood Academic, Amsterdam.

Stone, R. A. (1986). Neuropeptide Y and the innervation of the human eye. *Exp. Eye Res.* **42,** 349–355.

Stone, R. A., Tervo, T., Tervo, K., and Tarkkanen, A. (1986). Vasoactive intestinal polypeptide-like immunoreactive nerves to the human eye. *Acta Ophthalmol.* **64,** 12–18.

Ström, C., Lundberg, J. M., Ahlman, H., Dahlström, A., Fahrenkrug, J., and Hökfelt, T. (1981). On the VIP-ergic innervation of the uterotubal junction. *Acta Physiol. Scand.* **111,** 213–215.

Sugenoya, J., Iwase, S., Mano, T., Sugiyama, Y., Ogawa, T., Nishiyama, T., Nishimura, N., and Kimura, T. (1998). Vasodilator component in sympathetic nerve activity destined for the skin of

the dorsal foot of mildly heated humans. *J. Physiol. (Lond)* **507,** 603–610.

Sunderland, S., and Hughes, E. S. R. (1946). The pupilloconstrictor pathway and the nerves to ocular muscles in man. *Brain* **69,** 301–309.

Sundin, T., Dahlström, A., Norlen, L., and Svedmyr, N. (1977). The sympathetic innervation and adrenoceptor function of the human lower urinary tract in the normal state and after parasympathetic denervation. *Invest. Urol.* **14,** 322–328.

Sundler, F., Alumets, J., Håkanson, R., Ingemansson, S., and Fahrenkrug, J. (1977). VIP innervation of the gall bladder. *Gastroenterology* **72,** 1375–1378.

Sundler, F., Alumets, J., Håkanson, R., Fahrenkrug, J., and Schaffalitzky De Muckadell, O. B. (1978). Peptidergic (VIP) nerves in the pancreas. *Histochemistry* **55,** 173–176.

Suzuki, N., Hardebo, J. E., and Owman, C. (1988). Origins and pathways of cerebrovascular vasoactive intestinal polypeptide-positive nerves in rat. *J Cereb. Blood Flow Metab.* **8,** 697–712.

Suzuki, R., Oso, T., and Kobayashi, S. (1983). Cholinergic inhibitory response in the bovine iris dilator muscle. *Invest. Ophthalmol. Vis. Sci.* **24,** 760–765.

Suzuki, Y., McMaster, D., Lederis, K., and Rorstad, O. P. (1984). Characterization of the relaxant effects of vasoactive intestinal peptide (VIP) and PHI on isolated brain arteries. *Brain Res.* **322,** 9–16.

Szabo, G. (1967). The regional anatomy of the human integument with special reference to the distribution of hair follicles, sweat glands and melanocytes. *Philos. Trans. R. Soc. Lond., Ser. B* **252,** 447–485.

Szurzewski, J. H. (1981). Physiology of mammalian prevertebral ganglia. *Annu. Rev. Physiol.* **43,** 53–68.

Taborsky, G. J., Jr., Ahren, B., and Havel, P. J. (1998). Autonomic mediation of glucagon secretion during hypoglycemia: implications for impaired alpha-cell responses in type 1 diabetes. *Diabetes* **47,** 995–1005.

Tache, Y., Windgate, D. L., and Burks, T. E., (eds.) (1994). "Innervation of the Gut: Pathophysiological Implications." CRC Press, Boca Raton.

Tainio, H. (1993). Neuropeptidergic innervation of the human male distal urethra and intrinsic external urethral sphincter. *Acta Histochem.* **94,** 197–201.

Tainio, H. (1994). Peptidergic innervation of the human testis and epididymis. *Acta Histochem.* **96,** 415–420.

Tainio, H., Vaalasti, A., and Rechardt, L. (1986). The distribution of sympathetic adrenergic, tyrosine hydroxylase- and neuropeptide Y-immunoreactive nerves in human axillary sweat glands. *Histochemistry* **85,** 117–120.

Tajti, J., Moller, S., Uddman, R., Bodi, I., and Edvinsson, L. (1999). The human superior cervical ganglion: neuropeptides and peptide receptors. *Neurosci. Lett.* **263,** 121–124.

Talmage, E. K., Pouliot, W. A., Schemann, M., and Mawe, G. M. (1996). Structure and chemical coding of human, canine and opossum gallbladder ganglia. *Cell Tiss. Res.* **284,** 289–302.

Tamura, M., Kagawa, S., Kimura, K., Kawanishi, Y., Tsuruo, Y., and Ishimura, K. (1995). Coexistence of nitric oxide synthase, tyrosine hydroxylase and vasoactive intestinal polypeptide in human penile tissue—a triple histochemical and immunohistochemical study. *J. Urol.* **153,** 530–534.

Tasman, A. J., Bogatzki, B., Heppt, W., Hauser-Kronberger, C., and Fischer, A. (1998). Nitric oxide synthase in the innervation of the human nasal mucosa: correlation with neuropeptides and tyrosine hydroxylase. *Laryngoscope* **108,** 128–133.

Taton, G., Chatetlain, P., Delhaye, M., Camus, J. C., De Neef, P., Waelbroek, M., Tatemoto, K., Robberecht, P., and Christophe, J. (1982). Vasoactive intestinal peptide (VIP) and peptide having N-terminal histidine and C-terminal isoleucine amide (PHI) stimulate adenylate cyclase activity in human heart membranes. *Peptides* **3,** 897–900.

Taylor, I. L., and Feldman, M. (1982). Effect of cephalic vagal stimulation on insulin, gastric inhibitory polypeptide and pancreatic polypeptide released from humans. *J. Clin. Endocrinol. Metab.* **55,** 1114–1117.

Taylor, I. M., and Smith, R. B. (1971). Intrinsic innervation of the human foetal lung between the 35 and 140 mm crown-rump length stages. *Biol. Neonate* **18,** 193–202.

Taylor, S. M., Pare. P. D., and Schellenberg, R. R. (1984). Cholinergic and non-adrenergic mechanisms in human and guinea-pig airways. *J. Appl. Physiol.* **56,** 958–965.

Thune, A., Delbro, D. S., Nilsson, B., Friman, S., and Svanvik, J. (1995). Role of nitric oxide in motility and secretion of the feline hepatobiliary tract. *Scand. J. Gastroenterol.* **30,** 715–720.

Toccafondi, R. S., Brandi, M. L., and Melander, A. (1984). Vasoactive intestinal peptide stimulation of human thyroid cell function. *J. Clin. Endocrinol. Metab.* **58,** 157–160.

Toda, N. (1981). Non-adrenergic, non-cholinergic innervation in monkey and human cerebral arteries. *Br. J. Pharmacol* **72,** 281–283.

Toda N. and Okamura T. (1996). Neurogenic nitric oxide (NO) in the regulation of cerebroarterial tone. *J. Chem. Neuroanat.* **10,** 259–265.

Toda N., Ayajiki K., Tanaka T., and Okamura T. (2000a). Preganglionic and postganglionic neurons responsible for cerebral vasodilation mediated by nitric oxide in anesthetized dogs. *J. Cereb. Blood Flow Metab.* **20,** 700–708.

Toda N., Tanaka T., Ayajiki K., and Okamura T. (2000b). Cerebral vasodilatation induced by stimulation of the pterygopalatine ganglion and greater petrosal nerve in anesthetized monkeys. *Neuroscience.* **96,** 393–398.

Togari, A., Arai, M., Mizutani, S., Mizutani, S., Koshihara, Y., and Nagatsu, T. (1997). Expression of mRNAs for neuropeptide receptors and beta-adrenergic receptors in human osteoblasts and human osteogenic sarcoma cells. *Neurosci. Lett.* **233,** 125–128.

Tomita, R., Kurosu, Y., and Munakata, K. (1997). Relationship between nitric oxide and non-adrenergic non-cholinergic inhibitory nerves in human lower esophageal sphincter. *J. Gastroenterol.* **32,** 1–5.

Tomita, R., Tanjoh, K., Fujisaki, S., and Fukuzawa, M. (1999). The role of nitric oxide (NO) in the human pyloric sphincter. *Hepatogastroenterology* **46,** 2999–3003.

Tonini, M., De Giorgio, R., De Ponti, F., Sternini, C., Spelta, V., Dionigi, P., Barbara, G., Stanghellini, V., and Corinaldesi, R. (2000). Role of nitric oxide- and vasoactive intestinal polypeptide-containing neurones in human gastric fundus strip relaxations. *Br. J. Pharmacol.* **129,** 12–20.

Traurig, H. H., and Papka, R. E. (1993). Autonomic efferent and visceral sensory innervation of the female reproductive system: special reference to the functional roles of nerves in reproductive organs. *In* "Nervous Control of the Urogenital System" (C. A. Maggi, ed.), pp. 103–141. Harwood Academic, Chur.

Trumble, H. C. (1933-1934). The plan of the visceral nerves in the lumbar and sacral outflow of the autonomic nervous system. *Br. J. Surg.* **21,** 664–676.

Tsuboi, M., Furukawa, Y., Nakajima, K., Kurogouchi, F., and Chiba, S. (2000). Inotropic, chronotropic, and dromotropic effects mediated via parasympathetic ganglia in the dog heart. *Am. J. Physiol.* **279,** H1201–1207.

Uddman, R., and Sundler, F. (1979). Vasoactive intestinal peptide nerves in human upper respiratory tract. *Oto-Rhino-Laryngol. (Amsterdam)* **41,** 221–226.

Uddman, R., Fahrenkrug, J., Malm, L., Alumets, J., Håkanson, R., and Sundler, F. (1980a). Neuronal VIP in salivary glands: distribution and release. *Acta Physiol. Scand.* **110,** 31–38.

Uddman, R., Malm, L., and Sundler, F. (1980b). The origin of vasoactive intestinal polypeptide (VIP) nerves in the feline nasal mucosa. *Acta Ophthalmol.* **89,** 152–156.

Uddman, R., Tajti, J., Moller, S., Sundler, F., and Edvinsson, L. (1999). Neuronal messengers and peptide receptors in the human sphenopalatine and otic ganglia. *Brain Res.* **826,** 193–199.

Uemura, S., Pompolo, S., Furness, J. B., and Hardy, K. J. (1997). Nitric oxide synthase in neurons of the human gall-bladder and its colocalization with neuropeptides. *J. Gastroenterol. Hepatol.* **12,** 257–265.

Uemura, Y., Sugimoto, T., Kikuchi, H., and Mizuno, N. (1988). Possible origins of cerebrovascular nerve fibers showing vasoactive intestinal polypeptide-like immunoreactivity: an immunohistochemical study in the dog. *Brain Res.* **448,** 98–105.

Uno, H. (1977). Sympathetic innervation of the sweat glands and piloarrector muscles of macaques and human beings. *J. Invest. Dermatol.* 69, 112–120.

Uusitalo, H., Lehtosalo, J., Palkama, A., and Toivanen. M. (1984). Vasoactive intestinal polypeptide (VIP)–like immunoreactivity in the human and guinea-pig choroid. *Exp. Eye Res.* **38,** 435–437.

Vaalasti, A., and Hervonen, A. (1980). Autonomic innervation of the human prostate. *Invest. Urol.* **17,** 293–297.

Vaalasti, A., Tainio, H., and Rechardt, C. (1985). Vasoactive intestinal polypeptide (VIP)–like immunoreactivity in the nerves of human axillary sweat glands. *J. Invest. Dermatol.* **85,** 246–248.

Vaalasti, A., Tainio, H., Pelto-Huikko, M., and Hervonen, A. (1986). Light and electron microscope demonstration of VIP and enkephalin-immunoreactive nerves in the human male genito-urinary tract. *Anat. Rec.* **215,** 21–27.

Van Buskirk, C. (1945). The seventh nerve complex. *J. Comp. Neurol.* **82,** 303–326.

Van Campenhout, E. (1927). Contributions a l'etude de l'histogenese du pancreas chez quelque mammiferes. Les complexes sympathetico-insulaires. *Arch. Biol.* **37,** 121–171.

van der Velden, V. H., and Hulsmann, A. R. (1999). Autonomic innervation of human airways: structure, function, and pathophysiology in asthma. *Neuroimmunomodulation* **6,** 145–159.

Van der Werf, F., Baljet, B., Prins, M., Timmerman, A., and Otto, J. A. (1993). Innervation of the superior tarsal (Müller's) muscle in the cynomolgous monkey: a retrograde tracing study. *Invest. Ophthalm. Vis. Sci.* **34,** 2333–2340.

Van der Werf F., Baljet B., Prins M., and Otto J. A. (1996) Innervation of the lacrimal gland in the cynomolgous monkey: a retrograde tracing study. *J. Anat.* **188,** 591–601.

Van der Zypen, E., Kasselharst, G.. Merz. R., and Fillinger, H. (1974). Histochemische und elektronen-mikroskopische Untersuchungen an den intramuralen Ganglien des Herzens bei Mensch und Ratte. *Acta Anat.* **88.** 161–187.

Vanner, S., and Surprenant, A. (1996). Neural reflexes controlling intestinal microcirculation. *Am. J. Physiol.* **271,** G223–G230.

Van Sande, J., Dumont, J. E., Melander, A., and Sundler, F. (1980). Presence and influence of cholinergic nerves in the human thyroid. *J. Clin .Endocrinol. Metab.* **51,** 500–502.

Verchere, C. B., Kowalyk, S., Koerker, D. J., Baskin, D. G., and Taborsky, G. J., Jr. (1996). Evidence that galanin is a parasympathetic, rather than a sympathetic, neurotransmitter in the baboon pancreas. *Regul. Peptides* **67,** 93–101.

Vincent, N. J., Knudsen, R., Leith, D. E., Macklem, P. T., and Mead, J. (1970). Factors influencing pulmonary resistance. *J. Appl. Physiol.* **29,** 236–243.

von Heyden, B., Jordan, U., and Hertle, L. (1998). Neurotransmitters in the human urethral sphincter in the absence of voiding dysfunction. *Urol. Res.* **26,** 299–310.

Wagner, G., and Levin, R. J. (1980). Effect of atropine and methylatropine on human vaginal blood flow, sexual arousal and climax. *Acta Pharmacol. Toxicol.* **46,** 321–325.

Wallick, D. W., and Martin, P. J. (1990). Separate parasympathetic control of heart rate and atrioventricular conduction of dogs. *Am. J. Physiol.* **259,** H536–H542.

Wallin, B.G., and Elam, M. (1997). Cutaneous sympathetic nerve activity in humans. *In* "Autonomic Innervation of the Skin" (J. L. Morris and I. L. Gibbins, eds.), pp. 111–132, Harwood Academic, Amsterdam.

Wallin, B. G., and Fagius, J. (1988). Peripheral sympathetic neural activity in conscious humans. *Annu. Rev. Physiol.* **50,** 565–576.

Walsh, J. H. (1987). Gastrointestinal hormones. *In* "Physiology of the Gastrointestinal Tract" (L. R. Johnson, ed.), 2nd Ed., pp. 181–284. Raven Press, New York.

Walsh, J. H. (1988). Peptides as regulators of gastric acid secretion. *Annu. Rev. Physiol.* **50,** 41–63.

Walters, B. B., Gillespine, S. A., and Moskowitz, M. A. (1986). Cerebrovascular projections from the sphenopalatine and otic ganglia to the middle cerebral artery of the cat. *Stroke* **17,** 488–494.

Ward, S. M., Morris, G., Reese, L., Wang, X. Y., and Sanders, K. M. (1998). Interstitial cells of Cajal mediate enteric inhibitory neurotransmission in the lower esophageal and pyloric sphincters. *Gastroenterology* **115,** 314–329.

Ward, S. M., Beckett, E. A. H., Wang, X. Y., Baker, F., Khoyi, M., and Sanders, K. M. (2000). Interstitial cells of Cajal mediate cholinergic neurotransmission from enteric motor neurons. *J. Neurosci.* **20,** 1393–1403.

Warwick, R. (1954). The ocular parasympathetic nerve supply and its mesencephalic sources. *J. Anat.* **88,** 71–93.

Wattchow, D. A., Cass, D. T., Furness, J. B., Costa, M., O'Brien, P. E., Little, K. E., and Pitkin, J. (1987a). Abnormalities of peptide-containing nerve fibers in infantile hypertrophic pyloric stenosis. *Gastroenterology* **92,** 443–448.

Wattchow, D. A., Furness, J. B., Costa, M., O'Brien, P. E., and Peacock, M. (1987b). Distributions of neuropeptides in the human esophagus. *Gastroenterology* **93,** 1363–1371.

Wattchow, D. A., Furness, J. B., and Costa, M. (1988). Distribution and coexistence of peptides in nerve fibers of the external muscle of the human gastrointestinal tract. *Gastroenterology* **95,** 32–41.

Wattchow, D. A., Brookes, S. J., and Costa, M. (1995). The morphology and projections of retrogradely labeled myenteric neurons in the human intestine. *Gastroenterology* **109,** 866–875.

Wattchow, D. A., and Costa, M. (1996). Distribution of peptide-containing nerve fibres in achalasia of the oesophagus. *J. Gastroenterol. Hepatol.* **11,** 478–485.

Wattchow, D. A., Porter, A. J., Brookes, S. J., and Costa, M. (1997). The polarity of neurochemically defined myenteric neurons in the human colon. *Gastroenterology* **113,** 497–506.

Webber, R. H. (1955). An analysis of the sympathetic trunk, communicating rami, sympathetic roots and visceral rami in the lumbar region in man. *Ann. Surg. 141,* 398–413.

Webber, R. H. (1958). A contribution on the sympathetic nerves in the lumbar region. *Anat. Rec.* **130,** 581–604.

Webber, S. E., and Widdicombe, J. G. (1987). The effect of vasoactive intestinal peptide on smooth muscle tone and mucous secretion from the ferret trachea. *Br. J. Pharmacol.* 91, 139–148.

Wedel, T., Roblick, U., Gleiss, J., Schiedeck, T., Bruch, H. P., Kuhnel, W., and Krammer, H. J. (1999). Organization of the enteric nervous system in the human colon demonstrated by wholemount immunohistochemistry with special reference to the submucous plexus. *Anat Anz* **181,** 327–337 [published erratum appears in *Anat. Anz.* (1999) **181,** 565].

Weiss, H. D. (1972). The physiology of human erection. *Ann. Intern. Med.* **76,** 793–799.

Wharton, J., and Gulbenkian. S. (1987). Peptides in the mammalian cardiovascular system. *Experientia* **43,** 821–832.

Wharton, J., Gulbenkian, S., Merighi, A., Kuhn, D. M., Jahn, R., Taylor, K. M., and Polak, J. M. (1988). Immunohistochemical and ultrastructural localisation of peptide-containing nerves and myocardial cells in the human atrial appendage. *Cell Tissue Res.* **254,** 155–166.

Whitelaw, G. P., and Smithwick, R. H. (1951). Some secondary effects of sympathectom—with particular reference to disturbance of sexual function. *N Engl. J. Med.* **245,** 121–130.

Williams, G. A., Kukreja, S. C., Longley, R. S., Bowser, E. N., Hargis, G. K., Vora, N. M., and Henderson, W. J. (1985). Effect of the parasympathetic system on secretion of parathyroid hormone. *Metabolism* **34,** 612–615.

Willis, E. A., Otteson, B.. Wagner, G., Sundler, F., and Fahrenkrug, J. (1983). Vasoactive intestinal polypeptide (VIP) as a putative neurotransmitter in penile erection. *Life Sci.* **33,** 383–391.

Wilson, J. E. (1984). Pterygopalatine ganglion cytology in monkeys. *J. Anat.* **139,** 307–317.

Wilson, W. C. (1935). Observations relating to the innervation of the sweat glands of the face. *Clin. Sci.* **2,** 273–286.

Winding, B., Wiltink, A., and Foged, N. T. (1997). Pituitary adenylyl cyclase-activating polypeptides and vasoactive intestinal peptide inhibit bone resorption by isolated rabbit osteoclasts. *Exp. Physiol.* **82,** 871–886.

Wood, J. D., and Schultz, S.G., eds., (1989). "Handbook of Physiology, Section 6: The Gastrointestinal System; Vol. 1, Motility and Circulation." American Physiology Society, Bethesda.

Woods, S. C., and Porte, D. (1974). Neural control of the endocrine pancreas. *Physiol. Rev.* **54,** 596–619.

Wozniak, W., and Skowronska, U. (1967). Comparative anatomy of pelvic plexus in cat, dog, rabbit, macaque and man. *Anat. Anz.* **120,** 457–473.

Wrete, M. (1959). The anatomy of the sympathetic trunks in man. *J. Anat.* **93,** 448–459.

Xie, H., and Lautt, W. W. (1995). Induction of insulin resistance by cholinergic blockade with atropine in the cat. *J. Auton. Pharmacol.* **15,** 361–369.

Xue, C., Aspelund, G., Sritharan, K. C., Wang, J. P., Slezak, L. A., and Andersen, D. K. (2000). Isolated hepatic cholinergic denervation impairs glucose and glycogen metabolism. *J. Surg. Res.* **90,** 19–25.

Yamaguchi, N. (1992). Sympathoadrenal system in neuroendocrine control of glucose: mechanisms involved in the liver, pancreas, and adrenal gland under hemorrhagic and hypoglycemic stress. Can. *J. Physiol. Pharmacol.* **70,** 167–206.

Yamashita, Y., Ogawa. T., Ohnishi, N., Imamura, R., and Sugenoya, J. (1987). Local effect of vasoactive intestinal polypeptide in human sweat gland function. *Jpn. J. Physiol.* **37,** 929–936.

Yang, T., Jacobstein. M. D., and Levy, M. N. (1985). Sustained increases in heart rate induced by timed reptition of vagal stimulation in dogs. *Am. J. Physiol.* **249,** H703–H709.

Yasue, H., Horio, Y., Nakamura, N., Fujii, H., Imoto, N., Sonoda, R., Kugiyama, K.. Obata, K., Morikami, Y., and Kimura, T. (1986). Induction of coronary artery spasm by acetylcholine in patients with variant angina: possible role of the parasympathetic nervous system in pathogenesis of coronary artery spasm. *Circulation* **74,** 955–963.

Yasui T., Karita K., Izumi H., and Tamai M. (1997). Correlation between vasodilatation and secretion in the lacrimal gland elicited by stimulation of the cornea and facial nerve root of the cat. *Invest. Ophthalm. Vis. Sci.* **38,** 2476–2482.

Yoshida, K., and Toda, N. (1996). NADPH diaphorase-positive neurons in the intracardiac plexus of human, monkey and canine right atria. *Brain Res.* **724,** 256–259.

Yoshida, Y., Yoshida, K., Kimura, T., and Toda, N. (1995). Distribution of NADPH diaphorase–reactive nerves in the human female genital organ. *Acta Obstet. Gynecol. Scand.* **74,** 171–176.

Young, M. A., and Vatner, S. F. (1986). Brief review: regulation of large coronary arteries. *Circ. Res.* **59,** 579–596.

Zhang, Y.L., Tan, C.K., and Wong, W.C., (1994). The ciliary ganglion of the monkey: a light and electron microscopic study. *J. Anat.* **184,** 251–260.

CHAPTER

7

Spinal Cord: Cyto- and Chemoarchitecture

JEAN SCHOENEN
Department of Neuroanatomy and Neurology
University of Liège, Liège, Belgium

RICHARD L. M. FAULL
Department of Anatomy with Radiology
The University of Auckland, Auckland, New Zealand

Our present knowledge on the detailed anatomical organization of the mammalian spinal cord is derived mainly from nonhuman animal studies. There have been many studies on the anatomy of the mammalian spinal cord in the rat, cat, and monkey, with the most comprehensive and authoritative accounts being those provided by Rexed (1952, 1954, 1964) on the cytoarchitectonic organization, and by Scheibel and Scheibel (1966a, b, 1968, 1969a, b, 1970a) on the dendroarchitecture of the cat spinal cord. However, there has been no detailed overall analysis of the anatomical organization of the human spinal cord. In an attempt to redress this, we present here a detailed account of the cytoarchitectural, dendroarchitectural, and myeloarchitectural features of the human spinal cord that is based on the examination of Nissl-, Golgi-, and myelin-stained material of the developing and mature human spinal cord from 93 cases. We will also describe the general chemoarchitecture as seen in the normal spinal cord, and consider the regional chemoarchitecture as well as some functional implications as demonstrated, in part, from the study of human pathological cases.

CYTO- AND DENDROARCHITECTURE

The laminar cytoarchitectonic scheme, described by Rexed in the cat, has been extended *de facto* to mature and immature spinal cords of other animals, e.g., the dog (Buxton and Goodman, 1967), monkey (Chambers and Liu, 1958; Kuypers, 1964; Kuypers and Brinkman, 19670; Kuypers *et al.*, 1962; Miller and Strominger, 1973), and rat (Brichta and Grant, 1985). However, the presence of such a cytoarchitectural organization has been formally demonstrated only in mice (Sidman *et al.*, 1971). Truex and Taylor (1968) have suggested in an abstract that the laminar cytoarchitectonic scheme might be applied to the human spinal cord and their results are mentioned in Carpenter's *Human Neuroanatomy* (1976). In contrast, several authors do not refer to the laminar scheme and prefer to classify spinal neurons

according to one of the classical anatomical organizational schemes (Bossy and Ferratier, 1968; Waibl, 1973). Nevertheless, Rexed's schema has been adopted by most neuroanatomists and neurophysiologists because it offers a more comprehensive and uniform view of the spinal organization. In addition, it has some physiological and functional correlates.

In order to verify the presence of a laminar cytoarchitectural organization of the human, we have studied 46 adults and 12 immature spinal cords, using thick (100 μm) and fine (10 μm) Nissl- and myelin-stained transverse and longitudinal sections. The functional significance of Rexed's lamination was placed in doubt because it is based on a purely cytoarchitectonic approach, neglecting one of the principal morphological attributes of the neurons, the dendritic tree. It is justified to consider dendritic tree geometry as an important parameter in all neuronal classifications with functional perspectives (Leontovich, 1975). Golgi's analysis of the spinal cord, practically abandoned since Ramón y Cajál (1909), was revived in the 1960s. Most of these analyses were performed in newborn kittens (Gobel, 1975a, b; Scheibel and Scheibel, 1966a, b, 1968, 1969a, b). A few concentrated on the adult cat (Leontovich and Zhukova, 1963; Proshansky and Egger, 1977; Szentágothai, 1964; Szentágothai and Rethelyi, 1973) or monkey cord (Beal and Cooper. 1978). Certain authors have examined human spinal cords, but their results, other than those of Pearson (1952) on the substantia gelatinosa and those of Abdel-Maguid and Bowsher (1979) on motoneurons, have not been published in detail. Golgi studies have partially validated the laminar cytoarchitectural schema of Rexed by demonstrating that each of laminae I–IV of the dorsal horn (Beal and Cooper, 1978; Gobel, 1975a, b, 1978a, b; Scheibel and Scheibel, 1966b, 1969b, 1970a, b; Sterling and Kuypers, 1967b) are dendroarchitecturally distinguishable. However, the neurons of the intermediate gray matter were regrouped into an entity, called the "isodendritic core," and linked on a structural basis to the reticular formation of the brain stem, of which it would simply be a caudal extension (Ramon-Moliner and Nauta, 1966; Szentágothai and Rethelyi, 1973).

Since Sholl's work (1953, 1956) on the cerebral cortex it has been known that morphometric analyses of Golgi-impregnated material, although fastidious and therefore little exploited, are indispensable to discern certain details of the dendritic morphology (Ramon-Moliner, 1967). The rare quantitative dendroarchitectural studies of the nonhuman cord indicate some differences between the large and small neurons of the ventral horn (Aitken and Bridger, 1961; Gelfan *et al.*, 1970). Dendritic studies of human cord are sparse and purely qualitative (Laruelle, 1937, 1948; Pearson, 1952; Ramón y Cajál, 1909; van Lenhossek, 1895). The work of Abdel-Maguid and Bowsher (1979) on motoneurons is the only morphometric study completed on human material until the present. On the basis of dendritic field size and dendritic branching pattern, these authors have described two types of a and two types of γ motoneurons. However, Golgi studies have hardly brought forward any criteria permitting better identification of laminae V, VI, VII, and VIII neurons or even motoneurons belonging to different columns. One problem is that they fail to consider the spatial polarization of dendritic trees. This is indeed a major dendroarchitectural parameter that relates closely to the connection of neurons, as already defined by Ramón y Cajál's (1909) "Loi de la polarisation dynamique" and as confirmed by studies of the cerebellum (for a review, see Rakic, 1975), visual cortex (Valverde, 1968, 1970), and laminae IV–VI of the cat spinal cord (Proshansky and Egger, 1977).

We have performed qualitative and quantitative Golgi analyses on 23 human spinal cords taken at autopsy from patients free of any detectable neurological diseases. Our work is based largely on the rapid Golgi technique and therefore on specimens of fetal (26–38 weeks of gestation) or young infant (1 day to 7 years old) tissue. Adult material (22–92 years of age) was studied with different variants of the slow Golgi method. Certain steps of the ontogenesis of spinal dendritic organization could thus be analyzed. The morphometric methods used on camera-lucida-drawn impregnated cells has been described elsewhere (Schoenen, 1981b, 1982a, b). The results of morphometric analyses were compiled from the examination of drawings of 542 neurons distributed in the cytoarchitectural laminae of the gray matter and identified in spinal cord of different ages.

General Laminar Organization

The general organization of spinal neurons was examined on thick transverse sections of the lumbar enlargement. As is shown in Figure 7.1, several groups of neurons can be easily recognized. The tip of the dorsal horn is cuffed by gray matter with a low neuronal density. Neurons in this region are medium sized and some of them lie in close contact with Lissauer's tract. Ventral (deep) to this first neuronal group is a region with very high neuronal density. These neurons are small and spread throughout the width of the dorsal horn. This easily recognizable portion of gray matter corresponds to the "substantia gelatinosa" of Rolando. Several neurons of larger caliber occupy the whole width of the dorsal horn ventral to Rolando's substance. The transition zone between the

FIGURE 7.1 Photomontage of transversely cut (100 μm) human spinal gray matter at the L5 level. Cresyl violet–stained section of a normal 60-year-old. Magnification: ×28. C, D-L, and V-L are the central, dorsolateral, and ventrolateral columns of motoneurons, respectively; imm, intermediomedial nucleus.

substantia gelatinosa and these large neurons is occupied by a portion of gray matter where neurons are larger but fewer than in Rolando's substance. In the ventral horn, motoneurons, which are easily identified, are clustered in three columns: dorsolateral, central, and ventrolateral. On the medial aspect of the ventral horn, there is a crescent-shaped group of neurons of varying sizes. The space between this group and the motoneuronal columns is occupied by smaller cells. In the rest of the gray matter, precise delineation of neuronal groups is more difficult. Figure 7.1 shows that the base of the dorsal horn contains many neurons which, tend to segregate into a medial and lateral group. Small, densely packed neurons predominate in the medial portion, while larger and less densely packed neurons appear in the lateral region. The most laterally located neurons of the lateral group are intermingled with the longitudinal fiber fascicles of the "formatio reticularis." The base of the dorsal horn is not clearly demarcated from the central core of the spinal gray matter. However, the latter is characterized by a lower neuronal density and by differently shaped neurons. Finally, the central canal is surrounded by small neurons, in the vicinity of which a clustering of cells can be recognized on some sections, corresponding to the intermediomedial nucleus.

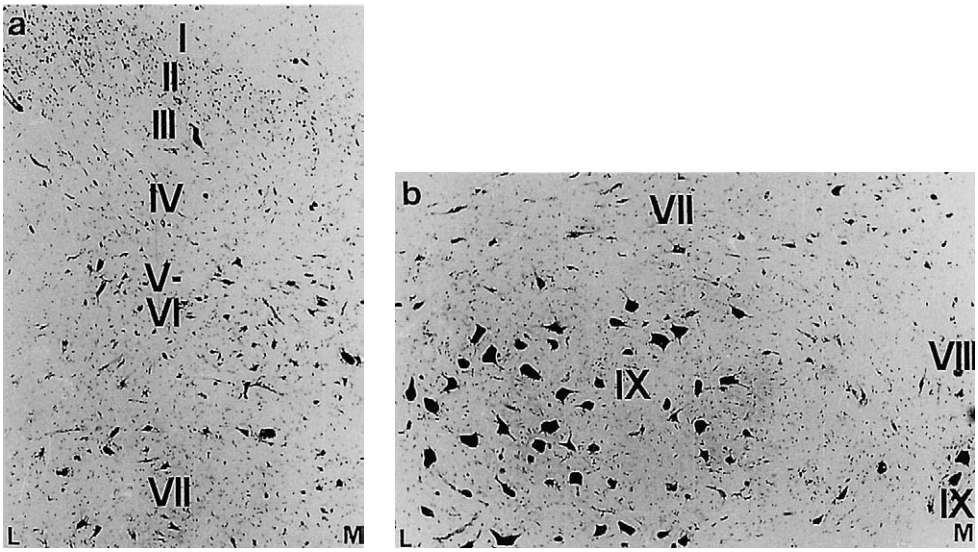

FIGURE 7.2 Transverse 10-µm Nissl-stained sections of a normal 72-year-old of the dorsal **(a)** and ventral **(b)** horns of human spinal segment L4. L, lateral, M, medial. Magnification: ×73.

Low-power examinations of thick transverse sections of the human spinal cord thus reveal a general cytoarchitectural organization that is fundamentally similar to that described by Rexed in the cat. The layer of marginal neurons cuffing the dorsal horn corresponds to lamina I. The substantia gelatinosa of Rolando and the region of large neurons in the center of the dorsal horn correspond to laminae II and IV, respectively. The transition zone between these two laminae is lamina III. The neurons located in the base of the dorsal horn correspond to laminae V and VI of Rexed's scheme. As described previously, these two laminae cannot be readily distinguished in the human spinal cord and contain neurons, which are cytologically similar. They can, however, be separated into a medial portion and a larger lateral portion. According to Rexed (1952), the asymmetries of medial and lateral portions can be used in the cat as a criterion for distinguishing lamina V from lamina VI, in addition to their different position in the dorsoventral axis. This criterion is not applicable to the human cord, so we have decided to call this region of the spinal gray "laminae V–VI." Ventral to laminae V–VI, the center portion of the spinal gray matter corresponds to lamina VII, which at the level of the cervical and lumbar enlargements extends up to the ventral border of the ventral horn. The group of neurons located medially in the ventral horn is lamina VIII. Finally, the columns of motoneurons form lamina IX and the neurons surrounding the central canal form lamina X.

The laminar cytoarchitectural organization described above is not limited to lumbar segments. Longitudinal sagittal sections indicate that the neuronal laminae extend throughout the rostrocaudal axis of the spinal cord. When the cord is cut sagittally, some neuronal laminae may not be in the plane of section because of their particular location (cf. Fig. 7.3). The cytoarchitectural organization of the cervical enlargement is similar to that of the lumbar enlargement. Segmental variations may occur at other levels and will be described. On thin histological sections, lamination of spinal neurons can be seen, but the borders between laminae are difficult to determine (Fig. 7.2).

The laminar organization of spinal gray matter occurs early during ontogenesis. It can be recognized as soon as neuroblasts migrate from the germinal plate laterally and differentiate. In the 6-week-old embryo, differentiated motoneurons can be identified in the ventral horn of the lumbar cord. In addition, neurons cluster on the medial aspect of the ventral horn to form lamina VIII. In the 10-week-old embryo, laminae V–IX can be readily recognized. Neuronal differentiation is less advanced in dorsal parts of the spinal gray, where the alar plate of the germinal zone remains present and laminae I–IV cannot be distinguished. From the age of 26 weeks *in utero* and onward, the cytoarchitectural organization of the spinal gray matter is similar to that of the adult cord except for greater neuronal density and development of myelinated structures. As illustrated in Figure 7.3, there is a clear laminar organization of spinal neurons in the sagittally cut cord of the 26-week-old fetus, although in this plane of section laminae VIII and X are not visualized. In the 5-month-old infant, neuronal density has declined in the gray matter and, as in the adult, the exact delineation of spinal laminae is difficult on thin sections (Fig. 7.3).

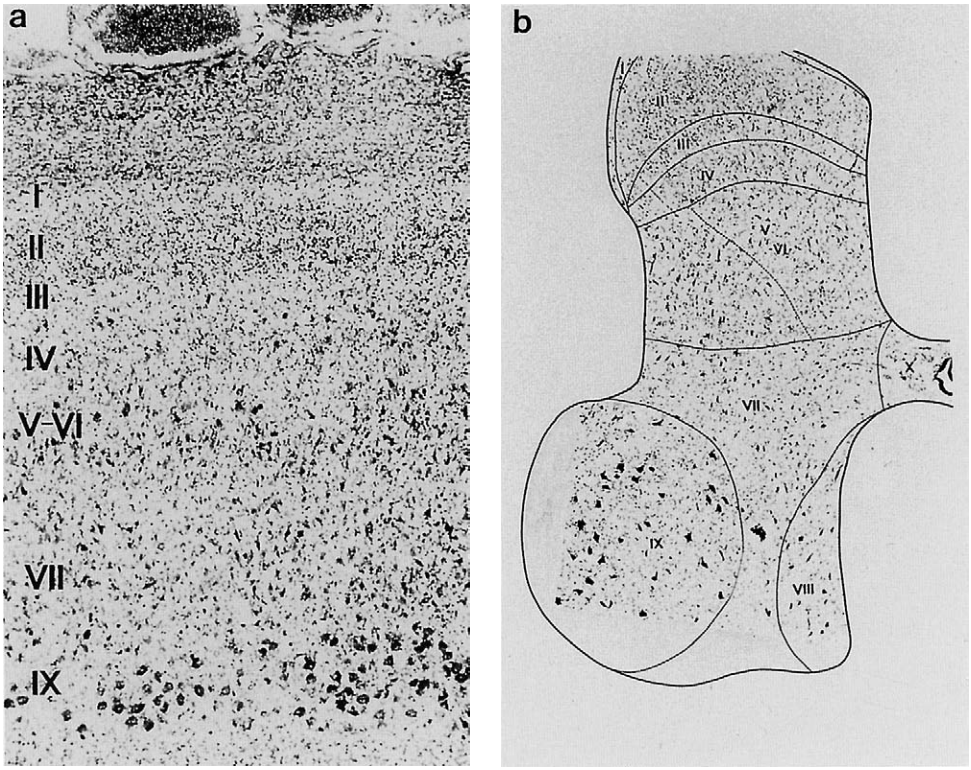

FIGURE 7.3 Spinal cytoarchitecture during development. **(a)** Sagittal Nissl-stained section at the lumbar level of a 26-week-old fetus. Note that laminae VIII and X are not in the plane of section. Magnification: ×48. **(b)** Photomontage of 10-µm transverse cresyl violet–stained sections of segment L5 of a 5-month-old neonate. Magnification: ×20.

Detailed Laminar Characteristics

Cell density and topography within the gray matter, as determined on thick histological section, are not the only criteria to identify cytoarchitectonic laminae. As already mentioned by Rexed, each lamina has in addition its own cytological characteristics. These can be most properly analyzed on Nissl-stained sections. The following cytological characteristics are derived from transverse and longitudinal sections of human spinal cord at the level of the enlargements. Moreover, for each lamina we will describe the dendroarchitectural features as well as morphometric data on dendritic trees.

Lamina I

Lamina I, which is horseshoe shaped and cuffs the tip of the dorsal horn, does not have a uniform thickness. It is thicker at the level of Lissauer's tract and on the lateral border of the dorsal horn. The neuropil of lamina I is loosely organized. Neuronal density is low, and most cells are found in the dorsolateral part, close to Lissauer's tract. Neurons are of variable sizes. Some are fusiform and tangentially oriented, but in the thicker part of the lamina most cells have a stellate, multipolar shape. Nissl bodies are inconspicuous in lamina I neurons.

In lamina I, the majority of dendrites are oriented tangentially to the edge of the dorsal horn. Besides transverse branches, the neurons have longitudinal dendrites that also follow the contour of the dorsal horn. Dendrites are not, however, restricted to the tangential plane; most cells also possess ventral dendrites. These are rami of longitudinal branches curving ventrally; in some cells, the majority of dendrites immediately take a ventral direction. The ventral dendrites which are found in both immature and adult material penetrate deeply into lamina II and can even reach lamina III and IV. Some neurons located in the lateral portion of lamina I have dendrites that penetrate into the white matter of the dorsolateral funiculus. Lamina I neurons are moderately covered with sessile or pedicled dendritic spines, which appear more numerous on the ventral dendrites.

Morphometric analyses confirm the tangential orientation of dendritic trees, but also show that the ventral orientation is far from negligible, since dendritic

spread in the ventral direction is comparable to that in the medial or lateral direction. Dendritic trees of lamina I neurons are poorly branched, and the ramification index (i.e., maximal number of dendritic intersections with 20-µm distant concentric circles from the perikaryon divided by the number of primary dendrites) of 1.60 is the lowest found in the human spinal cord. In adult material, the maximal dendritic extension (radius of the outermost circles crossing a dendrite) is 440 µm.

The tangential orientation of dendrites in lamina I is a classical finding from animal experimentation (Waldeyer, 1888; Ramón y Cajál, 1909; Scheibel and Scheibel, 1968; Gobel 1978a); it was described in humans by von Lenhossek (1895). In our study of the human spinal cord, dendrites perpendicular to the edge of the dorsal horn are a prominent finding. They may outnumber tangential dendrites and penetrate deeply into lamina II, some even reaching laminae II and IV. By contrast, Falls and Gobel (1976) reported that perpendicular dendrites do not exist in lamina I of the adult cat cord, but Ramón y Cajál (1909) pointed out their presence in the cord of the chick embryo and in the medulla of newborn rabbits. Gobel (1978a) thus suggested that they might be immature structures, disappearing during postnatal development. This is not the case in the human cord, where they can be found in fetal as well as in adult material. Lamina I contains projection neurons of the spinothalamic tract as well as proprioneurons (for a review, see Willis and Coggeshall. 1978). In humans, spinothalamic neurons can be identified in lamina I in cases of ventrolateral cordotomy; however, these neurons represent only a small percentage of the total cell population (Schoenen, 1981b; Smith 1976; see Chap 8). Input to this lamina is chiefly from peripheral nociceptors through A-delta and C fibers (for a review, see Cervero and Iggo, 1980; Lynn and Hunt, 1984). These afferents form a dense, tangentially oriented terminal plexus (Rethelyi, 1981) that should favor multiple contacts with dendrites, but not spatial discrimination of inputs. There is evidence from animal experiments that lamina I also contains polymodal neurons, i.e., cells responding to noxious as well as to innocuous tactile stimuli conveyed by A-beta fibers (Willis and Coggeshall, 1978). The latter are distributed mainly to the deeper laminae of the dorsal horn (Lynn and Hunt, 1984). In the human cord, at least, one has to consider the possibility that A-beta fibers might contact laminae I neurons on their ventral dendrites which penetrate deeply into laminae II, III, and IV. Moreover, these ventral dendrites lie within the rich neuropil of lamina II, where part of the control exerted by the substantia gelatinosa on nociceptor-driven projection neurons may be localized.

Lamina II

Lamina II occupies most of the head of the dorsal horn. On transverse section, it has a ventral concavity. It is thickest in its lateral portion, where it covers lamina III. Neuronal density is highest in lamina II, which accounts for the dark appearance of this lamina on Nissl-stained sections. In the human spinal cord there is no clear separation between an outer zone and an inner zone, whereas such a separation was described by Rexed in the cat. The neuronal population of lamina II appears homogeneous. Neurons are small, the largest diameter of their perikaryons reaching 20 µm. They contain only a few Nissl bodies located at either pool of the soma (Fig. 7.4). Horizontal sections indicate that most lamina II neurons are fusiform and oriented along the rostrocaudal axis.

Based on dendritic geometry and axonal course, lamina II contains four types of neurons (islet, filamentous, curly, and stellate cells; their dendroarchitecture is described in detail below (see Fig. 7.6).

Islet Cells These neurons are mainly found in the central parts of lamina II. They have primary dendrites only on a limited surface of the perikaryon. In the most characteristic samples, the first-order dendrites originate from tightly grouped points on the soma, then diverge by branching on diametrically opposite directions. The shape of the dendritic tree resembles a parasol pine. Recurrent dendrites are numerous. Other cells of this class have primary dendrites on two opposite poles of the soma. This cell type, exclusively oriented in the rostrocaudal axis of the cord, closely resembles the islet cells identified by Gobel (1975a, b) in the spinal trigeminal nucleus of the cat. Islet cells represent about 30% of the lamina II neuronal population in humans. They have sparse, irregularly distributed dendritic spines. The axon usually originates on the proximal segment of a primary dendrite. After a short course in the rostral or caudal direction, the axon bifurcates repeatedly at obtuse angles in the immediate vicinity of the neurons. Most axonal branches run longitudinally. Some of them are recurrent collaterals so that the axonal network extends to both sides of the perikaryon. Numerous "boutons en passant" and a few terminal boutons, sometimes grape shaped, can be observed. Rarely, islet cells emit two axons, one originating on the cell soma and the other on a dendrite.

Filamentous Cells These cells are located either in the inner or in the outer portion of lamina II. They are small and have two to three large-caliber dendrites which branch out into a limited number of daughter branches. The main characteristic of these cells is the presence of fine expansions of varied lengths,

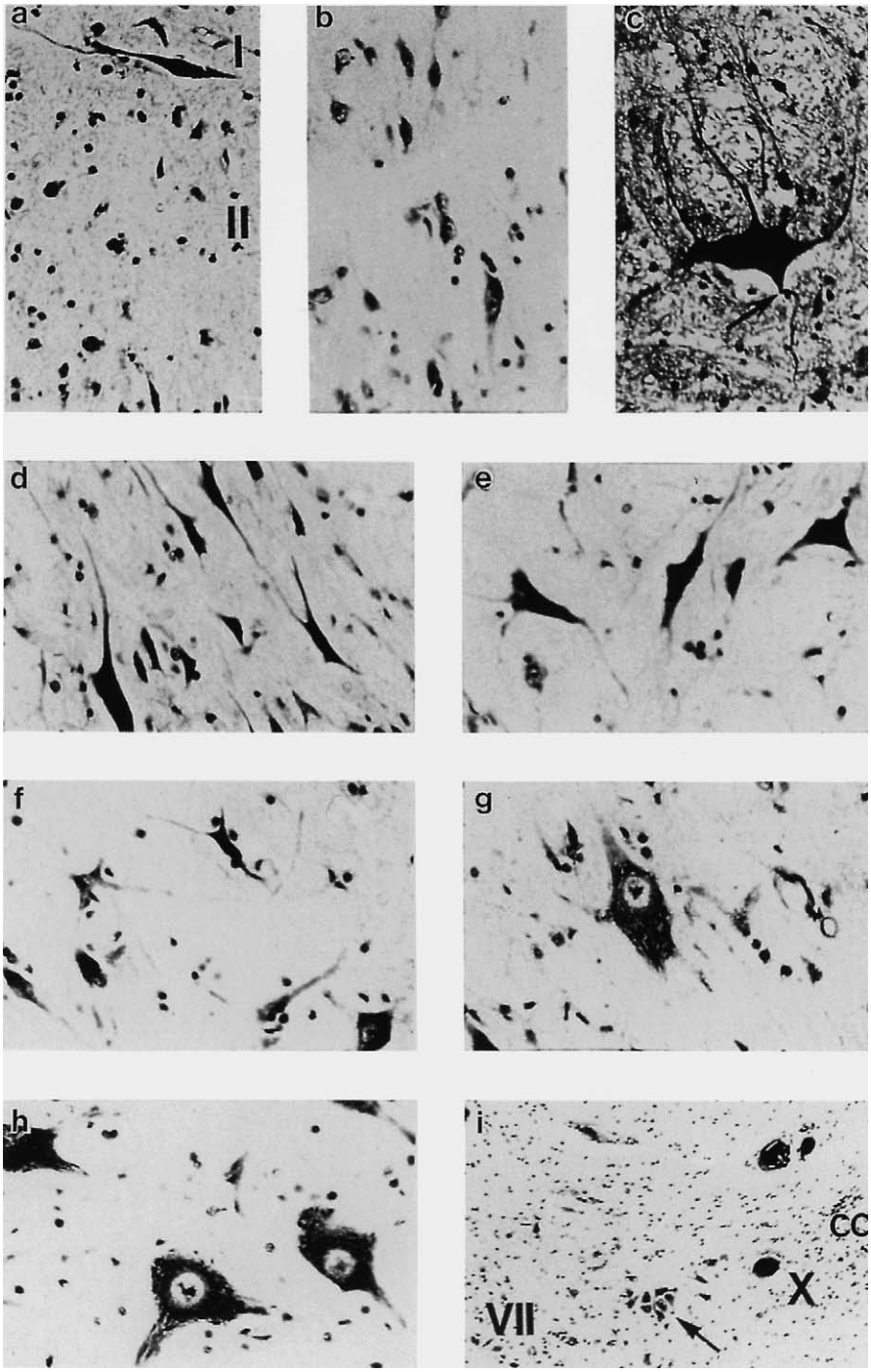

FIGURE 7.4 High-power photomicrographs of poorly differentiated Nissl-stained sections illustrating the cytological characteristics of neurons located in the 10 laminae of human spinal gray matter. **(a)** Transverse section of laminae I and II. A large, fusiform, tangentially oriented lamina I neuron can be seen. Magnification: ×455. **(b)** Horizontal section of lamina II. Note the rostrocaudal orientation of most perikarya. Magnification: ×500. **(c)** Transverse section of lamina IV. Note the large "antenna-like" neuron with a ventral axon *(arrow)*. Magnification: ×500. **(d)** Transverse section of the medial portion of laminae V–VI. Most neurons are fusiform. Magnification: ×455. **(e)** Transverse section of the lateral portion of lamina V–VI. Most neurons are multipolar. Magnification: ×455. **(f)** Transverse section of laminae VII. Neurons are multipolar, but smaller than in laminae V–VI. Magnification: ×455. **(g)** Transverse section of laminae VIII. Note the large neuron. Magnification: ×455. **(h)** Transverse section of lamina IX. Large motoneurons can be seen. Magnification: ×455. **(i)** Transverse section of lamina X. Glial and neuronal elements surround the central canal (cc). The intermediomedial nucleus *(arrow)* is located ventrally at the border between laminae VII and X. Magnification: ×125.

garnishing the entire dendritic tree and conferring the "filamentous aspects" to the cell. In most neurons, the dendritic tree is clearly asymmetrical, predominantly developed on one side of the cell soma. Certain neurons, however, have a bipolar dendritic organization. The orientation of filamentous neurons is always vertical. They represent approximately 20% of the neuronal population impregnated in lamina II. Dendritic spines are more numerous on the filiform branches than on the thick dendrites. The axon issues from the pole opposite to the dendritic tree, gives off a few local branches, then leaves lamina II to penetrate into lamina I or into Lissauer's tract. The axon has a dorsal direction both in dorsally and ventrally located cells.

Curly Cells Among human lamina II neurons, this cell type displays the most complex dendritic tree. Primary dendrites, few in number, give off large-caliber branches, coated with short filiform branches and stalk-like appendages. Most dendrites curve toward each other and thus intermingle to give the "curled" aspect that characterizes this cell type . Curly cells are the least numerous of the four cell types, representing about 10% of lamina II neurons. They are generally located in the outer substantia gelatinosa. Curly cells have abundant dendritic spines that are thin and stubby necked. The axon emerges from a first-order dendrite, runs straight toward the margin of the dorsal horn, and can often be seen to penetrate into lamina I or Lissauer's tract.

Stellate Cells These cells are characterized by a simple dendroarchitecture. Numerous primary dendrites issue from the entire surface of the perikaryon and branch in a rectilinear fashion in many directions within the sagittal plane. These neurons are of the isodendritic type while the other cells in lamina II belong to the allo- or idiodendritic class. The dorsoventral dendrites of stellate cells may cover the entire depth of lamina II and even penetrate a short distance into laminae I and III. Stellate cells preferentially occupy the inner portion of lamina II and represents about 40% of impregnated neurons. Dendritic spines are numerous and spread irregularly over the dendritic tree. The axon issues from the cell soma or, more rarely, from a primary dendrite; it has a ventral direction and one or several collaterals that penetrate deeply into underlying laminae III and IV. Within lamina II, there are some longitudinal axon collaterals.

Morphometric Analyses These confirm the distinct dendritic geometry of each of the four cell types. All lamina II neurons are small, the largest diameter of their perikaryon being around 20 µm. Islet neurons of the adult cord cover a longitudinal territory of 700–800 µm in the rostrocaudal axis. Their dorsoventral or mediolateral extension, however, is less than 50–80 µm. The vertical dendritic extension of filamentous cells can reach 300 µm. Their dendritic spread is greater in the sagittal (50–80 µm) than in the transverse plane (10–30 µm). This explains why, on the transverse plane of section, the visible portion of the dendritic tree is minimal. The dendrites of curly cells occupy a circular territory in the sagittal plane. Because of the curved trajectory of the majority of dendrites, the territorial diameter is low (less than 300 µm). The mediolateral expansion is negligible. The dendritic tree of stellate cells spreads radially in the sagittal plane. Maximal dendritic extension reaches 400 µm in the longitudinal axis, 300–350 µm in the vertical axis. All lamina II neurons have a high ramification index (3.75–4.42), but this is in part due to the presence of recurrent dendritic branches, particularly in islet and curly cells.

Ramón y Cajál (1909) was the first to call attention to the existence of two cell types in the substantia gelatinosa: the "cellule limitrophe" and the "cellule centrale et antérieure." In lamina II of the macaque spinal cord, Beal and Cooper (1978), using the Golgi–Cox method, described a large variety of neurons with different dendritic morphologies. They also proposed a subdivision of the substantia gelatinosa into three differently organized zones: the external zone, or the external portion of lamina II in the cytoarchitectural map of the cat (Rexed, 1964), which is characterized by numerous oblique and ventral dendrites; the middle zone, containing the internal portion of lamina II and the dorsal portion of lamina III, characterized by longitudinal dendrites; and the internal zone, corresponding to the ventral portion of lamina III in the cytoarchitectural scheme and containing principally oblique dorsal dendrites. In our human material, such a stratification of lamina II was not found. However, the four neuronal types described above (Fig. 7.6) do not have an identical topographic distribution. Gobel (1975a, b) described four cell types in lamina II of the cat spinal trigeminal nucleus. Islet cells are identical in his report and in our human studies. Gobel's "border cells" resemble stellate cells in lamina II, except that the axon of "border cells" branches within laminae I, II, and III, while the axon of stellate cells provides collaterals to lamina II and extends into lamina III and IV. The last two neuronal types described by Gobel in the cat, the "stalked cell" and the "abnormal cell" have not been found as such in humans. However, the stalked cell can be compared to the curly cell because of the short, stalk-like dendritic appendages, and the vertical orientation of dendrites is common to both the arboreal cells in the cat and the filamentous cells in

the human cord. Nevertheless, the dendritic tree of the latter is much less extensive, and its axon gives collaterals only to laminae I and II.

Finally, both Gobel's (1975b) results and our human studies have shown the presence of two axons on some lamina II islet cells. The existence of short-axoned Golgi type II neurons in lamina II is controversial. Golgi (1890) pointed out their abundance in the substantia gelatinosa. This observation was challenged by Ramón y Cajál (1909), who found that these neurons were very rare in this location, a finding supported by all subsequent studies of Rolando's substantia gelatinosa using the Golgi method in cats or monkeys (Beal and Cooper, 1978; Scheibel and Scheibel, 1968; Sugiura, 1975; Szentágothai, 1964). In the human cord, the dense axonal network of islet cells occupies the same territory as the dendritic tree. Therefore, unlike other neuronal types identified in lamina II, these cells probably correspond to Golgi type II neurons. This is in agreement with findings in the spinal trigeminal nucleus of the cat (Gobel, 1978b) but not of the monkey (Beal and Cooper, 1978). Interestingly, both the "gate control" (Wall, 1980) and the "reciprocal sensory interaction" theories (Cervero and Iggo, 1980) of modulation of nociceptive transmission in the dorsal horn assume the presence of inhibitory interneurons in lamina II.

Lamina III

Lamina III is poorly demarcated from adjacent laminae II and IV. However, it differs from lamina II by a lower neuronal density and by the occurrence of larger neurons. Conversely, its neuronal density is higher than that of lamina IV, where neurons are larger. Lamina III also presents a distinct myeloarchitecture, which will be described below.

Lamina III contains two neuronal types, which differ in size and dendritic geometry. The majority of impregnated neurons possess an asymmetrical dendritic tree, of which the dorsal branches are more developed. These branches rise vertically from the cell soma and penetrate deeply into the overlying lamina II, reaching 400 μm in length. Ventral dendrites are few and short. In its antenna-like dendritic geometry, this cell type resembles lamina IV neurons but distinguishes itself by its smaller size (perikaryal diameter of 30–50 μm).

The second neuronal type is characterized by a radial dendritic tree and a smaller size (perikaryal diameter of 20 μm or less). Most of its dendrites are located in the transverse and sagittal planes, with a slight preference for a ventrodorsal spread. This cell type is more abundant in the dorsal portion of lamina III, where it may be confused with lamina II stellate cells. It can, however, be distinguished from the latter by a less ramified dendritic tree, fewer dendritic spines, and a greater mediolateral spread.

In the cat, laminae II and III were together referred to as the "substantia gelatinosa" (Szentágothai, 1964) or "gelatinosal complex" (Scheibel and Scheibel, 1968). In the human spinal cord, the dendroarchitecture of lamina III is clearly distinct from that of lamina II. The suggestion that, in humans, laminae II and III are separated entities is also supported by the experimental work of Matsushita (1969) and Ralston (1968a, b, 1979), which showed that laminae II and III differ by their connections and ultrastructure.

Lamina IV

Lamina IV is thicker than lamina III but contains only a small number of neurons of varying size. The characteristic cell type of lamina IV antenna-like neurons (Szentágothai, 1964) can be readily recognized in poorly differentiated Nissl-stained sections (Fig. 7.4c). These larger neurons have the majority of their dendrites oriented dorsally while their axons originate from the ventral region of the perikaryon.

All impregnated neurons in this lamina possess the typical antenna-like dendritic organization, already described in the cat (Szentágothai and Rethelyi, 1973). Most dendrites originate on the dorsal face of the cell and spread dorsally toward the overlying lamina II and III (Fig. 7.5). The dendritic tree extends in both the transverse and sagittal planes. However, morphometric studies show that the mediolateral spread dominates the rostrocaudal spread. Lamina IV neurons can be separated into two groups: medium cells (25–40 μm), which are the most numerous, and large cells (50–75 μm). The length of dorsal dendrites exceeds 1000 μm in the large cells; therefore, these dendrites may cross lamina II out to its dorsal border. The average ramification index for lamina IV neurons is 7.28, which is slightly lower than that of lamina III neurons (7.36). Lamina IV neurons are richly covered with dendritic spines, which are most numerous on dorsal dendrites. When the axon hillock is visible it is always located at the ventral pole of the soma.

As in the cat (Leontovich and Zukova, 1963; Szentágothai and Rethelyi, 1973), all lamina IV neurons in humans, though differing in size, have the typical antenna-like morphology (Figs. 7.6 and 7.7). The mediolateral spread of dendritic trees is not symmetrical but is more marked in lateral directions. A similar asymmetry is found in the cat lamina IV (Proshansky and Egger, 1977) and may be related to the somatotopic organization of peripheral afferents in the dorsal horn where proximal fibers from large cutaneous receptive fields terminate most laterally (Sprague and Ha, 1964; Sterling and Kuypers, 1967a). The predomi-

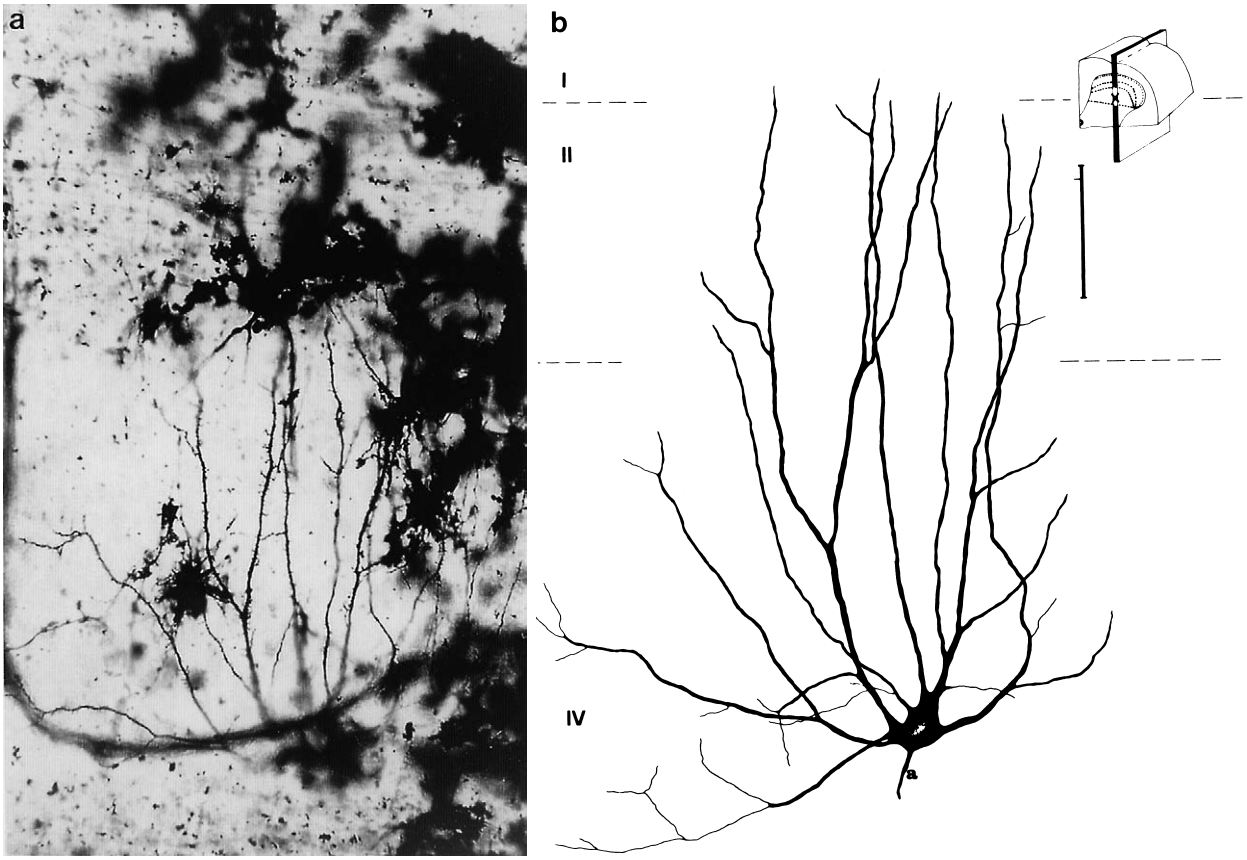

FIGURE 7.5 Large antenna-like neuron in lamina IV. Photomicrograph of Golgi preparation **(a)** and corresponding camera-lucida drawing **(b)** of a sagittal section at the lumbar level of a 1-day-old neonate. The perikaryon *(arrowhead)* is not in the plane of section. Dendritic spines are not drawn.

nantly lateral direction of horizontal dendrites may also provide for an input from corticospinal and lateral reticulospinal afferents, which may enable these effects to exert a powerful descending control on sensory mechanisms in the dorsal horn (Willis and Coggeshall, 1978; see Chapter 8). In animals, the axons of most lamina V neurons enter the spinocervical tract (Willis and Coggeshall, 1978). This tract is merely vestigial in humans (Truex *et al.*, 1970) and most projection neurons in human lamina IV are probably spinothalamic cells, as suggested by the findings in cordotomy cases (Schoenen, 1981b; Smith, 1976; see Chapter 8). The dorsal dendrites of large lamina IV neurons penetrate deeply into lamina II, some reaching the lamina I neuropil. A direct control on lamina IV projection neurons may thus be exerted by lamina II interneurons.

Laminae V and VI

Laminae V and VI occupy the base of the dorsal horn and have different characteristics in their medial and lateral portions. The medial portion contains fusiform or triangular-shaped neurons. These are medium sized and mostly dorsoventrally oriented (Fig. 7.4d). Neurons are less densely packed dorsally in laminae V and VI. Neuronal density is highest in the ventral parts of the medial portion.

The lateral portion of laminae V and VI is not well demarcated from the white matter of the dorsolateral funiculus. This part of the gray matter, corresponding to the "formatio reticularis," has its largest extension in the cervical enlargement. Most neurons are medium sized and multipolar (Fig. 7.4e).

Laminae V and VI have a very similar dendroarchitecture and therefore will be considered together. In transverse sections, neurons of laminae V and VI have a common vertical orientation of the dendritic tree. Dorsal and ventral dendrites extend symmetrically on both sides of the perikaryon in most neurons. According to the position of the soma, dorsal dendrites may cross lamina IV and extend as far as laminae III or II, while ventral dendrites may reach lamina VII. On frontal sections, only a few proximal dendritic stumps are visible, indicating that neurons in laminae V–VI have hardly any longitudinal branches.

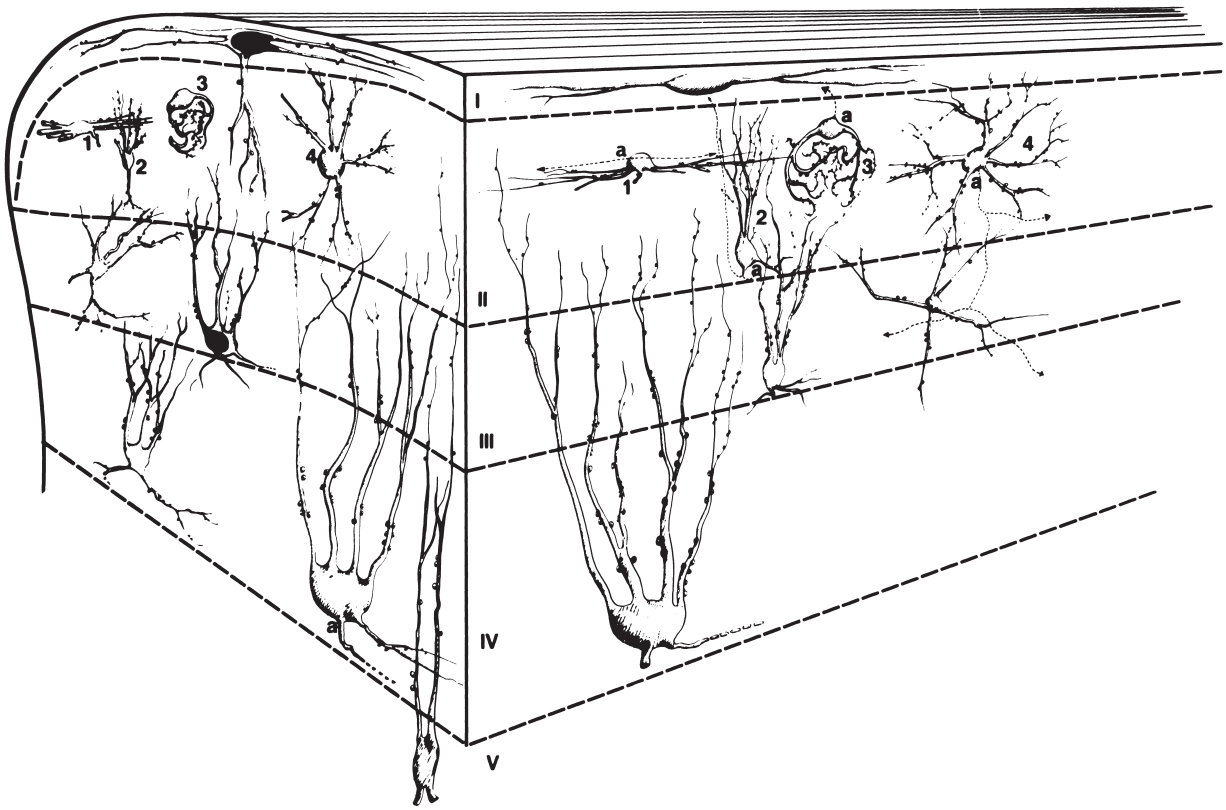

FIGURE 7.6 A representation of the various cell types identified on Golgi-impregnated transverse and sagittal sections in the dorsal horn of human spinal cord. 1, Islet cells; 2, filamentous cells; 3, curly cells; 4, stellate cells; a, axon. From Schoenen (1982a).

In addition to the general verticotransverse orientation of dendrites, some regional dendroarchitectural peculiarities need to be mentioned. There is a narrow mediolateral spread of dendritic trees in medial laminae V–VI neurons. Conversely, laterally located neurons possess a large number of horizontotransverse dendrites, some of which may reach the white matter of the dorsolateral funiculus. The mediolateral spread of dendrites is more marked in lamina VI, especially in its lateral portion. The neuronal population of lamina V is heterogeneous. In the central part of the lamina, the dorsal dendrites of some neurons may cluster and run in parallel with bundles of myelinated afferents penetrating the dorsal horn (Fig. 7.6). In its medial portion, lamina V contains cells that have a dendritic geometry reminiscent of lamina IV antenna-like neurons. Neurons of laminae V–VI have only a few dendritic spines; the initial axonal segment originates mostly from the ventral or lateral poles of the cell body.

Morphometric analyses confirm the preferential verticotransverse orientation of dendrites in these laminae. Mediolateral dendritic spread of the lateral cell population is greater than that of the medial neurons. The dorsoventral spread of medial neurons is greater than that of the lateral cells, while the dorsoventral extension of lamina VI neurons exceeds that of lamina V neurons. In the vertical axis, the total length of the dendritic tree of certain neurons can reach 1300 µm in adult material; its width in the transverse plane reaches 400 µm. The size of laminae V and VI neuronal perikarya varies between 30 and 60 µm. The ramification index is comparable in lateral (7.1) and medial (7.13) neurons, but lateral cells have fewer primary dendrites.

A similar general dendroarchitecture was thus found in laminae V and VI. Therefore, these laminae may comprise a single morphological entity, as suggested by cytoarchitectural studies of the human cord. However, the geometry of dendritic trees differs between medial and lateral portions of lamina V and VI. Mediolateral spread of dendrites is significantly larger in lateral neurons than in medial neurons. This is in accordance with the observations of Proshansky and Egger (1977) in the L6 segment of the cat and with the anatomical subdivision of Ramón y Cajál (1909).

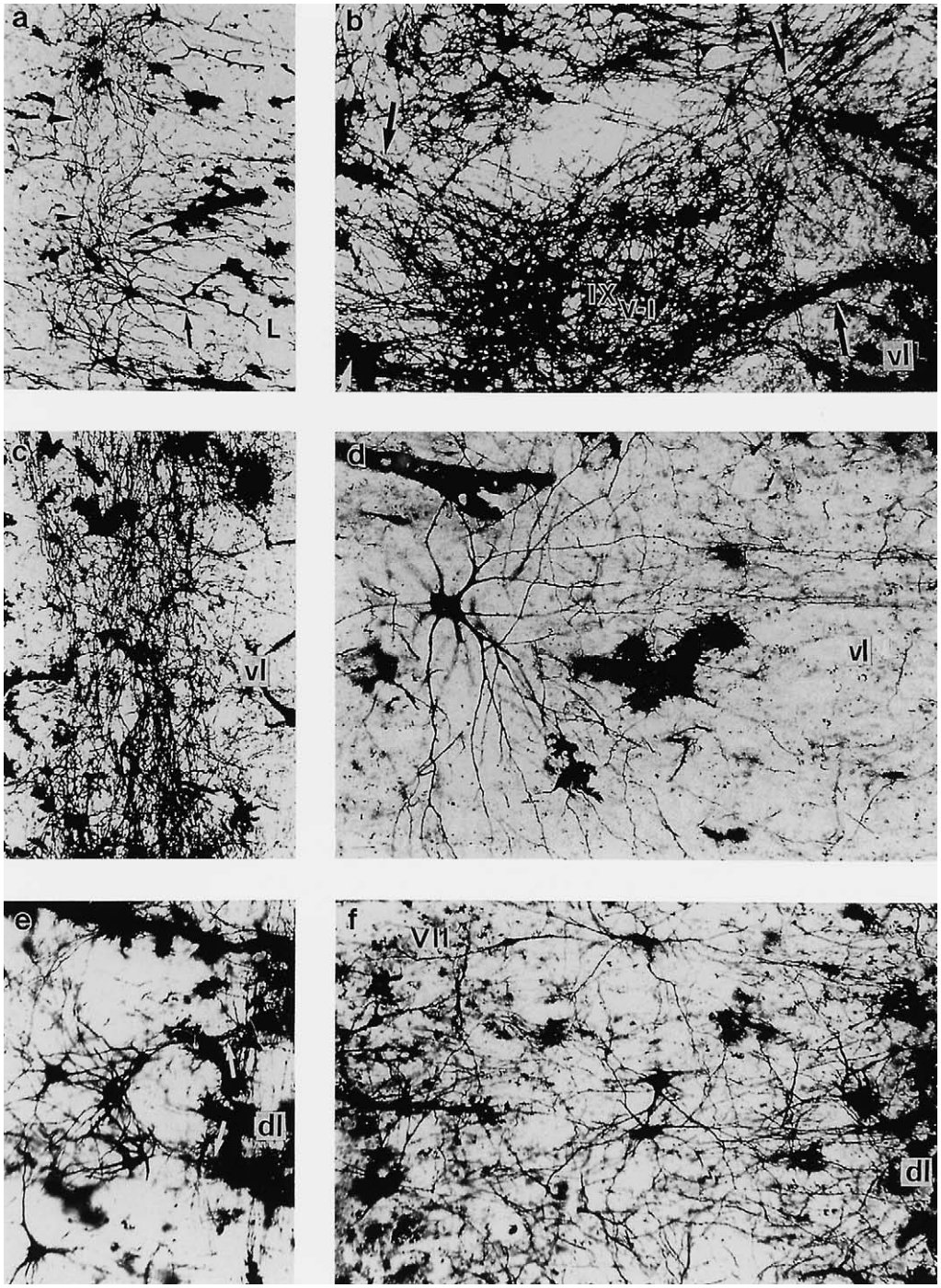

FIGURE 7.7 Golgi-impregnated central, ventrolateral, and dorsolateral motoneurons. **(a)** Horizontal section of the central motoneuronal column at the lumbar level of a 26-week-old fetus. Note the longitudinal dendritic plexus and beginning of bundling *(arrow)* of lateral dendrites (L). Magnification: ×77. **(b)** Transverse section at L5 of a 42-year-old adult. The ventrolateral column of motoneurons (IX_{v-l}) has medial and lateral dendritic bundles *(arrow)*. Magnification: ×73. **(c)** Sagittal section of the ventrolateral motoneuronal column at L5 of a 22-year-old adult. Note the loosely meshed longitudinal dendritic plexus. Magnification: ×50. **(d)** Horizontal section of a lateral motoneuron of the ventrolateral column at the lumbar level of a 1-year-old baby. Note the dendritic geometry characterized by rostral, caudal, and lateral branches, the latter penetrating the ventrolateral funiculus. Magnification: ×115. **(e)** Horizontal section at the lumbar level of a 36-week-old fetus. Shown are border cells of the dorsolateral column, forming short transverse bundles which reach the dorsolateral funiculus. Magnification: ×125. **(f)** Horizontal section of the dorsolateral motoneuronal column at the lumbar level of a 2-month-old infant. Note that most dendrites are transversely oriented. Magnification: ×115. Dl, Dorsolateral funiculus; vl, ventrolateral funiculus. From Schoenen (1982b).

From animal experiments it is known that laminae V and VI receive an important contingent of primary afferents of which the terminal arborizations are verticotransverse and avoid the longitudinal axis of the cord (Brown, 1977; Ramón y Cajál, 1909; Scheibel and Scheibel, 1969a; Sprague and Ha, 1964; Sterling and Kuypers, 1967a). The preferential dendritic orientation, as described above, could therefore be parallel to primary afferent terminals, which would favor spatial discrimination of peripheral inputs. In animals, primary afferents of the dorsal horn undergo a dual somatotopic organization. Fibers originating distally terminate in the medial portions of the cord while proximal afferents project onto the lateral portion (Sprague and Ha, 1964). In addition, in the dorsoventral axis of the dorsal horn, there is a progressive enlargement of peripheral receptor fields, with the most ventral neurons displaying the largest cutaneous territory (Applebaum *et al.*, 1975; Brown and Fuchs, 1975; Bryan *et al.*, 1973; Price and Mayer, 1974; Wall, 1967). In accordance with this somatotopic organization, Proshansky and Egger (1977) found in the cat a larger mediolateral dendritic spread in lateral laminae V–VI neurons as compared to medial neurons, and in lamina VI neurons as compared to lamina V cells. Lateral neurons also differ from medial neurons by a large supraspinal and propriospinal input in addition to peripheral afferents, as demonstrated in the cat (Kuypers, 1964; Liu and Chambers, 1964; Nyberg-Hansen and Brodal, 1963; Sterling and Kuypers, 1968) and in humans (Schoen, 1964; Schoenen, 1981b). The greater diversity of afferents could thus be responsible for the more radial morphology of dendritic trees, if one accepts such a causal relationship (Ramón-Moliner, 1967).

Lamina VII

Lamina VII has poorly defined borders. It differs from adjacent laminae V–VI by its lower neuronal density. All neurons are medium sized but vary widely in shape (Fig. 7.4f). Fusiform, mediolaterally oriented neurons predominate in lateral lamina VII, which lies close to the dorsolateral column of motoneurons. Multipolar cells are more frequently found in the central and dorsal regions of lamina VII, while triangular-shaped cells are more numerous in the ventral portion of lamina VII at the level of the enlargements.

In transverse sections, lamina VII is formed by an apparently homogeneous population of medium-sized multipolar neurons. Although these neurons are similar to neurons in laminae VI and VIII, the lamina VII neurons are characterized by a larger number of horizontal or oblique dendrites. These dendrites are the only branches visible in frontal sections; longitudinal dendrites are virtually absent (Fig. 7.8).

Regional dendroarchitectural differences are also found in lamina VII. There is a gradual modification of dendroarchitecture in passing from the lateral to the medial portion of the lamina. Some lateral neurons, adjacent to the dorsolateral column of motoneurons, possess a bipolar dendritic tree that is obliquely oriented in the transverse plane. Neurons located in

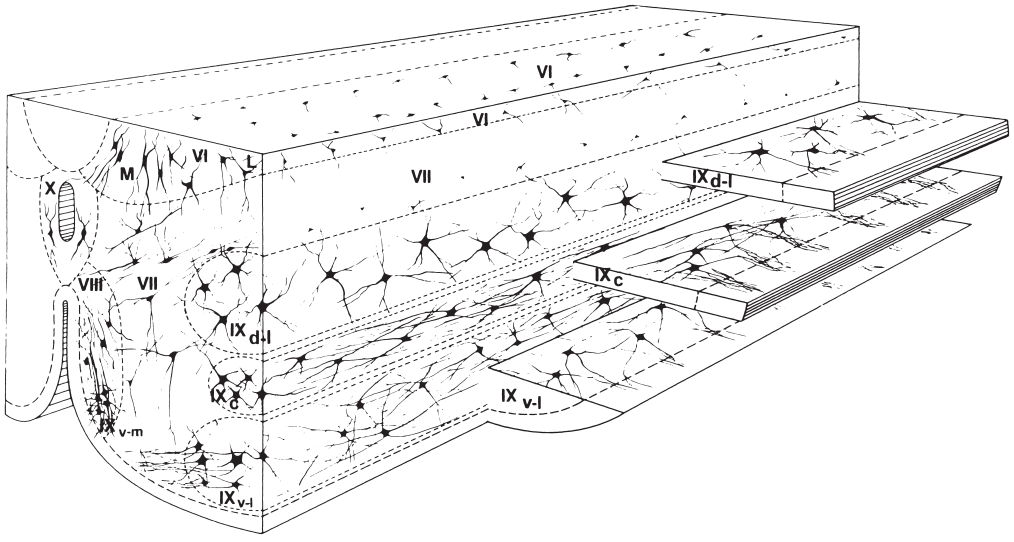

FIGURE 7.8 Three-dimensional representation of spinal dendroarchitecture in the intermediate gray matter and the ventral horn. $IX_{v\text{-}m}$. Ventromedial; $IX_{v\text{-}l}$, ventrolateral; IX_c, central; and $IX_{d\text{-}l}$, dorsolateral columns of motoneurons; M, medial; L, lateral. From Schoenen (1982b).

the central and ventral portions of lamina VII have, in addition, long though scarce ventral dendrites. On the contrary, medial cells X present a rich dorsal dendritic arborization. The dendritic spine density of lamina VII neurons lies between that of motoneurons, which have the lowest spine density, and neurons of overlying laminae. The position of the initial axonal segment is variable.

Morphometric data computed for the entire cell population of lamina VII indicates that dendrites extend mainly in medial and lateral directions. In addition, they show that on average, polarization of dendritic trees occurs along a slightly oblique horizontal transverse axis with a ventromedial and a dorsolateral pole. This is clearly distinct from dendritic polarization in laminae VI or VIII. The territory covered by transverse dendrites can be considerable, certain dendrites extending over the entire width of the gray matter from lamina X to the white matter of the dorsolateral funiculus, i.e., up to 2 mm. The ramification index of lamina VII neurons is 7.45, which is higher than that of lamina VIII or IX neurons.

Lamina VII receives a small contingent of primary afferents, originating chiefly from muscles and joints (Eccles *et al.*, 1954; Menetrey *et al.*, 1977). These afferents are concentrated in the medial portion, where they form small vertical bouquets corresponding to the "collatérales du noyau gris intermediaire" of Ramón y Cajál (1909; Sterling and Kuypers, 1967b). Interestingly, the dorsal dendritic tufts of lamina VII neurons in the human cord have a similar morphology and orientation. Supraspinal and propriospinal afferents terminate massively in lamina VII (see Chapter 8). Again, the preferential dendritic orientation of lamina VII neurons, oblique in the transverse plane, corresponds to the axis through which the major afferents penetrate this lamina: ventromedial course for dorsolateral afferents (i.e., lateral cortico- and reticulospinal, dorsolateral propriospinal) and dorsolateral course for ventromedial afferents (i.e., ventral cortico- and reticulospinal, ventromedial propriospinal).

Lamina VIII

Lamina VIII has, in contrast to the previously described laminae, a dorsoventral extension. It is characterized by cytological heterogeneity as it contains small-, medium-, and large-sized neurons of varying shapes. The larger multipolar neurons differ from motoneurons only by finer appearance of their Nissl bodies (Fig. 7.4g).

In transverse section the dendritic tree of lamina VIII neurons is predominantly vertically oriented. Most dendrites originate from either the ventral or dorsal pole of the soma. Dorsal dendrites are directed toward the ventral gray commissure without crossing the midline, or toward lamina VII. Ventral branches run toward the ventromedial tip of the ventral horn. A few dendrites penetrate into the white matter of the anterior funiculus. Lamina VIII neurons have no longitudinal dendrites. Dendritic spines appear more numerous than in lamina VII or IX and predominate on proximal dendrites. When impregnated, the axon hillock has a dorsal orientation.

Morphometric analyses confirm the dorsoventral polarization of dendritic trees in lamina VIII. In most neurons the vertical dendritic extension is symmetrical on either side of the soma, with minimal mediolateral spread. The vertical transverse territory covered by the dendritic tree may be more than 1 mm in the largest neurons. These large neurons have a perikaryal diameter of up to 80 µm, but small cells with a diameter not exceeding 30 µm are also found. The ramification index (3.12) of lamina VIII neurons is among the highest found in human spinal neurons.

According to observations in animals, most afferents to lamina VIII are oriented vertically in the transverse plane and thus parallel to the preferential orientation of dendritic trees found in the human cord. This is the case for the propriospinal fibers (Matsushita, 1969; Ramón y Cajál, 1909; Sterling and Kuypers, 1968), medial vestibulo- and reticulospinal fibers (Kuypers *et al.*, 1962), and primary afferents to the dorsal portion of the lamina (Scheibel and Scheibel, 1969a; Sterling and Kuypers, 1967a).

Lamina X

Lamina X corresponds to the periependymal gray matter and is characterized by the dense structure of its neuropil and a low cell body density. The lamina X neurons are small in contrast to those of adjacent laminae V–VI, VII, and VIII.

As shown in Fig. 7.4i, a cluster of small neurons may be seen at the border between lamina VII and lamina X. These form the intermediomedial nucleus. This nucleus does not form a continuous column along the rostrocaudal axis of the cord, but has a beaded structure, so that it is not identifiable on all sections.

Despite the low number of neurons impregnated on Golgi stains in this lamina, two cell types can be recognized. The first type is found in the mid- and dorsal portions of lamina X. These cells have a bipolar appearance with a fan-shaped dendritic tree branching from one, or rarely, two, primary dendrites located at the ventral and dorsal pole of the soma. Dorsal dendrites may reach the medial part of lamina VI, whereas ventral branches penetrate into lamina VIII. Dendritic spines are spare. The axon is frequently impregnated:

it is directed first laterally, then bifurcates into a dorsal branch crossing laminae VI and V and a ventral branch penetrating lamina VII. On morphometry, dendritic spread is clearly dorsoventral and limited to the transverse plane. Dorsoventral extension of dendritic trees does not exceed 600 µm in adult human material. The high ramification index of 4.16 underlines the richness of dendritic branching.

The second neuronal type is located is in the ventral portion of lamina X. Its dendritic tree is morphologically simple and poorly ramified. Primary and secondary dendrites are oriented along the rostrocaudal axis of the cord, parallel to the central canal. Dendritic spines are sparse and only the axon hillock is impregnated. Morphometric analyses show that this cell type is also bipolar, but dendritic polarization is longitudinal, in contrast to the first neuronal type. The total extension of the dendritic tree is considerable, reaching 1.5 mm in adult human material. The ramification index (7.3) is distinctly lower than in the first neuronal type. The perikarya of both lamina X cell types are of comparable size (30–35 µm).

The two cell types found in human lamina X can be compared to the "neurone fusiforme ou triangulaire" and the "cellule étoilée" described by Ramón y Cajál (1909) in the cat. Until recently, lamina X has received little attention from neuroanatomists and neurophysiologists. Interest in this lamina has been revived by the demonstration of a large number of afferents containing various neuropeptides (for a review, see Honda and Lee, 1985). Lamina X probably receives a strong visceral input and has a role in autonomic function.

Lamina IX (Motoneurons)

Lamina IX contains the motoneurons, which are grouped in several columns. Motoneurons are easily recognized by their large size, multipolar shapes, and abundance of large Nissl bodies (Fig. 7.4h). In accordance with the work of Massazza (1922, 1923, 1924), we have identified three columns of motoneurons at the L5 level: a dorsolateral, a ventrolateral, and a central column (Fig. 7.1). In addition, a ventromedial column of motoneurons is found at the L4 level, occupying the ventromedial tip of the ventral horn (Fig. 7.2). Motoneurons have been counted in the human lumbosacral cord by two research groups. The total number of motoneurons in segments L1 to S5 lies between 52,000 and 62,000, with segment L5 frequently containing the largest number of cells (around 10,000) and segment S1 showing the highest density of motoneurons per section (Irving *et al.*, 1974; Tomlinson *et al.*, 1973). In the L5 segment, the size distribution of lamina IX neurons is approximately as follows: 65% large-diameter cells (35–60 µm), 25% intermediate-diameter cells (25–35 µm), and 10% small-diameter cells (less than 25 µm) (Kawamura *et al.*, 1977). The number of motoneurons decreases with age, chiefly around 60 years (Tomlinson and Irving, 1977). It has been estimated that about 200 lamina IX neurons are lost per decade.

Laruelle (1937, 1948) was the first to call attention to the particular dendroarchitectural organization of motoneurons. Using the Bielchowski–Reumont silver impregnation technique in longitudinal sections of the cord, he showed that in various species the majority of motoneuron dendrites are rostrocaudally oriented. Unknown to earlier authors whose studies were exclusively based on transverse sections, this dendritic organization was later confirmed in the cat with the Golgi technique (Balthasar, 1952; Scheibel and Scheibel, 1966a, 1969b; Sterling and Kuypers, 1967b).

In 1970, the Scheibels (1970a, b) renewed interest in the anatomy of motoneurons by showing that their dendrites are gathered into bundles and suggesting that these dendritic bundles might play a role in certain motor programs in the cat. The Golgi method and morphometric analyses of dendritic orientation reveal distinct dendroarchitecture for each motoneuronal column.

Ventromedial Column On transverse sections, the ventromedial motoneurons present a characteristic configuration. One or two primary dendrites of large diameter arise from the dorsal surface of the neurons. These apical dendrites and their daughter branches cross lamina VIII toward the ventral gray commissure or, rarely, toward lamina VII. The ventral, or basal, pole of the perikaryon emits a large number of primary dendrites (three to five), which ramify entirely in a fanlike arrangement. On longitudinal sections, several dendrites from the ventral perikaryon are oriented rostrocaudally, but they are fewer and shorter than longitudinal branches in other motoneuronal columns. Dendritic spines appear most numerous on ventral dendrites. The axon generally arises from the basal pole of the perikaryon.

Ventromedial motoneurons form vertical and longitudinal dendritic bundles. Vertical bundles are composed of 10–30 dendrites, mostly secondary branches belonging to adjacent motoneurons. They are oriented dorsally, and penetrate lamina VIII to reach the ventral gray commissure, but do not cross the midline. During their course through lamina VIII they may receive dorsal or ventral dendrites from neurons within this lamina. The vertical dendritic bundles of ventromedial motoneurons are among the longest and thickest observed in the human cord. They may extend over

2–3 mm in the ventrodorsal axis and their thickness varies from 30–100 µm.

The longitudinal dendrites of ventromedial motoneurons intermesh within the rostrocaudal axis of the cord to form a dendritic plexus which is continuous over the entire length of the motoneuronal column and contains dendritic "microbundles." The latter are formed by five or less dendrites and do not exceed 5–10 µm in width and a few tens of micrometers in length. The dendrites are of variable thickness and order, belonging to neighboring or distant neurons. They may pass from one microbundle to another within the longitudinal dendritic plexus. Both vertical and longitudinal dendritic bundles of the ventromedial motoneurons are already well developed in the 26-week-old fetus.

Morphometric analyses of dendritic spread, i.e., vector analysis (for details, see Schoenen, 1982b), show that the ventromedial motoneurons are preferentially oriented in dorsal, rostral, and caudal directions, with a predominance of dorsal spread. The total length of longitudinal dendrites does not exceed 500–800 mm, even in adult material, which is much lower than in other motoneurons.

Central Column On transverse sections, motoneurons of the central column present a radial, multipolar dendritic tree. The characteristic dendroarchitecture of central motoneurons appears in longitudinal sections. The majority of dendrites are oriented along the rostrocaudal axis of the cord (Fig. 7.7 a).

After a short trajectory, dendrites arising from the medial surface of the perikaryon curve at right angles and spread into the longitudinal axis. In contrast, dendrites on the lateral face of the soma extend perpendicular to the longitudinal dendrites toward the lateral border of the ventral horn, penetrating, with few exceptions, into the white matter of the ventrolateral funiculus. Dendritic spines are scarce. The position of the initial axonal segment varies.

The central motoneuronal column is characterized by transverse and longitudinal dendritic bundles. The lateral dendrites of central motoneurons gather to form large dendritic bundles, which head toward the ventrolateral funiculus. These are formed at first- and second-order dendrites of adjacent motoneurons that join the bundles only at a distance of 50–100 µm from their soma of origin. These laterally oriented bundles contain several tens of dendrites and reach a thickness of 80 µm and a length of 2 mm. Unlike the vertical bundles of the ventromedial column, the lateral dendritic bundling of central motoneurons is inconspicuous in the 26-week-old fetus (Fig. 7.7a), but easily recognized from 36 weeks of fetal age onward.

Longitudinal dendrites of central motoneurons intermesh within the rostrocaudal axis of the cord to form a longitudinal dendritic plexus with microbundles comparable to that described in the ventromedial column. Longitudinal microbundles can be readily identified as early as 26 weeks *in utero* (Fig. 7.7a).

On morphometric analyses of the central column, lateral dendritic spread predominates in the transverse plane, while rostral and caudal spread is prominent in the sagittal plane, confirming the triple polarization of the dendritic tree. Lateral dendrites reach a length of 1300–1500 µm in the adult and penetrate the white matter of the ventrolateral funiculus. The length of longitudinal dendrites nears 900 µm in adult material; thus, the global span of the dendritic tree in the rostrocaudal axis can reach 1800 µm or more.

Ventrolateral Column Dendritic trees of ventrolateral motoneurons are radial in the transverse plane. In the lateral portion of the column, most dendrites are laterally oriented whereas their orientation in the medial portion is medial. Sagittal and frontal sections show that longitudinal dendrites are numerous and long. They run along the rostrocaudal axis as soon as they originate at the antipodes of the cell body (Fig. 7.7d).

Like motoneurons of the central column, those of the ventrolateral column form dendritic bundles in the transverse (Fig. 7.7b) and longitudinal planes (Fig. 7.7c). The morphological features, architecture, and ontogenesis of these bundles are comparable in central and ventrolateral motoneurons. The ventrolateral column is distinguished by the existence of both laterally and medially oriented bundles, in its lateral and medial portions, respectively (Fig. 7.7b), while only lateral bundles are present in the central column.

The vector analysis shows that longitudinal dendritic spread is very pronounced. The territory covered by longitudinal dendrites is the most extensive dendritic domain in human spinal gray matter, since it can reach a total length of 3 mm in the adult. In the transverse plane, vector analyses give varying results, depending on whether the medially or laterally situated neurons are studied. Medial dendritic spread dominates in the former, lateral extension in the latter. There are differences between the morphometric data obtained from ventrolateral motoneurons and those pooled from the other motoneuronal columns. For instance, ventromedial motoneurons have a lower number of primary dendrites and are less ramified, their ramification index (1.70) being lower than that of the other motoneurons (7.13). As a consequence, the radial distance from the soma to the maximal number of dendritic intersections (and thus the perisomatic volume containing most of the dendritic membrane area) is reduced in ventrolateral

motoneurons (60 μm) compared to other motoneurons (100 μm).

Dorsolateral Column In contrast to other motoneurons, those of the dorsolateral column mostly branch out in the transverse plane, showing a rich and multipolar dendritic tree. In frontal sections the dendritic tree is also radial without clear polarization (Fig. 7.7f). In the sagittal plane, the majority of dendrites have a ventrodorsal orientation. There are a few exceptions to the multipolar dendritic organization of dorsolateral motoneurons. These are found in the cervical enlargement, where some neurons bordering the white matter have a longitudinal orientation, and in segment S1, where some ventromedially located neurons may have a similar dendroarchitecture to that of neighboring cells of the central column.

Dendritic bundling is inconspicuous in the dorsolateral column. So-called spinal border cells, located in the vicinity of the dorsolateral funiculus, give rise to short (150–200 μm or less), laterally oriented dendritic bundles, which may penetrate several tens of micrometers into the white matter (Fig. 7.7e).

On morphometry, there is a predominance of dorsal and lateral dendritic spread on transverse sections, dorsal and lateral spread on sagittal sections, and a slight preference for the rostrocaudal axis on frontal sections.

Figure 7.8 is a three-dimensional representation of spinal dendroarchitecture in the intermediate gray matter and the ventral horn. Each motoneuronal column of human spinal cord has a distinct dendroarchitecture. The dendritic tree of *ventromedial* motoneurons has a pyramidal shape resembling that of cerebral cortex pyramidal cells. Apical, dorsally oriented dendrites are the longest; longitudinal dendrites are the most numerous, although shorter. The dendritic tree of *central* column motoneurons forms a T, the base of which is planted on the lateral border of the ventral horn. The majority of dendrites are oriented along the rostrocaudal axis of the cord. Longitudinal spread of dendrites is also dominant in the *ventrolateral* column. Schematically, the dendritic tree of these motoneurons can be compared to a cross in the frontal plane, of which the longest branch is oriented along the rostrocaudal axis of the cord. The *dorsolateral* motoneurons differ from other motoneurons by their multipolar dendritic morphology. Differences in the dendritic branching pattern have been reported between human α and γ motoneurons (Abdel-Maguid and Bowsher, 1979). Our morphometric analyses, based on a greater number of large neurons than small neurons, reveal a similar dendritic organization for small (30–50 μm) and large (50–80 μm) cells. Although there may be species differences, the general somatotopic arrangement of motoneurons is well known. Motoneurons innervating proximal musculature are found in a medial and ventral position, with the ventromedial column innervating axial muscles. On the other hand, the neurons for distal muscles occupy a lateral and dorsal position in the ventral horn (Burke *et al.*, 1977; Elliott, 1944; Romanes, 1951, 1964; Sharrard, 1955; Sprague, 1948, 1951; Sterling and Kuypers, 1967b). In the cat and monkey, it is well established that motoneurons innervating a single muscle are grouped into a single longitudinal column, and columns corresponding to synergic muscles line up in the rostrocaudal axis of the cord. Within a motoneuronal column of which the preferential dendritic orientation is longitudinal, the dendritic trees overlap over a long distance. Such a dendritic organization would thus favor spatial summation along the longitudinal axis of a motoneuronal column and, consequently, synchronization and synergy. The results in the human lumbosacral cord suggest that longitudinal dendritic spread is common to motoneurons of axial, proximal, and calf muscles. These muscles have primary functions in the maintenance of posture and upright position, where synchronization and synergy are required properties. These functional properties are reinforced by the parallel orientation to dendrites of most propriospinal and supraspinal afferents (Scheibel and Scheibel, 1966a, b; Sterling and Kuypers, 1968). In contrast to longitudinal motoneuronal columns, the radial dendritic organization of the dorsolateral column only allows slight interactions between motoneurons, since only dendrites of adjacent neurons are close to each other. This column innervates distal muscles involved in fine, delicate movements of the extremities, so that it is not surprising that its dendritic organization favors precise and selective contacts with afferents.

The literature concerning motoneuronal *dendritic bundles* and differences in these between species has been reviewed elsewhere (Schoenen, 1982b). It is worth mentioning that specialized contacts resembling "puncta adherentia" have been demonstrated at the ultrastructural level within dendritic bundles of human motoneurons (Schoenen, 1981a). The exact role of dendritic bundles is still unknown. However, they are eminently favorable structures for dendrodendritic interactions and ephaptic transmission or electrotonic coupling. It has been suggested that electrotonic contacts between dendrites, transmitting a particular type of information, would constitute within a group of neurons a network of local circuits (Horcholle-Bossavit, 1978) that could serve for central programming (Scheibel and Scheibel, 1975). One can hypothesize that the functional role of the longitudinal dendritic

plexus and microbundles of motoneurons is to favor synchronization within a motoneuronal pole and also synergy between motoneurons of agonist muscles. Moreover, these structures could form a network of local circuits for electrotonic currents that would influence the excitability and tonic activity of the motoneuronal column. Synchronization and synergy are favorable in axial and antigravity muscles, which also possess an important tonic activity. It is therefore interesting to note that the longitudinal plexus is tightest in ventromedial and central columns innervating axial and antigravity muscles, respectively. In contrast to longitudinal bundles, the transverse dendritic bundles clearly have a local, intrasegmental organization, since only adjacent motoneurons in the longitudinal axis participate in a given bundle. Therefore, they could act in phasic, focal modulation of the excitability of a motoneuronal pool. In this respect, it is noteworthy that the motoneurons of an antigravity muscles, where longitudinal as well as transverse dendritic bundles are found, function tonically in maintaining posture, but discharge phasically in other activities such as locomotion (Grillner, 1975). Another peculiarity of transverse dendritic bundles is their topography and orientation within the ventral horn. They are in a close spatial relationship with two principal groups of afferents, namely, the medial system of the brain stem (Kuypers, 1981) and the propriospinal system (Barilari and Kuypers, 1969; Nathan and Smith, 1959; Sterling and Kuypers, 1969; Szentágothai, 1964). These two systems play an important role in adjusting the center of gravity and in locomotion (Delwaide, 1977; Grillner, 1975; Grillner and Zangger, 1979; Kuypers, 1973). It is therefore tempting to attribute to the transverse dendritic bundles of motoneurons a function in centrally programmed activities, such as walking. In line with this hypothesis, one would expect a parallelism between the ontogenic development of these bundles and that of certain motor activities. Such a parallelism has already been established in the kitten (Scheibel and Scheibel, 1970b). In the human lumbar cord, transverse dendritic bundles of central and ventrolateral motoneurons cannot be identified before the fetal age of 36 weeks, while bundling in the ventromedial motoneurons is easily recognizable in the 26-week-old fetus. It is worth relating this anatomical observation to the development of motor function in the fetus. Automatic walking is well developed in the 36-week-old premature infant, whereas it is absent in the 26- to 28-week-old premature infant. In contrast, primitive reflex activities with a predominantly tonic component, such as an incomplete Moro reflex, are already elicitable by 26 weeks (Sher and Brown, 1975). This would thus suggest a developmental synchronism between the different types of motoneuronal dendritic bundles and specific motor programs.

Segmental Variations

In the previous sections, we have described the laminar cytoarchitectural organization of the spinal gray matter at the level of the enlargements. However, it is well known, that the volume and the shape of the spinal gray matter vary along the length of the cord. These variations are commonly used to identify specific spinal segments on histological sections. We have studied regional and segmental variations of spinal cytoarchitecture from C1 to the conus terminalis on serial sections of the spinal cord from a 45-year-old person.

All the neuronal laminae described previously are present throughout the length of the cord down to the lower sacral segments. However, certain laminae undergo important size variations according to the segmental level. As a consequence, the topography of other laminae may be modified. In addition, some neuronal groups such as the central cervical nucleus, the dorsal nucleus of Clarke, the intermediolateral nucleus, and the parasympathetic sacral nuclei, which are easily recognizable, are present only at certain segmental levels. For this reason, they are not included in the general lamina cytoarchitectonic scheme. Only the most significant segmental variations of spinal cytoarchitecture will be described below.

The volume of laminae V–VI is markedly reduced at the thoracic level due to the appearance of Clarke's column in its ventromedial portion (Fig. 7.10). Extension of lamina VII is maximal at the level of the enlargements where this lamina reaches the ventral border of the gray matter between lamina VIII and IX. This ventral portion of lamina VII disappears at thoracic levels. At these levels, lamina VIII, while confined to the medial aspect of the ventral horn in the enlargements, occupies the whole width of the central part of the ventral horn (Fig. 7.9). From thoracic level T1 to the lumbar segment L1, the intermediolateral nucleus can be found in the lateral tip of lamina VII. The central cervical nucleus is found lateral to lamina X at caudal levels of the pyramidal decussation and at cervical levels. It is evidenced by its acetylcholinesterase-clear background marked by stained vascular elements.

Lamina IX is most developed at the level of the enlargements, but the various motoneuronal columns are not found in all segments. The ventromedial column, for instance, can be identified from segments C1 to segment L4; it is the only motoneuronal column identifiable in superior cervical and thoracic segments.

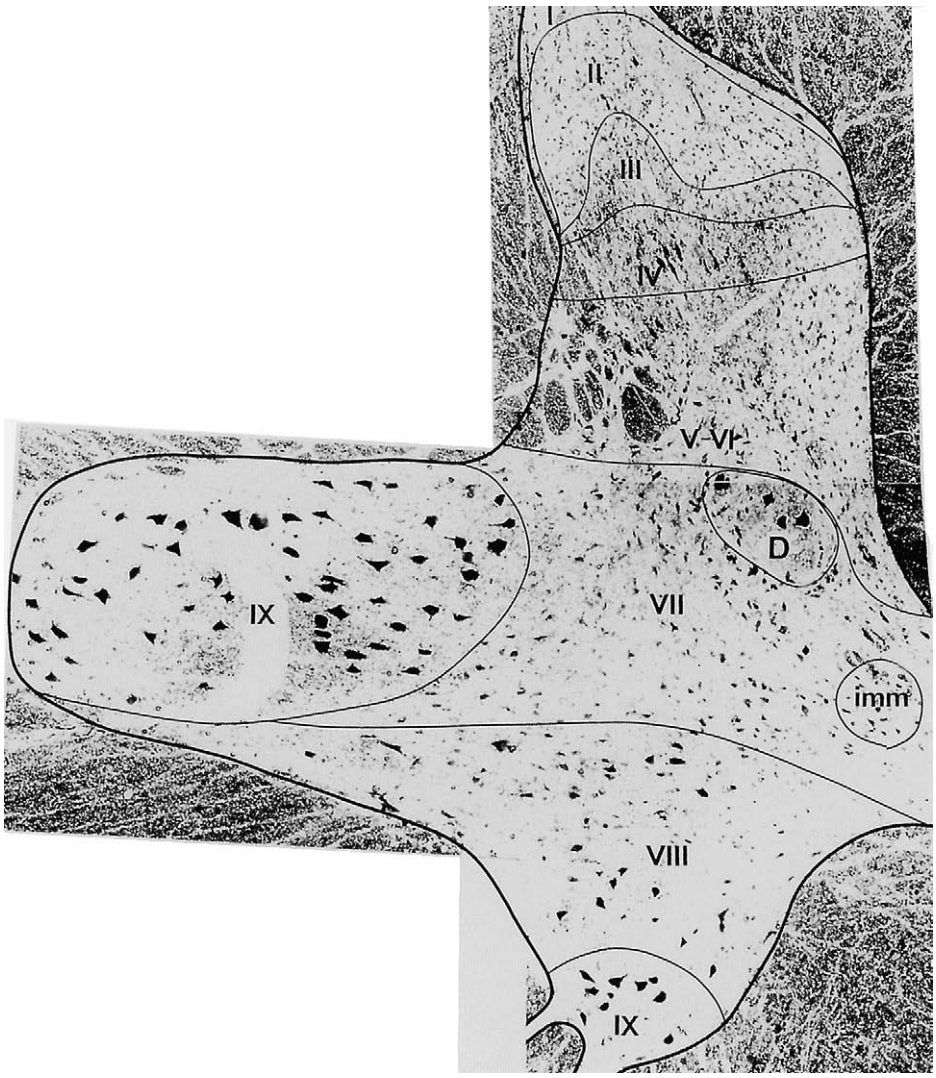

FIGURE 7.9 Photomontage of transverse cresyl violet–stained sections at level T1 illustrating the segmental variations of spinal laminar cytoarchitecture. The T1 segment belongs to the "transitional" cytoarchitectural type. It has features in common with the "thoracic" type [dorsal nucleus of Clarke (D), lamina VIII occupying the width of the ventral horn] and with the "enlargement" type (voluminous dorsolateral column of motoneurons); imm, intermediomedial nucleus. Magnification: ×13.5.

Below the fourth lumbar segment, the ventromedial column of motoneurons disappears.

Below the fourth sacral segment, the cytoarchitectonic laminae progressively vanish. From segment S3 on, there is a midline fusion of the gray matter of the dorsal horns. In addition, the last sacral segments are characterized by the parasympathetic nuclei. The conus terminalis only contains a few cells of glial morphology surrounding the terminal ventricle. At the opposite extremity of the cord, the laminar cytoarchitectural organization extends into the lower medulla where laminae I–IV can be identified in the caudal trigeminal complex. However, rostral to the spinomedullary junction these laminae rotate 90° around the central canal, so that their orientation becomes dorsoventral.

Figure 7.10 is a schematic illustration of the regional surface variations of the first nine cytoarchitectonic laminae from segment C1 to segment S4. From these studies, one may infer the existence of three main region-dependent cytoarchitectural types in the human spinal cord (detailed below) that are comparable to those described by Rexed in the cat:

1. *Enlargement type.* The enlargement type (C4–C8; L4–S2) (see Figs. 7.1 and 7.2) is characterized by expansive dorsal and ventral horns, a large lamina V–VI, a

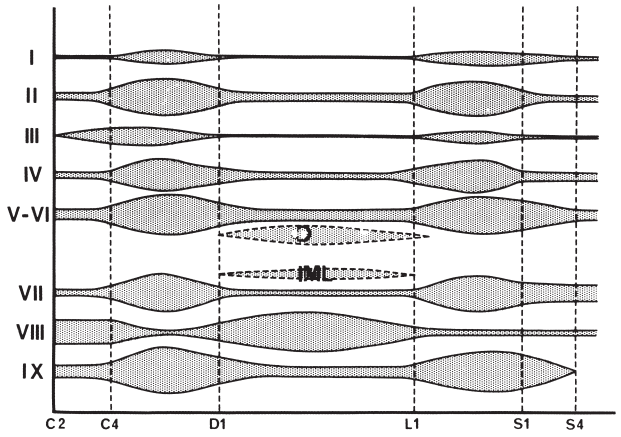

FIGURE 7.10 The surface variations of cytoarchitectural laminae from segment C2 to the sacral level. D, Dorsal nucleus of Clarke; IML, intermediolateral column.

ventrally extended lamina VII, a medially confined lamina VIII, and an extensive lamina IX comprising several motoneuronal columns.

2. *Thoracic type.* The thoracic type (T2–T12) is characterized by a much reduced gray matter, absence of large antenna-like neurons in lamina IV, partial replacement of laminae V–VI by Clarke's column, the presence of the intermediolateral nucleus, the spread of lamina VIII from the medial to the lateral border of the ventral horn, and the sole persistence of the ventromedial motoneuronal column.

3. *Transitional type.* The transitional type is characterized by an intermediate cytoarchitectural organization. This type is found in segments C1–C3, T1, L1–L3, S3, and S4. Figure 7.9 illustrates the cytoarchitectural organization of segment T1, which resembles the thoracic type by the presence of Clarke's column and the topography of laminae VII and VIII but, similar to the enlargement type, contains a well-developed dorsolateral column of motoneurons. From S1–S2 to S4, a supplementary column of motoneurons appears in the ventral horn. This is Onuf's nucleus, which lies at the most ventral border of the ventral horn medial to the other motoneuronal columns. Onuf's nucleus is divided into a dorsomedial cell group innervating the bulbocavernosus and ischiocavernosus muscles and a ventrolateral group innervating external anal and urethral sphincters. A sexual dimorphism has been found in the dorsomedial portion of Onuf's nucleus, which contains significantly more motoneurons in males than in females (Forger and Breedlove, 1986).

The various segmental types of the spinal cytoarchitecture can be readily recognized on high-resolution nuclear magnetic resonance (NMR) images (Solsberg *et al.*, 1990). Some regional variations are illustrated in the 3-Tesla NMR images of formalin-fixed spinal cords shown in Figure 7.11.

CHEMOARCHITECTURE

General Chemoarchitecture

This account of the general chemoarchitecture of the human spinal chord is based on results obtained by histochemical (including immunohistological) methods, receptor autoradiography, and topographical biochemical analyses. Because of obvious methodological problems, human data are still incomplete. We will therefore refer to results of animal experiments whenever appropriate. However, it must be kept in mind that species differences do occur in the spinal chemoarchitectural organization. Such differences are clearly evident when using histoenzymological methods (Schoenen, 1973, 1981). For instance, FRAP, the fluoro-resistant isoenzyme of acid phosphatase that characterizes a subpopulation of spinal ganglion cells in rats and mice, is not found in human spinal chord. Glutamate and succinate-semialdehyde dehydrogenase, which play a role in the metabolism of γ-aminobutyric acid (GABA), are heavily concentrated in lamina II of humans, but not of monkeys.

Acetylcholine

Cholinergic mechanisms appear to play a ubiquitous role in the spinal gray matter. However, the histoenzymological reaction for acetylcholinesterase, the hydrolyzing enzyme of acetylcholine, is strongest (Schoenen, 1973, 1977, 1981; R.L.M. Faull, unpublished observations) and the enzymatically determined levels of choline acetyltransferase, its synthesizing enzyme, are highest (Aquilonius *et al.*, 1981) in dorsal horn laminae I and II, in lamina IX of motoneurons, and in autonomic nuclei such as the intermediolateral nucleus or the sacral parasympathetic nuclei. Muscarinic cholinergic receptors are densely concentrated in laminae II and IX (Scatton *et al.*, 1984; Villiger and Faull, 1985; Whitehouse *et al.*, 1983). As reported in the rat, muscarinic receptors in the human spinal chord are predominantly of the M1 type in lamina II, but significant densities of both M1 and M2 receptor subtypes are present in the motoneuronal columns (Fig. 7.12) (Villiger and Faull, 1985). Therefore, motoneurons that use acetylcholine as a transmitter at the neuromuscular junction receive an important cholinergic input. This input has various origins, including recurrent collaterals from adjacent motoneurons and supra- and propriospinal fibers. Moreover, axon collaterals of motoneurons are the main afferents of Renshaw cells, which are responsible for recurrent

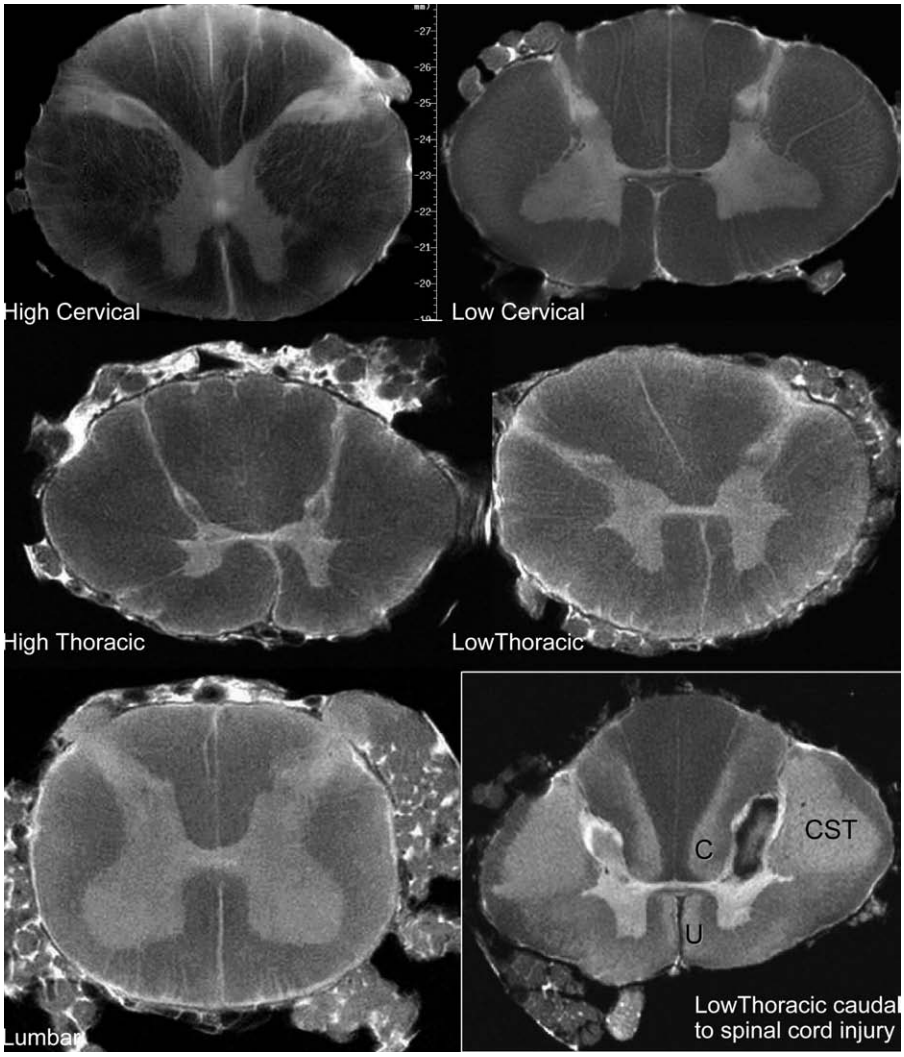

FIGURE 7.11 3T NMR images of formalin-fixed human spinal cords at high and low cervical and thoracic levels, and at the lumbar level. Myelin-rich white matter appears dark, while gray matter is lighter. In the dorsal horns, myelin-poor laminae I–II and Lissauer's tract contrast with surrounding white matter and underlying laminae III and IV. The lower right image shows demyelination in crossed (CST) and uncrossed (U) corticospinal tracts, and in Schultze's comma tract in a segment just caudal to a spinal cord injury. A necrotic lesion can be seen in the right dorsal horn. (Courtesy of Drs Kakulas-Univ of Perth-Australia, Martin & Scholtes-Univ of Liège-Belgium and Gelan-Univ of Limburg-Belgium.)

inhibition and possess cholinergic nicotinic receptors (for a review, see Krnjevic, 1979).

Monoamines

The monoaminergic projections to the spinal cord are well known in animals (for reviews, see Hunt, 1983, and Lindvall and Bjorklund, 1983). Noradrenaline-containing fibers to the dorsal horn and to the ventral horn originate, respectively, in the lateral tegmentum (A5 and A7 groups) and in the locus ceruleus and subceruleus. Serotonergic input to the dorsal horn comes from the raphe magnus nucleus, whereas the raphe obscurus and pallidus nuclei innervate the intermediate gray matter and the ventral horn. Dopamine-containing fibers are chiefly concentrated in the dorsal horn and originate from the diencephalic A11 cell group. There is also evidence in primates for a histamine-containing descending pathway (Ninkovic *et al.*, 1982). Cell bodies immunoreactive for histamine have been localized in the pons and medulla, and H1 histamine receptors have been found in dorsal and ventral horns but also over dorsal root ganglion cells.

In humans, the organization of spinal monoaminergic systems is poorly known. Topographical

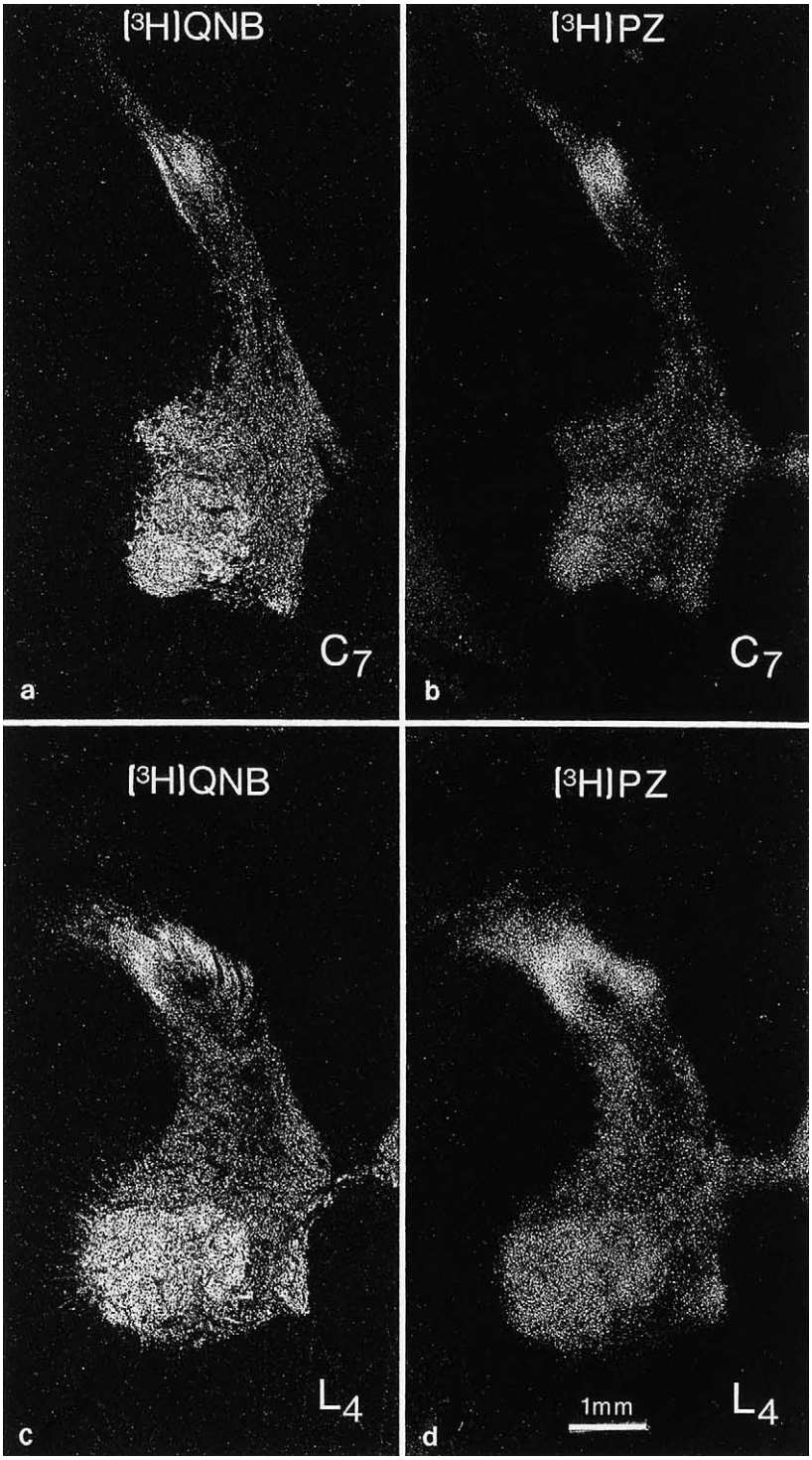

FIGURE 7.12 Autoradiograms showing the distribution of muscarinic cholinergic receptor subtypes (M1 and M2) in transverse hemisections of the human spinal chord at segment levels C7 (**a** and **b**) and L4 (**c** and **d**). **a** and **c** show the distribution of [^{3}H]quinuclidinyl bezilate ([^{3}H]QNB; a ligand with a high affinity for both M1 and M2 receptors) binding sites; **b** and **d** show the distribution of [^{3}H]pirenzepine ([^{3}H]PZ; a ligand with a high affinity for M1 sites and a low affinity for M2 sites) binding sites. The distance between sections a and b and that between sections c and d is 64 µm. In the autoradiograms, the region of dense labeling in the dorsal horn of the gray matter is located within lamina II, and the regions of moderate to heavy labeling in the ventral horn are localized to the regions of lower motor neuron nuclei which constitute lamina IX. Comparison of the density of [^{3}H]QNB and [^{3}H]PZ binding in laminae II and IX suggests that lamina I contains a high proportion of M1 receptors while lamina IX contains both M1 and M2 receptors. From Villiger and Faull (1985).

biochemical studios, using radioenzymatic assays or chromatography, have shown that the spinal levels of serotonin are much higher than those of noradrenaline and dopamine (Bennett *et al.*, 1986; Scatton *et al.*, 1986). Serotonin and noradrenaline are more abundant in the ventral horn, whereas dopamine predominates in the dorsal horn (Scatton *et al.*, 1986). Fibers immunoreactive for serotonin are most numerous in laminae I, II, VIII, and IX of human cord. They can be found in close contact with motoneuronal somata or proximal dendrites. Up to now, cell bodies containing serotonin, which have been described in lamina X of the monkey cord (LaMotte *et al.*, 1982), have not been identified in human materials. α2-Adrenergic receptors are very dense in lamina II and the intermediolateral nucleus (Unnerstall *et al.*, 1984). They have a low density in the ventral horn, as have β-adrenergic receptors (Hayashi *et al.*, 1981).

Amino Acids

Experimental data in animals suggest that amino acids such as glutamate, aspartate, glycine, and GABA are of paramount importance in spinal neurotransmission. Unfortunately, these substances are rapidly autolyzed after death, and this is a major obstacle to their study in human autopsy material.

Glutamate and Aspartate These amino acids are excitatory in spinal gray matter. There is some incomplete evidence from animal experiments that aspartate is the transmitter of certain peripheral afferents and interneurons, whereas glutamate may be used by Ia afferents and corticospinal fibers (see Krnjevic, 1979). In ventral gray matter of the human spinal cord, levels of aspartate exceed those of glutamate (Patten *et al.*, 1982).

Glycine Glycine is thought to be the principal inhibitory neurotransmitter in the ventral horn. It is known from studies in animals that Renshaw cells are glycinergic. These cells project on motoneurons but also on Ia interneurons and on other Renshaw cells. Ia interneurons, which inhibit antagonistic motoneurons when they are activated by Ia afferents coming from agonist muscles, might also use glycine as a neurotransmitter.

In the human spinal cord, glycine is detected biochemically at appreciable levels in the ventral gray matter (Boehme *et al.*, 1976; Patten *et al.*, 1982) Moreover, glycinergic receptor levels are high in homogenized ventral horns (Hayashi *et al.*, 1981). However, with *in vitro* autoradiography, glycinergic receptors appear more dense in lamina II than in lamina IX (J. Schoenen, unpublished observations).

γ-Aminobutyric Acid GABA is an inhibitory transmitter that has been implicated in presynaptic inhibition. Concentrations of GABA are high in the entire spinal gray matter, but especially in the dorsal horn. In the rat, neurons immunoreactive for glutamic acid decarboxlase (GAD), the synthesizing enzyme of GABA, are most numerous in the ventral horn (McLaughlin *et al.*, 1975).

In human autoradiographic studies, selective labeling of lamina II occurs with the use of tritiated muscimol, a preferential agonist of $GABA_A$ receptors (Fig. 7.13a and a'). Similarly, tritiated baclofen demonstrates that $GABA_B$ receptors have a higher density in this lamina (Fig. 7.13b and b') and this extends results obtained in the rat (Price *et al.*, 1984). Both $GABA_A$ (Whitehouse *et al.*, 1983) and $GABA_B$ receptors are scarce in human ventral horns, but they exist in appreciable amounts in lamina X (Fig. 7.13). Benzodiazepine receptors, which are linked to the $GABA_A$ receptor–chloride ionophore complex (Haring *et al.*, 1985; Schoch *et al.*, 1985), are very dense in lamina II (Fig. 7.14); in particular, as shown in Figure 7.14, the highest density of benzodiazepine receptors is localized in the inner segment of lamina II (Iii), and this region is flanked by moderate densities of receptors in the outer segment of lamina II (IIo) and in the immediately adjacent region of lamina III (Faull and Villiger, 1986.) Our autoradiographic studies and biochemical assays of membranes prepared from the lumbosacral cord show that these [^{3}H]flunitrazepam binding sites have high affinity and satisfy the pharmacological characteristics of the "central" type II benzodiazepine receptors (Faull and Villiger, 1986). Although the precise synaptic localization of benzodiazepine receptors in the human spinal cord has not been determined, physiological evidence from animals shows that benzodiazepines act by enhancing GABA-mediated presynaptic inhibition on primary dorsal root afferent terminals (Haefely *et al.*, 1983).

Neuropeptides

We have studied the differential distribution of 12 neuropeptides using immunocytochemical methods in spinal cords from 20 patients (25–70 years old) without neurological disease (Schoenen *et al.*, 1982, 1983, 1985a). We have also examined the spinal cord from a 32-week-old premature fetus. In half the cases, the sampling had to be limited to the lumbosacral enlargement. The unlabeled peroxidase–antiperoxidase complex method of Sternberger (1970) and the indirect fluorescent method of Coons (1958) were used. All primary antisera were tested for specificity using liquid- and solid-phase absorption tests. The methodology has been described elsewhere (Schoenen *et al.*, 1985a). Opiate receptors were studied with quantitative

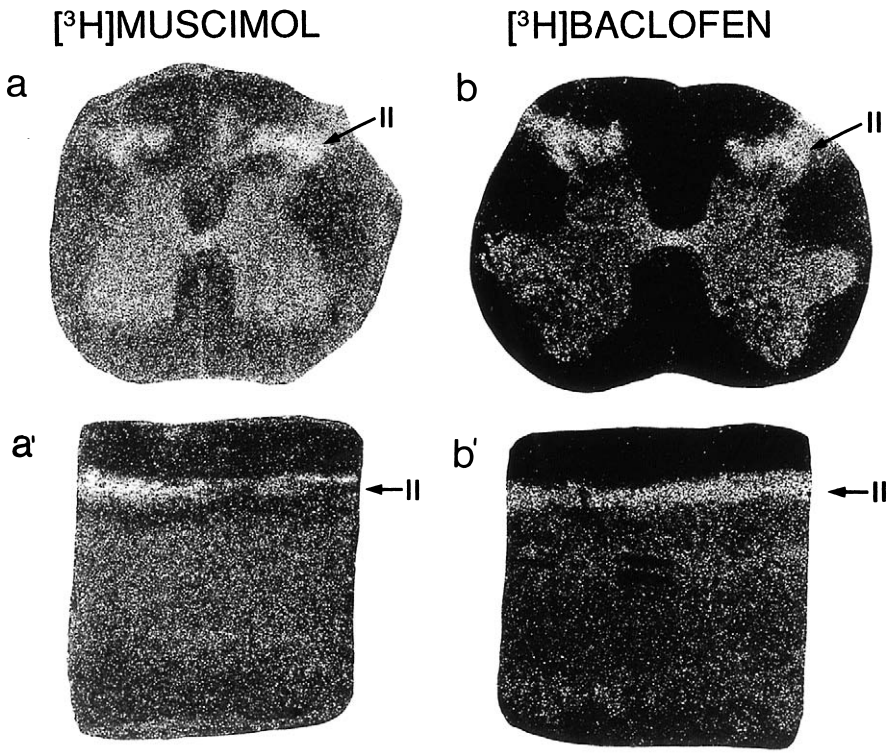

FIGURE 7.13 Autoradiographic localization of GABA receptor subtypes in the lumbar enlargement of human spinal cord using [^{3}H]muscimol (GABAA agonist) for a and a′ and [^{3}H]baclofen (GABAB agonist) for b and b′ as ligands. a and a′ transverse and sagittal sections at L4; b and b′, transverse and sagittal sections at S1. Magnification is ×10.

autoradiographic methods and [^{3}H]diprenorphine as a ligand in six cases aged 7–41 years. Preliminary results on localization of calcitonin gene–related peptide (CGRP) were obtained in two cases using ^{125}I-labeled CGRP. The results on the distribution of peptide immunoreactivities in the human spinal cord are summarized in Tables 7.1 (dorsal horn) and 7.2 (ventral horn.)

Substance P All spinal laminae contain substance P (SP)–positive, medium sized fibers with varicosities. A few fine fibers are also present. Lamina I shows the greatest immunoreactivity (Faull and Villiger, 1986, 1987; Schoenen *et al.*, 1985a). Fibers tend to cluster in dense bundles that are rostrocaudally oriented (Fig. 7.15). Dorsoventral fibers are numerous in the lateral part of lamina I neurons (Fig. 7.15b). Longitudinal and oblique fibers are seen in Lissauer's tract, some dividing into ascending and descending branches (Fig. 7.15b). Positive fibers are less densely packed in lamina II, where they are most numerous in its inner portion (IIi). These fibers are also longitudinal. The number of obliquely running fibers increases in deep lamina II (IIi) and lamina III (Fig. 7.15d). In their medial portions, laminae I to IV are crossed by dorsoventral bundles of SP-positive afferents (Fig. 7.15a). In contrast to lamina IV, laminae V–VI contains many fibers, most of which are oriented obliquely in the transverse plane. SP-positive fibers are less abundant in laminae VII, VIII, and IX but can be easily identified in all cases.

Some SP terminals appear in close association with the perikarya or the proximal dendrite of motoneurons. Lamina X contains a moderate number of positive fibers, with prominent commissural fibers dorsal to the central canal. There is a dense distribution of SP fibers to the intermediolateral column and the sacral parasympathetic nuclei. In the 38-week-old fetus, SP innervation is evident in the dorsal horn.

Cell bodies immunoreactive for SP can be identified in lamina III. Their dendrite are confined to the sagittal plane but spread in several directions, suggesting that they correspond to the "radiate" cell types described in Golgi material in the opening section (Fig. 7.19). SP receptors have been demonstrated in lamina II of the rat spinal cord (Danks *et al.*, 1986).

Opiates Substantial evidence indicates that the spinal cord is an important site for the action of

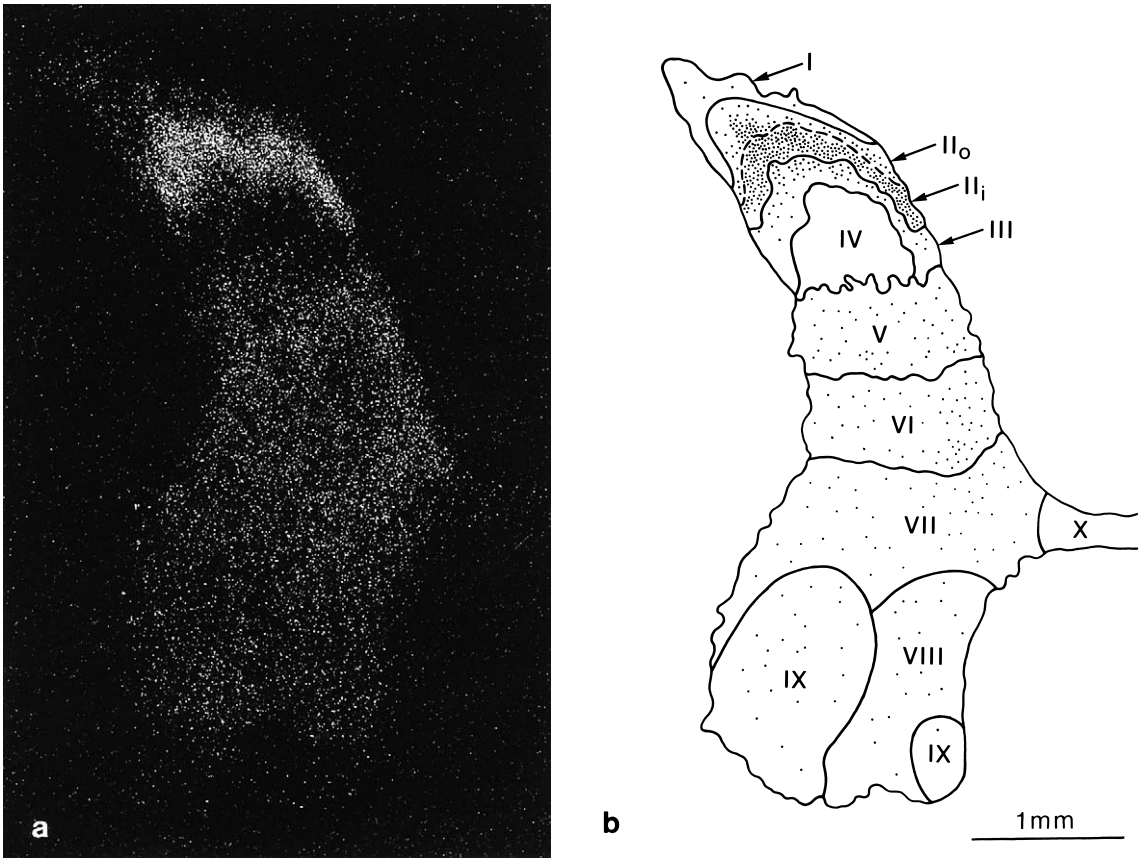

FIGURE 7.14 The distribution of benzodiazepine receptors in the third lumbar segment of the human spinal cord. **(a)** Autoradiogram of [^{3}H]flunitrazepam binding sites; **(b)** a detailed charting of this pattern of labeling on a diagram depicting the laminar subdivision of the spinal gray matter as demonstrated in sections stained for myelin, Nissl substance, and substance P (see Section and Villiger, 1986, for details). The highest density of benzodiazepine receptors is localized within the inner portion of lamina II (IIi) lying immediately adjacent to lamina III, whereas the remaining laminae of the spinal gray show a moderate to low level of receptor labeling. From Faull and Villiger (1986).

TABLE 7.1 Peptide-Containing Fibers in the Dorsal Horn of the Human Spinal Cord[a]

	Peptide[b]											
Lamina	**SP**	**M-ENK**	**L-ENK**	**SYN**	**CCK**	**CGRP**	**NPY**	**SOM**	**OXY**	**VASO**	**TRH**	**VIP**
I	****	**	**	*	***	****	**	*	*	0	0	**
IIo	**	****	****	***	*	***	**	*	0	*	**	*
IIi	***	***	***	**	**	***	*	**	0	*	**	0
III	**	**	**	*	*	***	*	*	*	*	0	0
IV	*	*	*	*	*	*	*	0	*	*	0	0
V-VI med	**	*	***	*	**	0	*	0	0	*	0	0
V-VI lat	**	****	****	***	***	0	*	0	0	0	0	0

[a]Distribution of immunoreactive peptidergic fibers in human dorsal horn: 0, no fibers seen; *, sparse; **, moderate; ***, dense; ****, very dense.
[b]SP, substance P; M-ENK, methionine–enkephalin; L-ENK, leucine–enkephalin; SYN, syn–enkephalin; CCK, cholecystokinin; CGRP, calcitonin gene–related peptide; NPY, neuropeptide Y; SOM, somatostatin; OXY, oxytocin; VASO, vasopressin; TRH, thyrotropin-releasing hormone; VIP, vasoactive intestinal polypeptide.

TABLE 7.2 Peptide-Containing Fibers in the Ventral Horn of the Human Spinal Cord[a]

	Peptide[b]											
Laminac	**SP**	**M-ENK**	**L-ENK**	**SYN**	**CCK**	**CGRP**	**NPY**	**SOM**	**OXY**	**VASO**	**TRH**	**VIP**
VII	*	*	*	*	**	0	*	0	0	0	*	0
VIII	*	*	**	*	***	0	**	0	0	0	0	0
IX	*	**	**	*	*	0 (MN*)	*	*	* (d-l)	0	*	0
ONUF	**	**	**	**	*	0	**	*	0	0	*	0
X	***	***	***	**	**	*	**	*	0	0	*	*
IML	***	***	***	**	***	*	**	*	0	0	*	*
PARA	***	**	**	*	**	**	**	*	0	0	0	**

[a]See Table 7.1 for the grading of the distribution of the immunoreactive fibers in human ventral horn and intermediate gray matter.
[b]See Table 7.1 for definitions of peptide abbreviations, MN, motoneurons contain CGRP; d-1, only the dorsolateral column of motoneurons contains OXY-positive fibers.
[c]ONUF, Onuf's nucleus; IML, intermediolateral column; PARA, sacral parasympathetic nuclei.

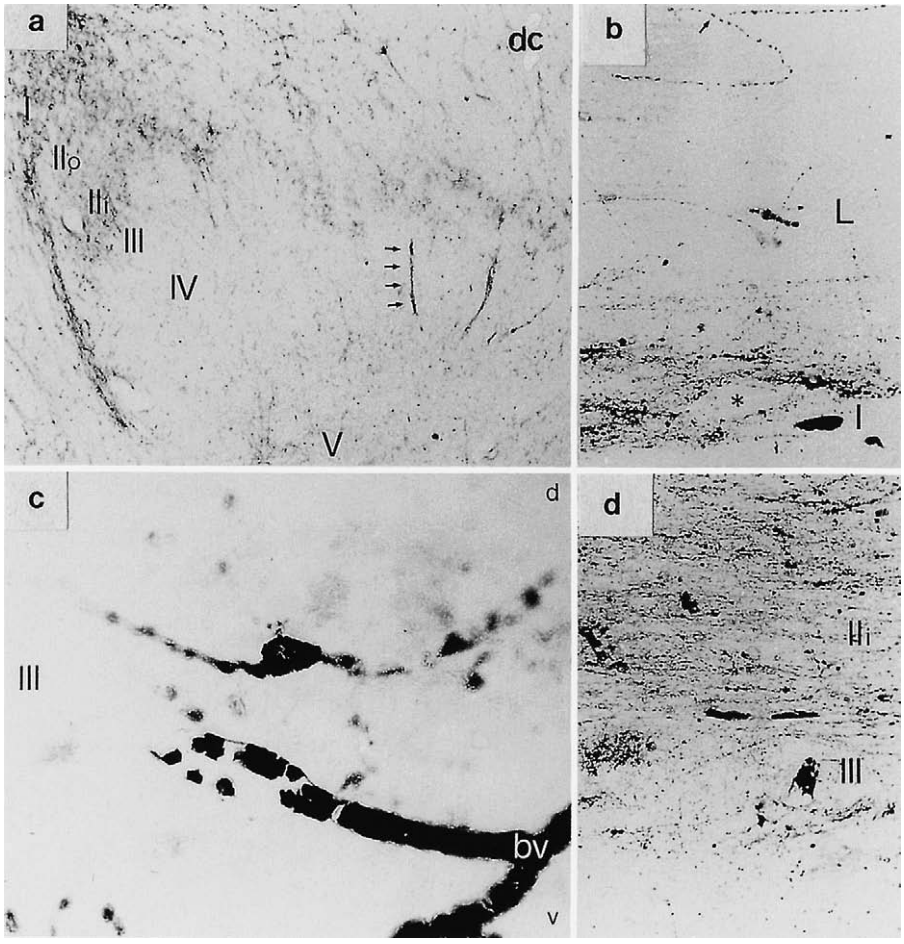

FIGURE 7.15 Substance P immunoreactivity in the dorsal horn of human spinal cord. **(a)** Transverse section at L5. Note dorsoventral bundles of SP fibers *(arrows)* running through laminae III and IV. Magnification is ×40. **(b)** Sagittal section at C8. A longitudinal fiber in Lissauer's tract (L) divides *(arrow)* into an ascending and a descending branch. A lamina I neuron (*asterisk)* is closely surrounded by SP terminals. Magnification is ×100. **(c)** Sagittal section at L4. A SP-positive lamina III neuron is visualized with its proximal dendrites. Magnification is ×200. **(d)** Sagittal section at C8. Note the numerous, chiefly longitudinal SP-positive fibers in inner lamina II (IIi) and less numerous, oblique fibers in lamina III. Magnification is ×100. d, Dorsal; v, ventral; bv, blood vessel with blood cell staining; dc, dorsal column.

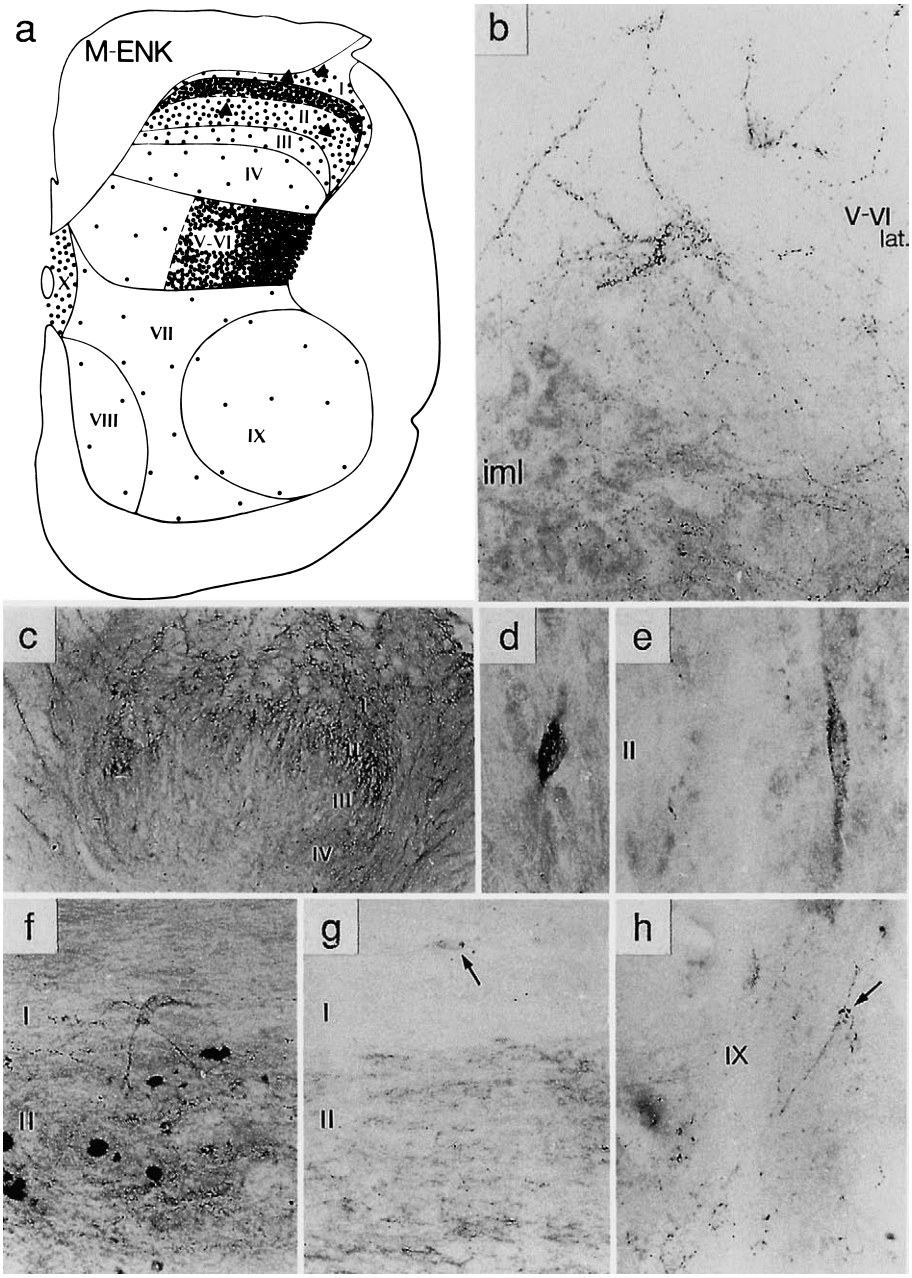

FIGURE 7.16 Methionine–enkephalin (M-ENK) immunoreactivity in human spinal cord. **(a)** Diagrammatic representation of M-ENK-positive fibers *(dots)* and cell bodies *(triangles)* in a transverse hemisection of lumbar human cord. **(b)** Sagittal section at L3 showing lateral part of laminae V–VI (V–VI lat.) and the intermediolateral column (iml). Magnification is ×100. **(c)** Transverse section at L4 through the dorsal horn. Magnification is ×40. **(d)** Sagittal section at C8 showing a M-ENK-positive cell body in lamina II. Magnification is ×200. **(e)** Transverse section at S1. M-ENK-positive neuron and proximal dendrites in lamina II. Magnification is ×200. **(f)** Sagittal section at L5. M-ENK-positive neuron in lamina I with ventral dendrites penetrating into lamina II. Magnification is ×75. **(g)** Sagittal section at C8 through the superficial dorsal horn. Note L-ENK-positive terminals surrounding a lamina I neuron *(arrow)*. Magnification is ×75. **(h)** Transverse section of the lumbar enlargement from a 32-week-old fetus. Note numerous M-ENK-positive fibers and terminal boutons *(arrow)* in lamina IX. Magnification is ×100. From Schoenen *et al*. (1985a).

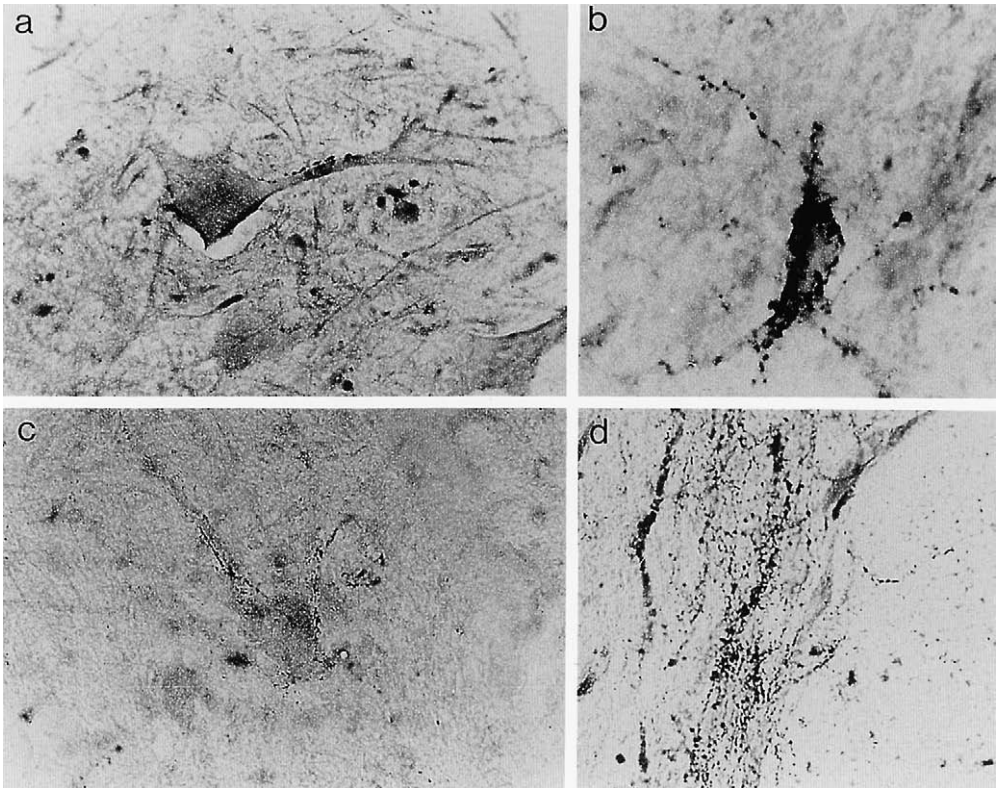

FIGURE 7.17 Peptide-containing terminals in human ventral horn. **(a)** TRH fiber lying in close contact with a proximal dendrite of a motoneuron belonging to the central column. Magnification is ×400. **(b)** SYN-containing fibers surrounding a large lamina VIII neuron. Magnification is ×400. **(c)** L-ENK-immunoreactive fibers covering the perikaryon and proximal dendrite of a motoneuron. Magnification is ×400. **(d)** CCK fiber network within lamina VIII. Magnification is ×200.

exogenous and endogenous opiates. Both methionine (M-ENK) and leucine (L-ENK) enkephalin immunoreactivies are found in small fibers with fine varicosities in the dorsal horn and in medium-sized, irregularly beaded fibers in the remaining gray matter (Fig. 7.16a). Since the density of M-ENK and L-ENK-immunoreactive fibers differs only in two laminae, medial V–VI and VII, the following description will account, with few exceptions, for both peptides. A moderate number of enkephalin-positive fibers is seen in lamina I, most of them running in the rostrocaudal direction (Fig. 7.16c, g). Immunoreactive dots, possibly representing terminal boutons, closely surround the soma and proximal dendrites of lamina I neurons (Fig. 7.16g.) Enkephalin immunoreactivity is much denser in lamina II, mainly in its outer zone (IIo) (Fig. 7.16c). Fiber density decreases markedly in laminae III and IV. Laminae V–VI contain various enkephalin-positive fibers which differ from those in the superficial laminae of the dorsal horn by their thicker caliber and their dorsoventral orientation. The lateral portions of laminae V–VI receive a very dense projection of enkephalin fibers, apparently coming from the dorsolateral funiculus (Fig. 7.16b). The medial portion contains chiefly L-ENK-positive fibers, which are also more numerous in lamina VIII. A substantial number of enkephalin fibers are found in lamina IX; these are in close contact with motoneuronal membranes (Figure 7.17); others can be followed deeply into the ventral white matter. Immunoreactivity for both enkephalins is very dense in lamina X and the intermediolateral column (Fig. 7.16b). In the 32-week-old fetus, enkephalin immunoreactivity is easily identified in the dorsal as well in the ventral horn (Fig. 7.16h).

A few faintly stained cell bodies have been identified only with the M-ENK antiserum. They are located in laminae I and II. Lamina I cells (Fig. 7.16f) present the characteristic ventral orientation of some dendrites. Labeled neurons in lamina II are bipolar and dorsoventrally oriented in transverse sections (Fig. 7.16d, e). This is the typical appearance of stellate cells in Golgi material (see introductory section and Fig. 7.19).

Syn-enkephalin (SYN) comprises 70 residues at the amino terminal of proenkephalin and was isolated

from bovine adrenal medulla and brain. In the human cord, the distribution of SYN immunoreactivity is comparable to that of M-ENK (Fig. 7.17b). However, its overall density is slightly lower and up to now no SYN-positive cell bodies have been detected (Schoenen *et al.*, 1986).

The high concentration of enkephalin immunoreactivity in laminae I and II of the dorsal horn closely correlates with the laminar distribution of opiate receptors in the human spinal cord, as demonstrated by our quantitative autoradiographic studies on the distribution of [^{3}H]diprenorphine (a ligand which binds to most of the opiate receptor subtypes; Chang *et al.*, 1981; Pfeiffer and Hertz 1982; Pfeiffer *et al.*, 1982) binding sites in six human cases aged 7–41 years (Faull and Villiger, 1987). As shown in Fig. 7.18, in these detailed anatomical studies covering 25 of the 31 segmental levels of the human spinal cord (Faull and Villiger, 1987), opiate receptors were found to be localized mainly within laminae I, II, and III of the dorsal horn and in Lissauer's tract, with the highest density of receptors localized within the inner portion of laminae II (see Fig. 7.18). These receptors appear to be principally of the k subtype (Faull and Villiger, 1987).

Cholecystokinin Cholecystokinin (CCK)–immunoreactive fibers are small to medium sized with regular varicosities. They are found in all spinal laminae. The distribution of CCK is comparable to that of SP, except for a heavier innervation of laminae VII and VIII. Fibers in lamina I are numerous and mainly longitudinal. Dorsoventral orientation predominates in the lateral portion of the lamina. Some fibers penetrate into lamina I from Lissauer's tract. Perisomatic terminals on marginal neurons are a frequent finding. CCK immunoreactivity is more dense in the inner than in the outer zone of lamina II. A moderate number of CCK fibers distributes to the medial portion of laminae V–VI and the dorsal part of lamina X. Innervation of lateral laminae V–VI is denser and thicker fibers are involved. A strong CCK immunoreactivity is found in lamina

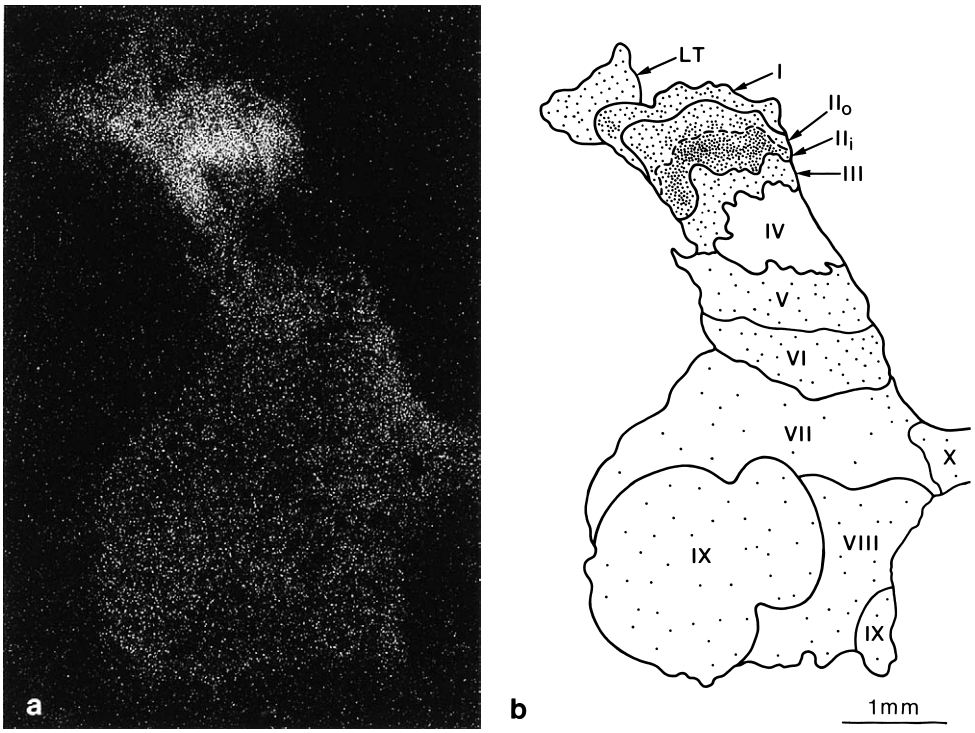

FIGURE 7.18 The distribution of opiate receptors in the fourth lumbar segment of the human spinal cord. **(a)** An autoradiogram of [^{3}H]diprenorphine binding sites; **(b)** a detailed charting of this pattern of labeling on a diagram depicting the laminar subdivision of the spinal gray matter as demonstrated in sections stained for myelin, Nissl substance, and substance P (see Sec. I and Faull and Villiger, 1987 for details). Opiate receptors are localized mainly within laminae I–III of the dorsal horn and in Lissauer's tract (LT), with the highest density of receptors localized within the inner portion of lamina II (IIi) lying immediately adjacent to lamina III; the remaining laminae of the spinal gray show much lower levels of receptor labelings. From Faull and Villiger (1987).

VIII, mainly in its dorsomedial part, at the level of enlargement (Fig. 7.17d). Scattered fibers can be seen in lamina IX in close association with motoneurons or penetrating the ventral funiculus.

It has recently been suggested that part of spinal CCK immunoreactivity may be due to the presence of CGRP (Ju *et al.*, 1986). This specificity problem is relevant mainly for peripheral afferents to the dorsal horn but awaits confirmation in humans.

Calcitonin Gene–Related Peptide CGRP is contained in medium-sized and thick fibers of the human gray matter. Characteristically, these fibers are confined to laminae I–IV of the dorsal horn, lamina X, the intermediolateral nucleus, and the sacral parasympathetic nuclei. In the dorsal horn, distribution of CGRP immunoreactivity is comparable, though not identical to that of SP. Indeed, CGRP fibers are most numerous in laminae I and II. In these laminae, they are chiefly longitudinal, whereas in deeper laminae III and IV they are oblique or dorsoventral in the transverse plane. Double-staining procedures indicate that strong staining for CGRP extends more ventrally in the dorsal horn than that for SP.

CGRP is until now, the only peptide identified within the perikarya of motoneurons. Only weak CGRP immunoreactivity can be found in motoneurons of the human cord. Demonstration of CGRP within motoneurons is easier in rat and other mammals (Gibson *et al.*, 1984). It has been demonstrated recently that CGRP may have a trophic action on cholinergic receptors of skeletal muscle (Fontaine *et al.*, 1986.)

CGRP receptors are most dense in lamina II, lamina X, and the intermediolateral column.

Neuropeptide Y Neuropeptide Y (NPY)–positive fibers are found in all laminae of human spinal gray matter. Dotlike immunoreactivity characterizes the superficial dorsal horn, whereas fibers are medium sized and beaded in other laminae. The densest NPY innervation is seen in laminae I and IIo, in the motoneuronal columns, and in the autonomic nuclei.

Somatostatin Somatostatin (SOM)–positive fibers are small with irregular varicosities. They are confined to the three superficial laminae of the dorsal horn, the motoneurons, lamina X, and the autonomic nuclei. The strongest concentration of SOM immunoreactivity is found in inner lamina II as a dense reticulum of longitudinal fibers. Several fibers in deep lamina II have a dorsoventral direction, penetrating into lamina III.

The greatest number of immunoreactive cell bodies demonstrated in our material contain SOM. These neurons are located in lamina II. Their dendritic organization (longitudinal polarization, few primary dendrites originating on one side of the perikaryon, presence of recurrent branches) suggest that they are of the islet cell type identified in this lamina with the Golgi method (Fig. 7.19).

Thyrotropin-Releasing Hormone Thyrotropin-releasing hormone (TRH) immunoreactivity is limited to certain specific regions of the human spinal gray matter: laminae II, VII, IX, X, and intermediolateral nucleus. TRH-positive fibers are small and punctiform in laminae II. Scattered beaded fibers are found in the other laminae. Some of these are closely opposed to the perikaryon or proximal dendrites of lamina VII neurons or motoneurons (Fig. 7.17). TRH receptors are dense in lamina II but less dense in lamina IX (Manaker *et al.*, 1985).

Other Peptides Oxytocin (OXY)–positive fibers have been detected only in four spinal laminae. Single elongated fibers run rostrocaudally in lamina I. In laminae III, IV, and IX, fibers are short and dorsoventrally oriented. OXY immunoreactivity in lamina IX is peculiar in that it is concentrated mainly in the dorsolateral motoneuronal column. Scattered vasopressin (VASO)–positive fibers are restricted to laminae II, III, IV, and medial V–VI.

As has been described in other mammals (Basbaum and Glazer, 1983) and in humans (Anand *et al.*, 1983), vasoactive intestinal polypeptide (VIP)–containing fibers are chiefly restricted to the lumbosacral cord. These thick, irregularly beaded fibers run tangentially in lamina I, mediolaterally in lamina X, and project to the intermediolateral column and the sacral parasympathetic preganglionic neurons.

During ontogenesis, peptidergic fibers appear early in the human spinal cord. Substance P and enkephalin-immunoreactive fibers can be identified in the dorsal horn as early as 12 weeks *in utero* (Charnay *et al.*, 1983, 1984).

VIP has a distinct distribution in the spinal gray matter. In humans, its concentration is very high in the lumbar and even more so in the sacral regions of the spinal cord (Anand *et al.*, 1983). VIP-containing fibers are mainly distributed to lamina I, IML, sacral parasympathetic preganglionic neurons, and lamina X (Table 7.2). There is good evidence from animal experiments that VIP is the transmitter in visceral afferents (for a review, see Basbaum and Glazer, 1983). Since VIP is also found within neuronal cell bodies in the IML and IMM nuclei in the monkey spinal cord (LaMotte, 1987), this peptide may have important functions in visceral autonomic reflex activities. VIP-containing lamina X neurons have been found to contact the cerebrospinal fluid along the surface of the

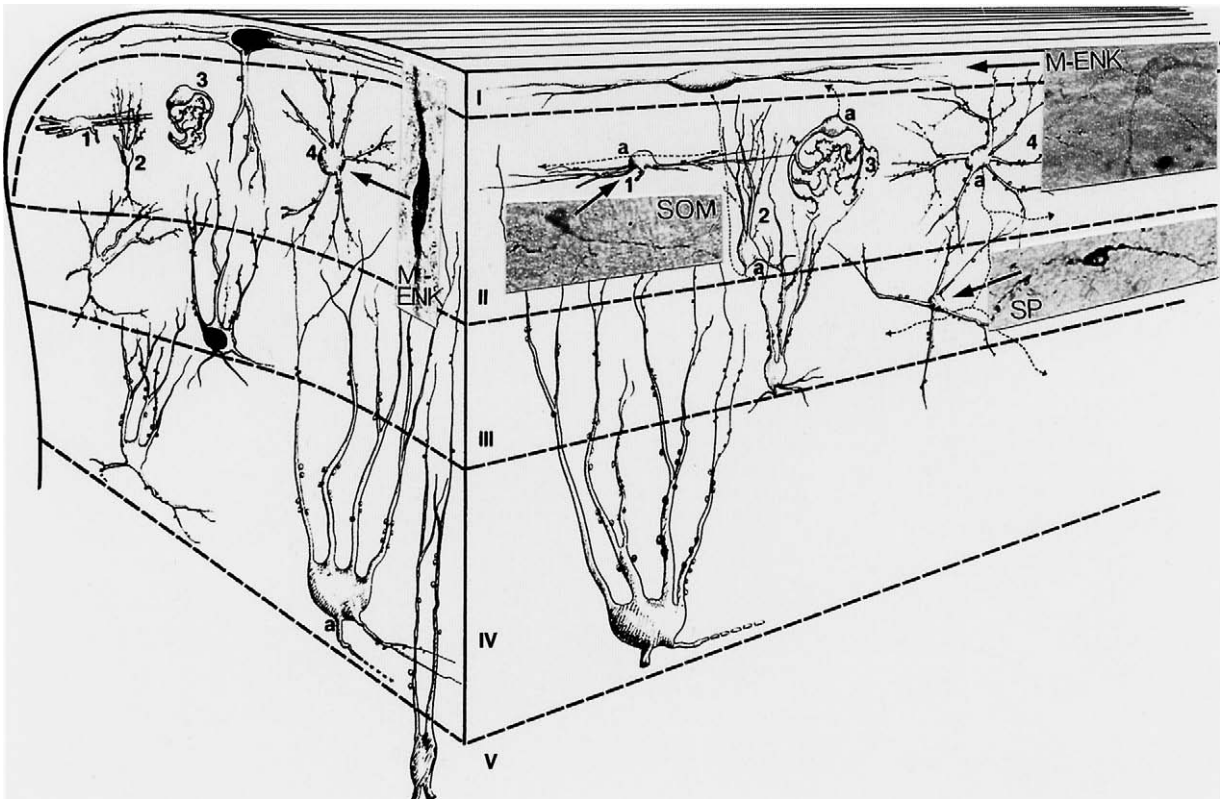

FIGURE 7.19 The dendritic cell types in human dorsal horn (see Schoenen and Faull, chapter 2) with superimposed photomicrographs of peptide-containing neurons. Comparison of dendritic geometries suggests that M-ENK-positive neurons correspond to marginal cells with ventral dendrites and to lamina II stellate cells (4), SOM-positive neurons correspond to lamina II islet cells (1), and SP-positive neurons correspond to lamina III radiate cells. 2, Filamentous cells; 3, curly cells; a, axon.

central canal in the cat and monkey (LaMotte, 1987). The biological role of these neurons remains obscure.

Others

Other chemicals characterize fibers and nerve cells in the human spinal cord. For examples, calcineurin is highly concentrated in small nerve cells and fibers of the substantia gelatinosa, whereas another Ca^{2+}-binding protein, synaptophysin, is distributed throughout the spinal gray matter with highest concentrations in the anterior horn, Clarke's column, and lamina II (Goto *et al.*, 1990; Zhang and Rosenblum, 1996).

Insulin-like growth factor-1 receptors have a concentration that is highest around the central canal and decreases from dorsal to ventral horns and white matter (Adem *et al.*, 1994). They are up-regulated in spinal cords from amyotrophic lateral sclerosis patients.

Glial-derived nemotrophic factor and neurotrophins as well as their receptor tyrosine kinases have been indentified in dorsal horn and motor neurons (Josephson *et al.*, 2001).

Regional Chemoarchitecture and Functional Considerations

We will now outline the overall chemical anatomy of the major functional subdivisions of the gray matter, i.e., the chemical characteristics of the "sensory" dorsal horn (laminae I–IV), the mixed "sensory–motor" intermediate gray (laminae V–VIII and X), and the "motor" ventral horn (laminae IX). Furthermore, from a functional viewpoint, it is interesting to consider how these chemicals may be involved in the processing of neuronal information in the spinal cord.

Dorsal Horn (Laminae I–IV)

From a functional point of view, the most interesting finding emerging from the studies reviewed above is that each of the laminae and the sublaminae of the dorsal horn has a distinctive chemoarchitecture (Table 7.1). The peptide-containing cell bodies, which are visualized in human autopsy material, are localized in the superficial spinal laminae (Fig. 7.19), with the exception of CGRP-positive motoneurons.

TABLE 7.3 Spinal Neuropeptide and 5-HT Immunoreactivity in Pathological Material[a]

Peptide	Site	Peripheral lesion (amputation)	Descending tract lesion (trauma, myelitis)	ALS
Substance P	Dorsal horn	↓↓	=	=
	Ventral horn	=	↓	↓↓
Enkephalin	Dorsal horn	↑	=	=
	Ventral horn	=	=	=
Somatostatin	Dorsal horn	↓	=	=
	Ventral horn	=	↓	=
Cholecystokinin	Dorsal horn	↓	=	=
	Ventral horn	=	=	=
Vasopressin	Dorsal horn	=	↓↓	=
Oxytocin	Dorsal horn	=	↓↓	=
	Ventral horn	=	↓↓	=
TRH	Dorsal horn	=	↓	=
	Ventral horn	=	↓↓	=
5-HT	Dorsal horn	=	↓	=
	Ventral horn	=	↓↓	=

[a]Shown are modifications of various putative neurotransmitter immunoreactivities in case of limb amputation, descending tract lesions, and amyotrophic lateral sclerosis (ALS): =, no change; ↓, slight reduction; ↓↓ massive reduction of immunoreactive fibers; ↑, slight increase of ENK immunoreactivity (only in a case of recent amputation).

In human material, information concerning the organization of transmitter systems can be gained by the study of selected pathological cases. Using immunocytochemistry, we have studied spinal cords from four patients who died at varying intervals after amputation: a below-knee (2 weeks delay), a below-hip (6 months delay), an arm (1 month delay), and a thumb (3 months delay). In all four cases, SP immunoreactivity was reduced but not abolished in the ipsilateral dorsal horn of the corresponding spinal segments (Table 7.3). Reduction was most pronounced in laminae I and II and especially in the medial portion of these laminae. Mediolateral extension of SP reduction was proportional to the deafferented peripheral territory; it was greatest in the case of the below-hip amputation and limited to a very narrow medial portion of the dorsal horn in the case of a thumb amputation. SP innervation of the intermediate gray and the ventral horn appeared normal. SOM and CCK immunoreactivities were also reduced in laminae I and II, but to a lesser degree. In contrast, enkephalin immunoreactivity was increased in these laminae but only in the case of a leg amputation performed 2 weeks before death. No asymmetries were observed in the staining for VASO, OXY, TRH, or serotonin.

These results confirm those obtained by Hunt *et al.* (1982) in two amputees and extend them to other neuropeptides. Reduction of peptide immunoreactivities is probably due to "transganglionic degeneration," which was first illustrated by the disappearance of FRAP in rat laminae II after transection of the sciatic nerve (Schoenen *et al.*, 1968). The data obtained in human pathological cases suggest also that the somatotopic arrangement of peripheral afferents to the dorsal horn is similar in humans and in animals, i.e., medial projection of distal afferents, lateral projection of proximal afferents.

On the other hand, we have studied immunocytochemically the lumbar enlargement in four pathological cases where most of the descending fibers had been interrupted at the cervical or thoracic level: two cases of complete traumatic section of the cord at C7 and T2 autopsied 2 and 5 years after the trauma, and two cases of transverse thoracic myelitis autopsied 2 and 5 months after the beginning of symptomatology. In all four cases, VASO- and OXY-immunoreactive fibers were absent in the lumbar gray matter. TRH- and serotonin-containing fibers were slightly reduced in the dorsal horn, whereas SP, SOM, CCK, or enkephalin fibers were unchanged in the dorsal laminae (Table 7.3).

It may be concluded from these studies that, as in the spinal cord of animals (Hökfelt *et al.*, 1975), most SP fibers to human laminae I and II originate from spinal ganglion cells. In contrast, there is no indication for a peripheral origin of enkephalinergic fibers to the dorsal horn. It remains to be determined why enkephalin immunoreactivity may increase after amputation. This may be due to accumulation of the neurotransmitter in terminals following the peripheral deafferentation, but our results suggest that this phenomenon could be

transitory. Parts of the SOM- and CCK- (or CGRP?) containing fibers in the human dorsal horn have a peripheral origin, whereas the totality of OXY and VASO immunoreactivity is provided by descending afferents. It is not clear at present whether the modifications of dorsal horn neuropeptides described above may play a role in the pathophysiology of phantom limb pain of amputees. The observation of a marked reduction of lamina II SP and synaptophysin immunoreactivities in patients suffering from familial dysautonomia or Riley-Day syndrome, who have a profound analgesia (Pearson *et al.*, 1982; Goto *et al.*, 1990), favors the hypothesis that SP is important for transmission of nociceptive input.

Intermediate Gray Matter (Laminae V–VIII, X, and Autonomic Nuclei)

It is well established that the intermediate gray matter as defined here contains neurons which are involved in the processing and relay of somatosensory information (nociceptive and deep-muscle mechanoreceptive functions—laminae V–VI), in the control of somatic motor functions (laminae V–VI, VII including the dorsal nucleus of Clarke, and VIII), and in autonomic sensory and motor functions (lamina VII including the intermediomedial nucleus, the intermediolateral nucleus, the sacral parasympathetic nucleus, and lamina X).

If one excludes the neuronal groups implicated in autonomic functions (intermediomedial nucleus, intermediolateral nucleus, sacral parasympathetic nucleus, periependymal gray matter), the distribution of the various putative neurotransmitters and their receptors that have so far been studied is rather nonselective. An interesting chemoarchitectural–functional correlation can be established from the findings of TRH innervation of medial lamina VII. It has been shown in human volunteers that TRH at low intravenous doses modifies excitability of motoneurons through an action on interneurons of the flexor reflex pathway (Delwaide and Schoenen, 1985). These interneurons are probably located in the medial portion of lamina VII, i.e., in a region where TRH terminals have been identified. Lamina VIII is characterized by a dense network of CCK- and serotonin-containing fibers. The functional significance of these findings is not known, but it is worth mentioning that lamina VIII contains interneurons and propriospinal neurons as well as some long projection neurons, which are implicated in the motor control of axial musculature. SP and enkephalin levels in laminae V–VI appear unchanged after lesions of peripheral (amputation) or descending (cord transection) afferents. In contrast, SP immunoreactivity in lamina VII is reduced below the spinal transection, whereas enkephalin immunoreactivity remains unchanged (Table 7.3). This suggest that, in laminae V–VI, SP and enkephalins are mainly of intrinsic origin, while in lamina VII the origin of SP is supraspinal and that of enkephalins is intrinsic.

The dorsal nucleus of Clarke is characterized by high levels of acetylcholinesterase (Schoenen, 1973) and muscarinic cholinergic receptors (R. L. M. Faull and J. W. Villiger, unpublished observations). These findings suggest that acetylcholine has a role to play in the dorsal spinocerebellar pathway. Furthermore, SP- and CGRP-containing fibers are found in close contact with neurons in the nucleus of Clarke, whereas other neuropeptides are virtually absent in this nucleus. This would indicate that Clarke's nucleus receives some small C or A delta peripheral afferents in addition to the large input by thick myelinated afferents.

The autonomic nuclei of the intermediate gray matter have a specific chemoarchitecture. The intermediolateral, intermediomedial, and sacral parasympathetic nuclei as well as lamina X are indeed characterized by high levels of muscarinic cholinergic receptor binding and high concentrations of several neuropeptides (SP, enkephalins, CCK, NPY, and VIP); with the exception of lamina X, acetylcholinesterase is also present in these structures. In addition, GABA and glycine receptors are found in lamina X. A similar profuse peptidergic innervation of autonomic nuclei and lamina X has been shown in animals (Honda and Lee, 1985; Hunt, 1983) and serotonin-containing lamina X neurons have been identified in the monkey (LaMotte *et al.*, 1982) and rat (Newton *et al.*, 1986). The high concentrations of muscarinic receptors and acetylcholinesterase in both autonomic sensory (IMM) and autonomic motor (IML) regions of the intermediate gray matter parallel their high concentration in somatic sensory (lamina II) and somatic motor (lamina IX) regions of adjacent dorsal and ventral horns, respectively. Acetylcholine and neuropeptides thus appear to have a major role in both sensory and motor autonomic functions.

Motor Nuclei (Lamina IX)

In agreement with numerous previous findings in animals suggesting that acetylcholine has a major role in lower motor neuron function. In the human, this region contains high concentrations of acetylcholinesterase (Engel, 1969; Schoenen, 1973), choline acetyltransferase (Aquilonius *et al.*, 1981), and muscarinic cholinergic receptor binding (Villiger and Faull, 1985). The latter is a mixed population of the M1 and M2 subtypes, contrasting with the high concentrations of M1 receptors in human lamina (Fig. 7.12). This suggests that M1 and M2 cholinergic receptors may be differentially involved in sensory and motor

TABLE 7.4 Reported Changes of Neurotransmitters and Their Receptors in ALS

Transmitter	Findings[a]	Tissue	Methods	Ref.
Acetylcholine	↓ Acetylcholinesterase	Neuropil ventral horn	Histochemistry	Friede (1969)
	↓ Choline acetyltransferase	Ventral horn	Enzymatic assay	Nagata *et al.* (1981)
		Entire gray matter	Enzymatic assay	Gillberg *et al.* (1982)
	↓ Muscarinic receptors (high affinity)	Lamina IX	Autoradiography	Whitehouse *et al.* (1983)
Glycine	↓ Glycinergic receptors	Ventral half	Spectrometry	Hayashia *et al.* (1981)
		Thoracic cord	Homogenized tissue	
		Lamina IX	Autoradiography	Whitehouse *et al.* (1983)
Substance P	Trend to ↓ content	Dorsal horn ventral	Radioimmunoassay	Gillberg *et al.* (1982)
	↓ Fibers	Lamina IX	Immunocytochemistry	Schoenen *et al.* (1985b)
TRH	↓ Content/wet weight	Ventral horn	Radioimmunoassay	Mitsuma *et al.* (1984)
	Normal content/protein	Ventral horn	Radioimmunoassay	Jackson *et al.* (1986)
	↑ His-Pro-DKP	Ventral horn	Radioimmunoassay	Jackson *et al.* (1986)
	↓ TRH receptors	Lamina XI II	Autoradiography	Manaker *et al.* (1985b)
IGF-1	↑receptors	Cervical and sacral segments	Immunocytochemistry, Autoradiography	Adam *et al.*, (1994)

[a] ↓, Slight reduction

functions in the human spinal cord (Villiger and Faull, 1985). Following degeneration of lower motoneurons in amyotrophic lateral sclerosis (ALS), there is a simultaneous reduction of acetylcholinesterase (Friede, 1969), choline acetyltransferase (Gillberg *et al.*, 1982; Nagata *et al.*, 1981), and muscarinic cholinergic receptors (Whitehouse *et al.*, 1983) in the ventral horn (Table 7.4). These findings are consistent with the concept that lower motoneurons utilize acetylcholine as a transmitter and also receive a cholinergic innervation. The latter may be provided by recurrent collaterals of motoneurons, and/or by supra- and propriospinal afferents.

Most of the inhibitory actions on motoneurons are probably mediated by glycine, the transmitter released by Renshaw cells and presumably Ia interneurons. The finding that motoneuron degeneration due to ALS results in the reduction of glycinergic receptors in the ventral horn (Hayashi *et al.*, 1981; Whitehouse *et al.*, 1983) provides further evidence that these receptors are located on motoneurons (Table 7.4).

Numerous animal studies have demonstrated that serotonin has a role in motor function in the ventral horn (for a review, see Krnjevic, 1979). Spinal reflexes and locomotor activity are facilitated in the spinal cat after injections of the serotonin precursor 5-hydroxtryptophan. This effect has been attributed to inhibition of inhibitory interneurons, but other mechanisms might be relevant. The finding of numerous serotonergic fibers in lamina IX of human spinal cord (Fig. 7.20) suggests that serotonergic neurons may also play a role in the control of spinal motor activity in humans. Since almost all these fibers disappear below spinal transections (Table 7.3), these neurons probably have a supraspinal localization. In addition to serotonin, noradrenaline has an action on motoneurons. Despite the high levels of noradrenaline in human ventral horn (Scatton *et al.*, 1986), its effect on motor functions is presumably mediated through an action on interneurons, since adrenergic receptors remain unchanged after degeneration of motoneurons in ALS (Hayashi *et al.*, 1981).

Finally, although the density of peptide-immunoreactive fibers in the ventral horn is relatively low in comparison to the dorsal horn, the fact that all peptides studied, except for CGRP, VASO, and VIP, are found in terminals closely apposed to motoneurons and that peptide receptors are also localized in this region suggests that various peptides may be involved in aspects of lower motor neuron control (Schoenen and Delwaide, 1985). Immunocytochemical studies in human pathological material have demonstrated the origin of some of the peptidergic fibers innervating lamina IX (Table 7.3). For example, a supraspinal origin for OXY, TRH, and, in part, SP and SOM fibers is indicated by the study of spinal transection cases. Conversely, the finding that enkephalins and CCK-immunoreactive fibers in this region are unaffected by descending tract degeneration suggests a predominantly local and/or dorsal root origin for these peptides in the human.

The modifications of spinal peptidergic innervation observed in ALS are especially interesting. In four cases of typical ALS, we have found a severe reduction or a total disappearance of SP-immunoreactive fibers in lamina IX (Fig. 7.20) (Schoenen *et al.*, 1985b). This reduction is obvious even at segmental levels where motoneuronal degeneration is inconspicuous, e.g., in the cervical enlargement of a patient with a lumbar

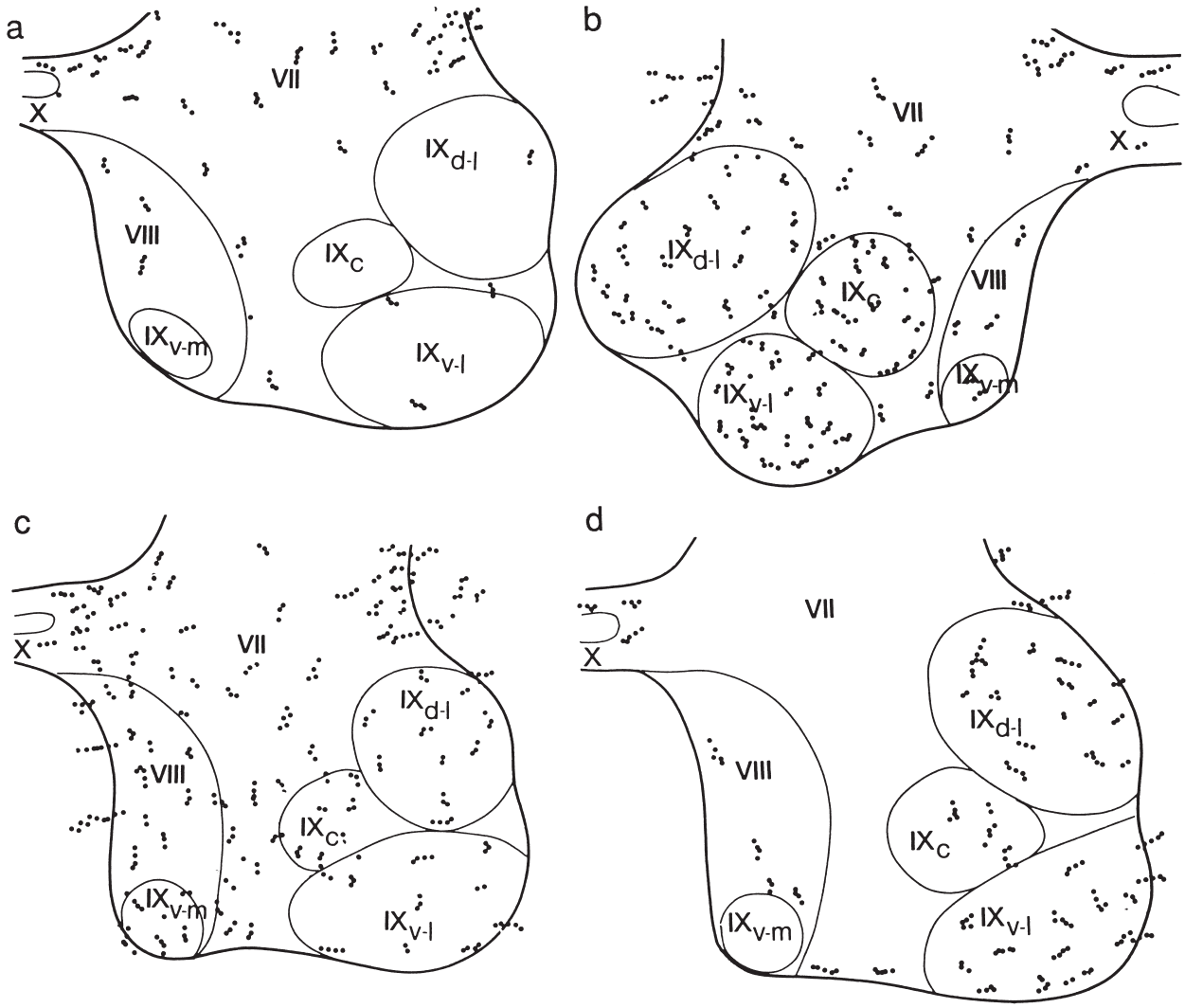

FIGURE 7.20 Camera-lucida mapping of immunoreactive fibers on three consecutive 30-mm-thick sections at L5. **(a)** ALS case, substance P; **(b)** normal case, substance P; **(c)** ALS case, metenkephalin; **(d)** ALS case, serotonin. IX_c, Central; IX_{d-l}, dorsolateral; IX_{v-l}, ventrolateral; and IX_{v-m}, ventromedial columns of motoneurons. From Schoenen *et al.* (1985b).

form of the disease. SP innervation remains normal, not only in the dorsal horn, but also in laminae VII and VIII. SP fibers are also normal in the entire spinal gray matter, including lamina IX in a case of motor neuron disease without pyramidal lesion. In the four ALS cases, immunoreactivity for other peptides (enkephalin, SOM, CCK, VASO, OXY, TRH) and for serotonin remained normal (see Fig. 7.20). This is of particular interest since there is evidence from animal experiments that SP, TRH, and serotonin can be colocalized in supraspinal afferents to lamina IX. Unlike other neurotransmitter changes, which are probably secondary to motoneuronal degeneration (Table 7.4), early loss of supraspinal SP afferents to motoneurons in ALS might be relevant to the pathogenesis of this disease, in which there is also an increase of IGF-1 receptors in cervical and sacral gray matter (Adem *et al.* 1994). For additional information on the distribution of receptors in the spinal cord, see Faull *et al.* (1991).

MYELOARCHITECTURE

There has been no previous detailed study on the myeloarchitecture of the gray matter in the human spinal cord. In our studies, the myeloarchitecture of the human spinal cord has been examined using 50-µm sections stained with osmium tetroxide (Fig. 7.21) and

FIGURE 7.21 The myeloarchitecture of the spinal gray matter in the fourth lumbar segment of the human spinal cord as demonstrated in a 50-µm section stained with osmium tetroxide.

10-µm sections stained using the Weigert method (Fig. 7.22). The myeloarchitectural characteristics of the various laminae in the spinal gray are described in detail below, followed by a general description of the major features in the white matter.

Dorsal Horn (Laminae I–IV)

The dorsal horn of the human spinal cord shows a very distinctive myeloarchitecture. In our studies on the human spinal cord, the myeloarchitectural characteristics of the dorsal horn are best seen in "thick" sections stained with osmium tetroxide (Fig. 7.21).

Lamina I

Lamina I caps the dorsal horn and is traversed by small numbers of quite finely myelinated fibers which give it a fine reticulated appearance in myelin-stained material (Fig. 7.21). It is generally easily distinguished from the surrounding white matter and the underlying lamina II.

Lamina II

Lamina II is the most distinctive lamina in myelin-stained material (Figs. 7.21 and 7.22). It is characterized and distinguished from adjacent laminae by the almost total lack of myelinated fibers, which results in its distinctive gelatinous appearance in fresh unfixed material. As shown in Figures 7.21 and 7.22, lamina II is so conspicuous in myelin-stained material that such preparations provide the best basis for accurately defining the precise boundaries of this lamina and for demonstrating its general morphological characteristics. Its ventral border describes an irregular serrated outline and is more clearly delineated than the dorsal border. The lamina shows considerable variation in size and shape from one level of the spinal cord to another. As can also be seen from Figures 7.21 and 7.22, lamina II is most extensive in the region of the cervical and lumbosacral enlargements (Fig. 7.22a, c, d) and is considerably thinner and more attenuated in the thoracic region (Fig. 7.22b). In the cervical (Fig. 7.22a) and lumbosacral (Figs. 7.21 and 7.22c ,d) enlargements, this myelin-poor lamina is frequently traversed by fascicles of heavily myelinated fibers passing in the dorsoventral direction to reach deeper laminae of the spinal gray.

Lamina III

Lamina III is also best distinguished by its myeloarchitecture (Fig. 7.21). It contains moderate numbers of myelinated fibers which clearly distinguish the lamina from the more superficial, nonmyelinated lamina II and the deeper, more heavily myelinated lamina IV.

Lamina IV

Lamina IV is characterized by an especially high concentration of myelinated fibers, the highest of any lamina in the spinal gray matter (Fig. 7.21). In osmium-stained material the myelinated fibers appear to be as densely packed as those in the adjacent spinal white matter, and in these preparations it is easy to delineate this lamina from the adjacent less densely myelinated laminae III and V.

Conclusions

The marked differences in the concentration of myelinated fibers in the laminae of the dorsal horn provide a sound basis for defining the precise boundaries between these laminae in the human spinal cord. Similar myeloarchitectural differences in other mammals have been used to assist in the delineation of the laminae of the dorsal horn (Hunt, 1983; Rexed,

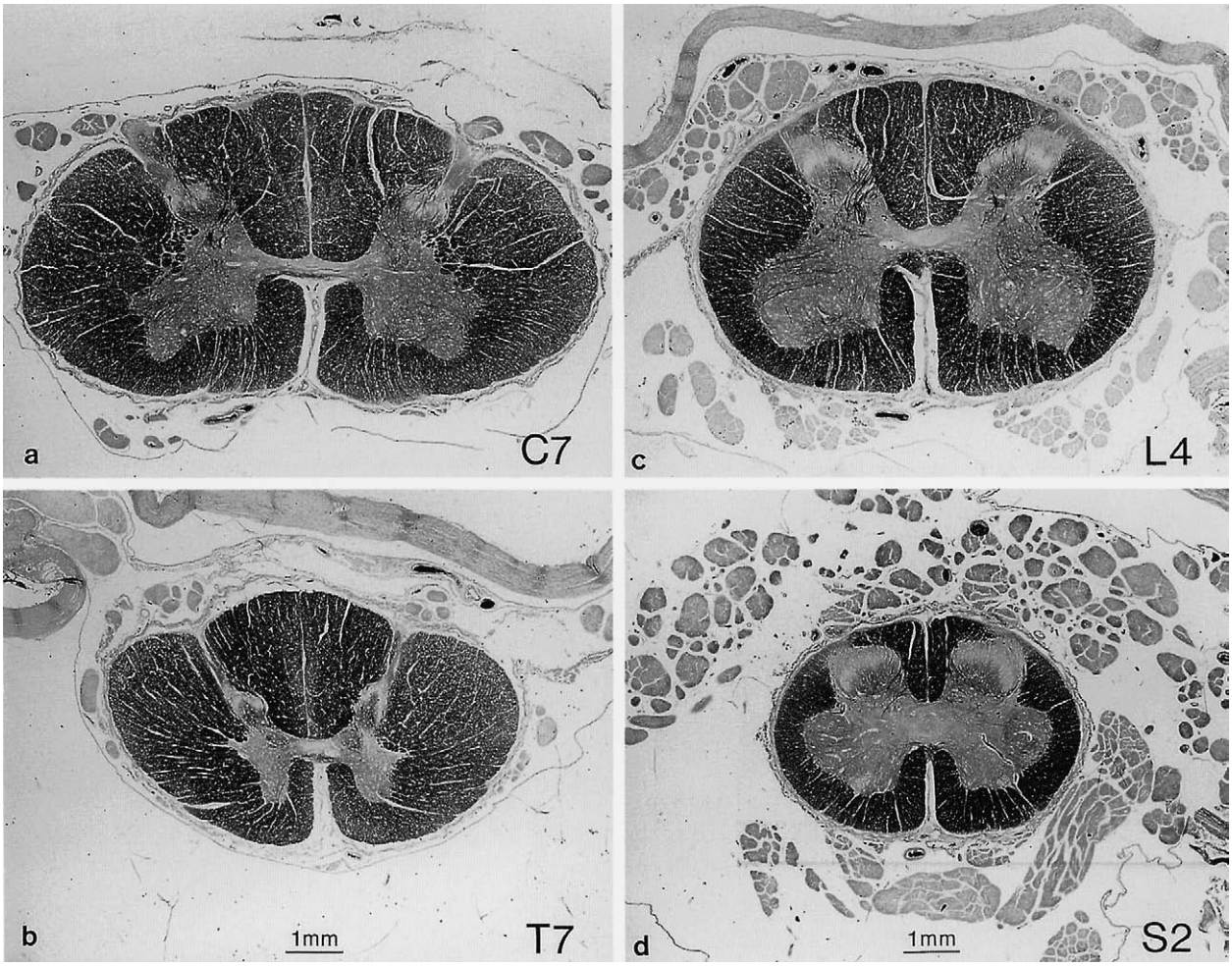

FIGURE 7.22 The myeloarchitecture of the human spinal cord at spinal levels **(a)** C7, **(b)** T7, **(c)** L4, and **(d)** S2, as demonstrated in 10-µm sections stained according to the Weigert procedure.

1964), particularly to show the border between laminae II and III (Molander *et al.*, 1984; Ralston, 1979; Rexed, 1964; Snyder, 1982) However, the laminar myeloarchitectural differences described in other mammals are generally not as marked or distinct as those observed in our osmium-stained "thick" sections of the human spinal cord (Fig. 7.21; see also Faull and Villiger, 1986, 1987). In particular, the subtle differences that we have observed in the myeloarchitecture between laminae III and IV in the human have not been reported in other mammalian species.

Intermediate Gray Matter (Laminae V–VIII and X)

Lamina V

On myeloarchitectural criteria, lamina V is easily separated from the more densely myelinated lamina IV but merges imperceptibly with lamina IV (Fig. 7.21). Within the lateral one-third of lamina V, longitudinally coursing bundles of myelinated fibers disrupt the gray matter and give it a distinctive reticulated appearance (Fig. 7.21); this is especially obvious at cervical levels of the human spinal cord (Fig. 7.22a). This reticulated lateral region of lamina V appears to be equivalent to the region designated as the lateral zone in the cat by Rexed (1952, 1964) and as the processus reticularis or formatio reticularis by earlier workers (see Rexed, 1964, for details). The larger remaining medial region of lamina V is characterized by the presence of heavily myelinated fiber bundles arching dorsoventrally from the dorsal funiculus to terminate either within this lamina or to reach the more ventrally located laminae of the spinal gray (Figs. 7.21 and 7.22). These fibers are presumably branches of the heavily myelinated fibers in the medial division of the dorsal root.

Lamina VI

Lamina VI is myeloarchitecturally similar to lamina V. It shows a comparable lateral reticular zone and a larger medial region where the dorsoventrally oriented fibers appear more dispersed (Figs. 7.21 and 7.22)

Lamina VII

Lamina VII shows a moderate concentration of myelinated fibers. Here the fibers generally have no preferred direction but are present in the form of an interlacing network of multidirectional myelinated biers (Fig. 7.21). Nevertheless, transversely directed fiber bundles are often clearly distinguished in lamina VII of the cervical and lumbar spinal enlargements (Fig. 7.22a, c, d). In the ventral region where lamina VII borders lamina IX, increased numbers of myelinated fibers are often present and here they skirt the lamina IX border, emphasizing and delineating the lamina VII/IX boundary (Fig. 7.21). Finally, in the dorsomedial region of lamina VII in the thoracic and upper lumbar segments, the round to oval dorsal nucleus of Clarke is conspicuously marked in myelin-stained material by the presence of a dense fine plexus of myelinated fiber terminals (Fig. 7.22b).

Lamina VIII

Lamina VIII is continuous with and myeloarchitecturally similar to lamina VII. Here the fibers are often oriented in the dorsoventral direction (Fig. 7.21).

Lamina X

Lamina X is distinguished by the relative lack of myelinated fibers. Thus, in myelin-stained material, it is easily distinguished from lamina VII laterally and from the anterior white commissure ventrally (Figs. 7.21 and 7.22).

Motoneurons (Lamina IX)

Lamina IX

Lamina IX generally shows a lower concentration of myelinated fibers than the adjacent laminae VII and VIII. In particular, as depicted in Fig. 7.21, the various component subnuclei of lower motoneurons which constitute this lamina are clearly demarcated by bordering fascicles of myelinated fibers. In addition, the neuropil of lamina IX is marked by the myelinated axons of lower motoneurons coursing ventrally toward the white matter; those myelinated fibers coalesce to form fascicles that traverse the adjacent white matter to form the emerging ventral rootlets of the spinal cord (Figs. 7.21 and 7.22).

White Matter

The white matter of the spinal cord consists of closely packed nerve fibers surrounding the gray matter (Fig. 7.21). It is divided into right and left halves by the posterior median septum and the anterior median fissure. At the base of the anterior median fissure the white matter on both sides of the cord is continuous via a slender lamina of decussating nerve fibers forming the anterior white commissure. Although the anterior white commissure is easily recognized at al spinal levels (Fig. 7.22), it appears to be most extensive at lumbosacral levels (Figs. 7.21 and 7.22c, d).

Because the number of nerve fibers in the ascending and descending spinal tracts is greatest at cervical levels, the white matter is best developed in the cervical segments (Fig. 7.22a) and progressively decreases in size at successive caudal levels of the spinal cord (Fig. 7.22b–d). These changes in the size of the white matter, together with variations in the gray matter, result in the spinal cord varying in size and shape from one region to another. Thus, the spinal cord is largest in the cervical region, where it is oval shaped (Fig. 7.22a), and smallest at sacral levels, where it is more circular in outline (Fig. 7.22d).

A sexual dimorphism in the relative proportion of white matter at the C5 level was described by Yuan *et al.* (1999), the area ratio of the white matter to the whole segment area being larger in males. The same authors found that with age, the area of gray matter decreased faster in males, but the area of white matter decrease faster in females.

The white matter is subdivided into three compartments: posterior, lateral, and anterior funiculi. The white matter between the posterior median septum and the attachment of the dorsal rootlets forms the posterior funiculus. The lateral funiculus lies between the attachment of the dorsal and ventral rootlets, and the anterior funiculus is formed by the white matter lying between the emerging ventral rootlets and the anterior median fissure. Rostral to midthoracic levels, the posterior funiculus and a lateral cuneate fasciculus (Fig. 7.22a); at levels caudal to T6 the posterior funiculus is represented only by the gracile fasciculus (Fig. 7.22b–d). The localization of the various fiber tracts in the spinal white matter is outlined by Schoenen and Grant in Chapter 11.

Acknowledgments

The work of Jean Schoenen was supported by grants from the National Fund for Scientific Research-Belgium and from the Research Fund of the Medical Faculty of the University of Liege. Richard Faull's

research is supported by grants from the Medical Research Council of New Zealand and the New Zealand Neurological Foundation.

Referenes

Abdel-Maguid, T.E., and Bowsher, D. (1979). Alpha and gamma-motoneurons in the adult human spinal cord and somatic cranial nerve nuclei: the significance of dendroarchitectronics studied by the Golgi method. *J. Comp. Neurol.* **186,** 259–270.

Adem, A., Ekblom, J., Sillberg, P.G., Jossan, S.S., Hoog, A., Winblad, B., Aquilonius, J.M., Wang, L.H., and Sara, V. (1994). Insulin-like growth factor – 1 receptors in human spinal cord changes in amyotrophic lateral sclerosis. *J. Neuro. Transm. Gen. Sect.* **97,** 73–84.

Aitken, J.T., and Bridger, J.E. (1961). Neuronal size and neuron population density in the lumbosacral region of the cat's spinal cord. *J. Anat.* **95,** 38–53.

Anand, P., Gibson, S.J., McGregor, G.P., Blank, M.A., Ghatei, M.A., Bacaresse-Hamilton, A.J., Polak, J.M., and Bloom, S.R. (1983). A VIP-containing system concentrated in the lumbosacral region of human spinal cord. *Nature (London)* **305,** 143–145.

Applebaum, A.E., Beall, J.E., Foreman, R.D. and Willis, W. D. (1975). Organization and receptive fields of primate spinothalamic tract neurons. *J. Neurophysiol.* **38,** 572–586.

Aquilonius, J.M., Eckernas, S.A., and Gillberg, P.G., (1981). Topographical localization of choline acetyltransferase within the human spinal cord and a comparison with some other species. *Brain Res.* **211,** 329–340.

Balthasar, K. (1952). Morphologie der spinalen Tibialis- und Peronaeus Kerne bei der Katze: Topographie, Architektonik, Axon- und Dendritenverlauf der Motoneurone und Zwischenneurone in den Segmenten L6-S7. *Arch. Psychiatr. Nervenkr.* **188,** 345–378.

Barilari, M.G. and Kuypers, H.G. J. M. (1969). Propriospinal fibers interconnecting the spinal enlargements in the cat. *Brain Res.* **14,** 321–330.

Basbaum, A.I., and Glazer, E.J. (1983). Immunoreactive vasoactive intestinal polypeptide is concentrated in the sacral spinal cord: a possible marker for pelvic visceral afferent fibers. *Somatosens. Res.* **1,** 69–87.

Beal, J.A., and Cooper, M.H. (1978). The neurons in the gelatinosal complex (laminae II and III) of the monkey (Macaca mulatta): a Golgi study. *J. Comp Neurol.* **179,** 89–127.

Bennett, G.W., Nathan, P.A., Wong, K.K., and Marsden, C.A. (1986). Regional distribution of immunoreactive-thyrotrophin-releasing hormone and substance P, and indoleamines in human spinal cord. *J. Neurochem.* **46,** 1718–1724.

Boehme, D.H., Marks, N., and Fordice, M.W. (1976). Glycine levels in the degenerated human spinal cord. *J. Neurol. Sci.* **27,** 347–357.

Bossy, J.G., and Ferratier, R. (1968). Studies of the spinal cord of *Galago senegalensis*, compared to that in man. *J. Comp. Neurol.* **132,** 485–498.

Brichta, A. M., and Grant, G. (1985). Cytoarchitectural organization of the spinal cord. *In* "The Rat Nervous System" (G. Paxinos, ed.), Vol. 2, pp. 293–301. Academic Press, Orlando, Florida.

Brown, A.G. (1977). Cutaneous axons and sensory neurones in the spinal cord. *Br. Med. Bull.* **33,** 109–117.

Brown, P.B., and Fuchs, J.L. (1975). Somatotopic representation of hindlimbs skin in cat dorsal horn. *J. Neurophysiol.* **38,** 1–9.

Bryan, R.N., Trevino, D.L., Coulter, J.D., and Willis, W.D. (1973). Location and somatotopic organization of the cells of origin of the spinocervical tract. *Exp. Brain Res.* **17,** 177–189.

Burke, R.E., Strick, P. L. Kanda, K., Kim, C. C., and Walmsley, B. (1977). Anatomy of medial gastrocnemius and soleus motor nuclei in cat spinal cord. *J. Neurophysiol.* **40,** 667–680.

Buxton, D.F., and Goodman, D.C. (1967). Motor function and corticospinal tracts in the dog and raccoon. *J. Comp. Neurol.* **129,** 341–360.

Cameron, W.D., Averill, D.B., and Berger, A.J. (1983). Morphology of cat phrenic motoneurons as revealed by intracellular injection of horseradish peroxidase. *J. Comp. Neurol.* **219,** 70–80.

Carpenter, M.B. (1976). "Human Neuroanatomy," 7th Ed. Williams & Wilkins, Baltimore.

Cervero, F., and Iggo, A. (1980). The substantia gelatinosa of the spinal cord. A critical review. *Brain* **103,** 717–777.

Chambers, W.W., and Liu, C.N. (1958). Cortico-spinal tract in monkey. *Fed. Proc., Fed. Am. Soc. Exp. Biol.* **17,** 24.

Chang, K.J., Hazum, E., and Cuatrecasas, P. (1981). Novel opiate binding sites selective for benzomorphan drugs. *Proc. Natl. Acad. Sci. U.S.A.* **78,** 4141–4145.

Charnay, Y., Paulin, C., Chayvialle, J.A., and Dubois, P.M. (1983). Distribution of substance P-like immunoreactivity in the spinal cord and dorsal root ganglia of the human foetus and infant. *Neuroscience* **10,** 41–55.

Charnay, Y., Paulin, C., Dray, F. and Dubois, P.M. (1984). Distribution of enkephalin in human fetus and infant spinal cord: an immuno-fluorescence study. *J. Comp. Neurol.* **223,** 415–423.

Coons, A.H. (1958). Fluorescent antibody methods. *In* "General Cytochemical Methods" (J. F. Danielli, ed.), pp. 399–427. Academic Press, New York.

Cullheim, S., Fleshman, J.W., Glenn, L.L., and Burke, R.E. (1987a). Membrane area and dendritic structure in type identified triceps surae alpha motoneurons. *J. Comp. Neurol.* **255,** 68–81.

Cullheim, D., Fleshman, J.W., Glenn, L.L., and Burke, R.E. (1987b). Three-dimensional architecture of dendritic trees in type-identified alpha-motoneurons. *J. Comp. Neurol.* **255,** 82–96.

Danks, J.A., Rothman, R.B., Cascieri, M.A., Chicchi, G.G., Liang, T., and Herkenham, M. (1986). A comparative autoradiographic study of the distributions of substance P and eledoisin binding sites in rat brain. *Brain Res.* **385,** 273–281.

Delwaide, P.J. (1977). Excitability of lower limb myotatic arcs under the influence of caloric labyrinthine stimulation: analysis of the postural effects in man. *J. Neurol., Neurosurg. Psychiatry* **40,** 970–974.

Delwaide, P.J., and Schoenen, J. (1985). The effects of TRH on F waves recorded from antagonistic muscles in human subjects. *Ann. Neurol.* **18,** 366–367.

Devor, M. and Wall, P.D. (1978). Reorganization of spinal cord sensory map after peripheral nerve injury. *Nature (London)* **275,** 75–76.

Eccles, J.C., Fatt, P., Landgren, S., and Winsbury, G.J. (1954). Spinal cord potentials generated by volleys in the large muscle afferents. *J. Physiol. (London)* **125,** 590–606.

Elliot, H.C. (1944). Studies on the motor cells of the spinal cord. IV. Distribution in experimental animals. *J. Comp. Neurol.* **81,** 97–103.

Emson, P.C. (1983). "Chemical Neuroanatomy," Raven Press, New York.

Engel, W.K. (1969). Motor Neuron histochemistry in ALS and infantile spinal muscular atrophy. *In* "Motor Neuron Disease: Contemporary Neurology Symposia" (F. H. Norris and L. T. Kurland, eds.), Vol. 2, pp. 218–234. Grune & Stratton, New York.

Falls, W., and Gobel, S. (1976). A Golgi and EM studies of the formation of dendritic and axonal arbors: the interneurons of the substantia gelatinosa of Rolando in newborn kittens. *J. Comp. Neurol.* **187,** 1–18.

Faull, R.L.M., and Villiger, J.W. (1986). Benzodiazepine receptors in the human spinal cord. A detailed anatomical and pharmacological study. *Neuroscience* **17,** 791–807.

Faull, R.L.M. and Villiger, J.W. (1987). Opiate receptors in the human spinal cord: a detailed anatomical study comparing the autoradiographic localization of 3H-diprenorphine binding sites with the laminar pattern of substance P, myelin and Nissl staining *Neuroscience* **20,** 395–407.

Faull, R.L.M., Dragunow, M., Jansen, K.L.R., Waldvogel, J.W., Villiger, J.W., Bullock, J.Y. and Williams, M.M. (1991). Receptors in the human spinal cord. In "Receptors in the Human Nervous System" (G. Paxinos and F. A. O. Mendelsohn, eds.), Academic Press, San Diego (in press).

Fontaine, B., Klarsfeld, A., Hokfelt, T., and Changeux, J.P. (1986). Calcitonin gene-related peptide, a peptide present in spinal cord motoneurons, increases the number of acetylcholine receptors in primary cultures of chick embryo myotubes. *Neurosci. Lett.* **71,** 59–65.

Forger, N. G., and Breedlove, S.M. (1986). Sexual dimorphism in human and canine spinal cord: role of early androgen. *Proc. Natl. Acad. Sci. U.S.A.* **83,** 7527–7531.

Friede, R.L. (1969). Enzyme histochemical observations in amyotrophic lateral sclerosis. *In* "Motor Neuron Disease: Contemporary Neurology Symposia" (F. J. Norris and L. T. Kurland, eds.), Vol. 2, pp. 235–241. Grune & Stratton, New York.

Gelfan, S. , Kao,, G., and Ruchkin, D.S. (1970). The dendritic tree of spinal neurons. *J. Comp. Neurol.* **139,** 385–417.

Gibson, S.J., Polak, J.M., Bloom, S.R., Sabate, I.M., Mulderry, PM., Ghater, M.A., Morrison, J.F.B., Kelley, J.S. and Rosenfeld, M.G. (1984). Calcitonin gene-related peptide (CGRP)-immunoreactivity in the spinal cord of man and of eight species. *J. Neurosci.* **4,** 3101–3111.

Gillberg, P.G., Aquilonius, S.M., Eckernas, S.A., Lundqvist, G., and Winbiad, B. (1982). Choline acetyltransferase and substance P-like immunoreactivity in the human spinal cord: changes in amyotrophic lateral sclerosis. *Brain Res.* **250,** 394–397.

Gobel, S. (1975a). Golgi studies of the substantia gelatinosa neurones in the spinal trigeminal nucleus. *J. Comp. Neurol.* **162,** 397–416.

Gobel, S. (1975b). Neurons with two axons in the substantia gelatinosa layer of the spinal trigeminal nucleus of the adult cat. *Brain Res.* **88,** 339–345.

Gobel, S. (1978a). Golgi studies of the neurons in layer I of the dorsal horn of the medulla (trigeminal nucleus caudalis). *J. Comp. Neurol.* **180,** 375–394.

Gobel, S. (1978b). Golgi studies of the neurons in layer II of the dorsal horn of the medulla (trigeminal nucleus caudalis). *J. Comp. Neurol.* **180,** 395–414.

Golgi, C. (1890). Über den feineren Bau des Rückenmarks. *Anat. Anz.* **5,** 372–396.

Goto S., Hirano A., Pearson J. (1990). Calcineurin and synaptophysin in the human spinal cord of normal individuals and patients with familial dysautonomia. *Act. Neuropathol.* **79,** 647–657.

Grillner, S. (1975). Locomotion in vertebrates: central mechanisms and reflex interaction. *Physiol rev.* **55,** 247–304.

Grillner, S., and Zangger, P. (1979). On the central generation of locomotion in the low spinal cat. *Exp. Brain Res.* **34,** 241–261.

Haefely, W., Pole, P., Pieri, L. Schaffner, R., and Laurent, J.P. (1983). Biological basis of the therapeutic effects of benzodiazepines. *In* "The Benzodiazepines: From Molecular Biology to Clinical Practice" (E. Costa, ed.), pp. 21–66. Raven Press, New York.

Haring, P., Stahli, C., Schoch, P. Takacs, B., Staehelin, T. and Mohler, H. (1985). Monoclonal antibodies reveal structural homogeneity of γ-aminobutyric acid/benzodiazepine receptors in different brain areas. *Proc. Natl. Acad. Sci. U.S.A.* **82,** 4837–4841.

Hayashi, H., Suga, M., Satake, M., and Tsubaki, T. (1981). Reduced glycine receptor in the spinal cord in amyotrophic lateral sclerosis. *Ann. Neurol.* **9,** 292–294.

Hökfelt, T., Kellerth, J.O., Nilsson, C., and Pernow, B. (1975). Experimental immunohistochemical studies on the localization and distribution of substance P in cat primary sensory neurons. *Brain Res.* **100,** 232–257.

Honda, C., and Lee, C. (1985). Immunohistochemistry of synaptic input and functional characterization of neurons near the spinal central canal. *Brain Res.* **343,** 120–128.

Horcholle-Bossavit, G. (1978). Transmission electronique dans le systeme nerveux central des mammiferes. *J. Physiol. (Paris)* **74,** 349–363.

Hunt, S.P. (1983). Cytochemistry of the spinal cord. *In* "Chemical Neuroanatomy" (P. C. Emson, ed.), pp. 53–84. Raven Press, New York.

Hunt, S.P., Rossor, M.N., Emson, P.c., and Clement-Jones, V. (1982). Substance P and enkephalins in spinal cord after limb amputation. *Lancet* **1,** 1023.

Irving, d., Rebeiz, J.J., and Tomlinson, B.E. (1974). The numbers of limb motor neurones in the individual segments of the human lumbosacral spinal cord. *J. Neurol. Sci.* **21,** 203–217.

Jackson, I.M.D., Adelman, L.S., Munsat, T.L., Forte, S. and Lechan, R.M. (1986). Amyotropic lateral sclerosis: thyrotropin-releasing hormone and histidyl proline diketopiperazine in the spinal cord and cerebrospinal fluid. *Neurology* **36,** 1218–1223.

Johansson, O., Hokfelt, T., Pernow, B. Jeffcoat, S.L., White, N. Steinbusch, H.W.M., Verhofstad, A.A.J., Emson, P.C. and Spindel, E. (1987). Immunohistochemical support for three putative transmitters in one neuron: Co-existence of 5-hydrozytryptamine, substance P and thyrotropin releasing hormone-like immunoreactivity in medullary neurons projecting to the spinal cord. *Neuroscience* **6,** 1857–1887.

Josephson, A., Widenfalk, J., Trifunovski, A., Widmer, H.R., Olson, L., Spenger, C. (2001). GDNF and NGF family members and receptors in human fetal and adult spinal cord and dorsal root ganglia. *J.Comp.Neurol.* **440,** 204–217.

Ju, G., Hokfelt, T., Fischer, J.A., Frey, P., Rehfeld, J.F. and Dockray, G.J. (1986). Does cholecystokinin-like immunoreactivity in rat primary sensory neurons represent calcitonin gene related peptide? *Neurosci. Lett.* **68,** 305–310.

Kawamura, Y., O'Brien, P., Okazaki, H., and Dyck, P.J. (1977). Lumbar motoneurons of man. II. The number and diameter distribution of large- and intermediate-diameter cytons in "motoneuron column" of spinal cord of man. *J. Neuropathol. Exp. Neurol.* **36,** 861–870.

Kierstead, S.A., and Rose, P.K. (1983). Dendritic distribution of splenius motoneurons in the cat: comparison of motoneurons innervating different regions of the muscle. *J. Comp. Neurol.* **219,** 273–284.

Krnjevic, K. (1979). Transmitters in motor systems. *In* "Handbook of Physiology," Sect. 1, Chapter 4, pp. 107–154. Am. Physiol. Soc., Washington, DC.

Kuypers, H.G.J.M. (1962). Corticospinal connections: postnatal development in the rhesus monkey. *Science* **138,** 678–680.

Kuypers, H.G.J.M. (1964). The descending pathways to the spinal cord, their anatomy and function. *Prog. Brain res.* **11,** 178–200.

Kuypers, H.G.J.M. (1973). The anatomical organization of the descending pathways and their contributions to motor control especially in primates. *In* "New Developments in Electromyography and Clinical Neurophysiology" (J.E. Desmedt, ed.), Vol. 3, pp. 38–68. Karger, Basel.

Kuypers, H.G.J.M. (1981). Anatomy of the descending pathways. *In* "Handbook of Physiology" (V. B. Brooks, ed.), Sect. 1, Vol. 2, pp. 597–665. Am. Physiol. Soc., Washington, D.C.

Kuypers, H.G.J.M., and Brinkman, J. (1970). Precentral projections to different parts of the spinal intermediate zone in the rhesus monkey. *Brain Res.* **24,** 29–48.

Kuypers, H.G.J.M., Fleming, W.R., and Farinholt, J.W. (1962). Subcortico-spinal projections in the rhesus monkey. *J. Comp. Neurol.* **118,** 107–137.

LaMotte, C.C. (1987). Vasoactive intestinal polypeptide cerebrospinal fluid-contracting neurons of the monkey and cat spinal central canal. *J. Comp. Neurol.* **258,** 527–541.

LaMotte, C.C. Johns, D.R., and de Lanerolle, N.C. (1982). Immunohistochemical evidence of indoleamine neurons in monkey spinal cord. *J. Comp. Neurol.* **206,** 359–370.

Laruelle, L. (1937). La structure de la moelle epinière en coupes longitudinales. *Rev. Neurol.* **44,** 695–725.

Laruelle, L. (1948). Etude d'anatomie microscopique du nevraxe sure coupes longitudinales. *Acta Neurol. Psychiatr. Belg.* **48,** 138–280.

Leontovich, T.A. (1975). Quantitative analysis and classification of subcortical forebrain neurons. *In* "Golgi Centennial Symposium" (M. Santini, ed.), pp. 101–127. Raven Press, New York.

Leontovich, T.A., and Zhukova, G.P. (1963. The specificity of the neuronal structure and topography of the reticular formation in the brain and spinal cord of carnivora. *J. Comp. Neurol.* **121,** 347–380.

Lindvall, O., and Björklund, A. (1983). Dopamine- and norepinephrine-containing neuron systems: their anatomy in the rat brain. *In* "Chemical Neuroanatomy" (P. C. Emson, ed.), pp. 229–256. Raven Press, New York.

Liu, C.N., and chambers, W.W. (1964). An experimental study of the corticospinal system in the monkey (Macaca Mulatta). The spinal pathways and preterminal distribution of degenerating fibers following discrete lesions of the pre- and post-central gyri and bulbar pyramid. *J. comp. Neurol.* **123,** 257–284.

Lynn, B., and Hunt, S.P. (1984). Afferent C-fibers: physiological and biochemical correlations. *Trends Neurosci.* **7,** 186–188.

Manaker, S., Winokur, A., Rhodes, C.H., and Rainbow, T.C. (1985a) Autoradiographic localization of thyrotropin-releasing hormone (TRH) receptors in human spinal cord. *Neurology* **35,** 328–337.

Manaker, S., Shulman, L.H., Winokur, A., and Rainbow, J.C. (1985b). Autoradiographic localization of thyrotropin releasing hormone receptors in amyotrophic lateral sclerosis spinal cord. *Neurology* **35,** 1650–1653.

Matsushita, M. (1969). Some aspects of the interneuronal connections in cat's spinal gray matter. *J. Comp. Neurol.* **136,** 57–80.

McLaughlin, B.J., Barker, R., Saito, K., Roberts, E., and Wu, J.Y. (1975). Immunocytochemical localization of glutamate decarboxylase in the rat spinal cord. *J. Comp. Neurol.* **164,** 305–327.

Menetrey, D., Giesler, G.J., and Besson, J.M. (1977). An analysis of response properties of spinal cord dorsal neurones to non-noxious and noxious stimuli in the spinal rat. *Exp. Brain Res.* **27,** 15–33.

Miller, R.A. , and Strominger, N.L. (1973). Efferent connections of the red nucleus in the brainstem and spinal cord of the rhesus monkey. *J. Comp. Neurol.* **152,** 327–346.

Mitsuma, T., Nagimori, T., Adachi, K., Mukoyama, M. and Ando, K. (1984). Concentrations of immunoreactive thyrotropin-releasing hormone in spinal cord of patients with amyotrophic lateral sclerosis. *Am. J. Med. Sci.* **287,** 34–36.

Molander, C., Xu, Q., and Grant, G. (1984). The cytoarchitectonic organization of the spinal cord in the rat. I. The lower thoracic and lumbosacral cord. *J. Comp. Neurol.* **230,** 133–141.

Nagata, Y., Okuya, M., and Honda, M. (1981). Regional distribution of choline acetyltransferase and acetylcholinesterase activity in spinal neurons of motor neuron disease patients. *Neurosci. Lett.*, Suppl. **6,** 71.

Nathan, P.W., and Smith, M.C. (1959). fasciculi proprii of the spinal cord in man. *Brain* **82,** 610–668.

Newton, B.W., Maley, B.E., and Hamill, R.W. (1986). Immunohistochemical demonstration of serotonin neurons in autonomic regions of the rat spinal cord. *Brain Res.* **376,** 155–163.

Ninkovic, M., Hunt, S.P., and Gleave, J. (1982). Localization of opiate and histamine H1-receptors in primate sensory ganglia and spinal cord. *Brain Res.* **243,** 197–206.

Nyberg-Hansen, R., and Brodal, A. (1963). Sites of termination of corticospinal fibers in the cat. An experimental study with silver impregnation method. *J. Comp. Neurol.* **120,** 369–391.

Patten, B., Kurlander, H., and Evans, B. (1982). Free amino acid concentrations in spinal tissue from patients dying of motor neuron disease. *Acta Neurol. Scand.* **66,** 594–599.

Pearson, A.A. (1952). Role of gelatinous substance of spinal cord in conduction of pain. *Arch. Neurol. Psychiatry* **68,** 515–529.

Pearson, J., Brandeis, L., and Cuello, A.C. (1982). Depletion of substance P-containing axons in substantia gelatinosa of patients with diminished pain sensitivity. *Nature (London)* **295,** 61–63.

Pfeiffer, A., and Herz, A. (1982). Discrimination of three opiate receptor binding sites with the use of a computerized curve-fitting technique. *Mol. Pharmacol.* **21,** 266–271.

Pfeiffer, A., Pasi, A., Mehraein, P., and Herz, A. (1982). Opiate receptor binding sites in human brain. *Brain Res.* **248,** 87–96.

Price, D.D. and Mayer, D.J. (1974). Physiological laminar organization of the dorsal horn of M. mulatta. *Brain Res.* **79,** 321–325.

Proshansky, e., and Egger, M.D. (1977). Dendritic spread of dorsal horn neurons in cats. *Exp. Brain Res.* **28,** 153–166.

Rakic, P. (1975). Role of cell interaction in development of dendritic patterns. *Adv. Neurol.* **12,** 117–134.

Rall, W. (1967). Distinguishing theoretical synaptic potentials computed for different soma-dendritic distributions of synaptic input. *J. Neurophysiol.* **30,** 1139–1167.

Rall, W., Burke, R.E., Smith, T.G., Nelson, P.G., and Frank, K. (1967). Dendritic location of synapses and possible mechanisms for the monosynaptic EPSP in motoneurons. *J. Neurophysiol.* **30,** 1169–1193.

Ralston, H.J. (1968a). The fine structure of neurons in the dorsal horn of the cat spinal cord. *J. Comp. Neurol.* **132,** 275–307.

Ralston, H.J. (1968b). Dorsal root projections to dorsal horn neurons in the cat spinal cord. *J. Comp. Neurol.* **132,** 303–330.

Ralston, H.J. (1979). The fine structure of laminae I, II and III of the macaque spinal cord. *J. Comp. Neurol.* **184,** 619–647.

Ramon-Moliner, E. (1967). A source of error in the study of Golgi stained materials. *Arch. Ital. Biol.* **105,** 139–148.

Ramon-Moliner, E., and Nauta, W.J.H. (1966). The isodendritic core of the brain stem. *J. Comp. Neurol.* **126,** 311–336.

Ramon y Cajál, S. (1909). *Histologie du systeme nerveux de l'Homme et des vertèbres*, Vol. 1. Maloine, Paris.

Rexed, B. (1952). The cytoarchitectonic organization of the spinal cord in the cat. *J. Comp. Neurol.* **95,** 415–495.

Rexed, B. (1954). A cytoarchitectonic atlas of the spinal cord in the cat. *J. Comp. Neurol.* **100,** 297–379.

Rexed, B. (1964). Some aspects of the cytoarchitectonics and synaptology of the spinal cord. *Prog. Brain Res.* **11,** 58–90.

Romanes, G.J. (1951). The motor cells columns of the lumbosacral cord of the cat. *J. Comp. Neurol.* **94,** 313–363.

Romanes, G.J. (1964). The motor columns of the spinal cord. *Prog. Brain Res.* **11,** 93–116.

Rose, P.K. (1981) Distribution of dendrites from biventer cervicis and complexus motoneurons stained intracellularly with horseradish peroxidase in the adult cat. *J. Comp. Neurol.* **197,** 395–409.

Scatton, B., Dubois, A., Javoy-Agid, F., and Camus, A. (1984). Autoradiographic localization of muscarinic cholinergic receptors at various segmental levels of the human spinal cord. *Neurosci. Lett.* **49,** 239–245.

Scatton, B., Dennis, T., L'Heureux, R., Monfort, J.C., Duyckaerts, C., and Javoy-Agid, f. (1986). Degeneration of noradrenergic and serotonergic but not dopaminergic neurones in the lumbar spinal cord of Parkinsonian patients. *Brain Res.* **380,** 181–185.

Scheibel, M.E. and Scheibel, A.B. (1966a). Terminal axonal patterns in cat spinal cord. I. The lateral corticospinal tract. *Brain Res.* **2,** 333–350.

Scheibel, M.E., and Scheibel, A.B. (1966b). Spinal motoneurons, interneurons and Renshaw cells. A Golgi study. *Arch. Ital. Biol.* **104,** 328–353.

Scheibel, M.E., and Scheibel, A.B. (1968). Terminal axonal patterns in cat spinal cord. II. The dorsal horn. *Brain Res.* **9,** 32–58.

Scheibel, M.E., and Scheibel, A.B. (1969a). terminal patterns in cat spinal cord. III. Primary afferent collaterals. *Brain Res.* **13,** 417–443.

Scheibel, M.E., and Scheibel, A.B. (1969b). A structural analysis of spinal interneurons and Renshaw cells. *In* "The Interneuron" (M. A. B. Brazier, ed.), pp. 159–208. Univ. of California Press, Los Angeles.

Scheibel, M.E., and Scheibel, A.B. (1970a). Organization of spinal motoneuron dendrites in bundles. *Exp. Neurol.* 28, 106–117.

Scheibel, M.E., and Scheibel, A.B.(1970b). Developmental relationship between spinal motoneuron dendrite bundles and patterned activity in the hindlimbs of cats. *Exp. Neurol.* **29,** 328–335.

Scheibel, M.E., and Scheibel, A.B. (1971). Developmental relationship between spinal motoneuron dendrite bundles and patterned activity in the forelimbs of cats. *Exp. Neurol.* **30,** 367–373.

Scheibel, M.E., and Scheibel, A.B. (1975). Dendrites as neuronal couplers: the dendritic bundle. *In* "Golgi Centennial Symposium" (M. Santini, ed.), pp. 347–354. Raven Press, New York.

Schoen, J.H. (1964). Comparative aspects of the descending fibre systems in the spinal cord. *Prog. Brain Res.* **11,** 203–227.

Schoenen, J. (1973). Etude histoenzymologique des couches cytoarchitectoniques de la moelle de diffèrents mammifères et de l'homme. *Bull. Assoc. Anat.* **58,** 415–425.

Schoenen, J. (1977). Histoenzymology of the developing rat spinal cord. *Neuropathol. Appl. Neurobiol.* **3,** 37–46.

Schoenen, J. (1981a). Dendritic bundles do exist in the human spinal cord. *Neurosci. Lett., Suppl.* **7,** S103.

Schoenen, J. (1981b). "L'organisation neuronale de la moelle epinière de l'homme." Editions Sciences et Lettres, Liege.

Schoenen, J. (1982a). The dendritic organization of the human spinal cord: the dorsal horn. *Neuroscience* **7,** 2057–2087.

Schoenen, J. (1982b). Dendritic organization of the human spinal cord: the motoneurons. *J. Comp. Neurol.* **211,** 226–247.

Schoenen, J., Budo, C., and Poncelet, G. (1968). Effet de la section du sciatique sur l'activité de l'isoenzyme fluororesistant de la phosphatase acide dans la moelle epiniere du rat. *C.R. Seances Soc. Biol. Ses Fil.* **162,** 2035–2037.

Schoenen, J., Vanderhaeghen, J.J., Lotstra, F., and Vierendeels, G. (1982). The differential distribution of substance P and enkephalins in the human spinal cord: an immunocytochemical analysis. *Neurology* **32,** 70.

Schoenen, J., Vanderhaeghen, J.J., Lotstra, F., and Vierendeels, G. (1983). Vasopressin, oxytocin, cholecystokinin and somatostatin in the human spinal cord: an immunocytochemical study. *Neurology* **33,** 70.

Schoenen, J. Lotstra, F. Vierendeels, G., Reznik, M., and Vanderhaeghen, J.J. (1985a). Substance P, enkephalins, somatostatin, cholecystokinin, oxytocin, and vasopressin in human spinal cord. *Neurology* **35,** 881–890.

Schoenen, J., Reznik, M., Delwaide, P.J., and Vanderhaeghen, J.J. (1985b). Etude immunocytochimique de la distribution spinale de substance P, des enkephalines, de cholecystokinine et de serotonine dans la sclerose latérale amyotrophique. *C.R. Seances Soc. Biol. Ses Fil.* **1179,** 528–534.

Schoenen, J., Lotstra, F., Liston, D., Rossier, J., and Vanderhaeghen, J.J. (1986). Synenkephalin in bovine and human spinal cord. *Cell Tissue Res.* **246,** 641–645.

Sharrard, W.J. (1955). The distribution of the permanent paralysis in the lower limb in poliomyelitis. *J. Bone Jt. Surg. Br.* **37B,** 540–558.

Sher, P.K., and Brown, S.B. (1975). The neurologic examination of the premature infant. *In* "The Practice of Pediatric Neurology" (K. F. Swaiman and F. S. Wright, eds.), Vol. 1, pp. 22–30. Mosby, St. Louis.

Sidman, R.L., Angevine, J., and Pierce, E. (1971). "Atlas of the Mouse Brain and Spinal Cord." Harvard Univ. Press, Cambridge, Massachusetts.

Smith, M.C. (1976). Retrograde cell changes in human spinal cord after anterolateral cordotomies. Location and identification after different periods of survival. *Adv. Pain Res. Ther.* **1,** 91–98.

Smith, R.G., and Appel, S.H. (1983). Extracts of skeletal muscle increase neurite outgrowth and cholinergic activity of fetal rat spinal motor neurons. *Science* **219,** 1079–1081.

Snyder, R.L. (1982). Light and electron microscopic autoradiographic study of the dorsal root projections to the cat dorsal horn. *Neuroscience* **7,** 1417–1437.

Solsberg, M.D., Lemaire, C., Resch, L., Potts, D.G. (1990). High-resolution MR imaging of the cadaveric human spinal cord: normal anatomy. *Am. J. Neuroradiol.* **11,** 3–7.

Sprague, J.M. (1948). A study of motor cell localization in the spinal cord of the rhesus monkey. *Am. J. Anat.* **82,** 1–26.

Sprague, J.M. (1951). Motor and propriospinal cells in the thoracic and lumbar ventral horn of the rhesus monkey. *J. Comp. Neurol.* **95,** 103–123.

Sprague, J.M., and Ha, H. (1964). The terminal fields of dorsal root fibers in the lumbosacral spinal cord of the cat and the dendritic organization of the motor nuclei. *Prog. Brain Res.* **11,** 120–154.

Sterling, P., and Kuypers, H.G.J.M. (1967a). Anatomical organization of the brachial spinal cord of the cat. I. The distribution of dorsal root fibers. *Brain Res.* **4,** 1–15.

Sterling, P., and Kuypers, H.G.J.M. (1967b). Anatomical organization of the brachial spinal cord of the cat. II. The motoneuron plexus. *Brain Res.* **4,** 16-37.

Sterling, P., and Kuypers, H.G.J.M. (1968). Anatomical organization of the brachial spinal cord of the cat. III. The propriospinal connections. *Brain Res.* **7,** 419–443.

Sternberger, L.A. (1970). The unlabelled antibody enzyme method of immunohistochemistry. *J. Histochem. Cytochem.* **8,** 315–325.

Sugiura, Y. (1975). Three dimensional analysis of neurons in the substantia gelatinosa Rolandi. *Proc. Jpn. Acad.* **51,** 336–341.

Szentágothai, J. (1964). Propriospinal pathways and their synapses. *Prog. Brain Res.* **11,** 155–177.

Szentágothai, J. and Rethelyi, M. (1973). Cyto- and neuropil architecture of the spinal cord. *In* "New Developments in Electromyography and Clinical Neurophysiology" (J. E. Desmedt, ed.), Vol. 3, pp. 20–37. Karger, Basel.

Tomlinson, B.E., and Irving, D. (1977). The numbers of limb motor neurons in the human lumbosacral cord through life. *J. Neurol. Sci.* **34,** 213–219.

Tomlinson, B.E., and Irving, D., and Rebeiz, J.J. (1973). Total numbers of limb motor neurones in the human lumbosacral cord and an analysis of the accuracy of various sampling procedures. *J. Neurol. Sci.* **20,** 313–327.

Truex, R.C., and Taylor, M.J. (1968). Gray matter lamination of the human spinal cord. *Anat. Rec.* **160,** 507.

Truex, R.C., Taylor, M.J., Smythe, M.G., and Gildenberg, P.J. (1970). The lateral cervical nucleus of cat, dog and man. *J. Comp. Neurol.* **139,** 93–103.

Unnerstall, J.R., Kopajtic, T.A., and Kuhar, M.J. (1984). Distribution of alpha2 agonist binding sites in the rat and human central nervous system: analysis of some functional, anatomic correlates

of the pharmacologic effects of clonidine and related adrenergic agents. B*rain Res. Rev.* **7,** 69–101.

Valverde, F. (1968). Structural changes in the area striata of the mouse after enucleation. *Exp. Brain Res.* **5,** 274–297.

Valverde, F. (1970). The Golgi method. A tool for comparative structural analysis. *In* "Contemporary Research Methods in Neuroanatomy" (W. J. H. Nauta and S. O. E. Ebbesson, eds.), pp. 12–31. Springer-Verlag, New York.

Vanner, S.J., and Rose, P.K. (1984). Dendritic distribution of motoneurons innervating the three heads of the trapezius muscle in the cat. *J. Comp. Neurol.* **226,** 96–110.

Villiger, J.W., and Faull, R.L.M. (1985). Muscarinic cholinergic receptors in the human spinal cord: differential localization of ^{3}H-pirenzepine and ^{3}H-quinuclidinylbenzilate binding sites. *Brain Res.* **345,** 196–199.

Von Lenhossek, M. (1895). "Der Feinere Bau des Nervensystems (im Lichte neuester Forschungen)," 2nd ed. Buchhandlung H. Kornfeld.

Waibl, H. (1973). Zur Topographie der Medulla spinalis der Albinoratte (Rattus norvegicus). *Adv. Anat. Embryol. Cell Biol.* **47**(6), 1–41.

Waldeyer, H. (1888). *Das Gorrilla Ruckenmark.* Abh. K. Akad. Wiss. Berlin., pp. 1–147.

Wall, P.D. (1967). The laminar organization of dorsal horn and effects of descending impulses. *J. Physiol. (London)* **188,** 403–423.

Wall, P.D. (1980). The substantia gelatinosa. A gate control mechanism set across a sensory pathway. *Trends Neurosci.* **3,** 221–224.

Whitehouse, P.J., Wamsley, J.K., Zarbin, M.A., Price, D.L., Tourtelotte, W.W., and Kuhar, M.J. (1983). Amyotrophic lateral sclerosis: alterations in neurotransmitter receptors. *Ann. Neurol.* **14,** 8–16.

Willis, W.D., and Coggeshall, R.E. (1978). "Sensory Mechanisms of the Spinal Cord," Plenum Publishers, New York.

Zhang, P.J., and Rosenblum, M.K. (1996). Synaptophysin expression in the human spinal cord. Diagnostic implications of an immunohistochemical study. *Am. J. Surg. Pathol.* **20,** 273–276.

CHAPTER

8

Spinal Cord: Connections

JEAN SCHOENEN
Department of Neuroanatomy and Neurology, University of Liège, Liège, Belgium
GUNNAR GRANT
Department of Neuroscience, Karolinska Institutet, Stockholm, Sweden

Thanks to modern tracing methods (antero- and retrograde transport labeling), which have complemented the classical fiber degeneration techniques, our knowledge of connections in the mammalian spinal cord has greatly expanded. Important contributions in this field have also been provided by electrophysiological experiments in animals using orthodromic or antidromic electrical stimulation. Extensive and competent reviews of the results of these experiments have been published by Willis and Coggeshall (1991), Kuypers (1981), Fyffe (1984), and Tracey (1986).

With human material, where the modern tracing methods are not applicable, one has to rely on data from the study of selected pathological cases with circumscribed lesions. In such cases, tracing of axons and identification of their terminals can be achieved by anterograde degeneration labeling (Marchi and Nauta techniques). Cells of origin of fiber systems can be detected by utilizing the chromatolytic changes that occur in neuronal cell bodies after transection of their axons (retrograde chromatolysis). The results of these human studies are often difficult to interpret and sometimes of limited value because of the low sensitivity of the methods used and the complexity of neurological pathology. Nevertheless, valid conclusions can be made about some of the important fiber connections in the human spinal cord. These will be reviewed below, but where appropriate, references will also be made to experimental findings in nonhuman mammalian cords. Indeed, it is known that certain spinal connections differ markedly between different species (e.g., corticospinal connections), while others have roughly the same organization in all mammals (e.g., descending brain stem pathways). In the following section we describe the intrinsic connections of the spinal cord, which are mainly represented by the propriospinal system. The second and third sections are devoted to afferent and efferent spinal pathways, respectively.

PROPRIOSPINAL PATHWAYS

Contrary to what has frequently been assumed, short-axoned neurons that distribute their fibers only through the gray matter to neighboring neurons are rare in the spinal cord. Such neurons probably only exist in the substantia gelatinosa (lamina II). The great majority of spinal neurons, especially those located in laminae V–VIII, are propriospinal in nature. On their way to the funiculi, they may establish connections with adjacent cells via collaterals of their main axons. Propriospinal neurons have a paramount role in spinal functions. For example, descending pathways are differentially distributed to subgroups of propriospinal neurons, which relay their action to motoneurons or other spinal cells.

White Matter Localization

The anatomy of the fasciculi proprii of the spinal cord in humans has been extensively reviewed by Nathan and Smith (1959). The portions of the spinal white matter bordering the central gray matter contain most of the axons of propriospinal neurons. According to Nathan and Smith, the following bundles of fibers need to be considered.

Ground Bundles

Anterior Ground Bundle The anterior ground bundle is present throughout the spinal cord, containing most fibers at the levels of the enlargements. It contains both ascending and descending fibers; these fibers vary in length, with some extending through the cord, and others covering one segment or less. The shortest fibers immediately surround the gray matter and the longer fibers are situated more peripherally. Most of the fibers are fine, with diameter of less than 3 μm. The cells of origin are poorly known, although they are probably located in the more medial and dorsal parts of the ventral horn, in the intermediate gray matter, and possibly in the dorsal horn. The fibers terminate in the ventral horn throughout the spinal cord, predominantly in their ventromedial portion. The anterior ground bundle is the first tract of the spinal cord to myelinate during ontogenesis.

Lateral Ground Bundle The lateral ground bundle is situated between the most lateral part of the ventral roots and the dorsal roots. It is also present throughout the cord and is most developed in the cervical and lumbar enlargements. It has both ascending and descending fibers; the fibers vary in length, and their cells of origin are mostly ipsilateral and located in the intermediate gray matter, the dorsal horn, and some in the ventral horn. Fibers in the lateral ground bundle have many collaterals and terminate throughout the gray matter. Most of the bundle is myelinated in the 5-month-old fetus.

Posterior Ground Bundle The posterior ground bundle designates the fine fibers of the fasciculi proprii scattered throughout the whole area of the dorsal columns. The presence of these propriospinal fibers is disputed. They probably arise from neurons in the medial parts of the dorsal horn, are short, and distribute to the gray matter of the medial part of the dorsal horn. These fibers are unmyelinated and small (0.5–2 μm).

Lissauer's Tract

Lissauer's tract is bound anteriorly (or ventrally) by lamina I and posteriorly (or dorsally) by the subpial neuroglia and the entering posterior roots. It is present throughout the cord, and is most developed in the upper cervical region and least developed in the thoracic cord. It is mainly composed of unmyelinated fibers but also contains fine myelinated fibers. The tract contains both ascending and descending fibers and both types extend for a few segments. In the monkey, the majority of these fibers have been found to be dorsal root afferents. The remaining fibers are intrinsic. The cells of origin of these intrinsic fibers and the cells around which they terminate are marginal neurons and neurons of the substantia gelatinosa. These neurons also receive terminals from the dorsal root afferent fibers.

Cornucommissural Tract

This tract, which is most developed in the lower lumbar region, lies against the medial aspect of the dorsal horn and along the dorsal commissure. It consists mainly of ipsilaterally running propriospinal ascending and descending fibers, which seem to connect the regions of subjacent gray matter to similar areas at other levels. It is apparently one of the earliest parts of the dorsal columns to show myelination during development.

Comma Tract

This comma-shaped collection of fibers lies in the cervical and upper thoracic cord between the fasciculi cuneatus and gracilis. Whether it consists of the descending division of dorsal root fibers or of intrinsic fibers has been a matter of discussion. According to Nathan and Smith (1959), the bulk of evidence indicates that the comma tract consists of the descending division of the cervical and upper thoracic dorsal roots.

Septomarginal Tract

This tract is situated along the posterior periphery of the cord but has a different location at different segmental levels. In the lumbar enlargement it extends along the median septum and may abut against the posterior commissure. It contains a mixture of both descending divisions of dorsal roots and intrinsic cord fibers. However, the evidence with respect to the latter is inconclusive.

Cells of Origin

While little is known regarding the distribution of propriospinal pathways in humans, a considerable number of data have been gathered in other mammals, especially in the cat and monkey, by means of the anterograde degeneration, retrograde degeneration, and the retrograde horseradish peroxidase (HRP)

transport techniques. The bulk of these data comes from the work of Barilari and Kuypers (1969) and Molenaar *et al.* (1974) and has been summarized by Kuypers (1981). The propriospinal neurons may be subdivided according to the length of their fibers into long, intermediate, and short propriospinal neurons. The long propriospinal neurons distribute their axons throughout the length of the spinal cord, mainly through the ventral funiculus and the ventrolateral fasciculus. They are concentrated in lamina VIII and the dorsally adjacent part of lamina VII. The fibers from the long propriospinal neurons in the cervical cord descend bilaterally, but those from the corresponding neurons in the lumbosacral cord ascend mainly contralaterally. The intermediate propriospinal neurons extend over shorter distances. They are located in the central and medial portions of lamina VII and project bilaterally but with an ipsilateral preponderance. The short propriospinal neurons that distribute their fibers over a distance of only six to eight segments are the main occupants of the lateral part of laminae V–VII; their fibers course primarily ipsilaterally through the lateral funiculus.

Distribution

The propriospinal fibers in the different parts of the ventral and lateral funiculi are distributed preferentially to different parts of the spinal gray matter. Recipient areas consist of both the intermediate gray matter and the motoneuronal columns. Propriospinal fibers in the dorsolateral fasciculus terminate mainly in the dorsal and lateral parts of the intermediate gray matter and in the dorsolateral motoneuronal column. These propriospinal fibers are thus distributed specifically to motoneurons of intrinsic hand and foot muscles. Conversely, propriospinal fibers in the ventral part of the ventrolateral fasciculus distribute to the central and medial parts of lamina VII and to ventromedial motoneurons, which innervate proximal extremity and girdle muscles. The third contingent of propriospinal fibers, those which run in the ventral funiculus, terminate mainly in the ventromedial part of the gray matter (lamina VIII and medial lamina VII), which contains long propriospinal neurons, and in the ventromedial motoneuronal column, which innervates axial and girdle muscles (Fig. 8.1).

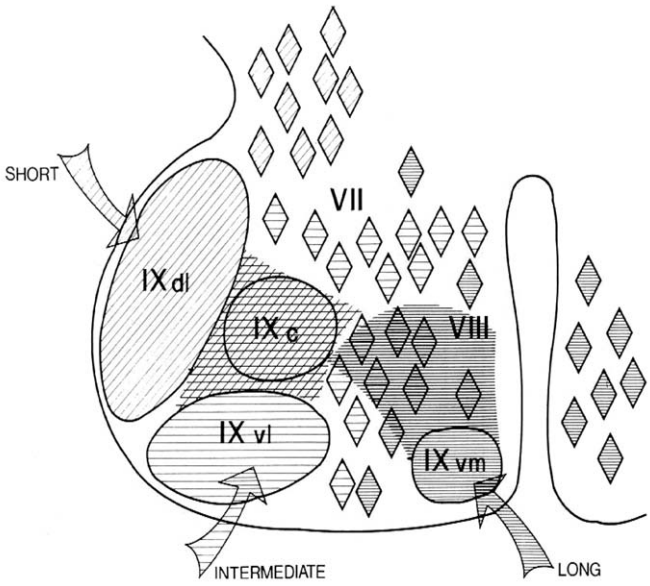

FIGURE 8.1 Cells of origin and terminal distribution area in ventral horn of long *(dark-shaded)*, intermediate *(horizontally shaded)*, and short (obliquely shaded) propriospinal neuron groups.

AFFERENT PATHWAYS

Primary Afferents

Primary afferent fibers reach the spinal cord via the dorsal roots. The question of whether some afferents also enter via the ventral roots has attracted interest in recent years, after unmyelinated sensory fibers were found in the ventral roots of various mammals including (probably) humans (see Coggeshall, 1986; Willis and Coggeshall, 1991). The cells of origin of these afferent fibers, like those of dorsal root afferents are in the dorsal root ganglia. Some of these fibers seem to be afferents making loops in the ventral root. They do not enter the spinal cord from its ventral side. Others are sensory afferents innervating the pia or the ventral surface of the spinal cord. They use the ventral roots on their way to reach the dorsal root ganglia. A third group may be afferents that actually enter the spinal cord from its ventral side, but conclusive evidence for this proposition is lacking.

The cells of origin of the primary afferent fibers are located in the dorsal root ganglia. These cells are unipolar and give rise to peripheral branches that are contained in the spinal nerves and to central branches entering the spinal cord. Peripherally, primary afferent fibers are usually related to different types of receptors; alternatively, they ramify as free nerve endings in skin, joints, muscle, and viscera. The central branches give rise to terminal ramifications in the dorsal column nuclei and/or the spinal gray matter.

Both myelinated fibers of different sizes and unmyelinated fibers are found among the primary afferents. Electron microscopic studies, carried out mainly in rats, have revealed that about two-thirds of

the afferent fibers are unmyelinated. It seems reasonable to assume that the situation would be similar in humans.

Cutaneous fibers are composed of the myelinated Aα/β and Aδ fibers, and of the unmyelinated, fine, slowly conducting C fibers. Joint and visceral afferents are classified in the same way as the cutaneous afferent fibers. In muscle nerves, however, the myelinated fibers are divided into groups I, II, and III, which have successively smaller diameters and slower conduction velocities, and group IV afferents, which are unmyelinated and have the slowest conduction velocities (see Chapter 5). The functional classes of afferent fibers and receptor types, both for cutaneous and for other types of afferents, have been reviewed by Kaas (Chapter 28; see also Willis and Coggeshall, 1991). They will therefore not be dealt with here. It should only be pointed out that methods are now available to characterize response properties of afferents in humans, using so-called microneurography, and to evoke sensations by electrical stimulation in nerves, thereby increasing our knowledge about sensory mechanisms in humans (see, e.g., Chapter 28). Such studies have led to the detection of specific C-fiber receptors for itch (Schmelz *et al.*, 1997) and also of tactile C afferents of a hitherto unknown type in humans (Vallbo *et al.*, 1999). Recently, in a unique patient lacking large myelinated afferents, it was found that activation of tactile C afferents produced a faint sensation of pleasant touch, suggesting their involvement in emotional aspects of tactile stimulation (Olausson *et al.*, 2002).

Dorsal Roots

The dorsal roots are segmentally arranged along the spinal cord. Peripherally, this segmental arrangement is reflected in the dermatomes. For humans, several extensive dermatomal maps have been published, constructed on the basis of different approaches. They are discussed by Kaas in Chapter 28 and will therefore not be dealt with further in this section (see also Dykes and Terzis, 1981). Suffice it to mention that, as a consequence of the anatomical arrangement, lesions affecting dorsal roots result in sensory loss within corresponding dermatomes.

In humans, there are usually 31 pairs of roots (8 cervical, 12 thoracic, 5 lumbar, 5 sacral, and 1 coccygeal), the largest being those of the lumbar and cervical enlargements. Occasionally, the first cervical dorsal root, which is normally very small, is missing. Because of the difference in length between the spinal cord and the vertebral column, the nerve roots of the lumbosacral spinal cord have a much longer distance to travel prior to reaching their respective foramina of exit from the vertebral canal. They are therefore much longer than those of the thoracic and cervical spinal cord. Each dorsal root fans out from the central end of the dorsal root ganglion into several rootlets that enter the spinal cord along the posterolateral sulcus.

About 1 million dorsal root fibers have been found on each side in the human adult. This figure is based on studies in which the silver impregnation technique was used (Arnell, 1933; see also Kjellgren, 1944). Although this technique reveals a higher number of fibers than myelin stains, the figure is certainly much too low. Considering the fact that about two-thirds of the afferent fibers may be unmyelinated, a more realistic number of dorsal root fibers should 2–2.5 million.

Caliber spectra of dorsal roots have been investigated in humans postnatally (Rexed, 1944). This was done with the Alzheimer–Mann–Häggqvist technique, which is used to stains myelinated fibers. A distinct development was found to take place that persisted for up to 5–9 years of age. There was one fine-caliber and one thick-caliber group, which in the adult had maximum diameters of 2–4 and 8–9 μm, respectively. In old persons, distinct signs of diminution in the number of the thick fibers were found commencing at the age of 50 years.

The myelin sheath of dorsal root fibers is produced by two types of cells, which meet at a transitional node. Peripherally, the myelin is produced by Schwann cells, centrally by oligodendrocytes. The transitional region which has several unique features, including astrocytic processes, has been studied in detail ultrastructurally in the cat (Carlstedt, 1977; see also Chapter 9), but not in humans.

A controversial question has been whether dorsal root fibers become segregated on the basis of their fiber diameter just before their entry into the spinal cord (Fyffe, 1984; Snyder, 1977). Early studies at the light microscopic level were not well suited for answering this question. In a comprehensive electron microscopic study, however, Snyder (1977) demonstrated convincingly that a reorganization of the fibers in the rootlet takes place central to the transitional region in the macaque monkey. In this species, as in the cat, small-caliber axons are randomly distributed in the peripheral part of the rootlet (as they are in the peripheral nerve). Centrally, however, in the monkey, but not in the cat, the small-caliber axons take a ventrolateral course in the rootlet and, as this merges with the dorsal columns, these axons form a single bundle on the ventral and lateral surface of the rootlet, which then merges with Lissauer's tract. These findings therefore indicate that a lateral division of the dorsal root is present in the monkey, but not in the cat. The situation in humans has been analyzed at the light microscopic level (Sindou *et al.*, 1974) but not electron microscopi-

cally, which would be necessary for disclosing all the unmyelinated fibers in the rootlet.

Dorsal Root Ganglia

The dorsal root ganglia (spinal ganglia) are usually located within the intervertebral foramina, immediately outside the points where the nerve roots perforate the dura mater. However, the C1 and C2 ganglia lie on the vertebral arches of the atlas and axis, those of the sacral nerves are inside the vertebral canal, and that of the coccygeal nerve is within the sheath of dura mater. The C1 ganglia are missing in some individuals. On the other hand, aberrant ganglia consisting of groups of nerve cells are sometimes found on the dorsal roots of the upper cervical nerves between the spinal ganglia and the spinal cord.

The ganglia are derived from the neural crest, and they contain the cell bodies of nearly all neurons conveying somatic and visceral input from the body to the spinal cord. The ganglion cells vary in diameter between about 10 and 100 μm. Each such cell is surrounded by satellite cells. These are also derived from the neural crest. They seem to be modified Schwann cells. The ganglion cell population has been divided into two groups, one group of large cells, which appear light in Nissl stains, giving rise to large-caliber fibers, and one group of small dark neurons, giving rise to small-caliber fibers. In recent years, attempts have been made, mainly in rats, to classify the two populations further in physiological, anatomical, and immunocytochemical terms (e.g., Dodd and Jessel, 1985, Lawson *et al.*, 1985, 1987; Lawson 1995, 2002; see also Chapter 9).

The ganglion cells are unipolar and are usually reported as giving rise to a single process that bifurcates into a peripheral and a central branch. Not infrequently, the proximal segment is highly coiled and this is then referred to as the glomerular segment. Some studies, mainly in the rat, suggest that one single dorsal root ganglion cell may in fact give rise to more than one peripheral branch, and also to more than one centrally projecting branch (see, e.g., Coggeshall, 1986). Evidence emanates mainly from studies in which two different labeling substances have been applied peripherally at different nerves and later both these substance were detected in the same dorsal root ganglion cells, and from studies in which axon counts have been made and compared with results of ganglion cell counts. In the first instance, only a small percentage of ganglion cells show both labels, indicating that double branching is infrequent. With respect to the counting studies, which have indicated a relationship of up to 2:1 between axons and ganglion cells, the results are critically dependent on the methods that have been used. Studies in the rat (Schmalbruch, 1987) indicate that previous investigations have given values for the number of dorsal root ganglion cells that are too low and that, in fact, the ganglion cell numbers compare well with the number of dorsal root axons. However, further investigations are necessary to answer this question, which is of interest also from a clinical point of view because the possible branching of peripheral axons has bearing on the problem of referred pain (Coggeshall, 1986).

Central Terminations

The termination of the primary afferent fibers in the spinal cord and dorsal column nuclei has been dealt with by Kaas in Chapter 28 (see also Chapters 7 and 9). Furthermore, the ascending dorsal column fibers have been discussed in the present chapter in connection with the ascending pathways. Therefore, only a few points will be made with regard to the primary afferent terminations, and they will be restricted to the spinal cord.

On the basis of studies across mammalian and nonmammalian species (Cervero, 1986; Fyffe, 1984; Grant, 1995), it seems justifiable to conclude that humans would also display two principles of organization for the spinal termination of primary afferent fibers. First, there is a somatotopic organization of incoming afferents mediolaterally in the dorsal horn. Distal parts of the limbs are "represented" medially and proximal parts laterally. For the thoracic region of the body, ventral parts are represented medially and dorsal parts laterally. Second, there is a ventrodorsal modality–related segregation principle superimposed on the somatotopic pattern. Fine-caliber fibers related to pain and temperature terminate in superficial parts of the dorsal horn (laminae I and II), whereas coarse-caliber fibers terminate in deeper parts, with some coarse-caliber proprioceptive afferents terminating in the ventral horn (Figs. 8.2 and 8.5). Furthermore, it seems from studies which have been made mainly in cats and rats that in the dorsal horn, the substantia gelatinosa (lamina II) receives primary afferent fibers almost exclusively from cutaneous receptors. Visceral afferents, as well as muscle afferent fibers, seem to have their terminations mainly in laminae I and V (see, e.g. Cervero, 1986; Molander and Grant, 1987; Sugiura *et al.*, 1993; Sugiura and Tonosaki, 1995).

Descending Pathways

The present knowledge on descending pathways in the human spinal cord is still fragmentary to the extent that the 1955 review by Nathan and Smith is still current. Most of the available data concern the corticospinal

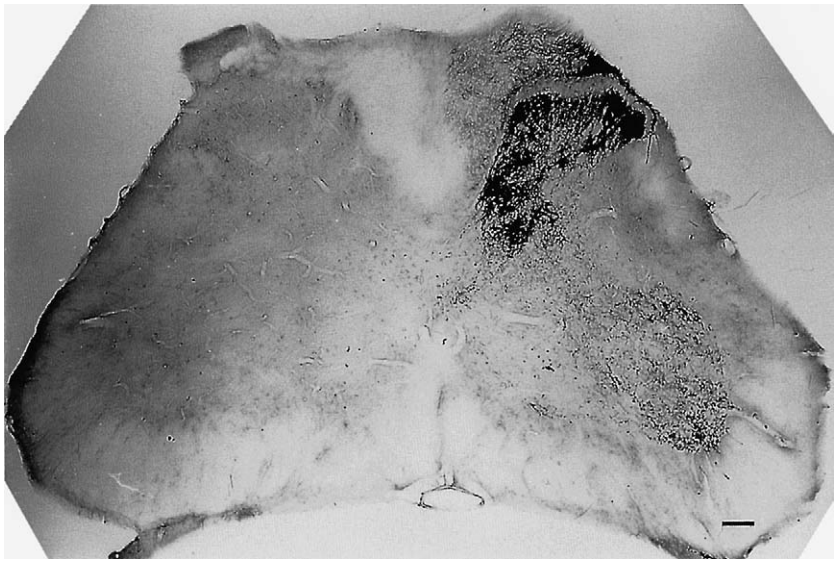

FIGURE 8.2 Distribution of coarse-caliber dorsal root fibers in the L4 segment of the spinal cord of the rat, following unilateral L4 dorsal root ganglion injection of horseadish peroxidase conjugated to the nontoxic B fragment of cholera toxin. Bar = 100 µm.

tract and have been obtained by the anterograde degeneration technique in selected pathological cases. Major contributions in this area have been made by Barnes (1901), Holmes and May (1909), Jane *et al.* (1967), Luhan (1959), Minckler *et al.* (1944), and Schoen (1964, 1969, 1972). Moreover, studies on the fiber composition and course of the pyramidal tract have been performed by Armand (1984), Bumke (1907), Fulton and Sheehan (1935), Giok (1956), Häggqvist (1937), Holstege and Kuypers (1982), Lankamp (1967), Lassek (1942a, b), Nyberg-Hansen and Rinvik (1963), and Swank (1934). An extensive review and analysis of all major work, as well as a compilation of experimental data on the corticospinal tract, has been published by Phillips and Porter (1977). Several comprehensive reviews of descending pathways to the spinal cord in mammals have been made by Kuypers (1964, 1973, 1981). We will first consider the corticospinal system, which has the highest level of development in higher primates, especially in humans. Subsequently, the other descending pathways, for which species differences are less pronounced, will be examined.

Corticospinal Tract

Cells of Origin The cells of origin of the corticospinal tract are located in the precentral gyrus, mainly in its upper two-thirds, and in the paracentral lobule. Brodmann's areas 4 (primary motor cortex) and 6 (nonprimary motor cortex) contribute 80% of the pyramidal tract fibers (see Chapter 27 for diagrammatic and pictorial representation of cortical regions, e.g., Fig. 27). In contrast to other mammals, contribution of corticospinal fibers from the postcentral gyrus is sparse in the human. Corticospinal fibers are not derived exclusively from the large lamina V Betz cells of area 4.

Number of Axons The number of axons in a pyramid is roughly proportional to body and brain weight. The corticospinal tract contains more axons in animals in which the pathway extends the entire length of the cord, compared to those species in which it terminates either at cervical or thoracic levels. In humans, there are approximately 1 million axons in each pyramid. Of these, 80% measure less than 2 µm in diameter and 90% range from 1 to 4 µm. The maximal fiber diameter may be as high as 20 µm. Thick fibers occur especially in species (such as humans) that possess many direct corticomotoneuronal connections.

Postnatal Development During postnatal development, myelination starts in the internal capsule and peduncles, where it is present in the 10- to 14-day-old neonate. Myelination is completed in the second year. It proceeds simultaneously in the lateral and ventral divisions of the tract. The axons from the paracentral lobule and from the upper third of the precentral gyrus myelinate before those from the middle third of this gyrus. Furthermore, a postnatal increase in diameter of corticospinal fibers has been observed in the human (Lassek, 1942b; Verhaart, 1950). In the

newborn rhesus monkey, virtually no cortical fibers are distributed to the motoneuronal cell groups, the full complement of corticospinal connections appearing around the age of 8 months. The increasing wide distribution of cortical fibers in the spinal gray matter with increasing age probably represents a true outgrowth of cortical fibers (Kuypers, 1962).

Trajectory and somatotopy The trajectory and somatology of corticospinal fibers is well known and will not be reviewed in detail here. After decussating in the caudal medulla, the bulk of corticospinal fibers continue in the dorsolateral fasciculus of the spinal cord as the lateral corticospinal tract. Some fibers do not cross in the medulla but continue into the cord in the ventral funiculus and then cross in the ventral white commissure. This is referred to as the ventral (uncrossed) corticospinal tract. The following features have been emphasized for corticospinal tracts in man (Nathan *et al.*, 1990). In the cervical cord, the lateral corticospinal tract covers an area of the white matter that extends anteriorly beyond the level of the central canal. At lower cervical cord levels, fibers separate from the main mass of the tract and reach the periphery of the anterolateral sector of the cord. There is a close anatomical relationship between the lateral corticospinal tract and the denticulate ligament in cervical segments. In most necropsy specimens the anterior uncrossed corticospinal tract is smaller on the left side because a greater number of corticospinal fibers cross to the right side. This accounts for the asymmetry of the two halves of the cord. Inconsistently, a small group of axons remains in the medulla and joins the lateral corticospinal tract. It must be emphasized that the pyramidal tract is subject to much anatomical variation from individual to individual. For instance, in some subjects, the ventral tract may be absent or not project into lumbosacral regions; the pyramidal decussation may be absent; a ventrolateral pyramidal tract may exist, or a Pick's bundle may be found, i.e., recurrent pyramidal fibers which, after decussating in the medulla, ascend in the bulbar lateral tegmental field.

Terminal Distribution The terminal distribution of corticospinal fibers in the human spinal gray matter has been determined by classical fiber degeneration methods in spinal cords of patients who died after suffering circumscribed central nervous system lesions such as cerebrovascular accidents (Schoen, 1964, 1969; Schoenen, 1981). Corticospinal fibers distribute mainly contralaterally to the lateral parts of laminae V–VI, VII, the dorsolateral motoneuronal column, and the lateral parts of the central and ventrolateral motoneurons (Fig. 8.3a, b). Terminals are also found contralaterally in the medial parts of lamina VII and bilaterally in lamina VIII (Schoen, 1969). A few cortical fibers are distributed to lateral lamina IV of the dorsal horn. This distribution pattern is similar throughout the length of the spinal cord, although it is more profuse in the enlargements.

Although at spinal levels fibers originating in different cortical areas are intermingled in the corticospinal tract, there is a clear difference in the terminal distribution of precentral and postcentral cortical fibers. Thus, the few fibers from the postcentral gyrus are distributed mainly to the dorsal gray matter (lamina IV, lateral part of laminae V–VI and VII) (Fig. 8.3c, d), while those from the precentral cortex project in a topographically organized fashion to the intermediate gray matter and the motoneuronal cell groups. According to studies in the monkey, the cortical areas carrying representations of axial and proximal limb movements give rise to few fibers to motoneuronal cell groups and characteristically project to those parts of the gray matter that contain propriospinal neurons with long axons (lamina VIII, medial lamina VII). In contrast, areas where distal extremity movements are represented, project to motoneuronal cell groups of distal extremity muscles and to those portions of the gray matter that mainly contain short and intermediate propriospinal neurons (laminae V–VI, lateral lamina VII) (Kuypers, 1981). The terminal distribution of corticospinal fibers in humans is clearly different from that observed in several other mammals. In more primitive species, such as elephants and marsupials, the corticospinal tract terminates in rostral cord segments and in the dorsal horn, suggesting that it chiefly has a sensory function. In more evolved species, such as rodents and carnivores, the corticospinal tract terminates at more caudal levels of the cord and in more ventral regions of the gray matter. In primates, and especially in humans, there is in addition a heavy projection of corticospinal fibers to the ventromedial part of gray matter containing long propriospinal neurons and to motoneuronal cell groups innervating distal and proximal extremity muscles. From a functional point of view, it is known from lesion experiments in which freely moving monkeys were used that the corticospinal pathway amplifies the motor control exerted by descending brain stem pathways (see below). Specifically, the direct corticomotoneuronal connections make possible the high degree of fractionation of movements such as individual finger movements (see Kuypers, 1981).

The motor deficits occurring after lesions of varying extent of the corticospinal tracts have been assessed in 44 patients having cordotomies for relief of cancer pain (Nathan, 1994). Only surgical incisions extending more posteriorly than the anterior quadrants of the cord

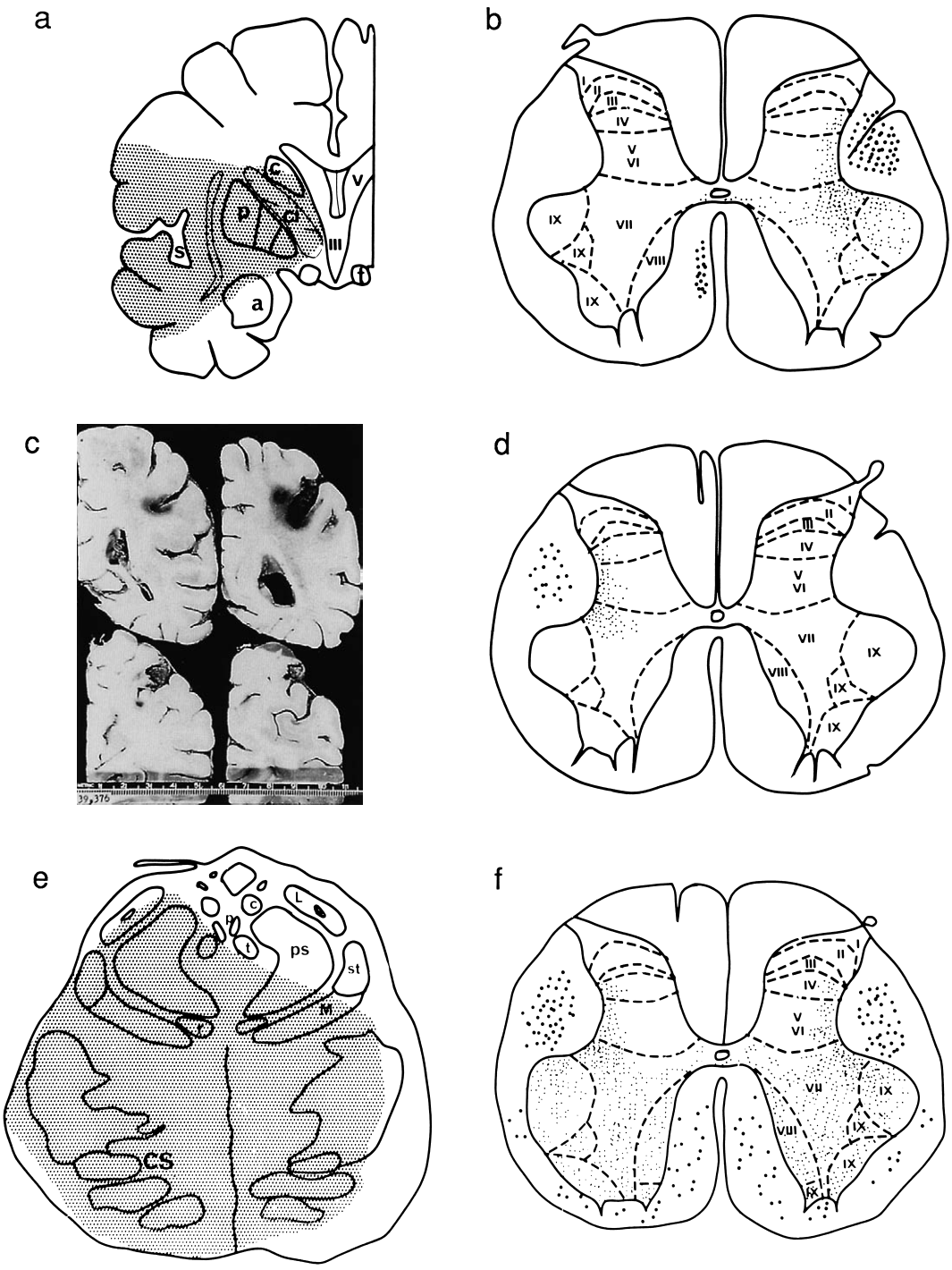

FIGURE 8.3 Distribution of cortico- and subcorticospinal fibers in human pathological cases determined with Albrecht–Fernström's variant of Nauta's technique. **(a)** Case 1: Outline of left sylvian infarction in a 70-year-old patient who presented a right hemiplegia and aphasia 2 weeks before death. a, Amygdala; c, caudate nucleus; ci, internal capsule; p, putamen; s, sylvian fissure; t, optic nerve; v, lateral ventricle. **(b)** Case 1: Degenerating fibers at segmental level L5. **(c)** Case 2: A small, right parietal, hemorrhagic infarction in a 67-year-old patient who had an embolus to the right ascending parietal artery 2 weeks before death. **(d)** Case 2: Degenerating fibers at L5. **(e)** Case 3: Outline of the territory occupied by a pontine fibrillary astrocytoma in a 21-year-old patient in whom tetraparesia and cranial nerve dysfunction evolved over 10 months before death. c, Locus coeruleus; CS, corticospinal tract; L, lateral lemniscus; M, medical lemniscus; ps, superior cerebellar peduncles; r, rubrospinal tract; st, spinothalamic tract; t, tectospinal tract. **(f)** Case 3: Degenerating fibers at L4.

caused motor disturbances. A large unilateral lesion dividing most of the lateral corticospinal tract, and the descending fibers anterior to it, caused flaccid paralysis of the ipsilateral lower limb, but voluntary movements started to return within hours. A thoracic incision cutting one lateral corticospinal tract and most of the opposite tract and reticulospinal fibers anterior to that tract caused total paraplegia; after 2 months, however, the patient was able to walk though with a severe spastic paraparesis. A unilateral division of the lateral corticospinal tract in the upper cervical cord was followed within 6 h by recovery of some ipsilateral finger and toe movements. Lesions of the anterior fibers of the lateral corticospinal tract above the cervical enlargement did not affect motility of the ipsilateral upper limb, suggesting that in more cranial segments fibers destined to the upper limb are in the more posterior part of the tract.

Descending Brain Stem Pathways

Most of the evidence regarding the cells of origin and the terminal distribution of these pathways comes from animal experiments (for recent studies, see Holstege, 1987a, b; Holstege and Kuypers, 1982; Holstege and Tan, 1987; see also Chapters 36 and 9). With few exceptions, only the white matter localization of some of the tracts descending from the brainstem to the spinal cord has been verified in human pathological material (for a review, see Nathan and Smith, 1955; Nathan *et al.*, 1996).

In the human spinal cord, reticulospinal fibers in general are scattered throughout the anterior and lateral columns. Contrary to their animal counterparts from which the description below is largely derived, they do not seem to form well-defined tracts. The following features characterized degenerating reticulospinal fibers in patients with brain stem lesions or anterolateral cordotomies (Nathan *et al.*, 1996). Reticulospinal fibers move posterolaterally as they descend and lie anterior to the lateral corticospinal tract. Their number decreases caudal to the cervical enlargement, their place being taken by propriospinal fibers, but some of them reach the sacral segments in the sulcomarginal fasciculus.

Medial Reticulospinal Tract The medial reticulospinal tract originates in the dorsal and central parts of the medulla and central pontine, medial tegmental field. Its fibers descend ipsi- and contralaterally in the ventral funiculus and ventrolateral fasciculus. These fibers give off multiple collaterals so that two-thirds of the reticulospinal neurons that distribute fibers to the cervical ventral gray also project to the lumbosacral cord. The terminal distribution of these reticulospinal fibers is especially dense in the enlargements and bilaterally involves the ventral gray matter, i.e., medial and central parts of lamina VII, lamina VIII, and the ventromedial motoneuronal column (Fig. 8.3e, f). The medullary reticulospinal fibers probably establish direct connections with motoneurons of neck and back muscles.

Vestibulospinal Tract

The vestibulospinal tract can be subdivided into a lateral component coming from the lateral vestibular (Deiters') nucleus and a medial component from the medial vestibular nucleus (see Chapter 33). Deiterospinal fibers descend ipsilaterally in the ventrolateral fasciculus at cervical levels and then shift into the medial part of the ventral funiculus at lower spinal levels. This population of neurons is somatotopically organized such that the fibers to the cervical cord are derived mainly from neurons in the rostroventral part of Deiters' nucleus, while those to the lumbosacral cord originate from neurons in its dorsocaudal part. Deiterospinal fibers terminate ipsilaterally in the ventromedial part of the gray matter, i.e., lamina VIII and medial part of lamina VII. A few fibers distribute contralaterally. It has been shown in cats that deiterospinal fibers establish polysynaptic excitatory connections with motoneurons of extensor muscles, monosynaptic connections with Ia inhibitory interneurons, and monosynaptic excitatory connections with motoneurons of neck and back muscles.

Medial vestibulospinal fibers pass via the medial longitudinal fasciculus in the spinal ventral funiculus. They descend bilaterally in the spinal cord with an ipsilateral dominance. Their termination area is more restricted than that of the deiterospinal fibers and comprises mainly lamina VIII and the dorsally adjoining part of lamina VII. Medial vestibulospinal fibers establish monosynaptic inhibitory connections with many motoneurons of neck and back muscles. For more details on the vestibulospinal pathways, see Chapter 33.

Interstitiospinal Tract

The interstitiospinal tract comprises fibers from the interstitial nucleus of Cajál that descend mainly ipsilaterally in the ventral funiculus of the spinal cord as far caudally as the sacral segments. These fibers distribute to the dorsal part of lamina VIII and the dorsally adjoining part of lamina VII.

Tectospinal Tract

The tectospinal tract originates in the deeper layers of the superior colliculus and distributes contralaterally only to the upper cervical cord. Its fibers descend in the ventral part of the ventral funiculus and terminate in the medial and lateral portions of the cervical ventral

horn. They establish multisynaptic connections with neck muscle motoneurons that are excitatory to contralateral muscles and inhibitory to ipsilateral ones.

Rubrospinal Tract

The rubrospinal tract is probably less developed in humans than in lower mammals. The cells of origin are located in the caudal magnocellular part of the red nucleus, which is extremely small in humans. According to findings in the cat and rat, the projections are somatotopically organized. Rubrospinal fibers cross in the ventral tegmental decussation of the midbrain and descend in the dorsolateral fasciculus of the spinal cord just ventral to the lateral corticospinal tract. They distribute to the lateral part of laminae V–VI and the dorsal part of lamina VII and, in the cat and monkey, to the dorsal part of lamina IX (Holstege, 1987a). Orthodromic electrical stimulation findings in the cat show that rubrospinal fibers excite flexor motoneurons and inhibit extensor motoneurons. In the rhesus monkey, rubrospinal fibers establish some direct connections with motoneurons of distal extremity muscles. In contrast to those of vestibulo- and medial reticulospinal fibers, the collaterals of rubrospinal fibers are largely restricted to specific levels.

Lateral Reticulospinal Tract

The lateral reticulospinal tract originates in the ventrolateral pontine tegmentum. Its fibers cross in the brain stem, descend through the dorsolateral fasciculus, and terminate in the spinal gray in laminae I and V (Holstege and Kuypers, 1982).

Other Descending Tracts

Fibers from solitary and retroambiguous nuclei descend mainly contralaterally in the ventrolateral and ventral white matter of the spinal cord, innervating phrenic motoneurons and thoracic motoneuronal cell groups. These pathways subserve respiratory activity, as exemplified by the fact that bilateral transection of the upper cervical ventrolateral fasciculus abolishes rhythmic respiration (Nathan, 1963; see also Chapter 15).

In man, the descending sympathetic fibers supplying preganglionic vasomotor and sudomotor neurons of the body caudal to the head and neck are located in the medial part of the white matter along the equatorial plane extending from the base of the posterior horn and the lateral horn. Projections are bilateral and fibers for vasomotor control probably leave the cord cranial to the Th 7 segment (Nathan and Smith, 1987).

According to animal experiments, catecholaminergic innervation of the spinal gray matter is provided by two pathways: (1) the cerulospinal noradrenergic projection, originating in the locus ceruleus and subceruleus and distributing to all parts of the gray matter (see Holstege and Kuypers, 1982); and (2) the tegmentospinal noradrenergic system originating from lateral pontine groups A5 and A7 and projecting to the intermediolateral column (adjoining parts of the intermediate gray) and the dorsal horn (Lindvall and Björklund, 1983).

Serotonergic fibers to the dorsal horn, considered to convey supraspinal control of nociception, come from the raphe magnus nucleus via the dorsolateral fasciculus and project to laminae I and V. The more caudally located nuclei raphe obscurus and pallidus innervate the intermediate and ventral horn via the ventral and ventrolateral white matter (Holstege and Kuypers, 1982; Hunt, 1983).

Conclusion

To summarize, Kuypers (1981) has proposed the subdivision of the descending brain stem pathways into two large groups on the basis of their terminal distribution and functional properties (Fig. 8.4).

Group A Group A (medial reticulospinal tract, vestibulospinal tract, interstitiospinal tract, tectospinal tract) is characterized by location in the ventral and ventrolateral white matter and, frequently, bilateral termination in the ventromedial part of the gray matter (an area that contains long and intermediate propriospinal neurons). These fibers display high degree of collateralization and have some direct connections with motoneurons of neck, back, and proximal extremity muscles. The cell groups of origin of group A pathways receive fibers mainly from cortical areas rostral to the precentral gyrus. Functionally, the system is concerned with the control of posture, synergistic whole-limb movements, and orientation movements of body and head. The distribution area of group A afferents overlaps mainly with that of ventral corticospinal fibers.

Group B Group B pathways (rubrospinal tract, pontospinal tract from the ventrolateral pontine tegmentum) comprise contralaterally descendings fibers which are situated in the spinal dorsolateral fasciculus and characterized by their termination in the dorsal and lateral parts of the intermediate gray matter, an area containing short propriospinal neurons. Group B pathways establish monosynaptic connections with motoneurons of distal extremity muscle in primates and cats. These pathways show a low degree of collateralization in contrast to group A pathways. Their area of termination overlaps chiefly with that of the lateral corticospinal or pyramidal tract. The cells of group B pathways, e.g., the red nucleus, receive mainly

Jean Schoenen and Gunnar Grant

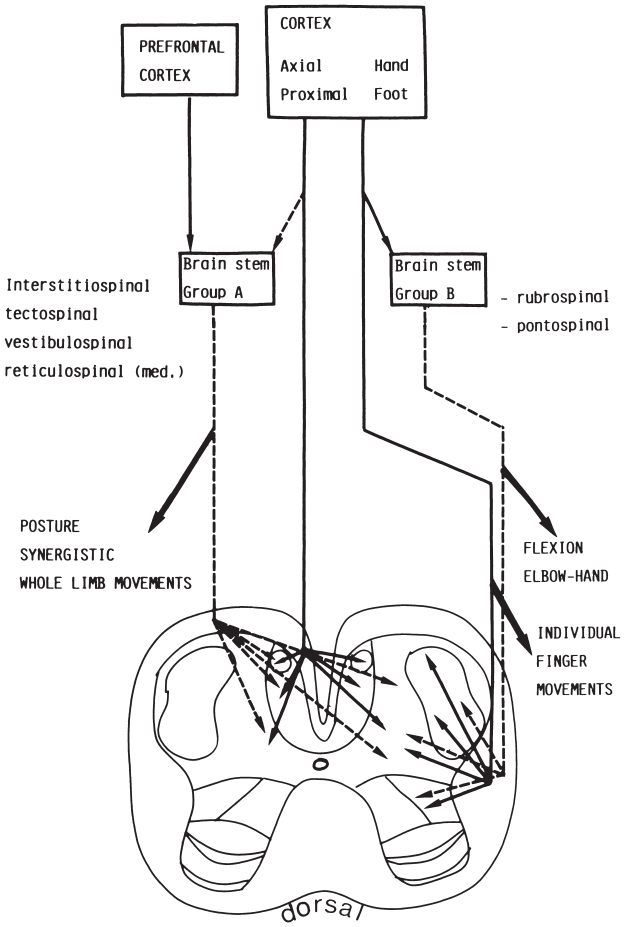

FIGURE 8.4 The major descending pathways to the spinal cord, their terminal distribution in the spinal gray matter, and their main functional roles.

cortical afferents from the precentral gyrus. In view of these anatomical data and functional findings in the freely moving monkey, group B brain stem pathways seem to supplement the control exerted by the group A pathways and provide the capacity for independent, flexion-biased movements of the extremities and the shoulder, but in particular of the elbow and hand.

Considering the pattern of spinal distribution of noradrenergic and serotonergic descending fibers from the brain stem, these pathways probably have a functional role in sensory processing in the dorsal horn, in autonomic activity, but also in motor control. In this respect, it is interesting to recall that electrical stimulation of the nucleus raphe magnus produces an analgesic effect as well as inhibition of interneurons in the spinal flexion reflex arc. Further research is needed to clarify the precise functions of the monoaminergic pathways to the spinal cord.

Finally, as illustrated in Figure 8.5, it is worth mentioning that within the spinal gray matter the majority of afferents are roughly parallel to the preferential dendritic orientation of spinal neurons (see above).

EFFERENT PATHWAYS

The well-known spinal output by somatic motoneurons and autonomic preganglionic cells will not be discussed here (see Chapter 5). We will review below the available data concerning the localization and the trajectory in the human spinal cord of so-called long projection neurons, which give rise to ascending pathways to supraspinal structures. Information in this field chiefly comes from the study of patients who had had ventrolateral cordotomies for the release of intractable pain or localized traumatic or inflammator spinal lesions. Since in such cases there is inevitably involvement of several white matter tracts, it is not possible to precisely determine the cells of origin of any given pathway. However, information can be obtained concerning the funicular localization of ascending axons from spinal neurons.

Ascending Pathways in Humans

Smith (1976) studied retrograde cell changes in 23 human spinal cords after ventrolateral cordotomies. She found that some fibers arising from all gray matter laminae, except laminae II and III, ascend the cord in the lateral funiculus. A larger proportion of fibers arises from laminae I, IV, V, and VII. The majority of those from lamina I have a course contralateral to that of their cells of origin, but a few have an ipsilateral course. More of the fibers arising from lamina I run in the ventrolateral than in the dorsolateral sector. The fibers arising from laminae IV and V run in both the ventrolateral and dorsolateral sectors, both contralateral and ipsilateral to their cells of origin. The major contributing fibers originating in lamina VII come from the nucleus dorsalis of Clarke. The fibers are located both in the dorsolateral and the ventrolateral fasciculi. Most of them are ipsilateral to their cells of origin. Some fibers arise from other cells in laminae V–VI and VII; they ascend both ipsilaterally and contralaterally in the ventrolateral fasciculus. Some neurons in laminae VIII and IX emit axons that run contralaterally in the ventrolateral fasciculus. In a study of five cases of ventrolateral cordotomy performed at upper cervical or thoracic levels between 3 weeks and 8 months before death, we have found (Schoenen, 1981) a low number of chromatolytic neurons contralaterally in

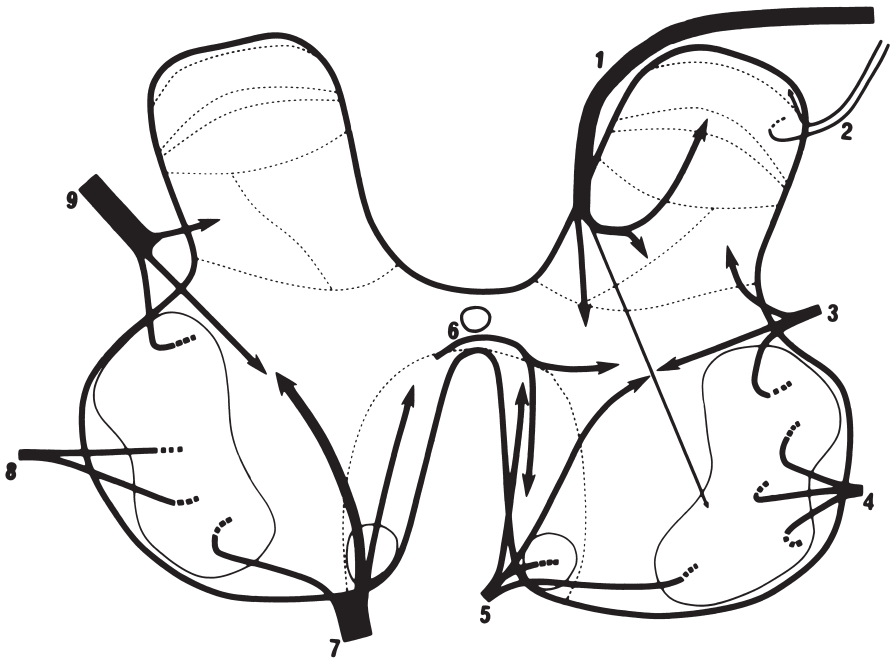

FIGURE 8.5 Illustration of the termination area and orientation of the main afferents to the spinal gray matter. Descending afferents are represented on the left, peripheral, and propriospinal afferents on the right. Fibers taking a longitudinal course are indicated by dashed lines. 1, Large-caliber dorsal root afferents; 2, small-caliber dorsal root afferents; 3, dorsolateral propriospinal afferents; 4, ventrolateral propriospinal afferents; 5, ventromedial propriospinal afferents; 6, commissural propriospinal afferents; 7, vestibulo- and medial reticulospinal afferents (brain stem group A); 8, rubro- and pontospinal afferents (brain stem group B); 9, lateral (crossed) corticospinal afferents.

laminae I and IV of the lumbar enlargement (Fig. 4.5). Conversely, in three patients dying after an acute transverse thoracic myelitis, chromatolytic neurons at the lumbar level were distributed bilaterally in laminae I and IV as well as in laminae VII and VIII and in the marginal part of the dorsolateral motoneuronal column (Fig. 8.6).

It is important to recall that ventrolateral cordotomies damage ascending fibers other than those of the spinothalamic tract, e.g., spinocerebellar, spinoreticular, spinomesencephalic, and propriospinal fibers. Nevertheless, the findings described above and those made by Kuru (1949) in three cordotomy cases suggest that in humans most of the cells of origin of the spinothalamic tract are located in contralateral laminae I and IV. This is at some variance with the results obtained in the cat and monkey, where spinothalamic neurons have been found in laminae I, V, and VII–VIII (Albe-Fessard *et al.*, 1975; Carstens and Trevino, 1978; Trevino and Carstens, 1975; Willis *et al.*, 1979; Apkarian and Hodge, 1989; Craig *et al.*, 1989). It may be surprising that such a low number of spinal neurons show retrograde changes in human cordotomy cases. This might be due to the low sensitivity of the retrograde degeneration method. Another explanation might be the existence of collaterals of the spinothalamic fibers in the spinal cord (Smith, 1976); on the other hand, it must be kept in mind that, as in the cat, the majority of lamina I neurons might be propriospinal in nature and not project into the spinothalamic tract (Cervero *et al.*, 1979) Regarding pain pathways in the human spinal cord, it is interesting to note that commissural myelotomy, another operation performed for relief of intractable pain, produces sensory changes that are not explicable on the basis of previous anatomical knowledge (Cook *et al.*, 1984). Although the purpose of this procedure has been to produce a loss of pain sensibility by dividing the spinothalamic and spinoreticulothalamic fibers as they decussate in the ventral commissure of the cord, this result is not always obtained. The patterns of sensory loss in this case have suggested that the lesion might involve intraspinal polysynaptic, i.e. propriospinal, pain-conducting pathways. Recent studies seem to have shed light on this problem, presenting evidence for a pathway in the posterior funiculus in humans responsible for the

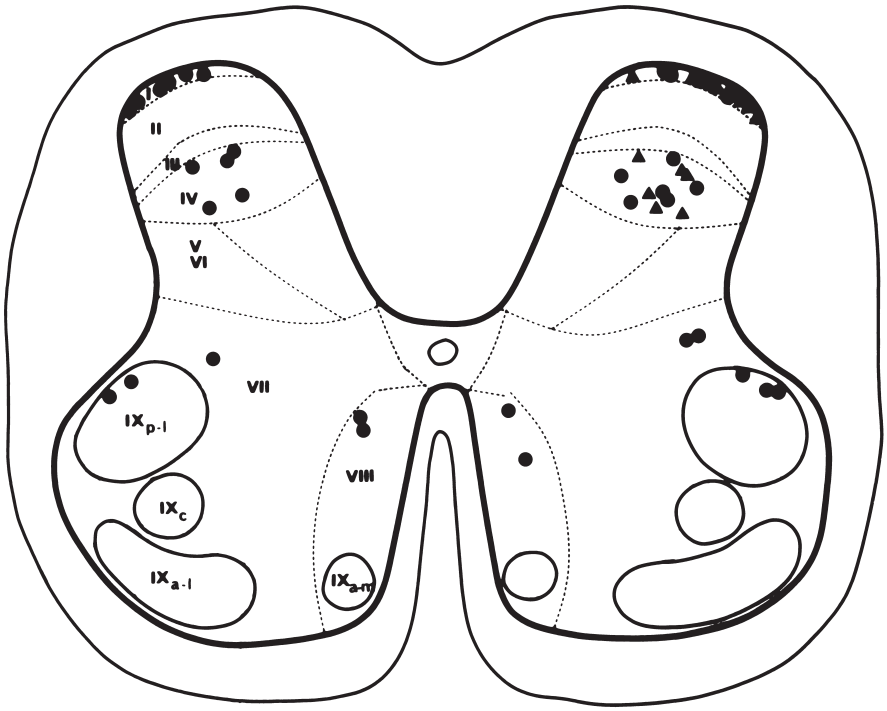

FIGURE 8.6 The distribution of chromatolytic neurons identified on five consecutive 15-mm sections of the lumbar enlargement in two cases of left ventrolateral cordotomy *(triangles)* and two cases of thoracic transverse myelitis *(solid circles)*. IX_{a-l}, Anterolateral; IX_{a-m}, anteromedial; IX_c, central; IX_{p-l}, posterolateral columns of motoneurons.

signaling of visceral pain (Hirschberg *et al.*, 1996). Axons in the medial part of the posterior funiculus at T10 seem to convey ascending nociceptive signals from pelvic visceral organs. This has stimulated a series of experimental studies in rats and monkeys giving evidence for a visceral nociceptive postsynaptic dorsal funiculus pathway, originating from cells in the spinal gray matter around the central canal and terminating in the dorsal column nuclei (Al-Chaer *et al.*, 1998, 1999; Wang *et al.*, 1999; see Willis and Westlund, Chapter 30).

According to Smith (1976), most of the spinocerebellar fibers, whether dorsolateral or ventrolateral, arise from the nucleus dorsalis of Clarke in humans. However, by analogy with experimental findings in the rat (Matsushita and Hosoya, 1979), cat (Burke *et al.*, 1971; Hubbard and Oscarsson, 1962; Matsushita *et al.*, 1979; Grant *et al.*, 1982), and monkey (Lafleur *et al.*, 1974; Petras, 1977; Sprague, 1953), some of the chromatolytic neurons found in laminae VII and VIII and the dorsolateral motoneuronal column ("spinal border cells"; Cooper and Sherington, 1940) after transverse myelitis (Fig. 8.6) may be cells of origin of the ventral spinocerebellar (Gowers') tract.

Ascending Pathways in Experimental Animals

Thanks to modern anatomical tracing methods and to electrophysiological experiments, data concerning the spinal ascending pathways are much more extensive and precise in animals than in humans. Findings have been comprehensively reviewed by a number of authors among whom are Willis and Coggeshall (1991), Clark (1984), Cook *et al.* (1984) and Tracey (1995). They are summarized below with emphasis on functional considerations. See also Kaas (Chapter 28) for the somatosensory system and Voogd *et al* (Chapter 11) for the spinocerebellar tracts.

Dorsal Columns

The dorsal columns comprise short, intermediate, and long systems of fibers. These fibers are from dorsal root afferent but also from second-order sensory neurons of the dorsal horn and the area around the central canal (see above). Less than 25% of the dorsal column fibers belong to the long system. The dorsal column pathway includes the gracile fasciculus, containing ascending branches of afferents supplying the lower part of the body and hindlimb, and the laterally located cuneate

fasciculus, which contains afferents from the upper part of the body and forelimb. The topographical anatomy of the dorsal columns in the human spinal cord has been studied by Smith and Deacon (1984). These authors conclude that the gracile and cuneate fasciculi should be considered as separate anatomical entities. The shape of each fasciculus is different in, and characteristic of, each of the upper thoracic and cervical segments. A certain degree of segmental lamination is present in the gracile fasciculus, but with extensive overlapping of fibers from different segments. The pattern of lamination in the cuneate fasciculus and the degree of overlapping of fibers resembles that in the caudal gracile fasciculus. The latter synapses in the gracile nucleus and the cuneate fasciculus in the cuneate nucleus (see Chapter 10). A small proportion of long ascending primary afferent fibers terminates in the dorsal horn at various segmental levels. Most of the axons of the second-order neurons, whose cells of origin are found mainly in laminae IV–V in the cat (but more dorsally in the rat and monkey) and also in the area around the central canal (see above), terminate in rostral portions of the ipsilateral dorsal column nuclei. It is interesting to note that large myelinated axons from muscle and joint receptors of the hindlimbs may leave the gracile fasciculus at lower lumbar levels and ascend through other systems (e.g., the dorsolateral fasciculus). This particular hindlimb projection terminates in nucleus Z, which is located immediately rostral to the gracile nucleus (see Kaas, Chapter 28).

Functional considerations regarding the dorsal column pathways have been revised dramatically over the past few years. It now appears that the dorsal column pathways are not particularly important for vibratory and joint sensations. Surgical lesions of the dorsal columns in humans can produce only minimal sensory deficits but affect visceral nociception, as discussed above. There is evidence that these pathways are involved in highly complex discriminative sensory tasks, such as two-point discrimination, judging the magnitude of cutaneous pressure, and the ability to detect the speed and direction of moving stimuli.

Ventrolateral Ascending Pathways

These pathways include portions of both the lateral and ventral funiculi. They contain spinothalamic and spinoreticular projections and convey pain, temperature, touch, and pressure information. The ventrolateral system is not compactly organized, but somewhat diffusely structured, intermingling with other ascending pathways. There is a general somatotopic tendency such that axons arising from lower segments are located in a more dorsolateral position and those from higher levels are more ventromedial in location.

Spinothalamic Tract

The spinothalamic tract in experimental animals originates from neurons in mainly contralateral laminae I, V, VII, and VIII. In the monkey, the majority of spinothalamic neurons are located in laminae I and V, while in the cat, spinothalamic neurons are more numerous in laminae VII and VIII. It has not been settled whether the decussation of spinothalamic tract axons is only in the ventral commissure of the cord or also in the dorsal commissure. Spinothalamic neurons in the human and monkey terminate in the ventral posterolateral thalamic nucleus (see Chapter 28) as well as in the central lateral nucleus of the intralaminar complex (see Chapter 20) and in the recently distinguished posterior ventromedial nucleus of the posterior group of nuclei (see Chapter 28). This latter nucleus has been identified in man as a specific pain and temperature relay receiving input from lamina I spinothalamic neurons (Craig *et al.,* 1995). In other mammals, e.g., cat, spinothalamic neurons terminate mainly in the posterior thalamic nuclear complex and the intralaminar nuclei. In a recent study in this animal species, evidence was presented for lamina I cells having different thalamic projection patterns for thermoreception and nociception (Craig and Dostrovsky, 2001).

Functionally, it has been demonstrated in humans that the spinothalamic tract conveys the accurate localization of pinprick and thermal stimuli. However, recovery of pain sensation after ventrolateral cordotomy indicates the potential for pathways in other parts of the cord (spinocervicothalamic tract, spinoreticular tract, intersegmental polysynaptic systems) than the ventrolateral fasciculus to transmit pain information. Division of the anterolateral pathways after cordotomy relieves pain and itch, but alters no form of tactile sensibility except for possible disturbance of discrimination (Nathan, 1990). A human case with a transection of all of the spinal cord except a superficial part of one ventral quadrant shows that this part of the cord carries sufficient information to permit touch and pressure sensation bilaterally, pain and temperature sensations contralaterally, and position sense at some joints ipsilaterally (Willis and Coggeshall, 1991). For the pain system, Chapter 30.

Spinoreticular Tract

The spinoreticular tract ascends in the ventral and lateral funiculi and ends in a number of nuclei of the reticular formation (see the anterolateral therapeutic cordotomy case in Figure 8.6). Its cells of origin are located bilaterally in the dorsal and the ventral horn. Many of its fibers are collaterals of spinothalamic tract neurons. In the primate, however, there is evidence that the spinoreticular projection is largely uncrossed.

The spinoreticular pathway responds to a wide variety of sensory stimulations.

Spinotectal Tract

The spinotectal tract consists of several components, including projections to the superior colliculus, the central gray, and the midbrain reticular formation. In the monkey, the cells of origin appear to be located in laminae I and IV–VII.

Spinocervicothalamic Tract

The lateral cervical nucleus, which is consistently found in lower mammals, is present only inconsistently in human cords (see Chapter 28). Afferent fibers to the lateral cervical nucleus arise at all cord levels from the ipsilateral dorsal horn, primarily from lamina IV. The axons travel in the dorsolateral fasciculus dorsally to the dorsal spinocerebellar tract. They synapse in the lateral cervical nucleus, which in turn projects through the contralateral medial lemniscus to the ventral posterolateral nucleus and the posterior nuclear complex of the thalamus. This system responds to a variety of sensory stimuli, primarily from cutaneous receptors. It seems to contribute to tactile conditioned reflexes, two-point discrimination, tactile and proprioceptive placing, and size discrimination. Recent studies indicate that it may be involved in nociception.

Spinocerebellar Tracts

The dorsal and the ventral spinocerebellar tracts project sensation related primarily to the lower extremities. For a more detailed account of the origin, route to the cerebellum, and lobular and zonal distribution, see Chapter 11.

Dorsal Spinocerebellar Tract

The dorsal spinocerebellar tract is located at the periphery of the dorsolateral fasciculus and arises from the ipsilateral nucleus dorsalis of Clarke. This nucleus is present from the first thoracic through the second lumbar spinal segments in humans, but is largest in the lower thoracic and upper lumbar segments. The pathway projects via the inferior cerebellar peduncle to the vermis and paravermal region of the cerebellum in the hindlimb regions. Functionally, the dorsal spinocerebellar tract conveys information from muscle spindles, Golgi tendon organs and joints, as well as from touch and pressure receptors of the lower extremities.

Ventral Spinocerebellar Tract The ventral spinocerebellar tract is located at the periphery of the ventrolateral fasciculus. Its cells of origin are distributed in laminae V and VII of the lumbosacral segments. The tract enters the superior cerebellar peduncle to terminate in the vermal and paravermal regions of the anterior lobe of the cerebellum. As a result of its numerous polysynaptic inputs and large receptive fields, the ventral spinocerebellar tract appears to relay information regarding the status of muscle groups and the entire extremity.

Cuneocerebellar Tract and Rostral Spinocerebellar Tract The cuneocerebellar tract and the rostral spinocerebellar tract are the upper extremity equivalents of, respectively, the dorsal and the ventral spinocerebellar tracts for the lower extremity.

Spinovestibular and Spinoolivary Tracts

These tracts are of uncertain existence in primates. An exception to this seems to be ascending fibers to group Z (nucleus Z) of the vestibular nuclear complex. As discussed in Chapter 28, this is a pathway for muscle spindle afferents from the hindlimb which projects further to the contralateral thalamus and cortex (see also Willis and Coggeshall, 1991).

It was thought previously that Helweg's tract, a small bundle of fine fibers located peripherally in the ventral part of the cervical ventrolateral fasciculus, contained spinoolivary fibers. This has been denied by Smith and Deacon (1981), who concluded that in the human cord Helweg's tract comprises a majority of descending fibers.

References

Albe-Fessard, D., Boivie, J., Grant, G., and Levante, A. (1975). Labelling of cells in the medula oblongata and the spinal cord of the monkey after injection of horseradish peroxidase in the thalamus. *Neurosci. Lett.* **1,** 75–80.

Al-Chaer, E. D., Feng, Y., and Willis, W. D. (1998). A role for the dorsal column in nociceptive visceral input into the thalamus of primates. *J. Neurophysiol.* **79,** 3143–3150.

Al-Chaer, E. D., Feng, Y., and Willis, W. D. (1999). Comparative study of viscerosomatic input onto postsynaptic dorsal column and spinothalamic tract neurons in the primate. *J. Neurophysiol.* **82,** 1876–1882.

Apkarian, A. V. and Hodge, C. J. (1989). Primate spinothalamic pathways: I. A quantitative study of the cells of origin of the spinothalamic pathway. *J. Comp. Neurol.* **288,** 447–473.

Armand, J. (1984). La voie pyramidale. *Rev. Neurol.* **140,** 309–329.

Arnell, N. (1933). Zur Kenntnis der Anzahi der Nervenfasern in den Wurzeln der spinalnerven des Menschen. *Upsala Laekarefoeren.* Foerh., [N.S.] **39.**

Barilari, M. G., and Kuypers, H. G. (1969). Propriospinal fibers interconnecting the spinal enlargements in the cat. *Brain Res.* **14,** 321–330.

Barnes, S. (1901). Degeneration in hemiplegia: With special reference to a ventrolateral pyramidal tract, the accessory fillet and Pick's bundle. *Brain* **24,** 463–501.

Bumke, O. C. E. (1907). Ueber Variationen im Verlauf der Pyramidenbahn. *Arch. Psychiatr. Nervenkr.* **42,** 1–18.

Burke, R., Lundberg A., and Weight, F. (1971). Spinal border cell origin of the ventral spinocerebellar tract. *Exp. Brain Res.* **12,** 283–294.

Carlstedt, T. (1977). Observations on the morphology at the transition between the peripheral and the central nervous system in the cat. *Acta Physiol. Scand., Suppl.* **446.**

Carstens, E., and Trevino, D. (1978). Laminar origins of spinothalamic projections in the cat as determined by the retrograde transport of horseradish peroxidase. *J. Comp. Neuron.* **182,** 151–166.

Cervero, F. (1986). Dorsal horn neurons and their sensory inputs. *In* "Spinal Afferent Processing" (T. L. Yaksh, ed.), pp. 197–216. Plenum, New York.

Cervero, F., Iggo, A., and Molony, V. (1979). Ascending projections of nocipceptor-driven lamina I neurones in the cat. *Exp. Brain Res.* **35,** 135–149.

Clark, R. G. (1984). Anatomy of the mammalian cord. *In* "Handbook of the Spinal Cord" (R. A. Davidoff, ed.), Vol. 2 and 3, pp. 1–45. Dekker, New York.

Coggeshall, R. E. (1986). Nonclassical features of dorsal root ganglion cell organization. *In* "Spinal Afferet Processing" (T. L. Yaksh, ed.), pp. 83–96. Plenum, New York.

Cook, A. W., Nathan, P. W., and Smith, M. C. (1984). Sensory consequences of commissural myelotomy. *Brain* **107,** 547–568.

Cooper, J. A., and Sherrington, C. S. (1940). Gower's tract and spinal border cells. *Brain Res.* **63,** 123–134.

Craig, A.D., and Dostrovsky, J. (2001). Differential projections of thermoreceptive and nociceptive lamina I trigeminothalamic and spinothalamic neurons in the cat. *J. Neurophysiol.* **86,** 856–870.

Craig, A. D., Bushnell, M. C., Chang, E. T., and Blomqvist, A. (1995). A thalamic nucleus specific for pain and temperature sensation. *Nature* **373,** 19–20.

Craig, A. D., Jr., Linington, A. J. and Kniffki, K. D. (1989). Cells of origin of spinothalamic tract projections to the medial and lateral thalamus in the cat. *J. Comp. Neurol.* **289,** 568–585.

Dodd, J., and Jessel, T. M. (1985). Lactoseries carbohydrates specify subsets of dorsal root ganglion neurons projecting to the superfacial dorsal horn of rat spinal cor. *J. Neurosci.* **5,** 3278–3294.

Dykes, R. W., and Terzis, J. K. (1981). Spinal nerve distributions in the upper limb: The organization of the dermatome and afferent myotome. *Philos. Trans. R. Soc. London. B Ser.* **293,** 509–554.

Fulton, J. F., and Sheehan, D. (1935). Uncrossed lateral pyramidal tract in higher primates. *J. Anat.* **69,** 181–187.

Fyffe, R. E. W. (1984). Afferent fibers. *In* "Handbook of the Spinal Cord" (R. A. Davidoff, ed.), Vol. 2 and 3, pp. 79–136. Dekker, New York.

Giok, S. P. (1956). "Localization of Fibre Systems Within the White Matter of the Medulla Oblongata and the Cervical Cord in Man." Eduardo Ydo, Leiden.

Grant, G. (1995). Primary afferent projections to the spinal cord. *In* "The Rat Nervous System" 2nd edition (G. Paxinos, ed.), pp. 61–66. Academic Press, San Diego, California.

Grant, G., Wiksten, B., Berkley, K. J., and Aldskogius, H. (1982). The location of cerebellar-projecting neurons within the lumbosacral spinal cord in the cat. An anatomical study with HRP and retrograde chromatolysis. *J. Comp. Neurol.* **204,** 336–348.

Häggqvist, G. (1937). Faseranalytische Studien uber die Pyramidenbahn. *Act Psychiatr. Neurol. Scand.* **12,** 457–466.

Hirschberg, R. M., Al-Chaer, E. D., Lawand, N. B., Westlund, K. N., and Willis, W. D. (1996). Is there a pathway in the posterior funiculus that signals pain? *Pain* **67,** 291–305.

Hökfelt, T., Kellerth, J. O., Nilsson, C., and Pernow, B. (1975). Experimental immunohistochemical studies on the localization and distribution of substance P in cat primary sensory neurons. *Brain Res.* **100,** 235–252.

Holmes, G., and May, W. P. (1909). On the exact origin of the pyramidal tracts in man and other mammals. *Brain* **132,** 1–43.

Holstege, G. (1987a). Anatomical evidence for an ipsilateral rubrospinal pathway and for direct rubrospinal projections of motoneurons in the cat. *Neurosci. Lett.* **74,** 2659–274.

Holstege, G. (1987b). Some anatomical observations on the projections from the hypothalamus to brain stem and spinal cord: An HRP autoradiographic tracing study in the cat. *J. Comp. Neurol.* **260,** 98–126.

Holstege, G., and Kuypers, H. G. J. M. (1982). The anatomy of brain stem pathways to the spinal cord in cat. A labeled amino acid tracing study. *Prog. Brain Res.* **57,** 145–175.

Holstege, G., and Tan, J. (1987). Supraspinal control of motoneurons innervating the striated muscles of the pelvic floor including urethral and anal spincters in the cat. *Brain* **110,** 1323–1344.

Hubbard, J., and Oscarsson, O. (1962). Localization of the cell bodies of the ventral spinocerebellar tract in lumbar segments of the cat. *J. Comp. Neurol.* **118,** 199–204.

Hunt, S. P. (1983). Cytochemistry of the spinal cord. *In* "Chemical Neuroanatomy" (P. C. Emson, ed.), pp. 53–84. Raven Press, New York.

Jane, J. A., Yashon, D., De Meyer, W., and Bucy, P. C. (1967). The contribution of the precentral gyrus to the pyramidal tract of man. *J. Neurosurg.* **26,** 244–248.

Kjellgren, K. (1944). Studien uber die Entwicklung der Neuronen nach der Geburt, ihre Regeneration und die Asymmetrien ihrer Verteilung beim Menschen. Quantitative und qualitative Analysen von Spinalganglien und Spinalnervenwurzeln. *Upsala Laekarefoeren.* **44,** 247.

Kuru, M. (1949). "Sensory Paths in the Spinal Cord and Brain Stem of Man." Sogensya, Tokyo.

Kuypers, H. G. J. M. (1962). Corticospinal connections: Postnatal development in the rhesus monkey. *Science* **138,** 678–680.

Kuypers, H. G. J. M. (1964). The descending pathways to the spinal cord, their anatomy and function. *Prog. Brain Res.* **11,** 178–200.

Kuypers, H. G. (1973). The anatomical organization of the descending pathways and their contributions to motor control especially in primates. *In* "New Developments in Electromyography and Clinical Neurophysiology" (J. E. Desmedt, ed.), Vol. 3, pp. 38–68. Karger, Basel.

Kuypers, H. G. J. M. (1981). Anatomy of the descending pathways. *In* "Handbook of Physiology" (V. B. Brooks, ed.), Sect. 1, Vol. II, Part I, pp. 597–665. Physiol. Soc. Washington, D.C.

Lafleur, J., de Lean, J., and Poirier, L. J. (1974). Physiopathology of the cerebellum in the monkey. Part I. Origin of cerebellar afferent nervous fibers from the spinal cord and brain stem. *J. Neurol. Sci.* **22,** 471–490.

Lankamp, D. J. (1967). "Fiber Composition of the Pedunculus cerebri (Crus cerebri) in Man." Luctor et Emergo, Leiden.

Lassek, A. M. (1942a). The human pyramidal tract. IV. A study of the mature, myelinated fibers of the pyramid. *J. Comp. Neurol.* **76,** 217–225.

Lassek, A. M. (1942b). The human pyramidal tract. V. Postnatal changes in the axons of the pyramids. *Arch. Neurol. Psychiatry* **47,** 422–427.

Lawson, S. N. (1992). Morphological and biochemical cell types of sensory neurons. *In* "Sensory Neurons. Diversity, Development and Plasticity" (S. A. Scott, ed.), pp. 27–59. Oxford University Press, New York.

Lawson, S. N. (2002). Phenotype and function of somatic primary afferent nociceptive neurones with C-, Adelta- or Aalpha/beta-fibres. *Exp. Physiol.* **87,** 239–244.

Lawson, S. N., Harper, E. I., Harper, A. A., Garson, J. A., Coakham, H. B., and Randle, B. J. (1985). Monoclonal antibody 2C5: A marker for a subpopulation of small neurons in rat dorsal root ganglia. *Neuroscience* **16,** 365–374.

Lawson, S. N., Waddell, P. J., and McCarthy, P. W. (1987). A comparison of the electrophysiological and immunocytochemical properties of rat dorsal root ganglion neurons with A and C fibers. *In* "Fine Afferent Nerve Fibers and Pain" (R. F. Schmidt, H. G. Schaible, and C. Vahle-Hinz, eds.), pp. 193–203. VCH Publishers, Weinheim and New York.

Lindvall, O., and Björklund, A. (1983). Dopamine- and Norepinephrine-containing neuron systems: Their anatomy in the rat brain. *In* "Chemical Neuroanatomy" (P. C. Emson, ed.), pp. 229–256. Raven Press, New York.

Luhan, J. A. (1959). Long survival after unilateral stab wound of medulla with unusual pyramidal tract distribution. *Arch. Neurol. (Chicago)* **1,** 427–434.

Matsushita, M., and Hosoya, Y. (1979). Cells of origin of the spinocerebellar tract in the rat, studied with the method of retrograde transport of horseradish peroxidase. *Brian Res.* **173,** 185–200.

Matsushita, M., Hosoya, Y., and Ikeda, M. (1979). Anatomical organization of the spinocerebellar system in the cat, as studied by retrograde transport of horseradish peroxidase. *J. Comp. Neurol.* **184,** 81–106.

Minckler, J. R., Kleme, R. M., and Minckler, D. (1944). The course of efferent fibers from the human premotor cortex. *J. Comp. Neurol.* **81,** 259–277.

Molander, C., and Grant, G. (1987). Spinal cord projections from hindlimb muscle nerves in the rat studied by transganglionic transport of horseradish peroxidase, wheat germ agglutinin conjugated horseradish peroxidase, or horseradish peroxidase with dimethylsulfoxide. *J. Comp. Neurol.* **260,** 246–255.

Molenaar, I. A., Rustioni, A., and Kuypers, H. G. (1974). The location of cells of origin of the fibers in the ventral and the lateral funiculus of the cat's lumbo-sacral cord. *Brain Res.* **78,** 239–254.

Nathan, P. W. (1963). The descending respiratory pathway in man. *J. Neurol., Neurosurg. Psychiatry* **26,** 487–499.

Nathan, P. W. (1990). Touch and surgical division of the anterior quadrant of the spinal cord. *J. Neurol. Neurosurg. Psychiatry* **53,** 935–939.

Nathan, P. W. (1994). Effects of movement of surgical incisions into the human spinal cord. *Brain* **117,** 337–346.

Nathan, P. W. (1996). Vestibulospinal, reticulospinal and descending propriospinal nerve fifres in man. *Brain* **119,** 1809–1833.

Nathan, P. W. and Smith M. C. (1987). The location of descending fibres to sympathetic preganglionic vasomotor and sudomotor neurons in man. *J. Neurol. Neurosurg. Psychiatry* **50,** 1253–1262.

Nathan, P. W. and Smith M. C., and Deacon, P. (1990). The corticospinal tracts in man. Course and location of fibres at different segmental levels. *Brain* **113,** 303–324.

Nathan, P. W., and Smith, M. C. (1955). Long descending tracts in man. I. Review of present knowledge. *Brain* **78,** 248–303.

Nathan, P. W., and Smith, M. C. (1959). Fasciculi proprii of the spinal cord in man. *Brain* **82,** 610–668.

Nyberg-Hansen, R., and Rinvik, E. (1963). Some comments on the pyramidal tract, with special reference to its individual variations in man. *Acta Neurol. Scand.* **39,** 1–30.

Olausson, H., Lamarre, Y., Backlund, H., Morin, C., Wallin, B. G., Starck, G., Ekholm, S., Strigo, I., Worsley, K., Vallbo, Å. B., and Bushnell, M. C. (2002). Unmyelinated tactile afferents signal touch and project to insular cortex. *Nature Neurosci.* **5,** 900–904.

Petras, J. M. (1977). Spinocerebellar neurons in the rhesus monkey. *Brain Res.* **130,** 146–151.

Philips, C. C., and Porter, R. (1977). "Corticospinal Neurones: Their Role in Movement," Monogr. Physiol. Soc. No. 34. Academic Press, London.

Rexed, B. (1944). Contributions to the knowledge of the postnatal development of the peripheral nervous system in man. A study of the bases and scope of systematic investigations into the fiber size in peripheral nerves. *Acta Psychiatr. Neurol., Suppl.* **33.**

Schmalbruch, H. (1987). The number of neurons in dorsal root ganglia L4–L6 of the rat. *Anat, Rec.* **219,** 315–322.

Schmelz, M., Schmidt, R., Bickel, A., Handwerker H. O., and Torebjork, H. E. (1997). Specific C-receptors for itch in human skin. *J. Neurosci.* **17,** 8003–8008.

Schoen, J. H. (1964). Comparative aspects of the descending fiber systems in the spinal cord. *Prog. Brain Res.* **11,** 203–222.

Schoen J. H. (1969). The corticofugal projection in the brain stem and spinal cord in man. *Psychiatr. Neurol. Neurochir.* **72,** 121–128.

Schoen, J. H. (1972). Some supplementary data concerning the central tegmental tract in man. *Acta Morphol. Neerl. Scand.* **10,** 380–381.

Schoenen, J. (1981). "L'organisation neuronale de la moelle epiniere de l'homme." Editions Sciences et Lettres, Liege.

Sindou, M., Quoex, C., and Baleydier, C. (1974). Fiber organization at the posterior spinal cord-rootlet junction in man. *J. Comp. Neurol.* **153,** 15–26.

Smith, M. C. (1976). Retrograde cell changes in human spinal cord after anterolateral cordotomies. Location and identification after different periods of survival. *Adv. Pain Res. Ther.* **1,** 91–98.

Smith, M. C., and Deacon, P. (1981). Helweg's triangular tract in man. *Brain* **104,** 249–277.

Smith, M. C., and Deacon, P. (1984). Topographical anatomy of the posterior columns of the spinal cord in man. The long ascending fibers. *Brain* **107,** 671–698.

Snyder, R. (1977). The organization of the dorsal root entry zone in cats and monkeys. *J. Comp. Neurol.* **174,** 47–70.

Sprague, J. M. (1953). Spinal 'border cells' and their role in postural mechanism (Schiff-Sherrington phenomenon). *J. Neurophysiol.* **16,** 464–474.

Sugiura, Y., Terui, N., Hosoya, Y., Tonosaki, Y., Nishiyama, K., and Honda, T. (1993) Quantitative analysis of central terminal projections of visceral and somatic unmyelinated (C) fibers in the guinea pig. *J. Comp. Neurol.* **15,** 315–325.

Sugiura, Y., and Tonosaki, Y. (1995). Spinal organization of unmyelinated visceral afferent fibers in comparison with somatic afferent fibers. *In* "Visceral Pain", Progress in Pain Research and Management, vol. 5, (G. F. Gebhart, ed.), pp. 41–59. IASP Press, Seattle.

Swank, R. L. (1934). The relationship between the circumolivary pyramidal fascicles and the pontobulbar body in man. *J. Comp. Neurol.* **60,** 309–317.

Tracey, D. J. (1995). Ascending and descending pathways in the spinal cord. *In* "the Rat Nervous System" 2nd edition (G. Paxinos, ed.), pp. 67–80. Academic Press, San Diego, California.

Trevino, D., and Carstens, E. (1975). Confirmation of the location of spinothalamic neurons in the cat and monkey by the retrograde transport of horseradish peroxidase. *Brain Res.* **98,** 177–182.

Vallbo, A. B., Olausson, H., and Wessberg, J. (1999). Unmyelinated afferents constitute a second system coding tactile stimuli of the human hairy skin. *J. Neurophysiol.* **81,** 2753–2763.

Verhaart, W. J. C. (1950). Hypertrophy of pes pedunculi and pyramid as result of degeneration of contralateral corticofugal fiber tracts, *J. Comp. Neurol.* **92,** 1–15.

Wang, C-C., Willis, W. D., and Westlund, K. N. (1999). Ascending projections from the area around the central canal: A Phaseolus vulgaris leucoagglutinin study in rats. *J. Comp. Neurol.* **415,** 341–367.

Willis, W. D., Jr. and Coggeshall, R. E. (1991). "Sensory Mechanisms of the Spinal Cord." 2nd edition, Plenum, New York.

Willis, W. D., Kenshalo, D. R., Jr., a d Leonard, R. B. (1979). The cells of origin of the primate spinothalamic tract. *J. Comp. Neurol.* **188,** 543–574.

CHAPTER

9

Spinal Cord in Relation to the Peripheral Nervous System

THOMAS CARLSTEDT
PNI Unit, The Royal National Orthopaedic Hospital, Stanmore, United Kingdom, and Karolinska Institutet, Stockholm, Sweden

STAFFAN CULLHEIM
Department of Neuroscience, Karolinska Institutet, Stockholm, Sweden

MÅRTEN RISLING
Department of Neuroscience, Karolinska Institutet, Stockholm, Sweden, and Department of Defence Medicine, Swedish Defence Research Agency (FOI), Stockholm, Sweden

There are profound differences between spinal cord and peripheral nerves in terms of their development, normal structure, organization and function, as well as in reactions to injury. The general principles in organization of the spinal cord and peripheral nerves differ with regards to the structure of the nerve–glia cell units and their surrounding extracellular space. In contrast to the quite arbitrary distribution of nerve fibers with different functional modalities in the peripheral nerves (Sunderland, 1945; see also Chapters 4–6), there is a clustering of nerve fibers according to function, modality, and somatotopy in the spinal cord (see Chapters 7 and 8). The condensed and advanced functional neuronal arrangements in the spinal cord are therefore quite different from the situation in the peripheral nerve.

All nerve fibers in the peripheral nervous system (PNS), except for those extending from postganglionic autonomic neurons, are also in part located in the central nervous system (CNS). Given the large differences in organization between the two compartments, most nerve fibers in the PNS show profound transformations when entering the CNS compartment. Although the conversion in cellular and histological organization from the peripheral nerve to the spinal cord occurs abruptly at the peripheral–central nervous interface in the transitional region (see below), somatotopic and functional characteristics change more gradually. Thus, there is a nerve fiber segregation by modality in the human nerve trunk (Hallin *et al.*, 1991). Closer to the spinal cord, in the spinal nerve roots, there is an even higher level of organization compared to the peripheral nerve trunk. The afferent sensory nerve

fibers are separated from the efferent fibers according to the law of Magendie (Cranefield, 1974), so that in principle, dorsal roots contain afferent nerve fibers, while efferent motor fibers are found in the ventral roots. At the junction between spinal cord and roots, there is a profound redistribution and reorganization of nerve fibers as well as of endoneural vessels.

THE SPINAL CORD-SPINAL NERVE ROOT JUNCTION

Gross Morphology

When approaching the spinal cord, the nerve root is at some distance split into several thinner components called rootlets, which in turn separate into still thinner minirootlets before joining the spinal cord. These entities are separated by pia and root sheath derivates. The rootlets and minirootlets of the dorsal root merge to form a socket of white matter at the junction with the spinal cord in the dorso-lateral sulcus, whereas in the ventral root, the minirootlets are less closely packed and enter the ventral aspect of the spinal cord as separate units (Fig. 9.1).

The segment of the spinal nerve root situated closest to the spinal cord, i.e., the root-spinal cord junction, contains a specific and specialized part of the nervous system where most of the translations between the peripheral nerve and spinal cord occurs (Carlstedt, 1977; Fraher, 1992, 2000). This part constitutes the PNS–CNS transitional region (TR). This region is characterized by the presence of a projection of CNS tissue from the spinal cord together with PNS tissue in the most proximal part of the root. The contour of the CNS projection is usually dome shaped with a peripherally oriented convexity (Berthold and Carlstedt, 1977). In cervical ventral roots the PNS–CNS interface is situated beneath the surface of the spinal cord (Fraher, 1978). A short length of the CNS projection into the rootlet makes its convexity less marked. The farther the CNS tissue extends into the root the more pointed it becomes. This CNS part of the root becomes longer in a caudal direction along the spinal cord. The CNS outgrowth is particularly conspicuous in the first sacral dorsal root (Tarlov, 1937). As a rule, the CNS part of the root is longer in sensory than in ventral roots.

Thus, the TR is the most proximal free part of the root which in one and the same cross-section contains both CNS and PNS tissue (Fig. 9.2).

The term transitional region has been chosen rather than "entry zone," "junction," or "border" because it gives greater emphasis to the conceptual importance of the structural changes that take place in association

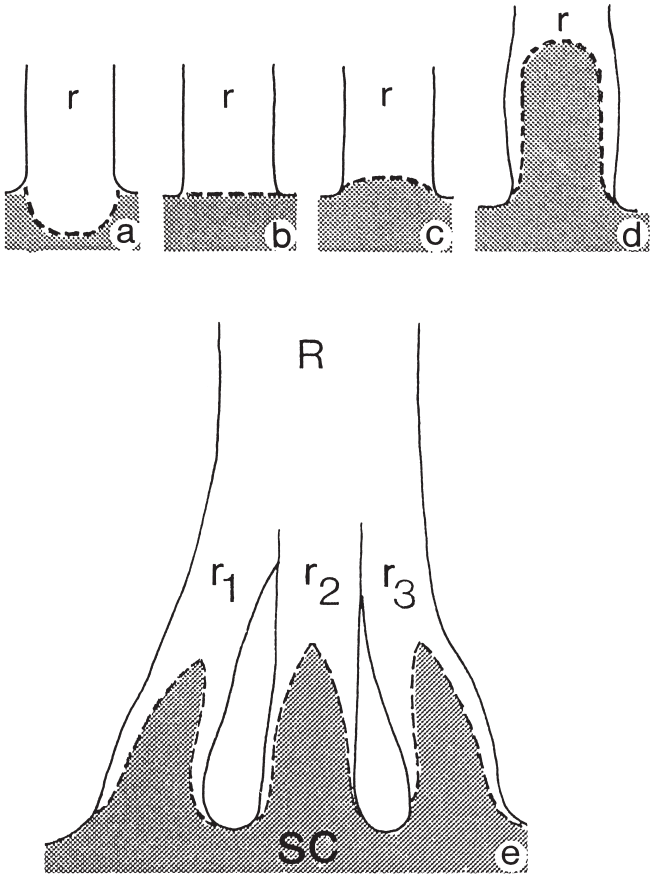

FIGURE 9.1 Schematic representation of the root–spinal cord junction with different PNS–CNS arrangements. **(a–c)** Concave, inverted flat, or slightly convex transitional region (TR) in cervical ventral roots. **(d)** Convex, dome-shaped, or pointed TR in dorsal roots in the caudal part of the spinal cord. The root splits into rootlets (r), each with its own TR and attaching separately to the spinal cord (SC; **e**). From Berthold, C. H., Carlstedt, T., Cornetrusson, O., Peripheral Neuropathy. 73–91, 198, 1993

with a more extended and spacious structure than is indicated by the other terms. When comparing PNS and CNS tissue, the PNS tissue is characterized by axon–Schwann cell units demarcated by a basement membrane suspended in a collagen-rich extracellular space, the endoneurial space. This is in contrast to the CNS tissue, in which the extracellular space is exceedingly small, collagen is lacking, and the axons are embedded in a complex network of oligodendrocyte and astrocyte processes. The interface between the axial CNS compartment and the surrounding PNS compartment is refered to as the CNS–PNS borderline, which is penetrated by nerve fibers. In this way, nerve fibers in the PNS extend into the CNS or vice versa and thus traverse the TR. This region therefore holds a position of conceptual importance with regard to neuronal organization as well as a model system for experi-

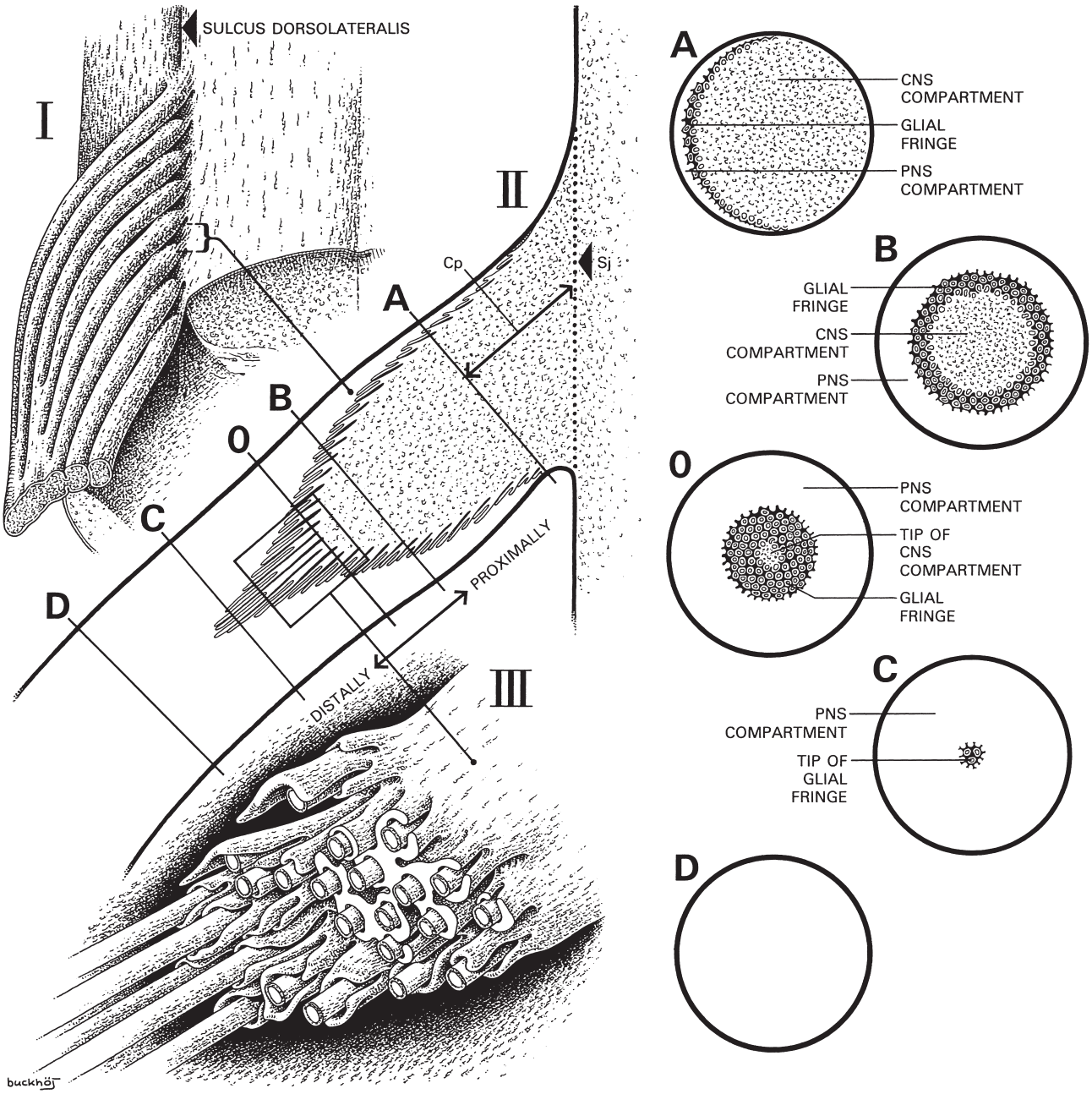

FIGURE 9.2 Schematic drawings showing the S1 dorsal root (I), a frontal section through the transitional region of a S1 doorsal rootlet (II), and the distal part of the glial fringe (III). **I.** The dorsal root S1 and part of its spinal cord segment as viewed from behind.The rootlet marked out by the bracket is present at higher magnification in II. **II.** Frontal section through the TR. The proximal and distal directions as well as the longitudinal axis of the rootlet are indicated. Five reference cross sections levels (A, B, C, D, and O) through the proximal part of the S1 dorsal rootlet are marked. The transitional region extends between levels A and C. The dotted line indicates the spinal cord–rootlet junction (Sj). The wedge shaped part of the rootlet situated between level A and the spinal cord–rootlet junction (Sj) is denoted the connecting piece (Cp). The tip of the cone-shaped CNS compartment is situated at level O. The tip of the glial fringe is located at level C. Level D runs through the stereotype part of the rootlet some 200–400 µm distal to the TR. The picture is not drawn to scale. **III.** Artistic view of glial fringe. Only myelinated fibers are indicated. From T. Carlstedt, Thesis 1977.

mental investigations regarding differences in reaction patterns within one and the same neuron in the two main parts of the nervous system.

Structural Elements in the PNS–CNS Transitional Tegion

The PNS compartment contains up to 100-µm-long extensions of fibrous astrocytic processes. These extend from the CNS compartment forming a fringe among the nerve fibers. The individual parts of this fringe are demarcated from the endoneurial space by a basement membrane. Similar to the organization in the glia limitans membrane, desmosomes, tight junctions, and gap junctions are common between individual astrocytic processes in the fringe. Closer, about 5–20 µm distal to the CNS compartment (the PNS–CNS borderline), the fringe becomes thicker, separating or enclosing individual myelinated nerve fibers in a tube- or holster-like fashion. In this way the most proximal PNS part of the myelinated nerve fiber, the paranode, is situated in an endoneural cul-de-sac that at the bottom contains a node of Ranvier. There is a hybrid transitional PNS–CNS node of Ranvier as the myelinated nerve fibers pass the TR (Fig. 9.3). The basement membrane coating the glial fringe is reflected over to the nerve fibers at the bottom of the various cul-de-sacs and continuous with the Schwann cell basement membrane. Here, there is a unique apposition between astrocytes and Schwann cells (Fig. 9.3). In the glial fringe there is an occurrence of a small uncharacterized cell type. Since such cells are invested by a basement membrane, they suggest an epithelial origin or may represent some sort of aberrant Schwann cells (see "Developmental Aspects").

The CNS compartment is dominated by fibrous astrocyte cell bodies and a dense network of astrocytic processes. The occurrence of astrocytes is about 10 times as high as for the white matter or the glia limitans. They seem to be concentrated at the transitional nodes of Ranvier for the larger myelinated fibers. Oligodendrocytes and microglia are rare. There are no vessels in the CNS compartment. The capillaries in the endoneural space of the PNS compartment do not cross the PNS–CNS borderline with the nerve fibers but deviate out from the rootlets to join vessels in the pia mater. Nor are there any vessels from the spinal cord proper in the CNS compartment. This indicates that the different permeability properties of vessels in the nerve and the spinal cord maintain different types of barriers, e.g., blood–nerve and brood–brain barriers, with different permeability properties. The lack of blood vessels means that the CNS compartment has to rely on diffusion of nutrients and waste products for a distance of sometimes more than 1 mm for a proper metabolism.

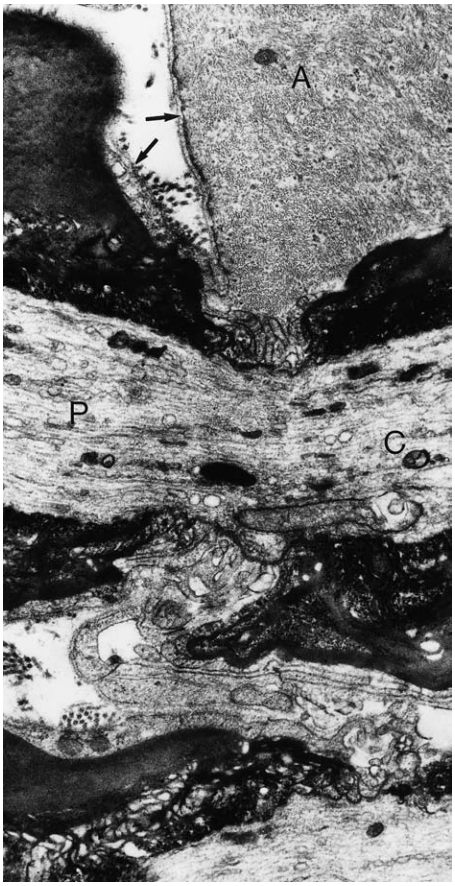

FIGURE 9.3 Electron micrograph of a longitudinal section through a transitional node of Ranvier. The proximal end of a part of the glial fringe surrounding the proximal peripheral paranode is seen outside the node gap. The Schwann cell basement membrane is continuous with that outlining the astrocyte outside the node gap (×25,000). From Berthold, C.H. and Carlstedt, T. *Acta Physiol Scand. Supp.* 446, 1977

Passage of Nerve Fibers through the Trasitional Region

There is an extensive reorganization particularly of dorsal root nerve fibers in the PNS compartment as they approach the CNS compartment. This part of the root seems to act as a sieve, organizing fibers according to size and function in preparation for their entrance into different fiber tracts of the spinal cord. The largest fibers become directed to the center of the root. The larger myelinated fibers in the dorsal root are known to project mono- or disynaptically to the motoneurons and to join the lemniscus pathways; some of them enter the posterior horn of the spinal gray matter and ramify.

The thinly myelinated and unmyelinated fibers are repositioned at the periphery of the root, aggregating just deep to the surface of the rootlet sheath and concentrated to the ventro-lateral zone of the rootlet. They therefore enter into the CNS close to the spinal cord. These fine fibers are aiming for the superficial layers of the dorsal horn, a segregation according to function occurring in the TR for adaptation of the peripheral nerve to the spinal cord. This segregation of the thin fibers, which mainly are concerned with pain, is the anatomical basis for the neurosurgical pain treatment of superficial rhizotomy (Sindou *et al.*, 1974; Berthold and Carlstedt, 1977). The myelinated fiber change from PNS to CNS type of organization occurs in a transitional node of Ranvier situated at the proximal end of a glial fringe cul-de-sac at the PNS–CNS borderline (Fig. 9.3). This node is a composite PNS–CNS node consisting of PNS components in its distal half, and CNS components in the proximal half. There is no change in size at the borderline passage. The larger unmyelinated fibers in the PNS part (>0.6 μm) become small myelinated fibers when crossing into the CNS compartment because of the different axon dimensions that initiate myelination in the PNS and the CNS, respectively. Thus, among the afferent nerve fibers there is conceptually a third group of nerve fibers being a hybride of a myelinated and unmyelinated axon. Fine unmyelinated fibers become invested by astrocyte processes rather than Schwann cells at the PNS–CNS crossing.

DEVELOPMENTAL ASPECTS

During early embryonic development the peripheral nerves and roots are formed by neurite outgrowth from neural tube and neural crest cells (Hamilton *et al.*, 1972; Horstadius, 1950; Pannese, 1974). Axons enter and exit the vertebrate spinal cord at specialized regions along the neuraxis. With a location at prospective exit and entry sites of the neural tube, just before axons arrive, a population of cells appear that have migrated from the neural crest. These cells form "boundary caps" delineating the site of presumptive exit–entry points (Golding *et al.*, 1997). They express a cell adhesion molecule, which is thought to be important for the adherence of these cells to the neural tube as well as to each other. The establishment of these exit–entry sites along the neural tube could be initiated by restricted domains of the neural tube basal lamina defining where the migrating boundary cap cells arrest and conglomerate or, alternatively, specific groups of neuroepithelial cells differentiate at the presumptive exit–entry points (Lumsden and Keynes, 1989). These cells would degrade the basal lamina by secreting proteases and create the attachment of neural crest cells. The boundary cap cells are acting as a potential source of chemoattractant, guiding early sensory axons to entry sites or motor axons to exits points (Guthrie and Lumsden, 1992; Niederlander and Lumsden, 1996). Schwann cell–astrocyte interfaces at the surface of the spinal cord are generated as a result of these interactions. Mostly these interfaces are segregated into distinct dorsal (afferent) entry and ventral (efferent) exit points. This segregation of the function of the dorsal and ventral nerve roots is often referred to as the law of Magendie (Cranefield, 1974). However, in addition to motor axons and preganglionic axons, ventral roots also contain unmyelinated or thin myelinated sensory axons and postganglionic sympathetic axons. Human ventral roots have been shown comprise a proportion of sensory axons (Phillips *et al.*, 2000), including some 15–30% unmyelinated axons (Coggeshall *et al.*, 1975). Many of these appear to represent pain transducing axons (Hosobuchi, 1980). It has therefore been assumed that ventral roots channel sensory axons to the CNS. However, observations in the cat indicate that these axons end blindly, enter the pia mater, or loop and return toward the periphery, and that these units reach the CNS via dorsal roots (Risling *et al.*, 1984). Thus, as it stands now, it seems that the law of Magendie still gives an accurate description of the function of the ventral and dorsal roots (see Hildebrand *et al.*, 1997). However, it cannot be excluded that these sensory axons may have a role in radicular root pain mechanisms since they seem to provide both the ventral roots and the ventral pia mater with mechanosensitive pain fibers (Frykholm *et al.*, 1953; White and Sweet, 1955).

Preceding the establishment of a Schwann cell–CNS glia, i.e., astrocyte, interface during early embryonic life, there is an outgrowth of neurites. Motoneuron axons leave the ventral horn in intramedullary bundles that cross the ventral white matter of the spinal cord. Dorsal root nerve fibers grow through the dorsal root to enter the spinal cord (Smith, 1983; Altman and Bayer, 1984; Mirnics and Koeber, 1995). Subsequently, there are different mechanisms governing the patterning of the central projections within the spinal cord (Fitzgerald *et al.*, 1993; Sharma *et al.*, 1994; Messersmith *et al.*, 1995; Puschel *et al.*, 1996; Redmond *et al.*, 1997). The first dorsal root nerve fibers to enter the spinal cord are the NT-3-dependent muscle sensory afferents.

The PNS–CNS border is initially situated at the very junction of the root to the spinal cord surface and there is no transitional region. Clusters of primitive Schwann or boundary cells cling to bundles of axons that pass through openings in the external glia limiting membrane of the spinal cord (Carlstedt, 1981) (Fig. 9.4). Schwann cell processes extend to the cord surface. The basement

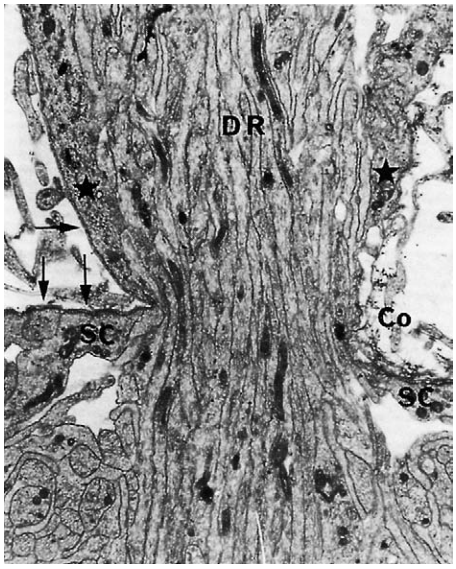

FIGURE 9.4 Electron micrograph of longitudinal section through the dorsal root (DR)–spinal cord (SC) junction during early embryonic life. There is not yet a TR developed. Bundles of immature neurites pass through an opening in an early glia limitans. The basement membrane of dorsal root satellite cells (*) is in continuity with that of the spinal cord *(arrows)* (×5000). Reproduced from T. Carlstedt, *J. Neurol. Sci.* **50,** 357–372, 1981, with permission from Elsevier Science.

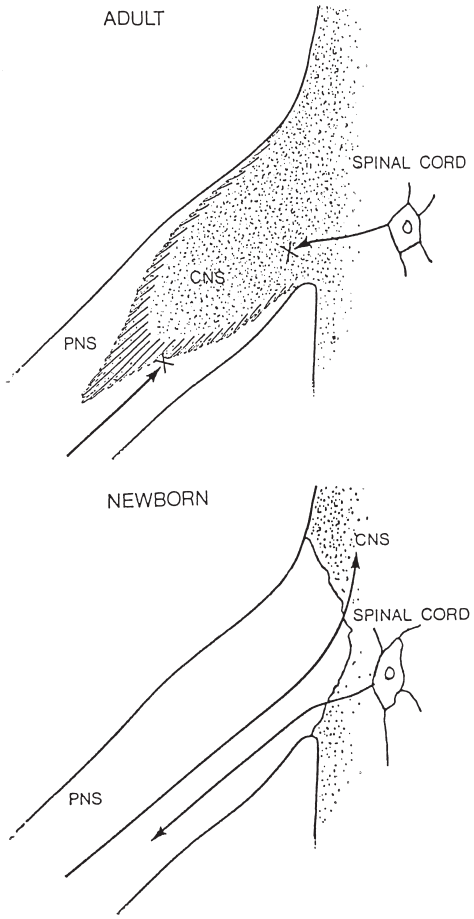

FIGURE 9.5 Schematic drawings. In the adult situation growth of lesioned dorsal root axons as well as intrinsic spinal cord neurites is impeded in the TR. A dorsal root injury that occurs before the TR has started to develop results in axon growth into as well as out from the spinal cord. Reproduced from T. Carlstedt *et al. Brain Res. Bull.* **22,** 93–102, 1989, with permission from Elsevier Science.

membrane of the root is continuous with that of the spinal cord. After nerve fiber separation by migrating Schwann and glia cells and the subsequent initial myelination, the first shallow "glia dome" is formed in the root. Since a CNS protrusion is in conflict with the already established PNS type of myelination of the nerve fibers a profound reorganization follows. Thus, there is a demyelination and disintegration of the most proximal PNS internodes, and a redistribution of detached Schwann cells to unmyelinated fibers as well as aberrant cells. The initial "PNS territory" is occupied by the rapidly extending CNS tissue until a cone of CNS tissue is formed and a TR is established in the most proximal part of the root. (Berthold and Carlstedt 1977, Carlstedt, 1981).

EXPERIMENTAL STUDIES OF THE TRANSITIONAL REGION

General aspects on regeneration through the Transitional Region

Historically, interest in the anatomy of the TR was derived from its involvement in various pathological processes, such as syphilis, acustic neuroma, amyloidosis, poliomyelitis, Werdinger–Hoffman disease, and herpes simplex virus infection. The segregation of axons that takes place in the TR has also served as a basis for certain neurosurgical procedures aimed at alleviation of pain (Sindou *et al.*, 1986). The TR is now used as a model to study the differentiated neuronal regenerative capacity in the PNS and CNS, respectively, as this region offers the unique opportunity to analyze within a limited area the same nerve fiber as it appears in the PNS and CNS.

In the mature mammal, neurons cannot negotiate an elongation across the transitional region and grow into or out of the spinal cord (Oorschot and Jones, 1990; Fig. 9.5). The astrocyte-rich CNS compartment is most effective in preventing regeneration. The lack of appropriate tissue components in the CNS, such as nerve growth factors and extracellular matrix molecules together with growth inhibitory molecules within the CNS are thought to be important in this failure

(Korsching, 1993; Schwab *et al.*, 1993). Thus, regenerating afferent axons are arrested, forming terminal enlargements or synaptoid endings indicating contact inhibition (Carlstedt, 1985). After dorsal root lesion, the astrocytes of the TR form a fibrous astrocytic scar to the same extent as after mechanical injury in the CNS compartment, but depending on the characteristics of the regrowing neurons, the astrocytes express different phenotypes, as well as disintegrate if regeneration of PNS neurites to the CNS root segment is prevented (Carlstedt *et al.*, 1989). Extension of neuronal processes from the spinal cord neurons into the root does not occur after a root lesion.

In the immature mammal, regrowth of severed root neurites as well as new growth from intrinsic spinal cord neurons may occur before the TR has been established. There is a rather sharp cutoff time limit coinciding with the establishment of astrocytes as the earliest CNS compartment in the root (Carlstedt, 1988). Thus, it has been claimed that reconnection between the spinal cord and the peripheral nerve is possible only before the TR has been established in early life (Carlstedt, 1988). However, in recent years regeneration between the CNS and PNS compartments have also been demonstrated in the adult stage. The first demonstration of this possibility came with the study of axon regeneration in spinal cord neurons after providing cut axons with a peripheral nerve graft (David and Aguayo, 1981). In this situation, new axons traversed the demarcation zone between CNS and PNS tissue and entered the denervated PNS graft. In another type of animal experiment, a remarkable regenerative capacity of motoneurons after a cut lesion in the ventral funiculus of the spinal cord with an ingrowth of axons through the lesion and into ventral roots could be demonstrated (Risling *et al.*, 1983). With these findings as a basis, a strategy to explore the possibility of repairing lesions where roots are avulsed from the spinal cord surface has been introduced.

Motoneuron Regeneration after Proximal Axon Injury

Like all other nerve cells, the motoneuron is dependent on interactions with its environment for its well-being and survival. Such interactions can be performed at synapses, between glial elements and the cell soma and dendrites in the CNS, but also along the peripheral axonal pathway. Special attention has been given to the relationship with the myelinating cells in the PNS, i.e., the Schwann cells, and the target muscle fibers in the skeletal muscles. By searching for molecules in these cell types, a number of putative substances with beneficial effects on motoneuron survival and regeneration have been identified. It is beyond the scope for this chapter to discuss the actions of these molecules, but it may be sufficient to conclude that the large number of molecules identified so far poses "an embarrassment of riches" (Oppenheim, 1996).

With the notion that spinal motoneurons are dependent on substances produced by Schwann cells and target muscle fibers for survival and axon regeneration, it may appear peculiar that an axotomy of the motor axon in a peripheral nerve does not seem to have any large influence on motoneuron survival if the lesion is induced in the adult stage (e.g., Schmalbruch, 1984; Lowrie and Vrbová, 1992). A similar lesion in young animals, such as rats in the early postnatal period, has a much more deleterious influence on the motoneurons, with virtually total elimination of motoneurons after a sciatic nerve transection at birth (e.g., Schmalbruch, 1984). Thus, it seems as if the immature motoneuron is much more vulnerable to a lesion of its axon than its adult counterpart, which may reflect a stronger dependency of extrinsic factors during early development. A situation that also appears to have a much more devastating effect on the motoneuron in the adult stage is the ventral root avulsion lesion. This lesion is followed by an extensive cell death (up to 90%) among affected motoneurons, with an occurrence mainly from 1 to 3 weeks post lesion (Koliatsos *et al.*, 1994; Novikov *et al.*, 1997; Piehl *et al.*, 1998). It is plausible to believe that the total lack of trophic support from target muscle fibers and Schwann cells in this case is a major cause of cell death. Another type of lesion in the adult mammal that seems to have a less harmful influence on the motoneuron than ventral root avulsion is, surprisingly, the central axotomy induced by an incision in the ventral funiculus of the spinal cord (Fig. 9.6). This axotomy is even more proximal than that produced by ventral root avulsion, but is followed by a larger proportion of motoneurons that survive (about 50%; Lindå *et al.*, 1993) and indeed also regenerate with new axons passing through the lesion area (Risling *et al.*, 1983). This unexpected regenerative activity may in part be a result of effects exerted by nearby denervated ventral roots and special properties of the motoneuron, but properties of the central scar tissue should also be of relevance (Risling *et al.*, 1989; Frisén *et al.*, 1995, 1998).

The potency of the regeneration of motor axons after an intramedullary lesion is illustrated by the fact that lesioned motoneurons may produce more than one myelinating axon-like process through the lesion area, and in some cases such axons may derive from distal dendrites ("dendraxons"; Lindå *et al.*, 1985). Remaining dendrites are reduced in size, and the number of synaptic connections with the lesioned cells

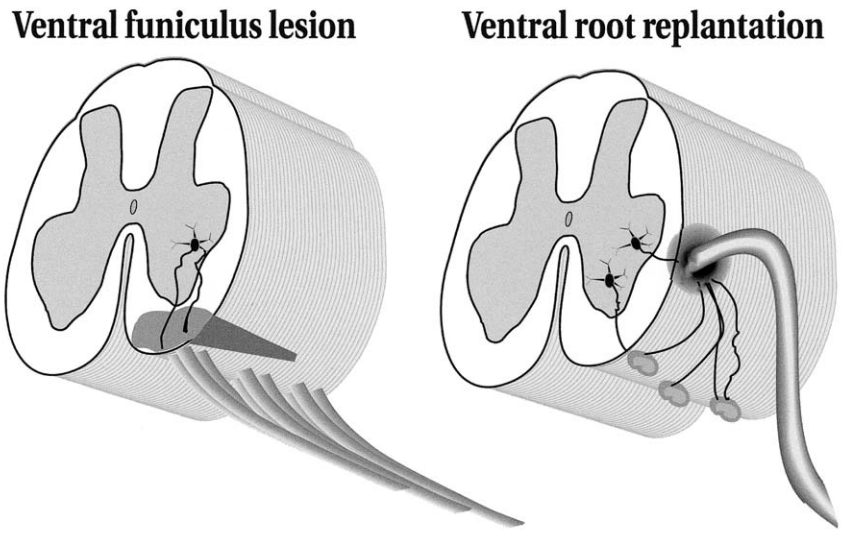

FIGURE 9.6 Schematic drawings of cross-sections through the spinal cord. Regenerative activity in spinal motoneurons is present both after an intramedullary lesion in the ventral funiculus of the cord and after replantation of avulsed ventral roots into the lateral aspect of the cord. From Risling, M. *et al.,* 1993 *Brain Res. Bull.* **30,** 405–411.

is diminished, especially on the cell body and proximal dendrites (Lindå *et al.,* 1992). There also seems to be a preferential loss of excitatory, glutamatergic inputs to the motoneuron in this situation, probably leaving the cells under an inhibitory influence during the repair process (Lindå *et al.,* 2000). These events may mirror a shift in the metabolism of the severed motoneurons from subserving the role for the motoneuron as a commander of muscle activity to a state where the primary goal is to survive and produce new axons.

Repair of Ventral Root Avulsion Lesions in Animals

With the background that spinal motoneurons can survive and regenerate even after a central lesion to their axons, one might expect that motoneurons could be rescued and produce new axons by offering them a peripheral nerve conduit after ventral root avulsion. The simplest and most obvious way to do so is to replant avulsed roots to their original position at the ventral root exit or at least to the spinal cord surface. Thus, after avulsion of lumbar ventral roots supplying the hindleg muscles in rat and cat, and the subsequent replantation of avulsed roots into the lateral part of the spinal cord (Fig. 9.6), it could be demonstrated morphologically after axonal uptake and retrograde transport of a tracer substance (horseradish peroxidase), or after direct intracellular labeling of single motoneurons, that a large number of neurons, presumably motoneurons, are able to let new axons grow out into the implanted roots (Carlstedt *et al.,* 1986; Cullheim *et al.,* 1989). By electrical stimulation of the operated roots it was also possible to show that such regenerating axons can make functional contact with denervated muscle and induce muscle contractions (Fig. 9.7).

A prerequisaite for a meaningful recovery of motor function after ventral root replantation is adequate connection of the motoneurons that reinnervate paralyzed muscles to other neurons. By intracellular recordings from single nerve cells it has been possible to demonstrate that regenerating motoneurons may be positioned in reflex arcs with excitatory and/or inhibitory effects on the motoneurons (Fig. 9.7b–d). With regard to the ability of the motoneurons to find the same muscle that they initially innervated, results from rat and cat studies suggest that there occurred a substantial degree of cross-innervation, with probable negative functional consequences (Carlstedt *et al.,* 1986; Cullheim *et al.,* 1989); (Fig. 9.7e).

The same type of operation in monkey with a change of location for the ventral root avulsion lesion to involve the lower part of cervical spinal cord with projections to the upper limb has shown that regenerating axons from a large number of motoneurons could be found in a small-muscle nerve (Carlstedt *et al.,* 1993). In fact, the number of labeled motoneurons was larger on the lesion side than on the intact side. This could be interpreted as if motoneurons after replantation of a ventral root produce several axons in different nerve branches. However, the most important result from these studies was that the monkeys, after an initial reinnervation phase with synkinesis of antagonistic musculature, with time were able to perform adequate voluntary

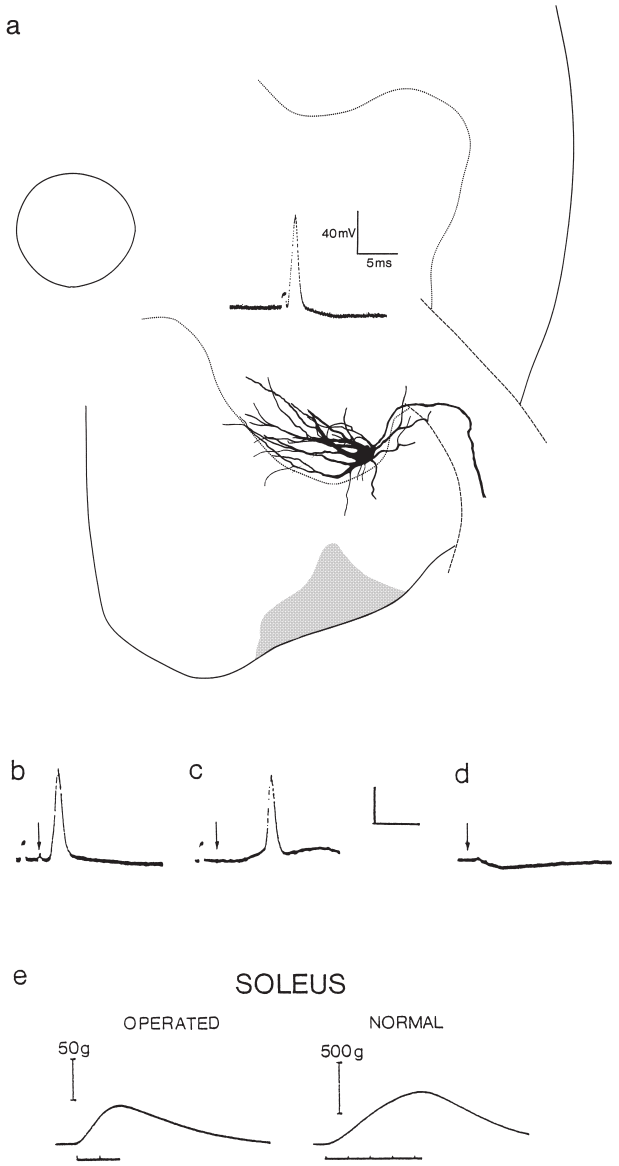

FIGURE 9.7 **(a)** A cat spinal lumbar motoneuron visualized by intracellular staining with horseradish peroxidase. After avulsion and reimplantation of a ventral root laterally a new axon has grown out into the implant. An action potential can be elicited by antidromic electrical stimulation of the ventral root. **(b–d)** Intracellular recordings from different motoneurons with axon outgrowth via implanted ventral roots. In (b) is shown an antidromically evoked action potential after stimulation of the implanted root. In (c) the same motoneuron has been activated orthodromically by stimulation of the tibial nerve in the popliteal fossa. In this way an excitatory postsynaptic potential (EPSP) is produced via primary afferent fibers. The EPSP in turn elicits an action potential. In yet another motoneuron **(d)** an inhibitory postsynaptic potential (IPSP) is elicited after stimulation of the tibial nerve. Scale bars: vertical, 20 mV, horizontal, 2 ms. **(e)** Electrical stimulation of an implanted ventral root gives rise to a contraction in the soleus muscle. The much faster contraction time in the operated animal than in the normal one strongly suggests that reinnervating motoneurons normally support fast-twitch muscle fibers. Reproduced from S. Cullheim, T. Carlstedt, and M. Risling, *Spinal Cord* **37,** 811–819, 1999, with permission from Nature Publishing Group.

movements in primarily proximal muscle groups in the arm (Carlstedt *et al.*, 1993; Hallin *et al.*, 1999).

The described approach rests on the fact that replantation of denervated ventral roots in the vicinity of motoneurons provides a favorable situation for motoneuron survival and regeneration after an axotomy at the CNS–PNS interface. As mentioned above, there is ample evidence that such a strategy may rescue the vast majority of lesioned motoneurons if it is performed within a rather short time from the time of lesion in the rat, but probably much later in the monkey (Hallin *et al.*, 1999). By the administration of substances with known trophic effects on the motoneurons, it may be possible to extend the time interval between lesion and surgery. Thus, it has been shown that intrathecal infusion of brain-derived neurotrophic factor may promote long-term survival of lesioned motoneurons and even induce abundant motor axon regeneration from the avulsion zone along the spinal cord surface, also in the absence of ventral root replantation (Novikov *et al.*, 1997; Novikova *et al.*, 1997). Therefore, a combination of ventral root reconstitution and treatment with neurotrophic factors may be a promising mean for the support of motoneuron survival and motor axon regeneration after ventral root lesions.

Repair of Human Cases of Ventral Root Avulsion Lesions

The technique to repair ventral root avulsion lesions as developed in animal experiments has been applied to humans. Thus, in patients who had sustained several spinal root avulsions, spinal cord implantation of the avulsed roots or nerve grafting was performed. Most patients, who have had spinal cord implantation, show signs of recovery. Electrophysiology has indicated regeneration through the reimplanted roots or nerve grafts by means of muscle reinnervation potentials about 9–15 months after surgery. This has been followed by muscle activity initially noted as muscle twitches (MRC grade 1) that increased in power over a period of 3–4 years (Carlstedt and Norén, 1995; Carlstedt *et al.*, 1995). Among the first 10 operated patients, 3 recovered a useful function due this surgery. In those successful cases there was a final muscle power of grade MRC 4 (Carlstedt *et al.*, 1995, 2000). Recovery occurred mainly in major proximal arm muscles containing large motor units. There was no functional restitution among the hand muscles with small motor units. However, also after a "classical" microsurgical repair of a proximal peripheral nerve injury there is a useful motor recovery limited to proximal arm muscles but rarely any recovery of hand function, probably basically due to a defective neurotropic axonal guidance to the

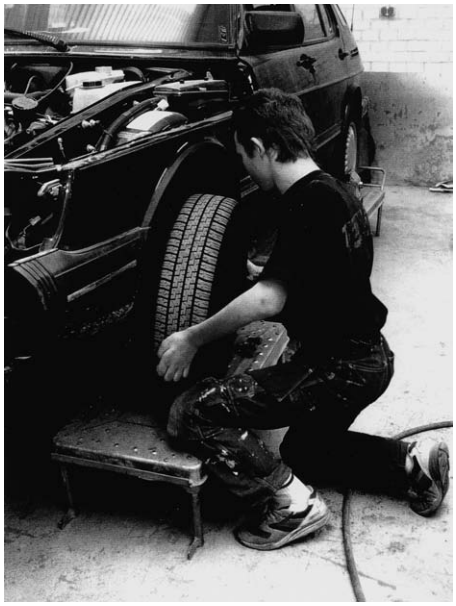

FIGURE 9.8 The first operated human case of ventral root avulsion lesion 2 years after the operation. The lesion engaged all ventral roots from C6 to T1 on the left side and there was initially a total paralysis of elbow and hand muscles. After recovery of especially elbow flexion, the patient could return to his work in a garage. Reproduced from S. Cullheim, T. Carlstedt, and M. Risling, *Spinal Cord* **37,** 811–819, 1999, with permission from Nature Publishing Group.

appropriate targets in the periphery (Brushart, 1988, 1993). Aberrant muscle reinnervation is therefore likely to result in no or poor function in the hand. In spite of this, a recovery of proximal arm function may still be of great value for the patient, exemplified by the first operation, where the recovery of function allowed the patient to go back to working in a garage (Fig 9.8).

A successful outcome occurred only in patients operated early after the injury (Carlstedt and Norén, 1995; Carlstedt *et al.*, 1995, 2000). Patients operated more than a month after the accident recovered little or nonuseful muscle power (MRC grade 1–2). This is consistent with the experimental findings of motoneuron loss after avulsion injury (see above), but also with the fact that cell programs for repair are available for a limited period and are effective if the severed axons are offered a conduit for regrowth (Skene and Willard, 1981; Tetzlaff *et al.*, 1991; Lefcourt *et al.*, 1992; Fawcett *et al.*, 1994). Therefore, if reconstruction is delayed, the growth-associated genes are down-regulated and the neurons become atrophic or die. With delay of repair there is also deterioration of the denervated muscles.

The surgical strategy to repair intraspinal and intramedullary motoneuron lesions does not account for the afferent system. Obviously the motor recovery depends on regrowth of the efferent or motor system only. The reinnervated muscles are probably deficient in proprioceptive innervation as the avulsed dorsal roots cannot be repaired (Carlstedt, 1997). It is difficult to appreciate how afferent sensory function is reintegrated with the motoneurons that have regenerated as a result of this surgical repair of ventral roots only. A central motor program alone may be sufficient to control learned simple movements, such as elbow flexion (Gandeviva and Burke, 1994). However, the afferent feedback system is essential when movements involve small precise contractions, such as finger movements (Gandeviva and Burke, 1994; Wolpert *et al.*, 1995), which do not recover in humans or in animals.

BRACHIAL AND LUMBOSACRAL PLEXUSES

Normal Anatomy

Several hundred thousand nerve fibers from the lower cervical and upper thoracic spinal cord segments interlace from the lateral aspect of the neck to the axilla forming the approximately 15-cm-long brachial plexus. It has the shape of a triangle with the base in parallel with the vertebral column and its apex in the axilla. This is the largest and most complex structure in the peripheral nervous system. It is also one of its most vulnerable parts. There are five components in the brachial plexus: five roots, three trunks, two divisions, three cords, and the nerves. The anterior primary rami of the lowest four cervical nerves (C5–C8) and the first thoracic nerve (T1) unite and branch (Fig. 9.9) in the lower part of the neck in between the anterior and middle scaleni muscles.

The most proximal muscles around the shoulder are innervated from the most proximal branches from the spinal nerves (the dorsalis scapula and the long thoracic nerves) before they started to form the brachial plexus. The trunks of the brachial plexus start at the lateral border of the scaleni muscles (upper trunk from C5 and C6, middle trunk from C7, and lower trunk from C8, and T1). From the upper trunk is the suprascapular nerve given off to innervate the rotator cuff muscles (supra- and infraspinatus). Each trunk splits behind the clavicle into an anterior and posterior division that form the cords that are situated below the clavicle and extend to the axilla. The anterior divisions form the lateral and medial cords—upper and middle trunks to lateral cord and lower trunk to the medial cord. The posterior divisions from all trunks merge into the posterior cord. The lateral and medial pectoral nerves are given off from the lateral and medial cords, respectively. The lateral pectoral nerve (being situated

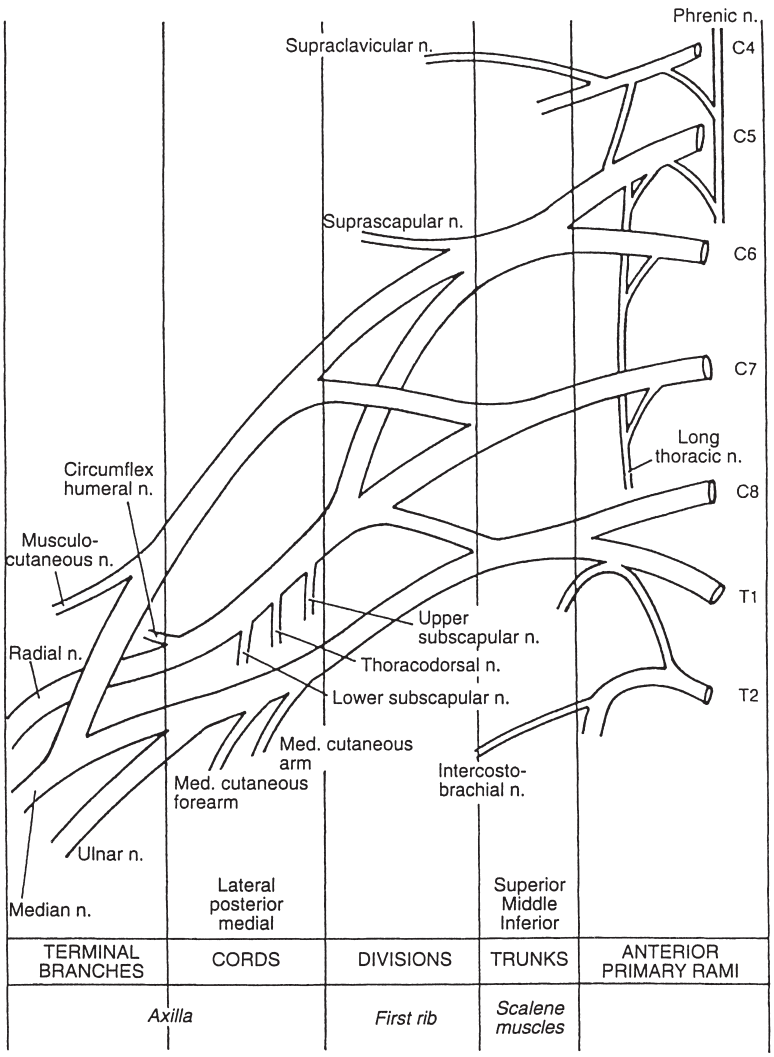

FIGURE 9.9 Schematic drawing of the human brachial plexus. Reproduced from R. Birch, G. Bonney, and C.B. Wynn Perry, "Surgical Disorders of the Peripheral Nerves," Churchill Livingstone, 1998, with permission from Dr. Rolfe Birch.

most medially of the two) is innervating the clavicular part of the pectoral muscle, while the medial pectoral nerve being more lateral innervates the sternal part of this muscle. The thoracodorsal nerve innervating the latissimus dorsi as well as teres and subscapular muscles branches from the posterior cord. At the distal end of the cords the different main nerves to the limb—median, ulnar, musculocutaneous, radial, and axillary are given off.

Thus, trunk and medial shoulder blade muscles are innervated from most proximal branches of the spinal nerves to the brachial plexus even before they have merged to form a plexus. From the trunks and the cords are nerve branches to the shoulder and proximal arm, whereas the muscles of the limb itself are innervated by branches from the main terminal nerves. This anatomical arrangement of nerve branches given off along the course of the length of the brachial plexus makes injury levels quite obvious when testing for muscle function.

The lumbosacral plexus is protected within the pelvic bony ring. Unlike the more exposed brachial plexus it is less subjected to injuries. It is less extensive and complex. Most nerves from the lumbosacral plexus are given off in the posterior abdominal or pelvic wall. The lumbar spinal nerve anterior rami form the lumbar plexus situated within the psoas major muscle in the posterior wall of the abdomen. The first to third sacral nerves form the sacral plexus on the posterolateral wall of the pelvis. Branches from the fourth lumbar ramus

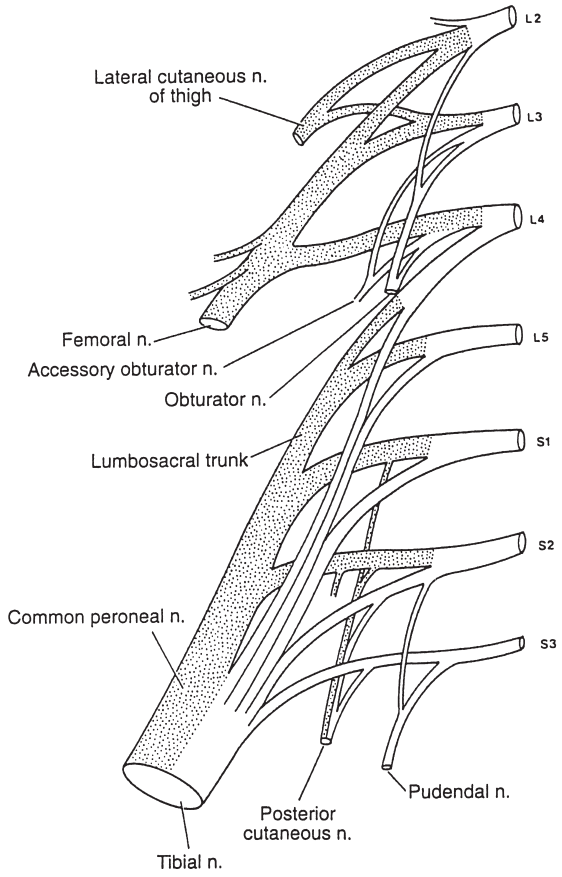

FIGURE 9.10 Schematic drawing of the human lumbosacral plexus. Reproduced from R. Birch, G. Bonney, and C.B. Wynn Perry, "Surgical Disorders of the Peripheral Nerves," Churchill Livingstone, 1998, with permission from Dr. Rolfe Birch.

and the entire fifth ventral ramus join to form the lumbosacral trunk, which emerges medial to the psoas major muscle to enter the pelvis and join the sacral plexus to form the lumbosacral plexus (Fig 9.10). Branches from the lumbar plexus innervate the skin and muscles of the lower part of the abdomen and the thigh.

The femoral nerve (L2–L4), after innervating the iliopsoas muscle, supplies the quadriceps muscle as well as skin of the thigh and the calf through the saphenous nerve. The obturator nerve (L2–L4) innervates medial muscles and skin in the thigh. Muscles in the buttock are innervated from the sacral plexus (superior and inferior gluteal nerves) as are muscles on the dorsal aspect of the thigh as well as in the calf and foot through the sciatic nerve. The organization is much less clear in the lumbosacral plexus than in the brachial plexus. Assessment of injuries as regards level of lesion in the lumbosacral plexus is obviously much more difficult by clinical means.

Plexus Lesions

One of the most devastating nerve injuries is a lesion of the brachial or the lumbosacral plexus. Restoration of limb function and control of pain after such injuries are formidable tasks. Prognosis for spontaneous recovery is often bleak, and several conditions can be recognized that make regeneration difficult (Carlstedt, 1998, Bonney, 1959, Birch *et al.*, 1998). Thus, in an injury like this, located in the most proximal part of the PNS, close to the neuron cell body, could give rise to significant neuronal death. If regeneration takes place, the new neurites would have to elongate for long distances. They would have to find their appropriate targets and form functional contacts without being sidetracked in the complex intrafascicular communications along the peripheral nerves.

The most common plexus lesion is the closed traction injury. It is usually sustained by young males following motor bike injury or children who had a complicated birth (the obstetrical brachial plexus lesion or birth palsy) (Birch *et al.*, 1998). The severity of the plexus lesion depends on the magnitude of the impact and can range from a temporary conduction block (neurapraxia), which recovers spontaneously, to a total severance (neurotmesis, avulsion) with a profound impairment of limb function, or partial lesions, sparing some activity in the limb. With regard to the brachial plexus, the injury is located supra- or infraclavicularly. The supraclavicular lesion is the most common type. In addition, there may be one or several spinal nerve roots avulsed from the spinal cord, root ruptures, or spinal nerve injuries. The birth palsy is usually sustained by a large child (> 4 kg) and located in the supraclavicular part of the brachial plexus. Most patients recover spontaneously, but severe injuries with several root avulsions may also occur. These injuries could have serious implications on the growth and development on the limb.

Detailed anatomical knowledge is the basis for diagnosis and treatment. By knowing the dermatomes and myotomes of different spinal nerves and where the peripheral nerves are leaving the plexus, a precise diagnosis of level and extension of the plexus injury can be reached. The surgical treatment should be swift and include nerve grafting to repair ruptures, as well as transfer of neighboring nerves (such as the accessory, dorsal scapular, and intercostal nerves) to reconstruct and augment function in parts of the plexus that have been severely damaged. In partial plexus lesion where hand function has been spared, it is possible to achive close to normal function with swift surgical reconstruction. In severe total lesions good supportive function and reduction of pain can be obtained by surgery (Birch *et al.*, 1998).

References

Altman, J., and Bayer, S.A. (1984).The development of the rat spinal cord. *Adv. Anat. Embryol. Cell Biol.* **85,** 1–168.

Berthold, C.H., and Carlstedt, T. (1977). General organization of the transitional region in S1 dorsal rootlets. *Acta Physiol. Scand. Suppl.* **446.**

Berthold, C.H., Carlstedt, T., and Cornetrusson, O. (1993). The Center-Peripheral Transition Zone in "Peripheral Neuropathy" (P.J. Dyck, P.K. Thomas, J.N. Griffin, P.A. Low, J.F.P Oduslo, eds.) pp 73–91. W.B. Saunders.

Birch, R., Bonney, G., and Wynn Parry, C.B. (1998). "Surgical Disorders of the Peripheral Nerves." Churchill Livingstone.

Bonney, G. (1959). Prognosis in traction lesions of the brachial plexus. *J. Bone Joint Surg.* **41,** 131–135.

Brushart, T.M. (1988). Preferential reinnervation of motor nerves by regenerating motor axons. *J. Neurosci.* **8,** 1026–1031.

Brushart, T.M. (1993). Motor axons preferentially reinnervate motor pathways. *J. Neurosci.* **13,** 2730–2738.

Carlstedt, T. (1977). Observations on the morphology at the transition between the peripheral and the central nervous system in the cat. Thesis, Karolinska Institutet, Stockholm.

Carlstedt, T. (1981). An electron-microscopical study of the developing transitional region in feline S1 dorsal rootlets. *J.Neurol. Sci.* **50,** 357–372.

Carlstedt, T. (1985). Regenerating axons form nerve terminals at astrocytes. *Brain Res.* **347,** 188–191.

Carlstedt, T. (1988). Reinnervation of the mammalian spinal cord after neonatal dorsal root crush. *J. Neurocytol.* **17,** 335–350.

Carlstedt, T. (1997). Surgical treatment of spinal nerve root injury. Current medical literature. *Neurol. Neurosurg.* **13,** 31–33.

Carlstedt, T. (1998). Brachial plexus injury. Current medical literature. *Neurol Neurosurg.***14,** 3–5.

Carlstedt, T., Anand, P., Hallin, R., Misra, P.V., Norén, G., and Seferlis, T. (2000). Spinal nerve root repair and reimplantation of avulsed ventral roots into the spinal cord after brachial plexus injury. *J. Neurosurg.* **93,** 237–247.

Carlstedt, T., Cullheim, S., Risling. M., and Ulfhake, B. (1989). Nerve fiber regeneration across the root-spinal cord junction. *Brain Res. Bull.* **22,** 93–102.

Carlstedt, T., Hallin, R.G., Hedström, K.G., and Nilsson-Remahl, I. (1993). Functional recovery in primates with brachial plexus injury after spinal cord implantation of avulsed ventral roots. *J. Neurol. Neurosurg. Psychiatry* **56,** 649–654.

Carlstedt, T., Lindå, H., Cullheim, S., and Risling, M. (1986). Reinnervation of hind limb muscles after ventral root avulsion and implantation in the lumbar spinal cord of the adult rat. *Acta physiol. scand.* **128,** 645–646.

Carlstedt, T., Grane, P., Hallin, R. G., and Norén, G. (1995). Return of function after spinal cord implantation of avulsed spinal nerve roots. *Lancet* **346,** 1323–1325.

Carlstedt, T., and Norén, G. (1995). Repair of ruptured spinal nerve roots in a brachial plexus lesion. *J. Neurosurg.* **82,** 661–663.

Coggeshall, R. E., Applebaum, M. L., Fazen, M., Stubbs, T. B., and Sykes, M. T. (1975). Unmyelinated axons in human ventral roots. *Brain* **98,** 157–166.

Cranefield, P. F. (1974). The way in and the way out. Futura, New York.

Cullheim, S., Carlstedt, T., Lindå, H., Risling, M., and Ulfhake, B. (1989). Motoneurons reinnervate skeletal muscle after ventral root implantation into the spinal cord of the cat. *Neuroscience* **29,** 725–733.

Cullifearn, S., Carlstedt, T. and Risling, M. (1991). Axon regeneration of spinal motoneuron following a lesion from the cord-ventral root interface. *Spinal Cord* **37,** 811–819.

David, S., and Aguayo, A.J. (1981). Axonal elongation into peripheral nervous system "bridges" after central nervous system injury in adult rats. *Science* **214,** 931–933.

Fawcett, J.W., Matthews, G., Housden, E., Goedert, M., and Matus, A. (1994). Regenerating sciatic nerve axons contain the adult rather than the embryonic pattern of microtubule associated proteins. *Neurosci.* **61,** 789–804.

Fitzgerald, M., Kwiat, G.C., Middleton, J., and Pini, A. (1993). Ventral spinal cord inhibition of neurite outgrowth from embryonic rat dorsal root ganglia. *Development* **117,** 1377–1384.

Fraher, J.P. (1978). The maturation of the ventral root-spinal cord transitional zone. An ultrastructural study. *J. Neurol. Sci.* **36,** 427–449.

Fraher, J.P. (1992). The CNS-PNS transitional zone of the rat. Morphometric studies at cranial and spinal levels. *Prog. Neurobiol.* **38,** 261–316.

Fraher, J.P. (2000). The transitional zone and CNS regeneration. *J. Anat.* **196,** 137–158.

Frisèn, J., Haegerstrand, A., Risling, M., Fried, K., Johansson, C.B., Hammarberg, H., Elde, R., Hökfelt, T., and Cullheim, S. (1995). Spinal axons in central nervous system scar tissue are closely related to laminin-immunoreactive astrocytes. *Neuroscience* **65,** 293–304.

Frisèn, J., Risling, M., Korhonen, L., Zirrgiebel, U., Johansson, C.B., Cullheim, S., and Lindholm, D. (1998). Nerve growth factor induces process formation in meningeal cells: implications for scar formation in the injured CNS. *J. Neurosci.* **18,** 5714–5722.

Frykholm, R., Hyde, J., Norlén, G., and Skoglund, C. R. (1953). On pain sensations produced by stimulation of ventral roots in man. *Acta Physiol. Scand.* **29,** 455–469.

Gandeviva, S.C., and Burke, D. (1994). Does the nervous system depend on kinesthetic information to control natural limb movements? *In* "Movement Control" (O. Cordo and S. Harnad, eds.), pp. 12–30. Cambridge University Press, New York.

Golding, J., Shewan, D., and Cohen, J. (1997). Maturation of the mammalian dorsal root entry zone—from entry to not entry. *Trends Neurosci.* **20,** 303–308.

Guthrie, S., and Lumsden, A. (1992). Motor neuron path finding following rhombomere reversals in the chick embryo hindbrain. *Development* **114,** 663–673.

Hallin, R.G., Carlstedt, T., Nilsson-Remahl, I., and Risling, M. (1999). Spinal cord implantation of avulsed ventral roots in primates; correlation between restored motor function and morphology. *Exp. Brain Res.* **124,** 304–310.

Hallin, R.G., Ekedahl, R., and Frank, O. (1991). Segregation by modality of myelinated and unmyelinated fibers in human sensory nerve fascicles. *Muscle Nerve* **14,** 157–165.

Hamilton, W.J., Boyd, J.D., and Mossman, H.W. (1972). "Human Embryology (Prenatal Development of Form and Function)," 4th Ed. W. Heffer and Sons, Cambridge, p. 437.

Hildebrand, C., Karlsson, M., and Risling, M. (1997). Ganglionic axons in motor roots and pia mater. Prog. Neurobiol. 51, 89–128.

Horstadius, S. (1950). "The Neural Crest." Oxford University Press, London.

Hosobuchi, Y. (1980). The majority of unmyelinated afferent axons in human ventral roots probably conduct pain. Pain 8, 167–180.

Koliatsos, V.E., Price, W.L., Pardo, C.A., and Price, D.L. (1994). Ventral root avulsion: an experimental model of death of adult motor neurons. *J. Comp. Neurol.* **342,** 35–44.

Korsching, S. (1993). The neurotrophic factor concept: a reexamination. *J. Neurosci.***13,** 2739–2748.

Lefcort, F., Venstrom, K., McDonald, J.A., and Reichardt, L.F. (1992). Regulation of expression of fibronectin and its receptor alpha 5 beta 1, during development and regeneration of peripheral nerve. *Development* **116,** 767–782.

Lindå, H., Cullheim, S., and Risling, M. (1992). A light and electron microscopic study of lumbar motoneurons after intramedullary axotomy in the adult cat. *J. Comp. Neurol.* **318,** 188–208.

Lindå, H., Risling, M., and Cullheim, S. (1985). "Dendraxons" in regenerating motoneurons in the cat: do dendrites generate new axons after central axotomy? *Brain Res.* **358,** 329–333.

Lindå, H., Risling, M., Shupliakov, O., and Cullheim, S. (1993). Changes in the synaptic input to lumbar motoneurons after intramedullary axotomy in the adult cat. In thesis by Hans LindÂ, Karolinska Institutet, Stockholm.

Lindå, H., Shupliakov, O., Örnung, G., Ottersen, O.P., Storm-Mathisen, J., Risling, M., and Cullheim, S. (2000). Ultrastructural evidence for a preferential elimination of glutamate immunoreactive synaptic terminals from spinal motoneurons after intramedullary axotomy. *J. Comp. Neurol.* **425,** 10–23.

Lowrie, M.B., and Vrbovà, G. (1992). Dependence of postnatal motoneurones on their targets: review and hypothesis. *Trends Neurosci.* **15,** 80–84.

Lumsden, A., and Keynes, R. (1989). Segmental patterns of neuronal development in the chick hindbrain. *Nature* **337,** 424–428.

Messersmith, E.K., Leonardo, E.D., Shatz, C.J., Tessier-Lavigne, M., Goodman, C.S., and Kolodkin, A.Z. (1995). Semaphorin III can function as a selective chemorepellant to pattern sensory projections in the spinal cord. *Neuron* **14,** 949–959.

Mirnics, K., and Koeber, H.R. (1995). Prenatal development of rat primary afferent fibers II. Central projections. *J. Comp. Neurol.* **335,** 601–614.

Niederlander, C., and Lumsden, A. (1996). Late emigrating neural crest cells migrate specifically to the exit points of cranial branchiomotor nerves. *Development* **122,** 2367–2374.

Novikov, L., Novikova, L., and Kellerth, J.-O. (1997). Brain-derived neurotrophic factor promotes axonal regeneration and long-term survival of adult rat spinal motoneurons in vivo. *Neuroscience* **79,** 765–774.

Novikova, L., Novikov, L, and Kellerth, J.-O. (1997). Effects of neurotransplants and BDNF on the survival and regeneration of injured spinal motoneurons. *Eur. J. Neurosci.* **9,** 2774–2777.

Oorschot, D.E., and Jones, D.G. (1990). Axonal regeneration in the mammalian central nervous system: a critique of hypotheses. *Adv. Anat. Embryol. Cell Biol.* **199,** 1–121.

Oppenheim, R.W. (1996). Neurotrophic survival molecules for motoneurons: an embarrassment of riches. *Neuron* **17,** 195–197.

Pannese, E. (1974). The histogenesis of the spinal ganglia. *Adv. Anat. Embryol. Cell Biol.* **47,** 7–97.

Phillips, L. H., 2nd, Park, T. S., Shaffrey, M. E., and Shaffrey, C. L. (2000). Electrophysiological evidence for afferent nerve fibers in human ventral roots. *Muscle Nerve* **23,** 410–415.

Piehl, F., Hammarberg, H., Tabar, G., Hökfelt, T., and Cullheim S. (1998). Changes in the mRNA expression pattern, with special reference to calcitinin gene-related peptide, after axonal injuries in rat motoneurons depend on age and type of injury. *Exp. Brain Res.* **119,** 191–204.

Puschel, A.W., Adams, R.H., and Betz, H. (1996). The sensory innervation of mouse spinal cord may be patterned by different expression of and differential responsiveness to semaphorins. *Mol.Cell Neurosci.* **7,** 419–431.

Redmond, L., Xie, H., Ziskind-Conhaim, L., and Hochfield, S. (1997). Cues intrinsic to the spinal cord determine the pattern and timing of primary afferent ingrowth. *Dev. Biol.* **182,** 205–218.

Risling, M., Cullheim, S., and Hildebrand, C. (1983). Reinnervation of the ventral root L7 from ventral horn neurons following intramedullary axotomy in the adult cat. *Brain Res.* **280,** 15–23.

Risling, M., Dalsgaard, C. J., Cukierman, A., and Cuello, A. C. (1984). Electron microscopic and immunohistochemical evidence that unmyelinated ventral root axons make U-turns or enter the spinal pia mater. *J Comp Neurol* **225:** 53–63.

Risling, M., Fried, K., Linda, H., Carlstedt, T., and Cullifearn, S. (1993). Regrowth of motor axons following spinal cord lesions: distribution of laminin and collagen in the CNS scar tissue. *Brain Res. Bull.* **30,** 405–411.

Risling, M., Lindå, H., Cullheim, S., and Franson P. (1989). A persistent defect in the blood–brain barrier after ventral funiculus lesion in adult cats: implications for CNS regeneration. *Brain Res.* **494,** 13–21.

Schmalbruch, H. (1984). Motoneuron death after sciatic nerve section in newborn rats. *J. Comp. Neurol.* **224,** 252–258.

Schwab, M.E., Kapfhammer, J.P., and Bandtlow, C.E. (1993). Inhibitors of neurite growth. *Annu. Rev. Neurosci.* **16,** 565–595.

Sharma, K., Korade, Z., and Frank, E. (1994). Development of specific muscle and cutaneous sensory projections in cultured segments of spinal cord. *Development* **120,** 1315–1323.

Sindou, M., Quoex, C., and Baleydier, C. (1974). Fiber organization at the posterior spinal cord-rootlet junction in man. *J. Comp. Neurol.* **153,** 15–26.

Skene, J.H.J.P., and Willard, M. (1981). Axonally transported proteins associated with axon growth in rabbit central and peripheral nervous systems. *J. Cell Biol.* **89,** 96–103.

Smith, C.L. (1983). The development and postnatal organization of primary affent projections into the rat thoracic spinal cord. *J. Comp. Neurol.* **220,** 29–43.

Sunderland, S. (1945). The intraneural topography of the radial, median and ulnar nerves. *Brain* **68,** 43–299.

Tarlov, I.M. (1937). Structure of the nerve root. II. Differentiation of sensory from motor roots: observations on identification of function in roots of mixed cranial nerves. *Arch. Neurol. Psychiatry.* **37,** 1338–1355.

Tetzlaff, W., Alexander, S.W., Miller, F.D., and Bisby, M.A. (1991). Response of facial and rubrospinal neurons to axotomy: changes in mRNA expression for cytoskeletal proteins and GAP-43. *J. Neurosci.* **9,** 3505–3512.

White, J. C., and Sweet, W. H. (1955). "Pain—Its Mechanisms and Neurosurgical Control." Charles C Thomas, Springfield, IL.

Wolpert, D.M., Ghahramani, Z., and Jordan, M.I. (1995). An internal model for sensorimotor integration. *Science* **269,** 1880–1882.

CHAPTER

10

Organization of Human Brain Stem Nuclei

YURI KOUTCHEROV
The Prince of Wales Medical Research Institute
The University of New South Wales
Sydney, Australia

XU-FENG HUANG
Department of Biomedical Sciences
University of Wollongong
Wollongong, Australia

GLENDA HALLIDAY
The Prince of Wales Medical Research Institute
The University of New South Wales
Sydney, Australia

GEORGE PAXINOS
The Prince of Wales Medical Research Institute
The University of New South Wales
Sydney, Australia

This chapter describes human homologues of nuclei identified in the brain stem of other mammals and attempts to extend to the human the overall organizational schemata that have been proposed for brain stem of other mammalian species. Structures of the brain stem are very diverse with respect to functions they participate in, neuroactive elements they contain, and neural pathways they accommodate. As a reflection, the anatomical organization of the human brain stem is a complex amalgam of compact neuronal groups and dispersed cell areas with varying cytoarchitecture. Many of these neurons, nuclei, and areas are given elaborate descriptions in separate chapters of this book that deal with associated functional networks, whereas the purpose of this chapter is to present an account of human brain stem nuclei and areas with discrete emphasis on the structural organization of the region, rather then functional, chemical, or pathological characteristics. It would have been inappropriate, however, to discount apparent functional characteristics of some brain stem structures, particularly when such characteristics can be used to systematize the diversity of brain stem neuronal groups. This chapter discusses a number of human brain stem structures in relation to autonomic function, vestibular system, visual system, auditory system, motor cranial nerves, or somatosensory system. However, many brain stem structures are not obviously related to a particular function, or are related to a number of functions or better known for their structural characteristics; thus, the reticular formation, precerebellar nuclei, red nucleus, locus coeruleus, and raphe nuclei are distinguished as complex structural entities and discussed in approximate rostro caudal order. This chapter also describes the distribution of some neuroactive chemicals to rationalize the details of structural delineations.

Following the original suggestion of Paxinos and Huang (1995), we also acknowledge that the radial arrangement of the human medulla with reference to the fourth ventricle (as King, 1980, proposed for the cat) is more tenable than the "quilt" pattern proposed by Olszewski and Baxter (1954). Thus, it appears that the human medulla is organized roughly in columns, commencing with a special afferent zone (vestibular nuclei) dorsolaterally and terminating in a general motor efferent zone ventromedially (hypoglossal). Intervening in a dorsal-to-ventral sequence are the somatic afferent column (spinal nucleus of the trigeminal), the visceral afferent column (solitary nucleus and the dorsolateral slab of the intermediate reticular zone), and the visceral or branchial efferent column (dorsal motor nucleus of vagus, ambiguus, and the ventromedial part of IRt). A scheme of organization along these lines was suggested by Herrick (1922) for the cranial nerve nuclei and is now

popularly used in many neuroanatomy text books.

Traditionally, nuclei have been identified using cytoarchitecture, myeloarchitecture, and connectivity. In the last 20 years, researchers have used developmental, functional, and, increasingly, chemoarchitectonic criteria to complement these traditional methods (Heimer and Wilson, 1975; Krettek and Price, 1978; Paxinos and Watson, 1998; Koutcherov *et al.*, 2000). We are of the view that for the establishment of homologies it is necessary that the human and rat brain stem be studied in parallel using the same criteria. The criteria used for establishing homologies in the present study were morphological and involve cytoarchitecture, chemoarchitecture, topography, and subnuclear organization.

Work based on chemoarchitectonic analysis began after Koelle and Friedenwald (1949) developed a simple histochemical method for revealing acetylcholinesterase (AChE), the degradative enzyme for acetylcholine. The application of AChE staining has subsequently proven very useful in distinguishing brain areas. A comprehensive delineation of the rat brain by Paxinos and Watson (1982) was done largely on the basis of AChE reactivity with Nissl staining used as a secondary criterion. In the last 30 years, AChE histochemistry was successfully used for delineation of the brain in many mammalian species. Most importantly, AChE histochemistry works well on the fresh (unfixed) postmortem human brain, which allows this method to be successfully applied to the neuroanatomical delineation of the human brain. For example, AChE staining was used in pathological studies of the brains of patients with Alzheimer's disease (Saper and German, 1987) and was recently employed to reveal the organization of the human hypothalamus (Koutcherov *et al.*, 2000). Because the AChE content of homologous nuclei is reasonably stable across mammalian species, this chapter relies mainly on AChE distribution to illustrate brain stem homologies. We have also considered cell morphology and the distribution of tyrosine hydroxylase (Chapter 14), phenylalanine hydroxylase (Chapter 13), substance P (Halliday *et al.*, 1988a), and neuropeptide Y (Halliday *et al.*, 1988c). Some connectivity data were available to us from therapeutic cordotomies (Mehler, 1974a). All findings reported here concern the human unless otherwise stated.

Abbreviations used in the Figures

10	dorsal motor nucleus of vagus
10Ca	dorsal motor nucleus of vagus, caudal part
10CaI	dorsal motor nucleus of vagus, caudointermediate part
10CeI	dorsal motor nucleus of vagus, centrointermediate part
10DI	dorsal motor nucleus of vagus, dorsointermediate part
10DR	dorsal motor nucleus of vagus, dorsorostral part
10n	vagus nerve
10Tr	vagal trigone
10VI	dorsal motor nucleus of vagus, ventrointermediate part
10VR	dorsal motor nucleus of vagus, ventrorostral part
11	spinal accessory nucleus
12	hypoglossal nucleus
12GH	hypoglossal nucleus, geniohyoid part
12L	hypoglossal nucleus, lateral part
12M	hypoglossal nucleus, medial part
12n	root of hypoglossal nerve
12V	hypoglossal nucleus, ventral part
12VL	hypoglossal nucleus, ventrolateral part
12VM	hypoglossal nucleus, ventromedial part
3	oculomotor nucleus
3n	oculomotor nerve or its root
4	trochlear nucleus
4n	trochlear nerve or its root
4V	fourth ventricle
6	abducens nucleus
6n	root of abducens nerve
7	facial nucleus
7D	facial nucleus, dorsal part
7I	facial nucleus, intermediate part
7L	facial nucleus, lateral part
7M	facial nucleus, medial part
7n	facial nerve or its root
7VL	facial nucleus, ventrolateral part
8vn	vestibular root of the vestibulocochlear nerve
9n	glossopharyngeal nerve
A1	noradrenaline cells A1
A1/C1	noradrenaline cells and/or adrenaline cells A1/C1
A2	noradrenaline cells A2
A2/C2	noradrenaline cells and/or adrenaline cells A2/C2
A5	noradrenaline cells A5
A8	dopamine cells
Acs5	accessory trigeminal nucleus
Acs7	accessory facial nucleus
AlI	alar interstitial nucleus
Amb	ambiguus nucleus
ami	amiculum of the olive
AP	area postrema
APT	anterior pretectal nucleus
Aq	aqueduct (Sylvius)
ar	acoustic radiation
Ar	arcuate nucleus of the medulla

AVC	anteroventral cochlear nucleus
b	beta nucleus of the inferior olive
B9	B9 5-hydroxytryptamine cells
basv	basal vein (drains into cavernous sinus)
bic	brachium of the inferior colliculus
BIC	nucleus of the brachium of the inferior colliculus
bsc	brachium of the superior colliculus
C1	C1 adrenaline cells
Cb	cerebellum
CC	central canal
CDPMn	caudal dorsal paramedian nucleus
CeC	central cervical nucleus
CGPn	central gray of the pons
chp	choroids plexus
CIC	central nucleus of the inferior colliculus
CIF	compact interfascicular nucleus
CLi	caudal linear nucleus of the raphe
CnF	cuneiform nucleus
cp	cerebral peduncle
Crb	cribiform nucleus
csc	commissure of the superior colliculus
CT	conterminal nucleus
ctg	central tegmental tract
cu	cuneate fasciculus
Cu	cuneate nucleus
CuR	cuneate nucleus, rotunda part
CuT	cuneate nucleus, triangular part
Cx	cerebral cortex
das	dorsal acoustic stria
DC	dorsal cochlear nucleus
DCIC	dorsal cortex of the inferior colliculus
DG	dentate gyrus
Dk	nucleus of Darkschewitsch
dlf	dorsal longitudinal fasciculus
DLG	dorsal lateral geniculate nucleus
DLL	dorsal nucleus of the lateral lemniscus
DLPAG	dorsolateral periaqueductal gray
DM5	dorsomedial spinal trigeminal nucleus
DMPAG	dorsomedial periaqueductal gray
dms	dorsomedian sulcus
DMSp5	dorsomedial spinal trigeminal nucleus
DMTg	dorsomedial tegmental area
DpG	deep gray layer of the superior colliculus
DPGi	dorsal paragigantocellular reticular nucleus
DpMe	deep mesencephalic nucleus
DPO	dorsal periolivary region
DpWh	deep white layer of the superior colliculus
DR	dorsal raphe nucleus
DRC	dorsal raphe nucleus, caudal part
DRD	dorsal raphe nucleus, dorsal part
DRI	dorsal raphe nucleus, interfascicular part
DRt	dorsal reticular nucleus of the medulla
DRV	dorsal raphe nucleus, ventral part
DRVL	dorsal raphe nucleus, ventrolateral part
DTg	dorsal tegmental nucleus
dtg	dorsal tegmental bundle
DTgC	dorsal tegmental nucleus, central part
DTgP	dorsal tegmental nucleus, pericentral part
E	ependyma and subependymal layers
EC	epicoeruleus nucleus
ECIC	external cortex of the inferior colliculus
EF	epifascicular nucleus
EL	endolemniscal nucleus
EO	epiolivary lateral reticular nucleus
EW	Edinger–Westphal nucleus
fr	fasciculus retroflexus
frpn	frontopontine fibers
FVe	F-cell group of the vestibular complex
γ	gamma pontine nucleus
g7	genu of the facial nerve
Ge5	gelatinous layer of the caudal spinal trigeminal nucleus
Gi	gigantocellular reticular nucleus
GiV	gigantocellular reticular nucleus, ventral part
Gia	gigantocellular reticular nucleus, alpha part
Gr	gracile nucleus
gr	gracile fasciculus
HIO	hilus of the inferior olive
I3	interoculomotor nucleus
I5	intertrigeminal nucleus
I8Ve	interstial nucleus of the vestibular nerve
ia	internal arcuate fibers
icp	inferior cerebellar peduncle (restiform body)
icv	inferior cerebellar vein
IF	interfascicular nucleus
IFH	interfascicular hypoglossal nucleus
II	intermediate interstitial nucleus of the medial longitudinal fasciculus
IMLF	interstitial nucleus of the medial longitudinal fasciculus
In	intercalated nucleus of the medulla
InG	intermediate gray layer of the superior colliculus
InWh	intermediate white layer of the superior colliculus
IO	inferior olive
IOA	inferior olive, subnucleus A of medial nucleus
IOB	inferior olive, subnucleus B of medial nucleus
IOC	inferior olive, subnucleus C of medial nucleus
IOD	inferior olive, dorsal nucleus
IODC	inferior olive, dorsal nucleus, caudal part
IODM	inferior olive, dorsomedial cell group

IOK	inferior olive, cap of Kooy of the medial nucleus
IOM	inferior olive, medial nucleus
IOPr	inferior olive, principal nucleus
IOVl	inferior olive, ventrolateral protrusion
IP	interpeduncular nucleus
IPA	interpeduncular nucleus, apical subnucleus
IPC	interpeduncular nucleus, caudal subnucleus
IPDM	interpeduncular nucleus, dorsomedial subnucleus
IPF	interpeduncular fossa
IPI	interpeduncular nucleus, intermediate subnucleus
IPL	interpeduncular nucleus, lateral subnucleus
IPo	interpositus
IPR	interpeduncular nucleus, rostral subnucleus
ipt	interpedunculotegmental tract
IRt	intermediate reticular nucleus
IS	inferior salivatory nucleus
jx	juxstarestiform body
KF	Kölliker–Fuse nucleus
LC	locus coeruleus
lcsp	lateral corticospinal tract
LDTg	laterodorsal tegmental nucleus
LDTgV	laterodorsal tegmental nucleus, ventral part
lfp	longitudinal fibers of the pons
ll	lateral lernniscus
LPAG	lateral periaqueductal gray
LPB	lateral parabrachial nucleus
LPBC	lateral parabrachial nucleus, central part
LPBD	lateral parabrachial nucleus, dorsal part
LPBE	lateral parabrachial nucleus, external part
LPCu	lateral pericuncate nucleus
LPGi	lateral paragigantocellular nucleus
LPtg5	lateral pterygoid subnucleus of the motor trigeminal
LR4V	lateral recess of the 4th ventricle
LRt	lateral reticular nucleus
LRtPC	lateral reticular nucleus, parvocellular part
LRtS5	lateral reticular nucleus, subtrigeminal part
lscb	lateral superior cerebellar artery (branch of superior cerebellar)
LSO	lateral superior olive
LT	lateral terminal nucleus of the accessory optic tract
LV	lateral ventricle
LVe	lateral vestibular nucleus
LVPO	lateroventral periolivary nucleus
m5	motor root of the trigeminal nerve
MA3	medial accessory oculomotor nucleus
Ma5	masseter subnucleus of the motor trigeminal
MB	mammillary body
mcp	middle cerebellar peduncle
Me5	mesencephalic trigeminal nucleus
me5	mesencephalic trigeminal tract
MG	medial geniculate nucleus
MGD	medial geniculate nucleus, dorsal part
MGM	medial geniculate nucleus, medial part
MGV	medial geniculate nucleus, ventral part
MHy5	mylohyoid subnucleus of the motor trigeminal
MiTg	microcellular tegmental nucleus
ml	medial lemniscus
mlf	medial longitudinal fasciculus
MnR	median raphe
Mo5	motor trigeminal nucleus
MPB	medial parabrachial nucleus
MPBE	medial parabrachial nucleus, external part
MPCu	medial pericuneate nucleus
MPOl	medial periolivary nucleus
MPtg5	medial pterygoid subnucleus of the motor trigeminal
MRF	mesencephalic reticular fields
MRt	medial reticular nucleus of the medulla
MRtV	medial reticular nucleus of medulla, ventral part
mscb	medial superior cerebellar artery (branch of superior cerebellar)
MSO	medial superior olive
MT	medial terminal nucleus of the accessory optic tract
mtg	medial tegmental tract
MVe	medial vestibular nucleus
MVeMC	medial vestibular nucleus, magnocellular part
MVePC	medial vestibular nucleus, parvicellular part
MVPO	medioventral periolivary nucleus
MZ	marginal zone
MZMG	marginal zone of the medial geniculate nucleus
oc	olivocerebellar tract
ocb	olivocerebellar bundle
ODPMn	oral dorsal paramedian nucleus
Op	optic nerve layer of the superior colliculus
opt	optic tract
P5	peritrigeminal zone
P7	perifacial zone
Pa5	paratrigeminal nucleus
Pa6	paraabducens nucleus
PaP	parapeduncular nucleus
PaR	pararaphales nucleus
PaS	parasubiculum
PaVe	paravestibular nucleus
PBG	prabigeminal nucleus

PBP	parabrachial pigmented nucleus
pc	posterior commissure
PC3	parvicellular oculomotor nucleus
PCRt	parvocellular reticular nucleus
PCRta	parvocellular reticular nucleus, a part
PCuMx	pericuneate matrix
PDTg	posterodorsal tegmental nucleus
Pe5	peritrigeminal nucleus
PF	parafascicular nucleus
pica	posterior inferior cerebellar artery
PIL	posterior intralaminar thalamic nucleus
PlGl	pleioglia periaqueductal gray
PLi	posterior limitans thalamic nucleus
pm	principal mammillary tract
PMn	paramedian reticular nucleus
PMnR	paramedian raphe nucleus
PN	paranigral nucleus
Pn	pontine nucleus
PnB	pontobulbar nucleus
PnC	pontine reticular nucleus, caudal part
pncb	pontocerebellar fibers
PnO	pontine reticular nucleus, oral part
Po	posterior thalamic nuclear group
PoDG	polymorph layer of the dentate gyrus
pof	post-olivary fissure
pola	paraolivary artery
polv	paraolivary vein
pos	preolivary sulcus
PoT	posterior thalamic nuclear group, triangular part
PP	peripeduncular nucleus
PPTg	pedunculopontine tegmental nucleus
PPTgC	pedunculopontine tegmental nucleus, compact part
PPTgD	pedunculopontine tegmental nucleus, diffuse part
Pr	prepositus nucleus
Pr5	principal sensory trigeminal nucleus
PRF	prerubral field
PrH	prepositus hypoglossal nucleus
PSol	parasolitary nucleus
ptpn	parietopontine fibers
Ptx	pyramidal decussation
Pul	pulvinar nuclei
PVC	posteroventral cochlear nucleus
PVM	posterior ventromedial thalamic nucleus
py	pyramidal tract
R7	retrofacial nucleus
Ramb	retroambiguus nucleus
Rbd	rhabdoid nucleus
RC	raphe cap
RDM	red nucleus, dorsomedial part
RIP	raphe interpositus nucleus
RLi	rostral linear nucleus
RMC	red nucleus, magnocellular part
RMg	raphe magnus nucleus
Ro	nucleus of Roller
ROb	raphe obscurus nucleus
RPa	raphe pontis nucleus
RPC	red nucleus, parvocellular part
RPn	raphe pontis nucleus
RPO	rostral periolivary region
RRF	retrorubal field
rs	rubrospinal tract
RtTg	reticulotegmental nucleus of the pons
RVL	rostroventrolateral reticular nucleus of the medulla
S	subiculum
s5	sensory root of the trigeminal nerve
Sag	sagulum nucleus
SC	superior colliculus
scol	supracollicular arterial network
scp	superior cerebellar peduncle
scpd	superior cerebellar peduncle, descending limb
SG	suprageniculate thalamic nucleus
SGe	suprageniculate nucleus
sl	sulcus limitans
smv	superior medullary velom
SNC	substantia nigra, compacta part
SND	substantia nigra, dorsal part
SNL	substantia nigra, lateral part
SNM	substantia nigra, medial part
SNR	substantia nigra, reticular part
SNV	substantia nigra, ventral part
SO	superior olive
Sol	nucleus of the solitary tract
sol	solitary tract
SolC	solitary nucleus, commissural subnucleus
SolD	solitary nucleus, dorsal subnucleus
SolDL	solitary nucleus, dorsolateral subnucleus
SolG	solitary nucleus, gelatinous subnucleus
SolI	solitary nucleus, interstitial subnucleus
SolIM	solitary nucleus, intermediate subnucleus
SolM	solitary nucleus, medial subnucleus
SolPaC	solitary nucleus, paracommissural part
SolV	solitary nucleus, ventral subnucleus
SolVL	solitary nucleus, ventrolateral subnucleus
Sp5	spinal trigeminal nucleus
sp5	spinal trigeminal tract
Sp5C	spinal trigeminal nucleus, caudal part
Sp5I	spinal trigerninal nucleus, interpolar part
Sp5O	spinal trigeminal nucleus, oral part
SPP	subpeduncular pigmented nucleus
spth	spinothalamic tract
SpVe	spinal vestibular nucleus
SSol	subsolitary nucleus
SSp	supraspinal nucleus
Su3	supraoculomotor nucleus
Su3C	supraoculomotor cap

SubB	subbrachial nucleus
SubC	subcoeruleus nucleus
SubCD	subcoeruleus nucleus, dorsal part
SubCV	subcoeruleus nucleus, ventral part
SuG	superficial gray layer of the superior colliculus
SuL	supralemniscal nucleus
SuM	supramammillary nucleus
SuVe	superior vestibular nucleus
Te5	temporalis subnucleus of the motor trigeminal
ts	tectospinal tract
tth	trigeminothalamic tract (trigeminal lemniscus)
Tz	nucleus of the trapezoid body
VCC	ventral cochlear cap
veme	vestibulomesencephalic tract
VLL	ventral nucleus of the lateral lemniscus
vlmv	ventrolateral medullary vein
VLPAG	ventrolateral periaqueductal gray
VLTg	ventrolateral tegmental area
VPI	ventral posterior inferior nucleus
VPM	ventral posteromedial thalamic nucleus
VPO	ventral periolivary nuclei
VRt	ventral reticular nucleus
vsc	ventral spinocerebellar tract
VTA	ventral tegmental area
vtg	ventral tegmental tract
VTg	ventral tegmental nucleus (Gudden)
VTgI	ventral tegmental nucleus, infrafascicular part
VTgP	ventral tegmental nucleus, principal part
VTgS	ventral tegmental nucleus, suprafascicular part
vtgx	ventral tegmental decussation
X	nucleus X
x4n	decussation of the trochlear nerve
xml	decussation of the medial lemniscus
xscp	decussation of the superior cerebellar peduncle
Y	nucleus Y
Z	nucleus Z
Zo	zonal layer of the superior colliculus

AUTONOMIC REGULATORY CENTERS

Dorsal Motor Nucleus of Vagus

Huang and colleagues (1993a, b) published a combined cyto- and chemoarchitectonic analysis depicting the human homologues of the subnuclei of the dorsal motor nucleus of vagus (10N) (Fig. 10.1–10.8). The caudal pole of the dorsal motor nucleus is found at the pyramidal decussation dorsolateral to the central canal (caudal to Fig. 10.1). At this level, it is a loose group of strongly AChE-positive cells. The cell bodies in 10N are prominent on a background of otherwise medium staining. This is in contrast with the hypoglossal nucleus, where the intense reaction in the neuropil obscures the equally intensely reactive cell bodies. The 10N is separated from the hypoglossal nucleus by the intercalated nucleus. The 10N almost reaches the periventricular gray matter at the level of the area postrema. It recedes from the ventricular surface together with the solitary nucleus, rostral to the hypoglossal nucleus. A cell-poor and AChE-negative fringe flanks the medial aspect of 10N. A few cells can be noticed within this zone, a number of which are pigmented and positive for AChE and tyrosine hydroxylase (A2 cell group). Rostrally, 10N persists as a minor medial companion to the ventrolaterally migrating solitary complex (Figs. 10.6–10.8). The compact rostral tip of the AChE-reactive 10N is succeeded by the salivatory nucleus—a scattering of AChE-positive neurons that persists until the level of the exiting fascicles of the facial nerve (Figs. 10.8 and 10.9).

In resent years several chemoarchitectonic studies demonstrated a high concentration of the somatostatin receptors (Carpentier *et al.*, 1996), cannabinoid receptors (Glass *et al.*, 1997), dopamine β-hydroxylase (Kitahama *et al.*, 1996), D2 and D4 dopamine receptors (Hyde *et al.*, 1996), and bombesin cells (Lynn *et al.*, 1996) in the human 10N.

Solitary Nucleus

The solitary tract is a heavily myelinated fiber bundle that extends from the level of the facial nucleus in the caudal pons to the spinomedullary junction. A large region of the dorsal tegmentum, mostly medial and dorsal to the tract, is the solitary nucleus. Early studies of the solitary tract in humans and experimental mammals have established that the tract is composed of fibers from the trigeminal and facial nerves rostrally (Nageotte, 1906), the glossopharyngeal nerve in the intermediate region and the vagus nerve caudally (Bruce, 1898; Papez, 1929; Pearson, 1947). Evidence from studies in experimental animals revealed the solitary nucleus (Sol) as the initial relay for baroreceptor, cardiac, pulmonary chemoreceptor, and other vagal and glossopharyngeal afferents (see Loewy, 1990). For example, the Sol in the rat is known to contain neurons activated by baroreflex afferents, while Sol projections to ventrolateral medulla are essential for baroreflex-induced sympathoinhibition and cardiovascular stimulation (Guyenet *et al.*, 1989). Further chemoarchitectonic analysis (Benarroch *et al.*,

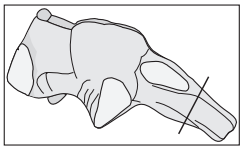

Figure 1

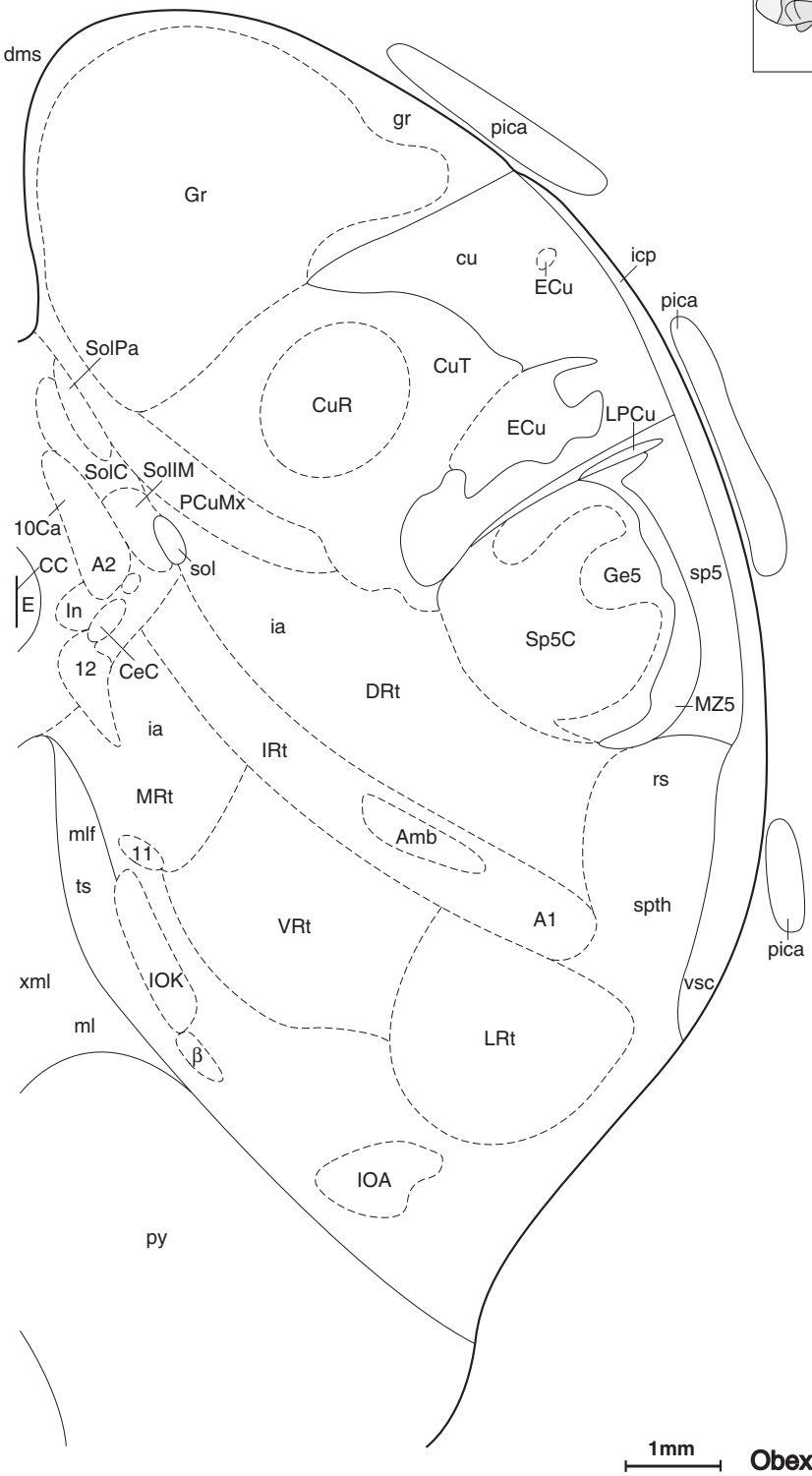

FIGURES 10.1–10.25 Coronal maps of the human brain stem presented in sections at 2-mm intervals. The medullary tissue depicted in plates 1–25 was obtained by Paxinos and Huang (1995) 4 h post mortem from a 59-year-old white male who died suddenly from a heart attack. The donor had no medical history of any neurological or psychiatric disease. The diagrams were reproduced from Paxinos, G., and Huang, X. F. *Atlas of the Human Brain Stem*, Academic Press, San Diego, 1995.

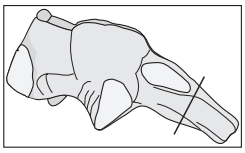

Figure 2

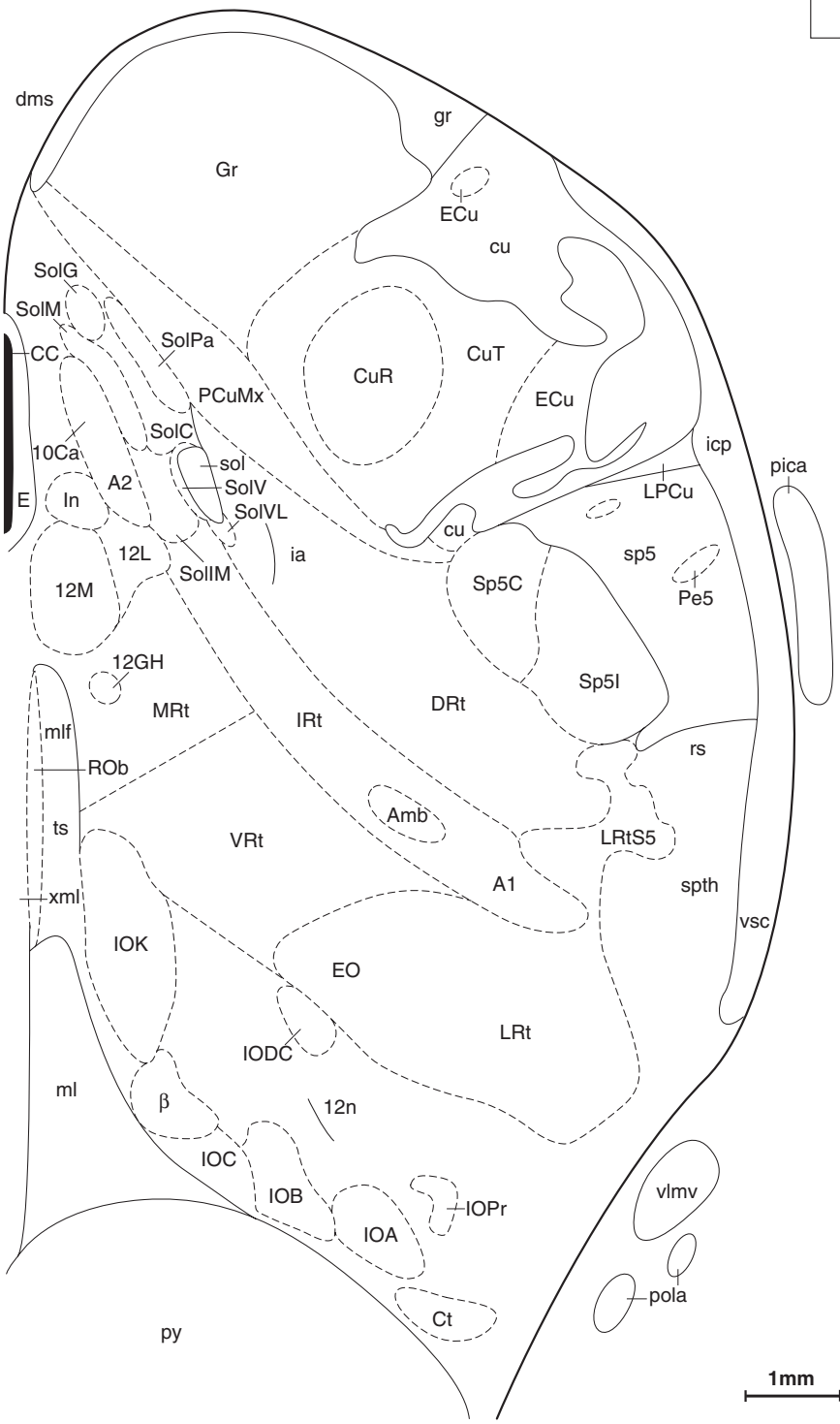

FIGURES 10.2

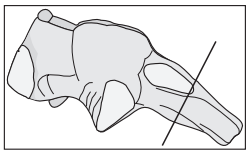

Figure 3

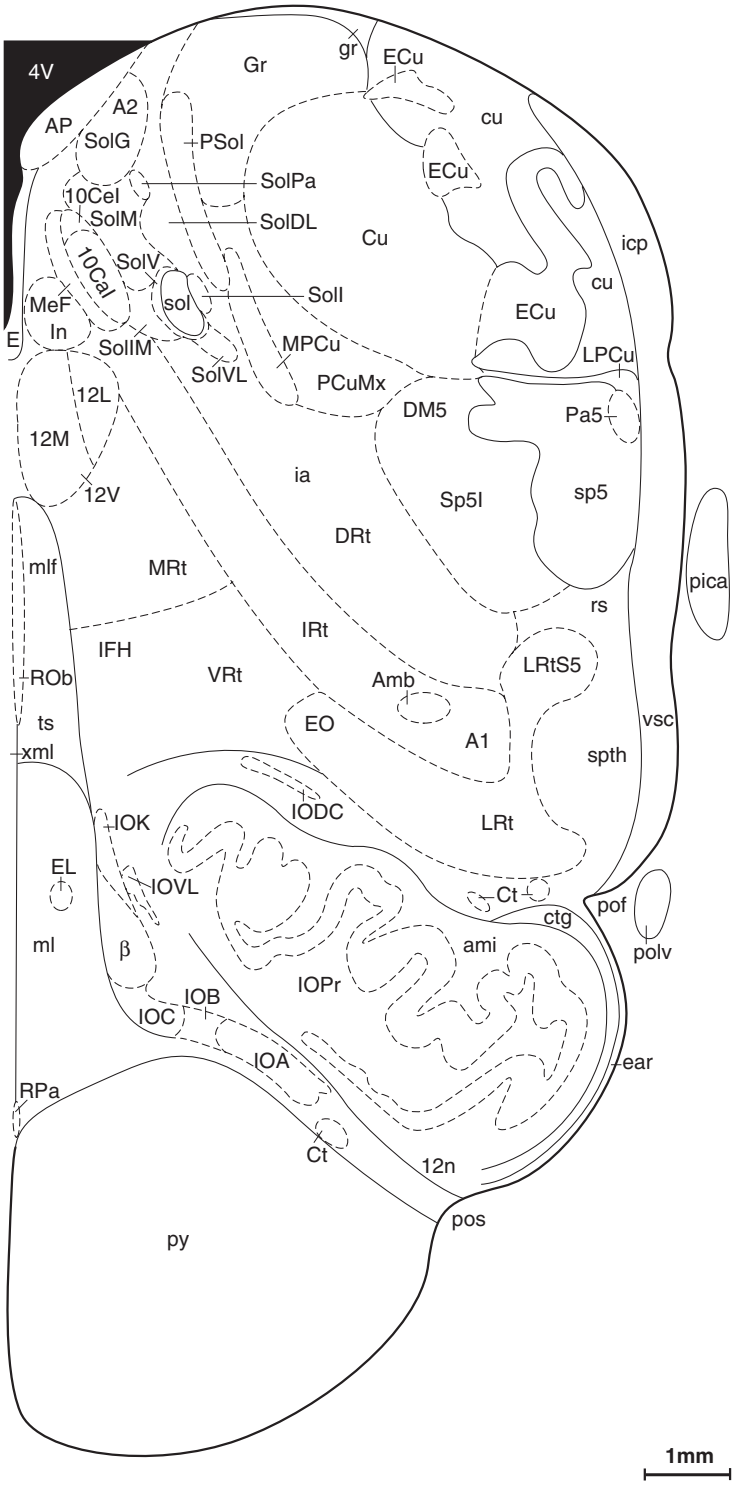

FIGURES 10.3

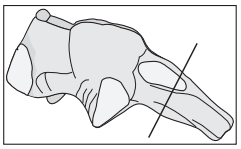

Figure 4

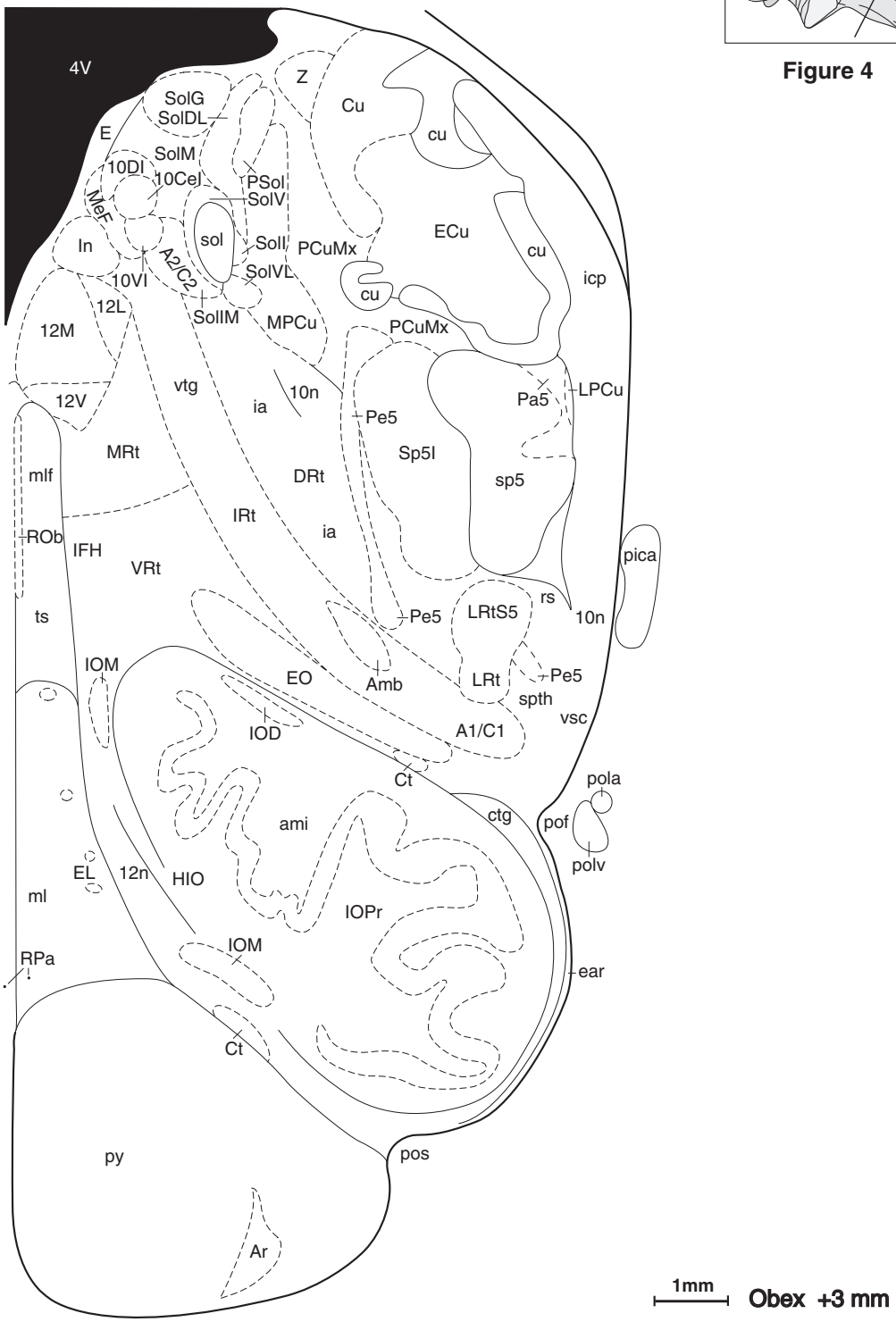

FIGURES 10.4

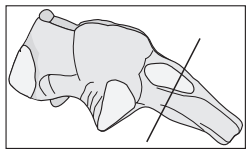

Figure 5

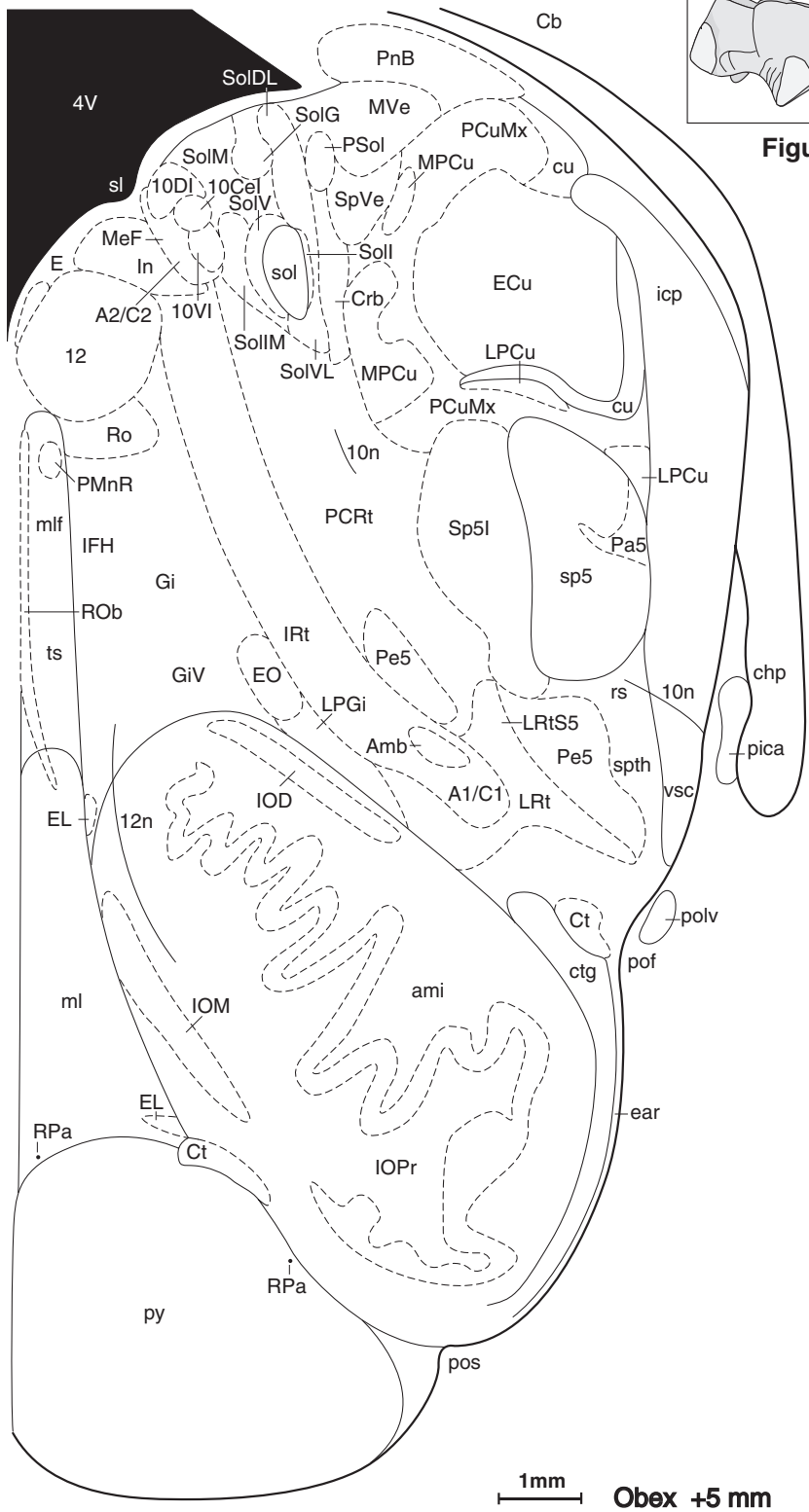

FIGURES 10.5

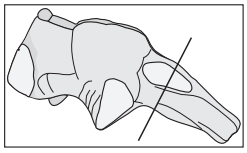

Figure 6

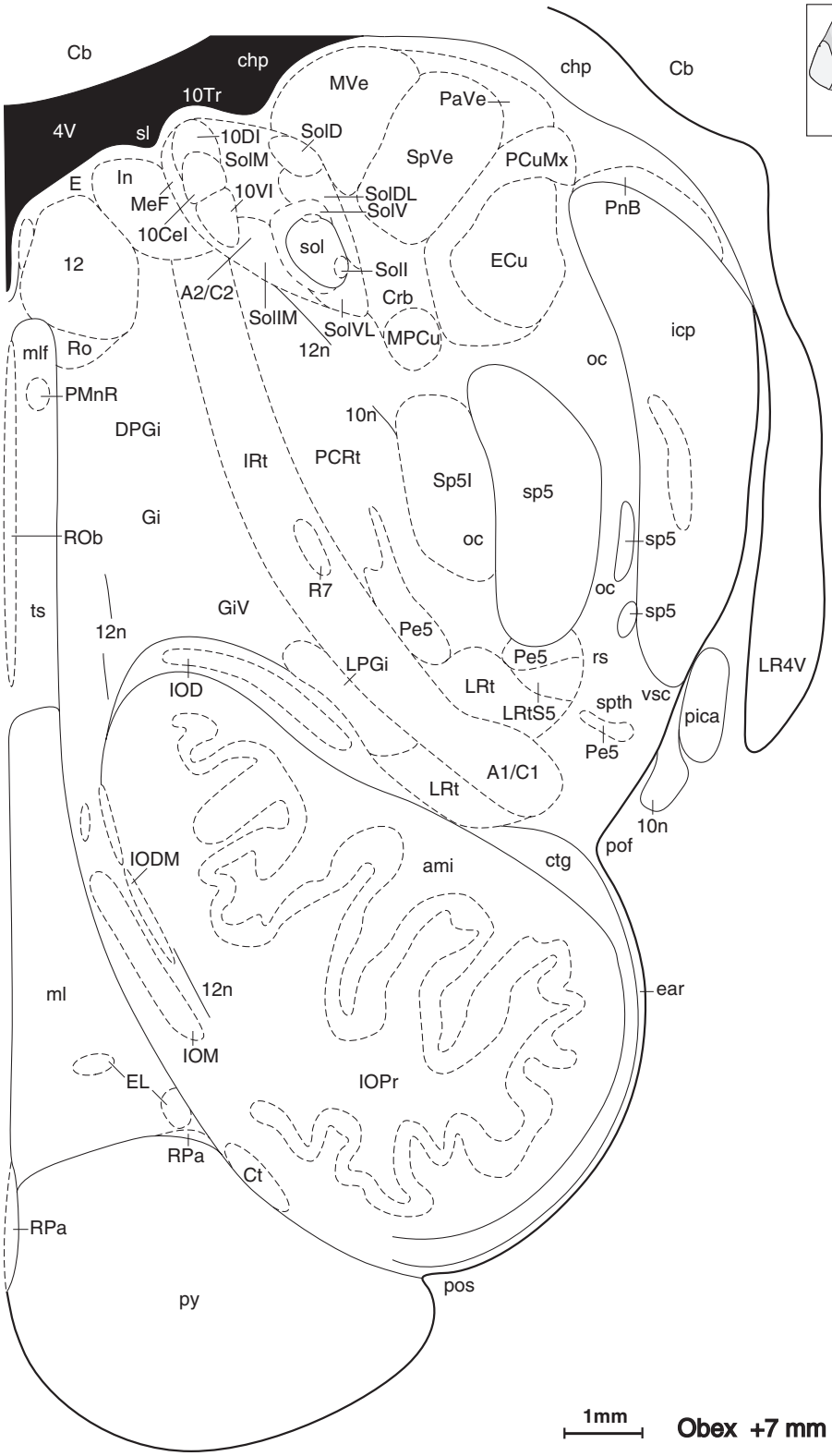

FIGURES 10.6

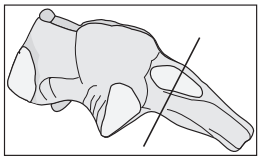

Figure 7

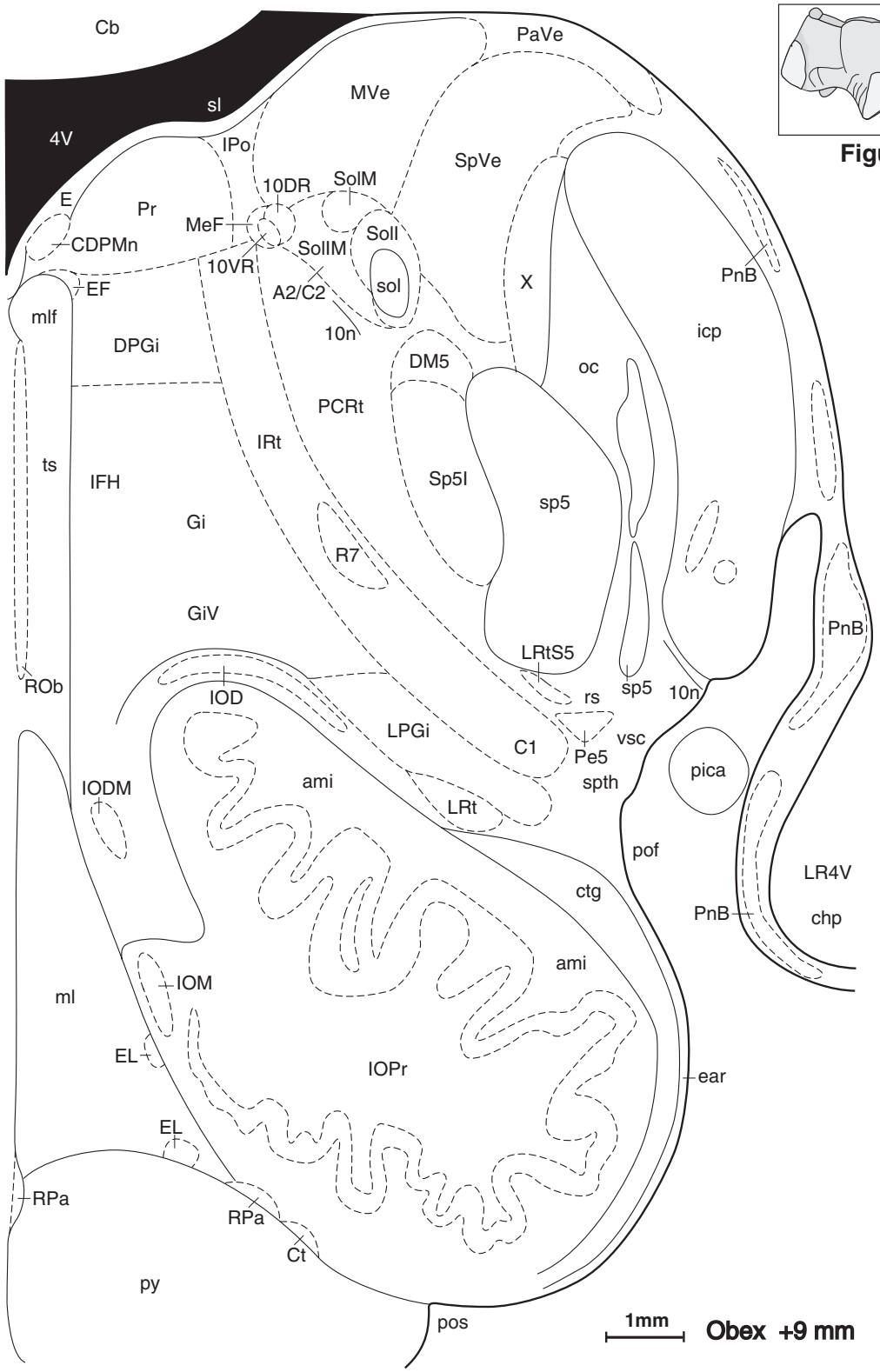

FIGURES 10.7

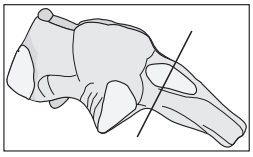

Figure 8

FIGURES 10.8

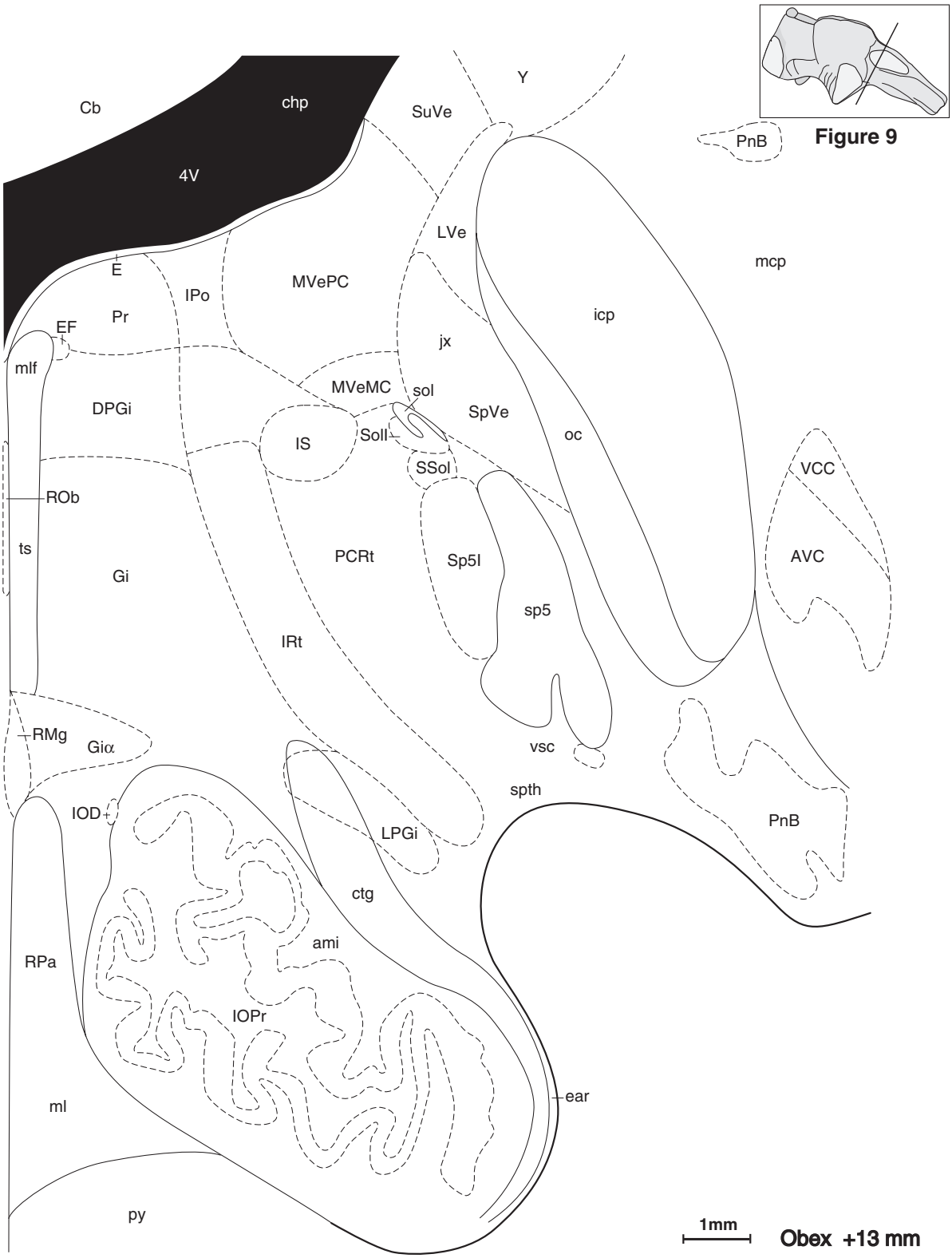
Figure 9
Cb
chp
4V
SuVe
Y
PnB
LVe
mcp
E
IPo
MVePC
Pr
EF
icp
jx
mlf
MVeMC
sol
DPGi
SpVe
IS
SolI
oc
SSol
VCC
ROb
ts
PCRt
Sp5I
AVC
Gi
sp5
IRt
RMg
Giα
vsc
spth
IOD
PnB
LPGi
ctg
RPa
ami
IOPr
ml
ear
py
1mm
Obex +13 mm

FIGURES 10.9

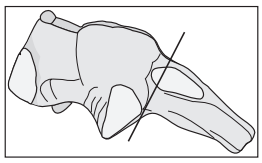

Figure 10

FIGURES 10.10

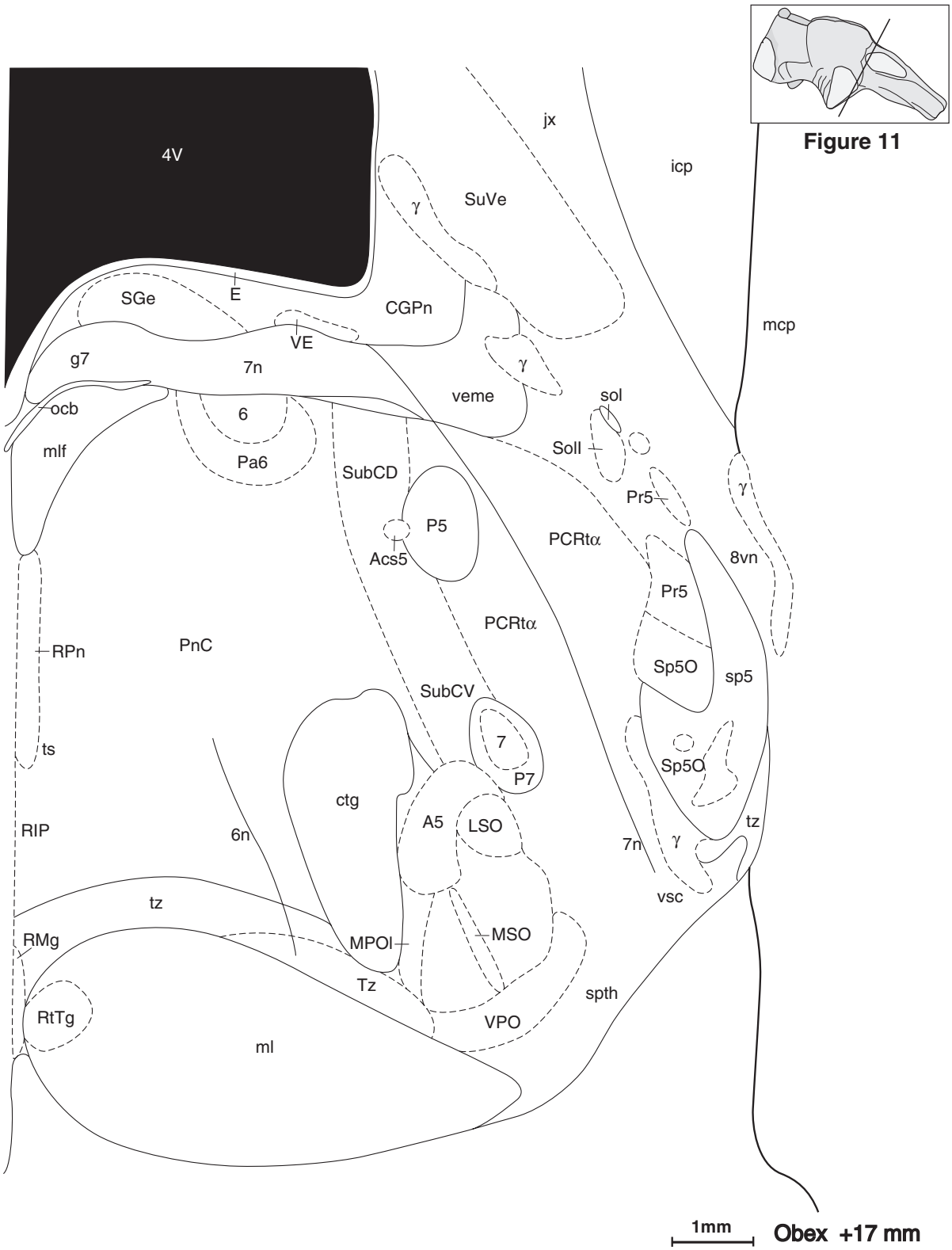

Figure 11

FIGURES 10.11

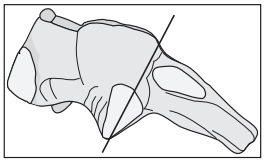

Figure 12

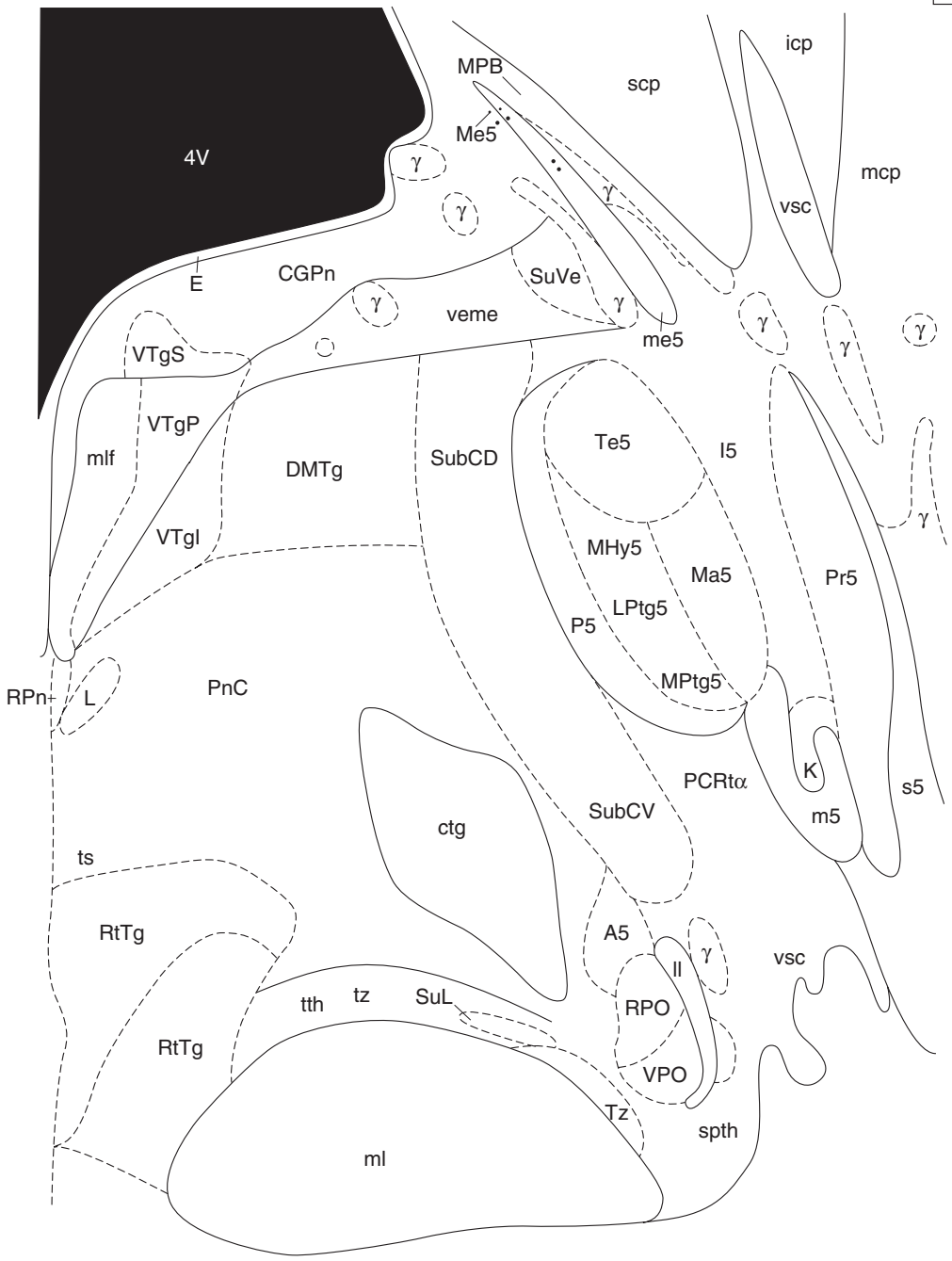

FIGURES 10.12

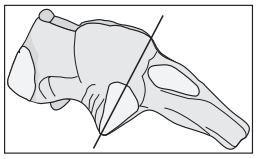

Figure 13

FIGURES 10.13

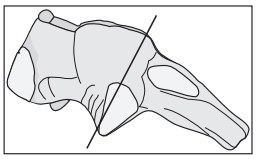

Figure 14

FIGURES 10.14

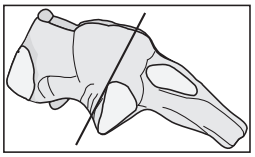

Figure 15

FIGURES 10.15

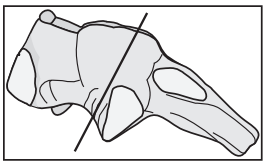

Figure 16

FIGURES 10.16

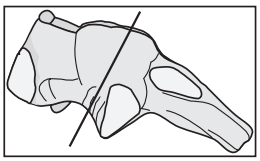

Figure 17

FIGURES 10.17

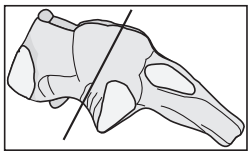

Figure 18

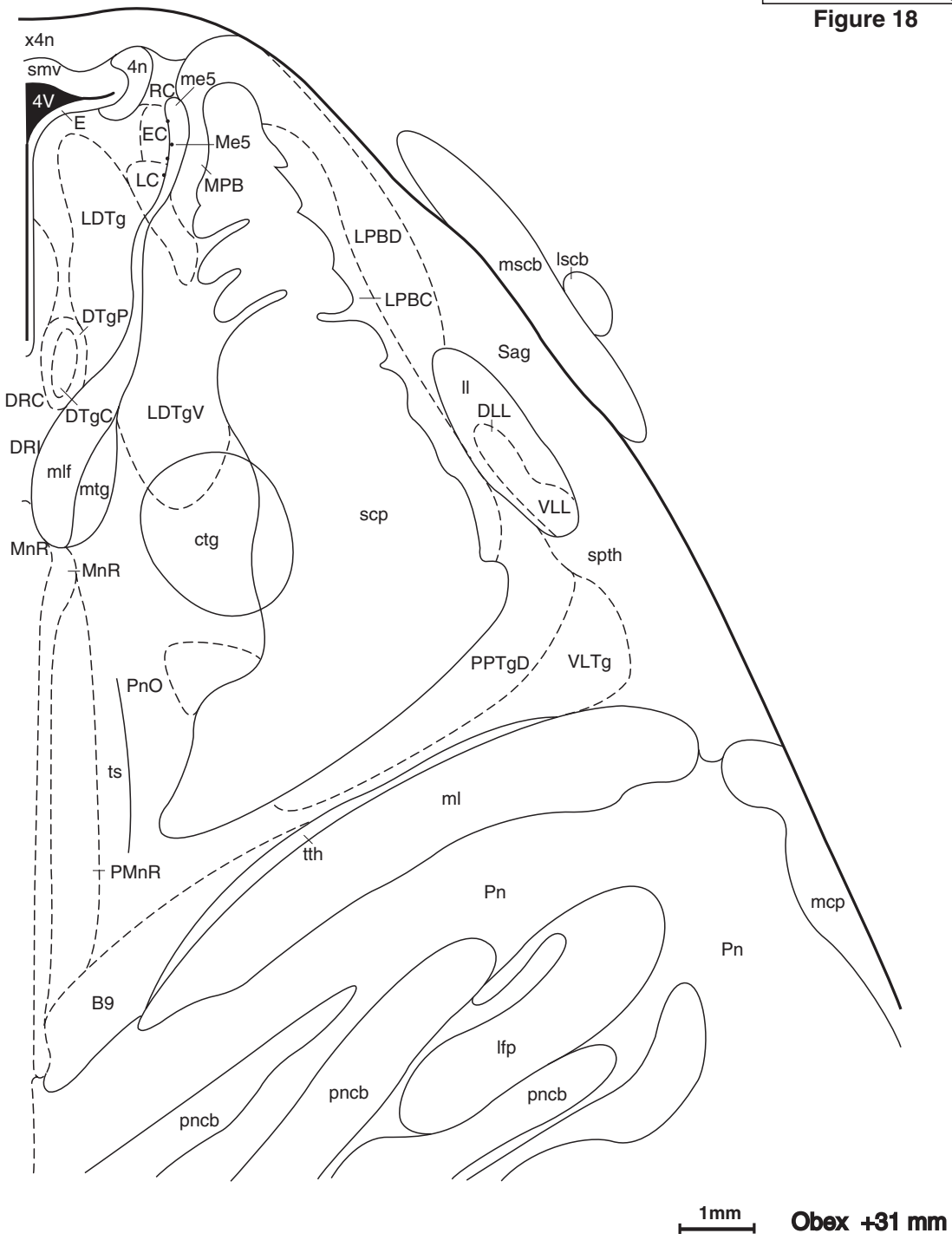

FIGURES 10.18

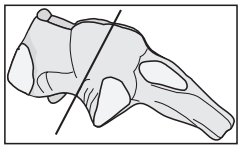

Figure 19

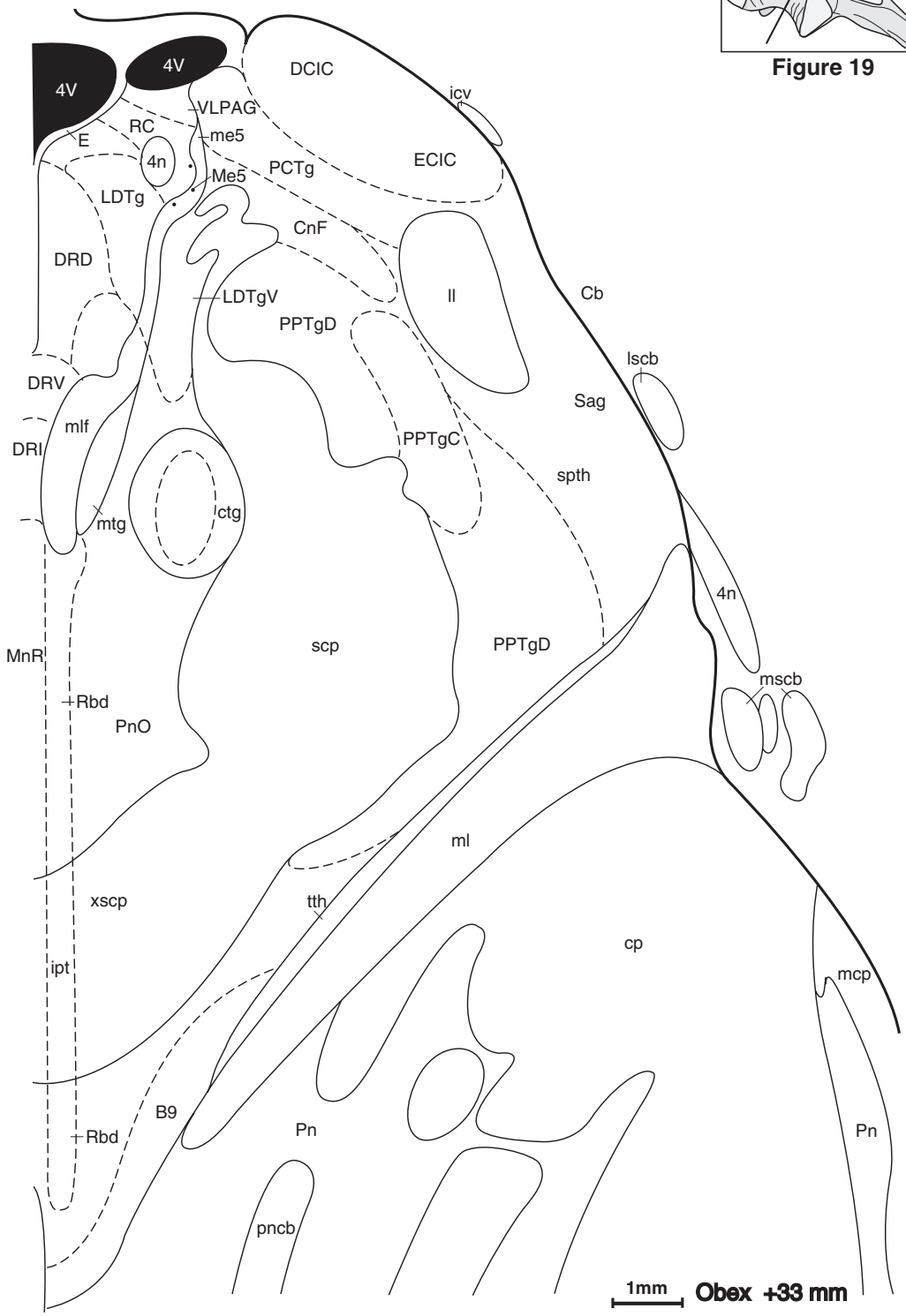

FIGURES 10.19

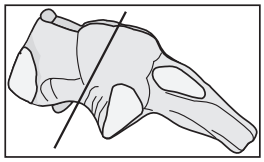

Figure 20

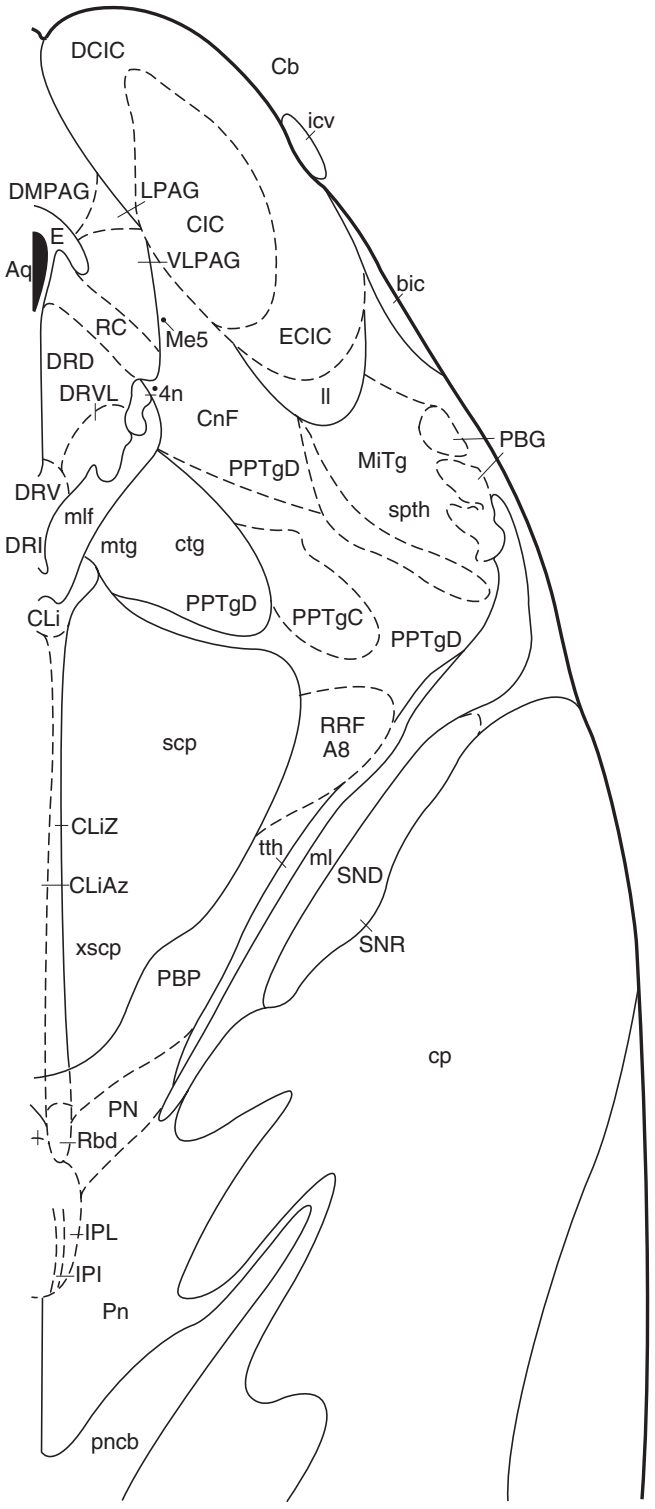

FIGURES 10.20

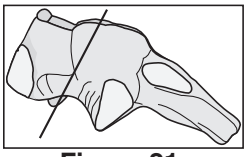

Figure 21

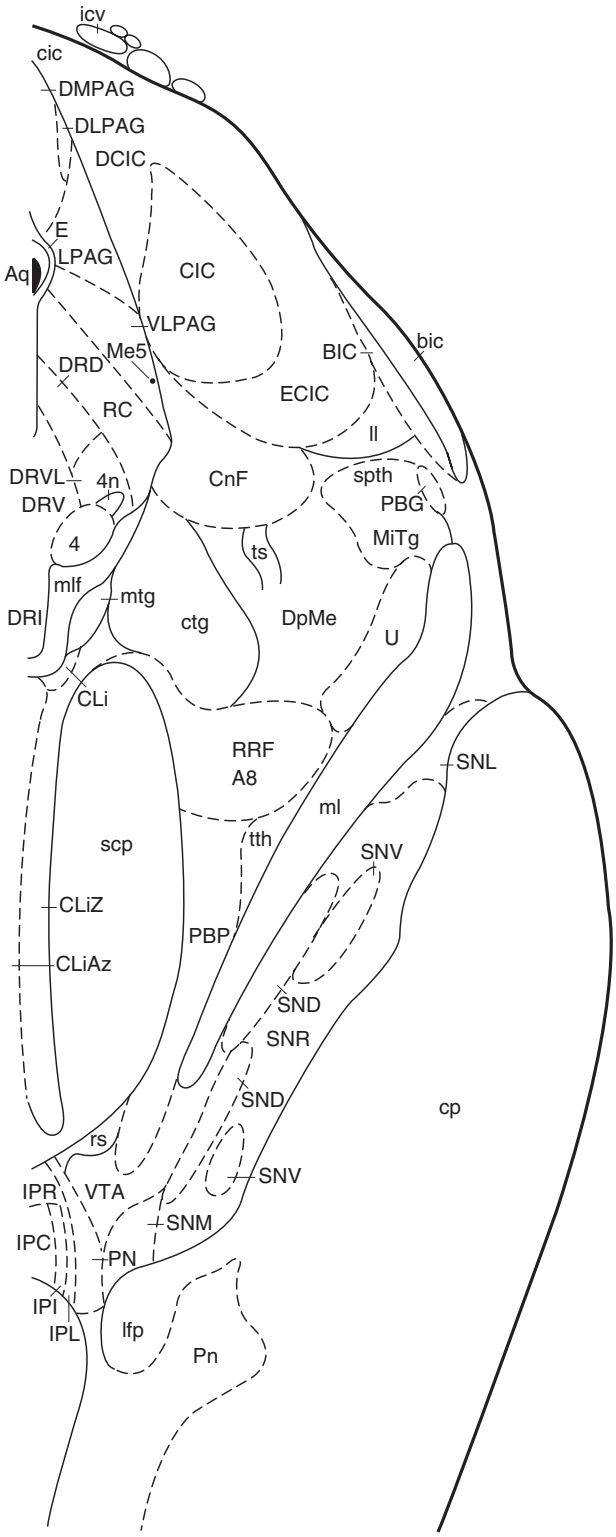

FIGURES 10.21

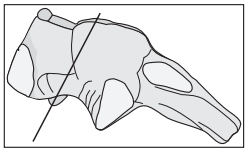

Figure 22

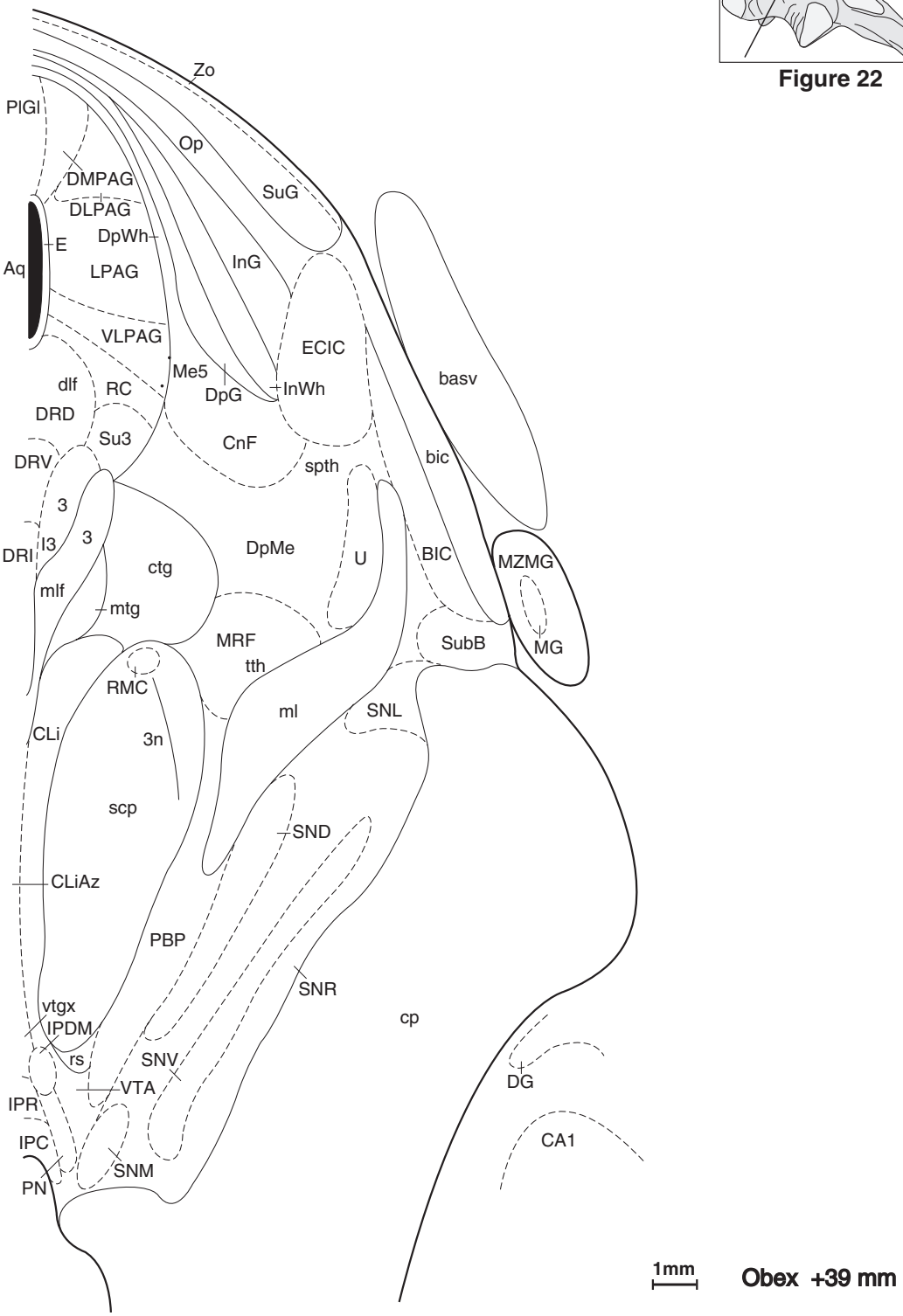

FIGURES 10.22

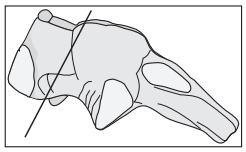

Figure 23

FIGURES 10.23

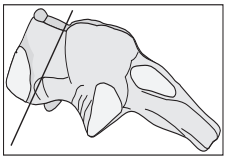

Figure 24

FIGURES 10.24

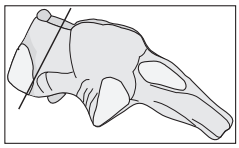

Figure 25

FIGURES 10.25

1995) revealed important topographic relationships between catecholamine and nitric oxide-synthesizing neurons, including innervation of intrinsic blood vessels (both tyrosine hydroxylase– and NADPH-diaphorase–reactive processes innervate intrinsic blood vessels in the Sol). Such topographic relationship may be associated with regulation of autonomic reflexes, sympathetic excitatory drive, and intrinsic control of cerebral blood flow in humans (Benarroch *et al.*, 1995). Recent study used postmortem horseradish peroxidase (HRP) tracing method to revealed the human Sol fiber trajectories forming three major bundles: through the intermediate reticular zone, across the dorsomedial reticular formation toward the dorsal raphe, and a ventral one toward the Gi. The terminals were shown within the Sol, dorsomotor nucleus of vagus, and reticular formation (Ruggiero *et al.*, 2000). Using chemoarchitecture, Törk and colleagues (1990), then McRitchie and Törk (1993, 1994) comprehensively delineated the human Sol (Figs. 10.1–10.9). The lowest levels of AChE reactivity are displayed by the ventrolateral, ventral, and intermediate nuclei of Sol. Slightly more reactivity is displayed by the dorsal, dorsolateral, and commissural nuclei. Intense reactivity is displayed by the gelatinous and medial nuclei. Extremely intense reactivity is displayed by the subsolitary and interstitial nuclei.

The paracommissural nucleus (SolPa) is the most caudal representative of Sol (Figs. 10.1–10.3). It appears at the level of the pyramidal decussation and ends with the advent of the gelatinous nucleus. The nucleus is conspicuous by its extremely reach AChE reactivity.

The interstitial nucleus (SolI) commences just caudal to the obex and persists until the accessory motor trigeminal nucleus, caudal to the main mass of the motor trigeminal nucleus; thus, it is the longest and the most rostral representative of Sol (Figs. 10.3–10.9). It is closely associated with the solitary tract, at times enveloping it and at times being enveloped by it. The SolI expands at its rostral pole. It is at these levels in the monkey and human that the nucleus has a gustatory function. Possible gustatory function more posteriorly is suggested by the contributions of the ninth and tenth nerves, but has not yet been confirmed. Pritchard and Norgren, in Chapter 31 provide a comprehensive review of the gustatory role of SolI. The subsolitary nucleus is found at the rostroventral border of the interstitial solitary nucleus. This cell group is characterized by extremely strong AChE reactivity (Paxinos and Huang, 1995). The intermediate, interstitial, ventral, and ventrolateral subnuclei of Sol reportedly contain light bombesin fiber/terminal staining in both the rat and the human brain (Lynn *et al.*, 1996).

Paxinos and Huang (1995) using AChE staining failed to identify the central subnucleus of the Sol in the human despite the prominent appearance of this structure in the rat brain stem. The human homologue of the central subnucleus was nevertheless identified on the basis of strong NADPH-diaphorase reactivity by Gai and Blessing (1996).

The commissural nucleus (SolC) lies ventromedial to the paracommissural nucleus and at its caudal end crosses the midline just dorsal to the central canal (Figs. 10.1 and 10.2). The SolC is composed of very small cells that tend to be mediolaterally oriented.

The gelatinous nucleus (SolG) appears in the lateral part of the solitary complex deep to the area postrema (Figs. 10.1–10.5). It contains extremely small cells that are spindle shaped and possess dendrites that are confined within the nucleus. Most cells are tyrosine hydroxylase positive, but are not pigmented and have been shown to be adrenergic (PNMT positive) (Kitahama *et al.*, 1985). The subnucleus is devoid of bombesin staining (Lynn *et al.*, 1996).

The dorsolateral nucleus (SolDL) (Figs. 10.3–10.6) displays fairly pale and patchy AChE reactivity. It contains small and medium-sized cells arranged in clusters, as well as large, darkly stained cells that are pigmented and tyrosine hydroxylase positive. The dorsolateral nucleus occupies the middle third of Sol rostral to the level of the obex.

The dorsal nucleus (SolD) (Fig. 10.6) is the rostral continuation of the dorsolateral nucleus but is distinguishable by its stronger and homogeneous AChE reactivity. Cytoarchitecturally it is heterogeneous, containing small and large cells. Clusters of bombesin-positive neurons were reported in the dorsal and ventrolateral subnuclei of the human Sol (Lynn *et al.*, 1996). Bombesin coexists with catecholamines in neurons in the dorsal subnucleus, a topographic association that may be relevant to the cardiovascular effects of bombesin.

The medial nucleus (SolM) (Figs. 10.2–10.7) is the strongly AChE-reactive region located between the dorsal, dorsolateral, ventral, and gelatinous nuclei. It is composed mainly of very small cells, although a few larger pigmented cells are also visible. The medial nucleus replaces the commissural nucleus rostrally (Fig. 10.2) and becomes a rectilinear shape as it occupies the full dorsolateral extent of Sol bordering 10 medially (Figs. 10.3–10.5). Further rostrally, it separates 10 from the interstitial nucleus of Sol. The medial nucleus disappears with the loss of 10 (Fig. 10.7). Chemoarchitectonic studies reported strong bombesin fiber/terminal staining in the medial subnucleus of Sol over its full rostral–caudal extent in both rat and human (Lynn *et al.*, 1996). Another study found the dopamine

D2 and D4 receptors to be almost exclusively concentrated in the intermediate and medial subnuclei of Sol (Hyde *et al.,* 1996).

The parasolitary nucleus (PSol) is a conspicuous, AChE-negative, banana-shaped nucleus (with a lateral concavity) featuring small, densely packed cells at the lateral border of Sol. It commences at about the level of the obex caudally and persists until the rostral third of the hypoglossal nucleus (Figs. 10.3–10.5).

Parabrachial Nuclei

The parabrachial nuclei (PB) are pivotal structures in autonomic control because they perform as an interface between the medullary reflex control mechanisms and the forebrain behavior and integrative regulation of central autonomic systems. While 13 distinct subnuclei have been identified in the rat PB (Fulwiler and Saper, 1984; Herbert *et al.,* 1990), only 5 have been discovered thus far in primates (Paxinos *et al.,* 2000). Relative to the rat, the human PB are cell poor and it is not obvious that there are human homologues to the numerous subdivisions described in the rat. Fortunately for the study of homologies, most of the PB subnuclei are chemically specified and project via somewhat distinct chemically coded lines to their terminations in the hypothalamus and medial part of the ventrobasal complex of the thalamus (see Chapter 31). The chemically coded afferent projections to the PB are also instructive in establishing subnuclei or homologies and their projection in the human. For example, consider the known catecholaminergic, cholecystokinin-, galanin-, and corticotropin-releasing hormone immunoreactive projections from Sol to the PB in the rat (Herbert and Saper, 1990; Phillips *et al.,* 2001). Somatostatin binding sites also indicate the presence of somatostatin receptors in PB (Carpentier *et al.,* 1996).

The central part of the human lateral PB contains AChE reactivity, while the dorsal part of the lateral PB is poorly stained for the enzyme. The external part of the lateral PB is also AChE positive and probably corresponds to the pigmented nucleus mentioned by Ohm and Braak (1987). The human homologue of the most medial part of the medial PB has also been identified by AChE staining.

The medial parabrachial (MPB) (Figs. 10.4–10.18) nucleus begins more caudally then the lateral parabrachial and is well displayed at the compact locus coeruleus pars alpha. The intensity of AChE staining varies between cell groups, but sometimes also between species; thus, unlike the rat, the human MPB is strongly AChE positive, especially in its juxtabrachial portion. It is limited rostroventrally by the central tegmental tract before the rostral end of the lateral parabrachial nucleus. The medial part of MPB directly overlies the ventromedial aspect of the superior cerebellar peduncle and is strongly reactive for AChE. The external part of MPB is distinguished by lower AChE reactivity than its medial part.

The lateral parabrachial nucleus (LPB) (Figs. 10.14–10.18) attains its full extent at the caudal pole of the dorsal tegmental nucleus. The AChE-positive central part of LPB succeeds the pedunculopontine tegmental nucleus caudally, which is distinguished by stronger AChE reactivity. The dorsal part of LPB is, in contrast, poorly stained for AChE. The external part of LPB is AChE positive. A quantitative autoradiographic study of human fetuses revealed a sharp decrease in the density of somatostatin binding sites on late stages of gestation (Carpenter *et al.,* 1997).

Calcitonin gene–related peptide (a neuromodulator in efferent projections from PB to the thalamus and amygdala in rats) was recently employed as a marker for ascending visceral sensory pathways in the human brain (le Lacalle and Saper, 2000). As well as in establishing affiliations of the human PB, chemoarchitecture of MPB and LPB may be of value in pathological investigation. For example, a recent study found that the density of somatostatin binding sites was significantly elevated in MPB and LPB in the sudden infant death syndrome (Carpentier *et al.,* 1998).

In the rat, the Kölliker–Fuse nucleus (KF) (Figs. 10.15 and 10.16) was proposed to harbor the most lateral cluster of the A7 noradrenergic group (Paxinos and Watson, 1998). We note, however, that KF does not form a well-circumscribed group in the rat, whereas in the cat, KF has been placed everywhere in the region between the superior cerebellar peduncle, the lateral lemniscus, and the motor trigeminal (see discussion by Berman, 1968). Paxinos and Huang (1995) depicted the location of the nucleus in the human brain stem (Fig. 10.16).

Fix (1980) identified a melanin-containing nucleus associated with the superior cerebellar peduncle. He labeled the nucleus –X, using inverted commas presumably to indicate that he did not wish this to be retained as its name. Ohm and Braak (1987) identified the same nucleus and called it the subpeduncular nucleus. This term can be easily confused with the subpeduncular tegmental nucleus (Paxinos and Watson, 1998); for this reason, Paxinos and Huang (1995) used the term subpeduncular pigmented nucleus, as did Ohm and Braak in the title of their abstract. The subpeduncular pigmented nucleus (SPP) is unmistakably AChE positive in neuropil and cell bodies. It has relatively large, tightly clustered, mostly pigmented cells presenting a globular profile in coronal section. Because SPP is attached to the ventrolateral edge of the

superior cerebellar peduncle, reaching the lateral lemniscus at the pontine surface, it has cell-poor and fibrous regions surrounding it. Caudally, it commences before the lateral parabrachial nucleus as a group of mainly nonpigmented cells ventral to the superior cerebellar peduncle. More rostrally, it is very favorably displayed and appears as a globular nucleus at the ventrolateral edge of the superior cerebellar peduncle with the majority of its cells pigmented. Further rostrally, it drifts dorsally and intrudes into LPB, tapering off as a row of cells on the dorsal part of PB. At this most rostral level, only a few pigmented cells are seen, but the characteristic AChE reactivity is present. The cells of SPP are polygonal with no specific orientation. Ohm and Braak (1987) observed neurofibrillary tangles in this nucleus in brains from Alzheimer's disease patients. Incidentally, considering their pivotal role within central autonomic regulatory systems, the nuclei of the pontine parabrachial region (MPB, LPB, SPP) together with the intermediate zone of the medullary reticular formation (IRt) are thought to be early targets of the Alzheimer's disease–related pathology (Rub *et al.*, 2001). The subpeduncular pigmented nucleus is not the homologue of the Köliker–Fuse nucleus or of any other known nucleus in experimental animals.

Periaqueductal Gray

Recent evidence suggests that the periaqueductal gray (PAG) is an important central relay in cardiovascular and other autonomic control. There is also substantial evidence for human homologies to the PAG subdivisons established in rat and cat (Bandler *et al.*, 1991; Beitz, 1995; see also Chapter 12). Thus, Paxinos and Huang (1995) identified dorsomedial, dorsolateral, lateral; and ventrolateral PAG columns in the human (Figs. 10.19–10.25). Another chemoarchitectonic investigation based on NADPH-diaphorase reactivity (Carrive and Paxinos, 1994) recognized the supraoculomotor cap in the human PAG. The posterior part of this cap was subsequently distinguished by AChE staining (Paxinos and Huang, 1995). Paxinos and Huang (1995) also outlined the human *pleoglial* PAG—a median structure above the rostral levels of the aqueduct. Like the parabrachial nucleus, the PAG forms an interface between the forebrain limbic system and medullary autonomic centers. It receives afferents from the hypothalamus and amygdala and in turn projects to the intermediate reticular zone of the medulla. Carrive *et al.* (1989) showed that the PAG autonomic control is compartmentally organized into PAG columns and coupled to defensive behavior in the rat. Paxinos and Huang (1995) showed a columnar arrangement for the human PAG, which is discussed in detail by Carrive and Morgan (in Chapter 12).

The nucleus of Darkschewitch (M) is found in the periaqueductal gray, dorsomedial to the interstitial nucleus of the medial longitudinal fasciculus at a level posterior to the ascending fasciculus retroflexus. It is nondistinct in AChE preparations. The human PAG displays certain AChE-reactive regions that have no apparent animal homology.

RETICULAR FORMATION

The keystone to the organizational plan of the medullary reticular formation offered in this chapter is the intermediate reticular zone (IRt). Rt is described in detail in Chapter 19 of this book.

Intermediate Reticular Zone

Historical Considerations

In 1986 the intermediate reticular nucleus of the rat was recognized as the zone between the gigantocellular and parvicellular reticular nuclei which contains large, medium, and small cells and is slightly more reactive for AChE than its neighbors (Paxinos and Watson, 1998, Figure 58–71). Presumably, this zone brackets the line separating the alar and basal plate derivatives in development. The line extends radially from the sulcus limitans in the floor of the fourth ventricle to the periphery of the brain stem where the vagal and glossopharyngeal rootlets emerge. Due to its cytoarchitecture and position, the zone was named the intermediate reticular nucleus. Allen *et al*. (1988) found a distinct punctuated distribution of angiotensin II receptors over cell bodies in what they proposed to be the human homologue of the rat intermediate reticular nucleus (see also Allen *et al.*, 1991). Halliday and colleagues (1988b, c), and later Huang and colleagues (1992), showed tyrosine hydroxylase, and neuropeptide Y (NPY) cell bodies and fibers in what in fact is the intermediate reticular nucleus.

Based on the evidence for the existence of the intermediate reticular zone in humans and, following mappings of tyrosine hydroxylase, serotonin, NPY, and substance P in this area, Paxinos and Huang (1995) proposed an extension of IRt boundaries. Given the heterogeneity of this area (see below), they changed its name from "intermediate reticular nucleus" to "intermediate reticular zone" (IRt). The hallmark of the cytoarchitecture of the intermediate reticular zone is the polarity of cell bodies and their major dendrites. These cells are oriented along the dorsomedial to ventrolateral axis, mirroring the shape of the zone in

coronal sections. This orientation predilection distinguishes the IRt from the adjacent gigantocellular and parvicellular reticular nuclei that contain neurons with various orientations.

Position

Caudally, the IRt separates the ventral and medial reticular nuclei from the dorsal reticular nucleus; rostrally, the IRt separates the gigantocellular from the parvicellular reticular nuclei (Figs. 10.1–10.10). The zone commences at the pyramidal decussation and extends to the facial nucleus. It is a convex arc with the convexity facing laterally in the rat but medially in the human (probably due to the enormity of the human inferior olive). Dorsally, outlying tyrosine hydroxylase–positive cells of this zone are found in the cell-poor region that caps the medial pole of the dorsal motor nucleus of vagus. Laterally, it has a variable extent. At caudal levels (Fig. 10.1), IRt reaches the lateral surface of the medulla dorsal to the lateral reticular nucleus (LRt). Somewhat rostrally (Figs. 10.2–10.6), IRt nearly bisects the LRt in its surge to the lateral surface. Further rostrally, it forms a slab dorsal to the lateral paragigantocellular nucleus and together they reach the lateral medullary surface (Fig. 10.9). Caudally, it harbors the retroambiguus, ambiguus, and Al noradrenaline cell groups. Rostrally, it harbors the ambiguus nucleus as well as the Cl adrenaline group.

Catecholamine Cells

Catecholamine cells are found throughout the IRt but are more prominent in the part ventrolateral to the ambiguus nucleus (Al and Cl). These regions of the IRt have been called the caudoventrolateral (CVL) and rostroventrolateral (RVL) reticular nuclei of the medulla (Arango *et al.,* 1988). This cell group is thought to be involved in control of sympathetic cardiovascular outflow, cardiorespiratory interactions, and reflex control of vasopressin release. For example, resent pathology study showed depletion of catecholaminergic tyrosine hydroxylase–positive neurons in patients with multiple-systems atrophy with autonomic failure (Benarroch *et al.,* 1998). The full extent of IRt can be clearly seen in Figure 4 of Arango *et al.,* which depicts tyrosine hydroxylase immunoreactivity in the medulla. This observation was later successfully used by Huang *et al.* (1992) for delimiting IRt on the basis of the distribution of the tyrosine hydroxylase–immunoreactive cells and fibers. The distribution of AChE-positive cells in the IRt resembles the distribution of the catecholamine-containing cells. The most distinct AChE positive neuropil is associated with RVL at levels where the ambiguus nucleus is most prominent. This AChE reactivity in the IRt (RVL) is associated with cell bodies and fibers and it nearly reaches the lateral surface of the brain.

Neuropeptide Y

NPY-reactive neurons are found throughout the rostrocaudal extent of the ventrolateral IRt, particularly at midolivary levels. Expression of NPY mRNA has also been reported in IRt (Pau *et al.,* 1997). Benarroch and Smithson (1997) described typosine hydrozylase (NADPH-diaphorase) distribution in the IRt. The distribution of NPY immunoreactivity overlaps typosine hydroxylase but not NADPH-diaphorase reactivity (Benarroch and Smithson, 1997), suggesting a possibility of further subdivision of human ventrolateral IRt.

Serotonin

Caudally, the lateral part of the IRt contains some serotonin cells intermixed with the catecholamine cells, though differentially concentrated. Many of these cells, particularly serotonin cells, are very close to the surface of the medulla. The more rostral regions of IRt contain only occasional serotonin cells. At rostral levels, most serotonin cells are distributed in the lateral paragigantocellular nucleus, immediately medioventral to IRt (Fig. 10.9).

At times, some chemically specified cell groups do not respect classical nuclear boundaries and no adjustment of boundaries can be made that can accommodate the new elements without violating other delineation criteria. However, the IRt has consistently appeared as an entity in the work of a number of investigators who have used retrograde or anterograde labels or different chemically specific stains. Having obtained an "afterimage" from the pattern of distribution of chemically specified elements, it is possible to detect, in Nissl-stained sections, fusiform cell bodies that are oriented in the direction of the axis that joins the dorsal motor nucleus/solitary complex dorsomedially with the Al/Cl cell groups ventrolaterally. The existence in the IRt of "independent" nuclei that do not share IRt properties prompted us to reclassify this region from a nucleus to a zone.

Substance P

Substance P is differentially distributed in the medullary reticular nuclei. IRt displays more substance P–positive fibers than adjacent nuclei. The distribution of substance P fibers in IRt is nonhomogeneous. Rostrally, IRt displays a band of substance P–positive fibers and cells near its border with the parvicellular reticular nucleus. The ambiguus nucleus is the most substance P–poor region of the IRt. Caudally, the IRt contains a few substance P–positive cell bodies that are larger than the substance P–positive cells in the parvi-

cellular reticular nucleus. All substance P cells in the IRt also contain adrenaline or noradrenaline. However, most (about 95%) of the catecholamine cells do not contain substance P (Halliday *et al.*, 1988a). Ni and Miller Jonakait (1988) have shown that substance P fibers excellently delineate Irt in the developing mouse.

Salmon Calcitonin Binding Sites

The IRt can also be delineated by the salmon calcitonin binding sites (Sexton *et al.*, 1994). It is important to mention, though, that these sites invade some regions of the parvicellular reticular nucleus and the gigantocellular nucleus.

Connections

There is evidence that cells contained in the IRt have both ascending and descending connections. For example, following small HRP injections into the parabrachial region in cats, King (1980) found separate sheets or layers of retrogradely labeled cells in '1ateral tegmental field" (Berman's, 1968) that ran parallel to the long axis of the lower brain stem and radially with respect to the ventricle. The more medial gamma and delta layers of labeled cells of King's (1980) description appear to occupy the medial region of the lateral tegmental fields [or parvicellular reticular formation (PCRt of our terminology)] that we have now incorporated into the IRt. Similarly, HRP injection into the caudal vagosolitary complex produced a comparable sheet of labeled cells extending the length of the cat's medulla in what Mehler (1983) also then called the medial part of the PCRt but which we now consider part of the IRt zone. Interestingly, anterograde tracer injection experiments involving IRt in the rat produce confirmatory evidence of ascending projections to the parabrachial region and descending projections to the solitary nucleus and the phrenic motoneuron pools at C4 (Yamada *et al.*, 1988).

In the monkey, injections of HRP into the cervical vagus nerve result in heavy retrograde labeling of neurons in the ipsilateral dorsal motor nucleus of the vagus and in the ambiguus nucleus. "Additionally, a few neurones are labeled in the intermediate zone between these two nuclei" (Gwyn *et al.*, 1985), i.e., in the IRt.

Retroambiguus and Ambiguus Nuclei

The RAmb commences below the pyramidal decussation as a scatter of AChE-positive cells embedded in the part of the IRt that is separated from the rest by the decussating corticospinal fibers. It extends to the level of the LRt, at which point it is succeeded by the Amb (Fig. 10.1). RAmb is characterized by diffuse spindle-shaped cells. Amb, by contrast, has large multipolar neurons that stain densely for AChE and display large Nissl granules. At area postrema levels the Amb is represented by only a few cells (Fig. 10.3). At the level of the caudal pole of the dorsal accessory olive (Fig. 10.4) it expands ventrolaterally to conform with the arcuate shape of the IRt. Near the level of the rostral pole of the hypoglossal nucleus it becomes a round cluster. It attains maximal size near the level of the roots of the glossopharyngeal nerve (Fig. 10.5). At this level, the AChE reactivity associated with the Amb engulfs the surrounding cell-poor zone.

Unlike other regions of IRt, RAmb and Amb do not possess catecholamine or NPY cells and are not invaded by catecholamine- or NPY-containing processes. On the other hands the human adult Amb contains serotonin immunoreactivity (Halliday *et al.*, 1990) and the human fetus Amb contains high concentrations of somatostatin receptors (Carpentier *et al.*, 1996). In addition, monoamine oxidase A, substance P, and receptors for angiotensin II are scarcest in the RAmb and Amb regions of the IRt (Paxinos *et al.*, 1990). The mode of integration of the RAmb and the Amb with the remainder of IRt is still unclear. A recent case description provided insight into the role of Amb, Sol and neighboring medullary reticular formation as well as the vagal dorsal motor nucleus in central control of swallowing. Thus, lateral medullary syndrome presented with numerous symptoms, including dysphagia, is associated with lesion in the upper medulla (Martino *et al.*, 2001).

Ventral, Medial, and Dorsal Reticular Nuclei

Considering that the existence of the IRt is accepted, the remainder of the reticular formation of the medulla can be subdivided in a scheme that is in harmony with the distribution of neuroactive compounds in this area.

The area ventral and medial to the IRt (previously known as medullary reticular nucleus, ventral part) features two distinct nuclei. These are a ventral nucleus with small and medium-sized cells that Paxinos *et al.* (1990) called the ventral reticular nucleus (VRt), and a medial nucleus with larger cells and greater AChE reactivity, which they called the medial reticular nucleus (MRt) (Figs. 10.1–10.4). The caudal pole of the VRt is found at a ventrolateral position below the retroambiguus nucleus (RAmb). Rostrally, it is displaced medially and dorsally by the advancing epiolivary lateral reticular nucleus (EO), which in turn is displaced medially and dorsally by the lateral paragigantocellular nucleus (LPGi) (Fig. 10.5). All these nuclei border the inferior olive (IO) ventrally and the IRt dorsally. Immunostaining for tyrosine hydroxylase reveals large catecholaminergic neurons in VRt.

The area dorsal and lateral to the IRt (previously known as medullary reticular nucleus, dorsal part [MdD]) contains smaller cells and fewer substance P fibers. To be consistent with the other terms in this region, Paxinos and Huang (1995) called it the dorsal reticular nucleus (DRt). The DRt contains large catecholaminergic neurons distinguishable by strong tyrosine hydroxylase immunoreactivity. It is thought that DRt servers a role of a primary pro-nociceptive center in the pain control system that integrates multiple excitatory and inhibitory actions for nociceptive processing (Lima and Almeida, 2002; Villanueva *et al.*, 2000). The parvicellular reticular nucleus is found dorsal to the IRt and rostral to DRt, from which it is difficult to distinguish.

Lateral Reticular Nucleus

The lateral reticular nucleus (LRt) consists of the lateral reticular nucleus proper, the subtrigeminal division, the epiolivary division, and the pravocellular division.

The LRt proper has AChE-positive neurons in a somewhat dense neuropil that is perforated by negative fibers with longitudinal orientation. It commences caudally at the rostral part of the pyramidal decussation (caudal to Fig. 10.1). According to Paxinos *et al.* (1990), the name "lateral reticular nucleus" is retained only for this part of the nucleus (without qualifiers such as "proper" or "prinicipal").

The subtrigeminal LRt (LRtS5) features large cells, well stained for AChE, in a dense AChE background. It commences caudal to the principal inferior olive (Figs. 10.1–10.3). At its rostral pole it becomes fractionated and discontinuous (Fig. 10.7). The LRtS5 also contains tyrosine hydroxylase–positive neurons. The LRtS5 together with VRt and DRt is thought to play a role of autonomic respiratory centers in the medulla. In support of this view, a recent study reported severe loss of catecholaminergic (tyrosine hydroxylase positive) neurons in LRtS5, VRt, and DRt in patients with myotonic dystrophy who suffered alveolar hypoventilation and respiratory insufficiency (Ono *et al.*, 1998).

The LRt extends medially over the caudal pole of the inferior olive. This epiolivary part becomes separated from the main LRt at the caudal pole of the dorsal accessory olive. Further rostrally, it shifts medially as a compact rectangular group (Figs. 10.1–10.7). Paxinos and colleagues (1990) noticed in the baboon a nucleus in a position similar to the epiolivary LRt that displays large retrogradely filled cells following thoracic HRP injections. This spinally projecting nucleus in the baboon cannot be assigned to LRt because it projects to the spinal cord rather than the cerebellum. Therefore, the epiolivary nucleus may not belong to LRt complex, although the two nuclei are nearly identical morphologically (Paxinos *et al.*, 1990). The similarity of the epiolivary nucleus to LRt was also recognized by Braak (1971).

The parvicellular part of LRt (LRtPC) betrays its presence in the rat by the extremely dense AchE reactivity. In the human, AChE reactivity is found in islets near the surface of the lateral medulla immediately external to LRt (Fig. 10.5). Small compact cells poorly stained for Nissl are associated with this reactivity is the homologue of LRtPC. In humans its size is clearly attenuated in comparision with that in the rat. For further details on LRt, see Walberg (1952).

Gigantocellular, Lateral Paragigantocellular, Gigantocellular Ventral Part, Gigantocellular Alpha Part, and Dorsal Paragigantocellular and Parvicellular Reticular Nuclei

The gigantocellular reticular nucleus (Gi) appears together with Roller's nucleus (Fig. 10.5). It extends to the level of the exiting facial nerve, where it is succeeded by the caudal part of the pontine reticular nucleus (PnC) (Figs. 10.10–10.11). Study of the cytoarchitectonic development of the human Gi suggested that immature Gi neurons appear by 16 weeks of gestation after migration and that the subsequent differentiation and maturation progresses gradually and monotonously during the latter half of gestation (Yamaguchi *et al.*, 1994).

The present description of the lateral paragigantocellular nucleus (LPGi) is based on the distribution of serotonin cells. LPGi first appears lateral to the rostral pole of the epiolivary LRt (Figs. 10.5–10.6). LPGi remains at a lateral position and always ventromedial to the IRt. When the dorsal accessory olive disappears, the LPGi expands medially (Figs. 10.7–10.8), where it persists until the rostral pole of the principal inferior olive. Along its entire length, LM features many fusiform serotonin-containing neurons. Beyond the caudal pole of LM, serotonin cells remain in the region but do not penetrate the epiolivary reticular nucleus; rather, they shift dorsally into the IRt and mingle with the tyrosine hydroxylase–positive cells of this zone. The spread of the LPGi as shown by Nissl staining matches that of the serotonin-positive cell bodies. More than 150 serotonin-positive cells can be seen on each side of a 50-µm section of the medulla. The serotonin-positive cells are larger in the LPGi (27 ± 4 µm) than in the caudal part of the intermediate reticular zone (19 ± 4 µm) (Halliday *et al.*, 1988a).

Substance P is found in many of the serotonin-containing cells in the LPGi (Halliday *et al.*, 1988b). A recent study examined proximal projections of LPGi using a bidirectional lipophilic fluorescent tracer, 1,1′-dioctadecyl-3,3.3′,3′-tetramethylindocarbocyanine perchlorate (DiI), in postmortem human fetuses and reported diffusion of DiI to the arcuate nucleus (Ar), nucleus raphe obscurus, hilus of the inferior olive, bilateral Gi and the intermediate reticular zone (IRt), vestibular and cochlear nuclei, cells and fibers at the floor of the fourth ventricle, medial lemniscus, lateral lemniscus, inferior cerebellar peduncle and cerebellar white matter, central tegmental tract, and capsule of the red nucleus (Zec and Kinney, 2001).

The Gi, ventral part (GiV) is an AChE-ppor area above the dorsal accessory olive. It borders the LPGi and IRt laterally and the Gi dorsally. Unlike the rat, cat, and monkey (see Chapter 8), the human GiV does not have giant cells. It is succeeded rostrally by the gigantocellular α part (Giα).

The Giα forms a cap over the raphe magnus (Figs. 10.9 and 10.10). It has small, medium, and large cells, many of which are oriented mediolaterally. It is bordered laterally by the central tegmental tract as the tract approaches the inferior olive. It is characterized by medium AChE reactivity and has AChE-positive cell bodies. In addition, serotonin-positive cells invade the ventral and lateral part of the GiA (see Chapter 30). The dorsal paragigantocellular nucleus (DPGi) is favorably seen in Fig. 10.10 as an AChE-poor region.

TEGMENTAL NUCLEI

Ventral Tegmental Nucleus

In 1884, von Gudden observed that in the rabbit the majority of the fibers of the mammilotegmental tract terminated in a distinct nucleus of the pontine tegmentum that he named after himself, "das Guddensche Ganglion." This nucleus is now known as the ventral tegmental nucleus (von Gudden, 1884) (VTg) and is a densely packed, conspicuous nucleus in all species studied except the human. On the basis of chemo- and cytoarchitecture, Paxinos *et al.* (1990) and, soon after, Huang *et al.* (1992) delineated VTg in humans as the large, AChE-reactive nucleus that succeeds rostrally the abducens nucleus, after allowing the root of the seventh nerve to interpose itself between the two nuclei. This area is not a rostral extension of the abducens nucleus because both nuclei taper prior to reaching either side of the root of the seventh nerve. The VTg is embedded in the lateral aspects of the medial longitudinal fasciculus (mlf), extending both ventrally into the tegmenturn and dorsally into the central gray of the pons. The extension into the central gray features slightly smaller cells and is slightly less AChE reactive than other portions of VTg. The cells of VTg are mainly large and well stained for Nissl. Its anteroposterior extent is about 2.4 mm. It is succeeded rostrally by the alar interstitial nucleus. The topography of the human VTg, as described by Huang *et al.* (1992) with a suprafascicular and a principal part, more closely resembles the arrangement of the nucleus in the hamster than that in the rat or cat (see Hayakawa and Zyo, 1983, for drawings of the VTg in a number of experimental animal species).

Dorsal Tegmental Nucleus

Caudally, the dorsal tegmental nucleus (DTg) commences at the level of the rostral pole of the reticular tegmental nucleus (Fig. 10.18). It was first identified by von Gudden (1889, cited by Berman, 1968). Chemo- and cytoarchitectonic study of the nucleus in the human (Huang *et al.*, 1992) delineated DTg as a circumscribed, compact, small-celled nucleus conspicuous by its relatively poor AChE reactivity, which contrasts sharply with the dense lateral dorsal tegmental nucleus (Fig. 10.18). It extends to the caudal pole of the pedunculopontine tegmental nucleus (PPTg). The DTg was erroneously considered to be part of the supratrochlear nucleus (dorsal raphe in current nomenclature) by Olszewski and Baxter (1954). The DTg is completely devoid of serotonin cells, and this supports the original classification of von Gudden (1889) that distinguished it from the raphe nuclei.

Posterodorsal Tegmental Nucleus

The posterodorsal tegmental nucleus has been identified by Huang *et al.* (1992) on the basis of chemo- and cytoarchitecture (Fig. 10.16). The nucleus is distinguished within PAG of the pons by strong AChE reactivity.

Lateral Dorsal Tegmental Nucleus

The lateral dorsal tegmental nucleus (LDTg) borders the locus coeruleus and the DTg through some of its course (Figs. 10.16–10.18). It outdistances the DTg caudally and, especially, rostrally where its ventral part persists until PPTg compact part is fully displayed (Fig.10.15). In humans, as in the rat, the ventral part of the LDTg (LDTgV) consists of AChE-positive cells that extend into the fibrous tegmentum ventral to PAG. The LDTgV mingles rostrally with PPTg. (For

the cholinergic nature of these nuclei, see Chapter 33). LDTg cells are extremely AChE positive but are usually concealed by the intense AChE neuropil of the nucleus. Substance P immunoreactivity is displayed by nearly all the large cells of the nucleus (Del Fiacco *et al.,* 1984; Nomura *et al.,* 1987).

Pedunculopontine Tegmental Nucleus

The PPTg contains AChE-positive cells and neuropil and rides the dorsal aspects of the superior cerebellar peduncle. The nucleus has a compact, large-celled part and a diffuse part (Figs. 10.19 and 10.20). It has cholinergic (see Chapter 33) and substance P-positive cells (see Chapter 32). It is likely that the compact part of the human PPTg is the homologue of the rat retrorubral nucleus.

In Figure 10.20, directly medial to the spinothalamic tract there is an area of AChE reactivity. Olszewski and Baxter outlined two nuclei in this position: the subcuneiform and the diffuse pedunculopontine tegmental. We believe that their scheme is not entirely correct, but we cannot at present make another proposal. This region is probably transversed by ascending AChE fibers of the PPTg. Riley (1943), referring to Ziehen (1934), included this region in "area U".

Microcellular Tegmental Nucleus

An extensive parvicellular and AChE-reactive nucleus has recently been identified medial to the parabigeminal nucleus of the rat (Paxinos, 1983, 1985; Paxinos and Butcher, 1986). It has been called the microcellular tegmental nucleus (MiTg). No nucleus of such intense AChE reactivity is found medial to the parabigeminal of the human. However, a parvicellular nucleus of low AChE reactivity is found in a position of the human tegmentum analogous to that occupied by the MiTg in the rat. On the basis of these observations, Paxinos *et al.* (1990) proposed that the MiTg exists in the human but has different AChE properties.

LOCUS COERULEUS

The locus coeruleus (LC) (Figs. 10.13–10.18) is characterized by large AChE-positive cells. Meesen and Olszewski (1949) identified in the rabbit a ventral extension of the LC, which they called LC alpha. This ventral extension included a compact portion and a more extensive diffuse part. In the human, Olszewski and Baxter included the compact portion of the pars alpha in their LC proper and the diffuse part in their subcoeruleus (SubC). Paxinos and Watson (1998) labeled the compact part of the LC that is ventral to PAG (in the fibrous tegmentum) as subcoeruleus alpha (SubCA). However, the cells more closely resemble those of the LC rather than those of the SubC; hence, the term "LC alpha" rather than "SubC alpha" in the present description. Unlike LC, which has relatively few spinal-projecting cells, the LC alpha exhibits numerous descending projections to the spinal cord as well as many ascending projections to the forebrain (W R. Mehler, unpublished observations; Satoh *et al.,* 1977). Resent report showed strong expression of NPY mRNA in the LC (Pau *et al.,* 1998). High concentration of somatostatin binding sites in the area also indicates presence of somatostatine receptors in the LC (Carpentier *et al.,* 1996). In Alzheimer's disease the LC sustains degeneration, but the LC alpha remains unaffected (Marcyniuk *et al.,* 1986a, b).

Epicoeruleus Nucleus

Unlike the rat, LC of humans confines itself to the ventrolateral corner of PAG and does not cling to the full dorsoventral extent of the mesencephalic tract of the trigeminal (Paxinos *et al.,* 1990). In humans, the space dorsal to the LC and medial to the mesencephalic tract of the trigeminal nerve is occupied by a group of medium cells, which Paxinos and Huang (1990) called the "epicoeruleus nucleus" (EC) (Figs. 10.15–10.18). In transverse section this nucleus has the shape of an isosceles triangle, with the base resting on the LC and a small-angle apex pointing dorsally. EC is best seen caudal to the caudal pole of DTg. It remains to be determined whether EC is a separate entity from the medial parabrachial nucleus.

Pathology of major depression was recently shown to be accompanied by altered norepinephrine transporter (NET) function (a membrane protein responsible for termination of the action of synaptic norepinephrine and a site of action of many antidepressants) in LC (Klimek *et al.,* 1997). Chemoarchitectonic evidence revealed the angiotensin II type 1 receptors in the human LC (Benarroch and Schmeichel, 1998) and somatostatin in the fetal human LC (Carpentier *et al.,* 1996), while the differential decrease in the density of somatostatin binding sites observed in the fetal LC during development supported the notion that the somatostatinergic systems in LC as well as in LPB may be involved in maturation of the respiratory control (Carpenter *et al.,* 1997). Recent study also localized strong human cocaine- and amphetamine-regulated transcript (CART) mRNA expression in the human LC (Hurd and Fagergren, 2000). The subcoeruleus nucleus is the AChE-positive area dorsolateral to the central

tegmental tract (ctg). For a description and pictorial representation of LC, subcoeruleus, and the A7 and A5 noradrenergic cell groups, see Chapter 14.

RAPHE NUCLEI

Raphe Obscurus and Magnus Nuclei

The raphe nuclei are described comprehensively in Chapter 13. The raphe obscurus (ROb) possesses AChE-positive cells and dendrites which form two paramedian bands at the divided midline medial to the medial longitudinal fasciculus and the predorsal bundle (Figs. 10.2–10.10).

The raphe magnus (RMg) caps the medial lemniscus and is most prominent at the rostral pole of the inferior olive (Figs. 10.9–10.11). At this level the raphe (the midline) is wide and colonized by two parallel chains of pontine nuclei (pararaphales nucleus). Cells of RMg tend to be oriented mediolaterally. The RMg neuropil shows medium AChE reactivity and is interrupted by the AChE-negative fibers of the medial lemniscus. About half of the raphe magnus cells are positive for serotonin and it is possible that serotonin cells are also AChE positive. Approximately 30% of serotonin cells in RMg and ROb also contain substance P (Halliday *et al.*, 1988a). In the rat, serotonergic cells in the medullary nucleus raphe magnus RMg and adjacent nucleus reticularis magnocellularis Gi are likely involved in modulation of nociceptive transmission, whereas nonserotonergic cells may modulate stimulus-evoked arousal or alerting as well as spinal autonomic and motor circuits involved in thermoregulation and sexual function (Mason, 2001).

Median and Paramedian Raphe Nuclei

In the rat, Paxinos and Watson (1998) used the term median raphe (MnR) to describe the midline nucleus containing large cells that are predominantly serotonin positive. The MnR cells differ from the remaining cells in what was formerly called the central superior medial nucleus (the region between the tectospinal tracts) in terms of morphology, chemoarchilecture, and connectivity. Paxinos and Watson abandoned the term "central superior medial nucleus" because this nucleus actually encompasses two heterogeneous nuclei. Taking Mehler's suggestion, Paxinos and Watson (1998) introduced the term "paramedian raphe nucleus" (PMR) to refer to the more laterally located non-serotonin-positive cells, which are distinct from MnR (see their figures 48–51).

In the human, the distribution of serotonin-positive cells is much more extensive than that of the rat. However, many (but not all) lateral serotonin cells of the human morphologically resemble the remainder of the reticular formation cells and do not present a specific dendritic orientation. The serotonin cells of MnR are characterized by their lack of laterally oriented dendrites. In the rat, an intense AChE-positive zone separates MnR from PMR. In humans, a similar AChE-positive zone shepherds the large median raphe cells rostrally but is invaded by the larger midline cells caudally (Paxinos and Huang, 1995). The shepherding zone, as well as MnR and PMR, display bowed boundaries that collectively give this region the appearance of a barrel with staves.

The MnR is found dorsal and rostral to RTg in the rostral pons and isthmus (Figs. 10.16–10.19). Hornung in Chapter 13 observes that in a narrow sense the raphe pontis nucleus is, in fact, the caudal pole of MnR and proposes to abandon the term "raphe pontis nucleus" as referring to a region harboring serotonin neurons. Rostrally, MnR is limited by the decussation of the superior cerebellar peduncle. Dorsal to the decussation, the nucleus merges with the caudal linear nucleus.

Raphe Pontis Nucleus

Unlike other raphe nuclei, the cells of raphe pontis nucleus are not serotonin positive. Buettner-Ennever and Horn describe this cell group in detail in Chapter 19 of this book.

Dorsal Raphe Nucleus

The dorsal raphe nucleus shows extreme AChE reactivity in the neuropil of its wings (Figs. 10.13–10.22). The median strip of cells is associated with less reactivity in the neuropil; consequently the cells, which display medium reactivity, can be visualized. An autoadiography study showed that neurons of dorsal raphe are characterized by NPY mRNA expression (Pau *et al.*, 1998). Recently, Hurd and Fagergren (2000) reported strong human CART mRNA expression in the dorsal raphe, though it is not clear whether the message is in serotonin-containing cells.

VENTRAL MESENCEPHALIC TEGMENTUM AND SUBSTANTIA NIGRA

Chapter 14 gives a comprehensive pictorial representation of the mesencephalic dopamine groups on the basis of tyrosine hydroxylase immunoreactivity.

Caudal Linear Nucleus

The caudal linear nucleus (CLi) is more extensive in the human than in the rat (Figs. 10.20–10.22). In humans, it extends from the medial longitudinal fasciculus dorsally to the interfascicular nucleus ventrally. Caudally, it rides on the rostral aspect of the decussation of the superior cerebellar peduncle until it joins the rostral tip of MnR. Some CLi cells infiltrate the decussation of the superior cerebellar peduncle to mingle with the median raphe. The caudal linear nucleus consists of a median and two paramedian corridors of cells that are strikingly different in their chemoarchitecture. The median corridor is AChE negative and contains serotonergic neurons, while the lateral corridors are AChE positive and contain numerous tyrosine hydroxylase–positive cells. Paxinos and Huang (1995) named the unpaired midline corridor featuring the serotonin cells—the *azygos* part of CLi. This azygos part succeeds MnR (with which it is continuous through cell bridges blasting through the superior cerebellar peduncle). The AChE-positive catecholaminergic corridor is the *zygos* part of CLi. The paramedian clusters do not extend as far caudally as the median cluster; thus, it is only the median cluster that meets MnR. The CLi borders the rhomboid nucleus and is succeeded rostrally by the rostral linear nucleus at approxi mately the point of the caudal pole of the red nucleus.

Interfascicular Nucleus

The interfascicular nucleus (IF) straddles the interpeduncular nucleus. Laterally, the IF is in contact with the paranigral nucleus. In contrast to rats, cats, and monkeys, in which the IF is a median cluster, the human IF is small and consists of two paramedian clusters that are connected only by cell bridges (Halliday and Törk, 1986). Compared to other nuclei of the ventral mesencephalic tegmentum, it has significantly smaller cells (Halliday and Törk, 1986). Both the cells and the neuropil are densely AChE positive.

Rostral Linear Nucleus

The rostral linear nucleus (RLi) consists of scattered pigmented AChE-reactive cells within and dorsomedial to the superior cerebellar peduncle as the peduncle encapsulates the red nucleus (Figs. 10.23–10.25).

Retrorubral Fields

The dopamine-containing (tyrosine hydroxylase-positive) retrorubral fields are found caudal and dorsal to the caudal pole of the red nucleus, at the level where the third nerve forces its way through the red nucleus. In drawing the borders of the human retrorubral fields it may be useful to consider the map of the pigmented cells in the human brain stem presented by Mai *et al.* (1987).

Paranigral Nucleus

In contrast to the rat, the paranigral nucleus (PN) of humans is extremely AChE reactive and abuts not on the interpeduncular nucleus as in the rat but on the medial pole of the substantia nigra (Figs. 10.20 and 10.21).

Parabrachial Pigmented Nucleus

The parabrachial pigmented nucleus (PBP) occupies the space between the substantia nigra compact part and the red nucleus (Figs. 10.20–10.25). It is characterized by AChE-positive neurons and a neuropil of medium to dense reactivity.

Substantia Nigra

The substantia nigra (SN) displays intense AChE reactivity in the cell bodies and neuropil of its compact (SNC) and lateral (SNL) parts (Figs. 10.20–10.25). In places, SNC divides or envelopes the reticular part. The dopamine-containing neurons are AChE positive but are not cholinergic (Butcher and Talbot, 1978). The reticular part of SN is less reactive than the compact part. For a comprehensive description of SN, see Chapter 31.

Interpeduncular Nucleus

The interpeduncular nucleus (IP) (Figs. 10.20–10.24) displays an AChE-dense zone that straddles a core of medium reactivity. This pattern is not readily comparable to that shown in the rat. As in the rat, the fasciculus retroflexus in humans displays an AChE-dense core surrounded by an AChE-negative area.

CRANIAL MOTOR NUCLEI

Hypoglossal Nucleus

The hypoglossal nucleus (12N) (Figs. 10.1–10.5) is one of the most AChE-reactive nuclei in the staining of both cell bodies and neuropil. Its caudal representative is the ventrolateral division (12VL). This division possesses large AChE-positive neurons found within the fibrous zone ventrolateral to the central canal, at

the medial border of MRt (see above). As in the rat (Krammer *et al.*, 1979), the 12VL disappears as soon as the dorsal division develops. In the rat, the 12VL innervates the geniohyoid muscle (Krammer *et al.*, 1979). The ventromedial division of 12N is the largest, and in the rat it innervates the genioglossus muscle (Krammer *et al.*, 1979). We are not confident about the homology of the dorsal division because another subnucleus (potentially a laterally displaced dorsal division) appears in the human. In the rat, the dorsal division innervates the styloglossus and hyoglossus muscles. The nucleus of Roller accompanies the rostral third of the hypoglossal nucleus.

Facial Nucleus

The facial nerve nucleus (7N) abuts the rostral end of IRt and persists until the level of the exiting facial nerve (Figs.10.10 and 10.11). In humans, as in the rat, the 7N contains AChE-reactive cell bodies and neuropil. Subdivision of the 7N in the human (see Figs. 10.10 and 10.11) (Pearson, 1947; Paxinos and Huang, 1995) is in conflict with this in the monkey (Satoda *et al.*, 1987). The accessory 7N are intensely reactive for AChE. Surrounding the 7N is an AChE-positive zone which was named the perifacial zone in the human and the rat brain (Paxinos and Huang, 1995). For more information on the nucleus, see also Chapter 16.

Accessory Facial Nucleus

The caudal pole of the accessory facial nucleus (Acs7) appears dorsomedial to the caudal third of the 7N. It assumes a compact pyramidal shape at its rostral pole immediately medial to the exiting facial nerve (Fig.10.10).

Motor Trigeminal Nucleus

The caudal pole of the motor trigeminal nucleus (Mo5) is represented by the accessory trigeminal nucleus (Acs5) (Fig. 10.11) and appears medial to the exiting root of the facial nerve. It extends rostrally to the dense caudal pole of LC. The Mo5 is strongly reactive for AChE (cells and neuropil) and the reactivity extends into the cell-poor peritrigeminal zone (Paxinos and Huang, 1995) (Fig. 10.13).

Abducens Nucleus

The abducens nucleus (6N) is located caudal to the horizontal limb of the exiting facial nerve (Figs. 10.10 and 10.11). The 6 has prominent AChE-positive cells but its neuropil is only of medium intensity. Rostrally, it is separated from the more reactive VTg by the horizontal limb of the facial nerve root. The nucleus is also discussed in Chapter 16.

Trochlear Nucleus

The trochlear nucleus (4N) is found in an invagination of the medial longitudinal fasciculus near the level of the junction of the inferior and superior colliculi (Fig. 10.21). Its motoneurons are AChE positive but its neuropil is only moderately reactive. The 4N is separated from the rostrally lying oculomotor nucleus by a small cell-free space. The two nuclei can be distinguished by the fact that 4N is embedded in the fasciculus while the oculomotor nucleus is cradled in it. In addition, unlike 4N, scattered oculomotor nucleus cells infiltrate the fasciculus. For additional details about 4N, see Chapter 16.

At the caudal pole of the trochlear nerve the midline between the two medial longitudinal fasciculi features a dense AChE segment (Paxinos *et al.*, 1990). This may correspond to the parvicellular "compact interfascicular nucleus" (CIF) of Olszewski and Baxter (1954).

Oculomotor Nucleus

Olszewski and Baxter (1954) report that the oculomotor nucleus (Figs. 10.22 and 10.23) is approximately 5 mm long. It extends from the trochlear nucleus to the unpaired anterior portion of the nucleus of Edinger–Westphal (Fig. 10.23). The caudal pole of the oculomotor nucleus is more reactive for AChE than the trochlear nucleus. The nucleus of Edinger–Westphal is reactive for AChE in both its cells and neuropil (Figs. 10.23 and 10.24).

SOMATOSENSORY SYSTEM

Gracile Nucleus

At the level of the pyramidal decussation, the tapering caudal pole of the gracile nucleus (Gr) appears as small clusters of AChE-positive cell bodies. Rostrally, the main body of Gr appears with the characteristic patches of AChE reactivity corresponding to clusters of cells separated by AChE-negative myelinated fibers (see Chapter 24). The Gr persists almost to the rostral pole of the area postrema (Figs. 10.1–10.3).

Cuneate Nucleus

The cuneate nucleus (Cu) first appears at midlevels of the pyramidal decussation (Fig. 10.3) and extends to

the rostral pole of the area postrema (Fig. 10.4). The Cu displays patches of AChE reactivity similar to those of Gr but of higher intensity. Attached to the borders of some compact bundles of the cuneate fasciculus are clusters of large cells that are well stained for Nissl (density near the brain surface on the border with the gracile nucleus in Fig. 10.4). The neuropil of these clusters is extremely reactive for AChE. It seems to correspond to the area reported to contain substance P fibers by Del Fiacco *et al.* (1984).

External Cuneate Nucleus

Unlike other species, the human external cuneate nucleus (ECu) occupies a greater area of the medulla than Cu or Gr (Figs. 10.1–10.6). It features large cells heavily stained for AChE on a pale background. It expands at the level of the obex and becomes the largest of the dorsal column nuclei rostral to the obex (Fig. 10.5). At its rostral pole it narrows and is found between the mediodorsal aspect of the inferior cerebellar peduncle, the spinal vestibular nucleus, and the spinal trigeminal nucleus. It terminates short of the rostral pole of 12 (Fig. 10.6).

Pericuneate, Peritrigeminal, X, and Paratrigeminal Nuclei

Medial Pericuneate Nucleus

At the level of the obex, a narrow zone of pale AChE reactivity appears in the neuropil ventral to the dorsal column nuclei (Figs. 10.2–10.4). Paxinos and colleagues (1990) named this zone the "medial pericuneate nucleus." This basal zone features small, medium, and occasionally large neurons that are AChE positive. The most medial part of this zone interposes itself between EC, solitary, and interpolar spinal trigeminal nuclei. This medial (basal) pericuneate zone (MPCu) was included in Cu by Olszewski and Baxter (1954), even though it can be seen in their photomicrographs to be separate from Cu proper and possess smaller cells (their plates 10 and 11). At levels caudal to the obex, cells in MPCu are diffuse and smaller. Rostral to the level of the area postrema (about 1 mm from the obex) these cells increase in number and become more heterogeneous in size and shape. At one point, MPCu cells appear as a triangular mass that merges rostrally with large, rounder cell clusters (Figs. 10.5 and 10.6). A comparable cell cluster is shown by Olszewki and Baxter in their plates 12 and 13, lateral to the solitary nucleus and medial to the spinal trigeminal nucleus. In AChE-stained sections, other small AChE-positive cells extend into the pale neuropil capping the oral pole of Cu (Fig. 10.5). This basal MPCu is coextensive in length with 12. There is no basal region ventral to the gracile nucleus, except for a few clusters at its oral pole.

Lateral Pericuneate Nucleus

Lateral and ventrolateral to the external cuneate nucleus there are variably shaped aggregates of chiefly large AChE-positive neurons intercalated in the medial edge of the inferior cerebellar peduncle. The most prominent group of these cells frequently forms a wedge separating the cervical dorsal roots surrounding ECu from the dorsal part of Sp5. This chain of cells extends from the level of the obex to the oral pole of ECu (Fig. 10.6), equivalent in length to the hypoglossal cell column. This cell group was described by Ziehen (1934) as the "promontorium" (Latin, "to jut out") and was considered part of the insular nuclei of ECu by Olszewski and Baxter (1954, their plate 10). This nucleus has been confused with nucleus X (described below). Paxinos and colleagues (1990) have called it the "lateral pericuneate nucleus"). Both LPCu and MPCu were identified as separate but related entities by Braak (1971). Braak adopted Ziehen's (1934) term "promontorium" for the lateral group and coined the term "repagulum cuneati" (Greek, *pagus,* "something fixed or fastened together") for the medial group of cells basal to Cu.

Peritrigeminal Nucleus

The peritrigeminal nucleus (Pe5) is in places continuous with LPCu and is found lateral, ventral, and medial to Sp5. Caudally, it commences at the level of the caudal pole of the dorsal accessory olive (Fig. 10.2) and extends to the rostral pole of 12. Olszewski and Baxter (1954) included the lateral segment of Pe5 in their insula cuneati lateralis (their plate 10). The ventral part of Pe5 is usually found between Sp5 and the subtrigeminal LRt. At times, however, it is found ventral or lateral to the subtrigeminal nucleus. A ventromedial cluster that receives anteroventral quadrant fibers has been labeled the paravagal nucleus by Braak (1971) (small-celled nucleus between the labels Amb and IRt). The Pe5 has a medial extension that intercedes between Sp5 and the LRt.

Afferent Connections of the Pericuneate and Peritrigeminal Nuclei

In experimental animals, the pericuneate and Pe5 receive ascending anterolateral spinal quadrant fiber connections (via the inferior cerebellar peduncle) and do not receive dorsal root primary fibers (Mehler, 1969). Nucleus X and the paratrigeminal nucleus (Pa5) project to the cerebellum (Mehler, 1977; Somana and Walberg, 1979). The MPCu cells may receive afferents from the same ascending fiber system that projects to LPCu. Cervical dorsal root connections to the pericuneate

cells cannot be ruled out. Cortical input to the basal dorsal funicular nuclear region has been verified in humans (Kuypers, 1960); rubrobulbar connections with the region have also been described (Holstege and Tan, 1988). The MPCu cells are believed to have connections with the overlying dorsal column nuclei that function as an intermediate zone (Kuypers and Turek, 1964). Differential studies of retrograde cell labeling, following HRP injections into the ventral posterior lateral thalamic nucleus, demonstrated that many cells in the medial basal pericuneate zone (PCu) that convey tactile information also project to the thalamus through the medial lemniscus with gracile and cuneate axons. However, Ostapoff *et al*. (1988) have concluded that what might be the homologues of the PCu cells in the racoon relay deep subcutaneous kinesthetic sensations ending chiefly in the ventral intermediate (Vim)–like shell region rostral to the tactile thalamic nucleus. They also confirmed that the caudally situated cells of subgroup X project to the cerebellum, but cells that they identified as rostrally situated subgroup X, like nucleus Z, also project to the thalamic shell region.

In animal experiments, cells capping the oral pole of Cu project to the cerebellum and do not join the medial lemniscus (Mehler, 1977). Vestibular group F–like cells (FVe) intercalated in the ventral caudal pole of the spinal vestibular nucleus (SpVe) give rise to a third vestibulospinal pathway (see review by Mehler and Rubertone, 1986). The ascending spinal fibers that delineate both the lateral X group and the medial basal dorsal column nuclei also appear to make connections with group F–like cells at this level of transition between the oral pole of the cuneate nuclei and the caudal pole of the vestibular nuclei.

Nucleus X

Sadjadpour and Brodal (1968) identified nucleus X as a cell group related to the dorsal boundary of SpVe, extending from the rostral level of ECu to the caudal level of the dorsal cochlear nucleus. They describe nucleus X as a small triangular area just medial to the inferior cerebellar peduncle, featuring small, lightly stained cells. Paxinos and Watson identified nucleus X in *The Rat Brain in Stereotaxic Coordinates* (Paxinos and Watson, 1998) as the AChE-reactive rostral continuation of ECu. We observed a similar AChE-reactive cluster of small cells in the position described by Sadjadpour and Brodal. Larger cells invade or form a boundary around nucleus X and these cells may belong to SpVe (Sadjadpour and Brodal, 1968). We believe that the ventral part (between the spinal vestibular nucleus and the inferior cerebellar peduncle) is different from SpVe, but we have not grouped it with nucleus X because of the larger cells of this area and its poorer AChE reactivity. Nucleus X can be confused with the insulae cuneati lateralis of Olszewski and Baxter (our lateral pericuneate nucleus). If we accept Sadjadpour and Brodal's view, nucleus X is unlikely to extend this far ventrally (Fig. 10.7). In addition, LPCu has large cells whereas nucleus X, according to Sadjadpour and Brodal, has small cells.

Paratrigeminal Nucleus

In the rat, the paratrigeminal nucleus (Pa5) forms a crescent between the spinocerebellar tract and the spinal tract of the trigeminal, usually invading the latter. The Pa5 of the rat features small cells and is characterized by light AChE and dense substance P reactivity. Some of its cells are substance P positive (Chan-Palay, 1978a, b). While we accept Chan-Palay's definition of this nucleus in the rat, we disagree with her on the human homologue of the Pa5. She considers the insulae cuneati lateralis of Olszewski and Baxter to be the Pa5 of the human. Paxinos and colleagues (1990) have grouped the dorsal insula cuneati lateralis with LPCu and the ventral insula with the peritrigeminal zone. They suggested that the human Pa5 may be, in fact, a string of cells contained primarily within the spinal tract and based their parcellation on the basis that the Pa5 of the rat has small cells in agreement with the parvicellular clusters within the human spinal tract and in contradistinction to the lateral pericuneate zone, which has large cells. An inconsistency in the homology is that the AChE reactivity of the proposed Pa5 of the human is lower than that displayed in the rat.

Spinal Trigeminal Nucleus

The caudal spinal trigeminal nucleus (Sp5) is characterized by strong AChE reactivity in the superficial layers, including the substantia gelatinosa (Figs. 10.1 and 10.2). The marginal zone of the caudal part of Sp5 can be distinguished because it is less AChE reactive than the gelatinous nucleus but more than the spinal tract. Some AChE-reactive cells are found totally within the cuneate fasciculus, yet strong AChE reactivity suggests that they most likely belong to the gelatinous part of the caudal Sp5 rather then to the cuneate system. Also, a recent study revealed NPY mRNA expression within the nucleus (Pau *et al.*, 1998).

The oral Sp5 (Sp5O) has a concentric pattern of AChE reactivity with an extremely AChE dense core (Figs. 10.10 and 10.11). It is succeeded rostrally by the less reactive principal sensory nucleus of the trigeminal nerve. In the principal sensory trigeminal nucleus the AChE reactivity is distributed in small patches adulterated by negative areas.

In the principal sensory trigeminal nucleus the AChE reactivity is distributed in small patches adul-

terated by negative areas. The interpolar nucleus (Sp5I) (Figs. 10.3–10.9) displays moderate AChE reactivity, although there are occasional extremely intense patches that correspond to parvicellular regions. In the ventral part of the nucleus a rodlike structure appears (circular in cross-section), featuring small compact neurones and extremely AChE-dense neuropil. No such structure appears in the rat. Both Sp5O and Sp5I are reported to contain significant number of somatostatin receptors as revealed by somatostatin binding sites (Carpentier *et al.*, 1996).

Mesencephalic Trigeminal Nucleus

The mesencephalic nucleus of the trigeminal nerve (Me5) features prominent AChE-reactive cells and, as in the rat, its cells and axons form a thin sheet that circumscribes the cylindrically shaped periaqueductal PAG from LC almost to the level of the posterior commissure (Figs. 10.12–10.24).

Endolemniscal Nucleus

At caudal medullary levels, long islands of cells strongly reactive for AChE separate dense fascicles of the medial lemniscus. The islands appear just rostral to the caudal pole of the principal nucleus of the inferior olive. Caudally, they are wholly confined within the medial lemniscus. However, rostrally they unite and flank the lateral side of the medial lemniscus. These cell groups resemble the medial accessory olive but are clearly more medial to it. Given their position, Paxinos *et al.* (1990) called them the "endolemniscal nucleus".

B9 and Supralemniscal Nucleus

The B9 is identified as a group of serotonergic cells lying above the medial lemniscus. This cell group also contains a region of extremely strong AChE reactivity that is distinguished as the supralemniscal nucleus (Fig. 10.16).

VESTIBULAR NUCLEI

Medial Vestibular Nucleus

The medial vestibular nucleus (MVe) succeeds the gracile nucleus rostrally at the level at which the gelatinous solitary nucleus is most prominent and persists rostrally to the level of the abducens nucleus (Figs. 10.5–10.10). It has a mottled appearance in AChE. Caudally, embedded in the medial part of MVe, are two clusters of larger cells, the neuropil of which stains strongly for AChE (Fig. 10.5). It is important to point out that a group of large neurons positioned ventrally and medially to the main body of MVe is currently considered to be part of the medial rather then lateral vestibular nucleus, as it was previously thought.

Spinal Vestibular Nucleus

The spinal vestibular nucleus (SpVe) overlaps the rostral pole of the external cuneate and subsequently replaces it (Figs. 10.5–10.9). It is rectangular in cross-section and is located dorsolateral to the solitary and spinal trigeminal nuclei. The SpVe is also characterized by the passage of the lateral vestibulospinal tract which, being AChE negative, contrasts with the medium density of the neuropil of the SpVe. Distribution of somatostatin binding revealed that both MVe and SpVe contain numerous somatostatin receptors (Carpentier *et al.*, 1996). The area above the spinal and dorsal vestibular nucleus is identified as the paravestibular nucleus. Nucleus Y is allocated an area above the inferior cerebellar peduncle prior to ascendance of the peduncle to the cerebellum.

Lateral Vestibular Nucleus

The lateral vestibular nucleus (LVe) replaces SpVe rostrally (Figs. 10.9 and 10.10). It displays large AChE-positive cells and has lighter neuropil than the rest of the vestibular nuclei. The superior vestibular nucleus is not optimally displayed in our plates.

Interstitial Nucleus of the Eighth Nerve

The eighth nerve is AChE negative but its interstitial nucleus displays AChE-positive cell bodies and neuropil.

Nucleus of Origin of Vestibular Efferents

The nucleus of origin of vestibular efferents is a human homologue of the paragenual nucleus of the rat, which was first identified in proximity of the genu of the seventh nerve by Paxinos and Watson (1998) and later by Swanson (1992). In the human, as in the rat, the nucleus is distinguished as a group of AChE-positive neurons riding on top of the horizontal limb of the root of the seventh nerve.

AUDITORY SYSTEM

Ventral Cochlear Nucleus

The ventral cochlear nucleus (VC) displays AChE-positive cell bodies against a light neuropil. It can be

distinguished from the pontobulbar nucleus, which is located more medially and which displays high AChE reactivity in its neuropil. The VC also features a cap that is slightly reactive in the neuropil. The dorsal cochlear nucleus is more reactive in AChE preparations than VC. At the same time the superficial glial zone of the nucleus is less AChE reactive then the nucleus itself.

Superior Olive

The superior olive (SO) is the AChE-poor area rostroventral to the facial nucleus (Figs. 10.10 and 10.11). The most conspicuous feature of SO in Nissl preparations is the medial superior olive (MSO). It consists of medium-sized, slightly AChE-positive cells and is surrounded by AChE-positive vascular elements that are themselves encircled by an AChE-negative zone. The lateral superior olive is extremely negative in AChE preparation but features some moderately stained capillaries. A conspicuous characteristic of the lateral superior olive is its significantly greater size relative to the size of the entire superior olive nucleus in the rat or the mouse.

The periolivary nuclei surround SO. The dorsal periolivary nucleus is the most AChE-reactive structure in the SO complex (Fig. 10.11). The position of the dorsal periolivary nucleus is betrayed by MSO, which points directly to it. The dorsal periolivary nucleus probably contains the bulk of the cells that provide the cochlear efferents. The human homologues of the mediocentral and lateroventral periolivary nuclei are AChE positive.

The human homologue of the superior paraolivary nucleus remains an enigma. In the rat, this nucleus is contiguous with MSO. In the human at this position, we noticed a vertically oriented stream of cells. These cells are medium sized and AChE positive, but do not display the dense AChE neuropil that characterizes the dorsal periolivary nucleus. Judging from the maps of retrogradely labeled cells following HRP injections into the cat cochlea, these cells may also belong to the cholinergic efferent projection. For a comprehensive account of the human auditory system and superior olive, see Chapter 34.

Trapezoid Nucleus

Identification of the human homologue to the trapezoid nucleus (Tz) has been elusive (Chapter 27). Stromberg and Hurwitz (1976) and Richter *et al.* (1983) suggested tentatively that an attenuated homolog of Tz in the human at the level of the exiting trochlear nerves. Indeed, Paxinos and colleagues (1990) found Tz at the level of the exiting sixth nerve in the shape of a golf club, with most of its cells underlying the central tegmental tract and bordering the medioventral periolivary nucleus. The cells of Tz are large, with weak AChE reactivity, and are found among the caudal crossing fibers of the trapezoid body (Figs. 10.11 and 10.12). It has been pointed out by Paxinos and colleagues (1990) that Tz in the human is much less cellular than in the rat.

Nuclei of the Lateral Lemniscus

The ventral nucleus of the lateral lemniscus (VLL) succeeds SO rostrally (Figs. 10.17 and 10.18). The VLL can be distinguished from SO by its slightly larger cells and by the fact that the cell group, after tapering to an elongated rostral pole, becomes larger and more cellular. In addition, the cells of the VLL are slightly more AChE reactive than those of SO. The VLL commences at the level of the oral pole of the motor nucleus of the trigeminal. The nuclei of the lateral lemniscus reach the caudal pole of the pedunculopontine tegmental nucleus. For a quantification of the human nuclei of the lateral lemniscus, see Ferraro and Minckler (1977).

Inferior Colliculus

As in the rat (Paxinos and Watson, 1998), the inferior colliculus (IC) of the human displays light AChE reactivity that features slightly denser patches, especially in the external cortex (ECIC) (Figs. 10.19–10.22). In the central nucleus of IC, blood vessels are visible as wavy lines of some AChE positivity. For more details regarding IC, see Chapter 34.

Nucleus of the Brachium of the Inferior Colliculus

The nucleus of the brachium of the inferior colliculus (BIC) (Figs. 10.21–10.23) shows pale AChE reactivity but is recognizable because the surrounding dorsolateral tegmentum is AChE negative. Rostrally, the subbrachial nucleus is found beneath the BIC.

Medial Geniculate

The medial geniculate (MG) displays weak and blotchy AChE reactivity (Figs. 10.22–10.25). By homology with the monkey (Pandya *et al.*, 1994), Paxinos and Huang (1995) recognized the AChE-negative ventral and the AChE-positive medial subnuclei of MG, as well as the strongly AChE-reactive and large-celled suprageniculate nucleus.

VISUAL SYSTEM

The visual system is covered in detail in Chapter 35 of this book, but some elements of the visual pathways represent integral structural parts of the brain stem and as such are presented in this chapter.

Superior Colliculus

Laemle (1983) has provided a Golgi analysis of the human superior colliculus (SC). Morphologically, SC can be divided into (1) a superficial division consisting of the zonal, superficial, and optic layers; (2) an intermediate division consisting of the intermediate gray and white layers, and (3) a deep division consisting of the deep gray and deep white layers (Figs. 10.22–10.25). The AChE reactivity of the human SC resembles that of the rat. The superficial gray layer is the most intensely reactive. The zonal layer is also reactive except for its most superficial strip. The optic nerve layer shows less reactivity than that of the surrounding superficial and intermediate gray layers and is, as a result, cospicuous. The intermediate gray and white layers show intense reactivity. The intermediate white layer displays periodic patches of AChE reactivity as observed in the rat (Paxinos and Watson, 1998). Lattices of high cytochrome oxidase or succinate dehydrogenase activity have been observed in the human SC (Wallace, 1988). The anterior pretectal area is densely reactive for AChE and so is the subadjacent parafascicular nucleus. A number of enigmatic patches of AChE reactivity appear below SC.

Parabigeminal Nucleus

The parabigeminal nucleus (PBG), while somewhat inconspicuous in Nissl preparations, is all too evident in AChE-stained sections (Figs. 10.20 and 10.21). It is present in the region at which the compact pedunculopontine tegmental nucleus achieves its greatest size.

Medial Terminal Nucleus of the Accessory Optic Tract

The existence of the medial terminal nucleus (MT) of the accessory optic tract is ambiguous in humans. On the basis of observations on the monkey, Fredericks *et al*. (1988) proposed that MT should be present in the human at a position transversed by the lateral rootlets of the oculomotor nerve. MT is an AChE-negative area (as in the rat) transversed by the most rostrally exiting oculomotor fibers.

Alar Interstitial Nucleus

At the caudal pole of LC, fibers from the vestibular nuclei travel rostromedially to gather in the medial longitudinal fasciculus proper (mlf). In these wings of the mlf is found an AChE-reactive nucleus with medium-sized cells. Paxinos *et al*. (1990) called this nucleus the alar interstitial nucleus of the mlf (AIl). It appears rostral to the rostral pole of the ventral tegmental nucleus and is approximately 1.5 mm in length (Fig. 10.14).

The alar interstitial nucleus is succeeded rostrally by the more medially placed interstitial nucleus of Cajal (see Buttner-Ennever and Horn, Chapter 19 of this book), AchE reactive cells and neuoropil wholly embedded in the mlf proper (Fig. 10.15). It is found at levels caudal to the dorsal tegmental nucleus.

PRECEREBELLAR NUCLEI AND RED NUCLEUS

Chapter 11 of this book includes a comprehensive description of the cytoarchitecture and connectivity of the precerebellar nuclei.

Inferior Olive

Medial Accessory Olive

AChE is differentially distributed in the medial accessory olive. The lateral part of the medial accessory olive (IOA) displays some of the densest AChE reactivity found in the medulla (Figs. 10.1–10.3). Both the neuropil and the cell bodies are densely reactive. IOA is the group that appears at the caudal pole of the olive and, rostrally, greatly outdistances the other nuclei of the medial accessory olive. Subnucleus B is slightly less reactive (Fig. 10.4). Subnucleus C is less densely stained in the neuropil and the cell bodies are clearly visible. In this respect, it resembles the beta nucleus that it borders.

Beta Nucleus

The beta nucleus (IOB) in the cat stains poorly for AChE and is confined to the caudal one-third of the olive (Marani *et al*., 1977). In the monkey, IOB disappears prior to the full development of the principal nucleus (Brodal and Brodal, 1981). In our human material, IOB appears as one of the caudal representatives of the olive but vanishes well before the appearance of the rostral division of the dorsal accessory olive (Figs. 10.2 and 10.3).

Dorsomedial Cell Column

The dorsomedial cell column (IODM) is best described as a dorsomedial satellite of IOA in the rostral part of the latter (Figs. 10.6–10.8). The IODM is small and usually ovoid; it is depicted in the monkey by Brodal and Brodal (1981; in their figure 1) and in the cat by Marani *et al.* (1997, in their figure 4A).

Ventrolateral Outgrowth

The ventrolateral outgrowth (IOVL) is actually the nuclei "g" and "h" of Olszewski and Baxter (1954) and of Braak (1970). The alternative term is consistent with the nomenclature now commonly used in studies with monkeys (Bowman and Sladek, 1973; Brodal and Brodal, 1981), cats (Marani *et al.*, 1977), and rats (Paxinos and Watson, 1998). The ventrolateral outgrowth is serpentine in the transverse plane, with its head (nucleus h) pointing dorsomedially (Fig. 10.3). It commences slightly more caudally than IODM and ends considerably short of the rostral pole of IODM. It is parallel to the IOA and interposes itself between IOA and IOPr.

Cap of Kooy

The cap of Kooy (IOK) is present at the caudal pole of the olive and represents the most dorsal extension of the complex at that level. It shows moderate AChE reactivity (Figs. 10.1–10.3).

Dorsal Accessory Olive

Olszewski and Baxter (1954) and Braak (1970) included in the dorsal accessory olive (IOD) two heterogeneous and discontinuous groups of cells. Paxinos and colleagues (1990) reserved the name IOD for the larger eyebrow-shaped rostral part that caps the dorsomedial aspects of the principal olive. This part persists until the frontal pole of the olive, where it has the shape of a comma (Figs. 10.4–10.9). The smaller, caudal subnucleus of the IOD (IODC) is rod shaped (round in cross-section) and, compared with IOD proper, has denser AChE reactivity and features smaller cells. The IODC commences prior to the principal nucleus and continues until the epiolivary lateral reticular nucleus becomes very prominent, at which point it briefly attains a horizontally oriented spindle shape (Figs. 10.2 and 10.3). It is succeeded rostrally by the IOD after a small hiatus. Paxinos and colleagues (1990) called the posterior part "caudal dorsal accessory olive." The inferior olive, including the caudal dorsal accessory olive, was excellently displayed by Kooy (1916).

Principal Olive

The principle subnucleus (IOPr) shows homogeneous medium staining for AChE neuropil and cell bodies (Figs. 10.3–10.9).

Conterminal Nucleus

The conterminal nucleus (Ct) is located on the lateral surface of the amiculum of the olive and displays intense AChE reactivity in cell bodies and neuropil (Figs. 10.2–10.7).

Arcuate Nucleus

The arcuate nucleus (Ar) appears on the anterior surface of the medulla, extending dorsally at the midline and partly surrounding the pyramid (Fig. 10.4). The Ar reacts densely for AChE, as do the pontine nuclei of which it is presumed to be a displaced kin (Mikhail and Ahmed, 1975; Olszewski and Baxter, 1954). A recent pathology study found that sudden infant death syndrome is associated with high-frequency hypoplasia, characterized by a volume reduction and neuronal depletion of Ar (Matturri *et al.*, 2002).

Paramedian and Dorsal Paramedian Nuclei

Brodal and Gogstad's (1957) paramedian groups correspond to the clusters of AChE-positive cells and neuropil seen within the predorsal bundle at the rostral pole of the hypoglossal nucleus. Olszewski and Baxter's dorsal paramedian groups resemble the pontine nuclei in cytoarchitecture and AChE reactivity. The caudal dorsal paramedian (CDPMn) is distinguishable from the subadjacent 12, which is extremely AChE reactive. The CDPMn is most prominent at the rostral pole of the 12 (Figs. 10.7 and 10.8). The CDPMn is succeeded rostrally by its oral companion (ODPMn).

Intercalated Nucleus

The intercalated nucleus (In) commences caudal to the obex and persists until the rostral pole of the hypoglossal nucleus, where it is succeeded by the prepositus hypoglossal nucleus. The intercalated nucleus displays medium AChE reactivity, and some positive cells can be detected through the neuropil. It starts as a narrow wedge between the 12 and the 10 but expands rostrally to fill the vacuum created by the lateral migration of the 10 (Figs. 10.1–10.6). Although In is characterized by small cells, at its rostral pole a dense cluster of larger cells appears at the border with 10. These cells are probably the ones that react for tyrosine hydroxylase (see Chapter 31).

Prepositus Hypoglossal and Interpositus Nuclei

The prepositus hypoglossal nucleus (Pr) succeeds the intercalated nucleus rostrally and displays a light AChE core surrounded by a region of greater reactivity (Figs. 10.7–10.9). A distinct cluster of large cells well stained for Nissl is found in the ventromedial tip of the Pr. The Pr is bordered medially by the oral dorsal paramedian and laterally by the interpositus nucleus (IPo) (Figs. 10.7–10.9). Rostrally, Pr is succeeded by the AChE-dense region found immediately caudal and medial to the abducens nucleus. This AChE-positive region may correspond to the pontine paramedian reticular nucleus involved in horizontal gaze. Dorsal to the 10, Olszewski and Baxter outlined IPo to separate Pr from the medial vestibular nucleus. Dorsal and rostral to the oral pole of Pr the supragenicular nucleus can be detected by medium AChE reactivity.

Cribriform Nucleus

The cribriform nucleus (Crb) was identified by Paxinos and Huang (1995) as the area lateral to the solitary nucleus and medial to the dorsal column nuclei and spinal vestibular nucleus. This area is generally AChE positive while characteristically perforated by AChE-negative fibers (Fig. 10.6).

Pontine Nuclei

The pontine nuclei (Pn) attain their maximal relative size in the human, nearly throttling the dorsal pontine tegmentum. Their outposts are distinguishable by the intense AChE reactivity of cell bodies and neuropil. As in other species, their main mass is found below the medial lemniscus. However, in the human, unlike the rat, there are pontine-like nuclei encircling and bisecting the rostral medulla. The pontobulbar nucleus (PnB) lies outside the inferior cerebellar peduncle and appears caudally at the rostral pole of the external cuneate nucleus, presenting a triangular profile at this level (Fig. 10.6). At more rostral levels, the pontobulbar nucleus spreads to engulf this peduncle laterally and ventrally. Further rostrally, it is broken up into large islands in the ventrolateral aspects of the medulla (Figs. 10.7–10.9). These islands are intermingled with the vestibular division of the vestibulocochlear nerve. The nuclei pararaphales constitute two paramedian chains of islands of pontine-like cells that bisect the medulla at rostral levels (Figs. 10.7–10.9) (see also Olszewski and Baxter, 1954).

The reticular tegmental nucleus (RtTg) is located above the medial lemniscus. It is found immediately rostral to the exiting sixth nerve and it is replaced by MnR rostrally (Figs. 10.11–10.16). The nucleus consists of many scattered tight clusters of cells usually engulfed in AChE-reactive neuropil. Some cell clusters are associated with weak reactivity, though the cell bodies are positive. The cells are distinguishable from those of the pontine nuclei because they are larger and stain more intensely in Nissl preparations.

Olszewski and Baxter (1954) recognized a "processus grisium pontis supralemniscalis." The AChE reactivity in the lateral part of this nucleus is extreme and thus similar to that of the pontine nuclei. However, the AChE reactivity of the medial part is light, resembling some of the lighter clusters of RtTg. The two parts of the processus grisium pontis supralemniscalis are often separated by fiber bundles. Olszewski and Baxter depicted more densely stained and larger cells in the lateral part. For the above reasons, Paxinos and colleagues (1990) allocated the medial part to RtTg and retained "processus grisium pontis supralemniscalis" only for the lateral part.

Red Nucleus

The red nucleus is found at the level of the substantia nigra as a sphere encapsulated within the ascending superior cerebellar peduncle (Figs. 10.22–10.25). Unlike the rat, the magnocellular part of the red nucleus is relatively small in the human, occupying only the caudal pole (Fig. 10.22) (Wollard, 1927, cited by Jerath. 1964). A number of large cells in this region, however, are pigmented and therefore must be ectopically placed cells of the parabrachial pigmented nucleus, of the mesencephalic reticular formation, or of the caudal linear nucleus. At rostral levels, the fasciculus retroflexus penetrates the red nucleus, separating a dorsomedial portion. The dorsomedial portion displays higher AChE reactivity. Recent immunohistochemical studies revealed the presence of parkin (Parkinson disease related protein) (Zarate-Lagunes *et al.*, 2001), somatostatin receptors sst (4) (Selmer *et al.*, 2000), as well as P2Y(1) purinergic receptor (Moore *et al.*, 2000) in the red nucleus of the human. The nucleus is relatively big and current resolution of MRI and PET scans allows depiction of the red nucleus in the brain of the conscious human. For the connections of the red nucleus, see Voogd, Chapter 11.

CONCLUSION

This overview presents a comprehensive classification of the human brain stem structures which include most of neuronal cell groups in the human brain stem.

The most significant conclusion of this overview is a glaring structural similarity of brain stem across species reflected by an impressive number of homologies recognised between the brain stem of the human and that of other animals. While it can be hypothesised that there are human homologues to nearly every nucleus identified in the rat brain stem, species differences and even strain differences occur, and this compels us to establish homologies not by extrapolation but by direct observation of human tissue.

Then again, this overview presents a comprehensive classification of the human brain stem structures which are, at this time, best characterised by trivial structural similarity to corresponding homologues in the brain stem of experimental animals. Functional mechanisms of the human brain stem, on the other hand, remain hidden in connections, chemoarchitecture and physiology of neuronal groups. These characteristics are emerging from encouraging noninvasive imaging studies and expanding creative application of chemical analysis of the human brain. At that, a comparative structural plan of the brain stem forms an excellent fundament to interpret, convey, and compare these findings.

References

Allien, A. M., McKinley, M. J., Paxinos, G., Oldfield, B. L., and Mendelsohn, E A. O. (1991). Angiotensin II receptors in the human nervous system. *In* G. Paxinos and E A. O. Mendelsohn (Eds.). "Receptors in the Human Nervous Systern." Academic Press, San Diego. (in press).

Allien, A. M., Siew, Y. C., Clevers, J., McKinley, M. L, Paxinos, G., and Mendelsohn, E A. O. (1988). Localization and characterization of angiotensin II receptor binding and angiotensin converting enzyme in the human medulla obliongata. *J. Comp. Neurol.* **269,** 249–M4.

Arango, V., Ruggiero, D. A., Callaway, J. L., Anwar, M., Reis, D. L., and Mann, J. J. (1988). Catecholamine neurons in the ventrolateral medulla and nucleus of the solitary tract in the human. *J. Comp. Neurol.* **273,** 224–240.

Benarroch, E. E., and Schmeichel, A. M. (1998). Immunohistochemical localization of the angiotensin II type 1 receptor in human hypothalamus and brain stem. *Brain Res.* **812,** 292–296.

Benarroch, E. E., Smithson, I. L., Low, P. A., and Parisi, J. E. (1998). Depletion of catecholaminergic neurons of the rostral ventrolateral medulla in multiple systems atrophy with autonomic failure. *Ann. Neurol.* **43,** 149–151.

Benarroch, E. E., Smithson, I. L., and Low, P. A. (1995). Localization and possible interactions of catecholamine- and NADPH-diaphorase neurons in human medullary autonomic regions. *Brain Res.* **684,** 215–220.

Benarroch, E. E., and Smithson, I. L. (1997). Distribution and relationships of neuropeptide Y and NADPH-diaphorase in human ventrolateral medulla oblongata. *J. Auton. Nerv. Syst.* **62,** 143–146.

Berman, A. L. (1968). "The Brain stem of the Cat: A Cytoarchitectonic Atlas with Stereotaxic Coordinates." University of Wisconsin Press, Madison.

Bogerts, B. (1981). A brain stem atlas of catecholamine neurons in man using melanin as a natural marker. *J. Comp. Neurol.* **197,** 63–80.

Bowman, J. P., and Sladek, J. R. (1973). Morphology of the inferior olivary complex of the rhesus monkey *(Macaca mulatta). J. Comp. Neurol.* **152,** 299–316.

Braak, H. (1970). Uber die kerngebiete des menschlichen hirnstammes. I. Oliva inferior, *Nucleus conterminalis* und *Nucleus vermigormis Corporis restiformis. Z. Zellforsch. Mikrosk. Anat.* **105,** 442–456.

Braak, H. (1971). Uber die kerngebiete des menschlichen hirnstammes. IV. Der *Nucleus reticularis lateralis* und seine satelliten. *Z. Zellforsch. Mikrosk. Anat.* **122,** 145–159.

Brodal, A., and Gogstad, A. C. (1957). Afferent connections of the paramedian reticular nucleus of the medulla oblongata in the cat. An experimental study. *Acta Anat.* **30,** 133–151.

Brodal, P., and Brodal, A. (1981). The olivocerebellar projection in the monkey. Experimental studies with the method of retrograde tracing of horseradish peroxidase. *J. Comp. Neurol.* **239,** 163–175.

Bruce, A. (1898). On the dorsal or so-called sensory nucleus of the glossopharyngeal nerve and on the nuclei of the trigeminal nerve. *Brain* **21,** 383–387.

Butcher, L. L., and Talbot, K. (1978). Acetylcholinesterase in rat nigra–neostriatal neurons: experimental verification and evidence for cholinergic–dopaminergic interactions in the substantia nigra and caudate-putamen complex. *In* "Cholinergic–Monoaminergic Interactions in the Brain" (L. L. Butcher, ed.), pp. 25–95. Academic Press, New York.

Buttner-Ennever, J. A., Buttner, U., Cohen, B., and Baurngartner, G. (1982). Vertical gaze paralysis and the rostral interstitial nucleus of the medial longitudinal fasciculus. *Brain* **105,** 125–149.

Buttner-Ennever, J. A., and Buttner, U. (1978). A cell group associated with vertical eye movements in the rostral mesencephalic reticular formation of the monkey. *Brain Res.* **151,** 31–47.

Carpentier, V., Vaudry, H., Laquerriere, A., Tayot, J., and Leroux, P. (1996a). Distribution of somatostatin receptors in the adult human brain stem. *Brain Res.* **734,** 135–148.

Carpentier, V., Vaudry, H., Mallet, E., Laquerriere, A., Tayot, J., and Leroux, P. (1996b). Anatomical distribution of somatostatin receptors in the brain stem of the human fetus. *Neuroscience* **73**(3), 865–879.

Carpentier, V., Vaudry, H., Mallet, E., Tayot, J., Laquerriere, A., and Leroux, P. (1997). Ontogeny of somatostatin binding sites in respiratory nuclei of the human brain stem. *J. Comp. Neurol.* **381,** 461–472.

Carpentier, V., Vaudry, H., Mallet, E., Laquerriere, A., and Leroux, P. (1998). Increased density of somatostatin binding sites in respiratory nuclei of the brain stem in sudden infant death syndrome. *Neuroscience* **86,** 159–166.

Chan-Palay, V. (1978a). The paratrigeminal nucleus. I. Neurons and synaptic organization. *Neurocytology* **7,** 405–418.

Chan-Palay, V. (1978b). The paratrigeminal nucleus. II. Identification and inter-relations of catecholamine axons, indoleamine axons, and substance P immunoreactive cells in the neuropil. *Neurocytology* **7,** 419–442.

Del Fiacco, M., Dessi, M. L., and Levanti, M. C. (1984). Topographical localization of substance P in the human post-mortem brain stem. An immunohistochemical study in the newborn and adult tissue. *Neuroscience* **12,** 591–611.

Eden, A. R., Chandross, K. L., Laitman, J. L., and Gannon, P. J. (1988). The salivatory nuclei of Macacafascicularis. *Soc. Neurosci. Abstr.* **14**(2), 1318.

Ferraro, J. A., and Minckler, J. (1977). The human lateral lemniscus and its nuclei. The human auditory pathways: a quantitative study. *Brain Language* **4,** 277–294.

Fix, J. D. (1980). A melanin-containing nucleus associated with the superior cerebellar peduncle in man. *J. Hirnforsch.* **21,** 429–436.

Fredericks, C. A., Giolli, R. A., Blanks, R. H. I., and Sadun, A. A. (1988). The human accessory optic system. *Brain Res.* **454,** 116–122.

Fulwiler, C. E., and Saper, C. B. (1984). Subnuclear organization of the efferent connections of the parabrachial nucleus in the rat. *Brain Res. Rev.* **7,** 229–259.

Gai, W. P., and Blessing, W. W. (1996). Nitric oxide synthesising neurons in the central subnucleus of the nucleus tractus solitarius in humans. *Neurosci. Lett.* **204,** 189–192.

Glass, M., Dragunow, M., and Faull, R. L. (1997). Cannabinoid receptors in the human brain: a detailed anatomical and quantitative autoradiographic study in the fetal, neonatal and adult human brain. *Neuroscience* **77**(2), 299–318.

Gwyn, D. G., Leslie, R. A., and Hopkins, D. A. (1985). Observation on the afferent and efferent organization of the vagus nerve and the innervation of the stomach in the squirrel monkey. *J. Comp. Neurol.* **239,** 163–175.

Halliday, G. M., and Tork, 1. (1986). Comparative anatomy of the ventromedial mesencephalic tegmentum in the rat, cat, monkey and human. *J. Comp. Neurol.* **252,** 423–445.

Halliday, G. M., Li, Y. W., Joh, T. H., Cotton, R. G. H., Howe, P. R. C., Geffen, L., and Blessing, W. W. (1988a). The distribution of substance P–like immunoreactive neurons in the human medulla oblongata, colocalization with monoamine synthesizing neurons. *Synapse* **2,** 353–370.

Halliday, G. M., Li, Y. W., Joh, T. H., Cotton, R. G. H., Howe, P. R. C., Geffen, L. B., and Blessing, W. W. (1988b). Distribution of monoamine synthesizing neurons in the human medulla oblongata. *J. Comp. Neurol.* **273,** 301–3l7.

Halliday, G. M., Li, Y. W., Oliver, J. R., Joh, T. H., Cotton, R. G. H., Howe, P. R. C., Geffen, L., and Blessing, W. W. (1988c). The distribution of neuropeptideY-like immunoreactive neurons in the human medulla oblongata. *Neuroscience* **26,** 179–191.

Hayakawa, I., and Zyo, K. (1983). Comparative cytoarchitectonic study of Gudden's tegmental nuclei in some mammals. *J. Comp. Neurol.* **216,** 233–244.

Heimer, L., and Wilson, R. D. (1975). The subcortical projections of the allocortex: similarities in the neural associations of the hippocampus, the piriform cortex, and the neocortex. *In* "Colgi Centennial Symposium" (M. Santini, ed.), pp. 177–193. Raven Press, New York.

Herrick, C. J. (1922). "An Introduction to Neurology," 3rd Ed. W. B. Saunders, Philadelphia.

Holstege, G., and Kuypers, H. G. J. M. (1977). Propribulbar fiber connections to the trigeminal, facial and hypoglossal motor nuclei. 1. An anterograde degeneration study in the cat. *Brain* **100,** 239–264.

Holstege, G., and Tan, J. (1988). Projections from the red nucleus and surrounding areas to the brain stem and spinal cord in the cat. An HRP and autoradiographical tracing study. *Behav. Brain Res.* **28,** 33–57.

Hurd, Y. L., and Fagergren, P. (2000). Human cocaine- and amphetamine-regulated transcript (CART) mRNA is highly expressed in limbic- and sensory-related brain regions. *J. Comp. Neurol.* **425,** 583–598.

Hyde, T. M., Knable, M. B., and Murray, A. M. (1996). Distribution of dopamine D1-D4 receptor subtypes in human dorsal vagal complex. *Synapse* **24**(3), 224–232.

King, G. W. (1980). Topology of ascending brain stem projections to nucleus parabrachialis in the cat. *J. Comp. Neurol.* **191,** 615–638.

Kitahama, K., Pearson, J., Denroy, L., Kopp, N., Ulrich, J., Naeda, I., and Jouvet, N. (1985). Adrenergic neurons in human brain demonstrated by immunohistochemistry with antibodies to phenylethanolamine-N-methyltransferase (PNMT): discovery of a new group in the nucleus tractus solitarius. *Neurosci. Lett.* **53,** 303–308.

Kitahama, K., Sakamoto, N., Jouvet, A., Nagatsu, I., and Pearson, J. (1996). Dopamine-beta-hydroxylase and tyrosine hydroxylase immunoreactive neurons in the human brain stem. *J. Chem. Neuroanat.* **10**(2), 137–146.

Klimek, V., Stockmeier, C., Overholser, J., Meltzer, H. Y., Kalka, S., Dilley, G., and Ordway, G. A. (1997). Reduced levels of norepinephrine transporters in the locus coeruleus in major depression. *J. Neurosci.* **17,** 8451–8458.

Koutcherov, Y., Ashwell, K. W. A. , Mai, J. K., and Paxinos, G. (2000). Organization of the human paraventricular hypothalamic nucleus. *J. Comp. Neurol.* **423**(2), 299–318.

Krammer, E. B., Rath, I, and Lischka, M. E. (1979). Sornatotopic organization of the hypoglossal nucleus: a HRP study in the rat. *Brain Res.* **170,** 533–537.

Kretteck, J. E., and Price, J. L. (1978). A description of the amygdaloid complex in the rat and cat with observations on intra-amygdaloid axonal connections. *J. Comp. Neurol.* **178,** 225–280.

Kuypers, H. G. J. M. (1960). Central cortical projections to motor and somato-sensory cell groups. *Brain* **83,** 161–184.

Kuypers, H. G. J. M., and Turek, J. D. (1964). The distribution of the cortical fibers within the nuclei cuneatus and gracilis in the cat. *J. Anat.* **98,** 143–160.

Laernle, L. K. (1983). A Golgi study of cell morphology in the deep layers of the human superior colliculus. *J. Hirnforsch.* **24,** 297–306.

le Lacalle, S., and Saper, C. B. (2000). Calcitonin gene-related peptide-like immunoreactivity marks putative visceral sensory pathways in human brain. *Neuroscience* **100,** 115–130.

Lerath, L. (1964). The red nucleus in the mice, monkey and man. Indian *J. Physiol. Pharmacol.* **8,** 143–148.

Lima, D., dan Almeida, A. (2002). The medullary dorsal reticular nucleus as a proprioceptive centre of the pain control system. *Prog. Neurobiol.* **66,** 81–108.

Lynn, R. B., Hyde, T. M., Cooperman, R. R., and Miselis, R. R. (1966). Distribution of bombesin-like immunoreactivity in the nucleus of the solitary tract and dorsal motor nucleus of the rat and human: colocalization with tyrosine hydroxylase. *J Comp Neurol.* **369,** 552–570.

Marani, E., Voogd, J., and Bockee, A. (1977). Acetylcholinesterase staining in subdivisions of the cats inferior olive. *J. Comp. Neurol.* **174,** 209–226.

Marcyniuk, N. B., Mann, D. M. A., and Yates, P. O. (1986a). The topography of cell loss from locus coeruleus in Alzheimer's disease. *J. Neurol. Sci.* **76,** 335–345.

Marcyniuk, N. B., Mann, D. M., and Yates, P. O. (1986b). Loss of nerve cells from locus coeruleus in Alzheimer's disease is topographically arranged. *Neurosci. Lett.* **64**(3), 247–252.

Martino, R., Terrault, N., Ezerzer, F., Mikulis, D., and Diamant, N.E. (2001). Dysphagia in a patient with lateral medullary syndrome: insight into the central control of swallowing. *Gastroenterology* **121,** 420–426.

Matturri, L., Minoli, I., Lavezzi, A. M., Cappellini, A., Ramos, S., and Rossi, L. (2002). Hypoplasia of medullary arcuate nucleus in unexpected late fetal death (stillborn infants): a pathologic study. *Pediatrics* **109,** E43.

McRitchie, D., and Tork, I. (1989). In preparation.

Meessen, H., and Olszewski, J. (1949). "A Cytoarchitectonic Atlas of the Rhombencephalon of the Rabbit." Karger, New York.

Mehler, W. R. (1983). Observations on the connectivity of the parvicellular reticular formation with respect to a vomiting center. *Brain Behav. Evol.* **23,** 63–80.

Mehler, W. R, (1969). Some neurological species differences—a poster. *Ann. N. Y. Acad. Sci.* **167,** 424–468.
Mehler, W. R. (1974a). Central pain and the spinothalamic tract. *In* "Pain" (J. J. Bonica, ed). Raven Press, New York.
Mehler, W. R. (1974b). A comparative study of the cells of origin of cerebellar afferents in the rat, cat, monkey studied with horseradish peroxidase technique. 11. The vestibular nuclear complex. *Anat. Rec.* **187,** 653.
Mehler, W. R. (1977). A comparative study of cells of origin of cerebellar afferents in the rat, cat, and monkey studied with HRP technique: II. The vestibular nuclear complex. *Anat. Rec.* **187,** 653.
Mchler, W. R., and Rubertone, J. (1986). Anatomy of the vestibular nucleus complex. *In* "The Rat Nervous Systern" (G. Paxinos, ed.), Vol. 2. Academic Press, Orlando.
Mikhail, Y., and Ahmed, Y. Y. (1975). Outline of the arcuate nucleus in the human medulla oblongata. *Acta Anat.* **92,** 285–291.
Moore, D., Chambers, J., Waldvogel H., Faull, R., and Emson, P. (2000). Regional and cellular distribution of the P2Y(1) purinergic receptor in the human brain: striking neuronal localisation. *J. Comp. Neurol.* **421,** 374–384.
Nageotte, J. (1906). The pars intermedia of nervus intermedius of Wrisberg, and the bulbopontine gustatory nucleus in man. *Rev. Neurol. Psychiatry (Edinburgh)* **4,** 473–488.
Ni, L., and Miller Jonakait, G. (1988). Development of substance P–containing neurons in the central nervous system in mice: an immuncytochernical study. *J. Comp. Neurol.* **275,** 493–510.
Nomura, H., Shiosaka, S., and Tohyama, M. (1987). Distribution of substance P-like immunoreactive structures in the brain stem of the adult human brain: an immunocytochernical study. *Brain Res.* **404,** 365–370.
Ohm, T. and Braak, J. W. (1987). The pigmented subpeduncular nucleus (nucleus subpeduncularis pigmentosus) in the human brain. Normal morphology and pathological changes in Alzheimer's disease. *Neuroscience* **22,** S785.
Olszewski, J., and Baxter, D. (1954). "Cytoarchitecture of the Human Brain Stem." J. B. Lippincott, Philadelphia.
Ono, S., Takahashi, K., Jinnai, K., Kanda, F., Fukuoka, Y., Kurisaki, H., Mitake, S., Inagaki, T., Yamano, T., Shimizu, N., and Nagao, K. (1998). Loss of catecholaminergic neurons in the medullary reticular formation in myotonic dystrophy. *Neurology* **51,** 1121–1124.
Ostapoff, E. M., Johnson, J. I., and Albright, B. C. (1988). Medullary sources of projections to the kinesthetic thalamus in racoons: external and basal cuneate nuclei and cell groups X and Z. *J. Comp. Neurol.* **267,** 231–252.
Papez, J. W. (1929). "Comparative Neurology." Hadner, New York.
Pau, K. Y., Yu, J. H., Lee, C. J., Spies, H. G. (1998). Topographic localization of neuropeptide Y mRNA in the monkey brain stem. *Regul Pept* **75–76,** 145–153.
Paxinos, G. (1983). Evidence for the existence of a parvicellular nucleus medial to the parabigeminal (P13g) nucleus. *Neurosci. Lett., Suppl.* **14,** S276.
Paxinos, G. (1985). The microcellular tegmental nucleus (Mi). *Neurosci. Lett., Suppl.* **1–9,** 589.
Paxinos, G., and Butcher, L. L. (1986). Organizational principles of the brain as revealed by choline acetyltransferase and acetylcholinesterase distribution and projections. *In* "The Rat Nervous System" (G. Paxinos, ed.), Vol. 1, pp. 487–521. Academic Press, Orlando.
Paxinos, G., and Huang, X. F. (1995). Atlas of the Human Brainstem. Academic Press, San Diego.
Paxinos, G., and Watson, C. (1998). "The Rat Brain in Stereotaxic Coordinates," 3rd Ed. Academic Press, San Diego.
Paxinos, G., Tork, L., Halliday, G., and Mchler, W. R. (1988). The human intermediate reticular nucleus (IRt). *Soc. Neurosci. Abstr.* **14,** 1317.
Pearson, A. A. (1947). The roots of the facial nerve in the human embryos and fetuses. *J. Comp. Neurol.* **87,** 139–159.
Petrovicky, P. (1973). Structure and incidence of Gudden's tegmental nuclei in some mammals. *Acta Anat.* **80,** 273–286.
Richter, E. A., Norris, B. E., Fullerton, B. C., Levine, R. A., and Kiang, N. Y. S. (1983). Is there a medial nucleus of the trapezoid body in humans. *Am. J. Anat.* **168,** 157–166.
Riley, H. A. (1943). "An Atlas of the Basal Ganglia, Brain Stem and Spinal Cord Based on Myelin-Stained Material." Williams & Wilkins, Baltimore.
Rub, U., Del Tredici, K., Schultz, C., Thal, D. R., Braak, E., and Braak, H. (2001). The autonomic higher order processing nuclei of the lower brain stem are among the early targets of the Alzheimer's disease–related cytoskeletal pathology. *Acta. Neuropathol. (Berl.)* **101,** 555–564.
Ruggiero, D.A., Underwood, M.D., Mann, J.J., Anwar, M,. and Arango, V. (2000). The human nucleus of the solitary tract: visceral pathways revealed with an "in vitro" postmortem tracing method. *J. Auton. Nerv. Syst.* **79,** 181–190.
Sadjadpour, K., and Brodal, A. (1968). The vestibular nuclei in man. A morphological study in the light of experimental findings in the cat. *J. Hirnforsch.* **10,** 299–323.
Satoh, K., Tohyama, M., Yamamoto, I., Sakumoto, I., and Shimizu, N. (1977). Noradrenaline innervation of the spinal cord studied by horseradish peroxidase method combined with monoamine oxidase staining. *Exp. Brain Res.* **223,** 175–186.
Selmer, I. S., Schindler, M., Humphrey, P. P., Waldvogel, H. J., Faull, R. L., and Emson, P. C. (2000). First localisation of somatostatin sst(4) receptor protein in selected human brain areas: an immunohistochemical study. *Brain Res. Mol. Brain Res.* **82,** 114–125.
Somana, R., and Walberg, F. (1979). The cerebellar projection from the paratrigeminal nucleus in the cat. *Neurosci. Lett.* **15,** 49–54.
Stromberg, N. L., and Hurwitz, J. L. (1976). Anatomical aspects of the superior olivary complex. *J. Comp. Neurol.* **170,** 485–491.
Villanueva, L., Bouhassira, D., and Le Bars. D. (2000). The medullary subnucleus reticularis dorsalis (SRD) as a key link in both the transmission and modulation of pain signals. *Brain Res.* **873**(1), 131–134.
von Gudden, B. (1884). Uber das corpus mammillare und die sogenarinten schenkel des fornix. *Vers. Dtsch. Naturforsch., Magdeburg, Tagungsbls.* **57,** 126.
von Gudden, B. (1889). Ueber clas corpus mammillane und diesogenannten schenkel des fornix. *In* "Berhard von Gudden's gesammelte und hinterlassene Abhandlungen" (H. Grasbey, ed.), pp. 190–192. J. F. Bergman, Weisbaden.
Walberg, F. (1952). The lateral reticular nucleus of the medulla oblongata in mammals. A comparative-anatomical study. *J. Comp. Neurol.* **96,** 283–337.
Wallace, M. N. (1988). Lattices of high histochemical activity occur in the human, monkey, and cat superior colliculus. *Neuroscience* **25,** 569–583.
Westlund, K. N., Denney, R. M., Rose, R. M., and Abels, C. W. (1988). Localization of distinct monoamine oxidase A and monoamine oxidase B cell populations in human brain stem. *Neuroscience* **25,** 439–456.
Yamada, H., Ezure, K., and Manabe, M. (1988). Efferent projections of inspiratory neurons of the ventral respiratory group. A dual labeling study in the rat. *Brain Res.* **455,** 283–294.
Yamaguchi, K., Goto, N., and Honma, K. (1994). Development of the human gigantocellular reticular nucleus: a morphometric study. *Acta Anat. (Basel)* **150**(3), 191–197.

Zarate-Lagunes, M., Gu, W.J., Blanchard, V., Francois, C., Muriel, M. P., Mouatt-Prigent, A., Bonici, B., Parent, A., Hartmann, A., Yelnik, J., Boehme, G. A., Pradier, L., Moussaoui, S., Faucheux, B., Raisman-Vozari, R., Agid, Y., Brice, A., and Hirsch, E. C. (2001). Parkin immunoreactivity in the brain of human and non-human primates: an immunohistochemical analysis in normal conditions and in Parkinsonian syndromes. *J. Comp. Neurol.* **432,** 184–196.

Zec, N., and Kinney, H. C. (2001). Anatomic relationships of the human nucleus paragigantocellularis lateralis: a DiI labeling study. *Auton. Neurosci.* **89,** 110–124.

Ziehen, T. (1934). Centralnervensystem. *In* "Handbuch der Anatomie des Menschen" (V. Eggerling, ed.), Vol. 4. Fischer, Jena.

CHAPTER

11

Cerebellum and Precerebellar Nuclei

JAN VOOGD
Department of Neuroscience
Erasmus Medical Center Rotterdam, Rotterdam
and Neuroregulation Group, Department of Physiology
University of Leiden, Leiden, Holland

Recent interest in the nonmotor functions of the human cerebellum (Leiner *et al.*, 1986; Schmahmann, 1997) and the advances made in the molecular biology and physiology of the cerebellum (De Zeeuw *et al.*, 1997; Gerrits *et al.*, 2000) have raised renewed interest in its anatomy. In this chapter I have tried to make the data on the gross anatomy of the human cerebellum and its nuclei more accessible to its users and to emphasize the magnitude of the cerebrocerebellar connections in the human brain. The problem in this approach remains that the recent literature is almost restricted to the anatomy of the rodent and feline cerebellum, with some excursions to nonhuman primates, and that new information on the fiber connections of the human cerebellum is almost completely lacking. During the late 19th century and the first decades of the 20th century, the connections of the human cerebellum were extensively studied with the myelogenetic method (reviewed by Flechsig, 1927) and traced with Marchi staining of degenerated myelin (Marchi and Algeri, 1885) in human pathological material. But these studies stopped and were never resumed. This situation did not improve with the advent of the silver impregnation methods for degenerated axons (Nauta and Gygax, 1951, 1954). Among the hundreds of papers using the Nauta method in experimental studies of the cerebellum there are only a few on the afferent, intrinsic, or efferent connections of the human cerebellum. What is probably the most complete account of the fiber connections of the human cerebellum therefore remains von Bechterew's review of his myelogenetic studies of the human brain *Die Leitungsbahnen im Gehirn und Rückenmark* from 1899. As a consequence, much of the anatomy of the human cerebellum still rests on assumptions and interpretations of animal studies.

This chapter is based on the text as it appeared in the first edition of *The Human Nervous System* (Voogd *et al.*, 1990). Most of the data on connections from studies in rodents and carnivores have been omitted from this new edition. This information is available in

some recent reviews (Voogd, 1995, 1998, Voogd *et al.*, 1996b, Voogd and Glickstein, 1998). Some of the human cases used in this chapter were documented by the late Dr. Jaap Schoen from the Department of Anatomy of the University of Leiden. For details on these cases, the reader is referred to the first edition.

EXTERNAL FORM, DEVELOPMENT, AND SUBDIVISION OF THE HUMAN CEREBELLUM

Introduction

The shape of the human cerebellum differs from that of most other mammals, with the possible exception of the great apes, which have not been studied in great detail (Larsell, 1970). The most obvious features of the human cerebellum are its overall size, the depth of the transverse fissures, and the great mediolateral width and parallel orientation of the folia of the hemisphere. According to Langelaan (1919), "the great obstacle to the study of the morphology of the cerebellum lies in its nomenclature." This problem probably is caused by the nature of the nomenclature of the cerebellum, which is a mixture of purely descriptive names and terms with a comparative anatomical context. Most of the names attributed to the lobules of the vermis and hemisphere by Malacarne (1776; cited by Glickstein, 1987), Meckel (1817; cited by Larsell and Jansen, 1972) and Burdach (1822; cited by Larsell and Jansen, 1972) are still in common use (Fig. 11.1). Different nomenclatures for the human cerebellum, which are mainly of a historical interest, were reviewed by Angevine *et al.* (1961) and tabulated by Schmahmann *et al.* (1999). In the following description of the folial pattern of the human cerebellum, I will use the classical terminology and refer to Larsell's comparative anatomical nomenclature. Introduced for the rat (Larsell, 1952), this nomenclature, which indicates the lobules of the vermis with the roman numerals I–X and the lobules of the hemisphere with the same numbers and the prefix "H", was applied in its final form to the human cerebellum by Larsell and Jansen in 1972. The comparative anatomical and embryological implications of Larsell's nomenclature will be discussed at the end of this section. In a recently published magnetic resonance imaging (MRI) atlas of the human cerebellum in proportional stereotactic space (Schmahmann *et al.*, 1999, 2000) a modification of Larsell's nomenclature was adopted to indicate the lobules. The prefix "H" for the lobules of the hemisphere was discarded, the superior and inferior semilunar lobules (Larsell's lobules HVIIAa and Ab) were indicated as crus I and crus II of Bolk's (1902, 1906) ansiform lobule, and the names of the transverse fissures, as used by Larsell and Jansen (1972), were retained.

Gross Anatomy of the Human Cerebellum

In the descriptive anatomy of the human cerebellum a superior surface (facing the tentorium and indicated as the rostral surface, when the long axis of the brain stem is taken as reference) and an inferior (caudal) surface generally are distinguished. The rostral, caudal and ventral aspects of the cerebellum are illustrated in Figs. 11.2 and 11.3. The folial pattern of the cerebellum is best studied in serial parasagittal sections (Fig. 11.4). MR images from serial sagittal, horizontal, and coronal slices were illustrated by Schmahman *et al.* (1999, 2000). One of their reconstructions of the human cerebellum and one of their slices horizontal slices are reproduced in the Figs. 11.3 and 11.5.

In a midsagittal section (Fig. 11.1C) the primary fissure, which divides the cerebellum into anterior and posterior lobes, can be identified as the deepest fissure on the superior (rostral) surface. The anterior lobe is subdivided into the lingula (lobules I and II of Larsell), the lobulus centralis (lobule III), the culmen (lobules IV and V). The lingula, or its ventral sublobule when present, is embedded in the anterior medullary velum. The ventral surface of the anterior medullary velum is covered with ependyma and forms the rostral wall of the fastigium, the narrow protrusion of the fourth ventricle in the base of the cerebellum. The main fissure in the anterior lobe, which can be recognized in all mammals, is the preculminate fissure between lobulus centralis and culmen. The folial pattern of the lingula/lobulus centralis region and the subdivision of the culmen in lobules IV and V is subject to many variations (Larsell and Jansen, 1972). The subdivision of the region behind the primary fissure into the declive (lobule VI), the folium (lobule VIIAa of Larsell; VIIAf of Schmahmann *et al.*), and the tuber (lobule VIIAb and VIIB of Larsell; lobules VIIAf and VIIB of Schmahmann) can only be appreciated when taking the relations of this part of the vermis with the hemisphere into account. The pyramis (lobule VIII), the uvula (lobule IX), and the nodulus (lobule X), with their intervening prepyramidal, secondary, and posterolateral fissures, are easy to identify. The ependymal roof of the fourth ventricle is attached to the nodulus. Together with the rostral ependymal surface of the nodulus it forms the caudal wall of the fastigium.

The superior (rostral) surface of the cerebellum is relatively flat, with the culmen forming the higest point of the "monticulus," the small hill, which slopes downward as the declive. At the superior surface the

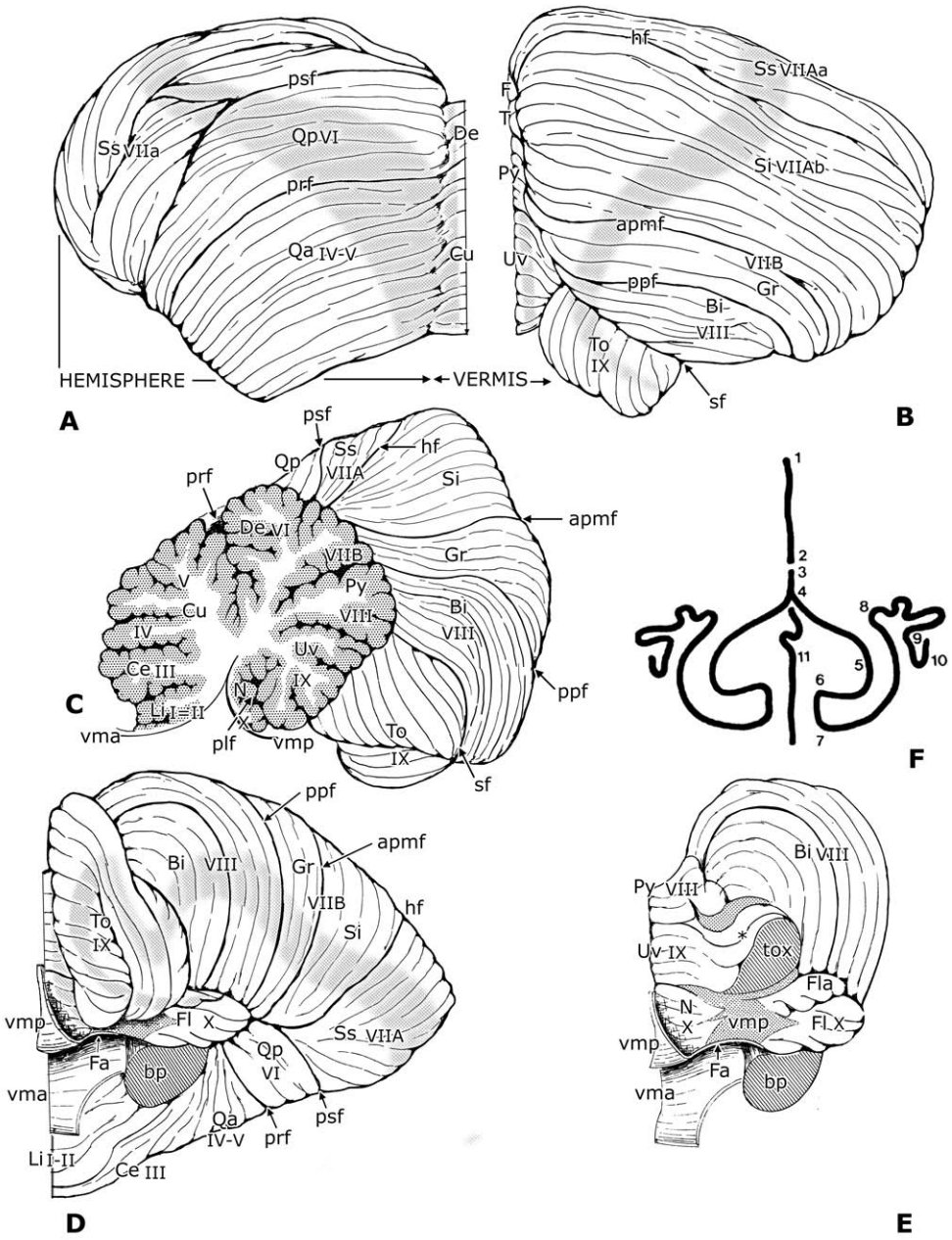

FIGURE 11.1 The human cerebellum. Semidiagramatic drawings of the anterior aspect **(A),** the posterior aspect **(B),** the midsagittal section **(C),** the ventral aspect **(D),** and the region of the nidus avis on the ventral aspect, after removal of the tonsilla **(E).** Bolk's (1906) wire diagram of the groundplan of the mammalian cerebellum is illustrated in **(F).** Areas without cortex in D and E are indicated by dots. The cross-sections of the brachium pontis and the peduncle of the tonsilla are hatched. The connection between the uvula and the tonsilla is indicated by an asterisk. The gray bands indicate the direction of the folial chains of the vermis and the hemisphere. Vermis and hemispheres separate in the posterior lobe. Two loops are present in the folial chain of the hemisphere: one at the level of the semilunar lobulus, one at the level of the tonsilla. This configuration corresponds to Bolk's (1906) groundplan of the mammalian cerebellum (F), which shows loops in the region of the ansiform lobule (4–5–6) and the paraflocculus (6–9). Lobules are indicated by abbreviations of their anatomical names and by Larsell's roman numerals. Abbreviations: apmf, ansoparamedian fissure; Bi, biventral lobule; bp, brachium pontis; Ce, central lobule; Cu, culmen; De declive; F, folium vermis; Fa, fastigium; Fl, flocculus; Fla, accessory paraflocculus of Henle; Gr, lobulus gracilis; hf, horizontal fissure; N, nodulus; plf, posterolateral fissure; ppf, prepyramidal fissure; prf, posterior superior fissure; psf, primary fissure; Py, Pyramis; Qa, anterior quadrangular lobule; Qp, posterior quadrangular lobule; sf, secondary fissure; Si, inferior semilunar lobule; Ss, superior semilinar lobule; T, tuber vermis; To, tonsilla; Tox, cross-section of the peduncle of the tonsilla; Uv, uvula; vma, anterior medullary velum; vmp, posterior medullary velum.

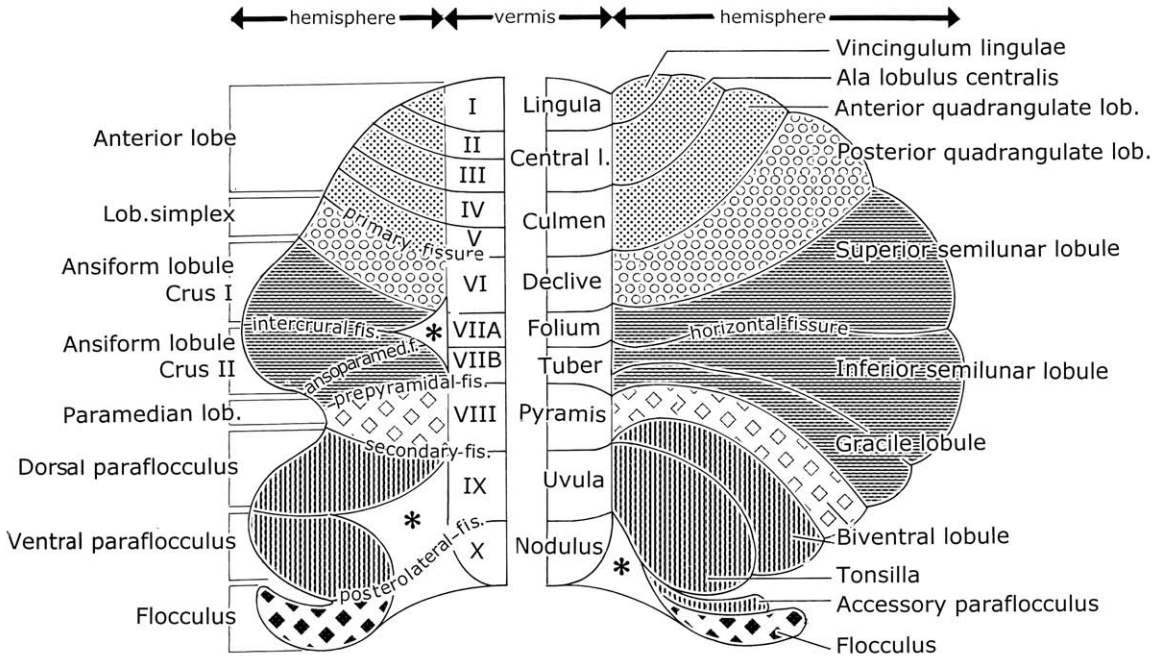

FIGURE 11.2 Comparative anatomical nomenclature of the cerebellum according to Bolk, with Larsell's roman numerals indicated in the vermis **(left),** and the classical nomenclature of the cerebellum **(right).** Possible homologies are indicated by identical hatchings in the two panels.

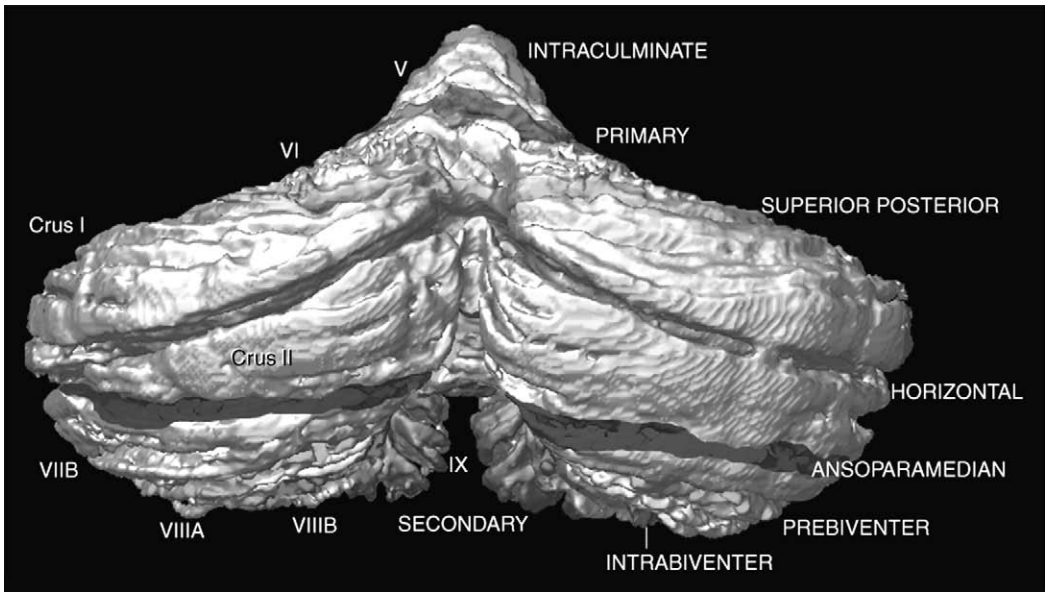

FIGURE 11.3 Three dimensional reconstructions of MR images, of the caudal surface of the cerebellum. The position of the ansoparamedian fissure, between the inferior semilunar lobule (Crus II) and the lobulus gracilis (VIIB), is asymmetric. The original color coding of the fissures has been omitted. Adapted from Schmahmann *et al.* (2000).

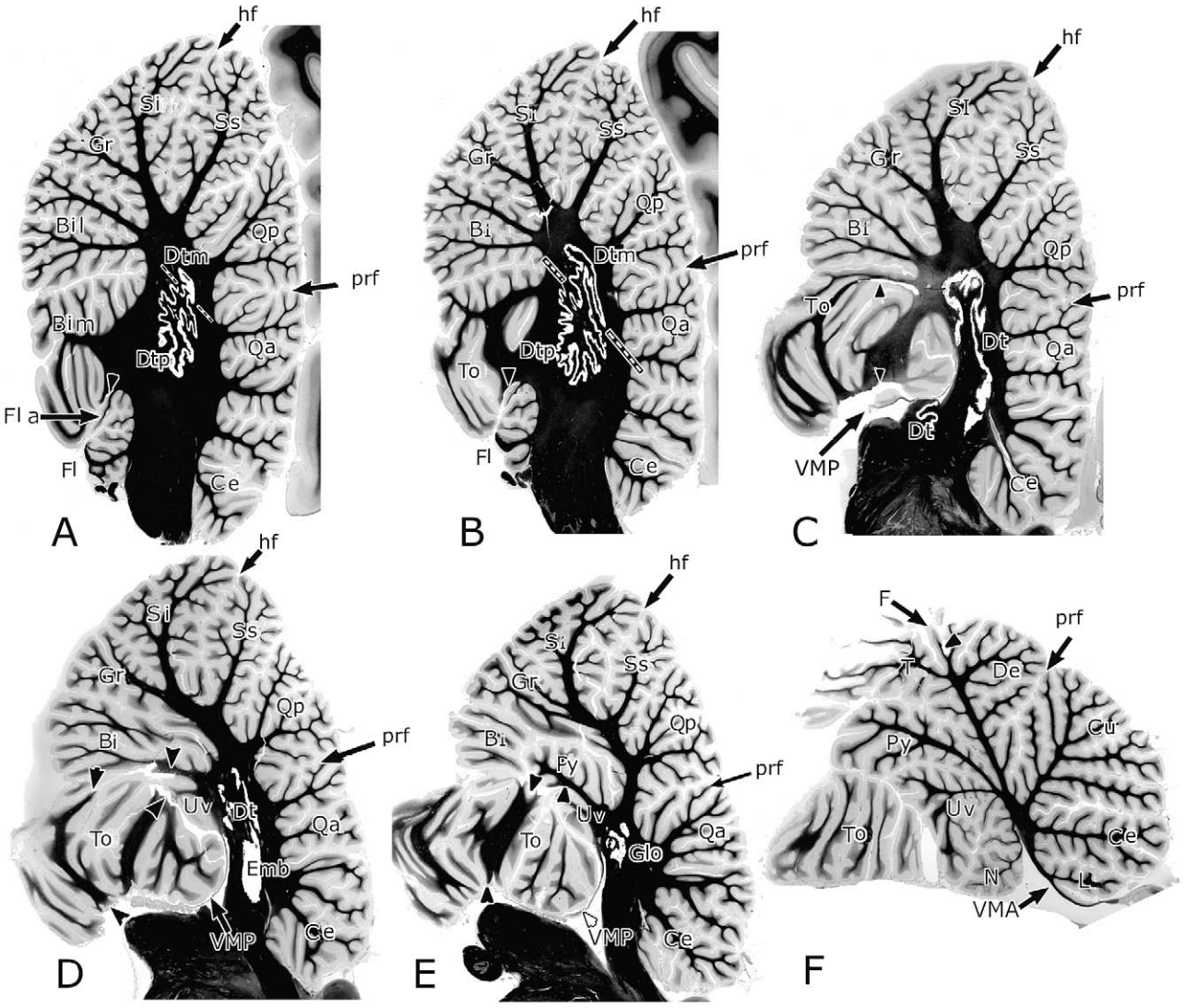

FIGURE 11.4 Six parasagittal sections through the cerebellum. A is the most lateral section, E passes through the paravermal region, F passes through the vermis. Arrowheads indicate areas without cortex between the tonsilla and the accessory paraflocculus/flocculus complex **(A, B),** the dorsal and ventral surface of the tonsilla **(C–E),** the transition from the pyramis into the biventral lobule (D), pyramis and uvula (E), and the base of the folium vermis **(F).** Compare with dissected area of nidus avis in Figure 11.1E. Scans with enhanced contrast from Weigert–Pal–stained sections from the Jelgerma Collection. Abbreviations: Bi, biventral lobule; Bil, lateral belly of the biventral lobule; Bim, medial belly of the biventral lobule; Ce, central lobule; Cu, culmen; De, declive; Dt, dentate nucleus; Dtm, magnocellular, dorsomedial portion of the dentate nucleus; Dtp, parvocellular, ventrolateral portion of the dentate nucleus; Emb, emboliform nucleus; F, folium vermis; Fl, flocculus; Fla, accessory paraflocculus of Henle; Glo, globose nucleus; Gr, lobulus gracilis; hf, horizontal fissure; N, nodulus; prf, primary fissure; Py, Pyramis; Qa, anterior quadrangular lobule; Qp, posterior quadrangular lobule; Si, inferior semilunar lobule; Ss, superior semilinar lobule; To, tonsilla; Tu, tuber vermis; Uv, uvula.; VMP, posterior medullary velum. Courtesy of Dr. Enrico Marani.

vermis is demarcated from the hemisphere by a shallow paramedian sulcus. Most fissures in the vermis of the anterior lobe and in the declive continue uninterruptedly into the hemisphere. A precise demarcation of the anterior vermis in sections is difficult if not impossible (Schmahmann *et al.*, 1999). These authors estimated the width of the anterior vermis at 14–20 mm, depending on the section and the definition of the surface markings. The hemispheral lobules on the superior surface generally can be traced from their vermal counterparts by following the transverse interlobular fissures. In this way the hemisphere of the lingula (the

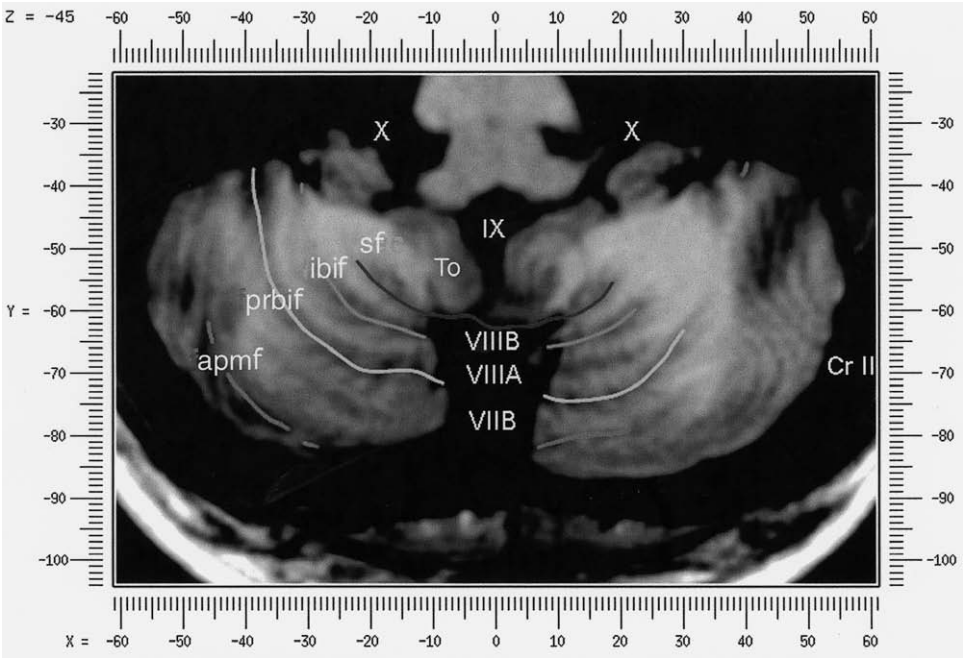

FIGURE 11.5 Horizontal MR image of a section passing through the ventrocaudal pole of the cerebellum. Note position of the tonsilla, as well as the presence of areas without cortex between the tonsilla (To) and the acessory paraflocculus/flocculus complex (X). Abbreviations: apmf, ansoparamedian fissure; Cr II, crus II; ibif, intrabiventral fissure; prbif, prebiventral fissure; sf, secondary fissure; To, tonsilla; VIIb–X, lobules VIIB–X of Larsell. From Schmahmann *et al*. (2000).

vinculum lingulae, Larsells lobule HI and HII), the hemisphere or "alae" of the lobulus centralis (HIII), and the hemisphere of the culmen (lobulus quadrangularis anterior, lobules HIV and HV) and of the declive (lobulus quadrangularis posterior, lobule HVI) can be delineated.

Morphologically the anterior lobe and the declive with its hemisphere form an entity characterized by the lack of a distinct vermis and the continuity of its transverse fissures. For the declive and its hemisphere this was emphasized by Bolk (1906), who coined the name "lobulus simplex" for this ensemble because he was unable to distinguish a clear border between vermis and hemispheres in this part of the cerebellum in most of the mammalian cerebella he examined. There are no stringent reasons to attach more importance to the primary fissure than to any other interlobular fissure. The subdivision of the cerebellum by the primary fissure into anterior and posterior lobes is of historical but not of great morphological significance.

A distinct vermis, bordered by deep paramedian sulci from the hemispheres, makes its appearence caudal to the lobulus simplex. The presence of a paramedian sulcus and the great expansion of the posterior hemisphere makes it more difficult to trace the interlobular fissures from the vermis into the hemisphere in this region. The posterior superior fissure constitutes the caudal border of the lobulus simplex and can be traced far laterally, caudal to the declive and the posterior quadrangular lobule (HVI) on the superior surface of the cerebellum. The deep horizontal fissure runs approximately along the border of the superior and inferior (caudal) surface of the hemisphere. Usually it can be traced into the vermis as the caudal border of the folium (lobule VIIAa of Larsell, VIIAf of Schmahmann). This vermal lobule may consist of a single, unfoliated lamina, caudal to the declive and located in the bottom of the deep cerebellar notch between the protruding hemispheres. Laterally it expands into the superior semilunar lobule (HVIIAa of Larsell, crus I of Bolk and Schmahmann).

At the inferior surface of the cerebellum the prepyramidal fissure forms the border between the tuber (lobule VIIB) and the pyramis (lobule VIII) at the level of the vermis, and between the lobulus gracilis (HVIIB) and the biventral lobule (HVIII) in the hemisphere. According to Larsell and Jansen (1972) and Schmahmann *et al*. (1999), the region of the hemiphere between the horizontal and prepyramidal fissures can be subdivided by the ansoparamedian fissure into the inferior semilunar lobule (lobule VIIAb of Larsell; crus II of Bolk and Schmahmann) and the lobulus gracilis (lobule VIIB of Larsell). However, the position of this fissure and its continuation in the tuber, is highly

variable, as shown by the asymmetry of these lobules in the specimen of the cerebellum illustrated by Schmahmann *et al.* (1999) (Fig. 11.3) and by the variations in the nomenclature for this region in their tabulated summary.

In the serially sectioned cerebellum illustrated in Fig. 11.4, I observed irregularities in the structure of the cerebellar cortex, with small areas where a cortex was completely lacking and white matter came to the surface, at the transition of the folium and the tuber into the hemisphere. Regions without cortex commonly are found in most mammals in the paramedian sulcus at sites of great expansion of the hemisphere, such as in the center of Bolk's ansiform lobule (Voogd, 1964, 1998).

The secondary fissure, located between the pyramis (VIII) and the uvula, laterally separates the biventral lobule (HVIII) from the tonsilla (HIX). The lateral part of the pyramis sometimes expands into a small folial rosette, known as the "Nebenpyramide" of Henle (1871). Laterally, most intralobular fissures of the pyramis become more shallow and disappear. An area without cortex replaces the cortex on the caudal (ventral) surface of the pyramis (Fig. 11.2E). At the junction with the biventral lobule, some folia that bridge the paramedian sulcus connect the rostral (dorsal) pyramis with the biventral lobule. Therefore, the intrabiventral fissure, which separates the lateral belly of the biventral lobule (lobules HVIIIAa and b) from the medial belly (lobules HVIIIAc and VIIIIB), continues into one of the intralobular fissures on the rostral (dorsal) surface of the pyramis.

The folia of the tonsilla (lobule HIX of Larsell) form a medially directed loop, which ends in the flocculus (Fig. 11.2D). Areas without cortex are found in the center of this loop, on the dorsal and the ventral surface of the uvula (Fig. 11.4C–E). In the bottom of the secondary fissure the cortex of the medial belly of the biventral lobule continues into the cortex covering the lateral aspect of the tonsilla. The distal part of the tonsilla is turned inward and is lodged next to the uvula and the nodulus in a deep recess, known as the nidus avis (Fig. 11.2E). The bottom of the nidus avis is formed by a medullary sheet, the posterior medullary velum. The posterior medullary velum is attached to the base of the nodulus medially and to the medullary stalk of the tonsilla and the floccular peduncle laterally. It serves as the attachment (taenia) of the plexus choroideus in the roof of the fourth ventricle and its lateral recess. The folia on the lateral aspect of the uvula taper and disppear. A foliated band (the "furrowed band" of Reil; Larsell and Jansen, 1972) connects the uvula with the tonsilla (asterisk in Fig. 11.2E, asterisk; Fig. 11.4D).

The cortex of the nodulus (lobule X) is not continuous with the flocculus (lobule HX) or the flocculus accessorius of Henle (1871) (lobule HIX of Larsell). Laterally its folia taper and disappear in the posterior medullary velum (Figs. 11.2E and 11.4A, D). Small islands of cerebellar cortex sometimes are present in the velum, between the nodulus and the flocculus. Laterally, the flocculus accessorius and the flocculus are located ventral to the tonsilla. The cortex of the flocculus accessorius remains separated from the cortex of the tonsilla by the area without cortex on the ventral tonsillar surface. The cortex of the flocculus and the flocculus accessorius are continuous in the bottom of the posterolateral fissure, which separates them. Variations in this region were studied by Tagliavini and Pietrini (1984).

Comparative Anatomical Considerations

The revised nomenclature for the human cerebellum, introduced by Schmahmann *et al.* (1999), is a modification of Larsell's nomenclature combined with some of the terms introduced by Bolk (1902, 1906). Bolk and Larsell are representatives of two quite different concepts on the morphology of the mammalian cerebellum, both based on studies of its comparative anatomy. Larsell (Larsell, 1967, 1970; Larsell and Jansen, 1972) emphasized the mediolateral continuity of fissures and the lobules of vermis and hemispheres. His descriptions are precise but rigid, acknowledging the continuity of each lobule of the vermis with its counterpart in the hemisphere. Bolk (1902, 1906; for reviews, see Glickstein and Voogd, 1995; Voogd, 1975) stressed the relative independance of vermis and hemispheres. His scheme is more flexible. Bolk contrasted the morphology of the anterior lobe and the lobulus simplex, where the transverse fissures continue uninterruptedly from the vermis into the hemispheres, and which lack a clearly defined vermis in many species, with the structure of more caudal parts of the cerebellum (Bolk's lobulus complicatus) characterized by a certain independance of the folial chains of vermis and hemispheres (Fig. 11.6). Both Larsell and Bolk acknowledged the classical subdivision of the vermis of the human cerebellum, although they introduced slight modifications and different nomenclatures for the lobules of the vermis in their comparative studies. Larsell subsequently traced the fissures separating the lobules of the vermis into the hemisphere, either during their development or in the adult. Bolk described his observations on adult mammalian cerebella in developmental terms. The anterior lobe and the lobulus simplex constitute a single "growth center"; the posterior vermis and its hemisphere behave as independent centers, which both expand in the sagittal plane. The folial chains of vermis and hemispheres can be subdivided into secondary centers, or segments, by the depth of

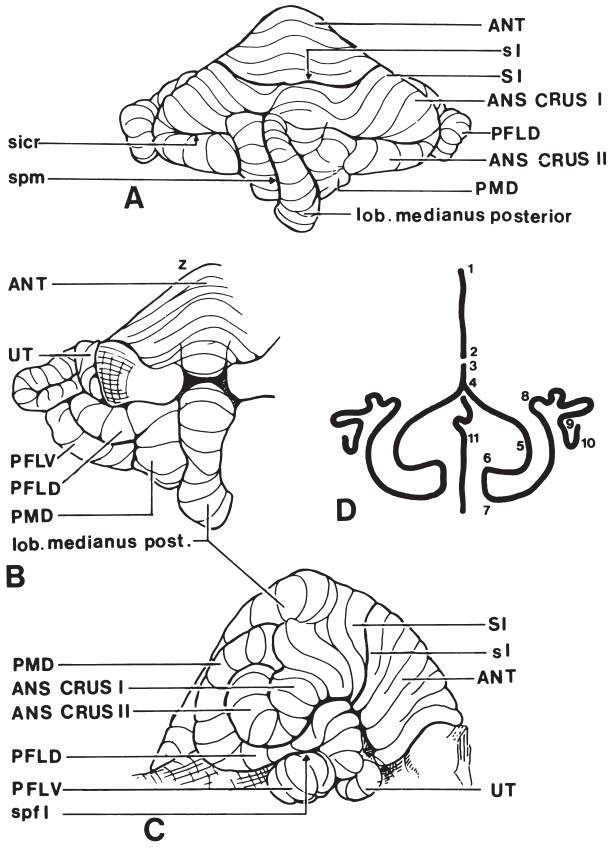

FIGURE 11.6 The cerebellum of *Lemur albifrons*. For the description of his basic plan of the mammalian cerebellum Bolk used the cerebellum of *L. albifrons*. This figure illustrates dorsal **(A),** ventral **(B)** and lateral **(C)** views of this cerebellum. Both the sulcus primarius and many of the intralobular fissures of the anterior lobe and the lobulus simplex can be traced to its lateral margin, and no indication can be found of paramedian sulci delimiting a vermis in these parts. The region behind the lobulus simplex (Bolk's lobulus complicatus) consists of the caudal vermis and the paired hemispheres separated by the deep paramedian sulci. The vermis consists of a long chain of narrow folia. The rostral and caudal segments of the folial chain of the hemisphere are thrown into loops: the lobulus ansiformis and the formatio vermicularis. The intermediate segment, the paramedian lobule, is located parallel to the vermis. The formatio vermicularis by Bolk consists of the paraflocculus (Stroud, 1895; divided into dorsal and ventral limbs, corresponding to the crus circumcludens and the pars floccularis of Bolk) and the flocculus (Bolk's uncus terminalis). The folial chain of the hemisphere, therefore, is "fragmented into secondary centres which differ in growth intensity." The segmentation of the folial chains of vermis and hemisphere is well illustrated in Bolk's wire diagram of the mammalian cerebellum (D:1–2: anterior lobe; 3–4: simple lobule; 4–6: ansiform lobule; 6–7: paramedian lobule; 7–9: crus circumcludens and pars floccularis, or paraflocculus; 10: uncus terminalis or flocculus; 11: caudal vermis). Abbreviations: ANS CRUS 1, Crus I of the ansiform lobule; ANS CRUS II, Crus II of the ansiform lobule; sI, sulcus primarius; SI, lobulus simplex; sicr, sulcus intercruralis; spfl, sulcus interparafloccularis; spm, sulcus ANT, anterior lobe; PFLD, paraflocculus dorsalis; PFLV, paraflocculus ventralis; PMD, lobulus paramedianus; sI, sulcus; UT, uncus terminalis (Bolk), flocculus. Redrawn from Bolk (1902).

the intervening fissures, or changes in the width or the direction of the folia. In the folial chain of the hemisphere Bolk distinguished two laterally directed loops, one in the region of the ansiform lobule and the other in the region of the paraflocculus. These loops also can be recognized in the human cerebellum (Fig. 11.1). The first loop is located in the region of the semilunar lobules, where folia emerge in a feather-like fashion from the horizontal fissure. The second loop is located in the tonsilla, the homologue of the mammalian paraflocculus. It the case of the human cerebellum it is directed medially.

In Bolk's descriptions the continuity within a folial chain (although he never verified the continuity of the cortex histologically) and the varying degrees of independance of vermis and hemisphere are the main elements. The precise location of the boundary fissures of a lobule, or the continuity between the fissures, separating the segments of the folial chain of the hemisphere, with their possible vermal counterparts, clearly is of less importance.The relative independence of vermis and hemispheres in the posterior lobe is supported by the mode of development of the principal transverse fissures and by interruption of the cortex between the expanding folial chains of vermis and hemispheres.

Most fissures, such as the posterior superior, intercrural (horizontal), ansoparamedian, secondary, and the posterolateral fissure develop independently in vermis and hemispheres and only become confluent at a later date. The only fissure in the posterior lobe, which is continuous from the vermis into the hemispheres from the beginning of development, is the prepyramidal fissure (Bolk, 1905a, b; Larsell, 1947; Larsell and Jansen, 1972).

Functionally, vermis and hemispheres are dissociated by the complete interruption of the cortex or the lack of a molecular layer in the center of the loops of the folial chains of the hemisphere (i.e., in the intercrural or horizontal fissure for the cortex between lobule VII and the ansiform lobule, and in the caudal paramedian sulcus for the cortex between the uvula/nodulus and the paraflocculus/flocculus). At these sites the parallel fibers, which represent the only means of transverse communication in the cerebellum, are either absent or reduced in number. The cortex within a folial chain always remains continuous between successive segments (Voogd, 1964, 1998). In most species the cortex of the pyramis is continuous with the hemisphere caudal to the prepyramidal fissure. The cortical bridge between pyramis, caudal paramedian lobule, and dorsal paraflocculus was identified by Ellioth Smith (1902, 1903) as the copula pyramidis. Interruptions of the cortex also were noticed in the human

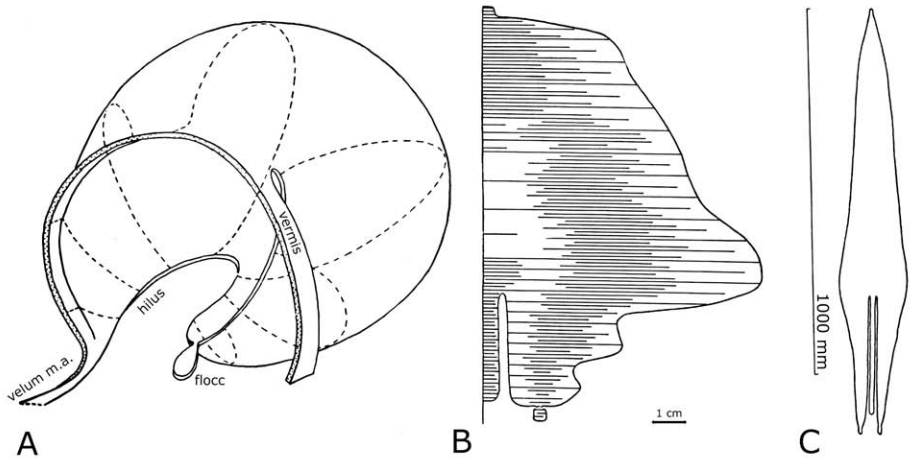

FIGURE 11.7 Braitenberg's graphical reconstructions of the cerebellar cortical sheet (Braitenberg and Atwood, 1958). **A.** Diagrammatic representation of right half of the human cerebellum as viewed from the medial side. For graphic purposes the discontinuous portion of the vermis is bent posteriorly. Dotted lines show direction of folia. The midline margin of the cerebellar sheet is cut. **B.** Plane representation of the right half of the cerebellar cortical sheet. Horizontal parallel lines have the actual measured length of the folia; three lines represent 10 folia. Actual vertical distances in this representation can be obtained by multiplying number of horizontal lines by 10 mm. **C.** Plane representation of human cerebellar cortical sheet, in which maximum length and width of the unfolded cortical sheet are represented in their true proportions (about 7:1).

cerebellum, in the lateral folium and tuber (VIIf and VIIt, Fig. 11.4F), and in the caudal paramedian sulcus in the region of the nidus avis (Figs. 11.2E and 11.4E, F). Striking illustrations of the independent expansion of the folial chains of vermis and hemispheres (which, however, ignore the continuity at the site of the copula pyramidis) were published by Braitenberg and Atwood (1958) (Fig. 11.7) for the human cerebellum and by Sultan and Braitenberg (1993) for many mammalian species. These figures also show to advantage the proportions of the folial chains, with their great length and relatively narrow width.

The nomenclatures of Bolk and Larsell as used in this chapter, are based on the comparative anatomy of the cerebellum. However, this does not guarantee the homology of fissures or fissures indicated with a name or number. These nomenclatures are primarily descriptive tools, based on criteria such as the developmental age and adult continuity of fissures, the general shape of lobules, or the apperence of the arbor vitae. The constancy of the paramedian sulcus and of some of the transverse fissures, such as the preculminate, primary, prepyramidal, secondary, and posterolateral fissures, is indicative of the homology of the intercalated lobules. However, homologies beyond this crude pattern generally remain uncertain. True homologies should be based on essential properties of the lobules, such as their zonal composition or on sound knowledge of the genetics and the developmental biology of the folial pattern (see Hatten and Heintz, 1995; Herrup and Kuemerle, 1997; Ozol *et al.*, 1999 for a discussion of this subject).

Homologies of the region of the biventral lobule, the tonsilla, and the flocculus with the paraflocculus and flocculus of the cerebellum of nonhuman primates have been notoriously difficult to establish. In monkeys (Fig. 11.8C) the cortex in the caudal paramedian sulcus, between uvula (lobule IX) and nodulus (X) and the hemisphere, is completely interrupted. The cortex of the pyramis (VIII) is continuous in the bottom of the paramedian sulcus with the caudal paramedian lobule (corresponding to the copula pyramidis). On the ventral surface (Fig. 11.8B) the cortex of the paramedian lobule is continuous with the folial chain of the dorsal paraflocculus. Rostrally the dorsal paraflocculus forms a laterally directed loop, the lobulus petrosus, which is lodged in the subarcuate fossa of the petrosal bone. At the rostral surface of the cerebellum a narrow bridge of cortex connects the rostral limb of the folial loop of the lobulus petrosus with the ventral paraflocculus (Fig. 11.8A). The deep, subfoliated posterolateral fissure separates the ventral paraflocculus from the flocculus, which includes the caudal 4 or 5 folia of the chain. Flocculus, (dorsal) paraflocculus, and paramedian lobule differ in their intrinsic zonal organization in most mammals (Voogd, 1998; see "Longitudinal Zonation of the Cerebellum" for more particulars). In monkeys the zonal organization of the flocculus and the ventral paraflocculus is very similar, sudden changes are observed at the transitions of the ventral paraflocculus

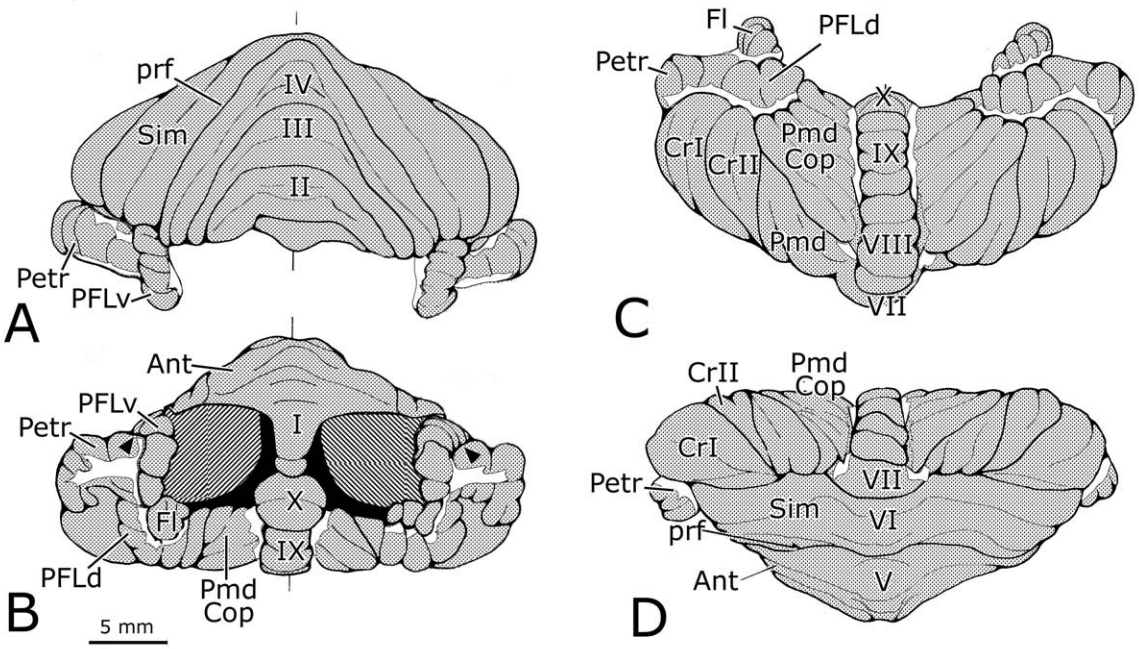

FIGURE 11.8 The cerebellum of *Macaca fascicularis*. **A.** Anterior aspect. **B.** Ventral aspect with cut surface of the cerebellar peduncles *(hatched)*. **C.** Caudal aspect. **D.** Dorsal aspect. Areas covered by cortex are shaded. The folial chains are bordered by white matter coming to the surface. Areas without cortex thus separate the ansiform and paramedian lobules from the caudal vermis, and from the dorsal paraflocculus and the petrosal lobule (in **B, C,** and **D**).White matter separates the rostral and caudal limbs of the petrosal lobule (in **B**) and the ventral paraflocculus with the flocculus from the dorsal paraflocculus (in **B** and **C**). The transition from the petrosal lobule into the ventral paraflocculus is indicated by arrowhead. Abbreviations: I–X, lobules I–X of Larsell; Ant, anterior lobe; Cop, copula pyramidis; CrI, crus I of the ansiform lobule; CrII, crus II of the ansiform lobule; Fl, flocculus; fps, fissura prima; Petr, petrosal lobule; PFLd, paraflocculus dorsalis; PFLv, paraflocculus ventralis; Pmd, lobulus paramedianus; Sim, lobulus simplex.

into the petrosal lobule and of the dorsal paraflocculus into the paramedian lobule (Figs. 11.49 and 11.50). A petrosal lobule and its subarcuate fossa are present in all monkeys of the old and the new world, but absent in homenoids, with the exception of *Hylobates* (Gannon *et al*., 1988).

Data on the gross anatomy of the cerebellum of the great apes are scarce (Larsell and Jansen, 1972), and the zonal organization of their cerebella and that of the human cerebellum has not yet been studied. The homology of the lobules in this region as stated by Bolk (1902, 1906) and Larsell (Larsell and Jansen, 1972) therefore remains uncertain. They maintain that the copula (lobule VIIIA) is represented by the lateral belly of the biventral lobule, the dorsal paraflocculus (lobule HVIIIB) by its medial belly, and the ventral paraflocculus by the tonsilla (lobule HIX). According to Larsell and Jansen (1972), the accessory paraflocculus (HIX; Loyning and Jansen, 1955) is connected to the tonsilla and separated from the flocculus proper (lobule HX). For several reasons these homologies appear unlikely.

In most mammals the dorsal and ventral paraflocculus can be distinguished as the two limbs of a continuous cortical loop, but they are certainly not homologous in different species (Fig. 11.49). In carnivores the dorsal paraflocculus and the proximal part of the ventral paraflocculus (in rodents and lagomorphs represented by the petrosal lobule) display the typical two- or three-zonal architecture of the paraflocculus. The distal part of the ventral paraflocculus [indicated in the cat as the ME, the medial extension of the ventral paraflocculus, by Gerrits and Voogd (1982)], corresponding to folium P in the rabbbit (Yamayoto, 1979), shares its zones with the flocculus. In monkeys these floccular zones extend over the entire ventral paraflocculus. Therefore, it appears unlikely that the huge tonsilla of the human cerebellum would represent the homologue of the ventral paraflocculus of monkeys; a homology with the dorsal paraflocculus seems much more likely. Whether pars of the biventral lobule should be included with the dorsal paraflocculus cannot be decided at present. The accessory paraflocculus probably is the homologue of ventral paraflocculus of monkeys. The

narrow cortical bridge between the ventral paraflocculus and the petrosal lobule in monkeys is not present in the human cerebellum, where white matter separates the accessory paraflocculus from the tonsilla and a petrosal lobule is absent.

CEREBELLAR NUCLEI

The four central cerebellar nuclei were first distinguished by Stilling (1864) in the human cerebellum (Fig. 11.9). Their morphology was extensively reviewed by Ziehen (1934) and more recently by Larsell and Jansen (1972). The cerebellar nuclei border on the fourth ventricle and the vestibular nuclei. The border with the vestibular nuclei is not distinct because the large cells of Deiters' nucleus, which are a prominent feature of this transitional area in lower mammals, are difficult to distinguish in the human brain (see Chapter 33).

The medial or fastigial nucleus is located next to the midline. It consists of several cell groups, which have not been named. Its rostral and dorsal parts are traversed by thick fibers of the uncinate tract, which decussates in between the fastigial nuclei of both sides. Laterally it is delimited by a cellular ridge, which extends in the cerebellar white matter of the vermis (Fig. 11.10B, C). In monkeys this ridge can be considered as part of the interstitial cell groups (Fig. 11.12).

The globose nucleus consists of several cell groups, separated by fiber bundles. It extends far caudally, where these cell groups fuse into a single mass. The emboliform nucleus has about the same rostrocaudal

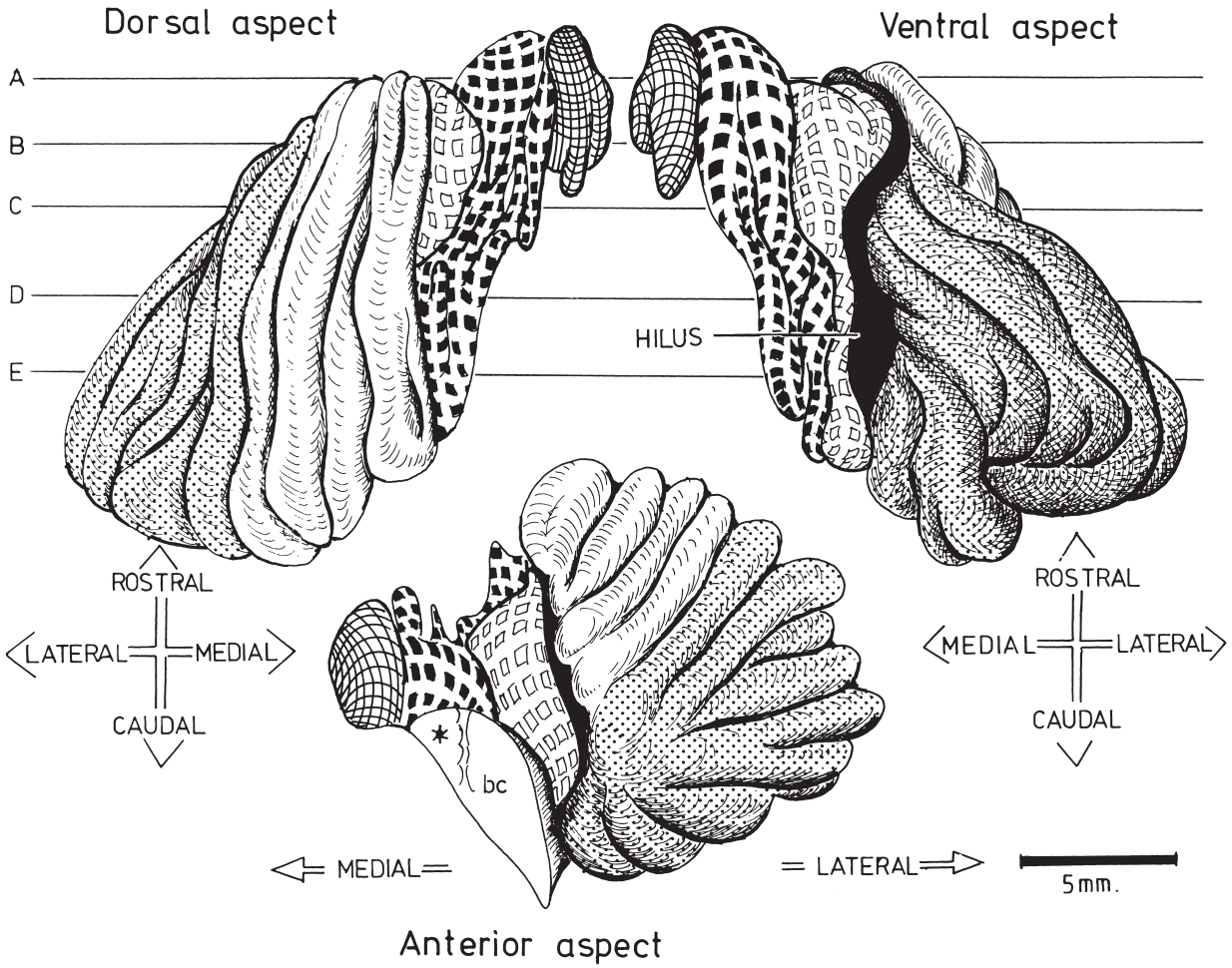

FIGURE 11.9 Graphical reconstructions of the central cerebellar nuclei of the human cerebellum. Dorsal, ventral and anterior views. Fastigial nucleus: double hatched; globose nucleus: filled squares; emboliform nucleus: open squares; the macrogyric, ventrolateral portion of the dentate is indicated by dots. The medial component of the brachium conjuctivum is indicated by an asterisk. The levels of the sections depicted in Figure 1.10A–E are indicated.

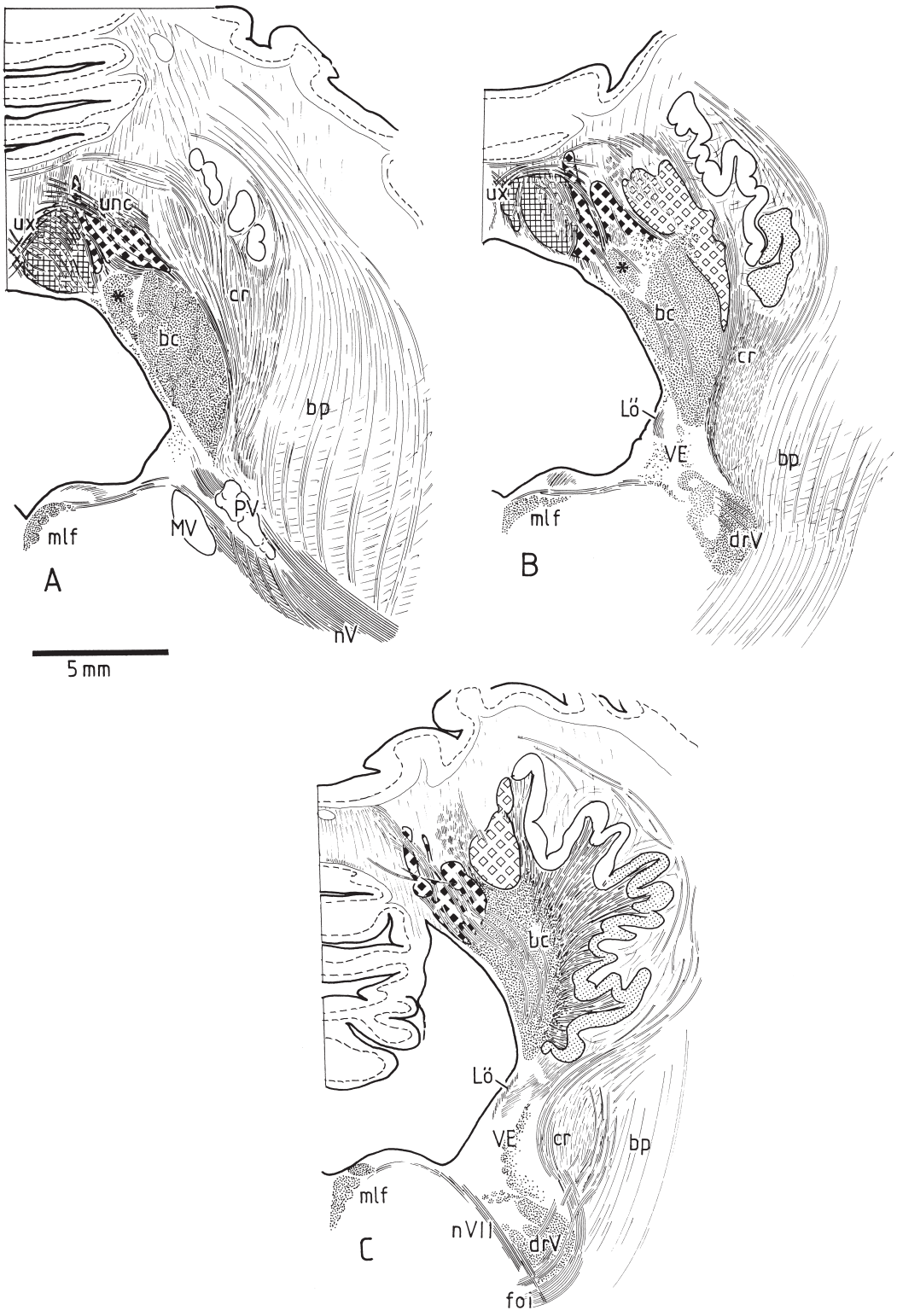

FIGURE 11.10 The cerebellar nuclei, drawn from Klüver-stained serial sections. Fastigial nucleus: double hatched; globose nucleus: filled squares; emboliform nucleus: open squares; the macrogyric part of the dentate is indicated by dots. **A:** Section through the rostral pole of the dentate nucleus. The medial component of the brachium conjunctivum is indicated with an asterisk. **B:** Section through the middle part of the fastigial nucleus. **C:** Section through the middle part of the emboliform and globose nuclei. *Continued*

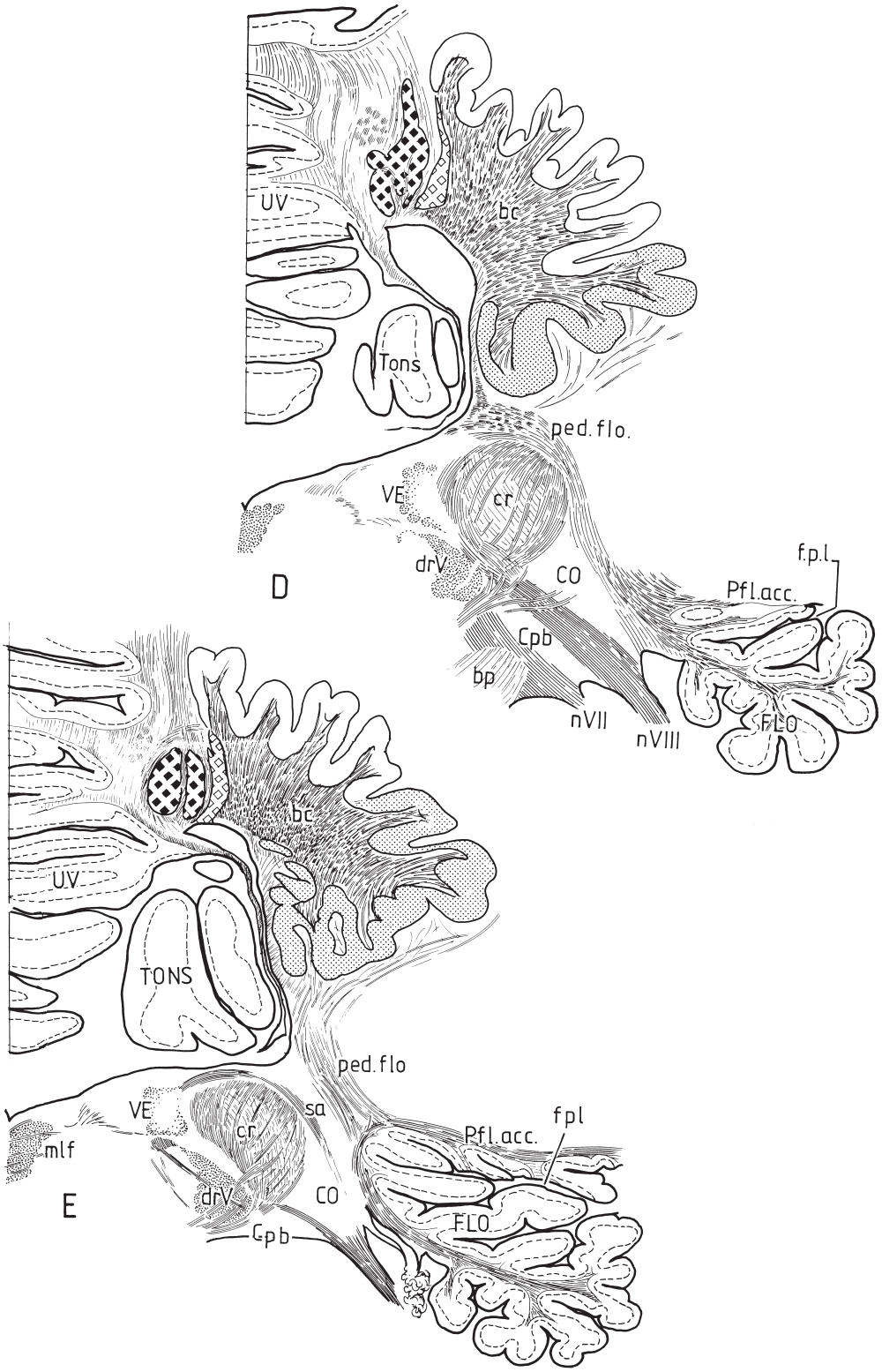

FIGURE 11.10 *Continued* **D:** Section through the floccular peduncle. **E:** Section through the caudal pole of the globose and emboliform nuclei. Abbreviations: CO, cochlear nuclei; Cpb, pontobulbar body; cr, restiform body; drV, spinal tract of the trigeminal nerve; f.p.l., posterolateral fissure; Foi, olivocerebellar fibers; Lö, bundle of Loewy; mlf, medial longitudinal fascicle; MV, motor nucleus of the trigeminal nerve; nV, trigeminal nerve; nVII. Facial nerve; Ped.flo, floccular peduncle; Pfl.acc., accessory paraflocculus of Henle; PV, principal sensory nucleus of the trigeminal nerve; sa, acoustic striae; Tons, tonsilla; UV, uvula; VE, vestibular nuclei.

extent as the globose nucleus. The two nuclei are completely separated by fiber bundles. The emboliform is a compact nucleus, which tapers caudally and fuses with the medial lamina of the dentate nucleus (Fig. 11.10D, E). The fastigial, globose, and emboliform nuclei contain cells of all sizes, but the larger cells are present in the emboliform nucleus.

The dentate nucleus has the shape of a "crumpled purse" (Chan-Palay, 1977) with its hilus directed ventromedially and rostrally. Two parts of the nucleus can be distinguished (Figs. 11.4A, B, 11.9 and 11.10). Its dorsomedial part is folded in rather narrow, rostrocaudally directed ridges. It is known as the microgyric part of the dentate nucleus. The ridges in the ventrolateral part of the nucleus are broad and subdivided, and the cell band in this part of the nucleus is wider than in the microgyric part. Their direction is obliquely laterally and caudally, and the ridges turn inward and can be followed at he ventral surface of the nucleus. Caudally the hilus is closed by the medial lamina of the dentate. The cells of the microgyric part of the dentate are larger than those in the macrogyric position of the nucleus (Demolé, 1927a, b), but both subdivisions also contain small neurons (Fig. 11.11).

The cerebellar nuclei of mammals can be subdivided according to Brunner (1919) into three mediolaterally arranged nuclei or according to Weidenreich (1899) and Ogawa (1935) in rostrolateral and caudomedial groups. Cytoarchitectonic criteria can be used to subdivide the cerebellar nuclei, but the presence of fiber bundles, and the disposition of their efferents in the nuclear hilus and in their efferent tracts are especially important in this respect. Brunner's (1919) mediolateral subdivision into the medial (fastigial), lateral (dentate), and interposed nuclei is based on the contours of the central nuclear mass. The three nuclei are part of a continuum and the nuclear borders therefore remain arbitrary. Although Brunner's concept of the cerebellar nuclei as a single mass has been disproved, his names for the nuclei have stuck. Weidenreich's (1899) comparative studies in mammals had already shown that fiber bundles subdivide the nuclei into a caudomedial group, which includes the fastigial nucleus and the caudal part of the Brunner's interposed nucleus (the nucleus interpositus posterior of Ogawa, 1935), and a rostrolateral group which is composed of the dentate nucleus and the rostral part of the interposed nucleus (the nucleus interpositus anterior). The nuclei within each group are interconnected by cell bridges. The subdivision of Weidenreich and Ogawa can be readily appreciated in lagomorpha (Ono and Kato, 1938; Snider, 1940), in carnivores (Flood and Jansen, 1961; Voogd, 1964), and in primates (Courville and Cooper, 1970; Chan-Palay, 1977). In rodents and insectivores the separation between the two nuclear groups is less

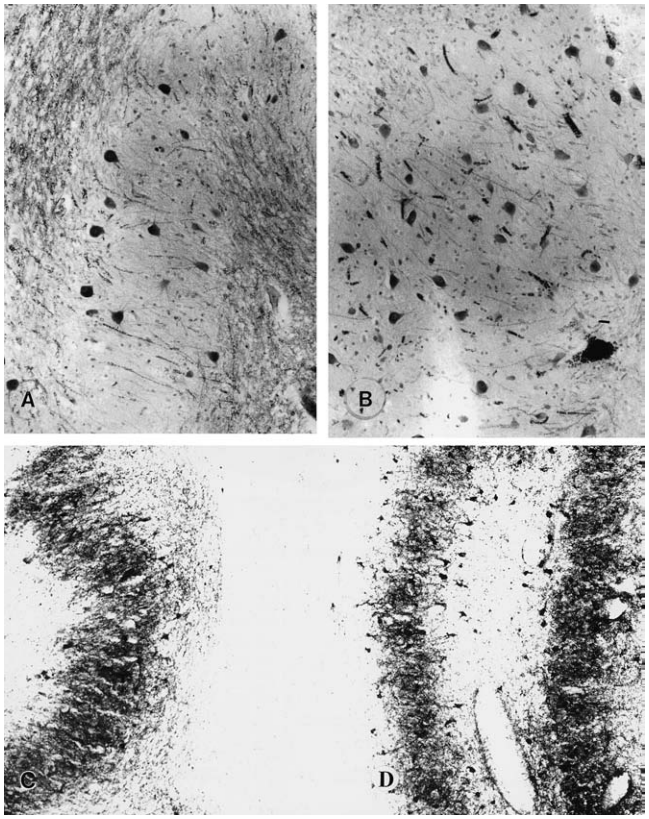

FIGURE 11.11 **A.** The dentate lamella. microgyric (magnocellular) part. Magnification 50×. **B.** Macrogyric (parvicellular) part. Same magnification. **C.** Section incubated with an antibody against glutamic acid decarboxylase. Small GABAergic cells and neuropil of the dentate lamella are stained. Magnification ×35. Courtesy of J. C. Adams and E. Mugnaini.

distinct and the connections between the nuclei of each group are more extensive (Korneliussen, 1968; Ohkawa, 1957).

The topographical relations of the fastigial, globose, and emboliform nuclei of man resemble those of the fastigial nucleus and the posterior and anterior interposed nuclei of nonhuman primates (Courville and Cooper, 1970). The fastigial nucleus of the monkey is broadly fused with the posterior interposed nucleus. Caudally this connection is U shaped (Fig. 11.12, section 120); rostrally it continues into a lateral "ridge" of the fastigial nucleus and scattered cells in the region between the fastigial and anterior interposed nuclei (Fig. 11.12, section 165). The U-shaped subnucleus probably is identical to the "interstitial cell groups," described by Buisseret-Delmas *et al.* (1993) in the same position in the rat. In the rat it is the recipient of the X zone, one of the Purkinje cell zones of the vermis (Fig. 11.46 in "Longitudinal Zonation of the Cerebellum"). The anterior interposed and dentate nuclei are interconnected in the same way as the emboliform and dentate nuclei in the human cerebellum. The

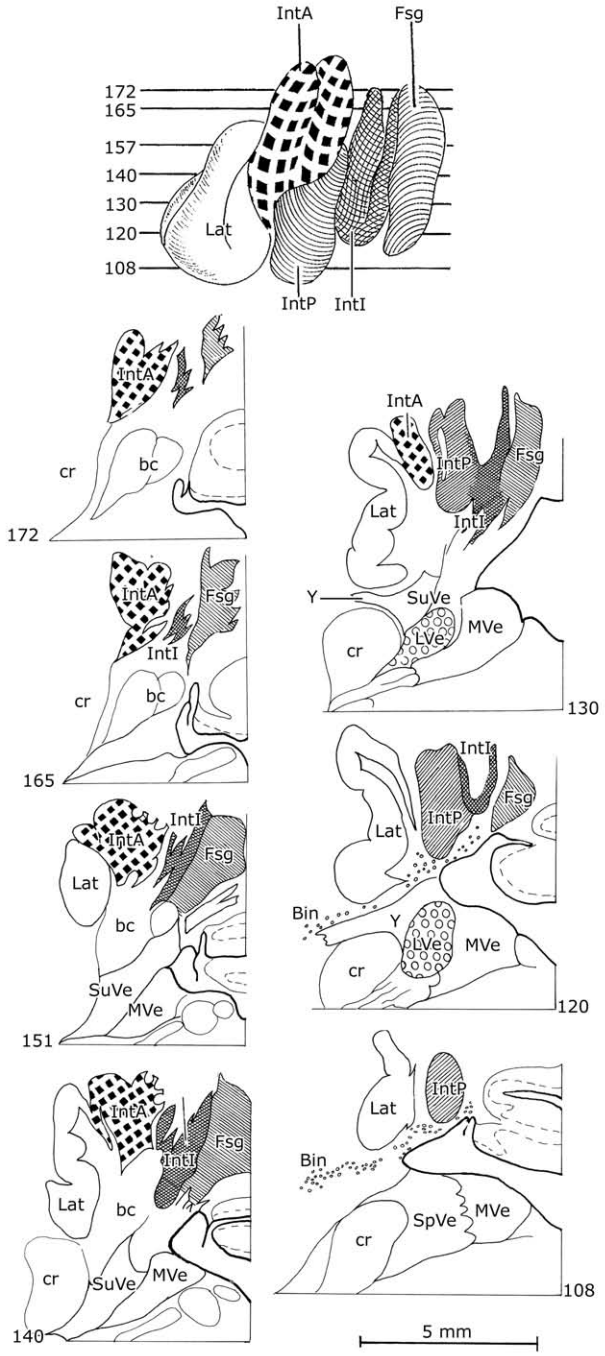

FIGURE 11.12 The cerebellar nuclei of the *Macaca fascicularis*. Upper diagram: graphical reconstruction of the dorsal aspect of the cerebellar nuclei. Levels of the diagrams are indicated by lines. Below are drawings of serial, acetylcholinesterase-stained sections. The U-shaped, intermediate cell group (IntI) located between the fastigial and interposed nuclei is indicated by double hatching. The basal interstitial nucleus of Langer (Bin) is indicated by dots. The medial component of the brachium conjunctivum is indicated with an asterisk. Abbreviations: bc, brachium conjunctivum; Bin, basal interstitial nucleus; bp, brachium pontis; cr, restiform body; Fsg, fastigial nucleus; IntA, anterior interposed nucleus; IntI, intermediate cell group; IntP, posterior interposed nucleus; Lat, lateral cerebellar nucleus; LVe, lateral vestibular nucleus of Deiters; Mve, medial vestibular nucleus; SpVe, spinal vestibular nucleus; SuVe, superior vestibular nucleus; Y, group Y.

anterior and posterior interposed nuclei in the monkey extend over approximately the same rostrocaudal extent (Fig. 11.12): therefore, the adjectives "anterior" and "posterior", are not entirely appropriate; they are derived from the situation in lower mammals, where the two nuclei occupy a rostral and a caudal position. The general shapes of the dentate nucleus and the lateral cerebellar nucleus of the monkey are the same, but a homology of their subdivisions is not yet possible.

One group of small neurons in the rhesus monkey, which was described by Langer (1985) under the name of the basal interstitial nucleus, displays uniform and strong AChE activity. These small cells lie dispersed in the white matter of the flocculus and the nodule and ventral to the dentate and the posterior interposed nucleus, in the roof of the fourth ventricle (Fig. 11.12). The basal interstitial nucleus is reciprocally connected with the flocculus and possibly projects to other lobules of the cerebellum (Langer, 1985). In this respect, it differs from the group Y (Brodal and Pompeiano, 1957), which is a lateral extension of the superior vestibular nucleus, located ventral to the dentate nucleus (Fig. 11.12). The group Y gives rise to projections to the oculomotor nuclei (Graybiel and Hartwieg, 1974; Sato *et al.*, 1984; Stanton, 1980b; Steiger and Büttner-Ennever, 1979; Yamamoto *et al.*, 1986). The group Y is large in monkeys but less conspicuous in the human brain (see Chapter 33). The basal interstitial nucleus has not been identified in the human cerebellum.

Two populations of neurons have been distinguished in all cerebellar nuclei. One consists of small GABAergic neurons, which project exclusively to the inferior olive (Graybiel *et al.*, 1973; Tolbert, 1976, Mugnaini and Oertel, 1981, 1985; see also "Afferent Systems of the Inferior Olive: The Nucleoolivary Projection"). These small GABAergic neurons also has been demonstrated in the human cerebellar nuclei (Mugnaini, personal communication) (Fig. 11.11C). The other population consists of excitatory relay cells with widespread, branching axons, terminating in the brain stem, spinal cord, and thalamus. They constitute a mixed population of cells of all shapes and sizes (Courville and Cooper, 1970). The possible excitatory neurotransmitters of the relay cells were reviewed by Voogd *et al.* (1996b). A third population of small interneurons was identified by Chan-Paly (1977) on morphological grounds in the monkey and by Chen and Hillman (1993) on the basis of their neurotransmitter content in the rat.

In the human cerebellum the dentate nucleus can be subdivided into ventromedial magnocellular and caudolateral parvocellular parts. These two regions also differ in their development, the rostromedial portion differentiating before the caudolateral dentate (De Sanctis, 1898, 1902/1903; Weidenreich, 1899; Vogt and Astzwazaturow, 1912; Brun, 1917/18a–c, 1925a, b), and

in the higher iron content of the caudolateral dentate (Gans, 1924). The latter observation probably constitutes first instance of a neurochemical differentiation within the cerebellum. The caudolateral dentate usually was involved in human cases of "neocerebellar atrophy," which mainly affected the hemisphere and spared the flocculus and the vermal and paravermal cortex and the other cerebellar nuclei, including the rostromedial dentate (Brouwer, 1913, 1915; Brouwer and Coenen, 1920, 1921; Brun, 1917/18a–c, 1925a, b). To express the differential vulnerability of the two parts of the human dentate nucleus they became known as the rostromedial palaeodentatum and the caudolateral neodentatum. The homology of the two parts of the human dentate with possible subdivisions of the dentate nucleus of monkeys is not clear. However, there are indications for a subdivision of the monkey dentate on the basis of the corticonuclear and efferent connections of this nucleus, which will be discussed in later sections of this chapter.

CEREBELLAR PEDUNCLES: TOPOGRAPHY OF PATHWAYS FROM THE HUMAN CEREBELLAR NUCLEI

Cerebellar Peduncles

Superior, inferior, and middle cerebellar peduncles generally are distinguished (Fig. 11.13). The superior peduncle contains a compact, sickle-shaped fiber bundle, the brachium conjunctivum, which consists of fibers from all the ipsilateral cerebellar nuclei. The middle cerebellar peduncle, or the brachium pontis, is located laterally. The middle peduncle is purely afferent. Its origin from the contralateral pontine nuclei was first demonstrated by Vejas (1885) in chronic experiments in the rabbit. The inferior peduncle consists of external and internal divisions: the restiform body and the juxtarestiform body (Stilling, 1846). The fiber bundles of the juxtarestiform body are located medial to the restiform body, within the lateral and spinal vestibular nuclei. They consist of the ascending and descending branches of the vestibular root fibers, intrinsic vestibular connections, crossed and uncrossed efferent pathways from the fastigial nucleus, and Purkinje cell axons that enter the juxtarestiform body from the flocculus and the vermis. The restiform body consists of afferent fibers

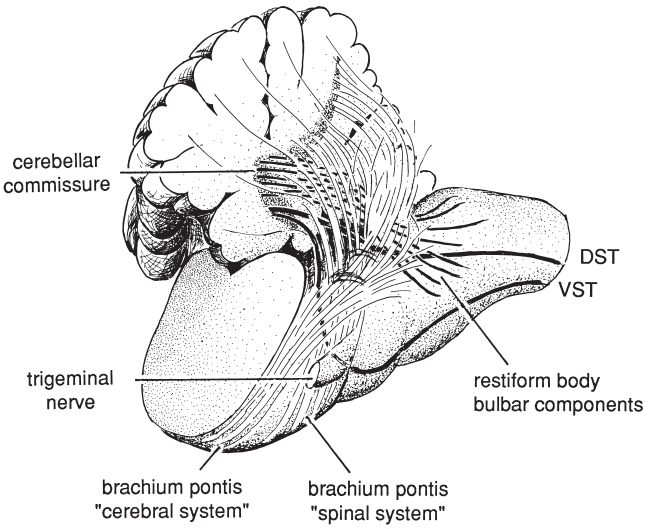

FIGURE 11.13 Diagram of the extra- and intracerebellar course of the main fiber systems terminating as mossy fibers in the cerebellum of the cat. *Thin lines:* pontocerebellar fibers. *Heavy lines:* bulbo- and spinocerebellar systems. The ventral spinocerebellar tract passes rostral to the root of the trigeminal nerve. From Voogd (1967).

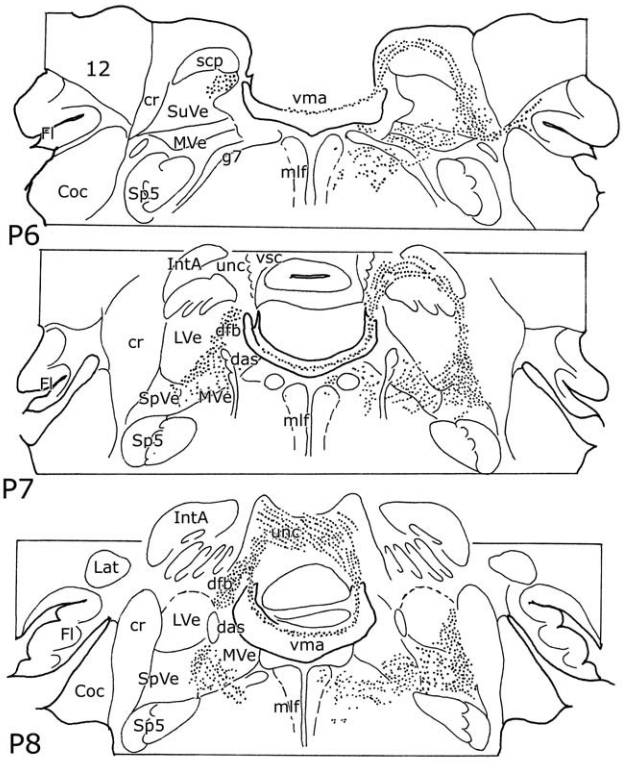

FIGURE 11.14 Diagram of the efferent pathways from the left fastigial nucleus in the cat. course of the direct fastigiobulbar tract **(left)** and the uncinate tract **(right)** in the stereotatic planes P.6–P.8. The situation in monkeys is very similar to the cat. Abbreviations: bp, brachium pontis; Coc, cochlear nuclei; cr, restiform body; das, acoustic striae; dfb, direct fastigiobulbar tract; Fl, flocculus; g7, genu of facial nerve; IntA, anterior interposed nucleus; Lat, lateral cerebellar nucleus; LVe, lateral vestibular nucleus of Deiters; mlf, medial longitinal fascicle; MVe, medial vestibular nucleus; scp, brachium conjunctivum; Sp5, spinal tract of the trigeminal nerve; SpVe, spinal vestibular nucleus; SuVe, superior vestibular nucleus; unc, uncinate tract; vma, anterior medullary velum; vsc, ventral spinocerebellar tract. Modified by Voogd (1964).

from the brain stem and the spinal cord that pass lateral to the spinal tract of the trigeminal nerve to enter the cerebellum in between the brachium pontis and the brachium conjunctivum. One group of spinocerebellar fibers does not join the restiform body but enters the cerebellum far rostrally, along the brachium conjunctivum, by passing ventral to the entering root of the trigeminal nerve (Fig. 11.13). At its emergence from the hilus of the cerebellar nuclei the brachium conjunctivum intersects with the juxtarestiform body. Bundles of Purkinje cell axons pass as perforating fibers through the brachium at its emergence from the hilus of the dentate nucleus (Fig. 11.10B, C).

Topography of Efferent Pathways from the Fastigial Nucleus

The efferent pathways of the fastigial nucleus have not been studied in man, fragmentary information is available from the myelogenetic studies of von Bechterew (1888, 1899) and De Sanctis (1898, 1902/03). Von Bechterew traced fibers from the fastigial nucleus to the superior olive. Obviously he mistook the early myelinating fibers of the olivocochlear bundle for the distal part of this pathway. The fibers crossing between the fastigial nuclei, which he saw arching over the brachium conjunctivum (Fig. 11.15, fos), clearly belong to the uncinate tract. In humans the decussating fibers of the uncinate tract occupy the dorsal and rostral periphery of the fastigial nucleus. Dorsally the decussation extends into the anterior medullary velum (Figs. 11.14 and 11.16). Fibers of the afferent component of the cerebellar commissure, which are thinner and are derived from the restiform body and the brachium pontis, occupy a more peripheral position.

In the cat (Fig. 11.14) the fibers of the uncinate tract subsequently arch over the brachium conjunctivum, to take up a position in the lateral part of the juxtarestiform body, traveling lateral to Deiters' nucleus, in the ventrolateral portion of the descending vestibular nucleus. A small bundle detaches from the uncinate tract, to ascend to the mesencephalon, dorsomedial to the brachium conjuctivum. The ascending limb of the uncinate tract was first described in the experimental studies of Probst (1902). In cat (Voogd, 1964) (Fig. 11.14) and monkey (Batton *et al,* 1977), a bundle of coarse fibers from the ipsilateral fastial nucleus passes medial to the brachium and Deiters' nucleus, to become located in the medial part of the juxtarestiform body. These "direct fastigiobulbar fibers" have not been observed in human material. The third, efferent pathway from the fastigial nucleus consists of fibers traveling in the medial third of the brachium conjuctivum. This component has been substantiated in the experimental studies of Voogd (1964) in the cat, and of Batton *et al.* (1974) and Asanuma *et al.* (1983c) in

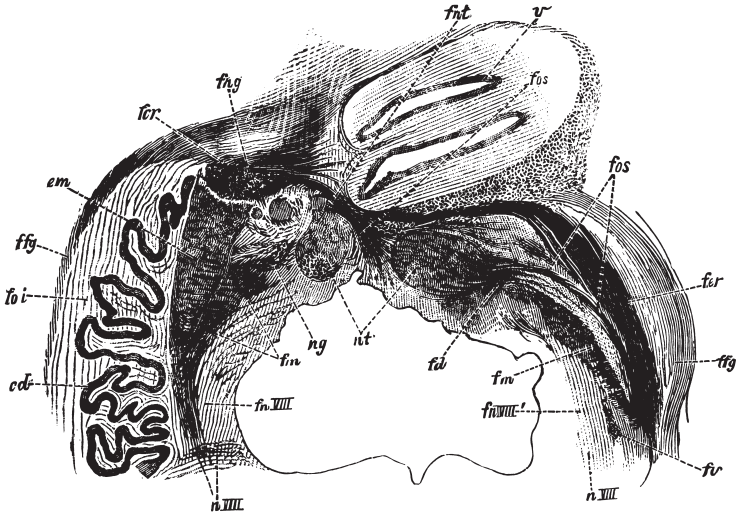

FIGURE 11.15 Myelin-stained section through the cerebellum of a human fetus of 44 cm. Abbreviations: cd, dentate nucleus; emboliform nucleus; fcr, spino-, cuneo-, and lateral reticulocerebellar fibers in restiform body; fd, fm, and fv, dorsal, medial, and ventral components of the brachium conjunctivum; ffg, external arcuate fibers; foi, unmyelinated olivocerebellar fibers; fng and fnt, fibers from central nucleus to the cortex; fos, fibers from fastigial nucleus to superior olive (uncinate tract); fnVIII', vestibulocerebellar fibers; nVIII, Von Bechterew's superior vestibular nucleus; ng, globose nucleus; nt, fastigial nucleus; v, vermis. From Von Bechterew (1899).

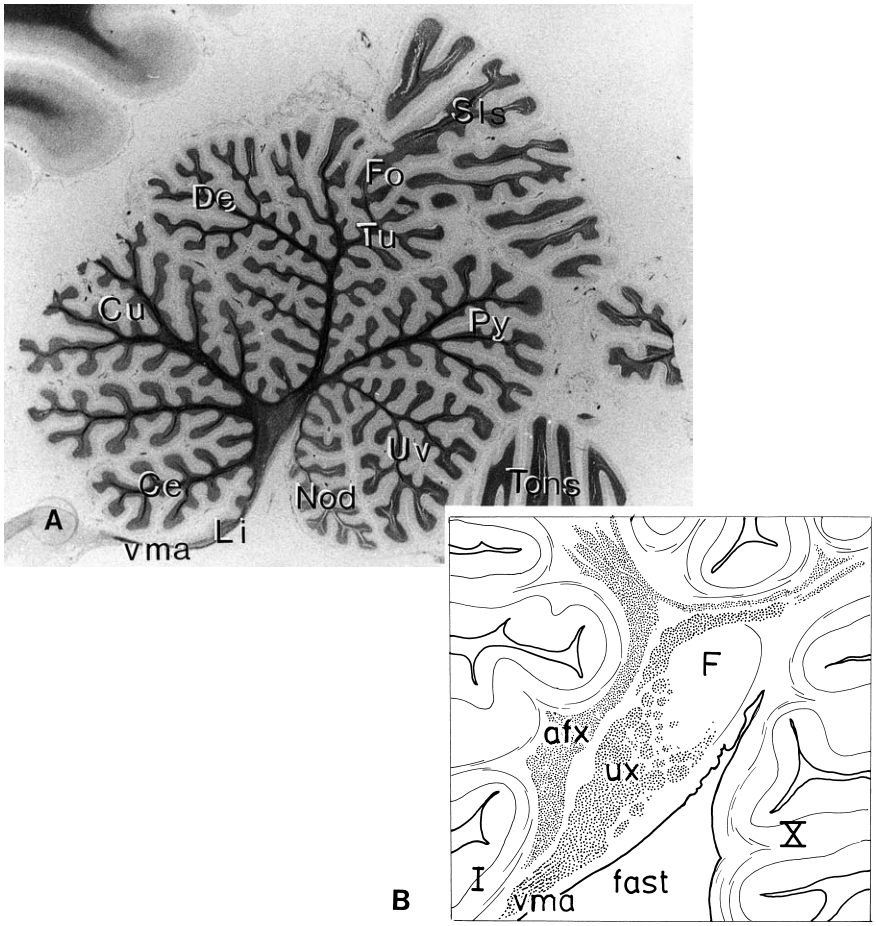

FIGURE 11.16 **A:** parasagittal section of the human cerebellum located near the midline. Klüver stain. **B:** Diagram of the afferent and uncinate components of the cerebellar commissure. Abbreviations: Ce, central lobule; Cu, culmen; De, declive; Fo; Folium vermis; Tu, tuber vermis; Py, pyramis; Sis, superior semilunar lobule; Uv, uvula; Nod, nodulus; Tons, tonsilla; vma, velum medullare anterior; afx, cerebellar comissure: afferent portion; ux, cerebellar commissure, uncinate tract; F, fastigial nucleus; Fast, fastigium.

monkeys. The fate of this fastigial efferent pathway is not known.

Origin, Course and Termination of the Brachium Conjunctivum in the Human Brain

The subdivision of the cerebellar nuclei by Weidenreich and Ogawa receives strong support from the localization of their efferent tracts in the brachium conjuctivum. A small medial and a large lateral portion can be distinguished in the brachium in most mammals at its exit from the cerebellar nuclei (Verhaart, l956b). Experiments in cats (Voogd, 1964) (Fig. 11.17A), rat (Haroian *et al.*, 1981), and monkey (Kievit, 1979; Stanton,1980a; Kalil, 1981) have shown that the medial part of the brachium takes its origin from the nuclei of the caudomedial group, the ipsilateral fastigial and posterior interposed nucleus, and the lateral portion from the ipsilateral anterior interposed and lateral cerebellar nucleus. The excitatory anterior canal—vestibulooculomotor neurons of the superior vestibular nucleus, and possibly from the group Y—occupy the extreme ventrolateral pole of the brachium conjunctivum (Highstein and Reisine, 1979; Lang *et al.*, 1979, Hirai and Uchino, 1984; Steiger and Büttner-Ennever, 1979).

In humans the brachium conjunctivum emerges from the hilus of the dentate and the ventral aspect of the emboliform nucleus. Its dorsomedial part contains a bundle of larger fibers embedded in a small fiber area (Verhaart, 1956b), which is separated from the rest of the brachium by an unmyelinated streak. This portion of the brachium seems to take its origin from the globose nucleus and possibly from the fastigial nucleus (Figs. 11.9 and 11.10A, B, *asterisk*). Such an origin would be in accord with the situation in lower

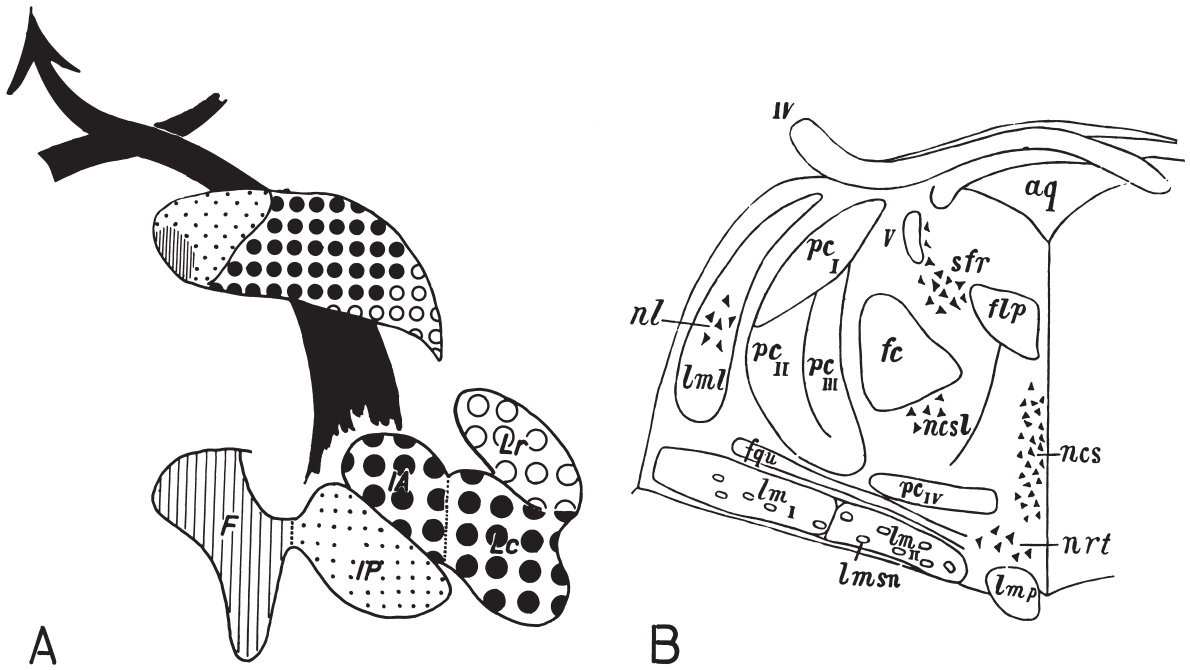

FIGURE 11.17 Components of the brachium conjunctivum. **A.** The brachium conjunctivum in the cat. Fibers from the fastigial and posterior interposed nucleus occupy its medial one-third; fibers from the anterior interposed and the dorsal part of the lateral nucleus (Lc) occupy the middle region of the brachium; fibers from the ventral part of the lateral nucleus (Lc) occupy its lateral pole. From Voogd (1964). **B.** The four components of the human brachium conjunctivum according to Von Bechterew (1888, 1899). pcI: early myelinating dorsal bundle from fastigial and globose nuclei (Fig. 11.15: fd); pcII: later myelinating fibers from emboliform nucleus (Fig. 11.15: fm); pcIII: fibers from dentate nucleus, myelinate postnatally (Fig. 11.15: fi); pcIV: fibers from the vestibular nuclei are the first to acquire their myelin sheaths (Fig. 11.15: fv). Abbreviations: aq, aqueduct; F, fastigial nucleus; Fc, central tegmental tract; Flp, medial longitidinal fascicle; IA, anterior interposed nucleus; IP, posterior interposed nucleus; IV, trochlear nerve; Lc, dorsocaudal part of lateral cerebellar nucleus; lmI, lmII, components of the medial lemniscus; Lr, ventromedial part of lateral cerebellar nucleus; msn, areae nebulosae in the medial lemniscus; Ncs, central superior nucleus; Ncsl, lateral part of the central superior nucleus; nrt, nucleus reticularis tegmenti pontis; sfr, locus coerulaeus; V, mesencephalic root of the trigeminal nerve.

mammals. Von Bechterew (1888, 1899), who studied the myelinization of the brachium conjunctivum in man, distinguished four components (Fig. 11.17B). The dorsal and middle components (PC-I and II) acquire their myelin rather early and are related to the fastigial nucleus, and the globose and emboliform nuclei, respectively. The PC-I component probably corresponds with the dorsomedial-, globose-; and fastigially derived portions of the brachium and the PC-II component includes the efferent pathway from the emboliform nucleus. The ventral component (PC-III) takes its origin from the dentate nucleus and acquires its myelin postnatally. The ventromedial position of the fibers of the dentate closely corresponds to their localization in the cat (Fig. 11.13A). The fourth component (PC-IV), which is the first to acquire its myelin, is related not to the cerebellar but to the vestibular nuclei. According to von Bechterew, it belongs to the vestibular commissure; in the pons these fibers decussate in the ventral part of the tegmentum. The ventral position of these fibers in the brachium and in its decussation are typical for the ascending vestibulooculomor fibers from von Bechterew's superior vestibular nucleus and the group Y, referred to above.

The decussation of the brachium conjunctivum consists of dorsal and ventral portions. In the ventral portion fibers from the ventral pole of the brachium cross dorsal to the interpedunclar nucleus; the dorsal portion contains decussating fibers of the dorsal and ventral brachium. Rostrally the two portions fuse and the decussation tapers out, ventral to the caudal pole of the red nucleus (Voogd, 1964). According to Chan-Palay (1977), the decussation in the monkey is incomplete: uncrossed fibers originate mainly from the caudal part of the dentate nucleus. Chan-Palay (1977) observed a dorsolateral fiber bundle, which detaches from the

brachium conjunctivum prior to its decussation, in all of her experiments with injections of tritiated methionine in the dentate nucleus. The fibers of this dorsolateral bundle decussate rostral to the main brachium and join the descending branch of the brachium conjunctivum. The course of the dorsolateral bundle in the monkey closely resembles the route followed by the nucleoolivary fibers from the interposed and dentate nuclei in cat (Legendre and Courville, 1987) and rat (Cholley *et al.*, 1989).

After their decussation the fibers of the brachium conjunctivum split in ascending and descending branches. The descending branch consists of collaterals from axons of cerebellar relay cells (Ramon y Cajal, 1909) and the nucleoolivary fibers of the dorsolateral bundle.

The fibers of the ascending branch ascend through and along the red nucleus. Apart from the red nucleus, terminations of the ascending branch include the central gray, the oculomotor nuclei, and the superior colliculus. The major ascending pathway leaves the red nucleus as a dorsolaterally directed bundle (the tegmental field H of Forel). In the subthalamus it passes through the external medullary lamina of the thalamus (field H1 of Forel) to terminate in the thalamus. This course was first described in the human brain by Forel (1877), who also coined the names for the tegmental fields (the "Haubenfeld"—tegmental field—which divides in the dorsal and the ventral "Haubenfeld," H1 and H2, with the zona incerta located in between).

The termination of the brachium conjunctivum in the thalamus in man has only been described in two studies using axonal degeneration techniques. The study of Probst (1901) used the Marchi method in a case with an isolated softening of the brachium conjunctivum. According to Probst, the decussation of the brachium is not complete, a few degenerated fibers ascend toward the ipsilateral red nucleus. The degenerated fibers traverse the red nucleus, where they are sparse in its dorsal part and where they constitute a ventromedial and lateral capsule of myelinated fibers. The dorsomedial part of the capsule of the red nucleus is formed by the emerging fibers of the central tegmental tract (Fig. 11.32; see "Afferent Systems of the Inferior Olive: The Nucleoolivary Projection"). In the subthalamus the degenerated fibers are located dorsal to the zona incerta in the external medullary lamina. Probst used von Monakow's (1895) subdivision of the thalamus. He traced some fibers into the internal medullary lamina, some of which pass through the ventral posterior nucleus (nucleus ventralis b of von Monakow) to terminate in the centre médian (nucleus medialis b). Most fibers terminate between the internal and external medullary laminae, rostral to the ventral posterior nucleus, in a region corresponding to the nucleus ventralis lateralis (nucleus ventralis a, nucleus lateralis b).

In the second study, the Nauta method was used in two cases with degeneration of the brachium conjunctivum (Gebbink, 1967). In one of these cases (H5739, Fig. 11.18) a hemorrhage destroyed the hilus of the dentate nucleus and extended into the medial half of the brachium conjunctivum (Fig. 11.19). The mesencephalon and the thalamus were sectioned sagittally. Degenerated fibers enter the thalamus from the red nucleus through the internal medullary lamina and the centre médian, where they terminate mediodorsally, and through the field of Forel, where they intermingle with the pallidal fibers from the fasciculus lenticularis. They pass rostroventral to the centre médian and dorsal to the zona incerta, which receives some degenerated fibers. Terminal degeneration is found rostral to the centre médian and rostral to the ventral posterior nucleus in the ventrolateral nucleus. Laterally and rostroventrally the amount of degeneration decreases. Some fibers enter the thalamus far rostrally from the reticular nucleus. The distribution in a second, horizontally sectioned case (H5753) with a large hemorrhage involving all cerebellar nuclei is essentially similar. In this case, degenerated fibers also were traced from the central gray into the periventricular region of the thalamus.

Gebbink (1967) also described the degeneration resulting from lesions of the globus pallidus. The sagittal sections from one of these cases (H5541, Nauta method) were redrawn together with the cerebellar degeneration in Figure 11.18. Degeneration is found in the fasciculus and ansa lenticularis, passing around the zona incerta, which did not receive a projection, into the fasciculus thalamicus. The terminations in the thalamus are located rostroventral and lateral to the main termination of the brachium conjunctivum, but there is some overlap of both projections. In addition, degeneration is present in the stria medullaris and the habenular nuclei. The centre médian is devoid of degenerated fibers.

Fibers of the descending branch of the brachium conjunctivum could be traced in the two cases with cerebellar lesions, which served as the basis for the description of the ascending branch by Gebbink (1967). One of these cases, H5739, is illustrated in Figure 11.19 (Schoen, unpublished observations). At the level of the entrance of the trigeminal nerve the degenerated descending branch occupies a triangular area in the ventromedial part of the tegmentum pontis; laterally it extends over the dorsal surface of the medial lemniscus and borders the ventromedial surface of the central tegmental tract. More caudally it intermingles with the

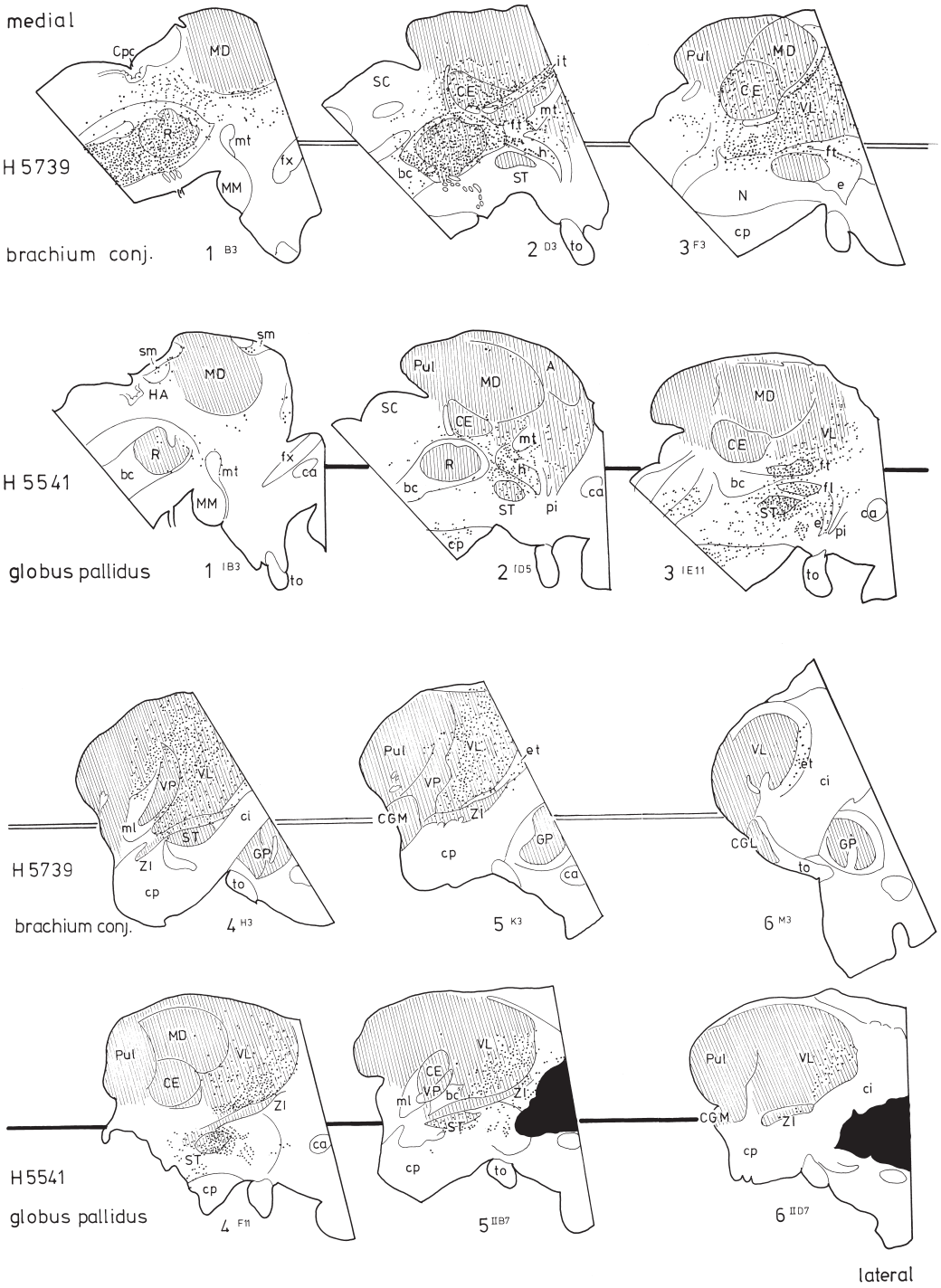

FIGURE 11.18 The termination of the ascending branch of the brachium conjunctivum in case H5739 and the fiber degeneration resulting from a lesion of the globus pallidus in case H5541. Nauta stain on sagittal sections. Lesion of the globus pallidus indicated in black. Abbreviations: Anterior thalamic nucleus; bc, brachium conjunctivum; ca, anterior comissure; CE, nucleus of the centre médian; CGL, lateral geniculate body; CGM, medial geniculate body; ci, internal capsule; cp, cerebral peduncle; Cpc, posterior commissure; e, Edinger's comb system; et, external medullary lamina; fl, fasciculus lenticularis; ft, fasciculus thalamicus; fx, fornix; GP, globus pallidus; h, tegmental field H of Forel; Ha, habenular nuclei; it, internal medullary lamina; MD, mediodorsal nucleus; ml, medial lemniscus; MM, corpus mamillare; mt, mamillothalamic tract; N, substantia nigra; pi, inferior thalamic peduncle; Pul, pulvinar; R, red nucleus; SC, superior colliculus; ST, subthalamic nucleus; to, optic tract; VL, ventral lateral nucleus; VP, ventral posterior nucleus; ZI, zona incerta. Redrawn from Gebbink (1967).

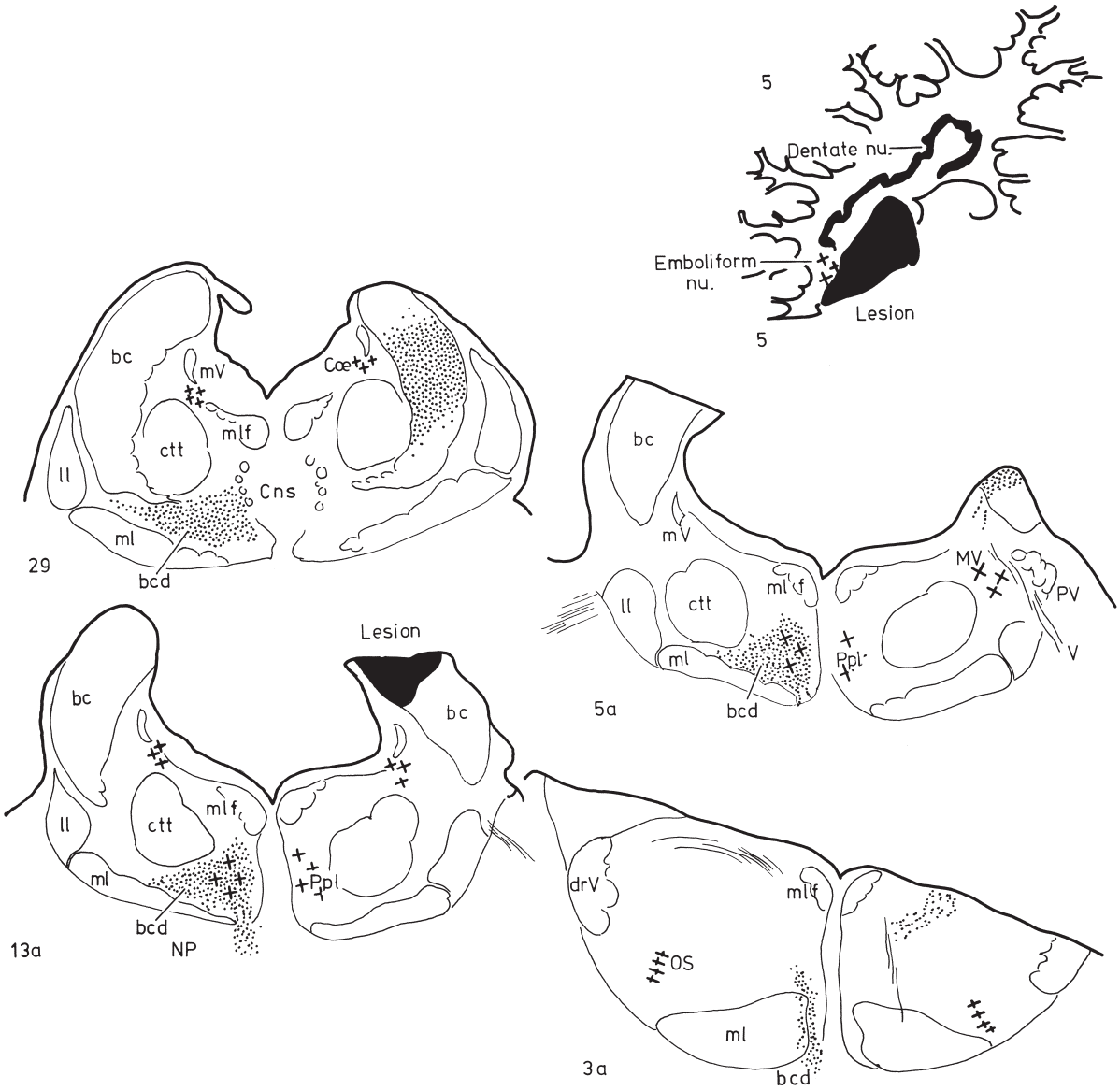

FIGURE 11.19 The termination of the descending branch of the brachium conjunctivum in the tegmentum pontis in case H5739. Nauta stain. Lesion indicated in black in a parasagittal section and in section 13a. (Schoen, unpublished). Abbreviations: bc, brachium conjunctivum; bcd, brachium conjunctivum descendens; Cns, central superior nucleus; Coe, locus coeryulaeus; ctt, central tegmental tract; drV, spinal tract of the trigeminal nerve; ll, lateral lemniscus; ml, medial lemniscus; mlf, medial longitudinal fascicle; mV, mesencephalic root of the trigeminal nerve; MV, medial vestibular nucleus; NP, basal pontine nuclei; nu, nucleus; OS, superior olive; Ppl papillioform nucleus (nucleus reticularis tegmenti pontis); PV, principal sensory nucleus of the trigeminal nerve; V, trigeminal nerve.

fibers of the medial part of the medial lemniscus. All of its fibers terminate around cells of the nucleus reticularis tegmenti pontis (NRTP, the nucleus papillioformis of Olszewski and Baxter, 1954), which lie scattered over the ventromedial pontine tegmentum, as well as in the processus medialis supralemniscalis grisei pontis. Some fibers end in the most dorsomedial pontine nuclei. Caudal to the level of the pons no more degenerated fibers of the brachium conjunctivum can be found.

The descending branch of the brachium conjunctivum was first described in the experimental studies of Thomas (1897) in cat and dog. In primates the descending branch can be traced caudally to the hilus of the inferior olive and beyond in the ventral funiculus

of the cord (Carpenter and Stevens, 1957; Chan-Palay, 1977). The absence of degeneration in the descending limb caudal to the pons in the case illustrated in Figure 11.19 is not so unusual. Some fibers of the descending branch were traced by most authors using the Nauta method in experimental studies, but the full extent of the nucleoolivary projection was not discovered until the application of tritiated amino acids in the tracing of this connection by Graybiel *et al.* (1973).

Cerebellar Projections to the Thalamus in Monkeys

The termination of the brachium conjunctivum in the thalamus in subhuman primates earlier was reviewed by Asanuma *et al.* (1983a–c), Kultas Ilinsky and Ilinsky (1986), Jones (1985), Mehler and Nauta (1974), Percheron *et al.* (1996), and Percheron (Chapter 20 of this volume). At present there is a consensus about the thalamic territory covered by the terminations of the cerebellar nuclei, but the parcellation and the extent of the cortical areas that receive their afferents from the cerebellar thalamus, the somatotopic organization and/or the presence of parallel pathways in the projection of the different cerebellar nuclei to the thalamus, and the question of segregation or overlap of the cerebellar, pallidal, and nigral projections to the thalamus are still being debated.

There is no doubt that the description of these connections has been complicated by the use of different nomenclatures for the nuclei of the thalamus and the areal subdivision of the cerebral cortex. The inconsistencies and the methodological drawbacks in the nomenclatures used to study the primate motor thalamus were pointed out in the critical reviews of Percheron here (Chapter 20) and elsewhere (Percheron *et al.*, 1996). Some papers on the cerebellar and thalamocortical projections stand out as landmarks in the desert. Kievit and Kuypers' 1977 paper offered "an alternate view of the organization of the thalamus" and suggested "that this structure contains a matrix of longitudinal cell columns which in some cases extend across specific nuclear borders" which "may represent the basic thalamic building blocks in respect to the thalamo-cortical connexions" (Kievit and Kuypers, 1977, p. 299). Medial thalamic columns project to rostral sectors in the frontal lobe; more lateral columns project to progressively more caudal regions in the frontal lobe. Kievit's (1979) thesis related the thalamic projections of the individual cerebellar nuclei to this thalamocortical matrix. Figure 11.20 is taken from Kievit's work. Chan-Palay (1977), Kalil (1981), Stanton (1980a), and Asanuma *et al.* (1983b) added new data on the thalamic of the individual cerebellar nuclei. Schell and Strick's paper of 1984 and Strick's subsequent studies on retrograde transneuronal transport from the cerebral cortex specified parallel projections from single cerebellar nuclei to different motor and nonmotor areas of the frontal lobe. Matelli *et al.* (1989, 1991), Matelli and Lupino (1996), Rouiller *et al.* (1994, 1999), Sakai *et al.* (1996, 2000), Yamamoto *et al.* (1992), and others compared corticothalamic projections with their cerebellar, pallidal, and nigral afferents in double- or multiple-labeling experiments. Finally, Nakano (1992), who published one of the few antegrade tracing studies of the projections of the motor thalamus in primates, made it possible to view the many retrograde labeling studies of this pathway in the right perspective.

Percheron (Percheron *et al.*, 1996; see also Chapter 20 of this volume) introduced a new nomenclature for the primate "motor thalamus" based on the existence of three discrete and nonoverlapping territories innervated from caudally to rostrally, by the cerebellar nuclei, the internal segment of the globus, pallidus and the substantia nigra. The three territories were indicated as the nucleus lateralis intermedius, oralis, and rostralis, respectively. On the basis of the data of Schell and Strick (1984), two "source spaces"were distinguished within the cerebellar nucleus lateralis intermedius, indicated as the nucleus lateralis intermedius lateralis and mediodorsalis. In Chapter 20 of this volume, Pecheron changed the prefix "lateralis" for the nuclei of the motor thalamus into "ventralis" and indicated the two nuclei as the ventrolateral (VImL) and dorsomedial subpartss (VImM) of the nucleus ventralis intermedius. His papers specify the invasion by spinothalamic and vestibular thalamic afferents of the cerebellar territory. Overlap of the cerebellar and pallidal projections, as documented in several recent publications (Fig. 11.21), is attributed to "plane, bidimensional, sections of the interdigitation of fringes that, in the absence of three-dimensional reconstruction, may indeed give the impression of a mixture" (Chapter 20). On the presence of overlap of the cerebellar and pallidal territiories in cat and rat, Percheron takes the somewhat unorthodox position that the pallidothalamic projection is a primate innovation. The entopeduncular nucleus in cat and rat does not represent the internal segment of the primate globus pallidus but would correspond to the lateral, intrapeduncular part of the substantia nigra.

Percheron's proposal is attractive in its logic and its simplicity. I have not attempted to use his nomenclature in my review because that would have detracted from the authenticity of the data from different authors, as cited in this section, especially where the possible overlap of cerebellar and pallidal thalamic afferents and the correspondance of cerebellothalamic and

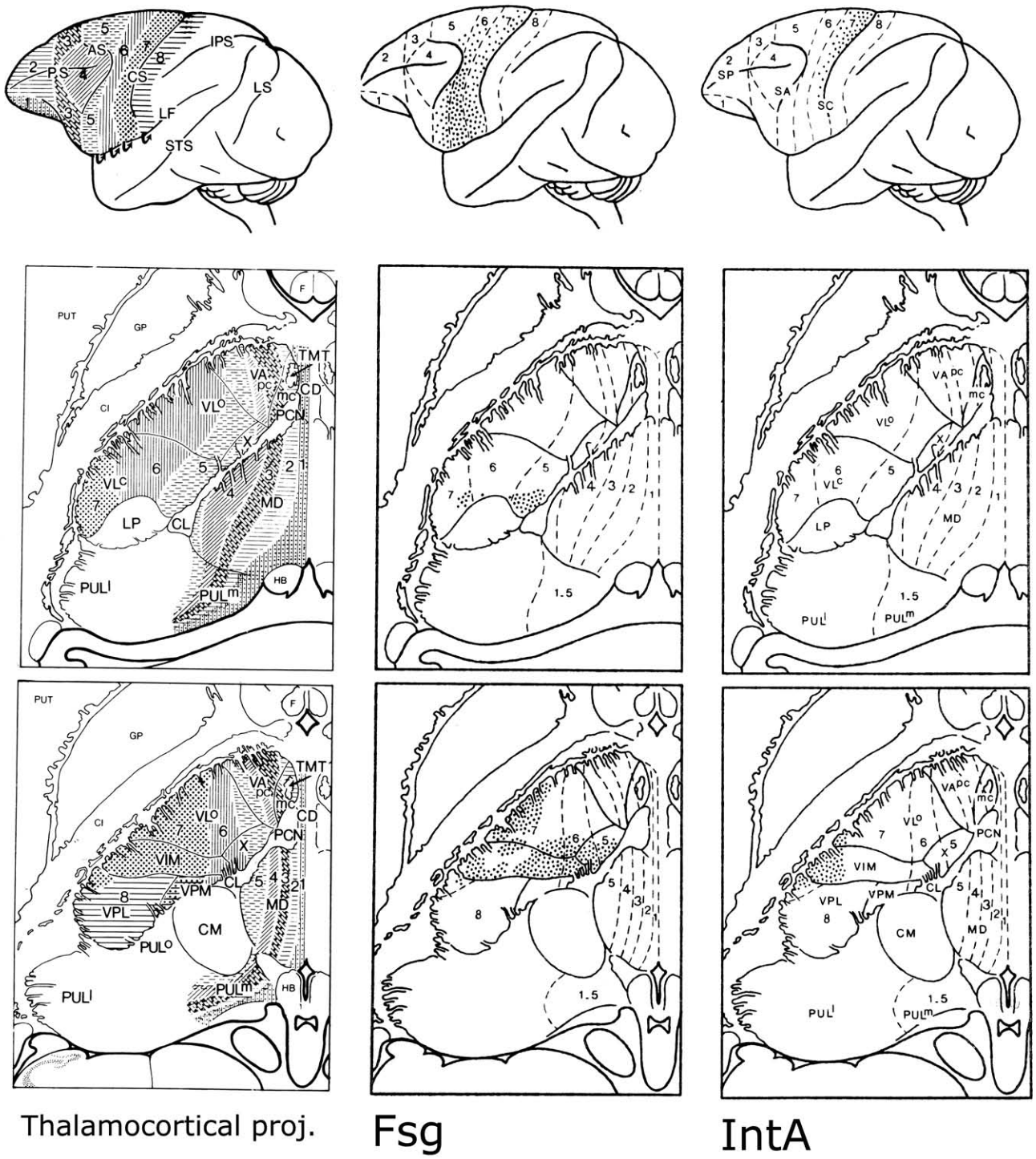

FIGURE 11.20 The cerebellothalamocortical projection in the rhesus monkey. **Upper row:** Diagrams of the left cerebral hemisphere. **Middle and lower rows:** Diagrams of dorsal and ventral horizontal sections through the thalamus. The thalamocortical projection is illustrated in the left-hand column. More caudally located cortical sectors of the frontal lobe receive their thalamic afferents from successively more lateral and ventral thalamic zones. These zones extend across the nuclear borders and the lamina medullaris interna. From Kievit and Kuypers (1977). The cerebello-thalamo-cortical projections of the individual cerebellar nuclei are illustrated in the four right-hand columns. (From Kievit, 1979.) The cortical target areas were reconstructed from the data of Kievit and Kuypers (1977). *Continued*

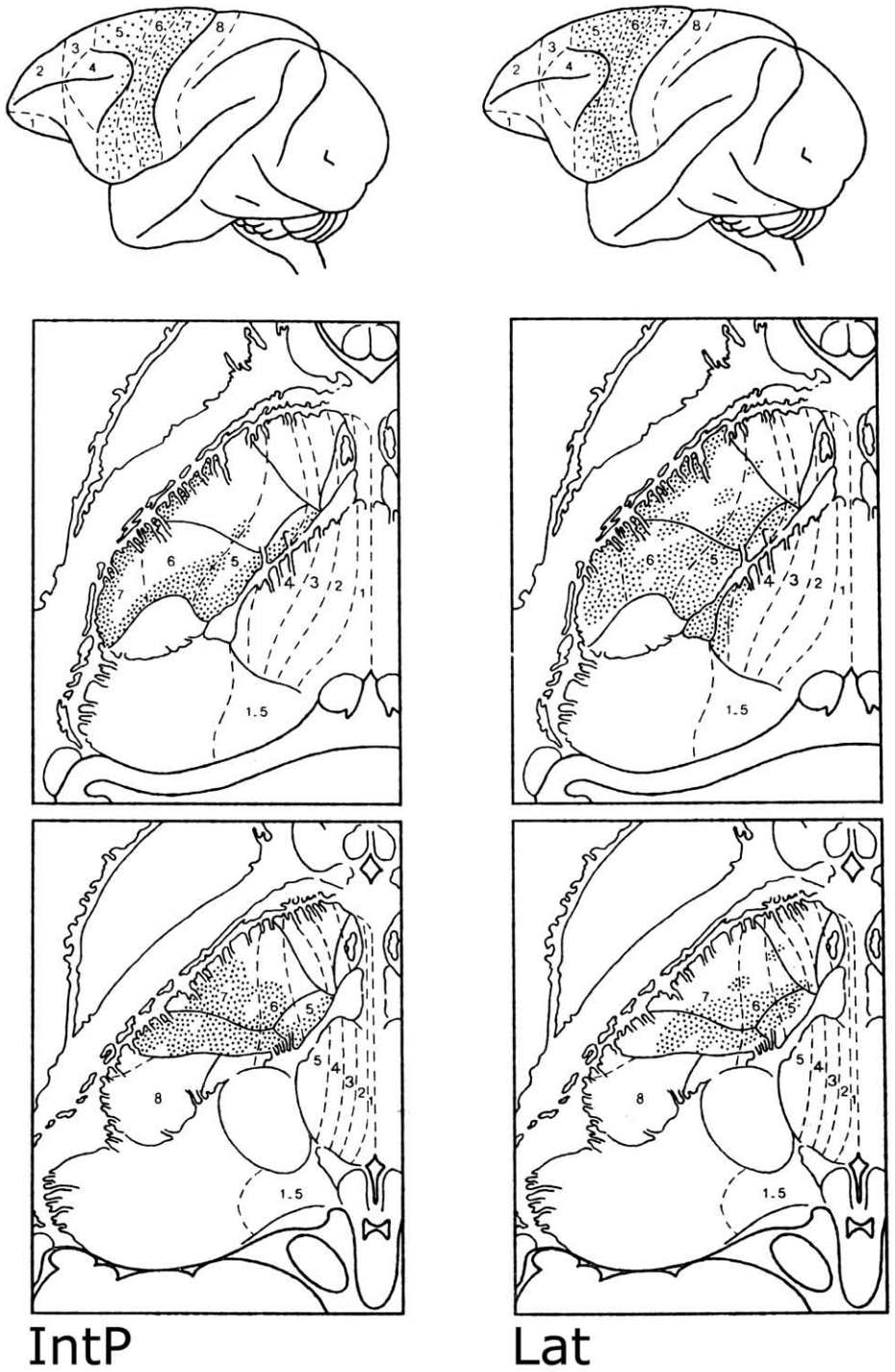

FIGURE 11.20 *Continued* Abbreviations: AS, ansate sulcus; CD, caudate nucleus: CI, internal capsule; CL, central lateral nucleus; CM, centre médian; CS, central sulcus; F, fornix; Fsg, fastigial nucleus; GP, globus pallidus; HB, habenulum; IntA, anterior interposed nucleus; IntP, posterior interposed nucfleus; IPS, intraparietal sulcus; Lat, lateral cerebellar nucleus; LF, lateral fissure; LP, lateral posterior nucleus; LS, lunate sulcus; MD, mediodorsal nucleus; PCN, nucleus paracentralis; PS, principal sulcus; PULl, lateral pulvinar; PULm, medial pulvinar; PUT, putamen; STS, superior temporal sulcus; TMT, mamillothalamic tract.

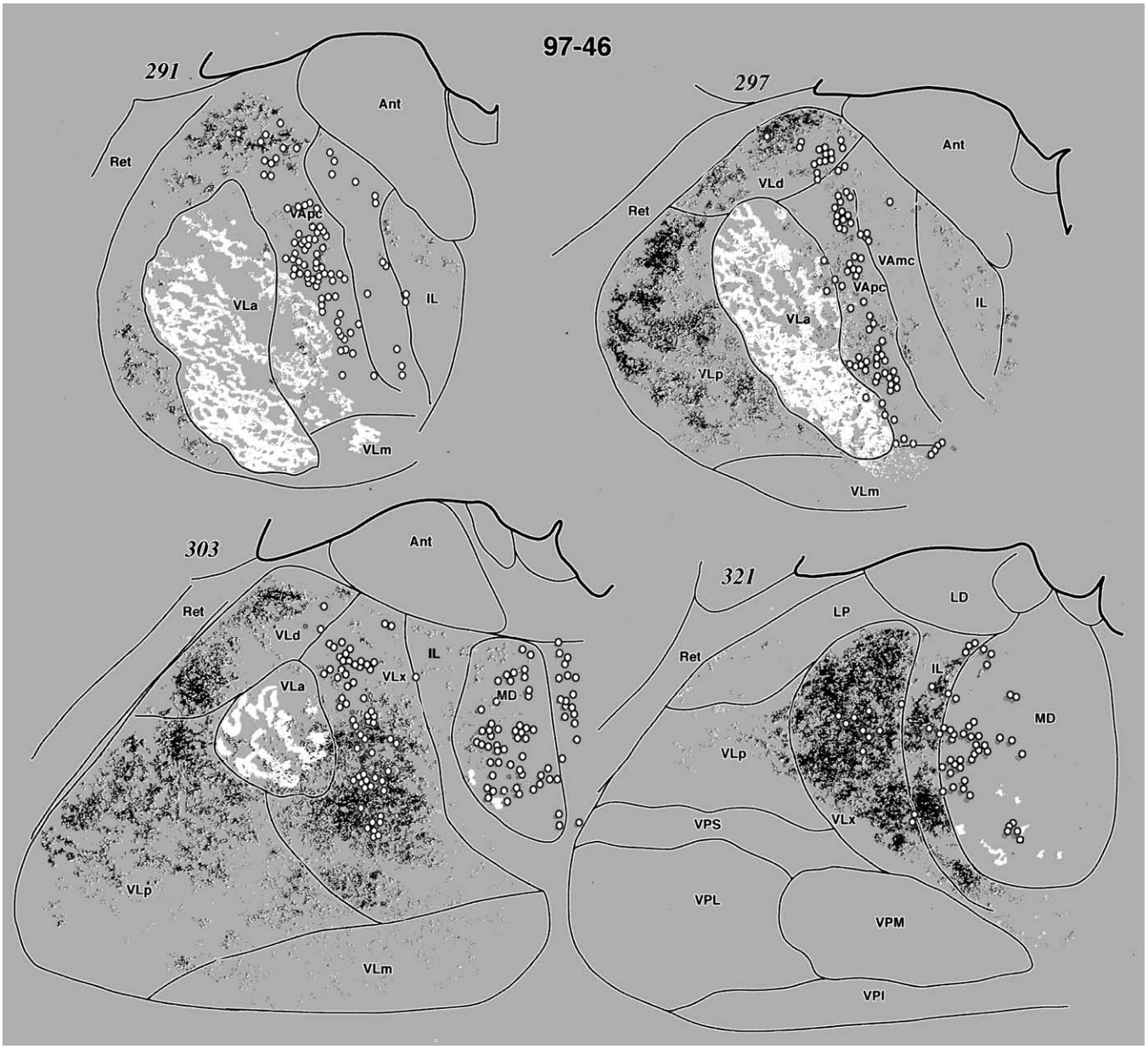

FIGURE 11.21 Drawing of coronal sections through the thalamus showing the distribution of pallidothalamic *(white)* and cerebellothalamic *(black)* anterograde label and the location of presupplementary motor area (SMA) projection neurons *(open circles)* in the owl monkey. Note the overlap of pallidal input with pre-SMA projecting neurons at the Vapc/Vla border (section 297) and cerebellar input with such neurons in VLx, VLd, and IL (sections 297–321). The anterior and posterior divisions of the ventral lateral nucleus (Vla, VLp) in the owl monkey correspond to the ventral lateral nucleus, pars oralis (Vlo) and the ventral posterior nucleus, pars oralis (VPLo) of Olszewski (1952) in the macaque monkey, respectively. Converted in gray scale with Photoshop from a color illustration from Sakai *et al.* (2000). In the conversion some of the detail of the original picture has been lost. Abbreviations: Ant, anterior nucleus; IL, intralaminar nuclei; LD, lateral dorsal nucleus; LP, lateral posterior nucleus; MD, mediodorsal nucleus; Ret, reticular nucleus; VAmc, ventral anterior nucleus, pars magnocellularis; VApc, ventral anterior nucleus, pars centralis; Vla, ventral lateral nucleus, pars anterior; VLd, ventral lateral nucleus, pars dorsalis; VLm, ventral lateral nucleus, pars medialis; VLp, nucleus ventralis lateralis, pars posterior; VLx, ventral lateral nucleus, area x; VPI, ventral posterior nucleus, pars inferior; VPL, ventral posterior nucleus, pars lateralis; VPM, ventral posterior nucleus, pars medialis.

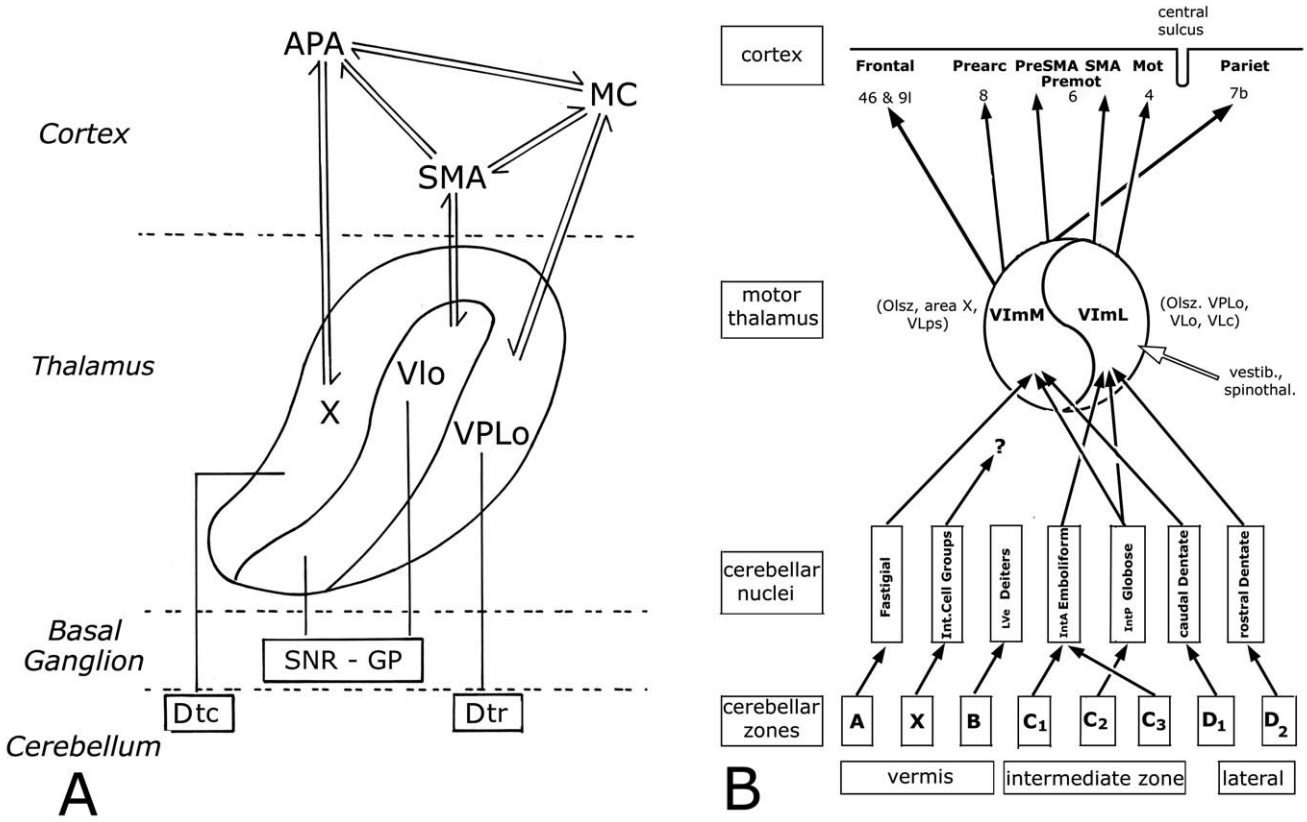

FIGURE 11.22 **A**. Diagram showing the connections of the basal ganglia and the cerebellar nuclei with the motor cortex (MC), the supplementary motor cortex (SMA), and the anterior premotor area (APA) and their relay nuclei in the thalamus. Note projection of rostral dentate nucleus (Dtr), through VPLo to the motor cortex, projection of caudal dentate nucleus (Dtc), through area X, to the premotor area and projections of the substantia nigra, pars reticulata (SNR) and the globus pallidus (GP), through Vlo, to the supplementary motor cortex. From Schell and Strick (1984). **B.** Diagram of parallel chanels in the cerebellothalamocortical projection. This diagram covers the same subject matter as Fig. 11.22A but incorporates Percheron's (Chapter 20) subdivision of the cerebellar territory of the motor thalamus (ventral intermedius nucleus) into ventrolateral (VImL) and dorsomedial subparts (VImM), and data on the connections of the individual cerebellar nuclei with the thalamus and the frontal and parietal cortices. The overlap of the vestibular and spinothalamic projections in the VImL (Chapter 20) is indicated. For details, see text. Abbreviations: IntA, anterior interposed nucleus; IntP, posterior interposed nucleus; Lve, lateral vestibular nucleus; Mot, primary motor area; Pariet., parietal lobe; prearc, prearcuate area; Premot, premotor area; preSMA, rostral part of supplementary motor area; SMS, supplementary motor area proper; VImL, lateral subpart of ventral intermedius nucleus; VImM, medial subpart of ventral intermedius nucleus; VLc, pars caudalis of nucleus ventralis lateralis; VLo, oral portion of nucleus ventralis lateralis; VLps, posterior superior part of nucleus ventralis lateralis; VPLo, oral portion of nucleus ventralis posterior lateralis.

thalamocortical projections are concerned. Percheron's interpretation of some of the same data can be found in his reviews and is summarized in Fig. 11.22B.

Figure 11.21, taken from the paper of Sakai *et al.* (2000), illustrates the distribution of cerebello- and pallidothalamic fibers in the owl monkey. In acordance with previous reports, the cerebellar afferents are directed to separate thalamic subdivisions (Asanuma *et al.*, 1983a–c; Schell and Strick, 1984; Kultas Ilinsky and Ilinsky, 1986; Sakai *et al.*, 1996, 1999; Percheron *et al.*, 1996). The internal segment of the globus pallidus projects to the anterior subdivision of the ventral lateral nucleus (VLa[1]), extending medially in its medial subdivision (VLm) and rostrally into the parvocellular division of the ventral anterior nucleus (Vapc), whereas

[1]The anterior division of the ventral lateral nucleus (VLa) in the owl monkey corresponds to the ventral lateral nucleus pars oralis (VLo) of Olszewski (1952).

the cerebellar projections primarily targeted the posterior motor thalamus, including the posterior division of the ventrolateral nucleus (VLp[2],) area X, and VLd. Both systems terminate in patches. Their terminations overlap or interdigitate in transitional regions between adjacent nuclei, such as the border region between the VLa and the VApc, with area X. The figure is an excellent ihelllustration of Scl and Strick's (1984) description of the cerebellothalamic territory as forming concentrations in lateral and medial areas of the motor thalamus, which are broadly connected by a band of terminals in the region immediately dorsal and rostral to the somatosensory ventral posterior nuclei.

Kievit's (1979) figure of the thalamic projections of the four cerebellar nuclei in *Macaca rhesus* illustrates the particulars in the projection of the four cerebellar nuclei (Fig. 11.20). Medially these projections occupy a position immediately lateral to the internal medullary lamina. Dentatothalamic fibers extend across the medullary lamina to terminate in the caudal, paralamellar portion of the dorsomedial nucleus (MD) and, possibly, in the caudal part of the intralaminar, central lateral nucleus (CL). Rostrally the medial region extends into the area X of Olszewski (1952) and the oral part of the ventral lateral nucleus (Vlo); caudally it includes medial parts of the caudal ventral lateral nucleus (VLc) and the pars posttrema of the VL nucleus. Laterally and caudally the cerebellar terminals occupy the oral portion of the lateral ventral posterior nucleus, the VPLo of Olszewski (1952), which corresponds to the ventral intermedius nucleus (VIM[3]), the term used in Kievit's figure, and the lateral parts of the Vlo, where they may extend into the lateral parvocellular portion of the ventral anterior nucleus (VApc). The projections of the fastigial and anterior interposed nuclei overlap with the dentate in ventral and caudal regions. The projection of the anterior interposed nucleus is restricted to a caudolateral region. The posterior interposed and dentate nuclei project to more extensive but, for the most part, overlapping areas, which include lateral and medial portions of the cerebellar territory. The projections extend into more dorsal, rostrolateral, and rostromedial portions of VLc, Vlo, and area X. The projection of the posterior interposed nucleus typically includes the medial zone of area X; the dentate projection extends into the paralamellar part of the MD nucleus. The cortical projections of the different cerebellar nuclei, as indicated in the diagrams of Fig. 11.20 were reconstructed from the data of Kievit and Kuypers (1977) on the matrix in the thalamocortical projection. These diagrams, though still valid, have been modified in subsequent, more detailed studies of the thalamocortical projection of Schell and Strick (1984) and others.

Schell and Strick (1984) criticized an earlier hypothesis of Asanuma *et al.* (1983b, c) and Jones (1985) that the thalamic regions that receive cerebellar inputs should be considered as a common nucleus (the cell-sparse zone of Asanuma *et al.*, 1983a) which influences only the primary motor cortex. They proposed instead the existence of at least two separate cerebellothalamic systems, which originate from the deep nuclei (Fig. 11.22). "One system, located in the rostral portion of the deep nuclei, projects largely to VPLo [which includes the VIM from Kievit's Figure 11.20] and therefore most directly influences the motor cortex. A second system in the caudal portions of the deep nuclei projects largely to area X and therefore most directly influences the arcuate premotor area," corresponding to the ventral part of area 6, located rostral to the primary motor area.[4] A third, supplementary motor area, located in dorsomedial area 6, receives a projection from the central and rostral Vlo, i.e., from a region located between the rostromedial and rostrolateral extensions of the cerebellar projection area. This part of the thalamus receives its projections from the globus pallidus and the substantia nigra (Figs. 11.21A and 11.22). Since the publication of this paper it has become clear that the medial thalamus, innervated by the caudal dentate and interposed nuclei, projects to more extensive regions of the frontal lobe, including certain premotor areas, and to the inferior parietal lobule (Fig. 11.22B). The medial and lateral territories innervated by the cerebellum were indicated as the lateral (VImL) and medial subparts (VImM) of the nucleus ventralis intermedius by Percheron (Chapter 20) (Fig. 11.22B).

Projections of the contralateral rostrodorsal dentate and the anterior interposed nucleus, through the VPLo, to the primary motor cortex (M1) have been confirmed in the retrograde transneuronal tracing studies of Wiesendanger and Wiesendanger (1985a, b), Oriolo and Strick (1989), Middleton and Strick (1997), and Hoover and Strick (1999). Transneuronally labeled neurons from the leg area of M1 were found in the rostral dentate, from the face area dorsally in its middle third and from the arm area in between (Fig. 11.23). In the anterior

[2]The posterior division of the ventral lateral nucleus (VLp) in the owl monkey corresponds to the ventral posterior nucleus pars oralis (VPLo, Olszewski, 1952) in macaque monkeys.

[3]The ventral intermedius nucleus was distinguished by Cécile Vogt (1903) as the termination of the cerebellar projection in monkeys.

[4]To be supplied.

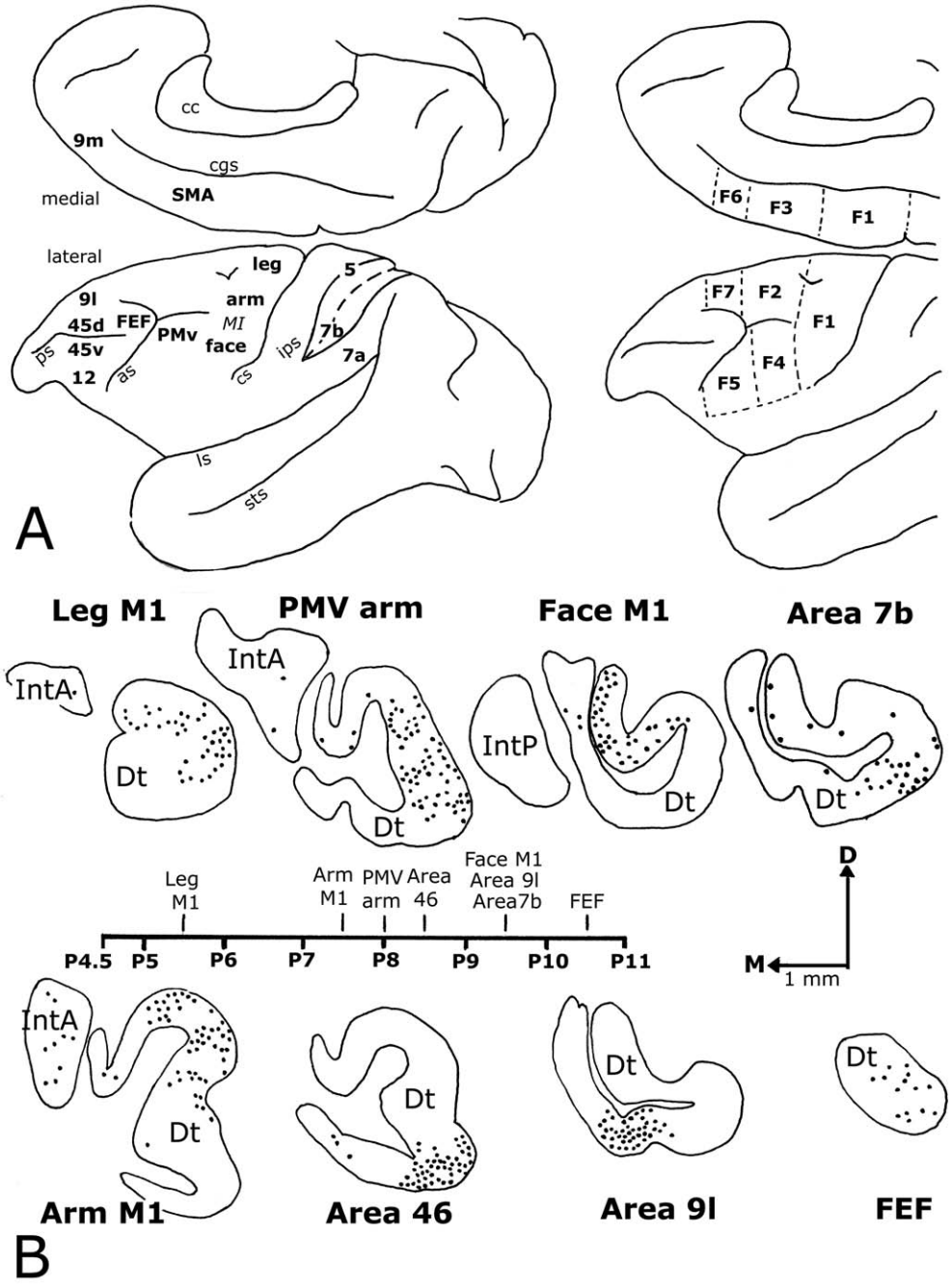

FIGURE 11.23 Transneuronal labeling of neurons in the contralateral cerebellar nuclei of the cebus monkey from injections of herpes simplex virus (HSV-1, McIntyre-B) in the cerebral cortex. **A.** Approximate locations of the injection sites are indicated in the left panel. **B.** The right panel illustrates the nomenclature of the agranular motor cortex introduced by Matelli *et al.* (1989) and Matelli and Lupino (1996). **C.** The location of labeled neurons in the cerebellar nuclei, in sections with the highest numbers of labeled cells. The approximate position of these sections is indicated on the P4.5–P11 bar representing the rostrocaudal extent of the cerebellar nuclei. Redrawn and relabeled from Hoover and Strick (1999), Middleton and Strick (2000, 2001), and Clower *et al.* (2001). Abbreviations: 46d,v, dorsal and ventral area 46; 5, superior parietal area 5; 7a, 7b, inferior parietal areas 7a and b; 9l,m, medial and lateral area 9; as, ansate sulcus; cc, corpus callosum; cgs, cingulate sulcus; cs, central sulcus; Dt, dentate nucleus; F1–F7, areas F1–F7 of Matelli *et al.* (1989) and Matelli and Lupino (1996); FEF, frontal eye field; IntA, anterior interposed nucleus; IntP, posterior interposed nucleus; ips, intraparietal sulcus (opened); ls, sylvian sulcus; M1, primary motor cortex; PMv, ventral premotor area; ps, principal sulcus; SMA, supplementary motor cortex; sts, superior temporal sulcus.

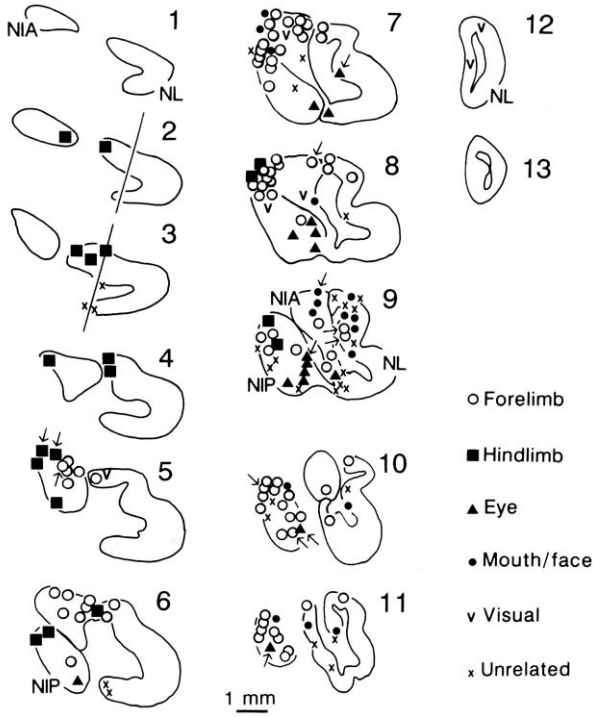

FIGURE 11.24 Somatotopic distribution of 134 movement-related neurons from two monkeys, plotted on equally spaced transverse sections through the cerebellar nuclei. Arrows indicate neurons with mixed movement relations. Lines through sections 2 and 3 indicate angle of the microelectrode penetrations. From Van Kan *et al.* (1993). Abbreviations: NIA, anterior interposed nucleus; NIP, posterior interposed nucleus; NL, dentate nucleus.

interposed nucleus the leg is represented rostromedially and the face caudally and laterally (Fig. 11.24). The posterior interposed nucleus also contained labeled neurons in the cases with M1 injections, but without a clear, somatotopical distribution. Labeled neurons from injections in medial area 6, in the rostral part of the supplementary motor area, were found in the VLc, in the Vapc, and in area X. Transneuronal labeling was observed in cells of the ventral and caudal dentate and the ventral posterior interposed nucleus, but not in the anterior interposed nucleus. The labeling in the cerebellar nuclei resulting from an injection including the caudal part of the supplementary motor area was more widespread (Wiesendanger and Wiesendanger, 1985a, b). Injections in the arcuate premotor area, corresponding to inferior area 6, retrogradely labeled the area X and were located in the rostromedial, ventral, and caudal dentate nucleus and in the caudal pole of the posterior interposed nucleus (Oriolo and Strick, 1989).

In subsequent studies, Strick and his collaborators retrogradely labeled neurons in the dentate, with a small number of cells in the adjacent interposed nuclei, from injections with a strain of the herpes simplex virus, in more rostral parts of the frontal lobe (Fig. 11.24). Injections in the frontal eye field (area 8) label cells in area X, in the ventral anterior and dorsomedial nuclei of the thalamus, and in the caudal dentate (Lynch *et al.*, 1994); injections in the prefrontal area 46 and 9 resulted in labeled neurons in a ventromedial region of the dentate, in the middle and caudal thirds of the ventrocaudal dentate nucleus. A few labeled cells were present in the posterior interposed and fastigial nuclei. Neurons labeled from area 46 tend to be located laterally to the labeled cells from area 9 (Middleton and Strick, 1997, 2001). Injections of inferior parietal area 7b labeled cells located ventrally in the contrlateral caudal third of the dentate (Clower *et al.*, 2001).

Cerebellar projections to the primary motor cortex generally have been confirmed in studies comparing multiple retrograde labeling from the cortex with data on the thalamic distributions of cerebellar and pallidal afferents. According to Rouiller *et al.* (1999), projections to the primary motor cortex mainly stem from the VPLo and remain segregated from the projection of the thalamus to other motor areas. Connections from the globus pallidus to the primary motor cortex are relayed by the Vlo (Rouiller *et al.*, 1994; Stepniewska *et al.*, 1994). According to Matelli *et al.* (1989), pallidal afferents are preferentially relayed to the rostral part of the primary motor cortex. The laminar patterns in the terminations from the VPLo and the Vlo are different. The corticothalamic projections from the Vlo terminate in superficial layer I of the cortex, whereas the projection from the VPLo innervates the deep layers III–V (Nakano *et al.*, 1992). The supplementary motor area (SMA), located on the mesial part of the hemisphere, receives corticothalamic fibers both from cerebellar and pallidal thalamic territories (Rouiller *et al.*, 1994). The thalamocortical projection to its caudal portion (SMA-proper, F3; see Fig. 11.23B for an explanation of the nomenclature of the motor areas) in the frontal lobe of Matelli *et al.* (1989) and Matelli and Lupino (1996) is very similar to the more ventrally located caudal premotor region (F2, F4). It receives projections from the rostrodorsal dentate and interposed nuclei, and the globus pallidus, which are relayed by the Vlo, VPLo, and VLc (Matelli and Lupino, 1996; Rouiller *et al.*, 1999; Sakai *et al.*, 1999). The rostral half of the SMA (F6) and the rostral premotor area (F5, F7) receive pallidal and cerebellar afferents from ventrocaudal parts of the dentate and interposed nuclei, relayed by area X, and the ventral anterior and mediodorsal nuclei (Matelli *et al.*, 1989, Matelli and Lupino, 1996; Rouiller *et al.*, 1999; Sakai *et al.* 2000) (Fig. 11.21). These thalamic nuclei innervate both deep (VA, area X) and superficial cortical layers (VA) of area 6 (Nakano *et al.*, 1992). The

supplementary eye field, located dorsally in F7, receives a preferential projection from lateral area X (Matelli and Lupino, 1996). The thalamic cerebellar territory also includes nuclei which project to prefrontal cortical areas. According to Yamamoto *et al.* (1992) and Rouiller *et al.* (1999), the prefrontal projections are relayed by the ventrolateral, paralamellar part of the mediodorsal nucleus. Middleton and Strick (2001) recently provided evidence that the projections to medial area 9 and 46 originate from the caudal VLc, the VLps, and area X.

Therefore, all motor areas in the monkey receive both cerebellar and pallidal afferents, be it in different proportions, but the cerebellar and pallidal inputs to the cortex are not equivalent. The cerebellothalamic connections are excitatory, whereas the pallidothalamic projections is GABAergic and inhibitory (for reviews, see Voogd *et al.*, 1996b and Gerfen and Wilson, 1996). Moreover, the input from the cerebellum and the globus pallidus to several cortical areas is distributed to different cortical laminae (Nakano *et al.*, 1992). In accordance with Schell and Strick's (1984) original proposal, the primary motor cortex is dominated by cerebellar afferents, derived from rostral dentate and interpositus. The caudal parts of the premotor (F2 and F4) and supplementary motor areas (F3) receive a mixture of cerebellar afferents from the same cerebellar nuclei and the pallidum. These premotor and supplementary motor areas receive substantial inputs from the parietal lobe (for references, see Matelli and Luppino, 1996) and maintain strong connections with the primary motor cortex. They give rise to corticospinal connections, to interneurons in the spinal intermediate zone, and to direct projections to the motoneurons, which are independent from similar projections from the primary motor cortex (Dum and Strick, 1991, 1996; He *et al.*, 1993, 1995). More rostral premotor and supplementary motor areas (F5, 6, and 7) receive afferents from the caudal dentate and interposed nuclei and a projection from the globus pallidus. These areas maintain strong connections with the prefrontal cortex. The most rostral prefrontal areas receiving cerebellar afferents include area 46 and 9 and, according to Lynch *et al.* (1994), the frontal eye field. Cerebellar projections to parietal areas (Sasaki *et al.*, 1976) recently were confirmed by Clower *et al.* (2001).[5]

Schell and Strick (1984) distinguished two parallel cerebellothalamic pathways from the rostral dentate and the anterior interposed nucleus and from the caudal dentate and the posterior interposed nucleus. The fastigial, anterior, and posterior interposed nuclei, however, should also be considered as independent target nuclei of different cerebellar modules, which receive projections by different Purkinje cell zones, and from different subnuclei of the inferior olive. The suggestion by Schell and Strick (1984) that the dentate nucleus consists of rostromedial and caudolateral subnuclei receives support from the observation that these subnuclei may serve as the targets for different Purkinje cell zones in the cerebellar hemisphere (see "Subdivision and Olivocerebellar Projection" and "Longitudinal Zonation of the Cerebellum"). As a consequence, at least five parallel cerebellothalamic pathways can be distinguished with systematically diverging and converging terminal fields in the thalamus and projections to different motor cortical areas (Fig. 11.22B). The terminations of these parallel paths are not limited to the thalamus but also include the brain stem and the upper cord.

Projections of Individual Cerebellar Nuclei to the Brain Stem in Monkeys

There are strong indications that the widely diverging projections of the cerebellar nuclei to the thalamus, the brain stem, and the cord are collaterals of the same highly branched axons of the relay cells of the cerebellar nuclei (Bentivoglio and Kuypers, 1982; Bharos *et al.*, 1981; Shinoda *et al.*, 1988, 1999; Tolbert *et al.*, 1978; Teune, 1999; Teune *et al.*, 1999, 2000). These branching axons are excitatory and should be distinguished from the GABAergic projection of the cerebellar nuclei to the inferior olive (see "Cerebellar Nuclei" and "Afferent Systems of the Inferior Olive: The Nucleoolivary Projection"). Apart from the thalamus, these projections include the vestibular nuclei, the reticular formation, and the tectum, where connections from visually dominated portions of the fastigial, dentate, and posterior interposed nuclei should be differentiated from regions of the cerebellar nuclei that are primarily somatomotor in function. In the mesencephalon, the cerebellar target nuclei include

[5]Connections to parietal areas from the cerebellar relay have also been reported in the cat. In a study, combining antegrade tracing from the cerebellar nuclei with retrograde tracing from areas 5 and 7. Hendry *et al.* (1979) and Sugimoto *et al.* (1981) observed some neurons in the cerebellar zone of termination to project to these parietal areas. Neurons in parietal association areas 5 and 7, located in the caudal bank of the ansate sulcus and the suprasylvian gyrus; responded to stimulation of the dentate and interposed nuclei. These effects were mediated by the VA-VL complex (Wannier *et al.*, 1992; Kakei *et al.*, 1995; Yamamoto and Oka, 1993). Some of these parietal neurons are corticocortical neurons with projections to the motor cortex (Kakei *et al.*, 1995). Another source of widespread projections to postrolandic areas would be the intralaminar, centrolateral nucleus, which is known to receive afferents from the cerebellar nuclei.

the red nucleus and the nucleus of Darkschewitsch and adjacent nuclei at the meso–diencephalic junction. These nuclei give rise to crossed descending rubrobulbar and rubrospinal pathways and uncrossed pathways to the inferior olive, which are part of a recurrent climbing fiber loop (see "Afferent Systems of the Inferior Olive: The Nucleoolivary Projection"). Similar recurrent loops, terminating as mossy fibers, are formed by cerebellar projections to the nucleus reticularis tegmenti pontis and the pontine nuclei, and the lateral reticular nucleus. These climbing fiber and mossy fiber recurrent loops also innervate the cerebellar nuclei. In the subthalamus cerebellar afferents terminate on the zona incerta.

The *fastigial nucleus* projects bilaterally and symmetrically to the vestibular nuclei and to the contralateral medial bulbar reticular formation and the cervical cord (Batton *et al.*, 1977). The magnocellular medial vestibular nucleus, the spinal vestibular nucleus, and the nucleus parasolitarius are among its main target nuclei. Crossed fibers from the uncinate tract and the ipsilateral fastigiobulbar tract pass lateral and medial to the lateral vestibular nucleus of Deiters but do not terminate there. The lateral vestibular nucleus receives a direct projection from Purkinje cells of the lateral B zone of the anterior vermis. The crossed ascending limb of the uncinate fascicle terminates in the mesencephalon in the dorsal reticular formation, in the central gray, deep and bilaterally in the intermediate layers of the superior colliculus, and in the nuclei of the posterior commissure. The bilateral projection to the intermediate layers is restricted to the rostral pole of the superior colliculus, i.e., corresponds to the foveal area of the contralateral hemifield (May *et al.*, 1990).

In the thalamus fastigial fibers terminate caudally in the suprageniculate nucleus, and ventrally, caudally, and bilaterally in the VPLo and the Vlo (Figs. 11.20 and 11.22B) (Kievit, 1979; Kievit and Kuypers, 1972; Asanuma *et al.*, 1983b), as described in previous paragraphs. Terminations in preolivary nuclei at the mesodiencephalic junction have not been found. Of the precerebellar nuclei with recurrent mossy fiber pathways, the dorsal part of the nucleus reticularis tegmenti pontis (NRTP), the dorsolateral basal pontine nuclei, and the magnocellular part of the lateral reticular nucleus receive projections from the fastigial nucleus.

The oculomotor region of the fastigial nucleus, located in the caudal part of the nucleus, receives Purkinje cell axons from visual areas of the vermis (lobules VII and VIc), which are characterized by a low threshold for evoking saccades (Noda *et al.*, 1990). Projections from the oculomotor region of the fastigial nucleus are not so different from the projections described from complete lesions or injections of this nucleus. They include the vestibular nuclei bilaterally. Contralaterally the oculomotor region projects to the paramedian pontine reticular formation (PPRF) and to a region caudoventral to the abducens nucleus. In the mesencephalon they terminate the intermediate layer of the superior colliculus and in the contralateral rostral interstitial nucleus of the medial longitudinal fascicle and the lateral part of the nucleus of Darkschewitsch. Projections to the PPRF and the preoculomotor nuclei in the mesencephalon are collaterals from the same neurons (Sato and Noda, 1991). The contralateral dorsomedial NRTP and the dorsomedial, rather than the dorsolateral basal pontine nuclei receive a projection from the oculomotor region (Noda *et al.*, 1990). Projections of the fastigial nucleus to the PPRF, the superior colliculus, and the paraoculomotor nuclei were also reported in a retrograde labeling study of Gonzalo-Ruiz *et al.* (1988), but the retrogradely labeled cells in this nucleus never were restricted to its oculomotor region.

The efferent connections of the *U-shaped nucleus*, located between the fastigial and interposed nuclei (Fig. 11.12), which supposedly corresponds to the interstitial cell groups in the rat (Buisseret-Delmas *et al.*, 1993; see "Cerebellar Nuclei"), have not been studied in primates. In cat and rat its neurons give rise to strong projections to the spinal cord, which also collateralize to the tectum and the thalamus (Bentivoglio and Kuypers, 1982; Matsushita and Hosoya, 1978).

Topographically the *posterior interposed nucleus* is closely related to the fastigial nucleus. After their decussation its fibers ascend medial to and through the red nucleus, to enter the central gray lateral to the oculomotor nuclei (Kievit, 1979). They terminate in deep layers of the contralateral superior colliculus (May *et al.*, 1990) and the nucleus of Darkschewitsch. Terminations in the magnocellular red nucleus were denied by Stanton (1980a) but found to be restricted to a caudal and medial shell of the caudal magnocellular part of the red nucleus by Kievit (1979). In the thalamus the projections from the posterior interposed nucleus cover a fairly broad region, which largely overlaps with the projection of the dentate nucleus (Fig. 11.20). The posterior interposed nucleus is the target nucleus of the C_2 zone (Fig. 11.46; see "Longitudinal Zonation of the Cerebellum"). A distinct somatotopical organization appears to be absent in the posterior interposed nucleus (Van Kan *et al.*, 1993) (Fig. 11.24). This corresponds to the characteristic lack of a somatotopical organization in the C_2 zone (Oscarsson, 1980). The projections to the red nucleus supposedly originate from the medial part of the nucleus. The lateral pole of the posterior interposed nucleus contains visual cells (Van Kan *et al.*, 1993) (Fig. 11.24). It is this region that gives rise to the projection to the tectum, which includes the entire

rostrocaudal extent of the nucleus and, therefore, corresponds to the entire contralateral hemifield (May *et al.*, 1990).

The thalamic projections of the posterior interposed nucleus cover both lateral and medial portions of the cerebellar territory (Fig. 11.22B, VImL and VImM). The medial region, corresponding to Percheron's (Chapter 20) medial subpart of the nucleus ventralis intermedius dorsomedialis, includes area X, which is a relay nucleus for the the frontal eye field (Lynch *et al.*, 1994) and the supplementary eye field (Matelli and Lupino, 1996). These projections may arise from the lateral, visual area of the posterior interposed.

One of the distinctive features of the posterior interposed nucleus in cat and rat is the absence of a projection to the NRTP (Voogd, 1964; Teune *et al.*, 1999). In primates this connection has not been studied with appropriate lesions or injection sites. Projections to the PPRF and the preoculomotor nuclei in the mesencephalon have not been reported.

The *anterior interposed nucleus* has a distinct somatotopical organization, with the lower extremity located rostrally and medially, the face laterally and caudally, and the upper extremity in between (Van Kan *et al.*, 1993) (Fig. 11.24). The presence of a detailed somatotopical organization is in accordance with the somatotopical, microzonal arrangement in C_1 and C_3 zones, which innervate this nucleus (Fig. 11.46A). The anterior interposed nucleus projects to the corresponding somatotopical subdivisions of the caudal magnocellular part of the red nucleus, with the leg area ventrally and laterally and the arm dorsomedially in the red nucleus (Fig. 11.25) (Stanton, 1980a; Van Kan, unpublished observations; Van Kan *et al.*, 1993). A representation of the face in the magnocellular red nucleus seems to absent. Neurons projecting to the motor nucleus of the facial nerve have been located in the dorsolateral parvocellular red nucleus (Burman *et al.*, 2000). It may correspond to a caudal region of the red nucleus in the cat, which projects to the upper cervical cord and receives afferents from the lateral anterior interposed and the rostromedial dentate nucleus (Pong *et al.*, 2002). Fibers from the anterior interposed nucleus proceed to the thalamus, where they are relayed by the ventrolateral and caudal regions of Percheron's (Chapter 20) lateral subpart of the nucleus ventralis intermedius (VImL), to the primary motor cortex (Figs. 11.20 and 11.22B) (Kievit, 1979; see also Asanuma *et al.*, 1983b, c). The nucleus projects to the NRTP, but connections with the preolivary nuclei at the meso–diencephalic junction have not been reported.

The *dentate nucleus* projects to the red nucleus, the interstitial nucleus of Cajal, the tectum and pretectum, the preolivary nuclei at the meso–diencephalic border, the prerubral filed, the zona incerta, and the thalamus. It contributes to the descending branch of the brachium conjunctivum, which terminates in the NRTP and the reticular formation. The connections of the dentate with the red nucleus generally have been stated to be limited to its rostral parvocellular portion (Miller and Strominger, 1977; Stanton, 1980a; Asanuma *et al.*, 1983d). However, fibers from the rostral dentate have been observed to ascend through and terminate in both the caudal magnocellular and the rostral parvocellular red nucleus (Chan-Palay, 1977; Kalil, 1980). The lateral, parvocellular portion of the red nucleus includes a dorsolateral group of neurons that contains a representation of the face and projects to the cord (Kennedy *et al.*, 1986; Burman *et al.*, 2000). Pong *et al.* (2002) noted in the cat that the dentate nucleus also established indirect connections with the parvocellular dentate nucleus, which were relayed by the zona incerta and the nucleus of the fields of Forel. The dentate nucleus shares this connection to the parvocellular red nucleus with the entopeduncular nucleus (the cat's homologue of the internal segment of the globus pallidus). Convergence of cerebellar and striatal sytems, therefore, also may occur at the level of the brain stem.

There are strong indications that the dentate nucleus consists of rostrodorsal and caudoventral subdivisions (Schell and Strick, 1984). The rostrodorsal subnucleus contains a representation of the hindlimb in the rostral part, of the face dorsally in the middle third of the dentate, and of the arm in between (Figs. 11.23 and 11.24) (Van Kan *et al.*, 1993; Wiesendanger and Wiesendanger, 1985b; Middleton and Strick, 1997). It projects to ventral, central, and dorsolateral parts of the parvocellular red nucleus (Fig. 11.25B) (Stanton, 1980a). Percheron's (Chapter 20) lateral subpart of the nucleus ventralis intermedius (VImL) is the thalamic relay nucleus for the somatotopically arrranged projection of the rostral denate to the primary motor cortex and the caudal premotor area (Figs. 11.22B and 11.23; see "Cerebellar Projections to the Thalamus in Monkeys"). The projection area in the red nucleus may include the dorsolateral part of the parvocellular subdivsion, which contains a representation of the face and preferentially projects to the upper spinal cord (Kennedy *et al.*, 1986).

The ventrocaudal dentate projects to the dorsomedial part of the parvocellular red nucleus (Fig. 11.25B). A projection to Darkschewitsch's nucleus was mentioned by Stanton (1980a) and Van Kan (unpublished), but its origin from the posterior interposed nucleus cannot be excluded. Projections of the ventrocaudal dentate to more rostral premotor and prefrontal areas (Fig. 11.23) (Middleton and Strick, 1997, 2001), which include the frontal eye field (Lynch *et al.*, 1994 and the inferior

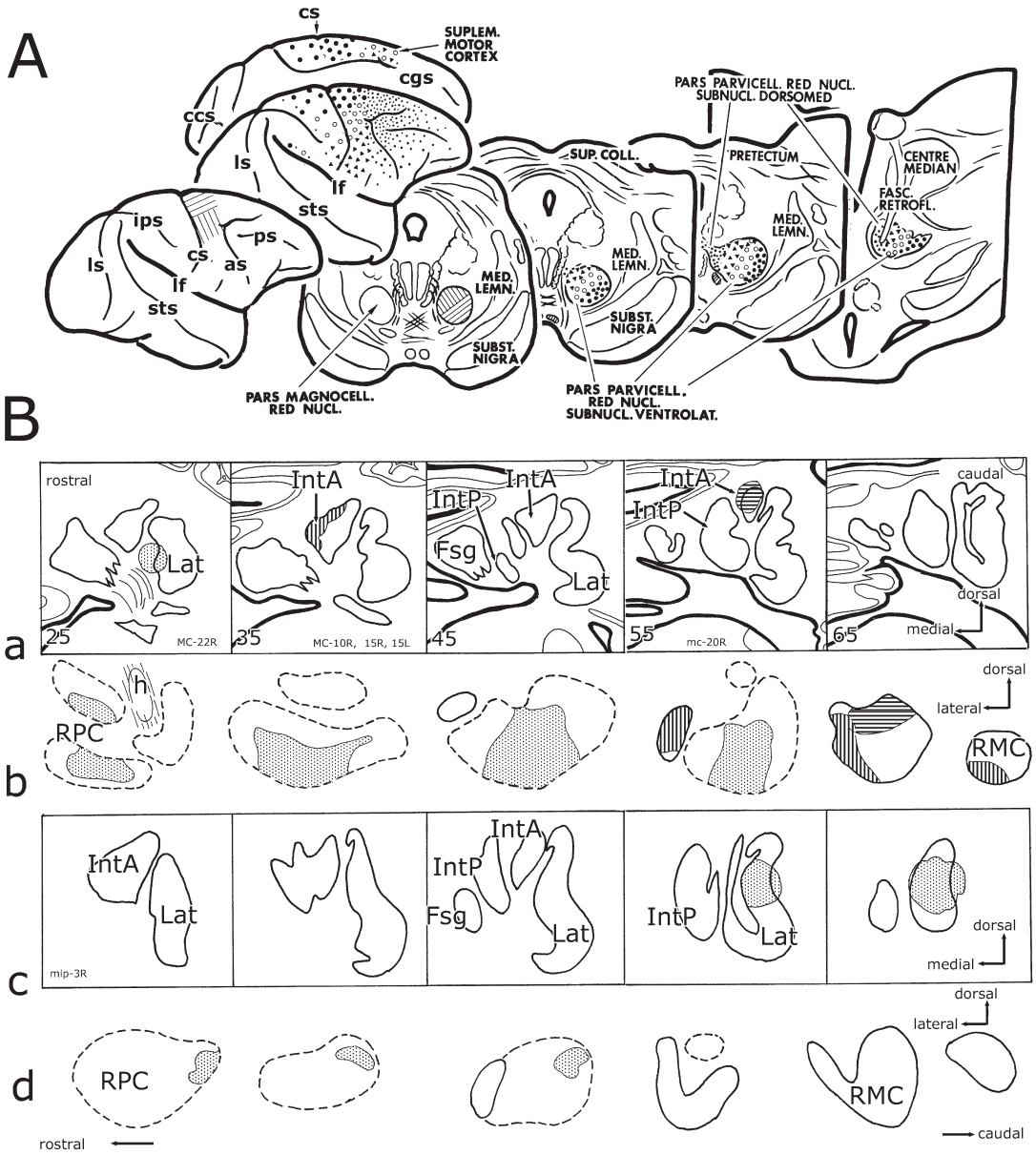

FIGURE 11.25 Afferent connections of the red nucleus in monkeys. **A.** The corticorubral projection. The origin of the corticorubral projections to the caudal, magnocellular portion of the red nucleus is restricted to arm and leg areas of the primary motor cortex. Somatotopically arranged projections from the primary motor cortex and the caudal premotor area terminate in the rostrolateral and caudal parvocellular red nucleus. More rostral frontal areas, including the frontal eye field, project to the rostromedial parvocellular red nucleus. From Kuypers and Lawrence (1967). **B.** Projections from the cerebellar nuclei to the red nucleus. Rows a and b were redrawn from Flumerfelt *et al.* (1973). Rows c and d were reproduced from unpublished materail of Van Kan. **a.** Lesion sites in the rostral dentate nucleus (section 25), three lesions in the rostromedial leg area of anterior interposed nucleus (section 35), and a lesion in the caudolateral, forelimb area of the anterior interposed nucleus (section 55). **b.** Localization of preterminal axonal degeneration from the lesion of the rostral dentate in the rostrolateral and caudal parvocellular red nucleus and of the termination of axons from leg and arm areas of the anterior interposed nucleus in the ventrolateral and dorsal parts of the magnocellular red nucleus. Contours of the parvocellular red nucleus are indicated with broken lines, of the magnocellular red nucleus with continuous lines. **c.** Lectin-coupled horseradish peroxidase injection in the caudal dentate nucleus. **d.** Resultant labeling in rostromedial parvocellular red nucleus. Abbreviations: as., ansate sulcus; ccs, calcarine sulcus; cgs., cingulate sulcus; cs., central sulcus; Fsg, fastigial nucleus; h, fasciculus retroflexus; IntA, anterior interposed nucleus; IntP, posterior interposed nucleus; ips, intraparietal sulcus; Lat, dentate nucleus; ls, lunate sulcus; ps., principal sulcus; RMC, magnocellular red nucleus; RPC, parvocellular red nucleus; sts., superior temporal sulcus.

parietal lobule (Clower *et al.*, 2001), are relayed by Percheron's (Chapter 20) medial subpart of the nucleus ventralis intermedius (VimM, Fig, 11.22B). The two subnuclei of the dentate presumably receive Purkinje cell afferents from different cortical zones in the hemisphere and are connected with different parts of the principal nucleus of the inferior olive (Figs. 11.46, 11.47, and "Longitudinal Zonation of the Cerebellum"). A precise border between the two subdivisions of the dentate cannot be drawn as yet. Their homology with the rostromedial microgyric and ventrolateral macrogyric portions of the human dentate has not been established.

Chan-Palay (1977) traced bilateral projections from the caudal dentate nucleus to the PPRF. These projections may take their origin from the eye movement area in the caudal dentate of Van Kan *et al.* (1993) (Fig. 11.24). The eye movement area in the caudal dentate shares these connections with oculomotor centers in the caudal fastigial nucleus and with the lateral oculomotor region in the posterior interposed nucleus Direct connections of the dentate nucleus with the neurons of the oculomotor nuclei (fibers of Klimoff, 1899 and Wallenberg, 1905) probably do not exist. These connections take their orgin from group Y. Stanton (1980a) traced connections from group Y, in the medial longitudinal fascicle, to the three ipsilateral eye muscle nuclei, and a crossed pathway, through the brachium conjunctivum, to the contralateral oculomotor nucleus.

AFFERENT FIBER SYSTEMS

Organization of Mossy and Climbing Fiber in the Cerebellum

Although most textbooks suggest otherwise, very little is known about the distribution of mossy and climbing fiber system in the cerebellum of humans and subhuman primates. Apart from one antegrade tracing study on the human spinocerebellar tracts, some papers on the pontocerebellar projection, and a few incomplete data on the zonal distribution of olivocerebellar fibers in monkeys, the available information is restricted to data on their origin from retrograde labeling experiments and human cases with damage to the cerebellar cortex. Supposedly the general rules on their distribution, which can be drawn from experimental studies in carnivores and rodents, also apply to the primate cerebellum. These rules are well illustrated by two recent papers of Wu *et al.* (1999) on the course and termination of individual mossy fibers from the lateral reticular nucleus and on the morphology of climbing fibers from single cells in the inferior olive (Sugihara and Shinoda, 1999), both in the rat.

Mossy fibers enter the cerebellum laterally in the restiform body or the brachium pontis, and sweep medially, as semicircular fibers, located rostral and dorsal to the cerebellar nuclei. A proportion of these mossy fibers cross in the rostral and dorsal portion of the cerebellar commissure and distribute bilaterally (Fig. 11.26A). They emit collaterals at certain preferential positions, which enter the white matter of the folia and terminate as ill-defined, longitudinal aggregates of mossy fiber rosettes in the granular layer (Fig. 11.26B). Mossy fibers preferentially influence Purkinje cells located immediately superficial to their terminal sites in the granular layer, by synapses on the ascending branches of the axons of the granule cells (the parallel fibers; Bower and Woolston, 1983). The multiple zonal pattern in the termination of the mossy fibers, therefore, will be reproduced at the level of the Purkinje cells. The transverse branches of the parallel fibers extend over large distances; over the entire width of the lobules of vermis and hemisphere in the rat. As a consequence, mossy fibers will exert a strong influence on certain longitudinal arrays of Purkinje cells and a weaker influence on the Purkinje cells in between. Some mossy fiber systems also provide the cerebellar nuclei with a collateral innervation.

In the case of the rat lateral reticular nucleus (Fig. 11.26B) (Sugihara and Shinoda, 1999), the striped termination pattern is symmetric and occupies the dorsal part of the anterior lobe (lobules IV and V, the lobulus simplex (VI), and the pyramis with the copula pyramidis (VIII). The terminal stripes, therefore, are not necessarily continuous from one lobule to the next; often they are restricted to the base or the apex of a folium. For other mossy fiber systems their distribution is mainly restricted to one side of the cerebellum, with only a few fibers crossing in the commissure. Similar, zonal patterns in their distribution to the cerebellum have been described for different spinocerebellar, cuneocerebellar, and secondary vestibulocerebellar mossy fiber systems in rabbit, rat and cat (Alisky and Tolbert, 1997; Chan-Palay *et al.*, 1977; Gerrits *et al.*, 1985; Gravel and Hawkes, 1999; Jasmin and Courville, 1987a, b; Künzle, 1975; Matsushita and Ikeda, 1987; Matsushita and Wang, 1987; Matsushita and Tanami, 1987; Matsushita and Yaginuma, 1989; Matsushita *et al.*, 1984, 1985, 1991; Oscarsson, 1976; Russchen *et al.*, 1976; Tolbert *et al.*, 1993; Tolbert and Gutting, 1997; Yaginuma and Matsushita, 1986a, b, 1987, 1989; Voogd, 1964, 1967, 1969).

Zonal patterns in the termination of vestibular root fibers and mossy fibers from the basal pons and

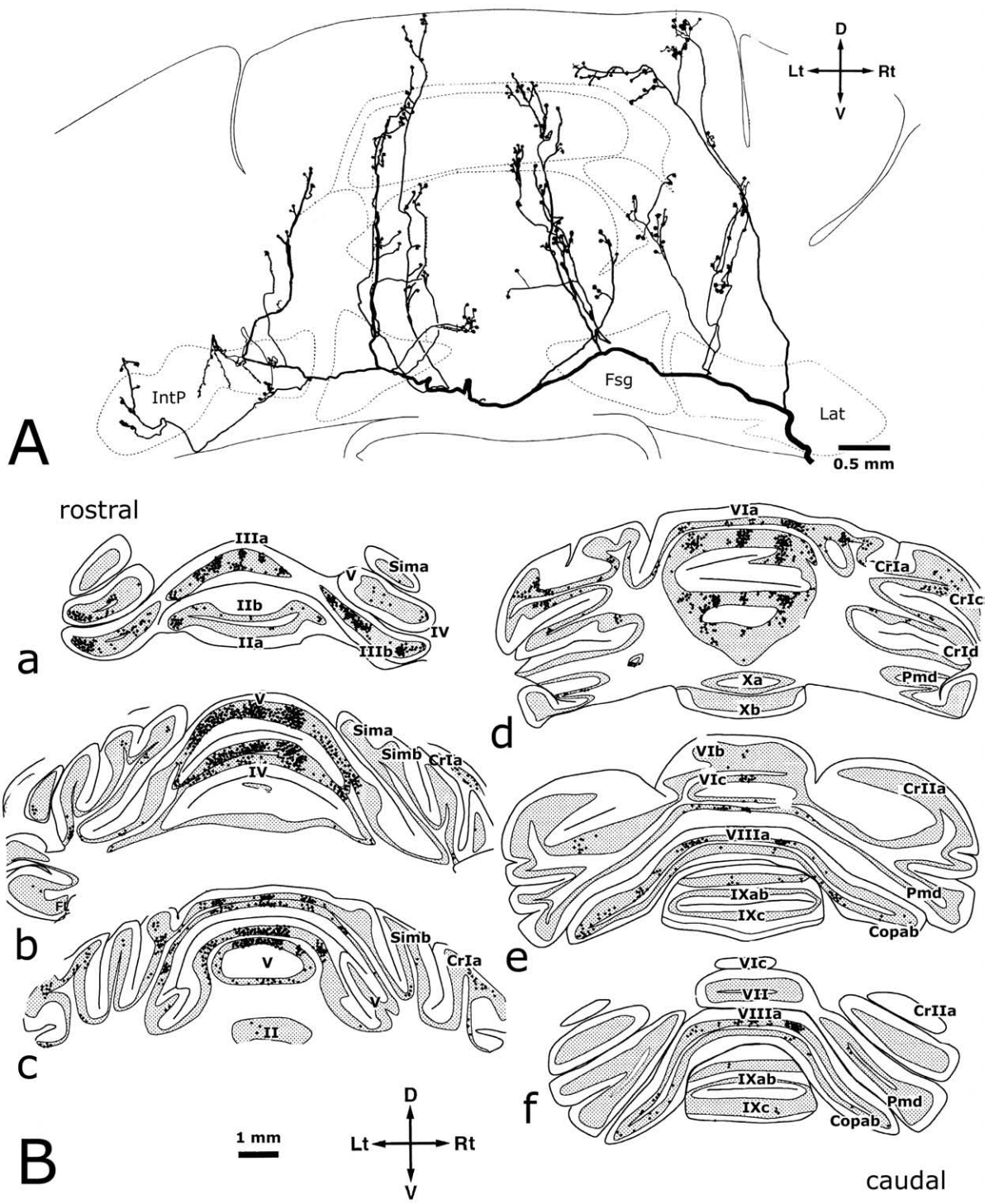

FIGURE 11.26 Course and termination of single mossy fibers in the cerebellum of the rat. **A.** Frontal view of a completely reconstructed, biotinylated dextran amine–labeled, single mossy fiber from the lateral reticular nucleus. The fiber entered the cerebellum through the ipsilateral restiform body, projected bilaterally to the cortex and the cerebellar nuclei and formed a multiple, longitudinal zonal projection pattern by its cortical arboresecnt collaterals. **B.** Mapping of mossy fiber rosettes in the cerebellar cortex after biotinylated dextran amine injection in the left lateral reticular nucleus, showing bilateral projction with ipsilateral predominance and zone-like terminal distribution in the cerebellar cortex. Modified and relabeled from Wu *et al.* (1999). Abbreviations: Copab, copula pyramidis, lobule ab; CrIa-c, Crus I a-c; CrIIa, Crus II a; D, dorsal; Fsg, fastigial nucleus; II-X, lobules II-X; IntP, posterior interposed nucleus; Lat, lateral cerebellar nucleus; Lt, left; Pmd, paramedian lobule; Rt, right; Sima,b, Simb, lobulus simplex, lolule a, b; V, ventral.

the nucleus reticularis tegmenti pontis are generally less conspicuous (however, see Voogd, 1969; Serapide *et al.*, 1994, 2001). Vestibular root fibers terminate in a continuous zone in the nodulus and the adjacent uvula and in patches in the bottom of the deep fissures (see Voogd *et al.*, 1996a for a review). Pontocerebellar fibers terminate diffusely in lateral parts of the cerebellum, in the apex of the medial lobules II–VI and VIII more medially, and massively in lobules VII and IX of the caudal vermis (Voogd, 1967; Gerrits and Voogd, 1986; Kawamura and Hashikawa, 1981).

The terminations of different mossy fiber systems in the cerebellum clearly overlap. Interesting observations on the mediolateral overlap and segregation of spinocerebellar and cuneocerebellar mossy fibers were made by Gravel and Hawkes (1990) and Alisky and Tolbert (1997) in the rat. The basoapical segregation of mossy fiber terminals, with vestibular root fibers located at the base, spinocerebellar terminals in the middle, and pontocerebellar fibers at the top would impart a characteristic mossy fiber profile to each individual lobule.

Collateral projections to the cerebellar nuclei have only been traced from the lateral reticular nucleus, the nucleus reticularis tegmenti pontis, the vestibular nuclei, and the spinal cord. These collaterals usually terminate bilaterally in multiple nuclei. The collateral projections of the two reticular nuclei appear to be complementary (Brodal, P., *et al.*, 1986; Dietrichs and Walberg, 1987; Gerrits and Voogd, 1987; Matsushita and Yaginuma, 1990, 1995; Mihailoff, 1993; Qvist, 1989a, b; Ruigrok *et al.*, 1995; Shinoda *et al.*, 1992; van der Want *et al.*, 1989). Other mossy fiber systems, such as the cuneocerebellar tract and the system from the basal pons seem to lack a collateral projection to the nuclei.

Olivocerebellar fibers only branch very sparingly. In the rat, one neuron of the inferior olive innervates ten Purkinje cells on the average (Schild, 1970; Sugihara *et al.*, 1999). Olivocerebellar fibers from subnuclei of the contralateral inferior olive distribute to discrete longitudinal zones and provide collaterals to the target nucleus of the Purkinje cells of this zone (Fig. 11.46; see also "Subdivision and Olivocerebellar Projection"). The precise topographical interrelations of mossy and climbing fiber zones have not been determined. One of the main conclusions of the ongoing discusssion about the spatial organization of mossy and climbing fibers holds that "mossy fiber and climbing fiber inputs to the cerebellar cortex are spatially coincident at the level of the single Purkinje cell" (Brown and Bower, 2000). Similar observations have been made by Ekerot and Larson (1972), and Garwicz *et al.* (1998). Therefore, the spatial and somatotopical organization of the mossy and climbing fibers should be congruent.

The Composition of the Restiform Body

The components of the restiform body, i.e., the dorsal spinocerebellar tract, the contribution of the dorsal column nuclei and the bulbar reticular nuclei, and the olivocerebellar fibers from the contralateral inferior olive, were already distinguished with the myelogenetic method in human fetal materal in the 19th century (von Bechterew, 1886; Darschewitsch and Freud, 1886). Darkschewitsch and Freud (1886) illustrated the dorsal and central position in the restiform body of the fibers from the dorsal column nuclei (1 and l′ in Fig. 11.27 and the more ventrally located dorsal spinocerebellar tract (indicated by "2" in the figure). The olivocerebellar fibers were just beginning to acquire their myelin sheath and could be followed from the contralateral olive, through and lateral to the spinal tract of the trigeminal nerve, into the periphery of the restiform body ("3" in Fig. 11.27A).

The position of the spinocerebellar tracts in the brain stem is indicated in Figure 11.13. The ventral spinocerebellar tract passes rostral to the entrance of the trigeminal nerve and enters the cerebellum along the superior cerebellar peduncle. The initial course of the olivocerebellar fibers is schematically indicated in Figure 11.28. The olivocerebellar fibers make their appearance as bundles of uniform 2-nm fibers passing through the lateral reticular nucleus and along the lateral margin of the spinal tract of the trigeminal nerve. More rostrally they also pass through this tract and its nucleus. In the restiform body the olivocerebellar fibers move through the central core of spino- and reticulocerebellar fibers to surround these mossy fiber systems at the entrance of the restiform body into the cerebellum. As a consequence, the olivocerebellar fibers become applied to the rostral and dorsal surface of the central cerebellar nuclei and their efferent tracts when they enter the cerebellum.

The early myelinating fibers of the dorsal spinocerebellar tract were traced to the cerebellum through the restiform body by Flechsig (1876) in human fetuses.[6] The separation of the spinocerebellar fibers into dorsal and ventral spinocerebellar tracts was first noted by Loewenthal (1885) in a Marchi study in the rabbit.[7] The course and termination of the spinocerebellar tracts in

[6]In the same paper that contains his famous description of the course of the degenerated pyramidal tract, Earlier Türck (1851) described following fiber degeneration from the dorsolateral funiculus of the spinal cord into the restiform body.

[7]It seems likely that the course of the ventral spinocerebellar tract was first described by Meynert (1872) as the "Hirnklappenschleife" (a lateral conmponent of the medial lemniscus, located ventral to the trigeminal spinal tract, which reaches the cerebellum along the "Hirnklappe," i.e., the anterior medullary velum).

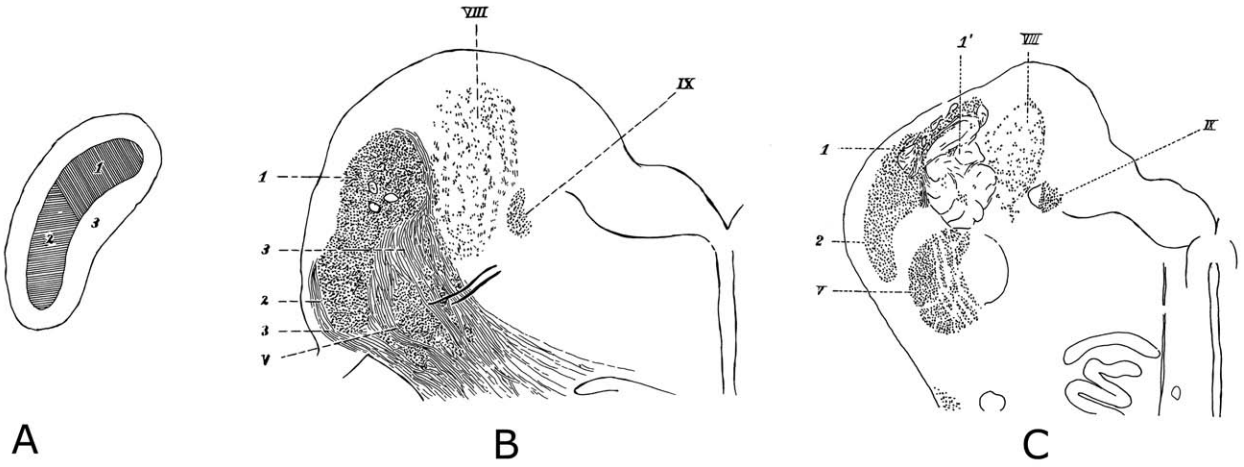

FIGURE 11.27 Myelinization of the restiform body in the human fetus. **A:** Diagram of the restiform body at a stage before myelinization of the olivocerebellar fibers has begun. The restiform body can be subdivided in a peripheral, unmyelinated portion (3) and a core with dorsal (1) and ventral parts (2). **B:** Section through the restiform body at a slightly later stage. Olivocerebellar fibers (3) now enter the restiform body through and ventral to the spinal root of the trigeminal nerve (V). **C.** Slightly more caudal section. The dorsal fibers of the early myelinating core of the restiform body (1) can be traced back to the cuneate nucleus (1′). Fibers from the dorsal spinocerebellar tract occupy its ventral portion (2). Abbreviations: n.XII, hypoglossal nerve; IX, solitary tract; VIII, juxtarestiform body. From Darkschewitsch and Freud (1886).

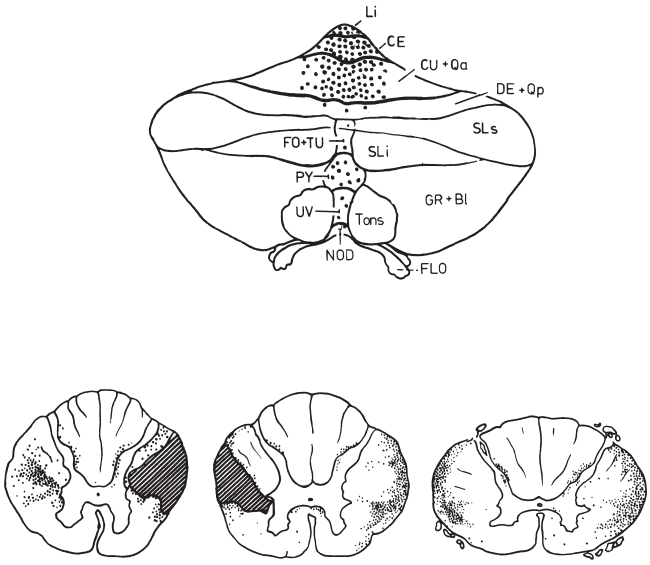

FIGURE 11.29 Termination of spinocerebellar fibers in the human cerebellum. Study using the Marchi method after a hemicordotomy at T.4–5. Lesions of the cord are hatched. Abbreviations: BI, biventral lobule; CE, central lobule; CU, culmen; DE, declive; FLO, flocculus; FO, folium vermis; GR, nucleus gracilis; Li, lingula; NOD, nodule; PY, pyramis; Qa, anterior quadrangular lobule; Qp, posterior quadrangular lobule; Sli, inferior semilunar lobule; SLs, superior semilunar lobule; Tons, tonsilla; UV, uvula. Adapted from Brodal and Jansen (1941).

the human cerebellum was described by Bruce (1898), Collier and Buzzard (1903), Hoche (1896), and Thiele and Horsley (1901), all with the Marchi method. In the most recent antegrade tracing study of the spinocerebellar tracts by Jansen and Brodal (1941), using the Marchi method in a case with bilateral thoracic cordotomies and ascending degeneration in both tracts, degenerated fibers were followed to the vermis of the anterior lobe, mainly in the central lobule and the ventral part of the culmen, less in dorsal culmen and lingula, until 1.5 cm out of the midline. In the posterior lobe degenerated fibers were found mostly in the pyramis, less in other lobules of the caudal vermis (Fig. 11.29). This paper is the last study of its kind in primates. The origin of spinocerebellar fibers was studied with retrograde tracing methods by Petras (1977), Petras and Cummings (1977), and Snyder *et al.* (1978). Recent papers on the distribution of spinocerebellar fibers in the cat were published by Tolbert *et al.* (1993) and Grant and Xu (1988).

The external cuneate nucleus has been described in man (Olszewski and Baxter, 1954; see also Chapter 10). Its disappearance has been noted in many pathological cases with cerebellar lesions, but details about the projection of the dorsal column nuclei to the cerebellum in primates are not available. The origin of the cuneocerebellar projection from the external cuneate nucleus was determined in experimental studies by Von Gudden (1882) and from the internal cuneate and

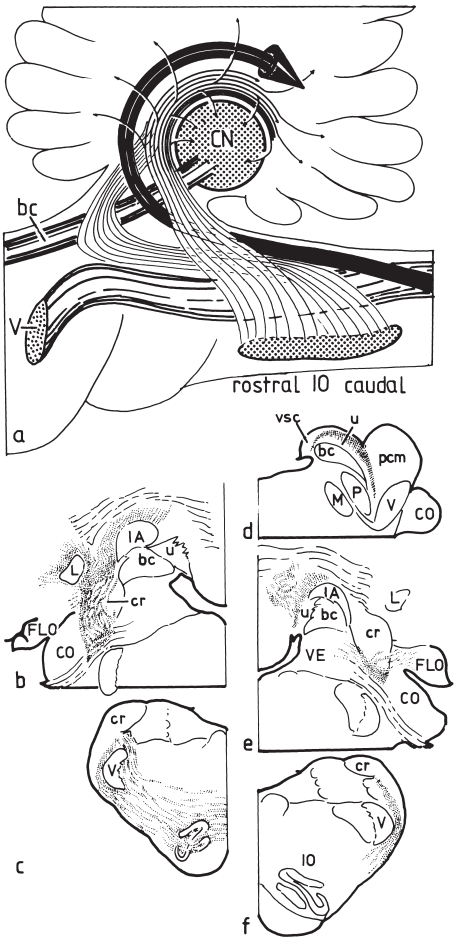

FIGURE 11.28 Lateral view of the localization of olivocerebellar fibers in the brain stem and cerebellum **(a)** Fibers from the caudal half of the inferior olive **(b–d)** pass lateral to the spinal tract (V) and ascend in the restiform body to enter the cerebellum medial to the spino-, cuneo-, and reticulocerebellar components of the restiform body *(thick arrow)*. Fibers from the rostral half of the inferior olive **(e, f)** enter the cerebellum lateral to these systems. In the cerebellum, olivocerebellar fibers become applied to the rostral and dorsal surface of the cerebellar nuclei and their efferent tracts. Abbreviations: bc, brachium conjunctivum; CN, cerebellar nuclei; CO, cochlear nuclei; cr, restiform body; FLO, flocculus; IA, anterior interposed nucleus; IO, inferior olive, L, lateral cerebellar nucleus; M, motor nucleus of the trigeminal nerve; P, principal sensory nucleus of the trigeminal nerve; pcm, brachium pontis; u, uncinate tract; V, trigeminal nerve; VE, vestibular nuclei; vsc, ventral spinocerebellar tract. From Voogd and Bigaré (1980).

gracile nuclei by Gordon and Seed (1961). The exteroceptive and proprioceptive components of the cuneocerebellar tract synapse in the internal and external cuneate nuclei, respectively (Cooke *et al.*, 1971). Data on the distribution of cuneocerebellar mossy fibers in the cat can be found in the papers of Alisky and Tolbert (1997), Gerrits *et al.* (1985), Jasmin and Courville (1987), and Tolbert and Gutting (1997).

The precerebellar reticular nuclei (see Chapter 10) are located in the caudal medulla, the lateral reticular nucleus in the lateral funiculus, and the paramedian reticular nucleus in the anterior funiculus (i.e., in the medial longitudinal fascicle, Fig. 11.32). The lateral reticular nucleus can be subdivided in most mammal into a lateral parvocellular, a medial magnocellular, and a subtrigeminal portion. A subdivision into a ventral main portion and a dorsal subtrigeminal part also is possible in man (Walberg, 1952). Parvocellular and magnocellular portions were difficult to identify. The lateral reticular nucleus is surrounded by the fiber systems of the lateral funiculus. In this position it was first described by Deiters (1865) in man. In human cordotomy cases, fiber degeneration in the lateral reticular nucleus always prevails in the lateral portion of the nucleus. In the cat the dorsal subtrigeminal portion of the lateral reticular nucleus is located in the center of the rubrospinal tract and receives collaterals from this system (Busch, 1961). In man the rubrospinal tract is not as well developed as in lower mammals (Verhaart, 1957). In cases with large lesions of the mesencephalon fibers can be traced to this location and were identified as rubrobulbar fibers terminating on the lateral reticular nucleus. Rubrospinal fibers cannot be traced caudal to the lateral reticular nucleus. The lateral reticular nucleus also receive cortical afferents in man (Kuypers, 1958; Schoen, 1964, 1969) (Fig. 11.40). Fibers from the lateral vestibulospinal tract that terminate in the medial extension of the lateral reticular nucleus in the cat (Ladpli and Brodal, 1968; Walberg *et al.*, 1985) and the projection of the fastigial nucleus to both parts of the nucleus (Walberg and Pompeiano, 1960) have not been identified in human material. The cerebellar projection of the lateral reticular and paramedian reticular nuclei have not been studied in primates. The literature on its distribution in rat and cat was reviewed by Wu *et al.* (1999). The literature on the collateral projection of the reticular nuclei to the cerebellar nuclei is included in the section "Organization of Mossy and Climbing Fiber in the Cerebellum" of this chapter.

Inferior Olive and Its Afferent Systems

Subdivision and Olivocerebellar Projection

The inferior olive in man was described and illustrated in the thesis of Kooy (1916, 1917), a phylogenetic and ontogenetic study on the subdivision of the inferior olive in vertebrates, and is discussed in Chapter 10 of this volume. It consists of dorsal (DAO) and medial (MAO) accessory olives and a principal nucleus (PO). The medial accessory olive is subdivided in rostral and

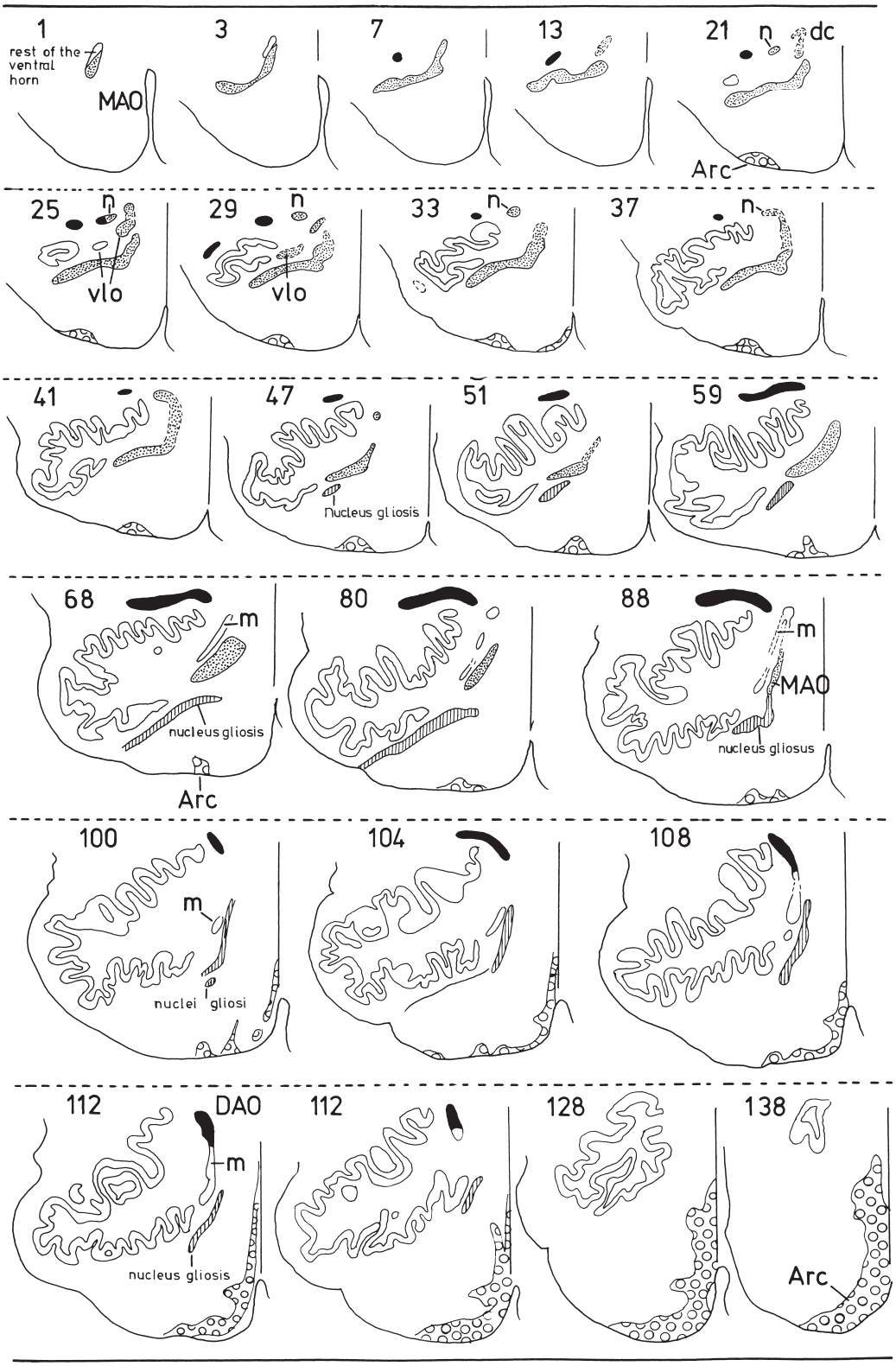

FIGURE 11.30 The human inferior olive. Dorsal accessory olive (DAO), black arreas; medial accessory olive (MAO), stippled areas; principal nucleus of the inferior olive (PO), unmarked areas; glial nuclei are hatched; arcuate nucleus is indicated with open circles. Abbreviations: m, medial leaf of the principal olive; n, connection between dorsal cap and the DAO; vlo, ventrolateral outgrowth. Adapted from Kooy (1916).

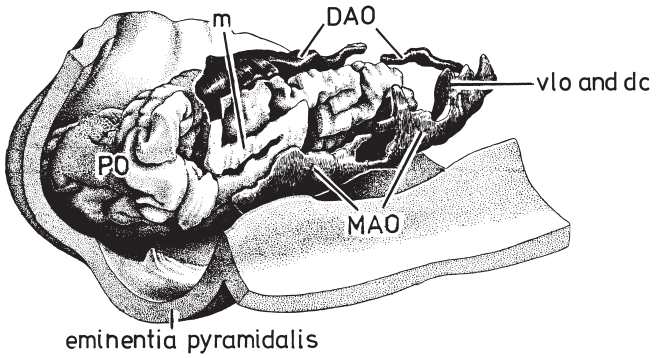

FIGURE 11.31 After a wax model of the human inferior olive. Abbreviations: see Fig. 11.30. From Kooy (1916).

caudal parts, separated by a narrow neck (Fig. 11.30, section 51; Fig. 11.31). The caudal pole of the MAO is located adjacent to the supraspinal nucleus, the rostral continuation of the ventral horn. The dorsal cap and the ventrolateral outgrowth are part of the vertical limb of the MAO (Fig. 11.30, sections 13–29; Figs. 11.31 and 11.32; the so-called Reticularisantheil of the medial accessory olive). The ventral part of the vertical limb was identified as the subnucleus β by Jansen and Brodal (1958). They also indicated a dorsomedial cell column, in the rostralmost parts of the olive. The dorsal accessory olive (DAO) caudally connects with the dorsal cap and rostrally with the medial lamina of the principal olive (PO). The connection of the DAO with either the dorsal or the ventral lamina of the PO is also observed in other mammals; the connections of the DAO with the dorsal cap is unusual. The continuity of the ventrolateral outgrowth with the ventral leaf of the PO, which is present in many other mammals, is also indicated in the human olive. The cell sheet of the principal olive is folded, except for its medial lamina. The PO of subhuman primates has a similar configuration, with strong folding of the dorsal and the lateral laminae, and an unfolded ventral lamina, which is continuous with the medial pole of the DAO (Whitworth and Haines, 1986b).

Knowledge of the olivocerebellar projection has progressed slowly. The decussation of the olivocerebellar fibers and their course and localization were well-known to the 19th century neurologists who described the composition of the restiform body (see "Composition of the Restiform Body"). The myelogenetic method and the Marchi technique, which visualizes degenerated myelin, are not suitable to trace the fine olivocerebellar fibers to their termination. The termination of the olivocerebellar fibers as climbing fibers was suggested in animal experiments by Szentagothai and Raikovits (1959). Desclin (1974) settled the sole origin of climbing fibers in the inferior

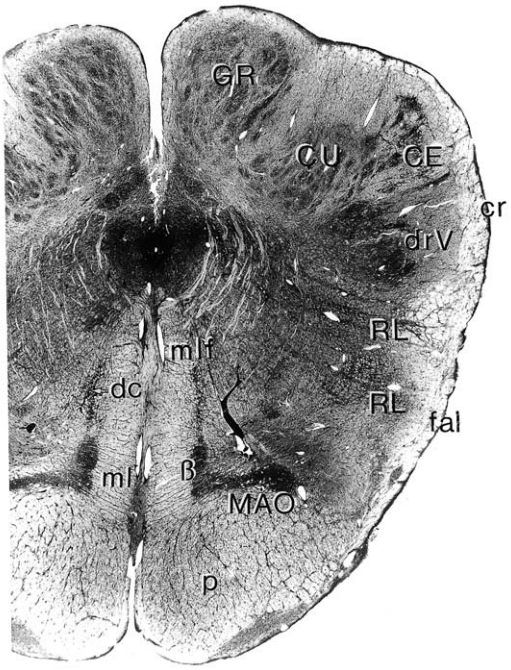

FIGURE 11.32 Häggqvist-stained section through the caudal pole of the medial accessory olive with the dorsal cap and group B. Abbreviations: CE, external cuneate nucleus; cr, restiform body; CU, cuneate nucleus; dc, dorsal cap; drV, spinal tract of the trigeminal nerve; fal, anterolateral fascicle; GR, nucleus gracilis; MAO, medial accessory olive; ml, medial lemniscus; mlf, medial longitudinal fascicle; p, pyramid; RL, retrolemniscal nucleus.

olive with Fink–Heimer modification of the Nauta technique after chemical destruction of the inferior olive of the rat with 3-acetylpyridine. The topography in the olivocerebellar projection had already been studied before the mode of termination of the olivocerebellar became known.

Brodal (1940) used retrograde changes, induced by localized lesions of the cerebellum, in cells of the inferior olive in young kittens and newborn rabbits (modified Von Gudden method) to map the olivocerebellar projection. His lesions were classified according to the lobules they involved, and in the interpretation of his results he made the assumption that a single olivary subnucleus usually projects to a single lobule or group of lobules. The rostral MAO was found to project to the flocculus and the caudal MAO to lobules of the anterior and posterior vermis. The projection of the DAO is restricted to the anterior lobe but extends beyond the vermis in the so-called pars intermedia. The hemisphere, including the hemisphere of the anterior lobe, receives olivocerebellar fibers from the PO. On the basis of these results he postulated the presence of three longitudinal zones in the anterior lobe: the vermis with projections from MAO and DAO, the pars

intermedia with projections from the DAO, and the hemisphere with projections from the PO. In later studies on the corticonuclear projection with Jansen (Jansen and Brodal, 1940, 1942) they described the corticonuclear projection of the three zones to the three cerebellar nuclei of Brunner (1919): the vermis to the fastigial nucleus, the intermediate zone to the interposed nucleus, and the hemisphere to the dentate. Projections to the cerebellar nuclei were found to arise from the dorsal cap and the ventrolateral outgrowth.

Brodal's (1940) lobular pattern in the olivocerebellar projection was challenged when Nauta's anterograde degeneration method was applied to study these connections. According to Voogd (1969), the olivocerebellar projection is organized in a strictly longitudinal zonal fashion: different subnuclei project to narrow longitudinal zones, which extend perpendicular to the long axis of the folia and which are continuous over many successive cerebellar lobules, sometimes including the entire cerebellum. It was postulated in the same paper, and later verified experimentally (Courville and Faraco-Cantin, 1976; Voogd and Bigaré, 1980) (Fig. 11.33), that these climbing fiber zones coexist with the corticonuclear projection zones, which contain Purkinje cells that project to a single cerebellar or vestibular nucleus (Fig. 11.46A). These observations were extended and confirmed using the anterograde tracing with [^{3}-H]leucine (Courville *et al.*, 1974; Gerrits and Voogd, 1982; Groenewegen and Voogd, 1977; Groenewegen *et al.*, 1979; Kawamura and Hashikawa, 1979; Voogd, 1982) and more recent antegrade tracer methods and electrophysiological techniques (Andersson and Oscarsson, 1978a, b; Atkins and App, 1997; Armstrong *et al.*, 1974; Buisseret-Delmas, 1988a, b; Buisseret-Delmas *et al.*, 1989, 1993; Jörntell *et al.*, 2000; Garwicz *et al.*, 1997; Oscarsson, 1969, 1973, 1980; Ruigrok *et al.*, 1992; Tan *et al.*, 1995a, b, c; Trott and Armstrong, 1987a, b; Trott *et al.*, 1998a, b; Voogd *et al.*, 1996). A single lobule therefore may receive its climbing fiber connections from as many as seven different olivary subnuclei, each of which provide one or more longitudinal zones of Purkinje cells with its climbing fibers. Projections to the cerebellar nuclei do not originate from separate subnuclei of the olive but as collaterals from the olivocerebellar fibers. They terminate in those cerebellar nuclei which receive the axons of the Purkinje cells which are innervated by climbing fiber collaterals from the same parent fibers (Ruigrok and Voogd, 2000; Sugihara and Shinoda, 1999; Van der Want and Voogd, 1987; Van der Want *et al.*, 1989). In an extensive series of experiments with retrograde tracers of Brodal and Walberg and their coworkers (reviewed by Brodal and Kawamura, 1980), these authors confirmed the longitudinal organization in the olivocerebellar projection.

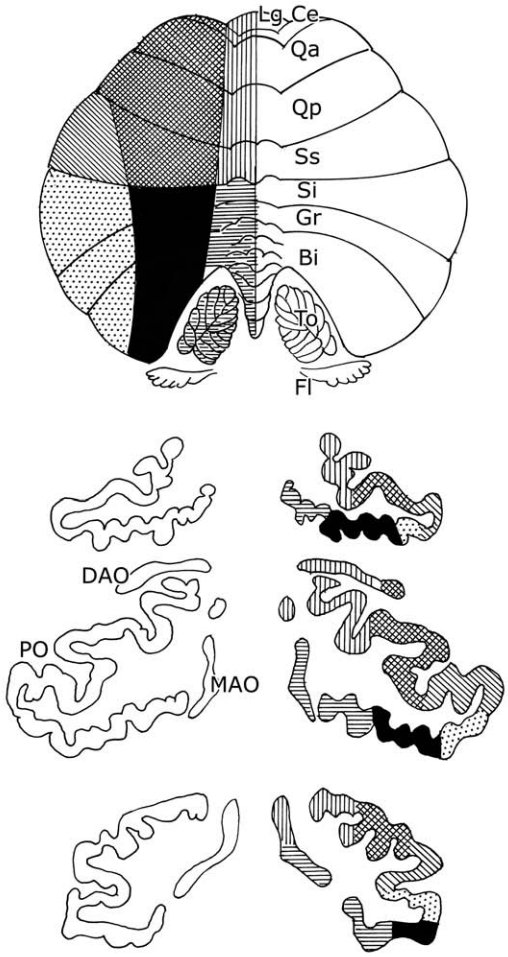

FIGURE 11.33 Diagram illustrating the topographical relations between the inferior olive and the human cerebellum. The dorsal accessory olive and the medial half of the dorsal leaf of the principal olive are connected with the cortex of the superior surface of the cerebellum. Olivocerebellar fibers from the ventral lamina of the principal olive and the ventral part of the medial accessory olive project to the tonsilla and the caudal vermis. Abbreviations: Bi, biventral lobule; Ce, central lobule; DAO, dorsal accessory olive; Fl, flocculus; Gr, lobulus gracilis; Lg, lingula; MAO, medial accesory olive; PO, principal olive; Qa, anterior quadrangular lobule; Qp, posterior quadrangular lobule; Si, inferior semilunar lobule; Ss, superior semilunar lobule; To, tonsilla. From Holmes and Stewart (1908).

The olivocerebellar projection in man was studied in many pathological cases with more or less restricted lesions of the cerebellum. Best known are the studies of Holmes and Stewart (1908)(Fig. 11.33). A topographical arrangement was proposed for the projections of the caudal ventral lamina of the PO and the medial accessory olive to the tonsilla and the caudal vermis, and of the medial part of the dorsal lamina and the dorsal accessory olive to the anterior lobe and the lobulus simplex. The longitudinal pattern in the olivocerebellar projection has not been investigated in man.

The scarce data from nonhuman primates indicated that the same longitudinal pattern that has been documented in carnivores is also present in the olivocerebellar projection in monkeys (Brodal and Brodal, 1981, 1982; Voogd *et al.*, 1987a; Whitworth and Haines, l986a).

One of the most vexing problems in the primate olivocerebellar projection remains the connections of the principal olive to the dentate nucleus and the cortex of the hemisphere. In carnivores Voogd (1969) distinguished two zones in the hemisphere, which are connected through separate white matter compartments, with different subdivisions of the dentate nucleus. Similar observations have been made in subhuman primates (Fig. 11.49; see "Longitudinal Zonation of the Cerebellum"). The medial D_1 zone is connected with the caudal dentate, the lateral D_2 zone with its more rostral portions. This relationship receives support from studies on the reciprocal connections between the dentate and the principal olive in cat and rat, which generally show that the target nucleus of the D_2 zone (the rostromedial dentate) is connected with the dorsal lamina and the lateral bend of the PO, and the target nucleus of D_1 (the ventrocaudal dentate) with its ventral, unfolded portion (Beitz, 1976; Dietrichs and Walberg, 1981; Courville *et al.*, 1983; Gerrits *et al.*, 1984, 1985a; Ruigrok and Voogd, 1990; Ruigrok *et al.*, 2000; Tolbert *et al.*, 1976). Similar observations have been published for monkeys (Chan-Palay, 1977; Kalil, 1979, Figure 36.3). However, the relationship of the ventral and the dorsal lamina of the PO with the D_1 and D_2 zones, as originally proposed by Voogd (1969), Groenewegen and Voogd (1977), and Provini (1982), was reversed in the studies in cat and rat by Brodal (Brodal and Kawamura, 1980; Azizi and Woodward, 1987; Buisseret-Delmas *et al.*, 1989). Therefore, the organization of the projection of the principal olive to the cortex of the the cerebellar hemisphere, which accounts for the major part of the olivocerebellar projections in primates, and the organization of the corticonuclear projection to the dentate nucleus remains undecided.

Afferent Systems of the Inferior Olive

Afferent systems of the inferior olive have been reviewed by Brodal and Kawamura (l980) and Saint-Cyr and Courville (1980) for the cat and by Martin *et al.* (1980) for the opossum. For the rat, the tabulated summery of its afferent connections in the paper of Brown *et al.* (1977) and the reviews by Flumerfelt and Hyrcyshyn (1985) and Ruigrok and Cella (1995) are useful. Afferent systems of the inferior olive can be subdivided into three groups: (1) excitatory projections from the spinal cord, certain brain stem nuclei, and the cerebral cortex; (2) GABA ergic nucleoolivary and vestibuloolivary projections; and (3) monoaminergic afferents. Monoaminergic and peptidergic projections to the inferior olive were reviewed by Voogd *et al.* (1996b).

Afferent Systems of the Inferior Olive: Ascending Connections Somatotopically arranged projections from the spinal cord, the dorsal column nuclei, and the sensory nuclei of the trigeminal nerve terminate in the entire DAO with the adjoining part of the dorsal lamina of the PO and in the caudal MAO, with the exception of the region of the nucleus β (Kalil, 1979; Mehler *et al.*, 1960; Whitworth and Haines, 1983). Spinoolivary fibers were already identified by Von Bechterew (1886). A portion of the caudal MAO, the group β and the dorsomedial cell column, receives afferents from the vestibular nuclei (reviewed by Voogd *et al.*, 1996a).

Afferent Systems of the Inferior Olive: Descending Connections. The Nucleus Ruber and Its Connections A major projection to the olive is derived from the so-called nuclei at the meso–diencephalic junction, which include the zona incerta, the pretectum, optokinetic centers such as the nucleus of the optic tract and the nuclei of the accessory optic tract, the central gray, the Darkschewitsch nucleus, the subparafascicular nucleus, the medial accessory nucleus of Von Bechterew, and the parvocellular red nucleus. The caudal magnocellular division of the red nucleus gives rise to rubrobulbar and rubrospinal tract but does not project to the inferior olive. In the cat, the descending fibers reach the olive through the medial and central tegmental tracts (Busch, l961; Ogawa, 1939; Onodera, 1984) and terminate in the rostral half of the MAO, in restricted parts of the caudal MAO, in the caudal DAO, and in the PO.

The central tegmental tract is especially well developed in man. It takes its origin from the parvocellular part of the red nucleus; the magnocellular portion is poorly developed in man. Its fibers emerge from the dorsomedial part of the red nucleus and traverse the capsule of brachium conjunctivum fibers in small fascicles of uniform 2- to 3-nm fibers in a dorsolateral direction. Together with similar fibers from the medial tegmental tract, which is located in the ventral part of the medial longitudinal fascicle, the central tegmental tract constitutes a single area characterized by its uniform fiber caliber in the mesencephalic tegmentum (Fig. 11.34). The uniform fiber pattern of the central tegmental tract makes it possible to trace it in normal, Häggqvist-stained sections (Verhaart, 1949, 1956a; Verhaart and Sie, 1958). Caudally the two tracts separate. The fibers of the central tegmental tract traverse the fibers of the brachium conjunctivum on

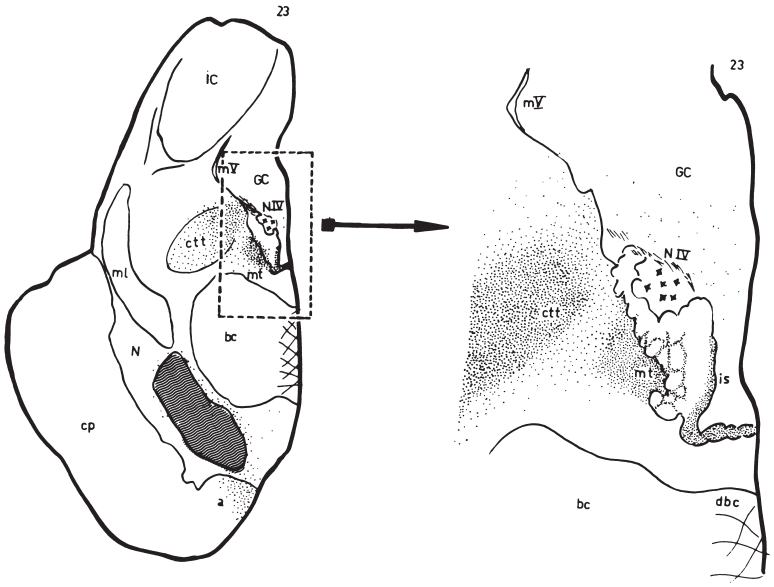

FIGURE 11.34 Localization of the central and medial tegmental and interstitiospinal tracts in the mesencephalon. Note the localization of the latter two tracts in the medial longitudinal fascicle. Drawing from degenerated Häggqvist-stained fibers in case H6486 (Fig. 11.37). Abbreviations: a, frontopontine tract of Arnold; bc, brachium conjunctivum; cp, cerebral peduncle; ctt, central tegmental tract; dcb, decussation of the brachium conjunctivum; GC, central gray; IC, inferior colliculus; is, interstitiospinal fibers; ml, medial lemniscus; mt., medial tegmental tract; mV, mesencephalic root of the trigeminal nerve; N, substantia nigra; NIV, nucleus of the trochlear nerve. Courtesy of Schoen (unpublished).

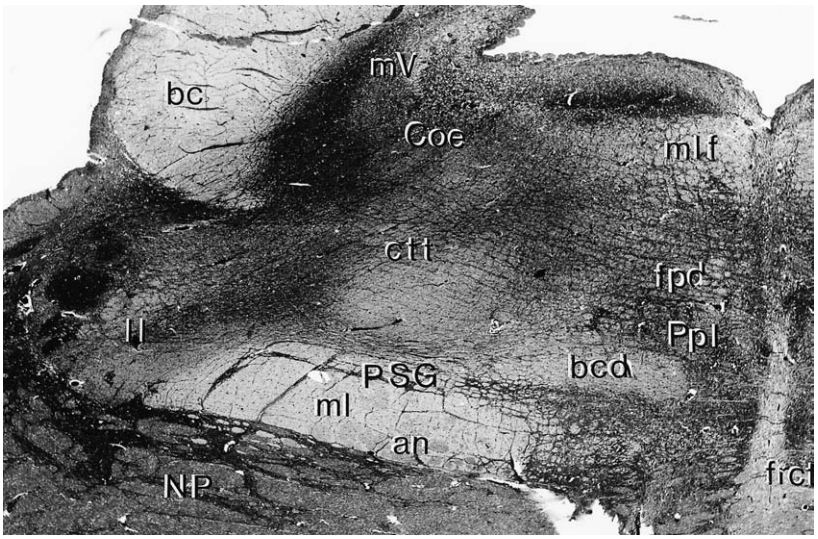

FIGURE 11.35 Section through the tegmentum pontis. Häggqvist stain. Note the central tegmental tract, the descending branch of the brachium conjunctivum (bc) and the papillioform nucleus. an, Areae nebulosae; bcd, descending branch of the brachium conjunctivum; Coe, locus coeruleus; ctt, central tegmental tract; fdp, predorsal fascicle; frc, fibrae rectae, predorsal fascicle; ll, lateral lemniscus; ml, medial lemniscus; mlf, medial longitudinal fasciculus; mV, mesencephalic root; NP, basal pontine nuclei; Ppl, papillioform nucleus; PSG, processus supralemniscalis grisei pontis.

their way to their decussation. They take up their characteristic central position as a comma-shaped tract in the tegmentum at the level of the pons (Fig. 11.35). Still more caudally they can be traced into the amiculum surrounding the inferior olive. The central tegmental tract was discovered by Von Bechterew (1899). The medial tegmental tract descends from its ventral position in the medial longitudinal fascicle, along the raphe to enter the olive dorsomedially (Ogawa, 1939; Busch, 1961; Onodera, 1984).

Termination of the tegmental tracts was reported in the autoradiographic tracing study of Strominger *et al.* (1979) in monkeys. The dorsomedial portion of the parvocellular red nucleus, located medial to the fasciculus retroflexus, projects to the ventral lamina of the PO. More lateral and caudal parts of this nucleus project to the lateral bend and dorsal lamina of the PO (Fig. 11.36, 1–2). The dorsomedial injection sites encroach on the central gray with Darkschewitsch's nucleus and invariably result in labeling in the rostral MAO. The distribution of the label in the cell band of the PO is discontinuous stripes of dense labeling alternating with regions with a lesser concentration (arrows in Fig. 11.36, 2). Similar but less detailed observations were made earlier in an axonal degeneration study of Courville and Otabe (1974). The projection of the nucleus of Darkschewitsch, which is located in the ventrolateral central gray at the level of the posterior commissure, through the medial tegmental tract to the rostral half of the MAO and the dorsomedial cell column is only known from studies in cat and rat (for reviews, see Busch, 1961; Onodera, 1984; Ruigrok and Cella, 1995).

The distribution of the labeling in the human cases depicted in Fig. 11.37 is in general accordance with the experimental data (Schoen, unpublished). Large lesions of the mesencephalon result in a descending degeneration of both tegmental tracts (Fig. 11.37, case 3). Fiber degeneration is found in and around the DAO, the MAO, and the PO over their entire rostrocaudal extent. Caudally degenerated fibers of the central tegmental tract proceed beyond the olive in the ventrolaterally located tract of Helweg. Its fibers are thinner than the fibers of the central tegmental tract at the level of the pons. In cases with medially located lesions of the central gray isolated degeneration of the medial tegmental tract is obtained. The fibers were found to terminate in the medial extremity of the ventral lamina of the PO and in the entire MAO (Fig. 11.37, case 1). A partial degeneration of the central tegmental tract is present in case H6486 (Fig. 11.37, case 2) with a hemorrhagic softening in the ventral part of the central gray matter, extending in the area of the medial and central tegmental tracts and the medial red nucleus. This resulted in degeneration in both medial tegmental tracts and in the medial half of the central tegmental tract. Termination is especially strong around the ventral lamella of the PO and in the entire MAO. The inclusion of the caudal MAO with the dorsal cap in these human cases may be due to the interruption by the large, less well-defined human cases of other descending fibers to the inferior olive, i.e., of fibers from the nucleus of the optic tract and the nuclei of the accessory optic tract to the dorsal cap and the ventral lateral outgrowth (for reviews, see Simpson, 1984 and Simpson *et al.*, 1988) or the interruption fibers from the superior colliculus to the medial part of the caudal MAO adjoining group β, which have been demonstrated in monkeys (Frankfurter *et al.*, 1976; Harting *et al.*, 1977) and other species. A projection of the central tegmental tract to the DAO was not reported in animal studies. Projections to the DAO originate from the pretectal nuclei in monkeys and other species (Sekiya and Kawamura, 1985; Bianchi and Gioia, 1990; for reviews, see Kitao *et al*, 1989 and Bull *et.al*, 1990). These pretectal projections may also exist in humans but in this case would include the entire DAO. It can be concluded that in humans the descending projections from the mesencephalon completely overlap with the ascending somatosensory projections to the accessory olive.

The parvocellular red nucleus and surrounding structures are links in corticoolivocerebellar climbing fiber paths, which are under control of the cerebral cortex. Direct corticoolivary connections exist, but they seem to be rather scanty (Saint-Cyr, 1983; Burman *et al.*, 2000). The corticorubral projection in monkeys seems to be limited to the frontal lobe and therefore is the mirror image of the cerebellothalamocortical projection. The corticorubral pathway to the parvocellular red nucleus in the monkey dominates over the projection to its magnocellular part (Fig. 11.25A). It arises from the entire motor cortex, the premotor cortex, the supplementary motor cortex and the cingulate motor areas, and the frontal eye field (areas 4, 6, 8, 23, and 24 of Brodmann, 1909). Connections from the parietal lobe are few or absent in the monkey. An origin from the prefrontal cortex was never mentioned in the literature but has not been systematically studied. The projection is mainly ipsilateral, with smaller, symmetric projections to the other side. Kuypers and Lawrence (1967), Hartmann-Von Monakow *et al.* (1979), Oriolo and Strick (1989), and Burman *et al.* (2000) established that the projection from the motor cortex occupies the lateral two-thirds of the rostral and the entire caudal portion of the parvocellular red nucleus (Fig. 11.25A). This projection is somatotopically arranged, with the hindlimb ventrolaterally and the face medially. Tokuno *et al.* (1995) observed a similar somatotopical

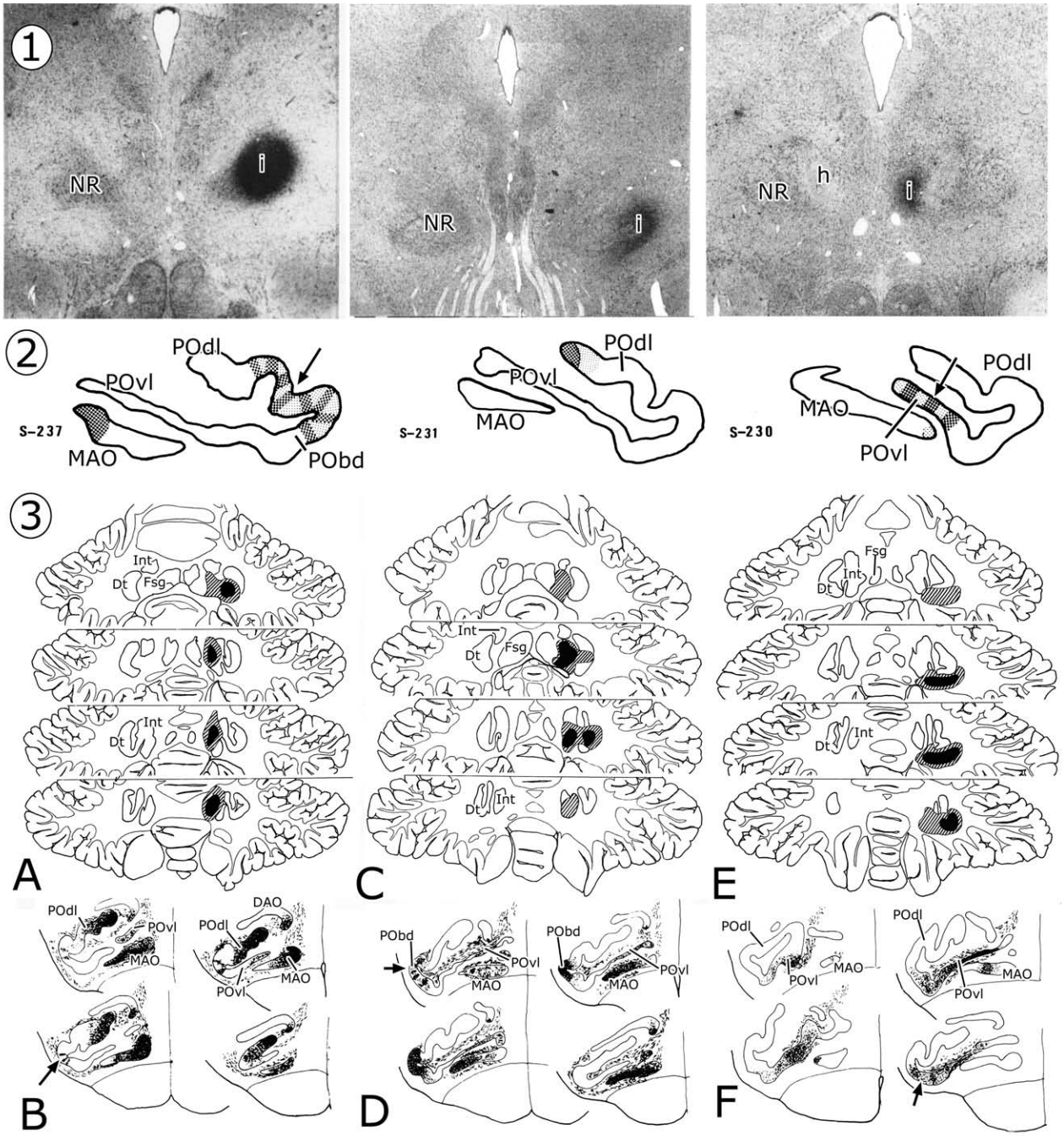

FIGURE 11.36 Afferent connections of the principal nucleus of the inferior olive in the monkey. **1, 2:** Injections of tritiated leucine in rostrolateral part of parvocellular red nucleus (S-237), caudal parvocellular red nucleus (S-231), and rostromedial parvocellular red nucleus (S-230) label a lateral part of the dorsal lamella and the bend of the principal olive, the medial pole of the dorsal lamella, and the ventral lamella of the ipsilateral principal olive, respectively. **3A–F:** Injections of tritiated proline in the rostral **(A),** lateral **(C),** and ventrocaudal **(E)** dentate mainly label the dorsal lamella **(B),** the lateral bend **(D),** and the ventral lamella **(F)** of the contralateral principal nucleus of the olive. Labeling in the rostral part of the medial accessory olive is caused by an extension of the injection into the posterior interposed nucleus. Terminals of both the the rubroolivary and the nucleoolivary projection display a periodicity in the lamella of the principal olive *(arrows).* Abbreviations: DAO, dorsal accesory olive; DAO, dorsal accessory olive; Dt, dentate nucleus; Fsg, fastigial nucleus; h, habenulointerpeduncular tract; i, injection site; Int, interposed nuclei; MAO, medial accessory olive; PObd, lateral bend of the principal nucleus of the inferior olive; POdl, dorsal lamella of the principal nucleus of the inferior olive; Povl, ventral lamella of the principal nucleus of the inferior olive; RN, red nucleus. Rows 1 and 2, from Strominger *et al*. (1979); rows 3A–F from Kalil (1979).

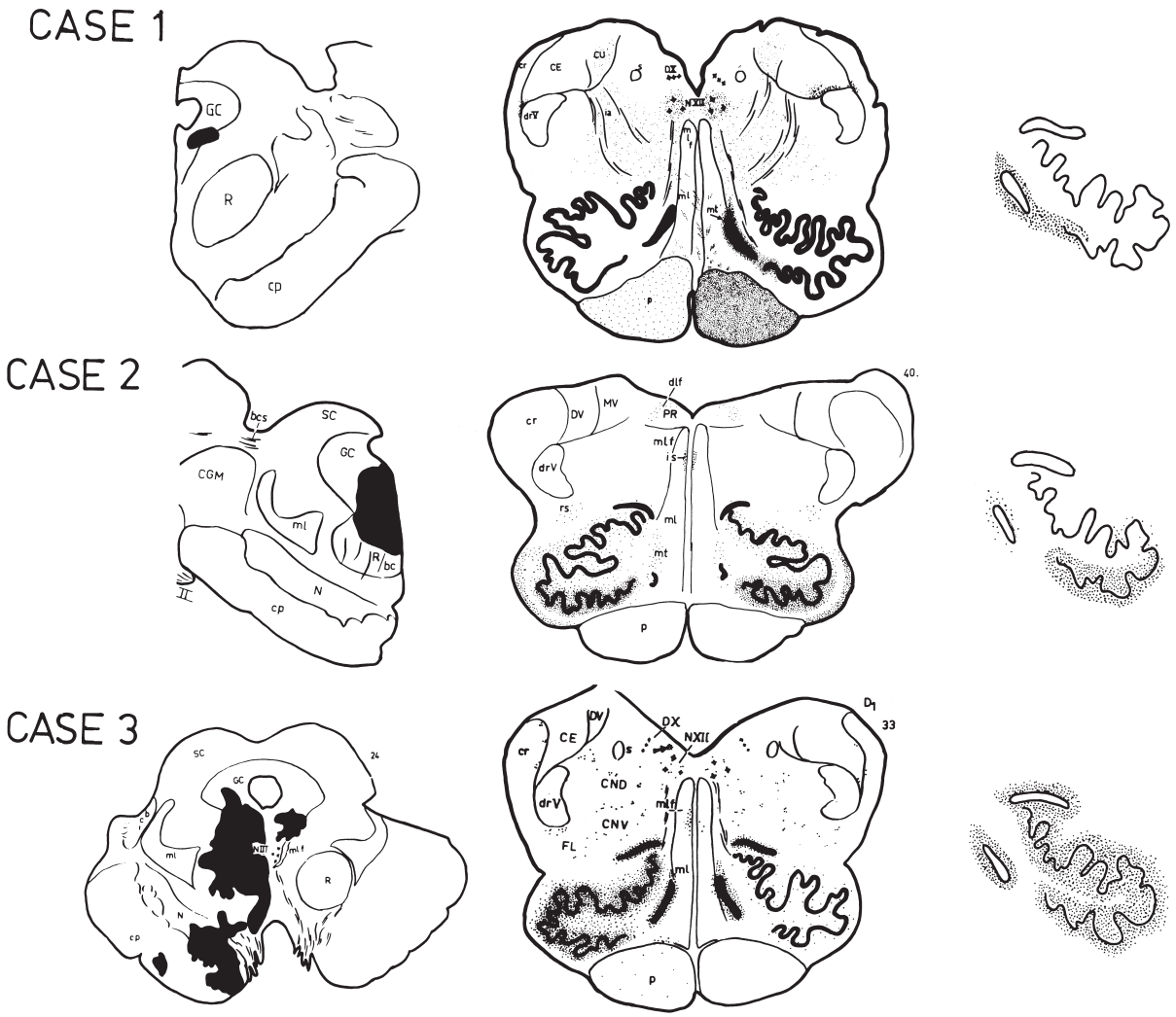

FIGURE 11.37 Lesions and fiber degeneration at the level of the inferior olive in three cases with axonal degeneration of the fibers of different components of the tegmental tracts. Case 1 (H6348) with degeneration of the medial tegmental tract; Case 2 (H6486) with a degeneration of the medial tegmental tract and a partial degeneration of the central tegmental tract, Case 3 (H6386) with a degeneration of the medial and central tegmental tracts. Lesions in the diagrams on the left are indicated in black. Nauta stain. Abbreviations: bc, brachium conjunctivum; bcs, brachium of the superior colliculus; cb, corpus bigeminum; CE, external cuneate nucleus; CGM, medial geniculate body; CND, central nucleus, pars dorsalis; CNV, central nucleus, pars ventralis; Cp, cerebral peduncle; CU, cuneate nucleus; dlf, dorsal fasciculus; drV, spinal tract of the trigeminal nerve; DV, spinal vestibular nucleus; DX, dorsal nucleus of the vagal nerve; FL, fasciculus anterolateralis; GC, central gray; ia, internal arcuate fibers; is, interstitiospinal fibers; m, medial longitudinal fascicle ; ml, medial lemniscus; mt, medial tegmental tract; N, substantia nigra; NIII, ocolomotor nerve; NXII, hypoglossal nerve (nucleus); p, pyramid; PR, nucleus prepositus hypoglossi; R, red nucleus; rs, rubrospinal tract; SC, superior colliculus. Courtesy of Schoen (unpublished).

pattern for the projection of the supplementary motor area. The rostral dorsomedial part of the parvocellular red nucleus, which extends medial to the fasciculus retroflexus, receives afferents from more rostral frontal areas, corresponding to the rostral part of the supplementary motor area (Hartmann-von Monakow *et al.*, 1979), the rostral and dorsal part of the premotor area (Kuypers and Lawrence, 1967; Hartmann-von Monakow *et al.*, 1979), the frontal eye field (Kuypers and Lawrence, 1967; Burman *et al.*, 2000), and the ventral premotor area (Hartmann-Von-Monakow *et al.*, 1979). Darkschewitsch's nucleus receives projections from arm and leg areas of the motor cortex, weakly from the premotor area and more strongly from the

frontal eye field (Kuypers and Lawrence, 1967; Leichnetz *et al.*, 1984a; Huerta *et al.*, 1986; Stanton *et al.*, 1988), and from posterior area 7 (Faugier-Grimaud and Ventre, 1989). The organization of the projections from the frontal lobe to the subdivisions of the inferior olive can be understood from a comparison with the data of Strominger on the rubroolivary projection (Fig. 11.36, 1–2). The corticorubral projections to the magnocellular red nucleus is uncrossed and derived from the primary motor cortex only. The leg area projects to the lateral part of the nucleus, the arm area medially. A projection from the face area is lacking (Fig. 11.25A).

The origin of most corticorubral fibers to the parvocellular red nucleus from superficial lamina Va pleads against their collateral origin from corticospinal fibers. Projections to the magnocellular red nucleus mainly arise from lamina Vb, and are part of a collateralizing system of corticospinal fibers, which also terminates in the medial reticular formation of the lower brain stem (Catsman-Berrevoets *et al.*, 1979; Humphrey *et al.*, 1984; Kuypers, 1987).

The parvocellular red nucleus and Darkschewitsch's nucleus and adjacent structures also receive strong projections from the cerebellar nuclei. Those terminating in the parvocellular red nucleus are derived from the dentate nucleus, with the rostral and dorsal dentate projecting to lateral and caudal parts of the red nucleus, and the caudal and ventral dentate to its rostral and dorsomedial portion. (see "Projections of Individual Cerebellar Nuclei to the Brain Stem in Monkeys" and Fig. 11.25). Projections to Darkschewitsch's nucleus originate preferentially from the posterior interposed nucleus (Voogd, 1964; Kievit, 1979).

The parietorubroolivary pathway, which seems to absent in primates, may be present in cats. Responses in the inferior olive, relayed by the red nucleus, were recorded after stimulation of parietal association areas in the suprasylvian gyrus (Oka *et al.*, 1979, 1988). The latencies of these responses were longer than those from stimulation of the motor cortex. This may be due to slower conducting axons arising from smaller pyramidal neurons in the parietal cortex projecting to the parvocellular red nucleus. Alternatively, they may have been transmitted by an indirect pathway, involving parietal layer III neurons with projections to the motor cortex, observed by Kakei *et al.* (1995). Projections of parietal association areas to the red nucleus have been reported repeatedly in the cat. However, according to Saint-Cyr (1987), these corticorubral fibers terminate in the magnocellular spinal projecting part of the red nucleus. In the cat, the cell groups at the meso–diencephalic junction that project to the inferior olive receive their cortical inputs primarily from precruciate areas 4 and 6, with only sparse contributions from postcruciate areas 3a, 3b, and perhaps 5. Precruciate and suprasylvian cortical afferents of Darkschewitsch's nucleus were confirmed by Rutherford *et al.* (1989) and Miyashita and Tamai (1989). The parietorubroolivary projection in the cat may be reciprocated by cerebello-parietal connections (see footnote 4).

Afferent Systems of the Inferior Olive: The Nucleo-Olivary Projection. The Inhibitory and Excitatory Feedback Loops Involving the Inferior Olive The cells in the central cerebellar nuclei that project to the inferior olive constitute a population of small, GABAergic neurons (see "Cerebellar Nuclei" and "Cerebellar Peducles"). GABAergic projections to certain subdivisions of the inferior olive also take their origin from the vestibular nuclei (Nelson and Mugnaini, 1989); the nucleus prepositus hypoglossi and the group Y project to the dorsal cap (De Zeeuw *et al.*, 1993, 1994) and the nucleus parasolitarius to the group β and the dorsomedial cell column (Barmack *et al.*, 1998).

The GABAergic nucleoolivary projection has a high resolution and displays an almost complete reciprocity, with the system of nuclear collaterals from the crossed olivocerebellar projection, apart from the presence of a minor, uncrossed nucleoolivary component (see Ruigrok *et al.*, 1990 for a review). The main features of the topical projection of the cerebellar nuclei to the olive have been confirmed in monkeys (Chan-Palay, l977; Kalil, 1979). Their main conclusions concern the projection of the ventrocaudal dentate to the ventral lamina of the PO, and of the rostral and dorsal portions of the nucleus to an extensive region in the dorsal lamina and the lateral bend of the nucleus (Fig. 11.36, 3). The reversal of the rostrocaudal axis in the projection of the dentate to the PO, as maintained by Chan-Palay (1977), or of the dorsoventral axis, as maintained by Lapresle and Ben Hamida (1965), has not been confirmed. The presence of a nucleoprojection from the fastigial nucleus to the caudal MAO has been questioned. The reciprocity with the olivocerebellar projection is less obvious for the vestibuloolivary paths because the existence of an olivovestibular projection (Balaban, l984, l988) is still debated. A remarkable but unexplained feature of the afferent connections of the principal olive from the parvocellular red nucleus and the dentate nucleus is the periodicity in their terminal labeling (arrows in Fig. 11.36).

Therefore, two kinds of recurrent cerebelloolivary loops, one inhibitory and the other excitatory, exist. The parvocellular red nucleus and the nucleus of Darkschewitsch are links in closed cerebellomesencephalic-olivary circuits that feed back into the cerebellum and presumably are excitatory.

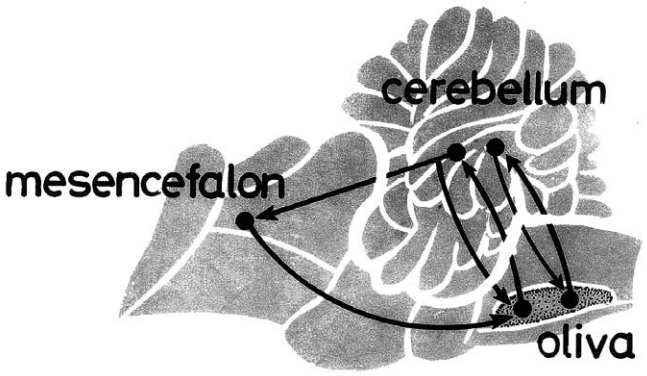

FIGURE 11.38 Diagram of the connections between the cerebellar nuclei and the inferior olive. The reciprocal olivonuclear and nucleoolivary projections and the cerebellomesencephaloolivary circuits are shown.

These multisynaptic loops are superimposed on the direct, inhibitory olivary projections from the same cerebellar cerebellar nuclei (Fig. 11.38). At the level of the inferior olive, these excitatory and inhibitory loops exert an opposite influence on electrotonic coupling of the olivary neurons; the nucleoolivary pathway decreases coupling, whereas the tegmental tracts enhance it (Ruigrok and Voogd, 1995).

When the data from the olivocerebellar projection ("Subdivision and Olivocerebellar Projection"; Figs. 11.36 and 11.46), the cerebellorubral projection ("Projection of Individual Cerebellar Nuclei to Brain Stem in Monkeys"; Fig. 11.25) and the cortico-olivary projection (Figs. 11.25 and 11.36) are combined, three multisynaptic recurrent loops can be distinguished One loop includes the posterior interposed nucleus, Darkschewitsch's nucleus, and the rostral MAO. The second loop includes the rostral and dorsal dentate nucleus, the caudal and lateral portion of the parvocellular red nucleus and the dorsal lamina, and the lateral bend of the principal nucleus of the inferior olive. The third loop consists of the caudal and ventral dentate nucleus, the rostromedial parvocellular red nucleus, and the ventral lamina of the principal olive. The cortical areas controlling each loop generally are the same as the areas that receive a projection from the cerebellar nucleus involved in the loop. It is of interest that the rostromedial part and the rostrolateral and caudal portion of the parvocellular red nucleus have been distinguished as separate subnuclei in the human brain stem (Papez and Stotler, 1940; Paxinos and Huang, 1995; see also Chapter 10).

Hypertrophy of the Inferior Olive Nucleoolivary projections have not been reported in humans, but this connection remains of particular importance because its existence was postulated by Trelles (1935) to explain the occurrence of hypertrophy of the inferior olive after lesions affecting the dentate nucleus. Olivary hypertrophy is a condition characterized by demyelinization of the amiculum of the olive (and apparent widening of the unmyelinated cell band of the olive: pseudohypertrophy) and swelling and vacuolization of its cells (true hypertrophy). In humans true hypertrophy of the inferior olive is associated with palatomyoclonus (Deuschl *et al.*, 1996; Wilms *et al.*, 1999).

Olivary hypertrophy can be induced in cats by ablation of the contralateral cerebellum with the cerebellar nuclei (Verhaart and Voogd, 1962; Boesten and Voogd, 1985; De Zeeuw *et al.*, 1990; Ruigrok *et al.*, 1990). The cellular changes are the same as in humans (Barron *et al.*, 1982). The cells swell, the nucleus is displaced to the periphery, the nucleolus is enlarged, and the rough endoplasmatic reticulum proliferates. The cisternae of the rough endoplasmatic reticulum are enlarged and may developed into vacuoles, filled with floccular material and globular inclusions. The hypertrophy does not subside but remains present for more than a year after the cerebellectomy.

Hypertrophy in the human cases is situated in the principal olive and the medial accessory olive, never in the dorsal accessory olive (Voogd *et al.*, 1990). The localization in the cat differs from that in human cases. In the cat hypertrophic cells are always present in the rostral medial accessory olive; the area that is involved appears to increase with longer survival times when hypertrophy is also present in the dorsal lamina of the PO. In other parts of the olive normal-looking cells or severe cellular atrophy may be present.

Different explanations for the occurrence of olivary hypertrophy have been forwarded. Interruption of the tegmental tracts, i.e., of the main excitatory input of the olive, has been associated with this condition. Trelles (1935) and, more recently, Lapresle and Ben Hamida (1965, 1967, 1968) concluded that hypertrophy is the consequence of lesions of the crossed nucleoolivary pathway, which as we have since, learned is inhibitory. A third explanation suggests that myoclonus, and by inference olivary hypertrophy, is caused by a reduction in the serotonergic innervation of the inferior olive (Welsh *et al.*, 1998).

None of these explanations alone is sufficient to explain the localization of the hypertrophic neurons in human pathological or in experimental cases. Interruption of the tegmental tracts, although often present, is not essential because hypertrophy can develop with an exclusive lesion of the contralateral dentate nucleus (Lapresle and Ben Hamida, 1965, 1967, 1968; Schoen, 1977). Lesions that damage the cerebellar nuclei or their nucleoolivary pathways are a more likely cause but do not fully explain the localization of the hypertrophy

in particular regions of the olive. Similarly, the distribution of serotonin in the inferior olive (Voogd *et al.*, 1996b) differs from the preferred localization of the hypertrophy.

The Pontocerebellar Projection

In 1885 Von Bechterew set the scene for the study of the corticopontocerebellar projection. The localization of the corticopontine fibers in the cerebral peduncle, with frontopontine fibers medially, fibers from the pericentral region, which form the pyramidal tract more caudally, in an intermediate position, and fibers from postrolandic cortex laterally, was already known from the studies of Arnold, Meynert, Charcot, and Flechsig (reviewed by Schmahmann *et al.*, 1992). In this review, Schmahmann uncovered the false attribution of the name of Türck, to the lateral, parietotemporal pontine component of the peduncle, and traced its subsequent history, including the important contributions of Dejerine (1885). In the same paper, von Bechterew (1885) also described the nucleus reticularis tegmenti pontis (NRTP) as a separate nucleus from the basal pontine nuclei. He distinguished two systems, one caudal ("spinal") and the other rostral ("cerebral"), in the pontocerebellar projection. The spinal system connects the NRTP and the pontine nuclei with the cortex of vermis and hemispheres of the superior surface of the cerebellum. It occupies the deep strata of the brachium pontis and acquires its myelin before birth (Fig. 11.39).

Von Bechterew was not always clear about the direction of the fibers; he believed that the spinal system originates from the cerebellum and terminates in the pons. The cerebral system is unmyelinated at birth. It originates from the contralateral pontine nuclei, which receive the lateral, parietotemporal pontine, and medial frontopontine components of the cerebral peduncle. It is distributed to caudal, basal, and lateral regions of the cerebellar hemisphere.

Von Bechterew's observations in the human brain were confirmed in the antegrade axonal degeneration study of Spitzer and Karplus (1907) in the monkey using Marchi's method. A lesion of the rostral one-fourth of the pons caused bilateral fiber degeneration in the dorsolateral periphery of the brachium pontis, which distributes to the caudal vermis and hemisphere of the posterior lobe. Fibers interrupted by a lesion of the caudal half of the pons, including the NRTP, distribute to the anterior vermis and hemisphere, from the dorsal lobulus centralis to the posterior superior fissure, with an especially heavy projection to the lobulus simplex. The flocculus receives a strong projection; the caudal vermis and the rest of the hemisphere remain free from label. The projection of the rostral pontine nuclei to the caudal cerebellum was studied in more detail in the antegrade tracing study of Glickstein *et al.* (1994). They followed labeled axons from injections in the rostrolateral pontine nuclei in monkeys. The fibers cross in the pons and terminate mainly in the contralateral dorsal paraflocculus, with moderate to scarce labeling in the paramedian lobule, and the crus II and I. Few fibers project to the ventral paraflocculus, none to the flocculus. There is a distinct projection to dorsal lobule IX. Afferents to the flocculus and the ventral paraflocculus were retrogradely traced from the NRTP. Some of these observations were later confirmed by Nagao *et al.* (1997).

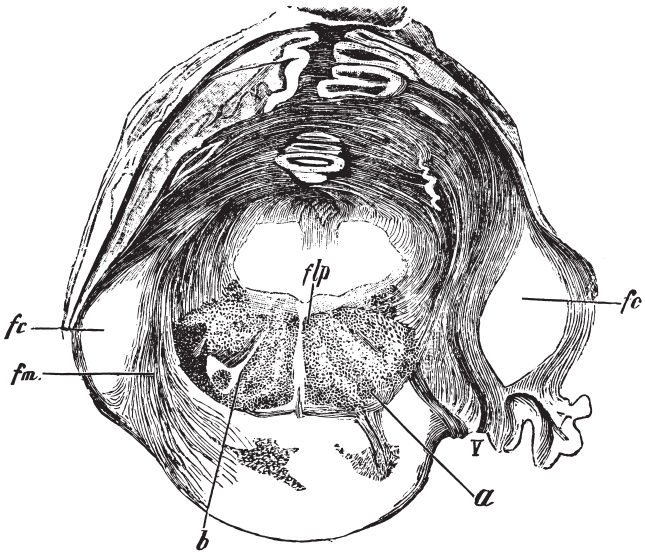

FIGURE 11.39 The "spinal" and "cerebral" pontocerebellar systems of Von Bechterew (1885). Myelin-stained section from the brain of a human infant. The cerebral system (fc) is still unmyelinated. Abbreviations: a, central tegtmental tract; b, fibers from Deiters' nucleus to the central tegmental tract; fc, late myelinating "cerebral system" of the brachium pontis; flp, medial longitudinal fascicle; fm, early myelinating "spinal system" of the brachium pontis; V, trigeminal root.

The corticopontine projection has been studied extensively in primates and other mammalian species. Patterns in the termination of corticopontine fibers have been variously described as patchy, columnar or lamellar, with a specific localization along the rostrocaudal, mediolateral, or dorsoventral axis of the pons. The mediolateral arrangement of frontopontine, pericentral, and parietotemperopontine fibers in the cerebral peduncle is reproduced in the pontine nuclei by their termination in medial, central, and lateral parts of the pontine nuclei (Fig. 11.40) (Schoen, unpublished). For a discussion of the subdivision of the pontine nuclei, the reader is referred to Chapter 10.

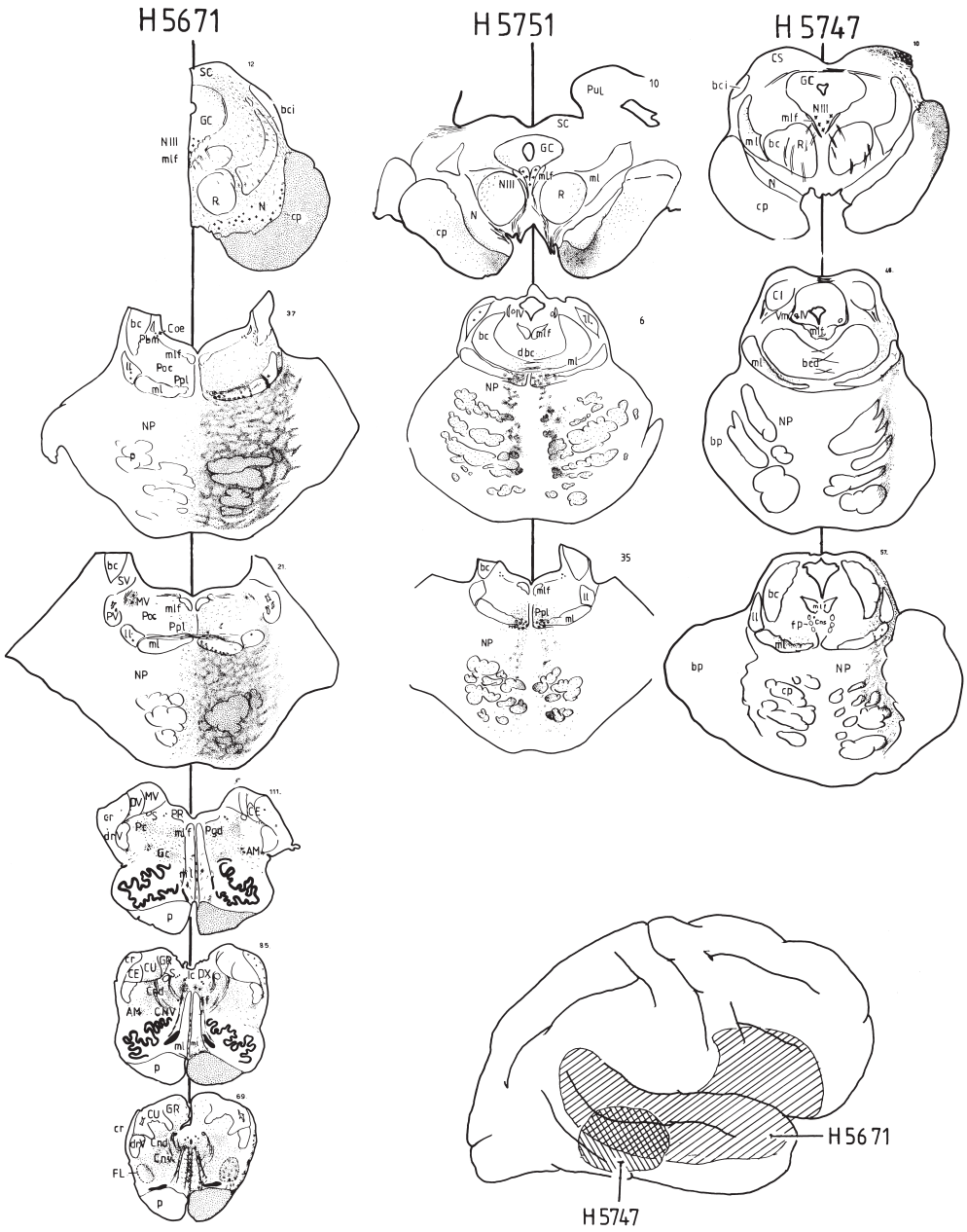

FIGURE 11.40 Corticofugal projections to pons and the lower brain stem. Case H5671: total degeneration of the cerebral peduncle, after an infarct including the basal ganglia and the internal capsule. From Schoen (1969). Case H5751: degeneration of the frontopontine tract. Case H5747: degeneration of the parietotempero-pontine tract. The extent of the lesions in two of the cases is indicated on a diagram of the right cerebral hemisphere. Nauta stain. Schoen, unpublished. Abbreviations: AM, nucleus ambiguus; bc, brachium conjunctivum; bci, brachium of the inferior colliculus; bp, brachium pontis; CE, external cunenate nucleus; CI, inferior colliculus; Cnd, nucleus centralis medullae oblongatae, pars dorsalis; CNV, nucleus centralis medullae oblongatae, pars ventralis; Coe, locus coerulaeus; cp, cerebral peduncle; cr, restiform body,; CU, nucleus cuneatus; dbc, decussation of the brachium conjunctivum; drV, spinal tract of the trigeminal nerve; DV, spinal vestibular nucleus; DX, dorsal nucleus of the vagal nerve; FL, nucleus reticularis lateralis; fP, predorsal fascicle; GC, central gray; Gc, nucleus gigantocellularis; GR, nucleus gracilis; IV, trochlear nerve; ll, lateral lemniscus; ml, medial lemniscus; mlf, medial longitudinal fascicle; MV, medial vestibular nucleus; N III, oculomotor nerve; N, substantia nigra; NP, pontine nuclei; p, pyramid; Pbm, parabrachial nuclei; Pgd, nucleus paragigantocellularis; Poc, nucleus pontis oralis, pars caudalis; Por, nucleus pontis oralis, pars rostralism; Ppl, papillioform nucleus (nucleus reticularis tegmenti pontis); PR, nucleus prepositus hypoglossi; PUL, pulvinard; PV, principal sensory nucleus of the trigeminal nerve; R, red nucleus; S, tractus solitarius; SC, superior colliculus; SV, superior vestibular nucleus.

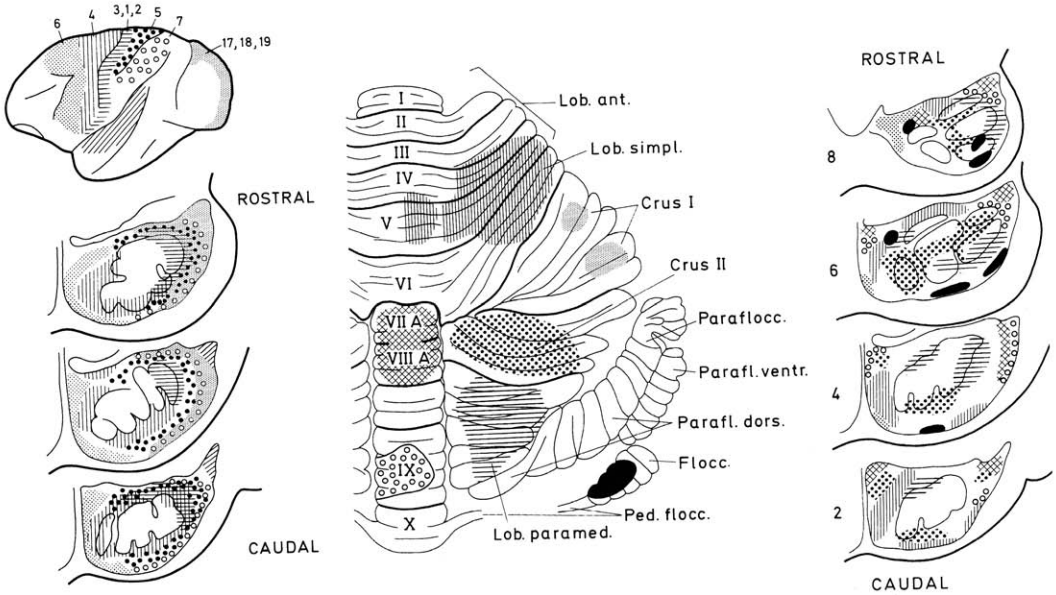

FIGURE 11.41 Diagram of the overall topography of corticopontine and pontocerebellar pathways of the monkey. From Brodal (1982).

Shifts in localization along the rostrocaudal and dorsoventral axis have been related to the mode of corticopontine development by Leergard *et al*. (1995) in the rat. They concluded that corticopontine fibers develop as collaterals of descending sytems and that they innervate a system of concentric shells in the pontine nuclei. These shells resemble the settling of pontocerebellar neurons during their migration, with early arriving neurons in the center and later arriving neurons in more external concentric layers (Altman and Bayer, 1987). Early arriving corticopontine fibers from ventral pericentral regions terminate in the core of the pons; collaterals from fibers from more frontal and occipital regions of the cortex, which arrive later, enter the pontine nuclei at rostral and caudal locations, and terminate in more external shells. Because the more external shells are thicker rostrally, the late-arriving corticopontine projections from more frontal or occipitotemporal regions predominate in the rostral pons. The distal branches of the descending corticofugal systems, which collateralize in the pons, may disappear later (Pittman and Tolbert, 1988; Tolbert, 1989).

The distribution of corticopontine fibers in the adult in more or less continuous lamellae is reminiscent of their development. The pericentral projection is located in and around the cerebral peduncle, and the more frontal and occipital projections ocupy more external lamellar spaces in the medial and lateral parts of the pons, respectively (Fig. 11.41). Similarly, lamellar shifts have been observed for the localization of pontine neurons projecting to different cerebellar lobules or folia (P. Brodal, 1978; Hartmann-Von Monakow *et al*., 1981; Brodal and Bjaalie, 1992; Bjaalie and Brodal, 1997). Still, the corticopontine terminals and the neurons projecting to a particular cerebellar region usually are discontinuous within multiple patches in a lamellar subspace. The corticopontine systems may terminate preferentially in the medial, lateral, rostral, or caudal pons, but smaller patches of terminals usually are present in a complementary region of the pons.

Corticopontine fibers originate from layer V pyramidal cells in large parts of the cerebral cortex (Glickstein *et al*., 1985) (Fig. 11.42). In descending order the densities of cells projecting to the pons were motor cortex (areas 4 and 6), parietal association cortex (areas 5 and 7), cingulate cortex (areas 23–25), somatosensory cortex (areas 3, 1, 2), frontal eye field (area 8 and dorsal frontal area 9, insular areas 13 and 14), and the striate and extrastriate visual cortex. There are large regions of the frontal cortex, the inferotemporal and occipital cortex that contained few or no cells with projections to the pons. The origin of the corticopontine projection was confirmed in the studies of Schmahmann and Pandya (1995, 1997a). The origin of the corticopontine projection in monkeys, therefore, includes postrolandic association areas, which are largely lacking from the origin of the corticorubral projection (Fig. 11.25) and from the region targeted by the cerebellar nuclei (Fig. 11.23).

The origin of pontocerebellar fibers from the prefrontal and premotor cortex in humans includes the lateral, medial, and dorsal aspects of the convexity

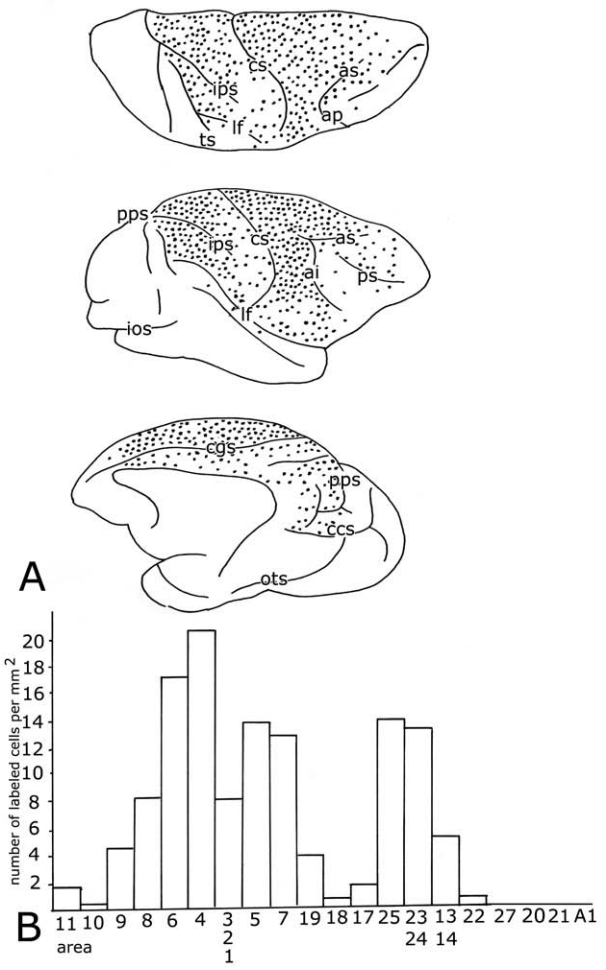

FIGURE 11.42 Distribution of corticopontine meurons in macaque monkeys. **A.** Distribution of retrogradely labeled neurons in the left cerebral hemisphere from a complete wheat germ agglutinin–coupled horseradish peroxidase filling of the pontine nuclei. **B.** Bar graphs illustrating the numbers of retrogradely labeled neurons in different cortical areas. Abbreviations: ai, ansate sulcus, inferior limb; as, ansate sulcus superior ilmb; ccs, calcarine fissure; cs, central sulcus; ios, inferior occipital sulcus; ips, intraparietal sulcus; lf, lateral fissure; ots occipitotemporal sulcus; pps, postparietal sulcus; ps, principal sulcus; ts, superior temporal sulcus. From Glickstein *et al.* (1985).

over its full anteroposterior length (areas 45, 46, 32, 24, and caudal area 9) and areas 8 (frontal eye field) and 6 (premotor cortex). The frontal pole, the ventrolateral convexity, and the orbital surface did not give rise to corticopontine fibers (Beck, 1950). Beck's observations are in accordance with the conclusions from experimental studies of Glickstein *et al.* (1985) and Schmahmann and Pandya (1995, 1997a). These frontopontine finers terminate, mainly rostrally, in medial, dorsomedial, and ventromedial regions of the pontine nuclei (Sunderland, 1940; Nyby and Jansen, 1951; P. Brodal, 1978; Hartmann-Von Monakow *et al.*, 1981; Leichnetz *et al.*, 1984b; Künzle and Akert, 1977; Künzle, 1978; Stanton *et al.*, 1988; Shook *et al.*, 1990; Schmahmann and Pandya, 1995, 1997b).

Pontocerebellar fibers from the pericentral region terminate centrally in the pons, in the pedunculular and peripeduncular region (Fig. 11.41). The motor cortex projects strongly to medial and less to lateral lamella–like areas, surrounding the peduncle in the caudal pons, with the face located rostrally and medially and the leg laterally and caudally. The somatotopically arranged projections of the primary sensory cortex are very similar to the motor cortex but favor more lateral peripeduncular regions (P. Brodal, 1978; Hartmann-Von Monakow *et al.*, 1981).

Postrolandic corticopontine projections, from parietal areas 5 and 7, peristriate, parahippocampal, and superior temporal cortices, mainly occupy the lateral pons. Area 5 projections are located most medially, partially overlapping the SI projection; striatal and peristriatal projections are located more dorso- and ventrolaterally, but also include a medial component; superior temporal projections, including area MT, occupy the extreme dorsolateral part of the pons (Fig. 11.41), (P. Brodal, 1978; Faugier-Grimaud and Ventre, 1989; Nyby and Jansen, 1951; Schmahmann and Pandya, 1989, 1991, 1993, 1997b; Sunderland, 1940).

The projection from the primary visual cortex (area 17) is restricted to a few cells in the caudal part of the calcarine fissure. However, many more corticopontine cells were found in the rostral end representing the visual periphery and the number of corticopontine cells decreased in an ordely way sucessively more caudally. Thus, there appears to be a systematic over-representation of the peripheral visual field in the corticopontine projections from striate cortex of monkeys (Glickstein *et al.*, 1983, 1985). Projections of moderate intensity arise from peristriate visual areas 18 and 19 including MT (Glickstein *et al.*, 1985). Striate and peristriate projections to the dorsolateral pons are located rostral to the termination of the uncrossed tectopontine tract from the superficial visual layers of the superior colliculus (Münzer and Wiener, 1902; Frankfurter, 1976; Harting, 1977; Wells *et al.*, 1989). Receptive fields of pontine visual neurons were large. Most cells responded to moving stimuli and were directionally selective (Baker *et al.*, 1976).

In accordance with their development as branches from long descending fiber tracts, many if not all corticopontine fibers should be considered as collaterals from corticofugal fibers terminating in other regions of the brain stem and the cord. Ugulini and Kuypers (1986) found retrogradely labeled collaterals from fibers of the pyramidal tract in the cat to be distributed in medial and lateral peripeduncular clusters, corresponding

with the region receiving pericentral cortical afferents and projecting to the anterior lobe and the lobulus simplex. Similarly, Baker *et al.* (1983) and Keizer *et al.* (1987) found up to 60% of the corticotectal neurons to project both to the tectum and the pons.

It can be concluded from the origin and distribution of the corticopontine projection that the main projections are derived from motor, premotor, somatosensory, parietal, and peristriate areas. Occipitotemporal and parietal projections are derived from areas included in the so-called dorsal visual stream of Ungerleider and Mishkin (1982) of visual and visually related cortical areas that contain representations of speed and direction of stimuli in the peripheral visual field and are concerned with the visual guidance of movements. Areas belonging to the "ventral visual stream," directed at the temporal lobe, which are concerned with object recognition, do not project to the pons. Prefrontal corticopontine connections are limited to dorsolateral and medial areas, related to kinesthetic, motivational, and spatially related functions, including spatial memory. Inferior and orbital prefrontal areas, related to autonomic and emotional response inhibition, stimulus sugnificance, and object recognition, do not project to the pons (Glickstein *et al.*, 1985; Schmahmann and Pandya, 1995, 1997a).

Much less is known about the pontocerebellar projection in primates. Pontocerebellar mossy fibers share a bilateral distribution with many other mossy fiber systems. Most of the ipsilaterally terminating fibers recross in the cerebellum (Rosina and Provini, 1984). Systematic collateralization of pontocerebellar mossy fibers, with terminations restricted to more or less discrete longitudinal zones, occasionally has been observed (Voogd, 1969; Voogd *et al.*, 1996b), but usually their distribution was reported to be a diffuse one. However, Serapide *et al.* (1994, 2001) recently observed zonally arranged projections to the paraflocculus and most other lobules of the cerebellum, from small injections of antegrade tracers in the pontine nuclei of the rat. With larger injections the zonal pattern gives way to diffuse labeling. The explanation of this phenomenon is not known.

In accordance with the classical observations of von Bechterew (1885) and Spitzer and Karplus (1907), caudal, peduncular, and peripeduncular regions of the pons containing a representation of the motor and somatosensory cortex project to the anterior lobe and the lobulus simplex (Fig. 11.41). More rostral, lateral, and medial regions of the pons mainly project to the hemisphere of the posterior lobe, with the more medial regions receiving frontopontine fibers, projecting rostrally to the ansiform lobule, and lateral regions receiving pontocerebellar fibers from parietal peristriate and superior temporal association cortex, projecting caudally to the dorsal paraflocculus and lobule IX of the caudal vermis. The target area of the tectopontine pathway in the caudal dorsolateral pons projects to the visual vermal area in lobule VII (P. Brodal, 1979, 1982; Glickstein *et al.*, 1994; Nagao *et al.*, 1997).

Collateral projections of the pontine nuclei to the cerebellar nuclei have been observed (Shinoda *et al.*, 1992), but most authors agree on their preferential origin from the NRTP. The NRTP receives a strong projection from the cerebellar nuclei, mainly from the anterior interposed and dentate nuclei ("Projection of Individual Cerebellar Nuclei to the Brain Stem in Monkeys") and afferents from the cerebral cortex, with parietal afferents located laterally, the motor cortex located centrally, and projections from the premotor cortex located laterally (P. Brodal, 1980; Hartmann-Von Monakow, 1981). In addition, it receives a crossed tectopontine projection from deep layers of the superior colliculus (Frankfurter, 1976; Harting, 1977; Wells *et al.*, 1989). In cat and rat the NRTP projects bilaterally to ventrocaudal regions of the dentate lateral regions of the posterior interposed nucleus and to the caudal visual area in the fastigial nucleus (Gerrits and Voogd, 1987; Mihailoff, 1993). This projection is complementary to the collateral projection of the lateral reticular nuclei to the cerebellar nuclei. Collateralization of (reticulopontine) pathways to the cerebellar nuclei has not been studies in primates.

THE VESTIBULOCEREBELLUM

The caudal part of the cerebellum, comprising the flocculus and the nodulus, often is indicated as the vestibulocerebellum. The arguments for this distinction recently were discussed by Voogd *et al.* (1996a). For references on this complicated topic, the reader is referred to this review. Generally, the typical distributions of cell types, primary and secondary vestibulocerebellar mossy fibers, climbing fibers from optokinetic and vestibular subnuclei of the inferior olive, and Purkinje cells with projections to the vestibular nuclei extend beyond the flocculus and the nodulus to include adjoining portions of the ventral paraflocculus and the uvula. In monkeys the entire ventral paraflocculus belongs to the vestibulocerebellum (see "Longitudinal Zonation of the Cerebellum").

One of the typical features of the vestibulocerebellum is the preferential distribution of unipolar brush cells in its cortex (Dino *et al.*, 1999). Primary vestibular root fibers terminate in the nodulus and the adjoining ventral uvula, but not in the flocculus.

Secondary vestibulocerebellar mossy fibers terminate bilaterally, in both divisions of the vestibulocerebellum; a subpopulation of these mossy fibers is cholinergic. The termination of primary and secondary vestibulocerebellar mossy fibers extends beyond the vestibulocerebellum, in the granular layer in the bottom of the deep transverse fissures and lobules I and II of the anterior lobe. The majority of the mossy fibers terminating in the flocculus are derived from the pontine reticular formation (cell groups of the paramedian tracts) (Büttner-Ennever and Horn, 1996) and the nucleus reticularis tegmenti pontis.

Climbing fibers to the flocculus and the adjoining ventral paraflocculus terminate in two pairs of alternating longitudinal zones (Fig. 11.46). In monkeys the most medial of these four zones seems to be lacking (Fig. 11.49). These climbing fibers are derived from the dorsal cap and the ventrolateral outgrowth, i.e., from optokinetic subnuclei of the inferior olive. These subnuclei also innervate the nodulus and adjacent parts of the uvula, but here the dorsal cap and ventrolateral outgrowth-innervated zones, alternate with strips that receive their climbing fibers from vestibular subnuclei of the inferior olive, such as the group β and the dorsomedial cell column.

The efferent projections of the nodulus and the flocculus are also arranged in a modular pattern. Zonal pairs in the flocculus, which receive optokinetic information about retinal slip in either the horizontal or an oblique vertical plane, project via the vestibular nuclei to the eye muscle nuclei, which move the eye in the corresponding plane. A more complicated arrangement in the corticonuclear projection involving both vestibular and cerebellar nuclei is present in the nodulus.

LONGITUDINAL ZONATION OF THE CEREBELLUM

The distinction of longitudinal zones in the cerebellar cortex is based on embryological and histochemical evidence and on anatomical and physiological studies of its afferent and efferent fiber connections (for reviews, see Hatten and Heintz, 1995; Herrup and Kuemerle, 1997; Hawkes and Eisenman, 1997; Hawkes, 1992; Voogd, 1998; Ozol *et al.*, 1999; Voogd *et al.*, 1996b; Voogd and Glickstein, 1998). Although it appears likely that a similar zonation is also present in the human cerebellum, there is no evidence available on this matter. Corticonuclear and afferent mossy and climbing fiber connections have not been studied in sufficient detail, and histochemical studies failed to demonstrate band patterns in the adult human cerebellum.

Direct evidence for zonation in the human cerebellum was obtained in studies of cerebellar development. Several authors noted that developing Purkinje cells are clustered in a number of parasagittal zones during early stages of cerebellar development, prior to the stage when the first fissures make their appearence (for reviews, see Sotelo and Wassef, 1991; Voogd *et al.*, 1996b). Purkinje cells and the cells of the cerebellar nuclei are generated in the ventricular layer (Jakob, 1928; Miale and Sidman, 1961). Purkinje cells migrate to the meningeal surface of the cerebellum where they settle in the cortical plate, deep to the external granular layer. Clustering of Purkinje cells in the cortical plate in human fetuses has been observed by several authors (Hochstetter, 1929; Korneliussen, 1968; Maat, 1978, 1981) (Fig. 11.43).

The significance of the clustering of Purkinje cells during early stages of cerebellar development has been clarified in animal studies. In monkey fetuses an interdigitating pattern of Purkinje cell clusters develops in the cortical plate between days 48 and 54 of gestation (Kappel, 1981; Voogd *et al.*, 1987b) (Figs. 11.44 and 11.45). The subsequent development of the first transverse fissures, and the inward migration of the granule cells, with the consequent increase of rostrocaudal extent of the meningeal surface of the cerebellum, transforms the Purkinje cell clusters in longitudinal zones. Cell strands connect these zones with the borders of the cerebellar nuclei (Fig. 11.44). The resulting zonal pattern is very similar to the patterns based on corticonuclear and olivocerebellar projection in adult mammals. With transformation of the multicellular clusters into a monolayer of Purkinje cells, the borders between the zones become lost around day 70 of gestation. The pattern that evolves from the position of the clusters in the cortical plate and their corticonuclear relations is very similar to the adult longitudinal patterns in the corticonuclear projection (Table 11.1). During similar developmental stages in rodents, Purkinje cell clusters show a transient heterogeneity for several Purkinje cell markers (for reviews, see Sotelo and Wassef, 1991; Voogd *et al.*, 1996b). The localization of these substances and the time course in their expression are modified in mouse mutants and transgenic mice, suggesting that these zonal patterns are under genetic control (Oberdick *et al.*, 1998).

The original observations on the zonal distribution of Purkinje cells of the cerebellar cortex were made on myelin-stained sections, which show a subdivision of the cerebellar white matter in parasagittal compartments, which contain one of the cerebellar nuclei (Voogd, 1964, 1969). These compartments serve as conduits for Purkinje cell axons from a longitudinal zone to their target nucleus and direct the olivocerebellar fibers to

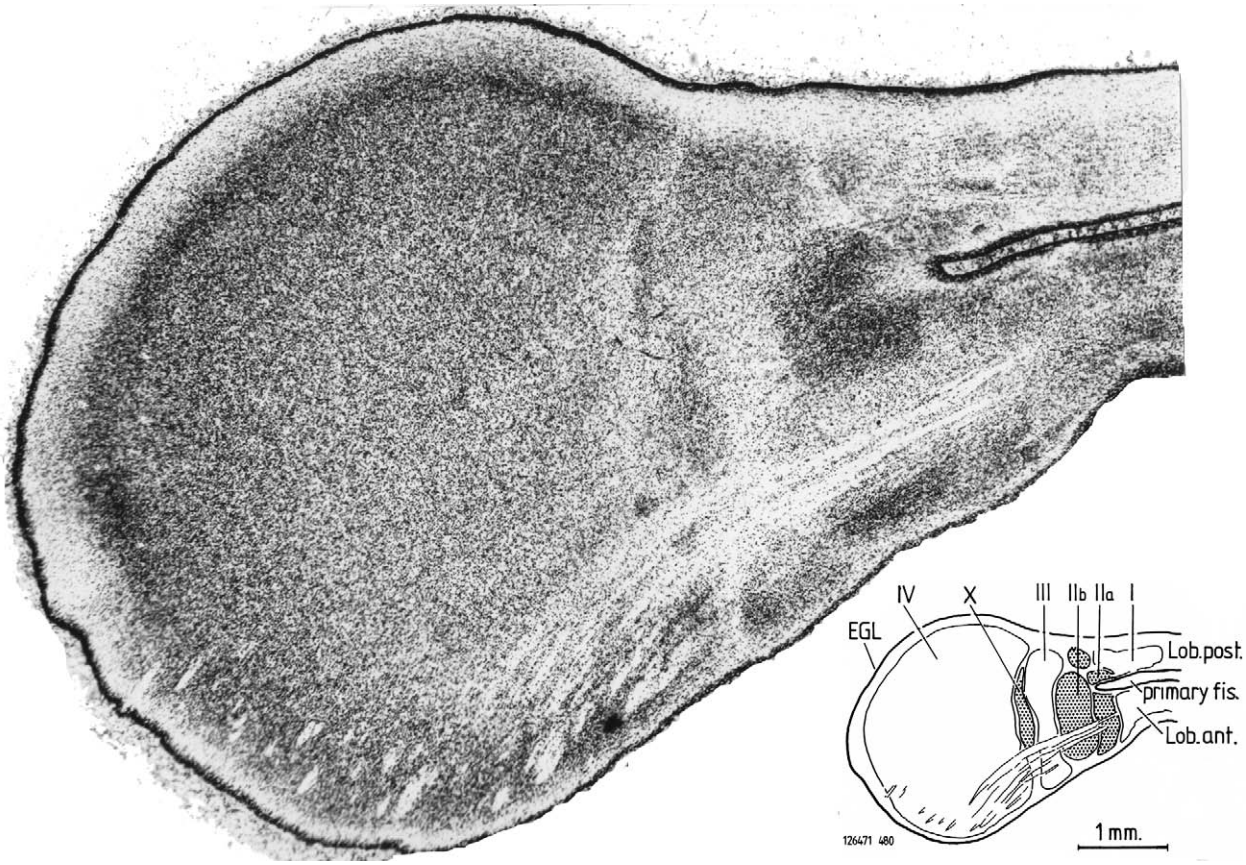

FIGURE 11.43 Coronal section through the cerebellum of a 65-mm human fetus, showing Purkinje cell clusters. The configuration of these clusters is very similar to their distribution in a 55-day-old monkey fetus, illustrated in Fig. 11.44A. Nissl stain. Abbreviations: see Fig. 11.44 and Table 11.1. Schenk collection, Department of Pathology, Erasmus University of Rotterdam.

TABLE 1 Nomenclature for Purkinje Cell Clusters in the Developing Cerebellum and Corresponding Purkinje Cell Zones with Their Target Nuclei in the Adult Cerebellum.

Cluster	Zone	Target Nucleus
I	A zone	Fastigial nucleus
IIa	B zone	Lateral vestibular nucleus
IIc	X zone	Interstitial cell group
IIb	C_1 zone	Anterior interposed nucleus
IIIa,b	C_2 zone	Posterior interposed nucleus
X	C_3 zone	Anterior interposed nucleus
IVa	D_1 zone	Dentate nucleus, caudal pole
IVb	D_2 zone	Dentate nucleus, rostral portion

Source: Kappel (1981).

the Purkinje cells on which they terminate. The organization and the conformity of corticonuclear and climbing fiber zones was established in subsequent experimental studies in carnivores and rodents (for references, see section "Subdivision and Olivocerebellar Projection") (Fig. 11.46). Haines studies on the corticonuclear projection (reviewed by Haines *et al.*, (1982) and the olivocerebellar projection in primates (Whitworth and Haines, 1986b) are especially important in this respect.

AchE histochemistry has proved a useful marker for the study of longitudinal zonation in the cortex and for the deliniation of the corresponding parasagittal compartments in the cerebellum of adult mammals (Fig. 11.47) (Marani and Voogd, 1977; Hess and Voogd, 1986; Boegman *et al.*, 1988; Voogd *et al.*, 1987a, b). The borders between the compartments are selectively stained with AChE and this staining is especially distinct in monkeys (Hess and Voogd, 1986). The image is reversed when the Purkinje cell axons are stained with Purkinje cell–specific markers, such as

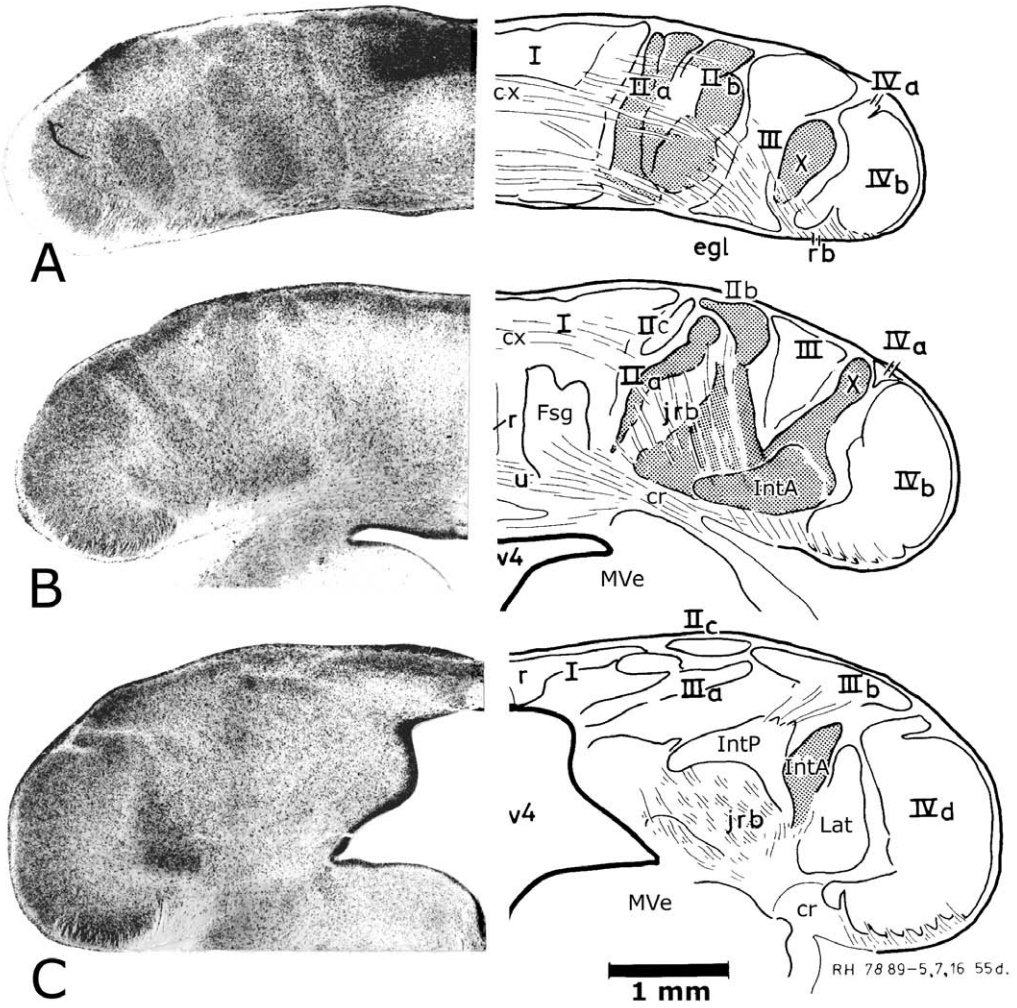

FIGURE 11.44 Three coronal sections through the cerebellum of a 55-day-old rhesus monkey fetus; **A** is the most rostral section. Purkinje cell clusters are indicated with roman numerals (see Table 11.1). Note superficial location of the Purkinje cells of the early arriving clusters I, III, and, IV, which still partially cover the later arriving deep clusters IIa, IIb, and X. Cell strands connect the clusters at this stage with their cerebellar target nuclei. Compare with the human fetus of the same developmental age illustrated in Fig. 11.43 and the reconstruction in Fig. 11.45. Abbreviations: cr, restiform body; cx, cerebellar commissure; egl, external granular layer; Fl, flocculus; I–IV, Purkinje cell clusters I–IV; IntA, anterior interposed nucleus; IntP, posterior interposed nucleus; jrb, juxtarestiform body; Lat, dentate nucleus; MVe, medial vestibular nucleus; prf, primary fissure; r, midline recess; v4, fourth ventricle.; X, Purkinje cell cluster X. From Kappel (1981).

calbindin. In this case the heavily stained interior of a compartment is delimited by a narrow unstained border zone (Voogd and Gerrits, 1997) (Figs. 11.50A, B). AChE histochemistry has not yet been used to study the cerebellum in human.

The antibodies zebrin I and II, developed by Hawkes, specifically stain a subset of Purkinje cells, distributed into multiple longitudinal zones and separated by zebrin-negative areas in rodents and marsupials (Hawkes *et al.*, 1985; Hawkes and Leclerc, 1987; Dore *et al.*, 1990). The zebrins are representative of a number of substances that show more or less the same distribution pattern. The first of these substances to be discovered was 5′-nucleotidase in the cerebellum of the mouse (Scott, 1964). In the squirrel monkey a similar zonal distribution was observed in the vermis (Leclerc *et al.*, 1990). In macaques antibodies against zebrin stain all Purkinje cells, and the resulting image is the same as found for Purkinje cell–specific markers, such as calbindin. Zebrin I has been applied to the human cerebellum, where it is heterogeneously distributed among the Purkinje cells. A clear arrangement in the distribution of these cells was not uncovered (Plioplys *et al.*, 1985).

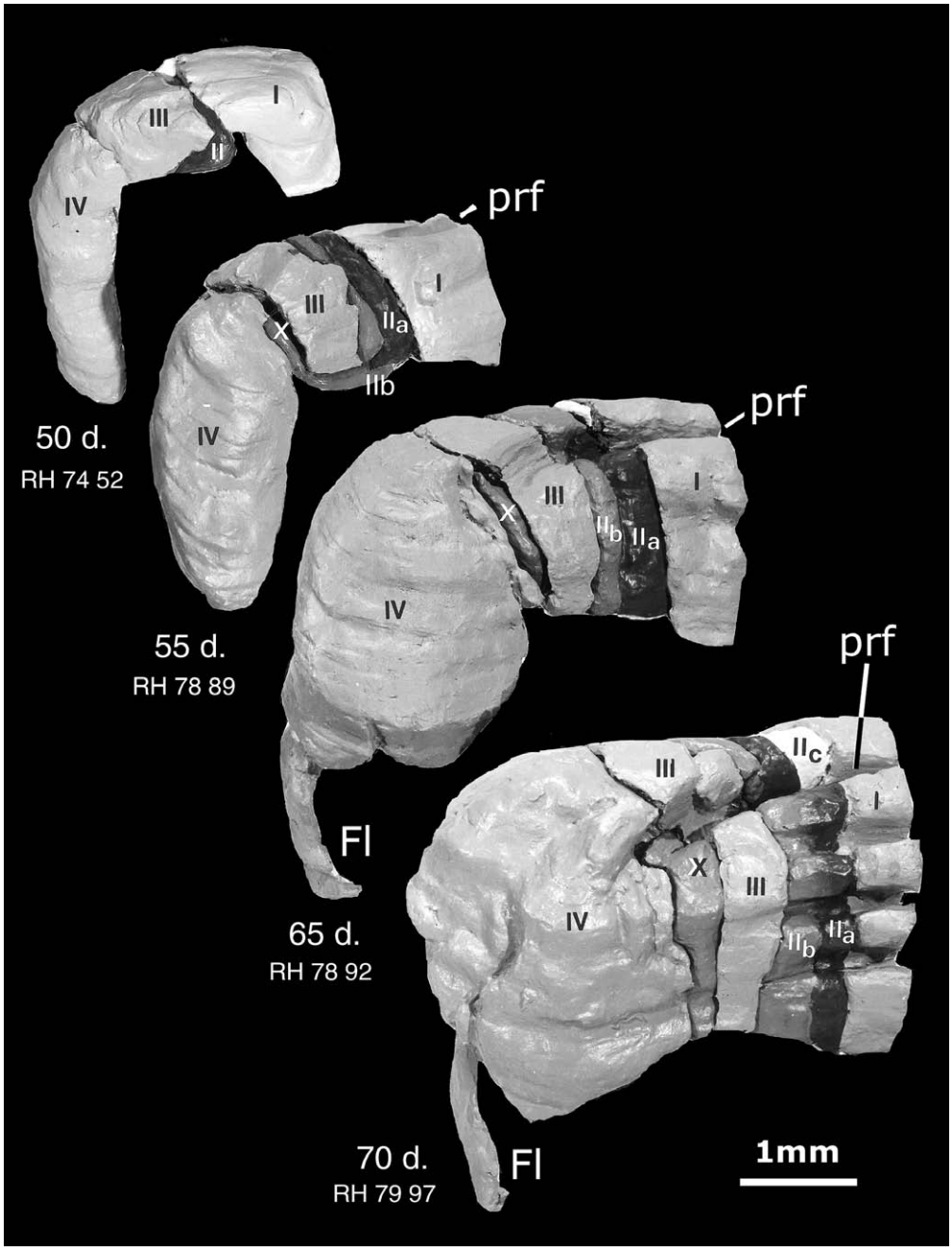

FIGURE 11.45 Photographs of the rostral aspect of reconstructions of the Purkinje cell layer of the cerebellum of four fetuses of the rhesus monkey. Clusters are indicate with different shadings. Note the superficial location of Purkinje cells of the early arriving clusters I, III, and IV in the youngest fetus, and the gradual emergence at the surface of the later arriving clusters IIa, IIb, and X. For explanation of nomenclature, see Table 11.1. Compare with sections of 55-day-old fetus in Fig. 11.44. From Kappel, 1981.

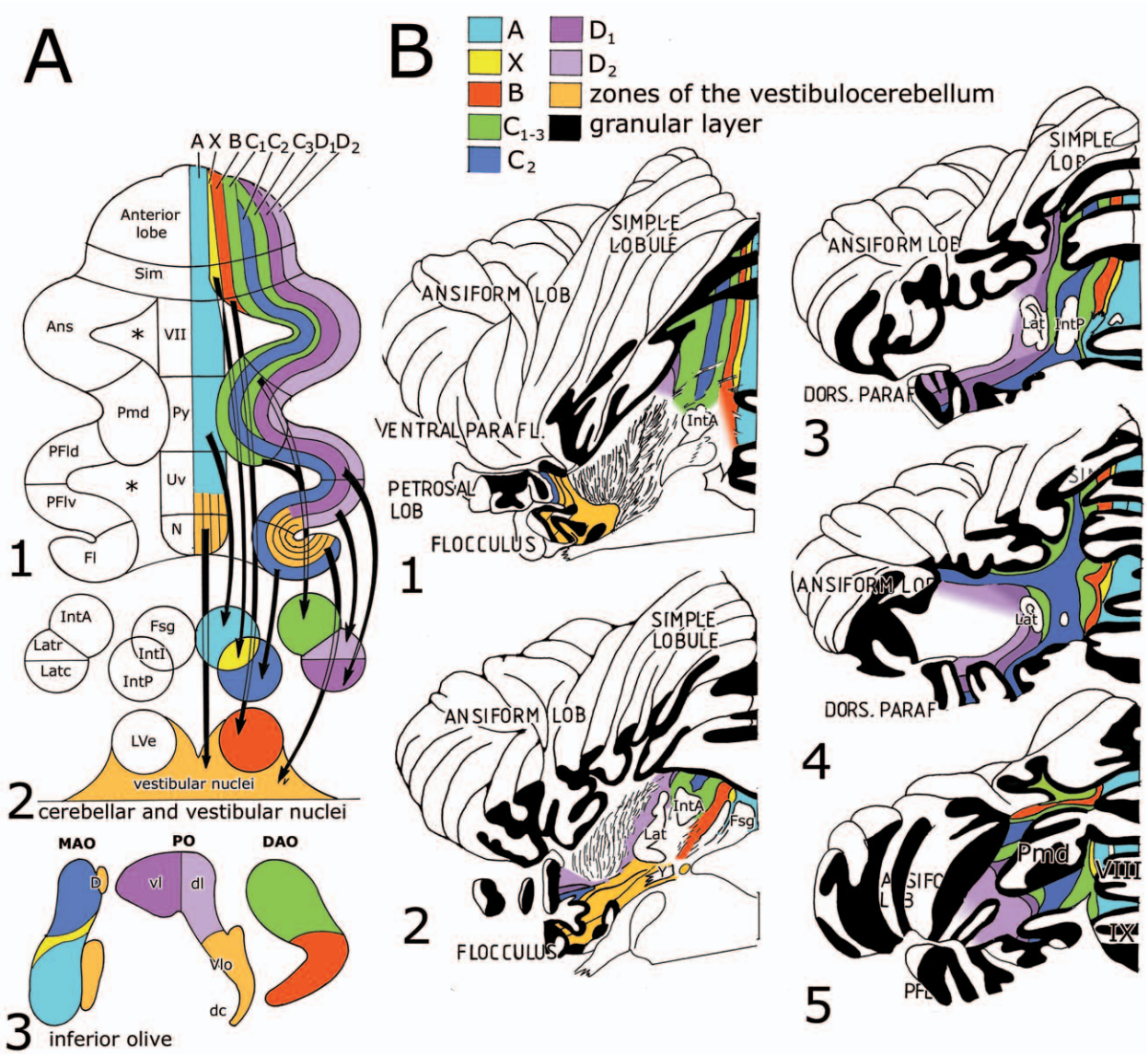

FIGURE 11.46 **A.** Diagram of the zonal organization in the corticonuclear and olivocerebellar projections in the cat. Modified from Groenewegen *et al*. (1979). **(1)** Diagram of the flattened cerebellar cortex. **(2)** Diagram of the cerebellar and vestibular nuclei. **(3)** Diagram of a projection of the inferior olive in the horizontal plane, constructed according to Brodal (1940). The longitudinal corticonuclear and olivocerebellar projection zones are indicated with capitals (A, X, B, $C_{1–3}$, $D_{1,2}$). The zones, their target nuclei, and the subnuclei of the inferior olive that project to these zones are indicated with the same colors. The diagram applies equally to the monkey cerebellum, with the exception of the floccular zones, the most medial one of which is lacking in the monkey. *Asterisks:* areas without cortex. **B.** Diagram of the white matter compartments in acetylcholinesterase-stained sections of the cerebellum of *Macaca fascicularis*. Compare Figs. 11.47, 11.48, and 11.50. Abbreviations: A, A zone; Ans, ansiform lobule; B, B zone; $C_{1–3}$, $C_{1–3}$ zones; D, dorsomedial cell column; $D_{1,2}$, $D_{1,2}$ zones; dc, dorsal cap;dl, dorsal leaf of principal olive; dl, dorsal lamina of the principal olive; Fl, flocculus; Fsg, medial cerebellar nucleus; IntA, anterior interposed nucleus; IntI, intermediate cell group; IntP, posterior interposed nucleus; Lat, lateral cerebellar nucleus; Latc, caudal lateral cerebellar nucleus; Latr, rostral lateral cerebellar nucleus; LVe, lateral vestibular nucleus; MAO, medial accessory olive; N, nodulus; PFld, dorsal paraflocculus; PFlv, ventral paraflocculus; Pmd, paramedian lobule; PO, principal nucleus of the inferior olive; PY, pyramis; Py, pyramis; Sim, lobulus simplex; Uv, uvula; VII–IX lobules VII–IX; vl, ventral leaf of principal olive; Vlo, ventrolateral outgrowth.

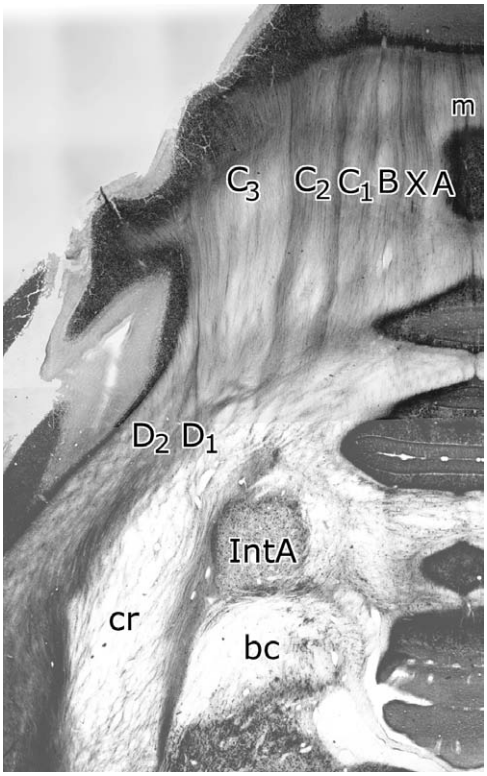

FIGURE 11.47 Coronal acetylcholinesterase-stained section through the anterior lobe of the cerebellum of *Macaca fascicularis*. The borders of the compartments A, X, B, C_{1-3}, D_1, and D_2 are heavily stained. Abbreviations: bc, brachium conjunctivum; cr, restiform body; IntA, anterior interposed nucleus; m, midline.

Compartments that were delineated and reconstructed from AChE-stained sections of Macaca fascicularis display the same configuration as the parasagittal compartments in cat and ferret (Figs. 11.46B–11.50). A, X, and B compartments can be distinguished in the anterior vermis. The A compartment is related to the fastigial nucleus, the X compartment to the U-shaped interstitial cell group located the fastigial and the posterior interposed nucleus (IntI: Fig. 11.12), and the B compartment leads to the lateral vestibular nucleus. In the hemisphere C_1 and C_3 compartments, which converge on the anterior interposed nucleus, are present in the anterior lobe and the lobulus simplex and in the paramedian lobule. C_1 continues into the ventral folia of the paramedian lobule; C_3 terminates more dorsally in this lobule. C_1 and C_3 fuse in the ventral anterior lobe. The C_2 compartment extends from the anterior lobe, throughout the hemisphere, into the flocculus. It converges on the posterior interposed nucleus. A narrow D_1 compartment is present, lateral to C_3, in the rostral parts of the cerebellum (Figs. 11.46A, B, 11.47). From the paramedian lobule, C_2, D_1, and D_2 compartments continue into the dorsal paraflocculus. The D_1 compartments converges on the caudal pole of the dentate nucleus (Fig. 11.48A). The most lateral D_2 compartment is narrow in the paraflocculus and much wider in the rest of the hemisphere. It is related to dorsal and rostral parts of

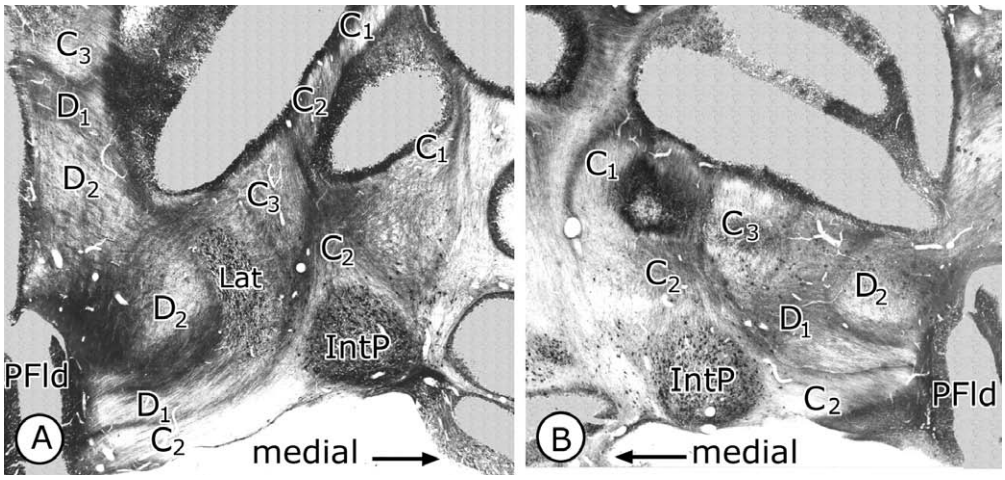

FIGURE 11.48 Left and right halves of a coronal acetylcholinesterase-stained section through the hemisphere of the posterior lobe of the cerebellum of *Saimiri sciureus*, approximately corresponding to level 6 in Fig. 11.46B. The borders of the white matter compartments are heavily stained. On both sides compartments C_2, D_1 and D_2 continue from the posterior white matter of the hemisphere into the dorsal paraflocculus. Compartments C_1, and C_3 terminate in the posterior white matter of the paramedian lobule. On both sides the caudal pole of the posterior interposed nucleus is lodged in the C_2 compartment. The caudal pole of the dentate nucleus appears in compartment D_1 on the left side. Abbreviations: C_{1-3}, compartments C_{1-3}; $D_{1,2}$, compartments $D_{1,2}$; IntP, posterior interposed nucleus; Lat, caudal pole of the dentate nucleus; PFld, dorsal paraflocculus.

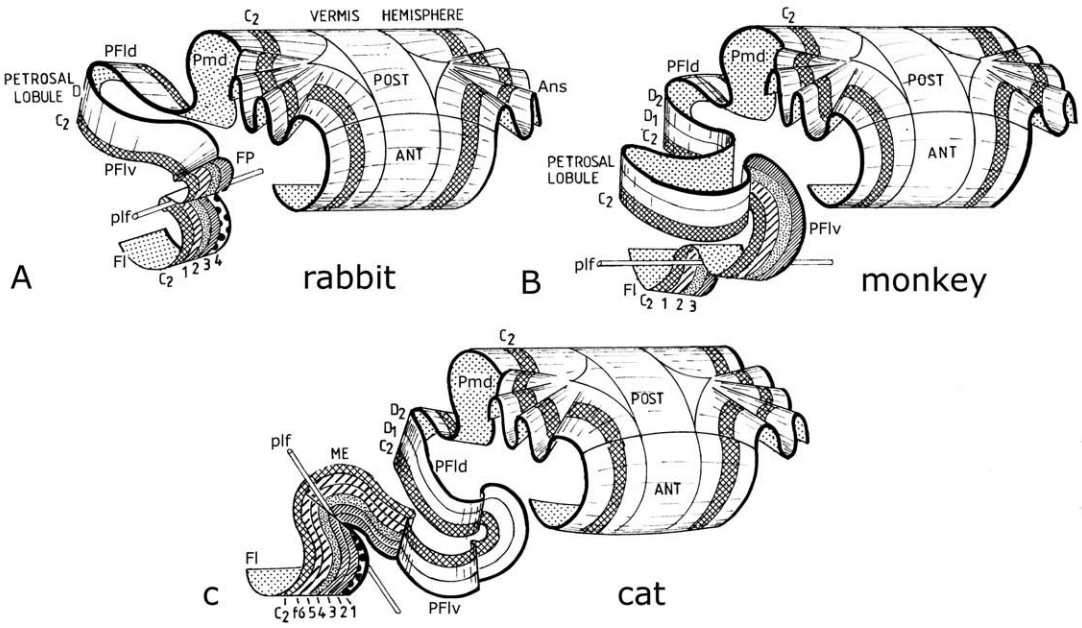

FIGURE 11.49 Diagrams illustrating the continuity of successive segments of the caudal folial chain of the hemisphere in different species. Two principal segments can be distinguished. The proximal segment is characterized by the presence of C_2 and D (D_1 and D_2) zones. It comprises the dorsal paraflocculus and the petrosal lobule in monkey, the dorsal paraflocculus and the proximal part of the ventral paraflocculus in cat, and the petrosal lobule in rat and rabbit. The distal segment consists of a C_2 zone and 3 (monkey), 6 (cat), or 4 (rat, rabbit) floccular zones with vestibular connections. It is represented by the ventral paraflocculus and the flocculus in monkeys, by the distal part (ME, medial extension) of the ventral paraflocculus and the flocculus in the cat, and by folium P and the flocculus in the rabbit. The relationship of the four floccular zones in rat and rabbit to the zonal configuration in cat and monkey is indicated by similar hatchings. Abbreviations: Ans, ansiform lobule; ANT, anterior lobe; C_2, zone C_2; D_1,D_2, zones D_1 and D_2; fl–f6, floccular zones f1–f6; Fl. flocculus; FP, folium P; ME, medial extension of the PFlv; PFld, dorsal paraflocculus; PFlv, ventral paraflocculus; plf, posterolateral fissure; Pmd, paramedian lobule; POST, posterior lobe. Based on data from Gerrits and Voogd (1982), Tan *et al.* (1995a–c), and unpublished observations in the monkey.

the dentate nucleus. The C_2 compartment contains the posterior interposed nucleus (Fig. 11.48A, B).

White matter compartments in the flocculus and he paraflocculus are especially clear in the monkey. Paraflocculus and flocculus are the last two segments of the folial chain of the hemisphere. The first part of the paraflocculus, which diverges from the paramedian lobule, is known as the dorsal paraflocculus (Fig. 11.49). It continues as the laterally directed loop of the petrosal lobule, which is lodged in the subarcuate fossa of the petrosal bone. The petrosal lobule continues as the rostrally directed rosette of the ventral paraflocculus and ends in the caudally directed flocculus. C_2, D_1, and D_2 compartments are present in the dorsal paraflocculus and the petrosal lobule (Fig. 11.46–11.50). The configuration of the ventral paraflocculus and the flocculus is completely different. Here four compartments can be distinguished. Compartments 2 and 4 continue as the floccular peduncle into the superior vestibular nucleus and the group Y. Compartment 3 gives rise to Löwy's angular bundle (Löwy, 1916), which runs in the caudal angle between the cerebellum and the brain stem to the medial vestibular nucleus. A medial compartment "1" is present in th rabbit and cat, but not in monkeys (Fig. 11.49). The fourth, most lateral compartment is connected with the posterior interposed nucleus. and represents the caudal extremity of the C_2 zone. Compartment 3 harbors many of the AChE-positive cells of Langer's (1985) basal interstitial nucleus. Only the C_2 compartment continues uninterruptedly from the dorsal ventral paraflocculus into the ventral paraflocculus and the flocculus (Fig. 11.50).

Therefore, the typical compartmentation of the flocculus is not limited to this lobule but is also present in the adjoining ventral paraflocculus (Fig. 11.49). An extension of the zonally arranged corticonuclear and olivocerebellar connections of the flocculus in the adjacent part of the ventral paraflocculus also was noted in cat (Voogd and Bigaré, 1980; Gerrits and Voogd, 1982), rat (Ruigrok *et al.*, 1992), rabbit (Yamamoto, 1979; Tan *et al.*, 1995a–c), and monkey (Gerrits and Voogd, 1989; Nagao *et al.*, 1997).

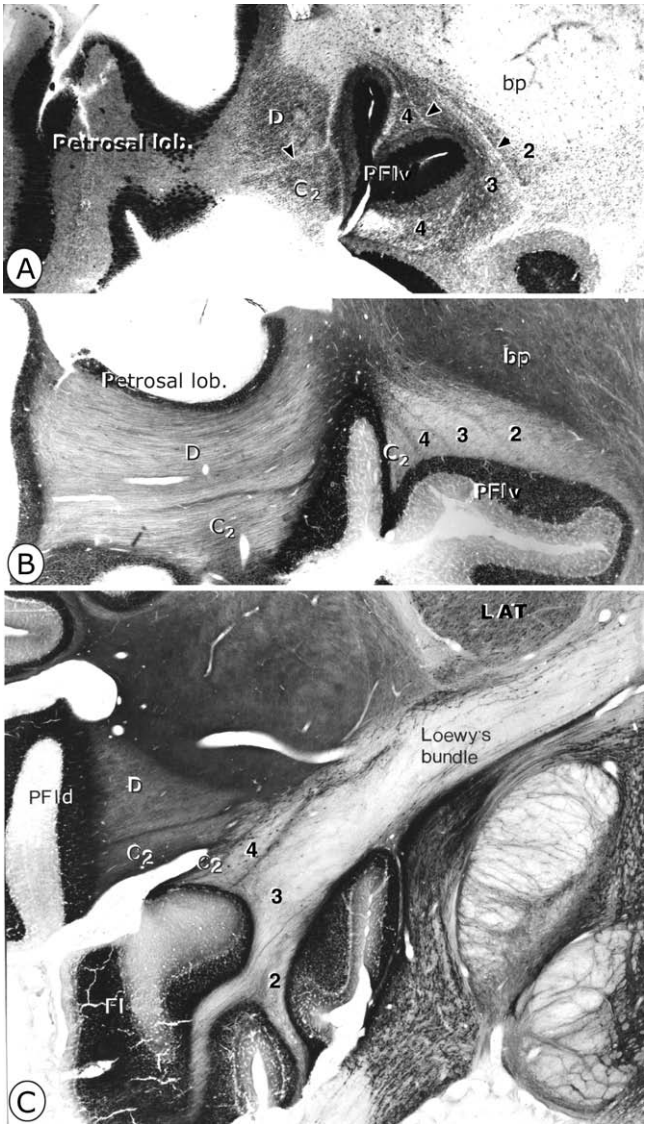

FIGURE 11.50 White matter in the flocculus and paraflocculus of *Macaca fascicularis*. **A.** Section through the petrosal lobule and the base of the ventral paraflocculus, reacted with an antbody against zebrin II. All Purkinjke cells and their axons are stained. Borders between compartments C_2 and D and between floccular compartments 2, 3, and 4 appear as unstained slits *(arrowheads)*. From Voogd and Gerrits (1997). **B.** A similar, acetylcholinesterase (AChE)–stained section, showing the AChE–stained borders between compartments C_2 and D, and between floccular compartments 2, 3, 4, and C_2. **C.** A more caudal AChE–stained section through the dorsal paraflocculus and the flocculus. Floccular compartment 3 continues into Loewy's bundle. Compartment 4 contains the AChE–positive cells of Langer's basal interstital nucleus. Abbreviations: bp, brachium pontis; C_2, C_2 compartment; $D_{1,2}$, $D_{1,2}$ compartment; Fl, flocculus; Lat, dentate nucleus; PFld, dorsal paraflocculus; PFlv, ventral paraflocculus; 2–4, floccular compartments 2–4.

Acknowledgments

I thank Eddy Dalm and Herman Chouffoer for their assistance in the preparation of the figures. Material for Figure 11.4 was on loan from the Neuroregulation Group of the Department of Physiology of the University of Leiden (Prof. Dr. Enrico Marani); acetylcholinesterase-stained monkey material was put at my disposal by Dr. Douglas T. Hess. Dr. Sharleen Sakai, Dr. Jeremy Schmahmann, Dr. Norman Strominger, and Dr. Peter van Kan made the originals of some of their figures available for reproduction in this chapter. Professor Yoshi Shinoda and Professor Mitchell Glickstein corrected the text on corticopontine and corticorubral connections. The responsibility for the statements contained therein remains mine.

References

Alisky, J.M., and Tolbert, D.L. (1997). Quantitative analysis of converging spinal and cuneate mossy fibre afferent projections to the rat cerebellar anterior lobe. *Neuroscience* **80,** 373–388.

Altman, J., and Bayer, S.A. (1987). Development of the precerebellar nuclei in the rat: IV. The anterior precerebellar extramural migratory stream and the nucleus reticularis tegmenti pontis and the basal pontine gray. *J Comp Neurol*. **257,** 529–552.

Andersson, G., and Oscarsson, O. (1978a). Projections to lateral vestibular nucleus from cerebellar climbing fiber zones. *Exp. Brain Res*. **32,** 549–564.

Andersson, G., and Oscarsson, O. (1978b). Climbing fiber microzones in cerebellar vermis and their projection to different groups of cells in the lateral vestbular nucleus. *Exp.Brain Res*. **32,** 565–579.

Angevine, J.B., Mancall, E.L., and Yakovlev, P.I. (1961). "The Human Cerebellum. An Atlas of Gross Topography in Serial Sections." Little Brown and Co., Boston.

Asanuma, C., Thach, W.T., and Jones, E.G. (1983a). Cytoarchitectonic delineation of the ventral lateral thalamic region in the monkey. *Brain Res. Rev.* **5,** 219–235.

Asanuma, C., Thach, W.T., and Jones, E.G. (1983b). Distribution of cerebellar terminations and their relation to other afferent terminations in the ventral lateral thalamic region of the monkey. *Brain Res. Rev*. **5,** 237–265.

Asanuma, C., Thach, W.T., and Jones, E.G. (1983c). Anatomical evidence for segregated focal groupings of efferent cells and their terminal ramifications in the cerebellothalamic pathway of the monkey. *Brain Res. Rev.* **5,** 267–297.

Asanuma, C., Thach, W.T., and Jones, E.G. (1983d). Brain stem and spinal projections of the deep cerebellar nuclei in the monkey, with observation on the brain stem projections of the dorsal column nuclei. *Brain Res. Rev.* **5,** 299–322.

Atkins, M.J., and Apps, R. (1997). Somatotopical organization within the climbing fibre projection to the paramedian lobule and copula pyramidis of the rat cerebellum. *J. Comp. Neurol*. **389,** 249–263.

Azizi, S.A., and Woodward, D.J. (1987). Inferior olivary nuclear complex of the rat: morphology and comments on the principles of organization within the olivocerebellar system. *J. Comp. Neurol*. **263,** 467–484.

Baker, J., Gibson, A., Glickstein, M., and Stein, J. (1976). Visual cells in the pontine nuclei of the cat. *J. Physiol*. **255,** 415–433.

Baker, J., Gibson, A., Mower, G., Robinson, F., and Glickstein, M. (1983). Cat visual corticopontine cells project to the superior colliculus. *Brain Res.* **265,** 227–232.

Balaban, C.D. (1984). Olivo-vestibular and cerebello-vestibular connections in albino rabbits. *Neuroscience* **12,** 129–149.

Balaban, C.D. (1988). Distribution of inferior olivary projections to the vestibular nuclei of albino rabbits. *Neuroscience* **24,** 119–134.

Barmack, N.H., Fredette, B.J., and Mugnaini, E. (1998). Parasolitary nucleus: a source of GABAergic vestibular information to the inferior olive of rat and rabbit. *J. Comp. Neurol.* **392,** 352–372.

Barron, K.D., Dentinger, M.P., and Koeppen, A.H. (1982). Fine structure of neurons of the hypertrophied human inferior olive. *J. Neuropathol. Exp. Neurol.* **41,** 186–203.

Batton R.R., III, Jayaraman, A., Ruggiero, D., and Carpenter, M.B. (1977). Fastigial efferent projections in the monkey: an autoradiographic study. *J. Comp. Neurol.* **174,** 281–306.

Bechterew, W. von (1885). Zur Anatomie der Schenkel des Kleinhirns. *Neurol. Centralbl.* **4,** 121–125.

Bechterew, W. von (1886). Ueber die Bestandtheile des Corpus restiforme. *Arch. Anat. Physiol. Anat. Abt.,* 403–411.

Bechterew, W. von (1887). Zur Frage uber den Ursprung des Hornerven und über die physiologische Bedeutung des N. vestibularis. *Neurol. Centralbl.* **6,** 193–198.

Bechterew, W. von (1888). Ueber die Bestandtheile des vorderen Kleinhirnschenkels. *Arch. Anat. Physiol. Anat. Abth.,* 195–204.

Bechterew, W. von (1899). "Die Leitungsbahnen im Gehirn und Ruckenmark." Leipzig Verlag von Arthur Georgi.

Beck, E. (1950). The origin, course and termination of the frontopontine tract in the human brain. *Brain* **73,** 368–391.

Beitz, A.J. (1976). The topographical organization of the olivo-dentate and dentato-olivary pathways in the cat. *Brain Res.* **115,** 311–317.

Bentivoglio, M., and Kuypers, H.G.J.M. (1982). Divergent axon collaterals from rat cerebellar nuclei to diencephalon, mesencephalon, medulla oblongata and cervical cord. A fluorescent double retrograde labeling study. *Exp. Brain Res.* **46,** 339–356.

Bharos, T.B., Kuypers, H.G., Lemon, R.N., and Muir, R.B. (1981). Divergent collaterals from deep cerebellar neurons to thalamus and tectum, and to medulla oblongata and spinal cord: retrograde fluorescent and electrophysiological studies. *Exp. Brain Res.* **42,** 399–410.

Bianchi, R., and Gioia, M. (1990). Accessory oculomotor nuclei of man. 1. The nucleus of Darkschewitsch: a Nissl and Golgi study. *Acta Anat. (Basel)* **139,** 349–356.

Bjaalie, J.G., and Brodal, P. (1997). Cat pontocerebellar network: numerical capacity and axonal collateral branching of neurones in the pontine nuclei projecting to individual parafloccular folia. *Neurosci. Res.* **27,** 199–210.

Boegman, R.J., Parent, A., and Hawkes, R. (1988). Zonation in the rat cerebellar cortex: patches of high acetylcholinesterase activity in the granular layer are congruent with Purkinje cell compartments. *Brain Res.* **448,** 237–251.

Boesten, A.J.P., and Voogd, J. (1985). Hypertrophy of neurons in the inferior olive after cerebellar ablations in the cat. *Neurosci. Lett.* **61,** 49–54.

Bolk, L. (1902). Hoofdlijnen der vergelijkende anatomie van het cerebellum der zoogdieren, voornamelijk in verband met den bouw der kleine hersenen van den mensch. *Psych. Neurol. Bladen* **3/4,** 1–43.

Bolk, L. (1905a). Over de ontwikkeling van het cerebellum bij den mensch. II. *Verslag Verg. Wis- en Natuurk. Afd. Kon. Akad. Wetensch. Amsterdam* **14,** 134–140.

Bolk, L. (1905b). On the development of the cerebellum in Man. II. *Proc. Kon. Akad. Wetensch., Amsterdam* **8,** 85–91.

Bolk, L. (1906). "Das Cerebellum der Saugetiere." F. Bohn, Fischer, Jena.

Bower, J.M., and Woolston, D.C. (1983). Congruence of spatial organization of tactile projections to granule cell and Purkinje cell layers of cerebellar hemispheres of the albino rat: vertical organization of cerebellar cortex. *J. Neurophysiol.* **49,** 745–766.

Braitenberg, V., and Atwood, R.P. (1958). Morphological observations on the cerebellar cortex. *J. Comp. Neurol.* **109,** 1–33.

Brodal, A. (1940). Experimentelle Untersuchungen uber die Olivo-Cerebellaren Lokalisation. *Z. Neur.* **169,** 1–153.

Brodal, A., and Jansen, J. (1941). Beitrag zur Kenntnis der spino-cerebellaren Bahnen beim Menschen. *Anat. Anz.* **91,** 185–195.

Brodal, A., and Kawamura, K. (1980). Olivocerebellar projection: A review. *Adv. Anat. Embryol. Cell Biol.* **64,** 1–137.

Brodal, A., and Pompeiano, O. (1957). The vestibular nuclei in the cat. *J. Anat. London* **91,** 438–454.

Brodal, P. (1978). The corticopontine projection in the rhesus monkey. Origin and principles of organization. *Brain* **101,** 251–283.

Brodal, P. (1979). The pontocerebellar projection in the rhesus monkey: an experimental study with retrograde axonal transport of horseradish peroxidase. *Neuroscience.* **4,** 193–208.

Brodal, P. (1980). The cortical projection to the nucleus reticularis tegmenti pontis in the rhesus monkey. *Exp. Brain Res.* **38,** 19–27.

Brodal, P. (1982). Further observations on the cerebellar projections from the pontine nuclei andthe nucleus reticularis tegmenti pontis in the rhesus monkey. *J. Comp. Neurol.* **204,** 44–55.

Brodal, P., and Brodal, A. (1981). The olivocerebellar projection in the monkey. Experimental studies with the method of retrograde tracing of horseradish peroxidase. *J. Comp. Neurol.* **201,** 375–393.

Brodal, P., and Brodal, A. (1982). Further observations on the olivocerebellar projection in the monkey. *Exp. Brain Res.* **45,** 71–83.

Brodal, P., and Bjaalie, J.G. (1992). Organization of the pontine nuclei. *Neurosci. Res.* **13,** 83–118.

Brouwer, B. (1913). Ueber Hemiatrophia neocerebellaris. *Arch. Psychiat.* **51,** 538–577.

Brouwer, B. (1915). Anatomische Untersuchung ueber das Kleinhirn des Menschen. *Psych. Neur. Bladen* **19,** 104–129.

Brouwer, B., and Coenen, L. (1920). Ueber die Oliva inferior. *J. Psychol. Neurol.* **25,** 52–71.

Brouwer, B., and Coenen, L. (1921). Untersuchungen uber das Kleinhirn. *Psych. Neur. Bladen* **25,** 201–228.

Brown, B.L. (1985). Changes in acetylcholinesterase staining in the molecular layer of the cat cerebellar cortex following climbing fiber destruction. *Anat. Rec.* **211,** 27A.

Brown, I.E., and Bower, J.M. (2001). Congruence of mossy fiber and climbing fiber tactile projections in the lateralhemispheres of the rat cerebellum. *J. Comp. Neurol.* **429,** 59–70.

Brun, R. (1917/18a). Zur Kenntnis der Bildungsfehler des Kleinhirns. *Schweiz Arch. Psychiat. Neurol.* **1,** 61–123.

Brun, R. (1917/18b). Zur Kenntnis der Bildungsfehler des Kleinhirns. *Schweiz Arch. Psychiat. Neurol.* **2,** 48–105.

Brun, R. (1917/18c). Zur Kenntnis der Bildungsfehler des Kleinhirns. *Schweiz Arch. Psychiat. Neurol.* **3,** 13–88.

Brun, R. (1925a). Das Cerebellum. Anatomie, Physiologie und Entwicklungsgeschichte. I. *Schweiz Arch. Psychiat. Neurol.* **16,** 183–197.

Brun, R. (1925b). Das Cerebellum. Anatomie, Physiologie und Entwicklungsgeschichte. *Arch. Psychiat. Neurol.* **17,** 89–108.

Brunner, H. (1919). Die zentrale Kleinhirnkerne bei den Saugetieren. *Arb. Neurol. Inst. Wiener Univ.* **22,** 200–272.

Buisseret-Delmas, C. (1988a). Sagittal organization of the olivocerebellonuclear pathway in the rat. I. Connections with the nucleus fastigii and the nucleus vestibularis lateralis. *Neurosci. Res.* **5,** 475–493.

Buisseret-Delmas, C. (1988b). Sagittal organization of the olivo-cerebellonuclear pathway in the rat. II. Connections with the nucleus interpositus. *Neurosci. Res.* **5,** 494–512.

Buisseret-Delmas, C., and Angaut, P. (1989). Sagittal organisation of the olivocerebellonuclear pathway in the rat. III. Connections with the nucleus dentatus. *Neurosci. Res.* **7,** 131–143.

Buisseret-Delmas, C., Yatim, N., Buisseret, P., and Angaut, P. (1993). The X zone and CX subzone of the cerebellum in the rat. *Neurosci. Res.* **16,** 195–297.

Bull, M.S., Mitchell, S.K., and Berkley, K.J. (1990). Convergent inputs to the inferior olive from the dorsal column nuclei and pretectum in the cat. *Brain Res.* **525,** 1–10.

Burman, K., Darian-Smith, C., and Darian-Smith, I. (2000). Macaque red nucleus: origins of spinal and olivary projections and terminations of cortical inputs. *J. Comp. Neurol.* **423,** 179–196.

Busch, H.F.M. (1961). An analysis of the white matter in the brain stem of the cat. Thesis, Van Gorcum, Assen.

Büttner-Ennever, J.A., and Horn, A.K.(1996). Pathways from cell groups of the paramedian tracts to the floccular region. *Ann. N. Y. Acad. Sci.* **781,** 532–540.

Cajal, S. Ramon y (1909). "Histologie du systeme nerveux." Maloine, Paris.

Carpenter, M.B., and Stevens, G.H. (1957). Structural and functional relationships between the deep cerebellar nuclei and the brachium conjunctivum in the rhesus monkey. *J. Comp. Neurol.* **107,** 109–152.

Catsman-Berrevoets, C.E., Kuypers, H.G.J.M., and Lemon, R.N. (1979). Cells of origin of the frontal projections to magnocellular and parvocellular red nucleus and superior colliculus in cynomolgus monkey. An HRP study. *Neurosci. Lett.* **12,** 41–46.

Catsman-Berrevoets, C.E., and Kuypers, H.J.G.M. (1981). A search for corticospinal collaterals to thalamus and mesencephalon by means of multiple retrograde flurorescent tracers in cat and rat. *Brain Res.* **218,** 15–33.

Chan-Palay, V. (1977). "Cerebellar Dentate Nucleus. Organization, Cytology and Transmitters." Springer-Verlag, Berlin.

Chen, S., and Hillman, D.E. (1993). Colocalization of neurotransmitters in the deep cerebellar nuclei. *J. Neurocytol.* **22,** 81–91.

Cholley, B., Wassef, M., Arsenio-Nunes, L., Brehier, A., and Sotelo, C. (1989). Proximal trajectory of the brachium conjunctivum in rat fetuses and its early association with the parabrachial nucleus. A study combining in vitro HRP anterograde axonal tracing and immunocytochemistry. *Dev. Brain Res.* **499,** 193–202.

Cintas, H.M., Rutherford, J.G., and Gwyn, D.G. (1980). Some midbrain and diencephalic projections to the inferior olive in the rat. *In* "The Inferior Olivary Nucleus," (J. Courville, C. De Montigny, and Y. Lamarre, eds.), pp. 73–96. Raven Press, New York.

Clower, D.M., West, R.A., Lynch, J.C., and Strick, P.L. (2001). The inferior parietal lobule is the target of output from the superior colliculus, hippocampus and cerebellum. *J. Neurosci.* **21,** 6283–629.

Collier, J., and Buzzard, E.F. (1903). The degeneration resulting from lesions of posterior nerve roots and from transverse lesions of the spinal cord in man. A study of twenty cases. *Brain* **26,** 559–591.

Condé, F., and Condé, H. (1982). The rubro-olivary tract in the cat, as demonstrated with the method of retrograde transport of horseradish peroxidase. *Neuroscience* **7,** 715–724.

Cooke, J.D., Larson, B., Oscarsson, O., and Sjölund, B. (1971). Origin and termination of cuneocerebellar tract. *Exp. Brain Res.* **13,** 339–358.

Courville, J., and Cooper, C.W. (1970). The cerebellar nuclei of *Macaca mulatta:* a morphological study. *J. Comp. Neurol.* **140,** 241–254.

Courville, J., and Faraco-Cantin, F. (1976). Cerebellar corticonuclear projection demonstrated by the horseradish peroxidase method. *Neurosci. Abstr.* **2,** 108.

Courville, J., Faraco-Cantin, F., and Diakiw, N. (l974). A functionally important feature of the distribution of the olivo-cerebellar climbing fibers. *Can. J. Physiol. Pharmacol.* **52,** 1212–1217.

Courville, J., and Otabe, S. (1974). The rubro-olivary projection in the macaque: an experimental study with silver impregnation methods. *J. Comp. Neurol.* **158,** 479–494.

Courville, J., Faraco-Cantin, F., and Legendre, A. (1983). Detailed organization of cerebello-olivary prokections in the cat. An autoradiographic study. *Arch. Ital. Biol.* **121,** 219–236.

Darkschewitsch, L., and Freud, S. (1886). Ueber die Beziehung des Strickkörpers zum Hinterstrang und Hinterstrangskern nebst Bemerkungen uber zwei Felden der Oblongata. *Neur. Centralbl.* **5,** 121–129.

Deiters, O. (1865). "Untersuchungen über Gehirn und Ruckenmark." Braunschweig.

Dejerine, J. (1985). "Anatomie des centres nerveux," Vol. 1. Rueff et Cie, Paris.

Demolé, V. (1927a). Structure et connexion des noyeaux dentelés du cervelet. I. *Schweiz Arch. Psychiat. Neurol.* **20,** 271–294.

Demolé, V. (1927b). Structure et connexion des noyeaux dentelés du cervelet. II *Schweiz Arch. Psychiat. Neurol.* **21,** 73–110.

Desclin, J.C. (1974). Histological evidence supporting the inferior olive as the major source of cerebellar climbing fibers in the rat. *Brain Res.* **77,** 365–384.

Deuschl, G., Toro, C., Valls-Sole, J., and Hallett, M. (1996). Symptomatic and essential palatal tremor. 3. Abnormal motor learning. *J. Neurol. Neurosurg. Psychiat.* **60,** 520–525.

De Zeeuw, C.I., Ruigrok, T.J., Schalekamp, M.P., Boesten, A.J., and Voogd, J. (1990). Ultrastructural study of the cat hypertrophic inferior olive following anterograde tracing, immunocytochemistry, and intracellular labeling. *Eur. J. Morphol.* **28,** 240–255.

De Zeeuw, C.I., Wentzel, P., and Mugnaini, E. (1993). Fine structure of the dorsal cap of the inferior olive and its GABAergic and non-GABAergic input from the nucleus prepositus hypoglossi in rat and rabbit. *J. Comp. Neurol.* **327,** 63–82.

De Zeeuw, C.I., Gerrits, N.M., Voogd, J., Leonard, C.S., and Simpson, J.I. (1994). The rostral dorsal cap and ventrolateral outgrowth of the rabbit inferior olive receive a GABAergic input from dorsal group Y and the ventral dentate nucleus. *J. Comp. Neurol.* **341,** 420–432.

De Zeeuw, C.I., Strata, P., and Voogd, J. (1997). The cerebellum from structure to control. *Prog. Brain Res.* **114.**

Dietrichs, E., and Walberg, F. (1987). Cerebellar nuclear afferents—where do they originate? A re-evaluation of the projections from some lower brain stem nuclei. *Anat. Embryol.* **177,** 165–172.

Dietrichs, E., Walberg, F., and Nordby, T. (1985). The cerebellar nucleo-olivary and olivo-cerebellar nuclear projections in the cat as studied with anterograde and retrograde transport in the same animal after implantation of crystalline WGA-HRP. I. The dentate nucleus. *Neurosci. Res.* **3,** 52–70.

Dino, M.R., Willard, F.H., and Mugnaini, E. (1999). Distribution of unipolar brush cells and other calretinin immunoreactive components in the mammalian cerebellar cortex. *J. Neurocytol.* **28,** 99–123.

Dore, L., Jacobson, C.D., and Hawkes, R. (1990). Organization and postnatal development of zebrin II antigenic compartmentation in the cerebellar vermis of the grey opossum, Monodelphis domestica. *J. Comp. Neurol.* **291,** 431–449.

Dum, R.P., and Strick, P.L. (1991). The origin of corticospinal projections from the premotor areas in the frontal lobe. *J. Neurosci.* **11,** 667–689.

Dum, R.P., and Strick, P.L. (1996). Spinal cord terminations of the medial wall motor areas in macaque monkeys. *J. Neurosci.* **16,** 6513–6525.

Edwards, S.B. (1972). The ascending and descending projections of the red nucleus in the cat: an experimental study using an autoradiographic tracing method. *Brain Res.* **48,** 45–63.

Ekerot, C.F., and Larson, B. (1972). Differential termination of the exteroceptive and proprioceptive components of the cuneo-cerebellar tract. *Brain Res.* **36,** 420–424.

Elliot Smith, G. (1902). The primary subdivision of the mammalian cerebellum. *J. Anat. London* **36,** 381–385.

Elliot Smith, G. (1903). Notes on the morphology of the cerebellum. *J. Anat. Physiol.* **37,** 329–332.

Faugier-Grimaud, S., and Ventre, J. (1989). Anatomic connections of the inferior parietal cortex (area 7) with subcortical structures related to vestibulo-ocular function in a monkey *(Macaca fascicularis). J. Comp. Neurol.* **280,** 1–14.

Flechsig, P. (1877). Notiz den "Strickkorper" betreffend. *Zentralbl. Med. Wiss.* **15,** 614–615.

Flechsig, P. (1927). "Meine myelogenetische Hirnlehre." Springer-Verlag, Berlin.

Flood, S., and Jansen, J. (1961). On the cerebellar nuclei in the cat. *Acta Anat.* **46,** 52–72.

Flumerfelt, B.A., Otabe, S., and Courville, J. (1973). Distinct projections to the red nucleus from the dentate and interposed nuclei in the monkey. *Brain Res.* **50,** 408–414.

Forel, A. (1877). Untersuchungen über die Haubenregion und ihre obere Verknüpfungen im Gehirn des Menschen und einiger Säugethiere mit Beiträgen zu den Methoden der Gehirnuntersuchung. *Arch. Psychiat.* **7,** 392–495.

Frankfurter, A., Weber, J.T., Royce, G.J., Strominger, N.L., and Harting, J.K. (1976). An autoradiographic analysis of the tecto-olivary projection in primates. *Brain Res.* **118,** 245–257.

Gannon, P.J., Eden, A.R., and Laitman, J.T. (1988). The subarcuate fossa and cerebellum of extant primates: comparative study of a skull-brain interface. *Am. J. Phys. Anthropol.* **77,** 143–164.

Gans, A. (1924). Beitrag zur Kenntnis des Aufbaus des Nucleus Dentatus aus zwei Teilen namentlich auf Grund von Untersuchungen mit der Eisenreaktion. Ztschr. *Ges. Neurol. Psychiat.* **93,** 750–755.

Garwicz, M. (1997). Sagittal zonal organization of climbing fibre input to the cerebellar anterior lobe of the ferret. *Exp. Brain Res.* **117,** 389–398.

Garwicz, M., Jörntell, H., and Ekerot, C.F. (1998). Cutaneous receptive fields and topography of mossy fibres and climbing fibres projecting to cat cerebellar C3 zone. *J. Physiol.* **512,** 277–293.

Gebbink, T.B. (1967). Structure and connections of the basal ganglia in man. Thesis Leiden. Van Gorcum & Comp. Assen.

Gerfen, C.R., and Wilson, C.J. (1998). The basal ganglia. *In:* "Handbook of Chemical Neuroanatomy, Vol. 12, Integrated systems of the CNS. Part III." (L.W. Swanson, A. Björklund, and T. Hökfelt, eds.), pp. 371–486. Elsevier, Amsterdam.

Gerrits, N.M., and Voogd, J. (1982). The climbing fiber projection to the flocculus and adjacent paraflocculus in the cat. *Neuroscience* **7,** 2971–2991.

Gerrits, N.M., and Voogd, J. (1986). The nucleus reticularis tegmenti pontis and the adjacent rostral paramedian reticular formation: differential projections to the cerebellum and the caudal brain stem. *Exp. Brain Res.* **62,** 29–45.

Gerrits, N.M., and Voogd, J. (1987). The projection of the nucleus reticularis tegmenti pontis and adjacent regions of the pontine nuclei to the central cerebellar nuclei in the cat. *J. Comp. Neurol.* **258,** 52–69.

Gerrits, N.M., and Voogd. J. (1989). The topographical organization of climbing and mossy fiber afferents in the flocculus and the ventral paraflocculus in rabbit, cat and monkey. In: "The Olivo-cerebellar System in Motor Control Strata," (P. ed.), pp. 26–29. Springer-Verlag, Berlin.

Gerrits, N.M., Voogd, J., and Magras, I.N. (1985a). Vestibular afferents of the inferior olive and the vestibulo-olivo-cerebellar climbing fiber pathway to the flocculus in the cat. *Brain Res.* **332,** 325–336.

Gerrits, N.M., Voogd, J., and Nas, W.S.C. (1985b). Cerebellar and olivary projections of the external and rostral internal cuneate nuclei in the cat. *Exp. Brain Res.* **57,** 239–255.

Gerrits, N.M, Ruigrok, T.J.H., and de Zeeuw, C.I. (2000). Cerebellar modules: molecules, morphology and function. *Prog. Brain Res.* **124.**

Glickstein, M. (1987). Structure and function of the cerebellum. A historical introduction to some current problems. *In:* "Cerebellum and Neuronal Plasticity." (M. Glickstein, Chr. Yeo, and J. Stein, eds.), pp. 1–13. NATO ASI Series A, Life Sciences Vol. 148.

Glickstein, M., May III, J.G., and Mercier, B.E. (1985). Corticopontine projection in the Macaque: the distribution of labelled cortical cells after large injections of horseradish peroxidase in the pontine nuclei. *J. Comp. Neurol.,* **235,** 343–359.

Glickstein, M., Gerrits, N., Kralj-Hans, I., Mercier, B., Stein, J., and Voogd, J. (1994). Visual pontocerebellar projections in the macaque. *J. Comp. Neurol.* **349,** 51–72.

Glickstein, M., and Voogd, J. (1995). Lodewijk Bolk and the comparative anatomy of the cerebellum. *Trends Neurosci.* **18,** 206–210.

Gonzalo-Ruiz. A., Leichnetz, G.R., and Smith, D.J. (1988). Origin of cerebellar projections to the region of the oculomotor complex, medial pontine reticular formation, and superior colliculus in new world monkeys: a retrograde horseradish peroxidase study. *J. Comp. Neurol.* **286,** 508–526.

Gordon, G., and Seed, W.A. (1961). An investigation of nucleus gracilis of the cat by antidromic stimulation. *J. Physiol. London* **155,** 589–601.

Grant, G., and Xu, Q. (1988). Routes of entry into the cerebellum of spinocerebellar axons from the lower part of the spinal cord. An experimental anatomical study in the cat. *Exp. Brain Res.* **72,** 43–61.

Gravel, C., and Hawkes, R. (1990). Parasagittal organization of the rat cerebellar cortex: direct comparison of Purkinje cell compartments and the organization of the spinocerebellar projection. *J. Comp. Neurol.* **291,** 79–102.

Graybiel, A.M., and Hartwieg, E.A. (1974). Some afferent connections of the oculomotor complex in the cat: an experimental study with tracer techniques. *Brain Res.* **81,** 543–551.

Graybiel, A.M., Nauta, H.J .W., Lasek, R.J., and Nauta, W.J.H. (1973). Experimental anatomical evidence for a cerebello-olivary pathway in the cat. *Anat. Rec.* **175,** 332.

Groenewegen, H.J., and Voogd, J. (1977). The parasagittal zonation within the olivocerebellar projection. I. Climbing fiber distribution in the vermis of cat cerebelllum. *J. Comp. Neurol.* **174,** 417–488.

Groenewegen, H.J., Voogd, J., and Freedman, S.L. (1979). The parasagittal zonation within the olivocerebellar projection. II. Climbing fiber distribution in the intermediate and hemispheric parts cat cerebellum. *J. Comp. Neurol.* **183,** 551–602.

Haines, D.E., Patrick, G.W., and Satrulee, P. (1982). Organization of cerebellar corticonuclear fiber systems. *Exp. Brain Res. Suppl* **6,** 320–367.

Haroian, A.J., Masopust, L.C., and Young, P.A. (1981). Cerebello-thalamic projections in the rat: an autoradiographic and degeneration study. *J. Comp. Neurol.* **197,** 217–236.

Harting, J.K. (1977). Descending pathways from the superior collicullus: an autoradiographic analysis in the rhesus monkey *(Macaca mulatta). J. Comp. Neurol.* **173,** 583–612.

Hartmann-von Monakow, K., Akert, K., and Kunzle, H. (1979). Projections of precentral and premotor cortex to the red nucleus and other midbrain areas in Macaca fascicularis. *Exp. Brain Res.* **34,** 91–105.

Hartmann-von Monakow, K., Akert, K., and Künzle, H. (1981). Projection of precentral, premotor and prefrontal cortex to the basilar pontine grey and to nucleus reticularis tegmenti pontis in

the monkey *(Macaca fascicularis). Arch Suisses Neurol. Neurochir. Psychat.* **129,** 189–208.
Hatten, and M.E., and Heintz, N. (1995). Mechanisms of neural patterning and specification in the developing cerebellum. *Annu. Rev. Neurosci.* **18,** 385–408.
Hawkes, R., and Eisenman, L.M. (1997). Stripes and zones: the origins of regionalization of the adult cerebellum. *Persp. Dev. Neurobiol.* **5,** 95–105.
Hawkes, R., and Leclerc, N. (1987). Antigenic map of the rat cerebellar cortex: the distribution of sagittal bands as revealed by monoclonal anti-Purkinje cell antibody mabQ113. *J. Comp. Neurol.* **256,** 29–41.
Hawkes, R., Colonnier, M., and Leclerc, N. (l985). Monoclonal antibodies reveal sagittal banding in the rodent cerebellar cortex. *Brain Res.* **333,** 359–365.
Hawkes, R. (1992). Antigenic markers of cerebellar modules in the adult mouse. *Biochem. Soc. Trans.* **20,** 391–395.
He, S.Q., Dum, R.P., and Strick, P.L. (1993). Topographic organization of corticospinal projections from the frontal lobe:motor areas on the lateral surface of the hemisphere. *J. Neurosci.* **13,** 952–980.
He, S.Q., Dum, R.P., and Strick, P.L. (1996). Topographic organization of corticospinal projections from the frontal lobe: motor areas on the medial surface of the hemisphere. *J. Neurosci.* **15,** 3284–3306.
Hendry, S.H., Jones, E.G., and Graham, J. (1979). Thalamic relay nuclei for cerebellar and certain related fiber systems in the cat. *J. Comp. Neurol.* **185,** 679–713.
Henle, J. (1871). "Handbuch der Nervenlehre des Menschen. *In:* Handbuch der systematischen Anatomie des Menschen." Vieweg, Braunschweig Bd 3, Abt. 2.
Herrup, K., and Kuemerle, B. (1997). The compartmentalization of the cerebellum. *Annu. Rev. Neurosci.* **20,** 61–90.
Hess, D.T., and Voogd, J. (1986). Chemoarchitectonic zonation of the monkey cerebellum. *Brain Res.* **369,** 383–387.
Highstein, S.M., and Reisine, H. (1979). Synaptic and functional organization of vestibulo-ocular reflex pathways. *Prog. Brain Res.* **50,** 431–442.
Hirai, M., and Uchino, Y. (1984). Superior vestibular neurones related to the excitatory vestibulo-ocular reflex of the anterior canal origin and their ascending course in the cat. *Neurosci. Res.* **1,** 73–79.
Hochstetter, F. (1929). "Beiträge zur Entwicklungsgeschichte des menschlichen Gehirns. II. Die Entwicklung des Mittel- und Rautenhirns." Franz Deuticke, Wien.
Holmes, G., and Stewart, T.G. (1908). On the connections of the inferior olives with the cerebellum in man. *Brain* **31,** 125–137.
Hoover, J.E., and Strick, P.L. (1999). The organization of cerebellar and basal ganlia outputs to primary motor cortex as revealed by retrograde transneuronal transport of herpes simplex virus type 1. *J. Neurosci.* **19,** 1446–1463.
Humphrey, D.R., Gold, R., and Reed, D.J. (1984). Sizes, laminar and topographical origins of cortical projections to the major divisions of the red nucleus in the monkey. *J. Comp. Neurol.* **225,** 75–94.
Jakob, A. (1928). "Das Kleinhirn. v. Möllendorff's Handbuch der mikroskopischen Anatomie des Menschen," Vol. 4, Part 1, pp. 674–916. Springer-Verlag, Berlin.
Jansen, J., and Brodal, A. (1940). Experimental studies on the intrinsic fibers of the cerebellum II. The cortico-nuclear projection. *J. Comp. Neurol.* **73,** 267–321.
Jansen, J., and Brodal, A. (1942). Experimental studies on the intrinsic fibers of the cerebellum. III. Cortico-nuclear projection in the rabbit and the monkey. *Norske Vid. Akad. Avh. 1 Math. Nat. Kl.* **3,** 1–50.
Jansen, J., and Brodal, A. (1958). Das Kleinhirn. In: "Handbuch der mikroskopischen Anatomie des Menschen," Vol. 4, Part 8 (Von Möllendorf, ed.), Springer-Verlag, Berlin.
Jasmin, L ., and Courville, J. (1987a). Distribution of external cuneate nucleus afferents to the cerebellum: I. Notes on the projections from the main cuneate and other adjacent nuclei. An experimental study with radioactive tracers in the cat. *J. Comp. Neurol.* **261,** 481–496.
Jasmin, L., and Courville, J. (1987b). Distribution of external cuneate nucleus afferents to the cerebellum: II. Topographical distribution and zonal pattern. An experimental study with radioactive tracers in the cat. *J. Comp. Neurol.* **261,** 497–514.
Ji, Z., and Hawkes, R. (1981). Topography of Purkinje cell compartments and mossy fiber terminal fields in lobules II and III of the rat cerebellar cortex: spinocerebellar and cuneocerebellar projections. *Neuroscience* **61,** 935–954.
Jones, E.G. (1985). "The Thalamus." Plenum Press, New York.
Jörntell, H., Ekerot, C., Garwicz, M., and Luo, X.L. (2000). Functional organization of climbing fibre projection to the cerebellar anterior lobe of the rat. *J. Physiol.* **522,** 297–309.
Kakei, S., Yagi, J., Wannier, T., Na, J., and Shinoda, Y. (1995). Cerebellar and cerebral inputs to corticocorical and corticofugal neurons in areas 5 and 7 in the cat. *J. Neurophysiol.* **74,** 400–412.
Kalil, K. (1979). Projections of the cerebellar and dorsal column nuclei upon the inferior olive in the rhesus monkey: an autoradiographic study. *J. Comp. Neurol.* **188,** 43–62.
Kalil, K. (1981). Projections of the cerebellar and dorsal column nuclei upon the thalamus of the rhesus monkey. *J. Comp. Neurol.* **195,** 25–50.
Kappel, R.M. (1981). The development of the cerebellum in *Macaca mulatta*. Thesis, Leiden.
Kawamura, K., and Hashikawa, T. (1979). Olivocerebellar projections in the cat studied by means of anterograde axonal transport of labeled amino acids as tracers. *Neuroscience* **4,** 1615–1633.
Kawamura, K., and Hashikawa, T. (1981). Projections from the pontine nuclei proper and reticular tegmental nucleus onto the cerebellar cortex in the cat. An autoradiographic study. *J. Comp. Neurol.* **201,** 395–413.
Keizer, K., Kuypers, H.G.J.M, and Ronday, H.K. (1987). Branching cortical neurons in cat which project to the colliculi and to the pons: a retrograde fluorescent double-labeling study. *Exp. Brain Res.,* **67,** 1–15.
Kennedy P.R., Gibson, A.R., and Houk, J.C. (1986). Functional and anatomic differentiation between parvicellular and magnocellular regions of red nucleus in the monkey. *Brain Res.* **364,** 124–136.
Kievit, J. (1979). Cerebello-thalamische projecties en de afferente verbindingen naar de frontaalschors in de rhesus aap. Thesis, Rotterdam.
Kievit, J., and Kuypers H.G.J.M. (1972). Fastigial cerebellar projections to the ventrolateral nucleus of the thalamus and the organization of the descending pathways. In: "Corticothalamic Projections and Sensorimotor Activities." (T. Frogyesi *et al*., eds.), pp. 91–114. Raven Press, New York.
Kievit, J., and Kuypers, H.J.G.M (1977). Organization of the thalamocortical connexions to the frontal lobe in the rhesus monkey. *Exp. Brain Res.* **29,** 299–322.
Kitao, Y., Nakamura, Y., Kudo, M., Moriizumi, T., and Tokuno, H. (1989). The cerebral and cerebellar connections of pretectothalamic and pretecto-olivary neurons in the anterior pretectal nucleus of the cat. *Brain Res.* **484,** 304–313.
Klimoff, J. (1899). Ueber die Leitungsbahnen des Kleinhirns. *Arch Anat. Physiol. Anat. Abt.* 11–27.
Kooy, F.H. (1916). The inferior olive in vertebrates. Thesis, Amsterdam.
Kooy, F.H. (1917). The inferior olive in vertebrates. *Folia Neurobiol.* **10,** 205–369.
Korneliussen, H.K. (1968). Comments on the cerebellum and its division. *Brain Res.* **8,** 229–236.

Kultas-Ilinsky, K., and Ilinsky, I.A. (1986). Neuronal and synaptic organization of the motor nuclei of mammalian thalamus. *Curr. Top. Res. Synapses* **3,** 77–145.

Künzle, H. (1975). Autoradiographic tracing of the cerebellar projection from the lateral reticular nucleus of the cat. *Exp. Brain Res.* **22,** 255-266.

Künzle, H. (1978). An autoradiographic analysis of the efferent connections from premotor and adjacent prefrontal regions (areas 6 and 9) in *Macaca fascicularis*. *Brain Behav. Evol.* **15,** 185–234.

Künzle, H., and Akert, K. (1977). Efferent connections of cortical area 8 (frontal eye field) in *Macaca fascicularis*. A reinvestigation using the autoradiographic technique. *J. Comp. Neurol.* **173,** 147–164.

Kuypers, H.G.J.M. (1958). Corticobulbar connections to the pons and lower brain stem in man. *Brain* **81,** 364–388.

Kuypers, H.G.J.M. (1987). Some aspects of the organization of the output of the motor cortex. *In:* "Motor Areas of the Cerebral Cortex," pp. 63–82. Ciba Foundation Symposium 132, Wiley, Chichester.

Kuypers, H.G.J.M., and Lawrence, D.G. (1967). Cortical projections to the red nucleus and the brain stem in the rhesus monkey. *Brain Res.* **4,** 151–188.

Ladpli, R., and Brodal, A. (1968). Experimental studies of commissural and reticular formation projections from the vestibular nuclei in the cat. *Brain Res.* **8,** 65–96.

Lang, W., Büttner-Ennever, J.A., and Büttner, U. (1979). Vestibular projections to the monkey thalamus: an autoradiographic study. *Brain Res.* **177,** 3–17.

Langelaan, J.W. (1919). On the development of the external form of the human cerebellum. *Brain* **42,** 130–170.

Langer, T.P. (1985). Basal interstitial nucleus of the cerebellum: cerebellar nucleus related to the flocculus. *J. Comp. Neurol.* **235,** 38–47.

Lapresle, J., and Ben Hamida, M. (1965). Correspondance somatotopique, secteur par secteur des dégénéresences de l'olive bulbaire consecutives à des lésions limitees du noyeau dentelé contra-lateral. *Revue Neurologique* **113,** 439–448.

Lapresle, J., and Ben Hamida, M. (1967). Contribution à la connaisssance de la voie dento-olivaire. Étude anatomique de deux cas de dégénérescence hypertrophique de l'olive bulbaire secondaire à un ramollissement limité de la calotte mésencéphalique. *Revue Neurologique* **117,** 574.

Lapresle, J., and Ben Hamida, M. (1968). Contribution à la connaissance de la voie dento-olivaire. Étude anatomique de deux cas de dégénérescence hypertrophique de l'olive bulbaire secondaire à un ramollissement limité de la calotte mésencéphalique. *Presse Med.* **76,** 1226–1230.

Larsell, O. (1952). The morphogenesis and adult pattern of the lobules and tissues of the cerebellum of the white rat. *J. Comp. Neurol.* **97,** 281–356.

Larsell, O. (1967). "The Comparative Anatomy and Histology of the Cerebellum from Myxinoids Through Birds," (J. Jansen, ed.), University of Minnesota Press, Minneapolis.

Larsell, O. (1970). "The comparative Anatomy and Histology of the Cerebellum from Monotremes Through Apes," (J. Jansen, ed.), University of Minnesota Press, Minneapolis.

Larsell, O., and Jansen, J. (l972). "The Comparative Anatomy and Histology of the Cerebellum. The Human Cerebellum, Cerebellar Connections, and the Cerebellar Cortex." University of Minnesota Press, Minneapolis.

Leclerc, N., Doré, L., Parent, A., and Hawkes, R. (1990). The compartmentalization of the monkey and rat cerebellar cortex: zebrin I and cytochrome oxidase. *Brain Res.* **506,** 70–78.

Leclerc, N., Schwarting, G.A., Herrup, K., Hawkes, R., and Yamamoto, M. (1992). Compartmentation in mammalian cerebellum: zebrin II and P-path antibodies define three classes of sagittally organized bands of Purkinje cells. *Proc. Natl. Acad. Sci. U.S.A.* **89,** 5006–5010.

Leergaard, T.B., Lakke, E.A., and Bjaalie, J.G. (1995). Topographical organization in the early postnatal corticopontine projection: carbocyanine dye and 3-D computer reconstruction study in the rat. *J. Comp. Neurol.* **361,** 77–94.

Legendre, A., and Courville, J. (1987). Origin and trajectory of the cerebello-olivary projection: an experimental study with radioactive and fluorescent tracers in the cat. *Neuroscience* **21,** 877–891.

Leichnetz, G.R., Spencer, R.F., and Smith, D.J. (1984a). Cortical projections to nuclei adjacent to the oculomotor complex in the medial dien-mesencephalic tegmentum in the monkey. *J. Comp. Neurol.* **228,** 359–387.

Leichnetz, G.R., Smith, D.J., and Spencer, R.F. (1984b). Cortical projections to the paramedian tegmental and basilar pons in the monkey. *J. Comp. Neurol.* **228**(3):388–408.

Leiner, H.C., Leiner, A.L., and Dow, R.S. (1986). Does the cerebellum contribute to mental skills. *Behav. Neurosci.* **100,** 443–454.

Linauts, M., and Martin, G.F. (1978). An autoradiographic study of midbrain-diencephalic projections to the inferior olivary nucleus in the opossum (Didelphis virginiana). *J. Comp. Neurol.* **179,** 325–354.

Loewenthal, N. (1885). Des dégénérations secondaires de la moelle épinière consecutives aux lésions experimentales medullaires et corticales. Thesis, Geneva.

Löwy, R. (1916). Ueber die Faseranatomie und Physiologie der Formatio vermicularis cerebelli. *Arb. Neurol. Inst. Wiener Univ.* **21,** 359–382.

Loyning, Y., and Jansen, J. (1955). A note on the morphology of the human cerebellum. *Acta Anat.* **25,** 309–318.

Lynch, J.C., Hoover, J.E., and Strick, P.L. (1994). Input to the primate frontal eye field from the substantia nigra, superior colliculus, and dentate nucleus demonstrated by transneuronal transport. *Exp. Brain Res.* **100,** 181–186.

Maat, G.J.R. (1978). Some aspects of the development of the cerebellar cortical layer in man. *Neurosci. Lett. Suppl* **1,** S150.

Maat, G.J.R. (1981). Histogenetic aspects of the cerebellar cortex in man. *Acta Morphol. Neerl. Scand.* **19,** 82–83.

Marani, E., and Voogd, J. (l977). An acetylcholinesterase band pattern in the molecular layer of the cat cerebellum. *J. Anat. London* **124,** 335–345.

Marchi, V., and Algeri, G. (1885). Sulle degenerazioni discendenti consecutive a lesioni sperimentale in diverse zone della corteccia cerebrale. *Riv. Sper. Freniatr. Med. Leg.* **11,** 492–494.

Martin, G.F., Henkel, C.K., and King, J.S. (1976). Cerebello-olivary fibers: their origin, course and distribution in the North American opossum. *Exp. Brain Res.* **24,** 219–236.

Martin, G.F., Culberson, J., Laxson, C., Linauts, M., and Panneton, M., and Tschismadia, I. (1980). Afferent connections of the inferior olivary nucleus with preliminary notes on their development: Studies using the North American Opossum. *In:* "The Inferior Olivary Nucleus: Anatomy and Physiology" (I. Courville, *et al.,* eds.), pp. 35–37. Raven Press, New York.

Matelli, M., and Luppino, G. (1996). Thalamic input to mesial and superior area 6 in the macaque monkey. *J. Comp. Neurol.* **372,** 59–87.

Matelli, M., Luppino, G., Fogassi, L., and Rizzolatti, G. (1989). Thalamic input to inferior area 6 and area 4 in the macaque monkey. *J. Comp. Neurol.* **280,** 468–488.

Matelli, M., Luppino, G., and Rizzolatti, G. (1991). Architecture of superior and mesial area 6 and of the adjacent cingulate cortex. *J. Comp. Neurol.* **311,** 445–462.

Matsushita, M., and Hosoya, Y. (1978). The location of spinal projection neurons in the cerebellar nuclei (cerebello-spinal tract neurons) of the cat. A study with the HRP technique. *Brain Res.* **142,** 237–248.

Matsushita, M., and Ikeda, M. (1987). Spinocerebellar projections from the cervical enlargement in the cat, as studied by anterograde transport of wheat germ agglutinin–horseradish peroxidase. *J. Comp. Neurol.* **263,** 223–240.

Matsushita, M., and Tanami, T. (1987). Spinocerebellar projections from the central cervical nucleus in the cat, as studied by anterograde transport of wheat germ agglutinin–horseradish peroxidase. *J. Comp. Neurol.* **266,** 376–397.

Matsushita, M., and Wang, C.L. (1987). Projection pattern of vestibulocerebellar fibers in the anterior vermis of the cat: an anterograde wheat germ agglutinin–horseradish peroxidase study. *Neurosci. Lett.* **74,** 25–30.

Matsushita, M., and Yaginuma, H. (1989). Spinocerebellar projections from spinal border cells in the cat as studied by anterograde transport of wheat germ agglutinin–horseradish peroxidase. *J. Comp. Neurol.* **288,** 19–38.

Matsushita, M., and Yaginuma, H. (1990). Afferents to the cerebellar nuclei from the cervical enlargement in the rat, as demonstrated with the *Phaseolus vulgaris* leucoagglutinin method. *Neurosci. Lett.* **113,** 253–259.

Matsushita, M., and Yaginuma, H. (1995). Projections from the central cervical nucleus to the cerebellar nuclei in the rat, studied by anterograde axonal tracing. *J. Comp. Neurol.* **353,** 234–246.

Matsushita, M., Tanami, T., and Yaginuma, H. (1984). Differential distribution of spinocerebellar fiber terminals within the lobules of the cerebellar anterior lobe in the cat: an anterograde WGA-HRP study. *Brain Res.* **305,** 157–161.

Matsushita, M., Ikeda, M., and Tanami, T. (1985). The vermal projection of spinocerebellar tracts arising from lower cervical segments in the cat: an anterograde WGA-HRP study. *Brain Res.* **360,** 389–393.

May, P.J., Hartwich-Young, R., Nelson, J., Sparks, D.L., and Porter, J.D. (1990). Cerebellotectal pathways in the macaque: implications for collicular generation of saccades. *Neuroscience* **36,** 305–324.

Mehler, W.R., and Nauta, W.J.H. (1974). Connections of the basal ganglia and of the cerebellum. *Confin. Neurol.* **36,** 205–222.

Mehler, W.R., Feferman M.E., and Nauta W.J.H. (1960). Ascending axon degeneration following anterolateral cordotomy. An experimental study in the monkey. *Brain* **83,** 718–751.

Meynert, T. (1872). Stricker's Handbuch der Lehre vom Geweben des Menschen und der Thiere. *In:* "Vom Gehirne der Saugethiere,". pp. 694–808. Leipzig.

Miale, I.L., and Sidman, R.L. (1961). An autoradiographic analysis of histogenesis in mouse cerebellum. *Exp. Neurol.* **4,** 277–296.

Middleton, F.A., and Strick, P.L. (1997). Cerebellar output channels. *Int. Rev. Neurobiol.* **41,** 61–82.

Middleton, F.A.,and Strick, P.L.(2001). Cerebellar projections to the prefrontal cortex of the primate. *J. Neurosci.* **21,** 700–712.

Mihailoff, G.A. (1994). Identification of pontocerebellar axon collateral synaptic boutons in the rat cerebellar nuclei. *Brain Res.* **648,** 313–318.

Mishkin, M., and Ungerleider, L.G. (1982). Contribution of striate inputs to the visuospatial functions of parieto-preoccipital cortex in monkeys. *Behav. Brain Res.* **6,** 57–77.

Miyashita, E., and Tamai, Y. (1989). Subcortical connections of frontal 'oculomotor' areas in the cat. *Brain Res.* **502,** 75–87.

Mugnaini, E., and Oertel, W.H. (1981). Distribution of decarboxylase positive neurons in the rat cerebellar nuclei. *Soc. Neurosci. Abstr.* **7,** 122.

Mugnaini, E., and Oertel, W.H. (1985). GABAergic neurons and terminals in the rat CNS as revealed by GAD immunohistochemistry. *In:* "GABA and Neuropeptides in the CNS: The Handbook of Chemical Neuroanatomy," Vol. 4, Part 1 (A. Bjorklund and T. Hokfelt, eds.), pp. 541–543. Amsterdam, Elsevier.

Münzer, E., and Wiener, H. (1902). Das Zwischen- und Mittelhirn des Kaninchens und die Beziehungen dieser Teile zum ubrigen Centralnervensystem, mit besondere Berücksichtigung der Pyramidenbahn und Schleife. *Mschr. Psychiat. Neurol.* **12,** 241–279.

Nagao, S., Kitamura, T., Nakamura, N., Hiramatsu, T., and Yamada, J. (1997). Differences of the primate flocculus and ventral paraflocculus in the mossy and climbing fiber input organization. *J. Comp. Neurol.* **382,** 480–498.

Nakano, K., Tokushige, A., Kohno, M., Hasegawa, Y., Kayahara, T., and Sasaki, K. (1992). An autoradiographic study of cortical projections from motor thalamic nuclei in the macaque monkey. *Neurosci. Res.* **13,** 119–137.

Nauta, W.J.H., and Gygax, P.A. (1954). Silver impregnation of degenerating axons in the c.n.s.: a modified technic. *Stain. Technol.* **29,** 91–93.

Nelson, B.J., and Mugnaini, E. (1989). Origins of GABAergic inputs to the inferior olive. *In:* "The Olivocerebellar System in Motor Control." (P. Strata, ed.), pp. 86–107. Springer-Verlag, Berlin.

Noda, H., Sugita, S., and Ikeda, Y.(1990). Afferent and efferent connections of the oculomotor region of the fastigial nucleus in the macaque monkey. *J. Comp. Neurol.* **302,** 330–348.

Nyby, O., and Jansen, J. (1951). An experimental investigation of the corticopontine projection in Macaca mulatta. *Skr. Norske Vidensk. Akad. I. Mat. Nat. Kl.* **3,** 1–47.

Oberdick, J., Baader, S.L., and Schilling, K.. (1998) From zebra stripes to postal zones: deciphering patterns of gene expression in the cerebellum. *Trends Neurosci.* **21,** 383–390.

Ogawa, T. (1935). Beitrage zur vergleichenden Anatomie des Zentralnervensystems der Wassersauge tiere: Ueber die Kleinhirnkerne der Pinnepedien und Cetaceen. *Arb. Anat. Inst. Sendai* **17,** 63–136.

Ogawa, T. (1939). The tractus tegmenti medialis and its connection with the inferior olive in the cat. *J. Comp. Neurol.* **70,** 181–190.

Ohkawa, K. (1957). Comparative anatomical studies of cerebellar nuclei of mammals. *Arch. Hist. Jpn.* **13,** 21–58.

Oka, H. (1988). Functional organization of the parvocellular red nucleus in the cat. *Behav. Brain Res.* **28,** 233–240.

Oka, H., Jinnai, K., and Yamamoto T. (1979). The parieto-rubro-olivary pathway in the cat. *Exp. Brain Res.* **37,** 115–125.

Olszewski, J. (1952). "The Thalamus of *Macaca mulatta*." Karger, Basel.

Olszewski, J., and Baxter, J. (1954). "Cytoarchitecture of the Human Brain Stem." Karger, Basel.

Ono, M., and Kato, H. (1938). Zur Kenntnis von den Kleinhirnkernen des Kaninchens. *Anat. Anz.* **86,** 245–259.

Onodera, S. (1984). Olivary projections from the mesodiencephalic structures in the cat studied by means of axonal transport of horseradish peroxidase and tritiated aminoacids. *J. Comp. Neurol.* **227,** 37–49.

Oriolo, P.J., and Strick, P.L. (1989). Cerebellar connections with the motor cortex and the arcuate premotor area: an analysis employing retrograde transneuronal transport of WGA-HRP. *J. Comp. Neurol.* **268,** 612–626.

Oscarsson, O. (1969). The sagittal organization of the cerebellar anterior lobe as revealed by the projection patterns of the climbing fiber system. *In:* "Neurobiology of Cerebellar Evolution and Development." (R. Llinas, ed.), pp. 525–537. AMA/ERF, Chicago.

Oscarsson, O. (1973). Functional organization of spinocerebellar paths. *In:* "Handbook of Sensory Physiology, Vol. 2, Somatosensory Systems." (A. Iggo, ed.), pp. 339–380. Springer-Verlag, Berlin.

Oscarsson, O. (1980). Functional organization of olivary projection to the cerebellar anterior lobe. *In:* "The inferior Olivary Nucleus:

Anatomy and Physiology," (J. Courville, C. de Montigny, and Y. Lamarre, eds.), pp. 279–289. Raven Press, New York.
Ozol, K., Hayden, J.M., Oberdick, J., and Hawkes, R. (1999). Transverse zones in the vermis of mouse cerebellum. *J. Comp. Neurol.* **412,** 95–111.
Papez, W., and Stotler, W.A. (1940). Connections of the red nucleus. *Arch Neurol. Psychiat.* **44,** 776–791.
Parenti R., Cicirata, F., Panto, M.R., and Serapide, M.F. (1996). The projections of the lateral reticular nucleus to the deep cerebellar nuclei. An experimental analysis in the rat. *Eur. J. Neurosci.* **8,** 2157–2167.
Paxinos, G., and Huang, X.F. (1995). "Atlas of the Human Brainstem." Academic Press, San Diego.
Percheron, G., François, C., Talbi, B., Yelnik, J., and Fénelon, G. (1996). The primate motor thalamus. *Brain Res. Rev.* **22,** 93–181.
Petras, J.M. (1977). Spinocerebellar neurons in the rhesus monkey. *Brain Res.* **130,** 146–151.
Petras, J.M., and Cummings, J.F. (1977). The origin of spinocerebellar pathways. II. The nucleus centro-basalis of the cervical enlargement and the nucleus dorsalis of the thoracolumbar spinal cord. *J. Comp. Neurol.* **173,** 693–716.
Pittman, T., and Tolbert, D.L. (1988). Organization of transient projections from the primary somatosensory cortex to the cerebellar nuclei in kittens. *Anat. Embryol. (Berlin).* **178,** 441–447.
Plioplys, A.V., Thibault, J., and Hawkes R. (1985). Selective staining of a subset of Purkinje cells in the human cerebellum with monoclonal antibody mabQ113. *J. Neurol. Sci.* **70,** 245–256.
Poirier, L.J., and Bouvier, G. (1966). The red nucleus and its efferent nervous pathways in the monkey. *J. Comp. Neurol.* **128,** 223–244.
Pong, M., Horn, K.M., and Gibson, A. (2002). Spinal projections to cat parvicellular red nucleus. *J. Neurophysiol.* **87,** 453–468.
Probst, M. (1901). Zur Kenntniss des Binderams, der Haubenstrahlung und des Regio Subthalamica. *Mschr. Psychiat. Neurol.* **10,** 288–309.
Probst, M. (1902). Zur Anatomie und Physiologie des Kleinhirns. *Arch. Psychiat.* **35,** 692–777.
Qvist, H. (1989). The cerebellar nuclear afferent and efferent connections with the lateral reticular nucleus in the cat as studied with retrograde transport of WGA-HRP. *Anat. Embryol. (Berlin).* **179,** 471–483.
Qvist, H. (1989). Demonstration of axonal branching of fibres from certain precerebellar nuclei to the cerebellar cortex and nuclei: a retrograde fluorescent double-labelling study in the cat. *Exp. Brain Res.* **75,** 15–27.
Ramon, Y., and Cajal, S. (1909). "Histologie du système nerveux." Maloine, Paris.
Rosina, A., and Provini, L. (1982). Longitudinal and topographical organization of the olivary projection to the cat ansiform lobule. *Neuroscience* **7,** 2657–2676.
Rosina, A., and Provini, L. (1984). Pontocerebellar system linking the two hemispheres by intracerebellar branching *Brain Res.* **296,** 365–369.
Rouiller, E.M., Liang, F., Balban, A., Moret, V., and Wiesendanger, M. (1994). Cerebellothalamocortical and pallidothalamocortical projections to the primary and supplementary motor cortical areas: a multiple tracing study in macaque monkeys. *J. Comp. Neurol.* **345,** 185–213.
Rouiller, E.M., Tanne, J., Moretm, V., and Boussaoudm, D. (1999). Origin of thalamic inputs to the primary, premotor, and supplementary motor cortical areas and to area 46 in macaque monkeys: a multiple retrograde tracing study. *J. Comp. Neurol.* **409,** 131–152.
Ruigrok, T.J., and Cella, F. (1995). Precerebellar nuclei and red nucleus. *In:* "The Rat Nervous System," 2nd ed. (G. Paxinos, ed.), pp. 277–308. Academic Press, San Diego.
Ruigrok, T.J., and Voogd, J. (1990). Cerebellar nucleo-olivary projections in the rat: an anterograde tracing study with *Phaseolus vulgaris*-leucoagglutinin (PHA-L). *J. Comp. Neurol.* **298,** 315–333.
Ruigrok, T.J., and Voogd, J. (1995). Cerebellar influence on olivary excitability in the cat. *Eur. J. Neurosci.* **7,** 679–693.
Ruigrok, T.J., and Voogd, J. (2000). Organization of projections from the inferior olive to the cerebellar nuclei in the rat. *J. Comp. Neurol.* **426,** 209–228.
Ruigrok, T.J., de Zeeuw, C.I., and Voogd, J. (1990). Hypertrophy of inferior olivary neurons: a degenerative, regenerative or plasticity phenomenon. *Eur. J. Morphol.* **28,** 224–239.
Ruigrok, T.J., Osse, R.J., and Voogd, J. (1992). Organization of inferior olivary projections to the flocculus and ventral paraflocculus of the rat cerebellum. *J. Comp. Neurol.* **316,** 129–150.
Ruigrok, T.J., Cella, F., and Voogd, J. (1995). Connections of the lateral reticular nucleus to the lateral vestibular nucleus in the rat. An anterograde tracing study with *Phaseolus vulgaris* leucoagglutinin. *Eur. J. Neurosci.* **7,** 1410–1413.
Russchen, F.T., Groenewegen, H.J., and Voogd, J. (1976). Reticulocerebellar fibers in the cat. An autoradiographic study. *Acta Morphol. Neerl. Scand.* **14,** 245–246.
Rutherford, J.G., Zulk-Harber, A., and Gwyn, D.G. (1989). A comparison of the distribution of the cerebellar and cortical connections of nucleus of Darkschewitsch (D) in the cat: a study using antegrade and retrograde HRP tracing techniques. *Anat. Emryol. (Berlin)* **180,** 585–496.
Saint-Cyr, J.A. (1983). The projection from the motor cortex to the inferior olive in the cat. *Neuroscience* **10,** 667–684.
Saint-Cyr, J.A. (1987). Anatomical organization of cortico-mesencephalo-olivary pathways in the cat as demonstrated by axonal transport techniques. *J. Comp. Neurol.* **257,** 39–59.
Saint-Cyr, J.A., and Courville, J. (1980). Projections from the motor cortex, mid-brain and vestibular nuclei to the inferior olive in the cat. Anatomical organization and functional correlates. *In:* "The inferior olivary Nucleus," (J. Courville, C de Montigny, and Y. Lamarre, eds.), pp. 97–124.
Saint-Cyr, J.A., and Courville, J. (1981). Sources of descending afferents to the inferior olive from the upper brain stem in the cat as revealed by the retrograde transport of horseradish peroxidase. *J. Comp. Neurol.* **198,** 567–581.
Saint-Cyr, J.A., and Courville, J. (1982). Descending projections to the inferior olive from the mesencephalon and superior colliculus in the cat. *Exp. Brain Res.* **45,** 333–348.
Sakai, S.T., Inase, M., and Tanji, J. (1996). Comparison of cerebellothalamic and pallidothalamic projections in the monkey *(Macaca fuscata):* a double anterograde labeling study. *J. Comp. Neurol.* **368,** 215–28.
Sakai, S.T., Inase, M., and Tanji, J. (1999). Pallidal and cerebellar inputs to thalamocortical neurons projecting to the supplementary motor area in *Macaca fuscata:* a triple-labeling light microscopic study. *Anat. Embryol. (Berlin).* **199,** 9–19.
Sakai, S.T., Stepniewska, I., Qi, H.X., and Kaas, J.H. (2000). Pallidal and cerebellar afferents to pre-supplementary motor area. Thalamocortical neurons in the owl monkey. A multiple labeling study. *J. Comp. Neurol.* **417,** 164–180.
Sanctis, De S. (1898). Untersuchungen uber den Bau der Markscheidenentwicklung des menschlichen Kleinhirns. *Mschr. Psychiat. Neurol.* **4,** 237–246.
Sanctis, De S. (1902/03). Richerche interno alle mielinizzazione del cerveletto umano. *Rich. Lab. Anat. Roma* **15,** 345–373.
Sasaki, K., Kawaguchi, S., Oka, H., Sakai, M., and Mizuno, N. (1976). Electrophysiological studies on the cerebellocerebral projections in monkeys. *Exp. Brain Res.* **24,** 495–507.

Sato, H., and Noda, H. (1991). Divergent axon collaterals from fastigial oculomotor region in mesodiencephalic junction and paramedian pontine reticular formation in macaques. *Neurosci. Res.* **11,** 41–45.

Schell, and G., and Strick, P.L. (1984). The origin of thalamic inputs to the arcuate premotor and supplementary motor areas. *J. Neurosci.* **4,** 539–560.

Schild, R.F. (1970). On the inferior olive of the albino rat. *J. Comp. Neurol.* **140,** 255–260.

Schmahmann, D.J.(1997). The cerebellum and cognition. *Int. Rev. Neurobiol.* Vol. **41,** 31–60.

Schmahmann, J.D., and Pandya, D.N. (1989). Anatomical investigation of projections to the basis pontis from posterior parietal association cortices in rhesus monkey. *J. Comp. Neurol.* **289,** 53–73.

Schmahmann, J.D., and Pandya, D.N. (1990). Anatomical investigation of projections from thalamus to posterior parietal cortex in the rhesus monkey: a WGA-HRP and fluorescent tracer study. *J. Comp. Neurol.* **295,** 299–326.

Schmahmann, J.D., and Pandya, D.N. (1993). Prelunate, occipitotemporal, and parahippocampal projections to the basis pontis in rhesus monkey. *J. Comp. Neurol.* **337,** 94–112.

Schmahmann, J.D., and Pandya, D.N. (1995). Prefrontal cortex projections to the basilar pons in rhesus monkey: implications for the cerebellar contribution to higher function. *Neurosci. Lett.* **199,** 175–178.

Schmahmann, J.D., and Pandya, D.N. (1997a). Anatomic organization of the basilar pontine projections from prefrontal cortices in rhesus monkey. *J. Neurosci.* **17,** 438–458.

Schmahmann, J.D., and Pandya, D.N. (1997b). The cerebrocerebellar system. *Int. Rev. Neurobiol.* **41,** 31–60.

Schmahmann, J.D., Nitsch, R.M., and Pandya, D.N. (1992). The mysterious relocation of the bundle of *Türck. Brain* **115,** 1911–1924.

Schmahmann, J.D., Doyon, J., McDonald, D., Holmes, C., Lavoie, K., Hurwitz, A.S., Kabani, N., Toga, A., Evans, A., and Petrides, M. (1999). Three dimensional MRI atlas of the human cerebellum in proportional stereotaxic space. *Neuroimage* **10,** 233–260.

Schmahmann, J.D., Doyon, J., Toga, A.W., Petrides, M., and Evans, A.C. (2000). "MRI Atlas of the Human Cerebellum." Academic Press, San Diego.

Schoen, J.H.R. (1964). Comparative aspects of the descending fibre systems in the spinal cord. *In:* "Progress in Brain Research," Vol. 11 (Eccles and Schade, eds.), pp. 203–222.

Schoen, J.H.R. (1969). The corticofugal projection on the brain stem and spinal cord in man. *Psychiat. Neurol. Neurochir.* **72,** 121–128.

Schoen, J.H.R. (1977). The olivary circuit of Guillain and Mollaret and olivary hypertrophy in man. *Exc. Med. Int. Congress Series* **427,** 183.

Scott, T.G. (1964). A unique pattern of localization within the cerebellum of the mouse. *J. Comp. Neurol.* **122,** 1–8.

Sekiya, H., and Kawamura, K. (1985). An HRP study in the monkey of olivary projections from the mesodiencephalic structures with particular reference to pretecto-olivary neurons. *Arch. Ital. Biol.* **123,** 171–183.

Serapide, M.F., Cicirata, F., Sotelo, C., Panto, M.R., and Parenti, R. (1994). The pontocerebellar projection: longitudinal zonal distribution of fibers from discrete regions of the pontine nuclei to vermal and parafloccular cortices in the rat. *Brain Res.* **644,** 175–180.

Serapide, M.F., Panto, M.R., Parenti, R., Zappala, A., and Cicirata, F. (2001). Multiple zonal projections of the basilar pontine nuclei to the cerebellar cortex of the rat. *J. Comp. Neurol.* **430,** 471–484.

Shinoda, Y., Futami, T., Mitoma, H., and Yokota, J. (1988). Morphology of single neurones in the cerebello-rubrospinal system. *Behav. Brain Res.* **28,** 59–64.

Shinoda, Y., Sugiuchi, Y., Futami, T., and Izawa, R. (1992). Axon collaterals of mossy fibers from the pontine nucleus in the cerebellar dentate nucleus. *J. Neurophysiol.* **67,** 547–560.

Shook, B.L., Schlag-Rey, M., and Schlag, J. (1990). Primate supplementary eye field: I. Comparative aspects of mesencephalic and pontine connections. *J. Comp. Neurol.* **301,** 618–642.

Simpson, J.I. (1984). The accessory optic system. *Annu. Rev. Neurosci.* **7,** 13–41.

Simpson, J.I., Leonard, C.S., and Soodak, R.E. (1988). The accessory optic system of rabbit. II. Spatial organization of direction selectively. *J. Neurophysiol.* **60,** 2055–2072.

Snider, R.S. (1940). Morphology of the cerebellar nuclei in the rabbit and cat. *J. Comp. Neurol.* **72,** 399–415.

Snyder, R.L., Faull, R.L.M., and Mehler, W.R. (1987). A comparative study of the neurons of origin of the spnocerebellar afferents in the rat, cat and squirrel monkey based on retrograde trnsport of horseradish peroxidase. *J. Comp. Neurol.* **181,** 833–852.

Sotelo, C., and Wassef, M. (1991). Cerebellar development: afferent organization and Purkinje cell heterogeneity. *Philos. Trans. R. So.c Lond. B. Biol. Sci.* **331**(1261), 307–313.

Spitzer, A., and Karplus, J.P. (1907). Ueber experimentelle Läsionen an der Gehirnbasis. *Arb. Neurol. Inst. Wiener Univ.* **16,** 348–436.

Stanton, G.B. (1980). Topographical organization of ascending cerebellar projections from the dentate and interposed nuclei in *Macaca mulatta:* an anterograde degeneration study. *J. Comp. Neurol.* **190,** 699–731.

Stanton, G.B. (1980). Afferents from oculomotor nuclei from area "y" in *Macaca mulatta:* an anterograde degeneration study. J. *Comp. Neurol.* **192,** 377–385.

Stanton, G.B., Goldberg, M.E., and Bruce, C.J. (1988). Frontal eye field efferents in the macaque monkey: II. Topography of terminal fields in midbrain and pons. *J. Comp. Neurol.* **271,** 493–506.

Steiger, H.J., and Büttner-Ennever, J.A. (1979). Oculomotor nucleus afferents in the monkey demonstrated with horseradish peroxidase. *Brain Res.* **160,** 1–15.

Stepniewska, I., Preuss, T.M., and Kaas, J.H. (1994). Thalamic connections of the primary motor cortex (M1) of owl monkeys. *J. Comp. Neurol.* **349,** 558–582.

Stilling, B. (1846). "Untersuchungen über den Bau und die Verrichtungen des Gehirns. I. Uber den Bau des Hirnknotens oder Varoli' schen Brucke." Jena.

Stilling, B. (1864). "Untersuchungen über den Bau des kleinen Gehirns des Menschen." Kassel.

Strominger, N.L., Truscott, C., Miller, R.A., and Royce, G.J. (1979). An autoradiographic study of the rubroolivary tract in the rhesus monkey. *J. Comp. Neurol.* **83,** 33–46.

Sugihara, I., and Shinoda, Y. (1999). Morphology of single olivocerebellar axons labeled with biotinylated dextran amine in the rat. *J. Comp. Neurol.* **414,** 131–148.

Sugimoto, T., Mizuno, N., and Itoh, K. (1981). An autoradiographic study on the terminal distribution of cerebellothalamic fibers in the cat. *Brain Res.* **215,** 29–47.

Sultan, F., and Braitenberg, V. (1993). Shapes and sizes of different mammalian cerebella. A study of quantitative comparative anatomy. *J. Hirnforsch.* **34,** 79-92.

Sunderland, S. (1940). The projection of the cerebral cortex on pons and cerebellum in the macaque monkey. *J. Anat. London* **74,** 201–226.

Swenson, R.S., and Castro, A.J. (1983a). The afferent connections of the inferior olivary complex in rat: A study using the retrograde transport of horseradish peroxidase. *Am. J. Anat.* **166,** 329–341.

Swenson, R.S., and Castro, A.J. (1983b). The afferent connections of the inferior olivary complex in rats. An anterograde study using autoradiographic and axonal degeneration techniques. *Neuroscience* **8,** 259–275.

Szentagothai, J., and Rajkovits, K. (1959). The origin of the climbing fibres of the cerebellum. *Anat. Entw. Gesch.* **121,** 130–141.

Tagliavini, F., and Pietrini, V. (1984). On the variability of the human flocculus and paraflocculus accessorius. *J. Hirnforsch.* **25,** 163–170.

Tan, J., Simpson, J.I., and Voogd, J. (1995a). Anatomical compartments in the white matter of the rabbit flocculus. *J. Comp. Neurol.* **356,** 1–22.

Tan, J., Gerrits, N.M., Nanhoe, R., and Simpson, J.I., and Voogd, J. (1995b). Zonal organization of the climbing fiber projection to the flocculus and nodulus of the rabbit: a combined axonal tracing and acetylcholinesterase histochemical study. *J. Comp. Neurol.* **356,** 23–50.

Tan, J., Epema, A.H., and Voogd, J. (1995c). Zonal organization of the flocculovestibular nucleus projection in the rabbit: a combined axonal tracing and acetylcholinesterase histochemical study. *J. Comp. Neurol.* **356,** 51–71.

Teune, T.M. (1999). Anatomy of cerebellar nuclear-bulbar projections in the rat. Thesis, Rotterdam.

Teune, T.M., van der Burg, J., van der Moer, J., Voogd, J., and Ruigrok, T.J. (2000). Topography of cerebellar nuclear projections to the brain stem in the rat. *Prog. Brain Res.* **124,** 141–172.

Thiele, F., and Horsley, V. (1901). A study of degenerations observed in the central nervous system in a case of fracture dislocation of the spine. *Brain* **24,** 519–531.

Thomas, A. (1897). "Le Cervelet." Steinheil, Paris.

Tokuno, H., Takada, M., Nambu, A., and Inase, M. (1995). Somatotopical projections from the supplementary motor area to the red nucleus in the macaque monkey. *Exp. Brain Res.* **106,** 351–355.

Tolbert, D.L. (1989). Somatotopically organized transient projections from the primary somatosensory cortex to the cerebellar cortex. *Dev. Brain Res.* **45,** 113–127.

Tolbert, D.L., and Gutting J.C. (1997). Quantitative analysis of cuneocerebellar projections in rats: differential topography in the anterior and posterior lobes. *Neuroscience* **80,** 359–371.

Tolbert, D.L., Massopust, L.C., Murphy, M.G., and Young P.A. (1976). The anatomical organization of cerebello-olivary projection in the cat. *J. Comp. Neurol.* **170,** 525–544.

Tolbert, D.L., Bantli, H., and Bloedel, J.R. (1978). Multiple branching of cerebellar efferent projections in cats. *Exp. Brain Res.,* **31,** 305–316.

Tolbert, D.L., Alisky, J.M., and Clark, B.R. (1993). Lower thoracic upper lumbar spinocerebellar projections in rats: a complex topography revealed in computer reconstructions of the unfolded anterior lobe. *Neuroscience* **55,** 755–774.

Trelles, J.O. (1935). "Les ramollissements protuberantiels." These Medicine, Paris.

Trott, J.R., and Armstrong, D.M. (1987a). The cerebellar corticonuclear projection from lobule Vb/c of the cat anterior lobe: a combined electrophysiological and autoradiographic study. I. Projections from the intermediate region. *Exp. Brain Res.* **66,** 318–338.

Trott, J.R., and Armstrong D.M. (1987b). The cerebellar corticonuclear projection from lobule Vb/c of the cat anterior lobe: a combined electrophysiological and autoradiographic study. II. Projections from the vermis. *Exp. Brain Res.* **68**(2), 339–354.

Trott, J.R., Apps, R., and Armstrong, D.M. (1998a). Zonal organization of cortico-nuclear and nucleo-cortical projections of the paramedian lobule of the cat cerebellum. 1. The C1 zone. *Exp. Brain Res.* **118,** 298–315.

Trott, J.R., Apps, R., and Armstrong D.M. (1998b). Zonal organization of cortico-nuclear and nucleo-cortical projections of the paramedian lobule of the cat cerebellum. 2. The C2 zone. *Exp. Brain Res.* **118,** 316–330.

Türck, L. (1851). Ueber secundare Erkrankung einzelnen Rückenmarksstrange und ihren Fortsetzungen zum Gehirne. *Sitzungsberichte Math. Nat. Classe Akad. Wissenschaften* **6,** 288–312.

Ugolini, G., and Kuypers, H.G.J.M. (1986). Collaterals of corticospinal and pyramidal fibres to the pontine grey demonstrated by a new application of the fluorescent fibre labelling technique. *Brain Res.* **365,** 211–227.

Van der Want, J.J.L., and Voogd, J. (1987). Ultrastructural identification and localization of climbing fiber terminals in the fastigial nucleus of the cat. *J. Comp. Neurol.* **25,** 81–90.

Van der Want, J.J., Wiklund, L., Guegan, M,. Ruigrok, T., and Voogd, J. (1989). Anterograde tracing of the rat olivocerebellar system with *Phaseolus vulgaris* leucoagglutinin (PHA-L). Demonstration of climbing fiber collateral innervation of the cerebellar nuclei. *J. Comp. Neurol.* **288,** 1–18.

Van Kan, P.L.E., Houk, J.C., and Gibson, A.R. (1993). Output organization of intermediate cerebellum of the monkey. *J. Neurophysiol.* **69,** 57–73.

Vejas, P. (1885). Experimentelle Beitrage zur Kenntnis der Verbindungsbahnen des Kleinhirns und das Verlauf der Fun. gracilis und cuneatus. *Arch. Psychiat.* **16,** 200–214.

Verhaart, W.J.C. (1949). The central tegmental tract. *J. Comp. Neurol.* **90,** 173–190.

Verhaart, W.J.C. (1956a). The fibre structure of the central tegmental tract in man, pongo, hylobates and macaca. *Acta Anatomica* **26,** 293–302.

Verhaart, W.J.C. (1956b). The fibrecontent of the superior cerebellar peduncle in the pons and the mesencephalon. *Acta Morphol. Neerl.-Scand.* **1,** 2–8.

Verhaart, W.J.C., and Sie, P.G. (1958). The fasciculus centralis tegmenti and the reticular formation fibre systems. *Acta Anat.* **33,** 257–272.

Verhaart, W.J.C., and Voogd, J. (1962). Hypertrophy of the inferior olives in the cat. *J. Neuropathol. Exp. Neurol.* **21,** 92–103.

Vogt, C. (1909). La myéloarchitecture du thalamus du cercopithèque. *J. Psychol. Neurol.* **12,** 285–324.

Vogt, H., and Astwazaturow, M. (1912). Ueber angeborene Kleinhirnerkrankungen mit Beitragen zur Entwicklungsgeschichte des Kleinhirns. *Arch. Psychiat.* **49,** 75–203.

Voogd, J. (1964). The cerebellum of the cat. Structure and fiber connections. Thesis, Van Gorcum, Assen.

Voogd, J. (1967). Comparative aspects of the structure and fibre connections of the mammalian cerebellum. *Prog. Brain Res.* **25,** 94–134.

Voogd, J. (1969). The importance of fiber connections in the comparative anatomy of the mammalian cerebellum. *In:* "Neurobiology of Cerebellar Evolution and Development," (R. Llinas, ed.), pp. 493–514. AMA-ERF Institute for Biomedical Research, Chicago.

Voogd, J. (1975). Bolk's subdivision of the mammalian cerebellum. Growth centres and functional zones. *Acta Morphol. Neerl. Scand.* **13,** 35–54.

Voogd, J. (1982). The olivocerebellar projection in the cat. *In* "The Cerebellum New Vistas." (S.T. Palay and V. Chan-Palay, (eds.), pp. 134–160. Springer-Verlag, Berlin.

Voogd, J. (1995). Cerebellum. In: "The Rat Nervous System," 2nd ed. (G. Paxinos, ed.), pp. 309–350. Academic Press, San Diego.

Voogd, J. (1998). Mammals. *In:* "The Central Nervous System of Vertebrates," Vol. 3 (R. Nieuwenhuys, H.J. ten Donkelaar, and C. Nicholson, eds.), pp. 1637–1844. Springer-Verlag, Berlin.

Voogd, J., and Bigaré, F. (1980). Topographical distribution of olivary and cortico-nuclear fibers in the cerebellum: a review. *In:* "The Olivary Nucleus. Anatomy and Physiology" (J. Courville *et al.,* eds.), pp. 207–234. Raven Press, New York.

Voogd, J., and Gerrits, N.M. (1997). Complementary distribution of acetylcholinesterase and calbindin-28K in the white matter of the primate cerebellum. *Neurosci. Abstr.,* **23,** 2365.

Voogd, J., and Glickstein, M. (1998). The anatomy of the cerebellum. *Trends Neurosci.* **21,** 370–375.

Voogd, J., and Ruigrok, T.J. (1997). Transverse and longitudinal patterns in the mammalian cerebellum. *Prog. Brain Res.* **114,** 21–37.

Voogd, J., Gerrits, N.M., and Hess, D.T. (1987a). Parasagittal zonation of the cerebellum in macaques: an analysis based on acetylcholinesterase histochemistry. *In:* "Cerebellum and Neuronal Plasticity." (M. Glickstein, Chr. Yeo, and J. Stein, eds.), pp. 15–39. Plenum Press, New York.

Voogd, J., Hess, D.T., and Marani, E. (1987b). The parasagittal zonation of the cerebellar cortex in cat and monkey. Topography, distribution of acetylcholinesterase and development. *In:* "New Concepts in Cerebellar Neurobiology" (J.S. King, and J. Courville, eds.), Alan Liss, New York.

Voogd, J., Feirabend, H.K.P., and Schoen, J.H.R. (1990). Cerebellum and precerebellar nuclei. *In:* "The Human Nervous System" (G. Paxinos, ed.), pp. 321–386. Academic Press, San Diego.

Voogd, J., Epema, A.H., and Rubertone, J.A. (1991). Cerebello-vestibular connections of the anterior vermis. A retrograde tracer study in different mammals including primates. *Arch. Ital. Biol.* **129,** 3–19.

Voogd, J., Gerrits, N.M., and Ruigrok, T.J. (1996a). Organization of the vestibulocerebellum. *Ann. N. Y. Acad. Sci.* **781,** 553–579.

Voogd, J., Jaarsma, D., and Marani, E. (1996b). The cerebellum, chemoarchitecture, and anatomy. I*n:* "Handbook of Chemical Neuroanatomy, Vol.12, Integrated Systems of the CNS, Part III, Cerebellum, Basal Ganglia, Olfactory System." (L.W. Swanson, A. Björklund, and T. Hökfelt, eds.), pp 1–369. Elsevier, Amsterdam.

Walberg, F. (1952). The lateral reticular nucleus of the medulla oblongata in mammals. *J. Comp. Neurol.* **96,** 283–342.

Walberg, F., and Nordby, T. (1981). A re-examination of the rubro-olivary tract in the cat, using horseradish peroxidase as a retrograde and an anterograde neuronal tracer. N*euroscience* **6,** 2379–2391.

Walberg, F., and Pompeiano, O. (1960). Fastigial fibers to the reticular nucleus. An experimental study in the cat. *Exp. Neurol.* **2,** 40–53.

Wallenberg, A. (1905). Sekundäre Bahnen aud dem frontalen sensiblen Trigeminuskerne des Kaninchens. *Anat. Anz.* **26,** 145–155.

Wannier, T., Kakei, S., and Shinoda, Y. (1992). Two modes of cerebellar input to the parietal cortex in the cat. *Exp. Brain Res.* **90,** 241–252.

Weidenreich, F. (1899). Zur Anatomie der zentralen Kleinhirnkerne der Säuger. Z. *Morphol. Anthropol.* **1,** 259–312.

Wells, G.R., Hardiman, M.J., and Yeo, C.H. (1989). Visual projections to the pontine nuclei in the rabbit: orthograde andretrograde tracing studies with WGA-HRP. *J Comp. Neurol.* **279,** 629–652.

Welsh, J.P., Chang, B., Menaker, M.E., and Aicher, A. (1997). Removal of the inferior olive abolishes myoclonic seizures associated with a loss of olivary serotonin. *Neuroscience* **82,** 876–897.

Whitworth, R.H., Jr., and Haines, D.E. (1983). The inferior olive of a prosimian primate Galago senegalensis. I. Conformation and spino-olivary projections. *J. Comp. Neurol.* **219,** 215–227.

Whitworth, R.H., Jr., and Haines, D.E. (1986a). The inferior olive of *Saimiri sciurus:* olivocerebellar projections to the anterior lobe. *Brain Res.* **372,** 55–72.

Whitworth, R.H., Jr, and Haines, D.E. (1986b). On the question of nomenclature of homologous subdivisions of the inferior olivary complex. *Arch. Ital. Biol.* **124,** 271–317.

Wiesendanger, R., and Wiesendanger, M. (1985a). The thalamic connections with medial area 6 (supplementary motor cortex) in the moneky *(Macaca fascicularis). Exp. Brain Res.* **59,** 91–104.

Wiesendanger, R., and Wiesendanger, M. (1985b). Cerebellar-cottical linkage in the monkey as revealed by transcellular labeling with the lectin wheat germ agglutinin conjugated to the marker horse-adish peroxidase. *Exp. Brain Res.* **59,** 105–117.

Wilms, H., Sievers, J., and Deuschl, G. (1999). Models of tremor. *Move. Disord.* **14,** 557–571.

Wu, H.S., Sugihara, I., and Shinoda, Y. (1999). Y Projection patterns of single mossy fibers originating from the lateral reticular nucleus in the rat cerebellar cortex and nuclei. *J. Comp. Neurol.* **411,** 97–118.

Yaginuma, H., and Matsushita, M. (1986a). The projection fields of spinal border cells in the cerebellar anterior lobe in the cat: an anterograde WGA-HRP study. *Brain Res.* **384,** 175–179.

Yaginuma, H., and Matsushita, M. (1986b). Spinocerebellar projection fields in the horizontal plane of lobules of the cerebellar anterior lobe in the cat: an anterograde wheat germ agglutinin–horseradish peroxidase study. *Brain Res.* **365,** 345–349.

Yaginuma, H., and Matsushita, M. (1987). Spinocerebellar projections from the thoracic cord in the cat, as studied by anterograde transport of wheat germ agglutinin–horseradish peroxidase. *J. Comp. Neurol.* **258,** 1–27.

Yaginuma, H., and Matsushita, M. (1989). Spinocerebellar projections from the upper lumbar segments in the cat, as studied by anterograde transport of wheat germ agglutinin–horseradish peroxidase. *J. Comp. Neurol.* **281,** 298–319.

Yamamoto, F., Sato, Y., and Kawasaki, T. (1986). The neuronal pathway from the flocculus to the oculomotor nucleus: an electrophysiological study of group y nucleus in cats. *Brain Res.* **371,** 350–354.

Yamamoto, M. (1979). Vestibulo-ocular reflex pathways of rabbits and their representation in the cerebellar flocculus. *Prog. Brain Res.* **50,** 451–457.

Yamamoto, T., and Oka, H. (1993). The mode of cerebellar activation of pyramidal neurons in the cat parietal cortex (areas 5 and 7): an intracellular HRP study. *Neurosci. Res.* **18,** 129–142.

Yamamoto, T., Yoshida, K., Yoshikawa, H., Kishimoto, Y., and Oka, H. (1992). The medial dorsal nucleus is one of the thalamic relays of the cerebellocerebral responses to the frontal association cortex in the monkey: horseradish peroxidase and fluorescent dye double staining study. *Brain Res.* **579,** 315-320.

Ziehen, T. (1934). Centralnervensystem. "Handb. Anat. Menschen," Part 4(2), pp. 1–1546. Fisher Verlag, Jena.

CHAPTER

12

Periaqueductal Gray

PASCAL CARRIVE
Department of Anatomy, School of Medical Sciences
The University of New South Wales, Sydney, Australia

MICHAEL M. MORGAN
Department of Psychology, Washington State University
Vancouver, Washington, USA

The periaqueductal gray (PAG) or central gray of the midbrain is the midline structure that encircles the mesencephalic aqueduct. It is a large structure made of poorly differentiated gray matter; it is rich in neuropeptides, and it forms an interface between the forebrain and the lower brain stem. There has been considerable attention focused on the PAG, especially the human PAG, because of its role in putative analgesic mechanisms. The aim of this chapter is to review and discuss the anatomical and functional aspects of the human PAG.

EXTERNAL BOUNDARIES OF THE PERIAQUEDUCTAL GRAY

The PAG is continuous with the periventricular gray of the third ventricle rostrally and with the pontine gray matter in the floor of the fourth ventricle caudally. The PAG starts approximately at the level of the posterior commissure and ends at the level of the locus coeruleus. Laterally it extends into the adjacent mesencephalic tegmentum but is separated from it by the streaming fibers of the tectospinal tract and the longitudinal fibers of the mesencephalic trigeminal tract. These fibers cast out the characteristic shapes of the PAG when viewed on cross-sections: first triangular (anteriorly), then round, and finally trapezoidal (posteriorly). These shapes are recognizable in all mammalian species and are best seen when the plane of section is perpendicular to the axis of the aqueduct. Dorsally, the PAG is bounded by the commissures of the superior and inferior colliculi.

To be exact, the PAG does not completely encircle the aqueduct. The region ventral to the aqueduct is not considered part of the PAG because it is occupied by well-differentiated nuclei with separate anatomical and functional attributes, i.e., the oculomotor-related nuclei (oculomotor, Edinger–Westphal, supraoculomotor and trochlear nuclei, nucleus of Darkschewitsch,

and interstitial nucleus of Cajal) and, more caudally, the dorsal raphe nucleus and laterodorsal tegmental nucleus. In other words, the PAG is more like a horseshoe than an annulus.

INTERNAL BOUNDARIES OF THE PERIAQUEDUCTAL GRAY

The question on how to subdivide the PAG has occupied neuroanatomists for a long time. The problem is that Nissl staining does not reveal any obvious boundaries within the PAG. Indeed, what characterizes the PAG when compared to the adjacent tectal and tegmental regions is the apparent lack of differentiation of its gray matter (see Chapter 10). Conventional myelin stains do not help either because the only fiber tract that traverses it is the loose and poorly myelinated dorsal longitudinal fasciculus (also known as Schütz bundle; see Schiller, 1984 for a historical review). However, behind this deceiving cytoarchitecture is a rich and complex chemoarchitecture that is gradually being revealed by more specific staining methods (i.e., histochemical, immunohistochemical, or receptor binding). The problem now is to extract meaningful subdivisions from this elaborate chemical mosaic. Ideally, as Blessing (1997) reminds us, subdivisions should be based on function rather than morphology (see also Chapter 15). Changes in morphology do not necessarily correspond to changes in function and vice versa.

Tracing and functional mapping studies in nonhuman mammalian species now suggest the existence of distinct identifiable functional units located in separate quadrants of the PAG. Interestingly, some of these functional units have corresponding chemoarchitectural features. Obviously, the only way these units can be transposed to the human PAG is through the use of chemical markers that are specific enough to consistently outline these subdivisions across species. NADPH-diaphorase, a constitutive enzyme, provides such a technique. The following sections describe how the human PAG subdivisions have evolved from early studies of Golgi and Nissl staining to more recent studies of NADPH-diaphorase staining.

Subdivisions Defined on the Basis of Cytoarchitecture

Golgi studies

Three Golgi studies have described the morphology of primate PAG neurons: Laemle (1979) and Gioia *et al.* (1998) in human and Mantyh (1982c) in the monkey. Mantyh described four types of neurons. The first type is the fusiform cell with two primary dendrites emerging from an elongated soma. Similar neurons have been described by Gioia *et al.* (1998). According to Beitz (1990), these fusiform cells correspond to the vertical and horizontal cells first mentioned by Laemle (1979). The second type is the multipolar cell with three to nine primary dendrites and extensive arborization that tend to spread in a coronal plane; these neurons also have been described by Gioia *et al.* (1998), who counted twice as many multipolar than fusiform cells in the human PAG. The third type, also described by Laemle (1979), is the stellate cell with an oval soma and three to six proximal dendrites. The fourth type is the pyramidal cell described only by Mantyh (1982c) and characterized by the most extensive arborization of all cells in the PAG. All four types are found throughout the PAG, although fusiform cells tend to be more prominent in medial regions near the aqueduct whereas pyramidal cells are more prominent in peripheral regions near the tegmentum or superior colliculus (Mantyh, 1982c).

These studies show that there is a great deal of variability in the cell types of the PAG. This variability is greater, for example, than in the adjacent superior colliculus or midbrain tegmentum. Most importantly, there does not seem to be obvious regional variations in the distributions of the different types to warrant a subdivisional scheme. In agreement with Ramon y Cajal (1909) and Kölliker (1896), Mantyh (1982c) concluded that the PAG is not subdivisible on the basis of distinct cell types.

Nissl Studies

The PAG is a cell-rich, myelin-poor structure (Mantyh, 1982c). Its neurons are small to medium with a diameter ranging from 10 to 35 μm (Mantyh, 1982c). In the human, 50% of cells in the lateral region of the PAG have a diameter between 15 and 25 μm and only 5% have a diameter greater than 25 μm (Laemle, 1979). One consistent feature of the mammalian PAG is the gradual increase in neuronal diameter, fiber size, degree of myelination, and packing density from the more medial to the more lateral regions of the PAG (Beitz, 1990; Mantyh, 1982c). Another consistent feature is the change in orientation of the neurons, from circular (parallel to the edge of the aqueduct) in the medial regions to radial (perpendicular to the edge of the aqueduct) in the more lateral regions (Beitz, 1990; Mantyh, 1982c).

The first cytoarchitectonic-based subdivisions of the human PAG were proposed by Olszewski and Baxter (1954) (Fig. 12.1). Three subdivisions were delineated as follows: (1) a narrow subnucleus dorsalis located on the midline above the aqueduct and characterized by a

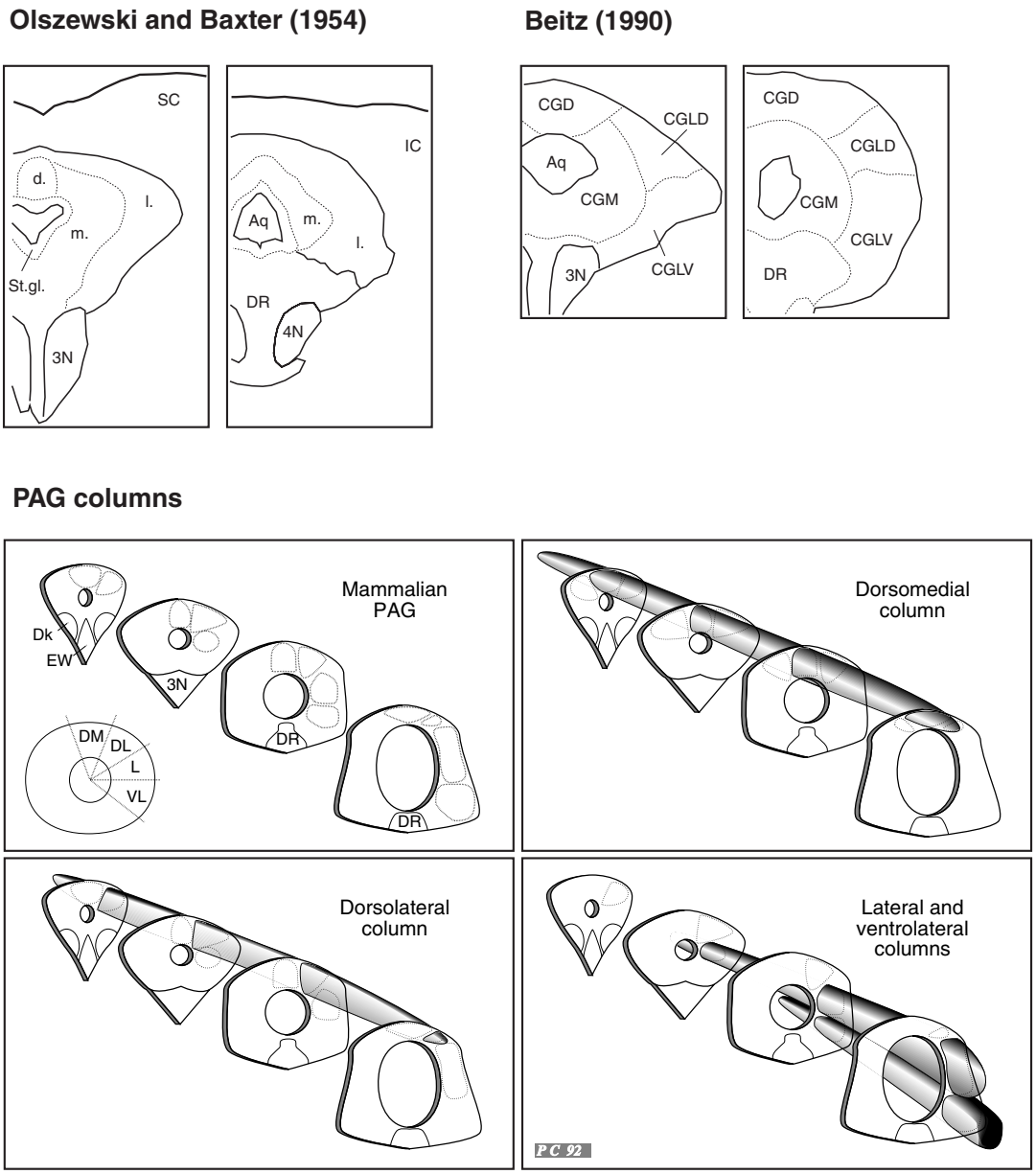

FIGURE 12.1 PAG subdivisions. **Upper left panel:** Subdivisions of the human PAG proposed by Olzewski and Baxter (1954). Abbreviations: Aq, aqueduct; d., subnucleus dorsalis of griseum centrale mesencephali; l., subnucleus lateralis; m., subnucleus medialis; St. gl. stratum gliosum subependymale; DR, dorsal raphe, 3N, oculomotor nucleus; 4N, trochlear nucleus. **Upper right panel:** Subdivisions of the human PAG proposed by Beitz (1990). Abbreviations: CGD, dorsal subdivision of central gray; CGLD, lateral dorsal subdivision; CGLV, lateral ventral subdivision; CGM, medial subdivision. **Lower panel:** PAG columns proposed by Carrive (1993) and Bandler (Bandler *et al.*, 1991b; Bandler and Shipley, 1994). Abbreviations: Dk, nucleus of Darkschewitsch; EW, Edinger–Westphall nucleus. Adapted from Olzewski and Baxter (1954), Beitz (1990), and Carrive (1993).

marked accumulation of glial cells; (2) a subnucleus medialis surrounding the aqueduct along its entire length and characterized by a low packing density; and (3) a subnucleus lateralis covering the lateral regions in the middle third of the PAG and characterized by a higher packing density. These subdivisions were verified and further refined by Beitz (1990) after an extensive quantitative study of neuronal size, shape, and packing density (Fig. 12.1). Beitz's dorsal subdivision, which was more extensive than Olszewski

and Baxter's subnucleus dorsalis, had on average the smallest neurons, the lowest neuronal packing densit, and the highest glia-to-neuron ratio. The medial subdivision was similar to the subnucleus medialis, although less extensive ventrolaterally. Its neurons had a medium neuronal packing density, were of small size, and had a circular orientation preference. The lateral subdivision was more extensive than Olszewski and Baxter's subnucleus lateralis and was characterized by a high neuronal packing density, larger neurons, and a preferential radial orientation of their soma. Beitz further subdivided the lateral division into lateral dorsal and lateral ventral subdivisions on the basis that the lateral dorsal part had a greater packing density, smaller neurons, and lower glia-to-neuron ratio than the lateral ventral part. His subdivisions were basically the same as those he had previously defined in the rat (Beitz, 1985).

Subdivisions Defined on the Basis of Connections and Functions

The current model of functional organization in the mammalian PAG proposes the existence of four basic longitudinal columns located parallel to the aqueduct (Fig 12.1). This columnar organization was originally proposed by Carrive (Carrive, 1989, 1991, 1993; Carrive and Bandler, 1991) on the basis of tracing and functional mapping studies with microinjections of excitatory amino acids in the decerebrate anaesthetized cat. The model has been further developed and documented by Bandler and collaborators (Bandler *et al.*, 1991a, b, 2000; Bandler and Shipley, 1994; Bernard and Bandler, 1998). The four columns are dorsomedial, dorsolateral, lateral, and ventrolateral, and were defined as follows: The dorsomedial, lateral, and ventrolateral columns all project directly to the lower brain stem, whereas the dorsolateral does not. The lateral and ventrolateral columns have similar connections but opposite effects on blood pressure and heart rate in the decerebrate cat (lateral is hypertensive; ventrolateral is hypotensive), and there is growing evidence that they coordinate different forms of defensive responses (lateral coordinates active defense; ventrolateral coordinates passive defense). Interestingly, the lateral and ventrolateral columns appear better separated in larger mammals and in some cases can be revealed as separate columns by neuronal tracers. A striking example is the pattern of termination of spinomesencephalic projections in the monkey (see Fig. 12.10).

These functional columns correspond to some extent to Beitz's cytoarchitectural subdivisions, although columns have better defined boundaries. Similarities include the dorsomedial and dorsolateral columns, which correspond relatively well to Beitz's dorsal and lateral dorsal subdivisions. The ventrolateral and lateral columns together also correspond approximately to Beitz's lateral ventral column. The main difference is that there is no equivalent to Beitz's medial subdivision. A gradient of cellular density may exist, but no obvious difference could be detected between the medial and lateral edges of the columns in terms of connectivity and function.

Subdivisions Defined on the Basis of a Chemical Stain, NADPH-Diaphorase

The enzyme NADPH-diaphorase (NADPH-d), the same enzyme as nitric oxide synthase (Hope *et al.*, 1991), has a remarkable distribution in the PAG. It reveals more subdivisions than any other chemical stain described so far and the boundaries that it reveals are consistent with the functional columns described in the nonhuman mammalian species. It is a simple and robust histochemical stain that reveals axons, terminals, dendritic processes, and neurons with as much resolution as a Golgi stain (Fig. 12.2). Its pattern of staining in the PAG was first described in the rat (Herbert and Saper, 1992; Onstott *et al.*, 1993).

Figure 12.3 is a series of camera lucida drawings showing the distribution of NADPH-d-stained neurons in the human PAG and adjacent tectum and tegmentum. The brain was from a male with no known neurological disease. Figure 12.4 compares this pattern across mammalian species at two rostrocaudal levels: intermediate and caudal. As can be seen, the pattern of staining is basically the same from rat to human. There are three areas within the PAG that contain NADPH-d

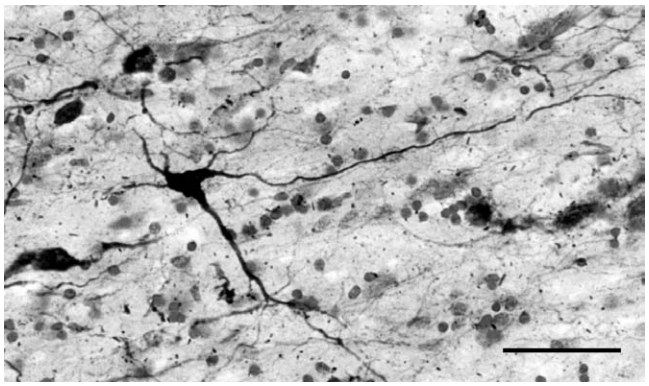

FIGURE 12.2 Microphotograph of an NADPH-diaphorase-stained neuron in the human dorsolateral PAG. The section has been counterstained with Nissl. Note the dense staining in soma and processes. Bar = 50 μm.

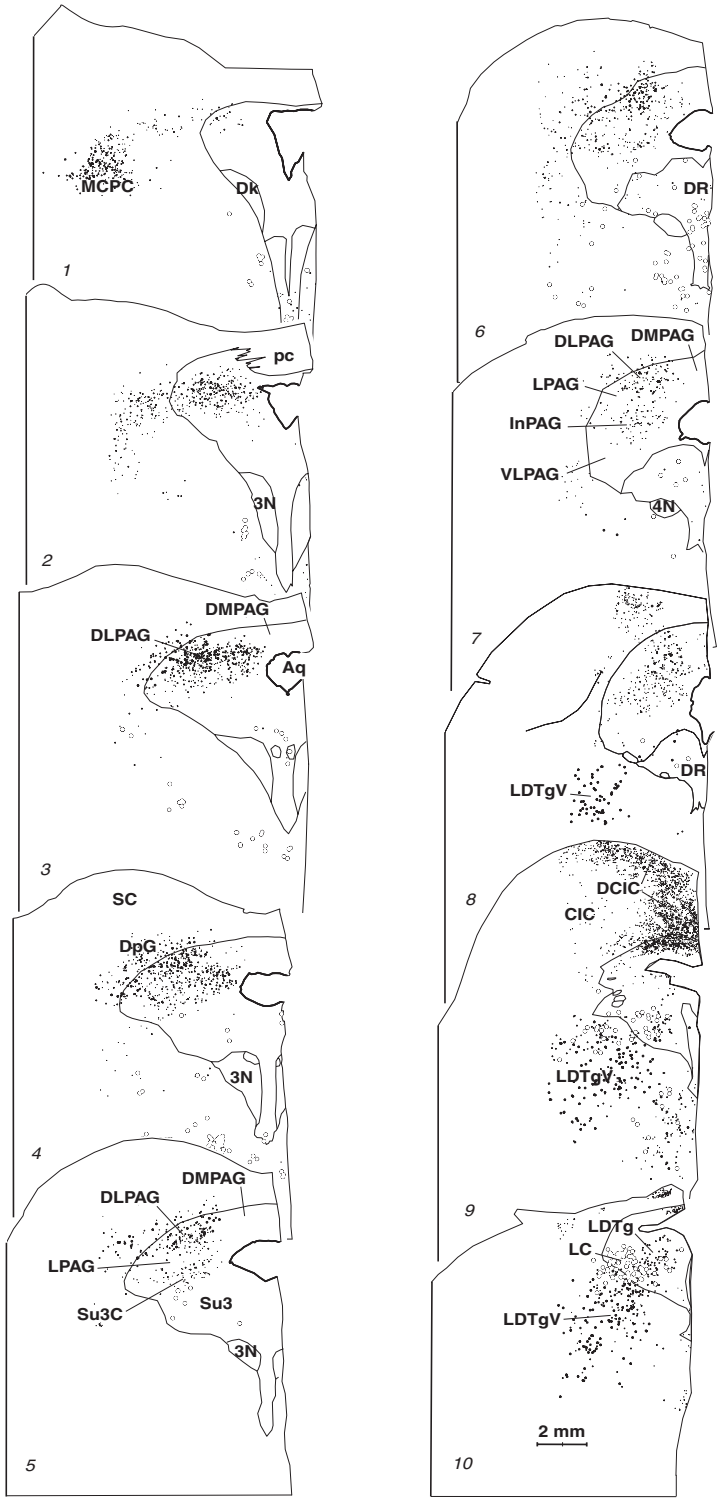

FIGURE 12.3 Camera lucida drawings of equidistant sections of a human midbrain showing the distribution of NADPH-diaphorase-stained neurons in and around the PAG from the level of the posterior commissure (section 1) to the level of the locus coeruleus (section 10). Abbreviations: 3N, oculomotor nucleus; 4N, trochlear nucleus ; Aq, aqueduct; CIC, central nucleus of inferior colliculus; Dk, nucleus of Darkschewitsch; DCIC, dorsal cortex of inferior colliculus; DLPAG, dorsolateral periaqueductal gray; DMPAG, dorsomedial periaqueductal gray; DpG, deep gray layers of superior colliculus; DR, dorsal raphe nucleus; IC, inferior colliculus; InPAG, intercalated PAG; LC, locus coeruleus; LDTg, laterodorsal tegmental nucleus; LTDgV, laterodorsal tegmental nucleus, ventral division; LPAG, lateral periaqueductal gray; MCPC, magnocellular nucleus of the posterior commissure; pc, posterior commissure; PPTg, pedunculopontine tegmental nucleus; SC, superior colliculus; Su3, supraoculomotor nucleus; Su3C, supraoculomotor cap; VLPAG, ventrolateral periaqueductal gray.

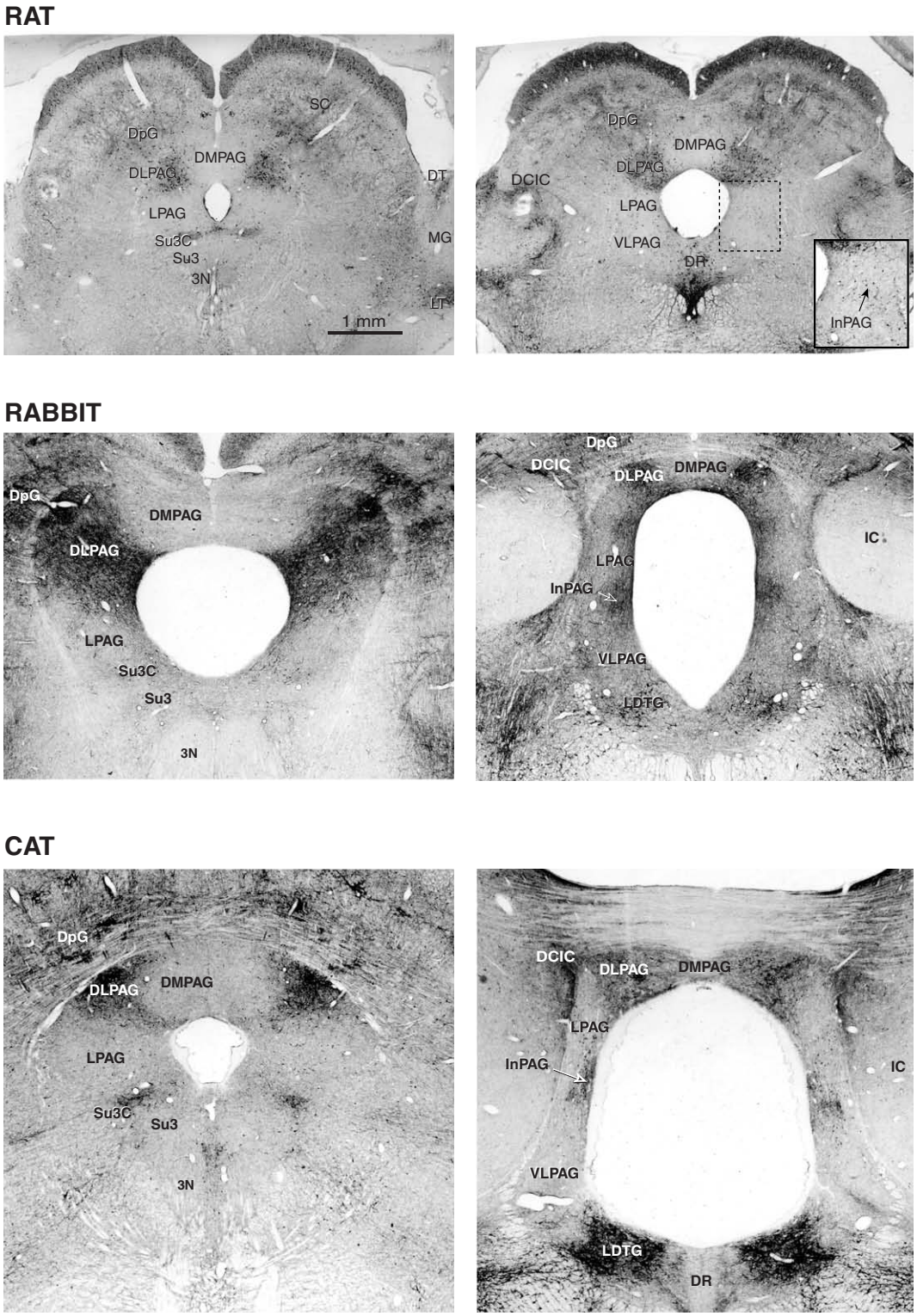

FIGURE 12.4 Comparison of NADPH-diaphorase staining of the PAG across mammalian species (rat, rabbit, cat, monkey, and human). Sections are shown at intermediate **(left)** and caudal **(right)** levels. All sections are shown at the same scale. Abbreviations: DT, dorsal terminal nucleus of the accessory optic tract; LT, lateral terminal nucleus of the accessory optic tract; MG, medial geniculate nucleus. For other abbreviations, see legend of Fig. 12.3.

Continued

MONKEY

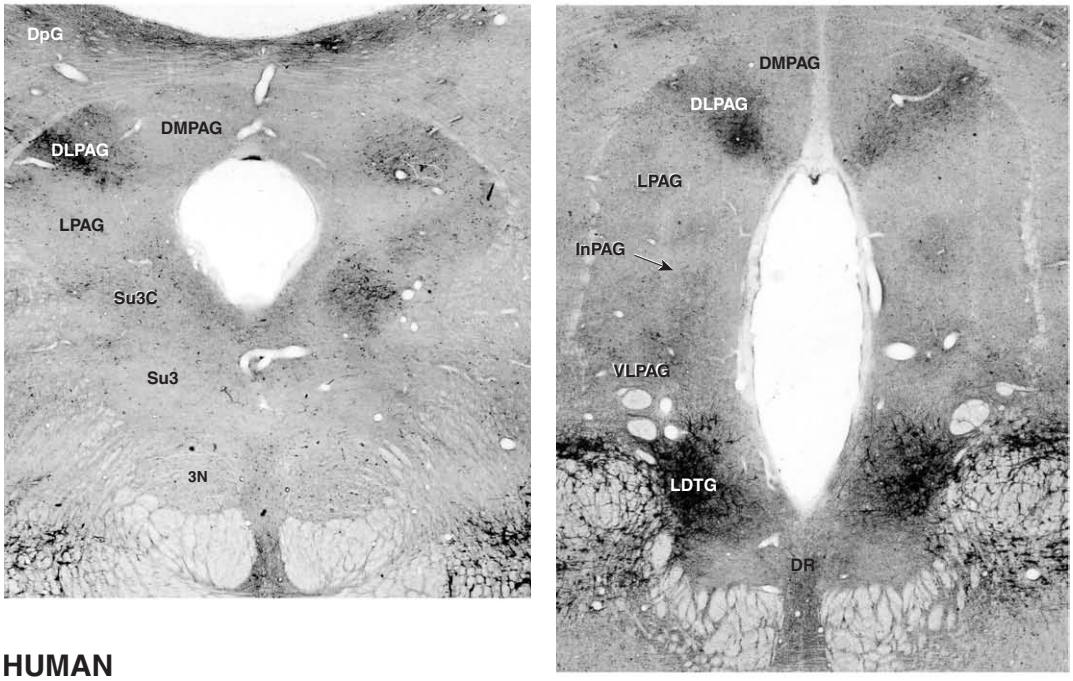

HUMAN

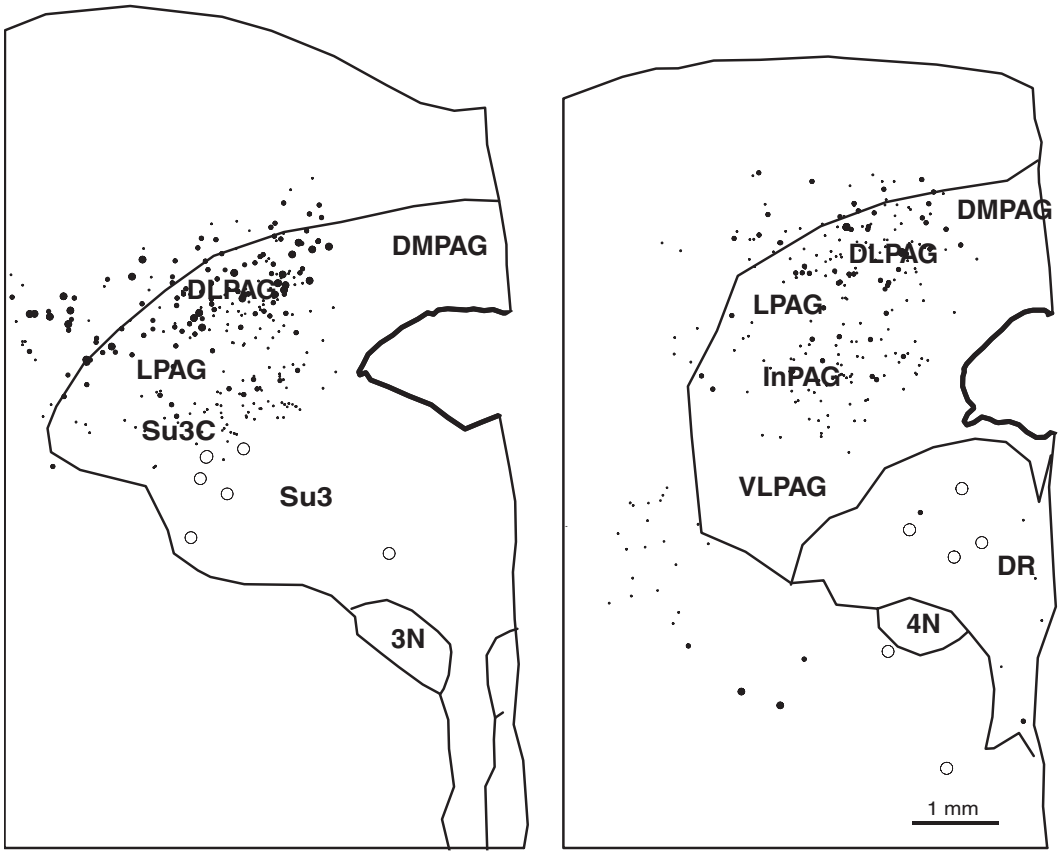

FIGURE 12.4 *Continued*

neurons: the dorsolateral column (DLPAG), the supraoculomotor cap (Su3C), and a small group of intercalated neurons that we will refer to as the "intercalated PAG" (InPAG).

The area of the PAG that stains best for NADPH-d corresponds to the dorsolateral column (Figs. 12.3 and 12.4). Approximately 17% of the neurons in the dorsolateral column are stained, and in some cases the stain is so dense that neurons are revealed in a Golgi-like manner (Fig. 12.2). Note also that the staining extends dorsally into the deep layers of the superior colliculus, suggesting some continuity between the dorsolateral column and the superior colliculus. Indeed, the dorsolateral column is largest at the level of the superior colliculus. Rostrally, the staining also seems to extend towards the magnocellular nucleus of the posterior commissure, which is NADPH-d positive (Fig. 12.3, section 1). Caudally, as the lateral column ends, it appears to merge with the NADPH-d neurons of the dorsal cortex of the inferior colliculus (lamina 1) (Fig. 12.3, section 8). However, this group of neurons is an extension not of the dorsolateral column but of the intercalated PAG (see below).

The second area that contains NADPH-d neurons is the Su3C in the intermediate PAG (Fig. 12.3, section 5). First described by Carrive and Paxinos (1994), the Su3C is located directly above the supraoculomotor nucleus and is also present in other species (Fig. 12.4). Although it is not identifiable on Nissl-stained material, it stains positively for acetylcholinesterase (Paxinos and Huang, 1995; see also Chapter 10). Nothing is known about its connectivity and function. Interestingly, closer examination of midbrain sections also suggests some continuity with clusters of NADPH-d neurons located in and next to the dorsal and lateral terminal nuclei of the accessory optic tract (Fig. 12.4, rat, DT and LT).

The third area is the InPAG, a band of stained neurons located in the caudal PAG, lateral to the aqueduct (Fig. 12.3, section 7 and Fig. 12.4). This band is also present in other species and can even appear as two distinct bands in rabbit and monkey. Interestingly, here again, there seems to be some continuity with more laterally placed NADPH-d groups of neurons, in this case the lamina 1 neurons of the dorsal cortex of the inferior colliculus which is found dorsomedial and ventromedial to the central nucleus of the inferior colliculus (Fig. 12.4, rat, rabbit, cat; see also Paxinos *et al.*, 1999).

In addition to these three PAG groups, NADPH-d staining reveals the large neurons of the laterodorsal tegmental nucleus on the ventral side of the caudal ventrolateral PAG. These darkly stained neurons merge with the neuromelanin neurons of the locus coeruleus.

The three separate groups of NADPH-d neurons described above strongly suggest that the PAG possesses a radial organization. Furthermore, the apparent continuity of these bands with more laterally placed structures also suggests that this radial organization is an architectural feature of the entire mammalian midbrain. Most importantly, it allows us to subdivide the undifferentiated gray of the PAG into quadrants of alternating NADPH-d positivity and negativity. Finally, these quadrants appear to correspond well to the functional columns identified in nonhuman species.

The dorsomedial column is thus defined as the NADPH-d-negative column between the two NADPH-d-positive dorsolateral columns; the lateral column is the NADPH-d-negative column between the NADPH-d-positive dorsolateral column and Su3C; and, finally, the NADPH-d-negative ventrolateral column is between the NADPH-d-positive InPAG and laterodorsal tegmental nucleus/dorsal raphe. This columnar organization is consistent across species and may reflect the basic functional/anatomical organization of the mammalian PAG.

Additional Subdivisions

Additional subdivisions can be added to this basic columnar organization. For example, Paxinos and Huang (1995) have delineated a pleioglial periaqueductal gray subdivision on the midline above the aqueduct in the center of the dorsomedial column (see Chapter 10). It contains a dense accumulation of glial cells and corresponds to Olszewski and Baxter's (1954) subnucleus dorsalis. Onstott *et al.* (1993) and others (Krout *et al.*, 1998) also recognize a juxtaaqueductal column surrounding the aqueduct. This area, characterized by a low neuronal density but a rich neuropil, may correspond to Olszewski and Baxter's (1954) subnucleus medialis but is much narrower. The lateral boundaries of this area are not well defined.

CHEMOARCHITECTURE OF THE PRIMATE PERIAQUEDUCTAL GRAY

Like other periventricular structures, the PAG is rich in neurochemicals. The most interesting and best studied are the neurotransmitters, neuromodulators, and their receptors. Despite the difficulty of detecting these neurochemicals in human tissue (problems with fixation, postmortem delays, size of the sections), information concerning their presence and distribution in the human PAG is nevertheless gradually accumulating. The following is an update on the neuro-

chemicals that have been identified in the human and monkey PAG so far. Parallels are drawn with studies in cat and rat when appropriate.

Monoamines and Acetylcholine

Catecholamines

Neurons. The human PAG contains scattered catecholamine-containing neurons in an area that corresponds to the ventrolateral column. These neurons were first revealed by aldehyde-induced catecholamine fluorescence (Nobin and Bjorklund, 1973) and later confirmed by tyrosine hydroxylase immunoreactivity (Pearson *et al.*, 1983, 1990). It is not clear if these neurons are dopaminergic or noradrenergic. The rostrally located neurons may be an extension of the dopaminergic neurons of the A10 group on the midline and the A8 group in the lateral tegmentum. There is evidence in the monkey of dopaminergic neurons in this area of the PAG (Arsenault *et al.*, 1988). In contrast, the caudally located neurons may be an extension of the noradrenergic neurons in the locus coeruleus.

Fibers and receptors. Epinephrine and norepinehrine are found in relatively high concentrations in the PAG, mainly in the ventrolateral part (Farley and Hornykiewicz, 1977; Mefford *et al.*, 1977). Immunoreactive tyrosine hydroxylase fibers are present in the ventrolateral PAG (Pearson *et al.*, 1983), and phenylethanolamine-*N*-methyltransferase is present there as well (Kopp *et al.*, 1979). The distribution of these fibers in the ventrolateral and lateral PAG has been described in greater detail in the rat (Herbert and Saper, 1992). These projections appear to originate from the adrenergic and noradrenergic groups of the lower brain stem (Herbert and Saper, 1992). *In vitro* autoradiographic studies showing α_2-adrenoceptor binding in the ventrolateral PAG is consistent with the location of these fibers (Pascual *et al.*, 1992).

Indoleamines

Apart from displaced dorsal raphe neurons in the ventrolateral area, the human PAG does not contain serotonergic neurons (Chen *et al.*, 2000; Nobin and Bjorklund, 1973; Takahashi *et al.*, 1986; Tork and Hornung, 1990). However, serotonin fibers and receptors are present in the PAG. In the rat, serotonin containing fibers are found mainly in the lateral PAG, are fewer in the ventrolateral PAG, and are rare in the dorsolateral and dorsomedial PAG (Halliday *et al.*, 1995). Receptors are found in moderate concentration in the human PAG, but no regional variation is apparent (Palacios *et al.*, 1983; Reddy *et al.*, 1996). These receptors are primarily of the 1A and 1B subtype, although not all subtypes have been investigated in the primate brain (Castro *et al.*, 1997; Pazos *et al.*, 1987a, b). In the rat, serotonin innervation of the PAG originates mainly from the pontine and medullary raphe nuclei (Beitz *et al.*, 1986).

Acetylcholine

The laterodorsal tegmental nucleus on the ventromedial border of the caudal ventrolateral PAG is a major cholinergic nucleus (Mesulam *et al.*, 1984). These neurons also stain positively for NADPH (Fig. 12.4). In contrast, an immunohistochemical analysis of choline acetyltransferase in the monkey indicates that the primate PAG does not contain cholinergic neurons (Mesulam *et al.*, 1984). However, the PAG is rich in muscarinic (Cortes, 1984, 1986; Reddy *et al.*, 1996) and nicotinic receptors (Adem *et al.*, 1989), with the muscarinic receptors located primarily in the dorsolateral PAG. The catabolizing enzyme acetylcholinesterase is also found in the PAG, where it appears to label the dorsolateral column and the supraoculomotor cap darker than the rest of the PAG (Graybiel, 1979; Paxinos and Huang, 1995; see also Chapter 10).

Amino Acids

Glutamate and Aspartate

Neurons. The two excitatory amino acids glutamate and aspartate are present in PAG neurons, and their distribution in the human PAG has been revealed by immunohistochemistry. Beitz (1990) reports glutamate-like immunoreactive neurons in the dorsomedial, lateral, and ventrolateral regions (as defined by the columns). There are fewer aspartate-like immunoreactive neurons. They are found in the dorsolateral, lateral, and ventrolateral regions. Thus, the distributions differ in the dorsal regions (Beitz, 1990). This pattern is the same in the rat (Clements *et al.*, 1987).

Receptors. Receptors for the glutamate agonist kainate have been reported in the human PAG (Reddy *et al.*, 1996) with the densest binding in the dorsolateral region. In the cat, the dorsolateral column is clearly more strongly labeled with glutamate receptors than the other columns (Gundlach, 1991).

GABA and Glycine

Neurons. The inhibitory amino acid γ-aminobutyric acid (GABA) has also been identified in PAG neurons by immunohistochemistry (Beitz, 1990). These neurons appear to have a similar distribution to the glutamate-like immunoreactive neurons in the human PAG. Much less is known about the distribution of the inhibitory amino acid glycine in human PAG neurons.

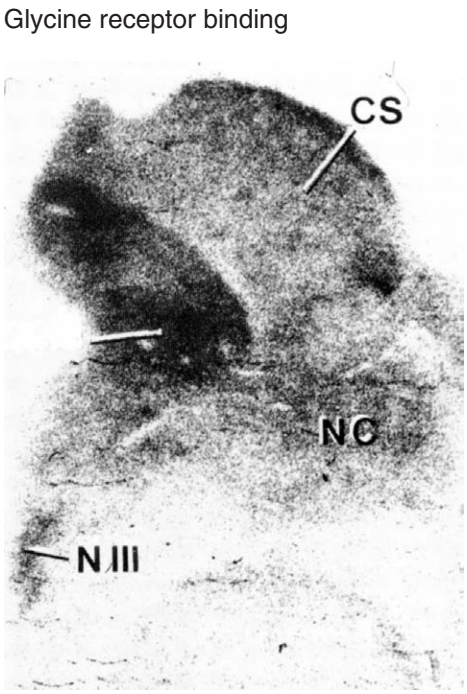

FIGURE 12.5 Bright-field photomicrograph of an autoradiogram of [^{3}H]strychnine binding to a human midbrain section. Dark regions in the dorsomedial and lateral PAG represent areas of high-density binding to glycine receptors. Note the light binding in the dorsolateral PAG. From Probst *et al.* (1986, figure 1, p. 13).

Receptors. The distribution of GABA receptors has not been described in the human PAG, but the closely related benzodiazepine receptor is found in high concentration (Doble *et al.*, 1987). In the cat, benzodiazepine binding is found throughout the PAG, with slightly denser binding in the dorsolateral column (Gundlach, 1991). Finally, glycine receptors display clear regional variations in the PAG. Thus, binding for strychnine is much denser in the dorsomedial, lateral, and ventrolateral columns than in the dorsolateral column (Probst *et al.*, 1986) (Fig. 12.5).

Neuropeptides

Opioids

There are three families of opioid neuropeptides: the enkephalins, the dynorphins, and the endorphins. They are derived from genetically distinct precursor genes: proenkephalin, prodynorphin, and proopiomelanocortin, respectively. The presence of the three opioid peptides—met-enkephalin, dynorphin, and β-endorphin—in the human PAG was first revealed by radioimmunoassay (Gramsch *et al.*, 1979, 1982). Subsequently, other derivatives of the proenkephalin precursor, the octapeptide [met]enkephalin-Arg-Gly-Leu and the heptapeptide [met]enkephalin-Arg-Phe, have been found in the human PAG (Pittius *et al.*, 1984). Of these three opioid families, the enkephalins are the most prevalent (Gramsch *et al.*, 1979, 1982; Pittius *et al.*, 1984).

Neurons. Immunohistochemical staining in colchicine-treated monkeys shows that the opioidergic neurons of the PAG are mainly enkephalinergic (Ibuki *et al.*, 1989). There are a few dynorphinergic neurons and no endorphinergic neurons (Ibuki *et al.*, 1989). *In situ* hybridization for proenkephalin and prodynorphin mRNA in humans confirms the high concentration of enkephalinergic neurons in the PAG but yields no evidence of dynorphinergic neurons (Hurd, 1996). Note that colchicine pretreatment (which blocks axonal transport) is necessary to increase peptide content in the cell sufficiently to be detected immunohistochemically. Because colchicine treatment is not possible in humans, *in situ* hybridization is the only labeling option. Although the columnar distribution of enkephalinergic neurons in the PAG has not been determined in the human, in the rat and cat these neurons are seen mainly in the dorsomedial, lateral, and ventrolateral columns (Conrath-Verrier *et al.*, 1983; Moss *et al.*, 1983; Smith *et al.*, 1994).

Fibers. The distribution of enkephalin- and β-endorphin-containing fibers has been studied by immunohistochemistry (colchicine is not required in this case). Enkephalin-like immunoreactive fibers are found in low density throughout the PAG (Bouras, 1986) but tend to be denser in the dorsolateral region (Pioro *et al.*, 1990). In contrast, β-endorphin-immunoreactive fibers avoid the dorsolateral PAG and target the dorsomedial, lateral, and ventrolateral PAG (Pilcher *et al.*, 1988). The same striking distribution is observed with two other derivatives of the proopiomelanocortin precursor adrenocorticotropic hormone (ACTH) (Buma *et al.*, 1989; Pilcher *et al.*, 1988) and corticotropin-like intermediate lobe peptide (CLIP) (Zaphiropoulos *et al.*, 1991) (Fig. 12.6). Note that this projection originates from a restricted region of the tuberal hypothalamus located in and around the arcuate nucleus (Pilcher *et al.*, 1988).

Receptors. An autoradiographic study shows naloxone binding throughout the adult human PAG with no obvious regional difference (Reddy *et al.*, 1996), and in the infant, naloxone binding is found preferentially in the dorsolateral column (Kinney *et al.*, 1998; Reddy *et al.*, 1996). Finally, competitive radioligand binding shows that the opiate receptors of the human PAG are mainly of the μ and κ types (46% μ, 41% κ and 13% δ type) (Pfeiffer *et al.*, 1982).

Substance P

Substance P neurons and fibers are found in high concentration in the human PAG (Bouras, 1986; Del

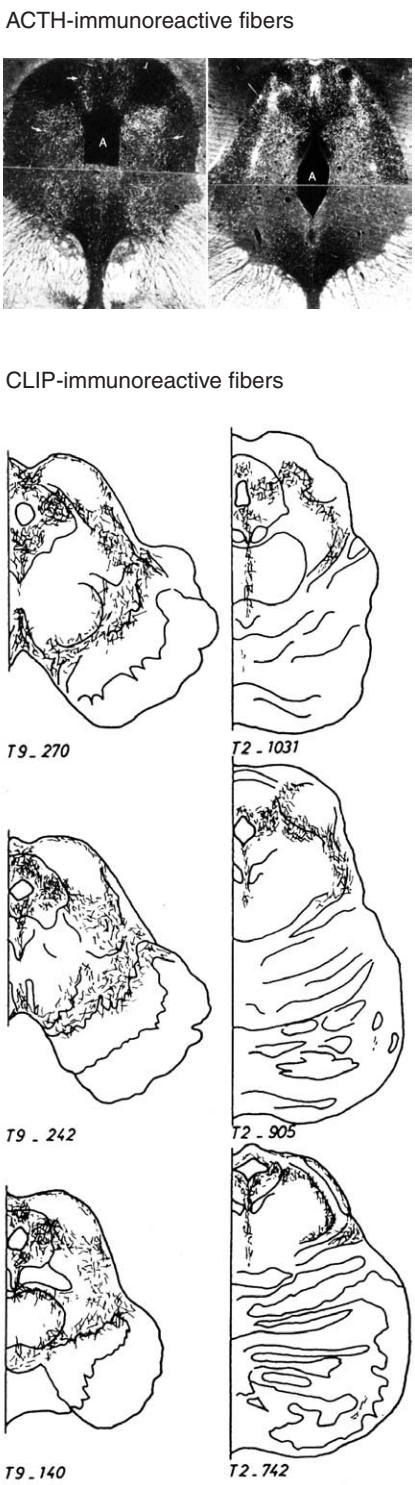

FIGURE 12.6 **Upper panel:** dark-field photomontage showing the distribution of ACTH-immunoreactive fibers and terminals in the human PAG at intermediate and caudal levels (ACTH labeling appears white on a black background). From Pilcher *et al.* (1988, figure 8, p. 627). **Lower panel:** distribution of corticotropin-like intermediate lobe peptide (CLIP)–immunoreactive fibers and terminals in the human midbrain. Adapted from Zaphiropoulos *et al.* (1991, figure 11a, p. 107). Note that in both cases the labeling is in the dorsomedial, lateral, and ventrolateral PAG and avoids the dorsolateral PAG. A, aqueduct.

Fiacco *et al.*, 1984; Halliday *et al.*, 1990; Hurd *et al.*, 1999; Nomura *et al.*, 1987; Pioro *et al.*, 1990). There is no obvious regional variation in the distribution of the neurons in the human or the rat (Smith *et al.*, 1994). However, although fibers are found throughout the PAG, they appear to be denser in the dorsolateral column (Pioro *et al.*, 1990). The same is observed in the rat (Halliday *et al.*, 1995).

Neurotensin

Neurotensin is found in high concentration in the human PAG (Mai *et al.*, 1987). Only a few neurons are revealed by immunostaining (Mai *et al.*, 1987). However, more neurons can be seen in colchicine treated rats, particularly in the dorsomedial, lateral, and ventrolateral regions (Shipley *et al.*, 1987). Most of the immunostaining is found in fibers that appear more densely distributed near the aqueduct (Mai *et al.*, 1987). In the rat, immunostained fibers are also denser near the aqueduct, but within the boundaries of the dorsomedial, lateral, and ventrolateral columns. Finally, the human PAG is rich in neurotensin binding sites; however, the columnar distribution has not been documented (Quirion *et al.*, 1987).

Somatostatin

Immunostaining for somatostatin- and prosomatostatin-derived peptides reveals the presence of both cell bodies and fibers within the human PAG (Bouras, 1986, 1987). In the rat, *in situ* hybridization shows that the cell bodies are found in all four columns of the PAG (Smith *et al.*, 1994).

Neurophysin, Oxytocin, and Vasopressin

Oxytocin, vasopressin, and their associated neurophysins (precursor proteins) are found in fibers in the human PAG (Sofroniew *et al.*, 1981; Unger and Lange, 1991). These peptides originate mainly from the parvicellular part of the paraventricular nucleus and target the dorsomedial, lateral, and ventrolateral regions (Unger and Lange, 1991) (Fig. 12.7).

Vasoactive Intestinal Polypeptide

Vasoactive intestinal polypeptide (VIP)–immunoreactive fibers are found in low density in the human PAG (Bouras, 1986). Moderately dense binding sites are also found in the monkey and appear stronger in the dorsolateral column (Dietl *et al.*, 1990). In the rat, VIP neurons are restricted to a narrow juxtaaqueductal zone (Smith *et al.*, 1994).

Calcitonin Gene–Related Peptide

Only a few fibers containing calcitonin gene–related peptide (CGRP) have been reported in the human PAG (Unger and Lange, 1991). In the monkey, moderate

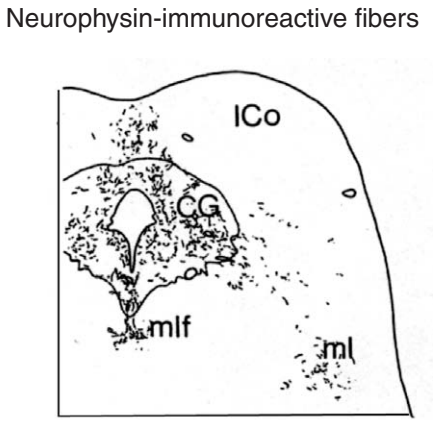

FIGURE 12.7 Distribution of neurophysin-immunoreactive fibers and terminals in the human midbrain. Note that the labeling is in the dorsomedial, lateral, and ventrolateral PAG and avoids the dorsolateral PAG. Adapted from Unger and Lange (1991, figure 1, p. 301). Abbreviations: CG, central gray; ICo, inferior colliculus; ml, medial lemniscus; mlf, medial longitudinal fasciculus.

CGRP binding is found in the dorsomedial, lateral, and ventrolateral columns (Paxinos *et al.*, 1995). Interestingly, calcitonin receptor binding in the monkey is found exclusively in the ventrolateral PAG (Christopoulos *et al.*, 1995; Paxinos *et al.*, 1995). *In situ* hybridization studies in the rat show that the PAG does not contain CGRP neurons (Smith *et al.*, 1994).

Neuropeptide Y

Neuropeptide Y neurons have been reported in the ventrolateral region of the human PAG by *in situ* hybridization (Pau *et al.*, 1998). However, comparison with the rat suggests that these neurons may actually be in the adjacent dorsal raphe nucleus (Smith *et al.*, 1994).

Others

Finally, cholecystokinin fibers and angiotensin-converting enzyme binding are found in low and moderate densities in the human PAG (Bouras *et al.*, 1986; Chai *et al.*, 1990).

Simple Gases

As indicated earlier, the enzyme that synthesizes nitric oxide (nitric oxide synthase) is the same as NADPH-d (Hope *et al.*, 1991). Thus, their identical distribution in the rat PAG is not surprising (Onstott *et al.*, 1993). The high concentration of NADPH-d in neurons of the dorsolateral PAG (Fig. 12.3) (Kowall and Mueller, 1988; Parvizi *et al.*, 2000) suggests that this gas plays an important role in this column. No information is yet available concerning carbon monoxide.

Summary

It will take time and the development of more refined tools before sense can be made of the chemical organization of the PAG. At this stage, the goal is to catalogue the presence or absence of transmitter systems and hope that patterns will emerge. For example, the information gathered so far supports the existence of distinct columns within the PAG. The dorsolateral column in particular is an area that stands out as the region with fewer shared features with the other three columns. This is apparent qualitatively, for example, with the presence of NADPH-d neurons or the absence of proopiomelanocortin (β-endorphin) and neurophysin fibers. It is also apparent quantitatively: for example, it stains darker for muscarinic receptors, substance P fibers, and benzodiazepine receptors. Interestingly, the chemical profile of the dorsolateral PAG is very similar to that of the deep layers of the superior colliculus (e.g., NADPH-d, substance P, and muscarinic receptors), suggesting that it is more closely related to the tectum than to the rest of the PAG. In contrast, the dorsomedial, lateral, and ventrolateral columns have many common features and may be considered more closely related to periventricular structures. For example, all three contain proopiomelanocortin (β-endorphin) and neurophysin fibers that originate from the hypothalamus. It is also difficult to detect quantitative differences between them for a number of markers (e.g., muscarinic and kainate receptors, substance P and neurotensin fibers). Nevertheless, subtle differences can be detected at least in some species. The dorsomedial column differs from the lateral and ventrolateral column in the rat in that it appears to have a lower density of serotonin and catecholaminergic fibers. The adjacent lateral and ventrolateral columns are more difficult to separate although there are differences in calcitonin binding and in the density of catecholaminergic fibers.

Finally, all the studies described so far have used tissue from humans who died of no known neurological diseases. However, cases involving neurological diseases are worth considering because the PAG columns may have different pathologies. This seems to be the case for Alzheimer's disease (Parvizi *et al.*, 2000). Parvizi *et al.* (2000) report that the ventrolateral column was mainly affected with dense core senile plaques, the dorsolateral and dorsomedial columns with diffuse senile plaques, and the lateral column with a mixture of diffuse and dense core senile plaques. No neurofibrillary tangles were found in the PAG but they were plentiful in the dorsal raphe nucleus. The juxtaaqueductal zone was not affected at all. Moreover, the dorsolateral and lateral columns

were the first affected in the progression of the disease and the dorsomedial column was last (Parvizi *et al.*, 2000). These interesting findings further support the existence of the columns and strongly suggest that they have different chemical and functional attributes.

CONNECTIVITY OF THE PRIMATE PERIAQUEDUCTAL GRAY

Although neuronal tract tracing is a powerful method, it is not applicable to humans because of methodological and ethical factors. Thus, the connections of the human PAG can only be inferred by homology with monkeys and other mammalian species. Fortunately, the patterns of afferent and efferent connections of the PAG seem to vary little across species and therefore are probably similar in human. The following describes what is currently known of the PAG connections in the monkey based on retrograde and anterograde tract tracing. These studies give an overall idea of what the PAG does and how it interacts with the rest of the brain. Moreover, these data are consistent with other data demonstrating the existence of PAG columns.

Periaqueductal Gray Afferents

From Forebrain

Forebrain afferents to the PAG arise from limbic structures, mainly from prefrontal cortex (see Chapters 24 and 25), insular cortex, amygdala (see Chapter 22), and hypothalamus (see Chapter 17). It does not receive any significant afferents from the parietal or occipital cortices, hippocampus, basal ganglia or thalamus (Mantyh, 1982b). These projections are mainly ipsilateral.

Cortical areas. The origins of cortical input to the monkey PAG were revealed by Hardy and Leichnetz (1981; see also Leichnetz *et al.*, 1981) and by Mantyh (1982b) using retrogradely transported horseradish peroxidase (HRP). The projection has recently been studied in greater detail by An *et al.* (1998). All three retrograde tracing studies show that cortical projections to the PAG originate principally from the prefrontal cortex. In particular, this input comes from the medial wall of the prefrontal cortex (areas 25, 32, 10m), the dorsomedial convexity of the medial wall (area 9) extending into the anterior cingulate cortex and the posterior orbitofrontal/anterior insular cortex (areas 13a, Iai, 12o, 12l) (An *et al.*, 1998). The lateral wall (areas 8 and 6) makes a minor contribution whereas the medial anterior part of the orbitofrontal cortex (areas 11, 13) does not project to the PAG. Caudal to the prefrontal cortex, other sources of cortical input are the posterior cingulate cortex (24b), the agranular and dysgranular parts of the insular cortex, and the dorsal bank of the superior temporal sulcus. The cortical projections arise from layer V and are predominantly ipsilateral.

The prefrontal projections have been verified by anterograde tracing with [^{3}H]amino acids, HRP, or biotinylated dextran amines (An *et al.*, 1998; Hardy and Leichnetz, 1981; Jürgens and Müller-Preuss, 1977; Müller-Preuss and Jürgens, 1976). Most importantly, anterograde tracing reveals that these afferents are organized along the same PAG columns described above (Fig. 12.8). Thus, the medial wall of the prefrontal cortex targets almost exclusively the dorsolateral column (Fig. 12.8, upper panel), the posterior orbitofrontal/anterior insular cortex targets preferentially the ventrolateral column (Fig. 12.8, lower panel), and the anterior cingulate gyrus targets mainly the lateral as well as the ventrolateral and dorsomedial columns (An *et al.*, 1998; Leichnetz *et al.*, 1981; Müller-Preuss and Jurgens, 1976). The significance of this topographical organization is not well understood, but given the well-known role of the prefrontal cortex in affect and mood, we can speculate that it corresponds to an organized network for processing and mediating the various motivational and emotional aspects of behavior (Bandler *et al.*, 2000). Whether this organization has been conserved with the massive expansion of the prefrontal cortex in humans cannot be known. However, these projections appear to be evolutionarily stable as indicated by the consistent pattern in the primate and rat (Floyd *et al.*, 2000).

Amygdala. The amygdala is another important source of input to the PAG although the projection is not as strong as from the prefrontal cortex (Mantyh, 1982b). Retrograde tracing shows that the projection originates from the central nucleus and the ventrolateral part of the basal nucleus mainly on the ipsilateral side (An *et al.*, 1998; Mantyh, 1982b). Anterograde tracing with [^{3}H]amino acids further shows that the PAG terminals of the central nucleus projection are in the dorsomedial, lateral, and ventrolateral column but not in the dorsolateral column (Price and Amaral, 1981) (Fig. 12.9). The PAG target of the ventrolateral basal nucleus has not been studied directly, but the retrograde studies of An *et al.* (1998) suggest input to the dorsolateral column. This pathway is interesting because the ventrolateral basal nucleus projects to the medial prefrontal cortex, which also targets the dorsolateral column (Bandler *et al.*, 2000; Ongur *et al.*, 1998). Given the well-known role of the amygdala in fear and defensive behavior, we can speculate that this organized projection is involved in the expression

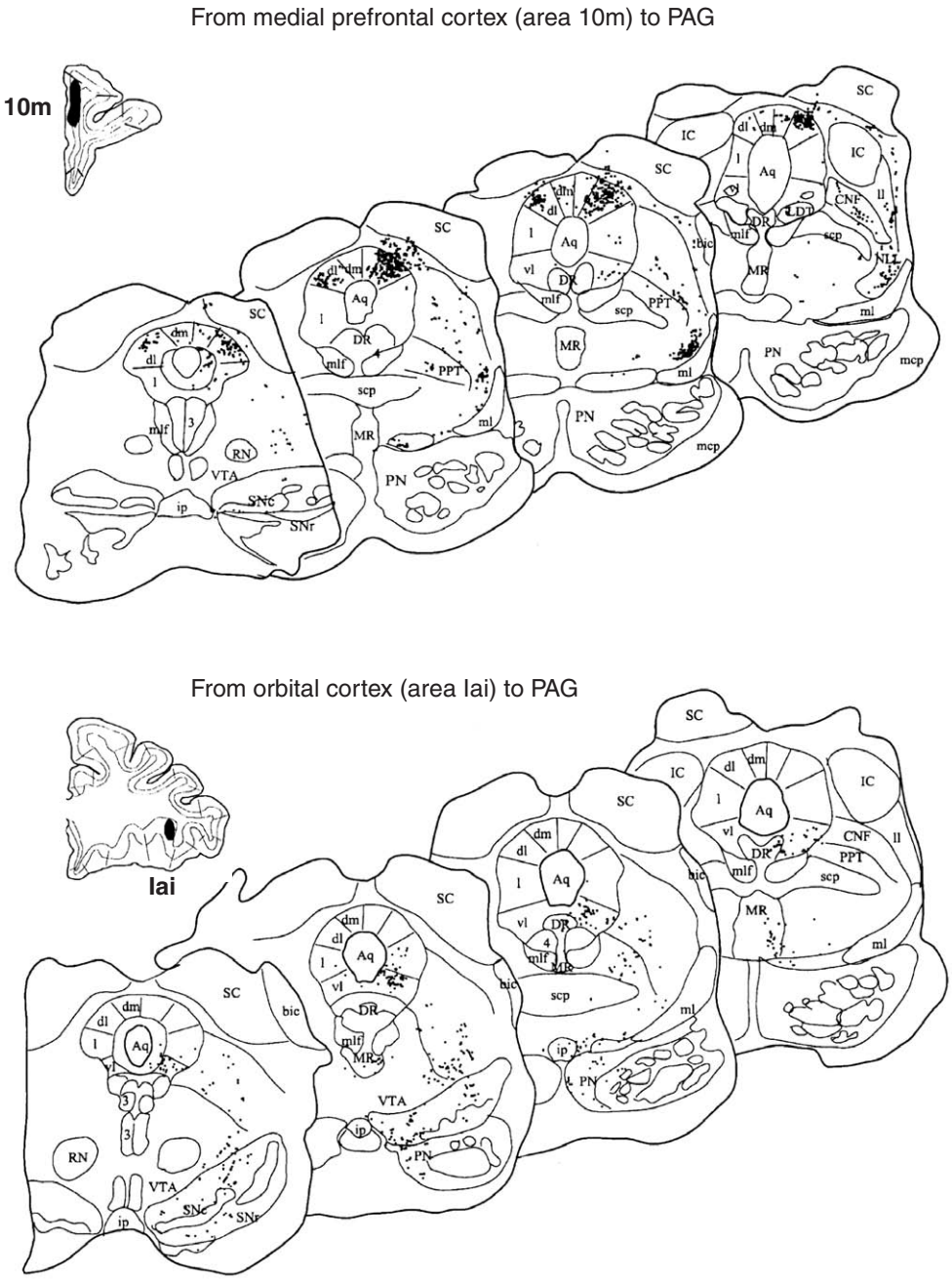

FIGURE 12.8 Distribution of axonal varicosities in the midbrain of the macaque monkey labeled following injections of the anterograde tracer biotinyilated dextran amine in the medial prefrontal cortex area 10m **(upper panel)** and orbital area Iai **(lower panel).** Afferents from medial prefrontal cortex terminate in the dorsolateral PAG column while afferents from the orbital cortex terminate in the ventrolateral PAG column. The frontal cortex diagrams depicting the injection sites are drawn at a lower magnification than the midbrain diagrams. The rostrocaudal axis for the midbrain sections is from left to right. Adapted from An *et al.* (1998, figure 9, p. 468; figure 12, p. 471; and figure 14, p. 473).

of emotional responses; however, the functional significance of the basolateral amygdala–dorsolateral PAG projection vs. amygdala–central dorsomedial/lateral/ventrolateral PAG is not clear at this stage.

Hypothalamus. HRP retrograde tracing shows that the PAG receives a massive input from the hypothalamus predominantly on the ipsilateral side (Mantyh, 1982c). Starting from the rostral hypothalamus, a heavy input originates from the medial preoptic area and the anterior hypothalamic area. In contrast, there is apparently little input coming from the supraoptic, paraventricular (magnocellular), and

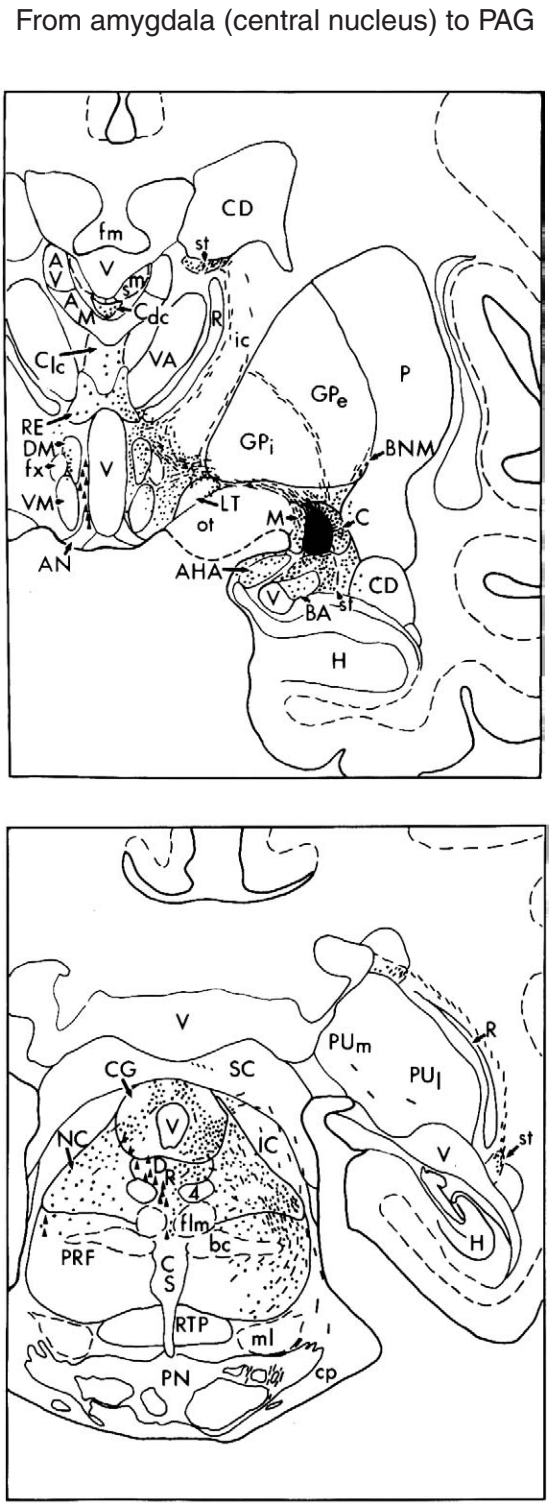

FIGURE 12.9 Distribution of autoradiographic silver grains in the midbrain of a macaque monkey following an injection of [^{3}H]amino acids in the central nucleus of the amygdala. Dots represent terminal fields or transversely cut axons. Note that the labeling is in the dorsomedial, lateral, and ventrolateral PAG and avoids the dorsolateral PAG. Small triangles represented on the left side represent neuromelanin-containing cells. Adapted from Price and Amaral (1981, figure 1, pp. 1244–1245).

suprachiasmatic nuclei. In the middle or tuberal region, the major inputs to PAG are the periventricular dorsal hypothalamus, ventromedial nucleus, and periarcuate region (just dorsal and lateral to the arcuate nucleus) together with the zona incerta laterally. PAG projecting neurons are also found throughout the rostrocaudal extent of the lateral hypothalamus, but few inputs are found from the arcuate nucleus itself. More caudally, the posterior hypothalamus and the supramammillary nucleus also represent major inputs. Most neurons project to the PAG via the periventricular bundle (Schütz bundle), except for those in the zona incerta, which travel more laterally in the medial forebrain bundle.

The specific PAG targets of some of these projections have been identified by anterograde tracing with [^{3}H]amino acids (Saper *et al.*, 1976, 1978; Veazey *et al.*, 1982). The anterior, posterior, and lateral hypothalamus areas project to the dorsomedial, lateral, and ventrolateral columns, but not to the dorsolateral column. The targets of the other areas of the hypothalamus have not been traced in the monkey. However, as mentioned earlier, β-endorphin, ACTH, and neurophysin projections—which arise from the region of the arcuate nucleus and paraventricular nucleus, respectively—terminate exclusively in the dorsomedial, lateral, and ventrolateral columns. Furthermore, studies in the rat indicate that with the exception of the dorsomedial part of the ventromedial nucleus, all areas of the hypothalamus project to the dorsomedial, lateral, and ventrolateral columns (Luiten *et al.*, 1987; Rizvi *et al.*, 1992; Roeling *et al.*, 1993; Veening *et al.*, 1991). The dorsomedial part of the ventromedial nucleus seems to be the only one that projects to the dorsolateral column (Canteras *et al.*, 1995; Veening *et al.*, 1991). These projections are likely to carry visceral, autonomic, and motivational information to the PAG, and to complement the limbic input coming from the prefrontal cortex and amygdala. It is worth noting here that many of these hypothalamic areas receive a reciprocal PAG input. This will be described later.

From Brain Stem

The brain stem afferents to the monkey PAG have been described by Mantyh (1982a) after retrograde transport of HRP. Here again the projections are predominantly ipsilateral. These afferents originate from the superior colliculus (mainly intermediate and deep layers) and the inferior colliculus (external layer) in the tectum, from the mesencephalic reticular formation and the cuneiform nucleus in the midbrain tegmentum, from the locus coeruleus and the parabrachial nucleus (lateral part) in the dorsal pons, and

from the ventromedial and ventrolateral medulla (raphe magnus and pallidus, the adjacent paragigantocellular area, and, more caudally the lateral tegmental field of the medulla). At this stage it is not known whether these afferents target specific columns. However, as mentioned earlier, the catecholaminergic projections that originate from the adrenergic and noradrenergic groups of the lower brain stem target the ventrolateral and, to some extent, the lateral columns. It is interesting to note that, like the hypothalamus, these brain stem areas are also major efferent targets of the PAG. These brain stem afferents could be part of feedback loops for proper integration of PAG outputs. Finally, projections from the solitary nucleus were not described by Mantyh (1982a). However, this could be due to placement of the HRP injection sites. Indeed, a small projection to the caudal ventrolateral PAG adjacent to the lateral parabrachial nucleus has been described after anterograde tracing with HRP and [^{3}H]amino acid injections into the solitary nucleus (Beckstead *et al.*, 1980). It is not known how important this projection is in the monkey, but in the rat there is a definite projection to the ventrolateral column (Herbert and Saper, 1992).

From Spinal Cord/Spinal Trigeminal Nucleus

Spinal projections to the PAG of the monkey were first demonstrated by Mehler (1969) using silver degeneration techniques. Retrograde tracing suggests the projection is sensory because it originates mainly from lamina 1 of the superficial dorsal horn and caudal trigeminal nucleus (Mantyh, 1982a; Wiberg *et al.*, 1987; Zhang *et al.*, 1990, see also Chapter 30). Other regions that contribute to the projection are the deep dorsal horn (lamina V), the lateral spinal nucleus, and, occasionally, the intermediate gray matter (lamina VII and X). These projections are predominantly contralateral, unlike the other afferent and efferent connections of the PAG. The spino-PAG projection has two other remarkable features that were revealed by anterograde tracing with the tracer wheat germ agglutinin–horseradish peroxidase (WGA-HRP) (Wiberg *et al.*, 1987; Yezierski, 1988) (Fig. 12.10). First, it terminates specifically in the lateral and ventrolateral columns and second, it is somatotopically organized (i.e., spinal trigeminal terminates at rostral PAG levels; cervical at intermediate levels, and lumbar at caudal levels) (Fig. 12.10). This latter feature suggests another level of organization within the PAG, this time along the rostrocaudal axis. Interestingly, this somatotopic organization is also present in other species, but it is clearest in the monkey (Blomqvist and Craig, 1991; Yezierski, 1988). There is very good evidence that the spinal neurons at the origin of this projection receive cutaneous, deep somatic, and visceral primary afferents and that they are readily activated by noxious stimulation (Clement *et al.*, 2000; Dougherty *et al.*, 1999; Yezierski, 1991). It also seems to be an important sensory projection given that it is much bigger than the better known spinothalamic projection. For example, a recent study in the cat shows that three times as many lamina I neurons project to the PAG than to the thalamus (Mouton and Holstege, 1998). All of this suggests that the PAG has an important role in processing and mediating responses to somatic and visceral noxious stimuli.

Periaqueductal Gray Efferents

To Forebrain

Anterograde tracing with [^{3}H]amino acids in the monkey shows that the forebrain targets of the PAG are in the diencephalon, mainly the hypothalamus and thalamus (Mantyh, 1983). The PAG does not project to any cortical region or to the hippocampus, amygdala, or basal ganglia. However, consistent labeling is found ventral to the aqueduct after retrograde tracing from these regions (Aggleton *et al.*, 1980; Amaral and Cowan, 1980; Porrino and Goldman-Rakic, 1982). These neurons clearly belong to the dorsal raphe and not to the PAG, but it is often a source of confusion.

Thalamus. The dorsal thalamus receives a substantial projection from the PAG, also predominantly ipsilateral (Mantyh, 1983). The targets are (1) the intralaminar nuclei, (2) the midline nuclei (central medial, central inferior, intramedial dorsal, reuniens, and paraventricular), and (3) the reticular nucleus. There is no input to the other main nuclei of the thalamus, including the ventrobasal complex. No retrograde study is available yet to know exactly how the different columns contribute to these projections in the monkey. However, a recent study in the rat (Krout and Loewy, 2000) showed that all four columns of the PAG contribute. Although no clear-cut demarcation was observed, the lateral and ventrolateral columns appear to provide the largest input. This is interesting because these two columns are the targets of the spino-PAG projection. Thus, the lateral/ventrolateral PAG connection with the intralaminar and midline nuclei may be an important link in the paleospinothalamic pathway (the polysynaptic ascending sensory system thought to mediate diffuse pain and its associated emotional overtones). Most importantly, the projection to the intralaminar and midline nuclei is a gateway to the cortex, especially limbic cortex and prefrontal cortex, and also to the amygdala and basal ganglia (Krout and Loewy, 2000; Mantyh, 1983). This may be the route by which the PAG accesses higher forebrain structures and is able to influence affect (e.g., fear). The reticular nucleus, on the other hand, does not project to any

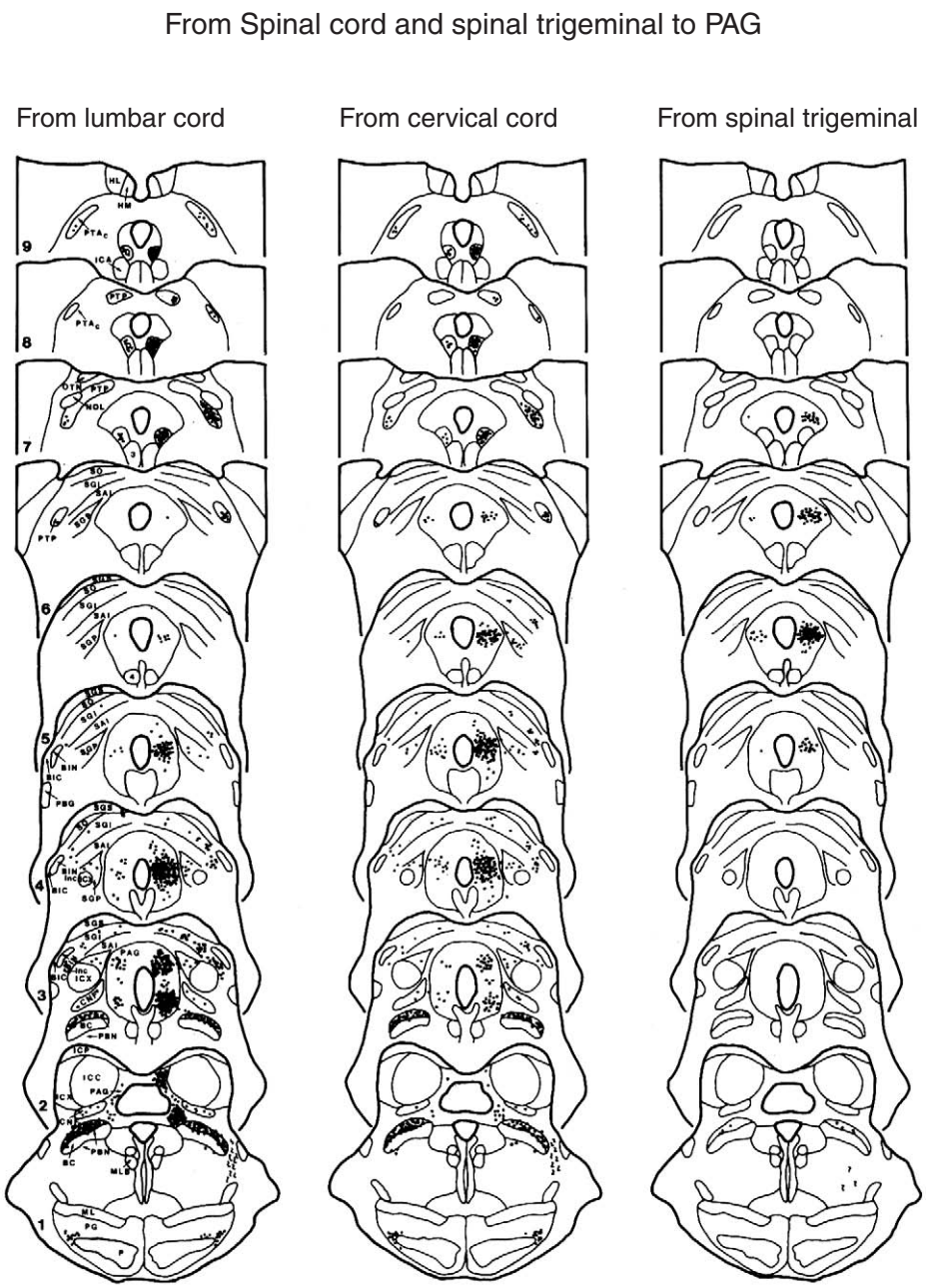

FIGURE 12.10 Distribution of axonal terminal labeling in the midbrain of macaque monkeys after injections of anterograde tracer wheat germ agglutinin–horseradish peroxidase (WGA-HRP) in the lumbar spinal cord, cervical spinal cord and laminar spinal trigeminal nucleus. All injections were on the left. Labeling is found in the contralateral lateral and ventrolateral PAG columns. Note also the somatotopic organization of the projections. Adapted from Wiberg *et al.* (1987, figure 2, p. 97).

cortical area, but regulates thalamic activity and controls thalamic output to the cortex. The input from PAG may represent a connection through which the PAG can modulate overall cortical activity (Mantyh, 1983).

Hypothalamus, substantia innominata, and zona incerta. The hypothalamus receives a heavy projection from the PAG that is predominantly ipsilateral (Mantyh, 1983). More specifically, the main targets in the rostral hypothalamus are the anterior medial areas and the substantia innominata. The supraoptic, paraventricular, and suprachiasmatic nuclei do not receive any afferents. In the intermediate hypothalamus, the projection is particularly dense, especially in the periventricular and dorsal nuclei. The ventromedial nucleus receives a moderate projection whereas the arcuate,

tuberal, and tuberomammillary nuclei do not appear to receive any input from the PAG. The posterior hypothalamus receives a heavy projection and blends with the periventricular bundle (Schütz bundle), which carries most of the connections between PAG and hypothalamus. Finally, the laterally located zona incerta also receives a heavy input from the PAG. Interestingly, many of these hypothalamic areas were already described as projecting to the PAG. There is indeed a high degree of reciprocity in this connection (Mantyh, 1983). However, it is not known whether this reciprocity extends to the level of the PAG columns. Nevertheless, the hypothalamus and the PAG are intricately related and appear to be key structures in the control of autonomic and behavioral responses (see also Chapter 17).

To brain Stem

The PAG projects to many structures in the brain stem, predominantly on the ipsilateral side (see also Chapter 30). Anterograde tracing (Mantyh, 1983) shows that the main PAG targets in the midbrain are the mesencephalic reticular formation laterally adjacent to the PAG, the superior colliculus (deep and intermediate layers but not superficial), and the cuneiform nucleus. In the dorsal pons, the locus coeruleus and the lateral parabrachial nuclei receive heavy projections, whereas the projections to the subcoeruleus nucleus and reticularis pontis oralis and caudalis are comparatively lighter. At this stage the efferent fibers move medially and ventrally to provide a heavy projection to a number of important structures in the caudal ventral pons and rostral ventral medulla, such as the median raphe nuclei (magnus and pallidus) and the paramedian gigantocellular and paragigantocellular nuclei. The more laterally placed parvicellular reticular nucleus receives a lighter projection. More caudally, there is a moderate-to-heavy projection to the retroambiguus nucleus and a lighter one to the surrounding reticular formation. Finally, no projection was found to the solitary nucleus or dorsal motor nucleus of the vagus (Mantyh, 1983).

Some of these projections to the raphe nuclei and paramedian reticular formation and to the retroambiguus nucleus have been verified by retrograde tracing (Chung *et al.*, 1983; Van der Horst *et al.*, 2000; Yezierski *et al.*, 1982). The projections to the raphe and paramedian reticular formation originate from the dorsomedial, lateral, and ventrolateral columns (Chung *et al.*, 1983; Yezierski *et al.*, 1982), and the projection to the retroambiguus nucleus originates from the lateral column, especially its intermediate part (Van der Horst *et al.*, 2000) (Fig. 12.11). This pattern of projection, which is very consistent across species, also indicates that the dorsolateral column does not project to the lower brain stem. The most caudal targets of the dorsolateral PAG, at least in the rat, appear to be the cuneiform nucleus (Redgrave and Dean, 1991; Redgrave *et al.*, 1988) and the adjacent superior lateral division of the parabrachial nucleus (Krout *et al.*, 1998). However, the cuneiform nucleus in turn projects to the lower brain stem (Korte *et al.*, 1992).

As pointed out by Holstege (1998), many of the PAG targets in the brain stem are premotor centers that in turn project to cranial nerve nuclei or to different groups of spinal interneurons (Fig. 12.12; see also Chapter 36). Some of these premotor centers have been well studied, and it is possible to understand their function. That the PAG projects to all these premotor centers suggests that it is an important integrating motor center for the coordinated expression of basic behavioral responses.

To Spinal Cord

Finally, the monkey PAG sends a moderate to light projection to the spinal trigeminal nucleus and into the spinal cord as far down as lumbar levels (Mantyh, 1983). However, these fibers end not in the superficial layers of the dorsal horn but in the deep layers and intermediate gray (V, VII, VIII) predominantly on the ipsilateral side. Thus, there is no reciprocity with the spino-PAG projection that originates from the superficial layers (mainly lamina I) on the contralateral side. The only way the PAG can access the superficial layers is via a relay in the rostral ventromedial medulla (e.g., raphe magnus). The PAG-spinal projection has been verified by retrograde tracing (Mantyh and Peschanski, 1982). It originates from a restricted region on the border between the lateral and ventrolateral columns. This projection is thought to target interneurons controlling motoneurons of the axial musculature (Mouton and Holstege, 1994) and some sympathetic preganglionic neurons (Fig. 12.12).

Summary

In summary, tracing studies reveal that the PAG is an important integrating center of the brain stem (Fig. 12.13). It is strategically located at the crossing of two systems: an ascending pain sensory system and a descending limbic (emotional) motor system (see Chapter 36). The two systems may modulate each other at the level of the PAG. Thus, the ascending sensory system, which relays noxious input from the spinal cord to the thalamus and then to the cortex and basal ganglia, can be modulated by limbic influence from prefrontal cortex and hypothalamus. This could lead, for example, to changes in the perception of pain

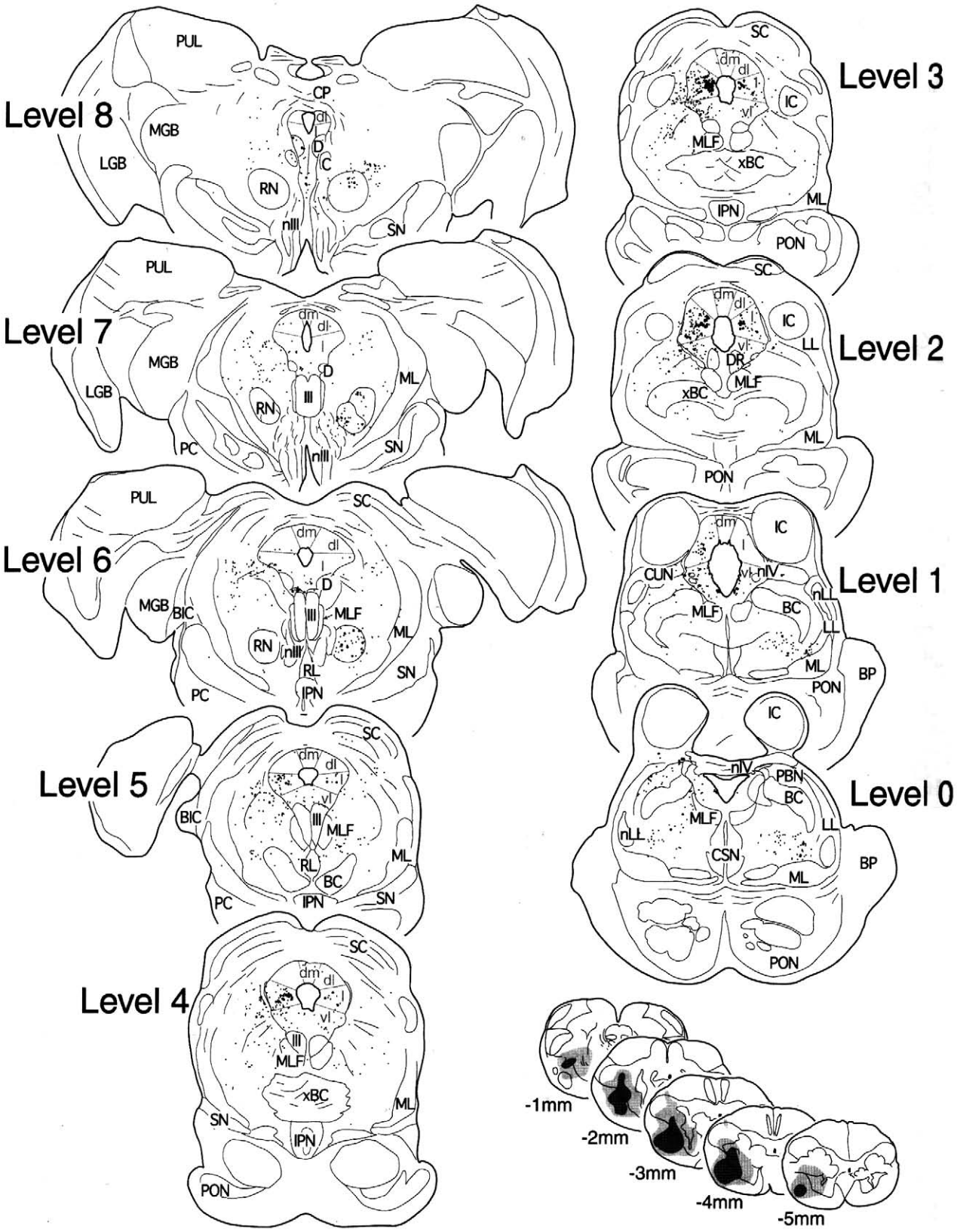

FIGURE 12.11 Distribution of retrogradely labeled neurons in the midbrain of a rhesus monkey after a wheat germ agglutinin–horseradish peroxidase (WGA-HRP) injection in the retroambiguus nucleus. The labeled cells are found mainly in the lateral PAG column. Adapted from Van der Horst *et al*. (2000, figure 3, p. 256).

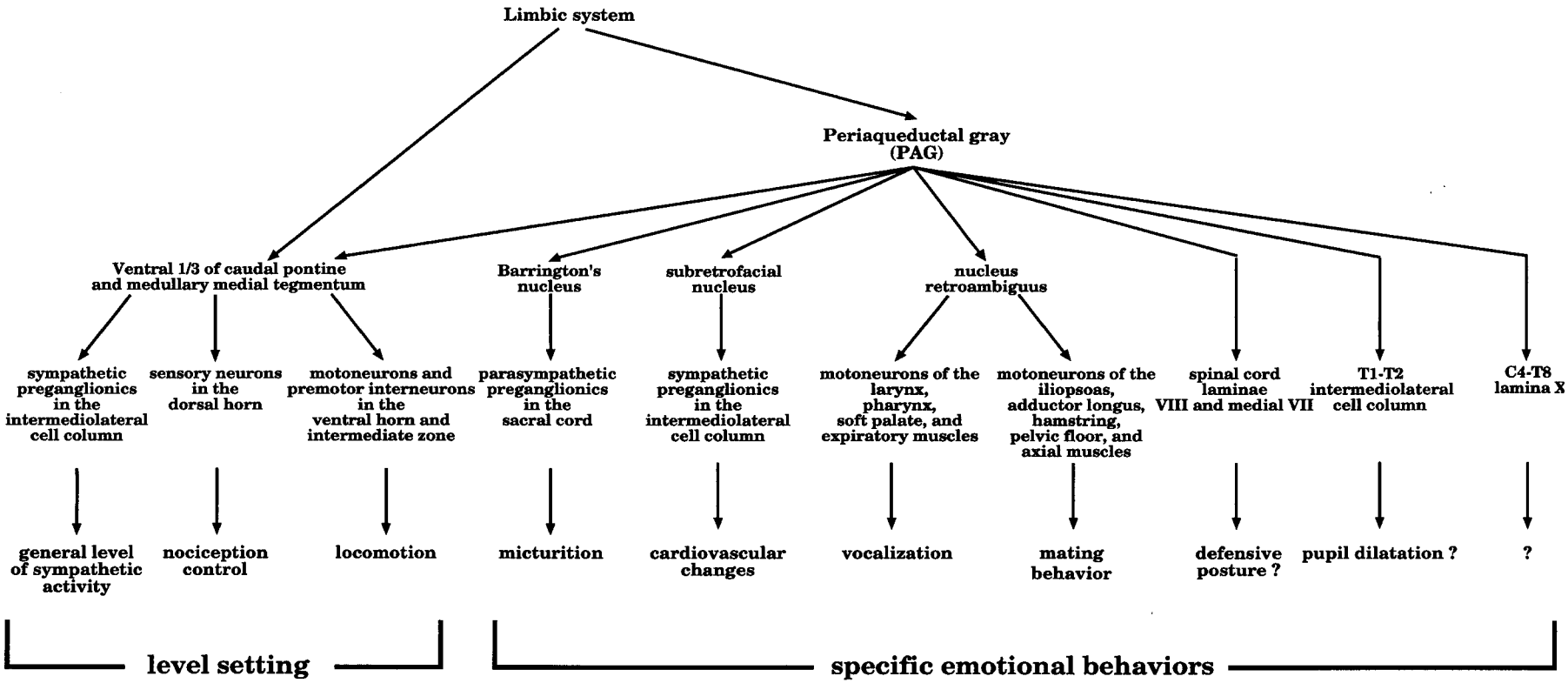

FIGURE 12.12 Schematic overview of the descending projections from the PAG to premotor centers of the caudal brain stem and to the spinal cord. The functions or possible functions of each projection is also indicated. From Holstege (1998, figure 2, p. 105).

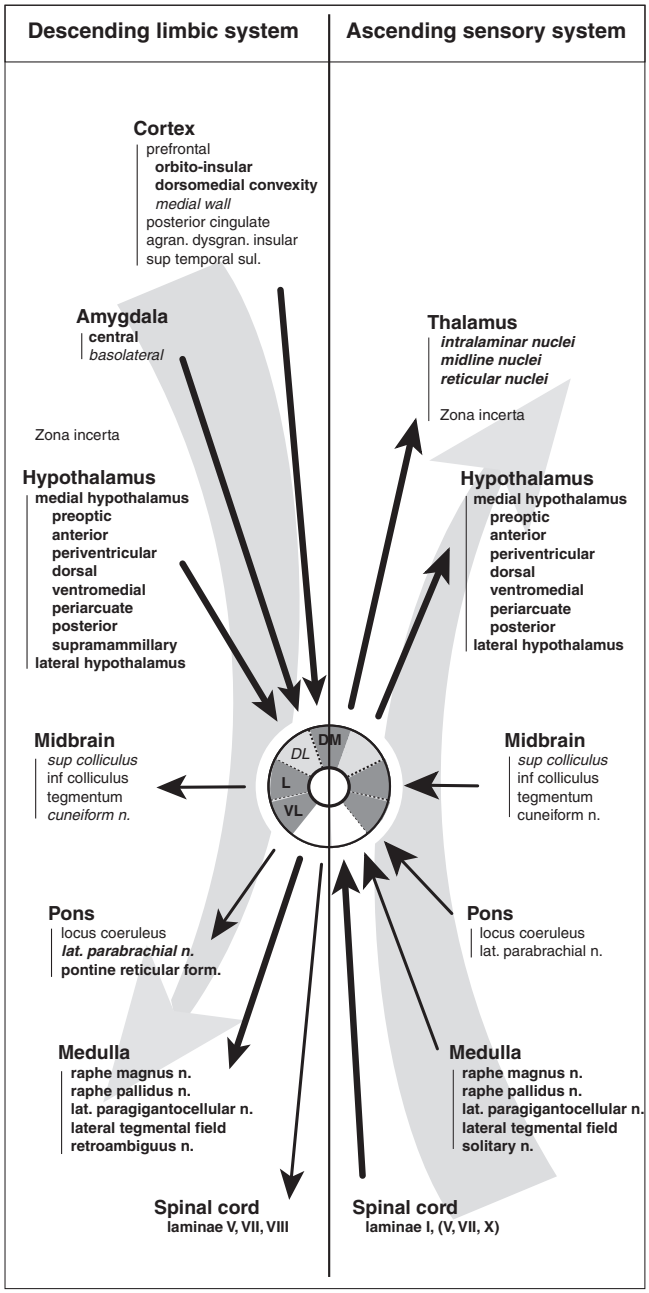

FIGURE 12.13 Schematic overview of the organization of PAG afferent and efferent connections. Represented on the left are the connections forming the descending limbic system and on the right are the connections forming the ascending sensory system. The two systems interact in the PAG. Structures indicated in **bold** are connected to either the dorsomedial, lateral or ventrolateral columns or two of them or all of them. Structures indicated in *italic* are connected to the dorsolateral column. Structures indicated in ***bold and italic*** are connected to all four columns. The specific connections of the structures indicated in regular style have not been established.

and other more subtle somatosensory stimuli. On the other hand, the descending limbic motor system, which controls basic but coordinated emotional responses by acting on premotor centers, can be modulated by sensory input coming from the external or internal (visceral) world. This could contribute to the transformation of mood or emotional state into different patterns of defensive reactions. It is important to bear in mind this basic organization when considering the different functional aspects of the PAG (i.e., pain modulation, fear, defensive behavior, vocalization, and reproductive behavior).

Tracing studies also support the existence of the columns and confirm the chemical disparity between the dorsolateral column and the other three columns established by chemoarchitecture. Thus, the lateral, ventrolateral, and, to some extent, the dorsomedial columns not only have common chemoarchitectural features; they also share common inputs and outputs. They are the integrating centers located at the crossing of the ascending sensory and descending limbic systems mentioned above (Fig. 12.13), and appear to be responsible for the best-known functions of the PAG. In contrast, the dorsolateral column stands out by its different chemical features and by a separate set of connections. It receives an important input from the prefrontal cortex but no direct somatosensory input, and only projects to the thalamus and caudal midbrain. The role of the dorsolateral column and the functional significance of its connections are still unknown.

FUNCTIONAL ASPECTS

Methodology and Limitations

The PAG appears to contribute to a wide range of behavioral reactions in animals. These include pain modulation, defensive reactions, cardiovascular regulation, vocalization, and reproductive behavior (Bandler and Shipley, 1994; Behbehani, 1995). Despite this diverse and extensive research, several problems have made a clear understanding of PAG function difficult to obtain. First, the PAG is an anatomically complex structure (see preceding sections). Second, the different subdivisions of the PAG (i.e., the columns) probably contribute to different behavioral reactions. Third, the widely held view of the PAG as an "analgesia center" has inhibited a broader understanding of its function.

Much of what is known about the function of the human PAG has been revealed by examining the effects of electrical stimulation. In the mid-1970s neurosurgeons began targeting the PAG with stimulating electrodes

as a means of treating chronic pain patients. Although some patients found pain relief, many refused stimulation because of unpleasant side effects. Regardless of the outcome, these stimulation studies revealed two things that have contributed to a better understanding of the function of the PAG. First, the unpleasant side effects revealed that the PAG is more than an "analgesia center." Second, the function of the PAG in humans appears consistent with reports of PAG function in animal studies (see below).

Additional insights into the function of the PAG have been revealed by examining patients with damage to that area (Collins *et al.*, 1995; Esposito *et al.*, 1999). However, these case reports must be viewed with caution because the deficits associated with PAG damage could be caused by damage to or activation of adjacent structures. In particular, damage to the PAG is often associated with ocular deficits because of the close proximity of ocular nuclei (e.g., Edinger–Westphal nucleus) and fibers traversing the PAG to these nuclei.

More recently, imaging technology such as positron emission tomography has been used to address questions about PAG function. For the most part, these studies have examined PAG activity in response to application of noxious stimuli or the anticipation of such stimuli. Although these studies have been interpreted as evidence that the PAG is part of an endogenous analgesia system, the significance of PAG activation in response to noxious stimuli is difficult to deduce from these data alone.

Role of the Periaqueductal Gray in Pain Modulation

The view of the PAG as an analgesia center dates back to a 1969 study in rats showing that PAG stimulation produced analgesia sufficient to perform abdominal surgery (Reynolds, 1969). Subsequent studies confirmed and extended this finding showing that (1) PAG stimulation inhibited the activity of nociceptive neurons in the dorsal horn of the spinal cord (Liebeskind *et al.*, 1973); (2) analgesia occurred in the absence of other behavioral effects (Mayer *et al.*, 1971); and (3) administration of the opiate antagonist naloxone attenuated PAG-mediated antinociception (Akil *et al.*, 1976). Although all three of these findings have been challenged (Cannon *et al.*, 1982; Gebhart and Jones, 1988; Klatt *et al.*, 1988; Morgan *et al.*, 1998; Thorn *et al.*, 1989), these early reports contributed to the view of the PAG as part of an endogenous analgesia system and led to the development of PAG stimulation as a treatment for chronic pain in humans (see also Chapter 30).

The first two papers describing PAG stimulation as a treatment for chronic pain reported positive results (Hosobuchi *et al.*, 1977; Richardson and Akil, 1977a). Not only did this enhance the view of the PAG as an analgesia center, but it encouraged other groups to target the PAG for stimulation as a treatment for chronic pain. Although the efficacy of brain stimulation to treat pain reported in subsequent studies varied greatly (Table 12.1), one point of agreement was that the more rostrally located periventricular gray (PVG) was a much more effective target than the PAG. Although the efficacy of brain stimulation is limited by medical problems caused by the electrode regardless of stimulation site (e.g., infection), the success of PAG stimulation is limited further by unpleasant side effects produced by the stimulation.

Table 12.1 shows that the long-term success rate for PAG stimulation is between 0 and 100%. Given that the goal is to reduce a patient's pain, the neurosurgeons optimize success using two approaches. First, surgery is carried out in awake patients so that the effects of stimulation at different sites can be determined and the electrode can be implanted in the most effective location. Second, multiple electrodes are implanted in each patient to maximize the chance of success. Optimistically high success rates may result when clear criteria for pain relief are not defined and when tests of efficacy are not carried out using blind procedures. Thus, the success of PAG stimulation in pain management is almost surely overstated. On the other hand, brain stimulation is only used to treat pain in the most severe cases, so that any success is noteworthy and of value to the patient. It should be noted that recent advances in intracerebroventricular and intrathecal administration of opioids has reduced the need for brain stimulation as a treatment for chronic pain (Gybels *et al.*, 1993).

Although the PVG and PAG form a seemingly continuous structure surrounding the third ventricle and aqueduct, the PVG has become the preferred site of stimulation because of the unpleasant side effects accompanying PAG stimulation. These effects can be so aversive that chronic pain patients refuse to stimulate the PAG despite a resultant reduction in pain (Boivie and Meyerson, 1982). Aversive reactions and antinociception also have been reported to co-occur with stimulation of the lateral and dorsal regions of the PAG in rats (Di Scala *et al.*, 1987; Fardin *et al.*, 1984; Morgan *et al.*, 1998; Prado and Roberts, 1985; Sandner *et al.*, 1987). However, these aversive reactions do not appear to cause analgesia (e.g., stress-induced antinociception) as has been postulated (Sandner *et al.*, 1987). Administration of the anxiolytic diazepam attenuates PAG evoked aversive reactions without

TABLE 12.1 Short and Long-Term Efficacy of Periaqueductal Gray Stimulation for the Management of Chronic Pain

Citation	Number of Patients	Initial Success[a]	Long Term Success	Notes
Hosobuchi *et al.*, 1977	6	6 (100%)	5 (83%)	
Hosobuchi, 1980	22		16 (73%)	Nociceptive pain patients
	17		0 (0%)	Deafferentation pain patients
Hosobuchi, 1983	11	11 (100%)	9 (82%)	PAG and thalamic electrodes
Hosobuchi, 1986	65	64 (98%)	50 (77%)	
Baskin *et al.*, 1986	7		7 (100%)	No distinction is made between PAG and PVG
Hosobuchi, 1987	7	7 (100%)	2 (29%)	Dorsal PAG stimulation
Young *et al.*, 1984	33	29 (88%)	22 (67%)	PAG and/or thalamus electrodes in 16 patients
Young *et al.*, 1985	42		33 (79%)	PAG/PVG and thalamus electrodes in 16 patients
Young and Brechner, 1986	17	16 (94%)	15 (88%)	Cancer pain patients
Young and Chambi, 1987	52	45 (87%)	33 (63%)	
Richardson and Akil, 1977a	5	5 (100%)		
Richardson and Akil, 1977b	4	1 (25%)		3 of 5 PVG sites were effective
Amano *et al.*, 1980	8	0 (0%)		PAG stimulation only lasted 10 s
Amano *et al.*, 1982	14	0 (0%)		PAG stimulation lasted 10–60 s
Levy *et al.*, 1987	52	30 (58%)	18 (35%)	Implants were near the posterior commissure
Cosyns and Gybels, 1979	3	0 (0%)		All 20 stimulation sites produced aversive reactions

[a]Initial success refers to the number of electrodes that were internalized as a result of pain inhibition during surgery.
PAG, periaqueductal gray; PVG, periventricular gray.

blocking stimulation-produced antinociception (Morgan *et al.*, 1987).

An important question is whether some regions of the human PAG will support stimulation-produced analgesia in the absence of unpleasant side effects. The anatomical subdivisions of the PAG described earlier in this chapter suggest functional differences. Because of ethical considerations, systematic mapping of the human PAG has not been carried out. Although the electrodes implanted into humans typically have four active sites, each separated by a millimeter or two, they are typically implanted in such a way that they are oriented along a single PAG column as opposed to across columns (see Gybels *et al.*, 1980; Richardson and Akil, 1977a). In the rat, pronounced differences in antinociception are produced simply by shifting stimulation from the lateral to ventrolateral column (Morgan, 1991). The most obvious difference is that activation of the lateral PAG in rats produces aversive reactions whereas activation of the ventrolateral PAG in the rat produces antinociception in the absence of any obvious aversive reaction (Fardin *et al.*, 1984; Morgan *et al.*, 1998).

In addition, differences in the characteristics of the antinociception mediated by the ventrolateral and more dorsal regions of the rat PAG have been reported (Morgan, 1991). The opioid antagonist naloxone attenuates the antinociception mediated by the ventrolateral but not more dorsal regions of the PAG (Cannon *et al.*, 1982; Thorn *et al.*, 1989). Another provocative difference is that the antinociception mediated by lateral and dorsal regions of the PAG appears resistant to tolerance in comparison with the antinociception mediated by the ventrolateral PAG. This has been demonstrated with both electrical stimulation (Morgan and Liebeskind, 1987) and morphine microinjections (Tortorici *et al.*, 1999). Finally, the ventrolateral PAG appears to modulate nociception via both ascending and descending pathways, whereas the antinociception mediated by the lateral and dorsal regions appear to follow a descending pathway only (Morgan *et al.*, 1989). If a similar functional organization exists in the human PAG, one might predict that stimulation of the ventrolateral PAG would produce more manageable pain relief than stimulation of the lateral PAG. It would be of great interest to carry out studies comparing stimulation of the lateral and ventrolateral PAG in humans.

Role of the Human Periaqueductal Gray in Emotion

The unpleasant sensations produced by PAG stimulation demonstrate that the PAG is much more than an analgesia center. Although the precise description of the sensations evoked by PAG stimulation vary from patient to patient and study to study (Table 12.2), the common element is an unpleasant sensation centered along the core of the

TABLE 12.2 Sensations Evoked from Periaqueductal Gray Stimulation

Nashold, Wilson, and Slaughter, 1969 (9 patients):
- "The patient also experienced an additional feeling described as fear which was so unpleasant that she was not willing to tolerate repeated stimulations."
- "… complain of vague bilateral sensations experienced as a 'choking' feeling referred into the chest."
- "In man, the feelings evoked from the central gray stimulation had a quality which he described as 'fearful,' 'frightful,' or 'terrible,' and he would not allow further stimulations."

Richardson and Akil, 1977 (4 patients):
- "… slight dizziness and shortness of breath …"
- "… numerous undesirable side effects, including nystagmus, nausea, vertigo, and a feeling of a 'rising vapor.'"
- "… increasing the stimulation above a certain level led to reports of poorly described noxious effects, such as discomfort, oppressiveness, or anxiety."

Cosyns and Gybels, 1979 (3 patients)
- "All patients displayed, on stimulation, an aversive emotional response which could outlast the stimulation itself."
- "The patients describe it as unpleasant and giving them feelings of anxiety and panic …"
- "All emotions were also bodily felt in the abdomen, chest, or head …"

Amano *et al.*, 1980 (8 patients):
- "… patients had a strong fear sensation on high frequency electrical stimulation …"
- "… patients complained of dizziness and unpleasant feeling … on low frequency stimulation …"

Amano *et al.*, 1982 (14 patients):
- "… substantial rise in pulse rate and systolic blood pressure (up to 50% increase). Bilaterally dilated pupils and flushing of the face were seen."
- "the patients suddenly expressed very strong fear sensation and a burning, hot feeling of the entire body. All of them appeared to be in a confused and acutely perplexed state."
- "The patients described themselves, 'Something horrible is coming', 'Somebody is now chasing me, I am trying to escape from him.'"
- "… he had an abrupt feeling of uncertainty 'just like entering into a long, dark tunnel.'"

Hosobuchi, 1987 (7 patients):
- "Five patients reported a significantly unpleasant sensation associated with stimulation …"
- "Five of the seven patients reported nausea, and four reported fright or a 'funny feeling' …"

body (from the bladder to inside the head). These sensations are so unpleasant that patients would rather endure chronic pain than receive stimulation of the PAG (Boivie and Meyerson, 1982). In contrast, stimulation of the more rostrally located PVG has been reported to have no effect (Hosobuchi, 1986) or to produce a warm or cold sensation throughout the body (Adams, 1977; Kumar and Wyant, 1985). These sensations are possibly a result of activation of the ascending sensory system, which relays in the lateral and ventrolateral PAG. As shown in Fig. 12.13, this system originates from lamina I of the spinal cord and terminates in the thalamus.

Fear and Defensive Behavior

PAG stimulation also produces sensations of fear, anxiety, and danger (Table 12.2). The stimulation was immediately stopped when these sensations occurred. Had they been prolonged they would certainly have led to strong behavioral responses. The co-occurrence of fear and antinociception suggests the PAG may contribute to defensive reactions. This hypothesis is supported by imaging studies showing that noxious stimulation or anticipation of a noxious stimulus activates the PAG (Hsieh *et al.*, 1996; Iadarola *et al.*, 1998; Kupers *et al.*, 2000). Noxious stimuli are threatening and have been shown to evoke defensive reactions (Fanselow, 1991). However, whether the noxious stimuli used in these studies are sufficient to evoke defensive reactions is debatable, so that these imaging data must be interpreted cautiously.

In contrast, behavioral studies in rats provide convincing evidence that the PAG contributes to defensive reactions. Fight-or-flight defense is evoked by attack from a predator or conspecific. A similar response consisting of explosive running and jumping is evoked upon activation of the lateral or dorsal regions of the caudal PAG (Fardin *et al.*, 1984; Morgan *et al.*, 1998; Sandner *et al.*, 1987). In addition, activation of the lateral PAG column produces cardiovascular changes consistent with defense. These include an increase in heart rate, blood pressure, and respiration, and a shift in blood flow from the viscera to the hindlimb muscles (Carrive and Bandler, 1991; Carrive *et al.*, 1987, 1989). Moreover, these coordinated responses can be evoked from precollicular decerebrate cats, indicating that such responses are integrated at the level of the PAG, not above. These responses are expressed via the lower part of the descending limbic system, i.e., the descending projections to the premotor centers of the lower brain stem, as indicated in Figure 12.12.

Fear can also induce a defensive reaction in rats known as freezing. Defensive freezing is a species-specific response produced by a threatening situation (Fanselow, 1991). A number of findings suggest that the ventrolateral column of the PAG contributes to this response. Activation of the ventrolateral PAG produces immobility (Depaulis *et al.*, 1994; Morgan *et al.*, 1998). Inactivation of the ventral PAG prevents the antinociception and immobility produced by placing

a rat in a frightening environment (Helmstetter and Tershner, 1994; Kim *et al.*, 1993; LeDoux *et al.*, 1988; Liebman *et al.*, 1970). Finally, placing a rat in an environment that induces defensive freezing activates neurons in the ventrolateral PAG as measured by c-fos-like immunoreactivity (Carrive *et al.*, 1997). Although the lateral and ventrolateral columns exist within the human PAG (see sections above), whether these regions correspond to functionally distinct types of defense as in the rat is open to speculation (Bandler *et al.*, 2000).

Vocalization and Reproductive Behavior

Although most of what is known about the PAG in humans focuses on analgesia and emotional reactions, animal studies indicate the PAG contributes to a number of other behaviors such as vocalization and reproduction (Fig. 12.12) (Bandler and Shipley, 1994; Behbehani, 1995; see also Chapter 36). The vocalization data are of particular interest because activation of the PAG evokes naturally occurring vocalizations in a wide range of species such as rat (Waldbillig, 1975), cat (Bandler and Carrive, 1988), and squirrel monkey (Jürgens and Ploog, 1970). Some of these vocalizations can be explained as part of PAG-mediated emotional (Table 12.2) and defensive responses (Bandler and Carrive, 1988), although stimulation of the ventrolateral PAG of the squirrel monkey elicits cooing and growling, vocalizations associated with comfort and dominance calls (Jürgens, 1991). PAG lesions also produce mutism in many species, including monkey (Jürgens, 1994) and human (Esposito *et al.*, 1999). Moreover, PAG lesions disrupt vocalizations evoked from higher brain structures such as the anterior cingulate cortex and amygdala (Jürgens and Pratt, 1979). In contrast, such lesions do not block vocal fold movements evoked from the facial motor cortex (Jürgens and Zwirner, 1996). Thus, two separate vocal pathways have been proposed: (1) a limbic one that relays in the PAG for nonverbal emotional vocal expression, and (2) a neocortical one that does not relay in PAG for the production of learned vocal patterns (Jürgens and Zwirner, 1996). The neocortical pathway is obviously crucial for human speech. However, the production of well-coordinated and intonated speech and in particular singing may require that the limbic pathway (the descending limbic system in Fig. 12.13) and the PAG be active as well (Davis *et al.*, 1996). As suggested by Davis *et al.* (1996), the role of the PAG may be to act as a generator and integrator of specific respiratory and laryngeal motor patterns to permit proper expression of the neocortical output. This would be made possible through the PAG's projections to the lower brain stem and in particular to the retroambiguus nucleus, which controls laryngeal motoneurons (Van der Horst *et al.*, 2000) (see Fig 12.12). This may be orchestrated by the lateral PAG column because it is a main target of the anterior cingulate gyrus and the amygdala and the main source of afferents to the retroambiguus nucleus (Fig. 12.13).

The PAG has been implicated in reproductive behavior in rat and cat, mainly as a coordinating center for mediating lordosis in the female (Pfaff *et al.*, 1994; Van der Horst and Holstege, 1998). This behavior, which may be seen as a form of emotional response, is thought to be mediated by PAG projections to the retroambiguus nucleus and rostral ventral medulla and to be the result of convergent influences in the PAG from limbic structures (especially hypothalamus), sex steroids, and sensory input from the perineum and pelvic viscera (Van der Horst and Holstege, 1998). Indeed, the sacral input to the PAG in the cat originates from dorsal horn regions that receive pelvic and pudendal sensory afferents (Van der Horst *et al.*, 1996). However, there is no evidence of any PAG involvement in reproductive behavior in the monkey and apparently no related comment has been made from human patients receiving PAG stimulation.

Finally it should be mentioned that the PAG has been implicated in micturition (Blok and Holstege, 1998) and that PET studies reveal activation of the PAG during micturition (Blok *et al.*, 1997).

CONCLUSION

In this chapter, we have presented anatomical evidences that the human PAG is not a homogeneous structure. Behind a deceiving cytoarchitecture lies a chemical organization that suggests the existence of four longitudinal columns located dorsomedial, dorsolateral, lateral, and ventrolateral to the aqueduct. The boundaries are revealed by a number of neurochemical markers like NADPH-diaphorase or ACTH-containing fibers. These columns appear to be important features as they are conserved across mammalian species. Furthermore, the afferent and efferent connections of the PAG are organized along these same columns. Although anatomical techniques prevent these connections from being demonstrated in humans, it is very likely that they exist because they are basically the same from rat to monkey. From these connections, it appears that the PAG is located at the crossroads of an ascending sensory system relaying noxious input and a descending limbic system organizing emotional responses. This seems clear at least for the lateral, ventrolateral, and dorsomedial columns, which share many common features. In

contrast, the dorsolateral PAG appears to have more in common with the deep and intermediate layers of the superior colliculus than with the other three columns. From a functional point of view, the PAG is one of the few brain structures that has been implanted with chronic electrodes and stimulated in awake human. The results of these studies indicate that the human PAG is involved in antinociception and aversive emotional responses—findings consistent with the anatomical connections. Although functional and anatomical data suggest the PAG is an important integrating center for coordinated emotional responses, the contribution of the various columns to these responses in human remains largely unknown. Such information requires the development of better functional imaging techniques with sufficient resolution to separate the different columns.

References

Adams, J. E. (1977). Technique and technical problems associated with implantation of neuroaugmentive devices. *Appl. Neurophysiol.* **40,** 111–23.

Adem, A., Nordberg, A., Jossan, S. S., Sara, V., and Gillberg, P. G. (1989). Quantitative autoradiography of nicotinic receptors in large cryosections of human brain hemispheres. *Neurosci. Lett.* **101,** 247–252.

Aggleton, J. P., Burton, M. J., and Passingham, R. E. (1980). Cortical and subcortical afferents to the amygdala of the rhesus monkey (Macaca mulatta). *Brain Res.* **190,** 347–368.

Akil, H., Mayer, D. J., and Liebeskind, J. C. (1976). Antagonism of stimulation-produced analgesia by naloxone, a narcotic antagonist. *Science* **191,** 961–962.

Amano, K., Kitamura, K., Kawamura, H., Tanikawa, T., Kawabatake, H., Notani, M., Iseki, H., Shiwaku, T., Suda, T., and Demura, H. (1980). Alterations of immunoreactive beta-endorphin in the third ventricular fluid in response to electrical stimulation of the human periaqueductal gray matter. *Appl. Neurophysiol.* **43,** 150-158.

Amano, K., Tanikawa, T., Kawamura, H., Iseki, H., Notani, M., Kawabatake, H., Shiwaku, T., Suda, T., Demura, H., and Kitamura, K. (1982). Endorphins and pain relief. Further observations on electrical stimulation of the lateral part of the periaqueductal gray matter during rostral mesencephalic reticulotomy for pain relief. *Appl. Neurophysiol.* **45,** 123–135.

Amaral, D. G., and Cowan, W. M. (1980). Subcortical afferents to the hippocampal formation in the monkey. *J. Comp. Neurol.* **189,** 573–591.

An, X., Bandler, R., Ongur, D., and Price, J. L. (1998). Prefrontal cortical projections to longitudinal columns in the midbrain periaqueductal gray in macaque monkeys. *J. Comp. Neurol.* **401,** 455–479.

Arsenault, M. Y., Parent, A., Seguela, P., and Descarries, L. (1988). Distribution and morphological characteristics of dopamine-immunoreactive neurons in the midbrain of the squirrel monkey (Saimiri sciureus). *J. Comp. Neurol.* **267,** 489–506.

Bandler, R., and Carrive, P. (1988). Integrated defence reaction elicited by excitatory amino acid microinjection in the midbrain periaqueductal grey region of the unrestrained cat. *Brain Res.* **439,** 95–106.

Bandler, R., and Shipley, M. T. (1994). Columnar organization in the midbrain periaqueductal gray: modules for emotional expression?. *Trends Neurosci.* **17,** 379–389.

Bandler, R., Carrive, P., and Depaulis, A. (1991a). Introduction. Emerging principles of organization in the midbrain periaqueductal gray matter. *In* "The Midbrain Periaqueductal Gray Matter. Functional, Anatomical and Neurochemical Organization" (A. Depaulis and R. Bandler, eds.), pp. 1–8. Plenum Press, New York.

Bandler, R., Carrive, P., and Zhang, S. P. (1991b). Integration of somatic and autonomic reactions within the midbrain periaqueductal grey: viscerotopic, somatotopic and functional organization. *Prog. Brain Res.* **87,** 269–305.

Bandler, R., Keay, K. A., Floyd, N., and Price, J. (2000). Central circuits mediating patterned autonomic activity during active vs. passive emotional coping. *Brain Res. Bull.* **53,** 95–104.

Baskin, D. S., Mehler, W. R., Hosobuchi, Y., Richardson, D. E., Adams, J. E., and Flitter, M. A. (1986). Autopsy analysis of the safety, efficacy and cartography of electrical stimulation of the central gray in humans. *Brain Res.* **371,** 231–236.

Beckstead, R. M., Morse, J. R., and Norgren, R. (1980). The nucleus of the solitary tract in the monkey: projections to the thalamus and brain stem nuclei. *J. Comp. Neurol.* **190,** 259–282.

Behbehani, M. M. (1995). Functional characteristics of the midbrain periaqueductal gray. *Prog. Neurobiol.* **46,** 575–605.

Beitz, A. J. (1985). The midbrain periaqueductal gray in the rat. I. Nuclear volume, cell number, density, orientation, and regional subdivisions. *J. Comp. Neurol.* **237,** 445–459.

Beitz, A. J. (1990). Central gray. *In* "The Human Nervous System" (G. Paxinos, ed.), pp. 307–320. Academic Press, San Diego.

Beitz, A. J., Clements, J. R., Mullett, M. A., and Ecklund, L. J. (1986). Differential origin of brain stem serotoninergic projections to the midbrain periaqueductal gray and superior colliculus of the rat. *J. Comp. Neurol.* **250,** 498–509.

Bernard, J. F., and Bandler, R. (1998). Parallel circuits for emotional coping behaviour: new pieces in the puzzle. *J. Comp. Neurol.* **401,** 429–436.

Blessing, W. W. (1997). "The Lower Brain Stem and Bodily Homeostasis." Oxford University Press, New York.

Blok, B. F. M., and Holstege, G. (1998). The central nervous system control of micturition in cats and humans. *Behav. Brain Res.* **92,** 119–125.

Blok, B. F. M., Willemsen, A. T. M., and Holstege, G. (1997) A PET study on the brain control of micturition in humans. *Brain* **120,** 111–121.

Blomqvist, A., and Craig, A. D. (1991). Organization of spinal and trigeminal input to the PAG. *In* "The Midbrain Periaqueductal Gray Matter. Functional, Anatomical and Neurochemical Organization" (A. Depaulis and R. Bandler, eds.), pp. 345–364. Plenum Press, New York.

Boivie, J., and Meyerson, B. A. (1982). A correlative anatomical and clinical study of pain suppression by deep brain stimulation. *Pain* **13,** 113–126.

Bouras, C., Magistretti, P. J., and Morrison, J. H. (1986). An immunohistochemical study of six biologically active peptides in the human brain. *Hum. Neurobiol.* **5,** 213–226.

Bouras, C., Magistretti, P. J., and Morrison, J. H., and Constantinidis, J. (1987). An immunohistochemical study of pro-somatostatin-derived peptides in the human brain. *Neuroscience* **22,** 781–800.

Buma, P., Veening, J., and Nieuwenhuys, R. (1989). Ultrastructural characterization of adrenocorticotrope hormone (ACTH) immunoreactive fibers in the mesencephalic central grey of the rat. *Eur. J. Neurosci.* **1,** 659–672.

Cannon, J. T., Prieto, G. J., Lee, A., and Liebeskind, J. C. (1982). Evidence for opioid and nonopioid forms of stimulation-produced analgesia in the rat. *Brain Res.* **243,** 315–321.

Canteras, N. S., Simerly, R. B., and Swanson, L. W. (1995). Organization of projections from the medial nucleus of the amygdala: a PHAL study in the rat. *J. Comp. Neurol.* **360,** 213–245.

Carrive, P. (1989). Functional organization of midbrain periaqueductal grey neurons mediating somatic and autonomic changes. PhD thesis *In* University of Sydney, Sydney, Australia.

Carrive, P. (1991). Functional organization of PAG neurons controlling vascular beds. *In* "The Midbrain Periaqueductal Gray Matter. Functional, Anatomical and Neurochemical Organization" (A. Depaulis and R. Bandler, eds.), pp. 67–100. Plenum Press, New York.

Carrive, P. (1993). The periaqueductal gray and defensive behavior: functional representation and neuronal organization. *Behav. Brain Res.* **58,** 27–47.

Carrive, P., and Bandler, R. (1991). Viscerotopic organization of neurons subserving hypotensive reactions within the midbrain periaqueductal grey: a correlative functional and anatomical study. *Brain Res.* **541,** 206–215.

Carrive, P., and Paxinos, G. (1994). The supraoculomotor cap: a region revealed by NADPH diaphorase histochemistry. *Neuroreport* **5,** 2257–2260.

Carrive, P., Dampney, R. A., and Bandler, R. (1987). Excitation of neurones in a restricted portion of the midbrain periaqueductal grey elicits both behavioural and cardiovascular components of the defence reaction in the unanaesthetised decerebrate *cat. Neurosci. Lett.* **81,** 273–278.

Carrive, P., Bandler, R., and Dampney, R. A. (1989). Somatic and autonomic integration in the midbrain of the unanesthetized decerebrate cat: A distinctive pattern evoked by excitation of neurones in the subtentorial portion of the midbrain periaqueductal grey. *Brain Res.* **483,** 251–258.

Carrive, P., Leung, P., Harris, J., and Paxinos, G. (1997). Conditioned fear to context is associated with increased Fos expresssion in the caudal ventrolateral region of the midbrain periaqueductal gray. *Neuroscience* **78,** 165–177.

Castro, M. E., Pascual, J., Romon, T., del Arco, C., del Olmo, E., and Pazos, A. (1997). Differential distribution of [3H]sumatriptan binding sites (5-HT1B, 5-HT1D and 5-HT1F receptors) in human brain: focus on brain stem and spinal cord. *Neuropharmacology* **36,** 535–542.

Chai, S. Y., McKenzie, J. S., McKinley, M.J. and Mendelsohn, F. A. O. (1990). Angiotensin converting enzyme in the human basal forebrain and midbrain visualized by in vitro autoradiography. *J. Comp. Neurol.* **291,** 179–194

Chen, C. P., Eastwood, S. L., Hope, T., McDonald, B., Francis, P. T., and Esiri, M. M. (2000). Immunocytochemical study of the dorsal and median raphe nuclei in patients with Alzheimer's disease prospectively assessed for behavioural changes. *Neuropathol. Appl. Neurobiol.* **26,** 347–355.

Christopoulos, G., Paxinos, G., Huang, X. F., Beaumont, K., Toga, A. W., and Sexton, P. M. (1995). Comparative distribution of receptors for amylin and the related peptides calcitonin gene related peptide and calcitonin in rat and monkey brain. *Can. J. Physiol. & Pharmacol.* **73,** 1037–1041.

Chung, J. M., Kevetter, G. A., Yezierski, R. P., Haber, L. H., Martin, R. F., and Willis, W. D. (1983). Midbrain nuclei projecting to the medial medulla oblongata in the monkey. *J. Comp. Neurol.* **214,** 93–102.

Clement, C. I., Keay, K. A., Podzebenko, K., Gordon, B. D., and Bandler, R. (2000). Spinal sources of noxious visceral and noxious deep somatic afferent drive onto the ventrolateral periaqueductal gray of the rat. *J. Comp. Neurol.* **425,** 323–344.

Clements, J. R., Madl, J. E., Johnson, R. L., Larson, A. A. and Beitz, A. J. (1987). Localization of glutamate, glutaminase, aspartate and aspartate aminotransferase in the rat midbrain periaqueductal gray. E*xp. Brain Res.* **67,** 594–602.

Collins, J. J., Berde, C. B., Grier, H. E., Nachmanoff, D. B., and Kinney, H. C. (1995). Massive opioid resistance in an infant with a localized metastasis to the midbrain periaqueductal gray. *Pain* **63,** 271–275.

Conrath-Verrier, M., Dietl, M., Arluison, M., Cesselin, F., Bourgoin, S., and Hamon, M. (1983). Localization of Met-enkephalin-like immunoreactivity within pain-related nuclei of cervical spinal cord, brain stem and midbrain in the cat. *Brain Res. Bull.* **11,** 587–604.

Cortes, R., Probst, A., Palacios, J. M. (1984). Quantitative light microscopic autoradiographic localization of cholinergic muscarinic receptors in human brain: brain stem. *Neuroscience* **4,** 1003–1026.

Cortes, R., Probst, A., Tobler, H. J., Palacios, J. M. (1986). Muscarinic cholinergic receptor subtypes in the human brain. II. Quantitative autoradiographic studies. *Brain Res.* **362,** 239–253.

Cosyns, P., and Gybels, J. (1979). Electrical central gray stimulation for pain in man. *In* "Advances in Pain Research and Therapy" (J. J. Bonica, ed.), Vol. 3, pp. 511–514. Raven Press, New York.

Davis, P. J., Zhang, S. P., Winkworth, A., and Bandler, R. (1996). Neural control of vocalization: respiratory and emotional influences. *J. Voice* **10,** 23–38.

Del Fiacco, M., Dessi, M. L., and Levanti, M. C. (1984). Topographical localization of substance P in the human post-mortem brain stem. An immunohistochemical study in the newborn and adult tissue. *Neuroscience* **12,** 591–611.

Depaulis, A., Keay, K. A., and Bandler, R. (1994). Quiescence and hyporeactivity evoked by activation of cell bodies in the ventrolateral midbrain periaqueductal gray of the rat. *Exp. Brain Res.* **99,** 75-83.

Di Scala, G., Mana, M. J., Jacobs, W. J., and Phillips, A. G. (1987). Evidence of Pavlovian conditioned fear following electrical stimulation of the periaqueductal grey in the rat. *Physiol. Behav.* **40,** 55–63.

Dietl, M. M., Hof, P. R., Martin, J. L., Magistretti, P. J., and Palacios, J. M. (1990). Autoradiographic analysis of the distribution of vasoactive intestinal peptide binding sites in the vertebrate central nervous system: a phylogenetic study. *Brain Res.* **520,** 14–26.

Doble, A., Malgouris, C., Daniel, M., Daniel, N., Imbault, F., Basbaum, A., Uzan, A., Gueremy, C., and Le Fur, G. (1987). Labelling of peripheral-type benzodiazepine binding sites in human brain with [3H]PK 11195: anatomical and subcellular distribution. *Brain Res. Bull.* **18,** 49–61.

Dougherty, P. M., Schwartz, A., and Lenz, F. A. (1999). Responses of primate spinomesencephalic tract cells to intradermal capsaicin. *Neuroscience* **90,** 1377–1392.

Esposito, A., Demeurisse, G., Alberti, B., and Fabbro, F. (1999). Complete mutism after midbrain periaqueductal gray lesion. *Neuroreport* **10,** 681–685.

Fanselow, M. S. (1991). The midbrain periaqueductal gray as a coordinator of action in response to fear and anxiety. *In* "The Midbrain Periaqueductal Gray Matter" (A. Depaulis and R. Bandler, eds.), Vol. 213, pp. 151–173. Plenum Press, New York.

Fardin, V., Oliveras, J. L., and Besson, J. M. (1984). A reinvestigation of the analgesic effects induced by stimulation of the periaqueductal gray matter in the rat. I. The production of behavioral side effects together with analgesia. *Brain Res.* **306,** 105–23.

Farley, I. J., and Hornykiewicz, O. (1977). Noradrenaline distribution insubcortical areas of the human brain. *Brain Res.* **126,** 53–62.

Floyd, N. S., Price, J. L., Ferry, A. T., Keay, K. A., and Bandler, R. (2000). Orbitomedial prefrontal cortical projections to distinct longitudinal columns of the periaqueductal gray in the rat. *J. Comp. Neurol.* **422,** 556–578.

Gebhart, G. F., and Jones, S. L. (1988). Effects of morphine given in the brain stem on the activity of dorsal horn nociceptive neurons. *Prog. Brain Res.* **77,** 229–243.

Gioia, M., Tredici, G., and Bianchi, R. (1998). Dendritic arborization and spines of the neurons of the cat and human periaqueductal gray: a light, confocal laser scanning, and electron microscope study. *Anat. Rec.* **251,** 316–325.

Gramsch, C., Hollt, V., Mehraein, P., Pasi, A., and Herz, A. (1979). Regional distribution of methionine-enkephalin- and beta-endorphin-like immunoreactivity in human brain and pituitary. *Brain Res.* **171,** 261–270.

Gramsch, C., Hollt, V., Pasi, A., Mehraein, P., and Herz, A. (1982). Immunoreactive dynorphin in human brain and pituitary. *Brain Res.* **233,** 65–74.

Graybiel, A. M. (1979). Periodic-compartmental distribution of acetylcholinesterase in the superior colliculus of the human brain. *Neuroscience* **4,** 643–650.

Gundlach, A. L. (1991). Regional subdivisions in the midbrain periaqueductal gray of the cat revealed by in vitro receptor autoradiography. *In* "The Midbrain Periaqueductal Gray Matter. Functional, Anatomical and Neurochemical Organization" (A. Depaulis and R. Bandler, eds.), pp. 449–464. Plenum Press, New York.

Gybels, J., Dom, R., and Cosyns, P. (1980). Electrical stimulation of the central gray for pain relief in human: autopsy data. *Acta Neurochir. Suppl.* **30,** 259–268.

Gybels, J., Kupers, R., and Nuttin, B. (1993). Therapeutic stereotactic procedures on the thalamus for pain. *Acta Neurochir.* **124,** 19–22.

Halliday, G. M., Gai, W. P., Blessing, W. W., and Geffen, L. B. (1990). Substance P-containing neurons in the pontomesencephalic tegmentum of the human brain. Neuroscience 39, 81–96.

Halliday, G., Harding, A., and Paxinos, G. (1995). Serotonin and tachykinin systems. *In* "The Rat Nervous System," 2nd ed. (G. Paxinos, ed.), pp. 929–974. Academic Press, San Diego.

Hardy, S. G., and Leichnetz, G. R. (1981). Cortical projections to the periaqueductal gray in the monkey: a retrograde and orthograde horseradish peroxidase study. *Neurosci. Lett.* **22,** 97–101.

Helmstetter, F. J., and Tershner, S. A. (1994). Lesions of the periaqueductal gray and rostral ventromedial medulla disrupt antinociceptive but not cardiovascular aversive conditional responses. *J. Neurosci.* **14,** 7099–7108.

Herbert, H., and Saper, C. B. (1992). Organization of medullary adrenergic and noradrenergic projections to the periaqueductal gray matter in the rat. *J. Comp. Neurol.* **315,** 34–52.

Holstege, G. (1998). The emotional motor system in relation to the supraspinal control of micturition and mating behavior. *Behav. Brain Res.* **92,** 103–109.

Hope, B. T., Michael, G. J., Knigge, K. M., and Vincent, S. R. (1991). Neuronal NADPH diaphorase is a nitric oxide synthase. *Proc. Nat. Acad. Sci. U.S.A.* **88,** 2811–2814.

Hosobuchi, Y. (1980). The current status of analgesic brain stimulation. *Acta Neurochir. Suppl.* **30,** 219–227.

Hosobuchi, Y. (1983). Combined electrical stimulation of the periaqueductal gray matter and sensory thalamus. *Appl. Neurophysiol.* **46,** 112–115.

Hosobuchi, Y. (1986). Subcortical electrical stimulation for control of intractable pain in humans. Report of 122 cases (1970-1984). *J. Neurosurg.* **64,** 543–553.

Hosobuchi, Y. (1987). Dorsal periaqueductal gray-matter stimulation in humans. *Pacing Clin. Electrophysiol.* **10,** 213–216.

Hosobuchi, Y., Adams, J. E., and Linchitz, R. (1977). Pain relief by electrical stimulation of the central gray matter in humans and its reversal by naloxone. *Science* **197,** 183–186.

Hsieh, J. C., Stahle-Backdahl, M., Hagermark, O., Stone-Elander, S., Rosenquist, G., and Ingvar, M. (1996). Traumatic nociceptive pain activates the hypothalamus and the periaqueductal gray: a positron emission tomography study. *Pain* **64,** 303–314.

Hurd, Y. L. (1996). Differential messenger RNA expression of prodynorphin and proenkephalin in the human brain [published erratum appears in Neuroscience 1996 Sep;74(1):293]. *Neuroscience* **72,** 767–783.

Hurd, Y. L., Keller, E., Sotonyi, P., and Sedvall, G. (1999). Preprotachykinin-A mRNA expression in the human and monkey brain: an *in situ* hybridization study. *J. Comp. Neurol.* **411,** 56–72.

Iadarola, M. J., Berman, K. F., Zeffiro, T. A., Byas-Smith, M. G., Gracely, R. H., Max, M. B., and Bennett, G. J. (1998). Neural activation during acute capsaicin-evoked pain and allodynia assessed with PET. *Brain* **121,** 931–947.

Ibuki, T., Okamura, H., Miyazaki, M., Yanaihara, N., Zimmerman, E. A., and Ibata, Y. (1989). Comparative distribution of three opioid systems in the lower brain stem of the monkey (Macaca fuscata). *J. Comp. Neurol.* **279,** 445–456.

Jürgens, U. (1991). Neurochemical study of PAG control of vocal behavior. *In* "The Midbrain Periaqueductal Gray Matter" (A. Depaulis and R. Bandler, eds.), Vol. 213, pp. 11–21. Plenum Press, New York.

Jürgens, U. (1994). The role of the periaqueductal gray in vocal behaviour. *Behav. Brain Res.* **62,** 107–117.

Jürgens, U., and Müller-Preuss, P. (1977). Convergent projections of different limbic vocalization areas in the squirrel monkey. *Exp. Brain Res.* **29,** 75–83.

Jürgens, U., and Ploog, D. (1970). Cerebral representation of vocalization in the squirrel monkey. *Exp. Brain Res.* **10,** 532–554.

Jürgens, U., and Pratt, R. (1979). Role of the periaqueductal grey in vocal expresssion of emotion. *Brain Res.* **167,** 367–378.

Jürgens, U., and Zwirner, P. (1996). Role of the periaqueductal grey in limbic and neocortical vocal fold control. *Neuroreport* **7,** 2921–2923.

Kim, J. J., Rison, R. A., and Fanselow, M. S. (1993). Effects of amygdala, hippocampus, and periaqueductal gray lesions on short- and long-term contextual fear. *Behav. Neurosci.* **107,** 1093–1098.

Kinney, H. C., Filiano, J. J., Assmann, S. F., Mandell, F., Valdes-Dapena, M., Krous, H. F., O'Donnell, T., Rava, L. A., and Frost White, W. (1998). Tritiated-naloxone binding to brain stem opioid receptors in the sudden infant death syndrome. *J. Auton. Nerv. Syst.* **69,** 156–163.

Klatt, D. S., Guinan, M. J., Culhane, E. S., Carstens, E., and Watkins, L. R. (1988). The dorsal raphe nucleus: a re-evaluation of its proposed role in opiate analgesia systems. *Brain Res.* **447,** 246–252.

Kölliker, A. (1896). "Handbuch der Gewebelehre des Menschen." Verlag von Wilhem Engelmann, Leipzig.

Kopp, N., Denoroy, L., Renaud, B., Pujol, J. F., Tabib, A., and Tommasi, M. (1979). Distribution of adrenaline-synthesizing enzyme activity in the human brain. *J. Neurol. Sci.* **41,** 397–409.

Korte, S. M., Jaarsma, D., Luiten, P. G., and Bohus, B. (1992). Mesencephalic cuneiform nucleus and its ascending and descending projections serve stress-related cardiovascular responses in the rat. *J. Auton. Nerv. Syst.* **41,** 157–176.

Kowall, N. W., and Mueller, M. P. (1988). Morphology and distribution of nicotinamide adenine dinucleotide phosphate (reduced form) diaphorase reactive neurons in human brain stem. *Neuroscience* **26,** 645–654.

Krout, K. E., and Loewy, A. D. (2000). Periaqueductal gray matter projections to midline and intralaminar thalamic nuclei of the rat. *J. Comp. Neurol.* **424,** 111–141.

Krout, K. E., Jansen, A. S., and Loewy, A. D. (1998). Periaqueductal gray matter projection to the parabrachial nucleus in rat. *J. Comp. Neurol.* **401,** 437–454.

Kumar, K., and Wyant, G. M. (1985). Deep brain stimulation for alleviating chronic intractable pain. *Can. J. Surg.* **28,** 20–22.

Kupers, R. C., Gybels, J. M., and Gjedde, A. (2000). Positron emission tomography study of a chronic pain patient successfully treated with somatosensory thalamic stimulation. *Pain* **87,** 295–302.

Laemle, L. K. (1979). Neuronal populations of the human periaqueductal gray, nucleus lateralis. *J. Comp. Neurol.* **186,** 93–107.

LeDoux, J. E., Iwata, J., Cicchetti, P., and Reis, D. J. (1988). Different projections of the central amygdaloid nucleus mediate autonomic and behavioral correlates of conditioned fear. *J. Neurosci.* **8,** 2517–2529.

Leichnetz, G. R., Spencer, R. F., Hardy, S. G., and Astruc, J. (1981). The prefrontal corticotectal projection in the monkey; an anterograde and retrograde horseradish peroxidase study. *Neuroscience* **6,** 1023–1041.

Levy, R. M., Lamb, S., and Adams, J. E. (1987). Treatment of chronic pain by deep brain stimulation: long term follow-up and review of the literature. *Neurosurgery* **21,** 885–893.

Liebeskind, J. C., Guilbaud, G., Besson, J., and Oliveras, J. L. (1973). Analgesia from electrical stimulation of the periaqueductal gray matter in the cat: behavioral observations and inhibitory effects on spinal cord interneurons. *Brain Res.* **50,** 441–446.

Liebman, J. M., Mayer, D. J., and Liebeskind, J. C. (1970). Mesencephalic central gray lesions and fear-motivated behavior in rats. *Brain Res.* **23,** 353–370.

Luiten, P. G., ter Horst, G. J., and Steffens, A. B. (1987). The hypothalamus, intrinsic connections and outflow pathways to the endocrine system in relation to the control of feeding and metabolism. *Prog. Neurobiol.* **28,** 1–54.

Mai, J. K., Triepel, J., and Metz, J. (1987). Neurotensin in the human brain. *Neuroscience* **22,** 499–524.

Mantyh, P. W. (1982a). The ascending input to the midbrain periaqueductal gray of the primate. *J. Comp. Neurol.* **211,** 50–64.

Mantyh, P. W. (1982b). Forebrain projections to the periaqueductal gray in the monkey, with observations in the cat and rat. *J. Comp. Neurol.* **206,** 146–158.

Mantyh, P. W. (1982c). The midbrain periaqueductal gray in the rat, cat, and monkey: a Nissl, Weil, and Golgi analysis. *J. Comp. Neurol.* **204,** 349–363.

Mantyh, P. W. (1983). Connections of midbrain periaqueductal gray in the monkey. I. Ascending efferent projections. *J. Neurophysiol.* **49,** 567–581.

Mantyh, P. W., and Peschanski, M. (1982). Spinal projections from the periaqueductal grey and dorsal raphe in the rat, cat and monkey. *Neuroscience* **7,** 2769–2776.

Mayer, D. J., Wolfle, T. L., Akil, H., Carder, B., and Liebeskind, J. C. (1971). Analgesia from electrical stimulation in the brain stem of the rat. *Science* **174,** 1351–1354.

Mefford, I., Oke, A., Adams, R. N., and Jonsson, G. (1977). Epinephrine localization in the human brain stem. *Neurosci. Lett.* **5,** 141–145.

Mehler, W. R. (1969). Some neurological species differences-a posteriori. *Ann. N. Y. Acad. Sci.* **167,** 424–468.

Mesulam, M. M., Mufson, E. J., Levey, A. I., and Wainer, B. H. (1984). Atlas of cholinergic neurons in the forebrain and upper brain stem of the macaque based on monoclonal choline acetyltransferase immunohistochemistry and acetylcholinesterase histochemistry. *Neuroscience* **12,** 669–686.

Morgan, M. M. (1991). Differences in antinociception evoked from dorsal and ventral regions of the caudal periaqueductal gray matter. *In* "The Midbrain Periaqueductal Gray Matter" (A. Depaulis and R. Bandler, eds.), Vol. 213, pp. 139–150. Plenum Press, New York.

Morgan, M. M., and Liebeskind, J. C. (1987). Site specificity in the development of tolerance to stimulation-produced analgesia from the periaqueductal gray matter of the rat. *Brain Res.* **425,** 356–359.

Morgan, M. M., Depaulis, A., and Liebeskind, J. C. (1987). Diazepam dissociates the analgesic and aversive effects of periaqueductal gray stimulation in the rat. *Brain Res.* **423,** 395–398.

Morgan, M. M., Sohn, J. H., and Liebeskind, J. C. (1989). Stimulation of the periaqueductal gray matter inhibits nociception at the supraspinal as well as spinal level. *Brain Res.* **502,** 61–66.

Morgan, M. M., Whitney, P. K., and Gold, M. S. (1998). Immobility and flight associated with antinociception produced by activation of the ventral and lateral/dorsal regions of the rat periaqueductal gray. *Brain Res.* **804,** 159–166.

Moss, M. S., Glazer, E. J., and Basbaum, A. I. (1983). The peptidergic organization of the cat periaqueductal gray. I. The distribution of immunoreactive enkephalin-containing neurons and terminals. *J. Neurosci.* **3,** 603–616.

Mouton, L. J., and Holstege, G. (1994). The periaqueductal gray in the cat projects to lamina VIII and the medial part of lamina VII throughout the length of the spinal cord. *Exp. Brain Res.* **101,** 253–264.

Mouton, L. J., and Holstege, G. (1998). Three times as many lamina I neurons project to the periaqueductal gray than to the thalamus: a retrograde tracing study in the cat. *Neurosci. Lett.* **255,** 107–110.

Müller-Preuss, P., and Jurgens, U. (1976). Projections from the "cingular" vocalization area in the squirrel monkey. *Brain Res.* **103,** 29–43.

Nashold, B. S., Jr., Wilson, W. P., and Slaughter, D. G. (1969). Sensations evoked by stimulation in the midbrain of man. *J. Neurosurg.* **30,** 14–24.

Nobin, A., and Bjorklund, A. (1973). Topography of the monoamine neuron systems in the human brain as revealed in fetuses. *Acta Physiol. Scand. Supple.* **388,** 1–40.

Nomura, H., Shiosaka, S., and Tohyama, M. (1987). Distribution of substance P-like immunoreactive structures in the brain stem of the adult human brain: an immunocytochemical study. *Brain Res.* **404,** 365–370.

Olszewski, J., and Baxter, D. (1954). "Cytoarchitecture of the Human Brain." Lippincott, Philadelphia.

Ongur, D., An, X., and Price, J. L. (1998). Prefrontal cortical projections to the hypothalamus in macaque monkeys. *J. Comp. Neurol.* **401,** 480–505.

Onstott, D., Mayer, B., and Beitz, A. J. (1993). Nitric oxide synthase immunoreactive neurons anatomically define a longitudinal dorsolateral column within the midbrain periaqueductal gray of the rat: analysis using laser confocal microscopy. *Brain Res.* **610,** 317–324.

Palacios, J. M., Probst, A., and Cortes, R. (1983). The distribution of serotonin receptors in the human brain: high density of [3H]LSD binding sites in the raphe nuclei of the brain stem. *Brain Res.* **274,** 150–155.

Parvizi, J., Van Hoesen, G. W., and Damasio, A. (2000). Selective pathological changes of the periaqueductal gray matter in Alzheimer's disease. *Ann. Neurol.* **48,** 344–253.

Pascual, J., del Arco, C. Gonzalez, A. M. and Pazos, A. Quantitative light microscopic localization of a2-adreniceptors in the human brain. *Brain Res.* **585,** 116–127.

Pau, K.-Y. F., Yu, J., Lee, C. J., and Spies, H. G. (1998). Topographic localization of neuropeptide Y in the monkey brain stem. *Regula. Peptides* **75–76,** 145–153.

Paxinos, G., Carrive, P. Wang, H. Q. and Wang, P.-Y. (1999). "Chemoarchitectonic Atlas of the Rat Brain Stem." Academic Press, San Diego.

Paxinos, G., and Huang, X.-F. (1995). "Atlas of the Human Brain Stem." Academic Press, San Diego.

Paxinos, G., Huang, X. F., Sexton, P., Toga, A., Wang, H. Q., and Carrive, P. (1995). Neurotransmitters as a tool for mapping the human brain. *In* "Neurotransmitters in the Human Nervous System; Advances in Behavioral Biology" (D. Tracey, G. Paxinos, and J. Stone, eds.), Vol. 43, pp. 1–24. Plenum Press, New York.

Pazos, A., Probst, A., and Palacios, J. M. (1987a). Serotonin receptors in the human brain—III. Autoradiographic mapping of serotonin-1 receptors. *Neuroscience* 21, 97–122.

Pazos, A., Probst, A., and Palacios, J. M. (1987b). Serotonin receptors in the human brain—IV. Autoradiographic mapping of serotonin-2 receptors. *Neuroscience* **21,** 123–139.

Pearson, J., Goldstein, M., Markey, K., and Brandeis, L. (1983). Human brain stem catecholamine neuronal anatomy as indicated by immunocytochemistry with antibodies to tyrosine hydroxylase. *Neuroscience* **8,** 3–32.

Pearson, J., Halliday, G., Sakamoto, N., and Michel, J.-P. (1990). Catecholaminergic neurons. *In* "The Human Nervous System" (G. Paxinos, ed.), pp. 1023–1050. Academic Press, San Diego.

Pfaff, D. W., Schwartz-Giblin, S., McCarthy, M. M. and Kow L. M. (1994). Cellular and molecular mechanisms of female reproductive behaviors. *In* "The Physiology of Reproduction," Vol. 2 (E. Knobil and J.D. Neill, eds.), pp. 107–220. Raven Press, New York.

Pfeiffer, A., Pasi, A., Mehraein, P., and Herz, A. (1982). Opiate receptor binding sites in human brain. *Brain Res.* **248,** 87–96.

Pilcher, W. H., Joseph, S. A., and McDonald, J. V. (1988). Immunocytochemical localization of pro-opiomelanocortin neurons in human brain areas subserving stimulation analgesia. *J. Neurosurg.* **68,** 621–629.

Pioro, E. P., Mai, J. K., and Cuello, A. C. (1990). Distribution of substance P- and enkephalin-immunoreactive neurons and fibers. *In* "The Human Nervous System" (G. Paxinos, ed.), pp. 1051–1094. Academic Press, San Diego.

Pittius, C. W., Seizinger, B. R., Pasi, A., Mehraein, P., and Herz, A. (1984). Distribution and characterization of opioid peptides derived from proenkephalin A in human and rat central nervous system. *Brain Res.* **304,** 127–136.

Porrino, L. J., and Goldman-Rakic, P. S. (1982). Brain stem innervation of prefrontal and anterior cingulate cortex in the rhesus monkey revealed by retrograde transport of HRP. *J. Comp. Neurol.* **205,** 63–76.

Prado, W. A., and Roberts, M. H. (1985). An assessment of the antinociceptive and aversive effects of stimulating identified sites in the rat brain. *Brain Res.* **340,** 219–228.

Price, J. L., and Amaral, D. G. (1981). An autoradiographic study of the projections of the central nucleus of the monkey amygdala. *J. Neurosci.* **1,** 1242–1259.

Probst, A., Cortes, R., and Palacios, J. M. (1986). The distribution of glycine receptors in the human brain. A light microscopic autoradiographic study using [3H]strychnine. *Neuroscience* **17,** 11–35.

Quirion, R., Welner, S., Gauthier, S., and Bedard, P. (1987). Neurotensin receptor binding sites in monkey and human brain: autoradiographic distribution and effects of 1-methyl-4-phenyl-1,2,3,6-tetrahydropyridine treatment. *Synapse* **1,** 559–566.

Ramón y Cajal, S. (1909). "Histologie du Système Nerveux de l'Homme et des Vertébrés. Traduit de l'espagnol par le Dr. L. Azoulay." Instituto Ramon y Cajal (1952), Madrid.

Reddy, S. C., Panigrahy, A., White, W. F., and Kinney, H. C. (1996). Developmental changes in neurotransmitter receptor binding in the human periaqueductal gray. *J. Neuropathol. Exp. Neurol.* **55,** 409–418.

Redgrave, P., and Dean, P. (1991). Does the PAG learn about emergencies from the superior colliculus? *In* "The Midbrain Periaqueductal Gray Matter. Functional, Anatomical and Neurochemical Oorganization" (A. Depaulis and R. Bandler, eds.), pp. 199–210. Plenum Press, New York.

Redgrave, P., Dean, P., Mitchell, I. J., Odekunle, A., and Clark, A. (1988). The projection from superior colliculus to cuneiform area in the rat. I. Anatomical studies. *Exp. Brain Res.* **72,** 611–625.

Reynolds, D. V. (1969). Surgery in the rat during electrical analgesia induced by focal brain stimulation. *Science* **164,** 444–445.

Richardson, D. E., and Akil, H. (1977a). Pain reduction by electrical brain stimulation in man. Part 1: Acute administration in periaqueductal and periventricular sites. *J. Neurosurg.* **47,** 178–183.

Richardson, D. E., and Akil, H. (1977b). Pain reduction by electrical brain stimulation in man. Part 2: Chronic self-administration in the periventricular gray matter. *J. Neurosurg.* **47,** 184–194.

Rizvi, T. A., Ennis, M., and Shipley, M. T. (1992). Reciprocal connections between the medial preoptic area and the midbrain periaqueductal gray in rat: a WGA-HRP and PHA-L study. *J. Comp. Neurol.* **315,** 1–15.

Roeling, T. A. P., Veening, J. G., Peters, J. P., Vermelis, M. E., and Nieuwenhuys, R. (1993). Efferent connections of the hypothalamic "grooming area" in the rat. *Neuroscience* **56,** 199–225.

Sandner, G., Schmitt, P., and Karli, P. (1987). Mapping of jumping, rearing, squealing and switch-off behaviors elicited by periaqueducatal gray stimulation in the rat. *Physiol. Behav.* **39,** 333–339.

Saper, C. B., Loewy, A. D., Swanson, L. W., and Cowan, W. M. (1976). Direct hypothalamo-autonomic connections. *Brain Res.* **117,** 305–312.

Saper, C. B., Swanson, L. W., and Cowan, W. M. (1978). The efferent connections of the anterior hypothalamic area of the rat, cat and monkey. *J. Comp. Neurol.* **182,** 575–599.

Schiller, F. (1984). When is posterior not dorsal but medial? *Neurology* **34,** 511–514.

Shipley, M. T., McLean, J. H., and Behbehani, M. M. (1987). Heterogeneous disribution of neurotensin-like immunoreactive neurons and fibers in the midbrain periaqueductal gray of the rat. *J. Neurosci.* **7,** 2025–2034.

Smith, G. S., Savery, D., Marden, C., Lopez Costa, J. J., Averill, S., Priestley, J. V., and Rattray, M. (1994). Distribution of messenger RNAs encoding enkephalin, substance P, somatostatin, galanin, vasoactive intestinal polypeptide, neuropeptide Y, and calcitonin gene-related peptide in the midbrain periaqueductal grey in the rat. *J. Comp. Neurol.* **350,** 23–40.

Sofroniew, M. V., Weindl, A., Schrell, U., and Wetzstein, R. (1981). Immunohistochemistry of vasopressin, oxytocin and neurophysin in the hypothalamus and extrahypothalamic regions of the human and primate brain. *Acta Histochem. Supplement* **24,** 79–95.

Takahashi, H., Nakashima, S., Ohama, E., Takeda, S., and Ikuta, F. (1986). Distribution of serotonin-containing cell bodies in the brain stem of the human fetus determined with immunohistochemistry using antiserotonin serum. *Brain Dev.* **8,** 355–365.

Thorn, B. E., Applegate, L., and Johnson, S. W. (1989). Ability of periaqueductal gray subdivisions and adjacent loci to elicit analgesia and ability of naloxone to reverse analgesia. *Behav. Neurosci.* **103,** 1335–1339.

Tork, I., and Hornung, J. P. (1990). Raphe nucei and the serotonergic system. *In* "The Human Nervous System" (G. Paxinos, ed.), pp. 1001–1022. Academic Press, San Diego.

Tortorici, V., Robbins, C. S., and Morgan, M. M. (1999). Tolerance to the antinociceptive effect of morphine microinjections into the ventral but not lateral-dorsal periaqueductal gray of the rat. *Behav. Neurosci.* **113,** 833–839.

Unger, J. W., and Lange, W. (1991). Immunohistochemical mapping of neurophysins and calcitonin gene-related peptide in the human brain stem and cervical spinal cord. *J. Chem. Neuroanato.* **4,** 299–309.

Van der Horst, V. G. J. M., Mouton, L. J., Blok, B. F. M. and Holstege G. (1996). Distinct cell groups in the lumbosacral cord of the cat project to different areas in the periaqueductal gray. *J. Comp. Neurol.* **376,** 361–385.

Van der Horst, V. G. J. M. and Holstege, G. (1998). Sensory and motor components of reproductive behavior: pathways and plasticity. *Behav. Brain Res.* **92,** 157–167.

Van der Horst, V. G., Terasawa, E., Ralston, H. J., 3rd, and Holstege, G. (2000). Monosynaptic projections from the lateral periaqueductal gray to the nucleus retroambiguus in the rhesus monkey: implications for vocalization and reproductive behavior. *J. Comp. Neurol.* **424,** 251–268.

Veazey, R. B., Amaral, D. G., and Cowan, W. M. (1982). The morphology and connections of the posterior hypothalamus in the cynomolgus monkey *(Macaca fascicularis).* II. Efferent connections. *J. Comp. Neurol.* **207,** 135–156.

Veening, J., Buma, P., Ter Horst, G. J., Roeling, T. A. P., Luiten, P. G. M., and Nieuwenhuys, R. (1991). Hypothalamic projections to the PAG in the rat: topographical, immuno-electromicroscopical and functional aspects. *In* "The Midbrain Periaqueductal Gray Matter. Functional, Anatomical and Neurochemical Organization" (A. Depaulis and R. Bandler, eds.), pp. 387–416. Plenum Press, New York.

Waldbillig, R. J. (1975). Attack, eating, drinking and gnawing elicited by electrical stimulation of rat mesencephalon and pons. *J. Comp. Physiol. Psychol.* **89,** 200–212.

Wiberg, M., Westman, J., and Blomqvist, A. (1987). Somatosensory projection to the mesencephalon: an anatomical study in the monkey. *J. Comp. Neurol.* **264,** 92–117.

Yezierski, R. P. (1988). Spinomesencephalic tract: projections from the lumbosacral spinal cord of the rat, cat, and monkey. *J. Comp. Neurol.* **267,** 131–146.

Yezierski, R. P. (1991). Somatosensory input to the periaqueductal gray: a spinal relay to a descending control center. *In* "The Midbrain Periaqueductal Gray Matter. Functional, Anatomical and Neurochemical Organization" (A. Depaulis and R. Bandler, eds.), pp. 365–386. Plenum Press, New York.

Yezierski, R. P., Bowker, R. M., Kevetter, G. A., Westlund, K. N., Coulter, J. D., and Willis, W. D. (1982). Serotonergic projections to the caudal brain stem: a double label study using horseradish peroxidase and serotonin immunocytochemistry. *Brain Res.* **239,** 258–264.

Young, R. F., and Brechner, T. (1986). Electrical stimulation of the brain for relief of intractable pain due to cancer. *Cancer* **57,** 1266–1272.

Young, R. F., and Chambi, V. I. (1987). Pain relief by electrical stimulation of the periaqueductal and periventricular gray matter. Evidence for a non-opioid mechanism. *J. Neurosurg.* **66,** 364–371.

Young, R. F., Feldman, R. A., Kroening, R., Fulton, W., and Morris, J. (1984). Electrical stimulation of the brain in the treatment of chronic pain in man. *In* "Advances in Pain Research and Therapy" (L. Kruger and J. C. Liebeskind, fds.), Vol. 6, pp. 289–303. Raven Press, New York.

Young, R. F., Kroening, R., Fulton, W., Feldman, R. A., and Chambi, I. (1985). Electrical stimulation of the brain in treatment of chronic pain. Experience over 5 years. *J. Neurosurg.* **62,** 389–396.

Zaphiropoulos, A., Charnay, Y., Vallet, P., Constantinidis, J., and Bouras, C. (1991). Immunohistochemical distribution of corticotropin-like intermediate lobe peptide (CLIP) immunoreactivity in the human brain. *Brain Res. Bull.* **26,** 99–111.

Zhang, D. X., Carlton, S. M., Sorkin, L. S., and Willis, W. D. (1990). Collaterals of primate spinothalamic tract neurons to the periaqueductal gray. *J. Comp. Neurol.* **296,** 277–290.

CHAPTER

13

Raphe Nuclei

JEAN-PIERRE HORNUNG
Institut de Biologie Cellulaire et de Morphologie
University of Lausanne, Lausanne, Switzerland

The *raphe nuclei* constitute a collection of cell groups distributed in the midline region of the tegmentum, from the rostral midbrain to the spinal cord transition at the pyramidal tract decussation. The term *raphe* refers to a seam or a ridge along the midsagittal plane of the body where left and right side structures fuse or join. In the brain stem, the union of both sides along the midline region is underlined by the crossing of numerous tracts, the most prominent ones being the decussation of the superior cerebellar tract in the mesencephalon, and, in the medulla oblongata, the medial lemniscal and the corticospinal decussations. As a result, cell density in raphe nuclei varies greatly between regions, with sharp cytoarchitectonic boundaries for the dorsal raphe nucleus and ill-defined limits for the midline caudal nuclei. Collectively, the raphe nuclei are part of the reticular formation bordering the midline, and are referred to as the *median division of the reticular formation* (Brodal, 1981; see also Chapter 10). At variance to the other raphe nuclei, the dorsal raphe nucleus is located dorsal to the medial longitudinal fasciculus, in the ventral periaqueductal gray.

Divisions of the raphe nuclei, first based on cytoarchitectonic features, were described in nonhuman species (Meessen and Olszewski, 1949; Taber *et al.*, 1960), and in humans (Olszewski and Baxter, 1954). With the availability of new histofluorescence techniques to reveal the bioamines in histological preparations, Dahlström and Fuxe (1964) reported that serotonergic neurons were mainly located near the midline in the brain stem. There has been thereafter an extension in the use of the term *raphe nuclei* to define the source of the serotonergic projections in the brain. Since the serotonin-containing cell groups revealed with this histochemical technique did not coincide entirely with known cytoarchitectonic divisions of the brain stem, these cell groups were designated B1–B9, ordered from caudal to rostral. It was demonstrated later by a range of methods and in various mammalian species that most serotonin-containing neurons are located in the raphe nuclei, with a population extending laterally in the medial and lateral reticular formation (Poitras and Parent, 1978; Wiklund, 1981; Steinbusch, 1981; Jacobs *et al.*, 1984; Törk, 1990; *et al.*, 1997). The higher proportion of serotonergic neurons positioned laterally to the median division of the

reticular formation is a characteristic feature of the primate brain, including human (Nobin and Björklund, 1973; Hubbard and diCarlo, 1974; Schoefield and Everitt, 1981; Schoefield and Dixon, 1982; Felten and Sladek, 1983; Azmitia and Gannon, 1986; Takahashi *et al.*, 1986; Hornung and Fritschy, 1988).

The presence in the human brain of serotonin and of its synthetic and degradation enzymatic systems had been well established (Costa and Aprison, 1958; Beskow *et al.*, 1976; Yamaguchi *et al.*, 1981) prior to its cytological localization. Direct visualization of serotonin in the human brain stem by histofluorescence or immunocytochemical techniques could not be applied to postmortem material because serotonin rapidly dissipates from the neurons after death. This applies to all monoamines and amino acids acting as neurotransmitters in the brain, whereas neuropeptides and enzymes specific for neurotransmitter metabolism could still be detected. The problem of postmortem serotonin dissipation could be circumvented by the use of fetal brain tissue, which could be rapidly frozen or fixed for histochemical (Nobin and Björklund, 1973; Olson *et al.*, 1973) or immunocytochemical (Takahashi *et al.*, 1986) studies. For the adult human brain, early studies relied on the aldehyde-fuchsin technique (Braak, 1970). Although not specific for the serotonergic neurons, it clearly delineated the cellular nuclei of the raphe. Alternatively, serotonergic neurons could be specifically stained by immunocytochemical detection of the degradation enzyme monoamine oxidase B (MAO B) (Konradi *et al.*, 1988) or antibodies recognizing the synthetic enzyme tryptophan hydroxylase (Haan *et al.*, 1987).

Since most serotonergic neurons are located in the raphe nuclei, "raphe" refers either to the cytoarchitectonic parcellation of the median division of the brain stem reticular formation, or to the chemoarchitectonic parcellation of the serotonergic neurons, in all mediolateral compartments of the brain stem. The raphe nuclei and the serotonergic system of common laboratory animals have been the subject of several detailed reviews that deal with the topography and aspects of the hodology of the serotonergic neural systems (Jacobowitz and MacLean, 1978; Wiklund *et al.*, 1981; Pecci-Saavedra *et al.*, 1983; Steinbusch and Nieuwenhuis, 1983; Jacobs *et al.*, 1984; Azmitia and Gannon, 1986; Hornung and Fritschy, 1988; Törk, 1995). In the raphe nuclei, the proportion of neurons synthesizing serotonin ranges from about 80% in the dorsal raphe nucleus to 10–20% in medullary raphe nuclei. Numerous neurotransmitters (amino acids, monoamines, peptides) have been localized in raphe neurons, some of them even colocalized in serotonergic neurons. In the present account, the cyto- and chemoarchitecture of the raphe nuclei will be systematically described, following the rostrocaudal axis. In addition, the median and lateral distribution of serotonergic neurons at each level of the brain stem will also be described. The connectivity of the raphe nuclei will be reported in a subsequent section.

The material used for the illustrations on this chapter came from publications describing the cyto- and chemoarchitecture of the human raphe nuclei (Halliday *et al.*, 1988a, 1990; Törk and Hornung, 1990; Baker *et al.*, 1991a, b). Human brain stem material was obtained from formalin-fixed autopsy material of patients without any clinical history of neurological disease. Adjacent sections were immunoreacted to visualize serotonin-synthesizing neurons or catecholamine-synthesizing neurons, stained for Nissl substance or for myelinated fibers. In the case of one brain stem, the immunohistochemically stained cells of every eighth section were plotted and digitized. In the reconstruction, the size and shape of the raphe nuclei could be visualized and the number of their neurons estimated (Hornung and Kraftsik, 1988). The serotonergic innervation of the human cerebral cortex was studied in freshly collected biopsies from patients surgically treated for brain tumors (Hornung and de Tribolet, 1995). Care was taken to collect samples at the margin of the resected pathological tissue, following a procedure in compliance with regulations of the local ethics committee.

DIVISIONS OF THE RAPHE NUCLEI

Caudal Linear Nucleus

The caudal linear nucleus (CLi) is a subnucleus of the ventral mesencephalic tegmentum (Halliday and Törk, 1986). It is located dorsal and caudal to the interpeduncular nucleus, on the midline between the two red nuclei. Posteriorly, the nucleus ends along the anterodorsal surface of the superior cerebellar peduncle decussation, which results in a ventral-to-dorsal shift of its caudal end. At the level of the medial longitudinal fasciculi, CLi merges with the interfascicular part of the dorsal raphe nucleus. The characteristic cytological feature of the CLi is the alignment of the dendrites parallel with the midline, with their major extensions in the rostral and caudal directions.

The CLi contains a large population of serotonergic neurons. This is the most rostral nucleus of the raphe system containing serotonin-synthesizing neurons in humans. The TPH-immunoreactive neurons are found between the levels of the red nuclei and the decussation of the superior cerebellar peduncles, with a gradual increase in cell density from rostral to caudal. These

neurons have small to medium soma and dendrites oriented parallel to the rostrocaudal axis. The most rostral serotonergic neurons in the human (Törk and Hornung, 1990), as in other primates (Azmitia and Gannon, 1986; Hornung and Fritschy, 1988), are located in the rostral part of the interpeduncular nucleus. These neurons have a distinctive multipolar dendritic morphology contrasting with the serotonergic neurons in the CLi.

Among the heterogeneous population of CLi neurons, there are pigmented dopaminergic neurons, immunoreactive for tyrosine hydroxylase (TH), and substance P (SP)–containing neurons. The latter are large-to-medium neurons with round or triangular somata (Halliday *et al.*, 1990).

Dorsal Raphe Nucleus

The dorsal raphe nucleus (DR) lies in the ventral part of the central gray matter of the mesencephalon and rostral pons (Fig. 12.1). It has long been recognized by its accumulation of large, darkly stained neurons in Nissl preparations (Kölliker, 1893). The main body of the DR lies dorsal to the caudal end of the oculomotor nucleus and to the trochlear nucleus (Baker *et al.*, 1992). The nucleus is subdivided in the midline region in a ventral part (DRV), at the bottom of the central gray, and an interfascicular part (DRI) between the trochlear nucleus and medial longitudinal fasciculus. The latter is continuous anteriorly with the CLi and stops caudally at the level of transition from the aqueduct to the rostral opening into the fourth ventricle. There are in addition three large subnuclei central to periaqueductal gray (PAG): the dorsal (DRD), the ventral (DRV), and the ventrolateral (DRVL) parts. Caudal to the isthmus of the brain stem, the portion of the DR in the PAG is reduced to two slits of neurons parallel to the ventricular surface of the anterior rhomboïd fossa, bordered laterally by the lateral tegmental nucleus, and extending caudally up to the level of the trigeminal motor nucleus; this is the caudal division of the DR (DRC). These subdivisions can be seen in Chapter 10.

The DR contains the largest population of serotonergic neurons in the human brain stem, amounting to an estimated 165,000 neurons (Baker *et al.*, 1991). Serotonergic neurons are found in all subdivisions of the DR, in different proportions of the total neuronal population estimated in adjacent Nissl-stained sections. Neurons rostral to the isthmus constitute the B7 group of Dahlström and Fuxe (1964), and those caudal to the isthmus the B6 group. The largest population of serotonergic neurons is in the DRD (28% of the total number of serotonergic neurons of DR, and 61% of all the DRD neurons). The remaining divisions of the DR amount to 16–22% of the total serotonergic population each. In the DRI, 100% of the neurons are serotonergic; in the DRV, 82%; and in the other divisions of the DR, around 60%. The serotonergic neurons in DRI have dendrites oriented parallel with the midline, a morphology similar to that of the serotonergic neurons in the CLi. This similarity is further accentuated by the fact that CLi is continuous with the DRI subdivision. Neurons in the DRVL are multipolar and densely packed. In the DRD, neurons are loosely arranged, medium sized, with radiating smooth dendrites. In the DRC, serotonergic neurons have smaller somatic diameter, with short dendrites often oriented parallel with the floor of the fourth ventricle.

Several neurotransmitters have been identified in the DR. Among the γ-aminobutyric acid (GABA)–containing neurons in the DR, very few colocalize with 5-hydroxytryptamine (Wang and Nakai, 1993; Stamp and Semba, 1995; Charara and Parent, 1998). The distribution of SP and catecholamine is restricted to the rostral DR (B7 group). There is a high proportion of large-to-medium SP-IR neurons with morphologies similar to the serotonergic neurons. The cumulative proportion of SP- and serotonin-containing neurons exceeds the total neuronal population estimated in Nissl-stained preparation of the DR. This is strong indirect evidence for the colocalization of serotonin and SP in the same neurons, this for almost 40% of the serotonergic neurons (Baker *et al.*, 1991b). There are only few catecholaminergic neurons, of variable morphologies, scattered in the rostral DR. There are also a few neurons containing the neuropeptides dynorphin, angiotensin, and enkephalin (Björklund and Hökfelt, 1985; Björklund *et al.*, 1990). In DRC, there is a dense and restricted population of neurotensin-containing neurons (Jennes *et al.*, 1982).

Median Raphe Nucleus and Pontomesencephalic Reticular Formation

Median Raphe Nucleus

The median raphe nucleus (MnR) extends from the decussation of the superior cerebellar peduncles to the middle pons at the level of the trigeminal motor nucleus. Dorsally, the MnR ends below the medial longitudinal fasciculus and ventrally at the bottom of the midline tegmental region (Baker *et al.*, 1991). The MnR is divided in a dorsal, midline, and paramedian cluster. In the caudal two-thirds of the MnR, the midline division is bordered by a paramedian cell cluster that lies at the medial border of the lateral cell cluster.

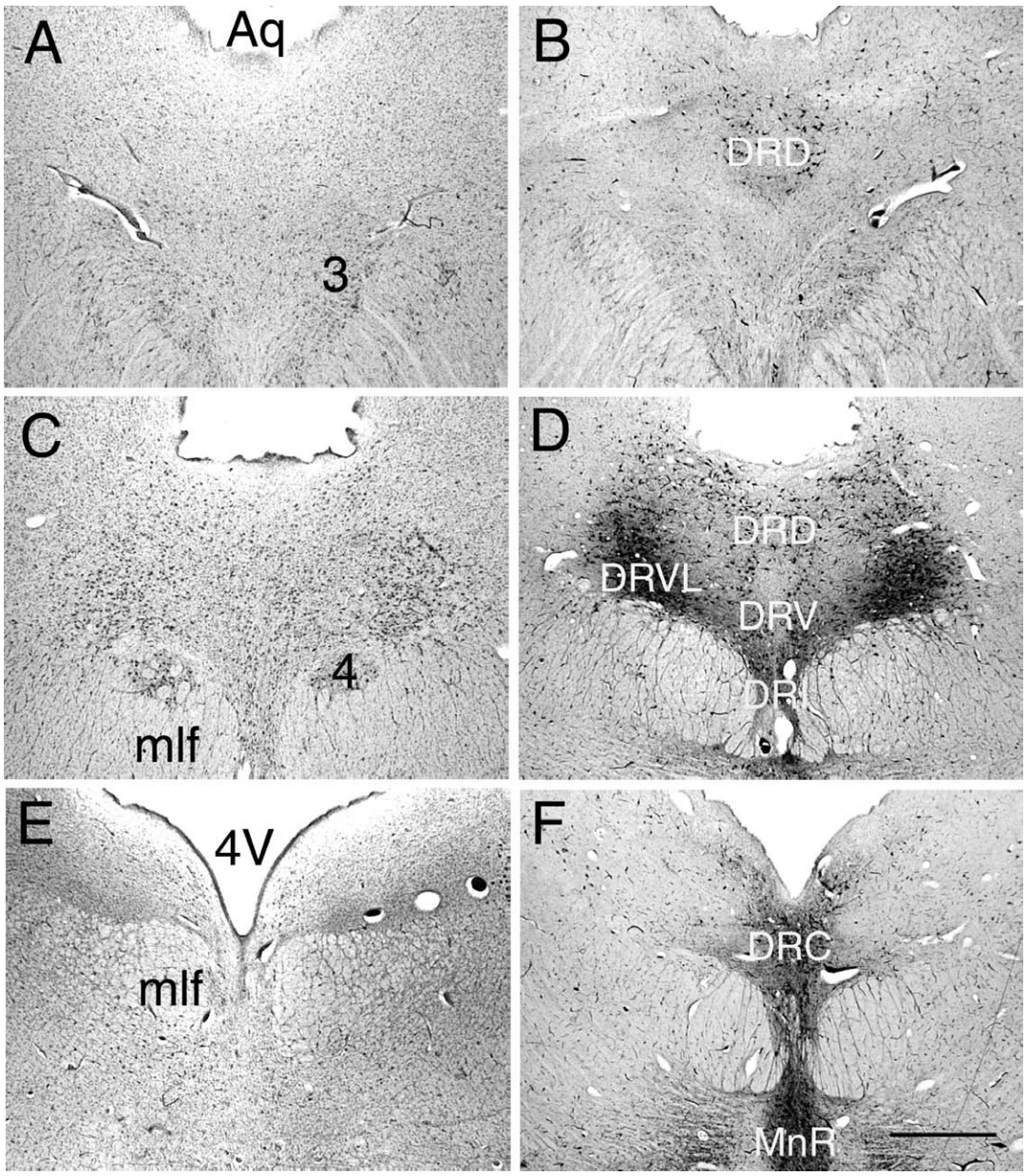

FIGURE 13.1 Transverse sections of the DR stained for Nissl substance **(A, C, E)** and the corresponding levels immunostained for TPH **(B, D, F).** The rostral division of DR (A, B) is at the level of the oculomotor nucleus (3). DR is most developed (C, D) at the level of the trochlear nucleus (4), and ist caudal extension (E, F) overlies the MnR. Scale bar: 1.5 mm.

Since the median and paramedian clusters are poorly myelinated in comparison with the lateral reticular formation, these divisions are also well delineated in myelin-stained sections, at the contrary to the dorsal raphe nucleus which is poorly delineated with such a staining. There is a change in structure from rostral to caudal levels of the MnR. Rostrally, the MnR is restricted to a thin dorsoventral slit of neurons near the midline of the mesencephalon. In the rostral pons, the midline group is segregated in a dorsal division, with densely packed neurons, and a ventral one, with more loosely organized neurons. At the most caudal levels of the MnR, the midline neurons are sparse and the paramedian neurons are more diffusely distributed than at the more rostral levels. In the MnR, most neurons have dendrites oriented in the rostrocaudal direction, reminiscent of the ventral division of the DR. Rostrally, the fact that the vicinity of the DRI neurons

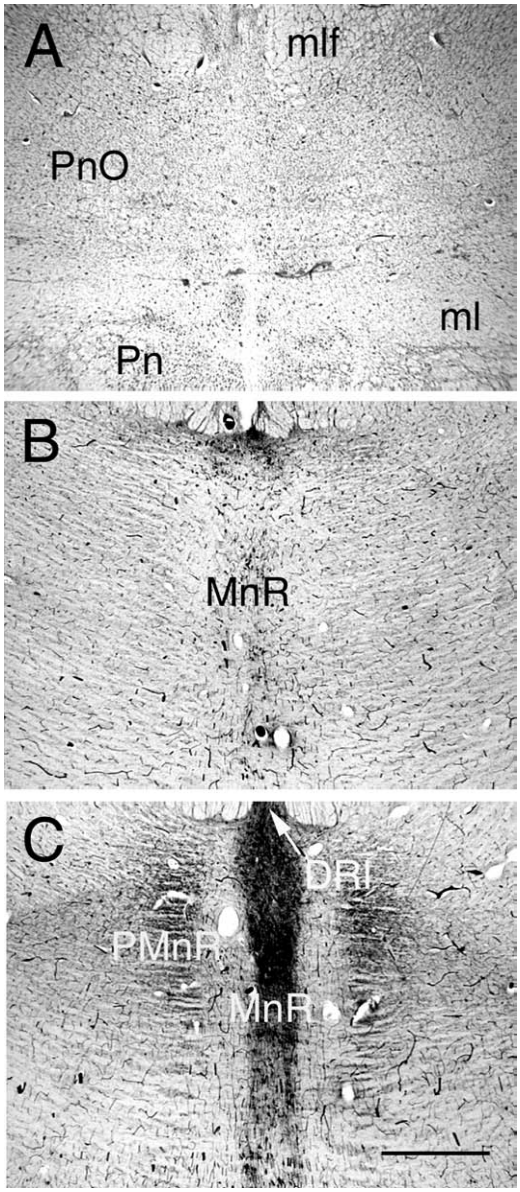

FIGURE 13.2 Transverse sections of the MnR at the level of the caudal mesencephalon **(A, B)** and the rostral pons **(C),** stained for Nissl substance (A) and immunostained for TPH (B, C). A: The MnR is bordered dorsally by the mlf, laterally by the PnO, and ventrally by the ml and the Pn. Rostrally (B), TPH-IR neurons are restricted to a midline stream of cells, whereas caudally (C), there is a major condensation of TPH-IR neurons on each side of the midline raphe (in PMnR) and scattered TPH-IR neurons are distributed even more laterally in the lateral reticular formation. Scale bar: 1.5 mm.

shares similar morphology makes the separation with the MnR somewhat arbitrary, although at most levels it is clearly delineated by small bundles of the medial longitudinal fasciculus. Neurons in the caudal division are characterized by a round somatic morphology and radially oriented dendrites (Fig. 12.2).

Serotonergic Neurons of the Pontomesencephalic Reticular Formation

In the pontomesencephalic region, serotonergic neurons have a wide distribution extending to two subdivisions of the lateral reticular region: the oral pontine nucleus (PnO) and the supralemniscal nucleus (SuL). The proportion of serotonergic neurons in the lateral reticular formation is highest in the primate brain, as compared to rodents and other mammalian species (Azmitia and Gannon, 1986), approaching amounts equal to the total number of serotonergic neurons in the MnR (Baker *et al.*, 1991). Serotonergic neurons in the lateral reticular formation are dispersed, with large radiating dendrites. There is a dorsal lateral extension of the serotonergic neurons surrounding the medial longitudinal fasciculus toward the lateral edge of the DR. This dorsal lateral extension spreads caudally toward the anteromedial limits of the locus coeruleus. The lateral extension of serotonergic neurons is reduced in the middle of the reticular formation traversed by the central tegmental tract. The ventral edge of the PnO is crossed by the fibers of the medial lemniscus. Serotonergic neurons are distributed laterally above the superior cerebellar peduncles in the ventral PnO. Ventrally relative to this peduncle, there is a second group of serotonergic neurons lying at the dorsal edge of the medial lemniscus in the SuL (Baker *et al.*, 1991a). In this latter location, neurons are often bipolar and their dendrites parallel with the dorsal limits of the medial lemniscus.

The division of the MnR and serotonin-synthesizing pontomesencephalic neurons corresponds to the B8 (MnR) and B9 (supralemniscal, SuL) groups. On the other hand, the neurons in PnO are mostly developed in the primates and were not named in Dalström and Fuxe's (1964) study on the rodent. Finally, in rodents a population of serotonergic neurons extends caudal to the MnR along the midline: the B5 group. There is no TPH-IR neurons caudal to the MnR in the caudal half of the pontine raphe. There are an estimated 125,000 serotonergic neurons in the mesopontine tegmentum, half of them in the MnR, a quarter in the PnO, and another quarter in the B9 group (Baker *et al.*, 1991a). In the midline subgroup of MnR, approximately 80% of the neurons are serotonergic, and in the paramedian subgroup, approximately 30%. Since the limits of the other subgroups are hardly distinguishable in Nissl preparations, such estimates are not available.

In the MnR, there are a few SP-IR neurons with small neuronal cell diameter (Baker *et al.*, 1991a). Several neuropeptides have been found in MnR neurons, e.g., cholecystokinin (Schiffmann and Vanderhaeghen, 1991) and, in lower abundance, dynorphin, enkephalin, and

neurotensin (Björklund and Hökfelt, 1985; Björklund *et al.*, 1990). Several observations have only been made in rodent brains.

Raphe Magnus Nucleus

The raphe magnus nucleus (RMg) is located in the caudal pons and the most rostral portion of the medulla (Fig. 12.3). It is restricted to the midline, overlying the medial lemniscus where its fibers are shifting from their ventromedial to a more lateral position as they enter the pons. The RMg is found at the same level as the facial nucleus. The first TPH-IR neurons of the RMg are loosely clustered on the midline in the ventral tegmentum, at the level of the genu of the facial nerve. Rostral to these neurons there is a gap of several millimeters nearly devoid of TPH-IR neurons, which segregates the raphe nuclei of the rostral group (CLi, DR, MnR, and the pontine tegmental nuclei PnO and SuL) from those of the caudal group (RMg, ROb, RPa). Caudally, the nucleus ends just caudal to the anterior tip of the inferior olivary nuclei. The serotonergic neurons have various morphologies ranging from bipolar to multipolar. The former ones predominate near the midline, whereas the latter are more abundant in the ventral and lateral divisions of the nucleus. Laterally in RMg, the major axis of dendritic arborization shifts from dorsoventral to mediolateral. At the level of the pontomedullary junction, TPH-IR neurons have a distribution extending laterally in the neighboring gigantocellular reticular nucleus, pars a (Giα). This population of serotonergic neurons extends laterally and caudally, arching over the dorsal boundary of the inferior olivary nuclei. These neurons bridge the RMg with a population of serotonergic neurons extending across the entire length of the medullary lateral reticular formation (see below). These neurons have elongated cell bodies with three to five dendrites extending within the axon bundles in the medial lemniscus and the reticular formation.

Substance P is found in many RMg neurons of the human brain stem, as well as in the terminals in the neuropil (Halliday *et al.*, 1988b; Rikard-Bell *et al.*, 1990). In rodents, substance P was shown to colocalize in RMg serotonergic neurons, as well as thyrotropin-releasing hormones (Poulat *et al.*, 1992; Wu *et al.*, 1993). Several neuropeptides (enkephalin, somatostatin, cholecystokinin) have also been identified in RMg neurons (Björklund and Hökfelt, 1985; Björklund *et al.*, 1990). A population of NPY-containing neurons has been described in the human RMg (Halliday *et al.*, 1988c).

Raphe Obscurus Nucleus

The rostrocaudal extent of the raphe obscurus nucleus (ROb) amounts to about 20 mm (Braak, 1970), second only in length to the DR. Rostrally, the nucleus appears at the level of the abducens nucleus, just below the medial longitudinal fasciculus. At this level, it overlaps with the RMg, which is located more ventrally. In the medulla, the ROb is restricted to the median division, extending dorsoventrally from the mlf to the dorsal edge of the inferior olivary nuclei. Caudally, the ROb ends in the intermediate division of the first cervical segment, where three to five TPH-IR

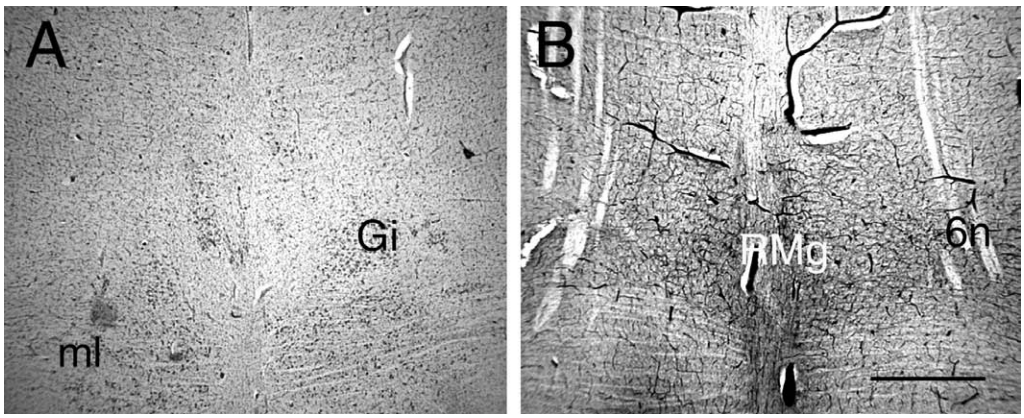

FIGURE 13.3 Transverse sections of the RMg at the level of the caudal pons stained for Nissl substance **(A)** and immunostained for TPH **(B).** The sections are located at the level of the nerve roots of the abducens (6n). The core of RMg is situated at the mediodorsal edge of ml, and is bordered laterally by a division of the reticular formation (Giα) in which TPH-IR neurons are bridging between the RMg and the serotonergic neurons of the lateroventral reticular formation of the medulla. Scale bar: 1.5 mm.

neurons per section flank laterally the pyramidal tract decussation. Neurons of the ROb form two separate paramedian columns of cells on either side of the midline. TPH-IR neurons have dendrites mainly dorsoventrally oriented, with a few of them crossing the midline into the contralateral ROb nucleus, and others oriented laterally, which penetrate in the medial nucleus of the medullary reticular formation.

Numerous SP-IR cell bodies have been reported in ROb of the human brain stem (Del Faccio *et al.*, 1984; Halliday *et al.*, 1988b, Rikard-Bell *et al.*, 1990), together with a dense network of SP-IR fibers surrounding ROb neurons. ROb neurons are very weakly labeled with MAO B antibodies (Westlund *et al.*, 1988). Scattered galanin-containing neurons have been described in the primate ROb (Blessing and Gai, 1997).

Raphe Pallidus Nucleus

The raphe pallidus nucleus (RPa) is the smallest of the human raphe nuclei. Its location in the atlas of Olszewski and Baxter (1954) has been mistaken for that of the RMg (see Braak, 1970). As a result, reference to RPa in some publications may actually refer to RMg or even ROb. The RPa is a narrow collection of cells close to the midline, at the border between the pyramidal tract and the overlying medial lemniscus. Its rostrocaudal extension corresponds roughly to that of the inferior olivary nuclei, starting, rostrally, from the level of the caudal tip of the RMg to the level of the obex, caudally. In our material, there was a clear accumulation of TPH-IR neurons at the pontomedullary junction at the medial side of the pyramids. However, these neurons were restricted to the rostral half of the cytoarchitectonic limits of the nucleus (Braak, 1970; Paxinos and Huang, 1995). TPH-IR neurons are slender, elongated neurons with few dendritic processes oriented predominantly dorsoventrally.

Serotonergic Neurons in the Medullary Reticular Formation

TPH-IR neurons are found in all transverse sections of the human medulla. Rostrally, there is a dense collection of serotonergic neurons in the Giα, at the lateral edge of the RMg. This column of neurons shifts laterally, in the caudal direction, into the lateral paragigantocellular reticular nucleus (LPGi). Further caudally, an additional population of TPH-IR neurons are located in the lateral reticular nucleus; these neurons surround in a U-shapped distribution the catecholaminergic groups (A1–C1) of the ventrolateral end of the intermediate reticular zone (Irt) (see Chapter 15). Serotonergic neurons are situated close to the medullary surface, in a location similar to that observed in other primate and nonprimate species (Chan-Palay, 1977; Steinbusch, 1981; Jacobs *et al.*, 1984; Azmitia and Gannon, 1988). The serotonergic and catecholaminergic neurons are two separate populations, with a limited number of neurons coexpressing serotonin- and catecholamine-synthesizing enzymes (Halliday *et al.*, 1998a) (Figs. 12.4 and 12.5).

In the Giα and the LPGi, TPH-IR neurons have multipolar morphology, and some of them colocalize with substance P, which is abundant in these nuclei (Halliday *et al.*, 1988b; Rikard-Bell *et al.*, 1990). Neurons in the lateral reticular formation have an elongated dendritic arborization, preferentially oriented in the transverse plane. A similar prominent distribution of serotonergic neurons in the lateral reticular nucleus of the medulla has been reported in several primates species (Azmitia and Gannon, 1988; Hornung and Fritschy, 1988). However, these cells fail, to stain with MAO B antibodies (Westlund *et al.*, 1988).

CONNECTIVITY

The tract-tracing methods available to demonstrate the connections in the mammalian brain have not been applied to the human raphe system. The pathways described are extrapolated from animal studies, though the existence of many has been confirmed in nonhuman primate studies. These data have been correlated with direct observations in human brain derived from histochemical or immunocytochemical studies of the serotonergic fibers, and from biochemical measurement of serotonin concentration or TPH activity in postmortem samples or biopsies.

The projections arising from the raphe nuclei are very extensive, as documented by the presence of serotonergic axons in virtually all brain regions. The raphe nuclei can be divided into two subgroups: the *rostral (oral) raphe nuclei* and the *caudal raphe nuclei* (Ohm *et al.*, 1989). The former ones are located in the mesencephalon and rostral pons, and send primarily ascending projections to the forebrain; the latter ones are located in the caudal pons and medulla, and send primarily projections to the lower brain stem and spinal cord (see below). These two regions of the raphe system are distinctly separated developmentally (Lidov and Molliver, 1982; Aitken and Törk, 1988).

The serotonergic axonal varicosities containing numerous synaptic vesicles are the main release sites for serotonin. Only a minority of them form classical chemical synapses with close apposition to the postsynaptic membrane. The incidence of conventional synapses at serotonergic terminals varies between the

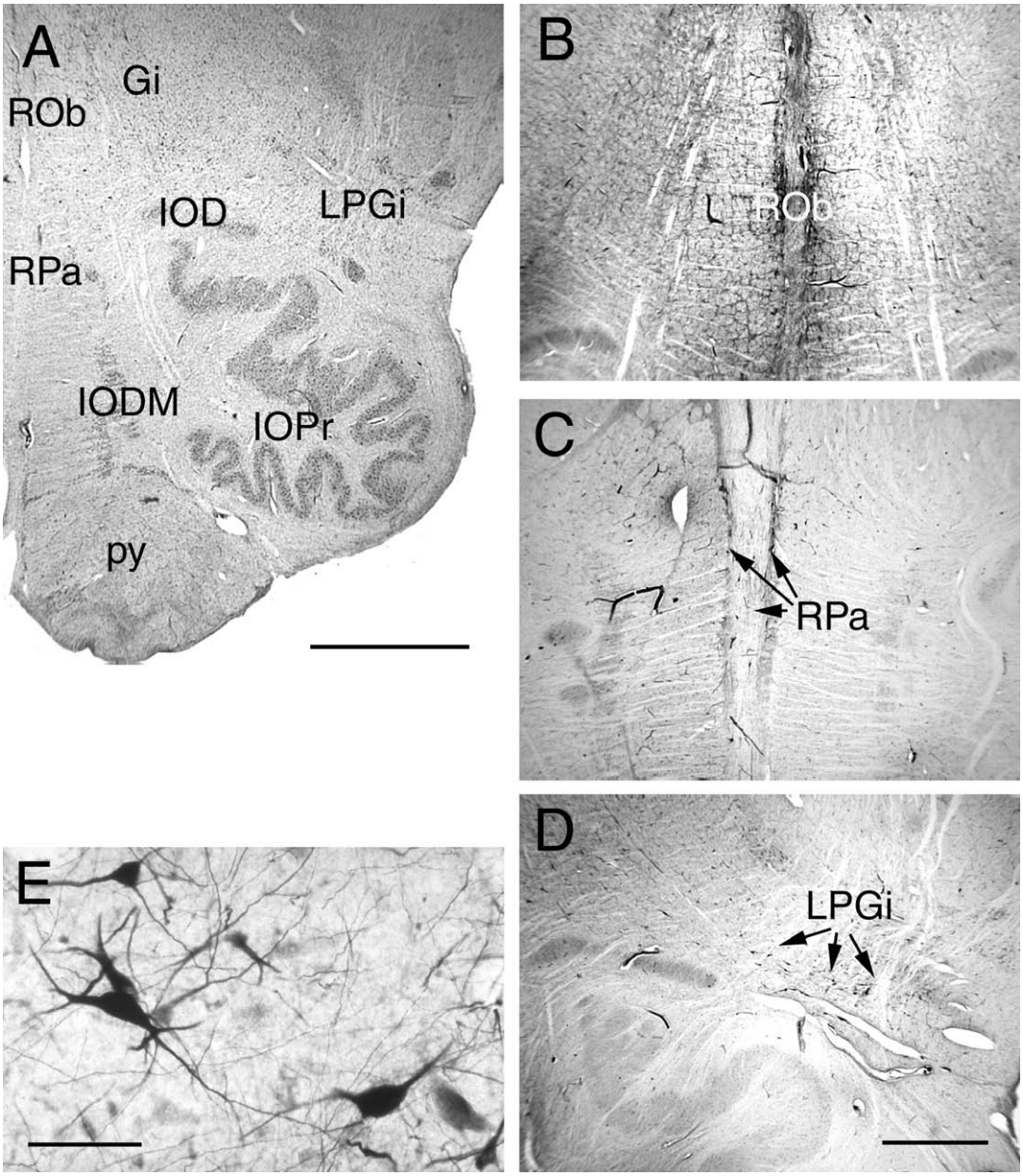

FIGURE 13.4 Transverse sections at the level of the rostral medulla stained for Nissl substance **(A)** and immunostained for TPH **(B–E).** The three serotonergic cell groups of the medulla are present at the rostral level of the inferior olive (A, B). TPH-IR neurons in the lateral reticular formation (LPGi) are bordering the dorsolateral edge of the IOPr. At high magnification (E), TPH-IR neurons in all divisions of the raphe display clearly the morphology of cell bodies, dendrites, and axons. Scale bars: (A) 3 mm, (B–D) 1.5 mm, (E) 40 mm.

sources of serotonergic projections, the brain regions, and the species. Serotonergic axons could be roughly subdivided into two groups: those bearing small or large varicosities (Kosofsky and Molliver, 1987; Ridet *et al.*, 1994). The former ones are associated with non-synaptic terminals whereas the latter ones often form classical chemical synapses (Törk, 1990; Ridet *et al.*, 1994; Smiley and Goldman-Rakic, 1996). For the ascending serotonergic projections, the source of the small varicose fibers is in DR and that of the large varicosities in MnR (Kosofsky and Molliver, 1987).

The Rostral Group

The rostral group is composed of the CLi, the DR, the MnR, and the pontomesencephalic neurons.

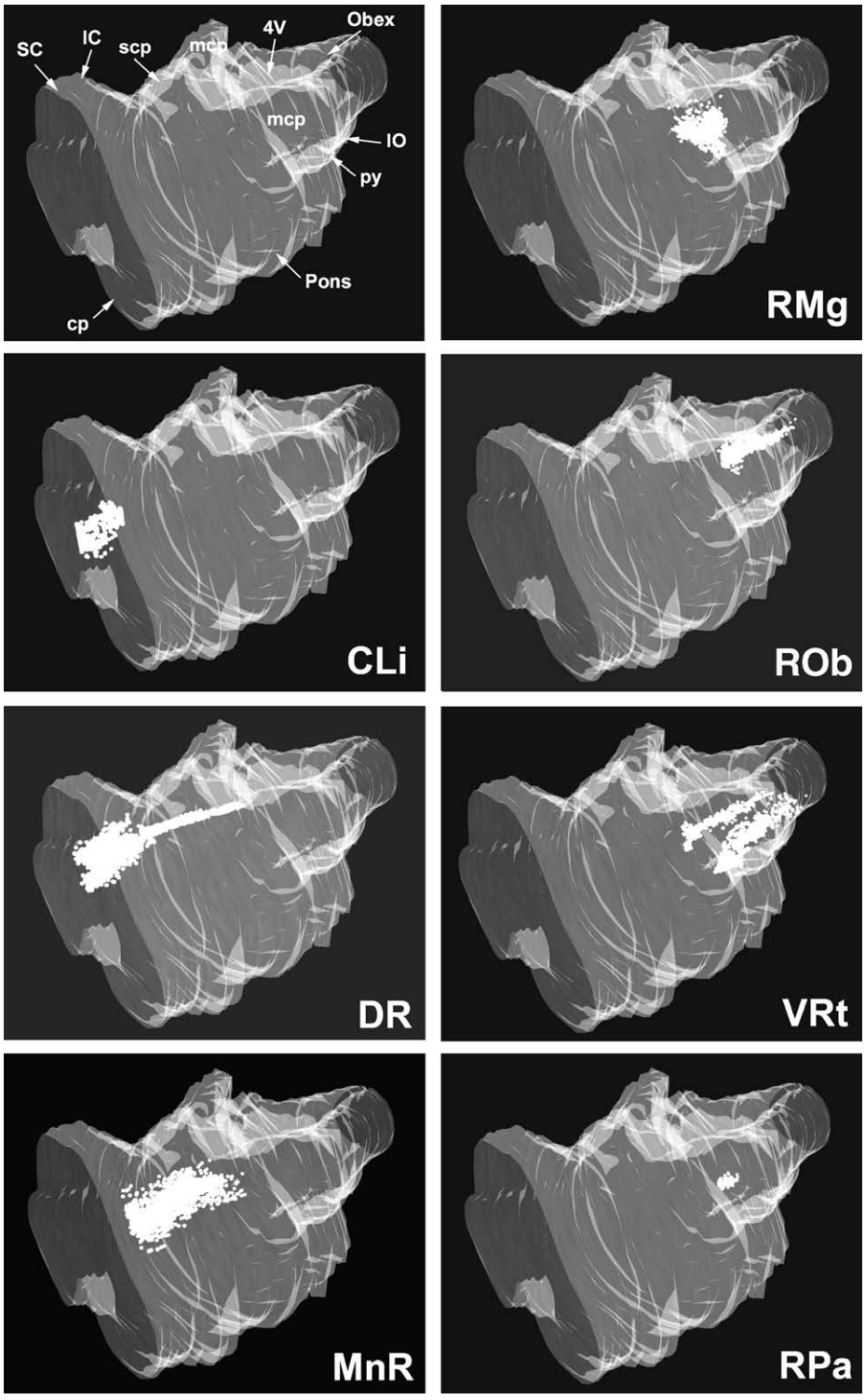

FIGURE 13.5 Three-dimensional representation of the reconstruction of brain stem from a series of transverse sections using the Solid View module of Neuroexplorer (Microbrightfield). The surface of the brain stem is represented in transparency, viewed from its anterior laterodorsal aspect. Top left panel points to the main structures of reference for orientation. The localization of TPH-IR neurons in every eighth section of the series has been plotted in reference to the outline of the brain stem. The distribution of the TPH-IR neurons in each raphe nucleus is illustrated separately in individual panels. Notice that the rostral group of the raphe neurons *(left panels)* are spatially segregated from the caudal group mostly restricted to the medulla *(right panels)*. The rostrocaudal length of the recontructed brain stem is 62 mm.

Collectively, the efferent projections of these nuclei are principally directed to the forebrain. Brodal *et al.* (1960) were the first to propose, using anterograde degeneration methods, that DR has a massive ascending projection to the forebrain, later confirmed by histofluorescence and immunocytochemical studies (Ungerstedt, 1971). More precise descriptions of the pathways of these ascending projections were obtained using anterograde transport of tritiated amino acids (Conrad *et al.*, 1974; Bobilier *et al.*, 1976; Taber-Pierce *et al.*, 1976; Azmitia and Segal, 1978; Moore *et al.*, 1978) or Phaseolus vulgaris (Halasy *et al.*, 1992; Acsády *et al.*, 1993; Datiche *et al.*, 1995), and retrograde transport of cholera toxin (Datiche *et al.*, 1995; Peyron *et al.*, 1998), fluorescent tracers (Kasakov *et al.*, 1993; Li *et al.*, 1993), or horseradish peroxidase (Kievit and Kuypers, 1975; Gonzalo-Ruiz *et al.*, 1995). Although the majority of the efferent targets are located in the upper brain stem and forebrain, there is evidence, for instance, of descending projections to the spinal cord from DR neurons with ascending axon collaterals (Kasakov *et al.*, 1993; Li *et al.*, 1993).

Efferent Projections

Efferent projections from the rostral serotonergic group ascend in two parallel pathways. A dorsal pathway running at the ventral side of the medial longitudinal fasciculus collects projections from DR and the dorsolateral cluster of MnR (Azmitia and Gannon, 1983, 1986). A ventral pathway starting at the level of the trochlear nucleus runs lateral of the MnR and reaches the mesencephalic ventral tegmental area near the dorsal limits of the interpeduncular nucleus. More rostrally, the ventral pathway extends into the medial forebrain bundle reaching the basal forebrain and the medial cortex. The dorsal pathway enters the internal capsule, heading for the lateral cerebral cortex. Fibers of the dorsal and ventral pathways intermingle at the midbrain–forebrain junction. In the monkey, the relative size of the dorsal bundle compared to the ventral one is increased, a feature possibly related to the increased size of the dorsal raphe nucleus and the cerebral cortex (Azmitia and Gannon, 1986). A minority of the serotonergic axons in the axon bundles are myelinated, in a proportion ranging from 0.7% in rodents to 25% in primates (Azmitia, 1987). The dorsal and the median raphe nuclei have distinct and partially overlapping projections, which will be considered separately. The ascending serotonergic projections to the cerebral cortex are described separately.

The projections of the dorsal raphe could be subdivided according to the rostral (B7; DRD, DRV, DRVL, and DRI) and caudal (B6; DRC) divisions of this nucleus on either part of the rhombencephalic isthmus (Azmitia and Segal, 1978; Jacobs *et al.*, 1978; De Olmos and Heimer, 1980; Fallon and Loughlin, 1982). The rostral division of the dorsal raphe nucleus projects principally to the cerebral cortex, neostriatum, amygdala, and substantia nigra (Steinbusch *et al.*, 1980; van der Kooy and Hattori, 1980; Waterhouse *et al.*, 1986; Corvaja *et al.*, 1993), whereas the caudal division projects to the hippocampus, entorhinal cortex, and locus coeruleus (Köhler and Steinbusch, 1982; Imai *et al.*, 1986; Datiche *et al.*, 1995). The dorsal raphe projects also to the thalamus (Westlund *et al.*, 1990; Gonzalo-Ruiz *et al.*, 1995), the ependyma and the subcommissural organ (Mikkelsen *et al.*, 1997), several brain stem nuclei (Li *et al.*, 1993; Thompson *et al.*, 1995; Steininger *et al.*, 1997), and the spinal cord (Kazakov *et al.*, 1993; Li e*t al.*, 1993). A projection from DR and CLi to the bed nucleus of the stria terminalis is made by neurons containing the vasoactive intestinal neuropeptide (Petit *et al.*, 1995). Multiple-tracing studies in rodents demonstrated that some serotonergic neurons could send axon collaterals in distinct divisions such as the cerebral cortex and the nucleus accumbens (Van Bockstaele e*t al.*, 1993), the lateral geniculate nucleus and the superior colliculus (Villar *et al.*, 1988), the trigeminal nucleus and the spinal cord (Li *et al.*, 1993), or even the cerebral cortex and the spinal cord (Kazakov *et al.*, 1993).

The main projections from the midline division of MnR are directed to the basal forebrain, the septal region, and the hippocampus (Azmitia and Segal, 1978; Vertes and Martin, 1988), with a majority of these projection neurons containing serotonin (up to 80%; Köhler *et al.*, 1982). The MnR also innervates also the cerebral cortex (Kievit and Kuypers, 1975; van der Kooy and Kuypers, 1979; Porrino and Goldman-Rakic, 1982; Tigges *et al.*, 1982). The dorsal region of MnR projects predominantly to the amygdala (Imai *et al.*, 1986). The lateral division of MnR in the PnO projects to more caudal structures (in the diencephalon and brain stem) than the midline division of MnR. There are serotonergic connections with the dopaminergic neurons of the substantia nigra, the intralaminar nucleus of the thalamus, and the mammillary nuclei (Vertes and Martin, 1988). Thus, MnR projections could modulate both the striatal system via its projections to the substantia nigra and the intralaminar nucleus of the thalamus, and the hippocampus via direct projections and indirect projections via the septal and mammillary nuclei (Baker *et al.*, 1991). The neurons in SuL project to the cerebellum (Brodal, 1982), functioning as an additional relay for cortical information forwarded to the cerebellum (Torigoe *et al.*, 1986). In addition to MnR, serotonergic projections to the cerebellum originate in the caudal raphe nuclei (Shinnar *et al.*, 1973; Bishop

and Ho, 1985). Neurons in SuL innervate the septal region (Köhler *et al.*, 1982) and the cerebral cortex, with 30% containing serotonin in rodents (O'Hearn and Molliver, 1984). This cortical projection is sparse in nonhuman primates (Kievit and Kuypers, 1975; Porrino and Goldman-Rakic, 1982; Tigges *et al.*, 1982).

The cerebral cortex receives dense parallel serotonergic projections from DR and MnR, which could be distinguished on the basis of several criteria: the morphology of the fibers, their areal and laminar distribution pattern, and their vulnerability to specific neurotoxins (O'Hearn *et al.*, 1988; Kosofsky and Molliver, 1987; Mamounas *et al.*, 1991). To summarize, axons originating in DR bear small varicosities (less than 1 μm in diameter), are widely distributed in the neocortex and hippocampus, and are highly sensitive to the application of amphetamine-derived neurotoxins, e.g., p-chloroamphetamine (PCA) and 3,4-methylenedioxymethamphetamine (MDMA, "ecstasy"). In contrast, axons originating in MnR bear large varicosities distributed predominantly in the hippocampus and in certain neocortical areas, and have little vulnerability to PCA and MDMA. The serotonergic innervation of the hippocampus originating in the dorsal raphe is diffuse across laminae and its activitation is likely to be mediated mainly by the activation of the serotonergic 5-HT_{1A} receptors (Mokler *et al.*, 1998), which are abundant in the hippocampus of all mammalian species studied, including nonhuman primates (Azmitia *et al.*, 1996) and humans (Burnet *et al.*, 1995; Pasqualetti *et al.*, 1996). The MnR projection to the hippocampus has been extensively studied with tract-tracing and immunocytochemical techniques in rodents and nonhuman primates. In rodents, this projection selectively innervates populations of GABAergic interneurons expressing calretinin or calbindin (two calcium-binding proteins), with numerous large axonal varicosities forming conventional synapses (Halasy *et al.*, 1992; Miettinen and Freund, 1992; Acsády *et al.*, 1993). Similar connections have been observed in the primate hippocampus (Hornung and Celio, 1992). Through this pathway, raphe neurons indirectly inhibit the activity of the pyramidal neurons of the hippocampus via a synaptic excitation of hippocampal GABAergic interneurons mediated by serotonergic 5-HT_3 receptors (Ropert and Guy, 1991; Maeda *et al.*, 1994; McMahon and Kauer, 1997) (Fig. 12.6).

A dense innervation by DR and MnR nuclei of the neocortex has been documented using both retrograde (Kievit and Kuypers, 1975; Porrino and Goldman-Rakic, 1982; Tigges *et al.*, 1982; O'Hearn and Molliver, 1984; Waterhouse *et al.*, 1986) and anterograde (Kosofsky and Molliver, 1987) tract-tracing techniques. The combination of these methods with serotonin immunodetection indicated that about 33–80% (100% for DRI) of the raphe projection neurons were serotonergic, depending on the nucleus of origin (O'Hearn and Molliver, 1984). The areal and laminar distribution of serotonergic axons in the neocortex is well differentiated in primates (Morisson *et al.*, 1982; Takeuchi and Sano, 1983; Campbell *et al.*, 1987; Berger *et al.*, 1988; DeFelipe and Jones, 1988; Hornung and Fritschy, 1990; Wilson and Molliver, 1991). There is a dense plexus of serotonergic axons in layer I in all areas, as well as in layer IV of the primary sensory areas (highest in the primary visual cortex). Layer IV innervation is also increased in density as compared to the neighboring supra- and infragranular layers in the associative cortices. In contrast in the agranular cortices (primary motor cortex, anterior cingulate cortex), the serotonergic axonal plexus is evenly distributed from layers II to VI. The laminar pattern of serotonergic innervation is complementary to that of the other aminergic afferent systems (Morisson *et al.*, 1982; Campbell *et al.*, 1987). Large varicose serotonergic axons are most

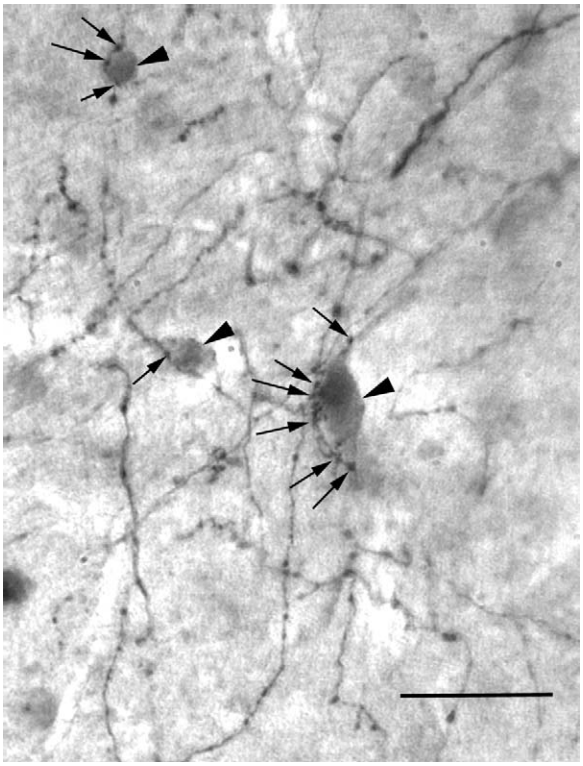

FIGURE 13.6 High-power micrograph of a transverse section of human cerebral cortex stained for 5-HT (black fibers) and for calbindin (gray cell bodies and dendrites, *arrowheads*). Note that serotonin-containing fibers form conspicuous large varicosities, several being in close apposition with the surface of calbindin-containing neurons *(arrows)*. Scale bar: 30 mm.

abundant in all divisions of the medial cortex and in the lateral cortex of the frontal lobe (Hornung *et al.*, 1990; Wilson and Molliver, 1991). These terminals have been shown to terminate preferentially on cortical interneurons (Smiley and Goldman-Rakic, 1996) and to form conspicuous pericellular baskets surrounding the soma and proximal dendrites of a subclass of inhibitory interneurons expressing the calcium-binding protein calretinin (Hornung and Celio, 1992). Immunocytochemical studies of the serotonergic innervation of the human cerebral cortex have been reported by a few groups (Kosofsky and Kowall, 1989; Hornung and de Tribolet, 1995; Trottier *et al.*, 1996). These studies confirmed that the cortical serotonergic innervation in the human brain is similar to that described in nonhuman primates with regard to the laminar distribution of the serotonergic fibers and their morphology (large and small varicose fibers) (Fig. 13.6). In addition, there is also evidence that large varicose fibers preferentially innervate calretinin-containing neurons in the frontal associative cortex (Fig. 13.6) (Hornung and de Tribolet, 1995). Ultrastructural analysis revealed that a minority of serotonergic terminals are engaged in conventional synapses, mostly those with varicosities of larger diameter (Beaudet and Descarries, 1978; Takeuchi and Sano, 1984; DeFelipe and Jones, 1988; De Lima *et al.*, 1988; Törk, 1990; Dori *et al.*, 1996; Smiley and Goldman-Rakic, 1996; Lambe *et al.*, 2000). Although several serotonin receptors have been identified in the cerebral cortex using mainly radioligand and *in situ* hybridization techniques, their cellular localization and function in cortical circuitry are only partially elucidated. Best characterized are the 5-HT_{1A}, 5-HT_{2A}, and 5-HT_3 receptors with a well-documented distribution in nonhuman primates (Lidow *et al.*, 1989; Azmitia *et al.*, 1996; Jakab and Goldman-Rakic, 1998, 2000) and in humans (Burnet *et al.*, 1995; Pasqualetti *et al.*, 1996). 5-HT_{1A} and 5-HT_{2A} receptors are expressed in all divisions of the cerebral cortex, with a predominant expression in pyramidal neurons of layers II, III, and V. There is also evidence for the expression of 5-HT_{2A} receptors in interneurons (Pasqualetti *et al.*, 1996; Jakab and Goldman-Rakic, 1998). In rodent piriform cortex, activation of 5-HT_2 receptors depolarizes layer II interneurons (Sheldon and Aghajanian, 1990; Gellman and Aghajanian, 1994) and hyperpolarizes pyramidal neurons (Sheldon and Aghajanian, 1990). Activation of 5-HT_{2A} receptors in the frontal cortex depolarizes pyramidal neurons (Aghajanian and Marek, 1997).

Afferents Projections

Our knowledge on the afferents to the raphe nuclei is based primarily on tract-tracing studies done on nonprimate mammalian species. The basic architecture of the connectivity of the raphe nuclei is likely to be common to all mammalian species. However, one could speculate that the organization of these pathways in primate and particularly human brains is more complex, since there is well-documented increasing complexity in the organization of the raphe nuclei themselves (see above). A large number of afferents are common to the DR and MnR. The major source of afferents to DR and MnR is the lateral habenula (Peyron *et al.*, 1998; Behzadi *et al.*, 1990), a pathway using excitatory amino acids (Behzadi *et al.*, 1990). There is a projection to both raphe nuclei from noncholinergic neurons of the medial septum and of the diagonal band nuclei (Kalén and Wiklund, 1989) and the ventral pallidum (Behzadi *et al.*, 1990; Peyron *et al.*, 1998). Several hypothalamic projections to the DR and MnR originate from nuclei in the medial and lateral preoptic areas, and the lateral, dorsal, and posterior divisions of the hypothalamus (Behzadi *et al.*, 1990; Peyron *et al.*, 1998). There is an abundant GABAergic innervation of DR neurons (Wang *et al.*, 1992), some of which are of hypothalamic origin (Peyron and Luppi, 1994). The projections from the lateral habenula, the interpeduncular nucleus, several hypothalamic nuclei, the ventral tegmental areas, the laterodorsal tegmentum nuclei, and the cingulate cortex are glutamatergic (Behzadi *et al.*, 1990). Medial prefrontal cortex innervates the DR and MnR nuclei, and stimulation of this pathway generates inhibition of the serotonergic (bursting) neurons in the midbrain (Hajòs *et al.*, 1998). The central nucleus of the amygdala projects to the DRV and DRD (Peyron *et al.*, 1998). Ascending projections to MnR originated from the RMg and RPa nuclei and from the nucleus prepositus hypoglossi (Behzadi *et al.*, 1990). Glycinergic projections to DR originate from the ventral and ventrolateral periaqueductal gray neurons and from neurons in the medullary rostral paragigantocellularis and rostral ventromedial reticular nuclei (Rampon *et al.*, 1999). Afferents from the medial nucleus of the solitary tract forward autonomic inputs to DR (Herbert, 1992).

The Caudal Group

The caudal group is composed of the RMg, the ROb, and the RPa. The group of serotonergic neurons in the medulla extends laterally from RMg in the Gia, the lateral paragigantocellular reticular nucleus (LPGi), and the lateral reticular nucleus.

Efferent Projections

Collectively, the efferent projections of these nuclei are principally directed to the caudal brain stem and spinal cord (Brodal *et al.*, 1960; Carlsson *et al.*, 1964; Skagerberg and Björklund, 1985). Combination of

retrograde labeling and immunocytochemistry reveals that about half of the spinally projecting midline raphe neurons contain serotonin, whereas this proportion falls to 28% in lateral medullary neurons (Jones and Light, 1992). Serotonergic axons to the spinal cord bear small varicosities in the dorsal horn and larger varicosities in the intermediate and ventral horns, the latter one forming conventional synaptic contacts with the spinal neurons (Ridet *et al.*, 1993). The serotonergic input to the somatic motor nuclei originates primarily from the ROb and the RPa, as demonstrated for the motor trigeminal nucleus (Li *et al.*, 1993, Ribeiro-do-Valle, 1997), the facial nucleus (Li *et al.*, 1993), the retrofacial and the ambiguus nuclei (Arita *et al.*, 1993, 1995), and the phrenic nucleus (Holtman *et al.*, 1990, Hosogai *et al.*, 1998). There is also a projection to the autonomic motor neurons of the parasympathetic (dorsal vagal nucleus) and sympathetic (thoracic intermediolateral column, IML) systems (Loewy and McKellar, 1981; Poulat *et al.*, 1992; Yang *et al.*, 1994; Manaker and Fogarty, 1995). Serotonergic projections to the autonomic motor neurons colocalize the neuropeptides thyrotropin-releasing hormone and SP (Poulat *et al.*, 1992; Wu *et al.*, 1993), whereas those to the somatic motoneurons lack SP (Wu *et al.*, 1993). The raphe projections to the dorsal horn and dorsal column nuclei originated primarily from the RMg, and its serotonergic axons are devoid of thyrotropin-releasing hormone and SP (Wu and Wessendorf, 1992). In the sensory relays, there is a dense serotonergic innervation of laminae I and II of the spinal trigeminal nucleus (Costa *et al.*, 1994) and the dorsal horn of the spinal cord (Ridet *et al.*, 1993). Following *p*-chloroamphetamine treatment, the fine varicose serotonergic innervation of the dorsal horn disappears while the large varicose serotonergic innervation is spared in all divisions of the spinal cord (Ridet *et al.*, 1994). Based on the distribution of the serotonergic fibers in the spinal cord, the fine varicose fibers originate primarily in RMg and the large varicose ones in ROb and RPa. The descending projections in the spinal cord follow two pathways: one lateral (and dorsal depending the authors) originates in the RMg and terminates in the dorsal horn, and one medial (and ventral) originates in the ROb and the RPa and terminates in the ventral horn and IML (Felten and Sladek, 1983; Azmitia and Gannon, 1986). There is a mixture of unmyelinated and partially myelinated descending serotonergic axons in the dorsolateral tract (Westlund *et al.*, 1992). Although most raphe projections are directed to caudal divisions of the brain, serotonergic and nonserotonergic neurons of the caudal raphe nuclei send axon collaterals to both the lumbar intermediate and ventral gray matter and the medial preoptic area of the hypothalamus (Leanza *et al.*, 1995).

Afferent Projections

Afferents to the anterior part of the caudal group (RMg, rostral Rpa, and Giα) originate in several hypothalamic nuclei, the dorsolateral periaqueductal gray, the central nucleus of the amygdala, the bed nucleus of the stria terminalis, and the medullary reticular formation (Zagon, 1993; Hermann *et al.*, 1997). Spinally projecting RMg and rostral RPa neurons receive direct catecholaminergic synaptic inputs (Tanaka *et al.*, 1994). The pneumotaxic area in the medial parabrachial area and the retrofacial nuclei have convergent inputs to the RMn (Gang *et al.*, 1993). There are also converging inputs onto RMg, Rob, and RPa midline raphe neurons from visceral sensory afferents and ventrolateral periaqueductal gray neurons (Snowball *et al.*, 1997).

FUNCTIONAL CONSIDERATIONS

The activity of raphe neurons, and of serotonergic neurons in particular, have been shown to be involved in a wide range of physiological and pathological functions. The following account summarizes some of the evidence for the involvement of serotonin in major brain functions, with some reference to nonserotonergic projections for which, however, little information on its contribution is available. This raises several issues that will require further investigation, such as the following: (1) Are the efferent and afferent projections of the non-serotonergic raphe neurons different from their serotonergic neighbors? (2) What is the organization of the intrinsic connections of the raphe and what is the degree of integration generated by this circuit? (3) Do the raphe nuclei constitute a system of their own or are some of their constituents integrative parts of the sensory, motor, or limbic systems? The functional mechanisms described below have been selected for their relevance to human neurobiology and pathology.

Sleep–Wake and Circadian Cycles

It has been known for several decades that the regulation of the sleep–wake cycles is in part modulated by serotonin (Jouvet, 1969) released by DR neurons projecting on the cholinergic laterodorsal tegmental nucleus (Steininger *et al.*, 1997). The activity of DR neurons is highest during waking, low during slow-wave sleep, and nearly abolished during paradoxical sleep (REM sleep) (McGinty and Harper, 1976), thus reducing the inhibition of serotonin on the cholinergic mesopontine neurons implicated in REM sleep generation (Luebke *et al.*, 1992; Thakkar *et al.*, 1998). During the sleep periods, there is a simultaneous increase in

dendritic release of serotonin in DR (Cespuglio *et al.*, 1990), which further inhibits serotonergic neurons activity by activation of 5-HT_{1A} autoreceptors (Sprouse and Aghajanian, 1987; Portas *et al.*, 1996). Inhibition of the DR during REM sleep is also dependent on GABAergic input, possibly originating from the periaqueductal gray and impinging on both the DR and the locus coeruleus, two structures with silent neurons during this phase of sleep (Nitz and Siegel, 1997a, b). The 5-HT_{2A} receptors participate in the control of slow-wave sleep (Dugovic *et al.*, 1989). The 5-HT_{1B} receptors are mainly located at terminals of axons and, for instance, at GABA and cholinergic terminals that are critical in sleep control. Pharmacological and electrophysiological study of the 5-HT_{1B}-deficient mouse demonstrated that this receptor participates in the regulation of paradoxical sleep (Boutrel *et al.*, 1999).

In mammals, the suprachiasmatic nucleus of the hypothalamus (SCh) is the primary circadian pacemaker of locomotor activity and various physiological functions (Hastings, 1997). It is richly innervated by serotonergic fibers (Leander *et al.*, 1998). Neurons in this nucleus have a rhythmic expression of several genes that regulate their cyclic activity (Dunlap, 1999). This intrinsic activity is modulated by photic and nonphotic manipulations. Among the nonphotic manipulations, injection of the serotonergic agonist 8-hydroxy-2(di-*n*-propylamino)tetralin (8-OH DPAT) shifts the rhythm of locomotor activity in the Syrian hamster (Tominaga *et al.*, 1992; Mintz, 1997). Electrical stimulations of DR and MnR induce phase shifts in SCh (Meyer-Bernstein and Morin, 1999). Serotonin application also shifts the activity of suprachiasmatic neurons maintained *in vitro* (Prosser *et al.*, 1993). These behavioral and physiological modifications correlate with the observation that 8-OH DPAT also modifies the rhythm of expression of two of the clock genes: *mPer1* and *mPer2* (Horikawa *et al.*, 2000).

Pain Control

The central modulation of noxious stimuli (opioid receptor–mediated analgesia) involves two structures lying in the raphe and its lateral extension: the ventro–lateral periaqueductal gray and the raphe magnus with the adjacent nucleus reticularis magnocellularis (Fields *et al.*, 1991). The periaqueductal region involves the contribution of DR (Wang and Nakai, 1994). Pain control occurs first at the synaptic relay of pain afferents in the dorsal horn and spinal trigeminal nucleus. It involves serotonergic and nonserotonergic populations of neurons in the rostromedial medulla (Skagerberg and Björklund, 1985). The contribution of serotonin in this descending pathway has recently been reevaluated years (Mason, 1999). This pathway suppresses pain transmission at the level of primary afferent synapses, with medullary serotonergic neurons responding by a tonic activity to noxious stimuli under stressful conditions (Milne and Gamble, 1990; Mitchell *et al.*, 1998). In unstressed conditions, the modulation of pain is regulated by nonserotonergic descending projections with inhibitory (off cells) and facilitatory (on cells) functions (Mason, 1997). The on cells are active during the awake and off cells during the sleep periods (Leung and Mason, 1999). In chronic pain situation, both on and off cells are active together (Montagne-Clavel and Oliveras, 1994). The bulbospinal projection for pain modulation originating from a raphe nuclei contains a mixture of serotonergic and nonserotonergic neurons. This projection illustrates a case where the two raphe neuron populations contribute to complementary and distinct functions.

Mood Disorders and Drug Addiction

Evidence for the involvement of serotonin in mood disorders and drug addiction stems from two main sources: (1) experimental studies on animals with pharmacologically or genetically modified neurotransmission, or (2) biochemical measurement of serotonergic metabolism, functional imaging, or therapeutic drug treatments on psychiatric or addicted patients. Of the abundant and controversial literature on the topic, the following account only reviews some of the issues relevant in the context of this chapter.

Hallucinogenic drugs, such as LSD or psilocibin, activate central neurons via 5-HT_{2A} receptors (Marek and Aghajanian, 1996; Vollenweider *et al.*, 1998). Mood disorders are managed with different drugs modulating serotonin metabolism (monoamine oxidase or serotonin transporter inhibitors, receptor agonists) (Meltzer, 1999). However, the biological substrate regulating the affective responses mediated by the action of 5-HT is still poorly understood The role of the receptor 5-HT_{2A} for the action of hallucinogens and antipsychotic drugs has been recently reported (Scruggs *et al.*, 2000), and the involvement of additional nonserotonergic receptors has been discussed in several reviews (Meltzer, 1999; Aghajanian and Marek, 2000; Harrison, 1999; Lewis and Lieberman, 2000). The activation of 5-HT_2 receptor in the frontal cortex has been studied by electrophysiological techniques in rat brain (Bergqvist *et al.*, 1999), and its expression was shown to be reduced in the brain of patients with major depression (Biver *et al.*, 1997). The genetic determinants of most psychiatric conditions are likely to be multiple genes contributing a fraction of the total genetic variance. The variance analysis of the promoter of the serotonin

transporter reveals evidence for polymorphism of the transporter associated with axiety and affective disorders (Lesch *et al.*, 1996; Greenberg *et al.*, 1998).

Serotonin, acting through a variety of receptors with distinct distributions, modulates differentially affective and cognitive responses. The 5-HT_{1A} agonists are used in the management of axiety disorders (Tunnicliff, 1991). Mice deficient for one of the serotonin receptors have been studied with the aim of identifing the mechanisms involved in the effect of the psychoactive drugs (Brunner and Hen, 1997). The knockout mice for the 5-HT_{1A} receptor have been reported to have anxiety or related disorders (Ramboz *et al.*, 1998). The knockout mice for the 5-HT_{5A} receptor have been reported to have increased locomotor activity and altered response to LSD (Grailhe *et al.*, 1999).

Elevated whole-blood serotonin levels have been reported in patients with autism (Cook *et al.*, 1996). Most individuals with autism who are treated with potent serotonin transporter inhibitors have a reduction of ritualistic behaviors and aggression (McDougle *et al.*, 1996). Genetic variants in this transporter have been linked with autism (Klauck *et al.*, 1997). On the other hand, reduction of serotonin function causes a worsening of stereotyped behaviors (McDougle *et al.*, 1996). A developmental abnormality associated with autism, such as decreased neurite branching in hippocampus (Raymond *et al.*, 1996), is similar to the reduced dendritic branching observed *in vitro* following stimulation of the 5-HT_{1A} receptor with the agonist 8-OH-DPAT (Sikich *et al.*, 1990).

The 5-HT_{1B} knockout mice are characterized by an elevated aggressivity in the resident-intruder paradigm (Saudou *et al.*, 1994). Mice deficient for the MAO A have an enhanced aggressive behavior in males (Cases *et al.*, 1995). In humans, similar behavior has been reported in male members of a family carrying a point mutation of MAO A (Brunner *et al.*, 1993). In rodents, agonists for several serotonin receptors decrease aggressive behavior (Olivier *et al.*, 1995). In genetic lines of mice selected for high or low offensive aggression, the density of 5-HT_{1A} receptors in low-aggressive mice was significantly higher in the hippocampus, lateral septum, and frontal cortex, but not in the DR (Korte, 1996). In small primate colonies deprived of a dominant male, a subordinate male with pharmacologically increased serotonergic function will acquire a dominant position and have lower levels of initiating aggressive behavior, whereas the opposite applies when the subordinate male has a pharmacologically lowered serotonergic function (Raleigh *et al.*, 1991). In humans, low brain serotonin correlates with aggressive behavior (Constantino *et al.*, 1997), and 5-HT receptor agonists reduce aggression (Bell and Hobson, 1994). There are, on the other hand, contradictory reports of elevated blood serotonin in humans with aggressive behavior (Cook *et al.*, 1995) and reduced aggressivity following 5-HT antagonist treatment (Shih *et al.*, 1999). Currently available evidence confirms that serotonin is involved in the regulation of aggressive behavior; however, its mechanism of action remains elusive. In knockout animal models, as in natural genetic deficiencies, the absence of a molecule during development could potentially indirectly affect other neurotransmitter systems or neuronal circuits, which in turn will be responsible for the modified phenotypes (Gingrich and Hen, 2000).

Among other neurotransmitters, serotonin was shown to participate in the circuitry of the reward pathways (Koob, 1992). Self-administration of cocaine by knockout mice with a deletion for the 5-HT_{1B} receptor demonstrated preexisting sensitization in these transgenic mice, resulting from a reduced inhibition by serotonin of the dopaminergic transmission at the level of both the ventral tegmental area and the accumbens nucleus (Rocha *et al.*, 1998).

Another study reported also an elevated self-administration of ethanol in these knock-out mice (Crabbe *et al.*, 1996). Thus, the 5-HT_{1B} receptor modulates the level of vulnerability to the reinforcing effects of certain addictive drugs and could possibly be involved in the individual variations of vulnerability to drugs of abuse.

Neurotoxicity of Amphetamine Derivatives

The recreational illicit drug 3,4-methylenedioxymethamphetamine (MDMA, or "ecstasy") is widely used for its hallucinogenic properties altering serotonergic functions and thus affecting mood states in which the serotonin system is involved (Green *et al.*, 1995). Early experimental studies in lower mammals (O'Hearn *et al.*, 1988) and primates (Wilson *et al.*, 1989) reported that MDMA had a neurotoxic effect on serotonin-containing axons. The effects are mediated by the action of MDMA on the membrane and vesicular serotonin transporters (Rudnick and Wall, 1992), and its neurotoxic action is prevented by prior serotonin depletion in terminals (Berger *et al.*, 1989). MDMA applied to mice lacking the serotonin transporter has no effect on the locomotor activation observed in wild-type animals receiving the same treatment (Bengel *et al.*, 1998). Serotonin neurotoxicity of MDMA has also been substantiated in humans (McCann *et al.*, 1994). The effect of MDMA is comparable to that of other amphetamine derivatives, such as *p*-chloroamphetamine (PCA) (Molliver *et al.*, 1990). The long-term reinnervation by

serotonergic axons in MDMA-treated rodents or primates demonstrated persistent abnormal projections such as a poor or missing reinnervation in the dorsal lateral neocortex and, on the opposite, hyperinnervation of more proximal targets such as the amygdala and hypothalamus (Fischer *et al.*, 1995). The reinnervation of the cerebral cortex by injured serotonergic axons following application of amphetamine neurotoxic drugs is strongly stimulated by the application of the neurotrophin brain-derived neurotrophic factor (Mamounas *et al.*, 2000). This effect is due to enhanced sprounting of spared axons but not an enhanced survival from a protective effect of the neurotrophin.

Motor Activity

Systemic application of serotonin precursors, agonists, or releasing agents induces a motor syndrome with characteristic head movements, tremors, and rigidity patterns (Jacobs, 1983). Alpha motor neurons in the brain stem and the spinal cord are surrounded by dense serotonergic plexuses, with the exception of those controlling finer motor activities such as for oculomotor and distal limb muscles (Steinbusch, 1981). Application of serotonin produces little or no effects on the motor neuron activity, but in combination with electrical stimulation or glutamate release, it produces a strong facilitation of neuronal activities, an effect mediated by the 5-HT_{2A} and 5-HT_{2C} receptors (Jacobs and Fornal, 1997). The activity of serotonergic neurons in all divisions of the raphe system is related to the state of the animal in the sleep–wake cycle (highest during waking and null during REM sleep) (Jacobs and Fornal, 1991). During waking, raphe neurons have a regular baseline activity, which increases dramatically in the rostral raphe in phase with repetitive complex motor activities such as orobuccal movements (chewing, licking, or grooming) (Fornal *et al.*, 1996), or in the caudal raphe in phase with treadmill-induced locomotion or hyperpnia induced by exposure to carbon dioxide (Veasey *et al.*, 1995). A recent case report describes a syndrome "fou rire prodromique" in which motor patterns for the laughing are generated in the absence of relevant behavioral or environmental association. This occured shortly after a vascular infarct restricted to a small area of the ventromedial pontomedullary region encroaching the RMg and anterior ROb nuclei (Assal *et al.*, 2000). Caudal raphe nuclei have also a modulatory role on the autonomic centers, as illustrated by the function of TRH-containing neurons in the raphe pallidus projecting onto the dorsal motor nucleus of the vagus in a loop regulating the physiology of the gastric mucosa (Kaneko *et al.*, 1998).

Modulatory Role of Serotonin During Brain Development

The early expression of serotonin and axonal growth in developing raphe neurons, prior to the cellular and synaptic differentiation of most of their target regions, led to the speculation that serotonin has a modulatory function in brain development (Lauder, 1993; Turlejsky, 1996). Application of synthetic enzyme inhibitors *in vivo* (Lauder and Krebs, 1978) or serotonin on cultured cells (Lavdas *et al.*, 1997) provides experimental evidence for a role of serotonin in cell proliferation and/or cell differentiation. During the early phase of embryonic development, the involvement of serotonin in cell migration has been well documented in neural crest cells (Moiseiwitsch and Lauder, 1995), by the activation of the 5-HT_{2B} receptor (Choi *et al.*, 1997). The dendritic growth of serotonergic neurons themselves is enhanced by the calcium-binding protein S-100β (Azmitia *et al.*, 1990), stored primarily in astroglia and released under stimulation of the 5-HT_{1A} receptor (Whitaker-Azmitia *et al.*, 1990). S-100β acts as a stabilizer of the cytoskeleton by inhibiting phosphorylation of brain cytoskeletal proteins such as MAP2, tau and GAP-43 (Sheu *et al.*, 1994; Nishi *et al.*, 2000). These mechanisms are involved in the serotonergic modulation of synaptic maturation in the dentate gyrus, where early serotonin depletion reduces the number dendritic spines (Yan *et al.*, 1997a, b; Wilson *et al.*, 1998). The anxiety-like behavior characteristic of the 5-HT_{1A} receptor knockout mouse (Ramboz *et al.*, 1998) has been shown to have a developmental origin since a conditional knockout mouse for this receptor showed anxiety-like behavior if the receptor was suppressed during the duration of development and restored in the adults whereas if the receptor was suppressed only in the adult, the animal had a phenotype similar to that of the wild type (Gross *et al.*, 2002).

In a transgenic mouse line with an inactivated gene for MAO A, there is a transient sevenfold increase in extracellular serotonin concentration during late embryonic and early postnatal life (Cases *et al.*, 1995). The morphological phenotype of this transgenic mouse is characterized by a lack of cytoarchitectonic differentiation in the barrel-field region of the somatosensory cortex (Cases *et al.*, 1995) and of ipsi-contralateral segregation of the retinal afferents in the thalamic lateral geniculate nucleus (Upton *et al.*, 1999). These glutamatergic pathways, among others, express transiently during the perinatal period the serotonin transporter, the vesicular monoamine transporter 2, and the 5-HT_{1B} receptor (Lebrand *et al.*, 1996, 1998). This results in a transient accumulation of serotonin in the thalamocortical and retinogeniculate pathways

(Cases *et al.*, 1996, 1998; Upton *et al.*, 1999). Serotonin acts at the thalamic and retinal terminals via the 5-HT_{1B} on the axon terminal, which reduces the amount of glutamate released, thus reducing the efficacy of the afferent terminals in processes of activity-dependent competition for synaptic targets. This hypothesis is supported by the recent study of the rescued morphological phenotype in the barrel-field cortex in double knockout mice for MAO A and the 5-HT_{1B} receptor, where the excess of serotonin is ineffective in absence of this receptor (Salichon *et al.*, 2001).

In the same transgenic mouse line, the maturation of the medullary respiratory rhythm generator is also altered (Bou-Flores *et al.*, 2000). This study demonstrates that cervical phrenic motor neurons develop abnormal dendritic morphologies, which correlates with a delayed maturation of a stable respiratory pattern. These data are relevant for the study of the sudden infant death syndrome, since victims of this syndrome have shown abnormally high cerebrospinal fluid levels of tryptophan and serotonin metabolites (Cann-Moisan *et al.*, 1999). The studies on the transgenic mouse strains illustrate the potential deleterious effects on brain development and functions of altered 5-HT metabolism, from genetic, metabolic, or pharmacological origin.

Neurodegenerative Disorders

In patients with Alzheimer's disease, there is a 70–80% reduction of the population of serotonergic neurons in the rostral group of the raphe, a reduction quantitatively similar in the DR and MnR nuclei (Halliday *et al.*, 1992). This neuronal reduction is corroborated with the reported reduction in serotonergic biochemical markers in brains of patients with Alzheimer's disease (D'Amato *et al.*, 1987). The reduction in serotonergic innervation is thought to be secondary to the cortical pathology of Alzheimen's patients (Mann and Yates, 1986). In brains of Parkinson's disease patients, there are several populations of serotonergic neurons severely affected, among which the MnR and ROb are characterized by the highest reduction in cell number (Halliday *et al.*, 1990). In primates with Parkinson-like symptoms induced by neurotoxic lesions, the loss in number of serotonergic cells parallels a reduction of 5-HT_{1A} receptor density in the hippocampus and other forebrain regions, except in the caudal striatum where an increase in receptor expression is observed (Frechilla *et al.*, 2001). In brains of Huntington's disease patients, the neurochemical alterations have been primarily investigated in the striatum. Parallel to a decrease in GABA, there is an increase in concentration of serotonin and its metabolites (Bird, 1980), which may be accounted for by the shrinkage following degeneration of striatal projection neurons (Kish *et al.*, 1987). Serotonin concentration is also increased in the cerebral cortex and the globus pallidus but not in the hippocampus (Reynolds and Pearson, 1987). In brains of chronic alcoholic patients, with or without Korsakoff's syndrome, the number of TPH-IR neurons in the raphe nuclei were substantially reduced in comparison to nonalcoholic controls (Halliday *et al.*, 1993). This difference was most pronounced in the caudal group of the raphe nuclei.

Acknowledgments

This chapter is dedicated to the memory of late Prof. Istvan Törk. This work was supported by grants of the National Health and Medical Research Council of Australia (to I. Törk) and by grants of the Swiss National Foundation (to J.-P. Hornung). Dr. R. G. H. Cotton and I. Jennings have generously provided the monoclonal antibody to label serotonergic neurons. The valuable assistance of R. Kraftsik and C. Lebrand for the preparation of this manuscript is gratefully acknowledged.

References

Aas, J.E., Brodal, P., Baughman, R.W., and Storm-Mathisen, J. (1990). Projections to the pontine nuclei from choline acetyltransferase-like immunoreactive neurons in the brain stem of the cat. *J. Comp. Neurol.* **300,** 183–195.

Acsády, L., Halasy, K., and Freund, T.F. (1993). Calretinin is present in non-pyramidal cells of the rat hippocampus—III. Their inputs from the median raphe and medial septal nuclei. *Neuroscience* **52,** 829–841.

Aghajanian, G.K. and Marek, G.J. (1997). Serotonin induces excitatory postsynaptic potentials in apical dendrites of neocortical pyramidal cells. *Neuropharmacology* **36,** 589–599.

Aitken, A.R., and Törk, I. (1988). Early development of serotonin-containing neurons and pathways as seen in wholemount preparations of the fetal rat brain. *J. Comp. Neurol.* **274,** 32–47.

Allen, G.V., and Cechetto, D.F. (1994). Serotoninergic and non-serotoninergic neurons in the medullary raphe system have axon collateral projections to autonomic and somatic cell groups in the medulla and spinal cord. *J. Comp. Neurol.* **350,** 357–366.

Antal, M., Petkó, M., Polgár, E., Heizmann, C.W., and Storm-Mathisen, J. (1996). Direct evidence of an extensive GABAergic innervation of the spinal dorsal horn by fibres descending from the rostral ventromedial medulla. *Neuroscience* **73,** 509–518.

Arai, R., Kimura, H., Nagatsu, I., and Maeda, T. (1997). Preferential localization of monoamine oxidase type A activity in neurons of the locus coeruleus and type B activity in neurons of the dorsal raphe nucleus of the rat: a detailed enzyme histochemical study. *Brain Res.* **745,** 352–356.

Arita, H., Sakamoto, M., Hirokawa, Y., and Okado, N. (1993). Serotonin innervation patterns differ among the various medullary motoneuronal groups involved in upper airway control. *Exp. Brain Res.* **95,** 100–110.

Arita, H., Ichikawa, K., and Sakamoto, M. (1995). Serotonergic cells in nucleus raphe pallidus provide tonic drive to posterior cricoarytenoid motoneurons via 5-hydroxytryptamine$_2$ receptors in cats. *Neurosci. Lett.* **197,** 113–116.

Assal, F., Valenza, N., Landis, T., and Hornung, J.P. (2000). Clinico-anatomical correlates of a Fou rire prodromique in a pontine infarction. *J. Neurol. Neurosurg. Psychiatry* **69,** 697–698.

Azmitia, E.C., and Segal, M. (1978). An autoradiographic analysis of the differential ascending projections of the dorsal and median raphe nuclei in the rat. *J. Comp. Neurol.* **179,** 641–668.

Azmitia, E.C., and Gannon, P.J. (1983). The ultrastructural localization of serotonin immunoreactivity in myelinated and unmyelinated axons within the medial forebrain bundle of rat and monkey. *J. Neurosci.* **3,** 2083–2090.

Azmitia, E.C., and Gannon, P.J. (1986). The primate serotonergic system: a review of human and animal studies and a report on *Macaca fascicularis*. *In* "Advances in Neurology," Vol. 43, Myoclonus (S. Fahn, ed.), pp. 407–468. Raven Press, New York.

Azmitia, E.C. (1987). The CNS serotonergic system: progression toward a collaborative organization. *In* "Psychopharmacology: The Third Generation of Progress," (H.Y. Meltzer, ed.), pp. 61–73. Raven Press, New York.

Azmitia, E.C., Gannon, P.J., Kheck, N.M., and Whitaker-Azmitia, P.M. (1996). Cellular localization of the 5-HT_{1A} receptor in primate brain neurons and glial cells. *Neuropsychopharmacology* **14,** 35–46.

Baker, K.G., Halliday, G.M., Hornung, J.P., Geffen, L.B., Cotton, R.G.H., and Törk, I. (1991a). Distribution, morphology and number of monoamine-synthesizing and substance P-containing neurons in the human dorsal raphe nucleus. *Neuroscience* **42,** 757–775.

Baker, K.G., Halliday, G.M., Halasz, P., Hornung, J.P., Geffen, L.B., Cotton, R.G., and Tork, I. (1991b). Cytoarchitecture of serotonin-synthesizing neurons in the pontine tegmentum of the human brain. *Synapse* **7,** 301–320.

Baker, K.G., Halliday, G.M., and Törk, I. (1992). Cytoarchitecture of the human dorsal raphe nucleus. *J. Comp. Neurol.* **301,** 147–161.

Beaudet, A., and Descarries, L. (1976). Quantitative data on serotonin nerve terminals in adult rat neocortex. *Brain Res.* **111,** 301–309.

Beaudet, A., and Descarries, L. (1978). The monoamine innervation of rat cerebral cortex: synaptic and nonsynaptic axon terminals. *Neuroscience* **3,** 851–860.

Bell, R., and Hobson, H. (1994). 5-HT1A receptor influences on rodent social and agonistic behavior: a review and empirical study. *Neurosci. Biobehav. Rev.* **18,** 325–338.

Bengel, D., Murphy, .L., Andrews, A.M., Wichems, C.H., Feltner, D., Heils, A., Mossner, R., Westphal, H., and Lesch, K.P. (1998). Altered brain serotonin homeostasis and locomotor insensitivity to 3,4-methylenedioxymethamphetamine ("Ecstasy") in serotonin transporter–deficient mice. *Mol. Pharmacol.* **53,** 649–655.

Berger, B., Trottier, S., Verney, C., Gaspar, P., and Alvarez, C. (1988). Regional and laminar distribution of the dopamine and serotonin innervation in the macaque cerebral cortex: a radioautographic study. *J. Comp. Neurol.* **273,** 99–119.

Berger, U.V., Grzanna, R., and Molliver, M.E. (1989). Depletion of serotonin using *p*-chlorophenylalanine (PCPA) and reserpine protects against the neurotoxic effects of *p*-chloroamphetamine (PCA) in the brain. *Exp. Neurol.* **103,** 111–115.

Bergqvist, P.B., Dong, J., and Blier, P. (1999). Effect of atypical anti-psychotic drugs on 5-HT_2 receptors in the rat orbito-frontal cortex: an *in vivo* electrophysiological study. *Psychopharmacology (Berl)* **143,** 89–96.

Bernheimer, H., Birkmayer, W., and Hornykiewicz, O. (1961). Verteilung des 5-hydroxytryptamine (serotonin) in Gehirn des Menschen und sein Verhalten bei Patienten mit Parkinsons-Syndrom. *Klin. Wochenschr.* **39,** 1056–1056.

Beskow, J., Gottfries, C.G., Roos, B.E., and Winblad, B. (1976). Determination of monoamine and monoamine metabolites in the human brain: post mortem studies in a group of suicides and in a control group. *Acta Psychiatr. Scand.* **53,** 7–20.

Bird, E.D. (1980). Chemical pathology of Huntington's disease. *Annu. Rev. Pharmacol. Toxicol.* **20,** 533-551.

Bishop, G.A., and Ho, R.H. (1985). The distribution and origin of serotonin immunoreactivity in the rat cerebellum. *Brain Res.* **331,** 195–207.

Biver, F., Wikler, D., Lotstra, F., Damhaut, P., Goldman, S., and Mendlewicz, J. (1997). Serotonin 5-HT2 receptor imaging in major depression: focal changes in orbito-insular cortex. *Br. J. Psychiatry* **171,** 444–448.

Bjarkam, C.R., Sorensen, J.C., and Geneser, F.A. (1997). Distribution and morphology of serotonin-immunoreactive neurons in the brain stem of the New Zealand white rabbit. *J. Comp. Neurol.* **380,** 507–519.

Björklund, A., and Hökfelt, T. (1985). "GABA and Neuropeptides in the CNS," Part I. Elsevier, Amsterdam.

Björklund, A., Hökfelt, T., and Kuhar, M.J. (1990). "Neuropeptides in the CNS," Part II. Elsevier, Amsterdam.

Blessing, W.W., and Gai, W.P. (1997). Caudal pons and medulla oblongata. *In* "The Primate Nervous System," Part I. (F.E. Bloom, A. Björklund, and T. Hökfelt, ed.), pp. 139–215. Elsevier, Amsterdam.

Bobilier, P., Seguin, S., Petitjean, F., Salvert, D., Touret, M., and Jouvet, M. (1976). The raphe nuclei of the cat brain stem: a topographical atlas of their efferent projections as revealed by autoradiography. *Brain Res.* **113,** 449–486.

Boutrel, B., Franc, B., Hen, R., Hamon, M., and Adrien, J. (1999). Key role of 5-HT1B receptors in the regulation of paradoxical sleep as evidenced in 5-HT1B knock-out mice. *J. Neurosci.* **19,** 3204–3212.

Braak, H. (1970). Uber die Kerngebiete des menschlichen Hinstammes II. Die Raphekerne. Z. Zellforsch **107,** 123–141.

Brodal, A. (1981). The reticular formation. *In* "Neurological Anatomy." (A. Brodal, ed.), pp. 411–447. Oxford University Press, Oxford.

Brodal, A., Taber, E., and Walberg, F. (1960). The raphe nuclei of the brain stem in the cat. II. Efferent connections. *J. Comp. Neurol.* **114,** 239–259.

Brunner, D., and Hen, R. (1997). Insights into the neurobiology of impulsive behavior from serotonin receptor knockout mice. *Ann. N.Y. Acad. Sci.* **836,** 81–105.

Brunner, H.G., Nelen, M.R., Breakefield, X.O., Ropers, H.H., and van Oost, B.A. (1993). Abnormal behavior associated with a point mutation in the structural gene for monoamine oxidase A. *Science* **262,** 578–580.

Burnet, P.W.J., Eastwood, S.L., Lacey, K., and Harrison, P.J. (1995). The distribution of 5-HT_{1A} and 5-HT_{2A} receptor mRNA in human brain. *Brain Res.* **676,** 157–168.

Büttner-Ennever, J.A., Cohen, B., Pause, M., and Fries, W. (1988). Raphe nucleus of the pons containing omnipause neurons of the oculomotor system in the monkey, and its homologue in man. *J. Comp. Neurol.* **267,** 307–321.

Campbell, M.J., Lewis, D.A., Foote, S.L., and Morrison, J.H. (1987). Distribution of choline acetyltransferase-, serotonin-, dopamine-β-hydroxylase-, tyrosine hydroxylase–immunoreactive fibers in monkey primary auditory cortex. *J. Comp. Neurol.* **261,** 209–220.

Cann-Moisan, C., Girin, E., Giroux, J.D., Le Bras, P., and Caroff, J. (1999). Changes in cerebrospinal fluid monoamine metabolites, tryptophan, and gamma-aminobutyric acid during the 1st year of life in normal infants. comparison with victims of sudden infant death syndrome. *Biol. Neonate* **75,** 152–159.

Carlsson, A., Falck, B., Fuxe, K., and Hillarp, N.A. (1964). Cellular localization of monoamines in the spinal cord. *Acta Physiol. Scand.* **60,** 112–119.

Cases, O., Seif, I., Grimsby, ., Gaspar, P., Chen, K., Pournin, S., Müller, U., Aguet, M., Babinet, C., Shih, J.C., and De Maeyer, E. (1995). Aggressive behavior and altered amounts of brain

serotonin and norepinephrine in mice lacking MAOA. *Science* **268,** 1763–1766.

Cases, O., Vitalis, T., Seif, I., De Maeyer, E., Sotelo, C., and Gaspar, P. (1996). Lack of barrels in the somatosensory cortex of monoamine oxidase A–deficient mice: role of a serotonin excess during the critical period. *Neuron* **16,** 297–307.

Cases, O., Lebrand, C., Giros, B., Vitalis, T., De Maeyer, E., Caron, M.G., Price, D.J., Gaspar, P., and Seif, I. (1998). Plasma membrane transporters of serotonin, dopamine, and norepinephrine mediate serotonin accumulation in atypical locations in the developing brain of monoamine oxidase A knock-outs. *J. Neurosci.* **18,** 6914–6927.

Chan-Palay, V. (1977). Indoleamine neurons and their processes in the normal rat brain and in chronic diet-induced thiamine deficiency demonstrated by uptake of ^{3}H-serotonin. *J. Comp. Neurol.* **176,** 467-494.

Charara, A., and Parent, A. (1998). Chemoarchitecture of the primate dorsal raphe nucleus. *J. Chem. Neuroanat.* **15,** 111–127.

Choi, D.S., Ward, S.J., Messaddeq, N., Launay, J.M., and Maroteaux, L. (1997). 5-HT2B receptor-mediated serotonin morphogenetic functions in mouse cranial neural crest and myocardiac cells. *Development* **124,** 745–1755.

Conrad, L.C.A., Leonard, C.M., and Pfaff, D.W. (1974). Connections of the median and dorsal raphe nuclei in the rat: an autoradiographic and degeneration study. *J. Comp. Neurol.* **156,** 179–206.

Constantino, J.N., Morris, J.A., and Murphy, D.L. (1997). CSF 5-HIAA and family history of antisocial personality disorder in newborns. *Am. J. Psychiatry* **154,** 1771–1773.

Cook, E.H., and Leventhal, B.L. (1996). The serotonin system in autism. *Curr. Opin. Pediatr.* **8,** 348–354.

Cook, E.H., Stein, M.A., Ellison, T., Unis, A.S., and Leventhal, B.L. (1995). Attention deficit hyperactivity disorder and wholeblood serotonin levels: effects of comorbidity. *Psychiatry Res.* **57,** 13–20.

Corvaja,N., Doucet, G., and Bolam, J.P. (1993). Ultrastructure and synaptic targets of the raphe-nigral projection in the rat. *Neuroscience* **55,** 417–427.

Costa, E., and Aprison, M.H. (1958). Studies of the 5-hydroxytryptamine (serotonin) content in human brain. *J. Nerv. Ment. Dis.* **126,** 289–293.

Costa, J.J.L., Averill, S., Saavedra, J.P., and Priestley, J.V. (1994). Serotonin innervation of enkephalin containing neurones in the rat spinal trigeminal nucleus. *Neurosci. Lett.* **168,** 167–171.

Crabbe, J.C., Phillips, T.J., Feller, D.J., Hen, R., Wenger, C.D., Lessov, C.N., and Schafer, G.L. (1996). Elevated alcohol consumption in null mutant mice lacking 5-HT$_{1B}$ serotonin receptors. *Nature Genet.* **14,** 98–101.

D'Amato, R.J., Blue, M.E., Largent, B.L., Lynch, D.R., Ledbetter, D.J., Molliver, M.E., and Snyder, S.H. (1987). Ontogeny of the serotonergic projection to rat neocortex: transient expression of a dense innervation to primary sensory areas. *Proc. Natl. Acad. Sci. U.S.A.* **84,** 4322–4326.

Dalhström, A., and Fuxe, K. (1964). Evidence for the existence of monoamine-containing neurons in the central nervous system. I. Demonstration of monoamines in the cell bodies of brain stem neurons. *Acta Physiol. Scand. 232 suppl.* **62,** 1–55.

Datiche, F., Luppi, P.-H., and Cattarelli, M. (1995). Serotonergic and non-serotonergic projections from the raphe nuclei to the piriform cortex in the rat: a cholera toxin B subunit (CTb) and 5-HT immunohistochemical study. *Brain Res.* **671,** 27–37.

De Lima, A.D., Bloom, F.E., and Morrison, J.H. (1988). Synaptic organization of serotonin-immunoreactive fibers in primary visual cortex of the macaque monkey. *J. Comp. Neurol.* **274,** 280–294.

De Olmos, J., and Heimer, L. (1980). Double and triple labeling of neurons with fluorescent substances. The study of collateral pathways in the ascending raphe system. *Neurosci. Lett.* **19,** 7–12.

DeFelipe, J., and Jones, E.G. (1988). A light and electron microscopic study of serotonin- immunoreactive fibers and terminals in the monkey sensory-motor cortex. *Exp. Brain Res.* **71,** 171–182.

Del Fiacco, M., Dessi, M.L., and Levanti, M.C. (1984). Topographical localization of substance P in the human postmortem brain stem. An immunohistochemical study in the newborn and adult tissue. *Neuroscience* **12,** 591–611.

Dori, I., Dinopoulos, A., Blue, M.E., and Parnavelas, J.G. (1996). Regional differences in the ontogeny of the serotonergic projection to the cerebral cortex. *Exp. Neurol.* **138,** 1–14.

Dugovic, C., Wauquier, A., Leysen, J.E., Marrannes, R., and Janssen, P.A. (1989). Functional role of 5-HT$_2$ receptors in the regulation of sleep and wakefulness in the rat. *Psychopharmacology (Berl)* **97,** 436–442.

Fallon, J.H., and Loughlin, S.E. (1987). Monoamine innervation of cerebral cortex and a theory of the role of monoamines in cerebral cortex and basal ganglia. *In* "Cerebral Cortex," Vol. 6. (E.G. Jones and A. Peters, eds.), pp. 41–127. Plenum Press, New York.

Felten, D.L., and Sladek, J.R., Jr. (1983). Monoamine distribution in primate brain V. Monoaminergic nuclei: anatomy, pathways and local organization. *Brain Res. Bull.* **10,** 171–284.

Fields, H.L., Heinricher, M.M., and Mason, P. (1991). Neurotransmitters in nociceptive modulatory circuits. *Ann. Rev. Neurosci.* **14,** 219–245.

Fischer, C., Hatzidimitriou, G., Wlos, J., Katz, J., and Ricaurte, G. (1995). Reorganization of ascending 5-HT axon projections in animals previously exposed to the recreational drug (±)3,4-methylenedioxymethamphetamine (MDMA, "ecstasy"). *J. Neurosci.* **15,** 5476–5485.

Fornal, C.A., Metzler, C.W., Marrosu, F., Ribiero-do-Valle, L.E., and Jacobs, B.L. (1996). A subgroup of dorsal raphe serotonergic neurons in the cat is strongly activated during oral-buccal movements. *Brain Res.* **716,** 123–133.

Frechilla, D., Cobreros, A., Saldise, L., Moratalla, R., Insausti, R., Luquin, M.R., and Del Rio, J. (2001). Serotonin 5-HT(1A) receptor expression is selectively enhanced in the striosomal compartment of chronic parkinsonian monkeys. *Synapse* **39,** 288–296.

Gang, S., Nakazono, Y., Aoki, M., and Aoki, N. (1993). Differential projections to the raphe nuclei from the medial parabrachial-Kolliker-Fuse (NPBM-KF) nuclear complex and the retrofacial nucleus in cats: retrograde WGA-HRP tracing. *J. Auton. Nerv. Syst.* **45,** 241–244.

Gellman, R.L., and Aghajanian, G.K. (1994). Serotonin$_2$ receptor–mediated excitation of interneurons in piriform cortex: antagonism by atypical antipsychotic drugs. *Neuroscience* **58,** 515–525.

Gingrich, J.A., and Hen, R. (2000). The broken mouse: the role of development, plasticity and environment in the interpretation of phenotypic changes in knockout mice. *Curr. Opin. Neurobiol.* **10,** 146–152.

Grailhe, R., Waeber, C., Dulawa, S.C., Hornung, J.P., Zhuang, X., Brunner, D., Geyer, M.A., and Hen, R. (1999). Increased exploratory activity and altered response to LSD in mice lacking the 5-HT$_{5A}$ receptor. *Neuron* **22,** 1–20.

Green, A.R., Cross, A.J., and Goodwin, G.M. (1995). Review of the pharmacology and clinical pharmacology of 3,4-methylenedioxymethamphetamine (MDMA or "Ecstasy"). *Psychopharmacology (Berl)* **119,** 247–260.

Greenberg, B.D., McMahon, F.J., and Murphy, D.L. (1998). Serotonin transporter candidate gene studies in affective disorders and personality: promises and potential pitfalls. *Mol. Psychiatry* **3,** 186–189.

Grimsby, J., Lan, N.C., Neve, R., Chen, K., and Shih, J.C. (1990). Tissue distribution of human monoamine oxidase A and B mRNA. *J. Neurochem.* **55,** 1166–1169.

Gross, C., Zhuang, X., Stark, K., Ramboz, S., Oosting, R., Kirby, L., Santarelli, L., Beck, S., and Hen, R. (2002). Serotonin 1A receptor acts during development to establish normal anxiety-like behaviour in the adult. *Nature* **416,** 396–400.

Haan, E.A., Jennings, I.G., Cuello, A.C., Nakata, H., Fujisawa, H., Chow, C.W., Kushinsky, R., Brittingham, J., and Cotton, R.G.H. (1987). Identification of serotonergic neurons in human brain by a monoclonal antibody binding to all three aromatic amino acid hydroxylases. *Brain Res.* **426,** 9–27.

Hajos, M., Richards, C.D., Szekely, A.D., and Sharp, T. (1998). An electrophysiological and neuroanatomical study of the medial prefrontal cortical projection to the midbrain raphe nuclei in the rat. *Neuroscience* **87,** 95–108.

Halasy, K., Miettinen, R., Szabat, E., and Freund, T.F. (1992). GABAergic interneurons are the major postsynaptic targets of median raphe afferents in the rat dentate gyrus. *Eur. J. Neurosci.* **4,** 144–153.

Halliday, G.M., and Törk, I. (1986). Comparative anatomy of the ventromedial mesencephalic tegmentum in the rat, cat, monkey and human. *J. Comp. Neurol.* **252,** 423–445.

Halliday, G.M., Li, Y.W., Joh, .H., Cotton, R.G.H., Howe, P.R.C., Geffen, L.B., and Blessing, W.W. (1988a). Distribution of monoamine-synthesizing neurons in the human medulla oblongata. *J. Comp. Neurol.* **273,** 301–317.

Halliday, G.M., Li, Y.W., Joh, T.H., Cotton, R.G.H., Howe, P.R.C., Geffen, L.B., and Blessing, W.W. (1988b). Distribution of substance *P*-like immunoreactive neurons in the human medulla oblongata: co-localization with monoamine-synthesizing neurons. *Synapse* **2,** 353–370.

Halliday, G.M., Li, Y.W., Oliver, J.R., Joh, T.H., Howe, P.R.C., Geffen, L.B., and Blessing, W.W. (1988c). The distribution of neuropeptide Y-like immunoreactive neurons in the human medulla. *Neuroscience* **26,** 179–191.

Halliday, G.M., Li, Y.W., Blumbergs, P.C., Joh, T.H., Cotton, R.G., Howe, P.R., Blessing, W.W., and Geffen, L.B. (1990). Neuropathology of immunohistochemically identified brain stem neurons in Parkinson's disease. *Ann.Neurol.* **27,** 373–385.

Halliday, G.M., Ellis, J., Heard, R., Caine, D., and Harper, C. (1993). Brain stem serotonergic neurons in chronic alcoholics with and without the memory impairment of Korsakoff's psychosis. *J. Neuropathol.Exp.Neurol.* **52,** 567–579.

Harrison, P.J. (1999). The neuropathology of schizophrenia. A critical review of the data and their interpretation. *Brain* **122** (Pt 4), 593–624.

Herbert, H. (1992). Evidence for projections from medullary nuclei onto serotonergic and dopaminergic neurons in the midbrain dorsal raphe nucleus of the rat. *Cell Tissue Res.* **270,** 149–156.

Hermann, D.M., Luppi, P.H., Peyron, C., Hinckel, P., and Jouvet, M. (1997). Afferent projections to the rat nuclei raphe magnus, raphe pallidus and reticularis gigantocellularis pars a demonstrated by iontophoretic application of choleratoxin (subunit b). *J. Chem. Neuroanat.* **13,** 1–21.

Hornung, J.-P., and Fritschy, J.-M. (1988). Serotoninergic system in the brain stem of the marmoset: a combined immunocytochemical and three-dimensional reconstruction study. *J. Comp. Neurol.* **270,** 471–487.

Hornung, J.-P., and Kraftsik, R. (1988). Three-dimensional reconstruction procedure using GKS primitives and software transformations for anatomical studies of the nervous system. *In* "Proceedings of the Computer Graphics International Meeting." (N. Magnenat-Thalmann and D. Thalmann, eds.), pp. 555–564. Springer-Verlag, Berlin.

Hornung, J.-P., Fritschy, J.-M., and Törk, I. (1990). Distribution of two morphologically distinct subsets of serotoninergic axons in the cerebral cortex of the marmoset. *J. Comp. Neurol.* **297,** 165–181.

Hornung, J.-P., and Celio, M.R. (1992). The selective innervation by serotonergic axons of calbindin-containing interneurons in the neocortex and hippocampus of the marmoset. *J. Comp. Neurol.* **320,** 457–467.

Hornung, J.-P., and de Tribolet, N. (1995). Chemical anatomy of the human cerebral cortex. *In* "Neurotransmitters in the human brain." (D. Tracey, G. Paxinos, and J.Stone, eds.), pp. 41–60.

Hosogai, M., Matsuo, S., Sibahara, T., and Kawai, Y. (1998). Projection of respiratory neurons in rat medullary raphe nuclei to the phrenic nucleus. *Respir. Physiol.* **112,** 37–50.

Hsu, S.M., Raine, L., and Fanger, H. (1981). Use of avidin-biotin-peroxidase complex (ABC) in immunoperoxidase techniques: a comparison between ABC and unlabeled antibody (PAP) procedures. *J. Histochem. Cytochem.* **29,** 577–580.

Hubbard, J.B., and Di Carlo, V. (1974). Fluorescence histochemistry of monoamine-containing cell bodies in the brain stem of the squirrel monkey (Saimiri sciureus) III. Serotonin-containing groups. *J. Comp. Neurol.* **153,** 385–396.

Imai, H., Steindler, D.A., and Kitai, S.T. (1986). The organization of divergent axonal projections from the midbrain raphe nuclei in the rat. *J. Comp. Neurol.* **243,** 363–380.

Jacobowitz, D.M. and MacLean, P.D. (1978). A brain stem atlas of catecholaminergic neurons and serotonergic perikarya in a pygmy primate (Cebuella pygmaea). *J. Comp. Neurol.* **177,** 397–416.

Jacobs, B.L., and Fornal, C.A. (1991). Activity of brain serotonergic neurons in the behaving animal. P*harmacol. Rev.* **43,** 563–578.

Jacobs, B.L., and Fornal, C.A. (1997). Serotonin and motor activity. *Curr. Opin. Neurobiol.* **7,** 820–825.

Jacobs, B., Gannon, P.J., and Azmitia, E.C. (1984). Atlas of serotonergic cell bodies in the cat brain stem: an immunohistochemical study. *Brain Res. Bull.* **13,** 1–31.

Jacobs, B.L., Foote, S.L., and Bloom, F.E. (1978). Differential projections of neurons within the dorsal raphe nucleus of the rat: a horseradish peroxidase (HRP) study. *Brain Res.* **147,** 149–153.

Jahng, J.W., Houpt, T.A., Wessel, T.C., Chen, K., Shih, J.C., and Joh, T.H. (1997). Localization of monoamine oxidase A and B mRNA in the rat brain by in situ hybridization. *Synapse* **25,** 30–36.

Jahng, J.W., Houpt, T.A., Joh, T.H., and Son, J.H. (1998). Differential expression of monoamine oxidase A, serotonin transporter, tyrosine hydroxylase and norepinephrine transporter mRNA by anorexia mutation and food deprivation. *Dev. Brain Res.* **107,** 241–246.

Jakab, R.L., and Goldman-Rakic, P.S. (1998). 5-Hydroxytryptamine$_{2A}$ serotonin receptors in the primate cerebral cortex: possible site of action of hallucinogenic and antipsychotic drugs in pyramidal cell apical dendrites. *Proc. Natl. Acad. Sci. U.S.A.* **95,** 735–740.

Jakab, R.L., and Goldman-Rakic, P.S. (2000). Segregation of serotonin 5-HT$_{2A}$ and 5-HT$_3$ receptors in inhibitory circuits of the primate cerebral cortex. *J. Comp. Neurol.* **417,** 337–348.

Jennes, L., Stumpf, W.E., and Kalivas, P.W. (1982). Neurotensin: topographical distribution in rat brain by immunohistochemistry. *J.Comp. Neurol.* **210,** 211–224.

Jones, S.L., and Light, A.R. (1992). Serotoninergic medullary raphespinal projection to the lumbar spinal cord in the rat: a retrograde immunohistochemical study. *J. Comp. Neurol.* **322,** 599–610.

Joseph, M.H., Baker, H.F., Crow, T.J., Riley, G.J., and Risby, D. (1979). Brain tryptophan metabolism in schizophrenia: a post mortem study of metabolites and kynurenine pathways in schizophrenic and control subjects. *Psychopharmacology* **62,** 279–285.

Kaneko, H., Kaunitz, J., and Tache, Y. (1998). Vagal mechanisms underlying gastric protection induced by chemical activation of raphe pallidus in rats. *Am. J. Physiol.* **275,** G1056–G1062.

Kapadia, S.E., De Lanerolle, N.C., and LaMotte, C.C. (1985). Immunocytochemical and electron microscopic study of

serotonin neuronal organization in the dorsal raphe nucleus of the monkey. *Neuroscience* **15,** 729–746.

Kazakov, V.N., Kravtsov, P.Y., Krakhotkina, E.D., and Maisky, V.A. (1993). Sources of cortical, hypothalamic and spinal serotonergic projections: topical organization within the nucleus raphe dorsalis. *Neuroscience* **56,** 157–164.

Kievit, J., and Kuypers, H.G.J.M. (1975). Subcortical afferents to the frontal lobe in the rhesus monkey studied by means of retrograde horseradish peroxidase transport. *Brain Res.* **85,** 261–266.

Kish, S.J., Shannak, K., and Hornykiewicz, O. (1987). Elevated serotonin and reduced dopamine in subregionally divided Huntington's disease striatum. *Ann. Neurol.* **22,** 386–389.

Kitahama, K., Kimura, H., Maeda, T., and Jouvet, M. (1987). Distribution of two types of monoamine oxidase–containing neurons in the cat medulla oblongata demonstrated by an improved histochemical method. *Neuroscience* **20,** 991–999.

Klauck, S.M., Poustka, F., Benner, A., Lesch, K.P., and Poustka, A. (1997). Serotonin transporter (5-HTT) gene variants associated with autism? *Hum. Mol. Genet.* **6,** 2233–2238.

Köhler, C., and Steinbusch, H. (1982). Identification of serotonin and non-serotonin-containing neurons of the mid-brain raphe projecting to the entorhinal area and the hippocampal formation. A combined immunohistochemical and fluorescent retrograde tracing study in the rat brain. *Neuroscience* **7,** 951–975.

Kölliker, A. (1893). "Handbuch der Gewebelehre des Menschen." Engelmann, Leipzig.

Konradi, C., Svoma, E., Jellinger, K., Riederer, P., Denney, R., and Thibault, J. (1988). Topographic immunocytochemical mapping of monoamine oxidase-A, monoamine oxidase-B and tyrosine hydroxylase in human post mortem brain stem. *Neuroscience* **26,** 791–802.

Koob, G.F. (1992). Drugs of abuse: anatomy pharmacology and function of reward pathways. *Trends Pharmacol. Sci.* **13,** 177–184.

Korte, S.M., Meijer, O.C., De Kloet, E.R., Buwalda, B., Keijser, J., Sluyter, F., van Oortmerssen, G., and Bohus, B. (1996). Enhanced 5-HT1A receptor expression in forebrain regions of aggressive house mice. *Brain Res.* **736,** 338–343.

Kosofsky,B.E., and Kowall, N.W. (1989), Demonstration of two morphologic classes of serotonergic fibers in human cortex. *Soc. Neurosci .Abstr.* **15,** 5–5.

Kosofsky, B.E., and Molliver, M.E. (1987). The serotoninergic innervation of cerebral cortex: different classes of axon terminals arise from dorsal and median raphe nuclei. *Synapse* **1,** 153–168.

Kosofsky, B.E., Molliver, M.E., Morrison, J.H., and Foote, S.L. (1984). The serotonin and norepinephrine innervation of primary visual cortex in the cynomolgus monkey *(Macaca fascicularis)*. *J. Comp. Neurol.* **230,** 168–178.

Lambe, E.K., Krimer, L.S., and Goldman-Rakic, P.S. (2000). Differential postnatal development of catecholamine and serotonin inputs to identified neurons in prefrontal cortex of Rhesus monkey. *J. Neurosci.* **20,** 8780–8787.

Lauder, J.M. (1993). Neurotransmitters as growth regulatory signals: role of receptors and second messengers. *Trends Neurosci.* **16,** 233–240.

Lauder, J.M., and Krebs, H. (1978). Serotonin as a differentiation signal in early neurogenesis. *Dev. Neurosci.* **1,** 15–30.

Lavdas, A.A., Blue, M.E., Lincoln, J., and Parnavelas, J.G. (1997). Serotonin promotes the differentiation of glutamate neurons in organotypic slice cultures of the developing cerebral cortex. *J. Neurosci.* **17,** 7872–7880.

Leander, P., Vrang, N., and Moller, M. (1998). Neuronal projections from the mesencephalic raphe nuclear complex to the suprachiasmatic nucleus and the deep pineal gland of the golden hamster (Mesocricetus auratus). *J. Comp. Neurol.* **399,** 73–93.

Leanza, G., Perez, S., Pellitteri, R., Russo, A., and Stanzani, S. (1995). Branching serotonergic and non-serotonergic projections from caudal brain stem to the medial preoptic area and the lumbar spinal cord, in the rat. *Neurosci. Lett.* **200,** 5–8.

Lebrand, C., Cases, O., Adelbrecht, C., Doye, A., Alvarez, C., El Mestikawy, S., Seif, I., and Gaspar, P. (1996). Transient uptake and storage of serotonin in developing thalamic neurons. *Neuron* **17,** 823–835.

Lebrand, C., Cases, O., Wehrlé, R., Blakely, R.D., Edwards, R.H., and Gaspar, P. (1998). Transient developmental expression of monoamine transporters in the rodent forebrain. *J. Comp. Neurol.* **401,** 506–524.

Lesch, K.P., Bengel, D., Heils, A., Sabol, S.Z., Greenberg, B.D., Petri, S., Benjamin, J., Muller, C.R., Hamer, D.H., and Murphy, D.L. (1996). Association of anxiety-related traits with a polymorphism in the serotonin transporter gene regulatory region. *Science* **274,** 1527–1531.

Leung, C.G., and Mason, P. (1999). Physiological properties of raphe magnus neurons during sleep and waking. *J. Neurophysiol.* **81,** 584–595.

Levine, E.S., and Jacobs, B.L. (1992). Neurochemical afferents controlling the activity of serotonergic neurons in the dorsal raphe nucleus: microiontophoretic studies in the awake cat. *J. Neurosci.* **12,** 4037–4044.

Lewis, D.A. and Lieberman, J.A. (2000) Catching up on schizophrenia. Natural history and neurobiology. *Neuron* **28,** 325–334.

Li, Y.-Q., Takada, M., and Mizuno, N. (1993). The sites of origin of serotoninergic afferent fibers in the trigeminal motor, facial, and hypoglossal nuclei in the rat. *Neurosci. Res.* **17,** 307–313.

Lidov, H.G.W., and Molliver, M.E. (1982). Immunohistochemical study of the development of serotonergic neurons in the rat CNS. *Brain Res.* **78,** 45–46.

Lidow, M.S., Goldman-Rakic, P.S., Gallager, D.W., and Rakic, P. (1989). Quantitative autoradiographic mapping of serotonin 5-HT_1 and 5-HT_2 receptors and uptake sites in the neocortex of the rhesus monkey. *J. Comp. Neurol.* **280,** 27–42.

Loewy, A.D., and McKellar, S. (1981). Serotonergic projections from the ventral medulla to the intermediolateral cell column in the rat. *Brain Res.* **211,** 146–152.

Luque, J.M., Kwan, S.W., Abell, C.W., Da Prada, M., and Richards, J.G. (1995). Cellular expression of mRNAs encoding monoamine oxidases A and B in the rat central nervous system. *J. Comp. Neurol.* **363,** 665–680.

Luque, J.M., Bleuel, Z., Hendrickson, A., and Richards, J.G. (1996). Detection of MAO-A and MAO-B mRNAs in monkey brain stem by cross-hybridization with human oligonucleotide probes. *Mol. Brain Res.* **36,** 357–360.

Maeda, T., Kaneko, S., and Satoh, M. (1994). Inhibitory influence via 5-HT_3 receptors on the induction of LTP in mossy fiber-CA3 system of guinea-pig hippocampal slices. *Neurosci. Res.* **18,** 277–282.

Maher, P., and Davis, J.B. (1996). The role of monoamine metabolism in oxidative glutamate toxicity. *J. Neurosci.* **16,** 6394–6401.

Mamounas, L.A., and Molliver, M.E. (1988). Evidence for dual serotonergic projections to neocortex: axons from the dorsal and median raphe nuclei are differentially vulnerable to the neurotoxin *p*- chloroamphetamine (PCA). *Exp. Neurol.* **102,** 23–36.

Mamounas, L.A., Altar, C.A., Blue, M.E., Kaplan, D.R., Tessarollo, L., and Lyons, W.E. (2000). BDNF promotes the regenerative sprouting, but no survival, of injured serotonergic axons in the adult rat brain. *J. Neurosci.* **20,** 771–782.

Manaker, S., and Fogarty, P.F. (1995). Raphespinal and reticulospinal neurons project to the dorsal vagal complex in the rat. *Exp. Brain Res.* **106,** 79–92.

Manaker, S. and Tischler, L.J. (1993). Origin of serotoninergic afferents to the hypoglossal nucleus in the rat. *J. Comp. Neurol.* **334,** 466–476.

Mann, D.M.A., and Yates, P.O. (1986). Neurotransmitter deficits in Alzheimer's disease and in other dementing disorders. *Human Neurobiol.* **5,** 147–158.

Mann, D.M.A., Yates, P.O., and Marcyniuk, B. (1984). Monoaminergic neurotransmitter systems in presenile Alzheimer's disease and in senile dementia of the Alzheimer type. *Clin. Neuropathol.* **3,** 199–205.

Mantyh, P.W., and Peschanski, M. (1982). Spinal projections from the periaqueductal grey and dorsal raphe in rat, cat and monkey. *Neuroscience* **11,** 2769–2776.

Marek, G.J., and Aghajanian, G.K. (1996). LSD and the phenethylamine hallucinogen DOI are potent partial agonists at 5-HT_{2A} receptors on interneurons in rat piriform cortex. *J. Pharmacol. Exp. Ther.* **278,** 1373–1382.

Mason, P. (1997). Physiological identification of pontomedullary serotonergic neurons in the rat. *J. Neurophysiol.* **77,** 1087–1098.

Mason, P. (1999). Central mechanisms of pain modulation. *Curr. Opin. Neurobiol.* **9,** 436–441.

May, P.J., Baker, H., Vidal, P.-P., Spencer, R.F., and Baker, R. (1987). Morphology and distribution of serotoninergic and oculomotor internuclear neurons in the cat midbrain. *J. Comp. Neurol.* **266,** 150–170.

McCann, U.D., Ridenour, A., Shaham, Y., and Ricaurte, G.A. (1994). Serotonin neurotoxicity after (±) 3,4-methylene dioxymethamphetamine (MDMA, "Ecstasy"): a controlled study in humans. *Neuropsychopharmacology* **10,** 129–138.

McDougle, C.J., Naylor, S.T., Cohen, D.J., Aghajanian, G.K., Heninger, G.R., and Price, L.H. (1996). Effects of tryptophan depletion in drug-free adults with autistic disorder. *Arch. Gen. Psychiatry* **53,** 993–1000.

McGeer, P.L., Eccles, J.C., and McGeer, E.G. (1987). "Molecular Neurobiology of the Mammalian Brain.' Plenum Press, New York.

McMahon, L.L., and Kauer, J.A. (1997). Hippocampal interneurons are excited via serotonin-gated ion channels. *J. Neurophysiol.* **78,** 2493–2502.

Meessen, H., and Olszewsky, J. (1949). "A Cytoarchitectonic Atlas of the Rhombencephalon of the Rabbit." S. Karger, New York.

Miettinen, R., and Freund, T.F. (1992). Convergence and segregation of septal and median raphe inputs onto different subsets of hippocampal inhibitory interneurons. *Brain Res.* **594,** 263–272.

Mikkelsen, J.D., Hay-Schmidt, A., and Larsen, P.J. (1997). Central innervation of the rat ependyma and subcommissural organ with special reference to ascending serotoninergic projections from the raphe nuclei. *J. Comp. Neurol.* **384,** 556–568.

Milne, R.J., and Gamble, G.D. (1990). Behavioural modification of bulbospinal serotonergic inhibition and morphine analgesia. *Brain Res.* **521,** 167–174.

Mitchell, J.M., Lowe, D., and Fields, H.L. (1998) .The contribution of the rostral ventromedial medulla to the antinociceptive effects of systemic morphine in restrained and unrestrained rats. *Neuroscience* **87,** 123–133.

Moiseiwitsch, J.R.D., and Lauder, J.M. (1995). Serotonin regulates mouse cranial neural crest migration. *Proc. Natl. Acad. Sci. U.S.A.* **92,** 7182–7186.

Mokler, D.J., Lariviere, D., Johnson, D.W., Theriault, N.L., Bronzino, J.D., Dixon, M., and Morgane, P.J. (1998). Serotonin neuronal release from dorsal hippocampus following electrical stimulation of the dorsal and median raphe nuclei in conscious rats. *Hippocampus* **8,** 262–273.

Molliver, M.E., Grzanna, R., Lidov, H.G.W., Morrison, J.H., and Olschowka, J.A. (1982). Monoamine systems in the cerebral cortex. *In* "Cytochemical Methods in Neuroanatomy." (V. Chan-Palay and S. L. Palay, eds.), pp. 256–277. Alan R. Liss, New York.

Molliver, M.E., Berger, U.V., Mamounas, L.A., Molliver, D.C., O'Hearn, E., and Wilson, M.A. (1990). Neurotoxicity of MDMA and related compounds: anatomic studies. *Ann. N.Y. Acad. Sci.* **600,** 640–664.

Montagne-Clavel, J., and Oliveras, J.L. (1994). Are ventromedial medulla neuronal properties modified by chronic peripheral inflammation? A single-unit study in the awake, freely moving polyarthritic rat. *Brain Res.* **657,** 92–104.

Morrison, J.H., Foote, S.L., Molliver, M.E., Bloom, F.E., and Lidov, H.G.W. (1982). Noradrenergic and serotonergic fibers innervate complementary layers in monkey primary visual cortex: an immunohistochemical study. *Proc. Natl. Acad. Sci. U.S.A.* **79,** 2401–2405.

Morrison, J.H., Foote, S.L., and Bloom, F.E. (1984). Regional, laminar, developmental and functional characteristics of noradrenaline and serotonin innervation patterns in monkey cortex. *In* "Monoamine Innvervation of Cerebral Cortex." (L.Descarries, T.R. Reader, and H.H. Jasper eds.), pp. 61–75. Alan R. Liss, New York.

Morrison, J.H., and Foote, S.L. (1986). Noradrenergic and serotoninergic innervation of cortical, thalamic, and tectal visual structures in old and new world monkeys. *J. Comp. Neurol.* **243,** 117–138.

Mulligan, K.A., and Törk, I. (1987). Serotonergic axons form basket-like terminals in cerebral cortex. *Neurosci. Lett.* **81,** 7–12.

Mulligan, K.A., and Törk, I. (1988). Serotonergic innervation of the cat cerebral cortex. *J. Comp. Neurol.* **270,** 86–110.

Nishi, M., Kawata, M., and Azmitia, E.C. (2000). Trophic interactions between brain-derived neurotrophic factor and s100beta on cultured serotonergic neurons. *Brain Res.* **868,** 113–118.

Nitz, D., and Siegel, J. (1997a). GABA release in the dorsal raphe nucleus: role in the control of REM sleep. *Am. J. Physiol.* **273,** R451–R455.

Nitz, D., and Siegel, J.M. (1997b). GABA release in the locus coeruleus as a function of sleep/wake state. *Neuroscience* **78,** 795–801.

Nobin, A., and Björklund, A. (1973). Topography of the monoamine neuron systems in the human brain as revealed in fetuses. *Acta Physiol. Scand.* **S388,** 1–40.

O'Hearn, E., Battaglia, G., De Souza, E.B., Kuhar, M.J., and Molliver, M.E. (1988). Methylenedioxyamphetamine (MDA) and methylenedioxymethamphetamine (MDMA) cause selective ablation of serotonergic axon terminals in forebrain: immunocytochemical evidence for neurotoxicity. *J. Neurosci.* **8,** 2788–2803.

Olivier, B., Mos, J., van Oorschot, R., and Hen, R. (1995). Serotonin receptors and animal models of aggressive behavior. *Pharmacopsychiatry 28 Suppl* **2,** 80–90.

Olson, L., Boréus, L.O., and Seiger, A. (1973). Histochemical demonstration and mapping of 5-hydroxytryptamine- and catecholamine-containing neuron systems in the human fetal brain. *Z. Anat. Entwickl.-Gesch.* **139,** 259–282.

Olszewski, J., and Baxter, D. (1954). "Cytoarchitecture of the Human Brain Stem." Karger, Basel.

Palmer, A.M., Francis, P.T., Benton, J.S., Sims, N.R., Mann, D.M.A., Neary, D., Snowden, J.S., and Bowen, D.M. (1987). Presynaptic serotonergic dysfunction in patients with Alzheimer's disease. *J. Neurochem.* **48,** 8–15.

Palmer, A.M., Wilcock, G.K., Esiri, M.M., Francis, P.T., and Bowen, D.M. (1987). Monoaminergic innervation of the frontal and temporal lobes in Alzheimer's disease. *Brain Res.* **401,** 231–238.

Parnavelas, J.G., Moises, H.C., and Speciale, S.G. (1985). The monoaminergic innervation of the rat visual cortex. *Proc. Roy. Soc. Lond. B* **223,** 319–329.

Pasqualetti, M., Nardi, I., Ladinsky, H., Marazziti, D., and Cassano, G.B. (1996), Comparative anatomical distribution of serotonin 1A, 1Dα and 2A receptor mRNAs in human brain postmortem. *Mol. Brain Res.* **39,** 223–233.

Paxinos, G., and Huang, X.F. (1995). "Atlas of the Human Brain Stem." Academic Press, San Diego.

Pecci-Saavadra, J., Pasik, T., and Pasik, P. (1983). Immunocytochemistry of serotonergic neurons in the central nervous system of monkeys. *In* "Neurotransmission. Learning and Memory." (R. Caputto and C. Ajmone-Marsan, eds.), pp. 81–96. Raven Press, New York.

Petit, J.-M., Luppi, P.-H., Peyron, C., Rampon, C., and Jouvet, M. (1995). VIP-like immunoreactive projections from the dorsal raphe and caudal linear raphe nuclei to the bed nucleus of the stria terminalis demonstrated by a double immunohistochemical method in the rat. *Neurosci. Lett.* **193,** 77–80.

Peyron, C., and Luppi, P. H. (1994). GABAergic afferents to the rat dorsal raphe nucleus. *Neurosci. Abstr.* 20, 291.

Poitras, D., and Parent, A. (1978). Atlas of the distribution of monoamine-containing nerve cell bodies in the brain stem of the cat. *J. Comp. Neurol.* 179, 699–718.

Porrino, L.J., and Goldman-Rakic, P.S. (1982). Brain stem innervation of prefrontal and anterior cingulate cortex in the rhesus monkey revealed by retrograde transport of HRP. *J. Comp. Neurol.* **205,** 63–76.

Poulat, P., Marlier, L., Rajaofetra, N., and Privat, A. (1992). 5-Hydroxytryptamine, substance P and thyrotropin-releasing hormone synapses in the intermediolateral cell column of the rat thoracic spinal cord. *Neurosci. Lett.* **136,** 19–22.

Raleigh, M.J., McGuire, M.T., Brammer, G.L., Pollack, D.B., and Yuwiler, A. (1991). Serotonergic mechanisms promote dominance acquisition in adult male vervet monkeys. *Brain Res.* **559,** 181–190.

Ramboz, S., Oosting, R., Amara, D.A., Kung, H.F., Blier, P., Mendelsohn, M., Mann, J.J., Brunner, D., and Hen, R. (1998). Serotonin receptor 1A knockout: an animal model of anxiety-related disorder. *Proc. Natl. Acad. Sci. U.S.A* **95,** 14476–14481.

Rampon, C., Peyron, C., Gervasoni, D., Pow, D.V., Luppi, P.H., and Fort, P. (1999). Origins of the glycinergic inputs to the rat locus coeruleus and dorsal raphe nuclei: a study combining retrograde tracing with glycine immunohistochemistry. *Eur. J. Neurosci.* **11,** 1058–1066.

Raymond, G.V., Bauman, M.L., and Kemper, T.L. (1996). Hippocampus in autism: a Golgi analysis. *Acta Neuropathol. (Berl.)* **91,** 117–119.

Reynolds, G.P., and Pearson, S.J. (1987). Decreased glutamic acid and increased 5-hydroxytryptamine in Huntington's disease brain. *Neurosci. Lett.* **78,** 233–238.

Ribeiro-do-Valle, L.E. (1997). Serotonergic neurons in the caudal raphe nuclei discharge in association with activity of masticatory muscles. *Braz. J. Med. Biol. Res.* **30,** 79–83.

Ridet, J.-L., Rajaofetra, N., Teilhac, J.-R., Geffard, M., and Privat, A. (1993). Evidence for nonsynaptic serotonergic and noradrenergic innervation of the rat dorsal horn and possible involvement of neuron-glia interactions. *Neuroscience* **52,** 143–157.

Ridet, J.-L., Geffard, M., and Privat, A. (1994). Light and electron microscopic studies of the effects of p-chloroamphetamine on the monoaminergic innervation of the rat spinal cord. *J. Comp. Neurol.* **343,** 281–296.

Rikard-Bell, G.C., Törk, I., Sullivan, C., and Scheibner, T. (1990). Distribution of substance P-like immunoreactive fibres and terminals in the medulla oblongata of the human infant. *Neuroscience* **34,** 133–148.

Rocha, B.A., Scearce-Levie, K., Lucas, J.J., Hiroi, N., Castanon, N., Crabbe, J.C., Nestler, E.J., and Hen, R. (1998) .Increased vulnerability to cocaine in mice lacking the serotonin-1B receptor. *Nature (Lond.)* **393,** 175–178.

Ropert, N., and Guy, N. (1991). Serotonin facilitates GABAergic transmission in the CA1 region of rat hippocampus in vitro. *J. Physiol.* **441,** 121–136.

Salichon, N., Gaspar, P., Upton, A.L., Picaud, S., Hanoun, N., Hamon, M., De Maeyer, E.E., Murphy, D.L., Mossner, R., Lesch, K.P., Hen, R., and Seif, I. (2001). Excessive activation of serotonin (5-HT) 1B receptors disrupts the formation of sensory maps in monoamine oxidase a and 5-HT transporter knock-out mice. *J. Neurosci.* **21,** 884–896.

Saudou, F., Amara, D.A., Dierich, A., LeMeur, M., Ramboz, S., Segu, L., Buhot, M.-C., and Hen, R. (1994). Enhanced aggressive behavior in mice lacking 5-HT_{1B} receptor. *Science* **265,** 1875–1878.

Scatton, B., Javoy-Agid, F., Rouquier, L., DuBois, B., and Agid, Y. (1983). Reduction of cortical dopamine, noradrenaline, serotonin and their metabolites in Parkinson's disease. *Brain Res.* **275,** 321–328.

Schiffmann, S.N., and Vanderhaeghen, J.J. (1991). Distribution of cells containing mRNA encoding cholecystokinin in the rat central nervous system. *J. Comp. Neurol.* **304,** 219–233.

Schlicker, E., Brandt, F., Classen, K., and Göthert, M. (1985). Serotonin release in human cerebral cortex and its modulation via serotonin receptors. *Brain Res.* **331,** 337–341.

Schoefield, S.P.M. and Dixon, A.F. (1982). Distribution of catecholamine and indoleamine neurons in the brain of the common marmoset *(Callithrix jacchus). J. Anat.* **134,** 315–338.

Schoefield, S.P.M., and Everitt, B.J. (1981). The organization of indoleamine neurons in the brain of the rhesus monkey *(Macaca mulatta). J. Comp. Neurol.* **197,** 369–383.

Sheldon, P.W., and Aghajanian, G.K. (1990). Serotonin (5-HT) induces IPSPs in pyramidal layer cells of rat piriform cortex: evidence for the involvement of a 5-HT_2-activated interneurons. *Brain Res.* **506,** 62–69.

Sheu, F.-S., Azmitia, E.C., Marshak, D.R., Parker, P.J., and Routtenberg, A. (1994). Glial-derived S100b protein selectively inhibits recombinant β protein kinase C (PKC) phosphorylation of neuron-specific protein F1/GAP43. *Mol. Brain Res.* **21,** 62–66.

Shinnar, S., Maciewicz, R.J., and Shofer, R.J. (1973). A raphe projection to cat cerebellar cortex. *Brain Res.* **97,** 139–143.

Sikich, L., Hickok, J.M., and Todd, R.D. (1990). 5-HT_{1A} receptors control neurite branching during development. *Brain Res. Dev. Brain Res.* **56,** 269–274.

Skagerberg, G., and Björklund, A. (1985). Topographic principles in the spinal projections of serotonergic and non-serotonergic brain stem neurons in the rat. *Neuroscience* **15,** 445–480.

Smiley, J.F., and Goldman-Rakic, P.S. (1996). Serotonergic axons in monkey prefrontal cerebral cortex synapse predominantly on interneurons as demonstrated by serial section electron microscopy. *J. Comp. Neurol.* **367,** 431–443.

Snowball, R.K., Dampney R.A., and Lumb, B.M. (1997). Responses of neurones in the medullary raphe nuclei to inputs from visceral nociceptors and the ventrolateral periaqueductal grey in the rat. *Exp. Physiol.* **82,** 485–500.

Stamp, J.A., and Semba, K. (1995). Extent of colocalization of serotonin and GABA in the neurons of the rat raphe nuclei. *Brain Res.* **677,** 39–49.

Steinbusch, H.W.M. (1981). Distribution of serotonin-immunoreactivity in the central nervous system of the rat-cell bodies and terminals. *Neuroscience* **6,** 557–618.

Steinbusch, H.W.M., and Nieuwenhuys, R. (1983). The raphe nuclei of the rat brain stem: a cytoarchitectonic and immunohistochemical study. *In* "Chemical Neuroanatomy." (P.C. Emson, ed.), pp. 131–207. Raven Press, New York.

Steinbush, H.W.M., van der Kooy, D., Verhofstad, A.A.J., and Pellegrino, A. (1980). Serotonergic and non-serotonergic projections from the nucleus raphe dorsalis to the caudate-putamen complex in the rat, studied by a combined immunofluorescence and fluorescent retrograde axonal labeling technique. *Neurosci. Lett.* **19,** 137–142.

Steininger, T.L., Wainer, B.H., Blakely, R.D., and Rye, D.B. (1997). Serotonergic dorsal raphe nucleus projections to the cholinergic and noncholinergic neurons of the pedunculopontine tegmental region: a light and electron microscopic anterograde tracing and immunohistochemical study. *J. Comp. Neurol.* **382,** 302–322.

Stone, J., Dreher, B., and Törk, I. (1987). "The neuroanatomist's Colouring Book." Maitland, Sydney. p. 123.

Tabaton, M., Schenone, A., Romagnoli, P., and Mancardi, G.L. (1985). A quantitative and ultrastructural study of substantia nigra and nucleus centralis superior in Alzheimer's disease. *Acta Neuropathol. (Berl.)* **68,** 218–223.

Taber-Pierce, E., Foote, W.E., and Hobson, J.A. (1976). The efferent connection of the nucleus raphe dorsalis. *Brain Res.* **107,** 137–144.

Taber, E., Brodal, A., and Walberg, F. (1960). The raphe nuclei of the brain stem in the cat. I. Normal topography and cytoarchitecture and cytoarchitecture and general discussion. *J. Comp. Neurol.* **114,** 161–187.

Takahashi, H., Nakashima, S., Ohama, E., Takeda, S., and Ikuta, F. (1986). Distribution of serotonin-containing bodies in the brain stem of the human fetus determined with immunohistochemistry using antiserotonin serum. *Brain Dev.* **8,** 355–365.

Takeuchi, Y., and Sano, Y. (1983). Immunohistochemical demonstration of serotonin nerve fibers in the neocortex of the monkey (Macaca fuscata). *Anat. Embryol.* **166,** 155–168.

Takeuchi, Y., and Sano, Y. (1984). Serotonin nerve fibers in the primary visual cortex of the monkey. Quantitative and immunoelectron-microscopical analysis. *Anat. Embryol.* **169,** 1–8.

Tanaka, M., Okamura, H., Tamada, Y., Nagatsu, I., Tanaka, Y., and Ibata, Y. (1994). Catecholaminergic input to spinally projecting serotonin neurons in the rostral ventromedial medulla oblongata of the rat. *Brain Res. Bull.* **35,** 23–30.

Thakkar, M.M., Strecker, R.E., and McCarley, R.W. (1998). Behavioral state control through differential serotonergic inhibition in the mesopontine cholinergic nuclei: a simultaneous unit recording and microdialysis study. *J. Neurosci.* **18,** 5490–5497.

Thompson, A.M., Moore, K.R., and Thompson, G.C. (1995). Distribution and origin of serotoninergic afferents to guinea pig cochlear nucleus. *J. Comp. Neurol.* **351,** 104–116.

Tigges, J., Tigges, M., Cross, N.A., McBride, R.L., Letbetter, W.D., and Anschel, S. (1982). Subcortical structures projecting to visual cortical areas in squirrel monkey. *J. Comp. Neurol.* **209,** 29–40.

Törk, I. (1985). Raphe nuclei and serotonin containing systems. *In* "The rat nervous system." (G. Paxinos, ed.), pp. 43–78. Academic Press (Australia), Sydney.

Törk, I., Hornung, J.-P., and Van der Loos, H. (1986). Synaptic connections of serotonergic axons in the molecular layer of the cat's neocortex. *Neurosci. Lett. Suppl.* **26,** S104.

Törk, I., and Hornung, J.-P. (1987). Serotonergic innervation of the human cerebral cortex. *Neuroscience Suppl.* **22,** S112.

Törk, I. (1990). Anatomy of the serotonergic system. *In* "Neuropharmacology of Serotonin." (P. Whitaker-Azmitia and S.J. Peroutka, eds.), pp. 1–35. New York Academy of Sciences, New York.

Trottier, S., Evrard, B., Vignal, J.P., Scarabin, J.M., and Chauvel, P. (1996). The serotonergic innervation of the cerebral cortex in man and its changes in focal cortical dysplasia. *Epilepsy Res.* **25,** 79–106.

Tunnicliff, G. (1991). Molecular basis of buspirone's anxiolytic action. Pharmacol. *Toxicol.* **69,** 149–156.

Turlejski, K. (1996). Evolutionary ancient roles of serotonin: long-lasting regulation of activity and development. *Acta Neurobiol. Exp.* **56,** 619–636.

Ungerstedt, U. (1971). Stereotaxic mapping of the monoamine pathways in the rat brain. *Acta Physiol. Scand. Suppl.* **367,** 1–48.

Upton, A.L., Salichon, N., Lebrand, C., Ravary, A., Blakely, R., Seif, I., and Gaspar, P. (1999). Excess of serotonin (5-HT) alters the segregation of ipsilateral and contralateral retinal projections in monoamine oxidase A knock-out mice: possible role of 5-HT uptake in retinal ganglion cells during development. *J. Neurosci.* **19,** 7007–7024.

Van Bockstaele, E.J., Biswas, A., and Pickel, V.M. (1993). Topography of serotonin neurons in the dorsal raphe nucleus that send axon collaterals to the rat prefrontal cortex and nucleus accumbens. *Brain Res.* **624,** 188–198.

Van den Pol, A.N., Herbst, R.S., and Powell, J.F. (1984). Tyrosine hydroxylase-immunoreative neurons of the hypothalamus: light and electron microscopic study. *Neuroscience* **13,** 1117–1156.

van der Kooy, D., and Hattori, T. (1980). Dorsal raphe cells with collateral projections to the caudate-putamen and substantia nigra: a fluorescent retrograde stud double labeling study in the rat. *Brain Res.* **186,** 1–7.

van der Kooy, D., and Kuypers, H.G.J.M. (1979). Fluorescent retrograde double labeling: axonal branching in the ascending raphe and nigral projections. *Science* **204,** 873–875.

Veasey, S.C., Fornal, C.A., Metzler, C.W., and Jacobs, B.L. (1995). Response of serotonergic caudal raphe neurons in relation to specific motor activities in freely moving cats. *J. Neurosci.* **15,** 5346–5359.

Vertes, R.P., and Martin, G.F. (1988). Autoradiographic analysis of ascending projections from the pontine and mesencephalic reticular formation and the median raphe nucleus in the rat. *J. Comp. Neurol.* **275,** 511–541.

Villar, M.J., Vitale, M.L., Hökfelt, T., and Verhofstad, A.A.J. (1988). Dorsal raphe serotoninergic branching neurons projecting both to the lateral geniculate body and superior colliculus: a combined retrograde tracing-immunohistochemical study in the rat. *J. Comp. Neurol.* **277,** 126–140.

Vollenweider, F.X., Vollenweider-Scherpenhuyzen, M.F., Babler, A., Vogel, H., and Hell, D. (1998). Psilocybin induces schizophrenia-like psychosis in humans via a serotonin-2 agonist action. *Neuroreport* **9,** 3897–3902.

Wang, Q.-P., and Nakai, Y. (1993). Enkephalinergic innervation of GABAergic neurons in the dorsal raphe nucleus of the rat. *Brain Res. Bull.* **32,** 315–320.

Wang,Q.-P. and Nakai,Y. (1994) The dorsal raphe: An important nucleus in pain modulation. *Brain Res.Bull.* **34,** 575-585.

Wang, Q.-P., Ochiai, H., and Nakai, Y. (1992). GABAergic innervation of serotonergic neurons in the dorsal raphe nucleus of the rat studied by electron microscopy double immunostaining. *Brain Res. Bull.* **29,** 943–948.

Waterhouse, B.D., Mihailoff, G.A., Baack, J.C., and Woodward, D.J. (1986). Topographical distribution of dorsal and median raphe neurons projecting to motor, sensorimotor, and visual cortical areas in the rat. *J. Comp. Neurol.* **249,** 460–476.

Westlund, K.N., Denney, R.M., Kochersperger, L.M., Rose, R.M., and Abell, C.W. (1985). Distinct monoamine oxidase A and B populations in primate brain. *Science* **230,** 181–183.

Westlund, K.N., Denney, R.M., Rose, R.M., and Abell, C.W. (1988). Localization of distinct monoamine oxidase A and monoamine oxidase B cell populations in human brain stem. *Neuroscience* **25,** 439–456.

Westlund, K.N., Sorkin, .S., Ferrington, D.G., Carlton, S.M., Willcockson, H.H., and Willis, W.D. (1990). Serotoninergic and

noradrenergic projections to the ventral posterolateral nucleus of the monkey thalamus. *J. Comp. Neurol.* **295,** 197–207.

Westlund, K.N., Lu, Y., Coggeshall, R.E., and Willis, W.D. (1992). Serotonin is found in myelinated axons of the dorsolateral funiculus in monkeys. *Neurosci. Lett.* **141,** 35–38.

Wiklund, L., Léger, L., and Persson, M. (1981). Monoamine cell distribution in the cat brain stem. A fluorescence histochemical study with quantification of indolaminergic and locus coeruleus cell groups. *J. Comp. Neurol.* **203,** 613–647.

Wilson, C.C., Faber, K.M., and Haring, J.H. (1998). Serotonin regulates synaptic connections in the dentate molecular layer of adult rats via 5-HT1a receptors: evidence for a glial mechanism. *Brain Res.* **782,** 235–239.

Wilson, M.A., and Molliver, M.E. (1991). The organization of serotonergic projections to cerebral cortex in primates: regional distribution of axon terminals. *Neuroscience* **44,** 537–553.

Wilson, M.A., Ricaurte, G.A., and Molliver, M.E. (1989). Distinct morphologic classes of serotonergic axons in primates exhibit differential vulnerability to the psychotropic drug 3,4-methylenedioxymethamphetamine. *Neuroscience* **28,** 121–137.

Wu, W., and Wessendorf, M.W. (1992). Organization of the serotonergic innervation of spinal neurons in rats—I. Neuropeptide coexistence in varicosities innervating some spinothalamic tract neurons but not in those innervating postsynaptic dorsal column neurons. *Neuroscience* **50,** 885–898.

Wu, W., Elde, R., and Wessendorf, M.W. (1993). Organization of the serotonergic innervation of spinal neurons in rats—III. Differential serotonergic innervation of somatic and parasympathetic preganglionic motoneurons as determined by patterns of co-existing peptides. *Neuroscience* **55,** 223–233.

Yamaguchi, T., Sawada, M., Kato, T., and Nagatsu, T. (1981). Demonstration of tryptophan 5-monooxygenase activity in human brain in highly sensitive high-performance liquid chromatography with fluorimetric detection. *Biochem. Int.* **2,** 295–303.

Yan, W., Wilson, C.C., and Haring, J.H. (1997a). 5-HT1A receptors mediate the neurotrophic effect of serotonin on developing dentate granule cells. *Dev. Brain Res.* **98,** 185–190.

Yan, W., Wilson, C.C., and Haring, J.H. (1997b). Effects of neonatal serotonin depletion on the development of rat dentate granule cells. *Dev. Brain Res.* **98,** 177–184.

Yang, H., Wu, S.V., Ishikawa, T., and Tache, Y. (1994). Cold exposure elevates thyrotropin-releasing hormone gene expression in medullary raphe nuclei: relationship with vagally mediated gastric erosions. *Neuroscience* **61,** 655–663.

Zagon, A. (1993). Innervation of serotonergic medullary raphe neurons from cells of the rostral ventrolateral medulla in rats. *Neuroscience* **55,** 849–867.

Zetzsche, T., and Chan-Palay, V. (1992). MAO A and B immunoreactivity in the hippocampus, temporal cortex and cerebellum of normal controls and of patients with senile dementia of the Alzheimer type. *Dementia* **3,** 270–281.

CHAPTER

14

Substantia Nigra and Locus Coeruleus

GLENDA HALLIDAY

Prince of Wales Medical Research Institute, The University of New South Wales
Sydney, Australia

There are two large nuclei containing neuromelanin-pigmented neurons in the human brain stem, the substantia nigra, and the locus coeruleus (Fig. 14.1). Although both nuclei contain neuromelanin-pigmented neurons (Fig.14.1), they have very little else in common; the locus coeruleus consists almost entirely of pigmented noradrenergic neurons (German *et al.*, 1988; Baker *et al.*, 1989), whereas the substantia nigra is a population of mixed neuron types that can be compartmentalized into at least three regions, one of which contains the largest group of dopaminergic neurons in the brain (Gibb and Lees, 1991; van Domburg and ten Donkelaar, 1991; Gibb, 1992; McRitchie *et al.*, 1996).

In humans mature dopaminergic and noradrenergic neurons contain considerable amounts of neuromelanin pigment distinguishing them from their surrounds. Surprisingly, the substantia nigra and locus coeruleus do not contain pigmented neuromelanin-containing cells at birth, but the pigment aggregates in the neurons of both regions during maturation and is clearly visible by eye at age 15–18 years (Mann and Yates, 1974). The brain stem of a 5-year-old child contains pigmented locus coeruleus neurons, with those in the substantia nigra remaining unpigmented (Olszewski and Baxter, 1954). The degree of pigmentation increases with age to reach a steady state within individual cells, and by age 30 a substantial proportion of the neurons in both regions contain neuromelanin pigment (Mann and Yates, 1974; Graham, 1984; Manaye *et al.*, 1995). Neuromelanin pigment is found in abundance only in the human brain stem. It was this characteristic that first drew attention to such neurons vulnerability to neurodegenerative diseases. Because of such vulnerability, both regions have been extensively studied in humans, with the bulk of attention on the changes found in the neuromelanin-containing neurons. Degeneration of the dopaminergic substantia nigra characterizes all parkinsonian conditions, with nondopaminergic nigral neurons also degenerating in selective movement disorders. Overactivity of noradrenergic locus coeruleus neurons is linked with neuropsychiatric conditions, whereas degeneration of this region occurs in diverse dementing and movement disorders. Dysfunction of these regions is common in the elderly.

The substantia nigra encompasses the most ventral part of the entire midbrain tegmentum, just dorsal to the cerebral peduncles (Fig. 14.1A; see also Chapter 10), whereas the locus coeruleus crowds the most lateral part of the pontine central gray matter, spilling over into the nearby tegmentum (Fig. 14.1B; see also Chapter 10). Consistent with other brain stem structures, these two nuclei are larger in their rostrocaudal extent than in cross-section. Research has established the locus coeruleus as a relatively homogeneous group of neurons, whereas the substantia nigra has a complex

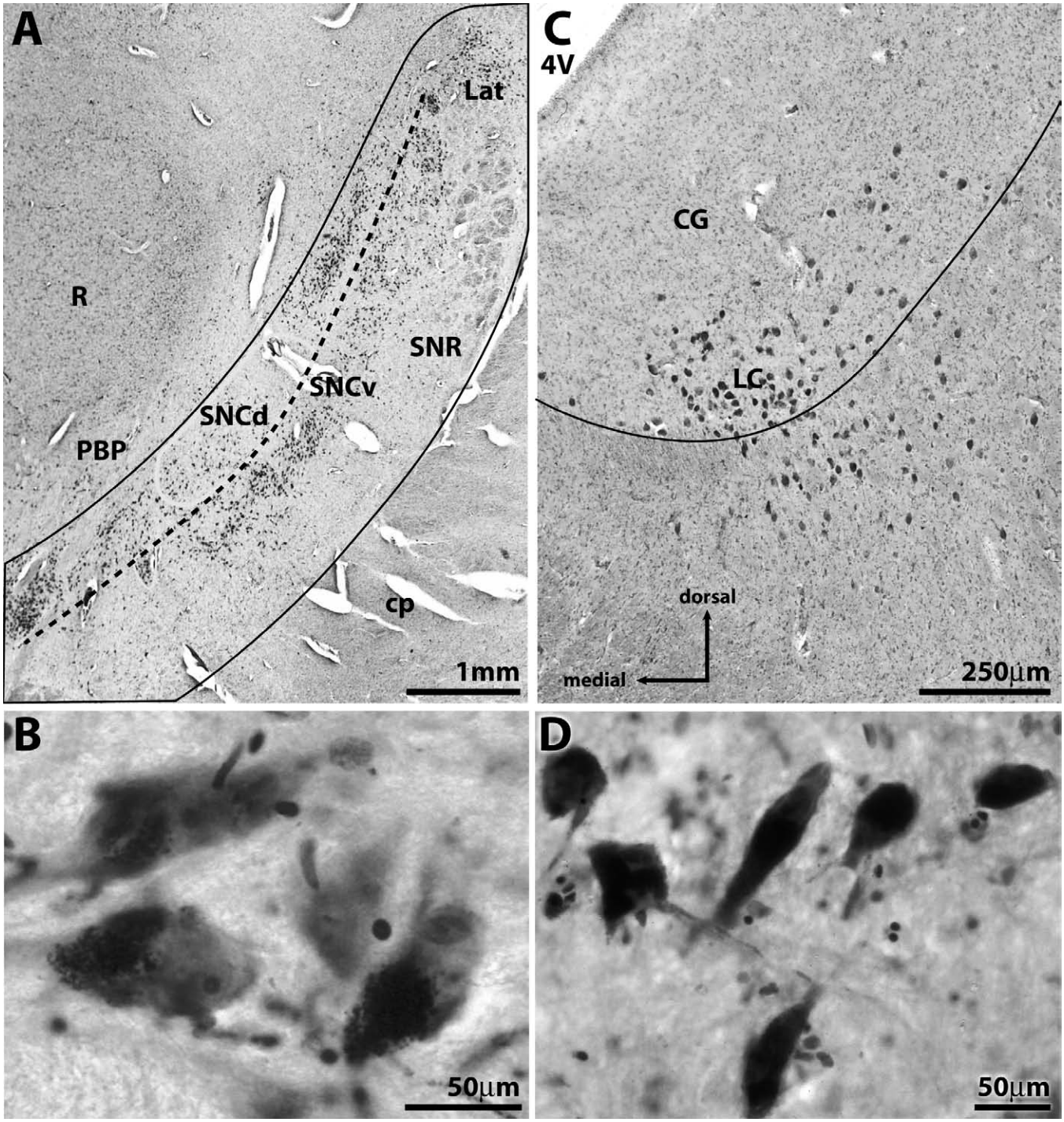

FIGURE 14.1 Photomicrographs of hematoxylin and eosin–stained transverse sections of the substantia nigra and locus coeruleus. These regions contain the highest densities of neuromelanin-pigmented neurons in the adult human brain. **A:** The substantia nigra is located in the ventral midbrain forming the bulk of tissue between the red nucleus (R) and the cerebral peduncle (cp). The nucleus has a three-tiered arrangement of neurons, a dorsal (SNCd) and ventral (SNCv) tier of the pars compacta neurons containing neuromelanin pigment, and the nonpigmented neurons of the pars reticulata (SNR) located more ventrally. It is separated from the red nucleus by the A10 cell cluster, the parabrachial pigmented nucleus (PBP). **B:** High magnification of neuromelanin-pigmented neurons of the substantia nigra. **C:** The locus coeruleus (LC) is located in the ventrolateral region of the central gray (CG) of the upper pons, and spills over into the nearby tegmentum. **D:** High magnification of neuromelanin-pigmented neurons of the locus coeruleus.

organization of multiple cell types. Neurons in the substantia nigra are arranged in a series of sheets or tiers, and within each tier are a series of columnar cell clusters. There is a complex topographical arrangement of carefully targeted projections to thalamic and brain stem sites as well as feedback circuits to the basal ganglia. This complex arrangement within the substantia nigra contrasts with the single-cell column structure of the locus coeruleus. The simplicity of the cellular arrangement of the locus coeruleus belies an extremely complex innervation pattern covering nearly the entire central nervous system.

SUBSTANTIA NIGRA
(see also Chapter 10 and 21)

The substantia nigra is considered an integral part of the basal ganglia, containing the dopaminergic neurons that provide a feedback loop to the striatum as well as the GABAergic neurons that relay basal ganglia output to the thalamus, colliculi, and tegmentum (Fig. 14.2; see also Chapter 21). It therefore plays a major role in the control of actions and thought.

Delineation

The boundaries of the human substantia nigra are not without contention, particularly its dorsal boundaries which interface with other cell clusters containing pigmented dopaminergic neurons. In particular, many works suggest that the substantia nigra extends dorsally to the red nucleus (Olszewski and Baxter, 1954; Hirsch *et al.*, 1988; German *et al.*, 1989; Damier *et al.*, 1999a). It was not until the technique of immunohistochemistry became a standard tool that the delineation of the borders of the human substantia nigra could be consistently identified by the dense neuropil immunostaining for substance P (Mai *et al.*, 1983; Gibb, 1992; McRitchie and Halliday, 1995; McRitchie *et al.*, 1995, 1996). The striatal axons innnervating the substantia nigra contain the tachykinin substance P (Ljungdahl *et al.*, 1978; Gerfen *et al.*, 1985; Pioro *et al.*, 1990), and this pathway identifies the midbrain relay neurons important for direct basal ganglia feedback (Fig. 14.2). Hence, the dense tachykinin staining of the substantia nigra can be used to define its boundaries, and covers a larger cross-sectional area of the ventral midbrain than similar dense immunostaining for either enkephalin or calbindin (Fig. 14.3), despite recent contrary assertions (Damier *et al.*, 1999a).

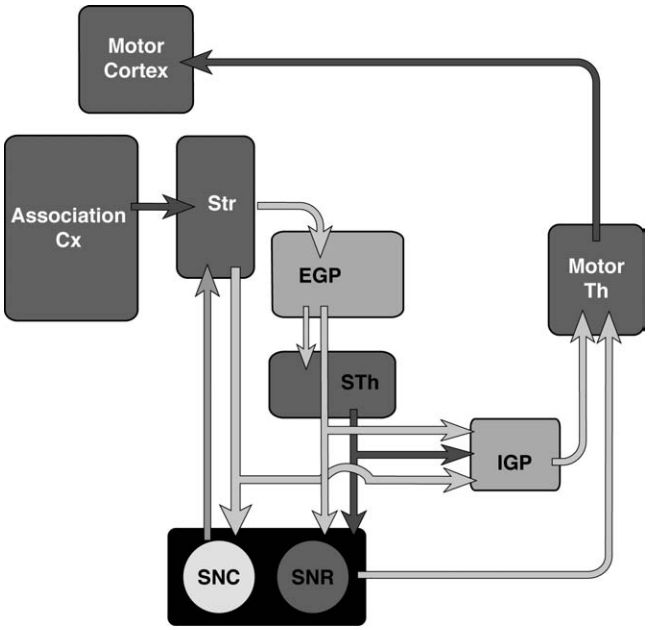

FIGURE 14.2 Schematic diagram of the main circuits of the basal ganglia (see Chapter xx for greater details). Information related to voluntary movement is channeled from the association cortices (Association Cx) to the caudate nucleus and putamen (together termed the striatum; Str). This information is then relayed directly or indirectly to the output nuclei of the basal ganglia (i.e., the internal globus pallidus, IGP; and the substantia nigra pars reticulata, SNR). The external globus pallidus (EGP) and subthalamic nucleus (STh) relay information from the striatum to the output nuclei, while the dopaminergic substantia nigra pars compacta (SNC) modulates striatal activity. The output nuclei project to the motor thalamus (MoTh), which in turn projects to the motor cortices (MoCx).

Neuronal Types

Tyrosine hydroxylase (TH)–positive pigmented neurons are typically medium sized to large, triangular, and multipolar, with a smaller proportion of spindle, bitufted neurons (Fig. 14.4). They contain variable amounts of neuromelanin pigment in the soma (Gibb, 1992) and substantial amounts of the high molecular weight nonphosphorylated neurofilament (Gai *et al.*, 1994) and microtubule-associated protein-2 (MAP 2) (D'Andrea *et al.*, 2001). They tend to have one large and two smaller primary dendrites, which become obscured by the local plethora of similar processes. Although there has been some contention in the literature (Parent *et al.*, 1996), few TH-positive pigmented neurons in the well-defined substantia nigra contain calbindin immunoreactivity (Gibb, 1992; McRitchie and Halliday, 1995; McRitchie *et al.*, 1996). These neurons carry the dopamine transporter (Ma *et al.*, 1999a) with some indication that the amount of this transporter

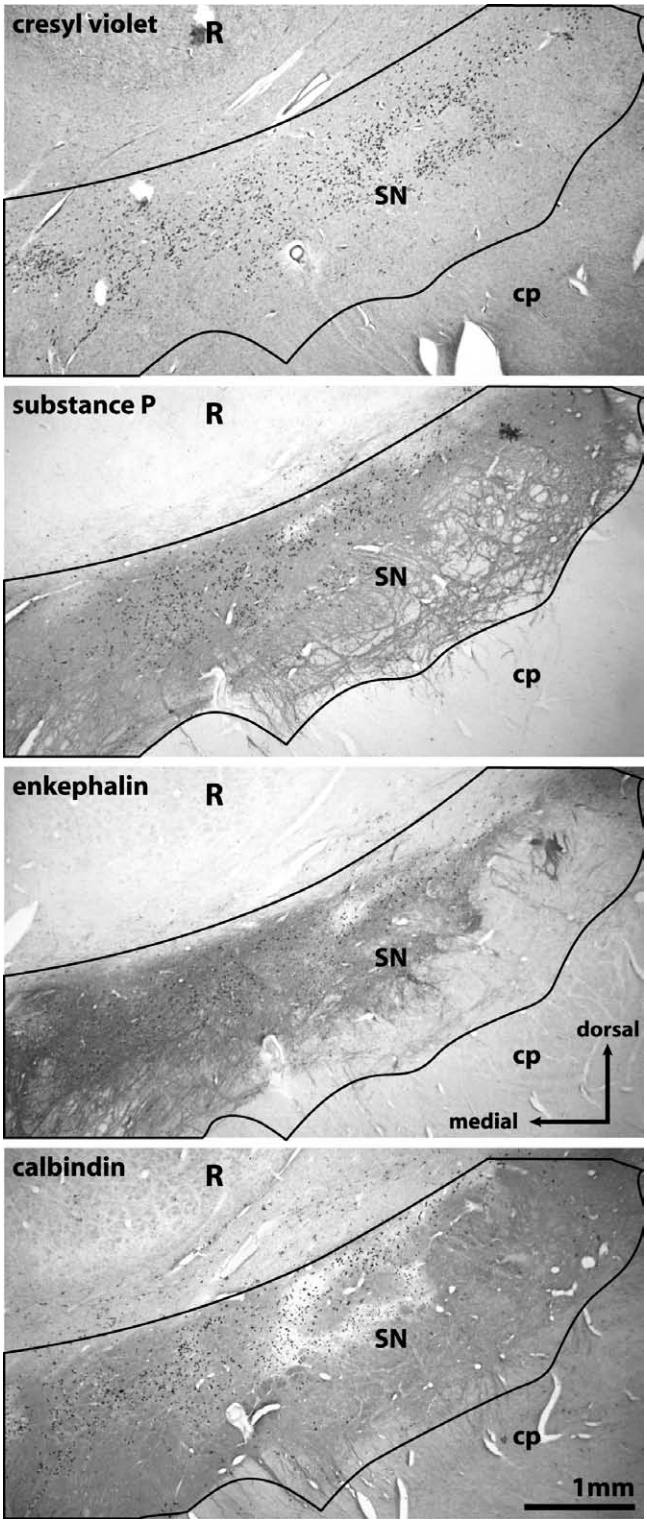

FIGURE 14.3 The substantia nigra can be defined as the midbrain region receiving striatal innervation. This innervation is clearly seen in immunohistochemical preparations identifying the peptide substance P. The dense substance P immunostaining consistently covers a larger cross-sectional area of the ventral midbrain than similar dense immunostaining for either enkephalin or calbindin.

within the soma region declines with age (Ma *et al.*, 1999a). In contrast to rats, human substantia nigra dopaminergic neurons express neurokinin-1 receptors rather than neurokinin-3 receptors (Whitty *et al.*, 1997). The effects of the striatal substance P and neurokinin A are thought to be mediated through this receptor (Whitty *et al.*, 1997). The neurons are also rich in α-synuclein and parkin (Solano *et al.*, 2000; Gavin *et al.*, 2001), as well as different growth factors (Walker *et al.*, 1998; Parain *et al.*, 1999; Howells *et al.*, 2000), synaptic and cellular proteins shown to be important for the survival and normal function of these neurons. The neurons also possess the appropriate trkB (Benisty *et al.*, 1998) and fibroblast growth factor (Walker *et al.*, 1998) receptors in high quantities.

The nonpigmented neurons in the human substantia nigra have not been analyzed with the same intensity. However, these neurons are known to be nondopaminergic as they do not display TH immunoreactivity (Hirsch *et al.*, 1988; Kubis *et al.*, 2000). The calcium-binding proteins calretinin and parvalbumin are found within the nonpigmented neurons of the human substantia nigra (McRitchie *et al.*, 1996). Neurons containing these calcium-binding proteins have been shown to be nondopaminergic in colocalization studies in other species (Parent *et al.*, 1995). Nonpigmented calretinin-containing neurons are typically bipolar, although some multipolar neurons also contain this calcium-binding protein (Fig. 14.4). The processes of these neurons have small varicosities at irregular intervals. Nonpigmented parvalbumin-containing neurons are small and typically multipolar, with round or triangular somas (Fig. 14.4). These neurons are similar in morphology to neurons in the globus pallidus (Yelnik *et al.*, 1987), with sparsely branching dendrites. These three major cell types are similar to those described using Golgi impregnation techniques (Braak and Braak, 1986; Yelnik *et al.*, 1987).

Cytoarchitecture

The substantia nigra contains three broad sheets or tiers of neuronal columns abutting the cerebral peduncle oriented ventromedial to dorsolateral in cross-section. In humans there is quite a complex arrangement of cell clusters in these regions, epitomized by the 21 subdivisions identified by Hassler (1937, 1938). The following descriptions are based on the broad agreement of the majority of studies in this area (Braak and Braak, 1986; Fearnley and Lees, 1991; Gibb and Lees, 1991; van Domburg and ten Donkelaar, 1991; Gibb, 1992; McRitchie and Halliday, 1995; McRitchie *et al.*, 1995, 1996) and incorporate the recent concepts using calbindin immmunostaining to define the

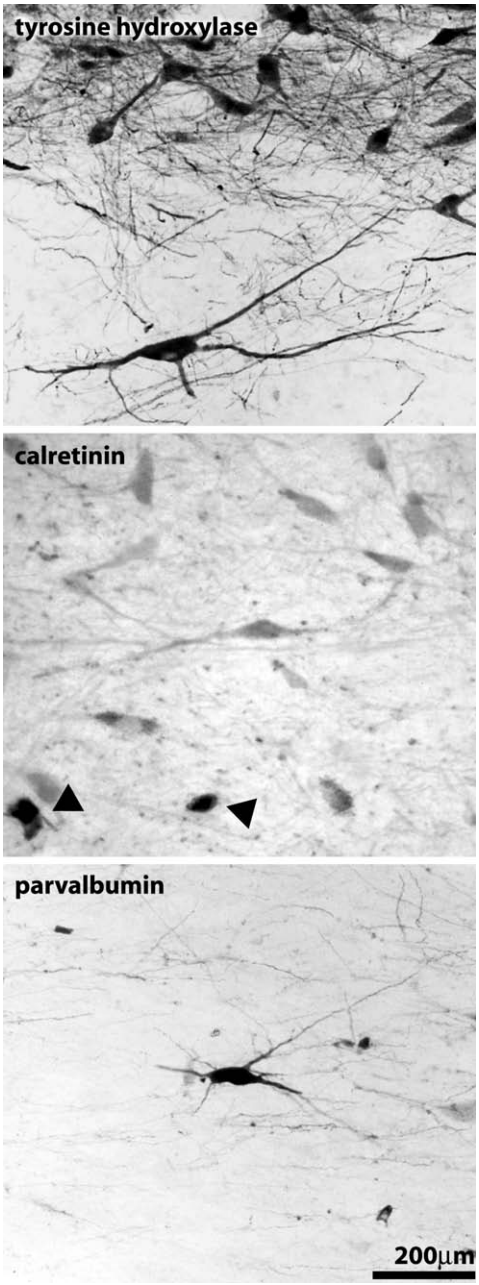

FIGURE 14.4 There are three basic types of neurons in the substantia nigra that can be identified immunohistochemically with tyrosine hydroxylase (TH), calretinin, or parvalbumin. The distinct morphology and distribution of these neurons suggests nonoverlapping populations. TH+ neurons are typically medium sized to large, triangular, and multipolar. They contain neuromelanin pigment and tend to have one large and two smaller primary dendrites, which usually become obscured within the local plethora of similar processes *(top of figure)*. Two types of nonpigmented, nondopaminergic neurons are found within the substantia nigra containing distinct calcium binding proteins. Nonpigmented calretinin-containing neurons are typically bipolar, whereas nonpigmented parvalbumin-containing neurons are typically multipolar, with round or triangular somas. Parvalbumin-containing neurons concentrate in the pars reticulata, while the calretinin-containing neurons are only found between the cell clusters of the pars compacta (pigmented neurons, *arrowheads*).

dopaminergic cell clusters in the substantia nigra (Damier *et al.*, 1999a).

Dorsally the closely related parabrachial pigmented nucleus is found between the substantia nigra and the red nucleus. This region has been recently called the substantia nigra pars dorsalis (Damier *et al.*, 1999a) and is easily distinguished cytoarchitecturally by the lower density of pigmented neurons and the ventromedial to dorsolateral orientation of their dendritic tree. Within the substantia nigra, the most ventral sheet of neurons largely comprises the GABAergic pars reticulata (288,000 ± 32,000 neurons in humans; Hardman *et al.*, 2002) while more dorsally there are two sheets of pigmented dopaminergic pars compacta neurons (totaling 382,000 ± 20,000 neurons in humans, Hardman *et al.*, 2002). These three sheets of neurons are squashed together at both the ventromedial and dorsolateral extremes (Fig. 14.5). These regions are called the pars medialis and pars lateralis. In these regions there is considerable mixing of neuron types.

Pars Compacta

The pars medialis, pars lateralis, and dorsal tier appear aligned along the dorsal border of the substantia nigra. The dorsal and ventral tiers of pigmented dopaminergic neurons are more conspicuous at different rostrocaudal levels (Fig. 14.5). The dorsal tier is significantly larger than the ventral tier and predominates both caudally and rostrally. The ventral tier is most noticeable at intermediate levels of the midbrain. Equal numbers of dopaminergic neurons are found in these tiers (Hardman *et al.*, 2002). In humans these tiers are arranged in longitudinal cell clusters with small bridges of pigmented neurons interspersed between the clusters (Fig. 14.6). These bridges comprise dorsomedial-to-ventrolateral aligned neurons, whereas there is a more random orientation of neurons and processes in the cell clusters. Both the dorsal and ventral tiers can be subdivided into medial, intermediate, and lateral longitudinal cell cluster regions based on the density and aggregations of pigmented neurons (Fig. 14.6). The densest cell clusters in the dorsal tier correspond to a dorsomedial column (McRitchie *et al.*, 1995), called nigrosome 2 (Damier *et al.*, 1999a), and a dorsolateral column (McRitchie *et al.*, 1995), called nigrosomes 4 and 5 (Damier *et al.*, 1999a). Nigrosome cell clusters are defined as having a significant decrease in fibers containing calbindin immunoreactivity around them (Damier *et al.*, 1999a). The dorsomedial column or nigrosome 2 is the most consistent and densely packed cell column, with the dorsolateral column (particularly nigrosome 5) always found at rostral levels (Fig. 14.6). Within the ventral tier, the intermediate and lateral cell columns (McRitchie

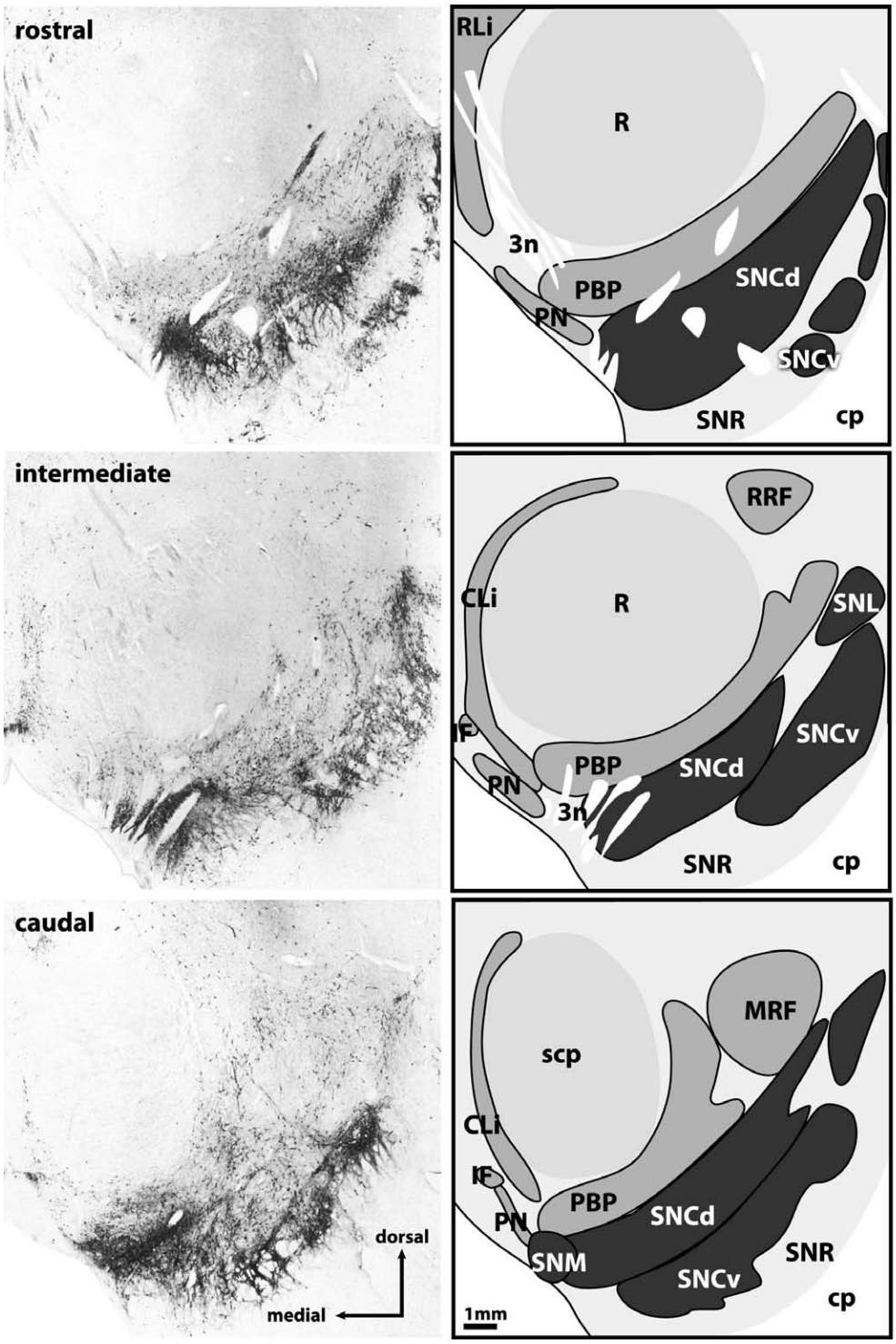

FIGURE 14.5 Three rostrocaudal transverse levels of the midbrain immunohistochemically stained for tyrosine hydroxylase (TH) showing the two dopaminergic tiers of the substantia nigra pars compacta (dorsal, SNCd, and ventral, SNCv) with the position of the more ventral pars reticulata (SNR) indicated. The pars lateralis (SNL) is located dorsolaterally within the substantia nigra, while the pars medialis (SNM) is located caudally on the dorsomedial border. The less cell-dense paranigral nucleus (PN, part of the A10 cell group) medially abuts directly onto this region of the substantia nigra. The very diffuse parabrachial pigmented nucleus (PBP) containing dopaminergic A10 cells can be seen dorsally between the red nucleus (R) and cerebral peduncle (cp). Other midbrain dopaminergic nuclei are indicated—rostral linear nucleus (A10 RLi), caudal linear nucleus (A10 CLi), interfasicular nucleus (A10 IF), and retrorubral fields (A8 RRF). 3n, third nerve; scp, superior cerebellar peduncle.

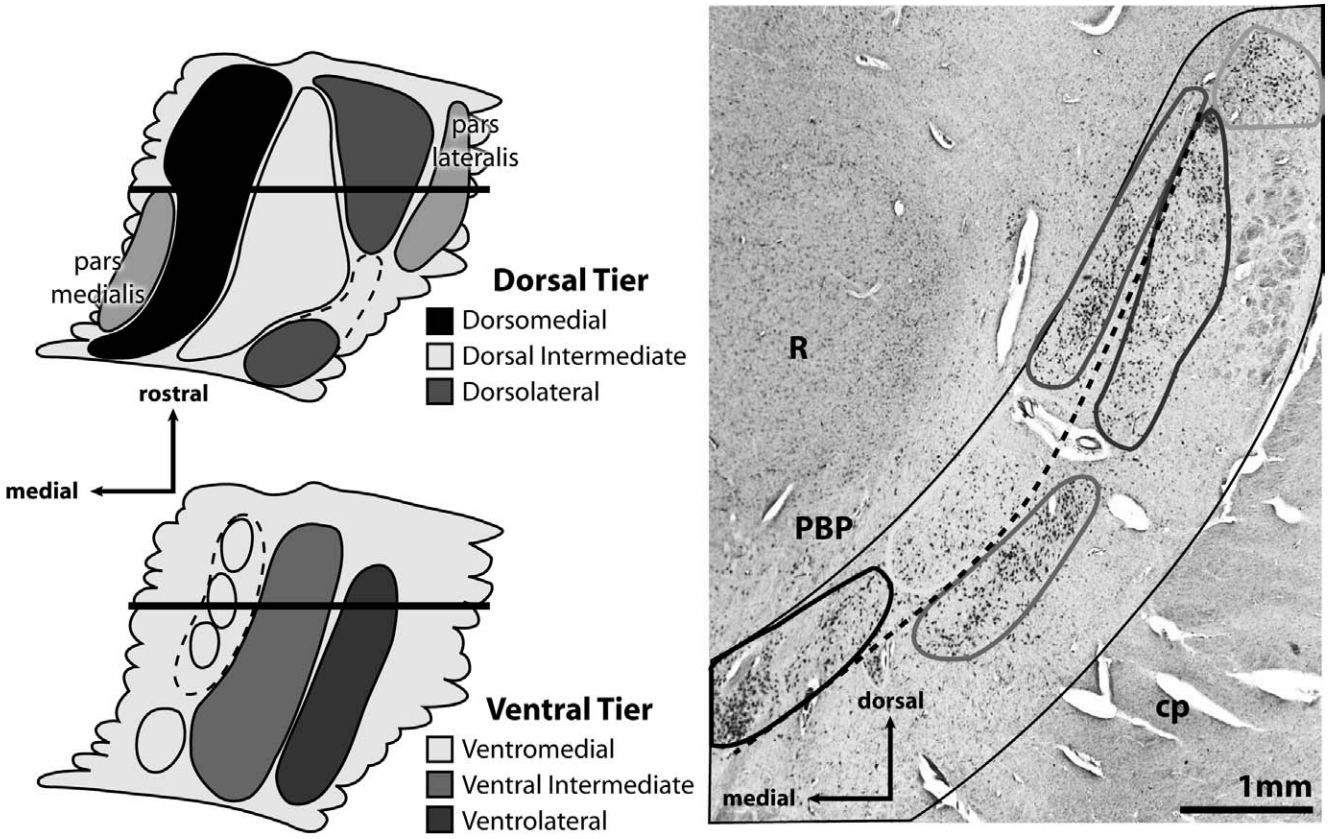

FIGURE 14.6 This diagram represents the consistently found cell clusters of the substantia nigra pars compacta as two-dimensional cell columns oriented obliquely as indicated by the dotted line on the cresyl violet–stained transverse section through this region. The diagrams were drawn from three-dimensional reconstructions of the cross-sections of the cell clusters, which clearly show that these clusters form longitudinal aggregations of neurons (McRitchie *et al.,* 1995). The level of the transverse section shown is indicated by the line. Shading gives some indication of the cell density with variable regions of cell clusters indicated by dotted lines. The dorsomedial column is equivalent to nigrosome 2, the dorsolateral column is equivalent to nigrosomes 4 caudally and 5 rostrally, the pars lateralis is equivalent to nigrosome 3, and the ventral intermediate and ventrolateral columns are equivalent to nigrosome 1 (Damier *et al.,* 1999).

et al., 1995), together called nigrosome 1 (Damier *et al.*, 1999a), have high cell densities, with the lateral cell column concentrating caudally (Fig. 14.6). The other cell columns (dorsointermediate and ventromedial) contain significantly fewer neurons (Fig. 14.6) and are found embedded within the calbindin-immunoreactive matrix (Damier *et al.*, 1999a).

The pars medialis is present only in the caudal midbrain within the dense substance P- and calbindin-immunoreactive striatonigral fiber matrix (Figure 14.6). This matrix separates the nigra from the medial A10 or ventral tegmental area cell clusters. The pars medialis is characterized by densely packed neurons that are smaller than the dorsal tier. Caudally the medial terminal nucleus of the accessory optic tract and the exiting third-nerve fibers separate the pars medialis from the dorsal tier. A proportion of pigmented neurons in the pars medialis contain calbindin or calretinin immunoreactivity. The pars lateralis (McRitchie *et al.*, 1995), called nigrosome 3 (Damier *et al.*, 1999a), is found at the dorsolateral extreme of the substantia nigra (Fig.14.6), lateral to the corticonigral and pallidonigral fiber tracts, and has a significantly decreased cell packing density compared to the dorsal tier. In addition to pigmented dopaminergic neurons, the pars lateralis contains nonpigmented parvalbumin-containing TH-positive neurons.

Pars Reticulata

In humans, neurons of the pars reticulata aggregate rostrally and ventrally (Fig. 14.7), although nonpigmented neurons are also found between the dense cell clusters of the nigra. The nonpigmented neurons between the clusters of pigmented cells contain either

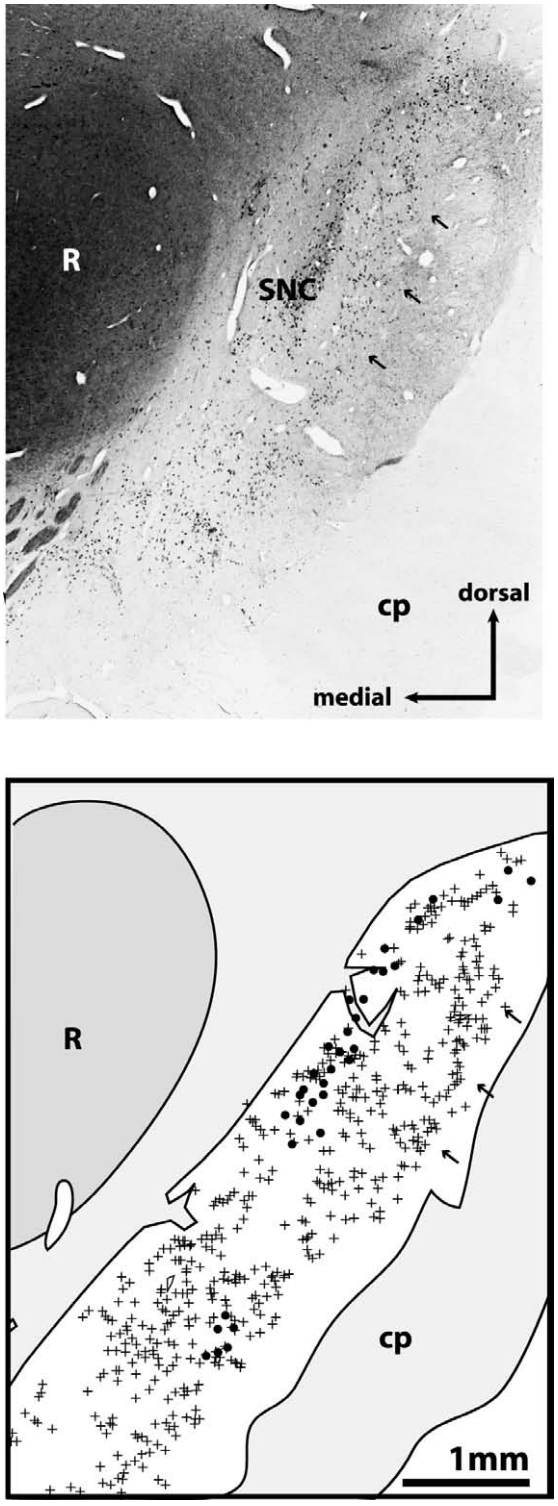

FIGURE 14.7 Parvalbumin-immunoreactive transverse section of the rostral midbrain and distributional plot of the immunoreactive neurons *(crosses)* within the substantia nigra. While many immunoreactive neurons are found in the pars reticulata *(arrows)*, these neurons are widely dispersed within the substantia nigra (pigmented cells indicated by *black circles*). Note the high neuropil immunostaining for parvalbumin in the red nucleus (R). cp, cerebral peduncle.

calretinin or parvalbumin immunoreactivity, whereas the neurons comprising the ventral sheet of reticulata neurons contain only parvalbumin immunoreactivity (Fig. 14.7).

Functional Connections

As stated above, the substantia nigra is an integral part of the basal ganglia, which regulates the pyramidal system (Fig. 14.2; see also Chapter 21). The basal ganglia system may be viewed as a system collecting and processing information from almost the whole extent of the cortex in order to finally furnish adequate information to the only cortex involved in movement preparation and execution. The dopaminergic substantia nigra pars compacta regulates the incoming cortical information at the level of the striatum (see Chapter 21). The GABAergic pars reticulata is one of the two major output nuclei of the basal ganglia, channeling information to thalamocortical relays and brain stem targets (see also Chapters 20 and 21).

Pars Compacta (see also Chapter 21)

While the dopaminergic pars compacta neurons form an integral feedback system to the striatum, the striatonigrostriatal loop is set up to disseminate such feedback (about 100 striatal neurons for each TH-positive nigral neuron) (Percheron *et al.*, 1994). Pars medialis dopaminergic neurons receive projections from the medial limbic striatum (nucleus accumbens) and project to multiple limbic sites, including the accumbens nucleus and limbic cortices (Porrino and Goldman-Rakic, 1982; Swanson, 1982; Loughlin and Fallon, 1984; Takada and Hattori, 1986; Haber *et al.*, 2000). Dorsal tier neurons receive projections from the striatal regions innervated by association cortices (caudate and anterior putamen). These neurons project back to the striatal association regions innervating them (Haber *et al.*, 2000). Ventral tier neurons receive innervation from both associative and sensorimotor regions of the striatum. These ventral neurons, particularly the lateral cell group, nearly selectively innervate sensorimotor innervated regions of the striatum (intermediate and posterior putamen) (Haber *et al.*, 2000). Pars lateralis dopaminergic neurons receive innervation from the caudate region innervated by visual and oculomotor cortical regions. This lateral region projects directly to the inferior and superior colliculi (Francois *et al.*, 1984; Tokuno *et al.*, 1993; Harting *et al.*, 2001).

Pars Reticulata (see also Chapters 20 and 21)

The nondopaminergic neurons in the pars reticulata project to the thalamus, with two smaller proportions projecting to the colliculi (located rostrally and

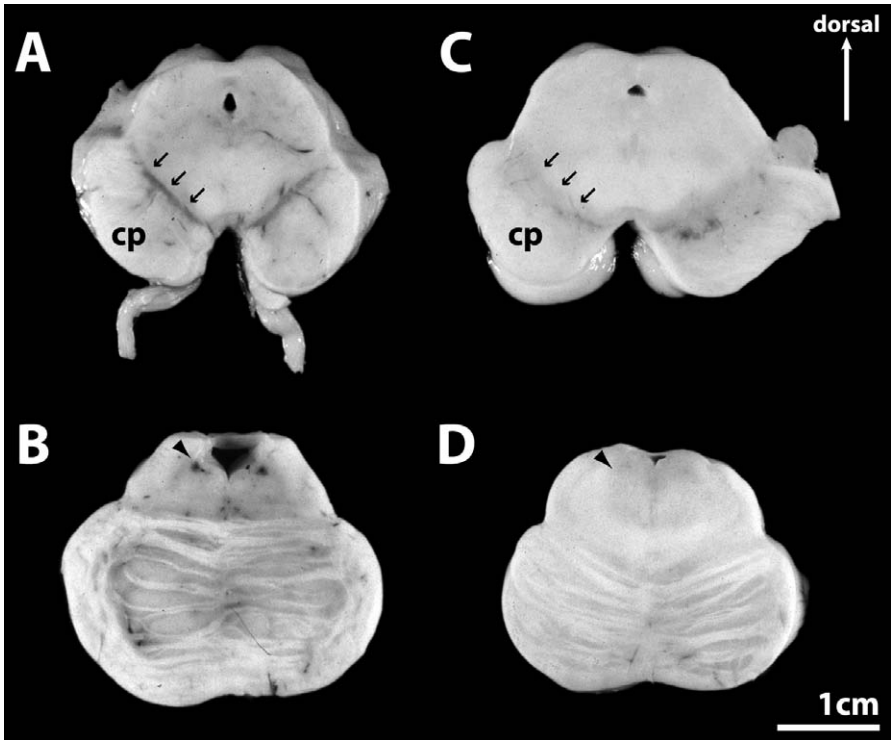

FIGURE 14.8 Macroscopically, the pigmented nuclei of the midbrain and pons are obvious in transverse sections of the normal human brain. **(A)** The pigmented substantia nigra is found in the midbrain just dorsal to the cerebral peduncle (cp). **(B)** The pigmented locus coeruleus is found in the dorsolateral pontine central gray. In Parkinson's disease, both the substantia nigra and locus coeruleus are severely depigmented **(C, D).**

laterally) or the reticular formation (located caudally) (Beckstead, 1983; Francois *et al.*, 1984; Percheron *et al.*, 1994). These projections are largely nonoverlapping in primates.

Change with Age and Human Disease

There is no consistent finding of cell loss with age in the substantia nigra pars compacta (pars reticulata not analyzed). Cross-sectional studies that include people ranging from 40 to 110 years of age consistently find no neuronal loss with age (Halliday *et al.*, 1996; Muthane *et al.*, 1998; Kubis *et al.*, 2000), whereas studies that include people younger than 25 years find age-related neuronal loss (Fearnley and Lees, 1991; Ma *et al.*, 1999b). The differences between studies may suggest that younger people may have an expanded substantia nigra pars compacta. Further studies and larger cohorts are required.

Despite some contention over the presence of age-related cell loss in the dopaminergic substantia nigra, the catastrophic loss of dopaminergic nigral neurons in patients with parkinsonism is without dispute. Thus, the degree of any age-related change is miniscule compared to diseases that impact on this region (Fig. 14.8). The most widely recognized disease affecting this region of the substantia nigra is Parkinson's disease. The definitive analysis of the involvement of the pars compacta in Parkinson's disease was performed by Hassler in 10 cases (Hassler, 1938). He found a constant cell loss with fibrous glial reaction in the central cell groups of the pars compacta and confirmed the presence of Lewy bodies as a defining lesion. Since then a large number of studies have confirmed this finding, which underlies current treatment strategies for this disease (Lozano *et al.*, 1998). Several studies have shown the highly selective nature of the cell loss as impacting most on the ventral intermediate and lateral cell groups of the pars compacta (Fearnley and Lees, 1991; Halliday *et al.*, 1996; Damier *et al.*, 1999b). The reason for this selective vulnerability of only a fraction of the dopaminergic neurons in the substantia nigra remains unknown. No apparent difference in a range of critical measures has been found, e.g., dopamine synthesis capacity (Kingsbury *et al.*, 1999), dopamine transporter gene expression (Counihan and Penney, 1998), and growth factor receptors (Benisty *et al.*, 1998; Walker *et al.*, 1998), although a loss of brain

derived growth factor (Parain *et al.*, 1999; Howells *et al.*, 2000) and nonphosphorylated neurofilament (Gai *et al.*, 1994) occurs in surviving dopaminergic neurons in patients with Parkinson's disease.

The dopaminergic substantia nigra is affected in all parkinsonian conditions, and not just in Parkinson's disease (Jellinger, 1998). Other conditions include dementia with Lewy bodies, multiple-system atrophy, Pick's disease, parkinsonism–dementia complex of Guam, progressive supranuclear palsy, corticobasal degeneration, and postencephalitic parkinsonism. These last three disorders impact severely on both the dopaminergic and nondopaminergic regions of the substantia nigra, depositing tau-positive neurofibrillary tangles in the few surviving compacta and reticulata neurons (Hardman *et al.*, 1997; Jellinger, 1998; Oyanagi *et al.*, 2001). All of these disorders affect multiple brain regions, with the substantia nigra only one of many regions involved in the disease processes.

LOCUS COERULEUS AND SUBCOERULEUS
(see also Chapter 10)

By far the largest group of noradrenergic neurons in the human brain are those located in the locus coeruleus and adjacent subcoeruleus (German *et al.*, 1988; Baker *et al.*, 1989). This relatively homogeneous compact nucleus contains 45,000–50,000 neurons bilaterally in the lateral central gray and another 5000–10,000 neurons in the lateral aspects of the central pontine tegmentum (Baker *et al.*, 1989). These neuronal clusters form a continuous column extending some 15 mm rostrocaudally in the upper lateral pontine central gray of adult humans (Fig. 14.9).

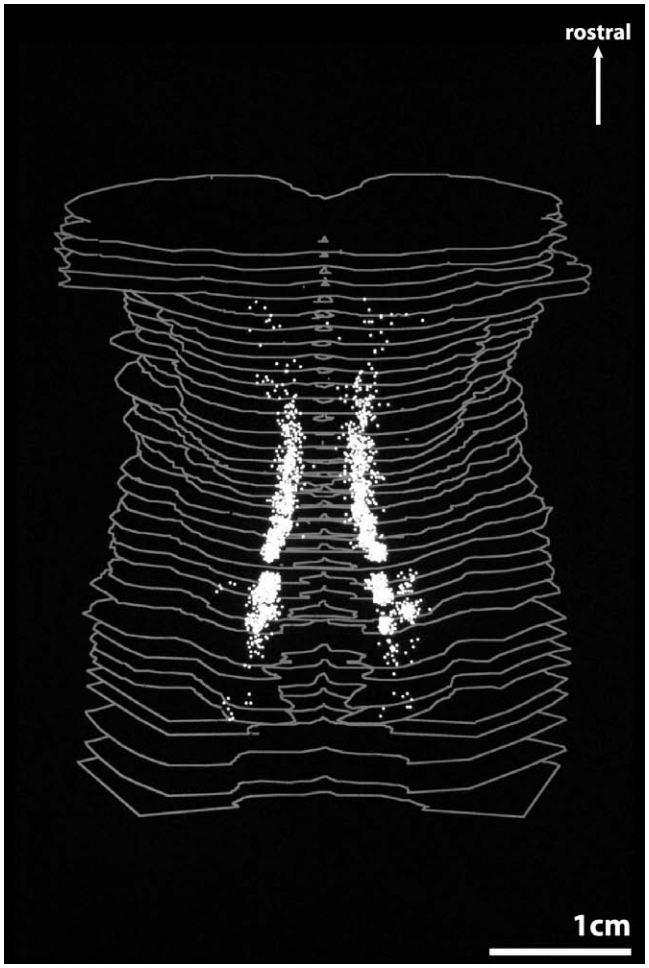

FIGURE 14.9 Three-dimensional reconstruction of transverse cell plots of pigmented locus ceoruleus and subcoeruleus neurons. One in 15 cells is shown with transverse sections spaced 750 μm apart. The locus coeruleus and subcoeruleus form a continuous cell column in the upper pons and caudal midbrain.

Delineation

The definition of the locus coeruleus is without dispute. Its characteristic neuromelanin-pigmented neurons (Fig. 14.1) have been successfully identified in a myriad of studies for nearly a century (Maeda, 2000).

Neuronal Types

Neurons in the locus coeruleus are nearly all pigmented and considered noradrenergic on the basis of their neurochemistry (German *et al.*, 1988; Baker *et al.*, 1989). They possess α_2-adrenoceptors (Klimek and Ordway, 1996), with some indication that the amount of this receptor declines with age (Klimek and Ordway, 1996). Medium (35–45 μm in diameter) and small (15–25 μm in diameter) pigmented neurons are found in this nucleus. The medium-sized locus coeruleus neurons are multipolar and tend to have round or oval somata (Fig. 14.10). Each cell usually has three or four long, thin, cylindrical dendrites that branch once or twice a short distance from the cell. The dendrites are up to 1 mm in length and often extend beyond the nucleus into surrounding structures. The small pigmented neurons are more spindle shaped with two tufts of dendrites (Fig. 14.10). These neurons concentrate in the subcoeruleus, although many medium-sized neurons are also found here, particularly in the rostral subcoeruleus. An unusal feature of the pigmented neurons in the human locus coeruleus is the deeply embedded axosomatic synapses possessed by these neurons (Iwanaga *et al.*, 1995). The anatomical arrangement of these synapses allows neurochemical interactions at previously unsuspected cellular sites.

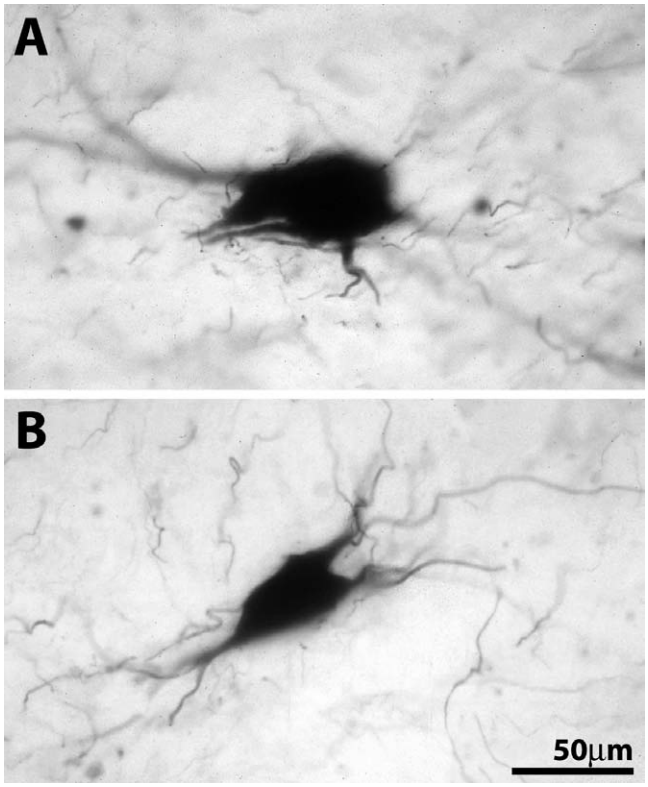

FIGURE 14.10 There are two main types of noradrenergic locus coeruleus neurons. The photomicrographs show TH-immunoreactive neurons of the locus coeruleus **(A)** and subcoeruleus **(B).** Medium-sized neurons are multipolar and tend to have round or oval somata with long cylindrical dendrites (A). Smaller neurons are more spindle shaped, with two tufts of dendrites (B).

A small number of pigmented neurons contain neuropeptide Y and/or galanin (Fodor *et al.*, 1992; Miller *et al.*, 1999).

Cytoarchitecture

Rostrally, locus coeruleus neurons are dispersed in the ventrolateral region of the gray matter, medial to the mesencephalic tract of the trigeminal nerve (Fig. 14.11). At its greatest density at the level of the superior medullary velum, the nucleus is divided into two distinct regions—dorsomedially the neurons are packed closely together whereas ventrolaterally the cells are more dispersed (Fig. 14.11). By midpontine levels the ventrolateral region has extended to form the subcoeruleus proper within the central tegmental regions (Fig. 14.11). The nucleus persists in a caudal direction until few neurons are found in the central gray region and only the subcoeruleus remains (Fig. 14.11). Caudally, scattered neurons extend to the level of the facial nerve whereas rostrally the nucleus tapers at the level of the decussation of the trochlear nerve continuing as scattered neurons in the midbrain periaqueductal gray (Fig. 14.9).

Functional Connections

The locus coeruleus is unique in the brain, being unsurpassed in the divergence and ubiquity of its projections through the central nervous system (Jones, 1991). In this regard it shares certain characteristics with peripheral sympathetic noradrenergic neurons. Nearly all levels of the central nervous system are innervated by this relatively small set of neurons, with the locus coeruleus providing the sole noradrenergic innervation of the cerebral, limbic, and cerebellar cortices. In contrast to this remarkable divergence, there are limited major inputs to the soma of locus coeruleus neurons from the ventral and dorsal medullary relays of sympathetic control and behavioral orienting responses found in the paragigantocellular nucleus and the prepositus hypoglossal nucleus (Aston-Jones *et al.*, 1991). Other afferents (cortical and subcortical) concentrate on the distal dendrites of these neurons, only affecting neuronal output with significant impulse trains (Aston-Jones *et al.*, 1991, 1994, 1999). This unique anatomical arrangement of restricted dominant and diverse weaker afferents along with divergent efferent projections is not found in any other brain stem region. Although it has been difficult to find consensus on the role of this nucleus in the brain, several studies now support the concept that this region is important for vigilance, particularly focused or selective attention and behavioral flexibility or scanning attentiveness (Aston-Jones *et al.*, 1994, 1999).

Change with Age and Human Disease

Similar to research on the substantia nigra, there is no consistent finding of cell loss with age in the locus coeruleus. Cross-sectional studies using modern three-dimensional counting techniques consistently find no neuronal loss with age (Mouton *et al.*, 1994; Ohm *et al.*, 1997), whereas studies using density counts find age-related neuronal loss (Vijayashanker and Brody, 1979; German *et al.*, 1988; Marcyniuk *et al.*, 1989; Manaye *et al.*, 1995). These latter studies emphasize the topographic location of the age-related cell loss (rostral rather than caudal), a finding that is not possible to dissect out using the modern sampling techniques. This location of cell loss is thought to correspond to regions featuring more cortically projecting neurons.

As with the substantia nigra, the degree of cell loss in disease states is an order of magnitude different from that observed with age. The number of conditions affecting the locus coeruleus appears to be more

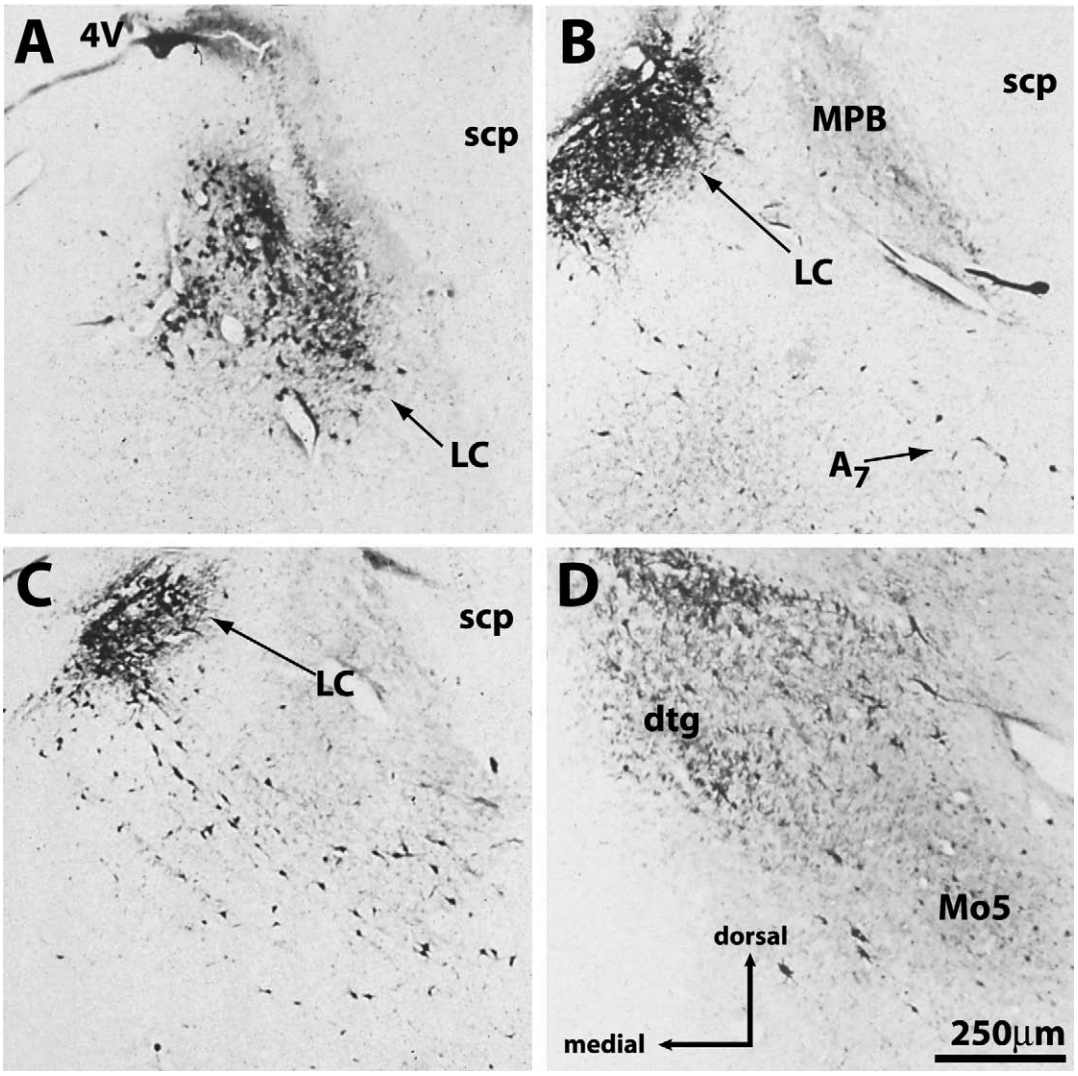

FIGURE 14.11 Photomicrographs of transverse sections through the locus coeruleus at different rostrocaudal levels. 4V, fourth ventricle; dtg, dorsal tegmental tract; MPB, medial parabrachial nucles; Mo5, motor trigeminal nucleus; scp, superior cerebellar peduncle. **A:** Rostrally, locus coeruleus neurons are dispersed in the ventrolateral region of the central gray, around the mesencephalic tract of the trigeminal nerve. **B:** At the level of the superior medullary velum, dorsomedially neurons are packed closely together, whereas ventrolaterally the cells are more dispersed. **C:** At mid-pontine levels, the ventrolateral region has extended to form the subcoeruleus proper within the central tegmental region. **D:** The nucleus persists in a caudal direction until few neurons are found within the central gray region and only the subcoeruleus remains.

diverse, covering both neurodegenerative dementing conditions and movement disorders (German *et al.*, 1992; Hoogendijk *et al.*, 1995). Considering the diverse projections of these neurons, it is not difficult to understand that many neurodegenerative conditions would impact on this region, if only in a retrograde fashion. In addition, a number of nondegenerative psychiatric conditions are suggested to impact on the locus coeruleus. In particular, the levels of TH and binding to α_2-adrenoceptors are increased in neurons of the locus coeruleus in depressed patients (Ordway *et al.*, 1994; Ordway, 1997; Zhu *et al.*, 1999), and a major treatment for depression is the use of tricyclic antidepressants, which reduces locus coeruleus activity. These medications are also effective for panic attacks (Mountjoy *et al.*, 1977).

The majority of research on this region has occurred in patients with Alzheimer's disease or Parkinson's disease. A substantial reduction in noradrenergic locus coeruleus neurons occurs in Alzheimer's disease (German *et al.*, 1992; Hoogendijk *et al.*, 1995), with the small number of remaining neurons containing

galanin (Miller *et al.*, 1999). These remaining neurons up-regulate both their activity (Hoogendijk *et al.*, 1999) and noradrenaline production (Szot *et al.*, 2000) to compensate for the loss of neurons. The cell loss in this region in Alzheimer's disease occurs over decades secondarily to the formation of neurofibrillary tangles (Busch *et al.*, 1997). The significant cell loss of the locus coeruleus in Parkinson's disease (Fig. 14.8) has now been incorporated, along with the substantia nigra, into current diagnostic criteria for this disorder (Gelb *et al.*, 1999). There is even some suggestion that the premature loss or dysfunction of locus coeruleus neurons could exacerbate the selective vulnerability of the dopaminergic nigral neurons (Gesi *et al.*, 2000), although the topographic nature of any neuronal loss has not been factored into this hypothesis. Patients with Parkinson's disease have slow thought reflexes (Gelb *et al.*, 1999), which could suggest a disruption to pathways involved in vigilance. Whether the levodopa medication commonly perscribed for Parkinson's disease can also be utilized in noradrenergic neurons is unresolved.

References

Aston-Jones, G., Chiang, C., and Alexinsky, T. (1991). Discharge of noradrenergic locus coeruleus neurons in behaving rats and monkeys suggests a role in vigilance. *Prog. Brain Res.* **88,** 501–520.

Aston-Jones, G., Rajkowski, J., and Cohen, J. (1999). Role of locus coeruleus in attention and behavioural flexibility. *Biol. Psychiatry* **46,** 1309–1320.

Aston-Jones, G., Rajkowski, J., Kubiak, P., and Alexinsky, T. (1994). Locus coeruleus neurons in monkey are selectively activated by attended cues in a vigilance task. *J. Neurosci.* **14,** 4467–4480.

Baker, K. G., Tork, I., Hornung, J.-P., and Halasz, P. (1989). The human locus coeruleus: an immunohistochemical and three dimensional reconstruction study. *Exp. Brain Res.* **77,** 257–270.

Beckstead, R. M. (1983). Long collateral brainches of substantia nigra pars reticulata axons to thalamus, superior colliculus and reticular formation in monkey and cat. Multiple retrograde neuronal labeling with fluorescent dyes. *Neuroscience* **10,** 767–779.

Benisty, S., Boissiere, F., Faucheux, B., Agid, Y., and Hirsch, E. C. (1998). trkB messenger RNA expression in normal human brain and in the substantia nigra of parkinsonian patients: an in situ hybridization study. *Neuroscience* **86,** 813–826.

Braak, H., and Braak, E. (1986). Nuclear configuration and neuronal types of the nucleus niger in the brain of the human adult. *Human Neurobiol.* **5,** 71–82.

Busch, C., Bohl, J., and Ohm, T. G. (1997). Spatial, temporal and numeric analysis of Alzheimer changes in the nucleus coeruleus. *Neurobiol. Aging* **18,** 401–406.

Counihan, T. J., and Penney, J. B. (1998). Regional dopamine transporter gene expression in the substantia nigra from control and Parkinson's disease brains. *J. Neurol. Neurosurg. Psychiatry* **65,** 164–169.

D'Andrea, M. R., Ilyin, S., and Plata-Salaman, C. R. (2001). Abnormal patterns of microtubule-associated protein-2 (MAP-2) immunolabeling in neuronal nuclei and Lewy bodies in Parkinson's disease substantia nigra brain tissue. *Neurosci. Lett.* **306,** 137–140.

Damier, P., Hirsch, E. C., Agid, Y., and Graybiel, A. M. (1999a). The substantia nigra of the human brain. I. Nigrosomes and the nigral matrix, a compartmental organization based on calbindin D28K immunohistochemistry. *Brain* **122,** 1421–1436.

Damier, P., Hirsch, E. C., Agid, Y., and Graybiel, A. M. (1999b). The substantia nigra of the human brain. II.Patterns of loss of dopamine-containing neurons in Parkinson's disease. *Brain* **122,** 1437–1448.

Fearnley, J. M., and Lees, A. J. (1991). Ageing and Parkinson's disease: substantia nigra regional selectivity. *Brain* **114,** 2283–2301.

Fodor, M., Görcs, T. J., and Palkovits, M. (1992). Immunohistochemical study on the distribution of neuropeptides within the pontine tegmentum—particularly the parabrachial nuclei and the locus coeruleus of the human brain. *Neuroscience* **46,** 891–908.

Francois, C., Percheron, G., and Yelnik, J. (1984). Localization of nigrostriatal, nigrothalamic and nigrotectal neurons in ventricular coordinates in macaques. *Neuroscience* **13,** 61–76.

Gai, W. P., Vickers, J. C., Blumbergs, P. C., and Blessing, W. W. (1994). Loss of non-phosphorylated neurofilament immunoreactivity, with preservation of tyrosine hydroxylase, in surviving substantia nigra neurons in Parkinson's disease. *J. Neurol. Neurosurg. Psychiatry* **57,** 1039–1046.

Gavin, J. E., Schuck, T. M., Lee, V. M., and Trojanowski, J. Q. (2001). Differential expression and distribution of alpha-, beta-, and gamma-synuclein int he developing human substantia nigra. *Exp. Neurol.* **168,** 347–355.

Gelb, D. J., Oliver, E., and Gilman, S. (1999). Diagnostic criteria for Parkinson's disease. *Arch. Neurol.* **56,** 33–39.

Gerfen, C. R., Baimbridge, K. G., and Miller, J. J. (1985). The neostriatal mosaic: Compartmental distribution of calcium-binding protein and parvalbumin in the basal ganglia of the rat and monkey. *Proc. Natl. Acad. Sci. U.S.A.* **82,** 8780–8784.

German, D. C., Walker, B. S., Manaye, K., Smith, W. K., Woodward, D. J., and North, A. J. (1988). The human locus coeruleus: computer reconstruction of cellular distribution. *J. Neurosci.* **8,** 1776–1788.

German, D. C., Manaye, K., Smith, W. K., Woodward, D. J., and Saper, C. B. (1989). Midbrain dopaminergic cell loss in Parkinson's disease: computer visualization. *Ann. Neurol.* **26,** 507–514.

German, D. C., Manaye, K. F., White, C. L., Woodward, D. J., McIntire, D. D., Smith, W. K., Kalaria, R. N., and Mann, D. M. A. (1992). Disease-specific patterns of locus coeruleus cell loss. *Ann. Neurol.* **32,** 667–676.

Gesi, M., Soldani, P., Giorgi, F. S., Santinami, A., Bonaccorsi, I., and Fornai, F. (2000). The role of the locus coeruleus in the development of Parkinson's disease. *Neurosci. Biobehav. Rev.* **24,** 655–668.

Gibb, W. R. G. (1992). Melanin, tyrosine hydroxylase, calbindin and substance P in the human midbrain and substantia nigra in relation to nigrostriatal projections and differential neuronal susceptibility in Parkinson's disease. *Brain Res.* **581,** 283–291.

Gibb, W. R. G., and Lees, A. J. (1991). Anatomy, pigmentation, ventral and dorsal subpopulations of the substantia nigra, and differential cell death in Parkinson's disease. *J. Neurol. Neurosurg. Psychiatry.* **54,** 388–396.

Graham, D. G. (1984). Catecholamine toxicity: a proposal for the molecular pathogenesis of manganese neurotoxicity and Parkinson's disease. *Neurotoxicology* **5,** 83–96.

Haber, S. N., Fudge, J. L., and McFarland, N. R. (2000). Striatonigrostriatal pathways in primates form an ascending spiral from the shell to the dorsolateral striatum. *J. Neurosci.* **20,** 2369–2382.

Halliday, G. M., McRitchie, D. A., Cartwright, H. R., Pamphlett, R. S., Hely, M. A., and Morris, J. G. L. (1996). Midbrain neuropathology in idiopathic Parkinson's disease and diffuse Lewy body disease. *J. Clin. Neurosci.* **3,** 52–60.

Hardman, C. D., Halliday, G. M., McRitchie, D. A., Cartwright, H. R., and Morris, J. G. L. (1997). Progressive supranuclear palsy affects

both the substantia nigra pars compacta and reticulata. *Exp. Neurol.* **144,** 183–192.

Hardman, C. D., Henderson, J. M., Finkelstein, D. I., Horne, M. K., Paxinos, G., and Halliday, G. M. (2002). Comparison of the basal ganglia in rats, marmosets, macaques, baboons, and humans; volume and neuronal number for the output, internal relay, and striatal modulating nuclei. *J. Comp. Neurol.* **445,** 238–255.

Harting, J. K., Updyke, B. V., and Van Lieshout, D. P. (2001). The visual-oculomotor striatum of the cat: functional relationship to the superior colliculus. *Exp. Brain Res.* **136,** 138–142.

Hassler, R. (1937). Zur Normalanatomie der Substanita nigra. Versuch einer architektonischen Gliederung. *J. Psychol. Neurol.* **47,** 1–55.

Hassler, R. (1938). Zur Pathologie der Paralysis agitans und des postenzephalitischen Parkinsonismus. *J. Psychol. Neurol.* **48,** 387–476.

Hirsch, E., Graybiel, A., and Agid, Y. (1988). Melanized dopaminergic neurons are differentially susceptible to degeneration in Parkinson's disease. *Nature* **334,** 345–348.

Hoogendijk, W. J. G., Pool, C. W., Troost, D., van Zwieten, E., and Swaab, D. F. (1995). Image analyser-assisted mmorphomtry of the locus coeruleus in Alzheimer's disease, Parkinson's disease and amyotrophic lateral sclerosis. *Brain* **118,** 131–143.

Hoogendijk, W. J., Feenstra, M. G., Botterblom, M. H., Gilhuis, J., Sommer, I. E., Kamphorst, W., Eikelenboom, P., and Swaab, D. F. (1999). Increased activity of surviving locus coeruleus neurons in Alzheimer's disease. *Ann. Neurol.* **45,** 82–91.

Howells, D. W., Porritt, M. J., Wong, J. Y., Batchelor, P. E., Kalnins, R., Hughes, A. J. ,and Donnan, G. A. (2000). Reduced BDNF mRNA expression in the Parkinson's disease substantia nigra. *Exp. Neurol.* **166,** 127–135.

Iwanaga, K., Takahashi, H., Yamada, M., and Ikuta, F. (1995). Synaptic terminals wrapped in the somatic cytoplasm of pigmented neurons in the human locus coeruleus. *Neurosci. Lett.* **188,** 147–150.

Jellinger, K. A. (1998). Neuropathology of movement disorders. *Neurosurg. Clin. North Am.* **2,** 237–262.

Jones, B. E. (1991). Noradrenergic locus coeruleus neurons: their distant connections and their relationship to neighboring (including cholinergic and GABAergic neurons) of the central gray and reticular formation. *Prog. Brain Res.* **88,** 15–30.

Kingsbury, A. E., Marsden, C. D., and Foster, O. J. (1999). The vulnerability of nigral neurons to Parkinson's disease is unrelated to their intrinsic capacity for dopamine synthesis: an in situ hybridization study. *Mov. Disord.* **14,** 206–218.

Klimek, V., and Ordway, G. A. (1996). Distribution of alph 2-adrenoceptors in the human locus coeruleus. *Brain Res.* **741,** 263–274.

Kubis, N., Faucheux, B. A., Ransmayr, G., Damier, P., Duyckaerts, C., Henin, D., Forette, B., Le Charpentier, Y., Hauw, J.-J., Agid, Y., and Hirsch, E. C. (2000). Preservation of midbrain catecholaminerigc neurons in very old human subjects. *Brain* **123,** 366–373.

Ljungdahl, Å., Hökfelt, T., and Nilsson, G. (1978). Distribution of substance P-like immunoreactivity in the central nervous system. *Neuroscience* **3,** 861–943.

Loughlin, S. E., and Fallon, J. H. (1984). Substantia nigra and ventral tegmental area projections to cortex: topography and collateralization. *Neuroscience* **11,** 425–435.

Lozano, A. M., Lang, A. E., Hutchison, W. D., and Dostrovsky, J. O. (1998). New developments in understanding the etiology of Parkinson's disease and its treatment. *Curr. Opin. Neurobiol.* **8,** 783–790.

Ma, S. Y., Ciliax, B. J., Stebbins, G., Jaffer, S., Joyce, J. N., Cochran, E. J., Kordower, J. H., Mash, D. C., Levey, A. I., and Mufson, E. J. (1999a). Dopamine transporter–immunoreactive neurons decrease with age in the human substantia nigra. *J. Comp. Neurol.* **409,** 25–37.

Ma, S. Y., Röyttä, M., Collan, Y., and Rinne, J. O. (1999b). Unbiased morphometrical measurements show loss of pigmented neurones with ageing. *Neuropath. Appl. Neurobiol.* **25,** 394–399.

Mai, J. K., Stephens, P. H., Hopf, A., and Cuelli, A. C. (1986). Substance P in the human brain. *Neuroscience* **17,** 709–739.

Maeda, T. (2000). The locus coeruleus: history. *J. Chem. Neuroanat.* **18,** 57–64.

Manaye, K. F., McIntire, D. D., Mann, D. M. A., and German, D. C. (1995). Locus coeruleus cell loss in the aging human brain: a non-random process. *J. Comp. Neurol.* **358,** 79–87.

Mann, D. M. A., and Yates, P. O. (1974). Lipoprotein pigments- their relationship to ageing in the human nervous system. II. The melanin content of pigmented nerve cells. *Brain* **97,** 489–498.

Marcyniuk, B., Mann, D. M., and Yates, P. O. (1989). The topography of nerve cell loss from the locus caeruleus in elderly persons. *Neurobiol. Aging* **10,** 5–9.

McRitchie, D. A., and Halliday, G. M. (1995). Calbindin D28K-containing neurons are restricted to the medial substantia nigra in humans. *Neuroscience* **65,** 87–91.

McRitchie, D. A., Halliday, G. M., and Cartwright, H. (1995). Quantitative analysis of the variability of substantia nigra cell clusters in the human. *Neuroscience* **68,** 539–551.

McRitchie, D. A., Hardman, C. D., and Halliday, G. M. (1996). Cytoarchitectural distribution of calcium binding proteins in midbrain dopaminergic regions of rats and humans. *J. Comp. Neurol.* **364,** 121–150.

Miller, M. A., Kolb, P. E., Leverenz, J. B., Peskind, E. R., and Raskind, M. A. (1999). Preservation of noradrenergic neurons in the locus coeruleus that coexpress galanin mRNA in Alzheimer's disease. *J. Neurochem.* **73,** 2028–2036.

Mountjoy, C. O., Roth, M., Garside, R. F., and Leitch, I. M. (1977). A clinical trial of phenelzine in anxiety, depression and phobic neuroses. *Br. J. Psychiatry* **131,** 486–492.

Mouton, P. R., Pakkenberg, B., Gundersen, H. J. G., and Price, D. L. (1994). Absolute number and size of pigmented locus coeruleus neurons in young and aged individuals. *J. Chem. Neuroanat.* **7,** 185–190.

Muthane, U., Yasha, T. C., and Shankar, S. K. (1998). Low numbers and no loss of melanized nigral neurons with increasing age in normal human brains from India. *Ann. Neurol.* **43,** 283–287.

Ohm, T. G., Busch, C., and Bohl, J. (1997). Unbiased estimation of neuronal numbers in the human nucleus coeruleus during "Cytoarchitecture of the Human Brain Stem." Karger, Basel.

Ordway, G. A. (1997). Pathophysiology of the locus coeruleus in suicide. *Ann. N.Y. Acad. Sci.* **836,** 233–252.

Ordway, G. A., Smith, K. S., and Haycock, J. W. (1994). Elevated tyrosine hydroxylase in the locus coeruleus of suicide victims. *J. Neurochem.* **62,** 680–685.

Oyanagi, K., Tsuchiya, K., Yamazaki, M., and Ikeda, K. (2001). Substantia nigra in progressive supranuclear palsy, corticobasal degeneration, and parkinsonism-dementia complex of Guam: specific pathological features. *J. Neuropathol. Exp. Neurol.* **60,** 393–402.

Parain, K., Murer, M. G., Yan, Q., Faucheux, B., Agid, Y., Hirsch, E., and Raisman-Vozari, R. (1999). Reduced expression of brain-derived neurotrophic factors protein in Parkinson's disease substantia nigra. *Neuroreport* **10,** 557–561.

Parent, A., Cote, P.-Y., and Lavoie, B. (1995). Chemical anatomy of the primate basal ganglia. *Prog. Neurobiol.* **46,** 131–197.

Parent, A., Fortin, M., Côté, P.-Y., and Cicchetti, F. (1996). Calcium-binding proteins in primate basal ganglia. *Neurosci. Res.* **25,** 309–334.

Percheron, G., François, C., Yelnik, J., Fénelon, G., and Talbi, B. (1994). The basal ganglia–related system of primates: definition,

description and informational analysis. *In* "The Basal Ganglia IV" (G. Percheron, J. S. McKenzie and J. Féger, eds.), pp. 3–20. Plenum Press, New York.

Pioro, E. P., Mai, J. K., and Cuello, C. A. (1990). Distribution of substance P- and enkephalin-immunoreactive neurons and fibres. *In* "The Human Nervous System" (G. Paxinos, eds.), pp. 1051–1094. Academic Press, San Diego.

Porrino, L. J., and Goldman-Rakic, P. S. (1982). Brain stem innervation of prefrontal and anterior cingulate cortex in the rhesus monkey revealed by retrograde transport of HRP. *J. Comp. Neurol.* **205,** 63–76.

Solano, S. M., Miller, D. W., Augood, S. J., Young, A. B., and Penney, J. B. (2000). Expression of alpha-synuclein, parkin, and ubiquitin carboxy-terminal hydrolase L1 mRNA in human brain: genes associated with familial Parkinson's disease. *Ann. Neurol.* **47,** 201–210.

Swanson, L. W. (1982). The projections of the ventral tegmental area and adjacent regions: a combined fluorescent retrograde tracer and immunofluorescence study in the rat. *Brain Res. Bull.* **9,** 321–353.

Szot, P., Leverenz, J. B., Peskind, E. R., Kiyasu, E., Rohde, K., Millar, M. A., and Raskind, M. A. (2000). Tyrosine hydroxylase and norepinephrine transporter mRNA expression in the locus coeruleus in Alzheimer's disease. *Brain Res. Mol. Brain Res.* **84,** 135–140.

Takada, M., and Hattori, T. (1986). Collateral projections from the substantia nigra to the cingulate cortex and striatum in the rat. *Brain Res.* **380,** 331–335.

Tokuno, H., Takada, M., Kondo, Y., and Mizuno, N. (1993). Laminar organization of the substantia nigra pars reticulata in the macaque monkey, with special reference to the caudato-nigrotectal link. *Exp. Brain. Res* **92,** 545–548.

van Domburg, P. H. M. F., and ten Donkelaar, H. J. (1991). The human substantia nigra and ventral tegmental area. *Adv. Anat.* **121,** 1–132.

Vijayashanker, N., and Brody, H. (1979). A quantitative study of the pigmented neurons in the nuclei locus coeruleus and subcoeruleus in man as related to aging. *J. Neuropathol. Exp. Neurol.* **38,** 490–497.

Walker, D. G., Terai, K., Matsuo, A., Beach, T. G., McGeer, E. G., and McGeer, P. L. (1998). Immunohistochemical analysis of fibroblast growth factor receptor-I in the human substantia nigra. Comparison between normal and Parkinson's disease cases. *Brain Res.* **794,** 181–187.

Whitty, C. J., Paul, M. A., and Bannon, M. J. (1997). Neurokinin receptor mRNA localization in human midbrain dopamine neurons. *J. Comp. Neurol.* **382,** 394–400.

Yelnik, J., Francois, C., Percheron, G., and Heyner, S. (1987). Golgi study of the primate substantia nigra. I. Quantitative morphology and typology of nigral neurons. *J. Comp. Neurol.* **265,** 455–472.

Zhu, M. Y., Klimek, V., Dilley, G. E., Haycock, J. W., Stockmeier, C., Overholser, J. C., Meltzer, H. Y., and Ordway, G. A. (1999). Elevated levels of tyrosine hydroxylase in the locus coeruleus in major depression. *Biol. Psychiatry* **46,** 1275–1286.

CHAPTER

15

Lower Brain Stem Regulation of Visceral, Cardiovascular, and Respiratory Function

WILLIAM W. BLESSING
Departments of Physiology and Medicine
Centre for Neuroscience
Flinders University
Adelaide, SA, Australia

The overall structural organization of the human lower brain stem is described in chapter 10 of this book. In this chapter I outline the functional organization of lower brain stem neurons regulating various aspects of homestatic function in humans. This is a somewhat speculative task since we have almost no functional information and little neuroanatomical information concerning the actual connectivity and function of brain stem circuitry in humans. The scant information we do have concerning the nonhuman primate brain is summarized in Blessing and Gai (1997). Studies correlating clinical dysfunction in humans with the site of brain stem lesions (demonstrated by imaging procedures or by postmortem examination) have not been especially helpful in identifying brain stem nuclei controlling basic homeostatic functions. Unilateral lower brain stem lesions may not cause clinically obvious dysfunction, and bilateral lesions are usually fatal. Damage to fibers of passage may confound the clinicopathological interpretation of any particular lesion.

This difficulty of interpreting even the most carefully conducted studies of the human brain stem is illustrated in a recent investigation of breathing after unilateral infarction of the medulla oblongata in the territory of the posterior inferior cerebellar artery (Morrell *et al.*, 1999). Ventilatory sensitivity to CO_2 was reduced in these patients. Ventilation was normal in

awake patients, but potentially impaired during sleep. The dorsoventral extent of the lesions was difficult to determine on the basis of either the clinical signs or the magnetic resonance image. At least some functional recovery (e.g., the ability to swallow) usually occurred between the time of the stroke and the time of respiratory investigation, so that ventilatory sensitivity might have been more severely affected if the investigation was conducted at an earlier stage. The authors also note the difficulties encountered when comparing effects of lesions in humans and experimental animals. The different shape of the human brain stem reflects the massive development of the inferior olives, the pyramidal tracts, and the corticopontocerebellar tracts that constitute the ventral pons.

It is clear, nevertheless, that large portions of the brain stem are quite similar in humans and experimental animals. Moreover, the basic homeostatic functions subserved are also similar in humans and experimental animals. Thus, for each of the functions to be discussed in this chapter, the first step will involve presentation of a summary of our understanding derived from studies on experimental animals. Most of the primary references are cited in "The Lower Brain stem and Bodily Homeostasis" (Blessing, 1997b), a book that summarizes the relevant evidence from animal studies. The task is to transfer this understanding to the human brain stem, principally on the basis of neuroanatomical homologies. Little weight will be placed on the idea that different nervous systems mediate separate aspects of bodily functions. The traditional practice of delineating two relatively independent nervous systems, "autonomic" and "somatic," differentially regulating bodily functions has hindered efforts to understand control of bodily homestasis by the central nervous system (Blessing, 1997a).

Natural selection has molded functionally integrated organisms, so that interactions with the external environment (e.g., catching and eating prey) are coordinated with control of the internal environment (e.g., digesting and absorbing prey). Programs enabling such integrated control are contained at different levels of complexity within different levels of the nervous system, with brain stem circuitry capable of organizing quite complex integrated responses. Neilsen and Sedgwick (1949) describe an anencephalic infant who proved to have no neural tissue above the midbrain when autopsied after 85 days survival. "The patient startled in the presence of loud noises. … If we handled the patient roughly he cried weakly, but otherwise like any other infant, and when we coddled him he showed contentment and settled down in our arms. When a finger was placed into his mouth he sucked vigorously. … He would sleep after feeding and awaken when hungry, expressing his hunger by crying." Clearly this infant also had adequate respiratory, cardiovascular, and gastroenterological control, with functioning bladder and bowel even if there was no normal continence.

PRINCIPLES OF FUNCTIONAL NEUROANATOMICAL ORGANIZATION IN THE BRAIN STEM

Brain stem neuronal groups can be viewed as belonging to one of the categories described below. In this chapter every effort is made to discuss brain stem neurons according to their membership of one these categories. Cells belonging to categories 2–7, and some cells in category 1, are principle constituents of the brain stem region referred to as the reticular formation.

Categories of brain stem neurons

1. Somatic motoneurons with efferent axons distributed via the motor cranial nerves.
2. Somatic premotoneurons that function to coordinate the different striated muscles involved in integrated activities such as swallowing.
3. Parasympathetic preganglionic motoneurons with axons exiting in cranial nerves III, VII, IX, and X. The "preganglionic"epithet reflects the historical definition of autonomical neurons with respect to the peripheral ganglia.
4. Presympathetic motoneurons, with axons descending to innervate sympathetic preganglionic neurons in the thoracic and upper lumbar spinal cord.
5. Preparasympathetic neurons, with axons descending to innervate parasympathetic preganglionic neurons in the sacral spinal cord, especially those concerned with genitourinary and bowel eliminative functions. Other brain stem preparasympathetic motoneurons have intra-brain stem axons innervating cranial parasympathetic preganglionic motoneurons in the brain stem.
6. Prephrenic and prethoracic inspiratory and expiratory motoneurons.
7. Interneurons with increasing orders of complexity, capable of producing the patterned somatic and visceral effector responses involved in an integrated activity such as breathing or the crying response that occurs in infants born with no forebrain (anencephalics).
8. Secondary sensory (afferent) neurons in the various dorsally and dorsolaterally situated sensory nuclei. Projection targets of secondary sensory neurons include brain stem interneurons and premotor neurons, and motoneurons. Some interneurons (e.g., those in

the pontine parabrachial nuclei) are probably closer to the afferent than to the efferent side of the brain stem neuronal organization.

CARDIOVASCULAR FUNCTION

The guiding principle in neural regulation of cardiovascular function is that the different bodily tissues should receive a blood supply appropriate to their involvement in the various activities that constitute the individual's daily life. During ingestion of food, for example, the salivary glands require a greatly increased blood supply so that sufficient saliva can be secreted. During sexual activity, there is increased blood supply to the genital organs. In diving animals, sudden submersion in water triggers a coordinated cardiovascular response that involves extreme bradycardia and intense vasoconstriction in many of the peripheral beds. These responses are mediated by coordinated, patterned activity of the different peripheral nerves, both parasympathetic and sympathetic. The patterns are contained in neural circuitry contained in the brain stem and in the basal forebrain.

All the specifically patterned cardiovascular responses occur on a general background, which requires an adequate arterial blood pressure so that the brain itself constantly receives an adequate blood supply. In humans, if the system fails for more than a few seconds, the individual slumps to the ground unconscious. To provide early warning of such failures, sensory nerve endings with specialized pressure receptors (baroreceptors) innervate the origin of the internal carotid artery (carotid sinus) and the ascending aorta (aortic arch baroreceptors). When arterial pressure rises, increased activity in the baroreceptor primary afferents activates medullary pathways that reduce arterial pressure by inhibition of sympathetic vasomotor activity and reduce the heart rate by activation of parasympathetic cardiac vagal efferents. When arterial pressure falls, reduced baroreceptor activation leads to increased sympathetic vasomotor activity and decreased cardiac vagal activity.

Excitatory Presympathetic Neurons in the Rostral Ventrolateral Medulla

Work in animals has established that discharge of excitatory presympathetic neurons in the rostral ventrolateral medulla oblongata (RVLM) maintains activity in peripheral sympathetic vasomotor and cardiomotor nerves so that arterial pressure and heart rate are in the physiological range. The pivotal role of these neurons is summarized in Fig. 15.1, and their role in the baroreceptor–vasomotor reflex is detailed below. The relevant RVLM presympathetic vasomotor neurons may be cardiovascular pacemaker neurons, or they may constitute the final bulbospinal outflow of a pacemaker network of neurons located in the lower brain stem. In animals, damage to the RVLM neurons or to their descending bulbospinal axons causes a loss of peripheral sympathetic vasomotor and cardiomotor activity, so that arterial pressure suddenly falls to the levels observed in "spinal shock." In animals, damage to the midbrain or forebrain does not cause this cardiovascular syndrome. Clinical observation confirms that the same is true in humans, so that it is likely that the fundamental organization of cardiovascular circuitry is similar in humans and other mammals.

In animals, approximately 50% of the excitatory presympathetic vasomotor neurons in the RVLM belong to the C1 group of catecholamine-synthesizing neurons present in this medullary region. The remaining RVLM vasomotor neurons, also bulbospinal but not catecholamine synthesizing, are scattered in the same anatomical region of the medulla. At present we have no reliable histological markers for the non-catecholamine vasomotor neurons. The catecholamine cells contain tyrosine hydroxylase (TH), dopamine β-hydroxylase (DBH, the enzyme that synthesizes noradrenaline), and, in most species, phenylethanolamine N-methyltransferase (PNMT), the enzyme that converts noradrenaline to adrenaline.

Although at present there is little functional evidence that adrenaline acts as a neurotransmitter in the intermediolateral column of the spinal cord, the presence of PNMT in the presympathetic neurons in the RVLM of animals is important because there is a prominant group of PNMT-containing neurons in the region of the human medulla corresponding to the RVLM in experimental animals (Arango *et al.*, 1988; Halliday *et al.*, 1988b; Gai *et al.*, 1993). Similarly situated neurons in the human also contain neuropeptide Y (Halliday *et al.*, 1988a). Neuroanatomical studies in nonhuman primates have established that at least some RVLM PNMT-containing cells have spinal projections (Carlton *et al.*, 1987, 1989). It is therefore likely that PNMT-containing neurons in the human medullary region shown in Fig. 15.2 (see also Table 15.1) at least partially constitute the sympathoexcitatory presympathetic vasomotor neurons responsible for activity in vasomotor and cardiomotor sympathetic axons, so that arterial pressure is maintained at a reasonable level. Animal studies indicate that peripheral vascular beds controlled by RVLM presympathetic neurons, including the PNMT-positive cells, include those in skeletal muscle, in kidney, and in the gastrointestinal tract. Loss of RVLM presympathetic vasomotor neurons may contribute to the postural hypotension

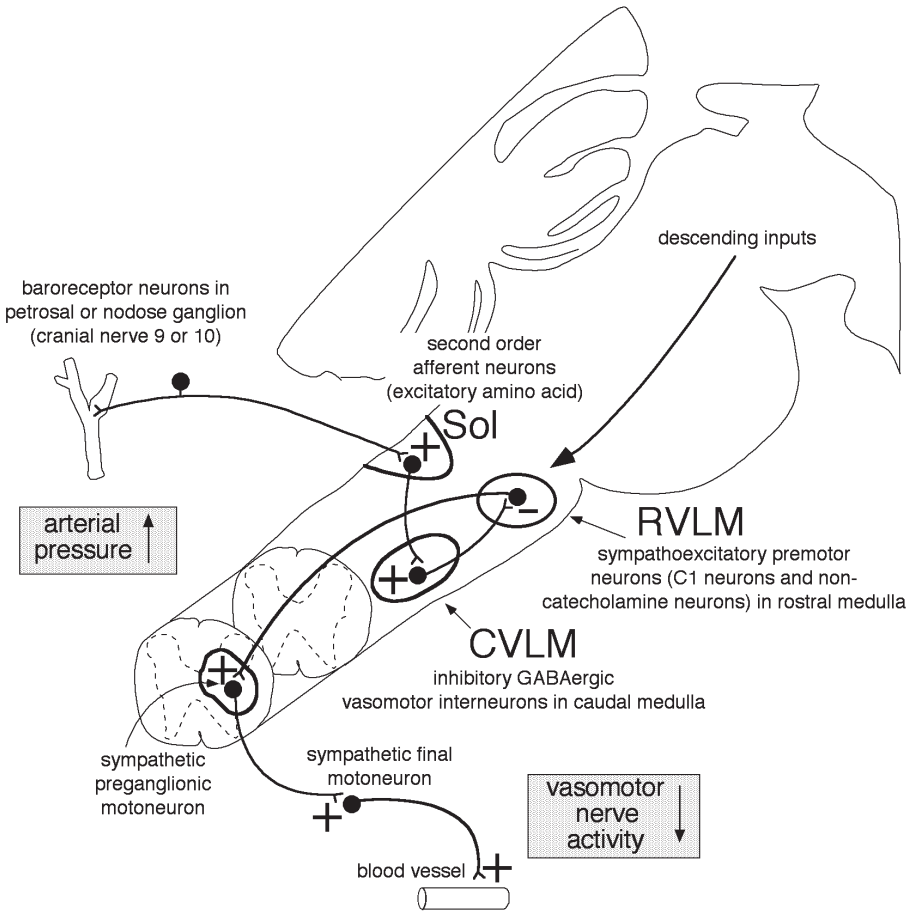

FIGURE 15.1 Diagram of central neural pathway mediating baroreceptor–vasomotor reflex. An inhibitory central link is provided by GABAergic interneurons in the caudal ventrolateral medulla (CVLM). These neurons increase their discharge when arterial pressure increases, thereby reducing the discharge of presympathetic vasomotor neurons in the rostral ventrolateral medulla (RVLM). Modified with permission from figure 5.18 of Blessing (1997b).

that sometimes occurs in patients with Parkinson's disease (Gai *et al.*, 1993) and with multiple systems atrophy with autonomic failure (Benarroch *et al.*, 1998).

Inhibitory Vasomotor Neurons Present in the Caudal Ventrolateral Medulla

In the caudal ventrolateral medulla (CVLM) region in experimental animals, there is a group of GABA-synthesizing vasomotor interneurons that tonically inhibit the RVLM sympathoexcitatory neurons by a short ascending axon. In animals the CVLM inhibitory vasomotor neurons are found intermingled with the A1 noradrenaline-synthesizing neurons, as well as in the region between the A1 cells and the ambiguus nucleus. So far there are no studies of the distribution of GABAergic neurons in the human medulla, and it is not easy to interpret clinical studies of altered arterial pressure following medullary lesions. There are reports of a patient with hypertension related to vagal rootlet–medullary compression by an arterial loop (Fein and Frishman, 1980; Jannetta *et al.*, 1985; Naraghi *et al.*, 1994) and another patient whose hypertension resolved following surgical removal of a soft-tissue mass that compressed the CVLM (Dickinson *et al.*, 1993), possibly interfering with the function of the inhibitory vasomotor neurons. The human medullary region likely to contain the inhibitory GABAergic vasomotor interneurons is shown in Figure 15.3.

Medullary Neural Circuitry Mediating the Baroreceptor–Vasomotor Reflex

A sudden rise in arterial pressure stimulates the baroreceptors in the carotid sinus and aortic arches, resulting in increased discharge in the primary afferent baroreceptor nerves entering the brain stem as part of the glossopharyngeal and vagus nerves (cranial 9 and 10). The paired nuclei of the solitary tract (Sol), particularly their caudal halves, are the principal

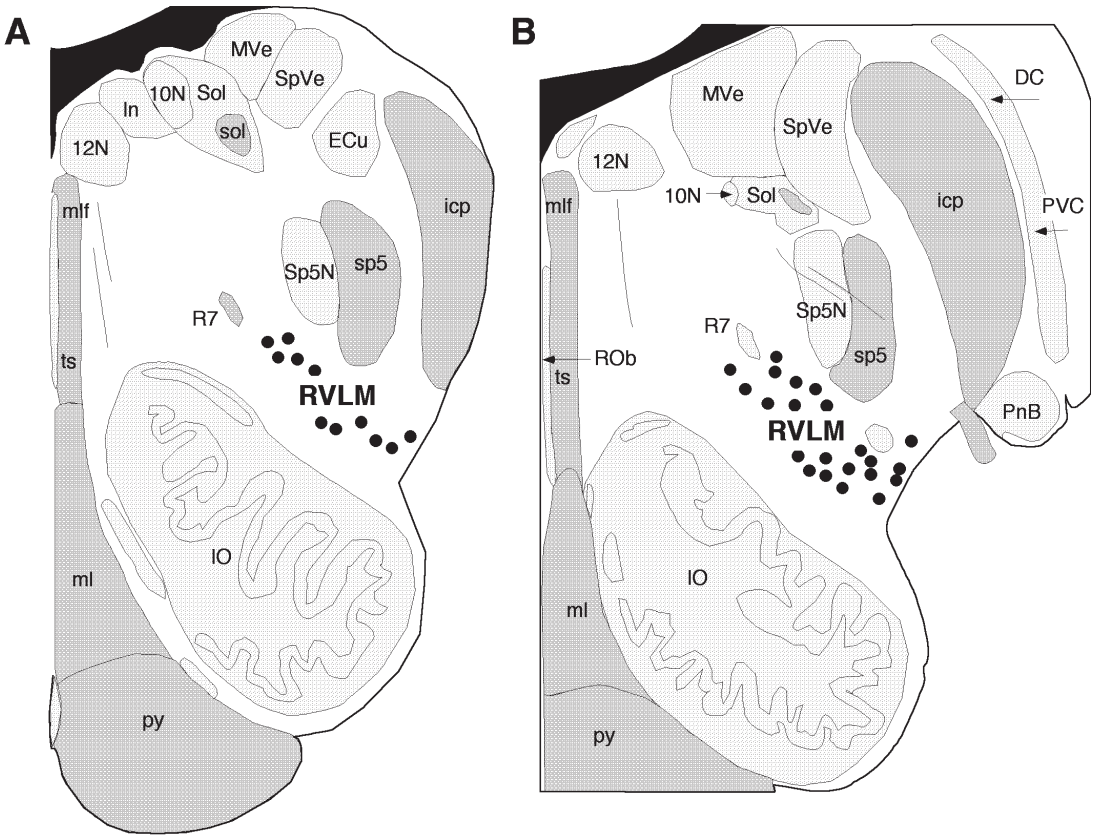

FIGURE 15.2 Distribution of PNMT-positive presympathetic (C1) neurons *(filled circles)* in the human rostral ventrolateral medulla (RVLM). The figure outlines **(A, B)** are based on figures 24 and 28 of Paxinos and Huang (1995). Abbreviations are listed in Table 15.1.

central termination sites of the baroreceptor afferents. In experimental animals, termination sites are concentrated in the dorsal and dorsolateral portions of Sol, near the border with the cuneate nucleus. Presumably this anatomical arrangement is similar in the human. Interruption of baroreceptor afferent input to Sol (or damage to secondary baroreceptor neurons in the Sol itself) would explain the fulminant hypertension sometimes observed in experimental animals and in humans with lesions near or within Sol (Reis, 1984; Doba and Reis, 1973).

As noted, in the case of sympathetic vasomotor activity, baroreceptor afferents operate in a negative-feedback fashion. Since the primary afferents excite the relevant secondary sensory neurons in Sol, there must be an inhibitory interneuron between Sol and the sympathetic preganglionic neurons in the spinal cord. The present consensus for experimental animals is that the inhibitory (GABAergic) vasomotor neurons in the CVLM fulfill this role. Thus, baroreceptor inputs to Sol activate an excitatory neuron (one that uses an excitatory amino acid as a neurotransmitter) that, by a ventrolateral projection, increases the discharge of the CVLM GABAergic neurons. This inhibits the excitatory presympathetic vasomotor and cardiomotor neurons in the RVLM (see Fig. 15.1), thereby reducing excitation of spinal preganglionic sympathetic vasomotor neurons and lowering arterial pressure.

Medullary Neural Circuitry Mediating the Baroreceptor–Cardiomotor (Vagal Efferents) Reflex

Less is known concerning the bradycardiac component of the baroreceptor reflex mediated by vagal efferents. Presumably the relevant central pathway is via a direct excitatory projection from sol to vagal parasympathetic cardiomotor neurons. In amimals these are acetylcholine-synthesizing neurons concentrated in the ambiguus nucleus at, and just caudal to, the level of the obex. They have not been definitely identified in humans but presumably are located in the region of the ambiguus nucleus region.

TABLE 15.1 Abbreviations

10N	dorsal motor nucleus of vagus	LVe	lateral vestibular nucleus
12N	hypoglossal nucleus	ml	medial lemniscus
6N	abducens nucleus	mlf	medial longitudinal fasciculus
7N	facial nucleus	MVe	medial vestibular nucleus
7n	facial nerve or its root	Pn	pontine nuclei
A5	A5 noradrenaline cells	PnB	pontobulbar nucleus
Acs5	accessory trigeminal nucleus	Pr	prepositus nucleus
Amb	ambiguus nucleus	prBo	pre-Bötzinger group of respiratory neurons
AP	area postrema	PVC	posteroventral cochlear nucleus
Ar	arcuate nucleus of the medulla	py	pyramidal tract
Ar	Arcuate nucleus	R7	retrofacial nucleus
Bo	Bötzinger group of respiratory neurons	RMg	raphe magnus nucleus
ctg	central tegmental tract	ROb	raphe obscurus nucleus
cu	cuneate fasciculus	RPn	raphe pontis nucleus
Cu	cuneate nucleus	rs	rubrospinal tract
CVRG	caudal respiratory group of neurons	RtTg	retrotrapezoid nucleus
DC	dorsal cochlear nucleus	RVRG	rostral ventral respiratory neurons
DRG	dorsal respiratory group	SGe	supragenicular nucleus
ECu	external cuneate nucleus	SON	superior olive
EO	epiolivary lateral reticular nucleus	sol	solitary tract
g7	genu of the facial nerve	Sol	solitary nucleus
gr	gracile fasciculus	sp5 s	pinal trigeminal tract
Gr	gracile nucleus	Sp5N	spinal trigeminal nucleus
icp	inferior cerebellar peduncle (restiform body)	spth	spinothalamic tract
In	intercalated nucleus of the medulla	SpVe	spinal vestibular nucleus
IO	inferior olive	ts	tectospinal tract
IV	fourth ventricle	tz	trapezoid body
LRt	lateral reticular nucleus	vsc	ventral spinocerebellar tract

Parasympathetic Preganglionic Motoneurons Regulating Cerebral Vasculature

The intracranial portions of the cerebral blood vessels are densely innervated by parasympathetic postganglionic fibers arising from cell bodies in the sphenopalatine and otic ganglia. The functional role of this innnervation is still not understoood. Presumably the relevant brain stem preganglionic parasympathetic neurons are among those normally grouped together as "salivary" nuclei (see below).

Medullary Raphe Magnus/Pallidus Neurons and Sympathetic Control of the Cutaneous Circulation

A subpopulation of raphe magnus/raphe pallidus neurons function as presympathetic vasomotor neurons regulating the cutaneous vascular bed and, in rats, the production of heat by brown fat (Blessing and Nalivaiko, 2001; Morrison *et al.*, 1999). Activity of these neurons is of importance in the regulation of body temperature. In addition, their activity probably mediates the cutaneous vasoconstriction that occurs when the individual detects a painful or potentially dangerous environmental stimulus (Blessing and Nalivaiko, 2000). Although we have no evidence that medullary raphe neurons fulfil a similar function in humans, the animal findings are important because they constitute the first evidence for regulation of a specific peripheral vascular bed by a group of brain stem presympathetic neurons outside the RVLM. Serotonin is one of the neurotransmitters in the raphe bulbospinal neurons, and drugs that elevate body temperature by acting on serotonin pathways (e.g., MDMA, "ecstasy") could affect the activity of these cells. The neurotransmitter in the relevant raphe bulbospinal neurons mediating cutaneous vasocon-

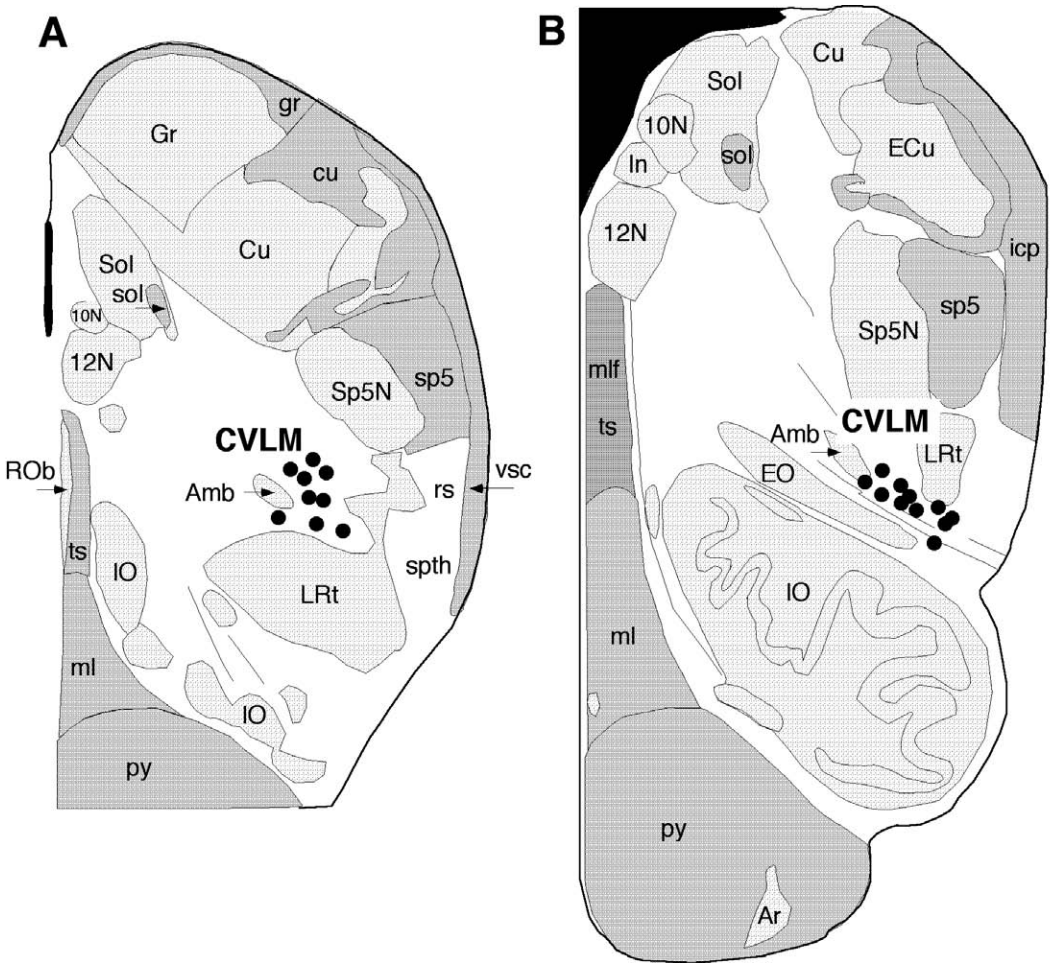

FIGURE 15.3 Human medullary region likely to contain GABAergic inhibitory vasomotor interneurons *(filled circles)* in caudal ventrolateral medulla (CVLM). The figure outlines **(A, B)** are based on figures 16 and 20 of Paxinos and Huang (1995). Abbreviations are listed in Table 15.1.

striction in response to surprising or painful stimuli in animals has not been identified. It is possible that the same neurons, by a descending projection to the dorsal horn of the spinal cord, are responsible for some of the antinociceptive functions thought to be mediated by medullary raphe neurons (Mason, 1999).

RESPIRATORY FUNCTION

Neural Circuitry Controlling Respiration

Intrathoracic pressures responsible for the to-and-fro passage of air are generated by the respiratory pump muscles. Other respiratory muscles with a valvelike function coordinate movements of the jaw, lips, tongue, pharynx, and larynx so that the airway is patent only at the appropriate time.

Inspiratory and expiratory pump muscles are innervated by somatic motor nerves (including the phrenic nerves) with cell bodies located in the C-3 and C-4 segments of the cervical spinal cord. Since lung tissue is elastic the lungs deflate by themselves, so that the first part of expiration is passive. The final part of normal expiration, as well as lung deflation during forced expiration, depends on active contraction of the expiratory muscles. Transection of the upper cervical cord isolates spinal respiratory neurons from descending control, so that respiration ceases. In contrast, breathing is maintained in patients with severe midbrain damage, but with an intact pons and medulla.

Thus, basic neural circuitry regulating respiration is present in the lower brain stem. Brain stem respiratory control was originally interpreted in terms of pneumotaxic, apneustic, inspiratory, and expiratory centers. However, these centers remained as poorly

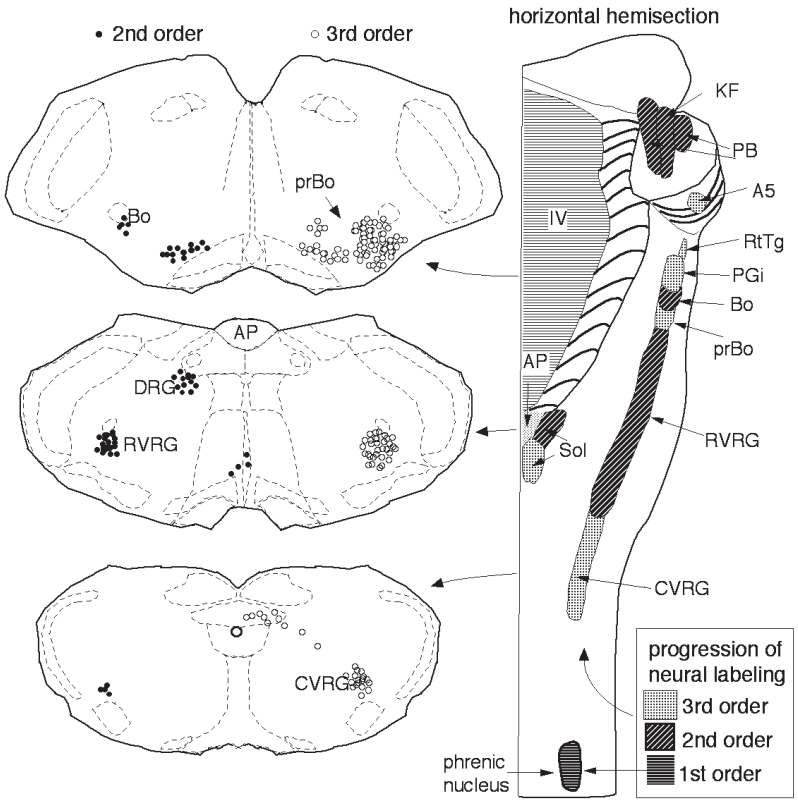

FIGURE 15.4 Transverse sections and horizontal hemisection through the medulla and lower pons, summarizing the successive distribution of virus-containing neurons after application of pseudorabies virus to one phrenic nerve. The different respiratory groups are explained in the text. Modified with permission from figure 4.3 of Blessing (1997b), based on the work of Dobbins and Feldman (1994). Abbreviations are listed in Table 15.1.

characterized hypothetical constructs, only vaguely related to actual brain stem regions. They did not provide an adequate theoretical framework for modern studies so that there is little to be gained by trying to identify these centers in the human lower brain stem. Summaries of neural circuitry mediating brain stem respiratory control can be found in Blessing (1997b) and in Dempsey and Pack (2000).

Animal studies have established that inspiratory pump premotoneurons (excitatory cells) projecting from the lower brain stem to the cervical spinal cord are located in the medulla oblongata, in the so-called rostral ventral respiratory group (RVRG). In turn, activity of RVRG neurons depends on net excitation from other medullary neurons either from the combined activity of a network of respiratory neurons or from the pacemaker activity of a particular group of respiratory neurons. These potential pacemaker cells are called pre-Botzinger cells. They are located in the ventrolateral medulla rostral to the RVRG cells.

During expiration, activity in RVRG neurons ceases so that the diaphragm and other inspiratory chest wall muscles no longer contract. These muscles are also innervated by spinal motoneurons activated by descending inputs from special expiratory motoneurons in the medulla oblongata. These inhibitory cells, discharging during expiration, are called the Botzinger group of expiratory neurons. A second group of expiratory neurons is located in the the caudal ventral respiratory group (CVRG). The distribution of the different groups in the rat is summarized in Figure 15.4.

Neurotransmitter-related antigens present in respiratory neurons are now being investigated (McCrimmon *et al.*, 1995). The pre-Botzinger cells are likely to use an excitatory amino acid as a neurotransmitter. The Botzinger cells may be GABAergic or glycinergic cells (Schreihofer *et al.*, 1999). It is not yet possible to use neurotransmitter anatomy to identify homologous neurons in the human brain. If the human system is similar to that being described in experimental animals, and if the relevant cells are located in similar regions of the human brain stem, the distribution of neurons regulating respiration may be as shown in Figure 15.5.

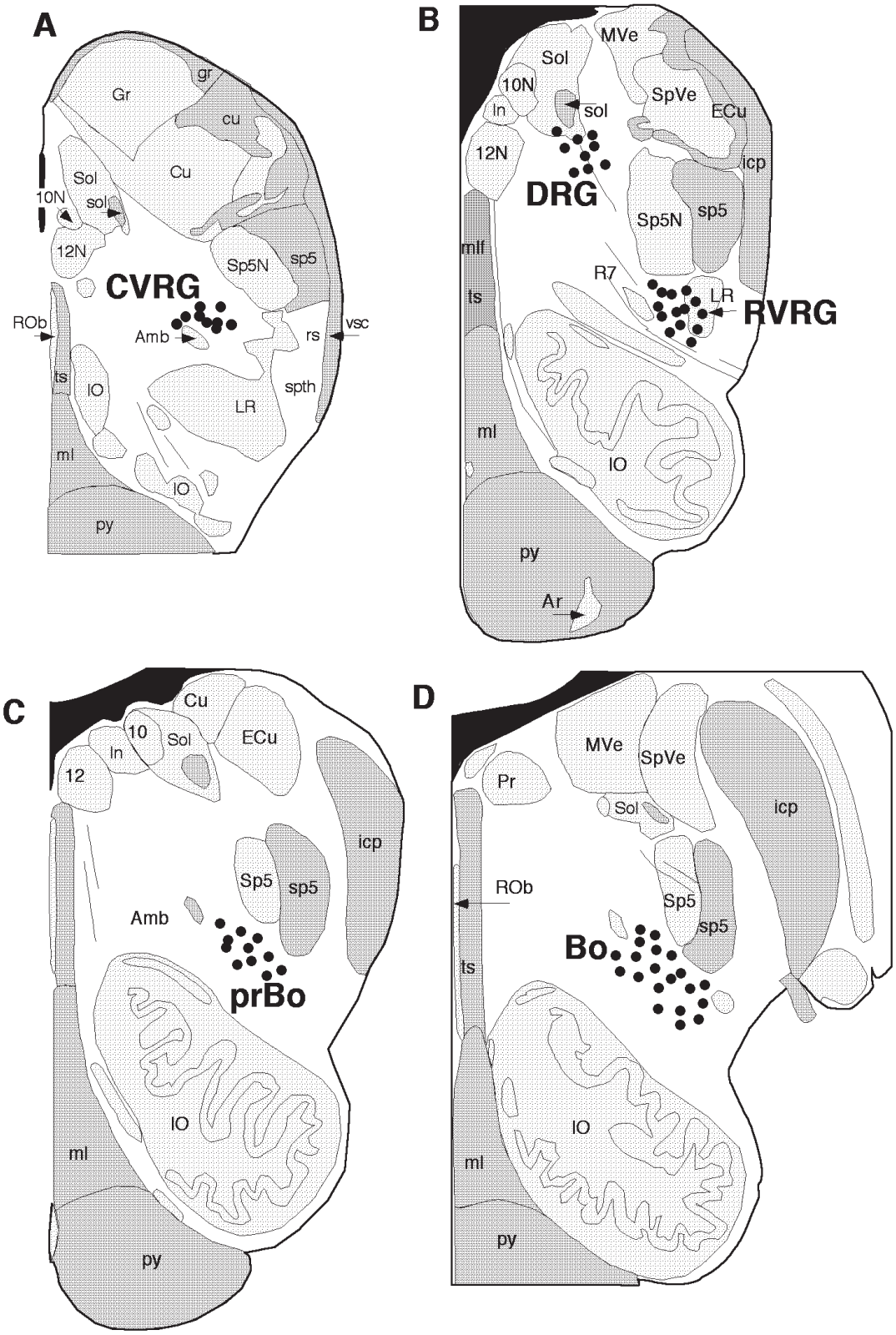

FIGURE 15.5 Human medullary regions likely to contain the different groups of respiratory interneurons and premotor neurons *(filled circles)*. The figure outlines **(A–D)** are based on figures 16, 20, 24, and 28 from Paxinos and Huang (1995). Abbreviations are listed in Table 15.1.

Responses to Hypercarbia and Hypoxia

Peripheral chemoreceptors in carotid and aortic bodies detect changes in blood levels of oxygen and carbon dixode–hydrogen ions. Primary afferent neurons in the nodose and petrosal ganglia transmit this information to the brain stem, especially to the solitary nucleus. Some primary afferents, probably chemoreceptor afferents, project beyond Sol to the ventrolateral medulla. Presumably these afferents make synaptic connections with various components of the central respiratory network, and with brain stem parasympathetic and presympathetic neurons mediating cardiovascular responses to hypercarbia and hypoxia (Guyenet, 2000).

The brain stem location of central chemoreceptors, and their cellular nature, has been the subject of many investigations in experimental animals commencing with the work of Loeschcke who studied the respiratory and cardiovascular effects of pharmacological agents applied to the ventral surface of the medulla oblongata. In recent years this approach has been supplemented by immunohistochemical demonstration of fos protein in neurons activated by appropriate respiratory-related stimuli (Sato *et al.*, 1992; Teppema *et al.*, 1997). Nattie (1999) has written a helpful review on this subject.

Ischemia of the lower brain stem, with consequent changes in tissue oxygen and carbon dioxide partial pressures and tissue acidity, elicits intense peripheral vasoconstriction and an increase in ventilation. The intense vasoconstriction is preserved after midpontine transection (Guyenet, 2000) and virtually eliminated by lesions of the presympathetic vasomotor neurons in the RVLM (Dampney and Moon, 1980). The RVLM neurons may act as the final bulbospinal pathway for sympathetic activation or could themselves have a chemosensitive function.

The arcuate nuclei are groups of small neurons scattered near the ventrolateral medulla surface, in the region medial to the corticospinal tract, and within the tract itself. The arcuate nuclei contain a subpopulation of neurons that synthesize serotonin, and they may be displaced components of raphe magnus/pallidus neurons. Kinney and colleagues have found various abnormalities in receptor binding studies focused on this region, and in the midline medullary raphe nuclei, in brains of infants dying of sudden infant death syndrome (Kinney *et al.*, 1992; Panigrahy *et al.*, 2000b; Harper *et al.*, 2000; Nachmanoff *et al.*, 1998). Studies in experimental animals also indicate that raphe serotonin cells may be chemosensitive, with a special relationship to intramedullary branches of the basilar artery, so that they sample the acidity of the blood supplying the medulla and thus act as central chemoreceptors (Iravani *et al.*, 2000).

It is possible that glial elements, as well as neurons, near the ventral surface of the medulla and in the midline raphe nuclei are sensitive to acidity and oxygen tension. Filiano and colleagues (1990) have described "thickened marginal glia" bordering the surface of the human ventrolateral medulla, associated with the clusters of small neurons identified as belonging to the arcuate nucleus.

SALIVATION, SWALLOWING, AND GASTROINTESTINAL FUNCTION, NAUSEA, AND VOMITING

Neural Circuitry Controlling Salivation

The brain stem location of preganglionic neurons regulating salivation in experimental animals is reasonably well established, thanks particularly to the work of Norgren and colleagues (e.g., Contreras *et al.*, 1980). Their findings indicate that the traditional distinction into superior and inferior salivary subnuclei is not based on firm experimental evidence. Salivary neurons with axons traveling in the facial nerve have a brain stem distribution virtually indistinguishable from that of salivary neurons with axons traveling in the glossopharyngeal nerve and its branches. The neurons are found dorsal and lateral to the facial nucleus, with scattered cells situated more dorsally, around the intramedullary fibers of the facial nerve within the caudal pons. In experimental animals, these intrapontine parasympathetic motoneurons stain strongly for NADPH and nitric oxide synthetase (NOS) (Zhu *et al.*, 1996).

In humans, neurons staining strongly for NADPH and NOS are found in corresponding regions of the pons (Gai and Blessing, 1996a), so that these cells are also presumably parasympathetic motoneurons (see Fig. 15.6 and Paxinos, *et al.*, 1999). Presumably many of the cells are salivary preganglionics, but similar neurons may also control lacrimation and secretion of nasal and paranasal mucosal cells. In addition, the neurons usually bundled together as "salivary" probably also make a major contribution to the regulation of the extra- and intracranial vasculature. The fluid in saliva is rapidly filtered from the blood, so that increased salivation is acccompanied by increased blood flow to the relevant salivary gland.

Neural Circuitry Controlling Swallowing

The lower brain stem contains neural circuitry sufficiently complex to initiate the appropriately coordinated contraction of jaw, facial, largygeal, pharyngeal,

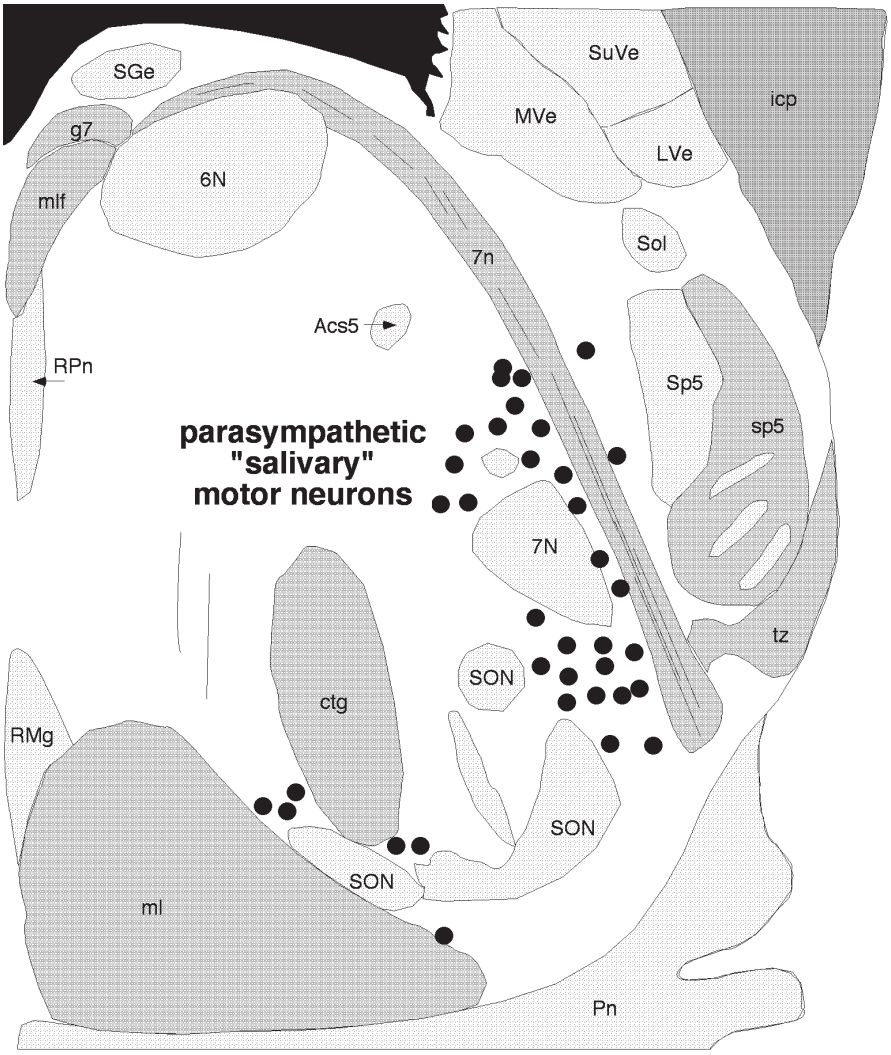

FIGURE 15.6 Human medullary regions likely to contain parasympathetic preganglionic motoneurons with axons exiting in cranial nerves 7 and 9 *(filled circles)*. The group is commonly referred to as the "salivary nucleus," but functions other than salivation are also controlled by parasympathetic motoneurons in this region. The figure outline is based on figure 33 from Paxinos and Huang (1995). Abbreviations are listed in Table 15.1.

tongue, and cervical muscles, with accompanying inhibition of respiration. Patients with severe forebrain damage can swallow if food or water is placed directly into the mouth, a stimulus that activates primary afferents in trigeminal, facial (nervus intermedius), glossopharyngeal, and vagal cranial nerves. These afferents synapse in sensory brain stem nuclei, including the principal sensory nucleus of V, the spinal nucleus of V, and the nucleus of the solitary tract (Sol). The taste afferents synapse in the rostral half of Sol. From these secondary sensory nuclei there must be projections to interneurons and premotor neurons appropriately connected to the relevant motoneurons in cranial nerves 5, 7, 9–12, and to the brain stem respiratory premotor neurons. There must be a complex degree of integration even within Sol since, in experimental animals, electrical stimulation of superior larygneal afferents can initiate swallowing.

At present there is only indirect evidence concerning the location of properties of the swallowing interneurons and premotor neurons. Live virus, applied to the hypoglossal nerve in experimental animals, spreads transneuronally from the hypoglossal nucleus to neurons (presumably premotor neurons) just lateral and a little ventral to this nucleus (Ugolini, 1995). Additional evidence from both anterograde and retrograde intraaxonal tracing studies indicates that neurons in this region have selective projections to motoneurons

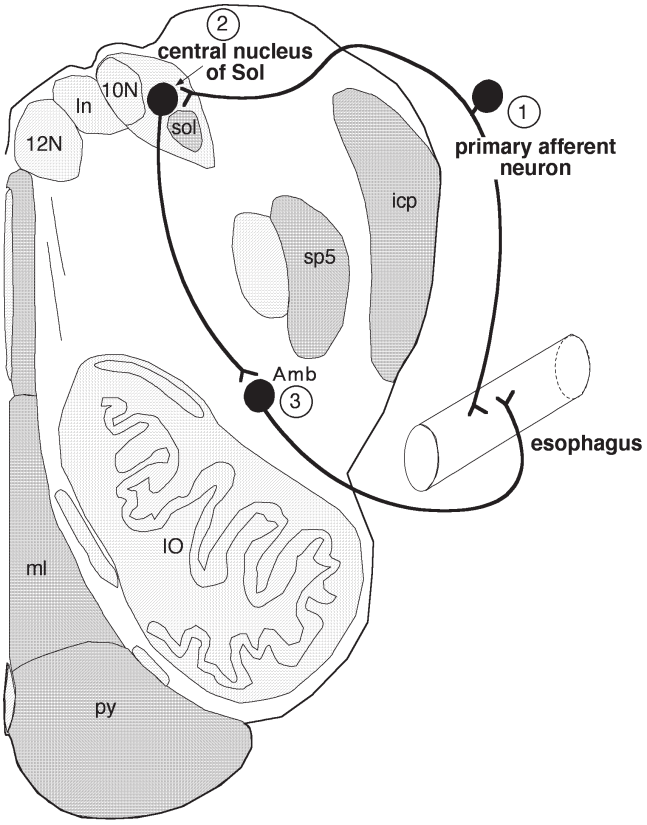

FIGURE 15.7 Diagram summarizing a single interneuron CNS pathway mediating esophago-esophageal reflexes. Neuron 1, the primary sensory neuron in the nodose ganglion, projects into the brain and synapses on neuron 2, a nitric oxide–synthesizing neuron in the central nucleus of Sol. This neuron projects directly to a nucleus ambiguus motoneuron (neuron 3), which innervates the esophageal striated muscle. Modified with permission from figure 7.6 of Blessing (1997b).

in cranial nerves 5, 7, and 9–12, so that neurons in this region lateral to the hypoglossal nucleus could function as premotor neurons regulating the integrated act of swallowing.

Vagal afferents originating in the lower esophagus synapse in a relatively newly recognized subdivision of Sol, just rostral to the obex, termed the central subnucleus of Sol. This central subnucleus contains a densely packed group of NOS-positive neurons, both in experimental animals and in humans (Gai and Blessing, 1996b). In experimental animals these cells project monosynaptically to preesophageal motoneurons in the nucleus ambiguus (Cunningham and Sawchenko, 1990; Gai *et al.*, 1995). Thus, it is likely that this central NOS-positive cell functions as a secondary sensory neuron, an interneuron, and a premotor neuron. A diagram summarizing this simple central connection is shown in Figure 15.7.

Neural Circuitry Controlling Gastric and Intestinal Function

Preganglionic parasympathetic motoneurons regulating the secretory and absorptive functions of the stomach and the intestine are located in the dorsal motor nucleus of the vagus (10). Axons project in the vagus nerve to ganglia in the wall of the gastrointestinal tract (the enteric nervous system) and to other parasympathetic ganglia located in proximity to the various abdominal viscera. Inputs to the dorsal motor nucleus of the vagus come from the adjacent Sol and other brain regions. Inputs to 10 from medullary raphe neurons [containing 5-hydroxytryptamine (5-HT), substance P, and thyrotropin-releasing factor] contribute to vagal regulation of gastric function, particularly to the regulation of gastric mucosal resistance to acid injury (Taché *et al.*, 1995). Damage to neurons in 10 in Parkinson's disease may be relevant to weight loss and gastrointestinal disturbances that may occur in this condition (Gai *et al.*, 1992).

LOWER BRAIN STEM REGULATION OF VOMITING

In both experimental animals and in humans activation of 5-HT_3 receptors on the distal terminals of abdominal vagal afferents may lead to the behavioral and physiological syndrome associated with vomiting (and with nausea in humans). These vagal afferents, originating in the lower esophagus, the stomach, or the upper small bowel, synapse in the gelatinous subnucleus of Sol. In animals there are additional inputs to the area postrema, so that cells in this specialized region are affected both by circulating factors and by vagal afferents. Nauseated humans secrete large amounts of vasopressin from the neurohypophysis. The neural pathways regulating this process are summarized in Figure 15.8 and in the following section.

LOWER BRAIN STEM REGULATION OF HYPOTHALAMOHYPOPHYSEAL SECRETION

The solitary nucleus (Sol) contains the A2 noradrenaline-synthesizing neurons and the caudal ventrolateral medulla contains the A1 noradrenaline-synthesizing neurons, present in humans as well as in experimental animals. Both these noradrenergic cell groups, via their direct axonal projections to neuro-

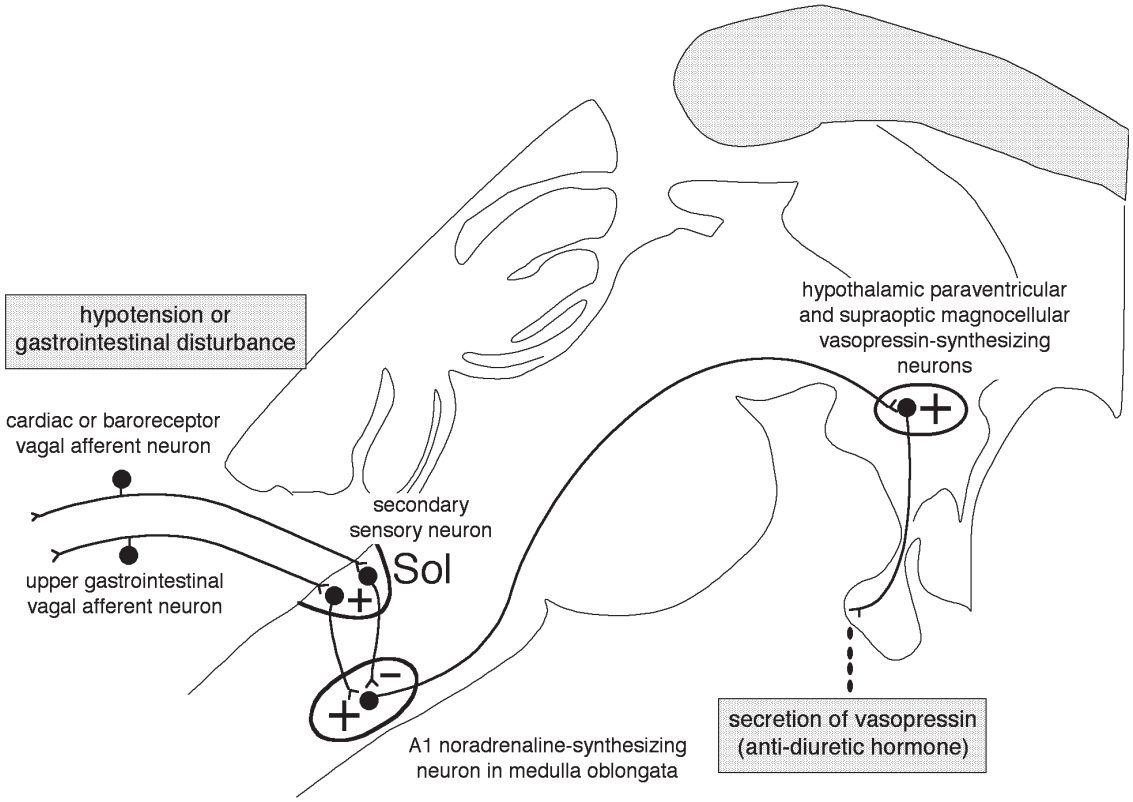

FIGURE 15.8 Central neural pathway mediating secretion of vasopressin in response to hemorrhage and in response to activation of abdominal vagal afferents. Baroreceptor afferents excite a Sol neuron (probably a GABAergic cell), which inhibits the A1 noradrenaline neurons in the caudal ventrolateral medulla. Hemorrhage causes a withdrawal of this inhibition, with consequent vasopressin secretion. Abdominal vagal afferents excite different Sol neurons, which excite the A1 cells, thereby increasing the secretion of vasopressin associated with nausea and vomiting. Modified with permission from figure 5.26 of Blessing (1997b).

endocrine cells in the paraventricular and supraoptic nuclei of the hypothalamus, regulate secretion of either vasopressin or oxytocin into the systemic circulation (Fig. 15.8).

In addition, axon terminals of A1 and A2 noradrenaline cells, as well as terminals of a subpopulation of C1 cells, innervate paraventricular neurons containing corticotrophin-releasing-factor (CRF). Activation of the medullary neurons (by internal bodily stresses reaching Sol via glossopharyngeal and vagal afferents) increases the discharge of the hypothalamic neurons so that CRF is secreted into the portal circulation. The medullary neurons thereby elicit secretion of adrenocorticotrophic hormone from the anterior pituitary in response to the internal bodily stesses.

The A1 and A2 neurons also have major inputs to luteinizing hormone–secreting cells in the medial preoptic area of the hypothalamus, so that changes in the activity of the medullary noradrenaline-synthesizing neurons are integrated into cyclical physiological changes related to the menstrual cycle.

LOWER BRAIN STEM REGULATION OF PELVIC VISCERA

Brain stem contains neurons (preparasympathetic neurons) with direct projection to either cranial or sacral parasympathetic preganglionic neurons. The latter group of neurons contributes to CNS control of pelvic visceral function, including micturition and defecation.

Existence of a pontine micturition center was initially suggested by the urinary effects of lesions of the dorsolateral pons in the cat. Modern studies in the rat (Valentino *et al.*, 1999) have identified a distinct cluster of neurons lying ventromedial to the rostral pole of the locus coeruleus and lateral to the dorsolateral tegmental nucleus. This cluser of neurons, termed Barrington's nucleus, is now known to constitute the pontine micturition center. The neurons, containing corticotropin-releasing factor (CRF) and atrial natriuretic peptide, project to the sacral column of parasympathetic preganglionic neurons, including neurons that control

the function of the urinary bladder. Transneuronal viral transport studies show that neurons in Barrington's nucleus have descending projections to sacral parasympathetic neurons controlling the function of the distal colon, the urethra and the urethral sphincter, the prostate, the penis, and the clitoris (see references in Valentino *et al.*, 1999). Thus, neurons in the "pontine micturition center" are likely to have a broad range of functions, controlling all pelvic viscera, not just the bladder. Consistent with this view, Barrington's nucleus also includes neurons that project to the dorsal motor nucleus of the vagus, innervating parasympathetic preganglionic cells with projections to ascending colon, transverse colon, and rectum.

Functional imaging studies (see references in Valentino *et al.*, 1999 and Blok and Holstege, 1998) suggest that micturition is controlled by a homologous dorsomedial pontine region in humans.

Acknowledgments

I thank Robyn Flook for help with preparation of this Chapter. My experimental work has been supported by the National Health and Medical Research Council and by the National Heart Foundation of Australia.

References

Arango, V., Ruggiero, D.A., Callaway, J.L., Anwar, M., Mann, J.J., and Reis, D.J. (1988). Catecholaminergic neurons in the ventrolateral medulla and nucleus of the solitary tract in the human. *J. Comp. Neurol.* **273,** 224–240.

Benarroch, E.E., Smithson, I.L., Low, P.A., and Parisi, J.E. (1998). Depletion of catecholaminergic neurons of the rostral ventrolateral medulla in multiple systems atrophy with autonomic failure. *Ann. Neurol.,* **43,** 156–16.

Blessing, W.W. (1997a). Inadequate frameworks for understanding bodily homeostasis. *Trends Neurosci.* **20,** 235–239.

Blessing, W. W. (1997b). "The Lower Brain stem and Bodily Homeostasis." Oxford University Press, New York.

Blessing, W. W., and Gai, W. P. (1997). Caudal pons and medulla oblongata. *In* "The Primate Nervous System, Part 1, Handbook of Chemical Neuroanatomy, Vol. 13" (F. E. Bloom, A. Björklund, and T. Hökfelt, eds.), pp. 139–186. Elsevier, Amsterdam.

Blessing, W.W., and Nalivaiko, E. (2000). Regional blood flow and nociceptive stimuli in rabbits: patterning by medullary raphe, not ventrolateral medulla. *J. Physiol.* **524,** 279–292.

Blessing, W.W., and Nalivaiko, E. (2001). Raphe magnus/pallidus neurons regulate tail but not mesenteric arterial blood flow in rats. *Neuroscience* **105,** 923–929, 2001.

Blok, B.F., and Holstege, G. (1998). The central nervous system control of micturition in cats and humans. *Behav Brain Res* **92,** 119–125.

Carlton, S.M., Honda, C.N., and Denoroy, L. (1989). Distribution of phenylethanolamine N-methyltransferase cell bodies, axons, and terminals in monkey brain stem: an immunohistochemical mapping study. *J. Comp. Neurol.* **287,** 273–285.

Carlton, S.M., Honda, C.N., Denoroy, L., and Willis, W.D.,Jr. (1987). Descending phenylethanolamine-*N*-methyltransferase projections to the monkey spinal cord: an immunohistochemical double labeling study. *Neurosci. Lett.* **76,** 133–139.

Contreras, R.J., Gomez, M.M., and Norgren, R. (1980). Central origins of cranial nerve parasympathetic neurons in the rat. *J. Comp. Neurol.* **190,** 373–394.

Cunningham, E.T.,Jr., and Sawchenko, P.E. (1990). Central neural control of esophageal motility: a review. *Dysphagia* **5,** 35–51.

Dampney, R.A., and Moon, E.A. (1980). Role of ventrolateral medulla in vasomotor response to cerebral ischemia. *Am. J. Physiol.* **239,** H349–H358.

Dempsey, J. A., and Pack, A. I., (2000). "Regulation of Breathing." Marcel Dekker, New York.

Dickinson, L.D., Papadopoulos, S.M., and Hoff, J.T. (1993). Neurogenic hypertension related to basilar impression. *J. Neurosurg.* **79,** 924–928.

Doba, N., and Reis, D.J. (1973). Acute fulminating neurogenic hypertension produced by brain stem lesions in the rat. *Circ. Res.* **32,** 584–593.

Dobbins, E.G., and Feldman, J.L. (1994). Brain stem network controlling descending drive to phrenic motoneurons in rat. *J. Comp. Neurol.* **347,** 64–86.

Fein, J.M., and Frishman, W. (1980). Neurogenic hypertension related to vascular compression of the lateral medulla. *Neurosurgery* **6,** 615–622.

Filiano, J.J., Choi, J.C., and Kinney, H.C. (1990). Candidate cell populations for respiratory chemosensitive fields in the human infant medulla. *J Comp. Neurol.* **293,** 448–465.

Gai, W.P., Blumbergs, P.C., Geffen, L.B., and Blessing, W.W. (1992). Age-related loss of dorsal vagal neurons in Parkinson's disease. *Neurology* **42** 2106–2111.

Gai, W.P., Geffen, L.B., Denoroy, L., and Blessing, W.W. (1993). Loss of C1 and C3 epinephrine-synthesizing neurons in the medulla oblongata in Parkinson's disease. *Ann Neurol* **33,** 357–367.

Gai, W.P., Messenger, J.P., Yu, Y.H., Gieroba, Z.J., and Blessing, W.W. (1995). Nitric oxide–synthesising neurons in the central subnucleus of the nucleus tractus solitarius provide a major innervation of the rostral nucleus ambiguus in the rabbit. *J Comp. Neurol.* **357,** 348–361.

Gai, W.P., and Blessing, W.W. (1996a). Human brain stem preganglionic parasympathetic neurons localized by markers for nitric oxide synthesis. *Brain* **119,** 1145–1152.

Gai, W.P., and Blessing, W.W. (1996b). Nitric oxide synthesising neurons in the central subnucleus of the nucleus tractus solitarius in humans. *Neurosci. Lett.* **204,** 189–192.

Guyenet, P.G. (2000). Neural structures that mediate sympathoexcitation during hypoxia. *Respir. Physiol.* **121,** 147–162.

Halliday, G.M., Li, Y.-W., Oliver, J.R., Joh, T.H., Cotton, R.G.H., Howe, P.R.C., Geffen, L.B., and Blessing, W.W. (1988a). The distribution of neuropeptide Y-like immunoreactive neurons in the human medulla oblongata. *Neurosci.* **26,** 179–191.

Halliday, G.M., Li, Y.W., Joh, T.H., Cotton, R.G.H., Howe, P.R.C, Geffen, L.B., and Blessing, W.W. (1988b). Distribution of monoamine-synthesizing neurons in the human medulla oblongata. *J. Comp. Neurol.* **273,** 301–317.

Harper, R.M., Kinney, H.C., Fleming, P.J., and Thach, B.T. (2000). Sleep influences on homeostatic functions: implications for sudden infant death syndrome. *Respir. Physiol.* **119,** 123–132.

Iravani, M.M., Asari, D., Patel, J., Wieczorek, W.J., and Kruk, Z.L. (2000). Direct effects of 3,4-methylenedioxymethamphetamine (MDMA) on serotonin or dopamine release and uptake in the caudate putamen, nucleus accumbens, substantia nigra pars reticulate, and the dorsal raphe nucleus slices. *Synapse* 275–285, 2000.

Jannetta, P.J., Segal, R., Wolfson, S.K.J., Dujovny, M., Semba, A., and Cook, E.E. (1985). Neurogenic hypertension: etiology and surgical

treatment. II. Observations in an experimental nonhuman primate model. *Ann Surg* **202,** 253–261.

Kinney, H.C., Filiano, J.J., and Harper, R.M. (1992). The neuropathology of the sudden infant death syndrome. A review. *J Neuropathol. Exp. Neurol.* **51,** 115–126.

Mason, P. (1999). Central mechanisms of pain modulation. *Curr. Opin. Neurobiol.* **9,** 436–441.

McCrimmon, D. R., Dekin, M. S., and Mitchell, G. S. (1995). Glutamate, GABA and serotonin in ventilatory control. *In* "Regulation of Breathing" (J. A. Dempsey and A. I. Pack, eds.), pp. 151–217. Marcel Dekker, New York.

Morrell, M.J., Heywood, P., Moosavi, S.H., Guz, A., and Stevens, J. (1999). Unilateral focal lesions in the rostrolateral medulla influence chemosensitivity and breathing measured during wakefulness, sleep, and exercise [see comments]. *J. Neurol. Neurosurg. Psychiatry* **67,** 637–645.

Morrison, S.F., Sved, A.F., and Passerin, A.M. (1999). GABA-mediated inhibition of raphe pallidus neurons regulates sympathetic outflow to brown adipose tissue. *Am. J. Physiol.* **276,** R290–R297.

Nachmanoff, D.B., Panigrahy, A., Filiano, J.J., Mandell, F., Sleeper, L.A., Valdes-Dapena, M., Krous, H.F., White, W.F., and Kinney, H.C. (1998). Brain stem 3H-nicotine receptor binding in the sudden infant death syndrome. *J Neuropathol. Exp Neurol.* **57,** 1018–1025.

Naraghi, R., Geiger, H., Crnac, J., Huk, W., Fahlbusch, R., Engels, G., and Luft, F.C. (1994). Posterior fossa neurovascular anomalies in essential hypertension. *Lancet* **344,** 1466–1470.

Nattie, E. (1999). CO_2, brain stem chemoreceptors and breathing. *Prog. Neurobiol.* **59,** 299–331.

Neilsen, J.M., and Sedgwick, R.P. (1949). Instincts and emotions in an anencephalic monster. *J. Nerv. Ment. Dis.* **110,** 387–394.

Panigrahy, A., Filiano, J., Sleeper, L.A., Mandell, F., Valdes-Dapena, M., Krous, H.F., Rava, L.A., Foley, E., White, W.F., and Kinney, H.C. (2000a). Decreased serotonergic receptor binding in rhombic lip–derived regions of the medulla oblongata in the sudden infant death syndrome. *J. Neuropathol. Exp. Neurol.* **59,** 377–384.

Panigrahy, A., Rosenberg, P.A., Assmann, S., Foley, E.C., and Kinney, H.C. (2000b). Differential expression of glutamate receptor subtypes in human brain stem sites involved in perinatal hypoxia-ischemia. *J. Comp. Neurol.* **427,** 196–208.

Paxinos, G., and Huang, X. -F., (1995). "Atlas of the Human Brain stem." Academic Press, San Diego.

Paxinos, G., Carrive, P., Wang, H.Q., and Wang, P.Y. (1998). "A Chemoarchitectonic Atlas of the Rat Brain stem." Academic Press, San Diego.

Reis, D.J. (1984). The brain and hypertension: reflections on 35 years of inquiry into the neurobiology of the circulation. *Circulation* **70,** III-31–III-45.

Sato, M., Severinghaus, J.W., and Basbaum, A.I. (1992). Medullary CO_2 chemoreceptor neuron identification by c-*fos* immunocytochemistry. *J. Appl. Physiol.* **73,** 96–100.

Schreihofer, A.M., Stornetta, R.L., and Guyenet, P.G. (1999). Evidence for glycinergic respiratory neurons: Botzinger neurons express mRNA for glycinergic transporter 2. *J. Comp. Neurol.* **407,** 583–597.

Taché, Y., Yang, H., and Kaneko, H. (1995) Caudal raphe–dorsal vagal complex peptidergic projections: role in gastric vagal control. *Peptides* **16,** 431–435.

Teppema, L.J., Veening, J.G., Kranenburg, A., Dahan, A., Berkenbosch, A., and Olievier, C. (1997). Expression of c-fos in the rat brain stem after exposure to hypoxia and to normoxic and hyperoxic hypercapnia. *J Comp. Neurol.* **388,** 169–190.

Ugolini, G. (1995). Specificity of rabies virus as a transneuronal tracer of motor networks: transfer from hypoglossal motoneurons to connected second-order and higher order central nervous system groups. *J. Comp. Neurol.* **356,** 457–480.

Valentino, R.J., Miselis, R.R., and Pavcovich, L.A. (1999). Pontine regulation of pelvic viscera: pharmacological target for pelvic visceral dysfunctions. *Trends. Pharmacol. Sci.* **20,** 253–260.

Zhu, B.S., Gai, W.P., Yu, Y.H., Gibbins, I.L., and Blessing, W.W. (1996). Preganglionic parasympathetic salivatory neurons in the brain stem contain markers for nitric oxide synthesis in the rabbit. *Neurosci. Lett.* **204,** 128–132.

CHAPTER

16

Reticular Formation: Eye Movements, Gaze, and Blinks

JEAN A. BÜTTNER-ENNEVER and ANJA K. E. HORN
Institute of Anatomy, Ludwig Maximilian University
Munich, Germany

The human brain stem reticular formation was first recognized as a cytoarchitectonic entity by August Forel (1877). The word *reticular* is derived from the Latin word *rete*, meaning "net", and refers to its characteristically diffuse structure, a network of loosely packed multipolar neurons, embedded in a dense neuropil. The reticular formation has no distinct cytoarchitectural boundaries, and forms the central core of the brain stem, in which other brain stem nuclei, with clearly outlined cytoarchitectural boundaries, are embedded, e.g., the red nucleus (RPC) or nucleus reticularis tegmenti pontis (RtTg). It stretches throughout the length of the brain stem, from the mesencephalon through the pons to the medulla oblongata (Fig. 16.1). In the spinal cord, the intermediate zone, i.e., Rexed's laminae V–VIII, is recognized through its cytoarchitecture as the continuation of the reticular formation into the spinal cord (see Chapter 7). There are subtle regional differences in the brain stem reticular formation cytoarchitecture, which led Jerzy Olszewski and his colleagues to subdivide it into nuclei (Olszewski and Baxter, 1954). These subdivisions have become the accepted classical standard, although the generally accepted nomenclature has evolved to include the word *reticular*, which Olszewski rigorously avoided. For example, Olszewski used the term "nucleus centralis pontis caudalis"; but presently, mostly due to the work of Brodal (1957) and Taber (1961), the same area is now usually referred to as nucleus reticularis pontis caudalis (PnC). Homologies of the subdivisions seen in the human reticular formation can be readily recognized in lower animals (for review, see Brodal, 1981). The typical wide dendritic fields of the multipolar reticular cells collect afferent signals from multiple sources (Scheibel and Scheibel, 1958) and funnel them onto nearby output structures, such as the trigeminal, facial, or oculomotor

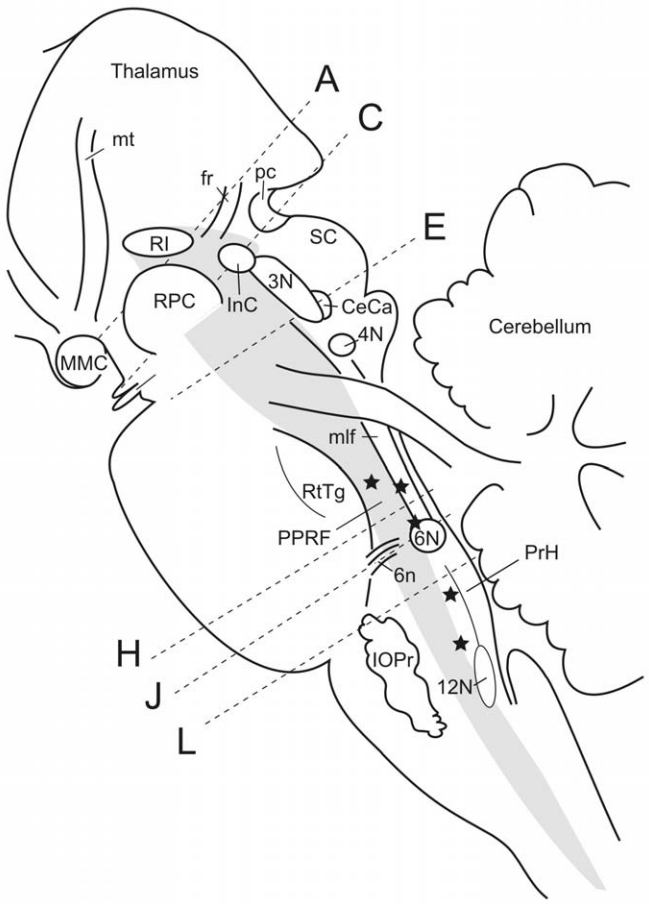

FIGURE 16.1 A sagittal view of the human brain stem showing the location of the reticular formation *(shaded area)* and several structures essential for the control of eye movements and gaze. The dashed lines indicate the levels of the transverse sections shown in Figures 16.3 and 16.4. The stars indicate the location of the cell groups of the paramedian tract (section I). Abbreviations: 3N, oculomotor nucleus; 4N, trochlear nucleus; 6N, abducens nucleus; 6n, abducens nerve; 12N, hypoglossal nucleus; CeCa, central caudal nucleus; fr, fasciculus retroflexus; InC, interstitial nucleus of Cajal; IO, inferior olive; mlf, medial longitudinal fasciculus; MMC, medial mammillary nucleus; mt, mammillothalamic tract; pc, posterior commissure; PPRF, paramedian pontine reticular formation; PrH, prepositus hypoglossal nucleus; RPC, red nucleus; RI, rostral interstitial nucleus of the medial longitudinal fasciculus; RtTg, reticulotegmental nucleus of the pons; SC, superior colliculus.

nuclei, or via descending pathways to motoneurons in the spinal cord.

Over the last years much progress has been made in the identification and characterization of functional cell groups within the reticular formation and their connectivity, either by single-cell recording in behaving animals, or with immunohistochemical and tract tracing techniques. Localized reticular cell groups, without any obvious cytoarchitectonic features, have been found to have highly specific functions and connections; therefore, in no way do they conform to the old idea that the reticular formation is part of a "diffuse arousal network" (Morruzi and Magoun, 1949), although one has to admit that it looks as though it should. Presently this concept has been replaced by the demonstration of highly localized functions within the reticular formation, while the role in arousal can be attributed to compact brain stem nuclei such as locus coeruleus (LC) or pedunculopontine tegmental nucleus (PPTg) whose cells have enormous axon terminal fields extending up to, and including, the cerebral cortex (Saper, 1987; Steckler *et al.*, 1994). In parallel to these experimental studies attempts have been made to identify the homologous cell groups in humans not only by their location and cytoarchitecture, but also by their histochemical properties, e.g., cytochrome-oxidase activity, acetylcholinesterase activity, and expression of calcium-binding proteins, such as parvalbumin (Paxinos *et al.*, 1990; Paxinos and Huang, 1995; Horn *et al.*, 1996).

The reticular formation of the pons and medulla can be divided into a lateral and a medial tegmental field (Holstege, 1991). The *lateral tegmental field* contains smaller cells, which are interneurons, or premotor neurons, for the trigeminal, facial, vagal, and hypoglossal motor nuclei. In addition it houses the premotor neurons with long descending axons to motor neurons of the spinal cord involved in respiration, abdominal pressure, micturition, and blood pressure (Holstege, 1991; see Chapter 15). The *medial tegmental field* contains the premotor circuitry for eye and head movements, and gives rise to descending pathways involved in postural orientation. These pathways are separate and distinct from the serotonergic raphe nuclei (see Chapter 13), which have widespread connections to the spinal gray matter and modulate or set, the firing level of the sensory or motor spinal circuits (for review, see Holstege 1991). The brain stem nuclei involved in the generation of eye and head movements, blinks, gaze holding, or postural orientation lie mostly in the medial tegmental field, and their functional neuroanatomy is the subject of this chapter.

EYE AND HEAD MOVEMENTS

General Concepts

The orientation of the eyes, head, and body toward a point of interest plays a central role in survival. The superior colliculus is essential for the generation of these responses, in particular the deep layers (Sparks and Hartwich-Young, 1989; for review, see Isa and Sasaki, 2002). It receives afferents from higher centers, brain stem, and spinal cord (Huerta and Harting, 1982; Harting *et al.*, 1992) and relays the commands to the

specific regions of the medial reticular formation that control the eyes, head, and postural muscles via tectoreticulospinal pathways. A rapid eye movement, called a *saccade,* is generated through the medial reticular pathways, possibly in combination with a head movement and postural adjustment, to orient the body to the object of interest. There are several different types of eye movements: saccades, vestibular ocular reflexes, optokinetic responses, smooth pursuit, vergence, and even gaze holding. Each of these is generated through circuits that are relatively separate from each other but converge at the level of the motoneuron to drive the eye movements (Büttner and Büttner-Ennever, 1988; Büttner-Ennever and Horn ,1997; Sharpe, 1998; Leigh and Zee, 1999). Although this is an oversimplification, it is an approach that enables us to schematically represent eye movements as in Figure 16.2, and to assign functions to several brain stem nuclei.

1. Saccades. A simple description of the premotor circuits for saccadic eye movements is as follows (see also Figs. 16.1 and 16.8): immediate premotor burst neurons (EBNs and IBNs), in the paramedian pontine reticular formation (PPRF) for horizontal saccades or in the rostral interstitial nucleus of the medial longitudinal fasciculus (RI) for vertical saccades, activate the eye muscle motoneurons in the abducens (6N), trochlear (4N), and oculomotor (3N) nuclei during a saccade. During slow eye movements and fixation the burst neurons are inhibited by omnipause neurons in the nucleus raphe interpositus (RIP) (for review, see Scudder *et al.*, 2002). Burst neurons and omnipause neurons receive afferents from the superior colliculus (SC), while the frontal eye fields of the cerebral cortex appear only to contact the omnipause neurons (Moschovakis *et al.*, 1996; Büttner-Ennever *et al.*, 1999).

2. The vestibuloocular reflex. The vestibuloocular reflex (VOR) is generated by sensory signals from the labyrinthine canals and otoliths, relayed through the vestibular nuclei (see Chapter 33), where the signals are modulated by the cerebellum, then fed to the extraocular muscle motoneurons in the oculomotor, trochlear, and abducens nucleus via the medial longitudinal fasciculus (mlf) or the brachium conjunctivum (Büttner-Ennever, 1992, 2000). This reflex is a slow

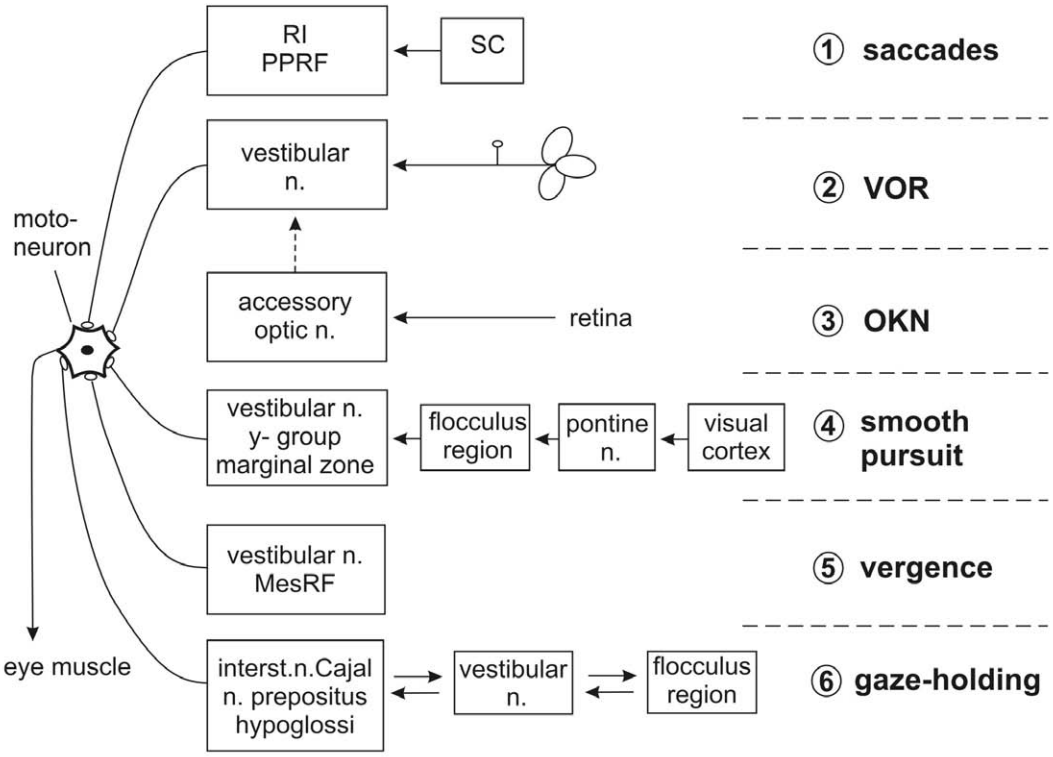

FIGURE 16.2 A simplified diagram of the premotor networks subserving five different types of eye movements, and gaze holding. All the relatively independent networks converge at the level of the motoneurons of the extraocular eye muscles. Abbreviations: MesRF, mesencephalic reticular formation; n., nucleus; OKN, optokinetic response; PPRF, paramedian pontine reticular formation; SC, superior colliculus; VOR, vestibuloocular reflex.

compensatory eye movement, and during a period of continuous stimulation it is interrupted by fast resetting saccades, giving rise to the typical fast and slow phases of vestibular nystagmus (Leigh and Zee, 1999).

3. The optokinetic response. Optokinetic responses are elicited by the movement of large visual fields across the retina, which generate responses in the retinorecipient accessory optic nuclei of the mesencephalon: the dorsal, medial, lateral, and interstitial terminal nuclei (DT, MT, LT, and IT). These nuclei, along with the nucleus of the optic tract (OT) in the pretectum, feed the information to the vestibular-oculomotor circuits through which the eye movement response, the optokinetic response, is generated (Fuchs and Mustari, 1993; Büttner-Ennever *et al.*, 1996a).

4. Smooth pursuit. Smooth-pursuit pathways receive retinal information through two parallel afferent pathways: a motion-sensitive "magnocellular pathway", and a form- and color-sensitive "parvicellular pathway" (see Chapter 35). The two inputs supply posterior parietal cortical areas with information concerning object motion in space (the dorsal stream), in contrast to the inferotemporal region more involved in the analysis of form (the ventral stream). Descending projections from the posterior parietal cortex relay in the dorsolateral pontine nuclei (May *et al.*, 1988), which project to the dorsal and ventral paraflocculus and the caudal vermis of the cerebellum. Cerebellar efferents via the vestibular complex or other relays reach the oculomotor nuclei to generate smooth-pursuit eye movements (Leigh and Zee, 1999).

5. Vergence. Vergence premotor neurons have been found in the medial mesencephalic reticular formation dorsal to the oculomotor nucleus and in the pretectum, which provide the vergence command to the oculomotor nuclei (Mays and Gamlin, 1995; for review, see Sharpe 1998). Recently, Chen-Huang and McCrea (1998) showned that a vergence signal proportional to the viewing distance during horizontal linear acceleration is carried by the ascending tract of Deiters to medial rectus motoneurons in the oculomotor nucleus. The ascending tract of Deiters originates in the rostral third of the vestibular complex (see Chapter 33).

6. Gaze holding. In addition, perhaps gaze holding, involving the velocity to position integrator, should be included in the list of eye movement types. Gaze holding is also subtended by a relatively separate group of neural circuits: the interstitial nucleus of Cajal (InC) for vertical, and the prepositus hypoglossal nucleus (PrH) for horizontal gaze holding with their reciprocal vestibular and cerebellar connections (Fukushima *et al.*, 1992; see also Chapter 33). A current hypothesis suggests that the cell groups of the paramedian tracts may provide the cerebellum with the motor feedback signal essential for maintaining gaze position (Büttner-Ennever and Horn, 1996).

In the following sections of this chapter the anatomy, histochemistry, connectivity, and functional and clinical significance are described for brain stem regions involved in the generation of eye and head movements, as well as lid movements. The line drawing in Figure 16.1 shows the location of these brain stem regions and indicates the planes of cutting for the transverse sections in Figures 16.3 and 16.4. Where possible, a reference is made to the plates in the human brain stem atlas of Paxinos and Huang (1995) or to the rhesus monkey atlas of Paxinos *et al.* (2000).

Abducens Nucleus (6N)

Structure and function

The abducens nucleus (6N) lies in the pontomedullary brain stem beneath the floor of the fourth ventricle as a round nucleus adjacent to the medial longitudinal fasciculus (Figs. 16.1 and 16.4J, K) (Paxinos and Huang, 1995, figures 31–34; Paxinos *et al.*, 2000, figures 95–100). It contains at least three functional cell groups: (1) motoneurons innervating the twitch and nontwitch muscle fibers of the lateral rectus muscle; (2) internuclear neurons, and (3) floccular-projecting neurons in the rostral cap, which belong to the paramedian tract neurons (see below; Büttner-Ennever and Horn, 1996). The motoneurons controlling the fast, twitch muscle fibers are scattered throughout the motor nucleus, but those controlling the slow, nontwitch fibers (unique to eye muscles) are arranged around the periphery of the nucleus in monkey (Büttner-Ennever *et al.*, 2001). Motoneurons and internuclear neurons exhibit the same burst-tonic firing pattern during eye movements (Fuchs *et al.*, 1988). However, only motoneurons, and not the internuclear neurons, carry conjugate- and vergence-related signals (Delgado-Garcia *et al.*, 1986; Zhou and King, 1998).

Histochemistry

In contrast to the cholinergic motoneurons, identified internuclear neurons are not cholinergic (Spencer and Bakers *et al.*, 1986; Carpenter *et al.*, 1992), but use glutamate and aspartate as transmitter (Nguyen and Spencer, 1999). The abducens nucleus receives inhibitory glycinergic afferents from inhibitory burst neurons in the contralateral dorsal paragigantocellular nucleus (DPGi) , the prepositus hypoglossi nucleus, and the ipsilateral medial vestibular nucleus (Spencer *et al.*, 1989). In addition, the motoneurons and, to a lesser extent, the internuclear neurons receive a GABAergic input, which in cat originates in part from internuclear

neurons in and above the oculomotor nucleus (de la Cruz *et al.*, 1992). The motoneurons contain the calcium-binding protein parvalbumin, but in the cat at least 80% of the internuclear neurons contain a different calcium-binding protein, calretinin, which could serve as a histological marker for internuclear neurons in this species (de la Cruz *et al.*, 1998).

Connections

The internuclear neurons of the abducens nucleus project to the motoneurons of the medial rectus muscle in the contralateral oculomotor nucleus, thereby forming the anatomical basis for conjugate eye movements (Büttner-Ennever and Akert, 1981). The motoneurons and internuclear neurons receive bilateral afferents from secondary vestibuloocular neurons in the medial vestibular nuclei, the prepositus hypoglossi nucleus (PrH), the excitatory and inhibitory saccadic burst neurons in the caudal pontine reticular nucleus (PnC) and dorsal paragigantocellular nucleus (DPGi), and from internuclear neurons of the oculomotor nucleus (Evinger, 1988).

Clinical Aspects

Lesions of the abducens nerve (6n) cause a motor paralysis of the lateral rectus muscle of the same side, resulting in horizontal diplopia (for review, see Smith, 1998; Leigh and Zee, 1999). Lesions of the abducens nucleus can be distinguished from abducens nerve palsy, since the nucleus contains not only motoneurons but also internuclear neurons that project to the medial rectus motoneurons of the contralateral side via the medial longitudinal fascicle. Therefore, damage to the nucleus results in a palsy of both muscles and an ipsilateral conjugate gaze palsy. This is often accompanied by a facial nerve palsy owing to the close proximity of the abducens nucleus (6N) and the facial genu (g7) (see Fig. 16.4J, K). A third group of neurons in the abducens nucleus, the paramedian tract neurons, which project to the flocculus, may contribute to a defect in gaze holding, if they, or their efferent or afferents inputs, are damaged (Büttner *et al.*, 1995; Büttner-Ennever and Horn, 1996).

Trochlear and Oculomotor nucleus (4N, 3N)

Structure and Function

The trochlear nucleus (4N) lies in the midbrain ventral to the aqueduct (Figs. 16.1 and 16.4A, B) (Paxinos and Huang, 1995, figures 53 and 54; Paxinos *et al.*, 2000; figures 82–84). It has been observed in human that the trochlear nucleus consists of one large group "sunken into the mlf; and several smaller groups of motoneurons further caudally" (Olszewski and Baxter, 1954). It contains only motoneurons of the contralateral superior oblique muscle. The motoneurons innervating the slow nontwitch muscle fibers lie in a tight cluster in the the dorsal cap of the nucleus (Büttner-Ennever *et al.*, 2001). The oculomotor nucleus (3N) (Figs. 16.3E, F and 16.6E, F) contains the motoneurons innervating the ipsilateral inferior rectus, inferior oblique, and medial rectus muscles and those for the contralateral superior rectus muscle. The motoneuron subgroups are organized in a topographic map (Evinger, 1988). In primates there are three clusters of medial rectus muscle motoneurons: ventrally the A group, dorsolaterally the B group, and dorsomedially at the border of the oculomotor nucleus the C group, consisting of smaller motoneurons (Büttner-Ennever and Akert, 1981). Recent experiments in the monkey show that the motoneurons of the C group innervate slow, nontwitch muscle fibers of both medial rectus and inferior rectus muscle. Small motoneurons on the midline between the oculomotor nuclei innervate the slow, nontwitch muscle fibers of the inferior oblique and superior rectus muscles (Büttner-Ennever *et al.*, 2001). In humans this region is often referred to as the nucleus of Perlia (Olszewski and Baxter, 1954); here it is termed interoculomotor nucleus (I3) (Paxinos and Huang, 1995, figures 56–58). Several populations of internuclear neurons with diverse projection targets, such as the spinal cord, the cerebellum, and the abducens nucleus, have been identified in and around the oculomotor nucleus (for review, see Evinger, 1988). So far little is known about their physiology and function.

Histochemistry

The motoneurons in the oculomotor and trochlear nuclei are cholinergic (e.g., Wang and Spencer, 1996) and express parvalbumin immunoreactivity (de la Cruz *et al.*, 1998). In contrast to the abducens nucleus, the motoneurons of vertical pulling eye muscles in the oculomotor and trochlear nuclei receive a strong GABAergic but a rather weak glycinergic input (de la Cruz *et al.*, 1992; Spencer and Baker, 1992). These results have led to the concept that inhibition in horizontal eye movement pathways is provided by glycine, whereas those for vertical eye movement pathways utilize GABA. GABAergic afferents to the oculomotor and trochlear nucleus originate from inhibitory secondary vestibuloocular neurons in the ipsilateral superior vestibular nucleus (rabbit: Wentzel *et al.*, 1995; cat: de la Cruz *et al.*, 1992; for review, see Spencer and Baker, 1992) and, at least in the cat, from the rostral interstitial nucleus of the mlf (RI) (see above; Spencer and Wang, 1996). The contralateral excitatory afferents from secondary vestibuloocular neurons in

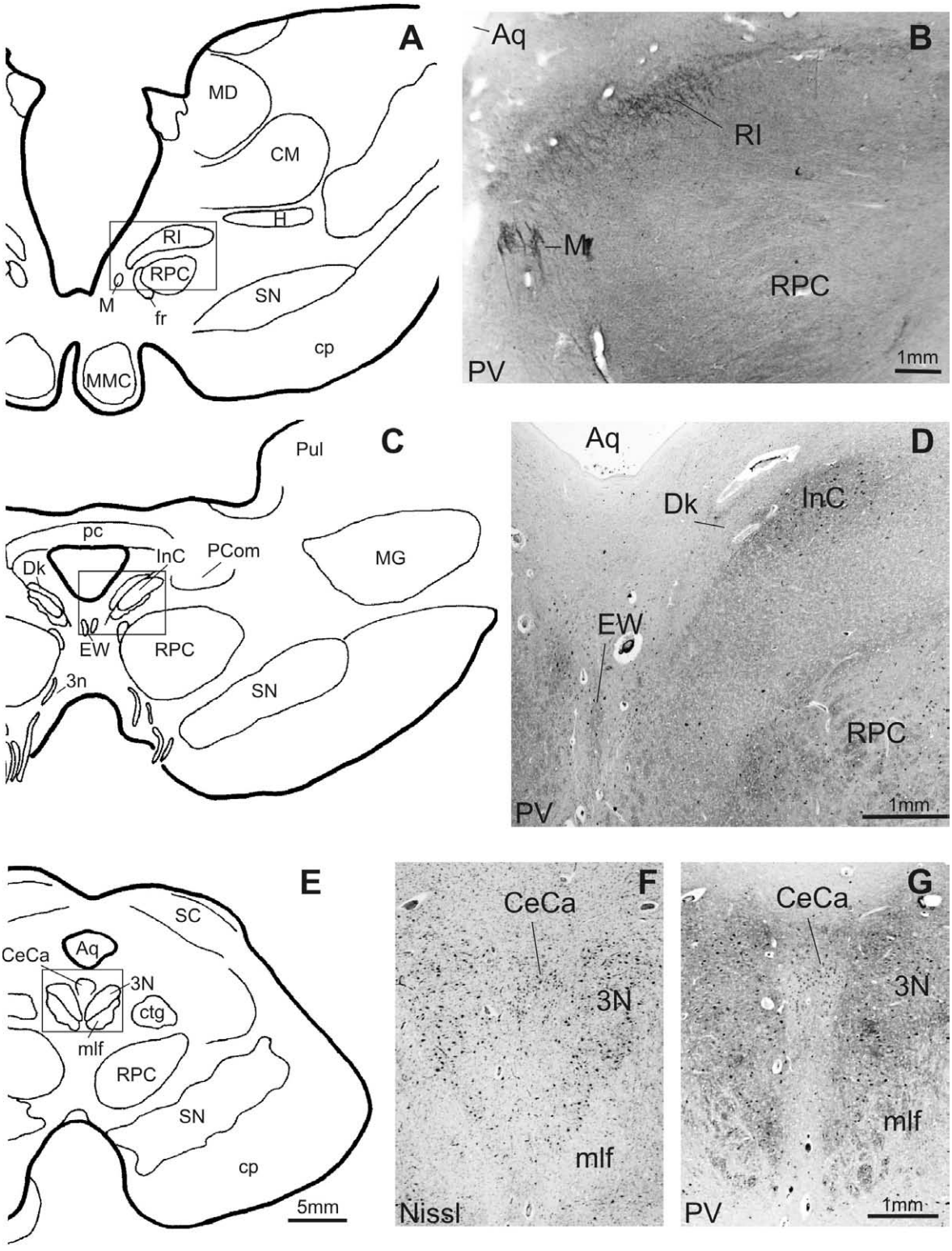

FIGURE 16.3 AND 16.4 Low-power drawings of transverse sections through the human brain stem taken from the levels indicated in Figure 16.1 (A, C, E, H, J, and L) from rostral to caudal. Adjacent, a medium-power photomicrograph with the section, stained for parvalbumin (Pv). This stain highlights several regions of the reticular formation important in the control of eye movements: In B the premotor region for vertical saccades, the rostral interstitial nucleus of the medial longitudinal fascicle (RI) and the lid premotor region (M), In D the interstitial nucleus of Cajal (InC) important for gaze holding in the vertical plane. In G the oculomotor nucleus (3N) and medially, the central caudal nucleus (CeCa) containing the motoneurons of the levator palpebrae muscle (F is taken from an adjacent Nissl-stained section). In I, the arrow marks the cluster of Pv-positive excitatory burst neurons in the dorsomedial tegmental area (DMTg) dorsomedial to the caudal pontine reticular nucleus (PnC). In K the strongly Pv-positive abducens nucleus (6N) under the facial genu (g7) and at the midline between the rootlets of the abducens nerve (6n) the nucleus raphe interpositus (RIP) consisting of Pv-immunoreactive neurons. In M, the arrow indicates darkly stained inhibitory burst neurons of the saccadic system in the dorsal paragigantocellular nucleus (DPGi). *Continued*

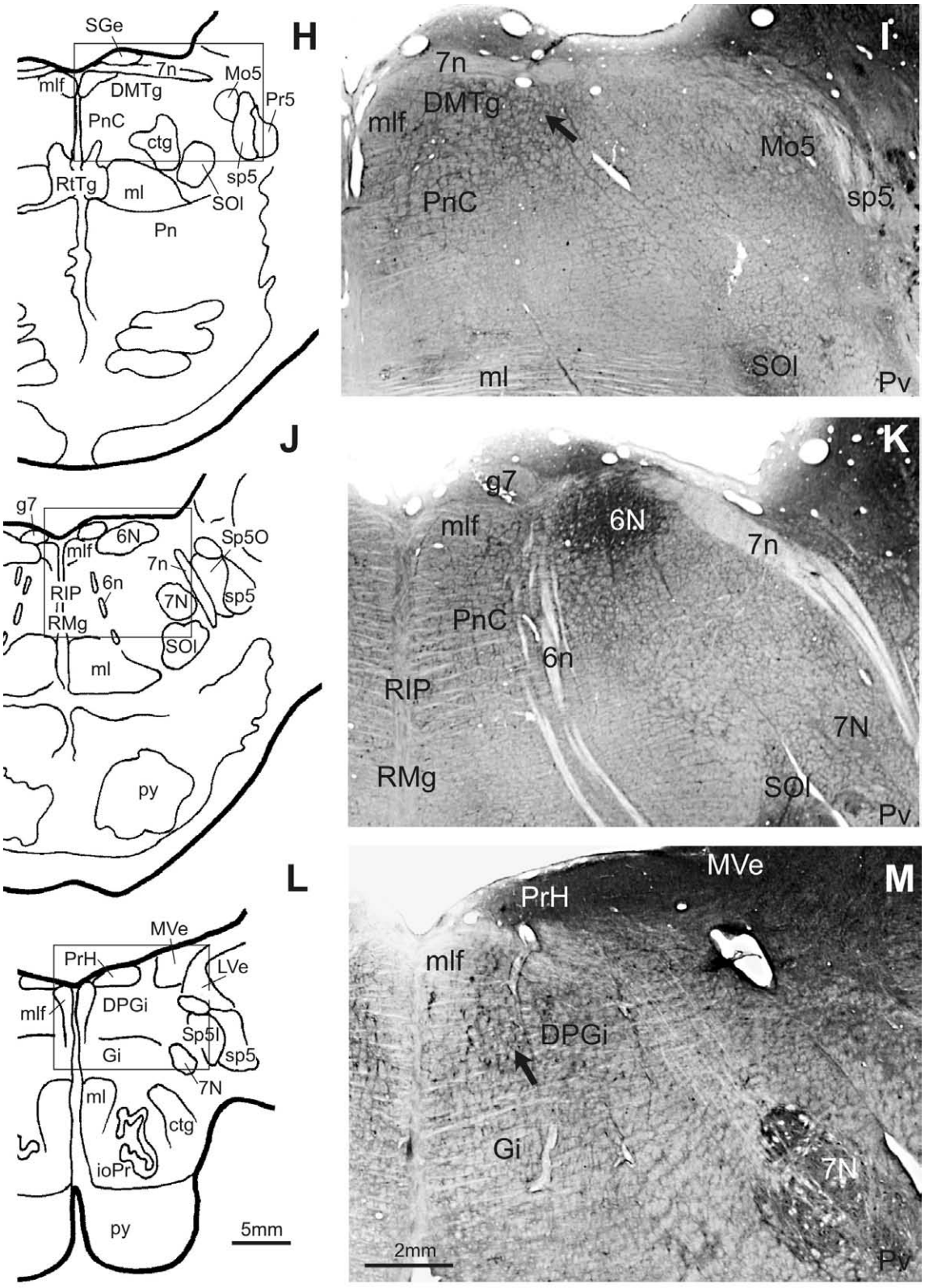

FIGURE 16.3 AND 16.4 *Continued* Abbreviations: 7N, facial nucleus; 7n, facial nerve; Aq, aquaeduct; CM, centromedian thalamic nucleus; ctg, central tegmental tract, Dk, nucleus of Darkschwitsch, DMTg, dorsomedial tegmental area, EW, Edinger–Westphal nucleus; fr, fasciculus retroflexus; Gi, gigantocellular nucleus; IO, inferior olive; LVe, lateral vestibular nucleus; M, M-group; MD, medial dorsal thalamic nucleus; MG, medial geniculate nucleus; ml, medial lemniscus; mlf, medial longitudinal fascicle; MMC, mammillary nucleus, magnocellular part; Mo5, motor trigeminal nucleus; Mve, medial vestibular nucleus; pc, posterior commissure; PCom, nucleus of the posterior commissure; Pr5, principal sensory trigeminal nucleus; Pul, pulvinar; py, pyramidal tract; RMg, raphe magnus nucleus; RPC, red nucleus, parvocellular part; SGe, supragenual nucleus; SN, substantia nigra; SOl, superior olive; Sp5O, spinal trigeminal nucleus, oral part; Sp5I, spinal trigeminal nucleus, interpolar part; sp5, spinal trigeminal tract.

the medial and superior vestibular nuclei most probably use glutamate as transmitter (Dememes and Raymond, 1982). Recent anatomical studies in the cat indicate that excitation to medial rectus motoneurons from the internuclear neurons of the contralateral abducens nucleus is mediated by glutamate and aspartate, whereas the afferents from the ascending tract of Deiters use only glutamate as transmitter (Nguyen and Spencer, 1999).

Connections

The medial rectus subgroup in the oculomotor nucleus receives afferents via the medial longitudinal fasciculus (mlf) from the internuclear neurons of the contralateral abducens nucleus (Büttner-Ennever and Akert, 1981) and from the ipsilateral ascending tract of Deiters, a vestibular pathway presumably involved in the control of vergence (Baker and Highstein, 1978; Chen-Huang and McCrea, 1998). Electrophysiological recording have identified neurons in the mesencephalic reticular formation, just lateral to the oculomotor nucleus, which carry a premotor-like signal for vergence (Mays, 1984), and theoretically should project to medial and inferior rectus motoneurons; however, these cells have not yet been visualized anatomically. Secondary vestibulooculomotor projections target the motoneurons of vertical pulling eye muscles, i.e., inferior rectus, inferior oblique, superior rectus, and superior oblique muscle, via excitatory fibers from the superior and medial vestibular nuclei from the contralateral side, and via inhibitory fibers from the superior vestibular nucleus of the the ipsilateral side (for review, see Büttner-Ennever, 2000; see also Chapter 33). These vestibular pathways can be visualised with transsynaptic retrograde tract tracers (Büttner-Ennever *et al.*, 1981). In the monkey the most striking input to vertical oculomotor neurons comes from the y group. The motoneurons of vertical pulling eye muscles in the oculomotor and trochlear nuclei also receive bilateral projections from the interstitial nucleus of Cajal (InC; see "Interstitial Nucleus of Cajal"), and predominantly ipsilateral projections from the rostral interstitial nucleus of the medial longitudinal fasciculus (RI; see "Rostral Interstitial Nucleus of the Medial Longitudinal Fasciculus") (Horn and Büttner-Ennever, 1998a).

Clinical Aspects

The trochlear nucleus and nerve innervate the superior oblique muscle. Damage to the nerve accounts for most cases of acquired vertical diplopia. Lesions in either nerve or nucleus result in a vertical or oblique diplopia, which is largest when there is attempted gaze in the "down and medial" quadrant of vision. Hence, a patient with trochlear palsy frequently complains of "difficulty walking down stairs" (Henn *et al.*, 1982, for review, see Smith, 1998; Leigh and Zee, 1999). The oculomotor nucleus and nerve rootlets innervate four muscles and the levators. Lesions of this small area often cause multiple palsies in which there is insufficient resolution to distinguish between nerve or nuclear damage (for review, see Smith, 1998; Leigh and Zee, 1999). Only the superior rectus muscle has a crossed innervation. A central unilateral oculomotor lesion is rare, but it will cause bilateral superior rectus muscle palsy, because it damages both the ipsilateral motoneurons and the fibers from the contralateral motoneurons crossing through the nucleus. Damage to this area may also affect the parasympathetic fibers arising from the Edinger–Westphal complex (EW; Fig. 16.3C), that provide the preganglionic neurons innervating the ciliary ganglion in the orbit (Erichsen and May, 2002). The ciliary ganglion supplies the pupillary sphincter and ciliary muscles for lens accomodation (for review, see Leigh and Zee, 1999; Sun and May, 1993). The supraoculomotor nucleus (Su3C; Paxinos and Huang, 1995, figure 58) and the supraoculomotor cap (Su3; Paxinos and Huang, 1995, figure 58) are probably part of this poorly defined group of cells.

Rostral Interstitial Nucleus of the Medial Longitudinal Fasciculus (RI)

Structure and function

The rostral interstitial nucleus of the medial longitudinal fasciculus (RI) contains the premotor burst neurons, which are essential for generation of vertical and torsional saccades (Büttner *et al.*, 1977; Vilis *et al.*, 1989; Crawford and Vilis, 1992). In addition, this region contains premotor neurons with projections to the motoneurons of dorsal neck muscles participating in eye–head or only head movements, at least in the cat (Isa and Sasaki, 1992; Isa *et al.*, 1992; for review, see Isa and Sasaki, 2002). The rostral interstitial nucleus of the RI lies in the mesencephalic reticular formation and forms the medial part of the H fields of Forel (Figs. 16.1 and 16.3A, B) (Paxinos *et al.*, 2000, figures 68–72). In transverse sections it forms a wing-shaped nucleus ventromedial to the third ventricle and borders the parvocellular portion of the red nucleus (RPC) dorsomedially (Fig. 16.3A, B). The RI adjoins directly the rostral end of the interstitial nucleus of Cajal (InC) from which it is separated by the traversing fibers of the fasciculus retroflexus (fr). Its rostral end is roughly demarcated by the traversing fibers of the mamillothalamic tract (mt) (Büttner-Ennever and Büttner, 1988). In frontal sections the posterior thalamosubthalamic artery serves as a helpful landmark, which borders the

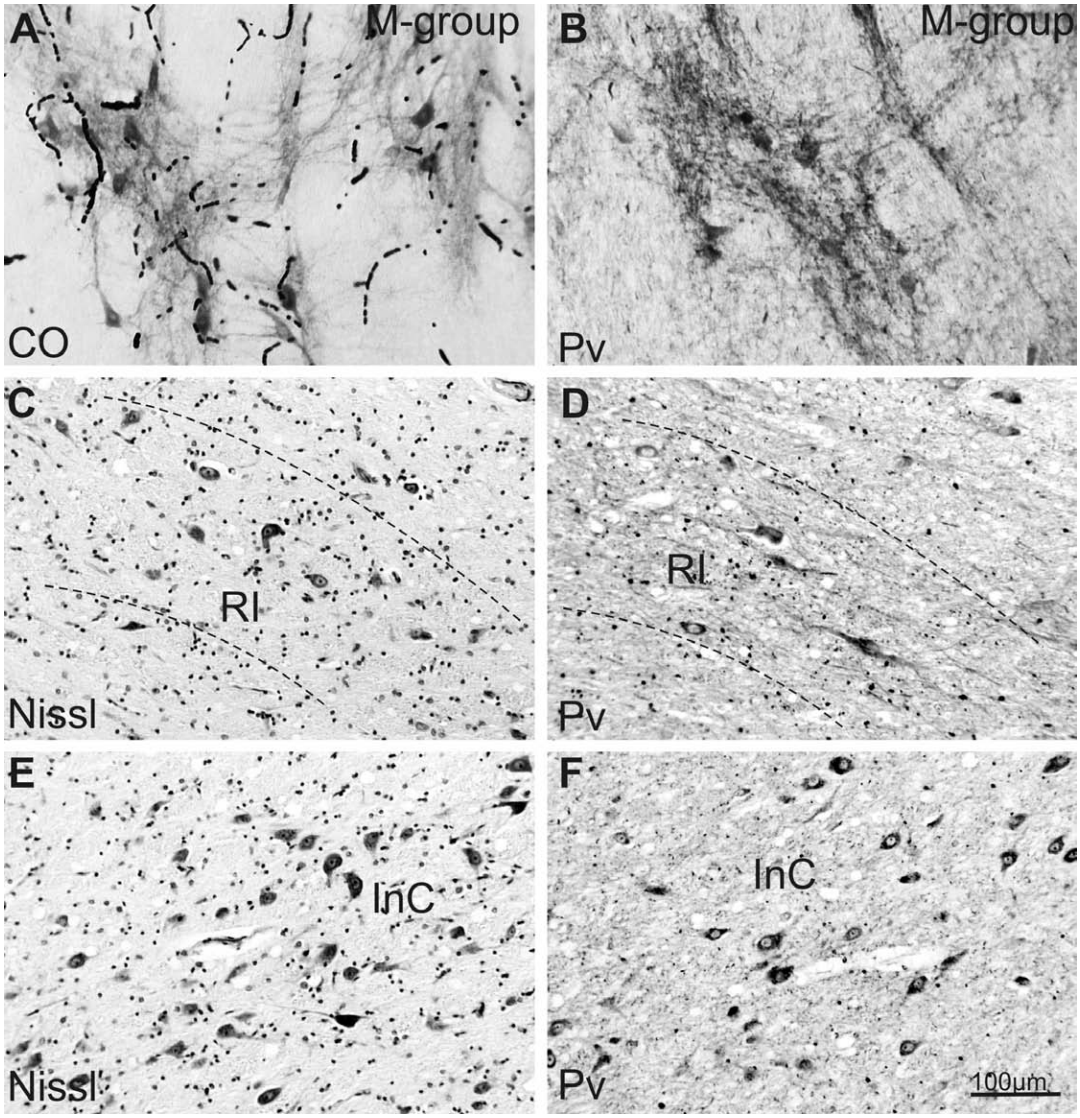

FIGURE 16.5 High-power photomicrographs of the M-group **(A, B),** the rostral interstitial nucleus of the mlf (RI) **(C, D),** and the interstitial nucleus of Cajal (InC) **(E, F),** stained for cytochrome oxidase (CO), parvalbumin (Pv), or with a Nissl stain, to show the characteristics of individual cell type.

RI dorsomedially like an eyebrow (Büttner-Ennever *et al.*, 1982). The RI is composed of several morphological cell types, enclosing small to medium-sized neurons, which are embedded in the fibers of the medial longitudinal fasciculus, resulting in its reticulated appearance (Fig. 16.5C, D; Crossland *et al.*, 1994).

Histochemistry

Recent work in monkey and human showed that the neuropil of the RI is highlighted within the mesencephalic reticular formation by its strong cytochrome oxidase activity and parvalbumin expression (Figs. 16.3B and 16.5D) (Horn and Büttner-Ennever, 1998a; Horn *et al.*, 2000). In addition, most of the parvalbumin-immunoreactive neurons in the RI express calretinin and are ensheathed by perineuronal nets as revealed by *Wisteria floribunda* agglutinin binding and chondroitin sulfate proteoglycan immunohistochemistry in monkeys and humans (Horn *et al.*, 2003). Similarly, the RI can be well visualized by immunostaining with the SMI32 antibody as shown in the atlas of Paxinos and Huang (2000; Petrides *et al.*, figure 34), where it is labeled as prerubral fields (PRFs). Anatomical studies in the RI of the cat revealed the presence of GABA-immunoreactive neurons within the dorsomedial part, which project to the oculomotor nucleus (Spencer and Wang, 1996). In contrast, the RI of the monkey contains only few small GABA-immunoreactive neurons, which

are not premotor burst neurons (Carpenter *et al.*, 1992). The RI receives a strong innervation by GABA- and glycine-immunoreactive terminals (Horn *et al.*, 1994). Combined anterograde tracing and immunocytochemical methods indicated that projection neurons from the RI to the oculomotor and trochlear nucleus use aspartate and/or glutamate as transmitter (Spencer and Wang, 1996).

Connections

The burst neurons, which make up all of the medium-sized neurons within the rostral interstitial nucleus of the mlf (RI), project monosynaptically to the motoneurons of the vertical pulling extraocular eye muscles in the oculomotor and trochlear nuclei (Moschovakis *et al.*, 1991a, b; Horn and Büttner-Ennever, 1998a; Wang and Spencer, 1996a). Additional targets are the RI of the contralateral side, the interstitial nucleus of Cajal (InC), the paramedian tract neurons (see "Interstitial Nucleus of Cajal"); and sparsely the spinal cord (Moschovakis *et al.*, 1991a, b; Wang and Spencer, 1996b; Holstege and Cowie, 1989). The burst neurons in the RI receive strong input from the inhibitory, glycinergic omnipause neurons in the pontine reticular formation (Horn *et al.*, 1994). In addition, the RI receives afferents from the interstitial nucleus of Cajal (InC) and the deep layers of the superior colliculus (Nakao *et al.*, 1990; Kokkoroyannis *et al.*, 1996). A minor projection from the medial vestibular nucleus targets mainly the mediocaudal part of the RI (Büttner-Ennever and Lang, 1981; Matsuo *et al.*, 1994).

Clinical Aspects

Unilateral experimental lesions in macaque monkeys lead to deficits of torsional saccades and produce a spontaneous torsional nystagmus (Crawford and Vilis, 1992; Suzuki *et al.*, 1995; Helmchen *et al.*, 1996b). Bilateral lesions result in a complete vertical gaze paralysis, but vertical gaze holding, vestibular eye movements, and pursuit are preserved, as are horizontal saccades (for review, see Leigh and Zee, 1999; Kömpf *et al.*, 1979; Suzuki *et al.*, 1995). In patients a rare pure isolated downgaze paralysis can be observed only after discrete bilateral lesions of the RI, whereas a combined up- and downgaze paralysis is seen after unilateral RI lesions, often but not always involving the posterior commissure (Büttner-Ennever *et al.*, 1982; Pierrot-Deseilligny *et al.*, 1982; Ranalli *et al.*, 1991; Riordan-Eva *et al.*, 1996; Helmchen *et al.*, 1998).

Interstitial Nucleus of Cajal (InC)

The Interstitial Nucleus of Cajal (InC) is elsewhere called the interstitial nucleus of the medial longitudinal fasciculus (IMLF). However, use of the term IMLF is not recommended by the authors of this chapter.

Structure and Function

The cells of the interstitial nucleus of Cajal (InC) lie within the medial longitudinal fasciculus (mlf) and form a rather well-circumscribed nucleus in the mesencephalic reticular formation lateral to the rostral pole of the oculomotor nucleus at the border of the periaqueductal gray. It consists of small to medium-sized neurons with few large polygonal cells intermingled (Figs. 16.3D and 16.5E, F) (Bianchi and Gioia, 1991) and lies just beneath the nucleus of Darkschewitsch (Dk), which contains more elongated, spindle-shaped, strongly Nissl-stained cells (Olszewski and Baxter, 1954; Bianchi and Gioia, 1990). The interstitial nucleus of Cajal is a well-known structure and has been described in many species. According to most investigations, it is clearly associated with a role in eye and head movements. In a recent description of a cell group representing the premotor center for vertical saccades, which lies immediate rostral and adjacent to InC, the name "rostral intersitial nucleus of the mlf (RI)" was chosen. Therefore, we suggest not using the name "interstitial nucleus of the mlf" for the interstitial nucleus of Cajal, because it might lead to much confusion with the RI (Figs. 16.1 and 16.3C, D) (Paxinos and Huang, 1995, figures 59–63, abbreviated as iMLF; Paxinos *et al.*, 2000, figures 72–78), as well as with some other structures, e.g., the intermediate and caudal interstitial nuclei of the mlf (Blanks 1990).

The interstitial nucleus of Cajal (InC), like the rostral interstitial nucleus of the mlf (RI), participates in vertical and torsional eye movements, but the InC is more involved in vertical gaze holding (Fukushima *et al.*, 1992) and eye–head coordination (Fukushima, 1987) rather than generation of eye movements. The InC contains several functional cell groups related to eye movements (for review, see Helmchen *et al.*, 1996a): Burst-tonic and tonic neurons encode the eye position and they are involved in the vertical integrator function (for review, see Fukushima *et al.*, 1992). Other neurons apparently participate in eye–head movements in the vertical and torsional plane, since stimulation of the InC results in an ipsilateral ocular tilt reaction consisting of an ipsilateral head tilt, with compensatory eye movements (Westheimer and Blair, 1975; Lueck *et al.*, 1991).

Histochemistry

In monkey and human the InC is highlighted by its strong parvalbumin immunoreactivity (Fig. 16.3D) and its cytochrome oxidase activity, and thereby is sharply separated from the dorsally adjacent nucleus

of Darkschewitsch (Dk), which exhibits much less parvalbumin immunoreactivity especially of the neuropil (Fig. 16.3D); (Horn and Büttner-Ennever, 1998a). Parvalbumin expression is confined to the medium-sized and large neurons in the InC, some of which are projection neurons to the motoneurons of vertical extraocular eye muscles, presumed premotor burst-tonic neurons (Fig. 16.5F) (Horn and Büttner-Ennever, 1998a). Using *in situ* hybridization methods for the detection of the messenger RNA of the GABA-synthetizing enzyme glutamate decarboxylase, there is evidence that the InC of the monkey contains numerous small and medium-sized GABAergic neurons, which in part project to the motoneurons of vertical eye muscles (Horn *et al.* 2003). The InC contains many GABA-immunoreactive terminals, some of which could arise from collaterals of the inhibitory secondary vestibulo oculomotor projections of the ipsilateral superior vestibular nucleus, which were shown to be GABAergic (De la Cruz *et al.*, 1992).

Connections

There are three main efferent projections systems leaving the interstitial nucleus of Cajal (INC) (Kokkoroyannis *et al.*, 1996): First, the ascending system has strong projections to the ipsilateral mesencephalic reticular formation, including the RI and zona incerta (ZI), weaker projections to the ipsilateral centromedian (CMn) and parafascicular (PF) thalamic nuclei and bilateral to the mediodorsal (MD), central medial (CM), and lateral nuclei of the thalamus. Second, the descending system projects through the medial longitudinal fasciculus (mlf) and innervates the ipsilateral oculomotor and trochlear nucleus, the ipsilateral paramedian pontine reticular formtion, and the rostral cap of the abducens nucleus as part of the paramedian tract groups (Büttner-Ennever *et al.*, 1989; Büttner-Ennever and Horn, 1996). Further, descending projections terminate in the vestibular nuclei, the prepositus hypoglossal nucleus, the gigantocellular portion of the reticular formation, which mediates head movements (Cowie and Robinson, 1994; Cowie *et al.*, 1994), the inferior olive, and the ventral horn of C1 to C4. The commissural system projects via the posterior commissure (pc) to the nucleus of the posterior commissure (PCom), the contralateral InC, and the contralateral oculomotor and trochlear nuclei to innervate only the motoneurons of vertical-pulling eye muscles (Kokkoroyannis *et al.*, 1996). In addition, the InC receives inputs from premotor neurons that encode eye or head velocity signals, e.g., from secondary vestibuloocular neurons (Iwamoto *et al.*, 1990) and from nucleus Y of the vestibular nuclei (Fukushima *et al.*, 1986; for review, see Leigh and Zee, 1999). Projections from the RI, presumably originating from premotor burst neurons, target most probably the burst-tonic and tonic neurons in the InC (Moschovakis *et al.*, 1991a, b).

Clinical Aspects

Unilateral lesions of the InC lead to a contralateral head tilt with torsion of the eyes to the contralateral side, but a torsional nystagmus to the ipsilateral side (Halmagyi *et al.*, 1994; for review, see Leigh and Zee, 1999). Bilateral lesions of the InC result in an upbeat nystagmus and neck retroflexion (Fukushima, 1987; Helmchen *et al.*, 1998, 2002), clinical signs characteristic of progressive supranuclear palsy (Fukushima-Kudo and Fukushima, 1987). A lesion of the posterior commissure (pc), which contains the crossing fibers of the burst-tonic and tonic neurons, leads to the inability to hold eccentric gaze after vertical saccades (Partsalis *et al.*, 1994).

Paramedian Pontine Reticular Formation

Structure and Function

Originally the term "paramedian pontine reticular formation (PPRF)" was introduced in macaque monkeys to define the brain stem site where lesions produce a horizontal gaze palsy (Fig. 16.1) (Cohen and Komatsuzaki, 1972). It includes several functional cell groups in the pontine and medullary reticular formation, which were found to be important for the generation of eye and head movements: excitatory and inhibitory burst neurons for horizontal eye movements, as well as omnipause neurons and saccadic long-lead burst neurons that participate directly in the generation of horizontal saccadic eye movements. Reticulospinal neurons are involved in eye–head movements, and paramedian tract neurons may have a role in gaze stabilization.

Anatomically, the paramedian pontine reticular formation is composed of the oral pontine reticular nucleus (PnO), and the caudal pontine reticular nucleus (PnC), including the dorsomedial tegmental area (DMTg). The PnO begins rostrally at the caudal end of the trochlear nucleus and extends caudally to the level of the caudal end of the locus coeruleus (LC) (Paxinos and Huang, 1995, figures 37–49). The caudal pontine reticular nucleus (PnC) adjoins the PnO caudally and extends to the caudal pole of the facial nucleus (7N), and the dorsomedial tegmental area (DMTg) stretches throughout the dorsal paramedian pontine reticular formation (Paxinos and Huang, 1995, figures 33–36; Paxinos *et al.*, 2000; figures 94–96). The PnC and the PnO consist of small to medium-sized cells. An additional few large reticulospinal neurons are scattered in the PnC, whereas the PnO is characterized by the presence

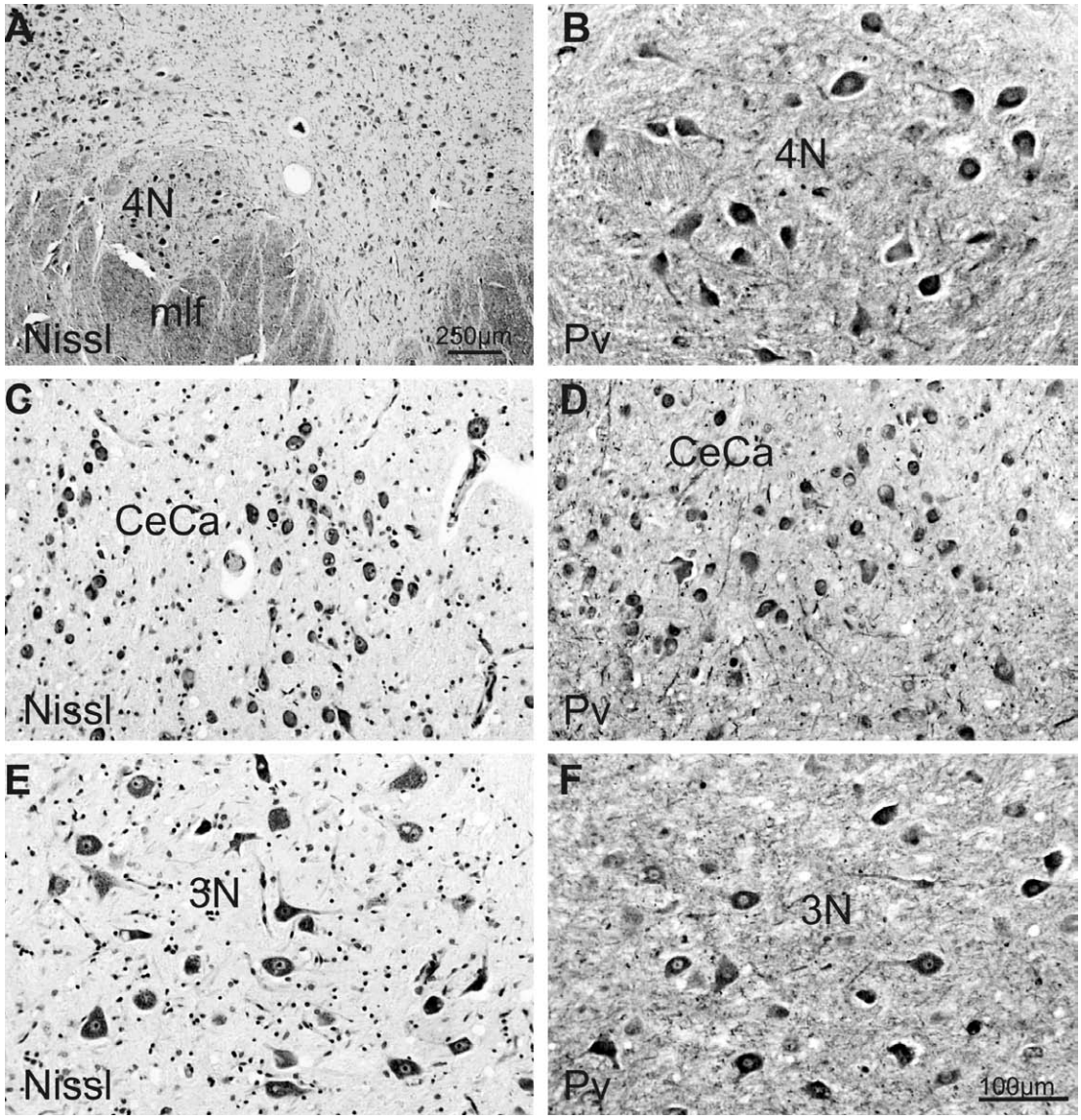

FIGURE 16.6 High -power photomicrographs to show the characteristics of individual cell types: **A,** (Nissl) and **B,** (Pv) the superior oblique muscle motoneurons in the trochlear nucleus (4N); in **C** (Nissl) and **D** (Pv), the levator palpebrae muscle motoneurons in the central caudal nucleus (CeCa); and in **E** (Nissl) and **F** (Pv), the extraocular muscle motoneurons in the oculomotor nucleus (3N).

of plump neurons and a more cellular appearance in Nissl-stained sections (Olszewski and Baxter, 1954; Martin and Holstege, 1990).

Saccadic Burst Neurons There are several types of saccade-related burst neurons in the PPRF (Figs. 16.7 and 16.8) (for review, see Leigh and Zee, 1999; Scudder *et al.*, 2002). Excitatory (EBNs) and inhibitory burst neurons (IBNs) exhibit a high-frequency burst during horizontal saccades and are otherwise silent being inhibited by omnipause neurons (OPNs). EBNs excite the motoneurons and internuclear neurons in the ipsilateral abducens nucleus, thereby also activating the medial rectus motoneurons in the contralateral oculomotor nucleus, which results in a saccade to the ipsilateral side (Fig. 16.8). At the same time IBNs are driven by the EBNs, and they inhibit the motoneurons in the contralateral abducens nucleus in order to evoke a conjugate saccade (Strassman *et al.*, 1986b). Saccade-related long-lead burst neurons (LBNs) exhibit an additional irregular low-frequency activity before the saccade-related burst, and they presumably activate the premotor burst neurons (for review, see Moschovakis *et al.*, 1996).

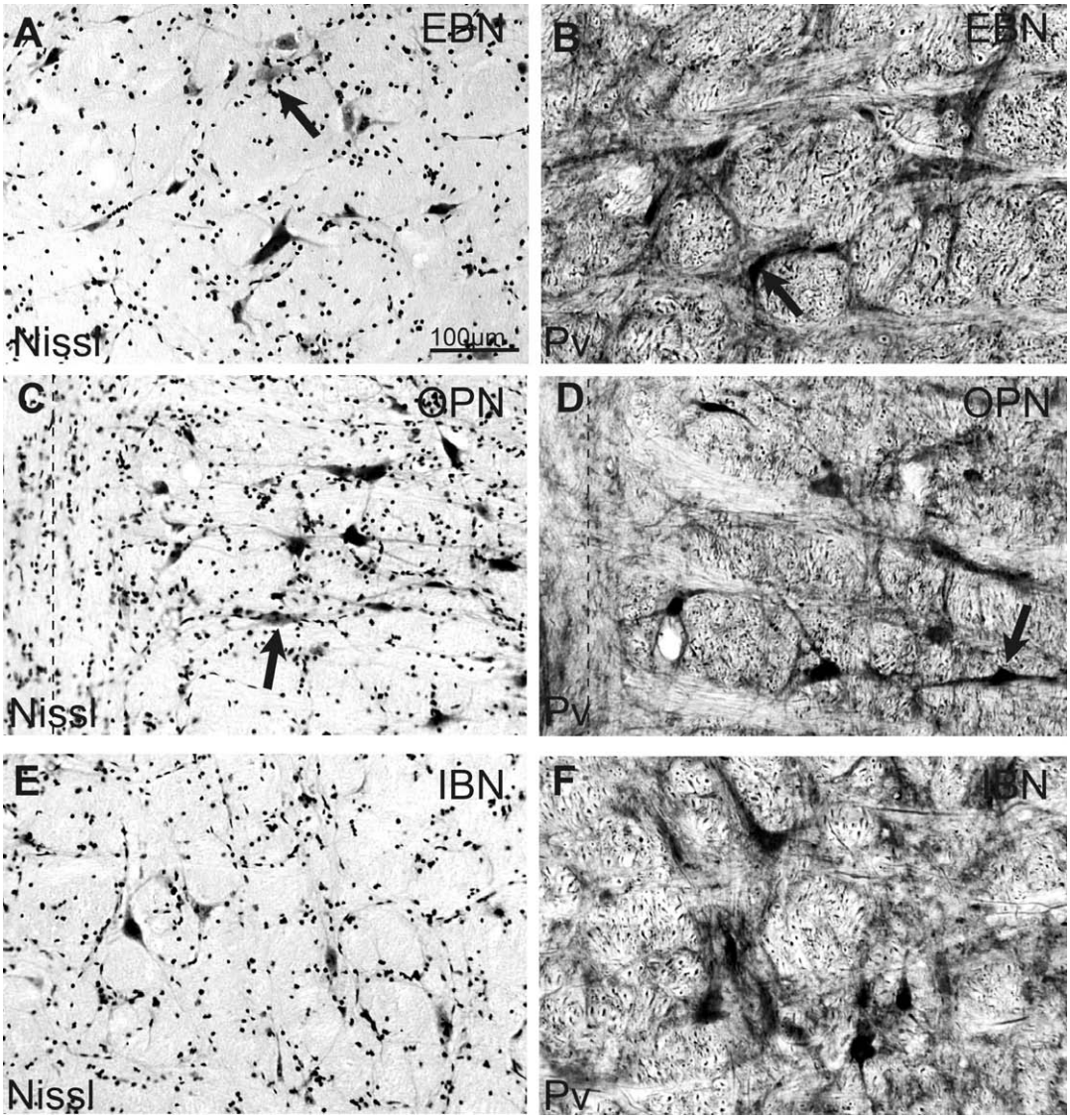

FIGURE 16.7 High-power photomicrographs of the excitatory burst neurons (EBNs; *arrow*) in the caudal pontine reticular nucleus **(A, B),** the omnipause neurons (OPNs) in the nucleus raphe interpositus (**C, D;** *arrows*), and the inhibitory burst neurons (IBNs) in the dorsal paragigantocellular nucleus **(E, F)** in either Nissl- or parvalbumin (Pv)–stained transverse sections, to show the characteristics of each individual cell type. Dotted lines in C and D indicate the midline.

Excitatory burst neurons (EBNs) Tract tracing experiments in the monkey showed that the excitatory burst neurons for horizontal saccades lie as a compact group within the dorsomedial part of the caudal pontine reticular nucleus (PnC) just rostral to the saccadic omnipause neurons (Fig. 16.4H, I) (Strassman *et al.*, 1986a; Langer *et al.*, 1986; Horn *et al.*, 1995). The burst neurons belong to the medium-sized cell population, which in addition express parvalbumin (Fig. 16.7A, B) (Horn *et al.*, 1995). Based on the parvalbumin-immunostaining pattern the homologue of the EBN area was described in humans, as an area of about 2.5 mm width and 2 mm height adjacent to the medial longitudinal fasciculus (mlf) that corresponds to the dorsomedial tegmental area (DMTg) (Paxinos and Huang, 1995, figure 35) (Fig. 16.4H, I, *arrow;* Horn *et al.*, 1995, 1996).

Inhibitory burst neurons (IBN) In monkey the premotor inhibitory neurons for horizontal saccades are located ventromedially to the abducens nucleus in the dorsal paragigantocellular nucleus (DPGi). They belong to the medium-sized cell population that expresses parvalbumin immunoreactivity and helped

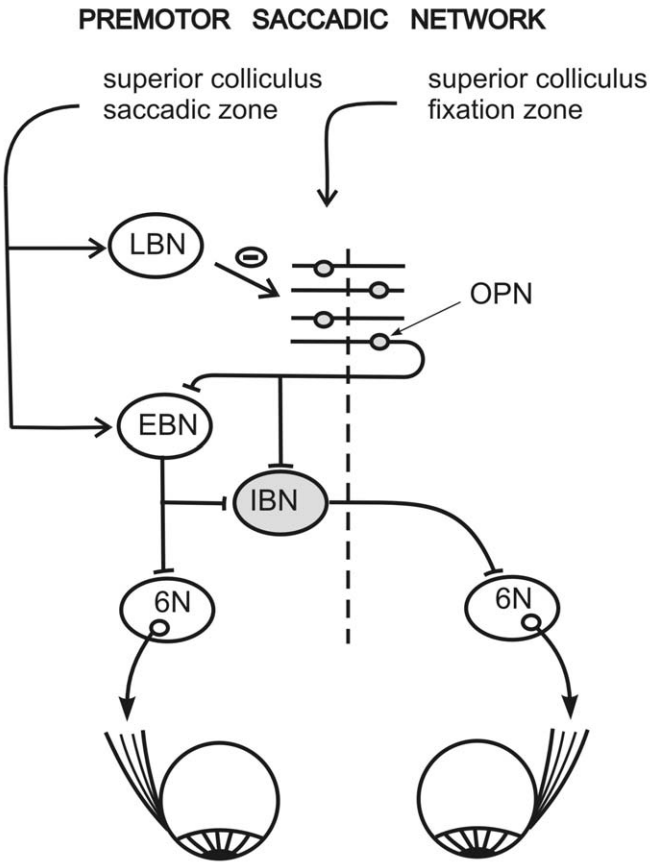

FIGURE 16.8 A simplified diagram of the arrangement of the excitatory burst neurons (EBNs), the glycinergic omnipause neurons (OPNs), and the glycinergic inhibitory burst neurons (IBNs) that constitute the premotor circuitry in the paramedian pontine reticular formation controlling the generation of horizontal saccades. The shaded elements are inhibitory neurons. 6N, abducens nucleus; LBN, long-lead burst neurons.

to outline the homologue region in human as well (Fig. 16.4L, M, *arrow;* Fig. 16.7E, F) (Horn *et al.*, 1995, 1996; Paxinos and Huang, 1995, figures 30–31).

Long-lead burst neurons (LBNs) Saccadic long-lead burst neurons are found at several locations in the brain stem (Fig. 16.8): pontine LBNs lie within the nucleus reticularis pontis caudalis (PnC), intermingled with premotor excitatory burst neurons, and more rostrally in the nucleus reticularis pontis oralis (PnO). They also lie in the reticulotegmental nucleus of the pons (RtTg) (Scudder *et al.*, 1996b) and intermingled with inhibitory burst neurons in the dorsal paragigantocellular nucleus (DPGi) (Scudder *et al.*, 1988).

Reticulospinal neurons In the cat, another class of excitatory saccade-related neurons in the PPRF was described, the reticulospinal neurons (for review, see Martin and Holstege, 1990; Grantyn *et al.*, 1992). They project via the medial reticulospinal tract to the spinal cord and give off collaterals to the abducens nucleus. The reticulospinal neurons are activated during eye movements and neck muscle activity during gaze shifts to the ipsilateral side (Grantyn *et al.*, 1987). Reticulospinal neurons were found in the vicinity of the abducens nucleus and in the nucleus reticularis pontis caudalis (PnC) intermingled with EBNs (Grantyn *et al.*, 1987). In the monkey, gaze-related neurons were recorded in the DPGi, the PnC, and the oral pontine reticular nucleus (PnO), which might have projections to the spinal cord with collaterals to the abducens nucleus (Whittington *et al.*, 1984; May and Porter, 1992; Robinson *et al.*, 1994).

Omnipause neurons (Fig. 16.7C, D) Saccadic omnipause neurons (OPNs) act as triggers for the initiation of saccadic eye movements in all directions (Fuchs *et al.*, 1985). During fixation and slow eye movements the OPNs exert a tonic inhibition on premotor burst neurons in the pontine reticular formation (see above) and the rostral interstitial nucleus of the mlf (RI). During a saccade the OPNs are inhibited, thereby enabling an activation of the burst neurons from the superior colliculus (for review, see Moschovakis and Highstein, 1994; Scudder *et al.*, 2002). The basic circuitry for the generation of horizontal saccades is shown in Figure 16.8. In cat OPNs not only trigger saccadic eye movement, but participate in gaze control, i.e., combined eye and head movements (Paré and Guitton, 1990, 1998). However, in primates the OPNs apparently control only that portion of gaze movement, that involves the eye movement (Phillips *et al.*, 1999). In addition, OPNs may form a link to the premotor circuit of the blink system, since stimulation of the OPNs suppresses reflex blinks (see "Blink–Saccade Interaction") (for review, see Sibony and Evinger, 1998).

Combined physiological and anatomical experiments showed that the saccadic omnipause neurons lie within a distinct nucleus at the ventrocaudal border of nucleus raphe pontis (RPn) and dorsal to the nucleus raphe magnus (RMg), which was termed nucleus raphe interpositus (RIP) (Figs. 16.4J, K and 16.7C D) (Paxinos and Huang, 1995, figures 33–34; Paxinos *et al.*, 2000, figures 93 and 94, Büttner-Ennever *et al.*, 1988). In monkey the RIP forms two vertical columns adjacent to the midline, consisting of medium-sized neurons, which are horizontally oriented with well-developed dendrites reaching across the midline. In all species so far studied, including humans, the RIP lies at the level where the traversing fibers of the abducens nerve (6n) rootlets appear (Fig. 16.4J, K) (Büttner-Ennever *et al.*, 1988; Horn *et al.*, 1994).

Histochemistry

There are only few reports on the histochemistry of the functional cell groups within the pontine reticular formation. Excitatory (EBNs) and inhibitory (IBNs) saccadic burst neurons and omnipause neurons (OPNs) are parvalbumin-immunoreactive and express cytochrome oxidase activity (Büttner-Ennever *et al.*, 1988; Horn *et al.*, 1994, 1995). The nucleus raphe interpositus shows positive staining for acetylholinesterase activity (see Paxinos and Huang, 1995, figure 34). The transmitter of the EBNs, RSNs, and LBNs is not known, but the IBNs use glycine as a transmitter (Spencer *et al.*, 1989). In contrast to its neighboring raphe nuclei, nucleus raphe interpositus (RIP), which is composed of OPNs, does not contain 5-HT-immunoreactive neurons (Büttner-Ennever *et al.*, 1988; Horn *et al.*, 1994; see also Chapter 13). Immunocytochemical studies in monkey showed that the neurons of the RIP are glycinergic, and that they receive a similar strong supply of glycine- and GABA-immunoreactive terminals on their somata and proximal dendrites, whereas glutamatergic afferents are confined to the dendrites (Horn *et al.*, 1994). Although embedded in a network of 5-HT and catecholaminergic fibers, only few immunostained varicosities are associated with RIP neurons (Horn *et al.*, 1994). In addition, the neurons of the RIP are ensheathed with prominent perineuronal nets (Horn *et al.*, 2003).

Connections

The excitatory burst neurons (EBNs) project directly to the motoneurons and internuclear neurons in the abducens nucleus and to the inhibitory burst neurons (IBNs) in the dorsal paragigantocellular nucleus (DPGi) of the same side, thereby providing the neuroanatomical basis for conjugate horizontal saccades (Fig. 16.8) (Strassman *et al.*, 1986a). In addition, the EBNs and IBNs send projections to the paramedian tract neurons (Strassman *et al.*, 1986a, b; Büttner-Ennever and Horn, 1996).

Recent work in monkey showed that the DPGi and PnC containing IBNs, EBNs, and reticulospinal neurons receive a strong afferent input from the intermediate layers of the superior colliculus motor map mediating large horizontal saccades, which could be accompanied by head movements (Büttner-Ennever *et al.*, 1999).

The omnipause neurons in the nucleus raphe interpositus (RIP) of the monkey project directly to the vertical burst neurons in the rostral interstitial nucleus of the mlf (RI) , the horizontal burst neurons (EBN) in the dorsomedial nucleus reticularis pontis caudalis (PnC), and the dorsal paragigantocellular nucleus (DPGi) (Fig. 16.8) (Ohgaki *et al.*, 1989; Strassman *et al.*, 1987; for review, see Moschovakis *et al.*, 1996). Axons of the majority of omnipause neurons cross the midline. In the monkey, the omnipause neurons receive direct afferents from the deep layers of the rostral superior colliculus, which represents the fixation area (Büttner-Ennever *et al.*, 1999; Everling *et al.*, 1998). Only a few omnipause neurons project to the spinal cord (Robinson *et al.*, 1994). Single-cell reconstructions of horseradish peroxidase–filled, electrophysiologcially identified saccadic long-lead burst neurons (LBNs) in the oral pontine reticular nucleus (PnO) of the monkey revealed projections to the dorsomedial part of the PnC and the DPGi, which correspond to the EBN and IBN area, respectively, the nucleus reticularis tegmenti pontis (RtTg), and the nucleus reticularis gigantocellularis (Gi), which contains premotor neurons for head movements (Cowie *et al.*, 1994; Scudder *et al.*, 1996b).

Clinical Aspects

Experimental unilateral lesions of the saccadic burst neuron region in the pontine reticular formation result in ipsilateral gaze paralysis (Henn *et al.*, 1984; for review, see Zee, 1998). Selective experimental and pharmacological lesions of the omnipause neurons in monkey resulted in slowed saccades but not oscillations (Kaneko, 1996; Soetedjo *et al.*, 2002). From clinicopathological studies in human, it is not clear whether the slowing of saccades is due to lesions of the omnipause neurons or the adjacent excitatory burst neurons (Johnston *et al.*, 1993; Hanson *et al.*, 1986; Kato *et al.*, 1994). Theoretically, it is also possible that restricted lesions of the omnipause neurons may result in oscillations (ocular flutter and opsoclonus) (Leigh and Zee, 1999; Schon *et al.*, 2001). On the other hand, the analysis of cases with opsoclonus in patients who had suffered from lung carcinoma did not reveal any significant deficits of omnipause neurons (Büttner-Ennever and Horn, 1994; Wong *et al.*, 2001).

Nucleus of the Posterior Commissure (PCom)

Structure and Function

The nucleus of the posterior commissure (PCom) lies rostral to the deep layers of the colliculus superior and is closely associated with the fibers of the posterior commissure (Fig. 16.3C) (Paxinos and Huang, 1995, figures 63 and 64). Based on the cytoarchitecture and relationship to the fibers of the posterior commissure, five different cell groups were identified in the PCom of monkey and human (Kuhlenbeck and Miller, 1949; Carpenter and Peter, 1970): the principal part, the medially adjacent magnocellular part, which borders on the periaqueductal gray; and the rostral, subcommissural, and infracommissural parts, which all lie

within the periaqueductal gray. Usually in the oculomotor literature the term "nucleus of the posterior commissure" refers to the two largest groups, the magnocellular and principle parts. All parts consist of small and medium-sized neurons; only in the magnocellular part are large cells predominant (Bianchi and Gioia, 1993).

On the basis of clinical observations, the nucleus of the posterior commissure (PCom) has long been suspected as being involved in the generation of upward eye movements, since lesions in patients resulted in upward gaze paralysis (Christoff, 1974). To date the role of the PCom in vertical gaze has not been fully explained. In addition, lesions of the PCom result in lid retraction, indicating a role in the premotor control of the upper eyelid (Schmidtke and Büttner-Ennever, 1992; Averbuch-Heller, 1997).

Recording experiments in the macaque monkey revealed neurons in the PCom, which fire with upward saccades. In contrast to the burst neurons in the rostral interstitial nucleus of the mlf (RI), these saccade-related PCom neurons do not project to motoneurons of extraocular eye muscles but target on neurons in the contralateral PCom, the InC, the RI, and intralaminar thalamic nuclei. They are thought to play a role in modulating the vertical gaze integrator (Moschovakis *et al.*, 1996). The PCom has moderate acetylcholinesterase activity (Paxinos and Huang, 1995, figures 63 and 64). It contains GABAergic neurons, which project to the superior colliculus in the cat (Appell and Behan, 1990).

Connections

Fibers of the magnocellular part of the PCom project through the ventral part of the posterior commissure to the contralateral interstitial nucleus of Cajal (InC), the magnocellular part of the PCom, the rostral interstitial nucleus of the mlf (RI), and the supraoculomotor area (Su3), which is the region immediately dorsal to the oculomotor nucleus (Carpenter *et al.*, 1970; Grantyn, 1988, Büttner-Ennever and Büttner, 1988). In addition, descending fibers terminate in the paramedian pontine reticular formation, but sparsely in the spinal cord at cervical levels (Benevento *et al.*, 1977; Holstege, 1988; Satoda *et al.*, 2002). The PCom has reciprocal connections with the superior colliculus, and receives a strong input from the frontal eye fields of the cortex and the dentate nucleus of the cerebellum (Huerta and Harting, 1982; Leichnetz, 1982; Sugimoto *et al.*, 1982; Grantyn, 1988; Stanton *et al.*, 1988).

Clinical Aspects

In macaque monkeys experimental lesions of the PCom lead to an upward gaze paralysis often combined with lid retraction (Pasik *et al.*, 1969; Carpenter *et al.*, 1970). The same symptoms were observed in patients with lesions of the Pcom (Christoff, 1974). The reanalysis of clinicopathological cases with vertical gaze paralysis and lid retraction showed that the common lesioned area involved the posterior commissure and the PCom, whereas the lesions in cases with only vertical gaze paralysis and no lid retraction spared the nuclei and the fibers of the posterior commissure (Schmidtke and Büttner-Ennever, 1992).

Central Mesencephalic Reticular Formation

Structure and Function

A specific area of the mesencephalic reticular formation lateral to the oculomotor nucleus has been distinguished on account of its involvement in the control of saccades and was designated as central mesencephalic reticular formation (cMRF) (for review, see Cohen *et al.*, 1986). The cMRF lacks distinctive boundaries, but the saccade-related region lies caudal to the posterior commissure (pc) and overlaps the rostral portion of nucleus subcuneiformis in monkeys (Waitzman 2000a). It has been recently visualized, at least in part, by Chen and May (2000) using retrograde tracer substances: its rostral pole lies dorsolateral to the anterior tip of the red nucleus and ventrolateral to the interstitial nucleus of Cajal (InC). Stimulation in cMRF induces contralateral saccadic eye movements, and lesions cause transient deficits in contralateral gaze shifts (Cohen and Büttner-Ennever, 1984; Waitzman *et al.*, 1996). Single-unit recordings and the microinjection of a reversible inactivator (muscimol) revealed two subregions of the mesencephalic reticular formation (Waitzman, 2000a, b). The first was a ventrocaudal region corresponding to cMRF, from which inactivation caused contraversive, upward saccade, hypermetria, as well as destabilization of gaze fixation and head tilts. The more rostral subregion lay in the mesencephalic reticular formation lateral to the interstitial nucleus of Cajal (InC), and inactivation there caused hypometria of vertical saccades. The functional role of cMRF in gaze control is not clear, but three different hypotheses have been put forward: (1) saccade triggering; (2) a feedback system informing the superior colliculus about dynamic changes in gaze; or (3) a feedforward system from superior colliculus to pontine gaze centers. It may be that there are multiple functions connecting this region with cell populations supporting several different functions. As is often the case, descending afferents from the limbic structures have been seen to avoid the oculomotor-related regions of the reticular formation (Büttner-Ennever and Holstege, 1986; Holstege, 1990; figure 55). There is some evidence supporting the GABAergic nature of some neurons within cMRF (Chen and May, 2000).

Connections

A study of the efferent projections from the mesencephalic reticular formation in cat was reported by Edwards and de Olmos (1975). The cMRF has been shown to be a major target for superior colliculus output (Cohen and Büttner-Ennever, 1984; Harting *et al.,* 1980; Huerta and Harting, 1984; Chen and May, 2000), and reciprocal connections back to the superior colliculus were emphasized by Moschovakis *et al.* (1988a, b) and Chen and May (2000)—features that have an important role in the feedforward or feedback hypotheses. Additional afferents to cMRF arise from the paramedian pontine reticular formation (PPRF), and in the light of more recent research cMRF efferents are seen to project to the omnipause neurons (Büttner-Ennever, personal observation).

Superior Colliculus (SC)

Structure and Function

The superior colliculus (Fig. 16.1) is essential for the generation of an orienting response to an object of visual or auditory interest (Grantyn *et al.,* 1993). Pathways from the superior colliculus to the saccade generator and reticulospinal cells groups generate the eye and head movements, and have been documented in many studies (Harting, 1977; Harting *et al.,* 1980; Moschovakis, 1996; Moschovakis *et al.,* 1996; Olivier *et al.,* 1993; Isa and Sasaki, 2002). Electrical stimulation and recording studies in the superior colliculus demonstrate a topographical motor map for the saccadic eye movements (Robinson, 1972). Large saccades are represented caudally and small saccades rostrally, and rostrolaterally lies the "rostral pole of the saccadic motor map," a region described as the fixation zone in behavioral experiments (Munoz and Guitton, 1991; Munoz and Wurtz, 1993; Paré *et al.,* 1994). These physiological studies in cat and monkey report regional specializations in the rostral pole considered to promote gaze fixation, and there is some neuroanatomical evidence supporting this (Büttner-Ennever *et al.,* 1999; Sato and Ohtsuka, 1996; Ohtsuka and Nagasaka, 1999).

Histochemistry

The superior colliculus of monkeys and humans contains numerous neurons immunoreactive for the calcium-binding proteins calretinin, calbindin, and parvalbumin, but with differing distribution patterns throughout the layers (Leuba and Saini, 1996; McHaffie *et al.,* 2001; Soares *et al.,* 2001). Whereas the small calbindin-positive neurons represent predominantly interneurons, some of which are GABAergic, many of the large and medium-sized parvalbumin-containing neurons in the deep layers of the superior colliculus are projection neurons including predorsal bundle fibers, which innervate neurons of the saccadic premotor network in the pontine reticular formation (Mize, 1992, 1996). The deep layers of the superior colliculus contain fiber patches seen with acetylcholinesterase histochemistry (see Paxinos and Huang, 1995, figure 58). These patches overlap with neuron clusters that give rise to the tectoreticular pathways controlling the orientation of eye and head to alerting stimuli (Jeon and Mize, 1993; Mize, 1996). These neuron clusters were shown to receive transmitter specific afferents from the pedunculopontine tegmental nucleus (PPT) associated with attention (Zweig *et al.,* 1987), which contain acetylcholine and nitric oxide, and from the GABAergic cells in the substantia nigra pars reticulata (Harting *et al.,* 1991, 1992, 1997), which impose a tonic inhibition on the superior colliculus that pauses during saccades (Hikosaka and Wurtz, 1983). In cat, equal numbers of tectotectal fibers are GABAergic or glutamatergic with identical topographical distribution within the contralateral SC (Olivier *et al.,* 1993; Hardy, 2000).

Connections

The intermediate and deep layers of the superior colliculus are the origin of the tectospinal system. The descending collicular fibers decussate below the oculomotor nucleus in the "dorsal tegmental decussation" and run close to the midline in the "predorsal bundle." Collicular terminals were found in the nucleus reticularis tegmenti pontis (RtTg), the caudal pontine reticular nucleus (PnC), and the medullary reticular formation mainly ipsilaterally (Sparks and Hartwich-Young, 1989), and they project directly to upper cervical motoneurons in the spinal cord (May and Porter, 1992). Ascending projections target the interstitial nucleus of Cajal (InC) and the rostral interstitial nucleus of the mlf (RI). The premotor neurons of the levator palpebrae muscle in the M-group receive afferents only from the medial part of the SC, which mediates upgaze (Horn and Büttner-Ennever, 1998b). Afferents to the superior colliculus arise from many regions: cortical areas, thalamus, sensory trigeminal nucleus (including afferents related to the blink system), pedunculopontine tegmental nucleus, and substantia nigra. The afferents terminate in specific tiers, or sublayers, of the superior colliculus intermediate layer, and also are arranged in discrete clusters, whereby the sensory- and motor-related terminal clusters are interdigitated.

Clinical Aspects

In general, the superior colliculus has very little clinical significance, and drastic cell loss is not an unusual finding in geriatric material. Theoretically the degeneration of the superior colliculus should severely

affect the generation of saccades and postural changes during orienting responses. This is the case in "progressive supranuclear palsy" (PSP), where the superior colliculus is known to degenerate early in the course of the disease. PSP patients have severe difficulty in orienting to alerting stimuli (Rafal *et al.*, 1988).

Theoretically, the loss of fixation and occurrence of square-wave jerks reported in PSP patients (Fisk *et al.*, 1982) could also be a result of the degeneration of the superior colliculus in the "fixation zones"; but this association has not been investigated. Experiments have demonstrated that bicuculine injections into the rostral superior colliculus block the effects of GABA on superior colliculus neurons and cause intrusion saccades (Munoz and Wurtz, 1993).

Prepositus Hypoglossi Nucleus

Structure and Function

The prepositus hypoglossal nucleus (PrH) lies in the floor of the fourth ventricle between the abducens and the hypoglossal motor nuclei (Figs. 16.1 and 16.4L, M) (Brodal, 1983; Paxinos and Huang, 1995, figures 25–30; Paxinos *et al.*, 2000; abbreviated as Prin; figures 101–108). Caudally it contains two distinct regions. One consists of small neurons and merges into the nucleus intercalatus of Staderini (In; Paxinos and Huang, 1995, figures 20–24). The second is a large-celled region that joins with the nucleus of Roller (Ro; Paxinos and Huang, 1995, figures 21–25). The ubiquitous connections of prepositus to and from oculomotor structures have earned it the nickname "nucleus preposterous." These studies, along with physiological studies of cell activity in behaving animals, have led to the hypothesis that the PrH has an important roll in stabilizing horizontal components of eye movements, i.e., is part of the velocity-to-position integrator (McCrea, 1988; for review, see Fukushima and Kaneko, 1995).

Histochemistry

Immunocytochemical staining revealed few GABAergic small neurons scattered throughout the PrH in cat and monkey, but a high density of GABAergic terminals (Yingcharoen *et al.*, 1989; Straube *et al.*, 1991). Some GABAergic neurons might send projections to the superior colliculus (cat: Appell and Behan, 1990) or the dorsal cap of the inferior olive (de Zeeuw *et al.*, 1993). A major GABAergic projection from the PrH to the locus coeruleus is only shown in rat so far (Aston-Jones *et al.*, 1991). The Purkinje cells of the cerebellar flocculus provide one source of GABAergic afferents to the PrH (Yamamoto, 1978). In cat, approximately 30% of the neurons the PrH are glycine (GLY)–immunoreactive, most of them being small neurons representing local circuit and commissural neurons (McCrea and Baker, 1985; Yingcharoen *et al.*, 1989). Medium-sized glycinergic neurons in the PrH were shown to project to the contralateral abducens nucleus (Spencer *et al.*, 1989). Glycinergic terminals are found throughout the PrH deriving from intrinsic commissural connections, but also from saccadic inhibitory burst neurons of the dorsal paragigantocellular nucleus and the ipsilateral medial vestibular nucleus (Spencer *et al.*, 1989). The PrH of the monkey contains cholinergic neurons, some of which might represent projection neurons to the oculomotor nucleus (Carpenter *et al.*, 1992). In addition, a cholinergic projection from the PrH to the contralateral inferior olive has been demonstrated in rat and monkey (Barmack *et al.*, 1993), and to the contralateral cerebellar flocculus and ventral paraflocculus in rat and rabbit (Barmack *et al.*, 1992). Interestingly, numerous neurons in the PrH of cat and monkey express nitric oxide synthetase immunoreactivity, a marker for nitric oxide–releasing neurons (Satoh *et al.*, 1995; Moreno-Lopez *et al.*, 2001), which is required for the correct performance of eye movements (Moreno-Lopez *et al.*, 1996).

Connections

The small cells in the PrH are predominantly commissural or interneurons; the larger cells give rise to the projections to the oculomotor cell groups, such as the vestibular nuclei, the inferior olive, the superior colliculus, and the motor nuclei. Prepositus afferents supply the cerebellum and terminate in the vermis (lobuli VII, IX, and X), the flocculus ventral paraflocculus (tonsilla), and fastigial nuclei (McCrea, 1988; Belknap and McCrea, 1988). All areas that project to the abducens nucleus also project to the prepositus hypoglossal nucleus. In addition, it receives afferents from the fastigial nucleus, the pregeniculate nucleus of the diencephalon—which controls the flow of information entering and leaving the visual striate pathways via the lateral geniculate nucleus (see Chapter 33).

Clinical Aspects

A unilateral muscimol injection in the PrH of the cat resulted in a bilateral gaze-holding failure (Mettens *et al.*, 1994). Lesions involving the PrH in humans often lead to an upbeat or horizontal gaze-evoked nystagmus (for review, see Leigh and Averbuch-Heller, 1998).

Paramedian Tract Neurons

Structure and Function

Paramedian tract neurons (PMTs) are defined as groups of cerebellar-projecting neurons that lie around the midline fiber bundles of the pons and medulla. The

PMT groups have been brought to the attention of oculomotor neuroanatomists on account of their projection to the flocculus and ventral paraflocculus region, demonstrated in experimental tract-tracing experiments (Sato *et al.*, 1983; Blanks *et al.*, 1983; Langer *et al.*, 1985; Blanks, 1990). The homologue of the cell groups has not been described in humans, although nucleus pararaphales of Olszewski and Baxter (1954) may be part of it. The PMT groups could provide the flocculus and ventral paraflocculus of the cerebellum and other areas of the brain with a motor efference copy of the oculomotor output signal. Damage could lead to a disturbance in gaze holding (Büttner *et al.*, 1995).

There are at least six relatively separate PMT groups scattered in the medial longitudinal fasciculus, rostral to, and even within, the abducens nucleus. They continue back to the level of the hypoglossal nucleus (stars in Fig. 16.1). In cat, rat, and monkey they have been given different names by different investigators; we use the individual terms introduced by Langer and colleagues. The use of the nomenclature "medial" and "caudal" interstitial nuclei of the mlf for the PMT groups rostral or caudal to the abducens nucleus is unsatisfactory (as well as unwieldy), partly because they overlook fine differences in the cell grouping, at least in the primate, and also because often the prefix "medial" or "caudal" is dropped and then there is total confusion with the vertical premotor neurons of the rostral interstitial nucleus of the mlf (RI) and interstitial nucleus of Cajal (InC) (see "Interstitial Nucleus of Cajal").

Histochemistry

The transmitter content of the PMT groups is unknown: however, we have found that the cell somata are not serotonergic or catecholaminergic (Büttner-Ennever and Horn, personal observation). In addition, the PMT groups contain high levels of cytochrome oxidase and acetylcholinesterase. The neurons are chromophilic, medium-sized cells that lie immediately lateral to the smaller-celled raphe nuclei. The difference between them can be demonstrated by immunocytochemical stainings with serotoninantibodies, the raphe nuclei are labeled but the PMT groups are not.

Connections

Aside from their projection to the flocculus and ventral paraflocculus, the PMT groups have been shown to receive an afferent input from all the premotor brain stem nuclei known to project to oculomotor motoneurons (Büttner-Ennever and Büttner, 1988; Büttner-Ennever *et al.*, 1989; Büttner-Ennever and Horn, 1996). Several projections from oculomotor or vestibular structures to the PMT groups are mistakenly described in the literature as projections to raphe nuclei (e.g., nucleus raphe obscurus; see Chapter 33).

Clinical Aspects

Theoretically the PMT cell groups are thought to contribute to gaze holding (Büttner-Ennever and Horn, 1996). Lesions of the midline brain stem often cause nystagmus, and in some cases it is likely to be due to lesions of the PMT neurons rather than "lesions of vestibular structures," which is the usual hypothesis put forward (Baloh and Yee, 1989; Janssen *et al.*, 1998). Recently, reversible chemical lesions to PMT cell groups in cat caused a nystagmus, which fits well to the above hypothesis (Nakamagoe *et al.*, 1998). Therefore, PMT cell groups should be taken more into account in future clinical analyses of brain stem nystagmus.

EYELID AND BLINK

In humans and monkeys the oculomotor system interacts with the eyelid system: (1) Blink-evoking stimuli elicit transient eye closure, along with movements of the eye (e.g., Collewijn *et al.*, 1985; Evinger *et al.*, 1984). (2) Blinks coincide with large saccades, combined with head movements (Evinger *et al.*, 1991, 1994) and may affect vergence movements as well (Rambold *et al.*, 2002). (3) Vertical eye movements are accompanied by synchronous movements of the upper eyelid (Becker and Fuchs, 1988).

The function of the eyelids is to protect the eyeball without interfering with vision and to keep the eyes wet, which is achieved by intermittent spontaneous brief blinks in the alert state, or by lid closing during sleep. The eyelids are mainly moved by the interaction of two muscles: the levator palpebrae muscle, which elevates the lid, and the orbicularis oculi muscle, which closes the eye. A third muscle, the smooth superior tarsal muscle (Müller`s muscle), contributes to retraction of the upper lid and is innervated by the sympathetic superior cervical ganglion (Van der Werf *et al.*, 1993; for review, see Sibony and Evinger, 1998). In the awake state the levator palpebrae motoneurons receive a tonic excitatory input (of unknown origin), which keeps the eye open. With increasing fatigue the activity of levator palpebrae motoneurons drops, resulting in eye closure, and indicating a change in the influence of the afferent limbic signals on levator palpebrae motoneurons. On top of this basic behavior the levator palpebrae motoneurons receive excitatory signals that synchronize lid movements with vertical eye movements, which are only interrupted during blinks. Whereas some data on the premotor circuitry of the eye closing orbicularis oculi muscle are available, information about the premotor control of the levator

palpebrae muscle during different types of lid movements is still scarce (Fig. 16.9A, B).

Lid–eye Movements (Fig. 16.9A)

During all types of vertical eye movements the upper eyelid closely follows the globe, providing protection but avoiding obstruction of vision. Thereby, the upper eyelid is elevated by activation of the levator palpebrae muscle, but lowered exclusively by passive downward forces resulting from a decrease in levator palpebrae activity without involvement of the orbicularis oculi muscle (for review, see Sibony and Evinger, 1998). The close coordination of lid movements with vertical eye movements must be mediated by common premotor neurons. Recently, a premotor cell group was identified in the rostral mesencephalon, termed M-group, which projects to motoneurons of the upper eyelid and those of upward pulling eye muscles and is therefore proposed as a structure controlling lid–eye coordination in upgaze (Figs. 16.3A, B and 16.5A, B) (Horn *et al.*, 2000).

Blinks (Fig. 16.9B)

In mammals blinking occurs through the interaction of two lid muscles, the levator palpebrae muscle and the orbicularis oculi muscle. During a blink the nervous system briefly inhibits the tonic activity of the levator palpebrae motoneurons, which is followed by a transient activity burst in the motoneurons of the orbicularis oculi muscle resulting in a fast eye closure. When the orbicularis oculi motoneurons cease discharging, the levator palpebrae motoneurons resume their tonic activity (for review, see Sibony and Evinger, 1998). The orbicularis oculi muscle response in the (trigeminally evoked) blink reflex consists of two electromyographic components, an early R1 and a late R2 response, which are both generated by the same orbicularis oculi muscle motoneurons, with the R2 component producing most of the lid closure in human (Shahani and Young, 1972). Both components are mediated by different routes: an oligosynaptic path through the sensory trigeminal nuclei for R1 and a polysynaptic path involving neurons in the reticular formation for R2 (for review, see Sibony and Evinger, 1998). A blink can be evoked by different stimuli, e.g., auditory, visual, or tactile, all of whose pathways project on premotor neurons of the orbicularis oculi muscle lying in the trigeminal nuclei, in the lateral part of the pontine reticular formation, in the medullary reticular formation, and in the red nucleus (for review, see Holstege, 1990, 1991; Sibony and Evinger 1998. Since the primates do not have a retractor bulbi muscle, which is present in most mammals and pulls the eyes back into the orbit during blinks, the connections of its motoneurons are not considered here (for review, see Holstege, 1990).

Central Caudal Nucleus (CeCa)

Structure and Function

In primates, the levator palpebrae motoneurons lie in the central caudal nucleus (CeCa), a compact unpaired nucleus situated dorsal to the caudal pole of the oculomotor nucleus in human (Schmidtke and Büttner-Ennever, 1992) (Fig. 16.1; Fig. 16.3E–G; Fig. 16.6C, D). Within the CeCa the motoneurons of both eyelids appear intermixed. There are conflicting reports as to whether some levator palpebrae motoneurons innervate the muscles of both sides (Sekiya *et al.*, 1992; van der Werf *et al.*, 1997), or whether each motoneuron innervates only the levator palpebrae of one side (Porter *et al.*, 1989).

Histochemistry

The central caudal nucleus (CeCa) is discernible in parvalbumin immunostaining, with less involvement of the neuropil compared to the motoneurons of the extraocular eye muscles (Fig. 16.6D). In addition, the motoneurons in the CeCa neurons are smaller than those of the extraocular eye muscles (Figs. 16.3F, G and 16.6C, D). The motoneurons receive a strong supply of GABA-immunoreactive terminals and are very specifically associated with glycine transporter immunoreactivity, indicating glycinergic afferents (Horn, personal observations).

Connections

In the primate the central caudal nucleus was shown to receive afferents from the interstitial nucleus of Cajal, from the nucleus of the posterior commissure (May, 1995), and from a small group medial to the rostral interstitial nucleus of the mlf (RI), which was called M-group (Fig. 16.3A, B) (Horn *et al.*, 2000). Studies in rabbit and monkey revealed projections from neurons at the rostral border of the principal and spinal trigeminal nucleus (pars oralis) to the central caudal nucleus, which presumably provide the inhibition during blinks (May, 1995).

Clinical Aspects

Midbrain lesions affecting the central caudal nucleus lead to ptosis, which is usually bilateral (Averbuch-Heller, 1997; Büttner-Ennever *et al.*, 1996b). A lesion anywhere in the brain stem sympathetic chain or superior cervical ganglion affects the innervation of

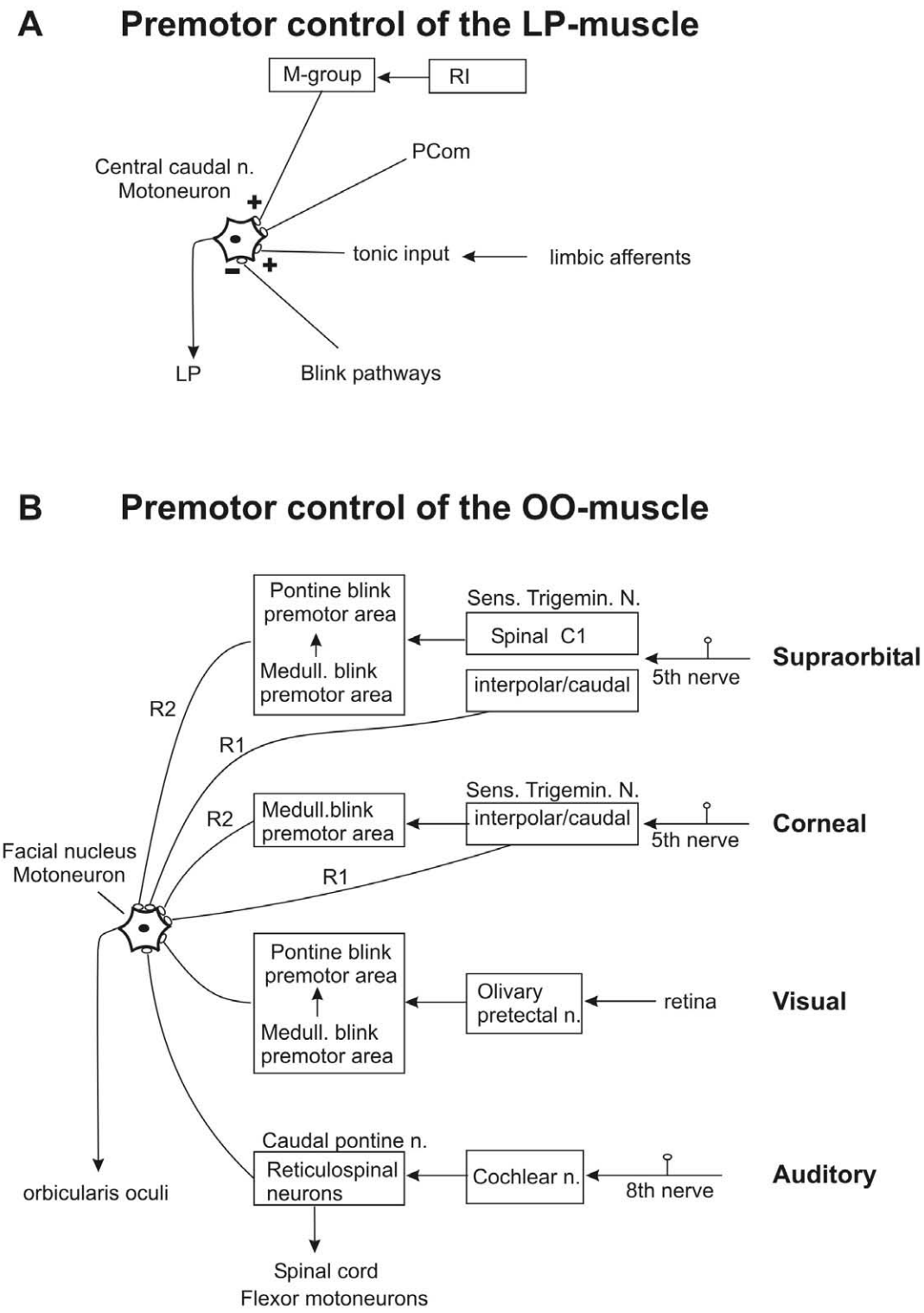

FIGURE 16.9 **A:** Diagrammatic representation of the premotor inputs controlling levator palpebrae motoneurons. **B:** A summary diagram of the premotor networks controlling the orbicularis oculi muscle in blink reflex generation. The blink response of the supraorbitally and corneally evoked blink reflex consists of a short-latency R1 response mediated by a three-neuron arc, whereas the long-latency R2 response uses polysynaptic connections for activation of the orbicularis oculi muscle. LP, levator palpebrae muscle; N., nucleus; PCom, nucleus of the posterior commissure; RI, rostral interstitial nucleus of the medial longitudinal fascicle.

the superior tarsal muscle (Müller`s muscle) and produces Horner`s syndrome, which is characterized by a mild, unilateral ptosis (for review, see Sibony and Evinger, 1998).

Facial Nucleus (7N)—Orbicularis Oculi Motoneurons

Structure and Function

The facial nucleus (7N) lies in the caudal pontine tegmentum lateral and ventral to the abducens nucleus (6N), medial to the spinal trigeminal nucleus, and dorsal to the nuclei of the superior olive (Fig. 16.4J, M) (Paxinos and Huang, 1995, figures 31–33). It is divided into several groups extending through the rostrocaudal length of the nucleus, each containing the motoneurons of the ipsilateral individual facial muscles. All subnuclei contain small and large neurons, presumably representing γ motoneurons innervating muscle spindles and α-motoneurons, respectively (Welt and Abbs, 1990). Retrograde tracing experiments in macaque monkeys demonstrated that the motoneurons of the orbicularis oculi muscle lie in the rostral two-thirds of the nucleus within the dorsal subgroup (Satoda *et al.*, 1987; Porter *et al.*, 1989; Welt and Abbs, 1990), those for the frontalis muscle in the dorsomedial subdivision (Welt and Abbs, 1990). Using the nomenclature of Courville, the motoneurons of the orbicularis oculi muscle lie in the intermediate nucleus in human (Courville, 1966; Paxinos and Huang, 1995, figure 31; Olszewski and Baxter, 1954, plate 18).

Histochemistry

As other motor nuclei, the facial nucleus can be easily identified by its strong acetylcholinesterase activity pattern (Paxinos and Huang, 1995, figure 32). The nucleus expresses moderate cytochrome oxidase activity, primarily in the neuropil. The parvalbumin immunoreactivity of the neurons is more confined to the cell bodies and does not involve the neuropil as in the oculomotor nuclei (Fig. 16.4M). The neurons of the facial nucleus of the cat receive catecholaminergic afferents from the locus coeruleus and nucleus parabrachialis lateralis, cholinergic afferents from an area ventral to the nucleus of the solitary tract, and methionine-, enkephalin-, and substance P–immunoreactive afferents (Fort *et al.*, 1989). In addition, the facial nucleus receives a dense supply with serotonergic fibers and terminals, which originate from neurons in the raphe magnus, raphe obscurus, and raphe pallidus and may adjust the excitability of facial motoneurons (McCall and Aghajanian, 1979; Fort *et al.*, 1989; Aghajanian and McCall, 1980).

Connections

There is anatomical evidence that the facial nucleus contains not only motoneurons innervating the facial muscles but also smaller neurons projecting to the cerebellar flocculus (Roste, 1989), which mainly arise from caudal parts of the facial nucleus in the monkey (Langer *et al.*, 1985). Retrograde tracing studies in different animals revealed several pools of neurons in the brain stem, which innervate the facial nucleus. Here only those projecting to orbicularis oculi motoneurons are considered (for review, see Sibony and Evinger, 1998; Holstege, 1990): the ventrolateral part of the spinal trigeminal nuclei, the dorsolateral pontine tegmentum, the ventral part of the lateral pontine tegmental field, the medial tegmentum at levels of the hypoglossal nucleus, and the red nucleus (Holstege *et al.*, 1986a, b). A recent transneuronal study in the rat describes a stronger input from the reticular regions than from trigeminal nuclei, in addition to afferents from the parabrachial nuclei, from the interpositus nucleus of the cerebellum, and from the dorsolateral quadrant of the red nucleus (Morcuende *et al.*, 2002). In the rat, facial motoneurons receive collaterals from descending fibers, which originate in giant neurons in the caudal pontine reticular formation and activate motoneurons of the flexors in the spinal cord. These giant reticular neurons receive direct projections from the cochlear nucleus and may represent part of the afferent limb of the circuit for auditory evoked blink reflexes as part of a more general startle response to loud noises (Fig. 16.9B) (for review, see Sibony and Evinger, 1998).

M-Group

Structure and Function

Recently, a small cell group was identified in the rostral mesencephalon of the primate, which contains premotor neurons of the upward-pulling extraocular eye muscles, superior rectus and inferior oblique muscles, and of the levator palpebrae muscle, which elevates the upper eyelid, as well as the frontalis muscle motoneurons. The premotor cells were termed M-group (Fig, 16.3A, B) (Horn *et al.*, 2000). The observed projection pattern implicates a role in the coordinated activation of the upper eyelid during vertical eye movements.

In macaque monkeys and humans the M-group lies as a separate cell group immediate medially to the caudal third of the rostral interstitial nucleus of the mlf (RI), whereas in cat the homologue premotor neurons were identified within the medial RI (Chen and May, 2002) (Fig. 16.3A, B). In contrast to the neurons of

the RI, which belong to the mesencephalic reticular formation, the M-group is part of the central gray, which surrounds the third ventricle and is composed of more densely packed cells. As the RI the M-group is highlighted by its strong cytochrome oxidase activity and its high parvalbumin content mainly of the neuropil, which was used to identify the homologue in the human brain as well (Figs. 16.3B and 16.5A, B) (Horn *et al.*, 2000).

Connections

Anterograde tract tracing experiments in macaque monkeys showed that the M-group projects to the motoneurons of the levator palpebrae muscle in the central caudal nucleus and the motoneurons of the superior rectus and inferior oblique muscle, that elevate the eye, but not those that depress the eye. Additional weaker projections target the dorsomedial group of the facial nucleus containing motoneurons of the frontalis muscle, which participates in extreme upward gaze (Welt and Abbs, 1990; Sibony and Evinger, 1998; Horn *et al.*, 2000). The M-group receives a strong projection from the medial part of the deep layers of the superior colliculus, which encodes upward saccades. Additional weaker afferent projections arise from the medial and superior vestibular nuclei and the interstitial nucleus of Cajal (Horn and Büttner-Ennever, 1998b).

Clinical Aspects

A selective destruction should lead to a dissociation of lid and eye movements, manifesting as pseudoptosis on attempted downgaze or lid lag during vertical gaze, as is indeed seen in a patient with a lesion involving the M-group region (Galetta *et al.*, 1996). The post-mortem analysis of a case with downgaze paralysis and ptosis, but preserved upgaze, revealed a partial RI lesion, which included the M-group. Since upgaze was not affected, these results show that the M-group is not alone generating upward eye movements (Büttner-Ennever *et al.*, 1996b).

Sensory Trigeminal Nuclei

Structure and Function

The sensory trigeminal complex is composed of several nuclei, from rostral to caudal: the principal sensory nucleus (Pr5) lying lateral to the motor trigeminal nucleus (Paxinos and Huang, 1995, figures 35–37) and the spinal trigeminal nucleus consisting of the oral part (Sp5O), the interpolar part (Sp5OI) (Paxinos and Huang, 1995, figures 17–30), and the caudal part (Sp5C) (Paxinos and Huang 1995, Appendix Liu, figures 6–16, see Chapters 29 and 28).

Primary afferents from the cornea terminate heavily in the ventrolateral portion at the junction of the interpolar and caudal spinal trigeminal nuclei, and only sparsely in the dorsal horn of the spinal cord of C1–C3, and not in the principal trigeminal nucleus (Panneton and Burton, 1981). The afferents from the supraorbital nerve supplying periocular structures terminate also primarily at the junction of the interpolar and caudal spinal trigeminal nucleus, but in addition to the principal trigeminal nucleus and the spinal cord dorsal horn at C1. The principal oral and interpolar parts of the sensory trigeminal nuclei are interconnected and send direct projections to the orbicularis oculi muscle motoneurons in the facial nucleus (Fig. 16.9B), representing the central link of the three-neuron arc, which contributes to the early R1 component of the blink response. The late R2 response is presumably initiated at the dorsal horn of the spinal cord at C1 and involves polysynaptic pathways involving the medullary reticular formation (for review, see Sibony and Evinger, 1998). In humans the principal trigeminal nucleus is suspected to be the source of afferents to the orbicularis oculi muscle motoneurons (Ongerboer de Visser, 1983).

Connections

In general, the principal and spinal trigeminal nucleus projects to the thalamus, the cerebellar cortex and the nucleus interpositus, the dorsal red nucleus, and the deep layers of the superior colliculus (Holstege *et al.*, 1986b). Neurons in the interpolaris and caudal part of the spinal trigeminal nucleus project to the orbicularis oculi motoneurons in the facial nucleus (Fig. 16.9) (Tamai *et al.*, 1986; Pellegrini *et al.*, 1995) This pathway is presumably excitatory, since no glycinergic or GABAergic projection neurons to the facial nucleus were found in the rat (Li *et al.*, 1997). Anterograde tracing experiments in the rabbit revealed projections from the principal sensory trigeminal nucleus and interpolar part of the spinal trigeminal nucleus to orbicularis oculi muscle motoneurons in the facial nucleus *and* to the region of levator palpebrae motoneurons in the oculomotor nucleus (van Ham and Yeo, 1996). The trigeminofacial projections in cat lack a parallel input to levator palpebrae motoneurons (Holstege, 1990). The blink interneurons in the sensory trigeminal nuclei are modulated by inhibitory inputs from serotoninergic projections from the nucleus raphe magnus, which in turn is controlled by afferents from the superior colliculus (for review, see Sibony and Evinger, 1998).

Clinical Aspects

Lesions involving the spinal trigeminal nucleus at the interpolaris/caudalis border and the adjacent reticular formation disrupt corneal reflex blinks in

human (Ongerboer de Visser, 1980, 1983). In Parkinson's disease, the blink rate is increased, presumably due to an increased excitability of the facial motoneurons. The following hypothesis is suggested: The dopamine deficit in the substantia nigra results in an increased inhibition of the superior colliculus by the GABAergic projections from the substantia nigra pars reticulata. This results in reduced excitation of the raphe magnus from the superior colliculus leading to reduced inhibition of the spinal trigeminal nucleus from the serotonergic neurons of the raphe nuclei, which produces increased excitability of the trigeminally evoked blink reflex (Basso and Evinger, 1996a; Basso *et al.*, 1996b; for review, see Sibony and Evinger, 1998).

Pontine Lateral Tegmental Field (Pontine Blink Premotor Area)

Structure and Function

Retrograde tracer injections in the facial nucleus, including the orbicularis oculi subdivision, revealed premotor neurons in the ventrolateral pontine tegmental field at the level of the motor trigeminal nucleus ventral to it, but not in the sensory trigeminal nuclei (Holstege, 1990). This area was called the pontine blink premotor area (Holstege *et al.*, 1986a) and together with the medullary blink premotor area is proposed to contribute to the R2 response.

Connections

In the rabbit neurons of the lateral pontine tegmental field *(pontine blink premotor area)* and the ventral sensory trigeminal nucleus project to levator palpebrae and superior rectus motoneuronal groups in the oculomotor nucleus (Guerra-Seijas *et al.*, 1993). A similar projection is described in cats and primates arising from neurons forming a continuous column at the rostral border of the principal and oral part of the sensory trigeminal nuclei (May, 1995). Data from the rat and cat suggest that this projection is inhibitory (Li *et al.*, 1997) and could provide the inhibition of levator palpebrae motoneurons during blinks.

In cat the pontine blink premotor area receives inputs from the olivary pretectal nucleus, which is innervated by retinal afferents, and may function as a luminance detector (Gamlin *et al.*, 1995), thereby forming the afferent arc of the visually evoked blink reflex (Takada *et al.*, 1984) (see Fig. 16.9B). In all nonprimate species the pretectal olivary nucleus has direct projections to facial motoneurons (Takada *et al.*, 1984). In addition, the pontine blink premotor area receives afferents from the facial motor cortex (for review, see Sibony and Evinger, 1998).

Medullary Medial Tegmental Field (Medullary Blink Premotor Area)

Structure and Function

In the cat the medullary medial tegmental field containing premotor neurons of the orbicularis oculi muscle lies ventral to the hypoglossal nucleus around the midline, and was called medullary blink premotor area (Holstege, 1990). Like the *pontine blink premotor area,* it does not include the spinal trigeminal nucleus. Lesion studies in humans (Kimura and Lyon, 1972; Ongerboer de Visser and Kuypers, 1978) and experimental studies (Pellegrini *et al.*, 1995) indicate that this region along with the *pontine blink premotor area* is important for the generation of the R2 response.

Connection

The medullary medial tegmental field, which might include the *medullary blink premotor area,* receives afferent projections from the intermediate and deep layers of the superior colliculus (for review, see Holstege, 1990). In addition, the medullary medial tegmental field projects to the *pontine blink premotor area,* mainly bilateral (Holstege *et al.*, 1986b). A strong afferent input to the *medullary blink premotor area* arises from the paramedian pontine reticular formation and the upper medullary medial tegmentum. Both structures receive afferent projections from the superior colliculus, thereby forming a possible anatomical link for blink–saccade interaction (for review, see Holstege, 1990; Sibony and Evinger, 1999).

Red Nucleus

Structure and Function

The red nucleus (RPC) is a large round cell group in the mesencephalon dorsomedial to the substantia nigra (Figs. 16.1 and 16.3C). It is composed of a magnocellular part, which is very small in the human, occupying only the caudal pole, and a parvocellular part, from which a dorsomedial portion with more densely packed cells can be separated (Paxinos and Huang, 1995, figure 63). Experimental data suggest that the red nucleus is more involved in the learned blink response, after classical conditioning with neutral stimuli (visual, auditory), since lesions of the red nucleus abolish the conditioned, but not the unconditioned, blink reflex (for review, see Holstege, 1991).

Connections

Tracing studies (for review, see Holstege, 1991) in the cat revealed a weak projection from the dorsal part of the red nucleus, which corresponds to the facial

part of the red nucleus, to the *pontine* and *medullary blink premotor areas* areas. In addition, a weak direct projection to the orbicularis oculi muscle portion of the facial nucleus was found in the cat (Holstege and Tan, 1988). The dorsolateral part of the red nucleus receives afferent projections from the trigeminal nucleus and the interpositus nucleus of the cerebellum, thereby providing a pathway for the conditioned blink response (Holstege *et al.*, 1986b).

Blink–Saccade Interaction

Large saccadic gaze shifts are accompanied by blinks (Evinger *et al.*, 1991, 1994). Several observations in patients indicate an interaction between blink and saccadic circuits; a blink can induce oscillations in saccades (Hain *et al.*, 1986), or patients with abnormally slow saccades can facilitate their saccadic eye movements with voluntary blinks (Leigh *et al.*, 1983; Zee *et al.*, 1983). Although the circuits for gaze-evoked blinks are unknown, there is some evidence that saccadic omnipause neurons (OPNs; see "Pontine Lateral Tegmental Field Britine Blink Premotor Area") may act on blink circuits: microstimulation of OPNs suppresses reflex blinks in monkeys (Mays and Morrisse, 1995) and rats (Basso *et al.*, 1996a) and the activity of OPNs pauses during blinks in the same way as during saccades (Mays and Morrisse, 1994). Recent data indicate that the blink circuits may act at the level of the superior colliculus, since the activity of saccade-related burst neurons in the deep layers of the superior colliculus is transiently suppressed if a reflex blink is evoked (Goossens and van Opstal, 2000a, b). Electrical stimulation studies showed that the least effective site in the superior colliculus for eliciting blink suppression is the rostral pole—a region associated with fixation and accommodation and possessing direct projections to the OPNs (Gnadt *et al.*, 1997; Ohtsuka and Nagasaka, 1999; Büttner-Ennever *et al.*, 1999).

References

Aghajanian, G. K., and McCall, R. B. (1980). Serotonergic synaptic input to facial motoneurons: localization by electronmicroscopic autoradiography. *Neuroscience.* **5,** 2155–2162.

Appell, P. P., and Behan, M. (1990). Sources of subcortical GABAergic projections to the superior colliculus in the cat. *J. Comp. Neurol.* **302,** 143–158.

Aston-Jones, G., Shipley, M.T., Chouvet, G., Ennis, M., van Blockstaele E.J., Pieribone, V.A., Shiekhattar, R., Akaoka, H., Drolet, G., Astier, Bl., Charlety, P. Valentino, R.J., and Williams, J.T. (1991). Afferent regulation of the locus coeruleus neurons: anatomy, physiology and pharmacology. *Prog. Brain Res.* **88,** 47–75.

Averbuch-Heller, L. (1997). Neurology of the eyelids. *Curr. Opin. Ophthalmol.* **8,** 27–34.

Baker, R., and Highstein, S. M. (1978). Vestibular projections to medial rectus subdivision of oculomotor nucleus. *J. Neurophysiol.* **41,** 1629–1646.

Barmack, N.H., Baughman, R.W., and Eckenstein, F.P. (1992). Cholinergic innervation of the cerebellum of rat, rabbit, cat, and monkey as revealed by choline acetyltransferase activity and immunohistochemistry *J. Comp. Neurol.* **317,** 233–249.

Barmack, N.H., Fagerson, M., and Errico, P. (1993). Cholinergic projection to the dorsal cap of the inferior olive of the rat, rabbit, and monkey. *J. Comp. Neurol.* **328,** 263–281.

Baloh, R. W., and Yee, R. D. (1989). Spontaneous vertical nystagmus. *Rev. Neurol.* (Paris) **145,** 527–532.

Basso, M.A., and Evinger, C. (1996a). An explanation for blink reflex hyperexcitability in Parkinson's disease. II. Ncl. raphe magnus. Superior colliculus. *J. Neurosci.* **16,** 7318–7330.

Basso, M.A., Powers, A.S., and Evinger, C. (1996b). An explanation for blink reflex hyperexcitability in Parkinson's disease. I. Superior colliculus. *J .Neurosci.* **16,** 7300–7317.

Becker, W., and Fuchs, A.F. (1988). Lid–eye coordination during vertical gaze changes in man and monkey. *J. Neurophysiol.* **60,** 1227–1252.

Belknap, D. B., and McCrea, R. A. (1988). Anatomical connections of the prepositus and abducens nuclei in the squirrel monkey. *J. Comp. Neurol.* **268,** 13–28.

Benevento, L. A., Rezak, M., and Santos-Anderson, R. (1977). An autoradiographic study of the projections of the pretectum in the rhesus monkey *(Macaca mulatta):* evidence for sensorimotor links to the thalamus and oculomotor nuclei. *Brain Res.* **127,** 197–218.

Bianchi, R., and Gioia, M. (1990). Accessory oculomotor nuclei of man. 1. The nucleus of Darkschewitsch: a Nissl and Golgi study. *Acta Anat.* **139,** 349–356.

Bianchi, R., and Gioia, M. (1991). Accessory oculomotor nuclei of man. 2. The interstitial nucleus of Cajal—a Nissl and Golgi study. *Acta Anat.* **142,** 357–365.

Bianchi, R., and Gioia, M. (1993). Accessory oculomotor nuclei of man. 3. The nuclear complex of the posterior commissure—a Nissl and Golgi study. *Acta Anat.* **146,** 53–61.

Blanks, R. H. I. (1990). Afferents to the cerebellar flocculus in cat with special reference to pathways conveying vestibular, visual (optokinetic) and oculomotor signals. *J. Neurocytol.* **19,** 628–642.

Blanks, R. H. I., Precht, W., and Torigoe, Y. (1983). Afferent projections to the cerebellar flocculus in the pigmented rat demonstrated by retrograde transport of horseradish peroxidase. Exp. *Brain Res.* **52,** 293–306.

Brodal, A. (1981). "Neurological Anatomy." Oxford University Press, Oxford.

Brodal, A. (1983). The perihypoglossal nuclei in the macaque monkey and the chimpanzee. *J. Comp. Neurol.* **218,** 257–269.

Brodal, A. (1957) "The Reticular Formation of the Brain Stem. Anatomical Aspects and Functional Correlations." The William Ramsay Henderson Trust, London.

Büttner, U., and Büttner-Ennever, J. A. (1988). Present concepts of oculomotor organization. *In* "Neuroanatomy of the Oculomotor System" (J.A. Büttner-Ennever, ed.), pp. 3–32. Elsevier, Amsterdam.

Büttner, U., Helmchen, C., and Büttner-Ennever, J. A. (1995). The localizing value of nystagmus in brain stem disorders. *Neuro-Ophthalm.* **15,** 283–290.

Büttner, U., Büttner-Ennever, J. A., and Henn, V. (1977). Vertical eye movement related activity in the rostral mesencephalic reticular formation of the alert monkey. *Brain Res.* **130,** 239–252.

Büttner-Ennever, J. A. (2000). Overview of the vestibular system: Anatomy. *In* "Neurochemistry of the Vestibular System." (A.J. Beitz, and J.H. Anderson, eds.), pp. 3–24. CRC Press, Boca Raton.

Büttner-Ennever, J. A., and Akert, K. (1981). Medial rectus subgroups of the oculomotor nucleus and their abducens internuclear input in the monkey. *J. Comp. Neurol.* **197,** 17–27.

Büttner-Ennever, J.A., and Büttner, U. (1988). The reticular formation. *In* "Neuroanatomy of the Oculomotor System" (J.A. Büttner-Ennever, ed.), pp. 119–176. Elsevier, Amsterdam.

Büttner-Ennever, J. A., and Holstege, G. (1986). Anatomy of premotor centers in the reticular formation controlling oculomotor, skeletomotor and autonomic motor systems. *Prog. Brain Res.* **64 ,** 89–98.

Büttner-Ennever, J. A., and Horn, A. K. E. (1994). Neuroanatomy of saccadic omnipause neurons in nucleus raphe interpositus. *In* "Contemporary Ocular Motor and Vestibular Research: A Tribute to David A. Robinson. [Session VII]," (A.F. Fuchs, *et al.,* eds.), pp. 488–495. Thieme Medical, New York.

Büttner-Ennever, J. A., and Horn, A. K. E. (1996). Pathways from cell groups of the paramedian tracts to the floccular region. *N. Y. Acad. Sci.* **781,** 532–540.

Büttner-Ennever, J. A., and Horn, A. K. E. (1997). Anatomical substrates of oculomotor control. *Curr. Opin Neurobiol.* **7,** 872–879.

Büttner-Ennever, J. A., and Lang, W. (1981). Vestibular projections to the monkey thalamus and rostral mesencephalon: an autoradiographic study. "The Vestibular System: Function and Morphology," Vol. 8 (T. Gualtierotti, ed.), pp. 130–143. Springer-Verlag, Berlin.

Büttner-Ennever, J.A., Grob, P., Akert, K., and Bizzini, B. (1981). Transsynaptic retrograde labeling in the oculomotor system of the monkey with 125I tetanus toxin BIIb fragment. *Neurosci. Lett.* **26,** 233–238.

Büttner-Ennever, J. A., Büttner, U., Cohen, B., and Baumgartner, G. (1982). Vertical gaze paralysis and the rostral interstitial nucleus of the medial longitudinal fasciculus. *Brain* **105,** 125–149.

Büttner-Ennever, J. A., Cohen, B., Pause, M., and Fries, W. (1988). Raphe nucleus of the pons containing omnipause neurons of the oculomotor system in the monkey, and its homologue in man. *J. Comp. Neurol.* **267,** 307–321.

Büttner-Ennever, J. A., Horn, A. K. E., and Schmidtke, K. (1989). Cell groups of the medial longitudinal fasciculus and paramedian tracts. *Rev. Neurol. (Paris)* **145,** 533–539.

Büttner-Ennever, J. A., Cohen, B., Horn, A. K. E., and Reisine, H. (1996a). Efferent pathways of the nucleus of the optic tract in monkey and their role in eye movements. *J. Comp. Neurol.* **373,** 90–107.

Büttner-Ennever, J.A., Jenkins, C., Armin-Parsa, H., Horn, A.K.E., and Elston, J.S. (1996b). A neuroanatomical analysis of lid–eye coordination in cases of ptosis and downgaze paralysis. *Clin. Neuropathol.* **15,** 313–318.

Büttner-Ennever, J.A., Horn A.K.E., Henn, V., and Cohen B. (1999). Projections from the superior colliculus motor map to omnipause neurons in monkey. *J. Comp. Neurol.* **413,** 55–67.

Büttner-Ennever, J.A., Horn A.K.E., Scherberger, H., and d`Ascanio, P (2001). A dual motor innervation of extraocular muscles from the abducens, trochlear and oculomotor nuclei of monkey. *J. Comp. Neurol.* **438,** 318–335.

Cannon, S.C., and Robinson, D.A. (1987). Loss of the neural integrator of the oculomotor system from brain stem lesions in monkey. *J. Neurophysiol.* **57,** 1383–1409.

Carpenter, M. B., and Peter, P. (1970). Accessory oculomotor nuclei in the monkey. *J. Hirnforsch.* **12,** 405–418.

Carpenter, M. B., Harbison, J. W., and Peter, P. (1970). Accessory oculomotor nuclei in the monkey: projections and effects of discrete lesions. *J. Comp. Neurol.* **140,** 131–154.

Carpenter, M. B., Periera, A. B., and Guha, N. (1992). Immunocytochemistry of oculomotor afferents in the squirrel monkey *(Saimiri Sciureus). J. Hirnforsch.* **33,** 151–167.

Chen-Huang, Ch., and McCrea, R. A. (1998). Contribution of vestibular nerve irregular afferents to viewing distance-related changes in the vestibulo-ocular reflex. *Exp. Brain Res.* **119,** 116–130.

Chen, B., and May, P.J. (2000). The feedback circuit connecting the superior colliculus and central mesencephalic formation: a direct morphological demonstration. *Exp. Brain Res.* **131,** 10–21.

Chen, B., and May, P.J. (2002). Premotor circuits controlling eyelid movements in conjunction with vertical saccades in the cat: I. The rostral interstitial nucleus of the medial longitudinal fasciculus. *J. Comp. Neurol.* **450,** 183–202.

Christoff, N. (1974). A clinicopathologic study of vertical eye movements. *Arch. Neurol.* **31,** 1–8.

Cohen, B., and Büttner-Ennever, J. A. (1984). Projections from the superior colliculus to a region of the central mesencephalic reticular formation (cMRF) associated with horizontal saccadic eye movements. *Exp. Brain Res.* **57,** 167–176.

Cohen, B., and Komatsuzaki, A. (1972). Eye movements induced by stimulation of the pontine reticular formation. Evidence for integration in oculomotor pathways. *Exp. Neurol.* **36,** 101–117.

Cohen, B., Waitzmann, D. M., Büttner-Ennever, J. A., and Matsuo, V. (1986). Horizontal saccades and the central mesencephalic reticular formation. *Brain Res.* **64,** 243–255.

Collewijn, H., van der Steen, J., and Steinman, R. M. (1985). Human eye movements associated with blinks and prolonged eyelid closure. *J. Neurophysiol.* **54,** 11–27.

Courville, J. (1966). The nucleus of the facial nerve: the relation between cellular groups and peripheral branches of the nerve. *Brain Res.* **1,** 338–354.

Cowie, R.J., and Robinson, D.L. (1994) Subcortical contributions to head movements in macaques. I. Contrasting effects of electrical stimulation of a medial pontomedullary region and the superior colliculus. *J. Neurophysiol.* **72,** 2648–2664.

Cowie, R. J., Smith, M. K., and Robinson, D. L. (1994). Subcortical contributions to head movements in macaques. II. Connections of a medial pontomedullary head-movement region. *J. Neurophysiol.* **72,** 2665–2682.

Crawford, J. D., and Vilis, T. (1992). Symmetry of oculomotor burst neuron coordinates about listing's plane. *J. Neurophysiol.* **68,** 432–448.

Crossland, W. J., Hu, X. J., and Rafols, J. A. (1994). Morphological study of the rostral interstitial nucleus of the medial longitudinal fasciculus in the monkey, Macaca mulatta, by Nissl, Golgi, and computer reconstruction and rotation methods. *J. Comp. Neurol.* **347,** 47–63.

De la Cruz, R. R., Pastor, A. M., Martinez-Guijarro, F. J., Lopez-Garcia, C., and Delgado-Garcia, J. M. (1992). Role of GABA in the extraocular motor nuclei of the cat: a postembedding immunocytochemical study. *Neuroscience* **51,** 911–929.

De la Cruz, R. R., Pastor, A. M., Martinez-Guijarro, F. J., Lopez-Garcia, C., and Delgado-Garcia, J. M. (1998) Localization of parvalbumin, calretinin, and calbindin D-28K in identified extraocular motoneurons and internuclear neurons of the cat. *J. Comp.Neurol.* **390,** 377–391.

Delgado-Garcia, J. M., Del Pozo, F., and Baker, R. (1986). Behavior of neurons in the abducens nucleus of the alert cat—II. Internuclear neurons. *Neuroscience* **17,** 953–973.

Dememes, D., and Raymond, J. L. (1982). Radioautographic identification of glutamic acid labeled nerve endings in the cat oculomotor nucleus. *Brain Res.* **231,** 433–437.

De Zeeuw, C.I. Wentzel, P.R., and Mugnainini, E., (1993). Fine structure of the dorsal cap of the inferior olive and its GABAergic and non-GABAergic input from the nucleus prepositus hypoglossi in the rat and rabbit. *J. Comp. Neurol.* **327,** 63–82.

Edwards, S. B., and de Olmos, J. S. D. (1975). Autoradiographic studies of the projections of the midbrain reticular formation: ascending projections of nucleus cuneiformis. *J. Comp. Neurol.* **165,** 417–-432.

Erichsen, J.T., and May, P.J. (2002). The pupillary and ciliary components of the cat Edinger–Westphal nucleus: a transsynaptic transport investigation. Vis. *Neurosci.* **19,** 15–29.

Everling, S., Paré, M., Dorris, M. C., and Munoz, D. P. (1998). Comparison of the discharge characteristics of brain stem omnipause neurons and superior colliculus fixation neurons in monkey: implications for control of fixation and saccade behavior. *J. Neurophysiol.* **79,** 511–528.

Evinger, C. (1988). Extraocular motor nuclei: location, morphology and afferent. *In* "Neuroanatomy of the Oculomotor System" (J.A. Büttner-Ennever, ed.), pp. 81–118. Elsevier, Amsterdam.

Evinger, C., Shaw, M. D., Peck, C. K., Manning, K. A., and Baker, R. (1984). Blinking and associated eye movements in humans, guinea pigs, and rabbits. *J. Neurophysiol.* **52,** 323–338.

Evinger, C., Manning, K. A., and Sibony, P. A. (1991). Eyelid movements. Mechanisms and normal data. Invest. *Ophthalmol.* **32,** 387–400.

Evinger, C., Manning, K. A., Pellegrini, J. J., Basso, M. A., Powers, A. S., and Sibony, P. A. (1994). Not looking while leaping: The linkage of blinking and saccadic gaze shifts. *Exp. Brain Res.* **100,** 337–344.

Fisk, J. D., Goodale, M. A., Burkhart, G., and Barnett, H. J. M. (1982). Progressive supranuclear palsy: the relationship between ocular motor dysfunction and psychological test performance. *Neurology* **32,** 698–705.

Forel, A. (1877). Untersuchungen über die Haubenregion und ihre oberen Verknüpfungen im Gehirn des Menschen und einiger Säugetiere, mit Beiträgen zu den Methoden der Gehirnuntersuchungen. *Arch. Psychiatry.* **7,** 1–495.

Fort, P., Sakai, K., Luppi, P.-H., Salvert, D., and Jouvet, M. (1989). Monoaminergic, peptidergic, and cholinergic afferents to the cat facial nucleus as evidenced by a double immunostaining method with unconjugated cholera toxin as a retrograde tracer. *J. Comp. Neurol.* **283,** 285–302.

Fuchs, A. F., and Mustari, M. J. (1993) The optokinetic response in primates and ist possible neuronal substrate. *In* "Visual Motion and Its Role in the Stabilization of Gaze" (F.A. Miles, and J. Wallman, eds.), pp. 343–369. Elsevier, Amsterdam.

Fuchs, A. F., Kaneko, C. R., and Scudder, C. A. (1985). Brain stem control of saccadic eye movements. *Annu. Rev. Neurosci.* **8,** 307–337.

Fuchs, A.F., Scudder, C.A., and Kaneko, C.R. (1988). Discharge patterns and recruitment order of identified motoneurons and internuclear neurons in the monkey abducens nucleus. *J. Neurophysiol.* **60,** 1874–1895.

Fukushima, K., and Kaneko, C.R. (1995). Vestibular integrators in the oculomotor system. *Neurosci Res.* **22,** 249–258.

Fukushima, K. (1987). The interstitial nucleus of Cajal and its role in the control of movements of head and eyes. *Prog. Neurobiol.* **29,** 107–192.

Fukushima, K., Takahashi, K., Fukushima, J., Ohno, M., Kimura, T., and Kato, M. (1986). Effects of lesion of the interstitial nucleus of Cajal on vestibular nuclear neurons activated by vertical vestibular stimulation. *Exp. Brain Res.* **64,** 496–504.

Fukushima-Kudo, J., Fukushima, K., and Tashiro, K. (1987). Rigidity and dorsiflexion of the neck in progressive supranuclear palsy and the interstitial nucleus of Cajal. *J. Neurol. Neurosurg. Psychiatry.* **50,**1197–1203.

Fukushima, K., Kaneko, C. R., and Fuchs, A. F. (1992). The neuronal substrate of integration in the oculomotor system. *Prog. Neurobiol.* **39,** 609–639.

Galetta, S. L., Raps, E. C., Liu, G. T., Saito, N. G., and Kline, L. B. (1996). Eyelid lag without eyelid retraction in pretectal disease. *J. Neuro-Ophthalmol.* **16,** 96–98.

Gamlin, P. D. R., Zhang, H. Y., and Clarke, R. J. (1995). Luminance neurons in the pretectal olivary nucleus mediate the pupillary light reflex in the rhesus monkey. *Exp. Brain Res.* **106,** 177–180.

Gnadt, J. W., Lu, S. M., Breznen, B., Basso, M., Henriquez, V. M., and Evinger, C. (1997). Influence of the superior colliculus on the primate blink reflex. *Exp. Brain Res.* **116,** 389–398.

Goossens, H.H.L.M., and van Opstal, A.J. (2000a). Blink-perturbed saccades in monkey. I. Behavioral analysis. *J. Neurophysiol.* **83,** 3411–3429.

Goossens, H.H.L.M., and van Opstal, A.J. (2000b). Blink-perturbed saccades in monkey. II. Superior colliculus activity. *J. Neurophysiol.* **83,** 3430–3452.

Grantyn, A., Ong-Meang Jacques, V., and Berthoz, A. (1987). Reticulospinal neurons participating in the control of synergic eye and head movements during orienting in the cat. II. Morphological properties as revealed by intaaxonal injections of horseradish peroxidase. *Exp. Brain Res.* **66,** 355–377.

Grantyn, A., Berthoz, A., Hardy, O., and Gourdon, A (1992). Contribution of reticulospinal neurons to the dynamic control of head movements: presumed neck bursters. *In* "The Head–Neck Sensory Motor System" (A. Berthoz, W. Graf, and P.P. Vidal, eds.), pp. 328–329. Oxford University Press, New York.

Grantyn, A., Olivier, E., and Kitama,T. (1993). Tracing premotor brain stem networks of orienting movements. *Curr.Opin. Neurobiol.* **3,** 973–981.

Grantyn, R. (1988). Gaze control through superior colliculus: structure and function. *In* "Neuroanatomy of the Oculomotor system." (J.A. Büttner-Ennever, ed.), pp. 273–333. Elsevier, Amsterdam.

Guerra-Seijas, M.J., Labandeira-Garcia, J.L., Tobio, J., and Gonzalez, F. (1993). Neurons located in the trigeminal sesnory complex in the lateral pontine tegmentum project to the oculomotor nucleus in the rabbit. *Brain Res.* **601,** 1–13.

Hain, T. C. (1986). Blink-induced saccadic oscillations. *Ann. Neurol.* **19,** 299–301.

Halmagyi, G. M., Aw, S. T., Dehaene, I., Curthoys, S. I., and Todd, M. J. (1994). Jerk-waveform see-saw nystagmus due to unilateral meso-diencephalic lesion. *Brain* **117,** 789–803.

Hanson, M. R., Hamid, H. A., Tomsak, R. L., Chou, S. S., and Leigh, R. J. (1986). Selective saccadic palsy caused by pontine lesions: clinical, physiological, and pathological correlations. *Ann. Neurol.* **20,** 209-217.

Harting, J. K. (1977). Descending pathways from the superior colliculus: an autoradiographic analysis in the rhesus monkey *(Macaca mulatta). J. Comp. Neurol.* **173,** 583–612.

Harting, J. K., Huerta, M. F., Frankfurter, A. J., Strominger, N. L., and Royce, G. J. (1980). Ascending pathways from the monkey superior colliculus: an autoradiographic analysis. *J. Comp. Neurol.* **192,** 853–882.

Harting, J. K., Lieshout, D. P. v., and Feig, S. (1991). Connectional studies of the primate lateral geniculate nucleus: distribution of axons arising from the thalamic reticular nucleus of galago crassicaudatus. *J. Comp. Neurol.* **310,** 411–427.

Harting, J. K., Updyke, B. V., and van Lieshout, D. P. (1992). Corticotectal projections in the cat—anterograde transport studies of 25 cortical areas. *J. Comp. Neurol.* **324,** 379–414.

Harting, J. K., Feig, S., and Van Lieshout, D. P. (1997). Cortical somatosensory and trigeminal inputs to the cat superior colliculus: light and electron microscopic analyses. *J. Comp. Neurol.* **388,** 313–326.

Helmchen, C., Glasauer, S., Bartl, K., and Büttner, U. (1996a). Contralesionally beating torsional nystagmus in a unilateral rostral midbrain lesion. *Neurology* **47,** 482–486.

Helmchen, C., Rambold, H., and Büttner, U. (1996b). Saccade-related burst neurons with torsional and vertical on- directions in the interstitial nucleus of cajal of the alert monkey. *Exp. Brain Res.* **112,** 63–78.

Helmchen, C., Rambold, H., Fuhry, L., and Büttner, U. (1998). Deficits in vertical and torsional eye movements after uni- and bilateral muscimol inactivation of the interstitial nucleus of Cajal of the alert monkey. *Exp. Brain Res.* **119,** 436–452.

Helmchen, C., Rambold, H.C., Kempermann, U., Büttner-Ennever J.A., and U. Büttner. (2002) Localizing value of torsional nystagmus in small midbrain lesions. *Neurology* **59,** 1956–1964.

Henn, V., Büttner-Ennever, and Hepp, K. (1982). The primate oculomotor system. I. Motoneurons. *Hum. Neurobiol.* **1,** 77–85.

Henn, V., Lang, W., Hepp, K., and Reisine, H. (1984). Experimental gaze palsies in monkeys and their relation to human pathology. *Brain* **107,** 619–636.

Hikosaka, O., and Wurtz, R. H. (1983). Effects on eye movements of a GABA agonist and antagonist injected into monkey superior colliculus. *Brain Res.* **272,** 368–372.

Holstege, G. (1988). Brain stem-spinal cord projections in the cat, related to the control of head and axial movements. *In* "Neuroanatomy of the Oculomotor System" (J.A. Büttner-Ennever, ed.), pp. 431–470. Elsevier, Amsterdam

Holstege, G. (1990). Neuronal organization of the blink reflex. *In* "The Human Nervous System" (G. Paxinos, ed.), pp. 287–296. Academic Press, San Diego.

Holstege, G. (1991). Descending motor pathways and the spinal motor system: limbic and nonlimbic components. *Prog. Brain Res.* **87,** 307–421.

Holstege, G. (1990). Neuronal organization of the blink reflex. *In* "The Human Nervous System" (G. Paxinos, ed.), pp. 287–296. Academic Press, San Diego.

Holstege, G.. and Cowie, R. J. (1989). Projections from the rostral mesencephalic reticular formation to the spinal cord. *Exp. Brain Res.* **75,** 265–279.

Holstege, G., van Ham, J. J., and Tan, J. (1986a). Afferent projections to the orbicularis oculi motoneuronal cell group. An autoradiographical tracing study in the cat. *Brain Res.* **374,** 306–320.

Holstege, G., Tan, J., Vanham, J. J., and Graveland, G. A. (1986b). Anatomical observations on the afferent projections to the retractor bubli motoneuronal cell group and other pathways possibly related to the blink reflex in the cat. *Brain Res.* **374,** 321–334.

Horn, A. K. E., and Büttner-Ennever, J. A. (1998a). Premotor neurons for vertical eye-movements in the rostral mesencephalon of monkey and man: the histological identification by parvalbumin immunostaining. *J. Comp. Neurol.* **392,** 413–427.

Horn, A. K. E., and Büttner-Ennever, J. A. (1998b). Premotor control of the upper eyelid: afferent projections to the M-group in macaque monkey. *Soc. Neurosci. Abstr.* **24,**1889.

Horn, A. K. E., Büttner-Ennever, J. A., Wahle, P., and Reichenberger, I. (1994). Neurotransmitter profile of saccadic omnipause neurons in nucleus raphe interpositus. *J. Neurosci.* **14,** 2032–2046.

Horn, A. K. E., Büttner-Ennever, J. A., Suzuki, Y., and Henn, V. (1995). Histological identification of premotor neurons for horizontal saccades in monkey and man by parvalbumin immunostaining. *J. Comp. Neurol.* **359,** 350-–363.

Horn, A. K. E., Büttner-Ennever, J. A., and Büttner, U. (1996). Saccadic premotor neurons in the brain stem: functional neuroanatomy and clinical implications. *Neuro-Ophthalmal.* **16,** 229–240.

Horn, A. K. E., Büttner-Ennever, J. A., Gayde, M., and Messoudi, A. (2000). Neuroanatomical identification of mesencephalic premotor neurons coordinating eyelid with upgaze in the monkey and man. *J.Comp.Neurol.* **420,** 19–34.

Horn, A.K.E., Brückner, G., Härtig, W., and Messoudi, A. (2003). Saccadic omnipause and burst neurons in monkey and human are ensheathed by perineuronal nets but differ in their expression of calcium-binding proteins. *J. Comp. Neurol.* **455,** 341–352.

Horn, A.K.E., Helmchen, C., Wahle, P. (2003) Gabaergic neurons in the rostral mesencephalon of the macaque monkey that control eye movements. *Ann. N. Y. Acad. Sci.* (in press).

Huerta, M. F., and Harting, J. K. (1982). Projections of the superior colliculus to the supraspinal nucleus and the cervical spinal cord gray of the cat. *Brain Res.* **242,** 326–331.

Huerta, M. F., and Harting, J. K. (1984). The mammalian superior colliculus: studies of its morphology and connections. *In* "Comparative Neurology of the Optic Tectum" (H. Vanegas, ed.), pp. 687–773. Plenum Publishing Corporation, New York.

Isa, T., and Sasaki, S. (1992). Mono- and disynaptic pathways from Forel's field H to dorsal neck motoneurones. Exp. *Brain Res.* **88,** 580–593.

Isa, T., and Sasaki, S. (2002). Brain stem control of head movments during orienting; organization of the premotor circuits. *Prog. Neurobiol.* **66,**205–241.

Isa, T., Itouji, T., and Sasaki, S. (1992). Control of vertical head movement via Forel's field H. *In* "The Head–Neck Sensory Motor System" (A. Berthoz, P.P. Vidal, and W. Graf, eds.), pp. 345–350. Oxford University Press, Oxford.

Iwamoto, Y., Kitama, T., and Yoshida, K. (1990). Vertical eye movement-related secondary vestibular neurons ascending in medial longitudinal fasciculus in cat. II. Direct connections with extraocular motoneurons. *J. Neurophysiol.* **63,** 918–935.

Janssen, J.C., Larner, A.J., Morris, H., Bronstein, A.M., and Farmer, S.F. (1998). Upbeat nystagmus: clinicoanatomical correlation. *J. Neurol. Neurosurg. Psychiatry.* **65,** 380–381.

Jeon, C.J., and Mize, R.R. (1993). Choline acetyltransferase immunoreactive patches overlap specific efferent cellgroups in the cat superior colliculus. *J. Comp. Neurol.* **337:**127–150.

Johnston, J. L., Sharpe, J. A., Ranalli, R. J., and Morrow, M. J. (1993). Oblique misdirection and slowing of vertical saccades after unilateral lesions of the pontine tegmentum. *Neurology* **43,** 2238–2244.

Kaneko, C.R. (1996). Effect of ibotenic acid lesion of the omnipause neurons on saccadic eye movements in rhesus macaques. *J. Neurophysiol.* **75,** 2229–2242.

Kaneko, C. R. (1997). Eye movement deficits following ibotenic acid lesions of the nucleus prepositus hypoglossi in monkey. I. Saccades and fixation. *J. Neurophysiol.* **78,**1753–1768.

Kato, I., Nakamura, T., Kanayama, R., and Aoyagi, M. (1994). Slow saccades and quick phases of nystagmus after pontine lesions. *Acta Oto-Laryngol. Suppl.* **511,** 95–98.

Kimura, J., and Lyon, L.W. (1972). Orbicularis oculi reflex in the Wallenberg syndrome: alteration of the late reflex by lesions of the spinal tract and nucleus of the trigeminal nerve. *J. Neurol. Neurosurg. Psychiatry.* **35,** 228–233.

Kokkoroyannis, T., Scudder, C. A., Balaban, C. D., Highstein, S. M., and Moschovakis, A. K. (1996). Anatomy and physiology of the primate interstitial nucleus of Cajal. 1. Efferent projections. *J. Neurophysiol.* **75,** 725–739.

Kömpf, D., Pasik, T., Pasik, P., and Bender, M. B. (1979). Downward gaze in monkeys: stimulation and lesion studies. *Brain* **102,** 527–558.

Kuhlenbeck, H., and Miller, R. N. (1949). The pretectal region of the human brain. *J. Comp. Neurol.* **91,** 369–407.

Langer, T. P., Fuchs, A. F., Scudder, C. A., and Chubb, M. C. (1985). Afferents to the flocculus of the cerebellum in the rhesus macaque as revealed by retrograde transport of horseradish peroxidase. *J. Comp. Neurol.* **235,** 1–25.

Langer, T. P., Kaneko, C. R., Scudder, C. A., and Fuchs, A. F. (1986). Afferents to the abducens nucleus in the monkey and cat. *J. Comp. Neurol.* **245,** 379–400.

Leichnetz, G. R. (1982). Connections between the frontal eye field and pretectum in the monkey: an anterograde/retrograde study using HRP gel and TMB neurohistochemistry. *J. Comp. Neurol.* **207,** 394–404.

Leigh, R.J., and Averbuch-Heller, L. (1998). Nystagmus and related ocular motility disorders. *In* "Clinical Neuro-ophthalmology" (N.R. Miller, and N.J. Newman, eds.), pp. 1461–1505. Wiliams & Wilkins, Baltimore.

Leigh, R.J., and Zee, D.S. (1999). "The Neurology of Eye Movements," 3rd ed. Contemporary Neurology Series, Oxford University Press, New York.

Leigh, R.J., Newman, S.A., Folstein, S.E., Lasker, A.G., and Jensen, B.A. (1983). Abnormal ocular motor control in Huntington's disease. *Neurology* **33,** 1268–1275.

Leuba, G., and Saini, K. (1996). Calcium-binding proteins immunoreactivity in the human subcortical and cortical visual structures. *Vis. Neurosci.* **13,** 997–1009.

Li, Y. Q., Takada, M., Kaneko, T., and Mizuno, N. (1997). Distribution of GABAergic and glycinergic premotor neurons projecting to the facial and hypoglossal nuclei in the rat. *J. Comp. Neurol.* **378,** 283–294.

Lueck, C. J., Hamlyn, P., Crawford, T. J., Levy, I. S., Brindley, G. S., Watkins, E. S., and Kennard, C. (1991). A case of ocular tilt reaction and torsional nystagmus due to direct stimulation of the midbrain in man. *Brain* **114,** 2069–2079.

Martin, G.F., and Holstege, G. (1990) Reticular formation of the pons and medulla. *In* "The Human Nervous System" (G. Paxinos, ed.), pp. 203–220, Academic Press, San Diego.

Matsuo, S., Hosogai, P., and Nakao, S. (1994). Ascending projections of posterior canal-activated excitatory and inhibitory secondary vestibular neurons to the mesodiencephalon in cats. *Exp. Brain Res.* **100,** 7–17.

May, P.J. Sources of premotor input directing primate eyelid motoneurons. (1995) Invest. Ophthalmol. *Vis. Sci.* **37,** 154.

May, P.J., and Porter, J.D. (1992). The laminar distribution of macaque tectobulbar and tectospinal neurons. *Vis. Neurosci.* **8,** 257–276.

May, J., Keller, E.L., and Suzuki, D.A. (1988). Smooth-pursuit eye movement deficits with chemical lesions in the dorsolateral pontine nucleus of the monkey. *J. Neurophysiol.* **59,** 952–957.

Mays, L. E. (1984). Neural control of vergence eye movements: convergence and divergence neurons in midbrain. *J. Neurophysiol.* **51,** 1091–1108.

Mays, L.E., and Gamlin, P.D.R. (1995). Neuronal circuitry controlling the near response. *Curr. Opin. Neurobiol.* **5,** 763–768.

Mays, L. E.. and Morisse, D. W. (1995). Electrical stimulation of the pontine omnipause area inhibits eye blink. *J. Am. Optom. Assoc.* **66,** 419–422.

McCall, R.B., and Aghajanian, G.K. (1979). Serotonergic facilitation of facial motoneuron excitation. *Brain Res.* **169,** 11–27.

McCrea, R.A. (1988) The nucleus prepositus. *In* "Neuroanatomy of the Oculomotor System" (J.A. Büttner-Ennever, ed.), pp. 203–224. Elsevier, Amsterdam

McCrea, R.A., and Baker, R. (1985). Anatomical connections of the nucleus prepositus of the cat. *J. Comp. Neurol.* **237:**377–407.

McHaffie, J.G., Anstrom, K.K., Gabriele, M.L., and Stein, B. (2001). Distribution of the calcium-binding proteins calbindin D-28K and parvalbumin in the superior colliculus of adult and neonatal cat and rhesus monkey. *Exp. Brain Res.* **141,** 460–470.

Mettens, P, Godaux, E., Cheron, G., and Galiana, H.L. (1994). Effect of muscimol microinjections into the prepositus hypoglossi and the medial vestibular nuclei on the eye cat movements. *J. Neurophysiol.* **72,** 785–802.

Mize, R. R. (1992). The organization of GABAergic neurons in the mammalian superior colliculus. *Prog. Brain Res.* **90,** 219–248.

Mize, R. R. (1996). Neurochemical microcicuitry underlying visual and oculomotor function in the cat superior colliculus. *Prog. Brain Res.* **112,** 35–55.

Morcuende, S., Delgado-Garcia, J.M., and Ugolini, G. (2002). Neuronal premotor networks involved in eyelid responses: retrograde transneuronal tracing with rabies virus from the orbicularis oculi muscle in the rat. *J. Neurosci.* **22,** 8808–8818.

Moreno-Lopez, B., Escudero, M., Delgado-Garcia, J.M., and Estrada, C. (1996). Nitric oxide production by brain stem neurons is required for normal performance of eye movements in alert animals. *Neuron* **17,** 739–745.

Moreno-Lopez, B., Escudero, M., de Vente, J., and Estrada, C. (2001). Morphological identification of nitric oxide sources and targets in the cat oculomotor system. *J. Comp. Neurol.* **435:**311–324.

Moruzzi, G., and Magoun, H. W. (1949). Brain stem reticular formation and activation of the EEG. *Electroencephalogr. Clin. Neurophysiol.* **1,** 455–473.

Moschovakis, A. K. (1996). The superior colliculus and eye movement control. *Curr. Opin. Neurobiol.* **6,** 811–816.

Moschovakis, A. K., and Highstein, S. M. (1994). The anatomy and physiology of primate neurons that control rapid eye movements. *Annu. Rev. Neurosci.* **17,** 465–488.

Moschovakis, A. K., Karabelas, A. B., and Highstein, S. M. (1988a). Structure–function relationships in the primate superior colliculus. I. Morphological classification of efferent neurons. *J. Neurophysiol.* **60,** 232–262.

Moschovakis, A. K., Karabelas, A. B., and Highstein, S. M. (1988b). Structure–function relationships in the primate superior colliculus. II. Morphological identity of presaccadic neurons. *J. Neurophysiol.* **60,** 263–301.

Moschovakis, A. K., Scudder, C. A., and Highstein, S. M. (1991a). The structure of the primate oculomotor burst generator. I. Medium-lead burst neurons with upward on-directions. *J. Neurophysiol.* **65,** 203–217.

Moschovakis, A. K., Scudder, C. A., Highstein, S. M., and Warren, J. D. (1991b). The structure of the primate oculomotor burst generator. II. Medium-lead burst neurons with downward on-directions. *J. Neurophysiol.* **65,** 218–229.

Moschovakis, A. K., Scudder, C. A., and Highstein, S. M. (1996). The microscopic anatomy and physiology of the mammalian saccadic system. *Prog. Neurobiol.* **50,** 133–133.

Munoz, D. P., and Guitton, D. (1991). Control of orienting gaze shifts by the tectoreticulospinal system in the had-free cat. II Sustained discharges during motor preparation and fixation. *J. Neurophysiol.* **66,** 1624–1641.

Munoz, D. P., and Wurtz, R. H. (1993). Fixation cells in monkey superior colliculus. I. Characteristics of cell discharge. *J. Neurophysiol.* **70,** 559–575.

Nakamagoe, K., Iwamoto Y., and Yoshida, K. (1998). Chemical inactivation of cell groups of the paramedian tracts impairs gaze holding in the cat. *Soc. Neurosci. Abstr* **24,** 1499

Nakao, S., Shiraishi, Y., Li, W. B., and Oikawa, T. (1990). Mono- and disynaptic excitatory inputs from the superior colliculus to vertical saccade-related neurons in the cat Forel's field H. *Exp. Brain Res.* **82,** 222–226.

Nguyen, L.T., and Spencer, R.F. (1999). Abducens internuclear and ascending tract of Deiters inputs to medial rectus motoneurons in the cat oculomotor nucleus: neurotransmitters. *J. Comp. Neurol.* **411,** 73–86.

Ohgaki, T., Markham, C. H., Schneider, J. S., and Curthoys, I. S. (1989). Anatomical evidence of the projection of pontine omnipause neurons to midbrain regions controlling vertical eye movements. *J. Comp. Neurol.* **289,** 610–625.

Ohtsuka, K., and Nagasaka, Y. (1999). Divergent axon collaterals from the rostral superior colliculus to the pretectal accommodation-

related areas and the omnipause neuron area in the cat. *J. Comp. Neurol.* **413,** 68–76.

Olivier, E., Grantyn, A., Chat, M., and Berthoz, A. (1993). The control of slow orienting eye movements by tectoreticulospinal neurons in the cat—behavior, discharge patterns and underlying connections. *Exp. Brain Res.* **93,** 435–449.

Olivier, E., Corvisier, J., Pauluis ,Y., and Hardy, O. (2000). Evidence for glutamatergic tectotectal neurons in the cat superior colliculus: a comparison with GABAergic tectotectal neurons. *Eur. J. Neurosci.* **12,** 2354–2366.

Olszewski, J., and Baxter, D. (1954). "Cytoarchitecture of the Human Brain stem." Karger, New York.

Ongerboer de Visser, B. W. (1980). The corneal reflex: electrophysiological and anatomical data in man. *Prog. Neurobiol.* **15,** 71–83.

Ongerboer de Visser, B.W. (1983). Anatomical and functional organization of reflexes involving the trigeminal system in man: jaw reflex, blink reflex, corneal reflex, and exterozeptive suppression. *In* "Motor Control Mechanisms in Health and Disease" (J.E. Desmedt, ed.), pp. 727–738. Raven Press, New York.

Ongerboer de Visser, B. W., and Kuypers, H. G. J. M. (1978). Late blink reflex changes in lateral medullary lesions. An electrophysiological and neuro-anatomical study of Wallenberg`s syndrome. *Brain* **101,** 285–294.

Panneton, W. M., and Burton, H. (1981). Corneal and periocular representation within the trigeminal sensory complex in the cat studied with gansganglionic transport of horseradish peroxidase. *J. Comp. Neurol.* **199,** 327–344.

Paré, M., and Guitton, D. (1998). Brain stem omnipause neurons and the control of combined eye- head gaze saccades in the alert cat. *J. Neurophysiol.* **79,** 3060–3076.

Paré, M., and Guitton, D. (1990). Gaze-related activity of brain stem omnipause neurons during combined eye-head gaze shifts in the alert cat. *Exp. Brain Res.* **83,** 210–214.

Paré, M., Crommelinck, M., and Guitton, D. (1994). Gaze shifts evoked by stimulation of the superior colliculus in the head-free cat conform to the motor map but also depend on stimulus strength and fixation activity. *Exp. Brain Res.* **101,** 123–139.

Partsalis, A. M., Highstein, S. M., and Moschovakis, A. K. (1994). Lesions of the posterior commissure disable the vertical neural integrator of the primate oculomotor system. *J. Neurophysiol.* **71,** 2582–2585.

Pasik, P., Pasik, T., and Bender, M. B. (1969). The pretectal syndrome in monkey. I. Disturbances of gaze and body posture. *Brain* **92,** 521–534.

Paxinos, G., and Huang, X.F. (1995). "Atlas of the Human Brain." Academic Press, San Diego.

Paxinos, G., Törk, I., Halliday, G., and Mehler, W.R. (1990). Human homologs to brain stem nuclei identified in other animals as revealed by acetylcholinesterase. *In* "The Human Nervous System" (G. Paxinos, ed.), pp. 149–201. Academic Press, San Diego.

Paxinos, G., Huang, X.F., and Toga, A.W. (2000). "The Rhesus Monkey Brain in Stereotaxic Coordinates." Academic Press, San Diego.

Pellegrini, J.J., Horn, A.K. E., and Evinger, C. (1995). The trigeminally evoked blink reflex. I. Neuronal circuits. *Exp. Brain Res.* **107,** 166–180.

Pierrot-Deseilligny, C. H., Chain, F., Gray, F., Serdaru, M., Escourolle, R., and Lhermitte, F. (1982). Parinaud's syndrome: electro-oculographic and anatomical analyses of six vascular cases with deductions about vertical gaze organization in the premotor structures. *Brain* **105,** 667–696.

Porter, J. D., Burns, L. A., and May, P. J. (1989). Morphological substrate for eyelid movements: innervation and structure of primate levator palpebrae superioris and orbicularis oculi muscles. *J. Comp. Neurol.* **287,** 64–81.

Rafal, R.D., Posner, M.I., Friedman, J.H., Inhoff, A.W., and Bernstein, E. (1988). Orienting of visual attention in progressive supranuclear palsy. *Brain* **111,** 267–280.

Rambold, H., Sprenger, A., and Helmchen, C. (2002). Effects of voluntary blinks on saccades, vergence eye movements, and saccade–vergance interactions in humans. *J. Neurophysiol.* **88,** 1220–1233.

Ranalli, P.J., Sharpe, J.A., and Fletcher, W.A. (1988). Palsy of upward and downward saccadic, pursuit, and vestibular movements with a unilateral midbrain lesion: pathophysiologic correlations. *Neurology* **38,** 114–122.

Riordan-Eva, P., Faldon, M.E., Büttner-Ennever, J.A., Gass, A., Bronstein, A.M., and Gresty, M.A. (1996). Abnormalities of torsional fast phase eye movements in unilateral rostral midbrain disease. *Neurology* **47,** 201–207.

Robinson, D.A. (1972). Eye movements evoked by collicular stimulation in the alert monkey. *Vis. Res.* **12,** 1795–1808.

Robinson, F.R., Phillips, J.O., and Fuchs, A.F. (1994). Coordination of gaze shifts in primates: brain stem inputs to neck and extraocular motoneuron pools. *J. Comp. Neurol.* **346,** 43–62.

Roste, G. K. (1989). Non-motoneurons in the facial and motor trigeminal nuclei projecting to the cerebellar flocculus in the cat. *Exp. Brain Res.* **75,** 295–305.

Saper, C.B. (1987). Function of locus coeruleus. *Trends Neurosci.* **10,** 343–344.

Sato, A. and Ohtsuka, K. (1996). Projection from the accommodation-related area in the superior colliculus of the cat. *J. Comp. Neurol.* **367,** 465-476.

Sato, Y., Kawasaki, T., and Ikarashi, K. (1983). Afferent projections from the brain stem to the three floccular zones in cats. II. Mossy fiber projections. *Brain Res.* **272,** 37–48.

Satoda, T., Takahashi, O., Tashiro, T., Matsushima, R., Uemura-Sumi, M., and Mizuno, N. (1987). Representation of the main branches of the facial nerve within the facial nucleus of the Japanese monkey *(Macaca fuscata). Neurosci. Lett.* **78,** 283–287.

Satoda, T., Matsumoto, H., Zhou, L., Rose, P.K., and Richmond, F.J.R. (2002). Mesencephalic projections to the first cervical segment in the cat. *Exp. Brain Res.* **144,** 397–413.

Satoh, K., Arai, R., Ikemoto, K, Narita, M., Nagai, T., Ohshima, H., and Kitahama, K. (1995). Distribution of the nitric oxide synthase in the central nervous system of *Macaca fuscata:* subcortical regions. *Neuroscience* **3,** 685–696.

Scheibel, M.E., and Scheibel, A.B. (1958). Structural substrates for integrative patterns in the brain stem reticular core. *In* "Reticular Formation of the Brain." (H.H. Jasper, and L.D. Proctor, eds.), pp. 31–55. Little, Brown, Boston.

Schmidtke, K., and Büttner-Ennever, J.A. (1992). Nervous control of eyelid function: a review of clinical, experimental and pathological data. *Brain* **115,** 227–247.

Schon, F., Hodgson, T.L., Mort, D., and Kennard, C. (2001). Ocular flutter associated with a localized lesion in the paramedian pontine reticular formation. *Ann. Neurol.* **50,** 413–416.

Scudder, C. A., Fuchs, A. F., and Langer, T. P. (1988). Characteristics and functional identification of saccadic inhibitory burst neurons in the alert monkey. *J. Neurophysiol.* **59,** 1430–1454.

Scudder, C. A., Moschovakis, A. K., Karabelas, A. B., and Highstein, S. M. (1996a). Anatomy and physiology of saccadic long-lead burst neurons recorded in the alert squirrel monkey. I. Descending projections from the mesencephalon. *J. Neurophysiol.* **76,** 332–352.

Scudder, C. A., Moschovakis, A. K., Karabelas, A. B., and Highstein, S. M. (1996b). Anatomy and physiology of saccadic

long-lead burst neurons recorded in the alert squirrel monkey. II. Pontine neurons. *J. Neurophysiol.* **76,** 353–370.

Scudder, C.A., Kaneko, C.R.S., and Fuchs, A.F. (2002). The brain stem burst generator for saccadic eye movements. *Exp. Brain* Res. **142:**349–462.

Sekiya, H., Kojima, Y., Hiramoto, D., Mukuno, K., and Ishikawa, S. (1992). Bilateral innervation of the musculus levator palpebrae superioris by single motoneurons in the monkey. *Neurosci. Lett.* **146,** 10–12.

Shahani, B.T., and Young, R.R. (1972). Human orbicularis oculi reflexes. *Neurol.* **22,** 149–154.

Sharpe, J.A. (1998). Neural control of oculomotor systems. *In* "Clinical Neuro-ophthalmology" (N.R. Miller, and N.J. Newman, eds.), pp. 1101–1167. Williams & Wilkins, Baltimore.

Sibony, P.A., and Evinger, C. (1998). Normal and abnormal eyelid function. *In* "Clinical Neuro-Ophthalmology" (N.R. Miller, and N.H. Newman, eds.), pp. 1509–1592. Williams & Wilkins, Baltimore.

Smith, C.H. (1998). Nuclear and infranuclear ocular motility disorders. *In* "Clinical Neuro-ophthalmology" (N.R. Miller, and N.J. Newman, eds.), pp. 1189–1281, Williams & Wilkins, Baltimore.

Soares, J.C.M., Bothelho, E.P., and Gattass, R. (2001). Distribution of calbindin, parvalbumin and calretinin in the lateral geniculate nucleus and superior colliculus in Cebus apella monkeys. *J. Chem. Neuroanat.* **22,** 139–146.

Soetedjo, R., Kaneko, C.R.S., and Fuchs, A.F. (2002). Evidence that the superior colliculus participates in the feedback control of saccadic eye movements. *J. Neurophysiol.* **87,** 679–695.

Sparks, D.L., and Hartwich-Young, R. (1989). The deep layers of the superior colliculus. *In* "The Neurobiology of Saccadic Eye Movements" (R.H. Wurtz, and M.E. Goldberg, eds.), pp. 213–255. Elsevier, Amsterdam

Spencer, R.F., and Baker, R. (1986). Histochemical localization of acetylcholinesterase in relation to motor neurons and internuclear neurons of the cat abducens nucleus. *J. Neurocytol.* **15,** 137–154.

Spencer, R. F., and Baker, R. (1992). Gaba and glycine as inhibitory neurotransmitters in the vestibuloocular reflex. *In* "Sensing and Controlling Motion" (B. Cohen, D.L. Tomko, and F. Guedry, eds.), pp. 602–611. New York Academy of Science, New York.

Spencer, R.F., and Wang, S.F. (1996). Immunohistochemical localization of neurotransmitters utilized by neurons in the rostral interstitial nucleus of the medial longitudinal fasciculus (riMLF) that project to the oculomotor and trochlear nuclei in the cat. *J. Comp. Neurol.* **366,** 134–148.

Spencer, R.F., Wenthold, R.J., and Baker, R. (1989). Evidence for glycine as an inhibitory neurotransmitter of vestibular, reticular, and prepositus hypoglossi neurons that project to the cat abducens nucleus. *J. Neurosci.* **9,** 2718–2736.

Stanton, G.B., Goldberg, M.E., and Bruce, C.J. (1988). Frontal eye field efferents in the macaque monkey: II. Topography of terminal fields in midbrain and pons. *J. Comp. Neurol.* **271,** 493–506.

Steckler, T., Inglis, W., Winn, P., and Sahgal, A. (1994). The pedunculopontine tegmental nucleus: A role in cognitive processes. *Brain Res. Rev.* **19,** 298–318.

Strassman, A., Highstein, S. M., and McCrea, R. A. (1986a). Anatomy and physiology of saccadic burst neurons in the alert squirrel monkey. I. Excitatory burst neurons. *J. Comp. Neurol.* **249,** 337–357.

Strassman, A., Highstein, S.M., and McCrea, R.A. (1986b). Anatomy and physiology of saccadic burst neurons in the alert squirrel monkey. II. Inhibitory burst neurons. *J. Comp. Neurol.* **249,** 358–380.

Strassman, A., Evinger, C., McCrea, R.A., Baker, R.G., and Highstein, S.M. (1987). Anatomy and physiology of intracellularly labelled omnipause neurons in the cat and squirrel monkey. *Exp. Brain Res.* **67,** 436–440.

Straube, A., Kurzan, R., and Büttner, U. (1991). Differential effects of bicuculline and muscimol microinjections into the vestibular nuclei on simian eye movments. *Exp. Brain Res.* **86,** 347–358.

Sugimoto, T., Mizuno, N., and Uchida, K. (1982). Distribution of cerebellar fiber terminals in the midbrain visuomotor areas: an autoradiographic study in the cat. *Brain Res.* **238,** 353–370.

Sun, W.S., and May, P.J. (1993). Organization of the extraocular and preganglionic motoneurons supplying the orbit in the lesser galago. *Anat.Rec.* **237,** 89–103.

Suzuki, Y., Büttner-Ennever, J.A., Straumann, D., Hepp, K., Hess, B.J.M., and Henn, V. (1995). Deficits in torsional and vertical rapid eye movements and shift of Listing`s plane after uni- and bilateral lesions of the rostral interstitial nucleus of the medial longitudinal fasciculus. *Exp. Brain Res.* **106,** 215–232.

Taber, E. (1961). The cytoarchitecture of the brain stem of the cat. I. Brain stem nuclei of the cat. *J. Comp. Neurol.* **116,** 27–70.

Takada, S., Itoh, K., Yasui, Y., Mitani, A., Nomura, S., and Mizuno, N. (1984). Distribution of premotor neurons for orbicularis oculi motoneurons in the cat, with particular reference to possible pathways for blink reflex. *Neurosci. Lett.* **50,** 251–255.

Tamai, Y., Iwamoto, M., and Tsujimoto, T. (1986). Pathway of the blink reflex in the brain stem of the cat: interneurons between the trigeminal nuclei and the facial nucleus. *Brain Res.* **380,** 19–25.

Van der Werf, F., Baljet, B., Prins, M., and Otto, J.A. (1993). Innervation of the superior tarsal (Müller`s) muscle in the cynomolgous monkey: a retrograde tracing study. Invest. Ophthalmol. *Vis. Sci.* **34:**2333–2340.

Van der Werf, F., Aramideh, M., Ongerboer de Visser, B.W., Baljet, B., Speelman, J.D., and Otto, J.A. (1997). A retrograde double fluorescent tracing study of the levator palpebrae superioris muscle in the cynomolgus monkey. *Exp. Brain Res.* **113,** 174–179.

van Ham, J.J., and Yeo, C.H. (1996). Trigeminal inputs to eyeblink motoneurons in the rabbit. *Exp. Neurol.* **142 ,** 244–257.

Vilis, T., Hepp, K., Schwarz, U., and Henn, V. (1989). On the generation of vertical and torsional rapid eye movements in the monkey. *Exp. Brain Res.* **77,** 1–11.

Waitzman, D.M., Silakov, V.L., and Cohen, B. (1996). Central mesencephalic reticular formation (cMRF) neurons discharging before and during eye movements. *J. Neurophysiol.* **75,** 1546–1572.

Waitzman, D.M., Silakov, V.L., DePalma-Bowles, S., and Ayers, A.S. (2000a). Effects of reversible inavtivation of the primate mesencephalic reticular formation. I. Hypermetric goal-directed saccades. *J. Neurophysiol.* **83,** 2260–2283.

Waitzman, D.M., Silakov, V.L., DePalma-Bowles, S., and Ayers, A.S. (2000b). Effects of reversible inavtivation of the primate mesencephalic reticular formation. II. Hypometric vertical saccades. *J. Neurophysiol.* **83,** 2285–2299.

Wang, S.F., and Spencer, R.F. (1996a). Morphology and somadendritic distribution of synaptic endings from the rostral interstitial nucleus of the medial longitudinal fasciculus (riMLF) on motoneurons in the oculomotor and trochlear nuclei in the cat. *J. Comp. Neurol.* **366,** 149–162.

Wang, S.F., and Spencer, R.F. (1996b). Spatial organization of premotor neurons related to vertical upward and downward saccadic eye movements in the rostral interstitial nucleus of the medial longitudinal fasciculus (riMLF) in the cat. *J. Comp. Neurol.* **366,** 163–180.

Welt, C., and Abbs, J.H. (1990). Musculotopic organisation of the facial motor nucleus in macaca fascicularis: a morphometric and retrograde tracing study with cholera toxin B-HRP. *J. Comp. Neurol.* **291,** 621–636.

Wentzel, P.R., Dezeeuw, C.I., Holstege, J.C., and Gerrits, N.M. (1995). Inhibitory synaptic inputs to the oculomotor nucleus from vestibulo-ocular-reflex–related nuclei in the rabbit. *Neurosci.* **65,** 161–174.

Westheimer, G., and Blair, S.M. (1975). The ocular tilt reaction—a brain stem oculomotor routine. Invest. *Ophthalmol.* **14,** 833–839.

Whittington, D.A., Lestienne, F., and Bizzi, E. (1984). Behavior of preoculomotor burst neurons during eye-head coordination. *Exp. Brain Res.***55:** 215–222.

Wong, A.M.F., Musallam, S., Tomlinson, R.D., Shannon, P., and Sharpe, J.A. (2001). Opsoclonus in three dimensions: oculographic, neuropathologic and modelling correlates. *J. Neurol. Sci.* **189,** 71–81.

Yingcharoen, K., Rinvik, E., Storm-Mathisen, J., and Ottersen, O.P. (1989). GABA, glycine, glutamate, aspartate and taurine in the perihypoglossal nuclei: an immunocytochemical investigation in the cat with particular reference to the issue of amino acid colocalization. *Exp. Brain Res.* **78:**345–357.

Zee, D.S. (1998). Supranuclear and internuclear ocular motor disorders. *In* "Clinical Neuro-Ophthalmology" (N.R. Miller, and N.J. Newman, eds.). pp. 1283–1349. Williams & Wilkins, Baltimore.

Zee, D.S., Chu, F.C., Leigh, R.J., Savino, P.J., Schatz, N.J., Reingold, D.B., and Cogan, D.G. (1983). Blink–saccade synkinesis. *Neurology* **33:**1233–1236.

Zhou, W., and King, W. M. (1998). Premotor commands encode monocular eye movements. *Nature* **393,** 692–695

Zweig, R.M., Whitehouse, J.P., Casanova, M.F., Walker, L.C., Jankel, W.R., and Price, D.L. (1987). Loss of pedunculopontine neurons in progressive supranuclear palsy. *Ann. Neurol.* **22,** 18–25.

CHAPTER

17

Hypothalamus

CLIFFORD B. SAPER

Department of Neurology and Program in Neuroscience
Beth Israel Deaconess Medical Center, Harvard Medical School
Boston, Massachusetts, USA

An enormous amount of information has been obtained about the organization of the hypothalamus in general, and the human hypothalamus in particular, since the first edition of this book was published. As a result of the gains in understanding over the last decade, the organization of this chapter in the last edition, which was strictly along the lines of cytoarchitecture, fiber connections, and chemoarchitecture, would no longer be appropriate. Instead, the current chapter focuses to a much greater extent than was possible in the past on the *functional organization* of the hypothalamus.

In taking this leap, this chapter will rely to a great extent on data that have been derived over the last decade in other species, most commonly in rodents. In some cases, where parallel data on monkeys or human exist, this will be emphasized. However, the functions of the hypothalamus are so basic that its plan and organizational patterns have, to a great degree, been conserved throughout the mammalian spectrum. As a result, even when data in humans or monkeys are still sketchy, it is useful to view what we know in a functional context that is derived in large part from other sources.

It is particularly appropriate to review the hypothalamus from this functional perspective in a book that emphasizes structure because the methods used to dissect the functions of the hypothalamus have relied heavily on new ways to localize physiologically driven gene expression at specific sites in the brain. This revolution, which has largely taken place in the last decade, has extended our ability to make structure–function correlations. Our functional knowledge about the hypothalamus has relied so heavily on morphological approaches because of the extraordinarily small size and functional complexity of this region. Occupying just 4 g of the approximately 1200 to 1400-g adult human brain weight, or just a fraction of 1% of the brain (Le Gros Clarke, 1938), the hypothalamus contains the integrative systems that support life, including such activities as fluid and electrolyte balance, food ingestion and energy metabolism, thermoregulation and immune response, and, of course, emotional expression and reproduction. All of these functional systems have in common a wide variety of sensory inputs; a set of specific types of regulatory drives and setpoints; and a range of specific types of effector mechanisms.

These complex mechanisms are subserved by an equally complicated array of cell groups and fiber pathways, packed into a very small space. As a result, studying the function of the hypothalamus requires placing it into anatomical context, and the current

generation of methods, which allow a cellular level of resolution of function, have finally allowed us to make headway in understanding the functional organization of the hypothalamus.

The sections that follow will first review the overall plan of the cytoarchitecture and the major fiber pathways of the hypothalamus. The following sections will focus on the functional organization of the hypothalamus. Current knowledge about the chemoarchitecture of the hypothalamus will be integrated, to the greatest extent possible, into that context.

CYTOARCHITECTURE OF THE HUMAN HYPOTHALAMUS

The cytoarchitectural plan of the human hypothalamus has been well understood for many years, although the exact terminology has often been controversial. The most exhaustive description of the human hypothalamus is that of Brockhaus (1942), who divided the hypothalamus into many more subdivisions than can be justified on the basis of the material used to prepare this chapter. Braak and Braak (1987) employed the method of pigmentoarchitectonics, identifying several additional cell groups that are poorly distinguished in Nissl-stained preparations. While recognizing these antecedants, the terminology to be used here will follow, insofar as possible, that of Nauta and Haymaker (1969). This system of nomenclature is largely derived, in turn, from that of Gagel (1927), Grünthal (1933), LeGros Clark (1936, 1938), and Rioch *et al.* (1939). For comparison with the nomenclature of early workers, the reader is referred to the extensive tables of terminologies prepared by Laruelle (1934) and Koikegami (1937).

One major reason for the differences in nomenclature in descriptions of the human hypothalamus is that the nuclear masses in this part of the brain are rarely as well differentiated as in most other mammalian species. LeGros Clark (1936), who was the first to distinguish among the medial hypothalamic nuclei in humans, relied extensively on preparations from the human fetus, where these cell groups are much better defined (see also Koutcherov *et al.*, 2002).

A second major problem in delineating cell groups in the human hypothalamus is the extreme variability of the plane of section. The human skull is foreshortened in the anteroposterior direction, in comparison with other mammalian species. As a result, the pituitary gland lies directly under the hypothalamus rather than posterior to it. In addition, the foreshortening of the face results in the rather abrupt decussation of the optic fibers in the chiasm almost as soon as they exit the optic foramen. This landmark limits the anterior extent of the hypothalamus. The effect of these two anatomical restrictions is that, depending on the exact shape of the skull, the pituitary stalk and the attached tuberal hypothalamus may be retroflexed, virtually straight, or even anteroflexed. Thus, there is as much as a 45-degree variation in the angle at which the tuberal part of the hypothalamus is cut, even if great pains are taken to block the forebrain in a standard plane.

As in other species, the human hypothalamus can be divided in Nissl-stained material into three major regions in the anteroposterior direction, and also into three zones in the mediolateral direction (Fig.17.1). The most anterior part of the hypothalamus, bordered rostrally by the lamina terminalis and caudally by the posterior edge of the optic chiasm, is the preoptic division. In the human brain the anterior wall of the third ventricle, containing the ventral part of the preoptic area, is often quite thinned and may extend for several millimeters between the dorsal surface of the optic chiasm and the floor of the septal region (Fig.17.2). Neurosurgeons have used this anatomical feature to place ventriculostomy incisions to drain the cerebrospinal fluid from the third ventricle. The next more caudal portion of the hypothalamus is the tuberal division. This gray swelling (tuber cinereum in Latin) along the base of the brain gives rise in the midline to the pituitary stalk. The lateral surface of the tuberal region may be raised by small bumps, representing the surface protrusions of the lateral tuberal nuclei (see LeGros Clark, 1936). Finally, the level of the mammillary bodies defines the posterior hypothalamic division. The mammillary recess, a small extension of the third ventricle trapped ventrally between the mammillary bodies in the midline, is common in other species but generally absent in humans.

Periventricular Zone

The most medial part of each of the anterioposterior divisions of the hypothalamus is the periventricular zone, bordering the wall of the third ventricle. At the level of the preoptic area, the organum vasculosum of the lamina terminalis is seen at the anteroventral end of the third ventricle, a vascularized area containing medium-sized, medium-staining cells. The organum vasculosum merges dorsally with the median preoptic nucleus and laterally with the anteroventral periventricular nucleus, both of which are composed of similar-appearing neurons. In rodents, the median preoptic nucleus can be followed dorsally, over the anterior surface of the anterior commissure, along the lamina terminalis, to the subfornical organ, but this

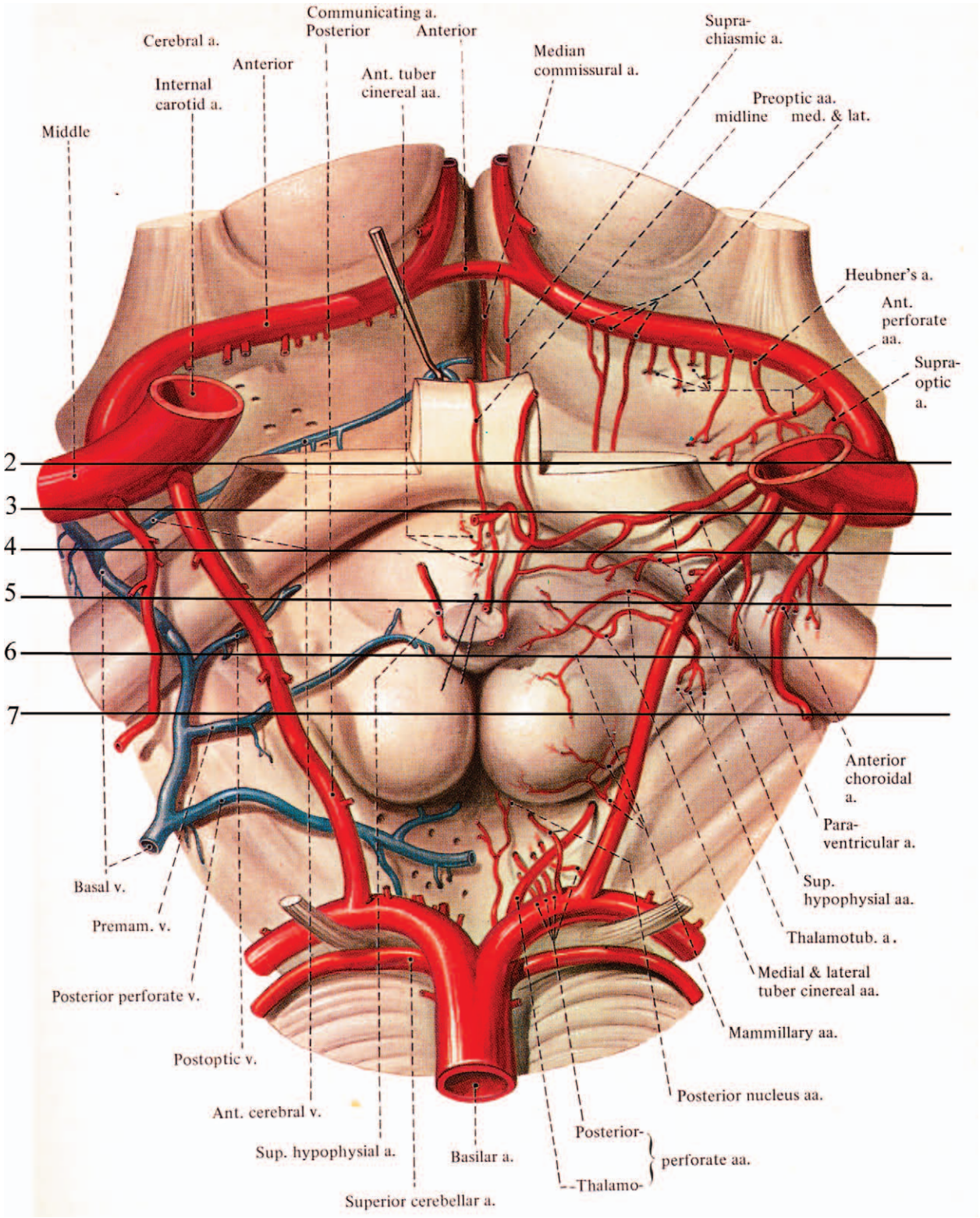

FIGURE 17.1 A drawing of the base of the brain, emphasizing the relationship of the hypothalamus to the circle of Willis. The approximate levels of the sections depicted in Figures 17.2–17.7 are shown. Modified from Nauta and Haymaker, 1969 with permission.

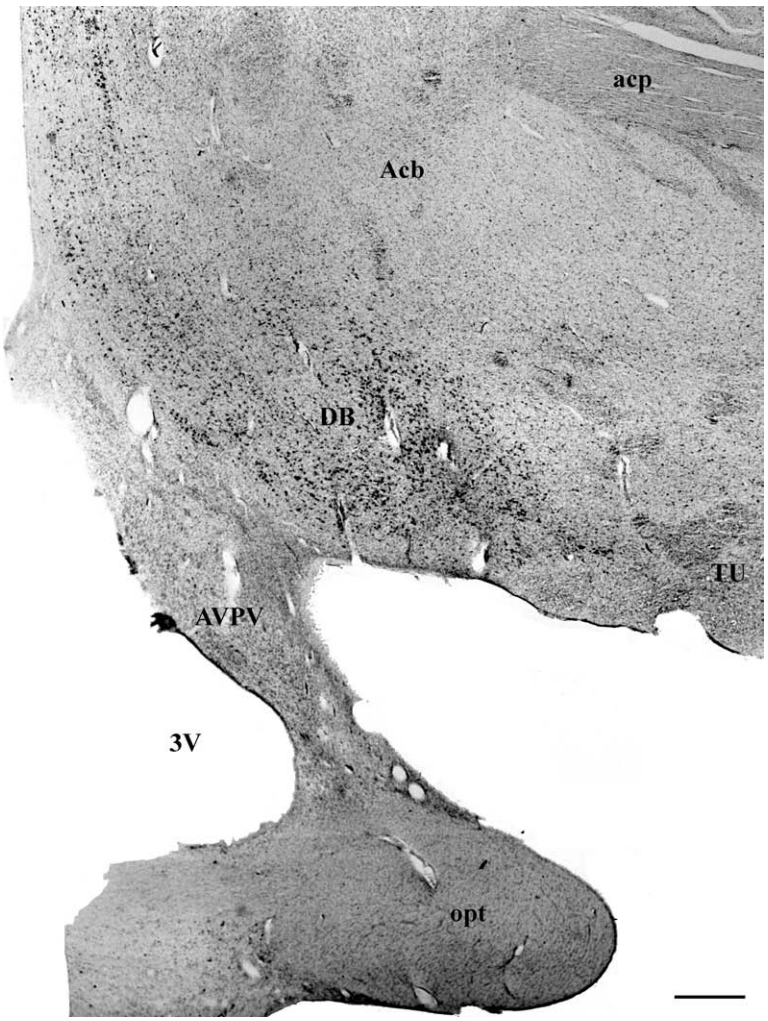

FIGURE 17.2 A photomicrograph taken at the level of the most rostral tip of the third ventricle. The preoptic area begins as an expansion of the tissue separating the optic chiasm from the base of the telencephalon. Scale = 1 mm.

extension is usually not apparent in humans. Both the subfornical organ and the organum vasculosum lack a blood–brain barrier (see Chapter 19). In rats there is evidence that angiotensin, and perhaps other blood-borne hormones, may act on neurons in these regions, which in turn project to the hypothalamus (Lind *et al.*, 1982, 1984).

At the foot of the third ventricle, just above the optic chiasm in the most rostral part of the preoptic area, lies a condensation of small, medium-staining neurons, the suprachiasmatic nucleus (Fig. 17.3). This cell group is less impressive in humans than in many other mammalian species and may be difficult to recognize in Nissl-stained material. The homology of this cell group with the suprachiasmatic nucleus, which is responsible for maintaining circadian rhythms in other species, was questioned until the application of immunohistochemical and pigmentoarchitectonic methods (Braak and Braak, 1987; Lydic *et al.*, 1980; Stopa *et al.*, 1984; Swaab *et al.*, 1985; Mai *et al.*, 1991). The shape of this cell group has been reported to be elongated in females and more spherical in males (Swaab *et al.*, 1985), although other investigators have not reported any sexual dimorphism in its structure (Braak and Braak, 1992).

The remainder of the periventricular zone in the preoptic area (Fig. 17.3) consists of a narrow strip of medium-sized to small, medium-staining neurons, the periventricular preoptic nucleus, which merges imperceptibly with the hypothalamic periventricular nucleus at the tuberal level. At the foot of the third ventricle in the tuberal region there is marked lateral

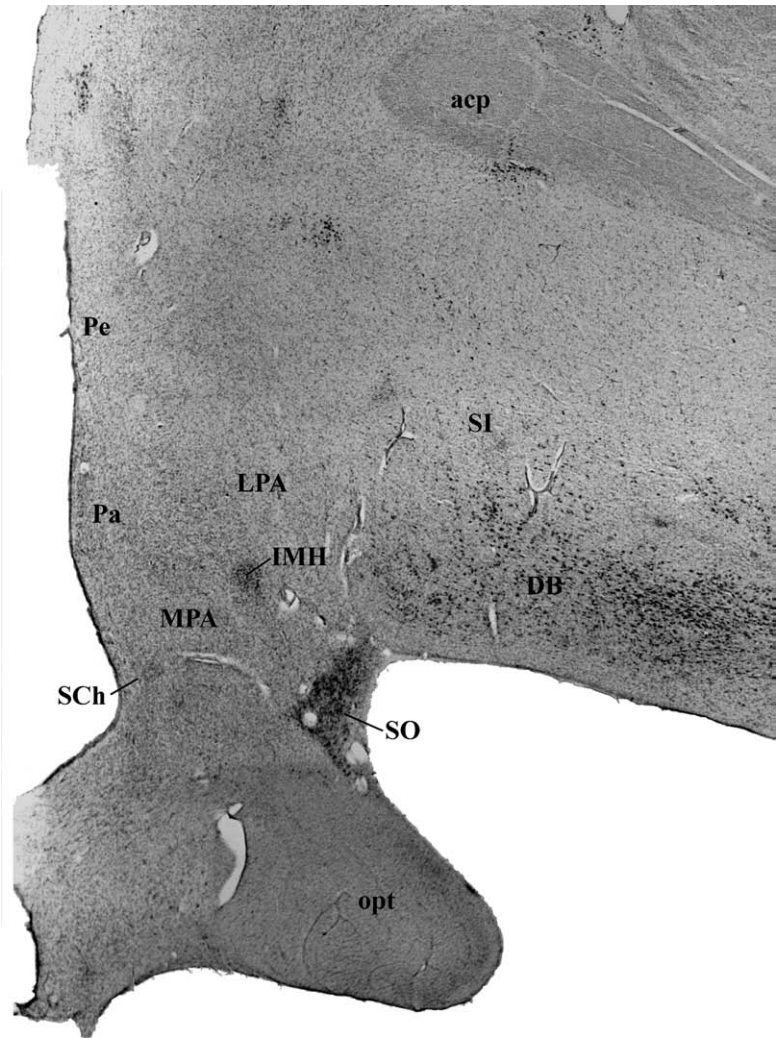

FIGURE 17.3 A photomicrograph taken at the level of the preoptic area, showing the most rotral portions of the supraoptic and paraventricular nuclei. The suprachiasmatic nucleus and the intermediate nucleus are also clearly seen at this level. Scale = 1 mm.

extension of the periventricular cell group, the arcuate nucleus (Figs. 17. 4 and 17.5). The arcuate nucleus overlies the median eminence, which forms the floor of the third ventricle at this level. Some arcuate neurons can be followed down into the median eminence itself. Unlike many other mammalian species, the median eminence in primates (including humans) does not form a neatly laminated structure; rather, the limited anteroposterior extent causes the neurohemal contact zone containing the hypophysial portal vessels to form a ball-like structure, whereas the axons of the neurohypophysial tract course along the surface of the infundibulum, toward the posterior pituitary gland.

At the posterior hypothalamic level, the periventricular zone expands laterally to become the posterior hypothalamic area (Figs. 17.6 and 17.7). This region is invaded along its lateral border by large, darkly staining neurons from the lateral hypothalamic area and the fields of Forel. Many of these neurons belong to the orexin- and melanin-containing hormone-containing populations (Elias *et al.*, 1998), which at tuberal levels occupy mainly the lateral hypothalamic area. The posterior hypothalamic area becomes continuous dorsally and caudally with the periventricular gray matter of the caudal third ventricle and the periaqueductal gray matter. Similarly, there is a well-defined cell group termed the supramammillary nucleus in rats, which lies between the posterior hypothalamic area and the dorsal surface of the mammillary body. However, in humans, there is no clear distinction between the supramammillary area and the posterior hypothalamic area.

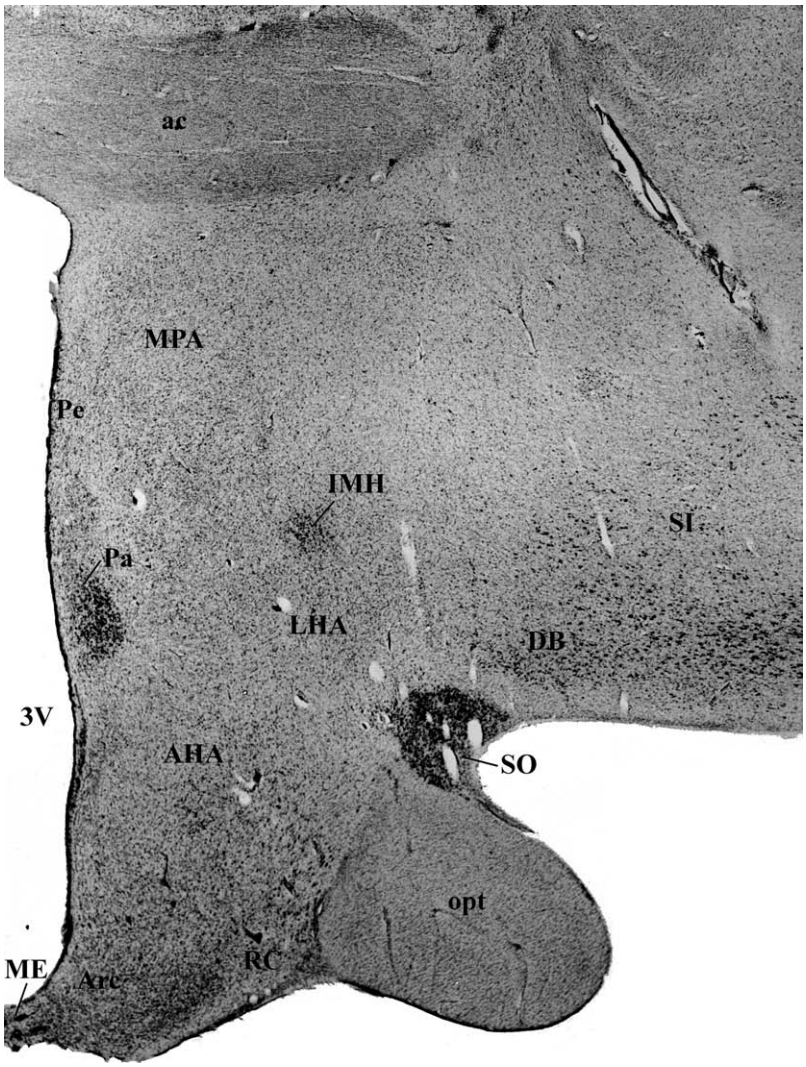

FIGURE 17.4 A photomicrograph taken at the level of the anterior hypothalamic area and the crossing of the anterior commissure. The section is slightly angled so that the dorsal part is roughly at the same anteroposterior level as Figure 17.3, while the ventral portion is closer to the level of Figure 17.5. This disparity in the orientation of the hypothalamus in the coronal plane is typical of human brains, in which the position of the pituitary stalk in relation to the optic chiasm may cause substantial topographical deformation of the relationship of the nuclei. Scale = 1 mm.

Medial Zone

The next more lateral portion of the hypothalamus, the medial zone, contains the most well-differentiated cell groups in the hypothalamus. At the preoptic level, the paraventricular nucleus can be seen near the foot of the third ventricle (Fig. 17.3). More caudally, the paraventricular nucleus appears to rise along the wall of the third ventricle, reaching nearly to the hypothalamic sulcus, which demarcates the hypothalamus from the thalamus at tuberal levels (Figs. 17.4–17.6). The paraventricular nucleus contains both large, darkly staining neurons as well as smaller, medium-staining cells. Unlike rodents, where these populations form discrete subnuclei, the subdivisions of the paraventricular nucleus in the human brain are not clear-cut. However, a number of homologies at the subnuclear level do exist (Koutcherov *et al*., 2000). For example, the larger neurons (the magnocellular neurosecretory cells that secrete oxytocin and vasopressin from their terminals in the posterior pituitary gland) tend to congregate most densely in the ventrolateral quadrant of the nucleus, generally avoiding the area just adjacent to the third ventricle (see Fig. 17.8).

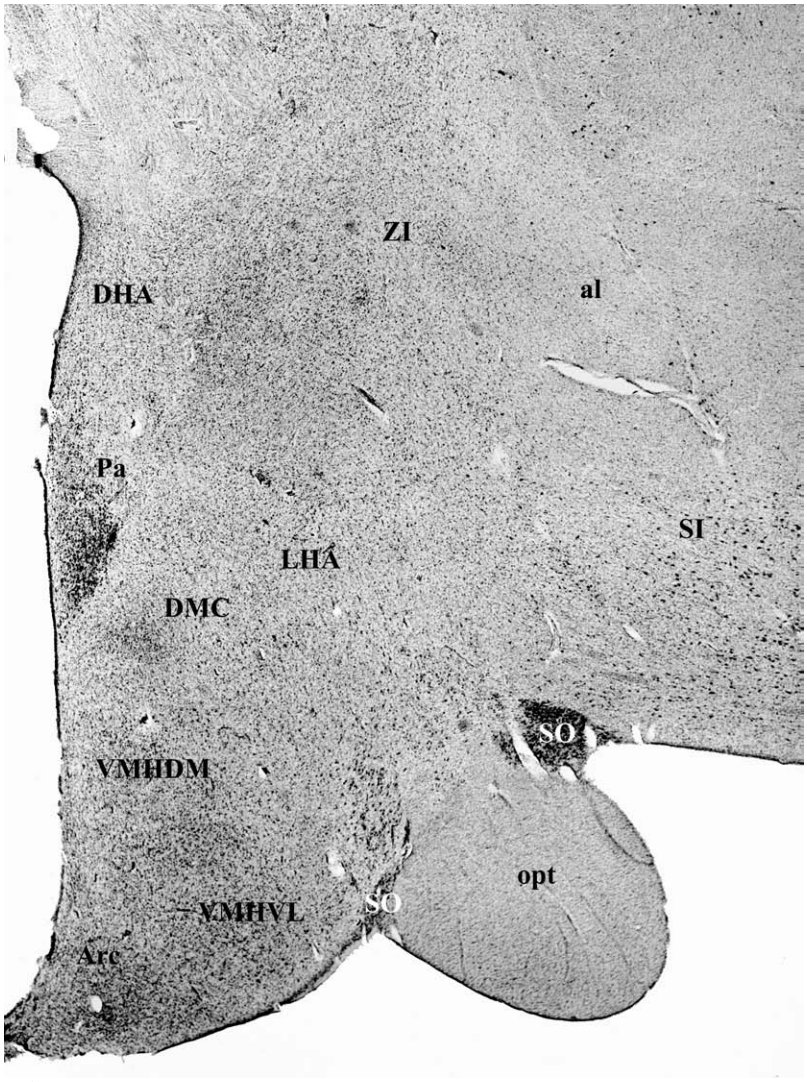

FIGURE 17.5 A photomicrograph taken at the level of the ventromedial nucleus of the hypothalamus. The dorsomedial and ventrolateral components of the ventromedial nucleus can be clearly seen, as can the compact portion of the dorsomedial nucleus of the hypothalamus. Scale = 1 mm.

Similar large, darkly staining neurons, without admixed smaller cells, are seen in the supraoptic nucleus. In humans, the largest part of the supraoptic nucleus is contained in a single well-defined cluster of neurons just dorsolateral to the optic tract. Additional supraoptic neurons are found spilling medially over the optic tract, to form a smaller cluster just ventromedial to the optic tract. Numerous scattered neurons are seen in the retrochiasmatic area, along the floor of the tuberal region.

At the rostral preoptic level, the supraoptic and paraventricular nuclei come to lie nearly adjacent to one another, reflecting their origin from the same embryological anlage. Here one often sees clusters of accessory neurosecretory neurons, running along the surface of penetrating blood vessels, bridging the gap between the two magnocellular nuclei (Figs. 17.3 and 17.4). It has been recognized since the work of Gagel (1927) that the main bodies of the paraventricular and supraoptic nuclei are also unusually heavily vascularized. This vascular relationship of magnocellular neurosecretory neurons, which is also seen in other species, may reflect their role in regulating blood osmolarity and electrolyte composition.

Just dorsal and medial to the supraoptic nucleus, another cluster of darkly staining neurons must be distinguished from the accessory neurosecretory nuclei. These cells are not quite as large as the magnocellular neuroendocrine neurons, nor is their cytoplasm as coarsely granular. Unlike the latter perikarya,

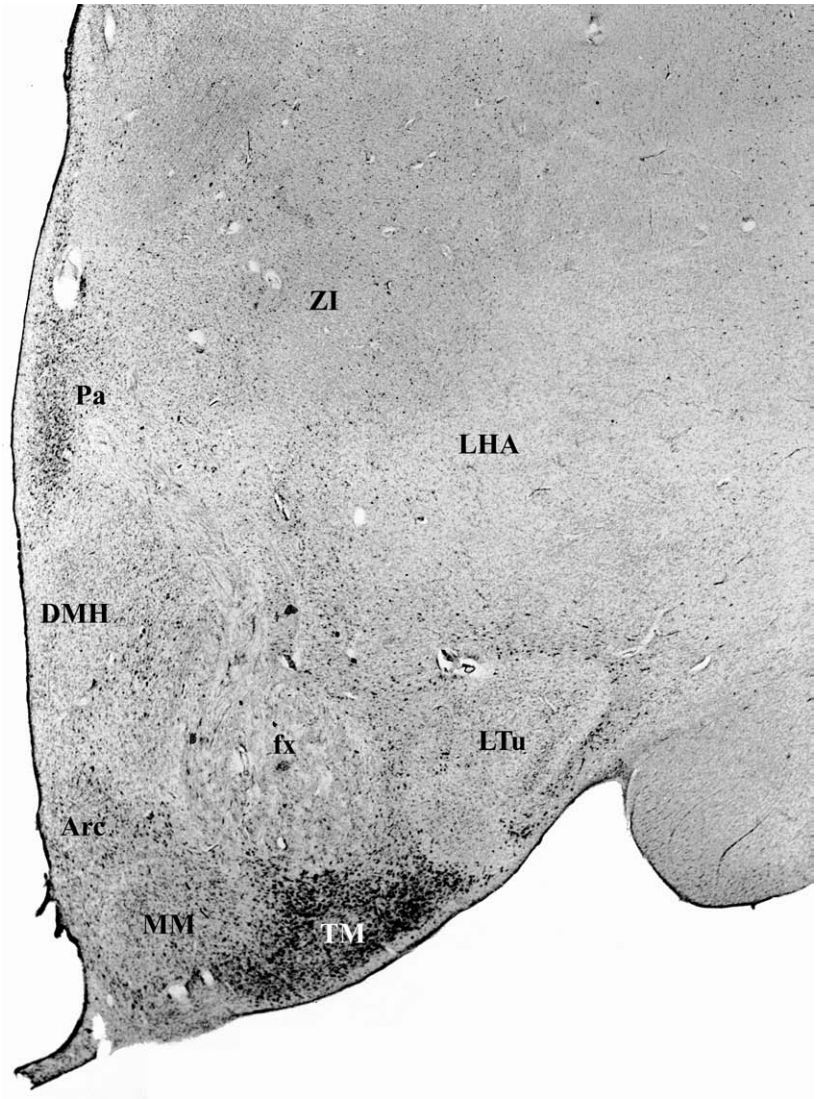

FIGURE 17.6 A photomicrograph taken at the premammillary level of the hypothalamus, demonstrating the tuberomammillary nucleus. Scale = 1 mm.

they do not stain immunohistochemically for posterior pituitary hormones, and they stand out as unstained with the aldehyde fuchsin stain for lipofuchsin pigment. Brockhaus (1942) and Braak and Braak (1987) termed this group the intermediate nucleus. This cell group, which is clearly seen in Nissl preparations, is often mistaken for a component of the accessory neurosecretory system, although its neurons are different in appearance and tend to become displaced progressively more dorsally at caudal preoptic levels (Fig. 17.3). Recent work has demonstrated that the neurons of the intermediate nucleus contain galanin mRNA, suggesting that they may represent the homologue of the ventrolateral preoptic nucleus, a cell group involved in sleep regulation (see below).

In the medial preoptic area of other species, there is considerable sexual differentiation of the pattern of innervation and cellular formations (see Simerly *et al.*, 1986, for review). Swaab and Fliers (1985) identified a sexually dimorphic nucleus in the human preoptic area, which has roughly twice as many neurons in men as in women. This cell group appears identical with the intermediate nucleus of Brockhaus (1942) and Braak and Braak (1987) and with the interstitial nucleus of the anterior hypothalamus 1 (INAH 1) of Allen and Gorski (1982). Allen and Gorski also described three other very small cell clusters in the medial preoptic region in humans, which they called INAH 2–4. They reported finding differences between the sexes in the size only of INAH 2 and INAH 3. LeVay (1991) found

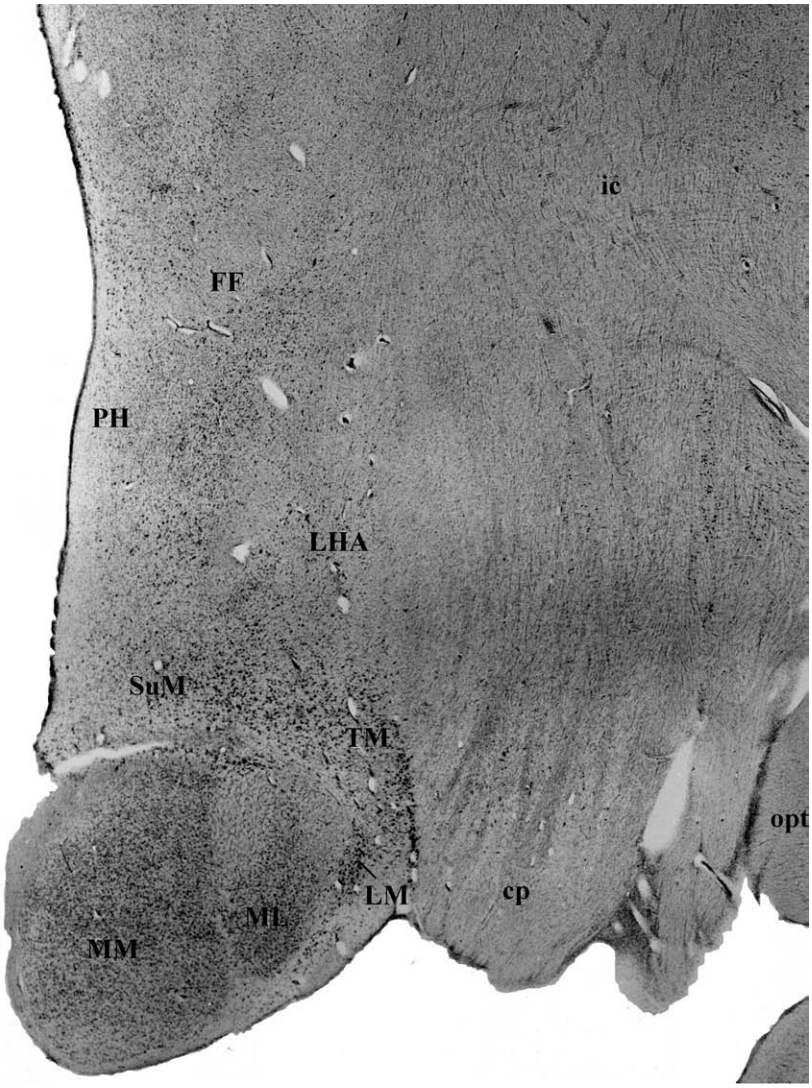

FIGURE 17.7 A photograph taken at the level of the midportion of the mammillary body, illustrating the relationships of the different mammillary nuclei. Scale = 1 mm.

no gender-based difference in the overall area of the INAH 1, 2, or 4 groups, but did confirm an increase in the size of INAH 3 in heterosexual males compared to females. LeVay also reported that INAH 3 in homosexual males was smaller than in heterosexual males, and about the same size as in females (who were not characterized for their gender preference). Byne and coworkers (2000) confirmed the sexually dimorphic nature of INAH 3, but not INAH 1.

The remainder of the medial preoptic area in the human brain is relatively undifferentiated. The ventromedial preoptic nucleus, a cell group that has been associated with thermoregulation in rats (Elmquist *et al.*, 1996), is not clearly demarcated in human brains. Ventral to the paraventricular nucleus, the anterior hypothalamic area blends with the medial preoptic area rostrally and with the dorsomedial hypothalamic nucleus caudally.

At the tuberal level, the ventromedial nucleus forms a dense cellular condensation, bordered ventromedially by the arcuate nucleus and dorsally by the dorsomedial nucleus. The ventromedial nucleus has a relatively cell-poor capsule (Fig. 17.5), and in some humans can be seen to form dorsal and ventral cell aggregations, as in other species (see Saper *et al.*, 1976b, 1979). In rats and monkeys, these subdivisions have distinct connections, with most of the long efferents of the ventromedial nucleus arising from the ventrolateral part. In monkeys, neurons in this same area bind sex steroids (Keefer and Stumpf, 1975).

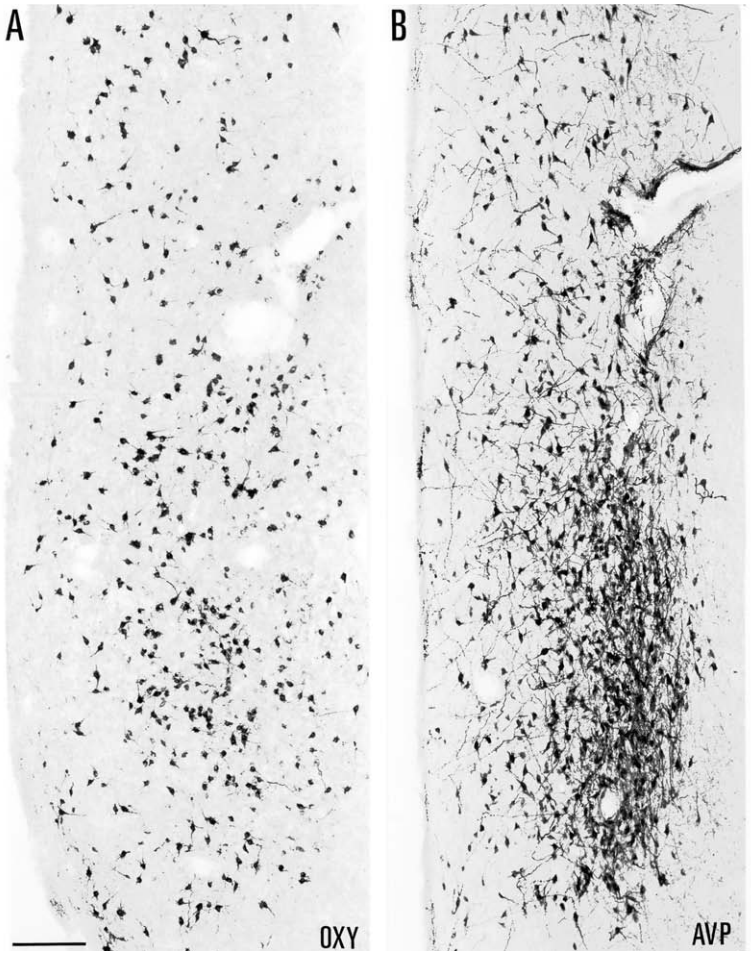

FIGURE 17.8 A pair of photomicrographs illustrating the distribution of oxytocin **(A)** and vasopressin **(B)** neurons in the human paraventricular nucleus. Note that the vasopressin cells form a dense cluster in the ventrolateral quadrant of the paraventricular nucleus, whereas the oxytocin neurons tend to avoid this region, instead clustering along its borders. Scale = 250 μm.

Immediately dorsal to the ventromedial nucleus and ventral to the caudal extension of the paraventricular nucleus lies the dorsomedial nucleus. This cell group is poorly differentiated in the human brain, consisting of loosely organized medium-sized, medium-staining neurons, so that it is best defined by its borders with neighboring structures. Its lateral margin can be arbitrarily marked at the edge of the fornix, although at this border the nucleus is often invaded by larger neurons from the lateral hypothalamus. Conversely, some dorsomedial nucleus cells spill over laterally past the descending column of the fornix. As in other species, embedded within the diffuse part of the dorsomedial nucleus is a cluster of smaller, more darkly staining and densely packed neurons, the compact part of the dorsomedial nucleus (Fig. 17.5). In humans the dorsomedial nucleus is clearly seen in acetylcholinesterase preparations (Koutcherov *et al.*, 2002).

At the caudal tuberal level, just rostral to the appearance of the mammillary nuclei, rodents such as rats show clearly defined dorsal and ventral premammillary nuclei. Similar cell groups cannot be adequately delineated in human brain with current data. However, like the suprachiasmatic nucleus, which was difficult to define on a cytoarchitectonic basis before it could be stained for characteristic chemical markers, it is possible that advances in determining the chemoarchitecture of these nuclei may make it possible to identify them within the tuberal hypothalamic gray level.

The mammillary body is the most prominent component of the medial hypothalamus at the posterior level (Figs. 17.1, 17.6 and 17.7). In human brains, the medial portion of the medial mammillary nucleus reaches prodigious proportions, causing the bulging shape in the floor of the hypothalamus that gave this region its suggestive name. The lateral part of the medial

mammillary nucleus forms a much smaller cluster that is often split off from the lateral margin of the medial subnucleus by a sheet of fornix fibers (Fig. 17.7). The neurons in the lateral part of the medial mammillary nucleus are identical in size (medium), shape (multipolar), and staining characteristics (moderately dense, relatively granular Nissl substance) to those in the medial part of the nucleus. Nevertheless, they have frequently been identified as a separate cell group: Gagel (1927), Grünthal (1933), and LeGros Clark (1936) called this the "lateral mammillary nucleus." This term is unfortunate because it suggests homology with the lateral mammillary nucleus in other species (such as rats), in which the lateral mammillary neurons are much larger and more darkly staining than those in the medial mammillary nucleus. In addition, the lateral mammillary nucleus in rodent species has distinct connections (e.g., a bilateral projection to the anterodorsal nucleus of the thalamus; see "Fiber Connections of the Hypothalamus"). The anterodorsal thalamic nucleus is not distinct in humans, and the lateral mammillary nucleus similarly is much less prominent. In our own material, a collection of larger, more darkly staining neurons located along the lateral edge of the medial mammillary nuclei can be distinguished (Fig. 17.7). This cluster of cells, which is of variable size and distinctiveness, has been designated the lateral mammillary nucleus.

Surrounding the mammillary body along its rostroventral, lateral, and caudodorsal borders is a diffuse population of slightly larger, intensely staining neurons (Figs. 17.6 and 17.7). This latter cell group, which first appears along the floor of the hypothalamus at the premammillary level (Fig. 17.6), was originally named the mammilloinfundibular nucleus by Malone in 1910. Later, he changed the name to the tuberomammillary nucleus (see Malone, 1916) because it was more closely related to the lateral tuberal region than the infundibulum. Several authors have, in fact, included the tuberomammillary nucleus within the mammillary complex, referring to it as the "nucleus intercalatus" (LeGros Clark, 1936; Brockhaus, 1942), whereas others have applied this same term to what is here called the lateral mammillary nucleus (Gagel, 1927; Malone, 1916). It seems preferable, in light of this confusion, to adopt a terminology that is similar to that used in other species and avoid the term "nucleus intercalatus" entirely.

Some authors have followed the suggestion of Bleier *et al.* (1979), who termed the tuberomammillary nucleus the "caudal magnocellular nucleus," to emphasize its cytological similarity to the more rostrally situated magnocellular neurons of the supraoptic nucleus. Malone noted this same similarity in 1916 but pointed out that the two structures could be distinguished on cytological grounds. Recent connectional and immunohistochemical observations in rats support this view. The supraoptic nucleus consists of oxytocin and vasopressin neurons that project to the posterior pituitary gland (Swanson and Kuypers, 1980). In contrast, tuberomammillary neurons stain immunohistochemically for a variety of neurotransmitters or their related enzymes, including histamine, adenosine deaminase, γ-aminobutyric acid (GABA), and galanin (Köhler *et al.*, 1985; Staines *et al.*, 1987). Furthermore, the tuberomammillary nucleus gives rise to widespread connections that are reminiscent of other monoamine cell groups, including innervation of the entire cortical mantle. For these reasons, the term "tuberomammillary nucleus" introduced by Malone is preferred.

In Malone's (1910, 1916) original descriptions, and the later ones of Grünthal (1933), LeGros Clark (1936), and Brockhaus (1942), the tuberomammillary nucleus was described as including similar cells located more dorsally in the tuberal and posterior lateral hypothalamus (Figs. 17.6 and 17.7). Although these populations appear continuous with the tuberomammillary nucleus in human brains, connectional studies in other species and immunocytochemical studies in humans indicate that they can be separated into several distinct cell groups (see "Functional Organization of the Hypothalamus").

Lateral Zone

The most lateral part of the hypothalamus, the lateral zone, comprises a continuum that runs from the lateral preoptic area rostrally through the anterior, tuberal, and posterior parts of the lateral hypothalamic area caudally. The large and relatively diffusely organized neurons of the lateral hypothalamic area are interspersed among the fibers of the medial forebrain bundle, which run longitudinally through the lateral hypothalamus, connecting the autonomic and limbic regions of the forebrain above with the hypothalamus and the brain stem below. The large lateral hypothalamic neurons also provide much of the long projections from the hypothalamus to the cerebral cortex and the brain stem (see "Fiber Connections of the Hypothalamus").

At the tuberal level, two distinctive cell groups can be seen embedded in the lateral hypothalamus. The lateral tuberal nuclei consist of several fiber-encapsulated clusters of small, medium-staining, parvalbumin-immunoreactive neurons embedded in a gelatinous-appearing matrix (Fig. 17.6). The lateral tuberal nuclei form small bulges along the floor of the caudal lateral hypothalamus that, in favorable cases, can be seen as distinct bumps on the surface of the

brain (LeGros Clark, 1936). The lateral tuberal nucleus can be identified on the basis of its staining for a variety of chemical markers, including corticotropin-releasing factor, somatostatin, and muscarinic cholinergic receptors (Kremer, 1994). This cell group also contains heavy staining with the Alz-50 antibody (Rye *et al.*, 1993; Kremer, 1994), but this is most likely cross-reactivity for somatostatin (Nelson and Saper, 1995). The lateral tuberal nucleus shows cytoskeletal pathology in Pick's disease and in argyrophilic grain disease, but only occasional Lewy bodies in Parkinson's disease and no characteristic changes in Alzheimer's disease (Braak and Braak, 1998; Schultz *et al.*, 1998; Kremer, 1994). A homologous structure has been identified in rhesus monkeys (Narkiewicz *et al.*, 1994; Paxinos *et al.*, 2000), and a similar-appearing cluster of parvalbumin-immunoreactive neurons has been identified in rats (Celio and Saper, 1999). Bleier and Byne (1986) also used this name for a cell group in rats, but it probably is a distinct nucleus not related to the human lateral tuberal nucleus.

A second feature of the tuberal lateral hypothalamus is the abrupt appearance of large, darkly staining neurons with coarse cytoplasm that are seen scattered throughout the region and invading the lateral edges of the medial nuclei. Similar-appearing cells can be followed caudally through the posterior level of the lateral hypothalamic area, where they invade the lateral part of the posterior hypothalamic area in large numbers. In Nissl-stained sections, these cell groups merge imperceptibly with the tuberomammillary nucleus, and with a collection of large, darkly staining neurons in the fields of Forel that encroaches on the lateral part of the posterior hypothalamic nucleus. In rats, similar-appearing cell groups are better differentiated from one another, and have distinct immunohistochemical properties (see "Functional Organization of the Hypothalamus"). In rats, all four groups (large neurons in the tuberal lateral hypothalamus, posterior lateral hypothalamus, tuberomammillary nucleus, and fields of Forel) project upon the cerebral cortex (see "Functional Organization of the Hypothalamus"). The apparent expansion of these cell groups in human brains is consistent with their role in innervation of the cerebral cortex in humans as well (see "Fiber Connections of the Hypothalamus").

FIBER CONNECTIONS OF THE HYPOTHALAMUS

The synaptic connections of the hypothalamus will be reviewed below in the context of their functions. However, it is useful first to gain an overview of the layout of hypothalamic connections. In addition, we still do not understand the functions of some of the most prominent fiber pathways of the hypothalamus. The larger myelinated hypothalamic pathways, in particular, would be otherwise overlooked if reviewed only in a functional context.

Afferents

The hypothalamus receives three main sources of neuronal input. *Descending* pathways originate in the cerebral cortex, hippocampal formation, septum, and extended amygdala. *Ascending* pathways arise from a variety of spinal and brain stem sources, including prominent inputs from brain stem sensory and monoaminergic systems. *Intrinsic connections,* meanwhile, connect the different hypothalamic nuclei with one another, allowing them to carry out their carefully orchestrated integrative functions.

Descending Pathways from the Forebrain

The input to the hypothalamus from the *hippocampal formation* forms one of the most heavily myelinated and easily identified fiber bundles in the brain, i.e., the fornix. The course of the fornix includes a long arching pathway that is a remnant of the developmental history of the hippocampal formation. The development of the temporal lobe in the primate brain carries the hippocampal formation, which occupies the most medial extreme of the cortical mantle in the embryonic brain, far from its site of origin near the lamina terminalis. As a result, the fimbria of the fornix recapitulates this migration. At the foramen of Monro, the fornix takes a sharp turn, bending back in a stately column that brushes past the posterior margin of the anterior commissure. The column of the fornix appears to form a solid structure as it pierces the hypothalamus, running slightly laterally as it moves caudally and inferiorly toward the dorsal surface of the mammillary body. Microscopic examination, by contrast, shows that the column of the fornix consists of rather loosely organized bundles of heavily myelinated axons. In rats (Guillery, 1955; Powell *et al.*, 1957; Swanson and Cowan, 1977; Canteras and Swanson, 1995; Canteras and Swanson, 1992; Kishi *et al.*, 2000) and in monkeys (Valenstein and Nauta, 1956), many axons lose their myelination and peel off the fornix to innervate the medial hypothalamic nuclei and lateral hypothalamic area.

Although the hippocampus proper is often considered to be the origin of the fornix projection, most of the axons that originate in the hippocampus travel no further than the septal nuclei in rodents. The projections to the hypothalamus, particularly the dense projections to the shell of the ventromedial nucleus

and to the mammillary body, originate primarily from the subiculum in both rats and monkeys, although the presubiculum may also contribute in primates (Swanson and Cowan, 1975; Krayniak *et al.*, 1979; see also Chapter 23).

Septal afferents to the hypothalamus originate mainly from the lateral septal nucleus. Although there is an extensive projection from the lateral septal nucleus to the hypothalamus in rats, including the medial preoptic, anterior hypothalamic, and lateral hypothalamic and preoptic areas, as well as the shell of the ventromedial nucleus and the ventral premammillary nucleus (Risold and Swanson, 1997), this structure has not received similar study in primates. There are also afferents, primarily to the lateral hypothalamic area, from the shell region of the nucleus accumbens in rats and cats (Powell and Leman, 1976; Mogenson *et al.*, 1983; Groenewegen and Ruschen, 1984; Heimer *et al.*, 1991; Zahm and Heimer, 1993; Usuda *et al.*, 1998); similar pathways have been reported in monkeys (Haber *et al.*, 1990), but these have not been studied in comparable detail.

The main inputs from the *amygdala* to the hypothalamus in rodents arise from the corticomedial and central nuclei. The cortical, medial, basomedial, and posterior nuclei innervate the medial preoptic and anterior and lateral hypothalamic areas and the ventromedial and ventral premammillary nuclei (Coolen and Wood, 1998; Canteras *et al.*, 1992, 1995; Gomez and Newman, 1982; Petrovich *et al.*, 1996). These pathways have been implicated in relaying the olfactory influence on reproductive behavior (Lehman and Winans, 1982). The central nucleus mainly projects to the lateral hypothalamic area (Krettek and Price, 1978; Price and Amaral, 1981) and has been implicated in the amygdaloid influence on the autonomic system (Schwaber *et al.*, 1982). In rats, fibers from the amygdala reach the hypothalamus via two pathways: a short, direct projection over the surface of the optic tract (the ventral amygdalofugal pathway, a component of the ansa peduncularis) and a long, looping projection through the stria terminals. The latter fiber bundle runs through the floor of the lateral ventricle just across from the free edge of the fornix. It then passes through (and extensively innervates) the bed nucleus of the stria terminalis before residual fibers enter the medial forebrain bundle, through which it distributes largely to the medial preoptic and hypothalamic nuclei. The organization of these pathways is similar in monkeys (Nauta, 1961; Price and Amaral, 1981), although the stria terminalis projection could not be followed as far caudally as the tuberal hypothalamus. Little is known about the functional significance of these pathways in primates. Lesions of the stria terminalis combined with interruption of the fimbria of the fornix in monkeys have been reported to impair visual memory (Mishkin, 1982), but it is not clear that it is the hypothalamic portion of these pathways that is important for this function.

The bed nucleus of the stria terminalis provides extensive projections to the hypothalamus in rodents that largely overlap those from the amygdala (see Numan and Numan, 1996; Dong *et al.*, 2000). However, this region has received little study in primates. The dorsal part of the substantia innominata also projects to the lateral hypothalamic area in monkeys (Kim *et al.*, 1976). In rats, the dorsal part of the substantia innnominata has projections consistent with its role as a part of the extended amygdala, innervating the medial preoptic and anterior hypothalmic areas, and the paraventricular, dorsomedial, ventromedial, arcuate, and ventral premammillary nuclei (Grove, 1988).

Cortical inputs to the hypothalamus in rats arise primarily from insular, lateral frontal, infralimbic, and prelimbic fields (Kita and Oomura, 1982; Saper, 1982; Tucker and Saper, 1984; Sesack *et al.*, 1989). In addition, there are afferents from olfactory cortical areas, including the primary olfactory cortex and anterior olfactory nucleus (see below and Chapter 32). Projections from the prelimbic and infralimbic areas in monkeys (areas 32 and 25) most heavily innervate the anterior hypothalamic area, perifornical region, and ventromedial nucleus, whereas the orbitoinsular area (including areas 13a, 12o, and Iai) projects to the lateral hypothalamic area most densely (Ongur *et al.*, 1998; Friedman *et al.*, 2000; Rempel-Clower and Barbas, 1998; Barbas *et al.*, 2000). Frontal cortical projections to the ventromedial nucleus and mammillary body have been reported in Glees-stained specimens from frontal leukotomy patients. However, it appears probable that this result was an artifact of the method used (see Nauta and Haymaker, 1969, for discussion). Nevertheless, corticohypothalamic projections similar to those described above in monkeys are likely to exist in humans as well.

The cortical and olfactory inputs to the hypothalamus form the anterior roots of the *medial forebrain bundle.* This fiber pathway, which runs longitudinally through the lateral hypothalamic area linking the hypothalamus with the forebrain rostrally and the brain stem caudally (Veening *et al.*, 1982), is really misnamed. Although it is medial to the internal capsule (the "lateral forebrain bundle"), the medial forebrain bundle is actually quite laterally placed in the hypothalamus. It also does not form a "bundle" in the strict sense. Most of the fibers are unmyelinated, and they are difficult to pick out in myelin-stained preparations. The axons of the medial forebrain bundle are widely dispersed across the lateral hypothalamus, intercalating themselves among the

neuronal populations, rather than forming a discrete fiber bundle (e.g., like the column of the fornix). Finally, some prominent components of the medial forebrain bundle have little to do with the hypothalamus, e.g., the nigrostriatal bundle.

Ascending Pathways from the Brain Stem

The ascending inputs to the hypothalamus from the brain stem originate in a wide variety of sources, including the nucleus of the solitary tract and ventrolateral reticular formation in the medulla; the parabrachial nucleus, locus coeruleus, and raphe nuclei in the pons; and the periaqueductal gray matter and ventral tegmental area in the midbrain. Each of these will be discussed in more detail below. These ascending pathways enter the hypothalamus via three main pathways. Many of the axons form the ascending root of the *medial forebrain bundle.* Afferents from monoaminergic and sensory systems, discussed below, contribute to this pathway. Another important component of the lateral hypothalamic ascending system is the *ventral supraoptic commissure* pathway. The ventral supraoptic commissure refers to axons that cross the midline of the hypothalamus along the caudal edge of the optic chiasm, then follow the optic tract back through the lateral hypothalamus (Nauta and Haymaker, 1969). Axons from a various sensory systems, particularly those concerned with pain (Cliffer *et al.*, 1991; see also Chapter 30), reach the hypothalamus from the brain stem by passing just medial to the lateral geniculate nucleus and following the medial surface of the optic tract back into the hypothalamus. Some hypothalamic intrinsic pathways also cross the midline in this path.

A third major pathway for brain stem afferents to the hypothalamus is the *periventricular fiber system* (Sutin, 1966). This tract was originally termed the dorsal longitudinal fasciculus of Schütz, on the basis of myelin-stained material, but most of the axons are not myelinated, and they do not form a bundle nor are they dorsally located. Rather, they penetrate diffusely through the periaqueductal gray matter of the midbrain into the periventricular third ventricular white matter. Some older textbooks still use the archaic term, but the more descriptive name proposed by Sutin is preferable.

A classical myelinated ascending input to the mammillary body, the mammillary peduncle, arises from the dorsal and ventral tegmental nuclei in the midbrain in rats (Cowan *et al.*, 1964). The mammillary peduncle is difficult to identify in the human brain, but just caudal to the mammillary body a myelinated bundle can be seen on the ventral surface of the midbrain, just medial to the cerebral peduncle. These fibers appear to enter the capsule of the mammillary body, although it is not possible to trace them caudally to their origin.

Each of the classes of monoamine cell groups in the rat brain stem provides innervation to the hypothalamus through both the medial forebrain bundle and the periventricular pathways. The origins and distribution of noradrenergic projections from the locus coeruleus and the medulla to the hypothalamus in rats has received considerable study (Sawchenko and Swanson, 1982; Tucker *et al.*, 1987). The organization of both noradrenergic and serotonergic cell groups in the brain stems of monkeys (Felten *et al.*, 1974; Garver and Sladek, 1975; Sladek *et al.*, 1982) and humans (Saper and Petito, 1982; J. Pearson *et al.*, 1983, 1990) is quite similar to that of rats, but little is known about the hypothalamic projections of these fiber systems in primates.

Projections to the hypothalamus from brain stem autonomic areas may be organized somewhat differently in monkeys than in rats. Both the nucleus of the solitary tract and the parabrachial nucleus project extensively to the lateral hypothalamic area, and the dorsomedial, paraventricular, and median preoptic nuclei in rats (Ricardo and Koh, 1978; Saper and Loewy, 1980; Bester *et al.*, 1997). There is also a separate projection from the parabrachial nucleus to the ventromedial nucleus (Fulwiler and Saper, 1984, 1985; Bester *et al.*, 1997). In monkeys, the projections from both the nucleus of the solitary tract and the parabrachial nucleus to the hypothalamus have been described as less intense than in rats (Beckstead *et al.*, 1980; Pritchard *et al.*, 2000). However, both of these studies employed the transport of tritium-labeled amino acids, which is less sensitive than modern tracer methods, so it is possible that these projections may be more extensive than earlier studies could demonstrate.

The periaqueductal gray matter in monkeys projects to the hypothalamus mainly via a periventricular route (Mantyh, 1983). The axons innervate most of the medial hypothalamic nuclei, including the medial preoptic, the anterior and posterior hypothalamic areas, and the ventromedial and dorsomedial nuclei, as well as the lateral hypothalamic area.

Intrinsic Connections of the Hypothalamus

Most studies of hypothalamic connections have concentrated on long-range connections in rodents. Often nearby connections are either obscured by the spread of tracer from the injection site or not emphasized in the analysis. Unfortunately, even less is known about hypothalamic intrinsic connections in primates. However, studies in rats, particularly those using the anterograde tracer *Phaseolus vulgaris* leucoagglutinin, have demonstrated some features of intrahypothalamic connections.

The structures in the medial part of the preoptic region in rats, including the median preoptic, medial preoptic, anteroventral periventricular, ventromedial preoptic, and periventricular preoptic nuclei, primarily project to the medial tuberal hypothalamus, including the paraventricular, ventromedial, and arcuate nuclei (Saper and Levisohn, 1986; Simerly and Swanson, 1988). The suprachiasmatic nucleus projects extensively into the medial part of the anterior hypothalamic area (the "subparaventricular zone") and back into the dorsomedial nucleus (Watts *et al.*, 1987), and similar projections have been confirmed by postmortem tracing in human brains (Dai *et al.*, 1998b; Abrahamson *et al.*, 2001). The anterior hypothalamic area projects into the perifornical part of the lateral hypothalamic area, as well as to the ventromedial and dorsal premammillary nuclei and the posterior hypothalamic area (Risold *et al.*, 1994). Smaller numbers of fibers enter the dorsomedial nucleus and the retrochiasmatic area. At the tuberal level, the arcuate nucleus projects to the paraventricular nucleus and lateral hypothalamic area both in rats and in humans (Elias *et al.*, 1998; Broberger *et al.*, 1998). The dorsomedial part of the ventromedial nucleus projects into the anterior hypothalamic area (including the subparaventricular zone), while the ventrolateral part projects to the medial preoptic and ventral premammillary nuclei as well as the lateral hypothalamic area (Canteras *et al.*, 1994; Saper *et al.*, 1979b; Elmquist *et al.*, 1998). The dorsomedial nucleus projects heavily to the paraventricular nucleus and less intensely to the median preoptic, medial preoptic, and anteroventral periventricular nuclei, and the lateral hypothalamic and retrochiasmatic areas (Thompson *et al.*, 1996; Elmquist *et al.*, 1998). The dorsal premammillary nucleus primarily projects to the anterior hypothalamic area (Canteras and Swanson, 1992), and the ventral premammillary nucleus to the ventrolateral part of the ventromedial nucleus and the medial preoptic nucleus (Canteras *et al.*, 1992).

In general, much less is known about intrinsic hypothalamic connections in humans or monkeys, although what is known suggests that they are similar to those documented in rats. The medial hypothalamic nuclei in monkeys provide the greatest amount of intrinsic connections, whereas the lateral hypothalamus is the major source of long ascending and descending projections (Saper *et al.*, 1978, 1979). Sketchy information available on the projections of the ventromedial nucleus of monkeys (Saper *et al.*, 1979a) is consistent with that from rats but relies on information from autoradiographic studies that are less sensitive than modern tracers. Recent studies of the chemically defined projections containing agouti-related protein, neuropeptide Y, or α-melanocyte-stimulating hormone, from the arcuate nucleus to the lateral hypothalamic area in human brain, shows that this pathway to orexin and melanin-concentrating neurons is virtually identical to that found in rats (Elias *et al.*, 1998).

Efferents

The efferent projections from the hypothalamus, like the afferents, consist of both ascending and descending projections. Both projections include components that follow the medial forebrain bundle, as well as periventricular components.

The ascending projections from the hypothalamus to the *cerebral cortex* have been examined using retrograde transport in both rats and monkeys (Kievet and Kuypers, 1975; Köhler and Swanson, 1984; Mesulam *et al.*, 1983; Porrino and Goldman-Rakic, 1982; Saper, 1985; Shiosaka *et al.*, 1984; Tigges *et al.*, 1983; Rempel-Clower and Barbas, 1998). In rats, four separate hypothalamocortical cell groups can be distinguished (see Saper, 1985): (1) Tuberal lateral hypothalamic neurons innervate the entire cortical mantle, including the hippocampal formation and the amygdala, in a crudely topographical manner. As we will discuss below, many of these neurons contain either melanin-concentrating hormone or orexin/hypocretin peptides. (2) The posterior lateral hypothalamus contains a separate population of neurons whose neurotransmitters are not yet known but that similarly project to the entirety of the ipsilateral cortex. The posterior lateral hypothalamic projection is organized in a strictly topographical manner. (3) Cortically projecting neurons in the fields of Forel have the narrowest range, innervating only the ipsilateral frontal and paralimbic fields in a loosely topographical fashion. (4) By contrast, tuberomammillary neurons on each side of the brain innervate the entire cortical mantle bilaterally but are not topographically organized. The tuberomammillary neurons contain histamine, as well as GABA, and galanin in both rats (Panula *et al.*, 1984; Vincent *et al.*, 1983; Staines *et al.*, 1986) and humans (Chan-Palay and Jentsch, 1992; Panula *et al.*, 1990).

Anterograde tracing studies in rats demonstrate that hypothalamic neurons project to the cerebral cortex via the medial forebrain bundle (Saper, 1985). At the level of the preoptic area, one group of fibers turns laterally, running ventral to the globus pallidus and the putamen, to enter the external capsule from which they are distributed to the cortex of the lateral wall of the hemisphere, including much of the temporal lobe outside the hippocampus. The remaining hypothalamocortical fibers follow the medial forebrain bundle rostrally, run along the dorsal surface

of the diagonal band nucleus, and then rostrally and dorsally. One bundle of axons enters the fornix and travels along back along it to innervate the hippocampal for mation. The other bundle runs over the genu of the corpus callosum into the cingulate bundle, from which its axons are distributed to the cortex of the medial wall of the cerebral hemisphere.

In several species of monkeys, investigators have noted retrogradely labeled neurons in the tuberal and posterior lateral hypothalamus (probably including the tuberomammillary nucleus, although this has not been separately identified) following injections into the frontal, parietal, and occipital cortex (Kievet and Kuypers, 1975; Porrino and Goldman-Rakic, 1982; Tigges *et al.*, 1983; Mesulam *et al.*, 1983; Rempel-Clower and Barbas, 1998). Although the data are less extensive than in rats, the medial-to-lateral topography of the lateral hypothalamic projection to the cerebral cortex appears to be preserved in monkeys (Rempel-Clower and Barbas, 1998). By staining melanin-concentrating hormone, orexin/hypocretin, and histaminergic neurons immunocytochemically in human brains, it has been possible to confirm the origins and pathways for these portions of the hypothalamocortical projection (Elias *et al.*, 1998 and unpublished observations; Panula *et al.*, 1990). The neurons of each of these populations are more widely dispersed in humans than in rats, occupying an overlapping region of the tuberal and posterior lateral hypothalamus (Fig. 17.9). However, the orexin- and melanin-concentrating hormone-containing neurons form interlacing clusters of cells rather than diffusely overlapping one another's distribution (Elias *et al.*, 1998). The ascending fiber pathways, and even the diffuse terminal distribution, favoring the deeper layers of the cerebral cortex, are much the same in human and rat brain.

Many hypothalamic nuclei also provide inputs to *the septum* or to *the extended amygdala*, including the bed nucleus of the stria terminalis and the substantia innominata. The ventromedial nucleus in monkeys projects to the capsule of the central nucleus of the amydgala, the substantia innominata (including the basal nucleus of Meynert), and the lateral part of the bed nucleus. The ventromedial nucleus also projects to the ventral lateral septal nucleus, whereas the lateral hypothalamic area projects to the medial septal nucleus (Saper *et al.*, 1979a).

The hypothalamus also provides afferents to the *thalamus* in rats (Risold *et al.*, 1997). Many of the medial nuclei project through the periventricular pathway to the paraventricular nucleus of the thalamus. These same cell groups give off collaterals to the nucleus reuniens, midline thalamic nuclei, and intralaminar nuclei as well. In addition, the lateral preoptic area sends a projection through the *stria medullaris* to the lateral habenular nucleus, in the epithalamus.

However, the most prominent hypothalamic projection to the thalamus is the mammillothalamic tract. These fibers leaves the mammillary body from its dorsomedial surface in a shallow ascending arc. Many of these axons bifurcate, giving rise to the mammillotegmental tract in rats (Fry and Cowan, 1972); similar studies have not been done in primates. The mammillothalamic fibers run in a dense bundle dorsally into the internal medullary lamina before entering the anterior thalamic nuclei. Unlike other species, the human anterior thalamic nuclei are not easily separated into distinct cell groups (Armstrong, 1990; see also Chapter 1). This lack of differentiation may reflect the fact that the most cytologically distinctive component of the anterior nuclei in other species, the anterodorsal nucleus, which primarily receives the output of the lateral mammillary nuclei, has not been identified in adult human brains. Comparative studies indicate that the mammillary body, the mammillothalamic tract, and the anterior thalamic nuclei reach their greatest state of development in anthropoids (see Armstrong, 1986, 1990). However, the increase in size primarily involves the medial mammillary nucleus, while the lateral nucleus remains quite small, its very existence being controversial (see above). Therefore it seems likely that the anterior thalamic nuclei of the human brain represent primarily the anteroventral, anteromedial, and laterodorsal nuclei, which receive medial mammillary inputs (Veazey *et al.*, 1982).

Although these pathways have received only limited study in primates, the projections from the ventromedial nucleus and anterior hypothalamic area to the midline and intralaminar thalamic nuclei have been confirmed (Saper *et al.*, 1978; 1979a). The projections from the medial mammillary nucleus to the anteroventral, anteromedial, and laterodorsal thalamic nuclei, and from the lateral mammillary nucleus to the anterodorsal nucleus, have also been identified in monkeys (Veazey *et al.*, 1982), and the mammillothalamic tract is among the most easily identified myelinated pathways in human brains.

The *descending projections* from the hypothalamus through the *periventricular* pathway originate widely from virtually all of the medial and periventricular hypothalamic nuclei in monkeys, much as they do in rats (Saper *et al.*, 1978, 1979a). These axons descend through the peraqueductal gray matter, but most terminate before the aqueduct opens into the fourth ventricle. Some axons via this pathway may reach as far as the rostral pole of the locus coeruleus.

The bulk of the descending pathway from the hypothalamus travels through the medial forebrain bundle

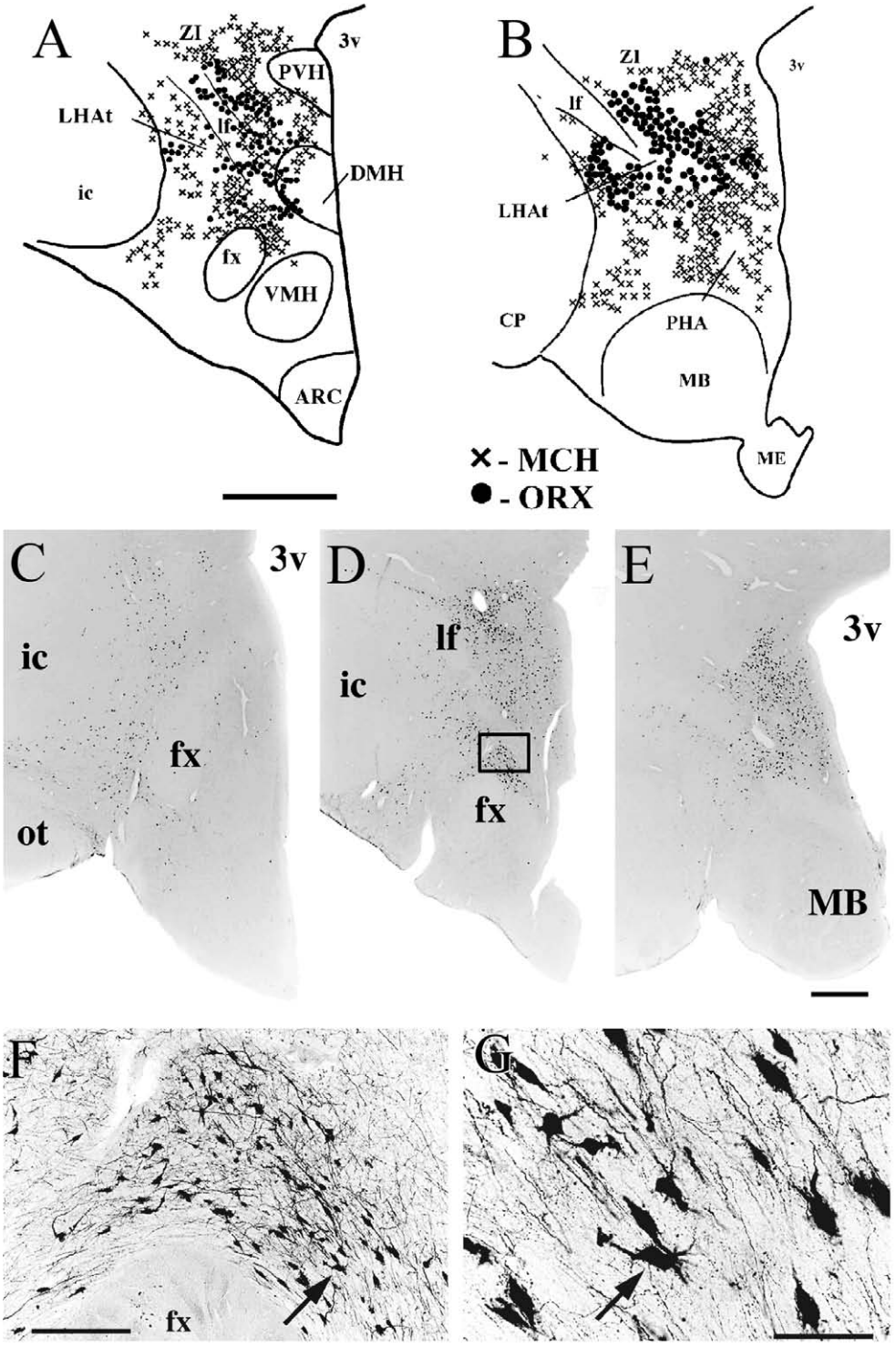

FIGURE 17.9 A series of drawings **(A, B),** and photomicrographs **(C–G)** illustrating the melanin-concentrating hormone and orexin neurons in the human lateral hypothalamus. In panels A and B, the distribution of neurons that are immunoreactive for the two peptides has been plotted from adjacent sections onto a single plane. Note that clusters of neurons containing each peptide are interlaced with clusters containing the other peptide. Panels C–D show the pattern of melanin-concentrating hormone neurons at low magnification in a series of sections roughly corresponding to Figures 17.5–17.7. Panel F shows a magnified view of the boxed area in panel D, and panel G shows a higher magnification of the area indicated by the arrow in panel F. Note the clustering of these neurons in the perifornical region. Scales = 3 mm for A; 2.4 mm for B; 1.5 mm in C–E; 200 μm in D; 100 μm in E. Modified from Elias *et al.*, 1998, with permisson.

and runs laterally at the level of the ventral tegmental area, to take a lateral position within the brain stem tegmentum. These fibers travel along the dorsal surface of the substantia nigra, and some may communicate with neurons of the ventral tegmental area or the substantia nigra (Saper *et al.*, 1978, 1979a). Many axons from medial hypothalamic cell groups such as the ventromedial nucleus terminate in the midbrain reticular formation, dorsal to the substantia nigra.

Only a relatively modest number of hypothalamic cell groups provide axons that descend further to the lower brain stem and the spinal cord. In rats, many of these axons terminate in autonomic or somatic sensory nuclei, such as the nucleus of the solitary tract, the parabrachial nucleus, or the outer laminae of the trigeminal or spinal dorsal horn, where they may modulate ascending afferents. Others end in the ventrolateral reticular formation or the spinal intermediate gray matter, where they may be involved in the modulation of brain stem or spinal reflexes, particularly those involved in autonomic and respiratory control. A similar pathway has been observed after large injections of anterograde tracers into the lateral hypothalamus and the paraventricular nucleus in monkeys (Saper *et al.*, 1976). The hypothalamic projections to the parasympathetic and sympathetic preganglionic cell groups in rats have been studied by retrograde transport (Saper *et al.*, 1976a; Swanson and Kuypers, 1980; Cechetto and Saper, 1988; Elias *et al.*, 2000; Zhang *et al.*, 2000) and viral transneuronal transport (Jansen *et al.*, 1992, 1997). This projection originates from the paraventricular and dorsomedial nuclei and the lateral hypothalamic area, as well as the lateral part of the arcuate nucleus and the adjacent retrochiasmatic area. In monkeys, similar studies have been done only using the less sensitive horseradish peroxidase retrograde tracing method. Nevertheless, these observations have confirmed projections from the paraventricular and dorsomedial nuclei and the lateral hypothalamic area to the medullary and spinal preganglionic cell groups (Saper, 1976a).

Likewise, studies tracing the hypothalamo-autonomic pathways in the anterograde direction have not been repeated using more sensitive modern tracers in primates. In monkeys, the descending projection from the hypothalamo-autonomic cell groups has been examined using very large injections of tritiated amino acids into the paraventricular nucleus and adjacent lateral hypothalamus (Saper *et al.*, 1976a). As in rats and cats, the descending pathway runs through the medial forebrain bundle into the lateral part of the brain stem tegmentum. One branch innervates the parabrachial nucleus in the pons, while the other traverses the ventrolateral medulla (just dorsolateral to the inferior olivary complex) to enter the dorsal lateral funiculus of the spinal cord. Fibers turn dorsally from this pathway in the medulla to innervate the nucleus ambiguus, the nucleus of the solitary tract, and the dorsal motor vagal nucleus. In the spinal cord, hypothalamic fibers can be traced to the sympathetic and parasympathetic preganglionic cell columns in the thoracic and sacral intermediolateral columns. The details of this spinal projection in monkeys have been demonstrated in the greatest detail by immunohistochemical staining for one of its neurotransmitters, oxytocin (see next section). The existence of a similar pathway in humans can be inferred from the presence of an ipsilateral sympathetic deficit following injury to the hypothalamus, lateral brain stem tegmentum, or spinal lateral funiculus (Nathan and Smith, 1986).

FUNCTIONAL ORGANIZATION OF THE HYPOTHALAMUS

The functional organization of the hypothalamus can be best appreciated in terms of its role as an *integrative* structure. By nature, it receives a wide variety of different afferent inputs which modulate specific drive states, and it controls autonomic, endocrine, and behavioral outputs which allow it to accomplish those goals. This section will describe circuitry along the same lines, beginning with the different sensory inputs, and how they are used to assess *homeostatic*, *allostatic*, and *circadian* needs. It will then review briefly what is known about the circuitry underlying regulation of autonomic, endocrine, and behavioral responses. Finally, it will review several functional systems, including feeding and energy metabolism; fluid and electrolyte control; reproduction; thermoregulation and fever; and wake–sleep regulation.

Sensory Afferent Inputs to the Hypothalamus

Although it was once thought that sensory afferents reach the hypothalamus only through multisynaptic and rather indirect pathways (see Nauta and Haymaker, 1969), work in recent decades has identified direct sensory inputs to the hypothalamus from nearly every sensory system. Much of this work was originally done in rodents, but in some cases correlative studies have been done in monkey or human brains.

Olfactory input arrives in the hypothalamus in rodents via relays in the olfactory tubercle, anterior olfactory nucleus, corticomedial amygdala, and olfactory cortex (Lehman and Winans, 1982; Switzer *et al.*, 1986; Price *et al.*, 1991), although in primates the main olfactory relays may include the nucleus accumbens and

septal nuclei (Tazawa *et al.*, 1987; see also Chapter 32). Olfactory afferents terminate throughout the lateral hypothalamus. In rodents there is an especially dense projection to the gemini nuclei in the premammillary part of the lateral hypothalamus from the polymorphic layer of the olfactory tubercle (Price *et al.*, 1991). A homologous projection has been identified in monkeys (Veazey *et al.*, 1982) but has not yet been described in humans (see also Chapter 32). In rodents, which have a well-developed vomeronasal organ that samples pheromones, the accessory olfactory system relays in the cortical and medial nuclei of the amygdala to provide inputs to the medial preoptic and ventromedial nuclei (Lehman and Winans, 1982; Coolen and Wood, 1998). Although it has recently been established that humans also have a vomeronasal organ, very little is known of its central connectivity (Jhanke and Merker, 2000; see Chapter 22, for additional discussion of this issue).

Visual afferents reach the hypothalamus via a direct retinal projection. In all mammalian species, including humans, some retinal fibers leave the optic chiasm and pass dorsally into the hypothalamus, where they innervate the suprachiasmatic nuclei (Sadun *et al.*, 1984; Moore, 1993; Dai *et al.*, 1998a). In addition, in rodents many retinal fibers bypass the suprachiasmatic nucleus and distribute more widely in the subparaventricular zone, the ventrolateral preoptic nucleus, and the lateral hypothalamic and retrochiasmatic areas (Johnson *et al.*, 1988; Lu *et al.*, 1999). Similar pathways have been described in nonhuman primates (Costa *et al.*, 1999; Reuss and Fuchs, 2000) and, to a lesser extent, in humans (Dai *et al.*, 1998a).

Somatic sensory information reaches the hypothalamus via a direct route: a projection to the lateral hypothalamic area from wide-dynamic-range mechanoreceptive and thermoreceptive neurons in the spinal and trigeminal dorsal horn has been reported in both rats and monkeys (Burstein *et al.*, 1987). These afferents have been traced anterogradely in rats, in which they reach the hypothalamus via the ventral supraoptic commissure pathway and provide afferents to the medial preoptic region and the lateral hypothalamic area (Cliffer *et al.*, 1987).

Visceral sensory inputs to the hypothalamus, including taste, arise from the nucleus of the solitary tract, which projects directly to the hypothalamus in rats (Ricardo and Koh, 1978). Similar experiments using injections of tritiated amino acids in monkeys have failed to provide evidence for such a projection (Beckstead *et al.*, 1980; see also Chapter 31), although studies using modern and more sensitive tracers have not been reported. Visceral sensory information from the nucleus of the solitary tract may, however, be relayed to the hypothalamus via projections of the solitary nucleus to the ventrolateral medullary reticular formation, the parabrachial nucleus, or the periaqueductal gray matter. The projection from the ventrolateral medulla to the hypothalamus arises predominantly from noradrenergic and adrenergic neurons in the A1 and C1 cell groups in rats (Tucker *et al.*, 1987) but has not received similar study in primates. The projection from the nucleus of the solitary tract to the parabrachial nucleus is very substantial both in rats and in monkeys (Beckstead *et al.*, 1980; Ricardo and Koh, 1978). The parabrachial projection to the hypothalamus is quite extensive in rats (Saper and Loewy, 1980; Fulwiler and Saper, 1984; Bester *et al.*, 1997). Evidence from experiments tracing the pathway with tritiated amino acid suggest a more restricted distribution in monkeys (Pritchard *et al.*, 2000), including dense inputs mainly to the lateral hypothalamic area, dorsomedial and ventromedial nuclei, and the preoptic area, and only light innervation of the arcuate and paraventricular nuclei. However, it is possible that more sensitive methods may demonstrate more extensive parabrachial projections to the hypothalamus in primates. For example, one recent study that used immunohistochemical staining of calcitonin gene–related protein to trace parabrachial projections to the forebrain in humans (de Lacalle and Saper, 2000) demonstrated more extensive projections to the thalamus, amygdala, and bed nucleus of the stria terminalis than were reported in monkeys. The projection from the nucleus of the solitary tract to the periaqueductal gray matter originates mostly from noradrenergic neurons in the A2 catecholamine cell group (Herbert and Saper, 1992). The periaqueductal gray matter, in turn, provides extensive projections to the nuclei of the medial hypothalamus in monkeys (Mantyh, 1983; see also Chapter 12).

Despite extensive study, no direct projection to the hypothalamus from the *auditory* system has been identified (LeDoux *et al.*, 1985). Nevertheless, it is clear that auditory information, like visual and somatic sensory input, may influence the firing of hypothalamic neurons in both rats and monkeys (Burstein *et al.*, 1987; Fisher and Almli, 1984; Oomura *et al.*, 1983; Rolls *et al.*, 1976). Many hypothalamic neurons respond best to complex sensory stimuli, suggesting that the sensory information that drives them is highly processed (Oomura *et al.*, 1983; Rolls *et al.*, 1976). It is likely, therefore, that much of the sensory information that reaches the hypothalamus travels by polysynaptic routes involving convergence of cortical sensory pathways in the amygdala, hippocampus, and cerebral cortex (Jones and Powell, 1970; Turner *et al.*, 1980; van Hoesen *et al.*, 1972).

Circuitry Supporting Hypothalamic Drive States

Homeostatic drives require both access to sensory inputs from the body, as described above, as well as *interoceptors,* or neuronal receptors that are internal to the brain. These include neurons within the hypothalamus that are especially responsive to local temperature (Boulant and Bignall, 1973; Hori *et al.,* 1986), glucose (Oomura, 1988; Shiraishi *et al.,* 1999; Lee *et al.,* 1999), osmolality (Bourque and Oliet, 1998), or sodium (Voisin *et al.,* 1999), as discussed below. In addition, the brain must have access to information about the levels of various nutrients and hormones in the bloodstream. Direct access for these molecules to the brain is prohibited by the blood–brain barrier, consisting of tight junctions between capillary endothelial cells that lack fenestrations. This arrangement prevents any hydrophilic compounds from entering the brain from the bloodstream unless they are specifically transported in. To overcome this barrier, the brain maintains a set of small "windows" on the circulation. These *circumventricular organs* are specialized neurohemal contact zones, along the borders of the ventricular system of the brain (Broadwell and Brightman, 1976; see also Chapter xx). The subfornical organ at the foramen of Monro, the organum vasculosum of the lamina terminalis at the anteroventral tip of the third ventricle, the median eminence at the midline in the floor of the tuberal hypothalamus, and the area postrema at the caudal end of the fourth ventricle all have fenestrated capillaries. Even large proteins in the bloodstream can enter the circumventricular organs, where they can interact with neurons that are just outside the blood–brain barrier (Broadwell and Brightman, 1976). Small amounts of blood-borne substances can penetrate the borders of the circumventricular organs and enter the brain for 1–2 mm, but most of the substances that gain entry are washed away in the cerebrospinal fluid. Specific homeostatic signals and their targets will be discussed below as we consider different functional systems in the hypothalamus.

Circadian rhythms in the brain are organized by the suprachiasmatic nucleus. This structure is difficult to identify in Nissl-stained sections of human brain, as it is far less prominent than it appears in rats and even in other primate brains (Moore, 1997). However, many neurons in the suprachiasmatic nucleus in rats contain vaspressin or vasoactive intestinal polypeptide, and the same peptide may be used as a marker for identifying the human suprachiasmatic nucleus as well (Stopa *et al.,* 1984; Mai *et al.,* 1991; Hofman *et al.,* 1996; Dai *et al.,* 1997).

Lesions of the suprachiasmatic nucleus result in loss of daily rhythms of wake–sleep activity, feeding, body temperature, and a variety of hormones, including melatonin and cortisol (see Moore, 1997). However, humans (e.g., shift workers) and animals (e.g., when food availability is restricted to normal sleeping hours) can entrain to activity cycles that are dictated by social or physiological necessity, rather than the light cycle. These observations suggest that, while the suprachiasmatic nucleus may be the pacemaker for circadian activity, there may be mechanisms downstream that are capable of modifying the output of the circadian clock and reorganizing activity, metabolic, and hormonal patterns.

One candidate for this function is the subparaventricular zone. In rats, the suprachiasmatic nucleus projects massively to the subparaventricular zone, which stretches from the dorsal surface of the suprachiasmatic nucleus, back into the area just ventral to the paraventricular nucleus, and caudally into the dorsomedial nucleus (Watts *et al.,* 1987). A similar pathway has been identified using postmortem tracing in human brains (Dai *et al.,* 1998). This column of tissue receives intense input from the suprachiasmatic nucleus throughout its course. Recent work in rodents suggests that lesions in the subparaventricular zone can profoundly interrupt circadian cycles of wakefulness and sleep, activity, and body temperature (Lu *et al.,* 2001). However, similar work in primates is so far lacking.

Allostatic drives are activated by perception of physiological challenges that are discrete and potentially of overwhelming importance (as opposed to the graded and often smaller challenges that constitute homeostatic challenges). McEwen (2000) defines allostatic challenges as those that produce stress, and which require change rather than return to equilibrium. Attack by a predator or competitor could be examples of allostatic challenges, but so could the presence of a potential mate. Such external allostatic challenges are detected by the classical sensory systems and identified by higher cognitive systems in the cerebral cortex. Access to the hypothalamus in primates is likely to involve cortical, amygdaloid, or hippocampal pathways.

Other allostatic challenges may be of internal origin. For example, extensive tissue injury or blood loss is sensed by visceral afferent systems. However, responses to invading microorganisms require additional sensory mechanisms. In response to a variety of immune challenges, white blood cells in various parts of the body make cytokines (see Breder and Saper, 1994). These hormones, which attract and recruit other immune system cells to battle the invader, also act on

the nervous system. Prostaglandins play a key role in this process, as inhibiting their synthesis blocks most of the CNS response to inflammation (Elmquist *et al.*, 1997). Prostaglandins made in various organs may act on local sensory branches of the vagus nerve, thus signaling the brain. In addition, circulating cytokines or other inflammatory signals may cause secretion of prostaglandins by the endothelial cells and perivascular microglia lining small venules at the borders of the brain (Laflamme *et al.*, 1999). Prostaglandins are lipids, and they can diffuse across the blood–brain barrier to activate CNS responses, which will be described below.

Autonomic and Endocrine Efferents of the Hypothalamus

The hypothalamus controls the autonomic nervous system by means of a series of both direct and relayed inputs to the parasympathetic and sympathetic preganglionic neurons in the medulla and the spinal cord. The origins of this pathway, in the paraventricular nucleus, arcuate nucleus, and lateral hypothalamic area, are described in the section on descending pathways above, as is the course of the pathway to the brain stem and the spinal cord. Oddly, the same pattern of retrograde labeling is seen in the hypothalamus from injections of retrograde tracers at virtually every spinal level in both rats and monkeys (Saper *et al.*, 1976a; Saper and Cechetto, 1988). Injections of pseudorabies virus for retrograde transneuronal labeling have demonstrated only minor variations in the pattern of retrograde labeling in the paraventricular nucleus after injections into different peripheral targets (Bamshad *et al.*, 1998; Smith *et al.*, 1998; Jansen *et al.*, 1997, 1992; Haxhiu *et al.*, 1993; Schramm *et al.*, 1993; Spencer *et al.*, 1990; Strack *et al.*, 1989). Recent studies in rats, however, have found that different patterns of hypothalamospinal neurons show Fos protein expression after specific physiological stimuli. For example, after injection of leptin, nearly all of the hypothalamospinal cells that show Fos expression are found in the arcuate nucleus (Elias *et al.*, 1998), whereas after administration of an immune stimulus such as lipopolysaccharide, nearly all of the hypothalamospinal cells that show Fos expression are in the dorsal parvicellular part of the paraventricular nucleus (Zhang *et al.*, 2000). These studies suggest that the unit of functional organization of the hypothalamic projection to the preganglionic nuclei may be functional, with neurons that participate in a specific response clustering together in one of the cell groups that constitute the hypothalamospinal system. These cells appear to project down the entire length of the sympathetic preganglionic column, specifically innervating those neurons necessary for that response at multiple spinal levels. Such a plan of organization would be consistent with widespread retrograde transport from any single organ (which can be involved to a greater or lesser degree in a wide range of physiological responses).

The neurons in the different cell groups that give rise to the hypothalamospinal pathway contain distinct peptide transmitters. The spinally projecting neurons in the paraventricular nucleus in the rat mainly contain oxytocin or vasopressin. Early immunohistochemical studies in rats found that fewer than 5% of cell bodies that project to the spinal cord stained for these peptides (Swanson and Sawchenko, 1983). However, unlike the magnocellular oxytocin and vasopressin neurons, which project to the pituitary gland but not the spinal cord (Swanson and Kuypers, 1980) (Fig. 17.8), the hypothalamospinal neurons are much smaller, and they are much less intensely stained for vasopressin or oxytocin. After colchicine administration, a much larger number of paraventriculospinal neurons stain for these peptides: about 25% of the retrogradely labeled neurons stained for oxytocin and up to 35% for vasopressin (Cechetto and Saper, 1988). Studies using *in situ* hybridization have found that about 40% of paraventriculospinal neurons contains vasopressin (Hallbeck and Blomqvist, 1999), suggesting that the immunocytochemical methods employed in most earlier studies were not adequately sensitive. Immunocytochemical studies in both rats (Teclemariam-Mesbah *et al.*, 1997; Motawei *et al.*, 1999) and monkeys (Swanson and McKellar, 1979) confirm that large numbers of oxytocin and vasopressin terminals appose sympathetic preganglionic neurons.

In contrast, many of the neurons in the arcuate nucleus that project to the spinal cord contain both proopiomelanocortin and its derivatives (such as α-melanocyte stimulating hormone (α-MSH) and β-endorphin) as well as the peptide known as CART (cocaine and amphetamine–regulated transcript) (Elias *et al.*, 1998). Early studies on the lateral hypothalamic projection to the spinal cord in rats showed that they stain with certain antisera against α-MSH (Cechetto and Saper, 1988). However, these cells did not not stain with other antisera against proopiomelanocortin derivatives, and many α-MSH antisera did not recognize them (see Saper *et al.*, 1986), suggesting that this staining represented cross-reactivity with an unidentified protein. More recently, it has been shown that many lateral hypothalamic neurons that project to the spinal cord contain either orexin/hypocretin or MCH (Bittencourt and Elias, 1998; van den Pol, 1999; Date *et al.*, 2000). A large percentage of the latter

neurons also contain CART (Broberger, 1999). The roles of these different peptides in the spinal cord have received only limited attention. Both oxytocin and vasopressin in the hypothalamospinal projection are probably excitatory (Ma and Dun, 1985; Desaulles *et al.*, 1995: Kolaj and Renaud, 1998), as is orexin/hypocretin (van den Pol, 1999).

None of these pathways has been studied in similar detail in primates. The best data are available for the oxytocin pathway, which has been described by the use of immunohistochemistry in monkeys (Swanson and McKellar, 1979). The distribution of oxytocin terminals in the intermediolateral cell column varies markedly at different levels of the thoracic and sacral spinal cord. This inhomogeneous distribution may reflect the uneven dispersion of preganglionic cell bodies along the column, or it may be due to oxytocin fibers innervating preferentially only certain functional classes of preganglionic neurons.

The hypothalamic control of the endocrine system is mediated by three main mechanisms. First, *magnocellular neuroendocrine* neurons in the paraventricular and supraoptic nuclei send their axons directly to the posterior pituitary gland, where they release these peptides from their terminals. Both types of neurons are found in both nuclei (Saper, 1990; Ishunina and Swaab, 1990; Koutcherov *et al.*, 2000) (see Fig. 17.8). In humans as in other species, the vasopressin neurons tend to cluster in the ventrolateral quadrant of the paraventricular nucleus, whereas the oxytocin neurons tend to surround this cluster and are more diffusely organized. Within the supraoptic nucleus the neurons of each type tend to cluster, but the topography of their mixing is more complex. Axons from the paraventricular nucleus run laterally, around the fornix, and then arch toward the supraoptic nucleus, with whose axons they merge on the way to the median eminence. The magnocellular axons form the hypothalamohypophysial tract, which runs in rat brain through the inner layer of the median eminence. The primate median eminence is a more complex spherical structure, with the hypothalamohypophysial axons coursing along the surface. Many additional peptides have been found to colocalize with oxytocin or vasopressin neurons in the hypothalamus of rats (Meister *et al.*, 1990), but similar data are not available for humans.

The *parvicellular neuroendocrine* neurons are those that contain peptides that are secreted into the hypothalamohypophysial portal circulation to control the anterior pituitary gland. In rats, retrograde transport studies demonstrate that these neurons are located in the periventricular zone of the hypothalamus and preoptic area (Lechan *et al.*, 1982; Swanson *et al.*, 1982). Similar studies have not been performed in other species.

Another approach has been the use of antisera for the immunohistochemical localization of the releasing hormones. The greatest amount of information is available for the rat. Each releasing factor investigated has been found within a spatially distinct population of neurons in the periventricular zone. The axons contribute to the tuberoinfundibular tract, which can be traced to the median eminence, where immunoreactive axons contact hypophysial portal vessels that carry the releasing hormones to the anterior pituitary gland. In most cases these releasing hormones are also found in other CNA pathways, where they are presumably used as neuromodulators. Thus, the pattern of immunohistochemical staining (where it can be applied in humans) does not, of itself, delineate the parvicellular neurosecretory system (i.e., those cells that secrete releasing hormones into the portal circulation). Nevertheless, this method provides the opportunity for establishing homology with other species in which connectional studies can be done.

Several releasing hormones have been localized immunohistochemically in human brains. Growth hormone–releasing hormone (GRH) has a rather limited distribution (Bloch *et al.*, 1984; Pelletier *et al.*, 1986). The only immunoreactive cell bodies seen in the human brain are in the arcuate nucleus, extending dorsally into the periventricular nucleus and laterally into the retrochiasmatic area. Occasional cells invade the borders of the ventromedial and lateral tuberal nuclei. GRH-immunoreactive fibers are seen in the periventricular region and in the neurovascular region of the median eminence.

Neurons that are immunoreactive for luteinizing hormone–releasing hormone (LHRH) are also found mainly in the hypothalamic periventricular and arcuate nuclei (Barry, 1977; Dudas *et al.*, 2000). Additional LHRH-immunoreactive cells are found extending rostrally through the periventricular preoptic area as far as the lamina terminalis and up into the septum. Other LHRH-immunoreactive cells are found extending caudally into the premammillary area and into the retromammillary region and the rostral midbrain. LHRH-immunoreactive fibers contribute to the tuberoinfundibular tract, ending on portal vessels in the median eminence, and among the capillaries of the organum vasculosum of the lamina terminalis (Barry, 1977). There is an increase in LHRH mRNA in the arcuate neurons in women who have undergone menopause (Rance and Uswandi, 1996).

Corticotropin-releasing hormone (CRH)–immunoreactive parvicellular neuroendocrine neurons are found primarily in the paraventricular nucleus in humans (Kruseman *et al.*, 1984; Mouri *et al.*, 1984; Pelletier *et al.*, 1983). The population of small CRH-immunoreactive cells is distinct from the magnocellular neurons that

secrete oxytocin and vasopressin. In rats, following adrenalectomy, some of the small CRH-immunoreactive neurons can be stained with antisera against vasopressin (Sawchenko and Swanson, 1985). It is not known if the content of these peptides is regulated in a similar fashion in humans.

In humans and other primates, somatostatin-(SOM-) and prosomatostatin-immunoreactive neurons are also found in the typical hypophysiotrophic distribution, in the arcuate and periventricular nuclei, with fibers extending into the neurohemal contact zone in the median eminence (Bennett-Clarke and Joseph, 1986; Bouras *et al.,* 1987; Filby and Gross, 1983). However, both SOM-immunoreactive cell bodies and fibers are also far more widely distributed. Immunoreactive cell bodies are found in the medial septal/diagonal band nuclei and magnocellular basal nucleus, the striatum and the bed nucleus of the stria terminalis, as well as in the amygdala, the periaqueductal gray matter, and the brain stem reticular formation (Bouras *et al.,* 1987). SOM-immunoreactive innervation is widespread throughout the basal forebrain, striatum, and brain stem tegmentum (Bouras *et al.,* 1987). Using autoradiography, SOM binding sites have been localized in most of these same sites in the human brain (Reubi *et al.,* 1986).

Dopamine also serves as a releasing hormone, inhibiting the secretion of prolactin by the anterior pituitary gland. It is possible to identify dopaminergic neurons in the human hypothalamus either by their content of melanin or by their immunoreactivity for the catecholamine synthetic enzyme tyrosine hydroxylase (Saper and Petito, 1982; Spencer *et al.,* 1985). In human brains these neurons are found in two clusters in the periventricular zone, corresponding to the A12 and A14 cell groups in rat and monkey (Saper and Petito, 1982; Spencer *et al.,* 1985). Other tyrosine hydroxylase–immunoreactive neurons are found extending more laterally into the zona incerta, possibly corresponding to the A11 catecholamine group in rats. Many immunoreactive neurons are also found in the supraoptic nucleus.

Finally, the hypothalamus also exerts influence over the endocrine system by means of autonomic innervation of the endocrine organs. For example, both sympathetic and parasympathetic innervation of the pancreas can influence secretion of insulin and glucagon (Havel *et al.,* 1994; Ahren, 2000). However, the central organization of this control system has not received much study in primates.

Behavioral Efferents of the Hypothalamus

The mechanisms by which the hypothalamus controls behavior remain among the least understood aspects of hypothalamic function. Early conceptualization of the hypothalamus containing specific behavioral "centers" that would independently elicit complex behaviors is almost certainly too simplistic (Stellar and Corbit, 1973). Rather than organizing full-blown behaviors, as one might conceive the cerebral cortex doing in a primate, the hypothalamus may more accurately be conceived as influencing behaviors by means of a range of efferent projections.

It has been tempting to assume that ascending projections to thalamus or cortex might mediate behavioral responses from the hypothalamus. Certainly the extensive projections to the cerebral cortex, reviewed above, could subserve the activation of specific behaviors. However, the cortical projections from the hypothalamus are widespread and diffusely organized, rather than being focused on specific cortical areas that might produce a discrete behavior. Even the projections from the lateral hypothalamic area, which are roughly topographic, are not organized in a way that indicates a major role in directly eliciting a specific behavior, such as feeding. Rather, the hypothalamocortical and hypothalamothalamic projections appear to be more important in regulating the level of cortical arousal and perhaps behavioral responsiveness (Risold *et al.,* 1997). This influence may be of importance in specific behaviors. For example, a hungry animal must be both awake and restless, so that it is stimulated to forage for food.

Descending hypothalamic projections to the brainstem reticular formation may play a role in facilitating specific behavioral responses. For example, a decerebrate rat, with no nervous system above the midbrain, can still chew and swallow if food is placed in its mouth (Kaplan *et al.,* 2000). The pattern generators for oropharyngeal behaviors that are associated with eating are located in the reticular areas around the cranial nerve (facial, trigeminal, hypoglossal, and ambiguus) motor nuclei that produce these movements (Travers *et al.,* 2000). By facilitating these movements and reducing the threshold for their production, the hypothalamus may be able to increase the probability of feeding, reduce its latency, and prolong its course (Stellar and Shrager, 1985).

Finally, the importance of autonomic responses in behavioral regulation cannot be overlooked. Among the most important cues for drinking is dryness of the mouth, which is due to reduced salivary outflow under hypothalamic control (Brunstrom *et al.,* 2000). Similarly, humans find that "hunger pangs," which consist of gastric motility and acid secretion, are important cues for feeding (Martyn *et al.,* 1984; Stricker and Verbalis, 1991). These sensory signals are thought to reach conscious appreciation through the pathway from the nucleus of the solitary tract to the parabrachial

nucleus to the visceral sensory thalamic nucleus and relay to the visceral sensory cortex in the insular area (Cechetto and Saper, 1987; de Lacalle and Saper, 2000). These relevant sensory stimuli may then be used by the cerebral cortex to plan specific behaviors.

While the concept that the hypothalamus mechanistically biases behavior toward specific outcomes may be less romantic and satisfying than "behavioral centers" that can produce full-blown and complex behaviors, the former view is almost certainly more accurate. There are very few studies of these problems in primates, but recent studies using functional imaging indicate that even simple behaviors in humans are supported by the activation of widespread networks of cortical and subcortical neurons (Tataranni *et al.*, 1999; Gordon *et al.*, 2000). It is unlikely that a hypothalamic "command neuron" can produce the complex sequence of responses necessary to drive specific behaviors in humans. Nevertheless, the ability of hypothalamic projections to influence behaviors ranging from seeking a warmer environment to feeding to sexual behavior is almost certainly as profound and pervasive in humans as it is in other mammalian species.

Organization of Specific Functional Systems

Feeding

The earliest view on the role of the hypothalamus in feeding came from observations of patients with Froehlich's syndrome, consisting of obesity and lack of sexual maturation (see review in Elmquist *et al.*, 1999). These patients were shown to have pituitary tumors impinging on the medial basal hypothalamus. Whereas such luminaries as Harvey Cushing thought that the disorder was due to the pituitary lesion, others argued that it only appeared when the lesions damaged the overlying hypothalamus. The issue was finally settled in studies done by Hetherington and Ranson (1939) who placed stereotaxic lesions in the medial basal hypothalamus in rats. Although the hyperphagia and obesity they produced has often been called the "ventromedial nucleus syndrome", and it has been observed in many other species, including man (Reeves and Plum, 1969), Hetherington and Ranson were careful to indicate that the region that produced the syndrome was considerably larger than the ventromedial nucleus, including the arcuate, dorsomedial, and ventral premammillary nuclei. Other studies showed that small focal lesions, primarily confined to the ventrolateral part of the ventromedial nucleus, do not cause hyperphagia or obesity (see Elmquist *et al.*, 1999, for review). However, lesions in the lateral hypothalamic area dramatically reduced feeding.

These observations can now be explained by a dramatic series of findings in the late 1990s, beginning with the identification of the gene defect in the *obese* mouse as a functional deletion of the hormone leptin (see Halaas *et al.*, 1995; Elmquist *et al.*, 1999 for reviews). Leptin is released by white adipose tissue during times of metabolic substrate availability. Absence of leptin causes profound hyperphagia, reminiscent of the ventromedial nucleus syndrome. When the distribution of the leptin receptor was mapped in the brain, neurons containing the highest levels of receptor were found to cluster in a group of nuclei that are located within about 1 mm of the median eminence, in the arcuate nucleus, dorsomedial part of the ventromedial nucleus, posterior dorsomedial nucleus, and ventral premammillary nucleus (Elmquist *et al.*, 1998), i.e., precisely the same region in which Hetherington and Ranson found the lesions cause hyperphagia and obesity.

Subsequent studies have confirmed that systemic leptin enters the CNS via the median eminence and binds in this same region (Banks *et al.*, 1996). The leptin receptor belongs to a family of cytokine receptors that use the JAK-Stat signaling system (Bjorbaek *et al.*, 1998; Hübschle *et al.*, 2001). Activation of theses receptors simultaneously causes transcription of members of the SOCS (suppressors of cytokine signaling) family. Leptin causes translocation of STAT3 to the cell nucleus and expression of SOCS-3 in cells whose receptors have been activated. It also activates expression of Fos protein in many (but not all) cells that show STAT3 or SOC-3 expression (Elias *et al.*, 1999, Hübschle *et al.*, 2001). By mapping the expression of these transcription factors after administration of intravenous leptin, it has been possible to show that leptin acts in part by stimulating neurons in the arcuate nucleus that contain both α-MSH and CART (Fig. 17.10), as well as by inhibiting neurons that contain both neuropeptide Y (NPY) and agouti-related protein (AgRP) (Fig. 17.11) (Elias *et al.*, 2000).

The α-MSH neurons are important for suppressing feeding, as demonstrated by the hyperphagia and obesity shown by animals that lack the melanocortin-4 receptor (Huszar *et al.*, 1997), for which α-MSH is the preferred agonist. Interestingly, AgRP is an antagonist at this same receptor (Fan *et al.*, 1997; Elmquist *et al.*, 1999). Animals that overexpress agouti protein, which also blocks the MC-4 receptor, are also obese. The α-MSH- and AgRP-containing neurons in the arcuate nucleus project to overlapping terminal fields in the paraventricular nucleus and the lateral hypothalamic area (Figs. 17.10–17.12), where they are believed to have mutually antagonistic effects (Elias *et al.*, 1998, 2000; Broberger *et al.*, 1998). The paraventricular nucleus is

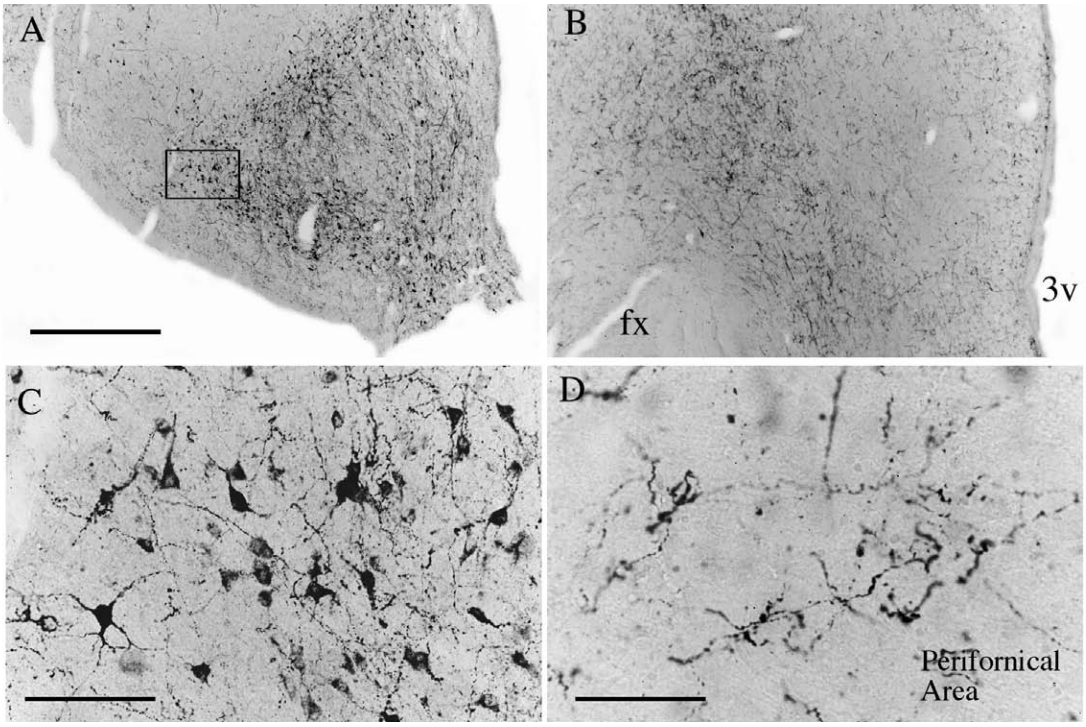

FIGURE 17.10 A series of photomicrographs illustrating α-melanocyte-stimulating hormone–immunoreactive neurons in the human hypothalamus. Note that nearly all immunoreactive cell bodies are in the arcuate nucleus and adjacent retrochiasmatic area **(A, C).** Immunreactive axons and terminals are distributed densely in the perifornical region **(B, D).** C is a higher magnification of the boxed area in panel A; D is a higher magnification of panel B. Scales = 750 μm in A and B; 100 μm in C; 50 μm in D. Modified from Elias *et al.,* 1998, with permission.

thought to be important in promoting feeding, as the injection of NPY and AgRP into it can increase feeding (Yokosuka *et al.,* 1999; Wirth and Giraudo, 2000), whereas α-MSH or CART injections decrease feeding (Wang *et al.,* 2000; Wirth *et al.,* 2001). Interestingly, transection of the vagus nerve below the diaphragm can abrogate the overeating response to ventromedial nucleus lesions (Cox and Powley, 1981). Thus, the projections from the medial basal hypothalamus through the autonomic control system are probably of great importance in the regulation of feeding.

The lateral hypothalamic area contains two separate populations of neurons that express peptides: orexin/hypocretin and melanin-concentrating hormone (MCH) (Figs. 17.9 and 17.12) (Elias *et al.,* 1998), whose transcription is increased during starvation, and decreased during food repletion or following leptin administration (Qu *et al.,* 1996; Sakurai *et al.,* 1998). Orexin/hypocretin knockout animals have minimal changes in feeding (Chemelli *et al.,* 1999). However, transgenic animals in which the orexin promoter drives the ataxin-3 gene, causing death of the orexin cells, are hypophagic but have an increased body weight (Hara *et al.,* 2001). In contrast, animals in which the MCH gene is deleted show hypophagia and decreased body weight (Shimada *et al.,* 1998). Thus, both the orexin/hypocretin and the MCH neurons, which are confined to the lateral hypothalamus, are involved in feeding and metabolism; both are also innervated by both the α-MSH/CART and the AgRP/NPY neurons in the arcuate nucleus (Fig. 17.12) (Elias *et al.,* 1998; Broberger *et al.,* 1998).

Although most of this work has been done in rats, the validity of its application to humans has been strikingly confirmed by observations showing that the same projections from the α-MSH/CART and the AgRP/NPY neurons in the arcuate nucleus project to both the orexin/hypocretin and the MCH neurons in the human hypothalamus (Figs. 17.11 and 17.12) (Elias *et al.,* 1998). The presence of the same chemically defined systems in the same relationships in the human brain provides strong evidence for the conservation of circuitry regulating feeding and body weight among mammals.

Reproduction

Evidence from the leptin system also suggests that reproductive pathways are highly conserved between

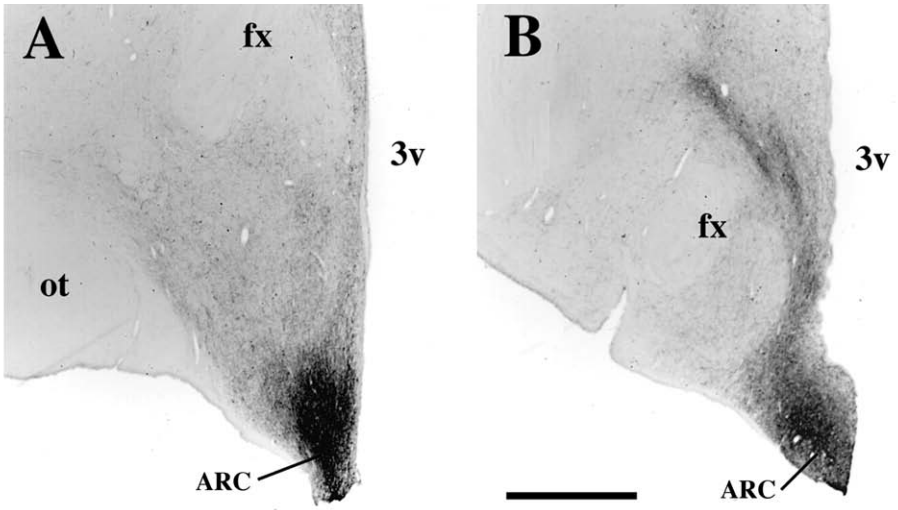

FIGURE 17.11 A pair of photomicrographs illustrating the immunostaining in the human hypothalamus with antiserum against agouti-related protein. Note the dense collection of cell bodies and fibers in the arcuate nucleus, which is the only source of this peptide in human brains. A dense bundle of fibers can be traced into the paraventricular nucleus **(A)** and the perifornical region of the lateral hypothalamus **(B).** Scale = 2 mm. Reproduced from Elias *et al.,* 1998, with permission.

humans and other mammals. Animals with absence of leptin or its receptor are both hyperphagic and hypogonadotropic, similar to the original description of Froehlich's syndrome (see Elmquist *et al.,* 1999, for review). Similarly, women who are marathon runners often have low body fat (and hence low leptin levels), which may contribute to loss of menstrual cycling (Shangold and Levine, 1982). This relationship presumably reflects the importance of adequate food supplies for reproduction. This response is thought to represent the influence of leptin-responsive neurons in the ventral premammillary, ventromedial, and arcuate nuclei on gonadotropin-releasing hormone neurons in the arcuate and periventricular regions (Rance *et al.,* 1994).

The medial preoptic nucleus in rats and other rodents contains a sexually dimorphic population of neurons, which are more prominent in males (Arendash and Gorski, 1983; Simerly *et al.,* 1986; Byne and Bleier, 1987). There is also a sexual dimorphism in monoaminergic innervation of this region rats (Simerly *et al.,* 1985, 1986). The identification of a homologous region of sexual dimorphism in the human hypothalamus has been controversial. Swaab and colleagues reported that there are about twice as many neurons in the intermediate nucleus in male compared to female human brains, and that the suprachiasmatic nucleus was more elongated in women and more spherical in men (Swaab and Fliers, 1985; Swaab *et al.,* 1985). Swaab and Hoffman later reported that the suprachiasmatic nucleus also had about twice as many neurons in homosexual as in heterosexual men (Swaab and Hofmann, 1990). However, Allen and Gorsky reported finding four interstitial nuclei of the anterior hypothalamus, or INAH groups, in human hypothalamus. Their INAH-1 corresponds to the intermediate nucleus, but they did not find any sexual dimorphism in this cell group. On the other hand, INAH-2 and INAH-3 were at least twice as large (as measured by volume) in male than in female brains (Allen *et al.,* 1989). LeVay (1991) subsequently reported finding that INAH-3 has about twice the volume in heterosexual men than women, with no difference in INAH-1 or INAH-2. In homosexual men, however, INAH-3 was the same size as in female brains. Byne (1998) confirmed that of the INAH cell groups, only INAH-3 is sexually dimorphic in both humans and rhesus monkeys. While the role of INAH-3 as a sexually dimorphic nucleus in humans seems secure, its correspondence with the sexually dimorphic preoptic nuclei in rat, which has been much more carefully studied, remains conjectural. In addition, the INAH-1 and INAH-2, each has been found to be sexually dimorphic by one group but not by two or three others. However, the age and reproductive status of the subjects may have affected the results, as may the disorders from which they eventually succumbed (as the subjects died of varying causes).

Physiological studies in rats and monkeys indicate that the sexually dimorphic medial preoptic nucleus is critical for male sexual performance (Arendash and Gorski, 1983; Lloyd and Dixson, 1988). Single cell recordings from the medial preoptic area in male and female monkeys (Oomura *et al.,* 1983; Aou *et al.,* 1988)

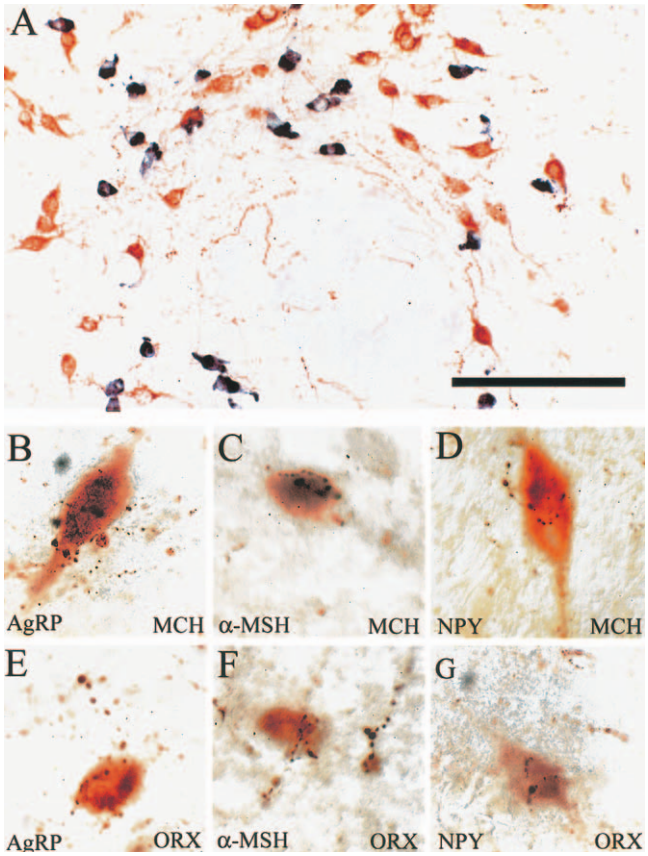

FIGURE 17.12 A series of color micrographs illustrating the melanin-concentrating hormone (MCH) and orexin (ORX) neuron systems in the hypothalamus. Panel **A** illustrates the mixing of neurons that stain with antiserum against ORX (brown) and with a digoxygenin-labeled probe for MCH mRNA (blue) in the perifornical region of a rat. Although the two types of neurons cluster closely with one another around the edge of the fornix, there is virtually no colocalization within individual neurons. Panels **B–G** illustrate the close relationship of axons that stain immunohistochemically for agouti-related protein (AgRP, panels B, E), α-melanocyte-stimulating hormone (α-MSH, panels C, F), or neuropeptide Y (NPY, panels D, G), with cell bodies in human brains that are immunoreactive for MCH (B–D) and ORX (E–G). Scale = 100 μm in A; 25 μm in panels C–G. Modified from Elias *et al.*, 1998, with permission.

have likewise shown a close relationship of neuronal firing with sexual behavior.

In rats, the medial preoptic nucleus is reciprocally connected with the ventrolateral part of the ventromedial nucleus and the ventral premammillary nucleus (Canteras *et al.*, 1992, 1994). Recordings from the ventromedial nucleus in female monkeys demonstrate that neuronal firing increases during sexual stimulation (Auo *et al.*, 1988). Lesions in the ventrolateral part of the ventromedial nucleus disrupt lordosis behavior in female rats (Pfaff and Sakuma, 1979). This response is thought to be mediated by projections from the ventromedial nucleus to the periaqueductal gray matter (Canteras *et al.*, 1994; Kow and Pfaff, 1998). There is also a high concentration of gonadotrophic steroid receptors in the preoptic area and ventromedial and arcuate nuclei in monkey and human brain, a pattern that is highly conserved across mammalian species (Pfaff *et al.*, 1976; Clancy *et al.*, 1992: Herbison *et al.*, 1995; Michael *et al.*, 1995; Choate *et al.*, 1998).

Thermoregulation and Fever

The medial preoptic region in rats and in monkeys is also enriched in neurons that respond to local brain temperature (Hardy and Boulant, 1974; Griffin and Boulant, 1995; Hori *et al.*, 1987). All neurons are temperature sensitive to some extent because the biophysical processes that account for neuronal firing increase in rate with temperature. However, a subset of preoptic and anterior hypothalamic neurons are especially warmth sensitive, increasing their firing rate more than 1 Hz for each 0.8°C of local warming. A large proportion of these warmth sensitive neurons also respond to skin temperature, lending support to their function as warmth receptive (Hardy and Boulant, 1974). Interestingly, a small proportion of preoptic neurons in intact animals is also found to be cold sensitive, increasing their firing with cooling of the local brain. However, very few such neurons are found in hypothalamic slice preparations, suggesting that this activity pattern results from axonal connections that are severed in a slice, e.g., inputs from warmth sensitive neurons that inhibit the firing of tonically active cells (Dean and Boulant, 1989).

The importance of the medial preoptic region in thermoregulation in humans is hinted at by a rare disorder, i.e., paroxysmal hypothermia (van Uitert and Plum, 1980). This disorder consists of intermittent attacks of decreased body temperature, to as low as 27°C. It typically occurs in individuals who have had a developmental lesion of the anterior wall of the third ventricle, which includes the medial preoptic region.

The mechanisms by which the preoptic neurons regulate body temperature still are poorly understood. There is evidence both in rats and in humans that medial preoptic neurons serve a thermostatic set point function. Lesions of this tissue cause loss of the fine regulation of body temperature, although crude thermoregulation, within a much broader range, is preserved (Satinoff *et al.*, 1982; Johnson *et al.*, 1990; Kubota *et al.*, 1991; Lu *et al.*, 2000). In rats, there is evidence that the descending pathways from the preoptic area that regulate thermogenesis involve projections through the ventrolateral part of the lateral hypothalamic area to the periaqueductal gray matter (Zhang *et al.*, 1997; Chen *et al.*, 1998). The periaqueductal

gray matter in turn innervates the medullary raphe nuclei (Hermann *et al.*, 1997), which have a profound effect on thermoregulation (Morrison, 1999). It is likely that a similar set of polysynaptic pathways plays a role in thermoregulation in primates, but thus far specific evidence for many of these steps is lacking.

While body temperature does not respond to heating or cooling the posterior hypothalamic area, electrical or chemical stimulation in this region can produce shivering and thermogenesis (Refinetti and Carlisle, 1986; Thornhill and Halvorson, 1994; Chou and Saper, unpublished observations). Similar studies in primates would be of great interest.

Fever is a hypothalamically mediated increase in body temperature in response to an inflammatory stimulus. Recent work, primarily in rats, shows that when a variety of immune stimuli, ranging from lipopolysaccharide to cytokines such as interleukin-1β and tumor necrosis factor-α, reach the brain, they cause endothelial cells and perivascular microglia along venules at the edges of the brain to express cyclooxygenase-2 (COX-2) (Elmquist *et al.*, 1997; Rivest *et al.*, 2000). COX is the key enzyme in the synthesis of prostaglandins, and COX-2 is the form that is produced in response to inflammatory stimuli. COX-2 synthesizes prostaglandin H_2, which is rapidly converted to prostaglandin E_2 in the same cells that express COX-2 (Yamagata *et al.*, 2001). Prostaglandin E_2 acts on EP receptors located in the preoptic area to produce a fever response (Scammell *et al.*, 1996, 1998). Recent studies in rats indicate that there are four different EP receptors, of which three (EP1, 3, and 4) are expressed in the hypothalamus (Oka *et al.*, 2000). Gene deletion studies have indicated that deletion of the EP3 receptors, but not the EP1 or EP4 receptors can prevent the production of fever with either an intravenous interleukin-1 or intracerebroventricular prostaglandin E_2 stimulus (Ushikubi *et al.*, 1998). Neurons that express the EP3 receptor cluster around the anteroventral tip of the third ventricle, in the median preoptic nucleus (Oka *et al.*, 2000; Ek *et al.*, 2000). Similarly, in monkeys there is binding of prostaglandin E_2 along the anteroventral tip of the third ventricle (Watanabe *et al.*, 1988) suggesting a similar locus for the pathogenesis of prostaglandin-mediated fever in primates.

Further experiments in rats have attempted to map the pathways involved in producing a fever response by examining the pattern of expression of the immediate early gene, Fos, after either intravenous injection of lipopolysaccharide or interleukin-1β (Ericsson *et al.*, 1994; Elmquist *et al.*, 1996). There is expression of Fos protein in the ventromedial preoptic nucleus, the paraventricular nucleus of the hypothalamus, and the nucleus of the solitary tract and ventrolateral medulla, at all time points and dosages of lipopolysaccharides that produce a fever (Elmquist *et al.*, 1996). The Fos expression in the ventromedial preoptic nucleus is colocalized with EP4 expression (Oka *et al.*, 2000). However, lesions of the ventromedial preoptic nucleus do not prevent fever responses (Lu *et al.*, 2000). In the paraventricular nucleus, Fos-positive neurons also express EP4 receptors (Oka *et al.*, 2000). In fact, there is an increase in EP4 receptor expression in the paraventricular nucleus after intravenous lipopolysaccharides (Zhang and Rivest, 1999; Oka *et al.*, 2000). Lesions of the paraventricular nucleus substantially block fever responses (Horn *et al.*, 1994; Lu *et al.*, 2000). Thus, the fever response appears to rely on a relay from the medial preoptic region to the paraventricular nucleus (Levisohn and Saper, 1983).

To identify the source of input to sympathetic preganglionic neurons during a fever, Zhang and colleagues (2000) combined retrograde transport from the sympathetic preganglionic column in the spinal cord with Fos staining after intravenous administration of lipopolysaccharides. Of the hypothalamic cell groups that were retrogradely labeled from the spinal cord, only neurons in the dorsal parvicellular subnucleus of the paraventricular nucleus were double labeled in these experiments. This same pattern of double labeling was present after injections of retrograde tracer at each level of the spinal cord. These observations suggest that the pattern generator for the sympathetic response associated with a fever may reside in a small population of paraventricular neurons that innervate multiple pools of preganglionic neurons involved in producing a fever response. Unfortunately, comparable data are not available for primates.

Sleep

Unlike many areas of neuroscience, in which discoveries made in experimental animals are applied to humans, the study of hypothalamic lesions that produce alterations of sleep was initiated by studies in humans. During World War I, there was a worldwide pandemic of a presumed viral illness that had not been reported before, and has not been seen since, known as *encephalitis lethargica*. The illness was studied closely by an Austrian physician, Baron Constantin von Economo (1930), who reported that victims with lesions of the posterior lateral hypothalamus and the adjacent midbrain would fall into a deep, sleeplike state, from which they could be transiently awakened. However, they would sleep most of the day, for up to several weeks. A second group of victims, who had lesions in the basal forebrain including the lateral preoptic area, showed the opposite response, demonstrating prolonged wakefulness or insomnia.

Subsequent lesion studies in rats (Nauta, 1946), cats (Sterman and Clemente, 1964), and monkeys (Ranson, 1939) confirmed von Economo's observations. Electrical recording studies demonstrated sleep-active neurons in the lateral preoptic area and adjacent basal forebrain (Alam *et al.*, 1995; Szymusiak *et al.*, 1998) and wake-active neurons in monoaminergic nuclei whose axons pass through the lateral hypothalamic area, including the noradrenergic locus coeruleus (Aston-Jones and Bloom, 1981; Rajkowski *et al.*, 1994), the serotonergic dorsal and median raphe nuclei (Trulson and Jacobs, 1979; Rasmussen *et al.*, 1994), and the histaminergic tuberomammillary nucleus (Steininger *et al.*, 1999). However, the exact source of neither the waking nor the sleeping influences from the hypothalamus were located until the last few years.

By studying afferents to the tuberomammillary nucleus, two different sets of hypothalamic neurons with important influences on the regulation of wakefulness and sleep were pinpointed (Sherin *et al.*, 1996). One group of neurons was located diffusely in the lateral hypothalamus. The other was clustered in the ventrolateral preoptic nucleus (VLPO). The VLPO neurons were also found to show Fos expression specifically during sleep, and about 80% of them contained both GABA and the inhibitory peptide transmitter, galanin (Sherin *et al., 1998*). Although many of the neurons with these properties were located in a dense cluster, almost half were found scattered dorsally and medially from the cluster, in a formation called the extended VLPO (Lu *et al.*, 2000). Excitotoxic amino acid lesions of the VLPO demonstrated that the loss of neurons in the VLPO cluster correlated with loss of non-REM sleep, which exceeded 70% in some animals. Loss of neurons in the extended VLPO correlated with a similar degree of loss of REM sleep. Recent observations have identified a set of sleep-active, galanin-containing neurons in the VLPO in mice, degus (a diurnal rodent), and cats (Gaus *et al.*, 2001). A homologous galanin-containing cell group has been identified in monkeys and in humans, verifying von Economo's observations.

The second source of afferents to the tuberomammillary nucleus consists mainly of orexin/hypocretin and MCH neurons (see Figs. 17.9 and 17.12) in the lateral hypothalamic area (Peyron *et al.*, 1998; Bittencourt *et al.*, 1998; Chemelli *et al.*, 1999). Although animals with MCH gene deletion do not have an obvious deficit of sleep or waking (Qu *et al.*, 1996), mice with deletion of the orexin/hypocretin gene (Chemelli *et al.*, 1999), or dogs with mutations in the orexin-2 receptor (Lin *et al.*, 1999), show a complex sleep disturbance known as narcolepsy. These individuals have sudden sleep attacks during their waking periods, in which they rapidly fall into REM sleep. They also have episodes of cataplexy, in which they show the atonia associated with REM sleep, against a waking background. Both of these traits are characteristic of humans with narcolepsy. Recent studies show that human narcoleptics have low levels of orexin/hypocretin in their spinal fluid (Nishino *et al.*, 2000), and that they lack orexin-producing neurons in the lateral hypothalamus, although MCH neurons are intact (Thannickal *et al.*, 2000) (Fig. 17.13). However, few human narcoleptics have mutations of either the orexin/hypocretin or orexin-2 receptor genes (Peyron *et al.*, 2000). Rather the loss of neurons in the lateral

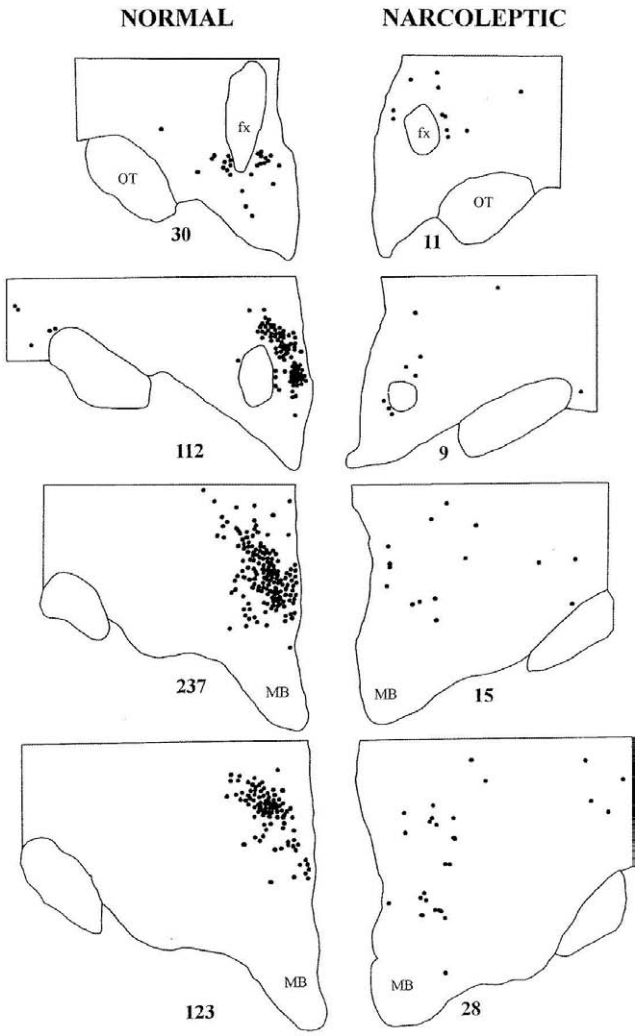

FIGURE 17.13 A series of drawings illustrating the numbers of orexin-immunoreactive neurons in a series of sections through the hypothalamus a normal individual **(left)** and in a similar series of sections through the brain of an individual with narcoleptic **(right).** Note the profound loss of orexin neurons in the narcoleptic brain. Reproduced from Thannickal *et al.*, 2000, with permission.

hypothalamus appears to be a degenerative process (occurring in the second or third decade of life).

Because both the MCH and orexin/hypocretin neurons can be identified by immunohistochemistry in normal human autopsy brains (Figs. 17.9–17.12), both the location of these neurons and many of their connections can be observed directly in humans (Elias *et al.*, 1998). The remarkable conservation of the details of this circuitry throughout the mammalian line, up to and including humans, underscores its importance. As with many hypothalamic neuronal systems that subserve basic life-supporting functions, the information available from study of animals is likely to be applicable to understanding human neuroanatomy and physiology.

References

Abrahamson, E.E., Leak, R.K., and Moore, R.Y. (2001). The suprachiasmatic nucleus projects to posterior hypothalamic arousal systems. *Neuroreport* **12,** 435–440.

Ahren, B. (2000). Autonomic regulation of islet hormone secretion—implications for health and disease. *Diabetologia* **43,** 393–410.

Allen, L.S., Hines, M., Shryne, J.E., and Gorski, R.A. (1989). Two sexually dimorphic cell groups in the human brain. *J. Neurosci.* **9,** 497–506.

Amaral, D.G., Veazey, R.B., and Cowan, W.M. (1982). Some observations on hypothalamo-amygdaloid connections in the monkey. *Brain Res.* **252,** 13–27.

Aou, S., Oomura, Y., and Yoshimatsu, H. (1988). Neuron activity of the ventromedial hypothalamus and the medial preoptic area of the female monkey during sexual behavior. *Brain Res.* **455,** 65–71.

Arendash, G.W., and Gorski, R.A. (1983). Effects of discrete lesions of the sexually dimorphic nucleus of the preoptic area or other medial preoptic regions on the sexual behavior of male rats. *Brain Res. Bull.* **10,** 147–154.

Armstrong, E. (1986). Enlarged timbic structures in the human brain: the anterior thalamus and medial mammary body. *Brain Res.* **362,** 394–397.

Aston-Jones, G., and Bloom, F.E. (1981). Activity of norepinephrine-containing locus coeruleus neurons in behaving rats anticipates fluctuations in the sleep–waking cycle. *J. Neurosci.* **1,** 876–886.

Bamshad, M., Aoki, V.T., Adkison, M.G., Warren, W.S., and Bartness, T.J. (1998). Central nervous system origins of the sympathetic nervous system outflow to white adipose tissue. *Am. J. Physiol.* **275,** R291–R299.

Banks, W.A., Kastin, A.J., Huang, W., Jaspan, J.B., and Maness, L.M. (1996). Leptin enters the brain by a saturable system independent of insulin. *Peptides* **17,** 305–311.

Barbas, H. (2000). Connections underlying the synthesis of cognition, memory, and emotion in primate prefrontal cortices. *Brain Res. Bull.* **52,** 319–330.

Barry, J. (1977). Immunofluorescence study of LRF neurons in man. *Cell Tissue Res.* **181,** I141.

Beckstead, R.M., Morse, J.R., and Norgren, R. (1980). The nucleus of the solitary tract in the monkey: projections to the thalamus and brain stem nuclei. *J. Comp. Neurol.* **1,** 259–282.

Bennett-Clarke, C.A., and Joseph, S.A. (1986). Immunocytochemical localization of somatostatin in human brain. *Peptides (N.Y.)* **7,** 877–884.

Bester, H., Besson, J.M., and Bernard, J.F. (1997). Organization of efferent projections from the parabrachial area to the hypothalamus: a *Phaseolus vulgaris*-leucoagglutinin study in the rat. *J. Comp. Neurol.* **383,** 245–281.

Bittencourt, J.C., Elias, C.F. (1998). Melanin-concentrating hormone and neuropeptide EI projections from the lateral hypothalamic area and zona incerta to the medial septal nucleus and spinal cord: a study using multiple neuronal tracers. *Brain Res.* **805,** 1–19.

Bittencourt, J.C., Frigo, L., Rissman, R.A., Casatti, C.A., Nahon, J.L., and Bauer, J.A. (1998). The distribution of melanin-concentrating hormone in the monkey brain (Cebus apella). *Brain Res.* **804,** 140–143.

Bjorbaek, C., Elmquist, J.K., Frantz, J.D., Shoelson, S.E., and Flier, J.S. (1998), Identification of SOCS-3 as a potential mediator of central leptin resistance. *Mol. Cell* **1,** 619–625.

Bleier, R., and Byne, W. (1986). The septum and hypothalamus. *In* "The Rat Nervous System" (G. Paxinos, ed.), Vol. 1, pp. 87–118. Academic Press, Orlando.

Bleier, R., Cohn, P., and Siggelkow, 1.R. (1979). A cytoarchitectonic atlas of the hypothalamus and hypothalamic third ventricle of the rat. *In* "Anatomy of the Hypothalamus. Handbook of the Hypothalamus" (P.J. Morgane and J. Panksepp, eds.), Vol. 1, pp. 137–220. Marcel Dekker, New York.

Bloch, B., Gaillard, R.G., Brazeau, P., Lin, H.D., and Ling, N. (1984). Topographical and ontogenetic study of the neurons producing growth hormone-releasing factor in human hypothalamus. *Regul Peptides* **8,** 21–31.

Bouras, C., Magistretti, P. J., Morrison, J. H., and Constantinidis, J. (1987). An immunohistochemical study of pro-somatostatin-derived peptides in the human brain. *Neuroscience* **22,** 781–800.

Boulant, J.A., and Hardy, J.D. (1974). The effect of spinal and skin temperatures on the firing rate and thermosensitivity of preoptic neurones. *J. Physiol.* **240,** 639–660.

Braak, H., and Braak, E. (1987). The hypothalamus of the human adult: chiasmatic region. *Anat. Embryol.* **176,** 315–330.

Braak, H., and Braak, E. (1992). Anatomy of the human hypothalamus (chiasmatic and tuberal region). *Prog. Brain Res.* **93,** 3–14; discussion 14–6: 3–14.

Braak, H., and Braak, E. (1998). Pick's disease: cytoskeletal changes in the hypothalamic lateral tuberal nucleus. *Brain Res.* **802,** 119–124.

Breder, C.D., Dinarello, C.A., and Saper, C.B. (1988). Interieukin-1 immunoreactive innervation of the human hypothalamus. *Science* **240,** 321–324.

Broadwell, R.D., and Brightman, M.W. (1976). Entry of peroxidase into neurons of the central and peripheral nervous systems from extracerebral and cerebral blood. *J. Comp. Neurol.* **166,** 257–283.

Broberger, C. (1999). Hypothalamic cocaine- and amphetamine-regulated transcript (CART) neurons: histochemical relationship to thyrotropin-releasing hormone, melanin-concentrating hormone, orexin/hypocretin and neuropeptide Y. *Brain Res.* **848,** 101–113.

Brockhaus, H. (1942). Beitrag zur normalen Anatomie des Hypothalamus und der Zona incerta beim Menschen. *J. Psychol. Neurol.* **51,** 96–196.

Brunstrom, J.M., Tribbeck, P.M., and MacRae, A.W. (2000). The role of mouth state in the termination of drinking behavior in humans. *Physiol. Behav.* **68,** 579–583.

Burstein, R., Cliffer, K.D., and Giesler, G.J. (1987). Direct somatosensory projections from the spinal cord to the hypothalamus and telencephalon. *J. Neurosci.* **7,** 4159–4164.

Byne, W., and Bleier, R. (1987). Medial preoptic sexual dimorphisms in the guinea pig. I. An investigation of their hormonal dependence. *J. Neurosci.* **7,** 2688–2696.

Byne, W. (1998). The medial preoptic and anterior hypothalamic regions of the rhesus monkey: cytoarchitectonic comparison with the human and evidence for sexual dimorphism. *Brain Res.* **793,** 346–350.

Byne, W., Lasco, M.S., Kemether, E., Shinwari, A., Edgar, M.A., Morgello. S., Jones. L.B., and Tobet, S. (2000). The interstitial nuclei of the human anterior hypothalamus: an investigation of sexual variation in volume and cell size, number and density. *Brain Res.* **856,** 254–258.

Canteras, N.S., and Swanson, L.W. (1992a). Projections of the ventral subiculum to the amygdala, septum, and hypothalamus: a PHAL anterograde tract-tracing study in the rat. *J. Comp. Neurol.* **324,** 180–194.

Canteras, N.S., and Swanson, L.W. (1992b). The dorsal premammillary nucleus: an unusual component of the mammillary body. *Proc. Natl. Acad. Sci. U.S.A.* **89,** 10089–10093.

Canteras, N.S., Simerly, R.B., and Swanson, L.W. (1992a). Connections of the posterior nucleus of the amygdala. *J. Comp. Neurol.* **324,** 143–179.

Canteras, N.S., Simerly, R.B., and Swanson, L.W. (1992b). Projections of the ventral premammillary nucleus. *J. Comp. Neurol.* **324,** 195–212.

Canteras, N.S., Simerly, R.B., and Swanson, L.W. (1994). Organization of projections from the ventromedial nucleus of the hypothalamus: a *Phaseolus vulgaris*-leucoagglutinin study in the rat. *J. Comp. Neurol.* **348,** 41–79.

Canteras, N.S., Simerly, R.B., and Swanson, L.W. (1995). Organization of projections from the medial nucleus of the amygdala: a PHAL study in the rat. *J. Comp. Neurol.* **360,** 213–245.

Cechetto, D.F., and Saper, C.B. (1987). Evidence for a viscerotopic sensory representation in the cortex and thalamus in the rat. *J. Comp. Neurol.* **262,** 27–45.

Cechetto, D.F., and Saper, C.B. (1988). Neurochemical organization of the hypothalamic projection to the spinal cord in the rat. *J. Comp. Neurol.* **272,** 579–604.

Chan-Palay, V.L., and Jentsch, B. (1992). Galanin tuberomammillary neurons in the hypothalamus in Alzheimer's and Parkinson's diseases. *Prog. Brain Res.* **93,** 263–270.

Chemelli, R.M., Willie, J.T., Sinton, C.M., Elmquist, J.K., Scammell, T., Lee, C., Richardson, J.A., Williams, S.C., Xiong, Y., Kisanuki, Y., Fitch, T.E., Nakazato, M., Hammer, R.E., Saper, C.B., and Yanagisawa, M. (1999). Narcolepsy in orexin knockout mice: molecular genetics of sleep regulation. *Cell* **98,** 437–451.

Chen, X.M., Hosono, T., Yoda, T., Fukuda, Y., and Kanosue, K. (1998). Efferent projection from the preoptic area for the control of non-shivering thermogenesis in rats. *J. Physiol.* **512,** 883–892.

Chiba, T., Kayahara, T., and Nakano, K. (2001). Efferent projections of infralimbic and prelimbic areas of the medial prefrontal cortex in the Japanese monkey, *Macaca fuscata*. *Brain Res.* **888,** 83–101.

Choate, J.V., Slayden, O.D., and Resko, J.A. (1998). Immunocytochemical localization of androgen receptors in brains of developing and adult male rhesus monkeys. *Endocrine* **8,** 51–60.

Clancy, A.N., Bonsall, R.W., and Michael, R.P. (1992). Immunohistochemical labeling of androgen receptors in the brain of rat and monkey. *Life Sci.* **50,** 409–417.

Cliffer, K.D., Burstein, R., and Giesler, G.J. (1991). Distributions of spinothalamic, spinohypothalamic, and spinotelencephalic fibers revealed by anterograde transport of PHA-L in rats. *J. Neurosci.* **11,** 852–868.

Coolen, L.M., and Wood, R.I. (1998). Bidirectional connections of the medial amygdaloid nucleus in the Syrian hamster brain: simultaneous anterograde and retrograde tract tracing. *J. Comp. Neurol.* **399,** 189–209.

Costa, M.S., Santee, U.R., Cavalcante, J.S., Moraes, P.R., Santos, N.P., and Britto, L.R. (1999). Retinohypothalamic projections in the common marmoset *(Callithrix jacchus):* a study using cholera toxin subunit B. *J. Comp. Neurol.* **415,** 393–403.

Cowan, W.M., Guillery, R.W., and Powell, T.P.S. (1964). The origin of the mammillary peduncle and other hypothalamic connexions from the midbrain. *J. Anat.* **98,** 345–363.

Dai, J., Swaab, D.F., Buijs, R.M. (1997). Distribution of vasopressin and vasoactive intestinal polypeptide (VIP) fibers in the human hypothalamus with special emphasis on suprachiasmatic nucleus efferent projections. *J. Comp. Neurol.* **383,** 397–414.

Dai, J., Van d, V., Swaab, D.F., and Buijs, R.M. (1998a). Human retinohypothalamic tract as revealed by *in vitro* postmortem tracing. *J. Comp. Neurol.* **397,** 357–370.

Dai, J., Swaab, D.F., Van der Vliet, J., and Buijs, R.M. (1998b). Postmortem tracing reveals the organization of hypothalamic projections of the suprachiasmatic nucleus in the human brain. *J. Comp. Neurol.* **400,** 87–102.

Date, Y., Mondal, M.S., Matsukura, S., and Nakazato, M. (2000). Distribution of orexin-A and orexin-B (hypocretins) in the rat spinal cord. *Neurosci Lett.* **288,** 87–90.

de Lacalle, S., and Saper, C.B. (2000). Calcitonin gene-related peptide-like immunoreactivity marks putative visceral sensory pathways in human brain. *Neuroscience* **100,** 115–130.

Dean, J.B., and Boulant, J.A. (1989). *In vitro* localization of thermosensitive neurons in the rat diencephalon. *Am. J. Physiol.* **257,** R57–R64.

Desaulles, E., Reiter, M.K., and Feltz, P. (1995). Electrophysiological evidence for oxytocin receptors on sympathetic preganglionic neurones—an *in vitro* study on the neonatal rat. *Brain Res.* **699,** 139–142.

Dong, H., Petrovich, G.D., and Swanson, L.W. (2000). Organization of projections from the juxtacapsular nucleus of the BST: a PHAL study in the rat. *Brain Res.* **859,** 1–14.

Dudas, B., Mihaly, A., and Merchenthaler, I. (2000). Topography and associations of luteinizing hormone-releasing hormone and neuropeptide Y-immunoreactive neuronal systems in the human diencephalon. *J. Comp. Neurol.* **427,** 593–603.

Ek, M., Arias, C., Sawchenko, P., and Ericsson-Dahlstrand, A. (2000). Distribution of the EP3 prostaglandin E(2) receptor subtype in the rat brain: relationship to sites of interleukin-1-induced cellular responsiveness. *J. Comp. Neurol.* **428,** 5–20.

Elias, C.F., Lee, C., Kelly, J., Aschkenasi, C., Ahima, R.S., Couceyro, P.R., Kuhar, M.J., Saper, C.B., and Elmquist, J.K. (1998a). Leptin activates hypothalamic CART neurons projecting to the spinal cord. *Neuron* **21,** 1375–1385.

Elias, C.F., Saper, C.B., Maratos-Flier, E., Tritos, N.A., Lee, C., Kelly, J., Tatro, J.B., Hoffman, G.E., Ollmann, M.M., Barsh, G.S., Sakurai, T., Yanagisawa, M., and Elmquist, J.K. (1998b). Chemically defined projections linking the mediobasal hypothalamus and the lateral hypothalamic area. *J. Comp. Neurol.* **402,** 442–459.

Elias, C.F., Aschkenasi, C., Lee, C., Kelly, J., Ahima, R.S., Bjorbaek, C., Flier, J.S., Saper, C.B., and Elmquist, J.K. (1999). Leptin differentially regulates NPY and POMC neurons projecting to the lateral hypothalamic area. *Neuron* **23,** 775–786.

Elias, C.F., Kelly, J.F., Lee, C.E., Ahima, R.S., Drucker, D.J., Saper, C.B., and Elmquist, J.K. (2000). Chemical characterization of leptin-activated neurons in the rat brain. *J. Comp. Neurol.* **423,** 261–281.

Elmquist, J.K., Scammell, T.E., Jacobson, C.D., and Saper, C.B. (1996). Distribution of Fos-like immunoreactivity in the rat brain following intravenous lipopolysaccharide administration. *J. Comp. Neurol.* **371,** 85–103.

Elmquist, J.K., Scammell, T.E., and Saper, C.B. (1997). Mechanisms of CNS response to systemic immune challenge: the febrile response. *Trends Neurosci.* **20,** 565–570.

Elmquist, J.K., Ahima, R.S., Elias, C.F., Flier, J.S., and Saper, C.B. (1998a). Leptin activates distinct projections from the dorsomedial and ventromedial hypothalamic nuclei. *Proc. Natl. Acad. Sci. U.S.A.* **95,** 741–746.

Elmquist, J.K., Bjorbaek, C., Ahima, R.S., Flier, J.S., and Saper, C.B. (1998b). Distributions of leptin receptor mRNA isoforms in the rat brain. *J. Comp. Neurol.* **395,** 535–547.

Elmquist, J.K., Elias, C.F., and Saper, C.B. (1999). From lesions to leptin: hypothalamic control of food intake and body weight. *Neuron* **22,** 221–232.

Ericsson, A., Kovacs, K.J., and Sawchenko, P.E. (1994). A functional anatomical analysis of central pathways subserving the effects of interleukin-1 on stress-related neuroendocrine neurons. *J. Neurosci.* **14,** 897–913.

Fan, W., Boston, B.A., Kesterson, R.A., Hruby ,V.J., and Cone, R.D. (1997). Role of melanocortinergic neurons in feeding and the agouti obesity syndrome. *Nature* **385,** 165–168.

Felten, D., Laties, A., and Carpenter, M. (1974). Localization of monoamine-containing cell bodies in the squirrel monkey brain. *Am. J. Anat.* **139,**153–166.

Filby, A.B., and Gross, D.S. (1983). Distribution of immunoreactive somatostatin in the primate hypothalamus. *Cell Tissue Res.* **233,** 69–80.

Fisher, R.S., and Almli, C.R. (1984). Postnatal development of sensory influences on lateral hypothalamic neurons of the rat. Dev. *Brain Res.* **12,** 55–75.

Freedman, L.J., Insel, T.R., and Smith, Y. (2000). Subcortical projections of area 25 (subgenual cortex) of the macaque monkey. *J. Comp. Neurol.* **421,** 172–188.

Fry, F.J., and Cowan, W.M. (1972). A study of retrograde cell degeneration in the lateral mammillary nucleus of the cat, with special reference to the role of axonal branching in the preservation of the cell. *J. Comp. Neurol.* **144,** 1–24.

Gagel, 0. (1927). Zur Topik und feineren Histologie der vegetativen Kerne des Zwischenhirns. *Z. Anat. Entwicki ungs gesch.* **37,** 548–584.

Garver, D., and Sladek, J.R. (1975). Monoamine distribution in primate brain. 1. Catecholamine-containing perikarya in the brain stem of *Macaca speciosa*. *J. Comp. Neurol.* **159,** 289–304.

German, D.C., White, C.L., and Sparkman, D.R. (1987). Alzheimer's disease: neurofibrillary tangles in nuclei that project to the cerebral cortex. *Neuroscience* **21,** 305–312.

Gomez, D.M., and Newman, S.W. (1992). Differential projections of the anterior and posterior regions of the medial amygdaloid nucleus in the Syrian hamster. *J. Comp. Neurol.* **317,** 195–218.

Gordon, C.M., Dougherty, D.D., Rauch, S.L., Emans, S.J., Grace, E., Lamm, R., Alpert, N.M., Majzoub, J.A., and Fischman, A.J. (2000). Neuroanatomy of human appetitive function: a positron emission tomography investigation. *Int. J. Eat. Disord.* **27,** 163–171.

Griffin, J.D., and Boulant, J.A. (1995). Temperature effects on membrane potential and input resistance in rat hypothalamic neurones. *J. Physiol.* **488,** 407–418.

Groenewegen, H.J., and Russchen, F.T. (1984). Organization of the efferent projections of the nucleus accumbens to pallidal, hypothalamic, and mesencephalic structures: a tracing and immunohistochemical study in the cat. *J. Comp. Neurol.* **223,** 347–367.

Grove, E.A. (1988). Efferent connections of the substantia innominata in the rat. *J. Comp. Neurol.* **277,** 347–364.

Grünthal, E. (1933). Uber das spezifisch Menschliche im Hypothalamusbau. *J. Psychol. Neural.* **45,** 237–263.

Guillery, R. W. (1955). A quantitative study of the mammary bodies and their connexions. *J. Anat.* **39,** 19–32.

Haber, S.N., Wolfe, D.P., and Groenewegen, H.J. (1990). The relationship between ventral striatal efferent fibers and the distribution of peptide-positive woolly fibers in the forebrain of the rhesus monkey. *Neuroscience* **39,** 323–338.

Haglund, L., Swanson, L.W., and Köhler, C. (1984). The projection of the supramammillary nucleus to the hippocampal formation: sn immunohistochemical and anterograde transport study with the lectin PHA-L in the rat. *J. Comp. Neurol.* **229,** 171–185.

Halaas, J.L., Gajiwala, K.S., Maffei, M., Cohen, S.L., Chait, B.T., Rabinowitz, D., Lallone. R.L., Burley, S.K., and Friedman, J.M. (1995). Weight-reducing effects of the plasma protein encoded by the obese gene. *Science* **269,** 543–546.

Hallbeck, M., and Blomqvist, A. (1999). Spinal cord-projecting vasopressinergic neurons in the rat paraventricular hypothalamus. *J. Comp. Neurol.* **411,** 201–211.

Hara, J., Beuckmann, C.T., Nambu, T., Willie, J.T., Chemelli, R.M., Sinton, C.M., Sugiyama, F., Yagami, K., Goto, K., Yanagisawa, M., and Sakurai, T. (2001). Genetic ablation of orexin neurons in mice results in narcolepsy, hypophagia, and obesity. *Neuron* **30,** 345–354.

Havel, P.J., Parry, S.J., Stern, J.S., Akpan, J.O., Gingerich, R.L., Taborsky, G.J., and Curry, D.L. (1994). Redundant parasympathetic and sympathoadrenal mediation of increased glucagon secretion during insulin-induced hypoglycemia in conscious rats. *Metabolism* **43,** 860–866.

Haxhiu, M.A., Jansen, A.S., Cherniack, N.S., and Loewy, A.D. (1993). CNS innervation of airway-related parasympathetic preganglionic neurons: a transneuronal labeling study using pseudorabies virus. *Brain Res.* **618:** 115–134.

Hedreen, J.C., Struble, R.G., Whitehouse, P.J., and Price, D.L. (1984). Topography of the magnocellular basal forebrain systems in human brain. *J. Neuropathol. Exp. Neurol.* **43,** 1–21.

Heimer, L., Zahm, D.S., Churchill, L., Kalivas, P.W., and Wohltmann, C. (1991). Specificity in the projection patterns of accumbal core and shell in the rat. *Neuroscience* **41,** 89–125.

Herbert, H., and Saper, C.B. (1992). Organization of medullary adrenergic and noradrenergic projections to the periaqueductal gray matter in the rat. *J. Comp. Neurol.* **315,** 34–52.

Herbison, A.E., Horvath, T.L., Naftolin, F., and Leranth, C. (1995). Distribution of estrogen receptor-immunoreactive cells in monkey hypothalamus: relationship to neurones containing luteinizing hormone-releasing hormone and tyrosine hydroxylase. *Neuroendocrinology* **61,** 1–10.

Hermann, D.M., Luppi, P.H., Peyron, C., Hinckel, P., and Jouvet, M. (1997). Afferent projections to the rat nuclei raphe magnus, raphe pallidus and reticularis gigantocellularis pars alpha demontrated by iontophoretic application of choleratoxin (subunit b). *J. Chem. Neuroanat.* **13,** 1–21.

Hofman, M.A., Zhou, J.N., and Swaab, D.F. (1996). Suprachiasmatic nucleus of the human brain: an immunocytochemical and morphometric analysis. *Anat. Rec.* **244,** 552–562.

Hori ,T., Kiyohara, T., Oomura, Y., Nishino, H., Aou, S., and Fujita, I. (1987). Activity of thermosensitive neurons of monkey preoptic hypothalamus during thermoregulatory operant behavior. *Brain Res. Bull* .**18,** 649–655.

Horn, T., Wilkinson, M.F., Landgraf, R., and Pittman, Q.J. (1994). Reduced febrile responses to pyrogens after lesions of the hypothalamic paraventricular nucleus. *Am. J. Physiol.* **267,** R323–R328.

Hübschle T., Thom E., Watson A., Roth J., Klaus S., Meyerhof W. (2001) Leptin-induced nuclear translocation of STAT3 immunoreactivity in hypothalamic nuclei involved in body weight regulation. *J Neurosci* **21,** 2413-2424.

Huszar, D., Lynch, C.A., Fairchild-Huntress,V., Dunmore, J.H., Fang, Q., Berkemeier, L.R.Gu, W., Kesterson, R.A., Boston, B.A., Cone, R.D., Smith, F.J., Campfield, L.A., Burn. P., and Lee. F. (1997). Targeted disruption of the melanocortin-4 receptor results in obesity in mice. *Cell* **88,** 131–141.

Ishunina, T.A., and Swaab. D.F. (1999). Vasopressin and oxytocin neurons of the human supraoptic and paraventricular nucleus: size changes in relation to age and sex. *J. Clin. Endocrinol. Metab.* **84,** 4637–4644.

Jahnke, V., and Merker, J.H. (2000). Electron microscopic and functional aspects of the human vomeronasal organ. *Am. J. Rhinol.* **14,** 63–67.

Jansen, A.S., Ter Horst, G.J., Mettenleiter, T.C., and Loewy, A.D. (1992). CNS cell groups projecting to the submandibular parasympathetic preganglionic neurons in the rat: a retrograde transneuronal viral cell body labeling study. *Brain Res.* **572,** 253–260.

Jansen, A.S., Hoffman, J.L., and Loewy, A.D. (1997). CNS sites involved in sympathetic and parasympathetic control of the pancreas: a viral tracing study. *Brain Res.* **766,** 29–38.

Johnson, R.H., Delahunt, J.W., and Robinson, B.J. (1990). Do thermoregulatory reflexes pass through the hypothalamus? Studies of chronic hypothermia due to hypothalamic lesion. *Aust. N.Z. J. Med.* **20,** 154–159.

Jones, E.G., and Powell, T.P.S. (1970). An anatomical study of converging sensory pathways within the cerebral cortex of the monkey. *Brain* **93,** 793–820.

Jones, E.G., Burton, H., Saper, C.B., and Swanson, L.W. (1976). Midbrain, diencephalic and cortical relationships of the basal nucleus of Meynert and associated structures in primates. *J. Comp. Neurol.* **167,**385–420.

Kaplan, J.M., Roitman, M., and Grill, H.J. (2000). Food deprivation does not potentiate glucose taste reactivity responses of chronic decerebrate rats. *Brain Res.* **870,** 102–108.

Keefer, D.A., and Stumpf, W.E. (1975). Atlas of estrogen-concentrating cells in the central nervous system of the squirrel monkey. *J. Comp. Neurol.* **160,** 419–442.

Khachaturian, H., Lewis, M.E., Tsou, S., and Watson, S.J. (1985). Beta-endorphin, alpha-MSH, ACTH and related peptides. *In* "Handbook of Chemical Neuroanatomy" (T. Hökfelt and A. Bj6rklund, eds.), Vol. 4, pp. 216–272. Elsevier, Amsterdam.

Kievet, J., and Kuypers, H.G.J.M. (1975). Basal forebrain and hypothalamic connections to the frontal and parietal cortex of the rhesus monkey. *Science* **187,** 660–662.

Kim, R., Nakano, K., Jayaraman, A., and Carpenter, M.B. (1976). Projections of the globus pallidus and adjacent structures: an autoradiographic study in the monkey. *J. Comp. Neurol.* **169,** 263–290.

Kishi, T., Tsumori ,T., Ono, K., Yokota, S., Ishino, H., and Yasui, Y. (2000). Topographical organization of projections from the subiculum to the hypothalamus in the rat. *J. Comp. Neurol.* **419,** 205–222.

Kita, H., and Oomura, Y. (1982). An HRP study of the afferent connections to rat lateral hypothalamic region. *Brain Res. Bull.* **8,** 63–71.

Köhler, C., and Swanson, L.W. (1984). Acetylcholinesterase-containing cells in the lateral hypothalamic area are imrnunoreactive for alpha-melanocyte stimulating hormone (alpha-MSH) and have cortical projections in the rat. *Neurosci. Lett.* **49,** 39–43.

Köhler, C., Haglund, L., and Swanson, L.W. (1984). A diffuse a-MSH-immunoreactive projection to the hippocampus and spinal cord from individual neurons in the lateral hypothalamic area and zona incerta. *J. Comp. Neurol.* **223,** 501–514.

Köhler, C., Swanson, L.W., Haglund, L., and Wu, J.Y. (1985). The cytoarchitecture, histochemistry and projections of the tubero-mammillary nucleus in the rat. *Neuroscience* **16,** 85–110.

Koikegami, H. (1937). Beitrage zur Kenntnis der Kerne des Hypothalamus bei Saugetieren. *Arch. Psychiatr. Nervenkr.* **107,** 742–774.

Kolaj, M., and Renaud, L.P. (1998). Vasopressin acting at V1-type receptors produces membrane depolarization in neonatal rat spinal lateral column neurons. *Prog. Brain Res.* **119,** 275–284.

Koutcherov, Y., Mai, J.K., Ashwell, K.W., and Paxinos, G. (2000). Organization of the human paraventricular hypothalamic nucleus. *J. Comp. Neurol.* **423,** 299–318.

Koutcherov, Y., May, J.K., Ashwell, K.W., and Paxinos, G. (2002). Organization of human hypothalamus in fetal development. *J. Comp. Neurol.* **446,** 301–324.

Kow, L.M., and Pfaff, D.W. (1998). Mapping of neural and signal transduction pathways for lordosis in the search for estrogen actions on the central nervous system. *Behav. Brain Res.* **92,** 169–180.

Krayniak, P.F., Siegel, A., Meibach, R.C., Fruchtman, D., and Scrimenti, M. (1979). Origin of the fornix system in the squirrel monkey. *Brain Res.* **160,** 401–411.

Kremer, H.P. (1992). The hypothalamic lateral tuberal nucleus: normal anatomy and changes in neurological diseases. *Prog. Brain Res.* **93,** 249-261.

Krettek, J.E., and Price, J.L. (1978). Amygdaloid projections to subcortical structures within the basal forebrain and brain stem in the rat and cat. *J. Comp. Neurol.* **178,** 225–254.

Kruseman, A.C.N., Linton, E.A., Ackland, J., Besser, G.M., and Lowry, P.J. (1984). Heterogeneous immunocytochemical reactivities of oCRF-41-like material in the human hypothalamus, pituitary and gastrointestinal tract. *Neuroendocrinology* **38,** 212–216.

Kubota, M., Shinozaki, M., Ishizaki, A., Kurata, K. (1991). Sodium regulation disorder, hypothermia, and circadian rhythm disturbances of the body temperature and sleep–wakefulness as sequelae of acute subdural hematoma. *No To Shinkei* **43,** 81–86.

Laflamme, N., Lacroix, S., and Rivest, S. (1999). An essential role of interleukin-1beta in mediating NF-kappaB activity and COX-2 transcription in cells of the blood–brain barrier in response to a systemic and localized inflammation but not during endotoxemia. *J. Neurosci.* **19,** 10923–10930.

Laruelle, M. L. (1934). Le système vdg6tatif meso-diencephalique. Partie anatomie. *Rev. Neural.* **1,** SW–842.

Lechan, R.M., Nestier, J.L., and Jacobson, S. (1982). The tubero-infundibular system of the rat as demonstrated by immuno-histochemical localization of retrogradely transported wheatgerm agglutinin (WGA) from the median eminence. *Brain Res.* **245,** 1–15.

LeDoux, J.E., Ruggiero, D.A., and Reis, D.J. (1985). Projections to the subcortical forebrain from anatomically defined regions of the medial geniculate body in the rat. *J. Comp. Neurol.* **242,** 182–213.

LeGros Clark, W.E. (1936). The topography and homologies of the hypothalamic nuclei in man. *J. Anat.* **70,** 203–216.

LeGros Clark, W.E. (1938). Morphological aspects of the hypothalamus. *In* "The Hypothalamus: Morphological, Functional, Clinical and Surgical Aspects" (W. E. LeGros Clark, J. Beattie, G. Riddoch, and N. M. Dott, eds.), pp. 1–68. Oliver Boyd, Edinburgh.

Lehman, M.N., and Winans, S.S. (1982). Vomeronasal and olfactory pathways to the amygdala controlling male hamster sexual behavior: autoradiographic and behavioral analyses. *Brain Res.* **240,** 27–41.

LeVay, S. (1991). A difference in hypothalamic structure between heterosexual and homosexual men. *Science* **253,** 1034–1037.

Lin, L., Faraco, J., Li, R., Kadotani, H., Rogers, W., Lin, X., Qiu, X., de Jong, P.J., Nishino, S., and Mignot, E. (1999). The sleep disorder canine narcolepsy is caused by a mutation in the hypocretin (orexin) receptor 2 gene. *Cell* **98,** 365–376.

Lind, R.W., Van Hoesen, G.W., and Johnson, A.K. (1982). An HRP study of the connections of the subfornical organ of the rat. *J. Comp. Neurol.* **210,** 265–277.

Lind, R.W., Swanson, L.W., and Ganten, D. (1984). Angiotensin 11 immunoreactivity in the neural afferents and efferents of the subfornical organ in the rat. *Brain Res.* **321,** 209–215.

Lloyd, S.A., and Dixson, A.F. (1988). Effects of hypothalamic lesions upon the sexual and social behaviour of the male common marmoset *(Callithrix jacchus). Brain Res.* **463,** 317–329

Lu, J., Shiromani, P., and Saper, C.B. (1999). Retinal input to the sleep-active ventrolateral preoptic nucleus in the rat. *Neuroscience* **93,** 209–214.

Lu, J., Greco, A.M., Shiromani, P., and Saper, C.B. (2001). Constrasting effects of lesions of the paraventricular nucleus and subparaventricular zone on circadian rhythms of sleep, body temperature, and activity. *J. Neurosci.* (in press).

Luiten, P.G.M., ter Horst, G.J., and Steffens, A.B. (1985). The course of paraventricular hypothalamic efferents to autonomic structures in medulla and spinal cord. *Brain Res.* **329,** 374–378.

Lydic, R., Schoene, W.C., Czeisler, C.A., and Moore-Ede, M.C. (1980). Suprachiasmatic region of the human hypothalamus: homolog to the primate circadian pacemaker? *Sleep* **2,** 355–361.

Lynch, W.C., Adair, E.R., and Adams, B.W. (1980). Vasomotor thresholds in the squirrel monkey: effects of central and peripheral temperature. *J. Appl. Physiol.* **48,** 89–96.

Ma, R.C., and Dun, N.J. (1985). Vasopressin depolarizes lateral horn cells of the neonatal rat spinal cord in vitro. *Brain Res.* **348,** 36–43.

Mai, J.K., Triepel, J., and Metz, J. (1987). Neurotensin in the human brain. *Neuroscience* **22,** 499–524.

Mai, J.K., Kedziora, O., Teckhaus, L. and Sofroniew M.V. (1991) Evidence for subdivisions in the human suprachiasmatic nucleus. *J. Comp. Neurol.* **305,** 508–525.

Malone, E.F. (1910). Uber die Kerne des Menschlichen Diencephalon. Abh. K. Preuss. Akad. Wiss., Berlin.

Malone, E.F. (1916). The nuclei tuberis laterales and the so-called ganglion opticum basale. *Johns Hopkins Hosp. Rep.* **17,** 441–511.

Mantyh, P.W. (1983). Connections of midbrain periaqueductal gray in the monkey. I. Ascending efferent projections. *J. Neurophysiol.* **49,** 567–581.

Martyn, P.A., Hansen, B.C., and Jen, K.L. (1984). The effects of parenteral nutrition on food intake and gastric motility. *Nurs. Res.* **33,** 336–342.

McEwen, B.S. (2000). Allostasis, allostatic load, and the aging nervous system: role of excitatory amino acids and excitotoxicity. *Neurochem, Res.* **25,** 1219–1231.

McKinney, M., Coyle, J.T., and Hedreen, J.C. (1983). Topographic analysis of the innervation of the rat neocortex and hippocampus by the basal forebrain cholinergic system. *J. Comp. Neurol.* **217,** 103–121.

Meister, B., Villar, M.J., Ceccatelli, S., and Hokfelt, T. (1990). Localization of chemical messengers in magnocellular neurons of the hypothalamic supraoptic and paraventricular nuclei: an immunohistochemical study using experimental manipulations. *Neuroscience* **37,** 603–633.

Mesulam, M.M., Mufson, E.J., Levey, A.I., and Wainer, B.H. (1983). Cholinergic innervation of cortex by the basal forebrain: cytochemistry and cortical connections of the septal area, diagonal band nuclei, nucleus basalis (substantia innominata) and hypothalamus in the rhesus monkey. *J. Comp. Neurol.* **214,** 170–197.

Michael, R.P., Clancy, A.N., and Zumpe, D. (1995). Distribution of androgen receptor-like immunoreactivity in the brains of cynomolgus monkeys. *J. Neuroendocrinol.* **7,** 713–719.

Mishkin, M. (1982). A memory system in the monkey. *Philos. Trans. R. Soc. London, Ser. B* **2,** 85–95.

Mogenson, G.J., Swanson, L.W., and Wu, M. (1983). Neural projections from nucleus accumbens to globus pallidus, substantia innominata, and lateral preoptic-lateral hypothalamic area: an anatomical and electrophysiological investigation in the rat. *J. Neurosci.* **3,** 189–202.

Moore, R.Y. (1993). Organization of the primate circadian system. *J. Biol. Rhythms* **8** Suppl, S3–S9.

Moore, R.Y. (1997). Circadian rhythms: basic neurobiology and clinical applications. *Annu. Rev. Med.* **48,** 253–266.

Morrison, S.F. (1999). RVLM and raphe differentially regulate sympathetic outflows to splanchnic and brown adipose tissue. *Am. J. Physiol.* **276,** R962–R973.

Motawei, K., Pyner, S., Ranson, R.N., Kamel, M., and Coote, J.H. (1999). Terminals of paraventricular spinal neurones are closely associated with adrenal medullary sympathetic preganglionic neurones: immunocytochemical evidence for vasopressin as a possible neurotransmitter in this pathway. *Exp. Brain Res.* **126,** 68–76.

Mouri, T., Suda, T., Sasano, N., Andoh, N., Takei, Y., Takase, M., Sasaki, A., Murakami, O., and Yoshinaga, K. (1984). Immunocytochemical identification of CRF in the human hypothalamus. *Tohoku J. Exp. Med.* **142,** 423–426.

Nagai, T., Pearson, T., Peng, F., McGeer, E.G., and McGeer, P.L. (1983). lmmunohistochemical staining of the human forebrain with monoclonal antibody to human choline acetyltransferase. *Brain Res.* **265,** 300–306.

Narkiewicz, O., Dziewiatkowski, J., and Morys, J. (1994). Lateral tuberal nucleus in man and macaca comparative morphometric investigations. *Folia Morphol (Warsz)* **53,** 1–12.

Nathan, P.W., and Smith, M.C. (1986). The location of descending fibers to sympathetic neurons supplying the eye and sudomotor neurons supplying the head and neck. *J. Neurol. Neurosurg. Psychiatry* **49,** 187.

Nauta, W.J.H. (1961). Fiber degeneration following lesions of the amygdaloid complex in the monkey. *J. Anat.* **95,** 515–531.

Nauta, W. J.H., and Haymaker, W. (1969). Hypothalamic nuclei and fiber connections. *In* "The Hypothalamus" (W. Haymaker, E. Anderson, and W.J.H. Nauta, eds.), pp. 136–209. Charles C Thomas, Springfield, Ill.

Nelson, P.T., Marton, L., and Saper, C.B. (1993). Alz-50 immunohistochemistry in the normal sheep striatum: a light and electron microscope study. *Brain Res.* **600,** 285–297.

Nilaver, G., Zimmerman, E.A., Wilkins, J., Michaels, J., Hoffman, D., and Silverman, A. J. (1980). Magnocellular hypothalamic projections to the lower brain stem and spinal cord of the rat. *Neuroendocrinology* **30,** 150–158.

Nishino, S., Ripley, B., Overeem, S., Lammers, G.J., and Mignot, E. (2000). Hypocretin (orexin) deficiency in human narcolepsy. *Lancet* **355,** 39–40.

Numan, M., and Numan, M. (1996). A lesion and neuroanatomical tract-tracing analysis of the role of the bed nucleus of the stria terminalis in retrieval behavior and other aspects of maternal responsiveness in rats. *Dev. Psychobiol.* **29,** 23–51.

Ongur, D., An, X., and Price, J.L. (1998). Prefrontal cortical projections to the hypothalamus in macaque monkeys. *J. Comp. Neurol.* **401,** 480–505.

Oomura, Y., Yoshimatsu, H., and Aou, S. (1983). Medial preoptic and hypothalamic neuronal activity during sexual behavior of the male monkey *Brain Res.* **266,** 340–343.

Osamura, R.Y., Komatsu, N., Watanabe, K., Nakai, Y., Tanaka, I., and lmura, H. (1982). lmmunohistochemical and immunocytochemical localization of gamma-melanocyte stimulating hormone (gamma-MSH)–like immunoreactivity in human and rat hypothalamus. *Peptides (N.Y.)* **3,** 781–787.

Panula, P., Yang, H.Y.T, and Costa, E. (1984). Histamine-containing neurons in the rat hypothalamus. *Proc. Natl. Acad. Sci. U.S.A.* **31,** 2572–2576.

Panula, P., Airaksinen, M.S., Pirvola, U., and Kotilainen, E. (1990). A histamine-containing neuronal system in human brain. *Neuroscience* **34,** 127–132.

Paxinos, G., and Watson, C. (1986). "The Rat Brain in Stereotaxic Coordinates," p. xii. Academic Press, Orlando.

Pearson, J., Goldstein, M., Markey, K., and Brandeis, L. (1983). Human brain stem catecholamine neuronal anatomy as indicated by immunocytochemistry with antibodies to tyrosine hydroxylase. *Neuroscience* **8,** 3–32.

Pearson, R.C.A., Gatter, K.C., Brodal, P., and Powell, T.P.S. (1983). The projection of the basal nucleus of Meynert upon the neocortex in the monkey. *Brain Res.* **259,** 132–136.

Pearson, R.C.A., Esiri, M.M., Hiorns, R.W., Wilcock, G.K., and Powell, T.P.S. (1985). Anatomical correlates of the distribution of the pathological changes in the neocortex in Alzheimer's disease. Proc. *Natl. Acad. Sci. U.S.A.* **82,** 4531–4534.

Pelletier, G., Desy, L., Cote, J., and Vaudry, H. (1983). Immunocytochemical localization of corticotropin-releasing factor-like immunoreactivity in the human hypothalamus. *Neurosci. Lett.* **41,** 259–263.

Pelletier, G., Desy, L., Kerkerian, L., and Cote, J. (1984). Immyocytochemical localization of neuropeptide Y (NPY) in the human hypothalamus. *Cell Tissue Res.* **238**, 203–205.

Pelletier, G., Desy, L., Cote, J., Lefevre, G., and Vaudry, H. (1986). Light-microscopic immunocytochemical localization of growth hormone–releasing factor in the human hypothalamus. *Cell Tissue Res.* **245,** 461-463.

Petrovich, G.D., Risold, P.Y., and Swanson, L.W. (1996). Organization of projections from the basomedial nucleus of the amygdala: a PHAL study in the rat. *J. Comp. Neurol.* **374,** 387–420.

Peyron, C., Tighe, D.K., van den Pol, A.N., de Lecea, L., Heller, H.C., Sutcliffe, J.G., and Kilduff, T.S. (1998). Neurons containing hypocretin (orexin) project to multiple neuronal systems. *J. Neurosci.* **18,** 9996–10015.

Peyron, C., Faraco, J., Rogers, W., Ripley, B., Overeem, S., Charnay, Y., Nevsimalova, S., Aldrich, M., Reynolds, D., Albin, R., Li, R., Hungs, M., Pedrazzoli, M., Padigaru, M., Kucherlapati, M., Fan, J., Maki, R., Lammers, G.J., Bouras, C., Kucherlapati, R., Nishino, S., and Mignot, E. (2000). A mutation in a case of early onset narcolepsy and a generalized absence of hypocretin peptides in human narcoleptic brains. *Nat. Med.* **6,** 991–997.

Pfaff, D.W., and Sakuma, Y. (1979). Deficit in the lordosis reflex of female rats caused by lesions in the ventromedial nucleus of the hypothalamus. *J. Physiol.* **288,** 203–210.

Pfaff, D.W., Gerlach, J.L., McEwen, B.S., Ferin, M., Carmel, P., and Zimmerman, E.A. (1976). Autoradiographic localization of hormone-concentrating cells in the brain of the female rhesus monkey. *J. Comp. Neurol.* **170,** 279–293.

Plum, F., and Van Uitert, R. (1978). Nonendocrine diseases and disorders of the hypothalamus. *In* "The Hypothalamus." Res. Publ. Assoc. Res. Nerv. Ment. Dis. (S. Reichlin, R. J. Baldessarini, and J. B. Martin, eds.), Vol. 56, pp. 415–473. Raven Press, New York.

Porrino, L.J., and Goldman-Rakic, P.S. (1982). Brain stem innervation of prefrontal and anterior cingulate cortex in the rhesus monkey revealed by retrograde transport of HRP. *J. Comp. Neurol.* **205,** 63–76.

Powell, E.W., and Leman, R.B. (1976). Connections of the nucleus accumbens. *Brain Res.* **105,** 389–403.

Powell, T.P.S., Guillery, R.W., and Cowan, W.M. (1957). A quantitative study of the fornix-mamillo-thalamic system. *J. Anat.* **91,** 419–437.

Powley, T.L., Opsahl, C.A., Cox, J.E., and Weingarten, H.P. (1980). The role of the hypothalamus in energy homeostasis. *In* "Behavioral Studies of the Hypothalamus. Handbook of the Hypothalamus" (P. J. Morgane and J. Panksepp, eds.), Vol. 3, Part A, pp. 211–298. Marcel Dekker, New York.

Price, J.L., and Amaral, D.G. (1981). An autoradiographic study of the projections of the central nucleus of the monkey amygdala. *J. Neurosci.* **1,** 1242–1259.

Price, J.L., and Stern, R. (1983). Individual cells in the nucleus basalis-diagonal band complex have restricted axonal projections to the cerebral cortex in the rat. *Brain Res.* **269,** 352–356.

Price, J.L., Slotnick, B.M., and Revial, M.F. (1991). Olfactory projections to the hypothalamus. *J. Comp. Neurol.* **306,** 447–461.

Pritchard, T.C., Hamilton, R.B., and Norgren, R. (2000). Projections of the parabrachial nucleus in the old world monkey. *Exp. Neurol.* **165,** 101–117.

Qu, D., Ludwig, D.S., Gammeltoft, S., Piper, M., Pelleymounter, M.A., Cullen, M.J., Mathes, W.F., Przypek, R., Kanarek, R., and Maratos-Flier, E. (1996). A role for melanin-concentrating hormone in the central regulation of feeding behaviour. *Nature* **380,** 243–247.

Rajkowski, J., Kubiak, P., and Aston-Jones, G. (1994). Locus coeruleus activity in monkey: phasic and tonic changes are associated with altered vigilance. *Brain Res. Bull.* **35,** 607–616.

Rance, N.E., and Uswandi, S.V. (1996). Gonadotropin-releasing hormone gene expression is increased in the medial basal hypothalamus of postmenopausal women. *J. Clin. Endocrinol. Metab.* **81,** 3540–3546.

Rance, N.E., Young, W.S., and McMullen, N.T. (1994). Topography of neurons expressing luteinizing hormone-releasing hormone gene transcripts in the human hypothalamus and basal forebrain. *J. Comp. Neurol.* **339,** 573–586.

Rasmussen, K., Heym, J., and Jacobs, B.L. (1984). Activity of serotonin-containing neurons in nucleus centralis superior of freely moving cats. *Exp. Neurol.* **83,** 302–317.

Reeves, A.G., and Plum, F. (1969). Hyperphagia, rage, and dementia accompanying a ventromedial hypothalamic neoplasm. *Arch. Neurol.* **20,** 616–624.

Refinetti, R., and Carlisle, H.J. (1986). Effects of anterior and posterior hypothalamic temperature changes on thermoregulation in the rat. *Physiol. Behav.* **36,** 1099–1103.

Rempel-Clower, N.L., and Barbas, H. (1998). Topographic organization of connections between the hypothalamus and prefrontal cortex in the rhesus monkey. *J. Comp. Neurol.* **398,** 393–419.

Reubi, J.C., Cortes, R., Maurer, R., Probst, A., and Palacios, J.M. (1986). Distribution of somatostatin receptors in the human brain: an autoradiographic study. *Neuroscience* **19,** 329–346.

Reuss, S., and Fuchs, E. (2000). Anterograde tracing of retinal afferents to the tree shrew hypothalamus and raphe. *Brain Res.* **874,** 66–74.

Ricardo, J.A., and Koh, E.T. (1978). Anatomical evidence of direct projections from the nucleus of the solitary tract to the hypothalamus, amygdala, and other forebrain structures in the rat. *Brain Res.* **153,** 1–26.

Rioch, D.M., Wislocki, G.B., and O'Leary, J.L. (1939). A precis of preoptic, hypothalamic and hypophyseal terminology with atlas. *In* "The Hypothalamus and Central Levels of Autonomic Function" Assoc. Res. Nerv. Ment. Dis. (J. F. Fulton, ed.), Vol. 20 pp. 3–30. Raven, New York.

Risold, P.Y., and Swanson, L.W. (1997). Connections of the rat lateral septal complex *Brain Res. Rev.* **24,** 115–195.

Risold, P.Y., Canteras, N.S., and Swanson, L.W. (1994). Organization of projections from the anterior hypothalamic nucleus: a *Phaseolus vulgaris*-leucoagglutinin study in the rat *J. Comp. Neurol.* **348,** 1–40.

Risold, P.Y., Thompson, R.H., and Swanson, L.W. (1997). The structural organization of connections between hypothalamus and cerebral cortex. *Brain Res. Rev.* **24,** 197–254.

Rivest, S., Lacroix, S., Vallieres, L., Nadeau, S., Zhang, J., and Laflamme, N. (2000). How the blood talks to the brain parenchyma and the paraventricular nucleus of the hypothalamus during systemic inflammatory and infectious stimuli. *Proc. Soc. Exp. Biol. Med.* **223,** 22–38.

Rolls, E.T., Burton, M.J., and Mora, R (1976). Hypothalamic neuronal responses associated with the sight of food. *Brain Res.* IU, 53–66.

Rye, D.B., Wainer, B.H., Mesulam, M. M., Mufson, E.J., and Saper, C.B. (1984). Cortical projections from the basal forebrain: a study of cholinergic and non-cholinergic components employing combined retrograde tracing and immunohistochemical localization of choline acetyltransferase. *Neuroscience* **13,** 627–643.

Rye, D.B., Leverenz, J., Greenberg, S.G., Davies, P., and Saper, C.B. (1993). The distribution of Alz-50 immunoreactivity in the normal human brain. *Neuroscience* **56,** 109–127.

Sadun, A.A., Schaechter, J.D., and Smith, L.E.H. (1984). A retinohypothalamic pathway in man: Light mediation of circadian rhythms. *Brain Res.* **302,** 371–377.

Saper, C.B. (1982). Convergence of autonomic and limbic connections in the insular cortex of the rat. *J. Comp. Neurol.* **210,** 163–173.

Saper, C.B. (1984). Organization of cerebral cortical afferent systems in the rat. I. Magnocellular basal nucleus. *J. Comp. Neurol.* **222,** 313–342.

Saper, C.B. (1985). Organization of cerebral cortical afferent systems in the rat. II. Hypothalamocortical projections. *J. Comp. Neurol.* **237,** 21–46.

Saper, C.B. (1987). Diffuse cortical projection systems: Anatomical organization and role in cortical function. *In* "Handbook of Physiology" (F. Plum, ed.), Sec. 1, Vol. V, pp. 169–210. *Am. Physiol. Soc.,* Washington, D. C.

Saper, C.B. (1988). Chemical neuroanatomy of Alzheimer's disease. *In* "Handbook of Psychopharmacology" (S. D. Iversen, L. L. Iversen, and S. H. Snyder, eds.), Vol. 20, pp. 131–156. Plenum Publishers, New York.

Saper, C.B., and Breder, C.D. (1994). The neurologic basis of fever. *N. Engl. J. Med.* **330,** 1880–1886.

Saper, C.B., and Chelimsky, T.C. (1984). A cytoarchitectonic and histochemical study of nucleus basalis and associated cell groups in the normal human brain. *Neuroscience* **13,** 1023–1037.

Saper, C.B., and German, D.C. (1987). Hypothalamic pathology in Alzheimer's disease. *Neurosci. Lett.* **74,** 364–370.

Saper, C.B., and Levisohn, D. (1983). Afferent connections of the median preoptic nucleus in the rat: anatomical evidence for a cardiovascular integrative mechanism in the anteroventral third ventricular (AV3V) region. *Brain Res.* **288,** 21–31.

Saper, C.B., and Petito, C.K. (1982). Correspondence of melanin-pigmented neurons in human brain with Al -A 14 catecholamine cell groups. *Brain* **W5,** 87101.

Saper, C.B., Loewy, A.D., Swanson, L.W., and Cowan, W.M. (1976a). Direct hypothalamo-autonomic connections. *Brain Res.* **U7,** 305–312.

Saper, C.B., Swanson, L.W., and Cowan, W.M. (1976b). The efferent connections of the ventromedial nucleus of the hypothalamus of the rat. *J. Comp. Neurol.* **169,** 409–442.

Saper, C.B., Swanson, L.W., and Cowan, W.M. (1978). The efferent connections of the anterior hypothalamic area of the rat, cat, and monkey. *J. Comp. Neurol.* **192,** 575–600.

Saper, C.B., Swanson, L.W., and Cowan, W.M. (1979a). Some efferent connections of the rostral hypothalamus in the squirrel monkey *(Saimiri sciureus)* and cat. *J. Comp. Neurol.* **184,** 205–242.

Saper, C.B., Swanson, L.W., and Cowan, W.M. (1979b). An autoradiographic study of the efferent connections of the lateral hypothalamic area in the rat. *J. Comp. Neurol.* **183,** 689–706.

Saper, C.B., Akil, H., and Watson, S.J. (1986). Lateral hypothalamic innervation of the cerebral cortex: immunoreactive staining for a peptide resembling but immunochemically distinct from pituitary/arcuate alpha-melanocyte stimulating hormone. *Brain Res. Bull.* **16,** 107–120.

Saper, C.B., Wainer, B.H., and German, D.C. (1987). Axonal and transneuronal transport in the transmission of neurological disease: potential role in system degenerations, including Alzheimer's disease. *Neuroscience* **23,** 389–398.

Saper, C.B., Hurley, K.M., Moga, M.M., Holmes, H.R., Adams, S.A., Leahy, K.M., and Needleman, P. (1989). Brain natriuretic peptides: differential localization of a new family of neuropeptides. *Neurosci. Lett.* **96,** 29–34.

Satinoff, E., Liran, J., and Clapman, R. (1982). Aberrations of circadian body temperature rhythms in rats with medial preoptic lesions. *Am. J. Physiol.* **242,** R352–R357.

Sawchenko, P.E., and Swanson, L.W. (1982). The organization of nordrenergic pathways from the brain stem to the paraventricular and supraoptic nuclei in the rat. *Brain Res. Rev.* **4,** 275–325.

Sawchenko, P.E., and Swanson, L.W. (1985). Localization, colocalization, and plasticity of corticotropin-releasing factor immunoreactivity in rat brain. *Proc. Fed. Am. Soc. Exp. Biol.* **44,** 221–227.

Scammell, T.E., Elmquist, J.K., Griffin, J.D., and Saper, C.B. (1996). Ventromedial preoptic prostaglandin E2 activates fever-producing autonomic pathways. *J. Neurosci.* **16,** 6246–6254.

Scammell, T.E., Griffin, J.D., Elmquist, J.K., and Saper, C.B. (1998). Microinjection of a cyclooxygenase inhibitor into the antero-ventral preoptic region attenuates LPS fever. *Am. J. Physiol.* **274,** R783–R789.

Schramm, L.P., Strack, A.M., Platt, K.B., and Loewy, A.D. (1993). Peripheral and central pathways regulating the kidney: a study using pseudorabies virus. *Brain Res.* **616,** 251–262.

Schultz, C., Koppers, D., Sassin, I., Braak, E., and Braak, H. (1998). Cytoskeletal alterations in the human tuberal hypothalamus related to argyrophilic grain disease. *Acta Neuropathol. (Berl.)* **96,** 596–602.

Schwaber, J.S., Kapp, B.S., Higgins, G.A., and Rapp, P.R. (1982). Amygdaloid and basal forebrain direct connections with the nucleus of the solitary tract and the dorsal motor nucleus. *J. Neurosci.* **2,**1424–1438.

Senba, E., Daddona, P.E., Watanabe, T, Wu, J.Y., and Nagy, J.1. (1985). Coexistence of adenosine deaminase, histidine decarboxylase, and glutamate decarboxylase in hypothalamic neurons of the rat. *J. Neurosci.* **5,** 3393–3402.

Sesack, S.R., Deutch, A.Y., Roth, R.H., and Bunney, B.S. (1989). Topographical organization of the efferent projections of the medial prefrontal cortex in the rat: an anterograde tract-tracing study with Phaseolus vulgaris leucoagglutinin. *J. Comp. Neurol.* **290,** 213–242.

Shangold, M.M., and Levine, H.S. (1982). The effect of marathon training upon menstrual function. *Am. J. Obstet. Gynecol.* **143,** 862–869.

Sherin, J.E., Shiromani, P.J., McCarley, R.W., and Saper, C.B. (1996). Activation of ventrolateral preoptic neurons during sleep. *Science* **271,** 216–219.

Sherin, J.E., Elmquist, J.K., Torrealba, F., and Saper, C.B. (1998). Innervation of histaminergic tuberomammillary neurons by GABAergic and galaninergic neurons in the ventrolateral preoptic nucleus of the rat. *J. Neurosci.* **18,** 4705–4721.

Shimada, M., Tritos, N.A., Lowell, B.B., Flier, J.S., and Maratos-Flier, E. (1998). Mice lacking melanin-concentrating hormone are hypophagic and lean. *Nature* **396,** 670–674.

Simerly, R.B., and Swanson, L.W. (1988). Projections of the medial preoptic nucleus: a Phaseolus vulgaris leucoagglutinin antero-grade tract-tracing study in the rat. *J. Comp. Neurol.* **270,** 209–242.

Simerly, R.B., Gorski, R.A., and Swanson, L.W. (1986). Neuro-transmitter specificity of cells and fibers in the medial preoptic nucleus: an immunohistochemical study in the rat. *J. Comp. Neurol.* **246,** 343–363.

Simerly, R.B., Swanson, L.W., and Gorski, R.A. (1985). The distribution of monoaminergic cells and fibers in a periventricular preoptic nucleus involved in the control of gonadotropin release: immunohistochemical evidence for a dopaminergic sexual dimorphism. *Brain Res.* **330,** 55–64.

Shiosaka, S., Shibasaki, T., and Tohyama, M. (1984). Bilateral a-melanocyte stimulating hormonergic fiber system from zona incerta to cerebral cortex: Combined retrograde axonal transport and immunohistochemical study. *Brain Res.* **309,** 350–353.

Sladek, J.R., Garver, D.L., and Cummings, J.P. (1982). Monoamine distribution in primate brain. 4. Indoleamine-containing perikarya in the brain stem of *Macaca-arctoides. Neuroscience* **7,** 477–493.

Smith, J.E., Jansen, A.S., Gilbey, M.P., and Loewy, A.D. (1998). CNS cell groups projecting to sympathetic outflow of tail artery: neural circuits involved in heat loss in the rat. *Brain Res.* **786,** 153–164.

Sofroniew, M.V. (1983). Morphology of vasopressin and oxytocin neurones and their central and vascular projections. *Prog. Brain Res.* **60,** 101–114.

Spencer, S., Saper, C.B., Joh, T., Reis, D.J., Goldstein, M., and Raese, J. (1985). Distribution of catecholamine-containing neurons in the normal human hypothalamus. *Brain Res.* **328,** 73–80.

Spencer, S.E., Sawyer, W.B., Wada, H., Platt, K.B., and Loewy, A.D. (1990). CNS projections to the pterygopalatine parasympathetic preganglionic neurons in the rat: a retrograde transneuronal viral cell body labeling study. *Brain Res.* **534,** 149–169.

Staines, W.A., Yamamoto, T., Daddona, P.E., and Nagy, J.1. (1986). Neuronal colocalization of adenosine deaminase, monoamine oxidase, galanin and 5-hydroxytryptophan uptake in the tuberomammillary nucleus of the rat. *Brain Res. Bull.* **17,** 351–366.

Staines, W.A., Daddona, P.E., and Nagy, J.1. (1987). The organization and hypothalamic projections of the tuberomammillary nucleus in the rat: an immunohistochemical study of adenosine deaminase-positive neurons and fibers. *Neuroscience* **23,** 571–598.

Steininger, T.L, Alam, M.N., Gong, H., Szymusiak, R., and McGinty, D. (1999). Sleep–waking discharge of neurons in the posterior lateral hypothalamus of the albino rat. *Brain Res,* **840,** 138–147.

Stellar, E., and Corbit, J.D. (1973). Neural control of motivated behavior. *Neurosci. Res. Prog. Bull.* **11,** 296–410.

Stellar, E., and Shrager, E.E. (1985). Chews and swallows and the microstructure of eating. *Am. J. Clin. Nutr.* **42,** 973–982.

Stopa, E.G., King, J.C., Lydic, R., and Schoene, W.C. (1984). Human brain contains vasopressin and vasoactive intestinal polypeptide neuronal subpopulations in the suprachiasmatic region. *Brain Res.* **297,** 159–163.

Strack, A.M., Sawyer, W.B., Platt, K.B., and Loewy, A.D. (1989). CNS cell groups regulating the sympathetic outflow to adrenal gland as revealed by transneuronal cell body labeling with pseudorabies virus. *Brain Res.* **491,** 274–296.

Stricker, E.M., and Verbalis, J.G. (1991). Caloric and noncaloric controls of food intake. *Brain Res. Bull.* **27,** 299–303.

Sutin, J. (1966). The periventricular stratum of the hypothalamus. *Int. Rev. Neurobiol.* **9,** 263–300.

Swaab, D.F., and Fliers, E. (1985). A sexually dimorphic nucleus in the human brain. *Science* **228,** 1112–1115.

Swaab, D.F., and Hofman, M.A. (1990). An enlarged suprachiasmatic nucleus in homosexual men. *Brain Res.* **537,** 141–148.

Swaab, D.F., Fliers, E., and Partiman, T.S. (1985). The suprachiasmatic nucleus of the human brain in relation to sex, age and senile dementia. *Brain Res.* **342,** 37–44.

Swanson, L.W. (1977). Immunohistochemical evidence for a neurophysin-containing autonomic pathway arising in the paraventricular nucleus of the hypothalamus. *Brain Res.* **128,** 346–353.

Swanson, L.W., and Cowan, W.M. (1975). Hippocampo-hypothalamic connections: origins in subicular cortex, not Ammon's horn. *Science* **189,** 303–304.

Swanson, L.W., and Cowan, W.M. (1977). An autoradiographic study of the organization of the efferent connections of the hippocampal formation in the rat. *J. Comp. Neurol.* **172,** 49–84.

Swanson, L.W., and Kuypers, H.G.J.M. (1980). The paraventricular nucleus of the hypothalamus: cytoarchitectonic subdivisions and organization of projections to the pituitary, dorsal vagal complex and spinal cord as demonstrated by retrograde double-labeling methods. *J. Comp. Neurol.* **194,** 555–570.

Swanson, L.W., and McKellar, S. (1979). The distribution of oxytocin and neurophysin-stained fibers in the spinal cord of the rat and monkey. *J. Comp. Neurol.* **188,** 87–106.

Swanson, L.W., and Sawchenko, P.E. (1983). Hypothalamic integration: organization of the paraventricular and supraoptic nuclei. *Annu. Rev. Neurosci.* **6,** 269–324.

Swanson, L.W., Sawchenko, P.E., Wiegand, S.J., and Price, J.L. (1982). Separate neurons in the paraventricular nucleus project to the median eminence and to the medulla or spinal cord. *Brain Res. M,* 207–212.

Switzer, R.C., de Olmos, J., and Heimer, L. (1986). Olfactory system. *In* "The Rat Nervous System" (G. Paxinos, ed.), Vol. 1, pp. 1–36. Academic Press, Orlando.

Tataranni, P.A., Gautier, J.F., Chen, K., Uecker, A., Bandy, D., Salbe, A.D., Pratley, R.E., Lawson, M., Reiman, E.M., and Ravussin, E. (1999). Neuroanatomical correlates of hunger and satiation in humans using positron emission tomography. *Proc. Natl. Acad. Sci. U.S.A.* **96,** 4569–4574.

Tazawa, Y., Onoda, N., and Takagi, S.F (1987). Olfactory input to the lateral hypothalamus of the old world monkey. *Neurosci. Res.* **4,** 357–375.

Teclemariam-Mesbah, R., Kalsbeek, A., Buijs, R.M., and Pevet, P. (1997). Oxytocin innervation of spinal preganglionic neurons projecting to the superior cervical ganglion in the rat. *Cell Tissue Res.* **287,** 481–486.

Thannickal, T.C., Moore, R.Y., Nienhuis, R., Ramanathan, L., Gulyani, S., Aldrich, M., Cornford, M. and Siegel, J.M. (2000). Reduced number of hypocretin neurons in human narcolepsy. *Neuron* **27,** 469–474.

Thompson, R.H., Canteras, N.S., and Swanson, L.W. (1996). Organization of projections from the dorsomedial nucleus of the hypothalamus: a PHA-L study in the rat. *J. Comp. Neurol.* **376,** 143–173.

Thornhill, J.A., and Halvorson, I. (1994). Electrical stimulation of the posterior and ventromedial hypothalamic nuclei causes specific activation of shivering and nonshivering thermogenesis. *Can. J. Physiol. Pharmacol.* **72,** 89–96.

Tigges, J., Walker, L.C., and Tigges, M. (1983). Subcortical projections to the occipital and parietal lobes of the chimpanzee brain. *J. Comp. Neurol.* **220,**106–115.

Travers, J.B., DiNardo, L.A., and Karimnamazi, H. (2000). Medullary reticular formation activity during ingestion and rejection in the awake rat. *Exp. Brain Res.* **130,** 78–92.

Trulson, M.E., and Jacobs, B.L. (1979). Raphe unit activity in freely moving cats: correlation with level of behavioral arousal. *Brain Res.* **163,** 135–150.

Tucker, D.C., Saper, C.B., Ruggiero, D.A., and Reis, D.J. (1987). Organization of central adrenergic pathways. I. Relationships of ventrolateral medullary projections to the hypothalamus and spinal cord. *J. Comp. Neurol.* **259,** 591–603.

Turner, B.H., Mishkin, M., and Knapp, M. (1980). Organization of the amygdalopetal projections from modality-specific cortical association areas in the monkey. *J. Comp. Neurol.* **191,** 515–543.

Ushikubi, F., Segi, E., Sugimoto, Y., Murata, T., Matsuoka, T., Kobayashi, T., Hizaki, H., Tuboi, K., Katsuyama, M., Ichikawa, A., Tanaka, T., Yoshida, N., and Narumiya, S. (1998). Impaired febrile response in mice lacking the prostaglandin E receptor subtype EP3. *Nature* **395,** 281–284.

Usuda, I., Tanaka, K., and Chiba, T. (1998). Efferent projections of the nucleus accumbens in the rat with special reference to subdivision of the nucleus: biotinylated dextran amine study. *Brain Res.* **797,** 73–93.

Valenstein, E.S., and Nauta, W.J.H. (1956). A comparison of the distribution of the fornix system in the rat, guinea pig, cat, and monkey. *J. Comp. Neurol.* **106,** 183.

van den Pol, A.N. (1999). Hypothalamic hypocretin (orexin): robust innervation of the spinal cord. *J. Neurosci.* **19,** 3171–3182.

van Hoesen, G.W., Pandya, D.N., and Butters, N. (1972). Cortical afferents to the entorhinal cortex of the rhesus monkey. *Science* **175,** 1471–1473.

Veazey, R.B., Amaral, D.G., and Cowan, W.M. (1982). The morphology and connections of the posterior hypothalamus in the Cynomolgus monkey *(Macaca fascicularis)*. II. Efferent connections. *J. Comp. Neurol.* **207,** 135–156.

Veening, J.G., Swanson, L.W., Cowan, W.M., Nieuwenhuys, R., and Geeraedts, L.M. (1982). The medial forebrain bundle of the rat. II. An autoradiographic study of the topography of the major descending and ascending components. *J. Comp. Neurol.* **206,** 82–108.

Vincent, S.R., Hökfelt, T., Skirboll, L.R., and Wu, J. Y. (1983). Hypothalamic gamma-amino butyric acid neurons project to the neocortex. *Science* **220,** 1309–1311.

Voisin, D.L., Chakfe, Y., and Bourque, C.W. (1999). Coincident detection of CSF Na^+ and osmotic pressure in osmoregulatory neurons of the supraoptic nucleus. *Neuron* **24,** 453–460.

Walker, L.C., Kitt, C.A., DeLong, M.R., and Price, D.L. (1985). Noncollateral projections of basal forebrain neurons to frontal and parietal neocortex in primates. *Brain Res. Bull.* **15,** 307–314.

Wang, C., Billington, C.J., Levine, A.S., and Kotz, C.M. (2000). Effect of CART in the hypothalamic paraventricular nucleus on feeding and uncoupling protein gene expression. *Neuroreport* **11,** 3251–325.

Watanabe, Y., Watanabe, Y., and Hayaishi, O. (1988). Quantitative autoradiographic localization of prostaglandin E2 binding sites in monkey diencephalon. *J. Neurosci.* **8,** 2003–2010.

Watson, S.J., and Akil, H. (1979). The presence of two A-MSH positive cell groups in rat hypothalamus. *Eur. J. Pharmacol.* **58,**101–103.

Watts, A.G., Swanson, L.W., and Sanchez-Watts, G. (1987). Efferent projections of the suprachiasmatic nucleus: I. Studies using anterograde transport of *Phaseolus vulgaris* leucoagglutinin in the rat *J. Comp. Neurol.* **258,** 204–229.

Wirth, M.M., and Giraudo, S.Q. (2000). Agouti-related protein in the hypothalamic paraventricular nucleus: effect on feeding. *Peptides* **21,** 1369–1375.

Wirth, M.M., Olszewski, P.K., Yu, C., Levine, A.S., Giraudo, S.Q., Sakurai, T., Amemiya, A., Ishii, M., Matsuzaki, I., Chemelli, R.M., Tanaka, H., Williams, S.C., Richardson, J.A., Kozlowski, G.P., Wilson S., Arch, J.R., Buckingham, R.E., Haynes, A.C., Carr, S.A., Annan, R.S., McNulty, D.E., Liu, W.S., Terrett, J.A., Elshourbagy, N.A., Bergsma, D.J., and Yanagisawa, M. (1998). Paraventricular hypothalamic alpha-melanocyte-stimulating hormone and MTII reduce feeding without causing aversive effects orexins and orexin receptors: a family of hypothalamic neuropeptides and G protein–coupled receptors that regulate feeding behavior. *Cell* **92,** 573–585.

Yamagata, K., Matsumura, K., Inoue, W., Shiraki, T., Suzuki, K., Yasuda, S., Sugiura, H., Cao, C., Watanabe, Y., and Kobayashi, S. (2001). Coexpression of microsomal-type prostaglandin E synthase with cyclooxygenase-2 in brain endothelial cells of rats during endotoxin-induced fever. *J. Neurosci.* **21,** 2669–2677.

Yokosuka, M., Kalra, P.S., and Kalra, S.P. (1999). Inhibition of neuropeptide Y (NPY)–induced feeding and c-Fos response in magnocellular paraventricular nucleus by a NPY receptor antagonist: a site of NPY action. *Endocrinology* **140,** 4494–4500.

Zahm, D.S., and Heimer, L. (1993). Specificity in the efferent projections of the nucleus accumbens in the rat: comparison of the rostral pole projection patterns with those of the core and shell. *J. Comp. Neurol.* **327,** 220–232.

Zhang, J., and Rivest, S. (1999). Distribution, regulation and colocalization of the genes encoding the EP2- and EP4-PGE2 receptors in the rat brain and neuronal responses to systemic inflammation. *Eur. J. Neurosci.* **11,** 2651–2668.

Zhang, Y.H., Hosono, T., Yanase-Fujiwara, M., Chen, X.M., and Kanosue, K. (1997). Effect of midbrain stimulations on thermoregulatory vasomotor responses in rats. *J. Physiol.* **503,** 177–186.

Zhang, Y.H., Lu, J., Elmquist, J.K., and Saper, C.B. (2000). Lipopolysaccharide activates specific populations of hypothalamic and brain stem neurons that project to the spinal cord. *J. Neurosci.* **20,** 6578–6586.

CHAPTER

18

Hypophysis

LUCIA STEFANEANU
Department of Laboratory Medicine and Pathobiology, St. Michael's Hospital
University of Toronto, Toronto, Ontario, Canada

GEORGE KONTOGEORGOS
Department of Pathology
G. Gennimatas General Hospital of Athens, Athens, Greece

KALMAN KOVACS, and EVA HORVATH
Department of Laboratory Medicine and Pathobiology, St. Michael's Hospital
University of Toronto, Toronto, Ontario, Canada

The pituitary, the master gland and conductor of the endocrine orchestra, is located in the sella turcica in close approximation to several vital structures such as the brain, vessels, nerves, bone, and connective tissue. Thus, it is not surprising that pituitary lesions can cause several local symptoms which, if not properly treated, may induce irreversible tissue damage, may be life threatening, and may even lead to the demise of the patient. Pituitary abnormalities are common. Numerous lesions may arise in or spread to the sella turcica and to the pituitary gland. The most frequently occurring pituitary abnormalities are the various types of pituitary adenomas. Small adenomas can be found in approximately 20% of unselected adult autopsies.

The pituitary gland is composed of several cell types and produces several hormones, which regulate the endocrine activities of the thyroid, adrenal cortices, and gonads. Beside affecting hormone secretion of these peripheral endocrine organs, the pituitary influences practically every function in the body, including growth, water and electrolyte balance, and protein, carbohydrate, and lipid metabolism. It influences sleep, sexual activity, muscle strength, and immune functions. In pituitary-related studies unprecedented progress was achieved during the last decade. Application of modern cellular and molecular methods increased our understanding on the pathogenesis of various pituitary lesions, shed light on their progression and prognosis, and obtained a deeper insight into structure–function correlations and treatment. Although advances were spectacular, the novel findings raised many new questions that are still unresolved at present.

ANATOMY OF THE HYPOPHYSIS

Gross anatomy

The hypophysis or pituitary is a small, bean-shaped endocrine gland measuring approximately 4 × 6 × 8 mm and weighting about 500–600 mg in adults. There are no major size differences between genders in adults (Kovacs and Horvath,1986). The hypophysis is located in the sella turcica, a depression in the superior

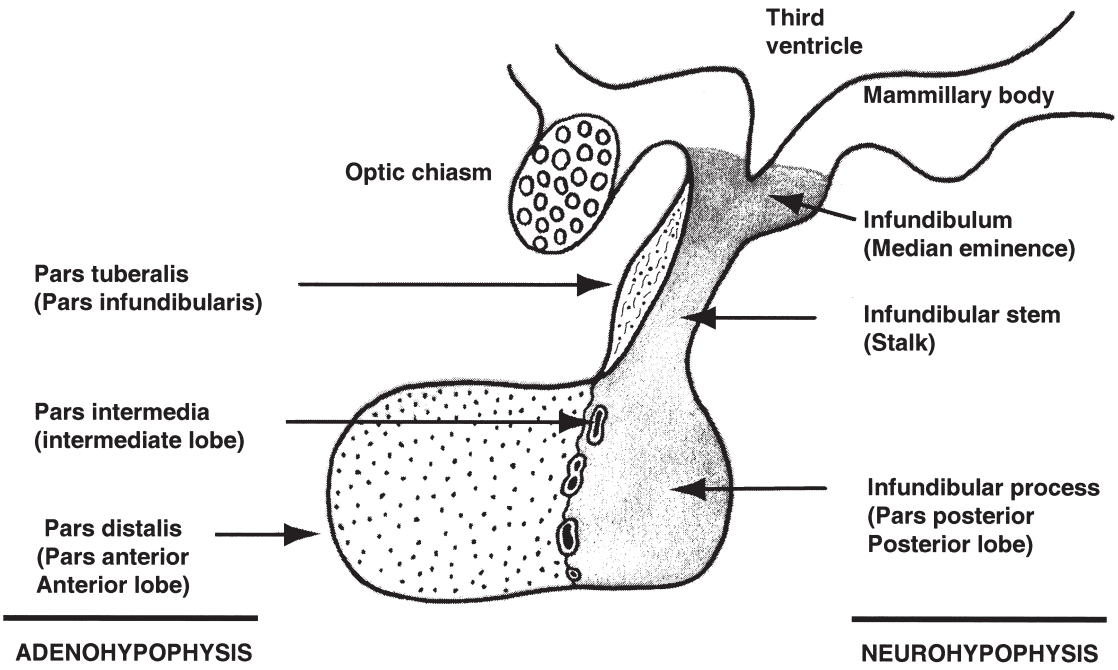

FIGURE 18.1 Diagram of the anatomical components of the hypophysis.

surface of the sphenoid bone. The gland is connected to the hypothalamus by the pituitary stalk through a small central opening of the diaphragma sellae, which forms the roof of the sella turcica. The hypophysis is in proximity to the optic chiasm and cranial nerves III, IV, V, and VI. Anatomically, the pituitary is divided into the adenohypophysis or anterior pituitary comprising approximately 80% of the gland and of the neurohypophysis or posterior pituitary. Anterior and posterior pituitaries represent two separate compartments of different embryology, anatomy, and structure. The adenohypophysis consists of three parts: the pars distalis (anterior lobe or pars glandularis), the pars intermedia (intermediate lobe), and the pars tuberalis (pars infundibularis). The adenohypophysis is of ectodermal origin and develops from an evagination of Rathke's pouch growing upward from the oral cavity. The neurohypophysis arises from the brain and also consists of three parts: the infundibulum, a funnel-shaped downgrowth projection of the tuber cinereum; the pituitary stalk; and the posterior lobe or pars nervosa (Fig. 18.1). The posterior lobe abuts the median wedge.

Blood Supply

The adenohypophysis has a highly dense and complex vascular network. The arterial supply is scarce, whereas the majority of blood reaches the parenchyma through the portal veins (Fig. 18.2). Pairs of the superior and inferior hypophysial arteries, both branches of the internal carotid arteries, enter the median eminence and form the superficial external plexus that gives rise to a network of capillaries and the gomitoli (also named internal plexus). Gomitoli are 1- to 2-mm-long arteries surrounded by a thick layer of muscle and capillaries. The internal plexus gives rise to long veins that contribute to the formation of the portal system. The long portal vessels originate in the proximal part of the hypophysial stalk and terminate in fenestrated capillaries within the pars distalis. The long portal vessels supply the adenohypophysis with 70–90% of blood and carry the hypothalamic releasing and inhibiting hormones that regulate secretion and multiplication of hormone-producing cells. The short portal vessels arise in the lower part of the stalk and in the posterior lobe. They provide the adenohypophysis the remaining 10–30% of the blood. The neurohypophysis receives arterial supply from the middle hypophysial (loral) arteries. They also provide arterial blood to the capsule of the pituitary and the superficial cells of the adenohypophysis. Given that capillaries of the pituitary are fenestrated, they lie outside the blood-brain barrier. Pituitary veins drain the blood from the pituitary to the cavernous sinus (Bergland and Page, 1978, 1979; Gorczyca and Hardy, 1987).

Innervation

Except for a few sympathetic nerve fibers along the vessels, the adenohypophysis has practically no innervation.

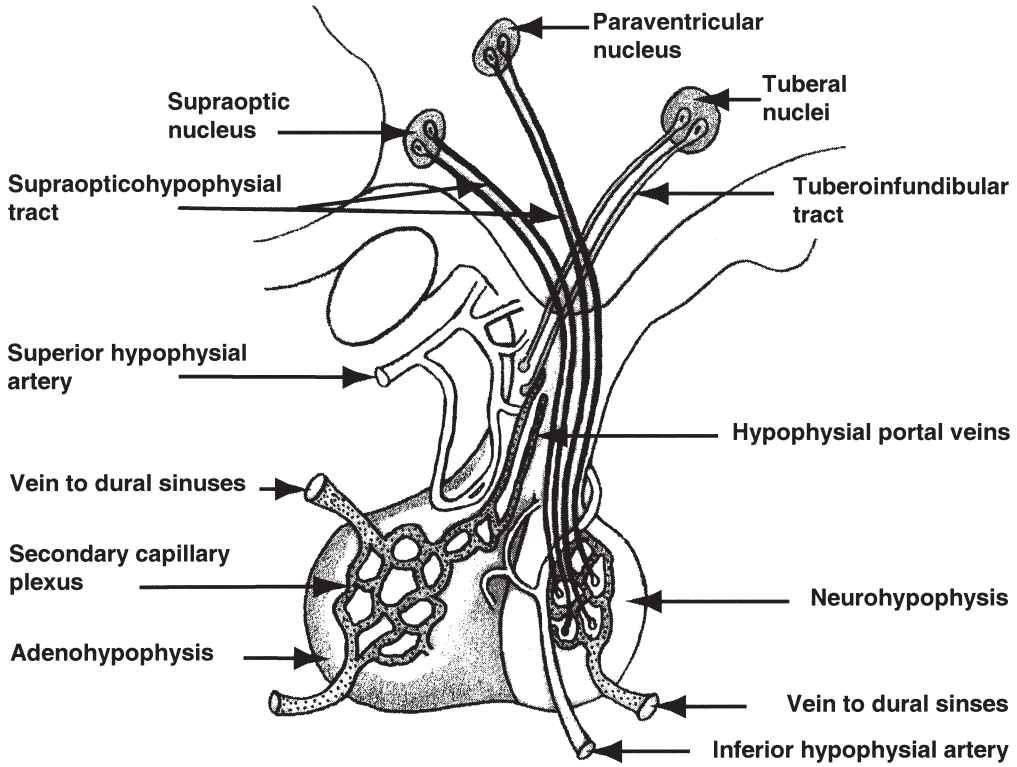

FIGURE 18.2 Diagram of the hypophysial portal system, supraopticohypophysial tract, and tuberoinfundibular tract.

IMAGING OF THE HYPOPHYSIS

Magnetic resonance images (MRI) can easily differentiate the two pituitary lobes of the hypophysis in adults. The adenohypophysis shows similar signal intensity to cerebral white matter on all pulse sequences (Fig. 18.3a, b). The fact that the hypophysis receives both arterial and venous blood can explain the different enhancement rate on dynamic scans after intravenous administration of contrast agents (Kucharczyk *et al.*, 1996). In pregnancy the adenohypophysis shows a hyperintense signal on T1-weighted images; the signal intensity ratio is positively correlated with the gestational age (Miki *et al.*, 1993). The neurohypophysis is markedly hyperintense on T1-weighted images. Both neurohypophysis and pituitary stalk show enhanced

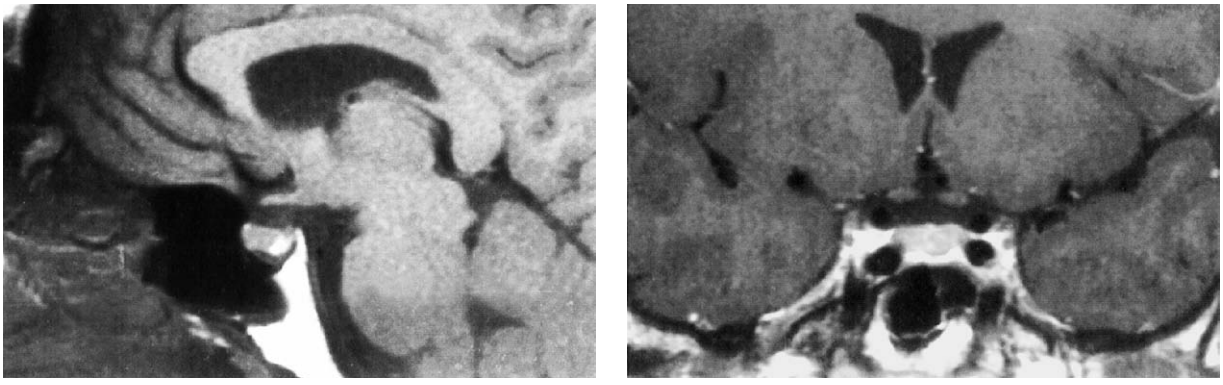

FIGURE 18.3 Midline sagittal T1-weighted **(a)** and coronal T1-weighted **(b)** MRI of the skull base of an adult. The adenohypophysis is approximately isointense to cerebral white matter whereas the neurohypophysis shows a markedly hyperintense signal.

intensity after intravenous contrast administration. Interestingly, the fetal hypophysis is hyperintense on T1-weighted MR images like the posterior lobe. In neonates the anterior lobe is brighter than in adults; 2 months later this brightness starts diminishing and by about 6 months of age becomes similar to that of adults (Kucharczyk *et al.*, 1996).

Imaging studies show that the size of pituitary gland increases progressively during fetal life. At puberty, particularly in females, the gland is significantly enlarged. During pregnancy the hypophysis enlarges and may reach 10 mm. At the immediate postpartum period the gland may measure up to 12 mm, but beyond the first week of postpartum it rapidly returns to normal size regardless the status of breast-feeding (Elster *et al.*, 1991).

HISTOLOGY

Anterior Pituitary (Adenohypophysis)

The adenohypophysis is divided by fibrous trabeculae into two lateral wings and the central mucoid wedge area, which can be seen on horizontal cross-section. The anterior lobe is composed mainly of hormone-producing cells grouped in acini delineated by a basement membrane, a delicate reticulin network, and capillaries. On hematoxylin and eosin (H&E)–stained sections, three types of cells can be distinguished: the acidophils disposed especially in the lateral wings, the basophils localized mainly in the mucoid wedge region, and the chromophobes scattered throughout the anterior lobe (Fig. 18.4). Immunocytochemistry for adenohypophysial hormones identifies five main cell types: growth hormone (GH) cells, prolactin (PRL) cells, adrenocorticotropin (ACTH) cells, thyrotropin (TSH) cells, and gonadotropin (follicle-stimulating hormone and luteinizing hormone) cells.

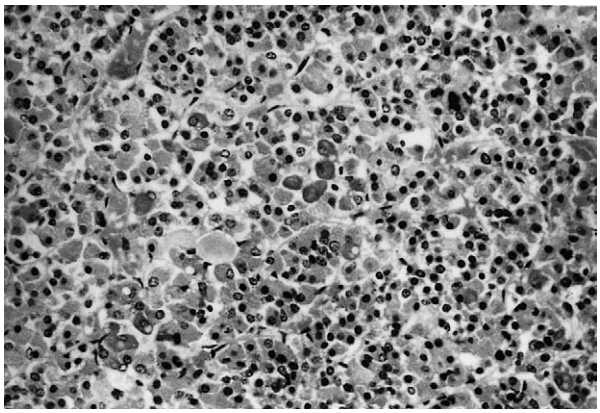

FIGURE 18.4 Hematoxylin and eosin–stained section of an autopsy pituitary shows the presence of acidophilic, basophilic, and chromophobic cells forming acini and a follicle.

GH cells or somatotrophs, situated mainly in the lateral wings, are acidophilic on H&E preparations, negative with periodic acid–Schiff (PAS) stain, and represent 40–50% of the cells (Fig. 18.5a, b). PRL cells, also called lactotrophs or mammotrophs are chromophobic or acidophilic on H&E-stained sections and PAS negative. PRL cells are distributed all over the anterior lobe, and are abundant especially in the posterolateral rim of adenohypophysis (Fig. 18.5c, d). The number of PRL cells varies in function of sex, age, parity and hormonal status (15–25%) (Asa *et al.*, 1982). Mammosomatotrophs, which are bihormonal cells that secret GH and PRL, are present in normal pituitary (Lloyd *et al.*, 1988). The increased number of mammosomatotrophs during pregnancy supports the concept of transformation of GH cells into PRL cells (Stefaneanu *et al.*, 1992). ACTH cells (corticotrophs) are located primarily in the central mucoid wedge and constitute 10–15% of adenohypophysial cells (Fig. 18.5e, f). ACTH is derived from the precursor protein proopiomelanocortin (POMC). These basophilic cells are easily identified with PAS stain. Enigmatic bodies located in the vicinity of nuclei correspond to large phagolysosomes at ultrastructural level and are useful markers of these cells. The number and size of enigmatic bodies increases with age (Sano *et al.*, 1993). The inhibited corticotrophs have a special feature in human hypophysis, the progressive accumulation of type 1 microfilaments, known as Crooke's hyalinization. The filaments are immunoreactive for cytokeratin. TSH cells (thyrotrophs), accounting for 5% of the adenohypophysial cells, are distributed preferentially in the anteromedian zone of the mucoid wedge (Fig. 18.5g, h). They are angular or polyhedral cells, stained by basic dyes. PAS stains small cytoplasmic globules corresponding ultrastructurally to phagolysosomes. They are immunoreactive for TSH-β and the α subunit of glycoprotein hormones. Gonadotropin cells (gonadotrophs) are basophilic and represent about 15–20% of adenohypophysial cells. The majority of gonadotrophs are bihormonal cells that can be demonstrated by immunocytochemistry for β subunits of follicle-stimulating hormone (FSH-β) and luteinizing hormone (LH-β) (Fig. 18.6). They are situated in the lateral wings and central mucoid wedge intermingled with other cell types and often are closely apposed to lactotrophs. The functional status of FSH/LH-immunoreactive cells is altered by age, sex, and various phases of the menstrual cycle.

Folliculo stellate (stellate) cells are nongranulated cells with a star shape due to long, thin cytoplasmic processes surrounding hormone-producing cells. S-100

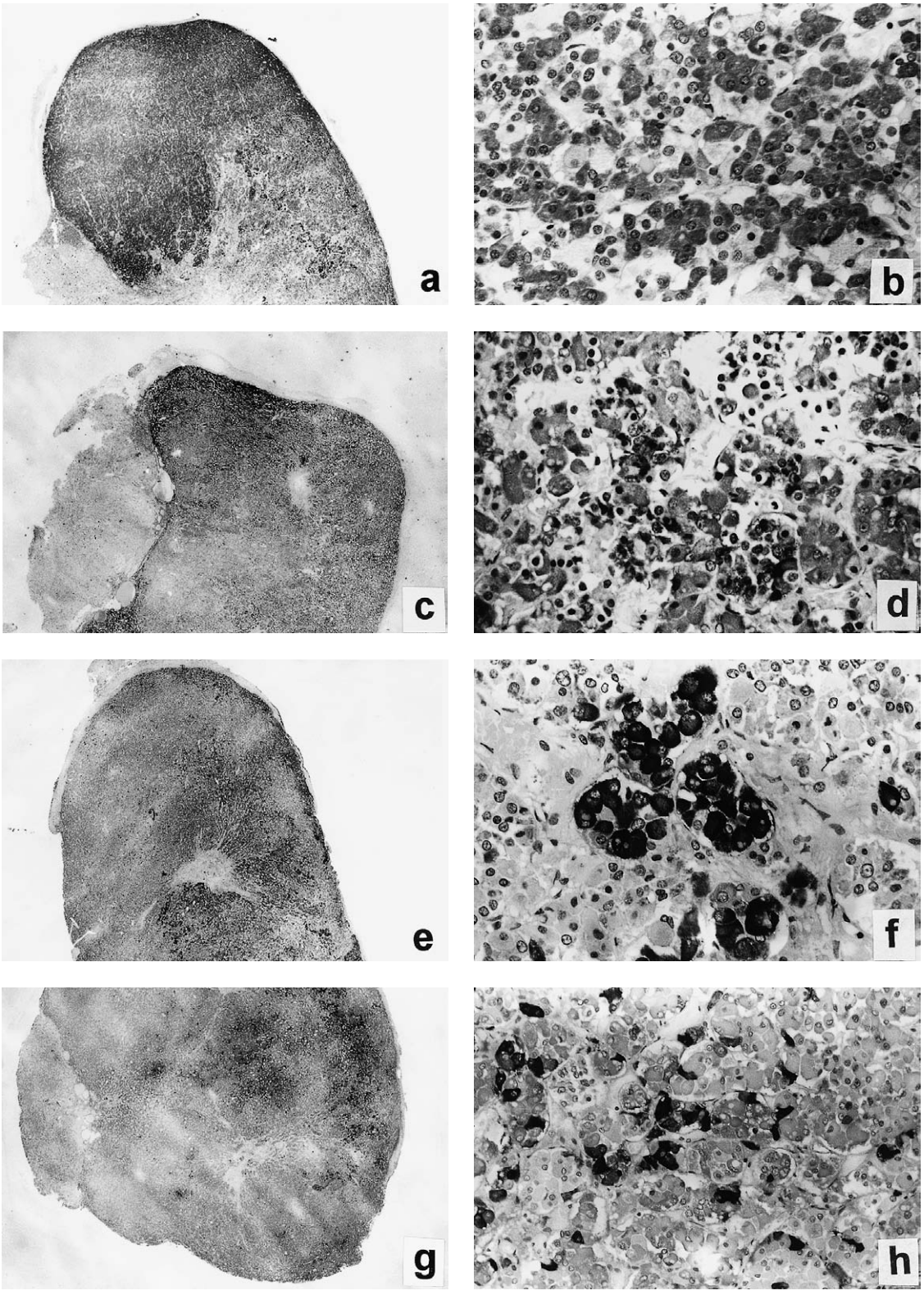

FIGURE 18.5 Horizontal cross-section of an autopsy pituitary depicts the preferential disposition of GH-immunoreactive cells in the lateral wing **(a);** GH-immunoreactive cells are middle sized with polyhedral or round contour **(b);** PRL-immunoreactive cells are distributed throughout the adenohypophysis but are especially abundant in the posterolateral wings **(c);** they are angular or polyhedral cells with the PRL immunoreactivity as a paranuclear dot or diffuse in the cytoplasm **(d);** horizontal cross-section of an autopsy pituitary shows the disposition of ACTH-immunoreactive cells in the mucoid edge **(e);** ACTH cells are polyhedral or ovoid and are often seen in cluster **(f);** TSH-immunoreactive cells are found in the mucoid edge that is shared with ACTH cells **(g);** TSH cells are angular or polyhedral with long cytoplasmic processes **(h).**

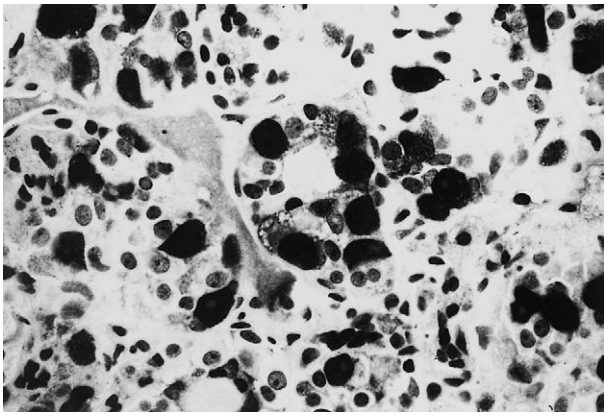

FIGURE 18.6 Gonadotrophs depicted by immunocytochemistry for LHβ are scattered throughout the adenohypophysis, and frequently participate to follicle formation.

protein is a useful immunocytochemical marker of this cell type (Fig. 18.7). It was suggested that stellate cells have phagocytic, paracrine, immune, and supporting roles (Inoue *et al.*, 1999; Marin *et al.*, 1992).

The pars intermedia (intermediate lobe) is part of the adenohypophysis located between the pars distalis and the posterior lobe. In the fetal and newborn pituitary the intermediate lobe is a distinctive structure of the pituitary, which in adults is assumed to be represented by cells scattered throughout the pars distalis (Horvath *et al.*, 1999; McNicol, 1986). They are immunoreactive for ACTH and other POMC-derived peptides. In aging people, the asymptomatic hyperplasia of these cells is more common in men than women (Horvath *et al.*, 1999). Some basophils immunoreactive for POMC peptides, and considered to represent intermediate lobe cells, extend into the posterior lobe. This process, referred to as "basophil invasion," may become prominent with age. At the border of anterior and posterior lobes, there are a variable number of heterogeneous cysts considered to be remnants of Rathke's pouch or vestigial intermediate lobe structures.

The pars tuberalis (tuberal lobe) surrounds the distal portion of the stalk, especially its anterior surface, and is covered by the arachnoid membranes. Pars tuberalis is formed by hormone-producing cells disposed along the longitudinally oriented portal vessels embedded in a loose connective tissue. The cells are immunoreactive for FSH and LH and occasionally for TSH or ACTH. Nests of squamous cells are also present.

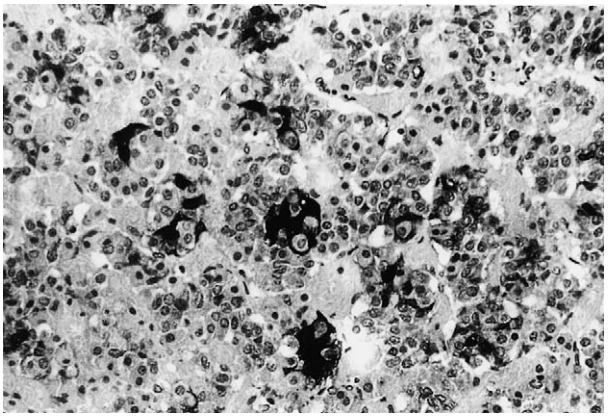

FIGURE 18.7 Folliculostellate cells demonstrated by immunocytochemistry for S-100 protein are angular with long cytoplasmic processes disposed among hormone-secreting cells.

Posterior Pituitary (Neurohypophysis)

The posterior lobe of the neurohypophysis is composed mainly of pituicytes that are glial cells with a supporting role. The pituicytes are inconspicuous on routinely stained sections and can be easily recognized by immunostaining for glial fibrillary acidic protein. These elongated cells possess long cytoplasmic processes and in aging people contain yellow brown pigment granules. Unmyelinated nerve fibers originating in the supraoptic and paraventricular nuclei of the hypothalamus are intermingled with the pituicytes and capillaries. The vasopressin (antidiuretic hormone) and oxytocin are transported by neurophysin carrier proteins along the axons and can be visualized by immunocytochemistry in the dilated axon terminals called Herring bodies.

ULTRASTRUCTURE

Somatotrophs are mostly middle-sized ovoid cells; the large polyhedral forms are less common. The rough endoplasmic reticulum (RER) occurs as slender cisternae; the Golgi apparatus is globoid and contains immature secretory granules. Most somatotrophs are densely granulated displaying an unusually wide range of granule sizes (200–1000 nm) (Horvath and Kovacs, 1988). The enormous GH cell population probably represents more subsets, which ultrastructurally overlap and blend into a virtual continuum. The most common type is ovoid with spherical, evenly electron dense secretory granules measuring up to 500 nm (Fig. 18.8). If the granule sizes are larger (exceeding 600 nm), ovoid and irregular forms and those with uneven electron density occur as well. This variant may show exocytosis (granule extrusion) suggesting mammosomatotroph differentiation. At the other end of the spectrum, immunoelectron microscopy may

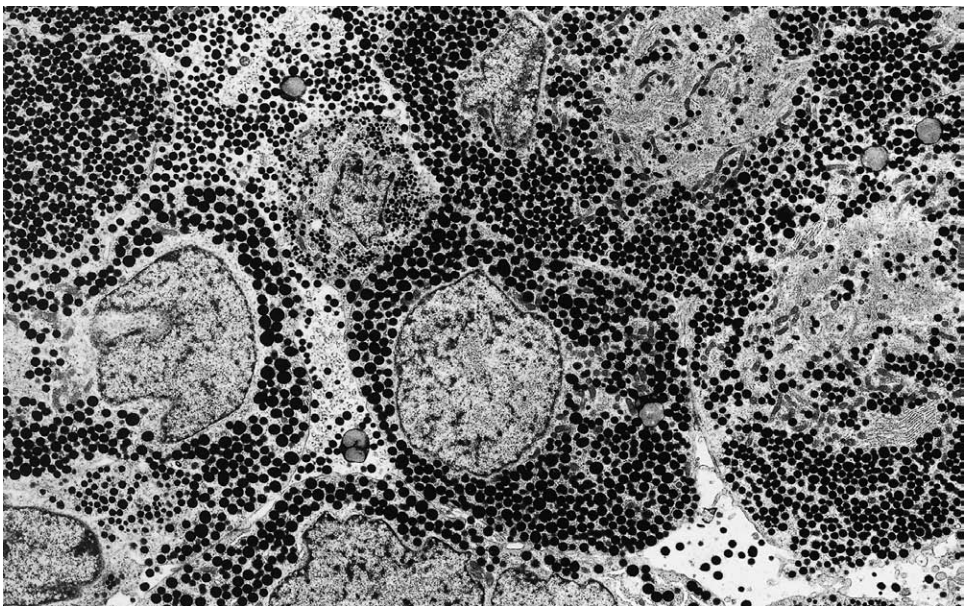

FIGURE 18.8 Ultrastructurally, the GH cells are filled with electron-dense secretory granules of 400–500 nm and well-developed Golgi apparatus; ×3800.

detect small, sparsely granulated cells possessing 100- to 200-nm GH-immunoreactive granules, further widening the range (Horvath and Kovacs, 1988). Functional stimulation or suppression of GH cells results in only subtle alterations of their ultrastructure.

Somatotrophs are assumed to represent a reserve cell type with potential for taking up hormonal functions of the other cell types (Childs, 2000). In the human gland, the best example is gestational PRL cell hyperplasia; many of the PRL-producing cells are recruited from the GH cell population (Stefaneanu *et al.*, 1992). Similar transdifferentiation occurs in cases of idiopathic or secondary PRL hyperplasia (Horvath, 1988), whereas transformation of GH cells into thyroid deficiency cells (stimulated thyrotrophs) takes place in hypothyroid subjects (Vidal *et al.*, 2000).

Lactotrophs are small to middle-sized polyhedral cells localized in the central part of acini, whereas their cytoplasmic processes extend to the basal lamina. Their cytoplasm contains parallel arrays of slender RER cisternae and juxtanuclear Golgi complex harboring spherical as well as pleomorphic (fused) granules and sparse, mostly spherical secretory granules ranging up to 300 nm (Fig. 18.9). Extrusion of secretory granules may take place along both basal and lateral cell membranes. PRL cells respond briskly to changing functional demand (Horvath and Kovacs, 1988). Stimulation results in enlargement of cytoplasm due chiefly to accumulation of RER and increased size of highly active Golgi complex containing most of the secretory granules. Functional suppression (presence of PRL cell adenoma, treatment with dopaminergic drugs) leads to dramatic shrinkage of cytoplasm owing to severe involution of RER and Golgi complex. Recently, it was shown that in GH cell hyperplasia due to ectopic overproduction of growth hormone–releasing hormone, PRL cells become bihormonal producing GH as well (Vidal *et al.*, 2001).

POMC-producing cell population of the pars distalis includes the corticotrophs as well as the more elusive, functionally yet uncharacterized pars intermedia–derived cells (Horvath *et al.*, 1999). Due to overlaps in their morphology and immunocytochemical profiles, clear distinction of these cell types is rarely possible (Horvath *et al.*, 1999).

Corticotrophs reside chiefly in the anterior two-thirds of the median wedge. The middle-sized ovoid cells have relatively electron opaque cytoplasm, moderately developed and unevenly dilated RER, fairly prominent Golgi complex, and a large heterogeneous lysosomal body. The secretory granules, ranging up to 500 nm, are not only numerous but characteristic being spherical as well as notched, irregular, and heart shaped. The other marker of the cell type is the presence of cytokeratin filaments first appearing in the perinuclear cytoplasm (Fig. 18.10) (Horvath and Kovacs, 1988).

Functional stimulation is not known to alter the ultrastructure of corticotrophs, whereas suppression (intrinsic or extrinsic hypercortisolism) results in the

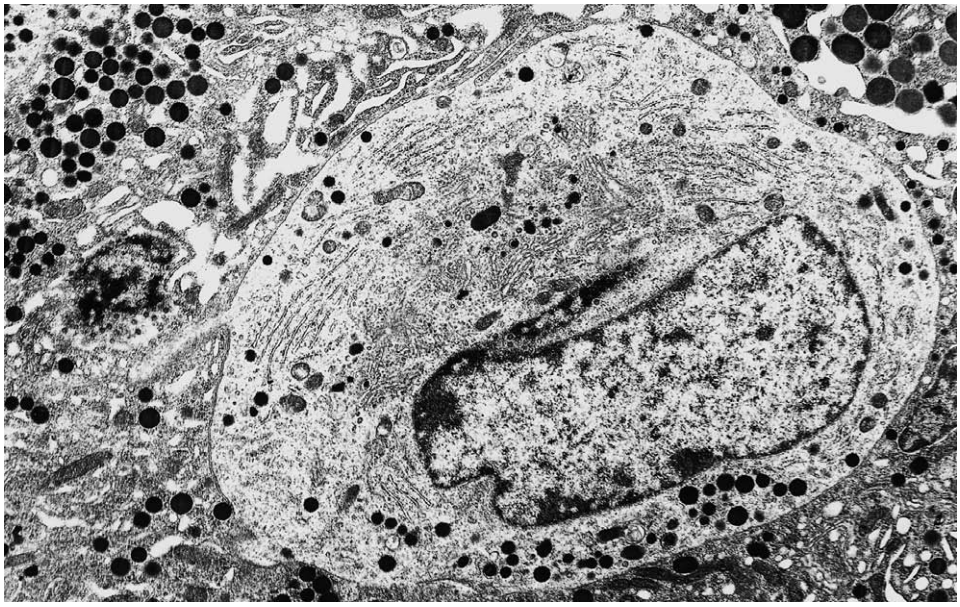

FIGURE 18.9 By electron microscopy, the PRL cells contain a few secretory granules, some seen in the process of formation inside the Golgi apparatus, and prominent rough endoplasmic reticulum in parallel arrays; ×6300.

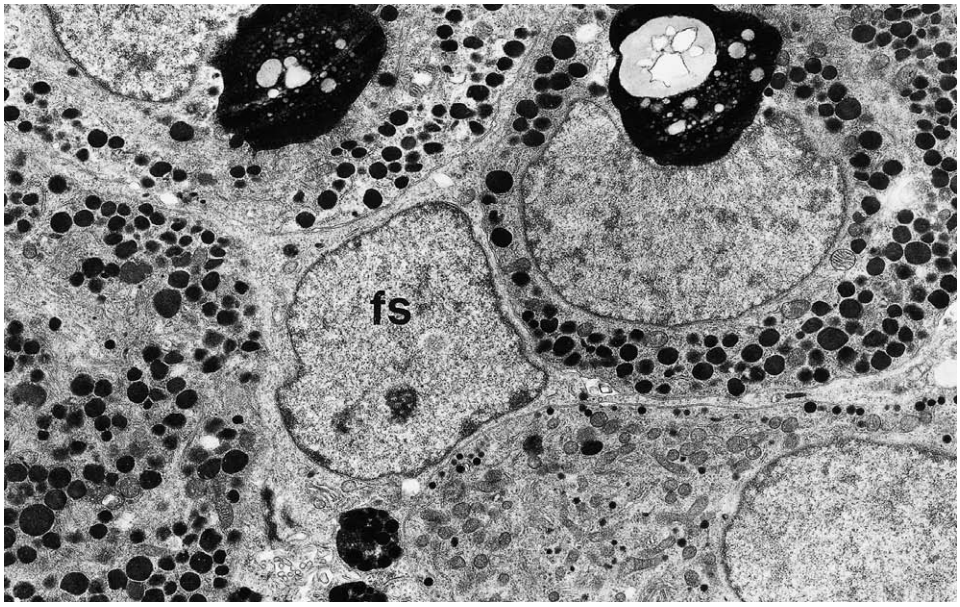

FIGURE 18.10 Ultrastructurally, the ACTH cells are easily recognized due to the presence of bundles of type 1 microfilaments and the prominent phagolysosome in the vicinity of the nucleus; the abundant secretory granules of about 500 nm have irregular contour. Note the presence of a folliculostellate cell (fs) sending slender processes among granulated cells; ×6900.

excessive accumulation of cytokeratin filaments known as Crooke's hyalinization (Fig. 18.11) (Horvath and Kovacs, 1988).

Pars intermedia–derived cells, which can be reliably identified within the posterior lobe, isolated from other adenohypophysial cell types, are morphologically indistinguishable from corticotrophs.

Thyrotrophs represent the least popular cell type and are largely restricted to the anteromedial rim of the pars distalis. The middle-sized to large, characteristically

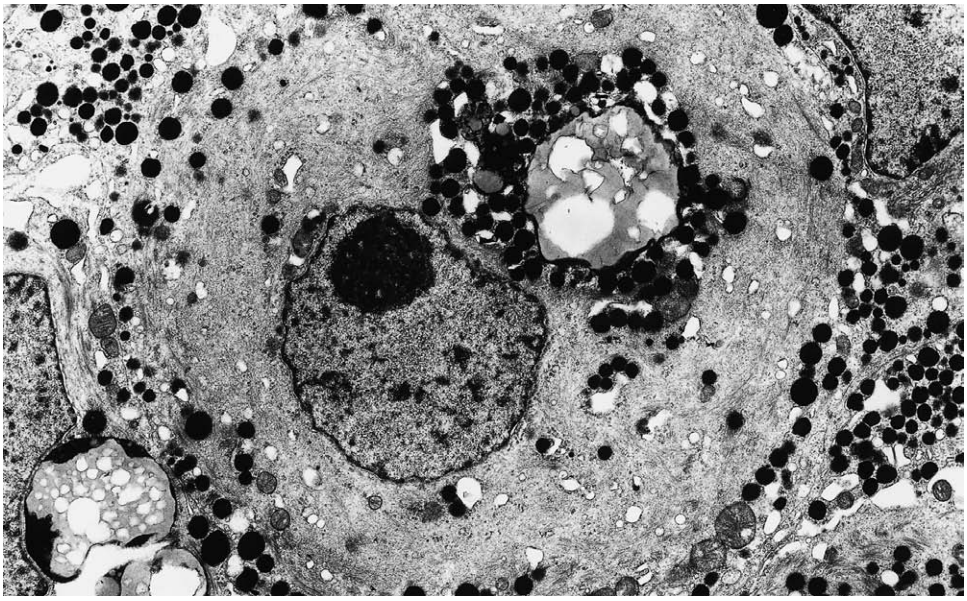

FIGURE 18.11 Ultrastructurally, the Crooke's cells are characterized by a large cytoplasm occupied by the microfilaments that push the secretory granules at the periphery; some secretory granules are engulfed by phagolysosomes; ×6900.

FIGURE 18.12 TSH cell with euchromatic nucleus, well-developed cytoplasm containing small secretory granules, prominent Golgi apparatus, and a few phagolysosomes is commonly seen; ×7800.

angular cells often lie on the basal lamina. They have a spherical nucleus with low heterochromatin content. The RER may be slightly dilated; the roughly spherical Golgi region includes numerous tiny Golgi vesicles. The well-defined secretory granules are small, ranging up to 250 nm. If sparse, they tend to form a single layer beneath the plasmalemma. Groups of heterogeneous lysosomes are often noted (Fig. 18.12).

Long standing hypothyroidism, i.e., sustained stimulation, results in hyperplasia comprising the highly characteristic thyroid deficiency cells (Vidal *et al.*, 2000). The cells possess a spherical euchromatic

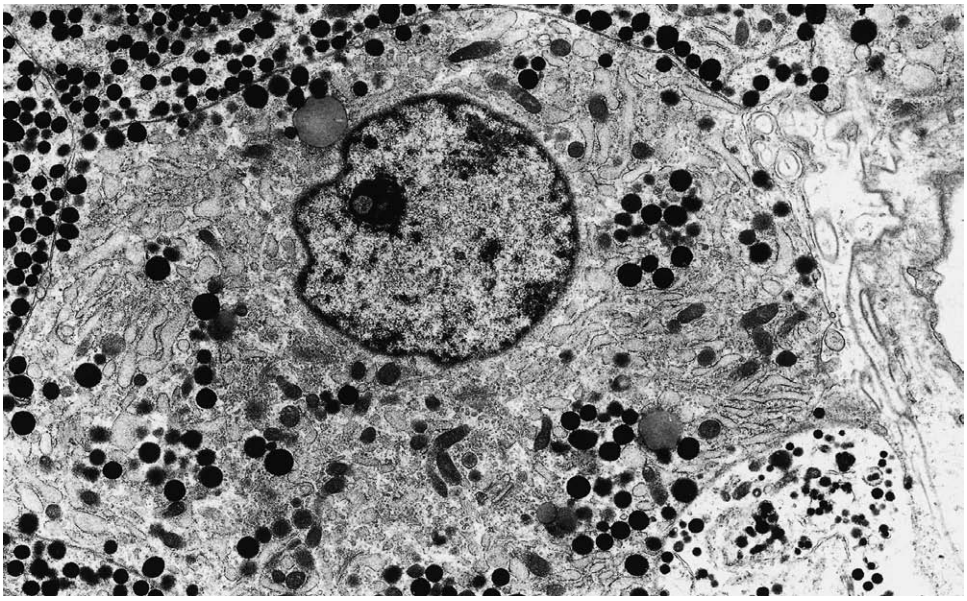

FIGURE 18.13 A gonadotroph with ovoid shape contains typical short, slightly dilated cisternae of rough endoplasmic reticulum and several secretory granules with variable electron density; ×7800.

nucleus, as well as enormous cytoplasm occupied chiefly by hyperplastic, markedly dilated RER filled with low-density proteinaceous substance. The prominent Golgi apparatus harbors few developing granules; packaging of secretory material appears to be bypassed in the highly stimulated cells. Accordingly, the number of cytoplasmic secretory granules diminishes as the hyperplastic changes progress. Thyroid deficiency cells usually harbor large, electron-dense lysosomal bodies readily noted as PAS-positive globules at the light microscopic level. In functional suppression (hyperthyroidism, presence of TSH-producing tumor) thyrotrophs become uncharacteristic: the small cells are packed with lysosomes and have few, small secretory granules and poorly developed membranous organelles.

Gonadotrophs, the cells of various sizes producing FSH and LH, are ovoid, have a large interface with the epithelial basal lamina, and are often surrounded by PRL cells (Horvath and Kovacs, 1988). Gonadotrophs have largely euchromatic spherical nucleus, slightly dilated RER with a nearly homogeneous content of low electron density, prominent ring-shaped Golgi apparatus and variable numbers of 250- to 600-nm secretory granules. The latter are spherical or slightly irregular with a variably electron dense, often uneven matrix (Fig. 18.13).

Functional stimulation (primary hypogonadism, ablation of gonads) leads to development of gonadal deficiency or castration cells (Horvath, 1988). Similar to thyroidectomy cells, castration cells display enlargement of cytoplasm and marked proliferation of dilated RER. With advancing change, the degree of dilation progresses, often leading to formation of a single large vacuole ("signet ring cell"). The number of secretory granules also decreases with time. The ultrastructure of hormonally inactive gonadotroph (seen in hypogonadotropic hypogonadism) is not sufficiently studied.

Folliculo stellate cells (FSCs), joined by terminal bars at their apical portion and projecting slender processes between hormone-producing cells, are essential parts of the acini of the human pituitary. The FSC are not demarcated by basal lamina, but they join directly the hormone-producing cells. The FSC are simple cells having unremarkable elongate nucleus, few RER membranes, small Golgi complex, fair number of mitochondria, and sometimes fine vimentin-like filaments. Lysosomal bodies may be present (Fig. 18.10). The activated form of FSC seen, for instance, in lymphocytic hypophysitis (Horvath *et al.*, 2001) is characterized by enlarged, rounded nucleus harboring prominent inclusions (spheridia), enlarged cytoplasm containing increased quantity of RER and free polyribosomes, sometimes copious amounts of filaments possibly including both vimentin and cytokeratin, variable number of lysosomes, and, less frequently, glycogen β particles.

References

Asa, S.L., Penz, G., Kovacs, K., and Ezrin, C. (1982). Prolactin cells in the human pituitary. A quantitative immunocytochemical analysis. *Arch. Pathol. Lab. Med.* **106,** 360–363.

Bergland, R.M., and Page, R.B. (1978). Can the pituitary secrete directly to the brain? (Affirmative anatomical evidence). *Endocrinology* **102,** 1325–1338.

Bergland, R.M., and Page, R.B. (1979). Pituitary–brain vascular relations: a new paradigm. *Science* **204,** 18–24.

Childs, G.V. (2000). Growth hormone cells as co-gonadotropes: partners in the regulation of the reproductive system. *Trends Endocrinol. Metab.* **11,** 168–175.

Elster, A.D., Sanders, T.G., Vines, F.S., and Chen, M.Y. (1991). Size and shape of the pituitary gland during pregnancy and post partum: measurement with MR imaging. *Radiology* **181,** 531–535.

Gorczyca, W., and Hardy, J. (1987). Arterial supply of the human anterior pituitary gland. *Neurosurgery* **20,** 369–378.

Horvath, E. (1988). Fine structural cytology and immunohistochemistry of the nonadenomatous pars distalis of the human pituitary. *Pathol. Res. Pract.* **183,** 631–633.

Horvath, E., and Kovacs, K. (1988). Fine structural cytology of the adenohypophysis in rat and man. *J. Electron Microsc. Tech.* **8,** 401–432.

Horvath, E., Kovacs, K., and Lloyd, R.V. (1999a). Pars intermedia of the human pituitary revisited: morphologic aspects and frequency of hyperplasia of POMC-peptide immunoreactive cells. *Endocr. Pathol.* **10,** 55–64.

Horvath, E., Kovacs,K., and Scheithauer, B.W. (1999b). Pituitary hyperplasia. *Pituitary.* **1,** 169–179.

Horvath, E., Vidal, S., Syro, L.V., Kovacs, K., Smyth, H.S., and Uribe, H. (2001). Severe lymphocytic adenohypophysitis with selective disappearance of prolactin cells: a histologic, ultrastructural and immunoelectron microscopic study. *Acta Neuropathol. (Berl)* **101,** 631–637.

Inoue, K., Corich, E.F., Takano, K., and Ogawa, S. (1999). The structure and function of folliculo-stellate cells in the anterior pituitary gland. *Arch. Histol. Cytol.* **62,** 205–218.

Kovacs, K., and Horvath, E. (1986). "Tumors of the Pituitary Gland," Second series, Fascicle 21 ed. Armed Forces Institute of Pathology, Washington, D.C.

Kucharczyk, W., Montanera, W.J., and Becker, L.E. (1996). The sellar and parasellar region. *In* "Magnetic Resonanace Imaging of the Brain and Spine" (S.W. Atlas, ed.), pp. 871–890. Lippincott-Raven Publishers, Philadelphia.

Lloyd, R.V., Anagnostou, D., Cano, M., Barkan, A.L., and Chandler, W.F. (1988). Analysis of mammosomatotropic cells in normal and neoplastic human pituitary tissues by the reverse hemolytic plaque assay and immunocytochemistry. *J. Clin. Endocrinol. Metab* **66,** 1103–1110.

Marin, F., Kovacs, K., Stefaneanu, L., Horvath, E., and Cheng, Z. (1992). S-100 protein immunopositivity in human nontumorous hypophyses and pituitary adenomas. *Endocr. Pathol.* **3,** 28–38.

McNicol, A.M. (1986). A study of intermediate lobe differentiation in the human pituitary gland. *J. Pathol.* **150,** 169–173.

Miki, Y., Asato, R., Okumura, R., Togashi, K., Kimura, I., Kawakami, S., and Konishi, J. (1993). Anterior pituitary gland in pregnancy: hyperintensity at MR. *Radiology* **187,** 229–231.

Sano, T., Kovacs, K.T., Scheithauer, B.W., and Young, W.F., Jr. (1993). Aging and the human pituitary gland. *Mayo Clin. Proc.* **68,** 971–977.

Stefaneanu, L., Kovacs, K., Lloyd, R.V., Scheithauer, B.W., Young, W.F., Jr., Sano, T., and Jin, L. (1992). Pituitary lactotrophs and somatotrophs in pregnancy: a correlative *in situ* hybridization and immunocytochemical study. *Virchows Arch. B Cell Pathol. Incl. Mol. Pathol.* **62,** 291–296.

Vidal, S., Horvath, E., Kovacs, K., Cohen, S.M., Lloyd, R.V., and Scheithauer, B.W. (2000). Transdifferentiation of somatotrophs to thyrotrophs in the pituitary of patients with protracted primary hypothyroidism. *Virchows Arch.* **436,** 43–51.

Vidal, S., Horvath, E., Kovacs, K., Lloyd, R.V., and Smyth, H.S. (2001). Reversible transdifferentiation: interconversion of somatotrophs and lactotrophs in pituitary hyperplasia. *Mod. Pathol.* **14,** 20–28.

CHAPTER

19

Circumventricular Organs

MICHAEL J. McKINLEY
Howard Florey Institute of Experimental Physiology and Medicine
University of Melbourne, Victoria, Australia

IAIN J. CLARKE
Prince Henry's Institute of Medical Research
Melbourne, Australia

BRIAN J. OLDFIELD
Howard Florey Institute of Experimental Physiology and Medicine
Victoria, Australia

The subfornical organ (SFO), vascular organ of the lamina terminalis (OVLT), median eminence, neurohypophysis, pineal gland, subcommissural organ, area postrema, and choroid plexus compose the circumventricular organs (CVOs) of the human brain (Fig. 19.1 and 19.2). They are a group of specialized structures within the brain, so named because they occupy strategic positions along the surface of the brain ventricles (Hofer, 1958). In lower vertebrates, a number of other structures, including the saccus vasculosus, paraventricular organ, and paraphysis, have also been classified in this grouping of CVOs but are not found in adult mammalian brain. Kuhlenbeck (1970) subdivided the mammalian CVOs into two groups, namely, paraependymal CVOs and ependymal CVOs. The paraependymal CVOs are the subfornical organ, OVLT, neurohypophysis, median eminence, pineal gland, and area postrema. They are characterized in regard to their neuroectodermal component by subependymal elements that differ considerably from the ependymal cells. The paraependymal CVOs have been further categorized by Gross and Johnson (1990) into sensory (subfornical organ, OVLT, and area postrema) and secretory circumventricular organs

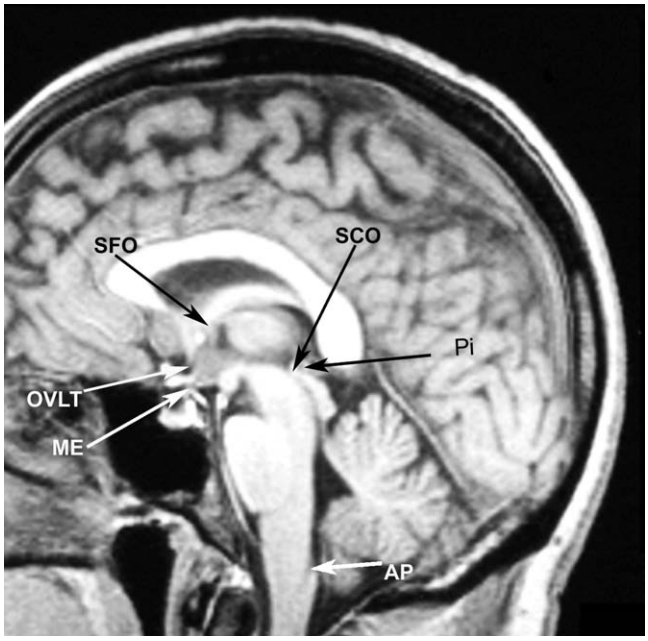

FIGURE 19.1 The position of human circumventricular organs *(arrowed)* on a midsagittal magnetic resonance image of the human brain. AP, area postrema; ME, median eminence; OVLT, vascular organ of the lamina terminalis; Pi, pineal gland; SCO, subcommissural organ; SFO, subfornical organ.

(neurohypophysis, median eminence, and pineal gland). The ependymal CVOs are the choroid plexus and subcommissural organ. They are characterized by one or more layers of ependymal cells which may be modified and vascularized.

All the CVOs of mammalian brains lie along the midline of the brain ventricular system, except for the lateral wings of the area postrema and parts of the choroid plexus, which extend to the lateral and fourth ventricles. CVOs are made up of neural, glial, and ependymal elements derived from the neuroectoderm, combined with leptomeningeal and vascular tissue of mesodermal origin. A number of morphological features characterize these structures.

1. The ependymal cells are irregular, flattened, or elongated columnar cells that contrast with the regularly apposed cuboidal cells of most of the surface of the ventricular system. In addition, they lack or have very few cilia, unlike the ciliated ependymal cells of other regions (Kuhlenbeck, 1970; Leonhardt, 1980; Weindl, 1973).
2. CVOs are highly vascularized structures with unusual vascular arrangements and capillary loops reaching almost to the ependymal surface (Duvernoy and Koritke, 1964; Hofer, 1957; Weindl, 1973).
3. With the exception of the subcommissural organ (Weindl and Joynt, 1973), the blood–brain barrier is absent due to fenestrations in the capillary endothelium of CVOs (Leonhardt, 1980; Weindl, 1973; Wislocki and Leduc, 1952).
4. Extensive perivascular spaces surround many of the capillary beds (Leonhardt, 1980; Weindl and Joynt, 1971).
5. Tight junctions between adjacent ependymal cells of these structures form a circumventricular organ–cerebrospinal fluid barrier (Krisch *et al.*, 1978; Weindl, 1973).
6. Supraependymal cells are often observed at the ventricular surface of CVOs (Brizzee and Klara, 1984; McKinley *et al.*, 1987b; Weindl, 1973).

In early studies of the CVOs, a major factor leading to their identification in animals was the feature of having an altered blood–brain barrier. It was discovered that intravitally administered colloidal dyes (e.g., trypan blue) stained such regions but not the remainder of the brain (Behnsen, 1927; Wislocki and King, 1936; Wislocki and Putnam, 1920). While the overwhelming bulk of evidence pertaining to the lack of a blood–brain barrier comes from experiments in animals, there is indirect evidence that the blood–brain barrier is also absent in human CVOs. This comes from postmortem observations that ingested silver salts, or iron pigments in hemochromatosis patients, are deposited in human CVOs but not in most other brain regions (Cammermeyer, 1947a; Landas *et al.*, 1985). Some investigators term the CVOs *neurohemal regions* because they provide an effective interface for exchange of substances between the blood "milieu" and the central nervous system (CNS). Some CVOs are sites of neurosecretion where substances synthesized in the brain can be delivered via the circulation to the periphery, e.g., median eminence, OVLT. There is also exchange of substances from the circulation to the brain in these organs, and it is likely that CVOs are sites of sensors whereby changes in the composition of the blood can be detected by the CNS. The CVOs are also receptor regions where certain humoral agents from the periphery (e.g., angiotensin II, atrial natriuretic peptide, relaxin) can act on the brain to exert centrally mediated effects (McKinley and Oldfield, 1998; Simpson, 1981; Weindl, 1973).

SUBFORNICAL ORGAN

General Characteristics and Comparative Studies

Located in the dorsal aspect of the midline anterior wall of the third ventricle, the subfornical organ is a prominent feature in coronal sections of the nonhuman

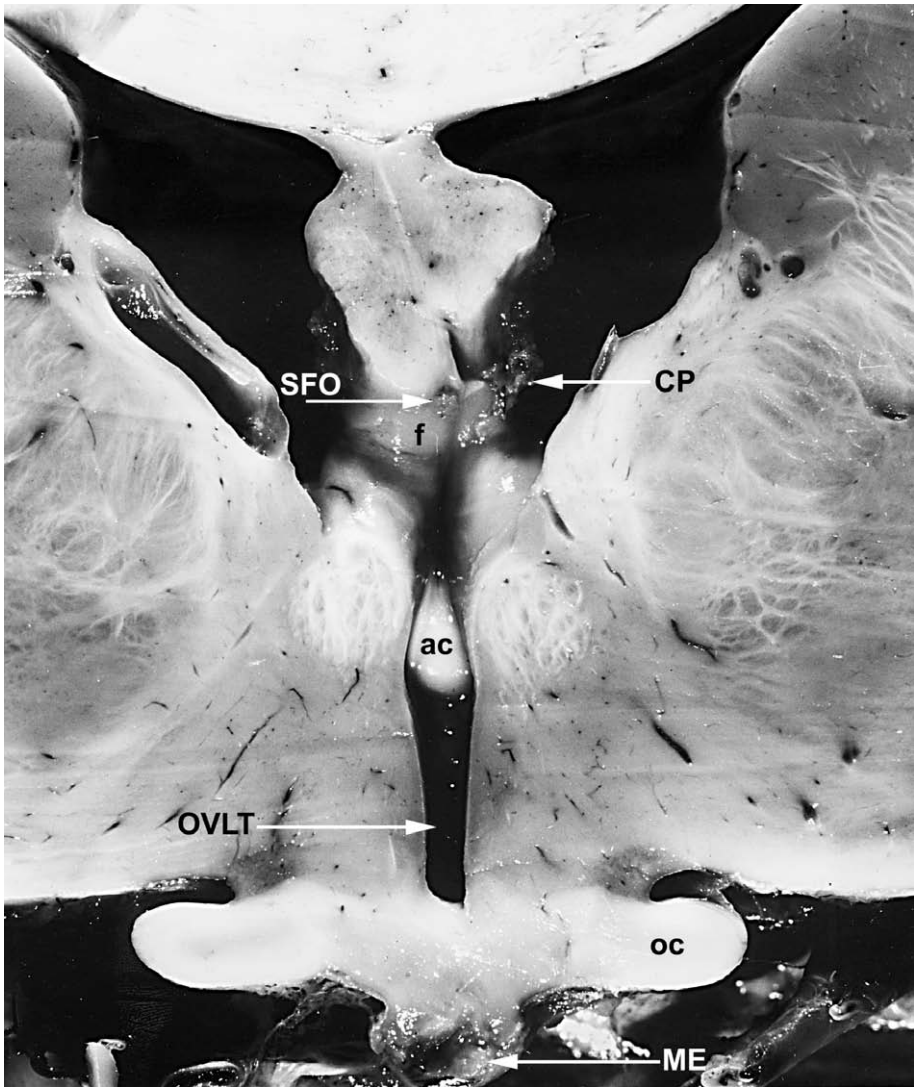

FIGURE 19.2 The position of the subfornical organ (SFO), choroid plexus of the lateral ventricle (CP), vascular organ of the lamina terminalis (OVLT) and median eminence seen in a coronally sectioned human brain. ac, anterior commissure; oc, optic chiasm.

mammalian brain at the level of the interventricular foramen. Bulging into the third ventricle at the confluence of the two interventricular foramina and ventral to the junction of the two fornical columns (Fig. 19.2 and 19.3A), this highly vascularized structure develops from the dorsal extremity of the lamina terminalis. Akert *et al*. (1961) made a comparative study of the subfornical organ that included a description of it in a primate, the squirrel monkey. They distinguished three distinct zones: the dorsal stalk, which comes in contact with the tela choroidea; the main body of the organ, which bulges into the ventricle; and a ventral stem merging into the median preoptic nucleus. Rostrally, the subfornical organ is bounded by the nucleus triangularis of the septum and hippocampal commissure. There have been many investigations into the cytological and ultrastructural characteristics of the subfornical organ of animals and these have been comprehensively reviewed (Dellman and Simpson, 1979; Dellman, 1998). In summary, four neuronal subtypes have been identified in the subfornical organ, despite earlier proposals that it lacked neuronal perikarya. Like other CVOs, glial cells are plentiful and the ependyma of the subfornical organ is modified. The ependymal cells either lack or have few cilia at their ventricular surface. Although there is considerable species variability in the appearance of the ependymal surface of the subfornical organ, and not all species have been shown to have fenestrated capillary endothelium (Weindl, 1973), a rich vascularization is

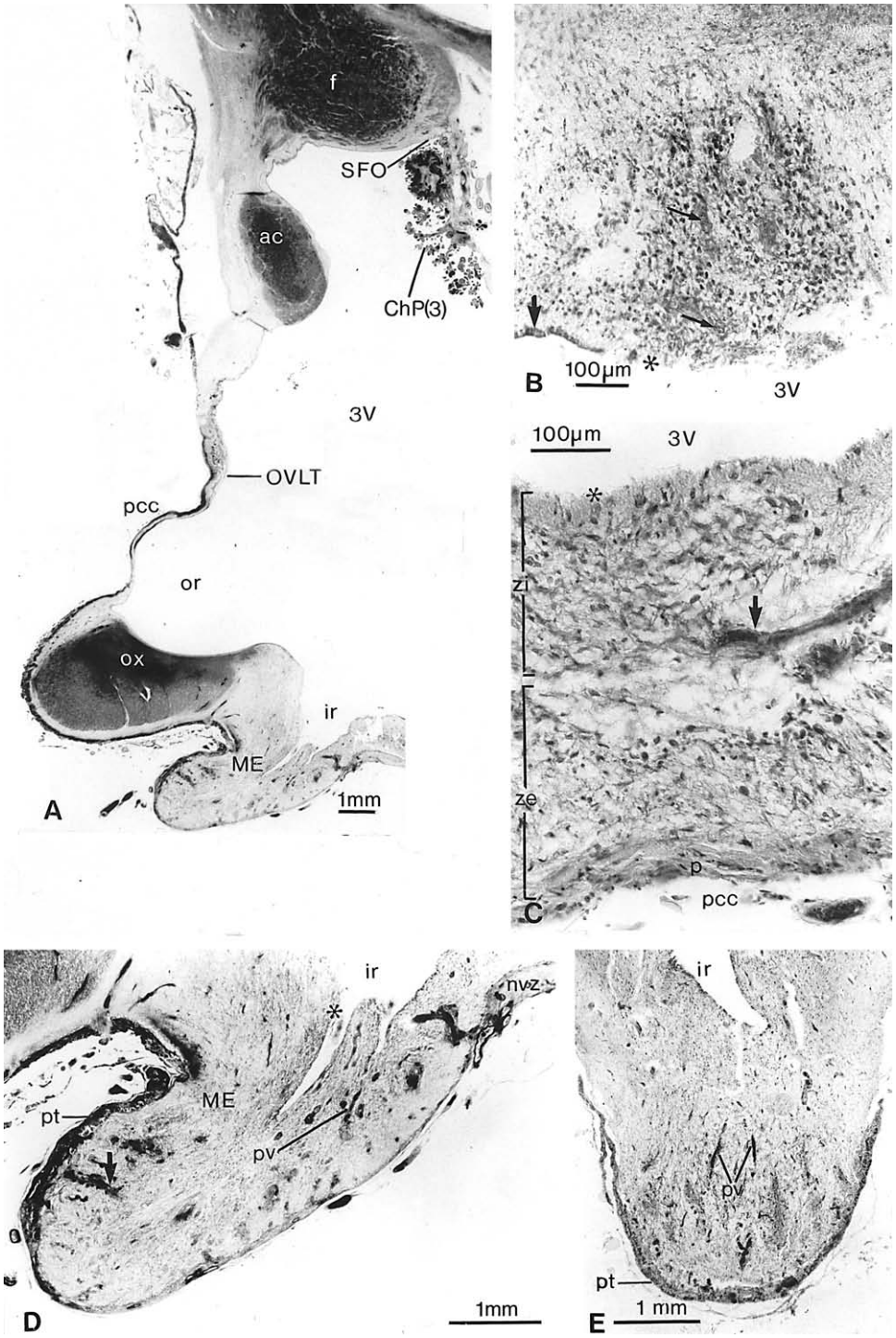

FIGURE 19.3 Forebrain circumventricular organs. **(A)** Midsagittal low-power photomicrograph showing human subfornical organ (SFO), vascular organ of the lamina terminalis (OVLT), median eminence (ME), and choroid plexus of the third ventricle (ChP(3)) on the saggital plane as in Figure 19.1. **(B)** Coronal section through the human subfornical organ. Note flattened ependyma *(asterisk)*, normal cuboidal ependyma on adjacent tissue *(large arrow)*, blood vessels *(small arrows)*, and numerous cell bodies. **(C)** Horizontal section of OVLT *(human)*. Arrow indicates a blood vessel. **(D)** Coronal section of median eminence (ME) (human). **(E)** Midsaggital section of median eminence (human). A capillary coil of the primary plexus is arrowed. Ac, Anterior commissure; f, fornix; ir, infundibular recess; nvz, neurovascular zone; or, optic recess; ox, optic chiasm; p, pia mater; pcc, prechiasmatic cisterna; pt, pars tuberalis; pv, portal vessels; ze, external zone; zi, internal zone; 3V, third ventricle; *, flattened ependyma.

always observed. The arterial sources to the subfornical organ form a capillary network with capillary loops reaching near to the ependymal surface, especially in the central part of the organ.

Human Subfornical Organ

Location

The subfornical organ in the human brain is much less prominent than that of many species in that, relative to overall brain size, it occupies less space. Putnam (1922) gave one of the early descriptions of the human subfornical organ, or intercolumnar tubercle as he called it, describing it as a rounded, pearly gray translucent nodule bulging into the third ventricle. It is found in the midline anterior wall of the third ventricle at the level of the superior border of the interventricular foramina (of Monro) (Mai *et al.*, 1997). Being adjacent to the tela choroidea, the subfornical organ is concealed by the overhanging choroid plexus (Fig. 19.3A), but if this is retracted it can be directly viewed ventral to the point where the two columns of the fornix meet (Duvernoy and Koritke, 1969b). The human subfornical organ is more easily seen in unfixed brains, in which it retains its pearly gray translucent character, making it stand out against the white matter of the fornix (Mark and Farmer, 1984; Putnam, 1922). It is ellipsoid with a diameter of only 1 mm, which caused Mark and Farmer (1984) to describe it as "miniscule". It has been observed at gestational week 16 and does not reach full structural and cytological development until the neonatal period (Castaneyra-Perdomo *et al.*, 1992).

Cellular Elements

The subfornical organ in humans (Fig. 19.3B) comprises a loose fibrillary network containing many neurons and glial cells (Castaneyra-Perdomo *et al.*, 1992; Mark and Farmer, 1984; Putnam, 1922). Typical neuronal perikarya of this structure are large and triangular, having round or ovoid nuclei with an eccentrically placed nucleolus. The cytoplasm stains faintly for Nissl. The ultrastructure of cells in the subfornical organ of the human has been examined by Mark and Farmer (1984). Many unmyelinated axons and dendrites are present and axodendritic and axosomatic synapses are plentiful, with presynaptic clear vesicles of 20–45 nm diameter and occasional larger granulated vesicles (80–150 nm). Nonsynaptic axonal dilatations are also noted to contain dense core granules of 100–175 nm.

The ependyma of the human subfornical organ is modified into flattened, squamous cells (Kuhlenbeck, 1955), and this can be seen in Fig. 19.3B. Astrocytes are numerous throughout the subfornical organ, particularly near blood vessels. Fewer oligodendrocytes and microglia are present. Channels lined by ciliated ependymal cells with microvilli have also been observed to infiltrate this organ (Mark and Farmer, 1984).

Vasculature

Branches of the anterior cerebral artery and posterior choroidal artery anastomose to form the capillary network of the subfornical organ. The network is particularly dense in the central part of the organ where groups of capillary loops extend toward the ependyma, coming close to the ventricular surface (Duvernoy and Koritke, 1964; Putnam, 1922). These capillaries exhibit extensive perivascular spaces and drain laterally into a wide vein on each side of the fornix, which eventually leads to the great cerebral vein. Arterioles in the subfornical organ of the human exhibit thick smooth muscle sheaths (Weindl, 1973). Some authors report vascular connections with the adjacent choroid plexus in certain species (Duvernoy and Koritke, 1964; Krisch and Leonhardt, 1980); however, this is not so in the human subfornical organ (Duvernoy and Koritke, 1969b; Putnam, 1922).

Neural Connectivity

Afferent Connections

The subfornical organ has both afferent and efferent neural projections and they are summarized in Table 19.1. The earliest indication of the nature of these projections came from the studies of Lewis and Shute (1967), who demonstrated in the rat that, acetylcholinesterase-containing fibers originating in the septum entered the subfornical organ. Many of the subsequent studies of its connections have involved experimental procedures, including placement of lesions with degeneration and silver impregnation techniques, axonal transport of tracers, and electrophysiological manipulations. Therefore, the most detailed information has necessarily arisen from experimental animals rather than postmortem human material. Hernesniemi *et al.* (1972) used lesion techniques as well as Golgi methods to study neural afferents to the subfornical organ, and found projections from the nucleus triangularis (of the septum) and the median preoptic nucleus. This projection from the median preoptic nucleus to the subfornical organ has subsequently been confirmed by both anterograde and retrograde transport of injected horseradish peroxidase into the subfornical organ (Lind *et al.*, 1982) and the median preoptic nucleus (Oldfield *et al.*, 1986), respectively. Other afferents to the subfornical organ arise from the medial septal nucleus, the OVLT, the medial preoptic area, hypothalamic para-

TABLE 19.1 Direct Neural Connections of the Subfornical Organ

Efferents (terminal fields listed)	Afferents (origins listed)	Ref.
Telencephalon		
Substantia innominata	Medial septal n.	Lind *et al.*, 1982; Swanson & Lind, 1986
Medial septal n.		Miselis *et al.*, 1987, Lind, 1987
Lamina terminalis		Miselis *et al.*, 1979; Lind *et al.*, 1982;
Median preoptic n.	Median preoptic n.	Saper & Lewisohn, 1983;
OVLT	OVLT	Miselis *et al.*, 1979; Oldfield *et al.*, 1992; Gu and Simerly, 1997
Limbic structures		
Infralimbic cortex	Infralimbic cortex	Swanson & Lind, 1986; Miselis *et al.*, 1987
Bed n. stria terminalis	Bed n. stria terminalis	Swanson & Lind, 1986; Lind, 1987; Miselis *et al.*, 1987
Central and median n. amygdala		Miselis *et al.*, 1987
Preoptic region		
Lateral preoptic area	Dorsal preoptic nucleus	Lind *et al.*, 1982
Anteroventral periventricular n.	Anteroventral periventricular n.	Swanson & Lind, 1986; Lind 1987
Medial preoptic area	Medial preoptic area	Miselis *et al.*, 1987; Lind *et al.*, 1982
Preoptic periventricular n.		Miselis *et al.*, 1987
Hypothalamus		
Arcuate n.	Arcuate n.	Rosas-Arellano *et al.*, 1996; Miselis *et al.*, 1987; Krout *et al.*, 2001
	Anterior hypothalamic area	Lind *et al.*, 1982
Dorsal perifornical area	Dorsal perifornical area	Lind *et al.*, 1984; Miselis, 1981
Dorsomedial hypothalamic n	Dorsomedial hypothalamic n.	Swanson & Lind, 1986;
Lateral hypothalamus	Lateral hypothalamus	Miselis 1981;
Median eminence		Miselis *et al.*, 1987
Periventricular stratum		Miselis 1981
Paraventricular n.	Paraventricular n.	Miselis 1981; Larsen *et al.*, 1991
Supraoptic n.		Miselis 1981
Suprachiasmatic n.		Miselis *et al.*, 1987
Zona incerta	Zona incerta	Swanson & Lind, 1986
Thalamus		
Centromedial n.		Miselis *et al.*, 1987
Paraventricular n.		Miselis *et al.*, 1987
Reuniens n.	Reuniens n.	Lind *et al.*, 1984; Swanson & Lind, 1986
Midbrain	Locus coeruleus	Miselis *et al.*, 1987;
	Lateral parabrachial n.	Gu & Ju, 1995
	Dorsal raphe	Lind, 1987
	Median raphe	Lind, 1987
Hindbrain		
	Nucleus of the solitary tract	Zardetto-Smith & Gray, 1987; Ciriello *et al.*, 1996; Kawano & Masuko, 2001
	Ventrolateral medulla	Kawano & Masuko, 2001

ventricular nucleus, anterior hypothalamus, and thalamic nuclei, including the paraventricular nucleus of the thalamus and the reuniens nucleus (Lind *et al.*, 1982). Of these, the projections from the perifornical region of the lateral hypothalamus as well as the rostral zona incerta and thalamic reuniens nucleus utilize angiotensin II and enter the organ via the columns of the fornix or along the lamina terminalis (Lind *et al.*, 1984; Tanaka *et al.*, 1986).

Efferent Connections

The efferent neural pathways of the subfornical organ have been well documented by anatomical (Lind *et al.*, 1982, 1984; Miselis, 1981; Miselis *et al.*, 1979; Saper and Levisohn, 1983; Swanson and Lind, 1986) and electrophysiological (Sgro *et al.*, 1984; Ferguson, 1997; Tanaka *et al.*, 1986) techniques, and there is generally close agreement on the trajectory of fibers and the areas innervated. Fibers emanating from the subfornical organ essentially take either of two courses. The first is a precommissural pathway and involves fibers that leave the organ via its ventral stalk and travel toward the median preoptic nucleus passing rostral to the anterior commissure. A few fibers split off at this point to innervate the medial preoptic area, whereas the major bundle continues to the OVLT,

suprachiasmatic nucleus, and supraoptic nucleus. The neurons giving rise to these fibers are found mainly around the periphery of the subfornical organ, while a group of neurons in the core of the subfornical organ sends a prominent efferent projection to the bed nucleus of the stria terminalis (Swanson and Lind, 1986).

The postcommissural pathway, on the other hand, travels with the columns of the fornix and the medial corticohypothalamic tract to innervate areas in the hypothalamus, including the paraventricular nucleus. Electrophysiological studies have indicated that efferents from the subfornical organ to the paraventricular and supraoptic nuclei change the excitability of vasopressin and oxytocin neurons projecting to the neurohypophysis (Ferguson *et al.*, 1984a; Sgro *et al.*, 1984) and, in the case of the paraventricular nucleus, vasopressin-containing neurons projecting to the dorsomedial medulla (Ferguson *et al.*, 1984b). More recent studies combining neural pathway tracing with immunohistochemical identification of Fos (the protein encoded by the immediate early gene *c-fos*, which is a marker of increased neuronal activity) in the rat show that neurons in the periphery of the subfornical organ that project to the supraoptic and paraventricular nuclei can be activated by hypertonicity or the circulating hormones angiotensin II and relaxin (Larsen and Mikkelsen, 1995; Oldfield *et al.*, 1994; Sunn *et al.*, 2001). Other regions found to be innervated by the subfornical organ were the infralimbic area of the prefrontal cortex, septal region, substantia innominata, zona incerta, and lateral hypothalamus (Swanson and Lind, 1986).

Tracing studies in the rat, which utilized injections of the neurotropic virus pseudorabies into peripheral sites, have shown that there are polysynaptic neural pathways from the subfornical organ and other parts of the lamina terminalis to many peripheral organs and tissues (Hubschle *et al.*, 1998; Sly *et al.*, 1999; Westerhaus and Loewy, 1999). These data indicate that neurons in the subfornical organ may influence sympathetic nerves supplying many peripheral organs, being an integral part of a visceral neuraxis as proposed by Miselis *et al.* (1987).

Function

As previously mentioned, experimental evidence of passage of intravenously administered horseradish peroxidase or intravitally administered dyes (Broadwell and Brightman, 1976; Weindl, 1973; Wislocki and Leduc, 1952) into the subfornical organ suggests that there is an altered permeability of the blood–brain barrier at this site. Such permeability of the vasculature to circulating agents provides the basis for its function as a site of receptors (AT_1 receptors) for circulating angiotensin II (Giles *et al.*, 1999). This octapeptide, which does not cross the blood–brain barrier (Ganten *et al.*, 1976), should be able to gain access to the subfornical organ from the circulation, and increased neuronal activity (shown by *c-fos* expression) occurs in neurons of the rat subfornical organ following intravenous infusion of angiotensin II (McKinley *et al.*, 1992). Physiological studies in animals have established that the subfornical organ is a site of receptors which are stimulated by circulating angiotensin II to induce water drinking, vasopressin secretion, and a centrally mediated pressor response (Simpson *et al.*, 1978, 1981). Consistent with these physiological findings is autoradiographic evidence of high-affinity binding of radiolabeled angiotensin II to the subfornical organ in animals and humans (Fig. 19.4D) (Allen *et al.*, 2000; McKinley *et al.*, 1987a; Mendelsohn *et al.*, 1984; Speth *et al.*, 1985), and both immunohistochemical and *in situ* hybridization histochemical evidence of high concentrations of angiotensin AT_1 receptors in the subfornical organ of the rat (Giles *et al.*, 1999; Lenkei *et al.*, 1997). In regard to angiotensin, significant levels of angiotensin-converting enzyme (ACE) are found in the human subfornical organ (Chai *et al.*, 1990), suggesting that local generation of angiotensin II within the subfornical organ may be of importance. Consistent with this notion is evidence in rats that circulating ACE inhibitors such as captopril or enalapril, at concentrations that are effective at inhibiting peripheral conversion of angiotensin I to angiotensin II, are ineffective in the subfornical organ. As a consequence, high levels of blood-borne angiotensin I reach the subfornical organ and are there converted to angiotensin II. This results in the activation of neurons in this CVO and stimulation of thirst (McKinley *et al.*, 1997). Binding sites in the subfornical organ of rats for other circulating hormones, such as somatostatin, atrial natriuretic peptide, calcitonin, and relaxin (Osheroff and Phillips 1991; Patel *et al.*, 1986; Quirion *et al.*, 1984; Rouleau *et al.*, 1984), have also been demonstrated, suggesting that angiotensin II may not be the only blood-borne agent acting at this site. Relaxin, a hormone secreted during pregnancy, directly stimulates neurons of the subfornical organ (Sunn *et al.*, 2001). Nitric oxide synthase (NOS) is also abundant in the rat subfornical organ, and NO donors depress the activity of the subfornical organ (Rauch *et al.*, 1997). In addition to being a receptor zone, morphological evidence suggests that hormones such as luteinizing hormone–releasing hormone (LHRH), somatostatin, or angiotensin II (of central origin) may be released by neurosecretion into the bloodstream by the subfornical organ (Krisch and Leonhardt, 1980; Lind *et al.*, 1985; Oldfield and McKinley, 1989).

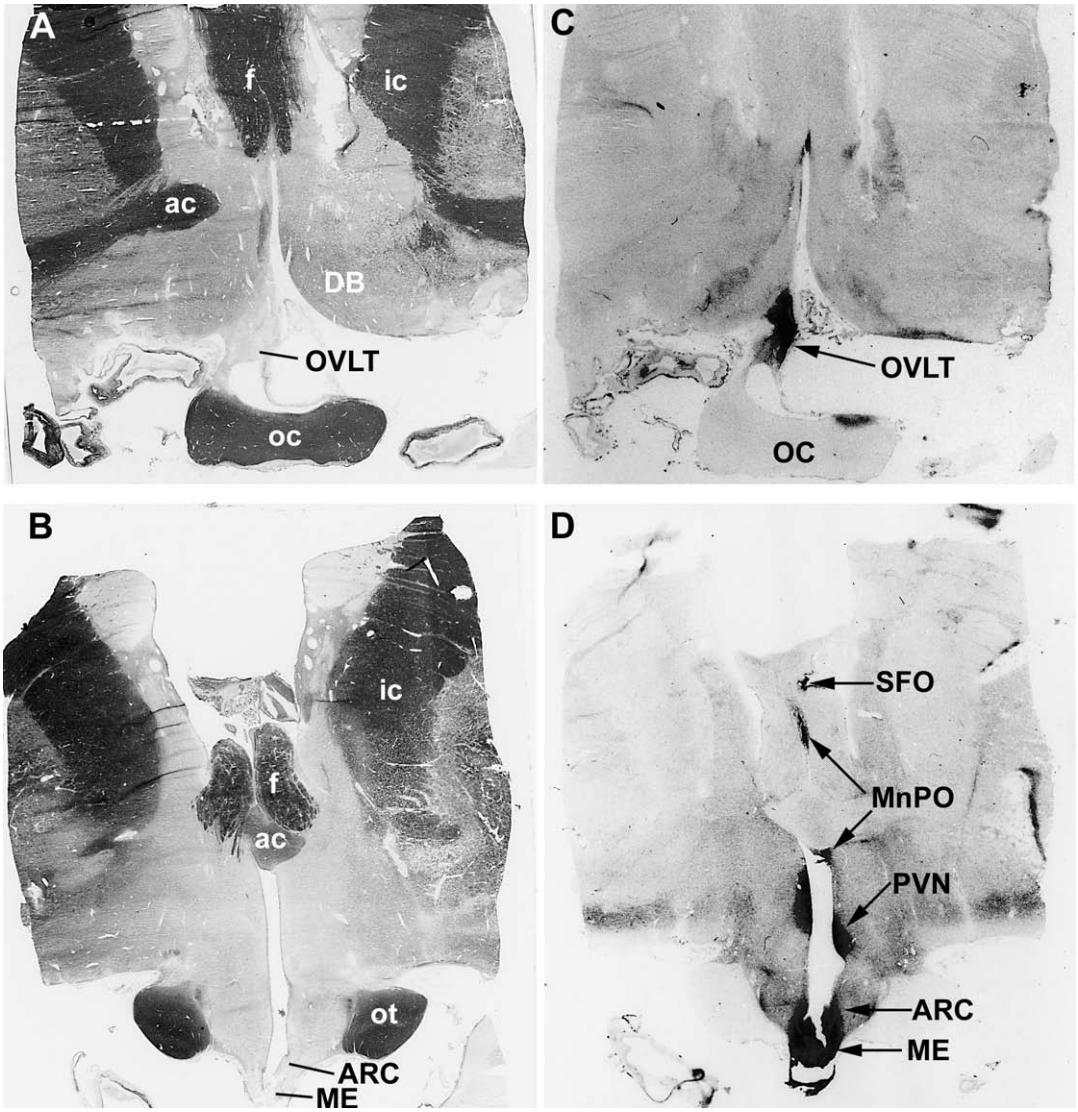

FIGURE 19.4 Coronal sections through the OVLT (**A** and **C**), and subfornical organ and median eminence (**B** and **D**) of the human brain showing *in vitro* autoradiographic binding (**C** and **D**) of an angiotensin II ligand (^{125}I-[Sar1,Ile^{8}]angiotensin II). Ligand binding is seen as the black regions arrowed in **C** and **D.** Adjacent frozen sections stained with cresyl violet and luxol fast blue showing anatomical features are shown in **A** and **B.**

VASCULAR ORGAN OF THE LAMINA TERMINALIS

General Characteristics and Comparative Studies

Situated in the anterior wall of the third ventricle between the optic chiasm and anterior commissure is another CVO, the vascular organ of the lamina terminalis or OVLT (an abbreviation derived from its Latin designation *organon vasculosum laminae terminalis*). Other terms that have been used for the OVLT are supraoptic crest, preoptic organ, medial (vascular) prechiasmatic gland, and Sclussplattenorgan (terminal plate organ). This region, initially described by Behnsen (1927) and then by Wislocki and King (1936) on the basis of its selective permeability to intravitally administered trypan blue, has been observed in many vertebrate species of fish, reptiles, birds, and mammals (McKinley *et al.*, 1987b; Weindl, 1973; Wenger and Tork, 1968).

While there is considerable variation between species in the morphology of the ependymal cells and

in the proportion of the lamina terminalis ventral to the anterior commissure that is occupied by the OVLT (McKinley *et al.*, 1987b), the general structural elements of the OVLT are quite similar throughout vertebrates (Wenger and Tork, 1968). Situated in the lamina terminalis immediately dorsal to the optic chiasm, the OVLT is characterized by a special vascular arrangement. This CVO separates two cerebrospinal fluid–containing spaces, the prechiasmatic cisterna rostrally and the optic recess of the third ventricle caudally, and has characteristics somewhat reminiscent of the median eminence, particularly the rich intrapial plexus of blood vessels of the OVLT which gives rise to a network of capillary loops with fenestrated endothelial cells and extensive perivascular spaces (Duvernoy and Koritke, 1964; Hofer, 1957; Wenger and Aros, 1971). While the precise functions of the OVLT have yet to be fully elucidated, the similarity in organization of this region to the median eminence has led several authors to suggest a neurosecretory role for the OVLT (Weindl, 1973), particularly in the release of LHRH (Wenger *et al.*, 1981).

Recent studies in a number of species have suggested that OVLT has (1) a sensor role as an osmoreceptor (McKinley *et al.*, 1982; Oldfield *et al.*, 1994; Thrasher and Keil, 1987), (2) a role as a mediator of the febrile (fever) response (Blatteis *et al.*, 1983, 1987), and (3) a receptor role for blood-borne angiotensin II and relaxin to stimulate the CNS (Johnson, 1985; McKinley *et al.*, 1992, 1997; Giles *et al.*, 1999).

Human OVLT

Location and Structural Organization

In humans, the OVLT is at its greatest extent in the lamina terminalis approximately midway between the optic chiasma and anterior commissure (Fig. 19.3A). Kuhlenbeck (1954) first described the human OVLT as a slight thickening in the lamina terminalis. He divided it into two zones, an outer one situated beneath the pia mater lining the prechiasmatic cisterna and an inner zone reaching to the ependymal lining of the optic recess of the third ventricle (Fig. 19.3C). He observed in the superficial lamina of the external zone a rich vascular plexus of sinusoidal vessels. Deeper to this lamina are the cellular elements of the external zone, while in the inner zone densely packed cells and a network of fibers running at right angles abutted the modified ependymal surface (Kuhlenbeck, 1970). Like other CVOs, the ependymal cells of the OVLT are flattened and have few, if any, cilia. Channels or canals lined by ependymal cells extending into the body of the OVLT have been reported (Wenger and Torö, 1971), and these also occur in the subfornical organ (Mark and Farmer, 1984).

Vasculature

Duvernoy *et al.* (1969) made a detailed study of the vascular architecture of the human OVLT and found that it received its arterial supply from four sources: (1) a superior median source branching from the anterior communicating artery, (2) and (3) two lateral sources coming from arteries which branch off from each anterior cerebral artery below the anterior communicating artery, and (4) an inferior median source ascending from below the optic chiasm (Fig. 19.5A). These sources anastomose and branches twig off to enter the pia mater and supply a dense superficial capillary network in the external zone of the OVLT. From this superficial network, a secondary deep capillary network extends into the body of the OVLT in the form of sinusoidal capillary loops and coils (Fig. 19.5B). This deep network, which drains the superficial capillary network, is denser in the inferior zone of the OVLT. There many anastomoses unite the capillary loops of the deep network (Fig. 19.5C). The venous drainage of the deep network is in a lateral direction to veins coming from adjacent hypothalamus and proceeding to the anterior cerebral veins (Duvernoy *et al.*, 1969).

Extensive perivascular spaces of 0.1–0.3 μm width may surround the blood vessels of the rich vascular network that extends from the pia mater into the organ. Unlike other species, fenestrations in the capillary endothelial cells have not been observed in the human OVLT (Wenger and Torö, 1971). However, reports of selective entry into the OVLT and other CVOs of endogenous iron deposits observed postmortem in cases of hemochromatosis (Cammermeyer, 1947a) and entry of imbibed silver (for cosmetic purposes) into the OVLT (Landas *et al.*, 1985) suggest altered blood–brain barrier characteristics in the human OVLT. The junctional complexes joining ependymal cells have not been studied.

Cellular Elements

With regard to its cellular elements, many glial cells can be seen in the deeper layer of the external zone. Neither Kuhlenbeck (1968) nor Wenger and Torö (1971) were able to discern neuronal cell bodies in the human OVLT; however, Landas and Phillips (1987) report the presence of small "primitive neurons" in the OVLT of humans analogous to those observed in the rabbit, the so–called parenchymal cells (Weindl *et al.*, 1968).

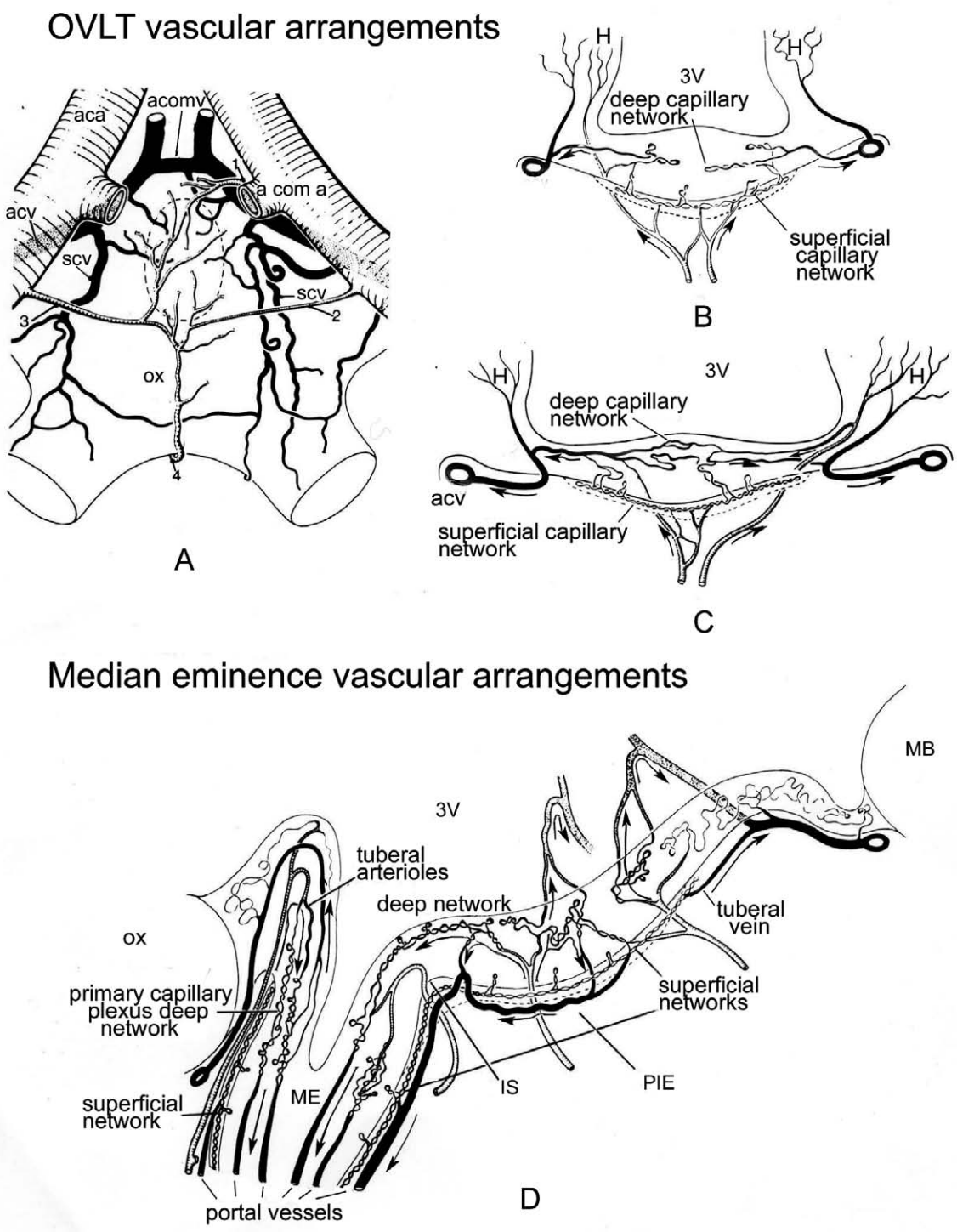

FIGURE 19.5 Vascular arrangements of the human OVLT and median eminence. **(A)** diagram of frontal view of blood vessels which anastomose to enter the OVLT. 1, Superior median arterial pedical; 2 and 3, left and right lateral arterial pedicals; 4, median inferior arterial pedical; aca, anterior cerebral artery; a coma, anterior communicating artery; a comv, anterior communicating vein; acv, anterior cerebral vein; ox, optic chiasm; scv, superior chiasmatic vein. From Duvernoy *et al.*, 1969, with permission. **(B, C)** Diagrams of capillary networks of human OVLT in horizontal sections. B is a more dorsal part of the OVLT than C. acv, Anterior cerebral vein. From Duvernoy *et al.*, 1969, with permission. **(D)** Diagram of capillary networks in the human median eminence. From Duvernoy, 1972, with permission. Arrows indicate the direction of the blood flow. IS, Infundibular sulcus; MB, mamillary body; ME, median eminence; ox, optic chiasm; PIE, post-infundibular eminence; 3V, third ventricle.

TABLE 19.2 Direct Neural Connections of the OVLT

Efferents (terminal fields listed)	Afferents (Origins listed)	Ref.
Lamina terminalis		
Median preoptic n.	Median preoptic n.	Saper & Lewisohn, 1983; Miselis, 1981;
Subfornical organ	Subfornical organ	Lind *et al.*, 1982, Gu & Simerly, 1982; Oldfield *et al.*, 1992
Limbic structures		
Cingulate cortex		Camacho & Phillips, 1981
Bed n. stria terminalis		Sunn, McKinley, & Oldfield (unpublished)
Preoptic region		
Parastrial nucleus		Gu & Simerly, 1997
Lateral preoptic area		Uschakov *et al.*, 2001
Medial preoptic area	Medial preoptic area	Gu & Simerly, 1997
Hypothalamus		
Supraoptic n.	Anterior hypothalamic area	Miselis, 1979; Camacho & Phillips, 1981
Arcuate n.	Dorsomedial hypothalamic n.	Gu & Simerly, 1997
Periventricular n.	Ventromedial hypothalamic n.	Camacho & Phillips, 1981
Lateral hypothalamus	Lateral hypothalamus	Uschakov *et al.*, 2001
Paraventricular n.	Paraventricular n.	Sunn *et al.*, 2001; Larsen *et al.*, 1991
Zona incerta		
Thalamus		
Paraventricular n.		Uschakov *et al.*, 2001
Midbrain		
Periaqueductal gray	Locus coeruleus	Gu & Simerly, 1997
Lateral parabrachial n.	Periaqueductal gray	Camacho & Phillips, 1981
Hindbrain		
Raphe pallidus		Uschakov *et al.*, 2001

Neural Connectivity

Afferent Connections

Based on the few studies in experimental animals (e.g., rat, sheep) utilizing the axonal transport of marker molecules such as tritiated amino acids and horseradish peroxidase, which have investigated the neural connectivity of the OVLT (summarized in Table 19.2), this CVO appears to be part of a neural network within the lamina terminalis and hypothalamus that is involved in the regulation of fluid balance (McKinley *et al.*, 1996, 1999; Miselis, 1981; Thrasher and Keil, 1987). The major afferent inputs to the OVLT appear to come from the subfornical organ (Camacho and Phillips, 1981; Miselis, 1981), locus coeruleus, central gray, medial preoptic, median preoptic, lateral preoptic, and anterior, lateral, dorsomedial, and ventromedial hypothalamic nuclei (Camacho and Phillips, 1981; Palkovits *et al.*, 1978; ter Horst and Luiten, 1986).

Efferent Connections

The efferent fibers emanating from neurons within the OVLT have not been studied in detail; however, it is clear from studies in the rat that there are strong projections to the median preoptic nucleus immediately dorsal to the OVLT and to the supraoptic nucleus (Camacho and Phillips, 1981; Gu and Simerly, 1997; Miselis, 1981; Oldfield *et al.*, 1986; Saper and Levisohn, 1983; Sunn *et al.*, 2001). Camacho and Phillips (1981) have suggested that the strong projection from the OVLT to the adjacent lateral preoptic region may be of more significance than the aforementioned pathways. Using anterogradely transported tritiated amino acids or horseradish peroxidase that had been microinjected into the OVLT of the rat, they also described projections to the limbic system via fibers that travel to the septum and spread out to continue to the hippocampus and cingulate cortex. Some terminate there in the dentate gyrus; however, these connections have yet to be confirmed by experiments using retrogradely transported neural tracers injected into these regions. There are also efferent projections to both magnocellular and parvocellular parts of the hypothalamic paraventricular nucleus (Sunn *et al.*, 2001) and also to the lateral hypothalamic region, lateral septal nucleus, parastrial nucleus of the preoptic region, bed nucleus of the stria terminalis, periaqueductal gray, and lateral parabrachial nucleus (Gu and Simerly, 1997; Uschakov *et al.*, 2001). Transneuronal viral tracing studies show that neurons in the OVLT may also be connected

polysynaptically to the autonomic nervous system (Hubschle *et al.*, 1998; Sly *et al.*, 1999; Westerhaus and Loewy, 1999).

Functions

Studies in animal species have suggested that the OVLT is of importance as a neurohemal neurosecretory and/or receptor zone. There are very few functional investigations in humans, although LHRH has been detected in the human OVLT (Okon and Koch, 1977). Consistent with neurosecretion into the bloodstream are reports that LHRH, angiotensin II–, somatostatin–, and atrial natriuretic peptide–immunoreactive fibers terminate in the OVLT (Barry and Carette, 1975; Kawata *et al.*, 1985; Lind *et al.*, 1985; Zimmerman and Antunes, 1976), and that there are dense core vesicles in nerve endings near perivascular spaces (Weindl and Schinko, 1975). Using *in vitro* autoradiography, we have observed dense binding of radioiodinated analogs of angiotensin II to the human OVLT (Fig. 19.4C) (Allen *et al.*, 2000; McKinley *et al.*, 1987a). This is similar to findings in animal species showing high concentrations of angiotensin AT_1 receptors in the OVLT (Allen *et al.*, 2000; McKinley *et al.*, 1986; Mendelsohn *et al.*, 1984; Speth *et al.*, 1985) and is consistent with the notion that the OVLT is a site at which blood-borne angiotensin II may act on the CNS to influence the regulation of fluid balance and arterial blood pressure (Camacho and Phillips, 1981; Johnson, 1985; McKinley *et al.*, 1992). Very high levels of ACE are observed in the human OVLT (Chai *et al.*, 1989), indicating that local generation of angiotensin II may occur there.

Experimental studies in animals using lesioning techniques, electrophysiology, and immunohistochemical identification of Fos show that the OVLT is a major osmoreceptor site for vasopressin secretion and thirst (McKinley *et al.*, 1988, 1994; Oldfield *et al.*, 1994; Richard and Bourque, 1993; Thrasher and Ramsay, 1987). Lack of thirst in some rare conditions reported in humans with either surgical damage, tumors, or cysts in the region of the OVLT (Robertson, 1991) is consistent with this view. The OVLT is also a site at which blood-borne relaxin directly stimulates neurons (Sunn *et al.*, 2001), consistent with the presence of relaxin binding sites in this CVO (Osheroff and Phillips, 1991). Neuronal NOS is also at a high level in the rat OVLT (Alm *et al.*, 1997), as are binding sites for peptides such as amylin, atrial natriuretic peptide, calcitonin, calcitonin gene–related peptide (CGRP), interleukin-1, endothelin, somatostatin, and vasopressin (Eriksson *et al.*, 1995; Murone *et al.*, 1997; Patel *et al.*, 1986; Saavedra *et al.*, 1992; Tribollet *et al.*, 1992; Sexton *et al.*, 1986, 1994).

MEDIAN EMINENCE AND NEUROHYPOPHYSIS

General Characteristics and Comparative Studies

In nonprimate mammalian species, the term *median eminence* refers to that tissue that is midline, immediately caudal to the optic chiasm and rostral to the mamillary bodies. Its name accords to the median position and the fact that it forms a protruberance from the surface of the brain. It is connected to the pituitary stalk. The median eminence includes the neural tissue that lies below the ependyma of the floor of the third ventricle. Two recesses are found in the ventricle at this level: the infundibular recess and the mamillary recess. The former is a central indentation of the median eminence. Diagrammatic representation of the ovine median eminence with photomicrographs is shown in Figure 19.6. The innermost layer of the median eminence (internal zone) contains cells of the arcuate nucleus in most nonprimate mammalian species. The nerve fibers of the hypothalamoneurohypophysial tract (traveling from the cell bodies of the magnocellular neurons to the posterior lobe of the pituitary) traverse the median eminence at this level. These axons of the oxytocin and vasopressin neurons, originating from the hypothalamic supraoptic and paraventricular nuclei, project to the neurohypophysis and secrete into the peripheral blood system. The next layer of the median eminence is the external zone (sometimes called the palisade layer because of its histological appearance). It is into this layer that the hypophysiotropic neurons project and come in close proximity to the primary plexus of the hypothalamohypophysial portal blood system. The cell bodies of the hypophysiotropic neurons are found in various nuclei of the hypothalamus and preoptic area and project to the external zone of the median eminence. In addition, there are projections from the arcuate nucleus and other regions as far away as the brain stem of nonhypophysiotropic neuropeptides (e.g., neuropeptide Y and substance P) and monoamines (Palkovits, 1984; Mai *et al.*, 1986). Secretion from these nonhypophysiotropic systems into the portal blood appears to vary between species, since there is good evidence for the secretion of significant levels of neuropeptide Y into the portal system of the rat (Sutton *et al.*, 1988) but not in the sheep (Clarke *et al.*, 1993). On the other hand, there is good evidence that noradrenaline is secreted directly into the portal system (Thomas *et al.*, 1989). While there is substantial evidence that dopamine is released into the portal blood of rats and serves as a prolactin inhibiting factor (Pan, 1996), there

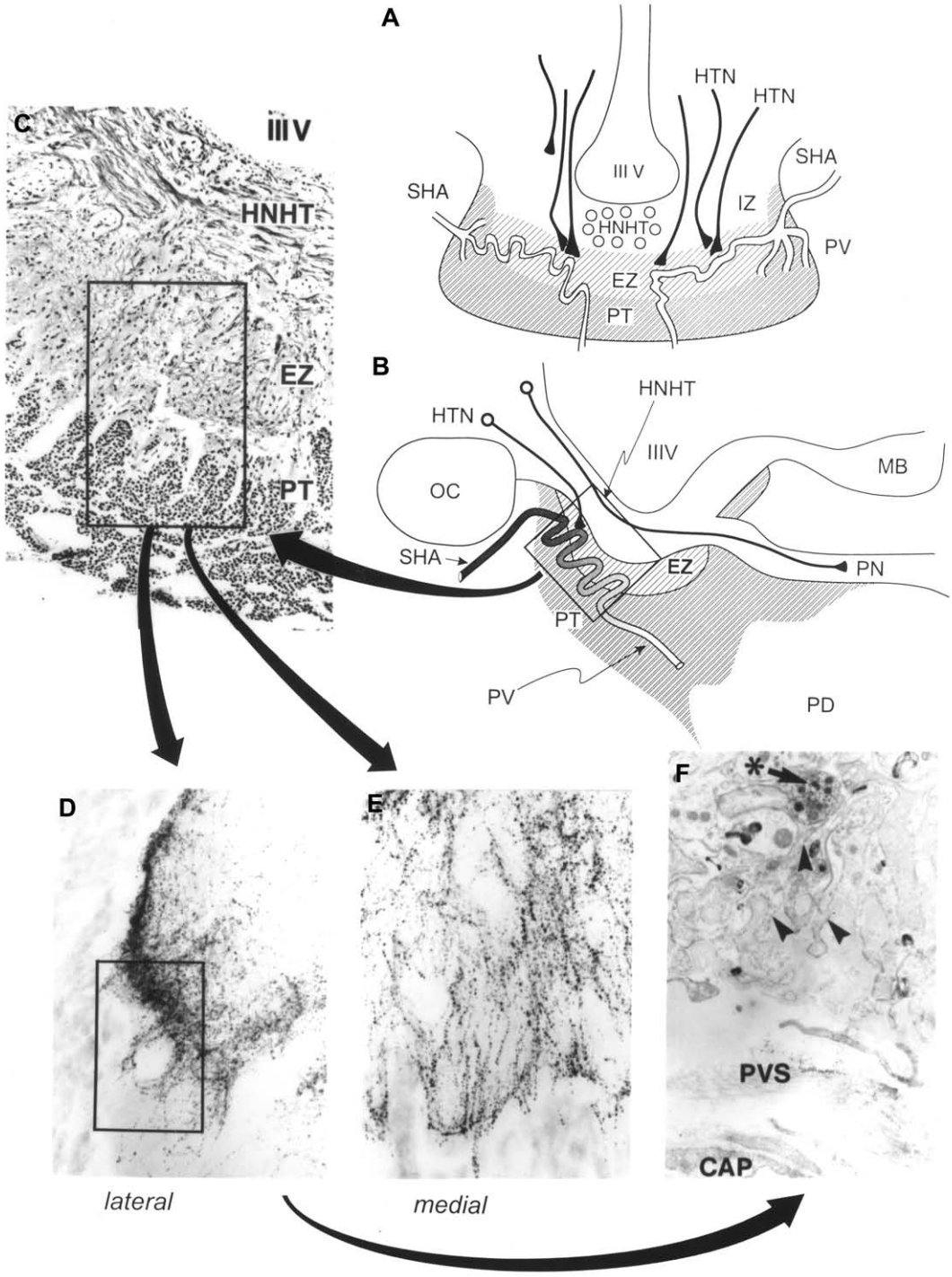

FIGURE 19.6 The ovine median eminence. **A.** Diagram of a frontal section of the sheep median eminence showing the processes of the hypophysiotrophic neurons (HTN) terminating in the external zone (EZ). The hypothalamoneurohypophysial tract (HNHT) is shown in the internal zone (IZ) en passant to the pars nervosa (neurohypophysis) of the pituitary gland. The pars tuberalis (PT) wraps around the entire structure. The portal vessels (PV) arise from the superior hypophysial artery (SHA). IIIV, third ventricle. **B.** Diagram of the sheep median eminence in saggital section. OC, optic chiasma; PD, pars distalis; PN, pars nervosa; MB, mamillary body. **C.** Sagittal section through the sheep median eminence showing the neurosecretory external zone (EZ) (see part B). The HNHT can be seen coursing through the IZ of the median eminence. The distinctive appearance of EZ is largely due to the portal vessels that loop through this region to come into close proximity to the terminals of HNT (×280) **D.** Lateral region of the median eminence showing fibers immunostained for GnRH in the EZ (×840). **E.** Medial region of the median eminence showing fibers immunostained for GnRH in the EZ (×840). **F.** Electron micrograph taken from the lateral region of the median eminence (see D) showing an immunreactive GnRH terminal (*). These terminals are generally surrounded by glial processes *(arrowheads)* that extend to the perivascular space (PVS) that is seen between the neural tissue and the fenestyrated capillaries (CAP). (×10,000).

are a number of discrepancies that require careful consideration before this doctrine is unequivocally accepted. These include sex differences and inconsistent relationships between the levels of dopamine in the median eminence/portal blood and peripheral prolactin levels. In the sheep, a differential in the plasma levels of dopamine cannot be demonstrated between the portal and peripheral circulation (Thomas *et al.*, 1989). In spite of this, dopamine is a highly effective inhibitor of prolactin secretion in a wide range of species, including man.

There is some degree of regionalization of projections from hypophysiotropic neurons into the median eminence. For example, the gonadotropin-releasing hormone terminals are found predominantly in the lateral regions of the external zone whereas the terminals of the somatostatin neurons are found mainly in the medial region. The neuronal terminals of the hypophysiotropic neurons are surrounded by glial elements (Fig. 19.6), and there is some degree of rearrangement under normal physiological conditions, e.g., across the seasons in seasonally breeding animals (Xiong *et al.*, 1997). In general, the terminals are found some distance from the fenestrated capillaries of the primary plexus, so that secreted stimulatory and inhibitory factors need to traverse an extravascular space prior to uptake into the primary plexus capillaries. Most hypophysiotropic hormones are secreted in a pulsatile manner (Clarke, 1996) and the presence of degrading enzymes in the median eminence (Smith *et al.*, 1997) might be a mechanism whereby such pulsatile secretion is maintained as a discrete rather than a prolonged signal to the anterior pituitary gland.

The outermost layer of the median eminence is the pars tuberalis, which is of nonneural origin and an upgrowth of the pituitary gland. The pars tuberalis is of a different embryonic origin to the pars distalis and contains cells that have a distinct profile. For example, the homeobox gene *Pit1* is expressed in the pars tuberalis to a much greater extent than in pars distalis cells (Lin *et al.*, 1994), and the cells of the pars distalis also express melatonin receptors at a very high level (Morgan, 2000).

The median eminence and the neurohypophysis (pars nervosa or posterior pituitary gland) contain a common neurohypophysial capillary bed (Page and Bergland, 1977). The hypophysial portal system arises from the superior hypophysial artery that supplies the primary capillary bed in the external zone of the median eminence. The superior hypophysial artery arises from both internal carotid arteries (Page and Bergland, 1977). Within the external zone of the median eminence the capillaries of the primary plexus of the portal system form loops, giving rise to the palisade appearance of the structure. These capillaries then drain into the portal vessels that travel through the pars tuberalis and pituitary stalk to the pars distalis of the pituitary gland; these are the long portal vessels (Xuereb *et al.*, 1954b). At the level of the pars tuberalis there is further opportunity for the secretion of factors that might influence the function of the cells of the pars distalis. Indeed, current work indicates that the cells of the pars tuberalis secrete a factor that regulates prolactin secretion (Morgan, 2000) and melatonin action on the pars tuberalis cells appears to mediate seasonal changes in prolactin secretion in sheep (Lincoln and Clarke, 1998). Vascular casts of the hypophysial portal system in a variety of species may be found in Page (1978). The inferior hypophysial artery supplies blood to the caudal end of the neurohypophysial capillary bed, but the capillaries of the median eminence and the neurohypophysis are confluent, allowing for variations in flow between the two, depending on the relative pressure with which blood is delivered via the superior and inferior hypophysial arteries (Page, 1987). A dense bed of short portal vessels connects the neurohypophysis to the pars distalis of the pituitary gland (Daniel and Prichard, 1975). The blood supply to the median eminence and neurohypophysis constitutes the sole blood supply to the pituitary gland and hypophysial stalk section results in substantial infarction of the pars distalis (Clarke *et al.*, 1983). The degree to which this occurs depends on the extent to which blood is supplied by the inferior hypophysial arteries in different species (Daniel and Prichard, 1975).

The median eminence is a masterpiece of physiology. Very small quantities of hypophysiotropic hormone (pg/mL levels) are secreted into the portal system to act on pituitary cells that then secrete large amounts of hormone (achieving peripheral concentrations in the order of ng/mL). The secondary bed of this portal system is the sinusoids of the pars distalis, where each hypophysiotropic signal can interact with the relevant cell type. Not only does this allow for substantial signal amplification, but the pulsatile nature of hypophysiotropic hormone secretion allows for fine modulation of both frequency and amplitude of pulsatile release of hormone. In this way the median eminence translates a neural signal into an hormonal signal. The portal system is able to carry multiple signals from the different hypophysiotropic systems and yet achieve specificity at the level of the pars distalis; each pituitary cell type responds specifically to the relevant releasing/inhibiting factor by way of specific receptors. Detailed dissertations on the significance of the junction between the brain and the endocrine system by way of the median eminence and the hypophysial

portal system can be found in Donovan (1978) and Flerko (1980).

Human Median Eminence

Location and Structural Organization

While the arrangement of the human median eminence follows the aforementioned general pattern, a number of modifications have evolved to give it distinct features worthy of comment. In its gross anatomy, the eminence on the brain surface that is equivalent to the median eminence of lower mammals is no longer evident in the ventral surface of the human hypothalamus. As a result of the increase in size of the human forebrain, the long axis of the infundibulum from hypothalamus to pituitary shifts its orientation so that it runs forward (see Chapter 17) and becomes elongated (Fig. 19.3A), and is not a caudally directed column as in nonprimates. Thus, the surface eminence disappears and the median eminence becomes incorporated into the upper part of the infundibular stem (Daniel and Pritchard, 1975). Unlike many species, there is no strict delineation of this region into internal and external zones in the developed human brain. However, there has been designation of an upper infundibular stem located in a suprasellar region and a lower infundibular stem which is the part of the infundibulum that is adjacent to the adenohypophysis and which has fibers leading in a caudal direction to the infundibular process (Daniel and Pritchard, 1975; Xuereb *et al.*, 1954a). The pars tuberalis forms the most rostral surface boundary of the median eminence (Figs. 19.3D, E), and the stalk of the infundibulum passes through an opening in the diaphragma sellae, an extension of the dura mater that closes over the pituitary fossa. At the caudal joining of the infundibular stem to the brain, a superficial layer termed the neurovascular zone extends in the midline postinfundibular eminence toward the mammillary body (Fig. 19.3E). At the junction of the neurohypophysis with the pars distalis, a pars intermedia can be discerned in many species; however, in the human pituitary gland, this feature is not present and cystic spaces and epithelial cells are observed in the analogous region (Daniel and Pritchard, 1975).

Vasculature

Perhaps the most distinguishing feature of the human neurohypophysis and median eminence is the specialized configuration of the vascular arrangement that pervades the neural tissue of the median eminence, which is so important for its neuroendocrine function. The blood supply to these regions comes from the superior hypophysial and inferior hypophysial arteries that arise from the internal carotid arteries. Some branches of the superior hypophysial artery descend within the pars tuberalis along the rostral and lateral surface of the infundibulum and give rise to arterioles, which enter the infundibulum and bend upward toward the median eminence to form complex capillary loops in both the superficial and deeper parts of the infundibulum (Fig. 19.5D). These capillary arrangements form the primary capillary complex of the median eminence in the upper infundibular stem. The continuation of these capillary coils gives rise to the long portal veins from their lower end which deliver blood to the pars distalis (Fig. 19.5D). These portal veins travel down the surface (pars tuberalis) and interior of the infundibulum to supply the sinusoids of the pars distalis (Xuereb *et al.*, 1954a, b). Other descending branches of the superior hypophysial artery break up into a capillary plexus within the pars tuberalis, the so-called mantle plexus from which some superficial capillary loops enter the infundibulum. Although the long portal veins are the major venous drainage of the median eminence, a few veins pass back to the pars tuberalis and reach surface retrochiasmatic veins and the hypothalamus (Fig. 19.5D). Similar capillary plexuses also occur in the caudal part of the median eminence, where there is a superficial plexus in the neurovascular zone of the postinfundibular eminence and arterioles giving rise to a deep network of capillary coils that drain into long portal vessels that supply the pars distalis (Duvernoy, 1972). A group of portal vessels is also found in the lower infundibular stem. These are the short portal vessels that arise from capillary loops in the neural tissue adjacent to the pars distalis and that supply the sinusoids of this tissue. The associated capillary loops receive their arteriolar input from the artery of the trabecula which links the inferior and superior hypophysial arteries.

The portal blood vessels which emanate from the median eminence and neurohypophysis provide the exclusive blood supply of the pars distalis (adenohypophysis) (Xuereb *et al.*, 1954a). The hypothalamic releasing factors and inhibitory agents secreted from nerve endings in the vicinity of capillary loops are delivered to the pars distalis by the portal vessels to influence the secretion of hormones by this gland. Histologically, the capillaries of the primary plexus are easily observed, being surrounded by extensive fibrous reticulum sheaths and bundles of nerve fibers of the neurohypophysial tract. Long processes from specialized ependymal cells (tanycytes) that line the floor of the infundibular recess also pass into this tissue.

Human Neurohypophysis (see also Chapter 18)

Location

The infundibular process of the neurohypophysis (posterior pituitary, pars nervosa) is situated in the most caudal part of the pituitary fossa. It is here that the majority of axons of the hypothalamoneurohypophysial tract terminate to release oxytocin and vasopressin. This most distal part of the neurohypophysis is characterized by rich vascularity, nerve endings, Herring bodies, and pituicytes.

Cellular Elements and Vasculature

The distribution of pituicytes (which may be analogous to astrocytes) varies within the neurohypophysis. Ultrastructurally, these cells have large nuclei and sparse perinuclear cytoplasm with processes that terminate near perivascular spaces (Lederis, 1965). The capillaries within the infundibular process receive a blood supply directly from numerous arteries of lateral and medial branches of the inferior hypophysial arteries, and the capillaries drain into venous channels to enter the systemic circulation via the posterior intracavernous sinus or a posterior venous network or the vein accompanying the inferior hypophysial artery (Green, 1957; Xuereb *et al.*, 1954a). These capillaries have fenestrated endothelial cells and extensive perivascular spaces containing collagen fibers and occasional fibroblasts surrounded by a basement membrane. Numerous nerve endings are found in this region together with pituicyte processes. The nerve endings contain elementary granules that are 90–200 nm in diameter and also some smaller vesicles, 20–50 nm in diameter, which may contain the neurosecretory products of the hypothalamoneurohypophysial tract (Bergland and Torack, 1969; Lederis, 1965).

Neural innervation of the Median Eminence and Neurohypophysis (see also Chapter 17)

The infundibulum or pituitary stalk receives neural input from two major fiber pathways. The first of these is the neurohypophysial tract or magnocellular system. The second neural input to the infundibulum is the tuberoinfundibular tract or parvocellular system. The neurohypophysis does not contain neuronal perikarya. Thus, the projections to the neurohypophysis/median eminence are of a neurosecretory nature. The neurohypophysial tract has its origin in the magnocellular neurons of the supraoptic and paraventricular nuclei in the hypothalamus and accessory internuclear cells in the bridging tissue between these two nuclei. Fibers from the paraventricular nucleus proceed through this tissue toward the supraoptic nucleus, joining its axonal outflow to the neurohypophysis, where they terminate around blood vessels in the lower infundibular stem and infundibular process to release oxytocin and vasopressin (Defendini and Zimmerman, 1978; Weindl and Sofroniew, 1985; Zimmerman and Antunes, 1976). Saper (see Chapter 17) presents sections through the human hypothalamus that favorably display the supraoptic and paraventricular nuclei as seen with Nissl staining (Figs. 17.2–17.7). He also presents a comprehensive account of the neuroactive compounds released by the magnocellular and parvocellular neurosecretory nuclei.

The axons of the tuberoinfundibular tract have as their origin parvocellular neurons in a number of brain regions, including the arcuate nucleus (or infundibular nucleus), the paraventricular nucleus, preoptic region, periventricular hypothalamic region, and ventromedial hypothalamus. These fibers terminate in the median eminence and lower infundibular stem in the vicinity of capillary loops to release a number of peptides (releasing hormones) and monoamines, which have been mentioned previously in this chapter and which influence the secretion of hormones from the anterior pituitary gland.

PINEAL GLAND

General Characteristics and Comparative Studies

The modern view of the mammalian pineal that has emerged is that the pinealocytes, the secretory cells of the pineal in mammals, have developed phylogenetically from photoreceptor cells of lower vertebrates but are no longer directly sensitive to light. The pinealocytes, though evolving from neurons, are not true neurons and do not have axonal projections to other brain regions or the periphery but secrete locally synthesized molecules such as melatonin into the circulation. Although not directly photosensitive, pinealocytes in mammals indirectly receive neural signals from the eye conveying information regarding the day–night cycle (Kappers, 1981; Korf *et al.*, 1998).

Stimulation of pineal secretion is dependent on the sympathetic innervation of the gland. This neural input to pinealocytes comes from the superior cervical ganglion. A daily rhythm in melatonin production is observed in many species, with darkness being stimulatory and light inhibitory to melatonin synthesis. It appears that melatonin has a role in the regulation of sleep and reproductive activities, although the precise mechanisms are not yet understood (Tamarkin *et al.*, 1985; Korf *et al.*, 1998).

Human Pineal Gland

Location and Structural Organization

The pineal gland in humans is a solid organ located in the midline roof of the third ventricle and joined by peduncles to the habenular commissure rostrally and posterior commissure caudally (Fig. 19.7A). From a dorsal aspect, it occupies a niche between the lobes of the superior colliculi. This cone-shaped structure of the epithalamus, which increases in size until the age of 2 years, is quite variable in size among individuals (Sumida *et al.*, 1996). It has the following dimensions: length 5–9 mm, width 3–8 mm, and thickness 2–4 mm (Kappers, 1962).

The pineal develops from a thickening of the ependyma around the pineal recess, a diverticulum of the thin roof of the dorsocaudal third ventricle. As it develops, two types of cells can be differentiated. These are small, fibrous cells that are thought to develop into astrocytic glial cells and larger cells with dark-staining nuclei that differentiate into pinealocytes by the eighth month of life (Kappers, 1962). A capsule derived from the pia also develops around the pineal anlage. From this connective tissue sheath there develop intrusions into the parenchyma that form septa breaking the organ into lobules (Tapp, 1979). Blood vessels and nerve fibers distribute within the pineal through these septa (Reyes, 1982). The central part of the human pineal is highly vascularized by sinusoidal capillaries, whereas its periphery is sparsely supplied with small, fine vessels (Duvernoy *et al.*, 2000). Its arterial sources are several pineal arteries branching from the medial posterior choroidal artery, whereas lateral pineal veins drain into the great cerebral vein of Galen (Duvernoy *et al.*, 2000).

Cellular Elements

With the development of the pineal to maturity, the pinealocyte, the cell intrinsic to this organ, becomes the major cell type. These cells, which are innervated and thought to be the major functional unit of the pineal, become arranged in cords or lobules of cells embedded in a matrix of neuroglia surrounded by the septa (Scharenberg and Liss, 1965). Pinealocytes having a large, round to oval nucleus, with a prominent nucleolus and scarcity of heterochromatin, are easily recognized and exhibit a number of cytoplasmic processes (Vollrath, 1984). These processes have been shown to be variable in length, narrow into fine strands, and possess club-shaped endings (del Rio Hortega, 1932; Scharenberg and Liss, 1965). There has been great interest from a functional point of view as to the sites where these club-shaped endings terminate. Vollrath (1984) suggested four terminal regions: the perivascular spaces, in the septa and capsule, between pinealocytes, and near calcified regions.

In regard to the glial cells found in the human pineal, astrocytes form a dense matrix enveloping the pinealocytes, perivascular areas, and septa. These cells are of the fibrous astrocyte type, and their long cytoplasmic processes are in close proximity with pinealocyte processes and fill much of the space between pinealocytes (Reyes, 1982). Ependymal cells of the pineal recess of the third ventricle cover the ventricular surface of the pineal.

Calcification and Cysts

An interesting aspect of pineal morphology is the presence of calcareous concretions (also termed acervuli, corpora arenacea, brain sand, pineal concrements, or psammoma bodies). These mulberry-like concretions, which consist mainly of hydroxyapatite and calcium phosphate, are found in the extracellular space of the parenchyma and septa (Reyes, 1982; Vollrath, 1984). There is great variability between individuals regarding the degree of calcification that occurs; however, concretions can be observed in the pineals of individuals of all age groups (Tapp and Huxley, 1971; von Heidel, 1965). Although this feature may occur in as many as 50% of children (von Heidel, 1965), its incidence increases with age and can be detected radiologically. The cause of pineal calcification is unknown; however, there is no evidence that pineal concretions diminish the secretory function of the pineal. Cysts are also commonly found in the pineal gland. It is considered that cysts with a lumen lined by ciliated ependymal cells are probably cutoff remnants of the original pineal diverticulum. Other cysts lined by neuroglial processes may be caused by degeneration of pineal tissue with a glial plaque surrounding a fluid-filled cyst (Kappers, 1962).

Neural Connectivity

Afferent Connections

The major neural input to the pineal gland comes from the peripheral nervous system. This is a sympathetic input from the superior cervical ganglion (Kappers, 1965). The innervation of the human pineal has been reviewed by Kenny (1985). These sympathetic fibers travel in the nervus conarii, which in humans is bilaterally represented, and enter the pineal at its posterior pole after coursing rostrally beneath the floor of the great cerebral vein of Galen from the dura mater of the tentorium cerebelli. Fibers of the nervus conarii enter the pineal at a number of sites on its posterior pole and extend through the septa and parenchyma of

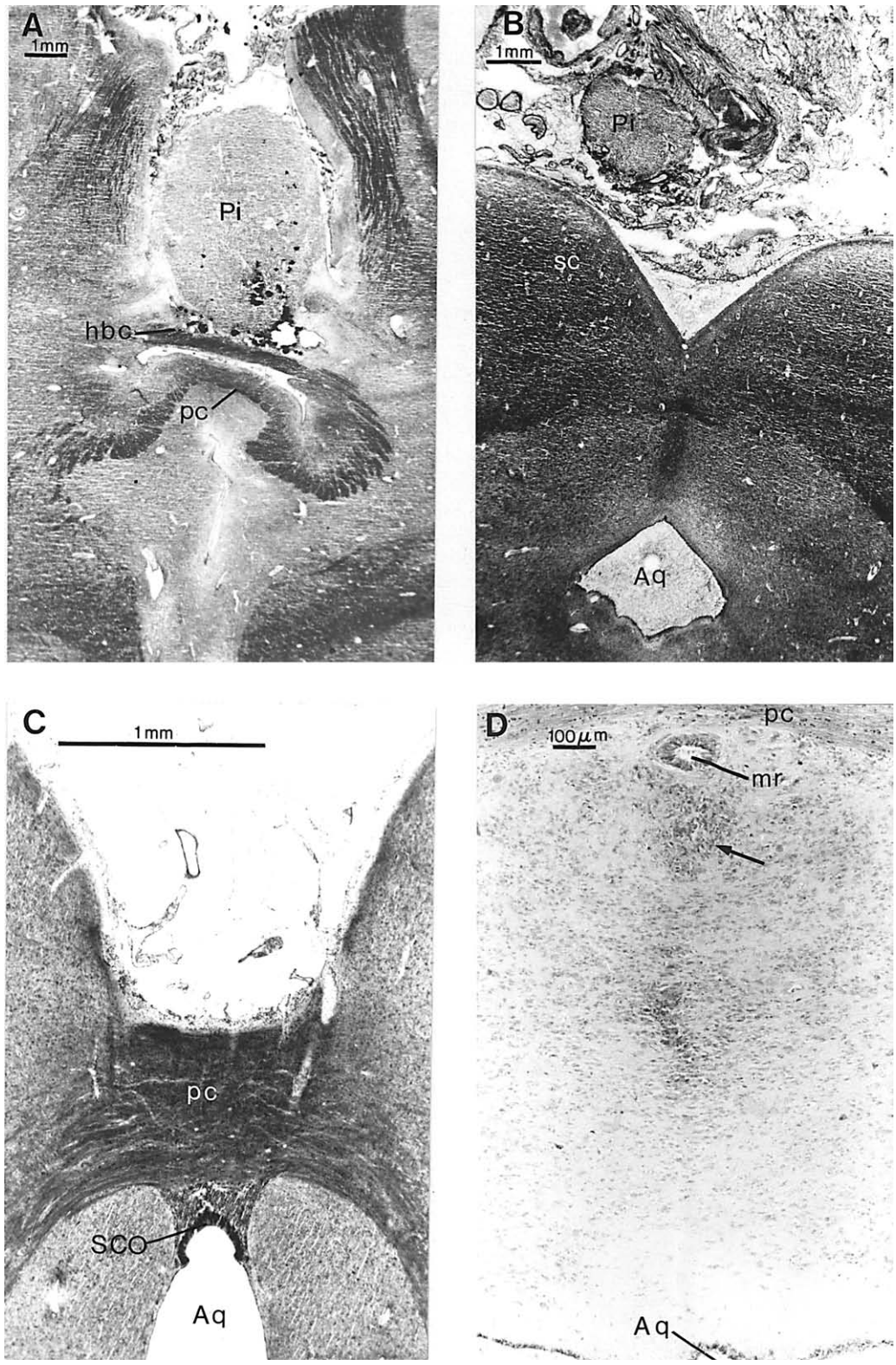

FIGURE 19.7 Coronal sections, stained with luxol fast blue and cresyl violet, through the pineal gland (Pi) of the human brain. **A** shows its attachment to the posterior (pc) and habenular commissures (hbc). **B** is a more caudal section with the superior colliculus (SC) evident. **(C)** Coronal section showing the subcommissural organ (SCO) of the sheep. **(D)** Coronal sections through the enclosed cavity of the mesocelic recess (mr) in an adult human brain. Possible remnants of SCO tissue are indicated by the arrow. Aq, aqueduct of Sylvius.

the gland (Kenny, 1965; Scharenberg and Liss, 1965).

The functional significance of the sympathetic innervation of the pineal and the central pathway linking it to the retina has been described in the rat by several investigators. By means of a series of lesions and knife cuts along the proposed pathway, they obtained evidence that signals from the retina are transmitted via the retinohypothalamic tract to the suprachiasmatic nuclei. From there, information is relayed to the hypothalamic paraventricular nucleus, then to the intermediolateral cell column of the spinal cord, where neurons innervate the superior cervical ganglion, which provides neural input to the pineal gland and its melatonin-secreting cells (Klein *et al.*, 1983; Moore and Klein, 1974; Pickard and Turek, 1983). This pathway has been confirmed and the cell groups involved more precisely defined by recent studies using the transneuronal viral tracer pseudorabies injected into the pineal of rats. The results show that the retinohypothalamic pathway to the suprachiasmatic nucleus is followed by synaptic relays in the dorsal, medial, and lateral parvocellular subdivisions of the hypothalamic paraventricular nucleus, intermediolateral nucleus, and central canal region of the upper thoracic spinal cord and superior cervical ganglion to provide the sympathetic innervation of the pineal (Larsen *et al.*, 1998; Teclamariam-Mesbah *et al.*, 1999). It is by this pathway that information regarding changes in the day–night cycle and seasonal alterations in illumination is transmitted from the eyes to the pineal gland to regulate melatonin secretion (Tamarkin *et al.*, 1985). There is also evidence that information regarding magnetic field changes is also relayed to the pineal from the eye (Olcese, 1990).

Direct input to the pineal originating in the CNS has also been reported from the habenular and posterior commissures (Korf and Moller, 1985). The sources of these fibers have been shown to be the paraventricular hypothalamic nucleus, medial and lateral habenular nuclei, posterior commissural nucleus, superior colliculi, and dorsal nucleus of the lateral geniculate (Guerillot *et al.*, 1982; Korf and Moller, 1985). Nerve fibers coming from the habenular and posterior commissures have also been observed to enter the pineal in humans (del Rio Hortega, 1932; Scharenberg and Liss, 1965).

The tracing studies using the neurotropic virus pseudorabies also produced evidence of a parasympathetic innervation of the pineal. Following infection of the pineal with pseudorabies virus in rats with bilateral superior cervical ganglionectomy, virally labeled neurons were observed in the sphenopalatine ganglion, nucleus of the solitary tract, and salivatory nucleus in the medulla oblongata, suggesting that these latter two medullary regions relayed signals to the pineal via the parasympathetic sphenopalatine ganglion (Larsen *et al.*, 1998). The presence of nerve cells in small (suggesting parasympathetic innervation) ganglia at the periphery of the human pineal has been reported by a number of investigators; neurons that were considered to be the origin of parasympathetic nerve fibers have also been reported in the primate (macaque) brain, the preganglionic parasympathetic fibers having traveled with the nervous conarii. However, such intrapineal neurons are rare in humans (Kenny, 1985).

SUBCOMMISSURAL ORGAN

General Characteristics and Comparative Studies

The term *subcommissural organ* was used by Dendy and Nicholls (1910) to designate a structure that they had observed in a number of mammalian species and that others had previously described in vertebrate classes ranging from cyclostomes to primates. In mammals, the subcommissural organ is situated on the rostral and ventral surfaces of the posterior commissure and forms the initial part of the midline dorsal roof of the aqueduct of Sylvius (Fig. 19.7C). The subcommissural organ is composed of modified ependymal cells that become elongated into a layer(s) of columnar epithelium. In some species, hypendymal cells situated in the subependymal tissue are also classified as part of this organ. Intimately associated with the subcommissural organ is Reissner's fiber, originally described as a threadlike structure that appears to originate as thin strands emanating from subcommissural cells into the cerebrospinal fluid and that aggregate to run caudally the entire length of the central canal of the spinal cord. Reissner's fiber is a noncellular aggregation of glycoproteins continuously secreted by the subcommissural cells (Gobron *et al.*, 1999; Sterba *et al.*, 1981). Although devoid of neuronal somata, ependymocytes of this organ may be neurally innervated (Oksche, 1962; Wiklund *et al.*, 1977). Many investigators have been impressed by the secretory aspect of the subcommissural organ, and such innervation may regulate glandular activity at both apical and basal surfaces of the ependymal cells. While there have been many propositions regarding the function of the subcommissural organ and Reissner's fiber, its function is still the subject of speculation. One of the more widely held views is that the molecules secreted in Reissner's fiber have a role in guiding the development of the brain and spinal cord.

Duvernoy and Koritke (1964, 1969a) studied the vascular arrangement of the subcommissural organ and reported that there is large variability between species. Some animals, including dog, cat, and monkey, have a richly vascularized subcommissural organ whereas others, such as rabbit, have only low vascular density. In the former case, a hypendymal capillary network extending along the organ arises from small arteries branching from the posterior cerebral arteries. These capillaries are extensively linked and may be in contact with the base of the columnar ependymal cells of the organ. Large capillary dilatations and occasionally capillary loops are observed. Venous drainage is mainly by way of a large vein on each side of the lateral wall of the third ventricle which drains other regions such as the habenula nuclei and which may join the great cerebral vein of Galen. A few vascular links with the pineal vessels have also been observed (Duvernoy and Koritke, 1969a).

Human Subcommissural Organ

Location and Structural Organization

Unlike other mammals, the human subcommissural organ is only clearly evident in the fetus and newborn. In the adult it has almost completely disappeared, although remnants of this tissue have been observed by some authors (Gilbert, 1960; Oksche, 1961; Galarza, 2002). There are no reports of Reissner's fiber in the adult human brain and only one report of it in a human fetus (Keene and Hewer, 1935), but there are suggestions that glycoprotein components of Reissner's fiber such as SCO-spondin are conserved in the human genome (Gobron *et al.*, 1999). The subcommissural organ has been discerned in the embryo as early as the second month of gestation in a 27–mm embryo (Castaneyra-Perdomo *et al.*, 1985; Keene and Hewer, 1935). In older fetuses, the subcommissural organ extends from the infrapineal recess caudally along the dorsolateral wall of the roof of the aqueduct of Sylvius to the mesocelic recess. It consists of elongated columnar ependymal cells that are found in the midline roof of the third ventricle around the posterior commissure and extend caudally as far as and including the mesocelic recess, which is a dorsal invagination of the aqueduct of Sylvius with blind-ending pockets in some instances. This recess is found immediately caudal to the posterior commissure in the fetal human brain, and most authors have considered its columnar ependymal cells to be part of the subcommissural organ (Castaneyra-Perdomo *et al.*, 1994; Dendy and Nicholls, 1910; Keene and Hewer, 1935; Rakic, 1965). This point is significant when considering the subcommissural organ in the adult brain because it has been proposed that the only remnant of this organ is the tissue that surrounds a vestige of the mesocelic recess (Dendy and Nicholls, 1910; Galarza, 2002). The mesocelic recess is prominent in the fetus but has virtually disappeared by the second year of life (Rakic, 1965). Dendy and Nicholls (1910) reported finding an irregular midline cavity with no opening to the aqueduct of Sylvius in the tissue over the caudal part of the posterior commissure. They regarded it as the blind termination of the mesocelic recess, the opening to the aqueduct having previously closed. Dendy and Nicholls (1910) reported that columnar ependymal cells of the subcommissural type lined this cavity. Although there are few other similar reports, we have observed such a mesocelic cavity in the adult brain (Fig. 19.7D), and Keene and Hewer (1935) presented evidence that epithelial cells plug the mesocelic recess to variable degrees, possibly leaving cavities in some instances. Rakic (1965) in a study of more than 300 cerebrums remarked on the great variability in size, configuration, and degree of regression of the mesocelic recess over the course of gestation; however, it had all but disappeared 1 year after birth. After this time, the midline ependymal lining of the infrapineal recess and the roof of the aqueduct of Sylvius below the posterior commissure is no longer of the elongated columnar type, and it appears that the subcommissural organ has almost completely regressed.

AREA POSTREMA

General Characteristics and Comparative Studies

The most caudal of the CVOs, the area postrema, is located bilaterally in the medulla oblongata in the walls of the fourth ventricle. In most mammalian species (carnivores, ruminants, and primates), it has the appearance of two convex humps bulging out from the lateral walls of the fourth ventricle. The two wings of the area postrema are positioned over the adjacent nucleus of the solitary tract and converge toward each other as the most posterior part of this CVO is reached at the obex (Fig. 19.8A). Two exceptions to this general description are the areas postrema of the rat and rabbit which, in coronal sections, take the form of a single midline quadrant of spongy tissue over the opening of the central canal. The area postrema is not present in fish or amphibians (Brizzee and Klara, 1984; Wilson, 1906; Wislocki and Putnam, 1920). It has a modified ependyma with few cilia, but some supraependymal cells. Although it was originally suggested that

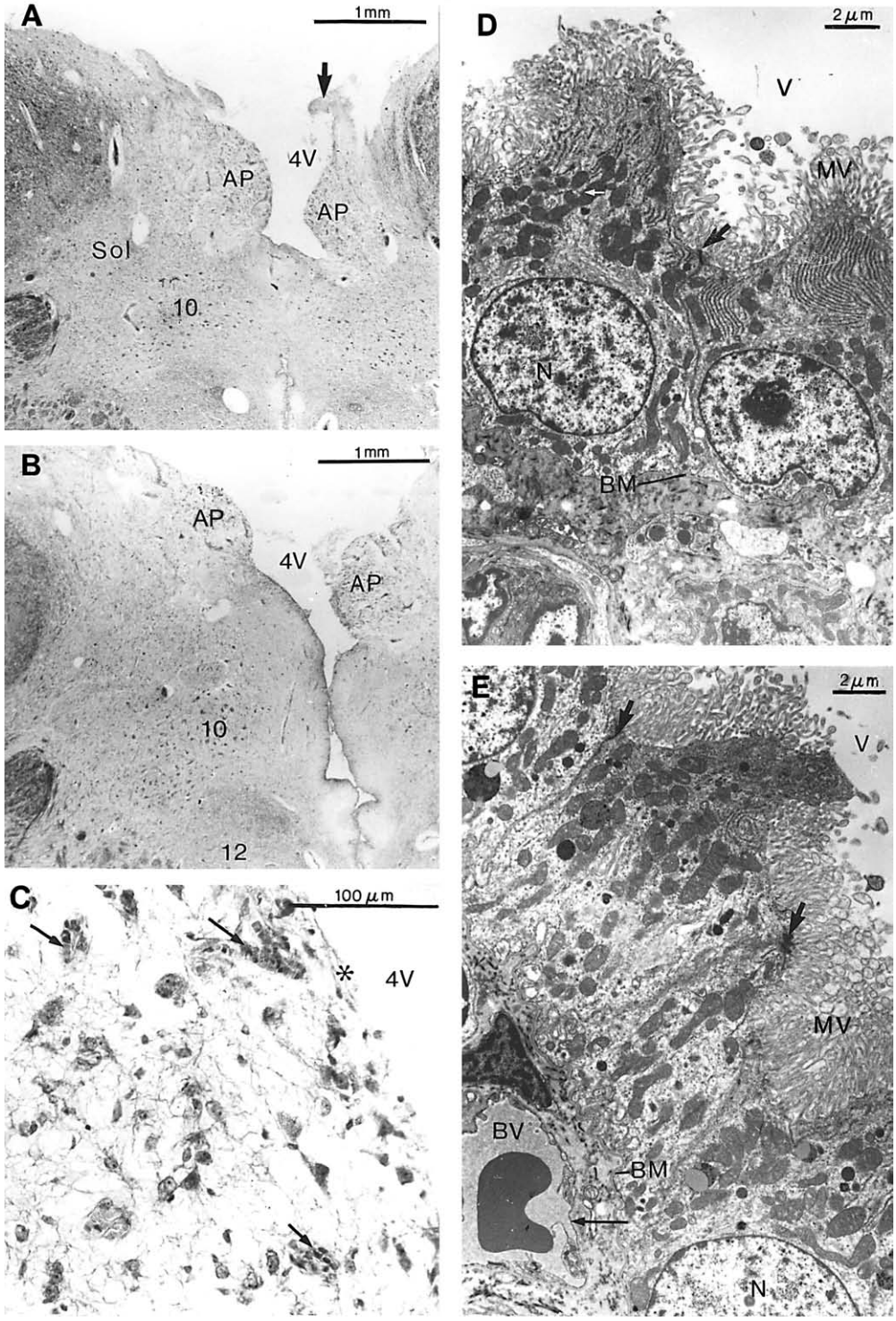

FIGURE 19.8 Low-power photomicrographs of coronal sections, stained with luxol fast blue and cresyl violet, through the human area postrema. The section in **A** is more caudal than that in **B.** AP, area postrema; Sol, nucleus of solitary tract; 10, dorsal motor nucleus of the vagus; 12, hypoglossal nucleus; 4V, fourth ventricle. **(C)** High-power photomicrograph of the human area postrema. Asterisk denotes flattened ependyma, arrows indicate blood vessels. Note the loose network of glial processes and neuronal perikarya. **(D, E)** Transmission electron micrographs of the choroid plexus of a cynomologous monkey. BM, basement membrane; BV, blood vessel; MV, microvilli; N, nucleus; V, ventricle. The thick black arrow in D indicates the zonula occludens, and the thin black arrow in E indicates a fenestrated blood vessel. Note the extensive rough endoplasmic reticulum *(large white arrow)* and mitochondria *(small white arrow)* in D.

neuronal perikarya were lacking in the area postrema of several species (Wislocki and Putnam, 1924), this proposition is no longer tenable. Neurons are situated in a mesh of astroglia, fibers, and numerous blood vessels, the latter exhibiting fenestrations in their endothelium, with two classes of capillaries identified in the rat area postrema (Gross, 1991).

Human Area Postrema

Location and Structural Organization

In humans the area postrema is found in the dorsomedial medulla oblongata and can be observed as two convex prominences bulging into the most caudal part of the fourth ventricle (Fig 19.8A). Longitudinally, the area postrema is a V-shaped structure diverging from an apex at the obex to a separation of 1.5–2 mm in a rostral direction while always overlying the nucleus of the solitary tract. Caudally, the area postrema can be observed bulging out from the lateral walls of the opening of the central canal. Rostrally, the bilateral prominences of the area postrema move dorsally and laterally in relation to the floor of the fourth ventricle (Fig. 19.8B) and at their lateral edges become attached to the pial membranes that form the roof of the ventricle and the tela choroidea. The human area postrema is immediately dorsal to the subpostremal nucleus, which separates the nucleus of the solitary tract proper from the area postrema (Hyde and Miselis, 1992). In the early 20th century, Wilson (1906) noted that there were variations in the human area postrema. In some individuals, the two wings of the area postrema coalesce to form the roof of the central canal, whereas in others there is no fusion of these wings. This latter situation is also observed in a number of animal species, e.g., monkey, sheep, and dog.

Cellular Elements

Morphologically, the area postrema shares many features with the subfornical organ and the OVLT, including rich vascularity, modified ependyma, and a network of neuroglia (Fig. 19.8C). The ependymal surface of the area postrema has been found to differ from the columnar ciliated ependyma of the adjacent ala cinerea in most species. In humans, ependymal cells of the area postrema are flattened to resemble a mesothelium or squamous epithelium, exhibiting few if any cilia (Kuhlenbeck, 1955). The body of this CVO consists of a loose network of neuroglia through which many blood vessels course (Fig. 19.8C). Prominent among the vascular profiles are arterioles with thickened perivascular sheaths of vascular smooth muscle and thin-walled veins or sinusoids (Cammermeyer, 1947b; Wilson, 1906; Wislocki and Putnam, 1920). The ventral boundary of the area postrema with the nucleus of the solitary tract is marked by a prominent array of glial cells, the funiculus separans of Retzius (Wislocki and Putnam, 1920). Fibroblasts and neuroglia occur throughout the area postrema, and Cammermeyer (1947b) reported that mast cells close to the ependyma can be detected with particular staining techniques in the human area postrema.

Although there has been some doubt expressed regarding the presence of neurons in the area postrema (Wislocki and Putnam, 1924), most authors now consider that neuronal profiles occur throughout the region, with their shape and size varying greatly (Cammermeyer, 1947b). Olszewski and Baxter (1982) noted that their appearance altered with age. In children, these cells had little or no cytoplasm around darkly stained, rounded or oval nuclei although a few cells with large clear nuclei were observed with some cytoplasm. In older subjects, more cells with cytoplasm are distinguishable and the ovoid-to-round nuclei tend to be eccentrically placed near the periphery of one side of the cell. In adults, black melanin pigment (in unstained sections) accumulates in the cytoplasm of nearly all neurons, but this is rarely seen in infants or children (Cammermeyer, 1947b).

Vasculature

The area postrema is supplied by a number of thin slender arteries coming from the pyramidal branches of the posterior inferior cerebellar arteries that run along the lateral edge of the area postrema and send arterioles across it to form a rich capillary bed (Wislocki and Putnam, 1920). This capillary bed is extensively linked with capillary loops, tufts, and tendrils and wide sinusoidal vessels. Some of these vessels reach close to the ependymal surface of the ventricle. The capillary bed drains into longitudinally running veins along the mesial edge. It is doubtful whether any vascular connections with the choroid plexus of the fourth ventricle are formed (Cammermeyer, 1947b; Duvernoy and Koritke, 1969b).

Neural Connectivity

Afferent Connections

Details of the neural connections associated with the area postrema come from studies in rats that have examined anterograde and retrograde transport of horseradish peroxidase and its conjugates, and these details are summarized in Table 19.3. The area postrema receives some innervation from the lateral parabrachial nucleus and from the caudal nucleus of the solitary tract (Shapiro and Miselis, 1985; van der Kooy and Koda, 1983). In addition, Hosoya and Matsushita (1981)

TABLE 19.3 Direct Neural Connections of the Area Postrema

Efferents (terminal fields listed)	Afferents (Origins listed)	Ref.
Hypothalamus		
	Paraventricular n.	Shapiro & Miselis, 1985
	Dorsomedial hypothalamic n.	Shapiro & Miselis, 1985
	Perifornical region	Shapiro & Miselis, 1985
Midbrain		
Lateral parabrachial n.	Lateral parabrachial n.	van der Kooy & Koda, 1983; Shapiro & Miselis, 1985; Herbert *et al.*, 1991; Cunningham *et al.*, 1994
Periaqueductal gray		Shapiro & Miselis, 1985
Mesencephalic n. 5th nerve		
Pericentral dorsal tegmental n.		van der Kooy & Koda, 1983
Dorsal tegmental n.		van der Kooy & Koda, 1983
Cerebellum		Shapiro & Miselis, 1985
Hindbrain		
N. of the solitary tract	N. of the solitary tract (NTS)	Shapiro & Miselis, 1985; Cunningham *et al.*,1994
Dorsal motor vagal n.		Shapiro & Miselis, 1985
Ambiguus n.		Shapiro & Miselis, 1985
A1 region of the caudal ventrolateral medulla	Shapiro & Miselis, 1985	
Rostral ventrolateral medulla		Blessing *et al.*, 1987; Badoer *et al.*, 1994
Paratrigeminal n.		Shapiro & Miselis, 1985
Spinal trigeminal n.		Shapiro & Miselis, 1985

produced evidence of diencephalic projections to the area postrema. These projections have been precisely mapped by Shapiro and Miselis (1985), who show that a group of neurons in the lateral parvocellular subnucleus of the paraventricular hypothalamic nucleus as well as in the subadjacent dorsomedial nucleus and perifornical area project to the area postrema. This CVO also receives a small number of direct peripheral inputs from the vagus, glossopharyngeal, and trigeminal nerves (Beckstead and Norgren, 1979; Kalia and Welles, 1980; Miselis *et al.*, 1987).

Efferent Connections

In regard to its efferent pathways, the area postrema has axonal contact with a number of other medullary regions including the neighboring nucleus of the solitary tract, the ambiguus nucleus, the noradrenergic neurons of the caudal ventrolateral medulla, spinal trigeminal nucleus, and paratrigeminal nucleus and midbrain periaqueductal gray. There are other connections to the cerebellar vermis and dorsolateral tegmental nucleus of the pons, and a particularly strong projection to the dorsal lateral parabrachial nucleus (Shapiro and Miselis, 1985).

Function

From a functional viewpoint, there is still considerable speculation as to the precise role of the area postrema. It has long been considered that this CVO may be a chemoreceptor trigger zone for vomiting (Borison and Brizzee, 1951). Ablation of the area postrema in animals also interferes with the taste aversions which become associated with nausea-producing stimuli (Berger *et al.*, 1973; Coil and Norgren, 1981). More recently, evidence has accrued suggesting that 5-HT_3 receptors in the area postrema have a role in vomiting and nausea, and it is blockade of these receptors (by agents such as odansetron) in the area postrema as well as on vagal afferent neurons that is effective in reducing the nausea associated with cancer chemotherapy (Miller and Leslie, 1994; Tyers and Freeman, 1992). Like the OVLT, subfornical organ, and median eminence, there is evidence that the area postrema may be a site of action of blood-borne angiotensin II, particularly with regard to centrally mediated cardiovascular effects of angiotensin II (Joy and Lowe, 1971), which may reset the baroreceptor reflex to a higher level of arterial pressure (Bishop and Sanderford, 2000). Although there are binding sites for angiotensin II in the area postrema of the rat and dog (Mendelsohn *et al.*, 1984; Speth, 1985), in the human area postrema, binding sites for angiotensin II were undetectable (Allen *et al.*, 1988), suggesting that it may not be a receptor zone for angiotensin II in humans. Vasopressin is another peptide hormone that has been shown to bind to the area postrema of the rat (Phillips *et al.*, 1988), and recent experimental evidence suggests

that the area postrema may be the central site at which blood-borne vasopressin acts to cause sympatho-inhibition and facilitate the baroreflex (Undesser *et al.*, 1985; Hasser *et al.*, 2000). Other effects consequential to the production of lesions in the area postrema of rats are loss of body weight, altered appetite, and altered sodium and water intake and excretion (Miselis *et al.*, 1987). Such results have not yet permitted a clear delineation of the exact roles which the area postrema may play in homeostatic mechanisms regulating fluid and electrolyte balance. However, its unique position in the medulla oblongata at the point of entry of visceral sensory information and lack of a blood–brain barrier exposing it to circulating humoral factors give the area postrema the potential to integrate or modulate homeostatic responses (Miselis *et al.*, 1987). In relation to some of the humoral or neurochemical agents which may influence area postrema functions, the rat area postrema displays binding sites for tritiated amino-clonidine, substance P, vasoactive intestinal polypeptide, bradykinin, cholecystokinin, opiates, atrial natriuretic peptide, somatostatin, neuropeptide, pancreatic poly-peptide, calcitonin, and insulin (Chen *et al.*, 2000; Gibson *et al.*, 1986; Helke *et al.*, 1984; Hilton *et al.*, 1995; Martel *et al.*, 1986; Moran *et al.*, 1986; Patel *et al.*, 1986; Shaffer and Moody, 1986; Tranh *et al.*, 1996; Walmsley *et al.*, 1982). In addition, immunohistochemistry has revealed noradrenaline-, enkephalin-, serotonin-, and cholecystokinin-containing neurons and adrenaline-, noradrenaline-, amylin-, and substance P-containing afferent fibers in the rat area postrema (Armstrong *et al.*, 1981; D'Este *et al.*, 2000; Lanca and van der Kooy, 1985; Newton and Maley, 1985). In the human area postrema, galanin, substance P, CGRP, dynorphin B, cholecystokinin, and neurophysin have been immuno-histochemically identified in nerve fibers (Fodor *et al.*, 1994; Unger and Lange, 1991), and serotonin in neuronal cell bodies (Azmitia *et al.*, 1991). In addition, muscarinic cholinergic and 5-HT_3 serotonergic receptor binding sites have been identified in the human area postrema (Hyde *et al.*, 1988; Ohuoha *et al.*, 1994). The 5-HT_3 receptors may be of relevance to the induction of nausea and vomiting (Ohuoha *et al.*, 1994). Finally, neurons sensitive to glucose and sodium have been identified in the area postrema by means of electro-physiological techniques (Adachi and Kobaski, 1985).

CHOROID PLEXUS

The choroid plexus has also been classified as a CVO (Hofer, 1958; Kuhlenbeck, 1970) and will be briefly considered here. Found in the body, collateral trigone, and inferior horn of the lateral ventricle (Fig. 19.2), the roof of the third ventricle (Fig. 19.3A), and also in the fourth ventricle, the choroid plexus has somewhat different features from the other CVOs. In common with the other CVOs, it is made up of elements from the leptomeninges and the ependyma. Highly vascularized tela choroidea of the medial surface of the cerebrum evaginates and acquires an epithelium to form the choroid plexus. The commonly accepted role of the choroid plexus in the formation of a major portion of cerebrospinal fluid (CSF) may be only one of a number of functions of this CVO (Davson, 1967; McComb, 1983).

When the morphological features of the choroid plexus are examined, the enormous surface area that results from the extensively folded surface and microvilli (Fig. 19.8D) of this tissue is consistent with a reabsorptive function as well as a secretory role (McComb, 1983). In addition to the transport of ions and water into the CSF, there is evidence that molecules such as thyroid hormones, leptin, and insulin-like growth factor I are also transported into the CSF from blood (Banks *et al.*, 1996; Schreiber *et al.*, 1990; Walter *et al.*, 1999). The choroid plexus consists of a core of vascularized connective tissue that is interfaced with an epithelium of low columnar or cuboidal cells by a basement membrane at their abluminal surface (Fig. 19.8D). The "capillaries" of this tissue have larger diameters (10–20 μm) than regular capillaries and have been designated as sinusoids (Kuhlenbeck, 1970). At an ultrastructural level, fenestrations can be seen in the vascular endothelium. Large spherical nuclei, microvilli at the luminal surface, abundant mito-chondria, and tight junctions (zonula occludens) between adjacent cells characterize the choroid epithelial cells (Fig. 19.8E).

The choroid plexus of several mammals, including primates, is innervated by cholinergic (from the vagus nerve) and adrenergic (from the superior cervical ganglion) nerves. Some nerve endings are associated with blood vessels whereas others may end at epithelial cells (Edvinsson *et al.*, 1974; Kuhlenbeck, 1970; Lindvall *et al.*, 1977). A number of peptides have been identified by immunohistochemical techniques in these nerve endings. They include substance P and vasoactive intestinal polypeptide (Edvinsson *et al.*, 1983).

In addition to these neurally derived peptides in the choroid plexus, many other peptides may be synthe-sized in the epithelial cells of the choroid plexus. These may be either secreted into the CSF for transport to cerebral targets, or act as local paracrine factors, a function supported by the presence of many peptide receptors within the choroid plexus (Chodobski and Szmydynger-Chodobska, 2001).

References

Adachi, A., and Kobashi, M. (1985). Chemosensitive neurons within the area postrema of the rat. *Neurosci. Lett.* **55,** 137–140.

Åkert, K., Potter, H. D., and Anderson, J. W. (1961). The subfornical organ in mammals. *J. Comp. Neurol.* **116,** 1–14.

Allen, A. M., Chai, S. Y., Clevers, J., McKinley, M. J., Paxinos, G., and Mendelsohn, F. A. O. (1988). Localization and characterization of angiotensin II receptor binding and angiotensin converting enzyme in the human medulla oblongata. *J. Comp. Neurol.* **269,** 249–264.

Allen, A.M., Oldfield, B.J., Giles, M.E., Paxinos, G., McKinley, M.J., and Mendelsohn, F.A.O. (2000). Localization of angiotensin receptors in the nervous system. *In* "Handbook of Chemical Neuroanatomy, Vol 16: Peptide Receptors, Part I" (R. Quirion, A. Bjorklund, and T. Hokfelt, eds.), pp. 79–124. Elsevier Science, Amsterdam.

Alm, P., Skagerberg, G., Nylen, A., Larsson, B., and Andersson, K.E. (1997). Nitric oxide synthase and vasopressin in rat circumventricular organs. An immunohistochemical study. *Exp. Brain Res.* **117,** 59–66.

Armstrong, D. M., Pickel, V. M., Joh, T. H., Reis, D. J., and Miller, R. J. (1981). Immunocytochemical localization of catecholamine synthesizing enzymes and neuropeptides in area postrema and medial nucleus tractus solitarius of rat brain. *J. Comp. Neurol.* **196,** 505–517.

Azmitua, E.C., and Whitaker-Azmitua P.M. (1991). Awakening the sleeping giant: anatomy and plasticity of the brain serotonergic system. *J. Clin. Psychiatry* **52 Suppl,** 4–16.

Badoer, E., McKinley, M.J., Oldfield, B.J., and McAllen, R.M. (1994). Localization of barosensitive neurons in the caudal ventrolateral medulla which project to the rostral ventrolateral medulla. *Brain Res.* **657,** 258–268.

Banks, W.A., Kastin, A.J., Huang, W., Jaspan, J.B., and Maness, L.M. (1996). Leptin enters the brain by a saturable system independent of insulin. *Peptides* **17,** 305–311.

Barry, J., and Carette, B. (1975). Immunofluorescence study of LRF neurons in primates. *Cell Tissue Res.* **164,** 163–178.

Beckstead, R. M., and Norgren, R. (1979). An autoradiographic examination of the central distribution of the trigeminal, facial, glossopharyngeal and vagal nerves in the monkey. *J. Comp. Neurol.* **184,** 455–472.

Behnsen, G. (1927). Uber die Farbstoffspeicheruing im Zentralnervensystem der weissen Maus in verschiedenen Alterszustanden. *Z. Zeliforsch. Mikrosk. Anat.* **4,** 515–572.

Berger, B. D., Wise, C. D., and Stein, L. (1973). Area postrema damage and bait shyness. *J. Comp. Physiol. Psychol.* **82,** 475–479.

Bergland, R. M., and Torack, R. M. (1969). An electron microscopic study of the human infundibulum. *Z. Zellforsch. Mikrosk. Anat.* **99,** 1–12.

Bishop, V.S., and Sanderford, M.G. (2000). Angiotensin II modulation of the arterial baroreflex: role of the area postrema. Clin. *Exp. Pharmacol. Physiol.* **27,** 428–431.

Blatteis, C. M., Bealer, S. L., Hunter, W. S., Llanos-O. J., Ahokas, R. A., and Mashburn, T. A. (1983). Supression of fever after lesions of the anteroventral third ventricle in guinea pigs. *Brain Res. Bull.* **11,** 519–526.

Blatteis, C. M., Hales, J. R. S., McKinley, M. J., and Fawcett, A. A. (1987). Role of anteroventral third ventricle region in fever in sheep. Can. *J. Physiol. Pharmacol.* **65,** 1255–1260.

Blessing, W.W., Hedger, S.C., Joh, T.H., and Willoughby, J.O. (1987). Neurons in the area postrema are the only catecholamine-synthesizng cells in the medulla or pons with projections to the rostral ventrolateral medulla (C1 – area) in the rabbit. *Brain Res.* **419,** 336–340.

Borison, H. L., and Brizzee, K. R. (1951). Morphology of emetic chemoreceptor trigger zone in cat medulla. *Proc. Soc. Exp. Biol. Med.* **77,** 38–42.

Brizzee, K. R., and Klara, P. M. (1984). The structure of the mammalian area postrema. *Fed. Proc. Fed. Am. Soc. Exp. Biol.* **43,** 2944–2948.

Broadwell, R. D., and Brightman, M. W. (1976). Entry of peroxidase into neurons of the central and peripheral nervous systems from extracerebral blood. *J. Comp. Neurol.* **166,** 257–284.

Camacho, A., and Phillips, M. L. (1981). Horseradish peroxidase study in rat of the neural connections of the organum vasculosum of the lamina terminalis. *Neurosci. Lett.* **25,** 201–204.

Cammermeyer, J. (1947a). Deposition of iron in paraventricular areas of the human brain in haemochromatosis. *J. Neuropathol. Exp. Neurol.* **6,**111–127.

Cammermeyer, J. (1947b). Is the area postrema a neurovegetative nucleus. *Acta Anat.* **2,** 294–319.

Castaneyra-Perdomo A., Meyer, G., and Ferres-Torres, I. (1985). The early development of the human subcommissural organ. *J. Anat.* **143,** 195–200.

Castanreyra-Perdomo, A., Meyer, G., and Heylings, D.J. (1992). Early development of the human area postrema and subfornical organ. *Anat. Rec.* **232,** 612–619.

Castaneyra-Perdomo A., Meyer, G., Carmono-Calero E., Banuelos-Pineda, J., Mendez-Medina R., Ormazabal-Ramos, C., and Ferres-Torres, I. (1994).

Chai, S.Y., McKenzie, J.S., McKinley, M.J., and Mendelsohn, F.A.O. (1990). Angiotensin converting enzyme in the human basal forebrain and midbrain visualized by *in vitro* autoradiography. *J. Comp. Neurol.* **291,** 179–194, 1990.

Chen, E.Y., Emerich, D.F., Bartus, R.T., and Kordower, J.H. (2000). B2 bradykinin receptor immunoreactivity in rat brain. *J Comp. Neurol.*

Chodobski, A., and Szmydynger-Chodobska, J. (2001). Choroid plexus: target for polypeptides and site of their synthesis. *Microsci. Res. Tech.* **52,** 65–82.

Ciriello, J., Rosas-Arellano, M.P., and Solano-Flores, L.P. (1996). Direct projections to subfornical organ from catecholaminergic neurons in the caudal nucleus of the solitary tract. *Brain Res.* **726,** 227–232.

Clarke, I.J. (1996). Effector mechanisms of the hypothalamus that regulate the anterior pituitary gland. *In* "The Autonomic Nervous System" (K. Unsicker, ed.), pp 45–88. Harwood, London.

Clarke, I.J., Cummins, J.T., and de Kretser, D.M. (1983). Pituitary gland function after disconnection from direct hypothalamic influences in the sheep. *Neuroendocrinology* **36,** 376–384.

Clarke, I.J., Jessop, D.S., Millar, R.P., Morris, M., Bloom, S.R., Lightman, S.L., Coen, C., Lew, R.A., and Smith, A.I. (1993). Many peptides that are present in the external zone of the median eminence are not secreted into the hypophysial portal blood of sheep. *Neuroendocrinol.* **57,** 765–775.

Cunningham, E.T., Miselis, R.R., and Sawchenko. P.E. (1994). The relationship of efferent projections from the area postrema to vagal motor and brain-stem catecholamine-containing cell groups: an axonal transport and immunohistochemical study in the rat. *Neuroscence* **58,** 635–648.

Daniel, P. M., and Pritchard, M. M. L. (1975). Studies of the hypothalamus and the pituitary gland with special reference to the effects of transection of the pituitary stalk. *Acta Endocrinol. (Copenhagen)* **80,** Suppl. 201, 1–210.

Daniel, P.M., and Pritchard, M.M.L. (1975). "Studies of the Hypothalamus and the Pituitary Gland with Special Reference to the Effects of Transection of the Pituitary Stalk." Alden Press, Oxford.

Davson, H. (1967). "Physiology of the Cerebrospinal Fluid." Churchill, London.

Defendini, R., and Zimmerman, E. A. (1978). The magnocellular neurosecretory system of the mammalian hypothalamus. *Res. Publ. Assoc. Res. Nerv. Ment. Dis.* **56,** 137–154.

Dellman, H.D. (1998). Structure of the subfornical organ: a review. *Microsci. Res. Tech.* **41,** 85–97.

Dellman, H. D., and Simpson, J. B. (1979). The subfornical organ. *Int. Rev. Cytol.* **58,** 333–421.

del Rio Hortega, P. (1932). Pineal gland. *In* "Cytology and Cellular Pathology of the Nervous System" (W Penfield, ed.), pp. 637–703. Harper (Hoeber), New York.

Dendy, A., and Nicholls, G. E. (1910). On the occurrence of a mesocoelic recess in the human brain, and its relation to the subcommissural organ of lower vertebrates; with special reference to the distribution of Reissner's fiber in the vertebrate series and its function. *Proc. R. Soc. London, Ser. B.* **82,** 515–529.

Donovan, B.T. (1978). The portal vessels, the hypothalamus and the control of reproductive function. *Neuroendocrinology* **25,** 1–21.

Duvernoy, H. (1972). The vascular architecture of the median eminence. *In* "Brain Endocrine Interaction" (K. M. Knigge, D. E. Scott, and A. Weindl, eds.), pp. 79–108. Karger, Basel.

Duvernoy, H., and Koritke, J. G. (1964). Contribution a etude de angioarchitectonic des organes circumventriculaires. *Arch. Biol.* **75,** Suppl., 849–904.

Duvernoy, H., and Koritke, J. G. (1969a). The vascular architecture of the subcommissural organ. *In* "Zirkumventrikulare Organe und Liquor" (G. Sterba, ed.), pp. 41–43. Fischer, Jena.

Duvernoy, H., and Koritke, J. G. (1969b). Concerning the relationships of the circumventricular organs and their vessels with the cavity of the ventricles. *In* "Zirkumventrikulare organe und liquor" (G. Sterba, ed.), pp. 113–115. Fischer, Jena.

Duvernoy, H., Koritke, J. G., and Monnier, G. (1969). Sur la vascularisation de la lame terminale humaine. *Z. Zeliforsch. Mikrosk. Anat.* **102,** 49–77.

Duvernoy, H.M., Paratte, B., Tatu, L., and Vuiller, F. (2000). The human pineal gland: relationships with surrounding structures and blood supply. *Neurol. Res.* **22,** 747–790.

Edvinsson, L. Nielsen, K. C. Owman, C., and West, K. A. (1974). Adrenergic innervation of the mammalian choroid plexus. *Am. J. Anat.* **139,** 299–308.

Edvinsson, L., Rosendal-Helgesen, S., and Voldman, R. (1983). Substance P: localization, concentration and release in cerebral arteries, choroid plexus and dura mater. *Cell Tissue Res.* **234,** 1–7.

Eriksson, A., Liu, C., Hart, R.P., and Sawchenko, P.E. (1995). Type 1 interleukin-1 recptor in rat brain: distribution, regulation and relationship to sites of IL-1 induced cellular activation. *J. Comp. Neurol.* **361,** 681–698.

Ferguson, A.V., and Bains, J.S. (1997). Electrophysiology of the circumventricular organs. *Front Neuroendocrinol.* **17,** 440–475.

Ferguson, A. V., Day, T. A., and Renaud, L. P. (1984a). Subfornical organ efferents influence the excitability of neurohypophysial and tuberoinfundibular paraventricular nucleus neurons in the rat. *Neuroendocrinology* **39,** 423–428.

Ferguson, A. V, Day, T A., and Renaud, L. P. (1984b). Subfornical organ stimulation excites paraventricular neurones projecting to dorsal medulla. *Am. J. Physiol.* **247,** R1088–R1092.

Flerko, B. (1980). The hypophysial portal circulation today. *Neuroendocrinology* **30,** 56–63.

Galarza, M. (2002). Evidence of the subcommissural organ in humans and its association with hydrocephalus. *Neurosurg. Rev.* **25,** 205–215.

Ganten, D., Hutchinson, J. S., Schelling, P., Ganten, U., and Fischer, H. (1976). The isorenin angiotensin systems in extrarenal tissue. Clin. *Exp. Pharmacol. Physiol.* **3,** 103–126.

Gibson, T. R., Wildey, G. M., Manaker, S., and Glembotski, C. C. (1986). Autoradiographic localization and characterization of atrial natriuretic peptide binding sites in the rat central nervous system and adrenal gland. *J. Neurosci.* **6,** 2004–2011.

Gilbert, G. J. (1960). The subcommissural organ. *Neurology* **10,** 138–142.

Giles, M.E., Fernley, R.T., Nakamura, Y., Moeller, I., Aldred, G.P., Ferraro, T., Penschow, J.D., McKinley, M.J., and Oldfield, B.J. (1999). Characterisation of a specific antibody to the rat angiotensin II AT1 receptor. *J. Histochem. Cytochem.* **47,** 507–516.

Gobron, S., Creveaux, I., Meiniel, R., Didier, R., Dastugue, B., and Meiniel, A. (1999). SCO-spondin is evolutionary conserved in the central nervous system of the caudate phylum. *Neuroscience* **88,** 655–664.

Green, H. T. (1957). The venous drainage of the human hypophysis cerebri. *Am. J. Anat.* **100,** 435–469.

Gross, P.M. (19xx). Morphology and physiology of capillary systems in subregion of the subfornical organ and area postrema. Can. *J. Physiol. Pharmacol.* **69,** 1010–1025.

Gu, G.B., and Ju, G. (1995). The parabrachio-subfornical organ projection in the rat. *Brain Res. Bull.* **38,** 41–47.

Gu, G.B., and Simerly, R.B. (1997). Projections of the sexually dimorphic anteroventral periventricular nucleus in the female rat. *J. Comp. Neurol.* **384,** 142–164.

Guerillot, C., Pfister, A., Muller, L., and De Lage, C. (1982). Récerche d'origine des fibers nerveuses extraorthosympathetiques innervant épiphyse du rat (étude du transport retrograde de la peroxidase de Raifort). *Reprod. Nutr. Dev.* **22,** 371–378.

Hasser, E.M., Cunningham, J.T., Sullivan, M.J., Curtis, K.S., Blaine, E.H., and Hay, M. (2000). Area postrema and sympathetic nervous system effects of vasopressin and angiotensin II. *Clin. Exp. Pharmacol. Physiol.* **27,** 432–436.

Haywood, J. R., Fink, G. D., Buggy, J, Phillips, M. L., and Brody, M. J. (1980). The area postrema plays no role in the pressor action of angiotensin in the rat. *Am. J. Physiol.* **239,** H108–H113.

Heike, C. J., Shults, C. W, Chase, T. N., and O'Donohue, T. L. (1984). Autoradiographic evidence of substance P receptors in rat medulla: effect of vagotomy and nodose ganglionectomy. *Neuroscience* **13,** 215–223.

Herbert, H., Moga, M.M., and Saper, C.B. (1991). Connections of the parabrachial nucleus with the nucleus of the solitary tract and the medullary reticular formation of the rat. *J. Comp. Neurol.* **293,** 540–58-.

Hernesniemi, L., Kawana, E., Bruppacher, H., and Sandri, C. (1972). Afferent connections of the subfornical organ and supraoptic crest. *Acta Anat.* **81,** 321–326.

Hilton, J.M., Chai, S.Y., and Sexton, P.M. (1995). *In vitro* auroradiographic localization of the calcitonin receptor isoforms, C1a and C1b, in rat brain. *Neuroscience* **69,** 1223–1237.

Hofer, H. (1957). Circumventrikulare organe des Zwischenhirns. *Primatologia* **2,** 1–104.

Hofer, H. (1958). Zur morphologie der circumventrikularen organe des zwischenhirns der saugeticre. *Verh. Dsch. Zoo. Ges.* **8,** 202–251.

Hosoya, Y., and Matsushita, M. (1981). A direct projection from the hypothalamus to the area postrema in the rat, as demonstrated by the HRP and autoradiographic methods. *Brain Res.* **214,** 144–149.

Hubschle T., McKinley, M.J., and Oldfield, B.J. (1998). Efferent connections of the lamina terminalis, the preoptic area and the insular cortex to submandibular and sublingual gland of the rat traced with pseudorabies virus. *Brain Res.* **806,** 219–231.

Hyde, T.M., and Miselis, R.R. (1992). Subnuclear organization of the human caudal nucleus of the solitary tract. *Brain Res. Bull.* **29:** 95–109.

Hyde, T.M., Gibbs, M., and Peroutka, S.J. (1988). Distribution of muscarinic cholinergic receptors in the dorsal vagal complex and other selected nuclei in the human medulla. *Brain Res.* **447,** 287–292.

Johnson, A. K. (1985). The periventricular anteroventral third ventricle (AV3V): its relationship with the subfornical organ and neural systems involved in maintaining body fluid homeostasis. *Brain Res. Bull.* **15,** 595–601.

Johnson, A.K., and Gross, P.M. (1993). Sensory circumventricular organs and brain homeostatic pathways. *FASEB J.* **7,** 678–686.

Joy, M. D., and Lowe, R. D. (1970). Abolition of the central cardiovascular effects of angiotensin by ablation of the area postrema. *Clin. Sci.* **39,** 3P.

Kalia, M., and Welles, R. V. (1980). Brain stem projections of the aortic nerve in the cat: a study using tetramethyl benzidine as the substrate for horseradish peroxidase. *Brain Res.* **188,** 23–32.

Kappers, J. A. (1962). Epiphysis. *In* "Correlative Anatomy of the Nervous Systern" (E. C. Crosby, T. Humphrey, and E. W Lauer, eds.), pp. 268–271. Macmillan, New York.

Kappers, J. A. (1965). Survey of the innervation of the epiphysis cerebri and the accessory pineal organs of the vertebrates. *Prog. Brain Res.* **10,** 87–153.

Kappers, J. A. (1981). A survey of advances in pineal research. *In* "The Pineal Gland" (R. J. Reiter, ed.), Vol. 1, pp. 1–26. CRC Press, Boca Raton.

Kawano, H., and Masuko, S. (2001). Tyrosine hydroxylase-immunoreactivity projections from the caudal ventrolateral medulla to the subfornical organ in the rat. *Brain Res.* **903,** 154–161.

Kawata, M., Nakao, K., Morii, N., Kiso, Y. Yamashita, H., Imura, H., and Sano, Y. (1985). Atrial natriuretic polypeptide: topographical distribution in the rat brain by radioimmunoassay and immunohistochemistry. *Neuroscience* **16,** 521–546.

Keene, M. E L., and Hewer, E. E. (1935). The human subcommissural organ and the mesocoelic recess in the human brain together with a note on Reissner's fiber. *J. Anat.* **69,** 501–507.

Kenny, G. C. T. (1965). The innervation of the mammalian pineal body (a comparative study). *Proc. Aust. Assoc. Neurol.* **3,** 133–140.

Kenny, G. C. T. (1985). Structural and ultrastructural analysis of the pineal in primates; its innervation. *In* "The Pineal Gland: Current State of Pineal Research" (B. Mess, Cs. Ruzsas, L. Tima, and P. Pevet, eds.), pp. 341–345. Elsevier, Amsterdam.

Klein, D.C., Smoot, R., Weller, J.L., Higa, S., Markey, S.P., Creed, G.J., and Jacowitz, D.M. (1983). Lesions of the paraventricular nucleus area of the hypothalamus disrupt the suprachiasmatic-spinal cord circuit in the melatonin rhythm generating system. *Brain Res. Bull.* **10,** 647–652.

Korf, H.-W., and Moller, M. (1985). The central innervation of the mammalian pineal gland. *In* "The Pineal Gland: Current State of Pineal Research" (B. Mess, Cs. Ruzsas, L. Tima, and P. Pevet, eds.), pp. 47–69. Elsevier, Amsterdam.

Korf, H-W., Schomerus, C., and Stehle, J.H. (1998).The pineal organ, its hormone melatonin, and the photoneuroendocrine system. *Adv. Anat. Embryol. Cell Biol.* **146,** 1–100.

Krisch, B., and Leonhardt, H. (1980). Luliberin and somatostatin fiber-terminals in the subfornical organ of the rat. *Cell Tissue Res.* **210,** 33–45.

Krisch, B., Leonhardt, H., and Buchheim, W. (1978). The functional and structural border between the CSF- and blood milieu in the circumventricular organs (organum vasculosum laminae terminalis, subfornical organ, area postrema) of the rat. *Cell Tissue Res.* **195,** 485–497.

Krout, K.E., Kawano, J., Mettenleiter, T.C., and Loewy, A.D. (2001). CNS inputs to the suprachiasmatic nucleus of the rat. *Neuroscience* **110,** 73–92.

Kuhlenbeck, H. (1954). The supraoptic crest in the human *brain. Anat. Rec.* **118,** 396.

Kuhlenbeck, H. (1955). Observations on some normal and pathological histological variations of ventricular lining structures in the human brain. *Anat. Rec.* **121,** 325.

Kuhlenbeck, H. (1968). Further observations on the lamination pattern in the supraoptic crest in man. *Anat. Rec.* **160,** 480.

Kuhlenbeck, H. (1970). "The Central Nervous System of Vertebrates," Vol. 3, Part 1, pp. 299–367. Karger, Basel.

Lanca, A. J., and van der Kooy, D. (1985). A serotonin-containing pathway from the area postrema to the parabrachial nucleus in the rat. *Neuroscience* **14,** 1117–1126.

Landas, S., and Phillips, M. 1. (1987), Comparative anatomy of the organum vasculosum of the lamina terminalis. *In* "Circumventricular Organs and Body Fluids" (P. Gross, ed.), Vol. 1, pp. 131–156. CRC Press, Boca Raton.

Landas, S., Fischer, J., Wilkin, L. D., Mitchell, L. D., Johnson, A. K., Turner, J. W., Theriac, M., and Moore, K. C. (1985). Demonstration of regional blood–brain barrier permeability in human brain. *Neurosci. Lett.* **57,** 251–256.

Larsen, P.J., and Mikkelsen, J.D. (1995). Functional identification of central afferent projections conveying information of acute stress to the hypothalamic paraventricular nucleus. *J. Neurosci.* **15,** 2609–2627.

Larsen, P.J., Moller, M., and Mikkelson, J.D. (1991). Efferent projections from the periventricular and medial parvicellular subnuclei of the hypothalamic paraventricular nucleus to circumventricular organs of the rat: a *Phaseolus vulgaris*-leucoagglutinin (PHA-L) tracing study. *J. Comp. Neurol.* **306,** 462–479.

Larsen, P.J., Enquist, L.W., and Card, J.P. (1999). Characterisation of the multisynaptic neuronal control of the rat pineal gland using viral transneuronal tracing. *Eur. J. Neurosci.* **10,** 128–145.

Lederis, K. (1965). An electron microscopical study of the human neurohypophysis. *Z. Zellforsch. Mikrosk. Anat.* **65,** 847–868.

Lenkei, Z., Palkovits, M., Corvol, P., and Llorens-Cortes, C. (1997). Expression of the angiotensin type 1 (AT1) and type 2 (AT2) receptor mRNAs in the adult rat brain: a functional neuroanatomical review. *Front. Neuroendocrinol.* **18,** 383–439.

Leonhardt, H. (1980). Ependym und circumventriculare Organ. *In* "Handbuch der mikroskopischen Anatomie des Menschen" (A. Oschke and L. Vollrath, eds.), Vol. 4, Part 1, pp. 362–666. Springer-Verlag, Berlin.

Lewis, P. R., and Shute, C. C. (1967). The cholinergic limbic system: projections to hippocampus formation, medial cortex, nuclei of the ascending cholinergic reticular system, and the subfornical organ and the supraoptic crest. *Brain* **90,** 521–550.

Lin, S-C., Li, S., Drolet, D.W., and Rosenfeld, M.G. (1994). Pituitary ontogeny of the Snell dwarf mouse reveals Pit-1 independent and Pit-1-dependent origins of the thyrotrope. *Development* **120,** 515–522.

Lincoln, G.A., and Clarke, I.J. (1998). Absence of photoperiodic modulation of gonadotrophin secretion in HPD rams following chronic pulsatile infusion of GnRH. *J. Neuroendocrinol.* **10,** 461–471.

Lind, R.W. (1987). Neural connections. *In* "Circumventricular Organs and Body Fluids" (P. Gross, ed.), Vol. 1, pp. 28–42. CRC Press, Boca Raton.

Lind, R. W, Van Hoesen, G. W., and Johnson, A. K. (1982). An HRP study of the connections of the subfornical organ of the rat. *J. Comp. Neurol.* **210,** 265–277.

Lind, R. W, Swanson, L. W., and Ganten, D. (1984). Angiotensin II immunoreactive cells in the neural afferents and efferents of the subfornical organ of the rat. *Brain Res.* **321**, 209–215.

Lind, R. W, Swanson, L. W., and Ganten, D. (1985). Organization of angiotensin II immunoreactive cells and fibers in the rat central nervous system. *Neuroendocrinology* **43,** 2–24.

Lindvall, M., Edvinsson, L., and Owman, C. (1977). Histochemical study on regional differences in the cholinergic nerve supply of the choroid plexus from several laboratory animals. *Exp. Neurol.* **55,** 155–159.

Mai, J.K., Stephens, P.H., Hopf, A., and Cuello, A.C. (1986). Substance P in the human brain. *Neurosci.* **17,** 709–739.

Mai, J.K., Assheuer, and J., Paxinos, G. (1997). "Atlas of the human brain." Academic Press, San Diego.

Mark, M. H., and Farmer, P. M. (1984). The human subfornical organ: an anatomic and ultrastructural study. *Ann. Clin. Lab. Sci.* **14,** 427–442.

Martel, J. C., St. Pierre, S., and Quirion, R. (1986). Neuropeptide Y receptors in rat brain: autoradiographic localization. *Peptides (N. Y.)* **7,** 55–60.

McComb, J. G. (1983). Recent research into the nature of cerebrospinal fluid formation and absorption. *J. Neurosurg.* **59,** 369–383.

McKinley, M. J., Denton, D. A., Leksell, L. G., Mouw, D. R., Scoggins, B. A., Smith, M. H., Weisinger, R. S., and Wright, R. D. (1982). Osmoregulatory thirst in sheep is disrupted by ablation of the anterior wall of the optic recess. *Brain Res.* **236,** 210–215.

McKinley, M. J., Congiu, M., Denton, D. A., Park, R. G., Penschow, L., Simpson, J. B., Tarjan, E., Weisinger, R. S., and Wright, R. D. (1984). The anterior wall of the third ventricle and homeostatic responses to dehydration. *J. Physiol. (Paris)* **79,** 421–427.

McKinley, M. J., Allen, A., Clevers, J., Denton, D. A., and Mendelsohn, F. A. O. (1986). Autoradiographic localization of angiotensin receptors in sheep brain. *Brain Res.* **375,** 373–376.

McKinley, M. J., Allen, A. M., Clevers, J., Paxinos, G., and Mendelsohn, F. A. O. (1987a). Angiotensin receptor binding in human hypothalamus: autoradiographic localization. *Brain Res.* **420,** 375–379.

McKinley, M. J., Clevers, J., Denton, D. A., Oldfield, B. J., Penschow, J., and Rundgren, M. (1987b). Fine structure of the organum vasculosum of the lamina terminalis. *In* "Circumventricular Organs and Body Fluids" (P. Gross, ed.), Vol. 1, pp. 111–130. CRC Press, Boca Raton.

McKinley, M.J. Badoer, E., and Oldfield, B.J. (1992). Intravenous angiotensin II induces Fos-immunoreactivity in circumventricular organs of the lamina terminalis. *Brain Res.* **594,** 295–300.

McKinley, M.J., Hards, D.K., and Oldfield, B.J. (1994). Identification of neural pathways activated in dehydrated rats by means of Fos-immunohistochemistry and neural tracing. *Brain Res.* **653,** 305–314.

Mendelsohn, F. A. 0., Quirion, R., Saavedra, J. M., Aguilera, G., and Catt, K. J. (1984). Autoradiographic localization of angiotensin If receptors in rat brain. *Proc. Natl. Acad. Sci. U.S.A.* **81,** 1575-1579.

Miller, A.D., and Leslie, R.A. (1994). The area postrema and vomiting. *Front. Neuroendocrinol.* **15,** 301–320.

Miselis, R. R. (1981). The efferent projections of the subfornical organ of the rat: A circumventricular organ within a neural network subserving fluid balance. *Brain Res.* **230,** 1–23.

Miselis, R. R., Shapiro, R. E., and Hand, P. H. (1979). Subfornical organ efferents to neural systems for control of body water. *Science* **205,** 1022–1025.

Miselis, R. R., Shapiro, R. E., and Hyde, I. M. (1987a). The area postrema. In "Circumventricular Organs and Body Fluids" (P. Gross, ed.), Vol. 2, pp. 185–207. CRC Press, Boca Raton.

Miselis, R.R., Weiss, M.L., and Shapiro, R.E. (1987b). Modulation of the visceral neuraxis. *In* "Circurnventricular Organs and Body Fluids" (P. Gross, ed.), Vol. 3, pp. 143–162. CRC Press, Boca Raton.

Morgan, P. (2000). The pars tuberalis: the missing link in the photoperiodic regulation of prolactin secretion? *J. Neuroendocrinol.* **12,** 287–295.

Moore, R. Y., and Klein, D. C. (1974). Visual pathways and the central neural control of a circadian rhythm in pineal N-acetyl transferase activity. *Brain Res.* **71,** 17–33.

Moran, T. H., Robinson, P. H., Goldrich, M. S., and McHugh, P. R. (1986). Two brain cholecystokinin receptors: Implications for behavior actions. *Brain Res.* **362,** 175–179.

Murone, C., Paxinos, G., McKinley, M.J., Oldfield, B.L., Muller-Esterle W., Mendelsohn, F.A.O., and Chai, S.Y. (1997). Distribution of bradykinin B2 receptors in sheep brain visualised by in vitro autoradiography. *J. Comp. Neurol.* **381,** 203–218, 1997.

Newton, B. W., and Maley, B. E. (1985). Cholecystokinin-octapeptide like immunoreactivity in the area postrema of the rat and cat. *Regul. Peptides* **13,** 31–40.

Ohuoha, D.C., Knable, M.B., Wolf, S.S., Kleinma, J.E., and Hyde, T.M. (1994). The subnuclear distribution of 5-HT3 receptors in the human nucleus of the solitary tract and other structires of the caudal medulla. *Brain Res.* **637,** 222–226.

Okon, E., and Koch, Y. (1977). Localisation of gonadotropin releasing hormone in the circumventricular organs of human brain. *Nature (London)* **268,** 445–447.

Oksche, A. (1961). Verglei chende untersuchungen uber die sekretorische Activatat des Subkonimissuralorgans und den Gliacharakter Seiner *Zellen. Z. Zellforsch. Mikrosk. Anat.* **54,** 549–612.

Oksche, A. (1962). Histologische, histochemische und experimentelle Studien am Subkorrimissuralorgans von Anuran. *Z. Zellforsch. Mikrosk. Anat.* **54,** 240–326.

Olcese, J.M. (1990)The neurobiology of magnetic field detection in rodents. *Prog. Neurobiol.* **35,** 325–330.

Oldfield, B. L., and McKinley, M. J. (1987). An electron microscopic inimunocytochemical study of angiotensin 11 in the rat brain. *Neurosci. Lett. Suppl.* **27,** S111.

Oldfield, B. L, Clevers, J., and McKinley, M. (1986). A light and electron microscopic study of the projections of the nucleus medianus with special reference to inputs to vasopressin neurones. *Soc. Neurosci. Abst.* **12,** 445.

Oldfield, B.J., Oldfield, B.J., Hards, D.K., and McKinley, M.J. (1994). Fos production in retrogradely-labelled neurons of the lamina terminalis following intravenous infusion of either hypertonic saline or angiotensin II. *Neuroscience* **60,** 255–262.

Olszewski, H., and Baxter, D. (1982). "Cytoarchitecture of the Human Brain Stern," 2nd ed., pp. 142–143. Karger, Basel.

Osheroff, P.L., and Phillips, H.S. (1991). Autoradiographic localization of relaxin binding sites in rat brain. *Proc. Natl. Acad. Sci. U.S.A.* **88,** 6413–6417.

Page, R. B. (1986). The pituitary portal system. *Curr. Top. Neuroendocrinol.* **7,** 1–47.

Page, R.B. (1987). Pituitary blood flow. *Am. J. Physiol.* **243,** E427–E442.

Page, R.B., and Bergland, R.M. (1977). The neurohypophysial capillary bed. I Anatomy and arterial supply. *Am. J. Anat.* **148,** 345–358.

Page, R.B., Leure-Dupree, A., and Bergland, R.M. (1978). The neurohypophysial capillary bed. II Specializations within the median eminence. *Am. J. Anat.* **153,** 33–66.

Palkovits, M., Mezey, E., Ambach, G., and Kivoviks, P. (1978). Neural and vascular connections between the organum vasculosum laminae terminalis and preoptic nuclei. *In* "Brain–Endocrine Interaction" (D. E. Scott, G. P. Kozlowski. and A. Weindl, eds.), Vol. 3, pp. 302–312. Karger, Basel.

Palkovits, M. (1984). Neuropeptides in the hypothalamo-hypophysial system: lateral retrochiasmatic area as a common gate for neuronal fibers towards the median eminence. Peptides 5, 35–39.

Pan, J.T. (1996). Neuroendocrine functions of dopamine. *In* "CNS Neurotransmitters and Neuromodulators; Dopamine" (T.W. Stone, ed.), pp. 213–232. CRC Press, Boca Raton.

Patel, Y. C., Baquiran, G., Srikant, C. B., and Postier, B. I. (1986). Quantitative in vivo autoradiographic localization of [^{125}I-Tyrl somatostatin-14 and [Leu8, D-Trp22-^{125}I-Tyr25] somatostatin28 binding sites in rat brain. *Endocrinology (Baltimore)* **119,** 2262–2269.

Phillips, P. A., Abrahams, J. M., Kelly, J., Paxinos, G., Grzonka, Z., Mendelsohn, F. A. O., and Johnston, C. I. (1988). Localization of

vasopressin binding in rat brain by in vitro autoradiography using a radioiodinated V, receptor antagonist. *Neuroscience* **27,** 749–775.

Pickard, G.E., and Turek, F.W. (1983). The hypothalamic paraventricular nucleus mediates the photoperiodic control of reproduction but not the effects of light on the circadian rhythm of activity. *Neurosci. Lett.* **43,** 67–72.

Putnam, T. J. (1922). The intercolumnar tubercle: an undescribed area in the anterior wall of the third ventricle. *Bull. Johns Hopkins Hosp.* **38,** 181–182.

Quirion, R., Dalpe, M., De Lean, A., Gutkowska, L., Cantin, M., and Genest, J. (1984). Atrial natriuretic factor binding sites in brain and related structures. *Peptides (N. Y.)* **5,** 1167–1172.

Rakic, P. (1965). Mesocoelic recess in the human brain. *Neurology* **15,** 709–715.

Rauch, M., Schmid, H.A., deVente, J., and Simon, E. (1997). Electrophysiological and immunocytochemical evidence for a cGMP-mediated inhibition of subfornical organ neurons by nitric oxide. *J. Neurosci.* **17,** 363–371.

Reyes, P. F. (1982). Age related histologic changes in the human pineal gland. *In* "The Pineal and Its Hormones" (R. J. Reiter, ed.), pp. 253–261. Alan R. Liss, New York.

Richard, D., and Bourque, C.W. (1993). Synaptic activation of rat supraoptic neurons by osmotic stimulation of the organum vasculosum of the lamina terminalis. *Neuroendocrinology* **55,** 609–611.

Robertson, G.L. (1991). Disorders of thirst in man. *In* "Thirst: Physiological and Psychological Aspects" (D.J. Ramsay and D.A. Booth, eds), pp. 453–477. Springer-Verlag, London.

Rosas-Arellano, Solano-Flores L.P., and Ciriello, J. (1996). Neurotensin projections to subfornical organ from arcuate nucleus. *Brain Res.* **706,** 323–327.

Rouleau, M. E, Warshawsky, H., and Goltzinan, D. (1984). Specific receptors for calcitonin in the subfornical organ of the brain. *Brain* **107,** 107–114.

Saavedra, J.M., Zorad, S., and Tsutsumi, K. (1992). Localization of atrial natriuretic peptide B and C receptors in rat brain. *In* "Handbook of Chemical Neuroanatomy," Vol 11 (A. Bjorklund, T. Hokfelt, and M.J. Kuhar, eds.), pp. 39–53. Elsevier, Amsterdam.

Saper, C. B., and Levisohn, D. (1983). Afferent connections of the median preoptic nucleus in the rat: anatomical evidence for a cardiovascular integrative mechanism in the anteroventral third ventricular (AV3V) region. *Brain Res.* **288,** 21–31.

Scharenberg, K., and Liss, L. (1965). The histologic structure of the human pineal body. *Prog. Brain Res.* **10,** 193–217.

Schreiber, G., Aldred, A.R., Jaworoski, A., Nilsson, C., Achen, M.G., and Segal, M.B. (1990). Thyroxine transport from blood to brain via transthyretin synthesis in choroid plexus. *Am. J. Physiol.* **258,** R338–R345.

Sexton, P.M., McKenzie, J.S., Mason, R.T., Moseley, J.M., Martin, T.J., and Mendelsohn, F.A.O. (1986). Localization of binding sites for calcitonin gene related peptide in rat brain by *in vitro* autoradiography. *Neuroscience* **19,** 1235–1245.

Sexton, P.M., Paxinos, G., Kenney, M.A., Wookey, P.J., and Beaumont, K. (1994). *In vitro* autoradiographic localization of amylin binding sites in rat brain. *Neuroscience* **62,** 553–567.

Sgro, S., Ferguson, A. V., and Renaud, L. P. (1984). Subfornical organ–supraoptic connections: an electrophysiological study in the rat. *Brain Res.* **303,** 7–13.

Shaffer, M. M., and Moody, T. W. (1986). Autoradiographic visualization of CNS receptors for vasoactive intestinal peptide. *Peptides (N. Y.)* **7,** 283–288.

Shapiro, R. E., and Miselis, R. R. (1985). The central neural connections of the area postrema of the rat. *J. Comp Neurol.* **234,** 344–364.

Simpson, J. B. (1981). The circumventricular organs and the central actions of angiotensin. *Neuroendocrinology* **32,** 248–256.

Simpson, J. B., Epstein, A. N., and Camardo, J. S. (1978). Localization of receptors for the dipsogenic action of angiotensin II in the subfornical organ of the rat. *J. Comp. Physiol. Psychol.* **92,** 2676–2682.

Sly, D.J., Colvill, L., McKinley, M.J., and Oldfield, B.J. (1999). Identification of neural projections from the forebrain to the kidney, using the virus pseudorabies. *J. Auton. Nerv. Syst.* **77,** 73–82.

Smith, A.I., Clarke, I.J., and Lew, R.A. (1997). Post-secretory processing of peptide signals: a novel mechanism for the regulation of peptide hormone receptors. *Biochem. Soc. Trans.* **25,** 1011–1014.

Speth, R. C, Walmsley, J. K., Gehlert, D. R., Chernicky, C. L., Barnes, K. L., and Ferrario, C. L. (1985). Angiotensin II receptor localization in the canine CNS. *Brain Res.* **326,** 137–143.

Sterba, G., Cleim, L., Naumann, W., and Petter, H. (1981). Immunocytochemical investigation of the subcommissural organ in the rat. *Cell Tissue Res.* **218,** 659–662.

Sumida, M., Barkovick, A.J., and Newton, T.H. (1996). Development of the pineal gland: measurement with *MR. Am. J. Neuroradiol.* **17,** 233–236.

Sunn, N., McKinley, M.J., and Oldfield, B.J. (2001). Identification of efferent neural pathways from the lamina terminalis activated by blood-borne relaxin. *J. Neuroendocrinol.* **13,** 1–7.

Sutton, S.W., Toyama, T.T., Otto, S., and Plotsky, P.M. (1988). Evidence that neuropeptide Y released into the hypophysial–portal circulation participates in priming gonadotropes to the effects of gonadotropin releasing hormone (GnRH). *Endocrinology* **123,** 1208–1210.

Swanson, L. W., and Lind, R. W (1986). Neural projections subserving the initiation of a specific motivated behaviour in the rat: new projections from the subfornical organ. *Brain Res.* **379,** 399–403.

Tamarkin, L., Baird, C. L., and Almeida, O. E X. (1985). Melatonin: a coordinating signal for mammalian reproduction. *Science* **227,** 714–720.

Tanaka, L, Kaba, H., Saito, H., and Seto, K. (1986). Lateral hypothalamic area stimulation excites neurons in the region of the subfornical organ with efferent projections to the hypothalamic paraventricular nucleus of the rat. *Brain Res.* **379,** 200–203.

Tapp, E. (1979). The histology and pathology of the human pineal gland. *Prog. Brain Res.* **52,** 481–499.

Tapp, E., and Huxley, M. (1971). The weight and degree of calcification of the pineal gland. *J. Pathol.* **105,** 31–39.

Teclemariam-Mesbah, R., Ter Horst G.J., Postema, F., Wortel, J., and Buijs, R.M. (1999). Anatomical demonstration of the suprachiasmatic nucleus-pineal pathway. *J. Comp. Neurol.* **406,** 171–182.

ter Horst, G. J., and Luiten, P. G. (1986). The projections of the dorsomedial hypothalamic nucleus in the rat. *Brain Res. Bull.* **16,** 231–248.

Thomas, G.B., Cummins, J.T., Smythe, G.A., Gleeson, R.M., Dow, R.C., Fink, G., and Clarke, I.J. (1989). Concentrations of dopamine and noradrenaline in hypophysial portal blood in the sheep and the rat. *J. Endocrinol.* **121,** 141–147.

Thrasher, T. N., and Keil, L. C. (1987). Regulation of drinking and vasopressin secretion: Role of organum vasculosum laminae terminalis. *Am. J. Physiol.* **253,** R108–R120.

Tribollet, E. (1992). Vasopressin and oxytocin receptors in the rat brain. *In* "Handbook of Chemical Neuroanatomy," Vol 11 (A. Bjorklund, T. Hokfelt, and M.J. Kuhar, eds.), pp. 289–320, Elsevier, Amsterdam.

Tyers M.B., and Freeman, A.J. (1992). Mechanism of the anti-emetic activity of 5-HT_3 receptor antagonists. *Oncology* **49,** 263–268.

Undesser, K. P., Hasser, E., Haywood, J. R., Johnson, A. K., and Bishop, V. S. (1985). Interactions of vasopressin with the area

postrema in arterial baroreflex function in conscious rabbits. *Circ. Res.* **56,** 410–417.

Uschakov, A., McAllen, R.M., Oldfield, B.J., and McKinley, M.J. (2001). Efferent projections of subpopulations of neurons in the lamina terminalis. *Soc. Neurosci. Abstracts* (in press).

van der Kooy, D., and Koda, L. Y. (1983). Organization of the projections of a circumventricular organ: the area postrema in the rat. *J. Comp. Neurol.* **219,** 328–338.

Volrath, L. (1984). Functional anatomy of the human pineal gland. *In* "The Pineal Gland" (R. Reiter, ed.), pp. 285–322. Raven Press, New York.

von Fleidel, G. (1965). Die Haufigkeit des Vorkornmens von Kalkkonkrementern in Corpus pineale des Kindes. *Anal. Anz.* **116,** 139–154.

Walmsley, J. K., Zarbin, M. A., Young, W. S., and Kuhar, M. J. (1982). Distribution of opiate receptors in the monkey brain; an autoradiographic study. *Neuroscience* **7,** 595–613.

Walter, H.J., Berry, M., Hill, D.J., Cwyfan-Hughes, S., Holly, J.M., and Logan, A. (1999). Distinct sites of insulin-like growth factor (IGF)-II expression and localization in lesioned rat brain: possible roles of IGF binding proteins (IGFBPs) in the mediayion of IGF-II activity. *Endocrinology* **140,** 520–532.

Weindl, A. (1973). Neuroendocrine aspects of circumventricular organs. *In* "Frontiers in Neuroendocrinology" (W. E Ganong and L. Martini, eds.), pp. 3–32. Oxford University Press, Oxford.

Weindl, A., and Joynt, R. J. (1972). The median eminence as a circumventricular organ. *In* "Brain Endocrine Interaction" (K. M. Knigge, D. E. Scott, and A. Weincil, eds.), pp. 280–297. Karger, Basel.

Weindl, A., and Joynt, R. J. (1973). Barrier properties of the subcommissural organ. Arch. Neurol. (Chicago) **29,** 16–22.

Weindl, A., and Schinko, I. (1975). Vascular and ventricular neurosecretion in the organum vasculosum of the lamina terminalis of the golden hamster. *In* "Brain Endocrine Interaction" (K. M. Knigge, D. E. Scott, and H. Kobayasha, eds.), Vol. 2, pp. 190–203. Karger, Basel.

Weindl, A., and Sofroniew, M. (1985). Neuroanatomical pathways related to vasopressin. *In* "Neurobiology of Vasopressin" (D. Ganten and D. Pfaff, eds.), pp. 137–196. Springer-Verlag, Berlin.

Weindl, A., Schwink, A., and Wetzstein, R. (1968). Der Feinbaudes GefaBorgans der Lamina terminalis beim Kaninchen. II. Das neuronale und gliale Gewebe. *Z. Zellforsch. Mikrosk. Anal.* **85,** 552–600.

Wenger, T., and Aros, B. (1971). Studies on the organon vasculosum laminae terminalis. III. Vascularization of the organon vasculosum laminae terminalis in the rat. *Acta Morphol. Acad.* Sci. *Hung.* **19,** 141–149.

Wenger, T., and Tork, I. (1968). Studies on the organon vasculosum laminae terminalis. II. Comparative morphology of the organon vasculosum laminae terminalis of fishes, amphibia, reptilia, birds and mammals. *Acta Biol. Acad. Sci. Hung.* **19,** 83–96.

Wenger, T., and Torö, I. (1971). Studies on the organon vasculosum laminae terminalis. IV. Fine structure of the organon vasculosum laminae terminalis in man. *Acta Biol. Acad. Sci. Hung.* **22,** 331–342.

Wenger, T, Kerdelhue, B., and Halasz, B. (1981). Does the organum vasculosum of the lamina terminalis play a role in the regulation of reproduction. *Acta Physiol. Acad. Sci. Hung.* **58,** 257–267.

Westerhaus, M.J., and Loewy, A.D. (1999). Sympathetic-related neurons in the preoptic region of the rat identified by viral transneuronal labelling. *J. Comp. Neurol.* **414,** 361–378.

Wiklund, L., Lundberg, J. J., and Mollgard, K. (1977). Species differences in serotonergic innervation and activity of rat, gerbil, mouse and rabbit subcommissural organ. *Acta Physiol. Scand. Suppl.* **452,** 27–30.

Wilson, J. T. (1906). On the anatomy of the calamus region. in the human bulb; with an account of a hitherto undescribcd "nucleus postremus." Parts I and II. *J. Anal. Physiol.* **40,** 210–241, 357–386.

Wislocki, G. B., and King, L. S. (1936). The permeability of the hypophysis and hypothalamus to vital dyes, with a study of the hypophysial vascular supply. *Am. J. Anal.* **58,** 421–472.

Wislocki, G. B., and Leduc, E. H. (1952). Vital staining of the hemato-encephalic barrier by silver nitrate and trypan blue and cytological comparisons of the neurohypophysis, pineal body, area postrema, intercolumnar tubercle and supraoptic crest. *J. Comp. Neurol.* **96,** 371–413.

Wislocki, G. B., and Putnam, T. J. (1920). Note on the anatomy of the area postremae. *Anat. Rec.* **19,** 281–285.

Wislocki, G. B., and Putnam, T. J. (1924). Further observations of the area postremae. *Anat. Rec.* **27,** 151–156.

Xiong, J-J., Karsch, F.J., and Lehman, M.N. (1997). Evidence for seasonal plasticity in the gonadotropin-releasing hormone (GnRH) system of the ewe: changes in synaptic inputs onto GnRH neurons. *Endocrinology* **138,** 1240–1250.

Xuereb, G. R., Prichard, M. M. L., and Daniel, P. M. (1954a). The arterial supply and venous drainage of the human hypophysis cerebri. *Q. J. Exp. Physiol. Cogn. Med. Sci.* **39,** 199–217.

Xuereb, G. P., Prichard, M. M. L., and Daniel, P. M. (1954b). The hypophysial portal system of vessels in man. *Q. J. Exp. Physiol. Cogn. Med. Sci.* **39,** 219–230.

Zardetto-Smith, A.M., and Gray, T.S. (1987). A direct neural projection from the nucleus of the solitary tract to the subfornical organ in the rat. *Neurosci. Lett.* **80,** 163–166.

Zimmerman, E. A., and Antunes, H. L. (1976). Organization of the hypothalamic pituitary system: current concepts from immunohistochemical studies. *J. Histochem. Cytochem.* **24,** 807–815.

CHAPTER

20

Thalamus

GERARD PERCHERON
Institut National de la Santé et de la Recherche Medicale
Paris, France

GENERAL CONSIDERATIONS

Macroscopical Anatomy and Topography

The thalamus is a diencephalic symmetrical oval-shaped mass located between the brainstem below and the telencephalon above, from the posterior commissure to the foramen of Monro (Fig. 20.1A). The medial aspect is observable after a sagittal section through the third ventricle (3V; Fig. 20.1A). The stria medullaris thalami (Fig. 20.1) starting from the ganglion habenulae goes up to the anterior tubercle with the taenia thalami (or habenulae). This is the line of attachment of the tela that forms the roof of the third ventricle. This line, up to cercopithecidae, constitutes the upper corner of the thalamus. Appearing first in chimpanzees, owing to the large dorsal increase of the thalamus, this is no more the case in the human brain. The medial view of the thalamus (Fig. 20.1A) shows two parts in relation to the line of attachment: below (ventricular or periventricular) and above ("extra-ventricular"). In many species, there is in the third ventricle an adhaesio interthalamica (Adh, Fig. 20.1A, or massa intermedia or commissura grisea, see para-median region). This is missing in 30% of the human cases (Rabl, 1958, and own material), not depending on gender or age. When present, the size of the adhesio, generally small, is variable, but the position of its anteroinferior pole is stable (aAd, Fig. 20.1A). The posterior part of the foramen of Monro corresponds to the anterior border of the thalamus (aTh, Fig. 20.1A). Placed between the midline and the internal capsule,

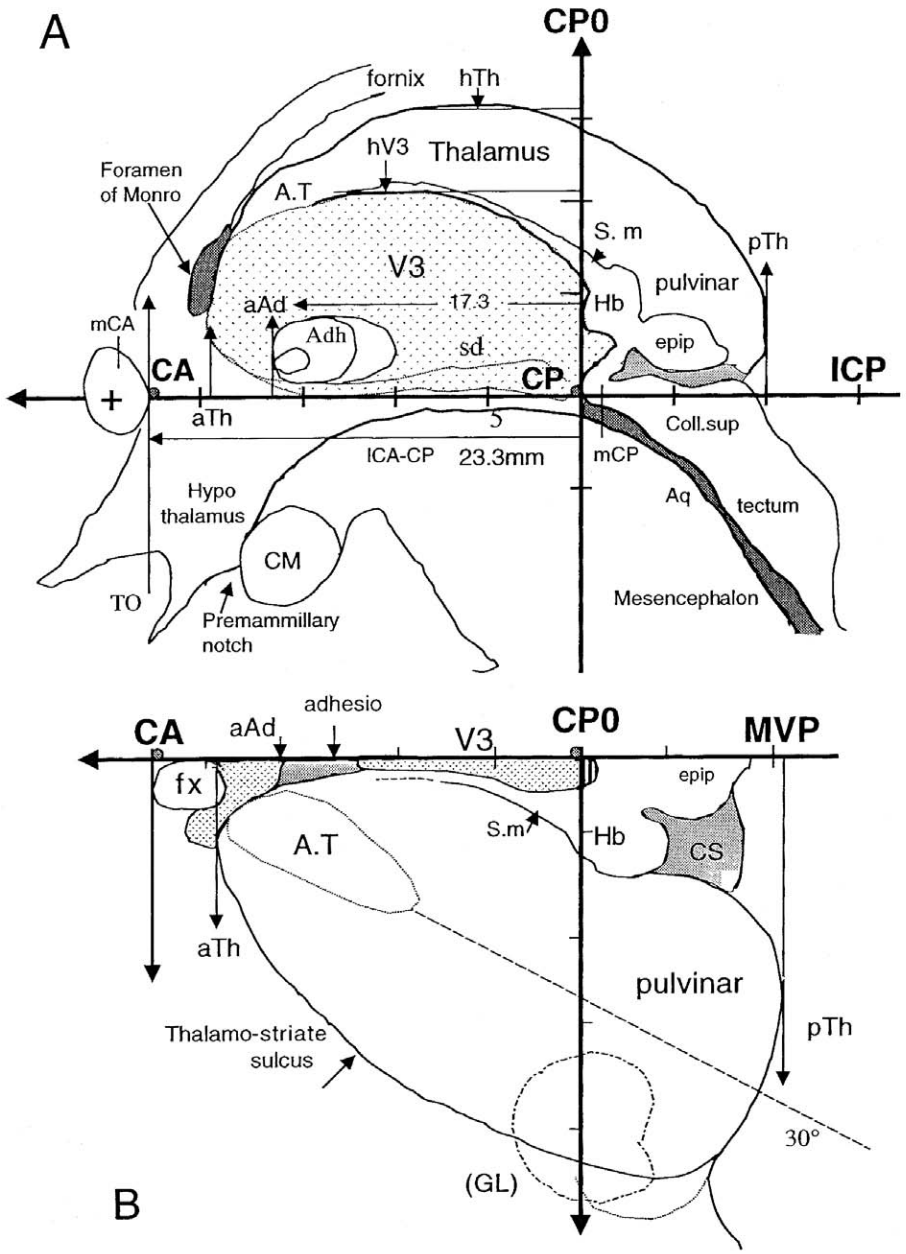

FIGURE 20.1 **(A)** Medial view after a midsagittal section through the third ventricle (V3). Position of the thalamus in relation to other parts of the brain and to the CA-CP, CP0, system of coordinates. This is based on two ventricular points observable on ventriculograms and histological sections, CA and CP located at the maximal protrusion of the border of the commissures where the distance between the two (lCA-CP) is minimum. The intercommissural plane (ICP) is the plane perpendicular to the midsagittal plane (MVP) passing through the two commissural points. CP0 is the plane perpendicular to both MVP and ICP and passing through CP. lCA-CP is the intercommissural length, giving the size of the ventricle allowing individual corrections in the posteroanterior dimension. The dotted area is the ventricular part of the thalamus, delineated dorsally by the stria medullaris medialis (sm) with the taenia habenulae corresponding to the line of attachment of the tela choroidea, the roof of the third ventricle. In man, a great part of the thalamus is extraventricular dorsally and posteriorly. Anteriorly, the anterior pole of the thalamus (aTh) corresponds to the posterior border of the foramen of Monro. Its position is statistically stable and may be used for size measurements. In humans, the adhesio interthalamica (Adh) is missing in 30% of the cases and of limited variable extent in others. The position of the anterior pole of the adhesio (aAd) is rather stable (not the posterior). Ventrally, the border partially follows the sulcus diencephalicus (sd) going from the foramen to the aqueduct of Sylvius (Aq). The posterior pole of the thalamus, pTh is directly observable in ventriculograms. The length of the posterior part of the thalamus CP-pTh is not linked to lCA-CP. The height of the ventricle (hV3) is not linked to its length. The height of the thalamus (hTh) is not linked to that of the ventricle (hV3), thus not offering metrical corrections. Other abbreviations: coll.sup, colliculus superior; CM, corpus mammillare; epip, epiphysis; Hb, ganglion habenulae; TO, tractus opticus. **(B)** Superior view of the thalamus after resection of the corpus callosum, fornix, and choroid plexuses. The thalamostriate sulcus constitutes the lateral border of the superior face. T.A, anterior tubercle. The third ventricle (V3) is shown with an adhesio interthalamica. The midventricular plane MVP passes through the middle of the ventricle. CP and CA are shown. CP0 is the plane of reference for anteriorities in the thalamus. Those of the anterior and posterior thalamic poles are indicated as aTH and pTh and that of the adhesio, as aAd. Back to the ventricle, the habenula (epithalamus)(Hb), the stria medialis or habenulae (s.m) and the epiphysis overhang the superior colliculus (cs). The main axis of the thalamus is not parallel to the midventricular plane and makes an angle of about 30°. Transverse and sagittal sections are thus not orthogonal to the anatomical thalamic axes. GL, lateral geniculate body and the lateral border of the pulvinar.

some faces of the thalamus are "adherent" and others are "free." The lateral face is adherent, to the capsule. The superior, posterior and infero-posterior faces, continuous and smooth, are visible after the removal of the corpus callosum or after pushing the temporal lobe laterally. The dorsomedial side shows the anterior tubercle in front (see superior region) and the dorsal part of the pulvinar in the back (Fig. 20.1B, see posterior region). The inferior side is made up of the superficial faces of the geniculate bodies in front and of the pulvinar posteriorly.

Thalamic Topometry and Cartography

There is general agreement for accepting the orientation and size of the third ventricle as the base for thalamic cartography and stereotaxy. Personal statistical analyses (Meder *et al.*, 1993, unpublished) on ventricular and thalamic average sizes made from 215 ventriculograms (135 from Ohye, 60 from Meder, and 20 from Nguyen) showed that the most practical (since observable in histology and radiography) and reliable CA-CP plane is that of Amador *et al.* (1959, in Schaltenbrand's atlas) (also the most reliable in macaques, Percheron, 1975), not Talairach's. This plane (Fig. 20.1A) links the most anterior point of the posterior commissure (CA) to the most posterior of the anterior (CP) (i.e., the shortest distance between the two) (Percheron, 1975; Meder *et al.*, 1993). Statistical analyses of the individual CA-CP distances (lCA-CP, length of the ventricle) measured on ventriculograms on Japanese and French samples (Meder *et al.*, 1993) led to an average of 23.3 ± 1.3 mm, with no differences between women and men or youngest and oldest. The mean distance from CP to the anterior part of the adhesio (CP-aAd), when present, is also stable (17.33 ± 1.2 mm). This material was compared to anatomical data resulting in about same values. Comparisons with 30 CT (from Ohye, 23.2±1.5) and 200 MRI pictures led to a slightly lower average, around 23 mm. The rule of using the closest commissural point (instead of the abstract middle ventricular plane) improves precision. CPO is the best initial plane for the thalamus (corresponding for instance to the posterior border of the central region, Percheron, 1975, 1997). Thalamic cartography thus relies on a simple cartesian system based on the midventricular plane (MVP), the intercommissural plane (ICP), and the plane perpendicular to the two preceding passing through the CPO point. Most of our figures are maps since following two mandatory rules: they are oriented in relation to a precise, immutable, system of coordinates, and they are scaled. These two properties are necessary for reconstruction in other planes. When the individual value of lCA-CP of the observed brain is less than ± 0.5mm in comparison to the reference, no correction is needed. In the reverse case, as already proposed by Tasker *et al.* (1982), a size correction using the ratio of the CA-CP length of the atlas of reference and of the observed one, improves precision (Percheron, 1975; Meder *et al.*, 1994). Variations of the highest point of the ventricle are not linked to variations in the anteroposterior dimension (as is also the case in macaques, Percheron 1975). Variations in the inferosuperior and in the lateral dimensions cannot be corrected. The CA-CP system of coordinates is not universal as, for instance, another ventricular system is preferable for the amygdala (Percheron, 1997). Some previous atlases of the human thalamus were performed in relation to exactly the same planes and identical CA and CP points: Schaltenbrand and Bailey (1959), Emmers and Tasker (1975) and Schaltenbrand and Wahren (1977). Atlases of Van Buren and Borke (1972), Mai *et al.* (1997); and Morel *et al.* (1997) using the center of the commissures (mCA and mCP, Fig. 20.1A) have the same horizontal plane and can be used with a simple anteroposterior correction (mCA-mCP is about 25 mm). The midsagittal plane, which was not precisely placed in the first Schaltenbrand's atlas (Niemann *et al.*, 1994; Morel *et al.*, 1997), was corrected later. The horizontal plane of section in Schaltenbrand's atlases was oriented at 7° from ICP and the series of horizontal sections cannot be used. The atlases of Talairach and Szickla (1967), Talairach and Tournoux, (1988) using other points of the commissures, or from Brierly and Beck (1959), Andrew and Watkins (1969), and Hassler *et al.* (1979) using the foramen of Monro, cannot be directly compared because they have different reference horizontal planes.

The study of the internal constitution of the human thalamus is made difficult by two geometrical particularities. First, the main axis makes an angle of about 30° (25° to 35°) (Figs. 20.1B and 20.2D) in relation to the midventricular plane (MVP, less than in macaques, 45°). Second, the main axis of the lateral region is strongly curved, its anterior part being almost perpendicular to the midventricular plane (Fig. 20.2D). The effect is such that anterior transverse sections are cut at almost a right angle to posterior (75°, Fig. 20.2D). When looking at histological sections or plates, it is imperious to think in terms of three-dimensional objects having complex forms that have been cut. A single level cannot be used as a proof for a separation or a mixture of elements. The recent progress of cerebral cartography has highly improved the precision of the description and the comparison of data. Sagittal views or slices show the geometrical complexity of the separating elements.

Topological Analysis

Usual concepts used today for the description of the cerebral organization are inherited from the end of the 19th century with their limitations. To understand the thalamic anatomofunctional structure, but also to better interprete experimental results, it is important today to distinguish neuronal sets and neuronal set spaces (Percheron, 1979; Percheron *et al.*, 1991, 1996) (Fig. 20.3A). Neuronal typology uses simple and reliable methods (Yelnik *et al.*, 1991). The founding neuronal set is the neuronal species: the set of neurons whose dendritic arborizations are statistically similar on topological, metrical, and geometrical parameters. Species and their parts are generally located in a given metrical space. There are thus distinct neuronal spaces shown on Fig. 20.3: nucleus, patria, basin, and territory. These spaces were implicitly understood to always coincide with thalamic nuclei, which is often not the case. The recent important changes in the conception of the thalamus come from the application of this rule. Neuronal sets have own internal organization (spatial distribution of items). That of a basin is an output map or outmap (Fig. 20.3); that of a territory is an input map or inmap. The transfer from one to the other forms the connectional map, using various combinatory possibilities. The ones shown on Fig. 20.3. are extreme cases among many intermediary situations. Topological closely linked to the experimental methods. Retrograde labeling disclose basins. Partial injections do not give the same result in the various mappings. Different in- and outmaps do not imply discrepant results.

Phylogenetic Problems

The anatomical description of the human thalamus is limited by the fact that it is still not possible to trace detailed connections in man. The most reliable tracing techniques rely on axonal flows, making necessary the resort to living animals. This had and has serious effects. Many conflicts in the description and nomenclature of the thalamus have come from different standpoints in relation to phylogenesis. The Vogt school (C. Vogt, 1909; Friedemann, 1911; Mussen, 1923; Vogt, 1941, and later Hassler, 1949, 1959; Hopf *et al.*, 1971) essentially worked on the human thalamus, resorting to monkeys for experimental data. Its parcellation and nomenclature were used by most stereotactic atlases, at first that of Hassler (1959, in Schaltenbrand and Bailey's celebrated book). Widely used by neurosurgeons, Hassler's partition was excessively complex with disputable functional attributions. Andrew and Watkins' (1969), van Buren and Borke's (1972), Emmers and Tasker's (1975) atlases are much simpler but, unfortunately, had less success. The "Michigan school" (named so by Walker, 1938) was a school of comparative neurology (Huber and Crosby, 1929), stemming from Le Gros Clark in London and starting with studies on early primate (Le Gros Clark) or nonprimate species (Gurdjian, 1927; Rioch, 1929). The partition and nomenclature were transferred to macaque brains by Le Gros Clark himself, and then by Crouch (1934), Aronson and Papez (1934), and Walker (1937, 1938). This nomenclature was used for the human brain by Sheps (1945), Toncray and Krieg (1946), and Dekaban (1955) and has been recently reintroduced in human brain stereotactic atlases (Talairach and Tournoux, 1988; Morel *et al.*, 1997; Mai *et al.*, 1997), raising problems of equivalence. Keeping the same name for thalamic elements throughout the phylogenesis of the thalamus is a belief in a general mammalian thalamus whose description would suffice for any species including ours. This minimizes evolutionary trends and changes and, as will be seen for the human thalamus, does not always allow the precise description of one species. There are noticeable changes from monkeys to man: thalamic parts have disappeared, others have appeared, and some have considerably developed. Within thalamic parts, the numbers of neurons (particularly of local circuit microneurons) and the complexity of connectivity increase (Kultas-Ilinsky and Ilinsky, 2001). Phylogenetic changes are linked to systemic modifications that must be considered as a whole. The large increase of the cerebral cortex and the differentiation of major afferent systems such as the basal ganglia system have strong thalamic effects that must be taken into account. The recent observation that afferent territories can be indirectly delineated by using immunochemistry has significantly improved the possibility of comparison. The recent understanding of some phylogenetic changes makes it possible to reunite the historic choices of major schools in a new synthesis.

DIENCEPHALON

There remains confusion concerning which cerebral elements really belong to the thalamus. The tradition relied on large ontogenic, embryologic subdivisions. Recent studies, using gene expression, favor the "neuromeric model" (Puelles and Rubinstein, 1993; Mueller and O'Rahilly, 1997, O'Rahilly and Mueller, 1999). In this model, the hypothalamus is no more diencephalic. The embryological lamina limitans of Kuhlenbeck (1920) forms the hin lamina medullaris

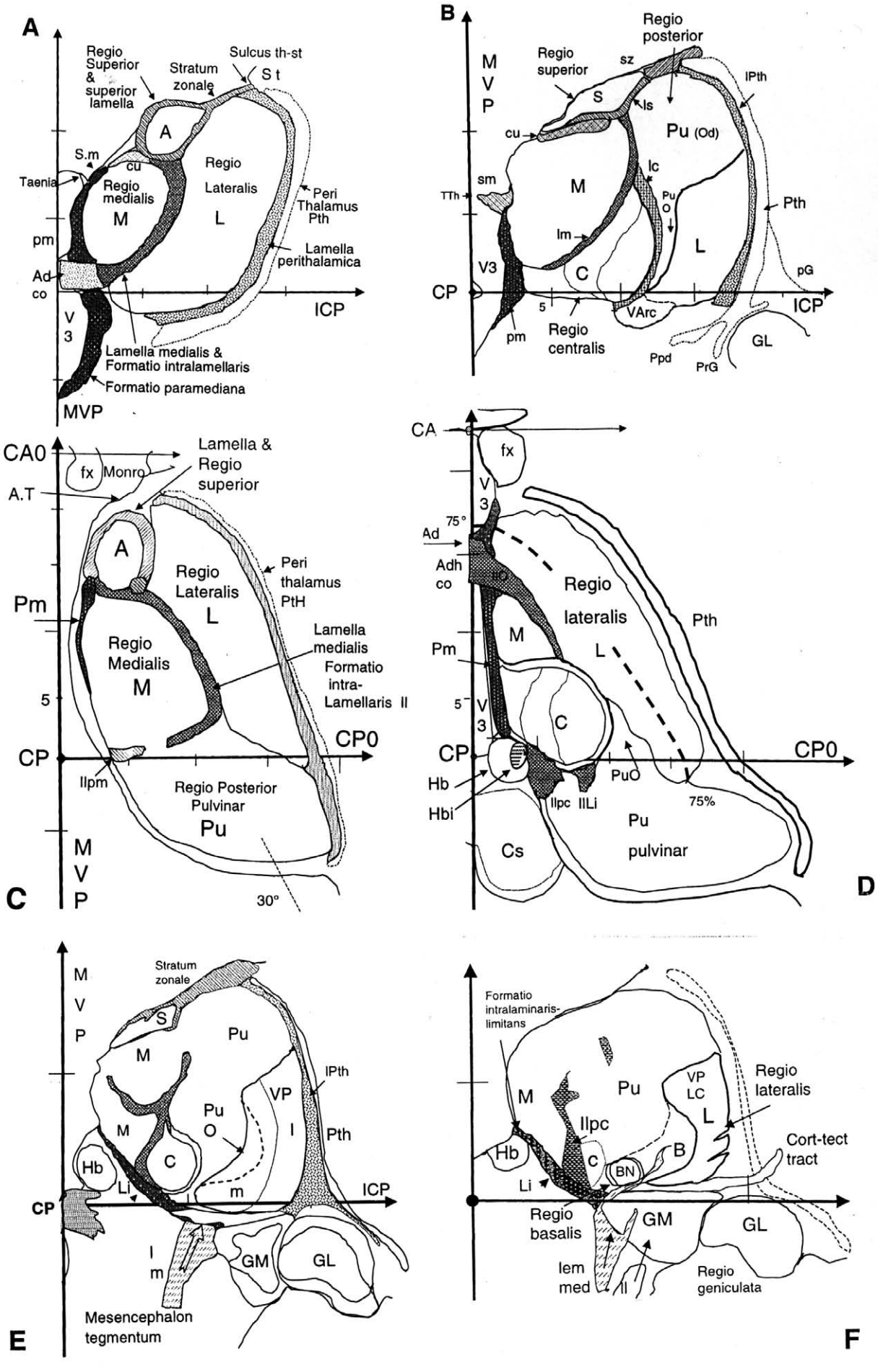
A
Regio Superior & superior lamella
Stratum zonale
Sulcus th-st
S t
A
S.m
cu
Taenia
Regio medialis
M
Regio Lateralis
L
Peri Thalamus Pth
pm
Lamella perithalamica
Ad
co
ICP
V 3
Lamella medialis & Formatio intralamellaris
Formatio paramediana
MVP
B
Regio posterior
M V P
Regio superior
sz
IPth
S
ls
Pu (Od)
cu
lc
sm
TTh
M
Pu O
Pth
lm
L
V3
C
pG
CP
5
VArc
ICP
pm
Regio centralis
GL
Ppd
PrG
C
CA0
Lamella & Regio superior
fx
Monro
A.T
A
Peri thalamus PtH
Regio Lateralis
L
Pm
Regio Medialis
M
Lamella medialis
Formatio intra-Lamellaris II
5
CP0
CP
IIpm
Regio Posterior Pulvinar
Pu
M V P
30°
D
CA
fx
V 3
75°
Ad
Adh co
Regio lateralis
Pth
M
L
Pm
5
V 3
C
CP
CP0
Hb
PuO
Hbi
IIpc IILi
75%
Pu pulvinar
Cs
E
M V P
Stratum zonale
S
Pu
M
IPth
VP
Pu O
M
I
Pth
Hb
C
Li
m
ICP
CP
I m
GM
GL
Mesencephalon tegmentum
F
Formatio intralaminaris-limitans
M
Pu
VP LC
Regio lateralis
L
IIpc
Hb
B
Cort-tect tract
c
BN
Li
Regio basalis
GM
GL
lem med
II
Regio geniculata

FIGURE 20.2 Lamellae and the classical model. **(A)** Transverse section (+12, Hassler *et al.*, 1979, modified) showing separating lamellae. Lamella perithalamica separates dorsal thalamus, or thalamus, from perithalamus (ventral thalamus). Myelinated lamellae separate large thalamic regions: lamella medialis (or interna), surrounding the medial region (regio medialis), and lamella superior, continuous with stratum zonale, surrounding superior region (regio superior, separating it from M and L). Neurons within lamellae form the intralaminar formation (Il) continued medially in the adhesial or commissuralis (Ad co) part, dorsally in cucullaris (cu) making a circle around the nucleus medialis (Grunthal n.circularis, Hassler's involucrum). Medially, regio paramediana or periventricular (dark) is a thin layer covering the ventricular wall. **(B)** Transverse section, more posterior. Perithalamus in continuity with "peripeduncular nucleus" (Ppd) and "nucleus pregeniculatus" (PrG). Appearance of regio centralis (C) and lamella centralis (lc) laterally separating it from the pulvinar and the lower part of the regio lateralis (Varc, nucleus ventralis arcuatus). Intralaminar neurons present in the lamella medialis not in the lamella centralis. **(C)** Slice of horizontal sections (9.7 from Van Buren and Borke's atlas modified). Superior region is surrounded by the lamella superior. Paramedian formation is reduced. The intralamellar lamina includes the intralaminar formation separates regio Medialis from Lateralis. Separation from the pulvinar is incomplete. **(D)** Slice of horizontal sections +2.7 to –0.9 from same (also modified), including the two commissures, the adhesio and the medial continuation of the intralaminar formation, (Adh Co), habenula (Hb) and habenulointerpeduncular bundle (Hbi). Regio centralis (C) strongly modifies the picture. Intralaminar-type groups of neurons are posterior to it: Ilpc, intralamellaris postcentralis and limitans (IlLi). PuO, wedge-shaped forward extension of the pulvinar. The main axis of the lateral region is curved. Its anterior part curves medially almost perpendicular to the midline (75°). **(E)** Transverse slice (Schaltenbrand and Bailey's atlas Fp 13 and 14 modified), close to the posterior commissure (CP) with the habenula (Hb). The lamella medialis still separates central **(C)** from medial region (M). Laterally, lamella centralis is devoid of neurons. Contiguity of intralaminar and limitans ensemble (Li) is made up of similar neurons though not in a lamella. Lm, lemniscus medialis. **(F)** Transverse slice (Fp 14 and 15, modified), posterior to the central region (c, central capsule). The irregular islands are no longer in a lamella with incomplete separation of M and Pu. Continuity of intralaminar elements with the limitans, constituting the intralaminar-limitans formation. Appearance of the regio basalis (B). It is not limited dorsally by a lamina. The presence of the lemniscus medialis (lm) and lateralis (ll) perturbs architecture.

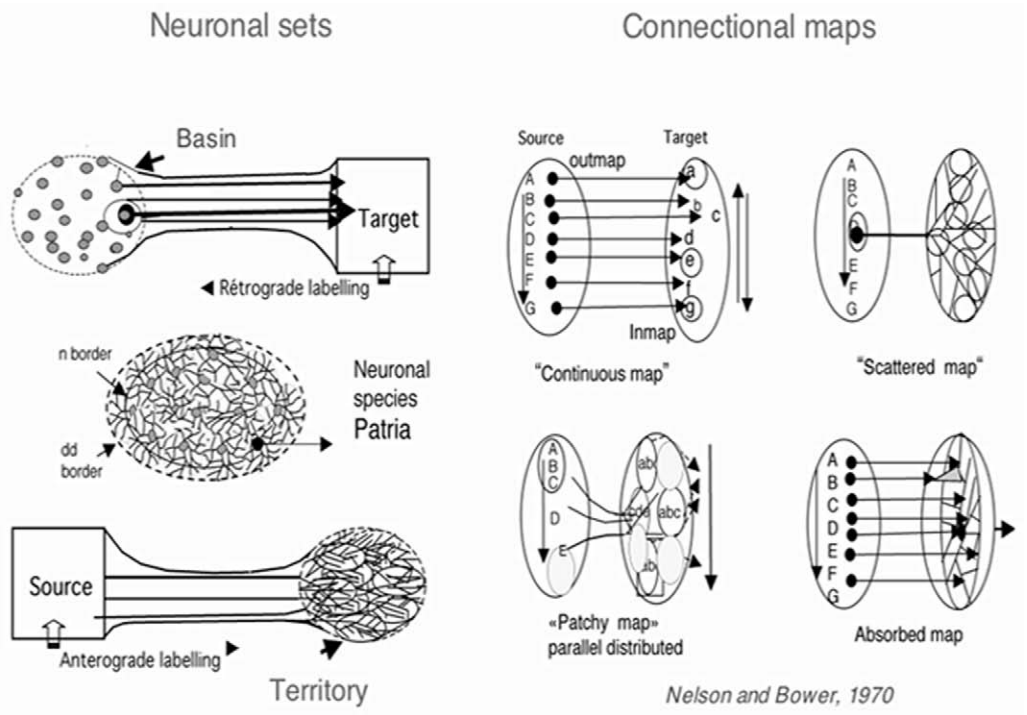

FIGURE 20.3 On the left, neuronal set spaces. The nucleus is the metrical space of all somata of one neuronal species. The patria is that of all dendritic arborizations of one neuronal species. The two borders do not necessarily always coincide. The basin is the metrical spaces containing all origins of neurons sending axons to one target. The territory is the space covered by all axonal arborizations from one source. On the right, connectional maps. Differentiated items may be differentiated in a source (basin). This inner order is an (output map) outmap. Differentiated items may distributed in a target. Their order is an (input map) inmap. The transfer of the outmap to the target may be made in different ways. Nelson and Bower (1990) distinguished three kinds: continuous, scattered, and patchy mappings. The first is the preservation of the discrete order present in the source by an ordered distribution in the target. In the upper left, the order of the source outmap is similar in the target inmap. A reverse order is still the same map. For getting such a distribution, in neuronal set terms, the space covered by one axonal arborization must be small enough (a) in comparison to the whole size of the target to maintain a distinct item of information and an about equal number of differentiated zones. This implies that the receiving dendritic arborizations of the targets is small enough to maintain about the same number of distinct items of information. This is observed in sensory systems. The outmap can be completely lost in the case where every separate element of the source is able to send information to any element of the target (scattered). This is also obtained when every neuron in a target is able to receive information from any distinct items of the source (absorbed). A frequent case in the brain uses islands or subgroups. The outmap is broken in several subparts. Each may give two or several inmaps in the target. This is a possible substrate for parallel distributed processing.

Continued

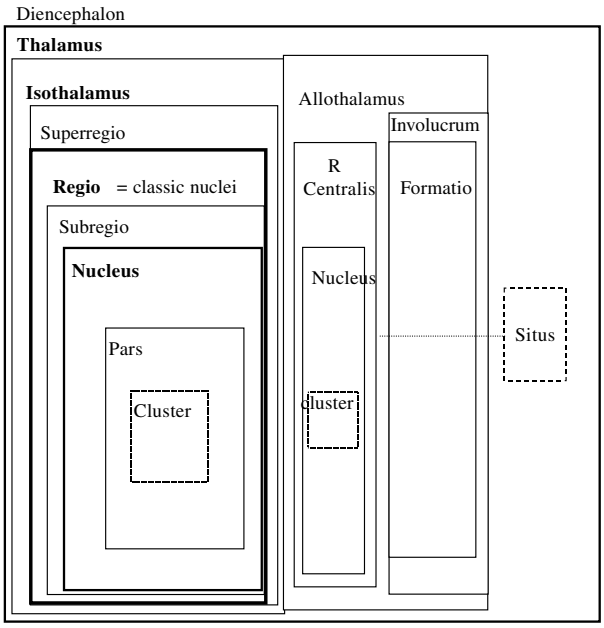

FIGURE 20.3 *Continued* Diagram of the hierarchical subdivision of the thalamus. As for zoological taxonomy, all levels are not filled. A site is not a formal subdivision and simply a distinctive topographic indication.

lateralis or lamella perithalamica (Fig. 20.2A) separating the "ventral thalamus," which is in fact lateral to the "dorsal thalamus" or better perithalamic (Ramon-Moliner, 1962, 1975) from the bulk of the thalamus. The geniculate bodies, ancient "metathalamus," leave early the thalamic mass but are parts of the dorsal thalamus considered here as the thalamus. The main subdivisions of the diencephalon are thus the thalamus and two nonthalamic elements, the epithalamus (habenula) and the perithalamus.

Epithalamus

In Rose and Woolsey's classical concept (1949), the "epithalamus" comprised the "paraventricular complex, habenular complex and the pretectal group of nuclei" not linked to the cortex. Only the habenular complex will be evoked. Habenula (small habena) means belt. This described the stria. The cellular part, commonly designated today as the "habenula" was the "ganglion habenulae" (Sachs, 1909; Hb, Figs. 20.1 and 20.2). This is made up of two nuclei (nuclei habenulae, Nomina anatomica): the nucleus habenulae medialis (HbM) and lateralis (Hbl) with contrasted neuronal types and immunochemical properties. The medial is densely stained by Nissl techniques with small round somata. The main afferent system comes through the stria medullaris (sm, Fig. 20.1). This is a bundle of myelinated axons, a noticeable part of which are pallidohabenular (Nauta and Mehler, 1966; Percheron *et al.*, 1996; Parent *et al.*, 2001). This major connection, in number of axons, is not understood yet. The major efferent bundle is the habenulointerpeduncular tract (fasciculus retroflexus of Meynert, 1872). Arising from the two habenular nuclei, it passes medially and then below the caudal pole of the medial nucleus of the thalamus, and then through the central complex and through the red nucleus to end in the interpeduncular nucleus. Part of this bundle is made up of cholinergic axons. The habenular system offers strong topographical marks for the analysis of the thalamus. The "stria medullaris thalami" (sm, Fig. 20.1 and 20.2) and the taenia thalami form the line of attachment of the tela choroidea and mark the superior roof of the third ventricle.

Perithalamus

As will be seen later, the classical subdivision of the thalamus was done using reference to myelinic lamellae. Arnold's (1838), the first, described a "stratum reticulatum" (reticulate not "reticular"), lateral to the thalamic mass. It was separated from it by the lamella perithalamica or "lamina medullaris externa" pursuing the embryological lamina limitans of Kuhlenbeck that thickens by the addition of various axons. Kuhlenbeck (1948) described a "ventral thalamus" (opposed to the dorsal one) comprising various elements: the reticulate nucleus, the zona incerta of Forel (1877), the pars ventralis of the lateral geniculate body, and the peripeduncular nucleus (ppd, Fig. L14. The ensemble in fact forms a continuous sheet, wrapping the external face of the thalamus (including that of the lateral geniculate body Fig. 20.3E, F). Below the thalamus, it widens and becomes fuzzy medially to form Forel's (1877) "zona incerta," that, as indicated by its name, has no clear border with the upper mesencephalic reticular formation. Posteriorly the so-called GL ventralis (or "ventral part of the lateral geniculate body") is in fact dorsal and lateral and a perithalamic part in primates. Peripeduncular and perigeniculate extensions are observable (Figs. 20.3B and 20.23B). The whole perithalamus is made up of very large neurons with large dendritic arborizations (leptodendritic, Ramon Moliner, 1969, which is a factor of wide convergence) that are flat and intertwined (Fig. 20.25). There are also a few local circuit neurons (about 15%, Dewulf, 1971). The majority of the large neurons contain parvalbumin (Münzle *et al.*, 1999) making a characteristic dark ring around the thalamus (allowing its differentiation from the motor thalamus in its anterior part). Bungarotoxin (alpha BTX) binding is particularly high with islands of higher concentration.

Other islands of cells and axonal endings are rich in calretinin (Ciccheti *et al.*, 1998; Fortin et al., 1998). The meaning of such islands is unknown. The topological position of the perithalamus in relation to the thalamus on one hand and the cortex on the other hand has been well established by the Scheibels (Scheibel and Scheibel, 1966b), (Fig. 20.5). The perithalamus is linked to the thalamus by collaterals from both thalamocortical and corticothalamic axons. One circuit shown by the Scheibels is short. The thalamocortical neuron sends axonal branches to a perithalamic neuron that sends back an axonal branch to the thalamic neuron (Fig. 20.5A). Another, longer, circuit involves the corticothalamic connection. A corticothalamic axon of a cortical pyramidal neuron sends a collateral to the perithalamic neuron that sends its axon to the thalamocortical neuron, which in turn sends a collateral to the perithalamic neuron. This offers the possibility for short circuits that may be the substrate of rhythmic activities. There is a significant literature about perithalamic degeneration in many species. It has been known for long that the perithalamus partially degenerates after cortical lesions together with the adjoining nuclei, at a date later than the thalamocortical neurons (as is also the case for internal circuit microneurons). The perithalamus also receives many cholinergic axonal endings (Heckers *et al.*, 1992). Perithalamic neurons have only one target, the thalamus. The perithalamothalamic axons, usually not much branched, have rather long trajectories through the thalamus, often ignoring the boundaries of nuclei. The anterior pole in macaques gives off more branched axons (Ilinsky *et al.*, 1999). In a comparison of eight species including man, Arcelli *et al.* (1997) showed that the perithalamic formation is a recessive structure (which is evident even between monkeys and human beings). In the human brain, the perithalamus is relatively thin, in some places difficult to delineate, with only few neurons. Arcelli *et al.* (1997) contrast this decline with the large increase in number of local circuit microneurons in the thalamus (Fig. 20.5). Both are GABAergic (inhibitory) and give branches to projection neurons. Perithalamic axons end on thalamocortical or local circuit neurons with long asymmetric synapses. At least 50% of terminal endings from the polar part of the perithalamus end on GABAergic local circuit neurons of the motor thalamus of macaques (Ilinsky *et al.*, 1999). In cats, the perithalamic nucleus is involved in the production of cerebral rhythms. Arcelli *et al.* (1997) made the hypothesis that "with the increase in the number of local circuit neurons in the dorsal thalamus, the Rt role becomes more focused in the regulation of sleep-waking cycle, and/or in acting as a thalamic pacemaker, rather than in direct thalamic inhibition."

THALAMUS

Lamellae and Classic Nuclei. Burdach's Model

The observation of thalamic lamellae was made as early as 1786 by Vicq d'Azyr who noted a "reddish spot" (current medial nucleus) surrounded by a "white circle." Burdach (1822) was the first to use the term "lamina medullaris interna" (lamella medialis, Fig. 20.2A, C) as the reference mark for the topographical distinction of "Kerne" or nuclei, his "innerer Kern" (internus) being medial and his "äusserer" (externus) lateral to it. Two other main subdivisions were the superior (anterior) nucleus and the posterior nucleus or pulvinar. In 1865, Luys added his "centre médian" surrounded by a capsule. A further addition, that of the semilunaris (Dejerine, 1895), cupuliform (von Tschisch, 1896), or arcuatus (Kölliker, 1896) nucleus, to which was linked a middle lamina medullaris, is no longer retained (not being "separating"). Déjerine (1895) insisted on the fact that his "noyau anterieur" was wrapped by a myelinic capsule with two parts: one dorsal, made up of the "stratum zonale," and one ventral, for him a particular thalamic lamella, the "lamina superior or anterior," isolating the anterior (superior) region from the rest (Fig. 20.2A, C). In 1941, the Vogts noted that the term "lamina" (usually designating a set of neurons lying in a row) was misleading and proposed that of lamella (also a recommendation of the Louvain symposium, 1963; Dewulf, 1971), which is followed here. Vogt (1909) and the Vogts (1941) indicated that only the superior part of the capsule surrounding the centre médian (supracentral) was the ventral continuation of the lamella medialis (their La.m., lm, Fig. 20.2B). The lateral part was said to form a distinct entity, their lamella intermedia (La.im, lamella centralis, lc, Fig. 20.2B). This is important for the interpretation of the central region (see regio centralis). Burdach's lamellar system, completed by Luys, forms the "classic model," separating what may be called the "classic nuclei" by the classic lamellae. This model was referred to for decades in works by Forel (1877), Sachs (1909), and Malone (1910). Figure 218 of Foix and Nicolesco (1925) shows the system of laminae that was generally used. At the Louvain meeting, it was recommended that the classic nuclei (separated by lamellae) be denoted "regions" or "formations".

Limiting Elements. Allo- and Isothalamus

The early use of staining techniques following Nissl showed that parts of the lamellae were not simple myelinic entities and contained neurons (Malone,

1910, "nucleus reuniens"). Classical nuclei were thus separated or surrounded by darker elements, particularly making a circle (rather a shell) around the medial nucleus—Foix and Nicolesco's (1925), "formation circulaire hyperchromique," Grünthal's (1934) "nucleus circularis," or Hassler's "involucrum" (or "enveloppe")(see Figs. 20.2 and 20.4). These limiting elements (in the lamellae and elsewhere) have neuronal genera different from those of the bulk of the nucleate thalamus. This is composed of similar neurons organized in the same manner and thus said to form the isothalamus (Percheron *et al.*, 1996; Fig. 20.4). By contrast, the limiting elements are said to constitute the allothalamus. Starting from Louvain's recommendation, it was proposed to reserve the term "regio" for classic nuclei and that of "formatio" for separating elements (Percheron *et al.*, 1996). The central region raises a particular problem because it is both a classical nucleus and allocortical. It is considered here as a region. For practical reasons, the study of the allothalamus is placed at the end of the chapter. To understand the spatial distribution of the limiting elements (particularly intralaminar-limitans), the reader could benefit from looking at Figure 20.24, on which the intralaminar system seems to stem from the adhesio, surrounds the medial nucleus, and ends in a complex way posteriorly to the central region. The lamellar system and the classic model with classical nuclei interpreted from these bases are shown on Fig. 20.2 on transverse sections (A, B, E, F) and two horizontal (C, D). The lamellar system ends at about one half of the length of the thalamus (Figs. 20.2C and 20.7A). There is no complete separation of the medial and posterior regions. All classic nuclei are not delineated by lamellae. For instance, there is no lamella between the posterior part of the lateral and the posterior regions. Anyway, the classic model remains a satisfactory base for the description of the thalamus, allowing to start from major classical works.

The analysis of pathological cases and the use of new techniques, anatomical and physiological, soon showed that some classic nuclei were composed of several anatomofunctional elements. For a long period, these were given the name of "nucleus." The reliance on a single elemental entity, the nucleus, sometimes subdivided in pars, led to a great confusion in the description of the thalamus.

The naming of thalamic parts must take into account the hierarchy of neuronal sets: cerebral part, diencephalon, thalamus. The belonging to either the iso- or the allothalamus leads to different categories. The isothalamus is subdivided into regions, representing the large classical "nuclei." These furnish the first adjective and acronym. The regions may correspond to one nucleus but more often correspond to several subregions. Subregions, are structurofunctional parts of regions. In the case of the lateral region, they are elements of the posteroanterior sequence of territories denoted by the second adjective. As for the zoological system, all levels are not necessarily filled. A regio or subregio may be made of a single nucleus (medialis for instance) and may be simply described as nucleus. Parts (of a nucleus) are designated by the third adjective medial or lateral, inferior or superior. A nucleus can have no pars. Clusters are elements such as rods, lamellae, and islands. Siti (sites) denote topographical places not necessarily positioned in the hierarchy (though often at pars level). They are characterized by their situation, have been often described as nuclei, but may not be a distinct subdivision.

ISOTHALAMUS. CONSTITUTION, ARCHITECTURE, AND FUNCTION

Contrary to its division into smaller masses and to the diversity of the afferent systems, the basic histological constitution of the bulk of the thalamus is made up of the same kinds of elements throughout. The parts of the thalamus built with these elements form the isothalamus (Percheron *et al.*, 1996). This is made up of two neuronal genera: the Golgi type I, "bushy" neuron (Kölliker's Buschzellen, 1898) (Fig. 20.4A) and the Golgi type II (von Monakow's Schaltzellen, 1895; McLardy's microneurons) (Fig. 20.4B). The first is the thalamocortical neuron having a long and robust axon aimed at its outer (cortical) target. The second is devoted to local circuitry. The two are engaged in particular relations. Dendritic arborizations of "tufted." "radiate," "bushy," "principal," thalamocortical, Golgi type I neurons are so peculiar as to be easily recognized in almost all mammalian species and particularly in man. Their graph theoretical analysis (Percheron, 1979, 1982) indicates the abundance of branches, measured by the number of dendritic tips, among the highest in the brain, increasing in evolution (Percheron *et al.*, 1996). There is a rather high number of stems. These stems are the origin of as many radtrees (Percheron, 1979, 1982). Topological parameters are different in individual nuclei and animal species but stable in the same place and animal species, which allows the identification of neuronal species. Metrical features of dendritic arborizations also are noteworthy. While terminal branches, twigs, are long, internodes and stems are usually short. Most nodes are close to the soma. The result is that there are grossly two zones, one proximal (somatic and proximal dendritic) and one distal. Distal inputs run on the longest distance on

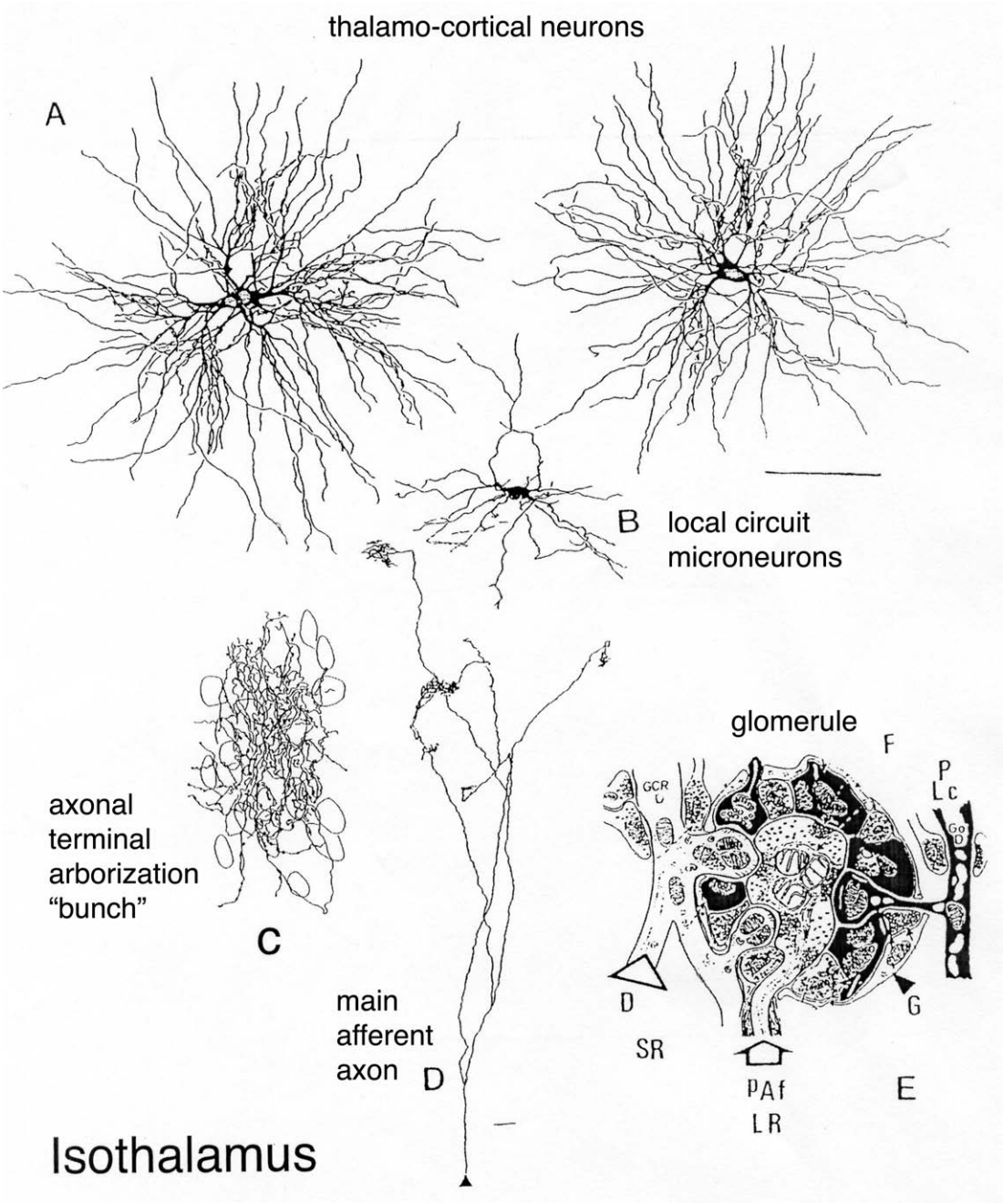

FIGURE 20.4 Elements of the isothalamus. **(A)** Upper row (from Percheron *et al.,* 1996). Two fully reconstructed bushy thalamocortical neurons. Note their high degree of branching. The number of branches and the diameter of arborizations vary with the location in the thalamus and with animal species (growing in evolution). Thick dendritic stems give dendritic subtrees branching close to the soma. Numerous and close branching give these neurons a very recognizable look and specific properties. The presence of such neurons suffices for defining the isothalamus. **(B)** Local circuit microneuron with few short branches and axonlike processes. The percentage of these neurons depends on thalamic parts and animal species (increasing in evolution, maximum in man and "associative" parts). (**C** and **D**) Afferent axon (pallidal) from Arrechi-Bouchhioua *et al.,* 1996). Fully reconstructed pallidal axon from its entrance to its ending in the thalamus. This species of axons gives several long branches and separate terminal axonal arborizations . These "bunches" are dense. The magnification is different from that of A and B. Several of them are thus necessary for covering one dendritic arborization (bringing convergence). One important component, corticothalamic endings, should have been added. **(E)** Early representation by Szentagothai *et al.* (1966) of a thalamic synaptic complex, here a glomerulus (in the GL of a cat), representing an extreme in differentiation of thalamic synaptology. One axonal ending of the principal afference (pAf) gives a large round bouton (LR) synapsing with the dendrite of a bushy thalamocortical neuron (D) and with endings of local circuit neurons (Lc). The glomerulus is closed by a glial capsule (G). The endings of corticothalamic neurons giving SR boutons are usually located more distally on the dendritic arborizations of the thalamocortical neurons. Two other types are F flattened for perithalamic axons (and others) and P from local circuit microneurons.

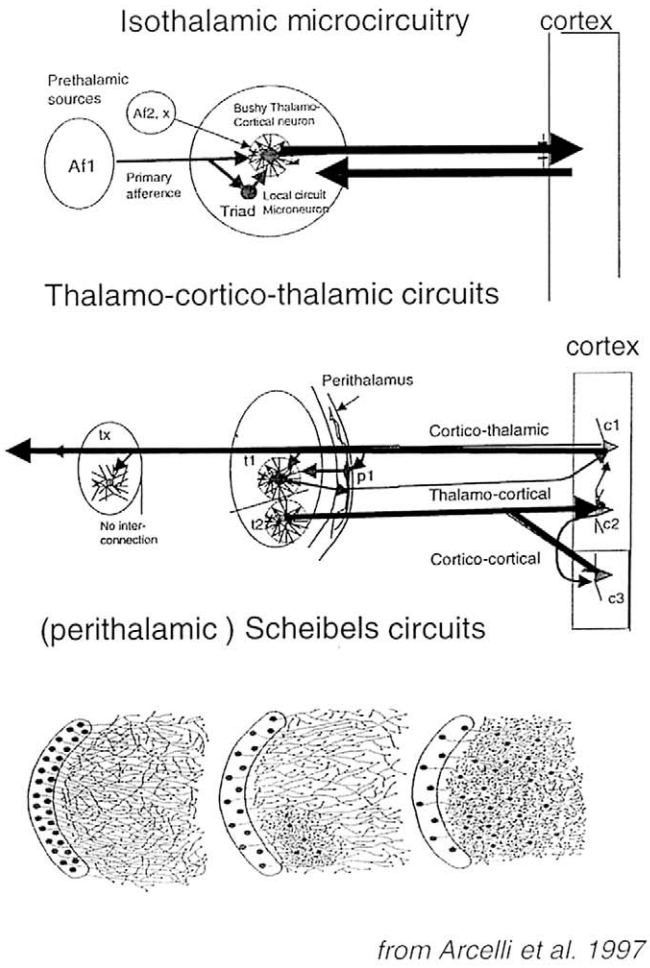

FIGURE 20.5 Topological positions of the perithalamus and local circuit neurons in relation to the cortex and thalamus. The perithalamic neuron with a very large (flat) arborization receives collaterals from the thalamocortical neuron (t1). Perithalamic neurons (p1) have a single target, the thalamus, to which they send an inhibitory message. There is thus a first Scheibels' minicircuit (t1-p1-t1). Another, which is longer, introduces the pyramidal corticothalamic neuron (c1). t1 sends an axon to c1. This, in turn, sends a collateral to the perithalamic neuron (p1), which sends back its axon toward thalamic bushy neurons (t1, thus t1-c1-p1-t1). There is no direct thalamothalamic (t1-t2) but extended corticocortical (c1-c2) interconnections. Thalamocortical neurons generally have several targets (t2 to c2+c3). Corticothalamic axons are generally modestly branched and overpass the nuclear boundaries, usually reaching other thalamic targets (tx). Within the same isothalamic region, a primary afference (Af1) gives synapses to the principal, bushy, thalamocortical neuron and to a local circuit neuron. This sends back synapses to the bushy neuron, forming a triad. The thalamic neuron thus receives two consecutive messages the first (excitatory or inhibitory) from the primary afference and the second, inhibitory, from microneuron. Bottom row. shows the progressive replacement in evolution of perithalamic by local circuit neurons (Arcelli *et al.,* 1997, Fig. 10).

twigs without encountering other afferent branches. Confluence of flows is made only very close to the soma and trigger zone. The three-dimensional geometry of the dendritic arborizations are usually spherical, sometimes modified by local factors and, except for the lateral geniculate body and some arborizations in the lemniscal relay, have no privileged orientation in relation to axonal afferents. The diameter of the arborizations is moderate, around 350 to 500 µm in the "basic" isothalamus, but can be larger in some nuclei. Another remarkable morphological feature of bushy, thalamocortical, neurons in Golgi preparation and in injected neurons is that their long, thick, myelinated axon does not emit initial collaterals (which is not so common) (Fig. 20.5). This means that a given thalamic neuron at one thalamic place does not communicate its leaving information to neighbor neurons (Fig. 20.5). On the contrary, all neurons give *en passant* collaterals

to the perithalamus (Fig. 20.5). Isothalamic neurons do not survive the transsection or serious lesioning of their axon. Their soma degenerates and dies (von Gudden's retrograde degeneration). The terminal axonal arborizations are generally dense in one or several successive bunches ending in layer IV in the eugranular cortex or in the lower part of layer III corresponding to "specific axonal endings." The mediator used by the thalamocortical neurons is glutamate. They stain for CAM II K alpha (Benson *et al.*, 1991; Jones, 1994), evocative of the presence of an exitatory aminoacid (Steriade *et al.*, 1997). They also stain for either calbindin or parvalbumin "and virtually never for both" (Jones and Hendry, 1989); the staining is used to differentiate neuronal groups and nuclei. Jones (1998) elaborated a theory differentiating islands of parvalbumin positive neurons among a "matrix" of calbinding positive neurons, the first projecting to deep layers of the cortex and the other to its superficial layer I. They were presented as constituting two classes of thalamocortical neurons, which is disputable.

The second type of isothalamic neurons is the "local circuit neuron," "interneuron," intrinsic, Golgi type II neuron (Fig. 20.4). They have a small soma (McLardy's, 1963, "microneurons") and short dendritic arborizations, around 250 µm. These arborizations are irregular in topology and three-dimensional geometry, apparently dependant on local conditions. They sometimes have one (or several) distinct axon that branches close to the dendritic arborizations. However, more generally, there are many thin axonal appendages stemming from dendrites, even from their distal part or their tips (the dendrite seems to end as an axon). The thalamic microneurons are GABAergic (inhibitory). Letinik and Rakic (2001) recently found that a part of them is of telencephalic origin in the human, and only in our species, which would serve to increase their number. Microneurons survive longer after cortical lesions but, after several months, do not survive the death of the thalamocortical neurons. The relative percentage between the two isothalamic genera was measured by Dewulf *et al.* (1973), Dom (1976), and Braak and Weindl (1985) in the human and Hunt *et al.* (1991) in the monkey. The ratio increases in evolution (Ilinsky and Ilinsky, 1993) from back to front in the formatio lateralis. The numbers given by Dewulf *et al.* (1973) should be corrected by a supplementary correction of 10–15% for stereological reasons argued by Hunt *et al.* (1991). All studies show that the relative percentage of microneurons is high, about 25% in many nuclei, up to 50 or 60% in the superregio medioposterior of the human brain. This ratio is an index of complexity.

Three kinds of afferent axons are distinguished: the "primary," supplementary, and corticothalamic axons (Fig. 20.4). Primary afferent axons from "prethalamic" sources belong to large afferent bundles and are numerous, usually with abundantly branched terminal arborizations forming dense territories. This is the case for sensory afferences (optic, auditory, gustatory, somesthetic), cerebellar, pallidal, nigral, mamillary, and fornical. The other afferent axons end usually as coafferences within primary territories, often in an insulate manner. They may completely cover or not the territory filled by the axonal arborizations of the primary source. Concerning cortical afferences, a forgotten law is that every isothalamic part receives many more axons from the cortex than it sends thalamocortical axons. This increases noticeably in the phylogenetic scale. Not only does the thalamus inform the cortex, but a strong influence is also exerted upon the thalamus.

The "principle of reciprocity" (Diamond *et al.*, 1969; Jones, 1985), asserting that every part of the cortex that receives axons from one thalamic subdivision sends back its axons to this cortical focus, is generally true but not absolute. The layer receiving thalamic axonal arborizations (IV), being different from that of the corticothalamic neurons (usually in layer VI), Crick and Koch (1998) proposed their "no-strong loops theory" (in fact circuits) made up of "driving" (thalamocortical) and "modulating" connections. Usual corticothalamic axons (Rockland's type 1, Rockland, 1994, 1996) are very sparsely branched and make connections with dendritic arborizations along an almost straight direction (see Yen in Jones 1985; Rockland, 1994), but can go deeply into the thalamus. This leads to feeding information on a long distance with a very low density. Corticocortical connections can transfer the receiving thalamic information to another focus (Fig. 20.5). The ultrastructural study of the isothalamus, started in the sixties (mainly in the lateral geniculate body where degeneration could be easily obtained, Szentagothai, 1960, 1962; Colonnier and Guillery, 1964; Szentagothai *et al.*, 966; Peters and Palay, 1966; Jones and Powell, 1969; Harding, 1971, to select only some), established a peculiar pattern of connectivity that appeared to be also observable in other isothalamic nuclei including the "associative" pulvinar (Mathers, 1972a). Four types of presynaptic terminals are described. The first corresponds to the so-called RL (Guillery, 1969, for round large) or LR (Harding, 1971; Fig. 20.4) terminals, which are electron dense with large mitochondria and round vesicles forming asymmetrical synapses. It is the primary afferent terminal (terminal of the principal prethalamic afferents, pAf, Fig. 20.5E). A frequent type—designated as small round terminals, RS or SR, or small, electron-dense that also forms asymmetrical synapses—is mainly located on the distal part of dendritic arborizations. Many SR

terminals are corticothalamic but not all, for many remain not degenerated after decortication (Mathers, 1972; Harding, 1973). F (for flattened) terminals are relatively electron lucent and form symmetrical synapses. They are GABAergic and end close to the soma. All perithalamothalamic terminals and some local circuit microneurons are of this type. P (Harding, 1972, PSD) terminals are also electron lucent, contain flattened vesicles, are GABAergic, and form symmetric synapses. They are terminals of local circuit neurons. The terminals are organized according to particular patterns. One is the "triad" (Fig. 20.5). It consists of a synaptic connection from the primary afferent (pAf, 5) to dendritic portions of both the thalamocortical and the local circuit microneuron and a synaptic connection from the latter to the former. Triads lead to particular functional properties (Labos *et al.*, 1990). A major pattern is the "glomerulus" (Szentagothai, 1963; Majorossy *et al.*, 1965) (or "archipelago," in case of numerous terminals and combinations), made up of a dense group of synaptic boutons distributed around the large bouton (LR) of the primary afference (Fig. 20.5). It is completely or more often partially ensheathed by glial profiles (G, Fig. 20.5, "ensheating processes"). The main bouton (T1 in sensory systems) ends on a large, central, dendritic segment (D1) of the thalamocortical neuron. The principal afferent terminals (and glomeruli) are often on the soma or on the stems or proximal dendritic segments. Also included in glomeruli are axonal endings of microneurons (P). There are dendrodendritic synapses and synapses between interneurons that may form complex patterns. A particular case is met in the "associative" isothalamus where there is no prethalamic (primary) afference (to be discussed in regio posterior). The extraglomerular part of the isothalamus ("interglomerular neuropil") is made up of the same elements with variously complex arrangements. The most frequent profiles there are the SR boutons. Another indicator of the complexity of isothalamic synaptology is the existence of synapses and minicircuits between local neurons. This characteristic increases in evolution and from back to front in the lateral region (Ilinsky and Kultas-Ilinsky, 1993). The general pattern of isothalamic synaptology is organized in different ways in the nuclei receiving various modalities of information. The glial sheath is more or less closed. The terminal endings of the primary afference are more or less numerous, as well as secondary afferences or local circuit neurons elements. But, to some extent, as already noted by Szentagothai (as early as 1970), the design of the (iso)thalamic machinery may be said to be about the same, depending on the afferent system, only by particular modifications of the general pattern.

The isothalamus works with essentially two mediators. Glutamate, the mediator of the thalamocortical neurons, is also that of the corticothalamic neurons (showing that a binary circuit may be built with the same transmittor) and that of the main afferences—cerebellar and lemniscal. GABA, the mediator of local circuit microneurons is also that of the perithalamothalamic connection and of two main afferences—pallidal and nigral. The "three types of ionotropic glutamate receptors (AMPA, KA and NMDA subtypes) are present and are distributed rather uniformly" but "little is known about metabotropic glutamate receptors" (Kultas-Ilinsky and Ilinsky, 2001). Some other mediators are added by particular afferences, e.g., acetylcholine or enkephalin.

The isothalamus is a fine-grain structure. Thalamic dendritic arborizations of both bushy neurons and microneurons are relatively small, less than 500 μm, making possible the separate distribution of many distinct items of information. Bushy neurons not emitting local collaterals, and microneurons having only short branches, there is no possibility for direct intrathalamic internuclear connections. Specific terminal axonal arborizations are about the same size. There is thus a framework for separate channels for different modalities. Thalamocortical neurons have in common the sending of their axons to the isocortex, with also a general pattern. The isothalamic device probably everywhere does the same basic information processing, giving the access of prethalamic information to the cerebral cortex. The first role of the isothalamus seems to be to filter and format the various kinds of arriving messages in a form "readable" by the cortex. This is helped by the cortex itself, which sends important corticothalamic feedback. The isothalamus would thus be at first a translator. It also distributes and combines in space and time the output to several cortical targets. The second function of the isothalamus would be thus that of a distributor or selector to particular and possibly various areas of the cortex.

REGIO SUPERIOR

This thalamic region links together elements that were united at the beginning and inappropriately separated later, for decades. The nucleus superior of Burdach (1822) or nucleus anterior (Dejerine, 1895; Sachs, 1909; Foix and Nicolesco, 1925) extended posteriorly, as far as there was a lamella superior. Later, the posterior part of this nucleus was removed and misleadingly linked to the lateral (or dorsal) nuclei, as the nucleus "lateralis dorsalis." The knowledge about the constitution and connections of this element led

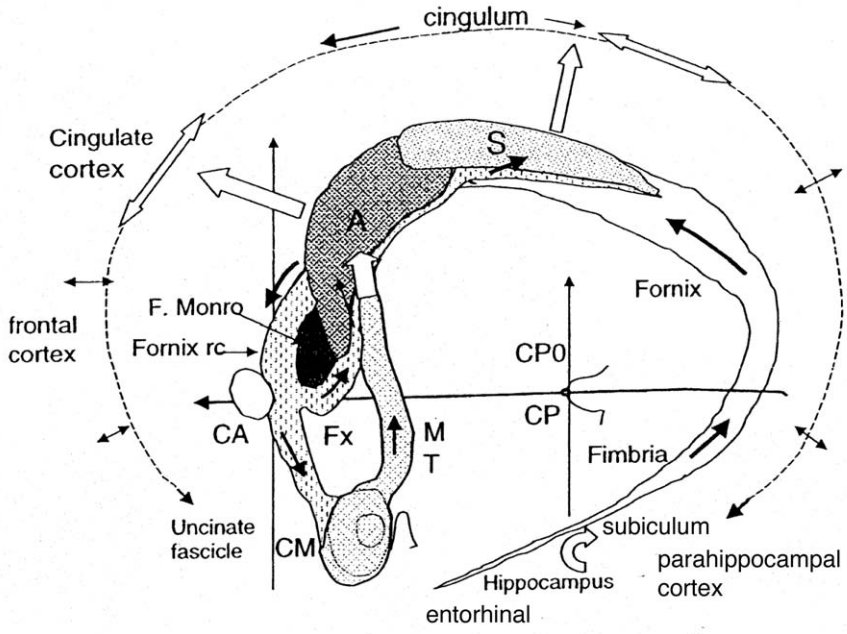

FIGURE 20.6 Regio superior. The two elements of the superior region (A, nucleus anterior; S, nucleus superficialis or superior) are shown in their positions with the complex trajectory of the afferent system from the hippocampus, fimbria, and fornix. After turning around the superior face of the thalamus, the fornix arrives as the anterior pilar close to the anterior commissure. There, a retrocommissural component passes dorsally to the commissure and divides into two parts. The first continues ventrally and reaches the mammillary body (corpus mammillare, CM). From there, a major bundle is emitted, the mammillothalamic tract of Vicq d'Azyr (MT). After a dorsalward sinuous trajectory, this reaches the inferior part of the anterior nucleus where it forms (in part) the lamella superior. The other component of the retrocommissural fornix turns round the inferior border of the foramen of Monro. It also reaches the anterior nucleus but through the superior lamella and essentially runs to the nucleus superficialis. The two nuclei have almost similar connections from the hippocampal system: the nucleus anterior, indirectly through the mamillary body, and the superficial directly. The two nuclei receive axons also from the cortex, at first cingular but not simply. The anterior nucleus has connections with the frontal cortex, and the superficial, with the parietal cortex. Both contribute to a major bundle, the cingulum, which links together many cortical regions and comes back to the parahippocampic cortex.

some to link it again to the anterior nucleus (Yakovlev *et al.*, 1960, 1966; Locke *et al.*, 1961, 1964; Van Buren and Borke, 1972). The regio superior (Percheron, 1969; Percheron *et al.*, 1996) is thus simply the classic anterior or superior nucleus, located above the lamella superior. It is superficial and may be observed on the dorsal surface as the protruding "anterior tubercle" ("tuberculum anterior") (already shown by Vicq d'Azyr, 1786, Fig. 20.1B). The region, larger in this anterior part, is elongated in the anteroposterior dimension. Starting at the anterior part of the thalamus, it ends progressively and merges into the pulvinar. The region constitutes a clearly distinct entity, as it is almost everywhere separated from both the medial and lateral regions by the lamella superior (Fig. 20.2). The "capsule of the anterior nuclei" and the internal lamina differentiate at about 104 mm (Dekaban, 1954). The superior lamella derives from the stratum zonale (Fig. 20.2A) downward with the addition of mamillo- and hippocampothalamic axons. The capsule makes superior elements "closed nuclei" (Mannen, 1960) and more precisely "enclosed nuclei" (Percheron *et al.*, 1996). The presence of a capsule between the nuclei anterior and superficialis separates two "enclosed nuclei" (Fig. 20.6A, 23 L6) one completely, the other only partly. The human "regio superior" is thus divided in two nuclei: anterior and superficialis or superior.

The anterior nucleus (Dejerine's 1906 and Foix and Nicoleco, 1925, "noyau antérieur"; "nucleus anterior" Sachs, 1909; Grünthal, 1934; McLardy, 1950; Russel, 1954; Feremutch and Simma, 1955, 1971; Van Buren and Borke, 1972) is the major ("nucleus anterior principalis", Apr., Vogt and Vogt, 1941), most traditional, nucleus. It has an inverted piriform shape in sagittal sections. In nonhuman species, the nucleus has been often subdvivided into two or three parts: anteroventalis or anterior ventralis (AV), anteromedialis or anterior medialis (AM), and anterodorsalis (AD) said to constitute as many nuclei. The presence and extent of these parts greatly changed in evolution. The subdivision of the anterior nucleus between the antero-

ventral (AV in fact dorsal) and anteromedial (AM) nuclei, already unnecessary in macaques, no longer appears to persist in man (except for coarse SP terminals exclusively observed in AV, Mai *et al.*, 1986). The nucleus anterodorsalis in nonhuman primates is a flat, oblong nucleus lying on the mediodorsal side of the nucleus anterior, from which it is separated by a lamella. In nonhuman primates, the cytoarchitecture of AD has darker cell bodies. It is not certain whether such a nucleus persists in man. Not considered by Toncray and Krieg (1946), the Vogts (1941) gave it the simple status of an accessory nucleus (nucleus anterior accessorius, Aac.). In many individuals, it is indeed made up of the same kind of neurons as the principal part. In macaques, the still obvious anterodorsal nucleus is known to receive afferences from the two (ipsi- and controlateral) mamillary bodies (Veazey *et al.*, 1982). The disappearance of this subdivision means a stricter lateralization of the system. The "anterior nuclear group" of textbooks usually meant AV + AM + AD but did not include the nucleus superficialis.

The nucleus superficialis or superior (S) ("nucleus lateralis dorsalis," LD), is today bound to the anterior group and more appropriately named "Superficiale" (Sf) by the Vogts (1941, II), "nucleus dorsalis superficialis" (D.sf, Hassler, 1959; Van Buren and Borke, 1972) or more simply nucleus superficialis (S. Percheron, 1966; 1996) or superior. It begins anteriorly just before the anterior nucleus ends (Fig. 20.6). It is in the same general topographic position as the anterior nucleus. Posteriorly, it remains superficial, becomes thinner, often makes irregular islands ("nuclei disseminati," Sachs, 1909; Riley, 1960), and moves laterally where it seems to fuse with the pulvinar. It must not be confused with Hassler's Pu.sf, which is more medial and is in fact a part of the pulvinar. The neurons of the two superior nuclei are typically isothalamic, radiate, and "bushy," with rather small dendritic fields. There is a rather large number of microneurons (32% in the anterior and 26% in the nucleus superficialis, Dewulf *et al.*, 1969, 1971, up to 42% GAD-IR neuirons, likely local circuits neurons, (Dixon and Harper, 2001), while they are only very few of them in rats (Dekker, 1976). The anterior nucleus is not covered by the perithalamus anteriorly and dorsolaterally (Fig. 20.2C, 13 L 6). It is rich in cholineric endings (Heckers *et al.*, 1992) in man and heavily stains for acetylcholinesterase (Jones, 1985). One of the characteristic of the region is its staining for calretinin (mainly fibers, Morel *et al.*, 1997; Fortin *et al.*, 1998; Münzle *et al.*, 1999). The (3H) nicotine binding is high, which would represent a significant difference of distribution between rat and monkey (Spurden *et al.*, 1997). There are GABA neurons, mainly local circuit microneurons (Hunt *et al.*, 1991) and a GABAergic innervation, with BZ GABA receptors more frequent in the monkey than in the cat (Bentivoglio *et al.*, 1993). As for other isocortical parts, axonal terminations of mamillary neurons are mainly located on proximal dendrites, while those of the hippocampus and cingulate cortex end on distal dendrites (in the rat, Dekker and Kuypers, 1976; Fig. 20.4 of Bentivoglio *et al.*, 1993).

The main afference to the regio superior is hippocampal, either directly or indirectly, through the fornix and the mamillary body (Fig. 20.6). The axons come from the subiculum ("subiculum proper" Krayniak *et al.*, 1977; Aggleton *et al.*, 1986; Van Hoesen *et al.*, 1993), prosubiculum (Aggleton *et al.*, 1986) and to a lesser extent from CA1 (Van Hoesen *et al.*, 1993) and presubiculum (Krayniak *et al.*, 1979; Aggleton *et al.*, 1986). Subicular axons gather in the fimbria, continue over the thalamus via the fornix, a large bundle increasing in size in evolution. When it arrives close to the foramen of Monro and the surface of the third ventricle, the fornix forms its "anterior pilar" supplying the main part of the "post commissural component" (Figs. 20.1 and 20.2C, D). From there, axons separate into two bundles: one proceeds to the mamillary body—and from there to the superior region—and the other directly to the latter regions in turning around the inferior border of the foramen of Monro (Poletti and Creswell, 1977; Fig. 20.6). The connection from the mamillary body to the anterior nucleus was identified a long time ago. The mammillothalamic tract is so obvious in man that it was dissected and first described in 1786 (Vicq d'Azyr, Pl. XXV; see also Cooper, 1950; Crosby *et al.*, 1962). "Vicq d'Azyr's bundle," as it became named, usually makes a double curve in the sagittal dimension first convex to the rear and then concave (Fig 20.6) and reaches the anterior nucleus at its inferior and lateral border participating in the lamina superior and making the border of the region particularly visible (Veazey *et al.*, 1982; Fig. 20.6). In simians, the main afferent system to the mamillary body is through the fornix (Powell, 1973; Poletti and Creswell, 1977; Aggleton *et al.*, 1986). In man, the mamillary body, the mammillothalamic tract, and the anterior nucleus system make up a major neuronal system that increases in evolution, even in comparison to monkeys (while the lateral mamillary nucleus disappeared in man, Crosby *et al.*, 1962). The system is important in size and in numbers of elements. The ratio between mamillary neurons (411,600) and anterior thalamic neurons (1,069,400) in man is 2.6 (Armstrong, 1986), indicating a limited numeric divergence. While the number of mamillary neurons does not increase from nonhuman anthropoids to human, the number of anterior thalamic neurons does (Armstrong, 1986) (the ratio moving from 1 to 2.6). The anterior nucleus is also furnished by direct hippo-

campal afferents bypassing the mamillary body through fibers of the postcommissural fornix turning round the inferior border of the foramen (Poletti and Creswell, 1977; Mikol *et al.*, 1984, Aggleton *et al.*, 1986). In addition, the anterior nucleus receives afferences from the anterior cingulate cortex through a direct route, round the caudate nucleus (Powell, 1973, Fig. 20.8) and from the posterior cingulate cortex (Vogt *et al.*, 1987). The projection of the anterior nucleus to the anterior cingulate cortex was identified over a century ago, first on human pathological material (Dejerine, 1895), by dissection (Bossy and Lacroix, 1968), and later experimentally (Mufson and Pandya, 1984; Vogt *et al.*, 1987; Bachevalier *et al.*, 1997). The anterior nucleus also sends axons to the posterior cingulate area (Vogt *et al.*, 1987), to the medial cortex dorsal to the gyrus cinguli, to the upper parietal (Niimi, 1962), to the prefrontal, the orbital (Barbas *et al.*, 1991; Carmichael and Price, 1995) and the retrosplenial cortex (Mufson and Pandya, 1984; Vogt *et al.*, 1987).

The nucleus superior does not receive axons from the mamillary body and receives only direct hippocampal afferents through the fornix. This afference was observed in man (van Buren and Borke, 1970; Mikol and Brion, 1975). Axons come essentially from the subiculum (Krayniak *et al.*, 1977; Aggleton *et al.*, 1986) and also, contrary to the anterior nucleus, from the entorhinal cortex (Aggleton *et al.*, 1986). The axons, passing below the foramen of Monro, run in the stratum zonale and reach the anterodorsal part of the nucleus above the anterior nucleus (Poletti and Creswell, 1977; Mikol *et al.*, 1977; Aggleton *et al.*, 1986) (Fig. 20.8). It receives axons from the posterior cingulate cortex (Mikol *et al.*, 1984) and inferior parietal lobule (Asanuma *et al.*, 1985). The nucleus superficialis sends axons to the posterior cingulate cortex (Yakovlev *et al.*, 1960; Locke *et al.*, 1964; Bossy and Lacroix, 1968; Mikol *et al.*, 1977, 1984; Mufson and Pandya, 1984) in continuity with the projection of the anterior nucleus to the anterior cingulate cortex, with some overlap at the junction (Yakovlev *et al.*, 1966). In fact, in man, the nucleus superficialis seems to project strongly also to the anterior cingulate area (Locke *et al.*, 1961). It also sends axons to the retrosplenial cortex, the subiculum (Mikol *et al.*, 1984), the presubiculum (Mufson and Pandya, 1984), the parietal cortex ("area 7"; Niimi and Tutsui, 1962) and the precuneus (7 and 31; Bossy and Lacroix, 1968; Mikol and Brion, 1975; Mikol *et al.*, 1977), which means more than "limbic areas."

The regio superior is an isothalamic region particular by its topography and its links with the historic Broca (1878) "limbic lobe" (cingulate and parahippocampic convolutions). In 1937, Papez described a circuit that started from the hippocampus reaching the mamillary body, the anterior nucleus, and the cingulate cortex and reached through the cingulum, the parahippocampal cortex, coming back to the hippocampus (Fig. 20.6). As already stressed by Shipley (1974), for decades, Papez circuit was not closed (at the hippocampal level). Dagi and Poletti (1983) claimed that "the cingulate cortex is not a prominent link in the Papez circuit." In spite of its success, the Papez circuit is only one among others. The superior region intervenes in these circuits according to complex combinatorics. The shortest are usually thalamocortical two-circuits with the subiculum and the cingulate cortex. One three-circuit is subiculum–mamillary body–anterior nucleus and back to the subiculum. The superficial nucleus receives direct afferences from the entorhinal cortex; another three-circuit is subiculum–superficial nucleus–entorhinal cortex–subiculum. The "Papez circuit" was linked by its author to the "mechanism of emotion". MacLean's included it later in his "visceral brain" (1949), which became his "limbic system" (1952). This led to many ulterior elaborations (see Brodal's, 1981, and Kötter and Meyer's, 1992, critical reviews). Rather than on emotion, the main effects of lesions or stimulation of the superior region provoke memory disturbances. Lesions of the mamillary bodies, Vicq d'Azyr bundle, or anterior and superficial nuclei, bilaterally, cause amnestic deficits such as the "anterograde amnesia" of Korsakoff's syndrome. Lesions of the hippocampal and parahippocampal cortex produce deficit of short-term memory (Penfield and Milner, 1958).

One element of the Papez circuit, the cingulum, is a huge parasagittal bundle of about constant thickness, higher in the posterior cingulate region (Bossy and Lacroix, 1968), that runs above the corpus callosum in the depth of the cingulate gyrus (Yakovlev and Locke, 1961). It links together the two anterior and posterior cingulate areas, the precallosal and retrosplenial regions, and, below the splenium of the corpus callosus, the parahippocampal gyrus. In fact, most axons do not make the whole turn. Most of those from the anterior nucleus do not reach the parahippocampal gyrus, and those from the superficial nucleus do not reach the subgenual or frontal areas (Mufson and Pandya, 1984). The cingulum also contains axons from the oculomotor and inferior parietal cortex (Mufson and Pandya, 1984). The "cingulum related system" is not closed and interconnected with the surrounding frontal (prefrontal and orbital, Vogt and Pandya, 1987; Van Hoesen *et al.*, 1993), parietal and oculomotor (Mufson and Pandya, 1984), and even premotor and motor (Arikuni *et al.*, 1994). The cingulum cannot be reduced to an element of the Papez circuit.

Yakovlev *et al.* (1960, 1966), Locke *et al.* (1961), Vogt and Gabriel (1993), and Bentivoglio *et al.* (1993) defined a "limbic thalamus" as the part of the thalamus that

sends axons to the cingulate, limbic, and cortex. This set, in addition to the superior region, would comprise the medial part of the nucleus medialis, the anterior part of the lateral region (VA), intralaminar, middline nuclei, and even the medial pulvinar (Yakovlev *et al.*, 1966; Vogt *et al.*, 1987; Bentivoglio *et al.* 1993), that is, a heterogeneous anatomical set without known functions. The benefit of such a grouping is not self-evident. The superior region is not so much "limbic" as the thalamic hippocampal territory.

REGIO MEDIALIS

The presence of a round nucleus in the middle part of the thalamus was already noted two centuries ago (Vicq d'Azyr, 1796, for instance). Using the lamella medialis as a landmark, (see "General Considerations"), Burdach (1822) described his "innerer Kern," the "noyau interne" of Dejerine, (1895), Cajal, *et al.* (1925), latinized into nucleus medius (Kölliker, 1895 and 1898) or medialis (Sachs, 1909, Malone, 1910; Nomina anatomica). This has been the term in common use in stereotactic and topographic atlases (Hassler, 1959; Hassler *et al.*, 1979; Andrew and Watkins, 1969; Van Buren and Borke, 1972) and the recommendation of the Louvain symosium (1963). The addition of the adjective "dorsalis" came after the unfortunate consideration, by von Monakow (1895) and C. Vogt (1909), of a "medial part of the thalamus" comprising in addition to the "classical medial nucleus" (C. Vogt, 1909) elements ventral such as the central region, having nothing in common with it. The terms "nucleus medialis dorsalis," "mediodorsal" (MD), "mediale dorsale" (Vogt and Vogt, 1941), and "dorsomedialis" (Sheps, 1945) introduced a persisting confusion that may be avoided by coming back to the initial nucleus medialis. From the beginning, this nucleus was observed to be almost everywhere separated from its surroundings, particularly laterally by the lamella medialis containing intralaminar neurons. Medially, there is a clear border with the formatio paramediana. The main problem is encountered at the posterior pole where there is no continuous frontier with the pulvinar (Fig. 20.2, 13 L9). Dejerine (1895), and many authors since, underlined that they have the same morphological aspect and no clear border. Golgi staining (VanBuren and Borke, 1972, personal material) shows that thalamocortical neurons have similar dendritic arborizations with the same size and shapes. Both regions have the highest number of micro-neurons in the thalamus (36–60.4% in the nucleus medialis, depending on samples or subregions, and 36–50% in the pulvinar, Dewulf *et al.*, 1972), which is considerable. Tracings between the medial nucleus and main pulvinar are carried out by "arbitrarily joining the cell islands of the n. intralamellaris " (Van Buren and Borke, 1972).

The medial nucleus was not divided in man over a long period (Dejerine, 1895; Foix and Nicolesco, 1925; Vogt and Vogt, 1941; Andrew and Watkins, 1969; Van Buren and Borke, 1972; Feremutch and Simma, 0000; Krieg, 1973). A separation was established in lower species (Rioch, 1929; Le Gros Clark, 1932; Crouch, 1934; Walker, 1938a; Olszewski, 1952) into a medial, magnocellular, and lateral parvocellular part. There is a visible "magnocellular" medial part in monkeys. The existence of afferences from the amygdala to this part is well documented in macaques (Nauta, 1961; Porrino *et al.*, 1981; Aggleton and Mishkin, 1984; Russchen *et al.* 1985; personal material). Walker (1938c) found the medial "magnocellular part very reduced in chimpanzees." This subdivision was found missing in more than 50% in human brains (Feremutsch and Simma, 1955). Foix and Nicolesco described a "sensibly unique type" of neurons in man. Cytometric studies made independantly by Dewulf (1971), Van Buren and Borke (1972), and Percheron (1966) did not show significant differences or any mediolateral gradient in somatic size between the medial and lateral parts. These data mean that there is no properly "magnocellular" part in man. This lack of a magnocellular part could cast a doubt on the existence of the amygdalar connection in man. But this connection is likely to persist as Klingler and Gloor (1960) dissected a bundle from the amygdala to the nucleus. However, there is no base yet for tracing the contour of an amygdalar territory in man. Another "lower" connection comes from the ensemble made up of the nucleus basalis, the nucleus of the diagonal band, and the medial septal nucleus (Hreib *et al.*, 1988) sometimes refered to as the "extended amygdala" including Brockhaus' (1938) "supra-amygdala." Vogt (1909), Walker (1938), and Akert (1964), in cercopithecidae described a third, "para-lamellar," subdivision, lateral and close to the lamella medialis—interpreted by some as belonging to the intralaminar formation. For Akert, the three parts—medial magnocellular, lateral parvocellular, and most lateral paralamellar—were three distinct sources of separate thalamocortical connections in macaques (Fig. 20.7). In cercopithecidae, there are in fact two paralamellar parts, not similar in cytoarchitecture: one anterior, in front of the central region, and the other posterior, dorsal to it. They correspond to parts of different territories. The posterior paralamellar site in macaques (pars multiformis of Olszewski, 1952) is a part of the cerebellar territory (Percheron, 1977; Fig. 20.7) with neurons resembling those of the cerebellar

territory in the neighboring lateral region VIm. The anterior paralamellar site, located in front and separate from the preceding, in macaques, receives nigral axons (from the pars reticulata, see subregio rostralis VA) (Ilinsky *et al.*, 1985; Percheron *et al.*, 1996). This part of the nigral territory looks like that located just on the other side of the lamella in VA (see lateral rostral subregion VA). No paralamellar part is described in chimpanzees (Heiner, 1960; Sakamoto, 1964; deLucchi *et al.*, 1965) or (except for a small Mpl for Hassler and pl for Morel *et al.*, 1997) in man. As conceded in the Louvain symposium, most proposed subdivisions in the human nucleus medialis were made on purely myeloarchitectonic differences (more myelinated fascicles being present laterally, Vogt, 1909; Hassler's 1959, 1977, 1979), which was criticized by Krieg, Feremutch, and Simma in Dewulf (1971). Van Buren and Borke (1972) conclude their examination of individual brains at the same level by considering "the n. medialis as a single entity." Immunostaining does not provide a much better tool for subdividing the nucleus. The medial nucleus does not stain for parvalbumin (or weakly, Morel *et al.*, 1997), calbindin or calretinin (Jones and Hendry, 1989; Morel *et al.*, 1977, personal material). Other stainings (e.g., acetylcholinesterase; Hirai and Jones, 1989a; Jones, 1997; Heckers *et al.*, 1992) brings out irregular islands. The topography of such clusters and their relation with cytoarchitectonic differentiation is not established. The lack of visible division in man raises the question whether there are still afferences from the cerebellum, nigra, and tectum in man. The most probable hypothesis today is that the lamella could be not the absolute separator postulated in Burdach's model, allowing territories to straddle it (leading to Feremutsch's heterotopy, 1973). Because of major changes at cortical levels, the two paralamellar sites corresponding to cerebellar and the nigral afferences could have withdrawn to the lateral region. The paralamellar sites and VA of monkeys are reciprocally linked to the frontal eye field (Akert, 1964; Künzle *et al.*, 1976; Akert and Hartman-von Monakow, 1980). The change in cortical oculomotor areas is such that the observed thalamic modifications would not be surprising. The separation between medial and lateral regions being greater in man, connections attributed to the nucleus medialis in macaques, when in its paralamellar part, must not be infered too hastly for humans.

It has been known for a long time that the major afferents to the nucleus medialis are cortical, particularly from the frontal cortex (Nauta, 1964; Akert and Hartman-von Monakow, 1980), according to a reciprocal pattern. This is not exclusive. The anterior cingulate cortex, for instance, projects dorsally, and the precentral motor cortex (Akert and Hartman-von Monakow, 1980), laterally. On the other hand, the medial nucleus is not the simple thalamic target of the medial face of the frontal cortex. Medial frontal cortex also projects to the anterior nucleus and the medial pulvinar.

Most of the knowledge about the efferent connection from the medial nucleus to the cortex came from human pathological material. As is true for other isothalamic elements, the medial nucleus degenerates locally after cortical lesions (von Gudden degeneration). This property was intensively used in the considerable literature devoted to brain examination after leucotomy. After Meyer *et al.* (1947) and Freeman and Watts (1947), McLardy (1950) came to the conclusion that there was a "general circumferential organization such that adjacent regions in the nucleus project to adjacent areas in the cortex." Van Buren and Borke (1972) came to about the same "circumferential" organization (see Fig. 20.7). Contrary to accepted ideas about the medial nucleus, Van Buren and Borke (1972) insisted on projections to cortical regions other than frontal, particularly to the precentral cortex. In macaques, an abundant literature is dealing with the main target of the medial nucleus, the frontal cortex. The intramedial organization of the sources to the various frontal cortical regions was examined by Mettler (1947), Nauta (1962), Leonard (1972), Tobias (1975), Passingham (1975), Goldman-Rakic and Porrino, (1985), Barbas *et al.* (1991), Ray and Price (1993), Bachevalier *et al.* (1997), and Cavada *et al.* (2000). As elsewhere in the isothalamus (see "General Considerations"), mediocortical axons have no local collaterals (Goldman-Rakic and Porrino, 1985). This means that distinct neuronal sources specifically project to distinct targets. In monkeys, the internal distribution was also said to be "circumferential" (Goldman-Rakic and Porrino's, 1985; Fig. 20.7). Kievit and Kuypers (1975) and Kievit (1979) insisted rather on a sagittal organization of the neurons projecting to the frontal cortex. Long stripes of neurons were found to extend not only from the anterior to the posterior pole of the medial nucleus but also anteriorly to the anterior part of the lateral region and posteriorly to the medial pulvinar. These stripes do not contradict the "circumferential" order observed in the medial nucleus since they are also parasagittal. Such stripes are in fact discontinuous (Goldman-Rakic and Porrino, 1985), forming islands with very irregular contours (Rouiller *et al.*, 1999). The frontal cortex had been "defined as the projection area of the mediodorsal nucleus"(Rose and Wolsey, 1948). This is no longer true in both directions. In macaques, the medial nucleus also sends axons to cortical regions other than the frontal: cingulate (Vogt *et al.*, 1979; Baleydier and Mauguière, 1980; Goldman-Rakic and Porrino, 1985; Vogt *et al.*, 1987), insular

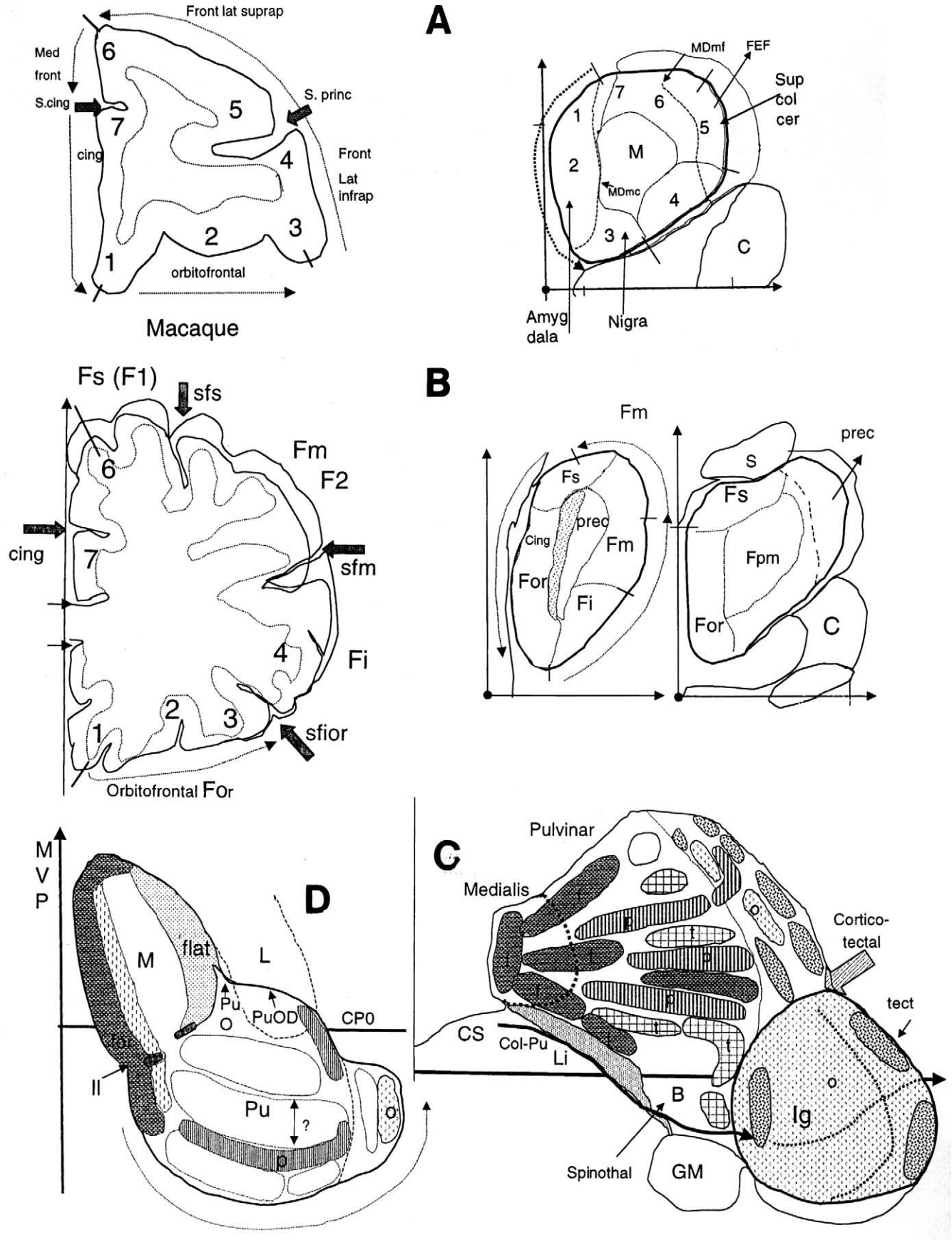
Front lat suprap
Med front
S.cing
cing
S. princ
Front Lat infrap
orbitofrontal
Macaque
A
MDmf
FEF
Sup col cer
M
MDmc
C
Amyg dala
Nigra
Fs (F1)
sfs
Fm F2
cing
sfm
Fi
sfior
Orbitofrontal For
B
Fm
prec
Fs
Cing
prec
Fm
For
Fi
S
Fs
Fpm
For
C
M V P
D
M
flat
L
Pu O
PuOD
CP0
For
II
Pu
?
p
o
C
Pulvinar
Medialis
Cortico-tectal
tect
CS
Col-Pu
Li
B
Ig
Spinothal
GM

FIGURE 20.7 Regio medialis and pulvinar. **(A)** Macaque. *Left,* transverse section of the frontal pole (Fig. 19 of Goldman-Rakic and Porino, 1985; inverted from right to left, midline is on the left). Numbers indicate cortical positions in a circular sequence in relation to cortical faces and main sulci. S.Princ, sulcus principalis. S. cing, sulcus cinguli. *Right*. Part of Section XXX from Olszewski's atlas corresponding to Goldman-Rakic and Porino's level. Position of the sources to different parts of the frontal cortex—"circumferential organization". The cytoarchitectonic borders drawn by Olszewski of the pars magnocellularis medially and pars multiformis laterally are shown. The contours of the nuclei, and subnuclei, not those of the sources placed in relative positions; are topographically mapped. Only the pars magnocellularis could coincide with the source to the orbital cortex. In macaque, the pars paralamellaris receiving tectal and cerebellar afferences projects to the frontal eye field. **(B)** Man. *Left,* transverse sections from Dejerine (Figs. 137 and 138) corresponding to that of the macaque in A. The sulci are indicated according to Bailey and von Bonin (1951). Cing, sulcus cinguli. Sfs, sulcus frontalis superior. Sfm, sulcus frontalis medius. Sfior, sulcus frontalis inferior orbitalis. *Right,* two levels show that the organization remains the same from anterior to posterior and from medial to lateral. The position of the sources are those described by VanBuren and Borke (1972). The spatial organization is also "circumferential," with the source for the orbitofrontal cortex (For) medially. The medial nucleus is not the only thalamic nucleus sending and receiving afferences from the frontal cortex nor the only furnisher of the frontal cortex. It sends axons to the cingular, precentral, and oculomotor cortex. The presence of a pars paralamellaris is not accepted by all in man (see note in the text). **(C)** Organization of the pulvinar in macaques. The position and contours are from Olszewski's (1952) plate XLII. *Left,* the end of the nucleus medialis is continuous with the pulvinar. Four frontal islands f, from Goldman-Rakic and Porino (1985) are radiating from one to the other. The three parietal islands (p) are from Hardy and Lynch (1992). The temporal islands are from Webster *et al.* (1991). The location of collicular islands is from Harting *et al.* (1980), Benevento and Standage (1983). Col-pu indicates the trajectory of tectothalamic axons. The visual pulvinar mainly corresponding to the intergeniculatus (Ig) or inferior part is delineated according to Bender's data. It is retinotopically organized with the limit of the four quadrants indicated by thick lines. The pictures, even not precisely mapped metrically, show that there is no clear mediofrontal border. B is Basal region receiving spinothalamic axons. **(D)** Medial-pulvinar superregion seen from above in man. (thick slice from VanBuren and Borke's 1972 atlas, 2,7 to 13.2). Anterior overlap of the pulvinar oralis dorsalis (PuOD) over lateral formation (L) and cuneiform PuO. Islands of nucleus medialis and pulvinar form a continuous system projecting to the associative cortex. The anteroposterior thickness of pulvinar stripes is not known and likely makes layers in this dimension.

(Roberts and Akert, 1963; Wirth, 1973; Mufson and Mesulam, 1984), parietal (Kasdon and Jacobson, 1978), premotor (Schell and Strick, 1984; Ilinsky *et al.*, 1985; Goldman-Rakic and Porrino, 1985; Matelli and Luppino, 1993; Rouiller *et al.*, 1999), inferior premotor (Matelli and Luppino, 1993), motor accessory (SMA; Goldman-Rakic and Porrino, 1985; Matelli and Luppino, 1993; Rouiller *et al.*, 1999), and preSMA and supplementary eye field, (SEF; Matelli and Luppino, 1993).

REGIO POSTERIOR

The name "pulvinar" comes from Galenus and means pillow or cushion in Latin. Its medial border, medial inferior and superior faces, which may be observed directly after the removal of the corpus callosum, is indeed rounded and smooth (Figs. 20.1 and 20. 7). The pulvinar constitutes the posterior pole of the thalamus. Its posterior border is observable on ventriculograms since they form the posterior curve of the lateral ventricle. As noted in the preceding paragraph, the pulvinar has no complete border with the nucleus medialis. Ventrally, the limit with the limitans is obvious. More laterally, the various tracings of the limit with the basal region (see "Regio Basalis") indicate that this border is not obvious. Two bundles, the tractus corticotectalis (Riley, 1960); (Figs. 20.2F and 20.9C), crossing the pulvinar almost horizontally, and the brachium colliculi superioris are topographic landmarks for the estimation of the anteroposterior position of transverse sections. The pulvinar was undivided in classical studies (Dejerine, 1895; Malone, 1910; Foix and Nicolesco, 1925). Kuhlenbeck (1951) and Dekaban (1953) introduced divisions previously established in lower species (Crouch, 1934; Walker, 1938): a pulvinar medialis (PuM), lateralis (PuL), and inferior (PuI partly equivalent to intergeniculatus). The problem of the subdivision of this large neuronal mass remains difficult and is not yet fixed. As for the medial nucleus, cytoarchitectonics being of no use, the subdivision was made essentially in relation to myeloarchitectonic traits (Vogt, 1909), the lateral part having more myelinated fascicles than the medial. The great variety of tracings exemplifies the difficulty of delineating a border between the "medial pulvinar" and the lateral. For Van Buren and Borke (1972), these "pulvinar divisions are largely areal designations of convenience."

Chemoarchitectonics, except for the particular parts analyzed below, do not lead to precise borders. The level of epinephrin is low (Oke *et al.*, 1997). The irregular concentration of 5-hydroxytryptamin apparently does not fit with subdivisions. On the other hand, some parts have particular topographic characteristics, including some previously described as distinct "nuclei," linked or not to the pulvinar. This was at first the case for the so-called "nucleus lateralis posterior." It was wrongly linked to the lateral region, for which it constituted the emblematic representative of the "dorsal nuclei"

(denoted at that time as "lateral," Aronson and Papez, 1934) as opposed to ventral. The delineation of the "dorsal nuclei", as already explained (Percheron *et al.*, 1996), was based on one effect of the complex three-dimensional shape of the territories of the lateral region, where the preceding ends over its successor. The nucleus lateralis posterior of nonhuman primates—or nucleus dorsalis caudalis (DC ; Vogt and Votg, 1941, and Van Buren and Borke, 1972), in man—is, to a large extent, a creation of transverse sections. Dorsal to the somesthetic nucleus, it contrasted, and still contrasts with it, the posterior lateral subregion VP being parvalbumin–positive, while the pulvinar-LP is not. In sagittal or horizontal sections (Figs. 20.2 and 20.23 L9), the lateral posterior "nucleus" has no border with the pulvinar. All authors already noted that the cyto- and dendroarchitecture of the LP and the pulvinar were similar, not to say the same. This similarity was such that the LP was frequently linked to the pulvinar in the "pulvinar-LP complex" (title of Cooper *et al.*'s 1974 book). Van Buren and Borke (1972) finally wondered "whether [their DC] should not be more simply considered as a division of the pulvinar." Lower mammals do not have a prominent posterior mass (i.e., a pulvinar) and a lateral posterior nucleus. This nucleus "of primitive mammals" was said to be the origin of the pulvinar (Harting *et al.*, 1972). This appears in early primates: bush baby (Galago, Harting *et al.*, 1972), marmoset (Stephan *et al.*, 1980), and cebideae (Emmers and Akert, 1963). The later phylogenetic development of the pulvinar is almost explosive, the number of neurons being said to exceed the total number of neurons of all other nuclei. This increase happens in posterior, dorsal, and anterior directions placing a part of pulvinar over the lateral region (denoted LP). The distribution of afferences and basins in continuous slabs (Asanuma *et al.*, 1985) adds further evidence for consideration of the past LP as a particular topographical site of the pulvinar, the pulvinar oralis dorsalis (PuOD, Percheron et al., 1996). In macaques, chimpanzees, and human beings, a particular cuneiform expansion between the central region medially and the lemniscal nuclei laterally was recognized by the Vogts (1941) as the oral pulvinar (PuO). It is dorsolaterally linked to the pulvinar oralis dorsalis (Figs. 20.2B and 20.21 VVB 1.6) and posteriorly to the bulk of the pulvinar, without any boundary (Fig. 20.23 L14).

Pulvinar Principalis (including lateralis posterior)

The ensemble made up of the "medial pulvinar," the middle, the "pulvinar oral," and the "lateral posterior," which does not receives major lower afferences, constitutes the principal pulvinar (as opposed to the intergeniculatus or inferior and lateral). The lack of major lower afferent territories shaping and separating distinct subdivisions, the general organization of this ensemble is subtle and cannot be analyzed in the same way as other regions. There are no true "nuclei" or even parts. The inner organization is made up of more or less coincident basins to and territories from the cortex. The main pulvinar and nucleus medialis have common connections, in continuous stripes. They constitute together a large isothalamic superregio medio-posterior, which represents some sort of an "associative" thalamus ("association region," Dewulf *et al.*, 1973), involving more than one half of the whole thalamic volume in man. Like the medial nucleus, the pulvinar essentially receives from and sends axons to the cortex. Thalamocortical neurons have rather small dendritic arborizations. Local circuit neurons are particularly abundant, up to 50% in the main part. Large local circuit neurons have complex dendritic endings and clusters of dendritic appendages (Ogren and Hendrickson, 1979). Early observations (Szentagothai, 1970; Mathers, 1972a) noted a remarkable feature. In the absence of lower primary subcortical afferences, special cortical axonal endings take their place as central LR terminals, generalizing in this curious manner the general isothalamic model. Rockland *et al.* (1999) described "pulvinocortical" axons and their endings in the cortex. They emit several branches dividing into several successive subtrees finally innervating rather large cortical surfaces, in layer 3 (and variably layers 4, 5, and 6). Rockland (1996, 1998) has shown two types of corticopulvinar terminal axons. The first ("type 1" "elongate"), emitted by usual pyramidal neurons of layer 5 corresponds to the common corticothalamic pattern. The second ("type 2" "round"), much less numerous, is emitted by giant pyramidal neurons. The first is spread over long distances without respecting ordinary subdivisions. The second is not greatly branched and has a small very dense arborization reaching only few dendritic arborizations.

One reason why the pulvinar cannot be easily subdivided into (medial to lateral) parts is that its internal organization is in fact pseudo-laminated, with horizontal parallel stripes made up of aggregations of islands joined together in parallel stripes, "slab-like" (Grieve *et al.*, 2000) separated by others (Fig. 20.7). The contours of basins and territories often coincide, thus constituting two-circuits, probably obeying Crick and Koch's (1998) "no-strong-loops" rules. At the same time where the nucleus medialis was said to be the single furnisher of the frontal cortex, the main pulvinar was traditionally seen as the main supplier of the parietal and temporal cortex. It is true that the

pulvinar has stong connections with the latter. Hardy and Lynch (1992) showed that the shape and organization of the basins of neurons projecting to the inferior parietal lobule (7a and LIP) in macaques were horizontal and alternate. Such parallel bands (or layers, their anteroposterior extent remaining unknown) already observable in DeVito and Simmons (1976), DeVito's (1978) and Asanuma *et al.*'s (1985) plates, are mainly located in the middle of the pulvinar and extended over about one half of its width (islands p in Fig. 20.7). The source to LIP is sandwiched between two parallel horizontal bands to 7A. The connection to (and from) the temporal cortex is mainly the superior temporal, including auditory areas (Trojanowski and Jacobson, 1975; Burton and Jones, 1976; Mauguière and Baleydier 1978; Yeterian and Pandya, 1988,1991; Kosmal, *et al.,* 1997). They form bands similar to the parietal with an alternation of sources to "TE" and "TEO" (Webster *et al.,* 1993). These could be superposed or, more likely, sandwiched by parietal islands (islands t, Fig. 20.7). In addition to parietal and temporal projections, as well as the medial nucleus, the pulvinar has significant connections with the frontal cortex: orbital (Bos and Benevento, 1975; Trojanowski and Jacobson, 1974; Goldman-Rakic and Porrino, 1985; Yeterian and Pandya, 1988; Romanski *et al.,* 1997; Cavada *et al.,* 2000), frontal polar (Cavada *et al.,* 2000), medial (located ventrally, Barbas *et al.,* 1991; Romanski *et al.,* 1997), principal (Goldman-Rakic and Porrino, 1985), and lateral dorsal (Kievit, 1977 ; Barbas *et al.,* 1991; Romanski *et al.,* 1997). While in the medial nucleus, the frontal layers are parasagittal (Kievit, 1977; Fig. 20.7D), in the pulvinar, they radiate from the most medial part and undergo a rotation (Goldman-Rakic and Porrino, 1985; Kuypers and Kievit, 1977), which places them horizontally (Goldman-Rakic and Porrino, 1985) (Fig. 20.7C). They extend laterally up to the suprageniculate area (B) (Barbas *et al.,* 1991; Romanski *et al.,* 1997). They may coincide with parietal layers (7a, Asanuma *et al.,* 1985). The main pulvinar has various connections with still other parts of the cortex: the anterior, (Vogt *et al.,* 1987) posterior cingulate, retrosplenial (Baleydier and Mauguière, 1985, 1987; Yeterian and Pandya, 1988), parahippocampic (Baleydier and Mauguière,1985; Yeterian and Pandya, 1988), and insular cortex (Burton and Jones, 1976; Wirth, 1970; Mufson and Mesulam, 1984; Romansky *et al.,* 1997). It is important to stress the connection with the oculomotor cortex, in particular with the frontal eye field FEF (Trojanowski and Jacobson, 1974; Bos and Benevento, 1975; Huerta *et al.,* 1986; Stanton *et al.,* 1988; Shook *et al.,* 1991). Oculomotor stripes (Barbas *et al.,* 1991; Romanski *et al.,* 1997) interdigit with or superpose to parietal and parietal with temporal. The set of cortical areas connected with the main part of the pulvinar resembles that projecting to the associative striatum: mixing together classical associative (frontal, parietal, temporal), so-called limbic (cingulate), and oculomotor areas. The dorsal and oral pulvinar (PuOD) has the same connections, in continuity with those of the main mass, with rostral parietal area 5 (DeVito, 1978; Asanuma *et al.,* 1985), the parietal opercule (DeVito, 1978), the "vicinity of the parietal operculum" (Van Buren and Borke, 1972, in humans), the anterior extremity of the first temporal gyrus (Whitlock and Nauta, 1956; Klinger and Gloor, 1960). In the most anterior part of the pulvinar, the cuneiform oral pulvinar (PuO) has also about the same connections. A problem is raised by its proximity with the lateral caudal subregion VP and the basal region, both somatosensory. This could explain the description of connections from and to the somesthetic cortex (DeVito, 1978; Cusick and Gould, 1990). The pulvinar and the medial nucleus form a continuum that could grossly represent the cerebral cortex: frontal medially, then parietal and temporal laterally. Two problems concerning pulvinar-cortical connections remain to be solved. The first is the determination of exactly which neurons from what source are really mixed in islands or separated. The second concerns the distribution in the cortex. A single injection indeed leads to a discontinuous ribbon in the frontal, anterior cingulate, insular, polar, superior temporal (Romanski *et al.,* 1997), posterior cingulate, and parahippocampal cortex (Baleydier and Mauguière, 1985). Stimulations of the left pulvinar (and left deep parietal area) led to anomia showing the role of the thalamocortical circuits in "higher functions."

Nucleus Intergeniculatus and Pulvinar Lateralis

As previously stated, another place generally considered as a part of the pulvinar, the "pulvinar inferior," raises a problem. In fundamental opposition to the main part of the thalamus, it receives lower afferences, namely tectal axons. This creates an important systematic difference that should be reflected in the thalamic division. For instance, it does not belong to the superregio medioposterior defined by not receiving lower afference and having simply corticothalamic afference. It is thus proposed to formally distinguish it from the main pulvinar. The superior colliculus is one major, underesteemed source to the thalamus. Its multiple thalamic targets makes its introduction difficult in a systematic description of the thalamus. In macaques, the terminal arborizations of tectothalamic axons occupy an important territory in

the inferolateral part the classic pulvinar, located anteriorly between the two geniculate bodies. This explains the term nucleus (or pulvinar) intergeniculatus Ig (Vogt and Vogt, 1941). It is also inferior, below the corticotectal tract, hence pulvinar inferior PuI (Crouch, 1934; Partlow *et al.*, 1977; Harting *et al.*, 1980; Benevento and Standage, 1983). The direct retinal projection to the pulvinar, documented in the tree shrew (Tupaia, Somogyi *et al.*, 1982) and old world monkeys (Itaya and Van Hoesen, 1983), no longer exists in macaques (Hendrikson *et al.*, 1970; Trojanowski and Jacobson, 1975) and thus likely no longer in man. The collicular, tectal afference, found in nonhuman primates, is, conversely, likely to persist in the human brain. Collicular axons arise from tectal neurons of superficial layers and follow the lower border of the thalamus parallel to the inferior border of the limitans ("colpu," Fig. 20.7c). The tectal or (superior) collicular afference composes a continuous and dense territory in the inferior part of the pulvinar in the squirrel monkey (Mathers, 1971). This is no more the case in macaques (Benevento and Fallon, 1975; Trojanowski and Jacobson, 1975; Partlow *et al.*, 1977; Harting *et al.*, 1980; Benevento and Standage, 1983) where the territory is made up of several islands. The tectal axonal islandic terminal fields form bands along the lateral border of the pulvinar up to its dorsal border (Harting *et al.*, 1980; Benevento and Standage, 1983; Fig. 20.7). Acetylcholinesterase was found to allow the delimitation of the tectal (collicular) territory in macaques (Lysakowski *et al.*, 1986) not respecting "classically defined thalamic boundaries." Calbindin and Cat 301 brought out variegated pictures that led Gutierrez *et al.* (1995) and Gray *et al.* (1999) to subdivide the inferior pulvinar of squirrel monkeys and macaques into four subparts. Superior collicular axonal endings, as other principal afferents, form central boutons LR (Partlow *et al.*, 1977). They are not numerous in comparison to cortical ones (Ogren and Hendrickson, 1979). Physiological data established the existence of a complete visuotopic map (Bender, 1981, 1982), isolating a clear functional entity. The map does not reach the inferior border of the pulvinar and extends slightly above the corticotectal bundle in macaques. In a further paper, Bender (1983) specified that the visuotopic map was not due to collicular but to cortical, occipital, afferences. The intergeniculate nucleus Ig (pulvinar inferior, PuI) receives cortical axons from the primary visual (Ogren and Hendrickson, 1979), preoccipital (18 and 19, Asanuma *et al.*, 1985), middle temporal and occipitotemporal cortex (Rockland, 1996) and the accessory visual area MT (also projecting to the superior colliculus) specialized in the analysis of visual motion (Ungerleider *et al.*, 1982). The intergeniculate nucleus sends thalamo-cortical axons to the visual and perivisual cortex (17 to 19), to the posterior temporal TEO, area MT (Benevento and Rezak, 1976) and to the inferior temporal cortex (Webster *et al.*, 1993). The morphology of the axonal arborisation of pulvinarocortical neurons, detailed by Rockland *et al.* (1999), showed that projections to MT and V5 are narrower than others.

In addition to the main pulvinar medially and the intergeniculate nucleus inferiorly, there remains a lateral and dorsal part in the pulvinar also receiving (less densely) islandic collicular afferents but not participating in the retinotopic map (Fig. 20.7). Collicular patches are parallel to the lateral border (Benevento and Standage, 1983). The inner organization is almost vertical, with stripes parallel to the lateral border of the thalamus. This part stains more densely for cholinesterase and is sufficiently stained for parvalbumin to allow its delineation (Morel *et al.*, 1997). The lateral pulvinar (PuL) would be restricted to this upper part in man, corresponding to the most laterodorsal part delineated by myelinated bundles in Hassler's and Dewulf's atlases. This part sends to and receives axons from visual areas including the striate cortex (Ogren and Henderson, 1976) and the prestriate area 18 (Curcio and Harding, 1978). It projects to the inferior parietal cortex (Hardy and Lynch, 1992).

Tectal axonal terminations are not restricted to the intergeniculate nucleus and lateral pulvinar. Collicular axonal islands for instance also end in the posterior intralaminar formation (see Formatio intralaminaris-limitans). In old world monkeys, tectal axons end in the posterior paralamellar site (Partlow *et al.*, 1977; Harting *et al.*, 1980), lateral to the nucleus medialis and medial to the lamella medialis (see discussion in regio medialis), along with cerebellar axons. Another place of tectal endings in monkeys is the rostral subregion of the lateral region VA. In macaques, the posterior paralamellar site and VA are both reciprocally linked with the frontal eye field (Akert, 1964; Künzle *et al.*, 1976; Akert and Hartman-von Monakow, 1980). Using transynaptic labeling, Lynch *et al.* (1994) showed that this "frontal eye field" receives confluent afferents from the dentate nucleus, the superior colliculus, and the nigra, indicating at least two tectothalamo-FEF subsystems: one through Vim (mixed with cerebellar axons) and the other through VA (mixed with nigral). See evolutive changes in the lateral region.

REGIO BASALIS

The anatomical demonstration of the ending of spinal axons in the thalamus of man is ancient (Quensel, 1898; Golstein, 1910; see Mehler 1962, 1966; Chapter 30). The classical spinothalamic tracts were

the tractus spinothalamicus anterior and lateralis (Nomina anatomica), both located in the anterolateral quadrant of the spinal cord, the first anteriorly to the second. To these two, forming the ventral spinothalamic tract (VSTT), a dorsal tract has been added, the dorsal spinothalamic tract (DSTT) runing in the dorsal quadrant. The pain and thermal components arise from the lamina I of the cord and ascend, as classically known (Dejerine, 1914), into the anterolateral quadrant. The proprio- and enteroceptice components arise from layer V and deeper parts of the spinal cord. The first experimental approach using an anterograde method in monkeys was Mehler's *et al.*, (1960) celebrated paper. The dorsal extension of the spinothalamic territory is not the same in all accounts in monkeys (Burton and Jones, 1976; Burton and Craig, 1983; Mantyh, 1983; Gingold *et al.*, 1991; Ralston and Ralston, 1992). Later, Mehler (1966) traced the spinothalamic axons in one human case after anterolateral tractotomy (Fig. 20.8). The intrathalamic distribution of spinothalamic afferences is multiple. A first target is the somesthetic lemniscal nucleus (VP). Spinothalamic islands form a "matrix" containing lemniscal "rods." Jones (1998) saw the matrix as a diffuse fundamental system having particular cortical projections (Raussell and Jones, 1991). The matrix is made up of smaller somata. It is calbindin positive (Raussel *et al.*, 1992; Blomqvist *et al.*, 2000) and contains tachykinin and enkephalin (Hirai and Jones, 1989). In front of the lemniscal subregion, spinothalamic islands, probably from lamina V, also reach the cerebellar territory (see subregio Intermedia of the lateral region, VIm-VL). In macaques, spinothalamic axons also end in the posterior paralamellar zone (Burton and Craig, 1983). The affinity of spinothalamic endings for the posterior part of the intralaminar formation (that excludes the central formation) is well known (Mehler *et al.*, 1960; Mehler, 1966): particularly in the supracentral (above the central region) and postcentral (Ilrc Fig. 20.8) sites (Mehler, 1966; Gingold *et al.*, 1991; Greenan and Strick, 1986; Apkarian and Shi, 1994) (see "Formatio Intralaminaris-limitans"). This is also true for the limitans itself, in macaques (Mantyh, 1983) and man (Blomqvist *et al.*, 2000). Some irregular "limitans" islands, visible with acetylcholinesterase staining, may be observed up to the medial corner of the medial geniculate nucleus. The extension of the limitans to more lateral sites in nonhuman primates as in Friedemann's (1911) "pars supragenicula nuclei limitantis" or human as in Hassler's (1959) "Limitans opticus" and "Limitans portae" ("Li.por.") is however not legitimate. The neurons of "Li.por" are indeed of a different neuronal family (isothalamic). There is thus no "limitans-supragenicule complex" or "nucleus."

The description of the thalamic place(s) where spinothalamic axons end elsewhere than in the lateral region (VP, VIm) or the intralaminar-limitans-retrocentral formation (IL) has been a longstanding problem. Two elements, "Vcpor" (Hassler, 1959) and "VPI" (Vcpce), raised the problem of their belonging to the ventral nuclei of the lateral region. Crouch (1934) described Friedemann's (1911) "ventralis parvicellularis" vp as the nucleus ventralis inferior (VPI), but specified that "its scarcity of cells makes one doubtful as to whether it should be called a nucleus." This was also Mehler's (1966) and our opinion (Percheron *et al.*, 1996). Hassler's (1959) Vcpce, Van Buren and Borke's (1972) VCV, Emmers and Akert's (1963), or Lenz (1995) Vci are equivalent to VPI by two characteristics: made up of small neurons and located below VP. The inferior border of VP is fuzzy; some islands or even individual VP larger neurons are located almost in the lemniscus, medially to the medial geniculate nucleus. In contradiction with its name, Hassler's (1959) "ventralis caudalis portae" Vcpor, having a different cytoarchitecture, as already admitted by Van Buren and Borke (1972) and Morel *et al.* (1997), is not a "ventral" element. Vcpor, continuous to VPI (Vcpce), was located posteriorly to the nucleus ventralis posterior medialis (Figs. 20.2 and 20.23 L11 to 14). This explains why it has been attributed by some to its posterior part as VPMpo (Koyoma *et al.*, 1998) or its "cap" ("s", Raussel *et al.*, 1992). The upper border of Vcpor (Hassler's Plate 66) was delineated much too high so that the "nucleus" included some extent of the oral pulvinar (PuO). The participation of the pulvinar oralis, evoked by Jones (1985), may be ruled out since it has not been demonstrated to receive spinothalamic axons and is more dorsal (Fig. 20.9). VPI, Vcpor, VPMO are simple topographical sites of a larger entity not belonging to the nucleus ventralis posterior VP or more largely to the lateral region. Jones' (1985) "posterior complex of nuclei" was composed of two elements: the "supragenicule-limitans nucleus" and the "posterior nucleus." The limitans being removed, two parts remain, "supragenicule" and the "posterior nucleus." The name supragenicule was given by Crouch (1934), in macaques to a place dorsal (in fact medial and posterior) to the medial geniculate nucleus. Its ancestor, the nucleus parageniculatus of Lewandowsky (1904) was linked by Friedemann (1911) to the medial geniculate nucleus. Olszewski's (1952) "supragenicule nucleus" (SG) was said to have no clear border with GM or the pulvinar. Crouch's nucleus, made up of small isothalamic neurons resembling those of the pulvinar, was said to correspond to C.Vogt's "noyau basal." This being said by C.Vogt to correspond to Déjerine's "region du ruban de Reil median" was clearly not a part of the geniculate body. In addition to

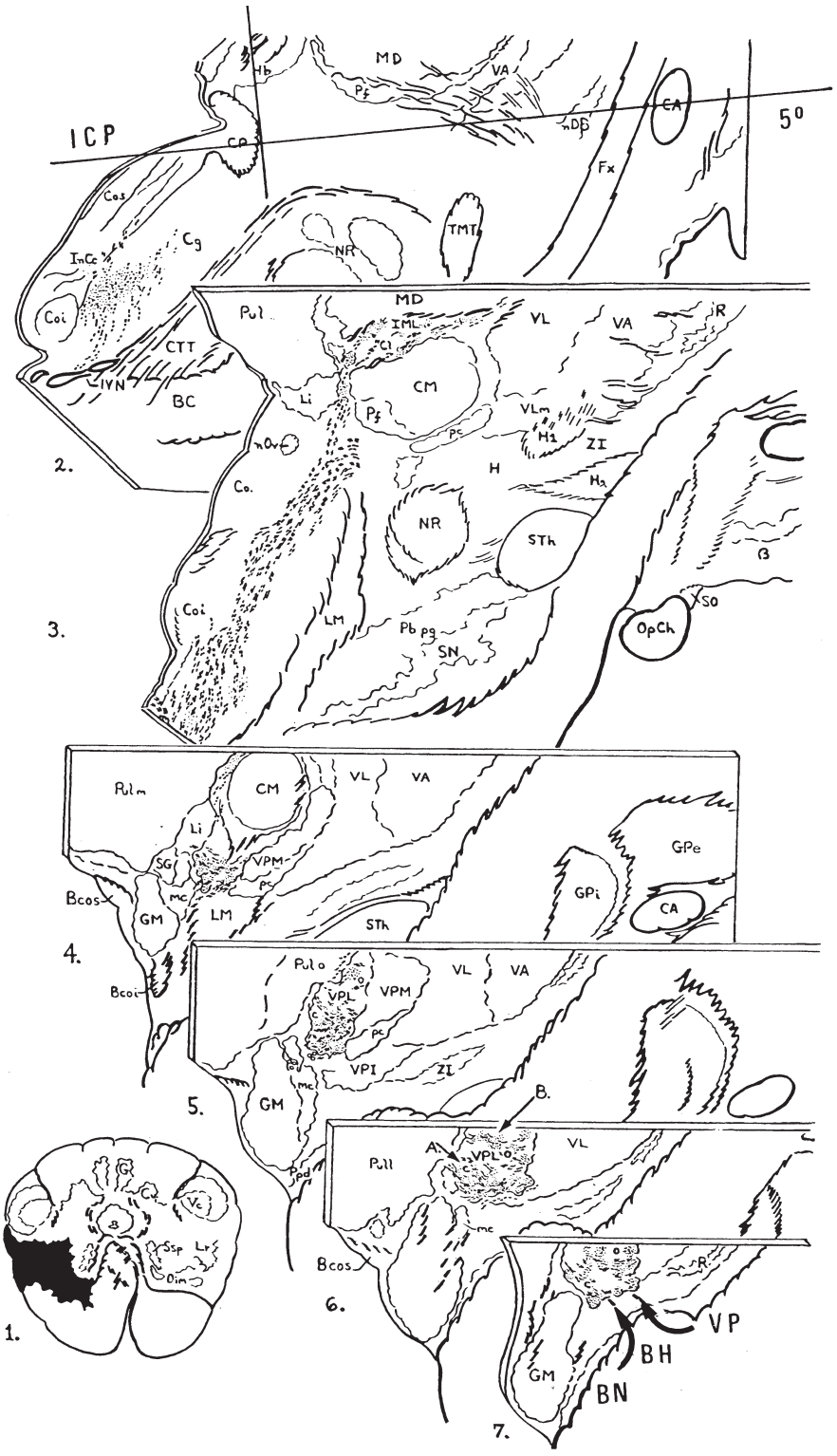

FIGURE 20.8 From Mehler (1966). Trajectory and termination of spinothalamic axons after a medullary lateral tractotomy in man. Sagittal sections. CA-CP line added on the upper section. The central formation (CM and Pf) is devoid of any ending. Intralaminar elements receiving spinothalamic endings are supracentral, dorsal and posterior (3), posterior and ventral (4) and lateral (5 to 7) to the central formation. The place indicated "c" in levels 5 to 7, lateral to CM is distinct from the limitans (Li), suprageniculate (SG) and medial magnocellular part of GM (mc). It corresponds to the nucleus basalis nodalis BN surrounded by a visible halo with few endings (and few neurons) BH. Dorsally to BH, the inferior part of VP.

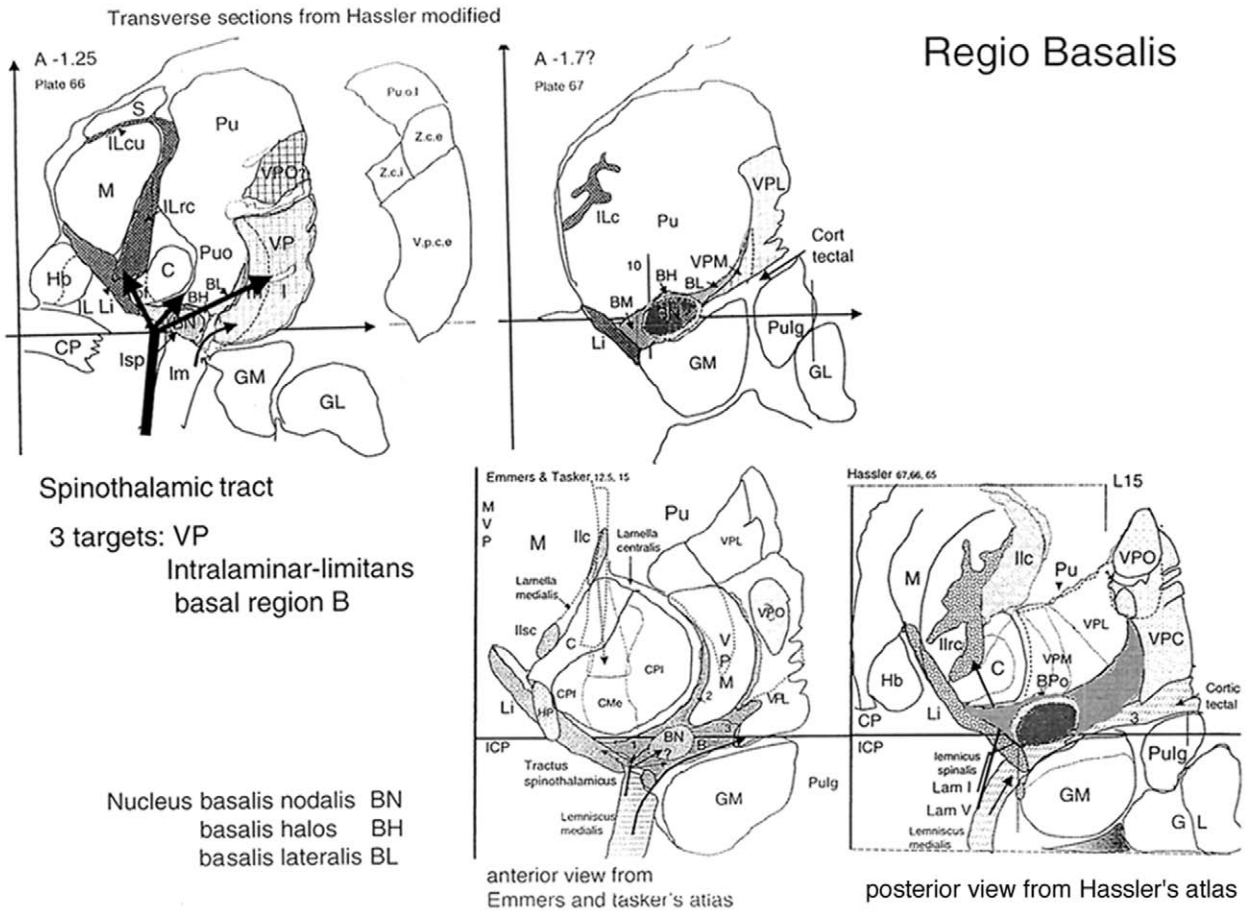

FIGURE 20.9 Regio basalis B. *Upper row.* Two transverse sections from Hassler's atlas. A -1,25 is located at about the posterior pole of the central region, with the medial nucleus surrounded by the intralaminar-limitans formation (limitans clearly visible), the anterior part of the main pulvinar, the posterior part of the lateral region and the appearing basal region. The spinothalamic tract reaches three targets: medially the intralaminar-limitans formation, laterally the somesthetic nucleus VP, and the basal region. At the more posterior -1,7 section, at the bottom of the pulvinar, one may observe a denser element (nucleus basalis) surrounded by a clearer halo (nucleus basalis halos). The ensemble is located in a region extended from the limitans to the VP with a part medial to BN (nucleus basalis medialis) and another one lateral (basalis lateralis) equivalent to VPI. The region is just posterior to the inferior part of the somesthetic cutaneous VP. *Inferior row.* Slice made by superposing several transverse sections from Emmers and Akert's atlas showing the basal part of the thalamus, seen from front. The central region is surrounded medially and ventrally by elements of the intralaminar-limitans formation: caudal Ilc (located dorsally to the central formation), supracentral Ilsc (dorsal to it, in the ventral part of the lamella medialis or interna), and retrocentral (posterior to the central formation). There is no intralaminar elements (and no spinothalamic endings) in the lamina centralis forming the lateral wall of the central formation. The slice made by superposing several transverse sections from Hassler's atlas is, this time, seen from the back in order to unveil the retroventral part C is the posterior pole of the formatio centralis.

the suprageniculate "nucleus," the "posterior complex of nuclei" of Jones (1985) or "posterior region" of Burton and Jones's (1976), comprised a more lateral "posterior nucleus". The physiological literature in macaques mentions a "Po" (DeVito and Simmons, 1976; Applebaum *et al.*, 1979; Asanuma *et al.*, 1983; Burton and Craig, 1983) or "posterior complex," "posterior nucleus" (Apkarian and Shi, 1994) or "posterior group PO/SG" (for suprageniculate posterior, Ralston *et al.*, 1995). The adjective "posterior" is confusing since "regio posterior" designates the pulvinar (e.g., Crouch, 1934) and the term ventralis posterior (VP), the lemniscal territory. Contrary to what might have been expected from a system presented as assuming an "archaic" function, the ensemble is highly evolutive. Burton and Jones' (1976) posterior region was said to exist in early mammals, for instance in marsupials (Rockell *et al.*, 1972) but "best appreciated in sections of higher primates" (Jones, 1985). In the cat, "Po" was divided into two parts—Pom and PoL (Jones, 1985). PoL, said to receive tectal afferents, could have given the intergeniculate, inferior pulvinar of primates (indeed

receiving tectal axons, see "Pulvinar Principalis"). The primate site receiving spinothalamic axons could be a derivative from the single Pom.

Because of its position, shape and unclear inhomogeneous cytoarchitecture, the analysis of the suprageniculate-posterior ensemble is made difficult by the presence of the numerous thick afferent axons of the medial lemniscus (as stressed by Dejerine's name: "region du ruban de Reil median," 1895, or Hassler's "portae," 1959) and of the spinothalamic fascicle (see Fig. 20.9). In addition, small ascending vessels disturb the pictures. The spinothalamic territory not included in the intralaminar-limitans or the lateral regions forms an irregular but continuous ensemble extended from the limitans (excluded) medially to the corner of the medial geniculate body laterally (excluded), passing posteriorly to the VPM to which its sends anterior fringes up to posteriorly and inferiorly to the VPL. This covers several sites, previously described as nuclei, shown in Fig. 20.9, "suprageniculate" (1), retroventral posterior (2) and "VPI" (3). This ensemble is not a part of the ventralis posterior (VP) defined as the lemniscal territory (parvalbumin-positive). Not limited by lamellae, it is thus not a classical region. Refering to the "noyau basal" of C. Vogt (1909), it is said to form the Regio Basalis (B).

The situation has changed recently. In macaques, the pain component of the spinothalamic tract arising from lamina I has been claimed to end in a particular thalamic place separated from others modalities (Zhang and Craig, 1997), Spinothalamic axons arising from layer I of the spinal cord can be selectively stained by calbindin immunochemistry, in rat, monkey, and man (Craig *et al.*, 1994; Blomqvist *et al.*, 2000). Using this tool, Blomqvist *et al.* (2000) found a new nucleus with a particular cytoarchitecture, composed of a dense core and a halo, or shell. This ensemble was already observable in Mehler's (1966) drawings (levels 4 to 7, reproduced in Fig. 20.9), unfortunately named "pars caudalis of the ventralis posterior lateralis" (VPLc) (in a caption a "nucleus basalis" B). The nucleus and the halo are clearly observable in the monkey (e.g., in Friedemann's (1911) Fig. 5, Burton and Jones' (1976) Figs. 18, 19 and 23, and Jones' (1985) Fig. 11.2). In man, the two are easily traced on Hassler's large magnification pictures, in transverse as well as in sagittal plates (drawn in Fig. 20.9), where, partly but indisputably, they correspond to "Li.por." In both planes, one nucleus is round or ovoid and is surrounded by a clearer ring. This contains few neurons and is partly made by neighboring bundles or fascicles (medial lemniscus, corticotectal and spinothalamic tracts) that are exploited for a nuclear closure. For reasons analyzed later, the denotation by Craig *et al.* (1994) and Blomqvist *et al.* (2000) of the nucleus as "VMpo" ("posterior division of ventromedial nucleus," Giesler, 1995), is not tenable. The regio being named basalis, it is proposed to denote "Vmpo" the nucleus Basalis Nodalis (BN; expressing its central position and its look), and its schell ("Po" of Blomqvist *et al.*, 2000) the nucleus Basalis Halos (BH, not conjugated in Greek). As observable in successive transverse plates of Fig. 20.9, the nodalis complex is at the same time in a suprageniculate position and posterior to the medial part of VP (VPM). The stereotactic coordinates given by Craig *et al.* 1994; (A –0.5 to +2, L 12 to 16, H-1 to +1) are about those found in our tracings on Hassler's plates, except for the lateral dimension (not firm in Hassler's atlas). The neurons of the nucleus basalis nodalis are calbindin-positive and form clusters, some of them substance P-positive. The neurons respond to painful heat (Lenz *et al.*, 1993). Their stimulations induce pain (Dostrowski *et al.*, 1992; Lenz, 1995). The surrounding is calbindin negative and CGRP-positive (calcitonin gene-related peptide)(deLacalle and Saper, 2000). Its afferent axons come from the vagal-solitary-parabrachial ensemble, which brings a different, enteroceptive, visceral information (Blomqvist *et al.*, 2000). The assessement that lamina I axon end only in the nucleus basalis nodalis BN is contested by Willis and colleagues (2001) and Ralston (2003). The injection of a retrograde marker into VP indeed shows numerous labeled neurons in lamina I in the macaque. It is clearly too soon for attributing to the BN/BH ensemble the exclusive processing of pain messages. This does not call into question its anatomical observation and topographical description. The ensemble is evolutive. In cats and rats, only "a primordial homologous region may exist" (Blomqvist *et al.*, 2000). Observed in cebideae (Blomqvist *et al.*, 1996) or cercopithecideae, it is nowhere as clear as in man (Blomqvist *et al.*, 2000). As could be also the case for the tectal intergeniculate nucleus, this could be made by a late differentiation of the ventral part of the pulvinar. An argument could be that some pulvinar neurons are furnished in primates (Rakic and Sidman, 1969) and some local circuit neurons only in man (Letinik and Rakic, 2001) by the telencephalic "ganglionic," or ventricular eminence.

In L11 sagittal section, the BN/BH ensemble in the mediolateral dimension, is in a central, intermediate, position in the basal region. This has thus one medial (BM, medial to BH) and one lateral (BL) additional parts not exactly corresponding to previous subdivisions. The nucleus basalis lateralis, BM, posterior to the taste relay, could be furnished by quintothalamic axons. The nucleus basalis lateralis BL (including "VPI") is likely

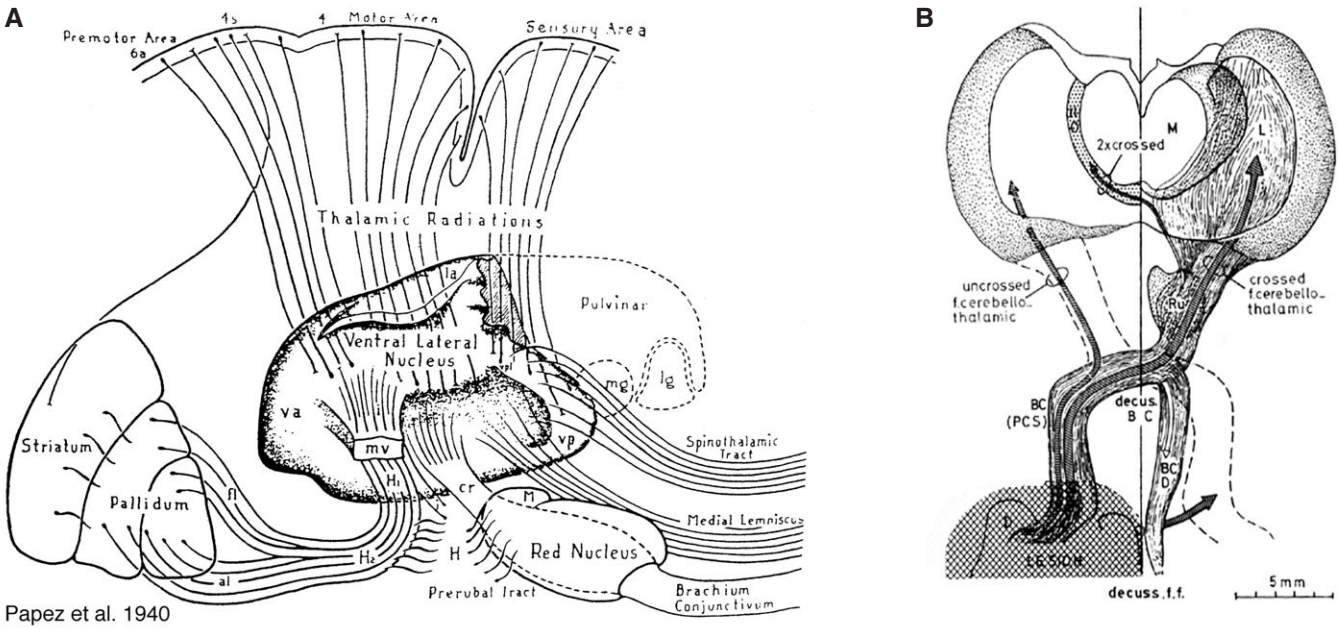

FIGURE 20.10 **(A)** Figure from Papez *et al.* (1940), sketching the thalamic organization in relation to the main afferent systems. The pulvinar and geniculate bodies are shown. The sequence matches C. Vogt's scheme (with three "radiations") and the spinothalamic tract posterior to the medial lemniscus. The latter formed Vogt's "lemniscal radiation." In front of it, Vogt's "prelemniscal radiation" is furnished by the brachium conjunctivum. It ends in a part of the ventral lateral nucleus. In front is the "thalamic fascicle" H1 field of Forel (Vogt's "lenticular radiation"). In front of the last, "va" is not shown to receive lower afferences, today the nigral territory. To the prethalamothalamic organization corresponds a thalamocortical distributed over the two sides of the central sulcus. **(B)** Figure from Percheron (1977). The brachium conjunctivum is reconstructed from series of sections in a macaque. The brachium arises from the cerebellar nuclei, mainly from the dentate nucleus. It ascends in the superior cerebellar peduncle PCS. Then it crosses at the decussatio brachiorum conjunctivorum (decus BC) and divides. The brachium conjunctivum descendens BCD goes down in the brainstem. The brachium conjunctivum ascendens is the cerebellothalamic tract. Ascending in the superior cerebellar peduncle (BCA), it crosses and is lateral to the red nucleus (Ru) before ending in the lateral intermediate subregion of the thalamus. Some axons do not cross the midline.

supplied by axons from lamina V of the spinal cord conveying other modalities that pain and thermaestesia. What was said about VPI may be transferred to BL: own somatotopic map and possibly modulatory (Chapter 28). The thalamocortical connections of the regio would comprise efferents to the superior temporal cortex (Kosmal *et al.*, 1997), frontal cortex and above all the anterior insula (Craig, 1995) or in an area of the granular insula (Ig) located between the the secondary somatosensory SII above and the primary auditory area AI (Burton and Jones, 1976; Jones and Burton, 1976).

REGIO GENICULATA

The two "geniculate bodies" once thought to form the metathalamus are in fact isothalamic elements detached from the thalamic mass early in embryonic life that later get a strong morphofunctional differentiation. The two nuclei are ventral, posterior, and lateral (Figs. 20.1B and 20.2E, F), located below the pulvinar.

Nucleus Geniculatus Lateralis

The nucleus geniculatus lateralis (GL), usually named lateral geniculate nucleus, is inferior in the thalamus, inferolateral to the lateral region. It has a superficial face that may be observed by dissection. Its anterior border is round. The nucleus geniculatus lateralis, everywhere except medially, is surrounded by thick myelinated bundles (thus forming an enclosed nucleus). The separation is complete. It is covered by the nucleus pregeniculatus Pr in Fig. 20.2. This thin element (the "ventral geniculate") is in fact an extension of the perithalamus. Ventral in nonprimates—even in lemurians—it is dorsal in higher primates. Part of the perithalamus, the pregeniculate does not belong to the regio geniculata. The lateral geniculate nucleus in primates is made up several cellular layers separated by axonal layers (the lamination, still not observable with the unaided eye in lemurians, appears after enucleation). There are six layers, numbered from the inferior surface, often subdivided into magno-

cellular layers I and II and mediocellular from III to VI. The first two contain a low percentage of local circuit neurons (14%; Dewulf, 1973), yet higher than in the other layers (4.5%). Layers II, III, and V are furnished by axons from the ipsilateral eye, and layers I, IV and VI, by the controlateral hemifield of the retina. The dendritic arborizations of the thalamocortical neurons are flattened or elongated in axes perpendicular to the layers. They do not cross their border. They however belong to the general bushy thalamocortical genus. The fine structure of the geniculate body has been the subject of extensive research for several decades as a kind of prototype of thalamic structure. It constitutes the extreme in nuclear separation and differentiation. The lateral geniculate nucleus has a particularly rich innervation in cholinergic afferents. It is particularly dark in cholinesterase staining. It is important to point out that the lamination observed in the geniculate body is different from that of the stratolaminate histotype (observed for instance in the cortex) since it is not underbased and covered. The lateral geniculate is the primary visual relay receiving axons from the retina through the optic nerves and tracts, thus the retinal territory. It contains a retinotopic map. Its voluminous efferent system is the optic radiation in direction to the primary visual cortex.

Nucleus Geniculatus Medialis

The nucleus geniculatus medialis GM (medial geniculate nucleus) is more medial and more anterior than the lateral. It is also superficial. Contrary to the lateral it still adheres to the thalamic mass and that fact creates problems of delineation and inclusion particularly dorsomedially. Posteriorly it is separated from the lateral geniculate body by the intergeniculate part of the pulvinar (Figs. 20.10B and 20.17). The main problem is raised by the so-called magnocellular part neighboring the formatio basalis. This is located just medial to the entrance of the medial lemniscus. Some large neurons appear to be neurons from the VPL located ventrally. The medial geniculate nucleus is parvalbumin positive with some calbindin positive islands (Jones, 1998) and poorly stained in acetylcholinesterase. More medially and posteriorly the "magnocellular part" with larger calbindin positive neurons (Molinari *et al.*, 1995) is contiguous to the part receiving spinothalamic axons (B, see VIII). The medial geniculate nucleus receives its afferents from the lateral lemniscus. It is made up of cellular "laminae." It contains a cochleotopic-tonotopic map. It is analyzed with the auditory system (see Chapter 34). The medial geniculate sends most of its axons to the primary auditory area (AI, AA1) (Mesulam and Pandya, 1973) and fewer to the second (AA1) and third (AA3; Kosmal *et al.*, 1997) auditory cortex. AI is located in the posterior part of the superior temporal gyrus, Bailey and von Bonin's (1952) "regio supratemporalis," more precisely in the transverse gyrus or gyri of Hesch. The auditory cortex, alike others primary sensory cortex, is a koniocortex surrounded by a perikoniocortex (area 41, TC or Kam and Kalt).

REGIO LATERALIS

Generalities

The regio lateralis (Louvain, 1963) corresponds to the classic lateral nucleus ("äusserer Kern" of Burdach, 1822, "noyau externe" of Dejerine, 1901, "nucleus lateralis thalami" of Riley, 1960), that is, the thalamic region topographically lateral to the lamella medialis, medial to the lamella perithalamica, and anterior to the posterior region (pulvinar). It extends up to and forms the anterior pole of the thalamus. The main recipient of major "prethalamic" afferences and the place of thalamic stereotaxy, it has been the subject of an important literature.

For a long time, there has been a lack of data on the precise topography of afferent territories. This has led to an excessive reliance on cytoarchitectural signs. Cytoarchitectonic "nuclei" with no precise definition have been drawn in an excessive number with various boundaries and names. The opposition made by Meynert (1872) between "ventral" versus "dorsal" nuclei introduced a longstanding misinterpretation. Techniques at hand for tracing connections were not able to show axonal endings. Only ventral elements were observed to receive "lower afferences." "Ventral nuclei" were thus declared to be "relay nuclei" as opposed to "dorsal" "associative nuclei" of the same group as the pulvinar. The use of the von Gudden technique (retrograde degeneration) for studying thalamocortical connections, extensively used in Walker's celebrated work (1938), did not result in clear subdivisions.

Territories Rather Than "Nuclei"

The major change in the understanding of the lateral region occurred with the consideration of territories. The subdivision of the lateral region using the separation of territories of identified afferences was effected as early as 1909 by C. Vogt. Her postero-anterior sequence of three "radiations" was lemniscal (caudal VC), "prelemniscal," cerebellar (intermediate VI, Vim in 1941), and "lenticular" pallidal (oral VO). The presence of a nigrothalamic connection was not known, only demonstrated in the 1960s. After its confirmation by Shuster (1936) and Kornyey (1926) in newborns and partly by Le Gros Clark (1936) experi-

mentally in the macaque, this scheme was supported by Papez *et al.* (1940) who added the more posterior "spinobulbothalamic tract" (Fig. 20.10). While mentioning the overlap of spinothalamic and medial lemniscal endings, they insisted on the separation of the other, somesthetic, cerebellar, and pallidal places of termination. This was illustrated by their Fig 4B (reproduced in Fig. 20.10). Bailey and von Bonin (1951) accepted this sequence. "The three systems i.e., the somesthetic tracts, the cerebellothalamic and the pallidothalamic systems, appear to end in different parts of the 'ventral nucleus.' " Bailey and von Bonin (1951) added that "the distinction into three systems that we recognized remains valid for the thalamocortical radiation", (i.e., the prethalamothalamic order had a corticothalamic correspondent). Sheps (1945) adopting Walker's scheme in man admitted that this and the one of the Vogts "agree in general." A curious scientific turn occurred in the 1950s. Thalamic subdivisions were no longer asked to correspond to particular afferent territories. A cytoarchitectonicist era rose up. Following Nissl and Jacobsohn's tradition, Olszewski and Baxter (1954) claimed that "the criteria used for cytoarchitectonic subdivisions are of biological importance." Olszewski's atlas (1952), during decades the common document of reference for experimenters on macaques, was not founded on precise afferences. This atlas, histologically and topographically careful, has been the tool used for establishing faulty attributions. It is now admitted that Olszewski's VPLo was not a part of VPL but, along with "Area X" (telling its uncertain belonging), a major part of the cerebellar territory. Olszewski's most unfortunate choice has been the attribution of what is known to be the pallidal territory to VL. This nucleus includes only a small part of the cerebellar territory (post VLc and ps) and the major part of the pallidal territory (his Vlo, VLm and the anterior part of VLc) and excludes important parts (VPLo and "area X"). VA was considered to receive no lower afferences. The identification and proof of the separation of the main territories has been arduous. The separation between the lemniscal and cerebellar territories was demonstrated by C.Vogt (1909) and then by Van Buren and Borke (1971) and Asanuma *et al.* (1983); that between the cerebellar and the two basal ganglia territories, by Percheron (1977), Asanuma *et al.* (1983), and Ilinsky and Kultas-Ilinsky (1987); and that of the pallidal and nigral, by Carpenter and Strominger (1967), Ilinsky *et al.* (1985), and Percheron *et al.* (1993, 1996). Finally, by tracing and using cartographic methods, it was shown that a restricted number of main afferent territories, often covering several cytoarchitectonic nuclei, separate one from the others, making a simple, functional, parcellation possible. The main territories have four geometrical properties (Figs. 20.17 and 20.18). First, they are continuous. Second, they have complex three-dimensional shapes. Third, their caudal part overhangs dorsally the next more caudal element (Percheron *et al.*, 1996; Fig. 20.17) explaining the classical (improper) separation between ventral and dorsal elements essentially made on transverse sections. Fourth, their borders are strongly irregular in some places with long fringes (already noted by Asanuma *et al.*, 1983, and the Ilinskys, 1987, 1993; Fig. 20.18). The now general agreement that territories are everywhere separate has been challenged by some recent studies insisting on a possible peripheral overlap (Rouiller *et al.*, 1994, or Sakai *et al.*, 1999, 2000). Some are the result of phylogenetic reasons (cebideae lacking complete separation), others to plane, bidimensional, sections of the interdigitation of fringes that, in the absence of three-dimensional reconstruction, may give the impression of a mixture. To our knowledge, no study has ever proven at the ultrastructural level the innervation of a single thalamic neuron by two distinct main sources. A major, recent advance has come from the observation that certain territories have particular immunocytochemical properties (particularly in calcium-binding and acetylcholinesterase histochemistry). This led to the possibility of tracing presumably similar entities in other species like the *Macaca*, particularly for man, in the absence of direct experimental data.

Lateral Rather Than Ventral and Dorsal

As already explained ("General Considerations"), two rival systems were used to name the parts of the lateral region. Both accepted Meynert's (1872) opposition between dorsal and ventral elements. The Vogt school (Vogt, 1909; Friedemann, 1911; Mussen, 1923; Vogt and Vogt, 1941) named the dorsal elements "dorsalis," but the so-called Michigan school (Walker, 1938), "lateralis." A major result of performing tracing methods has been that (at least for three of them) the main territories are not simply ventral but also dorsal, reaching the dorsal border of the lateral region. Thus, as already criticized at Louvain's symposium, "to indicate the formatio lateralis, the term ventralis is no longer desirable" (Drooglever Fortuyn 1963, in Dewulf, 1971). At the end of our studies on the topography of the main territories (Percheron *et al.*, 1996), we proposed to give to all elements of the lateral region the first adjective Lateralis (L). This remains the more rational and less confusing. However, a strong reluctance appeared to abandon the term "ventral." Ventralis is thus accepted as the first adjective, with one condition. The equivalence of ventral and lateral elements is possible if and only if there is no other "ventral" and "lateral" nuclei (e.g., no longer lateralis

dorsalis and lateralis posterior), which can be done on other arguments.

Evolutive Changes in the Lateral Region

The disputes in conception and nomenclature, perceived as cultural, as already mentioned in "General Considerations," were to a large extent linked to different standpoints toward phylogenesis. The so-called Michigan school was at first a school of comparative anatomy with no particular consideration for the human brain. The Vogt school, after works on nonhuman primates intensively worked on the human thalamus (1941). Hassler's atlas (1959) was used for decades by stereotacticians. Phylogenetic changes at the thalamic level must be interpreted in the larger frame of the evolution of neuronal systems, where relative numbers of constituents, volume, and internal organization vary. In the lemniscal territory, the separation of cutaneous and kinaesthetic afferents led to the differentiation of a particular thalamic area. In the cerebellar territory, the differentiation of the motor cortex developed a specialized lateral subpart. The changes in the basal ganglia system had even heavier effects. In sauropsids, the "pallidum" (pale, in the topographic position of the lateral pallidum of upper primates) sends most of its axons to the tectum (Reiner *et al.*, 1984). In nonprimate genera, the sequence is restricted to the few intracapsular neurons forming the "entopeduncular nucleus" (not an equivalent yet of the medial pallidum) and the substantia nigra. In catarhineae (from cercopithecideae to man), the full lateromedial sequence of the striatal targets is lateral pallidum, medial pallidum, nigra lateralis, and nigra reticulata (including dendrites of the compacta) (Percheron *et al.*, 1994). The first and the third have no thalamic outputs, the lateral pallidum projecting, among other targets, to the subthalamic nucleus and the nigra lateralis to the tectum. The second and fourth elements are the origins of two separate prethalamothalamic subsystems. The development, differentiation, and separation of the medial pallidum go with that of the pallidothalamic bundle and the selective projection to the supplementary motor area (SMA) (see Fig. 20.19 and VO pallidal subregion). This chain adds to the lemniscal, cerebellar, nigral, and pallidal territory, VO, a fourth thalamic territory. The complete separation with the nigral territory has led to the disappearance of "VM." No VM existed in the founding literature on monkeys (Vogt, 1909; Mussen, 1923; Crouch, 1934; Walker, 1938). Aronson and Papez (1934), in a brain cut very obliquely, described a VM said to be similar to that described by Rioch (1929) in dogs. In the cat, VM (along with VL) is known to receive both cerebellar (e.g., Hendry *et al.*, 1979; Kultas-Ilinsky *et al.*, 1980) and nigral afferences (Hendry *et al.*, 1979). A ventral and medial thalamic part, located just in front of the central formation, called VMp by Jones (1985, 1995), is actually a topographical part of the nigral territory; thus included in VA (see "Subregio Lateralis Rostralis. Nigral Territory"). Since the convergence of cerebellar and nigral afferences in the VM no longer exists, it may be said that there is no longer a VM in upper primates. Jones's VMb (Asanuma *et al.*, 1983; Jones, 1985, 1995) and followers (Craig *et al.*, 1994; Morel *et al.*, 1997; Blomqvist *et al.*, 2000) was a totally different thalamic entity, the taste relay, belonging to the lateral region ("Subregio Arcuata"). Still another part, the relay of the spinothalamic system conveying pain (Craig *et al.*, 1994; Blomqvist *et al.*, 2001) has been recently labeled Vmpo. It does not belong to the lateral region but to the spinothalamic receiving basal region (see "Regio Basalis."). Other major thalamic changes came with the evolution of the oculomotor systems (see Chapter 33). In macaques, one important thalamic source to the oculomotor cortex is located in the paralamellar site of the medial region receiving tectal and cerebellar axons. This is likely to have disappeared in apes and man and to have moved to the lateral region. In macaques, the frontal eye field (FEF, area 8) is anatomically defined as dysgranular and linked to the arcuate sulcus. This no longer true in chimpanzees. The arcuate sulcus has disappeared and the frontal eye field has moved far anteriorly (Grunbaum and Sherrington, 1901; Leyton and Sherrington, 1917; Hines, 1940) and FDT of Bailey *et al.* (1950) is isocortical. In man, the delineation of area 8 led to a great discrepancy between Brodman (1909), Vogt and Vogt (1926), and von Economo and Koskinas (FC, 1925). Stimulations by Foerster (1939), Penfield and Brodley (1937), Rasmussen and Penfield (1948), Penfield and Rasmussen (1957) led to a more posterior position than in the chimpanzee, close to the precentral sulcus. There would be in fact at least two oculomotor areas (Tehovnik *et al.*, 2000). FEF would be located at the posterior part of the middle frontal gyrus. This is more inferior than for Paus (1996). The varying positions of FEF must not be seen as the mere displacement of one cortical spot but as a sign of deep and fast evolutive changes. With such cortical changes, thalamic interspecific differences are not surprising.

Subdvision and Nomenclature

The discovery and description of main afferent territories brought out the necessity of having to name four of them: from back to front at first the lemniscal territory (with posterior, cutaneous, and anterior kinaesthetic parts), the cerebellar territory (with lateral and a mediodorsal parts), the pallidal, and, finally, the most anterior, nigral territory. For the second topo-

graphic adjective (after ventral or dorsal), the Vogts' school used caudal, intermediate, and oral. The Michigan system used posterior and anterior (both acceptable by the Nomina Anatomica). Kievit (1979) and Stanton (1980) accepted the "VL-Vim" equivalence for naming the cerebellar territory. The late discovery of the nigral territory opened a problem. In Cecile Vogt's account, a subdivision ("fasciculaire") was located in front of the pallidal territory (Vo). In Papez' *et al.*'s drawing (1940; Fig. 20.10), va was in front of the pallidal afferences, making possible an attribution to a rostral (nigral) territory. The VL-VA system of the Michigan school had only two adjectives for three subdivisions (cerebellar, pallidal, nigral) in primates. This could have two possible interpretations. That of Jones (1985; Hirai and Jones, 1989; Morel *et al.*, 1997), continuing Olszewski's choice, had two VL (VLp, cerebellar and VLa, pallidal) and one VA-VM. The attribution of the same label (VL) to two obviously distinct anatomofunctional territories, having different properties, one excitatory (cerebellar) and the other inhibitory (pallidal), is hardly defensible. The other system, that of Ilinsky and Kultas-Ilinsky (1987, 1993, 2001) has one VL (cerebellar), two VA, one pallidal (Vadc, a new naming), and one nigral (Vamc). The two distinct (pallidal and nigral) territories have some features in common: their belonging to the basal ganglia system, and their receiving GABAergic, inhibitory messages. They have, however, different sources and different staining properties. The pallidal territory is acetylcholinesterase positive. Only somata in the nigral territory are calbindin positive with a different ultrastructure. Above all, the separation of the nigral and pallidal territories in upper primates expresses the separation at the thalamic level of two thalamocortical subsystems: one rather "motor" (MI, SMA) and the other rather "associative" (frontal and cingulate) and "oculomotor" (FEF, SEF) (Fig. 20.20). The placement of the pallidal territory into a single VA perpetuates the continuous neglect of the nigral territory. The two territories must be distinguished with two different names.

In the last decades, some attempts have been made to homogenize the thalamic nomenclature for monkeys to human beings (Louvain symposium, 1963; Percheron, 1969, 1977; Jones, 1985; Ilinsky and Kultas-Ilinsky, 1987; Hirai and Jones, 1989; Percheron *et al.*, 1994, 1996; Macchi and Jones, 1997). During the writing of this chapter, competent colleagues were asked for their opinion about the nomenclature for thalamic subdivisions of the human thalamus (and more generally to the catharinian thalamus). After the acceptance of ventralis for lateralis for denoting elements of the lateral region, the basis for an agreement for the second adjective was mainly the anterior-posterior system ("Michigan" choice, with VO added). In catarhinians primates (and man), from back to front, the sequence of territories is as follows (Fig. 20.18). The lemniscal territory is the nucleus ventralis posterior VP (Kaas *et al.*, 1984), with two parts. The most caudal, cutaneous, is the nucleus ventralis posterior caudalis (VPC). The, more oral, kinaesthetic, is the nucleus ventralis posterior oralis VPO with its own map. Taking into account the rejection by some of any reference to VL for the cerebellar territory in man, it is proposed that the choice be between VL (in the Ilinsky's conception) or ventralis intermedius, either VI (Crouch, 1934; Kusama and Mabuchi, 1970; Percheron, 1977, in macaques) or VIm (Vogt and Vogt, 1941; Hassler 1959 in man). The problem of the pallidal territory (Fig. 20.18) may be simply solved by accepting that it requires its own name. Part of the ventral oral nucleus of C. Vogt and the anterior part of VO (Voa) for Hassler (1959) were retained together with VA at the Louvain symposium. The pallidal territory may thus be the nucleus ventralis oralis VO. The sequence is continued by the nigral territory, which, in spite of deep phylogenetic changes, could be the nucleus ventralis anterior VA. The third adjectives, in thalamic nomenclature, usually denote parts (of nuclei). The Vogt school used externus and internus (that also meaning inside and outside are not adequate, Louvain, Dewulf 1971). Parts are thus medial or lateral or inferior or superior. VPC has two subparts VPL and VPM (ventralis posterior lateralis and medialis), with a single map. The cerebellar territory is subdivided into two parts: one lateral Vim L or VLL and one medial VimM or VLM. The sequence (VP-Vim-VO-VA) may bring a common language to both stereotacticians and neuropathologists on the one hand and neuroanatomists and physiologists working on the primate thalamus (starting from cercopithecideae) on the other.

SUBREGIO LATERALIS ARCUATA. NUCLEUS VENTRALIS ARCUATUS. VArc

The posterior part of the lateral region has a clear-cut boundary with the pulvinar. This is true in cytoarchtectonics and in Golgi impregnation where dendritic arborizations bend, forming a dendritic wall. In immunocytochemistry, the border is observable using parvalbumin immunoreactivity, the lemniscal territory, not the pulvinar, being parvalbumin positive. The most posterior part of the lateral region is not entirely simple. Medial to the caudal nucleus (vc), a crescent-shaped part surrounding the central formation of Luys was described: the nucleus "semilunaris" (Dejerine, 1895), cupuliform (von Tschisch 1896), or

arcuatus (Kölliker, 1896). Its macroscopic contrast with the lateral caudal nucleus, particularly in myelin stains, was such that it was considered only as "accessory" to the lateral region (Dejerine, 1895). A lateral lamella was described, but it was not a true one because it was not separating (see "Lamellae and Classic Nuclei. Burdach's Model"), but rather was made by a sheet of lemniscal axons. Another problem is due to the fact that only the dorsal part of the arcuate nucleus is somesthetic with one common map with the more lateral ventral posterior. The ventral part of the classical "arcuate nucleus" is the thalamic part receiving and processing gustatory information.

The most inferior and medial part of the classic nucleus arcuatus or semilunaris ventral and anterior to the central formation that it surrounds usually considered as a part of VPM (Vci) has particular cytoarchitectonic traits: small pale and round neurons (VPMpc parvocellularis; see Mai *et al.*, 1986; Chapter 31). Because it does not receive lemniscal axons, it is not a part of the lemniscal territory that defines VP. It prolongs the representation of the tongue in the adjoining ventralis posterior but does not belong to the somatotopic map of the lemniscal nuclei. A particular nucleus that is so strongly stained for calbindin makes its observation and differentiation easy. It is proposed to denote it nucleus ventralis arcuatus Varc (Aronson and Papez, 1934; Papez *et al.*, 1940, "arc"). Bowman and Combs (1969) found a projection of hypoglossal afferents to VPM without precision about the parvocellular part but likely in Varc. Becksteadt *et al.* (1980) showed a selective afference from the nucleus of the solitary tract, which receives axons from the vagus (X). In macaques, Roberts and Akert (1963) and Wirth (1973) showed a projection to the insula. Concerning the thalamocortical connections, see Chapter 31. The primary gustatory area is known to be located below the primary somesthetic area, in the opercule up to the insular cortex (Sanides, 1968).

SUBREGIO LATERALIS CAUDALIS. LEMNISCAL TERRITORY

This subregion is analyzed in Chapter 28, which is devoted to the somatosensory system. Its general shape is rather simple (Fig. 20.15). The posterior curvature corresponds to the anterior border of the central region. One problem is raised by the presence of a subpart devoted to "deep" afferents. As established in macaques by Mountcastle and Henneman (1952) and Poggio and Mountcastle (1963), it is agreed today that the cutaneous and kinaesthetic representations of the body are separate in the primate thalamus, the second being more dorsal and more anterior. The physiological separation is sharp. The anatomical delimitation on cytoarchitectural criteria is difficult. In any case, it is necessary to distinguish two nuclei VPC and VPO.

Nucleus Ventralis Posterior Caudalis. VPC

The traditional (cutaneous) part VP is usually subdivided in two formal parts being given the status of nuclei, one medial (VPM) and one lateral (VPL). In opposition to their histological contrast, the lateral part VPL and the superior part of the arcuate nucleus VPM constitute a single nucleus with a single cutaneous somatotopic map: the nucleus ventralis posterior caudalis (VPC; Hassler's Vcp). This is made up of two subparts: the lateral corresponding to the classical VPL and the medial to the upper part of the arcuate ensemble VPM. This is composed of CO-rich rods in a CO-weak "matrix" (Raussel and Jones, 1991a, b). VPL has less obvious but similar elements (Raussel *et al.*, 1992). Only the parvalbumin positive CO-rich rods would receive lemniscal afferent. The CO-weak matrix would receive spinothalamic axons. The reception of lamina I spinothalamic axons, in the VP has recently been reassessed by Willis *et al.* (2001). This input is said to act in "the sensory-discriminative processing of nociceptive information." The source toward the somatic sensory cortex is "onion-like" with "lamellae" for small cortical fields (Jones *et al.*, 1979). The cortical projection asks for a short presentation of the perirolandic cortex. This is a zone of strong morphological (and functional) differentiation, myelinating early in ontogenesis (Flechsig). This led Bailey and von Bonin (1951) to distinguish it as the "sector" or "regio centralis." Because the presence of scissurae, sulci, and gyri, cortical points have three topological positions: gyral on the surface, sulcal on the ridge, and fundic in the bottom of the sulcus (Von Economo, 1927; Krieg, 1963). The central sulcus is the origin of two, pre- and postrolandic, opposed morphogenetic gradients (Sanides, 1966, 1968). In the depth of the central sulcus (fundic) is the "transitory" area 3a (Vogt and Vogt, 1919; Jones and Porter, 1980) or intermediate sensorimotor area (Ism; Sanides 1967). The posterior bank of the central sulcus is sensory. Most primary sensory areas (somesthetic, visual, auditory, and gustatory) are sulcal, on the ridge of a gyrus, often not visible on the surface in man. Primary sensory afferences are strong morphogenetic agents of cortical differentiation. They form koniocortical (Von Economo, 1927; from *konios*) dust, linked to the presence of many "granular neurons" in layers IV and III or hypergranular gradients. The koniocortex (area 3b of Brodmann, somatic koniocortical area, Ks, Sanides, 1967) is surrounded by the perikoniocortical area 1 (Brodmann's order does not follow the arithmetic order). The "area 3b" (PB1,

Von Economo) and "area 1" (PC) constitute the primary somesthetic cortex SI. It is followed by the gyral area 2. The eugranular parietal cortex starts with area 5. The cutaneous VPC (VPL + VPM) projects somatotopically to the postcentral, sulcal, composed of "area 3b" (PB1) and and "area 1" (PC)(Jones and Powell, 1970; Jones *et al.*, 1979; Jones and Friedman, 1982). The CO-rich lemniscal rods would project to the deep layers of SI. The CO-poor matrix would project to its superficial layer.

Nucleus Ventralis Posterior Oralis. VPO

The segregation of thalamic neurons responsive to different somesthetic modalities (cutaneous, tactile versus deep, kinaesthetic) was observed first in macaques by Mountcastle and Henneman (1952). The individuality and precise intrathalamic location of the kinaesthetic group has been the subjects of debates for several decades. In macaques, Maendly *et al.* (1981) observed a "narrow zone with a maximal longitudinal extent of 3mm" in the "rostral cap" of the VPL with "short-latency field potentials evoked by group I muscle afferents," Jones and Friedeman's (1982) opposed a kinesthetic "shell" (anterosuperior) to a cutaneous "core" in the nucleus ventralis posterior. The aspect and topography of the kinaesthetic zone were not easily established. Walker (1938) yet had made an exact description of an "anterior part of the nucleus ventralis posterior" forming "a quite narrow, almost vertical, sheet of cells which are distinguished by their large size and deep staining. It extends posteriorly tail-like over the dorsal part of the nucleus ventralis posterior pars lateralis for some distance" (p. 46). This concerned a "nucleus ventralis intermedius," evidently different from that of C. Vogt (cerebellar), which Walker no longer mentioned and was forgotten by its followers. The situation in sane monkeys was however relatively clear: the kinaesthetic group was located in the lemniscal nucleus ventralis posterior. The problem was more complex in man because of the lack of distinction between sane and pathological conditions. On cyto- and myeloarchitectonic differences, Hassler's (1959, followed by Emmers and Tasker, 1975) distinguished two parts in the nucleus ventralis caudalis (Vc equivalent to ventralis posterior): V.c.a. and V.c.p (each with medial and lateral subparts) surmounted by Zc (zonalis caudalis). In 1966, Albe-Fessard *et al.* showed the location of a zone in the human thalamus receiving information "from deep tissue, joints and we believe from Group I muscle afferents." illustrated on a modified Hassler's map (their Fig. 1 reproduced in Fig. 20.27). This zone, crescent-shaped over the cutaneous VPM, involved V.im and a region dorsal to the somesthetic nucleus (Z.c, Fig. 20.27). The selected reference L15 plane was unfortunately too medial. The transfer of the data to planes L16 of the same atlas, L16 of Van Buren and Borke (1972) or L16.7 of Morel *et al.* (1997) shows that the kinesthetic zone likely was in Hassler's Vc.a.e and Zce. The two elements, not seen in continuity, actually form a sort of comma in front and above the cutaneous VP (Fig. 20.28 from L14 to 18.5). The kinaesthetic zone was not described earlier because of its misleading cytoarchitecture, appearing even more "cerebellar" than the cerebellar territory itself, with particularly large neurons, distant one from the other. In horizontal sections, Hirai and Jones (1989) delineated a subdivision having cell-sparse large neurons looking like the cerebellar territory but staining for cholinesterase (like the lemniscal). This part, equated to the Vcae of Hassler (1959), was said to form an anterior part of the lemniscal territory, renamed VPLa (in opposition to the cutaneous VPLp). Hassler's Zc was not considered. In the squirrel monkey, Kaas *et al.* (1984) and Kaas (1988) later described two subnuclei: one nucleus ventralis posterior oralis (VPO) located in front of the cutaneous VP (thus potential equivalent to V.c.a.e) "relaying muscle spindle information" and projecting to area 3a and one nucleus ventralis posterior superior (VPS), superior to it (thus potential equivalent to Zc), relaying "deep receptor" (articulation, tendon) input to area 2. This separation is now said to be "inconclusive in primates" (Chapter 28), leading to a single subdivision (VPS, Kaas). VPS privileged a ventrodorsal sequence (VPI-VP-VPS) when the kinesthetic part is located in a general caudooral sequence (VPC-VPO-Vim-VO-VA) previously acknowledged in Hassler's Vca or Jones VPLa. VPO is thus preferable. This anterior part of the lemniscal territory is embedded between the cutaneous and the cerebellar territories (horizontal sections, Fig. 20.16; transverse, Fig. 20.17 A 4.2 to –1.25; sagittal, Fig. 20.23, L14 and Fig. 20.15 L15 and 16). It does not mix with the cerebellar territory or the cutaneous, from which it is separated by an irregular spacing strip. The kinesthetic nucleus has been the subject of many physiological studies in man (Albe-Fessard *et al.*, 1966; Jasper and Bertrand 1966; Bertrand *et al.*, 1967; Ohye *et al.*, 1972, 1990; Tasker *et al.*, 1982; Lenz *et al.*, 1988, and 1990; Seike, 1993). Lenz *et al.* (1988) insisted on the fact that "kinaesthetic" axons had lemniscal physiological characteristics. The kinaesthetic part has its own complete somatotopic map, thus forming a separate complete nucleus. The kinesthetic nucleus VPO projects to the fundic, intermediate sensorimotor (Ism; Sanides, 1967), area 3a (Jones and Friedman, 1982; Darian-Smith *et al.*, 1990; Darian-Smith and Darian-Smith, 1993; Kaas *et al.*, 1984) and to "area 2."

SUBREGIO LATERALIS INTERMEDIA. CEREBELLAR TERRITORY

Nucleus Ventralis Intermedius Lateralis. VimL or VLL, and Nucleus Ventralis Intermedius Medialis. VimM or VLM

The ending of cerebellar axons in the lateral part of the thalamus is known for long. C. Vogt (1909), after the destruction of the dentate nucleus in a monkey, showed cerebellothalamic axons forming her "prelemniscal radiation." This was located in front of the medial lemniscus and posterior to her lenticular radiation, thus in an intermediate position explaining the term "n. intermédiaire," latinized as nucleus intermedius (Crouch, 1934)(V.im for the Vogt and Vogts, 1941). The radiation was also observed during myelinization (Vogt, 1909; Kornyey, 1926). Crouch and Thomson (1938) and Walker (1938), in macaques, experimentally confirmed the location of the cerebellar territory, Walker adding that it is not simply ventral but also dorsal caudally. Van Buren and Borke (1971) found the same position in chimpanzees and Larson *et al.* (1982) in man. A series of experimental studies in macaques using anterograde degeneration extended the distribution of the territory (Mehler, 1971; Kusama *et al.*, 1971; Kievit and Kuypers, 1972) but thought that it overlapped with the more anterior pallidal territory. Our first topographic studies (Percheron, 1975, 1977) showed the high density, continuous, and complex three-dimensional shape of the territory. The comparison with previously published maps indicated that the cerebellar territory was separate from the pallidal and nigral territories, which was not accepted at that time. Further works (Chan-Palay, 1977; Berkley, 1980; Stanton, 1980; Kalil, 1981; Asanuma *et al.*, 1983; Ilinsky and Kultas-Ilinsky, 1987) confirmed the thalamic extent of the territory and its spatial separation from the lemniscal territory. Three-dimensional studies, rotations, and reslicing (Ilinsky *et al.*, 1993; Percheron *et al.*, 1996) showed the complex three-dimensional shape of the territory and its fundamental position for the analysis of motor thalamus (Fig. 20.17).

The cerebellar source to the thalamus is in all cerebellar nuclei (dentate, emboliform, globose and fastigial) (see Chapter 11). Transynaptic studies (Wiesendanger and Wiesendanger, 1985; Orioli and Strick, 1989; Hoover and Strick, 1999), however, specified that the main component of nucleocerebellar-thalamic connection was from the dentate nucleus (75–90%; Hoover and Strick, 1999), only 15–20% from the interposed nucleus and very few from the fastigial nucleus. Asanuma *et al.* (1983) put forward a somatotopic organization of the cerebellar nuclei with the face caudally and the leg anteriorly. Hoover and Strick (1999) showed instead a gross somatotopical organization only in the dorsal third of the dentate nucleus in monkeys having transynaptic links with the motor cortex M1. This part of the dentate nucleus would contain multiple somatic maps. Other, more ventral, parts of the dentate nucleus transynaptically project to other cortical areas. The two parts of the interpositus nucleus (nucleus interpositus anterior or emboliformis-emboliform nucleus and nucleus interpositus posterior or nucleus globosus-globose nucleus) together would contain another single complete somatotopic map.

The trajectory of cerebellothalamic axons is well known (Percheron 1977; Fig. 20.12A; Percheron *et al.*, 1996), through the superior cerebellar peduncle, decussating in the decussatio brachium conjunctivum and the brachium conjunctivum ascendens (Fig. 20.10B). This crosses the lateral part of the red nucleus and reaches the inferior border of the lateral region of the thalamus from which it spans to form the thalamic territory.

The cerebellar territory is intercalated between the nigral and pallidal territories anteriorly and the lemniscal territory posteriorly, thus intermediate: "nucleus ventralis intermedius" or "V.im". The description of its topography is made difficult by its complex geometry (Fig. 20.18). It is strongly curved sagittally (Figs. 20.17 and 20.18, 20.23). The anterior border with the pallidal territory is sinuous with long fringes, even peninsulae (Fig. 20.23 L11 and 12). Sections, may lead to misinterpretations about mixture, only avoided by three-dimensional reconstruction. The territory ends dorsally over the lemniscal territory (Fig. 20.23, L14). In horizontal sections (Fig. 20.21), the territory, oblique, is located medially to the pallidal, which is a noticeable difference with the monkey. The cerebellar territory expands ventrally and dorsally (Fig. 20.23 L8). Posteriorly, the border with the lemniscal subregion is rather smooth (Fig. 20.21 H1 0,9 to 7 and Fig. 20.23 L11 to 14). The intermediate subregion makes a clear contrast with the smaller cells of the posterior region and the dense islands of the pallidal subregion (also Hirai *et al.*, 1982). There are difficulties for delineating the cerebellar from the more anterior "magnocellular" neurons of the nigral subregion and the more caudal lemniscal subregion that also have large cells. The last, however, has more densely packed neurons mixed with small and middle-sized neurons (see "Subregio Caudalis. Lemniscal Territory"). The cerebellar territory stains for parvalbumin, which allows its delineation from the more anterior calbindin positive pallidal (also acetylcholinesterase positive) and nigral territories and from the poorly stained posterior region (pulvinar),

FIGURE 20.11 Cerebellar territory. Twenty transverse levels from Percheron *et al.* (1996), from among 32, placed in CA-CP coordinates and regularly spaced, *Macaca fascicularis*. The brachium conjunctivum is visible from 3.9 to 2.65. At first frontal levels, the territory starts as two—one medial and one lateral—islands. The two join posteriorly, and the territory becomes ventral. Starting from CP 3,65, pushed by the VP, it goes up dorsally and ends posteriorly in the upper lateral corner as the postremus site Lips. Note the dorsal place left for the pallidal territory. The territory does not respect the posterior part of the lamella medialis end and includes the paralamellar site that looks like a medial extension of the lateral region (l)I. LC, lateral caudal, lemniscal territory (LCL = VPL, LCM = VPM); LI, lateral intermediate, cerebellar subregion (of the lateral region), with two parts LIL (VImL or VLL) and LIM (VimM or VLM); LO, lateral oral subregion pallidal (VO) pallidal; LR, lateral rostral subregion nigral (VA); Larc, lateralis arcuatus, taste relay; Lu n, subthalamicus of Luys; C, regio centralis; M , nucleus medialis; Pu, pulvinar with PuO pulvinar oralis and PuOd pulvinar oralis dorsalis (ex LP).

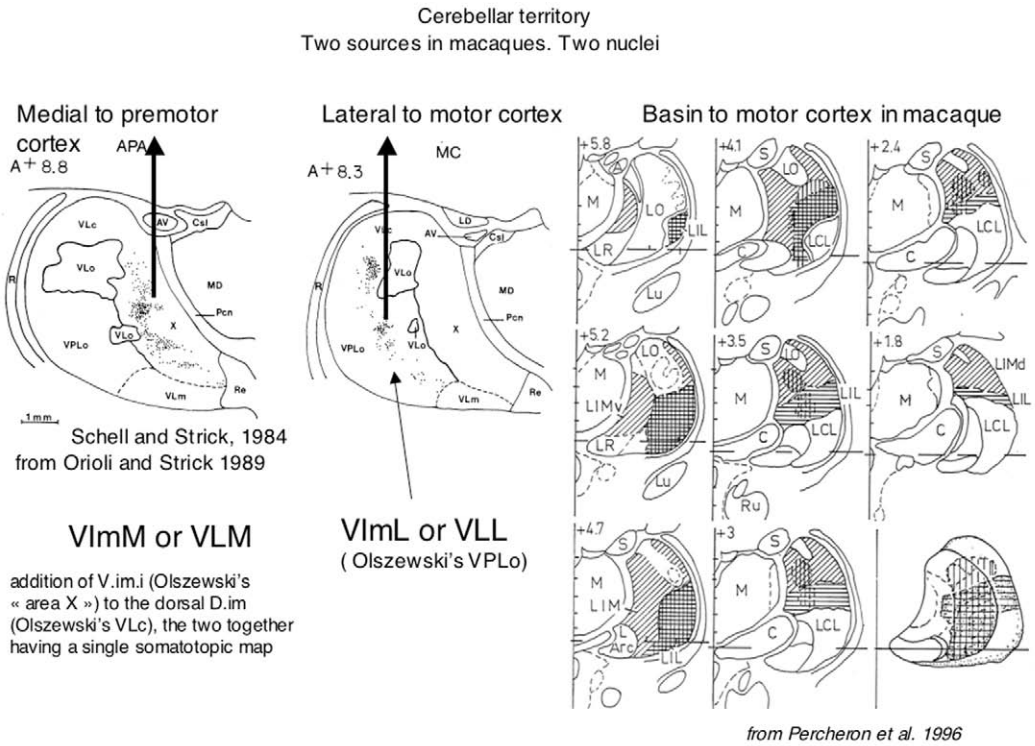

FIGURE 20.12 Subdivision of the cerebellar territory. *Left:* Picture from Orioli and Strick (1989) showing that there are distinct basins for the motor and premotor cortex. There are two parts generally separated ventrally in the macaque (VPLo and areaX) and man (Vim;e and V.im.i). The dorsal site is a continuation of the medial with a single somatotopic map. There are thus two nuclei: V.Im.L (o VLL) projecting to the motor cortex and V.Im.M (or VLM) projecting to the premotor. V.Im.L is strongly magnocellular with sparse neurons. *Right:* Picture from Percheron *et al.* (1996). This character is plotted using horizontal hatching on eight transverse sections of one monkey. The extent of the basin to the motor cortex (in vertical hatching) is traced on data from several works from literature. The two coincide essentially anteriorly where the separation of the two parts is visible.

but not simply from the lemniscal territory also parvalbumin+. The cerebellar region is, however, less dark with curved fascicles in sagittal sections.

The, intermediate, cerebellar subregion is not homogeneous, having some cytoarchitectonic diversity more or less coinciding with several previously delineated "nuclei." It has been known for a long time that the lateroventral part is made up of particularly large neurons, confirmed by cytometric studies (Dewulf, 1971; Van Buren and Borke, 1972; Hirai *et al.*, 1982, 1989). In Golgi staining, the dendritic arborizations of these neurons are larger than in the rest of the thalamus; about 500 to 600 µm in diameter (Hirai *et al.*, 1989; Percheron *et al.*, 1996). This part (VImL-VLL) also has a particularly low density of neurons giving a quite distinguishable aspect. The mediodorsal ensemble (VImM-VLM) contains smaller neurons. It is denser than the lateroventral part but still relatively poor in neurons; the whole cerebellar-receiving territory forming Asanuma *et al.*'s (1983) "cell sparse zone." As will be seen later, the distinction of two subparts in the cerebellar territory is not primarily based on cyto- or myeloarchitectonic criteria. The fine structure of the cerebellar territory has been analyzed by Kultas-Ilinsky and Ilinsky (1991) who found interspecific differences with few or no glomeruli and only few triads in macaques.

Contribution of the Different Cerebellar Nuclei and Distribution of Cerebellonuclear Axons

The cerebellar territory is at first the controlateral dentate territory, alone covering all its extent (Chan-Palay, 1977; Stanton, 1980; Asanuma *et al.*, 1983) and acting as the main territory with cerebellar and other coterritories. The distribution within the dentate territory is composed of onion-like layered curved laminae (Thach and Jones, 1979). Individual dentate axons emit one or only a few bunches of terminal twigs, ovoid or conical in shape, whose length and width is about 200 µm (Percheron, 1977). This points to rather focused input information and the possibility for the distribution of many separate items. But one point of the dentate nucleus may project to many laminae (Thach and Jones, 1979). The territories from others cerebellar sources such as the ipsilateral dentate or interposed territories are included within the main territory, often as spread islands. So does the fastigial

territory (Kievit and Kuypers, 1972; Asanuma *et al.*, 1983). The distribution of the axons from various cerebellar sources within the cerebellar territory must be analyzed according to neuronal paths starting from precerebellar afferents, cerebellar zones, and ("deep") cerebellar nuclei (Chapter 11). The zonation also involves the accessory vestibular nucleus of Deiters, the "nucleus X," and the interstitial nuclei. The interposed nuclei through the cerebellar cortex receive spinal afferences from spinocerebellar tracts conveying "deep" information from muscle (Allen *et al.*, 1977, 1978), articulations, tendons, and skin pressure.

Coterritories. Vestibulothalamic Coterritory

For a long time, the topography of the vestibular afference was not fixed. It is extended over the whole extent of the cerebellar territory and more abundantly posteriorly in macaques (Büttner-Ennever and Büttner, 1978; Lange *et al.*, 1979; Asanuma *et al.*, 1980, 1983), and man (Havrylyshyn *et al.*, 1978); (see Chapter 33).

Spinothalamic Coterritory

The spinothalamic coterritory also has a predilection for the posterior part of the nucleus (Mehler, 1969, 1971; Mehler and Nauta, 1974; Applebaum *et al.*, 1979; Boivie, 1979; Burton and Craig, 1983; Asanuma *et al.*, 1983; Berkley, 1980, 1983; Jones, 1983; Mantyh, 1983; Greenan and Strick, 1986; Apkarian and Hodge, 1989; Apkarian ans Shi, 1994). Spinothalamic axons end in other thalamic places (see "Regio Basalis."), but their presence among cerebellar afferents raises important problems that, in spite of their pathophysiological importance, have not been solved yet. The intervention of the spinothalamic system in the emission of messages to the motor cortex has been ruled out by Greenan and Strick (1986) based on the lack of register between islands of spinothalamic axons and of motor cortex-projecting neurons. There are strong indications that, in addition to the interposed contribution, the spinothalamic afferents bring deep information from articulations, muscles, and tendons that are recorded in the motor cortex (Goto *et al.*, 1968). For Mackel (2001), the sensory imput to VImVL could be important in the recovery from cerebellar motor deficits.

Tectothalamic Connection

The tectothalamic coterritory of the cerebellar territory also raises unanswered questions. In macaques, collicular endings are observed in the paralamellar part of the medial region (see discussion on paralamellar site in "Regio Medialis"), a part of the cerebellar territory with larger somata. This part is no longer observable on cyto- or immunoarchitectural signs in man. Morel *et al.* (1997) delineated a "VLpl" (nucleus ventralis lateralis paralamellaris), on unspecified criteria but indicated that it was a part of Olsewski's "area X" in macaques (i.e., a ventromedial part of the cerebellar territory, corresponding to Hassler's V.im.i in man—and not V.o.i).

The neurons in the cerebellar territory in macaques are sensible to passive limb manipulation or torque perturbation (Vitek, *et al.*, 1994) with no difference for fast or low movements (Strick, 1976; Goto *et al.*, 1968, in man). The internal organization of the cerebellar receiving zone of the lateral region is at least dual. Microstimulations in the ventrolateral part (Olszewski's "VPLo," VImL-LIL) in macaques (Anner-Baratti *et al.*, 1986; Buford *et al.*, 1986; Vitek *et al.*, 1996; Miall *et al.*, 1998) evoke movements of all parts of the body including orofacial ("lips, tongue, jaw, eyebrows and, occasionally, the eyes," Miall *et al.*, 1998) with a predilection for the production of proximal arm (shoulder and elbow) and face movements. The evoked movements are complex, multijoint (more complex than in the motor cortex and close to what is observed in SMA, Miall *et al.*, 1998). Considered separately, the medial (Olszewski's "area X" or Hassler's V.im.i) and dorsal elements (Vlc or DI) have incomplete maps (the first without leg, the second without face or eye representation). Together they make another map with about same topological organization (favoring their grouping together as VimM or VLM). The map in this ensemble is much less organized than in the lateral nucleus, the slabs being not well segregated, with some overlap for instance between arm and eye or face (Anderson and Turner, 1991; Vitek *et al.*, 1994). The cerebellothalamic system brings the necessary information for the coordination of movements in relation to the body ensemble and in space. There are task-specific differences in the macaques between the lateral VImL (VLL) and the medial VImM (VLM) in relation to internally triggered or visually guided movements (Miall *et al.*, 1998). One is preferentially driven by inner and the other by spatial environmental requests. Data in human are unfortunately not completely reliable in the absence of anatomical verification of trajectories but the functional organization of macaques is likely to be similar.

Efferences to the (sensorimotor) striatum have been shown only recently in macaques (McFarland and Haber, 2000). Conversely, it was known for a long time that the main target of the cerebellar receiving thalamic region was the primary motor cortex (Walker, 1938a, b; Strick, 1975; Jones, 1978; Myita and Sasaki, 1983; Gosh *et al.*, 1987). The anterior ridge of the central sulcus (of Rolando), then precentral or prerolandic, is shaped by an agranular gradient. The

motor cortex or primary motor cortex (MI, Mot., "area 4", Gig) is agranular and gigantopyramidal. In front of it are other agranular areas (past area 6). One is medial, the supplementary motor area (SMA), with a "preSMA" (Matzuzaka *et al.*, 1992). The other is lateral, the premotor cortex (Premot)(Wise, 1985a, b), often subdivided in macaques in dorsal PMd and ventral PMv parts. In macaques, in front of the premotor cortex is the dysgranular oculomotor cortex (frontal eye field, FEF, area 8) and an SEF (supplementary eye field) (Schlag and Schlag-Rey, 1987). These are histologically not obvious in chimpanzees and humans and not precisely located yet. Schell and Strick (1984) and Orioli and Strick (1989) found that the primary motor cortex is not furnished by the neurons of the whole cerebellar-receiving subregion (VIm/VL), and essentially by those of its lateroventral part (with larger neurons, i.e., Olszewski's "VPLo" or V.im.e; Fig. 20.12). Schell and Strick (1984) added that the medial part of the cerebellar subregion, in contrast, in macaques, sends its axons to the ventral premotor cortex ("postarcuate cortex," "APA"). This founded the proposed separation of the cerebellar subregion into one ventrolateral (VImL-VLL) and one dorsomedial (VImM-VLM) subparts (Percheron *et al.*, 1996). This differentiation, proper to upper primates, could be linked to the higher differentiation of the primary motor cortex (and of the pyramidal tract) and to the development and diversification of the premotor cortex. In a recent study, Dum and Strick (2003) found that a different part of the macaque dentate nucleus transynaptically project to different cortical areas. The thalamic lateral nucleus (VimL) projects essentially to the motor cortex while the ventral premotor cortex, the parietal 7b and the frontal (46 and 9) areas are furnished by the medial nucleus (VimM). This indicates that the differentiation into two subsystems starts from the dentate, the thalamic separation being secondary, and adds a further weight to the formal anatomical separation. As noted by stereotacticians, VImL (V.im.e) is organized according to a clear, complete, somatotopic map. Vertically oriented slabs ("shell-like") correspond to the leg laterally and the arm and face medially (i.e., grossly the same map as that of the lemniscal territory). Microstimulations, however, show multiple points for digits and face together (Miall *et al.*, 1998). Shindo *et al.*, (1995) found adjacent but separate, insulate basins to distal or proximal representation in the motor cortex, indicating a highly complex system. In the motor cortex, the inmap privileges proximal over distal parts of the body (Vitek *et al.*, 1994). The distribution to the motor cortex is inhomogeneous, not point to point and patchy (Hoover and Strick, 1999). The output map from the cerebellar subregion was carefully analyzed by Matelli and Luppino (1993) after retrograde tracer injections into subdivisions delineated by Matelli *et al.* (1991). Recent works using multiple labeling in macaques showed that the selectivity for cortical targets is not absolute and that the connections are subtle and weighted. The ventrolateral subpart (VImL-VLL), main furnisher of the primary motor cortex, also sends some axons to the ventral and dorsal premotor cortex (PMv, Pmd, Rouiller *et al.*, 1999; Sakai *et al.*, 1999) and to the supplementary motor area (SMA proper, whose main afferentation is from the pallidal territory, Hoover and Strick, 1999; Sakai *et al.*, 1999; Rouiller *et al.*, 1999). The mediodorsal part (VImM-VLM), which receives neurons from the ventral premotor cortex, the main furnisher of the premotor cortex, ventral (PMv, PMvr and PMvc) and dorsal (PMd, rostral and caudal, Pmdr and Pmdc) also sends axons to the preSMA (Rouiller *et al.*, 1999) and to SMA itself (Shindo *et al.*, 1995; Rouiller *et al.*, 1999; Sakai *et al.*, 1999). The sources to the primary and the supplementary motor cortex are separate with little overlap. The dorsal part of the mediodorsal part (VImM-VLM) sends axons also to the parietal cortex (Miyata and Sasaki, 1983; Schmahmann and Pandya, 1990). The cerebellar- and tectal-receiving paralamellar region (see above) sends axons to the oculomotor cortex (frontal eye field, FEF and SEF, Scollo-Lavizzari and Akert, 1963; Akert, 1964; Huerta *et al.*, 1986). The paralamellar subpart of the cerebellar territory has the same projections as other VImM-VLM parts (i.e., to the premotor Pmv, Schell and Strick, 1984, and motor cortex, Gosh *et al.*, 1987). This is an argument for not separating a VLpl or VImpl from VimM.

In conclusion, on histological, hodological, and physiological arguments, there are likely (at least) two cerebellar thalamic nuclei in man: VImL-VLL, corresponding to the Vogts' V.im.e, (famous V.im), and VImM-VLM (V.im.i + DI). These cannot be delimited with certainty in man in the absence of a reliable way of delineating the source to the motor cortex. Only the magnocellular character of the somata could be used, allowing some differentiation anteriorly. Tracings on Figures 20.21 to 20.23, are just the most likely. In addition, motor thalamocortical connections having different weights and simian cortical subdivisions having neither clear equivalent nor firm assessment may be made about the situation in man.

SUBREGIO LATERALIS ORALIS. PALLIDAL TERRITORY

Nucleus Ventralis Oralis. VO

The history of the pallidothalamic connection is long, since the connection was first described by C. Vogt in 1909 and was still being discussed relatively

recently, starting with the pioneering experimental work by Nauta and Mehler (1966) in macaques. C. Vogt established the continuity of the pallidothalamic axons in the right sense. The works of the Ransons (1939, 1941), furnishing sufficient data, had been unjustly forgotten (see Percheron *et al.,* 1996). The pallidal territory corresponded to C. Vogt's "lenticular radiation" located in front of her "prelemniscal" (cerebellar) radiation. As previously explained ("Lateral Region. Generalities") the sequence, accepted by Papez *et al.* (1940; Fig. 20.10) and Bailey and von Bonin (1951), was no longer taken into account in the formal subdivision of the thalamus effected by Olszewski (1952) and further authors. This had long-lasting detrimental effects on the whole thalamic parcellation. After the works of Carpenter and colleagues (Kuo and Carpenter 1973; Kim *et al.,* 1976), DeVito and Anderson (1982) and from Ilinsky and Kultas-Ilinsky (1987), in macaques, our study (Percheron *et al.,* 1994, 1996) delineated the territory on 52 transverse levels (20 in Fig. 20.13) followed by three-dimensional reconstruction. This led to the consideration of the pallidal as one of the major territories of the primate motor thalamus. It cannot be analyzed without placing it into a larger system, a three-path (with three consecutive connections), which are nonexistent in nonprimate orders, composed of the medial pallidum, the thalamic pallidal territory, and the cortical supplementary motor area (SMA; Fig. 20.19). This ensemble appears in simians, increases in size and number of neurons and progressively segregates from other systems. The process is not achieved in cebideae since, in the squirrel monkey for instance (Sidibé *et al.,* 1997), a part of the pallidal territory is located in front of the central region (Fig. 20.19 L6) shown in macaques to receive only nigral afferences (Percheron *et al.,* 1996). The catarhinian pallidal territory cannot be named using nomenclatures devised for lower animal species. The initial name given by C. Vogt to the recipient of her "lenticular radiation" was the "ventral oral" nucleus (more precisely her "noyau ventral oral lateral" Vogt, 1909, later V.O.e, Vogt and Vogt, 1941). Hassler (1949, 1982) constantly mislocated the thalamic place where cerebellar afferents are ending, wrongly placing them in the posterior part of the Vogts' V.o.e to which he described two parts: one anterior V.o.a, pallidal, and one posterior V.o.p, cerebellar. This misinterpretation, illustrated in Fig. 20.23 L8 to L14, had heavy effects in stereotactical culture. The other part of the Vogts' Vo, V.o.i, medial, was within what is known to be the nigral territory (VA). There was and is only one pallidal nucleus ventralis oralis VO; a term retained together with VA by the Louvain committee.

The source of the pallidal territory is the medial pallidal nucleus alone (Parent and de Bellefeuille, 1982; Fénelon *et al.,* 1990). The main afference of the medial pallidum is the striatum through the striatopallidonigral fascicle (the striatum, the bundle and the direct targets, pallidum and nigra, constituting the "core of the basal ganglia," Percheron *et al.,* 1994). The striatum is subdivided into associative and sensorimotor striatum (Percheron *et al.,* 1984). The latter receives axonal intertwined islands from the somatosensory, motor, premotor cortex and accessory motor, SMA. The greatest part of the macaque medial pallidum (63%, François *et al.,* 1994) receives axons from the sensorimotor component. This must be tempered by the fact that the geometry of the communication between striatal and pallidal axons (Yelnik *et al.,* 1984; Percheron *et al.,* 1984) realizes a drastic compression of information. The dendritic arborizations of the pallidum are flat, discoid, very large, and perpendicular to the emitting striatal axons. One pallidal (or nigral) neuron is in the position to receive pieces of information from numerous upstream striatal axons and is able to combine them. The map of the striatum is thus greatly impoverished in the pallidum. Transynaptic studies using viruses have shown that the outmap of the medial pallidum is still subdivided into a main, ventral, sensorimotor part and a dorsomedial associative part. Projections through the thalamus to SMA, motor, and premotor cortex arise from the sensorimotor part, while the transynaptic connection to the frontal cortex does it from the associative part (Middleton and Strick (2000). In the sensorimotor part, there could be a crude somatotopic outmap, the neurons transynaptically projecting to the part of the motor cortex devoted to the leg being more dorsal than those projecting to the face (Hoover and Strick, 1993, 1999). In the sensorimotor part, pallidal neurons are activated by passive movements of the controlateral part of the body. They intervene before the initiation of movement with elective directions of movements and kinematics (Turner and Anderson, 1997).

Medial pallidal neurons have several other targets; the most remote one being the pedunculopontine complex (PPN, Parent *et al.,* 2001). On their way, they successively emit collaterals to the oral lateral subregion, the central complex, the "nucleus of the field of Forel" and finally the pedunculopontine complex PPN. Some axons reach all four targets. The majority of the neurons of the medial pallidum project to the lateral region of the thalamus (Fénelon *et al.,* 1991; Parent *et al.,* 2001). Axons ending in VO are all collaterals of pallidoperipeduncular axons in macaques. About one half of these axons give a collateral to the central complex (see Arrechi-Bouchiouia *et al.,* 1997), the other not (Fig. 20.14). In the pallidum, pallidal axons run anteriorly, medially, and ventrally. They arrive at the anteroinferior part of the medial pallidum

FIGURE 20.13 Pallidal territory. Twenty of the 52 levels from Percheron *et al*. (1996). Intrapallidal injection of H3 in a *Macaca fascicularis* at CP+6.75. The massive pallidothalamic bundle makes successively the three Forel's H2-H and H1 fields (the last is the classic "fasciculus thalamicus"). Lateral position of the territory in the initial sections with oblique oblong islands. Separation from nigral VA (shown as LR) and cerebellar V.Im (shown as LI) territories. Posteriorly, pushed by the cerebellar territory inferiorly, the territory ends dorsally far posteriorly.

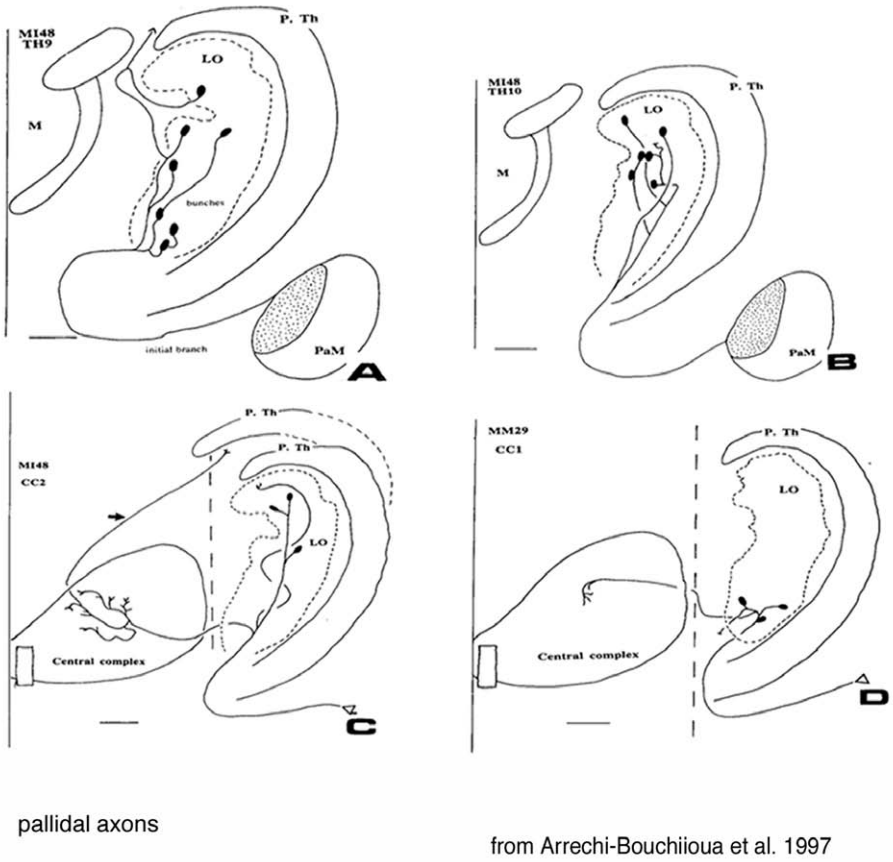

FIGURE 20.14 From Arrechi-Bouchhioua *et al.* (1997), showing the distribution of single pallidal axons labelled by biocytin. All of them reach the pallidal territory (here Lo). Long branches distribute widely rather small very dense glomerules of terminal endings ("bunches"). This spatial distribution makes unlikely the possibility for a somatotopic organisation. Two of the neurons emit a collateral to the central complex. Note that the mode of arborization is different in the two targets.

that they cover as a cap. The separation between the ansa lenticularis, inferior, and the fasciculus lenticularis, superior, argued at length by Nauta and Mehler (1966) is likely not necessary as they appear as mere aspects due to the section of an unique major bundle. Parent *et al.* (2001) showed that pallidal axons may give two branches, one horizontal and one ventral, that would have been said to run to the ansa or to the fasciculs. When pallidal axons arrive at the internal capsule, they cross it in separate elongated bundles forming Edinger's (1904) "Kamm-system" or "comb" (also containing cells). At the other side of the capsule, they gather together to reach the dorsal border of the subthalamic nucleus where they constitute the first part, H2, of the Forel's fields (1877). The pallido-thalamic bundle has a very peculiar three-dimensional trajectory that perturbed interpretations. Pallidal axons indeed go down in the hypothalamus. The so-sudden and so-sharp curve (about 350°) of the axons at "H," unusual in the brain, made unlikely that the two parts could belong to a single axonal system. Wilson (1914), for instance, believed that the descending branch corresponded to a lenticulorubral bundle (not existing but the main element of his "extrapyramidal system"). The continuity with the ascending "fasciculus thalamicus" (H1) and the direction were yet recognized by C. Vogt (1909) in the brain of a newborn (later confirmed by Kornyey, 1926, and Verhardt, 1938). The general shape of pallidal territory, relatively simple in horizontal sections (Fig. 20.19) is complex in three-dimension (Figs. 20.17 and 20.18). It is extended from the lower to the upper borders of the lateral region, thus neither ventral or dorsal and "lateral" (i.e., belonging to the lateral region). It is curved following the lateral border of the lateral region in the mediolateral dimension in frontal sections (Fig. 20.22, A 16.8 to 13). It is crescent-like in sagittal sections (Fig. 20.23 L9 to 12,), its dorsal and posterior part ending over the cerebellar territory. The medial and posterior border is highly sinuous with long

peninsulae (Percheron *et al.*, 1996; Kultas-Ilinsky *et al.*, 1997, Fig. 20.23 L8 and L11). This creates problems of interpretations on single sections without three-dimensional reconstruction. The irregularity of the contour must be considered along with the opposite nigral fringes. In transverse sections in macaques, there are oblique oblong islands densely containing small neurons. Bands in between have few neurons. Such bands are still visible in the most anterior transverse sections of the human brain (Fig. 20.22 A 16.8, 14.5) but are more evident in sagittal sections (Fig. 20.23 L9 to 12). They are interdigitated with similar ones of the nigral territory anteriorly and of the cerebellar territory posteriorly, mainly dorsally. The pallidal territory selectively stains for calbindin (Percheron *et al.*, 1996; Parent *et al.*, 2001), which is already the case at 23 weeks (Forutan *et al.*, 2001), where it is stained alone in the lateral region. Both neurons and "neuropil" are stained, allowing the delineation from the nigral territory in the absence of experimental methods. In addition, the pallidal territory stains for acetylcholinesterase. In man, the calbindin-positive territory is still anterior to the cerebellar. An internal change occurred in comparison with monkeys, as the nigral and the medial cerebellar territories seem to have moved anteriorly. What is medial to the pallidal territory in macaques is the nigral territory while in man it is the anteromedial part of the cerebellar territory (Fig. 20.21, H 3.9, Fig. 20.22, A 12 5 and 8.4). The pallidal axons arrive in great number at the inferior border of the lateral region (Fig. 20.23 L8 and 9). Their density leaves little room for neurons that led to the unnecessary isolation of a ventral subdivision (Vlm) (see "Lateral Region. Generalities"). In the pallidal territory, pallidal axons (Fig. 20.14) spread over large extents up to the dorsal border (Yelnik *et al.*, 1996; Arrechi-Bouchiouia *et al.*, 1997; Parent *et al.*, 2001). They emit several long distributing branches covering loosely the extent of the territory with no discernible order. At their extremity, they give off dense "bunches" (Arrechi-Bouchouaia *et al.*, 1996, 1997; Ilinsky and Kultas-Ilinsky, 1997; Parent *et al.*, 2001) or plexuses or baskets made by numerous axonal terminals (Fig. 20.7). Smaller than the receiving dendritic arborizations, such bunches bring a convergence and impoverishment of the thalamic map. Bunches are emitted in the inferior and dorsal part as well. This pattern offers little possibility for a somatotopic distribution if any. Thalamocortical neurons, which belong to a single neuronal species, are smaller than those of the more posterior intermediate neurons (Hirai *et al.*, 1982, 1985, 1989) and have medium-sized dendritic arborizations (VanBuren and Borke, 1972; Percheron *et al.*, 1996). Pallidal-receiving VO has the usual amount of local circuit neurons for the lateral region (24.5%, Dewulf, 1971). The pallidal boutons are mainly located on the somata and proximal dendrites (Kayahara and Nakano, 1996; Kultas-Ilinsky *et al.*, 1997; Ilinsky and Kultas-Ilinsky, 2001; Kultas-Ilinsky and Ilinsky, 2001). The mediator of the pallidothalamic connection is GABA (Aizawa *et al.*, 1999). Pallidal boutons contain pleimorphic vesicles and display synaptic contacts. Also ending on local circuit microneurons, they constitute triads (Ilinsky and Kultas-Ilinsky, 2001; see "Isothalamus. Constitution, Architecture, and Function") that are peculiar by the fact that they involve only inhibitory GABAergic neurons.

Pedunculopontine Coterritory

As already mentioned, the pallidal territory contains acetylcholinesterase-positive axons. These are likely of pedunculopontine origin. Since the medial pallidum directly sends axons to the pedunculopontine complex (Nauta and Mehler, 1966; Percheron *et al.*, 1996, Shink *et al.*, 1997, Parent *et al.*, 2001), the medial pallidum exerts a double influence on VO: one direct pallidothalamic, inhibitory, and the other indirect, medial pallidum- PPN-pallidal territory VO, excitatory.

The pallidal-receiving VO sends axons to the sensorimotor striatum in macaques (Nakano *et al.*, 1990; MacFarland and Haber, 2000; personal material) contributing to an important basal ganglia subsystem. The main cortical target of the pallidal receiving VO is the supplementary motor area (SMA; Strick, 1976; Jinnai *et al.*, 1983; Schell and Strick, 1984; Miyata and Sasaki, 1984; Wiesendanger and Wiesendanger, 1985, 1987; Wiesendanger *et al.*, 1987; Tokuno *et al.*, 1992; Hoover and Stick, 1993; Jinnai *et al.*, 1993; Matelli and Luppino, 1993; Nakano *et al.*, 1993; Shindo *et al.*, 1995; Sakai *et al.*, 1999). The pallidal three-path medial pallidum-pallidal territory-SMA very likely is still an important ensemble in man. SMA has been the subject of many works and reviews (see Goldberg, 1985; Tanji, 1994; Sakai *et al.*, 1999). SMA has numerous "functions" including motor preparation and sequential movement. Lesions there have major clinical effects (Laplane *et al.*, 1977). Some data have to be reconsidered after the discovery of the pre-SMA (Matuzaka *et al.*, 1992). It is today certain that VO also projects to the anterior part of the motor cortex M1 (Matelli and Luppino 1989; Shindo *et al.*, 1995; Kayahara and Nakano, 1996; Hoover and Strick 1999; Middleton and Stick, 2000). It also sends axons to the premotor cortex, dorsal (Pmd)(Kievit, 1968; Jinnai *et al.*, 1989, 1993; Nakano *et al.*, 1992, 1993) and ventral (Matelli *et al.*, 1986; Matelli and Luppino 1993; Hoover and Strick, 1993; Nakano *et al.*, 1993; Middleton and Stick, 2000). A

projection to the frontal cortex (principalis) has been observed by Middleton and Strick (1994, 2000). The pallidal territory has been postulated to be somatotopically organized, continuing orally the somatotopic order of the lateral cerebellar territory with three slabs, that of the leg laterally and that of the face more medially (Matelli and Luppino, 1993). In human patients, Hassler *et al.* (1979) drew a homunculus, which does not fit with Schaltenbrandt *et al.*'s (1971) observations and the axonal distribution described previously. One major difference with the efferences of the nigral subregion is the absence of projection to the orbital cortex (Cavada *et al.*, 2000).

The physiological analysis of the lateral oral subregion is made difficult by its indentation with the more posterior cerebellar territory (VIm-VL). Recent studies in the "pallidal receiving area" (found to be such after pallidal stimulation) are bringing rapid progress. In humans, neurons were said to be only weakly sensitive to passive movements (Vitek *et al.*, 1996) or do not respond to sensory stimulation at all (Jasper and Bertrand, 1966). VO neurons are sensitive to active movements (Vitek *et al.*, 1996). In human patients, some neurons have multiunit activity associated with arousal (e.g., sudden noise, unexpected taps, or sudden verbal instructions). But the most characteristic are "voluntary units" (or "voluntary motor cells," Jasper and Bertrand, 1966) firing only when voluntary movements are executed. This was discussed by Ohye (1990). Raeva (1986) found neurons whose activity was not rhythmic at rest but could become rhythmic during the initiation of movement and during the phase that follows motor tasks. The same author described the "triggered verbal command unit" increasing their activity after verbal commands for active movements, before the movement. The effects of microstimulation are disputed. Anner-Baratti *et al.* (1986), Bufford *et al.* (1996), and Vitek *et al.* (1996) found that it occasionally caused complex movements organized according to a somatotopic map. The reappraisal of their data led Miall *et al.* (1998) to the conclusion that microstimulations of pallidal-receiving neurons cannot produce movement (which would remain the property of the cerebellar-receiving neurons). The striatopallidal and the pallidothalamic connections being both inhibitory form an unusual path with a desinhibition well known by physiologists. The transient inhibition of the pallidum by injection of muscimol leads to an increase in the firing rate of thalamic neurons (Anderson *et al.*, 2001). The tonic inhibitory output of the medial pallidum would be of main importance for the maintenance of postural stability (Inase *et al.*, 1996). The medial pallidal system would contribute to the holding of the general and limb posture making the pyramidal system able to effect fine distal movements.

SUBREGIO LATERALIS ROSTRALIS. NIGRAL TERRITORY

Nucleus Ventralis Anterior. VA

The interpretation of the anterior part of the lateral region has raised many questions for a long time (discussed in Percheron *et al.*, 1992, 1993). In the beginning, the most anterior part of the lateral region has been separated from the rest on several assessed properties: (1) lack of projection to the cortex, as it did not degenerate (or degenerated incompletely) after hemidecortication (in macaques, Walker, 1935, 1938; Peacock and Combs, 1965); in chimpanzee, Walker, 1938; and in man, Powell, 1952; (2) lack of lower afferences (Jones, 1985 among others); (3) projection to the striatum (Walker, 1938); and (4) linkage to a diffuse system extending the reticular formation (Carmel, 1970) or to the limbic system (Angevine *et al.*, 1962a, b; Bentivoglio *et al.*, 1993). The long-standing interrogation concerning the polar part of the lateral region was partly linked to its unclear borders. This is caused by the strong curvature of the main axis of the lateral region, its anterior part ending not anteriorly but medially, almost perpendicular to the ventricle (Figs. 20.2D, 20.16). Another element of difficulty is the crossing of many fascicles breaking borders and cytoarchitecture. The neglect of the nigral territory for years, particularly at the time where the lateral region was being subdivided, had a detrimental effect on the whole structurofunctional subdivision of the thalamus that is still noticeable today. Cécile Vogt (1909) ignored the nigral territory as later did Crouch (1934), Walker (1938), and Olszewski (1952) among others. Hassler (1959, 1979, 1982) constantly rejected the existence of this afference, leading to its omission by stereotacticians. The acceptance of a nigrothalamic connection in primates appeared only after the work of Cole *et al.* (1964) using Nauta's method, followed by a series of works by Carpenter and colleagues (Carpenter and McMasters, 1964; Carpenter and Strominger, 1967; Carpenter and Peter, 1972; Carpenter *et al.*, 1976). These studies showed only the ventral part of the territory. The cartographic delineation of the whole extent of the territory was done only later (Ilinsky *et al.*, 1985; Ilinsky and Kultas-Ilinsky, 1987; Percheron *et al.*, 1993, 1996). These studies not only confirmed the connection but, as previously assessed by Carpenter and Strominger (1967), its separation from the pallidal territory, making it (with the cerebellar and the

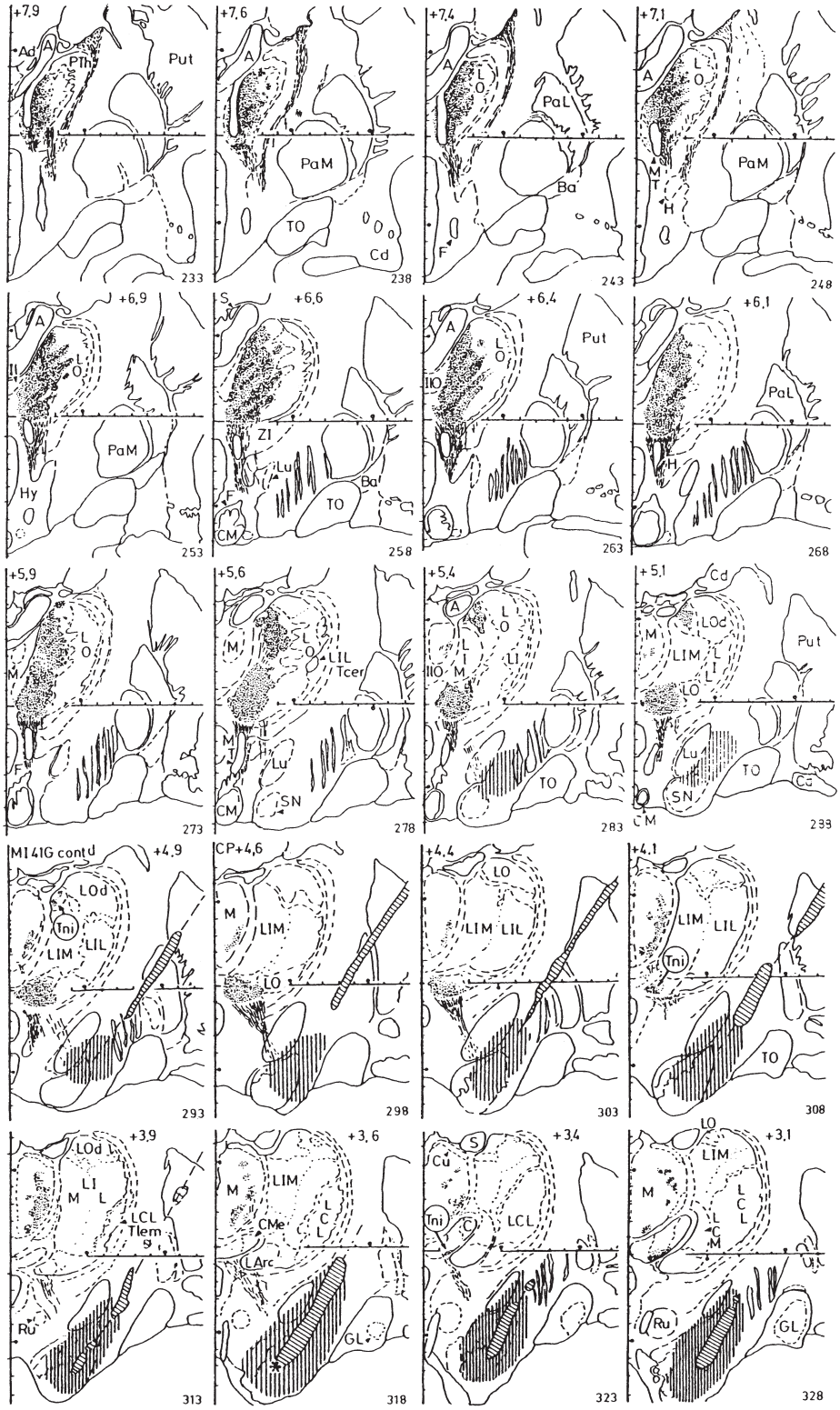

FIGURE 20.15 Nigral territory. Twenty levels on 41 from Percheron *et al.* (1996). The tip of the nigral injection with H3 is at CP+3.6 (star), with nigra almost entirely injected. The nigral territory, traversed by the mamillothalamic fascicle of Vicq d'Azyr, is medial and fills the anterior part of the lateral region not occupied by the pallidal territory LO (VO). The long indentations of the lateral border fit with sinuosities of the medial border of the pallidal territory. Posteriorly, the nigral territory is broken in its middle into ventral and dorsal parts by cerebellar territory. The ventral part continues far posteriorly up to the anterior pole of the central formation (CP+4.9 and 5.1) in a position sometimes separated as VM.

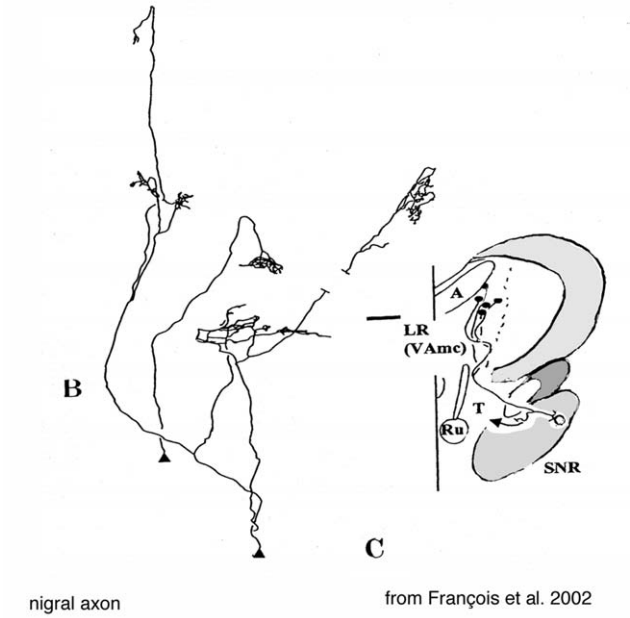

FIGURE 20.16 From François *et al.* (2002) modified showing the distribution of a single nigral axon in the nigral territory or rostral lateral subregion (LR) or VA. In B, one loose and widespread nigral arborization emits bunches similar to the pallidal, but they are less complex and less dense.

pallidal) the third major "motor" territory. Our study in macaques (Percheron *et al.*, 1996), where 41 successive maps were presented (20 in Fig. 20.15), brought out its three-dimensional extent, much larger than previously thought. The nigral territory also includes a place located just in front of the central region (Fig. 20.15, VA, Fig. 20.23, and Fig. 20.22, A12.5 and 13, L6), often isolated as a distinct lateral nucleus, the so-called "nucleus ventralis medialis." This, in higher primates, is the mere posterior continuation of the nigral territory (see "Lateral Region. Generalities"). The nigral territory contains patchy coterritories but has no other territory in front of it. It constitutes the anterior pole of the lateral region, being thus "polar" as for Hassler's nucleus lateralis polaris.

The source of nigral axons is located in the pars reticulata, lateralis, and mixta (above the compacta) (François *et al.*, 1984, 2002; Middleton and Strick, 1996). Nigral axons do not form a massive bundle; rather they form a continuous sagittal curtain through the hypothalamus, close and surrounding the mammillothalamic tract and avoiding the pallido-thalamic (H-H1 Forels fields) tract laterally (Percheron *et al.*, 1996; Fig. 20.17). Anteriorly and laterally it is surrounded by

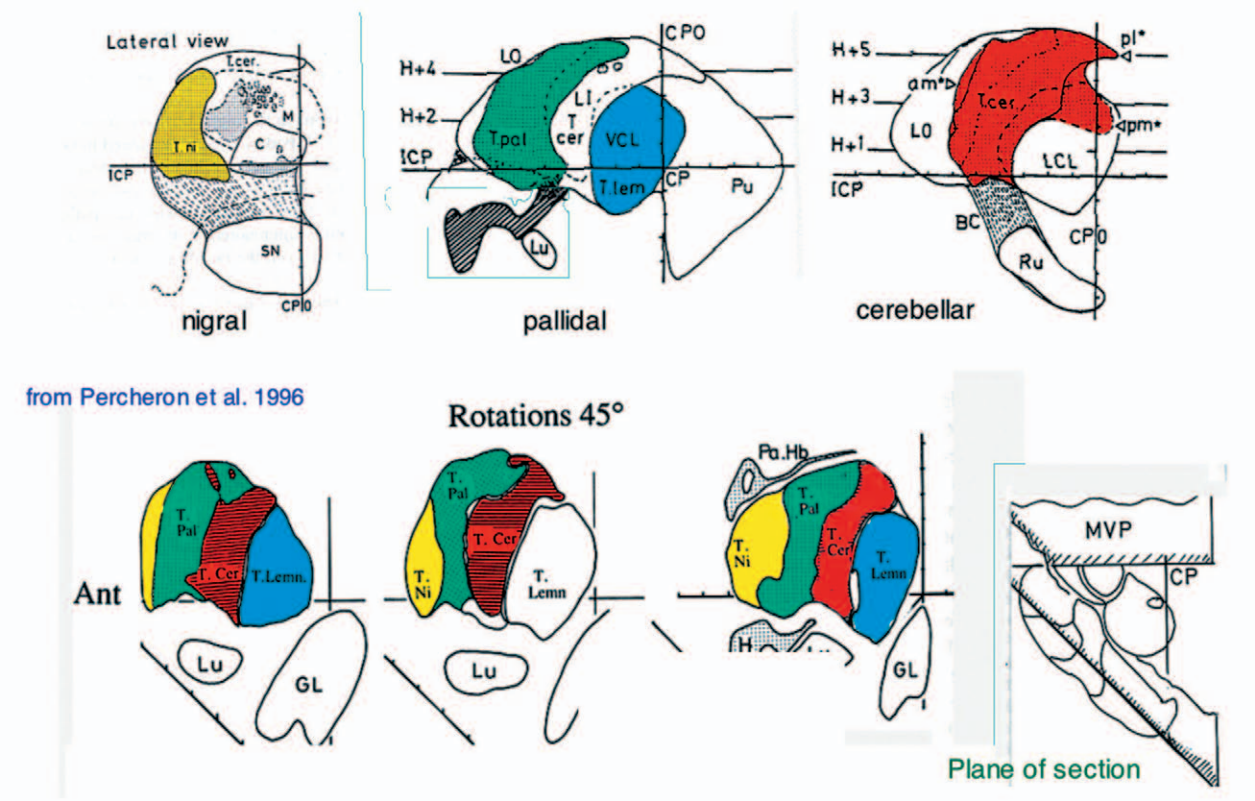

FIGURE 20.17 *Upper row.* From Percheron *et al.* (1996), colored. Sagittal reconstruction of the territories shown in Figures 20.15 (nigral), 20.13 (pallidal), and 20.11 (cerebellar) in *Macaca fascicularis*. The stong curvature of the territories may be observed convex to the front. The posterior part of the more anterior territory ends over the anterior part of the next territory. The three-dimensional geometry is complex. *Lower row.* "false sections" at 45° from the midventricular plane show a posteroanterior succession of territories: (retinal) lemniscal, cerebellar, pallidal, and nigral, still in macaques. This kind of section strongly reduces the curvature of territories.

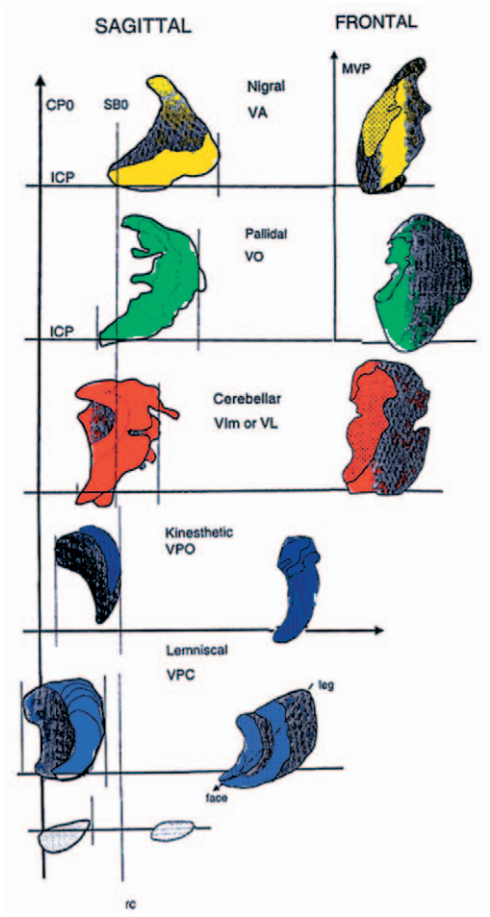

FIGURE 20.18 Sagittal reconstructions of the nigral, pallidal, cerebellar, kinaesthetic, cutaneous, and gustatory territories in human. The same curvature is observed as in the monkey. The relative position or sequence of territories is the same. Some borders are smooth but others, such as the pallidal and cerebellar, are strongly fringed, meaning sinuous borders whose section may create difficult interpretation.

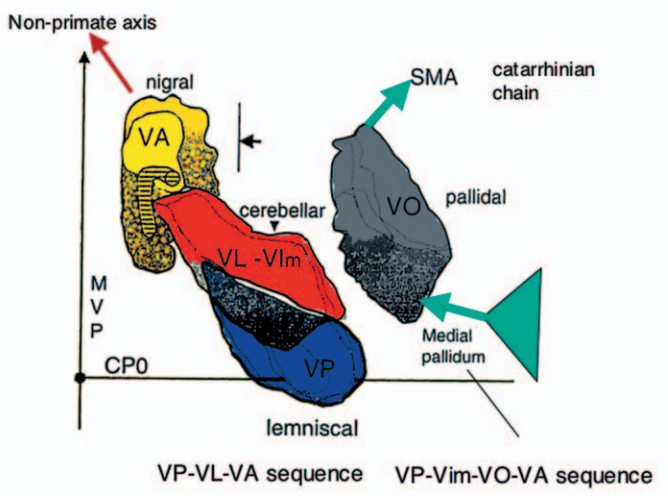

FIGURE 20.19 Three-dimensional reconstruction of subregions from horizontal sections in man. The sequence of the three, most medial subregions, is left in its position in relation to the CP0 system of coordinates. The pallidal subregion is moved apart laterally. The lemniscal, cerebellar, and nigral territories constitute a sequence observable in nonprimate species translated as the VPL-VL-VA sequence. The addition of the pallidal territory, which remains lateral, is particular to primates. It is linked to the development of a three-path: medial pallidum-pallidal territory-SMA. The pallidal territory deserves a particular name and acronym: VO. The nigral territory, crossed by the mammillothalamic tract, develops anteriorly. The cerebellar territory is pushed medially and reaches the posterior border of the nigral territory. The lemniscal territory has the same obliquity.

the perithalamus, which is particularly thick there. It is broken by the heavy myelinated fascicles that form oralwards the anterior thalamic peduncle. The territory is crossed through its whole ventrodorsal extent by the mammillothalamic tract of Vicq d'Azyr (Fig. 20.22 A14.5 and Fig. 20.23 L6). The posteromedial border of the nigral territory with the cerebellar territory is difficult to trace on cytoarchitectonic pictures in man since they both have large cells. This may be solved by using calcium-binding immunostaining, the nigral territory being not parvalbumin-positive. The border with the pallidal territory is sinuous with interdigitation in both frontal and sagittal sections (Fig. 20.23 L9). The nucleus ventralis anterior was said to be made up of several cytoarchitectonic nuclei: magnocellularis around the mammillothalamic tract, parvocellularis or principalis (or unspecified VA for Olszewski, 1952). The structure of the magnocellular part, proper to primates, has been analyzed by Ilinsky and Kultas-Ilinsky (1990) and Kultas-Ilinsky and Ilinsky (1990). The thalamocortical neurons are of various sizes and packed in subparts with no clear borders. The magnocellular differentiation, which is mainly medial, fades out laterally, dorsally, and ventrally in the less differentiated part. In humans, there is an obvious extension of this magnocellular differentiation, making its distinction from the large sparse-celled part of the cerebellar subregion more difficult than in macaques. Dekaban's (1953) VA, Andrew and Watkins' (1969) LOI, and VanBuren and Borke's (1972) Lpo did not contain any magnocellular subpart in man. At the reverse, a parvocellular differentiation is generally not taken into consideration. This part is more visible in man than in monkeys, which could expresses a further differentiation. It is made up of smaller somata and smaller dendritic arborizations (Van Buren and Borke, 1972). Ventromedial, it probably corresponds to the nucleus fasciculosus ("fasciculaire", Vogt, 1909) proposed by Van Buren and Borke (1972) to belong to the ensemble. For Ilinsky and Kultas-Ilinsky (1990), the magnocellular part Vamc would be the essential (or the only)

recipient of the nigral afferences. In fact, the parvocellular part also receives nigral afferences in macaques (Percheron *et al.,* 1996; Fig. 20.15; François *et al.,* 2002). The nigral territory in this genus covers different cytoarchitectural parts with apparently no care about cytoarchitectonics, giving no argument for making subdivisions on cytoarchitectonic criteria. The nigral territory does not stain for parvalbumin. Some of its neurons stain for calbindin, but much less than in the pallidal subregion from which it can be differentiated and which has no axons. The nigral territory is sagittally curved with a posterior and ventral part located just in front of the pole of the central region (Fig. 20.23 L6). At this level, it expands anterolaterally. The percentage of local circuit neurons is said to be only 10% in macaques (Ilinsky and Kultas-Ilinsky, 1990) but is 25% in the human thalamus (Dewulf *et al.,* 1973), the usual percentage in the lateral region. This indicates that VA is an evolutive part of the lateral mass. The nigral axonal endings within the nigral territory enter ventrally. From there, they climb on long distances, up to the superior border (Fig. 20.16). In their course, they irregularly emit long branches (Ilinsky *et al.,* 1993; François *et al.,* 1998, 2002; Fig. 20.14) that cover a great part of the territory. Many synapses are emitted *en passant,* all along the way of the axon (Ilinsky and Kultas-Ilinsky, 1990). There are, however, dense terminal axonal arborizations (François *et al.,* 2002) to some extent resembling the pallidal "bunches." Their average dimensions are 157 × 156 × 131 µm (François *et al.,* 2002); that is smaller than the average size of dendritic arborizations (about 400 µm). These sizes lead to the convergence of various axons on a single thalamocortical neuron not a simple transmission. The nigral boutons are similar to the pallidal and their distribution mainly on somata and proximal dendritic stems; however, they are less marked than in the pallidal territory (Ilinsky and Kultas-Ilinsky, 1990). Probably due to the low number of local circuit neurons in macaques, few triads and no glomeruli were observed (Ilinsky and Kultas-Ilinsky, 1990), which could be different in man with much more microneurons. The distribution of the axonal bunches is made in large extents of the nucleus, which does not offer a spatial substrate for a somatotopic organization. The physiological study of Vitek *et al.* (1994) did not find "a clear somatotopic picture" either. Studies in the posterior part of the nigral subregion in humans ("VOi") found either a partial (face and tongue, Hassler, 1968) or no somatotopy (Schaltenbrand *et al.,* 1971). The substantia nigra itself does not have a clear somatotopic organization. For DeLong *et al.* (1983, 1985) and Hoover and Strick (1999), the lateral part of the nigra would continue the outmap observed in the medial pallidum (orofacial). There is, however, no known somatotopic map in the nondopaminergic substantia nigra.

Amygdalar Coterritory

The anterior and medial part of the ventral anterior nucleus also receives axons from the basal nucleus of the amygdala in macaques (Percheron *et al.,* 1996). Amygdalar axons arrive anteriorly and branch without forming dense arborizations. Both the rostral part of the thalamic lateral subregion VA and amygdala have reciprocal connections with the cortex. The addition of the amygdalothalamic connection would create a link between the two. There is, however, no direct argument for the presence of this afference in human brains.

Tectal Coterritory

As already said in "Regio Basalis." and lateral intermediate subregion, terminal axons of the superior colliculus also end in the rostral subregion (Künzle and Akert, 1977; Harting *et al.,* 1980). They form islands within the nigral territory, not particularly in its magnocellular patch.

The three, nigral, collicular, and amygdalar sources make a peculiar set of afferences. All three have links or are parts of oculomotor systems. All three are sending axons in the nucleus medialis in macaques. But, as already mentioned, paralamellar subdivisions likely no longer exist in apes and humans. The topographically medial extensions of the tectal, nigral, and perhaps amygdalar territory of cercopithecidae could have moved partially or even completely in the lateral region namely in VA in man. The nigral subregion also receives abundant cortical afferences, from the frontal cortex in particular. Efferences from the nigral subregion VA to the striatum have been observed in macaques (Walker, 1938; Nakano *et al.,* 1990; Druga *et al.,* 1991; Fénelon *et al.,* 1991; McFarland and Haber, 2001), essentially to the associative striatum, thus participating in a subsidiary basal ganglia circuit. This connection was said to explain the lack of complete degeneration after cortical lesions. There is no argument for its persistence in the human brain where the polar region more clearly degenerates after cortical lesions (VanBuren and Borke, 1972). There would be projections to the anterior intralaminar complex (explaining the postulated link to the "non specific thalamic system," Carmel, 1970). Contrary to the initial claim, the efferences to the cortex are abundant. In contrast with the cerebellar and pallidal subregions, there is no projection to the motor cortex (Ilinsky *et al.,* 1985). The major projection of the nigral-

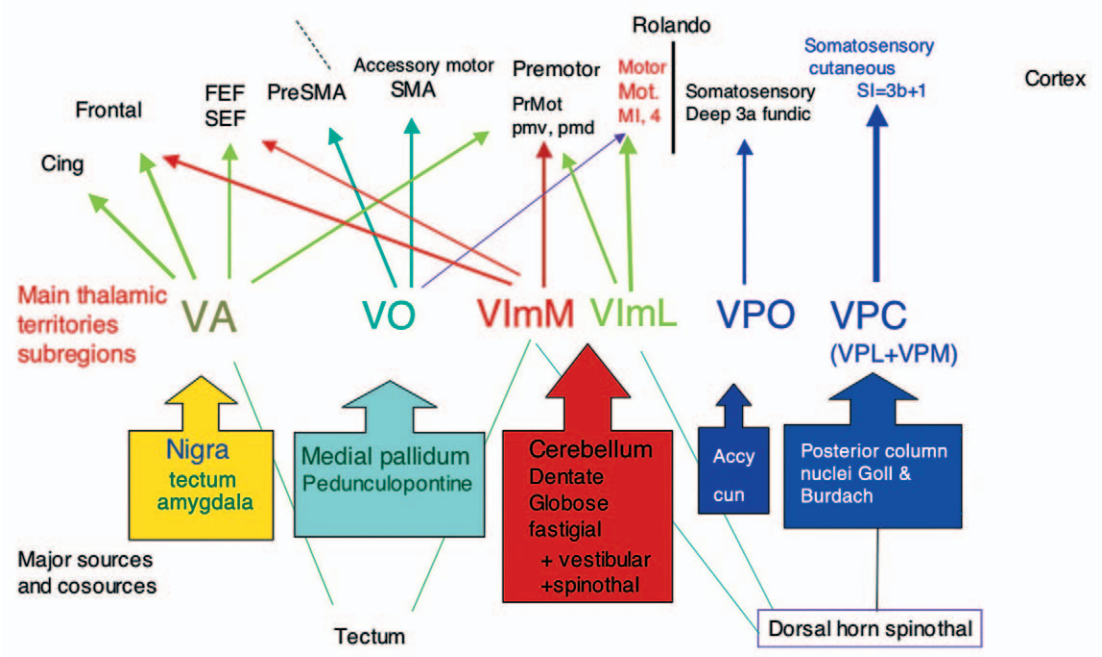

FIGURE 20.20 Flow chart of inputs to and outputs from the thalamus. In front of the central sulcus (Rolando) the number of cortical targets and the combinatorics increases. The separation of the pallidal and nigral territories leads to differentiated cortical targets and systems.

receiving VA, in partial continuity (on the other side of the lamella) with the anterior paralamellar part of the medial region is to the eugranular frontal cortex. Frontal targets are the superior, supraprincipalis (Rouiller *et al.*, 1999) and above all the inferior part from the principalis sulcus, infraprincipalis, and orbital (Carmel, 1970; Ilinsky *et al.*, 1985; Barbas *et al.*, 1991; Dermon and Barbas, 1994; Rouiller *et al.*, 1999; Middleton and Strick, 2000). Level 1 of Figure 4 of Cavada *et al.* (2000) shows that the source of projection to the orbital cortex exactly corresponds to the extent of the nigral territory (including fringes) and not the pallidal. There is a projection to the anterior cingulate area (Vogt *et al.*, 1987). In human brains a projection to the insula, considered as a major one, has been described by Angevine *et al.* (1962) and Van Buren and Borke (1972), not documented in macaques (Wirth, 1973). Another target is the inferior temporal cortex (TE; Middleton and Strick, 1996), known to be "critically involved in the recognition and discrimination of visual objects." There are projections to the premotor cortex (Ilinsky *et al.*, 1985; Nakano *et al.*, 1992, 1993), essentially in its dorsal part Pmd (Inase and Tanji, 1994; Pmdr and Pmdc, Rouiller *et al.*, 1999). Matelli and Luppino (1993) showed that there is no somatotopic outmap. There is also a projection to the supplementary motor cortex, SMA proper (Nakano *et al.*, 1992; Shindo *et al.*, 1995; Rouiller *et al.*, 1999) and preSMA (Rouiller *et al.*, 1999), which could concern essentially the last. VA thalamic axons also end in the temporal TE (Midleton and Strick, 2000). A particular discussion must deal with the projection to the oculomotor cortex. The neurons projecting to the frontal eye field (Huerta *et al.*, 1986; Lynch *et al.*, 1994; Middleton and Strick, 2000) and the supplementary motor eye field (Shook *et al.*, 1991) in macaques are located in the medial part of the nucleus. In this position, they can receive nigral, tectal, and perhaps amygdalar information. As already discussed, the evolution of the oculomotor cortex, from macaques, chimpanzees, to humans is such that it would have been surprising if the rostral lateral subregion (VA) had not changed. Very little is known concerning its physiology and physiopathology. There are almost no recordings of neurons in the nucleus. There are few data concerning microstimulations. One problem is linked to the abundance of crossing thalamocortical (thalamofrontal from the medial nucleus) fascicles, leaving little chance to avoid their excitation during the stimulation. Knowing the afferences (nigral, amygdalar, collicular) and the efferences to frontal, premotor, inferior temporal, and oculomotor cortex, the rostral subregion (VA) would be at first visuomotor likely more than that. This is one more argument for formally separating the two topographically distinct territories from basal ganglia sources and for giving the nigral territory its own space and identity.

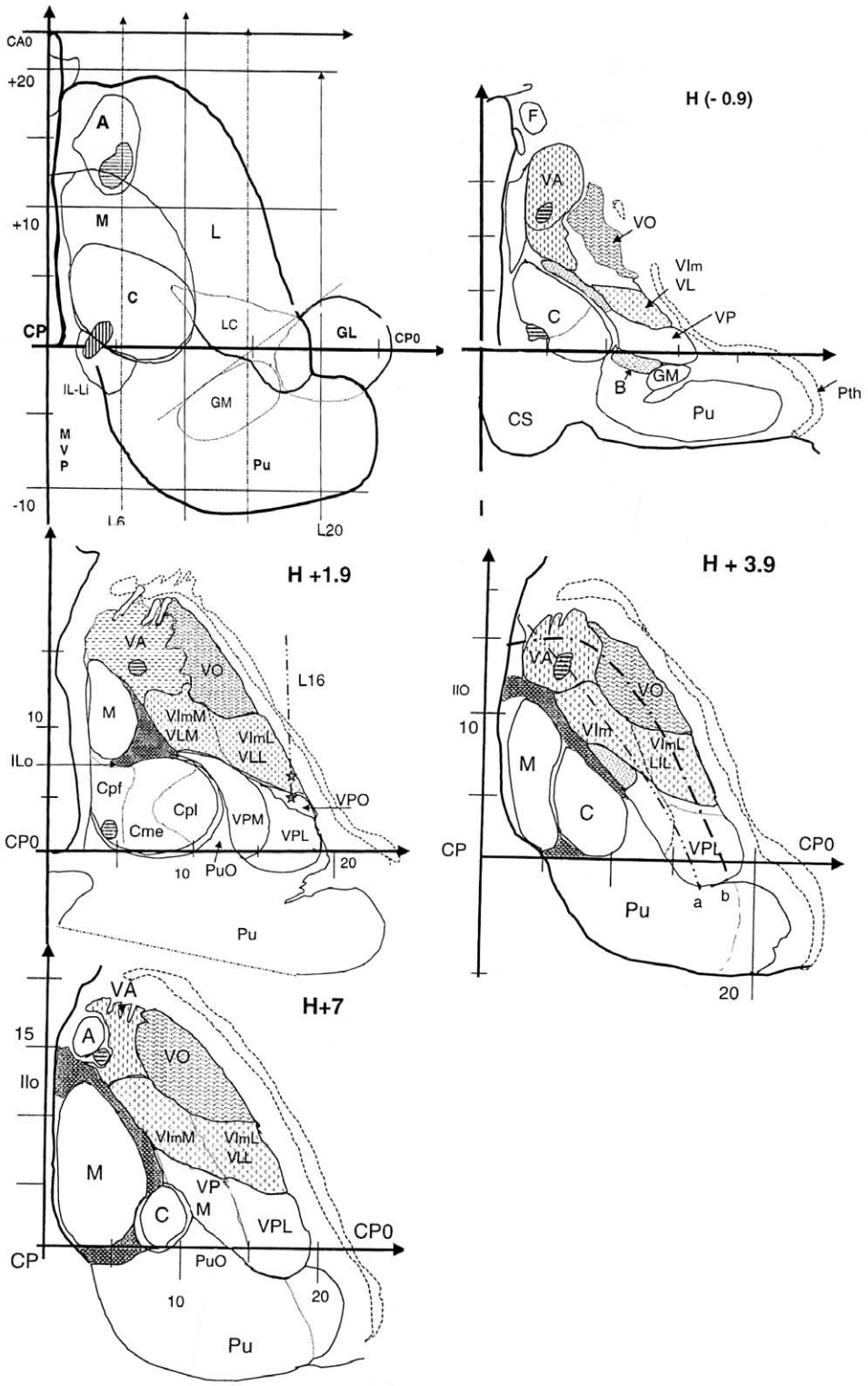

FIGURE 20.21 Horizontal sections and slices. *Upper left*. Horizontal projection (not an upper view) of the maximal contours plotted from the whole series of horizontal sections of Van Buren and Borke (1972) atlas. Contours do not correspond to any level but to their addition. C, central region; L, lateralis; M, medialis. The projection of the central region is included within that of the medialis. Projection of anterior nucleus overlaps with the anteromedial part of the lateral region. The projection of the two geniculate bodies (GL and GM) is shown. Horizontal sections from Van Buren and Borke atlas with reference to equivalent levels of Morel *et al.*'s atlas (1997)(Hassler's material was cut because of an improper angle). *H(–0.9), (V0.9 of Morel)* with the five elements of the lateral region, including Varc (arcuatus), gustatory nucleus. *H + 1.9 (D 1.8 Morel)*. Maximal extent of the central region. VA (lateral rostral subregion) is traversed by the mamillothalamic tract. The line at 16.5 corresponds to the frequent trajectory of stereotacticians for tremor alleviation. It visualizes a major problem of interpretation since the electrode crosses through VIm and/or anterior part of the VP receiving kinesthetic afferences (VPO). *H+ 3.9 (D3.6 Morel)* middle ventral level. Two lines are traced. The first (a) most medial, follows the main axis of the lateral region (here about 30°). From the posterior border of the lateral region, the sequence includes first VP (including face representation), then the cerebellar VL, and finally VA. This is the organization of nonprimate species where VA receives convergent afferences from both the nigra and entopeduncular nucleus. The second curve (b) follows the border of the lateral region at about equal distance and passes through an nucleus proper to primates, the pallidal territory VO over a long distance and ends in the nigral territory afferences VA (Lateral Rostral subregion). *H + 7 (D6.3 Morel)* transition plane. Appearance of the superior (A) and disappearance of the central (C) region.

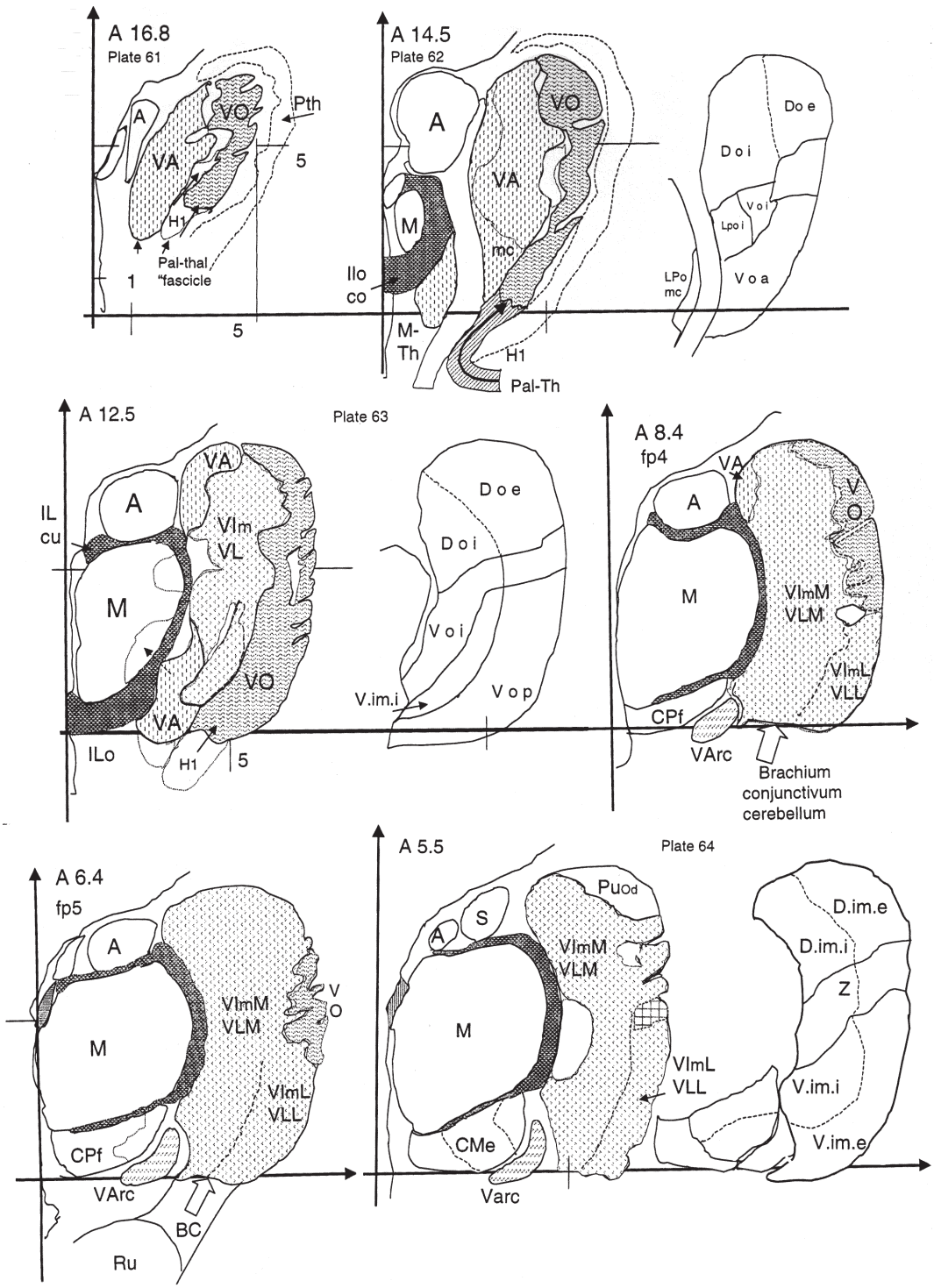

FIGURE 20.22 Series of transverse sections from Schaltenbrand and Bailey's atlas (from plate 61 to 67). The anterior position of each level from CP was calculated from its placement in relation to CP0. This series is unfortunately irregular with lacks at levels of transitions. Additional levels of the same and from Van Buren and Borke were used. Correspondance with Van Buren and Borke's and Mai *et al.*'s atlases are given. *A 16.8* (plate 61, corresp Van Buren and Borke's, 20.3, Mai +6.7 – 27). Border between nigral, on the left, and pallidal subregions, on the right, highly sinuous with interrupted spacing strips (myelinic or acellular). The perithalamus cut obliquely appears thick. *A 14.5* (plate 62) (Van Buren and Borke, 17.2, Mai +12 –31) passing through the mammillothalamic tract with the appearance of the medial nucleus. The nigral (VA) lateral rostral subregion has a maximal extent from the ventral to the dorsal border of the lateral mass and medially in front of the medial nucleus. The border with the pallidal (VO) lateral oral subregion is sinuous. This is broken laterally by oblique fascicles *A 12.5* (plate 63, corresp Van Buren and Borke's, 10.9, Mai+14.6 or 16 –33 or 34) Opening of the nigral territory VA (lateral rostral subregion) with two subparts—dorsal and ventral. The presumed cerebellar territory (VIm-VL, lateral intermediate subregion) is already well developed, with a differentiated subpart denoted V.im.i by Hassler. Parasagittal organization, with from medial to lateral, the nigral, cerebellar and pallidal subregions. *A 8.4.* (fpa, plate 38, corresp VanBuren and Borke 7.8, Mai +19.9 –37). Intermediary section the nigral territory disappearing and the cerebellar expanding. This covers the majority of the lateral region except for a pallidal border. The cerebellar territory is differentiated into a mediodorsal part, VImM-VLM, and a lateral, VImL-VLL, magnocellular that, in macaques, projects to the motor cortex. *A 6.4* (fp5, plate 39, corresp. Mai +21.2 38). The lateral region is almost entirely covered by the VL-VIm, cerebellar (lateral intermediate subregion). *A 5.5* (plate 64, M, corresp. Mai 22.6 –39) disappearance of the pallidal territory and appearance of the pulvinar dorsally. Hassler's "zonalis" (Z) corresponded to an almost acellular area.

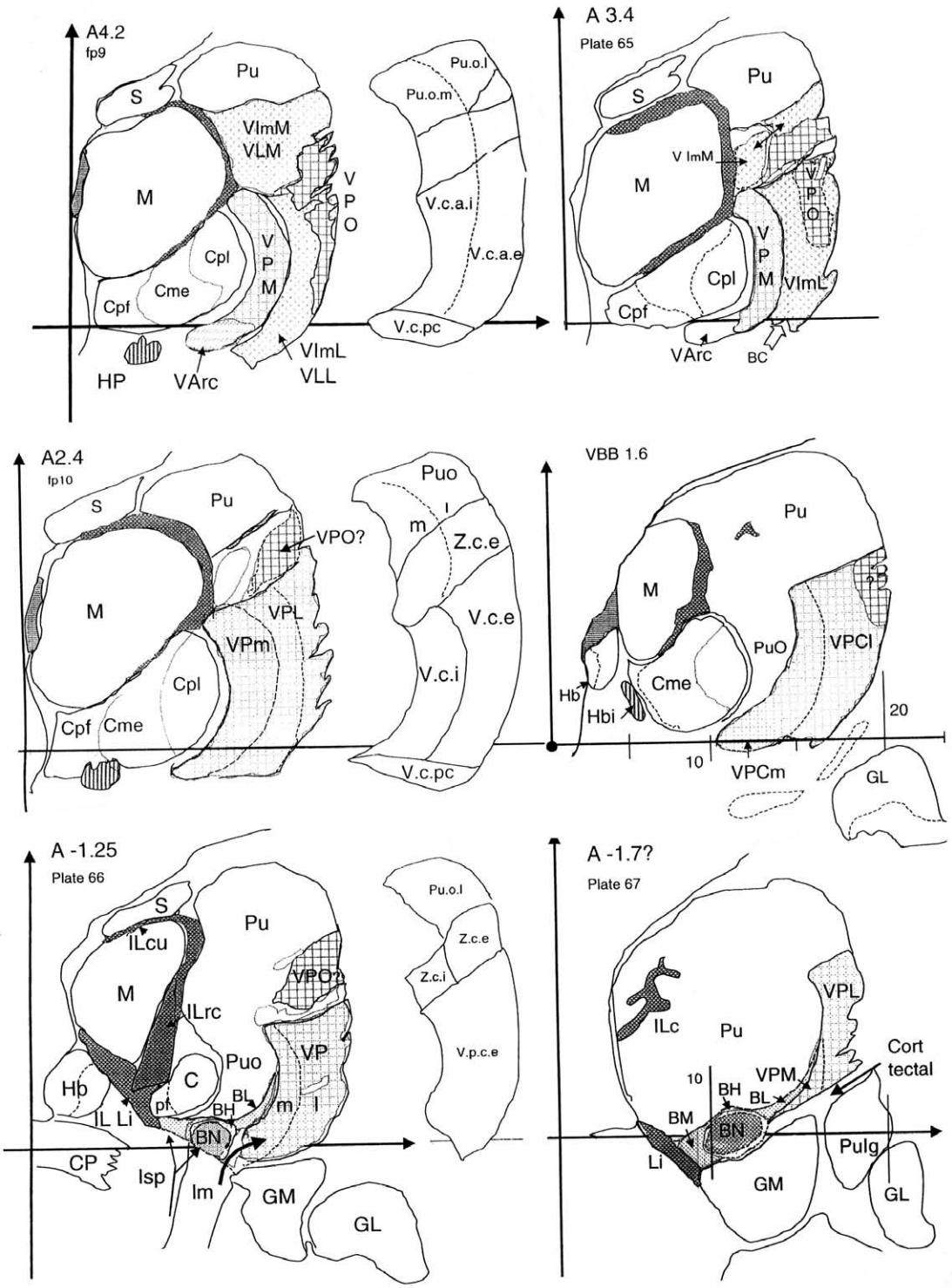

FIGURE 20.22 *Continued* Transverse series, posterior levels (with somesthetic nuclei). *A 4.2.* (fp9, plate 39, corresp Mai 23.9 –40). The sagittal pattern, still visible in the lower part is reinforced by the appearance of the lemniscal territory. The horizontal organization appears with the cerebellar subregion in the middle, the somesthetic ensemble below, and the pulvinar (oral dorsal) dorsally. Maximal extent of the classical arcuate nucleus whose upper part is VPM and lower, Varc. Laterally, magnocellular subdivision are likely attributable to the anterior part of the lemniscal kinesthetic "VPO". *A 3.4.* (Plate 65 corresp, Mai 25.2 –41, VanBuren and Borke 3.4– 25). Posterior end of the cerebellar subregion ventrally (VImL) and dorsally (VImM). The transition with the lemniscal (caudal subregion) is not topographically similar to that observed in the monkey. VimL appears relatively smaller. VPO is raising up. Dorsally, lowering of the pulvinar. *A 2.4.* (fp10, plate 39, corresp Mai 26.5). The dorsal magnocellular field is likely VPO. It goes up in a dorsal position in relation to VPL. Medially to VPO is an almost acellular field, a separating strip with the pulvinar. *VBB 1.6.* Additional map from Van Buren and Borke (corresp. Mai 27.8 –43) to fill the lack of a level showing the wedge-shaped oral pulvinar separating the central from the lateral region. This map brings out the imprecision in the laterality of transverse series of Schaltenbrand and Bailey's atlas, due to problems in the placement of the midventricular plane, MVP. *A-1.25.* (Plate 66). Posterior pole of the central formation C. The pulvinar is reaching the lower border. A patch of large neurons is still present over the VP, possibly the VPO. Appearance of the limitans. Retrocentral part of the intralaminar formation Ilrc. Appearance of regio basalis B with centrally located nucleus (N) and basalis nodalis (BN) receiving axons from spinothalamic tract forming the lemniscus spinalis (lsp). *A-1.7* (Plate 67). Section placed too posterior in the atlas. Corresponds to Van Buren and Borke 1.6–27, Morel *et al.* 1.8, Mai 29.2–44). End of VP, and of the lateral region, laterally. In the basal region, the n. basalis nodalis is surrounded by the n.basalis halos (BH). BL, n. basalis lateralis.

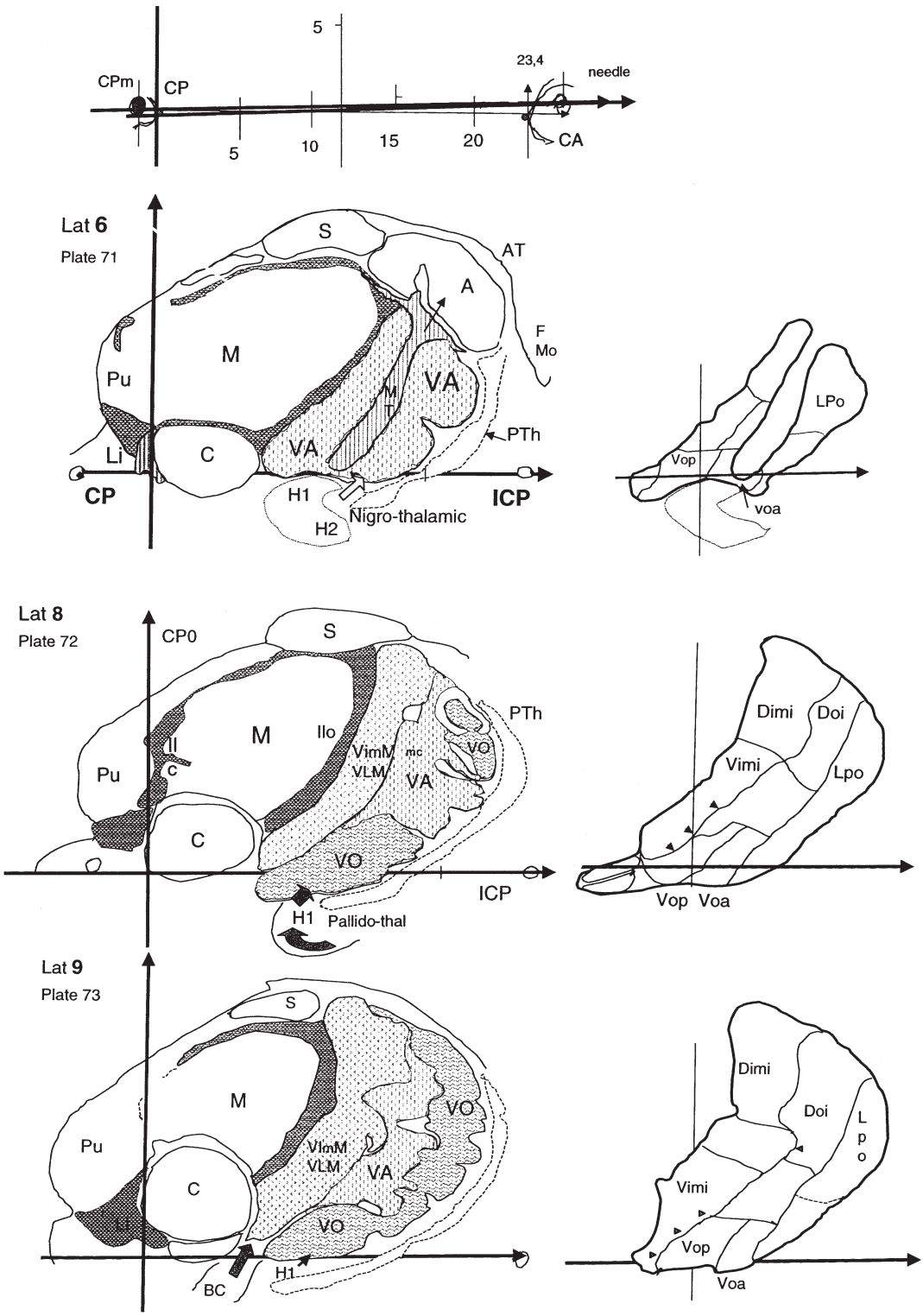

FIGURE 20.23 Sagittal sections. Series of sagittal sections redrawn on high magnification photos (plates 70 to 76) from Schaltenbrand and Bailey's atlas, on transparent sheets and reduced. *Upper drawing*, commissural landmarks and system of coordinates from plate 70 (L3). The two marks made by needles do not exactly correspond to CA and CP points. The two lines are traced. The only cartographic modification in this series is the use of CP as the 0 for anteroposterior positions (instead of Hassler's midcommissural point of poor topometric value). Successive plates may be compared to same levels of plates 44 to 47 from same authors. *L6* (plate 71). Medial section cutting the superior region with anterior nucleus and superficialis fragmented in nuclei disseminati, the medial nucleus and the central region. The lateral region is crossed all the way by the mammillo-thalamic tract (MT). The anterior part of the lateral region is similar to VA of macaques, presumed to correspond to the nigral territory and goes back up to the anterior pole of the central region. On the right, Hassler's tracings with the unjustified separation between ventral and dorsal elements. *L8* (plate 72). Anterior nucleus disappeared and replaced by the lateral region. Nigral territory also disappearing. Its lateral border and the medial border of the pallidal territory being curved, the section leaves still some VA at midheight. The pallidal territory appears ventrally and dorsally to it VO. Hassler's tracings coincide only at the border between the cerebellar (sparse large cells) and the pallidal territory (dense small cells; indicated by small arrows). *L9* (plate 73) complete filling by the lateral region replacing the anterior nucleus. Curved banana-shaped succession of three territories and lack of separation between ventral and dorsal elements. Hassler's Voa and Vop were one single thing belonging to the pallidal territory.

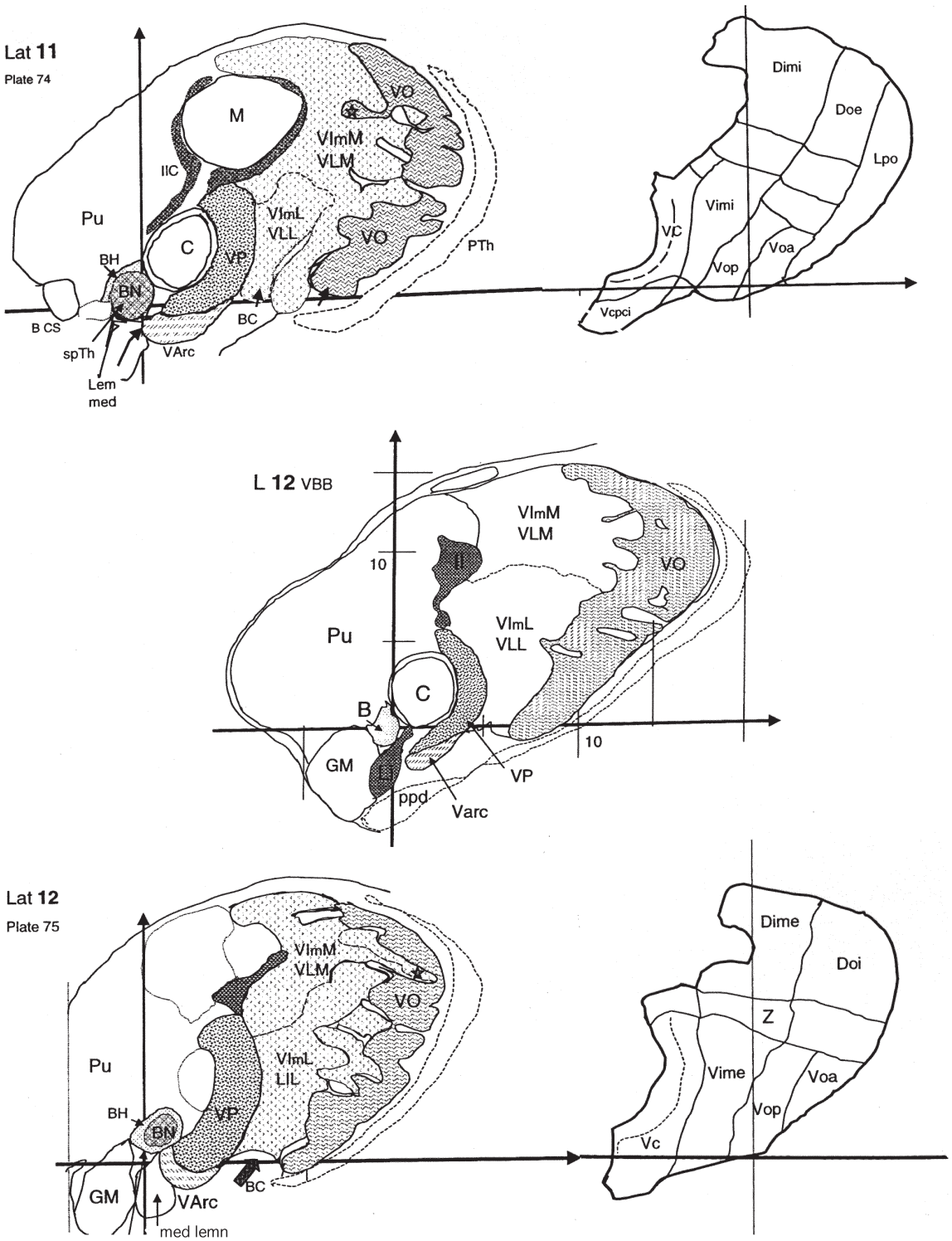

FIGURE 20.23 *Continued* Sagittal sections L11 and 12. *L11* (plate 74). Strong curvature of territories, dorsal parts of subregions passing over the more posteriorly located territory. Irregularity of territorial borders with long peninsulae (one shown by a star—pallidal within cerebellar). Two apparently ventral elements appear, one most posterior, lemniscal (also arcuate in this plane). On the right, Hassler's Vop was likely cerebellar. VImL-VLL distinguished by the presence of large cells, not necessarily corresponding to the place projecting to the motor cortex. Varc, gustatory nucleus made up of small neurons. The roundel of the basalis ensemble with BN and its halo BH is well observed. *L12 VBB* level 12 of Van Buren and Borke atlas giving metrics from CP illustrating individual variations in shape but a stable pattern. *L12* (plate 75). Section passing at the lateral borders of both the medial and central regions disturbing pictures dorsally. In lateral region, Hassler's Vop was very likely pallidal. The border between pallidal and cerebellar subregions is extremely sinuous. Long islands (such as the one with a star) correspond to section of fringres. Some are bordered by spacing strips (white places with no neurons separating territories). In Hassler's tracings, Z is zonalis (between ventralis and dorsalis, not founded). The roundel of BN-BH still observable. *Continued*

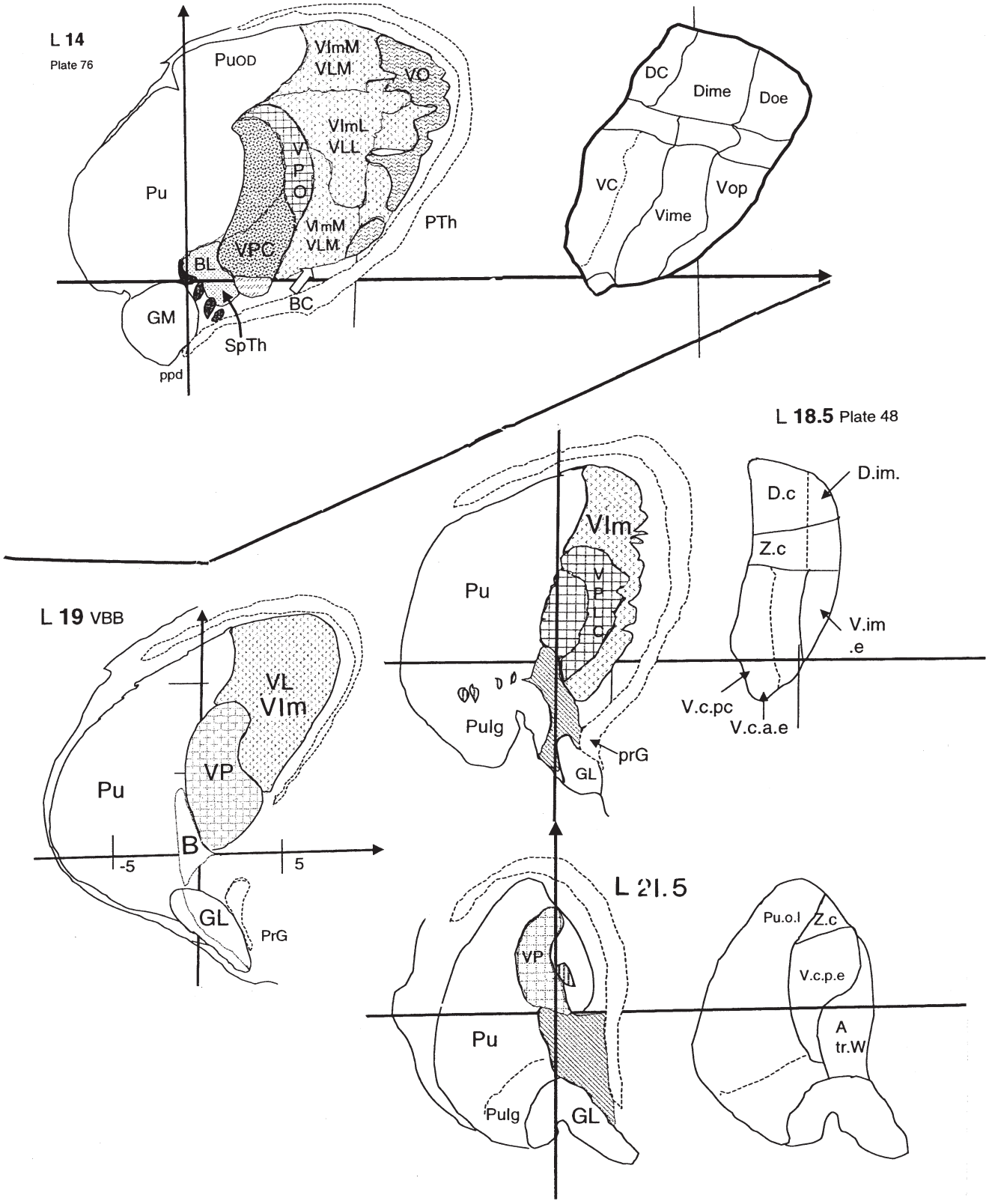

FIGURE 20.23 *Continued* L14 and most lateral sections, L18 to L21.5. Intermediary levels of the sagittal series showed in Figures 20.19 and 20.20. *L14* (plate 76). Pallidal subregion disappearing lemniscal expanding. Compared to Figure 20.2C stained for parvalbumin by Morel *et al.* (1997). The differentiation between what is designated as VLL-LIL or VLM-LIM, theoretically founded by different sources to the cortex, is based on magnocellular or less magnocellular parts. Appearance of a particular subdivision, also "magnocellular," adjacent to and more anterior than VLL-LIL, presumably VPO, the kinaesthetic part of the lemniscal subregion. The lateral region in most lateral sections, *L18,5 of Hassler and L19 of VanBuren and Borke,* with only the cerebellar (Vim or VL) and the lemniscal (VPL) territories. *L 21.5.* The lateral region is represented by the most lateral part of VPL.

ALLOTHALAMUS. INVOLUCRUM

As already discussed at the start of the chapter, some thalamic components surrounding the medial region have projection neurons morphologically different from those of the bulk of the thalamus and defined by contrast, which are said to constitute the allothalamus (Percheron *et al.*, 1996). This ensemble is not homogeneous. It may be divided in two different entities: the ensemble made up of the paramedian and intralaminar formations (involucrum or enveloppe) and the central region. Textbooks still frequently group the two in "the intralaminar nuclei," subdivided into an anterior (grossly intralaminar) and a posterior group (the central complex). This was detrimental for the understanding of the central region (Percheron *et al.*, 1991) and that of the intralaminar ensemble. The intralaminar elements were said to be a part of a system for the unspecific excitation of the cortex (see Steriade *et al*.). The central complex of primates has no known role in such function. Topographic analyses (Fig. 20.24) show a spatial separation of the intralaminar and central ensembles, the first wrapping around the second without any mixture. Today, many arguments, from neuronal types to connections are in favor of separating the two ensembles in man and upper primates.

The two first allothalamic components—the paramedian and intralaminar formations—have a common ontophylogenetic origin (Rose and Woolsey, 1949). Rose (1937), in the rabbit, grouped them into a "centrocommissural system." In the macaque, Olszewski (1952), described together "the midline and intralaminar nuclei." The two formations are continuous (or mixed) medially. They form a ring around the medial region, corresponding to Foix and Nicolesco's (1925), "formation circulaire hyperchromique", Grünthal's (1934) "nucleus circularis," or Hassler's "involucrum" (or "enveloppe"). The involucrum is commonly said to be made up of distinct (small) "nuclei". The existence of such nuclei (that imply some degree of closure) is highly disputable. The ensemble stain in the same way for Nissl, acetylcholinesterase, calbindin, and calretinin. It contains tachykinin- and enkephalin immunoreactive fibers (Hirai and Jones, 1989b). In addition to the two traditional paramedian and intralaminar formations, two other neuronal sets must be considered together. One is the "nucleus limitans" usually considered separately. The other, well visible in man posteriorly to the central formation, "retrocentral," can be linked to the intralaminar formation in the formatio intralaminaris-limitans IL.

Formatio Paramediana

The formatio paramediana is the ensemble of thalamic elements located close to the midline. It may be seen as the thalamic part of a much more extended neuronal ensemble starting from the periependymal gray of the spinal cord up to the periventricular gray of the third ventricle ending at the foramen of Monro and continued by the hypothalamus. Highly regressive, the thalamic paramedian formation is difficult to describe in the human brain. The adhaesio interthalamica or massa intermedia, present in all other species, still conspicuous in macaques, even in chimpanzees, has disappeared in 30% of human brains or is present just as a remnant. A certain number of afferent systems that cross the midline through the adhaesio in macaques can no more do it in man, implying a higher hemispheric lateralization. In the human brain, the paramedian formation is reduced to a rather thin layer forming the wall of the third ventricle, separating it from the rest of the thalamus, mainly the medial nucleus. The neuronal genus of the paramedian formation is known only in young rats (Scheibel and Scheibel, 1971), where it is not very different from the intralaminar and parafascicular types in this species (i.e., short leptodendritic). There are only a few local circuits, GABAergic, neurons (Hunt *et al.*, 1991), and none in lower species. Multiple cytoarchitectonic subdivisions have been proposed in the literature. Several levels may be distinguished, at first in relation to the taenia: ventricular, inferior to it, or supraventricular, superior to it (Fig. 20.1). In the ventricular part, the level of the adhaesio made by the junction of the two medial lamellae gives a reliable reference for distinguishing an interlamellar level (Ad co, Fig. 20.2A) corresponding to Rabl's (1958) nucleus reuniens or to Hassler's (1959) and Van Buren and Borke's (1972) nucleus commisuralis. The term situs commissuralis (co, Figs. 20.2 and 20.4 or adhesialis, or reuniens) of the intralaminar ensemble should be preferred to that of "nucleus centralis medialis" (CeM), leading to a confusion with the central region (centre médian, CM). The junction of elements of the two oral intralaminar nuclei is the only element (with glia) constituting the human adhaesio (Rabl, 1958). Inferior to the interlaminar level, Rabl (1958) distinguished a paramedianus inferior (nucleus endymalis, VanBuren and Borke, 1972), and superior to it, a nucleus paramedianus superior (paramedianus anterior, Van Buren and Borke 1972). Above the level of the stria (or taenia), a nucleus paratenialis or parataenialis is often described. A part located superior to the taenia and covering the dorsomedial corner of the medial region

joins the paramedian and intralaminar formations. Specific to primates (Macchi and Bentivoglio, 1988), its neuronal species being still unknown, the pars superior or Hassler's nucleus cucullaris (Cu, hat-shaped, Fig. 20.2A, B), could belong to one or the other formation. Immunochemistry does not allow much more precision. Some paramedian neurons are calretinin positive neurons (Ciccheti *et al.*, 1998), cholecystokinin CCK, SRIF, and substance P positive neurons (Molinari *et al.*, 1987). The paramedian formation receives afferences of the reticular type: serotoninergic from the raphe and norepinephrinergic from the locus coeruleus (Oke *et al.*, 1997). Paramedian neurons give axons to the striatum (Fénelon *et al.*, 1991; MacFarland and Haber, 2000). It is traditionally admitted that the paramedian region does not project to the cortex, since it does not degenerate after cortical lesions (Walker, 1935; Peacock and Combs, 1965). Van Buren and Borke (1972), however, described a complete degeneration four years after a large infarct. Kievit (1977) described a connection to the orbital cortex, and Bachevalier *et al.* (1997), to the frontal and anterior cingulate cortex. It is proposed that, except when there is an adhaesio with a visible adhesial bridge between the two lamellae or in the case of an evident particular afferent or efferent distribution, the paramedian formation be left undivided. Its real role is not known.

Formatio Intralaminaris-Limitans

For reasons developed later, this formation does not include the central complex (see "Regio Centralis"). The presence of neuronal groups within the medial lamina was observed in the human thalamus very early, for instance by Malone (1910, in his "nucleus reunions") and Foix and Nicolesco (1925). As already said, following the Vogts (1941), the Louvain symposium recommended that the term "lamella" be employed rather than the term "lamina". The term "lamella" is used for the fibrous components but, in order to come closer to common use (and in accordance with the Nomina anatomica), the adjective "intralaminar" is used for neuronal groups. The appearance of the lamella medialis, though considered as a major topographic key is relatively late in fetal life (Gilbert, 1934; Yakovlev, 1969). There is also no complete coincidence between the topography of the lamella and the topographic distribution of the neurons of the intralaminar neuronal genus. Not all parts of the lamellae contain intralaminar neurons. Not all neuronal groups of the intralaminar genus are within lamellae. This is particularly true posteriorly, back to the central region (Fig. 20.24). The evolution of the neuronal ensemble is only scarcely documented. Its constitution in the anterior part is rather stable as its topography in relation to the medial region remains similar. The presence of calretinin (and acetylcholinesterase activity), documented in rats and primates, makes equivalence possible. The purely intralaminar part is phylogenetically regressive in number and density of neurons. Moreover, the neuronal types change in primates. Equivalencies are particularly difficult posteriorly. The posterior elements, usually not considered among the intralaminar ensemble, show an evolutionary increase, suggesting that there could be a phylogenetic move of neurons of the anterior intralaminar set toward a position posterior to the central complex (see Fig. 20.24). The "nucleus limitans" (Friedemann, 1911; previously shown in man by Malone, 1910, as a part of his reuniens) was given this name because it separates the thalamus from the pretectum. In the rat, the parafascicularis nucleus has a lateral extension, the ethmoid nucleus (Eth, Paxinos and Watson, 1986), with a topography similar to that of the limitans but containing the parafascicular type of neurons (Deschênes *et al.*, 1996). Not described in the cat or in the tree-shrew, the limitans apparently appears with lemurians (Stephan *et al.*, 1980) and is obvious in simians. In human brains, cytoarchitectural similitude already led Malone (1910) and Feremutsch and Simma (1954) to classify this neuronal group among intralaminar elements. Some neurons observed in Golgi-impregnated specimen were seen to be of the intralaminar genus. Recently found properties make it reasonable to concur with the conclusion of the Louvain symposium (Dewulf, 1971), Jones (1997) and Steriade *et al.* (1997) and to link these elements to the continuous and extended intralaminar-limitans formation. Neuronal islands are generally described as nuclei. Steriade *et al.*, (1997) insist on a "compartmental organization" of different kinds of neurons and on the patchy distribution of afferent axons. From the little known about it, the ensemble with relatively short dendritic arborizations in fact constitutes a continuous layer (Fig. 20.24) with no delimited nuclei. The subparts may be described at most as parts or sites (see Fig. 20.3). The continuous intralaminar-limitans formation is extended from the adhaesio interthalamica medially, from which it seem to emanate, to the limitans site behind the central complex (Figs. 20.2 and 20.24). The formation is made up of two neuronal families. One is the local circuit neuron, close to that of the isothalamus but with a lesser percentage. In the human brain, Dewulf (1971) found numbers from 11 to 16% (paracentral, 11%, limitans 11, 3, centralis lateralis 14, 5, 15, 5), which are significantly less than those in

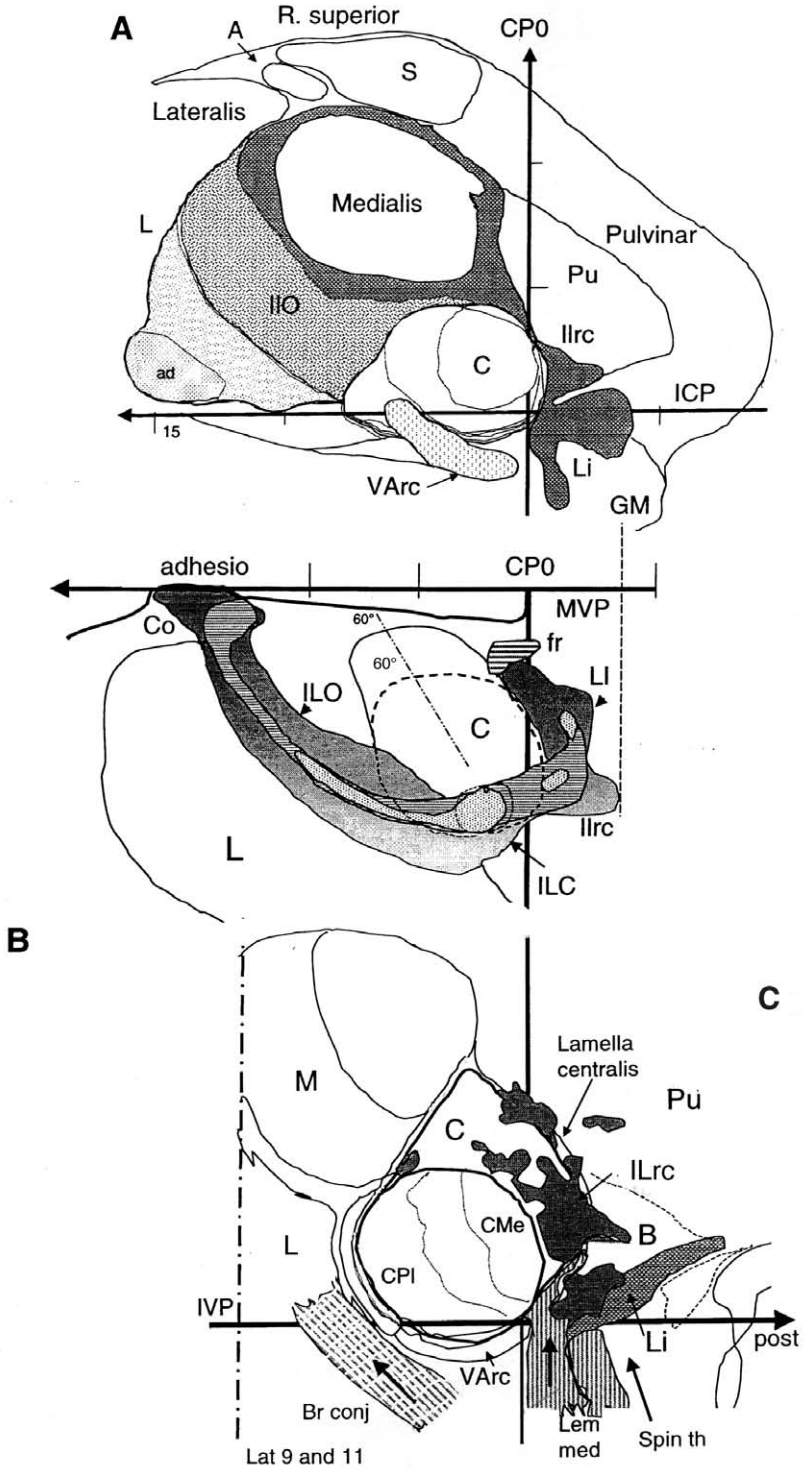

FIGURE 20.24 Separating elements. Formatio intralaminaris-limitans. Allothalamus. **(A)** Sagittal slice from VanBuren and Borke's atlas (up to L9 and 12). Lateral view showing the lamella medialis and intralaminar elements surrounding the medial nucleus in successive slice. A noticeable portion, generally not considered, is located posteriorly to the central region (C). The retrocentral intralaminar subnucleus (Ilrc) is continuous with the limitans (Li). These elements cover posteriorly the central region without penetrating it. Varc, part of the lateral region, the taste nucleus. **(B)** Slice of horizontal sections from the same atlas (not same brain). The continuous intralaminar-limitans formation seems to arise from the adhesio. The oral site (IlO, "paracentralis") turns around the medial nucleus. The supracentral, intralaminar caudal ILC ("centralis lateralis") surrounds the lateral part of the central complex. Fr is the retroflexus tract (habenulo-interpeduncular) of Meynert. The comparison of A and B shows that the rather thin band in B is in fact a continuous layer, with no obvious subdivisions other than topographical, extended from the adhesial or commissural place anteriorly (co, commissuralis crossing the midline when there is an adhesio) to the limitans posteriorly. C is the slice of sagittal sections from Emmers and Tasker's atlas. Medial view. Intralaminar elements surround (not penetrate) the central formation **(C)**, showing that this is not intralaminar. Dorsal islands of the traditional "nucleus centralis lateralis" are continuous with posterior retrocentral elements and the "nucleus limitans" not included in any lamina.

the central region. In macaques, Hunt *et al.* (1991), however, found a higher number of GABAergic neurons (25.4 and 27.9%), close to those of the lateral region. The projection neurons are different from those of the isothalamus (with fewer branched dendritic arborizations), and this difference explains their attribution to the allothalamus. These neurons hardly stain in Golgi variants, and no statistical neuronal typology is available. It is worthwhile stressing that the neuronal type found in the primate intralaminar ensemble (Fig. 20.25) differs from those described in rats and cats. In these orders, neurons are indeed leptodendritic (i.e., with scarcely branched arborizations, to some extent resembling those of the reticular formation; Scheibel and Scheibel, 1972; Ramon-Moliner, 1975; Tömböl *et al.*, 1990). In our material (Fig. 20.25), primate intralaminar dendritic arborizations appear shorter than those of cats and different from those of surrounding isothalamic neurons. These arborizations are often bitufted (Percheron *et al.*, 1978), with few stems (about four), often simply large extensions of the soma emitting several branches (Fig. 20.25). They are generally oriented in the direction of the lamella or obliquely in the direction of thalamocortical fascicles. In the anterior intralaminar site at least, their arborizations seldom, if ever, cross the border of the lamella. This fact would indicate that they could be partly closed nuclei (opposed to the reticulate histotype). Dorsally to the centralis complex there are no clear dendroarchitectonic boundaries. Along with intralaminar neurons, typical isothalamic bushy neurons are also found. When incompletely cut, these may lead to confusing pictures. Intralaminar neurons are dark in Nissl stains, heavily stained for calbindin (Jones and Hendry, 1989; personal material), calretinin (Ciccheti *et al.*, 1998; which is the reverse of the regio centralis, with a dense calretinin positive neuropil (Fortin *et al.*, 1998), and acetylcholinesterase (Poirier *et al.*, 1977; Heckers *et al.*, 1992). Some neurons contain cholecystokinin (CCK; Burgunder and Young, 1992).

The formation has been subdivided into many small entities, often with no precise criteria, according to animal species and the traditions of different schools. The central region being excluded, one may subdivide the intralaminar-limitans formation into several, not separate, topographical parts or sites: one oral, inside the well differentiated anterior part of the lamella medialis; a second more caudal, dorsal to the central complex; a third one corresponding to the limitans site; and a last one caudal to the central complex. The simplest situation is observed in the anterior lamellar subregion. The lamella is obvious and the intralaminar neuronal sets, well differentiated from their surrounding are located inside it. The situs intralaminaris oralis Ilo (i.la or "nucleus" paracentralis, or alaris) is sheet-shaped and wraps around the anterior part of the nucleus medialis (Figs. 20.2A, C, and 20.24). This intralaminaris oralis situs is continuous, ventrally and medially, with the pars or situs commissuralis (Ilco) (Figs. 20.2A and 20.24) linking in the adhaesio the left and right formations. Another element usually linked to the oral intralaminar site (already mentioned in "Formation Paramediana") is its dorsomedial continuation, in the superior lamina, over the upper border of the nucleus medialis, corresponding to Olszewski's centralis superior lateralis or to Hassler's cucullaris (as a hat; Figs. 20.2 and 20.3). This site cannot be attributed (as frequently labeled) to the nucleus centralis lateralis, which is more posterior. One reason for the complexity of the posterior part of the intralaminar formation comes from the important development of the regio centralis modifying topographical positions and from the fact that the posterior part of the lamella itself is fuzzy. The intermediate intralaminar site comprises at first an element located in the lamella medialis above the regio centralis, at the superolateral border of the regio medialis (ncl. intralaminaris caudalis Ilc. or "centralis lateralis"; Fig. 20.24). Traced in Nissl sections only with difficulty, it may be observed using calbindin, calretinin, and cholinesterase immunochemistry. It appears then significantly thinner than in Nissl or myelin stains. In man, it is irregular with interspersed islands. Another, more regular site is observed in the lower part of the lamella medialis located between the central and medial regions, the supracentral site (Fig. 20.24, Ilsc), with elongated islands intensly stained for calretinin. The most caudal elements of the formation are located behind the central region. Some elements are still in lamellae (such as the intralaminaris retrocentralis, Ilrc, Fig. 20.2D and 20.24). But the existence of neuronal groups not topographically intralaminar makes the description difficult. This generally neglected part of the formation is continuous with the intralamellar sheath wrapping around the posterior pole of the medial region. The so-called limitans nucleus (Fig. 20.2C) forms an oblique thin band starting from below the central region to the medial geniculate nucleus. After Friedemann's (1911) "pars supragenicula nuclei limitantis," Hassler (1959) described an excessively extended limitans comprising parts ("Li opt" and "Li.por") that are known today to belong to the basal region (see "Regio Basalis."). The situs limitans of the intralaminar-limitans formation having an intense staining for calretinin (Ciccheti *et al.*, 1998) is restricted to a thin discontinuous band extending from the medial border of the thalamus to islands

close to the medial corner of medial geniculate body (Fig. 20.2).

The intralaminar-limitans formation receives afferences of the reticular kind. This is particularly the case for very dense cholinergic afferences (Heckers *et al.*, 1992) contrasting with the surrounding isothalamus. The oral intralaminar site ("paracentral") and the limitans receive dense projections from brainstem cholinergic reticular sources (Olivier *et al.*, 1970; Paxinos *et al.*, 2000), the pedunculopontine complex (PPT) and the laterodorsal tegmental nucleus (LDT; Wainer and Mesulam, 1990) forming a single complex PPT/LDT (Steriade *et al.*, 1997). The formation also receives from this complex noncholinergic, glutamatergic axons with a colocalization of cholinesterase and glutamate (Lavoie and Parent, 1994). There are also tachykinin and enkephalin axons (Hirai and Jones 1989b). The intralaminar formation, in addition, receives other glutamatergic axons from the medulla, caudal pons, and midbrain and from the magnocellular bulbar reticular fields. Mainly in its posterior subregion, it still receives afferences from "lower" large afferences—at first spinothalamic. Axons from the spinothalamic tract end in the caudal part surrounding the central region (the pars caudalis, ILc, CL, supracentral and retrocentral, parts and limitans; Mehler, 1966a; Burton and Craig, 1983; Mantyh, 1983; Fig. 20.9). Another lower afference is cerebellar. Endings are observed essentially in the intralaminaris caudalis (ILc, CL) not in the supra or retrocentral nor in the limitans parts (Percheron, 1977; Percheron *et al.*, 1996). Yet another afference comes from the superior colliculus (Benevento and Fallon, 1975). This set of afference, spinothalamic, cerebellar, and collicular, is peculiar. Only the last also projects to the parafascicular part of the central region. The two others, in the cat, already do not completely coincide, and they form a less diffuse organization than ordinarily claimed (Bentivoglio *et al.*, 1988).

For a long time, the intralaminar ensemble was said to have no cortical connection, since it was observed to remain intact after cortical lesions. This was explained by its strong connection to the striatum (Nakano *et al.*, 1990; Fénelon *et al.*, 1991; MacFarland and Haber, 2000). Axons to the striatum come from the whole intralaminar-limitans formation including its limitans part (Nakano *et al.*, 1990), in continuity with the parafascicular part (CPf) of the central region. The destination of efferent axons to the striatum was considered by Jones (1997) and Steriade *et al.* (1997) as necessary for isolating "intralaminar" elements. In fact, other thalamic regions, even the lateral, also project to the striatum. Even incomplete degeneration is observed in macaques after hemidecortication (Peacock and Combs, 1960; Jones and Leavitt, 1974). Intralaminar-limitans neurons actually project to the cortex. The oral intralaminar neurons project abundantly to the frontal cortex according to the same spatial plane as that of the medial region (Van Buren and Borke, 1972) and to the supplementary motor area but not to the motor cortex (Shindo *et al.*, 1995). The limitans degenerates after large lesions, essentially parietooccipital (Powell and Cowan, 1967) or with additional deep lesions (VanBuren and Borke, 1972), rather densely to the insular cortex and to a lesser extent to the superior temporal cortex including the primary auditory area (Kosmal *et al.*, 1997). The axons of the intralaminar axons, presumably, as drawn by Lorente de No (1938), end primarily in layer I and VI and reach rather widespread cortical surface. But this remains a disputed point. Studies and experiments on "intralaminar nuclei" have been the subject of a considerable literature that (in spite of the claimed nucleation) finally led to the concept of diffuse or unspecific systems. The evolutionary decrease of intralaminar groups in primates and particularly in man is not easily compatible with their role in the unspecific excitation of the cortex, as their volume does not increase in proportion to the cortical surface. Considering the major anatomical changes in this part of the thalamus, it is very difficult today to assign functions to the intralaminar-limitans formation in human beings. It is proposed to consider the intralaminar-limitans ensemble IL or IlLi as a whole with mere topographical parts or sites, including purely intralaminar elements, the commissural, superior or cucullaris part (these two being thus excluded from the paramedian formation), the retrocentral part, the limitans and extralaminar islands.

REGIO CENTRALIS

Luys (1865) discriminated his "centre médian" on its whitish aspect on unstained human brain sections. The anatomical situation, the link with the fasciculus retroflexus or Meynert's bundle (Meynert, 1872) or habenulo-interpeduncular fascicle and the presence of a capsule were already observed at that time. The twin nucleus, medial to the habenulointerpeduncular fascicle was described later, in a cercopitheque, as the "champ parafasciculaire" (C. Vogt, 1909) or nucleus parafascicularis (Friedemann, 1911). Over time, the two nuclei were united into what has been named the "centre médian-parafascicular complex." Recent studies in cercopithecidae and human brains (Fénelon *et al.*, 1991, 1994, Percheron *et al.*, 1991) have stressed the necessity for replacing the

traditional binary opposition by a ternary partition of a "central complex," forming the central region or regio centralis. This stands out clearly from its surrounding. Its medial frontier with the periventricular gray is traced without much difficulty, on cytoarchitectonic differences. Above all, in man and upper primates, it is clearly separated by a myelin capsule, making it an almost enclosed nucleus (closed by a wall, Percheron *et al.*, 1991)(Figs. 20.24 and 20.25). This capsule first appears as C-shaped at about 9 (Cooper, 1950), 13–15, (Yakovlev, 1969), or 16 weeks (Forutan *et al.*, 2001), that is, much earlier than the intralaminar formation. The nature and components of this capsule have been already discussed (see mention of lamellae in "General Considerations"). It is made up of two parts (Fig. 20.2B). Only the dorsal, supracentral, separating it from the regio medialis is the ventral continuation of the lamina medialis or interna, alone containing intralaminar elements (see "Formatio Intralaminaris-limitans" and Fig. 20.24). The lateral part is the lamina centralis separating it laterally from the lateral region (its caudal somesthetic subregion) and caudally from the pulvinar (Fig. 20.2B). The myelinization of this lateral part (lc; Fig. 20.1B, 20.6A) is late, 30th week, 170 mm; Niimi *et al.*, 1960) and only complete at about 8 months postnatal (Yakovlev and Lecours, 1967) at the same time as the myelinization of the medial lemniscal axons.

The central region is hanging at the inferior part of the thalamus, overhanging the mesencephalic reticular formation, not covered by the perithalamic lamina and perithalamus (Fig. 20.2B). Its posterior pole, in macaques and humans, almost corresponds to the CP0 plane and its inferior border to the ICP plane. Its general shape is piriform with the largest part located caudally. Its main axis is oblique in relation to the midsagittal plane and curved (60° in Fig. 20.24). The complex is crossed in its medial third by the habenulointerpeduncular, or retroflexus, fascicle of Meynert. Oriented obliquely from back to front, its position in relation to the complex is a reliable landmark for the determination of anteroposterior positions. The primate regio centralis is also obvious with particular stains. It is strikingly unstained for calbindin, calretinin (Fortin *et al.*, 1996; Ciccheti *et al.*, 1998), or cytochrome-oxydase (Jones, 1997) and irregularly stained for parvalbumin (Jones and Hendry, 1989), with parvalbumin-stained somata (Munkle *et al.*, 1999), which is the reverse of truly intralaminar elements. The problem of the subdivision of the region is an old one. In 1941, the Vogts introduced a subdivision of the human centre médian into a dorsomedial pars magnocellularis (CeMc) and a ventrolateral pars parvocellularis (Cepc), endorsed by many successive authors working on the human brain (see Fénelon *et al.*, 1994, for a review). From phylogenetic arguments, Niimi *et al.* (1960, 1973) also retained a tripartition of the complex but interpreted the Vogts' magnocellular part as the lateral part of the parafascicular nucleus (Pfl), the parvicellular part only forming the centre médian "in a narrow sense." Braak (1971), though designating more subparts, showed that the lateral and the parafascicular parts are regular, one darker and the other lighter, when the intermediate is irregular with oblique stripes (also observable in the chimpanzee, Sakamoto, 1964). The phylogenesis of the region leads to conflicting conclusions concerning its subdivision. Today, following Nauta's opinion (1966), it is agreed that there is no centre médian in rodents, only a parafascicular nucleus. According to Mehler's interpretation (1966; concurred by Royce, 1987) a small centre médian would appear in carnivora, limited to the small lateral part receiving confluent afferences from the entopeduncular nucleus and the motor cortex. But this could be as well, in Niimi's conception, the lateral part of the parafascicular nucleus. In the prosimian Galago, a "centre médian," whose neuronal type is that of the macaque pars media, has increased and sends axons to the sensorimotor cortex (Pearson *et al.*, 1984). In cebideae, in the owl monkey (Aotus) there is apparently no sign of a lateral subdivision (Stepniewska *et al.*, 1994). In the squirrel monkey (Saimiri), while only two parts, including a dorsolateral part of the parafascicular nucleus receiving pallidal afferences, are described (Sadikot *et al.*, 1992; Sidibé *et al.*, 1997, 2002) there is in fact a curved slim, located at the most lateral part of the complex, not receiving pallidal axons, not projecting to the striatum and sending axons to the cortex, likely prefigurating the pars paralateralis. The development of the pars media (either lateral parafascicular or medial centre médian) is more than likely due to that of the medial pallidum (appearing in platyrhinians) from which its receives its main afferences. The appearance of the pars paralateralis becomes obvious only in cercopithecideae (that include macaques). Its tracing may be made on the fact that contrary to the two other parts it does not stain for acetylcholinesterase. In man, the paralateral part is voluminous, almost one half of the complex, which represents a massive increase. Having a particular neuronal type, particular staining properties and connections, and a huge development, it could be considered as the "centre médian" proper (Percheron, 1966). In such a case, it would be an old-world primate creation linked to modifications of corticosubcortical connections whose meaning is not known yet. For the traditional binary description of the region leading to dead ends for cercopithecidae

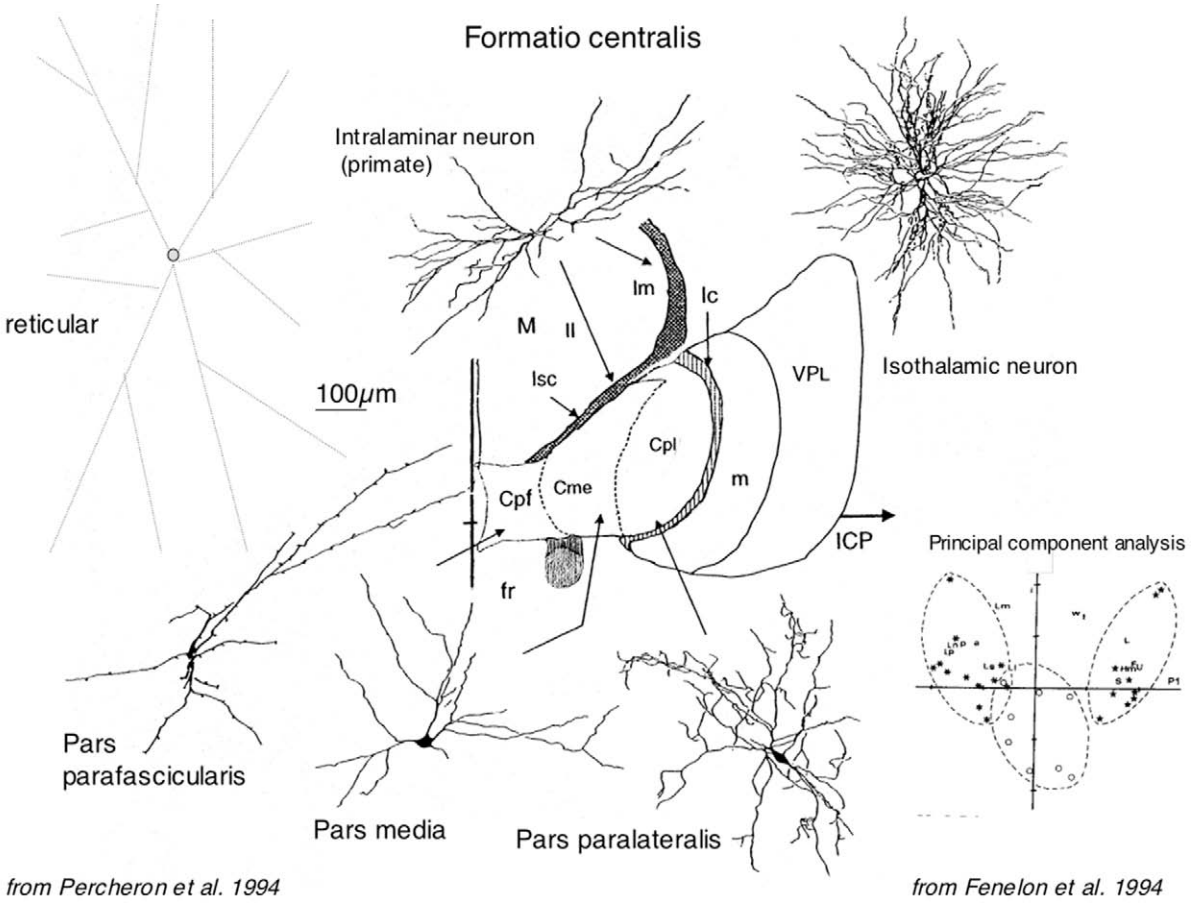

FIGURE 20.25 Regio centralis. Central region or central complex shown at is maximal extent on a slice made up Fp 7 to 10 from Schaltenbrand and Bailey's atlas. It is surrounded by a capsule composed of the supracentral part (lsc) of the lamella medialis (lm) dorsomedially (single continuation of the lamina medialis, containing intralaminar neurons) and the lamella centralis (lc) laterally. The complex is crossed by the habenulointerpeduncular (Meynert's) bundle (or retroflexus, fr). The central complex is made up of three parts, each with a particular neuronal species (lowere part of A). The pars parafascicularis (Cpf) has leptodendritic neurons (long and scarcely branched). Laterally, the pars paralateralis (Cpl, present only in upper primates) is made up of neurons with thinner and more branched arborizations with axonlike processes. The bar represents 100 μm. The intermediary pars media (Cme) is also intermediary in neuronal morphology (complete variations in Fénelon *et al.*, 1994). The principal component analysis shows that there is no gradient and a separation into three neuronal species. These species are clearly different from those of the isothalamus. The neuron on the upper right is a typical small bushy or tufted neuron much more branched with short stems. The region is thus allothalamic. Central neurons are not of the intralaminar neuronal genus shown dorsally, made up of bitufted elongated arborizations in primates (different from those of rat and cat). The complex is distinct from the intralaminar-limitans formation almost everywhere.

and human brains, a tripartition was proposed (Fénelon *et al.*, 1991, 1994; Percheron *et al.*, 1991) that is detailed now.

The regio centralis is made up of two distinct neuronal families: projection neurons and local circuit neurons. These are similar to the ones found in the isothalamus (i.e., microneurons with small somata, short dendritic arborizations, and axon-like appendages). Their proportion—19% in the parafascicular part and 25% in the lateral half (Dewulf *et al.*, 1969, 1971) in man and 28% and 27.4 of GABAergic neurons in macaques (Hunt *et al.*, 1991)—are higher than that in the intralaminar formation and close to numbers in the lateral region. In contrast, the cellular types of the projection neurons are clearly different from those of the isothalamus (Fig. 20.25), explaining their attribution to the allothalamus, and from those of the intralaminar formation (Fig. 20.25), explaining the removal from the so-called intralaminar group. Quantitative typology (on topological and metrical parameters) of dendritic arborizations of centralis neurons in macaques and humans (Fénelon *et al.*, 1994) showed that there are in fact three neuronal species, each for one of three subparts (Fig. 20.25): the medial pars parafascicularis (Cpf), with a lateral expansion below the next, the pars media (Cme), approximately

equivalent to the Vogts' Ce magnocellularis, Ce.mc or to Niimi's Pfl and the lateral pars paralateralis Cpl, (Niimi's, 1960, center median proper). CPf is made up of leptodendritic neurons (with scarcely branched dendritic arborizations, Fig. 20.25) similar to the neurons of the rat parafascicular nucleus (Scheibel and Scheibel, 1972; Deschênes *et al.*, 1996) of which 20% were seen to give initial collaterals. Cme, topographically intermediate, has neurons with intermediate dendritic characteristics (Fig. 20.25). Cpl, pars paralateralis, has richly ramified neurons bearing many axon-like processes. This differentiation is accentuated in human brains with larger and even more branched dendritic arborizations. In the two most lateral parts, electron microscopic studies (Harding, 1974; Balercia *et al.*, 1996) observed serial synapses and triads, but only a few glomeruli were not considered as typical elements. Immunohistochemistry brought new arguments. The two medial, Cpf and Cme, subparts are heavily stained for acetylcholinesterase (Olivier *et al.*, 1970) and for GABAa 1 (Huntsman *et al.*, 1996), while Cpl is weakly stained or unstained in human thalamus (Hirai and Jones, 1989; Heckers *et al.*, 1992; Jones, 1997; personal material) and stained for acetyltransferase (Heckers *et al.*, 1996) and GABAα5 and β3 (Huntsman *et al.*, 1996).

The connections of the complex point out its specificity. In opposition to surrounding intralaminar elements, there are no afferences from the spinothalamic tract or the brachium conjunctivum, just crossing through the complex for a more dorsal destination (Mehler, 1966; Percheron, 1977). Again in contrast with the surrounding intralaminar elements, the main subcortical afference comes from the system of the basal ganglia, at first the medial pallidum (Nauta and Mehler, 1966; confirmed by further works, François *et al.*, 1988; Percheron *et al.*, 1996). The intrapallidal distribution of the neurons that project to the complex overlaps with that of the neurons projecting to the lateral region (Parent and de Bellefeuille, 1983; Fénelon *et al.*, 1990). They are in fact collaterals of the axons targeted to this region (Arrechi-Bouchiouia *et al.*, 1997, Fig. 20.14). Branching is *effected* within the lateral region. Pallidocentral axons then go in a posterior direction, passing the central capsule. There are intraorder differences between macaques and cebideae (the last having endings in the parafascicularis and a particular dorsolateral PF, Sidibé *et al.*, 1997). In macaques, the intracentral territory of pallidal endings is mainly the pars media (François *et al.*, 1988; Percheron *et al.*, 1996; Fig. 20.6B). These endings are only sparsely ramified, with no dense arborizations (Arrechi-Bouchiouia *et al.*, 1997). Electron microscopic studies (Harding 1974; Balercia *et al.*, 1996) showed that the boutons of pallidal origin, calcium-binding protein negative, are not of LR (large round) type but of a subpopulation of F1 type boutons with symmetric, GABAergic synapses. They are often located on the dendritic stems, in any case close from the soma. LR boutons are different from those found in the isothalamus (Balercia *et al.*, 1996). Another afference from the basal ganglia system comes from the nigra lateralis and reticulata (Ilinsky *et al.*, 1985; Percheron *et al.*, 1996; François *et al.*, 2002; Fig. 20.26). Nigral axons selectively projecting to the pars parafascicularis including its ventrolateral extension below the pars media (François *et al.*, 2002; Sidibé *et al.*, 2002). The same parafascicular part also receives axons from the superior colliculus (Harting *et al.*, 1980). The parafascicular part of the complex, at least, is innervated by the brainstem reticular formation. The complex receives cholinergic axons from the pedunculopontine complex (Ch5; Lavoie and Parent, 1994) and lateral dorsal tegmental nucleus (Mesulam *et al.*, 1989), more intensively in the medial part, which likely explains the intense staining for acetylcholinesterase of the pars parafascicularis and media. It receives also glutamate afferents from the same pedunculopontine complex and from other reticular sources. The complex receives axons from extended portions of the perithalamus (Parent and de Bellefeuille, 1983). In addition to subcortical, the regio centralis receives cortical afferences. The afferences from the motor cortex to both paralateral (Cpl) and intermediate (Cme) parts are well documented (DeVito, 1969; Künzle, 1976, 1978; Jones *et al.*, 1979; Miyata and Sasaki, 1983; Leichneitz, 1986) and confirmed by Kuypers and Pandya (1966) in the chimpanzee. The topography of the endings of the axons from the premotor cortex, dorsal and ventral, is more medial since also involving the parafascicular part (Künzle, 1978; Miyata and Sasaki, 1983; Wiesendanger and Wiesendanger, 1985). There could be an evolutionary change as only the pars media receives premotor axons in chimpanzee (Kuypers and Pandya, 1966). The topography of the territory of the motor supplementary cortex (SMA) is even more extended as it comprises the three parts of the complex (DeVito and Smith, 1959; Wiesendanger and Wiesendanger, 1985). In addition, the pars parafascicularis selectively receives axons from the frontal eye field (Astruc 1971; Künzle and Akert, 1977; Akert and Harmann-von Monakow, 1980; Huerta *et al.*, 1986, Stanton *et al.*, 1988), from the supplementary frontal eye field (Huerta and Kaas, 1990) and from the associative frontal cortex (DeVito, 1969; supra and infraprincipalis, Künzle, 1978; Preuss and Goldmann-Rakic, 1987) and from the cingulate cortex (Van Hoesen *et al.*, 1993).

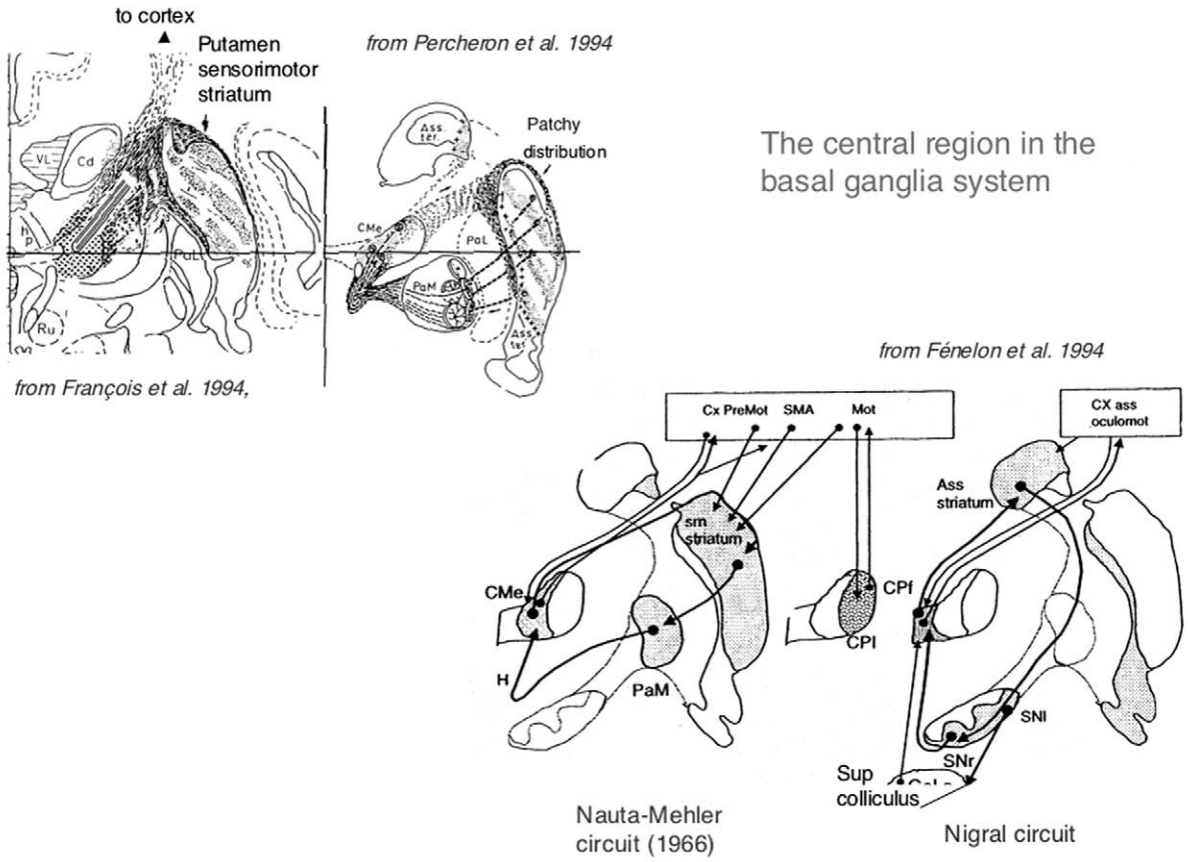

FIGURE 20.26 *Upper part* from François *et al*. (1994). Showing the connection from the central region to the striatum. The injection of tritiated amino acids shows that the tract is massive, reaching the upper border of the putamen. Central axons form separate oblique layers in the putamen. This constitutes the first part of the Nauta-Mehler circuit: striatum-medial pallidum-central region-striatum. Essentially sensorimotor. The striato-pallidal connection, due to the large dendritic arborizations of the pallidum represents a step of strong convergence (Percheron *et al.*, 1994). *Lower part*. The central region as a part of the system of the basal ganglia. Modified from Fenelon *et al.*'s (1994). The striatum of a macaque with its sensorimotor, mainly putaminal, and associative part, caudate and lower putamen. On the left, the pars media (Cme) receives afferences from the medial nucleus of the pallidum (PaM) through Forel's fields (H). CMe sends most of its axons to the sensorimotor striatum (Nauta-Mehler's circuit). Cpf receives afferences from the substantia nigra pars reticulata (SNr, in addition to superior colliculus, col s) and send its axons to the associative striatum, forming another subcortical circuit, the nigral circuit. Cpl receives some pallidal axons in macaques, does not send axons to the striatum and is mainly involved in reciprocal cortical connection, in particular with the primary motor cortex (mot).

Cortical endings form SR boutons making asymmetric synapses located distally on the dendrites of the centralis neurons (Balercia *et al.*, 1996).

The complex does not degenerate after cortical lesions in man and macaques (Peacock and Combs, 1960) and was thus said to receive no cortical efferences. The main efference, probably explaining this resistance, the striatum, was discovered on pathological material (Le Gros Clark and Russel, 1939; Vogt and Vogt, 1941). This projection was found to be ordered: the nucleus parafascicularis to the fundus, the dorsomedial Ce.mc., to the caudate nucleus and the inferolateral Ce.pc. to the putamen (Simma, 1951). The degeneration technique was also used experimentally in monkeys (Powell and Cowan, 1956). A lesion by Mehler (1966) and injections (François *et al.*, 1991; Sadikot *et al.*, 1990, 1992) in the middle and lateral part of the complex allowed to observe that the centralo-striatal connection is a major one, in terms of number of axons and density. Centralis axons cross obliquely through the lateral region and then the internal capsule and arrive at the superior border of the lateral pallidum where they either enter the lateral pallidal lamina or follow the lateral border of the putamen (François *et al.*, 1991)(Fig. 20.26). The pars media is the part that sends most axons to the sensorimotor striatum (Nakano *et al.*, 1990; Fénelon *et al.*, 1991; MacFarland and Haber, 2000), exclusively in the matrix. The axonal distribution is inhomogeneous (as already the case in rats, Deschênes *et al.*, 1996; cats,

Royce, 1987; squirrel monkeys, Sadikot *et al.*, 1992) in the form of dense irregular islands. In macaques, these make long oblique streaks following the direction of the somatotopic bands and forming long parasagittal bands (François *et al.*, 1991). The centralis complex is one element of the Nauta-Mehler's circuit (1966; striatum-medial pallidum-striatum; Fig. 20.26). This, mainly sensorimotor, circuit is doubled by another one, associative. The neurons of the pars parafascicularis indeed send axons to the associative striatum (Nakano *et al.*, 1990; Sadikot *et al.*, 1990, 1992; Druga *et al.*, 1991) comprising the caudate nucleus, the fundus and the ventral part of the putamen (Fig. 20.26) The complex finally covers irregularly (not including the spaces between streaks) the whole extent of the striatum. The centralostriatal connection is glutamatergic, excitatory. The presence of cholecystokinin in neurons of the three parts of the complex (Burgunder and Young, 1992) could be one source of CCK axons in the striatum. Centralis terminals form asymmetric synapses on dendrites (66%) and spines of the spiny neurons. In addition to the striatum, the central complex sends axons to the oral intralaminar nucleus (ILo including the IL cucullaris, see "Formatio intralaminaris-limitans") and to the formatio paramediana (Sadikot, 1992). Furthermore, it sends axons to other elements of the basal ganglia, lateral pallidum and subthalamic nucleus (Sadikot *et al.*, 1992, verified in macaques), and likely to the medial pallidum and nigra. The connection to the substantia nigra pars compacta appears selectively dense. The projection to the pedunculopontine complex would come from the pars Pf or from the adjacent reticular formation (Sadikot *et al.*, 1992). In the rat, the efferent connection from the pars parafascicularis to the different targets is effected by an arborescent connection distributing branches first to the perithalamus, the lateral pallidum, the striatum, and then the cortex (Deschênes *et al.*, 1996, 20% reaching all targets, others reaching only the pallidum). The projection to the cortex is constantly a collateral of the centro-striatal. In the cat (Macchi and Bentivoglio, 1985; Steriade *et al.*, 1997), the projection neurons were reported as either "striatally" or "cortically projecting," with some bifurcated axons (Jinnai and Matsuda, 1981). However, the bifurcated pattern could be in macaques the same as in rats (François, personal communication). Contrary to the classical assessment, the complex also projects to the cortex. The parafascicular part sends axons to the associative frontal orbital (Ilinsky *et al.*, 1985), "prefrontal" (Sadikot *et al.*, 1992; Rouiller *et al.*, 1999), oculomotor (frontal eye field), and anterior cingulate cortex (Vogt *et al.*, 1987). The efferences from the two lateral parts, CMe and CPl, are not different in macaques. They send axons to the motor cortex (Wiesendanger and Wiesendanger, 1985; Sadikot *et al.*, 1992; Rouiller *et al.*, 1999), the postarcuate premotor area (Shell and Strick, 1984), and the accessory motor cortex SMA (Wiesendanger and Wiesendanger, 1985; Shindo *et al.*, 1995; Rouiller *et al.*, 1999). The centralis axons end both in layers I and IV (Steriade *et al.*, 1997).

The functional meaning of the regio has varied in history. Luys' conception was sensory. As previously stated, the spinothalamic tract ends outside of it, dorsally and laterally (Mehler, 1966, Fig. 20.11), in the posterior intralaminar formation. Nociceptive responses in the parafascicular part observed after strong visceral stimulations (Berkley *et al.*, 1995) were attributed to a serotoninergic afference from the dorsal raphe (Reyes-Vazques *et al.*, 1989). This is documented in rats, not in primates. In the 1960s, the complex was a stereotactic target for the relief of central pain. Localized lesions there were rapidly shown to have no real effect, and this procedure was therefore abandoned. As assessed by Blomqvist *et al.* (2000), the postulated role in nociception was in fact very likely linked to the concomitant stimulation or lesion of the neighboring regio basalis (see "Regio Basalis."). The generally held interpretation of the function of the region, coming from LeGros Clark (1932, see above), is its belonging to the so-called intralaminar group, of which it was said to constitute the posterior or caudal part. The arguments in favor of such an ensemble was that both, intralaminar and central elements, are rich in cholinesterase (linked to an afference) and project to the striatum. The two criteria do not apply to the more lateral, paralateral, part. Furthermore, even if the bulk of the thalamic axons to the striatum in primates comes from the central or intralaminar formations, this is not their exclusivity since, in macaque at least, the paramedian and the motor isothalamus also send axons to the striatum (Nakano *et al.*, 1990; Fénelon *et al.*, 1991; McFarland and Haber, 2001). The central complex has more localized selective cortical connections than the intralaminar elements. Above all, the complex has its specific neuronal types and stains in a contrary way for calcium-binding proteins. On the other hand, in common with the isothalamus, the complex sends and receives axons to and from the perithalamic formation and has interneurons in about the same quantity and a nonidentical but close synaptic pattern. The intervention of the central region in nonspecific activation (sleep-wakening cycle or polysensory projection to the cortex, Jones, 1985; Steriade *et al.*, 1997) is unlikely. Lesions in the central complex in human brains do not lead to modification of consciousness or sleep. Thus, in spite of its persisting attribution to the intralaminar group, no argument is solid enough in comparison to its belonging to the

basal ganglia system as proposed in upper primates (see Percheron *et al.,* 1991). One reason, probably explaining the resistance to this attribution is that experimental and pathological lesions have no obvious motor effect. But anatomical data and systemic analyses are all concordant. The two Nauta-Mehler's and nigral circuits are major elements of the system of the basal ganglia. The second involves not only the usual associative elements but also the cingulate and oculomotor elements. The nigra lateralis projects to the superior colliculus. Considering the direct tectal afference to the pars parafascicularis and its cortical connections to FEF and SEF, this part was attributed a role in oculomotor control (Fénelon *et al.,* 1991; Sadikot *et al.,* 1992). The mixing with associative frontal, parietal, and temporal cortex indicates that its function would be more general. The most intriguing question remains, what is the functional role of the most lateral part (Cpl) receiving axons from the motor cortex?

The conclusion is that the central formation is not an element of the intralaminar formation and a major constituent of the basal ganglia system, which deserves to be studied as such.

THALAMIC STEREOTAXY

The principles and bases (at least cartographic) of stereotaxy have been explained in "Thalamic Topometry and Cartography". The resort to stereotaxy, a neurosurgical method allowing to reach deep structures with minimal cerebral damage, was introduced first in animals by Horsley and Clarke (1908; Clarke 1920) using bony landmarks. Because of large individual skull-brain variations, these were soon found to be unreliable in human. The resort to pineal calcifications (Spiegel and Wycis, 1952) was a step toward ventricular landmarks. A few years later, the reliance on the protrusion of the posterior commissure was durably exploited using ventriculography (Talairach and Szickla, 1967; Talairach *et al.*, 1957). The CA-CP system (see "General Considerations") became the usual reference. The most frequently used atlas in operation rooms was that of Hassler (1959, illustrated in Figs. 20.22, 20.23, 20.27 and 20.28 and later Hassler, 1967), on which observations and results were generally plotted, most often on sagittal sections. Among stereotactical techniques and apparatuses over at least 30 years, Leskell's ones became the most popular.

The main indications for thalamic lesions were intractable pain, tremor, and parkinsonian symptoms. Concerning the first, in the 1960s, many lesions were done in or around the central formation. The reappraisal of their inconstant effects led to the abandonment of this approach. As suggested by Craig *et al.* (1994) and Blomqvist *et al.* (2000), the lesions that had some positive effect probably included the nucleus basalis nodalis (see "Regio Basalis."), indeed close to the central region. The more precise topographic knowledge acquired during the last years could lead to a reappraisal of stereotactic possibilities in this domain. It is worthy to note that lesions of the central region never had observable motor consequence. The recent data from Henderson *et al.* (2000) showing primary degeneration in the central region of parkinsonian patients could lead to reconsider stereotactic possibilities.

The stereotaxy for the improvement of motor disorders has been preceded by neurosurgical hesitations. A vascular lesion of the capsule was already known by Charcot to improve parkinsonian symptoms. Later, the infarction of the territory of the anterior choroid artery, including the medial pallidum and its efferent bundles, had been observed to improve parkinsonian symptoms. The medial pallidum thus became the first neurosurgical target for parkinsonian-invalidating manifestations. Various surgical interventions targeted at the pallidum were proposed at that time, exposed in Cooper's treatise (1950). Later, the lesion of the internal capsule was thought to give better results than that of the pallidum. Continuing medially, finally the thalamus for some time became the usual selective target (Hassler *et al.,* 1979). A previous review (Percheron *et al.,* 1996) extensively analyzed the data on the location of thalamic sites whose stimulation or lesion were efficient in improving neurological motor symptoms and the possible mechanisms of their intervention (also a question, among others, for Marsden and Obeso, 1994). The best effects of lesioning were on tremor. Neurosurgical teams agree that the most efficient thalamic sites of lesion for alleviating or improving tremor, either "essential," cerebellar, or parkinsonian was always the same. They accepted that the "best target" was located at the lower part of the celebrate V.im, (Vogts 1941, Hassler's, V.im.e; Fig. 20.27; L 16), recipient of cerebellar afferences (see lateral intermediate subregion) where the axons of the brachium cunjunctivum are concentrated. This was understandable for the cases of cerebellar lesions or dysfunction (such as multiple sclerosis) but not in parkinsonian syndrome where the cerebellar system is anatomically intact. New interrogations had been raised by the discovery of "tremorosynchronous" neurons, whose firing rate was the same as that of the tremor, about 7–10 Hz (Albe-Fessard *et al.,* 1961). Tremor synchronicity became a major criterion for the selection of the target in parkinsonian tremor. The distribution of tremorosynchronous neurons was plotted by Albe-Fessard *et al.* (1961, 1966), Jasper and Bertand (1962), and

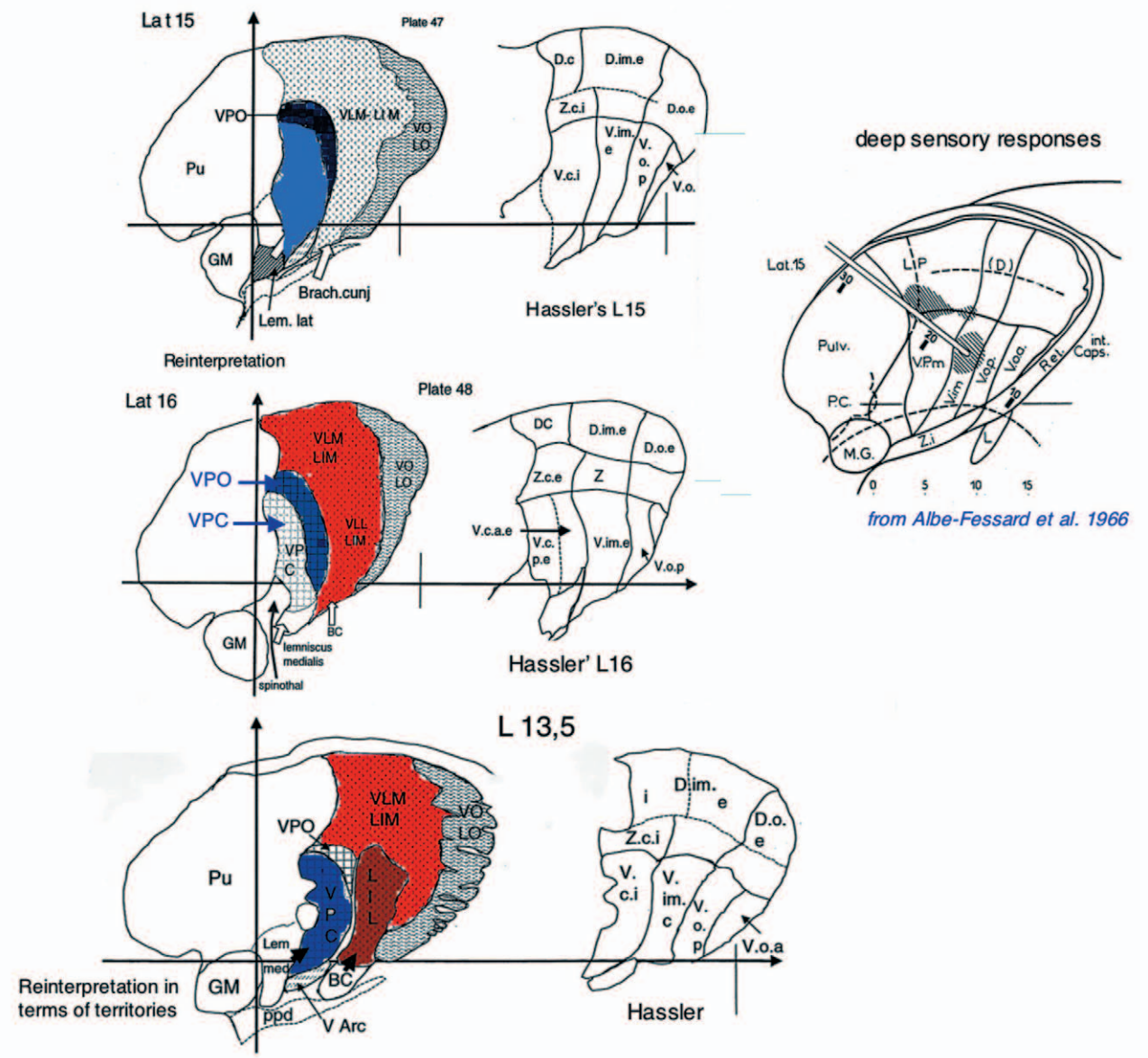

FIGURE 20.27 Stereotaxic data and additional sagittal sections. L15 and 16 from Schaltenbrand and Bailey's atlas—VPO. Drawing from Albe-Fessard *et al.* (1966) plotting points responding to deep stimuli (pressure, passive movement). One part is located dorsally in Hassler's Z.c.; the other, in his V.im.e. The comparison with the maps located above (L15) and below (L16) shows that the two could correspond to the curved VPO. *L-15.* Tracings from Hassler. The dorsal part of VPO is located in his Z.c.i (Hassler's interpretation). VPO is his anterior part of the lemniscal territory Vc (Vc a.e) and comprises also a part of Zc. Hassler's V.o.p at this level is part of the pallidal territory VO. The separation into zonal Z or dorsal D elements was artificial. DC was cerebellar like D.im. *L15.* Personal tracings. Appearance of VPO, the kinaesthetic part of the lemniscal territory (Kaas, VPS). Succession of three curved territories: pallidal VO, cerebellar VIm (or VL) and lemniscal (VP) with no ventrodorsal limits. The first two territories reach the dorsal border of lateral region.

Tasker *et al.* (1982; Fig. 20.19), essentially in Hassler's Vim. The nucleus ventralis intermedius (V.Im) has been the subject of much work particularly by Ohye (Ohye, 1978, 1982; Ohye and Albe-Fessard, 1978; Ohye and Narabayashi, 1979; Ohye *et al.*, 1972, 1976/77, 1977, 1989, 1990) including histological studies (Hirai *et al.*, 1982, 1989). The physiological characteristics of Vim were an intense activity with very large spikes (the highest in the thalamus, Fig. 20.28). The tremorosynchronous neurons were soon found to be sensitive to deep stimuli ("responses to passive and active movements of joint or muscle on the controlateral extremity but never to light stimuli," Ohye and Narabayashi, 1979). This led to a long-lasting confusion between pathologically tremorosynchronous and normal kinaesthetic neurons of sane monkeys and

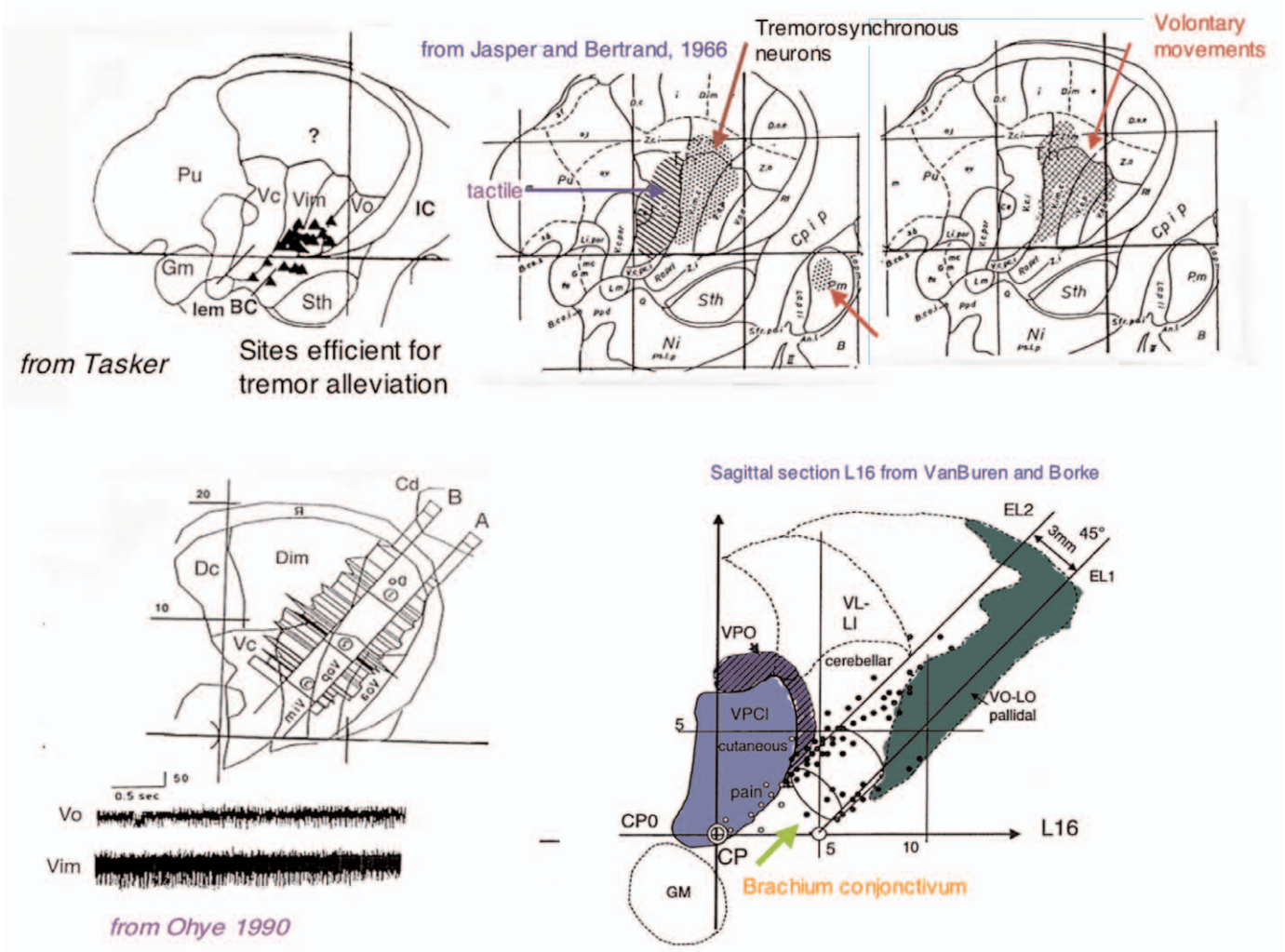

FIGURE 20.28 Stereotaxic data on tremorosynchronicity and the cure of tremor. *First row* from Tasker *et al.* (1982) and Jasper and Bertrand (1966). *Lower left* from Ohye *et al.* (1990). The surgical protocol is always the same. Two parallel electrodes 3 mm apart enter simultaneously at 45° from the intercommissural plane ICP. The lowest is targeted at the point located 5 mm in front of the posterior commissure on ICP. The activity on the upper electrode traversing Vim is much higher with larger spikes. That of the inferior electrode is that of the pallidal-receiving neurons. *Lower right.* Original drawing plotting of data from Ohye (Maebashi, Gunma) on level L16 of VanBuren and Borke's atlas (inverted and intentionally given larger magnification). The tracing of VPO is personal and made outside their VC. The points correspond to positions in 30 patients with parkinsonian tremor. Their anteroposterior position, as in Tasker *et al.* (1982), was corrected in relation to their individual CA-CP lengths. The open points, were those where stimulation evoked paraesthesia or pain. Neurons there are irresponsive to either active or passive movements. The black points are the positions of tremorosynchronous neurons also responding to deep information. Some are in the lower part of VPO. Still others are in the pallidal territory. The majority is located in the inferior part of the cerebellar territory. The cylinder shows the usual place of therapeutic lesions for alleviating parkinsonian tremor. It is located in the lower part of the cerebellar territory VIm, here VimL, projecting to the (primary) motor cortex, or at the entrance of cerebellar afferences (brachium conjunctivum, Brach. Cunj. in 15 and B.C in 16). The efficacy of lesions or stimulations is not linked to destruction or lesion of the set of neurons receiving deep information VPO but to another cause (see text).

men. From the beginning, it was admitted that there is no overlap between the somesthetic lemniscal and the cerebellar territory. The location of kinaesthetic neurons plotted in man by Albe-Fessard *et al.* (1966, 1967 on level 15, reproduced in Fig. 20.27), Jasper and Bertrand (1966), and Bertrand *et al.* (1967, Fig. 20.19) was considered to be outside the classic somesthetic nucleus (V.c), in the cerebellar territory (V.im) and dorsally to it (Z.c)(Figs. 20.19 and 20.20). In the "Albe-Fessard-Jasper-Ohye hypothesis" (see Percheron *et al.*, 1996), the intervention of the lemniscal system was ruled out because the denervation of limbs (rhizotomies) did not suppress thalamic rhythmic activity. The pathways conveying kinaesthetic information to Vim were

thought to be possibly the interposed component of the cerebellar input and the spinothalamic coafference, both forming islands interspersed in the dentate (cerebellar) territory (see "Subregio Lateralis Intermedia. Cerebellar Territory"). Starting from physiological data in sane monkeys and based on the fact that the afferents to the Vim have the characteristics of lemniscal axons, this was contested by the "Jones-Lenz hypothesis" according to which the tremorosynchronous neurons were simple kinaesthetic neurons passively driven by tremor. Recent topographic studies have added a nucleus between the cutaneous VP and the cerebellar Vim, receiving lemniscal kinaesthetic information, VPO (Kaas' VPS) (see "Subregio Caudalis. Lemniscal Territory") leading to other interpretations. This subdivision existed in Hassler's maps as the ventralis caudalis anterior externus Vcae at lateral levels 16 (Fig. 20.27) to 18.5 (Fig. 20.23), that is, in more lateral planes than the ones generally selected by neurosurgeons for plotting their points. A simple transfer to more lateral maps modifies the possible interpretation (see Fig. 20.27). Today it may be accepted that neurosurgeons looking for the most characteristic neurons could have preferentially selected VPO kinaesthetic neurons for their presentations. But the lesion of these neurons cannot explain alone the improvement of tremor. In Figure 20.27, data from 30 patients of Dr. Ohye at Maebashi were plotted on VanBuren and Borke L16 map on which a VPO was added. Tremor synchronous neurons are located anteriorly to the border of the cutaneous representation, VPC. The superior electrode skims the inferior border of VPO, likely lemniscal and kinaesthetic. However, the majority of tremorosynchronous neurons is more anterior, within the cerebellar (Vim-VL) and, to a lesser degree, the pallidal subregion (VO; Fig. 20.27). The location of lesions (Fig. 20.20, L16, cylinder) shows that the efficient places of lesions or stimulation for alleviation of parkinsonian tremor was not the kinaesthetic zone but V.im.e (VImL-VLL), known to project to the motor cortex. In the intermediate subregion (VIm), this receives massive "reciprocal" corticothalamic afferences from the motor cortex. The activity of the motor cortex is perturbed in the parkinsonian condition, overexcited and less selective. An explanation could be that cerebellar-receiving Vim neurons, normally not responding to deep stimuli, could do it in pathological conditions. Successive dynamic changes in neuronal systems also involving the basal ganglia and cortex might render thalamic neurons overexcited by lower afferents. The explanation for the improvement of tremor by thalamic lesions could be the interruption of perturbed messages. Another could be the suppression (lesion) or modification (stimulation) of perturbing messages to the motor cortex.

The presence of tremorosynchronous neurons in the medial pallidum was already known by Jasper and Bertrand (1966; Fig. 20.27). An abundant stereotactic literature underlines the fact that, if lesions in the VIm (cerebellar) improve parkinsonian tremor, more anterior lesions (in VO, pallidal territory) improve akinesia and rigidity. The pathophysiology of MPTP-induced parkinsonian syndromes, nowadays take into account that pallidal neurons are tremorosynchronous and perhaps tremorogenous (Raz *et al.*, 2000). These data open up a different view of the role of the thalamus in parkinsonian symptomatology and physiopathology. Surgical interventions in parkinsonism today include instead pallidal and subthalamic stimulation.

References

Aggleton, J.P., and Mishkin, M. (1984). Projections of the amygdala to the thalamus in the cynomolgus monkey. *J. Comp. Neurol.* **222,** 56–68.

Aggleton, J.P., Desimone, R., and Mishkin, M. (1986). The origin, course and termination of the hippocampothalamic projections in the macaque. *J. Comp. Neurol.* **243,** 409–421.

Aizawa, H., Kwak, S., Shimizu, T., and Mannen, T. (1991). Determination of GABAergic pallidothalamic termination in human brain. *J. Neurol. Sci.* **105,** 124–000.

Akert, K. (1964). Comparative anatomy of frontal cortex and thalamofrontal connections. *In* "The Frontal Granular Cortex and Behaviour" (J.M. Warren and K. Akert, eds.), pp. 372–394. McGraw Hill, New York.

Akert, K., and Harmann-von Monakow, K. (1980). Relationship of precentral, premotor and prefrontal cortex to the mediodorsal and intralaminar nuclei of the monkey thalamus. *Acta Neurobiol. Exp.* **40,** 7–25.

Albe-Fessard, D., Arfel, G., Guiot, G., Derome, P., and Guilbaud, G. (1967). Thalamic unit activity in man. *E.E.G. Clin. Neurophysiol. Suppl.* **25,** 132–142.

Albe-Fessard, D., Guiot, G., Lamarre, Y., and Arfel, G. (1966). Activation of thalamocortical projections related to tremorogenic processes. *In* "The Thalamus" (D.P. Purpura and M.D. Yahr, eds.), pp. 237–249. Columbia Univ. Press, New York.

Allen, G.I., Gibert, P.F.C., Marini, R., Schultz, W., and Yin, T.C.T. (1977). Integration of cerebral and peripheral inputs by interpositus neurons in monkey. *Exp. Brain Res.* **27,** 81–99.

Allen, G.I., Gibert, P.F.C., and Yin, T.C.T. (1978). Convergence of cerebral inputs onto dentate neurons in monkey. *Exp. Brain Res.* **32,** 151–170.

Amador, L.V., Blundell, J.E., and Wahren, W. (1959). Descriptions of coordinates of the deep structures. *In* "Introduction to Stereotaxis with an Atlas of the Human Brain" (G. Schaltenbrand and P. Bailey, eds.), pp. 16–28. Thieme, Stuttgart.

Anderson, M.E., and Turner, B.S. (1991). Activity of neurons in cerebellar-receiving and pallidal-receiving areas of the thalamus of the behaving monkey. *J. Neurophysiol.* **66,** 879–893.

Anderson, M.E., Ruffo, M., Buford, J.A., and Inase, M. (2001). Pallidal and thalamic determinants of thalamic activity. *In* "Basal Ganglia and Thalamus in Health and Movement Disorders" (I.A. Ilinsky and K. Kultas-Ilinsky, eds.), pp. 93–104. Plenum.

Andrew, J., and Watkins, E.S. (1969). "A Stereotaxic Atlas of the Human Thalamus and Adjacent Structures." Williams and Wilkins, Baltimore.

Angevine, J.B., Jr., Locke, S., and Yakovlev, P.I. (1962). Limbic nuclei of thalamus and connections of limbic cortex, *Arch. Neurol.* **7,** 518–528.

Angevine, J.B., Locke, S., and Yakovlev, P.I. (1962). Thalamocortical projection of the ventral anterior nucleus in man. *A.M.A. Arch. Neurol.* **7,** 518–528.

Angevine, J.B., Locke, S., and Yakovlev, P.I. (1963). Limbic nuclei of thalamus and connections of limbic cortex. V. Projection of the magnocellular medial dorsal nucleus to the orbital limbus of the hemisphere in man. *Trans. Am. Neurol. Ass.* 189–190.

Anner-Baratti, R., Allum, J.H.J., and Hepp-Reymond, M-C. (1986). Neural correlates of isometric force in the "motor" thalamus. *Exp. Brain Res.* **63,** 567–58.

Apkarian, A.V., and Hodge, C.J. (1989a) Primate spinothalamic pathways: I. A quantitative study of the cells of origin of the spinothalamic pathway. *J. Comp. Neurol.* **288,** 447-473.

Apkarian, A.V., and Hodge, C.J. (1989b). Primate spinothalamic pathways: II. The cells of origin of the dorsolateral and ventral spinothalamic pathways. *J. Comp. Neurol.* **288,** 474–492.

Apkarian, A.V., and Hodge, C.J. (1989c). Primate spinothalamic pathways: III. Thalamic terminations of the dorsolateral and ventral spinothalamic pathways. *J. Comp. Neurol.* **288,** 493–511.

Apkarian, A.V., and Shi, T. (1994). Squirrel monkey lateral thalamus. I. Somatic nociresponsive neurons and their relation to spinothalamic terminals. *J. Neurosci.* **14,** 6779–6795.

Applebaum, A.E., Leonard, R.B., Kenshalo, D.R., Jr., Martin, R.F., and Willis, W.D. (1979). Nuclei in which functionally identified spinothalamic tract neurons terminate. *J. Comp. Neurol.* **188,** 575–586.

Arcelli, P., Frassoni, C., Regondi, M.C., De Biasi, S., and Streafico, R. (1997). GABAergic neurons in mammalian thalamus: A marker of thalamic complexity? *Brain Res. Bul.* **42,** 27–37.

Armstrong, E. (1980). Quantitative comparison of the hominoid thalamus. II. Limbic nuclei anterior principalis and lateralis dorsalis. *Am. J. Phys. Anthrop.* **52,** 43–53.

Armstrong, E. (1986). Enlarged limbic structures in the human brain: The anterior thalamus and medial mamillary body. *Brain Res.* **362,** 394–397.

Arnold (1838–1842). "Handbuch der Anatomie." Zurich.

Aronson, L.R., and Papez, J.W. (1934). The thalamic nuclei of Pithecus (Macacus) rhesus. II. Dorsal thalamus. *Arch. Neurol. Psychiatr.* **32,** 27–44.

Arrechi-Bouchhioua, P., Yelnik, J., François, C., Percheron, G., and Tandé, D. (1996). Three-dimensional tracing of individual biocytin-labeled pallido-thalamic axons in the monkey. *Neuroreport* **7,** 981–984.

Arrechi-Bouchhioua, P., Yelnik, J., François, C., Percheron, G., and Tandé, D. (1997). Three-dimensional morphology and distribution of pallidal axons projecting to both the lateral region of the thalamus and the central complex in primates. *Brain Res.* **754,** 311–314.

Asanuma, C., Andersen, R.A., and Cowan, W.M. (1985). The thalamic relations of the caudal inferior parietal lobule and the lateral prefrontal cortex in monkeys: Divergent cortical projection from cell clusters in the medial pulvinar nucleus. *J. Comp. Neurol.* **241,** 357–381.

Asanuma, H., Larsen, K., and Yumiya, H. (1980). Peripheral input pathways to the monkey motor cortex. *Exp. Brain Res.* **38,** 349–355.

Asanuma, C., Thach, W.T., and Jones, E.G. (1983a). Cytoarchitectonic delineation of the ventral lateral thalamic region in the monkey. *Brain Res. Rev.* **5,** 219–235.

Asanuma, C., Thach, W.T., and Jones, E.G. (1983b). Distribution of cerebellar terminations and their relation to other afferent terminations in the ventral lateral thalamic region of the monkey. *Brain Res. Rev.* **5,** 237–265.

Asanuma, C., Thach, W.T., and Jones, E.G. (1983c). Anatomical evidence for segregated focal groupings of efferent cells and their terminal ramifications in the cerebellothalamic pathway in the monkey. *Brain Res. Rev.* **5,** 267–297.

Asanuma, C., Thach, W.T., and Jones, E.G. (1983d). Brainstem and spinal projections of the deep cerebellar nuclei in the monkey, with observations on the brainstem projections of the dorsal column nuclei. *Brain Res. Rev.* **5,** 299–322.

Astruc, J. (1971). Corticofugal connections of area 8 (frontal eye field) in Macaca mulatta. *Brain Res.* **33,** 241–256.

Bachevalier, J., Meunier, M., Lu, M.X., and Ungerleider, L.G. (1997). Thalamic and temporal cortex input to medial prefrontal cortex in rhesus monkey. *Exp. Brain Res.* **115,** 430–444.

Bailey, P., and von Bonin, G. (1952). "The Isocortex of Man." Univ. Illinois Press, Urbana.

Balercia, G., Kultas-Ilinsky, K., Bentivoglio, M., and Ilinsky, I.A. (1996). Neuronal and synaptic organization of the centromedian nucleus of the monkey thalamus: A quantitative ultrastructural study with tract tracing and immunohistochemical observations. *J. Neurocytol.* **25,** 267–288.

Baleydier, C., and Mauguière, F. (1980). The duality of the cingulate gyrus in monkey. Neuroanatomical study and functional hypothesis. *Brain* **103,** 525–554.

Baleydier, C., and Mauguière, F. (1985). Anatomical evidence for medial pulvinar connections with the posterior cingulate cortex, the retrosplenial area and the posterior parahippocampal gyrus in monkeys. *J. Comp. Neurol.* **232,** 219–228.

Baleydier, C., and Mauguière, F. (1987). Network organization of the connectivity between parietal area 7, posterior cingulate cortex and medial pulvinar nucleus: A double fluorescent tracer study in monkey. *Exp. Brain Res.* **66,** 385–393.

Barbas , H., and Pandya, D.N. (1987). Architecture and frontal cortical connections of the premotor cortex (area 6) in the rhesus monkey *J. Comp. Neurol.* **256,** 211–228.

Barbas, H., Haswell Henion, T.H., and Dermon, C.R. (1991). Diverse thalamic projections to the prefrontal cortex in the rhesus monkey. *J. Comp. Neurol.* **313,** 65–94.

Batton, R.R., Jarayaman, A., Ruggiero, D., and Carpenter, M.D. (1977). Fastigial efferent projections in the monkey: An autoradiographic study. *J. Comp. Neurol.* **174,** 281–306.

Becksteadt, R.M., and Frankfurter, A. (1982). The distribution and some morphological features of substantia nigra neurons that project to the thalamus, superior colliculus and pedunculopontine nucleus in the monkey. *Neuroscience* **7,** 2377–2388.

Becksteadt, R.M., Morse, J.R., and Norgren, R. (1980). The nucleus of the solitary tract in the monkey: Projections to the thalamus and brain stem nuclei. *J. Comp. Neurol.* **190,** 259–282.

Bender, D.B. (1981). Retinotopic organization of macaque pulvinar. *J. Neurophysiol.* **46,** 672–693.

Bender, D.B. (1982). Receptive-field properties of neurons in the macaque inferior pulvinar. *J. Neurophysiol.* **48,** 1–17.

Bender, D.B. (1983). Visual activation of neurons in the primate pulvinar depends on cortex but not colliculus. *Brain Res.* **279,** 258–261.

Benevento, L.A., and Fallon, J.H. (1975). The ascending projections of the superior colliculus in the rhesus monkey *(Macaca mulatta). J. Comp. Neurol.* **160,** 339–362.

Benevento, L.A., and Rezac, M. (1976). The cortical projections of the inferior pulvinar and adjacent lateral pulvinar in the rhesus monkey (macaca mulatta): An autoradiographic study. *Brain Res.* **108,** 1–24.

Benevento, L.A., and Standage, G.P. (1983). The organization and projections of the retinorecipient and nonretinorecipient nuclei of the pretectal complex and layers of the superior colliculus to the lateral and medial pulvinar in the macaque monkey. *J. Comp. Neurol.* **217,** 307–336.

Benson, D.L., Isaackson, P.J., Hendry, S.H.C., and Jones, E.G. (1991). Differential gene expression for glutamic acid decarboxylase and type II calcium-calmodulin-dependent protein kinase in basal ganglia, thalamus, and hypothalamus of the monkey. *J. Neurosci.* **11,** 1540–1564.

Bentivoglio, M., Kultas-Ilinsky, K., and Ilinsky, I.A.(1993). Limbic thalamus: Structure, intrinsic organization and connections. *In* "Neurobiology of Cingulate Cortex and Limbic Thalamus" (B.A. Vogt and M. Gabriel, eds.), pp. 72–122. Birkhauser, Boston.

Berkley, K.J. (1980). Spatial relationships between the terminations of somatic sensory and motor pathways in the rostral brainstem of cats and monkeys. I. Ascending somatic sensory inputs to lateral diencephalon. *J. Comp. Neurol.* **193,** 283–317.

Berkley, K.J. (1983a). Spatial relationships between the terminations of somatic sensory and motor pathways in the rostral brainstem of cats and monkeys. II. Cerebellar projections compared with those of the ascending somatic sensory pathways in lateral diencephalon. *J. Comp. Neurol.* **220,** 229–251.

Berkley, K.J. (1983b). Afferent projection to and near the ventrobasal complex in the cat and monkey. *In* "Somatosensory Integration in the Thalamus" (G. Macchi, A. Rustioni, and R. Spreafico, eds.), pp. 43–61. Elsevier, Amsterdam.

Berkley, K.J., Benoist, J., Gautron, M., and Guilbaud, G. (1985). Responses of neurons in the caudal intralaminar thalamic complex of the rat to stimulation of the uterus, vagina, cervix, colon and skin. *Brain Res.* **695,** 92–95.

Bertrand, G., Jasper, H., and Wong, A. (1967). Microelectrode study of the human thalamus: Functional organization in the ventrobasal complex. *Confin. Neurol.* **29,** 81–86.

Blomqvist, A., Ericson, A-C, Craig, A.D., and Broman, J. (1996). Evidence for glutamate as a neurotransmitter in spinothalamic tract terminals in the posterior region of owl monkeys. *Exp. Brain Res.* **108,** 33–44.

Blomqvist, A., Zhang, E-T., and Craig, A.D. (2000). Cytoarchitecture and immunohistochemical characterization of a specific pain and temperature relay, the posterior portion of the ventral medial nucleus, in the human thalamus. *Brain* **123,** 601–619.

Boivie, J. (1979). An anatomical reinvestigation of the termination of the spino-thalamic tract in the monkey. *J. Comp. Neurol.* **186,** 343–370.

Bos, J., and Benevento, L.A. (1975). Projections of the medial pulvinar to orbital cortex and frontal eye fields in the rhesus monkey (Macaca mulatta). *Exp. Neurol.* **49,** 487–496.

Bossy, J., and Lacroix, A. (1968). Aspect macroscopique du cingulum de l'homme adulte. *Bul. Ass. Anat.* **141,** 580–587.

Borke, R.C., and Van Buren, J.M. (1972). The cerebellosensory inflow to the large-celled lateroventral nuclei of the chimpanzee. *Anat. Rec.* **172,** 274.

Bowman, J.P., and Combs, C.M. (1969). The thalamic projection of hypoglossal afferents in the rhesus monkey. *Exp. Neurol.* **25,** 509–520.

Braak, H. (1971). Uber die kerngebiete des menschlichen hirnstammes. III. Centrum medianum thalami and nucleus parafascicularis. *Z. Zellforsch.* **114,** 331–343.

Brierley, J. B., and Beck, E.(1959). The significance in human stereotactic brain surgery of individual variation in diencephalon and globus pallidus. *J. Neurol. Neurosurg. Psychiat.* **22,** 287–298.

Brockhaus, H. (1938. Zur normalen and pathologischen anatomie des mandelkerngebietes. *J. Psychol. Neurol.* **49,** 1–136.

Brodal, A. (1981). "Neurological Anatomy." Oxford Univ. Press, London.

Brodman, K. (1905). Beiträge zur histologischen lokalisation der Grosshirn rinde. *J. Psychol. Neurol.* **4,** 177–226.

Browne, B., and Simmons, R.M.T. (1984). Quantitative studies of the evolution of the thalamus in primates. *J. Hirnforsch.* **25,** 261–274.

Brüggemann, J., Shi,T., and Apkarian, A.V. (1994). Squirrel monkey lateral thalamus. II. Viscerosomatic convergent representation of urinary bladder, colon, and esophagus. *J. Neurosci.* **14,** 6796–6814.

Burdach, K.F. (1822). "Von Baue und Leben des Gehirns," Dyk, Leipzig. 1819–1826.

Burgunder, J-M., and Young, W.S. (1992). Expression of cholecystokinin and somatostatin genes in the human thalamus. *J. Comp. Neurol.* **324,** 14–22.

Burton, H., and Craig, A.D. (1983). Spinothalamic projections in cat, raccoon and monkey: A study based on anterograde transport of horseradish peroxidase. *In* "Somatosensory integration in the Thalamus" (G. Macchi, A. Rustioni, and R. Spreafico, eds.), pp. 17–41. Elsevier, Amsterdam.

Burton, H., and Jones, E.G. (1976). The posterior thalamic region and its cortical projection in New world and Old world monkeys. *J. Comp. Neurol.* **168,** 249–301.

Büttner-Ennever, J.A., and Büttner, U. (1978). Vestibular projections to the monkey thalamus and rostral mesencephalon: An autoradiographic study. *In* "The Vestibular System, Function and Morphology" (T. Gualteirotti, ed.), pp. 130–143. Springer, Berlin.

Caparros-Lefebvre, D., Ruchoux, M.M., Blond, S., Petit, H., and Percheron, G. (1994). Long-term thalamic stimulation in Parkinson's disease: Postmortem anatomoclinical study. *Neurol.* **44,** 1856-1860.

Carmel, P.W. (1970). Efferent projections of the ventral anterior nucleus of the thalamus in the monkey. *Amer. J. Anat.* **128,** 159–184.

Carmichael, S.T., and Price, J.L. (1995). Sensory and premotor connections of the orbital and medial prefrontal cortex of macaque monkeys. *J. Comp. Neurol.* **363,** 642–664.

Carpenter, M.B. (1959). Lesions of fastigial nuclei in the rhesus monkey, *J. Comp. Neurol.* **104,** 1–33.

Carpenter, M.B. (1973). Comparisons of the efferent projections of the globus pallidus and substantia nigra in the monkey. *In* "Efferent Organization and the Integration of Behavior" (J.D. Maser, ed.), pp. 137–174. Academic Press, New York.

Carpenter, M.B., and McMasters, R.E. (1964). Lesions of the substantia nigra in the Rhesus monkey. Efferent fiber degeneration and behavioral observations, *Amer. J. Anat.* **114,** 293–320.

Carpenter, M.B., and Peter, P. (1972). Nigrostriatal and nigrothalamic fibers in the rhesus monkey, *J. Comp. Neurol.* **144,** 93–116.

Carpenter, M.B., and Strominger, N.L. (1964). Cerebello-oculomotor fibers in the rhesus monkey, *J. Comp. Neurol.* **123,** 211–230.

Carpenter, M.B., and Strominger, N.L. (1967). Efferent fiber projections of the subthalamic nucleus in the rhesus monkey. A comparison of the efferent projections of the subthalamic nucleus, substantia nigra and globus pallidus. *Amer. J. Anat.* **121,** 41–72.

Carpenter, M.B., Nakano, K., and Kim, R. (1976). Nigrothalamic projections in the monkey demonstrated by autoradiographic technics. *J. Comp. Neurol.* **165,** 401–416.

Cavada, C., Company, T., Hernandez-Gonzales, A., and Reinoso-Suarez, F. (1995). Acetylcholinesterase histochemistry in the

macaque thalamus reveals territories selectively connected to frontal, parietal and temporal association cortices., *J. Chem. Neuroanat*. **8,** 245–257.
Cavada, C., Company, T., Tejedor, J., Cruz-Rizzolo, R.J., and Reinoso-Suarez, F. (2000). The anatomical connections of the macaque monkey orbitofrontal cortex. *A review. Cereb. Cortex* **10,** 240–242.
Chan-Palay, V. (1977). "Cerebellar Dentate Nucleus. Organisation, Cytology and Transmitters." Springer, Berlin.
Ciccheti, F., Lacroix, S., Beach, T.G., and Parent, A. (1998). Calretinin gene expresssion in the human thalamus. *Mol. Brain Res.* **54,** 1–12.
Clarke, R.H. (1920). Investigation of the central nervous system. Methods and instruments . John Hopkins Hosp. Reports.
Cole, M., Nauta, W.J.H., and Mehler, W.R. (1964). The ascending efferent projections of the substantia nigra, *Trans. Am. Neurol. Ass.* **89,** 74–78.
Cooper, E.R.A. (1950). The development of the thalamus. *Acta Anat*. **9,** 201–226.
Cooper, I.S. (1956). "The neurosurgical Alleviation of Parkinsonism." Thomas, Springfield, IL.
Cooper, I.S., Riklan, M., and Rakic, P. (1974). The Pulvinar-LP complex. Thomas, Springfield, IL.
Craig, A.D. (1995). Supraspinal projections of lamina I neurons. In "Forebrain Areas involved in Pain Processing" (J.M. Besson, G.Guilbaud, and H. Ollat, eds.), pp. 13–25. John Libbey, Paris.
Craig, A.D., Bushnell, M.C., Zhang, E-T., and Blomqvist, A. (1994). A thalamic nucleus specific for pain and temperature sensation. *Nature* **372,** 770–773.
Crick, F., and Koch, C . (1998). Constraints on cortical and thalamic projections: The no-strong-loops hypothesis. *Nature* **391,** 245–250.
Crosby, E.C., Humphrey, T., and Lauer, E.W. (1962). "Correlative Anatomy of the Nervous System." MacMillan, New York.
Crouch, R.L. (1934). The nuclear configuration of the thalamus of Macacus rhesus. *J. Comp. Neurol.* **59,** 451-485.
Crouch, R., and Thompson, J.K. (1938). Termination of the brachium conjunctivum in the thalamus of the macaque monkey. *J. Comp. Neurol*. **69,** 449–452.
Crowell, R.M., Perret, E., Siegfried, J., and Villoz, J-P. (1968). "Movement units" and "tremor phasic units" in the human thalamus. *Brain Res.* **11,** 481–488.
Cusick, C.G., Scripter, J.L., Darensbourg, J.G., and Weber, J.T. (1993). Chemoarchitectonic subdivisions of the visual pulvinar in monkeys and their connectional relations with the middle temporal and rostral dorsolateral visual area, MT and DLr. *J. Comp. Neurol*. **336,** 1–30.
Dagi, T.F., and Poletti, C.E. (1983). Reformulation of the Papez circuit: Absence of hippocampal influence on cingulate cortex unit activity in the primate. *Brain Res*. **259,** 229–236.
Darian-Smith, C., and Darian-Smith, I. (1993a). Thalamic projections to areas 3a, 3b, and 4 in the sensorimotor cortex of the mature and infant monkey. *J. Comp. Neurol.* **335,** 173–199.
Darian-Smith, C., and Darian-Smith, I. (1993b). Ipsilateral cortical projections to areas 3a, 3b, and 4 in the macaque monkey. *J. Comp. Neurol*. **335,** 200–213.
Dejerine, J. (1901). "Anatomie des centres nerveux." Masson, Paris.
Dejerine, J. (1914). "Semiologie des affections du système nerveux." Masson, Paris.
Dejerine, J., and Roussy, G. (1906). Le syndrome thalamique. *Rev. Neurol*. **14,** 521–532.
Dekaban, A. (1953). Human thalamus. An anatomical developmental and pathological study. I. Division of the human adult thalamus into nuclei by use of the cyto-myelo-architectonic method. *J. Comp. Neurol.* **99,** 639–667.
Dekaban, A. (1954). II. Development of the human thalamic nuclei. *J. Comp. Neurol*. **100,** 63–97.
Dekker, J.J., and Kuypers, H.G.J.M (1976). Morphology of rat's AV thalamic nucleus in light and electron microscopy. *Brain Res.* **117,** 387–398.
DeLong, M.R., Crutcher, M.D., and Georgopoulos, A.P. (1983). Relations between movement and single cell discharge in the substantia nigra of the behaving monkey. *J. Neurosci*. **3,** 1599–1606.
Dermon, C.R., and Barbas, H. (1994). Controlateral thalamic projections predominantly reach transitional cortices in the rhesus monkey. *J. Comp. Neurol.* **344,** 508–531.
Deschênes, M., Bourassa, J., Doan, V.D., and Parent, A. (1996). A single-cell study of the axonal projections arising from the posterior intralaminar thalamic nuclei in the rat. *Eur. J. Neurosci.* **8,** 329–343.
DeVito, J.L. (1969). Projections from the cerebral cortex to intralaminar nuclei in monkey. *J. Comp. Neurol.* **136,** 193–202.
DeVito, J.L. (1978). A horseradish peroxidase-autoradiographic study in parietopulvinar connections in Saimiri sciureus. *Exp. Brain Res*. **32,** 581-590.
DeVito, J.L., and Anderson, M.E. (1982). An autoradiographic study of the efferent connections of the globus pallidus in *Macaca mulatta*. *Exp. Brain Res.* **46,** 107–117.
DeVito, J.L., and Simmons, D.M. (1976). Some connections of the posterior thalamus in monkey. **51,** 347–362.
DeVito, J., and Smith, O.A. (1959). Projections from the mesial frontal cortex (supplementary motor area) to the cerebral hemispheres and brain stem of the Macaca mulatta. *J. Comp. Neurol.* **111,** 261–277.
Dewulf, A. (1971). "Anatomy of the Normal Human Thalamus." Elsevier, Amsterdam.
Dixon, G., and Harper, C.G. (2001). Quantitative analysis of glutamic acid decarboxylase-immunoreactive neurons in the anterior thalamus of the human brain. *Brain Res.* **923,** 39–44.
Dostrowski, J.O., Wells, F.E.B., and Tasker, R.R. (1992). Pain sensations evoked by stimulation in human thalamus. *In* "Processing and Inhibition of Nociceptive Information" (R. Inoka, Y. Shinenaga, and M. Toyama, eds.), pp. 115–120. Excerpta Med.
Druga, R., Rokyta, R., and Benes, V. (1991). Thalamocaudate projections in the macaque monkey (a horseradish peroxidase study). *J. Hirnforsch*. **32,** 765–774.
Dum, R.P., and Strick, P.L. (2003). An unfolded map of the cerebellar dentate nucleus and its projections to the cerebral cortex. *J. Neurophysiol*. **89,** 634–639.
Edinger, L. (1900–1904). Vorlesungen uber den Bau der nervosen Centralorgane des Menschen.
Emmers, R., and Tasker, R.R. (1975). "The Human Somesthetic Thalamus with Maps for Physiological Target Localization during Stereotatic Neurosurgery." Raven Press, New York.
Fénelon, G., François, C., Percheron, G., and Yelnik, J. (1990). Topographic distribution of pallidal neurons projecting to the thalamus in macaques. *Brain Res*. **520,** 27–35.
Fénelon, G., François, C., Percheron, G., and Yelnik, J. (1991). Topographic distribution of the neurons of the central complex ("centre médian-parafascicular complex") and of other thalamic neurons projecting to the striatum in macaques. *Neurosci.* **45,** 495–510.
Fénelon, G., Yelnik, J., François, C., and Percheron, G. (1994). The central complex of the primate thalamus: A quantitative analysis of neuronal morphology, *J. Comp. Neurol*. **341**, 463–479.
Feremutsch, K., and Simma, K. (1954a). Strukturanalysen des Menschlichen Thalamus. II. Die intralaminaren kerne. *Mschr. Psychiat. Neurol.* **127,** 88.

Feremutsch, K., and Simma, K. (1956b). Strukturanalysen des Menschlichen Thalamus. III. Der lateralkerncomplex. *Mschr. Psychiat. Neurol.* **128,** 365–000.

Feremutsch, K., and Simma, K. (1955). Strukturanalysen des Menschlichen Thalamus. IV. Nucleus anterior, nucleus mediodorsalis, nucleus pulvinaris thalami. *Mschr. Psychiat. Neurol.* **130,** 347–359.

Flament, D., and Hore, J. (1988). Relations of motor cortex neural discharge to kinematics of passive and active elbow movements in the monkey, *J. Neurophysiol,* **60,** 1268–1284.

Foix, C., and Hillemand, P. (1925). Les artères de l'axe encéphalique jusqu'au diencéphale inclusivement. *Rev. Neurol.* **2,** 705–739.

Foix, C., and Nicolesco, J. (1925). "Les noyaux gris centraux et la région mésencéphalo-sous-optique." Masson, Paris.

Forel, A. (1877). Untersuchungen über die Haubenregion und ihre oberen Verknüpfungen im Gehirne des Menschen und einiger Saügethiere, mit Beiträgen zu den Methoden der Gehirnuntersuchung. *Arch. Psychiat. Nervenkr.* **7,** 393–495.

Foreman, R.D., Kenshalo, D.R., Schmidt, R.F., and Willis, W.D. (1979). Field potentials and excitation of primate spinothalamic neurones in response to volleys in muscle afferents. *J. Physiol.* **286,**197–213.

Fortin, M., Asselin, M-C., Gould, P.V., and Parent, A. (1998). Calretinin-immunoreactive neurons in the human thalamus. *Neurosci.* **84,** 537–548.

Forutan, F., Mai, J.K., Ashwell, K.W.S., Lensing-Höhn, S., Nohr, D., Voss, T., Boss, J., and Andressen. C. (2001). Organisation and maturation of the human thalamus as revealed by CD15. *J. Comp. Neurol.* **437,** 476–495.

François, C., Percheron, G., and Yelnik, J. (1984). Localization of nigrostriatal, nigrothalamic and nigrotectal neurons in ventricular coordinates in macaques. *Neurosci.* **13,** 61–76.

François, C., Percheron, G., Parent, A., Sadikot, A.F., Fenelon, G., and Yelnik, J. (1991). Topography of the projection from the central complex of the thalamus to the sensorimotor striatal territory in monkeys. *J. Comp. Neurol.* **305,** 17–34.

François, C., Percheron, G., Yelnik, J., and Tandé, D. (1988). A topographic study of the course of nigral axons and the distribution of pallidal axonal endings in the centre médian-parafascicular complex of macaques. *Brain Res.* **473,** 181–186.

François, C., Tandé, D., Yelnik, J., and Hirsch, E.C. (2002). Distribution and morphology of nigral axons projecting to the thalamus in primates. *J. Comp. Neurol.* In press

François, C., Yelnik, J., Percheron, G., and Fenelon, G. (1994a). Topographic distribution of the axonal endings from the sensorimotor and associative striatum in the macaque pallidum and substantia nigra. *Exp. Brain Res.* **102,** 305–318.

François, C., Yelnik, J., Percheron, G., and Tandé, D. (1994b). Calbindin D-28K as a marker for the associative cortical territory of the striatum in macaque. *Brain Res.* **633,** 331–336.

Freeman, W., and Watts, J.W. (1947). Retrograde degeneration of the thalamus following prefrontal lobotomy. *J. Comp. Neurol.* **86,** 65–93.

Fried, I., Katz, A., McCarthy, G., Sass, K.J., Williamson, P., Spencer, S.S., and Spencer, D.D (1991). Functional organization of human supplementary motor cortex studid by electrical stimulation. *J. Neurosci.* **11,** 3656–3666.

Friedemann, M. (1911). Die cytoarchitektonik des Zwishenhirns der Cercopitheken mit besonderer Berücksichtigung des Thalamus opticus. *J. Psychol. Neurol.* **18,** 309–378.

Friedman, D.P., and Jones, E.G. (1986). Thalamic input to areas 3a and 2 in monkeys, *J. Neurophysiol.* **45,** 59–85.

Friedman, D.P., and Murray, E.A. (1986). Thalamic connectivity of the second somatosensory area and neighboring somatosensory fields of the lateral sulcus of the macaque. *J. Comp. Neurol.* **252,** 348–373.

Gilbert, M.S. (1934). The early development of the human diencephalon. *J. Comp. Neurol.* **62,** 81–115.

Gingold, S.T., Greenspan, J.D., and Apkarian, A.V. (1991). Anatomic evidence of nociceptive inputs to primary somatosensory cortex: Relationship between spinothalamic terminals and thalamocortical cells in squirrel monkeys. *J. Comp. Neurol.* **308,** 467–490.

Goldberg, G. (1985). Supplementary motor area structure and function: Review and hypothese. *Behav. Brain Res.* **8,** 567–616.

Goldman-Rakic, P.S., and Porrino, L.J. (1985). The primate mediodorsal nucleus (MD) and its projection to the frontal lobe. *J. Comp. Neurol.* **242,** 535–560.

Gosh, S., Brinkman, C., and Porter, R. (1987). A quantitative study of the distribution of neurons projecting to the precentral motor cortex in the monkey (*M. fascicularis*). *J. Comp. Neurol.* **259,** 424–444.

Goto, A., Kosaka, K., Kubota, K., Nakamura, R., and Narabayashi, H. (1968). Thalamic potentials from muscle afferents in the human. *Arch. Neurol.* **19,** 302–309.

Greenan, T.J., and Strick, P.L. (1986). Do thalamic regions which project to rostral primate motor cortex receive spinothalamic input? *Brain Res.* **362,** 384–388.

Grieve, K.L., Acuna, C., and Cuderio, J. (2000). The primate pulvinar nuclei: Vision and action. *Trends Neurosci.* **23,** 35–39.

Grünthal, E. (1934). Der Zellbau im thalamus der Säuger und dem Menshen. Eine beschreibend und vergleichend anatomishe untersuchung. *J. Psychol. Neurol. (Lpz)* **46,** 41–112.

Guillery, R.W (1969). The organization of the synaptic interconnections in the dorsal lateral geniculate nucleus of cat and monkey. *Zeitschr. Zellforsch. mikro. Anat.* **96,** 1–38.

Gurdjian, E.S. (1927). The diencephalon of the albino rat. *J. Comp. Neurol.* **43,** 1–114.

Gutierrez, C.A., Yaun, A., and Cusick, C.G. (1995). Neurochemical subdivisions of the inferior pulvinar in macaque monkeys. *J. Comp. Neurol.* **363,** 545–562.

Harding, B.N. (1971). Dedro-dendritic synapses, including reciprocal synapses, in the ventro-lateral nucleus of the monkey thalamus. *Brain Res.* **34,** 181–185.

Harding, B.N. (1972). An electron microscopic study of afferent fibre connexions to the motor thalamus from motor cortex and basal ganglia. *J. Anat.* **111,** 503–504.

Harding, B.N. (1973). An ultrastructural study of the termination of afferent fibres within ventrolateral and centre median nuclei in the monkey thalamus. *Brain Res.* **54,** 341–346.

Harding, B.N., and Powell, T.P.S. (1977). An electron microscopic study of the centremedian and ventrolateral nuclei of the thalamus in the monkey. *Philos. Trans. R. Soc. B.* **279,** 357–412.

Harting, J.K., Hall, W.C., and Diamond, I.T. (1972). Evolution of the pulvinar. *Brain Behav. Evol.* **6,** 424–452.

Harting, J.K., Huerta, M.F., Frankfurter, A.J., Strominger, N.L., and Royce, G.J. (1980). Ascending pathways from the superior colliculus: An autoradiographic analysis. *J. Comp. Neurol.* **192,** 853–882.

Hardy, S.G.P., and Lynch, J.C. (1992). The spatial distribution of pulvinar neurons that project to two subregions of the inferior parietal lobule in the macaque. *Cereb. Cortex* **2,** 217–230.

Hassler, R. (1949). Uber die afferenten Bahnen und thalamuskerne des motorischen Systems des Grosshirns. *Arch. f. Psychiat.* **182,** 759–818.

Hassler, R. (1959). Anatomy of the thalamus. *In* "Introduction to Stereotaxic Operations with an Atlas of the Human Brain" (G. Schaltenbrand and P. Bailey, eds.), pp. 230–290. Thieme, Stuttgart.

Hassler, R. (1982). Cytoarchitectonic organization of the thalamic nuclei. *In* "Stereotaxy of the Human Brain" (G. Schaltenbrand and A.E. Walker, eds.), pp. 140–180. Thieme, Stuttgart.

Hassler, R., Mundinger, F., and Riechert, T. (1979). Stereotaxis in Parkinson syndrome. With an atlas of the basal ganglia in Parkinsonism. Springer, Berlin.

Havrylyshyn, P.A., Rubin, A.M., Tasker, R.R., Organ, L., and Fredrickson, J.M. (1978). Vestibulothalamic projection in man—A sixth primary sensory pathway. *J. Neurophysiol.* **41,** 394–401.

Head, H., and Holmes, G. (1911). Sensory disturbances from cerebral lesions. *Brain* **34,** 102–254.

Heckers, S., Geula, C., and Mesulam, M.-M. (1992). Cholinergic innervation of the human thalamus: Dual origin and differential nuclear distribution. *J. Comp. Neurol.* **325,** 68–82.

Henderson, J.M., Carpenter, K., Cartwright, H., and Halliday, G.M. (2000a). Degeneration of the centre médian-parafascicular complex in Parkinson's disease. *Ann. Neurol.* **47,** 345–352.

Henderson, J.M., Carpenter, K., Cartwright, H., and Halliday, G.M. (2000b). Loss of thalamic intralaminar nuclei in progressive supranuclear palsy and Parkinson's disease: Clinical and therapeutic implication. *Brain.* **123,** 1410–1421.

Hendrickson, A., Wilson, M.E., and Toyne, M.J. (1970). The distribution of the optic nerve fibers in *Macaca mulatta*. *Brain Res.* **23,** 425–427.

Hendry, S.H.C., Jones, E.G., and Graham, J. (1979). Thalamic relay nuclei for cerebellar and certain related fiber systems in the cat. *J. Comp. Neurol.* **185,** 679–714.

Hirai, T., and Jones, E.G. (1989a). A new parcellation of the human thalamus on the basis of histochemical staining. *Brain Res. Rev.* **14,** 1–34.

Hirai, T., and Jones, E.G. (1989b). Distribution of tachykinin immunoreactive fibers in the human thalamus. *Brain Res.* **14,** 35–52.

Hirai, T., and Jones, E.G. (1993). Comparative anatomical study of ventrolateral thalamic mass in humans and monkeys. *Stereotact. Funct. Neurosurg.* **60,** 6–16.

Hirai, T., Nagaseki, Y., Kawashima, Y., Wada, H., Tsukahara, Y., Imai, S., and Ohye, C. (1982). Large neurons in the thalamic ventro-lateral mass in humans and monkeys. *Appl. Neurophysiol.* **45,** 245–250.

Hirai, T., Ohye, C., Nagaseki, Y., and Matsumara, M. (1989). Cytometric analysis of the thalamic ventralis intermedius nucleus in humans, *J. Neurophysiol.* **61,** 478–487.

Holsapple, J.W., Preston, J.B., and Strick, P.L. (1991). The origin of thalamic inputs to the "hand" representation in the primary motor cortex. *J. Neurosci.* **11,** 2644–2654.

Hoover, J.H., and Strick, P.L. (1993). Multiple output channels in the basal ganglia. *Science* **259,** 819–821.

Hoover, J.E., and Strick, P.L. (1999). The organization of cerebellar and basal ganglia outputs to primary motor cortex as revealed by retrograde transneuronal transport of Herpes simplex virus. *J. Neurosci.* **19,** 1446–1463.

Hopf, A., Krieg, W.J.S., Feremutsch, K., Simma, K., and Macchi, G. (1971). Attempt at standardization of nomenclature. *In* "Anatomy of the Normal Human Thalamus" (A. Dewulf, ed.), pp. 121–138. Elsevier, Amsterdam pp. 121–138.

Horsley, V., and Clarke, R.H. (1908). The structure and functions of the cerebellum examined by a new method. *Brain,* **31,** 5–124.

Hreib, K.K., Rosene, D.L., and Moss, M.B. (1988). Basal forebrain efferents to the medial dorsal thalamic nucleus inthe rhesus monkey. *J. Comp. Neurol.* **277,** 365–390.

Huber, G.C., and Crosby, E.C. (1929). Somatic and visceral connections of the diencephalon. *Res. Nerv. Ment. Dis.* **9,** 199–248.

Huerta, M.F., Krubitzer, L.A., and Kaas, J.H. (1986). Frontal eye field as defined by intracortical microstimulation in squirrel monkeys, owl monkeys, and macaque monkeys: I. Subcortical connections. *J. Comp. Neurol.* **253,** 415–439.

Hunt, C.A., Pang, D.Z., and Jones, E.G. (1991). Distribution and density of GABA cells in intralalminar and adjacent nuclei of monkey thalamus. *Neurosci.* **43,** 185–196.

Huntsman, M.M., Leggio, M.G., and Jones, E.G. (1966). Nucleus-specific expression of GABA (A) receptor subunit mRNAs in monkey thalamus. *J. Neurosci.* **16,** 3571–3589.

Ilinsky, I.A. (1990). Structural and connectional diversity of the primate motor thalamus: Experimental light and electron microscopic studies in the rhesus monkey. *Stereotact. Funct. Neurosurg.* **54/55,** 114–124.

Ilinsky, I.A., and Kultas-Ilinsky, K. (1987). Sagittal cytoarchitectonic maps of the *Macaca mulatta* thalamus with a revised nomenclature of motor-related nuclei validated by observations on their connectivity. *J. Comp. Neurol.* **262,** 331–364.

Ilinsky, I.A., and Kultas-Ilinsky, K. (1990). Fine structure of the magnocellular subdivision of the ventral anterior thalamic nucleus (VAmc) of *Macaca mulatta*. I. Cell types and synaptology. *J. Comp. Neurol.* **294,** 455–478.

Ilinsky, I.A., and Kultas-Ilinsky, K. (1997). The mode of termination of pallidal afferent to the thalamus: A light and electron microscopic study with anterograde tracers and immunocytochemistry in *Macaca mulatta*. *J. Comp. Neurol.* **386,** 601–612.

Ilinsky, I.A., and Kultas-Ilinsky, K. (2001). Neuroanatomical organization and connections of the motor thalamus of primates. *In* "Basal Ganglia and Thalamus in Health and Movement Disorders" (I.A. Ilinsky and K. Kultas-Ilinsky, eds.), pp. 77–91. Plenum.

Ilinsky, I.A., Ambaderkar, A.V., and Kultas-Ilinsky, K. (1999). Organization of the projections from the anterior pole of the nucleus reticularis thalami (NRT) to subbdivisions of the motor thalamus: Light and electron microscopic studies in the rhesus monkey. *J. Comp. Neurol.* **409,** 369–384.

Ilinsky, I.A., Jouandet, M.L., and Goldman-Rakic, P.S. (1985). Organisation of the nigrothalamocortical system in the rhesus monkey. *J. Comp. Neurol.* **263,** 315–330.

Ilinsky, I.A., Toga, A.W., and Kultas-Ilinsky, K. (1982). Anatomical organisation of internal neuronal circuits in the motor thalamus. *In* "Thalamic Networks for Relay and Modulation" (D. Minciacchi, M. Molinari, G. Macchi and E.G. Jones, eds.), pp. 155–164. Pergamon Press, New York.

Inase, M., and Tanji, J. (1994). Projections from the globus pallidus to the thalamic areas projecting to the dorsal area 6 of the macaque monkey: A multiple tracing study. *Neurosci. Lett.* **180,** 135–137.

Inase, M., and Tanji, J. (1995). Thalamic distribution of projection neurons to the primary motor cortex relative to afferent terminal fields from the globus pallidus in the macaque monkey. *J. Comp. Neurol.* **353,** 415–426.

Itaya, S.K., and and Van Hoesen, G.W. (1983). Retinal projections to the inferior and medial pulvinar nuclei in the old-world monkey. *Brain Res.* **269**, 223–230.

Jasper H.H., and Bertrand, G. (1966). Thalamic units involved in somatic sensation and voluntary and involuntary movements in man. *In* "The Thalamus" (D.P. Purpura and M.D. Yahr, eds.), pp. 365–390. Columbia Univ Press, New York.

Jinnai, K., and Matsuda, Y. (1981). Thalamocaudate projection neurons with a branching axon to the cerebral cortex. *Neurosci. Lett.* **26,** 95–100.

Jinnai, K., Nambu, A., Tanibuchi, I., and Yoshida, S.-I. (1993). Cerebello- and pallidothalamic pathways to areas 6 and 4 in the monkey. *Stereotac. Funct. Neurosurg.* **60,** 70–79.

Jinnai, K., Nambu, A., and Yoshida, S.-I. (1989). Activity of thalamic neurons conveying the basal ganglia output to the motor cortex.

In "Neural Programming. 12th Tanaguchi Symposia on Brain Science" (M. Ito, ed.), pp. 111–121. Karger, Basel.

Joffroy, A.J., and Lamarre, Y. (1974). Single cell activity in the ventral lateral thalamus of the unanesthetized monkey, *Exp. Neurol.* **42,** 1–16.

Jones, E.G. (1983a). Lack of collateral thalamocortical projections to fields of the first somatic sensory cortex in monkeys. *Exp. Brain Res.* **52,** 375–384.

Jones, E.G. (1983). The nature of the afferent pathways conveying short-latency inputs to primate motor cortex. *In* "Motor Control Mechanisms in Health and Disease" (J.E. Desmedt, ed.), pp. 263–285. Raven Press, New York.

Jones, E.G. (1985). The *Thalamus*. Plenum Press, New York.

Jones, E.G. (1987). Ascending inputs to, and internal organization of, cortical motor areas. *In* "Motor Areas of the Cerebral Cortex," pp. 21–35. Wiley, Chichester.

Jones, E.G. (1990). Correlation and revised nomenclature of ventral nuclei in the thalamus of human and monkey. *Stereotact. Funct. Neurosurg.* **54/55,** 1–20.

Jones, E.G. (1997). A description of the human thalamus. *In* "The Thalamus" (E.G. Jones and D.A. Mc Cormick, eds.), Vol. II, Chap. 9. pp. 425–499. Elsevier, Amsterdam

Jones, E.G. (1998), View point: The core and matrix of thalmic organization. *Neurosci.* **85,** 331–345.

Jones, E.G., and Burton, H. (1976). Areal differences in the laminar distribution of thalamic afferents in cortical fields of the insular, parietal and temporal regions of primates. *J. Comp. Neurol.* **168,** 197–248.

Jones, E.G., and Friedman, D.P. (1982). Projection pattern of functional components of thalamic ventrobasal complex on monkey somatosensory cortex. *J. Neurophysiol.* **48,** 521–544.

Jones, E.G., and Hendry, S.H.C. (1989). Differential calcium binding protein immunoreactivity distinguishes classes of relay neurons in monkey thalamic nuclei. *Eur. J. Neurosci.* **1,** 222–246.

Jones, E.G., and and Leavitt, R.Y. (1974). Retrograde axonal transport and the demonstration of non-specific projections to the cerebral cortex and striatum from thalamic intralaminar nuclei in the rat, cat and monkey. *J. Comp. Neurol.* **154,** 349–378.

Jones , E.G., and Porter, R. (1980). What is area 3a? *Brain Res. Rev.* **203,** 1–43.

Jones, E.G., and Powell, T.P.S. (1970). Connexions of the somatic sensory cortex of the rhesus monkey. III. Thalamic connexions. *Brain* **93,** 37–56.

Jones, E.G., Friedman, D.P., and Hendry, S.H.C. (1982). Thalamic basis of place- and modality-specific columns in monkey somatosensory cortex: A correlative anatomical and physiological study. *J. Neurophysiol.* **48,** 545–568.

Jones, E.G., Schwark, H.D., and Callahan, P.A. (1986). Extent of the ipsilateral representation in the ventral posterior medial nucleus of the monkey thalamus. *Exp. Brain Res.* **63,** 310–320.

Jones, E.G., Wise, S.P., and Coulter, J.D. (1979). Differential thalamic relationships of sensory-motor and parietal cortical fields in monkeys. *J. Comp. Neurol.* **183,** 833–882.

Kaas, J.H. (1988). How the somatosensory thalamus is subdivided and interconnected with areas of somatosensory cortex in monkeys. *In* "Cellular Thalamic Mechanisms" (M. Bentivoglio and R. Spreafico, eds.), pp. 143–150. Excerpta Medica, Amsterdam.

Kaas, J.H., Nelson, R.J., Sur, M., Dykes, R.W., and Merzenich, M.M. (1984). The somatotopic organization of the ventroposterior thalamus of the squirrel monkey, *Saimiri sciureus. J. Comp. Neurol.* **226,** 111–140.

Kalil, K. (1981). Projections of the cerebellar and dorsal column nuclei upon the thalamus of the rhesus monkey. *J. Comp. Neurol.* **195,** 25–50.

Kasdon, D.L., and Jacobson, S. (1978). The thalamic aferents to the inferior parietal lobule of the rhesus monkey. *J. Comp. Neurol.* **177,** 685–706.

Kayahara, T., and Nakano, K. (1996). Pallido-thalamo-motor cortical connections: An electron microscopic study in the macaque monkey. **706,** 337–342.

Kievit, J. (1979). "Cerebello-thalamishe projecties en de afferente verbindingen naar de frontalshors in de rhesusaap." Bronder-offset, Rotterdam.

Kievit, J., and Kuypers, H.G.J.M. (1972). Fastigial cerebellar projections to the ventrolateral nucleus of the thalamus and the organization of the descending pathways. *In* "Corticothalamic Projections and Sensorimotor Areas" (T. Frigyesi, E. Rinyik, and M.D. Yahr, eds.), pp.91–111. Raven, New York.

Kievit, J., and Kuypers, H.G.J.M. (1975). Subcortical afferents to the frontal lobe in the rhesus monkey studied by means of retrograde horseradish peroxidase transport. *Brain Res.* **85,** 261–266.

Kievit, J., and Kuypers, H.G.J.M. (1977). Organization of the thalamo-cortical connections to the frontal lobe in the Rhesus monkey. *Exp. Brain Res.* **29,** 299–322.

Kim, R., Nakano, K., Jayaraman, A., and Carpenter, M.B. (1976). Projections of the globus pallidus and adjacent structures: An autoradiographic study in the monkey. *J. Comp. Neurol.* **169,** 263–290.

Klinger, J., and Gloor, P. (1960). The connections of the amygdala and of the anterior temporal cortex in the human brain. *J. comp. Neurol.* **115,** 333–369.

Kölliker, A. (1895, 1898). *Handbuch der Gewebelehre des Menschen und der Thiere.* Engelman, Leipzig.

Kornyey, S. (1926). Zur faseranatomie des striatum, der Zwischen- and Mittel-hirns auf grund der markreifung im der ersten drei Lebensmonaten. *Ztschr. Anat. Entwick.* **81,** 620–632.

Kosmal, A., Malinowska, M., and Kowalska, D.M. (1997). Thalamic and amygdaloid connections of the auditory cortex of the superior tem.poral gyrus in the rhesus monkey (*Macaca mulatta*). *Acta Neurobiol. Exp.* **57,** 165–188.

Kotter, R., and Meyer, N. (1992). The limbic system: A review of its empirical foundation. *Behav. Brain Res.* **52,** 105–127.

Koyoma, N., Nishikawa, Y., and Yokota, T. (1998). Distribution of nociceptive neurons in the ventrobasal complex of macaque thalamus. *Neurosci. Res.* **31,** 39–51.

Krieg, W.J.S. (1963). *Connections of the Ccerebral Cortex*. Brain Books, Evanston, IL.

Krubitzer, L.A., and Kaas, J.H. (1992). The somatosensory thalamus of monkeys: Cortical connections and a redefinition of nuclei in marmosets. *J. Comp. Neurol.* **319,** 123–140.

Kuhlenbeck, H. (1948). The derivatives of the thalamus ventralis in the human brain and their relation to the so-called subthalamus. *Milit. Surg.* **102,** 433–447.

Kuhlenbeck, H. (1951). The derivatives of the thalamus dorsalis and epithalamus in the human brain: Their relation to cortical and other centers. *Milit. Surg.* **108,** 205–256.

Kuhlenbeck, H. (1954). The human diencephalon. A summary of development structure, function and pathology. *Conf. Neurol. Suppl.* **14,** 1–230.

Kultas-Ilinsky, K., and Ilinsky, I.A. (1990). Fine structure of the magnocellular subdivision of the ventral anterior thalamic nucleus (VAmc) of *Macaca mulatta*. II. Organisation of nigrothalamic afferents as revealed with EM autoradiography. *J. Comp. Neurol.* **294,** 479–489.

Kultas-Ilinsky, K., and Ilinsky, I.A (1991). Fine structure of the ventral lateral nucleus (VL) of the *Macaca mulatta* thalamus: Cell types and synaptology. *J. Comp. Neurol.* **314,** 319–349.

Kultas-Ilinsky, K., and Ilinsky, I.A (2001). Neurotransmittors and receptors in thee primate motor thalamus and potential for plasticity. *In* "Basal Ganglia and Thalamus in Health and Movement Disorders" (I.A. Ilinsky, and K. Kultas-Ilinsky, eds.), pp. 215–224. Plenum.

Kultas-Ilinsky, K., Reising, L., Yi, H., and Ilinsky, I.A. (1997). Pallidal afferent territory of the *Macaca mulatta* thalamus: Neuronal and synaptic organization of the VAdc. *J. Comp. Neurol.* **386,** 573–600.

Kultas-Ilinsky, K., Warton, S., Tolbert, D.L., and Ilinsky, I.A. (1980). Quantitative and qualitative characteristics of dentate and fastigial afferents identified by electron microscopic autoradiography in the cat thalamus. *Brain Res.* **201,** 220–226.

Künzle, K. (1976). Thalamic projections from the precentral motor cortex in *Macaca fascicularis*. *Brain Res.* **105,** 253–268.

Künzle, K. (1977). Projections from the primary somatosenbsory cortex to basal ganglia and thalamus in the monkey. *Exp. Brain Res.* **30,** 481–493.

Künzle, K. (1978). An autoradiographic analysis of the efferent connections from premotor and adjacent prefrontal regions (areas 6 and 9) in *Macaca fascicularis*. *Brain Behav. Evol.* **15,** 185–234.

Künzle, K., and Akert, K. (1977). Efferent connections of cortical area 8 (frontal eye field) in *Macaca fascicularis*. A reinvestigation using the autoradiographic technique. *J. Comp. Neurol.* **173,** 147–164.

Kuo, J.-S., and Carpenter, M.B. (1973). Organization of the pallidothalamic projections in the rhesus monkey. *J. Comp. Neurol.* **151,** 201–236.

Kurata, K. (1994). Site of origin of projections from the thalamus to dorsal versus ventral aspects of the premotor cortex of monkeys. *Neurosci. Res.* **21,** 71–76.

Kusama, T., and Mabuchi, M. (1970). Stereotaxic Atlas of the Brain of Macaca fuscata. Univ. Tokyo Press, Tokyo.

Kusama, T., Mabuchi, M., and Sumino, T. (1971). Cerebellar projections to the thalamic nuclei in monkeys. *Proc. Japan Acad.* **47,** 505–510.

Labos, E., Pasik, P., Hamori, J., and Nogradi, E. (1990). On the dynamics of triadic synaptic arrangements: Computer experiments with formal neural nets of chaotic units. *J. Hirnforsch.* **31,** 715–722.

Lamarre, Y., and Joffroy, A.J. (1979). Experimental tremor in monkey: Activity of thalamic and precentral cortical neurons in the absence of peripheral feedback. *Adv. Neurol.* **24,** 109–122.

Lange, W., Büttner-Ennever, J.A., and Büttner, U. (1979). Vestibular projections to the monkey thalamus: An autoradiographic study. *Brain Res.* **177,** 3–18.

Laplane, D., Talairach, J. , Meininger, V., Bancaud, J., and Orgogozo, J.M. (1977). Clinical consequences of corticectomies involving the supplementary motor area in man. *J. Neurol. Sci.* **34,** 301–314.

Larson, S.J., Sances, A., and Wetzel, N (1982). Cerebello-pallidothalamic connections in man. *Appl. Physiol.* **45,** 549–562.

Lavoie, B., and Parent, A. (1994). Pedunculopontine nucleus in the squirrel monkey: Distribution of cholinergic and monoaminergic neurons in the mesopontine tegmentum with evidence of the presence of glutamate in cholinergic neurons. *J. Comp. Neurol.* **344,** 190–209.

Le Gros Clark, W.E.L. (1932). The structure and function of the thalamus. *Brain* **35,** 406–470.

Le Gros Clark, W.E.L. (1936). The termination of the ascending tracts in the thalamus of the macaque monkey. *J. Anat.* **81,** 7–40.

Le Gros Clark, W.E.L., and Boggon, R.H. (1935). Thalamic connexions of parietal and frontal lobes of the brain in the monkey, Phil. *Trans. Roy. Soc. B* **224,** 313–359.

Le Gros Clark, W.E.L., and Northfield, D.W.C. (1937). The cortical projection of the pulvinar in the macaque monkey. *Brain* **60,** 126–142.

Le Gros Clark, W.E.L., and Russel, W.R. (1939). Observation on the efferent connexions of the centre median nucleus. *J. Anat. (Lond)* **73,** 255–262.

Leichnetz, G.R. (1986). Afferent and efferent connections of the dorsolateral precentral gyrus (area 4, hand/arm region) in the macaque monkey, with comparisons to area 8. *J. Comp. Neurol.* **254,** 460–492.

Lenz, F.A. (1995). The region postero-inferior to the human thalamic principal sensory nucleus (Vc) may contribute to the affective dimension of pain through thalamocorticolimbic connections. *In* "Forebrain Areas Involved in Pain Processing" (J-M. Besson, G.H. Guilbaud, and H. Hollat, eds.), pp. 119–130. Libbey.

Lenz, F.A., Dostrowski, J.O., Tasker, R.R., Yamashiro, K., Kwan, H.C., and Murphy, J.T. (0000). Single-unit analysis of the human ventral thalamic nuclear group: Somatosensory responses. *J. Neurophysiol.* **59,** 299–316.

Lenz, F.A., Kwan, H.C., Dostrowski, J.O., Tasker, R.R., Murphy, J.T., and Lenz, Y.E. (1988). Single unit analysis of the human ventral thalamic nuclear group. Activity related to movement. *Brain* **113,** 1795–1821.

Lenz, F.A., Kwan, H.C., Martin, R.L., Tasker, R.R., Dostrowski, J.O., and Lenz, Y.E. (1994). Single unit analysis of the human ventral thalamic group. Tremor-related activity in functionally identified cells. *Brain* **117,** 531–543.

Lenz, F.A., Seike, M., Lin, Y.C., Baker, F.H., Rowland, L.H., Gracely, R.H., and Richardson, R.T. (1993). Neurons in the area of human thalamic neurons ventralis caudalis respond to painful heat stimuli. *Brain Res.* **623,** 135–240.

Lenz, F.A., Tasker, R.R., Kwan, H.C., Schnider, S., Kwong, R., Murayama, Y., Dostrowski, J.O., and Murphy, J.T. (1988). Single analysis of the human ventral thalamic nuclear group: Correlation of thalamic "tremor cells" with the 3–6 Hz component of Parkinsonian tremor, *J. Neurosci.* **8,** 754–764.

Leonard, C.M. (1972). The connections of the dorsomedial nuclei. *Brain Behav. Evol. 6,* 524–541.

Letinik, K., and Rakic, P. (2001). Telencephalic origin of human thalamic GABAergic neurons. *Nature Neurosci.* **4,** 931–936.

Lewandowsky, M. (1904). Untersuchungen uber die Leitungsbahnen des Truncus cerebri und ihren Zusammenhang mit der medulla spinalis und der cortex cerebri. *Neurobiologische Arbeiten.* Jena. (Quoted by Friedemann, 1911.)

Lin, C.S., and Kaas, J.H. (1979). The inferior pulvinar complex in owl monkeys : Architectonic subdivisions and patterns of input from the superior colliculus and subdivisions of visual cortex. *J. Comp. Neurol.* **187,** 655–678.

Locke, S., Angevine, J.B., and Yakovlev, P.I. (1961). Limbic nuclei of thalamus and connections of limbic cortex. II- Thalamo-cortical projections in the lateral dorsal nucleus in man. *Arch. Neurol.* **4,** 355–364.

Locke, S., Angevine, J.B., and Yakovlev, P.I. (1964). Limbic nuclei of thalamus and connections of limbic cortex. *Arch. Neurol.* **11,** 1–12.

Locke, S., Angevine, J.B., and Yakovlev, P.I. (1964). Thalamocortical projection of the lateral dorsal nucleus in cat and monkey. *Arch. Neurol.* **11,** 1–12.

Locke, S., and Kerr, C. (1974). The projection of nucleus lateralis dorsalis of monkey to basomedial temporal cortex. *J. Comp. Neurol.* **149,** 29–42.

Loe, P.R., Whitsel, B.L., Dreyer, D.A., and Metz, C.B. (1977). Body representation in ventrobasal thalamus of macaque: A single-unit analysis. *J. Neurophysiol.* **40,** 1339–1355.

Lorente de No, R. (1938). Cerebral cortex: Architecture, intracortical connections, motor projections. *In* "Physiology of the Nervous System" (J.F. Fulton, ed.), pp. 288–330. Oxford Univ. Press, New York.

Lu, M-T, Preston, J.B., and Strick, P.L. (1994). Interconnections between the prefrontal cortex and the premotor areas in the frontal cortex. *J. Comp. Neurol.* **341,** 375–392.

Luys, J-B. (1865). "Recherches sur systeme nerveux cerebrospinal." Baillère. Paris.

Lynch, J.C., Hoover, J.E., and Strick, P.L. (1994). Input to the primate frontal eye field from the substantia nigra, superior colliculus, and dentate nucleus demonstrated by transneuronal transport. *Exp. Brain Res.* **100,** 181–186.

Lysakowski, A., Standage, G.P., and Benevento, L.A. (1986). Histochemical and architectonic differentiation of zones of pretectal and collicular inputs to the pulvinar and dorsal lateral geniculate nuclei in the macaque. *J. Comp. Neurol.* **250,** 431–448.

Macchi, G., and Bentivoglio, M. (1985). The thalamic intralaminar nuclei and the cerebral cortex. In "Cerebral Cortex" (E.G. Jones, and A. Peters, eds.), Vol. 5, pp. 355–401. Plenum, New York.

Macchi, G., and Jones, E.G. (1997). Towards an agreement on terminology of nuclear and subnuclear subdivisions of the motor thalamus. *J. Neurosurg.* **86,** 77–92.

MacFarland, N.R., and Haber, S. (2000). Convergent inpus from thalamic motor nuclei and frontal cortical areas to the dorsal striatum in the primate. *J. Neurosci.* **20,** 3798–3813.

MacLardy, T. (1963). Thalamic microneurons. *Nature* **199,** 820–821.

MacLean, P.D. (1949). Culminating Development in the evolution of the limbic system: The thalamocingulate division. *In* "The Limbic System" (B.K. Doane and K.F. Livingstone, eds.), pp. 1–29. Raven, New York.

MacLean, P.D. (1970). The triune brain, emotion ans scientific bias. *In* "The Neurosciences 2d Study Program" (F.O. Schmitt, ed.), pp. 336–348. Rockefeller Univ. Press.

Macpherson, J.M., Rasmusson, D.D., and Murphy, J.T. (1980). Activities of neurons in "motor" thalamus during control of limb movement in the primate. *J. Neurophysiol.* **44,** 1128–0000.

Maddock, R.J. (1999). The retrosplenial cortex and emotion: New insight from functional neuroimaging of the human brain. *Trends Neurosci.* **22,** 310–316.

Maeda, T. (1989). Lateral coordinates of nucleus ventralis intermedius target for tremor alleviation. *Stereotac. Funct. Neurosurg.* **52,** 191–199.

Maendly, R., Rüegg, D.G., Wiesendanger, M., Wiesendanger, R., Lagowska, J., and Hes, B. (1981). Thalamic relay for group I muscle afferents of forelimb nerves in the monkey. *J. Neurophysiol.* **46,** 901–917.

Mai, J.K., Assheuer, J., and Paxinos, G. (1997). "Atlas of the Human Brain." Academic Press. San Diego

Majorossy, K., Rethelyi, M., and Szentagothai, J. (1965). The large glomerular synapses of the pulvinar. *J. Hirnforsch.* **7,** 415–432.

Malis, L.I, Pribram, K.H., and Kruger, L. (1953). Action potentials in "motor" cortex evoked by peripheral nerve stimulation. *J. Neurophysiol.* **16,** 161–167.

Malone, E. (1910). Uber die Kerne des menschlichen diencephalon. *Preuss. Akad.Wiss. Phys.-math.* 1–32.

Mannen, H. (1960). "Noyau fermé" et "noyau ouvert". Contribution à l'étude cytoarchitectonique du tronc cérébral envisagé du point de vue de l'arborisation dendritique. *Arch. Ital. Biol.* **98,** 330–350.

Mantyh, P.W. (1983). The spinothalmic tract in the primate: a re-examination using wheatgerm agglutinin conjugated to horseradish peroxidase. *Neurosci.* **9,** 847–862.

Manzoni, T., Conti, F., and Fabri, M. (1986). Callosal projections rom area SII to SI in monkeys: Anatomical organization and comparison with association projections. *J. Comp. Neurol.* **252,** 245–263.

Marsden, C.D., and Obeso, J.A. (1994). The functions of the basal ganglia and the paradox of stereotaxic surgery in Parkinson's disease. *Brain* **117,** 877–897.

Martin, J.J. (1970). Contribution à l'étude de l'anatomie du thalamus et de sa pathologie au cours des maladies dégénératives dites abiotrophiques. Pub. Act. Med. Belg. Bruxelles.

Matelli, M., and Luppino, G. (1993). Cortical projections of motor thalamus. *In* "Thalamic Networks for Relay and Modulation" (D. Minciacchi, M. Molinari, G. Macchi and E.G. Jones, eds.), pp. 165–174. Pergamon Press, Oxford.

Matelli, M., Camarda, R., Glickstein, M., and Rizzolatti, G. (1986). Afferent and efferent projections of the inferior area 6 in the macaque monkey. *J. Comp. Neurol.* **251,** 281–298.

Matelli, M., Luppino, G., Fogassi, L., and Rizzolati, G. (1989). Thalamic input to inferior area 6 and area 4 in the macaque monkey. *J. Comp. Neurol.* **280,** 468–488.

Mathers, L.H. (1971). Tectal projection to the posterior thalamus of the squirrel monkey. *Brain Res.* **35,** 295–298.

Mathers, L.H. (1972a). Ultrastructure of the pulvinar of the squirrel monkey. *J. Comp. Neurol.* **146,** 15–42.

Mathers, L.H.(1972b). The synaptic organization of the cortical projection of the pulvinar of the squirrel monkey. *J. Comp. Neurol.* **146,** 43–60.

Matuzaka, Y., Aizawa, H., and Tanji, J. (1992). A motor area rostral to the supplementary motor area (presupplementary motor area) in the monkey: Neuronal activity during a learned motor task. *J. Neurophysiol.* **68,** 653–662.

Mehler, W.R. (1962). The anatomy of the so-called « pain tract » in main: An analysis of the course and distribution of the ascending fiberds of the fasciculus anterolateralis. *In* "Basic Research in Paraplegia" (J.D. French and R.W. Porter, eds.), pp. 26–55. Thomas, Springfield.

Mehler, W.R. (1966a). Further note on the center median nucleus of Luys. *In* "The Thalamus" (D.P. Purpura and M.D. Yahr, eds.), pp. 109–122. Columbia University Press, New York.

Mehler, W.R. (1966b). The posterior thalamic region in man. *Conf. Neurol.* **27,** 18–29.

Mehler, W.R. (1969). Some neurological species differences, a posteriori. *Ann. N.Y. Acad. Sci.* **167,** 424–468.

Mehler, W.R. (1971). Idea of a new anatomy of the thalamus. *J. Psychiat. Res.* **8,** 203–217.

Mehler, W.R. (1974). Central pain and spinothalmic tract. *Adv. Neurol.* **4,** 127–146.

Mehler, W.R. (1980). Subcortical afferent connections of the amygdala in the monkey, *J. Comp. Neurol.* **190,** 733–762.

Mehler, W.R., and Nauta, W.J.H. (1974). Connections of the basal ganglia and of cerebellum. *Confin. Neurol.* **36,** 205–222.

Mehler, W.R., Feferman, M.E., and Nauta, W.F.H. (1960). Ascending axon degeneration following anterolateral cordotomy. An experimental study in the monkey, *Brain* **83,** 718–750.

Mesulam, M-M., and Pandya, D.N. (1973). The projection of the medial complex within the sylvian fissure of the Rhesus monkey. *Brain Res.* **60,** 315–333.

Mesulam, M-M., Geula, C., Bothwell, M.A., and Hersh, L.B. (1989). Human reticular formation: Cholinergic neurons of the pedunculopontine and laterodorsal tegmental nuclei and some cytochemical comparison to forebrain cholinergic neurons. *J. Comp. Neurol.* **22,** 611–623.

Mettler, F. A. (1947). Extracortical connections of the primate frontal cerebral cortex. I. Thalamo-cortical connections. *J. Comp. Neurol.* **86,** 95–118.

Meyer, A., Beck, E., and McLardy, T. (1947). Prefrontal leucotomy: A neuroanatomical report. *Brain* **70,** 18–49.

Meynert, T. (1872). "Vom Gehirn der Saugetiere." Engelman, Leipzig.

Miall, R.C., Price, S., Mason, R., Passingham, R.E., Winter, J.L., and Stein, J.F. (1998). Microstimulation of movements from cerebellar-receiving but not pallidal-receiving areas of the macaque thalamus under ketamine anaesthesia. *Exp. Brain Res.* **123,** 387–396.

Middleton, F.A., and Strick, P.L. (1994). Anatomical evidence for cerebellar and basal ganglia involvement in higher cognitive function. *Science* **266,** 458–461.

Middleton, F.A., and Strick, P.L. (1996). Basal ganglia and cerebellar output influences non-motor function. *Mol. Psychiat.* **1,** 429–433.

Middleton, F.A., and Strick, P.L. (2000). Basal ganglia and cerebellar loops: Motor and cognitive circuits. *Brain Res. Rev.* **31,** 236–250.

Mikol, J., and Brion, S. (1975). Connexions du noyau latero-dorsal du thalamus et du circuit limbique chez l'homme. *Rev. Neurol.* **131,** 469–490.

Mikol, J., Brion, S., Derome, P., de Pomery, J., and Galissot, M.C. (1977). Connections of laterodorsal nucleus of the thalamus. II. Experimental study in Papio papio. *Brain Res.* **138,** 1–16.

Mikol, J., Menini, M., Brion, S., and Guicharnaud, L. (1984). Connexions du noyau latero-dorsal du thalamus chez le singe. Etudes des efferences. *Rev. Neurol.* **140,** 615–624.

Miyata, M., and Sasaki, K. (1983). HRP studies on thalamocortical neurons related to the cerebellocerebral projection in the monkey. *Brain Res.* **274,** 213–224.

Miyata, M., and Sasaki, K. (1984). Horseradish peroxidase studies on thalamic and striatal connections of the mesial part of area 6 in the monkey. *Neurosci. Lett.* **49,** 127–133.

Molinari, M., Dell'Anna, M.E., Raussel, E., Leggio, M.G., Hashiwaka, T., and Jones, E.G. (1995). Auditory thalamo-cortical pathways defined in monkey by calcium binding protein immunoreactivity. *J. Comp. Neurol.* **362,** 171–194.

Molinari, M., Hendry, S.H.C., and Jones, E.G. (1987). Distribution of certain neuropeptides in the primate thalamus. *Brain Res.* **426,** 270–289.

Morel, A., Magnin, M., and Jeanmonod, D. (1997). Multiarchitectonic and stereotactic atlas of the human thalamus. *J. Comp. Neurol.* **387,** 588–630.

Mountcastle, V.B., and Henneman, E. (1952). The representation of tactile sensibility in the thalamus of monkey. *J. Comp. Neurol.* **97,** 409–431.

Muakkassa, K.F., and Strick, P. L. (1979). Frontal lobe inputs to primate motor cortex: Evidence for four somatotopically organized premotor areas. *Brain Res.* **177,** 176–182.

Mufson, E.J., and Mesulam, M-M. (1984). Thalamic connections of the insula in the rhesus monkey and comments on paralimbic connectivity in the medial pulvinar of the thalamus. *J. Comp. Neurol.* **227,** 109–120.

Mufson, E.J., and Pandya, D.N. (1984). Some observations on the course and composition of the cingulum bundle in the rhesus monkey. *J. Comp. Neurol.* **225,** 31–43.

Münzle, M.C., Walvogel, H.J., and Faull, R.L. (1999). Calcium-binding immunoreactivity delineates the intralaminar nuclei in the human thalamus. *Neurosci.* **90,** 485–491.

Münzle, M.C., Walvogel, H.J., and Faull, R.L. (2000). The distribution of calbindin, calretinin, and parvalbumin immunoreactivity in the human thalamus. *J. Chem. Neuroanat.* **19,** 155–173.

Mussen, A.T. (1923). A cytoarchitectural atlas of the brain stem of the Macacus rhesus. *J. Psychol. Neurol. (Lpz)* **29,** 451–518.

Nakano, K., Hasegawa, Y., Kayahara, T., Tokushige, A., and Kuga, Y. (1993). Cortical connections of the motor thalamic nuclei in the Japanese monkey Macaca fuscata. *Stereotact. Funct. Neurosurg.* **60,** 42–61.

Nakano, K., Hasegawa, Y., Tokushige, A., Nakagawa, S., Kayahara, T., and Mizuno, N. (1990). Topographical projections from the thalamus, subthalamic nucleus and pedunculopontine tegmental nucleus to the striatum in the Japanese monkey, Macaca fuscata. *Brain Res.* **537,** 54–68.

Nakano, K., Kayahara, T., Yasui, Y., and Kubawara, H. (1992). Thalamic region projecting to area 3a: An autoradiographic study in the monkey. *Neurosci.* **18,** 89–100.

Nakano, K., Tokushige, A., Kohno, M., Hasegawa, Y., Kayahara, T., and Sasaki, K. (1992). An autoradiographic study of cortical projections from the motor thalamic nuclei in the macaque monkey. *Neurosci. Res.* **13,** 119–137.

Nambu, A., Yoshida, S., and Jinnai, K. (1988). Projection on the motor cortex of thalamic neurons with pallidal input in the monkey. *Exp. Brain Res.* **71,** 658–662.

Nambu, A., Yoshida, S., and Jinnai, K. (1991). Movement-related activity of thalamic neurons with input from the globus pallidus and projection to the motor cortex in the monkey, *Exp. Brain Res.* **84,** 279–284.

Narabayashi, H., and Ohye, C. (1983). Pathological tremor: its generating mechanism and treatment. *In* "Current Concepts of Parkinson Disease and Related Disorders" (M.D. Yahr, ed.), pp. 47–55. Excerpta Medica.

Nauta, W.J.H. (1961). Fibre degeneration following lesions of the amygdaloid complex in the monkey. *J. Anat. (Lond.)* **95,** 515–531.

Nauta, W.J.H. (1962). Neural associations of the amygdaloid complex in the monkey. *Brain* **85,** 505–520.

Nauta, W.J.H. (1964). Some efferent connections of the prefrontal cortex in the monkey. *In* "The Frontal Granular Cortex and Behavior" (J.M. Warren and K. Akert, eds.), pp. 397–407. McGraw-Hill.

Nauta, W.J.H., and Mehler, W.R. (1966). Projections of the lentiform nucleus in the monkey, *Brain Res.* **1,** 3–42.

Nelson, M.E., and Bower, J.M. (1990). Brain maps and parallel computers. *Trends Neurosci.* **13,** 403–408.

Niemann, K., Naujokat, C., Pohl, G., Wolner, C., and Keyserligk, D.V. (1994). Verification of the Shaltenbrandt and Wahren stereotactic atlas. *Acta Neurochir.* **129,** 72–81.

Niimi, K. (1961). Anatomy of the human thalamus. *Brain and Nerve* **13,** 307–325.

Niimi, K., and Tsutsui, M. (1962). A contribution to the knowledge of the cortical connections of the anterior thalamic nuclei in the monkey. *Tokushima J. Exp. Med.* **9,**1–7.

Niimi, K., Katayama, K., Kanaseki, T., and Morimoto, K. (1960). Studies on the derivation of the centre median nucleus of Luys. *Tokushima J. Exp. Med.* **2,** 261–268.

Nissl, F. (1889). "Die Kerne des Thalamus beim Kanishens." D. Nat. Aert, Heidelberg.

Ogren, M.P., and Hendrickson, A.E. (1979). The structural organization of the inferior and lateral subdivisions of the Macaca monkey pulvinar. *J. Comp. Neurol.* **188,** 147–178.

Ohara, P.T., and Havton, L.A. (1994). Preserved features of thalamocortical projection neuron dendritic architecture in somatosensory thalamus of the rat, cat and macaque. *Brain Res.* **648,** 259–264.

Ohye, C. (1978). Anatomy and physiology of the thalamic nucleus ventralis intermedius. *In* "Integrative Control Functions of the Brain" (M. Ito, ed.), pp. 152–163. Kodansha, Tokyo.

Ohye, C. (1982). Depth microelectrode studies. *In* "Stereotaxy of the Human Brain" (G. Schaltenbrand and A.E. Walkerm, eds.), pp. 372–389. Thieme, Stuttgart.

Ohye, C. (1990). Thalamus. *In* "The Human Nervous System" G. Paxinos, ed.), pp. 439–468. Academic Press, New York.

Ohye, C., and Albe-Fessard, D. (1978). Rythmic discharges related to tremor in humans and monkeys. *In* "Abnormal Neuronal Discharges" (N. Chalazonitis, and M. Boisson, eds.), pp. 37–48. Raven Press, New York.

Ohye, C., and Narabayashi, H. (1979). Physiological study of the presumed ventralis intermedius neurons in the human thalamus. *J. Neurosurg.* **50,** 290–297.

Ohye, C., Fukamashi, A., and Narabayashi, H. (1972). Spontaneous and evoked activity of sensory neurons and their organization in the human thalamus. *Z. Neurol.* **203,** 219–234.

Ohye, C., Kawashima, Y., Hirato, M., and Satake, K. (1990). Lamellar distribution of kinesthetic neurons and its clinical implication. *Funct. Neurosurg.* **29,** 193–199.

Ohye, C., Maeda, T., and Narabayashi, H. (1976/1977). Physiologically defined VIM nucleus. Its special reference to control of tremor. *Appl. Neurophysiol.* **39,** 285–295.

Ohye, C., Shibazaki, T., Hirai, T., Kawashima, Y., Hirato, M., and Matsumara, M. (1993). Tremor-mediating thalamic zone studied in humans and in monkeys. *Stereotact. Funct. Neurosurg.* **60,** 136–145.

Ohye, C., Shibazaki, T., Hirai, T., Wada, H., Hirato, M., and Kawashima, Y. (1989). Further physiological observations on the ventralis intermedius neurons in the human thalamus. *J. Neurophysiol.* **61,** 488–500.

Ojeman, G.A., Fedio, P., and VanBuren, J.M. (0000). Anomia from pulvinar and subcortical parietal stimulation. **401,** 99–117.

Oke, A.F., Carver, L.A., Gouvion, C.M., and Adams, R.N. (1997). Three-dimensional mapping of norepinephrine and serotonin in human thalamus. *Brain Res.* **763,** 69–78.

Olivier, A., Parent, A., and Poirier, L. (1970). Identification of the thalamic nuclei on the basis of their cholinesterase content. *J. Anat.* **106,** 37–50.

Olszewski, J. (1952). "The Thalamus of the *Macaca mulatta.* An Atlas for Use with the Stereotaxic Instrument." Karger, Basel.

Orioli, P.J., and Strick, P.L. (1989). Cerebellar connections with the motor cortex and the arcuate premotor area: An analysis employing retrograde transneuronal transport of WGA-HRP. *J. Comp. Neurol.* **288,** 612–626.

Page, R.D., Sambrook, M.A., and Crossman, A.R. (1993). Thalamotomy for the alleviation of Levodopa-induced dyskinesia: Experimental studies in the 1-methyl-1,2,3,6-tetrahydropyridine-treated parkinsonian monkey. *Neurosci.* **55,** 147–165.

Papez, J.W. (1937). A proposed mechanism of emotion. *Arch. Neurol. Psychiat.* **38,** 725–743.

Papez, J.W., Bull, H.G., and Sloter, W.A. (1940). Cortical softening with atrophy of internal capsule and dorsal thalamus. Connections of ventral lateral nucleus of thalamus. *Arch. Neurol. Psych.* **44,** 979–989.

Parent, A., and de Bellefeuille, L. (1983). The pallidointralaminar and pallidonigral projections in primate as studied by retrograde double-labeling method. *Brain Res.* **278,** 11–27.

Parent, A., Mackey, A., and De Bellefeuille, L. (1983). The subcortical afferents to caudate nucleus and putamen in primate: A fluorescence retrograde double labeling study. *Neurosci.* **10,** 1137–1150.

Parent, M., Levesque, M., and Parent, A. (2001). Two types of projection neurons in the internal pallidum of primates: single axon tracing and three-dimensional reconstruction. *J.Comp. Neurol.* **439,** 162–175.

Parent, A., Smith, Y., and De Bellefeuille, L. (1984). The output organization of the pallidum and substantia nigra in primate as revealed by a retrograde double-labeling method. *In* "The Basal Ganglia" (J.S. McKenzie, R.E. Kemm, and L.N. Wilcock, eds.), pp. 147–160. Plenum Press, New York.

Partlow, G.D., Colonnier, M., and Szabo, J. (1977). Thalamic projections of the superior colliculus in the rhesus monkey, Macaca mulatta. A light and electron microscopy. *J. Comp. Neurol.* **171,** 285–318.

Passingham, R.E. (1987). From where does the motor cortex get its instructions? In "Higher Brain Functions" (S.P. Wise, ed.), pp. 67–97. Wiley, Chichester.

Passingham, R.E. (1989). Premotor cortex and the retrieval of movement. *Brain Behav. Evol.* **33,** 189–192.

Paxinos, G., and Watson, C. (1986). "The Rat Brain in Stereotaxic Coordinates." Academic Press, Sydney.

Paxinos, G., Huang, X-F., and Toga, A.W. (2000). The rhesus monkey brain in stereotactic coordinates. Academic Press.

Peacock, J.H., and Combs, C.M. (1965). Retrograde cell degeneration in diencephalic and other structures after hemidecortication of rhesus monkeys. *Exp. Neurol.* **11,** 367–399.

Percheron, G. (1966). Etude anatomique du thalamus de l'homme adulte et de sa vascularisation arterielle. Med. Thesis. Paris.

Percheron, G. (1969). "Présentation d'un modèle de division et d'une nomenclature raisonnée pour le thalamus de l'homme et des autres simioidés," pp. 7–19. C.G.R., Marseille.

Percheron, G. (1975a). Ventricular landmarks for thalamic stereotaxy in *Macaca. J. Med. Primatol.* **4,** 217–244.

Percheron, G. (1975b). The thalamic territory of cerebellar afferents in macaques. *Exp Brain Res. Suppl.* **23,** 160.

Percheron, G. (1976a). Les artères du thalamus humain. I. Artères et territoire thalamiques polaires de l'artère communicante postérieure. *Rev. Neurol.* **133,** 533–545.

Percheron, G. (1976b). Les artères du thalamus humain. II. Artères et territoires thalamiques paramédians de l'artère basilaire communicante. *Rev.* **132,** 309–324.

Percheron, G. (1977a). The thalamic territory of cerebellar afferents and the lateral region of the thalamus of the macaque in stereotactic ventricular coordinates. *J. Hirnforsch.* **18,** 375-400.

Percheron, G. (1977b). Les artères choroïdiennes et les artères thalamiques postérieures. Etude macroscopique des variations individuelles et systématisation. *Rev. Neurol.* **133,** 533–545.

Percheron, G. (1977c). Les artères du thalamus humain. Territoires des artères choroidiennes. III. Absence de territoire thalamique constitué de l'artère choroïdienne antérieure. IV. Artères et territoires thalamiques du système choroidien posteromedian. V. Artères et territoires thalamiques du système choroidien posterolateral. *Rev. Neurol.* **133,** 547–558.

Percheron, G. (1979a). Quantitative analysis of dendritic branching. I. Simple formulae for the quantitative analysis of dendritic branching. *Neurosci. Lett.* **14,** 287–293.

Percheron, G. (1979b). Quantitative analysis of dendritic branching. II. Fundamental dendritic numbers as a tool for the analysis of neuronal groups. *Neurosci. Lett.* **14,** 287–293.

Percheron, G. (1982a). Principles and methods of the graph-theoretical analysis of natural binary arborescences. *J. Theor. Biol.* **99,** 509–552.

Percheron, G. (1982b). Arterial suppy of the thalamus. *In* "Stereotaxy of the Human Brain" (G. Schaltenbrand, and A.E. Walker, eds.), pp. 219–232. Thieme, Stuttgart.

Percheron, G. (1991). The spatial organization of information processing in the striato-pallido-nigral system. *New Issues Neurosci.* **3,** 211–234.

Percheron, G. (1997). A reliable systrem of ventricular coordinates for the cartography and stereotaxy of the amygdala (and anterior hippocampus) in macaques. *J. Neurosci. Meth.* **75,** 5–14.

Percheron, G., Filion, M., Tremblay, L., Fénelon, G., François, C., and Yelnik, J. (1993). The role of the medial pallidum in the pathophysiology of akinesia in primates. *In* "Parkinson's Disease" (H. Narabayashi, T. Nagatsu, N. Yanagisawa, and Y. Mizuno, eds.), pp. 84–87. Raven Press, New York.

Percheron, G., François, C., Parent, A., Sadikot, A.F., Fénelon, G., and Yelnik, J. (1991). The primate central complex as one of the basal ganglia. *In* "The Basal Ganglia III" (G. Bernardi, M.B. Carpenter, G. Di Chiara, M. Morelli, and P. Stanzione, eds.), pp. 177–186. Plenum Press, New York.

Percheron, G., François, C., Talbi, B., Meder, J.-F., Fénelon, G., and Yelnik, J. (1993). The primate motor thalamus analyzed with reference to subcortical afferent territories. *Stereotact. Funct. Neurosurg.* **60,** 32–41.

Percheron, G., François, C., Talbi, B., Meder, J.-F., Yelnik, J., and Fénelon, G. (1996). The primate motor thalamus. *Brain Res. Rev.* **22,** 93–181.

Percheron, G., François, C., and Yelnik, J. (1986a). Instruments and techniques for the stereotactic surgery based on the CA-CP system of coordinates in monkeys. *J. Neurosci. Methods.* **17,** 89–99.

Percheron, G., François, C., and Yelnik, J. (1987). Spatial organization and information processing in the core of the basal ganglia. *In* "The Basal Ganglia II" (M.B. Carpenter and A. Jayaraman, eds.), pp. 205–226. Plenum Press, New York.

Percheron, G., François, C., Yelnik, J., Fénelon, G., and Talbi, B. (1994). The basal ganglia related system of primates: Definition, description and informational analysis. In "The Basal Ganglia IV. New Ideas and Data on Structure and Function" (G. Percheron, J.S.McKenzie, and J. Féger, eds.), pp. 3–20. Plenum Press, New York.

Percheron, G., François, C., Yelnik, J., Talbi, B., Meder, J.F., and Fénelon, G. (1993). The pallidal and nigral thalamic territories and the problem of the anterior part of the lateral region in primates. *In* "Thalamic Networks for Relay and Modulation" (D. Minciacchi, M. Molinari, G. Macchi, and E.G. Jones, eds.), pp. 145–154. Pergamon Press, Oxford.

Percheron, G., Yelnik, J., and François, C. (1986b). Systems of coordinates for stereotactic surgery and cerebral cartography: Advantages of ventricular systems in monkeys. *J. Neurosci. Meth.* **17,** 69–88.

Percheron, G., Yelnik, J., François, C., Fénelon, G., and Talbi, B. (1991). The spatial organisation of information processing in the striato-pallido-nigral system. *In* "Basal Ganglia and Movement Disorders" (A. Bignami, ed.), pp. 211–234. Thieme, Stuttgart.

Peters, A., and Palay, S.L. (1966). The morphology of laminae A and A1 of the dorsal nucleus of the lateral geniculate body of the cat. *J. Anat.* **100,** 451–486.

Poggio, G.F., and Mountcastle, V.B. (1963). The functional properties of ventrobasal thalamic neurons studied in unanesthetized monkeys. *J. Neurophysiol.* **26,** 775–806.

Poirier, L.J., Parent, A., Marchand, R., and Butler, L.L. (1977). Morphological characteristics of the acetylcholinesterase-containing neurons in the CNS of DFP-treated monkeys. Part I Extrapyramidal and related structures. *J. Neurol. Sci.* **31,** 181–198.

Poletti, C., and Creswell, G. (1977). Fornix system efferent projections in the squirrel monkey: An experimental degeneration study. *J. Comp. Neurol.* **175,** 101–127.

Porrino, L.J., Crane, A.M., and Goldman-Rakic, P.S. (1981). Direct and indirect pathways from the amygdala to the frontal lobe in Rhesus monkeys. *J. Comp. Neurol.* **198,** 121–136.

Powell, E.W. (1973). Limbic projections to the thalamus. *Exp. Brain Res.* **17,** 394–401.

Powell, T.P.S. (1952). Residual neurons in the human thalamus following hemidecortication. *Brain* **15,** 571–584.

Powell, T.P.S., and Cowan, W.M. (1967). The interpretation of the degenerative changes in the intralaminar nuclei of the thalamus. *J. Neurol. Neurosurg. Psychiat.* **30,** 140–153.

Prenfield, W., and Milner, B. (1958). Memory deficit produced by bilateral lesion in the hippocampal zone. *Arch. Neurol. Psychiat.* **79,** 475–497.

Preuss, T.M., and Goldman Rakic, P.S. (1987). Myelo- and cytoarchitecture of the granular frontal cortex and surrounding regions in strepsirhine primate Galago and the anthropoid primate macaque. *J. Comp. Neurol.* **310,** 429–474.

Price, J.L., and Amaral, D.G. (1981). An autoradiographic study of the projections of the central nucleus of the monkey amygdala. *J. Neurosci.* **11,** 1242–1259.

Proske, U., Schaible, H.-G., and Schmidt, R.F. (1988). Joint receptors and kinaesthesia. *Exp. Brain Res.* **72,** 219–224.

Puelles, L., and Rubinstein, L.R. (1993). Expression patterns of homeobox and other putative regulatory genes in the embryonic mouse forebrain suggest a neuromeric organization. *Trends Neurosci.* **16,** 472–479.

Rabl, R. (1958). Strukturstudien an der massa intermedia des thalamus opticus. *J. Hirnforsch.* **4,** 78–112.

Raeva, S.N. (1986). Localization in human thalamus of units triggered during "verbal commands" voluntary movements and tremor. *Electroenceph. Clin. Neurophysiol.* **63,** 160–173.

Raeva, S.N. (1990). Unit activity of the human thalamus during voluntery movements. *Stereotact. Funct. Neurosurg.* **54/55,** 154–158.

Ralston, H.J. (2003). Pain, the brain, and the calbindin stain. *J. Comp. Neurol.* **459,** 329–333.

Ralston, H.J., and Ralston, D.D. (1992). The primate dorsal spinothalamic tract: Evidence for a specific termination in the posterior nuclei (Po/SG) of the thalamus, *Pain* **48,** 107–118.

Ralston, H.J., Ohara, P.T., Meng, X.W., and Ralston, D.D. (1995). The organization of the spinothalamic tract circuitry in the macaque and the role of GABA information processing. *In* "Forebrain Areas Involved in Pain Processing" (J.M. Besson, G. Guilbaud, and H. Ollat, eds.), pp. 1–12. Libbey, London.

Ramon-Moliner, E. (1962). An attempt at classifying nerve cells on the basis of their dendritic patterns. *J. Comp. Neurol.* **119,** 211–227.

Ramon-Moliner, E. (1975). Specialized and generalized dendritic patterns. *In* "Golgi Centenial Symosium" (M. Santini, ed.), pp. 87–100. Raven Press, New York.

Rand, R.W. (1954). An anatomical and experimental study of the cerebellar nuclei and their efferent pathways in the monkey. *J. Comp. Neurol.* **101,** 167–224.

Ranson, S.W., and Ranson, M. (1939). Pallidofugal fibers in the monkey. *Arch. Neurol. Psychiat. (Chicago)* **42,** 1059–-1067.

Ranson, S.W., Ranson, S.W., Jr., and Ranson, M. (1941). Fiber connections of the corpus striatum as seen in Marchi preparations. *Arch. Neurol. Psychiat. (Chicago)* **46,** 230–249.

Rausell, E., and Jones, E.G. (1991). Histochemical and immunocytochemical compartments of the thalamic VPM nucleus in monkeys and their relationship to the representational map. *J. Neurosci.* **11,** 210–225.

Rausell, E., and Jones, E.G. (1991). Chemically distinct compartments of the thalamic VPM nucleus in monkeys relay principal and spinal trigeminal pathways to different layers of the somatosensory cortex. *J. Neurosci.* **11,** 226–237.

Rausell, E., Bae, C.S., Vinuela, A., Huntley, G.W., and Jones, E.G. (1992). Calbindin and parvalbumin cells in monkey VPL thalamic nucleus: distribution, laminar cortical projections, and relations to spinothalamic terminations. *J. Neurosci.* **12,** 4088–4111.

Ray, J.P., and Price, J.L. (1993). The organization of projections from the mediodorsal nucleus of the thalamus to orbital and medial prefrontal cortex in macaque monkeys. *J. Comp. Neurol.* **337,** 1–31.

Raz, A., V. Vaadia, E., and Bergman, H. (2000). Firing patterns and correlations of spontaneous discharge of pallidal neurons in the normal—and the tremulous 1-Methyl-4-phenyl-1,2,3,6-tetra-hydropyridine vervet model of Parkinsonism. *J. Neurosci.* **15,** 8559–85571.

Reiner, A., Brauth, S.E., and Karten, H.J. (1984). Evolution of the amniote basal ganglia. *Trends Neurosci.* **7,** 320–325.

Reyes-Vazquez, C., Qiao, J.T., and Dafny, N. (1989). Nociceptive responses in nucleus parafascicularis thalami are modulated by dorsal raphe stimulation and microiontophoretic application of morphin and serotonin. *Brain Res. Bul.* **23,** 405–411.

Riley, H.A. (1960). "An Atlas of the Basal Ganglia, Brain Stem, and Spinal Cord." Hafner, New York.

Rioch, D.M. (1929). Studies on the diencephalon of carnivora. Part I. The nuclear configuration of the thalamus, epithalamus and hypothalamus of the dog and the cat. *J. Comp. Neurol.* **49,** 1–119.

Roberts, T.S., and Akert, K. (1963) Insular and opercular cortex and its thalamic projection in *Macaca mulatta*. *Schweitz. Arch. Neurol., Neurochir. Psychiat.* **92,** 3–45.

Rockell, A.J., Heath, C.J., and Jones, E.G. (1972). Afferent connections to the diencephalon in the marsupial phalanger and the question of sensory convergence in the "posterior group" of the thalamus. *J. Comp. Neurol.* **145,** 105-130.

Rockland, K.S. (1994). Further evidence for two types of cortico-pulvinar neurons. *Neuroreport.* **3,** 1865–1868.

Rockland, K.S. (1996). Two types of corticopulvinar terminations: Round (type 2) and elongate (type 1). *J. Comp. Neurol.* **368,** 57–87.

Rockland, K.S., Andresen, J., Cowie, R.J. and Robinson, D.L. (1999). Single axon analysis of pulvinocortical connections to several visual areas in the macaque. *J. Comp. Neurol.,* **406:** 221-250.

Romanski, L.M., Giguere, M., Bates, J.F., and Goldman-Rakic, P. (1997) Topographic organization of medial pulvinar connections with prefrontal cortex in the rhesus monkey . *J. Comp. Neurol.* **379,** 313–332.

Rose, J., and Woolsey, C.N. (1949). Organization of the mammalian thalamus and its relationships to the cerebral cortex. *E.E.G. Clin. Neurophys.* **1,** 391–404.

Rose, M. (1935). Das Zwischenhirn des Kaninschen. *Mem. Acad. Pol. Sci.* N° 8.

Rouiller, E.M., Liang, F., Babalian, A., Moret, V., and Wiesendanger, M. (1994). Cerebellothalamocortical and pallidothalamocortical projections to the primary and supplementary motor cortical areas: A multiple tracing study in the Macaque monkeys. *J. Comp. Neurol.* **345,** 185–213.

Rouiller, E.M., Tanne, J., and Boussaoud, D. (1999). Origin of thalamic inputs to primary, premotor, and supplementary motor cortical areas and to area 46 in macaque monkeys : A multiple retrograde tracing study. *J. Comp. Neurol.* **409,** 131–152.

Rümler, B., Schaltenbrand, G., Spuler, H., and Wahren, W. (1972). Somatotopic array of the ventro-oral nucleus of the thalamus based on electrical stimulation during stereotactic procedures. *Confin. Neurol.* **34,** 197–199.

Russchen, F.T., Bakst, I., Amaral, D.G., and Price, J.L. (1985). The amygdalostriatal projections in the monkey. An anterograde tracing study. *Brain Res.* **329,** 241–257.

Russell, G.V. (1954). The dorsal trigemino-thalamic tract in the cat reconsidered as a lateral reticulo-thalamic system of connections. *J. Comp. Neurol.* **101,** 237–263.

Sachs, E. (1909). On the structure and functional relations of the optic thalamus. *Brain* **32,** 95–186.

Sadikot, A.F., Parent, A., and François, C. (1990). The centre médian and parafascicular thalamic nuclei project respectively to the sensorimotor and associative-limbic striatal territories in the squirrel monkey. *Brain Res.* **510,** 161–165.

Sadikot, A.F., Parent, A., and François, C. (1992). Efferent connections of the centromedian and parafascicular thalamic nuclei in the squirrel monkey. A PHA-L study of subcortical projections. *J. Comp. Neurol.* **315,** 137–159.

Sakai, S. (1967). Some observations on the cortico-thalamic fiber connections in the monkey. *Proc. Jap. Acad.* **43,** 822–826.

Sakai, S.T., Inase, M., and Tanji, J. (1996). Comparison of cerebello-thalamic and pallido thalamic projections in the monkey (Macaca fuscata): A double anterograde labeling study. *J. Comp. Neurol.* **368,** 215–228.

Sakai, S.T., Inase, M., and Tanji, J. (1999). Pallidal and cerebellar inputs to thalamocortical neurons projecting to the supplementary motor area in *Macaca fuscata:* A triple-labeling light microscopic study. *Anat. Embryol.* **199,** 9–19.

Sakai, S.T., Stanton, G.B., and Tanaka, D. (1983) The ventral lateral thalamic nucleus in the dog: Cerebellar afferents and acetyl-cholinesterase histochemistry. *Brain Res.* **271,** 1–19.

Sakai, S.T. Stepniewska, I., and Qi, H.X. (2000). Pallidal and cerebellar afferents to presupplementary motor area thalamo-cortical neurons of the owl monkey: A multiple tracing study. *J. Comp. Neurol.* **417,** 164–180.

Sakamoto, E. (1964). The dorsal thalamus of the chimpanzee. *Arb. Abt. Anat. Inst. Univ. Tokushima,* **10,** 1–36.

Sakata, H., Takaoka, Y., Kawarasaki, A., and Shibutani, H. (1973). Somatosensory properties of neurons in the superior parietal cortex (area 5) of the rhesus monkey. *Brain Res.* **64,** 85–102.

Sanides, F. (1964). The cyto-myeloarchitecture of the human frontal lobe and its relation to phylogenetic differentiation of the cerebral cortex. *J. Hirnforsch.* **6,** 269–282.

Sanides, F. (1968). The architecture of the cortical taste nerve areas in squirrel monkey (*Saimiri sciureus*) and their relationships to insular, sensorimotor and prefrontal regions. *Brain Res.* **8,** 97–124.

Schaltenbrand, G., and Bailey, P. (1959). "Introduction to Stereotaxis with an Atlas of the Human Brain." Thieme, Stuttgart.

Schaltenbrand, G., and Wahren, W. (1977). "Atlas for Stereotaxy of the Human Brain." Thieme, Stuttgart.

Schaltenbrand, G., and Walker, A.E. (1982). "Stereotaxy of the Human Brain." Thieme, Stuttgart.

Schaltenbrand, G., Spuler, H., Wahren, W., and Rümler, B. (1971). Electroanatomy of the thalamic ventro-oral nucleus based on stereotaxic stimulation in man. *Z. Neurol.* **19,** 259–276.

Scheibel, M.E., and Scheibel, A.B. (1966a). The organization of the nucleus reticularis thalami: *A Golgi study.* **1,** 43–62.

Scheibel, M.E., and Scheibel, A.B (1966b). Patterns of organization in specific and non specific thalamic fields. *In* "The Thalamus" (D.P. Purpura and M.D. Yahr, eds.), pp. 13–46. Columbia Univ. Press, New York.

Scheibel, M.E., and Scheibel, A.B. (1971). Input-output relations of the thalamic nonspecific system. *Brain Behav. Evol.* **6,** 332–358.

Scheibel, M.E., and Scheibel, A.B. (1972). Specialized organizational patterns within the nucleus reticularis thalami of the cat. *Exp. Neurol.* **34,** 316–322.

Scheibel, M.E., and Scheibel, A.B. (1976). Ontogenetic development of somatosensory thalamus I. Morphogenesis. *Exp. Neurol.* **51,** 392–406.

Schell, E.R., and Strick, P.L. (1984). The origin of thalamic inputs to the arcuate premotor and supplementary motor areas. *J. Neurosci.* **4,** 539–560.

Schlag, J., and Schlag-Rey, M. (1987). Evidence for a supplementary eye field. *J. Neurophysiol.* **57,** 179–200.

Schmahmann, J.D., and Pandya, D.N. (1990). Anatomical investigation of projections from thalamus to posterior parietal cortex in the rhesus monkey: A WGA-HRP and fluorescent tracer study. *J. Comp. Neurol.* **295,** 299–326.

Seike, M. (1993). A study of the area of distribution of deep sensory neurons of the human ventral thalamus. *Stereotact. Funct. Neurosurg.* **61,** 12–23.

Scollo-Lavizzari, G., and Akert, K. (1963). Cortical area 8 and its thalamic projection in macaca mulatta. *J. Comp. Neurol.* **121,** 259–270.

Sheps, J.G. (1945). The nuclear configuration and cortical connections of the human thalamus. *J. Comp. Neurol.* **83,** 1–56.

Shink, E., Sidibé, M., and Smith, Y. (1997). Efferent connections of the internal globus pallidus in the squirrel monkey: II. Topography and synaptic organization of pallidal efferents to the pedunculopontine nucleus. *J. Comp. Neurol.* **382,** 348–363.

Shinoda, Y. (1988). Input-output organization of the ventrolateral nucleus of the thalamus. *Neurosci. Res.* **32,** 398–410.

Shook, B.L., Schlag-Rey, M., and Schlag, J. (1991). Primate supplementary eye field. II. Comparative aspects of connections with the thalamus, corpus striatum, and related forebrain nuclei. *J. Comp. Neurol.* **307,** 562–583.

Shuster, P. (1936). Beitrage zur pathologie des thalamus opticus. *Arch.Psychiat.* **105,** I, 358–432; II, 550–622.

Sidibe, M., Bevan, M.D., Bolam, J.P., and Smith, Y. (1997). Efferent connections of the internal globus pallidus in the squirrel monkey. I. Topography and synaptic organization of the pallidothalamic connection. *J. Comp. Neurol.* **382,** 323–347.

Simma, K. (1951). Zur Projektion des centrum medianum und nucleus parafascicularis thalami beim Menschen. *Mschr. Psychiat. Neurol.* **122,** 32–46.

Simma, K. (1957). Der Thalamus des Menschenaffen. *Psych. Neurol.* **134,** 145–175.

Smith, Y., and Parent, A. (1986). Differential connections of caudate nucleus and putamen in the squirrel monkey *(Saïmiri sciureus). Neurosci.* **18,** 347–371.

Spiegel, E.A., and Wycis, H.T. (1952). "Stereoencephalotomy (Thalamotomy and Related Procedures." Grune and Stratton, New York.

Spurden, D.P., Court, J.A., Lloyd, S., Oakley, A., Perry, R., Pearson, C., Pullen, R.G., and Perry, E.K. (1997). Nicotinic receptor distriution in the human thalamus: Autoradiographical localization of (3H) nicotine and (125I) alpha-bungarotoxin binding. *J. Chem. Neuroanat.* **13,** 105–113.

Stanton, G.B. (1980). Topographical organization of ascending cerebellar projections from the dentate and interposed nuclei in *Macaca mulatta;* an anterograde degeneration study. *J. Comp. Neurol.* **190,** 699–731.

Stanton, G.B., Goldberg, M.E., and Bruce, C.J. (1988). Frontal eye field efferents in the macaque monkey: I. Subcortical pathways and topography of striatal and thalamic fields. *J. Comp. Neurol.* **271,** 473–492.

Stephan, H., Baron, G., and Schwerdtfeger, W.K. (1980). "The Brain of the Common Marmoset." Springer, Berlin.

Stepniewska, I., Preuss, T.M., and Kaas, J.H (1994). Architectonic subdivisions of the motor thalamus of owl monkeys: Nissl, acetylcholinesterase and cytochrome oxydase patterns. *J.Comp. Neurol.* **349,** 536–557.

Steriade, M., Jones, E.G., and McCormick, D.A. (1997). Thalamic organization and chemical anatomy. *In* "Thalamus" (M. Steriade, E.G. Jones, and D.A. McCormick, eds.), Vol. I, Chap. 2, pp. 31. Elsevier.

Stevens, R.T., London, S.M., and Appkarian, A.V. (1993). Spinothalamocortical projections to the secondary somatosensory cortex (SII) in squirrel monkey. *Brain Res.* **631,** 241–246.

Strick, P.L. (1975), Multiple sources of thalamic input to the primate motor cortex. *Brain Res.* **88,** 372–377.

Strick, P.L. (1976a). Anatomical analysis of ventrolateral thalamic input to primate motor cortex. *J. Neurophysiol,* **39,** 1020–1031.

Strick, P.L. (1976b). Activity of ventrolateral thalmic neurons during arm movement, *J. Neurophysiol.* **39,** 1032–1044.

Sugita, S., and Noda, H. (1991). Pathways and terminations of axons arising in the fastigial oculomotor region of macaque monkeys. *Neurosci. Res.* **10,** 118–136.

Szentagothai, J. (1963). The structure of the synapses in the lateral geniculate body. *Acta Anat.* **55,** 166–185.

Szenthagotai, J. (1970). Glomerular synapses, complex synaptic arrangements and their operational significance. *In* "The neurosciences. 2d Study Program."

Szentagothai, J, Hamori, J., and Tombol, T. (1966). Degeneration and electron microscope analysis of the synaptic glomeruli in the lateral geniculate body. *Exp. Brain Res.* **2,** 283–301.

Talairach, J., and Szickla, G. (1967). "Atlas d'anatomie stéréotaxique du télencéphale." Masson, Paris.

Talairach, J. and Tournoux, P. (1988). "Co-planar Stereotaxic Atlas of the Human Brain." Thieme, Stuttgart.

Talairach, J., David, M., Tournoux, P. Corredor, H., and Kvasina, T. (1957). "Atlas d'anatomie des noyaux gris centraux." Masson, Paris.

Tanji, J. (1994). The supplementary motor area in the cerebral cortex. *Neurosci. Res.* **19,** 251–268.

Tarlov, E. (1969). The rostral projection of the vestibular nuclei: An experimental study in macaque, baboon and chimpanzee. *J. Comp. Neurol.* **135,** 27–56.

Tasker, R.R., Organ, L.W., and Hawrylyshyn, P.A. (eds.), (1982). "The Thalamus and Midbrain of Man. A Physiological Atlas Using Electrical Stimulation." Thomas, Springfield.

Thach, W.T. (1987). Cerebellar inputs to motor cortex. *In* "Motor Areas of the Cerebral Cortex" pp. 201–220. Wiley, Chichester.

Thach, W.T., and Jones, E.G. (1979). The cerebellar dentatothalamic connection: terminal field, lamellae, rods and somatotopy. *Brain Res.* **169,** 168–172.

Tobias, T.J. (1975). Afferents to prefrontal cortex from the thalamic mediodorsal nucleus in the rhesus monkey. *Brain Res.* **83,** 191–212.

Tokuno, H., and Tanji, J. (1993). Input organization of distal and proximal forelimb areas in the monkey primary motor cortex: A retrograde double labeling study. *J. Comp. Neurol.* **333,** 199–209.

Tokuno, H., Kimura, M., and Tanji, J. (1992). Pallidal inputs to thalamocortical neurons projecting to the supplementary motor area. *Exp. Brain Res.* **90,** 635–638.

Tombol, T., Bentivoglio, M., and Macchi, G. (1990). Neuronal cell types in the intralaminar central lateral nucleus of the cat. *Exp. Brain Res.* **81,** 491–499.

Tomlinson, J.D.W., Watkins, E.S., and Andrew, J. (1969). Observations on the nomenclature and variabilities of the human thalamic nuclei. *In* "Third Symposium on Parkinson Disease" (F.F. Gilligan and I.M.C. Donaldson, eds.), pp. 76–82.

Toncray, J.E., and Krieg, W.J.S. (1946). The nuclei of the human thalamus: A comparative approach. *J. Comp. Neurol.* **85,** 421–455.

Tracey, D.J., Asanuma, C., and Jones, E.G. (1980). Thalamic relay to motor cortex: afferent pathways from brain stem, cerebellum, and spinal cord in monkeys, *J. Neurophysiol.* **44,** 532–554.

Trojanowski, J.Q., and Jacobson, S. (1974). Medial pulvinar afferents to frontal eye field in rhesus monkey demonstrated by horseradish peroxydase. *Brain Res.* **80,** 395–411.

Trojanowski, J.Q., and Jacobson, S. (1975). A combined horseradishperoxydase-autoradiographic investigation of reciprocal connections between superior temporal gyrus and pulvinar in squirrel monkey. *Brain Res.* **85,** 347–353.

Turner, R.S., and Anderson, M.E. (1997). Pallidal discharge related to kinematics of reaching movements in two dimensions. *J. Nezurophysiol.* **77,** 1051–1074.

Van Buren, J.M. (1974). Anatomic studies of pulvinar in human. *In* "The pulvinar-LP Complex" (I.S. Cooper, M. Riklan, and P. Rakic, eds.), pp. 67–79. Thomas, Sprigfield, IL.

Van Buren, J.M., and Borke, R.C. (1971). A re-evaluation of the "nucleus ventralis lateralis" and its cerebellar connections. A study in man and chimpanzee. *Intern. J. Neurol.* **8,** 155–177.

Van Buren, J.M., and Borke, R.C. (1972). "Variations and Connections of the Human Thalamus," 2 vol. Springer, Berlin.

Van Donkelaar, P., Stein, J.F., Passingham, R.E., and Miall, R.C. (1999). Neuronal activity in the primate motor thalamus during visually triggered and internally generated lim movements. *J. Neurophysiol.* **82,** 934–945.

Van Donkelaar, P., Stein, J.F., Passingham, R.E., and Miall, R.C. (2000). Temporary inactivation in the primate motor thalamus during visually triggered and internally generated limb movements. *J. Neurophysiol.* **85,** 2780–0000.

Veazey, R.B., Amaral, D.G., and Cowan, W.M. (1982). The morphology and connections of the posterior hypothalamus in the cynomolgus monkey *(Macaca fascicularis)* II. Efferent connections. *J. Comp. Neurol.* **207,** 135–156.

Verhaart, W.J.C. (1938). Comparison of the corpus striatum and the red nucleus as subcortical centra of the cerebral motor system. *Psychiat. Neurol.* bl., 42.

Vicq d'Azyr, R. (1786). "Traité d'anatomie et de physiologie avec des planches colorées." Didot, Paris.

Vitek, J.L., Ashe, J., DeLong, M.R., and Alexander, G.E. (1994). Physiologic properties and somatotopic organization of the primate motor thalamus, *J. Neurophysiol.* **71,** 1498–1513.

Vitek, J.L., Ashe, J., DeLong, M.R., and Kaneotke. (1996). Microstimulation of primate motor thalamus: Somatotopic organization and differential distribution of evoked motor responses among subnuclei. *J. Neurophysiol.* **75,** 2496–2495.

Vogt, B.A., and Pandya, D.N. (1987). Cingulate cortex of the rhesus monkey: Cytoarchitecture and thalamic afferents. *J. Comp. Neurol.* **262,** 256–270.

Vogt, B.A., Pandya, D.N., and Rosene, D.L. (1987). Cingulate cortex of the rhesus monkey. I Cytoarchitecture and thalamic afferents. *J. Comp. Neurol.* **262,** 256–270.

Vogt, B.A., Rosene, D.L., and Pandya, D.N. (1979). Thalamic and cortical afferents differentiate anterior from posterior cingulate cortex in the monkey. *Science* **204,** 205–207.

Vogt, C. (1909). La myélocytoarchitecture du thalamus du cercopithèque, *J. Psychol. Neurol.* **12,** 285–324.

Vogt, C., and Vogt, O. (1919a). Allgemeinere Ergebnisse unserer Hirforchung. *J Psychol Neurol.* **25,** 279–462.

Vogt, C., and Vogt, O. (1919b). Zur Kenntnis der pathologishen Veränderungen des striatum und des pallidum und zur Pathophysiologie des dabei auftretenden Krankheitserscheinungen. *S.B. Heidelb. Akad. Wiss.* **10,** 1–56.

Vogt, C., and Vogt, O. (1941). Thalamusstudien, *J. Psychol. Neurol.* **50,** 3–74.

Von Economo, C (1927). "L'architecture cellulaire normale de l'ecorce cérébrale." Masson, Paris.

Von Monakow, C. (1895). Experimentelle und pathologische-anatomische Untersuchungen über die Haubenregion, den Sehhügel und die Regio subthalamica, nebst Beiträgen zur Kenntnis früher-worbener Gross- und Kleinhirndefekte. *Archiv Psychiatr. Nervenkr.* **27,** 1–128.

Walker, A.E. (1935). The retrograde cell degeneration in the thalamus of macacus rhesus following hemidecortication. *J. Comp. Neurol.* **62,** 407–419.

Walker, A.E. (1936). An experimental study of the thalamocortical projection of the macaque monkey. *J. Comp. Neurol.* **64,** 1–39.

Walker, A.E. (1937). A note on the thalamic nuclei of Macaca mulatta. *J. Comp. Neurol.* **66,** 145–155.

Walker, A.E. (1938a). "The Primate Thalamus." Chicago University Press, Chicago.

Walker, A.E. (1938b). The thalamus of the chimpanzee. II Its nuclear structure, normal and following hemidecortication. *J. Comp. Neurol.* **69,** 487–507.

Walker, A.E. (1938c). The thalamus of the chimpanzee. IV. Thalamic projection to the cerebellar cortex. *J. Anat.* **73,** 37–93.

Walker, A.E (1940). The medial thalamic nucleus. A comparative anatomical, physiological and clinical study of the nucleus dorsalis medialis thalami. *J. Comp. Neurol.* **73,** 87–115.

Webster, M.J., Bachevalier, J., and Ungerleider, L.G. (1993). Subcortical connedctions of inferior temporal areas TE and TEO in macaque monkeys. *J. Comp. Neurol.* **335,** 73–91.

Whitlock, D.G., and Nauta, W.J.H. (1956). Subcortical projections from the temporal neocortex in Macaca mulatta. *J. Comp. Neurol.* **106,** 182–212.

Wiesendanger, M. (1986). Recent development in studies of the supplementary motor ara of primates. *Rev. Physiol. Biochem. Pharmacol.* **103,** 1–59.

Wiesendanger, R., and Wiesendanger, M. (1985a). Cerebello-cortical linkage in the monkey as revealed by transcellular labelling with the lectin wheat germ agglutinin conjugated to the marker horseradish peroxidase. *Exp. Brain Res.* **59,** 105–117.

Wiesendanger, R., and Wiesendanger, M. (1985b). The thalamic connections with medial area 6 (supplementary motor cortex) in the monkey *(Macaca fascicularis). Exp. Brain Res.* **59,** 91–104.

Wiesendanger, M., Hummelsheim, H., Bianchetti, M., Chen, D.F., Hyland, B., Maier, V., and Wiesendanger, R. (1987). Input and output organization of the supplementary motor area. *In* "Motor Areas of the Cerebral Cortex," pp. 40–61. Wiley, Chichester.

Wiesendanger, M., Wiesendanger, R., Maendly, R., and Ruëgg, D.G. (1979). Afferent input and cortical projection to the VPLo-VPLc border zone of the monkey's thalamus. *Neurosci. Lett., Suppl.* **1** S120.

Willis, W.D., Zhang, X., Honda, C.N., and Giesler, G.J. (2001). Projections from the marginal zone and deep dorsal horn to the ventrobasal nuclei of the primate thalamus. *Pain* **92,** 267–276.

Wilson, S.A.K. (1914). An experimental research into the anatomy and physiology of the corpus striatum. *Brain* **36,** 427–492.

Wirth, F.P. (1973). Insular diencephalic connections in the macaque, *J. Comp. Neurol.* **150,** 361–392.

Wise, S.P. (1985a). The primate premotor cortex fifty years after Fulton. *Behav. Brain Res.* **18,** 79–88.

Wise, S.P. (1985b). The primate premotor cortex: past, present and preparatory. *Ann. Rev. Neurosci.* **8,** 1–19.

Yakovlev, P.I. (1969). Development of nuclei of the dorsal thalamus and of the cerebral cortex. *In* "Modern Neurology" (Locke, ed.), pp. 15–53. Little Brown.

Yakovlev, P. I., and Lecours, A-R. (1967). The myelogenetic cycles of regional maturation of the brain. *In* "Regional Development of the Brain in Early Life" (W. Clowes, ed.), pp. 1–70.

Yakovlev, P.I., Locke, S., and Angevine, J.B. (1966). The limbus of the hemisphere, limbic nuclei of the thalamus, and the cingulum bundle. *In* "The Thalamus" (D.P. Purpura and M.D. Yahr, eds.), pp.77–91. Columbia Univ. Press, New York.

Yakovlev, P.I., Locke, S., Koskoff, D.Y., and Patton, R.A. (1960). Limbic nuclei of thalamus and connections of limbic cortex. I. Organization of the projections of the anterior group of nuclei

and of the midline nuclei of the thalamus to the anterior cingulate gyrus and hippocampal rudiment in the monkey. *Arch. Neurol.* **3,** 620–641.

Yamadori, T. (1961). The developmental study on the thalamic nuclei in japanese fetus. *Kobe J. Med. Sci.* **7,** 1–25.

Yamamoto, T., Yoshida, K., Yoshikawa, Y., Kishimoto, Y., and Oka, H. (1992). The medial dorsal nucleus is one of the thalamic relays of the cerebellocerebral response to the frontal association cortex in the monkey: Horseradish peroxidase and fluorescent dye double staining study. *Brain Res.* **579,** 315–320.

Yelnik, J., François, C., and Percheron, G. (1997). Spatial relatioships between striatal axonal endings and pallidal neurons in the macaque monkey. *Adv. Neurol.* **74,** 45–56.

Yelnik, J., François, C., Percheron, G., and Tandé, D. (1991). Morphological taxonomy of the neurons of the primate striatum. *J. Comp. Neurol.* **313,** 273–294.

Yelnik, J., Percheron, G., and François, C.(1984). A Golgi analysis of the primate globus pallidus. II. Quantitative morphology and spatial orientation of dendritic arborizations. *J. Comp. Neurol.* **227,** 200–213.

Yeterian, E.H., and Pandya, D.N. (1988). Corticothalamic connections of paralimbic regions in the rhesus monkey. *J. Comp. Neurol.* **269,** 130–146.

Zhang, E-T., and Craig, A.D. (1997). Morphology and distribution of spinothalamic Lamina I neurons in the monkey. *J. Neurosci.* **17,** 3274–3284.

CHAPTER

21

The Basal Ganglia

SUZANNE N. HABER
Department of Pharmocology and Physiology
University of Rochester School of Medicine
Rochester, New York, USA

MARTHA JOHNSON GDOWSKI
Department Neurobiology and Anatomy
University of Rochester School of Medicine
Rochester, New York, USA

The basal ganglia work in concert with cortex to orchestrate and execute planned, motivated behaviors requiring motor, cognitive, and limbic circuits. Their main driving force is cortex, as indicated by both a massive projection from cortex and the functional relationships associated with this input. Historically, the basal ganglia are best known for their motor functions. This functional association was established in large part by the neuropathology in the neurodegenerative disorders affecting the control of movement, such as that found in Parkinson's disease (PD) and Huntington's chorea. In addition, while receiving input from wide areas of cortex, basal ganglia pathways were thought to return primarily to motor cortex (Nauta and Mehler, 1966). In further support of the role of the basal ganglia in the control of movement, animal studies demonstrated several roles in motor control, including (but not limited to) regulation of posture or postural reflexes, as a center for automatic movements and as a source of inborn motor programs. Furthermore, the basal ganglia are involved in generating the necessary timing (ramp signals) for smooth guided movements (Denny-Brown, 1962; Kornhuber, 1974; MacLean, 1978). Later studies demonstrated basal ganglia involvement not only in motor execution but also in motor planning and in sensory-motor integration (Marshall *et al.*, 1971; Teuber, 1976; Marsden, 1984; Evarts *et al.*, 1985; Lidsky *et al.*, 1985; Marsden, 1985).

While a role for the basal ganglia in the control of movement is now clear, our concept of basal ganglia function has dramatically changed in the last 20 years, from a purely motor or sensory-motor one to a more complex and complicated set of functions that mediate the full range of goal-directed behaviors. Thus, in addition to their involvement in the expression of goal-directed behaviors through movement, the basal ganglia are also involved in the processes that lead to movement—in other words, the elements that drive actions, including emotions, motivation, and cognition. Indeed, regions within each of the basal ganglia nuclei

have been identified as serving not only a sensory-motor function but also limbic and cognitive ones. Ventral regions of the basal ganglia play a key role in reward and reinforcement (Heath *et al.*, 1968; Fibiger and Phillips, 1986; Everitt *et al.*, 1989; Robbins *et al.*, 1989; Wise, 1996; Schultz, 1997; Rolls, 2000) and are important in the development of addictive behaviors and habit formation (Kalivas *et al.*, 1993; Nestler *et al.*, 1993; Koob, 1999). More central basal ganglia areas are involved in cognitive functions such as procedural learning and working memory tasks (Mishkin *et al.*, 1984; Phillips and Carr, 1987; Jueptner *et al.*, 1997; Levy *et al.*, 1997; Jog *et al.*, 1999). Diseases affecting mental health, including schizophrenia, drug addiction, and obsessive compulsive disorder, are linked to pathology in the basal ganglia, albeit the ventral basal ganglia (Stevens, 1973; Kalivas *et al.*, 1993; Mogenson *et al.*, 1993; Swerdlow *et al.*, 1993; McGuire *et al.*, 1994; Breiter *et al.*, 1996; Koob and Nestler, 1997; Pantelis *et al.*, 1997). This is in contrast to diseases that interfere with motor control and primarily affect the dorsal basal ganglia. Thus, the role of the basal ganglia in cognitive and emotional behaviors is now as well accepted as is the role in motor control. Although several new theories of general function have emerged from the enormous progress in understanding the anatomy, physiology, and behaviors associated with the basal ganglia (Penney and Young, 1983; Nauta, 1986; Marsden, 1987; Hikosaka and Wurtz, 1989; DeLong and Georgopoulos, 1991; Kimura and Graybiel, 1995; Mink, 1996; Wise *et al.*, 1996; Wickens, 1997; Bergman *et al.*, 1998; Graybiel, 1998; Parent and Cicchetti, 1998; Schultz *et al.*, 1998; Boraud *et al.*, 2002), the actual role of the basal ganglia in executing goal-directed behaviors remains elusive. What is clear from the recent progress is that this set of subcortical nuclei work in tandem with cortex (particularly frontal cortex) via a complex corticobasal ganglia network to develop and carry out complex behaviors. The present review describes the organization of the primate basal ganglia from the perspective of cortical function in carrying out goal-directed actions. In some situations, when necessary, data are also presented from rodent work. We have attempted, whenever possible, to integrate the anatomical data with physiological and behavioral findings.

TOPOGRAPHY, CYTOARCHITECTURE, AND BASIC CIRCUITRY

Overview of Terminology and Basic Pathways

The basal ganglia (BG) refer to the large subcortical nuclear masses, the caudate nucleus, putamen, and the globus pallidus. In addition, two closely related structures, the substantia nigra (SN) and subthalamic nucleus (STh), are generally included as components of the basal ganglia. The caudate nucleus and the putamen form the neostriatum. The term "striatum" was assigned to these structures because of their striated appearance owing to the penetration by fascicles of dispersed corticofugal, striatofugal, and corticopetal axons. This region is also referred to as the dorsal striatum to distinguish it from the more recently identified ventral striatum (Fig. 21.1). The concept of the ventral striatum was introduced as the ventral extension of the striatum that included the nucleus accumbens, the medial and ventral portions of the caudate and putamen, and the striatal cells of the olfactory tubercle and anterior perforated substance. While the concept of a ventral extension of the striatum into the anterior perforated substance of the human was suggested some time ago (von Economo and Horn, 1930; Brockhaus, 1942; Macchi, 1951), it has been accepted relatively recently based on its connections, cell morphology, and histochemistry (Heimer, 1978; Heimer *et al.*, 1994).

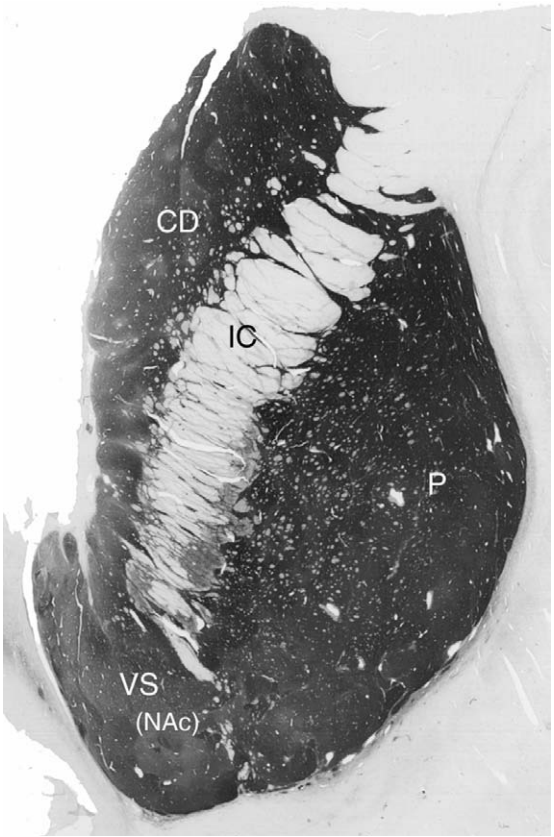

FIGURE 21.1 Photomicrograph of a acetylcholinesterase-stained coronal section through the rostral, human striatum. NAc. Accumbens; CD, caudate nucleus; IC, internal capsule; P, putamen; VS, ventral striatum.

The pallidal complex is comprised of the external (GPe) and internal segments (GPi) of the globus pallidus and the ventral pallidum. While the external and internal segments (together referred to as the dorsal pallidum) receive inputs from the caudate and putamen, their connections differ in important ways and are discussed in detail in a later section. They are separated by the internal medullary lamina. These two pallidal structures, along with the putamen, form the lentiform nucleus (Figs. 21.2 and 21.3). The ventral pallidum is located ventral to the anterior commissure and extends rostrally invading the parts of the ventral striatum (Fig. 21.2). Caudally it occupies the ventral and medial extremes of the external and internal pallidal segments (Parent, 1986; Haber *et al.*, 1993; Heimer *et al.*, 1999). The ventral pallidum receives its input from the ventral striatum and exhibits a combination of features of both the external and internal segments of the dorsal pallidum (Haber and Elde, 1981; Haber *et al.*, 1985, 1993). The STh nucleus can be considered an intrinsic nucleus of the basal ganglia (Fig. 21.4). It receives its input from the external pallidal segment and projects to both the internal and external pallidal segments. The connections and function of the STh are, of course, much more complicated, and its role in mediating basal ganglia function is central to some of the therapeutic treatment strategies for PD. These issues are addressed in detail in "The Subthalamic Nucleus." Finally, the substantia nigra and the adjacent ventral tegmental area (VTA) can also be considered intrinsic nuclei. The substantia nigra is divided into two parts, the pars compacta (SNC) and the pars reticulata (SNR) (Fig. 21.5). Dopamine neurons from both the pars compacta and VTA project to the striatum and the striatal output is directed toward both the dopamine neurons and the pars reticulata.

The striatum is the main input structure of the basal ganglia. It's afferent projections are derived from three major sources: (1) it receives a massive and topographic input from all of cerebral cortex; (2) the second

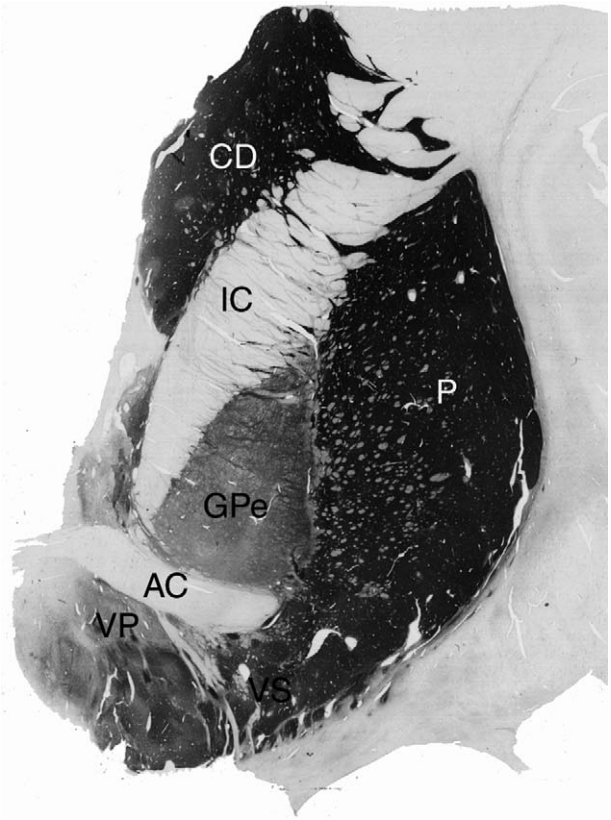

FIGURE 21.2 Photomicrograph of an acetylcholinesterase-stained coronal section through the human striatum at the level of the anterior commissure. Note the ventral extension of the striatum beneath the anterior commissure. AC, anterior commissure; CD, caudate nucleus; GPe, globus pallidus external segment; IC, internal capsule; P, putamen; VP, ventral pallidum; VS, ventral striatum.

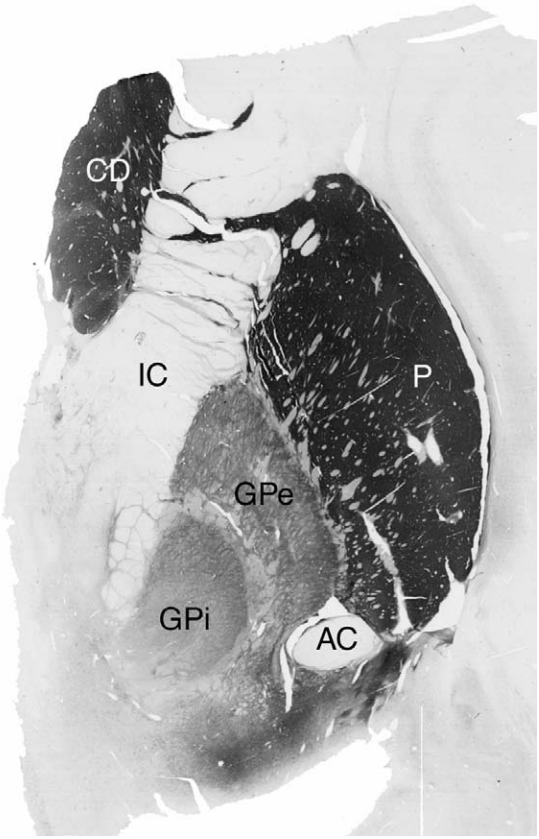

FIGURE 21.3 Photomicrograph of a acetylcholinesterase-stained coronal section through the central, human striatum. This level includes both the internal and external segments of the globus pallidus. AC, anterior commissure; CD, caudate nucleus; GPe, globus pallidus external segment; GPi, globus pallidus internal segment; IC, internal capsule; P, putamen.

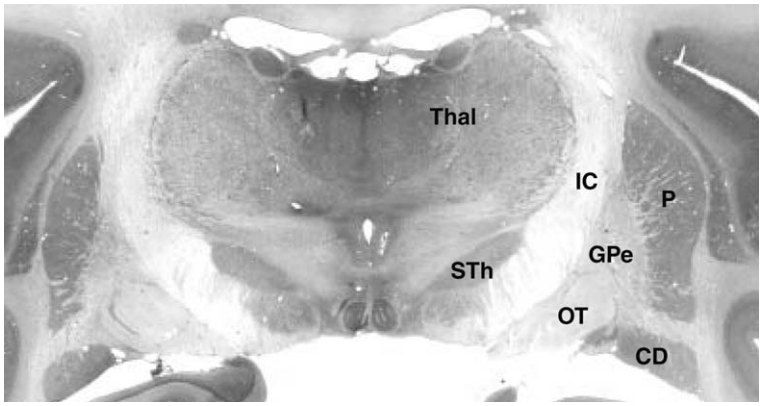

FIGURE 21.4 Photomicrograph of a Nissl-stained coronal section through the nonhuman primate brain at the level of the subthalamic nucleus. CD, caudate; GPe, globus pallidus internal segment; IC, internal capsule; P, putamen; OT, optic tract; STh, subthalamic nucleus; Thal, thalamus.

largest input is derived from the thalamus; and (3) the third main input is from the brainstem, primarily from both the dopaminergic cells of the midbrain and the serotonergic cells of the dorsal raphe nucleus. Afferent projections terminate in a functional topographic manner (Alexander *et al.*, 1986; Parent, 1986; Haber and McFarland, 1999a), such that the dorsolateral striatum receives cortical input from sensory-motor areas, central striatum receives input from associative cortical areas, and the ventromedial striatum receives input from limbic areas. Within this organization, afferent projections terminate in a patchy and interdigitated manner (Künzle, 1975, 1976; Goldman and Nauta, 1977; Künzle, 1977, 1978; Yeterian and Van Hoesen, 1978; Selemon and Goldman-Rakic, 1985; Kunishio and Haber, 1994; Chikama and Haber, 1995; Haber *et al.*, 1995b; Yeterian and Pandya, 1998; McFarland and Haber, 2001). The striatum, in turn, projects topographically to the pallidal complex and the substantia nigra, pars reticulata (Fig. 21.6) (Szabo, 1962, 1967, 1970; Parent *et al.*, 1984; Smith and Parent, 1986; Haber *et al.*, 1990b; Hazrati and Parent, 1992b; Parent and Hazrati, 1993; Lynd-Balta and Haber, 1994c; Parent and Hazrati, 1995; Smith *et al.*, 1998a). The outputs from the GPi and SNR are to the thalamus, which then projects back to the cortex, completing the basic corticobasal ganglia circuit. This is referred to as the "direct" pathway (Fig. 21.7A). Several investigators have successfully exploited the topographic corticostriatal organization of the several functionally distinct and separate BG circuits, demonstrating parallel corticosubcortical channels through the basal ganglia (see "The Direct and Indirect Basal Ganglia Pathways") (Alexander and Crutcher, 1990; Groenewegen *et al.*, 1990; Dum and Strick, 1991b; Middleton and Strick, 1997; O'Donnell *et al.*, 1997; Smith *et al.*, 1998b; Sidibe *et al.*, 2002). Other studies suggest a more complicated pattern of basal ganglia connections that indicate potential complex interactions between these channels (Percheron *et al.*, 1984b; Percheron and Filion, 1991; Joel and Weiner, 1994; Bevan *et al.*, 1996; Yelnik *et al.*, 1996; Joel and Weiner, 1997; Haber *et al.*, 2000; McFarland and Haber, 2002a). In reality, these two organizational schemes likely work together, rather than in conflict, allowing the coordinated behaviors to be maintained, and focused, but also to be modified and changed according the appropiate external and internal stimuli. Indeed, both the inability to maintain and to focus in the execution of specific behaviors, as well as the inability to adapt appropriately to external

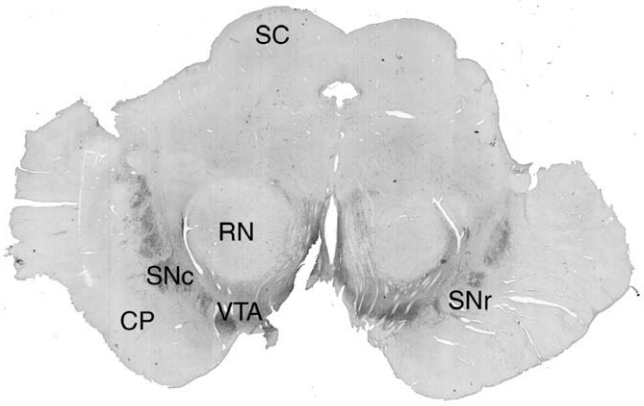

FIGURE 21.5 Photomicrograph of a tyrosine hydroxylase-stained coronal section through the midbrain of a human brain, illustrating the distribution of the dopamine cells in the substantia nigra and adjacent ventral tegmental area. CP, cerebral peduncle; RN, red nucleus; SC, superior colliculus; SNc, substantia nigra pars compacta; SNr, substantia nigra pars reticulata; VTA, ventral tegmental area.

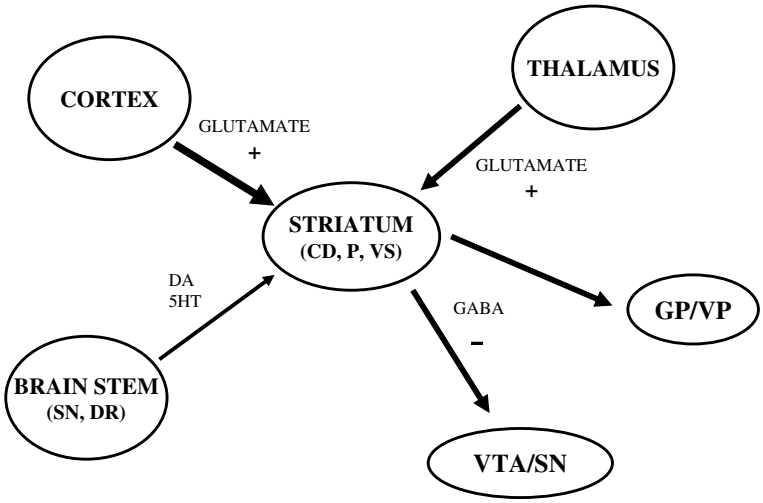

FIGURE 21.6 Diagram demonstrating the connections of the striatum. CD, caudate nucleus; DA, dopamine; DR, dorsal raphe; GP, globus pallidus; P, putamen; SN, substantia nigra; VP, ventral pallidum; VS, ventral striatum; VTA, ventral tegmental area; 5HT, serotonin.

and internal cues, are key deficits in basal ganglia diseases that affect these aspects of motor control, cognition, and motivation. We will return to this topic in "Functional Basal Ganglia Connections."

The GPe is part of the BG intrinsic circuitry and is reciprocally connected to the STh. The STh in turn projects to the GPi. This is referred to as the indirect pathway in contrast to the direct pathway described earlier (Fig. 21.7B). These two striatal output systems are associated with different transmitters and receptors, which are described in more detail later. The main extrinsic afferent projections to the BG are excitatory, using glutamate as the excitatory transmitter. Intrinsic connections (with the exception of the STh) are typically inhibitory, using gamma-amino-butyric acid (GABA) as the primary transmitter. Because of the

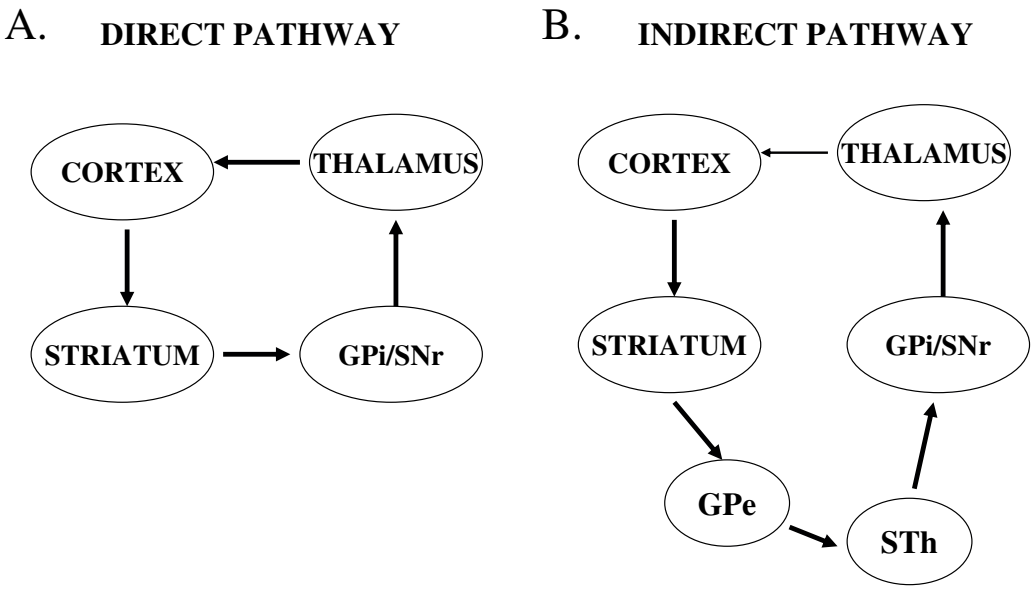

FIGURE 21.7 Diagram demonstrating the two corticobasal ganglia circuits: the direct and indirect pathways. **(A)** Direct pathway. **(B)** Indirect pathway involves a side loop, which includes the globus pallidus external segment and subthalamic nucleus. GPe, globus pallidus external segment; GPi, globus pallidus internal segment; SNr, substantia nigra pars reticulata; STh, subthalamic nucleus.

complex internal circuitry of the BG, the net effect of cortical and thalamic input to the striatum is to increase firing of striatal cells, which, in turn, inhibits (through the direct pathway) the relatively high rates of tonic activity in the pallidum and SN. This, in turn, serves to disinhibit thalamic firing and, consequently, increase thalamic stimulation of cortical activity. In contrast, through the indirect pathway, inhibition of the GPe disinhibits STh firing, which effectively stimulates GPi firing, thereby inhibiting thalamic stimulation of cortex. In this way, these two pathways have opposing actions on the thalamocortical activity: the direct pathway serves to reinforce cortico-BG activity, and the indirect pathway serves to inhibit cortico-BG activity (see Fig. 21.8). As with the parallel processing scheme mentioned earlier, the concept of direct and indirect pathways and associated transmitter-related molecules has stimulated a very productive area of research leading to important insights in basal ganglia function and therapies, particularly for PD. However, we also now recognize that the concept of direct and indirect pathways is likely to be far too simplistic, as a more complex organization emerges (Kawaguchi *et al.*, 1990; Parent *et al.*, 1995; Surmeier *et al.*, 1996; Smith *et al.*, 1998b; Reiner *et al.*, 1999). Finally, the dopamine cells of the midbrain (the SNC and VTA) also represent an intrinsic set of pathways. These cells project to the striatum and also receive striatal output. The control of dopamine on the striatal output cells is an area of intense research as the importance of this transmitter system is recognized for the normal (and abnormal) functioning of the BG (see Fig. 21.6).

The Striatum

In mammals with a more developed cortex, and especially in the human, the striatum is separated into the caudate nucleus and the putamen by the internal capsule. However, the separation is incomplete. This is particularly evident at rostral levels where the head of the caudate is joined to the putamen by the "striatal cell bridges," interspersed between the fibers of the internal capsule. The caudate nucleus forms an elongated nuclear mass, which is closely related to the

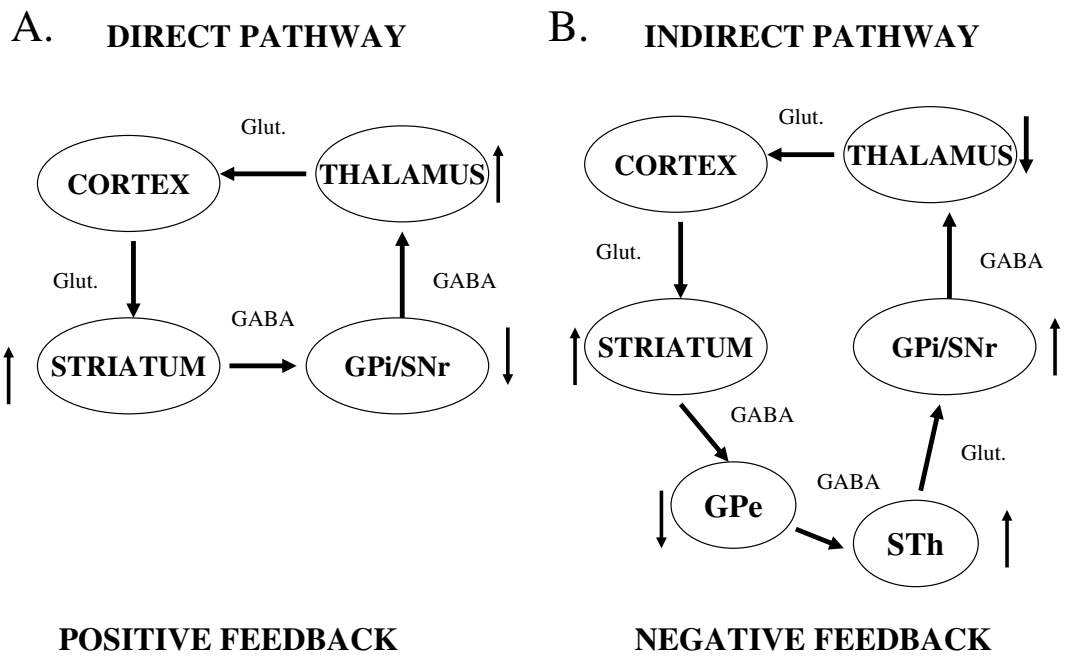

FIGURE 21.8 Diagram demonstrating the consequences of cortical activation of the direct and indirect pathways. Arrows indicate the direction of activation following an increase in cortical activity. Transmitters for each pathway are indicated in parenthesis. Glutamatergic (Glut.) excitation of the striatum via cortical inputs increases striatal activity in both pathways. **(A)** Increased striatal GABAergic activity reduces the output of GPi and/or SNr in the direct pathway. This reduction reduces the inhibition of thalamic neurons, resulting in an increase of glutamatergic thalamic activation of cortical neurons. This is then referred to as positive feedback to cortex via the direct pathway. **(B)** The consequences of cortical activation of the indirect pathway have the opposite effect on the indirect pathway. Increased striatal GABAergic activity reduces the output of GPe activity. This reduction reduces the inhibition of subthalamic neurons, resulting in an increase of glutamatergic subthalamic activation of the GPi/SNr. Activation of this inhibitory pathway reduces thalamic activation of cortical neurons. This is then referred to as negative feedback to cortex via the indirect pathway. GPe, globus pallidus external segment; GPi, globus pallidus internal segment; SNr, substantia nigra pars reticulata; STh, subthalamic nucleus.

lateral ventricle throughout its extent. Its thick anterior portion is referred to as the head of the caudate, which gradually narrows into the body of the caudate. The body is located in the floor of the central part of the lateral ventricle on the dorsolateral side of the thalamus. The body of the caudate gradually tapers off and becomes the tail of the caudate, as it curves along with ventricular system entering the temporal lobe caudal to the thalamus. The putamen, the largest part of the striatum in humans, forms the large lateral part of the lentiform nucleus and is separated from the globus pallidus by the external medullary lamina. The ventral border of the putamen cannot always be easily delineated in gross-anatomical preparations. Rostrally, it is continuous with the accumbens underneath the anterior limb of the internal capsule (see Fig. 21.1). At the level of the crossing of the anterior commissure, the putamen reaches towards the ventral surface of the brain. Caudally, the putamen merges in varying degrees with the tail of the caudate (Figs. 21.1–21.5).

The nucleus accumbens and the rostroventral most aspects of the caudate and putamen form the ventral striatum. In the human brain, the broad continuity between the caudate nucleus and putamen underneath the rostroventral aspect of the internal capsule is generally referred to as the fundus striati and includes the nucleus accumbens. At a slightly more caudal level underneath the lateral extension of the anterior commissure, the ventral striatum includes the ventral extension of the putamen, which reaches the surface of the brain in the region of the anterior perforated space. This ventral region, which had been included in the term, the "substantia innominata," has now been histochemically identified as a ventral extension of the striatum. In addition, the olfactory tubercle and the rostrolateral portion of the anterior perforated space adjacent to the lateral olfactory tract in primates are also included in the ventral striatum (Heimer *et al.*, 1999). The remainder of the anterior perforated space appears to be a mixed area with elements of the putamen, extended amygdala, the corticopetal cell complex, and the ventral extension of the pallidum.

Cell Types and Intrinsic Organization of the Striatum

The striatum (both dorsal and ventral) contains several cell types that are generally divided into two general groups: projection neurons and interneurons.

Projection Neurons Projection neurons are the most common cell type and are referred to as medium spiny neurons (MSN) or the principal neurons (also referred to as spiny I neurons) of the striatum: in nonprimate species they account for over 90% of the cells, and about 70% in primates (Fox *et al.*, 1971a; Kemp and Powell, 1971b; DiFiglia *et al.*, 1976, Difiglia *et al.*, 1982; Graveland and DiFiglia, 1985; Graveland *et al.*, 1985; DiFiglia and Carey, 1986). These are medium size, ovoid cells (14–20 μm) with four to seven radiating dendrites that are heavily covered with spines (Fig. 21.9). The axon emerges from the soma or the proximal part of a primary dendrite and gives rise to a dense collateral network (Wilson and Groves, 1980). Human striatal cells have a larger soma and dendritic radius compared with the monkey, but fewer spines (Graveland and DiFiglia, 1985). In addition, there is a second spiny neuron (type II spiny neuron which is relatively infrequent, (about 1%) and varies considerably in size (Graveland and DiFiglia, 1985; Graveland *et al.*, 1985; DiFiglia and Carey, 1986). The medium spiny neurons are the main efferent cells of the striatum, projecting to the globus pallidus, ventral pallidum, and substantia nigra (Szabo, 1962; Kemp and Powell, 1971a; Szabo, 1972; Grofova, 1975; Somogyi and Smith, 1979; Preston *et al.*, 1980; Bolam *et al.*, 1981; Chang, 1981; Parent *et al.*, 1984; Haber *et al.*, 1990b; Selemon and Goldman-Rakic, 1990; Lynd-Balta and Haber, 1994c). Axon collaterals also terminate within the striatum, onto both interneurons and other medium spiny cells (Somogyi *et al.*, 1981a; Bolam *et al.*, 1986; Pickel and Chan, 1990). Terminals of the medium spiny neurons are small to medium in size, densely packed with vesicles, and have few mitochondria. They form symmetrical synaptic contacts and contain GABA (Bolam *et al.*, 1985; Kita, 1993; Smith *et al.*, 1998b). These data, along with electophysiological data, indicate that the projection cells of the striatum are inhibitory (Wickens and Oorshcot, 2000). Based on histochemical localization of neuropeptides, there are two general types of medium spiny cells: one that co-contains substance P (SP) and GABA; and one that co-contains enkephalin (enk) and GABA. Substance P-containing medium spiny neurons project primarily to the internal segment of the GP and sustantia nigra, while the enkephalin-containing cells project primarily to the extenal segment of the GP (Pickel *et al.*, 1980; Haber and Elde, 1981; Bolam and Izzo, 1988; Bolam and Smith, 1990; Pioro *et al.*, 1990; Reiner *et al.*, 1999). In addition to these transmitter molecules, smaller subpopulations of the principal neurons also co-contain other neuropeptides (Haber, 1986; Graybiel, 1990; Reiner and Anderson, 1990). For a review of the histochemistry of the striatum, see Graybiel and Ragsdale (1983) and Holt *et al.* (1997).

The main extrinsic inputs to the medium spiny cells are derived from the cortex, thalamus, and brainstem. Cortical fibers primarily project to the dendritic spines, form asymmetric terminals, are glutamatergic

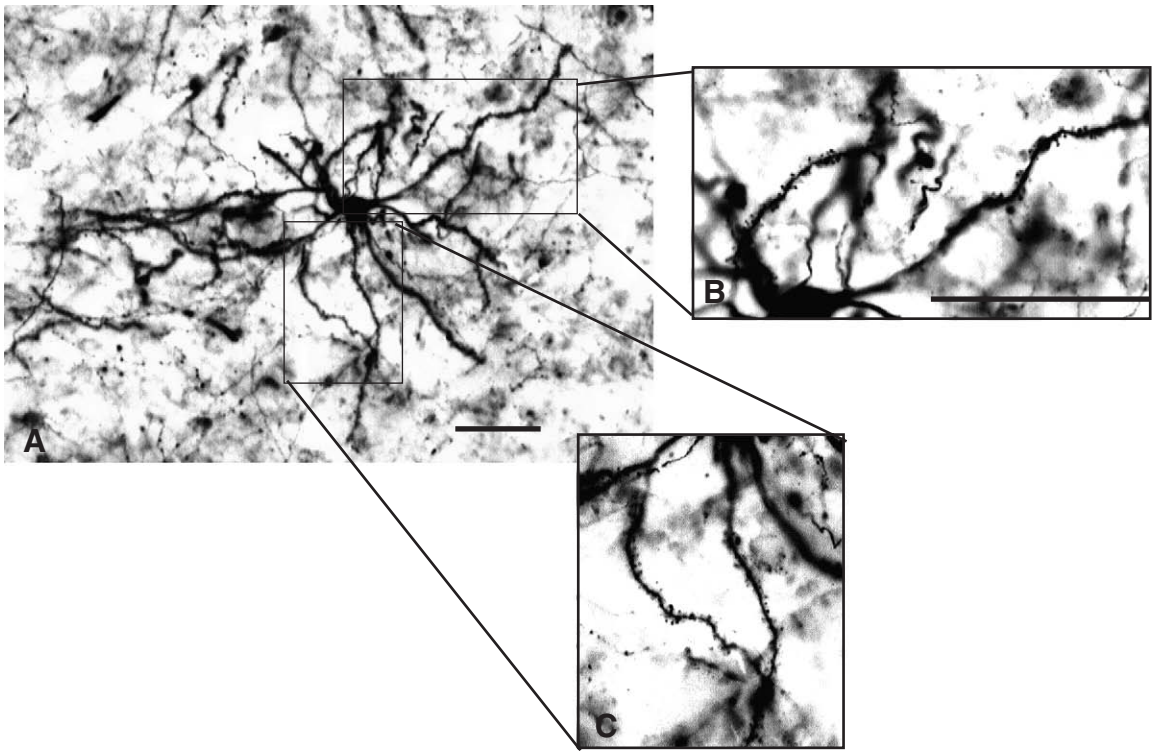

FIGURE 21.9 Photomicrograph of a medium spiny neuron (MSN) filled with Lucifer Yellow. Boxes in panel A are enlarged in panels B and C to reveal prominent spines on the dendritic processes. Scale bars = 50 μm.

and are excitatory (Kemp and Powell, 1971c; Somogyi *et al.*, 1981a; Smith and Bolam, 1990). Thalamic projections terminate primarily onto dendrites, are excitatory, and probably also are glutamatergic (Kemp and Powell, 1971c; Dubé *et al.*, 1988; Sadikot *et al.*, 1992b; Sidibe and Smith, 1996). In the striatum, as in other brain regions, glutamate binds to three receptor types, AMPA (AMPARs), NMDA (NMDARs), and metabotrophic glutamate receptors (mGluTRs). AMPA and NMDA receptors are ionotrophic receptors, mediating fast transmission. These receptors, particularly the NMDA receptors, are thought to be involved in the pathophysiology that leads to cell death during neurodegenerative diseases such as Huntington's disease (Beal *et al.*, 1991; Ferrante *et al.*, 1993; Young, 1993). AMPA and NMDA receptors are asssembled from several subunits, encoded by different genes. The combination of the different subunits determines specific membrane properties such as gating, permeability to Ca^{2+}, and Mg^{2+} sensitivity (Gotz *et al.*, 1997). The distribution, expression, and function of these subunits in the striatum demonstrate that the principal neurons express AMPA receptors that exhibit slow gating and moderate Ca^{2+} permeability. While the NMDA subunit expression differs between the principal neurons and interneurons, there is little functional variation between subunit configurations in the striatum (Landwehrmeyer *et al.*, 1995; Gotz *et al.*, 1997). The mGluRs couple to G proteins to modulate ion channels and intracellular signaling. The distribution of five cloned mGluRs demonstrates a differential distribution of these receptor subtypes throughout basal ganglia structures (Testa *et al.*, 1994; Tallaksen-Greene *et al.*, 1998; Testa *et al.*, 1998; Calabresi *et al.*, 2000b). The three glutamate receptor groups are involved in various aspects of longterm potentiation (LTP) and long-term depression (LTD), two forms of synaptic plasticity associated with learning and memory. Indeed, the striatum plays a central role in learning, and both LTP and LTD have been demonstrated at corticostriatal synapses (Calabresi *et al.*, 1992; Kombian and Malenka, 1994; Mori *et al.*, 1994; Gotz *et al.*, 1997; Calabresi *et al.*, 1999; Calabresi *et al.*, 2000b; Kerr and Wickens, 2001; Reynolds *et al.*, 2001).

Extracellular physiological recordings in awake, behaving monkeys show that the medium spiny neurons are phasically active neurons (PANs). Phasically active neurons have a very low spontaneous discharge rate (0.5–1 spike/s), but a relatively high firing rate associated with behavioral tasks. Phasically active

neurons are activated antidromically from either GPe or GPi, thus identifying them as the projection neurons. These cells exhibit phasic discharges that are time-locked to specific behaviors including movement, preparation for movement, and the performance of learned tasks (Crutcher and DeLong, 1984b; Kimura, 1990; Kimura *et al.*, 1996). Medium spiny neurons are bistable, shifting between two membrane states: an upstate and a downstate (Wilson and Kawaguchi, 1996; Plenz and Kitai, 1998). In the downstate, the membranes are hyperpolarized and cannot generate action potentials. In the upstate, the membranes are relatively depolarized and close to threshold for spike generation. Movement from a downstate to the upstate occurs in response to the combined effects of temporally coherent and convergent excitatory input from cortex and/or thalamus (Wilson, 1993; O'Donnell and Grace, 1995; Calabresi *et al.*, 2000b). Neurons in the upstate are primed to fire in reponse to further depolarization. However, in the absence of the coherent excitatory input, the membrane returns to the downstate. While the medium spiny neuron membrane is not intrinsicaly bistable, the successful transfer between states does depend on intrinsic membrane channels that mediate ion conductances (Wilson and Kawaguchi, 1996; Hernandez-Lopez *et al.*, 1997; Stern *et al.*, 1997; Kerr and Plenz, 2002). The distribution and function of the glutatmate receptor groups and their constituent subunit composition along the spiny dendrite have direct impact on complex regulation of the firing state of the principal neuron. Recently the bistable membrane properties of the MSN have also been demonstrated to exist in awake monkeys, further establishing that this important phenonmenon is likely to be relevant to most mammalian striatal cells including human. We will return to this topic later as we examine the role of the interneuron and dopamine in contributing to the regulation of MSN firing pattern.

Brainstem projections from the substantia nigra, pars compacta, and the VTA terminate onto the spines as well as the dendritic shafts of the medium spiny neurons (Bouyer *et al.*, 1984a, b; Freund *et al.*, 1984; Smith *et al.*, 1994b; Hanley and Bolam, 1997; Kung *et al.*, 1998). These projections are primarily dopaminergic. The distribution of dopamine terminals onto dendrites, soma, and spines has been studied by many investigators. The general conclusion of all these studies is that, for the dorsal striatum, there are few terminals onto the soma, but they are relatively evenly split between the spine and dendrite. In contrast, for the ventral striatum, particularly the shell of the nuc. accumbens, dopamine terminals are more commonly found on the dendrite than on the spine (Zahm, 1992). Early studies using fluorescence staining, and later studies using TH immunhistochemistry to mark the dopaminergic terminals, clearly demonstrated the dense distribution of dopamine fibers throughout the striatum (Felten and Sladek, 1983; Lavoie *et al.*, 1989). The topography of this projection from the midbrain is well documented by lesion studies, tracing studies, and the pathological material from Parkinson's disease patients (Szabo, 1979; Gerlach *et al.*, 1991; Pifl *et al.*, 1991; Lynd-Balta and Haber, 1994a, b). Five different dopamine receptor genes have been cloned, (D_1–D_5), which are divided into two distinct families, D1 and D2, based on pharmacological and molecular criteria (Civelli *et al.*, 1993; Sokoloff and Schwartz, 1995). Although within each family the receptor subtypes may involve different G-proteins and intracellular responses, their effect on cAMP is relatively consistent (for review see Sokoloff and Schwartz, 1995). D_1, D_2, and D3 are expressed in MSN and found in dendrites and spines (Gerfen *et al.*, 1990; Hersch *et al.*, 1995; Caille *et al.*, 1996). The D_3 receptor is primarily expressed in the ventral striatum, while the D_1 and D_2 receptors are expressed throughout the striatum. The D_2 receptor is also expressed in axons. The D1 family of receptors (including D_1 and D_5 receptor subtypes) activate G-proteins that stimulate cAMP. Medium spiny neurons that contain high mRNA expression levels for the D_1 receptors also co-contain mRNA for substance P. The D2 group (D_2, D_3, and D_4), acting through different G-proteins, inhibits cAMP. Cells that contain high mRNA expression levels for the D_2 receptor subtype also co-contain mRNA for enkephalin. The separation of receptor subtypes within different pathways, along with their different pharmacological actions and co-localized neuropeptides, has been particularly important in forming the functional framework of the direct and indirect pathways (Emson *et al.*, 1980; Haber and Elde, 1981; Inagaki and Parent, 1984; Albin *et al.*, 1989; Bolam and Smith, 1990; Gerfen *et al.*, 1990; Le Moine *et al.*, 1991; Harrington *et al.*, 1995; Lu *et al.*, 1998) (Fig. 21.10). Cells of the direct pathway contain mRNA for the D_1 receptor preprotachykinin and project to the internal pallidal segment and to the substantia nigra, pars reticulata. Cells of the indirect pathway contain mRNA for the D_2 receptor preproenkephalin and project to the external pallidal segment (see Fig. 21.11). However, the discovery of the $D_{3\text{-}5}$ dopamine receptor subtypes has complicated this notion. Recent studies have demonstrated subpopulations of medium spiny projection neurons that coexpress different complements of dopamine receptor subtypes, including the D_4 and D_5 receptors, as well as cells that colocalize substance P and enkephalin. Of particular interest here is the D_3 receptor subtype (part of the D2 family) which is often colocalized with

Pharmacologically-defined DA receptors:

D1-like receptors: **Activates G-proteins resulting in stimulation of cAMP.**

- **D_1 receptors: striatum, neocortex**
- **D_5 receptors: hippocampus, hypothalamus**

- **D2-like receptors:** **Activates G-proteins resulting in inhibition of cAMP.**
- **D_2 receptors: striatum, SN/VTA, pituitary**
- **D_3 receptors: NAc, olfactory tubercle, hypothalamus**
- **D_4 receptors: frontal cortex, medulla, midbrain**

FIGURE 21.10 Locations of pharmacologically defined dopamine (DA) receptor subtypes. cAMP, cyclic AMP; SN, substantia nigra; VTA, ventral tegmental area; NAc, nucleus accumbens.

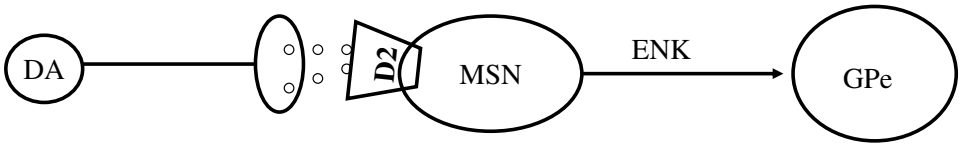

ENK-POSITIVE MSN (CONTAINING THE D2 R)
PROJECTS TO THE EXTERNAL SEGMENT

A.

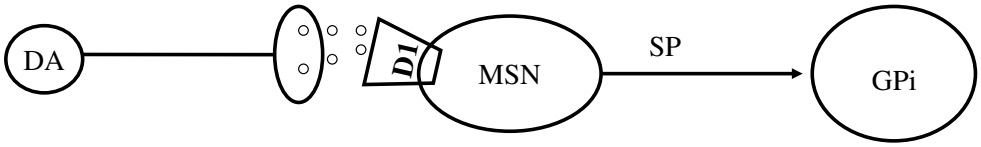

SP-POSITIVE MSN (CONTAINING THE D1 R)
PROJECTS TO THE INTERNAL SEGMENT

B.

FIGURE 21.11 Diagram demonstrating the two populations of medium spiny neurons. **(A)** One population contains high expression levels for D2 R and enkephalin and projects to the external pallidal segment. **(B)** One population contains high expression levels for D1 R and substance P and projects to the internal pallidal segment. DA, dopamine; D1 R, dopamine D1 receptor; D2 R, dopamine D2 receptor; ENK, enkephalin; GPe, globus pallidus external segment; GPi, globus pallidus internal segment; SP, substance P.

the D_1 receptors in the ventral striatum (Surmeier *et al.*, 1996; Aizman *et al.*, 2000; Nicola *et al.*, 2000).

The other main brainstem input arises from the dorsal and median raphe nuclei. This pathway uses serotonin as a transmitter. Unlike the distribution of dopaminergic terminals in the striatum, serotonergic terminals are not densely distributed throughout the striatum. Rather, they are more abundant in the ventral striatum (Lavoie and Parent, 1990). There are several serotonergic receptor subtypes, and their localization has been identified primarily in rats (Patel *et al.*, 1995; Ward and Dorsa, 1996). Inputs to the striatum also

5 Cell Types	Classical Name	Size	Transmitter	Dendrites	Axons	Inputs	Outputs
1	Aspiny I	Medium	GABA/PV	Arborize within 300um of the cell body	Collaterals are relatively local	Main input: Cortex; also from GPe.	Main target: MSN Terminals on proximal dendrites and cell bodies, forming pericellular baskets around MSN GAP Junctions
2		Medium to large	GABA/NPY/SOM +NOS			Cortex	MSN
3		Small to Medium	GABA/Calretinin				
4	Aspiny II	Large	Acetylcholine	Long dendrites, 400 um from cell extensive arborization	extensive	Thalamus, also from MSN, dopamine, (cortex)	MSN, other aspiny II cells
5	Aspiny III (infrequent)			Moderate branching	Few branches		

FIGURE 21.12 Features of the five subtypes of striatal interneurons. MSN, medium spiny neuron; GPe, globus pallidus external segment; PV, parvalbumin; NPY, neuropeptide Y; NOS, nitric oxide synthase; SOM, somatostatin.

include projections from other components of the basal ganglia including the external globus pallidus (and comparable region of the ventral pallidum), and the STh (Spooren *et al.*, 1996; Smith *et al.*, 1998b; Sato *et al.*, 2000b).

In addition to the extrinsic inputs, the projection neurons also receive input from interneurons and from local collaterals of other medium spiny cells. These terminate onto the spines, dendritic shafts, and soma of the medium spiny cells (Bishop *et al.*, 1982; DiFiglia and Aronin, 1982; Takagi *et al.*, 1983; Bolam *et al.*, 1985; Phelps *et al.*, 1985; Aronin *et al.*, 1986; DiFiglia, 1987; Izzo and Bolam, 1988; Kawaguchi *et al.*, 1990; Kita *et al.*, 1990; Pickel and Chan, 1990; Bennett and Bolam, 1994; Yung, 1996). The cholinergic interneurons terminate onto dendritic spines of the MSNs, which contain an enriched complement of muscarinic receptors. The m_1 and m_4 are the principal muscarinic receptors on the these neurons and play an important role in modulation of cortical effects on MSN spiking activity (Hersch *et al.*, 1994; Calabresi *et al.*, 1998, 2000a; Yan *et al.*, 2001). In addition, other interneurons also project to the MSN affecting their activity as well (Kawaguchi *et al.*, 1995; Kawaguchi, 1997; Calabresi *et al.*, 2000b). The relationships among these chemically identified cells and terminals reveal an intricate local network that forms the basis for the complex neuronal processing within the striatum (see section on microcircuitry).

Interneurons In addition to the spiny projection neurons, there are at least five distinct types of aspiny neurons, which are considered to be interneurons (Fox *et al.*, 1971b; Pasik *et al.*, 1976; Graveland and DiFiglia, 1985; Graveland *et al.*, 1985; Kawaguchi *et al.*, 1995) (Fig. 21.12). All are relatively less abundant compared to the medium spiny projection neurons and possess a relatively short axon, which is highly arborized into a rich local network. Aspiny type I cells are medium sized, round, and contain GABA. These are relatively frequent in the human striatum and constitute as many as 23% of the medium-sized cell population in the primate compared with less than 5% in the rat and mouse. The medium-sized interneurons give off two to five primary dendrites that branch profusely while remaining rather close to the soma. The axons of these cells also collateralize extensively relatively close to the parent cell, adding evidence that they are interneurons. These neurons have recently been further classified on the basis of histochemical markers and physiological properties (for review, see Kawaguchi

et al., 1995). One population co-contains GABA and the calcium-binding protein, parvalbumin (Gerfen *et al.,* 1985; Cowan *et al.,* 1990; Kita, 1993). These cells are slightly larger than the medium spiny projection neurons. Their dendrites arborize within 300 µm, and their axon collatoral arborization is relatively local. The parvalbumin-positive, GABA interneurons receive a powerful input from cortex (Lapper *et al.,* 1992; Kita, 1993). At least some of this cortical input is funneled to the substantia nigra via the MSN projection cells. Of particular interest is that these cells have gap junctions, indicating that they are coupled in a continuous network. Thus, while relatively few in number, their inhibition on medium spiny projection neurons is likely to be particularly effective (Kita, 1993; Jaeger *et al.,* 1994). The second type of aspiny, GABA-containing interneuron stains positively for the neuropeptides somatostatin, and neuropeptide Y, and co-contains nitric oxide synthase (NOS) (DiFiglia and Aronin, 1982; Takagi *et al.,* 1983; Vincent and Johansson, 1983; Vuillet *et al.,* 1989). These cells also receive cortical input (Kawaguchi *et al.,* 1995). Similar to the parvalbumin-immunoreactive cells, they synapse onto the soma and dendrites of the medium spiny projection neurons. The parvalbumin- and neuropeptide-containing interneurons differ in their intrinsic electophysiological properties (Kawaguchi *et al.,* 1995). The third type of GABA-containing medium-sized interneuron co-contains calretinin, a calcium-binding protein. Less is known about this group of medium aspiny interneurons.

Aspiny type II neurons are the largest of the striatal cells (30–40 µm) and represent approximately 1% of the population. These are the cholinergic interneurons. Compared to aspiny type I cells they have longer dendrites with extensive dendrite trees. They have 3–14 primary dendrites that branch frequently and extend to as much as 400 µm from the soma. Furthermore, their axonal fields are also more elaborate than other striatal cells (Braak and Braak, 1982; Graveland *et al.,* 1985; Yelnik *et al.,* 1993). These features have led to the hypothesis that the cholinergic interneurons play an important role in integrating inputs between functional or compartmental regions of the striatum (Kawaguchi *et al.,* 1995). Anatomical studies demonstrate that excitatory input is derived primarily from the thalamus (Meredith and Wouterlood, 1990; Lapper and Bolam, 1992) and is mediated in part by NMDA, AMPA, and mGluR receptors (Testa *et al.,* 1994; Landwehrmeyer *et al.,* 1995; Gotz *et al.,* 1997; Testa *et al.,* 1998; Pisani *et al.,* 2002). However, physiological examination of these cells also shows a cortical influence (Wilson *et al.,* 1990). The cholinergic interneurons have a complex relationship with the medium spiny projection cells, both receiving input from and projecting to them. Synaptic inputs from the medium spiny cells to the cholinergic cells terminate primarily onto the dendritic shafts and spines (Bolam *et al.,* 1986). Although synaptic inputs to the medium spiny cells from the cholinergic cells terminate onto cell bodies, they primarily target the dendritic shafts and spines (Izzo and Bolam, 1988). The cholinergic cells also receive dopaminergic input and have high expression levels of both the D_2 and D_5 receptor subtypes (Surmeier *et al.,* 1996). The central role for the functional balance between dopaminergic/cholinergic populations is well documented in both Parkinson's disease and in experimental animal models. Indeed, it had been assumed for some time that the cholinergic interneurons received direct input from the dopamine-containing fibers. However, more recently it has been demonstrated that while there is a direct input to the cholinergic cells, mostly mediated via D_2 receptors, much of the dopamine and cholinergic interaction likely takes place via converging inputs onto MSN (Lehmann and Langer, 1983; Kubota *et al.,* 1987; Chang, 1988b; Izzo and Bolam, 1988; Kawaguchi *et al.,* 1995).

The cholingergic interneurons are marked by their characteristic, spontaneous firing pattern and are referred to as tonically active neurons (TANs; Wilson *et al.,* 1990; Aosaki *et al.,* 1995). This firing pattern was observed in awake behaving primates in which pauses in the spontaneous cell firing occurred in conjunction with rewarded visuomotor behavioral tasks (Crutcher and DeLong, 1984a; Kimura *et al.,* 1984; Liles, 1985; Apicella *et al.,* 1991a). Tonically active neurons are thought to be involved in the detection of stimuli that have inherent motivational significance. These neurons respond to stimuli that have been conditioned, through behavioral training, to be associated with the delivery of primary rewards (Kimura *et al.,* 1984; Aosaki *et al.,* 1994b; Apicella *et al.,* 1997; Ravel *et al.,* 2001). In contrast to the membrane properties responsible for the physiological (up and down) states of the MSN, which are controlled in large part by extrinsic connections, the tonically active neurons' spontaneous firing patterns are by and large a function of the intrinsic membrane properties of the cholinergic cells (Bennett and Wilson, 1999; Bennett *et al.,* 2000). These properties are modified by synaptic inputs, which are influential in the temporal regulation of spikes sequences (Aosaki *et al.,* 1994b; Raz *et al.,* 1996). Unlike the MSN, tonically active neurons require relatively few extrinsic synaptic inputs to directly influence their spiking pattern (Wilson *et al.,* 1990).

The fifth class of interneurons includes small neurons with variable dendritic morphology that have only rarely been described. Nonetheless these may be

more prevalent in the human striatum than in other species (Graveland *et al.*, 1985). They have an average equivalent diameter of 10 µm, with aspiny to sparsely spiny moderate branching dendrites, which extend up to 130 µm from the soma. Axons are very fine and have few branches, which remain close to the parent soma. These cells in humans appear somewhat different from their closest counterpart in the monkey (Aspiny type III; DiFiglia *et al.*, 1976). The latter neurons have a more elaborate arborization, while in the human, axons for small cells were often absent, although failure to impregnate the axon could not be excluded. In this context it should be mentioned that in the primate, but not in the rat, significant numbers of small (8–12 µm) dopaminergic neurons have been reported at the dorsal, lateral, and ventral borders of the caudate and putamen (De la Torre, 1972; Felten and Sladek, 1983; Kohler *et al.*, 1983; Dubach *et al.*, 1987; Pearson, 1990).

Finally, Braak and Braak (1982) identified an additional large aspiny cell type (their type III), having long thick radiating dendrites and few branches. These cells are most probably not striatal, but rather are pallidal neurons that invade striatal territory (Haber, 1987; Heimer *et al.*, 1999).

Microcircuitry of the Striatum

The medium spiny neuron is the main target of extrinsic inputs to the striatum. The specificity of these inputs, derived from the cortex, thalamus, and brain stem and their spatial relationship to each other, in addition to interneuron contacts onto the spiny cells, dictates how projection neurons modify cortical information that passes through the basal ganglia. Present evidence suggests that, even though cortex and thalamus do project onto the spines and dendrites of the medium spiny cells, they may not terminate onto the same cells. The location of these glutamatergic synapses varies, with the cortex primarily terminating onto the heads of the spines and the thalamus primarily onto dendritic shafts (Dubé *et al.*, 1988; Smith and Bolam, 1990; Smith *et al.*, 1994b; Wang and Pickel, 2002). Tyrosine hydroxylase (TH)-positive terminals (presumably dopaminergic) also terminate onto both spines and shafts. Electronmicroscopic studies indicate that the dopaminergic terminals are optimally positioned relative to cortical afferent projections to specifically modulate cortical influence (Bouyer *et al.*, 1984b; Wang and Pickel, 2002). For example, cortical terminals are often found on the heads of spines, and dopaminergic terminals are found nearby, but on the dendritic shafts (Bouyer *et al.*, 1984a, b; Dubé *et al.*, 1988; Smith *et al.*, 1994b) (Fig. 21.13). The relationship between dopamine and thalamic terminals is less clear. However, the complexity of glutamatergic and dopaminergic interaction is further emphasized by ultrastructural studies that indicate DA release may be modulated by NMDA receptors (Gracy and Pickel, 1996).

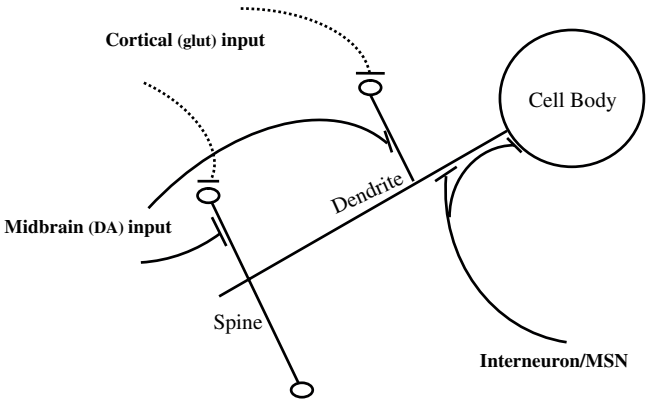

FIGURE 21.13 Schematic illustrating the arrangement of synaptic inputs to the medium spiny neurons. Cortical inputs generally terminate distal to the midbrain dopaminergic (DA) inputs. Interneurons and medium spiny neurons terminate closer to the cell body.

As mentioned earlier, in addition to extrinsic inputs, the medium spiny cells receive specific intrinsic inputs from the aspiny interneurons that terminate onto dendritic shafts, spines, and soma of medium spiny neurons (Izzo and Bolam, 1988). These synapses have an intricate relationship with dopaminergic inputs onto the medium spiny cells indicating a complex cholinergic-dopamine balance in mediating medium spiny neuron response. Finally, the medium spiny neurons receive input from other medium spiny cells (Aronin *et al.*, 1986; Bolam and Izzo, 1988; Pickel and Chan, 1990; Yung, 1996). Since most of the striatal cells (both interneurons and medium spiny neurons) use GABA and are considered inhibitory, their connections to the nearby projection neurons would theoretically indicate lateral inhibition. Little direct evidence has supported this concept (Jaeger *et al.*, 1994), so this remains an unsolved issue (Tunstall *et al.*, 2002).

The ability to record from single striatal cells, the cloning of receptor subtypes, and the development of selective receptor agonists and antagonists have lead to a greater appreciation of how receptor subtypes generate and modulate striatal firing activity. Furthermore, the ability to isolate and manipulate multiple ion channels has provided a clearer picture of how ionic conductances are modulated by a combination of voltage-dependent and ligand-dependent mechanisms to determine ultimately the spiking pattern of the projection cells. In particular, it is now realized that the idea that receptors either depolarize (excitatory response) or hyperpolarize (inhibitory response) is far

too simplistic. Rather, most postsynaptic responses to transmitter release onto MSN are complex and form part of a highly integrative system that ultimately will help determine the conditions under which the cell may fire. Indeed, many of the receptor subtypes do not inherently affect resting potential. In other situations, the postsynaptic response of a receptor may differ depending on other events taking place in the membrane. The D_1 receptor provides an excellent example of this phenomenon. D_1 activation can alter ion channel properties such that when the MSN is in a down-state, it is more difficult to transit into the up-state. However, if the MSN is in the up-state, then D_1 activation can enhance evoked activity. A similar case is made for the muscarinic receptors, in that they can affect synaptic transmission by altering various ion conductances (for reviews of these interactions, see Wilson, 1998; Calabresi *et al.,* 2000b; Nicola *et al.,* 2000).

Compartmentation of the Striatum

While overall the striatum was thought to be a relatively homogenous structure, it is now known that striatal neurons do form clusters, referred to as cell islands (Goldman-Rakic, 1982). Furthermore, histochemical and tracing studies demonstrate discontinuities in transmitter-related molecules, and of afferent terminal distribution patterns (Künzle, 1975; Goldman and Nauta, 1977; Jones *et al.,* 1977; Yeterian and Van Hoesen, 1978; Graybiel and Ragsdale, 1980). These patterns have formed the basis for many studies to investigate how these clusterings of cells, molecules, and terminals may be related to each other in an attempt to determine their functional significance. One of the first markers used to identify compartments chemically was acetylcholinesterase (AChE). AChE-poor striatal regions (termed striosomes) are surrounded by a densely stained 'matrix' (Graybiel and Ragsdale, 1978). The striosomes, embedded in the AChE-rich matrix, correspond to opiate receptor patches as well as to several other transmitter-related compounds (Kunzle, 1975; Künzle, 1977; Kalil, 1978; Herkenham and Pert, 1981; Ragsdale and Graybiel, 1981; Haber and Elde, 1982; Kelley *et al.,* 1982; Graybiel, 1983; Gerfen, 1984; Graybiel, 1984; Herkenham *et al.,* 1984; Gerfen, 1985; Donoghue and Herkenham, 1986; Joyce *et al.,* 1986; Gerfen, 1987; Gerfen *et al.,* 1987; Besson *et al.,* 1988; Gerfen, 1988; Groves *et al.,* 1988; Faull *et al.,* 1989; Zahm, 1989; Graybiel, 1990; Haber and Lu, 1992; Voorn *et al.,* 1994; McFarland and Haber, 2001). Within the striatum, the shape and extent of dendrites of some types of striatal neurons may be restricted by the size and shape of the striatal compartment in which they are found as well as by the proximity of individual cells to the borders of such compartments (Gerfen, 1985; Penny *et al.,* 1988). In contrast, the dendrites of large striatal interneurons (presumably cholinergic cells) readily cross striosomal/matrix boundaries, as do the medium-sized aspiny interneurons (medium-sized aspiny neurons). Thus, these interneurons may help to bridge compartments (Gerfen, 1984; Gerfen, 1985; Chesselet and Graybiel, 1986; Bolam and Izzo, 1988). This suggests that interneurons may function as assemblies that may have a greater impact on particular striatal channels than if these cells were randomly scattered throughout striatal areas. While several hypotheses have been put forth concerning the significance of the compartmental organization in the striatum, it continues to present a challenge in understanding the functional significance of this complex arrangement. For a review of this organization in primates and humans see Faull *et al.* (1989), Martin *et al.* (1993), Selden *et al.* (1994), Selemon *et al.* (1994), Ikemoto *et al.* (1995), Holt *et al.* (1996), and Holt *et al.* (1997).

Unique Features of the Ventral Striatum

Unique Cell Groups

The relative distribution of various striatal cell types differs somewhat between the dorsal and ventral striatum, with greater frequency of small neurons in the ventral striatum (Meyer *et al.,* 1989). The density of small cells is highest in the "fundus striati," while the density of large cells is lowest. Some of this difference may be attributed to the presence of the islands of Calleja in ventral striatal areas (see following discussion). However, clusters of smaller neurons outside the islands, while also found in the dorsal striatum, are particularly frequent in the ventral striatum (e.g., see Chronister *et al.,* 1981; Hedreen, 1981).

Embedded within parts of the ventral striatum are the islands of Calleja or cell islands, identifiable in all mammalian species by their dense core of granule cells (Fallon *et al.,* 1978; Fallon *et al.,* 1983; Meyer *et al.,* 1989). The largest island, Calleja Magna, forms the medial border of the nucleus accumbens. Additional, albeit smaller, islands (referred to as interface islands by Heimer *et al.,* 1999) are located in the basal forebrain in primates, including humans. These are found close to substance-P- and enkephalin-positive ventral pallidal fibers. The islands themselves also contain cholinergic, dopaminergic, and serotonergic fibers and terminals; epidermal growth factor (Fallon *et al.,* 1984) substance P; and glutamic acid decarboxylase (Fallon *et al.,* 1983; Oertel and Mugnaini, 1984; Young III *et al.,* 1984; Mugnaini and Oertel, 1985; Mai *et al.,* 1986; Pioro *et al.,* 1993). In addition, they also have estrogen and gonadotrophic hormone releasing hormone receptors (Fallon, 1983; Fallon *et al.,* 1983; Phelps and Vaughn,

1986). Together, these features have led to the suggestion that the islands may function as a type of "endocrine striatopallidal system." The granule cells in the islands are some of the smallest neurons in the brain (5–10 μm), which are nearly spherical and give rise to thin, mostly spine-sparse dendrites that are generally restricted to the island (Fallon *et al.*, 1978; Meyer and Wahle, 1986; Millhouse, 1987). There is an additional population of granule cells with spiny dendrites (Millhouse, 1987). Electron microscopic studies in rats show that some of these make "ephatic" junctions (Ribak and Fallon, 1982), which allow coupling of adjacent neurons in order to synchronize firing. In support of this morphological evidence that cells in the ventral striatum may communicate via gap junctions, Halliwell and colleagues recently demonstrated that these cells were physiologically coupled. Furthermore, the D3 receptor activation enhances gap junction in granule cells (Halliwell and Horne, 1998). The granule cells of the islands are arranged in a cuplike cluster with invaginations called the hilar area. Adjacent to the granule cells are striatal MSNs, whose dendrites invade the granule cell clusters. These cells stain positively for substance P and enkephalin (Fallon *et al.*, 1978; Fallon *et al.*, 1983; Millhouse, 1987). Although the connections of the islands of Calleja have been difficult to elucidate, ascending afferents include the dopamine, serotonin, and norepinephrine fibers from the substantia nigra, locus coeruleus, and dorsal and median (central superior) raphe nuclei of the brainstem (Azmitia and Segal, 1978; Fallon, 1978; Fallon *et al.*, 1978; Beckstead, 1979; Steinbusch *et al.*, 1981; Kohler *et al.*, 1982; Fallon, 1983; Bjorklund and Lindvall, 1984; Voorn *et al.*, 1986). It has been difficult to demonstrate projections for the granular cells beyond the immediate district of the cell cluster, and projections are thought to be limited to the dendrites that penetrate the islands from striatal cells.

Striatal cells located in and adjacent to the hilar regions stain positively for cholinergic markers and may account for the cholinergic innervation of granule cell clusters (Fallon *et al.*, 1983; Mesulam and Mufson, 1984; Young *et al.*, 1984; Phelps and Vaughn, 1986). Of particular interest is the fact that the cells in the islands are thought to contain quiescent immature cells that remain in the adult brain (Bayer, 1985; Meyer *et al.*, 1989; Heimer, 2000). In support of this idea, studies show that bcl-2 protein, a potent inhibitor of neuronal apoptosis (Zhong *et al.*, 1993; Farlie *et al.*, 1995) and promoter of axonal outgrowth and differentiation (Chen *et al.*, 1997), marks these islands (Bernier and Parent, 1998). Bcl-2 is most abundant in fetal neurons but persists in limited regions of the adult primate brain (Bernier and Parent, 1998; Yachnis *et al.*, 2000). One of the most prominent subcortical regions containing bcl-2 is the granular islands embedded within the ventral striatum. In addition to the small, immature-appearing bcl-2-positive cells, there are patches of larger size, more differentiated bcl-2-positive medium spiny cells within the ventral striatum (VS), at the border of the shell and core (Bernier and Parent, 1998; Fudge *et al.*, 2002).

The Shell and Core of the Ventral Striatum. Recently, a subterritory of the ventral striatum, the shell region, has been identified in rodents dividing the ventral striatum into two parts—a medial/ventral shell region and a central core region (Zaborszky *et al.*, 1985). Experiments aimed at delineating the functional significance of these two regions have been instrumental in understanding the circuitry underlying goal-directed behaviors, behavioral sensitization, and changes in affective states. Studies in rodents have been particularly important in demonstrating the organization of the shell and core and their relationship to distinct ventral striatal afferent and efferent projections. These studies provide critical information on how interactions between specific transmitter/receptor pathways mediate the transition between motivating stimuli and motor outcome (Heimer *et al.*, 1991b; Zahm and Brog, 1992; Brog *et al.*, 1993; O'Donnell and Grace, 1993; Pennartz *et al.*, 1994; Groenewegen *et al.*, 1996). While several transmitter and receptor distribution patterns distinguish the shell/core subterritories, lack of calbindin-positive staining is the most consistent marker for the shell across species (Meredith *et al.*, 1996).

In primates as in rodents, the ventral striatum is divided into two territories: the inner core which is calbindin-rich, and the outer crescent-shaped shell, which is calbindin-poor. Although a calbindin-poor region marks the subterritory of the shell, staining intensity of other histochemical markers varies both within the shell and in distinguishing it from the core. These markers include enkephalin; acetylcholinesterase; neurotensin; the μ opiate receptor; the growth associated protein, GAP-43; the AMPA subunits, GluR1, GluR2/3 & GluR4; the dopamine transporter; and serotonin (Haber and McFarland, 1999b) (Fig. 21.14). In general, compared to the core, the shell is rich in GluR1, GAP-43, acetylcholinesterase, μ receptor binding, serotonin, and Substance P (Alheid and Heimer, 1988; Martin *et al.*, 1991; Martin *et al.*, 1993; Hurd and Herkenham, 1995; Ikemoto *et al.*, 1995; Voorn *et al.*, 1996). Substance P is distributed in patches throughout the striatum, but it is particularly dense in the shell. Acetylcholinesterase is very dense in the medial part of the shell. More laterally, however, the

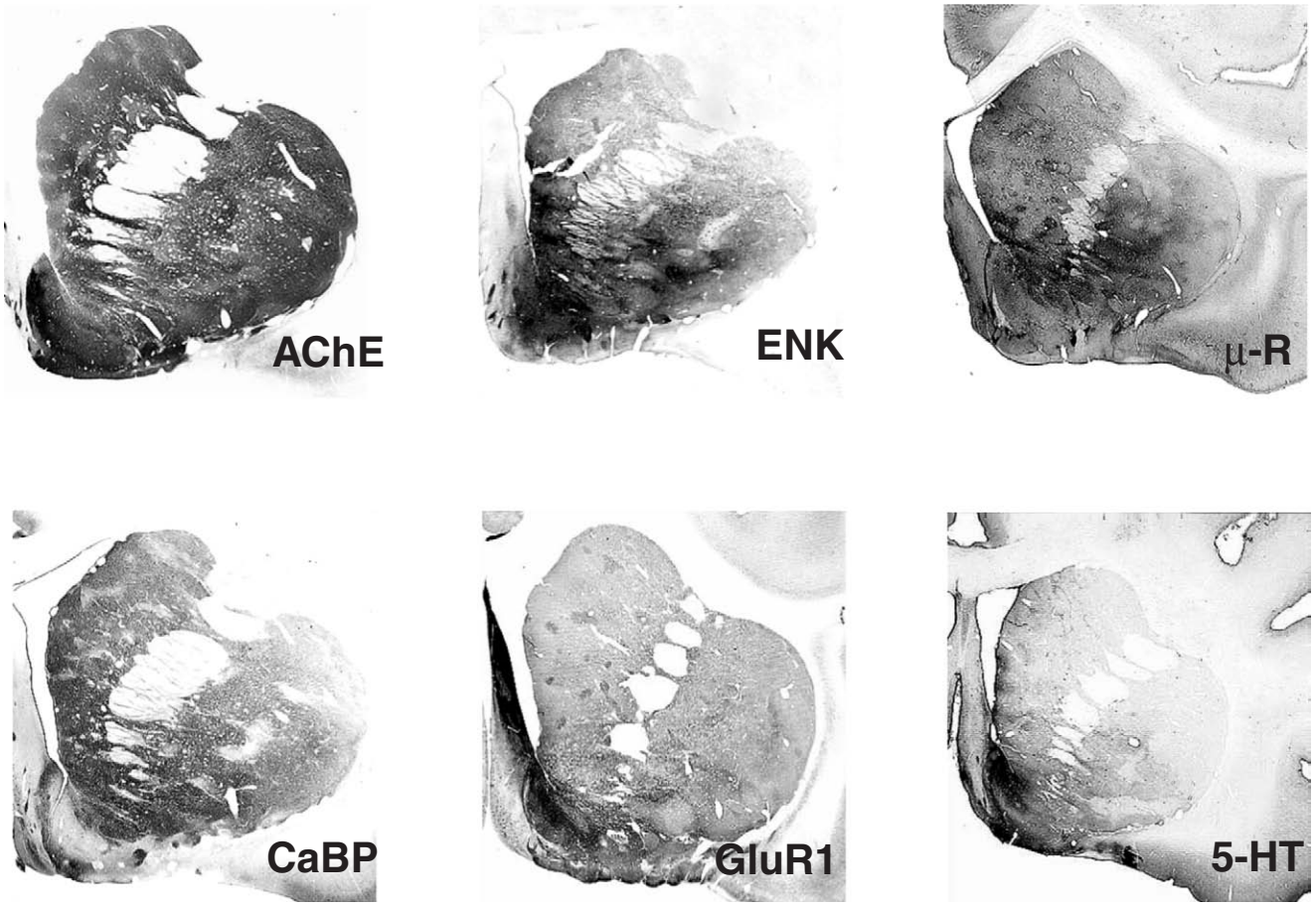

FIGURE 21.14 Photomicrographs of the striatum at the level of the shell and core, immunostained for various transmitter-related molecules. AchE, acetylcholinesterase; ENK, enkephalin; CaBP, calbindin-28; GluR1,GluR1 AMPA receptor subunit; μ-R, μ-opiate receptor; 5-HT, serotonin.

staining blends into the core and becomes indistinguishable from that observed in the remainder of the ventral striatum. Immunoreactivity for neurotensin is relatively low throughout the striatum; however, staining is dense in the medial rim of the shell. Enkephalin immunoreactivity is patchy throughout the striatum and does not show a remarkable differential pattern between the shell and core. Serotonin staining is dense in shell, with the highest immunoreactivity in the medial dorsal portion. The dopamine transporter is relatively low throughout the ventral striatum including the core. This pattern is consistent with the fact that the dorsal tier dopamine neurons express relatively low levels of mRNA for the dopamine transporter compared to the ventral tier (Haber *et al.*, 1995a). While GAP-43 immunoreactivity is found throughout the adult striatum, the shell region stands out with the strongest antisera reaction. The μ receptor distribution is dense but patchy in the ventral striatum. There are dense patches in the medial and ventral shell, with the remainder remarkably free of receptor. In contrast, the core shows numerous patches of immunoreactivity that extend into the medial wall of the ventral caudate. Most of the excitatory amino acid receptors do not distinguish the dorsal striatum and ventral striatum. However, the AMPA receptor subunits do. The GluR1 subunit shows particularly dense immunoreactivity in the shell, with patches of reactivity in the core. In contrast, the GluR4 subunit shows weaker immunoreactivity in the shell than in the rest of the striatum. Taken together, neurotransmitters and receptors help distinguish the ventral and medial borders of the ventral striatum and the shell/core subterritories within it. However, the dorsal and lateral boundaries are more problematic. Here, the ventral striatum merges imperceptibly with the dorsal striatum (see Fig. 21.14).

Afferent Projections of the Ventral Striatum. Finally, while the basic cortical BG loop is similar in all BG

circuits, the ventral striatum alone receives an additional subcortical input from the amygdala and from the hippocampus, for which there is no comprable input to the other basal ganglia territories (Russchen *et al.*, 1985; Fudge *et al.*, 2002) (see Fig. 21.22B).

The Pallidal Complex

Internal Structure, Morphology, and Organization of the Globus Pallidus

The primate globus pallidus forms the most medial cone-shaped portion of the lentiform nucleus for which the putamen forms a cap. In primates, the pallidum lies laterally to the internal capsule and appears as a very pale area in Nissl stains when compared to adjacent striatum. The globus pallidus is separated in part from the putamen by the external medullary lamina, a band of myelinated fibers capping the lateral aspects of globus pallidus (see Fig. 21.3). Dorsolaterally, pallidal neurons are, in general, confined within the border formed by the external medullary lamina, although occasional dendrites may extend into the putamen, and the possibility remains that occasional ectopic pallidal neurons may be found entirely within the striatum (see the previous discussion of striatal cell types). The ventral and rostral limit of the pallidum has been more difficult to define. Pallidal cells are often scattered in an interconnected network in basal forebrain that reaches quite near to the ventral surface of the brain.

The primate globus pallidus is divided by the internal medullary lamina into two zones—the external and internal pallidal segments. In most nonprimate mammalian species the internal pallidal segment extends into the internal capsule so that the bulk of neurons comprising this segment are completely surrounded by capsular fibers to form the entopeduncular nucleus. The distinction between the two segments of the dorsal pallidum can also be visualized with substance P and enkephalin immunohistochemistry (Haber and Elde, 1981)(Fig. 21.15A, B). As mentioned earlier, the internal segment receives striatal input from cells that express primarily substance P, while the external segment receives input from striatal cells that express primarily enkephalin (Del Fiacco *et al.*, 1982; Haber, 1986; Mai *et al.*, 1986; Reiner *et al.*, 1999). In primates, including humans, the separation of these two peptides into the two pallidal segments is not complete. Rather, the external segment contains substance P-positive immunoreactivity along the medial boundary. Likewise, enkephalin immunoreactivity is found in the medial portion of the internal segment (Haber and Elde, 1981; Haber, 1986; Reiner *et al.*, 1999). In humans, some cells of the internal segment may also be found embedded within the ventral portions of the internal capsule, although these might alternatively be considered rostral elements of the pars reticulata substantia nigra (Francois *et al.*, 1987). The internal pallidal segment is further divided into lateral and medial portions by an accessory medullary lamina produced by vertically running fibers of the ansa lenticularis. Furthermore, within the medial part of the internal pallidal segment in the human, a small, posteromedially located zone might be distinguished from the remainder of the internal pallidal segment by an absence of substance-P immunoreactivity. This

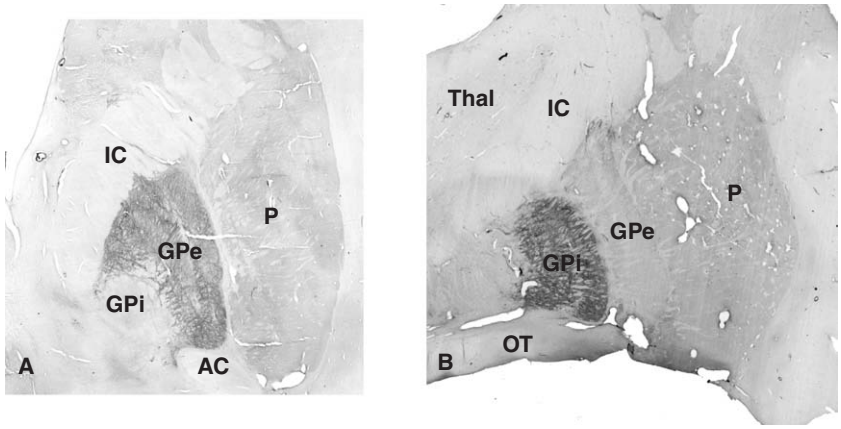

FIGURE 21.15 Photomicrographs of coronal sections through the human globus pallidus demonstrating the different distribution patterns of enkephalin and substance P immunostaining in the external and internal segments, respectively. **(A)** Enkephalin immunostaining of the globus pallidus external segment. **(B)** Substance P immunostaining of the globus pallidus internal segment. GPi, globus pallidus internal segment; GPe, globus pallidus external segment; IC, internal capsule; P, putamen; OT, optic tract; Thal, thalamus.

cone-shaped posteromedial subdivision, which in a sense could represent a fourth division of the globus pallidus, occurs in an area with somewhat increased density of myelinated fibers. The pattern of substance-P immunoreactivity demarcates this area in humans (see Mai *et al.,* 1986). Significant amounts of neurotensin immunoreactivity are also found in this posteromedial portion of the internal pallidal segment in humans (Michel *et al.,* 1986), which may correspond to similar intrapallidal neurotensin-rich territories noted in rodents (Uhl, 1982; Zahm and Heimer, 1988). The ability to divide the internal pallidal segment into several subdivisions may reflect the fact that projection neurons within this nucleus are more or less segregated based on their targets. Indeed, as we will see later, the topography of these output neurons to their targets is functionally arranged such that cortical representations in the striatum continue to be represented in the pallidal outputs to the subthalamus, thalamus, and brainstem (Carpenter, 1976; Parent, 1979; Carpenter *et al.,* 1981b; Parent and De Bellefeuille, 1982; Parent, 1986; Haber *et al.,* 1993; Hoover and Strick, 1993; Kayahara and Nakano, 1996; Arecchi-Bouchhioua *et al.,* 1997; Hoover and Strick, 1999; Sidibe *et al.,* 2002).

The cellular morphology of neurons in the globus pallidus is more uniform than that of the striatum. The globus pallidus is primarily made of relatively large, quite distinctive cells (20–60 μm) with triangular or polygonal cell bodies giving rise to thick, sparsely spined, poorly branching dendrites (Fox *et al.,* 1974; Schwyn and Fox, 1974; Iwahori and Mizuno, 1981; DiFiglia *et al.,* 1982a; Yelnik *et al.,* 1984; Braak and Braak, 1986). These dendrites are impressive, sometimes creating dendritic radii in excess of 2 mm in their principal plane with the very distal portions often branching elaborately to form complex dendritic endings (DiFiglia *et al.,* 1982a; Francois *et al.,* 1984b; Difiglia and Rafols, 1988). Complex dendritic endings appear to be more common in the external pallidal segment and in the substantia nigra than in the internal pallidal segment (Francois *et al.,* 1984b). The physiological significance of these specialized dendrites is not understood, although it has been suggested that they may contribute to local synapses between neighboring pallidal neurons (Francois *et al.,* 1984b; Yelnik *et al.,* 1984; Shink and Smith, 1995). Another feature of many large pallidal (and substantia nigra, pars reticulata) neurons, which is more frequently observed in humans than in nonhuman primates, is the fine, beaded, generally unbranched axonal-like processes originating at irregular intervals from pallidal dendrites. These extend for moderate distances (mean, 82 μm pallidum; 79 μm pars reticulata) and, in some instances, appear to contact the soma or dendrite of adjacent neurons (Francois *et al.,* 1984b; Yelnik *et al.,* 1987). As with the complex endings of pallidal cells, these thin processes appear to be more frequent within the lateral pallidal segment than in the medial segment (Francois *et al.,* 1984b).

The dendrites in the globus pallidus appear as a disclike territory oriented perpendicular to incoming striatal fibers. Thus each pallidal cell intercepts efferents originating in a column of striatal cells (Percheron *et al.,* 1984a, b). A significant feature of pallidal dendrites is their dense innervation by synapses, which at the electron microscopic level can be seen to cover the entire dendrite (Fox *et al.,* 1974; Schwyn and Fox, 1974; DiFiglia *et al.,* 1982a; Hassler and Chung, 1984; Difiglia and Rafols, 1988). The majority of these synapses represent striatopallidal terminals. Myelinated striatofugal axons cross perpendicular to pallidal dendritic fields and send thin unmyelinated collaterals parallel to pallidal dendrites with which they repeatedly synapse (Difiglia and Rafols, 1988). These axons and their dense field of terminal boutons in pallidal areas are immunopositive for either enkephalin (GPe) or substance P (GPi) (DiFiglia *et al.,* 1982b; Haber and Nauta, 1983; Chang, 1988a; Haber *et al.,* 1990a). The unique pattern of striatopallidal innervation as seen with peptide-postive staining has been termed "wooly fibers" and has been used to define the rostral and ventral extent of the ventral pallidum in rats and primates (Haber and Nauta, 1983; Haber, 1986; Haber *et al.,* 1990a; see discussion that follows).

Although the large cells account for the majority of pallidal neurons, there are other cell types that have been identified using Golgi and Nissl preparations. One type are small "microneurons" with few short thin dendritic processes. Another identified cell type is somewhat larger cells than the microneurons (15–21 μm) with more slender dendrites than the principal pallidal cells and shorter local axons. These two cell types presumably represent interneurons (Francois *et al.,* 1984b). A final cell type observed in the monkey but not in the human was intermediate in size between the small and large pallidal cells (23–34 μm) with slender but long radiating dendrites (Francois *et al.,* 1984b).

Ventral Pallidum

The pallidum, like the striatum, also extends ventrally, below the anterior commissure and into the anterior perforated space (see Fig. 21.2). This ventral extension of the globus pallidus was identified based on histological criteria and found to receive its primary input from the ventral striatum (Heimer, 1978). While determining the extent of the ventral

pallidum in normal Nissl and fiber stains is somewhat problematic, substance-P and enkephalin immunoreactivity are particularly useful for determining its boundaries and extent (Haber and Elde, 1981; DiFiglia *et al.*, 1982b; Haber and Nauta, 1983; Beach and McGeer, 1984; Haber and Watson, 1985; Mai *et al.*, 1986). In particular, the morphology of the peptide-stained fibers bears a stricking resemblence to Golgi-impregnated pallidal fibers (Fox *et al.*, 1974; Haber and Nauta, 1983). These fibers, which appear as tubular-like structures and are also referred to as wooly fibers, demonstrate the continuity of the dorsal and ventral pallidum. The ventral pallidum not only extends ventrally, but also rostrally to invade the rostral and ventral portions of the ventral striatum, sending finger-like extensions into the anterior perforated space. In addition, other histochemical markers such as endogneous iron demonstrate the continuity of the dorsal and ventral pallidum (Francois *et al.*, 1981; Switzer *et al.*, 1982; Alheid and Heimer, 1988; Dwork *et al.*, 1988). The ventral pallidum has common features of both the external and internal segments. It contains both enkephalin- and substance P-positive fibers, which, in turn, project to the STh and thalamus, respectively (Haber and Watson, 1985; Mai *et al.*, 1986; Russchen *et al.*, 1987; Haber *et al.*, 1990a; Haber *et al.*, 1993). Based on the preceding tracing and immunohistochemical studies in primates, the external pallidal component of the ventral pallidum lies ventral and rostral to the external segment. The internal segment component of the ventral pallidum lies primarily in the medial and rostral portion of the internal segment proper. In the human brain, the ventral pallidum extends far into the anterior perforated space, where the structure appears to be rapidly broken up into an interconnected lacework of pallidal areas, interdigitating with striatal cell islands and microcellular islands, including possibly deep islands of Calleja. In sagittal sections, the human ventral pallidum appears to be displaced somewhat more caudally by the nucleus accumbens than seems to be the case in the nonhuman primate. The realization and subsequent support of the concept of the ventral pallidum and striatum served to simplify the structural analysis of ventral forebrain (Heimer and Wilson, 1975; Heimer, 1978; Switzer *et al.*, 1982; Haber and Nauta, 1983; Haber *et al.*, 1985; Heimer *et al.*, 1985, 1987; Alheid and Heimer, 1988; Zahm and Brog, 1992). Thus, a large portion of the rostral forebrain that includes rostral, subcommissural substantia innominata can now be viewed as more or less continuous extensions of the better known dorsal striatopallidal complex.

Circuitry of the External, Internal, and Ventral Pallidum

While the projections of the two pallidal segments GPe and GPi (and the comprable parts of the ventral pallidum) differ, their main input is derived from the striatum (Fig. 21.16). In addition to this GABAergic striatal input, there is the well-characterized glutamatergic input from the STh nucleus to all palldial components (Nauta and Cole, 1978; Carpenter *et al.*, 1981a, b; Smith and Parent, 1988; Smith *et al.*, 1990; Hazrati and Parent, 1992a; Joel and Weiner, 1997). Terminals from STh intermingle with the much greater GABAergic innervation from the striatum (Shink and Smith, 1995). Striatal input to the GPi synapse all along the thick dendrites (Shink and Smith, 1995). All three glutamate receptor families are found in the pallidum. As observed in the striatum, the subunit composition of these receptors dictates the specific membrane properties. For example, AMPA receptors with high Ca^{2+} permeability are found in the globus pallidus (and the STh) in contrast to those with low Ca^{2+} permeability found in the medium spiny neurons of the striatum (Gotz *et al.*, 1997). Of particular interest is

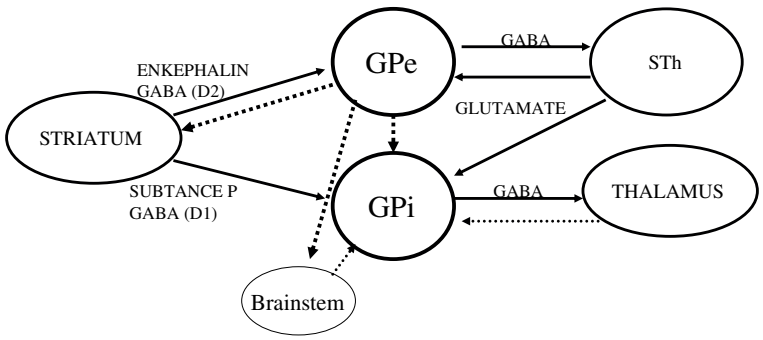

FIGURE 21.16 Diagram demonstrating the connections of the globus pallidus. The main connections (solid lines) and less prominent connections (dotted lines) are indicated. GPe, globus pallidus external segment; GPi, globus pallidus internal segment; STh, subthalamic nucleus.

the fact that glutamatergic receptors (metabotropic receptors) are found not only at postsynaptic specializations of asymmetric synapses but also at postsynaptic specializations of symmetric synapses, presummably formed by striatal GABAergic terminals. Hanson and Smith raised the interesting possibility that one role of these metabotropic receptors may be in modulating the GABAergic input from the striatum (Hanson and Smith, 1999). In addition to afferent input from the striatum and STh, the GPi also receives input from the GPe, which terminates close to, or on the somata (Hazrati *et al.,* 1990a; Shink and Smith, 1995; Smith *et al.,* 1998b). Other inputs to the GPi (and parts of the VP) are derived from the thalamus, brainstem pedunculopontine nucleus, and midbrain dopaminergic cells (Shink *et al.,* 1997; Francois *et al.,* 2000; Fig. 21.16).

It is important to remember that all pallidal neurons use GABA as their transmitter (Smith *et al.,* 1987; Ilinsky *et al.,* 1997). Projection fibers from the GPi are divided into three bundles—the ansa lenticularis, lenticular fasciculus, and pallidotegmental fibers (Nauta and Mehler, 1966; DeVito and Anderson, 1982). Fibers in the ansa lenticularis arise from the outer portion of the GPi, forming a clearly defined bundle that sweeps ventromedially and rostrally, around the internal capsule and continuing caudally to merge with Forel's field H. Fibers of the lenticular fasciculus arise from the medial portion of the GPi, traverse the internal capsule, and form a discete bundle, ventral to the zona incerta. This bundle joins the ansa lenticularis in Forel's field H and both fiber groups than become part of the thalamic fasciculus to terminate in different thalamic nuclei (Kuo and Carpenter, 1973; Carpenter, 1976). These projections are topographic in that they maintain their functional integrity in the thalamus. Thus, information carried via the two efferent fiber bundles is thought to differ somewhat functionally (Kuo and Carpenter, 1973; Carpenter, 1985; Baron *et al.,* 2001). The regions of the pallidum that receive sensorimotor-related input from the striatum project to the ventrolateral thalamic nucleus; those that receive input from association areas of the striatum project to the ventral anterior thalamic nucleus and mediodorsal nuc. of the thalamus, and those that receive input from limbic striatal regions (including the internal segment portion of the ventral pallidum) project to the mediodorsal nuc. and the lateral habenular nuc. (Kuo and Carpenter, 1973; DeVito and Anderson, 1982; Parent and De Bellefeuille, 1982; Haber *et al.,* 1985; Russchen *et al.,* 1987; Inase and Tanji, 1994, 1995; Kayahara and Nakano, 1996; Sidibe *et al.,* 1997; Hoover and Strick, 1999; Sakai *et al.,* 2000). GPi fibers projecting to the thalamic relay nuclei also give off collaterals that terminate in the intralaminar nuclei, the centromedian and parafasicular nuclei (Kuo and Carpenter, 1973; Kim *et al.,* 1976; Parent *et al.,* 2001). The third fiber bundle arising from the GPi, the palllidotegmental fibers, terminates in the pedunculopontine nuc. (Shink *et al.,* 1997). Recent studies using single cell reconstruction demonstrate that there appear to be at least two types of pallidal projection cells. Type I cells, which are centrally located and quite abundant and project to the pedunculopontine tegmentum, give off collateral branches that ascend and also terminate in the thalamus, in both the relay nuclei and in the intralaminar group. Type II cells project to the lateral habenular nucleus (Parent *et al.,* 2001). Pallidal fibers entering the thalamus give off several collaterals that form branches that terminate primarily onto the soma and proximal dendrites of thalamic projection cells. In addition, some synaptic contact is also made with local circuit neurons. This terminal organization indicates that, while pallidal projections to the thalamus are primarily inhibitory on thalamic relay neurons cells, they may also function to disinhibit projection cells via the local circuit neurons (Arecchi-Bouchhioua *et al.,* 1997; Ilinsky *et al.,* 1997). While projections from the GPi to the ventral tier nuclear group of the thalamus have been considered to be segregated from cerebellar inputs to the thalamus, recent evidence suggests that there may be some overlap between them (Middleton and Strick, 1994; Sakai *et al.,* 1996; Hoover and Strick, 1999; Sakai *et al.,* 2000).

The external segment of the globus pallidus projects primarily to the STh via the subthalamic fasciculus, a fiber system that carries both pallidosubthalamic axons and subthalamopallidal fibers (Fig. 21.16). However, in addition, this pallidal segment also projects to the striatum, the internal pallidal segment, and the midbrain. In addition, terminals have also been found from the GPe to synapse in the reticular nuc. of the thalmaus. As observed with the internal segment, these projections are also topographically organized to maintain functional continuity within the target structures (Kim *et al.,* 1976; DeVito and Anderson, 1982; Parent and DeBellefeuille, 1983; Hazrati *et al.,* 1990a; Hazrati and Parent, 1991; Haber *et al.,* 1993; Asanuma, 1994; Smith *et al.,* 1994a; Shink *et al.,* 1996; Sato *et al.,* 2000a). Neurons in the GPe segment have been further classified according to their projection target: those that target the STh and the SNR; those that target the internal segment and the STh; those that target the STh and SNR, and those that target the striatum (Sato *et al.,* 2000a). In general, projections from the GPe, as with the output from the GPi, terminate on the soma or proximal dendrites of its target sites. The two pallidal segments are central to the concept of the direct and indirect pathways through the basal

ganglia. As a result, teasing apart the complexity of these pallidal pathways has been an important avenue of research (see the section on "The Direct and Indirect Basal Ganglia Pathways").

Pallidal neurons are very tonically active cells. GPe and GPi have different firing patterns as indicated in nonhuman primate and human studies (DeLong, 1971; Georgopoulos *et al.*, 1983; DeLong *et al.*, 1985; Mitchell *et al.*, 1987; Filion and Tremblay, 1991; Mink and Thach, 1991a; Boraud *et al.*, 1996; Boraud *et al.*, 2000; Raz *et al.*, 2000). The resting discharge of GPi neurons is relatively homogeneous. They discharge at approximately 60–80 spikes/s during maintenance of a relaxed neutral posture. In contrast, GPe neurons can be divided into two populations based upon their discharge patterns. One population of GPe neurons discharges at relatively high frequencies (50–70 spikes/s) interrupted with long-duration pauses. In contrast, the second population of GPe neurons discharges at lower frequencies (<15 spikes/s) with intermittent, high-frequency bursts. Similar to GPi cells, these neurons change their firing in relationship to behavioral activity. During behavioral activity, all pallidal cells change their resting, tonic activity and either burst or pause. These changes are presumably the result of a combination of inhibitory, GABAergic inputs from the striatum and/or direct excitatory, glutamatergic inputs to the STh from the cortex through what has recently been named the "hyperdirect pathway" (Mink, 1996; Nambu *et al.*, 2002). These changes in firing patterns in association with behavioral activity are similar to those described by Basso and Wurtz (2002) for cells of the substantia nigra, pars reticulata. In addition to the cells that are typically identified as belonging to either GPe or GPi, there is a fourth population of neurons, referred to as "border cells." These are generally located near the perimeter of the pallidal segments or adjacent to, or in, the external or internal medullary laminae (DeLong, 1971). Border cells exhibit a medium-frequency, regular discharge pattern that is not unlike that recorded from the neurons located in the nearby substantia innominata, presumably the cholinergic cells of the nucleus basalis. While border cells have been shown to be modulated in association with movements related to reward, an understanding of their role in voluntary movement remains unclear.

The Subthalamic Nucleus

The subthalamic nucleus is a well-defined compact oval structure that takes the shape of a biconvex lens. It is located medial to the peduncular portion of the internal capsule at its rostral level and extends caudally to overlie the rostral part of the substantia nigra (Fig. 21.4). The principal neurons in the STh nucleus of the primate are medium to large cells (25–49 μm) and are pyramidal, or round in shape. Each cell gives rise to five to eight dendritic stems, which branch extensively to cover a large area of the nucleus (in primates approximately 20%). Secondary dendrites are thin and have varying numbers of dendritic spines ranging from sparse to very frequent (Rafols and Fox, 1976; Yelnik and Percheron, 1979; Hammond and Yelnik, 1983; Sato *et al.*, 2000b). There are important species differences in the extent to which the dendritic arbor innervates the nucleus. For example, in the rodent, the dendritic field of each cell is calculated to cover the entire nucleus, while in primates it covers only a fraction of it (Hammond and Yelnik, 1983). The projection neurons are divided into two groups—one that has axons that collateralize locally and one with axons that do not collatoralize extensively within the STh. Cells with collaterals within the STh terminate often beyond the dendritic radius of the parent cell (Kita *et al.*, 1983). Both types of subthalamic neurons give rise to a single axon that bifurcates, producing one ascending and one descending axon collateral. These axons terminate in pallidum and in pars reticulata substantia nigra, respectively (Kita *et al.*, 1983). Projection cells have been further divided according to their collateralization to target structues (Sato *et al.*, 2000b) (see discussion that follows). There are few interneurons in the STh (less than 5%). These interneurons are relatively small (12–16 μm) cells, with long dendrites that follow a more tortuous course than the radiating dendrites of the principal neurons (Rafols and Fox, 1976).

Connections of the STh include both intrinsic basal ganglia connections as well as extrinsic (Fig. 21.17). The external segment of the globus pallidus and parts of the ventral pallidum provide one of the most massive afferent projections. As seen with the other basal ganglia structures, these inputs terminate in a functionally topographic manner (Nauta and Mehler, 1966; Carpenter *et al.*, 1968; Kim *et al.*, 1976; Carpenter *et al.*, 1981a, b; Haber *et al.*, 1985). This GABAergic input is inhibitory and ensheaths the soma and dendrites of the STh cells (Smith *et al.*, 1990; Shink *et al.*, 1996; Bevan *et al.*, 1997). The main extrinsic inputs to the STN are from the cortex and brainstem. Cortical inputs are also topographically organized, which mirrors the functional organization of frontal cortex (Künzle, 1977; Kunzle and Akert, 1977; Kunzle, 1978; Monakow *et al.*, 1978; Carpenter *et al.*, 1981a; Matsumura *et al.*, 1992; Wichmann *et al.*, 1994; Nambu *et al.*, 1996; Nambu *et al.*, 1997; Takada *et al.*, 2001). Corticosubthalamic inputs make monosynaptic, glutamatergic, asymmetrical

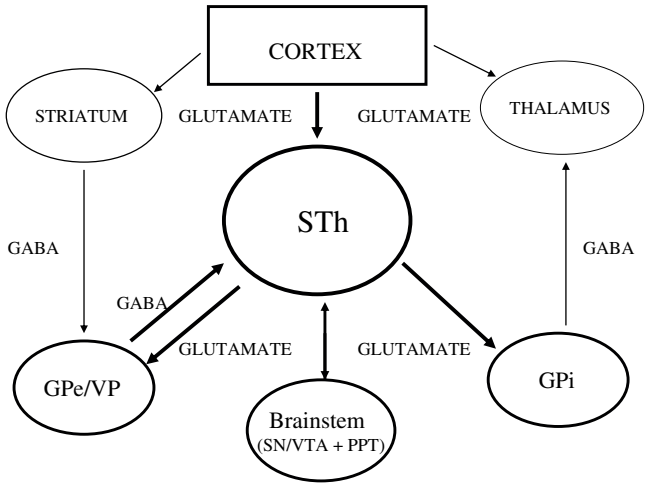

FIGURE 21.17 Diagram demonstrating the connections of the subthalamic nucleus (STh). Direct afferent and efferent projections of the STh are shown in bold lines. Connections between the other basal ganglia nuclei are also indicated. GPe, globus pallidus external segment; GPi, globus pallidus internal segment; PPT, pedunculopontine nucleus; SN, substantia nigra; VP, ventral pallidum; VTA, ventral tegmental area.

synapses onto the distal dendrites and spines of the STh neurons (Romansky *et al.*, 1979; Kitai and Deniau, 1981; Bevan *et al.*, 1995). The STh contains all three glutamatergic receptor subtypes. As with the other basal ganglia structures, the distribution and physiological effects of these have been described in the STh (Gotz *et al.*, 1997; Nambu *et al.*, 2000; Turner *et al.*, 2001). The composition of the different subunits for the AMPA and NMDA receptors emphasizes the functional properties of the different subunit compositions. In the STh, for example, neurons express receptor compositions which lead to highly Ca^{2+} permeable receptors (Gotz *et al.*, 1997). Afferent projections from the cortex and pallidum terminate onto the same dendrites in STh, indicating that these neurons process, simultaneously, information from both cortex and pallidum. However, it should be noted that the cortical input appears to be distal to that of the pallidum.

The idea that dopamine projects directly to the STh, first suggested by immunohistofluorescent staining demonstrating labeled dopamine fibers in the STh of rodents, has been further supported by immunohistochemical staining for tyrosine hydroxylase in the STh and tracing and functional studies (Brown *et al.*, 1979; Rinvik *et al.*, 1979; Bjorklund and Lindvall, 1984; Campbell *et al.*, 1985; Lavoie *et al.*, 1989; Hassani *et al.*, 1996; Hassani *et al.*, 1997; Cossette *et al.*, 1999; Hedreen, 1999). Support of the functional relevance of dopamine in the STh itself, rather than as passing fibers, comes from binding and *in situ* hybridization studies that demonstrate the presence of D_1, D_2, and D_3 receptors in the nucleus (Martres *et al.*, 1985; Weiner *et al.*, 1991; Mansour *et al.*, 1992; Flores *et al.*, 1999). Interest in the direct dopamine innervation of the STh has increased recently because of the recognition of its hyperactivity in Parkinson's disease (Bergman *et al.*, 1990; Limousin *et al.*, 1997; Rodriguez *et al.*, 1998; Francois *et al.*, 2000) and the fact that at least a subpopulation of the dopamine cells that project to the STh are vulnerable to degeneration in Parkinson's disease and in animal models of PD (Francois *et al.*, 2000).

Additional brainstem inputs to the STh are derived from cholinergic cells of the pedunculopontine region; more medially placed cells of the extrapyramidal area, which are noncholinergic; and cells from the laterodorsal tegmental nucleus (Rye *et al.*, 1987; Lavoie and Parent, 1994; Bevan and Bolam, 1995). It should be noted that projections from the PPTg are reciprocal.

The STh projects topographically to all pallidal regions including the GPe, GPi, and VP, and to the substantia nigra, primarily terminating in the pars reticulata. Single-cell labeling techniques, along with electrophysiological studies in rodents, demonstrate that these target structures receive input from collateral axons that the stem from the same cell (Van der Kooy and Hattori, 1980; Hammond *et al.*, 1983; Hammond and Yelnik, 1983; Kita *et al.*, 1983). A recent study in primates supports the notion that single STh cells send collateral fibers to the different output basal ganglia nuclei (Shink *et al.*, 1996). This study found several subpopulations of neurons, each with different branching patterns. One population projects to all three target regions, the GPi, GPe, and SN; a second population, the largest, sends axons to the GPi and

GPe; a third group of cells innervates only GPe; a fourth population innervates only the striatum; and finally a very small group of cells targets the GPe and SN (Sato *et al.,* 2000b). STh neurons use glutamate as the transmitter, and all the target regions of the STh show ultrastructural features that are consistent with an enriched glutatmatergic synaptic innervation. These terminals make synaptic contact along the entire cell and dendrites of the target structures (Shink and Smith, 1995; Smith *et al.,* 1998a). Other outputs of the STh include the striatum (as mentioned previously) and the pedunculopontine tegmental nuc.

As with the pallidal neurons, cells of the STh are tonically active, firing at a low frequency (approximately 24 spikes/s)(Georgopoulos *et al.,* 1983; DeLong *et al.,* 1985). Culture studies show that the rhythmic discharge pattern, albeit slow, is not dependent upon excitatory input, but rather on intrinsic membrane properties (Bevan and Wilson, 1999). Furthermore, the same group examined the intrinsic membrane properties of STh neurons *in vitro* using intracellular recording methods and pharmacological manipulation of the GABAa receptor and found that the diverse firing patterns manifest by STh neurons were likely to be the produced as a result of inhibitory input from GP in combination with the intrinsic membrane properties of STh cells (Bevan *et al.,* 2002). Both excitatory glutamatergic, cortical input and inhibitory GABAergic pallidal input are the main extrinsic sources that control the firing pattern of STh. Thus, when these cells respond with a burst firing pattern in association with the direction of movement, it is the result of a combination of intrinsic properties and the excitatory and inhibitory influences of cortex and the pallidus, respectively.

The Direct and Indirect Basal Ganglia Pathways

At this, point we can review the concept of the direct and indirect pathways (refer to Fig. 21.7; Albin *et al.,* 1989; Alexander and Crutcher, 1990; DeLong, 1990; Kato and Hikosaka, 1995; Joel and Weiner, 1997; Smith *et al.,* 1998b). This organizational scheme has played an important role in formulating the functional organization and underlying mechanisms of motor control through basal ganglia circuits (Kato and Hikosaka, 1995; Mink, 1996; Boraud *et al.,* 2002). While this concept has been further theoretically extended to the other BG functions, including cognition and emotion, the experimental data have been primarily focused on the control of movement and the pathophysiology that underlies movement disorders such as Parkinson's disease and Huntington's chorea (DeLong, 1990). Review of the pathways and transmitter-related compounds as described in previous sections (see Fig. 21.8) shows that (1) the direct pathway includes projections from the cortex (glutamatergic) that terminate onto MSN that primarily co-contain substance P and GABA, along with the D_1 dopamine receptor. Recall that this receptor increases cAMP but also has a number of important effects on the channel properties of the MSN. The MSNs of the direct pathway project primarily to the GPi. This inhibitory input to the GABAergic neurons of the GPi decreases the firing of these cells. Since the GPi also uses GABA and is inhibitory, the net effect of this striatal inhibition, and decreased GPi firing, is to disinhibit the thalamus (decreased inhibition of thalamic cells = increased thalamic firing). Thus, through the direct pathway cortical excitation of the striatum should result in promoting thalamic output back to cortex, thereby reinforcing cortical activity. In this way, the direct pathway retains and reinforces the cortico-basal ganglia activity. This can be further reinforced by the dopaminergic input (via the D_1 receptors), especially if the cortical drive is maintained with temporally coherent excitatory inputs, thus maintaining the MSN in an upstate. This activity can be further reinforced by the direct, excitatory thalamic input to MSN (Fig. 21.18).

The indirect pathway includes projections from the cortex (glutamatergic) that terminate onto the MSN, which primarily co-contain enkephalin and GABA, along with the D_2 receptor subtype (see Fig. 21.11). This receptor, we will recall, inhibits cAMP and therefore tends to be inhibitory. The MSNs of the indirect pathway project primarily to the GPe. This inhibitory influence on the GPe results in a decreased inhibition of the STh (or disinhibition), thereby causing an increased glutamatergic excitation of both pallidal segments. The increase in GPi output results in an inhibition of the basal ganglia thalamic relay nuclei, thereby decreasing its excitatory influence on cortex. The net result, therefore, of this pathway is the opposite of the direct pathway in that, rather than reinforcing cortico-basal ganglia activity, it decreases (or inhibits) it. The action of dopamine on this system is to further decrease the output, by reinforcing the inhibition of the striatopallidal output (Fig. 21.18). There are several excellent and detailed reviews of the direct and indirect pathways (Albin *et al.,* 1989; DeLong and Georgopoulos, 1991; Gerfen and Wilson, 1996; Smith *et al.,* 1998b). Less is known about the details of this organization for the ventral striatopallidal system, (Haber *et al.,* 1993; Groenewegen and Berendse, 1994b).

This scheme of two opposing pathways has led to the hypothesis that the balance between the direct and indirect pathways is critical for the smooth execution

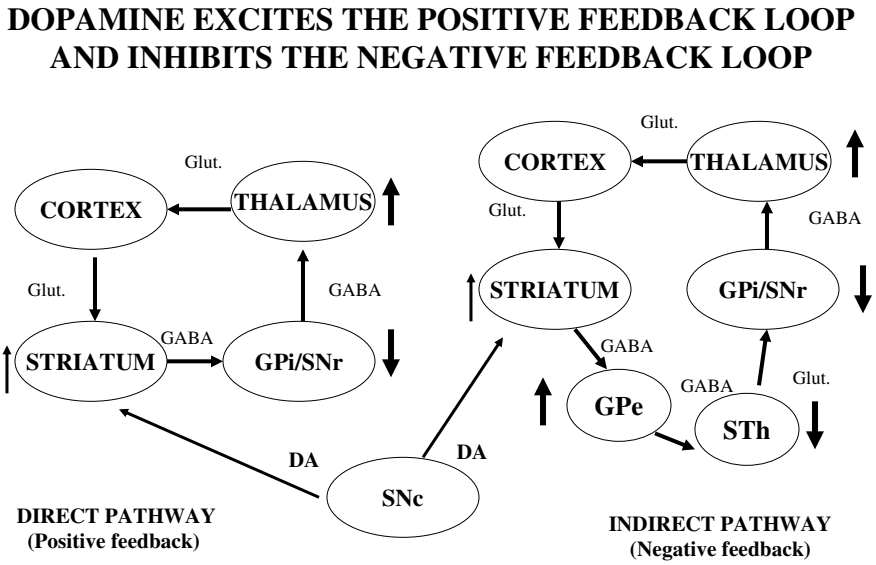

FIGURE 21.18 Diagram demonstrating how dopamine influences the direct and indirect pathways. Larger arrows indicate the changes of normal pathway interactions by DA modulation. The consequences of this DA modulation are to enhancement of the positive feedback to cortex through the direct pathway and inhibit the negative feedback to cortex through the indirect pathway. Glut, glutamate; GPe, globus pallidus external segment; GPi, globus pallidus internal segment; STh, subthalamic nucleus.

of behavior, and that in pathological situations, this equilibrium is disrupted. This core model for BG function has helped explain some of the pathophysiological mechanisms for both hypokinetic (Parkinson's disease) and hyperkinetic (Huntington's disease and hemibalismus) states in which there is either an increased inhibition of the thalamocortical pathway, resulting in hypokinetic disorders, or a decreased inhibition of thalamocortical output, resulting in hyperkinetic disorders (DeLong, 1990). The assumption that these two pathways are separate suggests two functional schemes: one in which the output from the indirect pathway merges at the cellular level with the direct pathway (in the GPi, or SNR); and one in which these two pathways remain separate and terminate on different neurons in the output nuclei (GPi or SNR). In the first situation, a temporal scaling of inputs onto the GPi/SNR cells results in an output that eventually drives the feedforward loop to the thalamus. In the second situation, it is the thalamus and/or cortex that collects these opposing inputs. In this scheme, two pathways send competing signals to the thalamus, one that broadly inhibits (via the indirect pathway), and one that focally stimulates (through the direct pathway), allowing what has been termed focused selection (Mink, 1996). In this model, the output of the two pathways effectively creates a "center-surround" inhibition, in which motor programs which underlie the desired movement are encouraged, while competing programs are inhibited. The model has the advantage of explaining some of the physiology associated with normal movement and the pathophysiology in PD. For example, the "focused-selection" model helps explain some of the timing of spike firing during movement. It also predicts that the majority of pallidal cells would be activated in movement-related activity (thereby inhibiting thalamocortical output), and the minority would be inactivated, (thereby "focusing" the thalamocortical ouput). Experimental evidence supports this prediction. Dopamine depletion results in the inability to disinhibit (thereby not releasing desired movements) through the direct pathway, and the inability to inhibit competing motor programs (thereby not inhibiting undesired movements) through the indirect pathway.

While the concept of the direct and indirect pathways has stimulated interesting and provocative models of BG function, recent studies show that there are anatomical, physiological, and cellular inconsistences with the idea that there are two completely separate pathways. These inconsistences force a reexamination of the role of a direct and indirect pathway as a fundamental feature that drives the BG. First, review of the anatomical data described in the previous section, shows that these two pathways are not completely separate. For example, there is a subpopulation of MSNs that project to the GPe (part of the indirect pathway) and also send collaterals to

either the GPi or to GPi and SNR (part of the direct pathway) (Kawaguchi *et al.,* 1990). Futhermore, MSNs of the direct and indirect pathways are interconnected via collaterals within the striatum (Aronin *et al.*, 1986; Yung, 1996) The GPe neurons (the indirect pathway) project directly to the GPi/SNR (the direct pathway) and collaterals from the STh project to all three striatal output structures (Hazrati *et al.,* 1990b; Smith *et al.,* 1994a; Parent *et al.,* 2000; Sato *et al.,* 2000a; Sato *et al.,* 2000b). Second, physiological experiments designed to test inhibition and disinhibition in the output pathways related to movement do not support the expected outcomes in all the structures. For example, there is little correlation of cell activitiy between the GPe and GPi during movement (Raz *et al.,* 2001). Furthermore, while hyperactivity in the GPi has been reported in dopamine-depleted animals (Wichmann *et al.,* 1999; Raz *et al.,* 2000), there is no evidence for hypoactivity in the GPe in these animals (Bezard *et al.,* 1999; Boraud *et al.,* 2001). Finally, molecular and immunohistochemical studies that demonstrate the transmitters and receptors assumed to be specific for each pathway are colocalized in some cells. As we have seen from the preceeding descriptions, several populations of MSN co-contain different dopamine receptor subtypes (Surmeier *et al.,* 1998; Aizman *et al.,* 2000). In addition, enkephalin is found in parts of the GPi and substance P is found in regions of the GPe (Haber and Elde, 1981; Haber and Watson, 1985; Reiner *et al.,* 1999).

Experiments directed at developing the functional utility of the direct and indirect pathway model are largely based on how motor programs are executed. As a result, while this models a microcircuit of function, it does not address the overall issue of how BG work with cortex to mediate goal-directed behaviors. In other words, it helps understand how, once a particular movement (or behavior) has been selected, it is carried out smoothly, without interference of "unwanted" actions. However, in reality, each action (or behavior) is made up of many decisions, both small (should I move slightly to the right to grasp the pencil?) and large (do I pay attention to the sweet smell coming from the bakery, turn and walk in to buy a treat?). While clearly many decisions are made at the cortical level, the BG play an important role in modifying behaviors based on reinforcement. This requires more than simple opposing pathways, mediating a particular outcome. It requires continual on-line adjustments, not only to keep a behavior on target, but also to be able to switch to accommodate adjustments. Consistent with this idea, the BG are now an accepted part of the learning process, plasticity, and reward acquistion, which requires immediate online modifications (Robbins *et al.,* 1989; Hikosaka, 1991; Everitt and Robbins, 1992; Saint-Cyr and Taylor, 1992; Kalivas *et al.,* 1993; Kombian and Malenka, 1994; Baev, 1995; Kimura, 1995; Kimura and Graybiel, 1995; Jueptner *et al.,* 1997; Kawagoe *et al.,* 1998; Schultz *et al.,* 1998; Wise, 1998; Bonci and Malenka, 1999; Jog *et al.,* 1999; Robbins and Everitt, 1999; Thomas and Malenka, 1999; Doya, 2000; Schultz *et al.,* 2000; Thomas *et al.,* 2000; Kerr and Wickens, 2001). As we will see later, the dopamine system plays an important role in these functions.

Another assumption that is made in most current models (including the direct and indirect pathway model) of BG function is that these pathways are organized in functionally discrete channels and that the model created for the motor system can than be applied to the other functional systems. A major drawback to this assumption is that most actions do not occur in isolation of motivation and cognition, and it is unlikely that the BG would operate to isolate these cortical functions. Several alternative schemes have been developed to address how the BG help cortex integrate information between these channels. An important issue here is not only the fact that there is potential cross-talk between different channels (Nauta *et al.,* 1978; Somogyi *et al.,* 1981b; Haber *et al.,* 1994; Bevan *et al.,* 1997), but how that information moves through the BG pathways to account for the development of coordinated, goal-directed behaviors (Bar-Gad *et al.,* 2000; Haber *et al.,* 2000, 2002; McFarland and Haber, 2002a, 2001). We will return to this topic in more detail later when we discuss the functional organization of BG circuits.

The Substantia Nigra and Ventral Tegmental Area

The substantia nigra appears as a flattened oval structure on the dorsal aspect of the base of the cerebral peduncle (Fig. 21.5). On the basis of cytoarchitectonic and chemical criteria, the substantia nigra is subdivided into two cell groups, the pars compacta (SNC) and the pars reticulata (SNR) (Olszewski and Baxter, 1982; Poirier *et al.,* 1983; Francois *et al.,* 1985; Halliday and Tork, 1986). This subdivision into two components is supported by the chemical anatomy of this nuclear complex. Some surveys in the monkey and human suggest further divisions—a pars lateralis and a mixed region at the dorsomedial surface of pars compacta (Francois *et al.,* 1984a; Francois *et al.,* 1987; Yelnik *et al.,* 1987 Percheron *et al.,* 1987). This latter subdivision contains some cells characteristic of the pars compacta and others more closely related to the pars reticulata, while the pars lateralis resembles for the most part the remainder of pars reticulata, except that cell bodies are somewhat larger and they may specifically target the

superior colliculus (Beckstead *et al.*, 1981; Beckstead and Frankfurter, 1982; Beckstead, 1983; Francois *et al.*, 1984a; Yelnik *et al.*, 1987; Paxinos *et al.*, 2000). In general, when using the term "pars reticulata," we will be referring to all of the cells not belonging to the dopaminergic, melatonin-rich class that composes the pars compacta.

The pars reticulata, while clearly a separate entity, is often considered a caudomedial extension of the internal pallidal segment based on morphology, connections, neurochemistry, and physiology (Fox *et al.*, 1974; DeLong and Georgopoulos, 1981; Percheron *et al.*, 1984a; Nauta, 1986; Francois *et al.*, 1987; Yelnik *et al.*, 1987; Percheron *et al.*, 1994). The pars compacta is part of an extensive midbrain dopaminergic system that includes the ventral tegmental area and the retrorubral group. The following discussion of the pars reticulata will be brief, since its characteristics are similar to that of the internal pallidal segment. In this section, we will discuss the entire midbrain dopamine system, including the ventral tegmental area (VTA) and retrorubral cell group.

Pars Reticulata Substantia Nigra

Even though the SNR can be considered as a caudomedial extension of the internal pallidal segment, it does not seem to be derived from the same developmental anlage as either the external or internal pallidal segments which appear to follow somewhat independent developmental courses (Marchand and Poirier, 1983; Marchand and Lajoie, 1986; Marchand *et al.*, 1986). The pars reticulata, like the pallidum, consists primarily of large neurons with long, thick dendrites, which are almost completely ensheathed with synaptic contacts (Kemp, 1970; Fox *et al.*, 1974; Francois *et al.*, 1987; Yelnik *et al.*, 1987). Histochemically, there are also striking similarities between the pars reticulata and the internal pallidal segment with dense substance P-positive woolly fibers (Beach and McGeer, 1984; Inagaki and Parent, 1984; Mai *et al.*, 1986; Haber and Groenewegen, 1989), as well as a dense histochemical reaction for iron (Francois *et al.*, 1981; Dwork *et al.*, 1988). As we have seen in the previous discussions, the connections of the pars reticulata are similar to those of the GPi. In addition, the SNR projects to the superior colliculus. This projection, which arises primarily from the lateral SNR, is important in the control of eye movements (Hopkins and Niessen, 1976; Beckstead, 1983; Hikosaka and Wurtz, 1983a; Vila *et al.*, 1996). The cell population of the pars reticulata contains predominantly GABAergic neurons, as can be shown with GAD or GABA immunohistochemistry (Oertel *et al.*, 1982; Mugnaini and Oertel, 1985). In primates, a clear demarcation between the pars compacta and the pars reticulata is often difficult to visualize, particularly in caudal regions, because of the invasion into the SNR by dopamine neurons and their dendritic arborizations.

Midbrain Dopamine Neurons (Pars Compacta and the VTA)

The midbrain dopamine neurons play a unique role in basal ganglia and cortical circuits modulating a broad range of behaviors from learning and "working memory" to motor control. Dopamine neurons are considered to be key for focusing attention on significant and rewarding stimuli, a requirement for the acquisition of new learned behaviors (Schultz *et al.*, 1997; Yamaguchi and Kobayashi, 1998; see also Wickelgren, 1997). Consistent with its role as a mediator of complex behaviors as a function of the environment (Ljungberg *et al.*, 1992; Schultz *et al.*, 1995), as we will see later, the dopamine pathways are in a position to provide an interface between cognitive, motor, and limbic functional domains of the forebrain, through complex forebrain neuronal networks (Haber *et al.*, 2000). Vicq d'Azyr first identified the substantia nigra in 1786, as "tache noire" or "locus niger crurum cerebri" (Vicq D'Azyr, 1786) when he described "black granules" (neuromelanin) in the human brainstem. It was then considered to be part of the oculomotor nerve because of its close proximity with the oculomotor nerve rootlets. The link between the substantia nigra and the motor system did not occur until the turn of the 19th century when several investigators associated this brainstem nucleus with Parkinson's disease (Brissaud, 1895; Bremer, 1920). This was later confirmed by Hassler's demonstration of progressive cell loss in the substantia nigra of Parkinson's patients (Hassler, 1938, 1939). The connection between the neurotransmitter dopamine and the substantia nigra was made by Ehringer and Hornykeiwicz's discovery that DA was depleted in Parkinson's disease patients (Ehringer and Hornykiewicz, 1960; Hornykiewicz, 1966). The hypothesis that DA is involved in the pathogenesis of major psychoses evolved in the early 1950s as a result of the empiric discovery that the phenothiazines could be effectively used for the treatment of psychosis (Baldessarini, 1985). Since that time the midbrain dopamine system has been linked to psychosis and behavioral disorders including schizophrenia, Gilles de la Tourette's disease, and drug abuse. Subpopulations of dopamine neurons have been associated with different functions and include reward, cognition, and motor control. Classically, these functions are related to the mesolimbic system, mesocortical system, and striatonigral pathways, respectively.

In the primate, dopaminergic neurons can be distinguished from the underlying pars reticulata by their content of melatonin, a dark pigment generally accumulated in catecholamine neurons, especially in the human brain (Braak and Braak, 1986). The colocalization of DA with neuromelanin, a byproduct of catecholamine metabolism, was first described in detail in 1967 (Bazelton *et al.*, 1967). Melanins are heterogeneous compounds that are formed oxidatively from various subunits such as tyrosine. Neuromelanin may be unique in that it is formed by autooxidation of dopamine, rather than enzymatically, and its synthesis generates free radicals. Quantitative examination of neuromelanin shows that it is found less in lower mammals but is very dense in primates (Bogerts, 1981; Marsden, 1983; McRitchie *et al.*, 1995). An important distinction between human and nonhuman primates may be a lower amount of neuromelanin per catecholamingeric cell in the nonhuman primates (Marsden, 1983; Herrero *et al.*, 1993). The neuromelanin content in midbrain neurons is age-dependent, increasing progressively until the sixth decade when it begins to decline, possibly because of neuronal degeneration of the pigmented cells (Mann and Yates, 1983; Marsden, 1983). Neuromelanin is particularly dense in the SNC cells.

Neurons of pars compacta are large in size (33 μm mean diameter) and larger than the adjacent cells of the pars reticulata (25 μm) or pars lateralis (28 μm) of substantia nigra (Yelnik *et al.*, 1987). Their dendrites are long and spine-poor, often radiating in a plane confined to pars compacta, but more frequently with dendrites extending into the underlying pars reticulata (Wassef *et al.*, 1981; Yelnik *et al.*, 1987). Pars compacta cells have been shown to make dendrodendritic synapses, releasing dopamine. Some of these intrinsic connections are electrotonically coupled. The D_2 dopamine receptor mRNA is high in the midbrain and functions here as an autoreceptor (Hajdu *et al.*, 1973; Groves *et al.*, 1975; Cheramy *et al.*, 1981; Grace and Bunney, 1983; Llinas *et al.*, 1984; Haber *et al.*, 1995a).

The midbrain dopamine neurons are divided into the substantia nigra pars compacta; the ventral tegmental area; and the retrorubral cell groups (Hokfelt *et al.*, 1984b) (Fig. 21.20, also see Fig. 21.5). The densely populated, relatively large melanin-containing pars compacta is mainly constituted by dopaminergic cell bodies. This was first visualized by dopamine- or TH-immunohistochemistry in rats (Ungerstedt, 1971; Bjorklund and Lindvall, 1984) and later in monkeys (Garver and Sladek, 1875; Hubbard and Di Carlo, 1974; Schofield and Everitt, 1981; Tanaka, 1982; Pearson *et al.*, 1983; Robert *et al.*, 1984). The SNC has been further divided into three groups: a dorsal group (the α group), also referred to as the pars dorsalis; a main, densocellular region (the β group); and a ventral group (the γ group), or the cell columns (Olszewski and Baxter, 1982; Poirier *et al.*, 1983; Francois *et al.*, 1985; Halliday and Tork, 1986; Haber *et al.*, 1995a). The dorsal group is composed of loosely arranged cells, extending dorsolaterally circumventing the ventral and lateral superior cerebellar peduncle and the red nucleus. These dorsal neurons are oriented horizontally, just dorsal to a dense cluster of neurons referred to as the densocellular region (Fig. 21.19). The dorsal cells merge with the immediately

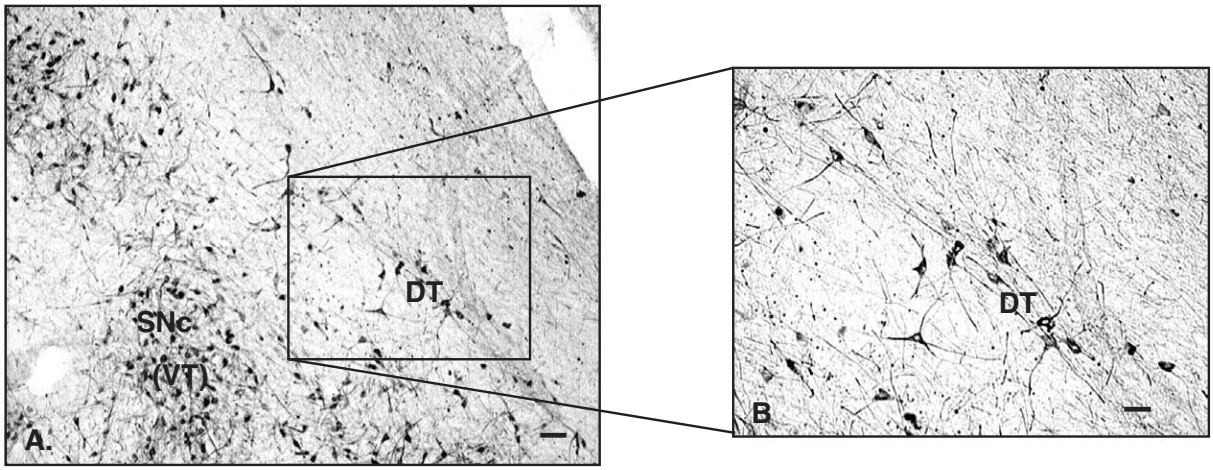

FIGURE 21.19 Photomicrograph of the tyrosine hydroxylase positive-staining in the midbrain. **(A)** TH-positive fibers and cells of dorsal and ventral tiers. Scale = 100 μm. The cells and processes of the dorsal tier indicated by the box are shown magnified in **(B)** revealing the horizontal arrangement of their dendritic processes. Scale = 50 μm. VT, ventral tier; DT, dorsal tier.

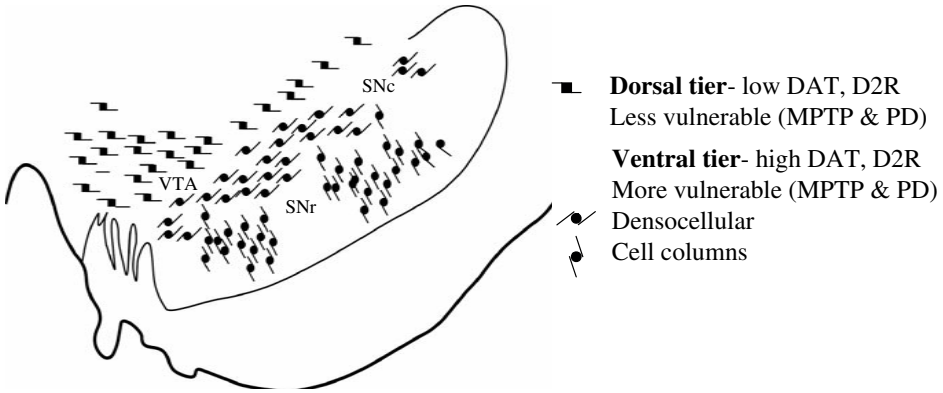

FIGURE 21.20 Schematic demonstrating the arrangement of the different dopaminergic cell groups in the midbrain. The dorsal tier includes the ventral tegmental area and the retrorubral cell groups; the ventral tier includes the densocellular cells and the cell columns. DAT, dopamine transporter; D2R, D2 dopamine receptor; MPTP, 1-methyl-4-phenyl-1,2,3,6,tetrahydropyridine; PD, Parkinson's disease; VTA, ventral tegmental area; SNr, substantia nigra pars reticulata; SNc, substantia nigra pars compacta.

adjacent dopamine cell groups of the ventral tegmental area to form a continuous mediodorsal band of cells. The dendrites of this dorsal group stretch in a mediolateral direction and do not extend into the ventral parts of the pars compacta or into the pars reticulata. Calbindin (CaBP), a calcium-binding protein, is an important phenotypic marker for both the VTA and the dorsal SNC.

In contrast, the ventral cell groups (the densocellular group and the cell columns) are calbindin-negative. Thus the distribution of calbindin-positive cells illustrates the continuity between the VTA and the dorsal SNC (Lavoie and Parent, 1991; Haber *et al.*, 1995a; McRitchie and Halliday, 1995). Furthermore, the dendritic arborizations of the densocellular region and cell columns are oriented ventrally and occupy the major portion of the pars reticulata in primates. These TH-labeled dendrites can be followed deep into the pars reticulata extending to, and in some instances into, the cerebral peduncle. The cell columns are finger-like extensions of cell clusters that lie within the pars reticulata and are particulaly prominent in primates. The densocellular group and the cell columns, in addition to being calbindin-negative, have high expression levels for dopamine transporter (DAT) and for the D2 receptor mRNAs.

Based on the phenotypic characteristics of the midbrain dopamine neurons, these cells can be divided into two tiers: a dorsal tier and a ventral tier (Fig. 21.20). The cells of the dorsal tier include both the dorsal SNC and the contiguous VTA. These cells are oriented horizontally and are calbindin-positive. The ventral tier cells include both the densocellular and the ventral group. They have dendrites that penetrate deep into the pars reticulata. Furthermore, the ventral tier cells are calbindin-negative and have relatively high levels of neuromelanin and expression of DAT and the D2 receptor mRNA. The ventral tier cells are more vulnerable to degeneration in Parkinson's disease and to *N*-methyl-4-phenyl-1,2,3,6-tetrahydropyridine (MPTP)-induced toxicity, while the calbindin-positive dorsal tier cell are selectively spared (Fallon and Moore, 1978; Gerfen *et al.*, 1985; Lavoie and Parent, 1991; Pifl *et al.*, 1991; Parent and Lavoie, 1993; Haber *et al.*, 1995a).

Finally, it should be noted that in some instances, particularly for cells in the ventral tegmental area, multiple transmitters coexist within the same neuron. For example, cholecystokinin or neurotensin may be found within cells that also contain dopamine (Hokfelt *et al.*, 1984a; Seroogy *et al.*, 1988).

Connections

Many of the dopamine connections (Fig. 21.21) with other structures in the basal ganglia have already been described in the previous sections and (other than the striatum) will only be briefly referred to later. In addition, to reciprocal connections with the striatum, pallidum, and STh, the dopamine cells also are linked to the cortex, hippocampus, and amygdala. Most of these projections are reciprocal and will therefore be discussed together.

The Striatum. The main target of the dopaminergic neurons is the striatum. Even though many tracing studies have not used double-labeling techniques demonstrating retrogradely labeled cells containing TH or other markers indicative of dopamine, since the majority of SNC cells are dopaminergic, projections from the ventral tier are presumed to be largely dopaminergic. The percentage of cells from the dorsal

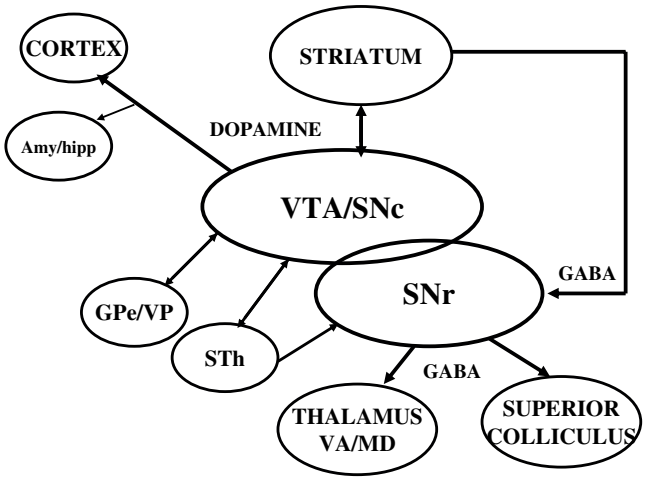

FIGURE 21.21 Diagram demonstrating the connections of the substantia nigra and ventral tegmental area. VTA, ventral tegmental area; SNc, substantia nigra pars compacta; SNr, substantia nigra pars reticulata; Amy, amygdala; hipp, hippocampus; GPe, globus pallidus external segment; VP, ventral pallidum; STh, subthalamic nucleus; VA, ventral anterior nucleus of the thalamus; MD, mediodorsal nucleus of the thalamus.

tier presumed to be dopaminergic may be somewhat less, in that there are a greater number of non-dopaminergic cells here. Both the dorsal and ventral tiers contribute to these pathways (Szabo, 1967, 1970; Johnson and Rosvold, 1971; Carpenter and Peter, 1972; Fallon and Moore, 1978; Nauta *et al.*, 1978; Szabo, 1979, 1980; Parent *et al.*, 1983; Francois *et al.*, 1984a; Parent *et al.*, 1984; Deutch *et al.*, 1986; Smith and Parent, 1986; Haber *et al.*, 1990b; Selemon and Goldman-Rakic, 1990; Hedreen and DeLong, 1991; Lynd-Balta and Haber, 1994b, c; Parent and Hazrati, 1994).

Szabo (1979, 1980) described the general topography of ascending striatal afferents demonstrating a mediolateral and rostrocaudal organization. He also described an inverse dorsoventral topography such that ventral compacta neurons project to the dorsal caudate nucleus and putamen and dorsal neurons project to the ventral parts of the striatum. These studies confirmed earlier ones that used fiber degeneration techniques (Carpenter and Peter, 1972). Parent *et al.* (1983) further extended these organizational studies by examining the relationship between nigral efferent projections to the caudate nucleus and to the putamen. They showed that retrogradely labeled cells projecting to either the caudate nucleus or the putamen are derived from different populations of pars compacta cells, thereby demonstrating that a single neuron did not send collaterals to both parts of the striatum. Retrogradely labeled cells from the caudate nucleus were distributed in clusters which interdigitate with clusters of retrogradely labeled cells from the putamen. These two populations of neurons were found throughout the extent of the substantia nigra.

The striatum projects massively back to the substantia nigra (Nauta and Mehler, 1966; Szabo, 1967, 1970; Johnson and Rosvold, 1971; Parent *et al.*, 1984; Haber *et al.*, 1990b; Selemon and Goldman-Rakic, 1990; Hedreen and DeLong, 1991; Lynd-Balta and Haber, 1994c; Parent and Hazrati, 1994). As described earlier, the striatonigral projection is GABAergic with subpopulations of cells co-containing primarily substance P, but also some populations co-contain enkephalin (DiFiglia *et al.*, 1981; Haber and Elde, 1982; Beach and McGeer, 1984; Inagaki and Parent, 1984; Pioro *et al.*, 1984; Inagaki *et al.*, 1986). Substance P-containing axons are found throughout the pars reticulata, whereas the enkephalinergic fibers are found in a more limited medial region. A common feature of the ventral and dorsal striatonigral connections is that all areas project throughout the rostro-caudal extent of the substantia nigra. Ventral striatonigral inputs terminate in the medial pars reticulata and much of the densocellular part of the pars compacta, whereas dorsolateral striatonigral inputs are concentrated in the ventrolateral pars reticulata. At the rostral level of the substantia nigra, ventral striatal fibers terminate medially. However, more caudally, these terminals spread dorsally and laterally to innervate the region of the densocellular SNC and, just ventral to it, in the SNR (Haber *et al.*, 1990b). Thus the ventral striatum not only projects throughout the rostrocaudal extent of the substantia nigra, but also covers a wide mediolateral range (Haber *et al.*, 1990b; Hedreen and DeLong, 1991). There are remarkably few ventral striatal terminals in the ventral tegmental area as compared to the heavy projections to the substantia nigra proper. The functional organization of the striatonigralstriatal pathway will be addressed in detail in "Functional Basal Ganglia Connections."

The Pallidum and Brain Stem. Both the external segment of the globus pallidus and the ventral pallidum project to the substantia nigra. The internal segment of the globus pallidus does not. The pallidal projection follows a similar organization as does the striatonigral projection. The region of the external segment that receives input from the sensorimotor part of the striatum projects ventrally to the pars reticulata. The more rostral regions of the pallidum that receive input from the association areas projects more dorsally in the region of, and just ventral to, the dopamine cells. Finally, the ventral pallidum projects dorsally, primarily to the densocellular region of the pars compacta (Haber *et al.*, 1993). Thus the pattern of projection from

the striatum to the pallidum and nigra is repeated again in the pallidal projection to the substantia nigra. In addition, the pedunculopontine nucleus terminates in the region of the dopaminergic cells bodies. At the light microscopic level, these fibers appear to form close contacts with the cells and dendrites of the dorsal pars compacta (Lavoie and Parent, 1994). Finally, studies demonstrate a serotonergic innervation from the dorsal raphe nucleus to the substantia nigra, though there is disagreement regarding whether fibers terminate primarily in the pars compacta or pars reticulata (Lavoie and Parent, 1990).

The Cortex. The presence of cortical dopamine and dopamine fibers in the cortex is clearly demonstrated using a variety of methods, including measurements of dopamine levels, immunohistochemistry for TH, dopamine uptake, specific antibodies against dopamine, and receptor autoradiography (Levitt *et al.,* 1984; Fallon and Loughlin, 1987; Lewis *et al.,* 1987; Gaspar *et al.,* 1989; Lidow *et al.,* 1991; Gaspar *et al.,* 1992; Verney *et al.,* 1993; Sesack *et al.,* 1998). The dopamine innervation of primate cortex is more extensive than in rats and found not only in granular areas but also in agranular frontal regions, parietal cortex, temporal cortex, and, albeit sparsely, occipital cortex. Dopamine terminals in layer I, which are prevalent throughout cortex, provide a rather general modulation of many cells at the distal apical dendrites. The terminals in layers V–VI, on the other hand, are found in specific cortical areas and are in a position to provide a more direct modulation of cortical efferent projections, including corticostriatal and corticothalamic projections. Dopamine fibers are also found in the hippocampus, albeit to a lesser extent than found in neocortex. The terminals are densest in the molecular layer and the hilus of the dentate gyrus and in the molecular layer and polymorphic layer of the subiculum (Samson *et al.,* 1990).

In rats, the majority of midbrain neurons projecting to the cortex arise from both the VTA and the medial half of the SNC, throughout its rostrocaudal extent. In primates, the majority of DA cortical projections are from the parabrachial pigmented nucleus of the VTA and the dorsal SNC (Amaral and Cowan, 1980; Porrino and Goldman-Rakic, 1982; Fallon and Loughlin, 1987; Gaspar *et al.,* 1992). The ventral tier does not project extensively to cortex. The VTA projects throughout prefrontal cortex including orbital, medial, and dorsolateral areas with fewer projections to motor areas. Midbrain projections to the hippocampus are also derived primarily from the VTA with few cells from the pars compacta proper terminating there. The dorsal SNC primarily innervates dorsolateral prefrontal cortex, motor, and premotor regions. The midbrain dopamine cells that project to functionally different cortical regions are intermingled with each other. Double label studies show that many cells send collateral axons to different cortical regions (Gaspar *et al.,* 1992). The nigrocortical projection appears to be a more diffuse system compared to the nigrostriatal system and can modulate cortical activity at several levels.

There is a general acceptance of descending cortical projections to the substantia nigra, based primarily on studies in rats and cats. Cortical lesions result in reduced glutamate content in the rat substantia nigra as well as fiber degeneration in the corticonigral pathway (Afifi *et al.,* 1974; Carter, 1980; Kornhuber, 1984). Retrograde tracing studies confirm these projections (Bunney and Aghajanian, 1976). However, these projections have been difficult to definitively demonstrate in primates (Leichnetz and Astruc, 1976; Kunzle, 1978). While descending corticonigral fibers have been demonstrated with fiber degeneration and anterograde tracing techniques in primates, the authors in both studies point out that the results must be interpreted with care. Neither technique clearly showed that fibers actually terminated in the substantia nigra.

In summary, the dorsal tier neurons (the VTA and the dorsal substantia nigra) are the source for the midbrain dopamine cortical projections. The ventral tier neurons, for the most part, do not contribute. Furthermore, this dorsal tier projection does not appear to be organized with respect to function. Cells projecting to functionally different cortical regions are intermingled with each other, many of which send collateral axons to different cortical regions. This is somewhat different than the nigrostriatal projection where some functional organization, although a rather loose one, does exist. The nigrocortical projection on the other hand is a diffuse system that can modulate cortical activity at several levels. Terminals in layer I, which are prevalent throughout cortex, provide a rather general modulation of many cells at the distal apical dendrites (Gaspar *et al.,* 1992). The terminals in layers V–VI, on the other hand, are found in specific cortical areas and are in a position to provide a more direct modulation of cortical efferent projections, including corticostriatal and corticothalamic projections. Thus, parts of the striatum can be influenced by dopamine directly via the nigrostriatal pathway and indirectly via a nigrocortical/striatal pathway.

Amygdala Projections. The basolateral complex and the central amydala nuclei are most consistently associated with projections to and from the midbrain. Dopamine fibers in the amygdala predominate in these areas supporting the midbrain projection here

(Sadikot and Parent, 1990). The densent innervation is in the central and medial part of the central nucleus. Projections to the amygdala arise from both the VTA and the adjoining dorsal pars compacta (Aggleton *et al.*, 1980; Mehler, 1980; Norita and Kawamura, 1980). These terminals form symmetric synapses primarily with spiny cells, indicating that direct contact is made with the projection neurons of the amygdala (Asan, 1997). Descending projections from the central nucleus of the amygdala terminate in a wide mediolateral region of dopamine cells (Price and Amaral, 1981; Fudge and Haber, 2000). These fibers descend in the ventral amygdalofuglal pathways and terminate primarily in the dorsal SNC and in the densocellular regions. In addition, there are projections to the VTA and the dorsomedial SNC from the bed nucleus of the stria terminalis and from the sublenticular substantia innominata (Price and Amaral, 1981; Parent and DeBellefeuille, 1983; Haber *et al.*, 1993; Lavoie and Parent, 1994; Fudge and Haber, 2000; Fudge and Haber, 2001). These fibers travel together with those from the amygdala, which travel together with those from the bed nucleus of the stria terminalis and the cells of the sublenticular substantia innominata, together forming the "extended amygdala" (Alheid and Heimer, 1988; Heimer *et al.*, 1991a).

FUNCTIONAL BASAL GANGLIA CONNECTIONS

The basal ganglia and frontal cortex operate together to execute goal-directed behaviors. This requires not only the execution of motor plans but also the behaviors that lead to this execution, including emotions and motivation that drive behaviors, cognition that organizes and plans the general strategy, motor planning, and finally the execution of that plan. Frontal cortex is organized in a hierarchical manner to mediate the smooth execution of behaviors (Fuster, 2001). Therefore, the connectivity of basal ganglia circuitry is best appreciated within the context of frontal cortical organization. The components of the frontal cortex that mediate behaviors, including the motivation and emotional drive, coupled with the planning and cognitive components to plan the action, and finally, the movement itself, are reflected in the organization, physiology, and connections between areas of frontal cortex and in their projections to striatum. The frontal cortex can thus be divided into several regions: the orbital and medial prefrontal cortex, involved in emotions and motivation; the dorsolateral prefrontal cortex, involved in higher cognitive processes or "executive functions"; the premotor areas, involved in different aspects of motor planning; and the motor cortex, involved in the execution of those plans. Since the basal ganglia are linked to each of these areas, we include a brief description of frontal cortical areas before turning to the associated BG circuitry (Fig. 21.22a). While the striatum receives input from other cortical areas, we focus on the frontal cortex because that receives the main BG output via the thalamus. Furthermore, inputs from other cortical areas are also functionally organized, such that they overlap with frontal projections in the striatum, which are both functionally related and closely connected with specific frontal regions (Yeterian and Van Hoesen, 1978; Selemon and Goldman-Rakic, 1985; Flaherty and Graybiel, 1993). As Yeterian and Van Hoesen suggested, "cortical areas related via reciprocal corticocortical connections project, in part, to similar areas within the caudate nucleus" (Yeterian and Van Hoesen, 1978; Van Hoesen *et al.*, 1981). The phenomenon of overlapping projections from reciprocally connected cortical areas often consists of interdigitated terminals rather then complete overlapping fields. However, the regional topography was similar (Selemon and Goldman-Rakic, 1985). We will briefly review these corticostriatal connections as appropriate along with the frontostriatal projections.

The Frontal Cortex

Recent studies of "motor" cortices have expanded the number of cortical areas involved in motor processing as well as the database of information on their physiology and connectivity—both cortical and subcortical (Dum and Strick, 1991a; Luppino *et al.*, 1991; Matelli *et al.*, 1991; Mushiake *et al.*, 1991; Dum and Strick, 1993; Luppino *et al.*, 1993; Lu *et al.*, 1994; Matelli and Luppino, 1996; Picard and Strick, 1996; Tanji and Mushiake, 1996; Strick *et al.*, 1998). Based on anatomical and physiological studies, motor areas are organized by connections and involvement in movement execution with regards to microexcitability and the temporal association between movement and neuronal reponse along with their involvement (or lack thereof) in cognitive motor processing (Schieber, 1999; McFarland and Haber, 2000). Caudal motor areas, including motor cortex (M1); supplementary motor area (SMA); cingulate motor area, caudal part (CMAc); and caudal premotor area (PM) areas are those areas most closely involved with movement execution. These areas also send a direct descending projection to spinal motor nuclei. They are highly microexcitable and closely timed to the execution of movment (Hutchins *et al.*, 1988; He *et al.*, 1993; Dum and Strick, 1996; Schieber, 1999). Rostral motor areas, including PreSMA, CMAr, and rostral PM areas, project to caudal motor areas and process more "cognitive" aspects of motor control,

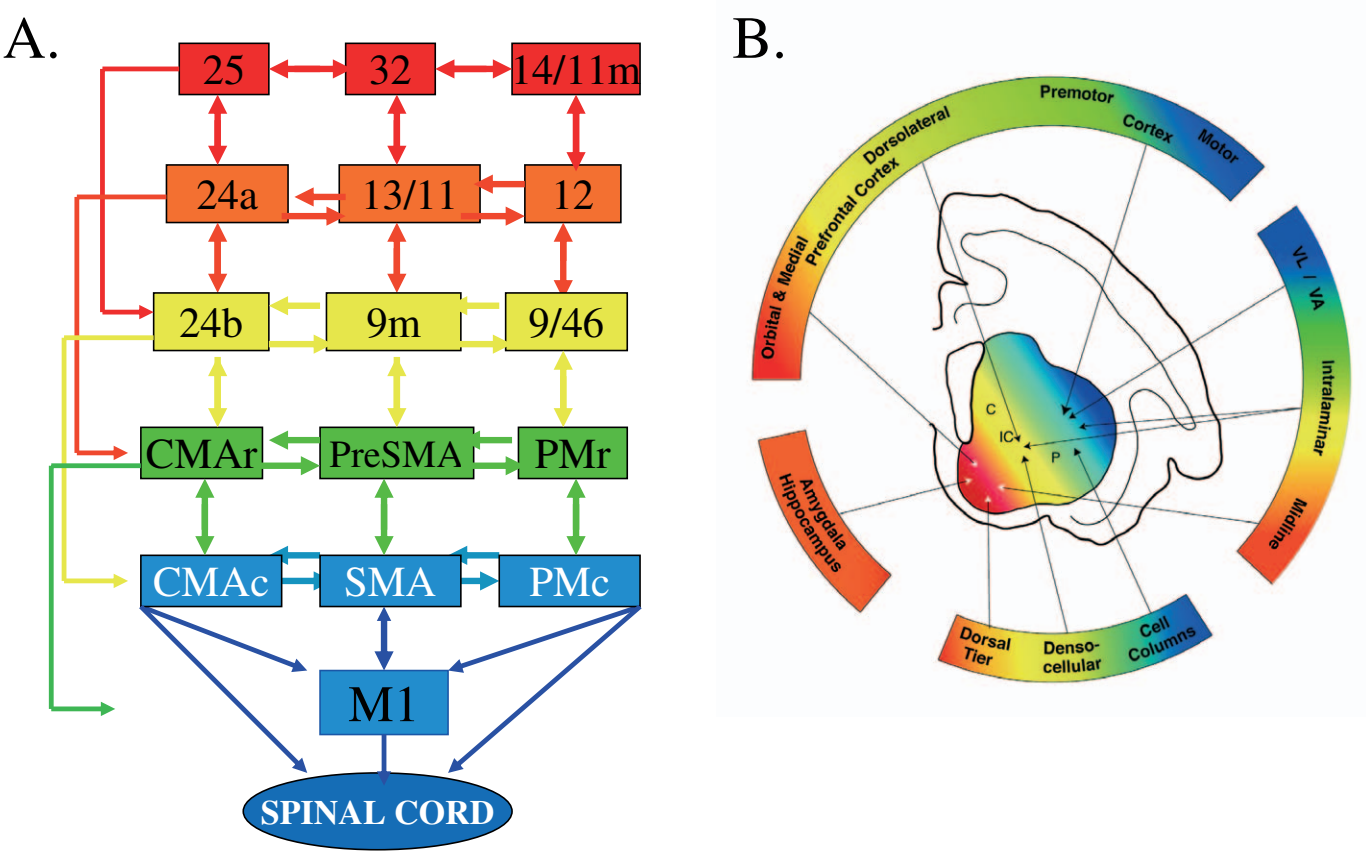

FIGURE 21.22 Diagram demonstrating the functional organization of frontal cortex and striatal afferent projections. **(A)** Schematic illustration of the functional connections linking frontal cortical brain regions. **(B)** Organization of cortical and subcortical inputs to the striatum. The colors denote functional distinctions. *Blue,* motor cortex, execution of motor actions; *green,* premotor cortex, planning of movements; *yellow,* dorsal and lateral prefrontal cortex, cognitive and executive functions; *orange,* orbital prefrontal cortex, goal-directed behaviors and motivation; *red,* medial prefrontal cortex, goal-directed behaviors and emotional processing.

such as sensorimotor integration, sequence generation, and motor learning. These areas are less microexcitable than the caudal motor areas, but more so than the prefrontal cortex. Furthermore, the temporal firing pattern of the rostral motor areas is less directly associated with movement than the caudal motor areas. In addition, although there are some direct connections to spinal cord, they are far fewer than those arising from the caudal motor areas. However, these areas are tightly connected both to caudal motor areas and to the prefronatal cortex (Bates and Goldman-Rakic, 1993; Lu *et al.,* 1994; Carmichael and Price, 1996a; Graziano *et al.,* 1997; Nakamura *et al.,* 1998). As we will see later, projections from this collective region of frontal cortex to the striatum define the striatal region associated most with the control of movement.

All three prefrontal cortical regions—dorsolateral, orbital, and medial—are the least microexcitable of frontal cortex (Fuster, 1997a). The dorsolateral prefrontal cortex, as mentioned earlier, is tightly linked to the rostral motor areas that are stimulation-responsive. Dorsal and lateral prefrontal cortical areas (DLPFC) are involved in working memory, set shifting, and strategic planning, often referred to as 'executive functions'. Delayed memory tasks are used as one measure of this function. These tasks require the subject to retain information during a delay period in which the stimuli have been removed. The DLPFC plays a critical role in this retention as has been demonstrated both experimentally and in patients with cognitive impairments (Goldman-Rakic, 1987; Jonides *et al.,* 1993; Smith and Jonides, 1997; Fuster, 2000, 2001). The most common deficit in this area following lesions is an inability to formulate a cohesive plan or sequence of actions that result in a desired goal. (Passingham, 1972a, b, 1975, 1995; Goldman-Rakic, 1994, 1996; Fuster, 1997b, 2000, 2001; Fuster *et al.,* 2000). The DLPFC has close connections with the orbital and medial prefrontal cortex. The orbital prefrontal regions are tightly linked to dorsolateral prefrontal areas (lateral 9 and 46) rostral and the dorsal cingulate cortex is tightly linked to rostral medial dorsal prefrontal areas, 9 and medial 10 (Carmichael and Price, 1996b; Fogassi *et al.,* 1996; Graziano *et al.,* 1997; Petrides and Pandya, 1999).

The medial prefrontal cortex, or anterior cingulate cortex, contains a number of different functional regions and has been divided into a ventral subgenual area (area 25) and two dorsal areas (24a/b and 24c). The subgenual region (area 25) is particularly important in the expression of emotion and, based on imaging studies, is associated with increased activity during depression (Mayberg *et al.,* 1999, 2000). It receives one of the densest innervations from the amygdala and the hypothalamus (Carmichael and Price, 1995). The more dorsal parts of cingulate cortex (area 24a/b), while also associated with emotion and motivation, and receiving amygdala input, are, in addition, closely connected to the dorsolateral prefrontal cortex (Carmichael and Price, 1996b). The most lateral and caudal areas of cingulate cortex (area 24c) are referred to as motor cingulate and are associated with premotor and motor areas (Dierssen *et al.,* 1969; Vogt and Pandya, 1987; Luppino *et al.,* 1991; Matelli *et al.,* 1991; Morecraft and VanHoesen, 1993; Showers, 1959). Orbital prefrontal cortex is involved in the development of reward-based learning and goal-directed behaviors. Consistent with its sensory inputs, coupled with those from the amygdala and other limbic-related regions, the orbital cortex has been linked with the development of reward-based behaviors (Benjamin and Burton, 1968; Butter and Snyder, 1972; Benevento *et al.,* 1977; Porrino *et al.,* 1981; Amaral, 1986; Mishkin and Bachevalier, 1986; Rolls and Baylis, 1994; Baylis *et al.,* 1995; Carmichael and Price, 1995, 1996a; Meunier *et al.,* 1997; Baxter *et al.,* 2000; Hikosaka and Watanabe, 2000; Schultz *et al.,* 2000). Lesions of the orbital and medical prefrontal areas result in an inability to initiate and carry out goal-directed behaviors and lead to socially inappropriate and impulsive behaviors (Butter, 1969; Rolls *et al.,* 1980; Eslinger and Damasio, 1985; Scott *et al.,* 1986; Fuster, 1989; Cummings, 1993, 1995; Filley, 1995; Schall, 1997). Furthermore, changes in the recruitment of activity in the orbitalfrontal and cingulate cortices are associated with several mental health disorders including anxiety, depression, drug addiction, and obsessive compulsive behaviors (Breiter *et al.,* 1996, 1997; Miguel *et al.,* 1997; Mayberg *et al.,* 1999, 2000). As we will see, together, the orbital and medial prefrontal cortical (OMPFC) projections to the striatum define the ventral striatum as that part of the striatum that mediates reward and motivation.

Afferent Connections to the Sriatum

Corticostriatal Projections

The origin of the neocortical striatal projection in primates is primarily derived from the pyramidal neurons of layer five (Jones *et al.,* 1977; Arikuni and Kubota, 1986; Goldman-Rakic and Selemon, 1986; Haber *et al.,* 1995b; McFarland and Haber, 2000). In addition, in some areas of cortex, layer three also contributes to the corticostriatal pathway (Jones *et al.,* 1977; Arikuni and Kubota, 1986; Goldman-Rakic and Selemon, 1986; Haber *et al.,* 1995b; McFarland and Haber, 2000). It has long been thought that corticostriatal projections arise as collaterals of other corticofugal axons. This certainly seems to be the case for many of the cortical afferents to striatum, based on examination of axons impregnated by the Golgi method and after intracellular filling of cortical neurons and their axons (Donoghue and Kitai, 1981; Ramón y Cajal *et al.,* 1988; Levesque *et al.,* 1996a, b). Corticothalamic fibers send a collateral projection to the striatum, and it is thought that all striatal projections indeed arise from these corticothalamic cells. However, it should be pointed out that not all cells that project to the thalamus send a collateral projection to the striatum. In addition, some evidence suggests that cells in layer three of cortex that give rise to corticocortical projections, also send collaterals to the striatum (Wilson, 1987). Cortical terminals within the striatum are distributed such that densely innervated areas are surrounded by areas relatively free of terminals. This patchy pattern is consistent with patterns found with other afferent projections as well as with transmitter-related compounds (see "Compartmentation of the Striatum").

Current views on the precise topography of corticostriatal connections are in a state of flux. The older idea is that the cortex projects in a more or less direct fashion to the closest portion of underlying striatum (Kemp and Powell, 1970). Moreover, behavioral, physiological, and clinical evidence has capitalized on this apparent topography to demonstrate functional similarities between particular areas of cortex and their "most closely" associated striatal subdivision (we will come back to this later). However, tracing studies have demonstrated a wide rostrocaudal projection area for each cortical region suggesting that corticostriatal innervation is organized in a longitudinal topography (Selemon and Goldman-Rakic, 1985). For example, prefrontal cortex projects not only to the head of the caudate but also to the body and tail of the caudate nucleus (Goldman and Nauta, 1977; Yeterian and Van Hoesen, 1978). Selemon and Goldman-Rakic (1985) concluded on the basis of such data that a significant feature of corticostriatal topography is a medial to lateral arrangement that extends throughout the length of the caudate including the head, body, and tail of this structure. More careful analysis of these pathways demonstrates that both schemes have merit. Projections from cortex to the striatum have a wider

rostrocaudal projection than initially described and indeed do project throughout a large extent of the striatum. However, while the extent is large, the main terminal region (as defined by the densest mediolateral, dorsoventral terminal area) is often found in a relatively localized rostrocaudal region and indeed in the most adjacent position to its cortical input. It is important to remember that the separation between the caudate nuc. and the putamen is merely a structural one, based solely on the interal capsule separation, not a functional one However, based on anatomical and physiological studies of the central and caudal aspects of the striatum, the putamen is mostly associated with the sensorimotor system, and the caudate, with association or prefrontal cortex. While these generalities are useful, we must be careful here because the rostral striatum does not fit well with this distinction.

Many of the tracing studies of BG circuitry have been done in primates, and, as such, we will focus on those. Perhaps the area that receives the most attention is that area associated with the motor system. The projections from motor and premotor cortices were some of the first to be identified (Kemp and Powell, 1970; Kunzle, 1975, 1978; McFarland and Haber, 2000). Projections from M1 terminate almost entirely in the putamen, in the dorsolateral and central region. There are some terminals, albeit few, rostral to the anterior commissure; however, the main projection lies caudal to the anterior commissure, with few terminals extending rostrally. Indeed, the motor cortex does not project to the rostral pole of the striatum or, in fact, to most of the area rostral to the anterior commissure. The caudal premotor area projects to a striatal region that is just adjacent to M1 projections. These terminals extend only slightly into the caudate nucleus. The rostral premotor areas terminate in both the caudate and putamen, bridging the two with a continuous projection. These premotor motor area terminals extend more rostrally than those from the motor cortex, although they do not extend into the rostral pole of the striatum. Both motor and premotor areas extend through much of the putamen caudally. This dorsolateral sector of the striatum also receives overlapping projections from parietal areas associated with somatosensory function. Furthermore, these parietal projections follow the same somatotopic organization (Künzle, 1977; Aosaki *et al.,* 1994b; Flaherty and Graybiel, 1994). Thus, the dorsolateral striatal region has been referred to as the sensorimotor striatal area (Alexander and Crutcher, 1990; Parent and Hazrati, 1995; McFarland and Haber, 2000). Physiological studies support the involvement of this region in sensorimotor control and motor plans. Within this area, a somatotopic map has been identified both through connectional as well as physiological studies demonstrating the somatotopic microexcitable striatal zones (Alexander and DeLong, 1985a, b). In addition, studies also show neuronal reponses to specific movement. For example, using arm-movement tasks in different behavioral paradigms, several investigators have demonstrated that neurons in the putamen fire in association with movement selection or initiation. Cells are also active during movement monitoring (DeLong and Strick, 1974; DeLong and Georgopoulos, 1979; Aldridge *et al.,* 1980b; DeLong and Georgopoulos, 1981; Alexander and DeLong, 1985a, b; Alexander and DeLong, 1986; Kimura, 1986, 1990; Flaherty and Graybiel, 1991b). Imaging studies in humans support these nonhuman primate physiological experiments revealing activity associated with repetitive and well-learned movements that require little cognitive effort, centered in both the caudal motor areas of cortex and in the lateral putamen. In contrast, activity recorded during the learning of sequential movements in both monkey physiological experiments and human imaging studies demonstrate activity in the rostral motor regions (pre SMA) and more anterior striatal areas including the caudate nucleus (Aizawa *et al.,* 1990; Kermadi and Joseph, 1995; Hikosaka *et al.,* 1996; Jueptner *et al.,* 1997; Miyachi *et al.,* 1997; Boecker *et al.,* 1998). The frontal eye fields send projections to the striatum that terminate in the central lateral part of the head and body of the caudate nucleus (Kunzle and Akert, 1977; Huerta *et al.,* 1986; Stanton *et al.,* 1988; Hikosaka *et al.,* 1989a). This area of cortex also contains a rostral region, referred to as the supplementary eye fields, which has a relationship to the frontal eye fields, with respect to learned acquistion of oculomotor behaviors, similar to that which the rostral and caudal motor regions have to learned behavioral sequences of hand movements (Chen and Wise, 1995). Finally, the motor cingulate cortex also sends an overlapping projection to the sensorimotor region of the striatum (Kunishio and Haber, 1994; McFarland and Haber, 2000). Taken together, the motor and premotor areas (and the frontal eye fields) mediate different aspects of motor behavior, including planning, learning, and execution, which are in turn reflected both anatomically and physiologically in the central and lateral caudate nuc. and in the central, dorsal, and lateral putamen, respectively. The pattern of neuronal discharge in these striatal regions that accompanies these behaviors has been proposed to underlie procedural learning. This corticostriatal interface has further been associated with the development of "habits", in which a discrete sequence of behaviors can be triggered by particular sets of stimuli (Hikosaka, 1991; Hikosaka *et al.,* 1995;

Kermadi and Joseph, 1995; Jueptner *et al.*, 1997; Graybiel, 1998; Jog *et al.*, 1999).

The DLPFC projects primarily to the rostral central region of the caudate nuc. However, the rostrocaudal extent of this projection is quite large and continues from the rostral pole of the striatum through its caudal extent (Selemon and Goldman-Rakic, 1985; Arikuni and Kubota, 1986). This innervation is one of the largest to the striatum and interfaces with several other cortical areas. These projections are organized somewhat topographically such that, for example, input from the rostral pole of frontal cortex terminates most densely in the rostral part of the striatum, including both the caudate and putamen. The entire DLPFC projection extends continuously throughout the caudate nuc., with few terminals in the central and caudal putamen (Selemon and Goldman-Rakic, 1985). The majority of this projection is centered in the head of the caudate nuc. As described earlier, the DLPFC plays an important role in executive functions, with delayed memory tasks as a classic measurement (Goldman-Rakic, 1987; Jonides *et al.*, 1993; Smith and Jonides, 1997; Fuster, 2000, 2001). Consistent with input from this cortical area, cells in the head of the caudate nuc. demonstrate spike-firing activity during the delayed portion of the task. This activity resembles that observed in the DLPFC (Hikosaka *et al.*, 1989b; Apicella *et al.*, 1992). Furthermore, imaging studies support the idea that the head of the caudate is instrumental in delayed tasks, particularly in specific working memory tasks (Levy *et al.*, 1997; Elliott and Dolan, 1999). Finally, lesions of the caudate nuc. in both human and nonhuman primates produce deficits in working memory as measured by delayed response tasks (Battig *et al.*, 1960; Butters and Rosvold, 1968; Partiot *et al.*, 1996). Taken together, the caudate nuc., and in particular the head of the caudate, is involved in working memory and strategic planning processes, working together with the DLPFC in mediating this function.

The orbital and medial prefrontal cortex projects primarily to the rostral striatum and includes terminals in the medial caudate nuc., the medial and ventral rostral putamen, and the nucleus accumbens (both the shell and the core). This projection extends caudally and occupies a small ventromedial portion of the caudate nuc. and the most ventral and medial part of the putamen (Pandya *et al.*, 1981; Kunishio and Haber, 1994; Haber *et al.*, 1995b; Chikama *et al.*, 1997; Ferry *et al.*, 2000; Freedman *et al.*, 2000). Indeed, the caudal, ventral putamen has been suggested as the caudal extension of the ventral striatum (Fudge and Haber, 2002). In addition, the ventral striatum receives input from the amygdala. The shell receives the densest innervation from medial areas 25, 14, and 32 and from agranular insular cortex areas involved in monitoring the internal mileu. Medial areas 24, 25, and 32, also project to the medial wall of the caudate nucleus. Projections from area 24 extend dorsally and somewhat more centrally into the caudate nuc. and overlap with inputs from the medial parts of the DLPFC (particularly rostral area 9). In addition, this medial area of the caudate nucleus receives a dense innervation from areas 13a/b and 14 and from parts of dysgranular insular cortex. In contrast, the central and lateral parts of the ventral striatum receive fewer inputs from medial prefrontal cortex. Their main input is derived from the lateral OMPFC regions, areas 13 and 12, and dysgranular insular cortex (Kunishio and Haber, 1994; Haber *et al.*, 1995b; Chikama *et al.*, 1997; Ferry *et al.*, 2000). These projections extend more centrally and overlap with inputs from the lateral aspects of the DLPFC. As noted previously, area 24, that part of the cingulate cortex closely connected to motor areas, does not project to the ventral striatum but rather to the dorsolateral striatum (Kunishio and Haber, 1994). As indicated earlier, these orbital and medial prefrontal areas are primarily associated with the development of reward-based behaviors. Physiological as well as imaging studies support the idea that the ventral striatum plays an important role in the aquistion and development of reward-based behaviors (Apicella *et al.*, 1991b; Apicella *et al.*, 1992; Bowman *et al.*, 1996; Tremblay *et al.*, 1998; Hassani *et al.*, 2001). This striatal area is a main focus of research in drug addiction and drug-seeking behaviors. These studies demonstrate activity changes in the ventral striatum during different aspects of addiction (Bowman *et al.*, 1996; Lyons *et al.*, 1996; Freeman *et al.*, 2001; Letchworth *et al.*, 2001). In addition, pharmacologic and molecular biological studies support the central role of the ventral striatum in drug addiction (Nestler *et al.*, 1993; Koob, 1999). That the ventral striatum is the striatal region most often associated with the limbic system, emotions, and motivation is supported by its central position in mediating reward-based learning (Everitt and Robbins, 1992; Kalivas *et al.*, 1993; Wise, 1998; Robbins and Everitt, 1999).

In summary, projections from frontal cortex form a functional gradient of inputs from the ventromedial sector through the dorsolateral striatum, with the medial and orbital prefrontal cortex terminating in the ventromedial part and the motor cortex terminating in the dorsolateral region (Fig. 21.22B). Within this gradient, the cortical projections to the striatum are quite precise. For example, the dorsolateral putamen receives input from the dorsal premotor, the dorsal primary motor, and the supplementary motor cortices. More ventral putamen areas receive input from the

ventrolateral premotor cortex and the lateral precentral gyrus (McFarland and Haber, 2000). In general, frontal projections from motor areas (areas 4, 6, and 8), but not from the medial and orbital prefrontal cortex, reach the dorsolateral striatum. In contrast, the medial and orbital prefrontal cortex projects to the ventral striatum but not to the dorsolateral striatum. Dorsolateral prefrontal cortex (areas 9, 46, and 45) project centrally, with little or no afferent projection to the calbindin-poor shell region or to the ventral rostral putamen, the ventral caudate nucleus, and the medial wall of the rostral caudate nucleus.

Fewer studies have focused on projections from other cortical areas to the striatum. As with the frontal lobe, temporal lobe projections terminate throughout wide areas of the striatum (Yeterian and Van Hoesen, 1978; Van Hoesen *et al.*, 1981; Selemon and Goldman-Rakic, 1985; Yeterian and Pandya, 1998). Superior temporal gyrus terminates primarily in the central half of the caudate nuc. and overlaps and interdigitates with inputs from DLPFC. Inferior temporal areas terminate more ventrally, including the caudal and ventral putamen. These inputs overlap to some extent with those from the medial and orbital prefrontal areas. Visual areas in the temporal lobe terminate primarily in the caudal part of the striatum. However, these projections reach quite rostrally into the medial part of the body of the caudate, extending into the tail of the caudate and reaching caudal parts of the putamen (Maioli *et al.*, 1983; Maunsell and van Essen, 1983). As mentioned earlier, projections from the parietal lobe terminate in striatal areas that complement those that are interconnected with frontal lobe projections. Finally, axons from visual cortex apparently terminate in posterior portions of the body of the caudate nucleus as it arcs ventrally into the temporal lobe (Saint-Cyr *et al.*, 1990).

Thalamostriatal Projections

Like the cortex, the thalamostriatal projection is topographically organized. Thalamic nuclei are associated with sensory, motor, association, and limbic systems by virtue of their connectivity with cortical and subcortical regions. Furthermore, as we will see later, comparison of the distribution of cortical and thalamic projections to the primate striatum demonstrates that interconnected thalamic and cortical areas project to the same region of the striatum (Künzle, 1975, 1977; Kunzle and Akert, 1977; Kunzle, 1978; Yeterian and Van Hoesen, 1978; Pandya *et al.*, 1981; Selemon and Goldman-Rakic, 1985; Flaherty and Graybiel, 1991a; Yeterian and Pandya, 1991; Parthasarathy *et al.*, 1992; Flaherty and Graybiel, 1994; Haber *et al.*, 1995b; Chikama *et al.*, 1997). Thus, afferents from these interconnected thalamic and cortical areas are likely to modulate the same striatal output circuits.

The midline and intralaminar nuclei are often referred to as part of the nonspecific thalamic cell groups. These are the source of the most widely reported thalamostriatal projections (Jones and Leavitt, 1974; Dubé *et al.*, 1988; Nakano *et al.*, 1990; Sadikot *et al.*, 1990; Fenelon *et al.*, 1991; Francois *et al.*, 1991; Sadikot *et al.*, 1992a; Smith *et al.*, 1994b; Giménez-Amaya *et al.*, 1995; McFarland and Haber, 1995; Nakano *et al.*, 1999; McFarland and Haber, 2000). These thalamic nuclei are associated with specific cortical areas, and, as such, with those cortical functions. Both the midline and the intralaminar nuclei are further subdivided. The midline and medial intralaminar nuclei (including central medial and medial parafascicular nuc.) project to medial prefrontal areas, the amygdala, hippocampus, and perihippocampal cortex. The rostral intralaminar nuclei and centromedian and parafascicular (CM/Pf) complex have connections with association areas, such as the prefrontal and posterior parietal cortices. The lateral CM nucleus projects to both the primary motor and sensory cortices (Herkenham, 1978, 1986; Groenewegen and Berendse, 1994a; Jones, 1998). These nuclei project topographically to the striatum such that the midline, medial parafascicular and central medial nuclei project mainly to ventral (limbic) striatal areas, whereas the more lateral intralaminar nuclei have connections with the dorsolateral (sensorimotor-association) caudate and putamen. A medial to lateral topography has been described for striatal projections from the CMPf complex in the squirrel monkey, such that the medial Pf projects to the ventral "limbic" striatum, the central part projects to association-striatum, and the lateral CM projects primarily to the sensorimotor putamen and dorsolateral caudate nucleus (Francois *et al.*, 1991; Sadikot *et al.*, 1992a; Giménez-Amaya *et al.*, 1995; McFarland and Haber, 2000). In this way, projections from the so-called nonspecific thalamic nuclei project to discete striatal areas that are consistent with the cortical area they are most associated with. This thalamostriatal projection thus maintains the functional distinction of different striatal regions.

In addition to intralaminar thalamic projections, there is an equally large projection to the dorsal striatum from the "specific" thalamic nuclei, including the mediodorsal (MD), ventral anterior and ventral lateral nuclei. While significant thalamostriatal projections from these areas are not observed in rodents, they are found in larger mammals, including primates (Jones and Leavitt, 1974; Parent *et al.*, 1983; Smith and Parent, 1986; Nakano *et al.*, 1990; Druga *et al.*, 1991; Fenelon

et al., 1991; Giménez-Amaya *et al.*, 1995; McFarland and Haber, 2000, 2001).

These thalamic nuclei are also intimately connected with specific frontal cortical areas (Akert and Hartmann-von Monakow, 1980; Goldman-Rakic and Porrino, 1985; Wiesendanger and Wiesendanger, 1985; Giguere and Goldman-Rakic, 1988; Matelli *et al.*, 1989; Nakano *et al.*, 1992; Dum and Strick, 1993; Matelli and Luppino, 1996). Thus, different regions of the ventral motor nuclei (VA-VL) have reciprocal projections with specific premotor, motor and cingulate cortices (Akert and Hartmann-von Monakow, 1980; Schell and Strick, 1984; Rouiller *et al.*, 1994; Matelli and Luppino, 1996). Different parts of the MD nucleus are linked to specific prefrontal areas (Akert and Hartmann-von Monakow, 1980; Goldman-Rakic and Porrino, 1985; Giguere and Goldman-Rakic, 1988). As with the midline and intralaminar nuclei, interconnected ventral thalamic and MD nuc. and cortical areas project to the same region of the striatum. For example, VPLo projects to M1 and most of the caudal "secondary" motor areas. These areas issue dense projections to the dorsolateral putamen. VLo projects densely to SMA and the dorsal part of CMAc. VLo and SMA projections converge in the dorsal, central putamen. VLc is predominately connected with PMd, but it also has connections with PMv and the ventral part of CMAc. VLc and PMd projections mainly target the dorsolateral caudate nucleus. Rostral motor areas, including PMdr, PreSMA, and CMAr, receive inputs from VApc. Striatal projections from these areas converge within the ventral putamen and dorsolateral caudate. These findings demonstrate a tight, anatomical and functional triad of basal ganglia input and output structures, involving the frontal motor cortices, the striatum, and the thalamic relay nuclei. Furthermore, these results also suggest that these thalamic projections play a dual role in basal ganglia circuitry: (1) relaying basal ganglia output to frontal cortical areas and (2) providing direct feedback to the striatum (McFarland and Haber, 2000, 2002a).

Midbrain Dopamine-Striatal Projections

Dopamine neurons, which comprise the majority of cells in the SN pars compacta, the VTA, and the retrorubral group, play a key role in the acquisition of newly acquired behaviors. The role of dopamine in reward has been well established (Fibiger and Phillips, 1986; Wise and Rompre, 1989); its primary function is to direct attention to important stimuli likely to bring about a desired outcome (Ljungberg *et al.*, 1991; Schultz, 1998). Dopamine cells discharge when presented with relevant stimuli for which a response is required (Grace and Bunney, 1995; Schultz, 1997). However, when the animal is overtrained, cells no longer respond, suggesting that it is not the movement but the relevance of the stimulus that is important (Schultz, 1992; Schultz *et al.*, 1993; Wilson *et al.*, 1995; Richardson and Gratton, 1996). While behavioral and pharmacological studies of dopamine pathways have lead to the association of the mesolimbic pathway and nigrostriatal pathway with reward and motor activity, respectively, more recently both of these cell groups have been associated with reward. Indeed, physiological experiments demonstrate that 75% of dopamine neurons (including neurons from the so-called nigrostriatal pathway) respond with burst firing activity when food is unexpectedly found (Romo and Shultz, 1990). These are not pure motor responses since the DA neurons are not modulated by the movements that are generated during exploratory behaviors performed in exclusion of touching the food reward. Instead, the DA neurons respond in association with identifying, obtaining, or predicting rewards. In contrast, DA neurons will pause if a predicted reward fails to occur (Schultz and Romo, 1990; Ljungberg *et al.*, 1991; Schultz, 1998; see also Schultz *et al.*, 2000). Thus, unlike the other major inputs to the striatum (the cortex and thalamus), the dopamine cells are more difficult to categorize based on their association with different cortical functions. Rather, as a group, they appear to mediate aspects of the reward response. In this respect, the dopamine system has been an intense focus of productive research in the development of reward-based learning, drug addiction, and plasticity (Weihmuller *et al.*, 1990; Anglade *et al.*, 1996; Montague *et al.*, 1996; Berridge and Robinson, 1998; Hollerman and Schultz, 1998; Bonci and Malenka, 1999; Contreras-Vidal and Schultz, 1999; Koob, 1999; Matsumoto *et al.*, 1999; Berke and Hyman, 2000; Calabresi *et al.*, 2000c; Song and Haber, 2000; Nestler, 2001). Therefore, from a functional perspective, the dopamine projection to the striatum is likely to have a similar impact on all striatal reigons.

You will remember that the dopamine synapses are in a position on the dendrites of the MSNs to modulate incoming cortical information. Therefore, with relatively few synapses, the impact of the dopaminergic innervation is nonetheless likely to be great. Striatal response to dopamine is heterogenous and, as described previously, determined by multiple variables including complex interactions between several receptors. Converging evidence indicates that tonic release of dopamine attenuates medium spiny neuronal response, while phasic release potentiates striatal response (Di Chiara *et al.*, 1994; Arbuthnott and Wickens, 1996; Cepeda and Levine, 1998; Calabresi *et al.*, 2000b; Wickens and Oorshcot, 2000). In this way, dopamine can both inhibit background corticostriatal input but

facilitate (and therefore "focus") specific corticostriatal synaptic transmission. Even though projections from the different dopamine cell groups are not as tightly arranged topographically as are inputs from the cortex and thalamus, there is an important organization to this input that underlies a mechanism for modulating the different striatal regions, both separately and across functional domains. This complex system includes both the dopamine-striatal pathway as well as the striatal input to the dopamine neurons. Here we will only address the dopamine input to the striatum and will return to the complexity of this interface later.

As previously described, the midbrain dopamine system is divided into the dorsal tier and ventral tier cells. The dorsal tier cells include the VTA, the retrorubral group, and the dorsal cells of the pars compacta. The ventral tier cells include the densocellular group and the cell columns that extend deep into the pars reticulata. In general, there is an inverse dorsal-ventral topographic organization to the midbrain projection to the striatum. The dorsal dopamine cells project to the ventral parts of the striatum, while the ventrally placed cells project to the dorsal parts of the striatum (Carpenter and Peter, 1972; Szabo, 1979, 1980; Parent *et al.*, 1983; Hedreen and DeLong, 1991; Lynd-Balta and Haber, 1994a, b; Haber *et al.*, 2000). Thus, the dorsal tier projects to the ventromedial striatum; the densocellular part of the ventral tier projects centrally and throughout different regions of the striatum; and the cell columns project primarily to the dorsolateral (sensorimotor) striatum. The shell region of the ventral striatum receives the most limited input, primarily derived from the VTA. The rest of the ventral striatum receives input from the entire dorsal tier. In addition, there are some afferent projections from the most medial region and dorsal part of the densocellular group. In contrast to the ventral striatum, the central striatal area (the region innervated by the DLPFC) receives input from a wide region of the densocellular group. The ventral tier projects to the dorsolateral striatum, with the cell columns projecting almost exclusively to there. The dorsolateral striatum receives the largest midbrain projection from cells throughout the ventral tier. In contrast to the dorsolateral region of the striatum, the ventral striatum receives the most limited dopamine cell input. Of this area, the shell is most limited in terms of relative distribution of cells projecting there. Thus, in addition to an inverse topography, there is also a differential ratio of dopamine projections to the different striatal areas. The input to the ventral striatum is derived from the most limited midbrain region, while the input to the dorsolateral striatum is derived from the largest midbrain area (Haber *et al.*, 2000).

Striatopallidal/Substantia Nigra Reticulata Connections

The striatum projects primarily to the pallidal complex and to the SNR. These projections are topographically organized, thus maintaining the functional organization of the striatum in its projections to the output nuclei of the basal ganglia (Szabo, 1962; Nauta and Mehler, 1966; Szabo, 1967, 1970, 1980; Carpenter *et al.*, 1981b; Parent *et al.*, 1984; Haber *et al.*, 1990b; Selemon and Goldman-Rakic, 1990; Hedreen and DeLong, 1991; Lynd-Balta and Haber, 1994c; Parent and Hazrati, 1994). Projections from the sensorimotor areas of the striatum terminate in the ventrolateral part of each pallidal segment. In the SNR they are also found in the ventrolateral part of the nucleus. Projections from the central striatum terminate more centrally in both the pallidum and the SNR. Finally, the ventral striatum terminates topographically in the ventral pallidum and in the dorsal part of the midbrain. The projection to the midbrain terminates both in the region of the dopamine neurons and in the pars reticulata (Parent *et al.*, 1984; Haber *et al.*, 1990b; Lynd-Balta and Haber, 1994c). Projection to the dopamine neurons has been considered one mechanism by which the limbic system can interface with the motor system through the basal ganglia pathways (Nauta and Domesick, 1978; Somogyi *et al.*, 1981b; Heimer *et al.*, 1982; Haber *et al.*, 2000). We will return to this concept later.

Physiological studies demonstrate the continuity of striatal functional areas in the pallidal complex. However, it must be recognized that here the functional organization within the pallidum is more complex than that of the striatum. This may, in part, be due to the fact that there is a certain amount of compression of terminals from a relatively large striatum to a much smaller pallidum (Oorshcot, 1996). It may also be the result of integrative networks linking different functional domains (Nauta *et al.*, 1978; Somogyi *et al.*, 1981b; Bevan *et al.*, 1997; Haber *et al.*, 2000; Haber, 2002; McFarland and Haber, 2002a). Pallidal neurons that receive information from motor cortical areas (via the striatum) are somatotopographically arranged such that, for example, those representing the face are located most ventrally and arm-related neurons are located more dorsally (DeLong *et al.*, 1985; Nambu *et al.*, 1990). Although the pallidal segments are differentiated anatomically and neurophysiologically, most behavioral studies have treated both segments as a single neural population. Studies have explored the relationship of pallidal response to different aspects of movement, including movement duration, movement direction, and movement amplitude or velocity. While most cells

increase their neural activity associated with motor tasks, a smaller proportion of cells do decrease (pause) their activity (Aldridge *et al.*, 1980a; Georgopoulos *et al.*, 1983; Anderson and Horak, 1985; Mitchell *et al.*, 1987; Anderson and Turner, 1991; Brotchie *et al.*, 1991b; Mink and Thach, 1991a; Mink and Thach, 1991b). Of particular interest is that these studies do not support the notion that GP neurons play a direct role in the initial activation of muscles to generate voluntary movement. Indeed, GP activity usually precedes muscle activation, but by too short a time increment to be instrumental in movement production. Taken together, these findings suggest that GP plays an integral role in the coordination of voluntary movement, but not necessarily in movement initiation. In fact, a growing body of evidence suggests that GP neurons are selectively modulated during movement behaviors performed in different behavioral contexts.

Experiments have also tested the potential role of the pallidum in learning paradigms. In one study, the investigators found that GPi neurons were modulated during the delay between the presentation of the visual instruction cue and the "go" cue signaling movement initiation. Furthermore, many of these cells were responsive during the novel cue condition suggesting that the pallidum participates in the association learning processes (Inase *et al.*, 2001). Other studies support the role of both pallidal segments in developing multiple-segment movement sequencing (Georgopoulos *et al.*, 1983; Brotchie *et al.*, 1991a; Jaeger *et al.*, 1993; Mushiake and Strick, 1995). These studies provide evidence for the diversity of neural activity that is exhibited by pallidal neurons in association with different behavioral conditions. Of particular importance is the change in response of these neurons in animal models of PD or in dopamine-depleted animals. These studies help explain some of the pathophysiological signs that become manifest as consequence of disease progression and may provide a mechanism to identify early cognitive and oculomotor deficits in nonhuman primates that may serve to facilitate early diagnosis in human patients (Nini *et al.*, 1995; Bergman *et al.*, 1998; Slovin *et al.*, 1999; Raz *et al.*, 2001). Furthermore, these animal models have been instrumental in developing and testing therapies that have proven to be useful in the treatment of humans with PD (Bergman *et al.*, 1990; Boraud *et al.*, 1996).

The neurons of the SNR are often related to oculomotor function. However, these cells not only are involved in the eye movement itself, but also are associated with the context in whch the movement occurs (Hikosaka and Wurtz, 1983b; Basso and Wurtz, 2002). For example, changes in modulation are observed when the eye movements were made within the constraints of the task, but not when the same eye movements were spontaneously generated (Hikosaka *et al.*, 1989b; Hikosaka and Watanabe, 2000).

Striatal Innervation of the Dopamine Neurons

While afferent control of dopaminergic neurons arises from a number of structures, the striatum is a major source. The striatum inhibits neurons in SNC. However, stimulation of the striatum can also lead to an increase in dopamine cell firing through inhibition of GABAergic interneurons (or pars reticulata cells) that terminate on dopaminergic cells and dendrites, resulting in disinhibition of pars compacta cells (Francois *et al.*, 1979; Grace and Bunney, 1979; Johnson and North, 1992; Grace and Bunney, 1995). This dual effect of both inhibition and disinhibition may be an important mechanism underlying the control of dopamine cell-firing patterns. Projections from the striatum to the midbrain are arranged in an inverse dorsal-ventral topography as are the ascending midbrain projections. Thus, the dorsal aspects of the striatum terminate in the ventral regions of the midbrain, while the ventral areas terminate dorsally (Szabo, 1967, 1970, 1980; Haber *et al.*, 1990b; Selemon and Goldman-Rakic, 1990; Hedreen and DeLong, 1991; Lynd-Balta and Haber, 1994c; Parent and Hazrati, 1994). Specifically, efferent projections to the midbrain from the ventromedial striatum, including the shell, terminate throughout an extensive dorsal region, including the VTA and the medial SNC, along with the medial pars reticulata. Thus the ventral striatum not only projects throughout the rostrocaudal extent of the substantia nigra but also innervates a wide mediolateral range of dopaminergic cells. At central and caudal levels, this projection field extends laterally and includes much of the densocellular SNc. The central striatum projection terminates more ventrally, primarily in the ventral densocellular region (and associated pars reticulata). The dorsolateral striatum projections to the midbrain terminate in the ventrolateral midbrain in the pars reticulata, which includes some of the dopaminergic cell columns that extend into this region.

You will remember that projections from the midbrain to the striatum differ in the proportion of cells projecting to each region of the striatum. Likewise, there are important differences in the extent of the terminal fields from each of the striatal regions to the midbrain. However, there is an inverse relationship to the extent of the midbrain innervation of the striatum. For example, in contrast to its relatively limited afferent midbrain input, the ventral striatum innervates a large area of the midbrain, including much of the dorsal tier and the densocellular area of the ventral tier and associated pars reticulata. On the other hand,

the dorsolateral striatum, which has a relatively extensive midbrain input, projects to a limited midbrain region, primarily to the ventrolateral pars reticulata and the cell columns that invade this area (Haber *et al.*, 2000). The central striatum terminates in both the densocellular region and the cell columns along with the pars reticulata associated with these areas. We can see from this relationship that there is a loose topographic organization demonstrating that the VTA and medial SN are associated with the limbic system, and the lateral and ventral midbrain are related to the associative and motor striatal regions, respectively. The ventral striatum receives a limited midbrain input but projects to a large region that includes dorsal and ventral tiers and the dorsal pars reticulata. In contrast, the dorsolateral striatum receives a wide input but projects to a limited region. This arrangement suggests that the ventral striatum influences a wide range of dopamine neurons but is itself influenced by a relatively limited group of dopamine cells. On the other hand, the dorsolateral striatum influences a limited midbrain region but is affected by a relatively large midbrain region. We will return to this later as we consider the role of the midbrain in integrating information flow across the functional domains of the striatum (Fig. 21.23).

Thalamus—The Final Basal Ganglia Link Back to Cortex

The ventral tier and mediodorsal thalamic nuclei receive the bulk of basal ganglia output (from the pallidum and substantia nigra). These BG thalamic relay nuclei are the source of the direct feedback to the cortex. The primate ventral anterior (VA) nucleus can be distinguished cytoarchitecturally from the ventral lateral nucleus. Both are composed of several distinct nuclear subdivisions (Ilinsky and Kultas-Ilinsky, 1987). The magnocellular portion of VA specifically receives nigral inputs and can be delineated by these projections (Ilinsky *et al.*, 1985). Moreover, the parvicellular and densocellular (VAdc, or VLo) portions receive pallidal projections (Kuo and Carpenter, 1973; Kim *et al.*, 1976; DeVito and Anderson, 1982; Parent and DeBellefeuille, 1983; Ilinsky *et al.*, 1993). In addition, the MD nucleus receives input from the SNR and from the ventral pallidum (Haber *et al.*, 1985; Ilinsky *et al.*, 1985). As we have seen in previous sections, the thalamus is linked to cortex both anatomically and physiologically. Areas of VL that receive the main ouput from motor regions of the pallidum terminate in motor areas of frontal cortex. Likewise VA nucleus is associated with premotor and DLPFC, and the MD nucleus is linked to the DLPFC and orbital and medial prefrontal cortex (Giguere and Goldman-Rakic, 1988).

Striato-nigro-striatal projections: a mechanism for integrating information across parallel pathways

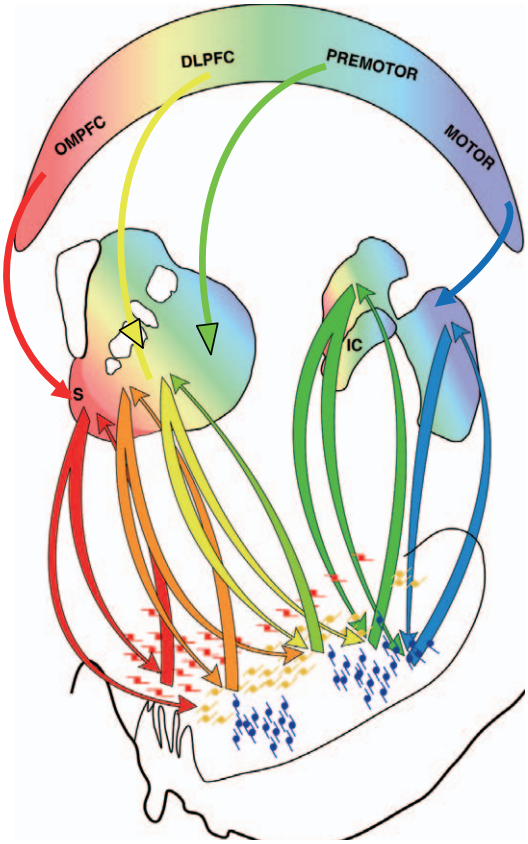

FIGURE 21.23 Diagram of the organization of striatonigrostriatal (SNS) projections (Haber *et al.*, 2000). The colored gradient in rostral and caudal schematics of the striatum illustrates the organization of functional corticostriatal inputs (see Fig. 21.22A). Midbrain projections from the shell target both the VTA and ventromedial SNc (red arrows). Midbrain projections from the VTA to the shell form a "closed," reciprocal SNS loop (red arrow). Projections from the medial SN feed-forward to the core forming the first part of a spiral (orange arrow). The spiral continues through the SNS projections (yellow and green arrows) with pathways originating in the core and projecting more dorsally (blue arrows). In this way, ventral striatal regions influence more dorsal striatal regions via spiraling SNS projections. IC, internal capsule; S, shell.

Thus, the functional topography of cortex is maintained from cortical connections to the striatum, from the striatum to the pallidum/SNR, from these output structures to the thalamus, and, finally, back to cortex.

FUNCTIONAL CONSIDERATIONS

As we have seen, the basal ganglia are connected with frontal cortex in a series of functional modules that maintain a relatively consistent anatomical and physiological organization. This organization has lead

to the concept of parallel processing of cortical information through segregated BG circuits. Parallel processing is based on the finding that each general functional area of cortex (limbic, associative, and sensorimotor) is represented in specific regions in each basal ganglia structure. Furthermore, within each of these three general circuits, additional channels have been proposed, each of which are linked to a subregion of frontal cortex (Alexander *et al.,* 1986; Hoover and Strick, 1993). This concept first arose in the late 1970s with the development of Heimer's classic concept of the ventral striatum (Heimer, 1978). While the basal ganglia was classically considered part of the motor control system, the inclusion of the ventral striatum and associated structures added an additional (and separate) functional loop within the basal ganglia. Indeed, tracing the pathways from the ventral striatum to the ventral pallidum, from the ventral pallidum to the thalamus and back to cortex was a fundamental discovery that pushed the field forward to consider other functional loops in addition to the motor circuit (Heimer *et al.,* 1982; Young *et al.,* 1984; Haber *et al.,* 1985). The idea of separate cortical loops in the basal ganglia was expanded in primates to include several parallel and segregated circuits based on frontal cortical regions (Alexander *et al.,* 1986). Collectively the studies reviewed in this chapter support the anatomical and general physiological organization of discrete cortical basal ganglia circuits and demonstrate three general regions: sensorimotor, associative, and limbic areas.

Superimposed on this model is the concept of direct and indirect pathways for each of these circuits. Together, these two organizational schemes (parallel processing and direct and indirect pathways) have helped us to formulate models concerning the role of the basal ganglia in processing cortical information within each circuit. The motor circuit has been commonly used to develop these models, which are then applied to each of the other circuits as well as to the general the overall function of the BG. Thus, the assumption is that, while each circuit mediates different behaviors (motor, cognition, motivation), the BG processes cortical information in a similar fashion within each circuit. One model that has received much attention focuses on the role of the BG in the selection and implementation of appropriate actions (or behaviors) while inhibiting unwanted ones. As you will recall, in the motor system this is viewed as inhibiting "unwanted" movements, while focusing on '"wanted and directed" movements. This model has been phrased in a number of different ways, including "focused selection," the modulation of action through temporal scaling and balance between the positive feedback via the direct pathway, and inhibition via the indirect pathway (Alexander and Crutcher, 1990; Mink, 1996; Wise *et al.,* 1996). Although helpful in understanding how the BG might play a role in the control of movement, it may not apply to the other circuits since these models are primarily based on the motor system and the execution of motor actions. Furthermore, since it is also based on parallel processing, this model does not address how information is transformed across functional regions to generate goal-directed behaviors. These two issues will be addressed later.

As mentioned in previous sections, in addition to the control of movement, the basal ganglia are now considered to be critical in the learning process. Indeed, based on experimental data and deficits caused by either cortical or basal ganglia disruption, several hypothesis that address the different roles for frontal cortex versus the basal ganglia in mediating the learning process now emerge. For example, based on comparing patients with frontal lesions with those suffering from PD, Owen and colleagues propose that the basal ganglia is critical for "shifting to" a new set of rules, while the frontal cortex is important for shifting from a new set of rules (Owen *et al.,* 1993). Wise and colleagues argue that frontal cortex is instrumental in learning new behaviors–guiding rules, while the basal ganglia potentates or reinforces those rules. Similarly, others have singled out the reward system of the basal ganglia for reinforcing cortically driven behaviors (Passingham, 1995). The role of reinforcement (particularly through the midbrain dopamine system) is now considered a critical component for basal ganglia function and is central to the newer models of BG function, which focus attention on its role in adaptation and adjustments to accommodate the past in predicting future outcomes and forming behavioral responses (Aosaki *et al.,* 1994a; Haber *et al.,* 2000; Bar-Gad and Bergman, 2001). This adaptability implies the necessity to evaluate continually and to adjust to stimuli throughout the execution of behaviors. This sort of "learning" has been physiologically demonstrated in several different tasks in which the firing pattern of BG neurons changes as during the learning process. Imaging studies further support the idea that different striatal cell groups change their activity during different phases of sequence learning (Grafton and Hazeltine, 1995; Hikosaka *et al.,* 1995; Jaeger *et al.,* 1995; Doyon *et al.,* 1997; Hikosaka *et al.,* 1998; Jog *et al.,* 1999). Thus, the emphasis is now on the role of the basal ganglia in the learning process, acquisition of new behaviors, and development of habits. The development of new behaviors and habits is dependent on response

learning (Passingham, 1995). That is, the ability of the animal to learn a new response, the learning rules, and the reinforcement of those behaviors. Indeed, the reinforcement properties of the dopamine system are critical for normal BG function. This, you will remember, is a neuronal system that primarily mediates different aspects of reward and affects all functional domains of the striatum (Aosaki *et al.*, 1994a; Schultz, 1997; Matsumoto *et al.*, 1999; Haber *et al.*, 2000; Bar-Gad and Bergman, 2001).

Most models of BG function rely on the concept of parallel processing. This is based on the idea that each cortical area mediates a parallel and segregated circuit through each of the BG structures. Therefore, these models do not address how information flows between circuits thereby developing new learned behaviors (or actions) from a combination of inputs from emotional, cognitive, and motor cortical areas. While frontal cortex is indeed divided based on specific functions, expressed behaviors are the result of a combination of complex information processing that involves all of the frontal cortex. The development and execution of appropriate responses to environmental stimuli require continual updating, as well as learning and adjusting to the response. Thus, response learning does not represent a separate motor, cognitive, and motivational tract, rather the combination of these areas working together forms a smoothly executed, goal-directed behavior. While the anatomical pathways appear to be generally topographic from cortex through BG circuits and there are some physiological correlates to the functional domains of the striatum, as we saw with the direct and indirect pathway concept, there are major points that argue against a strict parallel processing system. In this respect, a number of studies demonstrate that these pathways are not are as segregated as once thought (Nauta *et al.*, 1978; Somogyi *et al.*, 1981b; Bevan *et al.*, 1997; Haber *et al.*, 2000; Kolomiets *et al.*, 2001; McFarland and Haber, 2002a). As we've already seen, the dendrites and axons of the striatal interneurons often cross functional boundaries and have been suggested to be one mechanism that integrates information across regions. Furthermore, the dendritic arbors in the STh and in GP are extensive and cross functional boundaries. In this way, distal dendrites from another region invade an adjacent functional region. Finally, experiments have demonstrated that following injections of tracer molecules into different functional regions of the pallidum resulted in overlapping terminals at the interface between these two projection fields in the STh (Yelnik *et al.*, 1984; Wilson *et al.*, 1990; Percheron and Filion, 1991; Kawaguchi *et al.*, 1995; Bevan *et al.*, 1997). Electrophysiological studies support this notion of integration by demonstrating cell activation in response to unexpected types of stimuli within a functional region, or a lack of expected functional topography following specific stimuli (Kolomiets *et al.*, 2001). The fact that the adjacent areas overlap in function is not surprising. Many cortical areas are tightly linked to the immediately adjacent cortex. Thus, "edges" of functionally identified regions are likely to process mixed signals. Furthermore, the interface between functional circuits increases with the complexity of interconnections within the intrinsic BG circuitry and with the compression of pathways to successively smaller structures (Smith *et al.*, 1998b; Bar-Gad *et al.*, 2000).

However, interaction at the interface of functions may not be sufficient to link across circuits to accommodate adaptive responses during the learning process, or in response to new environmental cues. As such, mechanisms, by which information "flows" through functional circuits occurs, are less well understood, but fundamental for understanding how the execution of goal-directed actions evolves from reward and cognitive inputs. Recent anatomical evidence from primates demonstrates that the pathways within two basal ganglia subnetworks are in a position to move information across functional circuits (Haber *et al.*, 2000; McFarland and Haber, 2002a) (Figs. 21.23–21.25). The two networks are the striatonigrostriatal network and the thalamocorticothalamic network. Within each of these sets of connected structures, there are both reciprocal connections linking up regions associated with similar functions. However, in addition, there are nonreciprocal connections linking up regions that are associated with different cortical basal ganglia circuits. Each component of information (from limbic to motor outcome) sends both a feedback connection and a feedforward connection, allowing the transfer of information. Goal-directed behaviors require the processing of a complex chain of events beginning with motivation and proceeding through cognitive processing that shapes final motor outcomes. This sequence is reflected in the feedforward organization of both the striatonigral connections and the thalamocortical connections. Information is channeled from limbic to cognitive to motor circuits. Action decision-making processes are thus influenced by motivation and cognitive inputs, allowing the animal to respond appropriately to environmental cues.

Acknowledgments

This work was supported by NIH grants NS22311 and MH45573. We thank April Whitbeck for her excellent editorial help and Fernando Sergio Arana for photographic assistance. We would also like to thank

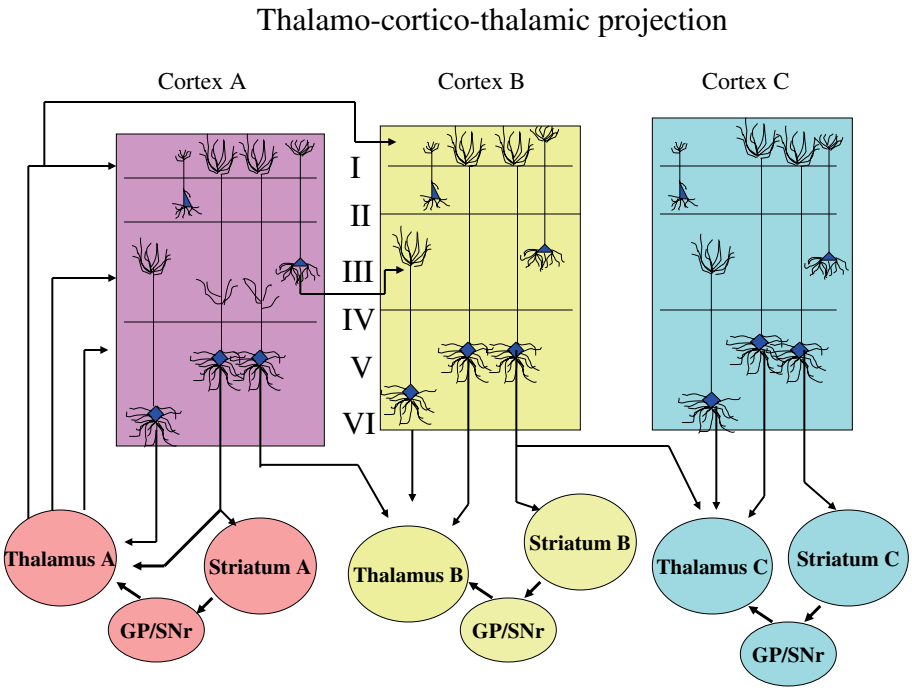

FIGURE 21.24 Summary diagram of thalamic terminal organization in cortical layers and information flow between thalamic relay nuclei and frontal cortical areas (McFarland and Haber, 2002b). Projections to the deep layers may interact with neurons that, in turn, project back to both the thalamus and striatum. These terminals therefore are in a position to reinforce directly information flow within a specific corticobasal ganglia circuit. In addition, through the nonreciprocal corticothalamic projection, terminals in layer V may also interface with other cortico-basal ganglia circuits by projecting into a thalamic region that is part of another circuit system. Thalamocortical projections to the superficial layers may also have this dual function. Projections may interact with the apical dendrites of layer V cells further reinforcing each parallel circuit. In addition, through corticocortical projections from layer III, these terminals may influence with adjacent circuits. GP, globus pallidus; SNr, substantia nigra pars reticulata.

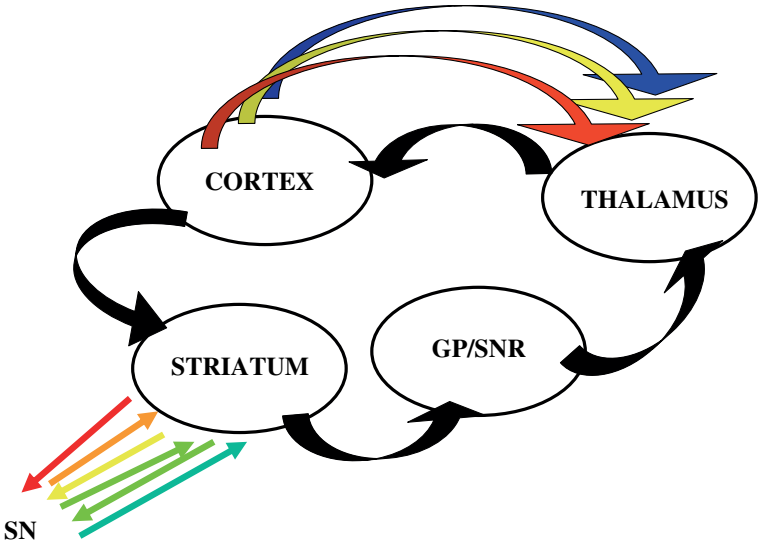

FIGURE 21.25 Schematic illustrating two potential mechanisms for relaying and integrating information within the cortico–basal ganglia circuitry. Information from distinct cortical regions could be processed separately and in parallel through functionally related neurons participating direct or indirect pathways *(black lines)*. Information from these distinct, parallel pathways could be integrated in two ways: (1) by spiraling connections between the midbrain dopamine cells and the striatum and (2) via thalamocorticothalamic projections.

Hagai Bergman and Yoland Smith for reading parts of this manuscript and their helpful comments. Finally, we thank George Alheid for his contributions to this chapter.

References

Afifi, A.K., Bahuth, N.B., Kaelber, W.W., Mikhael, E., and Nassar, S. (1974). The cortico-nigral fibre tract. An experimental Fink-Heimer study in cats. *J. Anat.* **118,** 69–476.

Aggleton, J.P., Burton, M.J., and Passingham, R.E. (1980). Cortical and subcortical afferents to the amygdala of the rhesus monkey (*Macaca mulatta*). *Brain Res.* **190,** 347–368.

Aizawa, H., Mushiake, H., Inase, M., and Tanji, J. (1990). An output zone of the monkey primary motor cortex specialized for bilateral hand movement. *Exp. Brain Res.* **82,** 219–221.

Aizman, O., Brismar, H., Uhlen, P., Zettergren, E., Levey, A.I., Forssberg, H., Greengard, P., and Aperia, A. (2000). Anatomical and physiological evidence for D1 and D2 dopamine receptor colocalization in neostriatal neurons. *Nat. Neurosci.* **3,** 226–230.

Akert, K., and Hartmann-von Monakow, K. (1980). Relationships of precentral, premotor and prefrontal cortex to the mediodorsal and intralaminar nuclei of the monkey thalamus. *Acta Neurobiol. Exp.* **40,** 7–25.

Albin, R.L., Young, A.B., and Penney, J.B. (1989). The functional anatomy of basal ganglia disorders. *Trends Neurosci.* **12** (10), 366–375.

Aldridge, J.W., Anderson, R.J., and Murphy, J.T. (1980a). The role of the basal ganglia in controlling a movement initiated by a visually presented cue. *Brain Res.* **192,** 3–16.

Aldridge, J.W., Anderson, R.J., and Murphy, J.T. (1980b). Sensory-motor processing in the caudate nucleus and globus pallidus: A single-unit study in behaving primates. *Can. J. Physiol. Pharmacol.* **58,** 1192–1201.

Alexander, G.E., and Crutcher, M.D. (1990). Functional architecture of basal ganglia circuits: neural substrates of parallel processing. *Trends Neurosci.* **13,** 266–271.

Alexander, G.E., and DeLong, M.R. (1985a). Microstimulation of the primate neostriatum. I. Physiological properties of striatal microexcitable zones. *J. Neurophysiol.* **53,** 1401–1416.

Alexander, G.E., and DeLong, M.R. (1985b). Microstimulation of the primate neostriatum. II. Somatotopic organization of striatal microexcitable zones and their relation to neuronal response properties. *J. Neurophysiol.* **53,** 1417–1430.

Alexander, G.E., and DeLong, M.R. (1986). Organization of supraspinal motor systems. *In* "Diseases of the Nervous System" (Asbury, McKhann, and McDonald, eds.), pp. 352–369. Ardmore Medical Books.

Alexander, G.E., DeLong, M.R., and Strick, P.L. (1986). Parallel organization of functionally segregated circuits linking basal ganglia and cortex. *Annu. Rev. Neurosci.* **9,** 357–381.

Alheid, G.F., and Heimer, L. (1988). New perspectives in basal forebrain organization of special relevance for neuropsychiatric disorders: The striatopallidal, amygdaloid, and corticopetal components of substantia innominata. *Neurosci.* **27,** 1–39.

Amaral, D.G. (1986). Amygdalohippocampal and amygdalocortical projections in the primate brain. *In* "Excitatory Amino Acids and Epilepsy" (R. Schwarcz and A. Yehezkel, eds.), pp. 3–17. Plenum.

Amaral, D.G., and Cowan, W.M. (1980), Subcortical afferents to the hippocampal formation in the monkey. *J. Comp. Neurol.* **189,** 573–591.

Anderson, M.E., and Horak, F.B. (1985). Influence of the globus pallidus on arm movements in monkeys. III. Timing of movement-related information. *J. Neurophysiol.* **54,** 433–448.

Anderson, M.E., and Turner, R.S, (1991). A quantitative analysis of pallidal discharge during targeted reaching movement in the monkey. *Exp. Brain Res.* **86,** 623–632.

Anglade, P., Blanchard, V., Raisman-Vozari, R., Faucheux, B.A., Herrero, M.T., Obeso, J.A., Mouatt-Prigent, A., Kastner, A., Strada, O., Javoy-Agid, F., Agid, Y., and Hirsch, E.C. (1996). Is dopaminergic cell death accompanied by concomitant nerve plasticity? *In* "Parkinson's Disease" (L. Battistin, G. Scarlato, T. Caraceni, and S. Ruggieri, eds.), pp. 195–208. Lippincott-Raven Publishers, Philadelphia.

Aosaki, T., Graybiel, A.M., and Kimura, M. (1994a). Effect of the nigrostriatal dopamine system on acquired neural responses in the striatum of behaving monkeys. *Science* **265,** 412–410.

Aosaki, T., Kimura, M., and Graybiel, A.M. (1995). Temporal and spatial characteristics of tonically active neurons of the primate's striatum. *J. Neurophysiol.* **73,** 1234–1252.

Aosaki, T., Tsubokawa, H., Ishida, A., Watanabe, K., Graybiel, A.M., and Kimura, M. (1994b). Responses of tonically active neurons in the primate's striatum undergo systematic changes during behavioral sensorimotor conditioning. *J. Neurosci.* **14,** 3969–3984.

Apicella, P., Legallet, E., and Trouche, E. (1997). Responses of tonically discharging neurons in the monkey striatum to primary rewards delivered during different behavioral states. *Exp. Brain Res.* **116,** 456–466.

Apicella, P., Ljungberg, T., Scarnati, E., and Schultz, W. (1991b). Responses to reward in monkey dorsal and ventral striatum. *Exp. Brain Res.* **85,** 491–500.

Apicella, P., Scarnati, E., and Schultz, W. (1991a). Tonically discharging neurons of monkey striatum respond to preparatory and rewarding stimuli. *Exp. Brain Res.* **84,** 672–675.

Apicella, P., Scarnati, E., Ljungberg, T., and Schultz, W. (1992). Neuronal activity in monkey striatum related to the expectation of predictable environmental events. *J. Neurophysiol.* **68** (3), 1–16.

Arbuthnott, G.W., and Wickens, J.R. (1996). Dopamine cells are neurones too [letter; comment]. *Trends Neurosci.* **19,** 279–280.

Arecchi-Bouchhioua, P., Yelnik, J., Francois, C., Percheron, G., and Tande, D. (1997). Three-dimensional morphology and distribution of pallidal axons projecting to both the lateral region of the thalamus and the central complex in primates. *Brain Res.* **754,** 311–314.

Arikuni, T., and Kubota, K. (1986). The organization of prefronto-caudate projections and their laminar origin in the macaque monkey: A retrograde study using HRP-gel. *J. Comp. Neurol.* **244,** 492–510.

Aronin, N., Chase, K., and DiFiglia, M. (1986). Glutamic acid decarboxylase and enkephalin immunoreactive axon terminals in the rat neostriatum synapse with striatonigral neurons. *Brain Res.* **365,** 151–158.

Asan, E. (1997). Ultrastructural features of tyrosine-hydroxylase-immunoreactive afferents and their targets in the rat amygdala. *Cell & Tissue Res.* **288,** 449–469.

Asanuma, C. (1994). GABAergic and pallidal terminals in the thalamic reticular nucleus of squirrel monkeys. *Exp. Brain Res.* **101,** 439–451.

Azmitia, E.C., and Segal, M. (1978). An autoradiographic analysis of the differential ascending projections of the dorsal and median raphe nuclei in the rat. *J. Comp. Neurol.* **179,** 641–668.

Baev, KV. (1995). Disturbances of learning processes in the basal ganglia in the pathogenesis of Parkinson's disease: A novel theory. *Neurol. Res.* **17,** 38–48.

Baldessarini, R.J. (1985). "Chemotherapy in Psychiatry. Principles and Practice," 2nd Ed. Harvard Uni. Press, Cambridge, MA.

Bar-Gad, I., and Bergman, H. (2001). Stepping out of the box: Information processing in the neural networks of the basal ganglia. *Current Opin. Neurobiol.* **11,** 689–695.

Bar-Gad, I., Havazelet-Heimer, G., Goldberg, J.A., Ruppin, E., and Bergman, H. (2000). Reinforcement-driven dimensionality reduction—A model for information processing in the basal ganglia. *J. Basic Clin. Physiol. Pharmacol.* **11,** 305–320.

Baron, M.S., Sidibe, M., DeLong, M.R., and Smith, Y. (2001). Course of motor and associative pallidothalamic projections in monkeys. *J. Comp. Neurol.* **429,** 490–501.

Basso, M.A., and Wurtz, R.H. (2002), Neuronal activity in substantia nigra pars reticulata during target selection. *J. Nuerosci.* **22,** 1883–1894.

Bates, J.F., and Goldman-Rakic, P.S. (1993). Prefrontal connections of medial motor areas in the rhesus monkey. *J. Comp. Neurol.* **336,** 211–228.

Battig, K., Rosvold, H.E., and Mishkin, M. (1960). Comparison of the effect of frontal and caudate lesions on delayed response and alternation in monkeys. *J. Comp. Physiol. Psychol.* **53,** 400–404.

Baxter, M.G., Parker, A., Lindner, C.C., Izquierdo, A.D., and Murray, E.A. (2000). Control of response selection by reinforcer value requires interaction of amygdala and orbital prefrontal cortex. *J. Neurosci.* **20,** 4311–4319.

Bayer, S.A. (1985). Neurogenesis in the olfactory tubercle and islands of calleja in the rat. *Int. J. Dev. Neurosci.* **3,** 135–147.

Baylis, L.L., Rolls, E.T., and Baylis, G.C. (1995). Afferent connections of the caudolateral orbitofrontal cortex taste area of the primate. *Neurosci.* **64,** 801–812.

Bazelton, M., Fenichel, G.M., and Randall, J. (1967). Studies on neuromelanin. I. A melanin system in the adult human brainstem. *Neurology* **17,** 512–519.

Beach, T.G., and McGeer, E.G. (1984). The distribution of substance P in the primate basal ganglia: An immunohistochemical study of baboon and human brain. *Neurosci.* **13,** 29–52.

Beal, M.F., Ferrante, R.J., Swartz, K.J., and Kowall, N.W. (1991). Chronic quinolinic acid lesions in rats closely resemble Huntington's disease. *J. Neurosci.* **11,** 1649–1659.

Beckstead, R.M. (1979). Convergent prefrontal and nigral projections to the striatum of the rat. *Neurosci. Lett.* **12,** 59–64.

Beckstead, R.M. (1983). Long collateral branches of substantia nigra pars reticulata axons to thalamus, superior colliculus and reticular formation in monkey and cat. Multiple retrograde neuronal labeling with fluorescent dyes. *Neurosci.* **10,** 767–779.

Beckstead, R.M., Frankfurter, A. (1982). The distribution and some morphological features of substantia nigra neurons that project to the thalamus, superior colliculus and pedunculopontine nucleus in the monkey. *Neurosci.* **7,** 2377–2388.

Beckstead, R.M., Edwards, S.B., and Frankfurter, A. (1981). A comparison of the intranigral distribution of nigrotectal neurons labeled with horseradish peroxidase in the monkey, cat, and rat. *J. Neurosci.* **1,** 121–125.

Benevento, L.A., Fallon, J., Davis, B.J., and Rezak, M. (1977). Auditory–visual interaction in single cells in the cortex of the superior temporal sulcus and the orbital frontal cortex of the macaque monkey. *Exp. Neurol.* **57,** 849–872.

Benjamin, R.M., and Burton, H. (1968). Projection of taste nerve afferents to anterior opercular-insular cortex in squirrel monkey. *Brain Res.* **7,** 221–231.

Bennett, B.D., and Bolam, J.P. (1994). Localization of parvalbumin-immunoreactive structures in primate caudate-putamen. *J. Comp. Neurol.* **347,** 340–356.

Bennett, B.D., Callaway, J.C., and Wilson, C.J. (2000). Intrinsic membrane properties underlying spontaneous tonic firing in neostriatal cholinergic interneurons. *J. Neurosci.* **20,** 8493–8503.

Bennett, B.D., and Wilson, C.J. (1999). Spontaneous activity of neostriatal cholinergic interneurons in vitro. *J. Neurosci.* **19,** 5586–5596.

Bergman, H., Feingold, A., Nini, A., Raz, A., Slovin, H., Abeles, M., and Vaadia, E. (1998). Physiological aspects of information processing in the basal ganglia of normal and parkinsonian primates. *Trends Neurosci.* **21** (1), 32–38.

Bergman, H., Wichmann, T., and DeLong, M.R. (1990). Reversal of experimental Parkinsonism by lesions of the subthalamic nucleus. *Science* **249,** 1436–1438.

Berke, J.D., and Hyman, S.E. (2000). Addiction, dopamine, and the molecular mechanisms of memory. *Neuron* **25,** 515–532.

Bernier, P.J., and Parent, A. (1998). Bcl-2 protein as a marker of neuronal immaturity in postnatal primate brain. *J. Neurosci.* **18,** 2486–2497.

Berridge, K.C., and Robinson, T.E. (1998). What is the role of dopamine in reward: Hedonic impact, reward learning, or incentive salience? *Brain Res. Rev.* **28,** 309–369.

Besson, M.J., Graybiel, A.M., and Nastuk. M.A. (1988). [^{3}H]SCH 23390 binding to D1 dopamine receptors in the basal ganglia of the cat and primate: Delineation of striosomal compartments and pallidal and nigral subdivisions. *Neurosci.* **26,** 101–119.

Bevan, M., Magill, P.J., Hallworth, N.E., Bolam, J.P., and Wilson, C.J. (2002). Regulation of the timing and pattern of action potential generation in rat subthalamic neurons in vitro by GABA-A IPSPs. *J. Neurophysiol.* **87,** 1348–1362.

Bevan, M.D., and Bolam, J.P. (1995). Cholinergic, GABAergic, and glutamate-enriched inputs from the mesopontine tegmentum to the subthalamic nucleus in the rat. *J. Neurosci.* **15,** 7105–7120.

Bevan, M.D., and Wilson, C.J. (1999). Mechanisms underlying spontaneous oscillation and rhythmic firing in rat subthalamic neurons. *J. Neurosci.* **19,** 7617–7628.

Bevan, M.D., Clarke, N.P., and Bolam, J.P. (1997). Synaptic integration of functionally diverse pallidal information in the entopeduncular nucleus and subthalamic nucleus in the rat. *J. Neurosci.* **17,** 308–324.

Bevan, M.D., Francis, C.M., and Bolam, J.P. (1995). The glutamate-enriched cortical and thalamic input to neurons in the subthalamic nucleus of the rat: Convergence with GABA-positive terminals. *J. Comp. Neurol.* **361,** 491–511.

Bevan, M.D., Smith, A.D., and Bolam, J.P. (1996). The substantia nigra as a site of synaptic integration of functionally diverse information arising from the ventral pallidum and the globus pallidus in the rat. *Neurosci.* **75,** 5–12.

Bezard, E., Boraud, T., Bioulac, B., and Gross, C.E. (1999). Involvement of the subthalamic nucleus in glutamatergic compensatory mechanisms. *Eur. J. Neurosci.* **11,** 2167–2170.

Bishop, G.A., Chang, H.T., and Kitai, S.T. (1982). Morphological and physiological properties of neostriatal neurons: An intracellular horseradish peroxidase study in the rat. *Neurosci.* **7,** 179–191.

Bjorklund, A., and Lindvall, O. (1984). Dopamine-containing systems in the CNS. *In* "Handbook of Chemical Neuroanatomy, Vol. II: Classical Transmitters in the CNS" (Bjorklund and Hokfelt, eds.), Part I, pp. 55–122. Elsevier, Amsterdam.

Boecker, H., Dagher, A., Ceballos-Baumann, A.O., Passingham, R.E., Samuel, M., Friston, K.J., Poline, J., Dettmers, C., Conrad, B., and Brooks, D.J. (1998). Role of the human rostral supplementary motor area and the basal ganglia in motor sequence control: Investigations with H2 15O PET. *J. Neurophysiol.* **79,** 1070–1080.

Bogerts, B. (1981). A brainstem atlas of catecholaminergic neurons in man, using melanin as a natural marker. *J. Comp. Neurol.* **197,** 63–80.

Bolam, J.P., and Izzo, P.N. (1988). The postsynaptic targets of substance P-immunoreactive terminals in the rat neostriatum with particular reference to identified spiny striatonigral neurons. *Exp. Brain Res.* **70,** 361–377.

Bolam, J.P., and Smith, Y. (1990). The GABA and substance P input to dopaminergic neurones in the substantia nigra of the rat. *Brain Res.* **529,** 57–78.

Bolam, J.P., Ingham, C.A., Izzo, P.N., Levey, A.I., Rye, D.B., Smith, A.D., and Wainer, B.H. (1986). Substance P-containing terminals in synaptic contact with cholinergic neurons in the neostriatum and basal forebrain: A double immunocytochemical study in the rat. *Brain Res.* **397,** 279–289.

Bolam, J.P., Powell, J.F., Totterdell, S., and Smith, A.D. (1981). The proportion of neurons in the rat neostriatum that project to the substantia nigra demonstrated using horseradish peroxidase conjugated with wheat germ agglutinin. *Brain Res.* **220,** 339–343.

Bolam, J.P., Powell, J.F., Wu, J.Y., and Smith, A.D. (1985). Glutamate decarboxylase-immunoreactive structures in the rat neostriatum: A correlated light and electron microscopic study including a combination of Golgi impregnation with immunocytochemistry. *J. Comp. Neurol.* **237,** 1–20.

Bonci, A., and Malenka, R.C. (1999). Properties and plasticity of excitatory synapses on dopaminergic and GABAergic cells in the ventral tegmental area. *J. Neurosci.* **19,** 3723–3730.

Boraud, T., Bezard, E., Bioulac, B., and Gross, C. (1996). High frequency stimulation of the internal Globus Pallidus (GPi) simultaneously improves parkinsonian symptoms and reduces the firing frequency of GPi neurons in the MPTP-treated monkey. *Neurosci. Lett.* **215,** 17–20.

Boraud, T., Bezard, E., Bioulac, B., and Gross, C.E. (2000). Ratio of inhibited-to-activated pallidal neurons decreases dramatically during passive limb movement in the MPTP-treated monkey. *J. Neurophysiol.* 83, 1760–1763.

Boraud, T., Bezard, E., Bioulac, B., and Gross, C.E. (2001). Dopamine agonist-induced dyskinesias are correlated to both firing pattern and frequency alterations of pallidal neurones in the MPTP-treated monkey. *Brain* **124,** 546–557.

Boraud, T., Bezard, E., Bioulac, B., and Gross, C.E. (2002). From single extracellular unit recording in experimental and human parkinsonism to the development of a functional concept of the role played by the basal ganglia in motor control. *Progr. Neurobiol.* **66,** 205–283.

Bouyer, J.J., Joh, T.H., and Pickel, V.M. (1984a). Ultrastructural localization of tyrosine hydroxylase in rat nucleus accumbens. *J. Comp. Neurol.* **227,** 92–103.

Bouyer, J.J., Park, D.H., Joh, T.H., and Pickel ,V.M. (1984b). Chemical and structural analysis of the relation between cortical inputs and tyrosine hydroxylase-containing terminals in rat neostriatum. *Brain Res.* **302,** 267–275.

Bowman, E.M., Aigner, T.G., and Richmond, B.J. (1996). Neural signals in the monkey ventral striatum related to motivation for juice and cocaine rewards. *J. Neurophysiol.* **75,** 1061–1073.

Braak, H., and Braak, E.(1982). Neuronal types in the striatum of man. *Cell & Tissue Res.* **227,** 319–342.

Braak, H., and Braak, E. (1986). Nuclear configuation and neuronal types of the nucleus niger in the brain of the human adult. *Hum. Neurobiol.* **5,** 71–82.

Breiter, H.C., Gollub, R.L., Weisskoff, R.M., Kennedy, D.N., Makris, N., Berke, J.D., Goodman, J.M., Kantor, H.L., Gastfriend, D.R., Riorden, J.P., Mathew, R.T., Rosen, B.R., and Hyman S.E. (1997). Acute effects of cocaine on human brain activity and emotion. *Neuron* **19,** 591–611.

Breiter, H.C., Rauch, S.L., Kwong, K.K., Baker, J.R., Weisskoff, R.M., Kennedy, D.N., Kendrick, A.D., Davis, T.L., Jiang, A., Cohen, M.S., Stern, C.E., Belliveau, J.W., Baer, L., O'Sullivan, R.L., Savage, C.R., Jenike, M.A., and Rosen, B.R. (1996). Functional magnetic resonance imaging of symptom provocation in obsessive-compulsive disorder. *Arch, Gen, Psychiatr.* **53,** 595–606.

Bremer, T. (1920). Encephalite lethargique avec syndrome parkinsonien et catatonie. *Rev. Neurol.* **27,** 772–770.

Brissaud, E. (1895). Nature et pathogenie de la maladie de Parkinson. *In* "Lecons sur les maladies nerveuses." Paris.

Brockhaus, H. (1942). The finer anatomy of the septum and of the striatum. *J. Psychol. Neurol.* **51,** 1–56.

Brog, J.S., Salyapongse, A., Deutch, A.Y., and Zahm, D.S. (1993). The patterns of afferent innervation of the core and shell in the "accumbens" part of the rat ventral striatum: Immunohistochemical detection of retrogradely transported fluoro-gold. *J. Comp. Neurol.* **338,** 255–278.

Brotchie, P., Iansek, R., and Horne, M.K. (1991a). Motor function of the monkey globus pallidus. I. Neuronal discharge and parameters of movement. *Brain* **114,** 1667–1683.

Brotchie, P., Iansek, R., and Horne, M. (1991b). A neural network model of neural activity in the monkey globus pallidus. *Neurosci. Lett.* **131,** 33–36.

Brown, L.L., Markman, M.H., Wolfson, L.I., Dvorkin, B., Warner, C., and Katzman, R. (1979). A direct role of dopamine in the rat subthalamic nucleus and an adjacent intrapeduncular area. *Science* **206,** 1416–1418.

Bunney, B.S., and Aghajanian, G.K. (1976). The precise localization of nigral afferents in the rat as determined by a retrograde tracing technique. *Brain Res.* **117,** 423–435.

Butter, C.M. (1969). Perseveration in extinction and in discrimination reversal tasks following selective fronal ablations in *macaca mulatta*. *Physiol. Behav.* **4,** 163–171.

Butter, C.M., and Snyder, D.R. (1972). Alterations in aversive and aggressive behaviors following orbital frontal lesions in rhesus monkeys. *Acta Neurobiol. Exp.* **32,** 525–565.

Butters, N., and Rosvold, H.E. (1968). Effect of caudate and septal nuclei lesions on resistance to extinction and delayed-alternation. *J. Comp. Physiol. Psychol.* **65** (3), 397–403.

Caille, I., Dumartin, B., and Bloch, B. (1996). Ultrastructural localization of D1 dopamine receptor immunoreactivity in rat striatonigral neurons and its relation with dopaminergic innervation. *Brain Res.* **730,** 17–31.

Calabresi, P., Centonze, D., Gubellini, P., and Bernardi, G. (1999). Activation of M1-like muscarinic receptors is required for the induction of corticostriatal LTP. *Neuropharmacology* **38,** 323–326.

Calabresi, P., Centonze, D., Gubellini, P., Marfia, G.A., Pisani, A., Sancesario, G., and Bernardi, G. (2000b). Synaptic transmission in the striatum: From plasticity to neurodegeneration. *Progr. Neurobiol.* **61,** 231–265.

Calabresi, P., Centonze, D., Gubellini, P., Pisani, A., and Bernardi, G. (1998). Endogenous ACh enhances striatal NMDA-responses via M1-like muscarinic receptors and PKC activation. *Eur. J. Neurosci.* **10,** 2887–2895.

Calabresi, P., Centonze, D., Gubellini, P., Pisani, A., and Bernardi, G. (2000a). Acetylcholine-mediated modulation of striatal function. *Trends Neurosci.* **23,** 120–126.

Calabresi, P., Gubellini, P., Centonze, D., Picconi, B., Bernardi, G., Chergui, K., Svenningsson, P., Fienberg, A.A., and Greengard, P. (2000c). Dopamine and cAMP-regulated phosphoprotein 32 kDa controls both striatal long-term depression and long-term potentiation, opposing forms of synaptic plasticity. *J. Neurosci.* **20,** 8443–8451.

Calabresi, P., Maj, R., Pisani, A., Mercuri, N.B., and Bernardi, G. (1992). Long-term synaptic depression in the striatum: Physiological and pharmacological characterization. *J. Neurosci.* **12,** 4224–4233.

Campbell, G.A., Eckardt, M.J., and Weight, F.F. (1985). Dopaminergic mechanisms in subthalamic nucleus of rat: Analysis using horseradish peroxidase and microiontophoresis. *Brain Res.* **333,** 261–270.

Carmichael, S.T., and Price, J.L. (1995), Limbic connections of the orbital and medial prefrontal cortex in macaque monkeys. *J. Comp. Neurol.* **363,** 615–641.

Carmichael, S.T., and Price, J.L. (1996a), Sensory and premotor connections of the orbital and medial prefrontal cortex of macaque monkeys. *J. Comp. Neurol.* **363,** 642–640.

Carmichael, S.T., and Price, J.L. (1996b). Connectional networks within the orbital and medial prefrontal cortex of Macaque monkeys. *J. Comp. Neurol.* **371,** 179–207.

Carpenter, M.B. (1976). Anatomical organization of the corpus striatum and related nuclei. *In* "The Basal Ganglia" (M.D. Yahr, ed.), pp. 1–36. Raven Press, New York.

Carpenter, M.B. (1985). "Core Text of Neuroanatomy," 3 ed. Williams & Wilkins, Baltimore.

Carpenter, M.B., and Peter, P. (1972). Nigrostriatal and nigrothalamic fibers in the rhesus monkey. *J. Comp. Neurol.* **144,** 93–115.

Carpenter, M.B., Baton, R.R., Carleton, S.C., and Keller, J.T. (1981b). Interconnections and organization of pallidal and subthalamic nucleus neurons in the monkey. *J. Comp. Neurol.* **197,** 579–603.

Carpenter, M.B., Carlton, S.C., Keller, J.T., Conte, P. (1981a). Connections of the subthalamic nucleus in the monkey. *Brain Res.* **224,** 1–29.

Carpenter, M.B., Fraser, R.A., and Shriver, J.E. (1968). The organization of pallidosubthalamic fibers in the monkey. *Brain Res.* **11,** 522–559.

Carter, C.J. (1980). Glutamatergic pathways from the medial prefrontal cortex to the anterior striatum, nucleus accumbens and substantia nigra. *Brit. J. Phermacol.* **70,** 50–51.

Cepeda, C., Levine, M.S. (1998). Dopamine and *N*-methyl-D-aspartate receptor interactions in the neostriatum. *Dev. Neurosci.* **20,** 1–18.

Chang, H.T. (1981). Single neostriatal efferent axons in the globus pallidus: A light and electron microscopic study. *Science* **213,** 915–918.

Chang, H.T. (1988a). Substance P-dopamine relationship in the rat substantia nigra: A light and electron microscopy study of double immunocytochemically labeled materials. *Brain Res.* **448,** 391–396.

Chang, H.T. (1988b). Dopamine-acetylcholine interaction in the rat striatum: A dual-labeling immunocytochemical study. *Brain Res. Bull.* **21,** 295–304.

Chen, D.F., Schneider, G.E., Martinou, J.C., and Tonegawa, S. (1997). Bcl-2 promotes regeneration of severed axons in mammalian CNS [see comments]. *Nature* **385,** 434—439.

Chen, L.L., and Wise, S.P. (1995). Supplementary eye field contrasted with the frontal eye field during acquisition of conditional oculomotor associations. *J. Neurophysiol.* **73,** 1122–1134.

Cheramy, A., Leviel, V., and Glowinski, J. (1981). Dendritic release of dopamine in the substantia nigra. *Nature* **289,** 537–542.

Chesselet, M.F., and Graybiel, A.M. (1986). Striatal neurons expressing somatostatin-like immunoreactivity: Evidence for a peptidergic interneuronal system in the cat. *Neuroscience* **17,** 547–571.

Chikama, M., and Haber, S.N. (1995). The primate striatal projections from the insula: A retrograde study. *Soc. Neurosci. Abst.*

Chikama, M., McFarland, N., Amaral, D.G., and Haber, S.N. (1997). Insular cortical projections to functional regions of the striatum correlate with cortical cytoarchitectonic organization in the primate. *J. Neurosci.* **17** (24), 9686–9705.

Chronister, R.B., Sikes, R.W., Trow, T.W., and DeFrance, J.F. (1981). The organization of the nucleus accumbens. *In* "The Neurobiology of the Nucleus Accumbens" (R.B. Chronister and J.F. DeFrance, eds.), pp. 97–146. Haer Institute, Brunswick, ME.

Civelli, O., Bunzow, J.R., and Grandy, D.K. (1993). Molecular diversity of the dopamine receptors. *Annu. Rev. Pharmacol. Toxicol.* **33,** 281–307.

Contreras-Vidal, J.L., and Schultz, W. (1999). A predictive reinforcement model of dopamine neurons for learning approach behavior. *J. Comput. Neurosci.* **6,** 191–214.

Cossette, M., Levesque, M., and Parent, A. (1999). Extrastriatal dopaminergic innervation of human basal ganglia. *Neurosci. Res. Suppl.* **34,** 51–54.

Cowan, R.L., Wilson, C.J., Emson, P.C., and Heizmann, C.W. (1990). Parvalbumin-containing GABAergic interneurons in the rat neostriatum. *J. Comp. Neurol.* **302,** 197–205.

Crutcher, M.D., and DeLong, M.R. (1984a). Single cell studies of the primate putamen. I. Functional organization. *Exp. Brain Res.* **53,** 233–243.

Crutcher, M.D., and DeLong, M.R. (1984b). Single cell studies of the primate putamen. II. Relations to direction of movement and pattern of muscular activity. *Exp. Brain Res.* **53,** 244–258.

Cummings, J.L. (1993). Frontal-subcortical circuits and human behavior [Review] [71 refs]. *Arch. Neurol.* **50,** 873–880.

Cummings, J.L. (1995). Anatomic and behavioral aspects of frontal-subcortical circuits [Review] [69 refs]. *Ann. N.Y. Acad. Sci.* **769,** 1–13.

De la Torre, J.C. (1972). Catecholamines in the human diencephalon: A histochemical fluorescence study. *Acta Neuropathol.* **21,** 165–168.

Del Fiacco, M., Paxinos, G., and Cuello, A.C. (1982). Neostriatal enkephalin-immunoreactive neurones project to the globus pallidus. *Brain Res.* **231,** 1–17.

DeLong, M.R. (1971). Activity of pallidal neurons during movement. *J. Neurophysiol.* **34,** 414–427.

DeLong, M.R. (1990). Primate models of movement disorders of basal ganglia origin. *Trends Neurosci.* **13,** 281–285.

DeLong, M.R., and Georgopoulos, A.P. (1979). Physiology of the basal ganglia—A brief overview. *Adv. Neurol.* **23,** 137–153.

DeLong, M.R., and Georgopoulos, A.P. (1981), Motor functions of the basal ganglia. *In* "Handbook of Physiology. I. The Nervous System" (J.M. Bookhard, V.B. Mountcastle, and V.B. Brooks, eds.), pp. 1017–1061. American Physiology Society, Bethesda.

DeLong, M.R., and Georgopoulos, A.P. (1991). Motor functions of basal ganglia. *In* "Handbook of Physiology—The Nervous System II" (Delong, ed.), pp. 1017–1061.

DeLong, M.R., and Strick, P.L. (1974), Relation of basal ganglia, cerebellum, and motor cortex units to ramp and ballistic limb movements. *Brain Res.* **71,** 327–335.

DeLong, M.R., Crutcher, M.D., and Georgopoulos, A.P. (1985). Primate globus pallidus and subthalamic nucleus: functional organization. *J. Neurophysiol.* **53,** 530–543.

Denny-Brown, D. (1962). "The Basal Ganglia." Oxford Univ. Press, Oxford.

Deutch, A.Y., Goldstein, M., and Roth, R.H. (1986). The ascending projections of the dopaminergic neurons of the substantia nigra, zona reticulata: A combined retrograde tracer-immunohistochemical study. *Neurosci. Lett.* **71,** 257–263.

DeVito, J.L., and Anderson, M.E. (1982). An autoradiographic study of efferent connections of the globus pallidus in *Macaca mulatta*. *Exp. Brain Res.* **46,** 107–117.

Di Chiara, G., Morelli, M., and Consolo, S. (1994). Modulatory functions of neurotransmitters in the striatum: ACh/dopamine/NMDA interactions. *Trends Neurosci.* **17,** 228–233.

Dierssen, G., Odoriz, B., and Hernando, C. (1969). Sensory and motor responses to stimulation of the posterior cingulate cortex in man. *J. Neurosurg.* **31,** 435–440.

DiFiglia, M. (1987). Synaptic organization of cholinergic neurons in the monkey neostriatum. *J. Comp. Neurol.* **255,** 245–258.

DiFiglia, M., and Aronin, N. (1982). Ultrastructural features of immunoreactive somatostatin neurons in the rat caudate nucleus. *J. Neurosci.* **2,** 1267–1274.

DiFiglia, M., and Carey, J. (1986). Large neurons in the primate neostriatum examined with the combined Golgi-electron microscopic method. *J. Comp. Neurol.* **244,** 36–52.

Difiglia, M., and Rafols, J.A. (1988). Synaptic organization of the globus pallidus. *J. Electron Microsc. Tech.* **10,** 247–263.

DiFiglia, M., Aronin, N., and Leeman, S.E. (1981). Immunoreactive substance P in the substantia nigra of the monkey: Light and electron microscopic localization. *Brain Res.* **233,** 381–388.

DiFiglia, M., Pasik, P., and Pasik, T. (1976). A Golgi study of neuronal types in the neostriatum of monkeys. *Brain Res.* **114,** 245–256.

DiFiglia, M., Pasik, P., and Pasik, T. (1982a). A golgi and ultrastructural study of the monkey globus pallius. *J. Comp. Neurol.* **212,** 53–75.

DiFiglia, M., Aronin, N., and Martin, J.B. (1982b). Light and electron microscopic localization of immunoreactive leu-enkephalin in the monkey basal ganglia. *J. Neurosci.* **2** (3), 303–320.

Difiglia, M., Pasik, T., and Pasik, P. (1982). Ultrastructure of Golgi-impregnated and gold-toned spiny and aspiny neurons in the monkey neostriatum. *J. Neurocytol.* **9,** 471–492.

Donoghue, J.P., and Herkenham, M. (1986). Neostriatal projections from individual cortical fields conform to histochemically distinct striatal compartments in the rat. *Brain Res.* **365,** 397–403.

Donoghue, J.P., and Kitai, S.T. (1981). A collateral pathway to the neostriatum from corticofugal neurons of the rat sensory-motor cortex: An intracellular HRP study. *J. Comp. Neurol.* **201,** 1–13.

Doya, K. (2000). Complementary roles of basal ganglia and cerebellum in learning and motor control. *Curr. Opin. Neurobiol.* **10,** 732–739.

Doyon, J., Gaudreau, D., Laforce, R., Jr., Castonguay, M., Bedard, P.J., Bedard, F., and Bouchard ,J.P. (1997). Role of the striatum, cerebellum, and frontal lobes in the learning of a visuomotor sequence. *Brain Cogn.* **34,** 218–245.

Druga, R., Rokyta, R., and Benes, V. (1991). Thalamocaudate projections in the macaque monkey (a horseradish peroxidase study). *J. Hirnforsch.* **6,** 765–774.

Dubach, M., Schmidt, R., Kunkel, D., Bowden, D.M., Martin, R., and German, D.C. (1987). Primate neostriatal neurons containing tyrosine hydroxylase: Immunohistochemical evidence. *Neurosci. Lett.* **75,** 205–210.

Dubé, L., Smith, A.D., and Bolam, J.P. (1988). Identification of synaptic terminals of thalamic or cortical origin in contact with distinct medium-size spiny neurons in the rat neurostriatum. *J. Comp. Neurol.* **267,** 455–471.

Dum, R.P., and Strick, P.L. (1991a). The origin of corticospinal projections from the premotor areas in the frontal lobe. *J. Neurosci.* **11** (3), 667–689.

Dum, R.P., and Strick, P.L. (1991b). Premotor areas: Nodal points for parallel efferent systems involved in the central control of movement. *In* "Motor Control: Concepts and Issues" (D.R. Humphrey and H-J. Freund, eds.), pp. 383–380. John Wiley & Sons, New York.

Dum, R.P., and Strick, P.L. (1993). Cingulate motor areas. *In* "Neurobiology of Cingulate Cortex and Limbic Thalamus: A Comprehensive Treatise" (B.A. Vogt and M. Gabriel, eds.), pp. 415–441. Birkhauser, Boston.

Dum, R.P., and Strick, P.L. (1996). Spinal cord terminations of the medial wall motor areas in macaque monkeys. *J. Neurosci.* **16,** 6513–6525.

Dwork, A.J., Schon, E.A., and Herbert, J. (1988). Nonidentical distribution of transferrin and ferric iron in human brain. *Neurosci.* **27,** 333–345.

Ehringer, H., and Hornykiewicz, O. (1960). Veteilung von Noradrenalin und Dopamine (3-hydro-xytyramin) im Gehirn des Menschen und ihr Verhalten bei Erkankungen des Extrapyramidalen Systems. Klin. *Wochenschr.* **38,** 1236–1239.

Elliott, R., and Dolan, R.J. (1999). Differential neural responses during performance of matching and nonmatching to sample tasks at two delay intervals. *J. Neurosci.* **19,** 5066–5073.

Emson, P.C., Arrequi, A., Clement, V-J., Sandberg, B.E.B., and Rossor, M. (1980). Regional distribution of methionine-enkephalin and substance P-like immunoreactivity in normal human brain and in Huntington's disease. *Brain Res.* **199,** 147–160.

Eslinger, P.J., and Damasio, A.R. (1985), Severe disturbance of higher cognition after bilateral frontal lobe ablation: Patient EVR. *Neurology* **35,** 1731–1741.

Evarts, E.V., Kimura, M., Wurtz, R.H., and Hikosaka, O. (1985). Behavioral correlates of activity in basal ganglia neurons. *In* "The Motor System in Neurobiology" (E.V. Evarts, S.P. Wise, and D. Bousfield , eds.), pp. 292–304. Elsevier Biomedical Press, Amsterdam.

Everitt, B.J., and Robbins, T.W. (1992). Amygdala-ventral striatal interactions and reward-related processes. *In* "The Amygdala: Neurobiological Aspects of Emotion, Memory, and Mental Dysfunction" (J.P. Aggleton, ed.), pp. 401–429. Wiley-Liss, Chichester.

Everitt, B.J., Cador, M., and Robbins, T.W. (1989). Interactions between the amygdala and ventral striatum in stimulus-reward associations: Studies using a second-order schedule of sexual reinforcement. *Neurosci.* **30** (1), 63–75.

Fallon, J.H. (1978). Catecholamine innervation of the basal forebrain. II. Amygdala, suprarhinal cortex and entorhinal cortex. *J. Comp. Neurol.* **180** (3), 509–532.

Fallon, J.H. (1983). The islands of Calleja complex of rat basal forebrain. II. Connections of medium and large sized cells. *Brain Res. Bull.* **10,** 775–793.

Fallon, J.H., and Loughlin. S.E. (1987). Monoamine innervation of cerebral cortex and a theory of the role of monoamines in cerebral cortex and basal ganglia. *In* "Cerebral Cortex" (E.G. Jones and A. Peters, eds.), pp. 41–109. Plenum Press.

Fallon, J.H., and Moore, R.Y. (1978). Catecholamine innervation of the basal forebrain. IV. Topography of the dopamine projections to the basal forebrain and neostriatum. *J. Comp. Neurol.* **180** (3), 545–580.

Fallon, J.H., Loughlin, S.E., and Ribak, C.E. (1983). The islands of Calleja complex of rat basal forebrain. III. Histochemical evidence for a striatopallidal system. *J. Comp. Neurol.* **218,** 91–120.

Fallon, J.H., Riley, J.N., Sipe, J.C., and Moore, R.Y. (1978). The islands of Calleja: Organization and connections. *J. Comp. Neurol.* **181,** 375–395.

Fallon, J.H., Seroogy, K.B., Loughlin, S.E., Morrison, R.S., Bradshaw, R.A., Knauer, D.J., and Cunningham, D.D. (1984). Epidermal growth factor immunoreactive material in the central nervous system: Location and development. *Science* **224,** 1107–1109.

Farlie, P.G., Dringen, R., Rees, S.M., Kannourakis, G., and Bernard, O. (1995). Bcl-2 transgene expression can protect neurons against developmental and induced cell death. *Proc. Natl. Acad. Sci. U.S.A.* **92,** 4397–4401.

Faull, R.L.M., Dragunow, M., and Villiger, J.W. (1989). The distribution of neurotensin receptors and acetylcholinesterase in the human caudate nucleus: Evidence for the existence of a third neurochemical compartment. *Brain Res.* **488,** 381–386.

Felten, D.L., and Sladek, J.R., Jr. (1983). Monoamine distribution in primate brain. V. Monoaminergic nuclei: Anatomy, pathways and local organization. *Brain Res. Bull.* **10,** 171–284.

Fenelon, G., Francois, C., Percheron, G., and Yelnik, J. (1991). Topographic distribution of the neurons of the central complex (Centre mèdian-parafascicular complex) and of other thalamic neurons projecting to the striatum in macaques. *Neurosci.* **45** (2), 495–510.

Ferrante, R.J., Kowall, N.W., Cipolloni, P.B., Storey, E., and Beal, M.F. (1993). Excitotoxin lesions in primates as a model for Huntington's disease: Histopathologic and neurochemical characterization. *Exp. Neurol.* **119,** 46–71.

Ferry, A.T., Ongur, D., An, X., and Price, J.L. (2000). Prefrontal cortical projections to the striatum in macaque monkeys: Evidence for an organization related to prefrontal networks. *J. Comp. Neurol.* **425,** 447–470.

Fibiger, H.C., and Phillips, A.G. (1986). Reward, motivation, cognition: psychobiology of mesotelencephalic dopamine systems. *In* "Handbook of Physiology. I. The Nervous System" (V.B. Mountcastle, F. Plum, and S.R. Geiger, eds.), pp. 647–674. American Physiological Society, Bethesda, MD.

Filion, M., and Tremblay, L. (1991). Abnormal spontaneous activity of globus pallidus neurons in monkeys with MPTP-induced parkinsonism. *Brain Res.* **547,** 142–151.

Filley, C.M. (1995). Frontal Lobe Syndromes. *In* "Neurobehavioral Anatomy," 1 ed., pp. 149–162. University Press of Colorado, Niwot.

Flaherty, A.W., and Graybiel, A.M. (1991a). Cortical transformations in the primate somatosensory system. Projections from physiologically mapped body-part representations. *J. Neurophysiol.* **66** (4), 1249–1263.

Flaherty, A.W., and Graybiel, AM. (1991b). Corticostriatal transformations in the primate somatosensory system. Projections from physiologically mapped body-part representations. *J. Neurophysiol.* **66,** 1249–1263.

Flaherty, A.W., and Graybiel, A.M. (1993). Two input systems for body representations in the primate striatal matrix: experimental evidence in the squirrel monkey. *J. Neurosci.* **13** (3), 1120–1137.

Flaherty, A.W., and Graybiel, A.M. (1994). Input-output organization of the sensorimotor striatum in the squirrel monkey. *J. Neurosci.* **14,** 599–610.

Flores, G., Liang, J.J., Sierra, A., Martinez-Fong, D., Quirion, R., Aceves, J., and Srivastava, L.K. (1999). Expression of dopamine receptors in the subthalamic nucleus of the rat: Characterization using reverse transcriptase-polymerase chain reaction and autoradiography. *Neurosci.* **91,** 549–556.

Fogassi, L., Gallese, V., Fadiga, L., Luppino, G., Matelli, M., and Rizzolatti, G. (1996). Coding of peripersonal space in inferior premotor cortex (area F4). *J. Neurophysiol.* **76,** 141–157.

Fox, C.A., Andrade, A.N., Hillman, D.E., and Schwyn, R.C. (1971a). The spiny neurons in the primate striatum: A Golgi and electron microscopic study. *J. Hirnforsch.* **13,** 181–201.

Fox, C.A., Andrade, A.N., Schwyn, R.C., and Rafols, J.A. (1971b). The aspiny neurons and the glia in the primate striatum: A golgi and electron microscopic study. *J. Hirnforsch.* **13,** 341–362.

Fox, C.H., Andrade, H.N., Du Qui, I.J., and Rafols, J.A. (1974). The primate globus pallidus. A Golgi and electron microscope study. *J. R. Hirnforschung.* **15,** 75–93.

Francois, C., Nguyen-Legros, J., and Percheron, G. (1981). Topographical and cytological localization of iron in rat and monkey brains. *Brain Res.* **215,** 317–322.

Francois, C., Percheron, G., and Yelnik, J. (1984a). Localization of nigrostriatal, nigrothalamic and nigrotectal neurons in ventricular coordinates in macaques. *Neurosci.* **13** (1), 61–76.

Francois, C., Percheron, G., Parent, A., Sadikot, A.F., Fenelon, G., and Yelnik, J. (1991). Topography of the projection from the central complex of the thalamus to the sensorimotor striatal territory in monkeys. *J. Comp. Neurol.* **305,** 17–34.

Francois, C., Percheron, G., Yelnik, J., and Heyner, S. (1979). Demonstration of the existence of small local circuit neurons in the Golgi-stained primate substantia nigra. *Brain Res.* **172,** 160–164.

Francois, C., Percheron, G., Yelnik, J., and Heyner, S. (1984b). A golgi analysis of the primate globus pallidus. I. Inconstant processes of large neurons, other neuronal types, and afferent axons. *J. Comp. Neurol.* **227,** 182–199.

Francois, C., Percheron, G., Yelnik, J., and Heyner, S. (1985). A histological atlas of the macaque *(macaca mulatta)* substantia nigra in ventricular coordinates. *Brain Res. Bull.* **14,** 349–367.

Francois, C., Savy, C., Jan, C., Tande, D., Hirsch, E.C., and Yelnik, J. (2000). Dopaminergic innervation of the subthalamic nucleus in the normal state, in MPTP-treated monkeys, and in Parkinson's disease patients. *J. Comp. Neurol.* **425,** 121–129.

Francois, C., Yelnik, J., and Percheron, G. (1987). Golgi study of the primate substantia nigra. II. Spatial organization of dendritic arborizations in relation to the cytoarchitectonic boundaries and to the striatonigral bundle. *J. Comp. Neurol.* **265,** 473–493.

Freedman, L.J., Insel, T.R., and Smith, Y. (2000). Subcortical projections of area 25 (subgenual cortex) of the macaque monkey. *J. Comp. Neurol.* **421,** 172–188.

Freeman, W.M., Nader, M.A., Nader, S.H., Robertson, D.J., Gioia, L., Mitchell, S.M., Daunais, J.B., Porrino, L.J., Friedman, D.P., and Vrana, K.E. (2001). Chronic cocaine-mediated changes in non-human primate nucleus accumbens gene expression. *J. Neurochem.* **77,** 542–549.

Freund, T.F., Powell, J.F., and Smith, A.D. (1984). Tyrosine hydroxylase-immunoreactive boutons in synaptic contact with identified striatonigral neurons, with particular reference to dendritic spines. *Neurosci.* **13,** 1189–1215.

Fudge, J.L., and Haber, S.N. (2000). The central nucleus of the amygdala projection to dopamine subpopulations in primates. *Neurosci.* **97,** 479–494.

Fudge, J.L., and Haber, S.N. (2001). Bed nucleus of the stria terminalis and extended amygdala inputs to dopamine subpopulations in primates. *Neurosci.* **104,** 807–827.

Fudge, J.L., and Haber, S.N. (2002). Defining the caudal ventral striatum in primates: cellular and histochemical features. *J. Neurosci.* **22,** 10078–10082.

Fudge, J.L., Kunishio, K., Walsh, C., Richard, D., and Haber, S.N. (2002). Amygdaloid projections to ventromedial striatal subterritories in the primate. *Neurosci.* **110,** 257–275.

Fuster, J. (1997a). "The Pre-frontal Cortex-Anatomy Physiology, and Neuropsychology of the Frontal Lobe," 3rd ed. Lippincott-Raven, Philadelphia.

Fuster, J.M. (1989). Lesion studies. *In* "The Prefrontal Cortex Anatomy, Physiology, and Neuropsychology of the Frontal Lobe," 2nd ed., pp. 51–82. Raven Press, New York.

Fuster, J.M. (1997b). Network memory. *Trends Neurosci.* **20,** 451–459.

Fuster, J.M. (2000). Prefrontal neurons in networks of executive memory. *Brain Res. Bull.* **52,** 331–336.

Fuster, J.M. (2001). The prefrontal cortex—an update: Time is of the essence. *Neuron* **30,** 319–333.

Fuster, J.M., Bodner, M., and Kroger, J.K. (2000). Cross-modal and cross-temporal association in neurons of frontal cortex. *Nature* **405,** 347–351.

Garver, D.L., and Sladek, J.R. (1875). Monoamine distribution in primate brain. I. Catecholamine-containing perikarya in the brain stem of macaca speciosa. *J. Comp. Neurol.* **159,** 289–304.

Gaspar, P., Berger, B., Febvret, A., Vigny, A., and Henry, J.P. (1989). Catecholamine innervation of the human cerebral cortex as revealed by comparative immunohistochemistry of tyrosine hydroxylase and dopamine-beta-hydroxylase. *J. Comp. Neurol.* **279,** 249–271.

Gaspar, P., Stepneiwska, I., and Kaas, J.H. (1992). Topography and collateralization of the dopaminergic projections to motor and lateral prefrontal cortex in owl monkeys. *J. Comp. Neurol.* **325,** 1–21.

Georgopoulos, A.P., DeLong, M.R., and Crutcher, M.D. (1983). Relations between parameters of step-tracking movements and single cell discharge in the globus pallidus and subthalamic nucleus of the behaving monkey. *J. Neurosci.* **3,** 1586–1598.

Gerfen, C.R. (1984). The neostriatal mosaic: Compartmentalization of corticostriatal input and striatonigral output systems. *Nature* **311,** 461–464.

Gerfen, C.R. (1985). The neostriatal mosaic. I. Compartmental organization of projections from the striatum to the substantia nigra in the rat. *J. Comp. Neurol.* **236,** 454–476.

Gerfen, C.R. (1987). The neostriatal mosaic: A reiterated processing unit. *In* "Interactions in the Basal Ganglia" (M. Sandler, C. Feuerstein, and B. Scatton, eds.). Raven Press, New York.

Gerfen, C.R. (1988). Synaptic organization of the striatum. *J. Electron Microsc. Tech.* **10,** 265–281.

Gerfen, C.R., and Wilson, C.J. (1996). The basal ganglia. *In* "Integrated Systems of the CNS" (Part III) (L.W. Swanson, A. Bjorklund, and T. Hokfelt, eds.), pp. 371–468. Elsevier Science.

Gerfen, C.R., Baimbridge, K.G., and Miller, J.J. (1985). The neostriatal mosaic: Compartmental distribution of calcium-binding protein and parvalbumin in the basal ganglia of the rat and monkey. *Proc. Nat. Acad. Sci. U.S.A.* **82,** 8780–8784.

Gerfen, C.R., Baimbridge, K.G., and Thibault, J. (1987). The neostriatal mosaic: III. Biochemical and developmental dissociation of patch-matrix mesostriatal systems. *J. Neurosci.* **7** (12), 3935–3944.

Gerfen, C.R., Engber, T.M., Mahan. L.C., Susel, Z., Chase, T.N., Monsma, F.J., Jr., and Sibley, D,R. (1990). D1 and D2 dopamine receptor-regulated gene expression of striatonigral and striatopallidal neurons. *Science* **250,** 1429–1432.

Gerlach, M., Riederer, P., Przuntek, H., and Youdim, M.B.H. (1991). MPTP mechanisms of neurotoxicity and their implications for Parkinson's disease. *Eur. J. Pharmacol.* **208,** 273–286.

Giguere, M., and Goldman-Rakic, P.S. (1988). Mediodorsal nucleus: Area 1 laminar and tangential distribution of afferents and efferents in the frontal lobe of rhesus monkeys. *J. Comp. Neurol.* **277** (2), 195–213.

Giménez-Amaya, J.M., McFarland, N.R., de las Heras, S., and Haber, S.N. (1995). Organization of thalamic projections to the ventral striatum in the primate. *J. Comp. Neurol.* **354,** 127–149.

Goldman, P.S., and Nauta, W.J. (1977). An intricately patterned prefronto-caudate projection in the rhesus monkey. *J. Comp. Neurol.* **72,** 369–386.

Goldman-Rakic, P.S. (1982). Cytoarchitectonic heterogeneity of the primate neostriatum: Subdivision into Island and Matrix cellular compartments. *J. Comp. Neurol.* **205,** 398–413.

Goldman-Rakic, P.S. (1987). Circuitry of the frontal association cortex and its relevance to dementia. *Arch. Gerontol. Geriatr.* **6,** 299–309.

Goldman-Rakic, P.S. (1994). Working memory dysfunction in schizophrenia. *J. Neuropsychiatry Clin. Neurosci.* **6,** 348–357.

Goldman-Rakic, P.S. (1996). The prefrontal landscape: Implications of functional architecture for understanding human mentation and the central executive. *Phil. Trans. Roy. Soc. Lon. Ser. B: Biol. Sci.* **351,** 1445–1453.

Goldman-Rakic, P.S., and Porrino, L.J. (1985). The primate mediodorsal (MD) nucleus and its projection to the frontal lobe. *J. Comp. Neurol.* **242,** 535–560.

Goldman-Rakic, P.S., and Selemon, L.D. (1986). Topography of corticostriatal projections in nonhuman primates and implications for functional parcellation of the neostriatum. *In* "Cerebral Cortex Vol. 5" (E.G. Jones and A. Peters, eds.), pp. 447–466. Plenum, New York.

Gotz, T., Kraushaar, U., Geiger, J., Lubke, J., Berger, T., and Jonas, P. (1997). Functional properties of AMPA and NMDA receptors expressed in identified types of basal ganglia neurons. *J. Neurosci.* **17,** 204–215.

Grace, A.A., and Bunney, B.S. (1979). Paradoxical GABA excitation of nigral dopaminergic cells: Indirect mediation through reticulata inhibitory neurons. *Eur. J. Pharmacol.* **59,** 211–218.

Grace, A.A., and Bunney, B.S. (1983). Intracellular and extracellular electrophysiology of nigral dopaminergic neurons—3. Evidence for electrotonic coupling. *Neurosci.* **10,** 333–348.

Grace, A.A., and Bunney, B.S. (1995). Electrophysiological properties of midbrain dopamine neurons. *In* "Psychopharmacology: The Fourth Generation of Progress" (F.E. Bloom and D.J. Kupfer, eds.), pp. 163–177. Raven Press, New York.

Gracy, K.N., and Pickel, V.M. (1996). Ultrastructural immunocytochemical localization of the *N*-methyl-D-aspartate receptor and tyrosine hydroxylase in the shell of the rat nucleus accumbens. *Brain Res.* **739,** 169–181.

Grafton, S.T., and Hazeltine, E. (1995). Functional mapping of sequence learning in normal humans. *J. Cog. Neurosci.* **7,** 497–510.

Graveland, G.A., and DiFiglia, M. (1985). The frequency and distribution of medium-sized neurons with indented nuclei in the primate and rodent neostriatum. *Brain Res.* **327,** 307–311.

Graveland, G.A., Williams, R.S., and DiFiglia, M. (1985). A Golgi study of the human neostriatum: Neurons and afferent fibers. *J. Comp. Neurol.* **234,** 317–333.

Graybiel, A.M. (1983). Compartmental organization of the mammalian striatum. *Prog. Brain Res.* **58,** 247–256.

Graybiel, A.M. (1984). Correspondence between the dopamine islands and striosomes of the mammalian striatum. *Neurosci.* **13,** 1157–1187.

Graybiel, A.M. (1990) Neurotransmitters and neuromodulators in the basal ganglia. *Trends Neurosci.* **13,** 244–254.

Graybiel, A.M. (1998). The basal ganglia and chunking of action repertoires. *Neurobiol. Learning & Memory* **70,** 119–136.

Graybiel, A.M., and Ragsdale, C.W. Jr. (1978). Histochemically distinct compartments in the striatum of human, monkeys, and cat demonstrated by acetylthiocholinesterase staining. *Proc. Nat. Acad. Sci. U.S.A.* **75,** 5723–5726.

Graybiel, A.M., and Ragsdale, C.W. Jr. (1980). Clumping of acetylcholinesterase activity in the developing striatum of the human fetus and young infant. *Proc. Nat. Acad. Sci. U.S.A.* **77,** 1214–1218.

Graybiel, A.M., and Ragsdale, C.W. (1983). Biochemical anatomy of the striatum. In "Chemical Anatomy" (P.C. Emson, ed.). Raven Press, New York.

Graziano, M.S., Hu, X.T., and Gross, C.G. (1997). Visuospatial properties of ventral premotor cortex. *J. Neurophysiol.* **77,** 2268–2292.

Groenewegen, H.J., and Berendse, H.W. (1994a). The specificity of the "nonspecific" midline and intralaminar thalamic nuclei. *Trends Neurosci.* **17,** 50.

Groenewegen, H.J., and Berendse, H.W. (1994b). Anatomical relationships between the prefrontal cortex and the basal ganglia in the rat. *In* "Motor and Cognitive Functions of the Prefrontal Cortex" (A.-M. T, ed.), pp. 51–77. Springer-Verlag, Berlin-Heidelberg.

Groenewegen, H.J., Wright, C.I., and Beijer, A.V.J. (1996), The nucleus accumbens: Gateway for limbic structures to reach the motor system? *In* "Progress in Brain Research" (G. Holstege, R. Bandler, and C.P. Saper, eds.), pp. 485–511. Elsevier Science.

Groenewegen, H.J., Berendse, H.W., Wolters, J.G., Witter, M.P., and Lohman, A.H.M. (1990). The anatomical relationship of the prefrontal cortex with the striatopallidal system, the thalamus and the amygdala: Evidence for a parallel organization. *In* "Progress in Brain Research," Vol. 85 (H.B.M. Uylings, ed.), pp. 95–118. Elsevier, Amsterdam.

Grofova, I. (1975). The identification of striatal and pallidal neurons projecting to substantia nigra. An experimental study by means of retrograde axonal transport of horseradish peroxidase. *Brain Res.* **91,** 286–291.

Groves, P.M., Wilson, C.J., Young, S.J., and Rebec, G.V. (1975). Self-inhibition by dopaminergic neurons. *Science* **190,** 522–528.

Groves, P.M., Martone, M., Young, S.J., and Armstrong, D.M. (1988). Three-dimensional pattern of enkephalin-like immunoreactivity in the caudate nucleus of the cat. *J. Neurosci.* **8,** 892–900.

Haber, S., and Elde, R. (1981). Correlation between met-enkephalin and substance P immunoreactivity in the primate globus pallidus. *Neurosci.* **6,** 1291–1298.

Haber, S.N. (1986). Neurotransmitters in the human and nonhuman primate basal ganglia. *Human Neurobiol.* **5**, 159–168.

Haber, S.N. (1987). Anatomical relationship between the basal ganglia and the basal nucleus of Maynert in human and monkey forebrain. *Proc. Natl. Acad. Sci. U.S.A.* **84,** 1408–1412.

Haber, S.N. (2002). Integrating motivation and cognition into the basal ganglia of action. *In* "Mental Dysfunction in Movement Disorders" (M.A. Bedard, Y. Agid, S. Chouinard, S. Fahn, A. Korczyn, and P. Lesperance, eds.), p. in press. Humana Press, Totowa, NJ.

Haber, S.N., and Elde, R. (1982). The distribution of enkephalin immunoreactive fibers and terminals in the monkey central nervous system: An immunohistochemical study. *Neurosci.* **7,** 1049–1095.

Haber, S.N., and Groenewegen, H.J. (1989). Interrelationship of the distribution of neuropeptides and tyrosine hydroxylase immunoreactivity in the human substantia nigra. *J. Comp. Neurol.* **290,** 53–68.

Haber, S.N., and Lu, W.X. (1992). High levels of enkephalin mRNA are found in the striatum and limbic-associated regions of the monkey telencephalon. In Preparation.

Haber, S.N., and McFarland, N.R. (1999a). The concept of the ventral striatum in nonhuman primates. *In* "Advancing from the Ventral Striatum to the Extended Amygdala" (J.F. McGinty, ed.), pp. 33–48. The New York Academy of Sciences, New York.

Haber, S.N., and McFarland, N.R. (1999b). The concept of the ventral striatum in nonhuman primates. *Ann. N.Y. Acad. Sci.* **877,** 33–48.

Haber, S.N., and Nauta, W.J.H. (1983). Ramifications of the globus pallidus in the rat as indicated by patterns of immunohistochemistry. *Neurosci.* **9,** 245–260.

Haber, S.N., and Watson, S.J. (1985). The comparative distribution of enkephalin, dynorphin and substance P in the human globus pallidus and basal forebrain. *Neurosci.* **4,** 1011–1024.

Haber, S.N., Fudge, J.L., and McFarland, N.R. (2000). Striatonigrostriatal pathways in primates form an ascending spiral from the shell to the dorsolateral striatum. *J. Neurosci.* **20,** 2369–2382.

Haber, S.N., Groenewegen, H.J., Grove, E.A., and Nauta, W.J.H. (1985). Efferent connections of the ventral pallidum. Evidence of a dual striatopallidofugal pathway. *J. Comp. Neurol.* **235,** 322–335.

Haber, S.N., Kunishio, K., Mizobuchi, M., Lynd-Balta, E. (1995b). The orbital and medial prefrontal circuit through the primate basal ganglia. *J. Neurosci.* **15,** 4851–4867.

Haber, S.N., Lynd, E., Klein, C., and Groenewegen, H.J. (1990b). Topographic organization of the ventral striatal efferent projections in the rhesus monkey: An anterograde tracing study. *J. Comp. Neurol.* **293,** 282–298.

Haber, S.N., Lynd-Balta, E., and Mitchell, S.J. (1993). The organization of the descending ventral pallidal projections in the monkey. *J. Comp. Neurol.* **329** (1), 111–129.

Haber, S.N., Lynd-Balta, E., and Spooren, W.P.T.M. (1994). Integrative aspects of basal ganglia circuitry. *In* "The Basal Ganglia IV" (G. Percheron, J.S. McKenzie, and J. Feger, eds.), pp. 71–80. Plenum Press, New York.

Haber, S.N., Ryoo, H., Cox, C., and Lu, W. (1995a). Subsets of midbrain dopaminergic neurons in monkeys are distinguished by different levels of mRNA for the dopamine transporter: Comparison with the mRNA for the D2 receptor, tyrosine hydroxylase and calbindin immunoreactivity. *J. Comp. Neurol.* **362,** 400–410.

Haber, S.N., Wolfe, D.P., and Groenewegen, H.J. (1990a). The relationship between ventral striatal efferent fibers and the distribution of peptide-positive woolly fibers in the forebrain of the rhesus monkey. *Neurosci.* **39,** 323–338.

Hajdu, F., Hassler, R., and Bak, I.J. (1973). Electron microscopic study of the substantia nigra and the strio-nigral projection in the rat. *Z. Zellforschung Mikroskop. Anatom.* **146,** 207–221.

Halliday, G.M., and Tork, I. (1986). Comparative anatomy of the ventromedial mesencephalic tegmentum in the rat, cat, monkey and human. *J. Comp. Neurol.* **252,** 423–445.

Halliwell, J.V., and Horne, A.L. (1998). Evidence for enhancement of gap junctional coupling between rat island of Calleja granule cells in vitro by the activation of dopamine D3 receptors. *J. Physiol.* **506,** 175–194.

Hammond, C., and Yelnik, J. (1983). Intracellular labelling of rat subthalamic neurones with horseradish peroxidase: Computer analysis of dendrites and characterization of axon arborization. *Neurosci.* **8,** 781–790.

Hammond, C., Rouzaire-Dubois, B., Feger, J., Jackson, A., and Crossman, A.R. (1983). Anatomical and electrophysiological studies on the reciprocal projections between the subthalamic nucleus and nucleus tegmenti pedunculopontinus in the rat. *Neurosci.* **9,** 41–52.

Hanley, J.J., and Bolam, J.P. (1997). Synaptology of the nigrostriatal projection in relation to the compartmental organization of the neostriatum in the rat. *Neurosci.* **81,** 353–370.

Hanson, J.E., and Smith, Y. (1999). Group I metabotropic glutamate receptors at GABAergic synapses in monkeys. *J. Neurosci.* **19,** 6488–6496.

Harrington, K.A., Augood, S.J., Faull, R.L., McKenna, P.J., and Emson, P.C. (1995). Dopamine D1 receptor, D2 receptor, proenkephalin A and substance P gene expression in the caudate nucleus of control and schizophrenic tissue: A quantitative cellular in situ hybridisation study. *Brain Res. Mol. Brain Res.* **33,** 333–342.

Hassani, O.K., Cromwell, H.C., and Schultz, W. (2001). Influence of expectation of different rewards on behavior-related neuronal activity in the striatum. *J. Neurophysiol.* **85,** 2477–2489.

Hassani, O.K., Francois, C., Yelnik, J., and Feger, J. (1997). Evidence for a dopaminergic innervation of the subthalamic nucleus in the rat. *Brain Res.* **749,** 88–94.

Hassler, R. (1939). Zur pathologischen anatomie des senilen und des parkinsonistischen tremor. *J. Psychol. Neurol.* 13–15.

Hassani, O-K., Mouroux, M., and Feger, J. (1996). Increased subthalamic neuronal activity after nigral dopaminergic lesion independent of disinhibition via the globus pallidus. *Neurosci.* **72,** 105–115.

Hassler, R., and Chung, Y.W. (1984). Identification of eight types of synapses in the pallidum externum and internum in squirrel monkey *(Saimiri sciureus). Acta. Anat.* **118,** 65–81.

Hazrati, L.N., and Parent, A. (1991). Projection from the external pallidum to the reticular thalamic nucleus in the squirrel monkey. *Brain Res.* **550,** 142–146.

Hazrati, L-N., and Parent, A. (1992a). Convergence of subthalamic and striatal efferents at pallidal level in primates: an anterograde double-labeling study with biocytin and PHA-L. *Brain Res.* **569,** 336–340.

Hazrati, L.N., and Parent, A. (1992b). The striatopallidal projection displays a high degree of anatomical specificity in the primate. *Brain Res.* **592,** 213–227.

Hazrati, L-N., Parent, A., Mitchell, S., and Haber, S.N. (1990a). Evidence for interconnections between the two segments of the

globus pallidus in primates: A PHA-L anterograde tracing study. *Brain Res.* **533,** 171–175.

Hazrati, L.N., Parent, A., Mitchell, S., and Haber, S.N. (1990b). Evidence for interconnections between the two segments of the globus pallidus in primates: A PHA-L anterograde tracing study. *Brain Res.* **533,** 171–175.

He, S.Q., Dum, R.P., and Strick, P.L. (1993). Topographic organization of corticospinal projections from the frontal lobe: Motor areas on the lateral surface of the hemisphere. *J. Neurosci.* **13,** 952–980.

Heath, R.G., John, S.B., and Fontana, C.J. (1968). The pleasure response, studies by stereotaxic technics in patients. *In* "Computers and Electronic Devices" (N. Kline and E, Laska, eds.), pp. 178–189. Grune and Stratton, New York.

Hedreen, J.C. (1981). Neurons of the nucleus accumbens and other striatal regions in rats. *In* "The neurobiology of the nucleus accumbens" (R.B. Chronister and J.F. de France, eds.), pp. 82–96. Haer Institute for Electrophysiological Research, Brunswick, ME.

Hedreen, J.C. (1999). Tyrosine hydroxylase-immunoreactive elements in the human globus pallidus and subthalamic nucleus. *J. Comp. Neurol.* **409,** 400–410.

Hedreen, J.C., and DeLong, M.R. (1991). Organization of striatopallidal, striatonigal, and nigrostriatal projections in the Macaque. *J. Comp. Neurol.* **304,** 569–595.

Heimer, L. (1978). The olfactory cortex and the ventral striatum. *In* "Limbic Mechanisms" (K.E. Livingston and O.Hornykiewicz, eds.), pp. 95–187. Plenum Press, New York.

Heimer, L. (2000). Basal forebrain in the context of schizophrenia. *Brain Res. Brain Res. Rev.* **31,** 205–235.

Heimer, L., and Wilson, R.D. (1975). The subcortical projections of the allocortex: similarities in the neural associations of the hippocampus, the piriform cortex, and the neocortex. *In* "Golgi Centennial Symposium: Perspectives in Neurobiology" (M. Santini , ed.), pp. 177–193. Raven Press, New York.

Heimer, L., Alheid, G.F., and Zaborszky, L. (1985). The basal ganglia. *In* "The rat nervous system" (G. Paxinos, ed.), pp. 37–74. Academic Press, Sydney.

Heimer, L., Alheid, G.F., and Zahm, D.S. (1994). Basal forebrain organization: An anatomical framework for motor aspects of drive and motivation. *In* "Limbic Motor Circuits and Neuropsychiatry" (P.W. Kalivas and C.D. Barnes, eds.). CRC Press, Boca Raton, FL.

Heimer, L., Switzer, R.D., and Van Hoesen, G.W. (1982). Ventral striatum and ventral pallidum. Components of the motor system? *Trends Neurosci.* **5,** 83–87.

Heimer, L., De Olmos, J.S., Alheid, G.F., Person, J., Sakamoto, N., Shinoda, K., Marksteiner, J., and Switzer, R.C. (1999). The human basal forebrain. Part II. *In* "Hanbook of Chemical Neuroanatomy" (F.E. Bloom, A. Bjorkland , and T. Hokfelt, eds.), pp. 57–226. Elsevier, Amsterdam.

Heimer, L., de Olmos, J., Alheid, G.F., and Zaborszky, L. (1991a). "Perestroika" in the basal forebrain: Opening the border between neurology and psychiatry. *In* "Progress in Brain Research," Vol. 87 (G. Holstege, ed.), pp. 109–165. Elsevier Science Publishers.

Heimer, L., Zahm, D.S., Churchill, L., Kalivas, P.W., and Wohltmann, C. (1991b). Specificity in the projection patterns of accumbal core and shell in the rat. *Neurosci.* **41** (1), 89–125.

Heimer, L., Zaborszky, L., Zahm, D.S., and Alheid, G.F. (1987). The ventral striatopallidothalamic projection: I. The striatopallidal link originating in the striatal parts of the olfactory tubercle. *J. Comp. Neurol.* **255,** 571–591.

Herkenham, M. (1978). The connections of the nucleus reuniens thalami: Evidence for a direct thalamo-hippocampal pathway in the rat. *J. Comp. Neurol.* **177,** 589–609.

Herkenham, M. (1986). New perspectives on the organization and evolution of nonspecific thalamochortical projections. *In* "Cerebral Cortex: Sensory-Motor Areas and Aspects of Cortical Connectivity' (E.G. Jones and A. Peters, eds.), pp. 403–445. Plenum Press, New York.

Herkenham, M., and Pert, C.B. (1981). Mosaic distribution of opiate receptors, parafascicular projections and acetylcholinesterase in rat striatum. *Nature* **291,** 415–418.

Herkenham, M., Moon Edley, S., and Stuart, J. (1984). Cell clusters in the nucleus accumbens of the rat, and the mosaic relationship of opiate receptors, acetylcholinesterase and subcortical afferent terminations. *Neurosci.* **11,** 561–593.

Hernandez-Lopez, S., Bargas, J., Surmeier, D.J., Reyes, A., and Galarraga, E. (1997). D1 receptor activation enhances evoked discharge in neostriatal medium spiny neurons by modulating an L-type Ca^{2+} conductance. *J. Neurosci.* **17,** 3334–3342.

Herrero, M.T., Hirsch, E.C., Kastner, A., Ruberg, M., Luquin, M.R., Laguna, J., Javoy-Agid, F., Obeso, J.A., and Agid, Y. (1993). Does neuromelanin contribute to the vulnerability of catecholaminergic neurons in monkeys intoxicated with MPTP? *Neurosci.* **56,** 499–511–499–510.

Hersch, S.M., Ciliax, B.J., Gutekunst, C.A., Rees, H.D., Heilman, C.J., Yung, K.K., Bolam, J.P., Ince, E., Yi, H., and Levey, A.I. (1995). Electron microscopic analysis of D1 and D2 dopamine receptor proteins in the dorsal striatum and their synaptic relationships with motor corticostriatal afferents. *J. Neurosci.* **15,** 5222–5237.

Hersch, S.M., Gutekunst, C.A., Rees, H.D., Heilman, C.J., and Levey, A.I. (1994). Distribution of m1-m4 muscarinic receptor proteins in the rat striatum: Light and electron microscopic immunocytochemistry using subtype-specific antibodies. *J. Neurosci.* **14,** 3351–3363.

Hikosaka, K., and Watanabe, M. (2000). Delay activity of orbital and lateral prefrontal neurons of the monkey varying with different rewards. *Cereb. Cortex* **10,** 263–271.

Hikosaka, O. (1991). Basal ganglia—possible role in motor coordination and learning. *Cur. Opin. Neurobiol.* **1,** 638–643.

Hikosaka, O., and Wurtz, R.H. (1983a). Visual and oculomotor functions of monkey substantia nigra pars reticulata. IV. Relation of substantia nigra to superior colliculus. *J. Neurophysiol.* **49** (5), 1285–1301.

Hikosaka, O., and Wurtz, R.H. (1983b). Visual and oculomotor functions of monkey substantia nigra pars reticulata. I. Relation of visual and auditory responses to saccades. *J. Neurophysiol.* **49,** 1230–1253.

Hikosaka, O., and Wurtz, R.H. (1989). The basal ganglia. *Rev. Oculomot. Res.* **3,** 257–281.

Hikosaka, O., Miyashita, K., Miyachi, S., Sakai, K., and Lu, X. (1998). Differential roles of the frontal cortex, basal ganglia, and cerebellum in visuomotor sequence learning. *Neurobiol. Learning & Memory* **70,** 137–149.

Hikosaka, O., Rand, M.K., Miyachi, S., and Miyashita, K. (1995). Learning of sequential movements in the monkey: Process of learning and retention of memory. *J. Neurophysiol.* **74,** 1652–1661.

Hikosaka, O., Sakai, K., Miyauchi, S., Takino, R., Sasaki, Y., and Putz, B. (1996). Activation of human presupplementary motor area in learning of sequential procedures: A functional MRI study. *J. Neurophysiol.* **76,** 617–621.

Hikosaka, O., Sakamoto, M., and Usui, S. (1989a). Functional properties of monkey caudate neurons I. Activities related to saccadic eye movements. *J. Neurophysiol.* **61** (4), 780.

Hikosaka, O., Sakamoto, M., and Usui, S. (1989b). Functional properties of monkey caudate neurons. III. Activities related to expectation of target and reward. *J. Neurophysiol.* **61,** 814–832.

Hokfelt, T., Everitt, B.J., Theodorsson-Norheim, E., and Goldstein, M. (1984a). Occurrence of neurotensinlike immunoreactivity in subpopulations of hypothalamic, mesencephalic, and medullary catecholamine neurons. *J. Comp. Neurol.* **222,** 543–559.

Hokfelt, T., Martensson, R., Bjorklund, A., Kleinau, S., and Goldstein, M. (1984b). Distributional maps of tyrosine-hydroxylase immunoreactive neurons in the rat brain. *In* "Handbook of Chemical Neuroanatomy, Vol. II: Classical Neurotransmitters in the CNS," Part I (A. Bjorklund and T. Hokfelt, eds.), pp. 277–379. Elsevier, Amsterdam.

Hollerman, J.R., and Schultz, W. (1998). Dopamine neurons report an error in the temporal prediction of reward during learning. *Nat. Neurosci.* **1,** 304–309.

Holt, D.J., Graybiel, A.M., and Saper, C.B. (1997). Neurochemical architecture of the human striatum. *J. Comp. Neurol.* **384,** 1–25.

Holt, D.J., Hersh, L.B., and Saper, C.B. (1996). Cholinergic innervation in the human striatum: a three-compartment model. *Neurosci.* **74,** 67–87.

Hoover, J.E., and Strick, P.L. (1993). Multiple output channels in the basal ganglia. *Science* **259,** 819–821.

Hoover, J.E., and Strick, P.L. (1999). The organization of cerebellar and basal ganglia outputs to primary motor cortex as revealed by retrograde transneuronal transport of herpes simplex virus type 1. *J. Neurosci.* **19,** 1446–1463.

Hopkins, D.A., and Niessen, L.W. (1976). Substantia nigra projections to the reticular formation, superior colliculus and central gray in the rat, cat, and monkey. *Neurosci. Lett.* **2,** 256–259.

Hornykiewicz, O. (1966). Metabolism of brain dopaine in human Parkinsonism: Neurochemical and clinical aspects. *In* "Biochemistry and pharmacology of the basal ganglia" (E. Costa, L.J. Côte, and M.D. Yahr, eds.), pp. 171–185. Raven Press, Hewlett NY.

Hubbard, J.E., and Di Carlo, V. (1974). Fluorescence histochemistry of monoamine-containing cell bodies in the brain stem of the squirrel monkey (*Saimiri sciureus*). II. Catecholamine-containing groups. *J. Comp. Neurol.* **153,** 369–384.

Huerta, M.F., Krubitzer, L.A., and Kaas, J.H. (1986). Fronal eye field as defined by intracortical microstimulaiton in squirrel monkeys, owl monkeys, and macaque monkeys. I. Subcortical connections. *J. Comp. Neurol.* **253,** 415–439.

Hurd, Y.L., and Herkenham, M. (1995). The human neostriatum shows compartmentalization of neuropeptide gene expression in dorsal and ventral regions: An *in situ* hybridization histochemical analysis. *Neurosci.* **64,** 571–586.

Hutchins, K.D., Martino, A.M., and Strick, P.L. (1988). Corticospinal projections from the medial wall of the hemisphere. *Exp. Brain Res.* **71,** 667–672.

Ikemoto, K., Satoh, K., Maeda, T., and Fibiger, H.C. (1995). Neurochemical heterogeneity of the primate nucleus accumbens. *Exp. Brain Res.* **104,** 177–190.

Ilinsky, I.A., and Kultas-Ilinsky, K. (1987). Sagittal cytoarchitectonic maps of the *Macaca mulatta* thalamus with a revised nomenclature of the motor-related nuclei validated by observations on their connectivity. *J. Comp. Neurol.* **262,** 331–364.

Ilinsky, I.A., Jouandet, M.L., and Goldman-Rakic, P.S. (1985). Organization of the nigrothalamocortical system in the rhesus monkey. *J. Comp. Neurol.* **236,** 315–330.

Ilinsky, I.A., Tourtellotte, W.G., and Kultas-Ilinsky, K. (1993). Anatomical distinctions between the two basal ganglia afferent territories in the primate motor thalamus. *Stereotactic & Functional Neurosurg.* **60,** 62–69.

Ilinsky, I.A., Yi, H., and Kultas-Ilinsky, K. (1997). Mode of termination of pallidal afferents to the thalamus: A light and electron microscopic study with anterograde tracers and immunocytochemistry in *Macaca mulatta*. *J. Comp. Neurol.* **386,** 601–612.

Inagaki, S., Kubota, Y., and Kito, S. (1986). Ultrastructural localization of enkephalin immunoreactivity in the substantia nigra of the monkey. *Brain Res.* **362,** 171–174.

Inagaki, S., and Parent, A. (1984). Distribution of substance P and enkephalin-like immunoreactivity in the substantia nigra of rat, cat and monkey. *Brain Res. Bull.* **13,** 319–329.

Inase, M., and Tanji, J. (1994). Projections from the globus pallidus to the thalamic areas projecting to the dorsal area 6 of the macaque monkey: A multiple tracing study. *Neurosci. Lett.* **180,** 135–137.

Inase, M., and Tanji, J. (1995). Thalamic distribution of projection neurons to the primary motor cortex relative to afferent terminal fields from the globus pallidus in the macaque monkey. *J. Comp. Neurol.* **353,** 415–426.

Inase, M., Li, BM., Takashima, I., and Iijima, T. (2001). Pallidal activity is involved in visuomotor association learning in monkeys. *Eur. J. Neurosci.* **14,** 897–901.

Iwahori, N., and Mizuno, N. (1981). A Golgi study on the globus pallidus of the mouse. *J. Comp. Neurol.* **197,** 29–43.

Izzo, P.N., and Bolam, J.P. (1988). Cholinergic synaptic input to different parts of spiny stratonigral neurons in the rat. *J. Comp. Neurol.* **269,** 219–236.

Jaeger, D., Gilman, S., and Aldridge, J.W. (1993). Primate basal ganglia activity in a precued reaching task: preparation for movement. *Exp. Brain Res.* **95,** 51–64.

Jaeger, D., Gilman, S., and Aldridge, J.W. (1995). Neuronal activity in the striatum and pallidum of primates related to the execution of externally cued reaching movements. *Brain Res.* **694,** 111–127.

Jaeger, D., Kita, H., and Wilson, C.J. (1994). Surround inhibition among projection neurons is weak or nonexistent in the rat neostriatum. *J. Neurophysiol.* **72,** 2555–2558.

Joel, D., and Weiner, I. (1994). The organization of the basal ganglia-thalamocortical circuits: Open interconnected rather than closed segregated. *Neurosci.* **63,** 363–379.

Joel, D., and Weiner, I. (1997). The connections of the primate subhalamic nucleus: indirect pathways and the open-interconnected scheme of basal ganglia-thalamocortical circuitry. *In* "Brain Research—Brain Research Reviews," pp. 62–78.

Jog, M.S., Kubota, Y., Connolly, C.I., Hillegaart, V., and Graybiel, A.M. (1999). Building neural representations of habits. *Science* **286,** 1745–1749.

Johnson, S.W., and North, R.A. (1992). Two types of neurone in the rat ventral tegmental area and their synaptic inputs. *J. Physiol.* **450,** 455–468.

Johnson, T.N., and Rosvold, H.E. (1971). Topographic projections on the globus pallidus and the substantia nigra of selectively placed lesions in the precommissural caudate nucleus and putamen in the monkey. *Exp. Neurol.* **33,** 584–596.

Jones, E.G. (1998). The thalamus of primates. *In* "The Primate Nervous System, Part II" (F.E. Bloom, A. Björklund, and T. Hökfelt, eds.), pp. 1–298. Elsevier Science, Amsterdam.

Jones, E.G., and Leavitt, R.Y. (1974). Retrograde axonal transport and the demonstration of non-specific projections to the cerebral cortex and striatum from thalamic intralaminar nuclei in the rat, cat and monkey. *J. Comp. Neurol.* **154,** 349–378.

Jones, E.G., Coulter, J.D., Burton, H., and Porter, R. (1977). Cells of origin and terminal distribution of corticostriatal fibers arising in the sensory-motor cortex of monkeys. *J. Comp. Neurol.* **173,** 53–80.

Jonides, J., Smith, E.E., Koeppe, R.A., Awh, E., Minoshima, S., and Mintun, M.A. (1993). Spatial working memory in humans as revealed by PET [see comments]. *Nature* **363,** 623–625.

Joyce, J.N., Sapp, D.W., and Marshall, J.F. (1986). Human striatal dopamine receptors are organized in compartments. *Proc. Natl. Acad. Sci. U.S.A.* **83,** 8002–8006.

Jueptner, M., Frith, C.D., Brooks, D.J., Frackowiak, R.S., and Passingham, R.E. (1997). Anatomy of motor learning. II. Sub-

cortical structures and learning by trial and error. *J. Neurophysiol.* **77,** 1325–1337.

Kalil, K. (1978). Patch-like termination of thalamic fibers in the putamen of the rhesus mokey; an autoradiographic study. *Brain Res.* **140,** 333–339.

Kalivas, P.W., Churchill, L., and Klitenick, M.A. (1993). The Circuitry Mediating the Translation of Motivational Stimuli into Adaptive Motor Responses. *In* "Limbic Motor Circuits and Neuropsychiatry" (P.W. Kalivas and C.D. Barnes, eds.), pp. 237–275. CRC Press, Boca Raton, FL.

Kato, T., and Hikosaka, O., eds. (1995). "Function of the Indirect Pathway in the Basal Ganglia Oculomotor System: Visuo-Oculomotor Activities of External Pallidum Neurons." Karger, Basel.

Kawagoe, R., Takikawa, Y., and Hikosaka, O.(1998). Expectation of reward modulates cognitive signals in the basal ganglia. *Nat. Neurosci.* **1,** 411–416.

Kawaguchi, Y. (1997). Neostriatal cell subtypes and their functional roles. *Neurosci. Res.* **27,** 1–8.

Kawaguchi, Y., Wilson, C.J., Augood, S.J., and Emson, P.C. (1995). Striatal interneurones: Chemical, physiological and morphological characterization. *Trends Neurosci.* **18,** 527–535.

Kawaguchi, Y., Wilson, C.J., and Emson, P.C. (1990). Projection subtypes of rat neostriatal matrix cells revealed by intracellular injection of biocytin. *J. Neurosci.* **10** (10), 3421–3438.

Kayahara, T., and Nakano, K. (1996). Pallido-thalamo-motor cortical connections: An electron microscopic study in the macaque monkey. *Brain Res.* **706,** 337–342.

Kelley, A.E., Domesick, V.B., and Nauta, W.J.H. (1982). The amygdalostriatal projection in the rat—An anatomical study by anterograde and retrograde tracing methods. *Neurosci.* **7,** 615–630.

Kemp, J.M. (1970). The termination of strio-pallidal and strio-nigral fibres. *Brain Res,* **17,** 125–128.

Kemp, J.M., and Powell, T.P. (1970). The cortico-striate projection in the monkey. *Brain* **93,** 525–546.

Kemp, J.M., and Powell, T.P. (1971a). The connexions of the striatum and globus pallidus: Synthesis and speculation. *Phil. Trans. Roy. Soc. Lond. Ser. B Biol. Sci.* **262,** 441–457.

Kemp, J.M., and Powell, T.P. (1971b). The structure of the caudate nucleus of the cat: Light and electron microscopy *Phil. Trans. Roy. Soc. Lond. Ser. B Biol. Sci.* **262,** 383-401.

Kemp, J.M., and Powell, T.P. (1971c). The termination of fibres from the cerebral cortex and thalamus upon dendritic spines in the caudate nucleus: A study with the Golgi method. *Phil. Trans. Roy. Soc. Lond. Ser. B Biol. Sci.* **262,** 429–439.

Kermadi, I., and Joseph, J.P. (1995). Activity in the caudate nucleus of monkey during spatial sequencing. *J. Neurophysi*ol. **74,** 911–933.

Kerr, J.N., and Wickens, J.R. (2001). Dopamine D-1/D-5 receptor activation is required for long-term potentiation in the rat neostriatum in vitro. *J. Neurophysiol.* **85,** 117–124.

Kerr, J.N.D., and Plenz, D. (2002). Dendritic calcium encodes striatal neuron output during up-states. *J. Neurosci.* **22,** 1499–1512.

Kim, R., Nakano, K., Jayaraman, A., and Carpenter, M.B. (1976). Projections of the globus pallidus and adjacent structures: An autoradiographic study in the monkey. *J. Comp. Neurol.* **169,** 263–290.

Kimura, M. (1986). The role of primate putamen neurons in the association of sensory stimulus with movement. *Neurosci. Res.* **3,** 436–443.

Kimura, M. (1990). Behaviorally contingent property of movement-related activity of the primate putamen. *J. Neurophysiol.* **63,** 1277–1296.

Kimura, M. (1995). Role of basal ganglia in behavioral learning. *Neurosci. Res.* **22,** 353–358.

Kimura, M., and Graybiel, A.M. (1995). Role of basal ganglia in sensory motor association learning. *In* "Functions of the Cortico-Basal Ganglia Loop" (M. Kimura and A.M. Graybiel, eds.), pp. 2–17. Springer-Verlag.

Kimura, M., Kato, M., Shimazaki, H., Watanabe, K., and Matsumoto, N. (1996). Neural information transferred from the putamen to the globus pallidus during learned movement in the monkey. *J. Neurophysiol.* **76,** 3771–3786.

Kimura, M., Rajkowski, J., and Evarts, E. (1984). Tonically discharging putamen neurons exhibit set-dependent responses. *Proc. Natl. Acad. Sci. U.S.A.* **81,** 4998–5001.

Kita, H. (1993). GABAergic circuits of the striatum. *Prog. Brain Res.* **99,** 51–72.

Kita, H., Chang, H.T., and Kitai, S.T. (1983). The morphology of intracellularly labeled rat subthalamic neurons: A light microscopic analysis. *J. Comp. Neurol.* **215,** 245–257.

Kita, H., Kosaka, T., and Heizmann, C.W. (1990). Parvalbumin-immunoreactive neurons in the rat neostriatum: A light and electron microscopic study. *Brain Res.* **536,** 1–15.

Kitai, S.T., and Deniau, J.M. (1981). Cortical inputs to the subthalamus: Intracellular analysis. *Brain Res.* **214,** 411–415.

Kohler, C., Chan-Palay, V., and Steinbusch, H. (1982). The distribution and origin of serotonin-containing fibers in the septal area: A combined immunohistochemical and fluorescent retrograde tracing study in the rat. *J. Comp. Neurol.* **209,** 91–111.

Kohler, C., Everitt, B.J., Pearson, J., and Goldstein, M. (1983). Immunohistochemical evidence for a new group of catecholamine-containing neurons in the basal forebrain of the monkey. *Neurosci. Lett.* **37,** 161–166.

Kolomiets, B.P., Deniau, J.M., Mailly, P., Menetrey, A., Glowinski, J., Thierry, A.M. (2001). Segregation and convergence of information flow through the cortico-subthalamic pathways. *J. Neurosci.* **21,** 5764–5772.

Kombian, S.B., and Malenka, R.C. (1994). Simultaneous LTP of non-NMDA- and LTD of NMDA-receptor-mediated responses in the nucleus accumbens. *Nature* **368,** 242–246.

Koob, (1999). Drug reward and addiction. *In* "Fundamental Neuroscience," pp. 1261–1279. Academic Press.

Koob, G.F., and Nestler, E.J. (1997). The neurobiology of drug addiction. *J. Neuropsychiatry Clin.Neurosci.* **9,** 482–497.

Kornhuber, H.H. (1974). Cerebral cortex, cerebellum, and basal ganglia: An introduction to their motor functions. *In* "The Neurosciences, Third Study Program" (F.O. Schmitt and F.G. Worden, eds.), pp. 267–288. MIT Press, Cambridge, MA.

Kornhuber, J. (1984). The cortico-nigral projection: Reduced glutamate content in the substantia nigra following frontal cortex ablation in the rat. *Brain Res.* **322,** 124–126.

Kubota, Y., Inagaki, S., Shimada, S., Kito, S., Eckenstein, F., and Tohyama, M. (1987). Neostriatal cholinergic neurons receive direct synaptic inputs from dopaminergic axons. *Brain Res.* **413,** 179–184.

Kung, L., Force, M., Chute, D.J., and Roberts, R.C. (1998). Immunocytochemical localization of tyrosine hydroxylase in the human striatum: A postmortem ultrastructural study. *J. Comp. Neurol.* **390,** 52–62.

Kunishio, K., and Haber. S.N .(1994). Primate cingulostriatal projection: Limbic striatal versus sensorimotor striatal input. *J. Comp. Neurol.* **350,** 337–356.

Kunzle, H. (1975). Bilateral projections from precentral motor cortex to the putamen and other parts of the basal ganglia. An autoradiographic study in *Macaca fascicularis. Brain Res.* **88,** 195–209.

Kunzle, H. (1978). An autoradiographic analysis of the efferent connections from premotor and adjacent prefrontal regions (areas 6 and 9) in *Macaca fascicularis. Brain Behav. Evol.* **15,** 185–234.

Kunzle, H., and Akert, K. (1977). Efferent connections of cortical, area 8 (frontal eye field) in *Macaca fascicularis*. A reinvestigation using the autoradiographic technique. *J. Comp. Neurol.* **173,** 147–164.

Künzle, H. (1976). Thalamic projections from the precentral motor cortex in *Macaca fascicularis*. *Brain Res.* **105,** 253–267.

Künzle, H. (1977). Projections from the primary somatosensory cortex to basal ganglia and thalamus in the monkey. *Exp. Brain Res.* **30,** 481–492.

Kuo, J., and Carpenter, M.B. (1973). Organization of pallidothalamic projections in the rhesus monkey. *J. Comp. Neurol.* **151,** 201–236.

Landwehrmeyer, G.B., Standaert, D.G., Testa, C.M., Penney. J.B., Jr., and Young, A.B. (1995). NMDA receptor subunit mRNA expression by projection neurons and interneurons in rat striatum. *J. Neurosci.* **15,** 5297–5307.

Lapper, S.R., and Bolam, J.P. (1992). Input from the frontal cortex and the parascicular nucleus to cholinergic interneurons in the dorsal striatum of the rat. *Neurosci.* **51** (3), 533–545.

Lapper, S.R., Smith, Y., Sadikot, A.F., Parent, A., and Bolam, J.P. (1992). Cortical input to parvalbumin-immunoreactive neurones in the putamen of the squirrel monkey. *Brain Res.* **580,** 215–224.

Lavoie, B., and Parent, A. (1990). Immunohistochemical study of the serotoninergic innervation of the basal ganglia in the squirrel monkey. *J. Comp. Neurol.* **299,** 1–16.

Lavoie, B., and Parent, A. (1991). Dopaminergic neurons expressing calbindin in normal and parkinsonian monkeys. *Neuroreport* **2** (10), 601–604.

Lavoie, B., and Parent, A. (1994). Pedunculopontine nucleus in the squirrel monkey: Projections to the basal ganglia as revealed by anterograde tract-tracing methods. *J. Comp. Neurol.* **344,** 210–231.

Lavoie, B., Smith, Y., and Parent, A. (1989). Dopaminergic innervation of the basal ganglia in the squirrel monkey as revealed by tyrosine hydroxylase immunohistochemistry. *J. Comp. Neurol.* **289,** 36–52.

Lehmann, J., and Langer, S.Z. (1983). The striatal cholinergic interneuron: Synaptic target of dopaminergic terminals? *Neurosci.* **10,** 1105–1120.

Leichnetz, G.R., and Astruc, J. (1976). The efferent projections of the medial prefrontal cortex in the squirrel monkey (*Saimiri sciureus*). *Brain Res.* **109,** 455–472.

Le Moine, C., Normand, E., and Bloch, B. (1991). Phenotypical characterization of the rat striatal neurons expressing the D1 dopamine receptor gene. *Proc. Natl. Acad. Sci. U.S.A.* **88,** 4205–4209.

Letchworth, S.R., Nader, M.A., Smith, H.R., Friedman, D.P., and Porrino, L.J. (2001). Progression of changes in dopamine transporter binding site density as a result of cocaine self-administration in rhesus monkeys. *J. Neurosci.* **21,** 2799–2807.

Levesque, M., Charara, A., Gagnon, S., Parent, A., and Deschenes, M. (1996b). Corticostriatal projections from layer V cells in rat are collaterals of long-range corticofugal axons. *Brain Res.* **709,** 311–315.

Levesque, M., Gagnon, S., Parent, A., and Deschenes, M. (1996a). Axonal arborizations of corticostriatal and corticothalamic fibers arising from the second somatosensory area in the rat. *Cereb. Cortex* **6,** 759–770.

Levitt, P., Rakic, P., and Goldman-Rakic, P. (1984). Region-specific distribution of catecholamine afferents in primate cerebral cortex: A fluorescence histochemical analysis. *J. Comp. Neurol.* **227,** 23–36.

Levy, R., Friedman, H.R., Davachi, L., and Goldman-Rakic, P.S. (1997). Differential activation of the caudate nucleus in primates performing spatial and nonspatial working memory tasks. *J. Neurosci.* **17.**

Lewis, D.A., Campbell, M.J., Foote, S.L., Goldstein, M., and Morrison, J.H. (1987). The distribution of tyrosine hydroxylase-immunoreactive fibers in primate neocortex is widespread but regionally specific. *J. Neurosci.* **7** (1), 279–290.

Lidow, M.S., Goldman-Rakic, P.S., Gallager, D.W., and Rakic, P. (1991). Distribution of dopaminergic receptors in the primate cerebral cortex: Quantitative autoradiographic analysis using [3H] raclopride, [3H] spiperone and [3H]sch23390. *Neurosci.* **40** (3), 657–671.

Lidsky, T.I., Manetto, C., and Schneider, J.S. (1985). A consideration of sensory factors involved in motor functions of the basal ganglia. *Brain Res.* **356,** 133–146.

Liles, S.L. (1985). Activity of neurons in putamen during active and passive movements of wrist. *J. Neurophysiol.* **53** (1), 217–236.

Limousin, P., Greene, J., Pollak, P., Rothwell, J., Benabid, A.L., and Frackowiak, R. (1997). Changes in cerebral activity pattern due to subthalamic nucleus or internal pallidum stimulation in Parkinson's disease. *Ann. Neurol.* **42,** 283–291.

Ljungberg, T., Apicella, P., and Schultz, W. (1991). Responses of monkey midbrain dopamine neurons during delayed alternation performance. *Brain Res.* **567,** 337–341.

Ljungberg, T., Apicella, P., and Schultz, W. (1992). Responses of monkey dopamine neurons during learning of behavioral reactions. *J. Neurophysiol.* **67** (1), 145–163.

Llinas, R., Greenfield, S.A., and Jahnsen, H. (1984). Electrophysiology of pars compacta cells in the in vitro substantia nigra—a possible mechanism for dendritic release. *Brain Res.* **294,** 127–132.

Lu, M-T., Preston, J.B., and Strick, P.L. (1994). Interconnections between the prefrontal cortex and the premotor areas in the frontal lobe. *J. Comp. Neurol.* **341,** 375–392.

Lu, X.Y., Ghasemzadeh, M.B., and Kalivas, P.W. (1998). Expression of D1 receptor, D2 receptor, substance P and enkephalin messenger RNAs in the neurons projecting from the nucleus accumbens. *Neurosci.* **82,** 767–780.

Luppino, G., Matelli, M., Camarda, R.M., Gallese, V., and Rizzolatti, G. (1991). Multiple representations of body movements in mesial area 6 and the adjacent cingulate cortex: An intracortical microstimulation study in the macaque monkey. *J. Comp. Neurol.* **311,** 463–482.

Luppino, G., Matelli, M., Camarda, R., and Rizzolatti, G. (1993). Corticocortical connections of area F3 (SMA-proper) and area F6 (pre-SMA) in the Macaque monkey. *J. Comp. Neurol.* **338,** 114–140.

Lynd-Balta, E., and Haber, S.N. (1994a). The organization of midbrain projections to the ventral striatum in the primate. *Neurosci.* **59,** 609–623.

Lynd-Balta, E., and Haber, S.N. (1994b). The organization of midbrain projections to the striatum in the primate: Sensorimotor-related striatum versus ventral striatum. *Neurosci.* **59,** 625–640.

Lynd-Balta, E., and Haber, S.N. (1994c). Primate striatonigral projections: A comparison of the sensorimotor-related striatum and the ventral striatum. *J. Comp. Neurol.* **343,** 1–17.

Lyons, D., Friedman, D.P., Nader, M.A. and Porrino, L.J. (1996). Cocaine alters cerebral metabolism within the ventral striatum and limbic cortex of monkeys. *J. Neurosci.* **16,** 1230–1238.

Macchi, G. (1951). The ontogenetic development of the olfactory telencephalon in man. *J. Comp. Neurol.* **95,** 245–305.

MacLean, P.D. (1978). Effects of lesions of globus pallidus on species-typical display behavior of squirrel monkeys. *Brain Res.* **149,** 175–196.

Mai, J.K., Stephens, P.H., Hopf, A., and Cuello, A.C. (1986). Substance P in the human brain. *Neurosci.* **17** (3), 709–739.

Maioli, M.G., Squatrito, S., Battaglini, P.P., Rossi, R., and Galletti, C. (1983). Projections from the visual cortical region of the superior

temporal sulcus to the striatum and claustrum in the macaque monkey. *Arch. Itali. Biol.* **121,** 259–266.

Mann, D.M.A., and Yates, P.O. (1983). Possible role of neuromelanin in the pathogenesis of Parkinson's disease. *Mech. Ageing Dev.* **21,** 193–203.

Mansour, A., Meador-Woodruff, J.H., Zhou, Q., Civelli, O., Akil, H., and Watson, S.J. (1992). A comparison of D1 receptor binding and mRNA in rat brain using receptor autoradiographic and *in situ* hybridization techniques. *Neurosci.* **46,** 959–971.

Marchand, R., and Lajoie, L. (1986). Histogenesis of the striopallidal system in the rat. Neurogenesis of its neurons. *Neurosci.* **17** (3), 573–590.

Marchand, R., and Poirier, L.J. (1983). Isthmic origin of neurons of the rat substantia nigra. *Neurosci.* **9,** 373–381.

Marchand, R., Lajoie, L., and Blanchet, C. (1986). Histogenesis at the level of the basal forebrain: The entopeduncular nucleus. *Neurosci.* **17** (3), 591–607.

Marsden, C.D. (1983). Neuromelanin and Parkinson's disease. *J. Neural Transm. Suppl.* **19,** 121–141.

Marsden, C.D. (1984). Function of the basal ganglia as revealed by cognitive and motor disorders in Parkinson's disease. *Can. J. Neurol. Sci.* **11,** 129–135.

Marsden, C.D. (1985). The enigma of the basal ganglia and movement. *In* "The Motor System in Neurobiology" (E.V. Evarts, S.P. Wise, and D. Bousfield, eds.), pp. 277–283. Elsevier, Medical Press, Amsterdam.

Marsden, C.D. (1987). What do the basal ganglia tell premotor cortical areas? *Ciba Found. Symp.* **132,** 282–300.

Marshall, J.F., Turner, B.H., and Teitelbaum, P. (1971). Sensory neglect produced by lateral hypothalamic damage. *Science* **174,** 523–525.

Martin, L.J., Blackstone, C.D., Huganir, R.L., and Price, D.L. (1993). The striatal mosaic in primates: striosomes and matrix are differentially enriched in ionotropic glutamate receptor subunits. *J. Neurosci.* **13,** 782–792.

Martin, L.J., Hadfield, M.G., Dellovade, T.L., and Price, D.L. (1991). The striatal mosaic in primates: Patterns of neuropeptide immunoreactivity differentiate the ventral striatum from the dorsal striatum. *Neurosci.* **43** (2/3), 397–417.

Martres, M.P., Bouthenet, M.L., Sales, N., Sokoloff, P., and Schwartz, J.C. (1985). Widespread distribution of brain dopamine receptors evidenced with and 2 over black square]; [1 and 2 over black square]25I]iodosulpride, a highly selective ligand. *Science* **228,** 752–755.

Matelli, M., and Luppino, G. (1996). Thalamic input to mesial and superior area 6 in the Macaque monkey. *J. Comp. Neurol.* **372,** 59–87.

Matelli, M., Luppino, G., Fogassi, L., and Rizzolatti, G. (1989). Thalamic input to inferior area 6 and area 4 in the macaque monkey. *J. Comp. Neurol.* **280,** 468–488.

Matelli, M., Luppino, G., and Rizzolatti, G. (1991). Architecture of superior and mesial area 6 and the adjacent cingulate cortex in the macaque monkey. *J. Comp. Neurol.* **311,** 445–462.

Matsumoto, N., Hanakawa, T., Maki, S., Graybiel, A.M., and Kimura, M. (1999). Nigrostriatal dopamine system in learning to perform sequential motor tasks in a predictive manner. *J. Neurophysiol.* **82,** 978–998.

Matsumura, M., Kojima, J., Gardiner, T.W., and Hikosaka, O. (1992). Visual and oculomotor functions of monkey subthalamic nucleus. *J. Neurophysiol.* **67,** 1615–1632.

Maunsell, J.H., and van Essen, D.C. (1983). The connections of the middle temporal visual area (MT) and their relationship to a cortical hierarchy in the macaque monkey. *J. Neurosci.* **3,** 2563–2586.

Mayberg, H.S., Brannan, S.K., Tekell, J.L., Silva, J.A., Mahurin, R.K., McGinnis S., and Jerabek, P.A. (2000). Regional metabolic effects of fluoxetine in major depression: Serial changes and relationship to clinical response. *Biol. Psychiatry* **48,** 830–843.

Mayberg, H.S., Liotti, M., Brannan, S.K., McGinnis, S., Mahurin, R.K., Jerabek, P.A., Silva, J.A., Tekell, J.L., Martin, C.C., Lancaster, J.L., and Fox, P.T. (1999). Reciprocal limbic-cortical function and negative mood: Converging PET findings in depression and normal sadness. *Am. J. Psychiatry* **156,** 675–682.

McFarland, N.R., and Haber, S.N. (1995). Organization of thalamic projections to the sensorimotor striatum in primates: A comparison to ventral striatum. *Soc. Neurosci. Abst.* **21,** 678.

McFarland, N.R., and Haber, S.N. (2000). Convergent inputs from thalamic motor nuclei and frontal cortical areas to the dorsal striatum in the primate. *J. Neurosci.* **20,** 3798–3813.

McFarland, N.R., and Haber, S.N. (2001). Organization of thalamostriatal terminals from the ventral motor nuclei in the macaque. *J. Comp. Neurol.* **429,** 321–336.

McFarland, N.R., and Haber, S.N. (2002a). Thalamic relay nuclei of the basal ganglia form both reciprocal and nonreciprocal cortical connections, linking multiple frontal cortical areas. *The J. Neurosci.* **22,** 8117–8132.

McFarland, N.R, and Haber, S.N. (2002b). Thalamic connections with cortex from the basal ganglia relay nuclei provide a mechanism for integration across multiple cortical areas. *J. Neurosci.* in press.

McGuire, P.K., Bench, C.J., Frith, C.D., Marks, I.M., Frackowiak, R.S., and Dolan, R.J. (1994). Functional anatomy of obsessive-compulsive phenomena. *Brit. J. Psychiat.* **164,** 459–468.

McRitchie, D.A., and Halliday, G.M. (1995). Calbindin D28K-containing neurons are restricted to the medial substantia nigra in humans. *Neurosci.* **65,** 87–91.

McRitchie, D.A., Halliday, G.M., and Cartwright, H. (1995). Quantitative analysis of the variability of substantia nigra pigmented cell clusters in the human. *Neurosci.* **68,** 539–551.

Mehler, W.R. (1980). Subcortical afferent connections of the amygdala in the monkey. *J. Comp. Neurol.* **190,** 733–762.

Meredith, G.E., and Wouterlood, F.G. (1990). Hippocampal and midline thalamic fibers and terminals in relation to the choline acetyltransferase-immunoreactive neurons in nucleus accumbens of the rat: A light and electron microscopic study. *J. Comp. Neurol.* **296,** 204–221.

Meredith, G.E., Pattiselanno, A., Groenewegen, H.J., and Haber, S.N. (1996). Shell and core in monkey and human nucleus accumbens identified with antibodies to calbindin-D28k. *J. Comp. Neurol.* **365,** 628–639.

Mesulam, M-M., and Mufson, E.J. (1984). Neural inputs into the nucleus basalis of the substantia innominata (Ch4) in the Rhesus monkey. *Brain* **107,** 253–274.

Meunier, M., Bachevalier, J., and Mishkin, M. (1997). Effects of orbital frontal and anterior cingulate lesions on object and spatial memory in rhesus monkeys. *Neuropsychologia* **35,** 999–1015.

Meyer, G., and Wahle, P. (1986). The olfactory tubercle of the cat. I. Morphological components. *Exp. Brain Res.* **62,** 515–527.

Meyer, G., Gonzalez-Hernandez, T., Carrillo-Padilla, F., and Ferres-Torres, R. (1989). Aggregations of granule cells in the basal forebrain (islands of Calleja): Golgi and cytoarchitectonic study in different mammals, including man. *J. Comp. Neurol.* **284,** 405–428.

Michel, J.P., Sakamoto, N., Kopp, N., and Pearson, J. (1986). Neurotensin immunoreactive structures in the human infant striatum, septum, amygdala and cerebral cortex. *Brain Res.* **397,** 93–102.

Middleton, F.A., and Strick, P.L. (1994). Anatomical evidence for cerebellar and basal ganglia involvement in higher cognitive function. *Science* **266,** 458–461.

Middleton, F.A., and Strick, P.L. (1997). New concepts about the organization of basal ganglia output. *In* "The Basal Ganglia and New Surgical Approaches for Parkinson's Disease, Advances in Neurology" (J.A. Obeso, M.R. Delong, C. Ohye, and C.D. Marsden, eds.), pp. 57–68. Lippincott-Raven, Philadelphia.

Miguel, E.C., Rauch S.L., and Jenike, M.A. (1997). Obsessive-compulsive disorder. *Psychiatric Clinics of North America* **20,** 863–883.

Millhouse, O.E. (1987). Granule cells of the olfactory tubercle and the question of the islands of Calleja. *J. Comp. Neurol.* **265,** 1–24.

Mink, J.W. (1996). The basal ganglia: Focused selection and inhibition of competing motor programs. *Prog.Neurobiol.* **50,** 381–425.

Mink, J.W., and Thach, W.T. (1991a). Basal ganglia motor control. I. Nonexclusive relation of pallidal discharge to five movement modes. *J. Neurophysiol.* **65,** 273–300.

Mink, J.W., and Thach, W.T. (1991b). Basal ganglia motor control. III. Pallidal ablation: Normal reaction time, muscle cocontraction, and slow movement. *J. Neurophysiol.* **65** (2), 330.

Mishkin, M., and Bachevalier, J. (1986). Differential involvement of orbital and anterior cingulate cortices in object and spatial memory functions in monkeys. *Soc. Neurosci. Abst.* **12,** 742–740.

Mishkin, M., Malamut, B., and Bachevalier, J. (1984). Memories and habits: Two neural systems. In "The Neurobiology of Learning and Memory" (J.L. McGaugh, G. Lynch, and N.M. Weinberger, eds.). Guilford Press, New York.

Mitchell, S.J., Richardson, R.T., Baker, F.H., and DeLong, M.R. (1987). The primate globus pallidus: Neuronal activity related to direction of movement. *Exp. Brain Res.* **68,** 491–505.

Miyachi, S., Hikosaka, O., Miyashita, K., Karadi, Z., and Rand, M.K. (1997). Differential roles of monkey striatum in learning of sequential hand movement. *Exp. Brain Res.* **115,** 1–5.

Mogenson, G.J., Brudzynski, S.M., Wu, M., Yang, C.R., and Yim, C.C.Y. (1993). From motivation to action: A review of dopaminergic regulation of limbic → nucleus accumbens → pallidum → pedunculopontine nucleus circuitries involved in limbic-motor integration. *In* "Limbic Motor Circuits and Neuroopsychiatry" (P.W. Kalivas and C.D. Barnes, eds.), pp. 193–236. CRC Press, Boca Raton.

Monakow, K.H., Akert, K., and Kunzle, H. (1978). Projections of the precentral motor cortex and other cortical areas of the frontal lobe to the subthalamic nucleus in the monkey. *Exp. Brain Res.* **33,** 395–403.

Montague, P.R., Dayan, P., and Sejnowski, T.J. (1996). A framework for mesencephalic dopamine systems based on predictive hebbian learning. *J. Neurosci.* **16** (5), 1936–1947.

Morecraft, R.J., and VanHoesen, G.W. (1993). Frontal granular cortex input to the cingulate (M3), supplementary (M2) and primary (M1) motor cortices in the Rhesus monkey. *J. Comp. Neurol.* **337,** 669–689.

Mori, A., Takahashi, T., Miyashita, Y., and Kasai, H. (1994). Two distinct glutamatergic synaptic inputs to striatal medium spiny neurones of neonatal rats and paired-pulse depression. *J. Physiol.* **476,** 217–228.

Mugnaini, E., and Oertel, W.H. (1985). An atlas of the distribution of GABAergic neurons and terminals in the rat CNS as revealed by GAD immunohistochemistry. *In* "Handbook of Chemical Neuroanatomy. Part I. GABA and neuropeptides in the CNS" (A. Bjorklund and T. Hokfelt, eds.), pp. 436–608. Elsevier Science Publishers BV, New York.

Mushiake, H., and Strick, P.L. (1995). Pallidal neuron activity during sequential arm movements. *J. Neurophysiol.* **74,** 2754–2758.

Mushiake, H., Inase, M., and Tanji, J. (1991). Neuronal activity in the primate premotor, supplementary, and precentral motor cortex during visually guided and internally determined sequential movements. *J. Neurophysiol.* **66,** 705–718.

Nakamura, K., Sakai, K., and Hikosaka, O. (1998). Neuronal activity in medial frontal cortex during learning of sequential procedures. *J. Neurophysiolo.* **80,** 2671–2687.

Nakano, K., Hasegawa, Y., Tokushige, A., Nakagawa S., Kayahara, T., and Mizuno, N. (1990). Topographical projections from the thalamus, subthalamic nucleus and pedunculopontine tegmental nucleus to the striatum in the Japanese monkey, *Macaca fuscata*. *Brain Res.* **537,** 54–68.

Nakano, K., Kayahara, T., and Chiba, T. (1999). Afferent connections to the ventral striatum from the medial prefrontal cortex (area 25) and the thalamic nuclei in the macaque monkey. *Ann.N.Y. Acad. Sci.* **877,** 667–670.

Nakano, K., Tokushige, A., Kohno, M., Hasegawa, Y., Kayahara, T., and Sasaki, K. (1992). An autoradiographic study of cortical projections from motor thalamic nuclei in the macaque monkey. *Neurosci. Res.* **13,** 119–137.

Nambu, A., Tokuno, H., Hamada, I., Kita, H., Imanishi, M., Akazawa, T., Ikeuchi, Y., and Hasegawa, N. (2000). Excitatory cortical inputs to pallidal neurons via the subthalamic nucleus in the monkey. *J. Neurophysiol.* **84,** 289–300.

Nambu, A., Tokuno, H., Inase, M., and Takada, M. (1997). Corticosubthalamic input zones from forelimb representations of the dorsal and ventral divisions of the premotor cortex in the macaque monkey: Comparison with the input zones from the primary motor cortex and the supplementary motor area. *Neurosci. Lett.* **239,** 13–16.

Nambu, A., Tokuno, H., and Takada, M. (2002). Functional significance of the cortico-subthalamo-pallidal 'hyperdirect' pathway. *Neurosci. Res.* **43,** 111–117.

Nambu, A., Takada M., Inase, M., and Tokuno, H. (1996). Dual somatotopical representations in the primate subthalamic nucleus: Evidence for ordered but reversed body-map transformations from the primary motor cortex and the supplimentary motor area. *J. Neurosci.* **16,** 2671–2683.

Nambu, A., Yoshida, S., and Jinnai, K. (1990). Discharge patterns of pallidal neurons with input from various cortical areas during movement in the monkey. *Brain Res.* **519,** 183–191.

Nauta, H.J.W. (1986). The relationship of the basal ganglia to the limbic system. *In* "Handbook of Clinical Neurology: Extrapyramidal Disorders" (P.J. Vinken, G.W. Bruyn, and J.J. Klawans, eds.), pp. 19–31. Elsevier Science Publishers, Amsterdam.

Nauta, H.J.W., and Cole, M. (1978). Efferent projections of the subthalamic nucleus: An autoradiographic study in monkey and cat. *J. Comp. Neurol.* **180,** 1–16.

Nauta, W.J.H., and Domesick, V.B. (1978). Crossroads of limbic and striatal circuitry: hypothalamic-nigral connections. *In* "imbic Mechanisms" (K.E. Livingston and O. Hornykiewicz, eds.), pp. 75–93. Plenum, New York.

Nauta, W.J., and Mehler, W.R. (1966). Projections of the lentiform nucleus in the monkey. *Brain Res.* **1,** 3–42.

Nauta, W.J.H., Smith, G.P., Faull, R.L.M., and Domesick, V.B. (1978). Efferent connections and nigral afferents of the nucleus accumbens septi in the rat. *Neurosci.* **3,** 385–401.

Nestler, E.J. (2001). Molecular basis of long-term plasticity underlying addiction. [erratum appears in *Nat. Rev. Neurosci.* (2001) **2** (3), 215]. *Nat. Rev. Neurosci.* **2,** 119–128.

Nestler, E.J, Hope, B.T., and Widnell, K.L. (1993). Drug addiction: A model for the molecular basis of neural plasticity [Review] [70 refs]. *Neuron* **11,** 995–1006.

Nicola, S.M., Surmeier, J., and Malenka, R.C. (2000). Dopaminergic modulation of neuronal excitability in the striatum and nucleus accumbens. *Annu. Rev. Neurosci.* **23,** 185–215.

Nini ,A., Feingold, A., Slovin, H., and Bergman, H. (1995). Neurons in the globus pallidus do not show correlated activity in the normal monkey, but phase-locked oscillations appear in the MPTP model of parkinsonism. *J. Neurophysiol.* **74,** 1800–1805.

Norita, M., and Kawamura, K. (1980). Subcortical afferents to the monkey amygdala: An HRP study. *Brain Res.* **190,** 225–230.

O'Donnell, P., and Grace, A.A. (1993). Dopaminergic modulation of dye coupling between neurons in the core and shell regions of the nucleus accumbens. *J. Neurosci.* **13** (8), 3456–3471.

O'Donnell, P., and Grace, A.A. (1995). Synaptic interactions among excitatory afferents to nucleus accumbens neurons: Hippocampal gating of prefrontal cortical input. *J. Neurosci.* **15,** 3622–3639.

O'Donnell, P., Lavin, A., Enquist, L.W., Grace, A.A., and Card, J.P. (1997). Interconnected parallel circuits between rat nucleus accumbens and thalamus revealed by retrograde transynaptic transport of pseudorabies virus. *J. Neurosci.* **17,** 2143–2167.

Oertel, W.H., and Mugnaini, E. (1984). Immunocytochemical studies of GABAergic neurons in rat basal ganglia and their relations to other neuronal systems. *Neurosci. Lett.* **47,** 233–238.

Oertel, W.H., Tappaz, M.L., Berod, A., and Mugnaini, E. (1982). Two-colour immunohistochemistry for dopamine and GABA neurons in rat substantia nigra and zona incerta. *Brain Res. Bull.* **9,** 463–474.

Olszewski, J., and Baxter, D. (1982). Cytoarchitecture of the Human Brain Stem, 2nd ed. S. Karger, Basel.

Oorshcot, D.E. (1996). Total number of neurons in the neostriatal, pallidal, subthalamic, and substantia nigral nuclei of the rat basal ganglia: a stereological study using the cavalieri and optical disector methods. *J. Comp. Neurol.* **366,** 580–599.

Owen, A.M., Roberts, A.C., Hodges, J.R., Summers, B.A., Polkey, C.E., and Robbins, T.W. (1993). Contrasting mechanisms of impaired attentional set-shifting in patients with frontal lobe damage or Parkinson's disease. *Brain* **116,** 1159–1175.

Pandya, D.N., Van Hoesen, G.W., and Mesulam, M-M. (1981). Efferent connections of the cingulate gyrus in the rhesus monkey. *Exp. Brain Res.* **42,** 319–330.

Pantelis, C., Barnes, T.R., Nelson, H.E., Tanner, S., Weatherley, L., Owen, A.M., and Robbins, T.W. (1997) Frontal-striatal cognitive deficits in patients with chronic schizophrenia. *Brain* **120,** 1823–1843.

Parent, A. (1979). Identification of the pallidal and peripallidal cells projecting to the habenula in monkey. *Neurosci .Lett.* **15,** 159–164.

Parent, A. (1986). "Comparative Neurobiology of the Basal Ganglia." John Wiley and Sons, New York.

Parent, A., and Cicchetti, F. (1998). The current model of basal ganglia organization under scrutiny [editorial]. *Movement Disorders* **13,** 199–202.

Parent, A., and De Bellefeuille, L. (1982). Organization of efferent projections from the internal segment of the globus pallidus in the primate as revealed by fluorescence retrograde labeling method. *Brain Res.* **245,** 201–213.

Parent, A., and DeBellefeuille, L. (1983). The pallidointralaminar and pallidonigral projections in primate as studied by retrograde double-labeling method. *Brain Res.* **278,** 11–27.

Parent, A., and Hazrati, L-N. (1993). Anatomical aspects of information processing in primate basal ganglia. *Trends Neurosci.* **16,** 111–115.

Parent, A., and Hazrati, L-N. (1994). Multiple striatal representation in primate substantia nigra. *J. Comp. Neurol.* **344,** 305–320.

Parent, A., and Hazrati, L.N. (1995). Functional anatomy of the basal ganglia. I. The cortico-basal ganglia-thalamo-cortical loop. *Brain Res. Brain Res. Rev.* **20,** 91–127.

Parent, A., and Lavoie, B. (1993). The heterogeneity of the mesostriatal dopaminergic system as revealed in normal and Parkinsonian monkeys. *Adv. Neurol.* **60,** 25–20.

Parent, A., Bouchard, C., and Smith, Y. (1984). The striatopallidal and striatonigral projections: Two distinct fiber systems in primate. *Brain Res.* **303,** 385–390.

Parent, A., Charara, A., and Pinault, D. (1995). Single striatofugal axons arborizing in both pallidal segments and in the substantia nigra in primates. *Brain Res.* **698,** 280–284.

Parent, M., Levesque, M., and Paren, A. (2001). Two types of projection neurons in the internal pallidum of primates: Single-axon tracing and three-dimensional reconstruction. *J. Comp. Neurol.* **439,** 162–175.

Parent, A., Mackey, A., and De Bellefeuille, L. (1983). The subcortical afferents to caudate nucleus and putamen in primate: A fluorescence retrograde double labeling study. *Neurosci.* **10** (4), 1137–1150.

Parent, A., Sato, F., Wu, Y., Gauthier, J., Levesque, M., and Parent, M. (2000). Organization of the basal ganglia: The importance of axonal collateralization. *Trends Neurosci* **23,** S20–27.

Parthasarathy, H.B., Schall, J.D., and Graybiel, A.M. (1992). Distributed but convergent ordering of corticostriatal projections: Analysis of the frontal eye field and the supplementary eye field in the macaque monkey. *J. Neurosci.* **12,** 4468–4488.

Partiot, A., Verin, M., Pillon, B., Teixeira-Ferreira, C., Agid, Y., and Dubois, B. (1996). Delayed response tasks in basal ganglia lesions in man: Further evidence for a striato-frontal cooperation in behavioural adaptation. *Neuropsychologia* **34,** 709–721.

Pasik, P., Pasik, T., and DiFiglia, M. (1976). Quantitative aspects of neuronal organization in the neostriatum of the macaque monkey. *Research Publications – Association for Research in Nervous & Mental Disease* **55,** 57–90.

Passingham, R. (1975). Delayed matching after selective prefronal lesions in monkeys *(Macaca mulatta). Brain Res.* **92,** 89–102.

Passingham, R.E. (1972a). Visual discrimination learning after selective prefrontal ablations in monkeys (*Macaca mulatta*). *Neuropsychologia* **10,** 27–39.

Passingham, R.E. (1972b). Non-reversal shifts after selective prefrontal ablations in monkeys (*Macaca mulatta*). *Neuropsychologia* **10,** 41–46.

Passingham, R.E. (1995). "The Frontal Lobes and Voluntary Action." Oxford Univ. Press, Oxford.

Patel, S., Roberts, J., Moorman, J., and Reavill, C. (1995). Localization of serotonin-4 receptors in the striatonigral pathway in rat brain. *Neurosci.* **69,** 1159–1167.

Paxinos, G., Huang, X.F., and Toga, A.W. (2000). "The Rhesus Monkey in Stereotaxic Coordinates." Academic Press, San Diego.

Pearson, J., Goldstein, M., Markey, K., and Brandeis, L. (1983). Human brainstem catecholamine neuronal anatomy as indicated by immunocytochemistry with antibodies to tyrosine hydroxylase. *Neurosci.* **8** (1), 3–32.

Pearson, J.H.G., Sakamoto, N., and Michel, J-P. (1990). Catecholaminergic neurons. *In* "The Human Nervous System" (G. Paxinos, ed.), pp. 1023–1050. Academic Press, San Diego.

Pennartz, C.M., Groenewegen, H.J., and Lopes da Silva, F.H. (1994). The nucleus accumbens as a complex of functionally distinct neuronal ensembles: An integration of behavioural, electrophysiological and anatomical data. *Prog. Neurobiol.* **42,** 719–761.

Penney, J.B., and Young, A.B. (1983). Speculations on the functional anatomy of basal ganglia disorders. *Annu. Rev. Neurosci.* **6,** 73–94.

Penny, G.R., Wilson, C.J., and Kitai, S.T. (1988). Relationship of the axonal and dendritic geometry of spiny projection neurons to the compartmental organization of the neostriatum. *J. Comp. Neurol.* **269,** 275–289.

Percheron, G., and Filion, M. (1991). Parallel processing in the basal ganglia: Up to a point. *Trends Neurosci.* **14,** 55–59.

Percheron, G., Francois, C., Yelnik, J., Fenelon, G., and Talbi, B. (1994). The basal ganglia related systems of primates: Definition, description and informational analysis. *In* "The Basal Ganglia IV" (G. Percheron, G.M. McKenzie, and J. Feger, eds.), pp. 3–20. Plenum Press, New York.

Percheron, G., Yelnik, J., and Francois, C. (1984a). A golgi analysis of the primate globus pallidus. III. Spatial organization of the striato-pallidal complex. *J. Comp. Neurol.* **227,** 214–227.

Percheron, G., Yelnik, J., and Francois, C. (1984b) The primate striato-pallido-nigral system: An integrative system for cortical information. *In* "The Basal Ganglia: Structure and Function" (J.S. McKenzie, R.E. Kemm, and L.N. Wilcock, eds.), pp. 87–105. Plenum Press, London.

Petrides, M., and Pandya, D.N. (1999). Dorsolateral prefrontal cortex: Comparative cytoarchitectonic analysis in the human and the macaque brain and corticocortical connection patterns. *Eur. J. Neurosci.* **11,** 1011–1036.

Phelps, P.E., and Vaughn, J.E. (1986). Immunocytochemical localization of choline acetyltransferase in rat ventral striatum: A light and electron microscopic study. *J. Neurocytol.* **15,** 595–617.

Phelps, P.E., Houser, C.R., and Vaughn, J.E. (1985). Immunocytochemical localization of choline acetyltransferase within the rat neostriatum: A correlated light and electron microscopic study of cholinergic neurons and synapses. *J. Comp. Neurol.* **238,** 286–307.

Phillips, A.G., and Carr, G.D. (1987). Cognition and the basal ganglia: A possible substrate for procedural knowledge. *Can. J. Neurol. Sci.* **14,** 381–385.

Picard, N., and Strick, P.L. (1996). Motor areas of the medial wall: A review of their location and functional activation. *Cereb. Cortex* **6,** 342–353.

Pickel, V.M, and Chan, J. (1990). Spiny neurons lacking choline acetyltransferase immunoreactivity are major targets of cholinergic and catecholaminergic terminals in rat striatum. *J. Neurosci. Res.* **25,** 263–280.

Pickel, V.M., Sumal, K.K., Beckley, S.C., Miller, R.J., and Reis, D.J. (1980). Immunocytochemical localization of enkephalin in the neostriatum of rat brain: A light and electron microscopic study. *J. Comp. Neurol.* **189,** 721–740.

Pifl, C., Schingnitz, G., and Hornykiewicz, O. (1991). Effect of 1-methyl-4-phenyl-1,2,3,6-tetrahydropyridine on the regional distribution of brain monoamines in the rhesus monkey. *Neurosci.* **44** (3), 591–605.

Pioro, E.P.J., Hughes, J.T., and Cuello, A.C. (1984). Loss of substance P and enkephalin immunoreactivity in the human substantia nigra after striatopallidal infarction. *Brain Res.* **292,** 339–347.

Pioro, E.P., Mai, J.K., and Cuello. A.C. (1990). Distribution of substance P- and enkephalin-immunoreactive neurons and fibers. *In* "The Human Nervous System" (G. Paxinos, ed.), pp. 1051–1094. Academic Press, San Diego.

Pioro, E.P., Maysinger, D., Ervin, F.R., Desypris, G., and Cuello, A.C. (1993). Primate nucleus basalis of meynert p75,NGFR-containing cholinergic neurons are protected from retrograde degeneration by the ganglioside GM1. *Neurosci.* **53** (1), 49–56.

Pisani, A., Bonsi, P., Catania, M.V., Giuffrida, R., Morari, M., Marti, M., Centonze, D., Bernardi, G., Kingston, A.E., and Calabresi, P. (2002). Metabotropic glutamate 2 receptors modulate synaptic inputs and calcium signals in striatal cholinergic interneurons. *J. Neurosci.* **22,** 6176–6185.

Plenz, D., and Kitai, S.T. (1998). Up and down states in striatal medium spiny neurons simultaneously recorded with spontaneous activity in fast-spiking interneurons studied in cortex-striatum-substantia nigra organotypic cultures. *J. Neurosci.* **18,** 266–283.

Poirier, L.J., Giguere, M., and Marchand, R. (1983). Comparative morphology of the substantia nigra and ventral tegmental area in the monkey, cat and rat. *Brain Res. Bull.* **11,** 371–397.

Porrino, L.J., and Goldman-Rakic, P.S. (1982). Brainstem innervation of prefrontal and anterior cingulate cortex in the rhesus monkey revealed by retrograde transport of HRP. *J. Comp. Neurol.* **205,** 63–76.

Porrino, L.J., Crane, A.M., and Goldman-Rakic, P.S. (1981). Direct and indirect pathways from the amygdala to the frontal lobe in rhesus monkeys. *J. Comp. Neurol.* **198,** 121–136.

Preston, R.J., Bishop, G.A., and Kitai, S.T. (1980). Medium spiny neuron projection from the rat striatum: An intracellular horseradish peroxidase study. *Brain Res.* **183,** 253–263.

Price, J.L., and Amaral, D.G. (1981). An autoradiographic study of the projections of the central nucleus of the monkey amygdala. *J. Neurosci.* **1,** 1242–1259.

Rafols, J.A., and Fox, C.A. (1976). The neurons in the primate subthalamic nucleus: A Golgi and electron microscopic study. *J. Comp. Neurol.* **168,** 75–111.

Ragsdale, Jr., C.W., and Graybiel, A.M. (1981). The fronto-striatal projection in the cat and monkey and its relationship to inhomogeneities established by acetylcholinesterase histochemistry. *Brain Res.* **208,** 259–266.

Ramón, Y., Cajal, S., DeFelipe, J., and Jones, E.G. (1988). "Cajal on the cerebral cortex: An Annotated Translation of the Complete Writings." Oxford Univ. Press, New York.

Ravel, S., Sardo, P., Legallet, E., and Apicella, P. (2001). Reward unpredictability inside and outside of a task context as a determinant of the responses of tonically active neurons in the monkey striatum. *J. Neurosci.* **21,** 5730–5739.

Raz, A., Feingold, A., Zelanskaya, V., Vaadia, E., and Bergman, H (1996). Neuronal synchronization of tonically active neurons in the striatum of normal and parkinsonian primates. *J. Neurophysiol.* **76,** 2083–2088.

Raz, A., Frechter-Mazar, V., Feingold, A., Abeles, M., Vaadia, E., and Bergman, H. (2001). Activity of pallidal and striatal tonically active neurons is correlated in mptp-treated monkeys but not in normal monkeys. *J. Neurosci.* **21,** RC128.

Raz, A., Vaadia, E., and Bergman, H. (2000). Firing patterns and correlations of spontaneous discharge of pallidal neurons in the normal and the tremulous 1-methyl-4-phenyl-1,2,3,6-tetrahydropyridine vervet model of parkinsonism. *J. Neurosci.* **20,** 8559–8571.

Reiner, A., and Anderson, K.D. (1990). The patterns of neurotransmitter and neuropeptide co-occurrence among striatal projection neurons: Conclusions based on recent findings. *Brain Res. Rev.* **15,** 251–265.

Reiner, A., Medina, L., and Haber, S.N. (1999). The distribution of dynorphinergic terminals in striatal target regions in comparison to the distribution of substance P-containing and enkephalinergic terminals in monkeys and humans. *Neurosci.* **88** (3), 775–793.

Reynolds, J.N., Hyland, B.I., and Wickens, J.R. (2001). A cellular mechanism of reward-related learning. *Nature* **413,** 67–70.

Ribak, C.E., and Fallon, J.H. (1982). The island of Calleja complex of rat basal forebrain. I. Light and electron microscopic observations. *J. Comp. Neurol.* **205,** 207–218.

Richardson, N.R., and Gratton, A. (1996). Behavior-relevant changes in nucleus accumbens dopamine transmission elicited by food reinforcement: An electrochemical study in rat. *J. Neurosci.* **16,** 8160–8169.

Rinvik, E., Grofova, I., Hammond, C., Feger, J., and Deniau, J.M. (1979). A study of the afferent connections to the subthalamic nucleus in the monkey and the cat using the HRP technique.

In "The extrapyramidal system and its disorders" (L.J. Poirier, T.L. Sourkes, and P.J. Bedard, eds.), pp. 53–70. Raven Press, New York.

Robbins, T.W., and Everitt, B.J. (1999). Motivation and reward. *In* "Sensory Systems," IV. Academic Press.

Robbins, T.W., Cador. M., Taylor, J.R., and Everitt, B.J. (1989). Limbic-striatal interactions in reward-related processes. *Neurosci. Biobehav. Rev.* **13,** 155–162.

Robert, O., Miachon, S., Kopp, N., Denoroy, L., Tommasi, M., Rollet, D., and Pujol, J.F. (1984). Immunohistochemical study of the catecholaminergic systems in the lower brain stem of the human infant. *Hum. Neurobiol.* **3,** 229–234.

Rodriguez, M.C., Guridi, O.J., Alvarez, L., Mewes, K., Macias, R., Vitek, J., DeLong, M.R., and Obeso, J.A. (1998). The subthalamic nucleus and tremor in Parkinson's disease. *Mov. Disord. 13 Suppl.* **3,** 111–118.

Rolls, E.T. (2000). The orbitofrontal cortex and reward. *Cereb. Cortex* **10,** 284–294.

Rolls, E.T., and Baylis, L.L. (1994). Gustatory, olfactory, and visual convergence within the primate orbitofrontal cortex. *J. Neurosci.* **14,** 5437–5452.

Rolls, E.T., Burton, M.J., and Mora, F. (1980). Neurophysiological analysis of brain-stimulation reward in the monkey. *Brain Res.* **194,** 339–357.

Romansky, K.V., Usunoff, K.G., Ivanov, D.P., and Galabov, G.P. (1979). Corticosubthalamic projection in the cat: An electron microscopic study. *Brain Res.* **163,** 319–322.

Romo, R., and Shultz, W. (1990). Dopamine neurons of the monkey midbrain: Contingencies of responses to active touch during self-initiated arm movements. *J.Neurophysiol.* **63,** 592–590.

Rouiller, E.M., Liang, F., Babalian. A., Moret, V., and Wiesendanger, M. (1994). Cerebellothalamocortical and pallidothalamocortical projections to the primary and supplementary motor cortical areas: A multiple tracing study in macaque monkeys. *J. Comp. Neurol.* **345,** 185–213.

Russchen, F.T., Amaral, D.G., and Price, J.L. (1987). The afferent input to the magnocellular division of the mediodorsal thalamic nucleus in the monkey, Macaca fascicularis. *J. Comp. Neurol.* **256,** 175–210.

Russchen, F.T., Bakst, I., Amaral, D.G., and Price, J.L. (1985). The amygdalostriatal projections in the monkey. An anterograde tracing study. *Brain Res.* **329,** 241–257.

Rye, D.B., Saper, C.B., Lee, H.J., and Wainer, B.H. (1987). Pedunculopontine tegmental nucleus of the rat: Cytoarchitecture, cytochemistry, and some extrapyramidal connections of the mesopontine tegmentum. *J. Comp. Neurol.* **259,** 483–528.

Sadikot, A.F., and Parent, A. (1990). The monoaminergic innervation of the amygdala in the squirrel monkey: An immunohistochemical study. *Neurosci.* **36,** 431–447.

Sadikot, A.F., Parent, A., and Francois, C. (1990). The centre median and parafascicular thalamic nuclei project respectively to the sensorimotor and associative-limbic striatal territories in the squirrel monkey. *Brain Res.* **510,**]161–165.

Sadikot, A.F., Parent, A., and Francois, C. (1992a). Efferent connections of the centromedian and parafascicular thalamic nuclei in the squirrel monkey: A PHA-L study of subcortical projections. *J. Comp. Neurol.* **315**, 137–159.

Sadikot, A.F., Parent, A., Smith, Y., and Bolam, J.P. (1992b). Efferent connections of the centromedian and parafascicular thalamic nuclei in the squirrel monkey: A light and electron microscopic study of the thalamostriatal projection in relation to striatal heterogeneity. *J. Comp. Neurol.* **320,** 228–242.

Saint-Cyr, J.A., and Taylor, A.E. (1992). The mobilization of procedural learning: The "key signature" of the basal ganglia. *In* "Neuropsychology of Memory," 2nd ed. (L.R. Squire nd N. Butters, eds.), pp. 188–202. The Guilford Press, New York.

Saint-Cyr, J.A., Ungerleider, L.G., and Desimone, R. (1990). Organization of visual cortical inputs to the striatum and subsequent outputs to the pallido-nigral complex in the monkey *J. Comp. Neurol.* **298,** 129–156.

Sakai, S.T., Inase, M., and Tanji, J. (1996). Comparison of cerebellothalamic and pallidothalamic projections in the monkey (*Macaca fuscata*): A double anterograde labeling study. *J. Comp. Neurol.* **368,** 215-228.

Sakai, S.T., Stepniewska, I., Qi, H.X., and Kaas, J.H. (2000). Pallidal and cerebellar afferents to pre-supplementary motor area thalamocortical neurons in the owl monkey: A multiple labeling study. *J. Comp. Neurol.* **417,** 164–180.

Samson, Y., Wu, J.J., Friedman, A.H., and Davis, J.N. (1990). Catecholaminergic innervation of the hippocampus in the cynomolgus monkey. *J. Comp. Neurol.* **298,** 250–263.

Sato, F., Lavallee, P., Levesque, M., and Parent, A. (2000a). Single-axon tracing study of neurons of the external segment of the globus pallidus in primate. *J. Comp. Neurol.* **417,** 17–31.

Sato, F., Parent, M., Levesque, M., and Parent, A. (2000b). Axonal branching pattern of neurons of the subthalamic nucleus in primates. J. Comp. Neurol. **424,** 142–152.

Schall, J.D. (1997). Visuomotor areas of the frontal lobe. *In* "Cerebral Cortex: Volume 12 Extrastriate Cortex in Primates," 1st ed. (K.S. Rockland, J.H. Kaas and A. Peters, eds.), pp. 527–638. Plenum Press, New York.

Schell, G.R., and Strick, P.L. (1984). The origin of thalamic inputs to the arcuate premotor and supplementary motor areas. *J. Neurosci.* **4,** 539–560.

Schieber, M.H. (1999). Voluntary descending control. *In* "Fundamental Neuroscience," pp. 931–949. Academic Press.

Schofield, S.P.M., and Everitt, B.J. (1981). The organization of catecholamine-containing neurons in the brain of the rhesus monkey (*Macaca mulatta*). *J. Anat.* **132,** 391–418.

Schultz, W. (1992). Activity of dopamine neurons in the behaving primate. *Seminars in the Neurosciences* **4,** 129–138.

Schultz, W. (1997). Dopamine neurons and their role in reward mechanisms [Review] [83 refs]. *Cur. Opin. Neurobiol.* **7,** 191–197.

Schultz, W. (1998). Predictive reward signal of dopamine neurons. *J. Neurophysiol.* **80,** 1–27.

Schultz, W., and Romo. R. (1990). Dopamine neurons of the monkey midbrain: contingencies of responses to stimuli eliciting immediate behavioral reactions. *J. Neurophysiol.* **63,** 607–624.

Schultz, W., Apicella, P., and Ljungberg, T. (1993). Responses of monkey dopamine neurons to reward and conditioned stimuli during successive steps of learning a delayed response task. *J. Neurosci.* **13,** 900–913.

Schultz, W., Dayan, P., and Montague, P.R. (1997). A neural substrate of prediction and reward [Review] [37 refs]. *Science* **275,** 1593–1599.

Schultz, W., Tremblay, L., Hollerman, J.R. (1998). Reward prediction in primate basal ganglia and frontal cortex. *Neuropharmacology* **37,** 421–429.

Schultz, W., Tremblay, L., and Hollerman, J.R. (2000). Reward processing in primate orbitofrontal cortex and basal ganglia. *Cereb. Cortex* **10,** 272–284.

Schultz, W., Romo, R., Ljungberg, T., Mirenowicz, J., Hollerman, J.R. and Dickinson, A. (1995). Reward-related signals carried by dopamine neurons. *In* "Models of Information Processing in the Basal Ganglia" (J.C. Houk, J.L. Davis and D.G. Beiser, eds.). MIT Press, Cambridge.

Schwyn, R.C., and Fox, C.A. (1974). The primate substantia nigra: A Golgi and electron microscopic study. *J. Hirnforsch.* **15,** 95–126.

Scott, T.R., Yaxley, S., Sienkiewicz, Z.J., and Rolls, E.T. (1986). Gustatory responses in the frontal opercular cortex of the alert cynomolgus monkey. *J. Neurophysiol.* **56,** 876–890.

Selden, N., Geula, C., Hersh, L., and Mesulam, M-M. (1994) Human striatum: Chemoarchitecture of the caudate nucleus, putamen and ventral striatum in health and Alzheimer's disease. *Neurosci.* **60,** 621–636.

Selemon, L.D., and Goldman-Rakic, P.S. (1985). Longitudinal topography and interdigitation of corticostriatal projections in the rhesus monkey. *J. Neurosci.* **5,** 776–794.

Selemon, L.D., and Goldman-Rakic, P.S. (1990). Topographic intermingling of striatonigral and striatopallidal neurons in the rhesus monkey. *J. Comp. Neurol.* **297,** 359–376.

Selemon, L.D., Gottlieb, J.P., and Goldman-Rakic, P.S. (1994). Islands and striosomes in the neostriatum of the Rhesus monkey: Non-equivalent compartments. *Neurosci.* **58,** 183–192.

Seroogy, K., Ceccatelli, S., Schalling, M., Hokfelt, T. Frey, P., Walsh, J., Dockray, G., Brown, J., Buchan, A., and Goldstein, M. (1988). A subpopulation of dopaminergic neurons in rat ventral mesencephalon contains both neurotensin and cholecystokinin. *Brain Res.* **455,** 88–98.

Sesack, S.R., Hawrylak, V.A., Melchitzky, D.S., and Lewis, D.A. (1998). Dopamine innervation of a subclass of local circuit neurons in monkey prefrontal cortex: Ultrastructural analysis of tyrosine hydroxylase and parvalbumin immunoreactive structures. *Cereb. Cortex* **8,** 614–622.

Shink, E., and Smith, Y. (1995). Differential synaptic innervation of neurons in the internal and external segments of the globus pallidus by the GABA- and glutamate-containing terminals in the squirrel monkey. *J. Comp. Neurol.* **358,** 119–141.

Shink, E., Bevan, M.D., Bolam, J.P., and Smith, Y. (1996). The subthalamic nucleus and the external pallidum: Two tightly interconnected structures that control the output of the basal ganglia in the monkey. *Neurosci.* **73,** 335–357.

Shink, E., Sidibé, M., and Smith, Y. (1997). Efferent connections of the internal globus pallidus in the squirrel monkey. II. Topography and synaptic organization of pallidal efferents to the pedunclulopontine nucleus. *J. Comp. Neurol.* **382,** 348–363.

Sidibe, M., and Smith, Y. (1996). Differential synaptic innervation of striatofugal neurones projecting to the internal or external segments of the globus pallidus by thalamic afferents in the squirrel monkey. *J. Comp. Neurol.* **365,** 445–465.

Sidibe, M., Bevan, M.D., Bolam, J.P., and Smith, Y. (1997). Efferent connections of the internal globus pallidus in the squirrel monkey. I. Topography and synaptic organization of the pallidothalamic projection. *J. Comp. Neurol.* **382,** 323–347.

Sidibe, M., Pare, J.F., and Smith, Y. (2002). Nigral and pallidal inputs to functionally segregated thalamostriatal neurons in the centromedian/parafascicular intralaminar nuclear complex in monkey. *J. Comp. Neurol.* **447,** 286–299.

Slovin, H., Abeles, M., Vaadia, E., Haalman, I., Prut, Y., and Bergman, H. (1999). Frontal cognitive impairments and saccadic deficits in low-dose MPTP-treated monkeys. *J. Neurophysiol.* **81,** 858–874.

Smith, A.D., and Bolam, J.P. (1990). The neural network of the basal ganglia as revealed by the study of synaptic connections of identifited neurones. *Trends Neurosci.* **13,** 259–265.

Smith, E.E., and Jonides, J. (1997). Working memory: A view from neuroimaging. *Cog. Psychol.* **33,** 5–42.

Smith, Y., and Parent, A. (1986). Differential connections of the caudate nucleus and putamen in the squirrel monkey (*Saimiri sciureus*). *Neurosci.* **18** (2), 347–371.

Smith, Y., and Parent, A. (1988). Neurons of the subthalamic nucleus in primates display glutamate but not GABA immunoreactivity. *Brain Res.* **453,** 353–356.

Smith, Y., Bennett, B.D., Bolam, J.P., Parent, A., and Sadikot, A.F. (1994b). Synaptic relationships between dopaminergic afferents and cortical or thalamic input in the sensorimotor territory of the striatum in monkey. *J. Comp. Neurol.* **344,** 1–19.

Smith, Y., Bevan, M.D., Shink, E., and Bolam, J.P. (1998b). Microcircuitry of the direct and indirect pathways of the basal ganglia. *Neurosci.* **86,** 353–387.

Smith, Y., Hazrati, L-N., and Parent, A. (1990). Efferent projections of the subthalamic nucleus in the squirrel monkey as studied by the PHA-L anterograde tracing method. *J. Comp. Neurol.* **294,** 306–323.

Smith, Y., Parent, A., Seguela, P., and Descarries, L. (1987). Distribution of GABA-immunoreactive neurons in the basal ganglia of the squirrel monkey (Saimiri sciureus). *J. Comp. Neurol.* **259,** 50–64.

Smith, Y., Shink, E., and Sidibe, M. (1998a). Neuronal circuitry and synaptic connectivity of the basal ganglia. *Neurosurgery Clinics of North America* **9,** 203–222.

Smith, Y., Wichmann, T., and DeLong, M.R. (1994a). Synaptic innervation of neurones in the internal pallidal segment by the subthalamic nucleus and the external pallidum in monkeys. *J. Comp. Neurol.* **343,** 297–318.

Sokoloff, P., and Schwartz, J.C. (1995). Novel dopamine receptors half a decade later. [see comments]. *Trends Pharmacol. Sci.* **16,** 270–275.

Somogyi, P., and Smith, A.D. (1979). Projection of neostriatal spiny neurons to the substantia nigra. Application of a combined Golgi-staining and horseradish peroxidase transport procedure at both light and electron microscopic levels. *Brain Res.* **178,** 3–15.

Somogyi, P., Bolam, J.P., and Smith, A.D. (1981a). Monosynaptic cortical input and local axon collaterals of identified striatonigral neurons. A light and electron microscopic study using the Golgi-peroxidase transport-degeneration procedure. *J. Comp. Neurol.* **195**, 567–584.

Somogyi, P., Bolam, J.P., Totterdell, S., and Smith, A.D. (1981b). Monosynaptic input from the nucleus accumbens-ventral striatum region to retrogradely labelled nigrostriatal neurones. *Brain Res.* **217,** 245–263.

Song, D.D., and Haber, S.N. (2000), Striatal responses to partial dopaminergic lesion: Evidence for compensatory sprouting. *J. Neurosci.* **20,** 5102–5114.

Spooren, W.P.J.M., Lynd-Balta, E., Mitchell, S., and Haber, S.N. (1996). Ventral pallidostriatal pathway in the monkey: Evidence for modulation of basal ganglia circuits. *J. Comp. Neurol.* **370** (3), 295–312.

Stanton, G.B., Goldberg, M.E., and Bruce, C.J. (1988). Frontal eye field efferents in the macaque monkey: I. subcortical pathways and topography of striatal and thalamic terminal fields. *J. Comp. Neurol.* **271,** 473–492.

Steinbusch, H.W.M., Nieuwenhuys, R., Verhofstad, A.A.J., and Van der Kooy, D. (1981). The nucleus raphe dorsalis of the rat and its projection upon the caudatoputamen. A combined cytoarchetectonic, immunohistochemical and retrograde transport study. *J. Physiol. Paris* **77,** 157–174.

Stern, E.A., Kincaid, A.E., and Wilson, C.J. (1997). Spontaneous subthreshold membrane potential fluctuations and action potential variability of rat corticostriatal and striatal neurons in vivo. *J. Neurophysiol.* **77**, 1697–1715.

Stevens, J.R. (1973). An anatomy of schizophrenia? *Arch. Gen. Psychiatry* **29,** 177–189.

Strick, P.L., Dum, R.P., and Picard, N. (1998). Motor areas on the medial wall of the hemisphere. *Novartis Foundation Symp.* **218,** 64–75; discussion 75–80.

Surmeier, D.J., Song, W-J., and Yan, Z. (1996). Coordinated expression of dopamine receptors in neostriatal medium spiny neurons. *J. Neurosci.* **16,** 6579–6591.

Surmeier, D.J., Yan, Z., and Song, W.J. (1998). Coordinated expression of dopamine receptors in neostriatal medium spiny neurons. *Adv. Pharmacol.* **42,** 1020–1023.

Swerdlow, N.R., Braff, D.L., Caine, S.B., and Geyer, M.A. (1993). Limbic cortico-striato-pallido-pontine substrates of sensorimotor gating in animal models and psychiatric disorders. *In* "Limbic Motor Circuits and Neuropsychiatry" (P.W. Kalivas and C.D. Barnes, eds.), pp. 311–328. CRC Press, Boca Raton, FL.

Switzer, R.C., Hill, T., and Heimer, L. (1982). The globus pallidus and its rostroventral extension into the olfactory tubercle of the rat: cyto and chemoarchitectural study. *Neurosci.* **7,** 1891–1904.

Szabo, J. (1962). Topical distribution of the striatal efferents in the monkey. *Exp. Neurol.* **5,** 21–36.

Szabo, J. (1967). The efferent projections of the putamen in the monkey. *Exp. Neurol.* **19,** 463–476.

Szabo, J. (1970). Projections from the body of the caudate nucleus in the rhesus monkey. *Exp. Neurol.* **27,** 1–15.

Szabo, J. (1972). The course and distribution of efferents from the tail of the caudate nucleus in the monkey. *Exp. Neurol.* **37,** 562–572.

Szabo, J. (1979). Strionigral and nigrostriatal connections. Anatomical studies. *Appl. Neurophysiol.* **42,** 9–12.

Szabo, J. (1980). Organization of the ascending striatal afferents in monkeys. *J. Comp. Neurol.* **189,** 307–321.

Takada, M., Tokuno, H., Hamada, I., Inase, M., Ito, Y., Imanishi, M., Hasegawa, N., Akazawa, T., Hatanaka, N., and Nambu, A. (2001). Organization of inputs from cingulate motor areas to basal ganglia in macaque monkey. *Eur. J. Neurosci.* **14,** 1633–1650.

Takagi, H., Somogyi, P., Somogyi, J., and Smith, A.D. (1983). Fine structural studies on a type of somatostatin-immunoreactive neuron and its synaptic connections in the rat neostriatum: A correlated light and electron microscopic study. *J. Comp. Neurol.* **214,** 1–16.

Tallaksen-Greene, S.J., Kaatz, K.W., Romano, C., and Albin, R.L. (1998). Localization of mGluR1a-like immunoreactivity and mGluR5-like immunoreactivity in identified populations of striatal neurons. *Brain Res.* **780,** 210–217.

Tanaka, C. (1982). Histochemical mapping of catecholaminergic neurons and their ascending fiber pathways in the rhesus monkey brain. *Brain Res. Bull.* **9,** 255–270.

Tanji, J., and Mushiake, H. (1996). Comparison of neuronal activity in the supplementary motor area and primary motor cortex. *Brain Res. Cog. Brain Res.* **3,** 143–150.

Testa, C.M., Friberg, I.K., Weiss, S.W., and Standaert, D.G. (1998). Immunohistochemical localization of metabotropic glutamate receptors mGluR1a and mGluR2/3 in the rat basal ganglia. *J. Comp. Neurol.* **390,** 5–19.

Testa, C.M., Standaert, D.G., Young, A.B., and Penney, J.B. (1994). Metabotropic glutamate receptor mRNA expression in the basal ganglia of the rat. *J. Neurosci.* **14,** 3005–3018.

Teuber, H.L. (1976). Complex functions of basal ganglia. *Research Publications—Association for Research in Nervous & Mental Disease* **55,** 151–168.

Thomas, M.J, and Malenka, R.C. (1999). NMDA receptor-dependent long-term depression in the nucleus accumbens. *Society of Neuroscience Abstract.*

Thomas, M.J., Malenka, R.C., and Bonci, A. (2000). Modulation of long-term depression by dopamine in the mesolimbic system. *J. Neurosci.* **20,** 5581–5586.

Tremblay, L., Hollerman, J.R., and Schultz, W. (1998). Modifications of reward expectation-related neuronal activity during learning in primate striatum. *J. Neurophysiol.* **80,** 964–977.

Tunstall, M.J, Oorschot, D.E., Kean, A., and Wickens, J.R. (2002). Inhibitory interactions between spiny projection neurons in the rat striatum. *J. Neurophysiol.* **88,** 1263–1269.

Turner, M.S., Lavin, A., Grace, A.A., and Napier, T.C. (2001). Regulation of limbic information outflow by the subthalamic nucleus: excitatory amino acid projections to the ventral pallidum. *J. Neurosci.* **21,** 2820–2832.

Uhl, G.R. (1982). Distribution of neurotensin and its receptor in the central nervous system. *Ann. N.Y. Acad. Sci.* **400,** 132–149.

Ungerstedt, U. (1971). Stereotaxic mapping of the monoamine pathways in the rat brain. *Acta Physiol. Scand.* **367,** 153–174.

Van der Kooy, D., and Hattori, T. (1980). Single subthalamic nucleus neurons project to both the globus pallidus and substantia nigra in rat. *J. Comp. Neurol.* **192,** 751–768.

Van Hoesen, G.W., Yeterian, E.H., and Lavizzo-Mourey, R. (1981). Widespread corticostriate projections from temporal cortex of the rhesus monkey. *J. Comp. Neurol.* **299,** 205–219.

Verney, C., Milosevic, A., Alvarex, C., and Berger, B. (1993). Immunocytochemical evidence of well-developed dopaminergic and noradernergic innervations in the frontal cerebral cortex of human fetuses at midgestation. *J. Comp. Neurol.* **336,** 331–344.

Vicq D'Azyr, F. (1786). "Traite d'Anatomie et de Physiologie, Tome Premier: Anatomie et Physiologie du Cerveau." Didot, Paris.

Vila, M., Herrero, M.T., Levy, R., Faucheux, B., Ruberg, M., Guillen, J., Luquin, M.R., Guridi, J., Javoy-Agid, F., Agid ,Y., Obeso, J.A., and Hirsch, E.C. (1996). Consequences of nigrostriatal denervation on the g-aminobutyric acidic neurons of substantia nigra pars reticulata and superior colliculus in parkinsonian syndromes. *Neurology* **46,** 802–809.

Vincent, S.R., and Johansson, O. (1983). Striatal neurons containing both somatostatin- and avian pancreatic polypeptide (APP)-like immunoreactivities and NADPH-diaphorase activity: A light and electron microscopic study. *J. Comp. Neurol.* **217,** 264–270.

Vogt, B.A., and Pandya, D.N. (1987). Cingulate cortex of the Rhesus monkey: II. Cortical afferents. *J. Comp. Neurol.* **262,** 271–289.

von Economo, C., and Horn, L. (1930). Uber Windungsrelief, Masse und Rindenarchitektonik der Supratemporalflache, ihre individuellen und ihr Seitenunterscheide, *Z. Gesamte Neurol. Psychiatry* **130,** 678–857.

Voorn, P., Brady, L.S., Berendse, H.W., and Richfield, E.K. (1996). Densitometrical analysis of opioid receptor ligand binding in the human striatum—I. Distribution of m opioid receptor defines shell and core of the ventral striatum. *Neurosci.* **75,** 777–792.

Voorn, P., Brady, L.S., Schotte, A., Berendse, H.W., and Richfield, E.K. (1994). Evidence for two neurochemical divisions in the human nucleus accumbens. *Eur. J. Neurosci.* **6,** 1913–1916.

Voorn, P., Jorritsma-Byham, B., VanDijk, C., and Buijs, R.M. (1986). The dopaminergic innervation of the ventral striatum in the rat: A light- and electron-microscopical study with antibodies against dopamine. *J. Comp. Neurol.* **251,** 84–99.

Vuillet, J., Kerkerian, L., Salin, P., and Nieoullon, A. (1989). Ultrastructural features of NPY-containing neurons in the rat striatum. *Brain Res.* **477,** 241–251.

Wang, H., and Pickel, V.M. (2002). Dopamine D2 receptors are present in prefrontal cortical afferents and their targets in patches of the rat caudate-putamen nucleus. *J. Comp. Neurol.* **442,** 392–404.

Ward, R.P., and Dorsa, D.M. (1996). Colocalization of serotonin receptor subtypes 5-HT2A, 5-HT2C, and 5-HT6 with neuropeptides in rat striatum. *J. Comp. Neurol.* **370,** 405–414.

Wassef, M., Berod, A., and Sotelo, C. (1981). Dopaminergic dendrites in the pars reticulata of the rat substantia nigra and their striatal input. Combined immunocytochemical localization of tyrosine hydroxylase and anterograde degeneration. *Neurosci.* **6,** 2125–2139.

Weihmuller, F.B., Bruno, J.P., Neff, N.H., and Hadjiconstantinou, M. (1990). Dopamine receptor plasticity following MPTP-induced nigrostriatal lesions in the mouse. *Eur. J. Pharmacol.* **180,** 369–372.

Weiner, D.M., Levey, A.I., Sunahara, R.K., Niznik, H.B., O'Dowd, B.F., Seeman, P., and Brann, M.R. (1991). D1 and D2 dopamine receptor mRNA in rat brain. *Proc. Nat. Acad. Sci. U.S.A.* **88,** 1859–1863.

Wichmann, T., Bergman, H., and DeLong, M.R. (1994). The primate subthalamic nucleus. I. Functional properties in intact animals. *J. Neurophysiol.* **72,** 494–506.

Wichmann, T., Bergman, H., Starr, P.A., Subramanian, T., Watts, R.L., and DeLong, M.R. (1999). Comparison of MPTP-induced changes in spontaneous neuronal discharge in the internal pallidal segment and in the substantia nigra pars reticulata in primates. *Exp. Brain Res.* **125,** 397–409.

Wickelgren, I. (1997). Getting the brain's attention. *Science* **278** (5335), 35–37.

Wickens, J. (1997). Basal ganglia: structure and computations. Network: *Comput. Neural Syst.* **8,** R77–R109.

Wickens, J.R., and Oorshcot, D.E. (2000). Neuronal dynamics and inhibition in the neostriatum: A possible connection. *In* "Brain Dynamics and the Striatal Complex" (R. Miller and J.R. Wickens, eds.), pp. 141–150. Harwood Academic Publishers, Australia.

Wiesendanger, R., and Wiesendanger, M. (1985). The thalamic connections with medial area 6 (supplementary motor cortex) in the monkey *(Macaca fascicularis). Exp. Brain Res.* **59,** 91–104.

Wilson, C., Nomikos, G.G., Collu, M., and Fibiger, H.C. (1995). Dopaminergic correlates of motivated behavior: Importance of drive. *J. Neurosci.* **15,** 5169–5178.

Wilson, C.J. (1987). Morphology and synaptic connections of crossed corticostriatal neurons in the rat. *J. Comp. Neurol.* **263,** 567–580.

Wilson, C.J. (1993). The generation of natural firing patterns in neostriatal neurons. *Prog. Brain Res.* **99,** 277–297.

Wilson, C.J. (1998). Basal ganglia. *In* "The Synaptic Organization of the Brain" (G.M. Shepherd, ed.), pp. 329–375. Oxford University Press, New York.

Wilson, C.J., and Groves, P.M. (1980). Fine structure and synaptic connections of the common spiny neuron of the rat neostriatum: A study employing intracellular inject of horseradish peroxidase. *J. Comp. Neurol.* **194,** 599–615.

Wilson, C.J., and Kawaguchi, Y. (1996). The origins of two-state spontaneous membrane potential fluctuations of neostriatal spiny neurons. *J. Neurosci.* **16,** 2397–2410.

Wilson, C.J., Chang, H.T., and Kitai, S.T. (1990). Firing patterns and synaptic potentials of identified giant aspiny interneurons in the rat neostriatum. *J. Neurosci.* **10,** 508–519.

Wise, R.A. (1996). Addictive drugs and brain stimulation reward. *Annu. Rev. Neurosci.* **19,** 319–340.

Wise, R.A. (1998). Drug-activation of brain reward pathways. *Drug & Alcohol Dependence* **51,** 13–22.

Wise, R.A., and Rompre, P.P. (1989). Brain dopamine and reward. *Annu. Rev. Psychol.* **40,** 191–225.

Wise, S.P., Murray, E.A., and Gerfen, C.R. (1996). The frontal cortex-basal ganglia system in primates. *Crit. Rev. Neurobiol.* **10,** 317–356.

Yachnis, A.T., Roper, S.N., Love, A., Fancey, J.T., and Muir, D. (2000). Bcl-2 immunoreactive cells with immature neuronal phenotype exist in the nonepileptic adult human brain. *J. Neuropathol. Exp. Neurol.* **59,** 113–119.

Yamaguchi, S., and Kobayashi, S. (1998). Contributions of the dopaminergic system to voluntary and automatic orienting of visuospatial attention. *J. Neurosci.* **18,** 1869–1878.

Yan, Z., Flores-Hernandez, J., and Surmeier, D.J. (2001). Coordinated expression of muscarinic receptor messenger RNAs in striatal medium spiny neurons. *Neurosci.* **103,** 1017–1024.

Yelnik, J., and Percheron. G. (1979). Subthalamic neurons in primates: A quantitative and comparative analysis. *Neurosci.* **4,** 1717–1743.

Yelnik, J., Francois, C., Percheron, G., and Heyner, S. (1987). Golgi study of the primate substantia nigra. I. Quantitative morphology and typology of nigral neurons. *J. Comp. Neurol.* **265,** 455-472.

Yelnik, J., Francois, C., Percheron, G., and Tande, D. (1996). A spatial and quantitative study of the striatopallidal connection in the monkey. *Neuroreport* **7,** 985–988.

Yelnik, J., Percheron, G., and Francois, C. (1984). A golgi analysis of the primate globus pallidus. II. Quantitative morphology and spatial orientation of dendritic arborizations. *J. Comp. Neurol.* **227,** 200–213.

Yelnik, J., Percheron, G., Francois, C., and Garnier, A. (1993). Cholinergic neurons of the rat and primate striatum are morpholgoically different. *In* "Progress in Brain Research" (G.W. Arbuthnott and P.C. Emson, eds.), pp. 25–33. Elsevier Science Publishers.

Yeterian, E.H., and Pandya, D.N. (1991). Prefrontostriatal connections in relation to cortical architectonic organization in Rhesus monkeys. *J. Comp. Neurol.* **312,** 43–67.

Yeterian, E.H., Pandya, D.N. (1998). Corticostriatal connections of the superior temporal region in rhesus monkeys. *J. Comp. Neurol.* **399,** 384–402.

Yeterian, E.H., and Van Hoesen, G.W. (1978). Cortico-striate projections in the rhesus monkey: The organization of certain cortico-caudate connections. *Brain Res.* **139,** 43–63.

Young, A.B. (1993). Role of excitotoxins in heredito-degenerative neurologic diseases. *Research Publications—Association for Research in Nervous & Mental Disease* **71,** 175–189.

Young III, W.S., Alheid, G.F., and Heimer, L. (1984). The ventral pallidal projection to the mediodorsal thalamus: a study with fluorescent retrograde tracers and immunohistofluorescence. *J. Neurosci.* **4,** 1626–1638.

Yung, K.S., A.D., Levey, A.I., and Bolam, J.P. (1996) Synaptic connections between spiny neurons of the direct and indirect pathways in the neostriatum of the rat: Evident from dopamine receptro and neuropeptide immostaining. *Eur. J. Neurosci.* **8,** 861–869.

Zaborszky, L., Alheid, G.F., Beinfeld, M.C., Eiden, L.E., Heimer, L., and Palkovits, M. (1985). Cholecystokinin innervation of the ventral striatum: A morphological and radioimmunological study. *Neurosci.* **14** (2), 427–453.

Zahm, D.S. (1989). The ventral striatopallidal parts of the basal ganglia in the rat. II. Compartmentation of ventral pallidal efferents. *Neuroscience* **30,** 33-50.

Zahm, D.S. (1992), An electron microscopic morphometric comparison of tyrosine hydroxylase immunoreactive innervation in the neostriatum and nucleus accumbens core and shell. *Brain Res.* **575,** 341–346.

Zahm, D.S., and Brog, J.S. (1992). On the significance of sub-territories in the "accumbens" part of the rat ventral striatum. *Neurosci.* **50,** 751–767.

Zahm, D.S., and Heimer, L. (1988). Ventral striatopallidal parts of the basal ganglia in the rat. I. Neurochemical compartmentation as reflected by the distributions of neurotensin and substance P immunoreactivity. *J. Comp. Neurol.* **272,** 516–535.

Zhong, L.T., Sarafian, T., Kane, D.J., Charles, A.C., Mah, S.P., Edwards, R.H., and Bredesen, D.E. (1993). Bcl-2 inhibits death of central neural cells induced by multiple agents. *Proc. Nat. Acad. Sci. U.S.A.* **90,** 4533–4537.

CHAPTER

22

Amygdala

JOSE S. DE OLMOS
Instituto De Investigacion Medica "Mercedes Y Martin Ferreyra"
Cordoba, Argentina

TERMINOLOGY

The primate amygdaloid body is a relatively large conglomerate of gray substance lying in the depth of the anteromedial temporal lobe ventral to the lentiform nucleus from which it is separated by the magnocellular basal forebrain neuronal complex (MCBFC) constituting the basal nucleus of Meynert and related cell groups, or the so-called substantia innominata sensu ampliori. Massive fiber systems separate the amygdala from the basal forebrain and form part of the telencephalic and diencephalotegmental radiations, bidirectionally connecting the amygdala and other gray formations of the temporal lobe with those in the basal and medial telencephalon, the diencephalon, the brain stem tegmentum, and even the spinal cord. Although the amygdala has been generally thought of as a single structure, it is actually a very heterogeneous one shown to be involved in the modulation of neuroendocrine functions, visceral effector mechanisms, and complex patterns of integrated behavior, such as defense, ingestion, aggression, reproduction, memory, and learning (Beltramino and Taleisnik, 1978, 1980; Benjamin and Jackson, 1974; Carrer, 1978; Carrer *et al.*, 1973, 1980; De Vito and Smith, 1982; Dunn, 1987; Fahrbach *et al.*, 1983; Fuchs and. Siegel, 1984; Fuchs *et al.*, 1985; Ghashghaei H.T., and Barbas, H., 2000, Gloor *et al.*, 1982, 1997; Lehman and Winans, 1982, 1983; Mishkin and Aggleton, 1981; Sarter and Markowitsch, 1985; ; Squire and Zola-Morgan, 1985; LeDoux, 1993; Maren, 1999; Adolphs, R., and Tranel, D., 2003; Hurd, 2002). This modulation is exercised, at least in part, through a vast network of connections with other brain regions, such as the hypothalamus. These other regions have been thought to have the most direct involvement in the regulation of these functions. Recent experimental anatomical, physiological, and behavioral data suggest that the amygdala is involved in more direct action than was previously suspected. This action is subserved by some of the nuclear groups into which the amygdala has been divided on the basis of cytoarchitectonic, histochemical, immunohistochemical, and hodological studies (de Olmos *et al.*, 1985; de Olmos, 1990; Alheid *et al.*, 1995; Heimer *et al.*, 1999). Furthermore, the amygdaloid complex has been shown to be significantly involved in a number of human neurodegenerative diseases, including Alzheimer's disease, the chorea of Huntington, and neuronal ceroid lipofuscinosis (Brockhaus, 1940; Cipollini and Corsellis, 1970; Herzog and Kemper, 1980; Braak and Braak, 1983, 1987, 1995; Brashear *et al.*, 1988; Brady and Mufson, 1989; Powers *et al.*, 1987; Benzing *et al.*, 1990, 1992; Hunger *et al.*, 1991, 1992; Emre *et al.*, 1993; Hudson *et al.*, 1993; Pitkänen *et al.*, 1998; Hurd, 2002; Heimer, 2002).

This review of the main anatomical and cytochemical features of the human amygdala is based on the thorough cytoarchitectonic studies of Brockhaus (1940), Crosby and Humphrey (1941), Hilpert (1928),

Sanides (1957b), and Stephan (l975), the pigmento-architectonic studies of Braak and Braak (1983, 1987) and Strenge *et al.* (l977), the histochemical reports by Svendsen and Bird (l98S), as well as on a recent descriptions by Sorvari *et al.* (1995–1996), Gloor (1977), and Heimer *et al.* (1999). In a previous version of this chapter, and in order to provide grounds for inferring connectional and functional meaning to the cytoarchitectonic and chemoarchitectonic human data reviewed here, a parallel though somewhat restricted account of information of the same concerning the nonhuman primate amygdala is given, since it is in these mammals—the closest phylogenetically speaking to the humans—that it has been possible to obtain by experimental means the connectional, physiological, and behavioral data mentioned above.

In analyzing the nuclear arrangement of the human amygdala and in critically reviewing the literature on the hodological relationships of the amygdala with the cerebral cortex, the basal ganglia, the diencephalic nuclei. and the tegmental grisea distributed along the brain stem and the spinal cord, the nomenclature employed will be based substantially on the seminal comparative neuroanatomical work of Johnston (l923), who examined the basal forebrain but more particularly the amygdala of the opossum, bat, rat, rabbit, macaque monkey, as well as human embryos. In many regards the terminology is also inspired by the work by Brockhaus (l938) on the human amygdala, and by that of Price *et al.* (1987) on the macaque monkey; finally, it is consistent with the terminology used in the last edition of Paxinos and Watson's (l997) stereotaxic atlas of the rat brain. In my view, this nomenclature is supported not only by well-established cyto- and fibro-architectonic criteria but also by ontogenetic, histochemical, immunohistochemical, and hodological data (Bayer, 1980; de Olmos *et al.*, 1985; Grove, 1988a, b; Barbas and de Olmos, 1991). In this regard, it is important to point out that Johnston (l923) used for the monkey and human amygdala the same terminology he proposed for the other subprimate mammals he examined. However, Johnston's proposition was only partially followed by Crosby and Humphrey (l94l) in describing the human amygdala and later by Lauer (l945) in his account of the macaque monkey amygdala. Lauer renamed Johnston's medial small-celled basal amygdaloid nucleus as the basal accessory amygdaloid, a term Johnston reserved for a completely different nucleus in the opossum amygdala and which he claimed was present only in this latter mammal [see also Young (l936) for the rabbit and Fox (1940) for the cat].

Nevertheless, this terminology eventually became common in American experimental neuroanatomical studies of primates and in evaluating of pathological changes in the human amygdala. However, hodological studies in the macaque monkey brain by Mehler (1980) encouraged me to suggest that the basal accessory amygdaloid nucleus of the primates is, at least in part, homologous to the basomedial amygdaloid nucleus in the rat and the cat [see also Barbas and de Olmos, 1990). On the other hand, Price (1981) not only accepted this possibility but also suggested that the medial small-celled basal nucleus (MB) [or *parvicellulare* basal amygdaloid nucleus (Bpc) of his own terminology] is homologous with the smaller celled part of the basolateral amygdaloid nucleus in the rat and the cat (see also Price *et al.*, 1987). On this basis, it seems more reasonable to maintain the earlier naming suggested by Johnston (1923) for the laterobasal nuclear complex (LBNC) and consider Crosby and Humphrey's (1941) medial basal nucleus as just one of the subdivisions of the basolateral amygdaloid nucleus.

In other order of subjects, it should be mentioned that our studies (de Olmos, 1990; Heimer *et al.*, 1999) have confirmed entirely the basic architectonic principle established by Brockhaus (1938). According to this plan (allowing for small variations in different species of monkeys), neurons within the LBNC, including the lateral amygdaloid nucleus as its third main member, tend to be arranged in such a manner that the smaller neurons are 1ocated closer to the walls of the inferior horn of the lateral ventricle and the largest ones are farther away, with the intermediate-sized neurons being located in an intermediate position within the respective members of the LBNC. Such a basic distribution pattern as well as a parallel variation in the density of the satellite glial cell population (i.e., densest around large-celled subdivisions, poorest at the smaller celled ones) provides the backbone of the subdivisions proposed here. On the other hand, at difference with what was done in the previous version of this chapter (de Olmos, 1990), the so-called "posterior amygdaloid nucleus" will be considered to be a subdivision (i.e., the posteromedial PM AHi) of now a larger amygdalo-hippocampal transition area (AHi), then recognizing the existence of only the anterior cortical nucleus as previously proposed by Price *et al.* (1987) and later by Price alone (1990). As a consequence, Johnston's (1923) cortical amygdaloid nucleus comes then to lie medio-ventrally to both ACo and AHi. Therefore, it is appropriately named the ventral cortical amygdaloid nucleus (VCo). Furthermore, in Johnston's description of the cortical amygdaloid nucleus, this structure does not seem to encompass what Crosby and Humphrey (1941, 1944) and Lauer (1945) labeled the corticoamygdaloid transition area, or what Humphrey (1968, 1972) later called the amygdalopiriform transition area (APir). By contrast, the "periamygdaloid cortex" of some authors (Rose, 1927; Koikegami, 1963; Mikami, 1952; Price *et al.*,

1987) encloses both the VCo and the amygdalopiriform transition area (APir) as here defined. Against the concept of the periamygdaloid cortex is the fact [shown in the thymidine autoradiographic studies by Bayer (1980) in the rat] that the cortical nucleus shows developmental features coincidental with those of a subcortical or nuclear gray formation. In addition, the neuronal maturation in APir seems to precede that of the surrounding structures (Hilpert, 1928; Brockhaus, 1940; Humphrey, 1968). In my view and in that of several colleagues (Barbas and de Olmos, 1990; Heimer *et al.,* 1999), these facts are compelling enough to permit consideration of APir as a separate anatomical entity from the VCo nucleus and to reaffirm the nuclear (rather than truly cortical) subcortical nature of the so-called periamygdaloid cortex. With these remarks in mind, I recognize in the human amygdala, as in the rat amygdala, four major nuclear groups: laterobasal amygdaloid nuclear complex, extended amygdala, superficial cortical-like olfactory amygdala; and non-assignable amygdaloid formations. By taking into consideration the hodological studies concerning the connectional relationships between the olfactory bulb and the amygdala in the macaque monkey (Turner *et al.,* 1978; Price 1990; Carmichael *et al.,* 1994) and by applying the modifications mentioned above with respect to the parcellation of the superficial nuclei of the amygdala, the superficial cortical-like secondary olfactory amygdala in humans at least will be considered to comprise the following three structures: the anterior (ACo) and ventral (VCo) cortical nuclei and the amygdalopirform transition (APir) areas.

With respect to the so-called medial nuclear group of the amygdala, it should be stressed that a division into medial "main olfactory" and "accessory" subgroups, as in the rat amygdala, does not apply to higher primates, including humans, since these mammals lack an accessory olfactory formation and, therefore, its corresponding fiber projection system, the accessory olfactory tract. This, together with the fact that the medial amygdaloid nucleus (Me) in primates does not seem to receive direct afferent projections from the main olfactory bulb, leaves this nuclear group outside the group of amygdaloid nuclei that are direct recipients of the lateral olfactory tract. In addition, as will be seen below, the Me nucleus is just a part of a major nuclear group, the medial extended amygdala (MExA) that comprises also the medial sublenticular extended amygdala (SLEAM) and the medial division of the bed nucleus of the stria (BSTM). The central extended amygdala group (CExA) consists of the central amygdaloid nucleus (Ce), the central sublenticular extended amygdala (SLEACn), the lateral division of the bed nucleus of the stria terminalis (BSTL), and the interstitial nucleus of the posterior limb of the anterior commissure (IPAC). Adding to either division of the extended amygdala is also medial (BSTSM) and lateral (BSTSL) supracapsular extent of the BST nucleus, respectively.

Although on the basis of structural organization and neurogenetic development (Bayer 1980, Bayer and Altman 1995), the amygdalohippocampal transition area (AHi) will be considered a member of the superficial cortical-like amygdaloid nuclei, this gray formation in humans does not seem to receive direct projections from the olfactory bulb. Therefore, it will be classified here as a putative nonolfactory component of the superficial cortical-like amygdaloid nuclei. However it is not possible to discard that it may receive olfactory information relayed through the superficial cortical-like secondary olfactory amygdala.

The laterobasal nuclear gray complex (LBNC), as mentioned before, is constituted by the lateral (La), basolateral (BL), basomedial (BM), and paralaminar (PL) amygdaloid nuclei and holds a deep juxtaventricular position within the amygdaloid complex. These four main members of the LBNC can in turn be divided into several subnuclei. Finally, the fourth group of amygdaloid nuclei, which includes the amygdalostriatal transition zone (AStr), the granular and parvicellular interface islands, the intercalated masses (ICMs), and the intramedullary griseum (IMG), is not clearly assignable to any particular amygdaloid group although the first two named cell groups have been considered to represent a transition to pallidostriatal formations (Heimer *et al.,* 1999) and the last two cell groups to the extended amygdala (de Olmos, 1969).

DESCRIPTION

This section is concerned with some of the main architectonic and histochemical features that distinguish each of the main nuclei and respective subnuclei, as well as main areas and corresponding subareas that form the amygdaloid body. This description is based on the examination of frontal, sagittal, and horizontal sections of normal human brains as well as macaque *(rhesus* and *fascicularis),* squirrel, and marmoset monkey brains, which were alternatively stained for the demonstration of Nissl substance (thionin, cresyl violet), myelinated fibers (Weigert), neurofibrillary frameworks (Bielschowsky–Gross modifications), acetylcholinesterase (AChE) activity [Geneser-Jensen and Blackstad's (1971) modification of the Koelle method], and heavy metals [Danscher's (1981) modification of the Timm method] or immunostained for neuropeptides such as substance P, somatostatin (SOM), and leu-enkephalin (ENK). It should be stressed here that a

wealth of the human and monkey material processed with the abovementioned histological procedures on which is partly based the present account, was generously placed at the disposition of the present writer by Drs. Lennart Hiemer and George A. Alheid during several visits to their Laboratory of Neuroanatomy in the Department of Neurosugery, Health Sciences Center of the UVA, in Charlottesville. Virginia, USA

Laterobasal Amygdaloid Nuclear Complex (LBNC)

The laterobasal amygdaloid complex constitutes the main part of the amygdaloid body and is regarded as "sensory input" to this structure. It has a very important role in so-called emotional memory and learning, which is particularly important in early developmental stages. It has been proposed that interference with its integrity at this particular time may cause psychiatric problems in later life, like neurosis, phobia, unconscious fear, or panic attacks. Furthermore, it has been established beyond doubt that the amygdala is one of the main sites of action for the clinically important antianxiety and anticonvulsant effects of benzodiazepines, and subsequent studies have shown that it is the basolateral portion of the amygdala (BL) which is critical for the anxiolytic actions of benzodiazepines. Recent studies have also raised the importance of the amygdala in the processing of facial expressions in humans (Morris *et al.*, 1996). Clinical and electrophysiological evidence indicates that the amygdala has an important role in the pathogenesis of the temporal lobe, and it has been demonstrated that γ-aminobutyric acid (GABA) function is disrupted in this condition (Hudson *et al.*, 1993; Wolf *et al.*, 1997).

Lateral Amygdaloid Nucleus (La)

It is clear that the lateral nucleus is the primary entry point for sensory information to the amygdala (Royer *et al.*, 1999; Stefanacci and Amaral, 2000), and although, as will be described shortly, its cholinergic innervation is one of the weakest in the human amygdala, it is the one that is most severely affected in Alzheimer's disease. It is sustained that many of the computations required to perform complex tasks are presumably initiated by the activation of neurons in the La nucleus via sensory inputs from the thalamus and from unimodal and polymodal sensory cortices (Le Doux, 1998). From the La nucleus, the information is conveyed to other amygdaloid nuclei through intra-amygdaloid connections, and finally relayed to motor, endocrine, and autonomic centers that elicit appropriate behavioral responses to sensory stimuli.

On the other hand, it has been reported that the La nucleus undergoes severe damage (mean neuronal loss: 50%) in most patients with temporal lobe epilepsy (Hudson *et al.*, 1993; Wolf *et al.*, 1997). These changes occur independently of any that occur in the hippocampus (Wolf *et al.*, 1997).

Topographical Landmarks The La nucleus is the largest among all the nuclei that make up the human amygdala, both as compared by direct measurements or by allometric procedures (Stephan *et al.*, 1977). It conforms an irregularly shaped, polygonal gray mass that occupies the rostral three fourths and the lateral one-third of the human amygdaloid complex (see Figs. 22.1a,b; 22.2–22.5a, 22.6a, 22.7a, 22.9–22.12). As such, it stretches between a plane cutting –0.6 mm rostrally to the midline crossing the anterior commissure (plane 0.0 mm) to another 10.7 mm caudally to it in Mai *et al.*'s (1997) *Atlas of the Human Brain*. In this manner, the La nucleus occupies approximately three-fourths of the rostrocaudal extent of the amygdala (Darvesh *et al.*, 1998). According to Murphy *et al.* (1987), the La nucleus is, of all of the amygdaloid nuclei, the one that contributes the most to the volumetric asymmetry existing between the amygdaloid nuclear complex of each hemisphere, since the right La nucleus was found significantly larger than its left counterpart.

The La nucleus is flanked laterally and ventrally by the temporal limb of the external capsule that interposes between it and the ventral claustrum [VCl in plates Kl B6 to Kl B9 in Sakamotos *et al.*'s (1999) collection of coronal sections through the human brain or the gray complex conformed by the laterocaudal extension of Mai *et al.*'s (1997) preamygdalar (PACl) and limitans(LiCl) divisions of their claustrum]. Transversally oriented branches of the external capsule detached from the main body of the external capsule also separate the La nucleus from the endopiriform nucleus [En, in the Kl B6 plate of Sakamoto *et al.*'s (1999) series, or the periamygdalar area, PAA, and more medial aspects of the PACl in plates 21–23 of Mai *et al.*'s (1997) atlas] rostrally as well as rostrodorsally. The rostrodorsal lateral pole of the La nucleus is almost completely separated from the main body of the nucleus by descending radiations of the temporal limb of the anterior commissure (Figs. 22.1a,b, 22.2, 22.5a, and 22.6a) giving place to the formation of characteristic cells columns that constitute what Brockhaus (1938) denominated the pars limitans of the amygdaleum profundum laterale, or Apl. More caudally the La nucleus is bordered by the amygdalostriatal transition zone [AStr, plates 26–30 of Mai *et al.*'s (1997) atlas]. Medially, the lateral medullary lamina separates the La nucleus from the basolateral amygdaloid nucleus (BL). Ventrally and rostrally small fascicles of fibers separates

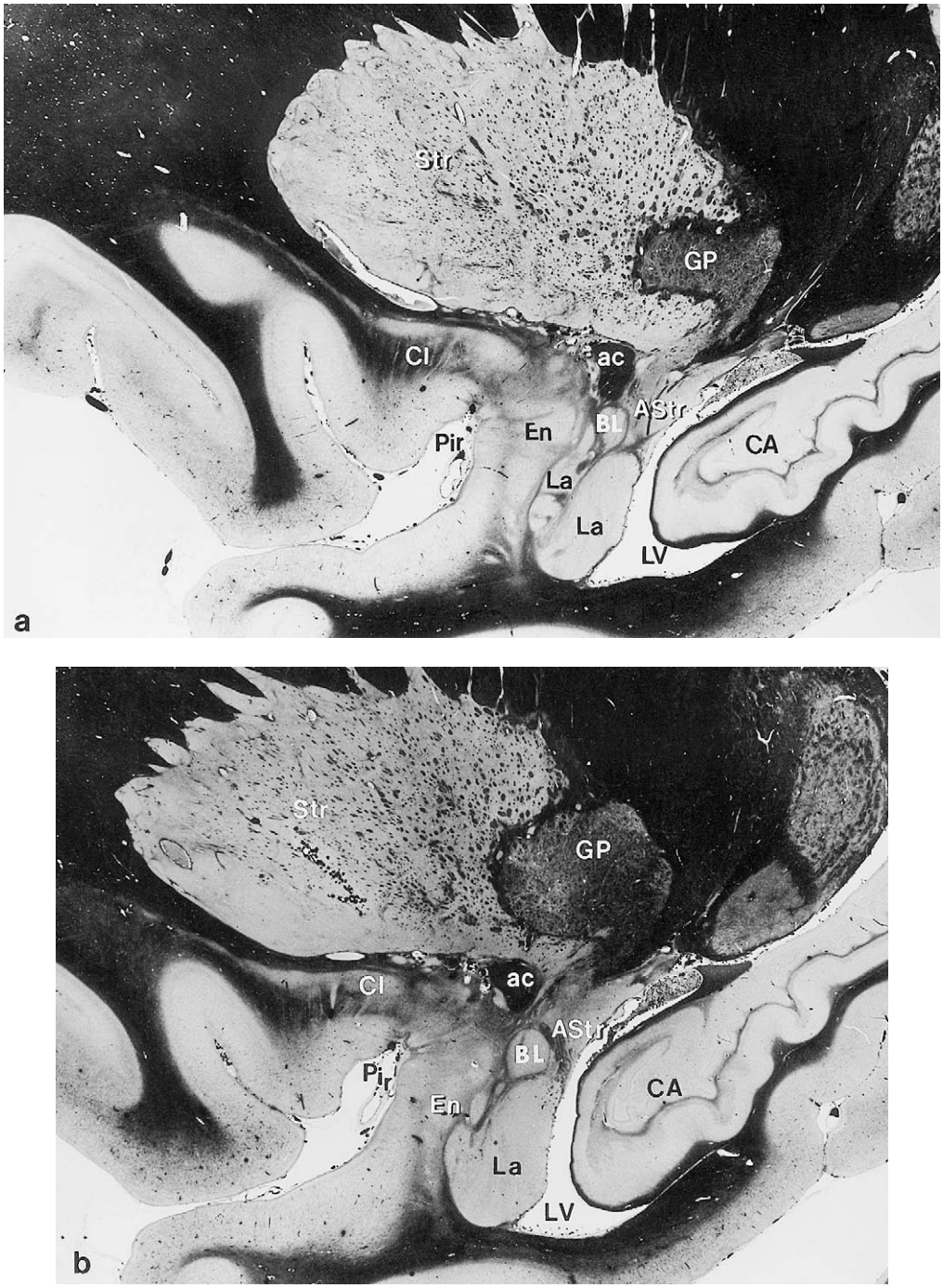

FIGURE 22.1 (a) Low-power photomicrograph of a sagittal section through the dorsal anterior portion of the lateral amygdaloid nucleus (La) showing its topographical relationships with the claustrum (Cl) rostrally, with the striatum (Str) and the amygdalostriatal zone (AStr) dorsocaudally, and the inferior horn of the lateral ventricle (LV) caudally. A fiber capsule surrounds the DL BL underneath the temporal limb of the anterior commissure (ac). (b) A more medial sagittal section showing the topographical relationships of the amygdaloclaustral area (ACA) with the basolateral amygdaloid nuclear group (BLNG) caudally, with the endopiriform (En) dorsally and ventrally, and the piriform cortex (Pir) rostrally. Even at this magnification the lobulations in the ventrolateral subdivision (VL) of the lateral amygdaloid nucleus (La) (white arrow) can be appreciated.

Continued

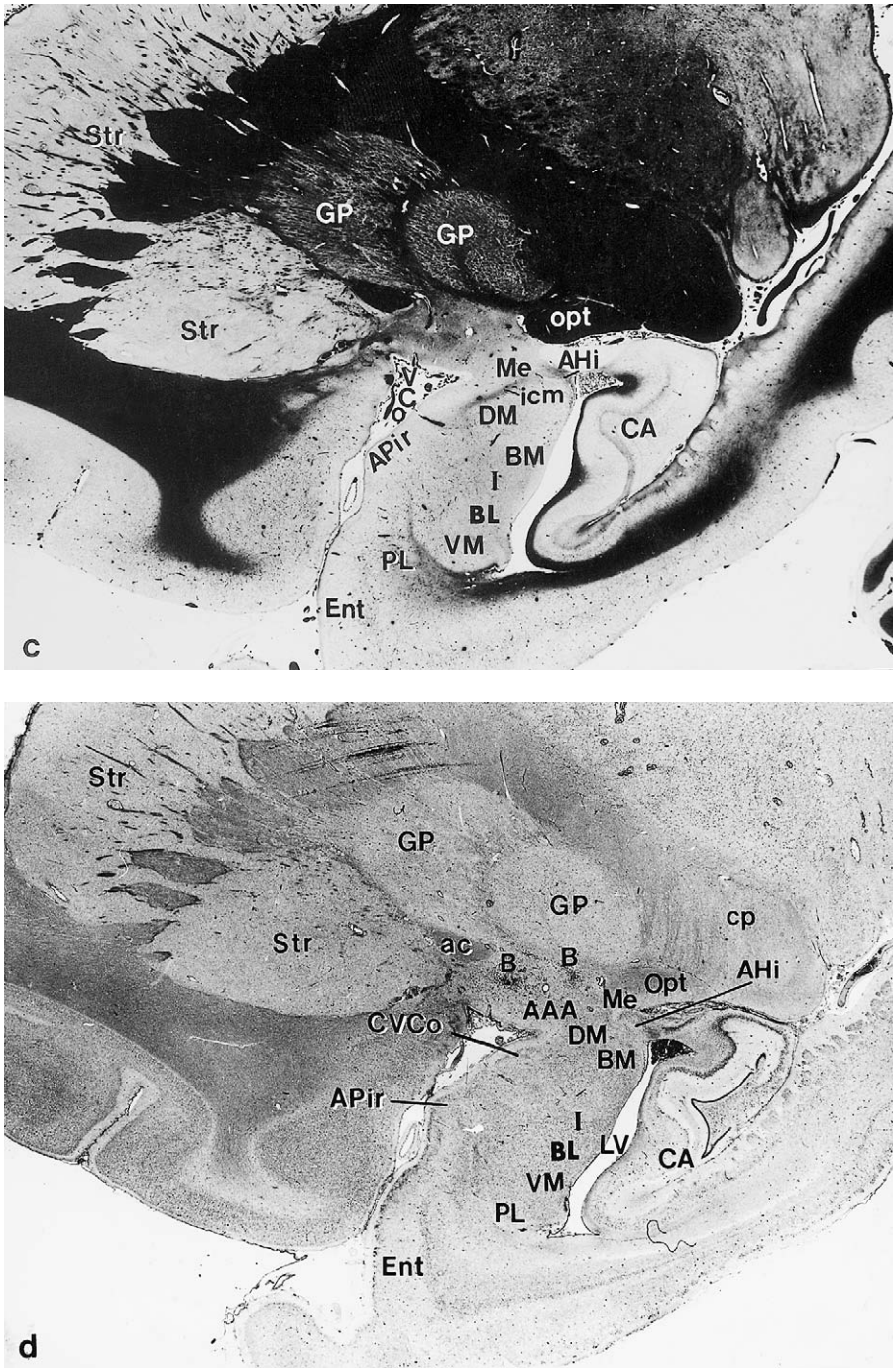

FIGURE 22.1 cont'd (c) A sagittal section close to the junction of the temporal pole with the basal telencephalon showing the intermediate caudomedial fiber masses (icm) as they form an oblique caudally coursing bundle in the interface between the superficial superior subdivision of caudal ventral cortical amygdaloid nucleus (CVCo) and medial amygdaloid nucleus (Me), on one side, and the deep lying dorsomedial division of BM (DM BM) on the other side. In the middle third of the basolateral nuclear group (BLNG) a densification marks the transitional region between the medium-celled I BL and the small-celled VM BL. Just rostral to it, the amygdalopiriform transition area (APir) forms a small eminence. (d) A Nissl-stained sagittal section cut approximately through the same plane as (c). Divisions of the nucleus basalis of Meynert (B) marks the approximate dorsal boundary of the Me and AAA.

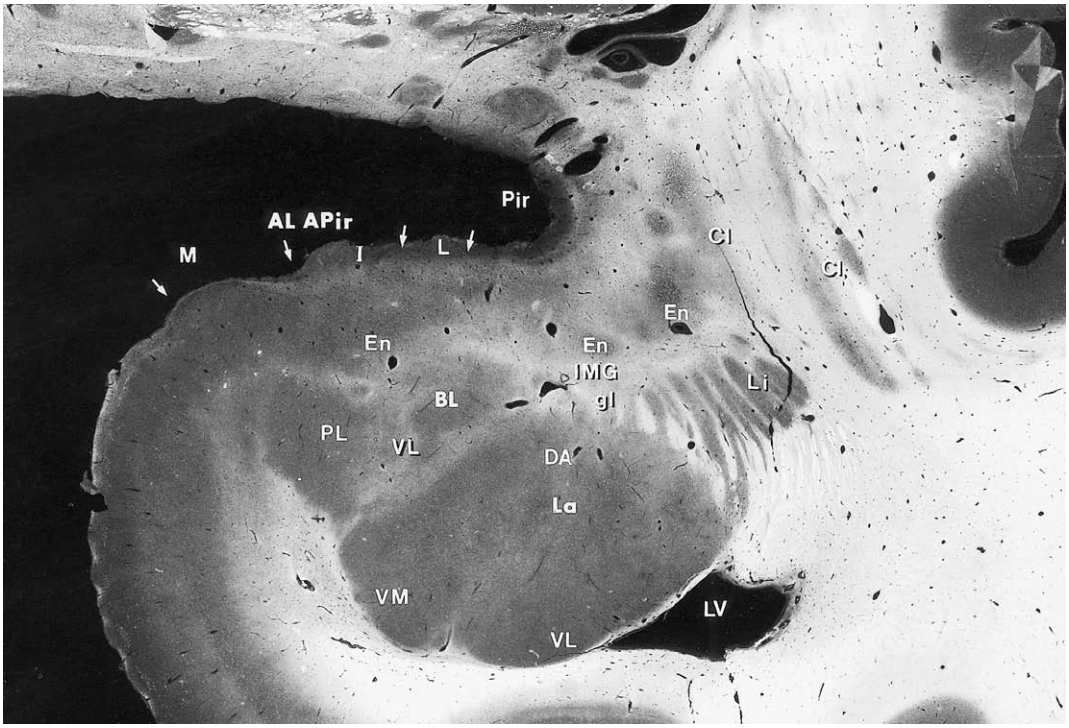

FIGURE 22.2 The human amygdala cut longitudinally at the rostral end of the BL to show the caudal sectors of the anterolateral APir and the expansion of PL BL as well as the broomlike arrangement of the limitans divisions of the La and its topographic relationships to the endopiriform-claustrum complex. The figure, like Figures 22.3–22.8, were prepared by projecting the image from a fixed, unstained, wet-mounted section onto a panchromatic photographic paper. This procedure displays all the medullary laminae separating the different gray nuclei of the human amygdala.

the La nucleus from island-like gray formations that constitute the lateral glomerular division of the paralaminar amygdaloid nucleus (PLgl) which is not delineated in Mai *et al.*'s (1997) atlas but can be found clearly depicted in de Olmos' (1990) Figure 22.5a. More caudally the La nucleus the ventral border of the lateral nucleus forms part of the roof of the temporal horn of the lateral ventricle (TLV, Plates 27–29 of Mai *et al.*'s atlas).

Cytoarchitectonics The La nucleus is made mostly of medium-sized to large neurons (Fig. 22.12), but it also includes within its neuronal population neurons of smaller size that become more numerous toward the ventricle. This feature, together with some correlative variability in the body shape and width of the fields covered by the branches of their dendritic trees, provides the nucleus a very characteristic cytoarchitectonic feature. By contrast, the glial cell population becomes more abundant away from the ventricle, i.e., rostrodorsally and parallel with an increase in the density of medullary nerve fibers. Horizontal and sagittal sections through this nucleus confirm an increased neuroglial density toward the ventricle, an arrangement already stressed by Brockhaus (1938).

As pointed out by Sorvari *et al.* (1995), the neuronal population in La is very heterogeneous even though they choose to reduce drastically its subdivision to just medial and lateral subdivisions in order to make it fit with that proposed by Price *et al.* (1995) for the monkey. However, according to the comparative appraisal of Koikegami (1963), who refers specifically to the findings reported by Mikami (1952), Sasagawa (1960a, b, 1961) and Koikegami (1963), the existence in this nucleus of a less simple grouping becomes meaningful when considering that some of the subdivisions that can be recognized in the human amygdala are not present in the monkey; such absences may have connectional implications. For this reason it seems necessary to insist on applying full fibro- and cytoarchitectonic criteria as well as topographical landmarks in describing the architectonical arrangement of La, and as a consequence to subdivide the nucleus, as was previously done (de Olmos, 1990), into five subnuclei: dorsal anterior (DA La), intermediate (I La), ventral [divisible into lateral (VL La) and medial (VM La) parts], dorsomedial

(DM La), and dorsolateral (DL La). On a similar basis, the broken-up laterorostral extension of DL La, on account of its close neighborhood with the claustrum and related grisea, merits to be labeled as the limitans (Li La) subdivision of La. The comb like appearance of Li La, the lobular disposition of VL La, and the tightness of the cells in DM La characterize well to all these subdivisions, as clearly as does the larger size of the neurons in DL La, the medium size of those in I La, and their smallness in VM La.

Fibroarchitectonics In myelin preparations the La nucleus appears as a poorly fibered nucleus, although in its caudomedial aspect a moderate number of myelinated fibers oriented in a dorsolateral to ventromedial direction [Brockhaus' (1940) fascicles laterales] traverse the nucleus, becoming more numerous near the lateral medullary lamella [lml] but decreasing in number and thickness rostrally. Numerous myelinated fibers cross the dorsolateral aspect of the La nucleus following a ventrolateral direction to join the white matter of the temporal lobe. The different subdivisions of La can also be distinguished in myelin preparations though not as clearly as in cell preparations. Thus, the dorsal anterior La subdivision can he distinguished from the intermediate La subdivision by a somewhat richer plexus of myelinated fibers. The ventral La subdivision has even fewer fibers than the dorsal and intermediate subdivisions of the La nucleus, and these fibers become less numerous at the level of its superficial lobulations, where the plexuses of myelinated fibers become more rare. In coronal sections stained with reduced silver for normal fibers, the neuropil formed by a dense network of fine fibers appears more homogeneously distributed except in the medial aspect of the intermediate (La I) and ventromedial (La VL/VM) subdivisions of the La nucleus, where fiber bundles of different thickness oriented in a dorsoventral direction can be seen. On the other hand, an abrupt change in fiber density at the level of the PL nucleus helps to identify the boundary between this latter and the ventral subdivisions of the La nucleus.

Chemoarchitectonics

Cupric Silver Stain In cupric silver preparations the La nucleus in macaque and squirrel monkeys, the La nucleus proper does not show, either in its neuropil or in its neuronal population, any argyrophilic reaction of the type seen at the level of the central division of the extended amygdala. However, at the boundary that separates the La nucleus from the striatum, which is lined by small to medium-sized spindle-shaped neurons with their main axis parallel to the boundary line, a granular argyrophilic neuropil is present extending along this interface.

Heavy Metals In Timm/Danscher's preparations of the marmoset monkey brain, the La nucleus shows a differential distribution of the silver disulfide precipitate which, though increasing in density from comparatively poorly labeled dorsolateral polar sectors of the nucleus, reaches very high levels in the medial, ventral, and caudal sectors of nucleus corresponding to approximately two-thirds or more of its extent. While in this latter aspect of the nucleus the silver sulfide precipitate shows a rather homogeneous distribution with very few profiles showing a rail-rod-like arrangement, this type of disposition becomes predominant in the above-mentioned rostrodorsolateral sectors of the nucleus (Fig. 22.23b). As happens in other amygdaloid nuclei showing this type of reaction, the neuronal perikarya remain free of precipitate.

Neurotransmitters

CHOLINERGIC MARKERS

ACETYLCHOLINESTERASE (ACHE) The neuropil of the La nucleus presents a generally weak to moderate AChE staining throughout its extent with an almost complete disregard for its cytoarchitectonic complexity (see also Sims and Williams, 1990; Emre *et al.,* 1993; de Olmos, 1990; Sorvary *et al.,* 1995; Heimer *et al.,* 1999). Such weakness and rather even staining contrasts sharply with the dense and nonhomogeneous reaction in the adjacent BL nucleus. The neuronal population in general remains unstained. However, Nitecka and Narkiewicz (1976) stressed that the AChE staining in the La nucleus varies topographically, with the intensity of the reaction decreasing in an anteroposterior direction, an observation that has been confirmed by other authors (Darvesh *et al.,* 1998; de Olmos, 1990; Simms and Williams, 1990). On the other hand, Svendsen and Bird (1985) were able to detect in *my* material a moderately stained ventral region that contrasted with a more lightly stained dorsolateral one. Finally, Darvesh *et al.* (1998) reported the detection of isolated small and medium-sized AChE-positive neurons with fusiform or triangular profiles which were loosely distributed within La.

CHOLINE ACETYLTRANSFERASE (CHAT) According to Emre *et al.,* (1993), the human La nucleus shows, in comparison with other amygdaloid nuclei, a low density of ChAT-ir fibers. Most of them are thin and varicose, whereas others are thick and straight. Although the general distribution of the ChAT-ir in these nucleus seems to match that of the AChE quite closely, its overall density appears to be somewhat higher in the posterior part of the nucleus. There are also patches with a higher density of ChAT-ir fibers.

In the macaque monkey, the La nucleus contains the lowest density of ChAT of all the deep amygdaloid

nuclei, and only the sector that has been labeled as Lvl shows appreciable staining for this enzyme. Occasional ChAT-positive neurons are found in the monkey La nucleus, but it corresponds to point out that within the area traversed by *fibers* that run along the lateral aspect of the nucleus ChAT-positive neurons can be found (Amaral and Basset, 1989), which would go along with the Lopez-Gimenez *et al*. (2001) findings according to which there is no specific signal for ChAT mRNA in this nucleus.

Irrespective of this apparent discrepancy in the distribution of the cholinergic markers, the point has been made that in Alzheimer's disease the La nucleus appears to display a more severe loss of ChAT-positive profiles than most other amygdaloid nuclei (Emre *et al*., 1993).

EXCITATORY AMINO ACIDS

GLUTAMATE (GLU) Retrograde tracing experiments made in rats using tritiated D-aspartate indicate that a considerable number of the La neurons would be source of GLU/ASPergic projections to the nucleus accumbens and olfactory tubercle (Fuller *et al*., 1987). According to Amaral and Insausti (1992), in the macaque monkey, injections of tritiated D-aspartate in the basal amygdaloid nucleus resulted in labeling of many scattered neurons throughout the La nucleus providing arguments for inferring that this nucleus would be a source of GLU/ASPergic intra-amygdaloid projections to the above-mentioned nucleus, giving further support to the concept that at least many of the extranuclear efferent projections originated from this nucleus are of a GLU/ASP nature.

On the other hand, this nucleus seems to be the target of GLU/ASPergic afferent projections coming from cortical fields after injections of tritiated D-aspartate in the medial aspect of the La nucleus, which also included the lateral aspect of the magnocellular basal lateral nucleus. Among the cortical areas involved in these projections are neurons in layers 5 and 6 of the entorhinal cortex, and neurons in layers 3 and 5 of the parainsular area, insular proper (agranular, disgranular, and granular), caudal portion of area 13a, area 13, cingulate areas 25 and 24, perirhinal areas 35 and 36, area TF, etc.

INHIBITORY AMINO ACIDS

γ-AMINOBUTYRIC ACID (GABA) No information is so far available until now about the distribution of this neurotransmitter for the human amygdala. According to Pitkänen and Amaral (1994), in the monkey amygdala the La nucleus shows the highest density of GABA-ir cells among the deep amygdaloid nuclei. These types of cells are distributed throughout the nucleus and with no obvious difference in distribution or density of the GABA-ir cells in the ventrolateral and dorsomedial divisions of the nucleus. In the La nucleus, and throughout the amygdala, the GABA-ir cells tend to be organized in small clusters separated by acellular regions. A gross estimate indicated that they account for approximately 20% of the neuronal population in the La nucleus. On the other hand, the GABA-ir fibers and terminals in the La nucleus are more densely distributed than in any other nucleus of the LBNC. The ventrolateral sector of the La nucleus apparently has a higher density of GABA-ir punctate neuropil and many non-ir neurons surrounded by GABA-ir varicosities.

MONOAMINE MARKERS

DOPAMINE β-HYDROXYLASE (DBH) According to Sadikot and Parent (1990), in the squirrel monkey the La nucleus displays light DBH-ir.

SEROTONIN (5-HT) According to Sadikot and Parent (1990), in the squirrel monkey, in the La 5-HT-ir is dense in the rostral one-third and moderate to dense in the caudal two-thirds, with 5-HT-ir terminal labeling being denser in the dorsolateral aspect of the nucleus.

TYROSINE HYDROXYLASE (TH) According to Pearson (1990) in the human amygdala, the La nucleus has a moderate network of catecholaminergic axons. In general, the TH-ir innervation diminishes anteriorly.

In the squirrel monkey, Sadikot and Parent (1990) describe for the La nucleus a dense terminal TH-ir in its rostral third, and density that remains heavy in its middle third except for a dorsomedial area of light density of varicose TH-ir fibers. At its caudal third, the La nucleus of the squirrel monkey shows a light density of varicose TH-ir fibers in all but its most dorsolateral aspect, where dense TH-ir can be seen.

NEUROPEPTIDES

CHOLECYSTOKININ (CCK) According to the findings by Savasta *et al*. (1990) in the human amygdala, the concentration of neurons containing cholecystokinin (CCK) mRNA was higher in this nucleus than in the BL, BM, or PL nuclei. In the macaque monkey, Sadikot *et al*. (1988) described the presence of CCK-ir fibers and CCK-ir cells bodies in the La, more particularly in its ventral subdivisions.

CHROMOGRANIN B According to Marksteiner *et al*. (1999), the human La nucleus contains a high-density PE-11-like ir consisting of varicose fibers with mixed-size varicosities. No PE-11-like ir neurons are present.

CORTICOTROPIN-RELEASING FACTOR (CRF) Although the La nucleus presents only a sparse population of

small CRF-ir bipolar cells, a significant reduction in the number of CRF-ir fibers have been reported to occur in AD (Powers *et al.*, 1987). On the other hand, highly dense plexus of corticotropin-like intermediate lobe peptide (CLIP) containing fibers with large varicosities and terminals could be detected in this nucleus (Zaphiropoulos *et al.*, 1991).

ENKEPHALIN (ENK) According to Piorio *et al.* (1990), the human La nucleus, like the rest of the LBNC, contains only lightly stained delicate networks of varicose fibers.

GALANIN (GAL) According to Kordower *et al.* (1992), in the macaque monkey amygdala this member of the LBNC, like all of its remaining components, does not contain GAL-ir cell bodies and few if any GAL-ir fibers.

NEUROTENSIN (NT) In the human La nucleus the density of the NT–ir is sparse and is made up exclusively of fibers since no NT-ir neurons could be detected. These NT-ir plexus in the La nucleus is made up of a mixture of both fine and coarsely-beaded fibers, which are more abundant in the ventral than in the dorsal regions of this nucleus (Benzing *et al.*,1992).

NEUROPEPTIDE Y (NPY) According to Mai *et al.* (1990), NPY-ir cells and fibers were numerous in the human La nucleus. As in the other members of the LBNC, NPY-ir cells appeared to be concentrated in dorsal regions of the nucleus, while the reverse is true concerning the distributions of NPY-ir fibers and terminals.

In the macaque monkey, the La nucleus would contain, broadly speaking, a moderate amount of NPY-ir neurons, with the highest concentration occurring in the dorsal portion of La. The NPY-ir neurons closely resemble SOM-ir neurons, which coincides with the extensive colocalization that is taking place in the monkey La amygdala. Both spiny and spine-sparse types (ovoid or fusiform) of neurons of diverse sizes exhibit NPY/SOM-ir, and they are thought to be a local circuit of neurons contributing to the formation of the peptide-containing neuropil present in the nucleus. Spiny NPY-ir and/or SOM-ir neurons appear primarily in the dorsal part of the La nucleus. As with other amygdaloid nuclei, the La nucleus contains NPY-ir fibers and puncta, which are particularly abundant in its ventral third while of moderate concentration in the remaining dorsal sectors.

SECRETONEURIN (SCR) The La nucleus shows rather poor if any SCR-ir either in its neuropil or in perikarya (Marksteiner *et al.*, 1995).

SOMATOSTATIN (SOM) In the human brain, Mufson *et al.* (1988) reported the presence of SOM-ir neurons in the La nucleus, but they did not provide further detail on the distribution pattern of cells and fibers within the nucleus. Bouras *et al.* (1987), in turn, described rather low densities of SOM-ir cell bodies and low to medium concentrations of SOM-ir fibers and terminals at the level of all the subdivisions of the amygdaloid body, but without giving more comprehensive data.

According to McDonald *et al.* (1995), the La nucleus in the amygdala of the macaque monkey would contain numerous SOM-ir neurons, but in the ventral portions of the nucleus where they outnumber the NPY-ir neurons. The dorsal part of La can be differentiated from the other amygdaloid nuclei because it is the only sector of the amygdala that contains a large population of SOM-ir neurons that do not exhibit NPY-ir.

In the squirrel monkey, the La nucleus shows a light to moderate SOM-ir in its neuropil with a ventrodorsal decreasing gradient. SOM-ir perikaria are abundant but increase in number caudally and toward its border with the large-celled BL nucleus (Desgardins and Parent, 1992).

SUBSTANCE P (SP) According to Piorio *et al.* (1990), the La nucleus, like in the rest of the LBNC except for their dorsal magnocellular part of the accessory basal nucleus (DM/CM BM, here), contains few scattered SP-ir neurons together with branching fibers and punctate material.

BRAIN–DERIVED NEUROTROPHIC FACTOR (BDNF) According to Murer *et al.* (1999), in the human amygdaloid complex all of their nuclear components show BDNF-ir neurons and fibers, but in contrast with the rest of the La nucleus contains abundant neurons with an intense cell body ir within a lightly ir plexus.

ENZYMES

ANGIOTENSIN-CONVERTING ENZYME (ACE) According to Chai *et al.* (1990), the La nucleus, in contrast to its immediate neighbor (the BL nucleus), shows a rather low binding level for ACE.

BUTYRYLCHOLINESTERASE (BUCHE) The lateral nucleus also contains numerous BuChE-containing neurons. Most of these neurons are medium sized to small and have round fusiform or triangular profiles and can be found throughout the rostrocaudal and dorsoventral extent of the nucleus. Some of these neurons have multiple branching processes that could be followed for a distance up to 150 µm from the cell body. These BuChE-positive neurons constitute approximately an 8% of the total neuronal population of the La (Darvesh *et al.*, 1998).

NICOTINAMIDE ADENINE DINUCLEOTIDE PHOSPHATE DIAPHORASE (NADPH-D) According to Sims and Williams (1990), in the human amygdala the NADPH-d staining is light and multipolar Golgi like cells are scattered throughout Li La (their pars externa). The DL/I/VL subdivisions (their lateral subdivision) would contain weakly stained, mostly pyramidal-shaped NADPH-d-containing neurons, but also a few bipolar ones. In the DM La (their dorsal subdivision) as well as in the VM La (their medial subdivision), the NADPH-d-containing neurons would present a similar immunoreactivity. In the La nucleus of the macaque monkey (Sorvari *et al.*, 1995), the NADPH-d-containing neurons show a similar appearance in all of its subregions, their perikaria being predominantly medium sized and presenting fusiform or stellate shape from which extend bipolar or multipolar dendrites. Furthermore, although they show a relatively homogeneous distribution, their presence is more prominent in the DL subdivision of the nucleus. As in other members of the laterobasal nuclear group, the La nucleus displays a very densely stained network of NADPH-d fibers and terminals (see also Brady *et al.*, 1992). This staining pattern is very similar to that observed in the squirrel monkey (*Saimiri sciureus*) (Brady *et al.*, 1992; Unger and Lange, 1992). Sorvari *et al.* (1995) estimated that in the monkey La nucleus, the multipolar NADPH-d-containing neurons in DL/Li/VL subdivisions closely resemble the type 2 multipolar PAV-ir neurons described by Pitkänen and Amaral (1993).

P450 AROMATASE (P450 AROM) According to Roselli *et al.* (2001), in the macaque monkey amygdala, the La nucleus presents a lesser expression of this enzyme than other amygdaloid nuclei, more particularly the superficial ones.

CALCIUM-BINDING PROTEINS

CALBINDIN-D28K (CAL) According to Sorvari *et al.* (1996b), the La nucleus has a moderate density of CAL-ir neurons. The density of CAL-ir neurons appears to be higher in the DM/VM La (their medial division) than in the DL/I/VL La (their lateral division). Morphologically, a large majority of the CAL-ir neurons in La belong to what they call the type 1 category, but numerous type 2 cells and a few type 3 cells were also reported. Typically, the primary dendrites emanating from the soma of immunopositive neurons were thin and straight and branched near the soma, giving off few secondary branches. Also, according these authors, the La nucleus contains a moderate to high density of CAL-ir fibers and terminals. In accordance with the density of the calbindin cells, the fiber and neuropil staining was higher in the DM/VM La than in the DL/I/VL La. The density of neuropil labeling in the La nucleus is, however, one of the lowest in the amygdala. (For more details, the reader is referred to the original paper by Sorvari *et al.*, 1998b.)

CALRETININ (CR) The density of CR-containing neurons in the La nucleus is considerably higher in its so-called medial division (i.e., DM/VM subdivisions of the present account) than in the lateral one (i.e., LD/Li/LV of the present account). Most of the neurons were small type 1 cells (i.e., small multipolar cells with typical spherical somata provide 3–11 dendrites of about equal thickness). The La nucleus, particularly its medial (DM/VM) subdivision, contains a high density of CR-ir fibers and terminals that are located near the clusters of CR-ir neurons. Thick varicose CR-ir fibers are found in the dorsal part of the La nucleus, probably fibers of passage. Finally, there is a gradient in the density of the neuropil so that it is low rostrally but increases lightly caudally. On the other hand, an analysis of the immunohistochemical data by Sorvari *et al.* (1996a) induces them to conclude that CR-ir and PAV-ir cells in the human amygdala constitute different subpopulations of nonpyramidal neurons. In another study, Sorvari *et al.* (1998a) were able to show that CR-ir terminals make synapses onto CAL-Dk28-ir neurons in the La nucleus. All synapses resemble symmetrical synapses (type II of Gray), which are typical of inhibitory synapses; this harmonizes with the fact that virtually all of the Cal-ir neurons in the La nucleus show morphological characteristics of local interneurons (Braak and Braak, 1983; Sorvari *et al.*, 1996a).

PARVALBUMIN (PAV) According to Sorvari *et al.* (1995, 1996c), the La nucleus has the highest density of PAV-ir neurons in the entire amygdala. Also, all the different types of PAV-containing neurons are present here. However, the PAV-ir neurons are unevenly distributed in the La nucleus. Their lateral division, which would include the DL, VL, and Li subdivisions in the present account, particularly its dorsal half, has a higher density of PAV-ir cells than their medial division, i.e., the DM, I, VM subdivisions of the present account. This nucleus also shows a high density of PAV-ir fibers and terminals and, as it happens with the PAV-ir neurons, their density is higher in their lateral division. In fact, the DL/Li shows, together with DL/D subdivisions of the BL nucleus, the highest density of PAV-ir fibers and terminals in the human amygdaloid complex. Furthermore, although the fiber density was lower in BM/I/VM, it was always higher in the VL/VM subdivisions of the adjacent *BL* nucleus. The DL/Li/VL subdivisions also contained a very large number of PAV-ir terminal cartridges than the medial subdivisions. This is also true for the pericellular

baskets, which, on the other hand, are more abundant in the dorsal sectors of the nucleus. It should be stressed that in recent studies in the human amygdala it was shown that PAV-ir terminals make synaptic contacts on the axon initial segments and somata of pyramidal cells (Sorvari *et al.*, 1996).

OTHER PROTEINS

DOPAMINE- AND ADENOSINE 3',5'-MONOPHOSPHATE (CAMP)–REGULATED PHOSPHOPROTEIN OF M, 32 KDA (DARPP-32) AND PHOSPHATASE INHIBITOR According to Barbas *et al.* (1998), in the macaque monkey, the DARP-32-ir and I-1-ir neurons are restricted to the ventral third of the La nucleus in some levels but extended up to the ventral half at other levels. Other parts of the nucleus contained fewer and more moderately stained DARPP-32-ir neurons. Among them, the dorsomedial third of the La nucleus contains few of this type of neuron but spares the dorsolateral sector. Though the distribution is similar for the two phosphoproteins, I-l-ir neurons can also be seen laterally.

DOPAMINE TRANSPORTER (DAT) The La nucleus, like the BM nucleus, presents markedly fewer DAT-containing axons than BL, although the DL region of the lateral had a higher density of axons than the rest of the subnucleus (Ciliax *et al.*, 1999).

LIMBIC SYSTEM–ASSOCIATED MEMBRANE PROTEIN (LAMP) According to Côté *et al.* (1996) in the macaque amygdala, LAMP-ir is very weak in the La nucleus. At midamygdaloid levels, the ventral one-third of the La nucleus shows intense LAMP-ir, and this staining is continuous medially with that of the small-celled division of the BL nucleus. In the caudal third of the La nucleus, the entire ventral half of this nucleus displays LAMP-ir that is as intense as that in the adjoining BL nucleus. At this level, the dorsal part of the La nucleus is devoid of LAMP-ir.

SMI32 NEUROFILAMENT PROTEIN (SMI32-IR) From the low magnification atlas published by Petrides *et al.* (2000), it seems that dorsal sectors of La contain some SMI32-ir.

RECEPTORS

ADENOSINE RECEPTOR (A–R) According to Svenningsson *et al.* (1997), the La nucleus contains a high concentration of A1 receptors, a potent modulator of cholinergic neurotransmission. No mention is made about the presence of A_2 receptors in this nucleus.

BENZODIAZEPINE RECEPTOR (BNZ-R) According to Zezula *et al.* (1988), the human La nucleus contains very high concentrations of BNZ-R.

CHOLINERGIC RECEPTORS

MUSCARINIC RECEPTOR (MACH-R) According to Cortés *et al.* (1987), the human La nucleus, in sharp contrast with the ICMs that surround it, presents one of the lowest densities in mACh-R.

GABAERGIC RECEPTORS (GABA-R)

GABA A /β 2 AND 3 SUBUNITS/BENZODIAZEPINE RECEPTOR (GABA A-R) In the macaque monkey, the neuropil of the La nucleus exhibits very dense immunoreactivity for the GABA A-R. This ir is also seen in neuronal perikarya and dendrites where it is localized to the cytoplasm and/or surface membrane. The cell type with the strongest ir is a subpopulation of small non-pyramidal neurons that had numerous thin dendrites. Other larger nonpyramidal neurons are also stained. In its whole, GABA A-R-containing neurons compose approximately 14% of the neuronal population of La (McDonald and Mascagni, 1996).

MONOAMINERGIC RECEPTORS

ADRENORECEPTOR α_1 According to Flügge *et al.* (1994), in the tree shrew, the La nucleus shows a strong binding of [^{3}H]PRA, an α-adrenoreceptor antagonist that indicates the presence of this type of adrenoreceptors.

ADRENORECEPTOR α_2 According to Flügge *et al.* (1994), in the tree shrew, the La nucleus shows a low number of [^{3}H]rauwolscine (α_2-adrenoreceptor antagonist) binding sites. The labeling in the La nucleus is nonuniform with a high number of binding sites at rostral levels and no binding sites at caudal ones.

SEROTONINERGIC RECEPTORS (5-HT-R)

SEROTONIN 2A RECEPTOR (5-HT_{2A}-R) According to Lopez-Gimenez *et al.* (2001), the dorsomedial subdivision of the La nucleus contains high densities of 5-HT_{2A} receptors.

NEUROPEPTIDE Y RECEPTOR (NPY-R) Double-labeling studies have found coexpression of NPY mRNA with the NPY-R2 but not with the NPY-R1 (Caberlotto *et al.*, 2000).

OPIOD RECEPTOR μ In the amygdaloid complex of cinomolgus monkeys, moderate to sparse densities of opioid receptors μ are distributed throughout the rostrocaudal extent of the dorsal sectors of the La nucleus, whereas much higher concentrations appear in the ventral sectors. Within the latter sectors, heavier concentrations are apparent in the posterior two-thirds of the La nucleus than in the anterior one-third (Daunais *et al.*, 2001). An approximately similar distribution pattern has been reported for the human La (Pilapil *et al.*, 1986; Quirion *et al.*, 1995), in which very

dense concentrations of μ receptors have been also observed in this sector. It should be mentioned than in humans, the μ receptors have been characterized with positron emission tomography, and, consistent with *in vitro* studies, high levels of ligand binding were found in the amygdala (Frost *et al.,* 1989). Moreover, the levels of opioid μ receptors in the amygdala have been shown to fluctuate with changes in circulating estradiol levels (Smith *et al.,* 1998), function of age and gender (Zubieta *et al.,* 1999), and in psychiatric (Mayberg *et al.,* 1991; Zubieta *et al.,* 1996) and neurological (Madar *et al.,* 1997) disease states.

At this point, it should be recalled that the ventral portions of the lateral nucleus have extensive connections with the small-celled VL/VM subdivisions of the BL as well as with the BM nucleus (Pitkanen and Amaral, 1998), each of which contains dense concentrations of μ binding sites. In contrast, the ventral small-celled La has few connections to the magnocellular sectors of both BL and BM, and with the central nuclei (Pitkanen and Amaral, 1998), each of which contains low levels of μ-receptor binding sites.

STEROID RECEPTORS

ESTROGEN RECEPTOR α (ER-α) According to Österlund *et al.* (2000), low ER-α mRNA labeling can be detected in the human La.

Basolateral Amygdaloid Nucleus (BL)

Pharmacobehavioral investigations in the 1970s indicated that the amygdala is one of the main sites of action for the clinically important antianxiety and anticonvulsant effects of benzodiazepines. Subsequent studies have shown that it is the basolateral portion of the amygdala (BL) that is critical for the anxiolytic actions of benzodiazepines.

Topographical Landmarks The basolateral amygdaloid nucleus (Figs. 22.1–22.12) [lamina 23 to lamina 32 (1.3–13.3 mm of Mai *et al.* (1997), *Atlas of the Human Brain*] lies medially but also dorsomedially to the La nucleus from which it is separated, throughout most of its extent, by a thin medullary lamina [lateral medullary lamina (lml)]. This nucleus occupies the central and the ventral third of the LBNC enclosing laterally and ventrally the BM amygdaloid nucleus from which it is separated by another septa of myelinated fibers, the medial medullary lamina (mml). In transverse sections cut at midcoronal levels of the amygdaloid gray complex, it stands out clearly from surrounding gray masses on account of its hook-like appearance (Figs. 26–28 of Mai *et al.,* 1997, *Atlas of the Human Brain*; Figs. 22.5a, 22.7b, 22.11, 22.4, 22.5, 22.6, 22.7a, 22.9, 22.10). Rostrally, however, this characteristic arrangement is lost, and the nucleus becomes then less clearly definable in part by reason of a looser arrangement of its cell components. Nevertheless, in both horizontal and sagittal unstained transilluminated sections, as well as on equally oriented sections stained with Weigert or reduced silver stain, it is possible also to appreciate its clear separation from surrounding rostrally located basal forebrain grisea by the interposition of dense fiber septa. Much less clearly definable is its separation from the paralaminar (PL) nucleus, more particularly at the level of its boundary with the medial division of this latter griseum. However, the existence of such separation is not only suggested by the presence of small collections of finely myelinated fibers in the interface between both cell aggregations and by the more transparent background of the PL divisions, but more specially by the larger size of the neuronal constituents of the BL VM subdivision.

Cytoarchitectonics Based on a stepped reduction of the cell size and stain ability as well as on a parallel increase in cell density, three major divisions can be recognized: large-celled dorsal (BL D), medium-celled intermediate (BL I), and small-celled ventral (BL V). An extreme dorsolateral extension of the dorsal division of the BL nucleus, which appears in many coronal sections as seemingly separated from the rest of the cell mass of this nucleus, has been referred to as the dorsolateral (DL) part (de Olmos, 1990) of the BL nucleus, even though it was admitted that its cytoarchitectonic features were entirely similar to that of the main dorsal division. Ventrally a different situation can be appreciated where the larger size and denser disposition of the neuronal perikarya in the medial sectors of the BL V division justifies its subdivision into lateral (BL VL) and medial (BL VM) subparts. This latter subdivision probably corresponds to the amygdaloideum profundum ventrale pyramidale of Brockhaus (1938).

Fiberarchitectonics In both myelin- or silver-stained sections the BL nucleus is characterized by the presence of numerous small bundles of fibers, most of them running diagonally in a dorsalateral to ventromedial direction which provides the nucleus a radiate appearance (Fig. 22.7). These bundles of fibers become denser medially at the level of the BL I division of the nucleus. The background network of fine fibers present throughout the nucleus is, however, less dense than that in the La nucleus or, more particularly, in the BM nucleus, while being denser than that in the PL nucleus—a feature that helps in tracing the boundary between the BL V division and the latter nucleus. The DL division of the BL nucleus, though heavily encapsulated by thick bundles of medullated fibers, shows in its core solely the presence of very few thin

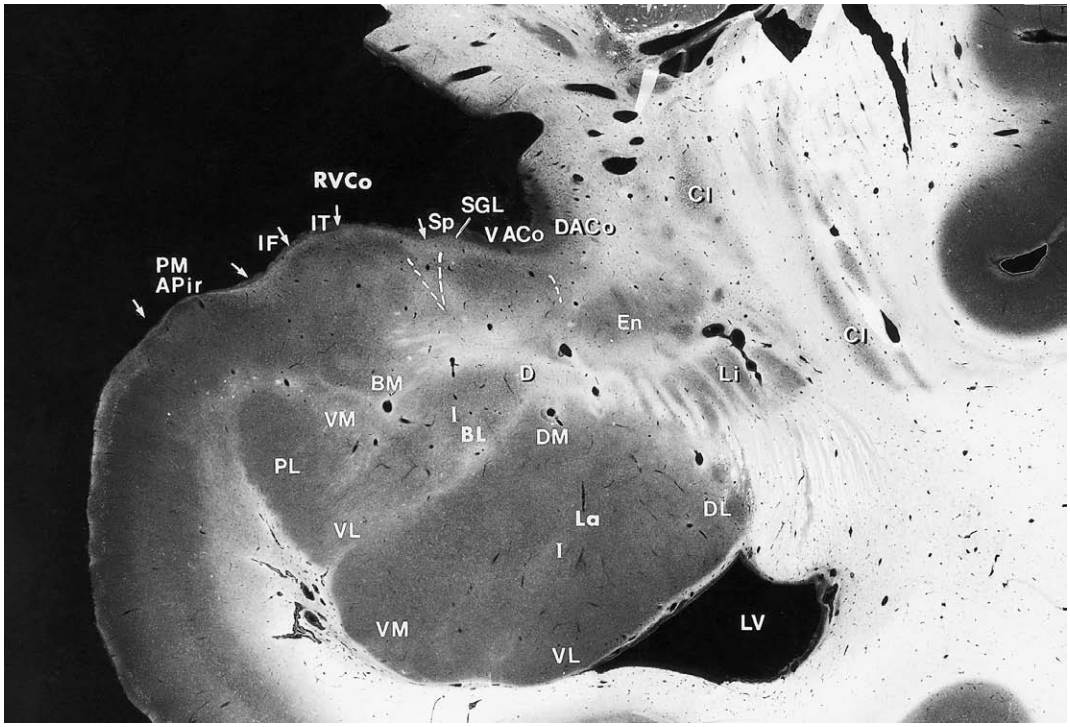

FIGURE 22.3 Low-power photomicrograph of the human amygdala at the level of the rostral pole of the ventral cortical amygdaloid nucleus (RVCo) showing its topographic relationships to the polar sectors of small-celled VL BM (Brockhaus' dense-celled division of his amygdalum profundum ventral). Already at this level the PM APir shows conspicuous development.

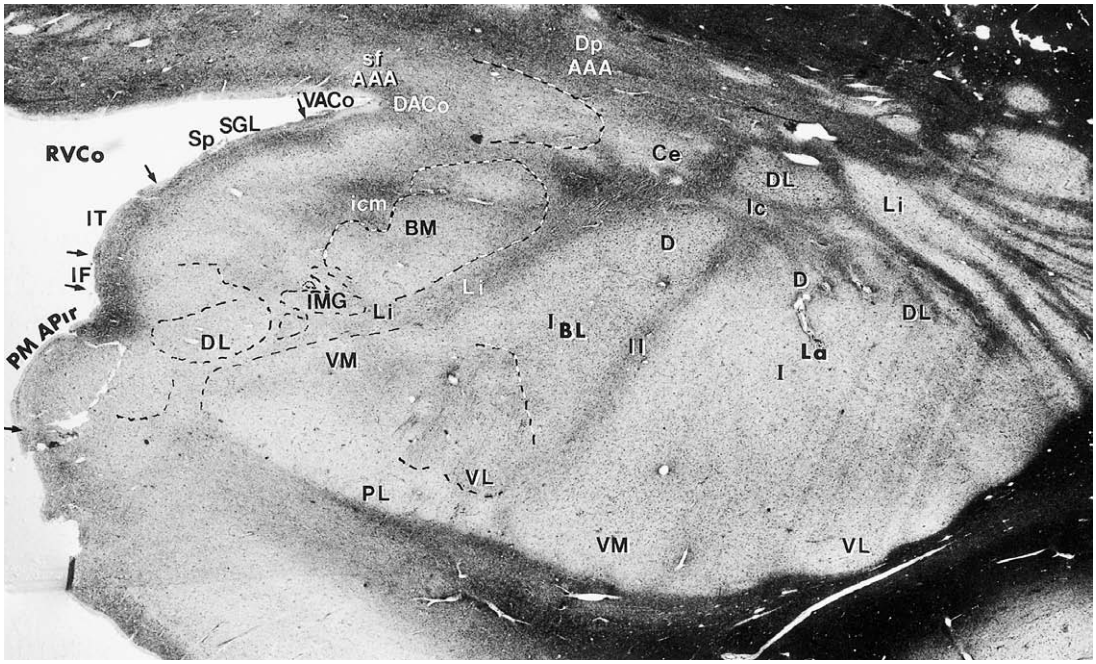

FIGURE 22.4 Low-power photomicrograph at the level of the rostralmost portion of the large-celled, dorsolateral division of the BL (DL BL). Individual subdivisions are clearly seen. Note the onset of the corridorlike bridge (SIsl) joining the Ce with the BSTL. A different method of transillumination was used by means of a microscope condenser and photographed directly with a reflex camera system.

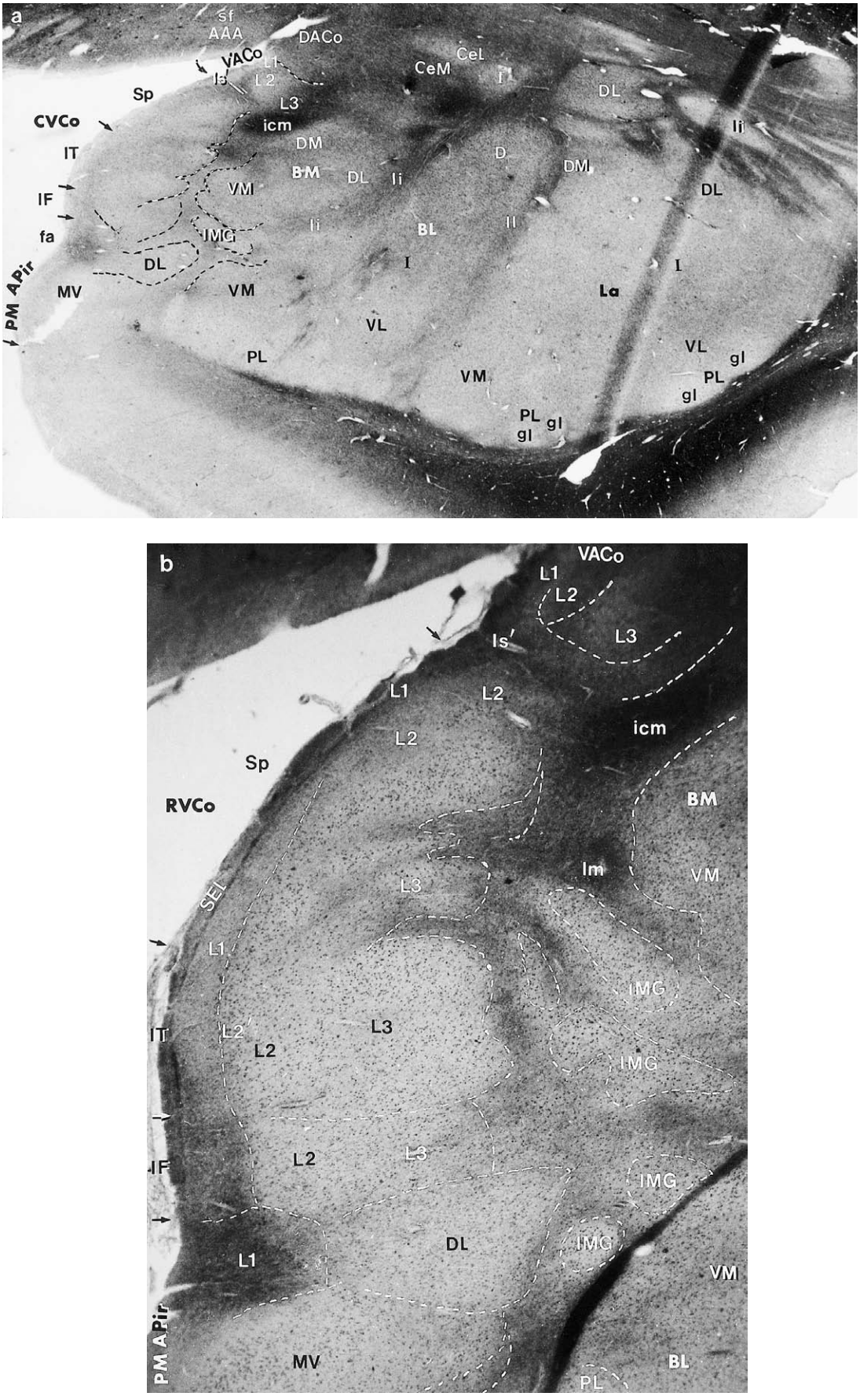

FIGURE 22.5 (a) Photomicrograph of a section slightly caudal to Figure 22.4 showing the subdivision of the VCo, the intramedullary grisea (IMG), the icm fiber system, as well as a more caudal segment of the SIsl as it fuses with the rostral pole of the Ce. (b) Medium-power photomicrograph providing a closer view of the intramedullary grisea (IMG) intervening between the BM and VCo. Note the lipofucsin-filled neurons in this amygdaloid region, and the clear boundaries that exist among the gray masses.

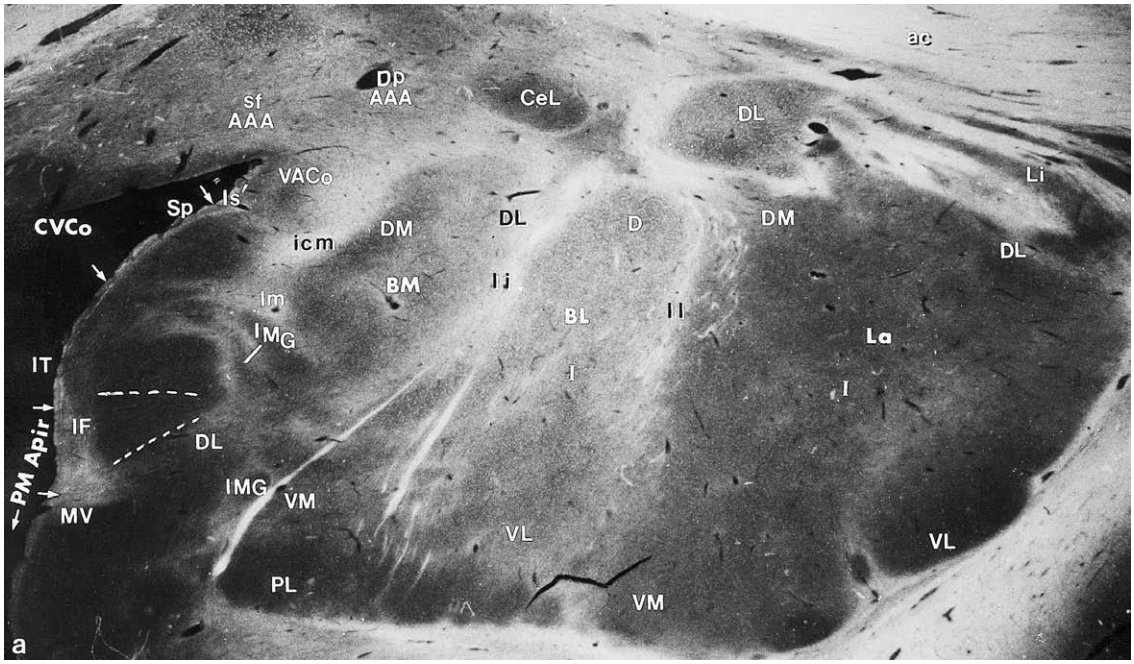

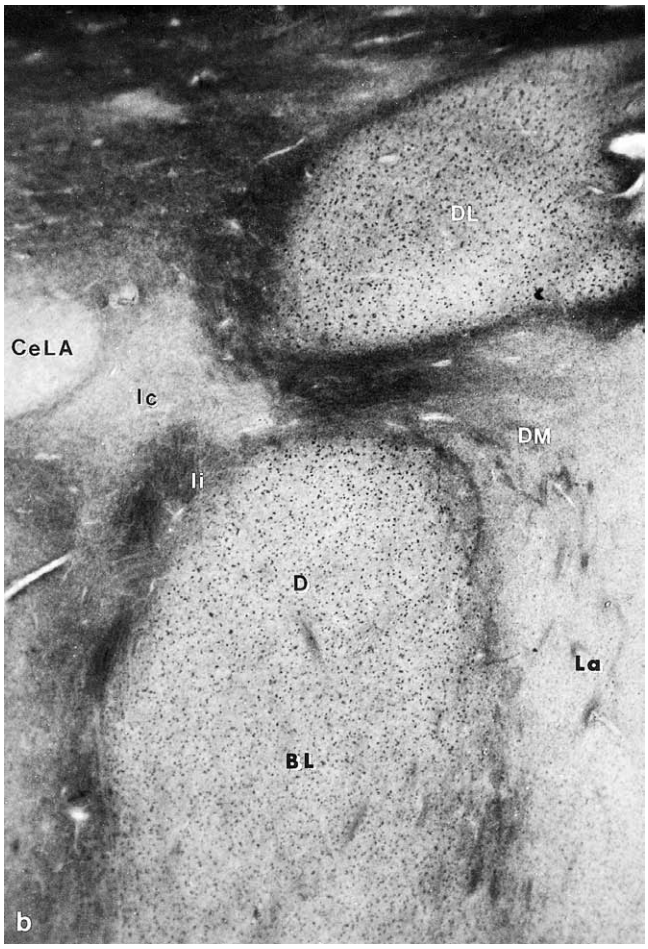

FIGURE 22.6 (a) Low-power photomicrograph at the level of the apical division of the central amygdaloid nucleus (CeLA) showing the clearly developed IMG intervening between the small-celled VM BM and the intermediate and inferior VCo medially, and the small-celled, ventromedial (VM) division of the BL laterally. The icm fiber system separates the large-celled DM BM from the ventral division of the ACo dorsomedially and the superior division of the VCo ventromedially. An intercalated mass (Ic) lies between the large-celled DL and D divisions of the BL laterally, and the Ce mediodorsally. (b) Medium-power magnification of the same section as in (a) but illuminated with the procedure indicated in Figure 22.4. It shows the different sizes of the lipofucsin deposits in the BL divisions and the small-celled, dorsomedial La. Lipofucsin deposits are absent in the intercalated masses (Ic) and in the CeLA.

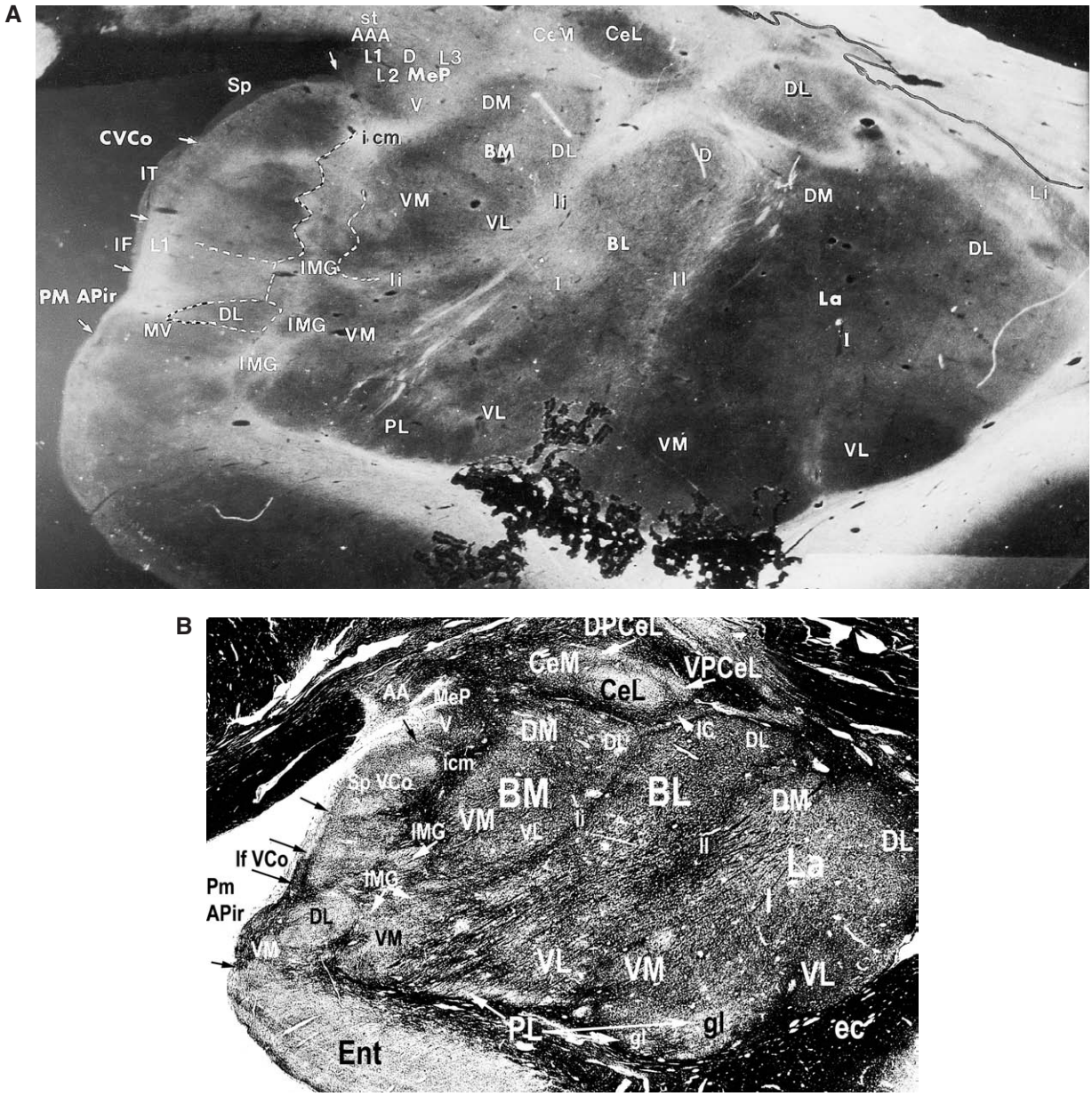

FIGURE 22.7 (a) Low-power photomicrograph of a transversal unstained section caudal to Figure 22.6 showing an almost vertical alignment of the intramedullary grisea (IMG) in the interface between the superficially located amygdaloid nuclei (IT CVCo, IF CVCo, DL PM APir, and MV PM APir on one side, and the medium-celled VM BM and small-celled VM BL and PL BL) on the other. A bigger IMG island lies between the VM BM and VM BL. (b) Low-power photomicropgraph of a transverse section taken at a plane just caudal to the that illustrated in figure 7a, which has been stained with a non-suppressive silver neurofibrillar stain. The image depicts a very close parallelism between the distribution pattern of optically dense medullated fibers seen in unstained sections with that provided by the silver stained material. The far more detailed demonstration provided by this latter procedure reinforces the parcellation proposed here for the human amygdala.

fiber bundles, a disposition that contrasts markedly with the radiated appearance in the rest of the nucleus. On the other hand, the dorsomedial tip of the BL VM subdivision shows a sharp drop in the number of radiating fiber bundles running through it that contrast markedly with their richness in the rest of the BL V division.

Chemoarchitectonics

Heavy Metals In Timm-Danscher's preparations of the marmoset monkey brain, the BL nucleus, like its other counterparts in the LBNC, shows a stepwise differential distribution of silver sulfide precipitate. Thus, while its dorsal sectors (DL D) show a comparatively poor reactivity, the middle sectors (BL I) display an

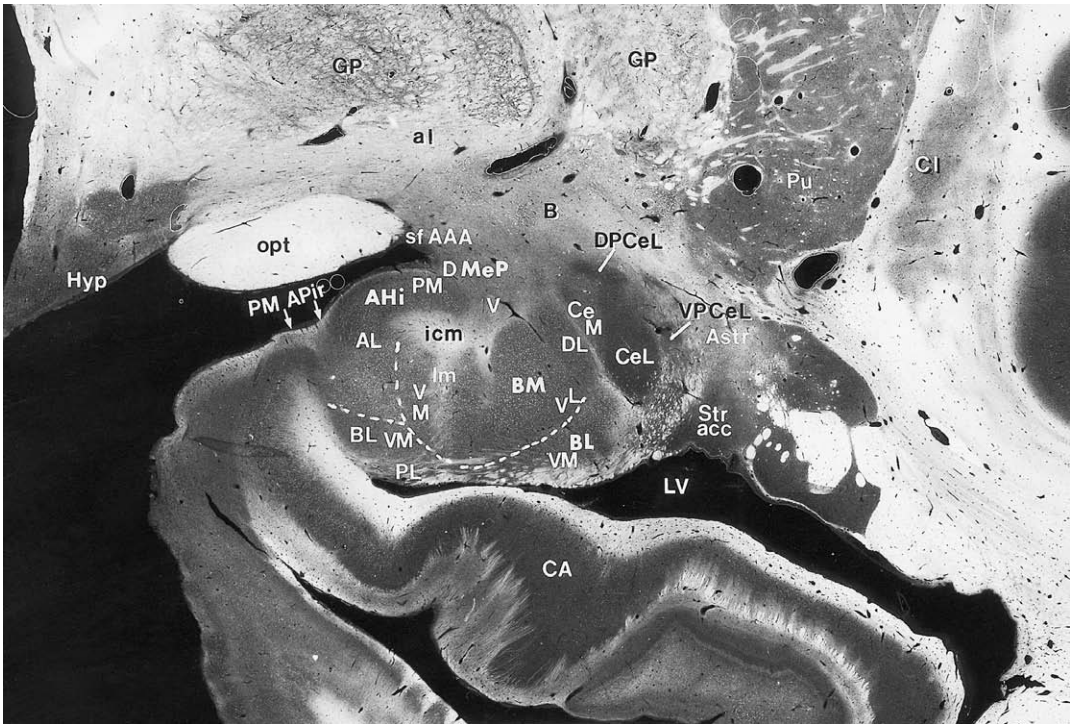

FIGURE 22.8 Low-power photograph at the caudal level of the amygdala showing the amygdalohippocampal-area (AHi) as well as some of the central amygdaloid nucleus subdivisions (Ce) and the relationship with the amygdalostriatal area. At this level the LA has disappeared and the BL is reduced to its small-celled VL and VM subdivisions which in turn are set apart by intervening portions of small-celled VL BM.

intermediate density and the ventral ones a heavy staining pattern that cannot be separated from that present in the PL nucleus (Fig. 22.23). Closer examination reveals that at difference with what happens in the La nucleus, most of the silver sulfide precipitate in the BL nucleus is distributed rather homogeneously throughout the nucleus but with patches of smaller density diffusely scattered in it. Rail rod-like images, although present here and there, are rather rare and difficult to locate within this generalized pattern of homogeneous distributed silver deposits and no Timm-Dancher-positive perikarya could be identified.

Neurotransmitters

CHOLINERGIC MARKERS

ACETYLCHOLINESTERASE (ACHE) This nucleus contains the most intensely stained AChE-positive neuropil in the amygdala with its intensity diminishing in a ventral direction (Nitecka and Narkiewicz, 1976; Svendsen and Bird, 1985; de Olmos, 1990; Darvesh *et al.*, 1998; Heimer *et al.*, 1999). There are only isolated AChE-containing neurons with fusiform or triangular-shaped perikarya representing approximately 1% of the total neuronal population.

CHOLINE ACETYLTRANSFERASE (CHAT) According to Emre *et al.* (1993), in the human amygdala all nuclei contain ChAT-ir axons and punctate varicosities, but there are substantial regional variations in the density of these axons and *neuropil*. In the BL nucleus the density of varicosities are so dense that individual fibers cannot be identified. These varicosities may be interpreted as preterminal specializations, consistent evidence has been found by these authors to show that the amygdala contains intrinsic ChAT-ir neurons except for few aberrant perikarya belonging to the nucleus basalis of Meynert. This was confirmed by Lopez-Gimenez *et al.* (2001b), who could not find any ChAT mRNA in this nucleus or in any other amygdaloid nucleus.

Emre *et al.* (1993) have stated that the BL nucleus contains the highest density of ChAT-ir profiles and is sharply delineated from its neighboring nuclei for that reason. The high density of the ChAT-ir in this nucleus remains unchanged along the anteroposterior extent of the BL nucleus but such density decreased toward the transition from the BL to the basomedial nucleus (here the small-celled subdivisions of the BL nucleus plus the PL nucleus). In the deep division of their basomedial nucleus (here VL/VM BL subdivision) as in their superficial division (here the PL nucleus), there are high to moderate ChAT-ir profiles, and this picture does not vary in its anteroposterior extent. However, it should be pointed out that, together with the VCo

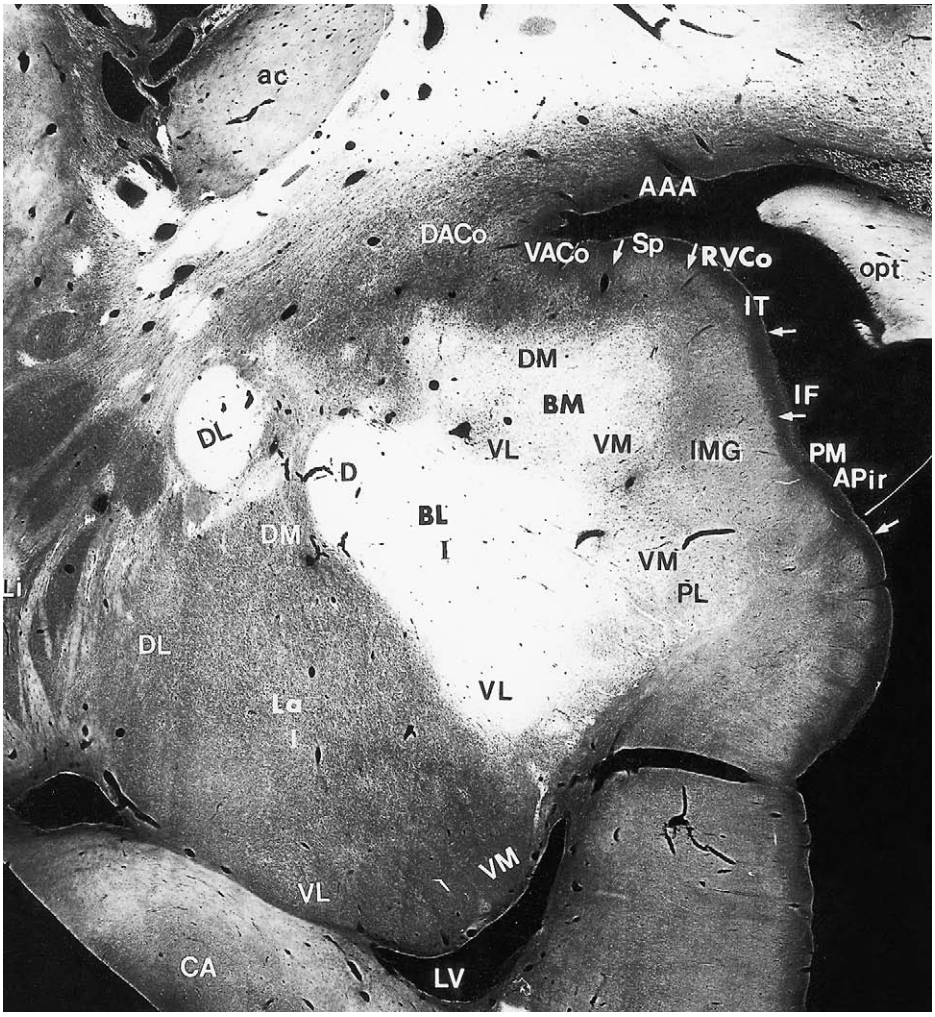

FIGURE 22.9 Low-power photomicrographs of transverse AChE-stained sections through the rostral third of the human amygdala showing the differential distribution of AChE activity in the amygdaloid nuclei. Same illumination system as in Figure 22.4.

nucleus and the BM nucleus, the small-celled VL/VM BL nucleus is ranked third in terms of the density of ChAT-ir fibers and varicosities.

In the macaque monkey, Amaral and Basset (1989) describe a picture very similar to the one present in the human amygdala, although, by recognizing a cytoarchitectonic different neuronal population in the interface between their classical magnocellular and parvicellular divisions of this nucleus, they have to introduce and fit their account to the new fact. Accordingly, their dorsally situated magnocellular division is said to contain an extremely dense and homogeneous amount of ChAT-ir fibers and terminals, while their intermediate subdivision bears ChAT fibers and terminals morphologically similar but that show a ChAT-ir density intermediate between that present in the dorsal magnocellular division and that existing in the ventral parvicellular division, which is substantially lower than in either of them.

EXCITATORY AMINO ACIDS

GLUTAMATE/ASPARTATE (GLU/ASP) Retrograde tracing experiments made in rats using tritiated D-aspartate indicate that a considerable number of the BL neurons could be the source of GLU/ASPergic projections to the nucleus accumbens and olfactory tubercle (Fuller *et al.*, 1987) and, even though in a very restricted manner, to the region of the paraventricular hypothalamic nucleus (Csáki *et al.*, 2000).

On the other hand, this nucleus seems to be the target of GLU/ASPergic afferent projections coming from cortical fields after injections of tritiated D-aspartate that involved the magnocellular and intermediate divisions of the BL nucleus. Among the cortical areas involved in these projections are neurons in the rostral two-thirds of the CA1 field of the hippocampus, in layers 5 and 6 of the entorhinal cortex, particularly its rostral olfactory division, and neurons in layers 3 and 5 of the insular cortex proper agranular (Ia), caudal

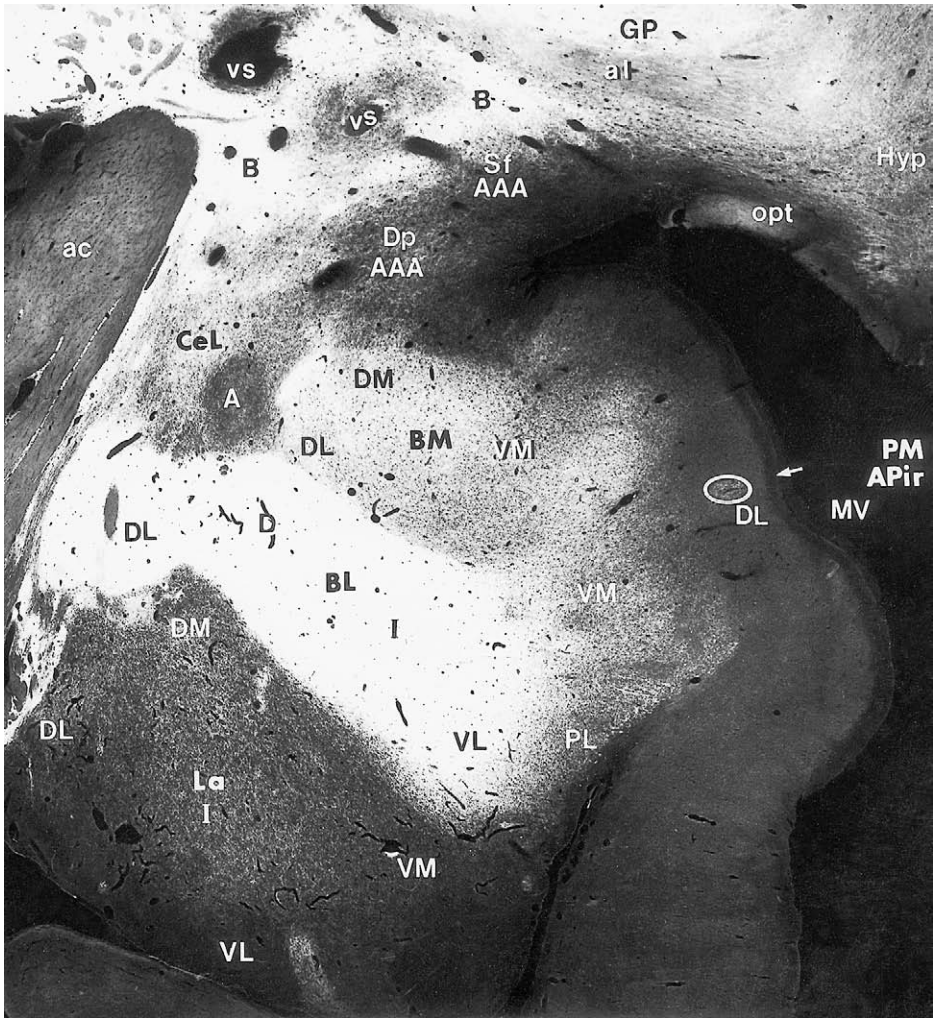

FIGURE 22.10 Low-power photomicrographs of transverse AChE-stained sections through the rostral third of the human amygdala showing the differential distribution of AChE activity in the amygdaloid nuclei. Same illumination system as in Figure 22.4.

portion of area 13a (14O), area 13 (13M and orbital periallocortex), cingulate areas 25 and 24, perirhinal areas 35 and 36, area TF and TH, etc. At the level of the amygdala itself, the most prominent intrinsic labeling with retrogradely transported tritiated D-aspartate occurs at the level of the PL nucleus neurons and not so markedly from the BST nucleus. From their schematic representation (Figs. 3 and 8A, B) it seems that the rostral and deep cell laminae of the AL AP-ir area (their periamygdaloid cortex sensu lato) contribute to the GLU/ASPergic neuropil in this nucleus.

INHIBITORY AMINO ACIDS

γ-AMINOBUTYRIC ACID (GABA) According to Pitkänen and Amaral (1994), in the macaque monkey the basal nucleus (here the BL nucleus) has a slightly lower density of GABA-ir cells than the La and BM nuclei. The density of GABA-ir cell is similar in the magnocellular (here large-celled DL/D BL) and intermediate (here medium-celled I BL) divisions and slightly higher in the parvicellular (here, small-celled VL/VM BL). Type 1 cells are most common throughout the BL nucleus, and type 2 cells are present mainly in the intermediate and parvicellular divisions. Very few type 3 cells can be found throughout the BL nucleus. The density of GAD mRNA-labeled cells is slightly lower in the BL nucleus than in the La and BM nuclei. Consistently with all this, the density of GABA-ir fibers and terminals in the BL nucleus is lower than in the La nucleus. Within the BL nucleus, a slightly higher density of GABA-ir fibers and terminals is present in the magnocellular and intermediate divisions than in the parvicellular division. A characteristic feature of the magnocellular division is the presence of numerous pericellular baskets surrounding non-ir large cell bodies.

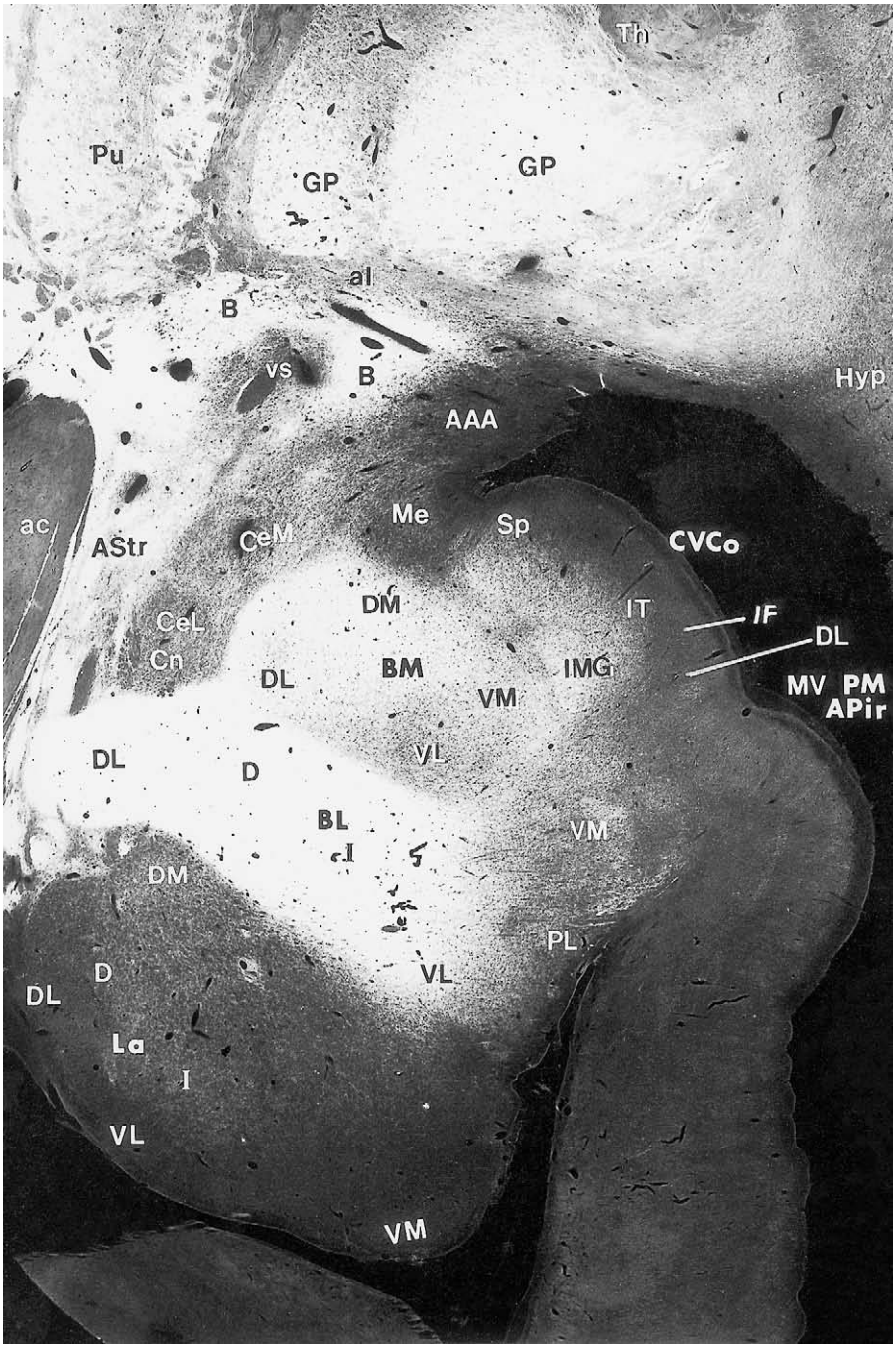

FIGURE 22.11 Low-power photomicrographs of transverse AChE-stained sections through the rostral third of the human amygdala showing the differential distribution of AChE activity in the amygdaloid nuclei. Same illumination system as in Figure 22.4.

MONOAMINE MARKERS

DOPAMINE-β-HYDROXYLASE (DBH) According to Sadikot and Parent (1990), in the squirrel monkey, the basal nucleus (here the BL nucleus) shows light DBH-ir in its magnocellular division (here the large-celled DL/D BL subdivision), and moderate ir in its parvicellular division (here the small-celled VL/VM BL subdivision), the latter appearing to fuse medially with the cortical transitional area. Note by the reviewer: It is possible that the parvicellular division of BL in the squirrel monkey, such as depicted by these latter authors, may also include the PL nucleus.

DOPAMINE TRANSPORTER (DAT) In the macaque monkey, Freedman and Shi (2001) have reported the presence of modest amounts of DAT-ir in the basal

FIGURE 22.12 High-power photomicrograph of a Nissl-stained section showing the smaller and more densely packed cells in the La as compared with the BL. Interposed between the La and BL is a dense group of very fine intercalated cells (Ic).

magnocellular amygdaloid nucleus, and they stress the fact that when DAT is present, outside striatum a network of very fine fibers of modest density is formed. Sadikot and Parent (1990) report that the basal nucleus (i.e., the BL nucleus) shows intranuclear gradients with dense TH-ir varicosities in the lateral aspect of the parvicellular division (here the VL/VM subdivisions of the BL nucleus) and moderate terminal density dorsally in its magnocellular division (here the DL/D of the BL nucleus).

SEROTONIN (5-HT) According to Freedman and Shi (2001), in the macaque monkey, there are relatively heavy concentrations of 5-HT-ir in the basal amygdaloid nucleus (here the BL nucleus).

After Sadikot and Parent (1990), in the squirrel monkey, the basal nucleus shows a gradient of 5-HT-ir ranging from moderate in the magnocellular division to dense in the lateral aspect of the parvicellular division (here the VL/VM BL subdivision). A patch of light 5-HT-ir is seen in the medial aspect of this division.

TYROSINE HYDROXYLASE (TH) According to Pearson (1990), the human BL nucleus contains a moderate amount of TH-ir axons and innervation that seems to diminish in density anteriorly.

Sadikot and Parent (1990) report that in the squirrel monkey the basal nucleus shows intranuclear gradients of TH-ir with denser TH-ir terminal varicosities in the lateral aspect of its parvicellular division and moderate TH-ir terminal density dorsally in its magnocellular division. A patch of light TH-ir is seen in the medial aspect of the parvicellular basal nucleus.

NEUROPEPTIDES

CHOLECYSTOKININ (CCK) The number of CCK mRNA-containing cell bodies in the BL nucleus seems to be rather modest (Savasta *et al.*, 1990).

CHROMOGRANIN B According to Marksteiner *et al.* (1999), the human BL nucleus contains a high-density PE-11-like ir that consists of varicose fibers and mixed-size varicosities. No PE-11-like ir neurons are present.

CORTICOTROPHIN-RELEASING FACTOR (CRF) Although the human BL presents only a sparse populations of small CRF-ir bipolar cells, the CRF-ir-containing fibers were highly conspicuous in this nucleus but not as dense as in BM (Powers *et al.*, 1987).

ENKEPHALIN (ENK) According to Piorio *et al.* (1990), in the human BL nucleus, as in the rest of the LBNC, only lightly stained delicate networks of varicose fibers are obscured.

GALANIN (GAL) According to Kordower *et al.* (1992), in the macaque monkey amygdala this member of the LBNC, like all of its remaining components,

does not contain GAL-ir cell bodies and few if any GAL-ir fibers.

NEUROPEPTIDE Y (NPY) According to Walter *et al.* (1990), in the human amygdala, NPY-ir fibers and cells are more numerous in all nuclei of the LBNC than in the medial superficial nuclei including Ce, Me, and VCo nuclei. On the other hand, as in other members of the LBNC, the NPY-ir perikarya appear to concentrate in the dorsal large-celled sectors of the BL nucleus, while the NPY-ir fibers appear highest in the ventral small-celled VL/VM subdivisions (i.e., their ventral *parvicellulare* subdivision of the nucleus profundus amygdalae intermedius).

According to McDonald *et al.* (1995), in the macaque monkey, the NPY-ir neurons resembled SOM-ir neurons in all nuclei of the LBNC, which is consistent with evidence for extensive colocalization of SOM-ir and NPY-ir. These "double" peptidergic neurons fall within two categories already mentioned to be present in the nuclei of the LBNC, i.e., spiny and spiny-sparse. (For more details, the reader is referred to the original paper by these authors.) As in the human amygdala fiber, labeling is most dense in the parvicellular basal nucleus, while it is much lighter in the magnocellular division though it still contains numerous NPY-ir fibers.

NEUROTENSIN (NT) Mai *et al.* (1987) reported that the human BL nucleus contains a much smaller density of NT-ir fibers than the corticomedial group of amygdaloid nuclei. According to Benzing *et al.* (1992), the large-celled BL nucleus (equivalent to DL/D BL and I BL of the present account) as a whole displays moderate densities of NT-ir, with the dorsal large-celled subdivisions (DL/D BL) containing a network of relatively short fine-beaded fibers and scattered dot-like puncta. In addition to the existence of a rostral-to-caudal gradient of increasing concentration of NT-ir, the fiber plexuses in the BL nucleus also show a dorsoventral gradient being densest in DL/D BL. By contrast, the NT-ir in their basal *parvicellulare* nucleus (equivalent to VL/VM BL of the present account) is described as being more dense than in DL/D-I BL and consisting of a network of fine and coarse fibers, with the fine ones strongly outnumbering the coarse ones.

SECRETONEURIN (SCR) The BL nucleus shows rather poor if any SCR-ir either in the neuropil or in perikarya of DL/D and I BL subnuclei, although what could be some expression of its presence can be found in the small-celled subdivisions of BL (see figure of Marksteiner *et al.*, 1995).

SOMATOSTATIN (SOM) In the human brain, Mufson *et al.* (1985) reported the presence of SOM-ir neurons in the BL nucleus (i.e., their laterobasal nucleus), but they did not provide further detail on the distribution pattern of cells and fibers within the nucleus.

According to Amaral *et al.* (1989), the density of SOM-ir cells is relatively low in the monkey BL nucleus, showing quite even distribution throughout the whole nucleus and varying sizes and shapes. By contrast, the density of SOM-ir fibers and terminals in the monkey BL nucleus follows a dorsoventral gradient, with their large-celled dorsal division showing the lowest level in the amygdala, the medium-celled intermediate division having a somewhat higher concentration, and the small-celled ventral division containing a fairly dense ir. According to McDonald *et al.* (1995), the BL nucleus, like the other amygdaloid nuclei, shows a moderate number of SOM-ir cell bodies (still more numerous than the NPY-ir cells). Since SOM-ir and NPY-ir colocalizes in significant numbers of neurons in this and other amygdaloid nucleus, this information should not be ignored. As can be inferred from these data, the density of SOM-ir fibers in the monkey BL nucleus parallels that of the NPY-ir fibers, although one has to keep in mind that SOM-ir neurons are always more numerous than NPY-ir neurons.

SUBSTANCE P (SP) According to Piorio *et al.* (1990), the BL nucleus, like in the rest of the LBNC, except their dorsal magnocellular part of the accessory basal nucleus (here DM/CM BM) contains few scattered SP-ir neurons together with branching fibers and punctate material.

NEUROTROPHINS

BRAIN-DERIVED NEUROTROPHIC FACTOR (BDNF) According to Murer *et al.* (1999), the human basal nucleus, i.e., the present BL nucleus, contains both BDNF-ir neurons and fibers, although showing a moderate staining intensity and rather modest density in number which contrast markedly with the much higher BDNF-ir in the neighboring Ce nucleus.

ENZYMES

ANGIOTENSIN-CONVERTING ENZYME (ACE) Moderate levels of binding for this enzyme are displayed by all the subdivisions, large celled and small celled, of the BL nucleus (Chai *et al.*, 1990), which contrast with the lower levels of binding shown by the other components of the LBNC.

BUTYRYLCHOLINESTERASE (BUCHE) The BL nucleus contains many BuChE-positive neurons being more numerous dorsally than ventrally. These neurons have round, fusiform, or triangular perikaria that give rise to numerous dendrites. According to Darvesh *et al.* (1998), approximately 10% of the neuronal population in the *BL* nucleus are BuChE.

NICOTINAMIDE ADENINE DINUCLEOTIDE PHOSPHATE DIAPHORASE (NADPH-D) As in other members of the basolateral nuclear group, the BL nucleus contains NADPH-d but with the particularity that here the concentration of this enzyme reaches its greatest expression involving neuronal perikarya, fibers, and terminals (Simms and Williams, 1990; Brady *et al.*, 1992). However, its general distribution in the nucleus is not homogeneous but follows a dorsoventral gradient attaining its maximal concentration at the level of the small-celled subdivisions of the BL nucleus, which sets these sectors apart from surrounding areas. The staining pattern in the human BL nucleus is very similar to that reported for a New World monkey, the *Saimiri sciureus* or squirrel monkey (Brady *et al.*, 1992).

P450 AROMATASE (P450 AROM) According to Roselli *et al.* (2001), in the macaque monkey amygdala, the BL nucleus (i.e., their basal nucleus) contains a moderate density of P450 AROM mRNA-labeled cells. Close examination of their illustrations indicates the existence of two separate labeled zones: one rostrally situated involving lateral sectors of the D and I subdivisions of the BL nucleus, and a caudal one that shifts toward the medial sectors of both subdivisions.

CALCIUM-BINDING PROTEINS

CALBINDIN-D28K (CAL) According to Sorvari *et al.* (1996b), the density of CAL-ir neurons in the DL/D (their magnocellular division) subdivision of the BL nucleus varies from low to moderate. The highest density of CAL-ir neurons was observed in the VL/VM subdivisions (their parvicellular division) of the BL nucleus. The I BL subdivision appears to contain higher density of neurons than the DL/D subdivision. The neurons are small and belong to mainly type 1 and type 2 categories. Characteristic of the I BL subnucleus is the presence of many large type 2 and type 3 cells, in addition to the smaller type 1 neurons. Lightly stained, pyramidal-shaped, immunopositive neurons are found only occasionally. The CAL-ir dendrites in the BL nucleus show a different appearance than those in the La nucleus. While the dendrites in this latter nucleus are thin and straight, the dendrites in the I BL and VL/VM subnuclei are thick and multibranched. In the VL/VM subdivision, the CAL-ir dendrites appear oriented in a dorsal-to-ventral direction and frequently extended to the PL nucleus. According to these authors, the intensity of neuropil CAL labeling in the BL nucleus was slightly higher than in the La and BMl nuclei, which helped define the borders between these areas. The I BL subnucleus of the BL nucleus appears to contain a substantially higher density of CAL-ir bundles than the VL/VM and DL/D subnuclei of the BL nucleus.

CALRETININ (CR) According to Sorvari *et al.* (1996a), the common feature for all divisions of their basal nucleus (here BL nucleus) is the presence of small-type CR-ir cells. On the other hand, the overall density of CR-ir neurons and the proportion of the three neuronal types they recognize varies in the different divisions. In their magnocellular division (here DL/D) the density of CR-ir neurons is said to be low and to be composed almost exclusively of small type 1 cells. In their intermediate division (here I BL), this type of neuron still is predominant but some type 3 cells are also reported. Characteristic of I BL is said to be the presence of very large type 2 cells, the largest CR-ir in the amygdaloid complex. The density of the CR-ir neuronal population in I BL as compared with the overall density of these cells in the amygdaloid complex is moderate. Moreover, the density of the CR-ir cells in their parvicellular division (here VL/VM) is lower than in IBL, and its CR-ir neuronal population consisted mainly of small type 1 cells. Some large type 2 cells and some small type 3 cells are present.

The intensity of the staining of CR-ir fibers, terminals, and neuropil is said to vary also in different divisions of the nucleus with I BL showing a higher density than DL/D BL or VL/VM BL. Compared with its neighboring laterobasal nuclear masses, the intensity of the fiber and neuropil staining in BL is lower than in the La nucleus but higher than in the BM nucleus.

PARVALBUMIN (PAV) According to Sorvari *et al.* (1995), the BL nucleus has more PAV-ir cells in its dorsal large-celled sectors than the intermediate and ventral small-celled subdivisions. The most common type of PAV-containing cell is the one constituted by neurons showing an angular and multipolar perikarya of variable size (their type 2 PAV-ir neurons). Some cells with stellate or spherical somata (their type 1 PAV-ir neurons) were detected particularly at the level of the intermediate subdivision of the BL nucleus. The BL nucleus also contains a high density of PAV-ir fibers that, as it happens in the La nucleus, follows a dorsoventral gradient though decreasing quite sharply at the border between the IBL and VLBM, with the latter and its medial counterpart, the VMBL subnucleus, displaying one of the lowest PAV-ir in the amygdala.

OTHER PROTEINS

DOPAMINE- AND ADENOSINE 3′,5′-MONOPHOSPHATE (CAMP)–REGULATED PHOSPHOPROTEIN OF M, 32 KDA (DARPP-32) AND PHOSPHATASE INHIBITOR 1 (I-1) According to Barbas *et al.* (1998), in the macaque monkey, there are fewer and less densely labeled neurons in the BLl nucleus than in the VCo, BMl, La, or Ce nuclei for I-l, and even fewer for DARPP-32.

The few and weakly stained DARPP-32-ir neurons can be found in its ventrolateral (VL BL) and, to a lesser extent, in its ventromedial sectors (VM BL). In contrast, I-l-ir neurons are more widely distributed in the VM sector of the nucleus, which abuts the BM nucleus. The ventrolateral zone of BL also contains I-l-ir neurons and, in a few sections, some can be noted in its central zone where the nucleus is narrow.

DOPAMINE TRANSPORTER (DAT) According to Ciliax *et al.* (1999), the human BL nucleus has the highest density of DAT-containing varicose axons, with a decreasing gradient from dorsomedial to ventrolateral regions providing a distinct boundary with both BM and La nuclei.

On the other hand, in the macaque monkey BL nucleus the number of DAT-ir fibers is modest, forming a very fine network (Freedman and Shi, 2001).

LIMBIC SYSTEM–ASSOCIATED MEMBRANE PROTEIN (LAMP) According to Côté *et al.* (1996), in the macaque amygdala, the BL nucleus is the most intensely stained nucleus of the primate amygdala. All divisions of the La nucleus express LAMP-ir, but the intensity of the ir differs among the various divisions and along the rostrocaudal extent of the nucleus. At the rostral pole, the BL nucleus consists of a single entity that displays very weak LAMP-ir. At slightly more caudal levels, a weak LAMP-ir occurs in the I BL and small-celled subdivisions of the BL nucleus but not in the large-celled division. At the midamygdaloid levels, the LAMP-ir is intense in the small-celled division, moderate in the I BL, and weak in the large-celled division. In the caudal one-third of the BL nucleus the LAMP-ir is weaker than at midamygdaloid levels. The magnocellular and intermediate divisions of the BL nucleus display a rather diffuse and moderate LAMP-ir.

SMI32 NEUROFILAMENT PROTEIN (SMI32-R) According to the Petrides *et al.* (2000) atlas on the distribution of the SMI32 neurofilament protein in the macaque monkey, this protein would be practically absent from most of the BL nucleus except at rostral levels where some SMI32-ir can be localized in the dorsal and intermediate subdivisions of this nucleus.

RECEPTORS

ADRENERGIC RECEPTORS

ADRENORECEPTOR α_2 According to Flügge *et al.* (1994), in the tree shrew, the basal nucleus shows a low number of [^{3}H]RAU binding sites, being RAU indicative of this type of receptor.

ADRENORECEPTOR β According to Flügge *et al.* (1994), in the tree shrew, the majority of the monoamine nonsertoninergic receptors present in the basal nucleus are β-adrenoceptors.

BENZODIAZEPINE RECEPTOR (BNZ-R) According to Zezula *et al.* (1988), the basal accessory nucleus in humans (here the BM nucleus) contains intermediate levels of BNZ-R.

ESTROGEN RECEPTOR α (ER-α) ER-α can be detected in this nucleus (Blurton-Jones *et al.*, 1999). Österlund *et al.* (2000) confirm these findings by detecting a low amount of ER-α mRNA–labeled nuclei in the large-celled D BL nucleus, a labeling not detected in monkeys.

GABA A RECEPTOR (GABA A-R) According to McDonald and Mascagni (1996), in the macaque monkey, the density of GABA A-R in the BL nucleus (i.e., their basal nucleus) is rather weak in both its large-celled and small-celled sectors.

OPIOID RECEPTOR (OR) According to Daunais *et al.* (2001), within the macaque monkey BL nucleus, different patterns of μ receptor binding were readily apparent in their magnocellular (here DL/D) and parvicellular (here VL/VM) portions of this nucleus. The concentration of binding sites is greatest in the VL/VM subnuclei, especially medially and at more caudal levels. Binding was considerably less intense in the intermediate division (I BL) and sparsest in the DL/D subnuclei.

SEROTONINERGIC RECEPTORS (5-HT-R)

5-HT$_{1A}$ RECEPTOR (5-HT$_{1A}$-R) According to Flügge *et al.* (1994), in the tree shrew, the basal nucleus is densely labeled by [^{3}H]DPAT, a specific agonist of the 5-HT$_{1A}$-R.

5-HT$_{2A}$ RECEPTOR (5-HT$_{2A}$-R) According to Lopez-Gimenez *et al.* (2001a), although the magnocellular DL and D sectors of the BL nucleus express mRNA for the 5-HT$_{2A}$-R, its density was rather low.

5-HT$_{2C}$ RECEPTOR (5-HT$_{2C}$-R) Based on an illustration presented by Lopez-Gimenez *et al.* (2001b), it seems that the BL nucleus as a whole does not contain this type of receptor.

VASOPRESSIN RECEPTOR (AVP-R) According to Loup *et al.* (1991), the dorsolateral part of the basal amygdaloid nucleus (here the BL nucleus) displays a weak AVP binding capacity.

Basomedial Amygdaloid Nucleus (BM)

This nucleus is one of the major outputs for projections to the hippocampal as well as to the

entorhinal and perirhinal cortices (see below). Since the hippocampal formation is strongly associated with memory and the amygdala has been shown to be involved in emotional memory (Halgreen, 1992), and since neurons containing estrogen receptors are heavily present in this nucleus, it is possible that the BM nucleus has a significant role in this function (Österlund *et al.*, 2000).

Topographical Landmarks The BM amygdaloid nucleus [BM in plates 22–32 (0.0–13.3 mm) of Mai *et al.*'s *Atlas of the Human Brain*, 1997] (Figs. 22.7b, 22.1c,d, 22.3–22.6a; 22.7a, 22. 23b, and 22.8–22.11) is a fairly oval gray mass that appears slightly caudal to the rostral pole of BL and extends posteriorly almost to the caudal end of the amygdaloid complex. Throughout much of its extent, the BM lies under the semilunar gyrus, separated from its surface by the stratified grisea of the VCo rostrally and the AHi caudally. The medial medullary lamina intervenes between the BM and the cortical-like divisions of the superficial amygdala. Another stratum of fibers, the intermediary medullary lamina, separates the BM from the BL, both laterally and ventrally. BM is overlaid with the ventral divisions of ACo rostrally and Me caudally, being separated from them by more or less diffusely arranged fibers, constituting branches of a larger fiber system. Dorsolaterally, the BM is separated from the Ce by the dorsomedial medullary lamina (longitudinal association bundle according to Gloor, 1997). The rostral end of the nucleus is marked not only by a clear change in the cytoarchitectonic arrangement where it borders with the AAA dorsally and with the preamygdalar sector of the endopiriform nucleus rostrally, but also by a sharp densification of the fiber plexus that separates BM from these two other gray formations. This is better appreciated in horizontal and sagittal sections of the amygdaloid region.

Cytoarchitectonics In cell preparations, the BM nucleus, like the other members of the LBNC, shows a gradual reduction in the size of its cells and a densification of its neuronal population, the largest element being located in the dorsomedial aspect of the nucleus and the smallest in the ventrolateral one. The glial population also shows a reduction in its density parallel with the reduction in the size of the neurons while density of the fiber plexuses in the nucleus follows a reverse pattern.

On cytoarchitectonic grounds, the BM can be divided into four major subnuclei: dorsomedial large-celled (BMDM), ventromedial medium-celled (BMVM), dorsolateral mixed-celled (BMDL), and ventrolateral small-celled (BMVL). To these (main) four subdivisions, a fifth less conspicuous one has to be added: the caudomedial dense-celled subnucleus (BMCM). However, many authors have chosen to blend them into two large medial (magnocellular) and lateral (parvicellular) subnuclei (Svendsen and Bird, 1985; Sorvari *et al.*, 1995, 1996a, b).

The dorsomedial division of the BM nucleus is composed in great part of gross pyramidal-like neurons similar to those in the dorsal large-celled part of the BL nucleus, showing a looser arrangement, darker staining, and smaller size than the latter. Smaller, thinner, pyramidal-like, round, or oval neurons are also present in the dorsolateral BM nucleus. Glial cells are evenly distributed, and satellite cells are rather scarce compared with the dorsal BL.

The dorsolateral division of the BM nucleus is located in the dorsolateral aspect of the BM nucleus, varying as much in length as in shape. Neurons are smaller and thinner than in the dorsomedial BM nucleus.

The ventromedial division of the BM nucleus is in the ventral and rostral aspects of the BM and is made up of smaller, lighter staining, more delicately outlined neurons also showing greater variations in shape and a looser arrangement than those in other subdivisions of the BM. It contains pyramid-like neurons, together with multiangular or spindle-shaped ones.

The ventrolateral division of the BM nucleus is in the ventrolateral corner of the BM nucleus and is composed of smaller and more closely packed pyramid-like cells, together with slender, spindle-shaped neurons. This subnucleus stretches the whole length of the BM and, contrary to the rest of the BM subdivisions, the rostral polar part of this subnucleus contains a relatively rich satellite cell population [Brockhaus' 1938) dense-celled BM].

The caudomedial division of the BM nucleus is located in the medial most aspect of the caudal one third of the BM nucleus, lying ventrally and medially to the caudomedial radiation of the intermediate (icm) stratum of fibers, being separated by the latter and by the medullary lamina (lm) from the AHi transition area, the caudal division of the VCo, and the posteromedial APir area. At levels at which fibers from the stria terminalis (st) join both the lm and the icm, the caudomedial division of the BM nucleus appears to be separated from the rest of the BM nucleus by a narrow, relatively poor cell band that joins with these fibers. The nerve cells in the caudomedial division of the BM nucleus are somewhat smaller and more closely packed than in the dorsomedial division of the BM nucleus. The pyramid-like neurons are also lighter staining and slender, sometimes showing a triangular outline.

Fibroarchitectonics In myelin preparations the fiber network in the BM nucleus shows a denser arrangement than in the BL nucleus. This is probably

why in dark-field illuminated unstained frozen sections (see Figs. 22.1–22.6a; 22.7a; 22.8) the former nucleus is denser. The myelin pattern in the BM nucleus shows some regional variations, being somewhat denser at the level of the dorsomedial division of the BM nucleus but definitely richer in the polar ventrolateral division of the BM nucleus. In the ventromedial divisions of the BM nucleus the myelin is substantially less dense than in the rest of the BM nucleus. The fiber network here is also much looser. In the caudal aspect of the BM, small bundles of fibers pass through the ventromedial division of the BM nucleus and display a fan-shaped distribution in the more medial aspect of the caudomedial BM. Thus, the dorsomedial and dorsolateral divisions of the BM nucleus show a less dense fiber network than in its ventromedial division, constituted mostly by fine to moderately thick single fibers lying on top of a faintly stained ground plexus of very fine fibers. Other single running fibers cut vertically or obliquely to the main fiber network. The great majority of the obliquely oriented fibers reach to or come from the capsular fiber system constituted by the icm and the lm, which intercalates between the BM and the deep layers of the superficial cortical-like amygdaloid grisea (VCo nucleus and the AHi, and posteromedial APir transitions area), and from Me nucleus medially, and by intermediate medullary lamina, which intervenes between the BM and the BL laterally, dorsally, and rostrally. Fibers detach from or enter the thick fiber capsule (i.e., the dorsomedial medullary lamella) that separates this part of the BM nucleus from the Ce nucleus, the AAA area, and the intercalated masses embedded in it. Ventrally, a sharp densification of the fiber plexus coincides with the cytoarchitectonic border between these subdivisions and the ventromedial division of the BM nucleus.

In neurofibrillar preparations (see Fig. 7b) these subdivisions appear to be denser in fibers than both the dorsomedial and dorsolateral divisions of the BM nucleus. It is crossed by small bundles of fine fibers oriented in a dorsomedial-to-ventrolateral direction. These fiber bundles are derived from the intermediate medullary lamina in the boundary with the dorsal subdivisions of the BM nucleus. A ground plexus of fine fibers enmeshes the perikarya of the neurons of this subdivision. Although the general picture is dominated by the obliquely running fibers, there are others, though fewer, coursing at a slight right angle.

Chemoarchitectonics

Heavy Metals In Timm-Danscher's preparations of the New World monkeys (squirrel and marmoset) the BM nucleus shows a stepwise increase of the density of the silver sulfide precipitate (Fig. 22.23b), which is expressed in the following ascending order according to a densitometric evaluation made at the level of its main subdivisions in these primates: DM, DL, VL, and VM. Accordingly, the DM BM large-celled subdivision would contain the weakest density of zinc-containing neuropil while the VM small-celled one, the highest, with the remaining sectors of the nucleus displaying moderate to dense deposits of silver sulfide. As in the BL nucleus, the silver precipitate shows a rather homogeneous distribution and the neuronal perikarya remains unstained.

Neurotransmitters

CHOLINERGIC MARKERS

ACETYLCHOLINESTERASE (ACHE) According to most authors, the BM nucleus contains a moderately stained (Figs. 22.9–22.11) AChE-positive neuropil with few AChE-containing fusiform or triangular neurons (Nitecka and Narkiewicz, 1976; Svendsen and Bird, 1985; de Olmos, 1990; Sims and Williams, 1990). According to Nitecka and Narkiewicz (1976), the AChE activity in their basal medial nucleus (here BM) is, as previously mentioned, moderately intense, but apart from that they recognize two areas of activity that fuse without clearly defined boundaries: a superomedial part (here DM BM) part of the nucleus which displays moderate AChE activity, and an inferior one (here VM/VL) with a weaker enzyme reaction. They also consider that the BM nucleus, like other amygdaloid nuclei, shows a rather diffuse though uneven AChE activity with no cellular involvement. Like these authors, Svendsen and Bird (1985) consider that the BM nucleus (i.e., their basal accessory nucleus) shows medial and lateral differences in staining with the lateral region showing the greatest AChE activity.

Benzing *et al.* (1992), on the basis of AChE stained sections, found that the dorsomedial divisions of the BM nucleus (i.e., their Abm) is the next most densely stained amygdaloid griseum after the BL nucleus (i.e., their Bmg nucleus). The VM BL (i.e., their Abp nucleus) like the BM nucleus (their Abm), was darkly stained and thus was readily differentiated from their ventrally adjacent and more lightly stained Bpv. According to Nakamura *et al.* (1992), this nucleus contained numerous AChE-positive axons, although fewer than in the basal nucleus.

According to Sorvari *et al.* (1995), the magnocellular division of their basal accessory nucleus has a moderate intensity of AChE staining compared to the parvicellular division, where the staining intensity is lower. A similar pattern of AChE staining in La has also been reported by others (Sims and Williams, 1990; Emre *et al.*, 1993; Sorvari *et al.* 1995).

CHOLINE ACETYLTRANSFERASE (CHAT) According to Emre *et al.* (1993), both divisions of the BM nucleus

(i.e., their AB nucleus), lateral (Abl) and medial (Abm), display moderate densities of ChAT-ir varicosities and fibers. Although thin fibers with varicosities predominated, there are also occasional thick nonvaricose fibers. The density of ChAT-ir was not uniform within the BM nucleus, and patches of slightly more intense staining are present. At anterior and midamygdaloid levels, dense collections of ChAT-ir fibers can be seen located at the junction of BM, VCo (i.e., their cortical nucleus Co) and VM BL, which, according to them, would correspond to intercalated masses (their Fig. 8a, IC), but here they are interpreted to correspond to the intramedullary grisea (IMG). Examination of their images also shows further differences in the density of the ChAT-ir plexuses in the BM nucleus so that its lateroventral one-third is clearly poorer than the rest of it, while the dorsomedial sector shows a higher density. According to Lopez-Gimenez *et al.* (2001), no ChAT mRNA could be observed in this nucleus. Together with the small-celled VL/VM BL nucleus and with the VCo nucleus, the BM nucleus ranks third concerning the density of ChAT-ir fibers and varicosities.

EXCITATORY AMINO ACIDS

GLUTAMATE/ASPARTATE (GLU/ASP) Experimental retrograde tracing data obtained in rats by use of tritiated D-aspartate indicate that a considerable number of the BM nucleus neurons give rise to GLU/ASPergic projections to all the members of the ventral striatum (Acb, Tu and IPAC) and to the ventral pallidum (Fuller *et al.*, 1987), or to the paraventricular hypothalamic nucleus or immediate surroundings (Csáki *et al.*, 2000).

INHIBITORY AMINO ACIDS

γ-AMINOBUTYRIC ACID (GABA) According to McDonald and Agustine (1993), in the macaque monkey, their basal accessory nucleus, like the other members of the LBNC, exhibit moderate levels of GABA-ir with some regional variations. These GABA-ir neurons represent a rather small neuronal subpopulation that is outnumbered by that constituted by non-ir pyramidal neurons. This GABA-ir neuronal subpopulation is accompanied by numerous GABA-ir puncta distributed in the neuropil and seems to represent axon terminals since they appear encapsulating the perikarya and apical dendrites of non-ir neurons. As in the other members of the LBNC, in the BM nucleus there is a pronounced tendency for the GABA-ir neurons to form clusters or be aligned in rows surrounding areas devoid of GABA-ir. In the same manner as for other members of the LBNC, the GABA-ir neurons in the BM nucleus are morphologically heterogeneous with most GABA-ir cells showing a round or oval soma that are smaller than those of the non-ir neurons. Usually they show only the initial segment of their apical dendrites, dendrites that are sparsely spined, and, for that reason, corresponding morphologically to non-pyramidal neurons (class II and III).

MONOAMINE MARKERS

DOPAMINE-β-HYDROXYLASE (DBH) According to Sadikot and Parent (1990), the squirrel monkey accessory basal nucleus shows very light DBH-ir terminal labeling in its magnocellular division and light DBH-ir in its parvicellular and "superficial" (?) divisions.

HISTAMINE (HA) According to Airaksinen *et al.* (1989), in the tree shrew, the BM nucleus, i.e., their nucleus basalis accessorius, which they do not include in their Table 1, would contain at least a similar amount of HA-ir fibers as other members of the LBNC, i.e., a fairly dense innervation.

SEROTONIN (5-HT) According to Sadikot and Parent (1990), in the squirrel monkey, the basal accessory nucleus shows a dense population of 5-HT-ir axonal varicosities in its magnocellular portion with a mild rostrocaudal gradient of decreasing density. The parvicellular and "superficial" (?) divisions show very light 5-HT-ir labeling, with some fibers of passage crossing the basal and cortical nuclei.

THYROSINE HYDROXYLASE (TH) According to Sadikot and Parent (1990), in the squirrel monkey the accessory basal nucleus (here BM) displays a striking paucity of TH-ir terminal labeling appearing in the one that is present in the form of preterminal fibers en route to the parvicellular basal nucleus and to the cortical transition area (here PM APir).

EXCITATORY AMINO ACIDS

GLUTAMATE/ASPARTATE (GLU/ASP) Retrograde tracing experiments made in rats using tritiated D-aspartate indicates that a considerable number of the BM neurons give rise to GLU/ASPergic projections to the ventral pallidum and in a lesser degree to the nucleus accumbens (Fuller *et al.*, 1987).

INHIBITORY AMINO ACIDS

γ-AMINOBUTYRIC ACID (GABA) According to Pitkänen and Amaral (1994), in the macaque monkey, all divisions of the basal accessory nucleus (here the BM nucleus) have a relatively high density of GABA-ir cells, most of them of type 1, though type 2 cells are also present. Cells expressing GAD mRNA are evenly distributed throughout the nucleus. Their density is

higher than in the BL nucleus but lower than in the adjacent VCo nucleus. The AB/BM nucleus has a medium-density GABA-ir neuropil with slightly higher density of GABA-ir fibers and terminals in the VM division.

NEUROPEPTIDES

COCAINE- AND AMPHETAMINE-REGULATED TRANSCRIPT (CART) The presence of a moderate CART mRNA signal has been reported for this nucleus (Hurd and Fagergren, 2000).

CHOLECYSTOKININ (CCK) The density of CCK mRNA-labeled cells in the BM nucleus is the highest after that in the La nucleus (Savasta *et al.*, 1990).

CHROMOGRANIN B According to Marksteiner *et al.* (1999), the human BM nucleus contains a high-density PE-11-like ir which consisted of varicose fibers and mixed-size varicosities. No PE-11-like ir neurons are present.

CORTICOTROPIN-RELEASING FACTOR (CRF) According to Powers *et al.* (1987), in the basolateral nuclear group there is a sparse populations of small, corticotropin-releasing factor immunoreactive (CRF-ir) bipolar cells, approximately 20 µm in length. In normal individuals CRF-ir axons, predominantly straight, thin, and unbranched, were present throughout the amygdala and were most conspicuous in the lateral and basolateral nuclei. However, according to their schematic representations these CRF-ir fibers will have a more homogeneous distribution in BM than in La, BL, or PL nuclei, although it seems that these fibers are more numerous in the middle sectors of the BM nucleus.

CORTICOTROPIN-LIKE INTERMEDIATE LOBE PEPTIDE (CLPI) Zaphiropoulos *et al.* (1991) reported that the highest accumulation of CLPI-ir fibers, varicosities and terminals present in the amygdaloid body take place at the level of the three major divisions of the basolateral amygdaloidal complex, i.e., La, BL, BM. In contrast, no CPLI-ir cell bodies were detected at any level of the amygdala.

ENKEPHALIN (ENK) According to Pioro *et al.* (1990), SP-ir neurons are clustered in their dorsal magnocellular part of the accessory basal nucleus (here DM/CM BM), but they are few and scattered in the rest of the amygdala.

GALANIN (GAL) According to Kordower *et al.* (1992), in the macaque monkey, amygdala this member of the LBNC, like all of its remaining components contains no GAL-ir cell bodies and few if any GAL-ir fibers.

NEUROKININ B (NKB) According to Chawla *et al.* (1997), the BM nucleus contains NKB-ir neurons that are scattered throughout the nucleus.

NEUROPETIDE Y (NPY) According to Walter *et al.* (1990), in the human amygdala, their nucleus profundus amygdalae mediale (here the BM nucleus), as in other members of the LBNC, the NPY-ir cells appeared to be concentrated in the dorsal (large-celled) regions whereas the reverse would be true concerning the distributions of NPY-ir fibers and terminals. Furthermore, according to Unger and Lange (1992), close to 90% of the NPY-ir neurons are also positive for NADPH-d.

NEUROTENSIN (NT) When the schematic drawings presented by Mai *et al.* (1987) are carefully examined, it becomes evident that the dorsomedial sectors of the BM nucleus (i.e., their nucleus amygdaloideus profundus, pars medialis) contains moderate amounts of NT-ir whereas ventrolateral sectors contain low levels. No NT-ir cell bodies were mapped by them, in agreement with Benzing *et al.* (1992), who reported that the BM nucleus (i.e., their basal accessory nucleus) contains collectively very little NT-ir with only few scattered fine- and coarse-beaded fibers expressing NT-ir. Apparently in their material there were no differences in density of NT-ir between their magnocellular (*my* DM/CM/DL subdivisions) and parvicellular (*my* VL/VM BM) divisions of their basal accessory nucleus. However, in a few cases a slight increase in NT-ir was observed in the extreme anterior aspect of the BM nucleus. This region likely represented a transition area between the posterior end of the AAA and the anterior BM; thus, the NT-ir fibers present here would likely be a caudal extension of the AAA rather than the BM proper.

SOMATOSTATIN (SOM) In the human brain, Mufson *et al.* (1981, 1988) reported the presence of SOM-ir neurons in the BM nucleus (i.e., their accessory basal nucleus) but did not provide further detail on the distribution pattern of cells and fibers within the nucleus. Bouras *et al.* (1987), in turn, reported rather low densities of cell bodies ir for somatostatin (SOM-ir) and low to medium concentrations of SOM-ir fibers and terminals at the level of all the subdivisions of the amygdaloid body. On the other hand, Unger and Lange (1992) established that close to 90% of the SOM-ir neurons are also positive for NADPH-d.

According to Amaral and Basset (1989) in the macaque monkey, their basal accessory nucleus (here

BM) shows a complementarity of SOM-ir fibers and cell body. SOM-ir fibers and terminals are very dense at the rostral parvicellular pole and continue caudally in the parvicellular sector of the nucleus where they seems to attain the highest density in the amygdala. Although the so-called accessory basal nucleus also contains SOM-ir cells, their density is not very high. While fibers and terminal labeling is quite low in the magnocellular division of the basal accessory nucleus, the density of SOM-ir cells is much higher than in the parvicellular division. This SOM-ir neuronal population is rather heterogeneous in shape and size. By contrast in the above-described picture, McDonald *et al.* (1995) describe a similar distribution.

SUBSTANCE P (SP) According to Piorio (1990), as in the remaining nuclei of the LBNC no SP-ir cells can be found, but a lightly stained delicate network of varicose SP-ir fibers can. However, Chawla *et al.* (1997) described the presence of scattered SP-ir neurons in the human amygdala.

NEUROTROPHINS

BRAIN-DERIVED NEUROTROPHIC FACTOR (BDNF) According to Murer *et al.* (1999), the human basal accessory nucleus, i.e., the present BM nucleus, contains both BDNF-ir neurons and fibers, although showing a moderate staining intensity and rather modest density in number, which contrasts markedly with the much higher BDNF-ir in the neighboring Ce nucleus.

ENZYMES

ANGIOTENSIN CONVERTING ENZYME (ACE) According to Chai *et al.* (1990), the BM nucleus (i.e., their basal accessory nucleus) displays lower levels of ACE binding than its counterpart, the BL nucleus.

BUTYRYLCHOLINESTERASE (BUCHE) This nucleus contains numerous BuChE-positive neurons that are of small size with round, fusiform, or triangular profiles. Some have several branching processes. The size of the BuChE-positive elements remains the same no matter its topographical location (Darvesch *et al.*, 1998).

NICOTINAMIDE ADENINE DINUCLEOTIDE PHOSPHATE DIAPHORASE (NADPH-D) According to Unger and Lange (1992), except for the relatively small AAA, in all nuclei of the amygdala there were numerous, relatively homogeneously distributed NADPH-d-positive cells and, concomitantly, a dense network of NADPH-d fibers that was distributed throughout the whole gray complex (see also Brady *et al.*, 1992). These NADPH-d-positive neurons were similar in all subregions, i.e., showing predominantly medium-sized cells sending out extended bipolar or multipolar dendritic branches. These authors also found that more than 90% of the SOM-ir and NPY-ir neurons are also NADPH-d positive.

With regard to the presence of a dense NADPH-d-positive neuropil in the BM nucleus, Sims and Williams (1990), in contrast to the above-cited report, found that the NADPH-d activity is nil in the neuropil of their dorsal large celled subdivision of the accessory basal nucleus (i.e., the DM/CM/DL BM), whereas it is characteristically positive in that of the ventral small-celled subdivision of the same nucleus (i.e., VM/VL BM), with only few scattered Golgi-like cells showing NADPH-d positivity.

P450 AROMATASE (P450 AROM) According to Roselli *et al.* (2001), in the macaque monkey amygdala, the BM nucleus (i.e., their basal accessory nucleus) contains very high density of P450 AROM mRNA containing cells. A close examination of their illustrations would indicate that the P450 AROM mRNA labeling is concentrated in the large-celled subdivision of the BM nucleus in rostral parts of the nucleus, but more caudally (Figs. 5B–D) the labeling shifts principally to the dorsolateral sector of BM and, but in a much lesser degree, to the ventral sectors of this nucleus, i.e., to places in the BM where the cell population is predominantly of the small celled.

PROTEINS

CALCIUM-BINDING PROTEINS

CALBINDIN (CAL) According to Sorvari *et al.* (1996b), the density of CAL-ir cells in the BM nucleus (their basal accessory nucleus) is high compared to other amygdaloid nuclei, particularly in the caudal portion of the large-celled dorsomedial subdivision (i.e., their magnocellular division). The small-celled DL and VL subdivisions and the medium-celled VM subdivision have slightly lower density of immunoreactive neurons than the DL. Most of the neurons in the DM and DL/VL parvicellular divisions were small type 1 neurons, although numerous type 2 and some type 3 cells were also observed. A few lightly stained pyramidal-shaped neurons have been also observed.

The highest density of CAL-positive fibers can be found in the VM BM. The density of CAL-ir neuropil in the BM nucleus is low. The DL/VL contained a moderate density of CAL-positive bundles. A slightly smaller number of bundles was found in the DM and VM subnuclei.

CALRETININ (CR) According to Sorvari *et al.* (1996a), the most common CR-ir neurons in their basal accessory nucleus (here BM nucleus) are small type 1 and 3 cells. They also found in their magnocellular division

(approximately DM/CM here) numerous type 2 CR-ir neurons. Their parvicellular division (approximately VL/VM here) contains a slightly higher density of CR-ir neurons than the previously described subdivision, but its lateral rim (VL BM?) was reported to contain fewer of these immunoreactive neurons. Their ventromedial subdivision (here IMG) is said to contain a moderate number of type 1 CR-ir neurons. On the other hand, the BM nucleus seems to contain the lowest fiber and neuropil staining in the human amygdaloid complex. Interestingly, the ventral part of the small-celled BM displays a moderate level of staining.

PARVALBUMIN (PAV) According to Sorvari *et al.* (1996c), the density of PAV-ir cells in this nucleus was lower than that in the magnocellular (here DL/D BL) and intermediate BL (here I BL).The largest number of PAV-ir cells could be found in their magnocellular subdivision (here DM/CM) of BM. All three types of cells were observed in moderate numbers, although the density of type 1 and type 2 cells was higher than that of type 3 cells.

As in other nuclei of the human and monkey amygdala, all of the PAV-positive neurons in BM belong to the aspiny or, in rare occasions, to the sparsely spiny categories (Pitkänen and Amaral, 1993; a, b), displaying spherical (type 1, 33%), angular, multipolar (type 2, 28%), and fusiform (type 3, 21%) shapes. The distribution of the PAV-positive cells was not uniform, showing a rostrocaudally decreasing gradient in their number.

Other Proteins

CALPASTATIN (CALPT) According to Mouatt-Prigent *et al.* (2000), large CALPT-ir neurons are present especially in the basal accessory nucleus (here the BM nucleus). A high proportion of these neurons are bipolar and strongly immunostained. They are surrounded by a dense plexus of CALPT-ir fibers and puncta very probably corresponding to nerve terminals.

DOPAMINE- AND ADENOSINE 3′,5′-MONOPHOSPHATE (CAMP)–REGULATED PHOSPHOPROTEIN OF M, 32 KDA (DARPP-32) AND PHOSPHATASE INHIBITOR 1 (I-1) According to Barbas *et al.* (1998), in the macaque monkey, the distribution of neurons DARPP-32-ir and I-1-ir is similar, though not identical, in the BM nucleus. For both phosphoproteins most ir neurons can be found in the medial half of the nucleus. However, I-1-ir neurons extended more ventrally and laterally than the DARPP-32-ir elements, suggesting only partial overlap in the two populations. The dorsolateral sector of the BM nucleus is relatively sparse in immunoreactive neurons, and those that can be detected are weakly labeled.

DOPAMINE TRANSPORTER (DAT) According to Ciliax *et al.* (1999), the BM nucleus has markedly fewer DAT-containing varicose axons than BL, a feature that helps its differentiation from this latter.

LIMBIC SYSTEM–ASSOCIATED MEMBRANE PROTEIN (LAMP) According to Côté *et al.* (1996), in the macaque amygdala, overall the BM nucleus stains much less intensely than does the adjoining BL nucleus. Rostrally, the BM nucleus is faintly LAMP-ir with only scattered ir punctate material in its small-celled division. More caudally, LAMP-ir is weak in the large-celled division, moderate in the small-celled one, and intense in the superficial division, this latter probably representing one of the large accumulations of intramedullary grisea of the present account. At its most caudal level, the BM nucleus shows a diffuse and moderate LAMP-ir.

SMI32 NEUROFILAMENT PROTEIN (SMI32-IR) From the low-magnification atlas on the distribution of this protein in the macaque brain published by Petrides *et al.* (2000), it is evident that the dorsal large-celled BM nucleus contains SMI32-ir while the ventral small-celled division seems to be relatively devoid of SMI32-ir.

RECEPTORS

BENZODIAZEPINE RECEPTOR (BZD) The BM nucleus apart from showing, together with La and PL BL, the highest concentrations of BZR in the amygdala, also shows anteroposterior variations in their density, so that the highest concentrations of BZD-R appear in the rostral sectors of the nucleus (Niehoff and Whitehouse, 1983). The existence of very high concentrations of BZR at the level of this nucleus in humans was confirmed by Zezula *et al.* (1988).

Cholinergic Receptors

MUSCARINIC RECEPTOR (MACH-R) According to Cortés *et al.* (1987), the human basal accessory nucleus (here the BM nucleus) contains one of the highest densities of mACh-R which belong predominantly to subtype 1 neuron. On the other hand, according to Smiley *et al.* (1999), the amygdala as a whole contains a low density of m2-ir neurons.

NICOTINIC RECEPTOR (NACH-R) No source of data is available to the present writer regarding the distribution of this type of receptors in the primate amygdala.

Monoamine Receptors

ADRENORECEPTORS α_1 According to Flügge *et al.* (1994), in the tree shrew, at mediorostral levels of the amygdala, the basal accessory nucleus (here BM) reveals

high numbers of [^{3}H]prazosin (α_1-adrenoreceptor antagonist) binding sites.

ADRENORECEPTORS α_2 According to Flügge *et al.* (1994), in the tree shrew, at mediorostral levels of the amygdala, the basal accessory nucleus (here BM) contains low numbers of [^{3}H]rauwolscine (α_2-adrenoreceptor antagonist).

ADRENORECEPTORS β_1 According to Flügge *et al.* (1994), in the tree shrew, the majority of the monoamine nonsertoninergic receptors present in the basal accessory nucleus (here BM) are adrenoreceptors of the beta 1 type.

SEROTONINERGIC RECEPTOR (5-HT-R)

5-HT$_{1A}$ RECEPTOR (5-HT$_{1A}$-R) According to Flügge *et al.* (1994), in the tree shrew, the basal accessory nucleus is strongly labeled by [^{3}H]DPAT, a specific agonist of 5-HT$_{1A}$-R.

5-HT$_{2C}$ RECEPTOR (5HT$_{2C}$-R) According to Lopez-Gimenez *et al.* (2001), high levels of 5-HT$_{2C}$-R mRNA are found in their basal accessory nucleus (i.e., the BM nucleus).

STEROID RECEPTORS

ESTROGEN RECEPTOR α (ER-α) According to Blurton-Jones *et al.* (1999), their accessory basal nucleus (here BM nucleus) displayed a large number of ER-α-labeled nuclei. According to Österlund *et al.* (2000), in both human and monkey brains, the mediodorsal part of both divisions (magnocellular and parvicellular) of the accessory basal nucleus (here the DM/MC/Mc VM nucleus) contain moderate amounts of ER-α-labeled nuclei.

OPIOID RECEPTOR (O-R) Daunais *et al.* (2001) divided the accessory basal nucleus (here the BM nucleus) into parvicellular (here VL/VM) and magnocellular divisions (here DM/CM), but found [^{3}H]DAMGO binding relatively uniform throughout these two subdivisions. They clearly noted an evident higher density of binding in what they called ventromedial subdivision (probably IMG, here), located along the medial border of the accessory basal nucleus.

SOMATOSTATIN RECEPTOR (SOM-R) According to Reubi *et al.* (1986), the BM nucleus contains a moderate amount of SOM-ir, which is lower than that present in the large-celled BL nucleus.

Neuropathology According to Kromer Vogt *et al.* (1990), the most pronounced density of neurofibrillar tangles (NTG), which are present in Alzheimers patients, are found in BM nucleus (i.e., their basal accessory nucleus) and cortical nuclei. According to Unger and Lange (1992), this nucleus, together with the corticomedial amygdala, shows the most dense accumulation of neuritic plaques (NP) in the amygdala of Alzheimer's patients. By contrast, this nucleus shows slight changes in patients suffering neuronal ceroid lipofuscinosis (Braak and Braak, 1987).

Paralaminar Amygdaloid Nucleus (PL)

For the sake of a greater conformity with the amygdaloid nomenclature more commonly used, I have decided to abandon the terminology I once used (paralaminar BL; de Olmos, 1990) for designating this part of the LBNC, not only because such naming implies that PL is a part of BL, as originally proposed by Crosby and Humphrey (1941) [i.e., their superficial part of the pars medialis (small-celled) of the basal nucleus], but because such implication conflicts with the cytoarchitectonic, chemoarchitectonic, and connectional data favoring segregation of these grisea.

Topographical Landmarks This nucleus (PL in Plates 28–30 (8.0–0.7 mm of Mai *et al.*'s *Atlas of the Human Brain*) (Figs. 22.1c,d; 22.2; 22.3; 22.4; 22.5a; 22.6a; 22.7a; 22.8–22.11; 22.3–22.6a; 22.7a,b; 22.8–22.10) lies superficially to the ventral small-celled sectors of both BL medially and La laterally. In sagittal sections it is possible to appreciate that this nucleus constitutes an incomplete dorsally opened shell around the rostral, ventral, and caudal borders of the nuclear mass formed by La, VL BL, and VM BL reaching farther dorsally in its rostral pole than in its caudal one.

Cytoarchitectonics On both topographic and cytoarchitectonic grounds, the PL nucleus can be divided into a larger and well-defined medial part, and a smaller lateral part, which, because of its insular arrangement, has been named the pars glomerularis by Brockhaus (1940), a name that is retained here. This part of the PL nucleus, which covers the ventromedial aspect of the La nucleus from the rostral pole to the more caudal sectors of the amygdala, tends to form cell strands and shell-shaped islands which, when the LBNC extends posteriorly for some distance into the roof of the lateral ventricle, lies immediately below the ventricle but never surfaces into it. The medial PL or PL nucleus proper, on the other hand, covers the ventral aspects of the two small-celled parts of the BL nucleus, i.e., the ventromedial and ventrolateral subdivisions (VM BL and VL BL), throughout their rostrocaudal extent as can be easily appreciated in sagittal sections. The cells of this sector of PL are smaller and more densely packed and hyperchromic than those

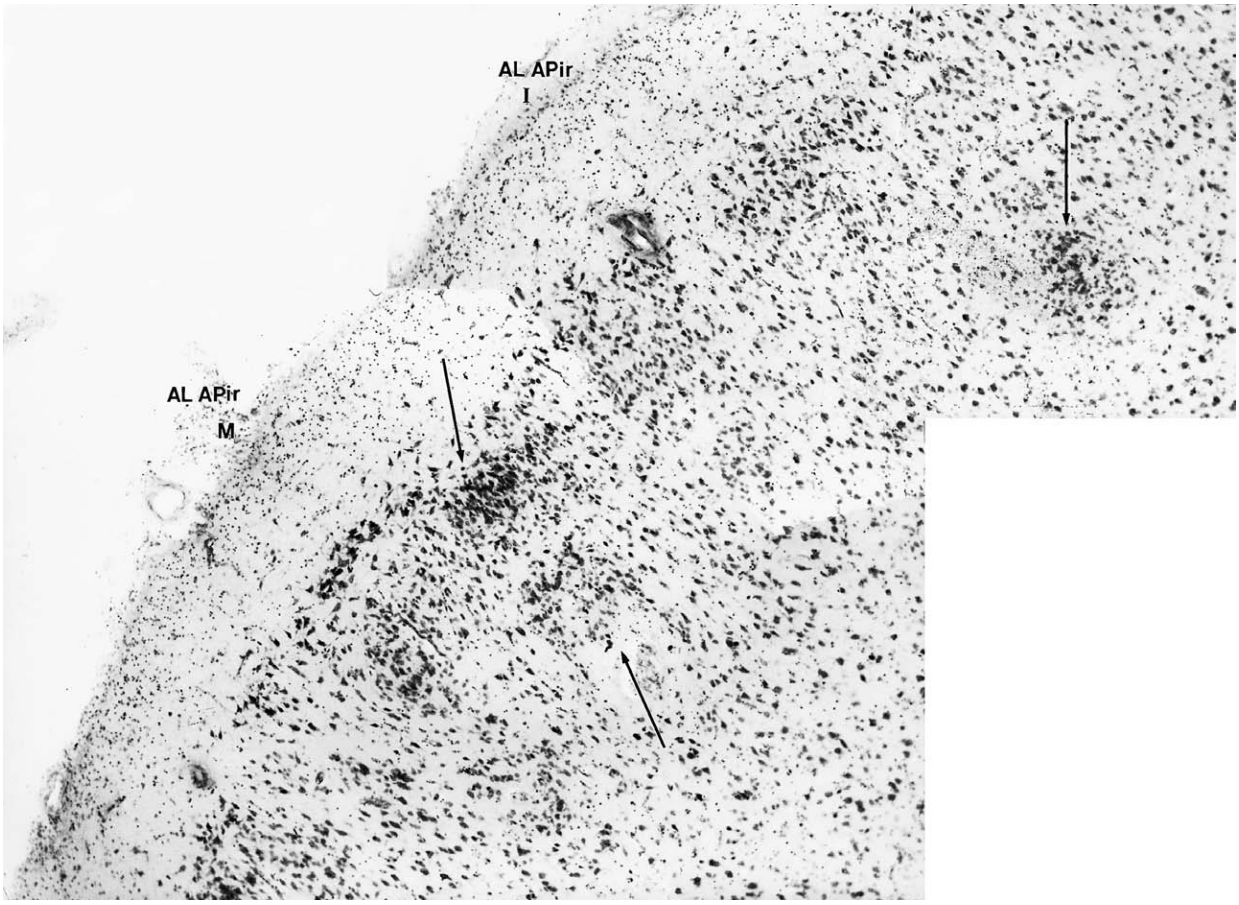

FIGURE 22.13 Medium-power photomontage of a Nissl-stained section through the anterolateral division (AL) of the amygdalopiriform area (Apir) showing the island of granule cells characterizing this transitional allocortical area. Arrows point to the islands of granule cells

in the neighboring small-celled BL nucleus, providing the division with a granular appearance. On the basis of cellular arrangement as well as differences in cell type, the medial PL division can be subdivided into anterior and posterior subparts. The anterior subpart (Brockhaus' amygdaloideum profundum ventrale supergrannulare) shows a tendency to break up into islands of different sizes, usually ovoid in shape (see also Brockhaus, 1940; Hilpert, 1928; Sanides, 1957b). The posterior subpart (Brockhaus' amygdaloideum profundum ventrale grannulare) presents, by contrast, a more compacted arrangement.

Finally, a characteristically cytoarchitectonic feature in PL, particularly appreciable in Nissl-stained sections, is the presence, along its whole extent, of numerous sharply delineated and deep staining nuclei resembling the naked nuclei of oligodendroglia cells that partially overlap the neuronal groups that constitute the nucleus. These naked nuclei tend to invade the deep layers of the amygdalopiriform transition area. It is interesting to point out that in a collection of macaque monkey brains at my disposition, this arrangement can be also found, whereas it is consistently absent in the squirrel monkey amygdala (unpublished observations).

According to Braak and Braak (1983), PL presents a characteristic pigmentation in aldehyde-stained sections different from that found in the other gray components of the LBNC, and which is due to the predominant presence in PL of small spiny neurons that store only moderate amounts of pigment granules. PL also contains pigment-laden aspiny or sparsely spiny neurons reminiscent of cortical stellate cells, and in addition sparsely pigmented small neurons that resemble morphologically similar neurons present in layer IV of the neocortex.

It should also be mentioned that, according to the embryological studies of several authors (Brockhaus, 1940; Humphrey, 1968, 1972; Mikami, 1952), PL is the last to be identifiable during the ontogenetic development of the amygdaloid nuclei. In addition to it, quantitative allometric studies by Stephan and Andy (1977) indicate that, among the various subdivisions of

the amygdala, PL is the most progressive structure. See Mueller and O'Rahilly (this volume).

Fibroarchitectonics In fiber preparations (Fig. 22.7b) the PL nucleus appears to have a less rich fiber network than that present in its companion nuclei of the LBNC, the La and BL nuclei, except in its island-like or glomerular-like (PL gl) sectors where the cell aggregations conforming them appear surrounded by relatively dense septa of fibers. The continuity of the lamina-like medial division of the PL nucleus is interrupted by small bundles of thin fibers traversing it almost perpendicularly to the temporal white matter running along its ventral surface.

Chemoarchitectonics

Heavy Metals In Timm-Danscher´s preparation of the marmoset and squirrel monkey brains (Fig. 22.23), the territory that is probably homologous to the PL nucleus in humans shows in most of its extent a dense silver sulfide precipitate similar to that described for its neighboring companions of the LBNC, except in some of the laterally located islands described above and the more medial sectors of the medial division of PL where the reactivity is apparently higher. As it happens with other amygdaloid nuclei showing a positive Timm-Dancher´s reaction, neuronal perikarya in the PL nucleus are negatively stained.

Neurotransmitters

CHOLINERGIC MARKERS

ACETYLCHOLINESTERASE (ACHE) According to Darvesh *et al.*'s (1998) histochemical data, the human PL (Figs. 22.9–22.11) would stand last concerning the AChE stainability as compared with the other nuclei of the LBNC. There are only isolated AChE-positive neurons in this nucleus with fusiform or triangular profiles, constituting less than 1% of the total neuronal population in this nucleus. With regard to the density of the AChE reaction at the level of this nucleus, Sorvari *et al.* (1995) claim that PL is slightly more intensely stained than the VL/VM BL nucleus (i.e., their parvicellular basal nucleus).

According to Amaral and Basset (1989), in the macaque brain, AChE preparations of the PL nucleus show a moderate pattern of fibrous staining similar to that present in their parvicellular basal nucleus (here small-celled VL/VM BL subnucleus). No AChE-positive cells can be detected in the PL nucleus. On the other hand, Flügge *et al.* (1994) reported that in the tree shrew the PL nucleus displays AChE reactivity from moderate to intense.

CHOLINE ACETYLTRANSFERASE (CHAT) According to Amaral and Basset (1989), in the macaque brain, the distribution of ChAT-ir fibers and terminals is very similar to that seen in the parvicellular basal nucleus (here VL/VM BL subnucleus) consisting of a thin plexus of ChAT-ir fibers and terminals.

EXCITATORY AMINO ACIDS

GLUTAMATE/ASPARTATE (GLU/ASP) According to Amaral and Insausti (1992), in the macaque monkey, injections of tritiated D-aspartate in the basal and lateral amygdaloid nuclei labeled a significant number of neurons along the whole PL nucleus, providing argument that the nucleus would be a source of glutamatergic intraamygdaloid projections to the above-mentioned nuclei.

INHIBITORY AMINO ACIDS

γ-AMINOBUTYRIC ACID (GABA) According to McDonald and Augustine (1993) and Pitkänen and Amaral (1994), in the macaque monkey PL nucleus, there is a marked reduction in the number of GABA-ir cells as compared with their density in the small-celled VL/VM BL nucleus, with most of the cells being type 1. This is also true for the labeling with GAD mRNA. The GABA-ir neuropil is also quite low in density.

MONOAMINE MARKERS

DOPAMINE β-HYDROXYLASE (DBH) From my own observations, at least in the squirrel monkey, DBH-ir fibers and terminals can be seen in this nucleus.

NEUROPEPTIDES

NEUROPEPTIDE Y (NPY) According to Walter *et al.* (1990), within the human amygdala the NPY-ir appear highest in the PL nucleus (i.e., the ventral parvicellular subdivisions of their nucleus profundus amygdalae ventralis).

According to McDonald (1995), in the macaque monkey PL nucleus, as in other components of the LBNC, the NPY-ir are numerous and the NPY-ir fiber plexus is dense. Likewise, the NPY-ir neuronal population in the PL nucleus includes spiny and spiny-sparse cells and many of them colocalize SOM-ir. The density of this plexus may be related to the fact that the NPY-ir spiny-sparse neurons are with all probability class II neurons possessing very dense local axonal arborizations.

NEUROTENSIN (NT) According to Benzing *et al.* (1990), the NT-ir in the human amygdaloid nucleus consists of a network of varicose fibers interspersed among a dense plexus of dot-like puncta. Although the density of the NT-ir in the PL nucleus is classified as high, as in the centromedial nuclei, it is, however, quite distinct.

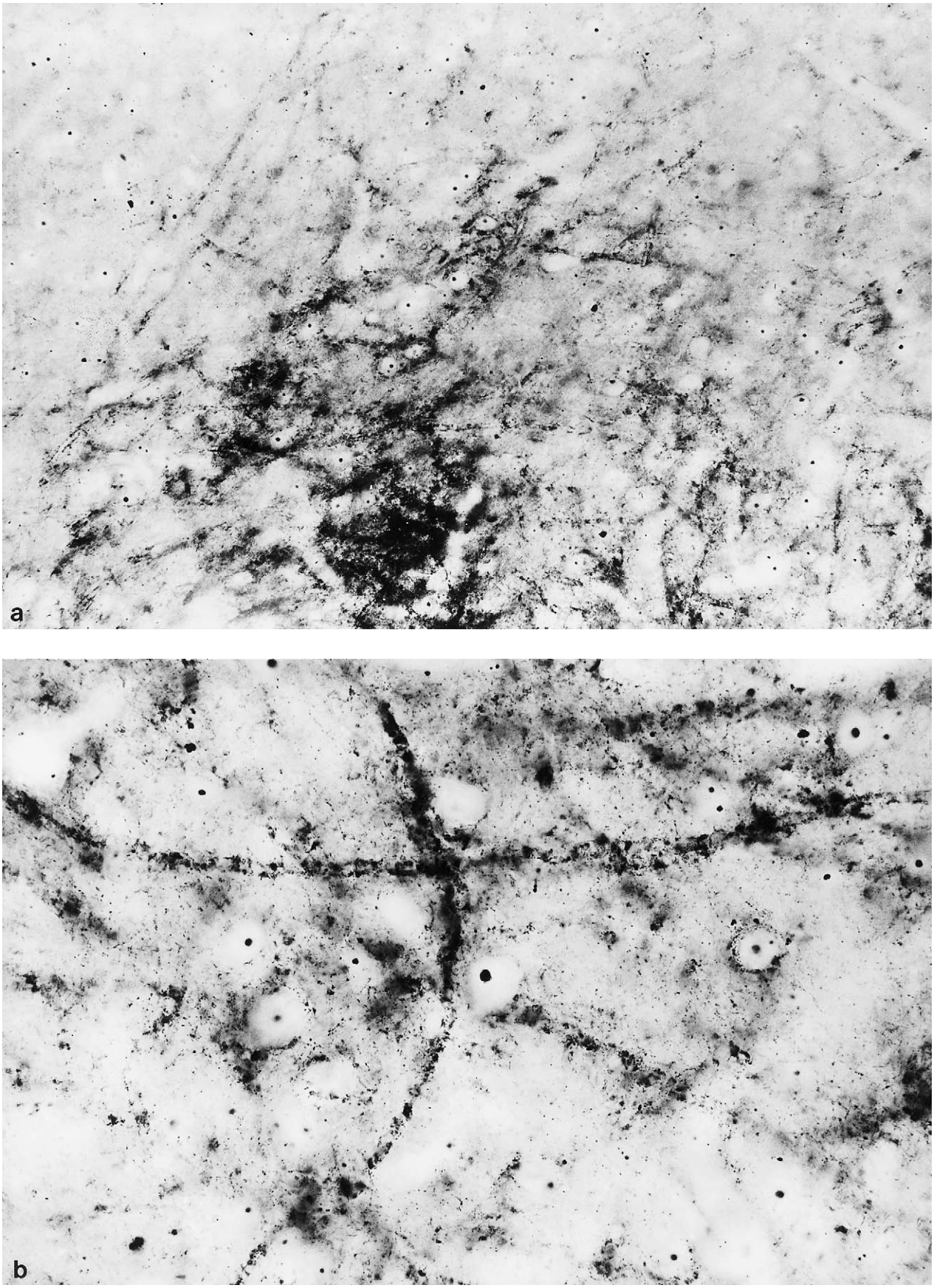

FIGURE 22.14 (a and b) Medium- and high-power photomicrographs of a cupric-silver stained coronal section through the sublenticular substantia innominata (SIsl) from a normal macaque monkey brain to show the heavily impregnated bistranded argyrophilic neuropil present at the level of the dorsal anterior division of this sector of the extended amygdala.

SOMATOSTATIN (SOM) In the monkey the PL is described as containing a fairly dense plexus of SOM-ir fibers and terminals that are similar in staining to that in the small-celled VL/VM BL nucleus. This nucleus is also described as containing numerous SOM-ir cell bodies especially at caudal levels of the amygdala (Amaral *et al.*, 1989). In McDonald *et al.* (1995) mapping of the localization of SOM-ir neurons also containing NPY can be seen to be more abundant in the medial subdivision of this nucleus while being more diffusely distributed in the lateral sector.

NEUROTROPHINS

BRAIN-DERIVED NEUROTROPHIC FACTOR (BDNF) According to Murer *et al.* (1999), in the human brain, all amygdaloid nuclei show BDNF-ir neurons and fibers, from which it can be inferred that PL nucleus is included though it is not specifically mentioned by the authors. Close examination of their minimally magnified Figure 4A suggests that this is so.

ENZYMES

BUTYRYLCHOLINESTERASE (BUCHE) According to Darvesh *et al.* (1998), in the human amygdala, the PL nucleus contains BuChE-positive neurons that are morphologically similar to the neurons in the BL nucleus, i.e., they are round, fusiform, or triangular in profile with many branching processes. Approximately, 6% of the neurons in the PL nucleus contain BuChE and none of them contains pigment.

CALCIUM-BINDING PROTEINS

CALBINDIN (CAB) According to Sorvari *et al.* (1996b), the PL nucleus contains one of the lowest densities of CAB-ir neurons in the human amygdaloid complex. Most of the CAB-ir neurons were small type 1 cells. A few small type 2 cells can be also found. The CAB-ir neurons are scattered around the PL nucleus and are mainly located outside the cell clusters, typical of this nucleus as seen in Nissl-stained preparations.

The density of the CAB-ir axons in the paralaminar nucleus is also low. In the medial part of the paralaminar nucleus, the few CAB-ir axons are located outside the neuronal clusters found in Nissl preparations. Some thick dendrites emanating from the CAB-ir somas located in the small-celled divisions of the BL nucleus (i.e., their parvicellular basal nucleus) extend to the PL nucleus. The intensity of the neuropil staining is similar to that in the BL nucleus. The lateral part of the PL nucleus located ventral to the La nucleus had more intense neuropil staining than this latter. Typical of the PL nucleus are thin, tortuous, and branched axonal plexuses. Such plexus are often observed near the soma of an CAB-ir type 1 neuron, which may have given rise to it. No CAB-ir bundles are observed in the PL nucleus.

CALRETININ (CR) According to Sorvari *et al.* (1996a), the PL nucleus contains the lowest density of CR-ir neurons in the human amygdaloid complex. A few CR-ir neurons are mostly located in the medial half of the PL nucleus. The CR-ir neurons are mainly small type 1 cells that seem to avoid the cell clusters that typify the nucleus in cell preparations. In the medial half of the PL nucleus the intensity of the CR-ir fiber and neuropil staining is similar to that found in the VL/VM BL (i.e., their parvicellular basal nucleus). Fibers are typically oriented dorsal to ventral and they tend to avoid the above-mentioned cell clusters**.** In the lateral part of the PL nucleus, CR-ir fibers and neuropil resemble that in the previously described medial division—a feature that facilitates its separation from the La CR-ir due to its denser staining.

PARVALBUMIN (PAV) According to Sorvari *et al.* (1995), only occasional PAV-ir cells can be found in the PL nucleus, and a low density of PAV-ir fibers and terminals. In the PL nucleus as well as in the border against the BL nucleus, the PAV-ir terminals form a small plexus enclosing several non-PAV-ir perikarya.

OTHER PROTEINS

LIMBIC SYSTEM–ASSOCIATED MEMBRANE PROTEIN (LAMP) According to Côté *et al.* (1996) in the macaque amygdala, the PL nucleus is devoid of LAMP-ir rostrally but shows moderate to intense staining at midamygdaloid levels. More caudally the moderate to intense LAMP-ir in the PL nucleus is continuous with the ir present in the I BL nucleus.

SMI32 NEUROFILAMENT PROTEIN (SMI32) From the low-magnification atlas published by Petrides *et al.* (2000), it seems that the PL nucleus, except for its most rostral extent where it borders rostrodorsally with the La and BL nuclei, does not contain any SMI32-ir. However, this rostral most sector of the PL seems to give one of the strongest positive signals on the amygdaloid complex.

RECEPTORS

BENZODIAZEPINE RECEPTOR (BNZ-R) According to Zezula *et al.* (1988), the granular nucleus (here the PL nucleus) contains very high concentrations of BNZ-R.

CCK RECEPTORS (CCK-R) CCK binding in macaque amygdala showed marked variation among nuclear subdivisions with laterally, ventrally, and medially placed nuclei more heavily labeled than those located

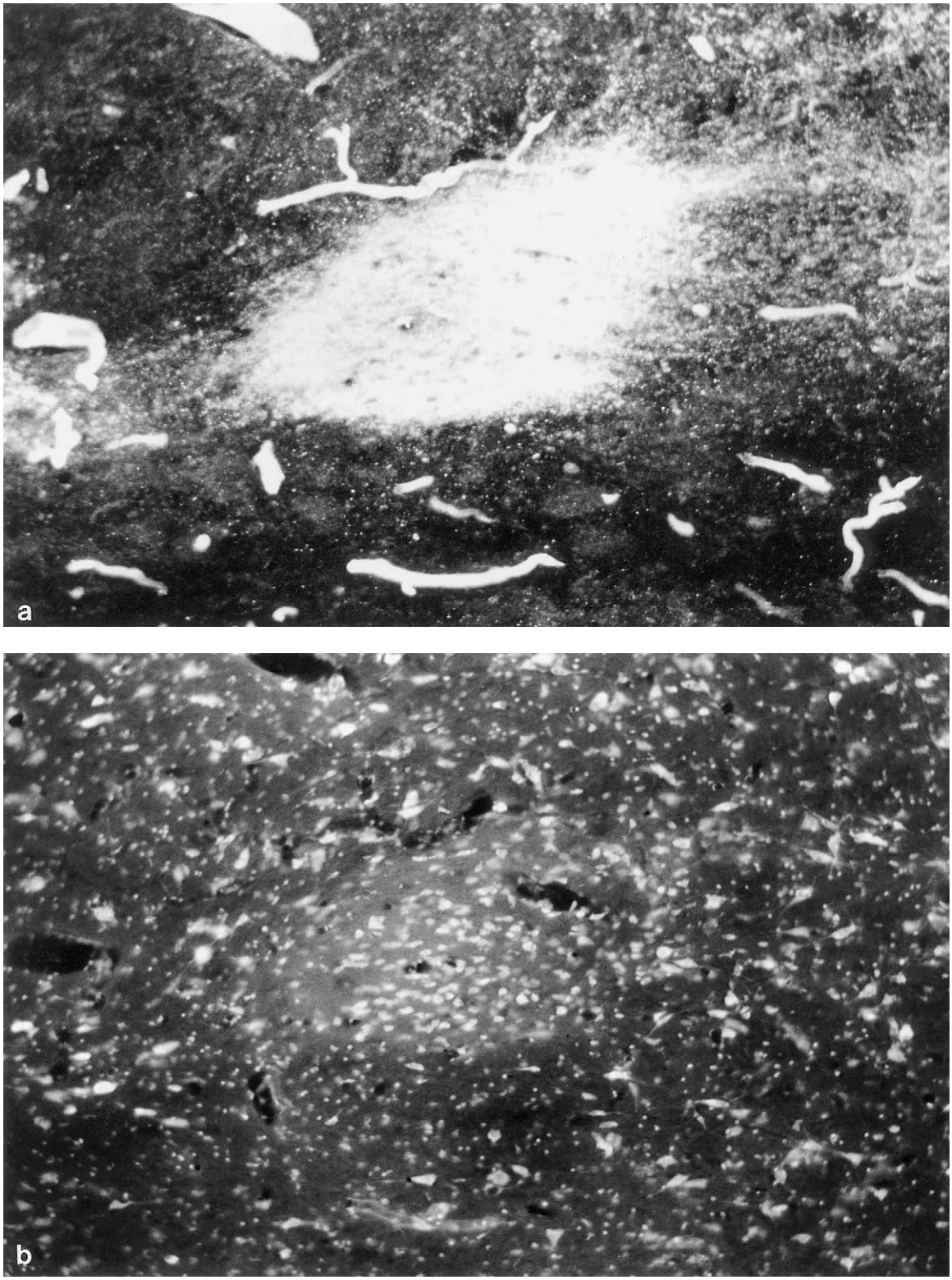

FIGURE 22.15 (a) Medium-power photomicrograph of a Timm's coronal section through the rostralmost extension of the dorsal anterior division of the sublenticular substantia innominata from a squirrel monkey brain. The very dense metal deposits are confined almost entirely to the small-celled neuronal island that is surrounded by the larger cells of the magnocellular basal forebrain complex (MCBFC). (b) The same section counterstained with ethidium bromide (micrograph courtesy of George Alheid).

more centrally and dorsally in the amygdaloid complex. Thus, the most prominent labeling was found over the endopiriform, cortical, mediobasal, and lateral nuclei, and in the parvicellular accessory basal nucleus. The magnitude of binding in the lateral and mediobasal nuclei showed parallels with cell density, i.e., the superficial or paralamellar portion of the mediobasal nucleus, characterized by small and densely packed cells (Crosby and Humphrey, 1941), was more densely labeled than the large-celled, deeper aspects of this nucleus.

CHOLINERGIC RECEPTORS

MUSCARINIC RECEPTOR (MACH-R) According to Cortés *et al*. (1987), the human granular nucleus (here the PL nucleus) contains one of the highest densities of mACh-R, which belong predominantly to subtype 1.

NICOTINIC RECEPTOR (NACH-R) This type of receptor as labeled by [^{3}H]ACh or [3H]nicotine, shows very low concentrations in all nuclei of the rat amygdaloid complex (Rainbow *et al*., 1984; Clarke *et al*., 1985).

MONOAMINERGIC RECEPTORS

ADRENORECEPTOR α_1 According to Flügge *et al*. (1994), in the tree shrew, the paralaminar nucleus forms a continuous band with the strongly labeled [^{32}H]PRA, an antagonist of this type of adrenoreceptor.

OPIOID RECEPTOR (OR) According to Daunais *et al*. (2001), the heaviest concentration of [3H]DAMGO binding sites in the amygdala was found in the PL nucleus. The distribution in this nucleus closely resembles the pattern reported for the small-celled VL and VM subdivisions of BL, in which the entire rostrocaudal extent was densely labeled.

Amygdaloclaustral Transition Area (ACA)

Topographical Landmarks According to Macchi (195l), the amygdaloclaustral transition area (ACA) (Fig. 22.1a) [caudodorsomedial part of PACl in plate 24 (2.7 mm) in Mai *et al*.'s (1997) *Atlas of the Human Brain*] is formed by islands of amygdaloid cells which constitute, together with the claustrum proper and the endopiriform nucleus, what he called the intercalated area. By contrast, many authors have considered this cell group either as part of the endopiriform nucleus [or claustrum preamygdaleum of Brockhaus (l938) or directly assigned to anterior amygdaloid area (see below)]. Actually, the ACA area is a well-circumscribed region made up of a rather homogeneous neuronal population located in the rostral portion of the amygdala, which as Macchi rightly thought is intercalated between the preamygdalar endopiriform nucleus rostrodorsally and laterally, and the lateral amygdaloid nucleus, ventrocaudally and medially, facing the temporal division of the piriform cortex and ACo nucleus in rostrocaudal succession. Groups of intercalated cells surround the nucleus dorsally, caudally, and ventrally, constituting a feature that assists its identification.

The topographical relationships of ACA coincide quite approximately with that given for the group Sorvari *et al*. (1995) labeled as anterior amygdaloid area, although in my material a direct topographical relationship with BL could not be as clearly seen. Furthermore, the cell population in ACA is not loosely packed but instead shows a far more coherent cell packing than that of AAA as here defined.

Cytoarchitectonics and Fiberarchitectonics It is composed predominantly of medium to large, rounded, darkly stained neurons surrounded by a rather scarce glial cell population, which contrasts markedly with the extremely rich glial framework in the neighboring preamygdalar endopiriform nucleus and the claustrum limitans. Groups of intercalated cells surround the nucleus dorsally, caudally, and ventrally. In fiber preparations its identification is facilitated by the rich fiber framework that surrounds this nucleus. Groups of intercalated cells surround the nucleus dorsally, caudally, and ventrally, constituting a feature that assists identification.

Chemoarchitectonics

Cholinergic Markers

ACETYLCHOLINESTERASE (ACHE) According to Amaral and Basset (1989), in the macaque monkey the ACA transition area (i.e., their anterior amygdaloid area) has a meager level of staining for AChE and can be distinguished by the large number of lightly to moderately stained AChE neurons that it contains. This can be confirmed in the Fig. 51 of the atlas of the rhesus monkey brain by Paxinos *et al*. (2000), in which the ACA transition area (i.e., their ventral endopiriform nucleus) appears wedged between the deep division of the AAA medially, the extended amygdala dorsally, and the La and BL nuclei ventrally. The area shows a very slightly higher content of AChE fibers than all of them, being bounded dorsally by the capsule of AChE positive fibers that encapsulates the extended amygdala, while ventrally AChE-rich ICMs mark the boundary with the nuclei of the LBNC.

CHOLINE ACETYLTRANSFERASE (CHAT) According to Amaral and Basset (1989), in the macaque monkey, the ACA transition area (i.e., their

anterior amygdaloid area) has a meager level of ChAT-ir consisting of a fine network of ChAT fibers.

EXCITATORY AMINO ACIDS

GLUTAMATE/ASPARTATE (GLU/ASP) No primate bibliographical data on the subject are available to the present writer.

INHIBITORY AMINO ACIDS

γ-AMINOBUTYRIC ACID (GABA) According to Pitkänen and Amaral (1994), in the macaque monkey, in their anterior amygdaloid area (i.e., the present ACA), the number of cells that are GABA-ir or that contain GAD mRNA is about equal to that observed in the deep amygdaloid nuclei. The GABA-ir neuropil staining of this field is also similar to that in the deep amygdaloid nuclei.

NEUROPEPTIDES

NEUROPEPTIDE Y (NPY) Although no direct reference to this structure is made by McDonald *et al.* (1995) in their description of the distributions of NPY-ir in the macaque monkey amygdala, in their Fig. 1B, and under the name of dorsal anterior amygdaloid nucleus, this ACA area is depicted as containing a moderate number of NPY-ir cells.

SOMATOTASTIN (SOM) According to Amaral *et al.* (1989), their anterior amygdaloid area (here the amygdaloclaustral transition area) demonstrated a low to moderate density of SOM-ir fibers and terminals and scattered labeled cells. They also speak about a certain similarity with the medial division of the central amygdaloid nucleus.

CALCIUM-BINDING PROTEINS

CALBINDIN (CAB) According to Sorvari *et al.* (1996b), their anterior amygdaloid area, which most probably corresponds to the present definition of ACA, contains a moderate density of CAB-ir neurons which correspond to their small type 1 and 2 cells. This territory also contains a moderate intensity of CAB-ir fibers and neuropil staining. The intensity of staining was slightly higher than in the surrounding areas, which helped them indicate the boundaries of the anterior amygdaloid area. No CAB-ir bundles of fibers are present here.

CALRETININ (CR) According to Sorvari *et al.* (1996a), the density of CR-ir neurons in the amygdaloid territory, which they termed the anterior amygdaloid area, is high, with the majority of cells corresponding to the their type 1 and small type 2 cells. The fiber and neuropil CR-ir is also dense.

PARVALBUMIN (PAV) According to Sorvari *et al.* (1995), in the region they termed the anterior amygdaloid area, the density of PAV-ir cells and fibers is low, and only an occasional small neuron can be detected.

OTHER PROTEINS

SMI32 NEUROFILAMENT PROTEIN (SMI32-IR) From the low-magnification atlas on the distribution of this protein in the macaque brain published by Petrides *et al.* (2000), it seems that this controversial nucleus does not contain any SMI32-ir.

Extended Amygdala (EXA)

Recent evidence supports the view held by Johnston (1923) that the bed nucleus of the stria terminalis (BST) and the central (Ce) and medial (Me) amygdaloid nuclei constitute an anatomical entity (e.g., de Olmos and Ingram, 1972; Holstege *et al.*, 1985; Price *et al.*, 1987), a concept that now has gained general acceptance (Alheid and Heimer, 1988; Grove, 1988a, b; Moga *el al.*, 1989; Gomez and Winans-Newman, 1992). Today's notion, however, expands that originally proposed concept by this pioneering worker, who conceived the continuity between the aforementioned structures as occurring only by way of gray matter accompanying the stria terminalis along its supra-, post-, and infra-capsular courses, bridging between these amygdaloid nuclei and their own paraseptal expansion. Based on cytoarchitecture, histochemistry, and hodology, the present expanded conception tells us that the anatomical entity formed by the BST, Ce, and Me should be added to the sublenticular portion of the so-called substantia innominata, now named the sublenticular extended amygdala (SLEA), and the interstitial nucleus of the posterior limb of the anterior commissure (IPAC). The extensive gray complex thus formed can be divided into two major subdivisions: one consisting of the medial bed nucleus of the stria terminalis (BSTM), medial division of the sublenticular extended amygdala (SLEAM) and the rostral Me amygdaloid nucleus; and one with the lateral bed nucleus of the stria terminalis (BSTL), the central division of the sublenticular extended amygdala (SLEACn), and the Ce amygdaloid nucleus (de Olmos *et al.*, 1985; Groove, 1988a, b; Moga *et al.*, 1989; de Alheid *et al.*, 1995; de Olmos and Heimer, 1999; Heimer *et al.*, 1999; Winans, 1999). This elaborate conceptualization of this part of the basal forebrain is derived from several lines of evidence, the earliest being provided by differential staining of the granular argyrophilic neuropil and neurons in cupric silver preparations of normal unlesioned brains (de Olmos, 1969, 1972). Subsequently, evidence was produced by

the backfilling of the neuronal continuum involving the Ce, the anterodorsal Slsl, and the BST after injections of retrograde tracers into the dorsal medulla and by placing fluorescent tracers into the accessory olfactory bulb. This results in the retrograde labeling of the neurons forming the continuum, stretching from the anterodorsal Me nucleus through the medial division of the sublenticular extended amygdala and the large-celled lateral part of the BSTM (de Olmos *et al.,* 1985). Evidence in favor of this hypothesis is discussed below and has been presented in several recent reports (de Olmos *et al.,* 1972, 1985; Holstege *et al.,* 1985; Hopkins and Holstege, 1978; Alheid and Heimer, 1988; Grove, 1988a, b; Moga *et al.,* 1989; Gomez and Winans-Newman, 1992; Alheid *et al.,* 1995; de Olmos and Heimer, 1999; Heimer *et al.,* 1999). Alheid and Heimer (1988), in their thorough morphological and functional analysis of the basal forebrain, coined the term extended amygdala in order to formalize very briefly the incorporation of the BST and the so-called substantia innominata into the amygdaloid complex.

Central Extended Amygdala (CExA)

Paraseptal Components of the Central Extended Amygdala From information that can be gathered from the wealth of data that will be discussed in the context of the present chapter, the classical segregation of the neuronal population of the bed nucleus of the stria terminalis into medial and lateral divisions continues to fit not only the recent cytoarchitectonic, hodological, and chemoarchitectonic information presently available, but also to the physiological and behavioral findings of most recent data. This conceptual advance has been possible largely due to the contribution made by tract tracing with modern procedures and, more particularly, to the hodological relationships between the amygdaloid nuclei and the BST nuclei. Although such contribution has played a key role in re-enforcing the soundness of the medial-to-lateral segregation, it is especially the striking similarities, morphological or otherwise, existing between the lateral group of BSTL nuclei and their counterparts in the central amygdala that justify their inclusion as a part of the central extended amygdala and, as a consequence, to be considered as its paraseptal components.

The following section describes the cytoarchitectonic features of the four subdivisions identified within the lateral division of the bed nucleus of the stria terminalis by using both classical neurohistological procedures applied to transverse, horizontal, and sagittal frozen sections, and nontraditional methods such as transillumination and the application of most recent histochemical and immunohistochemical staining procedures.

The Bed Nucleus of the Stria terminalis (BST)

Topographical Landmarks In the human brain the bed nucleus of the stria terminalis (BST) is a lengthy structure that stretches rostrally from the amygdaloid body to the paraseptal pericommissural region (Figs. 22.1b–22.26b). On topographical grounds the BST can be divided into intra-amygdaloid, supracapsular, and paraseptal sectors. In all mammals, including humans, the paraseptal sector undoubtedly constitutes the main part of the nucleus. It forms an elongated, irregularly shaped pyramid, with its basis over the anterior commissure and the preoptic region and its apical end resting on the dorsolateral aspect of the thalamus. This section lies caudal to the nucleus accumbens, immediately ventrolateral to the anterior horn of the lateral ventricle, caudoventrolateral to the lateral septal nucleus, lateral to the anterior pillars of the fornix, medial to the internal capsule, and rostral to the stria medullaris thalami. It also completely encircles the anterior commissure just before its crossing of the midline. On this basis, pre-, supra-, infra-, and postcommissural sections can be distinguished (Figs. 22.16–22.18, 22.24b, 22.23, 22.26a). Moreover, in their cytoarchitectonic studies of the human septal region, Andy and Stephan (1968) recognized three parts: anterior, internal, and external, the former two being small celled and the latter large celled. These gross divisions were also recognized by Brockhaus (1942a,b), who used different names for them in his cell studies of the hypothalamus and the striatum, and by Strenge *et al.* (1977) in their pigmentoarchitectonic analysis of the whole BST. Although the idea of such a division has held quite well, the markedly heterogeneous population of the BST itself suggests the possibility of further subdivisions. This has already been disclosed in rats with the application of classical histochemical techniques but has been reaffirmed by the introduction of immunohistochemical procedures for demonstrating neuropeptides and other neurotransmitters or neuromodulators. This has received additional support from the hodological information provided by fluorescent retrograde tracers and their combined use with the immunochemical procedures. Since most of this vast array of information comes from studies in the rat, it remains to be seen to what extent these results can be fully extrapolated to the human brain. However, close scrutiny of the literature and my own observations of human and monkey material indicate that several, but not all, of the major subdivisions of the paraseptal BST described for the rat brain are also present in the brains of these higher mammals. Consequently, I have

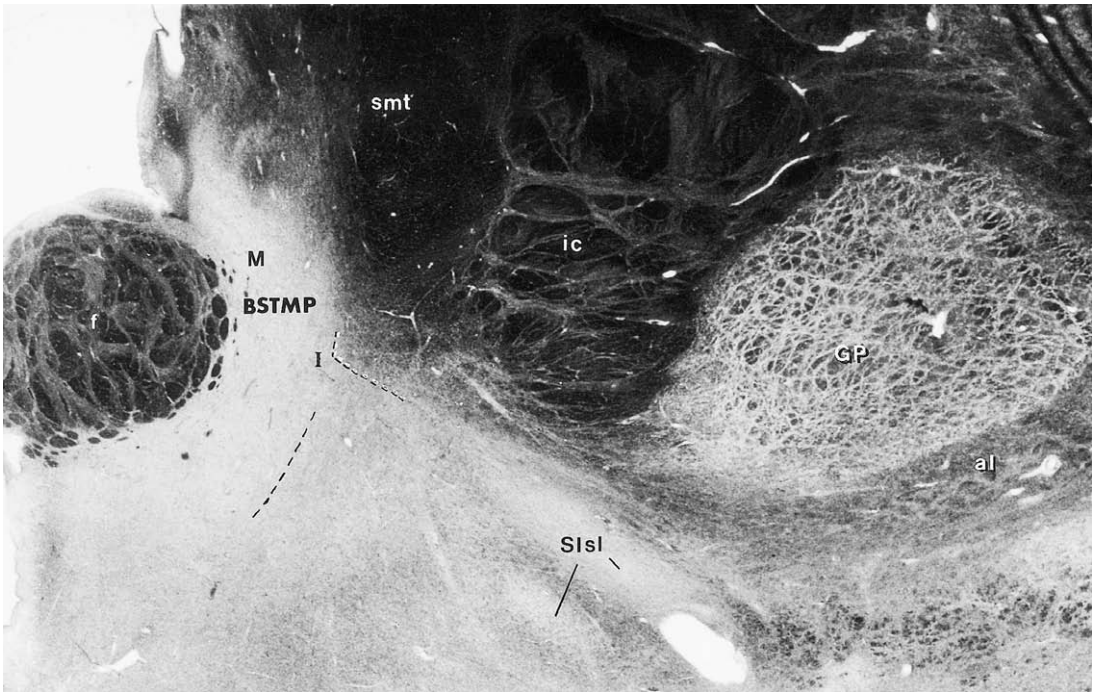

FIGURE 22.16 Low-power photomicrograph of a transverse section through the caudal portion of the BST in its preoptic extension. Note one of the junction bridges between the BST and SIsl. Such continuities have been demonstrated in human brain by immunohistochemical procedures for several neuropeptides (Som, CCK, LENK).

identified not only the two classical major divisions, the lateral (BSTL) and medial (BSTM) but also anterior- and posterior-derived subdivisions, in agreement with the morpho- and neurogenetic findings made by Bayer and Altman (l987) in the rat. In consequence, I include anteromedial, dorsolateral, and juxtacapsular BST subdivisions on the supracommissural plane; a ventral lateral BST subdivision on the infracommissural plane; and medial posterior and lateral posterior BST subdivisions on the postcommissural plane. As in the rat, the posterior medial BST subdivision can be further subdivided into small-celled medial, medium-celled intermediate, and large-celled lateral gray columns. By contrast, in Nissl sections of human brains, I was not able to identify with certainty the presence of a ventral BST subdivision on the medial infracommissural region of the human telencephalon, at least with the cytological characteristics the rat ventral BST presents (see below), nor could I detect a commissural division, whereas the intermediate division seems to be reduced to a thin lamina of scattered large neurons interposed between the intermediate and medial BST.

The Lateral Division of the Bed Nucleus of the Stria Terminalis (BSTL)

Cytoarchitectonic Characterization In cell preparations the BSTL is characterized by its heterogeneous neuronal population and its apparent division into fractions, or island-like cell aggregations, contributing to the difficulty of its analysis. This is partially circumvented by the fact that the island-like formations show a rather scarce population of glial cells and a lack of any particular orientation of the neurons that form them. Such a disposition contrasts with the greater density of the glial cell component in other subdivisions of the BSTL and with the consistent alignment of their neurons with the incoming fibers of the stria terminalis. Another feature worth mentioning here is the presence of small islands made up of tightly packed granular-like neurons [Sanides' (1957) insulae terminalaes] sprinkled at the level of the juxtacapsular and intermediate sectors of the BSTL. Finally, with the exception of its dorsal part, the BSTL contains large to very large neurons displaying different degrees of chromophilia, which are loosely dispersed singly or in clusters. Neurons displaying hyperchromatic staining probably correspond to the diffuse or interstitial component of the MCBPC (Hedreen *et al*., 1984; Mesulam and Geula, 1988; Saper and Chelimsky, 1984; Saper, 1990), whereas the relatively hypochromatic ones presumably represent vestigial elements of the intermediate BST as described in the rodent brain (de Olmos *et al*., 1985).

The dorsal subdivision of the BSTL division (BSTLD) is the largest of the cell aggregates forming

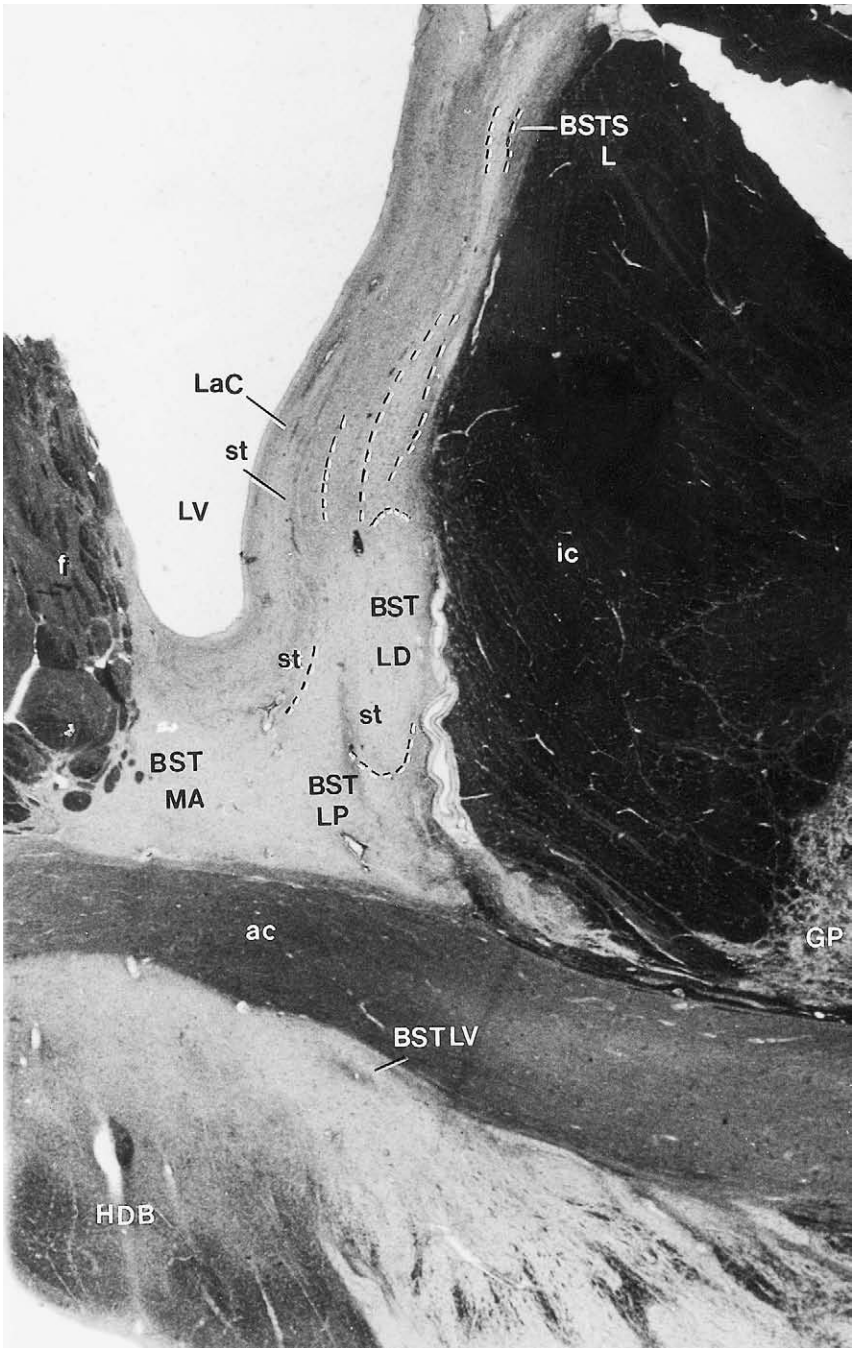

FIGURE 22.17 Low-power photomicrograph of a coronal section through the anterior commissure (ac) decussation showing the bed nucleus of the stria terminalis (BST) in its paraseptal expansion. The picture shows the supracapsular extension of this nucleus.

the supracommissural BST, stretching from the rostral end of the BST to a plane passing slightly caudal to the decussation of the anterior commissure. In transverse sections this subdivision of the BST appears composed of a number of cell islands or clusters, the largest of which is located centrally and dorsally within the supracommissural BST and adopts an elongated oval outline (Figs. 22.17, 22.22a, 22.23a, 22.24). The other, smaller islands appear rounded or semirounded. However, examination of sagittal and horizontal sections reveals that a majority of these islands are continuous with the main body of the dorsal subdivision. At its anteromedial border, the latter is separated from the ependermal lining of the lateral ventricle by a

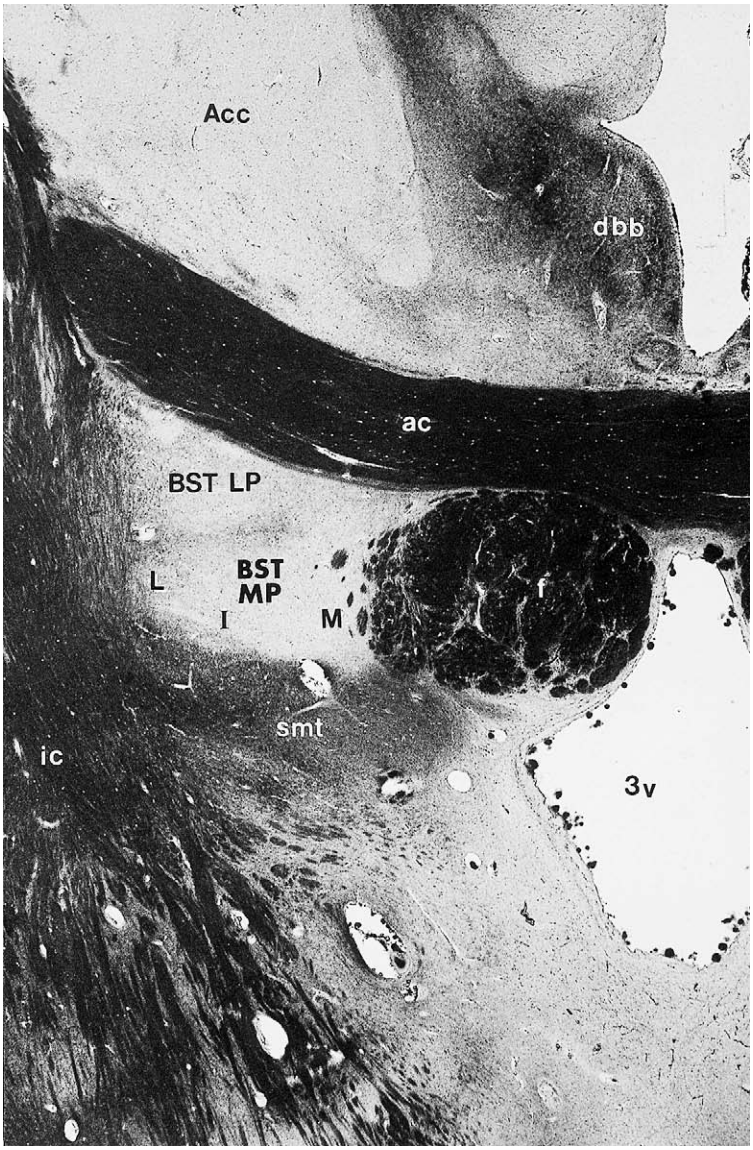

FIGURE 22.18 Low-power photomicrograph of a Weigert-stained horizontal section showing the topographical relationship between the various subdivisions of the posterior part of the medial BST. the nucleus appears completely enclosed by four great fiber systems (ac, f, ic, smt).

broad subependermal glial layer, the lamina cornea (Fig. 22.17). A narrow, sparsely celled zone separates the dorsal BST, rostrally and dorsally, from the striatum. Laterally, a caudoventral extension of the striatum and the juxtacapsular subdivision of BSTL intervenes between the BSTLD and the internal capsule (Figs. 22.22a, 22.23, 22.24a, 22.25). Caudally, medially, and ventrally the posterior subdivisions of BSTL replace the dorsal subdivision. In the interface between these two subdivisions of the BST appear occasional, very small islands of very small neurons, some made up of Sanides' (1957) gamma 1 cells (Figs. 22. 19a and 22.24) and, more often, of gamma 2 cells (Fig. 22.19b). Surrounding the main body of the BSTLD as well as its "peninsula-like" extensions there is a narrow, sparsely celled zone that is particularly clear in horizontal sections. On account of this feature it is reasonable to distinguish a central core and capsular subdivision in the BSTLD (Figs. 22.22a, 22.24a, and 22.25a).

In cell preparations, some cytological features facilitate identification of the BSTLD. These is a translucent background consequent to a poverty of glial cell nuclei, and a random orientation of the rather loosely packed medium-sized neuronal population of the central subdivision (Fig. 22.20). Within its capsular subdivision, cells are predominantly oriented parallel to

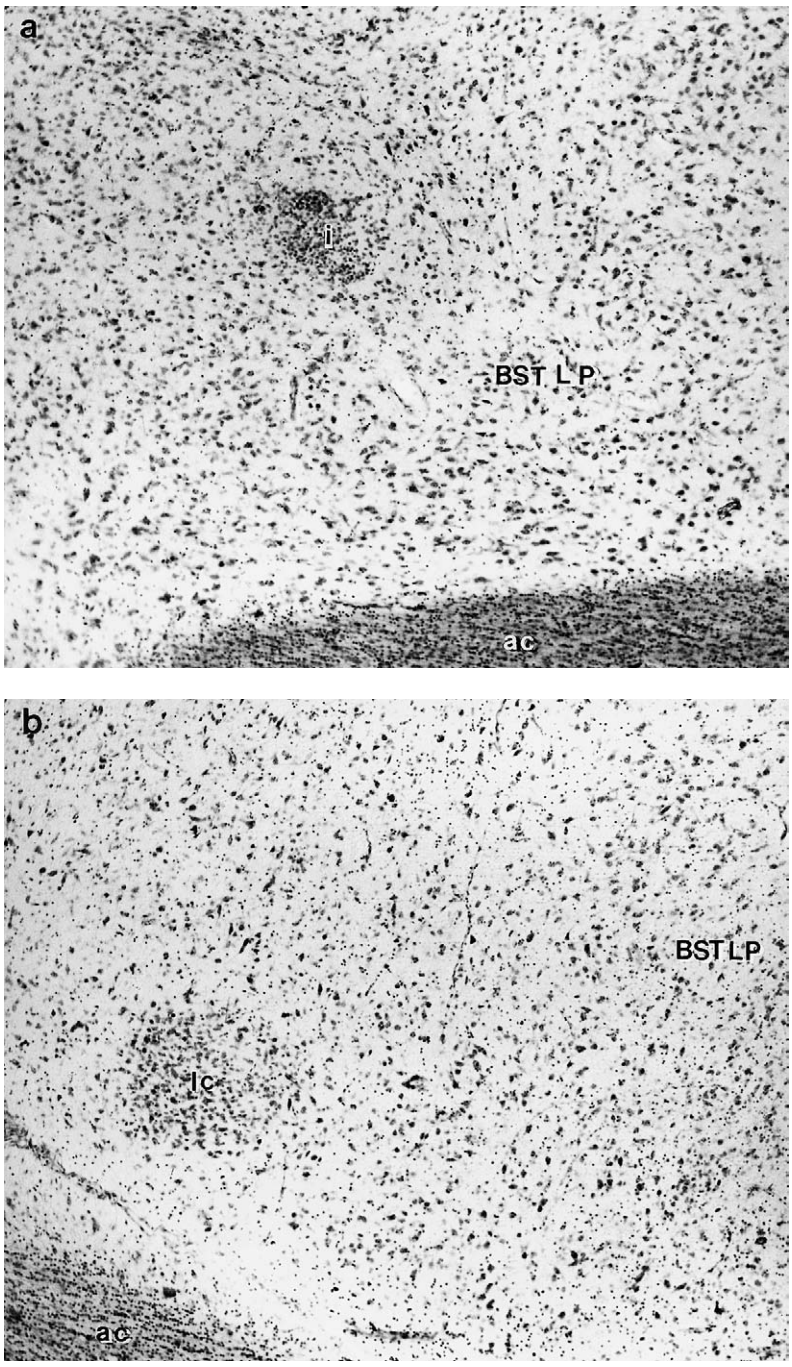

FIGURE 22.19 Photomicrographs of transverse Nissl-stained sections of the BST at the level of the anterior commissure (ac) decussation to show the neuronal clusters present in this nucleus. (a) Neuronal aggregate similar to the γ^1-cell islands (i) described by Sanides (1957). (b) Cell clusters reminiscent of intercalated masses (Ic) referred to as γ^2 islands by Sanides.

the contours of the BSTLD and tend to be larger and with a predominance of spindle-shaped neurons. Such an arrangement is better appreciated in sections processed for the immunohistochemical staining of neuropeptides (Bennett-Clarke and Joseph, 1986; Gaspar *et al.*, 1987; Martin *et al.*, 1988).

The posterior subdivision of the BSTL division (BSTLP) (Figs. 22.17, 22.19, 22.22a, and 22.23–22.26) extends ventrally, caudally, and medially to its dorsal counterpart until it meets the dorsally to ventrally coursing fibers of the stria terminalis. In doing so, it merges with the ventral subdivision of the BSTL just

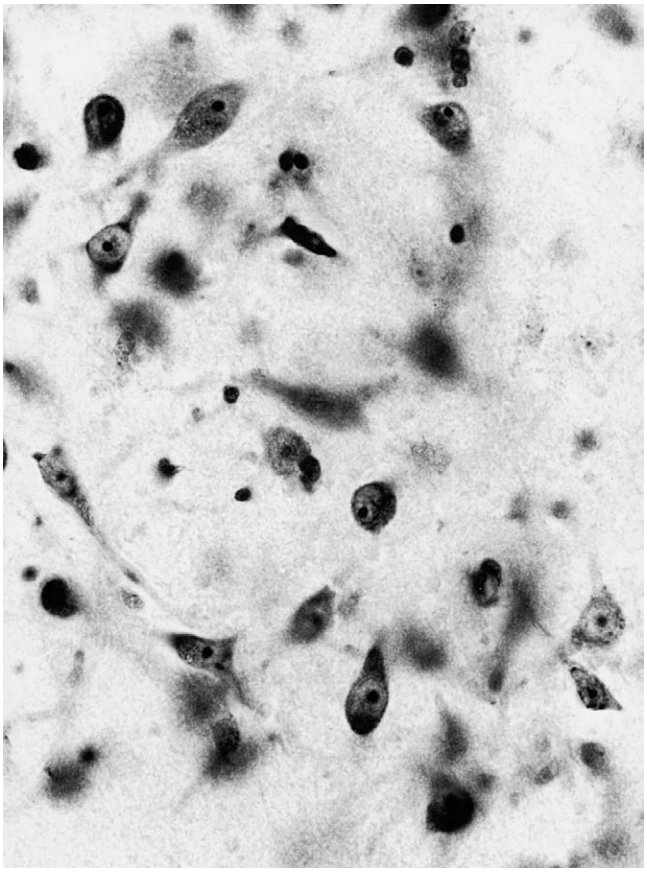

FIGURE 22.20 High-magnification photomicrograph of a Nissl-stained section showing the type of neurons present in BSTLD. Note the transparency of the background and the reduced number of glial nuclei characteristic of this division.

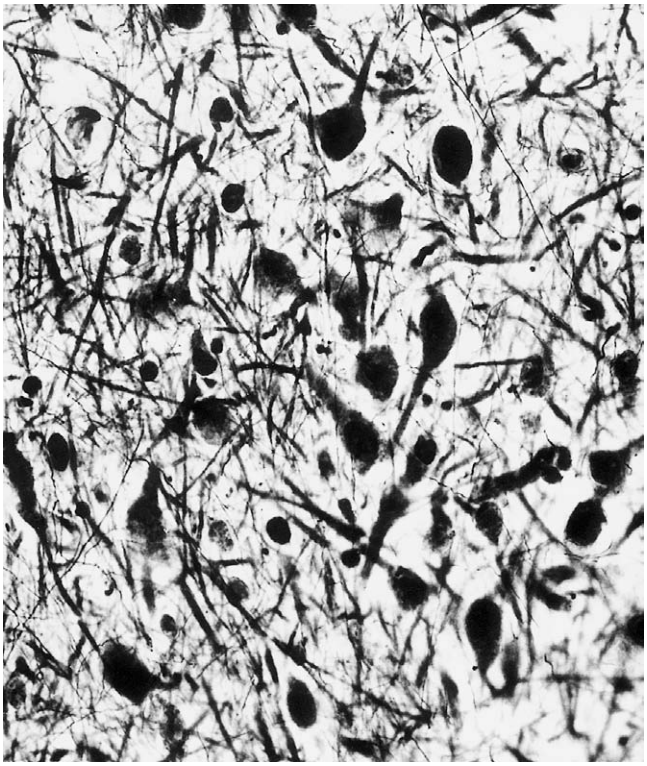

FIGURE 22.21 High-magnification photomicrograph of neurons in BSTLD of human brain using a modified Glees silver method, which demonstrates the dendritic processes of the leptodendritic neurons.

caudal to the decussating anterior commissure and fuses with the more rostral extent of the dorsal anterior division of the sublenticular substantia innominata (Fig. 22.26a). Along its supra- and postcommissural extent, the BSTLP is flanked by the previously mentioned rounded granular interface islands. The continuity of the former structure is occasionally interrupted by these islands (Figs. 22.19 and 22.24b). In contrast with the other subdivisions of BSTL, the BSTLP can be followed continuously to its merger with the supracapsular division of the BST nucleus. Cytoarchitectonically, neurons in the BSTLP can be differentiated from those on their dorsal counterpart by their smaller size, more slender profile, and the preferential dorsoventral orientation of their longer axes. Also, contrary to the BSTLD, the BSTLP can be characterized by its rather rich content of glial cell nuclei.

The juxtacapsular subdivision of the BSTL division (JXC) (Figs. 22.22a, 22.23, 22.24a, and 22.25) can be found in the supracommissural sector of the BST lying interposed between the internal capsule laterally and the dorsal and posterior subdivisions of the BSTL division medially. Anteriorly, it is bounded by the ventrocaudal extension of the caudate nucleus, while posteriorly it is eventually replaced by the most caudal extent of the posterior BSTL. Ventrally, the juxtacapsular BSTL borders with supracommissurally located granular and parvicellular interface (Sanides' gamma types 1 and 2, respectively). In cell preparations, the JXC appears to be made up of slender columns of neurons that are smaller, more darkly staining, and more densely packed than those in the remaining subdivisions of BSTL. Scattered among the core elements there are thin, triangular or spindle-shaped neurons showing a somewhat better defined tigroid substance. However, these medium-sized-to-large cells are considerably smaller than the large-celled neuronal component of the neighboring striatum or the singly lying ectopic neurons bordering the medial aspect of the internal capsule which belong to the MCBFC. As in the posterior BST, the JXC is also rich in glial cell nuclei, and the greater majority of its neurons are oriented in a dorsal-to-ventral direction, parallel to the medial border of the internal capsule. Here and there,

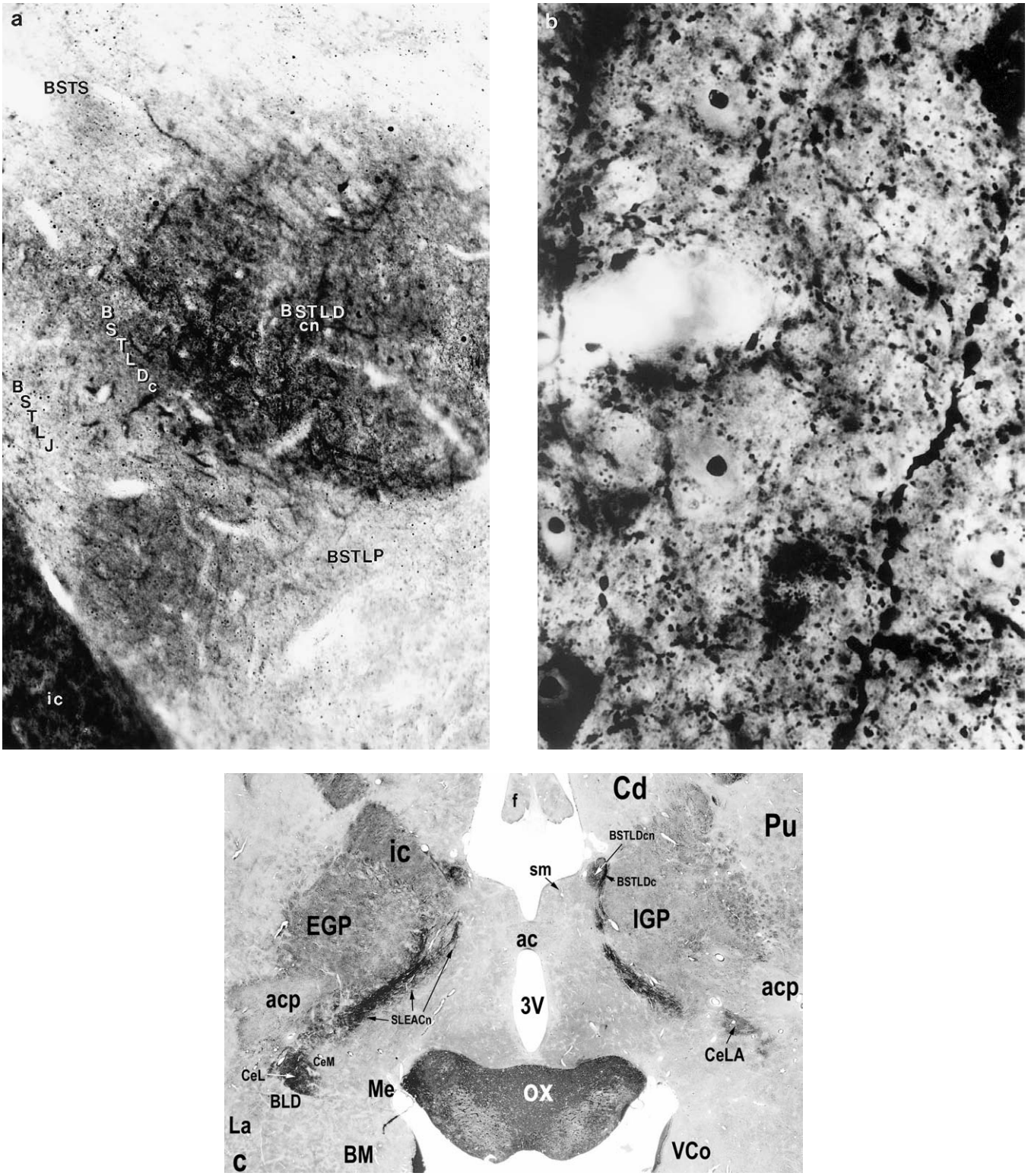

FIGURE 22.22 Medium-, high- and low power photomicrographs of cupric silver stained sections through the supra-commissural sector of the bed nucleus of the stria terminalis from a normal macaque to show in the first two illustrations the bi-stranded (a) and granular beaded (a and b) neuropil present at this level. At high power (b) it is possible to see at the level of the BSTLDcn the additional presence of rounded granular argyrophilic neurons which in general are not present in other divisions of the paraseptal BST nucleus except for few isolated slender spindle shaped neurons in its more medial and posterior sectors. Transverse sections in the squirrel monkey (c) stained with the same histological procedure allows to see even at low power and in just a single section the continuum conformed by the granular argyrophilic neuriopil which stretches from the lateral division of the central amygdaloid nucleus (CeL) through dorsal sublenticular sector of the basal forebrain until it reaches and invades the dorsolateral division (BSTLD) of the BST nucleus. Note that the members of the MEXA remain unstained, while the posterior division of the BSTL nucleus and the medial division of the Ce nucleus though positively stained too, it requires high magnification to be appreciated.

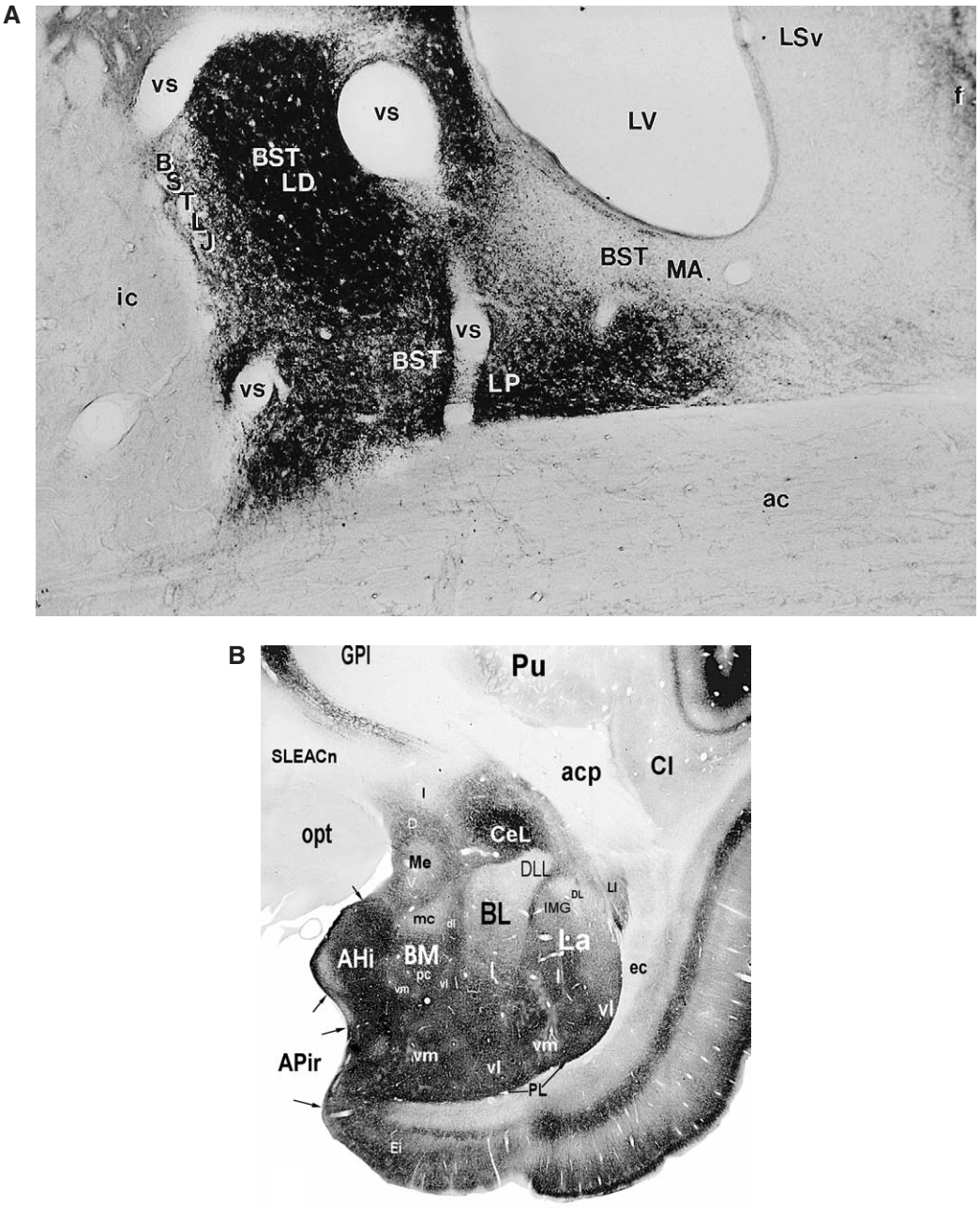

FIGURE 22.23 (a) Timm-stained coronal section (medium-low magnification) of the marmoset monkey BST at the level of the anterior commissural decussation to show the different intensity of silver selenite precipitate in the various divisions of the supracommissural sector of the nucleus (courtesy of George Alheid). (b) Low-power microphotograph of a Timm's stained transverse section through the squirrel monkey brain at a plane quite similar to that seen in Fig. 22.22c which shows that the silver sulphide precipitate in the CeL nucleus streaches through the central SLEA in direction to its final distribution in the BSTLD division of the BST nucleus as shown in Fig. 22.23a.

the continuity of the JXC is interrupted by the presence of very small granular and parvicellular interface islands (Sanides' gamma type 1 and type 2, respectively).

The ventral subdivision of the BSTL division (BSTLV) (Figs. 22.17, 22.22c and 22.26) in the human brain, as compared with the presumably homologous cell group in nonhuman primates, appears to be rather reduced in extent. In frontal sections it occupies a relatively narrow irregular triangular area below the anterior commissure close to the angle formed by the

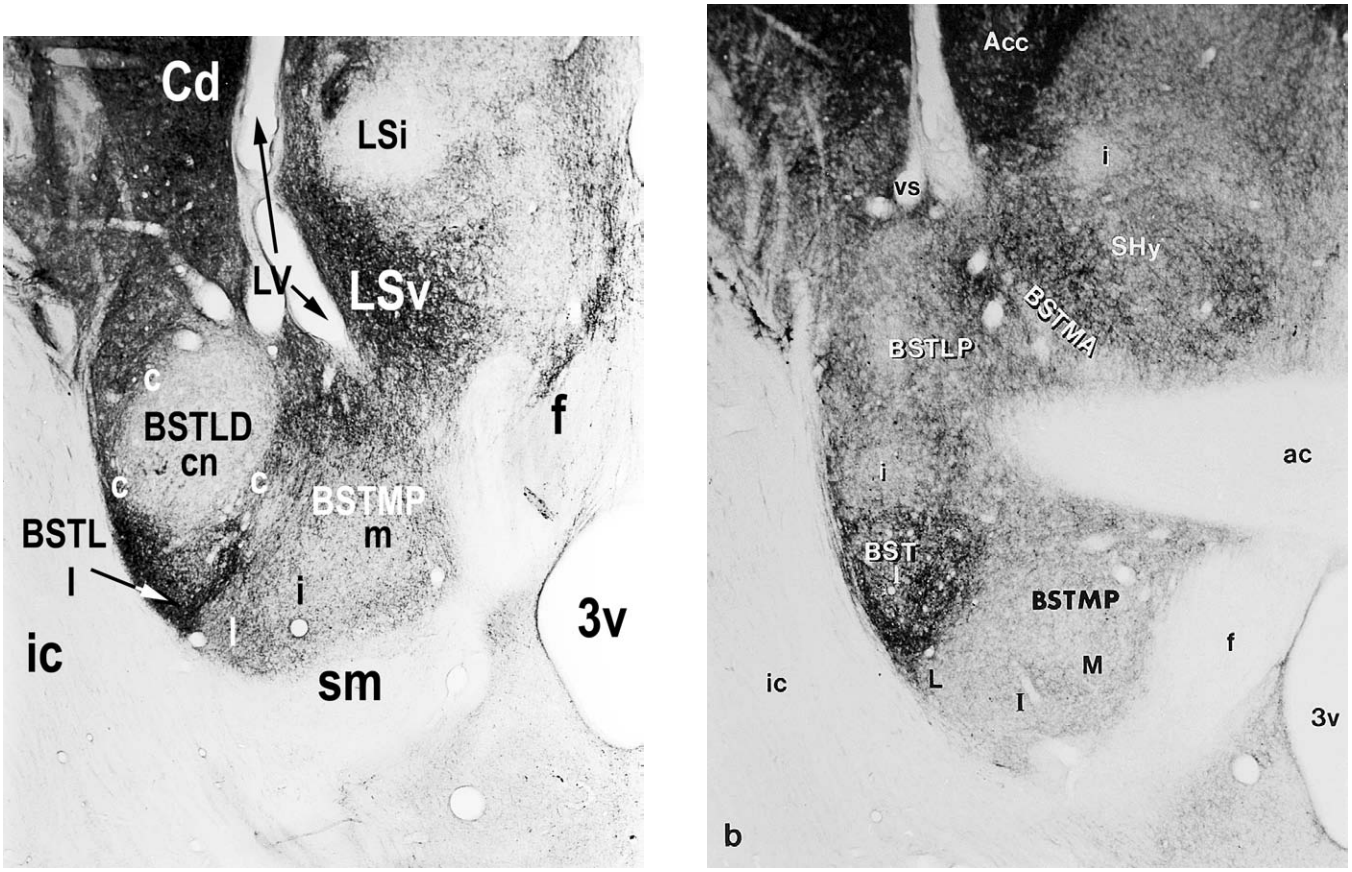

FIGURE 22.24 (a) Medium-power photomicrograph of an horizontal immunostained section from a squirrel monkey brain used for the demonstration of distribution of Substance P (SP) immunoreactivity at the supracomisural level of the BST nucleus. This plane of sectioning like the one that follows below, allows to appreciate the columnar arrangement of the SP-positive and SP-non-positive neuronal pools and neuropil existent on this paraseptal member of the Extended Amygdala. (b) Medium-power photomicrograph of an horizontal immunostained section from a squirrel monkey brain for the demonstration of the Substance P (SP) immunoreactivity present at the level of the anterior commissure crossing of the midline in the same monkey brain which allows to strengthen the columnar arrangement suggested by a sequence of serial sections not shown here.

latter and infracommissural coursing bundles detached from the internal capsule (Fig. 22.17). Caudally the BSTLV merges with the posterior division dorsally and with the dorsal anterior division of the sublenticular substantia innominata ventrolaterally (Figs. 22.22c and 22.26), while rostrally and medially it is replaced by the bed nucleus of the anterior commissure. In cell preparations, the BSTLV is made up of a loosely packed mixture of small to medium-sized neurons that are round to oval or spindle shaped, and by somewhat larger, more scattered, and more densely stained multiangular neurons. This last cell type, however, is smaller and more lightly staining than that in the neighboring ventral pallidum (laterally) or the lateral preoptic area (ventrally). The general orientation of neuronal population in the BSTLV tends to change from a horizontal direction rostrally to an oblique dorsomedial to ventrolateral one caudally. Along its rostrocaudal extent, the BSTLV is almost constantly flanked laterally by parvicellular interface islands (Sanides type 2).

Chemoarchitectonics

CUPRIC SILVER METHOD (CU–AG) In cupric silver–stained sections from normal marmoset, squirrel, and macaque brains, the dorsal and ventral divisions of the BSTL division and, to a much lesser degree, its posterior division (BSTLP) displays a typical argyrophilia in their neuropil (Figs. 22.22a–c). As will described for the Ce nucleus, this appears "granular" or in a "bistranded" arrangement, the former pattern being confined to the central subdivision of the BSTLD (Fig. 22.22), whereas the bistranded pattern can be observed at the level of the capsular subdivision of the BSTLD, and at the BSTLP and BSLTV. Together with

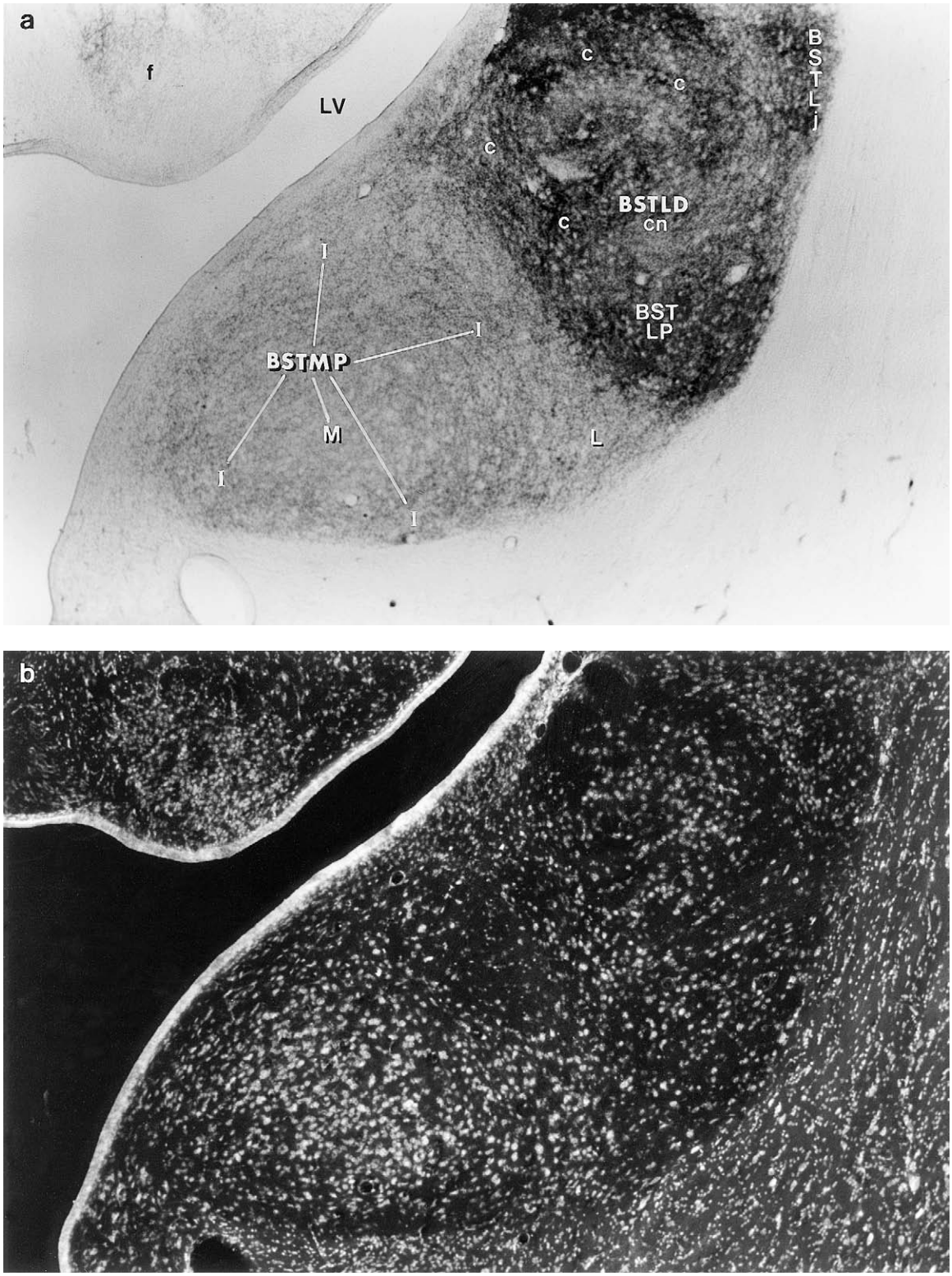

FIGURE 22.25 (a) Medium-power photomicrograph of a Timm's horizontal section through the supracommissural bed nucleus of the stria terminalis from a squirrel monkey brain, showing the differential distribution of heavy metals in the different divisions of the nucleus. The same section counterstained with ethidium bromide is shown in (b).

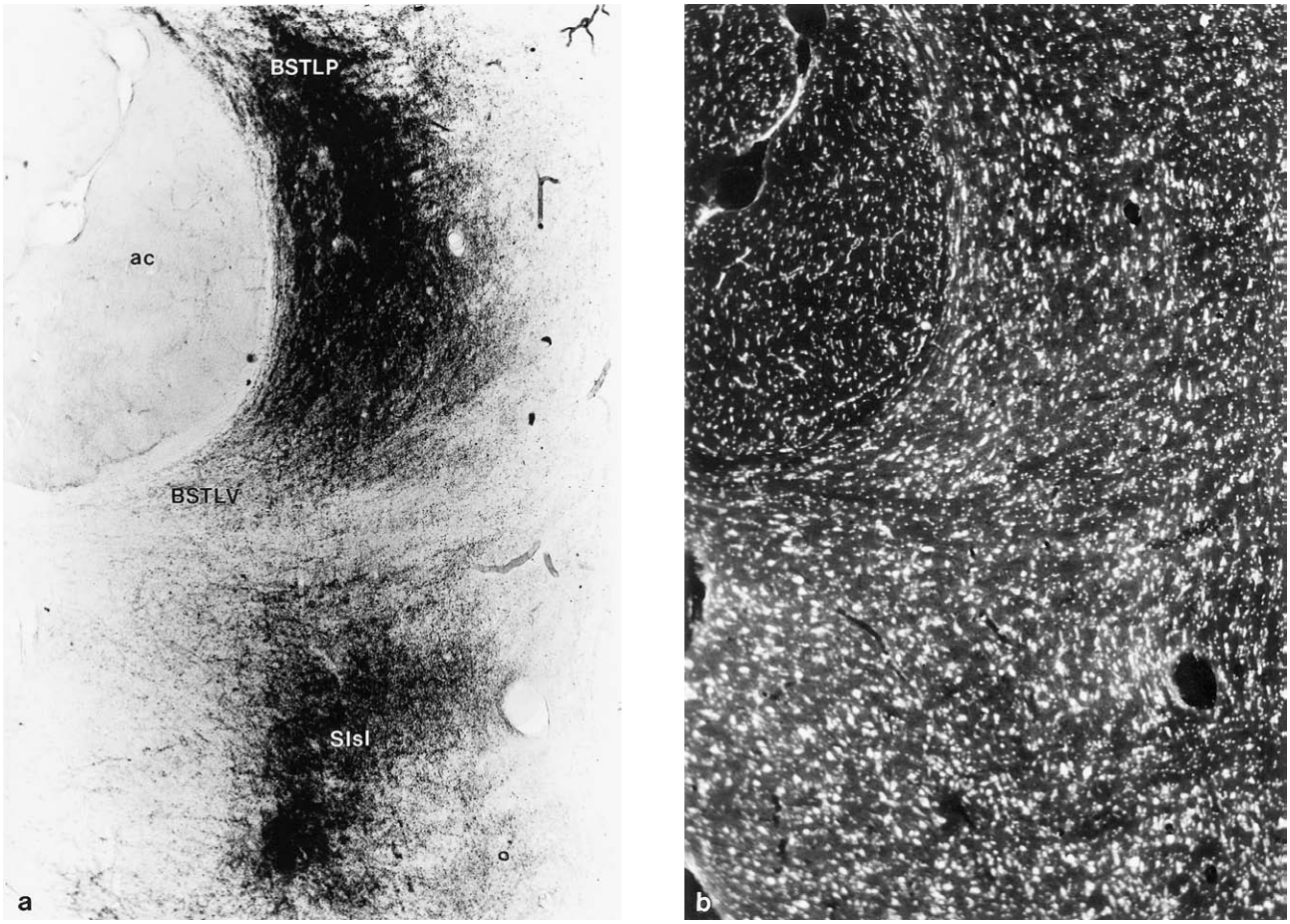

FIGURE 22.26 (a) Medium-power photomicrograph of a Timm-stained sagittal section through the retrocommissural sectors of the bed nucleus of the stria terminalis from a squirrel monkey brains, showing the nearly continuous metal deposits within the ventral and posterior parts of the lateral divisions of this nucleus and the DA SIsl. (b) The same section counterstained with ethidium bromide indicates that most of the metal deposits coincide with the location of the small- to medium-celled neuronal population in this nuclear complex. Note the almost complete lack of deposits in the neighboring larger-celled structures.

granular impregnation of its neuropil, the central subdivision of the BSTLD contains granular argyrophilic neurons displaying the same morphological features as those to be described for the central subdivision of the CeL division of the Ce nucleus (Fig. 22.22b). Both staining patterns can also be identified, although in discontinuous fashion, along the large-celled lateral column of the supracapsular BST.

HEAVY METALS It is unfortunate that until recently it has not been possible to obtain normal human material stained for the above-described silver procedure or with the Timm-Danscher procedure for heavy metals, for reasons that I will discuss here based on information provided by monkey material. Thus, in Timm-Danscher (1981) stained transverse sections of the amygdala of macaque, squirrel, and marmoset monkeys, the central subdivision of the BSTL division shows very dense silver deposits that are greater than in any other member of the group (Fig. 22.25a). Furthermore, a very strong reaction, though not as strong, covers all the space left laterally and ventrally to the dense core (Figs. 22.23 and 25.25a), which would correspond to the BSTLP subdivision of the BSTL nucleus. This precipitate also fills a very narrow representative of the BSTLV laterally just below of the anterior commissure decussation (not shown).

In Part 3 of the Heimer *et al.* "The Primate Nervous System" (1997), their Fig. 22C and D shows quite clearly the distribution of silver deposits, a product of the selenite reaction with heavy metals that occurs in axon terminals of presumably zinc containing glutamatergic pathways with most probable source in cortical regions, mostly of the allo-, periallo-, or proisocortical

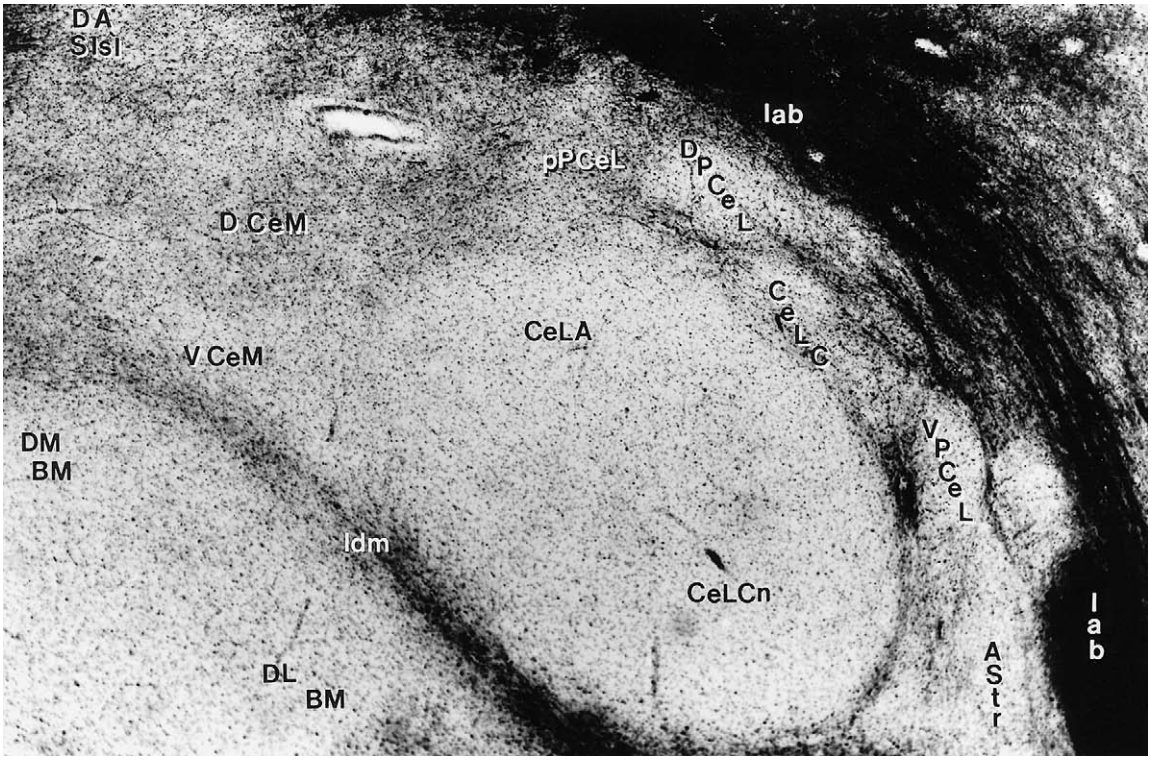

FIGURE 22.27 Medium-power photomicrograph of a Weigert-stained coronal section through the central amygdaloid nucleus from a human brain to show the different divisions of this nucleus.

type which are known to send projections to this particular sector of the rat brain (for reviews, see Olmos, 1985; Amaral *et al.*, 1992; McDonald *et al.*, 1999). In more posterior levels, it is possible to appreciate a direct continuation of the metal deposits present in these two subdivisions of the BSTL up to their continuation in the SLEA ventrally or in the supracapsular component of the BST nucleus dorsally. Such silver deposits correspond to those occurring at the level of the central amygdaloid nucleus, in this way forming a perfect ring around the internal capsule.

In unpublished rat experiments with iontophoretic injections of Na selenite in the area of the Ce/SLEACn carried out in collaboration with C. A. Beltramino in our laboratory, it was possible to establish the source of these zinc-laden projections from the temporal sector of the piriform cortex, the amygdalopiriform cortex, the lateral entorhinal cortex, the agranular insular cortex, etc., as well as from other amygdaloid nuclei, such as the posterolateral amygdaloid nucleus, posterior basolateral nucleus, ventral basolateral nucleus, and both divisions anterior and posterior of the basomedial amygdaloid nucleus. Since the presence of zinc in axons terminals has been associated with that of glutamate, it is probable that all of the above-listed structures, which are known by other tracing procedures to be a source of afferents to the extended amygdala, would be the right candidates for the glutamatergic innervation of the SLEACn and, therefore, of the whole extended amygdala.

CHOLINERGIC MARKERS

ACETYLCHOLINESTERASE (ACHE) In AChE-stained sections the BSTL presents a rather heterogeneous staining picture, where along with places in which the staining is strongly positive, as in its JCX, there are other places where the AChE activity is practically nil, as in the capsular subdivision of the BSTLD division, to moderate to strong in some of the oval-shaped cell clusters representing its central subdivision.

In the monkey material placed at my disposition (macaque, squirrel, and marmoset), the AChE staining pattern at the level of the BSTL division of the BST nucleus is somewhat complementary to that which can be observed in Timm-Danscher-stained section; that is to say that while the core shows a lighter staining, the capsule and the surrounding BSTLP and the BSTLV subdivisions show a heavier staining although the AChE reactivity in the capsular region and in the JCX appears much stronger.

MONOAMINERGIC MARKERS

DOPAMINE β-HYDROXYLASE (DBH) According to Gaspar *et al.* (1985), in the septal area in humans, the BSTL nucleus is sparsely innervated by DBH-ir fibers. In the macaque monkey the heaviest concentration of DBH lies in the BSTLV subnucleus while moderate amounts are also present in the BSTLD and BSTLP subdivisions (Freedman and Shi, 2001).

DOPAMINE TRANSPORTER (DAT) According to Freedman and Shi (2001), in the macaque monkey, the concentration of DAT throughout the EXA is generally far lower than in the striatum. Moderate amounts of DAT-ir fibers are present in the BSTLD and JXC subnuclei of the BSTL division. However, the JXC subnucleus shows somewhat higher DAT-ir than its neighboring BSTL subnuclei.

HISTAMINE (HA) According to Airaksinen *et al.* (1989), in the tree shrew (*Tupaia belangeri*), HA-ir fibers collected in dense bundles are seen at the level of the BST nucleus where they distribute forming a very dense plexus that reaches the highest density.

SEROTONIN (5-HT) According to Freedman and Shi (2001), in the macaque monkey, the heaviest concentration of 5-HT-ir fibers in the BST nucleus is in its BSTLD and BSTLV subnuclei with levels comparable to that found in the striatum. A moderate to heavy density of these fibers is also present in the JXC. In the heavily labeled BSTLD, multiple small puncta 5-HT-ir structures with relatively few fibers are present as is a diffuse background staining that is higher than structures without specific labeling.

SEROTONIN TRANSPORTER (SERT) According to Freedman and Shi (2001), in the macaque monkey, the distribution of the SerT in the BSTL largely parallels that of the 5-HT. SerT-ir fibers are present in moderate to heavy concentration in the BSTLD, BSTLV, and JXC subnuclei.

TYROSINE HYDROXYLASE (TH) Gaspar *et al.* (1985) demonstrated that within the human BST nucleus, the distribution of the TH-ir fibers adopts a topographical disposition that is complementary of that of the DBH-ir ones. Within the BSTL division of these paraseptal griseum, the TH-ir fibers show a patchy distribution, with densely innervated ovoidal areas neighboring others more lightly innervated. These dense TH-ir clusters are frequently aligned along the lateral edge of the BST nucleus or surrounding the dorsal and ventral aspects of the decussating anterior commissure. Within these clusters, fine dot-like varicose fibers are most abundant and frequently form basket-like pericellular arrangements. A rostrocaudal decreasing gradient of TH-ir terminals can also be observed, particularly caudally to the anterior commissure. Finally, a close correspondence seems to exist between these patches of TH-ir terminals and the intensely AChE stained islands present in the BST nucleus. In a later report in which a topographical analysis was made to determine the relationships between the TH-ir and the peptidergic innervation of the BST nucleus, Gaspar *et al.* (1987) arrived at the conclusion that there is an overlap between fields containing the characteristic dopaminergic pericellular baskets and the clusters of dense SOM-ir fibers and perikarya. However, Lesur *et al.* (1989), performing a similar analysis concluded that the aminergic and peptidergic inputs do not converge on the same neuronal components since none of the TH-ir pericellular baskets colocalized with SOM-ir or ENK-ir, even though TH-ir, ENK-ir, and SOM-ir profiles overlap coincidentally with the patchy cell organization present in the BSTL nucleus. Although TH-ir basket-like formations frequently surrounded SOM-ir perikarya, they did it more often on nonlabeled cell bodies. Finally, they found that in the infracommissural portion of the BST nucleus, TH-ir axons of smooth nonvaricose type not only are concentrated in its ventrolateral sector (i.e., the BSTLV subdivision), but tended to have the same orientation as the peridendritic plexuses.

On the other hand, in the macaque monkey, Freedman and Shi (2001) described that TH-ir fibers are most dense in the BSTLD and BSTLV subnuclei, with their concentration approaching that of the striatum, although the density decreases at the most caudal level.

EXCITATORY AMINO ACIDS

GLUTAMATE/ASPARTATE (GLU/ASP) Injections of tritiated aspartate in the BL nucleus of the macaque monkey amygdala produce the retrograde labeling at the level of the BST nucleus (Amaral and Insausti, 1992). Furthermore, in the rat, injections of tritiated D-aspartate in the ventral pallidum caused the retrograde labeling of a moderate number of cells in lateral and ventral aspect of BST (Fuller *et al.*, 1987), and also after similar of injections in the area of the paraventricular hypothalamic nucleus (Csáki *et al.*, 2000). These results favor of the existence of a subpopulation of glutamatergic neuron within this component of the CExA. These data also favor the concept of the extended amygdala, as it can be gathered from the fact that the Ce nucleus, but more particularly its medial division, also contributes to the putative glutamatergic innervation of the above-listed structures.

INHIBITORY AMINO ACIDS

γ-Aminobutyric Acid (GABA) According to Heimer *et al.* (1999), the BSTLD subdivision of the human BST nucleus contains significant concentrations of GAD as is shown in their illustrations (Figs. 6 and 13B), while the remaining sectors contain somewhat less dense concentrations.

NEUROPEPTIDES

Calcitonin Gene–Related Peptide (CGRP) According to De Lacalle and Saper (2000), in the human brain, the presence at the level of the BST nucleus of specific patterns of CGRP-ir innervation seems to be closely related to the subnuclear subdivisions of this nucleus. Although scattered CGRP-ir fibers and terminals can be found throughout the whole BST complex, the most prominent innervation involves the supracommissural BSTL division excepting its anterior portion (BSTA). On the other hand, the BSTLP subdivisions is rather loosely innervated by CGRP-ir fibers. Islands of Sanides γ cells are surrounded by dense bundle of CGRP-ir fibers. The most characteristic feature of the CGRP-ir innervation of the BST nucleus are the dense baskets of peridendritic and perisomatic CGRP-ir that outlines the contour of non-ir neuronal somata. No CGRP-ir cell bodies are detectable in the BST nucleus.

Cocaine- and Amphetamine-Regulated Transcript (CART) According to Hurd and Fagergren (2000), the human BST nucleus shows a moderate CART mRNA expression. Although no statement is made about the specific localization of this peptide, from the illustrations presented by them (Figs. 2B and 5), it seems that the strongest signals occur in the whole BSTL division.

Chromogranin B According to Marksteiner *et al.* (1999), in the human brain peptide PE-11-like ir can be found in the BST nucleus in high densities in the medial, lateral, and ventral parts of this nucleus. In the lateral part, a core of PE-11-like ir perikaria is surrounded by PE-11-like ir wooly-like fibers with intensely stained varicosities.

Corticotropin-Releasing factor (CRF) In the human amygdaloid complex, dense accumulation of CRF-ir fibers, with large varicosities, and terminals has been reported in almost all amygdaloid nuclei (Power *et al.*, 1987; Zaphiropoulos *et al.*, 1991). In the BST nucleus, a few fusiform lightly CRF-ir neurons are present (Powers *et al.*, 1987).

Dynorphin (DYN) The presence of fibers displaying DYN-ir has been detected (Haber and Watson, 1985) at the intersection between the internal capsule and the anterior commissure. After crossing the former fiber system, the fibers enter into the BST, forming a thin stratum that covers the medial surface of the internal capsule.

Enkephalin (ENK) According to Gaspar *et al.* (1987), only few ENK-ir perikarya are present in the BST nucleus. The peptidergic axons are always small, forming peridendritic terminal plexuses that give the appearance of thick granular or tubular fibers or strands, named "wooly fibers" by Haber and Nauta (1983). Following a pattern of nonoverlap of the same target, few of these ENK-ir fibers also label pericellular SOM-ir baskets. However, Lesur *et al.* (1989) were unable to determine if there is some colocalization in these circumstances. They also found that the ENK-ir plexuses are much more numerous than SOM-ir ones, that there are no basket-like formations within the cell clusters, and that while a few ENK-ir peridendritic plexuses can be detected, they are grouped in the lateral-most sector border near the internal capsule. With reference to the distribution of ENK-ir cell bodies, their location seemed not to follow any particular pattern within or outside the cell patches. According to these authors, their central division (here BSTLD) is delimited by ENK fibers that encircles it forming a shell (i.e., the present capsular subdivision of the BSTL subnucleus) of densely labeled ENK-ir peridendritic plexuses but with a moderate innervation of the central core (the central subdivision of the BSTLD subnucleus). The bulk of the ENK-ir basket-like pericellular formation seem to be concentrated in the BSTLD. Finally, according to these authors, very rare SOM-ir perikarya or pericellular basket formations can be detected in the BSTLV division of the BST nucleus that are characterized by very dense SOM-ir peridendritic plexuses of granular type. Many of them can be followed for long distances in a lateroventral direction toward the so-called substantia innominata.

According to Kaufmann *et al.* (1997), the woolly-like and varicose ENK-ir fibers are predominantly present in the BSTLP subdivision of BSTL nucleus. At infracommissural levels, just behind the crossing of the anterior commissure, ENK-ir can be detected ventromedially to the internal capsule and the ventral pallidum (Martin *et al.*, 1991). In this ventral part of the BST, i.e., the present BSTLV subnucleus, the ENK-ir consists of woolly-like fibers. From here woolly-like ENK-ir fibers extend laterally to the sublenticular substantia innominata, though to a lesser degree than the SECR-ir.

Haber and Watson (1985) described the presence in the macaque monkey forebrain of distinct clusters of

ENK-positive woolly fibers that invade the supracommissural BST nucleus. In this sector of the BST a dense swirl of these fibers encapsulates and to a lesser degree permeates BSTLD (ovoid) subnucleus, which contains numerous ENK-positive cell bodies.

GALANIN (GAL) According to Kordower *et al.* (1992) in the cebus monkey, numerous GAL-ir perikarya are seen throughout the BST with a preponderance of neurons in the anterior aspect of this nucleus. At this level the GAL-ir neurons are preferentially located in the medial (BSTMA), dorsolateral (BSTLD), and ventrolateral (BSTLV) subdivisions of the BST, as well as within the caudal temporal portion of the stria terminalis (BSTSl).

NEUROKININ B (NKB) Practically no SP-ir is present at the level of the BSTLD (ovoid nucleus), and very little in other sectors of the BST (Haber and Watson, 1985; Chawla *et al.*, 1997). By contrast, the presence of numerous small, oval-to-round, NKB-containing neurons were found in the BST. The illustrations (Fig. 3A–C) presented by Chawla *et al.* (1997) indicate that most of the NKB-containing neurons are more concentrated in the medial than in the lateral sectors of BST, and more in supracommissural than in infracommissural position.

NEUROPEPTIDE Y (NPY) According to Gaspar *et al.* (1987), the NPY-ir innervation of the human BST nucleus is essentially restricted to the lateral part of the nucleus, forming an elongated zone close to the internal capsule (i.e., BSTLD) and a smaller field medially close to the pillars of the fornix. NPY-ir perikarya are small to medium-sized, scarce, and almost exclusively located in the BSTL division in both supra- and infracommissural sectors. Ventrocaudally the NPY-ir fiber and terminal network can be seen to extend to the preoptic area and the substantia innominata. Comparison of SOM-ir and NPY-ir patterns demonstrates partly overlapping and partly complementary patterns of both peptidergic innervations. Thus, the central or dorsal SOM-ir clusters seem to contain only small amounts of NPY-ir fibers and practically no colocalization of these neuropeptides, whereas the lateral, caudal, and medial fields contain only moderate amounts of both peptides and only a few double-labeled neurons.

According to Walter *et al.* (1990), the supracommissural portion of the human BST nucleus contains bipolar NPY-ir cell bodies, are located exclusively along the boundary of the internal capsule (i.e., the BSTL division) and preferentially oriented ventrodorsally. NPY-ir fibers occur with no particular orientation. A column of very high fiber density lying laterally at the border of the internal capsule (here BSTLP division) is distinct from an intermediate zone of considerably less NPY-ir, corresponding to Brockhaus' (1942a) nucleus subcaudatus (here the BSTLD subnucleus). Moreover, they maintain that the subcommissural region (BSTLV) of the BST nucleus appears as a ventral extension of the BSTLP supracommissural, and contains both NPY-ir fibers and pericaria. This contingent seems to eventually join those in the basal telencephalon.

On the other hand, according to Bons *et al.* (1990), in the BST nucleus of the microcebus murinus (primate, lemurian), the NPY-ir axons form a dense plexus surrounding the anterior commissure and fornix. However, in contraposition to what has been described above, the NPY-ir perikarya seems to be predominantly located near the border of the lateral ventricle (i.e., BSTM).

NEUROTENSIN (NT) According to Mai *et al.* (1987), within the telencephalic regions studied, the BST nucleus that is close to the anterior commissure contains NT-ir cell groups. In this nucleus most of the NT-ir neurons accumulate laterally at the medial border of the internal capsule, i.e., the BSTL division. These authors establish likewise that the most conspicuous accumulation of NT-ir fibers within subcortical telencephalic structures occurs around the head of the anterior commissure, predominantly the septal area and the BST nucleus.

PREPROTACHYKININ A Intense PPT-A mRNA hybridization signals have been reported to be present in some neurons of the bed nucleus of stria terminalis. PPT-A mRNA-expressing cells also were scattered throughout the substantia innominata (sublenticular extended amygdala). Silver grains were seen predominantly over the medium-sized and small neurons, and not over the large neurons, within this area. No positive PPT-A hybridization signals were detected in the ventral pallidum or the globus pallidus, except in a few subjects under very long exposure time, and even then the signal was barely higher than the background.

SECRETONEURIN (SECR) According to Marksteiner *et al.* (1992) and Kaufmann *et al.* (1997), within the human supracommissural BSTL, its central core (BSTLD) shows the highest density of SECR-ir which contains perisomatic SECR-ir surrounding SECR-ir and non-SECR-ir oval-shaped neurons. This oval core appears in turn surrounded by SECR-ir woolly-like and SECR-ir varicose fibers. This SECR-ir is partially coexistent with ENK-ir and CAB-ir profiles but not with SP-ir ones. The posterior part of BSTL, i.e., the

present BSTLP, which shows a much less dense SECR-ir pattern, contains both SECR-ir varicose fibers and SECR-ir woolly-like fibers (type II) oriented dorsoventrally with an arrangement similar to that presented by ENK-ir profiles.

At infracommissural levels, just behind the crossing of the anterior commissure, SECR-ir can be detected ventromedially to the internal capsule and the ventral pallidum. In this ventral part of the BSTL division of the BST nucleus (here the BSTLV subdivision), the SECR-ir consists of a very high density of woolly-like fibers. From here a dense network of SECR-ir woolly-like type II fibers extends laterally into the sublenticular subtantia innominata, i.e., the present CSLEA.

SOMATOSTATIN (SOM) Mufson *et al.* (1988) and Bennet-Clarke and Joseph (1986) were the first group of researchers to describe the presence of SOM-ir neurons in the human BST nucleus, and they stress the tendency of SOM-ir fibers to form island-like clusters, which they were also able to detect at the level of the so-called substantia innominata. On the other hand, Gaspar *et al.* (1987) described the BST nucleus as the structure that contains the highest density SOM-ir innervation. SOM-ir perikarya and fibers were said to be present throughout the entire nucleus but were more densely grouped within oval or round clusters or fields forming a mosaic-like pattern. In the rostral BST nucleus, the clusters appear distributed in both the infra- (BSTLV) and supracommissural sectors of the nucleus, occupying the central and dorsal field (BSTLD). Caudally to the anterior commissure, the dense SOM-ir fields tend to be restricted to the ventral part of the BST nucleus and to small dorsal zones close to the stria terminalis. The clusters display dense packing of round or fusiform medium-sized SOM-ir perikarya, and also contain varicose fibers, isolated varicosities, and SOM-ir woolly-like fibers. A relatively large number of pericellular arrangements can also be seen, particularly in the BSTLV. Outside the clusters, in the lateral, caudal, and medial fields of the BST nucleus, SOM-ir perikarya and fine varicose fibers are far more scattered. Finally, the so-called SOM-ir woolly-like fibers,which are highly characteristic for this nucleus, become particularly abundant ventrally (BSTLV).

In a later report by Mufson *et al.* (1988), which extended their previously published preliminary data, they not only confirmed that the BST nucleus constitutes the forebrain area containing the heaviest concentration of SOM-ir perikarya, nerve fiber, and terminals, but more importantly they provided additional documentation in favor of the existence of a SOM-ir pathway connecting these SOM-ir with that in the Ce nucleus via the ansa peduncularis/ventral amygdalofuga1/sublenticular substantia innominata system of fibers and neurons.

Lesur *et al.* (1989) took another approach and reached the conclusion that aminergic and peptidergic inputs do not converge on the same neuronal components, so that none of the pericellular baskets formed by TH-ir fibers contained SOM-ir (or ENK), whereas a few SOM-ir pericellular baskets also contained ENK-ir profiles. SOM-ir woolly-like fibers were also found in continuity with pericellular baskets. Furthermore, according to these authors, very rare SOM-ir perikarya or pericellular basket formations can be detected in the BSTLV division of the BST nucleus that are characterized by very dense SOM-ir peridendritic plexuses of granular type. Many can be followed for long distances in a lateroventral direction toward the so-called substantia innominata.

In the macaque monkey, Amaral *et al.* (1989) found that the SOM-ir has much of the same appearance as that in the Ce nucleus. According to them, SOM-ir fiber and terminal are present in the lateral division of the nucleus where they tend to be substantially denser than in the medial division, a distribution pattern that coincides with that in the human BST. As happens in the Ce nucleus, dense clusters of SOM-ir neurons appear located in the lateral part of the BST, but are concentrated in the dorsolateral portion at the rostral pole of the nucleus.

There is a very important point here, since there are profound sexual behavioral consequences. These are related to the dimorphic difference in the peptidergic organization of the central BSTLD subdivision of the BSTL. According to recent studies in humans, it has been established quite firmly that SOM-ir neurons are more numerous in males than females (Kruijver *et al.*, 2000), which is consistent with the fact that this nucleus is larger in males (39%) than in females (Zhou *et al.*, 1995; Kruijver *et al.*, 2000; Chung *et al.*, 2002).

SUBSTANCE P (SP) According to Kaufmann *et al.* (1997), only a few single fibers can be detected at the level of the supracommissural BSTL, particularly in BSTLP. At infracommissural levels, just behind the crossing of the anterior commissure, where high SECR-ir can be detected ventromedially to the internal capsule and the ventral pallidum, no SP-ir could be detected.

VASOINTESTINAL PEPTIDE (VIP) According to Martin *et al.* (1991a), both in the human and monkey BST nucleus, VIP-ir fibers and terminals are heavily concentrated in the BSTLDcn (see also Chung *et al.*, 2002), This VIP-ir can also be followed in the rostral substantia innominata and anterior commissure region,

conditions that are strikingly demonstrated in the Heimer *et al.* (1999) illustrations. On the other hand, Martin *et al.* (1991a) were unable to identify VIP-ir perikarya in any sector of the two major divisions of the extended amygdala. It has been demonstrated (Chung *et al.*, 2002) that, as happens with the SOM-ir, there is dimorphic distribution of this peptide at the level of the BSTLDcn (larger VIP-ir area in human males than females), and this deserves as much special attention as that dedicated to the SOM-ir in view of their behavioral implications (Chung *et al.*, 2002) (see above).

NEUROTROPHINS

Brain-Derived Neurotrophic Factor (BDNF) According to Murer *et al.* (1999), in the human BST nucleus, BDNF-ir fibers form a dense and strongly ir plexus where several non stained neuronal cell bodies are completely enveloped by BDNF-ir terminals boutons and fibers. Furthermore, it can be inferred from their Fig. 3A that both supra- (BSTLP/BSTLD) and infracommissural (BSTLV) representatives of the lateral BST nucleus contain BDNF-ir.

CALCIUM-BINDING PROTEINS

Calbindin (CAB) According to Kaufmann *et al.* (1997), in the supracommissural BSTL, CAB-ir coexists with ENK-ir and SECR-ir but not with SP-ir. For the rat, Celio *et al.* (1990) provide a rather succinct description according to which the CAB-ir staining pattern is very similar to that of the lateral septum consisting of the presence of a myriad of small cells embedded in a rich CAB-ir fiber and terminal matrix. According to these authors, the medial division of the BST posesses a denser distribution than the lateral.

Calretinin (CR) No information concerning the distribution of this protein within the paraseptal components of the extended amygdala in humans or nonhuman primates is available at present. However, even though extrapolation from one mammalian specie to another is always a risk, the present writer considers it to be beneficial for the reader and for a greater consistency of this section to describe some observations made on material immunostained for this protein in transverse and sagittal section of the rat and guinea pig basal telencephalon. According to the information provided by this material, the rat lateral bed nucleus of the stria terminalis shows a lightly CR-ir core surrounded by a rich CR-ir background composed of fine granular CR-ir profiles enmeshing both scattered CR-ir perikarya and non-ir cell bodies. The more lightly CR-ir stained ovoidal core corresponds to the BSTLD subdivision of the rat BST nucleus, which appears more or less encapsulated ventrally, medially, dorsocaudally, and caudally by groups of more densely packed CR-ir cell bodies. The regions corresponding to the BSTLP and BSTLV subdivisions also show a rich CR-ir neuropil in which CR-ir cell bodies are distributed in a scattered manner. CR-ir fibers and scattered CR-ir cell bodies can be traced along the course of the stria terminalis, with most of them located in the BSTSl sector of the BSTS division of the BST nucleus. It goes without saying that the distribution of cells and fibers in the central amygdaloid nucleus conforms very closely to that seen in the lateral BST nucleus.

Parvalbumin (PAV) According to the schematic mapping illustrated by Celio *et al.* (1990), in the rat, the PAV-ir is nil in the BST nucleus.

OTHER PROTEINS

Calpastatin (CALPT) Although this division of the BST nucleus is not mentioned or listed among the telencephalic structures that show CALT-ir, examination of the Moutt-Prigent *et al.* (2000) Fig. 2A reveals that, at the level of the BSTL, an irregularly oval cluster of CALP-ir appears surrounded by a non-ir capsule, and below it another probable CALPT-ir formation that topographically corresponds to the BSTLP subdivision. Such property would support the fact that in the Ce nucleus its counterpart in the temporal lobe is also CALPT-ir stainable.

Limbic System–Associated Membrane Protein (LAMP) According to Côté *et al.* (1996) in the macaque amygdala, the LAMP-ir present in the dorsal part of the sublenticular substantia innominata, i.e., the SLEAC of the present account, becomes continuous with the LAMP-ir present in the BSTL division. This LAMP-ir is predominantly expressed in the dorsal subdivision of the extended amygdala (CExA), which extends in the form of strands from the Ce nucleus ventrolaterally to the dorsal part of the BST nucleus dorsomedially. According to these authors, the LAMP-rich dorsal continuum avoids the intensely CAB-ir basal forebrain magnocellular neurons, including the nucleus basalis of Meynert.

ENZYMES

P450 Aromatase The large number of cells expressing P450 aromatase mRNA in the BST (and in its amygdaloid counterparts) make it probable that testosterone (T) acts in large part through the aromatase pathway in these brain regions. These same regions have been also found to exhibit high levels of ER-α and ER-β, suggesting that locally formed estrogen

can act on cells in the immediate vicinity through ER-mediated mechanisms. Studies in other species have also demonstrated that a majority of neurons in the BST and its amygdaloid counterparts contain P450 aromatase and estrogen receptors (see Roselli *et al.*, 2001).

RECEPTORS

CHOLINERGIC RECEPTORS

MUSCARINIC RECEPTOR (MACH-R) According to Cortés *et al.* (1987), there is high concentration of mACh-R in the human BST nucleus, which presents densely labeled patches especially near the internal capsule and which is enriched in m_1 subtype. From their illustrations (Fig. 5A, B) it can be inferred that the most dense activity takes place in the BSTLD and JCX subnuclei of the BSTL, whereas lower labeling occurs at the level of the BSTLP and BSTLV subnuclei.

GALANIN RECEPTOR (GAL-R) According to Kohler and Chan Palay (1990), within the human telencephalon, high densities of [^{125}I]GAL-R are found in the BST nucleus.

GLUTAMATE RECEPTOR (GLUR) According to Ginsberg *et al.* (1995), in the macaque monkey, the laterodorsal subnucleus of the bed nucleus of the stria terminalis (here BSTLD), contain a high density of GluR 2/3-ir neurons and a lower density of GluR1-ir neurons but express minimal GluR4.

OPIOID RECEPTOR (OR) Both [^{3}H]DAMGO binding and DAMGO-stimulated G proteins were expressed in high densities in the medial portions of the bed nucleus, but moderately in the lateral cytoarchitecturally defined subdivisions (Daunais *et al.*, 2001).

OXYTOCIN RECEPTOR (OTR) For the human BSTL, Loup *et al.* (1991) made no mention of the presence of this type of receptor. However, according to Wilson *et al.* (1999), while a high level of oxytocin (OT) binding could be found in the Ce nucleus and associated BSTLD, the binding density was lower in the MeA nucleus and in the BSTMA. These authors also found that although the OT binding was the greatest in the nuclei of the CExA, the excitatory responses to OT did not match it, being greater in the MexA. However, it is important for the hypothesis of the EXA that the relative expression of OT binding sites and the patterns of response reflect these associations within the extended amygdala.

VASOPRESSIN RECEPTOR (AVP) According to Loup *et al.* (1991), in the human BST nucleus, the lateral and lateroventral divisions show inconsistent weak AVP binding.

Sublenticular Components of the Central Extended Amygdala (SLEAC)

Central Division of the Sublenticular Extended Amygdala (SLEACn)

Topographical Landmarks Basically, the SLEACn can be defined as the griseum that connects the BSTL division of the bed nucleus of the stria terminalis with the Ce amygdaloid nucleus (Figs. 22.14a,b, 22.15a,b, 22.16, 22.22c, 22.26b) [BSTCV in Plate 24 (2.7 mm) in Mai *et al.* (1997), *Atlas of the Human Brain*; EA (extended amygdala) in Plates/Figs. 50–55 (Interaural 18.30–16.05 mm) of Paxinos *et al.* (2000), *The Rhesus Monkey Brain in Stereotaxic Coordinates*]. At a closer look, the SLEACn appears constituted by cell columns corresponding to the dorsal (BSTLD), posterior (BSTLP), and ventral (BSTLV) parts of the lateral division of the BST nucleus, which become located in a sublenticular corridor that crosses the classically denominated substantia innominata while accompanying the ventral amygdalofugal pathways in their passage through these regions of the basal telencephalon. By doing so, these cell columns come to constitute in a broad way their bed nucleus. Along this route, they come to occupy what some authors (Martin *et al.*, 1991; Marksteiner *et al.*, 1993; Kaufman *et al.*, 1997) have denominated the anterodorsal and posterodorsal sectors of the so-called substantia innominata before meeting the Ce nucleus.

Cytoarchitectonics The neurons that form these bridges are loosely packed, medium sized, fusiform to triangular shaped, and more elongated than those in the SLEAM (Fig. 22.15b). Another feature that helps to identify them is that these sublenticular columns are eventually surrounded by magnocellular neurons at the point where the intermediate division of the basal nucleus of Meynert comes to be subdivided into intermediodorsal and intermedioventral parts. Groups of small, granule-like, tightly packed, and darkly stained neurons (parvicellular interface islands or Sanides' type 2 cells) are also found in the sublenticular sector of the so-called substantia innominata. These types of cells may be linked to the striatum (Heimer *et al.*, 1999) in which case they should not be considered to form part of any of the divisions of SLEA.

While in the macaque and squirrel monkeys the BSTL divisions of the BST nucleus and Ce amygdaloid nucleus appear to continue in each other as uninterrupted cell columns extending along the course of the stria terminalis dorsally and through the so-called substantia innominata ventrally (de Olmos, 1990; Martin *et al.*, 1991), this pattern does not seem to hold for

the human brain since the gray columns that connect them are more or less dislocated, particularly in the sublenticular sector of the EXA, probably by reason of their interruption by dense fibers of passage.

Freedman and Shi (2001), on the basis of their immunohistochemical tracing of the monaminergic innervation of the extended amygdala, concluded that the dorsal part of the substantia innominata appears similar to the medial subnucleus of the Ce amygdaloid nucleus, though they also stressed the existence of a more heterogeneous cell population in the SLEACn. Such apparent heterogeneity was considered to be probably due to the interdigitation of the true SLEACn cell constituents with other basal telencephalic with more or less diffusely arranged cell subpopulations.

As here defined SLEACn encloses Martin *et al.*'s (1991) anterodorsal (SIad) and posterodorsal (SIpd) branches of their sublenticular (BSTSL) division of the BST (see also Marksteiner *et al.*, 1993; Kaufman *et al.*, 1997).

Chemoarchitecture

CUPRIC SILVER STAIN (CU-AG) One of the intriguing staining properties of the SLEACn (Figs. 22.14a,b, 22.22, 22.26a) along with the Ce nucleus and the BSTL division of the BST nucleus is the specific manner in which silver impregnates to what I have called the granular argyrophilic neuropil and neurons. This application of the Cu-Ag procedure (de Olmos, 1981; de Olmos *et al.*, 1994) to normal brain tissue of many mammalian species, such as zariguella or South American opossum, armadillo, rat, rabbit, guinea pig, cat, dog, and Old (macaques) and New World (squirrel and marmoset) monkeys with this suppressive silver impregnation method (which does not allow the staining of normal fibers or matter whether myelinated or unmyelinated, or most normal neurons in the brain), consistently shows this specific reaction.

While few argyrophilic cell bodies can be detected in a lateral branch of this peculiar system of granular preterminal fibers that courses rostrally very close to the basal surface of the posterior limb of the anterior commissure (IPAC?, see below), another medially directed branch of greater size and density, which comes to occupy the sublenticular region (i.e., SLEACn), only shows peridendritic and perisomatic argyrophilic granules. High-magnification examination reveals that these images correspond to the terminal boutons issued by very thin argyrophilic preterminal fibers detectable just at the limit of the optical microscope resolution. This argyrophilic profile surrounds otherwise negatively stained dendrites and slender, fusiform perikarya of medium-sized neurons, and they never seem to get into contact of any kind with the large unstained cell bodies of the basal nucleus of Meynert. As can be appreciated, this staining pattern closely resembles that described for the many neuropeptides present in the same area.

NEUROTRANSMITTERS

Cholinergic Markers

ACETYLCHOLINESTERASE (AChE) In AChE preparations many of the interrupted columns and channels of the SLEACn appear to be far less reactive than the nearby MCBFC and the neuropil that surrounds them. Some authors have shown a granular, moderately AChE-positive neuropil that enmeshes AChE-negative neurons (see Perry *et al.*, 1984) bearing morphological characteristics seen in the BSTL division of the BST nucleus and of the Ce nucleus.

CHOLINE ACETYLTRANSFERASE (ChAT) No human or nonhuman primate information on this important point is available at present.

Excitatory Amino Acids

GLUTAMATE (GLU) No human or non-human primate information about this important point is available at present.

Inhibitory Amino Acids

γ-AMINOBUTYRIC ACID (GABA) According to Pitkanen and Amaral (1994), in the macaque monkey, this region of the brain presents insurmountable difficulties for identifying which are the true representatives of the continuum even if GABA-ir fibers can be identified in the region of the ventral amygdalofugal pathway.

MONOAMINE MARKERS

Dopamine-β-Hydroxylase (DBH) Sadikot and Parent (1990) report that in the squirrel monkey DBH-ir fibers enter the amygdala via the ansa lenticularis/ventral amygdaloid bundle that derive from DBH-ir fascicles running in the ventrolateral hypothalamus. The DBH-ir in the substantia innominata is light rostrally and increases progressively to moderate levels caudally.

Histamine (HA) According to Airaksinen *et al.* (1989), in the tree shrew the HA-ir fibers spread in the amygdaloid complex as a dense network including in this manner the SLEACn (see their Fig. 3G).

Phenylethanolamine-N-methyltransferase (PNMT) (Adrenaline/Epinephrine) According to Sadikot and Parent (1990), in the squirrel monkey, few PNMT-ir fibers are present in the ansa lenticularis/ventral amygdalofugal bundle. No further data are given.

SEROTONIN (5-HT) According to Sadikot and Parent (1990), in the squirrel monkey, 5-HT-ir fibers arrive from via the medial forebrain bundle in the lateral hypothalamus to reach the amygdala via the ansa peduncularis/ventral amygdaloid bundle in the sublenticular substantia innominata. These latter contains a large number of nonvaricose and varicose 5-HT-ir fibers showing profuse terminal arborizations.

TYROSINE HYDROXYLASE (TH) According to Sadikot and Parent (1990), in the squirrel monkey, the TH-ir fibers in their route toward their amygdaloid targets travel in the ansa peduncularis/ventral amygdalofugal pathway fiber system, which run in the sublenticular substantia innominata to turn ventrally toward the amygdala. Within this fiber system, fine TH-ir fibers, regularly spaced ovoid varicosities are interrupted by thicker, nonvaricose terminal fibers. Varicose and non-varicose TH-ir fibers cross the substantia innominata, with their number increasing in a rostrocaudal axis of this structure.

NEUROPEPTIDES

CALCITONIN GENE–RELATED PEPTIDE (CGRP) De Lacalle and Saper (2000), in the human brain, report the presence of a bundle of CGRP-ir fibers bridging between the Ce nucleus and the BST nucleus that crosses the so-called substantia innominata in a mediolateral and dorsoventral progression.

CHROMOGRANIN B According to Marksteiner *et al.* (1999), the sublenticular part of the so-called substantia innominata contained the highest density of PE-11-like ir. In the dorsal part of the substantia innominata and in the transition zone to the amygdala the PE-11-like ir is mainly composed of woolly-like fibers.

CHOLECYSTOKININ (CCK) According to Martin *et al.* (1991), who worked with human tissue, their sublenticular BST division (here the SLEACn) of the BST-amygdala continuum contains long, linear or curvilinear dendrites of non-ir neurons that are covered with CCK-ir boutons. These boutons are predominantly present on proximal dendrites and perikaryal surfaces of the nonreactive large, triangular, and fusiform neurons that build up this continuum.

CORTICOTROPIN RELEASING FACTOR (CRF) In the human amygdaloid complex, a dense accumulation of CRF-ir fibers, with large varicosities, and terminals has been reported to be present in almost all amygdaloid nuclei (Powers *et al.*, 1987; Zaphiropoulos *et al.*, 1991). This statement may be extendable to the so-called substantia innominata (Zaphiropolous *et al.*, 1991)

ENKEPHALIN (ENK) In the human brain, Haber and Watson (1985) described ENK-ir fibers of the so-called woolly type. Such fibers extend medially and laterally from a position beneath the ansa peduncularis, and from there they continue as a prominent group that curves around the lateral side of the Ce nucleus. Lesur *et al.* (1987), in turn, reported the presence of "islands" of very dense ENK-ir characterized by the presence of numerous ENK-ir plexuses of granular type, and propose the possibility that these peptidergic "islands" may represent a continuation of the BST nucleus ENK-ir with that of the amygdaloid nuclei via the sublenticular substantia innominata. Martin *et al.* (1991) reported likewise the presence of ENK-ir peridendritic and perisomatic fiber formations which they described either as ribbon-like structures, or as woolly-like, or as tubules as a characteristic of ENK-ir arrangement in the anterodorsal and posterodorsal SLSI (here SLEACn) (see also Haber and Watson, 1985; Mai *et al.*, 1986; Kaufmann *et al.*, 1997). In addition, they reported that peridendritic woolly-like type II fibers as well as ENK-ir varicose fibers extend from the ENK-ir lateral infracommissural BST (i.e., BSTLV) into their anterodorsal sublenticular substantia innominata (i.e., SLEACn). At more caudal levels, these ENK-ir profiles curve medially and ventromedially to the internal segment of the globus pallidus to get into the area of the ansa peduncularis and into the postero-dorsal substantia innominata (i.e., still SLEACn) to eventually reach the dorsal aspect of the amygdaloid body, closely imitating the distribution pattern of the SECR-ir (see below).

DYNORPHIN (DYN) According to Haber and Watson (1985), the human subtlenticular region contains only few DYN-ir fibers.

GALANIN (GAL) According to the mapping of the forebrain distribution of this neuropeptide presented in the cebus monkey amygdala (Kordower *et al.* 1992), this member of the CExA, like other components of this gray continuum, does not contain GAL-ir cell bodies but seems to contain small amounts of GAL-ir fibers, which are depicted in continuity with those at the level of the Ce nucleus, ventrolaterally and caudally. However, the pattern changes dramatically at the level of its paraseptal expansion, i.e., the BSTL division.

NEUROPEPTIDE Y (NPY) According to Walter *et al.* (1990), in the human brain, the area corresponding to the sublenticular extended amygdala contains fibers running in a uniform orientation parallel to the pial surface ventral to, and rarely within, magnocellular complex of the basal forebrain. Occasional NPY-ir

perikarya appear that seem to merge with NPY cells in the ventral part of the putamen accompanied by NPY-ir fibers. By comparison, McDonald *et al.* (1995) could not see NPY-ir peridendritic axonal configurations in the macaque monkey.

NEUROTENSIN (NT) According to Mai *et al.* (1987), NT-ir fibers forming the AA area are continuous with the claustrum striatale and the pedunculus lentiformis as well as with the sublenticular region, including the so-called substantia innominata. Some of the full picture concerning the distribution of NT-ir fibers in this region of the telencephalon form without doubt to the NT-ir component of the extended amygdala described by Martin *et al.* (1991), who described the existence of NT-ir peridendritic and perisomatic profiles which were considered to be characteristic in the anterodorsal and posterodorsal SLSI (here SLEACn).

PROSOMATOSTATIN-DERIVED PEPTIDE (PSDP) According to Bouras *et al.* (1987), the human substantia innominata contains moderate amounts of both PSDP-ir cell bodies and fibers.

SECRETONEURIN (SECR) According to Kaufmann *et al.* (1997), from the lateral infracommissural BST (i.e., the BSTLV) SECR-ir peridendritic woolly-like type II fibers as well as SECR-ir varicose fibers extend into the sublenticular substantia innominata (i.e., SLEACn). More caudally, these SECR-ir profiles curved medially and ventromedially to the internal segment of the globus pallidus to get into the area of the ansa peduncularis where they appear distributed in two areas separated by the large CAB-ir neurons of the nucleus of Meynert, neurons that do not express SECR-ir. More laterally and caudally, prominent SECR-ir can be observed throughout the posterodorsal substantia innominata (i.e., still SLEACn). SECR-ir peridendritic woolly-like fibers extend ventrolaterally beneath the caudal aspect of the anterior commissure to eventually reach the dorsal aspect of the amygdaloid complex and join the SECR-ir in the Ce nucleus.

SOMATOSTATIN (SOM) According to Candy *et al.* (1985), Bennet-Clarke and Joseph (1986), Lesur *et al.* (1987), Mufson *et al.* (1988), and Heimer *et al.* (1999) in the human brain, SOM-ir fibers and small fusiform, multipolar or bipolar SOM-ir perikarya can be seen to form island-like clusters, with some forming a continuous band up to the dorsolateral preoptic area, with SOM-ir processes present in every area containing SOM-ir perikaria. Gaspar *et al.* (1987) describe the SOM-ir woolly-like and other fine lone SOM-ir fibers coursing within the ansa peduncularis/ventral amygdalofugal pathway. Martin *et al.* (1991) confirmed these observations but also stressed the continuation of the BSTLV division of the BST into anterodorsal and posterodorsal sectors of the substantia innominata (here the SLEACn). They also found that this peptidergic sector of the substantia innominata is delineated by a dense band of overlapping immunoreactivity for several other neuropeptides.

Amaral *et al.* (1989), in the macaque monkey, specifically stressed the fact that the SOM-ir present in the Ce nucleus is continuous with the dense SOM-ir located in the so-called substantia innominata and BST nucleus, an observation that coincides with those of Mufson *et al.* (1988) in the human basal forebrain. They also remarked that this disposition parallels the projection of the Ce nucleus to the BST nucleus (see Fig.2B in Price and Amaral, 1981). These authors also pointed out the presence in this SOM-ir field within the sublenticular substantia innominata (i.e., the present SLEACn) of dense, fasciculated bundles of only slightly varicose SOM-ir fibers as well as large varicosities that formed single or double parallel profiles that, as in the Ce nucleus, outlined dendritic processes of non-ir neurons. Closely associated with them, Amaral and Prise (1988) also found patches of densely SOM-ir terminals. None of these latter seem to be associated with magnocellular neurons of the basal nucleus of Meynert, but rather with clusters of densely packed smaller neurons located within the sublenticular substantia innominata. Similar findings have been reported by McDonald *et al.* (1995).

According to Desjardin and Parent (1992), in the squirrel monkey, the areas corresponding to the EXA display a rather intense SOM-ir. In this New World primate, as in the macaque brain, within the SLEA groups of SOM-ir fibers form a dense bundle that course among the fibers of the ansa lenticularis, the inferior thalamic peduncle, and the adjoining BST nucleus. These fibers could be traced continuously within the so-called substantia innominata to the dorsal tier of the Ce nucleus. A large proportion of these fibers in the squirrel monkey brain are of the woolly-like type. It is interesting to point out that, according to these authors, in contrast to what happens with every component of the EXA, the entire pallidal complex in the squirrel monkey is largely devoid of SOM-ir.

SUBSTANCE P (SP) According to Haber and Watson (1985), in the humans sublenticular region, there are no SP-ir fibers.

VASOINTESTINAL PEPTIDE (VIP) Although Martin *et al.* (1991) have schematically mapped the presence of

this peptide in the sublenticular region of the BSTLD, the material illustrated with microphotographs by Heimer *et al.* (1999) provides a dramatic and convincing demonstration of the ventrolaterally directed VIP-ir continuum coming from the VIP-ir fibers and neuropil present in the BSTLD division of the BST nucleus to reach immediately after the SLEACn and later on the VIP-ir plexus in the central division of the Ce nucleus. This proof is especially significant given the fact that the VIP-ir is a specific marker for central extended amygdala since neither the BSTM division nor the Me or the SLEAM shows VIP-ir. The VIP-ir appears in these areas in the form of perisomatic and peridendritic profile.

CALCIUM-BINDING PROTEINS

CALBINDIN (CAB) According to Kaufmann *et al.* (1997), CAB-ir profiles are not present at any level of the anterodorsal sublenticular substantia innominata, i.e., the present SLEACn. Sorvari *et al.* (1996b) described CAB-ir in the ventral amygdalofugal pathway.

RECEPTORS

GALANIN RECEPTOR (GAL-R) According to Kohler and Chan Palay (1990), in the human telencephalon, [^{125}I]-galanin binding occurs in the so-called substantia innominata in the form of patches separated by areas of low or no specific binding.

SEROTONINERGIC RECEPTORS (5-HT-R)

5-HT$_{2C}$ RECEPTOR (5-HT$_{2C}$-R) According to Lopez-Gimenez *et al.* (2001), the sublenticular extended amygdala constitutes one of the forebrain structures showing the strongest hybridization signal with probes for 5-HT$_{2C}$-R mRNA.

Interstitial Nucleus of the Posterior Limb of the Anterior Commissure (IPAC) In the rat brain IPAC has been well delineated as a result of normal and experimental studies carried out in this macrosmatic mammal by Alheid and colleagues (Alheid *et al.*, 1994, 1995; Alheid and Heimer, 1996, Alheid *et al.* 1998; Heimer *et al.*, 1997a, b; Veinante and Freund-Mercier, 1997). This anatomical entity includes an area along the posterior limb of the anterior commissure that is continuous with the caudomedial accumbens and shares the histochemistry and close connections with the central division of the extended amygdala. At present it is not possible to specify with any precision the homologous area of the primate or human brain. However, some histochemical data presented by Heimer *et al.* (1999) suggest that portions of the human ventral striatum that are close to the temporal limb of the anterior commissure are differentiated from the overlying striatum and stain in a similar fashion as the ventrally adjacent elements of the extended amygdala (see their Figs. 26A, B for SECR-ir and CCK-ir).

CUPRIC SILVER STAIN Examination of transverse sections of the macaque and squirrel monkey brains stained with the cupric silver technique show that argyrophilic neuropil and a few granularly silver-stained neurons appear below and very briefly in front of the temporal limb of the anterior commissure of what might be a very reduced representation of this structure in nonhuman primates. If this is so, one can expect that this small and so peculiarly argyrophilic region will share the immuhistochemical characteristics of the rest of the equally argyrophilic SLEACn. Finally, it should be pointed out that in nonprimate macrosmatic mammals larger than the rat, such as the guinea pig, the rabbit, and the cat, the region of the ventral striatum located around or near the external capsule displays a similar picture to that observed in the above-mentioned monkeys.

Supracapsular Components of the Extended Amygdala

The Supracapsular Division of the Bed Nucleus of the Stria Terminalis (BSTS) and the Stria Terminalis Bundle (st) The neurons of the BSTS division of the BST nucleus form a more or less continuous column of cells along the stria terminalis extending from the BST nucleus to the centromedial or supra-amygdaloid sector of the amygdaloid complex (Figs. 22.17 and 22.22a) [BST/st in Plates 30–48 (10.7–34.6 mm) in Mai *et al.*, *Atlas of the Human Brain*, in Plates/Figs. 57–88 in Paxinos *et al.* (1997), "The Rhesus Monkey Brain in Stereotaxic Coordinates"]. In the human brain, this division appears to be composed mainly of two discontinuous columns of cells (however, see Martin *et al.*, 1991): medial (BSTSM) and lateral (BSTSl).

The BSTS subdivision of the supracapsular BST nucleus consists of a column of cells that at the level of the anterior thalamic nuclei, lies just medioventral to the stria terminalis bundles and, more caudally, comes to lie directly within the bundles themselves, where it is represented by relatively few neuronal elements. In general, the BSTS column is made up of small, spindle-shaped neurons with their longer axis oriented parallel to the course of the bundle resembling very much those in the BSTM division of the BST nucleus.

The more laterally located and complex BSTSL subdivision initially becomes evident at the same level as the just described BSTS, but located dorsolateral to the stria terminalis and within the border of the caudate nucleus. It continues in this position until it reaches the amygdaloid expansion of the BST nucleus. In an

intermittent fashion but still along the whole stretch of the supracapsular BST, small granular (Sanides' gamma type I) and parvicellular (Sanides' gamma type II) cells accompany this lateral component of the BSTS division. The more externally located, more continuous, larger celled lateral cell column constituted by the BSTSL proper when compared with the BSTS subdivision appears to be composed of somewhat more ovoid medium-sized neurons intermingled with a few larger and darkly staining neuronal elements scattered along the subdivision. These neurons are morphologically similar to those described for the BSTLD subnucleus of the lateral division of the BST nucleus.

The BSTS division of the bed nucleus of the stria terminalis as here defined in humans seems to be equivalent to that utilized by Martin *et al.* (1997), although the BSTSL subdivision of the present account seems to include their dorsal (BSTSld) and posterior (BSTlpl) subdivisions. According to these authors, the first cited subdivision would be a continuation of the BSTLD subdivision of the paraseptal BST nucleus, and the second cited one to the BSTLP subdivision.

Chemoarchitectonics

HEAVY METALS In Timm-Dansher's preparations of marmoset and squirrel monkey brains, it is possible to see a direct continuation of metal deposits present in the BSTL nucleus with those in the lateral large-celled column of the BSTSCn, which can be followed up to their final reunions with similar deposits at the level Ce nucleus. This evidence speaks in favor of a supracapsular continuation of the extended amygdala.

CUPRIC SILVER STAIN In cupric silver–stained transverse sections of macaque, squirrel, and marmoset monkey brains, it is possible to identify along the suprathalamic course of the stria terminalis pocket of granular argyrophilic perikarya and neuropil more or less closely adjacent to the lateral side of the compact medial bundle of the stria terminalis near the ventricular surface. The same can be seen near the entrance of the stria terminalis into the amygdaloid complex. Other times the pockets of argyrophilic perikarya and neuropil are found laterally in the angle between the stria terminalis and the thalamic radiation of the internal capsule, or within thin wedge-like septa of gray matter interposed between lateral and medial bundles of the stria terminalis when this fiber system travels below the optic tract, etc. Although this distribution pattern sometimes resembles that described for some neuropeptides, such as the CCK or SOM, it seems that there is no entire coincidence.

NEUROTRANSMITTERS OR NEUROMODULATORS

MONOAMINE MARKERS

DOPAMINE-β-HYDROXYLASE (DBH) According to Gaspar *et al.* (1985), in the human basal telencephalon the DBH-ir fibers, together with TH-ir ones, participate in a contingent of catecholaminergic fibers coming from the medial zone of the medial forebrain bundle into the septal region located around the anterior commissure decussation from which level a caudally oriented bundle branched from them runs dorsally toward the stria terminalis forming a vertically oriented axonal bundle that follows the lateral border of the BST nucleus medially to the internal capsule vertically. From this position abundant DBH-ir fibers branch off to concentrate in the medial portion (BSTM) of the BST nucleus while innervating very scarcely its lateral portion (BSTL).

In the squirrel monkey, DBH-ir fibers have been detected in the intra-amygdaloid portion of the stria terminalis (Sadikot and Parent, 1990).

HISTAMINE (HA) According to Airaksinen *et al.* (1989), in the tree shrew the stria terminalis contains a dense bundle of HA-ir fibers.

SEROTONIN (5-HT) In the squirrel monkey, 5-HT-ir fibers are present in the intra-amygdaloid portion of the stria terminalis (Sadikot and Parent, 1990).

TYROSINE HYDROXYLASE (TH) TH-ir fibers follow approximately the same course as DBH-ir fibers to become incorporated in the stria terminalis after innervating the BST nucleus in a complementary fashion with respect to that provided by the DBH-ir fibers, i.e., by innervating the lateral portion (BSTL) of the BST nucleus.

In the squirrel monkey, TH-ir fibers are present in the intra-amygdaloid portion of the stria terminalis (Sadikot and Parent, 1990).

INHIBITORY AMINO ACIDS

γ-AMINOBUTYRIC ACID (GABA) According to Pitkänen and Amaral (1994), GABA-ir fibers could be observed along the entire course of the stria terminalis. Some of the fibers entered the medially adjacent extension of the BST nucleus and developed a dense network there.

NEUROPEPTIDES According to Martin *et al.* (1991), the gray matter constituting caudal extension of the BST nucleus that accompanies the stria terminalis dorsally, i.e., its supracapsular division, contains neurons that are similar to those present in the main

body of this nucleus, so that the BSTS has features of the BSTLD, BSTLP, and BSTM divisions.

CHOLECYSTOKININ (CCK) According to Martin *et al.* (1991), both dorsolateral and posterolateral divisions as well as the medial division of the baboon and green monkey contain CCK-ir varicose fibers and punctate material. Only in the baboon are CCK-ir bodies present in the lateroposterior and medial divisions of the BSTS.

CHROMOGRANIN B According to Marksteiner *et al.* (1999), the stria terminalis displayed a high density of PE-11-like ir fibers.

ENKEPHALIN (ENK) According to Martin *et al.* (1991), both dorsolateral and posterolateral divisions of the BSTS division material of the macaque, baboon, and green monkeys contain ENK-ir cell bodies as well as of ENK-ir varicose fibers, peridendritic, perisomatic, and punctate material.

GALANIN (GAL) According to Kordower *et al.* (1992), in the cebus monkey, temporal segments of the stria terminalis and occasional small GAL-ir neurons can be detected.

NEUROPEPTIDE Y (NPY) According to Walter *et al.* (1990), human stria terminalis exhibits NPY-ir fibers in low to moderate amounts. Occasionally, small NPY-ir perikarya can be noted in the vicinity of these fibers.

NEUROTENSIN (NT) According to Martin *et al.* (1991), both dorsolateral and posterolateral divisions of the BSTS division of the macaque, baboon, and green monkey contain NT-ir cell bodies as well as of NT-ir varicose fibers, peridendritic, perisomatic, and punctate material.

OXYTOCIN (OXT) According to Caffé *et al.* (1989), in the macaque brain, thick, smooth OXT-ir fibers are present in the stria terminalis with origin very presumably in the magnocellular paraventricular hypothalamic nucleus.

PROSOMATOSTATIN-DERIVED PEPTIDE (PSDP) Bouras *et al.* (1987), in the human brain, were able to detect a high density of PSDP-ir fibers in the stria terminalis.

SECRETONEURIN (SECR) According to Kaufmann *et al.* (1997), this part of the BST complex displayed a high density of SECR-ir varicose fibers and is partially confluent with that of the stria terminalis. This bundle displayed the highest density of this neuropeptide compared with that of other neuropeptide markers.

SOMATOSTATIN (SOM) According to Gaspar *et al.* (1987), while a majority of the so-called SOM-ir woolly fibers are oriented to the sublenticular region of the basal telencephalon, a few course along the stria terminalis. Martin *et al.* (1991) have reported the presence of SOM-ir cells in the laterodorsal BSTS division, as well as of SOM-ir varicose fibers, peridendritic, perisomatic, and punctate material in both laterodorsal and lateroposterior subdivisions of the BSTS of the macaque and green monkeys.

VASOINTESTINAL PEPTIDE (VIP) According to the report by Martin *et al.* (1991), VIP-ir fibers are present in the laterodorsal subdivision of the macaque BSTS division.

VASOPRESSIN (VP) According to Caffé *et al.* (1989), in the macaque brain very thick, smooth VP-ir fibers are present in the stria terminalis, presumably having their origin in the magnocellular paraventricular hypothalamic nucleus

CALCIUM-BINDING PROTEINS

CALBINDIN (CAB) According to Sorvari *et al.* (1996b), the human stria terminalis contains CAB-ir fibers. However, they do not comment about the presence or absence of CAB-ir cell bodies.

CALRETININ (CR) According to Sorvari *et al.* (1996a), the human stria terminalis contains CR-ir fibers; however, they do not comment about the presence or absence of CR-ir cell bodies. In observations made in rat material processed in my laboratory for immunochemical demonstration of CR-ir, the CR-ir fibers tend to run predominantly in the ventral component of this bundle, being stronger in the lateral division of this component than in the medial one. CR-ir perikarya can be detected forming a small cluster along the course of the ventrolateral ST. Interestingly, no CR-ir fibers or cells are present in the commissural component of the ST bundle, which goes along with the very poor presence of CR-ir cells in the LOT nucleus.

PARVALBUMIN (PAV) According to Sorvari *et al.* (1995), in the human basal telencephalon, very few PAV-ir fibers can be found in the stria terminalis.

Temporal Lobe Components of the Central Extended Amygdala

Central Amygdaloid Nucleus (Ce) The Ce nucleus is the main output of the amygdala acting as an

integrator site that receives multimodal sensory information supplied by amygdaloid, paleo-, archi-, periallo- and neocortical structures, by the hypothalamus and thalamus, and by brain stem areas. As such, it is concerned with the elaboration of autonomic, endocrine, cardiovascular, immune, and behavioral functions, playing, for example, a crucial role in modulating cardiac changes associated with fear and anxiety, and with aggression. For this reason, it plays also a key role in fear-related responses, such as the increase of the arterial blood pressure and tachycardia that occurs in this type of behavior. It is also considered to be the main brain structure for conditioned fear-responses, accomplishing all of these functions through its direct and indirect efferent projections to thalamic, hypothalamic, brain stem, and even spinal cord effector centers.

Topographical Landmarks The Ce nucleus [Ce (plates 25–33, 4.0–14,6 mms in Mai *et al.* (1997) *Atlas of the Human Brain*] is the most deeply located amygdaloid nucleus seated in the angle formed by the BL and BM nuclei (Figs. 22.4, 22.5a, 22.6a,b, 22.7a,b, 22.8, 22.10, 22.11, 22.22c, 22.27). It extends within the posterior two-thirds of the amygdaloid complex, lying ventral to the base of the pallidum and putamen from which it is separated by numerous myelinated fiber bundles and by magnocellular neurons that are the caudal representatives of the diffuse and compact parts of the basal nucleus of Meynert (BC). The Ce extends until it reaches the posterior limit of the amygdala, though it remains separated from the ventricular wall by intra-amygdaloid fiber radiation of the stria terminalis together with the neurons that form their bed nucleus. The Ce nucleus is also bounded ventrally and laterally by dense fiber bundles [Broackhaus'(1938) lamellae dorsomedialis and dorsalateralis, respectively], although a less prominent fiber network surrounds the nucleus almost entirely forming a capsule. Rostrally the Ce nucleus is bordered dorsally by the SLEACn, with which it is continuous, and by the intermediate division of the nucleus basalis (BC). The Ce nucleus is also flanked laterally by the temporal limb of the anterior commissure (ac) and the amygdalostriatal transition area (AStr) by which it is partially replaced further caudally. As pointed out before ventrolaterally, the Ce nucleus is bounded by the DL subdivision of the BL nucleus and by intercalated cell islands of different size and shape, while ventrally the DM division of the BM nucleus provides the seat for this nucleus. Medially, the Ce nucleus is separated from the MeA nucleus by a narrow arm of the deep AAA that wedges between both nuclei. The rostral pole of the Ce abuts the deep AAA from which is separated by a thin but always present rostral extension of the capsular formation mentioned earlier. The existence of this fiber limit can be clearly seen in neurofibrillar preparations stained with nonsuppressive silver procedures. In this type of preparation it is possible to establish without doubt the existence of such limiting fiber barrier as well as the far less dense fiber network present in the Ce nucleus as compared with that seen in the deep AAA. Furthermore, in Nissl preparations, and contrary to the much insisted continuity of the Ce with the deep AAA, it is also easy to appreciate not only that the background staining in the Ce nucleus is more translucent than that in the deep AAA, but also that the glial population in this latter griseum is richer than in the Ce nucleus, a glioarchitectonic feature that very presumably reflects higher fiber density present in the deep AAA.

Just dorsal to the main mass of the Ce nucleus and even reaching beyond the rostral pole of it, neuronal islands appear that share some of the morphological characteristics of the Ce nucleus, such as chromophilic ground substance and light staining in both Nissl and Weigert preparations. These cell islands correspond to what Brockhaus (1938) labeled the "supraamygdala ventralis accessoria." In the present chapter they are called the paracapsular subdivision of the CeL (PC CeL). As pointed out in a previous version of this chapter, and accepted by other investigators (Martin *et al.*, 1991; Heimer *et al.*, 1999), these accessory formations may constitute peninsular extensions because they are attached to the main body by bridges of Ce tissue. Furthermore, these accessory formations, like the principal nucleus, are encircled by narrow capsular-like formation of cells and fibers that shares many of the morphological and chemical characteristics of the main capsular division of the Ce nucleus. It is important to add that similar disposition can be observed in the BSTL, supporting in this manner the principle of symmetry on which is based the morphological theory of the extended amygdala.

Cytoarchitectonics On the basis of its cytoarchitectonic arrangement, the Ce nucleus can be divided into two major divisions: medial (CeM) and lateral (CeL). Each one, in turn, can be subdivided into subnuclei: the former division into dorsal (D CeM) and ventral parts (V CeM), and the latter named division, which shows a far more complicated cell arrangement, into central (CeLCn), apical (CeLA), capsular (CeLC), paracapsular (PCeL), and periparacapsular (PPCeL) subdivisions.

The CeM, lies dorsomedially to the CeL subnucleus and is intercalated between this laterally, the deep AAA rostrally, the MeA nucleus medially, and the DM BM ventrally. CeM has a more heterogeneous

neuronal population made up of densely packed small and medium-sized neurons and, in general, contains a denser glial cell population than that in CeL. Furthermore, if differences in cell packing and topographic location are taken into account, the CeM division can be divided into dorsal (D CeM) and ventral (V CeM) subnuclei. While the neuronal population in the D CeM subnucleus is more densely arranged and the glial population richer than in the V CeM, this latter possesses a more loosely arranged and homogeneous cell composition.

Broadly speaking, the CeL division of the Ce is constituted by medium-sized, lightly stained cells, with those in the CeLCn being very similar in appearance to the cells in the BSTLDcn. These neurons show a well-defined round, fusiform, or triangular outline against a very typical translucent background in which very few glial cells can be observed, as compared with the glial population in surrounding structures. There are, however, some organizational differences in different sectors in several divisions of the CeL that justify its parcellation. Thus, the main body of CeL can be divided into a less extensive anterodorsally located apical part (CeLA) and a much larger central part (CeLCn) that lies posteroventrally to the former subdivision. Such subdivision results from a looser arrangement and orientation of the slightly larger and more darkly staining neurons in CeLCn subnucleus, but from the typically much sharper outline of their cell processes and perikarya. The neuronal population in the CeLA subnucleus is, on the other hand, more heterogeneous than that in the CeLCn subnucleus, in the sense that it contains a significanty larger number of pallidal-like neurons. On the basis of this and other morphological features to be dealt with later in this chapters, the CeLA subnucleus could be viewed as an extension of the capsular part of the CeL division.

The narrow neuron-poor and glial cell–rich CeLC is populated by loosely arranged, more darkly stained, usually fusiform neurons enmeshed in the fiber capsule that surrounds the CeLCn subnucleus, a disposition that is again very similar to that observed in the BSTLD. On topographical grounds, this subdivision of the CeL division can be parcelled into dorsal (D PCeLC), ventral (V PCeLC), and periparacapsular (P PCeLC) parts, although these latter two subdivisions may be continuous and constitute a structurally uniform sheet wrapping both the PCeL division and the dorsal and lateral aspects of the CeLCn. By contrast, the V PCeLC subdivision appears to be made of a more heterogeneous and larger-celled neuronal population. Peculiar to the capsular CeL is the orientation of its generally spindle-shaped neurons parallel to the locally predominant direction of the fiber fascicles in which they are enmeshed. Such features help to distinguish this division of the Ce nucleus from surrounding structures. (For further details, see de Olmos, 1990.)

The paracapsular sector (PCeL) of the Ce nucleus forms an irregularly shaped plate-like structure in which the central segment is, in general, thinner than its ends and discontinuous at times. It is this thinner portion that connects with or appears to be connected by cell bridges to the main body of the CeL division. The neurons in the paracapsular part are, in general, smaller and more densely packed than in the CeLCn and tend to be oriented parallel to the long axis of gray paracapsular formation to whose buildup they contribute. Like the rest of the CeL division, the PC CeL is poor in glial satellite cells and shows a translucent background staining.

On purely topographical grounds, the PCeL can be divided into dorsal (D PCeL) and ventral (V PCeL) parts. The D PCeL extends farther dorsally (and rostrally) and its ventral counterpart eventually becomes continuous with the SLEACn. The cells in this subdivision are regularly oval shaped with poorly outlined processes and weakly stained Nissl substance with a oval nucleus centrally located. The V PCeL is sharply delineated by the capsular formation that surrounds and separates it from the CeLCn, the AStr, and the ventral putamen.

Fibroarchitectonics In Weigert-stained sections or in neurofibrillar preparations (Fig. 22.27b), the CeM division can be distinguished from surrounding structures by the dense and random orientation of the fiber plexus present in it. Rostromedially and dorsally, the fiber plexus in the CeM division seems to merge into the deep AAA or in that related to the basal nucleus of Meynert. However, as pointed out at the beginning of this chapter, closer examination reveals that this division of the Ce nucleus is actually separated from the deep AAA by a thin fiber capsule barely visible in Weigert sections that becomes denser toward the BM nucleus. The D CeM subnucleus can be differentiated from the V CeM subnucleus by the greater density of its fiber plexuses.

The CeL division and its many subdivisions are more sharply defined in this type of preparation than in cell preparations. As was pointed out, the main body of the CeL division and its paracapsular extensions are easily recognized by their fiber-poor composition, which contrasts sharply with the richly fibered CeLC subdivision. Ventrally, however, this latter, which is poor in fibers, should not be mistaken for the dorsomedial medullary lamina that separates the Ce nucleus from the BM nucleus and in which are

embedded a few neuronal elements whose cytological characteristics are much like those in the CeM nucleus.

As here described, the Ce nucleus corresponds to the supra-amygdaleum profundum dorsale (sApd), supra-amygdaleum profundum ventrale (sApv), and supra-amygdaleum profundum ventrale accessorius (sApv acc) of Brockhaus (1938). The dorsolateral subdivision of the Ce nucleus by Sims and Williams (1990) probably corresponds to the PCeL subdivision of the present account; however, their ventrolateral subdivision seems to correspond to the AStr, and their interstitial subdivision most probably represents one of the intercalated nuclei that are always present around the Ce nucleus.

Chemoarchitectonics

CUPRIC SILVER STAIN In cupric silver–stained sections of macaque, squirrel, and marmoset monkey brains (Fig. 22.22c), silver deposits involve all divisions of the Ce nucleus, although such deposits assume different expressions according to the subdivision under examination. These silver precipitates, which occur in an otherwise normal tissue, display a granular and beaded appearance for which reason the name of granular argyrophilic neuropil was assigned. The central core of the Ce nucleus is characterized by its content of granular or punctate profiles that appear to represent mostly thickened terminals of granular argyrophilic axons. The diameter of argyrophilic axons is small and on most occasions the axons are not detected by the optical microscope. Embedded in this neuropil and having a tendency to be located ventrally and laterally within this part of the lateral Ce are granular argyrophilic neurons of rounded cell bodies with different degrees of argyrophilia. This argyrophilia is expressed by the accumulation of minute argyrophilic granules that almost fill their perikarya and that, on occasion, may also invade the proximal dendrites of these neurons and—more rarely—their axons (de Olmos, 1969; de Olmos *et al.*, 198l). These neurons are scattered throughout the core of the lateral paracapsular Ce, as well as in the rostral and caudal extensions of the central core and also involving the supracapsular–dorsolateral BST continuum or the SLEACn (see above). In the capsular lateral and apical lateral Ce, as well as the paracapsular extensions of the former, the argyrophilic profiles assume the ribbon-like or bistranded arrangement already described when dealing with the medial Ce. This argyrophilic pattern also extends beyond the boundaries of the just-mentioned subdivisions of the lateral Ce to continue into the supracapsular BST division caudally and into the SLEACn ventrolateral BST rostrally. Seldom are argyrophilic neurons seen in any of the subdivisions of the capsular lateral or apical lateral Ce.

HEAVY METALS In Timm-Dancher's-stained sections (see Fig. 22.23b) of macaque, squirrel, and marmoset monkey brains, the CeL division is densely impregnated with silver-sulfur granular deposits, while the CeM division shows a much lighter silver precipitate. Within CeL the staining is not homogeneously distributed but is denser on a medially located core (CeLCn) than on the lateral semiring (CeLC) that encloses the lateral and dorsal sides of the former. Interestingly, around the less densely stained semiring formation appears somewhat denser area suggesting a paracapsular division because of its more dense reaction. Adjacent sections stained for AChE show a point-to-point complementary staining pattern. Whatever the meaning of this histochemical heterogeneity, the point remains that this division of the Ce nucleus is most probably the target of zinc-containing pathways with source outside the nucleus. This reasoning is based on the fact that in rats microiontophoretic injections of sodium selenite in this Ce nucleus does not cause the labeling of the local neurons but occurs in neurons located in amygdaloid nuclei and in cortical structures known to have this nucleus as a target of their efferent projections (de Olmos and Beltramino, unpublished observations).

NEUROTRANSMITTERS

CHOLINERGIC MARKERS

ACETYLCHOLINESTERASE (ACHE) As pointed out by Gloor (1997), the various reports available in the literature concerning the presence in the Ce nucleus of cholinergic markers differ in detail, but there exists a general consensus that the neuropil of the Ce nucleus stains lightly and that some cells contain AChE (Nitecka and Narkiewicz, 1976; Sims and Williams, 1990). There are, however, some differences in the AChE reactivity within the Ce nucleus that deserve to be stressed, since this enzyme is more densely expressed in the CeM division than in the CeL division (Sorvari *et al.*, 1995; Heimer *et al.*, 1999). On the other hand, Darvesh *et al.* (1998) have claimed that they were not able to detect AChE-positive neurons in four of five brains, and in the only one that showed them, they were very few. Furthermore, the distribution pattern of the AChE activity within the CeL helps to distinguish the CeLCn subnucleus from the CeLC, being denser in the former and providing a clear picture of the more or less continuous AChE-negative sheet that encapsulates the CeLCn subnucleus (Benzing *et al.*, 1992; Heimer *et al.*, 1999).

In the macaque monkey brain AChE staining of the CeL division of the Ce nucleus is lighter than that of the CeM division. AChE staining in the CeL division is finer and slightly different in color than in other regions of the amygdala and there are few distinctly stained

fibers. The density of the staining is darker at caudal levels of the CeM division in which the AChE staining involved fiber and background. The dorsal half of the nucleus has higher levels of both types of staining. AChE-positive neuronal perikarya can frequently be detected adjacent to the fibers that surround the Ce nucleus as well as within the CeM division.

CHOLINE ACETYLTRANSFERASE (CHAT) According to Emre *et al.* (1993), the Ce nucleus in humans has a clearly delimited oval CeL that is surrounded by a non-ir fiber bundle and a less well-delineated CeM that merges into neighboring structures, such as the so-called substantia innominata. The density of varicose ChAT-ir profiles is high within the CeL division and slightly less intense within the CeM division. The density is slightly higher and more patchy in the more posterior levels, especially in the CeL division. In overall ranking the CeL division is second only to the large-celled DL/D BL nucleus concerning the density of ChAT-ir fibers and varicosities.

Amaral and Basset (1989) report that in the macaque monkey the CeL division contains a moderate density of diffuse ChAT-ir that has a finely granular appearance. A thin plexus of fine-caliber ChAT-ir fibers are also visible. Superimposed on the diffuse ChAT-ir are small patches of more dense ir that appears to be condensation of ChAT-ir terminals. The overall staining of the CeL division increases at more caudal levels. The ChAT-ir in the CeM division of Ce consists primarily of relatively coarse ChAT-ir fibers that appear largely to be running through the nucleus. There is also a little of a fine ChAT-ir indicative of terminal labeling. Thus, in ChAT preparations the CeL division tends to have a darker appearance. ChAT-ir neurons are not seen within the boundaries of the Ce nucleus.

EXCITATORY AMINO ACIDS

GLUTAMATE/ASPARTATE (GLU/ASP) In the rat, cells of the Ce nucleus have been said to contain a lesser amount of Glu/Asp than the nucleus of the laterobasal and superficial cortical amygdaloid formations (Ottersen *et al.*, 1986). However, experimental tracing data obtained by the use of tritiated D-aspartate indicate that a considerable number of the Ce neurons, mostly in its CeM, would be source of GLU/ASPergic projections to the ventral striatum (IPAC) and to the ventral pallidum (Fuller *et al.*, 1987), or to the paraventricular hypothalamic nucleus or immediate surroundings (Csáki *et al.*, 2000).

INHIBITORY AMINO ACIDS

γ-AMINOBUTYRIC ACID (GABA) According to McDonald and Augustine (1993), in the macaque monkey, the Ce nucleus in its lateral division displays a moderate to light GABA-ir which resembles that in the striatum, though the latter contains more intense GABA-ir. In the Ce nucleus, its medial neighbor, the MeA nucleus, contains a very dense array of GABA-ir puncta that appear to represent axon terminals whose density is greater than in the LBNC and that of most nuclei of the superficial pseudocortical amygdala while approximating that in the ACo nucleus. In both major divisions of the Ce nucleus it is possible to identify parallel rows of large GABA-ir puncta-encapsulating processes that appear to be dendrites. This type of image can be found more frequently in the lateral Ce nucleus than in the medial one. Finally, some encapsulated somata and dendritic processes exhibit light GABA-ir. The whole picture has been entirely confirmed in Pitkännen and Amaral's (1994) studies.

MONOAMINE MARKERS

DOPAMINE-β-HYDROXYLASE (DBH) (NORADRENALINE/NOREPINEPHRINE) The human forebrain regions that are innervated by the ascending norepinephrine-containing fibers display low to moderate concentrations of fine, varicose DBH-ir fibers, with sparse medium-sized, nonvaricose DBH-ir fibers intermixed. The most probable candidate as a source of the NET-containing fibers in the human forebrain appears to be the locus coeruleus (A6) (Basile *et al.*). On the other hand, according to Freedman and Shi (2001), in the macaque monkey, the concentration of DBH-ir fibers in the amygdaloid complex is generally lower than in the BSTLV subnucleus. Accordingly, there are moderate numbers of this type of fiber in the CeM division of this important member of the CExA.

In the squirrel monkey, both the CeM and CeL divisions of the Ce display moderately dense terminal DBH-ir with a slight decrease from medial to lateral (Sadikot and Parent, 1990).

HISTAMINE (HA) According to Airaksinen *et al.* (1989), in the tree shrew (*Tupaia belangeri*), HA-ir fibers collected in dense bundles along the stria terminalis continue to the amygdaloid complex to spread as a dense and diffusely distributed network in the amygdala. At the level of the Ce nucleus this network reaches a high density.

PHENYLETHANOLAMINE-*N*-METHYLTRANSFERASE (PNMT) (ADRENALINE/EPINEPHRINE) According to Sadikot and Parent (1990), in the squirrel monkey, PNMT-ir occurs only in the Ce nucleus as a very sparse terminal labeling. These PNMT-ir fibers are likely to arise from a few PNMT-ir fibers within the ansa lenticularis/ventral amygdalofugal bundle, although direct continuity is difficult to establish.

SEROTONIN (5-HT) Within the macaque monkey amygdala, the heaviest concentration of 5-HT-ir fibers is found in the dorsal part of the rostral CeLC subnucleus and in the more caudal parts of the CeLCn subnucleus. These heavily labeled gray formations contain multiple small punctate 5-HT-ir structures with relatively few fibers and a diffuse background staining that was higher than in structures without specific ir. The CeM division of this nuclear component of the CExA contain only moderate amounts of 5-HT-ir fibers.

In the squirrel monkey, the CeM division of the Ce nucleus display very dense to dense 5-HT-ir terminal labeling with a mediolateral gradient of decreasing 5-HT-ir. The CeL division shows moderately dense 5-HT-ir, although its extreme caudolateral and dorsal aspects display dense 5-HT-ir (Sadikot and Parent, 1990).

TYROSINE HYDROXYLASE (TH) (DOPAMINE) According to Freedman and Shi (2001), in the macaque monkey amygdala, the highest densities of TH-ir fibers are found in the Ce nucleus, particularly in the rostrodorsal and caudal CeLC subnucleus and in the more caudal parts of the CeLCn subnucleus, while there are modest amounts of TH-ir fibers in the CeM division. In the squirrel monkey, the CeM division of the Ce nucleus displays very dense TH-ir terminals at its medial sector that diminish to dense TH-ir laterally. The CeL division of the Ce nucleus shows a medial to lateral gradient, varying from moderate ir medially to a dense one at its extreme lateral and dorsal portion.

NEUROPEPTIDES

BRAIN-DERIVED NEUROTROPHIC FACTOR (BDNF) According to Murer *et al.* (1999), in the human amygdala, although BDNF-ir neurons and fibers are present in all amygdaloid nuclei, in the Ce nucleus they are only moderately represented by neurons displaying a rather strong staining. By contrast, BDNF-ir fibers form a very dense plexus within which some BDNF-ir neuronal cell bodies can be distinguished.

CALCITONIN GENE–RELATED PEPTIDE (CGRP) According to De La Calle and Saper (2000), in the human amygdala, the dorsal CeLC and CeLcn subdivisions of the Ce nucleus contain the densest concentration of CGRP-ir axons. At the rostral pole of the Ce nucleus there is an extremely dense CGRP-ir plexus that fills a distinct spherical region that corresponds to the CeL nucleus, which at caudal levels expands into the characteristic ovoid shape of the Ce nucleus. At these levels the CeM division of the Ce nucleus shows only a light to moderate plexus of CGRP-ir fibers that disperses throughout. Caudally and ventrally patches of CGRP-ir fibers bridge the Ce nucleus with the amygdalostriatal area.

CHROMOGRANIN B According to Marksteiner *et al.* (1999), the strongest intensity of PE-11-like ir is found in the Ce nucleus. This is the only amygdaloid nucleus that contains PE-11-like ir neuronal perikarya.

COCAINE- AND AMPHETAMINE-REGULATED TRANSCRIPT (CART) According to Hurd and Fagergren (2000), moderate CART mRNA signal can be demonstrated at the level of the Ce nucleus (primarily the anterior region).

CHOLECYSTOKININ (CCK) In the human brain, there is a concentration of CCK-ir puncta and varicose fibers in the central part of the CeL and a tendency for the labeling of peridendritic terminals to appear as tubular profiles, especially in the more dorsally located capsular part. CCK-ir varicose fibers and terminals, sometimes in typical peridendritic pattern, also characterize the para- and periparacapsular parts of the CeL division. In contrast, the Ce does not seem to contain CCK-ir neuronal perikarya (Heimer *et al.*, 1999), a negative finding that would agree with an apparent absence of CCK mRNA hybridization signal in this nucleus as can be inferred from its nonlisting among the amygdaloid nuclei showing it (Savasta *et al.*, 1990).

CORTICOTROPIN-RELEASING FACTOR (CRF) In the human amygdaloid complex, a dense accumulation of CRF-ir fibers with large varicosities and terminals has been reported in almost all amygdaloid nuclei (Power *et al.*, 1987; Zaphiropoulos *et al.*, 1991). This finding, together with the fact that the BST and the sublenticular substantia innominata (here SLEA) also contain a high density of CRF-containing fibers and terminals (Powers *et al.*, 1987; Zaphiropoulos *et al.*, 1991), speaks in favor of the existence of a similar distribution pattern in Ce. In contrast, the Ce nucleus seems to contain a rather sparse population of small bipolar CRF-ir neurons.

On the other hand, in rodents, the Ce nucleus has been shown to be the site of high concentrations of CRF-containing cell bodies that project to areas known to mediate endocrine, autonomic, and behavioral responses to stress. The presence of CRF–synthesizing neurons has been confirmed by the finding that, at least in rat brain, this nucleus is the place in the amygdala showing the maximal CRH mRNA expression; what

is of great significance is that this expression is significantly increased in response to stress (Hsu *et al.*, 1998).

DYNORPHIN (DYN) This endogenous opioid peptide, which in the rat is distributed in the neuropil of the Ce, seems to originate in part at least from DYN-containing neurons located in the lateral hypothalamic and perifornical areas of the hypothalamus (Zardetto-Smith *et al.*, 1985).

ENKEPHALIN (ENK) In the human amygdala, the ENK-ir is concentrated almost exclusively within the Ce, particularly in CeL (Pioro *et al.*, 1990). According to material presented by Heimer *et al.* (1999), the components of CeL division are characterized by strong or moderately strong ENK-ir. The central and apical parts of the CeL division contains a large number of ENK-ir puncta and varicose fibers in addition to some ENK-ir neuronal somata, whereas the capsular part (CeLC) is characterized by granular-type tubular profiles and puncta. The accessory parts of the Ce, i.e., the paracapsular and pericapsular subdivisions of the CeL, are surrounded by fiber-rich capsules characterized by tubular profiles in ENK-stained sections. CeM, on the other hand, shows a moderately strong reaction to ENK, which is similar to that present in the BSTLP. According to Sukhov *et al.* (1995), the human Ce contains a robust number of preproenkephalin (PENK) mRNA-containing neurons.

In the monkey ENK-ir fibers form a plexus of "woolly-like" fibers that surrounds the nucleus and extends into the substantia innominata (SLEAC) (Haber and Watson, 1985).

In the rat, the lateral division of the Ce nucleus, as in humans, also contains ENK-ir cells, and the administration of amphetamine in different experimental setups produced significant and synchronized changes in the c-fos mRNA expression both in ENK-ir cells of the CeL nucleus, and of its rostral extent, the BSLTLD (oval) nucleus (Day *et al.*, 2001).

It should be mentioned that in the rat, ENK-containing neurons located in the lateral and perifornical hypothalamic areas, though in rather scarce numbers contribute to ENKergic innervation of Ce (Zardetto-Smith *et al.*, 1985).

GALANIN (GAL) GAL-ir cell bodies are found mostly in the medial subdivision of the nucleus in the monkey (Köhler *et al.*, 1989a, b). However, according to mapping of the forebrain distribution of this neuropeptide presented by Kordower *et al.* (1992) in the macaque monkey amygdala, this member of the superficial amygdala, like its other components, would not contain GAL-ir cell bodies but seems to contain at least a small number of GAL-ir fibers.

NEUROPEPTIDE Y (NPY) According to Walter *et al.* (1990), in the human amygdala, the Ce nucleus shows a small number of cells in the lateral half of the CeL division.

According to McDonald *et al.* (1995), in the macaque monkey, the CeL division and the rostral CeM contains very few NPY-ir neurons, whereas moderate amounts of these type of neurons can be found in the caudal sectors of the CeM division. The NPY-ir cells in the Ce nucleus are small to medium sized with three to four sparsely branched dendrites. A distinct population of larger, richly spined NPY-ir neurons can be found around the dorsal, lateral, and ventral boundaries of the CeL division. These cells are endowed with three to four sparsely branched dendrites. It should be pointed out that all the NPY-ir cells in the Ce nucleus are also SOM-ir (McDonald *et al.*, 1995). Whether this also occurs in the human Ce nucleus is not known.

NEUROTENSIN (NT) Mai *et al.* (1987) describe the presence of NT-ir cell bodies in the transition zone between the LBNC (i.e., their amygdaloid body proper) and the anterocentromedial nuclear group (i.e., their supra-amygdaloid region) and in the Ce nucleus. They also reported that the strongest accumulation of NT-ir fibers and varicosities can be found in the corticomedial and anterocentromedial amygdala. According to Benzing *et al.* (1992), the Ce nucleus is densely NT-ir throughout its anteroposterior extent, although at caudal levels there is a greater density in the staining than at anterior levels. The CeM division, in turn, stains more intensely than the CeL, being one of the most intensely NT-ir structures in the whole amygdaloid complex. The NT-ir in the CeM division consists primarily of a dense matrix of puncta and interspersed fine-beaded fibers, and of numerous darkly staining bipolar and multipolar neurons randomly distributed throughout the nucleus. By contrast, the CeL division contains considerably less NT-ir than the medial one and appears encircled by a dense band of NT-ir fibers that is continuous with the NT-ir fiber plexus in the CeM division. The NT-ir neurons in the CeL division differ from those in the CeM division in that they consist of about equal numbers of multipolar, bipolar and unipolar, lightly or moderately stained cells, being more numerous in caudal levels of the division than anteriorly. Heimer *et al.* (1999) confirmed this description in general but also pointed out that the majority of the NT-ir neuronal perikarya are located in the CeM division rather than in the central part of the CeL division.

PROSOMATOSTATIN-DERIVED PEPTIDES (PSDP) According to Bouras *et al.* (1987), all of the nuclear divisions of the human amygdaloid complex contain PSDP-ir neurons as well as PSDP-ir fibers and terminals.

SECRETONEURIN (SECR) According to Kaufman *et al.* (1997), in the human amygdala the SECR-ir reaches particularly high levels of density, which stands out from the relatively SECR-ir poor LBNC. In the central subregion of the CeL division are numerous SECR-ir neurons that are very similar in size and shape to neurons in the central core of the BSTLD. Numerous SECR-ir and non-ir neurons are pericellularly stained. The CeLCn appears surrounded by SECR-ir granular, peridendritic, and perisomatic plexuses of the same type as those in the BSTLD and in the SLEAC. The CeM division displays a high density of SECR-ir varicose fibers with only scattered woolly-like fibers. The rostral part of the CeM divisions contains the most SECR-ir neurons.

SOMATOSTATIN (SOM) In humans, as in other primates and nonprimates, SOM-ir fibers and terminals are abundant in the Ce nucleus, though predominating in the CeL division. Some of these fibers can be followed directly into the so-called substantia innominata (here SLEAC) (Mai *et al.*, 1987; Mufson *et al.*, 1988).

In the monkey the Ce has been described as having the most distinctive pattern of SOM-ir, although the appearance of the fibers and terminals containing this neuropeptide varies with the type of antibody utilized. Irrespective of this fact, the lateral division (CeL) of the nucleus displays much denser fibers and terminals than the medial (CeM) one, and the soma and principal dendrites of several neurons appear heavily encrusted with large varicosities (Amaral *et al.*, 1989). Also, the majority of the SOM-ir neurons in Ce is located in the CeL (Amaral *et al.*, 1989; McDonald *et al.*, 1995) appearing tightly clustered in the ventromedial portion of the caudal pole of the nucleus. The cells were small and multipolar. It should be stressed again that many of the SOM-ir neurons in the CeM division are also ir for NPY (McDonald *et al.*, 1995). On the other hand, as pointed out by Amaral *et al.* (1989), a striking feature of the SOM-ir associated with the Ce nucleus is that the distinctive coarse varicose fiber staining is continuous with the dense SOM-ir detectable in substantia innominata (here SLEAC) and in the BSTL (Amaral *et al.*, 1989). Desjardins and Parent (1992) reported in the squirrel monkey amygdala that the medial and lateral divisions of the Ce nucleus are separated by a dense plexus of fine, vertically oriented, varicose, SOM-ir fibers. By contrast, the core of each division displayed a very light to light SOM-ir, whereas high SOM-ir occurs in the peripheral portion of this nuclear region. Overall, the Ce nucleus in the squirrel monkey seems to contain relatively few SOM-ir cell bodies.

SUBSTANCE P (SP) According to Mai *et al.* (1986), SP-ir fibers could be followed in the ventral amygdalofugal pathway and bands of punctate SP-ir are continuous with the supra- and periamygdaloid regions (here Ce, MeA, and AA). SP-ir is seen in scattered neuron branching fibers and punctate material throughout the human amygdala with no preference for the Ce nucleus. In the supra-amygdaloid area (here Ce), the substantia innominata (here SLEAC) contains rare SP-ir cell bodies (Pioro *et al.*, 1990). According to Heimer *et al.* (1999), CeL is lightly stained for SP as compared with the darker staining CeM.

TAKYKININS: NEUROKININ B (NKB) NKB is the predominant tachykinin in the Ce. Both NKB and SP neurons were scattered in the basomedial nucleus of the amygdala. More NKB neurons than SP neurons were observed in the BST and the Ce. Consequently, NKB is the predominant tachykinin in both the BST and Ce (Lucas *et al.*, 1992; Marksteiner *et al.*, 1992a). These data support the concept that these nuclei are part of a neuronal continuum extending through the substantia innominata (Alheid and Heimer, 1988; de Olmos, 1990; Martin *et al.*, 1991).

VASOINTESTINAL PEPTIDE (VIP) According to Heimer *et al.* (1999), VIP-ir, which is said to be an excellent marker of the central extended amygdala, is present in both CeLCn and CeLC as dense, fine granular, peridendritic, and perisomatic immunoreactivity.

VASOPRESSIN (VP) According to Sofroniev *et al.* (1981), in several primate species (tree shrew, macaque monkey), including human, it is possible to trace neurophysin/VP-ir fibers which distribute in the Ce nucleus via the stria terminalis from their source in the paraventricular hypothalamic nucleus. According to Caffé *et al.* (1989), in the macaque monkey, thick varicose VP-ir fibers are present in the MeA nucleus as well as in two types of VP-ir cell: one of ovoid shape that resembles the VP-ir cells in the BST nucleus is located at a level near to the hippocampal formation, and the other of multipolar appearance that resembles the VP-ir cells in the ventromedial BST nucleus and is present at more rostral levels of the MeA nucleus.

NEUROTROPHINS

BRAIN-DERIVED NEUROTROPHIC FACTOR (BDNF) According to Murer *et al.* (1999), in the human CeAN

nucleus BDNF-ir fibers form a very dense plexus within which some BDNF-ir neuronal cell bodies can be distinguished.

Enzymes

ANGIOTENSIN CONVERTING ENZYME (ACE) According to Chai *et al.* (1990), the Ce nucleus in the human amygdala contains low binding levels for ACE as would also happen with other members of the CExA.

BUTYRYLCHOLINESTERASE (BuChE) It contains few BuChE-containing small to medium-sized fusiform neurons. Approximately 1% of the neuronal population of Ce expressed this enzyme (Darvesh *et al.*, 1998).

NICOTINAMIDE ADENINE DINUCLEOTIDE PHOSPHATE DIAPHORASE (NADPH-d) The CeM division stains more intensely for NADPH-d than the CeL division, and there is a particularly intense staining for both the neuropil and the perikarya along the border with the BL and BM nuclei (Sims and Williams, 1990). In contrast, Brady *et al.* (1992) have stated that the NADPH-d–ir is minimal in the human Ce and squirrel monkey amygdala. These authors also described the existence of a pleomorphic population of NADPH-d-positive neurons that is divisible into two classes based on their staining characteristics: intensely or lightly stained neurons. In the macaque monkey, the Ce nucleus shows only a few NADPH-d-containing neurons and rather poor NADPH-d-containing fibers and neuropil (Pitkannen and Amaral, 1991b), which seems to concur with a similar finding in the squirrel monkey amygdala (Brady *et al.*, 1992).

Receptors

BENZODIAZEPINE RECEPTOR (BNZ-R) According to Zezula *et al.* (1988) the human Ce nucleus contains intermediate levels of BNZ-R.

ADRENORECEPTOR α_2 According to Flügge *et al.* (1994), in the tree shrew, the central amygdaloid nucleus shows a high amount of [^{3}H]RAU binding sites, RAU being indicative of this type of receptor.

GALANIN RECEPTOR (GAL-R) According to Kohler and Chan Palay (1990), in the human amygdala primarily the Ce and MeA nuclei harbored significant amounts of specific [^{125}I]-galanin-R.

MUSCARINIC RECEPTOR (mACh-R) According to Cortés *et al.* (1987), there is an intermediate to low concentration of mACh-R in the human Ce nucleus which is of the m_1 type. On the other hand, according to Smiley *et al.* (1999), the amygdala as a whole contains a low density of mACh-ir neurons.

NICOTINIC RECEPTOR (nACh-R) Hybridization signals for the α_4 and β_2 subunits of this ionic excitatory receptor can be found in virtually all parts of the rat amygdala. However, the signals for these subunits in Ce are rather weak, while practically no signals can be found for the subunits α_2 and α_3 (Wada *et al.*, 1989).

STEROID RECEPTORS

Estrogen Receptor α (ER-α) According to Österlund *et al.* (1999), the central amygdaloid nucleus in human and monkey brains does not show any ER-α mRNA signal.

Estrogen Receptor β (ER-β) In the rat, areas that expressed the greatest density of ER-β-ir cells included, among others, the Ce nucleus, and it is highly probable that this receptor colocalizes with PAV-ir neurons present in it (Blurton-Jones and Tuszinski, 2002).

MU OPIOID RECEPTOR (ORμ) According to Mansour *et al.* (1988), the density of the opioid receptors in the monkey Ce is moderate with predominance of the mu type although some of them are of the delta type. Daunais *et al.* (2001) have reported that in the cynomolgus monkey by far the lowest concentrations of [^{3}H]DAMGO binding sites are found in the Ce where there is a uniformly low binding within the lateral and medial divisions of this nucleus regardless of the anterior–posterior level considered. Similar low levels of μ receptors in the Ce nucleus has also been observed in rhesus monkeys (Daunais and Porrino, unpublished observations). On the other hand, in striking contrast to very low levels of [^{3}H]DAMGO binding found in this nucleus, moderate levels of DAMGO-stimulated [^{35}S]GTPγS binding are found in it.

SEROTONINERGIC RECEPTOR (5-HT-R)

5-HT$_{2C}$ Receptor (5-HT$_{2C}$-R) According to Lopez-Gimenez *et al.* (2001), one of the strongest hybridization signals with probes for the 5-HT$_{2C}$-R that can be found in the basal forebrain is the Ce nucleus, which is one of the components of the extended amygdala.

The Medial Extended Amygdala (MExA)

The medial amygdaloid nucleus has been classically considered to be part of the superficial or olfactory group of amygdaloid nuclei (see Figs. 22.1c, 22.7a,b, 22.8, 22.11, 22.16, 22.16, 22.18, 22.23b, 22.24b, 22.25, 22.28). Today it is generally accepted that this nucleus

should be considered a part—a very important part indeed—of the "medial extended amygdala." The forebrain gray continuum which bridges this was once considered a superficial nucleus, with the deep located medial bed nucleus of the stria terminalis in the paraseptal telencephalon (de Olmos *et al.*, 1985; Alheid and Heimer, 1988; de Olmos, 1999; Martin *et al.*, 1991). Furthermore, because of its strategic position the medial amygdaloid nucleus receives, handles and transfers olfactory-related information (Meyer and Allison, 1949; Allison, 1954, Heimer *et al.*, 1977; Turner *et al.*, 1978; Price, 1990; Carmichael *et al.*, 1994), adding emotionally relevant olfactory information to the inputs that reach the medial caudal aspect of the shell of the accumbens nucleus, or the medial hypothalamus, among other important targets of medial amygdaloid nucleus efferent projections. As was briefly stated at the beginning of this introductory section, the concept of the extended amygdala implies that the bed nucleus of the stria terminalis and the centromedial nuclei of the amygdala are parts of a single structure whose continuity is maintained by more or less uninterrupted columns of neurons. The cellular bridges that do that extend dorsally among the fibers of the stria terminalis and ventrally through the posteroventral sectors of the so-called substantia innominata, accompanying the ventral amygdalofugal/ansa peduncularis pathway, a gray matter/fiber bridge that is termed in this account the medial sublenticular extended amygdala. Morphological evidence demonstrates that in the forebrain of humans and monkeys, similarly to what occurs in nonprimate macrosmatic mammals like the rat, there is a neuronal continuity between the BST and the amygdala (Mufson *et al.*, 1981, 1988; Amaral and Basset, 1989b; Lesur *et al.*, 1989; de Olmos, 1990; Martin *et al.*, 1991, Heimer *et al.*, 1999; etc.). However, the functional relevance of the amygdalosublenticulostrial continuum in primates remains under question, but by assuming that there is some analogy with other species, this complex griseum may play an important role regarding species-typical behaviors associated with reproduction, feeding, emotion, etc. In addition, the medial amygdaloid nucleus, together with its partners that form the medial extended amygdala continuum, may interact with the visceroendocrine and autonomic system by way of their reciprocal connections with hypothalamic and brain stem centers, but also with motor systems through its efferent projections to the ventral striatum and certain mesencephalic motor regions (Alheid *et al.*, 1995).

As has been done with the description of the central division of the extended amygdala, this section will start with the description of the paraseptal components of the MExA to be followed by that of the sublenticular and supracapsular bridges and, finally, its temporal lobe components. A reason for doing this is the fact that, as reported by Stephan and associates (Andy and Stephan, 1976, Stephan and Andy, 1977; Stephan *et al.*, 1987), the bed nucleus of the stria terminalis is a progressive structure in humans and nonhuman primates, whereas the medial amygdaloid nucleus seems to be a regressive griseum in the primate phylogeny and the central amygdaloid seems to have just maintained its morphological and functional properties without showing signs of regression or progression.

Paraseptal Components of the Medial Extended Amygdala The medial nucleus in rodents and other nonprimate macrosmatic mammals is considered to be not only a part but rather the main component of the "medial extended amygdala," i.e., the forebrain gray continuum that bridges the medial amygdaloid nucleus and medial bed nucleus of the stria terminalis (de Olmos *et al.*, 1985; Alheid and Heimer, 1988; de Olmos, 1999; Martin *et al.*, 1991). As such, the medial amygdaloid nucleus mediates olfactory-related information (Price, 1973; Turner *et al.*, 1978), adding emotionally relevant olfactory information to the inputs that reach the shell of the accumbens nucleus, one of the targets of the Me nucleus efferent projections. According to the concept of the extended amygdala, the BST and the centromedial nuclei of the amygdala are parts of a single structure whose continuity is maintained by more or less uninterrupted columns of neurons. The cellular bridges extend dorsally among the fibers of the stria terminalis and ventrally through the posteroventral sectors of the so-called substantia innominata, a bridge that in this account is termed the medial sublenticular extended amygdala. Morphological evidence demonstrates that in the forebrain of humans and monkeys, as in nonprimate mammals like the rat, there is neuronal continuity between the BST and the amygdala (Mufson *et al.*, 1988; Amaral and Basset, 1989b; de Olmos, 1990; Martin *et al.*, 1991; Heimer *et al.*, 1999, etc.). However, the functional relevance of the BST–amygdala continuum in primates remains largely speculative, but by analogy with other species (Kondo Y and Sachs BD.,2002) may be important in species-typical behaviors associated with reproduction, feeding, and so forth. The medial amygdaloid nucleus as the main member of the medial extended amygdala continuum interacts jointly with visceroendocrine and autonomic systems through its connections with hypothalamic and brain stem autonomic centers, and with motor systems through its connections with basal ganglia and mesencephalic motor regions (Alheid *et al.*, 1995).

Interestingly, in humans, amygdala lesions localized mainly in the medially situated nuclei blunt emotions but not fear (Narabayashi and Shima, 1980) and the posterior Me nucleus has been related mainly to sexual behaviors (Kondo Y and Sachs BD.,2002), but the relevance to primates is not clear. On the other hand, the medial amygdaloid nucleus, which is one of the amygdaloid nuclei richest in P450 aromatase, not only has intrinsic connections within the amygdala but also projects to several of the so-called limbic areas of the allocortical (paleo- and archicortex) and periallocortical types such as the piriform cortex, the hippocampal formation, and the entorhinal cortex, to the nucleus accumbens septi in the ventral striatum, and to the hypothalamus. Thus, locally formed estrogen may be able to regulate and influence many of the so-called limbic functions and related behaviors such as emotion processing, sexual and social behavior, memory, learning, and cognition. Finally, it should be pointed out that, although in subprimates like rodents and in New World squirrel monkeys sexually dimorphic differences in the neuronal composition of the medial amygdaloid nucleus has been reported (Nishizula and Arai, 1981, 1983; Mizukami *et al.*, 1983; Arimatsu *et al.*, 1981; Bubenik and Brown, 1973), very careful statistical analysis does not support the existence of such sexual dimorphism in the medial amygdaloid nucleus of humans (Murphy, 1986).

In the description that follows, each member of the medial extended amygdala will be thoroughly examined by taking into account only their cytoarchitectonic, fibroarchitectonic, and chemoarchitectonic properties, and reference to their afferent and/or efferent connections will be made only when they may contribute substantially to the understanding of the intrinsic cell organization of the concerned structures. By no means, the present writer is not ignoring the great importance of such hodological data; however, limitations of space have placed a limit on how far it is possible to go with the enormous amount of information that the writer has to handle in trying to be fair regarding the scientific contribution of fellow investigators in the field of the neuroanatomy.

But before dealing with further details concerning intrinsic anatomical and cytochemical organization of the medial extended amygdala, it is necessary to first describe the topographical relationship of the brain formation which hosts the paraseptal ends of both medial and central divisions of the extended amygdala, the bed nucleus of the stria terminalis.

Medial Division of the Bed Nucleus of the Stria Terminalis (BSTM) In the human brain this sector of the paraseptal region represents the rostral end of a intermitently interrupted ring-like gray continuum that is here termed the medial extended amygdala (MExA) [BSTM, BSTP, BSTPL in Plates/Figs.19–25 (–2.0–4.0 mm) of Mai *et al.* (1997), *Atlas of the Human Brain*; BST, BSTMA, BSTMP, BSTMPI, BSTMPM, BSTMPL in Plates/Figs.46–56 (interaural 20.10–15.60 mm) of Paxinos *et al.* (2000), *The Rhesus Monkey Brain in Stereotaxic Coordinates*. In this division it is possible to recognize two main subdivisions: anterior and posterior. This is in agreement with the neurogenetic findings of Bayer and Altmann (1987) in the rat.

The **anterior subdivision of the BSTM** (Figs. 22.17, 22.23, and 22.24b) [BSTM in plates 19 to 22 (-2.0-0,0mm) of Mai *et al.´s Atlas of the Human Brain*, 1997] in humans occupies a medial position in the supracommissural BST immediately ventral to the inferior angle of the lateral ventricle and ventromedial to the ventral expansion of the lamina cornea. At its rostral pole it is bounded by the lateral septal nucleus, while more caudally it is flanked by the postcommissural fornix, lying in the angle formed by this bundle and the decussating anterior commissure. Caudally, it is replaced by the more dense, small-celled medial subdivision of the posterior BSTM. In all preparations the anterior division of BSTM can be further divided into dorsolateral small-celled and ventromedial large-celled parts. While the lighter staining cells in the dorsolateral part tend to be oriented parallel to the incoming fibers of the stria terminalis, the more darkly staining cells in the ventromedial part show a more random arrangement. In addition, the dorsolateral part has a much richer content of glial cells than the ventromedial one. At times islands of granular (Sanides' gamma type 1) and parvicellular (Sanides' gamma type two) interface islands appear at the lateral boundary of the ventromedial subdivision of the anterior BSTM division.

In the human brain, like in other mammals, the **posterior division of the BSTM** (Figs. 22.16 and 22.18) [BSTP, BSTPL in plates 23 to 26 (1,3-5.4mm) of Mai *et al.´s Atlas of the Human Brain*, 1997] lies caudal to the decussating anterior commissure flanking the descending columns of the fornix, medially while being separated from the ventral thalamus by the stria medullaris thalami, caudally, and from the internal-capsule by posterior division of the BSTL, laterally. Caudoventrally, the BSTMP division becomes continuous with the medial preoptic region. Like its predecessor, the BSTM division can be further divided into three so to say vertically oriented cell ciolumns, medial small-celled, intermediate medium celled, and lateral large-celled subdivisions. **The small-celled medial subdivision** of the posterior BST (Figs. 22.16, 22.18, 22.23–22.25), as in other nonhuman primate and

nonprimate mammalian species (G. Alheid and J. S. de Olmos, unpublished observations; de Olmos *et al.*, 1985; Moga *et al.*, 1989); constitutes a comparatively narrow, dorsally to ventrally oriented cell column that makes its appearance at a transverse plane just behind the decussating anterior commissure and the medial-most coursing bundles within the main body of the stria terminalis. Dorsally, the medial aspect of the small-celled subdivision of the posterior medial BST is first bounded by the lateral ventricle and then flanked by fornix bundles ventrally. This column appears surrounded on all its other sides by the medium-celled intermediate portion of the posterior BSTM (Figs. 22.16, 22.18, 22.24, and 22.25). In Nissl preparations the medial subdivision of the posterior BSTM appears to be composed of small, relatively densely packed round to oval, well-staining neurons. Scattered among them can be observed larger triangular, darkly staining neurons. Ventrally, the medial posterior BSTM subdivision can be followed within the medial preoptic region without major modifications in its cell constitution, as can be judged from the Nissl material available for the author. Finally, thin and discontinuous aggregates of much larger and more darkly staining cells appear intercalated between this column and the immediately adjacent intermediate posterior BSTM subdivision.

The **medium celled intermediate subdivision** of the posterior BSTM (Figs. 22.16, 22.18, 22.24–22.25), like its small-celled medial neighbor (which it almost completely surrounds), constitutes a cell column that fills most of the postcommissural BST. In doing so it also extends more dorsally and ventrally than the small-celled medial column, while at the same time it compresses the larger celled lateral component of the posterior BST into a rather thin, broken lamina. Throughout the great part of its intradiencephalic course, this column lies just rostral to and adjoining the stria medullaris. At its ventral end, it separates from the stria medullaris, becoming rostral and ventral to the descending columns of the fornix, where it seems to merge with similar cell types belonging to the medial preoptic–anterior hypothalamic region.

The medium celled, intermediate subdivision of the posterior BSTM is composed of more loosely arranged and lightly staining medium-sized spindle and angular-shaped neurons. Although most neurons are seen with the thin larger axis oriented parallel to the incoming fibers of the stria terminalis, many additional types of neurons are oriented obliquely or perpendicularly to them. Furthermore, this subdivision of the posterior BSTM, in contrast with the medial ones, shows not only a lesser content of glial cell nuclei but undergoes modifications in the density of its neuronal population, which becomes greater in a ventral direction.

The large-celled lateral subdivision of the posterior BSTM (Figs. 22.16, 22.18, 22.24–22.25) in the human brain appears to be limited to the middle sectors (dorsoventrally) of the postcommissural BST. It is represented by a heterogeneous population of loosely arranged neurons, many of which are larger than the largest ones scattered in the other two subdivisions of the posterior BSTM but smaller than ectopic neurons of the MCBFC.

Chemoarchitectonics

CUPRIC SILVER STAIN (CU-AG) As it happens with its companions, the Me nucleus and the SLEAM, the BSTM division of the macaque, squirrel, or marmoset BST nucleus does not show a Cu-Ag staining pattern of the type present in all of the components of the central extended amygdala. However, like its temporal lobe counterpart, the Me nucleus (see below) contains isolated bipolar, slender, strongly argyrophilic neurons with a very scattered distribution. As will be discussed below for the Me nucleus, these neurons show a very similar morphological appearance to the LH-ir neurons and also coincide with them in their hypothalamic distribution.

HEAVY METALS In sections from squirrel monkey brain, the staining pattern in the BSTM division of the BST nucleus has a heterogeneous distribution (Fig. 22.23a, b; 22.24a, b; 22.25) showing at a same level areas of high precipitate and other of very low precipitate; however, with a tendency for the amall-celled medial subdivision to stain lighter than the medium-celled subdivision that surrounds it almost entirely though, as a whole, the density of the silver precipitate is lower than in the BSTLD subdivision of the paraseptal BST nucleus.

NEUROTRANSMITTERS

CHOLINERGIC MARKERS

ACETYLCHOLINESTERASE (AChE) According to Heimer *et al.* (1999), most of the anterior and posterior division subsections of the medial division of the BST nucleus exhibit little AChE activity, especially dorsally (see Plates AChE 5-6 to 10, in Sakamoto *et al.*, 1999). In macaque brain (BST, BSTMA, BSTMP, BSTMI, BSTMPL) (Plates/Figs. 47, 49, 51, and 55 in Paxinos *et al.* (2000), *The Rhesus Monkey in Stereotaxic Coordinates* and in macaque monkey darkfield collection of low magnification microphotographic material put to my disposition by Drs. Heimer and Alheid, it is clear that the BSTM division in this nonhuman primate shows a lower density than the lateral one. Caudal patches of stronger AChE activity appear at the level of the medial subdivision (BSTMPm) of the posterior BSTM

division of the BST nucleus. It is also evident that the intermediate subdivision presents the lowest density of the three subdivisions identified in this posterior region of the BST nucleus.

Excitatory Amino Acids

GLUTAMATE/ASPARTATE (GLU/ASP) In the rat, injections of tritiated D-aspartate in the ventral pallidum caused the retrograde labeling of a moderate number of cells in the ventral subdivision of the BSTMA division of the BST nucleus and in the ventral sector of the lateral cell column of the BSTMP division of this nucleus (Fuller *et al.*, 1987). Furthermore, similar injections in the area of the paraventricular hypothalamic nucleus caused the retrograde labeling of neurons in the anterior (BSTMA) and ventral (BSTMV) subregions of the medial division of the BST nucleus (Csáki *et al.*, 2000). These results speak in favor of the existence of a subpopulation of glutamatergic neurons within this component of the medial extended amygdala. These data provide further support to the concept of the extended amygdala, as it can be inferred from the fact that in the same experiments Me nucleus also shows the presence of many [^{3}H]D-aspartate-labeled neurons, contributing this sector of the extended amygdala to the GLU/ASPergic innervation of pallidal and hypothalamic structures.

Inhibitory Amino Acids

γ-AMINOBUTYRIC ACID (GABA) Since in most regards the BSTM division of the bed nucleus of the stria terminalis as a component of the medial extended amygdala shares most of the chemoarchitectonic properties of its temporal lobe companion, the Me amygdaloid nucleus, one may be justified in extrapolating those properties to the BSTM.

Monoamine Markers

DOPAMINE-β-HYDROXYLASE (DBH) According to Gaspar *et al.* (1985), the human medial division of the BST contains abundant amounts of DBH-ir fibers. The terminal DBH-ir field in the BSTM division is continuous ventrally with that of the preoptic area and medially with that of the ventral lateral septal nucleus.

HISTAMINE (HA) According to Airaksinen *et al.* (1989), in the tree shrew (*Tupaia belangeri*), HA-ir fibers collected in dense bundles are seen at the level of the BST nucleus where they distribute forming a very dense plexus that reaches the highest density. Their illustrations (Fig. 3F, G) suggest that the denser concentration of HA-ir fibers occurs in supra-, infra-, and postcommissural sectors of the medial division of the BST.

TYROSINE HYDROXYLASE (TH) According to Gaspar *et al.* (1985, 1987), the TH-ir innervation of the BST nucleus is complementary to that by DBH-ir fibers, with little if any for the medial sector, except for a patch of TH-ir fibers and terminals located near the wall of the lateral ventricle at the level of the decussation of the anterior commissure.

Neuropeptides

COCAINE- AND AMPHETAMINE-REGULATED TRANSCRIPT (CART) According to Hurd and Fagergreen (2000), the human BST nucleus shows a moderate CART mRNA expression. No statement is made about the specific localization of this peptide, nor it is possible to gather this information from the illustrations presented.

CHOLECYSTOKININ (CCK) Martin *et al.* (1991) were unable to detect CCK-ir cell bodies in the human BSTM, although some seem to be present in the baboon monkey. CCK-ir varicose fibers and puncta show moderate density.

CHROMOGRANIN B Although Marksteiner *et al.* (1999) include this division of the BST nucleus as displaying PE-11-like ir, no detail is added beyond this citation.

DYNORPHIN (DYN) According to Sukhov *et al.* (1995), in the human amygdala, a moderate amount of small preprodynorphin (PDYN) containing neurons arranged in peripheral islands accompany the main core of the nucleus as it traverses the rostrolateral hypothalamus toward the amygdala. However, their number is small.

ENKEPHALIN (ENK) According to Lesur *et al.* (1989), the ENK-ir innervation of the BSTM is unconspicuous, being made up of varicose fibers of a moderate density. In addition, this division of the BST nucleus does not contain ENK-ir perikarya, a fact that was confirmed by Martin *et al.* (1991). By contrast, after Shukov *et al.* (1995), in the human basal telencephalon, there is abundant preproenkephalin (PENK) containing neurons at the level of the BST. Their illustrations indicate that the majority are located dorsally, ventrally, and caudally to the crossing of the anterior commissure, corresponding to BSTMA, BSTMV, and BSTI subdivisions of the BST nucleus. However, according to Kaufmann *et al.* (1997), confirming in part Gaspar *et al.*'s (1985, 1987) observations, the human medial BST does not contain ENK-fibers. In the material examined by Heimer and associates (1999), the ENK-ir is modest or very light in the anterior subregion of the

BSTM division, a pattern that is not maintained posteriorly where it becomes quite heterogeneous.

GONADOTROPHIN-RELEASING HORMONE–ASSOCIATED PEPTIDE (GAP) According to Song *et al.* (1987), in macaque and baboons, a few round or fusiform bipolar GAP-ir cells are found in the BST nucleus together with a similar scarcity of GAP-ir fibers.

GALANIN (GAL) Martin *et al.* (1991) detected few GAL-ir somata in the BSTM division of the human BST nucleus, but GAL-ir beaded fibers and puncta appeared prominent. According to Kordower *et al.* (1992) in the cebus monkey, numerous GAL-ir perikarya are seen throughout the BST, with a preponderance of neurons in the anterior aspect of this nucleus. At this level the GAL-ir neurons are preferentially located in the medial (BSTMA), dorsolateral (BSTLD), and ventrolateral (BSTLV) subdivisions of the BST, as well as in the caudal temporal portion of the stria terminalis (BSTSl).

Mufson *et al.* (1993) reported that the GAL-ir profiles appeared as either thin beaded or thick coarse fibers within the BST of apes (gorilla, chimpanzee, and gibbons). In addition, a small number of GAL-positive parvicellular neurons could also be detected in this region, and GAL-ir fibers appeared to coalesce within the territory of the so-called substantia innominata to form a major GALergic pathway that travels through this region en route to the hypothalamus, bed nucleus of the stria terminalis, and vertical limb of the diagonal band just as it has been described in the human telencephalon (Mufson, 1993). Within the BST, the similar distribution patterns of cell bodies and fiber staining are evident.

NEUROKININ B (NKB) Small, oval to round NKB-containing neurons were numerous in the BST nucleus. Examination of the illustrations (Figs. 3A–C) presented by Chawla *et al.* (1997) reveals that most NKB-containing neurons appear to be concentrated more in the medial than in the lateral sectors of BST, and more predominant on supracommissural than in the infracommissural ones.

NEUROPEPTIDE Y (NPY) According to Gaspar *et al.* (1987), innervation by NPY is essentially restricted to the lateral BST nucleus although in close proximity to the pillar of the fornix. NPY-ir is apparent in a small field of axons and terminals. NPY-ir perikarya are almost exclusively located in the lateral BST nucleus. On the other hand, and although the BSTM division of the human BST nucleus is not specifically mentioned in Walter *et al.*'s (1990) mapping of the NPY-ir distribution in this epencephalic structure, their Fig. 1c shows that both supracommissural and infracommissural sectors of the BSTM division contain NPY-ir profiles.

By comparison, Bons *et al.* (1990) reported that in the BST nucleus of the microcebus murinus (primate, lemurian), NPY-ir axons form a dense plexus surrounding the anterior commissure and fornix. Apart from that, NPY-ir perikarya could be visualized especially near the border of the lateral ventricle (BSTM), which does not seem to be the case in humans.

NEUROTENSIN (NT) Martin *et al.* (1991) were unable to detect NT-ir cell bodies in the BSTM division of the human BST nucleus, but a few could be detected in the macaque monkey.

OXYTOCIN (OXT) According to Caffé *et al.* (1989), in the macaque monkey, the BST nucleus contains OXT-ir fibers although their presence is not as dense as that in the cortical nucleus. No mention is made about the presence of OTX-ir cell bodies, although in their schematic representation of the distribution of OXT-ir cell bodies in Fig. 2, cells of this type are depicted close to the fornix pillars in an area that may belong to the medial cell column of the BSTMP division. This does not seem to be the case in the BST nucleus of the common marmoset where scattered OXT-ir neurons are present in the medial subdivisions of the anterior and posterior divisions (Wang *et al.*, 1997).

SECRETONEURIN (SECR) According to Marksteiner *et al.* (1993) and Kaufmann *et al.* (1997), the BSTM division contains a high density of SECR-ir varicosities and varicose fibers, which sometimes form pericellular arrangements, but only scattered peridendritic woolly-like type 2 fibers. This picture does not seem to vary with sex or age.

SOMATOSTATIN (SOM) According to Gaspar *et al.* (1985, 1987), in the human BSTM division, SOM-ir fibers and cell bodies are more diversely distributed than in the lateral division. Bennet-Clarke and Joseph (1986) partially confirmed the previous report by describing that SOM-ir perikarya not only are scattered throughout the BST nucleus but also invade the bed nucleus of the anterior commissure that is adjacent to the ventral border of the commissure, and that SOM-ir processes are seen in every area of the BST nucleus containing SOM-ir perikarya. By contrast, Martin *et al.* (1991) were unable to detect SOM-ir cell bodies in the BSTM division of the human BST nucleus or in that of several nonhuman primates.

SUBSTANCE P (SP) Martin *et al.* (1991) traced a continuum of SP-ir puncta and varicose fibers to the

BSTMA subdivision of the human BST nucleus, also detecting a few SP-ir cell bodies. Kaufmann *et al.* (1997), confirmed these findings but also stressed that the BSTM division as a whole contained only moderate densities of SP-ir when compared to the very high levels of SECR-ir present there. Heimer and associates' (Heimer *et al.*, 1999; Sakamoto *et al.*, 1999) human material shows that, while the SP-ir in the posterior sub-region of the BSTM division is somewhat heterogeneous, these SP-ir gradually increases in strength in the anterior part of the medial bed nucleus [see Plates SP5–SP9 in Sakamoto *et al.* (1999)].

VASOPRESSIN (VP) According to Fliers *et al.* (1986), in the human BST nucleus, few bipolar VP-ir cells can be identified, but not so in its amygdaloid companion, the Me nucleus. After their results, the bipolar VP-ir cells located in the rostral BST nucleus appear to be smaller than those of the magnocellular supraoptic and paraventricular hypothalamic nuclei. However, on more caudal levels, many VP-ir neurons can be found that show magnocellular features. Interestingly, the highest incidence of VP-ir fibers in the limbic system is found in the BST and BAC nuclei, but also in a very reduced number of telencephalic nuclei. Finally, there is no evidence of sex differences concerning the richness of the VP-ir innervation.

Caffé *et al.* (1989), working with macaque monkey brains, reported the existence in their BST nucleus of a VP-ir innervation pattern that seems to represent an extension from that present in the preoptic area, although with an increased density in the former. In addition, a very dense plexus of thick, highly varicose VP fibers appears to be confined to what they call the "BST nucleus proper," a well-defined cell aggregation located in the supracommissural part of the BST nucleus. Very probably this cell group corresponds to the BSTLD subnucleus of the present parcellation. Furthermore, they could determine that these types of VP-ir fibers are also found ventral to the anterior commissure corresponding most probably in location to the BSTLV subnucleus.

Medially to their BST nucleus proper and just adjacent to the lateral ventricle, a few ovoid bipolar VP-ir neurons could be identified (i.e., in the area corresponding to the medial subdivision of the BSTMP division). In addition, a moderate number of multipolar VP-ir cells exhibiting many short dendrites are also found in the ventromedial part of BST (i.e., the BSTMV subdivision).

On the other hand, Wang *et al.* (1997) studying the common marmoset (*Callithrix jacchus*) found a distribution pattern of VP-ir fibers and cells that closely imitated the distribution pattern of VIP-ir cells reported for the human brain, i.e., with VP-ir somata that remain confined to the supracommissural sector of both anterior and posterior subregions of the BSTM division, and with no VP-ir cell present in the Me nucleus. However, at variance with the human pattern, the subpopulation of VP-ir neurons presents in this animal dimorphic differences with respect to the number of VP-ir cells in the male versus the female BST.

VASOINTESTINAL PEPTIDE (VIP) According to Martin *et al.* (1991), in nonhuman primates, such as the macaque monkey among others examined, VIP-ir puncta and varicose fibers that are present in the dorsomedial nucleus accumbens extend caudally to merge with a similar disposition in the BSTMA subregion (their BSTA) and in the bed nucleus of the anterior commissure (BAC). No evidence for the existence of VIP-ir cell bodies in the BSTM division was found.

BRAIN-DERIVED NEUROTROPHIC FACTOR (BDNF) According to Murer *et al.* (1999), in the human BST nucleus, BDNF-ir fibers form a dense and strongly ir plexus where several nonstained neuronal cell bodies are completely enveloped by BDNF-ir terminals boutons and fibers. Isolated BDNF-ir neurons are rarely found in a region localized between the ventricular wall, the caudate nucleus, and the septum/BST region. It is a problem that the presented illustration (Fig. 3G) corresponds only to a sector within the BSTMA subnucleus according to the present parcellation of the EXA. Also from their Fig.3A it can be inferred that both supra- and infracommissural regions of the medial BSTM division of the BST nucleus contain BDNF-ir.

ENZYMES

P450 AROMATASE (P450 AROM) According to Roselli *et al.* (2001), in the macaque monkey, the BST nucleus contains P450 AROM with the heaviest labelling occurring in the medial anterior (BSTMA) and medial posterior (BSTMP) BST subnuclei, areas that have strong reciprocal connections with the hypothalamus and amygdala. Even though these authors reported scattered labelling in the substantia innominata, these data also speak in favor of the existence of a medial extended amygdala, since the Me nucleus also contains high concentrations of this enzyme.

CALCIUM-BINDING PROTEINS Since there is a paucity of data in the literature concerning the distribution of these types of proteins in the human or monkey BST nucleus, and since immunohistochemical information

from my own laboratory indicates that the rat BST nucleus presents staining patterns for these proteins that closely match that seen in the rat central and medial amygdaloid nuclei, these data will be given here to provide an approximate picture of what can happen in this nucleus in primates.

CALRETININ (CR) Examination of rat material processed immunohistochemically for the demonstration of this calcium-binding protein reveals a significant presence of a subpopulation of CR-ir neurons enmeshed in a dense CR-ir neuropil in both anterior and ventral subdivisions of the BSTMA subdivision of the BST nucleus as well as the intermediate medium-celled column of the BSTMP subdivision of this nucleus. This information acquires relevance when considering that in the rat both anterodorsal and anteroventral subnucleus of the Me nucleus contains an equally significant subpopulation of CR-ir neurons and that in experiments carried out in rats utilizing a double-labeling procedure (Krzywkowski *et al.*, 1995) it has been possible to determine that CR-ir neurons of both components of the medial extended amygdala send projections to the ventromedial hypothalamic nucleus. Such results fit very well to the theory of the extended amygdala.

RECEPTORS

CHOLINERGIC RECEPTORS

MUSCARINIC RECEPTOR (MACH-R) According to Cortés *et al.* (1987), there is a high concentration of mACh-R in the human BST nucleus. However, from their illustrations (Fig. 5A, B) it can be inferred that the densest activity takes place in the BSTLD and JCX subnuclei of the BSTL while lower labeling occurs at the level of the BSTM.

GLUTAMATE IONOTROPIC RECEPTOR (GLUR) According to Ginsberg *et al.* (1995), in the macaque monkey, the BSTM contains a high density of GluR2/3-ir neurons and a lower density of GluR1-ir neurons but expresses minimal GluR4 immunoreactivity.

ANDROGEN RECEPTOR (AR) According to two groups of researchers (Resko *et al.*, 2000; Roselli *et al.*, 2001), in the adult male macaque monkey, only moderate amounts of neurons expressing AR mRNAs appear to be present in the BSTMA and BSTMP. In contrast, these sectors of the BST appear to contain very high densities of strongly labeled aromatase-containing neurons. This distribution and labeling pattern coincides with those reported for the other end of the MExA, the Me nucleus. By contrast, a few aromatase-containing cells and no AR containing cells could be detected in the SLEA.

OXYTOCIN RECEPTOR (OT-R) Although Loup *et al.* (1991) made no mention of the presence of OT-R in the medial division of the BST nucleus, their Fig. 5 shows heavy OT binding in a sector of the human paraseptal region that, despite being considered to represent a dorsal part of the lateral septal nucleus (which they label as LSD), by all present criteria for the organization of the human basal telencephalon, should be assigned as the BSTMA division of the BST nucleus [see corresponding level in Plate/Fig. 22 of Mai *et al.*, 1997 *Atlas*]. It deserves to be mentioned that Wilson *et al.* (1999) found in rats that whereas the OT binding density is lower in the Me nucleus and in the BSTMA than in CExA representatives, the excitatory response to OT was greater in these representatives of the MExA than in the CExA. Nevertheless, what is important for the hypothesis of the EXA is that the relative expression of OT binding sites and the patterns of response reflect these associations within the extended amygdala.

STEROID RECEPTORS

ESTROGENIC RECEPTOR (ER)

Estrogen Receptor α (ER-α) According to Österlund *et al.* (2000), the medial division of the BST nucleus shows low ER-α mRNA in human and monkey brain.

Medial Division of the Sublenticular Extended Amygdala (SLEAM) This medial component of the SLEA extends from the BSTMPL, passing into the ventral sectors of the so-called sublenticular SI and eventually fusing with the superficial division of AAA rostrally and Me caudally. The cells that form this more ventral column, despite sharing most of the cytological characteristics seen in more dorsal sectors of the SLEA, show a rounder shape, in some parts arc-like. Coursing through the so-called substantia innominata, some ectopic elements detached from neighboring basal telencephalic structures and invade this structure, partly modifying its cytoarchitectonic characteristics.

Although the medial nucleus of the amygdala (Me) is cytologically similar to the medial division of the bed nucleus of the stria terminalis, the sublenticular cell bridges that connect them are by no means clearly identifiable in Nissl preparations. Some help is provided by the fact that this division of the sublenticular extended amygdala, like both the medial amygdaloid nucleus and the posterior division of the bed nucleus with which the medial sublenticular is continuous, are richer in their glial cell population than the representatives of the central sublenticular limb of the extended amygdala. Other neighboring neuronal populations not related to either continuum also share this cytoarchitectonic trait. The same can be said concerning

the morphological features of the cells that form this continuum: lightly staining, medium to small sized, slender, generally fusiform, and preferentially roughly transverse orientation of their cell body long axis. This allows us to distinguish them from the large, strongly staining cells that form the magnocellular gray complex of the basal telencephalon whose main representative is the basal nucleus of Meynert. SLEAM is not clearly distinguishable from its companion central limb of the SLEA or from other similar-looking cells belonging to other nearby gray formations, such as those in the ventral pallidum rostrally or the lateral preoptic region medially. Adhering to this difficulties is the fact that the region where this continuum extends is traversed by numerous fiber systems that disrupt the continuum into islands of varying size. This may also occur because of their adaptation to many variations in position and physical compression they undergo during early stages of their ontogenetic development. Although not all of these factors in the rat play this negative role as in higher mammals for the identification of the medial continuum, even in this relatively simple brain dissection of this component does not come easily. It is only with the help of a histochemical procedure such as the Timm-Dansher staining for heavy metals or the experimental application of retrograde tracing procedures that it has been possible to unravel the existence of this continuum (de Olmos *et al.*, 1985; Grover *et al.*, 1988a, b); neither procedure can be applied to the study of the human SLEA. At this point it should be pointed out that Martin *et al.* (1991) rightly emphasized that immunohistochemical procedures that were well suited for the demonstration of the SLEACn division did help in the delineation of the medial continuum (their anteroventral and posteroventral SLSI). However, as has been reported by Heimer *et al.* (1999), human brain sections stained for both CCK and NT (see their Figs. 27A, B) provide evidence of partly interrupted NT-ir/SOM-ir sublenticular columns close to the ventral brain surface. Another good marker of this medial continuum is the antibody for the demonstration of secretoneurin (Marksteiner *et al.*, 1993; Kaufmann *et al.*, 1997; Heimer *et al.*, 1999). This antibody was demonstrated to be very useful in immunostaining the extended amygdala in the sense that it labels both its central and medial divisions while leaving practically unstained the rest of the amygdaloid nuclei. However, it presents the disadvantage of also labeling the ventromedial parts of the striopallidal system, especially in places of the basal epencephalon where these adjoin the extended amygdala. However, the fact remains that both ends of the medial extended continuum, the BSTM division of the BST nucleus and the Me amygdaloid nuclei, are densely SECR-ir labeled (for a more detailed discussion, see Heimer *et al.*, 1999).

As here defined SLEAM corresponds to the Martin *et al.* (1991) and Kaufman *et al.* (1997) anteroventral subdivision (SIav) of their sublenticular BST, while their posteroventral subdivision corresponds to the amygdaloid sector or temporal end of the MExA, i.e., the superficial division of the AAA or the anterior division of the Me nucleus. Freedman and Shi (2001), on the basis of their immunohistochemical tracing of the monaminergic innervation of the extended amygdala, concluded that the ventral part of the substantia innominata (here the SLEAM division) appears similar to the medial subnucleus of the Ce nucleus, though stressing the greater density of the AChE staining in the formerly cited component of the EXA. As in the case of the SLEACn, this apparently greater heterogeneity of the SLEAM may be due to a similar interdigitation with elements detached form the main core of non-EXA telencephalic structures.

Chemoarchitecture

CUPRIC SILVER (CU–AG) Like the other members of the medial extended amygdala, the SLEAM does not show the Cu-Ag staining pattern that is present along the extent of the central extended amygdala, nor it has been possible to detect isolated argyrophilic cells of the type sometimes present in the Me nucleus or the BSTM division of the BST nucleus.

HEAVY METALS In sections stained by the Timm-Danscher method (Danscher, 1981) for heavy metals obtained from squirrel or marmoset brain, close examination reveals that the pattern of silver precipitate in the sublenticular region has two expressions. One of these is in the form of a dorsal, very dense column of thick silver selenite precipitate that detaches clearly from the dorsomedial aspect of the Ce nucleus. This column can be followed just ventral to the globus pallidus and internal capsule until it joins an equally densely stained region in the lateral posterior and ventral subdivisions of the BST nucleus. Another more or less compact and densely stained column apparently departs from the dorsomedial aspect of the Me amygdaloid nucleus and superficial AAA area to extend medially and dorsally until it reaches a comparatively similar weak-stained region in the lateroventral aspect of the posterolateral subdivision of the medial BST nucleus.

NEUROTRANSMITTERS

CHOLINERGIC MARKERS

ACETYLCHOLINESTERASE (ACHE) In the macaque brain [EA Plates/Figs. 51 and 55 in Paxinos *et al.* (2000),

The Rhesus Monkey in Stereotaxic Coordinates], and in macaque monkey darkfield collection of low-magnification microphotographic material generously provided to the author by Drs. Heimer and Alheid, it is clear that this sector of the monkey basal telencephalon shows a lower AChE activity than surrounding structures.

CHOLINE ACETYLTRANSFERASE (ChAT) No human or nonhuman primate data are available about the presence or absence of this enzyme in this sector of the SLEA.

EXCITATORY AMINO ACIDS

GLUTAMATE (GLU) No human or nonhuman primate data are available about the presence or not of this neurotransmitter in this sector of the SLEA; however, it is justifiable to assume that this sector of the SLEAM might imitate its representative in the temporal lobe, i.e., the Me nucleus, in containing subpopulation of GABA-ir neurons and its corresponding GABA-ir neuropil.

INHIBITORY AMINO ACIDS

γ-AMINOBUTYRIC ACID (GABA) No data available for the author from the literature are cited.

MONOAMINE MARKERS

DOPAMINE-β-HYDROXYLASE (DBH) According to Freedman and Shi (2001), there are moderate amounts of DBH-ir fibers in the ventral part of the so-called substantia innominata (here, SLEAM).

HISTAMINE (HA) According to Airaksinen *et al.* (1989), in the tree shrew the HA-ir fibers spread in the amygdaloid complex as a dense network including in this manner the SLEAM (see their Fig. 3G).

NEUROPEPTIDES

CORTICOTROPIN-RELEASING FACTOR (CRF) In the human amygdaloid complex, a dense accumulation of CRF-ir fibers, with large varicosities and terminals, has been reported to be present in almost all amygdaloid nuclei (Power *et al.*, 1987; Zaphiropoulos *et al.*, 1991). This statement may be extensible to the substantia innominata and more particular to this division, according to the mapping made for this region by Zaphiropolous *et al.* (1991).

CHOLECYTOKININ (CCK) Although according to Martin *et al.* (1991), the data provided by their human and nonhuman primate material did not provide evidence for a participation of CCK-ir neurons. Heimer *et al.* (1997), in contrast, found unmistakable evidence for the existence CCK-ir fibers and terminals in this region of the human extended amygdala continuum.

ENKEPHALIN (ENK) According to Martin *et al.* (1991), the data provided by their human and nonhuman primate material did not provide evidences for a participation of ENK-ir neurons or ENK-ir fibers and terminals in this part of the extended amygdala continuum.

GALANIN (GAL) According to the mapping of the forebrain distribution of this neuropeptide presented by Kordower *et al.* (1992) in the cebus monkey amygdala, this member of the MExA, like the other amygdaloid components of it, would not contain GAL-ir cell bodies, though it may contain small amounts of GAL-ir fibers. Instead, this pattern is shown to change dramatically toward the paraseptal expansion of the posteroventral continuum, i.e., the present SLEAM.

NEUROKININ B (NKB) Small to round NKB mRNA-containing neurons are numerous in the BST, which contrasts with the small number of SP-ir cells present there. NKB mRNA is also identifiable in small neurons scattered from the BST to the amygdala. These NKB neurons are occasionally seen aligned in small groups along fiber bundles (Chawla *et al.*, 1997).

NEUROTENSIN (NT) According to Heimer *et al.* (1999) evidence for the existence of the SLEAm is provided by partly interrupted sublenticular columns close to the ventral brain surface. This NT-ir islands contain NT-ir fibers and terminals as well as the typical medium-sized fusiform neuronal cell bodies that are part of a string of NT-ir islands that rostromedially form a continuous arch in apparent continuity with the posterolateral part of the BSTM division of the bed nucleus of the stria terminalis.

SECRETONEURIN (SECR) According to Kaufmann *et al.* (1997), in the human brain, their anteroventral and posteroventral parts of the so-called substantia innominata (here SLEAM) exhibit SECR-ir although such activity resided mainly in varicose fibers, not participating in the type of axonal peridendritic formation sometimes called woolly fibers.

SOMATOSTATIN (SOM) According to Martin *et al.* (1991), the data provided by their human and nonhuman primate material did not provide evidence for a participation of SOM-ir neurons or SOM-ir fibers and terminals in this part of the extended amygdala continuum.

SUBSTANCE P (SP) According to Martin *et al.* (1991), the data provided by their human and nonhuman primate material did not provide evidence for a participation of SP-ir neurons or SP-ir fibers and terminals in this part of the extended amygdala continuum.

VASOPRESSIN (VP) According to Caffé *et al.* (1989) in the macaque monkey, there is moderate innervation by thick varicose and thin beaded fibers. These fibers form a continuum with those in the BST nucleus and the amygdala.

ENZYMES

P450 AROMATASE (P450 AROM) According to Roselli *et al.* (2001), in the macaque monkey amygdala, scattered cells containing P450 AROM mRNA could be detected at the level of the substantia innominata.

CALCIUM-BINDING PROTEINS

CALRETININ (CR) In rat material processed in my laboratory for the immunostaining of this calcium-binding protein, it is possible to see that columns of CR-ir neurons and neuropil bridge sublenticularly the anterodorsal subdivision of the Me nucleus with the intermediate subdivision of the BSTMP division of the BST nucleus. Since in the human brain the medial amygdaloid nucleus shows, as will be described below, a rich CR-ir neuronal population that is enmeshed in a very dense CR-ir network of fibers and terminals, it is justifiable to assume that a CR-ir medial continuum of neurons and fibers is present in the human brain.

OTHER PROTEINS

SEROTONIN TRANSPORTER (SERT) According to Freedman and Shi (2001), in the macaque ventral substantia innominata (here SLEAM), there are moderate to high amounts of SerT-ir fibers. Unlike serotonin labeling, fibers as varicosities are well defined and tend not to have much diffuse background labeling.

RECEPTORS

CHOLINERGIC RECEPTORS

MUSCARINIC RECEPTOR (MACH-R) According to Cortés *et al.* (1987), there is an intermediate to low concentration of mACh-R in the so-called substantia innominata in the human telencephalon, which is of the m_1 subtype.

SEROTONINERGIC RECEPTORS (5-HT-R)

5-HT_{2C} RECEPTOR (5-HT_{2C}-R) According to Lopez-Gimenez *et al.* (2001), the sublenticular extended amygdala constitutes one of the forebrain structures showing the strongest hybridization signal with probes for 5-HT_{2C}-R mRNA.

STEROID RECEPTORS

ANDROGENIC RECEPTOR (AR) Although not mentioned in a report about testosterone action in the brain of the female macaque brains by Rees *et al.* (1986), their mapping (Fig. 1 A–D) indicates that at least this division of SLEA contains scattered [^{3}H]testosterone-labeled nuclei.

ESTROGENIC RECEPTORS (ER)

ESTROGEN RECEPTOR α (ER-α) According to Österlund *et al.* (2000), both in human and monkey brains, the ER-α transcript is widely distributed in neurons of the amygdala but predominantly in the more medial nuclei throughout the entire rostral to caudal continuum of the amygdaloid complex.

The Temporal Lobe Components of the Medial Extended Amygdala

Medial Amygdaloid Nucleus (Me)

Topographical Landmarks The medial amygdaloid nucleus (see Figs. 22.1c,d, 22.7, 22.8, 22.22c, 22.23b, 22.28, 22.29) [Me in Plates 26–33 (5.4–14.6 mm) of Mai *et al.* (1997), *Atlas of the Human Brain*; and Me in Plates/Figs. 49–65 (interaural 18.75–11.55 mm) in Paxinos *et al.* (2000) *The Rhesus Monkey Brain in Stereotaxic Coordinates*], which is continuous dorsomedially with the caudal superficial AAA, is an elongated mass of gray matter located in the superficial portion of the dorsomedial amygdala stretching throughout the caudal two-thirds of the amygdaloid complex. In coronally cut sections passing through the level of its main body, the Me nucleus shows a crescent-like shape whereas in sagittal sections cut along its main longitudinal axis, the nucleus appears as a very regular columnar formation. At its rostral one-third, the Me nucleus is located adjacent to the notch formed by the entorhinal sulcus, but near its caudal pole Me occupies only the ventral bank of this sulcus and eventually is displaced from that position by the amygdalohippocampal transition area (AHi) that wedges between this gray formation and the medial division of Ce. Along its extent Me borders ventrally, in successive sequence, with the caudal superior subdivision of the ventral cortical nucleus (CSpVCo) and the rostrodorsal pole of the posteromedial division of the amygdalohippocampal area (PM AHi); dorsolaterally, the narrow extension of the deep AAA wedges between Me and the medial division of Ce. Throughout most of its rostral to caudal extent Me is filled by a relatively dense stratum of fibers forming Brockhaus' (1938) intermediate central fiber masses (icm), which surround the nucleus dorsally, laterally, and, partly, ventrally. At its rostral pole this fiber system fades out coincidentally with the replacement of the Me nucleus by the ACo nucleus. Rostrally and ventrally, a small, round neuronal

griseum, probably representing the caudal-most end of the ventral subdivision of the ACo nucleus or the posterior part of the so-called nucleus of the lateral olfactory tract of some authors, intervenes between the Me nucleus and the superior subdivision of the VCo.

Cytoarchitectonics As with other superficial amygdaloid grisea, there is a tendency for the neurons of the Me nucleus to form layers, especially superficially, allowing the identification of a cell-poor molecular layer (L1), a superficial dense cell layer (L2), and a deep layer (L3) with somewhat less densely distributed neurons. On the basis of purely morphological criteria the Me can be divided into two major divisions: anterior (MeA) and posterior (MeP). The MeP division, in turn, can be further divided into dorsal (D MeP) and ventral subnuclei (V MeP). The MeA nucleus borders rostrally with the ACo nucleus, the superficial amygdaloid griseum which it replaces caudally until it is replaced by the dorsal subdivision of the MeP subnucleus. The latter stretches until it reaches the onset of the extra-amygdaloid portion of the stria terminalis at the posterior end of the amygdala. It is the V MeP subnucleus that is separated from the amygdalohippocampal transition area by a capsule of fibers detached from the medial medullary lamina whose density varies but that always intervenes between these two gray formations.

The MeA division (see Figs. 22.7 and 22.8), in contrast with MeP, still shows a rather wide molecular layer (L1) although not as wide as that in ACo. As in this latter nucleus, it is invaded, though in a very scattered fashion, by small, slender neurons of varying conformation and stainability. Deep to the molecular layer, the main cell layers, superficial (L2) and deep (L3), are clearly segregated from L1 and form a relatively homogeneous cell mass, although the neurons located in the superficial two-thirds show a tendency to lie more closely packed. Furthermore, the more deeply lying cells tend to be slightly larger and more darkly stained than the more superficially located ones. The neuronal population in the MeA division is rather heterogeneous being made up of pyramidal, multiangular, round, and spindle-shaped cells of different sizes, but still smaller than those in the neighboring Sp VCo, and more compactly and regularly arranged than those in AAA. The MeA can be differentiated from the rostral immediate neighbor, the ACo, by the greater cell density of L2, and a concomitant rarefaction of its deeper lying neuronal population as well as by the narrowing of its L1.

In the MeP division, its ventral subdivision (V MeP) occupies the most dorsal segment of the ventral bank of the entorhinal sulcus shortly before the optic tract meets its now narrow fundus. It is constituted by a rather narrow cell aggregate encapsulated ventromedially and laterally by the fiber septum which branches off from the intermediate caudomedial fiber masses (icm) described by Brockhaus (1938). It shows a well-defined superficial cell layer (L2) composed of medium-sized, darkly staining neurons that in more caudal sectors of the V MeP subnucleus tend to become more densely arranged toward the deep aspect of this griseum. The deep layer (L3) in the V MeP is even more densely populated and narrower than L2, containing a more darkly staining neuronal somata displaying no particular orientation. Finally, the deep aspect of the molecular layer (L1) of the V MeP appears invaded by small cells showing the same distribution pattern and general morphological features as those in L1 of the MeA division.

Dorsally the V MeP subnucleus merges with its dorsal counterpart (D MeP). This subnucleus lies for most of its extent immediately adjacent to the optic tract's lateroventral facet, intercalated between the V MeP subnucleus and the Sf AA. It contains a more homogeneous neuronal population of slightly larger, more densely packed, and darker staining neurons than the V MeP subnucleus. Its superficial cell layer (L2) contains slender radially oriented, oval to spindle-shaped neurons more densely packed than those in L3. The latter contains a more heterogeneous population of darkly staining neurons showing no particular orientation. Finally,the D MeP possess a richer glial population than its ventral counterpart.

No less important than the cell composition and arrangement as a means of delineating the different components of this member of the MEXA is its fibroarchitectonic arrangement. Thus, the MeA division shows a moderately rich plexus of randomly oriented myelinated fibers that become denser in its more superficial layers. This pattern changes dramatically at the level of the MeP division. Here the density of the myelinated fiber plexus increases sharply in both subnuclei of the MeP division but showing variations regarding its predominant orientation. Consequently, whereas the plexus of myelinated fibers in the D MeP subnucleus is dominated by transversely coursing fibers, the medullated fiber plexus in the PV subnucleus is made up of more randomly oriented fibers with some predominance of ventrodorsally coursing fibers radiating from the Brockhaus (1938) ism fiber masses. Furthermore, the presence of short bundles of densely myelinated fibers intercalated between the superficial cell layer an the lateral margin of the optic tract also marks the difference between both subnuclei of the MeP division. Corroborating the above-described myeloarchitectonic arrangement, neurofibrillar preparations

display a similar arrangement but with a far denser disposition.

As pointed out by Heimer *et al.* (1999), although the heterogeneous population of small to medium-sized, relatively lightly stained neurons and a significant number of glial cells in the Me is reminiscent of the situation in parts of the BSTM, it is not yet possible to closely correlate the various parts of the Me nucleus and the BSTM on the basis of cytoarchitectonics alone. Furthermore, the generally weak reaction for AChE, and ENK added to the stronger reaction for SP is consistent with the overall concept of the MExA, which is based in the premise of a general correspondence between the Me nucleus and the BSTM. As will be seen below, even more convincing evidence supporting the above-mentioned premise comes from the examination of human material stained for CCK, NT, and SECR.

Chemoarchitectonics

HEAVY METALS In sections of both squirrel and marmoset monkeys stained with the Timm-Danscher method, the medial amygdaloid nucleus shows a heterogeneous pattern of staining that varies both in the dorsoventral axis of the nucleus and in the anteroposterior one. As a whole, the density of the silver selenide deposits in this nucleus is significantly lower than in its ventral neighbor, the VCo nucleus, or its more laterally located component of the central extended amygdala, the Ce nucleus.

CUPRIC SILVER STAIN (CU-AG) In Cu-Ag-stained sections of macaque and squirrel monkeys brain the Me nucleus does not show an argyrophilic staining pattern like that obtainable in all members of the central extended amygdala. However, in the squirrel monkey material it was possible to detect the presence of isolated bipolar granular argyrophilic neurons of fusiform shape, with very slender perikarya that appear scattered along the medial surface and in the whole extent of the Me, ACo nuclei, and the superficial division of the AAA area, oriented mostly parallel to the brain surface. Neurons of the same morphological characteristics could be detected at the level of the BSTM division. Interestingly, argyrophilic neurons with exactly the same appearance as those just described are also present in the subfornical organ, the organum vasculosum laminae terminalis, the medial preoptic area, the infundibular arcuate nucleus, the ventral premammillary nucleus, and even the area of the interpeduncular nucleus just behind the mammillary bodies. On some occasions it was possible to follow one of their very thin processes for some distance. If one looks for similar images, the closest are those presented by LH-RH-ir neurons.

NEUROTRANSMITTERS AND NEUROMODULATORS

Cholinergic Markers

ACETYLCHOLINESTERASE (AChE) Me contains a lightly AChE stained neuropil and a few isolated AChE-containing neurons (Darvesh *et al.*, 1998; Sorvari *et al.*, 1995; Heimer *et al.*, 1999). Amaral and Basset (1989) have shown that in the macaque monkey the Me nucleus together with the ACo nucleus contains the lowest density of AChE-positive fibers. In contrast with these low levels of AChE activity, both nuclei, but more particularly the Me nucleus, contain large numbers of AChE positive neurons.

CHOLINE ACETYLTRANSFERASE (ChAT) According to Emre *et al.* (1993), the Me nucleus in humans has the lowest density of ChAT-ir profiles of all amygdaloid nuclei. Only a few ChAT-ir varicose axons are present in this nucleus. In agreement with this, Amaral and Basset (1989) found that in the macaque monkey amygdala, the medial amygdaloid nucleus can be distinguished by its extremely low ChAT-ir fibers and terminals, yielding in this nucleus the lowest density of this type of fiber in any amygdaloid areas.

Excitatory Amino Acids

GLUTAMATE (GLU/ASP) Retrograde tracing experiments made in rats using tritiated D-aspartate indicate that a considerable number of Me neurons, mostly the anterodorsal division, are a source of GLU/ASPergic projections to both the laterocaudal ventral striatum (IPAC?) and the ventral pallidum (Fuller *et al.*, 1987), as well as to the paraventricular hypothalamic nucleus or immediate surroundings (Csáki *et al.*, 2000).

Inhibitory Amino Acids

γ-AMINOBUTYRIC ACID (GABA) According to McDonald and Augustine (1993), in the macaque monkey the Me nucleus, despite containing some GABA-ir neurons, mostly contains non-ir neurons. Pitkännen and Amaral (1994) consider that in this nucleus the distribution pattern of the GABA-ir is very similar to that of the ACo nucleus and, therefore, confirmed the McDonald and Augustine data concerning the low numbers of GABA-ir cells present in Me. However, they found that the density of GAD mRNA-labeled neurons is very high. At anterior levels the cells are preferentially located in the superficial portion of L2 and in the deep portion of L3. In the caudal portions of the Me the labeled cells are more homogeneously distributed throughout L2 and L3.

The neuropil GABA-ir levels are among the highest in the monkey amygdaloid complex. Pericellular baskets in L2 are more prominent than in the ACo

nucleus. Finally, a bundle of dense GABA-ir fibers lies located immediately lateral to this nucleus.

Monoamine Markers

DOPAMINE-β-HYDROXYLASE (DBH) According to Freedman and Shi (2001), in the macaque monkey there are moderate amounts of DBH in the Me. In the squirrel monkey, the Me nucleus (plus ACo) shows moderate to dense DBH-ir at its caudal portion (the Me nucleus proper), but the DBH-ir becomes much lighter at its rostral-most portion (the ACo nucleus) (Sadikot and Parent, 1990).

HISTAMINE (HA) According to Airaksinen *et al.* (1989), in the tree shrew (*Tupaia belangeri*), HA-ir fibers collected in dense bundles along the stria terminalis continue to the amygdaloid complex to spread as a dense and diffusely distributed network within the amygdala. At the level of the Me nucleus this network reaches a high density (4 in a scale of 0–5).

SEROTONIN (5-HT) According to Freedman and Shi (2001), in the macaque monkey, there are moderate amounts of 5-HT-ir in the Me nucleus. In the squirrel monkey, the Me nucleus shows light 5-HT-ir terminal labeling (Sadikot and Parent, 1990).

TYROSINE HYDROXYLASE (TH) According to Freedman and Shi (2001), there are moderate concentrations of TH-ir fibers in the rostral part of the Me nucleus. In the squirrel monkey, the TH-ir terminal labeling is light to absent in the Me nucleus (Sadikot and Parent, 1990).

Neuropeptides

BRAIN-DERIVED NEUROTROPHIC FACTOR (BDNF) According to Murer *et al.* (1999), in the human amygdala, BDNF-ir neurons and fibers are present in all amygdaloid nuclei. No specific data are given concerning Me.

CHROMOGRANIN B According to Marksteiner *et al.* (1999), in the human brain, the Me nucleus displays a moderate density of PE-11-like ir. However, from their illustrations it seems that the most caudal part of the Me nucleus according the present parcellation contains a high density of this neuropeptide. Such ir is exclusively due to fibers and neuropil but not to cell bodies since only the Ce nucleus within the whole amygdaloid complex would contain them.

COCAINE- AND AMPHETAMINE-REGULATED TRANSCRIPT (CART) According to Hurd and Fagergren (2000), the highest CART mRNA expression can be found in the Me nucleus.

CORTICOTROPIN-RELEASING FACTOR (CRF) In the human amygdaloid complex a dense accumulation of CRF-ir fibers, with large varicosities, and terminals can be found in almost all amygdaloid nuclei. This finding, together with the fact that the bed nucleus of the stria terminalis and the sublenticular substantia innominata (here SLEA) contain a high density of CRF-containing fibers and terminals (Zaphiropoulos *et al.*, 1991), speaks in favor of the existence of a similar distribution pattern in Me.

GALANIN (GAL) According to the mapping of the forebrain distribution of this neuropeptide presented by Kordower *et al.* (1992), in the macaque monkey amygdala, this member of the superficial amygdala, like its other components, does not contain GAL-ir cell bodies but seems to contain at least a small number GAL-ir fibers.

GONADOTROPHIN-RELEASING HORMONE–ASSOCIATED PEPTIDE (GAP) According to Song *et al.* (1987), in macaque and baboon, a few GAP-ir fibers can be detected in the Me A nucleus.

LUTEINIZING HORMONE–RELEASING FACTOR (LHRF) According to Silverman *et al.* (1982), in the brain of macaque monkeys, a group of LHRF-ir round perikarya showing a short segment of their processes are situated in the Me nucleus. However, these cells seem to be rare.

NEUROPEPTIDE Y (NPY) According to McDonald *et al.* (1995), in the macaque monkey the highest densities of NPY-ir neurons are found in the Me nucleus. It is interesting that large globular uni- or multipolar NPY-ir neurons are also present in the Me nucleus of the lemur microcebus marinus (Bons *et al.*, 1990).

NEUROTENSIN (NT) Mai *et al.* (1987) stated that the Me nucleus together with the cortical nucleus and the so-called supra-amygdaloid areas (i.e., the Ce and AAA nuclei) contain the strongest accumulation of NT-ir fibers. This statement was confirmed by Benzing *et al.* (1992), who found that the Me nucleus contains a dense NT-ir that is distributed evenly across the anteroposterior extent of the nucleus. Most of the NT-ir is confined to dot-like puncta although many fine- and a few coarse-beaded fibers are present. In addition to the NT-ir fibers, numerous darkly stained bipolar neurons are distributed throughout the nucleus, but they are preferentially located in the deep (lateral) portions of the nucleus. As can be inferred from the illustrations and mapping of the amygdaloid nuclei presented by these authors, their anterior amygdaloid area (Fig. 1, AAA) not only comprises the AAA as here

defined but also the ACo, while their mapping of the medial amygdaloid nucleus (Fig. 1, Me) coincides approximately with the Me nucleus as defined here. It is interesting to point out differences in the density of the NT-ir shown between AAA and their Me (Figs. 3C and 4C, respectively), with the AAA stained least of the subnuclei of the centromedial group. Furthermore, according to Heimer *et al.* (1999), the NT-ir fibers and terminals intermingle with NT-ir perikarya and form a continuous column from the Me nucleus through the AAA and further medially to the NT-ir islands in the sublenticular region of the basal forebrain.

OXYTOCIN (OXT) According to Fliers *et al.* (1986), in the human Me nucleus, very few OXT-ir fibers and no OXT-ir cells are present. No mention of the presence of this type of fiber in the macaque Me nucleus is made by Caffé *et al.* (1989), while, according to Wang *et al.* (1997), in the common marmoset monkey amygdala a few OXT-ir cells are present in the dorsal aspect of the Me nucleus. In this latter animal, no sex difference seems to exist concerning the number of OXT-ir cells or the density of the OXT-ir innervation.

SOMATOSTATIN (SOM) In the macaque monkey the Me nucleus has been described as containing one of the most dense plexuses of SOM-ir fibers and terminals distributed throughout all layers of the nucleus, clearly demarcating the limits of the nucleus. The nucleus also contains numerous SOM-ir cells located in both the compact layer II and the more loosely organized layer III. The SOM-ir cells tend to be small, round, and similar in appearance to those located in ACo (Amaral *et al.*, 1989). In the squirrel monkey amygdala, Desjardins and Parent (1992) were able to detect SOM-ir beaded fibers coursing along the lateral side of the optic tract before reaching the Me nucleus, where they also found a very dense SOM-ir plexus. No SOM-ir-labeled cell bodies could be found in this nucleus. They also call attention to the fact that the ventral pallidum and other pallidal structures in this New World monkey are almost entirely devoid of SOM-ir.

SUBSTANCE P (SP) According to Bouras *et al.* (1986), in the human amygdaloid complex few medium-sized SP-ir cells can be seen in its dorsomedial sectors, particularly in the medial nucleus.

VASOPRESSIN (VP) According to Sofroniev *et al.* (1981), in several primate species, including humans, it is possible to trace VP-ir fibers that run laterally over the optic tract from their source in the medial hypothalamus—presumably from VP-ir neurons in the suprachiasmatic nucleus—to the Me nucleus, which appears densely innervated. By contrast, Fliers *et al.* (1986) found few VP-ir fibers and no VP-ir cells in the human Me nucleus. In harmony with this, in the common marmoset monkey, no VP-ir fibers or cells are present in the Me nucleus (Wang *et al.*, 1997).

ENZYMES

ANGIOTENSIN-CONVERTING ENZYME (ACE) Like other members of the superficial amygdala, the Me nucleus shows low labeling levels for this enzyme, sharing this rather negative attribute with the stria terminalis and its bed (Chai *et al.*, 1990). This contrasts markedly with high binding levels shown by every division of the pallidum, a structure with which some authors have proposed the Me should be compared.

BUTYRYLCHOLINESTERASE (BUCHE) The Me nucleus contains a few small to medium-sized triangular BuChE-positive neurons. Processes of some of these cells were also stained. Approximately 5% of the neurons were BuChE-positive and were found predominantly in the medial portion of the nucleus (Darvesh *et al.*, 1998). There was a slightly stained AChE-positive neuropil in this nucleus, with only isolated AChE-positive neurons.

NICOTINAMIDE ADENINE DINUCLEOTIDE PHOSPHATE DIAPHORASE (NADPH-D) Except for the AAA, a dense network of NADPH-d-ir fibers has been reported to be present throughout the remaining amygdaloid nuclei, conjointly with a rather homogeneous distribution of NADPH-d-ir cells. According to Brady *et al.* (1992), the Me nucleus shows a moderate NADPH-d activity in both human and squirrel monkey amygdala. Furthermore, these cells are said to be similar in all subregions, and there is an almost complete overlap between NADPH-d and SOM- or NPY-containing neurons (Unger and Lange, 1992).

P450 AROMATASE (P450 AROM) According to Roselli *et al.* (2001), in the macaque monkey amygdala, the Me nucleus contains a very high density of P450 AROM mRNA-labeled cells. Examination of their illustrations (Fig. 5) would indicate a strong labeling in the rostral amygdala (Fig. 5A), which corresponds to both dorsal and ventral subdivisions of ACo of the present parcellation.

P450 AROM mRNA expression has been found to be extensively distributed throughout the extended amygdala in the primate brain. In particular, P450 AROM mRNA is concentrated in the ventral division (the present MExA) composed of the medial components of BST, the ventral SI (the present SLEAM), and Me, where lower densities of AR-containing cells have been detected. The relative abundance of P450 AROM mRNA compared with ARE mRNA within this circuitry

in nonhuman primates suggests that the aromatization pathway plays a major role in mediating testosterone actions on BST and amygdala neurons. Furthermore, the expression of P450 AROM, ARE, as well as ER mRNA (Österlund *et al.*, 2000) has been reported to be low in the primate amygdala areas related to fear. The highest levels of P450 AROM, were detected in the BM, posteromedial AHi, and posterior Me. Estrogen receptor mRNA was reported to be abundant in all of these regions (Österlund *et al.*, 2000), whereas ARE mRNA expression was found predominantly in the If VCo.

CALCIUM-BINDING PROTEINS

CALBINDIN (CAB) According to Sorvari *et al.* (1996b), like the D ACo nucleus, the Me nucleus shows a high density of CAB-ir neurons in layer 2 and also in layer 3 (Fig. 3). However, layer 1, contained only a few neurons. At the caudal level, lamination of the CAB-ir neurons became less obvious. All three morphological cell types described by these authors are found in the Me nucleus, with the majority of the neurons being of the medium-sized type 2 cells. As in the D ACo nucleus, there were small, lightly stained cells in which only the proximal portions of the dendrites can be followed. The staining of the fibers and neuropil is similar in intensity to that in the D ACo nucleus.

The highest intensity of fibers and neuropil staining occurs in layer 2, followed by layer 3. The intense neuropil staining helped Sorvari *et al.* (1996b) to distinguish the Me nucleus from the neighboring nuclei, such as from the BM and PM AHi. As in the D ACo nucleus, no CAB-ir bundles of fibers can be observed in this nucleus.

CALRETININ (CR) According to Sorvari *et al.* (1996a), the Me nucleus contains considerablely fewer CR-ir cells than the D ACo nucleus. However, as in the D ACo nucleus, these cells are small and darkly staining, displaying all of the features of their type 1 cells with only the proximal part of their dendrites being stained. More lightly stained cells can be found scattered among the very darkly staining neuropil. The CR-ir in the Me nucleus is considerably higher than in the surrounding areas such as the BM nucleus and the PM AHi.

PARVALBUMIN (PAV) The human Me nucleus contains only a few small PAV-ir neurons with no visible dendrites or only short ones. Cells can be found mainly in layers 2 and 3. Furthermore, the density of PAV-ir fibers and terminals is very low, being distributed diffusely in all three layers. No basket-like or cartridges are found here (Sorvari *et al.*, 1995).

OTHER PROTEINS

DOPAMINE- AND ADENOSINE 3′,5′-MONOPHOSPHATE (CAMP)–REGULATED PHOSPHOPROTEIN OF M, 32 KDA (DARPP-32) AND PHOSPHATASE INHIBITOR 1 (I-L) According to Barbas *et al.* (1998), in the macaque monkey, the Me nucleus contains very few lightly stained DARPP-32-ir and I-l-ir neurons.

LIMBIC SYSTEM–ASSOCIATED MEMBRANE PROTEIN (LAMP) According to Côté *et al.* (1996), in the macaque amygdala, the caudal half of the medial amygdaloid nucleus, i.e., the Me nucleus of the present account, is weakly LAMP-ir. This is particularly obvious in the most superficial aspect of the nucleus.

PALLADIN (PALL) In the Me nucleus the pattern of distribution of the Pall-ir puncta is similar to that observed in the striatum (Hwang *et al.*, 2001). Most of the palladin was colocalized (60%), with synaptophysin in puncta distributed throughout the nucleus. It should be stressed that the Pall expression in the globus pallidus is one of the weakest in the forebrain, which contrasts with its very dense concentration in the Me nucleus, where it reaches the same level as that in the striatum. This protein is predominantly present in the excitatory synapses and is consistently present in glutamatergic ones (Hwang *et al.*, 2001).

SEROTONIN TRANSPORTER (SERT) According to Freedman and Shi (2001), in the macaque monkey moderate to heavy amounts of SerT-ir fibers are present in the Me nucleus.

SMI32 NEUROFILAMENT PROTEIN (SMI32-IR) From the low-magnification atlas on the distribution of this protein in the macaque brain published by Petrides *et al.* (2000), it is evident that the Me nucleus is practically devoid of SMI32-ir. This is in marked contrast to the high labeling occurring in the ventral pallidum, a structure with which this Me nucleus has been proposed as equivalent.

RECEPTORS

ADRENERGIC RECEPTORS

ADRENORECEPTOR α_1 According to Flügge *et al.* (1994), in the tree shrew, the medial nucleus show moderate levels of [^{3}H]PRA binding, an α-adrenoreceptor antagonist indicative of the presence of this type of adrenoreceptors.

ADRENORECEPTOR α_2 According to Flügge *et al.* (1994), in the tree shrew, the central nucleus shows a high density of [^{3}H]RAU binding sites, RAU being indicative of the presence of this type of receptor.

BENZODIAZEPINE RECEPTOR (BNZ-R) According to Zezula *et al.* (1988), the Me nucleus contains intermediate levels of BNZ-R.

CHOLINERGIC RECEPTORS

MUSCARINIC RECEPTORS (MACH-R) According to Cortés *et al.* (1987), the human Me nucleus presents one of the lowest concentrations of mACh-R. On the other hand, according to Smiley *et al.* (1999), the amygdala as a whole contains a low density of m_2-ir neurons.

SEROTONINERGIC RECEPTORS (5-HT-R)

5-HT_{1A} RECEPTOR (5-HT_{1A}-R) According to Flügge *et al.* (1994), in the tree shrew, the Me nucleus is faintly labeled by [^{3}H]DPAT, a specific agonist of the 5-HT_{1A}-R.

5-HT_{2C} RECEPTOR ($5HT_{2C}$-R) According to Lopez-Gimenez *et al.* (2001), one of the strongest hybridization signals with probes for the 5-HT_{2C}-R can be found in the basal forebrain of the Me nucleus, one of the components of the extended amygdala. It is interesting to point out that the pallidal grisea show no signal for this receptor.

STEROID RECEPTORS

ANDROGEN RECEPTOR (AR) In contrast with its high density of aromatase-containing neurons, the number of neurons AR mRNA containing neurons is modest (Roselli *et al.*, 2001).

ESTROGENIC RECEPTORS

Estrogen Receptor α (ER-α) According to Österlund *et al.* (1999), both in humans and in monkeys, the Me nucleus displays low ER-α mRNA but still compares well with the lack of this type of hybridization signal in the globus pallidus. It should be pointed out that the medial division of the bed nucleus of the stria terminalis, like the Me nucleus, shows low ER-α mRNA.

Estrogen Receptor β (ER-β) In the rat brain, areas that express the greatest density of ER-β-ir cells include, among others, the Me nucleus. Occasional ER-β/PAV-ir cells could be detected in this nucleus (Blurton-Jones and Tuszinski, 2002).

Anterior Amygdaloid Area (AAA)

Topographical Landmarks [AA in Plates/Figs. 23–27 (1.3–6.7 mm) of Mai *et al.* (1997), *Atlas of the Human Brain*]

According to the ontogenetic and phylogenetic literature so far available with respect to the basal forebrain territory bearing this name in the brains of nonprimate mammals, the AAA of the higher primates would be represented by the ill-defined area located at the cephalic pole of the amygdala, which, according to Crosby and Humphrey (1941), has differentiated into specific nuclear masses. As such, this territory comprises the heterogeneous transitional griseum that at the level of the rostral and rostrodorsal aspects of the amygdala fills the space lying just lateral and caudal to the horizontal limb of the anterior commissure. The griseum stretches caudomedially to the preamygdalar endopiriform nucleus (En) so as to even reach levels close to the exit of the stria terminalis where it is partly replaced by the Ce and the Me amygdaloid nuclei (see Figs. 22.1d, 22.4–22.11). For much of its rostrocaudal extent, it occupies the dorsal lip and superior part of the fundus of the sulcus hemisphericus (endorhinal sulcus), but it also fills the space intervening between the superficial nuclei of the amygdala (ACo and Me), the amygdaloclaustral transition area (ACA), and the medial division of Ce, successively.

Cytoarchitectonics The AAA, as in other mammals, can be divided into superficial (Figs. 22.4–22.7 and 22.10) (ventral) and deep (dorsal) parts or sectors. The superficial AAA is characterized by the presence in its molecular layer of a rich population of glial cells and a well-defined subpial granular layer, as well as the presence, in the inner half of this layer, of a scattered population of small, multiangular neurons. The feature is also found further caudally at the level of the ACo and allows individualization from other superficially lying structures. The cell layer proper shows no stratification and is composed of superficially, mostly lightly stained, spindle-shaped neurons mixed with many fewer large triangular neurons. This latter type of neuron becomes more numerous toward the depth of the AAA where the superficial sector blends gradually with the deep one. Medially and dorsally the AAA becomes continuous with cell corridors of the medial SLEA.

Fibroarchitectonics Apart from stretching for a longer distance than its superficial counterpart, the main characteristic of the deep AAA is the richness of the fiber network present in it, which is formed by a mixture of both fibers of passage and intrinsic axons. Embedded in this dense network lies a morphologically heterogeneous neuronal population in which, again, predominates cells of small and medium size but with a greater presence of bigger and more chromophilic multiangular neurons. However, these latter cells do not share the morphological characteristics of the nearby magnocellular grisea like the basal nucleus of Meynert (BC). All of these typifying features can be better appreciated in nonsuppressive silver-stained sections where the density of the fiber plexus found

in the AAA is not matched by that in any other amygdaloid structure. This observation is confirmed by computer-based semiquantitative densitometric analysis of amygdaloid tissue treated in this manner. Such fiber arrangements, added to the fact that even the biggest neurons in the AAA do not match the size or deep stainability of the neurons composing the so-called preamygdalar endopiriform nucleus (En), or of those making up the ACA, or their greater cell compactness, greatly contribute to differentiating AAA from both of them.

Golgi-Stained Sections At this point it should be stressed that in Golgi studies in the cat brain by Hall (1972) and Kamal and Tömbol (1975), the amygdaloid region that in this mammal shares most of the morphological features that have been applied here for defining the human AAA was found to contain a neuronal pool composed mainly by small or medium-sized projecting neurons displaying ovoid, fusiform, or multiangular perikarya that were provided with three to six richly arborized primary dendrites endowed with a moderate number of dendritic spines, with one of them giving origin to a long projecting axon. In the cat, as in other mammalian species, AAA also contains, but in lesser number, large triangular or multiangular neurons provided with beaded irregular dendritic trees and possessing long projecting axons. According to Kamal and Tömböl, these neurons appeared scattered in the superior half of the AAA. On the basis of their material these authors also described the presence in the cat AAA of fusiform cells typical of what they called the substantia innominata, as well as the existence of small neurons of the Golgi type I resembling those found in La and the so-called cortical amygdala (Hall, 1972). On the other hand, McDonald (1992) working with Golgi impregnated section of rat amygdala, arrived at the conclusion that the medium sized cells in the deep AAA, the substantia innominata (here SLEA), the Me, and the medial subdivision of Ce are similar.

The above description of AAA coincides with that given by Croby and Humphrey (1940), de Olmos (1990), Barbas and de Olmos (1990), Sims and Williams (1990), Benzing *et al.* (1992), Mai *et al.* (1997), and Heimer *et al.* (1999) for the human brain, and with the accounts or mappings of AAA in the monkey brain by Lauer (1945) and by Paxinos *et al.* (2000). Benzing *et al.* (1992), on the other hand, includes as part of AAA the amygdaloid region that here is considered to represent ACo nucleus. Furthermore, there is also a close correspondence of the present account with that reported by Brockhaus (1938) for his area perisupra-amygdalae dorsalis (psAd) and, by the same token, with that of the Koikegamis collaborators (Mikami, 1952a, b; Sasagawa, 1960a, b) on studies done on the brains of humans, chimpanzees, macaques, and New World monkeys. However, it should be pointed out that many of the authors who have described the AAA in humans or in monkeys do not concur with the above definition. While some of them consider that the preamygdalar endopiriform nucleus should be included in or simply homologized with AAA (Gloor, 1997, for humans; J imenez Castellanos, 1949 for the macaque monkey), others confine AAA to a well circumscribed griseum made up of darkly stained neurons that are somewhat smaller and paler than those in the endopiriform nucleus or in the neighboring claustrum [Sorvari *et al.* (1995, 1996) in humans; Amaral and Basset (1989), Amaral *et al.* (1992), and Pitkänen and Amaral (1993) in macaque monkeys]. The mappings and descriptions of their putative anterior amygdaloid area coincide almost entirely with what is here called the ACA (see Heimer *et al.*, 1999 for further details).

Chemoarchitectonics Because of the existing differences in terminology, it is far from clear to which point some of the histochemical and immunohistochemical findings reported by some authors concerning what they define as AAA can be applied to the amygdaloid territory defined here as such. Therefore, they will only be cited to the extent that, through examination of the illustrations presented, they seem to fit the morphological and topographical parameters that guide the present account.

HEAVY METALS/ZINC In Timm Na/selenite–stained section through the squirrel monkey brain, AAA shows homogeneous moderate to weak granular silver deposits that contrast markedly with their virtual absence in the neighboring interstitial nuclei of the horizontal limb of the diagonal band of Broca (HDB) or of the Meynert CB. This staining seems to be continuous with similarly dense silver deposits found along the cell corridors that form medial SLEA. However, it should be stressed that the density of the silver deposits are very weak in comparison with those occurring along the CExA or at both expanded ends (Me and BSTM) of the MexA. The AAA silver deposits probably are representative of terminal boutons belonging to axons coming from more caudally located zinc-rich glutamatergic neuronal somata. Similar observations could also be made in brains of Tamarin monkeys (Heimer *et al.*, 1999).

NEUROTRANSMITTERS

CHOLINERGIC MARKERS

ACETYLCHOLINESTERASE (AChE) According to the present author´ own material, this region is rather

poor in AChE activity, with AAA showing a weaker content of this enzyme than Dp AAA, a result that coincides with those reported by other authors (Svendsen and Bird, 1985; Simms and Williams, 1990; Benzing *et al.*, 1992).Weak AChE activity can be detected in the perikarya of spindle-shaped neurons that are oriented parallel to the brain surface at the level of AAsf, while a stronger reactivity can be seen in some much larger, polymorphic neurons that probably represent ectopic elements of the BC.

CHOLINE ACETYLTRANSFERAE (CHAT) In the human brain the AAA seems to contain only a moderate to low level of ChAT-ir fibers (Emre *et al.*, 1993). ChAT stained a section of the macaque brain (Amaral and Basset, 1989), i.e., an area corresponding approximately to what Barbas and de Olmos (1990) describe as the AAA.

MONOAMINE MARKERS

DOPAMINE-β-HYDROXYLASE (DBH) According to Sadikot and Parent (1990), in the squirrel monkey, the AAA area displays very light and moderate DBH-ir.

SEROTONIN (5-HT) According to Sadikot and Parent (1990), in the squirrel monkey, the AAA area shows a light density of 5-HT-ir terminals.

TYROSINE HYDROXYLASE (TH) According to Sadikot and Parent (1990), in the squirrel monkey, the classical AAA area displays a light density of terminal TH-ir varicosities, with preterminal fibers of passage seen en route to temporal lobe areas rostral and lateral to the amygdala.

INHIBITORY AMINO ACIDS

γ-AMINOBUTYRIC ACID (GABA) According to McDonald and Augustine (1993), in the macaque monkey, the AAA area would contain a subpopulation of GABA-ir neurons that varies in size and shape. Most cells are ovoid and the neuropil exhibits moderate levels of GABA-ir.

NEUROPEPTIDES

CHOLECYSTOKININ (CCK) Heimer *et al.*'s (1999) examination of the immunostained material for the demonstration of CCK shows quite clearly that AAA not only displays a moderate to heavy CCK-ir in its neuropil but also contains a few scattered CCK-ir neurons. At present it is not possible to establish if these neurons only provide for the local CCK innervation or if they also participate in the CCK pathway that courses medially toward the preoptic-hypothalamic region [see Heimer *et al.*'s (1999) Fig. 27A].

CHROMOGRANIN B Although not mentioned by Marksteiner *et al.* (1999), examination of their illustrations (Fig. 3b and c) shows that the human AAA area (not recognized as such in their Fig. 3B) contains moderate PE-11-like ir.

CORTICOTROPIN-RELEASING FACTOR (CRF) In the human amygdaloid complex, a dense accumulation of CRF-ir fibers, with large varicosities, and terminals has been reported in almost all amygdaloid nuclei (Power *et al.*, 1987; Zaphiropoulos *et al.*, 1991).

GALANIN (GAL) According to the mapping of the forebrain distribution of this neuropeptide presented by Kordower *et al.* (1992), in the macaque monkey amygdala, this member of the superficial amygdala, like its other components, does not contain GAL-ir cell bodies but seems to contain at least a small amount GAL-ir fibers.

NEUROTENSIN (NT) NT-immunoreactive cell bodies have been reported to be located in the transition area between the amygdaloid body proper and the supra-amygdaloid region of the human brain, including in this manner the region defined here as AAA. They are randomly scattered throughout the AAA and they are predominantly multipolar in shape although bipolar and unipolar neurons were observed as well. This transition area also contains one of the strongest accumulations of NT-ir fibers and these are continuous with those located in the substriatal claustrum, the lentiform peduncle, and the sublenticular region of the substantia innominata. However, the density of the NT-ir fiber plexus at the level of AAA, though greater than in some of its neighbors (i.e., the endopiriform, basolateral, and lateral nuclei), was less than in the centromedial group ((Mai *et al.*, 1987; Benzing *et al.*, 1992). Material available to me confirms these observations (see Heimer *et al.*, 1999). The AAA contains a light matrix of NT-ir fine-beaded fibers, dot-like puncta, and a small number of NT-ir neurons.

SECRETONEURIN (SECR) As illustrated by Heimer *et al.* (1999) [Figs. 28A] this rostral representative of the SLEAM show in human a strong SECR-ir which is higher in its superficial division. Such ir is a high as in the Me nucleus but lesser than that in the neighbor Ce nucleus. In the Tamarin monkey a similar picture can be appreciated [Fig. 20B, C and D of Heimer *et al.*, 1999].

SOMATOSTATIN (SOM) According to Mufson *et al.* (1988), in the human amygdala, the AAA area contains SOM-ir perikarya. On the basis of the illustrations

(Figs. 2A–F) presented by Amaral *et al.* (1989) on the distribution of SOM-ir in the macaque monkey amygdala, it seems that after the present parcellation is considered to represent the AAA area, containing high amounts of this neuropeptide though in lesser concentration than its neighboring ACo, MeA, and ACA nuclei. On the same basis it seems that the superficial sector of the AAA area contains higher amount of SOM-ir than the deep one this is particularly marked in the more caudal sectors of this amygdaloid undifferentiated area, where SOM-ir radiations seem to have as target the hypothalamic region.

SUBSTANCE P (SP) According Mai *et al.* (1986), SP-ir fibers could be followed along the ventral amygdalofugal pathway, and a band of punctate SP-ir within the sublenticular areas could be followed up to the supra- and periamygdaloid regions, including the AAA.

ENZYMES

ANGIOTENSIN-CONVERTING ENZYME (ACE) According to Chai *et al.* (1990), the AAA area displays low binding levels for this enzyme.

NICOTINAMIDE ADENINE NUCLEOTIDE PHOSPHATE DIAPHORASE (NADPH-D) The human AAA shows no or at most a rather poor NADPH-d immunoreactivity. (Sims and Williams, 1990; Unger and Lange, 1992).

CALCIUM-BINDING PROTEINS

CALRETININ (CR) According to Sorvari *et al.* (1996), mapping of the CR-containing neurons in the human amygdala (see their Figs. 1B, 2B, 3, 4B, and 5), AAA, i.e., the field covered by black points that has been depicted outside the line-encircled amygdaloid nuclei, seems to contain a lower density of this type of cell than its immediate neighbors, the ACo and MeA nuclei, but an equivalent concentration to that depicted for the CeM division of the Ce nucleus. Furthermore, although they did not label the sector they assigned to their version of the AAA area, they claimed that this sector contained a high amount of lightly stained CR-ir cells.

PARVALBUMIN(PAV) In the immunohistochemical maps of PAV-containing neurons built for the human amygdala by Sorvari *et al.* (1995; Figs. 1B, 3B, 5B), as in the case of those reconstructed by Pitkänen and Amaral (1993; Figs. 3A) for the macaque monkey amygdala, it is apparent that the density of the PAV-ir cells in AAA area, as here defined, matches quite closely that found in other two members of the EXA, the MeA nucleus and the CeM division of the Ce nucleus. This subpopulation of GABA-producing inhibitory cells has a rather poor representation in this part of the amygdala. By contrast with this pattern, the PAV-ir neuropil in the AAA area appears to be better developed, particularly in the more rostral aspects of this undifferentiated territory.

NEUROTROPHINS

BRAIN-DERIVED NEUROTROPHIC FACTOR (BDNF) According to Murer *et al.* (1999), in the human brain, all of the amygdaloid nuclei contain BDNF-ir neurons and fibers. However, from their Fig. 4A it is possible to infer that the density of the BDNF-ir is moderate in the AAA area as compared with that of the inferior subdivision of the VCo nucleus or that of the Ce nucleus, whereas it is comparable to that of the ACo nucleus according to the present parcellation of the amygdaloid complex in humans.

OTHER PROTEINS

DOPAMINE- AND ADENOSINE-3,5-MONOPHOSPHATE (CAMP)–REGULATED PHOSPHOPROTEIN OF M, 32 KDA (DARPP-32) AND PHOSPHATASE INHIBITOR 1 (I-L) According to Barbas *et al.* (1998), in the macaque monkey, very few DARP-32-ir or I-1-ir neurons can be found in the AAA area.

LIMBIC SYSTEM–ASSOCIATED MEMBRANE PROTEIN (LAMP) According to Côté *et al.* (1996), in the macaque amygdala, the AAA area is devoid of LAMP-ir.

NEUROFILAMENT PROTEIN SMI32 (SMI32) In the macaque brain, this region does not seem to contain any SMI32-ir (Petrides *et al.*, 2000), going along with what occurs with other members of the MExA.

RECEPTORS

ADRENERGIC RECEPTORS

ADRENORECEPTOR α_1 According to Flügge *et al.* (1994), in the tree shrew, the AAA area shows moderate levels of [^{3}H]PRA binding, an α-adrenoreceptor antagonist indicative of the presence of this type of adrenoreceptor.

ADRENORECEPTOR α_2 According to Flügge *et al.* (1994), in the tree shrew, the AAA area has a low number of [^{3}H]RAU binding sites, RAU being indicative of this type of receptor.

CHOLECYSTOKININ RECEPTOR (CCK-R) According to Kritzer *et al.* (1988), in contrast with the rest of the superficially located amygdaloid grisea, the AAA area of the macaque monkey shows minimal CCK binding.

μ OPIOID RECEPTOR (ORμ) According to Daunais *et al.* (2001), low to moderate concentrations of [^{3}H]DAMGO binding sites could be measured in the AAA area. Furthermore, the distribution of mu-stimulated [^{35}S]GTPγS binding also corresponds to the anatomical distribution of [^{3}H]DAMGO sites in the AAA area.

SEROTONIN RECEPTORS

5-HT$_{1A}$ RECEPTOR (5-HT$_{1A}$-R) According to Flügge *et al.* (1994), in the tree shrew, the ventral part of the AAA area is moderately labeled by [^{3}H]DPAT, a specific agonist of the 5-HT$_{1A}$-R.

STEROID RECEPTORS

ESTROGEN RECEPTOR α (ER-α) According to Österlund *et al.* (2000), in the human and monkey AAA area, no ER-α mRNA hybridization signal can be detected.

Superficial Cortical-like Secondary Olfactory Amygdala

In a detailed review of the rat amygdaloid gray complex, de Olmos *et al.* (1985) pointed out that the most characteristic feature of the "olfactory" nuclear group of the amygdala is that each member receives direct input not only from the mitral cells in the main olfactory bulb but from the whole primary olfactory cortex (including the prepiriform cortex, or eupaleocortex, and anterior olfactory or transitional entorhinal periarchicortex). In addition to the above olfactory projections, the olfactory amygdala receives important input from the interstitial nucleus of the horizontal limb of the diagonal band, a well-established source of cholinergic and GABA-ergic projections, the locus coeruleus (norepinephrine), and the raphe nuclei (serotonin). On the other hand, efferent projections from the olfactory amygdala reach back to the primary olfactory cortex and the fundus striati.

Within the amygdaloid complex itself, the olfactory amygdala, either into or though some of its members, projects heavily to MExA or CExA while it restricts its projections to the most ventral member of the LBNC, the ventral basolateral amygdaloid nucleus, which may be the homolog of the amygdaloclaustral transition area (ACA) of the nonhuman primate amygdala. On these grounds the olfactory amygdala could relay olfactory information to all these gray formations. With this in mind, it should be stressed that although many of the structures listed above may undergo regressive changes during the phylogenetic evolution leading to humans, some others seem to have remained unchanged and still others have even undergone some progression (Andy and Stephan, 1976; Stephan, 1975; Stephan and Andy, 1977; Stephan *et al.*, 1987).

As previously done by Alheid *et al.* (1995) for the rat amygdala, the term "cortical-like" is applied here for heuristic reasons and does not imply a strict equivalence with cortical structures. Even so, this subject is controversial and may need more attention than can be provided here. However, until this subject is fully resolved, what deserves consideration is the fact that, at least in the rat, for most of the "olfactory" superficial amygdaloid nuclei the earliest cells that appear developmentally are in the most superficial layers (Bayer, 1980b). This is in contrast to the prepiriform cortex, and the cortex in general, in which deep layers develop first, with superficial layer developing later (Angevine, 1965; Sidman and Angevine, 1961; Bayer, 1980, 1986). For this reason it has been argued that the "olfactory" amygdaloid nuclei should be considered subcortical zones**.** It is in this context that the term ventral cortical nucleus (VCo) was used by us in previous chapters about the human (de Olmos 1990, Heimer *et al.*, 1999) and macaque monkey (Barbas and de Olmos, 1990) amygdala, i.e., for the amygdaloid superficial structures identified as the "periamygdaloid cortex" in the amygdala of rats, monkeys, and humans by Price and coworkers (Krettek and Price, 1977; Price *et al.*, 1987; Amaral *et al.*, 1989; 1992; Pitkänen and Amaral, 1991-1994; Sorvari *et al.*, 1996–1998). In this context it may have especial meaning, concerning the existence of the so-called nucleus of the lateral olfactory tract in primates. In the rat, a macrosmatic animal in which the existence of such a nucleus is accepted without discussion, the cells in this structure follow a deep to superficial developmental sequence (Bayer, 1980) typical of cortical areas.

In a previous chapter on the human amygdala (de Olmos, 1990), the present writer applied to the human amygdala the same classificatory criterion used for the rat brain (de Olmos *et al.*, 1985). That is to say, the anterior amygdaloid area, the anterior, ventral, and posterior cortical amygdaloid nuclei, together with the amygdalopiriform transition area were grouped together as belonging to the olfactory amygdala. Although a nucleus of the lateral olfactory tract was included as part of that group, its existence as such was firmly questioned. For that reason, and in spite of controversy, in this chapter the cell group identified as such by other authors will be taken into account only when needed and always in the context of the ventral cortical nucleus parcellation. Furthermore, because connectional information derived from non primate mammals would favor the existence intimate hodological relationships between the amygdalohippocampal area on one side and the proper olfactory amygdaloid nuclei, as well as with primary olfactory cortex, on the other, it seems appropiate to incorporate

this superficial transitional cortical-like gray formation to the superficial cortical-like group of nuclei and therefore described in the same section. Furthermore, since histochemical information has become available that reinforces the arguments put against the existence of a so-called 'posterior cortical amygdaloid nucleus' in the caudal part of the superficial amygdala by Heimer and colleagues, and since that evidence suggests its inclusion as part of the amygdalohippocampal transition area, in the section that follows the description of the olfactory amygdaloid nuclei, the above-mentioned cells groups will not be recognized as entities by their own. On the other hand, as it has been already discussed in the section concerned with the medial extended amygdala, there are convincing histochemical, immunohistochemical, morphofunctional, and behavioral data for viewing the anterior amygdaloid area and the medial amygdaloid nucleus as temporal end of the medial extended amygdala. Since there is no clear evidence that both structures receive afferents from the olfactory bulb (for a thorough discussion, see Heimer *et al.*, 1999), these two anatomical entities will be treated together with the other members of this gray continuum.

Anterior Cortical Amygdaloid Nucleus (ACo)

Topographical Landmarks The ACo nucleus (Figs. 22.3–5, 22.6a, 22.7a, and 22.8) is located in the rostral half of the amygdala bordering the piriform cortex (Pir) rostrally, the Me nucleus caudally, and the superior subdivision of the VCo nucleus ventrally, from which it is separated by a superficial extension of the icm. In so doing, it extends rostrocaudally from the level of the APir claustrocortex and of the insular and temporal divisions of the piriform cortex, to a transverse plane passing through the rostral pole of the dorsolateral large-celled division of the BL nucleus and the rostral-most tip of the inferior horn of the lateral ventricle, at which level it is replaced by MeA nucleus. Throughout its extent ACo lies in the immediate vicinity of the fundus and the lower lip of the sulcus hemisphericus, being bound by the ventral cortical nucleus (VCo) ventromedially, by the BM nucleus ventrolaterally, from which is separated by the medial medullary lamina and by the AAA laterally and dorsally. When compared with other divisions of the olfactory amygdala, the ACo nucleus stands apart by displaying a sharp widening of the cell-poor layer that separates it from the brain surface and which can be considered a molecular layer (L1). Such widening starts at the border with Me caudally and attains its peak at the border zone with the piriform allocortex and particularly at the bottom of the sulcus hemisphericus. As in the superficial division of the AAA, it is characteristically bound at the outer border of the molecular layer by a prominent granular subpial layer and shows a richer glial cell population than the more caudal and ventral superficial amygdaloid nuclei.

Cytoarchitectonics On topographical and cytoarchitectonic grounds, the ACo nucleus can be divided into dorsal and ventral parts. The dorsal division of the anterior cortical nucleus (D ACo) occupies the fundus of the sulcus hemisphericus and therefore shows a wide molecular layer (L1) that also contains the rich glial cell population and a sharply marked subpial granular layer (described above). It is made up of small, lightly staining, loosely arranged neurons, among which predominate those of fusiform shape, whereas the less numerous pyramid-like neurons are slightly larger and more darkly staining. In the D ACo division the superficial and deep neurons practically form a gray continuum without any distinct boundary among them, constituting, in consequence, a homogeneous field.

The ventral division of the anterior cortical nucleus (V ACo) occupies that part of the lower lip of the sulcus hemisphericus that stretches from the dorsolateral border of the VCo nucleus to the beginning of the fundus of this sulcus. 1t appears caudally to the D ACo nucleus behind the lateral subdivision of the AL APir from which it is separated by a cell-poor zone [Brockhaus' (1938) 1" bundle] and stretches just beyond the boundary between the D ACo nucleus and the anterior division of the Me nucleus. Fibers detached from Brockhaus' (1938) intermediate caudomedial fiber masses (icm) surround the nucleus ventrally and medially. Those medially located form a relatively loose fiber septum that separates the V ACo nucleus from its ventromedially adjacent neighbor, the superior subdivision of the R VCo nucleus. Like its dorsal counterpart, the V ACo division possesses a well-defined subpial granular (glial) layer, but this and its L1 are substantially less wide than in the dorsal subdivision.

In Nissl preparations, the V ACo division appears more structured than its dorsal counterpart and presents a more clearly defined stratification. Within its molecular layer, small invading neurons, such as those seen in the D ACo division, are still present though in a more scattered fashion. This is in sharp contrast with the total absence of such cells in the neighboring VCo nucleus. Its superficial cell layer is made up of more loosely packed and darkly staining neurons than those in the D ACo division and tend to become clustered. Although these neurons present a variety of body shapes, they are slender and more

angular than those in the dorsal ACo nucleus but less so than in the adjacent VCo nucleus. The deep cell layer is made up of larger, more loosely arranged, predominantly pyramidal-shaped neurons showing a tendency to form scattered, loosely packed clusters.

Fibroarchitectonics In Weigert preparations, the D ACo division can easily be differentiated from its ventral counterpart by the presence of much denser plexuses of mostly transversely coursing fibers that are quite homogeneously distributed throughout this subdivision, although they are somewhat richer within its molecular (L1) and deep cell (L2–3) layers. However, the greatest difference occurs with respect to the fiber content in the superficial cell layer where the fiber plexuses in the V ACo division are far less dense than in its dorsal counterpart, and are composed of mostly randomly oriented fibers.

As here described and mapped, the ACo nucleus corresponds to the anterior portion of Crosby and Humphrey's (1940) medial nucleus, to Brockhaus' (1938) area perisupra-amygdalae intermedialis and ventralis, Stephan's (1975) area medialis as a division of this subregion periamygdalaris anteromedialis, the dorsal cortical nucleus of Gloor (1997), and the anterior part of the V ACo division plus the superficial part of AAAS in Plates/Figs. 46–48 (interaural 20.10–19.20 mm) of Paxinos *et al.* (2000) *The Rhesus Monkey Brain in Stereotaxic Coordinates*]. When comparing the present parcellation of the human cortical nucleus with that of the macaque monkey proposed by Price *et al.* (1987), Amaral and Basset (1989), and Amaral *et al.* (1989), it is clear that the former authors when describing the ACo nucleus did not differentiate it from the rest of the ventral subdivision that appears in the Paxinos *et al.* (2000) atlas of the rhesus monkey (Plate/Fig. 46), even if in Fig. 4 of Amaral and Basset's paper it is possible to appreciate the occurrence of a clear bending in the surface of the ACo nucleus that takes place a little before the border with the so-called nucleus of the lateral olfactory. Furthermore, in my estimation, the so-called 'nucleus of the lateral olfactory tract' (NLOT), according to Sorvary *et al.* (1996a, b), seems to involve both the ventral division of the ACo nucleus and the rostral intermediate and superior subdivisions of the VCo nucleus of the human amygdala, whereas in the monkey the representative of this nucleus (Pitkänen and Amaral, 1993a,b) seems to be confined to what Barbas and de Olmos (1990) termed the superior subdivision of the VCo nucleus. It is interesting that Price (1990) and Price *et al.* (1987) confine the extension of this nucleus in both human and monkey brain to a very small group of densely packed, darkly staining cells that lie in the interface between the ventral division of the ACo nucleus and the superior subdivision of the VCo nucleus. I have been able to detect this group of cells in my human and macaque monkey preparations, but I do not assign the homology with the NLOT of macrosmatic mammals.

Chemoarchitectonics

Heavy Metals In Timm-Danscher-stained sections from Old (macaque) and New World (squirrel, marmoset) monkeys, the ACo nucleus, together with the Me nucleus and the AAA area, shows low to moderate metal content as compared with other amygdaloid nuclei.

Neurotransmitters

CHOLINERGIC MARKERS The ACo has the very lowest levels of cholinergic markers in the amygdala, which helps to distinguish it from rostrally located piriform cortex that has moderate levels of AChE and ChAT staining (Amaral *et al.*, 1992).

ACETYLCHOLINESTERASE (AChE) In AChE sections from human brains, the ACo appears poorly stained, although a closer examination reveals a slightly higher activity than in the MeA nucleus.

According to Amaral and Basset (1989), in the macaque monkey, the ACo nucleus, like the MeA nucleus, can be distinguished by the extremely low level of AChE-positive fibers and terminals but, by contrast, contains a large number of AChE-positive neurons.

CHOLINE ACETYLTRANSFERASE (CHAT) Emre *et al.* (1993), in their description of the distribution of ChAT-ir in the human amygdala, do not mention the existence of an anterior cortical nucleus. Rather, they seem to include within the boundaries of their putative medial amygdaloid nucleus the present ACo nucleus. Therefore, this latter appears to share the low ChAT-ir displayed by the rest of the MeA nucleus. In comparing this with that described by Amaral and Basset (1989) in the macaque monkey, it is evident that in this non-human primate the ACo nucleus, like the MeA nucleus, displays an extremely low level of ChAT-ir fibers and terminals, although the level is somewhat higher than in the latter.

EXCITATORY AMINO ACIDS

GLUTAMATE (GLU) Retrograde tracing experiments in rats using tritiated D-aspartate indicate that a number of the ACo neurons would be a source of GLU/ASPergic projections to both the laterocaudal ventral striatum (IPAC) and the ventral pallidum (Fuller *et al.*, 1987).

INHIBITORY AMINO ACIDS

γ-AMINOBUTYRIC ACID (GABA) Although McDonald and Augustine (1993) reported that the ACo nucleus has a GABA-ir equivalent to that in the centromedial amygdaloid nuclei, their illustration in Fig. 1 seems to correspond rather to the more rostral portions of the MeA nucleus. By contrast, Pitkänen and Amaral (1994) have found that their ACo nucleus has one of the lowest densities of GABA-ir cells in the amygdala, most of them being of type 1 and located in L2 and L3. They are ovoid or spherical without visible processes. The density of GAD mRNA-labeled cells is one of the highest in the amygdala and consequently clearly higher than that of the GABA-ir cells. The density of the GABA-ir neuropil is quite high, and many of the GABA-ir fibers and varicosities in L2 formed basket-like plexuses around non-ir somata.

NEUROPEPTIDES

CHROMOGRANIN B Although Marksteiner *et al.* (1999) did not recognize this nucleus in their account of the distribution of this neuropeptide, a close examination of their illustrations (Fig. 3) indicates that they had included ACo as a part of their medial amygdaloid nucleus. If this observation is applied, then ACo will contain a moderate amount of PE-11-like ir.

CORTICOTROPIN-RELEASING FACTOR (CRF) According to Basset *et al.* (1992), in the macaque monkey, the density of CRF-ir fibers in the superficial and the so-called cortical regions of the amygdala seems to be light to moderate in relation to that observable in the Ce and La amygdaloid nuclei. The highest density of this type of fibers is seen in the MeA and ACo nuclei, with those in L1a showing the same appearance than in the molecular layer of the piriform cortex, i.e., darkly CRP-ir fibers on a more uniform background. Deeper in these nuclei the density of the CRF fibers decreases and a few CRF-ir small cell bodies with their dendritic processes can be seen.

NEUROPEPTIDE Y (NPY) In their mapping of the distribution of NPY in the human telencephalon, Walter *et al.* (1990) do not mention this nucleus. However, since they depict the Me nucleus as including within it the present ACo nucleus it can be inferred that it is devoid of NPY-ir fibers or cells. On the other hand, these authors stated that "labeled cells and fibers were more numerous in the nuclei amygdalae profundi of Brockhaus or the basolateral group in contrast with the nuclei corticali, medialis and centralis"—a comparison that implies the presence, though scarce, of this neuropeptide in some neurons of the superficially located nuclei.

In complete contrast with this picture, according to McDonald *et al.* (1995), in the macaque monkey, their ACo nucleus (probably equivalent to the dorsal division of the human ACo) is one of the amygdaloid nuclei showing the highest number of NPY-ir neurons. Although some NPY-ir neurons are found in L1, the vast majority are located in the deeper cellular layers. The perikarya and dendritic morphology of the NPY-ir neurons is essentially identical to that of the spine-sparse class seen in the LBNC. Furthermore, these peptidergic neurons are roughly the same size as the non-NPY-ir cells that form its pool of principal neurons.

The NPY-ir neurons in L1 possess dendrites that are oriented parallel to the pial surface, whereas many of the peptidergic neurons in the deep layers have their dendrites oriented to the pial surface.

NEUROTENSIN (NT) According to Benzing *et al.* (1992) mapping of the human amygdala, the ACo nucleus would be included within what these authors consider to be the human AAA area. According to such criterion, the ACo nucleus would share with the AAA area the type of NT-ir distribution pattern. Consequently, the NT-ir in the ACo nucleus would be prominent enough to differentiate it from neighboring nuclei, such as the endopiriform nucleus, and the BM and BL nuclei, but less dense than that in the temporal representatives of the MExA, the MeA and Ce nuclei. This NT-ir is represented mostly by a light matrix of fine-beaded NTR-ir fibers, dot-like puncta, and a small number of NT-ir multipolar perikarya that are randomly scattered throughout the nucleus.

SOMATOSTATIN (SOM) In the macaque monkey, this amygdaloid nucleus shows the highest number of SOM-ir neurons (McDonald *et al.*, 1995). When the ACo emerges from the caudal end of the piriform cortex, the density of SOM-ir fibers and terminals decreases slightly and preferentially involves L1. By contrast, the number of SOM-ir neurons increases, and they appear to be distributed more diffusely throughout all layers of ACo (Amaral *et al.*, 1989).

In the sector of the monkey V ACo that the above-mentioned authors have labeled as the NOLT there is no prominent SOM-ir and, much like the adjacent rostral APir, SOM-ir fibers are seen in L1 of this formation. Numerous SOM-ir neurons can be observed deep to this subdivision of the ACo nucleus (Amaral *et al.*, 1989).

VASOPRESSIN (VP) According to Caffé *et al.* (1989), in the macaque monkey, dense accumulations of VP-ir fibers are found in the cortical nucleus, which,

according to the present amygdaloid parcellation, includes among others the ACo nucleus.

Neurotrophins

Brain-derived neurotrophic factor (BDNF) According to Murer *et al.* (1999), in the human brain all of the amygdaloid nuclei contain BDNF-ir neurons and fibers. However, from their Fig. 4A it is possible to infer that the density of the BDNF-ir in the ACo nucleus is moderate in comparison with that of the inferior subdivision of the VCo nucleus or that of the Ce nucleus, while it is comparable to that of the AAA according to the present parcellation of the amygdaloid complex in humans.

Calcium-Binding Proteins

Calbindin (CAB) According to Sorvari *et al.* (1996b), there are virtually no CAB-ir neurons in layer 1 of their ACo nucleus, which corresponds to the present D ACo division. However, L2 contains a high density of CAB-ir neurons. In L3, the neuronal density is slightly lower than in L2. In L2 and L3, the cells are mostly medium sized or small type 2 cells with short dendrites. A few type 3 and type 1 cells can also be observed. In addition, there are numerous lightly stained small neurons that resembled type 1 and type 2 cells. Because of the intense neuropil labeling, the dendritic morphology of these neurons cannot be determined with certainty.

The above-mentioned authors consider L1 in the sector of the present V ACo division to represent the nucleus of the lateral olfactory tract; it contains a low density of CAB-ir neurons. L2 and L3 contain moderate densities of neurons. In layer 2, the small, darkly stained type 1 and 2 CAB-ir neurons form clusters corresponding to the cellular clusters in cell preparations. In L3, the density of diffusely scattered CAB-ir neurons is high. Characteristic of the CAB-ir neurons in this division would be their variable morphology, which ranged from small, darkly stained type 1 cells to large, lightly stained type 2 and 3 cells.

L2 contained the highest intensity of CAB-ir fibers. In L3, the intensity of CAB-ir is said to be lower than in L2, and L1 contains only a few CAB-ir fibers oriented perpendicular to the pial surface. While the CAB-ir of the neuropil is high in all three layers, it is highest in L2. A low density of CAB-ir fiber bundles can be observed in L2 and L3.

Calretinin (CR) According to Sorvari *et al.* (1996a), the density of CR-ir neurons in their ACo nucleus, here the D ACo division, is one of the highest in the human amygdala, with these neurons being mostly small and lightly staining and corresponding to their types 1 and 3 cells with only the proximal part of their dendrites being stained. The CR-ir cells are densely packed in L2 and L3, whereas L1 contains only a few neurons. The neuropil density in this division of the ACo nucleus is similar to that of the MeA nucleus reaching such high levels that it is not possible to distinguish individual fibers and terminals.

On the other hand, the cell aggregates they consider to be the human representative of the nucleus of the lateral olfactory tract of lower mammals that here is included as a part of the V ACo division, is said to contain a large number of small type 1 and some type 3 CR-ir neurons. The density of the CR-ir cells is higher in those places where there are higher concentrations of cells (L2) while they are more diffusely scattered in those with lesser aggregations. In contrast with what happens in the D ACo division, the density of CR-ir fibers and terminals is moderate but staining is as intense as in the MeA nucleus.

Parvalbumin (PAV) According to Sorvari *et al.* (1995), the very few PAV-ir cells that can be detected in their ACo nucleus, here the D ACo division, are small type 1 and 2 neurons with short dendritic processes located mainly in layers 1 and 2. The density of PAV-ir fibers is also very low with total absence of basket-like terminal plexuses or cartridges. On the other hand, their so-called nucleus of the lateral olfactory tract, which here is included as part of ACo or, better, its ventral division (V ACo), is described as containing a moderate number of type 2 and some type 1 PAV-ir cells. The location of most of these corresponds to cell clusters and columns in layers 2 and 3. The distribution of PAV-ir fibers and terminals also corresponds to the location of neuronal clusters in L2, while in L1 the fibers run perpendicularly to the pial surface and in L3 the PAV-ir fibers are diffusely scattered.

Other Proteins

Dopamine- and adenosine-3′,5′-monophosphate (cAMP)–Regulated Phosphoprotein of M, 32 kDa (DARPP-32) and Phosphatase Inhibitor 1 (I-1) Since the sector corresponding to the ACo nucleus in the macaque amygdala has been included by Barbas *et al.* (1998) within what they define as the medial amygdaloid nucleus, one should conclude, by taking into account their mapping of the distribution of this protein and their photomicrographs (e.g., Fig. 3A), that the presence of this protein here is negligible as in the Me nucleus itself.

Limbic System–Associated Membrane Protein (LAMP) According to Côté *et al.* (1996), in the macaque amygdala, the anterior half of their medial

amygdaloid nucleus and their ACo nucleus as well as their nucleus of the lateral olfactory tract, i.e., the two formerly cited entities representing together the main dorsal divisions of the ACo nucleus of the present account, and the remaining one the ventral division of the present ACo nucleus, all of them, are totally devoid of LAMP-ir.

SMI32 NEUROFILAMENT PROTEIN (SMI32-IR) From the low magnification atlas on the distribution of this protein in the macaque brain published by Petrides *et al.* (2000), that part of their Me nucleus (fig.27, section 567) that includes the ACo nucleus according to Price *et al.* (1987) is negatively stained for this protein.

RECEPTORS

ESTROGEN RECEPTOR α (ER-α) According to Österlund *et al.* (2000), the human ACo nucleus shows low signals of ER-α mRNA.

NEUROKININ-1 RECEPTOR (NK-1R) According to Mileusnic *et al.* (1999), in the human amygdala, the density of NK-ir shows the highest expression at the level of ACo nucleus and in the AHi area, but no mention is made of other superficial amygdaloid nuclei.

Ventral Cortical Amygdaloid Nucleus (VCo) and Nucleus of the Lateral Olfactory Tract (LOT)

Topographical Landmarks The VCo nucleus [ACoV plus part of PCo in Plates 24 to 28 (2.7–9.3 mm) in Mai *et al.* (1997), *Atlas of the Human Brain*; BAOT plus VCo in Plates/Figs. 46–57 (interaural 20.10–15.15 nn) in Paxinos *et al.* (2000), *The Rhesus Monkey Brain in Stereotaxic Coordinates*], i.e., the periamygdaloid cortex, PAC, of some authors (see below), constitutes the main component of the superficial amygdala (Figs. 22.1c,d; 22.3–22.6a; 22.7a–22.11; 22.22c). This heterogeneous group occupies most of the semilunar gyrus (SEL) and, in clear contrast with other components of the superficial group that lie rostrally and dorsally to it (the ACo nucleus and the AAA area), its superficial pyramidal cell layer appears clearly separated from the brain surface by a relatively cell-free molecular layer of varying wideness. This molecular layer is rich in transversally oriented fibers running parallel to the brain surface as can be easily appreciated in non-suppressive silver-stained sections.

Cytoarchitectonics and Fibroarchitectonics On the basis of cyto- and fibroarchitectonic criteria, it is possible to divide VCo into two major divisions, **rostral (RVCo)** and **caudal (CVCo)**, the latter being the larger of the two. Either division is, in turn, susceptible to further division into superior, intermediate, and inferior subnuclei, the laterodorsally located ones being less extensive and narrower than those forming the upper wall and the lip of the amygdaloid fissure and the adjacent convexity of the semilunar gyrus medioventrally.

All of these divisions have been basically visualized at least in part by different authors (see below), and they can be clearly seen in frozen sections under darkfield illumination or by projecting them onto a panatomic photographic paper with a photographic enlarger. These renditions are possible on account of the existence of heavily myelinated fiber systems forming septa between each of the subdivisions of the VCo nucleus mentioned above and by building fiber plexuses of different density that provide diverse degrees of transparency. This occurs particularly at the level of the inferior divisions, both caudal and rostral, of the VCo nucleus (Fig. 22.7b), differentiating them in their whole extent from the intermediate ones dorsally and from the dorsolateral and medioventral subdivisions of the posteromedial APir area. Such parcellation can also be detected in Nissl preparations and in neurofibrillar silver- or Weigert-stained sections appropriately oriented.

Irrespective of the type of staining procedure used, the two major divisions of the VCo nucleus, rostral and caudal, can be differentiated by some simple morphological features. These include the thinness of the dorsolateral sectors of the rostral VCo division, which, together with a gradual thickening in a ventromedial direction, provides this sector an inverted comma-like shape in transverse sections. These features contrast markedly with the rather abrupt thickening of every subdivision of the caudal VCo, imparting to the whole caudal VCo division a semioval shape. Furthermore, Nissl preparations reveal a much more organized arrangement of the neuronal elements in the caudal than in the rostral division. This increased organization has prompted some investigators to define this region as cortical, a definition that is inconsistent with ontogenetic data (Bayer, 1980). The rostral and caudal VCo exhibit some common cytoarchitectonic characteristics. For example, they have a relatively narrow but well-delineated superficial cell layer, followed by a deeper one less clearly delineated, particularly at its deepest boundary. The presence of cell islands (here called intramedullary grisea, IMG) (Figs. 22.4 and 22.7b), which are intercalated between the VCo nucleus and the deep amygdaloid nuclei, provides guidance concerning the point of separation.

Other morphological features shared by the two main divisions of the VCo nucleus are: (l) a relatively

narrow molecular layer overlaid by a rather thin granular subpial layer; (2) loosely arranged neurons in the superficial cell layer showing typical features, such as slenderness, pyramidal or spindle shape, and long, thin dendritic processes resembling the fork-shaped cells in the piriform cortex; and (3) the fact that the continuity of the deep cell layer is interrupted by cell-poor, wedge-like, elongated, narrow spaces.

In fiber preparations these spaces are occupied by fiber septa irradiating from the deeper dorsolateral to ventromedial fiber capsule that constitutes the medial medullary lamellae (Fig. 22.7b). On occasion, these fiber septa are accompanied by neurons that seem to be related to the intramedullary griseum system (IMG) rather than the VCo nucleus.

However, the rostral and caudal subdivisions of the VCo nucleus present several cyto- and fibroarchiteconic features which allow their distinction from each other as it will be appreciated from the following account.

As mentioned before, the **rostral VCo division** (RVCo in 22.3 and 22.4) con be is less clearly stratified than its caudal counterpart and like this latter it can be divided into superior, intermediate and inferior parts.

The **superior rostral VCo** (Sp RVCo in Figs. 22.3 and 22.4) abuts rostrally and laterally with the lateral subdivision of the anterolateral APir area and, more caudally, the ventral ACo nucleus, from both of which it is separated by a wide, superficially located cell gap. It is the thinnest of all of the VCo subdivisions, constituting the tail of the inverted comma-like rostral VCo divisions. In spite of this, the superficial cellular layer features a thin additional sublayer (L2′) made up of darkly staining, scattered, pyramidal and spindle-shaped neurons. The main axes of these neurons are oriented parallel to the brain surface. This accessory superficial cell layer, which is separated from L2 by a cell-free narrow interval, appears to be continuous, with a band of cells showing the same general features but located in a thin band perpendicular and medially adjacent to the cell gap mentioned above. Whether this group is the putative "nucleus of the lateral olfactory tract" of some authors could not be established with certainty. The main superficial cell layer of rostral VCo division is made up instead of lighter staining neurons, with their apical dendrites directed perpendicular to the brain surface. The deeper cellular layer (L3) lies separated from L2 by an ill-defined narrow space with few cells. Neurons here are somewhat smaller than those at the center of L3 but also made up of large, isolated polymorphic cells. Immediately deep to L3 lies a cell-free area corresponding to the intermediate caudomedial fiber system (icm) coursing between the superior rostral VCo subdivision and the large-celled dorsomedial division of the BM nucleus.

In fiber preparations the molecular layer (Ll) of the former, particularly near its rostral end, is rather wide compared with that of its more ventrally located counterpart, the intermediate rostral VCo subdivision. The superior rostral VCo subdivision is filled with tangentially running fibers whose richness diminishes toward this subdivision. The cell layers appear to be poorer in fiber content but more so L2. The **intermediate subdivision** of the rostral VCo nucleus (It RVCo in Figs. 22.3, 22.4, and 22.9) presents a superficial cell layer made up of more chaotically arranged pyramidal cells, although it blends without any transition with L2 in the superior rostral VCo nucleus. This layer in the intermediate rostral VCo subdivision widens gradually in a ventromedial direction to stop just beside L2 in the inferior rostral VCo subdivision. The superficial line of the latter lies more deeply than that of the superficial cellular layer in the intermediate rostral VCo subdivision. As a result, the molecular layer in the inferior rostral VCo subfield is wider than in any other VCo subfields, except its counterpart in the inferior caudal VCo subdivision. As in the more dorsally located superior subdivision of the rostral VCo nucleus, the deep cellular layer in the intermediate rostral VCo subarea is rather poorly celled, but not as much as in the former subnucleus. Cell islands deep to the intermediate subdivision are a feature that helps to identify this portion of the VCo nucleus.

These cell islands are made up of darker staining, more densely packed neurons whose main cell axes are oriented in the same direction as the fiber systems that surround them. This can be seen in fiber preparations but is also suggested by the myelin density pattern in unstained sections. These are most probably intramedullary grisea (IMG) which tend to be located around the ventromedial aspects of the neighboring BM nucleus (Figs. 22.5a and 22.6a).

In fiber preparations the molecular layer of the intermediate rostral VCo subdivision is less rich in fibers than the superior and inferior rostral VCo subdivisions between which it is interspersed. As is the case in these two subdivisions, L2 is poorer in fibers. In contrast, the deep cell layer (L3) is characterized by the presence of numerous obliquely coursing fibers that contribute to the buildup of a moderately rich fiber plexus. Many of the small bundles constituting these obliquely oriented fibers appear to be deflected from their ventrally directed course by the IMG (Fig. 22.7b).

Compared with the two dorsally located subdivisions, the **inferior division** of the rostral VCo nucleus (If RVCo in Figs. 22.3, 22.4, and 22.9) is characterized by wider L1 and L2 layers. The former is practically cell free and the latter is made up of slender, pyramidal neurons rather loosely but regularly arranged with

their apical dendrites, oriented perpendicular to the brain surface. The superficial cellular layer blends without transition into the deep cellular layer, from which it can be barely separated, although closer observation reveals that its neuronal population is of smaller size and less slender contours than those in the deep layer. These architectonic characteristics allow easy differentiation of the inferior rostral VCo subdivision from its immediate dorsal and ventral neighbors, the intermediate rostral VCo subdivision and the APir transition area, and from the IMG which at this level occupy a wedge between the BM and the small-celled ventromedial BL nucleus.

In fiber preparations the molecular layer of the inferior rostral VCo subdivision regains the richness of fibers seen in the superior rostral VCo subdivision. These are similarly oriented tangentially and cover the whole width of the layer. Here, however, the fibers show some stratification, with a dense fiber peripheral sublayer, an intermediate wider sublayer with few fibers, and another deeper one again densely fibrous. The superficial cellular sublayer is not well endowed in fibers. Radially oriented fibers are observed here, although they are not as dense as the similarly oriented plexus in the deeper cell layer (L3). This arrangement of the fiber component in the inferior rostral VCo facilitates its differentiation not only from its intermediate counterpart but more particularly from the AP-ir transitional area with which some authors have grouped it.

The **caudal VCo division** (CVCo in Figs. 22.5a, 22.6a, 22.7a, and 22.11) presents a more cortex-like arrangement of its cells and fibers than the rostral VCo division, which is particularly appreciable in its **superior subdivision** (Figs. 22.5a–22.6a, 22.7a–22.11). This latter part of the caudal VCo division lies intercalated between the superior rostral VCo subdivision rostrally and the AHi transition area caudally, and is separated dorsally from the ventral Me nucleus by a rather narrow fiber septum. Beneath an inconspicuous molecular layer the caudal VCo division shows a relatively wide superficial cell layer that appears to be much more organized than its counterpart in the rostral superior subnucleus of the VCo nucleus. As in the latter, the superior caudal VCo subdivision possesses an accessory superficial cellular sublayer, but in preparations examined personally this is less clearly defined. The main superficial layer is wider and denser than the equivalent layer in the superior rostral VCo subdivision and contains many fork-like cells oriented perpendicular to the brain surface. On the other hand, the far more well-developed deep cellular layer appears to be composed of somewhat smaller cells showing no particular orientation.

In fiber preparations the molecular layer is occupied by fibers coursing parallel to the brain surface all of its width, showing few signs of substratification. In neurofibrillar preparations many randomly oriented fibers form a still not well-differentiated network that appears to overlap the accessory superficial cellular layer. This network diminishes sharply in density at the level of the main cellular layer and becomes almost entirely made up of randomly oriented fibers at level L3. However, these are however, still denser than in the superficial layer (L2).

The **intermediate subdivision** of the caudal VCo division (Figs. 22.5–22.6a, 22.7a–22.11) has a molecular layer that becomes gradually wider as one moves away from the superior caudal VCo subdivision. The superficial cell layer appears to be more densely populated by darkly staining pyramid-like neurons although they are still more loosely arranged in a more disorderly way than in the more ventrally located inferior caudal VCo subdivision. Because of this it is difficult to recognize an accessory superficial cellular layer. Between the main (L2) and the deep (L3) cellular layer is a rarefication of the cell population, a zone that is at times occupied by larger, more deeply staining angular neurons. The deep layer, in turn, is made up of medium-sized, moderately staining neurons with no particular orientation, but which appear to be more densely arranged and smaller than their counterparts in the superior caudal VCo subdivision.

In fiber preparations the intermediate caudal VCo subdivision appears to be separated from the superior caudal VCo subdivision by a rather dense fiber septum. The fiber plexus at the level of the secondary superficial layer is better differentiated than its dorsal neighbor but still does not reach the density observed in the inferior caudal VCo subdivision. In the gap between the superficial and deep cellular layers, the fiber plexus is less dense but richer than in the deep layer, both layers being randomly arranged. However. a sharp increase in density takes place at the very border with the medial medullary lamina.

In the **inferior subdivision** of the caudal VCo (Figs. 22.5a, 22.6a, 22.7a–22.11), an increase in the width of its molecular layer causes further sinking of its superficial layer. This rarefication of its deep cell layer contributes to a sharper border with the intermediate caudal VCo subdivision. The inferior subdivision of the caudal VCo division is further characterized by a more homogeneous pattern in the cell layers, with the majority of cells oriented perpendicular to the surface. Accompanying its expansion one may observe in fiber preparations a clearer substratification of the molecular layer. This is readily subdivisible into a richly fibered outer sublayer (L la) and a poorly fibered inner one

(L lb). The fiber plexus at the superficial cellular layer, on the other hand, becomes even richer than in more rostral levels away from the superior caudal VCo subdivision. The superficial cell layer appears to be more densely populated by darkly staining pyramid-like neurons although they are still more loosely arranged in a more disorderly way than in the more ventrally located inferior caudal VCo subdivision. Because of this it is difficult to recognize an accessory superficial cellular layer. Between the main (L2) and the deep (L3) cellular layer is a rarefication of the cell population, a zone that is sometimes occupied by larger, more deeply staining angular neurons. The deep layer, in turn, is made up of medium-sized, moderately staining neurons with no particular orientation, but which appear to be more densely arranged and smaller than their counterparts in the superior caudal VCo subdivision.

As here described, the VCo corresponds to the cortical amygdaloid nucleus of Crosby and Humphrey (1940) and Humphrey (1968, 1972), the latter author having recognized in the human embryo medial (If VCo), intermediate (It VCo), and lateral (Sp VCo) subdivisions. The superior subdivisions of the rostral and caudal VCo correspond approximately to Hilpert's (1928) fields pa4 and 2, respectively; while the intermediate subdivisions of the rostral and caudal VCo correspond to the his fields pa3 and pa1, respectively. Finally, Hilperts's field 2 seems to correspond to both rostral and caudal parts of the inferior subdivisions of the VCo. On the other hand, the superior and intermediate subdivisions of the VCo nucleus correspond approximately to Brockhaus' (1938) periamygdaleum oralis dorsalis and amygdaleum superficialis dorsalis pars oralis and intermedium. The latter designation indicates the deep cell layers of the VCo. He further subdivided the periamygdaleum oralis into oral and caudal parts that are represented by the superficial layers of the rostral and caudal divisions of the VCo, respectively, of the present terminology. In the same line, this author subdivided his amygdaleum superficialis dorsalis into oral, intermediate, and caudal parts, where the oral and intermediate parts correspond to the deep cellular layers of the superior and intermediate subdivisions of the rostral and caudal VCo, respectively. The superficial layers of the inferior subdivisions of the rostral and caudal VCo correspond to Brockhaus' periamygdaleum oralis ventralis, while the deep layers of the VCo correspond to amygdaleum superficialis (pars oralis ventralis and pars intermedium ventralis medialis). All of these different terminologies and subdivisions proposed by the classical authors, reflect the complexity of this superficially located amygdaloid nucleus, complexity that seems to have defeated attempts to simplify it on the basis of cytoarchitectonic criteria alone. However, the situation has not changed much in the present time because modern authors who have depended on sophisticated immunohistochemical procedures have changed the parcellations which they themselves had used previously.

Chemoarchitectonics

Heavy Metals In Timm-Danscher-stained sections of macaque, squirrel, and marmoset brains, the entire VCo nucleus appears moderately to heavily stained. The silver granular deposits vary in decreasing order from maximal activity in the deepest layer to lowest activity in the superficial cell layer. The molecular layer appears to be homogeneously stained except at the level of the inferior subdivision of the caudal VCo nucleus, where a semilunar subpial blank area can be detected (Alheid and J.S. de Olmos, unpublished observations). This latter property allows a clear differentiation from the posteromedial division of the AHi area, which does not show this subpial negatively stained band that most probably corresponds to the place of termination of olfactory pathways coming from the main olfactory bulb or from other olfactory-related cortical and subcortical grisea.

It should be pointed out that iontophoretic injections of sodium selenite in some of the main targets of the rat APir area produce retrograde labeling of neurons in all cell layers of this transitional cortical field. As mentioned before, this experimental procedure allows the identification of zinc-containing neurons which usually use glutamate as a neurotransmitter.

Neurotransmitters and Neuromodulators

CHOLINERGIC MARKERS

ACETYLCHOLINESTERASE (ACHE) In AChE preparations are placed at the disposition of the present writer, the enzyme activity appears to be concentrated in the deep cellular layers of all subdivisions of the VCo nucleus. However, at the level of the inferior subdivision of the VCo nucleus the AChE activity seems to diminish ventrally, so that it contrasts markedly with that in the posteromedial division of the APir area and that in the nearby IMG, filling the wedge-like area between the medium-celled ventromedial BM nucleus and the small-celled ventromedial BL nucleus. According to Darvesh *et al.* (1998), the neuropil of the nucleus is lightly AChE positive at rostral levels, gradually increasing in a caudal direction. AChE-positive triangular perikarya of small to medium size are present, their number diminishing in a caudal direction (5% rostrally; just isolated neurons caudally). According to Amaral and Basset (1989), in the macaque monkey, the PAC3 division of their periamygdaloid

cortex (PAC) shows the lowest AChE positivity of the whole PAC.

CHOLINE ACETYLTRANSFERASE (CHAT) According to Emre *et al.* (1993), this nucleus displayed a moderate density of mostly varicose and thin ChAT-positive fibers. The density was higher at the periphery of the nucleus, but in a patchy fashion, and its density was slightly higher in the posterior parts of the nucleus.

Together with the small-celled VL/VM BL nucleus and with the BM nucleus, the VCo nucleus is ranked third concerning the density of ChAT-ir fibers and varicosities.

In the macaque monkey, Amaral and Basset (1989) PAC3 subdivision shows the lowest density of ChAT-ir fibers in what they define as periamygdaloid cortex (PAC). The ChAT-ir fibers are diffusely arranged and of about equal density in all of the layers. The low staining of this subdivision provides a clear boundary with PACs (here the PM APir area), which has the densest fiber and terminal ChAT-ir.

EXCITATORY AMINO ACIDS

GLUTAMATE/ASPARTATE (GLU/ASP) Experimental tract tracing data obtained in rats with tritiated D-aspartate indicates that a considerable number of neurons in layer II and III of the rat of the periamygdaloid cortex, i.e., the posterolateral cortical amygdaloid nucleus (see Paxinos), which would be the homolog of the present VCo nucleus, give rise to GLU/ASPergic projections to all components of the ventral striatum (Acb, Tu, and IPAC) and to the ventral pallidum (Fuller *et al.*, 1987).

INHIBITORY AMINO ACIDS

γ-AMINOBUTYRIC ACID (GABA) According to McDonald and Augustine (1993) and Pitkännen and Amaral (1994), in the macaque monkey, the distribution of GABA-ir neurons and neuropil is similar throughout what they term the periamygdaloid cortex, which includes (besides the present VCo nucleus) the APir area after the present parcellation. The latter-named authors also found that the density of GABA-ir neurons is high and the number of cells expressing GAD mRNA matches that of these ir neurons. Furthermore, the density of these GABA-ir cells is noticeably higher than that of similar type of cells in the deep amygdaloid nuclei. The same can be said about the GABA-ir neuropil.

MONOAMINE MARKERS

DOPAMINE-β-HYDROXYLASE (DBH) According to Sadikot and Parent (1990), in the squirrel monkey, the periamygdaloid cortex shows light to moderate DBH-ir, with denser staining at the subpial area.

HISTAMINE (HA) According to Airaksinen *et al.* (1989), in the tree shrew (*Tupaia belangeri*), HA-ir fibers collected in dense bundles along the stria terminalis continue to the amygdaloid complex to spread as a dense and diffusely distributed network of HA-ir fibers within the amygdala. At the level of the VCo nucleus this network reaches a moderate density (3 on an scale from 0 to 5).

SEROTONIN (5-HT) According to Sadikot and Parent (1990), in the squirrel monkey the periamygdaloid cortex shows high to moderate 5-HT-ir except for subpial regions where a moderate density of fine 5-HT-ir fibers can be observed.

TYROSINE HYDROXYLASE (TH) According to Sadikot and Parent (1990), in the squirrel monkey, the TH-ir terminal labeling is light to absent.

NEUROPEPTIDES

BRAIN-DERIVED NEUROTROPHIC FACTOR (BDNF) According to Murer *et al.* (1999), in the human amygdala, this nucleus together with the BM nucleus contains a lower density of BDNF-ir neurons and fibers than the rest of the amygdaloid nuclei.

CORTICOTROPIN-RELEASING FACTOR (CRF) According to Basset *et al.* (1992), in the macaque monkey, the density of CRF-ir fibers in the superficial and the so-called cortical regions of the amygdala seems to be light to moderate in comparison with that observable in the Ce and La amygdaloid nuclei. Within their periamygdaloid cortex and "nucleus of the lateral olfactory tract," darkly coarse CRF-ir fibers with numerous large varicosities are present that are confined to the most superficial portion of La. In addition, a lesser density of medium to coarse CRF-ir fibers and occasional CRF-ir neurons, similar to those present in the MeA, are present in the deeper layers.

CHROMOGRANIN B According to Marksteiner *et al.* (1999), in the human brain, this nucleus displays a high density of PE-11-like ir which consist of varicose fibers and mixed size varicosities, though it does not seem to contain PE-11-like ir neurons.

DYNORPHIN (DYN) According to Sukhov *et al.* (1995), the cortical amygdaloid nucleus (here VCo) contains PDYN-containing neurons.

GALANIN (GAL) According to the mapping of the forebrain distribution of this neuropeptide presented by Kordower *et al.* (1992), in the macaque monkey amygdala, this member of the superficial amygdala, like its other components, does not contain GAL-ir cell

bodies but seems to contain at least a small number of GAL-ir fibers.

NEUROPEPTIDE Y (NPY) In their mapping of the distribution of the NPY in the human telencephalon, Walter *et al.* (1990) do not mention this nucleus but they depict it in their mapping as devoid of NPY-ir fibers or cells. However, according to McDonald *et al.* (1995), in the macaque monkey NPY fibers and puncta can be observed in all amygdaloid nuclei, though their density varies from place to place, showing high concentrations in all superficial amygdaloid nuclei with NPY-ir fibers coursing near the surface of the brain tending to run parallel to the pial surface. Bons *et al.* (1990) found likewise that in the lemur *Microcebus murinus* the cortical nucleus exhibits a dense superficial network of NPY-ir fibers and terminals. The plexuses of this type of fiber are less compact in the deeper aspect of the nucleus. The nucleus presents a small number of NPY-ir perikarya exhibiting bipolar, spindle, or pyramidal shapes.

NEUROTENSIN (NT) According to Benzing *et al.* (1992), their cortical nucleus, which is equivalent in most regards to the present VCo nucleus, contains moderate levels of NT-ir sufficient for its clear delineation from the laterally adjacent, lightly staining BM nucleus (AB in their account). The NT-ir is exclusively located in the L2 and L3 of the nucleus, while the superficial L1 contains little if any NT-ir. Their dorsal division (Cod) (superior and intermediate subdivisions in the R and C VCo) shows a denser staining than their ventral one (inferior subdivisions in the R VCo and C VCo). In the whole nucleus the NT-ir consists mostly of fine beaded fibers although fewer coarse-beaded fibers as well as dot-like punta are also present. It should be stressed that both divisions are described as showing a distinct anterior to posterior gradient of NT-ir with the posterior level showing a denser staining.

OXYTOCIN (OXT) According to Caffé *et al.* (1989), in the macaque monkey, OXT-ir fibers accumulate in the cortical nucleus where there is most dense innervation. A similar VP-ir innervation takes place in the cortical nucleus of the common marmoset monkey (Wang *et al.*, 1997).

SECRETONEURIN (SECR) High density of SECR-ir has been detected in the cortical nuclei (Kaufman *et al.*, 1997). Examination of the illustration available in the literature allows differentiation of the three subdivisions suggested in the present account, characterized by the presence of a strong SECR-ir in L1 and L3 of the three subdivision, but absence in L2 of the superior and inferior subdivisions and dense presence in this layer in the intermediate subdivision. On the other hand, the relatively high levels of the SECR-ir in this nucleus, and the even higher concentration of this neuropeptide in the AHi area, allows clear delineation of the deep layer of the VCo from this latter area, separation not evident when using other, more current histological, histochemical, and immunocytochemical procedures. This latter fact is why in some published accounts of this superficial structures the deep layers of VCo has been included as part of the AHi area.

VASOPRESSIN (VP) According to Caffé *et al.* (1989), in the macaque monkey, dense accumulations of VP-ir fibers are found in the their cortical nucleus, which, according to the present amygdaloid parcellation, includes among others the VCo nucleus.

NEUROTROPHINS

BRAIN-DERIVED NEUROTROPHIC FACTOR (BDNF) According to Murer *et al.* (1999), in the human brain all of the amygdaloid nuclei contain BDNF-ir neurons and fibers. In the case of their cortical nucleus, the number of BDNF-ir neurons and the density of the BDNF-ir neuropil was said to be lower than that of the Ce nucleus. On the other hand, from examining their Fig. 4 A it is possible to infer that the density of the BDNF-ir in the inferior subdivision of the VCo nucleus is higher than its other two subdivisions but even higher than in the ACo according to the present parcellation of the amygdaloid complex in humans.

ENZYMES

ANGIOTENSIN-CONVERTING ENZYME (ACE) According to Chai *et al.* (1990), the VCo nucleus shows low binding levels for ACE.

BUTYROCHOLINESTERASE (BUCHE) The VCo nucleus contains many BuChE-containing neurons of small to medium in size with round, fusiform, or triangular perikarya. Some have multiple branching dendrites, their number dropping in the caudal direction (14%, 2%, and &% of the neuronal population) (Darvesh *et al.*, 1998).

NICOTINE ADENINE DINUCLEOTIDE PHOSPHATE DIAPHORASE (NADPH-D) According to Sims and Williams (1990), APir shows a moderate NADPH-d, an observation that has been confirmed for both the human and squirrel monkey amygdalae (Brady *et al.*, 1992).

P450 AROMATASE (P450 AROM) According to Roselli *et al.* (2001), in the macaque monkey amygdala, the VCo nucleus contains a very high density of

P450 AROM mRNA-containing cells. However, by examining their illustrations (Fig. 5), it seems that in rostral transverse sections (Fig. 5A) the P450 AROM labeling is restricted to the superior and ventral subdivisions of the rostral VCo, while further back (Fig. 5B) the labeling is restricted to intermediate subdivision, and even further back (Fig. 5C) back to the inferior division, labeling that is directly continuous with that taking place at the level of the PM AHi area, which these authors have included as part of their cortical nucleus.

CALCIUM-BINDING PROTEINS

CALBINDIN (CAB) According to Sorvari *et al.* (1996b), the PAC3 subdivision of their periamygdaloid cortex (i.e., the If subdivision of the both rostral and caudal divisions of the VCo nucleus) has a higher density of CAB-ir neurons than the adjacent PACs (i.e., the PM APir area of the present parcellation). The neurons are type 1 and 3 cells and their dendrites were oriented perpendicular to the pial surface. Compared to the dorsally located nucleus of the lateral olfactory tract (i.e., the superior and intermediate subdivisions of the rostral VCo nucleus), the CAB-positive neurons in PAC3 are smaller. The intensity of CAB-ir fiber and neuropil staining is slightly higher than in the adjacent PACs.

After the same authors, in their "nucleus of the lateral olfactory tract," as in other pseudocortical periamygdaloid areas, L1 contains a 1ow density of CAB-ir neurons. L2 and L3 contain by contrast a moderate density of CAB-ir neurons. In L2, the small, darkly stained type 1 and 2 CAB-ir neurons form clusters that corresponded to the cellular clusters seen in Nissl-stained preparations. In L3, the density of diffusely scattered ir neurons is high. Characteristic of the CAB-ir neurons in this part of the present R ACo nucleus is their variable morphology, which ranged from small, darkly stained type 1 cells to large, lightly stained type 2 and 3 cells. On the other hand, L2 of CAB-ir while in L3, the intensity of ir is lower than in L2; and L1 contains only a few CAB-ir fibers oriented perpendicular to the pial surface. While the immunoreactivity of the neuropil was high in all three layers, it was highest in layer 2. A low density of CAB-ir bundles was observed in L2 and L3.

CALRETININ (CR) According to Sorvari *et al.* (1996a), in the human amygdala, the CR-ir neurons are distributed in a laminar fashion at the level of their PAC3 subdivision (inferior subdivision of both rostral and caudal divisions of the VCo nucleus) of the periamygdaloid cortex. This part of the VCo nucleus, therefore, would have the same density of CR-Ir neurons than the ventrally located PACs (here, PM APir area). Most of the ir neurons are of the type 1 or small type 3 cells. Furthermore, their "nucleus of their nucleus of the lateral olfactory tract" in humans (here included within the superior and intermediate subdivisions of the R VCo nucleus) contains a large number of small type 1 and some type 3 CR-ir neurons. The density of CR-ir cells is higher in the cellular L2, while in L3 these types of cells are scattered distributed.

The CR fiber and neuropil has a higher density than in the PM APir area. Finally, the rostral part their "posterior cortical nucleus" (here the superior and intermediate subdivisions of the caudal division of the VCo nucleus) is described as containing a small density of CR-ir small type 1 and type 3 cells.

The CR-ir fiber, terminals, and neuropil distribution in this superficial structure, has been described as being higher in PACs than in the adjacent PACs, while that in their "nucleus of the lateral olfactory tract" is moderate and its intensity of staining is as high as in the MeA nucleus. Finally, the CR-ir pattern in the rostral part of their posterior cortical nucleus is differentiated from the caudal one (i.e., from PM AHi area) by the fact that more CR-ir fibers can be detected parallel to the pial surface in the former sector than in the latter one.

It is important to stress that since the so-called nucleus of the lateral olfactory tract has been proposed to be homologous with an equally named nucleus present in macrosmatic mammals, its comparison with that of the rat in this type of CR immunohistochemical preparation indicates the existence of an almost completely different staining pattern that contrasts for its scarcity, particularly when compared against the very rich one in the neighboring AAA (personal observation).

PARVALBUMIN (PAV) According to Sorvari *et al.* (1995), at rostral levels of their posterior cortical nucleus, [approximately equivalent to the superior and intermediate(Sp and It) subdivisions of the caudal VCo], the few PAV-ir cells present are mostly small, palely stained type 1 or 2 cells. Concordantly, the density of PAV-ir fiber and terminals is low, with some of them running parallel to the pial surface. According to the same authors, their PAC3 subdivision of the periamygdaloid cortex [approximately homologous to the inferior (rostral and caudal subdivisions of the VCo nucleus)] is said to contain some PAV-ir neurons in L2 and L3 which are small type 1 and type 2 cells, their density being higher toward the boundary with the SP VCo or with APir (their PACs).

Finally, their "nucleus of the lateral olfactory tract" (which in more medial and ventral sectors corresponds

approximately to the superior and intermediate subdivisions of the R VCo nucleus) is described as containing a moderate number of PAV-ir neurons of type 2 cells and some type 1 cells located mostly in L2 and L3 of this sector of the VCo.

OTHER PROTEINS

CALPASTATIN (CALPT) According to Mouatt-Prigent *et al.* (2000), large CALPT-ir neurons are present especially in the cortical nucleus, high proportion of these neurons are bipolar and strongly immunostained. They are surrounded by a dense plexus of CALPT-ir fibers and puncta corresponding very probably to nerve terminals.

DOPAMINE- AND ADENOSINE 3',5'-MONOPHOSPHATE (CAMP)–REGULATED PHOSPHOPROTEIN OF M, 32 KDA (DAPP-32) AND PHOSPHATASE INHIBITOR 1 (I-L) According to Barbas *et al.* (1998), in the macaque monkey, most of the DARP-32-ir and I-1-ir neurons can be detected in the VCo nucleus. Moderately or densely stained DARPP-32-ir and I-l-ir neurons can be seen in all cortical subdivisions, but their prevalence within each differed. DARPP-32-ir neurons are more numerous in the It VCo subnucleus while I-1-ir are more sparsely distributed in the If VCo subnucleus. The I-l-ir neurons are found in all parts of the VCo nucleus, with gaps noted in the central sector.

Within the VCo nucleus, DARPP-32-ir and I-l-ir neurons are present in layers 2 and 3, and there is some overlap in their laminar distribution. However, the DARPP-32-ir neurons are located superficially in layer 2 and in the deep part of layer 3, whereas I-1-ir neurons are concentrated primarily, though not exclusively, in the inner part of layer 2 and the upper part of layer 3.

LIMBIC SYSTEM-ASSOCIATED MEMBRANE PROTEIN (LAMP) According to Côté *et al.* (1996) in the macaque amygdala, their PAC2 subdivision of the periamygdaloid cortex, i.e., approximately the rostral division of the VCo, is devoid of LAMP-ir, while their PAC3 subdivision, i.e., the present caudal division of VCo, displays a light to moderate LAMP-ir.

NEUROFILAMENT PROTEIN SMI32 (SMI32) According to the low magnification atlas published by Petrides *et al.* (2000), the inferior subdivision of the posterior VCo contains some SMI32-ir, while the remaining subdivisions, except for a sector at the rostral pole of the nucleus, show a completely negative staining. Within the inferior subdivision of the P VCo, the distribution of the SMI32-ir is rather homogeneous not showing the stratified distribution apparent in those neocortical fields that show positively stained profiles. In the sector located at the rostral pole of VCo mentioned before, a very strong and stratified SMIR32-ir can be appreciated. The cells in the L2 of this sector stand out on account of the negative staining of layer 1 and 3 and of surrounding structures. This sector of the VCo, which has received different names, lies within what Barbas and de Olmos (1990) designated as the superior subdivision of the VCo nucleus, Price *et al.* (1987) as PAC 2, Turner *et al.* (1978) and Pitkannen and Amaral (1993) as NLOT, and Paxinos *et al.* (2000) as BAOT. As pointed out by Turner *et al.* (1978), this sector of the superficial amygdala of the macaque monkey receives a direct afferent supply into L1a from the main olfactory bulb, is strongly AChE positive, and displays a strong ChAT-ir (see above), meeting some of the hitochemical and immunohistochemical features of the NLOT in some subprimates mammals. However, it remains to be seen whether the full hodological characteristics that have been established for this nucleus in lower mammals are met by this so-called NLOT or BAOT.

RECEPTORS

BENZODIAZEPINE RECEPTOR The cortical amygdaloid nucleus has been reported to contain high densities of benzodiazepine receptors (Zezula *et al.*, 1988).

CCK RECEPTORS (CCK-R) According to Kritzer *et al.* (1988), keeping with the general pattern of CCK binding site concentration in the ventral medial margins of the macaque monkey amygdala, the VCo shows a prominent concentration of CCK-R.

CHOLINERGIC RECEPTORS

MUSCARINIC RECEPTOR (MACH-R) According to Cortés *et al.* (1987), the molecular layer of the human cortical nucleus (here the VCo nucleus) BM nucleus) contains one of the lowest densities of mACH-R. On the other hand, according to Smiley *et al.* (1999), the amygdala as a whole contains a low density of m_2-ir neurons.

NICOTINIC RECEPTORS (NACH-R) This type of receptor as labeled [^{3}H]ACh or [^{3}H]nicotine shows very low concentrations in all nuclei of the rat amygdaloid complex (Rainbow *et al.*, 1984; Clarke *et al.*, 1985). No other source of this type of data is available to the present writer about the distribution of this type of receptors in the primate amygdala.

OPIOID RECEPTORS (OR) According to Daunais *et al.* (2001), low to moderate concentrations of [^{3}H]DAMGO binding sites could be measured in the cortical nucleus.

STEROID RECEPTORS

ANDROGEN RECEPTOR (AR) The distribution of AR mRNA-containing cells in the amygdala was mainly confined to the cortical and basomedial amygdaloid nuclei (Roselli *et al.*, 2001).

ESTROGEN RECEPTOR α (ER-α) According to Österlund *et al.* (2000), in both human and monkey brains, their nucleus of the lateral tract, which corresponds according to their illustrations (Fig. 3A) to the superior subdivision of the rostral VCo of the present account, is described as having moderate amounts of ER-α mRNA-labeled nuclei. In their periamygdala cortex (here the VCo nucleus), the ER-α mRNA expression is most abundant in the human and monkey brains.

Amygdalopiriform Transition Area (APir)

Topographical Landmarks This extensive band-like gray formation (Figs. 22.1c, 22.2–22.6a, 22.7a–22.11) [CxA plus PHA in Plates 21–27 (-0.6–6.7 mm) of Mai *et al.* (1997), *Atlas of the Human Brain*; and APir in Plates/Figs. 45–62 (interaural 20.55 mm to 12.99 mm) of Paxinos *et al.* (2000), *The Rhesus Monkey Brain in Stereotaxic Coordinates*] occupies the fundus and lower lip of the semicircular (or semiannular s., sas) sulcus that lies intercalated mainly between the superficial amygdala, and the putative olfactory sector of the entorhinal cortex (Price *et al.*, 1987) (Ent; Plate 24, 2.7 mm), though at its rostral-most pole it becomes interposed between the temporal area of the (pre-) piriform paleocortex (PirT) and the rostral pole of the Ent (Plates 21–22) a relationship that is also maintained in the monkey bran [Figs. 41–45 of Paxinos *et al.* (2000)]. Likewise, the rostral end of APir will also bind with the temporopolar periallocortex (Fig. 42, TPPal in Paxinos *et al. Atlas of the Macaque Brain*), maintaining in this manner it transitional character with respect to the several expressions of the temporal periallocortex.

Furthermore, by comparing sections of the human brain with that of the macaque monkey, it is apparent that, at least in the human brain, this structure not only lies entirely confined to the above described territory but in conjunction with a clear topographical relationship with the semiannular sulcus (sas). It also seems to extend further caudally than in the monkey so as to end up abutting a transitional field of the hippocampal formation, Rosene and Van Hoesen's (1987) hippocampal–amygdaloid transition area (HATA)). On the other hand, it should be pointed out that in the macaque (Old World) and squirrel (New World) monkeys, APir has been generally depicted as covering not only the bottom and the lower lip of sas but also its dorsal lip (Price and colleagues PACs subdivision of their periamygdaloid cortex). However, closer fibroarchitectonical analysis reveals that even in these lower primates the dorsal lip of the sas is made up, at least in part, by the inferior division of the ventral cortical amygdaloid nucleus.

Cytoarchitectonics On account of some cytoarchitectonic variations that are more or less coincidental with successive intercalations among the different modalities of temporal periallocortex, APir can be divided into anterolateral (APir AL) and posteromedial (APir PM) portions. The former is further susceptible to be subdivided into lateral (APir ALl), intermediate (APir ALi), and medial (APir ALm). While APir is easily distinguishable from Pir T by an abrupt disappearance of the pattern of densely packed cells that characterizes the superficial pyramidal cell layer of this allocortex, its borders with the periallocortical fields of ambiens gyrus are that clear. The posteromedial division of APir has an oval or circular shaped area in transverse sections extending itself throughout much of the caudal half of the amygdaloid body. It has been said that the neurons that make up this formation belong to either an inward extension of the caudal VCo nucleus or a medial extension of the ventromedial subdivision of the BL nucleus. Caudally this transitional griseum is replaced posteriorly by the anteroventral division of the AHi area.

Fibroarchitectonics In neurofibrillar preparations, the APir area appears to be separated from neighboring structures by fiber septa of different densities and thicknesses, although this is more particularly the case in its posteromedial division.

As here described, the APir area corresponds to the claustrocortex preamygdaleum of Brockhaus (1940), the field sem 1 of Hilpert (1928), and the subfields PACo, PACs, and PAC1 of Price (1973) and to PACo (lateral AL APir 0) plus PAC1 (medial AL APir), the rostral (intermediate AL APir) and caudal (PM APir) PACs of Sorvari *et al.* (1995, 1996a,b).

Chemoarchitectonics

Heavy Metals In Old (macaque) and New World (squirrel, marmoset) monkeys, APir area as a whole shows as it can bee seen in all allo- and periallocortical formations as very strong Timm-Danscher-silver/selenide deposits in all of their layers except around the superficial cell layers, where the precipitate is only moderate. It deserves to be mentioned here that in rat experiments made in my laboratory of the present writer in which Na selenite was injected iontophoretically in the bed nucleus of the stria terminalis or in the region of the central amygdaloid nucleus/sublenticular substantia innominata, a dense retrograde labeling with silvered selenide of a dense population of neurons in

both superficial and deep layers of both anterolateral and posteromedial divisions of the APir occurs. Such findings may mean that this transitional formation may be one of the main sources of a zinc-reach glutamatergic innervation of the central extended amygdala.

Neurotransmitters

CHOLINERGIC MARKERS

ACETYLCHOLINESTERASE (AChE) In AChE preparations the APir area shows, in the material to my disposition, moderate to weak enzyme reactivity which seems to be slightly greater than that for the neighboring entorhinal periarchicortex. The laterodorsal subdivision of the PM division of this transitional gray formation shows however higher reactivity [Figs. 22.10 and 22.11). In the macaque monkey amygdala, APir stains intensely for AChE and ChAT (Amaral and Basset, 1989- their area PACs), but in humans Sims and Williams (1990) and Benzing *et al.* (1992) found virtually no AChE staining.

EXCITATORY AMINO ACIDS

GLUTAMATE (GLU) No human or nonhuman primate information is available to the present writer

INHIBITORY AMINO ACIDS

γ-AMINOBUTYRIC ACID (GABA) According to Pitkänen and Amaral (1994), the distribution of GABA-ir neurons and neuropil as well as the distribution of cells that contain GAD mRNA is quite similar throughout the periamygdaloid cortex (i.e., including PACs, equivalent to the present APir area). The density of the GABA-ir- and/or GAD mRNA-labeled neurons being high as that of the neuropil in where numerous pericellular baskets surrounding unstained cells can be observed.

NEUROPEPTIDES

CORTICOTROPIN-RELEASING FACTOR (CRF) Although it has been stated that all of the amygdaloid nuclei contain dense accumulation of CRF-ir fibers (Powers *et al.*, 1987; Zaphiropoulos *et al.*, 1991), with large varicosities and terminals, their density would not reach that detected at the level of the LBNC (Zaphiropoulos *et al.*, 1991).

NEUROPEPTIDE Y (NPY) Also in humans APir seem to contain NPY-ir cell bodies and fibers (Zech *et al.*, 1986).

NEUROTENSIN (NT) According to Zech *et al.* (1986), APir contains NT-ir positive perikarya and dense plexuses. According to Benzing *et al.* (1992), APir contains a moderate amount of NT-ir and is characterized mainly by coarse-beaded as well as some fine-beaded fibers. These fibers are similar in appearance to those found in the medial aspect of the VM BL nucleus, but the former contains more coarse fibers that the latter.

SOMATOSTATIN (SOM) In agreement with the suggested subdivisions into anterolateral and posteromedial sectors, the former appears to be densely innervated by SOM-containing fibers while the latter only contains a modest amount of these elements. This rather modest concentration of SOM-ir elements in APir helps to distinguish this transition field from the dorsally adjacent VCo.

According to Amaral *et al.* (1989), the SOM-ir at the level of what they define as periamygdaloid cortex (PAC) is widespread and does not distinguish between subdivisions. In general there is a dense SOM-ir fiber network and terminals in layer 1 which extended less densely in the deeper layers but is a lesser degree than in their PAC2 subdivision (approximately AL APir L here). The large-celled region of their PACs was described as containing a dense accumulation of SOM-ir neurons.

VASOPRESSIN (VP) According to Caffé *et al.* (1989), in the macaque monkey, dense accumulations of VP-ir fibers are found in the their cortical nucleus, which, according to the present amygdaloid parcellation, includes among others the PM APir area.

ENZYMES

NICOTINE ADENINE DINUCLEOTIDE PHOSPHATE DIAPHORASE (NADPH-D) According to Sims and Williams (1990), APir shows a moderate NADPH-d. Thus observation has been confirmed for both the human and squirrel monkey amygdalae (Brady *et al.*, 1992). Furthermore, according to Unger and Lange (1992), 90% of the NPY-ir and SOM-ir neurons and *neuropil* are positively ir for NADPH-d.

P450 AROMATASE (P450 AROM) A close examination of the illustrations (Fig. 5A–C) presented by Roselli *et al.* (2001) about the distribution of this enzyme in the macaque monkey amygdala would indicate that while the rostral PM subdivision of APir areas does not seem to contain any P450 AROM mRNA-labeled cells, in more caudal planes (Fig. 5 C), this area does, though to a lesser degree than the other superficial amygdaloid nuclei.

CALCIUM BINDING PROTEINS

CALBINDIN (CAB) According to Sorvari *et al.* (1996b), their "sulcal part of the periamygdaloid cortex" in humans (i.e., the PM APir of the present account), the CAB staining pattern, in accordance with

the cytoarchitectonic organization of this transition field, also reveals some differences between the dorsal and ventral parts of PACs. The dorsal part of the PACs contained a moderate density of CAB-ir neurons, which in L2 are mostly small type 1 cells. In L3, there were type 3 cells which have dendrites oriented perpendicular to the pial surface. In the ventral part of PACs (L2 and L3), CAB-ir neurons are not as clearly oriented as in the dorsal part. In addition, the ventra1 part contains a high number of lightly stained CAB-ir neurons, which resemble the pyramidal neurons found in the entorhinal cortex. The fiber bundle separating the ventral part of PACs from the entorhinal cortex contained several CAB-ir neurons. PACs contains a moderate density of CAB-ir fibers and CAB-ir neuropil. L2–L3 of the PACs are the only parts with few CAB-ir bundles.

CALRETININ (CR) According to Sorvari *et al.* (1996a), their "sulcal portion of the periamygdaloid cortex" (i.e., PM APir area) contains a low density of CR-ir neurons. L1 contains only few small type 1 neurons. Most of the CR-ir neurons in this territory are located in L2 and L3. In the ventral portion of PACs neurons of the small type 2 are also found. At the rostral level, the territory they assign to their "nucleus of the lateral olfactory tract" contains considerably more cells in L3 than in PACs. On the other hand, their PAC1 subdivision (i.e., the lateral and intermediate subdivisions of AL APir area) contains few CR-ir cells most of which are of the small type 1 and are located in L2 and L3. Finally, L1 and L2 of their PACo subdivision (i.e., the medial AL APir subarea) contain few CR-ir neurons but the clusters of cells in L2 that characterize this subdivision are free of CR-ir cells. A slightly higher density of CR-ir neurons is found in L3, which contains some small type 1 and 2 cells.

The CR-ir fibers and terminals as well as the neuropil in the PACs division is high and of equal density in both dorsal and ventral subdivisions. In L2 and in L3 fibers run perpendicularly to the pial surface. On the other hand, the CR-ir neuropil in PACo is dense throughout it, and CR-ir fibers in L3 run, like in PACs, perpendicularly to the pial surface. Both PACs and PACo are easily distinguished from the entorhinal cortex because the latter has a large number of CR-ir neurons in L3 and in L5 and the fiber bundle that runs between PACs and this periarchicortical field contains CR-ir fibers. Finally, in PAC1, the CR-ir neuropil I highly stained particularly in L2 and L3 but the number of CR-ir fibers is low.

PARVALBUMIN (PAV) According to Sorvari *et al.* (1995), the oral part of their periamygdaloid cortex (here AL APir M) almost completely lack PAV-ir neurons, and the density of PAVC-ir fibers and terminals is low. A similar picture is also applicable to their PAC1 subfield (here AL APir I+L). With respect to the subfield they label as PACs (sulcal portion of their periamygdaloid cortex; here PM APir), the picture does not seem to vary significantly since they observed a low density of lightly stained PAV-ir neurons. These neurons have no visible dendrites, and the cells in the ventral sector of this structure appeared less fusiform in shape than those in the more dorsal sectors. A low number of PAV-ir fibers and terminals were seen here, but this scarcity becomes apparently more pronounced in the ventral nonsulcal sector. In layers 2 and 3 of APir, the PAV-ir fibers appeared oriented perpendicularly to the brain surface, but at the level of the fundus of the sas, they formed in layer 1 of this field a triangular plexus.

OTHER PROTEINS

DOPAMINE- AND ADENOSINE-3′,5′-MONOPHOSPHATE (CAMP)–REGULATED PHOSPHOPROTEIN OF M, 32 KDA (DARPP-32) AND PHOSPHATASE INHIBITOR 1 (I-L) According to Barbas *et al.* (1998), in the macaque monkey, very few DARP-32-ir or I-1-ir neurons can be found in the APir, which when detected were very lightly labeled. This feature contrasts sharply with the relative preponderance of immunoreactive neurons demonstrable in the VCo nucleus, which is interposed between APir area and the MeA nucleus.

DOPAMINE TRANSPORTER (DAT) According to Ciliax *et al.* (1999), in humans APir contains a moderately dense concentration of varicose axons.

RECEPTORS

BENZODIAZEPINE RECEPTOR (BNZ-R) According to Zezula *et al.* (1988), the corticoamygdaloid area (here the APir area) contains high densities of BNZ-R.

CHOLECYSTOKININE RECEPTOR (CCK-R) According to Kritzer *et al.* (1988), keeping with the general pattern of CCK binding site concentration in the ventral medial margins of the amygdala, the APir area shows a prominent concentration of CCK-R.

MONOAMINERGIC RECEPTORS

ADRENORECEPTOR α_2 According to Flügge *et al.* (1994), in the tree shrew, the area semiannularis of the cortical amygdaloid nucleus shows a high density of [^{3}H]rawolscine (its antagonist) binding sites.

ADRENORECEPTOR β_1 According to Flügge *et al.* (1994), in the tree shrew, the area semiannularis of the cortical amygdaloid nucleus contain β_1-adrenoreceptors as revealed by its antagonist [^{3}H]iodocyanopindolol.

SEROTONIN RECEPTORS

5-HT_{1A} RECEPTOR (5-HT_{1A}-R) According to Flügge *et al.* (1994), in the tree shrew, the area semiannularis of the cortical nucleus (here the APir area) is strongly labeled by [^{3}H]8-hydroxy-2(di-*n*-propylamino) tetraline (a specific agonist of the 5-HT_{1A}-R).

STEROID RECEPTORS

ESTROGEN RECEPTOR α (ER-α) According to Österlund *et al.* (2000), in both the human and monkey APir, the ER-α mRNA expression is most abundant together with that seen in the other posterior superficial nucleus, i.e., their AHi and posterior amygdaloid nucleus (the present AP/AL AHi).

Superficial Cortical-like Tertiary Olfactory Amygdala

Amygdalohippocampal Area (AHi)

Topographical Landmarks The AHi area in humans, as in the monkeys [AHi plus PCo in Plates 30 and 31 (10.7–12.0 mm) of Mai *et al.* (1997), *Atlas of the Human Brain*; AhiMC plus AHiPC in Plates/Figs. 57–66 (interaural 15.15–11.10 mm) of Paxinos *et al.* (2000), *The Rhesus Monkey Brain in Stereotaxic Coordinates*], is the most caudal of all the amygdaloid nuclei, extending between the posterior aspect of the amygdaloid complex and the anterior portion of the uncus of the hippocampal formation. Rostrally it extends ventrocaudally to the posterior division of the Me nucleus to constitute an elongated mass of rather complex shape, cell composition, and special arrangement of the neuronal population that forms it. Thus, in the formation of the AHi area participate at least two somewhat differently arranged set of neurons that merge gradually with each other and are represented mainly by a deep, wider, and nonstratified anteroventral (AV AHi) division and a superficial, narrower, but stratified posteromedial division (PM AHi). Implied by this modified naming of the major divisions of the AHi area is the inclusion of both de Olmos'(1990) "amygdalo-hippocampal area" and "posterior cortical amygdaloid nucleus" (see Heimer *et al.*, 1999). As such, the AHi area, or more exactly its posteromedial division, is separated from the large-celled CM subdivision of the BM nucleus by the compact segment of the medial medullary lamina (ml) that occupies the space intercalated between them, while at its rostral tip it is separated from the posterior Me nucleus by a narrow acellular area through which run markedly less compactly arranged strands of fibers. Caudally, PM AHi area comes to occupy a rostral portion of the uncal bridge connecting the hippocampus with the amygdala. At this level a small gap marks the boundary with Rosene and Van Hoesen's (1987) "hippocampalamygdaloid transition area" which can be distinguished by the greater width of its molecular layer, by a less clear layering of the fiber plexus that contains a richer fiber content in its superficial cell layer (L2), and, finally, by a lack of sublayering in its deep cell layer (L3). The deeper, wider, and more heterogeneous AL AHi area, which ventrally replaces the PM AHi area, stands out among the superficial nuclei of the human amygdala on account of its wide cellular area consisting mostly of large, deeply staining, densely packed neurons. This sector of the AHi area in contrast to its posteromedial counterpart is not so clearly separated from the deeper-lying amygdaloid nuclei laterally, and from the deep layers of the VCo nucleus rostrally, with which apparently it merges.

Cytoarchitectonics The molecular layer (L1) of the AHi area, which varies in width in the different sectors of this transitional gray formation, is well delineated and in its deeper aspect displays superficially a well-developed granular pial lining (Fig. 22.30). The neurons in L1 are mostly oriented parallel to the brain surface, whereas most neurons in the deeper cell layers are oriented perpendicularly. The more superficial of these cell layers (L2), although made up in great part of large pyramidal cells, also contain smaller neurons of diverse shapes. Actually, the superficial cell layer can be subdivided into two sublayres. The more superficial one is very narrow and is formed by cells arranged more loosely and more lightly staining than those in the underlying L2 proper. Some of the latter have their main axis oriented parallel to the brain surface. The deep cell layer, in contrast with L2, consists mostly of medium–sized pyramidal neurons that stain more lightly and are more densely packed.

Because of cell composition and fibroarchitectonic characteristics, the AHi area in the human amygdala can be divided into anteroventral (AV AHi) and posteromedial (PM AHi) divisions. The former shows a less clear stratification than its counterpart, the posteromedial AHi division, which can be distinguished on account of a noticeable expansion of its deep layer and a gradually and by a gradual decrease in the size and stainability of its neurons toward its depth. Nevertheless, in general, neurons are smaller and more densely arranged in the posteromedial AHi division than in the anteroventral one.

The molecular layer of the PM AHi division is wider than that seen at the level of the superior subdivision of the caudal VCo nucleus, but, it is narrow when compared with the molecular layer of the anteroventral AHi division. At first sight the cell layer in the PM AHi subarea appears to be nonstratified, but closer examination reveals that the more superficially located

neurons in this layer are more scattered and randomly arranged than those in the deeper aspect of the area whose main axes are oriented perpendicular to the brain surface. Together with large rounded or spindle-shaped neurons, there are also medium-sized neurons of different shapes, including inverted pyramids. These deeper neurons are somewhat darker staining than the superficial ones, but not as intensely staining as those in the principal anteroventral sector of the AHi area. The presence of a third cell layer together with the widening of the molecular layer marks the boundary between the PM AHi subarea and the main AV AHi division. In addition, the granular subpial layer in the surface of this subarea is better developed than in the main AHi body.

Fibroarchitectonics In neurofibrillar preparations the PM AHi subarea appears to be characteristically encapsulated in both its dorsal and lateral deep portions and is therefore clearly separated from the ventral Me and the large-celled dorsomedial BM nucleus. These fibers eventually join the medullary fiber systems linked to the stria terminalis. At its rostral pole this fiber capsule separates this AHi subarea from the caudal division of the VCo nucleus; it is also at this level that the PM AHi division experiences a densification of its cell layer and shows a more cortical-like appearance than more caudally. Immediately superficial to the cell layer and occupying the whole width of the molecular layer are fine fibers running in every direction, forming a relatively rich network. The cell layer, on the other hand, is traversed by a not-so-rich system of radially oriented fibers that converge in the deep aspect of the nucleus to form a richer fiber plexus that constitutes part of the fiber capsule covering the nucleus laterally and dorsally.

As here described, the AHi area corresponds to Broackhaus' (1938) area periamygdalae caudalis ventralis and dorsalis or the greater part of Stephan's (1975) area parahippocampalis, and coincides with that defined by Gloor (1997). With respect to Sorvari *et al.* (1995–1996) mapping in the human brain of this transition field, the present parcellation of the AHi area corresponds to the caudal sector (here the AV AHi division) of the much larger area defined by them as such. As was been stated before, the present definition of AHi area includes their posterior cortical nucleus (here the PM AHi division).

Sasagawa (1960a) reports that in the chimpanzee the AHi area is identified as part of the periamygdaloid cortex (pam), with his subdivision Pam3 alpha corresponding to the AL AHi subfield and his subdivision Pam2 alpha, to the PM AHi subdivision of the present parcellation. This was also done in the woolly howling monkeys (Sasagawa, 1960) and in the macaque monkey (Mikami,1952). The AHi area as delimited by Barbas and de Olmos (1990) and by Paxinos *et al.* (2000) would probably correspond to its homonimous as here described.

Chemoarchitectonics

Heavy Metals The Timm-Danscher selenium pattern in monkeys shows a rather uniformly distributed Timm-positive neuropil throughout the nucleus, including the whole width of its molecular layer. This staining contrasts with the moderate to weak staining of the superficial cell layer in the main AHi, which is even more moderate than in the deeper aspects of this region. Also, though in a reverse manner, the heavier Timm-Danscher staining of the molecular layer in both divisions of the AHi area contrasts sharply with that in the subjacent superficial and deep layers of this transitional formation, so that when taken at its whole the main body of the AHi area appears enclosed by Timm-Danscher heavy silver deposits that are present in surrounding tissue. By generating such a picture, this histochemical procedure provides a very accurate means of separating the AHi area from surrounding superficial grisea such as the APir area and the VCo nucleus, more particularly from its deep cell layers which appear markedly densely stained (Alheid and de Olmos, unpublished observations). Is important to point out that in trying to find homologous brain structures among different mammalian species, in terms of the distribution pattern of the Timm-Dancher–positive staining in monkey material examined by us, a striking similarly in such distribution seems to take place in a presumably homologous division of the rat amygdala (de Olmos *et al.*, 1985). More specifically, as happens in the monkey brain, its molecular layer is totally filled with silver granules. Such disposition clearly contrast with the presence in both posteromedial (the posterior cortical nucleus of Canteras *et al.*, 1992) and posterolateral amygdaloid nuclei de Olmos *et al.*, 1985; Alheid *et al.*, 1995; Swanson, 1992), as also happens in the primary olfactory cortex of very sharply and negatively stained subpial laminae 1a intervening between brain surface and an otherwise densely stained sublamina 1b in the molecular layer of all these structures. Importantly, such a pattern is even more clearly displayed in the amygdala of Timm-Danscher's stained sections of the rabbit and guinea pig amygdala (unpublished observations).

Neurotransmitters

CHOLINERGIC MARKERS

ACETYLCHOLINESTERASE (ACHE) In AChE preparations of the human amygdala, Benzing *et al.* (1992)

described the AHi area as being moderately stained but nevertheless delineated from the anterior hippocampal formation and the nuclei of the posterior amygdala.

According to Amaral and Basset (1989) in the macaque monkey, the amygdalohippocampal area (here the AL AHi subdivision) contains the greatest density of cholinergic markers, showing a AChE staining that parallels the ChAT staining except for the occasional presence of AChE-positive cells.

CHOLINE ACETYLTRANSFERASE (CHAT) Although Emre *et al.* (1993) had a moderate density of ChAT-positive fibers, such a statement applies to a transition field that intervenes between the caudal end of the amygdalohippocampal area proper, which they labeled as cortical amygdaloid nucleus, and the hippocampal formation.

According to Amaral and Basset (1989), in the macaque monkey, the amygdalohippocampal area (here the AL AHi subdivision) contains the greatest density of cholinergic markers, showing a relatively dense ChAT-ir that has a particulate appearance similar to that seen in the nuclei of the LBNC.

EXCITATORY AMINO ACIDS

GLUTAMATE (GLU) No primate or nonhuman primate information is available to the present writer concerning this point. See, however, the section on heavy metals.

INHIBITORY AMINO ACIDS

γ-AMINOBUTYRIC ACID (GABA) According to Pitkänen and Amaral (1994), in the macaque monkey, the AHi area (here the anterolateral division of AHi) contains a high number of GABA-ir cells that are very similar to those in the VCo nucleus. Many GAD mRNA-labeled cells are evenly distributed in this transitional gray formation. The GABA-ir neuropil is also highly dense, and basket-like plexuses around non-ir somata are common. On the other hand, the caudal part of their posterior cortical nucleus, which here is considered to be part of the posteromedial division of the AHi area, also contains a very high number of GABA-ir neurons. There is a dense GABA-ir in the neuropil of this sector of the caudal amygdala which in the superficial aspect of L2 presents numerous basket-like profiles.

MONOAMINE MARKERS

DOPAMINE-β-HYDROXYLASE (DBH) (NORADRENALINE/NOREPINEPHRINE) According to Sadikot and Parent (1990), in the squirrel monkey, the AHi area shows only light DBH-ir.

SEROTONIN (5-HT) According to Sadikot and Parent (1990), in the squirrel monkey, the AHi area is notable for a very heavy concentration of 5-HT-ir terminal varicosities.

TYROSINE HYDROXYLASE (TH) According to Sadikot and Parent (1990), in the squirrel monkey the AHi area shows no TH-ir terminal varicosities.

NEUROPEPTIDES

CHROMOGRANIN B Although Marksteiner *et al.* (1999) do not mention this transitional field among the amygdaloid nuclei that express PE-11-like ir, their illustrations (Fig. 3C, D) clearly indicate that the whole extent of the AHi area contains high amounts of this neuropeptide.

COCAINE- AND AMPHETAMINE REGULATED TRANSCRIPT (CART) According to Hurd and Fagergren (2000), both their posterior cortical nucleus and amygdala–hippocampal area (corresponding jointly to the present AHi), together with MeA nucleus, show the highest CART mRNA expression in the human amygdala.

CORTICOTROPIN-RELEASING FACTOR (CRF) According to Basset *et al.* (1992), in the macaque monkey, the density of CRF-ir fibers in the superficial and the so-called cortical regions of the amygdala seems to be light-to moderate to that observable in the Ce and La amygdaloid. Within their posterior cortical nucleus (here the PM AHi subdivision) darkly coarse CRF-ir fibers with numerous large varicosities are present that are confined to the most superficial portion of L1a. In addition, a lesser density of medium to coarse CRF-ir fibers and occasional CRF-ir neurons similar to those present in the MeA are present in the deeper layers.

GALANIN (GAL) According to the mapping of the forebrain distribution of this neuropeptide presented by Kordower *et al.* (1992), in the macaque monkey amygdala, this member of the superficial amygdala, like its other components, does not contain GAL-ir cell bodies, although it seems to contain at least a light amount GAL-ir fibers.

NEUROPEPTIDE Y (NPY) In their mapping of the distribution of NPY in the human telencephalon, Walter *et al.* (1990) do not mention this nucleus. However, they depict it in their mapping (Fig. 1e) as containing a low number of NPY-ir fibers or cells.

NEUROTENSIN (NT) The AHi contains a light to moderate NT-ir that is homogeneously distributed

across its extent, consisting primarily of beaded fibers and dot-like puncta. NYT-ir neurons are not present in this transitional formation (Benzing *et al.*, 1992).

OXYTOCIN (OXT) Caffé *et al.* (1989) state that in the macaque brain the telencephalic are most densely innervated by the OXT-ir fibers is the cortical nucleus. However, from a close examination of their schematic mapping concerning the distribution of these fibers within the amygdala, it can be inferred that at least some of that innervation takes place in the PM AHi area.

SOMATOSTATIN (SOM) In the macaque monkey (Amaral *et al.*, 1989), the AL AHi area has a moderate plexus of SOM-ir fibers and terminals and scattered SOM-ir cell bodies. The dense fiber staining seen in layer 1 of other superficial amygdaloid nuclei also covers the superficial surface of AHi, which stops sharply at the boundary of the hippocampal formation [Rosene and van Hoesen's (1987) HATA]. In this animal, the caudal part of the so-called posterior cortical nucleus (here the PM AHi area) by Sorvari *et al.* (1996a, b) contains a dense plexus of fibers in L1 and relatively few scattered SOM-ir cell bodies.

VASOPRESSIN (VP) According to Caffé *et al.* (1989), in the macaque monkey, dense accumulations of VP-ir fibers are found in the cortical nucleus, which according to the present amygdaloid parcellation seems also to include, among others, the PM AHi subarea, though such presence may be due to fibers of passage with destiny to the hippocampal formation.

NEUROTROPHINS

BRAIN-DERIVED NEUROTROPHIC FACTOR (BDNF) According to Murer *et al.* (1999), in the human brain, all of the amygdaloid nuclei contain BDNF-ir neurons and fibers. However from their Fig. 4A and guided by topographical landmarks, it seems plausible that the density of the BDNF-ir in the AHi area is relatively high at least in its nonsuperficial anterolateral division.

ENZYMES

NICOTINAMIDE ADENINE DINOCLEOTIDE PHOSPHATE DIAPHORASE (NADHP-D) In Figs. 10D and 11D of Simms and Williams (1990) report on the distribution of this enzyme in the human amygdala, the AHi, both its posterior and anterolateral divisions, appears positively stained for NADHP-d included in the medial and lateral divisions of their cortical nucleus. In addition, their description of the NADHP-d–ir neuronal population corresponding to these divisions do not seem to correspond to the neuronal population proper of the posterior VCo but rather to the AHi neuronal pool. However, the existence of this type of neurons has been postulated for the whole amygdala by Unger and Lange (1992).

P450 AROMATASE (P450 AROM) Close examination of the illustrations presented by Roselli *et al.* (2001) indicates that these authors have included both the AL and PM divisions of the AHi in what they call the cortical amygdaloid nucleus. If this criterion is accepted, then the conclusion is that the AHi has the highest density of P450 AROM mRNA-labeled cells in the amygdaloid nucleus.

PROTEINS

CALCIUM-BINDING PROTEINS

CALBINDIN (CAB) According to Sorvari *et al.* (1996b), the caudal half of their amygdalohippocampal area (i.e., the AL AHi division) contains a high density of CAB-ir type 1 neurons. Numerous large type 2 and a few type 3 neurons with long, thick dendrites can be also observed. In the so-called posterior cortical nucleus (i.e., the PM AHi division), L1 contains virtually no CAB-ir cells. In L2, which is seen as a dark band of darkly stained angular cells in Nissl-sections, there are a moderate number of small and round type 1 CAB-ir neurons. In L3, the CAB-ir neurons are morphologically more heterogeneous. They consist of type 1 and 2 cells that are larger and have thicker and longer dendrites than the neurons in L2. A few type 3 neurons are also observed.

The intensity of CAB-ir fibers in the AL division of the AHi area is high and the CAB-ir of the neuropil is moderate, similar to that in the PM division of this transitional area. The AL division of the AHi area contains the highest density of CAB-ir bundles in the human amygdala. In the PM division of the AHi area, the density of the CAB-ir fibers and of the CAB-ir neuropil is high in L2 and L3; however, L1 contains significantly fewer fibers. Finally, L2 and L 3 have a moderate density of CAB-ir bundles, which are oriented perpendicular to the pial surface.

CALRETININ (CR) According to Sorvari *et al.* (1996a), their posterior cortical nucleus, which in their illustrations (Figs .2A, 4A, and 6A) includes the P AHi as well as the superior subdivisions of both rostral and caudal divisions of the VCo nucleus, contains a moderate density of small CR-ir neurons of their class 1 and 3. The density of the CR-ir fibers, terminal, and neuropil is stated to be moderately high, but not as high as in the MeA nucleus or in their AHi. A difference between the fiber distribution in rostral and caudal parts of their posterior cortical nucleus is noted.

Furthermore, their AHi includes Al AHi of the present account and also the intermediate subdivision of both rostral and caudal VCo contains their three types of CR-ir neurons. Their medial subdivision of AHi, most probably corresponding to the intermediate subdivisions of both rostral and caudal VCo in the present account, is said to contain numerous large type 2 and type 3 neurons with their main axis oriented perpendicularly or obliquely to the pial surface. Furthermore, the neuronal density in this medial part is higher than in their lateral part of AHi (AL AHi proper), and coincidentally with it, it is here the only place in the whole amygdala that displays CR-ir neurons showing dendritic spines. Finally, the density of the CR-ir fibers is moderate with the highest number of these fibers in their medial part.

PARVALBUMIN (PAV) According to Sorvari *et al.* (1995), in their posterior cortical nucleus, which corresponds to superior subdivisions of both rostral and caudal major divisions of the VCo nucleus, as well as de Olmos (1990), the number of PA-ir neurons is scarce, and such neurons are mostly small, palely stained type 1 and 2 cells. On the other hand, their AHi is said to contain all three types of PAV-ir neurons. The cell density is described as relatively high in their lateral part of AHi (here AL AHi), while the density in their medial AHi (i.e., the intermediate subdivisions of both rostral and caudal VCo here, is said to be lower. The density of PAV-ir cells increases toward the caudal end of AHi. Furthermore, the density of PAV-ir fibers correlates with the cell density. Consistent with that, the largest proportion of these fibers is found in the area corresponding to the caudal levels AL AHi.

Other Proteins

DOPAMINE- AND ADENOSINE-3′,5′-MONOPHOSPHATE (cAMP)–REGULATED PHOSPHOPROTEIN OF M, 32 KDA (DARPP-32) AND PHOSPHATASE INHIBITOR 1 (I-1) According to Barbas *et al.* (1998), in the macaque monkey, the AHi area contains both DARPP-32-ir and I-1-ir neurons, but the former are more numerous and more densely stained than the latter. I-1-ir fibers can be detected in the AHi area. The posterior cortical nucleus of this autors, i.e., the posteromedial division of AHi, is said to contain many I-1-ir and DARPP-32-ir neurons.

LIMBIC SYSTEM–ASSOCIATED MEMBRANE PROTEIN (LAMP) According to Côté *et al.* (1996), in the macaque amygdala, their amygdalohippocampal area and their posterior cortical nucleus, i.e., the anterolateral and posteromedial divisions of the AHi of the present account, display different LAMP-ir with the former being apparently devoid of this protein and the latter showing a moderate LAMP-ir.

SMI32 NEUROFILAMENT PROTEIN (SMI32-IR) From the low-magnification atlas on the distribution of this protein in the macaque brain published by Petrides *et al.* (2000), it seems that the most medial sectors of the AL AHi area contain some SMI32-ir whereas the PM AHi is completely devoid of SMI32-ir.

RECEPTORS

Cholinergic Receptors

MUSCARINIC RECEPTOR (M-R) From the mapping of the distribution of M-R in the human brain by Cortés *et al.* (1987), it is evident that in their Fig. 20 they include both divisions of the AHi in what they depict as the cortical nucleus. If this interpretation is correct, then AHi would contain moderate concentration of this receptor. On the other hand, according to Smiley *et al.* (1999), the amygdala as a whole contains a low density of m_2-ir neurons.

NICOTINIC RECEPTOR (N-R) No primate information is available to the present writer.

CCK RECEPTOR (CCK-R) According to Kritzer *et al.* (1988), keeping with the general pattern of CCK binding site concentration in the ventral medial margins of the macaque monkey amygdala, the AHi area shows a prominent concentration of CCK-R.

Steroid Receptors

ESTROGENIC RECEPTOR (ER)

Estrogen Receptor α (ER-α) According to Blurton-Jones *et al.* (1999), the AHi in humans can display a large, very dense population of ER-α-labeling nuclei (Fig. 3C). By contrast, at least in their studies, only rarely could this type of receptors be detected in the hippocampus proper. This confirms the studies of Osterlund *et al.* (2000), made in human and monkey brains, in which they also found a most abundant expression in their amygdalohippocampal area and their posterior cortical nucleus.

NEUROKININ-1 RECEPTOR (NK-1R) According to Mileusnic *et al.* (1999), in the human amygdala, the density of NK-1R shows the highest expression at the level of AHi and in the ACo, but no mention is made of other superficial amygdaloid nuclei.

Serotoninergic Receptors (5-HT-R)

5-HT_{1A} RECEPTOR (5-HT_{1A}-R) According to Flügge *et al.* (1994), in the tree shrew, the AHi area is strongly labeled by [^{3}H]DPAT, a specific agonist of 5-HT_{1A}-R.

5-HT_{2C} RECEPTOR (5-HT_{2C}-R) Examination of the illustration presented by Lopez-Gimenez *et al.* (2001) it seems that they have included the AHi as a part of their medial amygdaloid nucleus and as such this area would also contain a high density of this type of receptors.

Non Assignable Amygdaloid Formations

Amygdalostriatal Transition Zone (AStr)

The Amygdalostriatal transition zone (Figs. 22.1a, b, 22.8, 22.11, 22.28) [AStr in Plates 25 to 38 (4.0–21.2 mm) in Mai *et al.* (1997), *Atlas of the Human Brain*; not identified in Paxinos *et al.*'s (2000), The Rhesus Monkey Brain in Stereotaxic Coordinates"], named as IPAC in the *Atlas of the Human Brain*, as its name implies, is a transitional zone which at rostral levels of the amygdala appears intervening between the lateral division of the central amygdaloid nucleus (Ce) and the temporal limb of the anterior commissure and at caudal levels comes to lie between the lateral Ce and the striatum. This comparatively small-celled transitional area displays cytoarchitectonic features which, in Nissl sections, look like those of the main member of the nonassignable amygdaloid formations, making it difficult to distinguish the AStr from the latter. A closer look reveals that the neuronal population of the AStr zone is made up of somewhat smaller, rounder cells quite loosely arranged. In sections impregnated with a modification of the Glees procedure, the AStr neurons do not show the characteristic fishlike appearance of the central nucleus neurons, and this facilitates the distinction between these two grisea. Furthermore, it has been possible to establish that in monkeys of the New World at least, but not in macaque monkeys, AStr does not display, under normal conditions, the typical argyrophilic reaction described for the central division of the extended amygdala. This evidence is complemented by differential staining of these structures by the AChE procedure, being denser in AStr than in the lateral Ce. As described here, the AStr seems to be comparable to Brockhaus' (1940) striatum limitans.

Chemoarchitectonics

Heavy Metals In sections of the squirrel and marmoset brains stained by the Timm-Danscher (1981) procedure, it is apparent the less precipitate

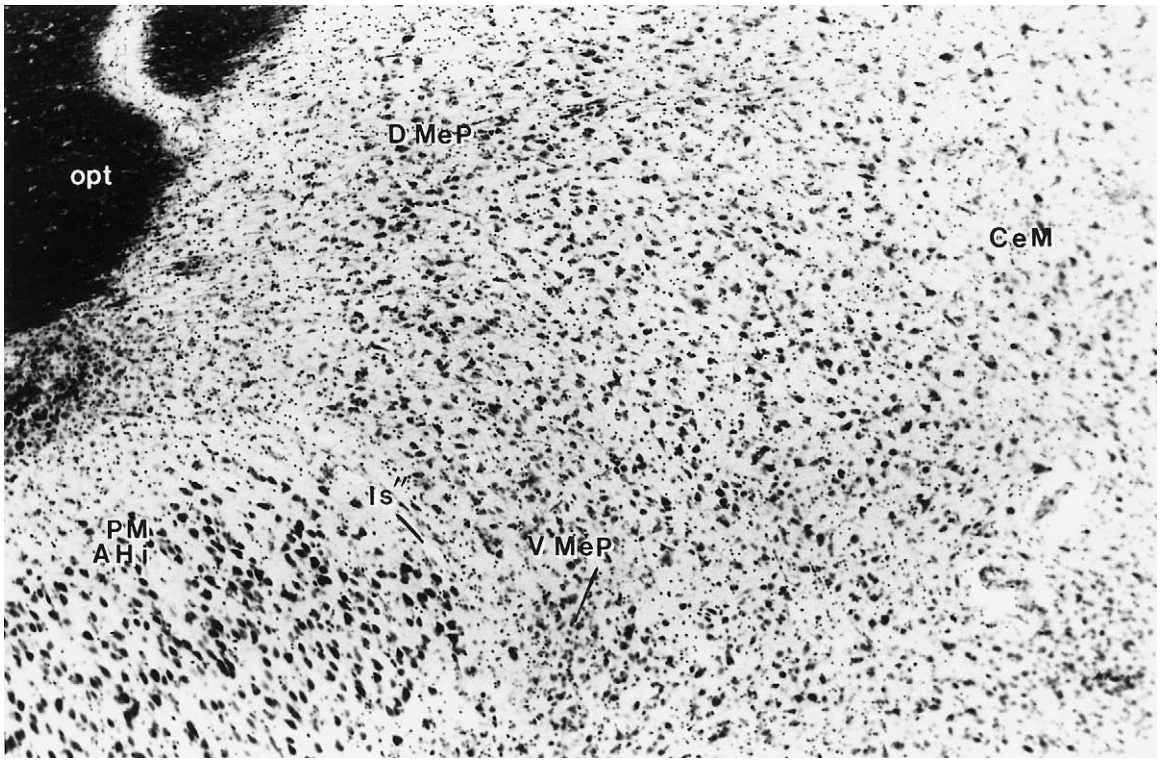

FIGURE 22.28 Medium power photomicrograph of a Cresyl violet-stained coronal section through the caudal portion of the human amygdaloid nuclear complex to show the topographical relationships between the two main members of the MeNG, the medial amygdaloid nucleus (D MeP and V MeP) and the amygdalohippocampal transition area (PM AHi).

distinguishes this structure from the heavily labeled central amygdaloid nucleus. On the other hand, the AStr zone stains darker than its neighbor, the ventral caudal putamen.

Neurotransmitters and Neuromodulators

CHOLINERGIC MARKERS

ACETYLCHOLINESTERASE (ACHE) While a denser AChE staining allows one to discriminate between the AStr zone and the central amygdaloid nucleus, the situation becomes reversed when comparing its level of AChE positivity with that of the striatum proper (more specifically, the ventral caudal putamen, a structure that shows a much higher AChE activity).

CHOLINE ACETYLTRANSFERASE (CHAT) No human or nonhuman primate data is available to the present writer.

MONOAMINE MARKERS

DOPAMINE-β-HYDROXYLASE (DBH) According to Sadikot and Parent (1990), in the squirrel monkey, the ventral striatum is difficult to distinguish from the CeL division on the basis of DBH immunochemistry due to the similar uniform and moderate DBH-ir present in the two areas. The amygdalostriatal area shows moderately dense DBH-ir terminal labeling.

DOPAMINE TRANSPORTER (DAT) According to Celiax *et al.* (1999), many DAT-expressing fibers were found in the human AStr. Punctate neuropil appears to consist of dense varicose axons and shows similar in appearance to that seen in striatum proper. However, the fibers were not as densely arranged as in the striatum. Consequently, many straight, branching, non-varicose axons were also seen through the neuropil.

SEROTONIN (5-HT) According to Sadikoy and Parent, in the squirrel monkey, the periamygdaloid ventral striatum (IPAC?) Shows a rostrocaudal gradient of increasing 5-HT-ir terminals ranging from dense at the amygdalostriatal area to very dense at the caudal interface with the CeL division of the Ce nucleus.

TYROSINE HYDROXYLASE (TH) According to Sadikot and Parent (1990), the intra-amygdaloid ventral striatum (IPAC?) shows dense terminal TH-ir rostrally at the amygdalostriatal area and at its caudal interface with the CeL division of the Ce nucleus.

NEUROPEPTIDES

CALCITONIN GENE–RELATED PEPTIDE (CGRP) According to De La Calle and Saper (2000), in the human brain, patches of CGRP-ir fibers bridge this area with the Ce nucleus.

CHOLECYTOKININ (CCK) In the baboon monkey, the AStr zone not only contains moderate amounts of CCK–ir varicose fibers and punctate profiles but also a few CCK–ir neurons (Martin *et al.*, 1991).

ENKEPHALIN (ENK) According to Heimer *et al.* (1999), the AStr zone in humans is strong in ENK-ir On the other hand, in three different monkeys (macaque, green monkey, and baboon), apart from containing a moderate density of ENK-ir varicose fibers and punctate profiles, the AStr zone also contains ENK–ir perikarya (Martin *et al.*, 1991).

NEUROTENSIN (NT) While the density of NT-ir varicose fibers and punctate profiles ranges from low to moderate in the AStr zone of the macaque, green, and baboon monkey AStr zone, few NT–ir neurons are present at least in the green and baboon monkeys (Martin *et al.*, 1991).

SECRETONEURIN (SECR) Although the AStr zone in the human brain contains SECR-ir fibers, their concentration is lower than in the central amygdaloid nucleus (Kaufman *et al.*, 1997).

SOMATOTASTIN (SOM) While in humans the CCK–ir at the level of the AStr zone seems to be limited to punctate profiles and even these are not abundant, in the macaque monkey, to the contrary, the density of SOM-ir varicose fibers and punctate profiles is significantly high (Martin *et al.*, 1991).

SUBSTANCE P (SP) According to Heimer *et al.* (1999), the AStr zone in human is poor in SP-ir.

CALCIUM BINDING PROTEINS

CALBINDIN (CAB) Although not mentioned by Sorvari *et al.* (1996) in their report of the distribution of this protein in the human amygdala, examination of their illustrations clearly shows that the area here assigned to the AStr zone in humans would contain both CAB-ir fibers and perikarya in clear contrast with the central amygdaloid nucleus, which almost completely lacks CAB-ir.

CALRETININ (CR) Although not mentioned by Sorvari *et al.* (1996) in their report on the distribution of this protein in the human amygdala, examination of their illustrations clearly shows that the area here assigned to the AStr zone in humans contains both CR-ir fibers and cell bodies, but no particular differences

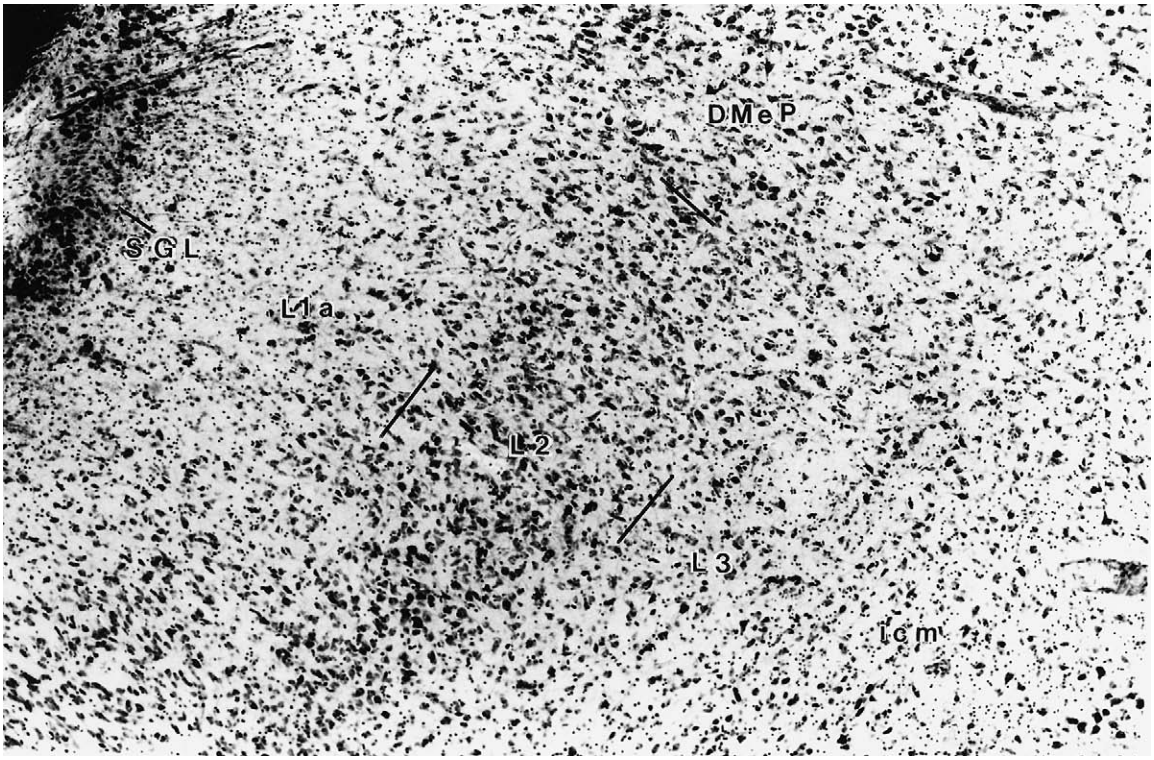

FIGURE 22.29 High-power photomicrograph of a more rostrally cut coronal section from the same brain stained with Cresyl violet showing the cytoarchitectural organization of the ventral part of the posterior division of the medial amygdaloid nucleus (V MeP).

in density of staining can be seen with respect to either the striatum or the central extended amygdala.

PARVALBUMIN (PAV) Although not mentioned by Sorvari *et al*. (1995) in their report on the distribution of this protein in the human amygdala, examination of their illustrations clearly shows that the area here assigned to the AStr zone in humans contains both PAV-ir fibers and cell bodies in clear contrast with their almost complete absence in the immediately adjacent central amygdaloid nucleus. At the same time, it is also visible that the AStr zone contains a lesser amount of PAV-ir than the ventral caudal putamen. The same appears to be true for the macaque AStr zone (Pitkänen and Amaral, 1993).

Interface Islands (IC)

The islands of granular neurons or interface islands (IC), a term shared by Sakamoto and Pearson (see Heimer *et al.*, 1999), are concentrated primarily in the ventral parts of the accumbens and putamen, and are constituted by numerous, more or less compact clusters of basal forebrain cells which are not related to the "islands of Calleja" in the macrosmatic animals, or to Sanides' (1957b) "terminal islands." As noted by Heimer *et al*. (1999), these islands are not restricted to the ventral striatal areas but are also found throughout much of the basal forebrain, especially in relation to the extended amygdala from which they are also components. In the amygdaloid body, where practically all islands are of the parvicellular variety, they are known as intercalated islands since they are located almost without exception between the extended amygdala and the rest of the amygdaloid body, or between components of the extended amygdala. These interface islands can be grouped on the basis of their cell composition in two groups: granular and parvicellular interface islands. The former, as their name indicates, are composed of granular cells, the best example of which are the gamma 1 insulae terminales of Sanides (1957). The second are constituted by somewhat larger and more heterogeneous neurons, the best example of which are the so-called gamma 2 and gamma 3 terminal islands of Sanides (for more details, see Heimer *et al.*, 1999).

From the archipelago-like chain of parvicellular ICs that extends caudally from the dorsomedial accumbens to the lateral bed nucleus of the stria terminalis, a string of this type of cell can be traced along the

supracommissural portion of the bed nucleus of the stria terminalis (BSTS), a route by which they eventually reach the amygdala. Along the course of the stria terminalis lying intercalated between the caudate nucleus and the BSTS grisea that accompanies it are prominent accumulations of interface islands, named paracaudate (interface islands by Heimer *et al.*, 1999) who provide a detailed report.

Chemoarchitectonics

Neurotransmitters and Neuromodulators

CHOLINERGIC MARKERS

ACETYLCHOLINESTERASE (AChE) Histochemical studies by Heimer *et al.* (1999) indicate that many of the parvicellular and granular interface islands show moderate to strong AChE reactivity. Although many interface islands can show AChE reactivity even stronger than surrounding striatal formations, there are, AChE-poor islands irregularly distributed in the human and monkey basal telencephalon. On the other hand, since the islands do not possess intrinsic cholinergic neurons, the AChE reactivity should be in fiber and terminals having presumably their source in some of the cholinergic cell groups in the basal telencephalon.

CHOLINE ACETYLTRANSFERASE (ChAT) Although no specific data deal with ChAT in the neuroanatomical literature consulted by the present writer, and in view of the general coincidence encountered when comparing AChE-stained sections with ChAT-immunostained sections, it is assumed here that the distribution pattern of ChAT-ir fibers and terminals would be consistent with such a pattern.

NEUROPEPTIDES

ENKEPHALIN (ENK) Within many of the parvicellular interface islands, many groups of cells distribution patterns that are complementary or not with that they possess for the SP-ir (Heimer *et al.*, 1999).

NEUROPEPTIDE Y (NPY) According to Walter *et al.* (1990), the parvicellular islands in the above-described chain are characterized by NPY-ir fibers and cell bodies which are in continuity with the NPY-positive region in the BSTL division of the bed nucleus of the stria terminalis. Both features allow its discrimination from the neighboring caudate nucleus.

CHOLECYSTOKININ (CCK) According to Heimer *et al.* (1999), in the human telencephalon the interface islands seems to be special targets for axons containing CCK. On the other hand, in the paracaudate interface island CCK-ir neuronal perikarya are also present.

SOMATOTASTIN (SOM) According to Heimer *et al.* (1999), in the human telencephalon, the interface islands seem to be special targets for axons containing SOM possibly coming from the Ce nucleus (Mufson *et al.*, 1988).

SUBSTANCE P (SP) According to Heimer *et al.* (1999), many of the parvicellular interface islands existing in the human basal telencephalon contain moderate to strong SP-ir processes and perikarya while others may have little or none.

Intercalated Cell Masses (ICMs)

As in nonhuman primates and subprimate mammals, the human amygdala contains groups of closely packed, granule-like neurons generally scattered among the different amygdaloid nuclei lying between, around, or within them. These groups of cells appear most prominently in the caudal half of the amygdaloid complex. In Nissl sections these groups of granule-like neurons show varying staining, so that in some of these masses the cells show somewhat light staining and in others even a prominently dark staining. The most outstanding ICM is located between the Ce and BM, and in appropriately oriented horizontal or sagittal sections it can be seen that, as in nonprimate mammals, one of these islands which is intercalated between the Ce and BM nuclei extends along the boundary line between them and eventually turns laterally around the back of Ce where it comes to lie between this nucleus and descending fascicles of the stria terminalis. Another conspicuous group is located between the ACo and Ce nuclei, or between this latter and the AStr, or between this transitional field and the La; or in the intersection between BM, VMBL, and VCo, etc. ICM are seen less often within the BM nucleus or the AAA area.

Chemoarchitectonics

Heavy Metals In Timm's/selenite-stained sections, the distribution of the silver precipitate shows exactly the inverse pattern as that observed for the AChE reaction. That is, while a majority of the ICM show heavy silver deposits, those around La appear rather weak.

Neurotransmitters

CHOLINERGIC MARKERS

ACETYLCHOLINESTERASE (AChE) Although most of the island-like gray formations stain negatively or show a rather weak AChE reaction, some of them, particularly those around La, present a high level of reactivity, the same as that located in the intersection between BM,VMBL, and VCo, and situated dorsally,

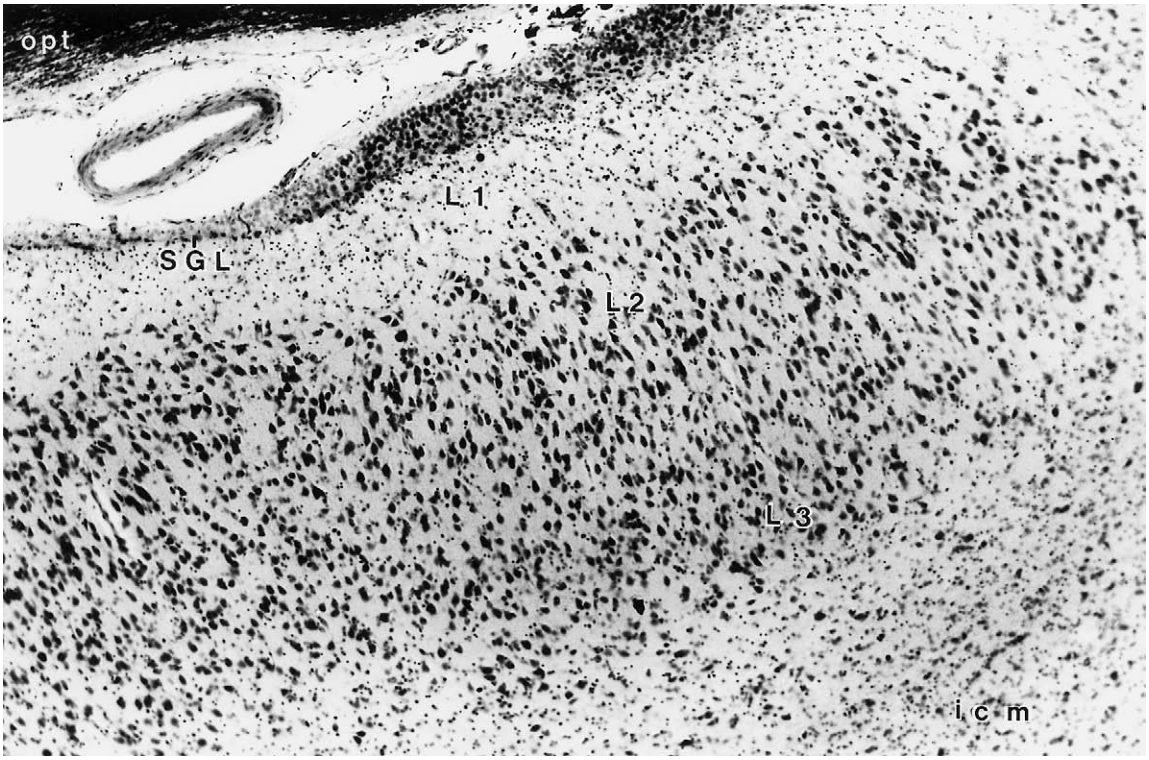

FIGURE 22.30 High-power photomicrograph of a Cresyl violet-stained coronal section through the posteromedial division of the amygdalohippocampal transition area of the human amygdala to show some details of its cytoarchitectonic organization.

caudally, and ventrally surrounding the ACA (see Simm and Williams, 1990; de Olmos, 1990; Heimer *et al.*, 1999).

According to Amaral and Basset (1989), in the macaque monkey most of the ICMs show a moderate AChE staining. However, some of these cell conglomerates contain high levels of this cholinergic marker. The ICMs located medially to the APir area contain a dense AChE activity. In the amygdala of the New World monkeys (i.e., squirrel monkey and marmoset), a similar distribution can be found according to AChE-stained material available to the present writer.

CHOLINE ACETYLTRANSFERASE (CHAT) According to Amaral and Basset (1989), in the macaque monkey most of the ICMs show a moderate ChAT-ir. However, as it happens in AChE-stained material, some of these cell aggregates show high levels of ChAT-ir. The ICMs located medially to the APir area likewise show a dense ChAT-ir.

MONOAMINE MARKERS

DOPAMINE-β-HYDROXYLASE (DBH) According to Sadikot and Parent (1990), in the squirrel monkey, the intercalated masses display very light and moderate DBH-ir terminal labeling.

HISTAMINE (HA) According to Airaksinen *et al.* (1989; Fig. 3), in the tree shrew, the ICM islands would be innervated by HA fibers.

SEROTONIN (5-HT) According to Freedman and Shi (2001), in the macaque monkey, there are relatively heavy concentrations of 5-HT-ir in an intercalated group ventromedial to Ce nucleus. In the squirrel monkey, the intercalated masses show a light density of 5-HT-ir terminal labeling.

TYROSINE HYDROXYLASE (TH) According to Sadikot and Parent (1990), in the squirrel monkey, the intercalated masses show a dense to moderately dense field of TH-ir terminal varicosities.

EXCITATORY AMINO ACIDS

GLUTAMATE/ASPARTATE (GLU/ASP) Retrograde tracing experiments made in rats using tritiated D-aspartate indicate that a considerable number of the ICMs ventral to the BL nucleus would be a source of

GLU/ASPergic strong projections to the ventral pallidum and olfactory tubercle and in a more reduced manner to the ventral striatum (Fuller *et al.*, 1987).

INHIBITORY AMINOACIDS

γ-Aminobutyric Acid (GABA) According to McDonald and Augustine (1993), in the macaque monkey all of the small cells but none of the large neurons present in the ICM nuclei are GABA-ir. These authors, together with Pitkännen and Amaral (1994), agree that most of the intercalate nuclei show a higher number of GABA-ir or GAD mRNA labeled cells than that present in the nuclei of the LBNC. A few intercalated nuclei present substantially fewer GABA-ir or GAD mRNA-labeled cells. The most distinctive feature of the intercalated nuclei is their very high density of GABA-ir fibers and terminals being the densest in the whole monkey amygdala.

NEUROPEPTIDES

Galanin (GAL) From the description and mappings presented by Kordower *et al.* (1992), on the basis of macaque monkey material, it does not seem that these cells contain any type of GAL-ir.

Neuropeptide Y According to McDonald *et al.* (1995), in the macaque monkey, very few NPY neurons are present in the ICMs.

Neurotensin (NT) According to Benzing *et al.* (1992), these island formations were densely NT-ir, consisting of a dense network of ir fibers and puncta. These formations are also characterized by the presence of numerous darkly stained and densely packed small to medium-sized multipolar or round neurons. The number of NT-ir neurons varies across the different IC accumulations both within and between cases.

Somatotastin (SOM) In the Macaque monkey the IC islands show light to moderate SOM-ir fibers and terminals as well as few SOM-ir cell bodies. McDonald *et al.* (1995) report few if any SOM-ir cell bodies in the ICMs. According to Desjardins, in the squirrel monkey, the intercalated masses display a neuropil staining whose intensity ranges from light to moderate.

CALCIUM-BINDING PROTEINS

Calbindin (CAB) According to Sorvari *et al.* (1996b), in the human amygdala, the amount of CAB-ir in the different intercalated nuclei varied. Most of the intercalated nuclei contained a large number of small, round, and densely packed CAB-ir neurons, while some of them contained few or no cells. Furthermore, the fiber and neuropil CAB-ir also varied greatly among the intercalated nuclei.

Parvalbumin (PAV) According to Sorvari *et al.* (1995), the PAV-ir varies slightly between the ICMs, with some nuclei showing only a few small PAV-containing neurons with short dendrites and others being completely negative. Moreover, the density of the PAV-ir-containing fibers and terminals was low.

OTHER PROTEINS

Dopamine- and Adenosine-3′,5′-monophosphate (cAMP)–Regulated Phosphoprotein of M, 32 kDa (DARPP-32) and Phosphatase Inhibitor 1 (I-l) According to Barbas *et al.* (1998), in the macaque monkey amygdala, many neurons moderately or robustly labeled for DARPP-32 or I-l can be found in the intercalated masses located between the medial, central, basolateral, and lateral nuclei. I-l-ir fibers can be found in the IC masses between the La and BL nuclei and between the BL and BM nuclei. These immunoreactive fibers joined laterally and continued through the central part of the basal forebrain.

Limbic System–Associated Membrane Protein (LAMP) According to Côté *et al.* (1996) in the macaque amygdala, the intercalated nuclei are devoid of LAMP-ir.

Neurofilament Protein SMI32 (SMI32) To judge from the low magnification in the Petrides *et al.* (2000) atlas on the distribution of the SMI32 neurofilament protein in the macaque monkey brain, these islands formations do not seem to contain any SMI32-ir.

RECEPTORS

Adrenergic Receptors

adrenoreceptor α_1 According to Flügge *et al.* (1994), in the tree shrew, the IC nuclei show a strong binding of [^{3}H]PRA, an α-adrenoreceptor antagonist indicative of the presence of this type of adrenoreceptor.

adrenoreceptor α_2 According to Flügge *et al.* (1994), in the tree shrew, IC nuclei show a high density of [^{3}H] RAU binding sites, RAU being indicative of the presence of this type of receptor.

benzodiazepine receptor (BNZ-R) According to Zezula *et al.* (1988), in the human amygdala, the IC cell masses contain very high concentrations of BNZ-R.

Cholinergic Receptors

muscarinic receptor (mACh-R) According to Cortés *et al.* (1987), in the human amygdala, the highest

densities in mACh-R can be detected in small cell masses lateral to the dorsal pole of the BL nucleus and along the ventrolateral surfaces of the La nucleus, which are identified as ICMs.

NICOTINIC RECEPTOR (NACH-R) This type of receptor, labeled as [^{3}H]ACh or [^{3}H]nicotine, shows very low concentrations in all nuclei of the rat amygdaloid complex (Rainbow *et al.*, 1984; Clarke *et al.*, 1985). No other source of this type of data is available to the present writer about the distribution of this type of receptor in the primate amygdala.

Intramedullary Griseum (IMG)

The intramedullary grisea (IMG) was first described for the rat amygdala as a narrow gray formation associated with the Ce. Such association was induced by the difficulty that it presented its full identification in the very narrow interface between the components of the LBNC themselves, on one side, and between them and the rest on the amygdaloid nuclei. However, in the guinea pig brain (unpublished personal observations) it is not as difficult to verify its existence, but this becomes far more evident in the amygdala of primates. Thus, whereas in the Nissl sections of the rat brain IMG appears represented by small, narrow clusters of neurons or even single neurons aligned along the fiber septa separating the Ce from the BL but becomes far more difficult to follow in its prolongation to other sectors of the amygdala, in the primate brain the IMG constitutes a much more generalized and easily traceable morphological entity.

IMG is composed of neurons of various sizes and shapes with well-defined perikarya but of varying stainability that are interspersed among the fibers of the medullary laminae, which are intercalated not only between the components of the LBNC but also among those less conspicuous fiber contingents lying interposed between this latter gray mass and the rest of the amygdaloid nuclei. At this point, however, it is convenient to stress that the intramedullary grisea that are intercalated between BL VM and BM, on one side, and the superficially located amygdaloid nuclei Me, ACo, VCo, and APir, on the other, show the same disposition than their more well-defined counterparts in the major medullary laminae. That is to say, they appear enmeshed by fibers running parallel to the deep border of the above-listed superficial nuclei, although at some places they become less obvious showing instead variable arrangements (see Figs. 22.4, 22.5a, b, 22.6a, 22.7a). Therefore, there is a question regarding the so-called morphological continuity between the superficial cortical nuclei and some of the representatives of the LBNC.

As in the previous version of this chapter (de Olmos, 1990), it is important to stress again the existence of several distinguishing cytoarchitectonic features that allow identification of the widely dispersed constituents of the IMG. These are as follows: (1) The cells making up the IMG, though of varying in size and shape, are always larger than those in the intercalated islands, but smaller and of more divergent shape than those shown by the main neuronal components of the LBGC. (2) The main cell body axes of the IMG cells are predominantly oriented parallel to the course of fiber bundles in which they are enmeshed, and many times this orientation contrasts sharply with the cells in the neighboring main nuclear divisions. This is particularly noticeable in horizontal sections showing the boundaries between VCo and BLVM.

On this basis it is possible to recognize the presence of the heterogeneous gray formation as strings of clusters forming real cell corridors intercalated between the various nuclei of the laterobasal complex separating them from each other as well as from the centromedial and cortical amygdaloid nuclei. However, at certain poinrs they form prominent accumulation of cells as is the case where they form a wedge between the BM VM, the BL VM, and the PCoV (lamina 27, plane 6.7 mm of Mai *et al. Atlas of the Human Brain*), i.e., where the lower medial end of the intermediate medullary lamina (li) meets the lower end of the medial medullary lamina (mm). This wedge-like area is filled with neuronal clusters which in the human amygdala may attain such a large volume that they have been considered by some authors to be subnuclei in their own right. As previously noted, the gray mass labeled Abvm in Sorvari *et al.* (1995) may be part of this extensive intramedullary grisea and at least one of the deep located subdivisions of Brockhaus (1940), i.e., their amygdala superficiale intermedia pars ventrolateralis, Asf ivl. Less conspicuous IMG clusters or even scattered neurons are found in the fiber strata separating BL from La, BM, ACA, and EN.

It is notable that this heterogeneous structure has escaped the attention of so many morphologists who, even if capable of identifying them, did not consider the IMG islands important enough to be differentiated from their neighboring nuclei. If this has been so, as will be shown below, these intramedullary grisea possess enough differentiating chemoarchitectonic and probably connectional features to speak strongly in favor of IMG as a separated anatomical entity.

Chemoarchitectonics

Cupric Silver Technique In cupric silver–stained sections of the amygdala of Old World (macaque) and New World (squirrel) monkeys, strips of lightly stained

granular neuropil can be found along the borders between the La and BL and BL and BM, i.e., overlapping the medullary strata separating these nuclei. This positive though light Cu-Ag reaction at the level of the IMG contrast with its total absence in the main components of the LBNC.

Heavy Metals

TIMM-DANSCHER PROCEDURE In Timm-stained New World monkey (squirrel) amygdala, many of the IMG islands show a moderate to strong reactivity, particularly those lying between BL and La.

Neurotransmitters

CHOLINERGIC MARKERS

ACETYLCHOLINESTERASE (AChE) In AChE preparations, the IMG islands show some staining variations, so that those located dorsal to La show strong AChE reactivity, whereas the greater part of the islands in the wedge-like region between BM and BL are negatively stained. The largest IMG island lying at the point of reunion of the medial and intermediate medullary laminae show instead a moderate to high AChE reactivity (Fig. 22.11, IMG). The same it occurs with some smaller IMG islands in the boundary region between BL VM, BM VM, and the inferior subdivision of the caudal VCo.

CHOLINE ACETYLTRANSFERASE (ChAT) In examining the ChAT material presented by Emre *et al.* (1993), it is possible to appreciate in their Fig. 2A and B a staining pattern close to the one just described above using AChE histochemistry. However, the isolation of this IMG island (interpreted by these authors as an intercalated island) from the main collections of amygdaloid neurons is much clearer.

MONOAMINE MARKERS

DOPAMINE-β-HYDROXYLASE (DBH) In the human amygdala, as in the squirrel monkey and even in a lower macrosmatic mammal like the rat, DBH-ir fibers detached from the ansa peduncularis/ventral amygdalofugal pathway can be seen to run in an almost preferential manner along the extent of the IMG elements sprinkled along the medullary laminae lying between the main nuclei of the LBNC or separating them from the cortical superficial nucleus. In their course these DBH-ir fibers show all the typical manifestations on the bouton en passage and even direct terminals.

NEUROPEPTIDES

CHOLECYSTOKININ (CCK) In IMG of the baboon monkey, Martin *et al.* (1991) reported the presence of CCK-ir varicose fibers and punctate profiles in moderate amounts, as well as the presence of CCK-ir neurons.

ENKEPHALIN (ENK) In all of the primates studied by Martin *et al.* (1991), fibers, punctate profiles, and cell bodies immunoreactive for ENK were detected.

NEUROTENSIN (NT) As with other neuropeptides, the IMGs show in primates a moderate amount of NT-ir (Martin *et al.*, 1991).

SOMATOTASTIN (SOM) Close examination of some of the images (Figs. 2A–F asterisks, and 6) published by Amaral *et al.* (1989) on the SOM-ir distribution in the macaque monkey amygdala, suggests the existence, along major medullary laminae that separate the main components of the LBNC or the BM nucleus from the superficial pseudocortical and superficial amygdaloid nuclei, of very thin fence-like SOM-ir deposits or island-like accumulations of varying size. These deposits vary in density, from being somewhat higher than in the nuclei it separates to places where they are almost completely negative. Unfortunately, because of the low magnification of the published material it is not possible to infer weather these formations contain SOM-ir cell bodies.

Acknowledgments

The author thanks Dr. Lennart Heimer and Dr. John Jane and the Department of Neurological Surgery, University of Virginia Health System, Charlottesville, VA, USA, for constant support and encouragement. To Dr. George Alheid for having collaborated in many projects which helped the writing of this chapter and Dr. Carlos Beltramino for advice and valuable comments. To Soledad de Olmos for all her technical support. I would also like to dedicate this chapter to my wife Esther de Olmos, for all her support and patience. This work has been supported by the Consejo Nacional de Investigaciones Cientificas y Tecnicas of Argentina (CONICET) PIP #02908, the Fundación Interior Argentina (FUNINAR), and the Fogarty International Research Award—IRO3TW00963. Dr. Jose S. de Olmos is a senior scientist of CONICET, Argentina.

Abbreviations

AAA anterior amygdaloid area
Dp AAA anterior amygdaloid area,deep division
Sf AAA anterior amygdaloid area, superficial division

ACA amygdaloclaustral transition area
ac anterior commissure
Acb nucleus accumbens septi
ACo anterior cortical nucleus
- **D ACo** anterior cortical nucleus, dorsal division
- **V ACo** anterior cortical nucleus, ventral division

AHi amygdalohippocampal area
- **AL AHi** anterolateral subdivision of amygdalohippocampal area
- **PM AHi** posteromedial subdivision of amygdalohippocampal area

al ansa lencticularis
APir amygdalopiriform transition area
- **AL APir** amygdalopiriform transition area, anterolateral division
  - **I AL** amygdalopiriform transition area, intermediate part of the anterolateral division
  - **L AL APir** amygdalopiriform transition area, lateral part of the anterolateral division
  - **M AL Apir** amygdalopiriform transition area, medial part of the anterolateral division
- **PM APir** amygdalopiriform transition area, posteromedial division
  - **DL PM Apir** amygdalopiriform transition area, dorsolateral part of the posteromedial division
  - **MV PM Apir** amygdalopiriform transition area, medioventral part of the posteromedial division

AStr amygdalostriatal transition Zone

B basal nucleus of Meynart
BL basolateral amygdaloid nucleus
- **D BL** basolateral amygdaloid nucleus, dorsal division
- **DL BL** basolateral amygdaloid nucleus, dorsolateral division
- **I BL** basolateral amygdaloid nucleus, intermediate division
- **VL BL** basolateral amygdaloid nucleus, ventrolateral division
- **VM BL** basolateral amygdaloid nucleus, ventromedial division

BM basomedial amygdaloid nucleus
- **CM BM** basomedial amygdaloid nucleus, caudomedial division
- **DL BM** basomedial amygdaloid nucleus, dorsolateral division
- **DM BM** basomedial amygdaloid nucleus, dorsomedial division
- **VL BM** basomedial amygdaloid nucleus, ventrolateral division
- **VM BM** basomedial amygdaloid nucleus, ventromedial division

BSTI bed nucleus of the stria terminalis intermediate division
BSTL lateral bed nucleus of the stria terminalis
- **BSTLD** bed nucleus of the stria terminalis, dorsal part of the lateral division
- **BSTLDc** bed nucleus of the stria terminalis, capsular subdivision of the dorsal part of the lateral division
- **BSTLDcn** bed nucleus of the stria terminalis, central subdivision of the dorsal part of the lateral division
- **BSTLP** bed nucleus of the stria terminalis, posterior part of the lateral division
- **BSTLV** bed nucleus of the stria terminalis, ventral part of the lateral division
- **BST JXC** bed nucleus of the stria terminalis, juxtacapsular part of the lateral division

BSTM bed nucleus of the stria terminalis medial division
- **BSTMA** bed nucleus of the stria terminalis; anterior part of the medial division
- **BSTMP** bed nucleus of the stria terminalis; posterior part of the medial division
  - **BSTMPi** bed nucleus of the stria terminalis, intermediate subdivision of the posterior part of the medial division
  - **BSTMPl** bed nucleus of the stria terminalis, lateral subdivision of the posterior part of the medial division
  - **BSTMPm** bed nucleus of the stria terminalis, medial subdivision of the posterior part of the medial division

BSTS bed nucleus of the stria terminalis, supracapsular division
- **BSTSl** bed nucleus of the stria terminalis, lateral column of the supracapsular division
- **BSTSm** bed nucleus of the stria terminalis medial column of the supracapsular division

CA cornu ammonis
Cd caudate nucleus
Ce central amygdaloid nucleus
CeL lateral subdivision of central amygdaloid nucleus
- **CeLA** central amygdaloid nucleus; apical part of the lateral division
- **CeLC** central amygdaloid nucleus; capsular part of the lateral division
- **CeLCn** central amygdaloid nucleus; central part of the lateral division
- **PCeL** central amygdaloid nucleus, paracapsular division
  - **D PCeL** central amygdaloid nucleus, dorsal subdivision of the paracapsular part of the lateral division

V PCeL central amygdaloid nucleus, ventral subdivision of the paracapsular part of the lateral division
PPCeL central amygdaloid nucleus, peri paracapsular part of the lateral division
CeM central amygdaloid nucleus, medial division
DCeM central amygdaloid nucleus, dorsal part of the medial division
VCeM central amygdaloid nucleus, ventral part of the medial division
Cl claustrum
cp cerebral peduncle

dbb diagonal band of Broca

En endopiriform nucleus
Ent entorhinal cortex

f fornix
fa amygdaloid fissure

GP globus pallidus
EGP external globus pallidus
IGP internal globus pallidus

HDB nucleus of the horizontal limb of the diagonal ban
Hyp hypothalamus

i island of gamma 1-cells
I intercalated masses
Ic intercalated cells
Ip paracapsular, intercalated cell clusters
ic internal capsule
icm intermediate caudomedial fiber masses
IMG intramedullary gray

La lateral amygdaloid nucleus
D La lateral amygdaloid nucleus, dorsal division
DA La lateral amygdaloid nucleus, dorsal anterior division
DL La lateral amygdaloid nucleus, dorsal lateral division
DM La lateral amygdaloid nucleus, dorsomedial division
I La lateral amygdaloid nucleus, intermediate division
Li La lateral amygdaloid nucleus, limitans division
VL La lateral anygdaloid nucleus, ventrolateral division
VM La lateral amygdaloid nucleus, ventromedial division
LBNC laterobasal nuclear complex
La C lamina cornea

lab longitudinal association bundle
ldm dorsomedial medullary lamina
li intermediate medullary lamina
ll lateral medullary lamina
lm medial medullary lamina
ls' superficial medullary lamina, first
ls" superficial medullary lamina, second
LS I lateral septal nucleus, intermediate division
LS V lateral septal nucleus, ventral division
LV lateral ventricle
L1 molecular layer
L2 superficial cell layer
L3 deep cell layer

MCBFC magnocellular basal forebrain complex
MeA medial amygdaloid nucleus
MeA medial amygdaloid nucleus, anterior division
MeP medial amygdaloid nucleus, posterior division
D MeP medial amygdaloid nucleus, dorsal part of the posterior division
V MeP medial amygdaloid nucleus, ventral part of the posterior division

opt optic tract

Pir piriform cortex
PL paralaminar nucleus
PL gl paralaminar nucleus, glomerular division
Pu putamen

sas semicircular amygdaloid sulcus
SGL subpial granular layer
SHy septohypothalamic nucleus
SLEA sublenticular extended amygdala
SLEAC central division of sublenticular extended amygdala
SLEAM medial division of sublenticular extended amygdala
smt stria medullaris thalami
st stria terminalis
Str acc striatum accessories

VCo ventral cortical amygdaloid nucleus
C VCo ventral cortical amygdaloid nucleus, caudal division
IF CVCo ventral cortical amygdaloid nucleus, inferior part of the caudal division
IT CVCo ventral cortical amygdaloid nucleus, intermediate part of the caudal division
Sp CVCo ventral cortical amygdaloid nucleus, superior part of the caudal division
R VCo ventral cortical amygdaloid nucleus, rostral division

IF RVCo ventral cortical amygdaloid nucleus, inferior part of the rostral division
IT RVCo ventral cortical amygdaloid nucleus, intermediate part of the rostral division
Sp RVCo ventral cortical amygdaloid nucleus, superior part of the rostral division
vs vessel
3v third ventricle

References

Adolphs, R., and Tranel, D. (2003). Amygdala damage impairs emotion recognition from scenes only when they contain facial expressions. *Neuropsychologia* **41,** 1281–1289.

Airaksinen, M.S., Flügge, G., Fuchs, E., and Panula, P. (1989). Histaminergic system in the tree shrew brain. *J. Comp. Neurol.* **286,** 289–310.

Alheid, G.F., de Olmos, J.S., and Beltramino, C.A. (1995). Amygdala and extended amygdala. *In* "The Rat Nervous System," 2nd. ed. (G. Paxinos, ed.), pp. 495–578, Academic Press, San Diego.

Alheid, G..F., and Heimer, L. (1988). New perspectives in basal forebrain organization of special relevance for neuropsychiatric disorders: the striopallidal, amygdaloid, and corticopetal components of substantia innominata. *Neuroscience* **27,** 1–39, 1988.

Alheid, G.F., and Heimer, L. (1996). Theories of basal forebrain organization and "the emotional motor system." *In* "The Emotional Motor System" (G. Holstege, R. Bandler, and C.B. Saper, eds.), pp 461–484.

Alheid, G.F., Beltramino, C.A., Braun, A., Miselis, R.R., Francois, Ch., and de Olmos, J. (1994). Transition areas of the striopallidal system with the extended amygdala in the rat and primate: observations from histochemistry and experiments with mono- and transsynaptic tracers. *In* "The Basal Ganglia," Part 4 (G. Percheron et al. eds.), pp. 95–107. Plenum, New York.

Alheid, C.A. Beltramino, J. de Olmos, M.S. Forbes, D.J.Swanson, and L.Heimer. (1998) The neuronal organization of the supracapsular part of the stria terminalis in the rat: the dorsal component of the extended amygdala. *Neuroscience* **84,** 967–996.

Amaral, D. G., and Price, J. L. (1984). Amygdalo-cortical projections in the monkey *(Macaca fascicularis). J. Comp. Neurol.* **230,** 463–496.

Amaral, D.G., Avendazo, C., and Benoit, R. (1989). Distribution of somatostatin-like immunoreactivity in the monkey amygdala. *J. Comp. Neurol.* **284,** 294–313.

Amaral, D.G., and Bassett, J.L. (1989). Cholinergic innervation of the monkey amygdala: an immunohistochemical analysis with antisera to choline acetyltransferase. *J. Comp. Neurol.* **281,** 337–361.

Amaral, D.G., and Insausti, R. (1992). Retrograde transport of D-[3H]-aspartate injected into the monkey amygdaloid complex. *Exp. Brain Res.* **88,** 375–388.

Amaral, D.G., Price, J.L., Pitkänen and Carmichael, S.T. (1992). Anatomical organization of the primate amygdaloid complex. *In* "The Amygdala; Neurobiological Aspects of Emotion, Memory and Mental Dysfunction" (J.P. Aggleton, ed.), pp. 1–66. Wiley-Liss, New York.

Amaral, D.G. (2002). The primate amygdala and the neurobiology of social behavior: implications for understanding social anxiety. *Biol. Psychiatry* **51,** 11–17.

Andy, O.J., and Stephan, H. (1976). Septum development in primates. *In* "The Septal Nuclei" (J.F. De France, ed.), pp. 3–36. Plenum, New York.

Andy, O.J., and Stephan, H. (1968). The septum in the human brain. *J. Comp. Neurol.* **133,** 383–410.

Angevine, J.B., Locke, S., and Yakolev, P.I. (1964). Limbic nuclei of thalamus and connections of limbic cortex. V. Thalamocortical projections of the magnocellular medial dorsal nucleus in man. *Arch. Neurol.* **10,** 165–180.

Angevine, J.B. (1965). Time of neuronal origin in the hippocampal region. *Exp. Neurol.* Suppl. 2: 1–70.

Angevine, J.B., and Sidman, R.L. (1961). Autoradiographic study of cell migration during histogenesis of cerebral cortex in the mouse. *Nature* **192,** 766–768.

Arimatsu, Y., Seto, A., and Amano, T. (1981). Sexual dimorphism in the α-bungarotoxin binding capacity in the mouse amygdala. *Brain Res.* **213,** 432–437.

Barbas, H., and de Olmos, J. (1990). Projections from the amygdala to basoventral and mediodorsal prefrontal regions in the rhesus monkey. *J. Comp. Neurol.* **300,** 549–571.

Barbas, H., Gustafson, E.L., and Greengard, P. (1998). Comparison of the immunocytochemical localization of DARPP-32 and I-1 in the amygdala and hippocampus of the rhesus monkey. *J. Comp. Neurol.* **334,** 1–18.

Basile, M.J., Heilman, C.J., Drash, G.W., Mou, K., Staley, J.K., Miller, G.-W., Mash, D.C., and Ciliax, B.C. (2000). The immunocytochemical distribution of the norepinephrine transporter in human brain. *Soc. Neurosc. Abstr.* **26(**2), 1429.

Basset, J.L., Shipley, M.T., and Foote, S.L. (1992). Localization of corticotropin-releasing factor-like immunoreactivity in monkey olfactory bulb and secondary olfactory areas. *J. Comp. Neurol.* **316,** 348–362.

Bayer, S. (1980). Quantitative 3H-thymidine autoradiographic analysis of neurogenesis in the rat amygdala. *J. Comp. Neurol.* **194,** 845–876.

Bayer, S.A. (1986). Neurogenesis in the anterior olfactory nucleus and its associated transition areas in the rat brain. *Int. J. Dev. Neurosci.* **4,** 225–249.

Bayer, S. (1987). Neurogenetic and morphogenetic heterogeneity in the bed nucleus of the stria terminalis. *J. Comp. Neurol.* **265,** 47–64.

Bayer, S.A., and Altman, J. (1987). Development of the preoptic area: time and site of origin, migratory routes, and settling patterns of its neurons. *J. Comp. Neurol.* **265,** 65–95.

Beltramino, C., and Taleisnik, S. (1978). Facilitatory and inhibitory effects of electrochemical stimulation of the amygdala on the release of luteinizing hormone. *Brain Res.* **144,** 95–107.

Beltramino, C., and Taleisnik, S. (1980). Dual action of electrochemical stimulation of the bed nucleus of the striha terminalis on the release of LH. *Neuroendocrinology* **30,** 238–242.

Benjamin, R.M., and Jackson, J.C. (1974). Unit discharges in the mediodorsal nucleus of the squirrel monkey evoked by electrical stimulation of the olfactory bulb. *Brain Res.* **75,** 181–191.

Bennet-Clarke, C., and Joseph, S.A. (1986) Immunohistochemical localization of somatotastin in human brain. *Peptides* **7,** 877–884.

Benzing, W.C., Mufson, E.J., Jennes, L., and Armstrong, D.M. (1990). Reduction of neurotensin immunoreactivity in the amygdala in Alzheimer's disease. *Brain Res.* **537,** 298–302.

Benzing, W.C., Mufson, E.J., Jennes, L., Stopa, E.G., and Amstrong, D.M. (1992). Distribution of neurotensin immunoreactivity within the human amygdaloid complex: a comparison with acetylcholinesterase- and Nissl-stained tissue sections. *J. Comp. Neurol.* **317,** 283–297.

Benzing, W.C., Kordower, J.H., and Mufson, E.J., (1993). Galanin immunoreactivity within the primate basal forebrain: evolutionary changes between monkeys and apes. *J. Comp. Neurol.* **336,** 31–39.

Blurton-Jones, M., and Tuszynski, M.H. (2002). Estrogen receptor-beta colocalizes extensively with parvalbumin-labeled inhibitory

neurons in the cortex, amygdala, basal forebrain, and hippocampal formation of intact and ovariectomized adult rats. *J. Comp. Neurol.* **452,** 276–287.

Blurton-Jones, M.M., Roberts, J.A., and Tuszynski, M.H. (1999). Estrogen receptor immunoreactivity in the adult primate brain: neuronal distribution and association with P75, *trka,* and choline acetyltransferase. *J. Comp. Neurol.* **405,** 529–542.

Bons, N., Mestre, N., Petter, A., Danger, J.M., Pelletier, G., and Vaudry, H. (1990). Localization and characterizetion of neuropeptide Y in the brain of *Microcebus murinus* (Primate, Lemurian). *J. Comp. Neurol.* **298,** 343–361.

Bouras, C., Vallet, P.G., Dobrinov, H., de St-Hilaire, S., and Constatinidis, J. (1986). Substance P neuronal cell bodies in the human brain: complete mapping by immunohistofluorescence. *Neurosci. Lett.* **69,** 31–36.

Bouras, C., Magistretti, P.J., Morrison, J.H., and Constatinidis, J. (1987). An immunohistochemical study of pro-somatotastin-derived peptides in the human brain. *Neuroscience* **22,** 781–800.

Braak, H., and Braak, E. (1983). Neuronal types in the basolateral amygdaloid nuclei of man. *J. Comp. Neurol.* **317,** 283–297.

Braak, H., and Braak, E. (1983). Neuronal types in the basolateral amygdaloid nuclei of man. *Brain Res. Bull.* **11,** 349–365.

Braak, H., and Braak, E. (1987). Projection neurons of basolateral amygdaloid nuclei develop meganeurites in juvenile and adult neuronal ceroid lipofuscinosis. *Clin. Neuropathol.* **6,** 116–119.

Brady, D.R., Carey, R.G., and Mufson, E.J. (1992). Reduced nicotinamide adenine dinucleotide phosphate-diaphorase (NADPH-d) profiles in the amygdala of human and New World monkey (*Saimiri sciureus*). *Brain Res.* **577,** 236–248.

Brashear, H.R., Godec, M.S., and Carlsen, J. (1988). The distribution of neuritic plaques and acetylcholinesterase staining in the amygdala in Alzheimer's disease. *Neurology* **38,** 1694–1699.

Brady, D.R., and Mufson, E.J. (1989). Amygdaloid pathology in Alzheimer's disease. *Anat. Rec.* **222,** 17A.

Brockhaus, H. (1938). Zur normalen und pathologischen Anatomie des Mandelkerngebietes. *J. Psychol. Neurol.* **49,** 1–136.

Brockhaus, H. (1940). Die Cyto- und Myeloarchitektonik des Cortex claustralis und des Claustrum beim Menschen. *J. Psychol. Neurol. (Lpz.)* **49,** 249–348.

Brockhaus, H. (1942a). Zur feineren Anatomie des Septum und des Striatum. *J. Psychol. Neurol.* **51,** 1–56.

Brockhaus, H. (1942b). Vergleichend-anatomische Untersuchungen über den Basalkern Komplex. *J. Psychol. Neurol.* **51,** 57–95.

Brog, J.S., Salyapongse, A., Deutch, A.Y., and Zahn, D.S. (1993). The patterns of afferent innervation of the core and shell in the accumbens part of the rat ventral striatum: immunohistochemical detection of retrogradely transported fluoro-gold. *J. Comp. Neurol.* **338,** 255–278.

Bubenik, G.A., and Brown, G.M. (1973). Morphological sex differences in primate brain areas involved in the regulation of reproductive activity. *Experientia* **29,** 619–620.

Caberlotto, L., Fuxe, K., and Hurd, Y.L. (2000). Characterization of NPY mRNA-expressing cells in the human brain: co-localization with Y2 but not Y1 mRNA in the cerebral cortex, hippocampus, amygdala, and striatum. *J. Chem. Neuroanat.* **20,** 327–337.

Caffé, A.R., Van Ryen, P.C., Van Der Woude, T.P., and Van Leeuwe, F.W. (1989). Vasopressin and oxytocin sistems in the brain and upper spinal cord of *Macaca fascicularis*. *J. Comp. Neurol.* **287,** 302–325.

Candy, J.M., Perry, R.H., Thompson, J.E., Johnson, M., and Oakley, A.E. (1985). Neuropeptide localization in the substantia innominata and adjacent regions of the human brain. *J. Anat.* **140,** 309–327.

Canteras. N.S., Simerly, R.B., and Swanson, L.W. (1992a). Connections of the posterior nucleus of the amygdala. *J. Comp. Neurol.* **324,** 143–179.

Canteras N.S., Simerly, R.B., and Swanson, L.W. (1992b). Projections of the ventral pre-mammilary nucleus. *J. Comp. Neurol.* **324,** 195–212.

Canteras, N.S., Simerly, R.B., and Swanson, L.W. (1995). Organization of projections from the medial nucleus of the amygdala: a PHAL study in the rat. *J. Comp. Neurol.* **360,** 213–245.

Card, J.P., Levitt, P., Enquist, L.W., and Rinaman, L. (1999). Retrograde transynaptic characterization of amygdaloid cell groups that modulate the output of the rat central nucleus. *Soc. Neurosci. Abstrs.* **25,** 2171.

Carlsen, J. (1988). Immunocytochemical localization of glutamate decarboxylase in the rat basolateral amygdaloid nucleus, with special reference to GABAergic innervation of the amygdalostriatal projection neurons. *J. Comp. Neurol.* **273,** 513–526.

Carmichael, S.T., Clugnet, M.C., and Price J.L. (1994). Central olfactory connections in the Monkey. *J. Comp. Neurol.* **346,** 403–434.

Carrer, H.F. (1978). Mesencephalic participation in the control of sexual behavior in the female rat. *J. Comp. Physiol. Psychol.* **92,** 877–887.

Carrer, H.F., Asch, G., and Aron, C. (1973). New facts concerning the role played by the ventromedial nucleus in the control of estrous cycle duration and sexual receptivity in the rat. *Neuroendocrinology* **13,** 129–139.

Carrer, H.F., Masco, D. H., and Aoki, A. (1980). Neural structures involved in the control of female sexual behaviour. *In* "Endocrinology" (A. Cumming, J. W. Funder, and F. A. O. Mendebhon, eds.), pp. 611–614. Aust. Acad. Sci., Canberra, Australia.

Celio, W.R. (1990). Calbindin D-28k and parvalbumin in the rat nervous system. *Neuroscience* **35,** 375–475.

Chai, S.Y., McKenzie, J.S., McKinley, M.J., and Mendelsohn, F.A. (1990). Angiotensin converting enzyme in the human basal forebrain and midbrain visualized by in vitro autoradiography. *J. Comp. Neurol.* **291,** 179–194.

Chawla, M.K., Gutierrez, G.M., Scott Young III, W., McMullen, N.T., and Rance, N.E. (1997). Localization of neuronal expressing substance P and neurokinin B gene transcripts in the human hypothalamus and basal forebrain. *J. Comp. Neurol.* **384,** 429–442.

Chung, W.C.J., de Vries, G.J., and Swaab, D.F. (2002). Sexual differentiation on the bed nucleus of the stria terminalis in humans may extend into adulthood. *J. Neurosci.* **22,** 1027–1033.

Ciliax, B.J., Drash, G.W., Staley, J.K., Haber, S., Mobley, C.J., Miller, G.W., Mufson, E.J., Mash, D.C., and Levey, A. I. (1999). Immunocytochemical localization of the dopamine transporter in human brain. *J. Comp. Neurol.* **409,** 38–56.

Clarke, P.B.S., Schwartz, R.D., Paul, S.M., Pert, C.B., and Pert, A. (1985). Nicotinic binding in the rat brain: autoradiographic comparison of [3H]acetylcholine, [3H]nicotine and [125I]bungarotoxine. *J. Neurosci.* **5,** 1307–1315.

Cortés, R., Probst, A., and Palacios, J.M. (1987). Quantitative light microscopic autoradiographic localization of cholinergic muscarinic receptors in the human brain: forebrain. *Neuroscience* **20,** 65–107.

Côté, P.Y., Levitt, P., and Parent, A. (1996). Limbic system-associated membrane protein (LAMP) in primate amygdala and hippocampus. *Hippocapus.* **6,** 483–494.

Crosby, E.C., and Humphrey, T. (1940). Studies of the vertebrate telencephalon. II. The nuclear pattern of the anterior olfactory nucleus, tuberculum olfactorium and the amygdaloid complex in adult man. *J. Comp. Neurol.* **74,** 309–352.

Crosby, E.C., and Humphrey, T. (1944). Studies of the vertebrate telencephalon. III. The amygdaloid complex in the Tress shrew (*Blarina brevicauda*). *J. Comp. Neurol.* **81,** 285–305.

Csáki, A., Kocsis, K., Halász, B., and Kiss, J. (2000). Localization of glutamatergic/aspartatergic neurons projecting to the hypothalamic paraventricular nucleus studied by retrograde transport of [3H]D-aspartate autoradiography. *Neuroscience* **101,** 637–655.

Danscher, G. (1981). Histochemical demonstration of heavy metals. A revised version of the sulphide silver method suitable for both light and electronmicroscopy. *Histochemistry* **71,** 1–16.

Darvesh, S., Grantham, D.L., and Hopkins, D.A. (1998). Distribution of butyrylcholinesterase in the human amygdala and hippocampal formation. *J. Comp. Neurol.* **393,** 374–390.

Daunais, J.B., Letchworth, S.R., Sim-Selley, L.J., Smith, H.R., Childers, S.R., and Porrino, L.J. (2001). Functional and anatomical localization of mu opioid receptors in the striatum, amygdala, and extended amygdala of the nonhuman primate. *J. Comp. Neurol.* **433,** 471–485.

Day, H.E.W., Badiani, A., Uslaner, J.M., Oates, M.M., Vittoz, N.M., Robinson, T.E., Watson, S.J., Jr, and Akil, A. (2001). Environmental novelty differentially affects c-fos mRNA expression induced by amphetamine or cocaine in subregions of the bed nucleus of the stria terminalis and amygdala. *J. Neurosci.* **21,** 732–740.

De Lacalle, S., and Saper, C.B. (2000). Calcitonin gene-related peptide-like immunoreactivity marks putative visceral sensory pathways in human brain. *Neuroscience* **100,** 115–130.

de Olmos, J.S. (1969). A cupric-silver method for impregnation of terminal axon degeneration and its further use in staining granular argyrophilic neurons. *Brain Behav. Evol.* **2,** 213–237.

de Olmos, J.S., and Ingram, W.R. (1972). The projection field of the stria terminalis in the rat brain. An experimental study. *J. Comp. Neurol.* **146,** 303–334.

de Olmos, J.S., Ebbesson, S.O.E., and Heimer, L. (1981). Silver methods for the impregnation of degenerating axoplasm. *In* "Neuroanatomical Tract-tracing Methods" (L. Heimer and M.J. RoBards, eds.), pp. 117–170. Plenum, New York.

de Olmos J.S., Alheid G.F., and Beltramino CA (1985). Amygdala. *In* "The Rat Nervous System" (G. Paxinos, ed.), pp. 223–334. Academic Press, Sydney.

de Olmos, J.S. (1990). Amygdala. *In* "The Human Nervous System" (G. Paxinos, ed.), pp. 583–710. Academic Press, San Diego.

de Olmos, J.S., Beltramino, C.A., and de Olmos, S. (1994). An amino-cupric-silver method for the early detection of degenerative and regressive changes in neuronal perikarya, dendrites, stem-axons and axon terminals caused by neurotoxicants and hypoxia. *Neurotoxicol. Teratol.* **16,** 545–561.

de Olmos, J.S., and Heimer, L. (1999). The concepts of the ventral striatopallidal system and extended amygdala. *In* "Advancing from the Ventral Striatum to the Extended Amygdala. Implications for Neuropsychiatry and Drug Abuse" (J.F. McGinty, ed.). *Ann. N.Y. Acad. Sci.* **877,** 1–32.

Desjardins, C., and Parent, A. (1992). Distribution of somatostatin immunoreactivity in the forebrain of the squirrel monkey: basal ganglia and amygdala. *Neuroscience* **47,** 115–133.

De Vito, J.L., and Smith, O.A. (1982). Afferent projections to the hypothalamic area controlling emotional responses (HACER). *Brain Res.* **252,** 213–226.

Drevets, W.C., Price, J.L., Bardgett, M.E., Reich, T., Todd, R.D., and Raichle, M.E. (2002). Glucose metabolism in the amygdala in depression: relationship to diagnostic subtype and plasma cortisol levels. *Pharmacol. Biochem. Behav.* **71,** 431-–447.

Dunn, J. D. (1987). Plasma corticosterone responses to electrical stimulation of the bed nucleus of the stria terminalis. *Brain Res.* **407,** 327–331.

Dunn, J.D., and Whitener, J. (1986). Plasma corticosterone responses to electrical stimulation of the amygdaloid complex: cytoarchitectural specificity. *Neuroendocrinology* **42,** 211–217.

Emre, M., Heckers, S., Mash, D.C., Geula, C., and Mesulam, M.M. (1993). Cholinergic innervation of the amygdaloid complex in the human brain and its alterations in old age and Alzheimer's disease. *J. Comp. Neurol.* **336,** 117–134.

Fahrbach, S.E., Morrell, J.I., and Pfaff, D.W. (1983). Estrogen-concentrating neurons in the medial preoptic area send axons to the ventral tegmental area and amygdala. *Soc. Neurosci. Abstr.* **9,** 516.

Fliers, E., Guldenaar, S.E.F., Wal, N.v.d., and Swaab, D.F. (1986). Extrahypothalamic vasopressin and oxytocin in the human brain; presence of vasopressin cells in the bed nucleus of the stria terminalis. *Brain Res.* **375,** 363–367.

Flugge G, Ahrens O, Fuchs E.(1994) Monoamine receptors in the amygdaloid complex of the tree shrew (*Tupaia belangeri*). *J. Comp. Neurol.* **343,** 597–608.

Fox, C.A. (1940). Certain basal telencephalic centers in the cat. *J. Comp. Neurol.* **72,** 1–62.

Freedman, L.J., and Shi, C. (2001). Monoaminergic innervation of the macaque extended amygdala. *Neuroscience* **4,** 1067–1084.

Friedman, D.P., Murray, E.A., O'Neill, J.B., and Mishkin, M. (1986). Cortical connections of the somatosensory fields of the lateral sulcus of macaques: evidence for a corticolimbic pathway for touch. *J. Comp. Neurol.* **252,** 323–347.

Frost, J.J., Douglass, K.H., Mayberg, H.S., Dannals, R.F., Links, J.M., Wilson, A.A., Ravert, H.T., Croozier, W.C., and Wagner, H.N. Jr. (1989). Multicompartmental analysis of [11C]-carfentanil binding to opiate receptors in humans measured by positron emission tomography. *J. Cereb. Blood Flow Metab.* **9,** 398–409.

Fuchs, S.A., and Siegel, A. (1984). Neural pathways tnediating hypothalamically elicited flight behaviour in the cat. *Brain Res.* **306,** 263–281.

Fuchs, S.A., Edinger, H.M., and Siegel, A. (1985). The organization of the hypothalamic pathways mediating affective defense behaviour in the cat. *Brain Res.* **330,** 77–92.

Fudge, J.L., Kunishio, K., Walsh, P., Richard, C., and Haber, S,N. (2002). Amygdaloid projections to ventromedial striatal subterritories in the primate. *Neuroscience*, **110,** 257–275.

Fuller, T.A., Russchen, F.T., and Price, J.L. (1987). Sources of presumptive glutamatergic/aspartergic afferents to the rat ventral striopallidal region. *J. Comp. Neurol.* **258,** 317–338.

Gaspar, P., Berger, B., Alvarez, C., Vigny, A. and Henry, J.P. (1985). Catecholaminergic innervation of the septal area in man: immunocytochemical study using TH and DBH antibodies. *J. Comp. Neurol.* **241,** 12–33.

Gaspar, P., Berger, B., Lesur, A., Borsoti, J.P., and Fervret, A. (1987). Somatostatin 28 and neuropeptide Y innervation in the septal area and related cortical and subcortical structures of the human brain. Distribution, relationships and evidence for differential coexistence. *Neuroscience* **22,** 49–73.

Gaspar, P., Duyckaerts, E., Fevrret, A., Benoit, R., Beck, B., and Berger, B. (1989). Subpopulation of somatostatin 28-immunoreactive neurons display different vulnerability in senile dementia of the Alzheimer type. *Brain Res.* **490,** 1–13.

Gaudreau, H., and Pare, D. (1996). Projection neurons of the lateral amygdaloid nucleus are virtually silent throughout the sleep–waking cycle. *J. Neurophysiol.* **75,** 1301–1305.

Geula, C., Schatz, C.R., and Mesulam, M.M. (1997). Differential localization of NADPH-diaphorase and calbindin-D28k within the cholinergic neurons of the basal forebrain, striatum and brainstem in the rat, monkey and human. *Neuroscience* **54,** 461–476.

Ghashghaei, H.T., and Barbas, H. (2002). Pathways for emotion: interactions of prefrontal and anterior temporal pathways in the amygdala of the rhesus monkey. *Neuroscience* **115,** 1261–1279.

Ginsberg, S.D., Price, D.L., Blackstone, C.D., Huganir, R.L., and Martin, L.J. (1995). Non-NMDA glutamate receptors are present throughout the primate hypothalamus. *J. Comp. Neurol.* **353,** 539–552.

Gloor, F., Olivier, A., Quesney, L.F., Andermann, F., and Horowitz, S. (1982). The role of the limbic system in experimental phenomena of temporal lobe epilepsy. *Ann. Neurol.* **12,** 129–144.

Gloor, P. (1997). "The Temporal Lobe and Limbic System," Oxford University Press, New York.

Gomez, D.M., and Winans-Newman, S. (1992). Differential projections of the anterior and posterior regions of the medial amygdaloid nucleus in the syrian hamster. *J. Comp. Neurol.* **317,** 195–218.

Grove, E.A. (1988a). Neural associations of the substantia innominata in the rat: afferent connections. *J. Comp. Neurol.* **277,** 315–346.

Grove, E.A. (1988b). Efferent connections of the substantia innominata in the rat. *J. Comp. Neurol.* **277,** 347–364.

Haber, S., and Elde, R.P. (1982). The distribution of enkephalin immunoreactive fibers and terminals in the monkey central nervous system: an immunohistochemical study. *Neuroscience* **7,** 1049–1095**.**

Haber, S.N., and Nauta, W.J.H. (1983). Ramifications of the globus pallidus in the rat as indicated by patterns of immunohistochemistry. *Neuroscience* **9,** 245–260.

Haber, S.N., and Watson, S.J. (1985). The comparative distribution of enkephalin, dynorphin and substance P in the human globus pallidus and basal forebrain. *Neuroscience* **14,** 1011–1024.

Halgreen, E. (1992). Emotional neurophysiology of the amygdala within the context of human cognition. *In* "The Amygdala Neurobiological Aspects of Emotion, Memory, and Mental Dysfunction" (J.P. Aggleton, ed.), pp. 191–228. Wiley-Liss, New York.

Hall, E., Haug, F.-M.S., and Ursin, H. (1969). Dithizone and sulphide silver staining of the amygdala in the cat. *Z. Zell- forsch.* **102,** 40–48.

Hall, E. (1972b). The amygdala of the cat; a Golgi study. *Z. Zellforsch.* **134,** 439–458.

Hedreen, J.C., Struble, R.G., Whitehouse, P.J., and Price, D.L. (1984). Topography of the magnocellular basal forebrain system in human brain. *J. Neuropathol. Exp. Neurol.* **43,** 1–21.

Heimer, L., Van Hoesen, G.W., and Rosene, D.L. (1977). The olfactory pathways and the anterior perforated substance in the primate brain. *Internatl. J. Neurol.* **12,** 42–52.

Heimer, L., and Alheid, G.F. (1991). Piecing together the puzzle of basal forebrain anatomy**.** *In* "The Basal Forebrain: Anatomy to Function" (T.C. Napier, P.W. Kalivas, and I. Hanin, eds.), pp. 1–42. Plenum, New York.

Heimer, L., de Olmos J.S., Alheid, G.F., and Záborszky, L. (1991). "Perestroika." *In* "The basal forebrain: Opening the border between neurology and psychiatry." *In* "Role of the forebrain in sensation and behavior" (G. Holstege, ed.), pp. 109–165. Elsevier, Amsterdam.

Heimer, L., Alheid, G.F., de Olmos, J.S., Groenewegen, H.J., Haber, S.N., Harlan, R.E., and Zahm, D.S. (1997a). The accumbens: Beyond the core-shell dichotomy. *J. Neuropsychol. Clin. Neurosci.* **9,** 354–381.

Heimer, L., Harlan, R.E., Alheid, G.F., Garcia, M., and de Olmos, J. (1997b). Substantia innominata: a notion which impedes clinical–anatomical correlations in neuropsychiatric disorders. *Neuroscience* **76,** 957–1006.

Heimer, L., de Olmos, J.S., Alheid, G.F., Pearson, J., Sakamoto, N., Shinoda, K, Marksteiner, J., and Switzer, R.C. (1999) The human basal forebrain, Part II. *In* "Hanbook of Chemical Neuroanatomy: The Primate Nervous System," Vol. 15, Part 3, (F.E. Bloom, A. Bjorklund, and T. Hokfelt, eds.), pp. 57–226.

Heimer, L. (2002). Basal forebrain in the context of schizophrenia *Brain Res. Rev.*, **31,** 205–235.

Hilpert, P. (1928). Der Mandelkern des Menschen. I. Cytoarchitektonik und Faserverbindungen. *J. Psychol. Neurol.* **36,** S. 44–77.

Holstege, G., Meiners, L., and Tan, T. (1985). Projections of the bed nucleus of the stria terminalis to the mesencephalon, pons, and medulla oblongata in the cat. *Exp. Brain Res.* **58,** 379–391.

Hopkins, D.A. (1975). Amygdalotegmental projections in the rat, cat and rhesus monkey. *Neurosci. Lett.* **1,** 263–270.

Hopkins, D.A., and Holstege, G. (1978). Amygdaloid projections to the mesencephalon, pons and medulla oblongata in the cat. *Exp. Brain Res.* **32,** 529–547.

Hsu, D.T., Chen, F.L., Takahashi, L.K., and Kalin, N.H. (1998). Rapid stress-induced elevations in corticotropin-releasing hormone mRNA in rat central amygdala nucleus and hypothalamic paraventricular nucleus: an in situ hybridization analysis. *Brain Res.* **788,** 305–310.

Hudson, L.P., MuZoz, D.G., Miller, L., Machlan, R.S., Girvin, J.P., and Blume, W.T. (1993). Amygdaloid sclerosis in temporal lobe epilepsy. *Ann. Neurol.* **33,** 622–631.

Humphrey, T. (1968). The development of the human amygdala during early embryonic life. *J. Comp. Neurol.* **132,** 135–166.

Humphrey, T. (1972). The development of the human amygdaloid complex. *In* "The Neurobiology of the Amygdala" (B.E. Eleftheriou ed.), pp. 21–77. Plenum Press, New York.

Hurd, Y.L., Keller, E., Sotonyi, P., and Sedvall, G. (1999). Preprotachykinin-A mRNA expression in the human and monkey brain: an in situ hybridization study. *J. Comp. Neurol.* **411,** 56–72.

Hurd, Y.L., and Fagergren, P. (2000). Human cocaine- and amphetamine-regulated transcript (CART) mRNA is highly expressed in limbic- and sensory-related brain regions. *J. Comp. Neurol.* **425,** 583–598.

Hwang, S.J., Pagliardini, Boukhelifa, S.M., Parast, M.M., Otey, C.O., Rustioni, A., and Valtschanoff, J.G. (2001). Palladin is expressed preferentially in excitatory terminals in the rat central nervous system. *J. Comp. Neurol.* **436,** 211–224.

Insausti, R., Amaral, D.G., and Cowan, W.M. (1987). The entorhinal cortex of the monkey: III. Subcortical afferents. *J. Comp. Neurol.* **264,** 396–408**.**

Iwai, E., and Yukie, M. (1987). Amygdalofugal and amygdalopetal connections with modality-specific visual cortical areas in macaques (*Macaca fudscata, M. mulatta,* and *M. fascicularis*). *J. Comp. Neurol.* **261,** 362–386.

Jacobowitz, D.M., and Winsky, L. (1991). Immunohistochemical localization of calretinine in the forebrain of the rat. *J. Comp. Neurol.* **304,** 198–218.

Jimenez-Castellanos, J. (1949). The amygdaloid complex in monkey studied by reconstructional methods. *J. Comp. Neurol.* **91,** 507–526.

Johnston, J.B. (1923). Further contribution to the study of the evolution of the forebrain. *J. Comp. Neurol.* **35,** 337–481.

Johnson, A.K., de Olmos, J., Pastukovas, C.V., Zardetto-Smith, A., and Vivas, L. (1999). The extended amygdala and salt appetite. *In* "Advancing from the Ventral Striatum to the Extended Amygdala" (J.F. McGinty, ed.), *Ann. N. Y. Acad. Sci.* **877,** 258–280.

Jolkkonen, E., and Pitkänen, A. (1998). Intrinsic connections of the rat amygdaloid complex: projections originating in the central nucleus. *J. Comp. Neurol.* **395,** 53–72.

Jongen-Relo, A.L. (1994). Immunohistochemical characterization of the shell and core territories of the nucleus accumbens in the rat. *Eur. J. Neurosci.* **6,** 1255–1264.

Kahn, I., Yeshurun, Y., Rotshtein, P., Fried, I., Ben-Bashat, D., and Hendler, T. (2002). The role of the amygdala in signaling prospective outcome of choice. *Neuron* **33,** 983–994

Kamal, A.M., and Tombol, T. (1975). Golgi studies on the amygdaloid nuclei of the cat. *J. Hirnforsch.* **16,** 175–201.

Kaufmann, W.A., Barnas, U., Maier, J., Saria, A., Alheid, G.F., and Marksteiner, J. (1997). Neurochemical compartments in the human forebrain: evidence for a high density of secretoneurin-like immunoreactivity in the extended amygdala. *Synapse* **26,** 114–130.

Koikegami, H. (1963). Amygdala and other related limbic structures: experimental studies on the anatomy and function. *Acta Med. Biol.* **10,** 161–277.

Köhler, C., Hallman, H., Melander, T. Hökfelt, T., and Norheim, E. (1989a). Autoradiographic mapping of galanin receptors in the monkey brain. *J. Chem. Neuroanat.* **2,** 269–284.

Köhler, C., Persson, A., Melander, T., Theodorsson, E., Sedvall, G., and Hökfelt, T. (1989b). Distribution of galanin-binding sites in the monkey and human telencephalon: preliminary observations. *Exp. Brain Res.* **75,** 375–380.

Kohler, C., and Chan-Palay, V. (1990). Galanin receptors in the postmortem human brain. Regional distribution of 125 I-galanin binding sites using the method of in vitro receptor autoradiography. *Neurosci. Lett.* **120,** 179–182.

Kondo, Y., and Sachs, B.D. (2002). Disparate effects of small medial amygdala lesions on noncontact erection, copulation, and partner preference. *Physiol. Behav.* **76,** 443–447.

Kordower, J.H., Piecinski, P., and Rakic, P. (1992). Neurogenesis of the amygdaloid nuclear complex in the rhesus monkey. *Dev. Brain Res.* **68**, 9–15.

Kosmal, A., Malinowska, M., and Kowalska, D.M., (1997). Thalamic and amygdaloid connections of the auditory association cortex of the superior temporal gyrus in rhesus monkey (*Macaca mulatta*). *Acta Neurobiol. Exp. (Warsz)* **57,** 165–188.

Krettek, J.E., and Price, J.L. (1977). Projections from the amygdaloid complex and adjacent olfactory structures to the entorhinal cortex and to the subiculum in the rat and cat. *J. Comp. Neurol.* **172,** 723–752.

Krettek, J.E., and Price, J.L. (1978). A description of the amygdaloid complex in the rat and cat with observations on intra-amygdaloid axonal connections. *J. Comp. Neurol.* **178,** 255–280.

Kritzer, M.F., Innis, R.B., and Goldman-Rakic, P.S. (1988). Regional distribution of cholecystokinin receptors in macaque medial temporal lobe determined by in vitro receptor autoradiography. *J. Comp. Neurol.* **276,** 219–230.

Kromer Vogt, L.J., Hyman, B.T., Van Hoesen, G.W., and Damasio, A.R. (1990). Pathological alterations in the amygdala in Alzheimer's disease. *Neuroscience* **37,** 377–385.

Kruijver, F.P.M., Zhou, J.N., Pool, C.W., Hofman, M.A., Gooren, L.J.G., and Swaab, D.F. (2000). Male-to-female transsexuals have female neuron numbers in a limbic nucleus. *J. Clin. Endocrinol. Metab.* **85,** 20–34.

Krzywkowski, P., Jacobowitz, D.M., and Lamour, Y. (1995). Calretinin-containing pathways in the rat forebrain. *Brain Res.* **705,** 273–294.

Lauer, E.W. (1945). The nuclear pattern and fiber connections of certain basal telencephalic centers in the macaque. *J. Comp. Neurol.* **82,** 215–254.

LeDoux, J. (1998). Fear and the brain: where have we been, and where are we going? *Biol. Psychiatry* **44,** 1229–1238.

Lesur, A., Gaspar, P., Alvarez, C., and Berger, B. (1989). Chemoanatomic compartments in the human bed nucleus of the stria terminalis. *Neuroscience* **32,** 181–194.

Lopez-Gimenez, J.F., Vilaró, M.T., Palacios, J.M., and Mengod, G. (2001a). Mapping of 5-HT^{2A} receptors and their mRNA in monkey brain: [3H]MDL100,907 autoradiography and in situ hybridization studies. *J. Comp. Neurol.* **429,** 571–589.

Lopez-Gimenez, J.F., Mengod, G., Palacios, J.M. and Vilaró, T. (2001b). Regional distribution and cellular localization of 5-HT 2C receptor mRNA in monkey brain: comparison with [3H] mesulergine binding sites and choline acethyltransferase mRNA. *Synapse* **42,** 12–26.

Loup, F., Tribollet, E., Dubois-Dauphin, M., and Dreifuss, J.J. (1991). Localization of high affinity binding sites for oxytocin and vasopressin in the human brain. An autoradiographic study. *Brain Res.* **555,** 220–232.

Lucas, L.R., Hurley, D.L., Krause, J.E., and Harlan, R.E. (1992). Localization of the tachykinin neurokinin B precursor peptide in rat brain by immunocytochemistry and in situ hybridization. *Neuroscience* **51,** 317–345.

Macchi, G. (1951). The ontogenetic development of the olfactory telencephalon in man. *J. Comp. Neurol.* **95,** 245–305.

Madar, I., Lesser, R.P., Krauss, G., Zubieta, J.K., Lever, J.R., Kinter, C.M., Ravert, H.T., Musachio, J.L., Mathews, W.B., Dannals, R.F., and Frost, J.J. (1997). Imaging of delta- and mu-opioid receptors in temporal lobe epilepsy by positron emission tomography. *Ann. Neurol.* **41,** 358–367.

Mai, J.K., Assheuer, J., and Paxinos, G. (1997). "Atlas of the Human Brain," Academic Press, San Diego.

Mai, J. K., Stephens, P. H., Hope, A., and Cuello, A. C. (1986). Substance P in the human brain. *Neuroscience* **17,** 709–739.

Mai, J.K., Thriepel, J., and Metz, J. (1987). Neurotensin in the human brain. *Neuroscience* **22,** 499–524.

Mansour, A., Khachaturian, H., Lewis, M.E., Akil, H., and Watson, S.J. (1988). Anatomy of CNS opioid receptors. *Trends Neurosci.* **11,** 308–314.

Maren, S. (1999). Long-term potentiation in the amygdala: a mechanism for emotional learning and memory. *Trends Neurosci.* **22,** 561–567.

Markowitsch, H. J., Emmans, D., Irle, E., Streicher, M., and Preilowski, B. (1985). Cortical and subcortical afferent connections of the primate's temporal pole: a study of rhesus monkeys and marmosets. *J. Comp. Neurol.* **242**, 425–458.

Marksteiner, J., Saria, A., and Krause, J.E. (1992). Comparative distribution of neurokinin B-, substance P- and enkephalin-like immunoreactivities and neurokinin B messenger RNA in the basal forebrain of the rat: evidence for neurochemical compartmentation. *Neuroscience* **51,** 107–120.

Marksteiner, J., Sara, A., Kirchmair, R., Pycha, R., Benesch, H., Fisher-Colbrie, R., Haring, C., Maier, H., and Ransmayr, G. (1993). Distribution of secretoneurin-like immunoreactivity in comparison with substance P and enkephalin-like immunorectivity in various human brain regions. *Eur. J. Neurosci.* **5,** 1573–1585.

Marksteiner, J., Bauer, R., Kaufmann, W.A., Weiss, E., Barnas, U., and Maier, H. (1999). PE-11, a peptide derived from chromogranin B, in the human brain. *Neuroscience* **91,** 1155–1170.

Martin-Elkins, C.L., and Horel, J. (1988). Parahippocampal gyrus afferent cortical connections as demonstrated by retrogradely labelling cells with WGA-HRP. *Soc. Neurosci. Abstr.* **14,** 1230.

Martin, L.J., Powers, R.E., Dellovade, T.L., and Price, D.L. (1991). The bed nucleus-amygdala continuum in human and monkey. *J. Comp. Neurol.* **309,** 445–485.

Martin, L.J., Hadfield, M.G., Dellovade, T.L., and Price, D.L. (1991a). The striatal mosaic in primates: patterns of neuropeptide immunoreactivity differentiate the ventral striatum from the dorsal striatum. *Neuroscience* **43,** 397–417.

Martin, L.J., Powers, R.E., Dellovade, T.L., and Price, D.L. (1991b). The bed nucleus-amygdala continuum in human and monkey. *J. Comp. Neurol.* **309,** 445–485.

Mayberg, H.S., Sadzot, B., Meltzer, C.C., Fisher, R.S., Lesser, R.P., Dannals, R.F., Lever, J.R., Winlson, A.A., Ravert, H.T., Wagner, H.N. Jr, Bryan, R.N., Cromwell, C.C. and Frost, J.J. (1991). Quantification of mu and non mu opiate receptor in temporal lobe epilepsy using positron emission tomography. *Ann. Neurol.* 30, 3–11.

McDonald, A.J. (1992). Cell types and intrinsic connections of the amygdala. *In* "The Amygdala. Neurobiological Aspects of Emotion, Memory and Mental Dysfunction" (J.P. Aggleton, ed.), pp. 67–96, Wiley- Liss, New York.

McDonald, A.J., and Agustine, J.R. (1993). Localization of GABA-like immunoreactivity in the monkey amygdala. *Neuroscience* **52,** 281–294.

McDonald, A.J., Mascagni, F., and Augustine, J.R. (1995). Neuropeptide Y and somatostatin-like immunoreactivity in neurons of the monkey amygdala. *Neuroscience* **66,** 959–982.

McDonald, A.J., and Mascagni, F. (1996). Immunohistochemical localization of the beta 2 and beta 3 subunits of the GABAA receptor in the basolateral amygdala of the rat and monkey. *Neuroscience* **75,** 407–419.

McDonald, A.J., Muller, J.F., and Mascagni, F. (2002). GABAergig innervation of alpha type II calcium/calmodulin dependent protein kinase immunoreactive pyramidal neurons in the rat basolateral amygdala. *J. Comp. Neurol.* **446,** 199–218.

McDonald, A.J., Shammah-Lagnado, S.J., Shi, C., and Davis, M. (1999). Cortical afferents to the extended amygdala. *In* "Advancing from the Ventral Striatum to the Extended Amygdala" (J.F. McGinty, ed.). *Ann. N.Y. Acad. Sci.* **877,** 309–338.

McGaugh, J.L., Cahill, L., and Roozendal, B. (1996). Involvement of the amygdala in memory storage: interaction with other brain systems. *Proc. Natl. Acad. Sci. U.S.A.* **93,** 13508–13514.

Mehler, W.R. (1980). Subcortical afferent connections of the amygdala in the monkey. *J. Comp. Neurol.* **190,** 733–762.

Mesches, M.H., Jongen-Relo, A.L., and Amaral, D.G. (1995). Are the projections from the central nucleus of the macaque monkey amygdala to the brain stem GABAergic? *Soc. Neurosci. Abstr.* **21,** 1666 (655).

Mesulam, M.M., and Geula, C. (1988). Nucleus basalis (Ch4) and cortical cholinergic innervation in the human brain; observations based on the distribution of acetylcholinesterase and choline acetyltransferase. *J. Comp. Neurol.* **274,** 216–240.

Meyer, M., and Allison, A.C. (1949). An experimental investigation of the connexions of the olfactory tracts in the monkey. *J. Neurol. Neurosurg. Psychiatry* **12,** 274–286.

Mikami, Y. (1952). A cytoarchitectonic study on the amygdaloid complex of the macaque monkey, especially on the differences compared with that of man. *Niigata Med. J.* **66,** 155–162.

Mileusnic, D., Lee, J.M., Magnuson, D.J., Hejna, M.J., Krause, J.E., Lorens J.B., and Lorens, S.A. (1999). Neurokinin-3 receptor distribution in rat and human brain: an immunohistochemical study. *Neuroscience* **89,** 1269–1290.

Mishkin, M., and Aggleton, J. (1981). Multiple functional contributions of the amygdala in the monkey. *In* "The Amygdaloid Complex" (Y. Ben-Ari, ed.), pp. 409–422. Elsevier/North-Holland, Amsterdam.

Mizukami, S., Nishizuka, M., and Arai, Y. (1983). Sexual difference in nuclear volume and its ontogeny in the rat amygdala. *Exp. Neurol.* **79,** 569–575.

Moga, M.M., Saper, C.B., and Gray, T.S. (1989). Bed nucleus of the stria terminalis: cytoarchitecture, immunohistochemistry, and projection to the parabrachial nucleus in the rat. *J. Comp. Neurol.* **283,** 315–332.

Morecraft, R.J., Geula, C., and Mesulam, M.-M. (1992). Cytoarchitecture and neural afferents of orbitofrontal cortex in the brain of the monkey. *J. Comp. Neurol.* **323,** 341–358.

Morris, J.S., Frith, C.D., Perret, D.I., Rowland, D., Young, A.W., Calder, A.J., and Dolan, R.J. (1996). A differential neural response in the human amygdala to fearful and happy facial expression. *Nature* **383**, 812–815.

Mouatt-Prigent, A., Karlsson, J.-O., Yeknik, J., Agid, Y., and Hirsch, E.C. (2000). Calpatastin immunoreactivity in the monkey and human brain of control subjects and patients with Parkinson's disease. *J. Comp. Neurol.* **419,** 175–192.

Mufson, E.J., Mesulam, M.-M., and Pandya, D.N. (1981). Insular interconnections with the amygdala in the rhesus monkey. *Neuroscience* **6,** 1231–1248.

Mufson, E.J., Benoit, R., and Mesulam, M.M. (1988). Immunohistochemical evidence for a possible somatotastinn-containing amygdalostriatal pathway in normal and Alzheimer's disease brain. *Brain Res.* **453,** 117–128.

Mufson, E.J., Cochran, E., Benzing, W., Kordower, J.H. (1993). Galaninergic innervation of the cholinergic vertical limb of the diagonal band (Ch_2) and bed nucleus of the stria terminalis in aging, Alzheimer's disease and Down's syndrome. *Dementia* **4,** 237–250.

Murer, M.G., Boissiere, F., Yan, Q., Hunot, S., Villares, J., Faucheux, B., Agid, Y., Hirsch, E., and Raisman-Vozari, R. (1999). An immunohistochemical study of the distribution of brain-derived neurotrophic factor in the adult human brain, with particular reference to Alzheimer's disease. *Neuroscience* **88**(4), 1015–1032.

Murphy, G.M., Inger, P., Mark, K., Lin, J., Morrice, W., Gee, C., Gan, S., and Korp, B. (1987). Volumetric asymmetry in the human amygdaloid complex. *J. Hirnforsch.* **28,** 281–289.

Murphy, G.M., Jr. (1986). The human medial amygdaloid nucleus: no evidence for sex differences in volume. *Brain Res.* **365,** 321–332.

Nakamura, S., Takemura, M., Suenaga, T., Akiguchi, I., Kimura, J., Yasuhara, O., Kimura, T., and Kitaguchi, N. (1992). Occurrence of acetylcholinesterase activity closely associated with amyloid beta/A4 protein is not correlated with acetylcholinesterase-positive fiber density in amygdala of Alzheimer's disease. *Acta Neuropathol.* **84,** 425–432.

Narabayashi, H. (1980). From experiences of medial amygdalotomy on epileptics. *Acta Neurochir. Suppl. (Wien)* **30,** 75–81.

Newman, S.W. (1999). The medial extended amygdala in male reproductive behavior: a node in the mammalian social behavior network. *In* "Advancing from the Ventral Striatum to the Extended Amygdala," *Ann. N.Y. Acad. Sci.* **877,** 242–257.

Niehoff, D.L., and Whitehouse, P.J. (1983). Multiple benzodiazepine receptors: autoradiographic localization in normal human amygdala. *Brain Res.* **276,** 237–245.

Nishizuka, M., and Arai, Y. (1981). Sexual dimorphism in synaptic organization in the amygdala and its dependence on neonatal hormone environment. *Brain Res.* **212,** 31–38.

Nishizuka, M., and Arai, Y. (1983). Regional difference in sexually dimorphic synaptic organization of the medial amygdala. *Exp. Brain Res.* **49,** 462–465.

Nitecka, L., and Narkiewicz, O. (1976). Localization of acethylcholinesterase activity in the amygdaloid body of man. *Acta Neurobiol. Exp.* **36,** 333–352.

Novotny, G.E.K. (1977). A direct ventral connection between the bed nucleus of the stria terminalis and the amygdaloid complex in the monkey (*Macaca fascicularis*). *J. Hirnforsch.* **18,** 271–284.

Österlund, M.K., Keller, E., and Hurd, Y.L. (2000). The human forebrain has discrete estrogen receptor α messenger RNA expression: high levels in the amygdaloid complex. *Neuroscience* **95,** 333–342.

Paxinos, G., and Watson, C. (1997). The rat brain*: In* "Stereotaxic Coordinates," 3rd ed. Academic Press, San Diego.

Paxinos, G., Huang, X-F., and Toga, A.W. (2000). The rehesus monkey brain. *In* "Stereotaxic Coordinates." Academic Press, San Diego.

Pearson, J., Halliday, G., Sakamoto, N., and Michel, J.Ph. (1990). Catecholaminergic neurons. *In* "The Human Nervous System" (G. Paxinos, ed.), pp. 1023–1049. Academic Press, San Diego.

Perry, R.H., Candy, J.M., Perry, E.K., Thompson, J., and Oakley, A.E. (1984). The substantia innominata and adjacent regions in the human brain: histochemical and biochemical observations. *J. Anat*. **140,** 309–327.

Petrides, M., Paxinos, G., Huang, X-F., Morris, R., and Pandya, D.N. (2000). Delineation of the monkey cortex on the basis of a neurofilament protein. *In* "The Rhesus Monkey Brain: In Stereotaxic Coordinates" (G. Paxinos *et al*., ed.), pp. 155–165. Academic Press, San Diego.

Pilapil, C., Welner, S., Magnan, J., Zamir, N., and Quirion, R. (1986). Mu opioid receptor binding sites in human brain. *NIDA Res. Monogr*. **75,** 319–322.

Pioro, E.P., Mai, J.K., and Cuello, A.C. (1990). Distribution of substance P- and enkephalin-immunoreactive neurons and fibers. *In* "The Human Nervous System" (G. Paxinos, ed.), pp. 1051–1094. Academic Press, San Diego.

Pitkännen, A., and Amaral, D.G. (1991). Distribution of reduced nicotinamide adenine dinucleotide phosphate diaphorase (NADPH-d) cells and fibers in the monkey amygdaloid complex. *J. Comp. Neurol*. **313,** 326–348.

Pitkännen, A., and Amaral, D.G. (1993a). Distribution of parvalbumin immunoreactive cells and fibers in the monkey temporal lobe: the amygdaloid complex. *J. Comp. Neurol*.**331,** 199–224.

Pitkännen, A., and Amaral, D.G. (1993b). Distribution of calbindin-D28k immunoreactive and fibers in the monkey temporal lobe: the amygdaloid complex. *J. Comp. Neurol*. **331,** 199–224.

Pitkännen, A., and Amaral, D.G. (1994). The distribution of GABAergic cells, fibers, and terminals in the monkey amygdaloid complex: an immunohistochemical and in situ hybridization study. *J. Neurosci*. **14,** 2200–2224.

Pitkännen, A., and Amaral, D.G. (1998). Organization of the intrinsic connections of the monkey amygdaloid complex: projections originating in the lateral nucleus. *J. Comp. Neurol*. **398,** 431–458.

Powers, R.E., Walker, L.C., De Zousa, E.B., Vale, W.W., Struble, R.G., Whitehouse, P.J., and Price, D.L. (1987). Immunohistochemical study of neurons containing corticotropin-releasing factor in Alzheimer's disease. *Synapse* **1,** 405–410.

Price, J.L. (1973). An autoradiographic study of complementary laminar patterns of terminations of afferent fibers to the olfactory system. *J. Comp. Neurol*. **150,** 87–108.

Price, J.L. (1990). Olfactory system. *In* "The Human Nervous System" (G. Paxinos, ed.). Academic Press, San Diego.

Price, J.L., and Amaral, D.G. (1981). An autoradiographic study of the projections of the central nucleus of the monkey amygdala. *J. Neurosci*. **11,** 1242–1259.

Price, J.L., Russchen, F.T., and Amaral, D.G. (1987). The limbic region. II. The amygdaloid complex. *In* "Handbook of Chemical Neuroanatomy, Vol. V, Integrated Systems of the CNS, Part I" (A. Björklund, T. Hokfelt, and L.W. Swanson, eds.), pp. 279–388. Elsevier, Amsterdam.

Quirion, R., Pipali C., Allaoua H., and Chaudieu I. (1995). Autoradiographic distribution of multiple opiod, sigma, and phencyclindine receptor binding sites in the human brain. *In* "Sites of Drug Action in the Human Brain" (Biegon, Volkow, eds.), pp. 117–141. CRC Press, Boca Raton, FL.

Ragsdale, C.W., and Graybiel, A.M. (1988). Fibers from the basolateral nucleus of the amygdala selectively innervate striosomes in the caudate nucleus of the cat. *J. Comp. Neurol*. **269,** 506–522.

Rainbow, T.C., Schwartz, R.D., Parsons, B., and Kellar, K.J. (1984) Quantitative autoradiography of nicotinic [3H]acetylcholine binding sites in the rat brain. *Neurosci. Lett*. **50,** 193–196.

Rees, H.D., Switz, G.M., and Michael, R.P. (1980). The estrogen-sensitive neura; system in the brain of female cats. *J. Comp. Neurol*. **193,** 789–804.

Resko, J.A., Pereyra-Martínez, A.C., Stadelman, H.L., and Roselli, C.E. (2000). Region-specific regulation of cytochrome P450 aromatase messenger ribonucleic acid by androgen in brains of male rhesus monkeys. *Biol. Reprod*. **62**, 1818–1822.

Reubi, J.C., Cortés, R., Maurer, R., Probst, A., and Palacios, J.M. (1986). Distribution of somatotastin receptors in the human brain: an autoradiographic study. *Neuroscience* **18,** 329–346.

Rose, M. (1927a). Der Allocortex bel Tier und Mensch. I. Teil. *J. Psychol. Neurol*. **34,** 1–112.

Rose, M. (1927b). Die sog. Riechrinde beim Menschen und beim Affen. II. Teil. Des "Allocortex bei Tier und Mensch." *J. Psychol. Neurol*. **34,** 261–401.

Roselli, C.E., Klosterman, S., and Resko, J.A. (2001). Anatomic relationship between aromatase and androgen receptor mRNA expression in the hypothalamus and amygdala of adult male Cynomolgus monkeys. *J. Comp. Neurol*. **439,** 208–223.

Rosene, D.L., and Van Hocsen, G.W. (1987). The hippocampal formation of the primate brain: some comparative aspects of architecture and connections. *In* "The Cortex" (E.G. Jones and A.A. Peters, eds.), pp. 345–456. Plenum Press, New York.

Royer, S., Martina, M., and Paré, D. (1999). An inhibitory interface gates impulse traffic between input and output stations of the amygdala. *J. Neurosci.* **19,** 10575–10583.

Russchen, F.T., Bakst, L., Amaral, D.G., and Price, J.L. (1985). The amygdalostriatal projections in the monkey. An anterograde tracing study. *Brain Res*. **329,** 241–257.

Sadikot, A.F., Smith, Y., and Parent, A. (1988). Chemical anatomy of the amygdala in primate. *Soc. Neurosci. Abstr.* **14,** 860.

Sadikot, A.F., and Parent, A. (1990). The monoaminergic innervation of the amygdala in the squirrel monkey: an immunohistochemical study. *Neuroscience* **36,** 431–447.

Sadikot, A.F., Parent, A., and Francois, C. (1992). Efferent connections of the centromedian and parafascicular thalamic nuclei in the squirrel monkey: a PHA-L study of subcortical projections. *J. Comp. Neurol*. **315,** 137–159.

Saha, S., Batten, T.F.C., and Henderson, Z. (2000). A GABAergic projection from the central nucleus of the amygdala to the nucleus of the solitary tract: a combined anterograde tracing and electron microscopic immunohistochemical study. *Neuroscience* **99,** 613–626.

Sakamoto, N., Pearson, J., Shinoda, K., Alheid, G.F., de Olmos, J.S., and Heimer, L. (1999). The human basal forebrain. Part I. An overview. *In* "The Handbook of chemical Neuroanatomy" (Bjorklund and Hokfelt, ed.), pp. 1–56. Vol. 15 of The Primate Nervous System, Part III. Elsevier, Amsterdam.

Sander, K., and Scheich, H. (2001). Auditory perception of laughing and crying activates human amygdala regardless of attentional state. *Brain Res. Cogn. Brain Res*. **12,** 181–98.

Sanides, F. (1957b). Die Insulae terminales des Erwachsenen Gehirns des Menschen. *J. Hirnforsch.* **3,** 243–273.

Santiago, A.C., and Shammah-Lagnado, S.J. (1999). Afferent connections of the amygdalopiriform transition area (apir) in the rat. *Soc. Neurosci. Abstrs*. **25,** 2171.

Saper, C.B. (1990). Colinergic system. *In* "The Human Nervous System" (G. Paxinos, ed.), pp. 1095–1113. Academic Press, San Diego.

Saper, C.B., and Chelimsky, T.C. (1984). A cytoarchitectonic and histochemical study of nucleus basalis and associated cell groups in the normal human brain. *Neuroscience* **13,** 1023–1037.

Sarter, M., and Markowitsch, H.J. (1985). The amygdala's role in human mnemonic processing. *Cortex* **21,** 7–24.

Sasagawa, H. (1960a). Amygdaloid nuclear complex of chimpanzee (Japanese text). *Niigata Igakkai Zassi (Niiguta Med J)* **74,** 1770–1785.

Sasagawa, H. (1960b). A cytoarchitectonic study on the amygdaloid nuclear complex of a woolly monkey-*Lagothrix lagothricha* Humboldt (Japanese text). *Niigata Igakkai Zassi (Niigata Med J)* **74,** 1815–1822.

Saunders, R.C., Rosene, D.L., and Van Hoesen, G. (1988). Comparison of the efferents of the amygdala and the hippocampal formation in the rhesus monkey: II. Reciprocal and nonreciprocal connections. *J. Comp. Neurol.* **271**, 185–207.

Savander, V., LeDoux, J.E., and Pitkanen, A. (1996). Topographic projections from the periamygdaloid cortex to select subregions of the lateral nucleus of the amygdala in the rat. *Neurosci. Lett.* **211,** 167–170.

Savasta, M., Palacios, J.M., and Mengod, G. (1990). Regional distribution of the messenger RNA coding for the neuropeptide cholecystokinin in the human brain examined by in situ hybridization. *Mol. Brain Res.* **7,** 91–104.

Schoel, M., Qpsahl, C.A., and Flynn, J.P. (1981). Afferent projections related to attack sites in the ventral midbrain tegmentum of the cat. *Brain Res.* **204,** 269–282.

Shammah-Lagnado, S.J., Alheid, G.F., and Heimer, L. (1999). Afferent connections of the interstitial nucleus of the posterior limb of the anterior commissure and adjacent amygdalostriatal transition area in the rat. *Neuroscience* **94,** 1097–1123.

Sidman, R.L.. and Angevine, J.B. (1962). Autoradiographic analysis of time of origin of nuclear versus cortical components of mouse telencephalon. *Anat. Rec.* **142,** 326–327.

Silverman, A.J., Antunes, J.L., Abrams, G.M., Nilaver, G., Thau, R., Robinson, J.A., Ferin, M., and Krey, L.C. (1982). The luteinizing hormone-releasing hormone pathways in rhesus (Macaca mulatta) and pigtailed (*Macaca nemestrina*) monkeys: new observations on thick embedded sections. *J. Comp. Neurol.* **211,** 309–317.

Sims, K.S., and Williams, R.S. (1990). The human amygdaloid complex: a cytologic and histochemical atlas using Nissl, myelin, acetylcholinesterase and nicotinamide adenine dinucleotide phosphate diaphorase staining. *Neuroscience* **36,** 449–472.

Simmons, D.A., and Yahr, P. (2002). Projections of the posterodorsal preoptic nucleus and the lateral part of the posterodorsal medial amygdala in male gerbils, with emphasis on cells activated with ejaculation. *J. Comp. Neurol.* **444,** 75–94.

Smiley, J.F., Levey, A.I., and Mesulam, M.M. (1999). m2 Mucarinic receptor immunolocalization in cholinergic cells of the monkey basal forebrain and striatum. *Neuroscience* **90,** 803–814.

Smith, Y., Zubieta, J., Del Carmen, M., Dannals, R., Ravert, H., Zacur, H., and Frost, J. (1998). Brain μ opioid receptor measurements by poistron emisión tomography in normal cycling women: relationships to LH pulsatility and gonadal steroid hormones. *J. Clin. Endocrinol. Metab.* **83,** 4498–4505.

Sofroniev, M.V., Weindle, A., Schrell, U., and Wetzstein, R. (1981). Immunohistochemistry of vasopressin, oxytocin and neurophysin in the hypothalamus and extrahypothalamic regions in the human and primate brain. *Acta Histochem.* Suppl. **24,** 79–85.

Song, T., Nikolics, K., Seeburg, P.H., and Goldsmith, P.C. (1987). GnRH-prohormone-containing neurons in the primate brain: immunostaining for the GnRH-associated peptide. *Peptides* **8,** 335–346.

Sorvari, H., Soininen, H., Paljärvi, L., Karkola, K., and Pitkänen, A. (1995). Distribution of parvalbumin-immunoreactive cells and fibers in the human amygdaloid complex. *J. Comp. Neurol.* **360,** 185–212.

Sorvari, H., Soininen, H., and Pitkänen, A. (1996a). Calretinin-immunoreactive cells and fibers in the human amygdaloid complex. *J. Comp. Neurol.* **369,** 188–208.

Sorvari, H., Soininen, H., and Pitkanen, A. (1996b). Calbindin-D28k-immunoreactive cells and fibers in the human amygdaloid complex. *Neuroscience* **75,** 421–433.

Sorvari, H., Miettinen, R., Soininen, H., and Pitkänen, A. (1996c). Parvalbumin-immunoreactive cells make inhibitory synapses on pyramidal cells in the human amygdala. *Neurosci. Lett.* **217,** 93–96.

Sorvari, H., Miettinen, R., Soininen, H., Paljäri, L., Karkola, K., and Pitkänen, A. (1998a). Calretinine-immunoreactive neurons in the lateral nucleus of the human amygdala. *Brain Res.* **783,** 355–356.

Sorvari, H., Miettinen, R., Soininen, H., Paljäri, L., Karkola, K., and Pitkänen, A. (1998b). Distribution of parvalbumin-immunoreactive cells and fibers in the human amygdaloid complex. *J. Comp. Neurol.* **360,** 185–212.

Squire, L.R., and Zola-Morgan, S. (1985). The neuropsychology of memory: new links between humans and experimental animals. *Ann. N.Y. Acad. Sci.* **444,** 137–149.

Stephan, H. (1975). "Handbuch der mikroskopischen Anatomie des Menschen. Allocortex," Vol. **4**/9. Springer-Verlag, Berlin.

Stephan, H., and Andy, O.J. (1977). Quantitative comparison of the amygdala in insectivores and primates. *Acat. Anat.* **98,** 130–153.

Stephan, H., Frahm, H.D., and Baron, G. (1987). Comparison of brain structure volumes in Insectivora and primates. VII. Amygdaloid components. *J. Hirnforschung.* **28,** 571–584.

Stefanacci, L., and Amaral, D.G. (2000).Topographic organization of cortical inputs to the lateral nucleus of the macaque monkey amygdala: a retrograde tracing study. *J. Comp. Neurol.* **421,** 52–79.

Strenge, H., Braak, E., and Braak, H. (1977). Über den Nucleus striae terminalis im Gehirn des erwachsenen Menschen. *Z mikrosk anat Forsch Leipzig* **91,** 105–118.

Striedter, G.F. (1997). The telencephalon of tetrapods in evolution. *Brain Behav. Evol.* **49,** 179–213.

Sukhov, R.R., Walker, L.C., Rance, N.E., Price, D.L., and Scott Young, W., III. (1995). Opioid precursor gene expression in the human hypothalamus. *J. Comp. Neurol.* **353,** 604–622.

Sun, N., Roberts, L., and Cassell, M.D. (1991). Rat central amygdaloid nucleus projections to the bed nucleus of the stria terminalis. *Brain Res. Bull.* **27,** 651–662.

Svendsen, C.N., and Bird, E.D. (1985). Acetylcholinesterase staining of the human amygdala. *Neurosci. Letts.* **54,** 313–318.

Svenningsson, P., Hall, H., Sedvall, G., and Fredholm, B.B. (1997). Distribution of adenosine receptors in the postmortem human brain: an extended autoradiographic study. *Synapse* **27,** 322–335.

Swanson, L.W. (1992). "Brain Maps: Structure of the Rat Brain." Elsevier, Amsterdam.

Swabb, D.F. (1997). Neurobiology and neuropathology of the human hypothalamus. *In* "Handbook of Chemical Neuroanatomy, Vol. 13, The Primate Nervous System, Part I," (F.E. Bloom, A. Börklunmd, and T. Hokfelt, eds.), pp. 39–137. Elsevier, Amsterdam.

Thomas, S.R, Assaf, S.Y., and Iversen, S.D. (1984). Amygdaloid complex modulates neurotransmission from the entorhinal cortex to the dentate gyrus of the rat. *Brain Res.* **307,** 363–365.

Turner, B.H., Gupta, K.C., and Mishkin, M. (1978). The locus and cytoarchitecture of the projection areas of the olfactory bulb in *Macaca mulatta*. *J. Comp. Neurol.* **177,** 381–396.

Unger, J.W., and Lange, W. (1992). NADHP-diaphorase positive cell populations in the human amygdala and temporal cortex: neuroanatomy, peptidergic characteristics and aspect of aging and Alzheimer's disease. *Acta Neuropathol.* **83,** 636–646.

Veinante, P., and Freund-Mercier, M.J. (1997). Distribution of oxytocin- and vasopressin-binding sites in the rat extended amygdala: a histoautoradiographic study. *J. Comp. Neurol.* **383,** 305–325.

Walter, A., Mai, J.K., and Jiménez-Härtel, W. (1990). Mapping of neuropeptide Y-like immunoreactivity in the human forebrain. *Brain Res. Bull*. **24,** 297–311.

Walter, A., Mai, J.K., Lanta, L., and Görcs, T. (1991). Differential distribution of immunohistochemical markers in the bed nucleus of the stria terminalis in the human brain. *J. Chem. Neuroanat*. **4,** 281–298.

Wang, Z., Moody, K., Newman J.D., and Insel, T.R. (1997). Vasopressin and oxytocin immunoreactive neurons and fibers in the forebrain of male and female common marmosets (*Callithric jacchus*), *Synapse* **27,** 14–25.

Wilson, B.C., Terenzi, M.G., and Ingram, C.D. (1999). Oxytocin binding and neuronal sensitivity in sub-nuclei of the amygdala and bed nuclei of the stria terminalis (BST). *Soc. Neurosci. Abstr.* **25,** 958.

Wolf, H.K., Aliashkevitch, A.F., Blümcke, I., Wiestler, O.D., and Zentner, J. (1997). Neuronal loss and gliosis of the amygdaloid nucleus in temporal lobe epilepsy. A quantitative analysis of 70 surgical specimens. *Acta Neuropathol*. **93,** 606–610.

Young, M.W. (1936). The nuclear pattern and fiber connections of the non-cortical centers of the telencephalon of the rabbit (*Lepus cuniculus*). *J. Comp. Neurol*. **65,** 295–401.

Yukie, M. (2002). Connections between the amygdala and auditory cortical areas in the macaque monkey. *Neurosci. Res*. **42,** 219–229.

Zald, D.H., and Pardo, J.V. (1997). Emotion, olfaction, and the human amygdala: amygdala activation during aversive olfactory stimulation. *Proc. Natl. Acad. Sci. U.S.A.* **94,** 4119–4124.

Zaphiropoulos, A., Charnay, Y., Vallet, P., Constatidinis, J., and Bouras, C. (1991). Immumohistochemical distribution of corticotropin-like intermediate lobe peptide (CLIP) immunoreactivity in the human brain, *Brain Res. Bull*. **26,** 99–111.

Zardetto-Smith, A.M., Moga, M., Magnuson, D., Watson, S.J., and Gray, T.S. (1985). Dynorhphin ceils in the lateral hypothalamus innervate the amygdala, central gray, parabrachial and dorsal vagal complex. *Soc. Neurosci. Abstr.* **1,** 1150.

Zardetto-Smith, A.M., Beltz, T.G., and Johnson, A.K. (1994). Role of the central nucleus of the amygdala and bed nucleus of the stria terminalis in experimentally induced salt appetite. *Brain Res.* Vol **645**(**1–2**): 123–134.

Zech, M., Roberts, G.W., Bogerts, B., Crow, T.J., and Polak, J.M. (1986). Neuropeptides in the amygdala of controls, schizophrenics and patients suffering from Huntington's chorea: an immunaohistochemical study. *Acta Neuropathol*. **71,** 259–266.

Zezula, J., Cortés, R., Probst, A., and Palacios, J.M. (1988). Benzodiazepine receptor sites in the human brain: autoradiographic mapping. *Neuroscience* **25,** 771–795.

Zhou, J.N., Hofman, M.A., Goooren, L.J.G., and Swaab, D.F. (1995). A sex difference in the human brain and its relation to transsexuality. *Nature* **378,** 68–70.

Zubieta, J., Dannals, R., and Frost, J. (1999). Gender and age influences on human brain μ receptor binding measured by PET. *Am. J. Psychiatry* **156,** 842–848.

CHAPTER

23

Hippocampal Formation

RICARDO INSAUSTI
University of Castilla-La Mancha, Spain

DAVID G. AMARAL
University of California, Davis, California, USA

It has been more than a decade since the first edition of this chapter appeared in the *Human Nervous System*. In the intervening period, there has been a burgeoning of interest in the functional organization of the human hippocampal formation. Much of this has been motivated by the use of noninvasive imaging techniques such as PET (positron emission tomography) or fMRI (functional magnetic resonance imaging). For the decade 1992–2002, the U.S. National Library of Medicine has no fewer than 8400 papers indexed under the keywords "human" and "hippocampus" Structural MRI has also become an integral component of diagnosis and assessing the progression of neurodegenerative processes in disorders such as Alzheimer's disease (e.g., Gosche *et al.*, 2002; Killiany *et al.*, 2002).

So, what has changed and what has stayed the same in the current chapter? Basically, the core of the previous version has not changed substantially. However, we have attempted to update areas where there have been new findings and revise other areas where our thinking about the structural organization of the hippocampal formation has changed somewhat. While we had previously addressed aspects of the gross anatomy of the hippocampal formation near the end of the chapter, we have moved that discussion to the front of the first section. This is due, in part, to our belief that gross anatomical features of the hippocampal formation are taking on increasing importance as landmarks in neuroimaging studies. The second section deals with the cytoarchitetonic organization of the hippocampus with a comparison to the rodent and nonhuman primate. The next section deals with the connectivity of the hippocampal formation (based on

experimental data obtained primarily from the nonhuman primate brain). The fourth section presents an overview of normal development of the human hippocampal formation, while the fifth section deals with pathological conditions that have a direct impact on human hippocampal formation. It necessarily provides just a brief overview of this area because there has been an explosion of research, both at the basic and clinical levels, dealing with topics such as Alzheimer's disease and the hippocampus. Finally, the last section briefly surveys the results obtained with modern neuroimaging techniques and how they have influenced thinking about the function of the hippocampal formation.

GROSS ANATOMICAL FEATURES

Rostrocaudal Extent of the Hippocampal Fields

The entire human hippocampal formation has a rostrocaudal extent of approximately 5 cm (Fig. 23.1). Fig. 23.4 provides an estimate of the location along the rostrocaudal axis of the different components of the hippocampal formation. The length of each one can be calculated from the distance to the anterior limit of the temporal pole. The rostrocaudal extent of the major portion of the hippocampal formation that is visible in the lateral ventricle (mostly CA1, CA2, and distal CA3) is approximately 4 cm (Figs. 23.2 and 23.4). The entorhinal cortex is the most rostrally situated of the hippocampal fields, and it can be identified slightly behind the limen insulae (frontotemporal junction). The entorhinal cortex (Fig. 23.1) begins rostrally approximately 2.0 cm from the temporal pole. The rostralmost 5 mm of the entorhinal cortex is located rostral to the amygdaloid complex. The next 5 mm lie in a position ventromedial to the amygdaloid complex. Thus, a full centimeter of the entorhinal cortex is located rostral to any other component of the hippocampal formation. The dentate gyrus, hippocampus, subiculum, presubiculum, and parasubiculum bend medially and then caudally at the rostral limit of the lateral ventricle. The dentate gyrus makes this bend most caudally and is not seen in coronal sections less than 6 mm from the anterior pole of the hippocampus. The last field to make the medial bend is the subiculum, which thus forms the most rostral portion of the hippocampal formation (excluding the entorhinal cortex). The medial or "uncal" region of the hippocampal formation makes up a large portion of what is commonly called the uncus (Figs. 23.1, 23.2, and 23.5–23.10). This uncal portion extends for a rostrocaudal distance of approximately 1 cm and, as we will discuss later, comprises several different hippocampal fields.

The various hippocampal fields also have different caudal termination points. The entorhinal cortex ends first, approximately 1.7 cm caudal to the anterior limit of the lateral ventricle and approximately 1.5 cm caudal to the start of the subiculum. The caudal border of the entorhinal cortex generally occurs approximately at the rostral limit of the lateral geniculate nucleus (if the plane of the section is orthogonal to a horizontal line through the anterior and posterior commissures). The parasubiculum ends at approximately the same level as the entorhinal cortex. However, the caudal border of the presubiculum is more difficult to determine precisely. This is because near the caudal border of the entorhinal cortex there is a subtle change in the cytoarchitectonic characteristics of the presubiculum, which, in the monkey (Insausti *et al.*, 1987a), marks the transition to a ventrotemporal extension of the retrosplenial cortex (Kobayshi and Amaral, 2001). It is likely that this occurs in the human brain as well.

As the remaining fields of the hippocampal formation curve dorsally to meet the retrosplenial region, their cytoarchitecture becomes increasingly difficult to interpret. As a general topographical rule, the hippocampal fields that make up the rostral extreme of the hippocampus (i.e., the subiculum and CA1 of the hippocampus) also make up the caudal extreme. Therefore, the remainder of the hippocampal fields (the dentate gyrus, CA3, and CA2) are enclosed at the rostral and caudal extremes by CA1 and the subiculum. For this reason, the dentate gyrus and CA2 and CA3 fields of the hippocampus appear to end at a more rostral level than the CA1 field and subiculum (Figs. 23.6–23.8 and 23.14). The dentate gyrus ends approximately 7 mm in front of the caudal pole of the hippocampal formation at a level that is just caudal to the emergence of the calcarine sulcus of the occipital lobe (Fig. 23.10).

Ventromedial Surface Anatomy

In the following paragraphs, we will describe the surface appearance of the temporal lobe regions that contain the hippocampal formation and associated structures. We will refer to illustrations showing the ventral and medial surfaces of the human brain (Figs. 23.1 and 23.3) and to illustrations showing dorsolateral views of the hippocampal formation as seen through dissection of the temporal lobe (Fig. 23.2). We will attempt to relate the gross anatomical features visible in these views to the familiar cytoarchitectonic terms

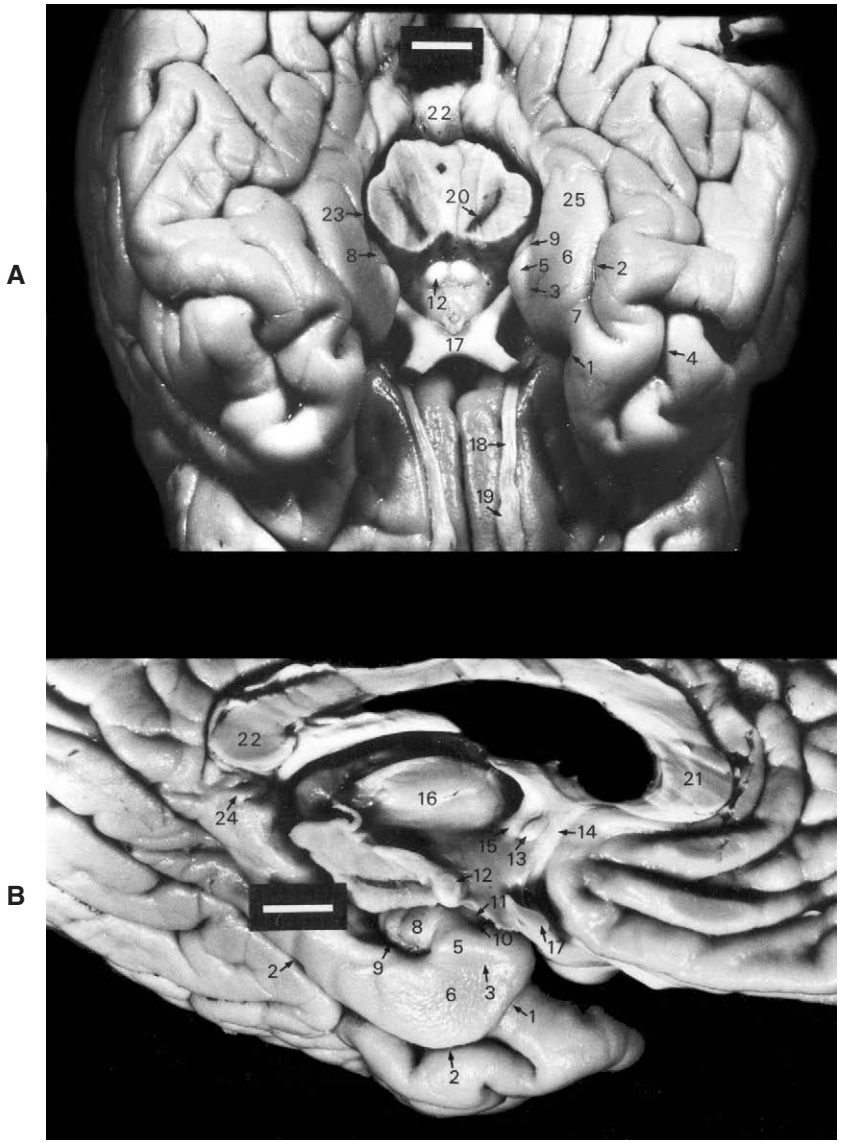

FIGURE 23.1 **(A)** The ventral surface of the human brain after removal of the brainstem and the cerebellum. The gyri and sulci of the ventral surface of the temporal lobe are clearly exposed and the relationships of the medial temporal lobe to other diencephalic and mesencephalic structures can be seen. **(B)** The ventromedial aspect of the left temporal lobe of the same brain after being bisected along the midline. The hippocampal structures situated at the medial and dorsal aspect of the temporal lobe that could not be demonstrated in the ventral view are now visible. The scale bar in both panels equals 1 cm. 1, rhinal sulcus; 2, collateral sulcus; 3, intrarhinal sulcus; 4, occipitotemporal sulcus; 5, gyrus ambiens; 6, entorhinal cortex; 7, perirhinal cortex (anterior portion); 8, uncus; 9, hippocampal fissure; 10, sulcus semiannularis; 11, gyrus semilunaris; 12, mammillary bodies; 13, anterior commissure; 14, precommissural fornix; 15, postcommissural fornix; 16, thalamus; 17, optic chiasm; 18, olfactory tract; 19, olfactory bulb; 20, substantia nigra; 21, corpus callosum (rostrum); 22, corpus callosum (splenium); 23, choroidal fissure; 24, gyri Andreae Retzii; 25, parahippocampal gyrus.

of the hippocampal fields. There is a rich heritage of gross anatomical analysis of the hippocampal formation dating back to Arantius (1587), who first described the appearance of human hippocampal formation and gave it the name hippocampus. Beautiful examples of illustrations of the gross anatomical appearance of the hippocampal formation were produced by Klingler (1948). This work, while rarely referenced, contains elegant drawings of various dissections of the human hippocampal formation.

FIGURE 23.2 Dorsolateral view of the human hippocampus after removal of the overlying structures. The preparation is seen from slightly different angles in A and B. The lateral ventricle (5) has been opened, thus exposing the shape of the hippocampus. It is possible to follow the hippocampal formation caudally as it ascends toward the retrosplenial region. Ultimately the fornix (3) extends rostrally and then ventrally to bifurcate around the anterior commissure (7) and innervate the septal nuclei and diencephalons. The lateral surface of the temporal lobe can be seen at the bottom of the two views. Scale bar equals 2 cm. 1, pes hippocampus; 2, hippocampus (body); 3, fimbria-fornix; 4, hippocampal commissure; 5, temporal horn of the lateral ventricle; 6, amygdala, 7, anterior commissure; 8, optic nerve; 9, corpus callosum.

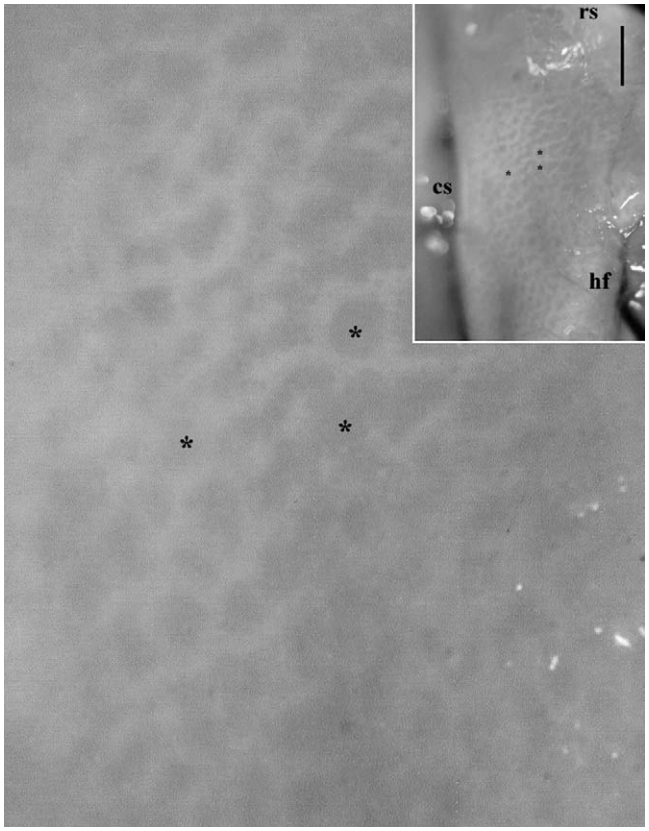

FIGURE 23.3 Unfixed surface of the human entorhinal cotex in a 72-year-old control case. Differences in density allow the clear appreciation of a latticework design that corresponds to cell islands in layer II. Note also the white matter surrounding the darker patches of layer II cell islands, the so-called substantia reticularis alba of Arnold. Scale bar equals 5 mm.

The ventral and medial surfaces of the temporal lobe are organized into strips by two prominent rostrocaudally oriented sulci. The more lateral of the two (Fig. 23.1) is the occipitotemporal sulcus (4) which is often broken forming small, transverse gyri. The more medial of the sulci, and the one that is more highly associated with the hippocampal formation, is the collateral sulcus (3) (Fig. 23.1). Not infrequently, both the collateral and the occipitotemporal sulcus are in continuity with each other. The collateral sulcus is usually continuous rostrally with the rhinal sulcus (41.9% of the cases according to Hanke, 1997), although there is a remarkable amount of individual variability in the configuration of these sulci [Insausti *et al.*, 1995; Heinsen *et al.*, 1994; Ono *et al.*, 1990; Figure 23.1(1)]. These two sulci form the lateral border of what has been classically termed the parahippocampal gyrus (Van Hoesen, 1995). The term "parahippocampal gyrus" or "parahippocampal region" (Scharfman *et al.*, 2000) has been used in different ways by different authors because the parahippocampal gyrus is a complex region that contains a number of distinct cytoarchitectonic fields. In recent years, the parahippocampal gyrus has been broken up into an anterior part that is mainly made up of the entorhinal cortex and associated perirhinal cortex and a posterior part

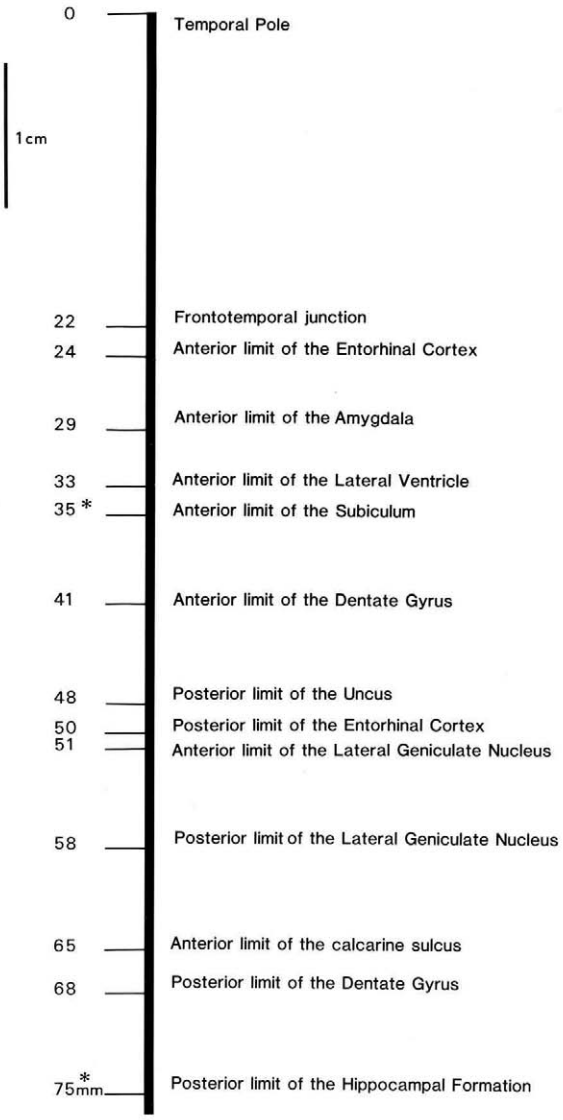

FIGURE 23.4 A representation of the approximate linear extents of each of the subdivisions of the hippocampal formation and related structures as reconstructed from a series of coronal sections through the temporal lobe of one brain. The numbers on the left are the distances in millimeters from the rostral pole of the temporal lobe to each of the anatomical points indicated on the right side of the bold vertical line. The distance between the asterisks indicates the length of all hippocampal fields excluding the entorhinal cortex.

(posterior parahippocampal cortex or PPH) that includes the TF and TH fields of Von Economo (1929; see Van Hoesen, 1982). In nonhuman primates, the parahippocampal gyrus consists of the TF and TH fields (Insausti *et al.*, 1987a). As we will describe in more detail in the cytoarchitectonic description, the collateral sulcus does not provide a discrete lateral boundary for the entorhinal cortex, which ends somewhere along the medial bank of the sulcus. The two fields of the perirhinal cortex (area 35, or more properly the perirhinal cortex, and area 36, or more properly the ectorhinal cortex, of Brodmann, 1909) actually form the remainder of the medial bank, fundus, and a portion of the lateral bank of the collateral sulcus (Fig. 23.14). The perirhinal cortex, in different brains, may or may not extend onto the most medial surface of the fusiform gyrus (the cortex located lateral to the collateral and/or occipitotemporal sulci). This appears to depend on the depth of the collateral sulcus. When the collateral sulcus is shallow, the perirhinal cortex not only covers all of the surface of the lateral bank but also extends a variable distance lateral to the collateral sulcus along the ventral surface of the temporal lobe (Insausti *et al.*, 1995).

The anterior portion of the classically defined parahippocampal gyrus is formed largely by the entorhinal cortex (Figs. 23.1 and 23.3). Much of the entorhinal cortex can actually be visually determined by identifying the conspicuous bumps [verrucae (or warts) gyri hippocampi; Klingler, 1948] that mark its surface, and that are best developed in humans, although they can be observed in apes as well (Van Hoesen, 1995). These bumps are located above the islands of cells that form layer II of the entorhinal cortex (Van Hoesen *et al.*, 1991). However, in unfixed specimens of the entorhinal cortex, discrete grayish patches are evident on the surface of the entorhinal cortex, surrounded by pale rims of white matter that give a lattice-like appearance (Fig. 23.3). The dorsomedial aspect of the entorhinal cortex (or anterior parahippocampal gyrus) is marked by a conspicuous mound or secondary gyrus that is referred to as gyrus ambiens (5) (Fig. 23.1). The lower limit of the gyrus ambiens is separated from the rest of the entorhinal cortex by a shallow sulcus that Retzius (1896) referred to as the inferior rhinal sulcus. Because this sulcus is entirely confined within the limits of the entorhinal cortex and is not related to the more prominent rhinal sulcus, we have referred to it as the intrarhinal sulcus. The position of this sulcus can be clearly seen in Figures 23.1–23.3. The location of the intrarhinal sulcus might be coincident with the imprint of the free edge of dura mater known as the tentorium cerebelli (Duvernoy, 1988; Hanke, 1997). The dorsomedial limit of the entorhinal cortex is marked by the shallow sulcus semiannularis (10) (Fig. 23.1). The gyrus semilunaris that is situated just dorsal to the sulcus semiannularis is made up of the periamygdaloid cortex (11) (Fig. 23.1).

There is a series of prominent bulges located caudal to the dorsomedial portion of the entorhinal cortex that is generally labeled as the uncus (or hook, 8) in gross anatomical descriptions (Figs. 23.1 and 23.7). The

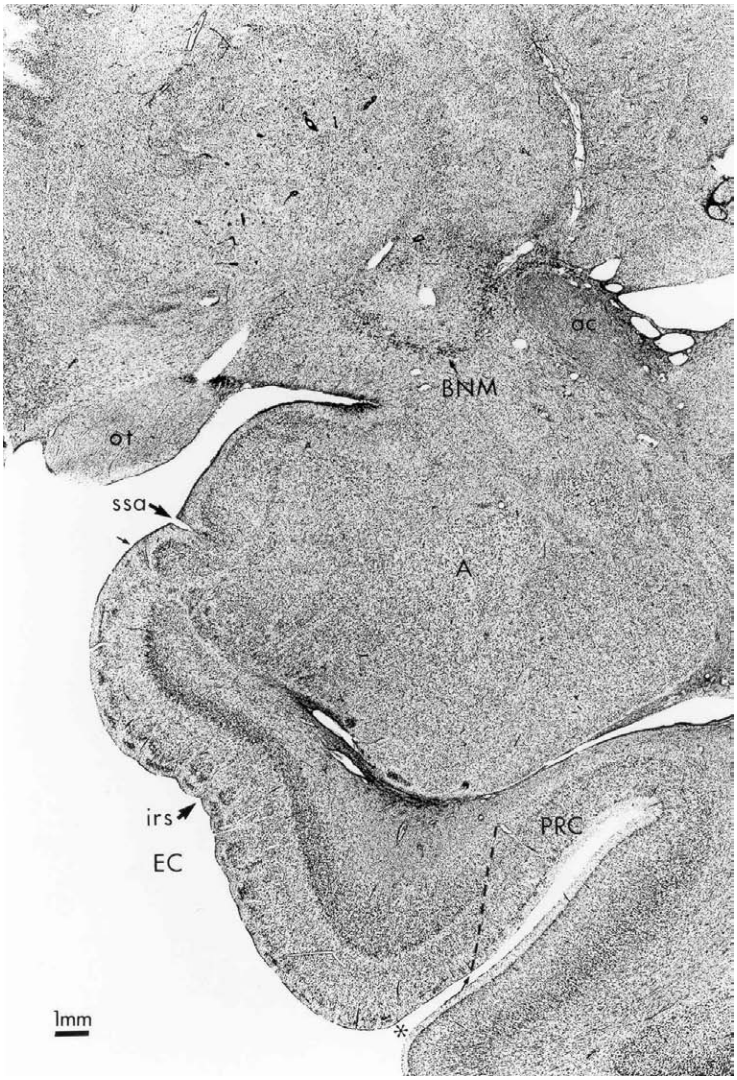

FIGURE 23.5–23.10 A representative series of coronal, thionin-stained sections [arranged rostrally (Fig. 23.5) to caudally (Fig. 23.10)] through the human hippocampal formation. A, Amygdaloid complex; a, alveus; ab, angular bundle; ac, anterior commissure; AHA, amygdalohippocampal area; BNM, nucleus basalis of Meynert; CA1, CA1 field of the hippocampus; CA2, CA2 field of the hippocampus; CA3, CA3 field of the hippocampus; cas, calcarine sulcus; cf, choroidal fissure; cos, collateral sulcus; DG, dentate gyrus; EC, entorhinal cortex; f, fimbria; gl, GL, granule cell layer of the dentate gyrus; hc, hippocampal commissure; hf, hippocampal fissure; irs, intrarhinal sulcus; LGN, lateral geniculate nucleus; 1-m, stratum lacunosum-moleculare of the hippocampus; ml, ML, molecular layer of the dentate gyrus; o, stratum oriens of the hippocampus; ot, optic tract; p, pyramidal cell layer of the dentate gyrus; PaS, Parasubiculum; PHG, parahippocampal gyrus (areas TF and TH); pl, PL, polymorphic layer of the dentate gyrus; PRC, perirhinal cortex (areas 35 and 36); Prs, presubiculum; r, stratum radiatum of the hippocampus; RSP, retrosplenial cortex; S, subiculum; ssa, sulcus semiannularis; V, temporal horn of the lateral ventricle.

FIGURE 23.5 A dashed line indicates the oblique border between the entorhinal cortex and the laterally adjacent perirhinal cortex. Here, and in Figures 23.4–23.7, small arrows mark the dorsomedial and ventrolateral extents of layer II of the entorhinal cortex and an asterisk marks the collateral sulcus.

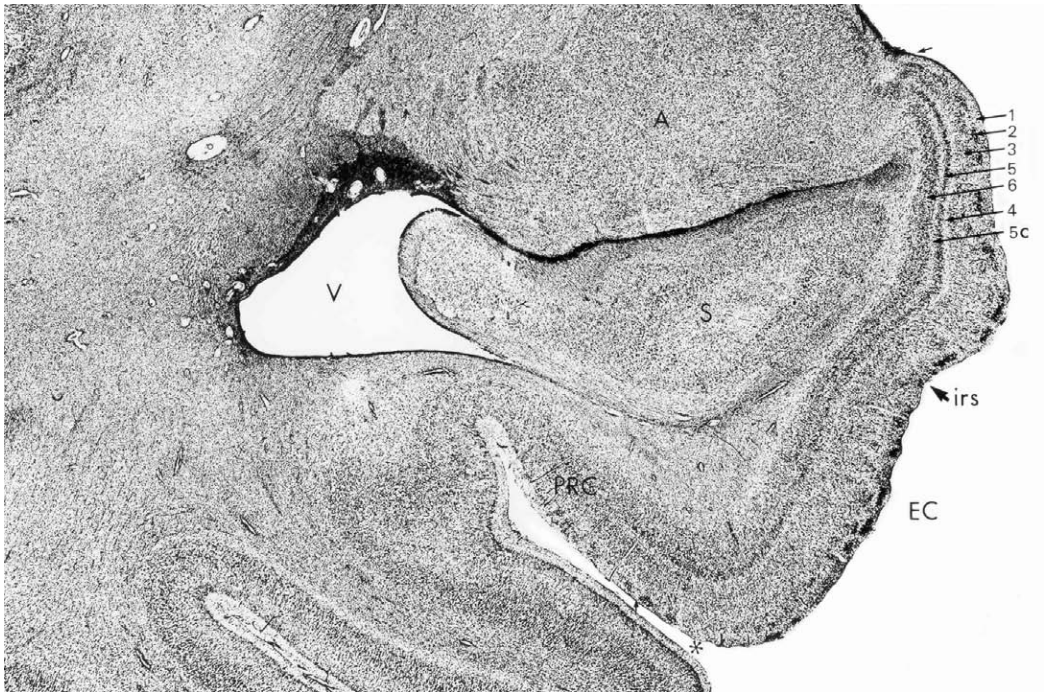

FIGURE 23.6 Numbers at the top right of this illustration indicate the layers of the entorhinal cortex. Note the shallow intrarhinal sulcus (irs) that is located in the entorhinal cortex.

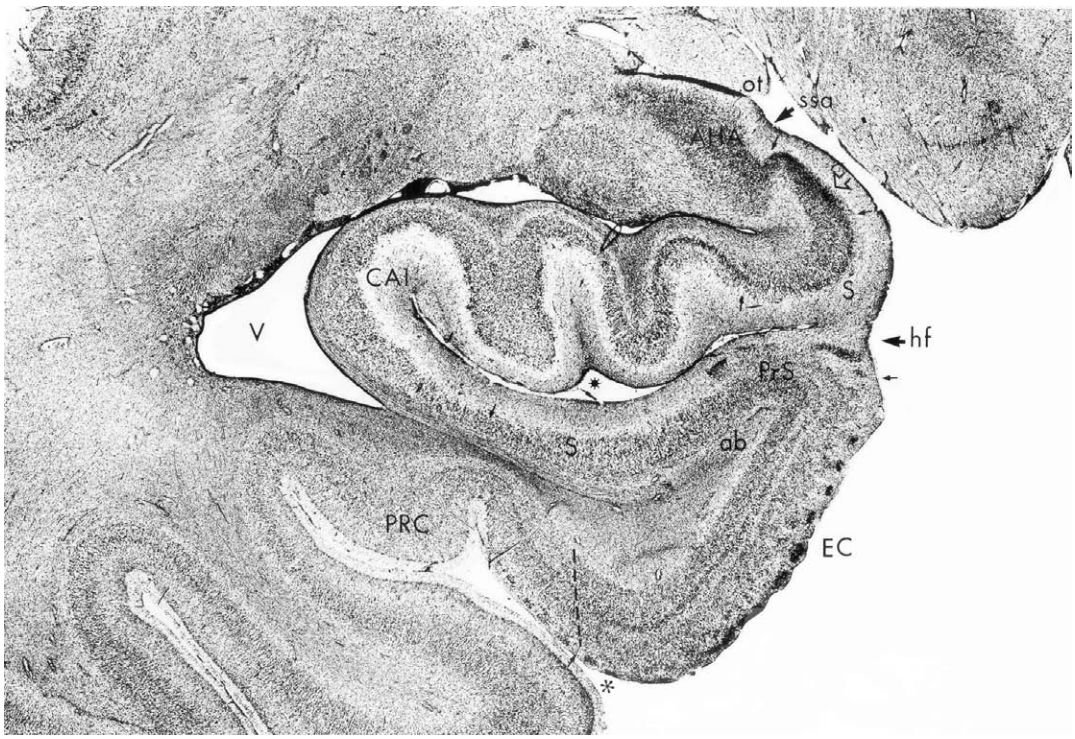

FIGURE 23.7 In Figures 23.5–23.8, small arrows mark the borders of each of the cytoarchitectonic fields of the hippocampal formation. A dashed line indicates the oblique border between the entorhinal cortex and the adjacent perirhinal cortex. The open arrow at top right indicates a transition region between the amygdala and hippocampal formation, which appears to be cytoarchitectonically distinct from other hippocampal fields. The asterisk in the center of the field marks the enclosed region of subarachnoid space called the diverticulum unci

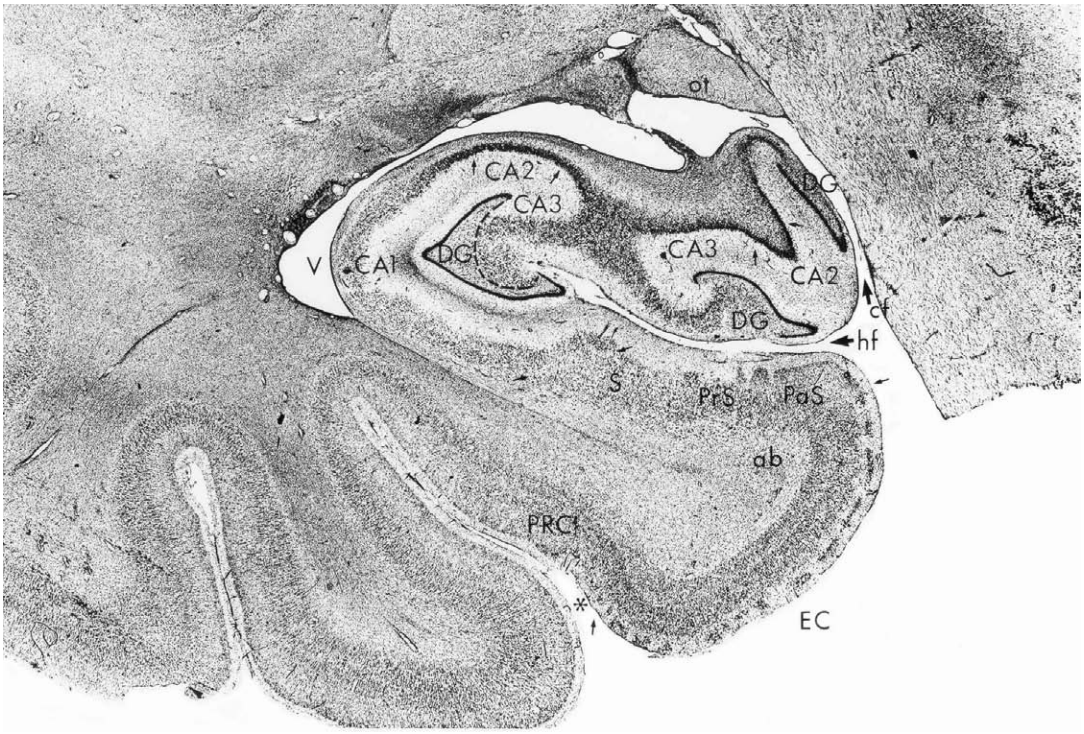

FIGURE 23.8 Dashed line in the dentate gyrus separates the polymorphic layer (hilus) of the dentate gyrus from the CA3 field of the hippocampus. Note that both the hippocampal fissure (hf) and the choroidal fissure (cf) are apparent at this level of the medial or uncal hippocampal formation. Note also that the border between CA1 and the subiculum (marked by arrows) is obliquely oriented relative to the pyramidal cell layer.

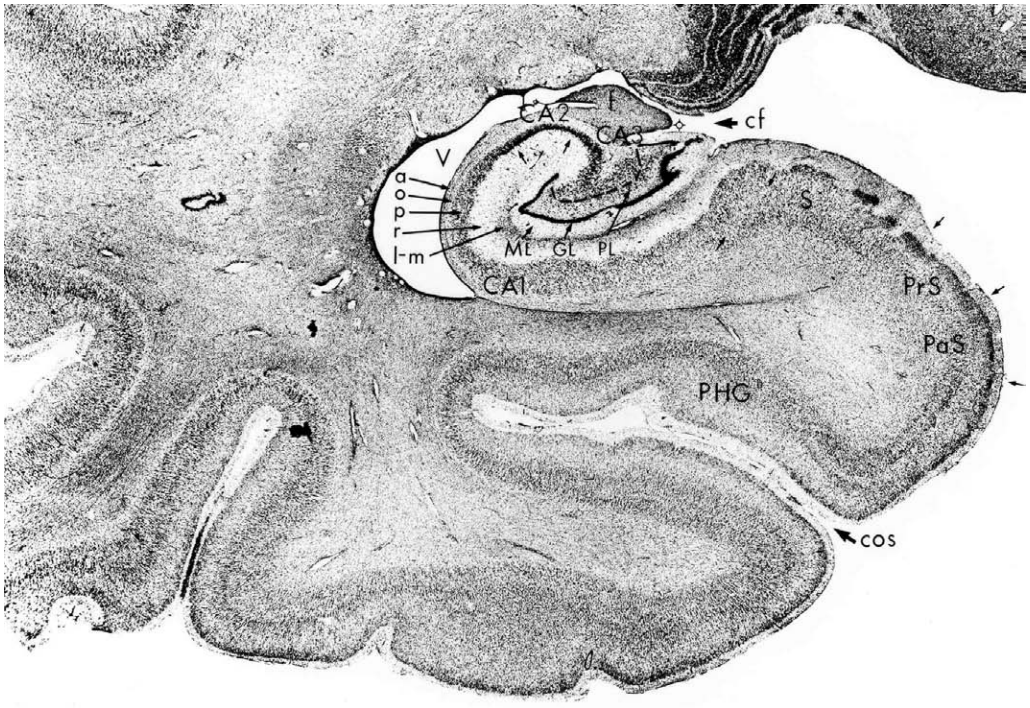

FIGURE 23.9 Dashed line in the dentate gyrus indicates the border between the polymorphic layer of the destate gyrus (PL) and the CA3 field of the hippocampus. Note that at this level the entorhinal cortex is no longer present and the parasubiculum (PaS) of the hippocampal formation abuts the parahippocampal cortex (PHG), which has replaced the perirhinal cortex. Note also that a small groove (target sign) called the fimbriodentate sulcus separates the molecular layer of the dentate gyrus from the fimbria.

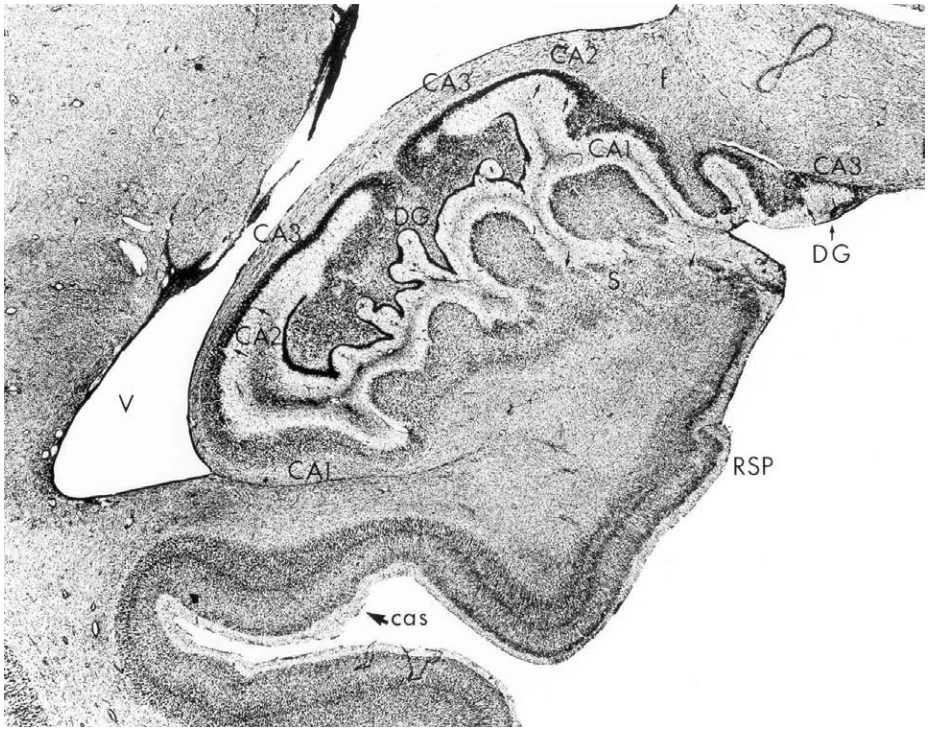

FIGURE 23.10 A coronal section near the caudal pole of the hippocampal formation. The hippocampal formation is bending dorsally and medially toward the corpus callosum. It is at about this level that the dentate gyrus and the CA2 and CA3 fields end though CA1 and the subiculum continue caudally for some distance. The presubiculum and parasubiculum are replaced by the retrosplenial cortex (RSP) and the collateral sulcus is replaced by the calcarine sulcus (cas). Fibers of the hippocampal commissure (hc) are apposed to the ventral surface of the corpus callosum.

most rostral of the uncal bulges is often separately labeled the gyrus uncinatus. In histological sections, the gyrus uncinatus is made up of the amygdalo-hippocampal region and the transition zone between the amygdala and hippocampus. The middle bulge is called the band or limbus of Giacomini and is generally composed of the most medial bend of the dentate gyrus (Fig. 23.8). The most caudal of the uncal bulges is called the gyrus intralimbicus and is composed mainly of field CA3 of the hippocampus. As seen in Figure 23.1, and in the coronal sections in Figures 23.5 and 23.6, the ventral boundary of the uncus is formed by the rostral extension of the hippocampal fissure (9), also known as the uncal sulcus (Fig. 23.1). Caudal to the level of the uncus, the hippocampal fissure (9) becomes attenuated (Fig. 23.1), and the choroidal fissure (23) marks the medial surface of the dentate gyrus and fimbria (Fig. 23.1). In this region, a small indentation can be seen between the fimbria and the molecular layer of the dentate gyrus that Gastaut and Lammers (1961) have called the fimbriodentate sulcus (Fig. 23.9, target sign). At rostral levels of the hippocampal formation, the hippocampal fissure extends laterally to separate the dentate gyrus or hippocampus from the underlying subiculum. Rostral to the medial closure of the hippocampal fissure, there is a narrow region of subarachnoid space between the hippocampus and the subiculum (Fig. 23.5). Klingler (1948) has labeled this ventricular pocket the diverticulum unci.

As the parahippocampal gyrus meets the retrosplenial region caudally, a group of small bumps known as the gyri Andreae Retzii (24) become noticeable (Fig. 23.1) on the medial surface. This irregular region of cortex marks the caudal limit of the hippocampal formation and is thus composed principally of the CA1 field of the hippocampus and the subiculum. Although they are difficult to see in Figure 23.1, two obliquely oriented small gyri are located deep to the gyri Andreae Retzii. The more medial one is known as the fasciola cinerea and corresponds to the caudalmost part of the dentate gyrus. The lateral gyrus is called the gyrus fasciolaris and corresponds to the end of the CA3 field. There is still some dispute about which of the fields of the hippocampal formation surround the splenium to

form the induseum griseum (or supracommissural hippocampal formation); however, our analysis indicates that the subiculum and field CA1 mainly form this small band of supracallosal tissue.

Dorsomedial Surface Anatomy

The classical gross anatomical image of the human hippocampal formation is of a prominent, bulging eminence in the floor of the temporal horn of the lateral ventricle (Fig. 23.2). As we have already described, and as seen in the histological coronal sections (Figs. 23.5–23.8), a number of distinct cytoarchitectonic fields, including the dentate gyrus, hippocampus, and subicular cortices, are included in this region.

The term "hippocampus" (or sea horse) was first applied to this region by the anatomist Arantius (1587), who considered the three-dimensional form of the grossly dissected human hippocampus to be reminiscent of this sea creature. It is actually unclear from the account of Arantius which particular aspect or surface of the hippocampal formation reminded him of the sea horse since he also likened the hippocampus to a silkworm. An historical and often amusing account of the etymology of the term "hippocampus" is provided by Lewis (1923). As he noted, others such as Winslow (1732) likened the hippocampus to a ram's horn, and de Garengeot (1742) named the hippocampus Ammon's horn after the mythological Egyptian god. The term Cornu Ammonis was appropriated by Lorente de Nó (1934) for his terminology of the hippocampus proper (CA1–CA4), and Ammon's horn has been used used synonymously with the hippocampus. Recent use appears to favor the term "hippocampus", however.

The ventricular portion of the hippocampal formation is seen in two slightly different views in Figure 23.2. This portion of the hippocampal formation is widest at its anterior extent where the structure bends toward the medial surface of the brain. The subtle gyri (digitations hippocampi) formed in this region (which can range from 2 to 5 in number; Gertz *et al.*, 1972) give it a footlike appearance and the name pes (foot) hippocampus (1) has classically been applied to this area (Fig. 23.2). The pes hippocampus is formed by several of the hippocampal fields, and the constituents differ at different rostrocaudal levels. Continuing caudally from the pes hippocampus, the unreflected "body" of the hippocampus (2) (Fig. 23.2) becomes progressively thinner as it bends upward toward the splenium of the corpus callosum.

The medial surface of the hippocampus is invested with a fringe of fibers called the fimbria. Fibers originating from the pyramidal cells of the hippocampus and subiculum travel in the white matter which sheaths the hippocampus (the alveus) and coalesce in the medially situated fimbria (3) (Fig. 23.2). At rostral levels, the fimbria is thin and flat, but it becomes progressively thicker caudally as fibers are continually added to it. The fibers in the fimbria, like those in the corticospinal tract, are given different names at different positions along their trajectory. As the fimbria leaves the caudal extent of the hippocampus, it fuses with the ventral surface of the corpus callosum and travels rostrally in the lateral ventricle. The region between the caudal limit or the hippocampal formation and the fusion with the corpus callosum is called the crus of the fornix, whereas the major portion of the rostrally directed fiber bundle is called the body of the fornix. At the end of its rostral trajectory, the body of the fornix descends and is called the column of the fornix. The fornix then divides around the anterior commissure to form the precommissural fornix, which innervates the septal region, and the postcommissural fornix, which terminates in the diencephalon (Fig. 23.2A). At about the point where the fimbria fuses with the posterior portion of the corpus callosum, fibers extend across the midline to form the hippocampal commissure. A variety of gross anatomical terms have been applied to this commissural projection but the term "psalterium" (alluding to an ancient instrument "psaltery" made of strings stretched over a board) is most common. As we will discuss in a future section, the primate hippocampal commissural connections are much more limited than in the rodent (Amaral *et al.*, 1984; Demeter *et al.*, 1985). Stereotaxic depth encephalography indicates that, as in the monkey, there is little commissural interaction of the human hippocampal formation (Wilson *et al.*, 1987). Gloor and colleagues have confirmed that the ventral hippocampal commissure is virtually absent in the human brain whereas the dorsal hippocampal commissure is similar to that observed in the nonhuman primate brain (Gloor *et al.*, 1993).

CYTOARCHITECTONIC ORGANIZATION OF THE HIPPOCAMPAL FORMATION

Introduction and Terminology

It would be relatively easy for someone familiar with rat or monkey neuroanatomy to identify the human hippocampal formation. The dentate gyrus is characteristically C-shaped and the fields that comprise the remainder of the hippocampal formation—

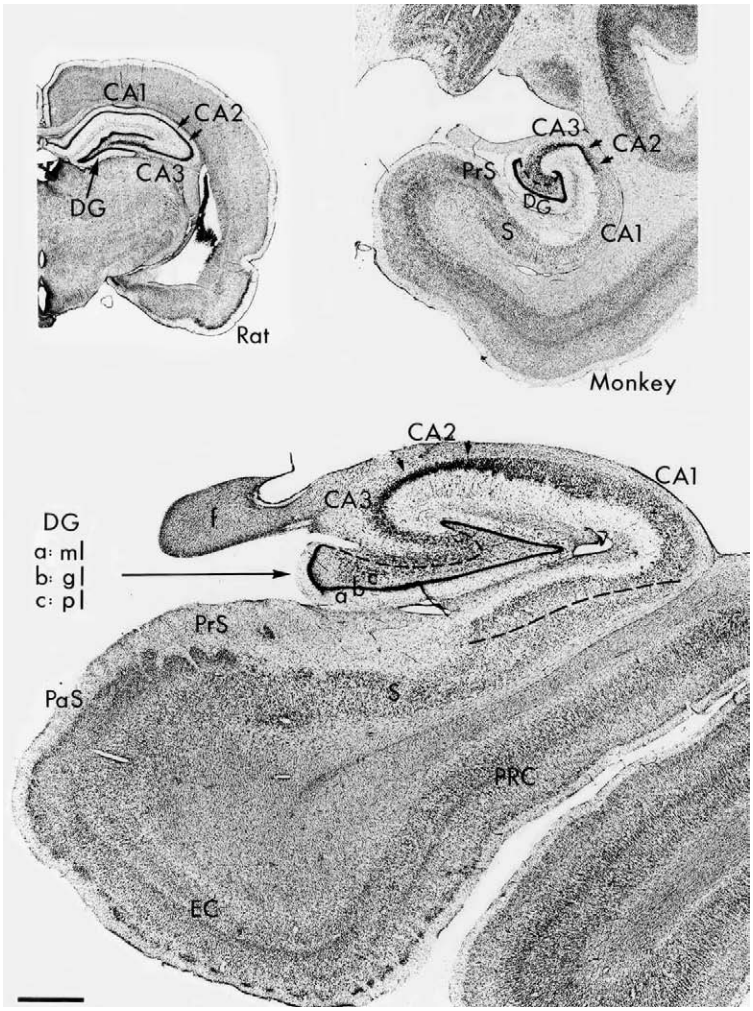

FIGURE 23.11 Coronal sections through the hippocampal formation of the rat, monkey, and human brains presented at the same magnification. Preparations are stained with thionin for the demonstration of neuronal cell bodies. The dashed line in the monkey and human dentate gyri separates the polymorphic layer of the dentate gyrus from the CA3 field of the hippocampus. In the human section, a dashed line also indicates the oblique border between field CA1 and the subiculum.

the hippocampus, subiculum, presubiculum and parasubiculum, and entorhinal cortex—are all reasonably recognizable (Fig. 23.11). Yet, even a cursory survey of the cellular infrastructure of the human hippocampal formation gives the impression that there are qualitative and quantitative differences in its organization relative to that in other species. Certain fields in the human hippocampal formation, such as CA1 of the hippocampus, appear to be disproportionately large. And, unlike in the rat where CA1 has a relatively homogeneous appearance, in humans it is characterized by a heterogeneity of cellular constituents that at some levels take on a multilaminate look (Fig. 23.11). Borders between the various fields of the human hippocampal formation are also more difficult to establish than in other species. This is due, in part, to the incessant overlapping of neuronal layers at the interfaces of fields. Rather than sharp, linear boundaries running perpendicular to the pial surface, demarcations between fields are often obliquely oriented (Figs. 23.5, 23.7, and 23.11).

Our perspective in revising this chapter ten years later has not substantially changed from the first edition. Although a number of studies have been reported in the literature, serious anatomical investigation of the human hippocampal formation is still meager, and it will be some time before the subtleties of its organization are completely understood. We describe the human hippocampal formation from a comparative point of view using the substantial data

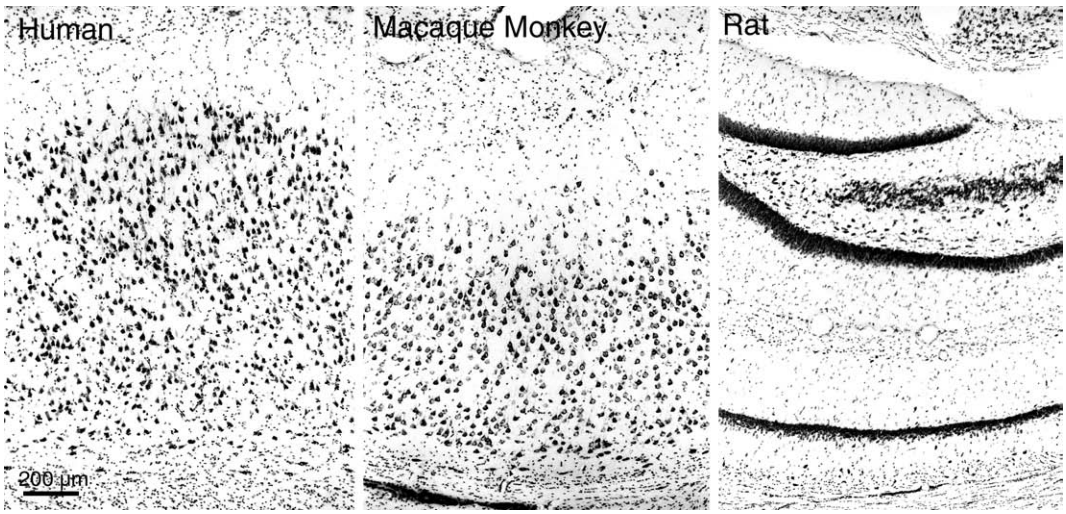

FIGURE 23.12 Higher magnification photomicrographs of approximately the same region of the CA1 field of the hippocampus in the rat, monkey, and human. This is a standard Nissl-stained preparation, and all of the images are at the same magnification. The calibration bar at the lower left applies to all three panels. Note that CA1 in the rat, which is the dark line at the bottom of the image, consists of three to five layers of tightly packed pyramidal cells (individual cells are difficult to resolve at this magnification). The monkey pyramidal cell layer, in contrast, is approximately 30 cell layers thick and there is a hint of sublamination with the top half of the layer having a slightly higher density of neurons. The pyramidal cell layer in the human CA1 field is even thicker and has a much more heterogeneous or laminated appearance.

from the rodent and monkey as the basis for our description of the general organizational features of the human hippocampal formation. Several detailed analyses of various morphological aspects of the human hippocampal formation are available in the literature. Most notable among these are the extensive pigmentoarchitectonic studies of Braak (1980, and references therein), the comparative morphometric studies of Stephan (1975, and references therein), "The Human Hippocampus" by Duvernoy (1988) and more recently, the comprehensive monograph of Gloor (1997) "The Temporal Lobe and Limbic System."

We will describe various aspects of the histological appearance of the human hippocampal formation. Where possible, we will relate conspicuous gross anatomical features of the human hippocampal formation to the underlying cytoarchitectonic structures. We will first survey the cytoarchitectonic characteristics and spatial organization of each of the fields of the hippocampal formation. This description will be referenced to a series of Nissl-stained coronal sections spaced throughout the rostrocaudal extent of the hippocampal formation (Figs. 23.5–23.10). The borders of the individual cytoarchitectonic fields are based on observations of adjacent Nissl- and fiber-stained coronal sections through several neurologically normal temporal lobes. This material was supplemented with histochemical preparations stained for the localization of acetylcholinesterase, by the Timm's sulfide silver method for the localization of heavy metals and by inmunohistochemical preparations using antisera directed against somatostatin, nonphosphorylated neurofilaments, or calcium-binding proteins.

We will also provide a brief summary of the connectivity of the hippocampal formation; more complete reviews can be found in Amaral (1987), Swanson *et al.* (1987), and Witter *et al.* (1989). Throughout this section, we will relate some of the more arcane terminology used in gross anatomical descriptions of the hippocampal formation to currently employed neuroanatomical terms.

The term "hippocampal formation" is usually applied to a group of cytoarchitectonically distinct fields associated with the hippocampus. The constituents of the group, however, vary with different authors. In this chapter, the term hippocampal formation includes the dentate gyrus, hippocampus, subiculum, presubiculum and parasubiculum, and entorhinal cortex. The major justification for grouping these fields together is that they are linked by prominent and largely unidirectional connections that appear to unite them as a functional entity (Figs. 23.16 and 23.17).

A variety of nomenclatures have been used to label the portions of the hippocampal formation. The use of one terminology rather than another has been dictated, in part, by what species is being described or

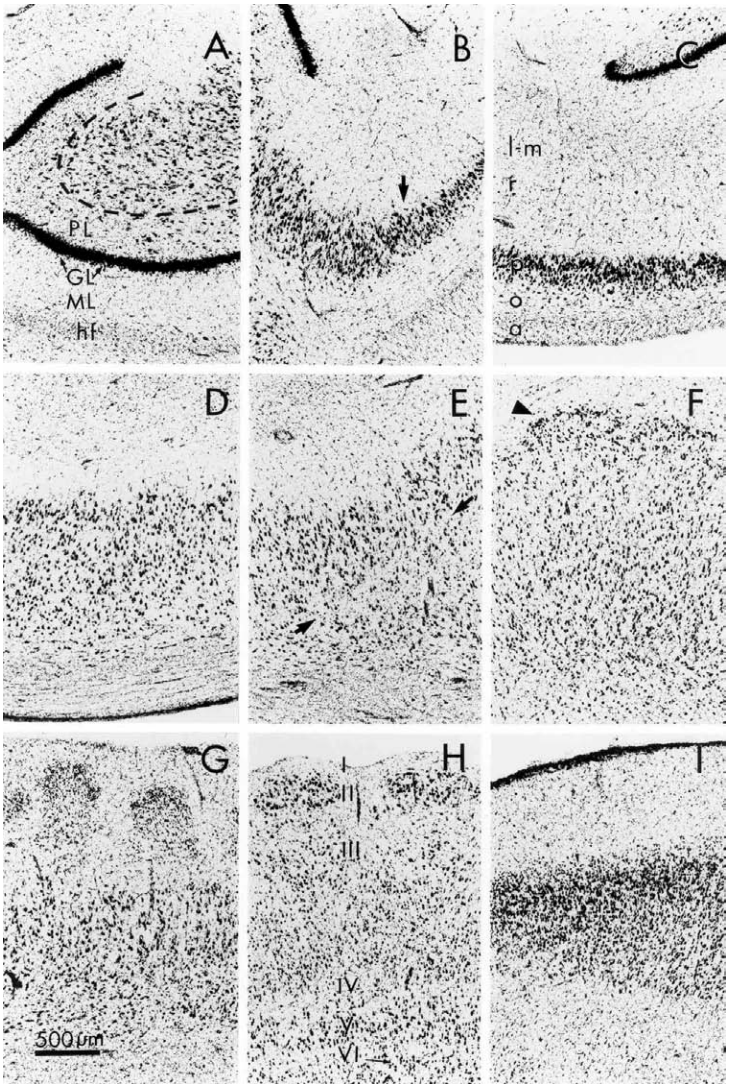

FIGURE 23.13 Higher-magnification photomicrographs to demonstrate the major cytoarchitectonic features of each of the fields of the human hippocampal formation. **(A)** the molecular (ML), granular (GL), and polymorphic (PL) layers of the dentate gyrus are indicated. The dashed line marks the border between CA3 of the hippocampus and the polymorphic layer. hf, huppocampal fissure. **(B)** Region of transition between the CA3 (on the left of the arrow) and CA2 (on the right) fields of the hippocampus. Note that the pyramidal cell layer in CA3 is both wider and more diffusely organized than in CA2. **(C)** Field CA2 of the hippocampus has the narrowest and most densely packed pyramidal cell layer of the hippocampal fields. The principal laminae of the hippocampus are also indicated: a, alveus; o, stratum oriens; p, pyramidal cell layer; r, stratum radiatum; l-m, stratum lacunosum-moleculare. **(D)** Field CA1 of the hippocampus has a wider pyramidal cell layer than fields CA3 or CA2 and the cells tend to be smaller and more widely separated. The most superficial pyramidal cells are more tightly packed, are somewhat larger, and stain somewhat darker than the deeper cells. **(E)** Transition region between CA1 (on left) and the subiculum (on right). A narrow cell-free zone (marked by arrows) often corresponds to the oblique border between the two fields. The region of overlap of the two pyramidal cell layers varies from brain to brain but in some cases can extend for several millimeters. **(F)** The pyramidal cell layer of the subiculum is often wider than of CA1. There are roughly two major layers of pyramidal cells, with the superficial ones being somewhat smaller than the deeper ones. The subicular pyramidal cell layer is also characterized by islands of small darkly stained cells (arrowhead) that lie at its superficial edge. **(G)** The presubiculum is characterized by a densely packed layer II that, at rostral levels (as illustrated in this photomicrograph), breaks up into spherical islands. The outer cap of layer II cells is more densely packed and somewhat darker staining than the cells in the remainder of the layer. (H) The entorhinal cortex is a multilaminate region that is generally considered to make up at least six distinct layers. The most distinctive feature of the entorhinal cortex is the islands of darkly stained modified pyramidal and stellate cells that make up layer II. In some regions, the surface of the entorhinal cortex forms bumps (verrucae or warts in the gross anatomical terminology) above the islands of layer II cells; these bumps are present in this section. Another distinguishing characteristic of the entorhinal cortex is the lack of an internal granular layer—layer IV. In its place through much of the entorhinal cortex is a cell-free space, the so-called lamina dissecans. (I) Transition region between the amygdala and hippocampus. This field is located in the rostral aspect of the uncal hippocampal formation (open arrow in Figure 23.5). Its small, darkly stained, and tightly packed neurons do not resemble those in any other hippocampal field.

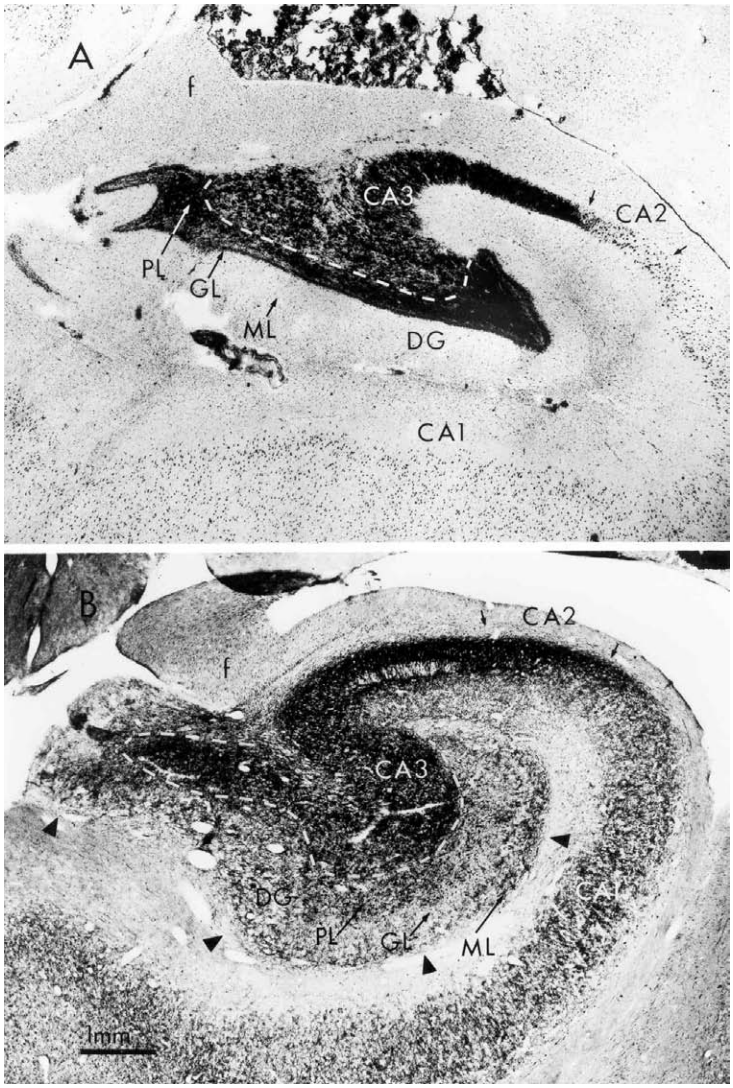

FIGURE 23.14 **(A)** A coronal section through the human hippocampal formation stained by the Timm's sulfide silver method for the demonstration of heavy metals. The section has also been counterstained with cresyl violet for the demonstration of neuronal cell bodies. Dark precipitate is confined to the polymorphic layer of the dentate gyrus and to the region within and immediately surrounding the CA3 pyramidal cell layer. The region of dark precipitate corresponds to the distribution of the mossy fiber axons arising from the granule cells of the dentate gyrus. Staining is attributable to the high level of zinc contained in the en passant presynaptic mossy fiber boutons. The termination of staining in the hippocampus marks the border between the CA3 and CA2 fields. This section was prepared and kindly made available to us by Carolyn Houser, University of California, Los Angeles. **(B)** A coronal hipppocampal section stained for the demonstration of AchE. In the dentate gyrus, staining is dense in the outer portion of the molecular layer (the superficial limit of which is marked with arrowheads) and in the polymorphic layer. There are numerous AchE-positive neurons in the polymorphic layer that distinguish it from the adjacent CA3 field. AchE staining is heavy in the CA3 field, especially in stratum oriens, and it gets somewhat darker in area CA2. There is a marked decrease in staining in CA1 and a further decrease in the subiculum.

to what discipline the description is directed. For the human hippocampus, the terminology first suggested by M. Rose (1926) is often used. Based on cytoarchitectonic criteria, he divided the human hippocampal formation into five fields and used labels H1–H5. While this nomenclature is still used in certain neuropathological communications, it has never been widely adopted for experimental animals and is difficult to apply to currently accepted subdivisions of the hippocampus. Perhaps the most commonly

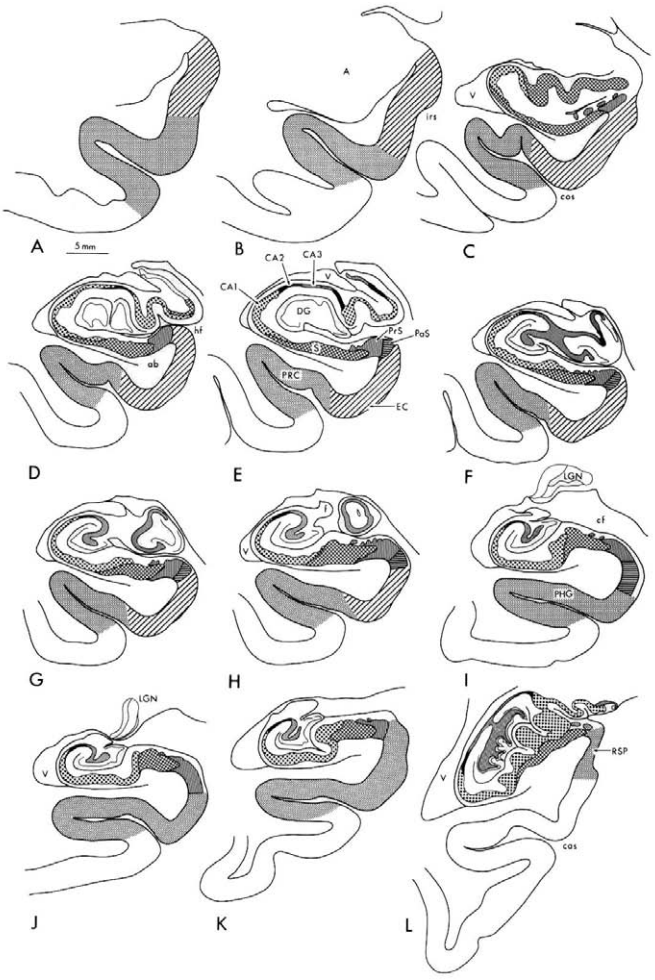

FIGURE 23.15 A series of coronal sections of the human temporal lobe arranged from rostral (A) to caudal (I). The various cytoarchitectonic fields of the hippocampal formation have been shaded with different hatching patterns (panel E is marked as a template) to show the varying extents of each of the fields at different rostrocaudal levels.

employed nomenclature for nonhuman primates and other experimental animals is that provided by Lorente de Nó (1934) based on his observations of Nissl, fiber, and Golgi preparations. He divided the hippocampus into four fields and labeled them CA1–CA4. While some lack of clarity in his description has led to confusion about the borders of some of the defined fields, the terms have the merit of common usage and can, with adequate presentation of criteria for boundaries, be easily employed in the human brain. There are several minor controversies concerning the naming of the other fields of the hippocampal formation, but they will be addressed during the description of the cytoarchitectonic characteristics of those fields.

Topographical Considerations

We presented a description of the topographical organization of the human hippocampal formation in the preceding section that should facilitate the interpretation of the cross-sectional photomicrographs shown in Figures 23.5–23.10. Much of the hippocampal formation lies in the floor of the temporal horn of the lateral ventricle (Fig. 23.2A, B). The individual fields of the hippocampal formation can be envisioned as adjacent bands of simple cortical tissue running rostrocaudally in the temporal lobe. The distinctive C-shape of the hippocampal formation is obtained when the fields fold over each other mediolaterally in an interlocking fashion. In its midportion or "body," the hippocampal formation has its simplest shape (Figs. 23.9 and 23.11). Each field is seen only once in coronal sections through this region. As the hippocampal formation approaches the rostral limit of the ventricle, however, it bends sharply in a medial direction and then in a caudal direction. The number of rostrocaudal flexures in this bend of the hippocampal formation varies substantially from individual to individual and can number as many as five (Gertz *et al.*, 1972). The photomicrographs (Figs. 23.6–23.8) of coronal sections through "uncal" (so called because of the bulge to which it contributes on the medial surface of the temporal lobe) levels show complex images of the hippocampal formation. It is difficult to determine solely on the basis of Nissl-stained coronal sections which fields of the hippocampal formation are seen at these levels. Only with the aid of other histochemical and inmunohistochemical series were we able to differentiate the fields that are designated in Figures 23.5–23.10, and schematically shown in Figure 23.15.

At caudal levels, the human hippocampal formation again loses its simple C-shaped organization. It bends dorsally as it ascends toward, and ultimately around, the splenium of the corpus callosum. Coronal sections through these caudal levels (Fig. 23.10) again provide complex images with discontinuous representations of several of its fields.

Dentate Gyrus

As in other species, the human dentate gyrus is a trilaminate cortical region. Its organization is most easily appreciated at mid rostrocaudal levels of the hippocampal formation (Figs. 23.9 and 23.11). Here it forms a C-shaped structure that is separated ventrally from the CA1 field of the hippocampus and the subiculum by the fused hippocampal fissure (Figs. 23.7 and 23.8). The principal cell layer of the dentate gyrus (the granule cell layer) is populated primarily by

one class of neuron, the granule cell, that sends a unipolar dendritic tree into the overlying molecular layer. Golgi-like staining of human granule cells show that dendrites extending into the molecular layer are invested with spines except for the most proximal 20–30 mm (Lim *et al.*, 1997a). Seress (1988) has estimated that the human dentate gyrus contains approximately 9×10^6 granule cells. More recent reports (West and Gundersen, 1990; West *et al.*, 1994; Simic *et al.*, 1997; Sá *et al.*, 1999) using unbiased stereological techniques have come up with figures that are substantially higher (i.e., 15×10^6 neurons in the granule cell layer of the human dentate gyrus). Interestingly, Sá *et al.* (1999) report a right–left asymmetry in the number of dentate granule cells, which are 20% more numerous on the right side. Human dentate granule cells often give rise to basal dendritic trees that extend into the subjacent polymorphic layer (Seress and Mrzljak, 1987). Lim *et al.* (1997a) note the presence of basal dendrites in 30% of the neurons they investigated. Such basal dendrites are rarely observed in nonprimates. The granule cell and molecular layers are sometimes referred to as the fascia dentata.

The third layer is generally called either the polymorphic layer or the hilus of the dentate gyrus. This is a complex region (Amaral, 1978), and there has been substantial confusion as to whether it should be included as a part of the dentate gyrus or is another, independent field of the hippocampus proper (the so-called field CA4). The situation is further complicated by the fact that the appearance of the region enclosed by the granule cell layer varies from species to species. With the use of powerful anatomical techniques in this region, there is increasingly convincing evidence in the rat and nonhuman primate that the polymorphic layer is a part of the dentate gyrus. Perhaps the most salient data come from connectional studies of the hilus, which indicate that its cells give rise to projections only to the dentate gyrus and not to any other field of the hippocampal formation (Laurberg and Sorensen, 1981). Connectional studies in the *in vitro* human hippocampal slice preparation also support the distinction of the polymorphic layer from the hippocampus; Lim *et al.* (1997a) demonstrated a dense plexus of fibers arising from the polymorphic layer that separates it from the remainder of CA3.

In the human dentate gyrus, it is not easy to differentiate the cells of the polymorphic layer from those of the hippocampus in standard Nissl preparations. Yet both Timm's stained preparations (Fig. 23.13A), which yield a patchy distribution of dark precipitate in the polymorphic layer, and acetylcholinesterase preparations (Fig. 23.13B), which demonstrate numerous precipitate-laden cells in the polymorphic layer, make the establishment of the border much easier. In Figures 23.8, 23.11, 23.12A, and 23.13A, B, a dashed line indicates the border of the polymorphic layer with the hippocampus.

The other question that commonly arises concerning this region is what to label the portion of the hippocampal pyramidal cell layer that is enclosed by the granule cell layer. As illustrated in Figures 23.8 and 23.9, these cells are rather numerous in the human hippocampal formation and are organized in a complex pattern. In fact, the pyramidal cell layer typically makes a sharp bend as it extends toward the hilus of the dentate gyrus and folds back on itself (the so-called end-blade). Lorente de Nó (1934) included some portion of the enclosed pyramidal cell layer as his field CA4. However, in some illustrations, he also appears to have applied the term "CA4" to the cells of the polymorphic layer of the dentate gyrus. Since that time, the term "CA4" has been applied either to the polymorphic layer or to the inserted portion of the pyramidal cell layer with about equal frequency in the literature. Because there is no cytoarchitectonic or connectional reason to distinguish the CA3 pyramidal cells enclosed within the granule cell layer from those that are outside it, we have dropped the use of the confusing term "CA4" and simply referred to all of the hippocampal pyramidal layer in this region as CA3.

Hippocampus

The human hippocampus can be divided into three distinct fields, which we have labeled CA3, CA2, and CA1 according to the nomenclature of Lorente de Nó (1934). In most respects, the overall organization of these fields is similar to that observed in the macaque monkey (Bakst and Amaral, 1984).

Field CA3 borders the hilus of the dentate gyrus, where it terminates in a complex fashion (as described earlier). At its other end, it borders field CA2. Cassell (1980) and Seress (1988) have estimated that there are about 2.1×10^6 neurons in the CA3 region and Cassell (1980) has estimated that there are about 0.22×10^6 pyramidal cells in CA2. More recent accounts of the number of neurons for CA3–CA2 combined derived using stereological techniques offer a figure of approximately 2.8×10^6 neurons (West and Gundersen, 1990; West *et al.*, 1994; Simic *et al.*, 1997; Sá *et al.*, 1999). Sá *et al.* (1999) reported hemispheric asymmetry so that CA3–CA2 contains 14% more neurons on the right side compared to on the left hippocampus. The CA3 pyramidal cells are the largest of the hippocampus and stain darkly in Nissl stains. While the layer is approximately 10 cells thick, it nonetheless has a relatively homogeneous appearance. There is no indication of

sublamination or marked variation of neuronal size or shape in different regions. The hallmark of CA3 is that its neurons receive input on their proximal dendrites from the axons of the dentate granule cells (the mossy fibers). The mossy fiber projection is located either within or immediately above the pyramidal cell layer in what is generally called stratum lucidum. The pattern of mossy fiber termination is best illustrated in Timm's silver sulfide preparations (Fig. 23.13A), in which the terminal varicosities of the mossy fibers are densely labeled with precipitate, presumably owing to their high content of zinc (Frederickson *et al.*, 1983). Lim *et al.* (1997a) analyzed the mossy fiber projection in slices of hippocampal tissue from human temporal lobe. Immunohistochemical stains have also been used to map the projections of the mossy fibers (see also Sloviter *et al.*, 1991; Seress *et al.*, 1993). Most of the dentate gyrus granule cells are immunoreactive for calbindin, as are interneurons in the external part of the molecular layer of the dentate gyrus (Seress *et al.*, 1993). The mossy fibers occupy the pyramidal cell layer and the stratum oriens. Fascicles of mossy fibers cross the pyramidal cell layer of CA3 to accumulate in the stratum lucidum, where they form the so-called end-bulb, and form presynaptic terminals to dendrites (mossy fiber giant boutons). Also, at this point intrahippocampal fibers travel for some distance along the longitudinal axis of the hippocampus.

Before proceeding, it might be appropriate to review the laminar nomenclature of the hippocampus. While it has essentially one cellular layer, the pyramidal cell layer, the plexiform layers above and below the pyramidal cell layer have all been given distinctive names. The limiting surface with the ventricular lumen deep to the pyramidal cell layer is formed by axons of the pyramidal cells and is called the alveus. Between it and the pyramidal cell layer is stratum oriens, which is occupied mainly by the basal dendrites of the pyramidal cells, though it also harbors a variety of neurons, many of which are interneurons. The region superficial to the pyramidal cell layer (toward the hippocampal fissure) contains the apical dendrites of the pyramidal cells and a number of interneurons. This plexiform region has historically been divided into a number of laminae. Stratum lucidum, in which the mossy fibers travel and form en passant synapses on the proximal dendrites of the pyramidal cells, is located immediately above the pyramidal cell layer in CA3. In the rat and monkey, stratum lucidum is apparent even in Nissl-stained sections owing to a noticeable decrease in glial staining. It is not as prominent in Nissl-stained sections of the human hippocampus because many of the mossy fibers also travel within the pyramidal cell layer and the difference in background glial staining is not as distinctive. Stratum lucidum is missing in fields CA2 and CA1 because pyramidal cells in these fields do not receive mossy fiber input. The remainder of the plexiform region is mainly occupied by stratum radiatum, and the most superficial portion (adjacent to the hippocampal fissure) is occupied by stratum lacunosum-moleculare. In stratum radiatum (as well as in stratum oriens), the CA3 and CA2 cells receive associational projections from other rostrocaudal levels as well as subcortical inputs from regions such as the septal nuclei and the supramammillary region. In CA1, the projections from CA3 and CA2 (the so-called Schaffer collaterals) terminate in stratum radiatum and stratum oriens.

The perforant pathway projection from the entorhinal cortex to the dentate gyrus travels, in part, in stratum lacunosum-moleculare of the hippocampus and makes en passant synapses on the distal apical dendrites of the hippocampal pyramidal cells.

The border between CA3 and CA2 is not readily apparent in Nissl-stained sections. This is because CA3 cells appear to extend under the border of CA2 for a short distance. The CA2 region has the most compact and narrow pyramidal cell layer of the hippocampus (Fig. 23.12C). Its cells are about as large and darkly stained as those in CA3, but there is far less space between the cell bodies. These characteristics, coupled with the lack of mossy fiber input, are the distinguishing features of the CA2 field. Even though the borders of CA2 are among the most difficult to establish with confidence, since CA2 has distinct connectional characteristics (in monkey, for example, it receives a particularly heavy input from the supramammillary region of the hypothalamus, Veazey *et al.*, 1982; and it is also recipient of a distinctive substance P projection from the hypothalamus, Nitsch and Leranth, 1994) and appears to be particularly insensitive to pathology (it is the so-called resistant sector of classical neuropathology, Brierly and Graham, 1984; Sloviter, 1994), it clearly deserves to be thought of as a distinct cytoarchitectonic field.

Field CA1 is unquestionably the most complex subdivision of the human hippocampus. According to Stephan (1983) and Stephan and Manolescu (1980), it is also one of the most phylogenetically progressive of the hippocampal fields. Not only does it appear to be populated by a far more heterogeneous group of neuronal elements than the other hippocampal fields, but its appearance also varies substantially along both its transverse (subiculodentate) and its rostrocaudal axes.

The border of CA1 with CA2 is not sharp because some CA2 pyramidal cells appear to extend over the emerging CA1 pyramidal cell layer. The boundary of

CA1 can be placed, however, shortly after the pyramidal cell layer starts to broaden. The border with the subiculum is equally difficult to place unless one is prepared to indicate a rather oblique border zone. As shown most clearly in Figures 23.8, 23.11, and 23.12E, the pyramidal cell layer of CA1 overlaps that of the subiculum for a considerable distance. There is often a cell-free zone between the two layers that helps to define the border (Fig. 23.12E). After the overlapping nature of this border is recognized, the boundary can then be fairly readily placed by using cytoarchitectonic criteria in Nissl-stained material.

Before describing the features of field CA1, we should discuss the origin and usefulness of the term "prosubiculum". Lorente de Nó (1934) used it to describe a field situated between CA1 and the subiculum. Analysis of his Figures 22 and 33 indicates that the area he illustrated as the prosubiculum is actually much of what contemporary authors consider to be the subiculum proper. Rosene and Van Hoesen (1987) continue to use the term "prosubiculum" to label the region of overlap of CA1 and the subiculum. However, we would agree with Braak (1972, see Fig. 23.1; Braak, 1974, see Fig. 23.2) and Cassell (1980) that overlap of elements from two adjacent fields does not constitute sufficient grounds for declaring the existence of a new field. If the cells in this region are ultimately shown to have input and output characteristics distinctly different from other parts of CA1 or the subiculum, then use of the term "prosubiculum" might be warranted. Until then, we have separated this border region into CA1 and subicular components.

According to Casell (1980) and Seress (1988), the CA1 field of the human hippocampus contains 4.6×10^6 to 4.7×10^6 neurons. Of these, Olbrich and Braak (1985) have estimated that 9.4% or approximately 430,000 are interneurons, and the remainder are pyramidal cells. More recent studies using nonbiased counting methods, yield counts that are three to four times larger, as reported by Sá *et al.* (1999, 11×10^6), West and Gundersen, (1990) and West *et al.* (1994, 14.4×10^6), and Simic *et al.* (1997, 20×10^6) without detectable differences between left and right sides of the hippocampus. As Braak (1974) pointed out, the human CA1 pyramidal cell layer can generally be subdivided into two main laminae that are each many cells thick. At many levels of the hippocampus, however, each of the sublayers also appears multilaminate. The pyramidal cell layer varies in thickness from about 10 cells to more than 30 cells. In general, the outer layer of pyramidal cells is more compact, and the cells tend to stain somewhat more darkly than the more deeply placed cells.

The CA1 pyramidal cell layer has a variable appearance at different rostrocaudal levels. And at any particular level, there is a gradient of changing organizational features along the transverse or subiculodentate axis. Close to the CA2 border, the CA1 pyramidal cell layer is at its thinnest, and the cells of both sublayers appear most tightly packed. Toward the subicular border, the pyramidal cell layer gets appreciably thicker and more loosely organized. It is often difficult to identify two discrete sublayers of CA1 in this region because the cells are often organized in a more patchy fashion. The stratum radiatum is much broader in the region of CA1 closest to CA2 and becomes much thinner toward the subiculum (Figs. 23.8, 23.9, and 23.11).

Subiculum

An early estimate of the number of pyramidal cells in the subiculum was approximately 2.55×10^6 (Cassell, 1980). However, more recent studies yield counts that are nearly twice as large (West *et al.*, 1994; Simic *et al.*, 1997), that is, around 5×10^6 neurons. The subiculum is the origin of major subcortical projections to the septal complex, nucleus accumbens, anterior thalamus, and mammillary nuclei, as well as projections to the entorhinal cortex. However, the precise organization of most of these projections is not well understood even in experimental animals. Moreover, the cellular and laminar organization of this region has nor yet been clearly delineated.

As noted earlier, the subiculum and field CA1 of the hippocampus overlap at their border (Figs. 23.8, 23.11, and 23.12E) The laminar organization of both regions is complex in this zone. More medially (i.e., closer to the presubiculum), the subiculum can easily be divided into three layers. Superficially there is a wide molecular layer into which the apical dendrites of the subicular pyramidal cells extend. The molecular layer of the human subiculum tends to be relatively wider than in the monkey and rat and, as in these species, is distinct from the stratum radiatum of CA1. At some levels, islands of what appear to be layer II presubicular cells invade the distal portions of the subicular molecular layer (Braak, 1972). The pyramidal cell layer of the subiculum is 30 or more cells thick and can be divided into at least two sublaminae. Relative to CA1, the subicular pyramidal cells tend to be somewhat larger and more widely spaced. Braak (1972) has labeled the two sublaminae of the pyramidal cell layer the external (nearest the molecular layer) and internal layers. The cells of the external pyramidal cell layer are larger than those in the internal layer, and many of the pyramidal cells contain a distinctive dense

accumulation of lipofuscin in the proximal portion of their apical dendrites. Neither of the subicular pyramidal cell layers is homogeneous. In particular, the superficial limit of the external pyramidal cell layer contains islands of small, darkly stained cells (Fig. 23.12F). This characteristic also distinguishes the subiculum from CA1, which contains large, darkly stained cells at its superficial limit (compare Fig. 23.12D and F). The deepest portion of the subicular pyramidal cell layer contains a variety of smaller neurons which appear to be analogous to the polymorphic layer identified in the monkey (Bakst and Amaral, 1984). As indicated in Figure 23.14, the subiculum makes up much of the uncal flexure of the hippocampal formation. We should note also that a unique field lies between the rostromedial subiculum and the amygdalohippocampal area of the amygdaloid complex (Fig. 23.7, open arrow). This transition region contains a high density of small, darkly stained cells (Fig. 23.12I) that are unlike neurons in any of the other hippocampal fields. This region has been termed hippocampoamygdaloid transitional area (HATA) by Rosene and Van Hoesen (1987).

Presubiculum and Parasubiculum

The laminar organization of the presubiculum and parasubiculum is complex and only poorly understood. It is perhaps most useful to consider that the presubiculum consists of a single, superficially located cellular layer (layer II), which is formed by densely packed, small, modified pyramidal cells.

Layer II of the presubiculum tends to be narrow and continuous at posterior levels of the hippocampal formation but breaks up into larger-diameter islands at more rostral levels. As in the monkey (Bakst and Amaral, 1984), layer II in the human can be further divided into a narrow, superficial rim that contains more densely packed and darkly stained neurons and a broader band of more widely separated cells. The parasubiculum also contains a single cellular layer that is difficult to clearly differentiate from the presubiculum. The layer II cells of the parasubiculum tend to be somewhat larger than those in the presubiculum and more widely spaced.

Entorhinal Cortex

The term "entorhinal cortex" was coined by Brodmann (1909) as a synonym for his area 28. More than any other hippocampal field, the entorhinal cortex has undergone substantial regional and laminar differentiation in the primate brain relative to the rodent (Stephan, 1983). In the rat, the entorhinal cortex is usually considered to comprise two regions (medial and lateral) that were originally proposed by Brodmann (1909, his areas 28a and 28b). In the macaque monkey, the entorhinal cortex demonstrates a marked gradient of cytoarchitectonic changes from its rostral to caudal extents and can be partitioned into at least seven different cytoarchitectonic fields (Amaral *et al.*, 1987; Fig. 23.15 upper part). The human entorhinal cortex has been studied by several authors (Braak, 1972; Macchi, 1951; Rose, 1927; Sgonina, 1938), who have partitioned it into as many as 23 fields (Rose, 1927; Sgonina, 1938). Our own studies suggest that the laminar organization of the human entorhinal cortex is not nearly as distinct as in the macaque monkey. Nonetheless, we have observed the same rostrocaudal gradient of cytoarchitectonic differentiation in the human entorhinal cortex and, using similar criteria, up to eight fields, largely comparable with those defined for the monkey, can be distinguished in the human (Insausti *et al.*, 1995; Fig. 23.15 lower part). Other cytoarchitectonic parcellations for the human entorhinal cortex have also been proposed, based either on the peculiarities of the pigment staining of layer II neurons (Hanke and Yilmazer-Hanke, 1997, 12 subfields) or more classical cyto- and myeloarchitectonic approaches (Krimer *et al.*, 1997, 9 subfields).

In the monkey, the entorhinal cortex is spatially associated with the amygdaloid complex rostrally and the other fields of the hippocampal formation caudally. It extends rostrally to about the mid rostrocaudal level of the amygdala and caudally to the level of the anterior limit of the lateral geniculate nucleus or about midway back through the hippocampus (Fig. 23.4). In the human, the entorhinal cortex appears to extend relatively more rostrally than in the monkey.

Structures that form the medial and lateral borders of the entorhinal cortex are different at various rostrocaudal levels. At rostral levels, the entorhinal cortex borders the periamygdaloid cortex medially, and the boundary is approximately marked by the location of the sulcus semiannularis (Fig. 23.5). As the other fields of the hippocampal formation emerge at more caudal levels of the entorhinal cortex, the medial boundary is formed either by the presubiculum or the parasubiculum. Unlike in the rat and monkey, where the lateral border of most of the entorhinal cortex is marked by the rhinal sulcus, there is no easily identifiable lateral limit of the human entorhinal cortex. In fact, the rhinal sulcus in the human is for the most part situated rostral to the entorhinal cortex. The collateral sulcus lies lateral to the entorhinal cortex for its full rostrocaudal extent but at no level does it form the lateral border of the entorhinal cortex. As in the

monkey, the human entorhinal cortex is laterally adjacent to the perirhinal cortex (areas 35 and 36 of Brodmann) for much of its rostrocaudal extent. In the monkey, we have found that area 35 forms the lateral border of rostral levels of the entorhinal cortex, whereas area 36 (which is differentiated from area 35 principally by the presence of a distinct layer IV) borders caudal levels. In the human brain, the lateral border of the entorhinal cortex is formed throughout its rostrocaudal extent by a cortical field that lacks a distinct layer IV and has many of the other cytoarchitectonic characteristics of area 35. However, the border between area 35 and the entorhinal cortex is not easily placed. As indicated in Figures 23.5 and 23.7, these two fields appear to have an obliquely oriented boundary. The deep layers of the entorhinal cortex appear to extend somewhat more laterally than the superficial layers. This distinctly angled border between area 35 and the entorhinal cortex has been emphasized by Braak (1980), who has labeled the region of overlap the "transentorhinal zone." The caudal limit of the human entorhinal cortex also presents a complex cytoarchitectonic appearance. In the monkey (Amaral *et al.*, 1987), the entorhinal cortex is continuous caudally with a lateral extension of what appears to be the parasubiculum and then with fields TH and TF of the parahippocampal gyrus. For some distance, however, neural elements from all these fields appear to be intermixed. A similar situation appears to hold for the human entorhinal cortex as well.

While the entorhinal cortex is a multilaminate structure, its cellular constituents and laminar organization are quite distinct from those of other neocortical regions. Several numbering schemes have been adopted for its various layers. According to Ramón y Cajal (1901–1902), Hammarberg (1895) provided the first account of entorhinal lamination and recognized five distinct layers. Ramón y Cajal (1901–1902) described seven cellular and plexiform layers in the entorhinal cortex while Lorente de Nó (1933) assigned six. Other authors (Braak, 1972; Sgonina, 1938; Heinsen *et al.*, 1994; Hanke and Yilmazer-Hanke, 1997) have not numbered the layers of the entorhinal cortex but simply divided it into two laminae, the laminae principalis externa and principalis interna, with a cell-free space, the lamina dissecans, interposed. By doing this, they stressed the perceived impropriety of associating layers of the entorhinal cortex with those of the neocortex. We (Amaral *et al.*, 1987) have adopted with minor modifications (Fig. 23.6) the scheme of layering proposed by Ramón y Cajal (1901–1902). Because there has been substantial confusion concerning the laminar organization of the human entorhinal cortex, it is worthwhile to review briefly the major characteristics of each of its laminae.

The entorhinal cortex can be conveniently divided into six layers (Fig. 23.12H). Layer I is an acellular or plexiform layer that tends to be somewhat thicker at more posterior levels. Layer II is a cellular layer made up of islands of relatively large and darkly stained modified pyramidal and stellate cells (Fig. 23.12H). Layer II is one of the most outstanding and distinguishing characteristics of the entorhinal cortex (see Fig. 23.3 for unfixed appearance). The islands are distributed all over the entorhinal cortex, although they tend to be thinner, more elongated, and less noticeable rostrally, at dorsal and medial portions (Braak, 1980, tangential sections; Insausti *et al.*, 1995; Hanke and Yilmazer-Hanke, 1997, tangential sections). In the fixed brain, the cell islands of layer II form small mounds (Fig. 23.12H) on the surface of the brain that can be observed with the naked eye (Figs. 23.1, 23.3, 23.5, and 23.8). These raised bumps on the surface of the entorhinal cortex (the verrucae hippocampi illustrated by Klingler, 1948) provide a useful macroscopic indication of the entorhinal location. The white strands surrounding layer II cell islands have been referred to as substantia reticularis alba of Arnold. The presence of modularity in the human entorhinal cortex has been suggested based on the demonstration of cytochrome oxidase activity in the upper layers of the human entorhinal cortex (Hevner and Wong-Riley, 1992). Interestingly, the cytochrome oxidase pattern loses the patchy appearance at the caudal limit of the entorhinal cortex. Further support for the presence of modules in the human entorhinal cortex is given by the immunoreactivity for nonphosphorylated neurofilaments and the calcium-binding proteins calbindin and parvalbumin (Beall and Lewis, 1992) and by a more detailed study using several techniques by Solodkin and Van Hoesen (1996). Although there are no reported studies of the ultrastructure of layer II neurons in the human entorhinal cortex, the study by Goldenberg *et al.* (1995) in the rhesus monkey shows differences along the rostrocaudal extent of the entorhinal cortex: rostrally (ER) neurons are grouped in clusters with frequent appositions of contiguous somata. These appositions were absent at intemediate and caudal levels. In contrast, axosomatic synapses and the presence of myelinated fibers increases caudally in the entorhinal cortex.

There is usually an acellular gap between layer II and the broad layer of medium-sized pyramidal cells that populate layer III. This gap increases at more posterior levels of the entorhinal cortex so that, in myelin-stained preparations, the layer II cell islands are conspicuous as negative images outlined by the dense fiber labeling in layer I and in the space between layers II and III. Layer III contains a relatively homogeneous population of pyramidal cells. Layer III

cells have a columnar appearance at caudal levels of the entorhinal cortex but tend to be arranged in large patches rostrally and medially. In myelin preparations, layer III contains delicate bundles of radially oriented fibers that run to the pial surface. These bundles of fibers are more noticeable at rostral levels of the entorhinal cortex, and they become particularly dense close to the boundary with the perirhinal cortex. Golgi studies of the monkey entorhinal cortex (Amaral *et al.*, 1987; Carboni *et al.*, 1990) show that dendrites of layer III pyramidal neurons bend and pass through the interstices of layer II cell islands, a morphological feature that has also been observed in the human entorhinal cortex after intracellular filling of neurons in fixed slices (Mikkonen *et al.*, 2000)

One of the most characteristic features of the entorhinal cortex in all species is the absence of an internal granule cell layer. In its place is an acellular region of dense fiber labeling, the lamina dissecans (Rose, 1927), which is most noticeable at mid rostrocaudal levels of the entorhinal cortex. In the entorhinal regions where the lamina dissecans is not prominent, layers III and V are apposed. Fiber preparations through these regions, however, still demonstrate a heavy plexus of fibers at the interface of the two layers. To emphasize the lack of a typical internal granule cell layer in the entorhinal cortex, the lamina dissecans has been labeled as layer IV. In some reports of the human entorhinal cortex (Hyman *et al.*, 1984), the term "layer IV" is applied to the layer of large pyramidal cells that lies deep to the lamina dissecans. To avoid the confusion that might arise from labeling a layer of large pyramidal cells with the same number typically applied to a layer of small cells in the neocortex, we have followed Ramón y Cajal's lead and labeled the large cells deep to lamina dissecans as layer V.

Layer V is about five or six cells deep and comprises primarily large and darkly stained pyramidal cells. At rostral levels of the entorhinal cortex, layer V merges with layer III while at mid levels the lamina dissecans clearly separates the two layers. Layer V becomes most highly developed at mid to caudal levels of the entorhinal cortex, and here three sublaminae can be differentiated. The most superficial layer (sublayer Va) contains the largest pyramidal cells in the entorhinal cortex, while the middle sublayer (Vb) contains somewhat smaller and more loosely arranged cells. The deep sublamina (layer Vc) contains fewer neurons and a fairly dense plexus of fibers (Figs. 23.6 and 23.7; Insausti *et al.*, 1995). At the same time that the lamina dissecans becomes less noticeable in the caudal half of the entorhinal cortex, layer Vc becomes much more pronounced, and it is easy to mistake Vc for a caudal extension of the lamina dissecans. At rostral levels of the entorhinal cortex, layer VI is not easily distinguished from layer V. Close to the border with the perirhinal cortex, layer VI is rather broad and diffuse. The border of layer VI with the white matter is not sharp rostrally, and there is a gradient of decreasing cell density from this layer into the white matter. Caudally, however, layer VI presents a sharp border at the transition with the white matter (Figs. 23.7 and 23.8). The subcortical white matter situated deep to the subicular complex is given the name angular bundle (Figs. 23.7 and 23.8) because of its trajectory in nonprimates. It is within this region that the perforan path fibers travel to caudal levels of the hippocampal formation. At the border of the entorhinal cortex with the perirhinal cortex, layer VI tends to fade out in a gradual fashion and finally ends somewhat more laterally than the termination of layer V. This contributes to the oblique orientation of the border between the entorhinal and perirhinal cortices that we discussed earlier.

Since the first writing of this chapter, several, studies have been conducted in order to estimate the number of neurons in the human entorhinal cortex (Heinsen *et al.*, 1994; Gómez-Isla *et al.*, 1996; West and Slomianka, 1998a; *corrigendum*, West and Slomianka, 1998b; Price *et al.*, 2001; Kordower *et al.*, 2001). The counts generally are carried out relative to layers but do not take the various subfields into consideration. The number of neurons of the human entorhinal cortex is on the order of 7×10^6 to 8×10^6 neurons. Of these, about 10% are in layer II, approximately 45% are located in layer III, about 15% of the total belong to layer V, and 31% are in layer VI.

A simple comparison of these figures has important implications for the understanding of the anatomical connections of the human hippocampal formation. For instance, these numbers, compared to those of the human hippocampus, emphasize how divergent the axonal projection of layer II neurons must be, both to the dentate gyrus and CA3 (West and Slomianska, 1998a, b). In addition, 6.1×10^6 neurons in layer III of the entorhinal cortex and 16×10^6 neurons in the human CA1 field of the hippocampus, yields a ratio of approximately 1:2.5. In other words, almost one half of the total number of neurons of the human entorhinal cortex might be projecting to CA1 (Witter and Amaral, 1991).

HIPPOCAMPAL CONNECTIVITY

Having reviewed the cytoarchitectonic organization of the human hippocampal formation, we now present a summary of its major connections. Virtually all the information we survey here was derived from experimental studies conducted in the rat, cat, or

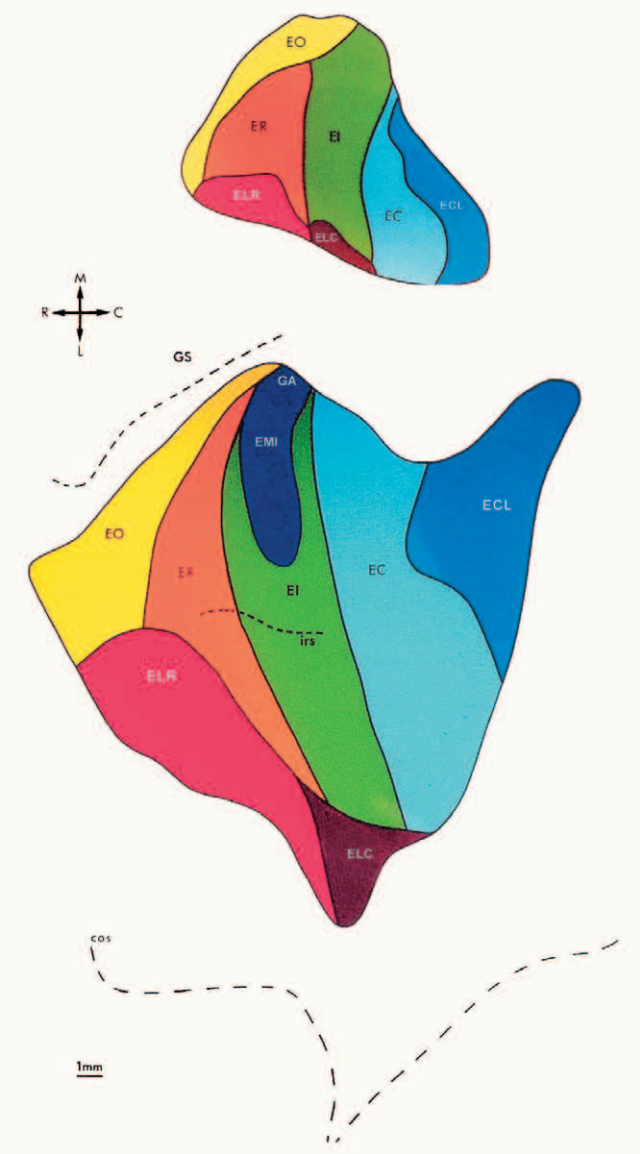

FIGURE 23.16 Two-dimensional unfolded maps of the entorhinal cortex in the nonhuman primate (*Macaca fascicularis* monkey, upper panel) and in the human brain (lower panel). In both cases, the same scale and orientation (arrows) applies to both species. While in the nonhuman primate, no special mention to adjacent sulci, the rhinal sulcus in particular, is made; in the case of the human entorhinal cortex, the location of the the gyrus semilunaris (GS) above the upper dashed line (sulcus semiannularis), the location of the intrarhinal sulcus (irs) in the middle of the mediolateral extent of the entorhinal cortex, and the fundus of the collateral sulcus (cs) separated some distance from the lateral border of the entorhinal cortex by the laterally adjacent perirhinal cortex are indicated. Subfields of the entorhinal cortex, which presumably share homology between both species, are color-coded in a similar way. Despite the fact that only one more subfield could be reliably identified, note the expanse of the caudal entorhinal portions of the human brain compared to nonhuman primates.

monkey. The fundamental intrinsic circuitry of the hippocampal formation and a listing of its major inputs and outputs is illustrated in Figure 23.16.

Intrinsic Connections

The dentate gyrus can, for convenience, be considered the first step in the intrinsic hippocampal formation circuit. It receives its major input from cells located primarily in layer II of the entorhinal cortex that give rise to the so-called perforant path (Andersen *et al.*, 1966; Hjorth-Simonsen, 1971, 1972; Hjorth-Simonsen and Jeune, 1972; Ruth *et al.*, 1982; Steward, 1976; Steward and Scoville, 1976; Witter and Groenewegen, 1984; Witter *et al.*, 1988a, 1989, Witter and Amaral, 1991). According to Witter and Amaral (1991), layer II neurons originate the projection to the molecular layer of the dentate gyrus and stratum lacunosum-moleculare of CA3, while layer III neurons project almost exclusively to CA1 and the subiculum. These fibers travel caudally from the entorhinal cortex in the angular bundle and ultimately perforate through the subiculum and hippocampus to terminate in the outer two-thirds of the molecular layer of the dentate gyrus. The course of the perforant path fibers is complex. Some of the fibers cross the obliterated hippocampal fissure to enter the dentate molecular layer directly from the subiculum, while others travel first through the stratum lacunosum-moleculare of CA1 and CA3 to enter the molecular layer at the tip of the dentate gyrus. As illustrated in Figure 23.16, the entorhinal fibers also terminate in the subiculum, CA1, and CA3 (Nafstad, 1967; Steward, 1976; Steward and Scoville, 1976; Van Hoesen and Pandya, 1975b). This direct projection to the hippocampus and subiculum has largely been neglected, though it is by no means trivial and is likely to be of substantial importance to the normal functioning of the hippocampal formation (Witter *et al.*, 1988a; Soltesz and Jones, 1995; Sybirska *et al.*, 2000). One of the few tracing studies conducted in the post-mortem human hippocampal formation reveals that specific entorhino-hipocampal (CA1, CA3 and subiculum) projections are present at 19 post-gestational weeks and originate in the appropriate layers, while entorhino-dentate projections lag a few weeks behind (Hevner and Kinney, 1996). The same study also reports that CA1 and subiculum contain retrogradely labeled neurons, similar to the connections of CA1 and subiculum of the monkey hippocampal formation (Kosel *et al.*, 1982; Insausti and Amaral, unpublished observations). Anterogradely DiI-labeled fibers were likewise demonstrated, although, in contrast to the monkey, the alvear path seemed more robust than in the monkey, while the

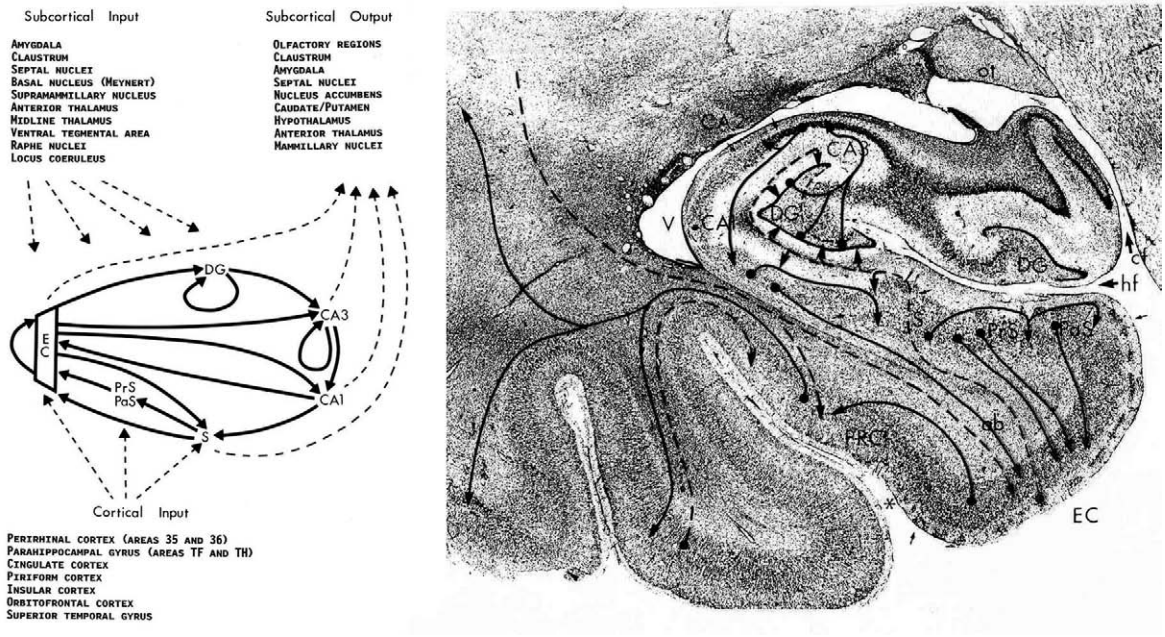

FIGURE 23.17 Illustration of the major connections of the hippocampal formation and a listing of prominent afferent and efferent connections (see text for details). Curved arrows in the dentate gyrus (DG) and in the CA3 field of the hippocampus indicate the presence of associational projections that link different levels of the fields. The curved arrow in the entorhinal cortex (EC) indicates the presence of associational projections between different levels of the field and projections from deep layers to superficial layers. Dashed lines at the right represent efferent projections carried by the fornix. Several of the subcortical afferents listed at the left enter the hippocampal formation through the fornix. A separate list of cortical outputs has not been included in this illustration. It is likely, however, that most, if not all, of the areas listed as afferents to the hippocampal formation receive return projections from the subiculum or entorhinal cortex.

labeling of the perforant path was similar to that reported in the monkey by Witter and Amaral (1991).

Cells of the dentate gyrus do not project outside of the hippocampal formation. Rather, the dentate granule cells project via their distinctive axons, the mossy fibers, upon cells of the dentate gyrus's own polymorphic layer (Clairbone *et al.*, 1986) and onto the proximal dendrites of the pyramidal cells of the CA3 region of the hippocampus (Blackstad *et al.*, 1970; Gaarskjaer, 1978, 1981; Rosene and Van Hoesen, 1977). The other main constituent of the granule cell layer is the dentate basket pyramidal cell that gives rise to a dense plexus of GABAergic fibers and terminals that surround the granule cell bodies (Ribak and Seress, 1983). The deep, or polymorphic layer of the dentate gyrus has a mixture of neuronal types that give rise to local and associational projections (Fig. 23.16). In nonprimates, cells in the polymorphic layer also contribute a commissural projection to the contralateral dentate gyrus, but this connection is largely vestigial in the monkey (Amaral *et al.*, 1984; Demeter *et al.*, 1985), as well as in humans (Wilson *et al.*, 1987; Gloor *et al.*, 1993). One class of cell, the mossy cell, originates a prominent associational system of fibers that terminates in the inner one-third of the molecular layer (Laurberg and Sorensen, 1981; Swanson *et al.*, 1978). Interestingly, this projection does not terminate locally (at the level of origin) but projects to distant portions of the dentate gyrus (Buckmaster and Amaral, 2001) and thus tends to associate different septotemporal (or rostrocaudal in the human) levels of the dentate gyrus. There is a second population of cells in the polymorphic layer, immunoreactive for the peptide somatostatin and for γ-aminobutyric acid (GABA), that gives rise to a fiber system that is complementary to the associational fibers. These fibers terminate in the outer two-thirds of the molecular layer and terminate most densely at a level close to the cells of origin (Bakst *et al.*, 1986). There are a number of other neuronal cell types in the dentate gyrus, many of which are immunoreactive for one or more peptides (Amaral and Campbell, 1986) or other transmitter candidates. The precise connectivity of most of these cells is not currently established.

Collaterals of single CA3 pyramidal cells project to other levels of CA3, to CA1, and to subcortical regions, especially the septal nuclei. CA3 pyramidal cells in the rat originate an extensive associational system that

projects widely along the septotemporal axis of the field (Ishizuka *et al.*, 1990; Swanson *et al.*, 1978). CA3 cells also contribute the mayor input system to CA1 (the Schaffer collaterals), which terminates throughout stratum radiatum and stratum oriens (Ishizuka *et al.*, 1990; Rosene and Van Hoesen, 1977; Swanson *et al.*, 1978; Lim *et al.*, 1997b). The CA3 field of the hippocampus also contains a number of nonpyramidal cells, many of which are interneurons, but the connectivity of these has not been well studied. CA1 pyramidal cells have a pattern of connections that is distinct from that of CA3. What is perhaps most striking is that CA1 pyramidal cells do not project significantly to other levels of CA1. Rather, CA1 pyramidal cells project predominantly to the subiculum (Finch and Babb, 1981; Finch *et al.*, 1983; Rosene and Van Hoesen, 1977; Swanson and Cowan, 1977). The subiculum, in turn, projects to the pre- and parasubiculum, and all three components of the subicular cortices project to the entorhinal cortex (Amaral *et al.*, 1984; Beckstead, 1978: Finch *et al.*, 1983; Köhler, 1984, 1985; Köhler *et al.*, 1978; Rosene and Van Hoesen, 1977; Shipley, 1974, 1975; Sorensen and Shipley, 1979).

As indicated in Figure 23.16, one of the more striking features of the intrinsic circuitry of the hippocampal formation is that it is largely unidirectional. The CA3 field does not project back to the granule cells of the dentate gyrus. Nor do CA1 pyramidal cells project back to CA3. Thus, aside from the initial entorhinal input that reaches all the hippocampal fields in parallel, information flow from the dentate gyrus through the other fields follows an obligatory serial and largely unidirectional pathway.

Extrinsic Connections

Until the mid 1970s, the prevailing view of the extrinsic connectivity of the hippocampal formation was largely that enunciated by Papez (1937). Papez suggested that the hippocampus was the recipient of sensory information from a variety of cortical regions (though the sources and pathways of these projections were only vaguely set forth). The hippocampus was thought to funnel this sensory information through the fimbria and fornix to the mammillary nuclei where it could marshal appropriate emotional responses. (The hippocampal projections to the septal nuclei and anterior thalamus were not experimentally demonstrated until the 1950s and early 1960s.) Because the fornix was such an obvious efferent pathway, alternative hippocampal efferents were largely overlooked. And because little was known about the specific connectivity of the individual hippocampal subdivisions, the fimbria was assumed to arise exclusively from the pyramidal cells of the hippocampus. It is now clear, however, that the subiculum, rather than the hippocampus proper, gives rise to the postcommissural projection to the mammillary complex. Moreover, recent studies conducted mainly in the primate brain have shown that the fornix is not the sole output pathway of the hippocampal system. Both CA1 and the subicular cortices form the non-entorhinal neocortical output of the hippocampal formation (Insausti and Muñoz, 2001), directed to polymodal association cortices (Barbas and Blatt, 1995; Blatt and Rosene, 1998; Ding *et al.*, 2000; Yukie, 2000; Insausti and Muñoz, 2001). Likewise, the entorhinal cortex projects to neighboring cortices such as the perirhinal and parahippocampal cortices and to more distant regions such as the orbitofrontal cortex. The concept has emerged that the interaction of the hippocampal formation with the neocortex is at least as important to its normal function as its subcortical interactions. The hippocampal formation can also influence a variety of brain regions through nonfimbrial projections to the amygdaloid complex and striatum. The literature on the extrinsic connectivity of the hippocampal formation is rapidly expanding, and it is beyond the scope of this chapter to review exhaustively this body of work. The following is intended to be an overview of the major extrinsic hippocampal connections.

Subcortical Connections

The fimbria and fornix form the classical efferent system of the hippocampal formation and the human fornix contains about 1.2 million fibers (Powell *et al.*, 1957). The precommissural fornix, which innervates primarily the lateral septal nucleus, arises mainly from cells of the hippocampus proper and to a lesser extent from the subiculum and entorhinal cortex (Alonso and Köhler, 1984; Siegel *et al.*, 1974, 1975; Swanson and Cowan, 1977). The cells of CA3, which project bilaterally to the septal complex, are the same cells that give rise to the Schaffer collaterals to CA1 (i.e., axon branches distribute terminals to both structures). The nucleus accumbens also receives a projection through the fornix that arises in the subiculum and entorhinal cortex (Groenewegen *et al.*, 1982; Kelley and Domesick, 1982; Lopes da Silva *et al.*, 1984; Sorensen, 1985; Swanson and Cowan, 1977). The subiculum and entorhinal cortex give rise to additional projections to the caudate nucleus and putamen (Groenewegen *et al.*, 1982; Sorensen, 1985; Sorensen and Witter, 1983). As noted previously, it is the subicular complex, rather than the hippocampus, is the origin of the postcommissural fiber system (Swanson and Cowan, 1975). Presubicular fibers innervate the anteromedial,

anteroventral, and lateral dorsal nuclei of the thalamus, and fibers originating in the subiculum and presubiculum provide the major extrinsic input to the mammillary nuclei (Chronister *et al.,* 1975; Edinger *et al.,* 1979; Irle and Markowitsch, 1982; Kaitz and Robertson, 1981; Meibach and Siegel, 1975, 1977: Poletti and Creswell, 1977; Raisman *et al.,* 1966; Rosene and Van Hoesen, 1977; Sherlock and Raisman, 1975; Simpson, 1952; Swanson and Cowan, 1975, 1977). The lateral mammillary nucleus is innervated by the subiculum and presubiculum, and the medial mammillary nucleus is innervated by the subiculum. In the rat and cat, the ventromedial nucleus of the hypothalamus is reciprocally connected with the ventral portion of the subiculum (Irle and Markowitsch, 1982; Krettek and Price, 1978; Swanson and Cowan, 1977), though this connection has not yet been confirmed in the primate.

Starting with the work of Krettek and Price (1977) in the rat and cat, it has become increasingly clear that the hippocampal formation is interconnected with several regions of the amygdala. They showed that the lateral nucleus of the amygdala gave rise to a prominent projection to layer III of the lateral entorhinal cortex. There were additional projections from the basal nucleus to the subiculum and parasubiculum. In the monkey, the lateral and basal nuclei also projects to the entorhinal cortex (Pitkänen *et al.,* 2002) and there are additional projections from the accessory basal nucleus to the subiculum (Aggleton, 1986; Amaral, 1986). The subiculum originates a return projection to the basal nucleus, while the entorhinal cortex projects to both the basal and lateral nuclei (Aggleton, 1986; Amaral, 1986). In the rat, the ventral portion of CA1 is reported to project to the lateral, basal, and cortical nuclei (Ottersen, 1982). (See Chapter 22 for further details on the connections of the amygdala with the hippocampal formation.) The entorhinal cortex is also reciprocally connected to the ventral part of the anterior claustrum (Insausti *et al.,* 1987b; Markowitsch *et al.,* 1984; Witter *et al.,* 1988b).

In addition to the amygdala and claustrum, a number of other subcortical structures project to the hippocampal formation. Most prominent among these are the septal complex and the supramammillary area. The septal projection to the hippocampal formation was first experimentally demonstrated in the early 1950s (Daitz and Powell, 1954; Morin, 1950), and numerous studies have subsequently been conducted to further define the projection (Fibiger, 1982; Meibach and Siegel, 1975; Milner *et al.,* 1983; Mosko *et al.,* 1973; Swanson, 1978; Swanson and Cowan, 1976; Amaral and Kurz, 1985). The septal projection arises from cells of the medial septal nucleus and the nucleus of the diagonal band of Broca and, in the rat brain, travels to the hippocampal formation via four routes: the fimbria, dorsal fornix, supracallosal stria, and a ventral route through the amygdala complex (Milner and Amaral, 1984). Septal fibers terminate in essentially all fields of the hippocampal formation but are most prominent in the dentate gyrus and the CA3 field of the hippocampal formation.

Lewis and Shute (1967; Lewis *et al.,* 1967) first proposed that the septohippocampal projection was cholinergic after showing that fimbrial sections led to a substantial loss of histochemical staining of the degradative enzyme acetylcholinesterase. Mesulam and colleagues, using inmunohistochemical procedures to demonstrate the specific cholinergic marker, choline acetylcholinesterase, in conjunction with retrograde tracer techniques (Mesulam *et al.,* 1983; Wainer *et al.,* 1985) found that 30–50% of the cells in the medial septal nucleus and 50–75% of the cells in the nucleus of the diagonal band that project to the hippocampal formation are cholinergic. Their retrograde tracer studies confirmed the long-held belief that the medial septal nucleus and the nucleus of the diagonal band give rise to the cholinergic innervation of the hippocampal formation but indicated that many cells, especially within the medial septal nucleus, that project to the hippocampal formation are not cholinergic. Many cells in the septal complex contain glutamic acid decarboxylase and are presumably GABAergic; at least some or these project to the hippocampal formation (Köhler *et al.,* 1984a). The entorhinal cortex is also innervated by cells of the medial septal nucleus and nucleus of the diagonal band (Alonso and Köhler, 1984; Insausti *et al.,* 1987b; Segal, 1977). These projections are similarly only partially cholinergic (Alonso and Köhler, 1984; Amaral and Kurz, 1985; see also Chapter 17).

The major hypothalamic projection to the hippocampal formation arises from a population of large cells that cap and partially surround the mammillary nuclei in a zone that has been named the supramammillary area (Amaral and Cowan, 1980; Pasquier and Reinoso-Suarez, 1977; Riley and Moore, 1981; Segal, 1979; Segal and Landis, 1974; Veazey *et al.,* 1982; Wyss *et al.,* 1979a, b; Insausti *et al.,* 1987b). The supramammillary projection terminates in many of the fields of the hippocampal formation but most heavily in the dentate gyrus, in fields CA2 and CA3 of the hippocampus, and in the rostral entorhinal cortex (Haglund *et al.,* 1984; Segal, 1979; Veazey *et al.,* 1982; Wyss *et al.,* 1979b; Nitsch and Leranth, 1993). A pathway containing calretinin and substance P has been reported to originate in the suprammamilary nucleus and terminates as a dense band in the inner

one-fourth of the molecular layer and uppermost granule cell layer of the dentate gyrus. Interestingly, in the adult human brain, this band of calretinin-positive fibers is restricted to the innermost portion of the dentate gyrus. This pathway has been proposed to play a role in the regulation of theta activity (Berger *et al.*, 2001). As already noted, the medial and lateral mammillary nuclei receive prominent projections from the subicular cortices, and the supramammillary projection provides one possible route for reciprocation. It is not presently known, however, whether cells of the supramammillary region receive linking projections from other components of the mammillary complex. In addition to the supramammillary cells, there are other cells scattered in several hypothalamic nuclei, many of which are in a perifornical position or within the lateral hypothalamic area, that project to the hippocampal formation. Taken together, these cells constitute a sizable input to the hippocampal formation. However, their diffuseness and lack of any distinguishing biochemical marker have made it difficult to study their projections. A subset of these cells demonstrate α-melanocyte-stimulating hormone-like inmunoreactivity and give rise to a diffusely distributed pathway to several fields of the hippocampal formation (Köhler *et al.*, 1984b; see Chapter 17).

Until recently, it was thought that the hippocampal formation received little or no thalamic input. More sensitive axonal tracing methods, however, have shown that it receives a substantial innervation from several thalamic nuclei. Projections to the hippocampal formation arise from all divisions of the anterior thalamic complex and associated lateral dorsal nucleus (Amaral and Cowan, 1980; Irle and Markowitsch, 1982; Niimi *et al.*, 1978; Wyss *et al.*, 1979a; Insausti *et al.*, 1987b). These nuclei project primarily to the subicular complex and more specifically to the presubiculum (Domesick, 1972; Niimi, 1978; Shipley and Sorensen, 1975). The "midline thalamic nuclei" (which include the parataenial nucleus, the anterior paraventricular nucleus, the nucleus centralis medialis, and the nucleus reuniens) also project to the hippocampal formation. The entorhinal cortex receives a particularly heavy projection from the paraventricular nucleus and a minor input from the dorsomedial portion of the medial pulvinar nucleus (Insausti *et al.*, 1987b). The nucleus reuniens projection terminates primarily in the stratum lacunosum-moleculare of CA1, in portions of the subicular cortices, and in the entorhinal cortex (Herkenham, 1978).

The hippocampal formation receives minor projections from several brainstem regions, including the ventral tegmental area, periaqueductal gray matter, and dorsal tegmental nucleus. Most hippocampally directed brainstem fibers, however, arise in the locus coeruleus, and in the raphe nuclei, mainly from the central superior and dorsal divisions. The locus coeruleus gives rise to the major noradrenergic input to the hippocampal formation (Kobayashi *et al.*, 1974; Koda *et al.*, 1978; Lindvall and Bjorklund, 1974; Loy *et al.*, 1980; Pasquier and Reinoso-Suarez, 1977; Segal and Landis, 1974; Swanson and Hartman, 1975), while the raphe nuclei give rise to its major serotonergic innervation (Azmitia and Segal, 1978; Conrad and Pfaff, 1976; Köhler and Steinbusch, 1982; Moore and Halaris, 1975). Both of these nuclei project to most of the hippocampal fields, with a particularly prominent innervation of the dentate gyrus. Histochemical (Hokfelt *et al.*, 1974) and inmunohistochemical data suggest that the hippocampus and subiculum may also be innervated by dopaminergic fibers (Pohle *et al.*, 1984: Verney *et al.*, 1985), many of which originate in the ventral tegmental area (Swanson, 1982). The entorhinal cortex of the monkey also likely receives dopaminergic projections from the ventral tegmental area (Insausti *et al.*, 1987b).

Commissural Connections

The classical neuroanatomists Kölliker (1896), Ramón y Cajal (1893), and Lorente de Nó (1934) all described prominent hippocampal commissures. The organization of the commissural connections was not experimentally analyzed, however, until the mid-1950s when Blackstad (1956) demonstrated a massive commissural system in the rat that interconnected most of the fields of the two sides of the hippocampal formation. Since Blackstad's publication, the commissural connections, particularly in rodents, have received intensive anatomical study (Fricke and Cowan, 1978; Gottlieb and Cowan, 1973; Hjorth-Simonsen, 1977; Hjorth-Simonsen and Laurberg, 1977; Laatsch and Cowan, 1966; Laurgerg, 1979; Laurberg and Sorensen, 1981; Raisman *et al.*, 1965; Shipley, 1975; Swanson *et al.*, 1980; West *et al.*, 1979). The commissural connections in the macaque monkey brain have also been studied (Amaral *et al.*, 1984; Demeter *et al.*, 1985). In the monkey, only the most rostral (or uncal) part of the hippocampus and associated dentate gyrus are connected by commissural fibers. This contrasts markedly with the rodent brain, where both CA3 and CA1 of the entire hippocampus receive a strong, topographically organized projection from the opposite CA3, and the dentate gyrus receives a major input from cells of the contralateral polymorphic layer. As in the rat, the monkey presubiculum gives rise to a substantial commissural projection that terminates in layer III of the contralateral entorhinal cortex. It would appear

that in primates, and presumably in humans, this projection constitutes the major link between the hippocampal formation of the two sides. This latter projection system appears to be conserved in the human brain. Gloor *et al.* (1993) studied post-mortem brains and identified a dorsal hippocampal commissue that had an appearance similar to that of the monkey. Also similar to the monkey, the ventral hippocampal commissure (through which dentate and hippocampal commissural connections travel in the rodent) is essentially eliminated.

Cortical Connections

Anatomical studies of the rat hippocampal formation have not uncovered many direct connections between the neocortex and the hippocampal formation. Only recently has it been shown, for example, that the rat subicular complex receives a projection from the perirhinal cortex (Kosel *et al.*, 1983), and even though it has been reported that only a restricted region of the rat entorhinal cortex projects to neocortical regions (Swanson and Köhler, 1986), more recent neuroanatomical studies in the rodent reveal that most of the entorhinal cortex gives rise to neocortical projections (Insausti *et al.*, 1997). In the cat and monkey, increasing evidence points to substantial and direct neocortical interconnections with both the subicular complex and the entorhinal cortex.

Van Hoesen and Pandya (1975a, b) and Van Hoesen *et al.* (1975) used degeneration techniques to study the connections of the macaque monkey entorhinal cortex. They found that several fields within the temporal lobe, especially areas TF and TH of the parahippocampal gyrus, the perirhinal cortex (area 35), and the temporal polar cortex (area TG) project to the lateral portion of the entorhinal cortex. More recently, Insausti *et al.* (1987a) reexamined the cortical input to the monkey entorhinal cortex using retrograde tracing techniques. This study largely confirmed Van Hoesen's findings but identified several additional cortical fields that project directly to the entorhinal cortex (Fig. 23.16). These included several fields along the dorsal bank of the superior temporal gyrus, the ventral or agranular insular cortex, the posterior orbitofrontal cortex (Walker's areas 14, 13, and 12), and, to a lesser extent, the dorsolateral frontal cortex (areas 9, 10, and 46). Sizeable projections were also found from the infralimbic and prelimbic portions of the medial frontal cortex (areas 25 and 32), the cingulate cortex (areas 24 and 23), and the caudally adjacent retrosplenial cortex (areas 29 and 30).

The efferent connections of the primate entorhinal cortex have not yet been intensively studied. There are indications that most, if not all, of the cortical areas that project to the entorhinal cortex receive return projections. In particular, entorhinal projections have been demonstrated to the perirhinal cortex, the temporal polar cortex, the caudal parahippocampal gyrus, and the caudal cingulate gyrus (Baleydier and Mauguiere, 1980; Kosel *et al.*, 1982; Van Hoesen, 1995; Suzuki and Amaral, 1994 for perirhinal–entorhinal connections; Good and Morrison, (1995) for connections with the polymodal area in the upper bank of the superior temporal gyrus; a comprenhensive account of efferent projections can be found in Muñoz and Insausti, submitted). At variance with the study on afferents to the primate entorhinal cortex of Insausti *et al.* (1987b), some projections from the anteroventral portion of unimodal visual association cortex, area TE, located medial to the anterior medial temporal sulcus seems to have reciprocal connections with the lateral portion of the entorhinal cortex, although it is not clear if perirhinal cortex (area 36) was included in some of the tracer deposits. Through these connections, the hippocampal formation is able to influence widespread regions of the temporal, parietal, and frontal lobes. As Van Hoesen (1982) has emphasized, the parahippocampal gyrus, in particular, gives rise to projections to virtually all the associational cortices of the primate brain.

Although available evidence indicates that the entorhinal cortex receives the most prominent cortical innervation, the subicular cortices also receive direct cortical input. Van Hoesen *et al.* (1979) first demonstrated that the temporal polar cortex, the perirhinal cortex, and the parahippocampal gyrus project to one or more divisions of the monkey subicular complex. A projection from the inferior parietal lobe to the medial portion of the caudal presubiculum has also been demonstrated (Seltzer and Pandya, 1984; Seltzer and Van Hoesen, 1979). The presubiculum receives additional inputs from the caudal cingulate cortex (Pandya *et al.*, 1973), the superior temporal gyrus (Amaral *et al.*, 1983), and the dorsolateral prefrontal cortex (Goldman-Rakic *et al.*, 1984). Interestingly, each of the cortical projections to the presubiculum terminates in a columnar fashion in a restricted rostrocaudal and mediolateral region. In addition to its subcortical projections to the anterior thalamus and mammillary nuclei, Rosene and Van Hoesen (1977) and Kosel *et al.* (1982) demonstrated that the monkey subicular cortices project to several cortical fields, including the perirhinal cortex, the parahippocampal gyrus, the caudal cingulate gyrus, and the medial frontal and medial orbitofrontal cortices. Widespread cortical connections have also been demonstrated from the subicular cortices of the cat and bush baby (Cavada

and Reinoso-Suarez, 1983; Irle and Markowitsch, 1982; Pritzel and Markowitsch, 1983). Recently, several studies in the nonhuman primate brain have shown that the subicular cortices, along with CA1 reciprocate the projections to most of these areas (Barbas and Blatt, 1995; Blatt and Rosene, 1998; Ding *et al.*, 2000; Yukie, 2000; Insausti and Muñoz, 2001) with those to the lateral frontal neocortex being least substantial. The precise relationship of this set of projections with the reported head-direction cell responses in the presubiculum (Robertson *et al.*, 1999) remains to be determined.

Chemical Neuroanatomy of the Hippocampal Formation

The ultimate goal of many neuroanatomists is an understanding of the neural circuitry of the human brain. Yet the lack of experimental approaches applicable to human neuroanatomy has forced most workers to conduct studies on experimental animals and extrapolate their findings to the human brain. Until recently, anatomical studies of the human brain had not advanced much beyond the cytoarchitectonic descriptions of the early part of the 20th century. Several new technologies have come together, however, to change this situation, and detailed neuroanatomical analysis of the human brain has once again become a fundamental aspect of modern neuroscience.

The development of noninvasive imaging techniques, including positron emission tomography (PET) and magnetic resonance imaging (MRI), has renewed interest in human neuroanatomy. These technologies allow hitherto unprecedented views of the functioning human brain. The final section of this chapter elaborates on neuroimaging. Perhaps even more important, however, is the development of new histological procedures such as immunohistochemistry, receptor autoradiography, and *in situ* hybridization that allow the direct comparison of the distribution of transmitter-specific or neuron-specific probes in the human brain and in the brains of experimental animals (i.e., Figure 23.18 that shows differences in the staining pattern to a specific marker—nonphosphorylated neurofilaments SMI-32—of the hippocampus in nonhuman primates and humans.

A comprehensive account of the chemical neuroanatomy in the nonhuman primate is provided in Kobayashi and Amaral (2001); therefore, the present account will deal with data elaborated on the human hippocampal formation. This is an area in which substantial progress has been made since the first version of this chapter.

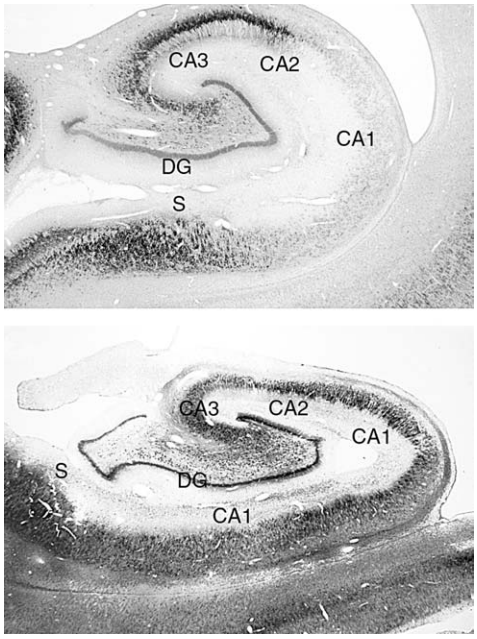

FIGURE 23.18 Brightfield photomicrographs of immunohistochemical preparations from the monkey *(top)* and the human *(bottom)* hippocampal formation stained for nonphosphorylated neurofilament (NF) with antibody SMI-32. Sections have been counterstained by the Giemsa method, which provides a Nissl-like stain. In the hippocampal formation, neurons in the CA3 and CA2 fields are heavily labeled whereas neurons in CA1 are completely unstained. Neurons in the subiculum are again very heavily stained, and the staining extends into the proximal apical and basal dendrites. Thus NF staining provides a very useful marker for the borders of the CA1 field. In the human, in contrast, NF staining appears to be much more generalized; in particular, cells in CA1 are heavily stained. In CA3 of the human, only some of the pyramidal cells are labeled, but the mossy fibers are stained. In the monkey, the mossy fibers are not stained. This human brain material had a postmortem interval to fixation of 6 hours. It is not clear whether the different staining patterns in the monkey and human are true species differences or are related to the differing fixation protocols used in the monkey (perfusion fixation) versus the human (immersion fixation 6 hours after death).

Green and Mesulam (1988) examined the distribution of cholinergic inputs to the human hippocampal formation by studying preparations stained histochemically for acetyl cholinesterase (AChE). The dentate gyrus shows little staining in the granular layer, a band in the innermost portion of the molecular layer of the dentate gyrus, and some neurons in the polymorphic cell layer. Fields CA3–CA1 have strong AChE activity in stratum oriens and the pyramidal cell layer, while stratum radiatum and lacunosum-moleculare display much lighter staining. Staining in the proximal (closer to CA1) part of the subiculum is far less dense than the adjacent CA1; thus, the oblique border between CA1 and the subiculum is quite noticeable. The presubiculum and parasubiculum

present moderate density in the external layer and weak reaction in the deep portion. The entorhinal cortex presents two bands of high AChE density, one corresponds to the layer II cell islands, and the other corresponds to layer V. More recently, De la Calle *et al.* (1994) carried out similar studies using the more specific cholinergic marker, choline acetyl transferase (ChAT). In general, the pattern of staining with ChAT was similar to that of AChE (as determined with an antibody against AChE), although some minor differences were observed such as higher density of ChAT positive fibers in the molecular layer of the parasubiculum. ChAT immunoreactivity in layer V of the entorhinal cortex is not as prominent as AChE activity. No ChAT positive somata were found in any subdivision of the hippocampal formation.

Akil and Lewis (1994) studied the distribution of TH immunoreactivity in the human entorhinal cortex. Marked gradients in the mediolateral and rostrocaudal axes were noted. The entorhinal cortex contained intense TH immunoreactivity in the deep portion of layer I and the superficial portion of layer II. TH fibers surrounded the cell clusters on the upper part of layer III at rostral levels. Layer V displayed the lowest density of TH positive fibers, and layer VI had again moderate density as well as some positive neurons.

Neither the noradrenergic nor the serotonergic innervation of the human hippocampal formation has been studied thus far.

A number of studies have been published in the last few years on the distribution of calcium-binding proteins, parvalbumin (Pv), calbindin (Cb), and calretinin (Cr) in the human hippocampal formation (Sloviter *et al.*, 1991; Braak *et al.*, 1991; Tuñón *et al.*, 1992; Seress *et al.*, 1993; Nitsch and Ohm, 1995; Mikkonen *et al.*, 1997). Parvalbumin mostly stains interneurons in the hippocampus. Braak *et al.*, (1991) describe up to 28 morphologically distinct interneurons in the dentate gyrus of the hippocampus. Electron microscopic examination of Pv-positive neurons show many similarities, despite the various morphological types (Seress *et al.*, 1993). Calbindin immunoreactivity is present in many granule cell neurons, as well as in nongranule neurons in the molecular layer of the dentate gyrus, but it does not appear as frequently in the polymorphic cell layer. In CA3, calbindin immunoreactivity is absent from the pyramidal cell layer but is coincident with that of the mossy fibers. Calbindin is not selective for the mossy fiber system, however, because other calbindin-positive interneurons can also be found (Lim *et al.*, 1997a). Many Cb-positive neurons are present in the pyramidal cell layer of CA2 and CA1, as well as in nonprincipal cells of the subicular cortices (Seress *et al.*, 1993). Calretinin immunoreativity in the human hippocampus has been studied by Nitsch and Ohm (1995). They found small Cr-positive neurons in the molecular layer of the dentate gyrus, as well as Cr-positive terminals both in the innermost part of the molecular layer of the dentate gyrus and around somata of CA2. The latter is similar in distribution to the hypothalamic-hippocampal afferents arising from the supramammillary region containing substance P (Nitsch and Leranth, 1993; Berger *et al.*, 2001). The distribution of calcium-binding proteins in the human entorhinal cortex has been described in several studies (Tuñón *et al.*, 1992; Solodkin and Van Hoesen, 1996; Mikkonen *et al.*, 1997). Only Mikkonen *et al.* (1997) present a comprehensive account of the pattern of distribution for Pv, Cb, and Cr in the various subfields of the entorhinal cortex. Rostral and medial portions of the entorhinal cortex display dense Cb and Cr immunoreactivity, while caudal and lateral portions are denser for Pv. Cr pyramidal cells were present in layers V and VI, while Cb neurons were present in layers II and III (Mikkonen *et al.*, 1997).

A number of peptide or candidate transmitter specific antibodies have also been used to examine the human hippocampal formation, and, in general, the distribution of identified elements is similar to that in experimental animals. Schlander *et al.* (1987), for example, demonstrated a distribution of glutamic acid decarboxylase (GAD, the GABA-synthesizing enzyme) activity in the human dentate gyrus that at the light and electron microscopic level appears similar to that in experimental animals. Cholecystokinin (CCK) immunoreactivity has also been reported in interneurons and fibers of several fields of the human hippocampal formation (Lotstra and Vanderhaeghen, 1987). CCK-immunoreactive fibers and terminals were most dense around the pyramidal cells of the CA2 and CA3 fields of the hippocampus and were also numerous in the molecular layer of the dentate gyrus. Antisera to neuropeptide tyrosine (neuropeptide Y) also identify a population of apparent interneurons in the polymorphic layer of the dentate gyrus, in CA1, subiculum, and entorhinal cortex of the human hippocampal formation (Chan-Palay *et al.*, 1986). Neuropeptide Y-immunoreactive fibers and terminals were most dense in the CA1 field, but other prominent plexuses occurred in the molecular layer of the dentate gyrus, presubiculum, and entorhinal cortex. Finally, Sakamoto *et al.* (1987) have found a fairly large population of neurons in the polymorphic layer of the human dentate gyrus that are immunoreactive for substance P. Substance P-immunoreactive terminals were found to innervate the granule cell layer heavily. In addition, they found fairly dense terminal labeling

among the cell bodies of CA2 and CA3 pyramidal cells with neuronal labeling in the subjacent stratum oriens. However, when they used antisera directed against 'Leu-enkephalin they found little staining in the human hippocampal formation. Characteristically, the distribution of opioid peptides in the hippocampal formation has varied markedly from species to species.

Receptor autoradiography has been conducted in the human hippocampal formation using probes compatible with the immunohistochemical studies cited previously. Often there are marked regional differences in receptor binding. Dietl *et al.* (1987) showed, for example, that the CA2 and CA3 fields, the subiculum, and the entorhinal cortex contain appreciable levels of CCK receptor binding, whereas CA1 has no detectable ligand binding. Similarly, Köhler *et al.* (1987) demonstrated high levels of neurotensin receptor binding in the presubiculum, entorhinal cortex, and polymorphic layer of the dentate gyrus whereas [3H]neurotensin binding was very low in the CA1 field and in the subiculum.

While it is beyond the scope of this chapter to survey the merits and pitfalls of the increasingly rich immunohistochemical and receptor autoradiography literatures, it is clear that these methodologies will play an increasingly important role in the functional neuroanatomical analysis of the human hippocampal formation. Because this analysis will depend on the comparison of human material with the more highly controlled experimental animal data, it becomes increasingly important to adopt a similar terminology for the cytoarchitectonic description of the hippocampal formation for all species.

A Note on the Development of the Human Hippocampal Formation

Taking into consideration the importance of the clinical problems for which a mechanism of failure in neuronal development or migration has been invoked as explanation, it seems timely to review data gathered so far and to present a synopsis of the development of the human hippocampal formation.

Classical accounts of the development of the hippocampal formation (Hines, 1922; Gastaut and Lammers, 1961; Humphrey, 1967) describe the main steps in the development of the hippocampus. A recent study by Arnold and Trojanowski (1996a) summarizes earlier details: by 9 weeks of gestation, the hippocampal anlage is located at the medial aspect of the developing cerebral hemisphere, and still it has not reached the doubly folded appearance of the more mature hippocampus. The hippocampal fissure does not appear until 10 weeks (Humphrey, 1967). By the middle of the second trimester (15–19 weeks), the hippocampal fields become apparent, and the subiculum is particularly clear at this time. The dentate gyrus demonstrates three layers, although they have an immature appearance. By the end of the second third of gestation (25 weeks), the hippocampal fissure is deeper, and the hippocampal fields have expanded. Still the border between CA1 and the subiculum is not distinct, but the layers of CA1 and CA2–CA3 are more evident. The dentate gyrus increases in cell density with many neurons still presenting immature features. By the last trimester of pregnancy (34 weeks), the hippocampal fissure is fused, and the border between CA1 and subiculum is present. CA1, CA2, and CA3 are all recognizable, and the pyramidal cell layer is more evident. The dentate gyrus takes on an adult appearance. In addition, the angular bundle is well defined and contains some myelin as determined by immunoreactivity to myelin basic protein. The hippocampus shows a decrease in cell density in the postnatal period, probably as a result of apoptotic processes and growth of neuronal processes and fibers. No significant morphological changes take place into adulthood, although the myelination is progressively more complete.

The development of the human entorhinal cortex has been studied by several authors (Macchi, 1951; Delmas, 1955; Kostovic *et al.*, 1993; Hevner and Kinney, 1996, Graterón *et al.*, 2002). The entorhinal cortex can be recognized as early as the 10th gestational week (Delmas, 1955, Kostovic *et al.*, 1993; Hevner and Kinney, 1996), and by week 13, the lamina dissecans is recognizable (Kostovic *et al.*, 1993). Hevner and Kinney (1996), by placing small amounts of the lipophilic tracer DiI in the surface of the foetal entorhinal cortex, demonstrated that by 17 weeks of gestation the entorhinal cortex is laminated and develops reciprocal connections with the CA1, while by the 19th week connections are established with the subiculum.

The postnatal development of the human entorhinal cortex has been analyzed by Graterón *et al.* (2002), who reported that all six layers of the entorhinal cortex are present at the time of birth. There is a gradient of differentiation such that at birth the lateral and caudal portions look more differentiated than rostral and medial parts. Moreover, deep layers (V and VI) develop prior to the superficial layers (II and III). The upper layers of the entorhinal cortex (II–III) look more mature by the end of the first postnatal year but do not reach adultlike morphology until the end of the second postnatal year. In contrast, the deep layers (V–VI) show little modification from their newborn appearance.

CLINICAL ANATOMY

Various clinical conditions result in morphological alterations of the human hippocampal formation. While the causative factors are not yet known for most of these disease states, it is clear that each of the different hippocampal cytoarchitectonic fields is more or less vulnerable to damage. In ischemia and temporal lobe epilepsy, for example, field CA1 of the hippocampus (the so-called Sommer's sector) suffers the greatest neuronal cell loss. In other neuropathological conditions, such as Alzheimer's disease, the pathological insult may actually demonstrate laminar specificity within some hippocampal fields.

Normal Aging Versus Alzheimer's Disease

A recurrent question in aging research is to what extent humans lose neurons as they grow older. Until a few years ago, the common assumption was that the hippocampus begins to lose neurons in midlife and the loss continues into old age. However, this view was not based on studies that used unbiased sampling strategies. Recent numerical counts by West and colleagues (West 1993; West *et al.*, 1994; Simic *et al.*, 1997) show that the hippocampal formation does not generally suffer any age-related loss of neurons. Only the subiculum (52% or 7.3% per decade) and the hilus of the dentate gyrus (31% or 4.2% per decade) demonstrate substantial cell loss in normal aging (West, 1993). In contrast, neuronal loss in the hippocampal formation of Alzheimer's disease patients is much higher, even in very mild cases (West *et al.*, 1994; Simic *et al.*, 1997; Price *et al.*, 2001). Studies on the entorhinal cortex (Price *et al.*, 2001) reveal a similar trend (0.7% of neuron loss per year, and, specifically 1.2% for layer II neurons). The analysis of the extent of atrophy in the human entorhinal cortex in normal aging (age range of the series, 12–110 years old) based on the areal measurement of two-dimensional reconstructions of the entorhinal cortex reveals a decrease up to 4% in size over the life range (Insausti *et al.*, 1998).

Among the many conditions that produce pathological changes in the hippocampal formation, Alzheimer's disease is probably the most devastating (Ball, 1977, 1978; Hyman *et al.*, 1984, 1986; Kemper, 1978; Van Hoesen and Damasio, 1987). Myriad studies have come to the clear conclusion that this disorder is distinctly different from an elaboration of normal aging. Alzheimer's disease is associated with four neuropathological correlates in the hippocampal formation: neuronal cell loss, neurofibrillary tangles, neuritic plaques, and granulovacuolar degeneration (for more information about each one of these lesions, see Tomlinson and Corsellis, 1984).

Corsellis (1970) first drew attention to the near complete cell loss in the CA1 field of the brains of Alzheimer's patients. Ball and colleagues have subsequently conducted systematic analyses of cell loss in the hippocampal formation, and they estimate that there is a decrease of some 56% in the number of hippocampal pyramidal cells (versus 12% in age-matched controls, Ball, 1977). These early studies have been confirmed by more recent studies using unbiased sampling procedures (West *et al.*, 1994; Simic *et al.*, 1997). They demonstrate that CA1 suffers a profound neuron loss (an average of 68%), in contrast to normal aging where neuron loss is negligible. Hyman *et al.* (1984, 1986) have emphasized that the cell loss is pronounced not only in CA1, but that the subiculum and layers II and V of the entorhinal cortex are also depleted. More recent studies (Price *et al.*, 2001) show that there is already profound neuron loss (35% in the entorhinal cortex as a whole, of which 50% is in layer II, and 46% in CA1, in mild clinical cases of Alzheimer's disease). Interestingly, despite the fact that neurons in layers II and V of the entorhinal cortex are nearly eliminated, layers III and VI have a relatively normal appearance.

Neurofibrillary tangles, while occasionally observed in the normal-aged brain, are more numerous in the Alzheimer's brain and are located in the same regions that undergo the greatest amount of cell loss (Ball, 1978; Kemper, 1983). Ball (1977) noted that a greater number of neurofibrillary tangles occur in the posterior part of the hippocampus. Neuritic plaques are spherical foci, 5–200 μm in diameter, that may have a central amyloid core surrounded by argyrophilic rods and granules. They are very numerous in the hippocampal formation of patients with Alzheimer's disease and show a preference for the molecular layer or the dentate gyrus (Burger, 1983; Hyman *et al.*, 1984). The fourth pathological correlate of Alzheimer's disease is granulovacuolar degeneration (Ball, 1983). Neurons demonstrating granulovacuolar degeneration contain one or more 3- to 5-μm vacuoles that hold a 0.5- to 1.5-μm agyrophilic granule. These profiles are numerous in the subiculum and CA1 of the Alzheimer's brain but are not frequently found in the entorhinal cortex.

As a result of the cell loss and other pathological sequelae of Alzheimer's disease, especially in the entorhinal cortex, it has been suggested that, as the disease develops, the hippocampal formation becomes, in essence, functionally disconnected from its major afferent and efferent interactions (Hyman *et al.*, 1984; see Braak and Braak, 1992 for a comprehensive review

of the human entorhinal cortex in various pathologies). Given the important role the hippocampal formation is known to play in certain forms of memory, it is likely that a major portion of the problems with memory function observed in Alzheimer's disease is attributable to damage of the hippocampal formation.

Epilepsy

Temporal lobe or complex partial epilepsy is another neurological disorder in which the hippocampal formation is severely affected (Meldrum and Corsellis, 1984). This most common form of epilepsy was first associated with damage to the hippocampal formation by Sommer (1880), who conducted the first postmortem microscopic examination of a brain from a long-term epileptic patient. Sommer noted a dramatic loss of neurons in the hippocampal formation that was relatively selective and involved a region that in modern terminology would encompass CA1 and part of the subiculum. During the first part of this century, it was generally believed that hippocampal pathology was a consequence of the epileptic seizures rather than their cause. Currently, however, increasing emphasis is being placed on the idea that disruption of normal hippocampal function may be an initiating factor in temporal lobe seizures (Babb *et al.*, 1984; Falconer, 1974), and a number of animal models have been established to study this possibility (Schwarcz and Ben-Ari, 1986).

In approximately two-thirds of the cases of temporal lobe epilepsy, the hippocampal formation is the only structure that shows pathological modifications (Cavanagh *et al.*, 1958; Meldrum and Corsellis, 1984). As Sommer initially described, cell loss is most consistently found in the CA1 field of the hippocampus, but in many cases cell loss is also observed in the dentate gyrus and CA3 and portion of the subiculum immediately adjacent to CA1 (Babb *et al.*, 1984; Mouritzen Dam, 1982). The CA2 field is usually preserved, and the remainder of the hippocampal formation (presubiculum, parasubiculum, and entorhinal cortex) is also reported to be much less susceptible to damage, altough neuronal loss in layer III of the entorhinal cortex has been reported (Du *et al.*, 1993). Other morphological changes are observed in the dentate gyrus of the epileptic brain such as dispersion of granule cells and a bilaminar organization of the granule cell layer (Houser *et al.*, 1992). Other changes include the absence of mossy cells and altered dendritic pattern in the polymorphic cell layer of the dentate gyrus (Blümcke *et al.*, 1999). In some cases of long-term epilepsy, cell loss is so striking that the gross appearance of the hippocampus is shrunken and the term "Ammon's horn sclerosis" is applied at this stage (for review see Sloviter, 1994) . Tissue characteristics are so modified at this point that the pathology can be detected by using magnetic resonance imaging (Kuzniecky *et al.*, 1987; Hogan *et al.*, 2000).

The sequence of events that leads to the initial establishment of a seizure-inducing focus in the hippocampal formation is not clear. Damage following infantile seizures is often invoked as a possibility (Meldrum and Corsellis, 1984; Delgado-Escueta and Walsh, 1985), but the exact metabolic alteration (ischemia, hypoxia, etc.) is not yet known. Using an animal model of epilepsy, Sloviter (1987) had advanced the interesting hypothesis that initial seizure episodes are particularly damaging to a class of hippocampal interneurons that are immunoreactive for somatostatin. The loss of this class of neuron could initiate a cascade of destabilizing events that ultimately leads to loss of the CA1 pyramidal cells. However, neurons containing the calcium-binding proteins parvalbumin and calbindin (see chemical neuroanatomy section) are among the surviving neurons in the hippocampal formation (Sloviter *et al.*, 1991). The process of cell loss in the hippocampal formation is accompanied by cell remodeling, as shown by Mikkonen *et al.* (1998) with respect to the cell adhesion molecule PSA-NCAM immunoreactivity increased not only in the dentate gyrus but in CA1 and the entorhinal cortex as well.

Ischemia, Schizophrenia, and Other Disorders

There are a number of other neurological or neuropsychiatric conditions in which the hippocampal formation may demonstrate pathology. Among these is the loss of neurons, primarily in CA1, consequent to the ischemia associated with cardiorespiratory arrest (Cummings *et al.*, 1984; Petito *et al.*, 1987; Zola-Morgan *et al.*, 1986). These patients demonstrate an anterograde memory impairment apparently resulting from the hippocampal damage (Zola-Morgan *et al.*, 1986). Much less clear-cut is the involvement of the hippocampal formation in major psychiatric disorders such as schizophrenia. It has been argued that developmental abnormalities in the hippocampal formation may be an important contributon to the symptoms of schizophrenia. Akbarian *et al.* (1993) reported a decrease of nicotinamide-adenine dinucleotide phosphate-diaphorase (NADPH-d) in the hippocampal formation of schizophrenic patients, although there was a tendency for an increase in NADPH-d positive cells in the white matter of the parahippocampal gyrus. The normal distribution of NADPH-d in the human hippocampal formation has been reported by Yan and Ribak (1997) in prenatal development and Sobreviela

and Mufson (1995) in the adult. Arnold *et al.* (1991) analyzed the expression of different neuronal cytoskeletal proteins and found that the rostral entorhinal cortex and subiculum had much lower expression of microtubule-associated proteins 2 and 5 (MAP2 and MAP5) in the schizophrenic brain.

A number of studies have highlighted the entorhinal cortex as one of the regions that present morphological changes in schizophrenic patients. Jakob and Beckmann (1986, 1994) and Arnold *et al.* (1997) proposed that the entorhinal cortex in schizophrenia presented disturbances in neuronal migration that could explain the disorganized appearance of layer II neurons and misplacement of these neurons into layer III. The role of a developmental problem in neuronal migration in the pathogenesis of schizophrenia awaits further confirmation.

There are some indications that the hippocampal formation has a significantly reduced volume in cases of schizophrenia (Bogerts *et al.*, 1985; Crow and Johnstone, 1987). No volumetric changes have been observed in the parahippocampal gyrus of schizophrenics compared to controls (Heckers *et al.*, 1990). While Falkai and Bogerts (1986) had found a significant loss of pyramidal cells in the CA fields of the hippocampus but not in the dentate gyrus or subicular cortices, more recent estimates of the number of neurons in the hippocampal formatioin (Heckers *et al.*, 1991) and in the entorhinal cortex (Krimer *et al.*, 1997) do not demonstrate differences between control and schizophrenic brains.

Pathological changes in the hippocampal formation have also been reported in several other dementing neurological diseases. Misuzawa *et al.* (1987), for example, found spongiform changes in the stratum lacunosum-moleculare of the hippocampus in three of five cases of Creutzfeldt-Jacob disease, a form of encephalopathy caused by a slow virus. The contribution of hippocampal impairment, however, to the overall behavioral deterioration in this disease is difficult to predict.

Neurodevelopmental Disorders

Autism and related disorders (for a recent review, see Lord *et al.*, 2000) is an increasingly common neurodevelopmental disorder for which abnormalities in the hippocampal formation have been described. Bauman and Kemper (1985) and Kemper and Baumann (1998) describe an increase in cell density in the CA3, CA2, and CA1 fields of the hippocampus, as well as in the entorhinal cortex, in addition to an "extra" lamina dissecans under layer II. Although these observations are interesting, they have not yet been independently confirmed. Moreover, structural imaging studies have produced highly conflictive findings on volume changes related to autism. This will clearly be an important area for future study.

FUNCTIONAL CONSIDERATION—THE EMERGENCE OF NEUROIMAGING

When this chapter first appeared in 1990, functional magnetic resonance imaging (fMRI) had not yet appeared as a tool for investigation of the human brain (Belliveau *et al.*, 1991). Since that time, hundreds of studies have been carried out using fMRI and PET to study the function of the hippocampal formation in awake behaving human subjects. Recent studies have even endeavored to fractionate component process of behavior to subfields of the hippocampal formation or to related cortical regions. In this final section, we will briefly provide an historical perspective on the function(s) of the hippocampal formation and then discuss some of the advances that the use of structural and functional imaging techniques has allowed. Given the intense activity in this area, this will necessarily provide only a sense of the issues that are being studied. However, we will refer to a number of recent review papers for further reading and references.

The hippocampal formation has historically been implicated in a variety of functions. Sommer (1880), for example, considered it to be a component of the motor system because he found that damage to the hippocampal formation highly correlated with the occurrence of temporal lobe epilepsy. For much of the first half of this century, the hippocampal formation was thought to be primarily related to olfactory function and was considered to be a prominent component of what was called the rhinencephalon or olfactory brain. This concept was put to rest by Brodal (1947), who indicated that the hippocampal formation was as prominent in anosmic species as in species that rely heavily on the sense of smell. Papez (1937) considered the hippocampal formation to be a central component in a system for marshaling emotional expression to sensory experiences. In his view, the hippocampus was something of a conduit by which perceptions could be channeled to the mammillary nuclei of the hypothalamus, where appropriate emotions could be effected. There has been very little substantiation of Papez's theory, and the role of modulator of emotional expression is now more closely linked to the amygdaloid complex than to the hippocampal formation.

Perhaps the most widely accepted and long-lived proposal of hippocampal function relates to its role in

memory (Milner, 1970; Squire, 1987). It has been known for nearly a century that damage to certain brain regions can result in an enduring, polysensory amnesic syndrome that is characterized by a complete, or near complete, anterograde amnesia with a variable degree of premorbid retrograde amnesia. Affected patients are incapable of recreating a record of day-to-day events though most past memories remain intact. Structures most commonly associated with this "global" or "general" form of amnesia are located either in the medial temporal lobe (the hippocampal formation and adjacent cortex) or in the diencephalon (the mammillary nuclei and mediodorsal nucleus of the thalamus) (Amaral, 1987; Ojemann, 1966; Squire, 1987). Until recently, there was no compelling evidence that damage isolated to any one of these structures leads to a clinically significant amnesia, though, in the last few years, the association between damage to the hippocampal formation and memory impairment has become substantially more established.

Bechterew (1900) was among the first to suggest that memory impairment could occur following damage to the temporal lobe. He based this conclusion on his studies of the brain of a 60-year-old man who had suffered from severe memory problems during the last 20 years of his life. Bechterew found that there was bilateral softening of the medial temporal lobe in this patient´s brain covering an area that included the amygdaloid complex and the hippocampal formation. Several decades later, Grunthal (1939) and Glees and Griffith (1952) published case reports of patients who had suffered vascular accidents that bilaterally damaged the hippocampal formation and parahippocampal gyrus. In both cases, memory function was compromised though formal testing was not carried out. In 1954, Scoville described a patient (H.M.) with severe anterograde amnesia resulting from bilateral surgical removal of the anterior medial temporal lobe that was intended to ameliorate intractable epilepsy. The resection involved the amygdaloid complex, the anterior two-thirds of the hippocampal formation, and portions of the adjacent parahippocampal gyrus. A recent and detailed MRI study has been reported (Corkin *et al.*, 1997). Interestingly, while the initial surgical report indicated that the entire hippocampal formation was removed, Corkin *et al.* (1997) found that only about half of the rostrocaudal extension of the hippocampus was removed. The entorhinal cortex, however, was totally removed so that the residual posterior hippocampus in H.M. is largely devoid of sensory input. From studies of H.M. and nine other patients with less extensive bilateral resection of the medial temporal lobe, Scoville and Milner (1957) concluded that damage to the hippocampal formation was necessary for the occurrence of the amnesic syndrome. They believed that damage confined to the amygdaloid complex did not produce amnesia.

This conclusion, however, has remained controversial. Horel (1978), for example, suggested that medial temporal lobe amnesia was not related to damage of the hippocampal formation or amygdaloid complex but rather to the interruption of efferent connections between the temporal neocortex and other cortical and subcortical regions. He suggested that the region just above the hippocampal formation in which these fibers travel, the so-called temporal stem, was damaged in the surgical approach followed by Scoville in patient H.M. At about the same time, Mishkin (1978) offered the alternative suggestion that amnesia results only when both the amygdala and hippocampal formation are damaged. He pointed out that in all human cases demonstrating medial temporal lobe amnesia, including case H.M., there was damage to both the amygdala and hippocampus. In experiments designed to test this hypothesis, Mishkin (1978) found that monkeys experimentally prepared with lesions of either the hippocampus or amygdala demonstrated only mild changes in memory performance whereas a conjoint lesion of both structures produced a profound memory impairment analogous to human global amnesia. While Zola-Morgan and Squire (1985, 1986) have confirmed that conjoint lesions produce a marked memory impairment, they found, in contrast to Mishkin (1978), that selective hippocampal lesions also result in a significant decrease in memory function. The question remained, therefore, whether damage to the human hippocampal formation alone would lead to a clinically significant amnesia.

A clinicopathological human case study (R.B.) of a patient with a selective hippocampal lesion indicates that this damage is sufficient to produce a clinically significant anterograde amnesia (Zola-Morgan *et al.*, 1986). R.B. was a retired, 52-year-old male postal worker who suffered a prolonged ischemic period following coronary bypass surgery. During his 5-year survival period, R.B. underwent extensive neuropsychological assessment. He exhibited marked anterograde amnesia, with little if any retrograde amnesia, and showed no signs of cognitive impairment other than memory. A postmortem histological analysis of the entire brain revealed a complete and bilateral loss of pyramidal cells in the CA1 field of the hippocampus; all other fields of the hippocampal formation had a normal appearance. While minor pathology was found elsewhere in the brain (patchy Purkinje cell loss in the cerebellum, gliosis in the left globus pallidus and internal capsule, infarct of the right postcentral gyrus), the only damage that could be reasonably

associated with the memory defect was the damage to the hippocampal formation. And, in this case, the amygdaloid complex, the mammillary nuclei, and the mediodorsal nucleus of the thalamus had an apparently normal appearance. Moreover, there was no widespread pathology in the temporal neocortex or in the region of the "temporal stem." Thus, this case provides strong evidence of amnesia following a lesion limited exclusively to the hippocampus.

While there is now fairly convincing evidence that the hippocampal formation plays a prominent role in the formation of enduring memories, the mechanism by which it exerts its influence is far from clear. Because damage to the hippocampal formation does not cause a loss of distant or well-established memories, it appears that the hippocampal formation cannot be the final repository for stored information. Rather, it appears that the hippocampal formation must interact with storage sites in other, presumably cortical, regions to consolidate ephemeral sensory experiences into long-term memory. The anatomical, physiological, and pharmacological bases for this interaction are among the most highly studied phenomena in current neuroscience. Yet, interestingly, the careful neuropsychological and histological analyses in studies of human cases have provided some or the most convincing evidence for the role of the hippocampal formation.

Spiers *et al.* (2001) have provided a comprehensive review of case studies of patients with medial temporal lobe lesions and resultant amnesia. They emphasized in this review that the human lesion studies are consistent in their conclusion that hippocampal damage leads to anterograde amnesia. They are less consistent in providing support for the role of the relationship between hippocampal damage and retrograde amnesia, deficits in semantic memory, or familiarity-based recognition. They also reiterated that there are suggestions that memory function is lateralized in human subjects. The left hippocampal formation is generally found to play a more prominent role in episodic or biographical memory, whereas the right hippocampal formation is more related to spatial memory processing.

One continuing controversial issue is whether the hippocampal formation is essential for semantic memory processing. Semantic memory is memory for factual knowledge devoid of the source of the information. Squire (1992) argued that the hippocampal formation is essential for encoding both semantic and autobiographical information. However, Vargha-Khadem and colleagues (Vargha-Khadem *et al.*, 1997; Gadian *et al.*, 2000) questioned this view. They studied children who had early ischemic/anoxic damage of the hippocampal formation. The surprising finding from this series of studies was that despite apparently near-normal learning of general information, these children had little or no autobiographical memory. This raised the prospect that regions outside and independent of the hippocampus might be able to support semantic memory processing. Interestingly, Maguire *et al.* (2001) demonstrated that the portion of the hippocampus that is not damaged in at least one of these children (Jon) can be activated in tasks of autobiographical memory. Therefore, it is not clear that these studies provide definitive evidence for nonhippocampal processing of semantic memory. This study, by Maguire and colleagues, provides an excellent example of how fMRI can provide information from patients with focal brain damage on which regions are supporting residual behavioral function (reviewed in Maguire, 2001).

Functional imaging studies have also dealt with the issue of retrograde amnesia. Retrograde amnesia is the loss of memories for events or information that was gained prior to the lesion. Both the existence and the duration of retrograde amnesia after hippocampal lesions has been hotly debated (Rosenbaum *et al.*, 2001; Nestor *et al.*, 2002). Haist *et al.* (2001) have used fMRI and the famous faces task to generate data indicating that the hippocampus proper may be involved only in the retrieval of memories that go back a few years. The entorhinal cortex, in contrast, demonstrates temporally graded changes in activity when viewing and identifying faces that extend back up to 20 years. Ryan *et al.* (2001) also carried out an fMRI study while subjects were asked to recall recent or distant past events in their lives. They found equivalent activation for both ages of events, which they argue disputes the notion of the hippocampus playing a role in long-term consolidation. These investigators, however, did not specifically examine the entorhinal cortex.

Another issue that has been profitably explored with fMRI is the role of the hippocampal formation in memory retrieval. It has been clear for some time that damage to the hippocampus impairs formation of new memories, but it was not thought that the hippocampus was an essential component of memory retrieval. However, a number of investigators have observed that the hippocampus is activated during the recollection of recently occurring facts and events (Stark and Squire, 2000). Lepage *et al.* (1998) carried out a meta analysis of PET activations of the hippocampus during encoding and retrieval on new information and found that encoding activations were predominantly in the anterior hippocampus and retrieval activations predominantly, in the posterior hippocampus. As attractive as this notion is, more

recent high-resolution fMRI studies have not been able to confirm this regions localization (Reber *et al.*, 2002).

Functional imaging technologies will undoubtedly become increasingly more powerful. Perhaps during the next decade, the functional significance of the complex yet elegant hippocampal neuroanatomy that has been the subject of this chapter will be determined.

Acknowledgments

Original work cited in this chapter was supported by NIH grants NS-16980 and MH-41470 to DGA and Grant FIS 86/1129 and 01/0688 from the Ministry of Health (Spain), and grant GC-02-022 of the Department of Science and Technology, Junta de Comunidades de Castilla-La Mancha (Spain) to RI. We would like to thank Janet Weber and Mary Ann Lawrence for superb histological assistance, Kris Trulock for splendid photographic help, and Belle Wamsely for secretarial and editorial help. We are also indebted to the Human Neuroanatomy Laboratory and CRIB components, Mª del Mar Arroyo, Pilar Marcos, Emilio Artacho, Alino Martínez, Mónica Muñoz, Xavier Blaizot, Alicia Mohedano, Sandra Cebada, Isabel Úbeda, and Carmen Ruiz for assistance in the elaboration of this chapter. Human brain material from which the histological preparations were made was obtained through the generous assistance of J. Martinez-Peñuela, T. Tuñon, A. Insausti, and T. Urrutia of the Department of Pathology, Hospital of Navarra, Pamplona, Spain.

References

Aggleton, J.P. (1986). A description of the amygdalo-hippocampal interconnections in the macaque monkey. *Exp. Brain Res.* **64,** 515–526.

Akbarian, S., Viñuela, A., Kim, J.J., Potkin, S.G., Bunney, W.E., and Jones, E.G. (1993). Distorted distribution of nicotinamide-adenine dinucleotide phosphate-diaphorase neurons in temporal lobe of schizophrenics implies anomalous cortical development. *Arch. Gen. Psychiatry* **50,** 178–187.

Akil, M., and Lewis, D.A. (1994). The distribution of tyrosine hydroxylase-immunoreactive fibers in the human entorhinal cortex. *Neurosci.* **60,** 857–874.

Alonso, A., and Köhler, C. (1984). A study of the reciprocal connections between the septum and the enthorhinal area using anterograde and retrograde axonal transport methods in the rat brain. *J. Comp. Neurol.* **225,** 327–343.

Amaral, D.G. (1978). A golgi study of the cell types in the hilar region of the hippocampus in the rat. *J. Comp. Neurol.* **182,** 851–914.

Amaral, D.G. (1986). Amygdalohippocampal and amygdalocortical projections in the primate brain. *In* "Excitatory Amino Acids and Epilepsy" (R. Schwarcz and Y. Ben-Ari, eds.), pp. 3–17. Plenum, New York.

Amaral, D.G. (1987). Memory: Anatomical organization of candidate brain regions. *In* "Handbook of Physiology" (F. Plum, ed.), Sect. 1, Vol. V, Part 2, pp. 211–294. Am. Physiol. Soc., Washington, D.C.

Amaral, D.G., and Campbell, M.J. (1986). Transmitter systems in the primate dentate gyrus. *Hum. Neurobiol.* **5,** 169–180.

Amaral, D.G., and Cowan, W.M. (1980). Subcortical afferents to the hippocampal formation in the monkey. *J. Comp. Neurol.* **189,** 573–591.

Amaral, D.G., and Kurz, J. (1985). An analysis of the origins of the cholinergic and non-cholinergic septal projections to the hippocampal formation of the rat. *J. Comp. Neurol.* **240,** 37–59.

Amaral, D.G., Insausti, R., and Cowan, W.M. (1983). Evidence for a direct projection from the superior temporal gyrus to the entorhinal cortex in the monkey. *Brain Res.* **275,** 263–277.

Amaral, D.G., Insausti, R., and Cowan, W.M. (1984). The commissural connections of the monkey hippocampal formation. *J. Comp. Neurol.* **224,** 307–336.

Amaral, D.G., Insausti, R., and Cowan, W.M. (1987). The entorhinal cortex of the monkey. I. Cytoarchitectonic organization. *J. Comp. Neurol.* **264,** 326–355.

Amaral, D.G., Insausti, R., and Campbell, M.J. (1988). Distribution of somatostatin immunoreactivity in the human dentate gyrus. *J. Neurosci.* **8,** 3306–3316.

Andersen, P., Holmquist, B., and Voorhoeve, P.E. (1966). Entorhinal activation of dentate granule cells. *Acta Physiol. Scand* **66,** 448–460.

Arantius, G. (1587). De humano foetu … Ejusdem anatomicorum observationum liber. Etc. Venice.

Arnold, S.E., and Trojanowski, J.Q. (1996a). Human fetal hippocampal development: I. Cytoarchitecture, myeloarchitecture, and neuronal morphologic features. *J. Comp. Neurol.* **367,** 274–292.

Arnold, S.E., and Trojanowski, J.Q. (1996b). Human fetal hippocampal development: II. The neuronal cytoskeleton. *J. Comp. Neurol.* **367,** 293–307.

Arnold, S.E., Lee, V.M.-Y., Gur, R.E., and Trojanowski, J.Q. (1991). Abnormal expression of two microtubule-associated proteins (MAP2 and MAP5) in specific subfields of the hippocampal formation in schizophrenia. *Proc. Natl. Acad. Sci.* **88,** 10850–10854.

Arnold, S.E., Ruscheinsky, D.D., and Han L.-Y. (1997). Further evidence of abnormal cytoarchitecture of the entorhinal cortex in schizophrenia using spatial point pattern analyses. *Biol. Psychiatry* **42,** 639–647.

Azmitia, E.C., and Segal, M. (1978). An autoradiographic análisis of the differential ascending projections of the dorsal and median raphe nuclei in the rat. *J. Comp. Neurol.* **179,** 941–668.

Babb, T. L., Lieb, J.P., Brown, W.J., Pretorius, J., and Crandall, P.H. (1984). Distribution of pyramidal cell density and hyperexcitability in the epileptic human hippocampal formation. *Epilepsia* **25,** 721–728.

Bakst, I., and Amaral, D.G. (1984). The distribution of acetylcholinesterase in the hippocampal formation of the monkey. *J. Comp. Neurol.* **225,** 344–371.

Bakst, I., Avendaño, C., Morrison, J.H., and Amaral, D.G. (1986). An experimental analysis of the origins of the somatostatin immunoreactive fibers in the dentate gyrus of the rat. *J. Neurosci.* **6,** 1452–1462.

Bakst, I., Morrison, J.H., and Amaral, D.G. (1985). The distribution of somatostatin-like immunoreactivity in the monkey hippocampal formation. *J. Comp. Neurol.* **236,** 423–442.

Baleydier, C., and Mauguiere, F. (1980). The duality of the cingulated gyrus in the monkey. Neuroanatomical study and functional hypothesis. *Brain* **103,** 525–554.

Ball, M.J. (1977). Neuronal loss, neurofibrillary tangles and granulovacuolar degeneration in the hippocampus with aging and dementia. *Acta Neuropathol.* **36,** 111–118.

Ball, M.J. (1978). Topographic distribution of neurofibrillary tangles and granulovacuolar degeneration in hippocampal cortex of aging and demented patients. A quantitative study. *Acta Neuropathol.* **42,** 73–80.

Ball, M.J. (1983). Granulovacuolar degeneration. *In* "Alzheimer's Disease" (B. Reisberg, ed.), pp. 62–68. Free Press, New York.

Barbas, H., and Blatt, G.J. (1995). Topographically specific hippocampal projections target functionally distinct prefrontal areas in the rhesus monkey. *Hippocampus* **5,** 511–533.

Bauman, M., and Kemper, T.L. (1985). Histoanatomic observations of the brain in early infantile autism. *Neurology* **35,** 866–874.

Beall, M.J., and Lewis, D.A. (1992). Heterogeneity of Layer II neurons in human entorhinal Cortex. *J. Comp. Neurol.* **321,** 241–266.

Bechterew, W. W. (1900). Demonstration eines Gehirs mit Zerstorung der vorderen und inneren Theile der Hirnrinde beider Schlafenlapen. *Neurol. Zentralbl.* **19,** 990–991.

Beckstead, R.M. (1978). Afferent connections of the entorhinal area in the rat as demonstrated by retrograde cell-labeling with horseradish peroxidase. *Brain Res.* **152,** 249–264.

Belliveau, J.W., Kennedy, D.N., McKinstry, C., et al. (1991). Functional mapping of the human visual cortex by magnetic resonance imaging. *Science* **254** (5032), 716–719

Berger, B., Esclapez, M., Alvarez, C., Meyer, G., and Catala M. (2001). Human and monkey fetal brain development of the supramammillary-hippocampal projections: A system involved in the regulation of theta activity. *J. Comp. Neurol.* **429,** 515–529.

Blackstad, T.W. (1956). Commissural connections of the hippocampal region in the rat, with special reference to their mode of termination. *J. Comp. Neurol.* **105,** 417–537.

Blackstad, T.W., Brink, K., Hem, J., and Jeune, B. (1970). Distribution of hippocampal mossy fibers in the rat. An experimental study with silver impregnation methods. *J. Comp. Neurol.* **138,** 433–450.

Blatt, G.J., and Rosene, D.L. (1998). Organization of direct hippocampal efferent projections to the cerebral cortex of the rhesus monkey: Projections from CA1, prosubiculum and subiculum to the temporal lobe. *J. Comp. Neurol.* **392,** 92–114.

Blümcke, I., Zuschratter, W., Schewe, J.-C., Suter, B., Lie, A.A., Riederer, B.M., Meyer, B., Schramm, J., Elger, C.E., and Wiestler, O.D. (1999). Cellular pathology of hilar neurons in ammon's horn sclerosis. *J. Comp. Neurol.* **414,** 437–453.

Bogerts, B., Meertz, E., and Schonfeldt-Bausch, R. (1985). Basal ganglia and limbic system pathology in schizophrenis. *Arch. Gen. Psychiatry* **42,** 784–791.

Braak, E., Strotkamp, B., and Braak H. (1991). Parvalbumin-immunoreactive structures in the hippocampus of the human adult. *Cell Tiss. Res.* **264,** 33–48.

Braak, H. (1972). Zur Pigmentarchitektonic der Grosshirnrinde des Menschen. I. Regio entorhinalis. *Z. Zellforsch. Mikrosk. Anat.* **127,** 407–438.

Braak, H. (1974). On the structure of the human archicocortex, I. The cornu ammonis. A Golgi and pigmentarchitectonic study. *Cell Tissue Res.* **152,** 349–383.

Braak, H. (1980). "Architectonics of the Human Telencephalic Cortex." Springer-Verlag, New York.

Braak, H., and Braak, E. (1992). The human entorhinal cortex: Normal morphology and lamina-specific pathology in various diseases. *Neurosci. Res.* **15,** 6–-31.

Brierley, J.B., and Graham, D.I. (1984). Hypoxia and vascular disorders of the central nervous system. *In* "Greenfield's Neuropathology" (J.H. Adams, J.A.N. Corsellis, and L.W. Duchen, eds.), 4th ed., pp. 125–207. Wiley, New York.

Brodal, A. (1947). The hippocampus and the sense of smell. A review. *Brain* **70,** 179–222.

Brodmann, K. (1909). "Vergleichende Lokalisationslehre der Groshirnrinde." Barth, Leipzig.

Buckmaster, P.S., and Amaral, D.G. (2001). Intracellular recording and labeling of mossy cells and proximal CA3 pyramidal cells in macaque monkeys. *J. Comp. Neurol.* **430,** 264–281.

Burger, P.C. (1983). The limbic system in Alzheimer's disease. *In* "Biological Aspects of Alzheimer's Disease" (R. Katzman, ed.), pp. 37–44. Cold Spring Harbor Lab., Cold Spring Harbor, New York.

Carboni, A.A., Lavelle, W.G., Barnes, C.L., and Cipolloni, P.B. (1990). Neurons of the lateral entorhinal cortex of the rhesus monkey: a Golgi, histochemical, and immunocytochemical characterization. *J. Comp. Neurol.* **291,** 583–608.

Cassell, M.D. (1980). The numbers of cells in the stratum pyramidale of the rat and human hippocampal formation. Ph.D. Thesis, University of Bristol, United Kingdom.

Cavada, C., and Reinoso-Suarez, F. (1983). Afferent connections of area 20 in the cat studied by means of the retrograde axonal transport of horseradish preoxidase. *Brain Res.* **270,** 319–324.

Cavanagh, J.B., Falconer, M.A., and Meyer, A. (1958). Some pathogenic problems of temporal lobe epilepsy. *In* "Temporal Lobe Epilepsy" (M. Baldwin and P. Bailey, eds.), pp. 140–148. Thomas, Springfield, Illinois.

Chan-Palay, V., Köhler, C., Haesler, U., Lang, W., and Yasargil, G. (1986). Distribution of neurons and axons immunoreactive with antisera against neuropeptide Y in the normal human hippocampus. *J. Comp. Neurol.* **248,** 360–375.

Chronister, R.B., Sikes, R.W., and White, L.E., Jr. (1975). Postcommissural fornix: Origin and distribution in the rodent. *Neurosci. Lett.* **1,** 199–202.

Conrad, L.C., and Pfaff, D.W. (1976). Autoradiographic tracing of nucleus accumbens efferents in the rat. *Brain Res.* **113,** 589–596.

Corkin, S., Amaral, D.G., González, R.G., Johnson, K.A., and Hyman, B.T. (1997). H.M.'s medial temporal lobe lesion: Findings from magnetic resonance imaging. *J. Neurosci.* **17,** 3964–3979.

Corsellis, J.A.N. (1970). The limbic areas in Alzheimer's disease and in other conditions associated with dementia. *In* "Alzheimer's Disease and Related Disorders" (G. E.W. Wolstenholme and M. O'Connor, eds.), pp. 37–50. Churchill, London.

Crow, T.J., and Johnstone, E.C. (1987). Schizophrenia: Nature of the disease process and its biological correlates. *In* "Handbook of Physiology" (F. Plum, ed.), Sect. 1, Vol. V, Part 2, pp. 843–869. Am. Physiol. Soc., Bethesda, Maryland.

Cummings, J.L., Tomiyasu, U., Read, S., and Benson, D.F. (1984). Amnesia with hippocampal lesions after cardiopulmonary arrest. *Neurology* **34,** 679–681.

Daitz, H.M., and Powell, T.P.S. (1954). Studies of the connexions of the fornix system. *J. Neurol. Neurosurg. Pychiatry* **17,** 75–82.

De la Calle, S., Lim, C., Sobreviela, T., Mufson, E.J., Hersh, L.B., and Saper, C.B. (1994). Cholinergic innervation in the human hippocampal formation including the entorhinal cortex. *J. Comp. Neurol.* **345,** 321–344.

Delgado-Escueta, A.V., and Walsh, G.O. (1985). Type I complex partial seizures of hippocampal origin: Excellent results of anterior temporal lobectomy. *Neurology* **35,** 143–154.

Delmas, A. (1955). Lobe ou complexe temporal. Considerations anatomiques et embryologiques sur le démembrement du lobe temporal. *In* "Les grandes activités du lobe temporal" (Alajouanine, ed.), pp 1–56. Masson, Paris

Demeter, S., Rosene, D.L., and Van Hoesen, G.W. (1985). Interhemispheric pathways of the hippocampal formation, presubiculum, and entorhinal and posterior parahippcampal cortex in the rhesus monkey: The structure and organization of the hippocampal commissures. *J. Comp. Neurol.* **233,** 30–47.

Dietl, M.M., Probst, A., and Palacios, J.M. (1987). On the distribution of cholecystokinin receptor binding sites in the human brain: An autoradiographic study. *Synapse* **1,** 169–183.

Ding, S.L., Van Hoesen, G., and Rockland, K.S. (2000). Inferior parietal lobule projections to the subiculum and neighboring ventromedial temporal cortical areas. *J. Comp. Neurol.* **425,** 510–530.

Domesick, V.B. (1972). Thalamic relationships of the medial cortex in the rat. *Brain, Behav. Evol.* **6,** 457–483.

Du, F., Whetsell, W.O., Jr., Abou Khalil, B., Blumenkopf, B., Lothman, E.W., and Schwarcz, R. (1993). Preferential neuronal loss in layer III of the entorhinal cortex in patients with temporal lobe epilepsy. *Epilepsy Res.* **16,** 223–233.

Duvernoy, H.M. (1988). "The Human Hippocampus." pp. 1–166. J.F. Bergman Verlag, München.

Edinger, E.M., Kramer, S.Z., Weiner, S., Krayniak, P.F., and Siegel, A. (1979). The subicular cortex of the cat: An anatomical and electrophysiological study. *Exp. Neurol.* **63,** 504–526.

Falconer, M.A. (1974). Mesial temporal (Ammon's horn) sclerosis as a common cause of epilepsy. Aetiology, treatment, and prevention. *Lancet* **2,** 767–770.

Falkai, P., and Bogerts, B. (1986). Cell loss in the hippocampus of schizophrenics. *Eur. Arch. Psychiatr. Neurol. Sci.* **263,** 154–161.

Fibiger, H.C. (1982). The organization and some projections of cholinergic neurons of the mammalian forebrain. *Brain Res. Rev.* **4,** 327–388.

Finch, D.M., and Babb, T.L. (1981). Demonstration of caudally directed hippocampal efferents in the rat by intracellular injection of horseradish peroxidase. *Brain Res.* **214,** 405–410.

Finch, D.M., Nowlin, N.L., and Babb, T.L. (1983). Demonstration of axonal projections of neurons in the rat hippocampus and subiculum by intracellular injection of HRP. *Brain Res.* **271,** 201–216.

Frederickson, C.J., Klitenick, M.A., Manton, W.I., and Kirkpatrick, J.B. (1983). Cytoarchitectonic distribution of zinc in the hippocampus of man and the rat. *Brain Res.* **273,** 335–339.

Fricke, R., and Cowan, W.M. (1978). An autoradiographic study of the commissural and ipsilateral hippocampo-dentate projections in the adult rat. *J. Comp. Neurol.* **181,** 253–269.

Gaarskjaer, F.B. (1978). Organization of the mossy fiber system of the rat studied in extended hippocampi. I. Terminal area related to number of granule and pyramidal cells. *J. Comp. Neurol.* **178,** 49–72.

Gaarskjaer, F.B. (1981). The hippocampal mossy fiber system of the rat studied with retrograde tracing techniques. Correlation between topographic organization and neurogenetic gradients. *J. Comp. Neurol.* **203,** 717–735.

Gadian, D.G., Aicardi, J., Watkins, K.E., Porter, D.A., Mishkin, M., and Vargha-Khadem, F. (2000). Developmental amnesia associated with early hypoxic-ischaemic injury. *Brain* **123,** 499–507.

de Garengeot. (1742). "Splanchnologie ou l'anatomie des visceres," 2nd ed., pp. 250–251. Paris.

Gastaut, H., and Lammers, J.H. (1961). Anatomie du rhinencephale. *In* "Les grandes activités dy rhinencéphale" (P.T. Alajouanine, ed.), Vol. 1. Masson, Paris.

Gertz, S.D., Lindenberg, R., and Piavis, G.W. (1972). Structural variations in the rostral human hippocampus. *Johns Hopkins Med. J.* **130,** 367–376.

Glees, P., and Griffith, H.B. (1952). Bilateral destruction of the hippocampus (Cornu ammonis) in a case of dementia. *Psychiatr. Neurol.* **123,** 193–204.

Gloor, P. (1997). "The Temporal Lobe and Limbic System." Oxford University Press, Oxford.

Gloor, P., Salanova, V., Olivier A., and Quesnay, L.F. (1993). The human dorsal hippocampal commissure. An anatomically identifiable and functional pathway. *Brain* **116,** 1249–1273.

Goldenberg, T.M., Bakay, R.A.E., and Ribak C.E. (1995). Electron Microscopy of Cell Islands in Layer II of the Primate Entorhinal Cortex. *J. Comp. Neurol.* **355,** 51–66.

Goldman-Rakic, P.S., Selemon, L.D., and Schwartz, M.L. (1984). Dual pathways connecting the dorsolaterl prefrontal cortex with the hippocampal formation and parahippocampal cortex in the rhesus monkey. *Neuroscience* **12,** 719–734.

Gomez-Isla, T., Price, J.L., McKeel, D.W., Morris, J.C., Growdon, J.H., and Hyman, B.T. (1996). Profound loss of layer II entorhinal cortex neurons distinguishes very mild Alzheimer's disease from nondemented aging. *J. Neurosci.* **16,** 4491–4500.

Good, P.F., and Morrison, J.H. (1995). Morphology and Kainate-receptor immunoreactivity of identified neurons within the entorhinal cortex projecting to superior temporal sulcus in the cynomolgus monkey. *J. Comp. Neurol.* **357,** 25–35.

Gosche, K.M., Mortimer, J.A., Smith, C.D., Markesbery, W.R., and Snowdon, D.A. (2002). Hippocampal volume as an index of Alzheimer neuropathology: Findings from the Nun Study. *Neurology* **58,** 1476–1482.

Gottlieb, D.I., and Cowan, W.M. (1973). Autoradiographic studies of the commissural and ipsilateral association connections of the hippocampus and dentate gyrus of the rat. *J. Comp. Neurol.* **149,** 393–420.

Graterón, L., Insausti, A.M., García-Bragado, F., Arroyo-Jiménez, M.M., Marcos, P., Martínez-Marcos, A., Blaizot, X., Artacho-Pérula, E., and Insausti, R. (2002). Postnatal development of the human entorhinal cortex. *In* "The parahippocampal gyrus" (M.P. Witter and F.G. Wouterlood, eds.), pp. 21–31. Oxford University Press, Oxford.

Green, R.C., and Mesulam, M.-M. (1988). Acetylcholinesterase fiber staining in the human hippocampus and parahippocampal gyrus. *J. Comp. Neurol.* **273,** 488–499.

Groenewegen, H.J., Room, P., Witter, M.P., and Lohman, A.H.M. (1982). Cortical afferents of the nucleus accumbens in the cat, studied with anterograde and retrograde transport techniques. *Neurosci.* **7,** 977–995.

Grunthal, E. (1939). Ueber das Corpus mamillare und den Korsakowschen Symtomen Komplex. *Confin. Neurol.* **2,** 65–95.

Haglund, L., Swanson, L.W., and Kohler, C. (1984). The projection of the supramammillary nucleus to the hippocampal formation: An immunohistochemical and anterograde transport study with the lectin PHA-L in the rat. *J. Comp. Neurol.* **229,** 171–185.

Haist, F., Bowden Gore, J., Mao, H. (2001). Consolidation of human memory over decades revealed by functional magnetic resonance imaging. *Nat Neurosci* **4,** 1139–1145.

Hammarberg, C. (1895). "Studien uber Klinik und Pathologie der Idiotie nebst Untersuchungen uber die normale Anatomie der Hirnrinde." Berling, Upsala.

Hanke, J. (1997). Sulcal pattern of the anterior parahippocampal gyrus in the human adult. *Ann Anat.* **179,** 335–339.

Hanke, J., and Yilmazer-Hanke, D. M. (1997). Pigmentarchitectonic subfields of the entorhinal region as revealed in tangential sections. *J. Brain Res.* **38,** 427–432.

Heckers, S., Heinsen, H., Geiger, B., and Beckmann, H. (1991). Hippocampal neuron number in schizophrenia. *Arch. Gen. Psychiatry* **48,** 1002–1008.

Heckers, S., Heinsen, H., Heinsen, Y., and Beckmann, H. (1990). Morphometry of the parahippocampal gyrus in schizophrenics and controls. Some anatomical considerations. *J. Neural Transm.* **80,** 151–155.

Heinsen, H., Henn, R., Eisenmenger, W., Götz, M., Bohl, J., Bethke, B., Lockemann, U., and Püschel, K. (1994). Quantitative investigations on the human entorhinal area: Left-right asymmetry and age-related changes. *Anat Embryol.* **190,** 181–194.

Herkenham, M. (1978). The connections of the nucleus reunions thalami: Evidence for a direct thalamo-hippocampal pathway in the rat. *J. Comp. Neurol.* **177,** 589–610.

Hevner, R.F., and Kinney, H.C. (1996). Reciprocal entorhinal-hippocampal connections established by human fetal midgestation. *J. Comp. Neurol.* **372,** 384–394.

Hevner, R.F., and Wong-Riley, M.T.T. (1992). Entorhinal Cortex of the Human, Monkey, and Rat: Metabolic Map as Revealed by Cytochrome Oxidase. *J. Comp. Neurol.* **326,** 451–469.

Hines, M. (1922). Studies in the growth and differentiation of the telencephalon in man. The fissura hippocampi. *J. Comp. Neurol.* **34,** 73–171.

Hjorth-Simonsen, A. (1971). Hippocampal efferents to the ipsilateral entorhinal area: An experimental study in the rat. *J. Comp. Neurol.* **177,** 589–610.

Hjorth-Simonsen, A. (1977). Distribution of commissural afferents to the hippocampus of the rabbit. *J. Comp. Nerol.* **176,** 495–514.

Hjorth-Simonsen, A., and Jeune, B. (1972). Origin and termination of the hippocampal perforant path in the rat studied by silver impregnation. *J. Comp. Neurol.* **144,** 215–231.

Hjorth-Simonsen, A., and Laurberg, S. (1977). Commissural connections of the dentate area of the rat. *J. Comp. Neurol.* **174,** 591–606.

Hogan, R.E., Mark, K.E., Wang, L., Joshi, S., Miller, M.I., and Bucholz, R.D. (2000). Mesial temporal sclerosis and temporal lobe epilepsy: MR imaging deformation-based segmentation of the hippocampus in five patients. *Radiology* **216,** 291–297.

Hokfelt, T., Fuxe, K., Johansson, O., and Ljungdahi, A. (1974). Pharmacohistochemical evidence of the existence of dopamine nerve terminals in the limbic cortex. *Eur. J. Pharmacol.* **25,** 108–112.

Horel, J. (1978). The neuroanatomy of amnesia: A critique of the hippocampal memory hypothesis. *Brain* **101,** 403–445.

Houser, C.R., Swartz, B.E., Walsh, G.O., and Delgado-Escueta, A.V. (1992). Granule cell disorganization in the dentate gyrus: possible alterations of neuronal migration in human temporal lobe epilepsy. *Mol. Neurobiol. Epilepsy* **9,** 41–49.

Humphrey, T. (1967). The development of the human hippocampal fissure. *J. Anat.* **101,** 655–676.

Hyman, B.T., Van Hoesen, G.W., Damasio, A.R., and Barnes, C.L. (1984). Alzheimers disease: Cell-specific pathology isolates the hippocampal formation. *Science* **225,** 1168–1170.

Hyman, B.T., Van Hoesen, G.W., Kromer, L.J., and Damasio, A.R. (1986). Perforant pathway changes and the memory impairment of Alzheimer's disease. *Ann. Neurol.* **20,** 472–481.

Insausti, R., and Muñoz, M. (2001). Cortical projections of the non-entorhinal hippocampal formation in the cynomolgus monkey (Macaca fascicularis). *Europ. J. Anat.* **14,** 435–451.

Insausti, R., Amaral, D.G., and Cowan, W.M. (1987a). The entorhinal cortex of the monkey. II. Cortical afferents. *J. Comp. Neurol.* **264,** 356–395.

Insausti, R., Amaral, D.G., and Cowan, W.M. (1987b). The entorhinal cortex of the monkey. III. Subcortical afferents. *J. Comp. Neurol.* **264,** 396–408.

Insausti, R., Herrero, M.T., and Witter, M.P. (1997). Entorhinal cortex of the rat: Cytoarchitectonic subdivisions and the origin and distribution of cortical efferents. *Hippocampus* **7,** 146–183.

Insausti, R., Insausti, A.M., Sobreviela, M.T., Salinas, A., and Martínez-Peñuela, J.M. (1998). Human medial temporal lobe in aging: Anatomical basis of memory preservation. *Microsci. Res. Tech.* **43,** 8–15.

Insausti, R., Tuñón, T., Sobreviela, T., Insausti, A.M., and Gonzalo, L.M. (1995). The human entorhinal cortex: A cytoarchitectonic análisis. *J. Comp. Neurol.* **355,** 171–198.

Irle, E., and Markowitsch, H.J. (1982). Single and combined lesions of the cat's mediodorsal nucleus and the mamillary bodies lead to severe deficits in the acquisition of an alternation task. *Behav. Brain Res.* **6,** 147–165.

Ishizuka, N., Weber, J., and Amaral, D.G. (1990). Organization of intrahippocampal projections originating from CA3 pyramidal cells in the rat. *J. Comp. Neurol.* **295,** 580–623.

Jack, C.R., Jr., Dickson, D.W., Parisi, J.E., Xu, Y.C., Cha. R.H., O'Brien, P.C., Edland, S.D., Smith, G.E., Boeve, B.F., Tangalos, E.G., Kokmen, E., and Petersen, R.C. (2002). Antemortem MRI findings correlate with hippocampal neuropathology in typical aging and dementia. *Neurology* **58,** 750–757.

Jakob, H., and Beckmann, H. (1986). Prenatal developmental disturbances in the limbic allocortex in schizophrenics. *J. Neural Transm.* **65,** 303–326.

Jakob, H., and Beckmann, H. (1994). Circumscribed malformation and nerve cell alterations in the entorhinal cortex of schizophrenics. *J. Neural Transm.* **98,** 83–106.

Kaitz, S.S., and Robertson, R.T. (1981). Thalamic connections with limbic cortex. II. Corticothalamic projections. *J. Comp. Neurol.* **195,** 527–545.

Kelley, A.E., and Domesick, V.B. (1982). The distribution of the projection from the hippocampal formation to the nucleus accumbens in the rat: An anterograde- and retrograde-horseradish peroxidase study. *Neurosci.* **7,** 2321–2335.

Kemper, T.L. (1978). Senile dementia: A focal disease in the temporal lobe. *In* "Senile Dementia: A Biomedical Approach" (K. Nandy, ed.), pp. 105–113. Elsevier/North-Holland, New York.

Kemper, T.L. (1983). Organization of the neuropathology of the amygdala in Alzheimer's disease. *Banbury Rep.* **15,** 31–35.

Kemper, T.L., and Bauman, M. (1998). Neuropathology of infantile autism. *J. Neuropathol. Exp. Neurol.* **57,** 645–652.

Killiany, R.J., Hyman, B.T., Gomez-Isla, T., Moss, M.B., Kikinis, R., Jolesz, F., Tanzi, R., Jones, K., and Albert, M.S. (2002). MRI measures of entorhinal cortex vs hippocampus in preclinical AD. *Neurology* **58,** 1188–1196.

Klingler, J. (1948). Die makroskopische anatomie der Ammonsformation. *Denkschr. Schweiz. Naturforsch. Ges.* **78,** Mem. 1, 1–80.

Kobayashi, Y., and Amaral, D.G. (2001). The hippocampal formation and perirhinal and parahippocampal cortices. *In* "The primate nervous system (F.E. Bloom, A. Bjorklund, and T. Hökfelt, eds.), pp. 285–401. Elsevier, Amsterdam.

Kobayashi, R.M., Palkovits, M., Kopin, I.J., and Jacobowitz, DM. (1974). Biochemical mapping of noradrenergic nerves arising from the rat locus coeruleus. *Brain Res.* **77,** 269–279.

Koda, L.Y., Schulman, J.A., and Bloom, F.E. (1978). Ultrastructural identification of noradrenergic terminals in rat hippocampus: Unilateral destruction of the locus coeruleus with 6-hydroxydopamine. *Brain Res.* **145,** 190–195.

Köhler, C. (1984). Morphological details of the projection from the presubiculum to the entorhinal area as shown with the novel PHA-L immunohistochemical tracing method in the rat. *Neurosci. Lett.* **45,** 285–290.

Köhler, C. (1985). Intrinsic projections of the retrohippocampal region in the rat brain. I. The subicular complex. *J. Comp. Neurol.* **236,** 504–522.

Köhler, C., and Steinbusch, H. (1982). Identification of serotonin and non-serotonin-containing neurons of the mid-brain raphe projecting to the entorhinal area and the hippocampal formation. A combined immunohistochemical and fluorescent retrograde tracing study in the rat brain. *Neurosci.* **7,** 951–975.

Köhler, C., Chan-Palay, V., and Wu, J.Y. (1984a). Septal neurons containing glutamic acid decarboxylase immunoreactivity project to the hippocampal region in the rat brain. *Anat. Embryol.* **169,** 41–44.

Köhler, C., Haglund, L., and Swanson, L.W. (1984b). A diffuse alpha-MSH-immunoreactive projection to the hippocampus and spinal cord from individual neurons in the lateral hypothalamic area and zona incerta. *J. Comp. Neurol.* **223,** 501–514.

Köhler, C., Radesater, A., and Chan.Palay, V. (1987). Distribution of neurotensin receptors in the primate hippocampal region: A quantitative autoradiographic study in the monkey and the postmortem human brain. *Neurosci. Lett.* **76,** 145–150.

Köhler, C., Shipley, M.T., Srebro, B., and Harkmark, W. (1978). Some retrohippocampal afferents to the entorhinal cortex. Cells of origin as studied by the HRP method in the rat and mouse. *Neurosci. Lett.* **10,** 115–120.

Kölliker, A. (1896). "Handbuch der Gewebelehre der Menschen." Engelmann, Leipzig.

Kordower, J., and Mufson, E.J. (1992). Nerve growth factor receptor-immunoreactive neurons within the developing human cortex. *J. Comp. Neurol.* **323,** 25–41.

Kordower, J.H., Chu, Y., Stebbins, G.T., Dekosky, S.T., Cochran, E.J., Bennett, D., and Mufson, E.J. (2001). Loss and atrophy of layer II entorhinal cortex neurons in elderly eople with mild cognitive impairment. *Ann. Neurol.* **49,** 202–213.

Kosel, K.C., Van Hoesen, G.W., and Rosene, D.L. (1982). Nonhippocampal cortical projections from the entorhinal cortex in the rat and rhesus monkey. *Brain Res.* **244,** 201–213.

Kosel, K.C., Van Hoesen, G.W., and Rosene, D.L. (1983). A direct projection from the perirhinal cortex (area 35) to the subiculum in the rat. *Brain Res.* **269,** 347–351.

Kostović, I., Zdravko, P., and Judaš, M. (1993). Early areal differentiation of the human cerebral cortex: Entorhinal area. *Hippocampus* **3,** 447–458.

Krettek, J.E., and Price, J.L. (1977). Projections from the amygdaloid complex and adjacent olfactory structures to the entorhinal cortex and to the subiculum in the rat and cat. *J. Comp. Neurol.* **172,** 723–752.

Krettek, J.E., and Price, J.L. (1978). A description of the amygdaloid complex in the rat and cat with observations on intraamygdaloid axonal connections. *J. Comp. Neurol.* **178,** 255–280.

Krimer, L.S., Hyde, T.M., Herman, M.M., and Saunders, R.C. (1997).The entorhinal cortex: An examination of cyto- and myeloarchitectonic organization in humans. *Cereb Cortex* **7,** 722–731.

Kuzniecky, R., de la Sayette, V., Ethier, R., Melanson, D., Andermann, F., Berkovic, S., Robitaille, Y., Olivier, A., Peters, A., and Feindel, W. (1987). Magnetic resonance imaging in temporal lobe epilepsy: pathological correlations. *Ann. Neurol.* **22,** 341–347.

Laatsch, R.H., and Cowan, W.M. (1966). Electron microscopic studies of the rat dentate gyrus. II. Degeneration of commissural afferents. *J. Comp. Neurol.* **130,** 241–262.

Laurberg, S. (1979). Commissural and intrinsic connections of the rat hippocampus. *J. Comp. Neurol.* **184,** 685–708.

Laurberg, S., and Sorensen, K.E. (1981). Associational and commissural collaterals of neurons in the hippocampal formation (hilus fasciae dentate and subfield CA3). *Brain Res.* **212,** 287–300.

Lepage, M., Habib, R., and Tulving, E. (1998). Hippocampal PET activations of memory encoding and retrieval: the HIPER model. *Hippocampus* **8,** 313–322.

Lewis, F.T. (1923). The significance of the term hippocampus. *J. Comp. Neurol.* **35,** 213–230.

Lewis, P.R., and Shute, C.C.D. (1967). The cholinergic limbic system: Projections to hippocampal formation, medial cortex, nuclei of the ascending cholinergic reticular system, and subfornical organ and supra-optic crest. *Brain* **90,** 521–590.

Lewis, P.R., Shute, C.C.D., and Silver, A. (1967). Confirmation from choline acetylase analysis of a massive cholinergic innervation to the rat hippocampus. *J. Physiol. (London)* **191,** 215–224.

Lim, C., Blume, H.W., Madsen, J.R., and Saper, C.B. (1997a). Connections of the hippocampal formation in humans: I. the mossy fiber pathway. *J. Comp. Neurol.* **385,** 325–351.

Lim, C., Mufson, E.J., Kordower, J.H., Blume, H.W., Madsen, J.R., and Saper, C.B. (1997b). Connections of the hippocampal formation in humans: II. The endfolial fiber pathway. *J. Comp. Neurol.* **385,** 352–371.

Lindvall, O., and Bjorklund, A. (1974). The organization of the ascending catecholamine neuron system in the rat brain. *Acta Physiol. Scan.* **412,** 1–48.

Lopes da Silva, F.H., Arnolds, D.E.A.T., and Neijt, H.C. (1984). A functional link between the limbic cortex and ventral striatum: Physiology of the subiculum accumbens pathway. *Exp. Brain Res.* **55,** 205–214.

Lord, C., Cook, E.H., Leventhal, B.L., and Amaral, D.G. (2000). Autism spectrum disorders. *Neuron* **28,** 355–363.

Lorente de Nó, R. (1933). Studies on the structure of the cerebral cortex. I. The area entorhinalis. *J. Psychol. Neurol.* **45,** 381–438.

Lorente de Nó, R. (1934). Studies on the structure of the cerebral cortex. II. Continuation of the study of the ammonic system. *J Psychol. Neurol.* **46,** 113–177.

Lotstra, F., and Vanderhaeghen, J. (1987). Distribution of immunoreactive cholecystokinin in the human hippocampus. *Peptides (N. Y.)* **8,** 911–920.

Loy, R., Koziell, D.A., Lindsey, J.D., and Moore, R. (1980). Noradrenergic innervation of the adult rat hippocampal formation. *J. Comp. Neurol.* **189,** 699–710.

Macchi, G. (1951). The ontogenetic development of the olfactory telencephalon in man. *J. Comp. Neurol.* **95,** 245–305.

Maguire, E.A. (2001). Neuroimaging studies of autobiographical event memory. *Philos. Trans. R. Soc. Lond. B. Biol. Sci.* **356,** 1441–1451.

Maguire, E.A., Vargha-Khadem, F., and Mishkin, M. (2001). The effects of bilateral hippocampal damage on fMRI regional activations and interactions during memory retrieval. *Brain* **124,** 1156–1170.

Markowitsch, H.J., Irle, E., Bang-Olsen, R., and Flindt-Egebak, P. (1984). Claustral efferents to the cat's limbic cortex studied with retrograde and anterograde tracing techniques. *Neurosci.* **12,** 409–425.

Meibach, R.C., and Siegel, A. (1975). The origin of fornix fibers which project to the mammillary bodies in the rat: A horseradish peroxidase study. *Brain Res.* **88,** 508–512.

Meibach, R.C., and Siegel, A. (1977). Efferent connections of the hippocampal formation in the rat. *Brain Res.* **124,** 197–224.

Meldrum, B.S., and Corsellis, J.A.N. (1984). Epilepsy. *In* "Greenfield's Neuropathology" (J.H. Adams, J.A.N. Corsellis, and L.W. Duchen, eds.), 4th ed., pp. 921–950. Wiley, New York.

Mesulam, M.M., Mufson, E.J., Levey, A.I., and Wainer, B.H. (1983). Cholinergic innervation of cortex by the basal forebrain: Cytochemistry and cortical connections of the septal area, diagonal band nuclei, Nucleus basalis (Substancia innominata), and hypothalamus in the rhesus monkey. *J. Comp. Neurol.* **214,** 170–197.

Mikkonen, M., Soininen, H., and Pitkänen, A. (1997). Distribution of Parvalbumin-. Calretinin-, and Calbindin-D28k-Immunoreactive Neurons and Fibers in the Human Entorhinal Cortex. *J. Comp. Neurol.* **388,** 64–88.

Mikkonen, M., Pitkänen, A., Soininen, H., Alafuzoff, I., and Miettinen, R. (2000). Morphology of spiny neurons in the human entorhinal cortex: intracellular filling with Lucifer yellow. *Neurosci.* **96,** 515–522.

Mikkonen, M., Soininen, H., Kälviäinen, R., Tapiola, T., Ylinen, A., Vapalahti, M., Paljärvi, L., and Pitkänen, A. (1998). Remodeling of neuronal circuitries in human temporal lobe epilepsy: Increased

expression of highly polysialylated neural cell adhesion molecule in the hippocampus and the entorhinal cortex. *Ann. Neurol.* **44,** 923–934.
Milner, B. (1970). Memory and the medial temporal regions of the brain. *In* "Biology of Memory" (K.H. Pribram and D.E. Broadbent, eds.), pp. 29–50. Academic Press, New York.
Milner, T.A., and Amaral, D.G. (1984). Evidence for a ventral septal projection to the hippocampal formation of the rat. *Exp. Brain Res.* **55,** 579–585.
Milner, T.A., Loy, R., and Amaral, D.G. (1983). An anatomical study of the development of the septo-hippocampal projection in the rat. *Dev. Brain Res.* **8,** 343–371.
Mishkin, M. (1978). Memory in monkeys severaly impaired by combined but not separate removal of amygdala and hippocampus. *Nature (London)* **273,** 297–298.
Misuzawa, H., Hirano, A., and Llena, J.F. (1987). Involvement of hippocampus in Creutzfeldt-Jakob disease. *J. Neurol. Sci.* **82,** 13–26.
Moore, R.Y., and Halaris, A.E. (1975). Hippocampal innervation by serotonin neurons of the midbrain raphe in the rat. *J. Comp. Neurol.* **164,** 171–184.
Morin, F. (1950). An experimental study of hypothalamic connections in the guinea pig. *J. Comp. Neurol.* **92,** 193–213.
Morrison, J.H., Benoit, R., Magistretti, P.J., Ling, N., and Bloom, F.E. (1982). Immunohistochemical distribution of prosomatostatin-related peptides in hippocampus. *Neurosci. Lett.* **34,** 137–142.
Mosko, S., Lynch, G., and Cotman, C.W. (1973). The distribution of septal projections to the hippocampus of the rat. *J. Comp. Neurol.* **152,** 163–174.
Mouritzen Dam, A. (1982). Hippocampal neuron loss in epilepsy and after experimental seizures. *Acta Neurol. Scand.* **66,** 601–642.
Mungas, D., Reed, B.R., Jagust, W.J., DeCarli, C., Mack, W.J., Kramer, J.H., Weiner, M.W., Schuff, N., and Chui, H.C. (2002). Volumetric MRI predicts rate of cognitive decline related to AD and cerebrovascular disease. *Neurology* **59,** 867–873.
Nafstad, P.H.J. (1967). An electron microscope study en the termination of the perforant path fibres in the hippocampus and the Fascia dentata. *Z. Zellforsch. Mikrosk. Anat.* **76,** 532–542.
Nestor, P.J., Graham, K.S., Bozeat, S., Simons, J.S., and Hodges, J.R. (2002). Memory consolidation and the hippocampus: Further evidence from studies of autobiographical memory in semantic dementia and frontal variant frontotemporal dementia. *Neuropsychologia* **40,** 633–654.
Niimi, M. (1978). Cortical projection of the anterior thalamic nuclei in the cat. *Exp. Brain Res.* **31,** 403–416.
Niimi, K., Niimi, M., and Okada, Y. (1978). Thalamic afferents to the limbic cortex in the cat studied with the method of retrograde axonal transport of horseradish persoxidase. *Brain Res.* **145,** 225–238.
Nitsch, R., and Leranth, C. (1993). Calretinin-immunoreactivity in the monkey hippocampal formation. II: Intrinsic GABAergic and hypothalamic non-GABAergic systems. An experimental tracing and coexistence study. *Neurosci.* **55,** 797–812.
Nitsch, R., and Leranth, C. (1994). Substance P-containing hypothalamic afferents to the monkey hippocampus: An immunocytochemical, tracing, and coexistence study. *Exp. Brain Res.* **101,** 231–240.
Nitsch, R., and Ohm, T.G. (1995). Calretinin immunoreactive structures in the human hippocampal formation. *J. Comp. Neurol.* **360,** 475–487.
Ojemann, R.G. (1966). Correlations between specific human brain lesions and memory changes. *Neurosci. Res. Program Bull.* **4,** 1–70.
Olbrich, H.G., and Braak, H. (1985). Ratio of pyramidal cells versus non-pyramidal cells in sector CA1 of the human Ammon's horn. *Anat. Embryol.* **173,** 105–110.
Ono, M., Kubik, S., and Abernathey, C.D. (1990). "Atlas of the cerebral sulci." Thieme Medical Publishers, Inc. Stuttgart, New York.
Ottersen, O.P. (1982). Connections of the amygdala of the rat. IV. Corticoamygdaloid and intraamygdaloid connections as studied with axonal transport of horseradish peroxidase. *J. Comp. Neurol.* **205,** 30–48.
Pandya, D.N., Van Hoesen, G.W., and Domesick, V.B. (1973). A cingulo-amygdaloid projection in the rhesus monkey. *Brain Res.* **61,** 369–373.
Papez, J.W. (1937). A proposed mechanism of emotion. *Arch. Neurol. Psychiatry* **38,** 725–743.
Pasquier, D.A., and Reinoso-Suarez, F. (1977). Differential efferent connections of the brain stem to the hippocampus in the cat. *Brain Res.* **120,** 540–548.
Petito, C.K., Feldmann, E., Pulsinelli, W.A., and Plum, F. (1987). Delayed hippocampal damage in humans following cardiorespiratory arrest. *Neurology* **37,** 1281–1286.
Pitkänen, A., Kelly, J.L., and Amaral, D.G. (2002). Projections from the lateral, basal, and accessory basal nuclei of the amygdala to the entorhinal cortex in the macaque monkey. *Hippocampus* **12,** 186–205.
Pohle, W., Ott, T., and Müller-Welde, P. (1984). Identification of neurons of origin providing the dopaminergic innervation of the hippocampus. *J. Hirnforsch.* **25,** 101–128.
Poletti, C.E., and Creswell, G. (1977). Fornix system efferent projections in the squirrel monkey: An experimental degeneration study. *J. Comp. Neurol.* **175,** 101–128.
Powell, T.P.S., Guillery, R.W., and Cowan, W.M. (1957). A quantitative study of the fornix-mamillo-thalamic system. *J. Anat.* **91,** 419–437.
Price, J.L., Ko, A.I., Wade, M.J., Tsou, S.K., Mckeel, D.W., and Morris, J.C. (2001). Neuron number in the entorhinal cortex and CA1 in preclinical Alzheimer disease. *Arch. Neurol.* **58,** 1395–1402.
Pritzel, M., and Markowitsch, H.J. (1983). Afferents from limbic-system-related regions to the frontal cortex in the bush baby. *Brain, Behav. Evol.* **23,** 110–120.
Raisman, G., Cowan, W.M., and Powell, T.P.S. (1965). The extrinsic afferent, commissural and association fibres of the hippocampus. *Brain* **88,** 963–997.
Raisman, G., Cowan, W.M., and Powell, T.P.S. (1966). An experimental analysis of the efferent projection of the hippocampus. *Brain* **89,** 83–108.
Ramón y Cajal, S. (1893). Estructura del asta de Ammon y fascia dentata. *Ann. Soc. Esp. Hist. Nat.* **22.**
Ramón y Cajal, S. (1901–1902). Sobre un ganglio especial de la corteza esfeno-occipital. *Trab. Lab. Invest. Biol. Univ. Madrid* **1,** 189-206.
Reber, P.J., Wong, E.C., and Buxton, R.B. (2002). Encoding activity in the medial temporal lobe examined with anatomically constrained fMRI analysis. *Hippocampus* **12,** 363–376.
Retzius, G. (1896). "Das Menschenhirn. Studien in der Makroskopischen Morphologie." Norstedt & Sohne, Stockholm.
Ribak, C.E., and Seress, L. (1983). Five types of basket cell in the hippocampal dentate gyrus: A combined Golgi and electron microscopic study. *J. Neurocytol.* **12,** 577–597.
Riley, J.N., and Moore, R.Y. (1981). Diencephalic and brainstem afferents to the hippocampal formation of the rat. *Brain Res. Bull.* **6,** 437–444.
Robertson, R.G., Rolls, E.T., Georges-François, P., and Panzeri, S. (1999). Head direction cells in the primate pre-subiculum. *Hippocampus* **9,** 206–219.
Rose, M. (1926). Der Allocortex bei Tier und Mensch. *J. Psychol. Neurol.* **34,** 1–99.

Rose, M. (1927). Die sog. Riechrinde beim Menschem und beim Aften. II. Teil des "Allocortex bei Tier und Mensch." *J. Psychol. Neurol.* **34,** 261–401.

Rosenbaum, R.S., Winocur, G., and Moscovitch, M. (2001). New views on old memories: Re-evaluating the role of the hippocampal complex. *Behav. Brain Res.* **127,** 183–197.

Rosene, D.L., and Van Hoesen, G.W. (1977). Hippocampal efferent reach widespread areas of cerebral cortex and amygdala in the rhesus monkey. *Science* **198,** 315–317.

Rosene, D.L., and Van Hoesen, G.W. (1987). The hippocampal formation of the primate brain. A review of some comparative aspects of cytoarchitecture connections. *In* "Cerebral Cortex" (E.G. Jones and A. Peters, eds.), Vol. 6, pp. 345–456. Plenum Press, New York.

Ruth, R.E., Collier, T.J., and Routtenberg, R. (1982). Topography between the entorhinal cortex and the dentate septotemporal axis in rats. I. Medial and intermediate entorhinal projecting cells. *J. Comp. Neurol.* **209,** 69–78.

Ryan, L., Nadel, L., Keil, K., Putnam, K., Schnyer, D., Trouard, T., and Moscovitch, M. (2001). Hippocampal complex and retrieval of recent and very remote autobiographical memories: Evidence from functional magnetic resonance imaging in neurologically intact people. *Hippocampus* **11,** 707–714.

Sá, M.J., Pereira, A., Paula-Barbosa, M.M., and Madeira, M.D. (1999). Anatomical asymmetries in the human hippocampal formation. *Acta Stereol.* **18/2,** 161–176.

Sakamoto, N., Michel, J.-P., Kopp, N., Tohyama, M., and Pearson, J. (1987). Substance P- and enkephalin-immunoreactive neurons in the hippocampus and related areas of the human infant brain. *Neurosci.* **22,** 801–811.

Salmon, E. (2002). Functional brain imaging applications to differential diagnosis in the dementias. *Curr. Opin. Neurol.* **15,** 439–444.

Scharfman, H.E., Witter, M.P., and Schwarcz, R. (2000). The parahippocampal region. Implications for neurological and psychiatric diseases. Introduction. *Ann. N.Y. Acad. Sci.* **911,** IX–XIII.

Schlander, M., Thomalske, G., and Frotscher, M. (1987). Fine structure of GABAergic neurons and synapses in the human dentate gyrus. *Brain Res.* **401,** 185–189.

Schwarcz, R., and Ben-Ari, Y., eds. (1986). "Excitatory Amino Acids and Epilepsy." Plenum, New York.

Scoville, W.B. (1954). The limbic lobe and memory in man. *J. Neurosurg.* **11,** 64–66.

Scoville, W.B., and Milner, B. (1957). Loss of recent memory after bilateral hippocampal lesions. *J. Neurol. Neurosurg. Psychiatry* **20,** 11–21.

Segal, M. (1977). Afferents to the entorhinal cortex of the rat studied by the method of retrograde transport of horseradish peroxidase. *Exp. Neurol.* **57,** 750–765.

Segal, M. (1979). A potent inhibitory monosynaptic hypothalamo-hippocampal connection. *Brain Res.* **162,** 137–141.

Segal, M., and Landis, S. (1974). Afferents to the hippocampus of the rat studied with the method of retrograde transport of horseradish peroxidase. *Brain Res.* **78,** 1–15.

Seltzer, B., and Pandya, D.N. (1984). Further observations on parieto-temporal connections in the rhesus monkey. *Exp. Brain Res.* **55,** 301–312.

Seltzer, B., and Van Hoesen, G.W. (1979). A direct inferior parietal lobule projection to the presubiculum in the rhesus monkey. *Brain Res.* **179,** 157–161.

Seress, L. (1988). Interspecies comparison of the hippocampal formation shows increased emphasis on the regio superior in the Ammon's horn of the human brain. *J. Hirnforsch.* **29,** 335–340.

Seress, L., and Mrzljak, L. (1987). Basal dendrites of granule cells are normal features of the fetal and adult dentate gyrus of both monkey and human hippocampal formations. *Brain Res.* **405,** 169–174.

Seress, L., Gulyás, A.I., Ferrer, I., Tunon, T., Soriano, E., and Freund, T.F. (1993). Distribution, morphological features, and synaptic connections of parvalbumin- and calbindin D28k-immunoreactive neurons in the human hippocampal formation. *J. Comp. Neurol.* **337,** 208–230.

Sgonina, K. (1938). Zur vergleichenden Anatomie der entorhinal- und Prasubikularresion. *J. Psychol. Neurol.* **48,** 56–163.

Sherlock, D.A., and Raisman, G. (1975). A comparison of anterograde and retrograde axonal transport of horseradish peroxidase in the connections of the mammillary nuclei in the rat. *Brain Res.* **85,** 321–324.

Shipley, M.T. (1974). Presubiculum afferents to the entorhinal area and the Papez circuit. *Brain Res.* **67,** 162–168.

Shipley, M.T. (1975). The topographical and laminar organization of the presubiculum's projection to the ipsi- and contralateral entorhinal cortex in the guinea pig. *J. Comp. Neurol.* **160,** 127–146.

Shipley, M.T., and Sorensen, K.E. (1975). On the laminar organization of the anterior thalamus projections to the presubiculum in the guinea pig. *Brain Res.* **86,** 473–477.

Siegel, A., Edinger, H., and Ohgami, S. (1974). The topographical organization of the hippocampal projection to the septal area: A comparative neuroanatomical analysis in the gerbil, rat, rabbit, and cat. *J. Comp. Neurol.* **157,** 359–378.

Siegel, A., Ohgami, S., and Edinger, H. (1975). Projections of the hippocampus to the septal area in the squirrel monkey. *Brain Res.* **99,** 245–260.

Šimić, G., Kostović, I., Winblad, B., and Bogdanović, N. (1997). Volume and number of neurons of the human hippocampal formation in normal aging and Alzheimer's disease. *J. Comp. Neurol.* **379,** 482–494.

Simpson, D.A. (1952). The efferent fibres of the hippocampus in the monkey. *J. Neurosurg. Psychiatry* **15,** 79–92.

Skoog, I. (2002). Magnetic-resonance imaging to assess Alzheimer's disease. *Lancet* **359,** 1538–1539.

Sloviter, R.S. (1987). Decreased hippocampal inhibition and a selective loss of interneurons in experimental epilepsy. *Science* **235,** 73–76.

Sloviter, R.S. (1994). The functional organizatin of the hippocampal dentate gyrus and its relevance to the pathogenesis of temporal lobe epilepsy. *Ann. Neurol.* **35,** 640–654.

Sloviter, R.S., Sollas, A.L., Barbaro, N.M., and Laxer, K.D. (1991). Calcium-binding protein (calbindin-D28K) and parvalbumin immunocytochemistry in the normal and epileptic human hippocampus. *J. Comp. Neurol.* **308,** 381–396.

Sobreviela, T., and Mufson, E.J. (1995). Reduced nicotinamide adenine dinucleotide phosphate-diaphorase/nitric oxide synthase profiles in the human hippocampal formation and perirhinal cortex. *J. Comp. Neurol.* **358,** 440–464.

Solodkin, A., and Van Hoesen, G.W. (1996). Entorhinal cortex modules of the human brain. *J. Comp. Neurol.* **365,** 610–627.

Soltesz, I., and Jones, R.S. (1995). The direct perforant path input to CA1: Excitatory or inhibitory? *Hippocampus* **5,** 101–103.

Sommer, W. (1880). Erkrankung des Ammonshorns als Aetiologisches moment der Epilepsie. *Arch. Psychiatr. Nervenkr.* **10,** 631-675.

Sorensen, K.E. (1985). Projections of the entorhinal area to the striatum, nucleus accumbens, and cerebral cortex in the guinea pig. *J. Comp. Neurol.* **238,** 308–322.

Sorensen, K.E., and Shipley, M.T. (1979). Projections from the subiculum to the deep layers of the ipsilateral presubicular and entorhinal cortices in the guinea pig. *J. Comp. Neurol.* **188,** 313–334.

Sorensen, K.E., and Witter, M.P. (1983). Entorhinal efferents reach the caudato-putamen. *Neurosci. Lett.* **35,** 259–264.

Spiers, H.J., Maguire, E.A., and Burgess, N. (2001). Hippocampal amnesia. *Neurocase* **7,** 357–382.

Squire, L.R. (1987). Memory: Neural organization and behavior. *In* "Handbook of Physiology" (F. Plum, ed.), Sect. 1, Vol. V, Part 2, pp. 295–371. Am. Physiol. Soc., Washington, D.C.

Stark, C.E., and Squire, L.R. (2000). Functional magnetic resonance imaging (fMRI) activity in the hippocampal region during recognition memory. *J. Neurosci.* **20,** 7776–7781.

Stephan, H. (1975). Allocortex. *In* Handbuch der mikroskopischen Anatomie des Menschen" (W. Bargmann, ed.), Vol. 4. Springer-Verlag, Berlin.

Stephan, H. (1983). Evolutionary trends in limbic structures. *Neurosci. Behav. Res.* **7,** 367–374.

Stephan, H., and Manolescu, J. (1980). Comparative investigation on hippocampus in insectivores and primates. *Z. Mikrosk. Anat. Forsch.* **94,** 1025–1050.

Steward, O. (1976). Topographic organization of the projections from the entorhinal area to the hippocampal formation of the rat. *J. Comp. Neurol.* **167,** 285–314.

Steward, O., and Scoville, S.A. (1976). Cells of origin of entorhinal cortical afferents to the hippocampus and fascia dentata of the rat. *J. Comp. Neurol.* **169,** 285–314.

Suzuki, W.A., and Amaral, D.G. (1994). Topographic organization of the reciprocal connections between the monkey entorhinal cortex and the perirhinal and parahippocampal cortices. *J. Neurosci.* **14,** 1856–1877.

Swanson, L.W. (1978). The anatomical organization of septohippocampal projections. *Ciba Found. Symp.* **58,** 25–48.

Swanson, L.W. (1982). The projections of the ventral tegmental area and adjacent regions: A combined fluorescent retrograde tracer and immunofluorescence study in the rat. *Brain Res. Bull.* **9,** 321–353.

Swanson, L.W., and Cowan, W.M. (1975). Hippocampo-hypothalamic connections: Origin in subicular cortex, not Ammon`s horn. *Science* **189,** 303–304.

Swanson, L.W., and Cowan, W.M. (1976). Autoradiographic studies of the development and connections of the septal aera in the rat. *In* "The Septal Nuclei" (J.W. DeFrance, ed.), pp. 37–64. Plenum, New York.

Swanson, L.W., and Cowan, W.M. (1977). An autoradiographic study of the organization of the efferent connections of the hippocampal formation in the rat. *J. Comp. Neurol.* **172,** 49–84.

Swanson, L.W., and Hartman, B.K. (1975). The central adrenergic system. An immunofluorescence study of the location of cell bodies and their efferent connections in the rat utilizing dopamine-beta-hydroxylase as a marker. *J. Comp. Neurol.* **163,** 467–506.

Swanson, L.W., and Köhler, C. (1986). Anatomical evidence for direct projections from the entorhinal area to the entire cortical mantle in the rat. *J. Neurosci.* **6,** 3010–3023.

Swanson, L.W., Köhler, C., and Bjorklund, A. (1987). The limbic region. I. The septohippocampal system. *In* "Handbook of Chemical Neuroanatomy" (A. Bjorklund, T. Hokfelt, and L. W. Swanson, eds.), Vol. 5, Part 1, pp. 125–277.

Swanson, L.W., Sawchenko, P.E., and Cowan, W.M. (1980). Evidence that the commissural associational and septal projections of the regio inferior of the hippocampus arise from the same neurons. *Brain Res.* **197,** 207–212.

Swanson, L.W., Wyss, J.M., and Cowan, W.M. (1978). An autoradiographic study of the organization of intrahippocampal association pathways in the rat. *J. Comp. Neurol.* **181,** 681–716.

Sybirska, E., Davachi, L., and Goldman-Rakic, P.S. (2000). Prominence of direct entorhinal-CA1 pathway activation in sensorimotor and cognitive tasks revealed by 2-DG functional mapping in nonhuman primate. *J. Neurosci.* **20,** 5827–5834.

Tomlinson, B.E., and Corsellis, J.A.N. (1984). Ageing and the dementias. *In* "Greenfield's Neuropathology" (J.H. Adams, J.A.N. Corsellis, and L.W. Duchen, eds.), 4th ed., pp. 951–1025. Wiley, New York.

Tuñón, T., Insausti, R., Ferrer, I., Sobreviela, T., and Soriano, E. (1992). Parvalbumin and calbindin D-28k in the human entorhinal cortex. An immunohistochemical study. *Brain Res.* **589,** 24–32.

Van Hoesen, G.W. (1982). The parahippocampal gyrus. New observations regarding its cortical connections in the monkey. *Trends Neurosci.* **5,** 345–350.

Van Hoesen, G.W. (1995). Anatomy of the medial temporal lobe. *Mag. Res. Imag.* **13,** 1047–1055.

Van Hoesen, G.W., and Damasio, A.R. (1987). Neural correlates of cognitive impairment in Alzheimer's disease. *In* "Handbook of Physiology" (F. Plum, ed.), Sect. 1, Vol. V, Part 2, pp. 871–898. Am. Physiol. Soc., Washington, D.C.

Van Hoesen, G.W., and Pandya, D.N. (1975a). Some connections of the entorhinal (area 28) and perirhinal (area 35) cortices of the rhesus monkey. I. Temporal lobe afferents. *Brain Res.* **95,** 1–24.

Van Hoesen, G.W., and Pandya, D.N. (1975b). Some connections of the entorhinal (area 28) and perirhinal (area 35) cortices of the rhesus monkey. III. Efferents connections. *Brain Res.* **95,** 39–59.

Van Hoesen, G.W., Hyman, B.T., and Damasio, A.R. (1991). Entorhinal cortex pathology in alzheimer's disesease. *Hippocampus* **1,** 1–8.

Van Hoesen, G.W., Pandya, D.N., and Butters, N. (1975). Some connections of the entorhinal (area 28) and perirhinal (area 35) cortices of the rhesus monkey. II. Frontal lobe afferents. *Brain Res.* **95,** 25–38.

Van Hoesen, G.W., Rosene, D.L., and Mesulam, M. M. (1979). Subicular input from temporal cortex in the rhesus monkey. *Science* **205,** 608–610.

Vargha-Khadem, F., Gadian, D.G., Watkins, K.E., Connelly, A., Van Paesschen, W., and Mishkin, M. (1997). Differential effects of early hippocampal pathology on episodic and semantic memory. *Science* **277,** 376–380

Veazey, C., Amaral, D.G., and Cowan, W.M. (1982). The morphology and connections of the posterior hypothalamus in the cynomolgous monkey. II. Efferent connections. *J. Comp. Neurol.* **207,** 135–156.

Verney, C., Baulac, M., Berger, B., Alvarez, C., Vigny, A., and Helle, K.B. (1985). Morphological evidence for a dopaminergic terminal field in the hippocampal formation of young and adult rat. *Neurosci.* **14,** 1039–1052.

Von Economo, C. (1929). "The Cytoarchitectonics of the Human Cerebral Cortex." Oxford Univ. Press, London and New York.

Wainer, B.H., Levey, A.I., Rye, D.B., and Mesulam, M.M. (1985). Cholinergic and non-cholinergic septohippocampal pathaways. *Neurosci. Lett.* **54,** 45–52.

West, J.R., Nornes, H.O., Barnes, C.L., and Bronfenbrenner, M. (1979). The cells of origin of the commissural afferents to the area dentata in the mouse. *Brain Res.* **160,** 203–216.

West, M.J. (1993). Regionally specific loss of neurons in the aging human hippocampus. *Neurobiol. Aging* **14,** 287–293.

West, M.J., and Gundersen, H.J.G. (1990). Unbiased stereological estimation of the number of neurons in the human hippocampus. *J. Comp. Neurol.* **296,** 1–22.

West, M.J., and Slomianka, L. (1998a). Total number of neurons in the layers of the human entorhinal cortex. *Hippocampus* **8,** 69–82.

West, M.J., and Slomianka, L. (1998b). Corrigendum. Total Number of Neurons in the Layers of the Human Entorhinal Cortex. *Hippocampus* **8,** 69–82.

West, M.J., Coleman, P.D., Flood, D.G., and Troncoso, J.C. (1994). Differences in the patterns of hippocampal neuronal loss in normal ageing and Alzheimer's disease. *The Lancet* **344,** 769–772.

Wilson, C.O., Isokawa-Akesson, M., Babb, T.L., Engel, J., Jr., Cahan, L.D., and Crandall, P.H. (1987). Comparative view of local and interhemispheric limbic pathways in humans: An evoked potential analysis. *In* "Fundamental Mechanisms of Human Brain Function" (J. Engel, Jr., G.A. Ojemann , H.O. Lüders, and P.D. Williamson, eds.), pp. 23–38. Raven Press, New York.

Winslow, J.B. (1732). "Exposition anatomique de la structure du corps humain." Paris.

Witter, M.P., and Amaral, D.G. (1991). Entorhinal cortex of the monkey: V. Projections to the dentate gyrus, hippocampus, and subicular complex. *J. Comp. Neurol.* **307,** 437–459.

Witter, M.P., and Groenewegen, H.J. (1984). Laminar origin and septotemporal distribution of entorhinal and perirhinal projections to the hippocampus in the cat. *J. Comp. Neurol.* **224,** 371–385.

Witter, M.P., Griffioen, A.W., Jorritsma-Byham, B., and Krijnen, J.L.M. (1988a). Entorhinal projections to the hippocampal CA1 region in the rat: An underestimated pathway. *Neurosci. Lett.* **85,** 193–198.

Witter, M.P., Room, P., Groenwegen, H.J., and Lohman A.H.M. (1988b). Reciprocal connections of the insular and piriform claustrum with limbic cortex: An anatomical study in the cat. *Neurosci.* **24,** 519–539.

Witter, M.P., Van Hoesen, G.W., and Amaral, D.G. (1989). Topograpical organization of the entorhinal projection to the dentate gyrus of the monkey. *J. Neurosci.* **9,** 216–228.

Wyss, J.M., Swanson, L.W., and Cowan, W.M. (1979a). Evidence for an input to the molecular layer and the stratum granulosum of the dentate gyrus from the supramammillary region of the hypotahalamus. *Anat. Embryol.* **156,** 165–176.

Wyss, J.M., Swanson, L.W., and Cowan, W.M. (1979b). A study of subcortical afferents to the hippocampal formation in the rat. *Neurosci.* **4,** 463–476.

Yan X., and Ribak, C.E. (1997). Prenatal development of nicotinamide adenine dinucleotide phosphate-diaphorase activity in the human hippocampal formation. *Hippocampus* **7,** 215–231.

Yukie, M. (2000). Connections between the medial temporal cortex and the CA1 subfield of the hippocampal formation in the japanese monkey (Macaca fuscata). *J. Comp. Neurol.* **423,** 282–298.

Zola-Morgan, S., and Squire, L.R. (1985). Medial temporal lesions in monkeys impair memory in a variety of tasks sensitive to amnesia. *Behav. Neurosci.* **99,** 22–34.

Zola-Morgan, S., and Squire, L.R. (1986). Memory impairment in monkeys following lesions of the hippocampus. *Behav. Neurosci.* **100,** 155–160.

Zola-Morgan, S., Squire, L.R., and Amaral, D.G. (1986). Human amnesia and the medial temporal region: Enduring memory impairment following a bilateral lesion limited to field CA1 of the hippocampus. *J. Neurosci.* **6,** 2950–2967.

CHAPTER

24

Cingulate Gyrus

BRENT A. VOGT[1], PATRICK R. HOF[2] and LESLIE J. VOGT[1]

[1]*Cingulum NeuroSciences Institute, Manlius, New York, and*
Department of Neuroscience and Physiology
SUNY Upstate Medical University
Syracuse, New York, USA

[2]*Kastor Neurobiology of Aging Laboratories, Fishberg Research Center for Neurobiology*
Department of Geriatrics and Adult Development
Mount Sinai School of Medicine
New York, New York, USA

The *cingulate gyrus* is the most prominent cortical feature on the medial surface of the human brain. It forms a cingulum or belt that extends from the lamina terminalis rostral to the anterior commissure, around the genu of the corpus callosum, over the body of the callosum, and just ventral to the splenium. The cingulate gyrus forms the dorsal component of the grand limbic lobe of Broca (1878) and has a major role in most theories of emotion (MacLean, 1993). Although it forms a single and continuous structure, the cingulate gyrus is structurally and functionally heterogeneous. Efforts to identify a structural motif that is responsible for the role of cingulate cortex in emotion and a limbic system have failed as have efforts to characterize a single cingulate function such as attention and its allocation. Because the structure of human cingulate cortex may uncover organizational principles that pertain to the entire brain, characterizing the structural heterogeneity of human cingulate cortex has been a major challenge for neuroscience.

The *cingulum bundle* is a white matter tract that underlies the cingulate cortex, and all connections entering and exiting the cingulate gyrus pass through this bundle. In addition, there are axons of passage that neither arise in the cingulate cortex nor terminate there. These pathways include projections between prefrontal and parahippocampal cortices (Nauta, 1964; Goldman-Rakic *et al.*, 1984) and projections to the median raphe nucleus that terminate in the dorsal

hippocampus (Azmitia and Segal, 1978). The cingulum bundle has been the target of neurosurgical procedures for the alleviation of chronic pain and psychiatric disorders including anxiety, major depression, and obsessive-compulsive disorder. When the primary target of the procedure is the cingulum bundle, the procedure is a *cingulumotomy*, and when the target is cingulate cortex itself and damage to the cingulum bundle is secondary to the procedure, the ablative technique is a *cingulotomy*. Finally, the term "cingulum" was used in the early part of the last millennium when Roman soldiers and clerics wore a belt or sash and woman wore an undergarment for breast support termed a cingulum. In the context of modern neuroanatomy, the cingulum bundle is the longitudinally oriented aggregate of myelinated axons that underlies cingulate cortex and looks like a belt or sash surrounding the corpus callosum when the overlying gray matter has been removed.

A *four-region neurobiological model of cingulate organization* incorporating key structure/function correlations requires the full armamentarium of neuroscience because no single methodology or theoretical framework has proven adequate to model it. Indeed, one of the jewels of cingulate neurobiology is evolving from imaging human cerebral activation under carefully controlled neuropsychological testing conditions. Even this body of work, however, cannot stand in a vacuum and must become part of a larger structure/function model. In the context of this model, regional designations are not simple statements of where activation sites are located on the gyrus. Instead, each region implicates specific cytologies, connections, functions, and disease vulnerabilities. For example, the designation perigenual anterior cingulate cortex is more than a location around the genu of the corpus callosum as is often stated in imaging studies. This region has differential inputs from the amygdala and parietal lobe, has unique projections to autonomic motor nuclei, a specific role in affect, and is selectively damaged in major depression. All these observations are an explicit part of the regional model.

The first and traditional model of the cingulate gyrus sought to localize key functions within a tripartite morphology of cortex with anterior cingulate, posterior cingulate, and retrosplenial cortices (Vogt *et al.*, 1992). In subsequent years that included a spate of human imaging research, this model was extended to the current four-region model (Vogt, 1993; Vogt *et al.*, 1997). These evolving models of medial cortical structure seek to identify the unique contributions of each of the 20 cingulate areas to particular functions. In the long run, such studies will yield a wealth of information about the mechanisms of neurodegeneration in brain diseases, the mechanisms of action of new drugs, and neurosurgical outcomes and for modulating consciousness with alternative mind/body methods.

The primary goal of this overview of the human cingulate gyrus is to characterize the cytoarchitectural features of each of its regions. In decades past, the cingulate gyrus was viewed as a relatively simple region with anterior and posterior divisions, and studies often assumed that Brodmann's (1909) maps of the medial surface were essentially correct. Recent macaque monkey connection studies, human functional imaging, and the cytoarchitectural work of Braak (1976, 1979a, b) have shown that the primate cingulate gyrus is more complex than envisioned by Brodmann. In most instances, the Brodmann areas are not cytologically uniform and do not perform a single function. This review begins with a consideration of the variations in the surface morphology of the cingulate gyrus and comments on brain maps that had a significant influence on current views of cingulate cytoarchitecture. Brodmann area "centroids" are identified, and histological features of each area shown in Nissl preparations to accommodate the lack of a full documentation supporting his maps. Most of the remaining text defines the cytological criteria for each area based on new human cases prepared for this review with immunohistochemical techniques not previously applied to the entire cingulate gyrus. During this analysis, new observations were possible, and they substantiated the evolving four-region neurobiological model of the cingulate gyrus. The cytological criteria for each area in the human cingulate gyrus are now available as are the patterns of transition that lead from adjacent allocortical areas to the fully developed isocortex. The heterogeneity of cingulate structure and function that baffled neuroscientists for generations is close to resolution, and this will provide a clear path to elucidating mechanisms of disease and their therapeutic amelioration through the study of the cingulate cortex.

SURFACE MORPHOLOGY

The surface features of human cingulate cortex are quite variable, and it is possible that each individual has his or her own "fingerprint" of medial surface features. To the extent that deep sulci are the most consistent, superficial or tertiary sulci may be excluded from surface feature classifications. Although Retzius (1896) performed the first systematic assessment of the surface cerebral morphology, the work of Ono *et al.* (1990) is more readily available and provides high-quality macrophotographs of the 25 postmortem

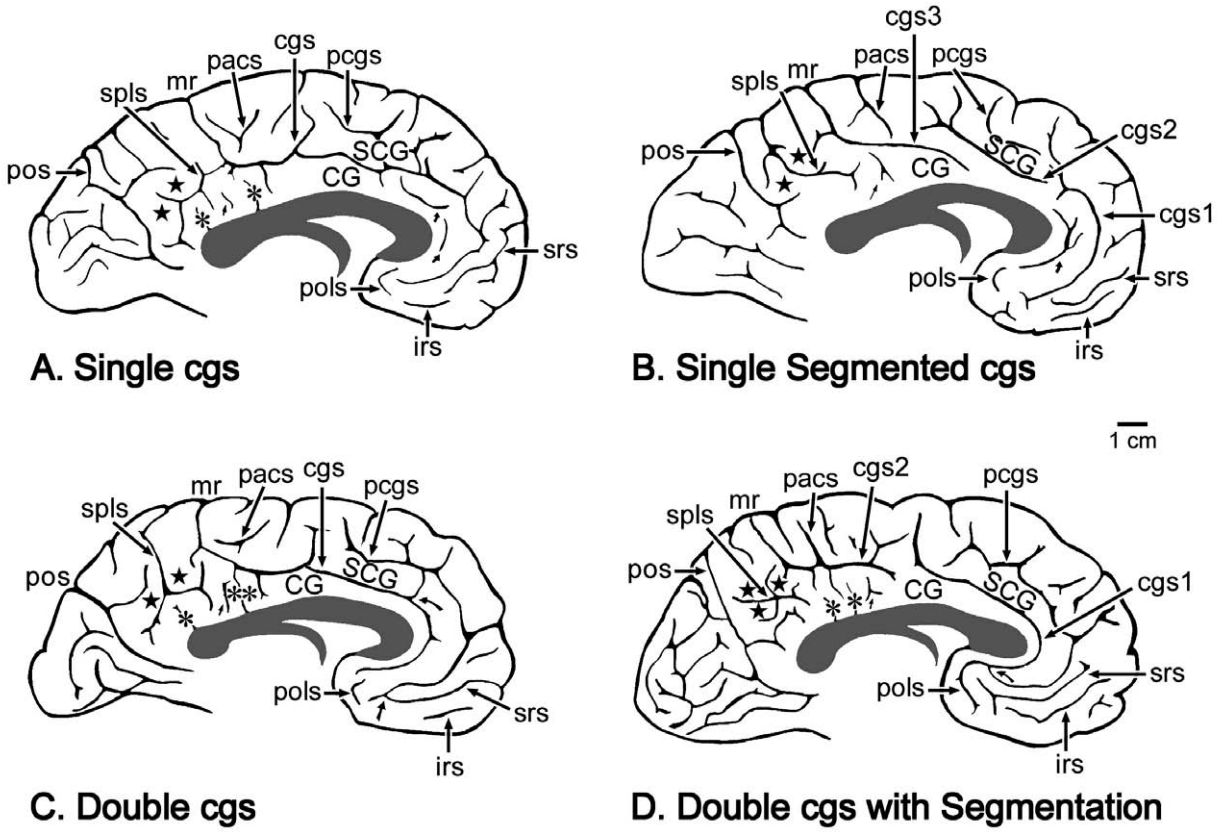

FIGURE 24.1 Sulcal patterns on the medial surface for the left hemispheres of four cases. The double parallel pattern differs from the single cgs in the extent of elaboration of pcgs. When there are just of few short branches of the pcgs, SCG cannot be identified, however, when the pcgs is fully developed, the double parallel pattern is well formed. Tertiary sulci in the anterior cingulate cortex (ACC) tend to lie parallel to the cas as shown by the short and curved arrows in A. In contrast, tertiary sulci in the posterior cingulate gyrus (PCG) are vertically oriented. Many of these sulci project directly from the callosal sulcus (cas, asterisks) and some are free (short, straight arrows). There are many connections between various sulci, however, none appear to be consistent. For example, the spls can connect with the cgs (A), the srs can connect with the pcgs (C, curved arrow), and the pcgs and cgs can attach (D). The stars around each spls identify the parasplenial sulci and are on the parasplenial lobules.

specimens in their analysis, which includes the cingulate gyrus. Ono *et al.* (1990) reported that the only large, main sulcus on the medial surface is the cingulate sulcus, which in usually not interrupted (58% of cases). The medial surface has a number of short, main sulci including the heavily branched splenial sulcus (spls) and the superior (srs) and inferior rostral (irs) sulci. Although Ono *et al.* use the term "subparietal sulcus" for the former sulcus, spls is used here because it is surrounded by dorsal and posterior cingulate area 31 and suggests an appropriate relation with the splenium. Parietal area 7m lies dorsal to area 31; thus, this sulcus is not subparietal, but rather it is intraposterior cingulate, and the cortex surrounding the spls forms folds called splenial lobules.

Although the single cingulate sulcus, with or without interruptions, is the most common form (76% on right or left hemispheres; Ono *et al.*, 1990), there are other patterns. The other most frequent pattern is the double parallel pattern where the paracingulate sulcus (pcgs) forms a long path dorsal to the cingulate sulcus (cgs). Ono *et al.* observed this in 24% of either hemisphere. Figure 24.1 presents a number of examples of these various patterns observed in our postmortem series. These include a single cgs without (Fig. 24.1A) or with (Fig. 24.1B) segmentation and the double parallel cgs without (Fig. 24.1C) or with (Fig. 24.1D) segmentation. Finally, even when the pcgs is not robust, there is a superior cingulate gyrus (SCG; Fig. 24.1).

The presence or absence of the pcgs is the primary basis for defining the single and double parallel sulcal patterns. In light of this variability, Paus *et al.* (1996) generated probabilistic maps for each hemisphere in 247 individuals and observed that the pcgs is more frequent in the left than right hemispheres. Ide *et al.* (1999) confirmed this observation by showing a significant hemispheric difference in the incidence of these two sulcal patterns. The single sulcus is more

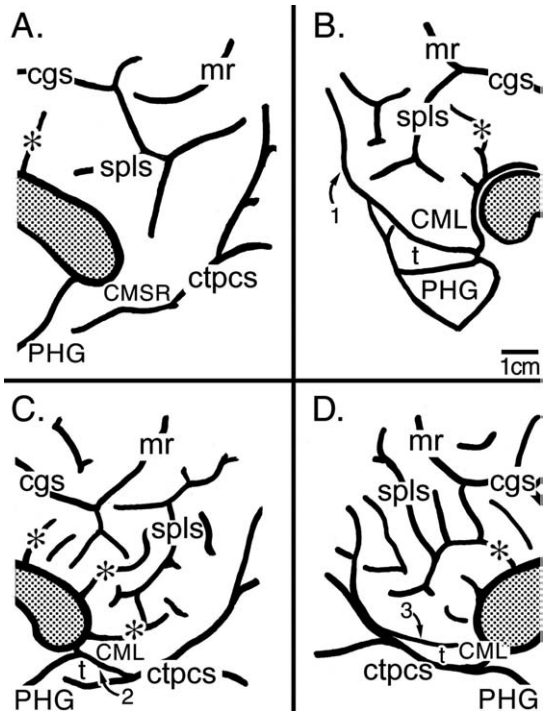

FIGURE 24.2 The perisplenial surface is shown for four cases. The asterisks identify some of the tertiary sulci that project directly from the cas and the splenium of the corpus callosum is shaded. (A) The PCG is continuous with the parahippocampal gyrus (PHG), and the caudomedial subregion (CMSR) is noted along this transition, but there is no identifying feature for the border between cingulate and parahippocampal areas. (B) Cortex below the ctpcs was removed at the arrow shown with #1, and this exposed the caudomedial lobule (CML), which is composed of the posterior cingulate areas 23 and 31. It also exposed a transitional PHGt, which contains the posterior divisions of the parahippocampal area 36′, and the PHG can be observed ventral to the PHGt. (C) Without dissection of the ventral bank of the ctpcs, the CML, PHGt, and PHG can be observed. The PHGt is formed by a branch of the ctpcs and is noted with the #2. (D) The CML is formed by the ctpcs; however, the PHGt is formed by a postsplenial dimple marked here, with the #3 and the posterior parahippocampal areas located ventral to this dimple.

frequent in the right (69%) than left (31%) hemispheres, while the double pattern is more frequent in the left (68%) than right (32%) hemispheres. Finally, Yücel *et al.* (2000) showed that males have a greater sulcal asymmetry in the left hemisphere with more prominent pcgs in 20% of males than is true for females who had a prominent pcgs in only 11% of left hemispheres.

The patterns of sulci in the posterior cingulate and caudomedial subregion are also quite variable. The angle or knee at the cgs and inflection of the marginal ramus (mr) is probably one of the deepest points in the cgs. The spls usually has two main vertical/oblique branches that are connected to form an H that can itself be connected to the cgs (Fig. 24.2A). The H form occurs in about 65% of spls in right or left hemispheres (Ono *et al.*, 1990), but many other variations have been reported including two or three branches projecting dorsally (Fig. 24.2D), connections with the cgs (Figs. 24.2A, B, D), free side branches, and branches that connect with the callosal sulcus (Cas; Figs. 24.2C, D). In light of the many vertical sulci, some projecting from the cas into the posterior cingulate gyrus, the specific morphology of the spls is of little note. Vertical sulci are a feature of most cases, and they provide for numerous interconnections between the cas, spls, and cgs. The patterns of these many vertical sulci may contribute to a relatively stable total cortical volume in this region. Brodmann (1909) used a case in which the spls had a typical pattern and showed that area 31 completely surrounds it. The vertical branches of this sulcus, however, are variable in length and can extend beyond the limits of area 31 to penetrate area 23b and sometimes area 23a. Thus, although all cases have a clear though variable spls, it does not mark the limits of particular cytoarchitectural areas. Indeed, the only gross structural feature in posterior cingulate cortex that consistently delineates a cytoarchitectural border is the cas at the apposition of the ventral apex of the CG and the cc where the border occurs between areas 23a and 30.

The surface of the posterior cingulate gyrus extends ventrally to form an isthmus with the posterior parahippocampal cortex, and the variable structure of this region is shown in Figure 24.2. In one case, a tongue of cortex provides no landmarks for transition from posterior cingulate cortex to the parahippocampal gyrus and the junctional cortex is simply termed the caudomedial subregion (Fig. 24.2A). In another case, a clear fold of tissue at the terminal part of the PCG may not be observed unless the ventral bank of the common truck is removed as at "1" (Fig. 24.2B). Upon removal of the ventral cortex, the ventral border of a lobule is noted as is a transitional fold of cortex termed the transitional PHG (PHGt or "t" in Fig. 24.2). Goldman-Rakic *et al.* (1984) referred to this consistent and terminal part of the monkey cingulate gyrus as the caudomedial lobule. When a CML is present in human cases, the common trunk of the parietooccipital and calcarine sulci (ctpos) often appears to interrupt the isthmus to form the CML (Fig. 24.2B). In other cases a branch of the ctpos extends to the cas to form a CML ("2" in Fig. 24.2C is the caudomedial branch of the ctpos). The PHGt lies ventral to the CML, in this instance, where it is formed by the terminal branch of the ctpos. In a fourth variant of CMSR, a postsplenial dimple ("3", Fig. 24.2D) extends into the CML and defines the border between posterior cingulate cortex and the transitional parahippocampal areas.

REGIONAL MORPHOLOGY: FOUR FUNDAMENTAL CINGULATE SUBDIVISIONS

Each part of the cingulate gyrus is designated according to the entire gyral surface and by its particular cytoarchitectural composition. The divisions are not based on a standardized coordinate system because each region cannot be defined with structural images. Rather, each region has specific architectures and this forms the basis for a neurobiological, structure/function model of the cingulate cortex. Traditionally, investigators identify an anterior cingulate region comprised of areas 25, 24 and 32, a posterior cingulate region with areas 23 and 31, and a retrosplenial region composed of areas 29 and 30. This approach failed to account for many observations gleaned over the past two decades and is undergoing major revisions. In the early 1990s it became clear that anterior cingulate cortex is not a single structural entity because amygdala and parietal projections into this region distinguished between its rostral and caudal parts. Figure 24.3 provides the two monkey cases that were pivotal to differentiating the organization of these two regions in primate brain. These reconstructions of the medial surface show the distribution of anterogradely labeled axon terminals throughout the CG following tritiated amino acid injections into the amygdala (Fig. 24.3A) and inferior and posterior parietal cortex (Fig. 24.3B) (Vogt and Pandya, 1987). Although the amygdala has widespread cortical connections including primary and secondary visual areas, the primary distribution of this input on the medial surface is to areas 25 and 32 and rostral area 24. There is little input to the midcingulate cortex (MCC; noted in Fig. 24.3 with two arrows) and none to the posterior cingulate cortex (PCC). In contrast, the parietal projection is massive throughout PCC and MCC but does not appreciably extend into the perigenual part of ACC. In view of the fundamentally different roles that the amygdala and parietal cortex play in brain function, it is likely that their differential projections to ACC represent a watershed boundary in ACC.

Another pivotal series of observations leading to new views of ACC were made by Heiko Braak. His primitive gigantopyramidal field (1976) was in the caudal part of ACC, and it was the first demonstration of a motor area in the cgs. This finding was corroborated in the macaque monkey when Biber *et al.* (1978) described its corticospinal projections, and later the details of somatotopically organized projections of cingulate motor cortex were described to the spinal cord (Dum and Strick, 1993) and motor and limbic cortices (Morecraft and Van Hoesen, 1992; Van Hoesen *et al.*, 1993). Heiko Braak (1979b) also detailed the pigmentarchitecture and location of the anterogenual magnoganglionaris area in the rostral sector of ACC and the visceromotor functions of subgenual cortex, and their projections to autonomic motor nuclei in the brainstem were identified by Neafsey *et al.* (1993). These cytoarchitecture and connection observations were considered from the overall perspective of cingulate organization; it was proposed that ACC be divided into a perigenual ACC (pACC) and a MCC (Vogt, 1993), the cytoarchitecture of ACC was assessed in each region in the human brain (Vogt *et al.*, 1995), and the rationale for functional distinctions along these lines was considered (Vogt *et al.*, 1997; Vogt and Sikes, 2000). The ACC duality was strengthened with numerous functional imaging studies reporting that the rostral and caudal parts of ACC provide substrates

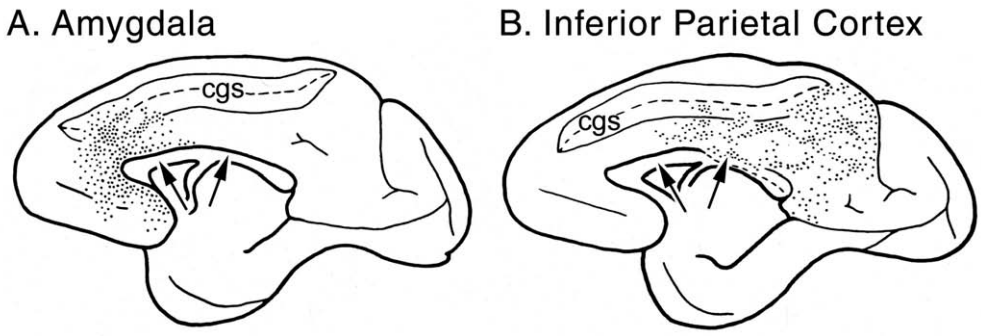

FIGURE 24.3 Differentiation of pACC and MCC by amygdala and inferior parietal cortex projections in the monkey shown with tritiated amino acid injections that label axon terminals in different parts of ACC (small dots emphasize limits of main terminal labeling). The midcingulate region is identified with two large arrows. **(A)** An injection mainly into the lateral and accessory basal nuclei of the amygdala heavily labels axon terminals throughout area 25 and the rostral part of area 24 or pACC. **(B)** An injection into inferior parietal cortex labels axon terminals throughout most of posterior cingulate cortex, and there is substantial termination in midcingulate cortex including the ventral bank of the cingulate sulcus. The details of injection location and laminar patterns of terminal labeling has been shown (Vogt and Pandya, 1987).

for different brain functions. An important delineation of these functional units was provided by Whalen *et al.* (1998) and Bush *et al.* (1998). In the former study, it was shown that the emotional-counting Stroop task activated pACC, while in the latter the counting Stroop activated MCC or their cognitive/motor region. Thus, the border between the rostral and caudal parts of ACC reflects important cytoarchitectural, connection, and functional differences. At the present time, pACC is equivalent to anterior ACC, MCC equates to posterior ACC, and each region has its own morphology. In the future the "p" will be removed and the term ACC will be used alone to refer only to the rostral part of ACC, and the four fundamental regions of cingulate cortex will be the following: ACC, MCC, PCC, and retrosplenial cortex (RSC).

The four primary cingulate regions and associated cytoarchitectural areas are shown in Figure 24.4. The pACC abuts the genu of the corpus callosum (gcc) and includes areas 25, 33, 32, and 24. Cortex ventral to the genu has also been termed subgenual or infragenual cortex and is comprised mainly of area 25 and caudoventral extensions of areas 12, 32, and 33. Because this region is likely engaged in expression of autonomic states through projections to the nucleus of the solitary tract and the dorsal motor nucleus of the vagus and the amygdala (Neafsey *et al.*, 1993), a separate subgenual subregion (SGSR) designation is provided. In view of its direct autonomic regulation and simple cytoarchitecture noted later, this region is true limbic cortex and the term "infralimbic" is not appropriate on functional or cytoarchitectural criteria.

The MCC is the middle one-third of the CG and includes the caudal parts of areas 33, 24, and 32, which are designated areas 33′, 24′, and 32′. Braak's primitive gigantopyramidal field is a caudal subdivision of area 24′ referred to as area 24d by Matelli *et al.* (1991). The MCC terminates before the inflection of the mr of the cgs. The PCC includes areas 23 and 31 on the PCG and the spls and surrounding cortex or suprasplenial lobules. The most caudal and ventral part of these areas forms the caudomedial subregion. Although the exact functions of this subregion are not known, it does have interesting connections with pACC (Vogt *et al.*, 1987; Fig. 24.5E, F, H) and is co-activated with the latter region in auditory-verbal memory tasks (Grasby *et al.*, 1993). RSC is areas 29 and 30, and they extend around the splenium of the corpus callosum (scc) and abut parahippocampal areas ventral to the ventral edge of the scc. Finally, PCC is not equivalent to the PCG because the ventral bank of the PCG contains RSC. Thus, the PCG comprises retrosplenial areas 29 and 30 in the cas, PCC on the posterior gyral surface with areas 23a/b and area 31 surrounding the spls,

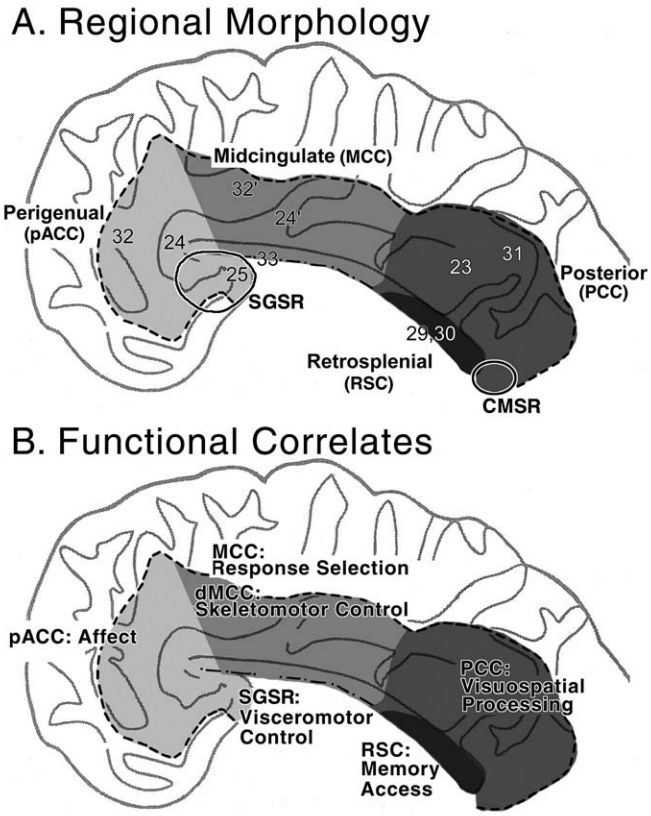

FIGURE 24.4 Four-region neurobiological model of the organization of the human cingulate gyrus. The model requires close correlations among the topology of cytoarchitectural areas, major afferent connections, regional composition, and functional properties. **(A)** pACC is comprised of areas 25, 33, 24, and 32 and includes a subgenual subregion. MCC includes areas 33′, 24′, 24d, and 32′, the PCC is areas 23 and 31 and the caudomedial subregion, and the RSC is areas 29 and 30. **(B)** The functional correlates are not derived from a single class of research, but rather a range of studies including electrical stimulation, stroke case reports, neuropsychological studies in monkey, and human functional imaging. In addition to the four regions, there are two subregions in pACC and MCC. These include the visceromotor control cortex in SGSR and the skeletomotor control subregion in dorsal MCC (dMCC). The dMCC includes area 32′ and the cingulate motor areas on the dorsal and ventral banks of the cingulate sulcus.

and area 23c in the depths of the PCG (i.e., the ventral part of the mr). Posterior cingulate cortex in the human refers to cortex on the gyral surface and that in the caudal part of the CG.

FUNCTIONAL CORRELATIONS OF THE FOUR CINGULATE REGIONS

The neurobiological model of cingulate cortex requires that each cytoarchitectural area and region be associated with different functions or structure/

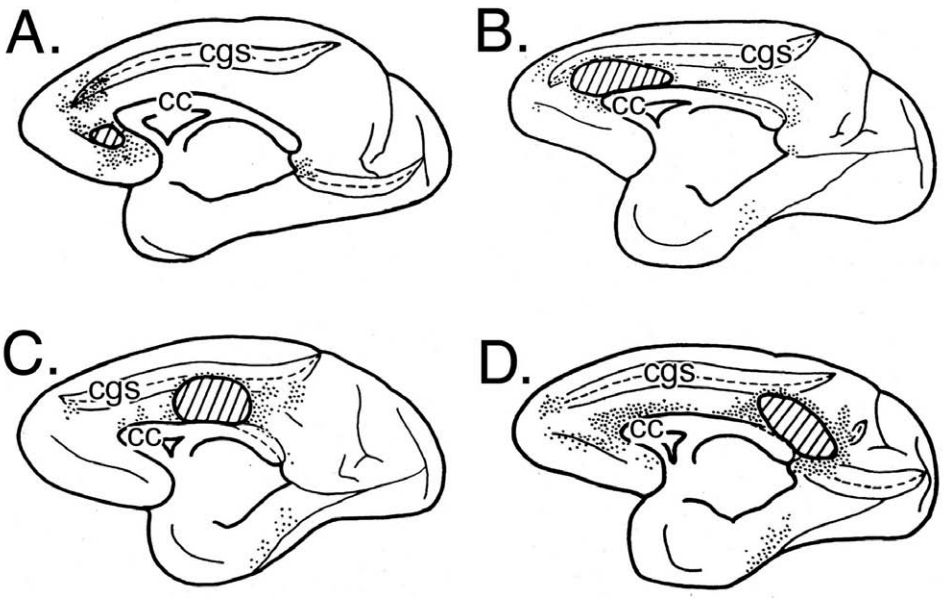

FIGURE 24.5 Four cases in which horseradish peroxidase was injected into the monkey cingulate gyrus and retrogradely labeled neurons plotted on the medial surface (each dot ≈ 3–5 labeled neurons). The intracingulate connections support substantial interactions between pACC and PCC (A, B, D), while the MCC (C) tends to have much less interaction with either of these regions.

function correlations. This does not imply that there is no functional overlap; rather, it means that each structurally distinct area makes a functionally unique contribution to brain activity. Identification of the cytoarchitectural border between areas 24 and 24′ (Vogt *et al.*, 1995) followed by its identification with functional imaging (Whalen *et al.*, 1998; Bush *et al.*, 1998) validates the importance of the neurobiological model based on structure/function correlations. Figure 21.4B presents the neurobiological model in the morphological context of four cingulate regions. As previously suggested (Vogt *et al.*, 1997), pACC is involved in affect, SGSR in visceromotor control, MCC in response selection including dMCC in skeletomotor control, PCC in visuospatial processing, and RSC in memory access.

Perigenual ACC and Subgenual Subregion in Affect

The perigenual areas are associated with affective experiences and are directly engaged in autonomic regulation. Electrical stimulation of dorsal perigenual cortex in humans produces fear, pleasure, and agitation (Meyer *et al.*, 1973). The most frequent response in this series was intense or overwhelming fear including one individual who reported the feeling that death was imminent. Electrical stimulation of different parts of ACC evokes different responses in epilepsy patients (Bancaud and Talairach, 1992). Stimulation of pACC produced the report, "I was afraid and my heart started to beat," whereas stimulation of MCC evoked the report, "I felt something, as though I was going to leave." The former report is of pure fear, while the latter is one of an early premotor planning with motivational characteristics. In another series of experiments, the SGSR had elevated blood flow when healthy women recalled sad experiences (George *et al.*, 1995) and the dorsal pACC had elevated blood flow when subjects were involved in a face recognition task and the faces expressed emotional content (George *et al.*, 1993). Finally, autonomic activity is a frequent correlate of emotional behaviors, and visceromotor changes are the most consistent responses evoked by electrical stimulation of areas 24 and 25. In humans these responses include increases and decreases in respiratory and cardiac rate and blood pressure, mydriasis, piloerection, and facial flushing (Pool, 1954; Escobedo *et al.*, 1973; Talairach *et al.*, 1973). Visceral responses include nausea, vomiting, epigastric sensation, salivation, or bowel or bladder evacuation (Pool and Ransohoff, 1949; Lewin and Whitty, 1960; Meyer *et al.*, 1973).

Perigenual ACC has important connections with structures that directly regulate autonomic activity. Area 25 projects to brainstem autonomic nuclei and has been termed the visceromotor control region by Neafsey *et al.* (1993). Projections of area 25 include those to the nucleus of the solitary tract, the dorsal motor nucleus of the vagus, and the sympathetic thoracic intermediolateral cell column. There are also projections to the periaqueductal gray and reciprocal connections with the amygdala, and detailed references for each projection have been provided (Vogt *et al.*, 1997); each of these connections likely contributes to the role of pACC in affect and autonomic regulation.

MCC in Response Selection

The MCC has a pattern of organization similar to pACC. Thus, pACC is primarily involved in affect, and it implements emotionally relevant, autonomic activity directly through the projections of area 25 to the various brainstem autonomic motor nuclei. In a similar way, MCC has a general role in response selection based on the motivational relevance of particular behaviors, and it implements these behaviors through cingulospinal and cortical motor and supplementary motor projections that arise in the cingulate motor areas. It is this fundamental dichotomy in which pACC regulates autonomic function and MCC regulates skeletomotor function that underpins the division of ACC into two parts.

Different functions have been ascribed to the MCC including attention-for-action (Posner *et al.,* 1988), response selection (Corbetta *et al.,* 1991; Bench *et al.,* 1992; Paus *et al.,* 1993), error detection (Gemba *et al.,* 1986), competition monitoring (Carter *et al.,* 1998), anticipation (Murtha *et al.,* 1996), and working memory (Petit *et al.,* 1998). Although it may be possible to accommodate all these functions with a single model of one area that incorporates many separate populations of neurons, the facts of cingulate cortex organization that suggest these various functions represent the activity in at least two divisions of MCC. Thus, MCC itself is composed of two subregions: the dMCC in the cgs that extends onto the superior cingulate gyrus and another on the surface of the CG.

The dMCC areas in the cgs have very large layer Vb neurons (Braak, 1976), project to the spinal cord (Biber *et al.,* 1978; Dum and Strick, 1993) and supplementrary and primary motor and limbic cortices (Morecraft and Van Hoesen, 1992; Van Hoesen *et al.,* 1993) and account for the many skeletomotor responses evoked by electrical stimulation. These latter responses include gestures such as touching, kneading, rubbing, or pressing the fingers or hands together and lip puckering or sucking (Escobedo *et al.,* 1973; Meyer *et al.,* 1973; Talairach *et al.,* 1973). These movements are often adapted to the environment; they can be modified by sensory stimuli and, at times, resisted. These areas contain neurons with premotor discharge properties (Shima *et al.,* 1991) that are coded according to the changing reward properties of particular behaviors (Shima and Tanji, 1998). Functional imaging studies show altered blood flow in this region during sequences of finger apposition movements (Schlaug *et al.,* 1994; Kwan *et al.,* 2000).

The dMCC, however, is not limited to regulating discrete motor activities, and functional imaging studies show that it has a major role in cognitive activity associated with the response selection process and not necessarily resulting in movement. Cognitive processes associated with divided attention (Corbetta *et al.,* 1991), selecting verbs to novel lists of nouns (Raichle *et al.,* 1994; Raichle, 2000), and Stroop interference tasks (Pardo *et al.,* 1990; Bench *et al.,* 1992) elevate blood flow in dMCC. Furthermore, generation of verbs to novel lists of nouns not only elevates flow in MCC but, as the task is practiced, blood flow returns to baseline in MCC, it is decreased in pACC, and PCC and medial parietal area 7m show an increase in activity (Raichle, 2000). Most importantly, altering the reward properties of particular outcomes elevates blood flow in dMCC (Bush *et al.,* 2002), and we predict that dMCC plays a pivotal role in reorganizing activity in a host of motor structures to produce new behavioral outputs that adapt to changing rewards. Thus, patterns of neuronal activity in the cingulate cortex reflect the differential contributions of each region to different aspects of task acquisition and performance as well as cognitive processing in the absence of movement.

Posterior Cingulate, Caudomedial, & Retrosplenial Cortices in Visuospatial/Memory Functions

Valenstein *et al.* (1987) presented a case with extensive anterograde and retrograde amnesia following removal of an arteriovenous malformation near the splenium and referred to the syndrome as *retrosplenial amnesia*. Since involvement of the fornix may have contributed to the presentation in this case, Parker and Gaffan (1997) placed massive cingulate cortical or anterior thalamic lesions in monkeys and tested object-in-place memory. Although cingulate lesions failed to show a significant deficit, there was substantial impairment in the anterior thalamic group. Because the anterior thalamic nuclei have as their primary projection to the RSC (Vogt *et al.,* 1987), it is surprising that no deficit was observed following cortical lesions. Explanations for the negative finding in the monkey are that the cortical lesions of RSC were incomplete owing to the effort to remove the entire gyrus in anterior and posterior cortices and/or the task was not sensitive to a cortical impairment. Other evidence links these cingulate gyral areas to memory and visuospatial functions.

Working memory tasks elevate glucose metabolism in the anterior thalamic nuclei (Friedman *et al.,* 1990), one of the highest levels of basal glucose metabolism in the monkey brain is in RSC, and glucose metabolism in RSC is elevated when performing a delayed-

response task (Matsunami *et al.*, 1989). We have compared the distribution of anterior thalamic inputs to RSC and basal glucose metabolism in the monkey, and there is a striking correlation between both (Vogt *et al.*, 1997). The tight link between anterior thalamic projections to RSC, high levels of basal glucose metabolism, and its modulation in both structures suggest that the anterior thalamic/RSC system is a pivotal player in memory.

Area 23a and RSC are adjacent to each other and reciprocally connected (Vogt and Pandya, 1987), and relationships between perigenual and perisplenial cortices are profound. Area 23a is heavily labeled following a horseradish peroxidase injection into pACC (Fig. 24.5A), and pACC is labeled after injections of anterograde tracers into posterior area 23 (Pandya *et al.*, 1981). Thus, the perigenual and perisplenial connection is reciprocal and involves only a small part of MCC as shown by tracer injections into different parts of the CG (Fig. 24.5B–D). It appears that the most profound intracingulate connections in these cases are reciprocal connections between pACC and PCC/CMSR, and it is possible that activation of both of these regions with a common auditory input (Grasby *et al.*, 1993) is strengthened by these reciprocal intracingulate connections. The linkage between pACC and the CMSR is even tighter when other cortical connections are considered. A limbic convergence zone in area 11m receives major inputs from both perigenual and perisplenial cortices with none from MCC (Carmichael and Price, 1995). Pericallosal cortex in both regions also receives direct subicular inputs that do not terminate appreciably in MCC (Rosene and Van Hoesen, 1977). Thus, primary sensory inputs, reciprocal intracingulate connections, and connections among limbic association areas preserve the functional integration of perigenual and perisplenial cortices to the exclusion of MCC.

The RSC and PCC are also involved in topographic and topokinetic memory. Olson *et al.* (1993) suggested that PCC is involved in large visual scene assessment, part of which is subserved by activity generated by the orbital position of the eye. Focal lesions that involve the right RSC impair memory of spatial positional relationships and are associated with topographic disorientation (Takahashi *et al.*, 1997). Furthermore, mental navigation along memorized routes elevates blood flow in PCC (Berthoz, 1997; Ghaem *et al.*, 1997; Maguire *et al.*, 1998). Thus, PCS, CMSR, and RSC have many interconnections that subserve memory and visuospatial functions, and their close relations to pACC suggest a coupling of the activity in these regions. It is possible, for example, that memories associated with emotional states are stored in pACC but their release for conscious consideration is mediated by the activity of RSC, PCC, and/or CMSR that have no specific role in emotion.

MAPS OF CINGULATE AREAS

Four maps of the areas on the human CG have been published over the past century that have been particularly important to understanding this region. von Economo and Koskinas (1925) identified areas LA2 and LA that share similarities with the distributions of pACC and MCC, and they viewed transitional changes on the medial surface as reflecting fundamental differences in the frontal lobe. Although Brodmann stated that area 32 is a dorsal and anterior cingulate area (1909), this area has transitional features that might also be termed cingulofrontal transition cortex. Areas LC1 and LC2 appear to be similar to Brodmann areas 31 and 23, although LC2 extends further rostrally than does area 23, while areas LD and LE are retrospelenial areas on the ventral bank of the CG. Finally, von Economo and Koskinas (1925) identified anterior ectogenual area LA3 and ectosplenial area LF that equate to Brodmann's areas 33 and 26, respectively.

The map of Sarkisov *et al.* (1955) identified parallel, ventral-to-dorsal subdivisions of areas 24 and 23 in human, and we observed them in monkey (Vogt *et al.*, 1987) and later in human (Vogt *et al.*, 1995). The major difference is that we observe only two gyral parts of each area (i.e., areas 24a and b and 23a and b), and the third subdivisions of each are areas 24c and 23c in the cgs. Area 23c is a caudal extension of cingulate sulcal cortex and we agree with Brodmann that area 31 surrounds the spls where this cortex forms the splenial lobules.

Brodmann (1909) discussed an intermediate cingulate area that might be similar to our MCC; however, he did not plot it on his map, he provides no unique subdivision of human area 24, and there is no histological description available comparing this region with rostral parts of ACC. Later we provide precise cytological information about the MCC region (i.e., not just a transitional zone where the cytoarchitecture is hard to define), relate this cortex to adjacent regions with immunohistochemical methods, employ a unique nomenclature, and plot the distribution of its areas.

Heiko Braak (1980) made a number of very important contributions to understanding cingulate cytoarchitecture. First, his map shows the prominent anterogenual magnoganglionic area in pACC, which suggests that the perigenual part of Brodmann's area 24 is distinct from its caudal extent. Indeed, it is

possible that the differences are responsible for a fundamental pattern of cortical differentiation as proposed by Braak. Second, the primitive gigantopyramidal field is located in the cgs and forms a cingulate motor area with corticospinal projections. Third, the retrosplenial areas are located on the ventral bank of the CG in the depths of the cas, while parasplenial isocortex surrounds RSC. It appears that parasplenial isocortex closely approximates, but is not equivalent to, area 23a.

The Brodmann map has become the most frequently used reference in human neuropathology and imaging studies partially because Talairach and Tournoux (1988) extrapolated it onto a standardized brain atlas. There are difficulties interpreting the Brodmann map because it was limited to a single case and the reconstruction was onto the convoluted cortex without delineation of areas in the sulcal depths, which accounts for about 50% of the cortical volume. To document Brodmann's views histologically, Figure 24.6 shows his map and the six circles reference points that are the topographic center of each area. These points were photographed at low magnification in the approximate center of each area in a case embedded in celloidin and stained with cresylecht violet. This centroid analysis serves as the basis for modifications made later to define structurally uniform subareas. In some instances, there is doubt as to which structure constituted a Brodmann area. For example, his area 33 could refer to an ectogenual area in the depths of the cas, it could refer to an area on the edge of the ventral bank of the CG (our area 24a), or it could be a combination of both. In this instance, we concur with Zilles (1990) in suggesting that it is an ectogenual area.

The Brodmann area centroids were located from his map by finding the approximate rostrocaudal and dorsoventral midpoint for each area and in equivalent locations in a celloidin-embedded/Nissl-stained case (Fig. 24.6). Area 33 wraps completely around the gcc and is likely an ectogenual area with a single layer of pyramidal neurons that abut the indusium griseum (IGr) and area 24 ventrally (Fig. 24.6A, B, D). Area 25 is agranular (lacks a layer IV) and has two principal layers of neurons; a superficial layer II/III that is relatively uniform in its density of medium-sized pyramidal neurons and a deep pyramidal layer of medium-large pyramids similar to those mainly in layer V; only a small layer VI is present (Fig. 24.6A). One of the most consistent features of cingulate architecture is the prominence of layer V, and the relative prominence of layer Va is most evident in area 24 (Fig. 24.6B/D, asterisks). Finally, area 32 is a dorsal, anterior cingulate area that surrounds rostral and dorsal area 24 and is dysgranular with a thin and variable layer IV (Fig. 24.6B/C).

The PCG is comprised of two regions, retrosplenial areas 29 and 30 on the ventral bank and posterior cingulate areas 23 and 31 on the cingulate gyral surface and depths of the caudal cgs. The ectosplenial area 26 is located at the fundus of the cas. Ectosplenial cortex is essentially a single, external layer of neurons that have a granular appearance and are similar to neurons in the external granular layer of retrosplenial area 29. Area 29 has a granular external pyramidal layer and undifferentiated layers V and VI (Fig. 24.6F). Brodmann referred to area 30 as "agranular," a concept that is challenged later. Finally, area 23 on the PCG surface is granular, while area 31 surrounds the spls and has the thickest and most granular layer IV in PCC (Fig. 24.6F and E, respectively). If immunohistochemical, connection, and functional studies observed homogeneity within each of these Brodmann areas, nothing more would need to be said about the architecture of the cingulate gyrus. However, almost none of the Brodmann areas are cytologically uniform, and a century of neuroscience requires a substantive modification.

CYTOLOGY OF CINGULATE AREAS

Before analyzing the details of cortical structure, a few overview comments will set the context for such an undertaking. First, although the border between areas 24 and 23 is not marked with a sulcus, this border comprises a fundamental change from an agranular anterior cortex to the granular posterior cortex. The presence of a layer IV in PCC suggests that there is an intermediate level of cortical processing between thalamic and cortical afferents that does not occur in MCC. The anterior areas have thalamic and cortical projections directly to the basal dendrites of layer III and the apical dendrites of layer V pyramidal neurons—presumably for more rapid processing and output functions (Vogt and Peters, 1981). Second, interpretation of cingulate cytoarchitecture is most productive in the context of cortical transition along the CG. This includes different cytological changes such as increases in neuron density in rostrocaudal and ventrodorsal directions, progressively greater expression of neurofilament proteins in layer IIIc pyramids and their "predecessors" in deep layer III, and elaboration of the basal dendrites of pyramidal neurons particularly in layers III and V throughout the retrosplenial areas. Third, although the Nissl stains were used productively over the past century, modern immunohistochemical techniques provide significant advancements. The antibody for neuron-specific nuclear binding protein (NeuN; Mullen *et al.*, 1992) is

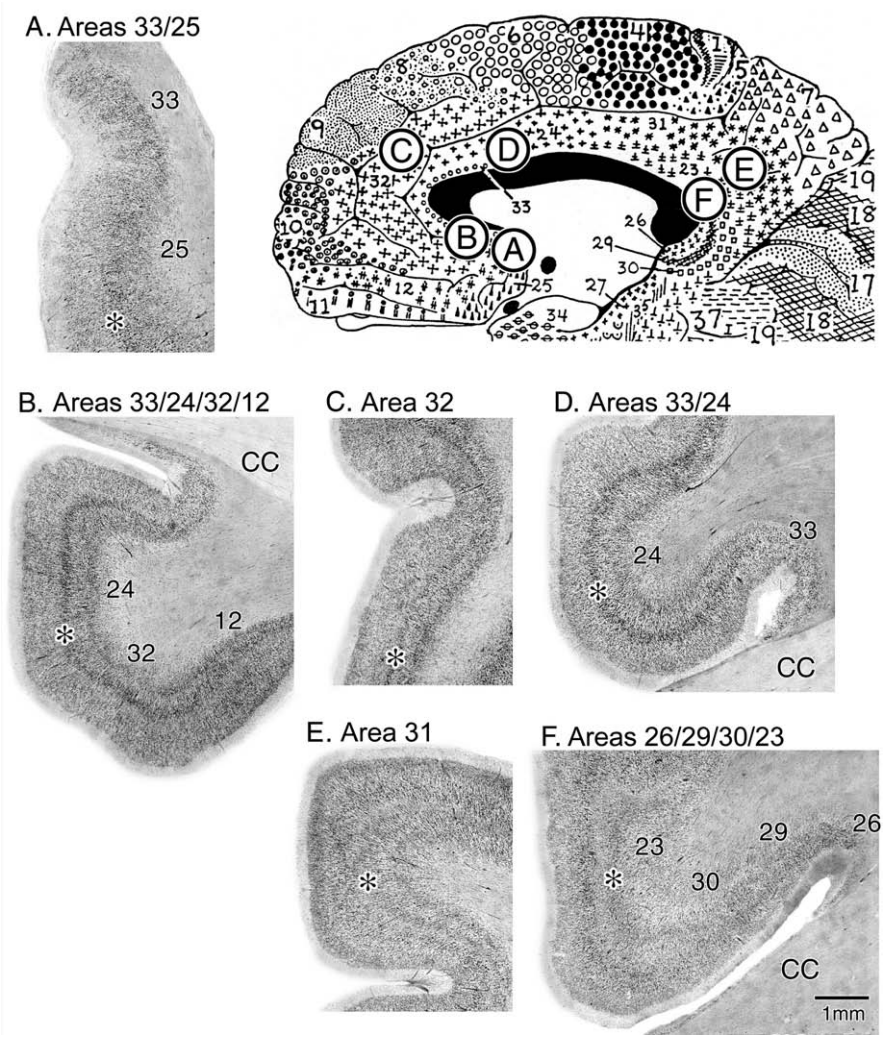

FIGURE 24.6 The Brodmann map (1909) is the most influential map of the medial surface. To assess the structure of each of these areas in celloidin-embedded and Nissl-stained sections, centroids (approximate centers) were identified for the major areas and photographed for levels A–F. The corpus callosum (cc) and layer V (asterisks) are identified and these centroid photographs provide benchmarks to which each cytoarchitectural area is compared in immunohistochemical preparations.

an important tool because it labels neurons and does not react with glial and vascular elements that add noise to the analysis of neuronal architectonics. In addition, the immunoreactivity is so intense that photographs have a high degree of contrast, and the laminar architecture can be shown with greater clarity at low magnifications than with Nissl staining. Another important antibody is SMI-32 for nonphosphorylated, intermediate neurofilament proteins (NFP-ir). This antibody is a valuable marker of unique neuronal phenotypes, and it is invaluable for identifying particular layers and area borders. It is most helpful in the granular layer of retrosplenial and ectosplenial cortices, layer IIIc in PCC, and layer Va throughout the entire cingulate gyrus including the cingulate motor areas in the cingulate sulcus.

Ectocallosal Region

The ectocallosal region is in the fundus of the entire callosal sulcus and is comprised of areas 33, 33′, and 26. Brodmann showed that area 33 surrounds the rostral one-third of the corpus callosum beginning in the subgenual subregion where it abuts area 25 and continues around the cc to terminate dorsal to the genu. Although he depicted area 26 as surrounding only the caudal end of the splenium and not abuting area 33 rostrally, these observations cannot be verified. Indeed, area 33 extends further caudally in the form of area 33′, area 26 extends rostrally above the splenium, and area 33′ and 26 abut each other at midcingulate levels in the form of an undifferentiated cortex. The ectocallosal areas are shown in Figure 24.7.

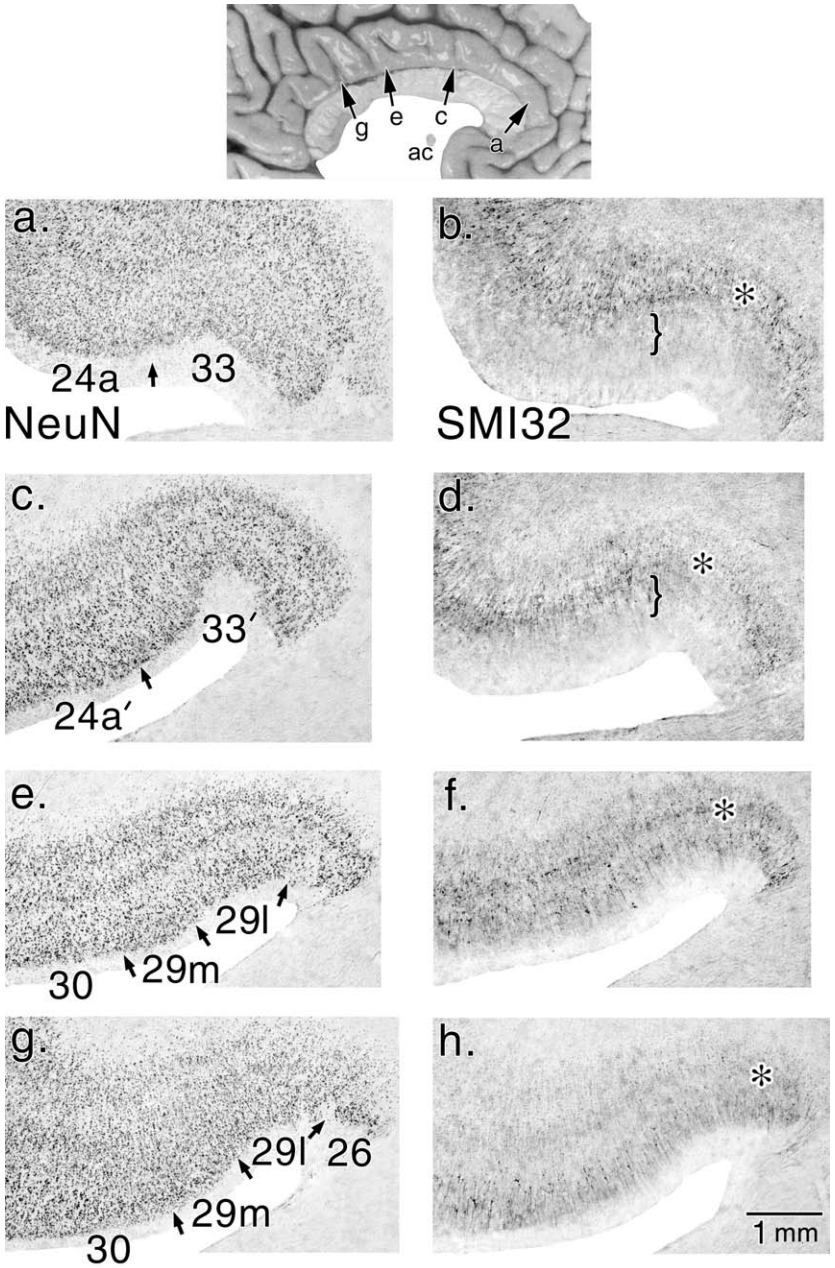

FIGURE 24.7 Ectocallosal areas immunoreacted with the NeuN and SMI32 antibodies. The levels begin rostrally just dorsal to the genu and extend to a caudal level. The asterisks indicate layer Va, and the bracket in d emphasizes that neurons in the deep part of layer III of area 33′ are NFP-ir, which serves as the basis for designating a caudal division of area 33. An undifferentiated area 29 appears in e and is identified by the substantially enhanced NFP in layer III that is not in areas 33′ or 24a′. An undifferentiated ectocallosal cortex continues along the full length of the cc.

Area 33 has broad and poorly differentiated layers II and III, a layer V with a moderate number of NFP-ir pyramids, and a layer VI of small neurons (Fig. 24.7a, b). There is an ectocallosal area in the depths of the cas at a midcingulate level (Fig. 24.7c, d.), but it has features that differentiate it from area 33. Area 33′ has a more clearly laminated structure, and layers II and III are thinner and contain somewhat smaller neurons, while the large neurons in the deep part of layer III are NFP-ir, as is not the case for area 33 (compare Fig. 24.7b and c in brackets). Finally, a small number of layer V neurons are NFP-ir, as is the case for area 33.

At a level just caudal to the midpoint in the cc (Fig. 24.7e), the external pyramidal layer contains small neurons with a granular appearance suggesting that this is one of the most rostral levels of area 29. There is a striking NFP-ir in pyramids throughout layer III of areas 29 and 30, and layer Va has many more NFP-ir pyramids than is the case for either area 33 or 33′. It is interesting that, at this rostral level of area 29, the neurons in the granular layer have not yet fully expressed NFP-ir as they do at caudal levels (e.g., Fig. 24.7h). It is also difficult at this transitional level of Figure 24.7e to identify the features of either area 33′ or area 26. Therefore, this poorly differentiated cortex lateral to area 29 is not designated in the figure. It appears that rather than a loss of ectosplenial cortex between areas 33′ and 26, there is a short distance of poorly differentiated and transitional cortex. The granular layer of area 26 and its heavily NFP-ir pyramids are shown in Figure 24.7g–h. Area 26, however, has almost no deep ganglionic pyramidal layer, and Braak (1979a) referred to these few neurons as essentially a layer VI of multiform cells. The few, deep-lying pyramids that are present express NFP-ir. The differentiation and extension of areas 29 and 30 along the ventral bank of the cingulate gyrus is also seen in Figure 24.7 but is described in more detail later as is the extension of area 26 around the splenium of the cc (Fig. 24.15). Thus, the ectocallosal areas form the fundus of the full rostrocaudal extent of the cas. Only at a level just caudal to the callosal midpoint is there a short stretch of undifferentiated cortex lacking the features of either areas 33′ or 26.

Perigenual Areas

The subgenual subregion is comprised of areas 33, 25, and 24a and the caudal extension of area 32. Area 25 is the principal component of this region and is of particular interest because of its projections to autonomic brainstem nuclei and its role as a visceromotor control region. The architecture of area 25 differentiates directly from area 33 (Figs. 24.7a, and 8A) where the broad and undifferentiated pyramidal layer of area 33 abuts area 25 and there is a broad and relatively uniform layer II/III of medium-sized pyramids. There is a slight intensification of layer Va in terms of both size and density of pyramidal neurons and a poorly differentiated layer VI. Small islands of layer II pyramidal neurons in caudal levels of area 25 have been observed (Vogt *et al.*, 1997); however, this feature is variable. Figure 24.8 shows two levels through this subgenual region. It appears that the dorsal and rostral parts of this cortex have the aggregations of neurons in layer II. Because this clumping is not a characteristic of area 24, this cortex is termed rostral area 25 (25r). Braak (1979b) referred to this as area anterogenualis simplex. There also appears to be scattered clumping of layer II neurons in area 33 in this subgenual region. Caudal to area 25r is the area Brodmann appears to have termed area 25. Figure 24.8B shows that this area has a clear layer II that is negative for NFP-ir. It has a layer III of medium-sized pyramids that are sparsely immunoreactive for NFP, a layer V of slightly larger neurons that are NFP-ir, and a layer VI of small neurons. Overall, this area is quite compact in comparison to area 25r. Because this area is caudal to area 25r, it is termed area 25c and equates to Brodmann's area 25.

Area anterogenual magnoganglionaris was identified by Braak (1979b) as a feature of cortex rostral to the genu. This provided one of the early arguments that area 24 does not surround the genu from its supracallosal position with a single architecture. Indeed, the broad layer Va of large pyramids that distinguishes this area 24b in pACC can be seen in Figure 24.9. Rostral and ventral to area 24b are areas 32 and 12. It is possible to identify components of areas 24a and 24b that have these magnocellular features, and this is one of the primary distinctions between rostral and caudal divisions of area 24 (i.e., area 24 vs. area 24′).

Area 24 architecture is shown in Figure 24.9 at a perigenual level. In the low-magnification photograph, the primary differences between areas 24a and 24b can be seen; area 24a has a less-dense layer II, thinner and less-dense layer Va, and a broad and less-neuron-dense layer VI when compared to area 24b. Each of these features are magnified where the subdivisions of layers V and VI are apparent as are a number of features of area 24b. The NeuN-ir section shows an interesting feature for both areas 24a and 24b and, as is noted later, for area 24′. Although layer III is not divisible with medium-sized neurons in the upper, large, and NFP-ir neurons in the deeper part, this layer does have neuron-dense-superficial and -sparse-deep parts. This fact is noted in Figures 24.9 and 24.10 with pairs of arrows between the NeuN and SMI32 sections. Another important feature of area 24b is that it has many small neurons intermingled with the large ones in layer Va. The neurons in layer Va tend to form aggregates and are NFP-ir. Layer Vb SMI32 immunostaining is magnified by a factor of 2 to show that neurons in this layer also form aggregates (asterisks); they are NFP-ir. Among these layer Vb neurons are the NFP-ir, spindle neurons of Nimchinsky (Nimchinsky *et al.*, 1995). These neurons are bipolar projection cells that are unique to limbic cortex including the insula; they are observed in human and great ape brains but not in monkeys (Nimchinsky *et al.*, 1999). Finally,

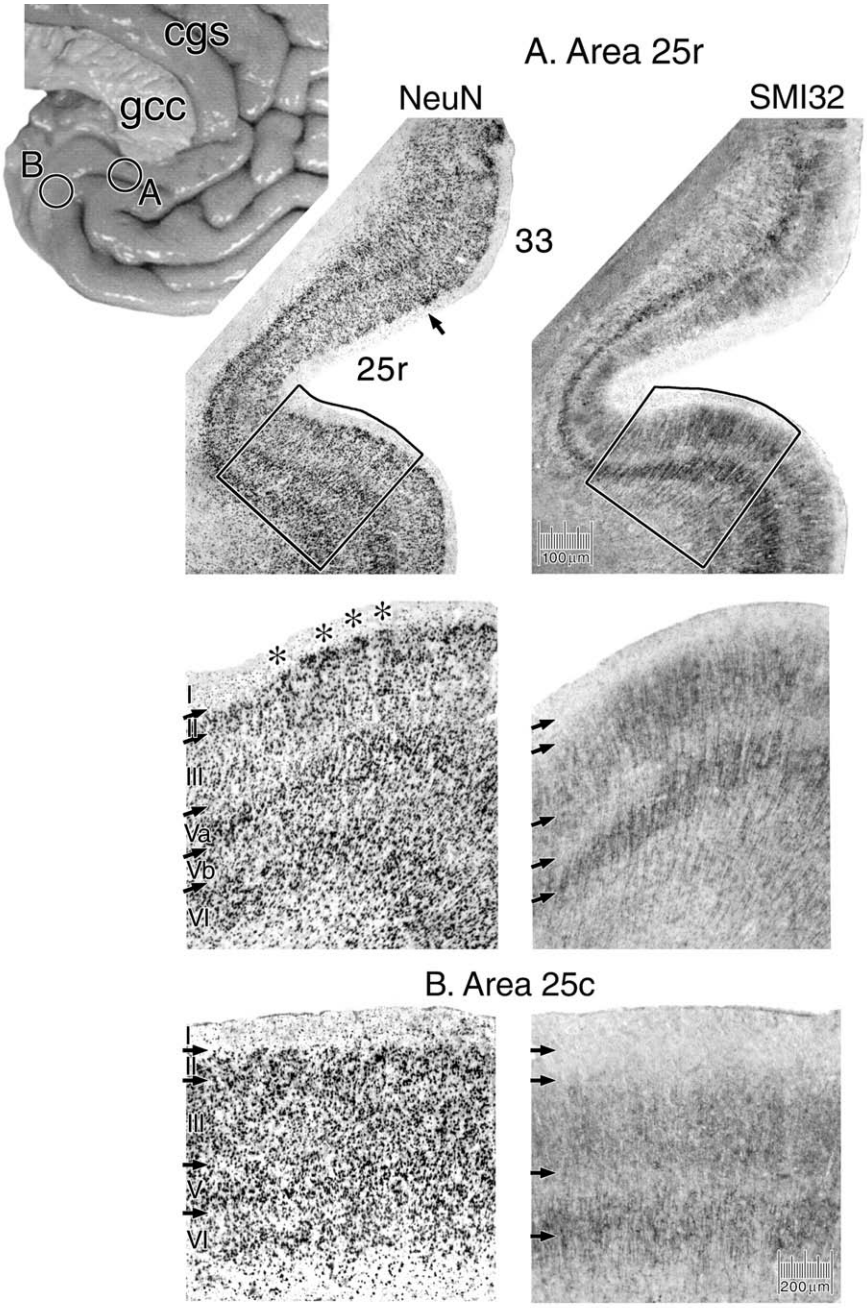

FIGURE 24.8 Area 25 is one of the main components of the SGSR, and its cytology is not uniform. The rostral part of area 25 (area 25r) is ventral to ectogenual area 33 and has some neuron aggregations in layer II and dense NFP-ir neuronal plexuses in layers III and V. Area 25c has a less differentiated structure with no subdivisions in layers III and V, a modest number of NFP-ir neurons in layer V, and few in layer III.

although layers Va and Vb are less neuron dense in area 24a, a similar clumping of NFP-ir pyramids is in both of these layers, but it is most prominent in layer Vb including the spindle neurons. These features of layer V distinguish area 24 from its caudal counterpart area 24′.

Midcingulate Gyral Areas

One of the primary features of MCC is the cingulate motor areas in the cingulate sulcus. Although this region has extensive connections with motor systems including direct projections to the spinal cord, the sulcal and gyral areas are not independent and may operate jointly under some circumstances. Pivotal to these interactions are direct and reciprocal connections identified in the monkey brain with anterograde tracer injections into gyral and sulcal areas. The greatest overall projections originate from the dorsal part of pACC, while injections into sulcal areas and midcingulate gyral cortex show limited projections primarily dorsal to the cc and rostral parts of PCC and often

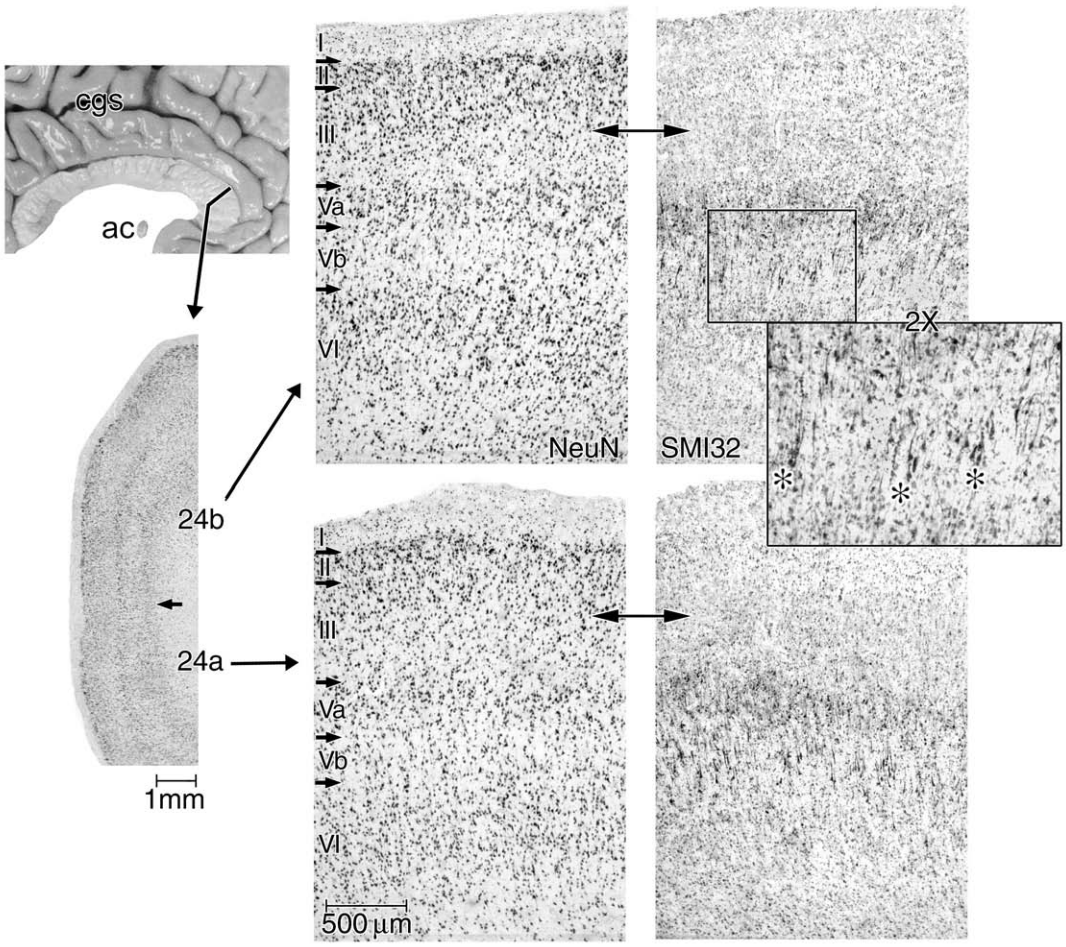

FIGURE 24.9 Although perigenual areas 24a and 24b both have a prominent layer Va and aggregations of NFP-ir neurons in layer Vb (asterisks in 2× pullout), layer Va is more dense in area 24b than it is in area 24a. Area 24b also has a more neuron-dense layer II. Although layer III is not divisible based on neuron sizes, there are fewer neurons in the deeper part of this layer in both areas (two-headed arrows).

limited to MCC itself (Van Hoesen *et al.*, 1993). Thus, even though the gyral areas do not themselves have projections to the spinal cord, the gyral areas are one step earlier in the premotor planning process—a processing stage that likely involves evaluation of the motivational consequences of particular motor outputs and, as such, is crucial in early premotor planning events.

In spite of the critical need to define the border between anterior and posterior parts of ACC in functional imaging studies, there are no objective methods to define this border with structural imaging and standardized atlases. This border can only be defined cytoarchitecturally and approximations made for the purposes of functional imaging. A comparison of the low-magnification photographs in Figures 24.9 and 24.10 makes a number of obvious points about the structure of area 24 in pACC and area 24′ in MCC. The MCC is thicker and has much broader layers II, III, Va, Vb, and VIa. A closer viewing of area 24b′ in Figure 24.10 shows that layer II neurons are in irregular groups rather than consistent islands as in area 25r. Although layer III does not have large pyramids in its deep aspect (i.e., no apparent layer IIIc), neurons are more sparse in the deep rather than superficial part of this layer, and there are a few NFP-ir cells scattered throughout deep layer III. There are, however, too few of these latter neurons to define a layer IIIc. Layer Va is broad, and the neurons have a very heterogeneous size profile with the typically large and NFP-ir pyramids in addition to many small and medium-sized pyramids. Although layer Vb neurons are sparse and NFP-ir, they do not form obvious aggregations as in area 24b. Finally, layer VI is quite broad, and about one-third of its small neurons are NFP-ir. Area 24a′ has thinner and less-neuron-dense layers II, III, and Va and it has a similar profile of NFP-ir neurons in all layers including III, V, and VI.

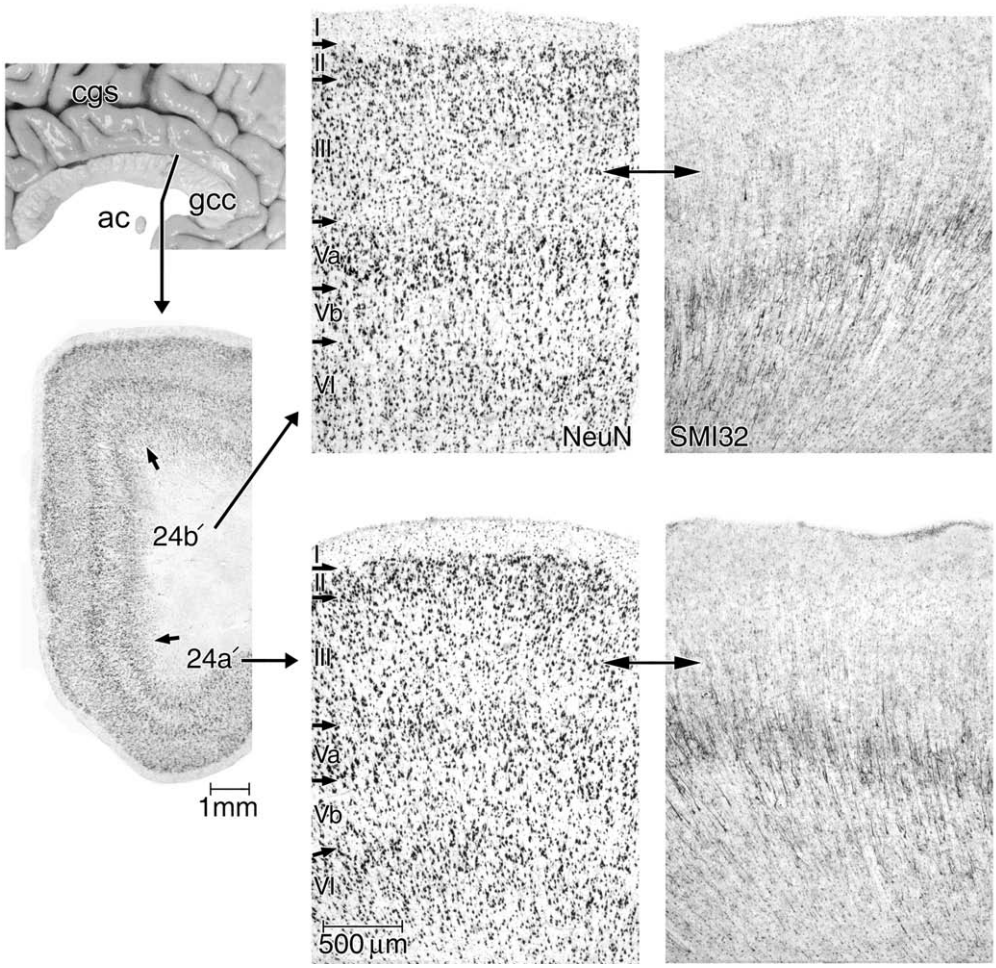

FIGURE 24.10 The gyral midcingulate areas 24a′/b′ are generally thicker than their pACC counterparts, they have a thicker layer Va, and there are more small neurons in layer Va. There also are more small neurons in the deep part of layer III and this layer does not yet have large enough neurons to specify a layer IIIc. There are almost no NFP-ir in layers II–III but quite a number in layers Va and Vb.

A study by Nimchinsky *et al.* (1997) makes a number of important points about the border between areas 24 and 24′ and that between areas 24′ and 23. First, the distribution of NFP-ir neurons in a horizontal section through the cingulate gyrus showed three levels of immunoreactivity. In pACC most staining was in layer Va, substantial staining in layer Vb, and none in layer III. In area 24′ the staining in layer Va was more focused (i.e., less in layer Vb), and there were moderate levels in layer III. In area 23 the staining was most intense in layer IIIc, less in layer Va, even less in layer Vb/VI, and nonexistent in layers II–IIIab. Second, an equally important differentiation could be made with a computer-generated map of the distribution of calretinin-ir pyramidal neurons. Most of these neurons are in the pACC and a moderate number in the rostral half of MCC, while there are none in area 23.

Perigenual and Midcingulate Sulcal Areas

Although it is well recognized that cortex in the depths of the cingulate sulcus projects to the spinal cord and has neurons with premovement discharges coding the reward properties associated with a movement, there is not complete agreement over the number and distribution of each cingulate motor area. Dum and Strick (1991, 1993) identify three areas with one in area 24c (CMAr), one in area 23c (CMAv), and one in area "6c" (CMAd). Their rostral border for area 23 extends quite far rostrally and it is unclear that the area 6c region is a CMA *per se*, particularly since a unique set of projections to primary motor cortex has not been identified for it (Nimchinsky *et al.*, 1996). Although Morecraft and Van Hoesen (1992, 1998) identify a CMA in area 23c, Luppino *et al.* (1991) and Rizzolatti *et al.* (1996) show no electrically evoked

activity from area 23c caudal to area 24d. A monkey cortex with features similar to Braak's primitive gigantopyramidal field appears to be part of the area 24d of Luppino *et al.* (1991); however, area 24d is more extensive than the primitive gigantopyramidal field and forms most of the dorsal and ventral banks of the cingulate sulcus (Nimchinsky *et al.*, 1996). It is fair to say that there is at least one, large cingulate motor area in area 24d. Finally, the concept of two motor areas with one rostral and one caudal is supported by Nimchinsky *et al.* (1996) who showed that the rostral one in area 24c' has projections to the primary motor cortex originating mainly in deep layers, while projections to the same area originate from both deep and superficial layers of area 24d. Chapter 26 discusses in fine detail the organization and functions of area 24d.

The present observations are based on a photographic series through 25 levels of the entire cingulate sulcus. Area 24c in the rostral cingulate sulcus appears to extend further caudal in immunohistochemical than in Nissl preparations. Area 24c has a thick layer II and a layer III with relatively uniform and medium-sized pyramids that thin out considerably toward its deeper part. Because there are no particularly large pyramidal neurons in deep layer III, a layer IIIc cannot be identified. Layer Va is quite dense with medium and large pyramidal neurons, many of which are NFP-ir. Indeed, there is a rich plexus of NFP-ir dendrites throughout layer Va (Fig. 24.11, SMI32). Interestingly, the architecture of area 24c is not constant in its mediolateral extent. At low magnification (Fig. 24.11A; asterisks) parts of layers Va and VI have an elevated number of larger neurons in comparison to the adjacent cortex. The edge of one of these aggregates is shown at high magnification to the right of a pair of asterisks (Fig. 24.11A, NeuN). Below layer Va there are many neurons in layer Vb, which is normally neuron-sparse. The neurons in layer VI under the layer Va/b aggregations are also larger. These subareal variations likely reflect differential organization of the innervation of different parts of the brainstem and spinal cord skeletomotor systems.

Area 24c' of MCC is cingulate motor cortex and is significantly thicker than its rostral counterpart. A number of significant changes occur in this cortex (Fig. 24.12). Layer III has more NFP-ir neurons, and relatively fewer are in layer V. Indeed, the dense plexus of dendrites characteristic of layer Va in area 24c is not in area 24'. The neurons in layer Va are generally smaller, while those in layer Vb are quite large and densely packed. In accordance with the trend in area 24 in which layer III neurons express higher levels of NFP-ir caudally, the posterior of two levels of SMI32 (Fig. 24.12B) has a higher density of large layer III neurons expressing NFP-ir than in the anterior section. The rostrocaudal trend toward increased numbers of NFP-ir neurons in layer III has been shown for sulcal (Nimchinsky *et al.*, 1996) and gyral (Nimchinsky *et al.*, 1997) cortex with full length, horizontal sections.

Very large pyramidal neurons in the deep part of layer V mark area 24d or the primitive gigantopyramidal field (Braak, 1976), and they are NFP-ir (Nimchinsky *et al.*, 1996). Area 24d has a broad layer II, relatively homogeneous layer III, deep layer Vb with the large pyramids, and a layer VI (Fig. 24.13). There are two unique aspects to layer V in area 24d. First, layer Va is parvicellular because it contains many small pyramids intermingled with larger neurons. This structure is not readily apparent in Nissl-stained preparations because of costaining of glial cells. Layer Va has many small neurons in the NeuN preparation, and it also has a dense plexus of NFP-ir dendrites and small neurons in the SMI32 preparation. Second, layer Vb contains the gigantopyramidal neurons of Braak that are NFP-ir, and aggregations of these neurons in layer Vb are particularly apparent in the SMI32 preparation of area 24d on the ventral bank of the sulcus (i.e., area 24dv). In addition, many of the large pyramids in layer III are NFP-ir, although a layer IIIc cannot be defined on the basis of neuronal size in comparison to superficial parts of layer III.

Cortex on the dorsal (area 24dd) and ventral (area 24dv) banks of the cgs share adequate similarities to be part of area 24d. The conclusion that area 24d extends onto the superior bank of the cgs means that the short extension of area 32' previously noted on the dorsal bank at this caudal level has been displaced. In this situation, area 32' inserts mainly between areas 24c' and area 6aβ. There are also some interesting differences between areas 24dd and 24dv (Fig. 24.13) that could have important functional consequences. First, area 24dd has a greater number of larger and NFP-ir neurons in layer III, and these neurons reach the point where a layer IIIc is defined. This is an important transitional feature to area 32' where layer III pyramids are a significant characteristic. Second, layer Va in area 24dd is much thicker than in area 24dv, although it appears to contain the same overall proportions of small and large pyramids. Third, layer Vb has slightly larger pyramids, and they are solitary rather than in groups as in area 24dv. Finally, the different morphologies of these two divisions of area 24d may relate to their differential involvement in skeletomotor and cognitive functions. Area 24dd mainly regulates muscles of the hindlimb and lower trunk, while area 24dv regulates mainly forelimb and upper trunk (Rizzolatti *et al.*, 1996).

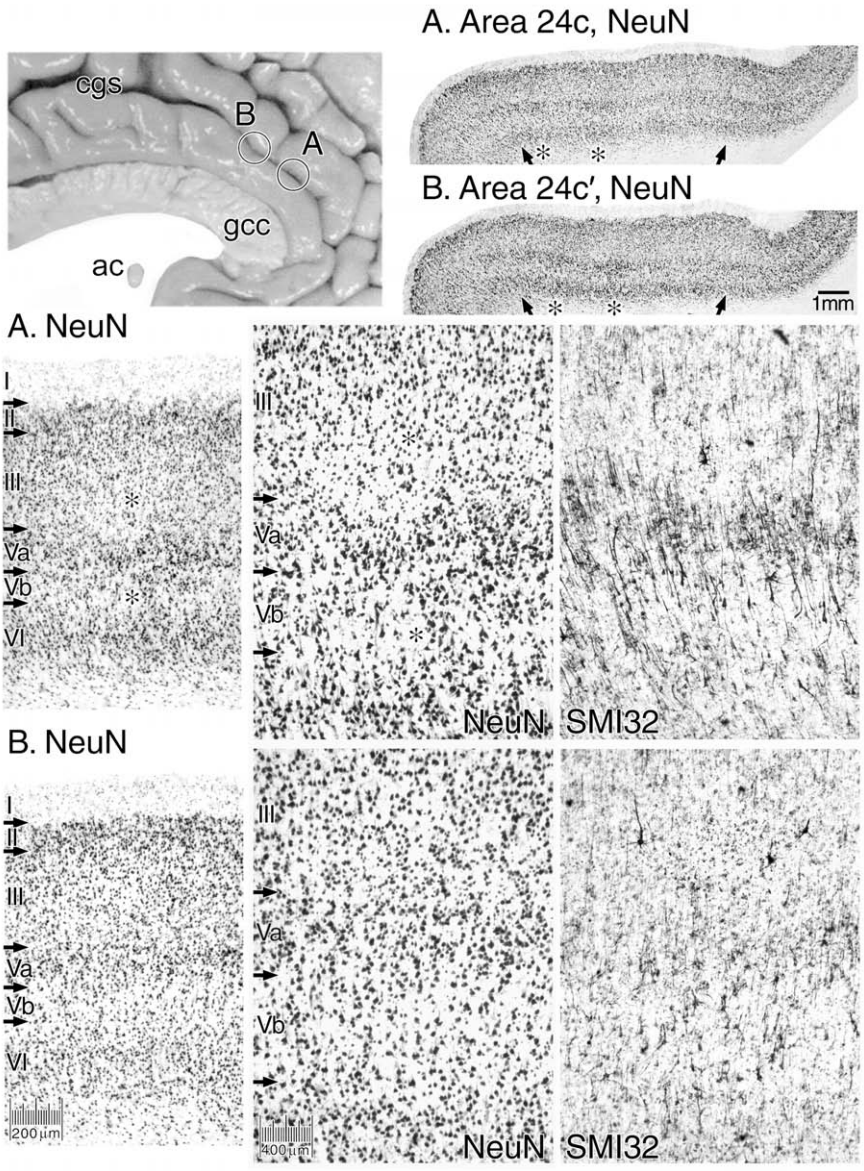

FIGURE 24.11 Areas 24c and 24c′ are shown in the depths of the rostral cingulate sulcus. In the low-magnification photographs, there are two aggregates of large neurons in layers Va and VI (above the asterisks). The NeuN section in A that is magnified further shows the border with one of these clumps with a pair of asterisks around layer Va and once again at the highest magnification. The distinction between layers Va and Vb are difficult, and many of these large neurons are NFP-ir. In this area, not only is layer III sparse in its deeper division but there are some large NFP-ir neurons therein, although an overt layer IIIc cannot be detected. Area 24c′ has a similar lamination pattern; however, layer V is substantially thicker, and the pattern of NFP-ir is quite different, as noted in Figure 24.12.

Areas 32 and 32′

Area 32 is a rostral and dorsal division of cingulate cortex that forms a belt around area 24. Although parts of it have been activated in a number of functional imaging studies associated with response selection such as generation of verbs to novel lists of nouns (Raichle *et al.*, 1994) and Stroop interference tasks (Pardo *et al.*, 1990; Bench *et al.*, 1992), its specific contributions to brain function are not fully understood. In view of its location between the cingulate motor areas ventrally and medial frontal areas dorsally, including the supplementary motor areas as well as reciprocal connections with these areas, it is reasonable to expect that this area plays a role in joining the activity of a number of frontal and cingulate motor areas. From a structural perspective, areas 32 and 32′ have features that are transitional to granular prefrontal cortex. In pACC, area 32 is transitional from area 24 to areas 12, 10, and 9, while area 32′ is transitional at

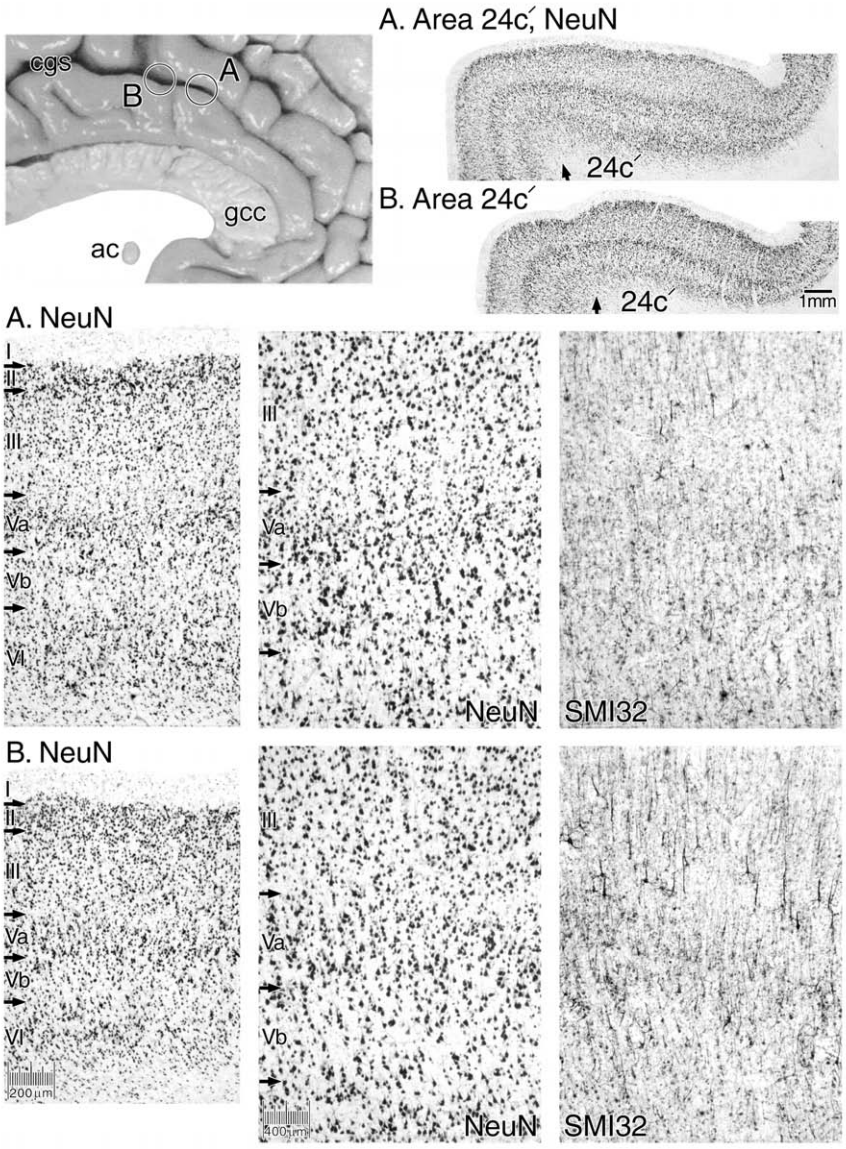

FIGURE 24.12 Two levels of area 24c′ show this area to have a very thick layer Va that is quite parvicellular. There are so many neurons in layers III-VI that are NFP-ir that the SMI32 preparations look almost homogeneous. The large though not gigantic layer Vb pyramids are clear in both preparations.

dorsal levels to area 9 and rostral area 6aβ. von Economo and Koskinas (1925) emphasized these transitional positions with adjacent frontal areas in their designations FhL, FeL, FdL, and FcL, although they did not recognize an area equivalent to area 32′. The cortex between areas 24c′ and 6ab is area 32′.

Area 32 has a well-developed layer IIIc with most large pyramids NFP-ir (Fig. 24.14A). Because these are the largest neurons in area 32, this inversion is a key transitional feature with area 24 where the largest and NFP-ir neurons are located in layer V. Layer IV is another transitional feature that contrasts sharply with the agranular areas 25 and 24. In area 32, layer IV is thin but continuous and is distinguished from the dysgranular organization of area 32′ where there are clear interruptions in layer IV. Finally, layers V and VI are unremarkable, although layer Vb seems to have more neurons than is usual in area 24.

Area 32′ of MCC inserts primarily between the supplementary motor area 6aβ and area 24c′. Area 32′ has a number of differences with area 32. Area 32′ has large layer IIIc pyramids that are NFP-ir; however, there are many fewer of these neurons (compare SMI32 for both in Fig. 24.14). Although there are fewer large layer IIIc pyramids, the overall neuron density in layer IIIc is lower than in area 32. Layer IV is more often interrupted by bridges of neurons requiring the designation of dysgranular as reported with Nissl

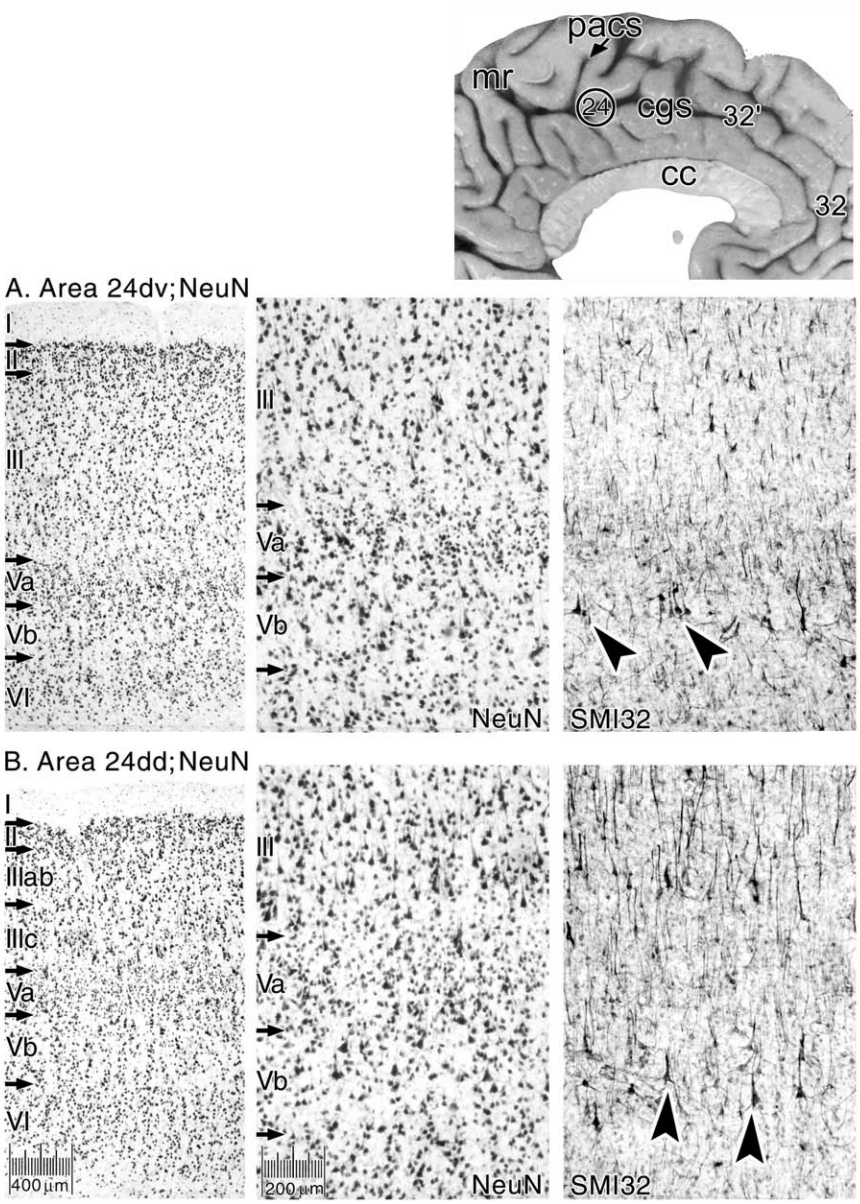

FIGURE 24.13 Electrical stimulation shows that the dorsal and ventral banks of the cingulate sulcus at this caudal level represent different parts of a somatotopically organized motor field; area 24dv (ventral) and 24dd (dorsal). Area 24d in these two locations represents an enlargement of this field from previous studies that relied on Nissl staining alone. The ventral bank has the hallmark aggregations of very large pyramidal neurons that are NFP-ir in layer Vb (A, two examples at arrowheads), while this layer in the dorsal division has solitary pyramids (B, two examples at arrowheads). There are also many more large and NFP-ir neurons in layer IIIc of area 24dd than in area 24dv.

preparations (Vogt *et al.*, 1995). In Figure 24.14B (area 32', NeuN), a level of this area is shown where one such interruption occurs at the pair of asterisks. Finally, although layers Va and Vb can be differentiated with large neurons in the former, layer Vb has a significant number of small and medium-sized neurons, and it is not neuron-sparse. This contrasts with area 24d, which has a more typically neuron-sparse layer Vb.

Ectosplenial and Retrosplenial Cortices

Each coronal section through RSC includes a segment of allocortical hippocampus and ectosplenial area 26. Above the splenium, the hippocampal rudiment (IGr) or areas LB2 and HF (von Economo and Koskinas, 1925) form a single layer of densely packed ganglion cells that are heavily NFP-ir (Fig. 24.15). Adjacent to the IGr is the subicular rudiment (Sub) or

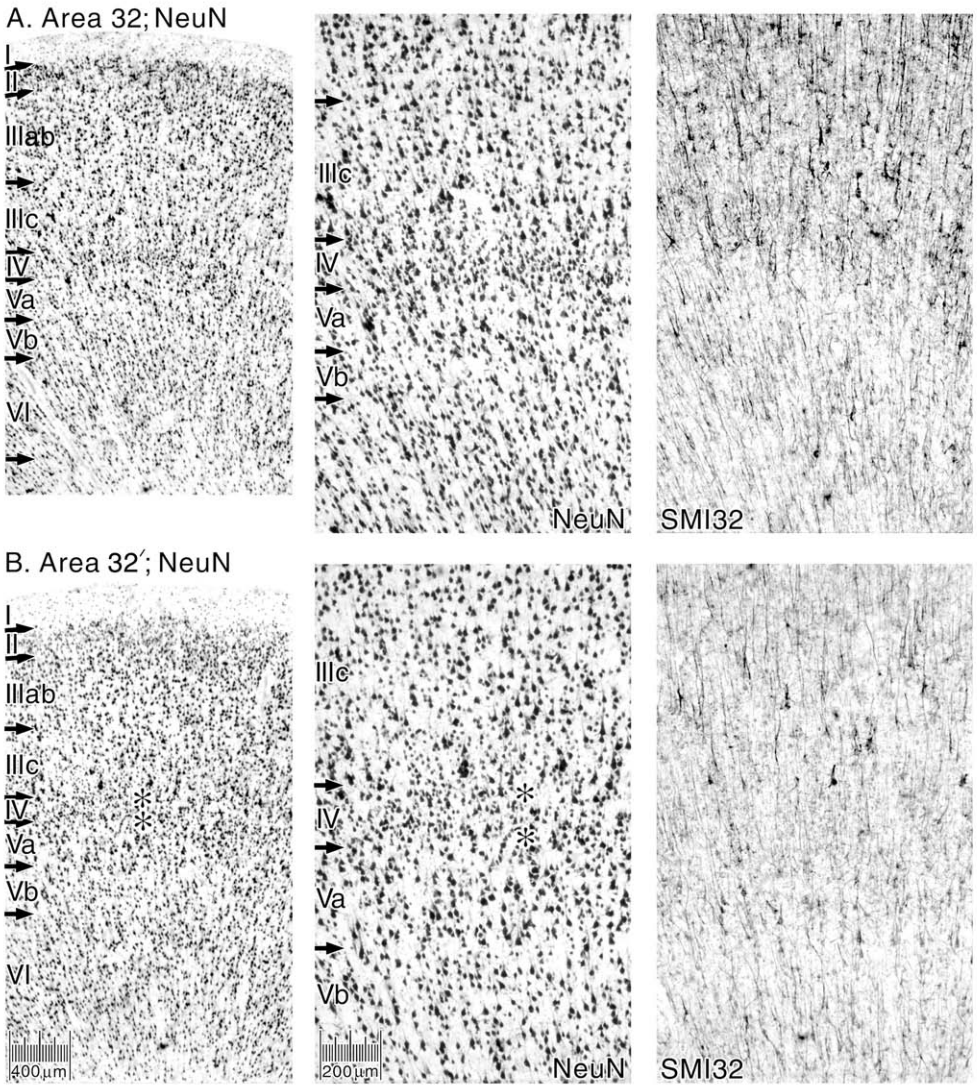

FIGURE 24.14 The rostral and dorsal cingulate areas 32 and 32′ are located in the pACC and MCC, respectively. The position of each photograph is shown in Figure 24.13. Area 32 has a continuous layer IV and large and heavily NFP-ir layer IIIc pyramids—characteristics of association areas in general (A). Area 32′ has a layer IV, but it is dysgranular because there are places where neurons in layers IIIc and Va abut each other as noted with asterisks in both magnifications of NeuN preparations (B). There are also substantially fewer layer III NFP-ir.

area HE of von Economo and Koskinas which has many fewer and more dispersed neurons. These two areas together form the fasciolate gyrus on the dorsal surface of the cc. Although the term "intralimbic" has been used for this small gyrus (Retzius, 1896), the concept of an intralimbic gyrus in this region requires that this cortex is limbic cortex; a view that has not been proven.

Ectosplenial Area 26

Area 26 of Brodmann (1909), area LF of von Economo and Koskinas (1925), and area es of Braak (1979a) have an architecture that is almost the inverse of that expressed by the IGr and subicular rudiment. Area 26 has a very dense layer of granular neurons most of which are NFP-ir, and there is a dense plexus of NFP-ir fibers in this layer (Fig. 24.15). Deep to the granular layer there are few pyramidal neurons, most of which are NFP-ir. This can be stated because the sections used for the SMI32 immunoreaction were counterstained with thionin, and there are no thionin-stained neurons that are not also SMI32+. Braak (1979a) observed that this deep layer was comprised of only the multiform neurons of layer VI.

Granular Area 29

The organization of the retrosplenial cortex presents a number of difficult problems. It undergoes many

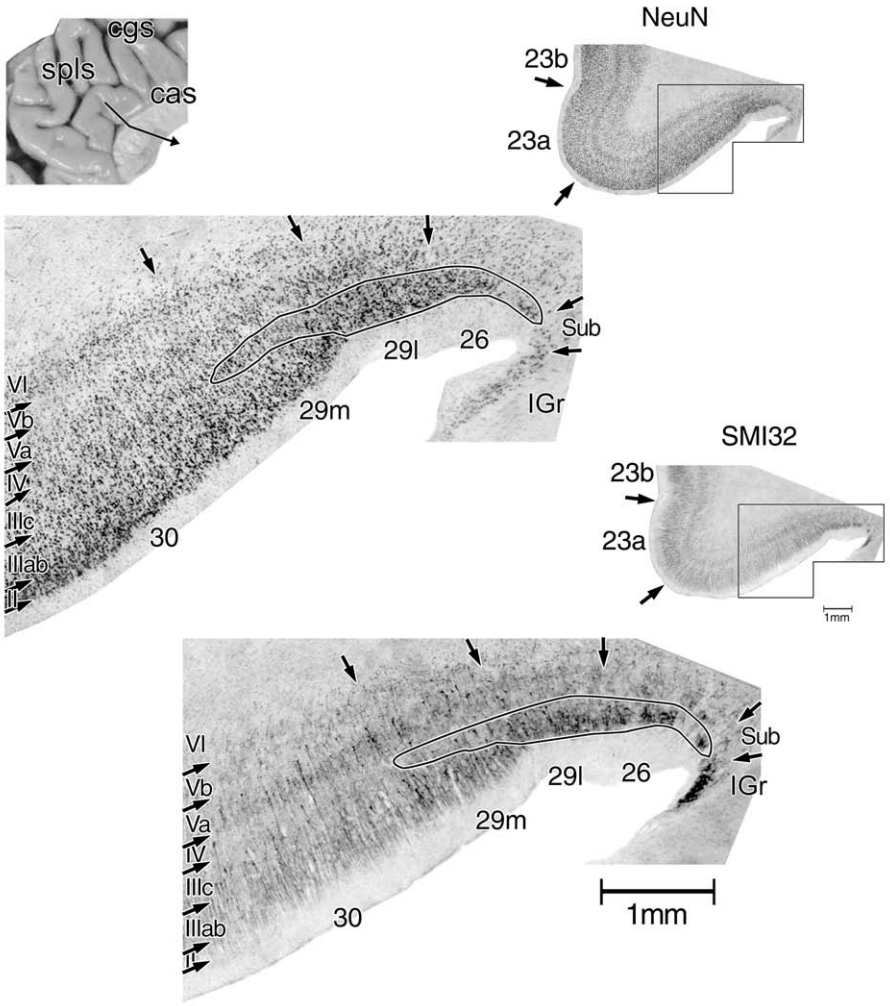

FIGURE 24.15 Coronal sections through the ventral bank of the posterior cingulate gyrus showing the posterior cingulate (23) and retrosplenial (29/30) cortices. The granular layer of areas 26 and 29 is outlined to emphasize the commonality of this layer to ectosplenial area 26 and granular retrosplenial area 29. Note that the overall density and sizes of neurons in this layer in area 29m is reduced because large neurons in layer III of area 29m separate from the granular layer, while in area 29l, such differentiation does not occur. In area 26 of both preparations, there are almost no neurons below the granular layer (i.e., there is essentially no internal pyramidal layer). Each layer in area 30 is shown to the left of the photographs including a variable layer IV.

transitions, and its structure must be interpreted in terms of differentiation trends. Also, it is convoluted around the splenium, and interpreting its organization and relationships with parahippocampal structures can be difficult. Finally, although the Brodmann map has been very influential, Talairach and Tournoux (1988) mislocated area 30 by transposing it to a posterior parahippocampal location. Although the architecture of RSC can be identified in Nissl-stained tissue (Vogt *et al.*, 1995, 1997, 2001), the details of cytological organization are more apparent with the NeuN and SMI32 antibodies, and Figure 24.15 shows a supraspleniał level of RSC. The unifying feature of the two subdivisions of area 29 is the granular layer that in lateral area 29l is directly adjacent to layer I, and in medial area 29m it is deep to a layer of medium-sized pyramidal neurons termed layer III. The granular layer is outlined in Figure 24.15 to emphasize its presence in areas 26 and 29. It is referred to as layer III/IV in areas 26 and 29l because it is an intermediate stage of differentiation of layers III and IV on the ventral bank of the cingulate gyrus (vCG). The granular layer contains many medium-sized pyramids that are NFP-ir, and the associated NFP-r dendritic plexus is prominent (Fig. 24.15, SMI32). Although this is also termed the granular layer, the neurons are not small and "granular" as they are in the monkey. In area 29m the density and sizes of neurons are reduced in layer IV because many medium-sized neurons are separated from this layer into a layer III (Figs. 24.15, 24.16, 24.21,

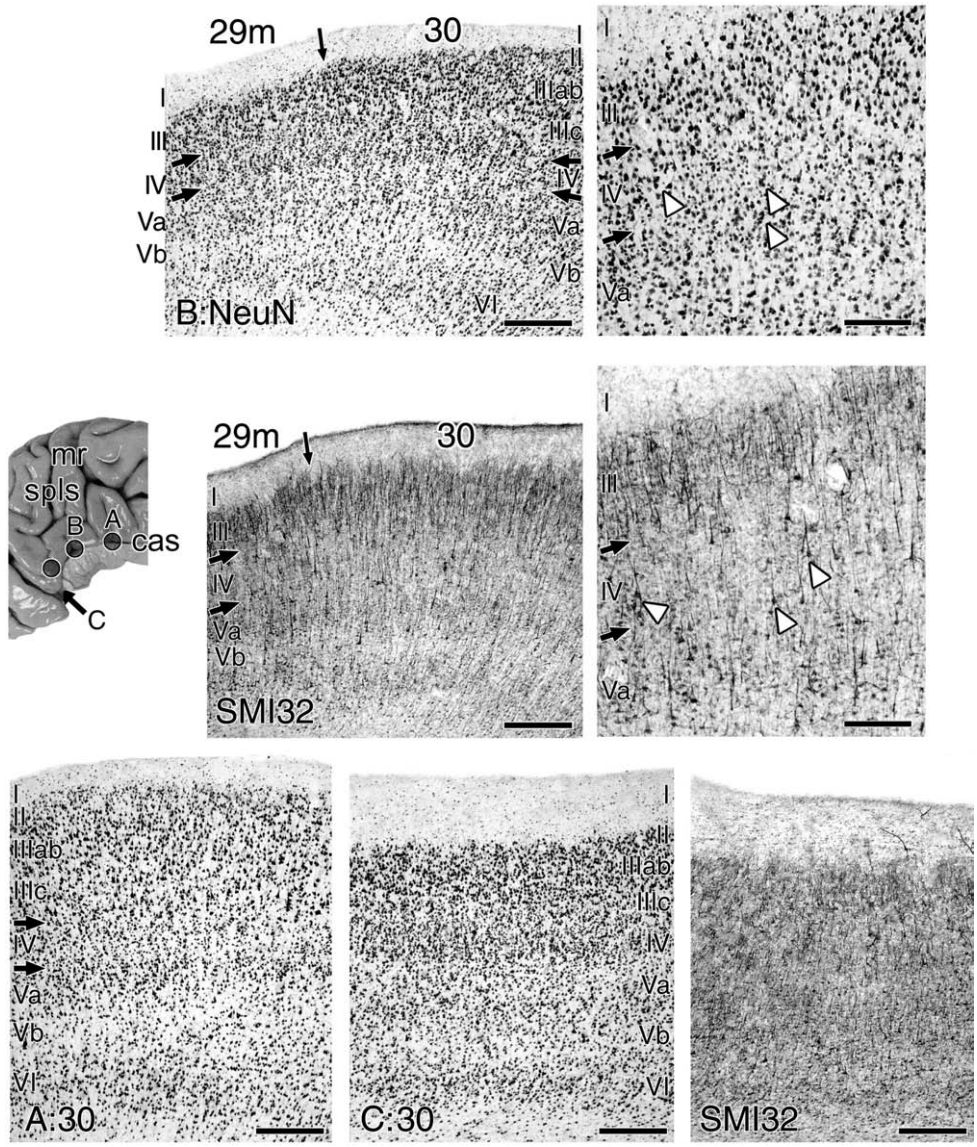

FIGURE 24.16 Three rostrocaudal levels of area 30 above the body of the corpus callosum (A), dorsal to the splenium (B), and caudal to the splenium and lateral to the CML as indicated with the arrow pointing below the CML (C). The medium-sized NFP-ir neurons in the parvicellular layer IV are demonstrated, and three in each preparation are emphasized with white arrowheads. The level of the section at C is noted with brackets in Figure 24.17: NeuN. This level of area 30 is transitional to area 29m at its most caudal level (i.e., this is the terminal end of area 30). At this point, area 30 has a more densely granular layers II and IV, and the sizes of layer III pyramids are reduced with less prominent NFP-ir dendrites. Scale bars, 1 mm.

and 24.22). Beneath the granular layer in area 29l are poorly differentiated layers V and VI, while in area 29m, layer V differentiates into layers Va and Vb. Many of the largest pyramids in area 29 are NFP-ir, and they are located mainly in the deeper part of layer V in area 29l and the deeper part of layer Va in area 29m. Finally, there are some NFP-ir neurons in layer VI throughout area 29, although the associated plexus in layer VI is much less dense than in layers IV and Va.

It may seem arbitrary to term the first neuronal layer adjacent to layer I in area 29m as layer III rather than layer II. This selection is not the result of a simple pia to white matter counting but rather is based on the facts of neuron structure and the principles of cortical transition in the posterior cingulate region. It has been suggested that this is not layer II in the monkey because these are not lancet-shaped neurons similar to those of layer II in area 23a and a distinct layer II appears only in the medial part of area 30 (Vogt, 1976). This fact is demonstrated later and confirms and extends observations in monkey RSC in the following ways. First, most neurons in layer III of area 29m are

NFP-ir, while almost none are NFP-ir in layer II of area 23a and medial area 30. Second, there is a reduction in the overall density of neurons and the NFP-ir dendritic plexus in the lateral part of area 30 that is adjacent to area 29m (Figs. 24.15 and 24.16). Third, the size and density of heavily NFP-ir neurons in layer III of area 29m contrasts with those in layer IIIc of area 30 (Fig. 24.15). It was concluded that neurons in layer III are most likely associated with layer IIIab as proposed for the monkey (Vogt, 1976). Thus, the cytoarchitecture of monkey and human cortices, Golgi studies in monkey, and immmunohistochemical studies in human all point to the fact that layer III of area 29 is similar to that of layer IIIab in neocortex rather than layers II, IIIc, or IV.

The parvicellular layer IV of area 29m contains not only small and medium-sized pyramidal neurons but also a number of large and solitary pyramids. These neurons are NFP-ir and are a distinguishing feature of area 29m along its full extent to its termination on the rostral bank of the CML. Examples of these pyramids are in Figure 24.16B (white arrowheads); at this magnification, it is clear that layer III is comprised of many medium-sized and large pyramidal neurons that are heavily NFP-ir. These latter neurons likely are the undifferentiated counterparts of pyramids of layers II and IIIab in adjacent areas 30 and 23a.

Dysgranular Area 30

Area 30 (Brodmann, 1909), LD (von Economo and Koskinas, 1925), Rsag (Rose, 1928), and rsm (Braak, 1979a) have been thoroughly analyzed histologically. At each point of transition from allocortex to isocortex throughout the primate telencephalon, there is at least one area with the features of a dysgranular cortex as is the case for orbitofrontal and insular cortices. In the insula, neurons in layer IV form islands, as is characteristic of a layer that is of irregular thickness (Mufson *et al.*, 1997). In orbitofrontal cortex, the intermediate area has a thin layer IV that can be difficult to detect where the layer III and V pyramids are particularly large (Hof *et al.*, 1995). Since cortex on the ventral PCG progresses through a number of transitions beginning with the allocortical indusium griseum and culminating in the isocortical area 23, the presence of a dysgranular cortex needs to be considered.

Brodmann (1909) referred to area 30 as agranular, and von Economo and Koskinas (1925) were quite explicit that area LD is not just agranular but that the "granulous" layer of area LE (Brodmann's area 29) is not continuous with the isocortical layer of area LC2 (Brodmann's area 23). Although there is no doubt that layer III/IV in area 29 is not equivalent to layer IV in area 23a, von Economo (1929, Fig. 50) vacillated on the presence of a layer IV in LD and showed a layer III(IV) below layer III. Furthermore, the granular layer IV of area 29m is continuous with layer IV in area 30 and layer IV in area 23a in immunohistochemical preparations invalidating von Economo's statement that they are not continuous (Vogt *et al.*, 2001).

Area 30 architecture is shown in Figure 24.16 for three rostrocaudal levels. It has layers IIIab and IIIc that differentiate from layer III of area 29m. Although some small neurons are at the border between layers I/II, a layer II is most apparent at the medial edge of this area. Small neurons aggregate in layer IV, and there are many instances where the layer is interrupted by bridges of neurons between layers IIIc and Va or where the small neurons interdigitate with those in layers IIIc and/or Va. The variability in layer IV thickness can be appreciated in Figure 24.16 where one level has a variable layer IV (B: NeuN), one has a thin but continuous layer (A: 30), and the granular neurons are either in a separate layer or intermingled with those in layer Va at the caudal level (C: 30). Area 30 has another feature that makes it stand out from adjacent areas. It has a high relative density of NFP-ir neurons in layer IIIab when compared to other layers. Although some large neurons in layers IIIc and Va are NFP-ir, they are infrequent when compared to area 23a. Although area 23b may have a similar number of NFP-ir neurons in layer IIIab, this area has the second highest density of NFP-ir neurons in layer IIIc (second only to area 31), and this contrasts strongly with the organization in area 30 where few of the layer IIIc neurons are NFP-ir. Finally, at caudal levels of area 30 (Fig. 24.16C: 30), the cortex is thinner, and there is a more homogeneous distribution of NFP-ir neurons.

Posterior Cingulate Cortex

The first isocortical area encountered in the transition that begins with the indusium griseum is area 23a. At its rostral border with area 24a', layer IV is thin, and there is an intermingling of small neurons with large pyramids in layer Va. Recall that area 24' does not have a layer IV but rather small neurons intermingled in layer Va. This feature, therefore, is a transitional aspect of rostral area 23a architecture. Caudally in area 23a, layer IV becomes more pronounced and, although a layer Va is present, the number of large neurons in it is surprisingly low. One of the key differences between areas 23a and 23b is that the latter area has a significantly greater number of neurons in layer Va (Fig. 24.17). The greatest number of NFP-ir neurons in area 23a are in layer IIIc that is in striking contrast to area 30 where most are in layer IIIab. A moderate population of large neurons in layer Va also

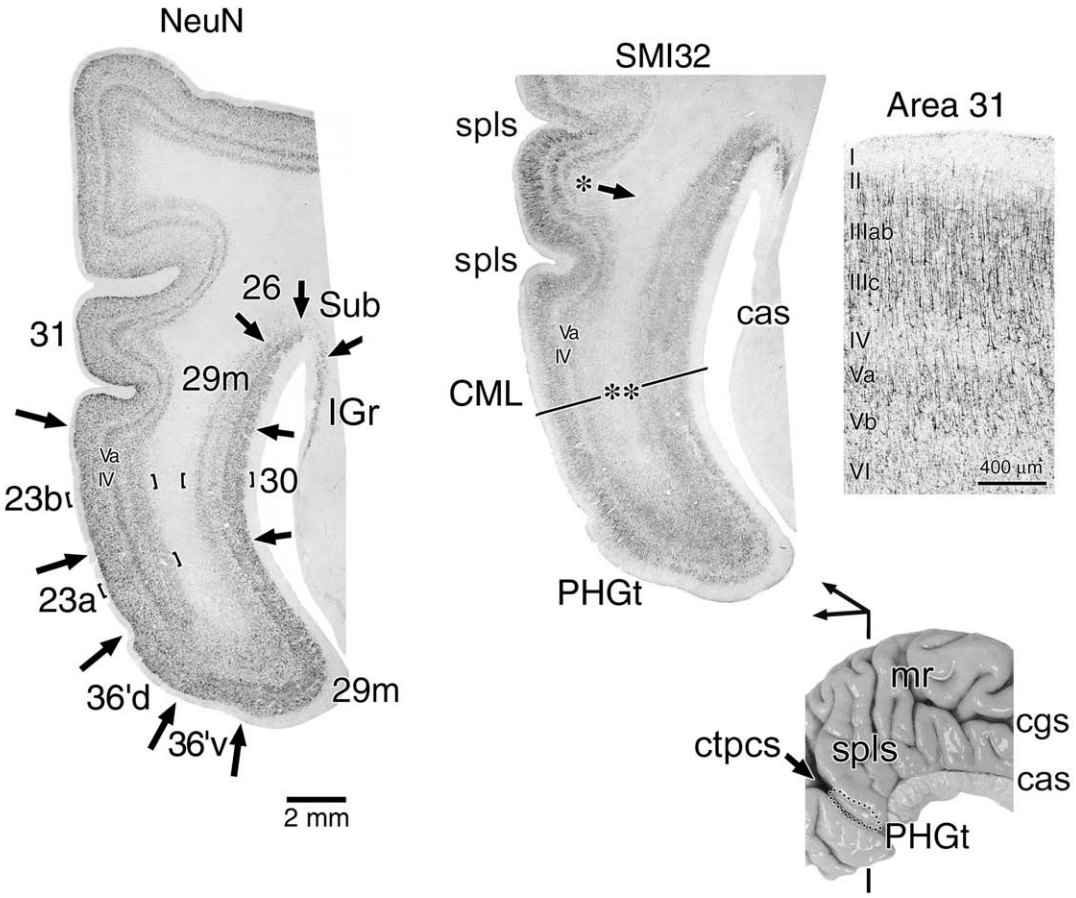

FIGURE 24.17 Microphotographs through the postsplenial posterior cingulate and retrosplenial regions and the junction with the PHGt. The surface reconstruction paradox of RSC in producing brain maps including that of Brodmann is clear because RSC is in the fundus of the cas lateral to the CML and not on the surface of the CML. The isocortical nature of areas 23a and 23b with their layer IV is apparent in both preparations and, as is true for most cingulate areas, layer Va is prominent even in isocortex. This case also demonstrates the clarity with which each area of CML can be assessed in standard coronal sections. Although area 29m does not appear on the CML, its border with parahippocampal area 36'd on the PHGt is demonstrated; the PHGt is outlined with a dotted line in the macrophotograph. Area 31 has not only the thickest layer IV of any cingulate area but also the highest level of NFP-ir in layer III that emphasizes its border with area 23b. The strip of area 31 cortex is a 3× magnification of the level in SMI32 marked with one asterisk and an arrow.

expresses NFP-ir and there is a fine mesh of NFP-ir dendrites throughout deep layer V and layer VI. As is the case for area 30, at caudal levels of area 23a there is a greater overall dispersion of NFP-ir neurons and dendrites that also includes some in layers II and IIIab.

The border between areas 23a and 23b is clearly marked by a significant increase in the number of layer Va neurons and the thickness of layer IV as shown in the CML (Fig. 24.17, NeuN). As is the case for area 23a, the rostral part of area 23b at its junction with area 24' has a thinner layer IV and a well-formed layer Va that does not contain many small neurons (Fig. 24.18A). One of the outstanding features of the dorsal and posterior cingulate areas is the very high density of NFP-ir neurons throughout layer III. There are so many of these cells that even layers II, IV, and VI have a high density of them (Fig. 24.18B, SMI32)

Area 31 forms lobules around the spls, and its structure is identified between the primary branches of these sulci. Area 31 has the thickest layer IV on the cingulate gyrus, and this layer can be compared with the same one in area 23b in Figure 24.17 in the NeuN preparation or as a negative image in the SMI32 section. Layer Va is also well developed and has the highest density of NFP-ir neurons in the posterior cingulate region (Fig. 24.17, SMI32). Finally, area 31 has the highest density of large NFP-ir neurons in layer III in the entire cingulate gyrus, and they are obvious even at low magnification (Fig. 24.17, SMI32). As shown in the subregional, postsplenial flat map (Fig. 24.20), area 31 forms the superior and posterior border of cingulate cortex and extends ventrally and caudally to area 23b along the posterior border of the caudomedial subregion.

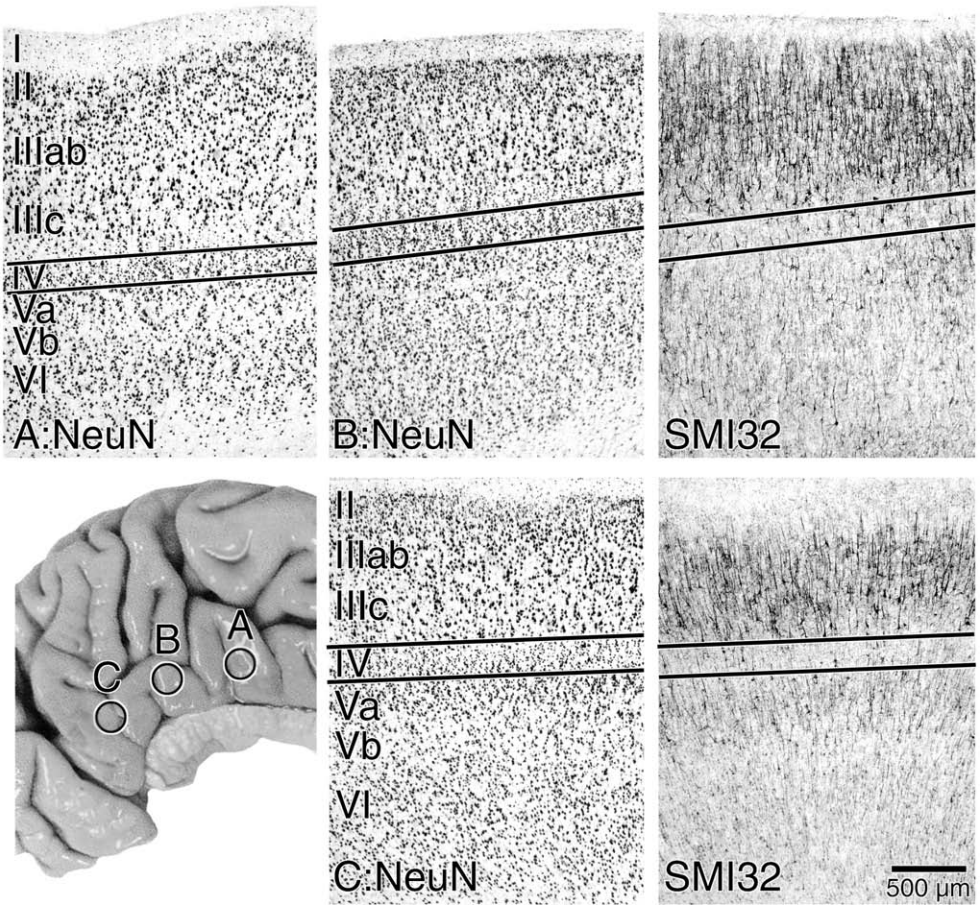

FIGURE 24.18 Three rostrocaudal levels of area 23b including a level at the dorsal part of the CML (C). Although the essential structure of area 23b is maintained throughout with heavily NFP-ir large neurons in layer III, a thick layer IV, and a robust layer Va with few NFP-ir neurons, the thickness of layer IV does decline close to the border with area 24, and a dysgranular architecture is apparent at some levels.

Caudomedial Subregion

Brodmann (1909) showed areas 26, 29, and 30 extending around the full extent of the splenium, while von Economo (1929, Fig. 58) provided a reconstruction of this region and showed that the retrosplenial areas terminated posterior to the splenium at a level just caudal to the ventral edge of the splenium rather than fully embracing it *per se*. Although there is no doubt about the von Economo conclusions because of his carefully drawn map of the region, the same cannot be said of the Brodmann map because it was reconstructed on the convoluted surface of the entire brain and represents compromises to show the topology of each area in sulci and on gyral surfaces. We evaluated these issues and concluded that the RSC in Brodmann's map does not extend far enough anteriorally, it does not extend onto the surface of the CML/CMSR, nor does it extend to the most ventral aspect of the splenium (Vogt *et al.*, 2001). Each of these issues has a significant impact on how functional imaging studies localize activation sites in this region. Indeed, the use of Brodmann's localizations without histological guidance led to a mislocation of retrosplenial area 30 on the surface of the CML/CMSR (Talairach and Tournoux, 1988).

The PCC and CMSR have variable surface features as detailed in Figure 24.2. In the monkey, there is a consistent pouch of cortex in the CMSR termed the CML (Goldman-Rakic *et al.*, 1984), and its surface is comprised mainly of areas 23a and 23b, while the rostral bank contains RSC (Vogt *et al.*, 1987, 1997; Vogt, 1993). Although a similar conclusion has been reached in human brain (Vogt *et al.*, 1995), the multiple gross morphologies of this cortex need consideration as do the details of transition to parahippocampal cortex. In instances in the human where a clearly defined CML is not present, the more general term CMSR is used. An overview of the posterior cingulate gyrus is provided in Figure 24.17, and the problem of reconstructing RSC on the convoluted surface of the human cortex is apparent therein because area 23 directly overlies the ectosplenial and retrosplenial areas in the cas. The isocortical layer IV of areas 23a and 23b can be seen in cortex on the surface of the CML, while areas 29 and 30 underlie this cortex in the depths of the cas and do not express a fully differentiated layer IV. It is not possible to reconstruct these areas accurately without flattening

the cortex to show areas in the fundus of the cas. At ventral levels, the CA1 sector of the hippocampus replaces the indusium griseum, and area 29m terminates adjacent to the caudal parahippocampal areas 36'd and 36'v.

Although histological studies have not shown area 30 on the gyral surface in the CML, two essential issues are raised by the atlas interpretations of Brodmann's map (Talairach and Tournoux, 1988). Does any gyral component of the CML/CMSR share cytoarchitectonic features with area 30 in the cas? How do the features of area 30 compare with those on the CML, including that area which most closely relates to area 30 cytoarchitectonics (i.e., area 23a) which it borders? In Figure 24.17, layer IV can be clearly identified at low magnification in areas 23 and 31. Since area 30 has a dysgranular layer IV that cannot be detected at this magnification, it is unlikely that area 30 is part of the gyral surface at the isthmus. Direct comparison of a supraspleniał level of area 30 (i.e., as in Fig. 24.16B) with cortex on the CML is provided in Figure 24.19, which has higher magnifications of layers IIIc–Va of area 30, and photographs of area 23a on the CML, which has the least differentiated layer IV in this region (i.e., between brackets in Fig. 24.17, NeuN). As noted earlier, area 30 has a layer IV that is interrupted by layer IIIc/Va neurons (asterisks in Fig. 24.19A, NeuN). There are some medium-sized, NFP-ir pyramidal neurons throughout layer IV in area 30 and this reduces the clarity with which layer IV can be identified with NFP-ir. In contrast, area 23a on the CML has a clear layer IV with only a few large and solitary layer IIIc or Va, NFP-ir neurons. There also are many more NFP-ir neurons in layer IIIc in area 23a than in area 30. As noted earlier, layer IIIc of area 30 has surprisingly few NFP-ir neurons in layer IIIc but the greatest relative density in layer IIIab. Finally, there are no neuronal bridges connecting layers IIIc and Va to the exclusion of a layer IV in area 23a, although layer IV in area 23a does have some solitary, NFP-ir neurons. Thus, area 30 is not expressed on the CML.

Another major component of the CMSR is area 23b. This area has such a well-defined layer IV that it is easily observed at low magnifications as in Figure 24.17, which shows both layers IV and Va. These layers show the two most important features of area 23b: thickness and neuron densities. Many large pyramidal neurons in layer Va, most of which are NFP-ir, easily distinguish this area from areas 23a and 30. Finally, the distinctions between areas 23a and 23b are enhanced by the extensive size and number of NFP-ir neurons throughout layers IIIab and IIIc in area 23b.

The differentiation of the retrosplenial areas from parahippocampal areas has been elegantly shown

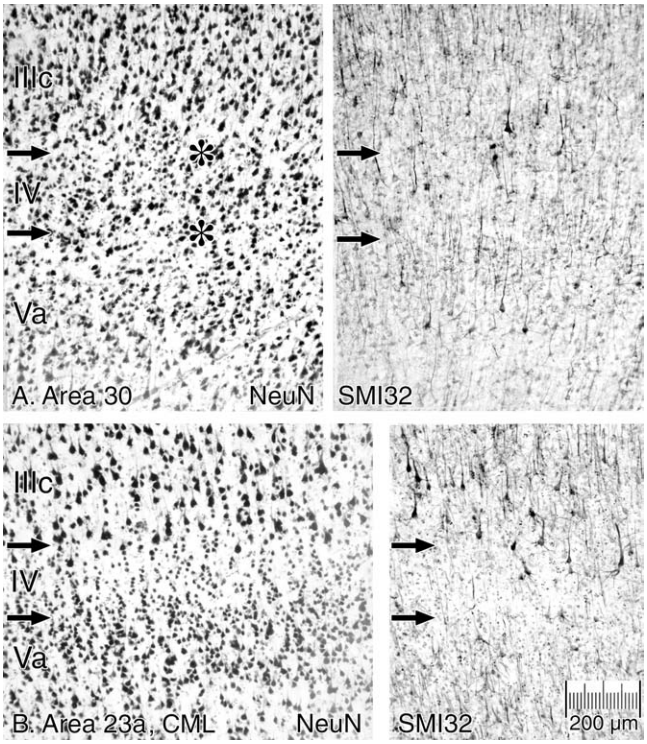

FIGURE 24.19 Area 30 dorsal to the splenium in the cas is compared with area 23a on the CML because no equivalent to area 30 has been identified in this latter region. The dysgranular nature of area 30 is emphasized at a point where layer IIIc and Va neurons intermingle (to the right of the double asterisks in A; NeuN). Area 30 also has a layer IV with many small and medium-sized NFP-ir neurons (SMI32). In contrast, area 23a has no neuron bridges across layer IV and only occasional solitary NFP-ir neurons in layer IV. Layer IIIc in area 23a has larger and more dense NFP-ir neurons than for area 30.

with immunohistochemical analyses of coronal sections in the monkey by Berger *et al.* (1997). This latter study showed that in the cas there is an arch of neurotensinergic neurons in the deep layer of areas 29 and 30, and the elaboration of these areas and their apposition to parahippocampal areas 27 and the parasubiculum. Although the retrosplenial and presubicular/parasubicular areas abut in the callosal sulcus just ventral to the splenium, in the human there is an intermediate level of transition between the posterior cingulate and more lateral parts of parahippocampal cortex. Ventral to posterior cingulate and retrosplenial cortices are two divisions of posterior parahippocampal cortex that share features with area 36. Area 36 has well-defined layers II and Va and a dense layer VI. Layer III is broad, and the pyramidal neurons are relatively uniform in size (Vogt *et al.*, 2001). The division of layer III into a superficial layer IIIab and deeper layer IIIc is possible, although

the neurons in layer IIIc do not reach the size and dispersion characteristic of the cingulate neocortical areas. The relative density of neurons in layer IV of area 29m increases around the splenium and to its termination either in the ventral part of the cas or the rostral lip of the CML/CMSR. The transition at this point is with area 36'v. The NFP-ir plexus in layers III and IV are apparent and disappear as area 29m merges with area 36'v. Area 36'v only has a NFP-ir plexus in layer V. Features of area 36'v that distinguish it from area 29m include broad layers II–III composed of more uniform, medium-sized pyramidal neurons, a poorly defined layer IV, and an infragranular layer dominated by a uniform layer V and a narrow layer VI.

Subregional Postsplenial Flat Map

Cytoarchitectural studies of human cortex require flat map reconstruction of the areas identified because 50% or more of the cortical surface is in the sulci, and this is particularly true for the posterior cingulate region. A flat map of the entire cingulate gyrus in which the fundus of the cas is represented and areas 29 and 30 are plotted on the ventral CG is available (Vogt *et al.*, 1995). As is true for flat maps of the entire brain, however, flat maps of the entire cingulate cortex result in significant distortions in all areas owing to the need to warp all areas to fit a two-dimensional space and still retain basic gross morphological relationships. Subregional flat maps alleviate this problem because they are limited to a subsector of cingulate cortex, flattening is performed in only one direction rather than two, and it is not influenced by flattening in other parts of cingulate cortex to form a full map. von Economo (1929, Fig. 58) provided the first posterior cingulate subregional map, although it was not flattened.

Figure 24.20 shows a case in which postsplenial cortex was sectioned in the plane of the flat map reconstruction to ensure precision in relating features on the map to histological observations. Asterisks on the convoluted surface on the left are used to orient the flat map at the right. The first one is at the cas and emphasizes that flattening was started at the fundus of the cas, while the second asterisk shows the rostral edge of the transitional PHG in both drawings. The depth of the cas was determined according to the curvature of the splenium and each area was represented according to the length of a line drawn through each area at a midcortical level between layers IV and V. Heavy lines in Figure 24.20 represent cortex on the ventral PCG (i.e., cortex in the cas) and the caudal edge of the CML, while in the ventral part of the map they represent the rostral and caudal limits of the

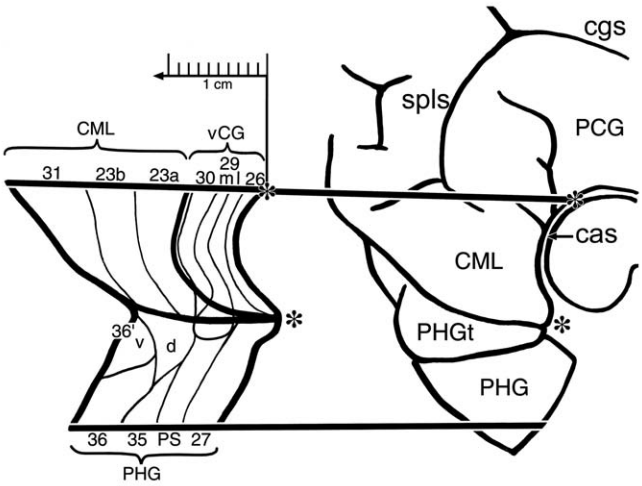

FIGURE 24.20 Subregional postsplenial flat map including the entire CML. This is a linear (one-dimensional) expansion of posterior cingulate, retrosplenial, and parahippocampal cortices in a single direction noted by the arrow on the scale bar (i.e., caudal from the fundus of the cas). The dorsal asterisk in the drawing on the right extends from the depths of the cas to an equivalent starting point on the flat map on the left, and the same is true for the rostral edge of the PHG/PHGt. Areas on the vCG are enclosed by thick lines on both sides of the callosal sulcus, while those on the gyral surface are extended to the left on the CML. The locations and interrelationships of RSC and transitional parahippocampal areas are clear with a transitional PHG.

PHGt and PHG. The direction and calibration of flattening in this case is shown with the arrow and scale bar, respectively. This map shows that almost all of RSC is on the ventral PCG in the cas. Area 30 ends just dorsal area 29m, and this case has a small termination of area 30 on the rostral edge of the CML. Because standardized atlases based on Brodmann's map show that most of the CMR is comprised of area 30, it is of interest to determine the actual extent of area 30 on the CML in this case. Because the map was flattened in only one dimension, it accurately represents the relative surface area for each area on the CML and cortex on the ventral CG. The surface area occupied by each cortical area was calculated directly from the flat map (Vogt *et al.*, 2001). Area 30 comprises 0.8% of CML, while it is 33% of area on the ventral CG at the level of the CML. In contrast, area 29m comprises 2.8% of the rostral edge of the CML, while it is 26% of cortex on the ventral CG. Thus, both areas 30 and 29m are almost entirely located within the cas, and all of areas 29l and 26 are in this sulcus. Finally, the PHGt contains a small rostral extension of area 29m and areas 36'd and 36'v, and neither area 29m or 30 appeared on the CML. Thus, area 30 does not comprise a substantive part of the CML.

COMPARISON OF THE BRODMANN AREAS WITH RECENT MODIFICATIONS THEREOF

Because only about 50% of the human cortical surface is represented on the convoluted brain surface, Brodmann had to make many compromises to render his interpretations of the entire cortex. The ectogenual, ectosplenial, and retrosplenial areas are buried within the callosal sulcus on the ventral bank of the cingulate gyrus. Indeed, area 24a extends into the callosal sulcus as well. Although one might imagine that Brodmann's area 24 extends into the cingulate sulcus, is that also true for area 32? What is the relationship between area 32 and the depths of the anterior cingulate sulcus? Area 24 is not uniform in either rostrocaudal or ventrodorsal orientations, and this has been documented in a number of species with architectural, connection, immunohistochemical, ligand binding and transmitter systems, and functional imaging analyses. Although the composition of the dorsal and ventral banks of the cingulate sulcus are a matter of conjecture for the Brodmann map, the assessment provided over the past 25 years by many investigators shows that it is comprised of areas 32, 32', 24c, 24c', 24d, and 23c. Each of these areas has a precise definition that is not just morphologically correct but also exacting in terms of their projections to the spinal cord and throughout the cerebral cortex, and the neuropsychological conditions under which they are most active.

Even when the same numerical designation has been used in the Brodmann and Vogt maps, there can be important differences in the topology of each area. Consider area 31 as an example. Although the centroid for area 31 is located on the splenial sulci and its architecture is easily defined, the monkey area 23 differentiates beyond the a/b designation on the gyral surface and forms area 23c in the ventral bank of the caudal cingulate sulcus that was not recognized by Brodmann. In this situation, the rostral border of area 31 is extended caudally, and area 23b extends dorsally to the level at which the marginal ramus is emitted from the cinguate sulcus. Thus, our area 31 does not extend as far rostral as does Brodmann's area 31. In another example, Brodmann's areas 29 and 30 completely surround the splenium and abut the parahippcampal areas, while our areas 29 and 30 extend more rostrally dorsal to the splenium and terminate caudally at a level that is adjacent but not ventral to the splenium. Finally, the structure of caudomedial cortex is very important, particularly in light of its reciprocal connections with pACC and functional imaging findings. One interpretation of Brodmann's area 30 is that it forms much of the CML and that areas 23 and 31 are excluded from this region. Our analysis of the cytoarchitecture of this region shows that areas 23a, 23b, and 31 form the surface of the CML, while the rostral bank of the CML is formed by areas 29l, 29m, and 30.

In conclusion, when an area of activation or other functional entity fully encompasses the location and extent of Brodmann's areas, "BA" designations are appropriate. However, when functional sites reflect a–c divisions of areas 24 or 23 or an area not recognized by Brodmann such as areas 23c, 24c', 25r/c, 32', 33', 29m, 29l, it is appropriate to use the designation "A" for area without the "BA." This provides a flexible nomenclature that can be modified over the coming decades in light of new anatomical and functional studies.

CORTICAL DIFFERENTIATION IN POSTERIOR CINGULATE GYRUS

Descriptions of a cortical region are most helpful when considered in terms of fundamental patterns of organization rather than only the unique features of a particular area. For example, area 29 has fewer than six layers, and simply counting from I to IV does not indicate which layers contain large ganglionic neurons similar to those in layer V, which layers contain primarily corticocortical projection neurons and are similar to layer III in other areas, nor which are most likely to receive thalamic afferents. Although one might speculate that such layers have no continuity or relationship with those in isocortex, this does not appear to be the case because layers of cortical neurons share common embryonic origins and axonal projections. From a developmental perspective, Nowakowski and Rakic (1981) showed that neurons in the hippocampus and deep layers of entorhinal cortex are generated in the subventricular zone. Thus, neurons throughout the indusium griseum and deep layers of the ventral bank of the cingulate gyrus likely share a similar origin. Furthermore, common projection sites provide another means of associating neurons in two different areas. The projections of layer VI neurons throughout the cingulate gyrus and including the retrosplenial areas are to the thalamus as shown in the monkey (Baleydier and Mauguiere, 1985). Thus, the deep layers of retrosplenial cortex share similarities in origin and projections that allow one to conclude that they are part of a similar differentiation scheme. Indeed, the concept of cortical differentiation is based on the principle that a common motif can be identified for all cortical areas such as layer V upon which

cortical differentiation proceeds to culminate in a fully elaborated isocortex.

Each area on the cingulate gyrus is transitional in nature because every area shares the cytoarchitectural features of its two or more neighbors. When there are transitions between cingulate and adjacent frontal or parietal cortices, the term transition designates the cingulofrontal transitional area 32 and the cingulo-parietal transitional area 31, respectively. Rather than speak in terms of transition from the perspective of single areas, we use this concept in relation to broad trends of cortical differentiation. Many students of cytoarchitecture have considered cortical trends of differentiation in the cingulate gyrus (e.g., von Economo and Koskinas, 1925; Vogt, 1976; Braak, 1979a; Braak and Braak, 1993), and this includes progressive alterations throughout the ectosplenial, retrosplenial, and posterior cingulate regions. The process begins with a substratum of densely packed neurons in the internal pyramidal layer. This stage is followed by the addition and differentiation of a granular external pyramidal and ends in the parietal and occipital association areas. A second trend includes the rostral agranular cortex and begins with the ectogenual areas and progresses through a differentiation pattern leading to the cingulate motor and supplementary motor areas. Here we consider some of the main issues related to transition on the posterior cingulate gyrus. The concepts of cortical differentiation are difficult conceptual issues as is their relation to ontogenetic events. Consult Chapter 27 for a thorough consideration of these issues.

Dysgranular Concept and Transition

At each point of transition from allocortex to isocortex throughout the primate telencephalon, there is at least one area with the features of a dysgranular cortex, and this is why the character of area 30 is important. In the insula, neurons in layer IV form islands as is characteristic of a layer that is of irregular thickness (Mufson *et al.*, 1997), while orbitofrontal cortex has an intermediate area with a thin layer IV, which can be difficult to detect where the layer III and V pyramids are particularly large (Hof *et al.*, 1995). Since we view area 30 as the dysgranular equivalent in posterior cingulate cortex, early perspectives need to be considered. Brodmann (1909) referred to area 30 as agranular, and von Economo and Koskinas (1925) were quite explicit in stating that area LD is not just agranular but that the "granulous" layer of area LE (Brodmann's area 29) is not continuous with the isocortical layer of area LC2 (Brodmann's area 23). Although there is no doubt that layer III/IV in area 29 is not equivalent to layer IV in area 23a, the following three points need to be considered. First, von Economo (1929, Fig. 50) vacillated on the presence of a layer IV in LD and showed a layer III(IV) below layer III therein. Second, the granular layer IV of area 29m is continuous with layer IV in area 30 and layer IV in area 23a with both NeuN and a negative image in an SMI32 preparation (Vogt *et al.*, 2001, Fig. 8). This does not mean that layer IV in each area is equivalent; however, von Economo's statement that they are not continuous is not supported. Finally, the dysgranular concept for a cortical area was not established during the early years of cytoarchitectonic analysis nor were immunohistochemical techniques available to clarify the concept. It is not surprising, therefore, that the dysgranular structure of area 30/LD was not appreciated by early neuroanatomists.

The dysgranular nature of area 30 in monkey and human brains has been documented with Nissl, Golgi, and immunohistochemical techniques (Vogt, 1976; Vogt *et al.*, 1995, 1997). Figures 24.15 and 24.19 show that layer IV is of variable thickness with points at which layers IIIc and Va join via neuronal bridges across layer IV, and a recent study demonstrated the dysgranular structure of layer IV in RSC using photomontages along the full lateromedial extent in area 30 (Vogt *et al.*, 2001). Another example of a dysgranular cortex is in ACC where area 32, which sits at the juncture of anterior cingulate and prefrontal cortices, was shown to have islands of neurons in layer IV (Vogt *et al.*, 1995). Thus, dysgranular cortices are both part of the transition of PCC as well as transitions to frontal cortical areas.

Retrosplenial Differentiation Pattern

The pattern of retrosplenial cortical differentiation is obvious in both the human and macaque monkey, and SMI32 preparations are particularly useful in demonstrating these patterns of change because the large pyramidal neurons are often NFP-ir. To the extent that NeuN preparations do not react with glial and endothelial elements, it is possible to analyze selectively small neurons in layers II and IV that contribute to the patterns of differentiation. Figure 24.21 provides a series of photographs through each area on the ventral bank of the PCG that are aligned at the border of layers III/IV and V or layers IV and V. The cell-dense layer of the indusium griseum and subiculum are NFP-ir. The addition of layer III/IV in area 26 is as prominent a change as is the overall reduction in the number of neurons in the deep layer. In area 29l, layer III/IV becomes less neuron-dense and the neurons are larger. The deep layer V is also

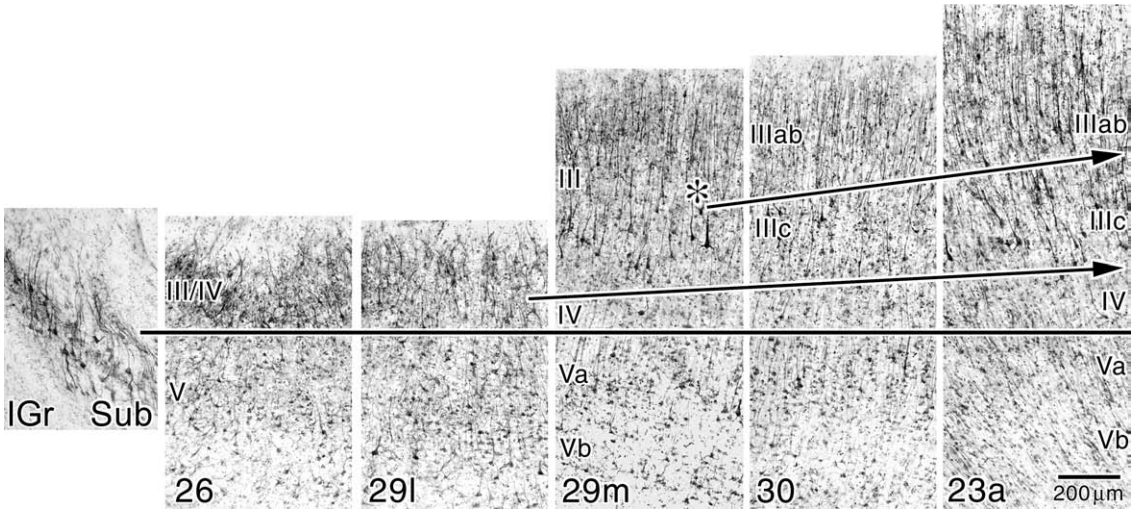

FIGURE 24.21 Cortical transition in humans is best shown for large neurons that are NFP-ir. Area 26 has an external granular layer and only a modest number of pyramids in deep layers. Differentiation of layer III/IV into layers III and IV occurs in area 29m. The asterisk marks the medial part of area 29m where a few large layer IIIc pyramids are first observed. The arrows in superficial layers draw the eye through the transitional events in areas 29m, 30, and 23a as discussed in the text.

populated by many more large and NFP-ir neurons than is true for area 26. Radical changes in morphology occur in area 29m including the addition of a thick layer of medium-sized to large pyramids in layer III, definition of a layer IV, and elaboration of layer Va. Some of the neurons in layer III are so large in the medial part of area 29m that they may presage those of layer IIIc in area 30 as shown in Figure 24.21 at the asterisk. Finally, layer III differentiates in area 30 in parts ab and c and in area 23a layer IV thickens to form an isocortical granular layer.

Elaboration of neuronal architecture and packing in layers II and IV are evident in the NeuN preparations where all neurons are immunoreactive rather than just a subset of large, NFP-ir pyramidal neurons. Figure 24.22 shows the ectosplenial, retrosplenial, and posterior cingulate areas aligned at the top of layer Va. The progressive elaboration of layer III/IV is evident, and it is even possible to identify a layer IV in area 29l that has not been done previously. It appears this differentiation is apparent in Figure 24.22 because a higher level of contrast was applied to the photographic reproduction to highlight neuronal somata. A parvicellular layer is clear in area 29m, and it becomes more pronounced in areas 30 and 23a. The demonstration of layer II addition over layer III is made by selecting the point in area 30 where layer II first appears as indicated with the asterisk. The lancet shape of these neurons appears in area 23a where layer IIIc also reaches a high degree of differentiation in contrast to the plump layer II neurons in area 30. The highest level of differentiation of layers IIIc and IV occurs in area 31. Although not shown in this figure, an SMI32 preparation of area 31 is magnified in Figure 24.17, as noted later. Thus, a combination of immunohistochemical techniques provides a compelling view of different aspects of cortical transition in the human posterior cingulate gyrus and provides a rationale for the nomenclature of each layer.

Area 31: Pinnacle of Cingulate Isocortical Differentiation

Area 31 represents the culmination of two important trends in cingulate cortical transition. The first differentiation trend is that of layer IIIc with a unique neuronal phenotype, and it is observed in the rostrocaudal dimension on the cingulate gyrus. Beginning with the anterior region, there is a progressive increase in the number of large layer III pyramidal neurons. Area 24 has only an undifferentiated layer III; area 24′ has more large neurons in this layer with progressively higher numbers of NFP-ir neurons, but there is only a decrease in neurons density and not a well-defined layer IIIc with large pyramidal neurons. Area 23 has a fully developed layer IIIc and a moderate to high density of NFP-ir neurons in this layer. Area 31 caps this trend with the most extensive layer IIIc and the highest density of NFP-ir neurons on the medial surface (Fig. 24.17). The second differentiation trend is that of layer IV, which occurs in the ventrodorsal dimension on the cingulate gyrus. This trend starts with layer III/IV of area 26. Layer III/IV of areas 26 and 29l differentiate into

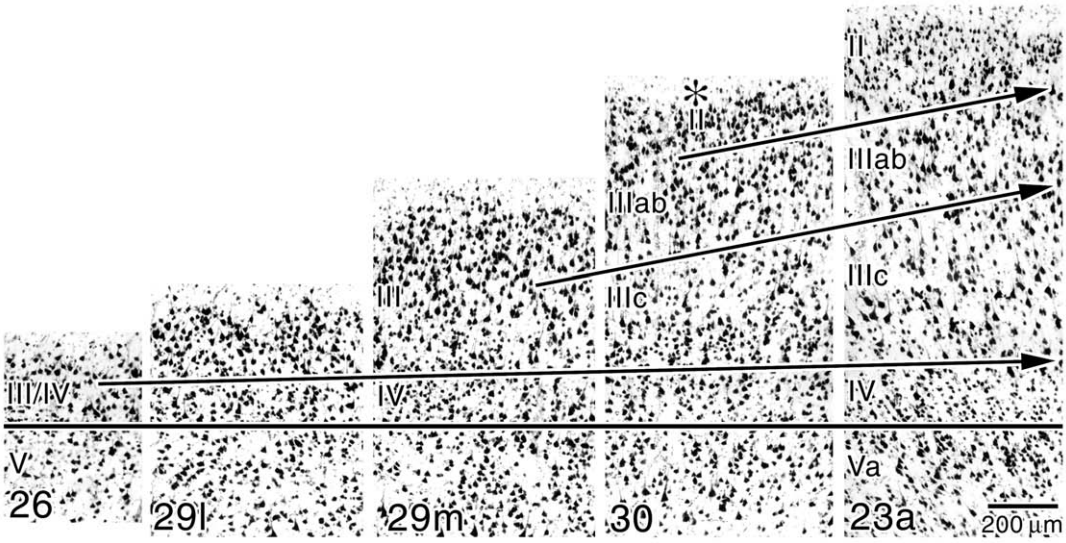

FIGURE 24.22 High-contrast prints of NeuN-immunoreacted tissue show changes in the superficial layers of the human retrosplenial areas that are not evident in SMI32—particularly layers II, IIIab, and IV that have few or no NFP-ir neurons. The rationale for not terming the granular layer of areas 26 and 29 layer II–IV is apparent; layer II is not present until the medial part of area 30 (asterisk, II). Differentiation of the superficial layers in terms of neuron densities and cell shapes is noteworthy in layer II where the plump versus lancet-shaped pyramids of areas 30 and 23a, respectively, are shown. Arrows are oriented to emphasize the direction of cortical transition and do not always fall on each laminar border.

layers III and IV in area 29m, while in area 30 there is the dysgranular layer IV. In area 23, layer IV reaches the isocortical thickness, but in area 31, layer IV is at the maximal thickness and overall neuron density. Thus, area 31 is the final and most differentiated form of granular cingulate cortex, and it forms the superior and caudal parts of the posterior cingulate gyrus.

THE FUTURE FOR CINGULOCENTRIC HYPOTHESES AND RESEARCH

One of the most frequently asked epistemological questions for a neuroscientist with interests in the structure and functions of cingulate cortex is: Why study cingulate cortex and what can be learned from such an undertaking? This question belies the fundamental sampling bias that pervades modern neuroscience with its emphasis on regions with neuronal discharges that are apparently simple and related to single sensory or motor events. For decades neurosurgeons ablated parts of cingulate cortex for the relief of pain and various psychiatric disorders such as obsessive-compulsive disorder and depression, yet research into the physiology of pain and premotor processing was limited to assessing the coding of noxious somatic stimuli in primary and secondary somatosensory cortices and the movement in primary and secondary motor cortices that have no known role in affect and motivation. The cingulocentric viewpoint brings new hypotheses to the scientific enterprise that are not possible in areas where motivation and affect are of little or no relevance. In another example, it is often striking to students of Alzheimer's disease that the cingulate gyrus would be of any interest to uncovering the etiology of this disease. Indeed, the first region to show glucose hypometabolism in patients suffering with their first memory deficit is posterior cingulate cortex (Minoshima *et al.*, 1997)—not entorhinal cortex as most would predict. At this point, the question might be reversed: Why would one study entorhinal cortex in individuals who have early signs of memory loss? Furthermore, there are cases of definite Alzheimer's disease with early signs of frontal lobe damage. Might it not make sense to study prefrontal cortex in these cases (Johnson *et al.*, 1999) and the cingulate motor areas (Vogt *et al.*, 1999)?

Indeed, the long-term consequences of precision anatomy and neurophsyiological studies of cingulate cortex are an understanding of many neurological and psychiatric diseases. There is substantial evidence that cingulate cortex is involved early in many diseases including Alzheimer's disease, schizophrenia, chronic pain, obsessive-compulsive disorder, irritable bowel syndrome, trigeminal neuralgia, post-traumatic stress disorder, and depression. Therefore, the challenge for research with a cingulocentric bias is to find the fundamental mechanisms of neurodegeneration and, ultimately, identify therapies that will stop disease progression by acting directly on the primary cause of each disease, possibly expressed in cingulate cortex.

Dedication and Acknowledgments

Dr. Brent A. Vogt would like to dedicate this work to his intellectual mentors: Dr. Helen Mahut at Northeastern University, Drs. Deepak N. Pandya and Gary W. Van Hoesen at the Harvard Neurology Unit of Boston City and Beth Israel Hospitals, and Drs. Alan Peters and Douglas L. Rosene at Boston University School of Medicine. Each provided the challenge, intellectual framework, resources, and understanding needed to undertake a lifetime study of the structure, functions, and pathologies of cingulate cortex.

The materials prepared, analyzed, and illustrated in this chapter were supported in part by NIH NINDS grants #NS38485 and #NS44222 (BAV) and NIA grant #AG05138 (PRH). We are grateful to Linda Arcure and Will Safrit for their assistance preparing the illustrations.

References

Azmitia, E.C., and Segal, M. (1978). An autoradiographic analysis of the differential ascending projections of the dorsal and median raphe nuclei in the rat. *J. Comp. Neurol.* **179,** 641–668.

Baleydier, C., and Mauguiere, F. (1985). Anatomical evidence for medial pulvinar connections with the posterior cingulate cortex, the retrosplenial area, and the posterior parahippocampal gyrus in monkeys. *J. Comp. Neurol.* **232,** 219–228.

Bancaud, J., and Talairach, J. (1992). Clinical semiology of frontal lobe seizures. *Adv. Neurol.* **57,** 3–58.

Bench, C.J., Frith, C.D., Grasby, P.M., Friston, K.J., Paulesu, E., Frackowiak, R.S.J., and Dolan, R.J. (1992). Patterns of cerebral activation during the Stroop colour word interference task: A positron emission tomography study. *Neuropsychologia* **31,** 907–922.

Berger, B., Alvarez, C., and Pelaprat, D. (1997). Retrosplenial/presubicular continuum in primates: A developmental approach in fetal macaques using neurotensin and parvalbumin as markers. *Devel. Brain Res.* **101,** 207–224.

Berthoz, A. (1997). Parietal and hippocampal contribution to topokinetic and topographic memory. *Phil. Trans. Royal Soc. London, Ser. B.* **352,** 1437–1448.

Biber, M.P., Kneisley, L.W., and LaVail, J.H. (1978). Cortical neurons projecting to the cervical and lumbar enlargements of the spinal cord in young and adult rhesus monkeys. *Exp. Neurol.* **59,** 492–508.

Braak, H. (1976). A primitive gigantopyramidal field buried in the depth of the cingulate sulcus of the human brain. *Brain Res.* **109,** 219–233.

Braak, H. (1979a). Pigment architecture of the human telencephalic cortex. IV. Regio retrosplenialis. *Cell Tissue Res.* **204,** 431–440.

Braak, H. (1979b). Pigment architecture of the human telencephalic cortex. V. Regio anterogenualis. *Cell Tissue Res.* **204**, 441–451.

Braak, H. (1980). "Architectonics of the Human Telencephalic Cortex." Springer-Verlag, Berlin.

Braak, H., and Braak, E. (1993). Alzheimer Neuropathology and Limbic Circuits. *In* "Neurobiology of Cingulate Cortex and Limbic Thalamus" (B.A. Vogt and M. Gabriel, eds.), pp. 606–626. Birkhäuser, Boston.

Broca, P. (1878). Anatomic comparée des circonvolutions cérébrales. Le grand lobe limbique et la scissure limbique dans la série des mammiféres. *Rev. Anthropol.* **1,** Ser 2, 456–498.

Brodmann, K. (1909). "Vergleichende Lokalisationslehre der Grosshirnrinde in ihren Prinzipien dargestellt auf Grund des Zellenbaues." Barth, Leipzig.

Bush, G., Vogt, B.A., Holmes, J., Dale, A.M., Greve, D., Jenike, M.A., and Rosen, B.R. (2002). Dorsal anterior cingulate cortex: A role in reward-based decision making. *Proc. Natl. Acad. Sci.* **99,** 523–528.

Bush, G., Whalen, P.J., Rosen, B.R., Jenike, M.A., McInerney, S.C., and Rauch, S.L. (1998). The counting Stroop: An interference task specialized for functional neuroimaging-Validation study with functional MRI. *Hum. Brain Map.* **6,** 270–282.

Carmichael, S.T., and Price, J.L. (1995). Limbic Connections of the orbital and medial prefrontal cortex in macaque monkeys. *J. Comp. Neurol.* **363,** 615–641.

Carter, C.S., Brauer, T.S., Barch, J.M., Botvinick, M.M., Noll. D., and Cohen, J.D. (1998). Anterior cingulate cortex, error detection, and on-line monitoring of performance. *Science* **280,** 747–749.

Corbetta, M., Miezin, F.M., Dobmeyer, S., Shulman, G.L., and Petersen, S.E. (1991). Selective and divided attention during visual discrimination of shape, color, and speed: Functional anatomy by positron emission tomography. *J. Neurosci.* **11,** 2383–2402.

Dum, R.P., and Strick, P.L. (1991). The origin of corticospinal projections from the premotor areas in the frontal lobe. *J. Neurosci.* **11,** 667–689.

Dum, R.P., and Strick, P.L. (1993). Cingulate motor areas. *In* "Neurobiology of Cingulate Cortex and Limbic Thalamus" (B. A. Vogt and M. Gabriel, eds.), pp. 415–441. Birkhäuser, Boston.

von Economo, C. (1929). "The Cytoarchitectonics of the Human Cerebral Cortex." Oxford University Press, London.

von Economo, C., and Koskinas, G.N. (1925). "Die Cytoarchitektonik der Hirnrinde des erwachsenen Menschen." Springer, Berlin.

Escobedo, F., Fernández-Guardiola, A., and Solis, G. (1973). Chronic stimulation of the cingulum in humans with behavior disorders. *In* "Surgical Approaches in Psychiatry" (L.V. Laitinen and K.E. Livingston, eds.), pp. 65–68. Lancaster (UK), MTP, Baltimore.

Friedman, H.R., Jana, J.D., and Goldman-Rakic, P.S. (1990). Enhancement of metabolic activity in the diencephalon of monkeys performing working memory tasks: A 2-deoxyglucose study in behaving rhesus monkeys. *J. Cog. Neurosci.* **2,** 18–31.

Gemba, H., Sasaki, K., and Brooks, V.B. (1986). 'Error' potentials in limbic cortex (anterior cingulate area 24) of monkeys during motor learning. *Neurosci. Lett.* **70,** 223–227.

George, M.S., Ketter, T.A., Gill, D.S., Haxby, J., Ungerleider, L.G., Herscovitch, P., and Post, R.M. (1993). Brain regions involved in recognizing facial emotion or identity: An oxygen-15 PET study. *J. Neuropsychiat. Clin. Neurosci.* **5,** 384–394.

George, M.S., Ketter, T.A., Parekh, P.I., Horwitz, B., Herscovitch, P., and Post, R.M. (1995). Brain activity during transient sadness and happiness in healthy women. *Am. J. Psychiatry* **152,** 341–351.

Ghaem, O., Mellet, O., Crivello, F., Tzourio, N., Mazoyer, B., Berthoz, A., and Denis, M. (1997). Mental navigation along memorized routes activates the hippocampus, precuneus and insula. *NeuroReport* **8,** 739–744.

Goldman-Rakic, P.S., Selemon, L.D., and Schwartz, M.L. (1984). Dual pathways connecting the dorsolateral prefrontal cortex with the hippocampal formation and parahippocampal cortex in the rhesus monkey. *Neurosci.* **12,** 719–743.

Grasby, P.M., Frith, C.D., Friston, K.J., Bench, C., Frackowiak, R.S.J., and Dolan, R.J. (1993). Functional mapping of brain areas implicated in auditory-verbal memory function. *Brain* **116,** 1–20.

Hof, P.R., Mufson, E.J., and Morrison, J. (1995). Human orbitofrontal cortex cytoarchitecture and quantitative immunohistochemical parcellation. *J. Comp. Neurol.* **359,** 48–68.

Ide, A., Dolezal, C., Fernández, M., Labbé, E., Mandujano, R., Montes, S., Segura, P., Verschae, G., Yarmuch, P., and Aboitiz, F. (1999). Hemispheric differences in variability of fissural patterns in parasylvian and cingulate regions of human brains. *J. Comp. Neurol.* **410,** 235–242.

Johnson, J.K., Head, E., Kim, R., Starr, A., and Cotman, C.W. (1999) Clinical and pathological evidence for a frontal variant of Alzheimer disease. *Arch. Neurol.* **56,** 1233–1239.

Kwan, C.L., Crawley, A.P., Mikulis, D.J., and Davis, K.D. (2000). An fMRI study of the anterior cingulate cortex and surrounding medial wall activations evoked by noxious cutaneous heat and cold stimuli. *Pain* **85,** 359–374.

Lewin, W. and Whitty, C.W. (1960). Effects of anterior cingulate stimulation in conscious human subjects. *J. Neurophysiol.* **23,** 447.

Luppino, G., Matelli, M., Camarda, R.M., Gallese, V., and Rizzolatti, G. (1991). Multiple representations of body movements in mesial area 6 and the adjacent cingulate cortex: An intracortical microstimulation study in the macaque monkey. *J. Comp. Neurol.* **311,** 463–482.

MacLean, P.D. (1993). Perspectives on cingulate cortex in the limbic system. *In* "Neurobiology of Cingulate Cortex and Limbic Thalamus" (B.A. Vogt and M. Gabriel, eds.), pp. 1–15. Birkhäuser, Boston.

Maguire, E.A., Frith, C.D., Burgess, N., Donnett, J.G., Pelaprat, D., and O'Keefe, J. (1998). Knowing where things are: Parahippocampal involvement in encoding object locations in virtual large-scale space. *J. Cog. Neurosci.* **10,** 61–76.

Matelli, M., Luppino, G., and Rizzolatti, G. (1991). Architecture of superior and mesial area 6 and the adjacent cingulate cortex in the macaque monkey. *J. Comp. Neurol.* **311,** 445–462.

Matsunami, K., Kawashima, T., and Satake, H. (1989). Mode of [^{14}C] 2-deoxy-D-glucose uptake into retrosplenial cortex and other memory-related structures of the monkey during a delayed response. *Brain Res. Bull.* **22,** 829–838.

Meyer, G., McElhaney, M., Martin, W., and McGraw, C.P. (1973). Stereotactic cingulotomy with results of acute stimulation and serial psychological testing. *In* "Surgical Approaches in Psychiatry" (L.V. Laitinen and K.E. Livingston, eds.), pp. 39–58. Lancaster (UK), MTP, Baltimore.

Minoshima, S., Giordani, B., Berent, S., Frey, R.A., Foster, N.L., and Kuhl, D.E. (1997). Metabolic reduction in the posterior cingulate cortex in very early Alzheimer's disease. *Ann. Neurol.* **42,** 85–94.

Morecraft, R.J., and Van Hoesen, G.W. (1992). Cingulate input to the primary and supplementary motor cortices in the rhesus monkey: Evidence for somatotopy in Areas 24c and 23c. *J. Comp. Neurol.* **322,** 471–489.

Morecraft, R.J., and Van Hoesen, G. (1998). Convergence of limbic input to the cingulate motor cortex in the rhesus monkey. *Brain Res. Bull.* **45,** 209–232.

Mufson, E.J., Sobreviela, T., and Kordoer, J.H. (1997). Chemical neuroanatomy of the primate insula cortex: Relationship to cytoarchitectonics, connectivity function, and neurodegeneration. *In* "Handbook of Chemical Neuroanatomy" (F.E. Bloom, A. Bjorklund and T. Hokfelt, eds.) vol. 13, Part 1, pp. 377–454. Elsevier, Amsterdam.

Mullen, R.J., Buck, C.R., and Smith, A.M. (1992). NeuN, a neuronal specific nuclear protein in vertebrates. *Development* **116,** 201–211.

Murtha, S., Chertkow, H., Beauregard, M., Dixon, R., and Evans, A. (1996). Anticipation causes increased blood flow to the anterior cingulate cortex. *Hum. Brain Mapp.* **4,** 103–112.

Nauta, W.J.H. (1964). Some efferent connections of the prefrontal cortex in the monkey. *In* "The Frontal Granular Cortex and Behavior" (J.M. Warren and K. Akert, eds.), pp. 397–409. McGraw-Hill, New York.

Neafsey, E.J., Terreberry, R.R., Hurley, K.M., Ruit, K.G., and Frysztak, R.J. (1993). Anterior cingulate cortex in rodents: Connections, visceral control functions, and implications for emotion. *In* "Neurobiology of Cingulate Cortex and Limbic Thalamus" (B.A. Vogt and M. Gabriel, eds.), pp. 207–223. Birkhäuser, Boston.

Nimchinsky, E.A., Gilissen, E., Allman, J.M., Perl, D.P., Erwin, J.M., and Hof, P.R. (1999). A neuronal morphologic type unique to human and great apes. *Proc. Natl. Acad. Sci.* **96,** 5268–5273.

Nimchinsky, E.A., Hof, P.R., Young, W.G., and Morrison, J.H. (1996). Neurochemical, morphologic, and laminar characterization of cortical projection neurons in the cingulate motor areas of the macaque monkey. *J. Comp. Neurol.* **374,** 136–160.

Nimchinsky, E.A., Vogt, B.A., Morrison, J.H., and Hof, P.R. (1995). Spindle neurons of the human anterior cingulate cortex. *J. Comp. Neurol.* **355,** 27–37.

Nimchinsky, E.A., Vogt, B.A., Morrison, J.H., and Hof, P.R. (1997). Neurofilament and calcium-binding proteins in the human cingulate cortex. *J. Comp. Neurol.* **384,** 597–620.

Nowakowski, R.S., and Rakic, P. (1981). The site of origin and route and rate of migration of neurons to the hippocampal region of the rhesus monkey. *J. Comp. Neurol.* **196**, 129–154.

Olson, C.R., Musil, S.Y., and Goldberg, M.E. (1993). Posterior cingulate cortex and visuospatial cognition: Properties of single neurons in the behaving monkey. *In* "Neurobiology of Cingulate Cortex and Limbic Thalamus" (B.A. Vogt and M. Gabriel, eds.), pp. 366–380. Birkhäuser, Boston.

Ono, M., Kubik, S., and Abernathey, C.D. (1990). "Atlas of the Cerebral Sulci." Georg Thieme Verlag, New York.

Pandya, D.N., Van Hoesen, G.W., and Mesulam, M-M. (1981). Efferent connections of the cingulate gyrus in the rhesus monkey. *Exp. Brain Res.* **42,** 319–330.

Pardo, J.V., Pardo, P.J., Janer, K.W., and Raichle, M.E. (1990). The anterior cingulate cortex mediates processing selection in the Stroop attentional conflict paradigm. *Proc. Natl. Acad. Sci. U.S.A.* **87,** 256–259.

Parker, A., and Gaffan, D. (1997). The effect of anterior thalamic and cingulate cortex lesions on object-in-place memory in monkeys. *Neuropsychologia* **35,** 1093–1102.

Paus, T., Petrides, M., Evans, A.C., and Meyer, E. (1993). Role of the human anterior cingulate cortex in the control of oculomotor, manual, and speech responses: A positron emission tomography study. *J. Neurophysiol.* **70,** 453–469.

Paus, T., Tomaiuolo, F., Otaky, N., MacDonald, D., Petrides, M., Atlas, J., Morris, R., and Evans, A.C. (1996). Human cingulate and paracingulate sulci: Pattern, variability, asymmetry, and probabilistic map. *Cereb. Cortex* **6,** 207–214.

Petit, L., Courtney, S.M., Ungerleider, L.G., and Haxby, J.V. (1998). Sustained activity in the medial wall during working memory delays. *J. Neurosci.* **18,** 9429–9437.

Pool, J.L. (1954). The visceral brain of man. *J. Neurosurg.* **11,** 45–63.

Pool, J.L., and Ransohoff, J. (1949). Autonomic effects on stimulating rostral portion of cingulate gyri in man. *J. Neurophysiol.* **12,** 385–392.

Posner, M.I., Peterson, S.E., Fox, P.T., and Raichle, M.E. (1988). Localization of cognitive operations in the human brain. *Science* **240,** 1627–1631.

Raichle, M.E. (2000). The neural correlates of consciousness: An analysis of cognitive skill learning. *In:* "The New Cognitive Neurosciences" (M.S. Gazzaniga, ed.), pp. 1305–1318. The MIT Press, Cambridge, Ma.

Raichle, M.E., Fiez, J.A., Videen, T.O., MacLeod, A.-M., Pardo, J.V., Fox, P.T., and Petersen, S.E. (1994). Practice-related changes in human brain functional anatomy during nonmotor learning. *Cereb. Cortex* **4,** 8–26.

Retzius, G. (1896). "Das Menschenhirn. Studien in der makroskopischen Morphologie." Norstedt Soner, Stockholm.

Rizzolatti, G., Luppino, G., and Matelli, M. (1996). The classic supplementary motor area is formed by two independent areas. *In* "Advances in Neurology" (H.O. Lüders, ed.), Vol. 70: Supplementary Sensorimotor Areas, pp. 45–56. Lippincott-Raven, Philadelphia.

Rose, M. (1928). Gyrus limbicus anterior and Regio retrosplenialis (Cortex holoprotoptychos quinquestratificatus). Vergleichende Architektonik bei Tier und Mensch. *J. Psychol. Neurol.* **35,** 65–173.

Rosene, D.L., and Van Hoesen, G.W. (1977). Hippocampal efferents reach widespread areas of cerebral cortex and amygdala in the rhesus monkey. *Science* **198,** 315–317.

Sarkisov, S.A., Filimonoff, I.N., Kononowa, E.P., Preobraschenskaja, I.S., and Kukuew, E.A. (1955). "Atlas of the cytoarchitectonics of the human cerebral cortex." Medgiz, Moscow.

Schlaug, G., Knorr, U., and Seitz, R.J. (1994). Inter-subject variability of cerebral activations in acquiring a motor skill: A study with positron emission tomography. *Exp. Brain Res.* **98,** 523–534.

Shima, K., and Tanji, J. (1998). Role for cingulate motor area cells in voluntary movement selection based on reward. *Science* **282,** 1335–1338.

Shima, K., Aya, K., Mushiake, H., Inase, M., Aizawa, H., and Tanji, J. (1991). Two movement-related foci in the primate cingulate cortex observed in signal-triggered and self-paced forelimb movements. *J. Neurophysiol.* **65,** 188–202.

Takahashi, N., Kawamura, M., Shiota, J., Kasahata, N., and Hirayama, K. (1997). Pure topographic disorientation due to right retrosplenial lesion. *Neurology* **49,** 464–469.

Talairach, J., and Tournoux, P. (1988). "Co-Planar Stereotaxic Atlas of the Human Brain." Thieme Medical Publishers, New York.

Talairach, J., Bancaud, J., Geier, S., Bordas-Ferrer, M., Bonis, A., and Szikla, G. (1973). The cingulate gyrus and human behavior. *Electroencephalogr. Clin. Neurophysiol.* **34,** 45–52.

Valenstein, E., Bowers, D., Verfaellie, M., Heilman, K.M., Day, A., and Watson, R.T. (1987). Retrosplenial amnesia. *Brain* **110,** 1631–1646.

Van Hoesen, G.W., Morecraft, R.J., and Vogt, B.A. (1993). Connections of the monkey cingulate cortex. *In* "Neurobiology of Cingulate Cortex and Limbic Thalamus" (B.A. Vogt and M. Gabriel, eds.), pp. 249–284. Birkhäuser, Boston.

Vogt, B.A. (1976). Retrosplenial cortex in the rhesus monkey: A cytoarchitectonic and Golgi study. *J. Comp. Neurol.* **169,** 63–98.

Vogt, B.A., and Pandya, D.N. (1987). Cingulate cortex of the rhesus monkey: II. Cortical afferents. *J. Comp. Neurol.* **262,** 271–289.

Vogt, B.A., and Peters, A. (1981). Form and distribution of neurons in rat cingulate cortex: Areas 32, 24, and 29. *J. Comp. Neurol.* **195,** 603–625.

Vogt, B.A., Pandya, D.N., and Rosene, D.L. (1987). Cingulate cortex of the rhesus monkey: I. Cytoarchitecture and thalamic afferents. *J. Comp. Neurol.* **262,** 256–270.

Vogt, B.A., Finch, D. M., and Olson, C.R. (1992). Functional heterogeneity of cingulate cortex: The anterior executive and posterior evaluative regions. *Cereb. Cortex* **2,** 435–443.

Vogt, B.A. (1993). Structural organization of cingulate cortex: Areas, neurons, and somatodendritic transmitter receptors. *In* "Neurobiology of Cingulate Cortex and Limbic Thalamus" (B.A. Vogt and M. Gabriel, eds.), pp. 19–70. Birkhäuser, Boston.

Vogt, B.A., Nimchinsky, E.A., and Hof, P.R. (1997a). Human cingulate cortex: Surface features, flat maps, and cytoarchitecture. *J. Comp. Neurol.* **359,** 490–506.

Vogt, B.A., Vogt, L.J., Nimchinsky, E.A., and Hof, P.R. (1997b). Primate cingulate cortex chemoarchitecture and its disruption in Alzheimer's disease. *In* "Handbook of Chemical Neuroanatomy, The Primate Nervous System" (F.E. Bloom, A. Björklund, and T. Hökfelt, eds.), Vol. 13, Part I, pp. 455–528. Elsevier, Amsterdam.

Vogt, B.A., Martin, A., Vrana, K.E., Absher, J.R., Vogt, L.J., and Hof, P.R. (1999). Multifocal cortical neurodegeneration in Alzheimer's disease. *In:* "Cerebral Cortex" (A. Peters and J.H. Morrison, eds.), pp. 553–601. Plenum, New York.

Vogt, B.A., and Sikes, R.W. (2000). The medial pain system, cingulate cortex, and parallel processing of nociceptive information. *In* "Progress in Brain Research" (E.A. Mayer and C.B. Saper, eds.), Vol. 122, The Biological Basis For Mind Body Interactions, pp. 223–235. Elsevier, Amsterdam.

Vogt, B.A., Vogt, L.J., Perl, D.P., and Hof, P.R. (2001). Cytology of human caudomedial cingulate, retrosplenial, and caudal parahippocampal cortices. *J. Comp. Neurol.* **438:** 353–376.

Whalen, P.J., Bush, G., McNally, R.J., Wilhelm, S., McInerney, S.C., Jenike, M.A., and Rauch, S.L. (1998). The emotional counting Stroop paradigm: An fMRI probe of the anterior cingulate affective division. *Biolog. Psychiatry* **44,** 1219–1228.

Yücel, M., Stuart, G.W., Maruff, P., Velakoulis, D., Crowe, S., Savage, G., and Pantelis, C. (2000). Hemisphere and gender-related differences in the gross morphology of the anterior cingulate/paracingulate cortex in normal volunteers: An MRI morphometric study. *Cereb. Cortex* **10,** 2–22.

Zilles, K. (1990). Cortex. *In* "The Human Nervous System" (G. Paxinos, ed.), pp. 757–802. Academic Press, Sydney.

CHAPTER

25

The Frontal Cortex

MICHAEL PETRIDES
Montreal Neurological Institute, McGill University
Montreal, Quebec, Canada, and
Department of Psychology, McGill University
Montreal, Quebec, Canada

DEEPAK N. PANDYA
Departments of Anatomy and Neurology, Boston University School of Medicine
Boston, Massachusetts, and
Harvard Neurological Unit, Beth Israel Hospital
Boston, Massachusetts, USA

In primate brains, the frontal cortex is the part of the cerebral mantle that lies anterior to the central sulcus and superior to the lateral (Sylvian) fissure. The sulcal and gyral morphology of the human cerebral cortex was the subject of intense investigation in the late 19th century culminating in the excellent surveys of Eberstaller (1890) and Cunningham (1892). It continued to be the focus of research during the first half of the 20th century (e.g., Landau, 1911, 1914; Shellshear, 1926, 1937; Connoly, 1950) but was relatively neglected during the latter part of this century, with some exceptions (e.g., Ono *et al.*, 1990). While standard textbooks of neuroanatomy and neuroradiology usually provide an adequate description of the sulci that define the precentral gyrus and the caudal part of the inferior frontal gyrus (i.e., the motor and premotor cortex and Broca's speech region, respectively), large parts of the remaining frontal cortex are described in terms of only a few sulci and gyri (e.g., superior frontal sulcus and inferior frontal sulcus).

The development of functional neuroimaging in recent years, leading to the demonstration of specific activation foci in many different parts of the human cerebral cortex, has given rise to the need for a more detailed description of the sulcal and gyral patterns of the human cerebral cortex than has typically been provided in recent textbooks of neuroanatomy. Consequently, the first part of this chapter will provide a description of the sulcal and gyral pattern of the cortex of the human frontal lobe. This description is based on the classical studies, as well as recent investigations in our laboratory of the sulcal and gyral patterns of the sulci of the frontal lobe. The second part of this chapter will provide a description of the cytoarchitectonic organization of the human prefrontal cortex. For a description of the motor and premotor cortex, see Chapter 26, and for the cingulate region, see Chapter 24. Finally, the third part of this chapter will briefly summarize current knowledge of the corticocortical connection patterns of the different prefrontal areas

based on experimental anatomical studies on the macaque monkey.

SULCAL AND GYRAL MORPHOLOGY OF THE FRONTAL CORTEX

Lateral Surface of the Frontal Lobe

The Precentral Region

The caudal limit of the frontal lobe is defined by the central sulcus (Figs. 25.1 and 25.2), a sulcus that runs in a primarily dorsoventral but more-or-less oblique direction, its dorsal end lying in a more posterior location than its ventral end. The superior (sprs) and inferior (iprs) precentral sulci that lie rostral to the central sulcus (cs) and, like the central sulcus, maintain a primarily dorsoventral direction define the rostral limit of the precentral gyrus (PrG). The central sulcus does not usually reach the lateral fissure and is separated from it by a short gyrus, the subcentral gyrus (SCG), which is formed by the fusion of the precentral and postcentral gyri in their ventralmost parts. This gyrus is also known as the central (Rolandic) operculum

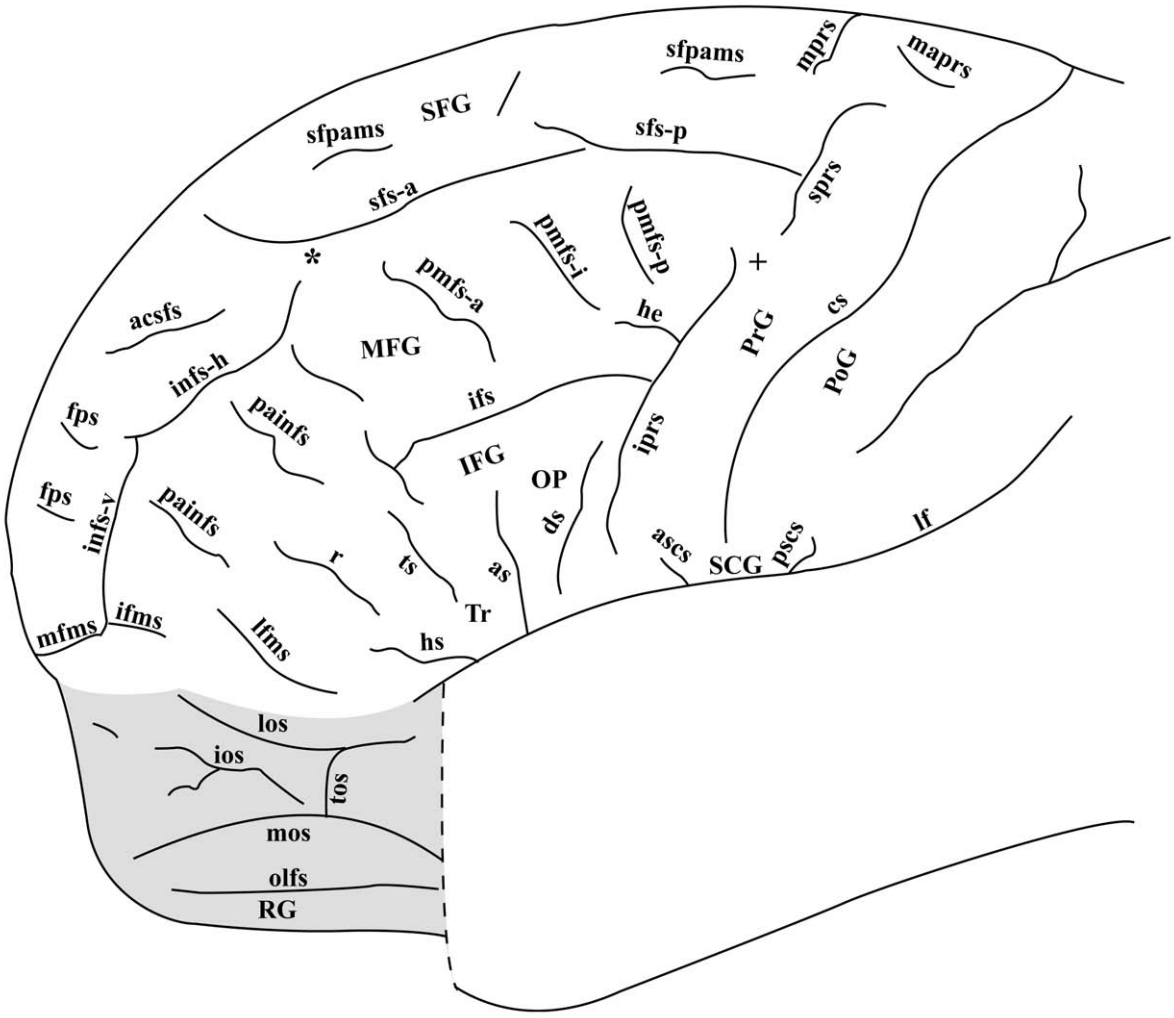

FIGURE 25.1 Diagrammatic representation of the lateral and orbital surfaces of the frontal lobe of the cerebral hemisphere to illustrate the location of the various sulci. The orbital surface is shaded in gray. Abbreviations: as, ascending sulcus (ascending ramus of the lateral fissure); acsfs, accessory superior frontal sulcus; ascs, anterior subcentral sulcus; cs, central sulcus; ds, diagonal sulcus; he, horizontal extension of the inferior precentral sulcus; hs, horizontal sulcus (horizontal ramus of the lateral fissure); infs-h, horizontal part of the intermediate frontal sulcus; infs-v, vertical part of the intermediate frontal sulcus; IFG, inferior frontal gyrus; ifms, intermediate frontomarginal sulcus; ifs, inferior frontal sulcus; ios, intermediate orbital frontal sulcus; iprs, inferior precentral sulcus; lf, lateral fissure; lfms, lateral frontomarginal sulcus; los, lateral orbital frontal sulcus; mfms, medial frontomarginal sulcus; mos, medial orbital sulcus; mprs, medial precentral sulcus; maprs, marginal precentral sulcus; MFG, middle frontal gyrus; pscs, posterior subcentral sulcus; olfs, olfactory frontal sulcus; OP, opercular part of inferior frontal gyrus (pars opercularis); RG, gyrus rectus; SFG, superior frontal gyrus; painfs, paraintermediate frontal sulci; pmfs-a, anterior posterior middle frontal sulcus; pmfs-i, intermediate posterior frontal sulcus; pmfs-p, posterior posterior frontal sulcus; PrG, precentral gyrus; SCG, subcentral gyrus; sfpams, superior frontal paramidline sulci; sfs-a, anterior branch of superior frontal sulcus; sfs-p, posterior branch of superior frontal sulcus; sprs, superior precentral sulcus; tos, transverse orbital sulcus; Tr, triangular part of inferior frontal gyrus (pars triangularis); ts, triangular sulcus; r, radiate sulcus of Eberstaller.

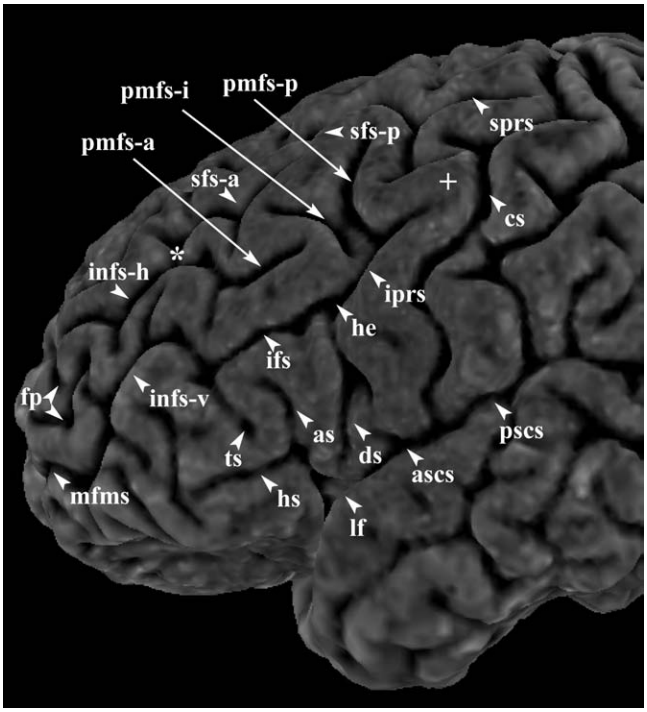

FIGURE 25.2 Three-dimensional reconstruction of the lateral surface of the frontal lobe based on a magnetic resonance image of a single human brain to illustrate the sulci. Abbreviations as in Figure 25.1.

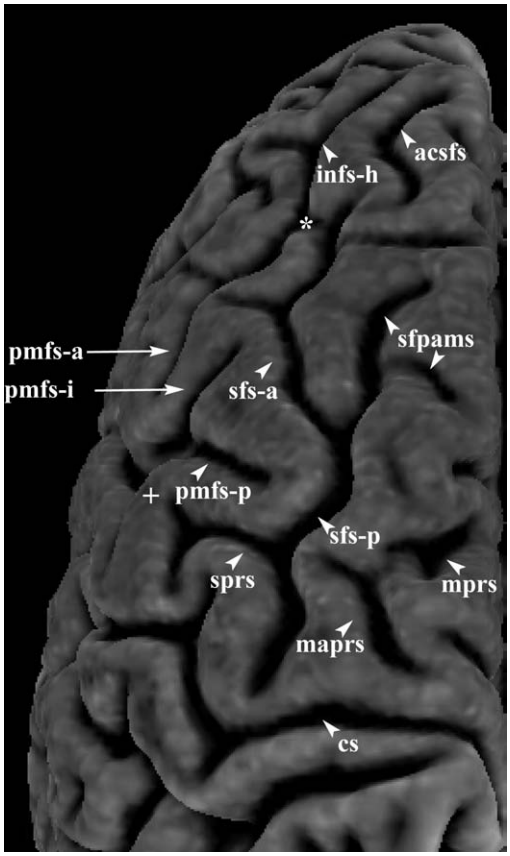

FIGURE 25.3 The dorsal view of the brain illustrated in Figure 25.2 to show the sulci in the dorsal frontal region. Abbreviations as in Figure 25.1.

or the inferior frontoparietal pli de passage. The subcentral gyrus is delimited in front and behind by the anterior (ascs) and posterior (pscs) subcentral sulci, respectively (Figs. 25.1 and 25.2). In some hemispheres, the subcentral gyrus is situated deep within the lateral fissure; in those cases, the central sulcus gives the impression of joining the lateral fissure (Fig. 25.2).

The superior and inferior precentral sulci form the rostral limit of the precentral gyrus and the caudal limit of the superior, middle, and inferior frontal gyri (SFG, MFG, IFG in Fig. 25.1). The inferior precentral sulcus, which is the longer one of the two precentral sulci, originates near the lateral fissure and courses dorsally for a considerable distance reaching the posterior margin of the middle frontal gyrus. The superior precentral sulcus lies, generally, caudal to the dorsalmost point of the inferior precentral sulcus and is often separated from it by a narrow gyral passage that joins the caudal part of the middle frontal gyrus with the precentral gyrus (see + in Figs. 25.1 and 25.2). In a few cases, this narrow gyral passage may be submerged; in those cases, the inferior and superior precentral sulci may fuse superficially giving the impression of a single uninterrupted sulcus. Frequently, there is a more or less horizontally directed extension (he) of the inferior precentral sulcus projecting into the middle frontal gyrus just above the caudal part of the inferior frontal sulcus (see Fig. 25.1). This short ramus sometimes merges with one of the adjoining sulci. In the brain shown in Figure 25.2, the horizontal extension (he) veers medially and merges with the inferior frontal sulcus (ifs) and can only be distinguished in coronal and horizontal sections through this region.

The superior precentral sulcus is shorter than the inferior precentral sulcus and frequently merges with the superior frontal sulcus. In some brains, a part of the superior or the inferior precentral sulcus may be separated; in these cases, one may speak of an intermediate precentral sulcus. However, this is not a useful distinction, and the separated part is best considered as belonging to either the superior or the inferior precentral sulcus.

Dorsal to the superior precentral sulcus, there is often a small dimple that Cunningham labeled the "sulcus precentralis marginalis" (maprs in Figs. 25.1 and 25.3). Rostral to this dimple and often cutting into the medial surface of the hemisphere is the "sulcus precentralis medialis" of Eberstaller. The medial precentral sulcus (mprs in Figs. 25.1 and 25.3) is not

really a medially located sulcus but rather a small sulcus located at the midline of the hemisphere that may extend for a variable distance onto the medial surface of the brain.

The Superior Frontal Gyrus

Anterior to the precentral gyrus, the gross morphology of the lateral surface of the frontal lobe is characterized by three horizontally directed gyri: the superior, middle, and inferior frontal gyri. The superior frontal sulcus is the lateral limit of the superior frontal gyrus (Figs. 25.1, 25.2, and 25.3). Rostral to its point of intersection with the superior precentral sulcus, the superior frontal sulcus runs in a more or less horizontal direction and in its rostral end approaches the midline of the hemisphere. Thus, the rostral end of the superior frontal sulcus is more medially located than its caudal end. The superior frontal sulcus is not a continuous sulcus but consists of two main branches that are either separated on the surface of the brain by an anastomotic fold or can be separated in the depths of the sulcus as can be seen in coronal or horizontal sections. Thus, one can speak of a posterior (sfs-p) and an anterior (sfs-a) superior frontal sulcus (Figs. 25.1, 25.2, 25.3). Rostral to the anterior branch of the superior frontal sulcus, there may be an additional short sulcus that we have called the accessory superior frontal sulcus (acsfs in Figs. 25.1 and 25.3).

The superior frontal sulcus is a deep sulcus that can clearly be identified in coronal or horizontal sections of the brain. Within the superior frontal gyrus, a number of shallow sulci are located approximately halfway between the midline of the brain and the superior frontal sulcus. Sometimes these shallow sulci have been referred to as the "medial frontal sulci" (e.g., Ono *et al.*, 1990), but this is a misnomer as these sulci are *not* lying on the medial surface of the hemisphere. We refer to them as the superior frontal paramidline sulci because they are located next to the midline of the hemisphere in the superior frontal gyrus (sfpams in Figs. 25.1 and 25.3).

The Middle Frontal Gyrus

The middle frontal gyrus is a wide gyrus that lies between the superior and the inferior frontal sulci, rostral to the precentral gyrus. The sulci of the middle frontal gyrus have generated a lot of confusion in the anatomical literature. In the anterior part of the middle frontal gyrus lies a deep sulcus that has been referred to as the middle frontal sulcus or the intermediate frontal sulcus. This sulcus was studied in detail by Eberstaller (1890). It originates in the rostral part of the middle frontal gyrus and runs in a horizontal direction initially (infs-h) and then veers ventrally (infs-v) to reach the medial frontomarginal sulcus (mfms) at the lower edge of the frontal pole (see Figs. 25.1 and 25.2). The horizontal and the vertical branches can be separate is some cases. The caudal end of the middle frontal sulcus begins close to the rostral end of the superior frontal sulcus. There is usually a narrow gyral passage that separates them (see * in Figs. 25.1, 25.2 and 25.3). In several cases, this narrow gyral passage may be collapsed; in these cases, the intermediate frontal sulcus may give the impression of joining the superior frontal sulcus. The superficial joining of these two sulci may lead to confusing the middle frontal sulcus as a continuation of the superior frontal sulcus when one relies on surface inspection of a brain. For instance, Ono *et al.* (1990, p. 51) reported that the superior frontal sulcus connects with the frontomarginal sulcus in 16% of the cases in the right hemisphere and 44% of the cases in the left hemisphere. In our studies, the superior frontal sulcus was never observed to join the frontomarginal sulcus, and we could always distinguish the anterior end of the superior frontal sulcus from the posterior end of the intermediate frontal sulcus in coronal or horizontal sections. Therefore, the statement that the superior frontal sulcus joins the frontomarginal sulcus in some cases has probably resulted from confusion of the intermediate frontal sulcus as a continuation of the superior frontal sulcus.

The anterior part of the middle frontal gyrus can be thought of as being divided into a dorsal and a ventral middle frontal tier by the horizontal part of the intermediate frontal sulcus. The caudal part of the middle frontal gyrus is divided into several smaller gyri by various short sulci that have not been the focus of an investigation before. In our recent examination of the sulcal patterns of the frontal lobe, three short sulci could usually be identified in the posterior middle frontal gyrus. These posterior middle frontal sulci are quite variable in their directions and may merge with each other creating confusing patterns. We have referred to these three sulci as the posterior (pmfs-p), the intermediate (pmfs-i), and the anterior (pmfs-a) posterior middle frontal sulci, proceeding in a caudorostral direction (Figs. 25.1, 25.2, and 25.3). The posterior and intermediate posterior middle frontal sulci can be more or less vertically oriented and directed toward the inferior precentral sulcus (Figs. 25.1, 25.2, and 25.3). It should be noted that a considerable extent of the frontal cortical region lies in the depth of the horizontal extension of the inferior precentral sulcus. Eberstaller (1890) noted that this is the deepest part of the lateral frontal cortex. The anterior posterior middle frontal sulcus is a sulcus that varies considerably in its direction and may approach the superior frontal sulcus and merge superficially with it.

Another set of short sulci can be identified in the anterior part of the middle frontal gyrus running next

to and lateral to the intermediate frontal sulcus. These sulci we refer to as the paraintermediate frontal sulci (painfs in Figs. 25.1 and 25.2). The dorsal one runs in a more or less vertical direction and lies just behind or below the caudal end of the intermediate frontal sulcus.

The Inferior Frontal Gyrus

The inferior frontal gyrus constitutes a large part of the ventrolateral surface of the prefrontal cortex. It is delimited dorsally by the horizontally directed inferior frontal sulcus (ifs) and ventrally by the rostral part of the lateral fissure (Figs. 25.1 and 25.2). In a caudorostral direction, the inferior frontal gyrus can be divided into three parts: the pars opercularis, the pars triangularis, and the pars orbitalis. The pars opercularis is delimited caudally by the inferior precentral sulcus and rostrally by the ascending sulcus (as; i.e., the ascending ramus of the lateral fissure). The pars triangularis lies between the ascending sulcus and the horizontal sulcus (hs), also known as the horizontal ramus of the lateral fissure. The pars orbitalis lies ventral to the horizontal sulcus as far as the lateral orbital sulcus. The pars opercularis is seen usually as a vertically oriented gyrus that is subdivided into a rostral and a caudal part by the diagonal sulcus (ds). In different brains, a variable extent of the caudal part of the pars opercularis is submerged into the inferior precentral sulcus (see Tomaiuolo *et al.*, 1999). Depending on the curvature of the pars opercularis and how much of it stays on the surface of the brain, the diagonal sulcus may appear to lie in the middle of the pars opercularis clearly separating it into two parts, or it may appear to join any of the surrounding sulci.

Within the pars triangularis, there is usually a small sulcus, the triangular sulcus (ts), also known as the incisura capitis. There may be an additional more rostrally located sulcus that is directed toward the pars triangularis, which Eberstaller (1890) named the sulcus radiatus (r). The inferior frontal sulcus originates, caudally, close to the inferior precentral sulcus; in many cases, there is a clear separation between these two sulci. In other cases, the narrow bridge of cortex that separates them may be submerged, and the inferior frontal sulcus and the inferior precentral sulcus merge superficially. Eberstaller (1890) pointed out that the inferior frontal sulcus extends rostrally until about the midportion of the dorsal edge of the pars triangularis of the inferior frontal gyrus. Our recent investigation of the frontal sulci in 80 cerebral hemispheres has confirmed Eberstaller's observations. In some textbooks (e.g., Ono *et al.*, 1990), the term "inferior frontal sulcus" has been used loosely to include additional sulci, such as the sulcus radiatus and the lateral frontomarginal sulcus, that lie anterior to it and, sometimes, abut superficially with it. The tendency to treat these distinct sulci as rostral extensions of the inferior frontal sulcus introduces considerable confusion in the identification of the frontal sulci. For instance, we observed that, although in some cases the sulcus radiatus and the lateral frontomarginal sulci may anastomose and appear to join superficially the rostral end of the inferior frontal sulcus, these three sulci could be clearly separated by careful examination of sections of the frontal lobe.

The Frontopolar Region

The term "frontomarginal sulcus" was first used by Wernicke (1876) to refer to a deep sulcus that is found at the ventralmost part of the frontal pole (Figs. 25.1, 25.2, and 25.4). Eberstaller (1890) and Economo and Koskinas (1925) recognized a complex of three distinct frontomarginal sulci that are running in the ventralmost part of the rostral frontal lobe along the edge with the orbital surface. These sulci are the medial frontomarginal sulcus (mfms), the intermediate frontomarginal sulcus (ifms), and the lateral frontomarginal

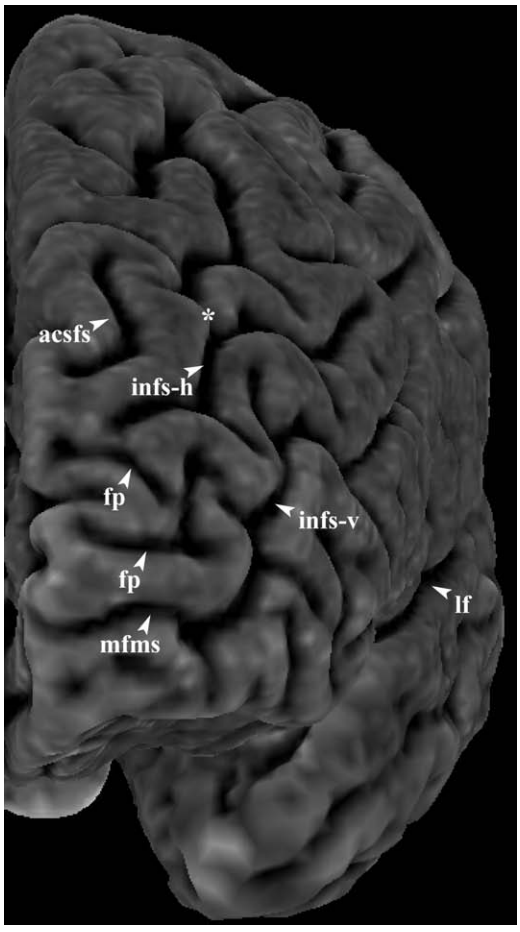

FIGURE 25.4 The frontopolar view of the brain illustrated in Figure 25.2 to show the sulci in this region. Abbreviations as in Figure 25.1.

sulcus (lfms) (Figs. 25.1, 25.2, and 25.4). The medial and intermediate frontomarginal sulci abut the ventralmost extension of the intermediate frontal sulcus (infs-v). The lateral frontomarginal sulcus lies rostral and lateral to the horizontal sulcus and is directed dorsally. In a recent atlas by Duvernoy (1991), the lateral frontomarginal sulcus was labeled as the lateral orbital sulcus. The term "lateral orbital sulcus" has been classically used by several investigators to refer to the lateral part of the H pattern of the sulcal complex that is lying on the orbital surface of the frontal lobe (e.g., Economo and Koskinas, 1925, pp. 28–31; Bailey and Bonin, 1951, p. 45). It must be emphasized here that the lateral frontomarginal sulcus lies lateral and dorsal to the lateral orbital sulcus and has been recognized as such by several major investigators such as Eberstaller (1890, p. 84) and Economo and Koskinas (1925, pp. 28–31).

The Orbital Surface of the Frontal Lobe

At the medialmost part of the orbital surface of the frontal lobe, one can identify the olfactory sulcus which is running in a rostrocaudal direction and delimits the gyrus rectus (RG), which lies medial to it (Figs. 25.1 and 25.5). Typically, the posterior end of the olfactory sulcus lies more lateral than its anterior end (Chiavaras and Petrides, 2000). Lateral to the olfactory sulcus, there are two longitudinally directed sulci, the medial (mos) and lateral (los) orbital sulci, which are joined together by the transverse orbital sulcus (tos) to form the impression of an H or a K pattern. The medial and lateral orbital sulci can be divided into rostral and caudal parts relative to the transverse orbital sulcus. The gyrus that lies between the olfactory sulcus and the medial orbital sulcus is often referred to as the medial orbital gyrus. The cortex lying rostral to the transverse orbital sulcus and between the medial and lateral orbital sulci can be referred to as the anterior orbital gyrus, and the cortex that lies caudal to it, as the posterior orbital gyrus. Lateral to the lateral orbital sulcus lies the orbital extension of the ventrolateral prefrontal cortex (i.e., the pars orbitalis of the inferior frontal gyrus).

One or two longitudinal sulci, named the intermediate orbital sulci (ios), may be lodged within the anterior orbital gyrus between the rostral parts of the medial and lateral orbital sulci. Similarly, in some cases one or two posterior orbital sulci can be observed behind the transverse orbital sulcus within the posterior orbital gyrus between the caudal parts of the medial and lateral orbital sulci. In some brains, a small dimple known as the sulcus fragmentosus can be identified between the olfactory sulcus and the medial orbital sulcus (Fig. 25.5).

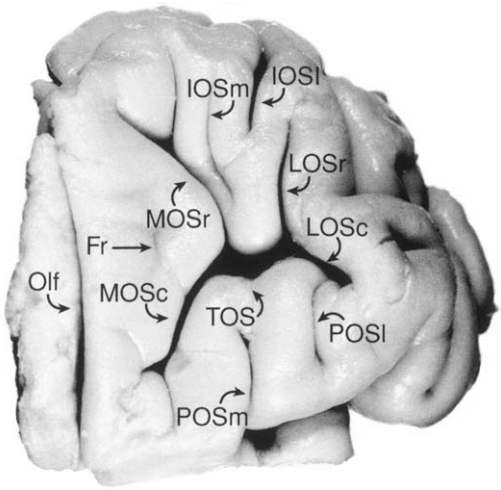

FIGURE 25.5 Photograph of the orbital frontal surface of a brain to show the sulci in this region. Abbreviations: Fr, sulcus fragmentosus; IOSm, medial intermediate orbital sulcus; IOSl, lateral intermediate orbital sulcus; MOSc, caudal part of medial orbital sulcus; MOSr, rostral part of medial orbital sulcus; LOSc, caudal lateral orbital sulcus; LOSr, rostral lateral orbital sulcus; Olf, olfactory sulcus; POSm, medial posterior orbital sulcus; POSl, lateral posterior orbital sulcus; TOS, transverse orbital sulcus.

ARCHITECTONIC ORGANIZATION

The cerebral cortex is not uniform in structure, but it can be divided into several distinct areas based on differential patterns of the neurons in the cortical layers. Cytoarchitectonic studies of the human cerebral cortex were initiated at the beginning of the 20th century. The first complete map to be published was that of Campbell (1905), who divided the cortex into a few general regions. A little later, Brodmann's map appeared in which a large number of cortical areas were identified (Brodmann, 1908, 1909, 1914) and labeled with distinct numbers (Fig. 25.6A). In 1925, Economo and Koskinas published a major atlas of the human cerebral cortex in which the different architectonic areas were labeled with letters (Fig. 25.6B), described in detail, and documented with excellent photomicrographs. In the 1950s, the maps of Bailey and Bonin (1951) and Sarkissov *et al.* (1955) (Fig. 25.6C) appeared. The map by Sarkissov is a modified version of the Brodmann map based on a survey of the cytoarchitecture of several brains. In 1962, Sanides published a monograph focused on the architecture of the human frontal lobe. The architecture of selected parts of the prefrontal cortex of the human brain has also been studied by Beck (1949), Rajkowska and Goldman-Rakic (1995), Amunts *et al.* (1999), and Semendeferi *et al.* (1998). Apart from these studies, other investigators have described the architecture of the cerebral cortex based on myelin (Vogt, 1910; Vogt and Vogt, 1919) or on pigment architecture (Braak, 1979).

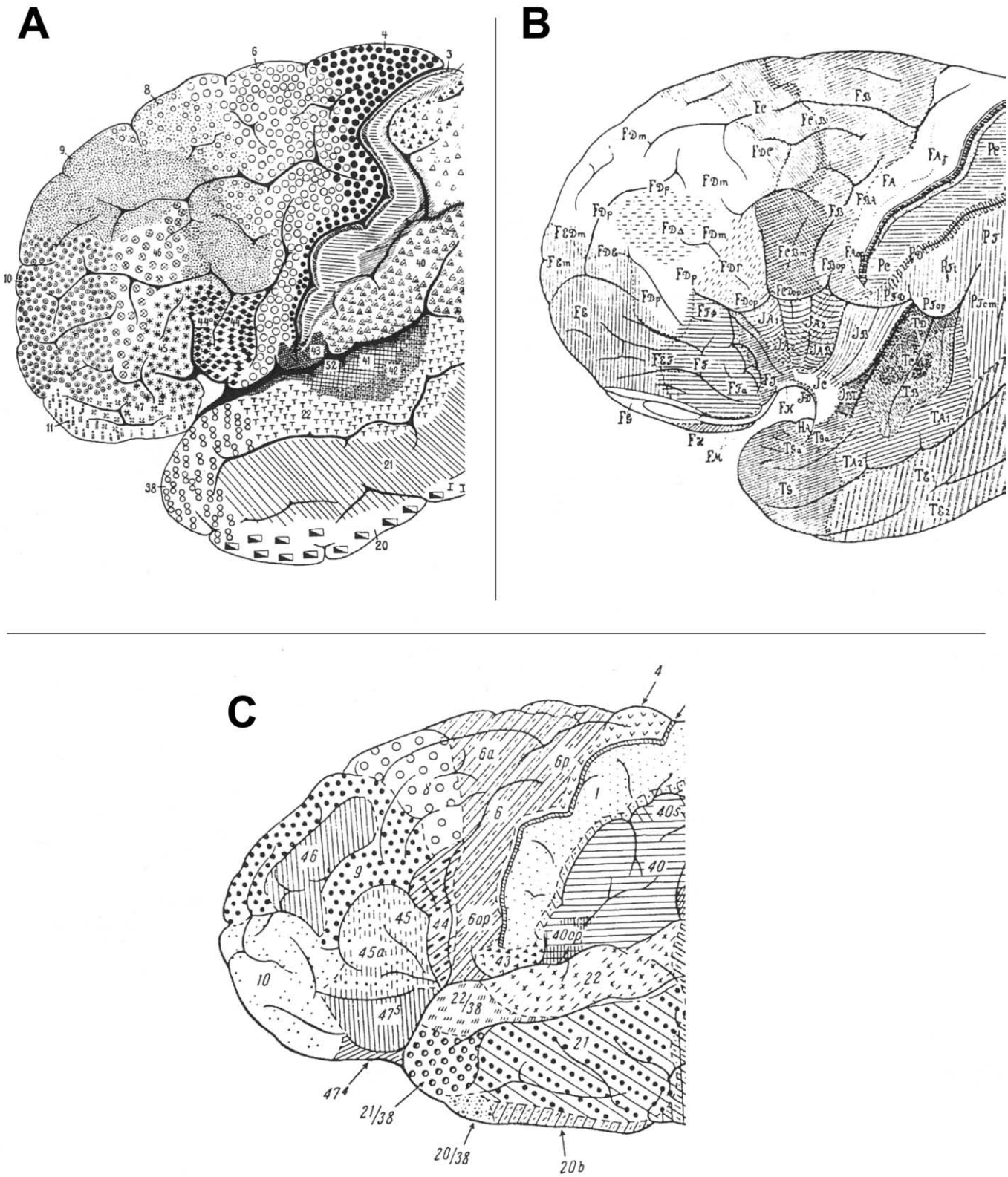

FIGURE 25.6 Cytoarchitectonic maps showing the human frontal cortex as parcellated by **(A)** Brodmann (1914), **(B)** Economo and Koskinas (1925), and **(C)** Sarkissov *et al.* (1955).

We have recently reexamined the architecture of the prefrontal cortex of the human brain in the context of a comparison with the architecture of the prefrontal cortex of the macaque monkey (Petrides and Pandya, 1994, 1999, 2002). Based on this comparative architectonic study, we modified somewhat the Brodmann scheme (Figs. 25.7 and 25.8). The description of the architecture of the human frontal cortex presented in this chapter follows our investigation. The present architectonic description is limited to the prefrontal cortex, namely the large region that lies rostral to the precentral motor region.

Dorsolateral Prefrontal Cortex

Area 8

Area 8 lies on the posterior part of the superior and middle frontal gyri and extends medially as far as the paracingulate sulcus (Fig. 25.7). Posteriorly, it abuts rostral area 6 and, anteriorly, area 9 on the superior frontal gyrus and area 9/46 on the middle frontal gyrus. Area 8 can be divided into two major subdivisions: area 8A and 8B. Area 8A lies on the middle frontal gyrus. It is characterized by a dense layer II that is clearly separated from layer III (Fig. 25.9). Layer III consists of medium and large pyramidal cells, as well as very large and darkly stained pyramidal neurons that occupy the lower part of this layer. Layer IV is also well developed. Layers V and VI contain medium to small pyramidal neurons, and Layer Va has a few darkly stained large pyramidal cells. The separation between layers Va and VI is marked by a thin and cell-sparse layer Vb. Area 8A can be divided into a ventral part (i.e., area 8Av), which occupies a small portion of the caudalmost middle frontal gyrus, and a dorsal part (i.e., 8Ad) extending into the superior frontal sulcus.

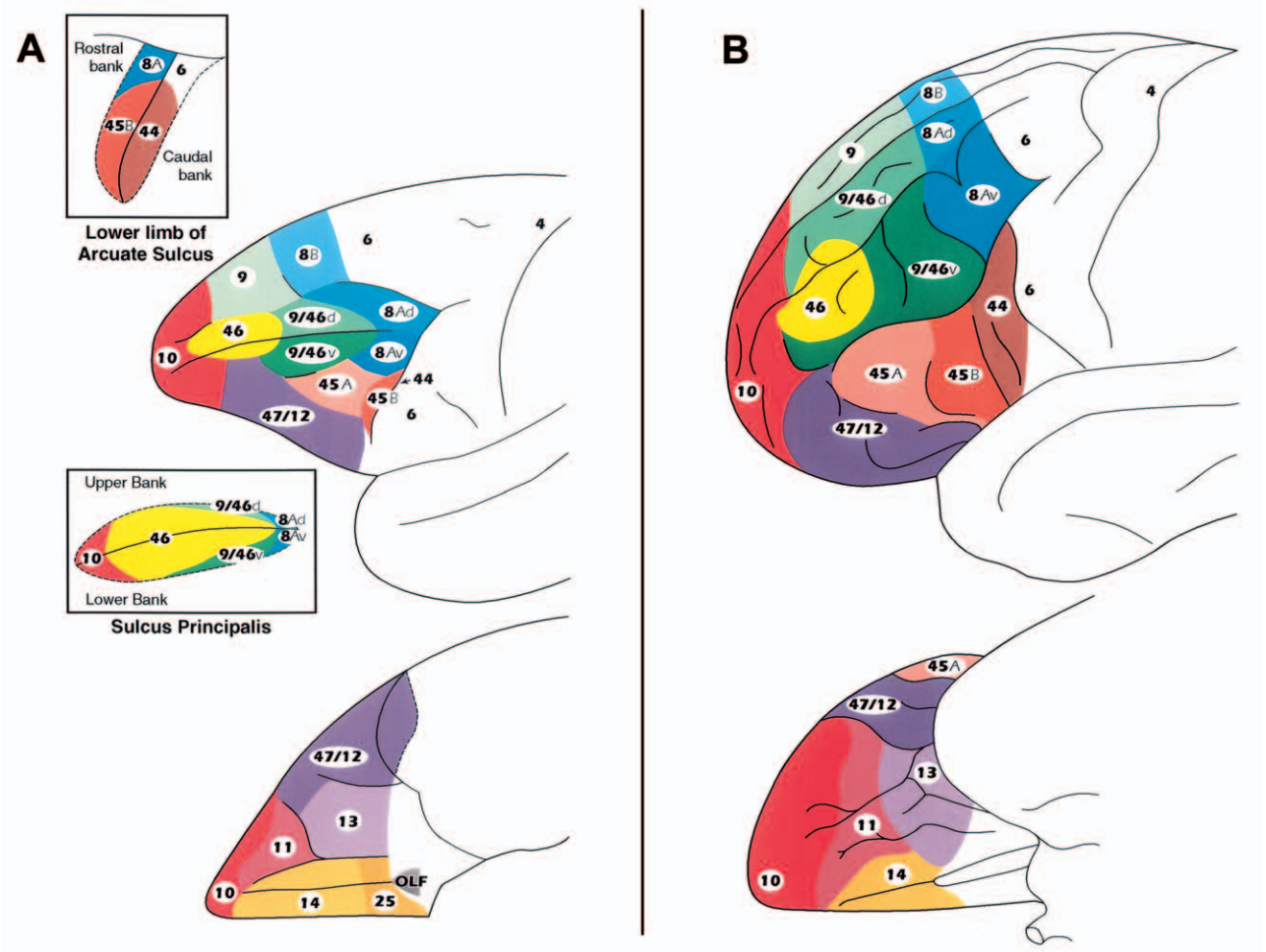

FIGURE 25.7 Cytoarchitectonic maps of the lateral and orbital surfaces of the frontal lobe of the macaque monkey **(A)** and the human **(B)** brains as parcellated by Petrides and Pandya (1994). In A, the inset diagrams display the region within the lower limb of the arcuate sulcus and the sulcus principalis to show the cytoarchitectonic areas lying within their banks.

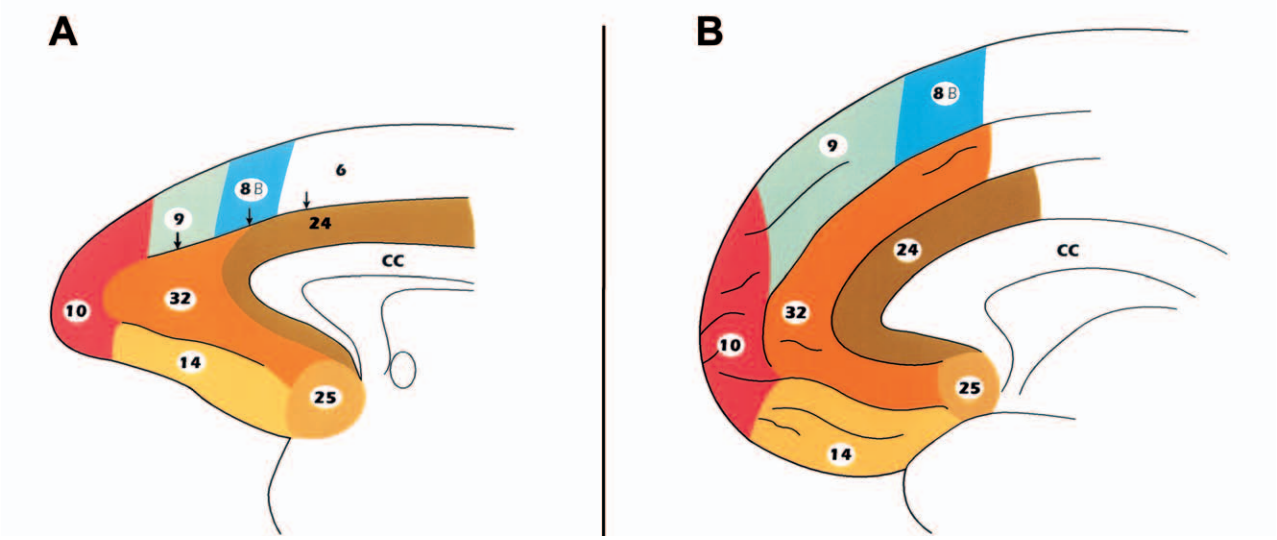

FIGURE 25.8 Cytoarchitectonic maps of the medial surface of the frontal lobe of the macaque monkey **(A)** and the human **(B)** brains as parcellated by Petrides and Pandya (1994).

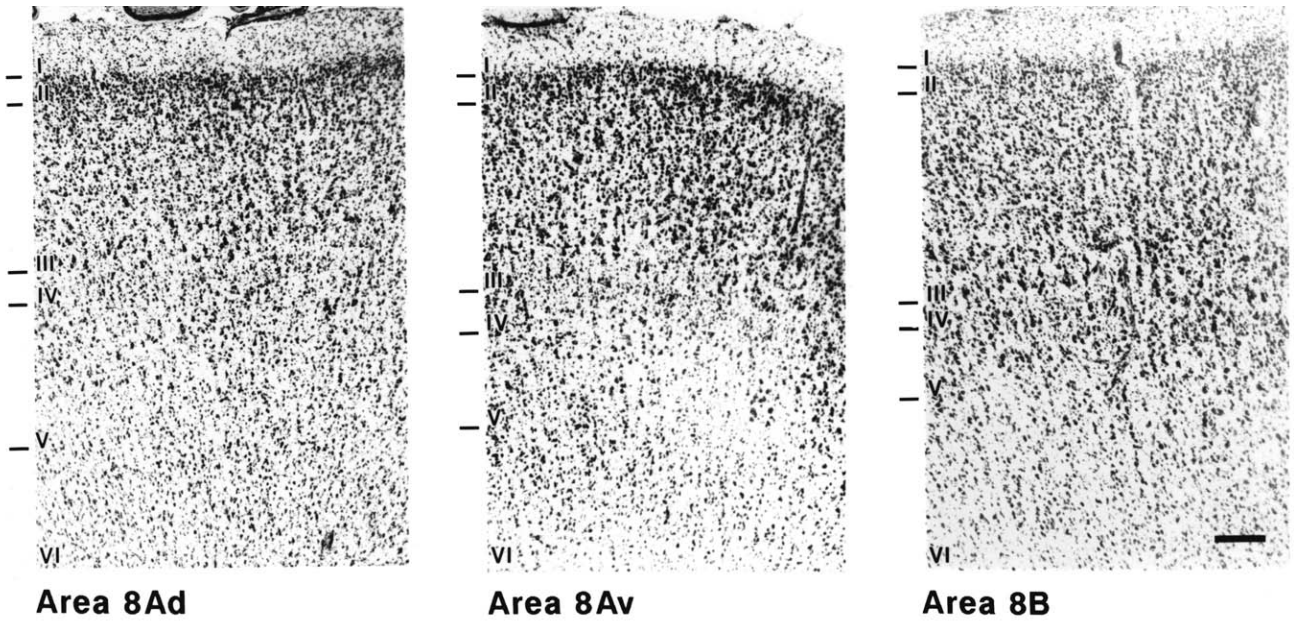

FIGURE 25.9 Photomicrographs of cortical areas 8Ad, 8Av, and 8B of the human frontal cortex. The roman numerals in each photograph indicate the cortical layers. The black bar in the photomicrograph of area 8B equals 1 mm.

The large pyramidal neurons in layer III are less dense in area 8Ad compared with area 8Av. Layer IV is somewhat more marked in area 8Av. Area 8B is located on the superior frontal gyrus and extends medially as far as the paracingulate sulcus. Area 8B has a relatively poorly developed layer IV and clusters of large neurons in the lower part of layer III. Area 8B resembles rostrally adjacent area 9 on the superior frontal gyrus that also has a poorly developed layer IV (see later).

Areas 9, 9/46, and 46

The dorsolateral frontal cortex at the midsection of the superior and middle frontal gyri is occupied by areas 9 and 46 in the map of Brodmann (1908, 1909) and Sarkissov *et al.* (1955) (Fig. 25.6A, C). In these maps, area 9 is shown to occupy both the superior frontal gyrus and a part of the middle frontal gyrus. Thus, area 46 (i.e., area FDΔ of Economo and Koskinas, 1925; Fig. 25.6B), which lies on the middle frontal

gyrus, is bordered dorsally and caudally by area 9. We observed that the architecture of the portion of the superior frontal gyrus designated as area 9 is different from that of the portion of the middle frontal gyrus also labeled as area 9 in the maps of Brodmann (1908, 1909) and Sarkissov *et al.* (1955). Indeed, the architecture of the portion of the middle frontal gyrus labeled as area 9 in the maps of Brodmann (1908, 1909) and Sarkissov *et al.* (1955) is more akin to area 46, which also lies on the middle frontal gyrus. Interestingly, this cortex corresponds in architecture to the cortex found in the caudal part of the sulcus principalis in the macaque monkey and that has been included with area 46 by Walker (1940). We have therefore labeled the portion of area 9 that lies on the middle frontal gyrus as area 9/46 (Fig. 25.7B) to acknowledge its architectonic similarity with area 46 and the fact that an equivalent cortical region was included as part of area 46 in the monkey by Walker (1940).

Area 9/46, which lies on the middle frontal gyrus, has a well defined layer II that is distinct from layer III (Fig. 25.10). Layer III contains a substantial number of large darkly stained pyramidal neurons in its lower part, a characteristic that sets it apart from area 46 (see later). Layer IV is well developed. Layer Va contains a number of medium pyramidal cells, and layer VI is separated from layer Va by a cell-sparse layer Vb. There is a slight difference between the ventral (9/46v) and dorsal (9/46d) parts of area 9/46. In area 9/46d, the large pyramidal cells in the lower part of layer III are less densely packed compared with those of area 9/46v, and layer IV is not as broad.

Area 9 lies on the superior frontal gyrus and extends medially to the paracingulate sulcus (Fig. 25.7). The main characteristic of area 9 that sets it apart from areas 46 and 9/46 is the fact that layer IV is not well developed (i.e., it is narrow and not very dense; Fig. 25.10). Area 9 has a compact layer II. The upper part of layer III is relatively dense, whereas the lower part is not as cell dense and has a number of large deeply stained pyramidal neurons.

Area 46 occupies the more anterior part the middle frontal gyrus (Fig. 25.7B). The extent of this area as seen from the surface of the brain can be deceptively small because a large part of it lies hidden in the depth of the intermediate frontal sulcus (Fig. 25.7B). In area 46, layer IV is well developed (i.e., it is broad, cell-dense, and easily identifiable; Fig. 25.10). Layer III of area 46 contains small and medium pyramidal cells, and the lower part of layer III lacks the large deeply stained pyramidal neurons found in areas 9 and 9/46. Layer Va contains pyramidal cells of medium size. Because of the relative absence of large neurons in layers III and V, and the rather even distribution of neurons in these layers, area 46 has a uniform appearance that distinguishes it from both areas 9 and 9/46.

Ventrolateral Prefrontal Cortex

Area 44

Rostral to the inferior precentral sulcus in the pars opercularis of the inferior frontal gyrus lies a cortical region labeled as area 44 by Brodmann (1908, 1909) or area FCBm by Economo and Koskinas (1925)

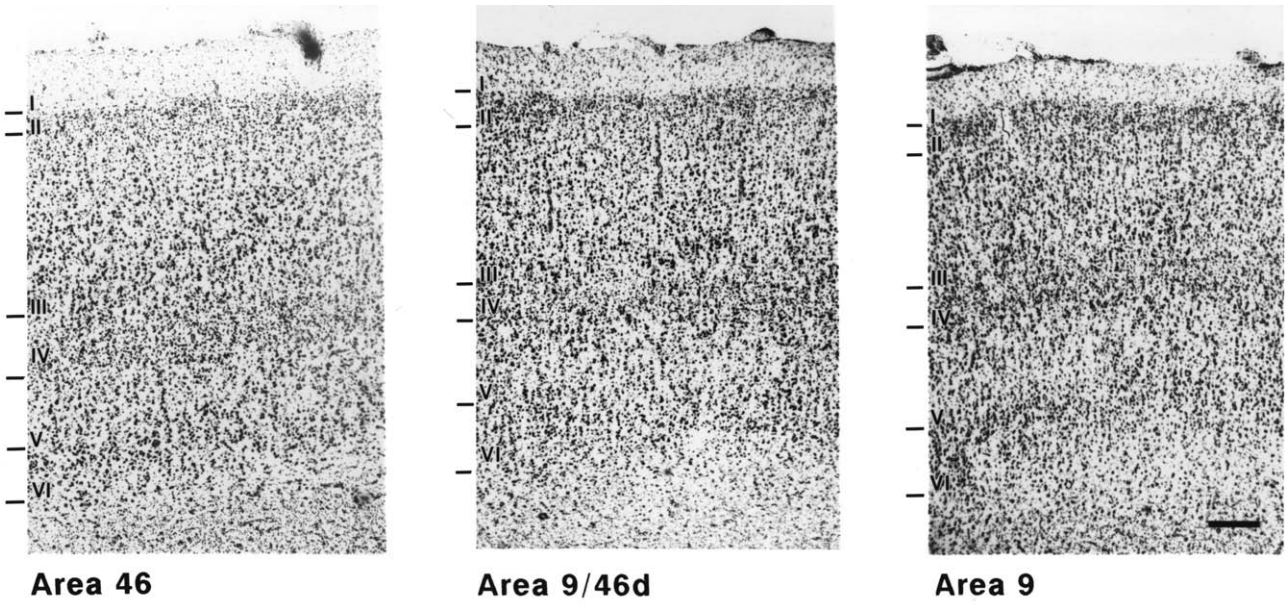

FIGURE 25.10 Photomicrographs of cortical areas 46, 9/46d, and 9 of the human frontal lobe. The roman numerals in each photograph indicate the cortical layers. The black bar in the photograph of area 9 equals 1 mm.

(Fig. 25.6A, B, and 25.7B). This area has been thought to constitute the main part of Broca's speech area. The pars opercularis often comprises two more or less vertically oriented small gyri that are separated by the diagonal sulcus. Area 44 has a densely packed layer II whose lower margin blends with layer III (Fig. 25.11). Layer III contains small and medium pyramidal cells mostly in its upper part. The lower half of this layer is occupied by deeply stained large pyramidal cells. Layer IV is dysgranular containing only a few neurons. Unlike the lower part of layer III, layer Va contains medium-sized pyramidal cells. Layer Vb contains fewer neurons than Va and layer VI is broad.

Area 45

Area 45 occupies the pars triangularis of the inferior frontal gyrus (Brodmann, 1908, 1909; Sarkissov *et al.*, 1955; Amunts *et al.*, 1999) (Fig. 25.6A, C). Economo and Koskinas (1925) have designated this area as FDΓ (Fig. 25.6B). In area 45, layer III contains small to medium pyramidal cells in its upper part and, in its lower part, has clusters of deeply stained and densely packed large pyramidal neurons (Fig. 25.11). Layer IV is well developed. The defining feature of area 45 that distinguishes it clearly from all adjacent areas are the clusters of large and deeply stained pyramidal neurons in the deeper part of layer III in combination with the well-developed layer IV. Layer Va contains medium pyramidal cells, and layer Vb is cell-sparse; therefore, layer VI is clearly separated from Va. Area 45 can be subdivided into a rostral and a caudal part, labeled areas 45A and 45B, respectively.

Area 47/12

In the classical maps of the human cerebral cortex, the cortical region rostroventral to area 45 has been labeled as area 47 (Fig. 25.6A, C). This region is shown to occupy the most rostral part of the inferior frontal gyrus (pars orbitalis), extending onto the caudal half of the orbitofrontal cortex (e.g., Sarkissov *et al.*, 1955; Beck, 1949). Brodmann (1909) pointed out that this region is heterogenous and that it can be further subdivided. Sarkissov *et al.* (1955) subdivided this large and architectonically heterogeneous region into five parts. In our comparative architectonic examination, we observed that the part of this large region that lies rostral and ventral to area 45 and extends as far as the lateral orbital sulcus has architectonic features comparable to those of Walker's area 12 in the monkey. We have therefore labeled this part as area 47/12 to denote the fact that this particular part of the previously labeled area 47 is comparable in architecture to Walker's ventrolateral area 12 in the monkey brain (Fig. 25.7A, B). By contrast, the remaining part of classical area 47 that occupies the caudal orbitofrontal cortex has different architectonic features that are similar to those of orbitofrontal area 13 of the monkey (see later).

The transition from area 45 to area 47/12 can be clearly defined. Basically, the conspicuously large and

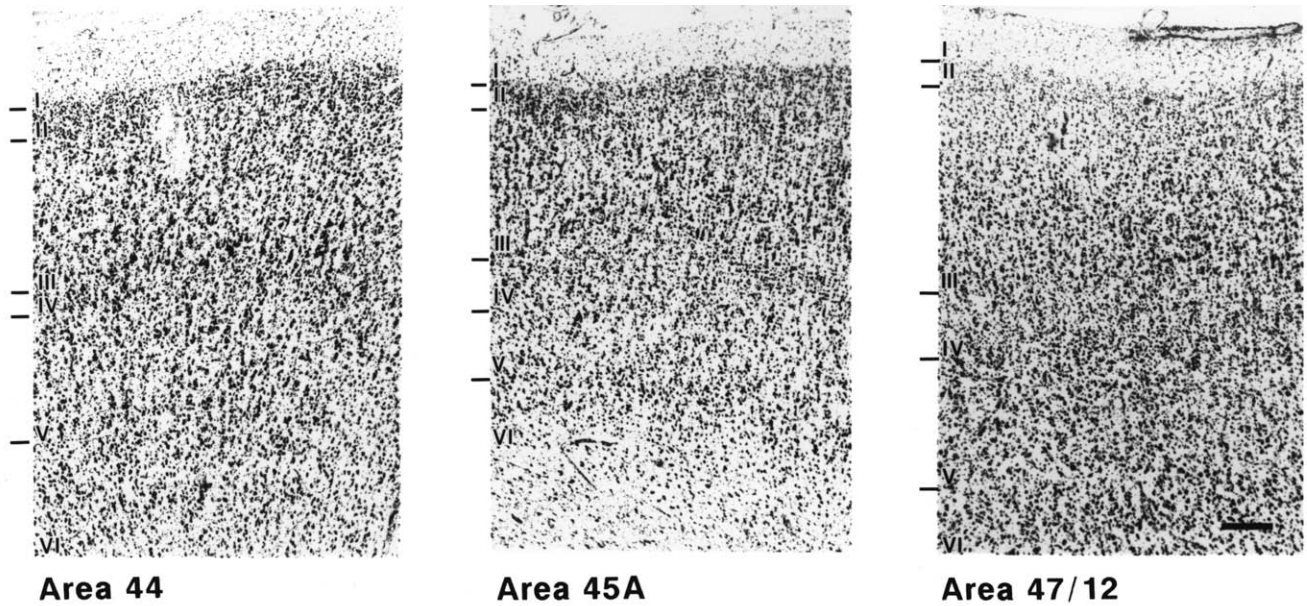

FIGURE 25.11 Photomicrographs of cortical areas 44, 45A, and 47/12 of the human frontal lobe. The roman numerals in each photograph indicate the cortical layers. The black bar in the photograph of area 47/12 equals 1 mm.

deeply stained pyramidal neurons in the deeper part of layer III, which are the defining feature of area 45, are replaced in area 47/12 by medium-sized neurons (Fig. 25.11). Thus, in area 47/12, layer III contains small and medium pyramidal cells in its upper part and medium and somewhat larger pyramidal neurons in its lower part. In area 47/12, layer IV is not as broad as in area 45. Layers V and VI contain densely packed medium to small pyramidal cells, and these infragranular layers are more prominent than those of adjacent area 45. The part of area 47/12 that extends onto the orbital surface differs slightly from the more lateral part in that layer IV is less well developed and, thus, one can speak of a lateral and an orbital part of area 47/12.

Orbital Frontal Cortex

As pointed out previously, Brodmann (1909) included a large region of the caudal orbitofrontal cortex as part of area 47 and labeled the remaining orbitofrontal cortex as area 11. He acknowledged, however, that these two large regions are architectonically heterogeneous and that they can be further subdivided. The caudomedial part of the region that Brodmann labeled as area 47 has architectonic characteristics comparable to those of Walker's area 13. We have therefore designated this region as area 13, distinguishing it from the more laterally located orbital extension of area 47/12, as well as the rostrally located area 11 and the medially located area 14 (Fig. 25.8A, B).

In area 13, layer II is clearly distinct, and layer III contains small to medium size pyramidal neurons (Fig. 25.12). The distinguishing feature of this area is the thin and irregular layer IV that characterizes it as a dysgranular type of cortex. Layer V contains mainly small pyramidal cells. Layer Vb blends with layer VI. Layer VI contains small to medium and densely packed pyramidal neurons.

Caudal to area 13 on the orbital frontal cortex lies the orbital proisocortex. This area is characterized by ill-defined layer II with an irregular outer margin. Layer III contains sparsely populated small pyramidal neurons. Layer IV is virtually absent, and layers V and VI contain deeply stained medium-sized pyramidal neurons. The orbital proisocortex has a bilaminated appearance that results from the juxtaposition of the deeply stained infragranular layers V and VI with the lightly stained sparse supragranular layers II and III.

The cortex that occupies the gyrus rectus on both its medial and orbital parts, as well as the remaining rostral part of the orbitofrontal cortex, was labeled by Brodmann (1909) as area 11 (Fig. 25.6A). Brodmann noted that, within this large region, the architecture of the cortex of the gyrus rectus is distinct from that of the remaining region. In our comparative architectonic examination, we noted that the cortex occupying the gyrus rectus has architectonic features comparable to those of Walker's cortical area 14 of the macaque monkey, which also occupies the gyrus rectus (Fig. 25.7A, B). We have therefore denoted the cortex of the gyrus rectus in the human brain as area 14. We have

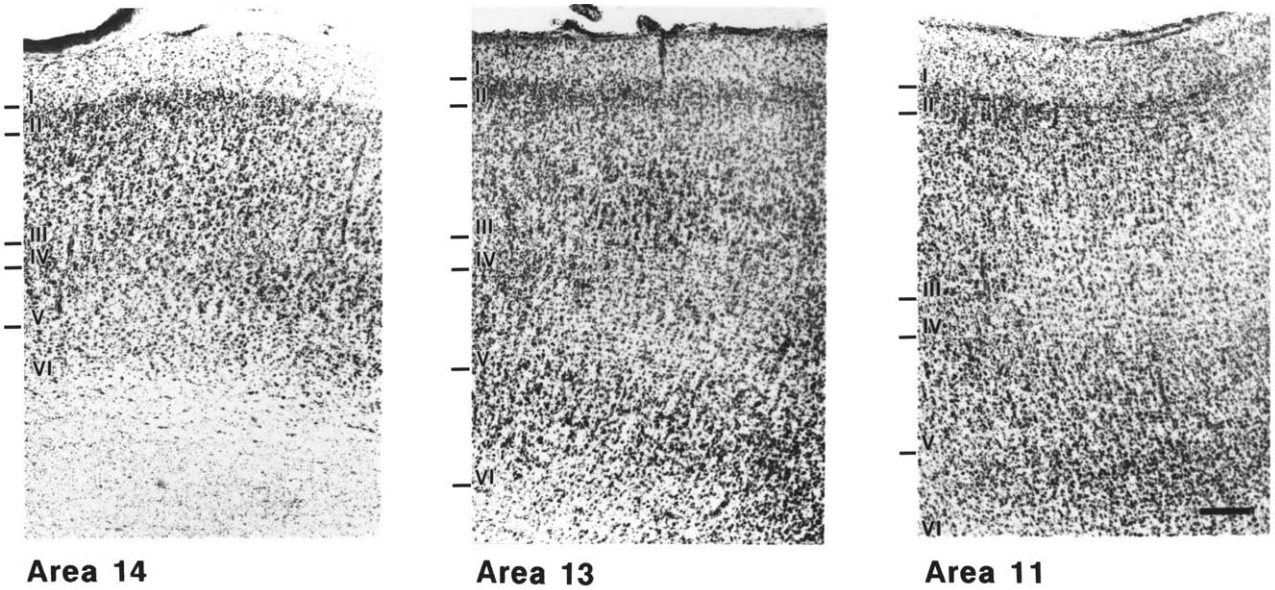

FIGURE 25.12 Photomicrographs of cortical areas 14, 13, and 11 of the human frontal lobe. The roman numerals in each photograph indicate the cortical layers. The black bar in the photograph of area 11 equals 1 mm.

restricted the term "area 11" to that part of the human orbital frontal cortex that is comparable in architecture to Walker's area 11 in the monkey (Fig. 25.7A, B).

In area 14, the outer border of layer II is irregular (Fig. 25.12). Layer III contains small to medium pyramidal cells that are uniformly distributed. Layer IV is thin but quite distinct. Layer Va contains densely packed, deeply stained medium-sized pyramidal cells, and Vb is sparsely populated with smaller neurons, clearly separating Va from VI. Layer VI contains deeply stained small and medium pyramidal neurons. Area 14 can be further subdivided into a medial and an orbital component.

Area 11 lies on the rostral part of the orbital frontal lobe in front of the transverse orbital sulcus. In area 11, layer II is thin. Layer III contains small to medium pyramidal cells that are uniformly arranged. Layer IV is well developed. Layer Va has medium-sized pyramidal cells and is somewhat denser than layer Vb. Layer VI contains small to medium-sized pyramidal cells that are faintly separated from Vb (Fig. 25.12).

Frontopolar Cortex

Area 10 occupies the frontal pole (Figs. 25.6A, C, and 25.7). On the lateral surface, it borders, caudally, with areas 9, 46, and 47/12. On the orbital surface, it borders areas 11 and 14, and on the medial surface, it borders areas 9, 32 and 14. In area 10, the cortex is overall cell-sparse and hence has a pale appearance as compared with the surrounding areas. Layer II is distinct from layer III (Fig. 25.13). Layer III is sparsely populated with small to medium-sized pyramidal neurons. Layer IV is narrow but distinct. Layer Va contains scattered medium-sized pyramidal cells, and layer VI has small to medium pyramidal neurons. The overall density of the supragranular (II and III) and the infragranular (V and VI) layers is about the same.

Medial Frontal Cortex

On the medial surface of the frontal lobe, the cingulate and paracingulate regions are occupied by areas 24 and 32, respectively (Fig. 25.8B). Dorsal to these areas, on the medial surface of the superior frontal gyrus, in a caudorostral direction, lie the medial extensions of areas 8B, 9, and 10. Ventrally, area 32 borders the medial part of area 14, and caudally it abuts area 25, which occupies the subcallosal gyrus.

In area 25, layer II has an irregular margin and is ill-defined (Fig. 25.13). Layer III contains small to medium-sized pyramidal cells that are sparsely distributed. Layers V and VI contain deeply stained neurons giving the infragranular layers a uniform appearance. Area 25, like area 24, is a proisocortical area by virtue of its prominent infragranular layers and the absence of layer IV.

In area 24, layer II has an irregular margin and is ill-defined. Layer III contains small to medium pyramidal cells that are sparsely distributed. The striking feature of area 24 is layer V, which contains deeply stained medium to large pyramidal cells. This layer abuts

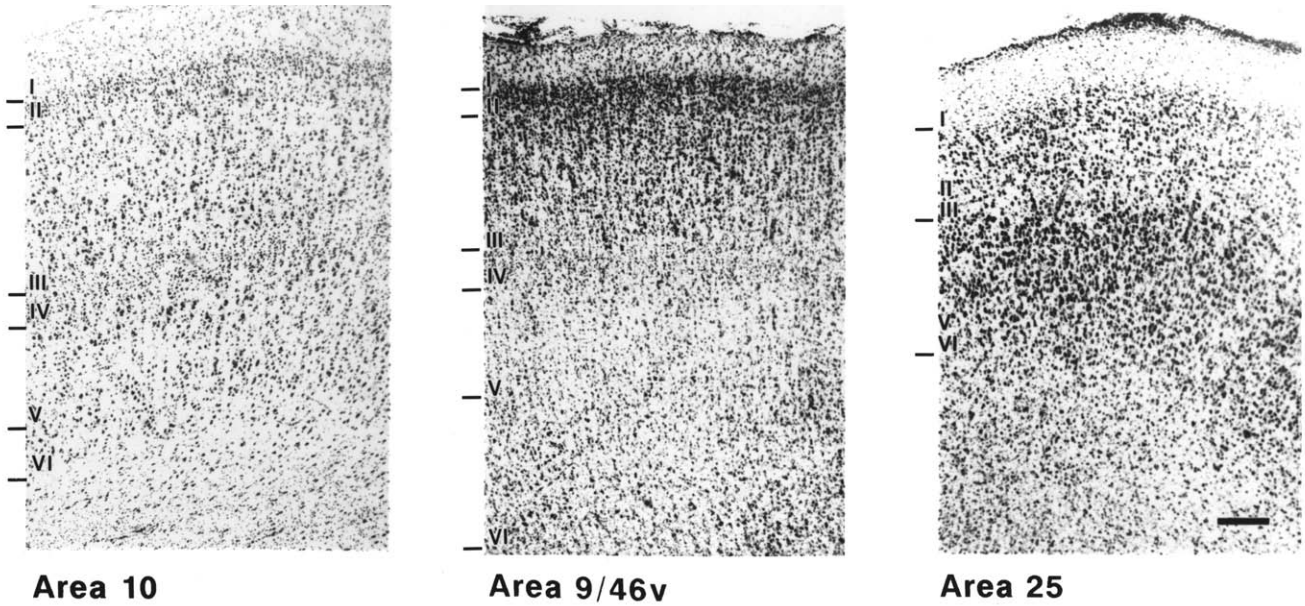

FIGURE 25.13 Photomicrographs of cortical areas 10, 9/46v, and 25 of the human frontal lobe. The roman numerals in each photograph indicate the cortical layers. The black bar in the photograph of area 25 equals 1 mm.

layer III because of the absence of layer IV. Layer Vb and VI blend and contain medium to small pyramidal cells. Like area 25, area 24 is a proisocortical region because of the overall prominence of the infragranular layers and the absence of layer IV.

Area 32 surrounds area 24 and occupies a region that is often referred to as the paracingulate gyrus (Fig. 25.8). In area 32, as in areas 24 and 25, the infragranular layers predominate. Layer III of area 32 contains small to medium pyramidal cells and is denser than that of area 24. There is an incipient layer IV in area 32. Layer Va contains deeply stained neurons that are more dispersed than those of area 24. Layers V and VI are slightly separated. Area 32 exhibits minor variations that have been recognized by both Economo and Koskinas (1925) and Sarkissov *et al.* (1955). Each subdivision exhibits some of the features of the neocortical areas adjoining it. Area 32 can be considered as a transitional type of cortex between the isocortex and the proisocortical areas 24 and 25. For a more detailed discussion of the cingulate areas, see Chapter 24.

Architectonic Trends

The prefrontal architectonic areas described previously can be conceptualized as belonging to one of two general groups or trends. This conceptualization is based on the notion of the dual origin of the cerebral cortex, which has been proposed by Dart (1934), Abbie (1940), Sanides (1969), Pandya and Yeterian (1990), and Barbas and Pandya (1989). According to this concept, one cortical architectonic trend originates from the paleocortical (olfactory) moiety, whereas the other trend originates in the archicortical (hippocampal) moiety. From each one of these two allocortical moieties, a progressive laminar differentiation can be traced, passing through periallocortex and proisocortex toward the development of the true six-layered isocortex.

For the frontal cortical areas, the sites of origin are (1) the allocortical, periallocortical and proisocortical areas in the caudal orbital frontal region and (2) the allocortical, periallocortical, and proisocortical areas in the cingulate region around the rostral part of the corpus callosum. From the proisocortex in the caudal orbital frontal region, which is characterized by a predominance of the infragranular layers and the absence of layer IV, the next stage of differentiation is area 13 which has an incipient layer IV. Next follow areas 14, 11, and orbital 47/12, which have a predominance of the infragranular layers V and VI and a better developed layer IV. Progressing further in terms of laminar differentiation are the adjacent cortical areas 10, lateral 47/12, and ventral portion of area 46, which are characterized by an approximately equal emphasis on the infra- and supragranular layers and further development of layer IV. Further differentiation within this trend can be seen in ventral area 9/46, ventral area 8 (i.e., 8Av), and area 45, all of which exhibit a predominance of the supragranular layers, prominent pyramidal neurons in layer III and highly developed layer IV.

The archicortical trend of prefrontal areas originates in the proisocortical areas 24, 25, and 32 in the anterior cingulate region. These areas exhibit a predominance of infragranular layers and virtually no layer IV. The next stage of differentiation is represented by the medial parts of isocortical areas 8B and 9, which have a poorly developed layer IV. The next stage of differentiation can be seen in lateral areas 8B, 9, and 10, which have a better developed layer IV and a relative equivalence of the infra- and supragranular layers. Finally, one observes areas 46, 9/46d, and 8Ad, which contain a highly developed layer IV and the predominance of supragranular layers. We would like to emphasize that within each stage of these two trends of architectonic differentiation, the various areas exhibit their own unique architectonic pattern. Although these two architectonic trends emerge from two distinct points of origin (i.e., the caudal orbitofrontal and the rostral cingulate regions), they come together in the region of the middle frontal gyrus.

CORTICOCORTICAL CONNECTION PATTERNS

Studies in the monkey have shown that the different architectonic areas have distinct cortical and subcortical connections. Although the connections of the different architectonic areas of the human frontal cortex cannot be studied directly, information about their connections can be inferred from experimental anatomical studies in the macaque monkey. Such an endeavor will be critically dependent on the extent to which architectonic areas have been defined by the same criteria in the monkey and the human frontal cortex. Cytoarchitectonic studies of the cortex of the monkey appeared at about the same time as those of the human cortex, but unfortunately the numerical designations employed were not always referring to areas with comparable architectonic features and location (see Petrides and Pandya, 1994, for discussion of this problem). As pointed out earlier, to circumvent this problem, we have reexamined the architecture of the human and the macaque monkey prefrontal cortex in a strictly comparative manner. Architectonic areas were defined in both species using the same criteria. Figures 25.7 and 25.8 shows the correspondence between

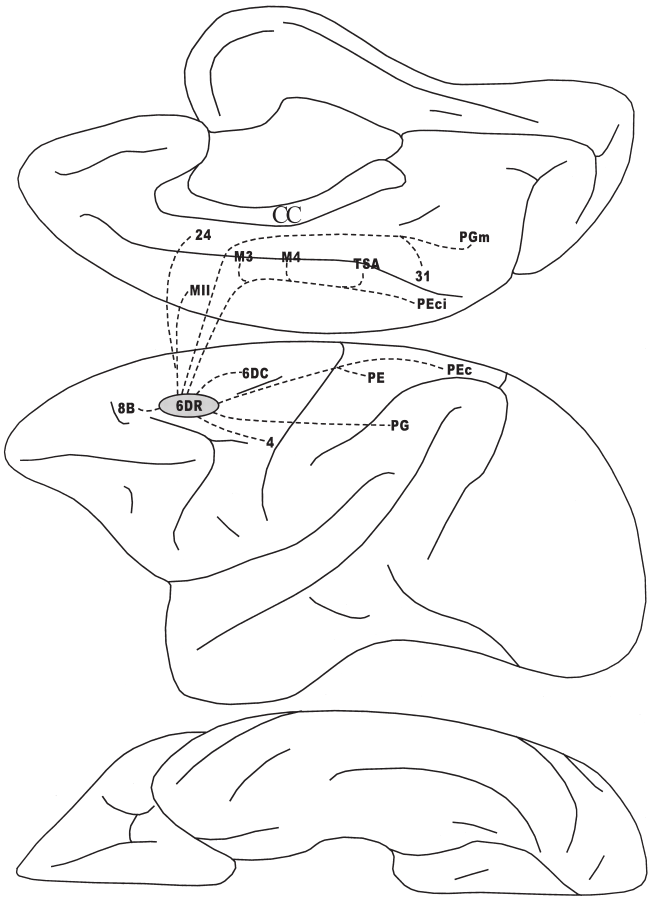

FIGURE 25.14 Diagrammatic representation of the medial, lateral, and orbital surfaces of the cerebral hemisphere of the macaque monkey to illustrate the connections of rostral dorsal area 6.

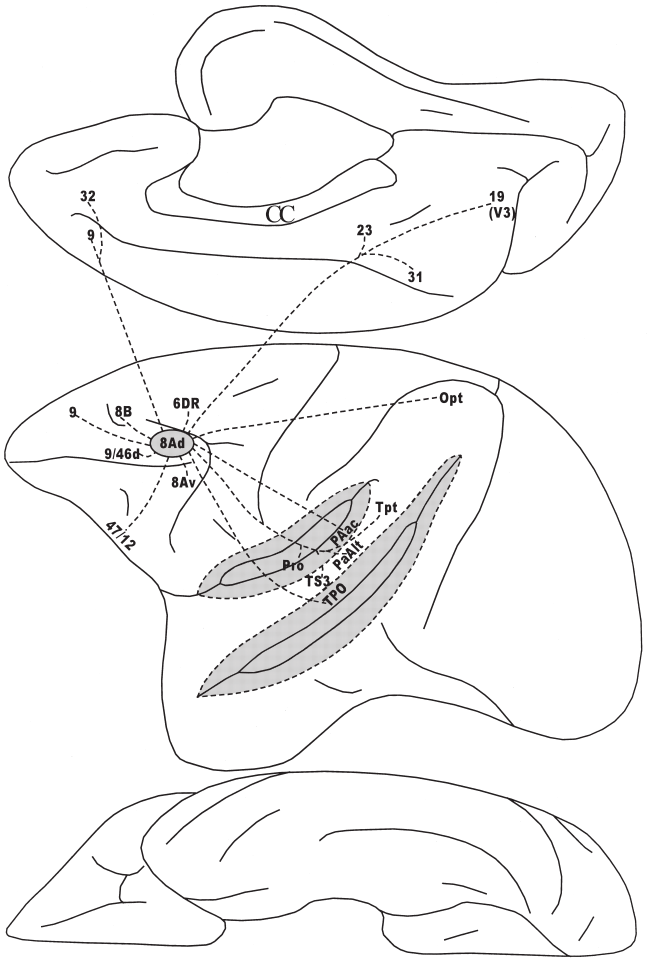

FIGURE 25.15 Diagrammatic representation of the medial, lateral, and orbital surfaces of the cerebral hemisphere of the macaque monkey to illustrate the connections of area 8Ad. The lateral fissure and the superior temporal sulcus have been opened up (shaded area) to show the connections within their banks.

the human and the monkey prefrontal cortical areas (Petrides and Pandya, 1994).

In the present description of the connections of the prefrontal cortex, data obtained from the experimental anatomical literature will be described using the architectonic areas of the prefrontal cortex as defined by Petrides and Pandya (1994). The following descriptions of the corticocortical connections of the different prefrontal areas are based on a synthesis of data presented in several studies using both anterograde and retrograde tracer techniques: Andersen *et al.* (1990), Barbas (1988), Barbas and Mesulam (1981, 1985), Barbas and Pandya (1987, 1989), Carmichael and Price (1995), Cavada and Goldman-Rakic (1989), Godschalk *et al.* (1984), Mesulam and Mufson (1982), Morris *et al.* (1999a, b), Petrides and Pandya (1984, 1988, 1999, 2002), Preuss and Goldman-Rakic (1989), Romanski *et al.* (1999), Schall *et al.* (1993, 1995), Seltzer and Pandya (1978, 1989).

Rostral Dorsal Area 6

The connections of the motor and premotor areas will not be described, except for those of the rostral part of area 6. Rostral dorsal area 6 (i.e., area 6DR) is connected with dorsal area 4, caudal area 6, supplementary motor area (i.e., MII), and cingulate motor areas M3 and M4 and, rostrally, with area 8B (Fig. 25.14). The long connections of rostral area 6 derive primarily from the posterior parietal region. There are connections from the lateral posterior parietal cortical areas PE, PEc, and PG and the medial parietal areas PEci (the supplementary sensory area, SSA), the transitional sensory area (TSA), area 31, and area PGm.

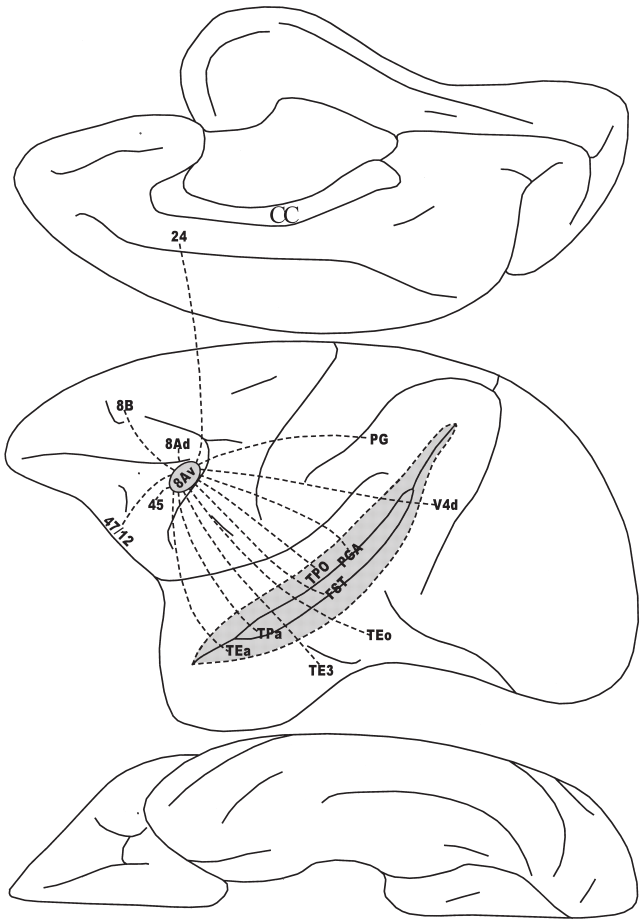

FIGURE 25.16 Diagrammatic representation of the medial, lateral, and orbital surfaces of the cerebral hemisphere of the macaque monkey to illustrate the connections of area 8Av. The superior temporal sulcus has been opened up (shaded area) to show the connections within its banks.

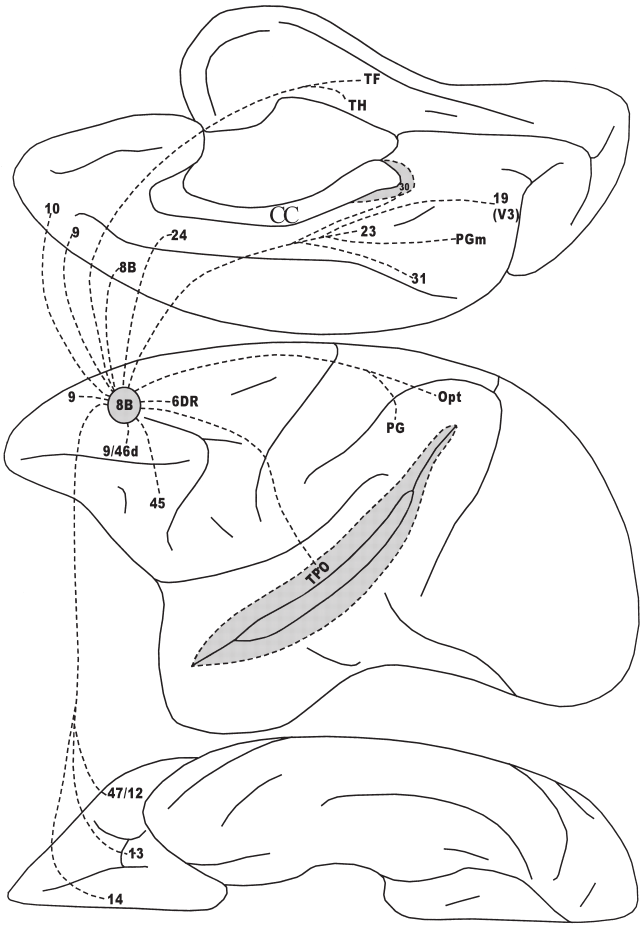

FIGURE 25.17 Diagrammatic representation of the medial, lateral, and orbital surfaces of the cerebral hemisphere of the macaque monkey to illustrate the connections of area 8B. The callosal sulcus around the splenium and the superior temporal sulcus have been opened up (shaded area) to show the connections within their banks.

Area 8Ad

Area 8Ad is connected with areas 6DR, 8B, 9, 9/46d, 8Av, and 47/12 and the cortex lying in the upper bank of the rostral cingulate sulcus (area 32 and 9) (Fig. 25.15). The long connections of area 8Ad originate from the caudalmost part of parietal cortex on the lateral surface (areas POa and Opt) and from areas 31, caudal area 23, and the medial portion of area 19 (V3). A substantial set of connections derive from the caudal superior temporal lobe (i.e., areas ProK, PAac in the supratemporal plane of the Sylvian fissure and areas Tpt, PAalt, and TS3 of the superior temporal gyrus and area TPO of the superior temporal sulcus).

Area 8Av

Area 8Av is connected locally with areas 8Ad, 8B, 45, and 47/12 (Fig. 25.16). There are also minor connections with area 24a. Its long connections are with the cortex of the multimodal cortex of the superior temporal sulcus (areas TPO and Pga) and the ventral bank of the superior temporal sulcus (areas IPa, TEa, and FST). Area 8Av is also connected with the caudal portion of inferotemporal and ventral occipital region (i.e., areas TE3, TEO, and V4d). A few connections exist between this area and area PG of the inferior parietal lobule.

Area 8B

Area 8B is connected locally with area 6DR, medial areas 10, 9, 8B, and 24; dorsolateral prefrontal areas 8B, 9, and 9/46d; ventrolateral prefrontal areas 45 and 47/12; and orbital areas 13 and 14 (Fig. 25.17). Its distant connections derive from the lateral parietal cortex (areas PG and Opt), the medial parietal areas 31

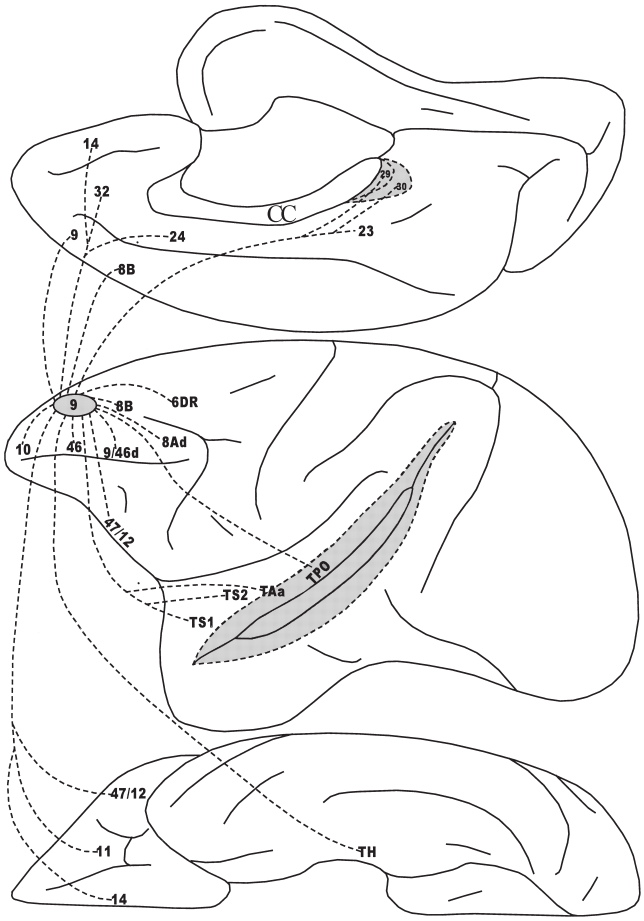

FIGURE 25.18 Diagrammatic representation of the medial, lateral, and orbital surfaces of the cerebral hemisphere of the macaque monkey to illustrate the connections of area 9. The callosal sulcus around the splenium and the superior temporal sulcus have been opened up (shaded area) to show the connections within their banks.

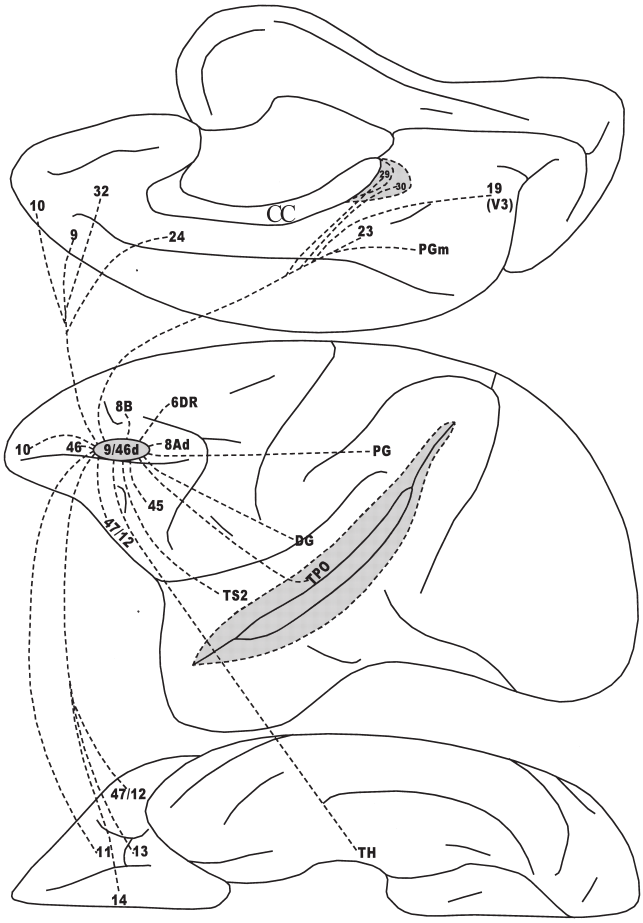

FIGURE 25.19 Diagrammatic representation of the medial, lateral, and orbital surfaces of the cerebral hemisphere of the macaque monkey to illustrate the connections of area 9/46d. The callosal sulcus around the splenium and the superior temporal sulcus have been opened up (shaded area) to show the connections within their banks.

and PGm, and the medial area 19 (V3). Area 8B is also linked with the multimodal areas TPO in the upper bank of the superior temporal sulcus. There are also connections with limbic areas, such the retrosplenial area 30, posterior cingulated area 23, and areas TH and TF of the parahippocampal gyrus.

Area 9

Area 9 has local connections with areas 6DR, 8B, 8Ad, 9/46d, dorsal 46, and 10 (Fig. 25.18). Area 9 is also linked with areas on the medial surface of the frontal lobe, namely areas 8B, 9, 32, 14, and 24. Area 9 is also connected with ventrolateral area 47/12 and areas 11 and 14 of the orbital frontal lobe. It has long connections with the rostral temporal area TS1, TS2 and TAa, as well as area TPO. Area 9 is connected with the limbic retrosplenial areas 29 and 30, caudal cingulate area 23, and the parahippocampal area TH.

Area 9/46d

Area 9/46d has local connections with areas 6DR, 8B, 8Ad, 46, and 10 (Fig. 25.19). It is linked with areas 10, 9, 32, and 24 of the medial prefrontal cortex and areas 45 and 47/12 of the ventrolateral prefrontal cortex. Area 9/46d has connections with areas 13, 11, and 14 in the orbital frontal cortex. Its long connections are with Ts2 of the superior temporal gyrus, area TPO of the superior temporal sulcus, and the dysgranular insula. The limbic connections are with areas 29, 30, and 23 in the posterior cingulate region, as well as

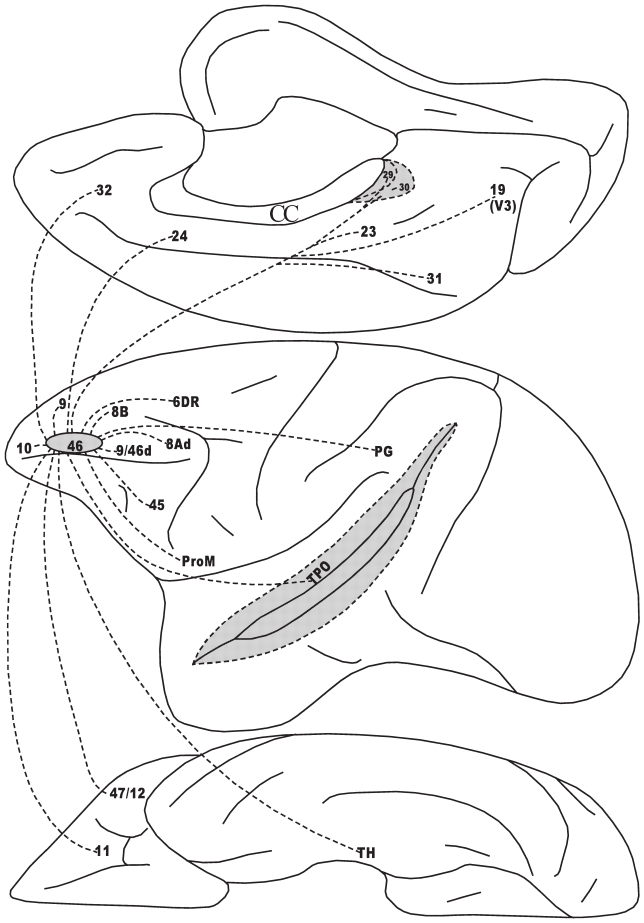

FIGURE 25.20 Diagrammatic representation of the medial, lateral, and orbital surfaces of the cerebral hemisphere of the macaque monkey to illustrate the connections of area 46. The callosal sulcus around the splenium and the superior temporal sulcus have been opened up (shaded area) to show the connections within their banks.

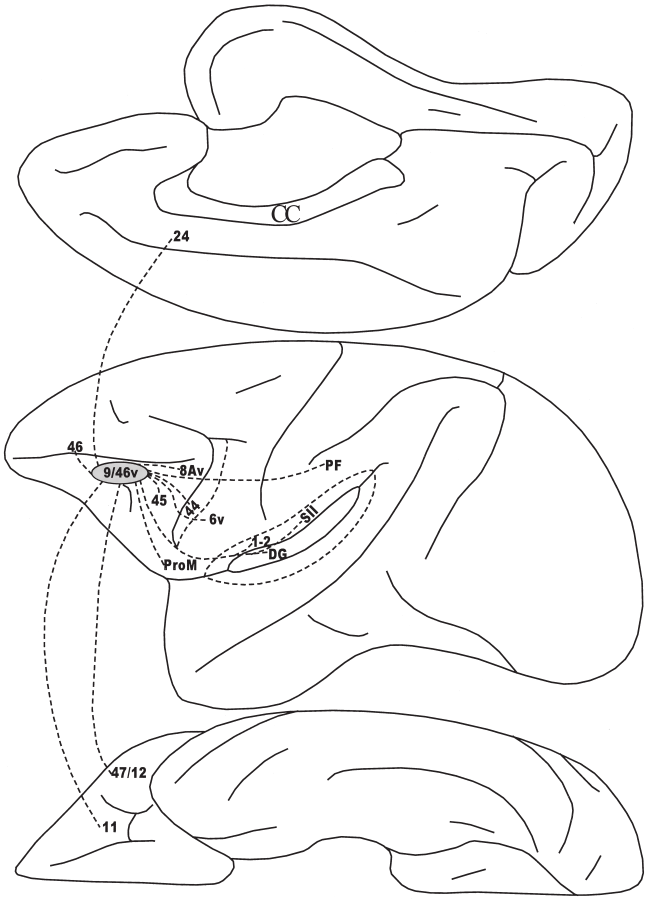

FIGURE 25.21 Diagrammatic representation of the medial, lateral, and orbital surfaces of the cerebral hemisphere of the macaque monkey to illustrate the connections of area 9/46v. The posterior bank of the lower limb of the arcuate sulcus and the lateral fissure have been opened up to show the connections within their banks.

area TH of the parahippocampal gyrus. There are also some connections with areas PG, PGm, and medial area 19. The connections of areas 46 and 9/46d are very similar, except that area 46 receives projections from ProM and is not connected with Ts2 and the insula (Fig. 25.20).

Area 9/46v

Area 9/46v is connected locally with area 8Av, ventral area 6, area ProM, and areas 47/12, 44, 45, and 46 (Fig. 25.21). It is also connected with area 11 of the orbitofrontal cortex and in a minor way with area 24. Significant long connections are with the dorsal Sylvian operculum (including area SII) and the dysgranular insula. Other areas connected with this region are the rostral inferior parietal lobule including areas PF and PFG.

Area 10

The frontopolar area 10 is connected with areas 8Ad, 8B, 9, 46, and 47/12 on the lateral frontal cortex and with areas 24, 32, and 9 on the medial surface of the frontal lobe (Fig. 25.22). Its connections with orbital frontal cortex are with areas 11, 13, and 14. Area 10 has long connections with retrosplenial area 30 and posterior cingulate area 23. Area 10 is also connected with dysgranular insula and parinsular region in the lateral fissure and temporal polar proisocortex. It also has connections with areas Ts1 and Ts2 of the superior temporal gyrus and areas TAa and TPO of the superior temporal sulcus.

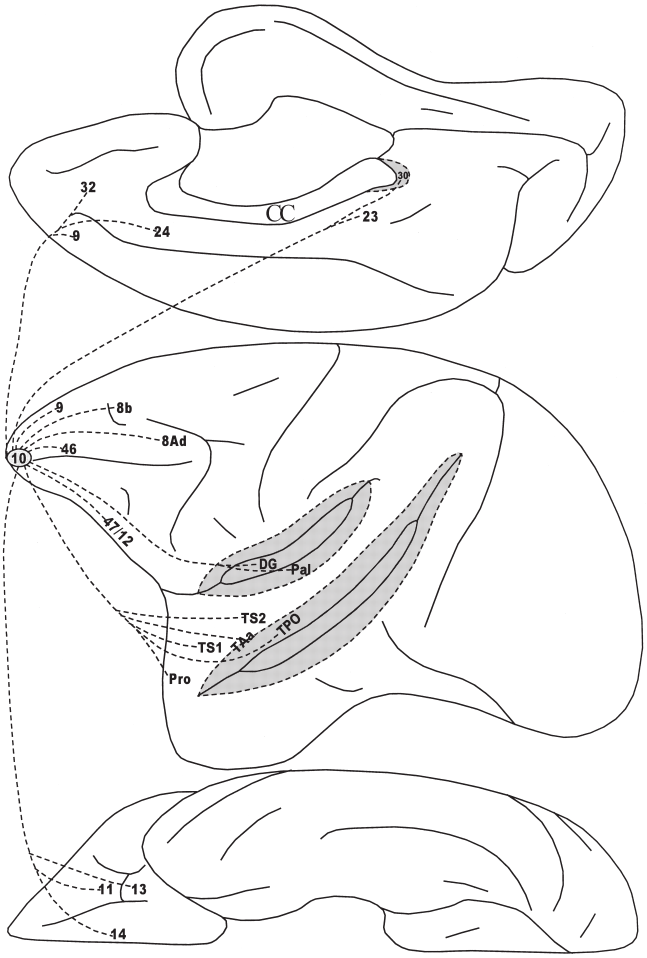

FIGURE 25.22 Diagrammatic representation of the medial, lateral, and orbital surfaces of the cerebral hemisphere of the macaque monkey to illustrate the connections of area 10. The lateral fissure and the superior temporal sulcus have been opened up (shaded area) to show the connections within their banks.

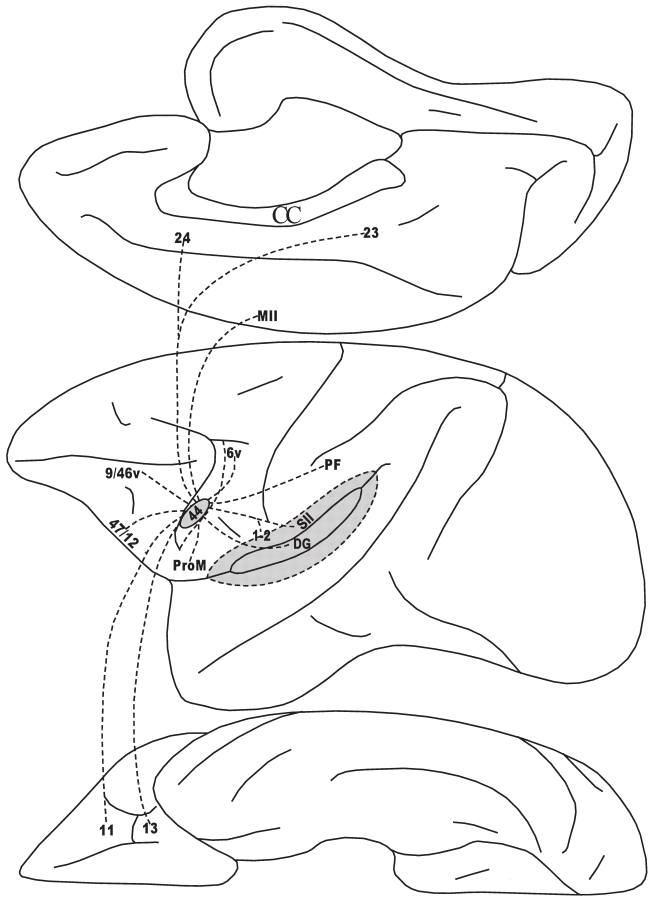

FIGURE 25.23 Diagrammatic representation of the medial, lateral, and orbital surfaces of the cerebral hemisphere of the macaque monkey to illustrate the connections of area 44. The lateral fissure has been opened up (shaded area) to show the connections within its banks.

Area 44

Area 44, which is the transitional area between ventral premotor and ventral prefrontal cortex, is linked locally with ventral area 6, area ProM, 9/46v and 47/12 (Fig. 25.23). This area also connected with areas 11 and 13 of the orbital frontal cortex and areas 24 and 23 of the cingulate gyrus, as well as the supplementary motor area. Its distant connections are with the Sylvian opercular cortex (i.e., areas 1 and 2 and SII). There are also some connections with the dysgranular insula. Strong connections exist with areas PF and PFG of the rotral part of the inferior parietal lobule.

Area 45

Area 45 is connected with many areas of the lateral prefrontal cortex: areas 8Av, 8Ad, 9/46v, 46, 10, 9, 8B, and 6DR (Fig. 25.24). Some connections exist between area 45 and medial frontal areas 10, 9, 8B, and 24. This area is also connected with area 47/12, 13, and 11 on the orbital frontal cortex. Long connections exist with dysgranular and granular insula and areas PaI and ProK of the supratemporal plane. There are major connections between the superior temporal region and area 45. These connections are with areas TS1, TS2, TS3, PAalt, and Tpt. There are also connections with areas TPO, PGa, and TEa and area FST in the superior temporal sulcus. Finally, there are connections with area SII in the parietal operculum and the midportion of the inferior parietal lobule (area PG).

Area 47/12

Area 47/12 is connected with areas 9/46v, 45, ProM, ventral area 6 and area 44, as well as with areas 11

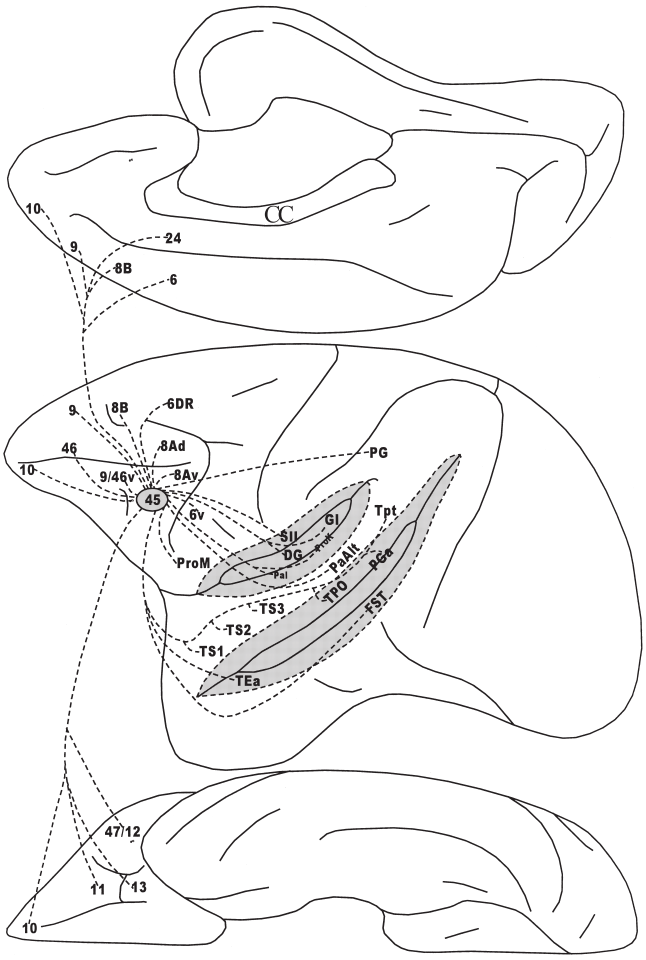

FIGURE 25.24 Diagrammatic representation of the medial, lateral, and orbital surfaces of the cerebral hemisphere of the macaque monkey to illustrate the connections of area 45. The lateral fissure and the superior temporal sulcus have been opened up (shaded area) to show the connections within their banks.

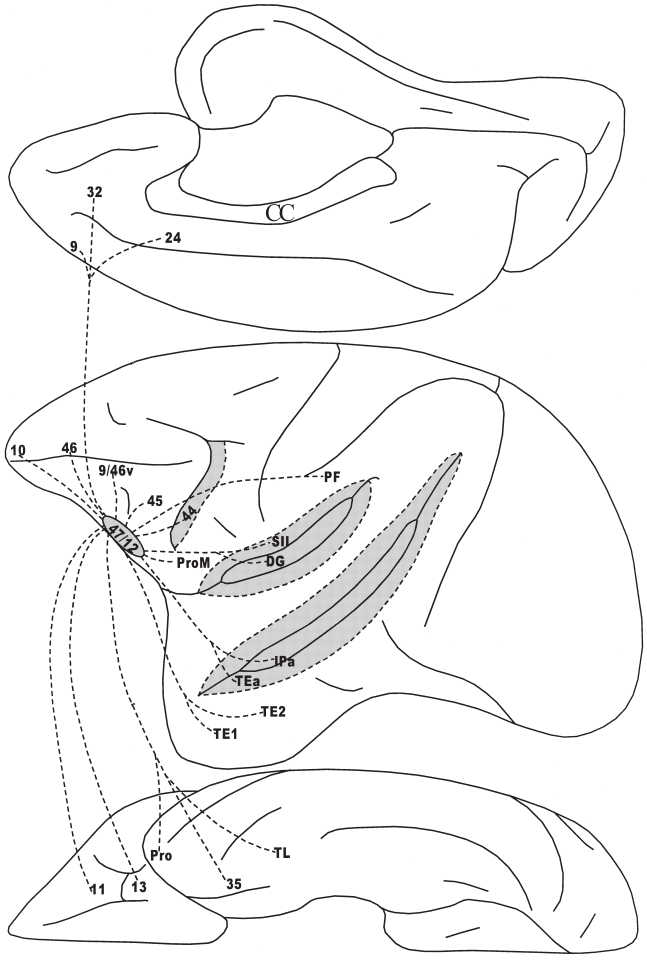

FIGURE 25.25 Diagrammatic representation of the medial, lateral, and orbital surfaces of the cerebral hemisphere of the macaque monkey to illustrate the connections of area 47/12. The posterior bank of the inferior limb of the arcuate sulcus, the lateral fissure, and the superior temporal sulci have been opened up (shaded area) to show the connections within their banks.

and 13 of orbital frontal cortex (Fig. 25.25). It is also connected with areas 24, 32, and 9 on the medial prefrontal cortex. Area 47/12 has long connections with area SII and the dysgranular insula. There is also a modest connection with the rostral part of the inferior parietal lobule. There are connections between area 47/12 and visual areas TEa, IPa, TE1, and TE2 of inferotemporal cortex and areas TL and 35 of the temporal proisocortex.

Area 13

The dysgranular area 13 at the caudal part of the orbital frontal cortex is connected with orbital proisocortex, areas 14, 11, and 47/12, as well as areas 46 and 10 on the lateral surface of the frontal cortex (Fig. 25.26). Area 13 is also connected with area ProM, the gustatory area, and the ventralmost parts of areas 3b, 1, and 2 around the Sylvian operculum as well as the agranular and dysgranular insula.

Area 11

Area 11 is connected locally with orbital proisocortex and areas 13, 14, 47/12, and 10 (Fig. 25.27). It is also connected with areas 46 and 10 on the lateral prefrontal cortex and areas 9, 10, 32, and 14 on the medial frontal cortex, as well as the rostral cingulate area 24 and the caudal cingulate areas 23 and 30. Long connections link area 11 with area SII and the agranular and dysgranular insula. Area 11 also receives projections from areas IPa and

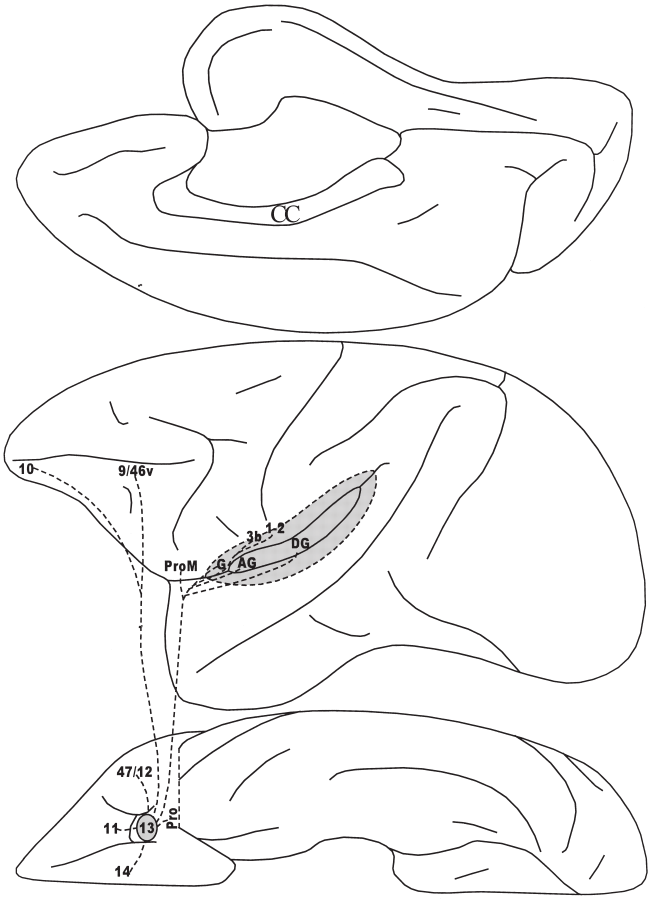

FIGURE 25.26 Diagrammatic representation of the medial, lateral, and orbital surfaces of the cerebral hemisphere of the macaque monkey to illustrate the connections of area 13. The lateral fissure has been opened up (shaded area) to show the connections within its banks.

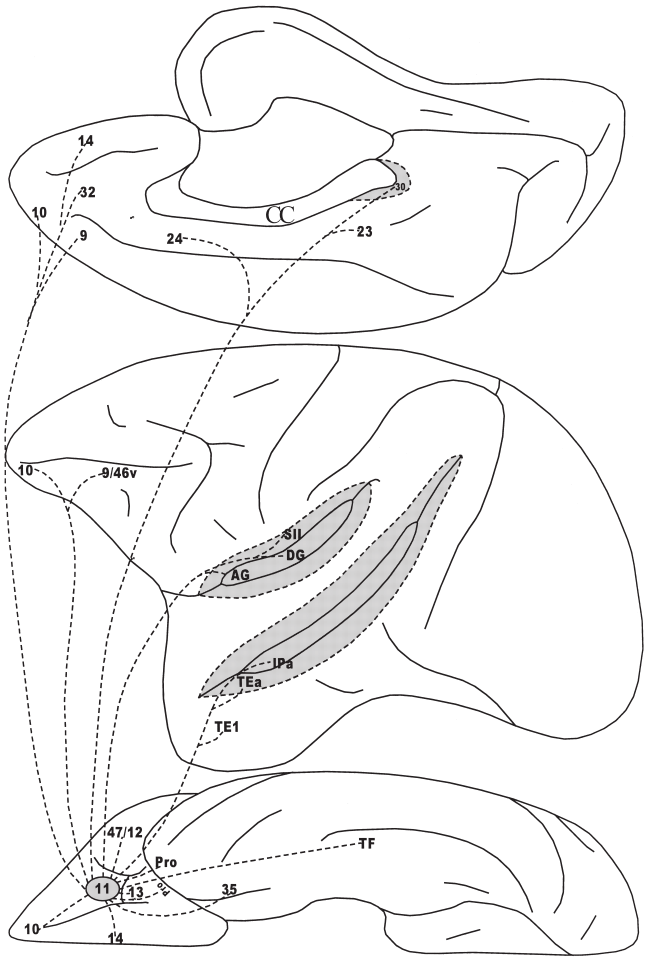

FIGURE 25.27 Diagrammatic representation of the medial, lateral, and orbital surfaces of the cerebral hemisphere of the macaque monkey to illustrate the connections of area 11. The callosal sulcus around the splenium, the lateral fissure, and the superior temporal sulcus have been opened up (shaded area) to show the connections within their banks.

TEa from the superior temporal sulcus as well as areas TE1 of the inferior temporal cortex. Finally, its limbic connections are derived from temporal proisocortex, area 35, and areas TF and TL.

Area 14

Area 14 on the gyrus rectus is linked locally with areas 13, 11, and the orbital proisocortex. It is also linked with medial areas 10, 9, 32, 25, and 24 (Fig. 25.28). There are also some connections with area 46. Its long connections are derived from agranular insula and the parinsular area PaI. Area 14 is also connected with the temporal polar proisocortex as well as adjoining areas TS1 and TS2. There are major connections between area 14 and the hippocampus and the presubiculum.

Orbital Proisocortex

The orbital proisocrtical area is locally connected with areas 13, 14, and 25 and the orbital periallocortex (Fig. 25.29). Its distant connections are with the gustatory area, the agranular insula, and the parinsular area PaI. The orbital proisocortex is also linked with the temporopolar proisocortex, as well as areas TS1 and TS2. It is also connected with rostral area TL and perirhinal area 35.

Acknowledgments

This work was supported by grants from the Canadian Institutes of Health Research. We thank Juergen Germann who prepared Figures 25.2, 25.3, and 25.4 and Helen Papageorgiou who prepared Figures 25.14 to 25.29.

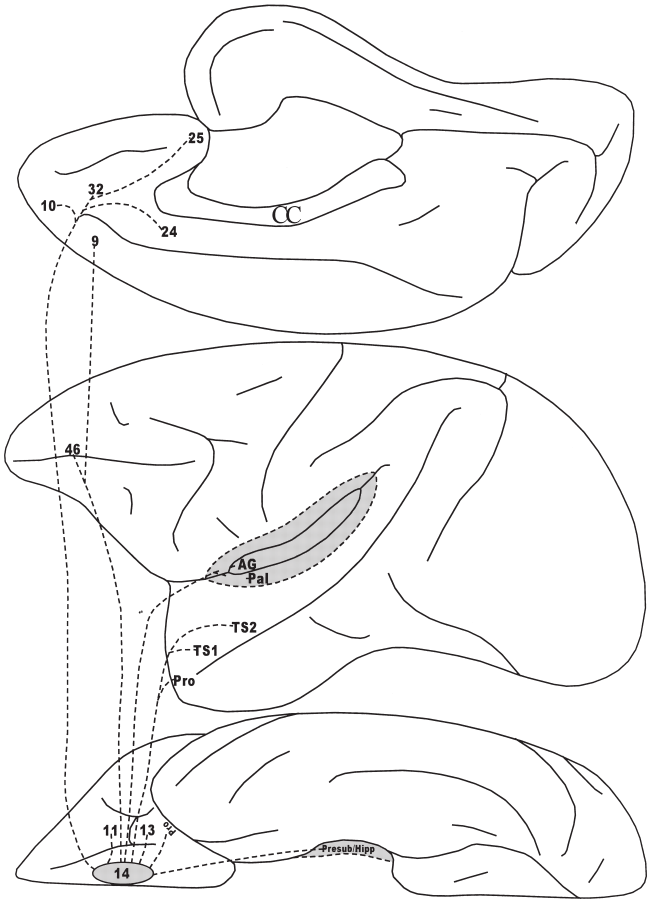

FIGURE 25.28 Diagrammatic representation of the medial, lateral, and orbital surfaces of the cerebral hemisphere of the macaque monkey to illustrate the connections of area 14. The lateral fissure has been opened up (shaded area) to show the connections within its banks.

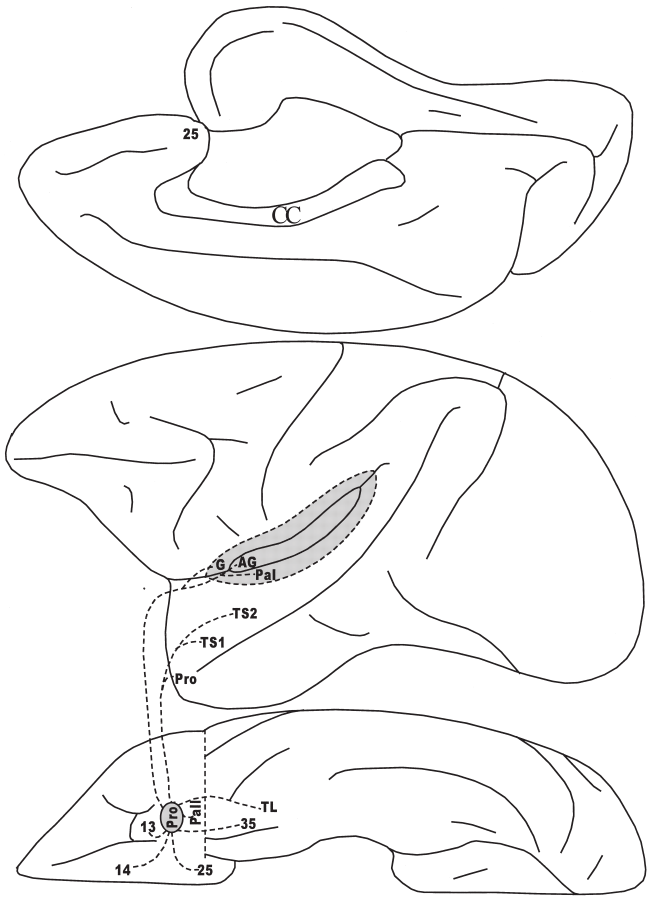

FIGURE 25.29 Diagrammatic representation of the medial, lateral, and orbital surfaces of the cerebral hemisphere of the macaque monkey to illustrate the connections of the orbital proisocortex. The lateral fissure has been opened up (shaded area) to show the connections within its banks.

References

Abbie, A.A. (1940). Cortical lamination in the monotremata. *J. Comp. Neurol*. **72,** 429–467.

Amunts, K., Schleicher, A., Burgel, U., Mohlberg, H., Uylings, H.B.M., and Zilles, K. (1999). Broca's region revisited: Cytoarchitecture and intersubject variability. *J.Comp. Neurol*. **412,** 319–341.

Andersen, R.A., Asanuma, C., Essick, G., and Siegel, R.M. (1990). Corticocortical connections of anatomically and physiologically defined subdivisions within the inferior parietal lobule. *J.Comp. Neurol*. **296,** 65–113.

Bailey, P., and Bonin, G. (1951). "The Isocortex of Man." University of Illinois Press, Urbana.

Barbas, H. (1988). Anatomic organization of basoventral and mediodorsal visual recipient prefrontal regions in the rhesus monkey. *J.Comp. Neurol*. **276,** 313–342.

Barbas, H., and Mesulam, M.-M. (1981). Organization of afferent input to subdivisions of area 8 in the rhesus monkey. *J.Comp. Neurol*. **200,** 407–431.

Barbas, H., and Mesulam, M.-M. (1985). Cortical afferent input to the principalis region of the rhesus monkey. *Neurosci*. **15,** 619–637.

Barbas, H., and Pandya, D. N. (1987). Architecture and frontal cortical connections of the premotor cortex (area 6) in the rhesus monkey. *J.Comp. Neurol*. **256,** 211–228.

Barbas, H., and Pandya, D. N. (1989). Architecture and intrinsic connections of the prefrontal cortex in the rhesus monkey. *J.Comp. Neurol*. **286,** 353–375.

Beck, E. (1949). A cytoarchitectural investigation into the boundaries of cortical areas 13 and 14 in the human brain. *J. Anat*. **83,** 147–157.

Braak, H. (1979). The pigment architecture of the human frontal lobe. I. Precentral, subcentral, and frontal region. *Anat. Embryol*. **157,** 35–68.

Brodmann, K. (1908). Beitraege zur histologischen Lokalisation der Grosshirnrinde. VI. Mitteilung: Die Cortexgliederung des Menschen. *J. Psychol. Neurol. (Lzp.)* **10,** 231–246.

Brodmann, K. (1909). Vergleichende Lokalisationslehre der Grosshirnrinde in ihren Prinzipien dargestellt auf Grund des Zellenbaues. Barth, Leipzig.

Brodmann, K. (1914). Physiologie des Gehirns. *In* "Neue Deutsche Chirurgie" (P. Bruns, ed.), Vol. 11, pp. 85–426. Enke, Stuttgart.

Campbell, A.W. (1905). "Histological Studies on the Localisation of Cerebral Function." University Press, Cambridge.

Carmichael, S.T., and Price, J.L. (1995). Sensory and premotor connections of the orbital and medial prefrontal cortex of macaque monkeys. *J.Comp. Neurol.* **363,** 642–664.

Cavada, C., and Goldman-Rakic, P.S. (1989). Posterior parietal cortex in the rhesus monkey. II. Evidence for segregated corticocortical networkds linking sensory and limbic areas with the frontal lobe. *J.Comp. Neurol.* **287,** 422–445.

Chiavaras, M. M., and Petrides, M. (2000). Orbitofrontal sulci of the human and macaque monkey brain. *J.Comp. Neurol.* **422,** 35–54.

Connolly, C.J. (1950). "External Morphology of the Primate Brain." Charles C Thomas, Springfield, Ill.

Cunningham, D.J. (1892). Contribution to the surface anatomy of the cerebral hemispheres. Royal Irish Academy of Science. Cunningham Memoirs, No. VII. Academy House, Dublin.

Dart, R.A. (1934). The dual structure of the neopallium: Its history and significance. *J. Anat.* **69,** 3–19.

Deacon, T.W. (1992). Cortical connections of the inferior arcuate sulcus cortex in the macaque monkey brain. *Brain Res.* **573,** 8–26.

Duvernoy, H. (1991). "The Human Brain: Surface, Three-Dimensional Sectional Anatomy and MRI." Springer-Verlag, Wien.

Eberstaller, O. (1890). "Das Stirnhirn." Urban & Schwarzenberg, Wien.

Economo, C., and Koskinas, G.N. (1925). "Die Cytoarchitektonik der Hirnrinde des erwachsenen Menschen." Springer, Wien.

Godschalk, M., Lemon, R.N., Kuypers, H.G.J.M., and Ronday, H.K. (1984). Cortical afferents and efferents of monkey postarcuate area: An anatomical and electrophysiological study. *Exp. Brain Res.* **56,** 410–-424.

Landau, E. (1911). Ueber die Grosshirnfurchen am basalen Teile des temporooccipitalen Feldes bei den Esten. *Ztschr. F. Morphol. u. Anthropol.* **13,** 423–438.

Landau, E. (1914). Ueber die Furchen an der Lateralflaeche des Grosshirns bei den Esten. *Ztschr. F. Morphol. u. Anthropol.* **16,** 239–279.

Mesulam, M.-M., and Mufson, E.J. (1982). Insula of the old world monkey. III: Efferent cortical output and comments on function. *J. Comp. Neurol.* **212,** 38–52.

Morris, R., Pandya, D.N., and Petrides, M. (1999a). Fiber system linking the mid-dorsolateral frontal cortex with the retrosplenial/presubicular region in the rhesus monkey. *J. Comp. Neurol.* **407,** 183–192.

Morris, R., Petrides, M., and Pandya, D.N. (1999b). Architecture and connections of retrosplenial area 30 in the rhesus monkey (macaca mulatta). *Eur. J. Neurosci.* **11,** 2506–2518.

Ono, M., Kubik, S., and Abernathey, C.D. (1990). "Atlas of the Cerebral Sulci." Georg Thieme, Stuttgart.

Pandya, D.N., and Yeterian, E.H. (1990). Architecture and connections of cerebral cortex: Implications for brain evolution and function. *In* "Neurobiology of Higher Cognitive Function" (A.B. Scheibel and A.F. Wechsler, eds,). The Guilford Press, New York.

Petrides, M., and Pandya, D.N. (1984). Projections to the frontal cortex from the posterior parietal region in the rhesus monkey. *J. Comp. Neurol.* **228,** 105–116.

Petrides, M., and Pandya, D.N. (1988). Association fiber pathways to the frontal cortex from the superior temporal region in the rhesus monkey. *J. Comp. Neurol.* **273,** 52–66.

Petrides, M., and Pandya, D.N. (1994). Comparative architectonic analysis of the human and the macaque frontal cortex. *In* "Handbook of Neuropsychology" (F. Boller and J. Grafman, eds.), Vol. 9, pp. 17–58, Elsevier, Amsterdam.

Petrides, M., and Pandya, D.N. (1999). Dorsolateral prefrontal cortex: comparative cytoarchitectonic analysis in the human and the macaque brain and corticocortical connection patterns. *Eur. J. Neurosci.* **11,** 1011–1036.

Petrides, M., and Pandya, D.N. (2002). Comparative architectonic analysis of the human and the macaque ventrolateral prefrontal cortex and corticocortical connection patterns in the monkey. *Eur. J. Neurosci.* **16,** 291–310.

Preuss, T.M., and Goldman-Rakic, P.S. (1989). Connections of the ventral granular frontal cortex of macaques with perisylvian premotor and somatosensory areas: Anatomical evidence for somatic representation in primate frontal association cortex. *J. Comp. Neurol.* **282,** 293–316.

Rajkowska, G., and Goldman-Rakic, P.S. (1995). Cytoarchitectonic definition of prefrontal areas in the normal human cortex. *Cereb. Cortex,* **5,** 307–322.

Romanski, L.M., Bates, J.F., and Goldman-Rakic, P.S. (1999). Auditory belt and parabelt projections to the prefrontal cortex in the rhesus monkey. *J. Comp. Neurol.* **403,** 141–157.

Sanides, F. (1962). "Die Architektonik des Menschlichen Stirnhirns." Springer-Verlag, Berlin.

Sarkissov, S.A., Filimonoff, I.N., Kononowa, E.P., Preobraschenskaja, I.S., and Kukuew, L.A. (1955). "Atlas of the Cytoarchitectonics of the Human Cerebral Cortex." Medgiz, Moscow.

Schall, J.D., Morel, A., and Kaas, J. (1993). Topography of supplementary eye field afferents to frontal eye field in macaque: Implications for mapping between saccade coordinate systems. *Visual Neurosci.* **10,** 385–393.

Seltzer, B., and Pandya, D.N. (1978). Afferent cortical connections and architectonics of the superior temporal sulcus and surrounding cortex in the rhesus monkey. *Brain Res.* **149,** 1–24.

Seltzer, B., and Pandya, D.N. (1989). Frontal lobe connections of the superior temporal sulcus in the rhesus monkey. *J. Comp. Neurol.* **281,** 97–113.

Semendeferi, K., Armstrong, E., Schleicher, A., Zilles, K., and Van Hoesen, G.W. (1998). Limbic frontal cortex in hominoids: A comparative study of area 13. *Am. J. Phys. Anthropol.* **106,** 129-155.

Shellshear, J.L. (1926). The occipital lobe in the brain of the Chinese with special reference to the sulcus lunatus. *J. Anat.* **61,** 1–13.

Shellshear, J.L. (1937). The brain of the Australian aboriginal. A study in cerebral morphology. *Phil. Trans. Roy. Soc. Lond. Ser. B* **227,** 293–409.

Tomaiuolo, F., MacDonald, J.D., Caramanos, Z., Posner, G., Chiavaras, M., Evans, A.C., and Petrides, M. (1999). Morphology, morphometry and probability mapping of the pars opercularis of the inferior frontal gyrus: An in vivo MRI analysis. *Eur. J. Neurosci.* **11,** 3033–3046.

Vogt, O. (1910). Die myeloarchitektonische Felderung des menschlichen Stirnhirns. *J. Psychol. Neurol. (Lpz.)* **15,** 000–000.

Vogt, C., and Vogt, O. (1919). Allgemeinere Ergebnisse unserer Hirnforschung. *J. Psychol. Neurol.* **25,** 279–462.

Walker, A.E. (1940). A cytoarchitectural study of the prefrontal area of the macaque monkey. *J. Comp. Neurol.* **73,** 59–86.

Wernicke, C. (1876). Das Urwindungssystem des menschlichen Gehirns. *Arch. F. Psychiat. u. Nervenkrktn.* **6,** 298–326.

CHAPTER

26

MOTOR CORTEX

MASSIMO MATELLI,[1] GIUSEPPE LUPPINO,[1]
STEFAN GEYER,[2] and KARL ZILLES[3]

[1]*Dipartimento di Neuroscienze, Sezione di Fisiologia*
Università di Parma, Parma, Italy

[2]*C. and O. Vogt Brain Research Institute*
University of Düsseldorf, Düsseldorf, Germany

[3]*Institute of Medicine, Research Center Jülich*
Jülich, Germany, and
C. & O. Vogt-Institute of Brain Research
University of Düsseldorf, Düsseldorf, Germany

In the second half of the 19th century, the prevailing view of the organization of the motor system was that all movements were controlled by the brainstem and the spinal cord. The cerebral cortex was thought to be involved only in mentation and other high-order cognitive functions. In those years, the British neurologist Hughlings Jackson, on the basis of his observations on the development of somatic seizures in patients with tumors or diseases affecting the cerebral cortex, formulated his revolutionary theory. Jackson's view was that the frontal cortex controls movements in different ways and in different combinations. He differentiated the *motor cortex proper*, that is the area that contains movement representations and sends direct and indirect projections to the spinal cord, and the *superimposed cortical areas*, which, although they contain similar movement representations, are connected with the spinal motor nuclei only indirectly via the motor cortex proper. Adapting his terminology to the principle of the hierarchy of the nervous system, Jackson ranked the motor cortex proper at the *middle level* and the superimposed cortical areas at the highest levels of the motor system (Jackson, 1931). Forty years later, Campbell (1905) suggested a possible anatomical counterpart of Jackson's functional organization of the cortical motor system. According to his cytoarchitectonic map of the cerebral cortex (Fig. 26.1), the precentral cortex should mediate the executive motor functions, while the intermediate precentral cortex should represent the level of the higher motor functions. Brodmann (1909) basically agreed with Campbell's view that there are two motor areas, area 4 and area 6, but provided a more detailed map of the frontal lobe

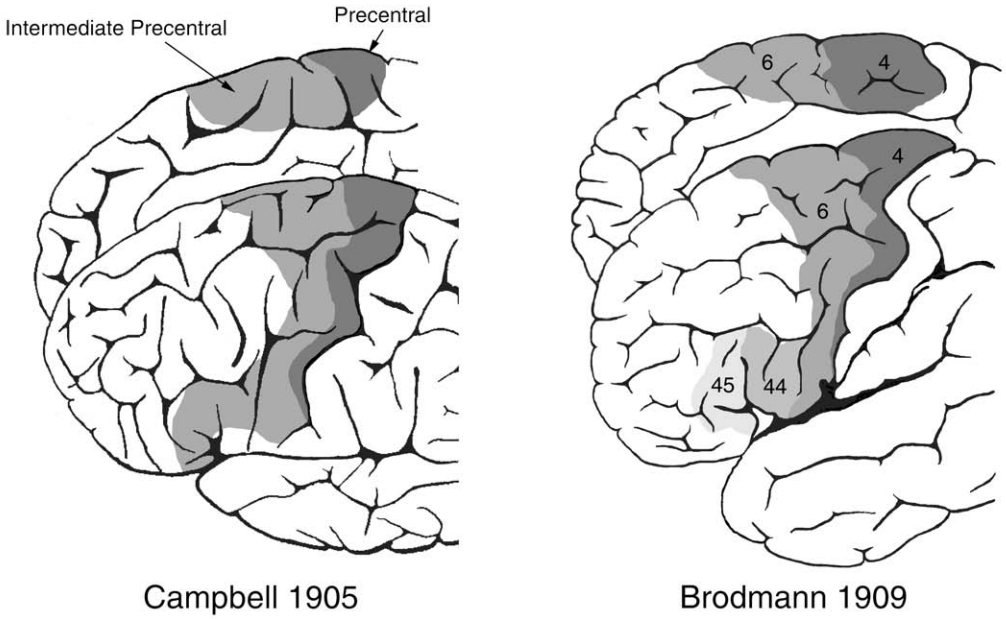

FIGURE 26.1 Cytoarchitectonic maps of the human frontal lobe, redrawn from Campbell (1905) and Brodmann (1909).

(Fig. 26.1). The notion that this architectonic subdivision could reflect functional differences was supported by Fulton (1935) who showed that ablation of area 6 (premotor cortex) produces, in addition to other symptoms, a specific deficit in the execution of skilled movements. Although these motor disturbances were described in several species of primates as in humans, some methodological weaknesses of Fulton's experiments, as well as some controversies concerning the architectonic correlates of the motor deficits hindered the acceptance of Fulton's ideas on the role of area 6.

Major criticism against architectonics arose, on the one hand, from Spanish anatomists who preferred the Golgi method in their studies of the cerebral cortex (Lorente de Nó, 1934) and, on the other hand, from psychologists (see Lashley and Clark, 1946). The idea that a boundless mind cannot be related to strictly bounded cortical areas appeared compelling for scientists devoted to understand the mind. Furthermore, in the1950s, the existence of a high-order motor area located in front of area 4 was challenged by electrophysiological studies employing surface electrical stimulation (Woolsey *et al.*, 1952). These studies, providing a detailed description of the somatotopy of the primary motor area, showed that the caudal part of area 6 is not an independent area but, together with area 4, forms the primary motor cortex (MI). In addition, the sector of area 6 located in the mesial wall of the frontal lobe was found to contain an additional somatotopically organized motor representation (the supplementary motor area, SMA). Finally, because the electrical stimulation of the rostral part of area 6 did not produce body movements, it was considered not to be involved in movement control. These data pointed against the validity of any cytoarchitectonic map, as stated by Woolsey in his influential paper: "no single cytoarchitectural area of any worker coincides with the extent of our precentral field" (Woolsey *et al.*, 1952).

A further source of skepticism on the functional validity of brain maps, derived from a large number of papers showing a great variability of the sulcal pattern among individual human brains, makes any generalization of cytoarchitectural subdivisions obtained mostly from single brains almost impossible. Given these technical and conceptual problems, the interest in anatomical research of the human brain declined, and, for a long time, the physiology of the motor system in human and nonhuman primates was largely dominated by the ideas of Woolsey. In recent years, however, neuroanatomical research in animals has significantly contributed to the study of brain circuitry and the characterization of cortical areas. Thanks to hodological and architectonic studies, there is now a general agreement that the monkey motor cortex is formed by several independent areas, each of which is identified and defined not only on the basis of its architectonic or histochemical characteristics but also on the basis of its connections, as well as its functional properties. In particular, careful studies on the descending pathways unequivocally showed that, rostral

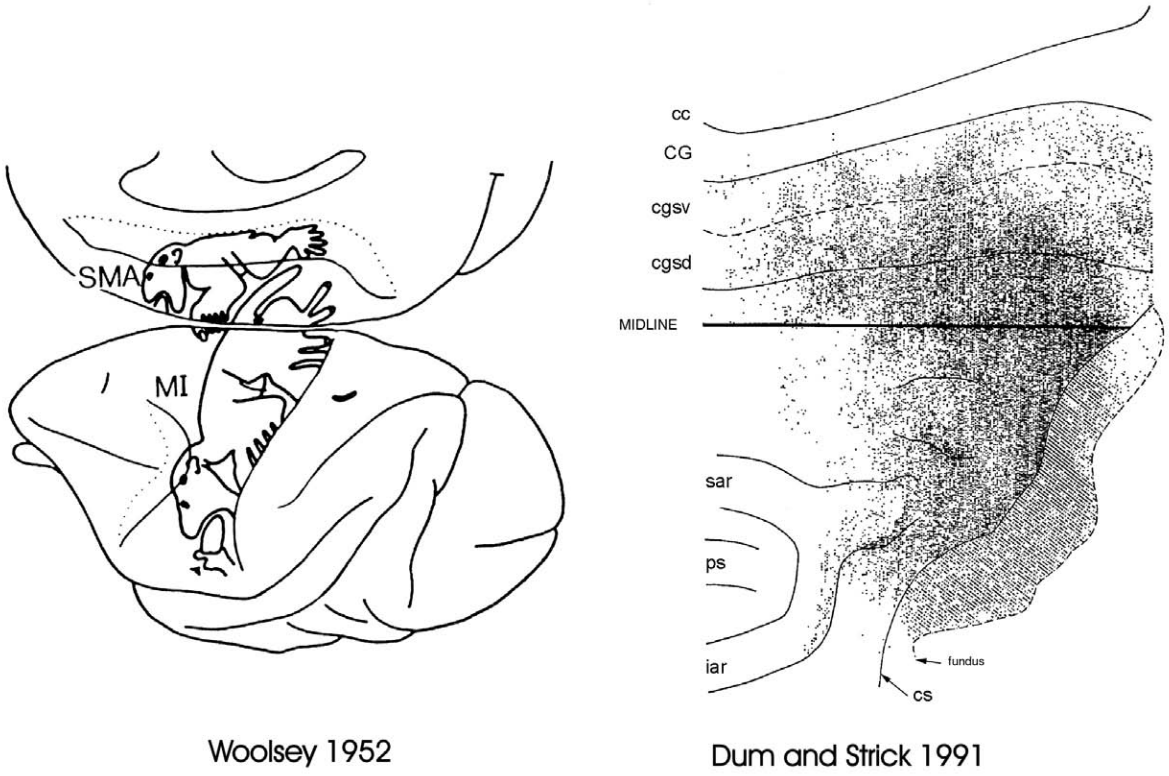

FIGURE 26.2 Mesial (top) and lateral (bottom) views of the macaque brain showing the extent of Woolsey's areas MI and SMA (Woolsey *et al.*, 1952) and a flat map of the distribution of corticospinal neurons (dots) in the frontal lobe (Dum and Strick, 1991). Abbreviations: cc, corpus callosum; CG, cingulate gyrus; cgsd, cingulate sulcus, dorsal bank; cgsv, cingulate sulcus, ventral bank; cs, central sulcus; iar, inferior arcuate sulcus; ps, principal sulcus; sar, superior arcuate sulcus.

to area 4, there are several areas projecting both to the brainstem and the spinal cord (Keizer and Kuypers, 1989). Therefore, it is quite clear today that Woolsey's MI is nothing else but a functional map of the corticospinal frontal territory and does not correspond to a single functional entity (Fig. 26.2). The aim of the present chapter is to present a modern view of the anatomical and functional organization of the agranular frontal cortex in monkeys and, by reviewing the available literature, to verify whether or not the same organizational principles are also valid for the human motor cortex.

MONKEY MOTOR CORTEX

Architectonic Subdivision of the Agranular Frontal Cortex

The agranular frontal cortex (henceforth referred to as the motor cortex) in the monkey occupies the caudal part of the frontal lobe between the fundus of the central and the fundus of the arcuate sulcus. According to the classical subdivision of Brodmann (1905), two large cytoarchitectonic areas, the caudally located area 4 and the rostrally located area 6, form the motor cortex. This subdivision was mainly based on the differential distribution, within the motor cortex, of giant pyramidal cells (Betz cells), which are abundant in area 4 but are rare or absent in area 6. Although Brodmann considered area 6 as a single entity, architectonic differences among its various parts were described in several subsequent studies (Vogt and Vogt, 1919; Bonin and Bailey, 1947; Barbas and Pandya, 1987). The possibility that architectonic subdivisions of area 6 have a functional correlate and, therefore, that architectonics can be a reliable technique for identifying functionally different motor areas has been a matter of debate for a long time. One strong argument against this possibility is the large variability among the various proposed parcellations in terms of size extent, and topography of cortical areas. Indeed, this variability results from different subjective criteria adopted by different investigators for defining borders between areas. For example, the most widely used criterion for defining

the border between areas 4 and 6 is the change in the number and density of giant pyramids in layer V. However, it is a quite common observation that these cells do not stop abruptly, but that their density decreases gradually, and that there is considerable interindividual variability among different monkeys. Therefore, if this criterion is used alone, the definition of the area 4/area 6 border becomes arbitrary. For example, this was the criterion used by Barbas and Pandya (1987) for delineating area 6DC, a cortical area, located just rostral to area 4 in the dorsal and mesial parts of the motor cortex, in which giant pyramids are scattered. Subsequent studies (see "Mesial Premotor Cortex"), however, clearly showed that this area does not correspond to any functionally independent entity and that its mesial part is nothing else but the leg field of the SMA. In contrast, when areas are defined on the basis of multiple criteria or different architectonic techniques, their definition becomes more objective and less sensitive to interindividual variability. Furthermore, it is now generally agreed that cortical areas can be identified, not only on an architectural basis but also on the basis of their connections and functional properties. If this multidisciplinary approach is adopted, maps of the monkey brain become much more reliable than they have been in the past. A clear example of the validity of this approach is the organization of the mesial sector of Brodmann's area 6. As it will be shown later in more detail (see "Mesial Premotor Cortex"), this cortical sector, once considered to be coextensive with the SMA (Woolsey *et al.,* 1952), is now almost unanimously considered to be formed by a caudal area F3 (SMA proper) and a rostral area F6 (pre-SMA, see Rizzolatti *et al.,* 1996c). The presence of an architectonic area, termed F3, occupying only the caudal part of mesial area 6 and independent from the adjoining dorsal sector of area 6, was first demonstrated by Matelli *et al.* (1985) with cytochrome-oxidase histochemistry. In a subsequent study (Matelli *et al.,* 1991), area F3 could be defined also on the basis of its cytoarchitectonic features and a new agranular area, rostral to F3, was identified and termed F6. The cytoarchitectonic border between these two newly identified mesial areas was defined on the basis of multiple criteria. For example, the caudal border of F3 with the mesial extension of area F1 (area 4) was mainly defined on the basis of clear changes in the density and arrangement of layers III and Va; therefore, the mesial part of area 6DC of Barbas and Pandya (1987) was included into a larger cytoarchitectonic entity (area F3). This subdivision of mesial area 6 was then corroborated by another completely independent approach, namely the receptor autoradiographic mapping of the binding sites of classical neurotransmitters (Geyer *et al.,* 1998). Hodological and functional data fully confirmed this subdivision and clearly demonstrated that F3 and F6 correspond to two functionally independent entities (Luppino *et al.,* 1993).

The results of the application of this kind of multidisciplinary approach to the parcellation of the whole extent of the motor cortex is represented by the map proposed by Matelli *et al.* (Fig. 26.3; Matelli *et al.,* 1985, 1991; see Rizzolatti *et al.,* 1998). This parcellation can also be found in the stereotaxic atlas of the rhesus monkey brain by Paxinos *et al.* (2000). The definition of the various motor areas of this map is mainly based on a combination of cytoarchitectonic histochemical, immunohistochemical, and neurochemical criteria but is also strongly corroborated by hodological and functional data. In this map, in analogy with von Economo and Koskinas (1925), the various areas are referred to with the letter "F." However, at variance with von Economo, numbers instead of letters, indicate the various motor areas. In this parcellation scheme, area F1 roughly corresponds to area 4, whereas each of the three main sectors of Brodmann's area 6—the mesial, the dorsal, and the ventral—is formed by a caudal and a rostral subdivision (Table 26.1).

It is quite clear, therefore, that the organization of the monkey motor cortex appears today much more

TABLE 26.1 Correspondence of Matelli *et al.*'s (1991) Nomenclature of the Agranular Frontal Areas with Brodmann's (1909) Nomenclature and the Most Widely Used Terminology in the Functional Literature

Matelli *et al.* nomenclature	Brodmann's nomenclature	Most widely used terminology in the functional literature
F1	Area 4	Primary motor cortex
F2	Dorsal sector of area 6, caudal part	Dorsal premotor cortex, caudal part (PMDc)
F3	Mesial sector of area 6, caudal part	Supplementary motor area proper (SMA proper)
F4	Ventral sector of area 6, caudal part	Ventral premotor cortex, caudal part (PMVc)
F5	Ventral sector of area 6, rostral part	Ventral premotor cortex, rostral part (PMVr)
F6	Mesial sector of area 6, rostral part	Presupplementary motor area (Pre-SMA)
F7	Dorsal sector of area 6, rostral part	Dorsal premotor cortex, rostral part (PMDr)

complex than previously thought. The motor cortex is, in fact, a mosaic of at least seven distinct areas that contains a multiplicity of body movement representations, playing a differential role in motor control.

In the next sections, the basic organizational principles of the anatomic connections of the various motor areas will be examined in order to better elucidate the functional differences among the various motor areas.

Classes of Motor Areas and General Pattern of Cortical Connectivity

Tract tracing experiments with modern neuroanatomical techniques can unravel in details the anatomic connections of each motor area with other cortical areas or subcortical structures. These data, then, provide crucial information about the functional interpretation of the role of each of these areas in motor control. Taken together, these data indicate that each frontal motor area has a specific pattern of anatomical connections. However, if the general pattern of connectivity is considered, it becomes obvious that the various frontal motor areas can be grouped into two major classes (see Luppino and Rizzolatti, 2000). The caudal motor areas F1, F2, F3, F4, and F5 form the first class. Their unifying feature is that these areas receive a primary cortical input from the parietal lobe; therefore, this class will be referred to as parieto-dependent motor areas. The rostral areas F6 and F7 form the second class. Their unifying feature is that their primary cortical input originates from the prefrontal cortex; therefore, this class will be referred to as prefronto-dependent motor areas.

Connections with the Spinal Cord and Intrinsic Motor Connections

The organization of the corticospinal projection is in agreement with the subdivision of the motor areas into two classes. Corticospinal projections originate from a large cortical territory that includes, in the frontal lobe, area 4 and the caudal part of area 6 and that, basically, corresponds to Woolsey's areas M1 and SMA. The origin of the corticospinal tract has been recently studied in great detail by Strick and co-workers (Dum and Strick, 1991; He *et al.*, 1993, 1995). These data (Fig. 26.2), when compared with the subdivision of the motor cortex, show that corticospinal projections originate from all the caudal motor areas, that is from F1, F2, F3, part of F4, and that part of F5 buried in the dorsal part of the inferior arcuate sulcus (F5 of the arcuate bank, F5ab). It is interesting to note that F2, F3, F4, and F5ab send connections also to F1 and are also connected with each other in a somatotopic manner. These data indicate that, although F1 is the only motor area provided with a rich direct access to the motor neuron pools (Porter and Lemon, 1993), all the caudal areas can be involved in movement execution, either directly, through their independent access to the spinal cord, or indirectly via F1.

In contrast, the organization of the prefronto-dependent motor areas is radically different. F6 (pre-SMA) and F7 do not project to the spinal cord, but their descending input terminates in various parts of the brainstem (Keizer and Kuypers, 1989). Furthermore, these areas are not connected with F1 and, especially in the case of F6, have more widespread connections with other motor areas. An exception is the dorsal and rostral part of F7, corresponding to the supplementary eye field (SEF; Schlag and Schlag-Rey, 1987), which has very poor connections with other motor areas but is strongly interconnected with the frontal eye field (FEF; Schall *et al.*, 1993). These data indicate that prefronto-dependent motor areas cannot control movement directly. They may control it indirectly through their subcortical relays or their connections with the parieto-dependent motor areas rostral to F1.

Connections with Other Cortical Areas

Cortical afferents to the frontal motor areas originate from three main regions: parietal cortex (primary somatosensory cortex, S1, and posterior parietal cortex), prefrontal cortex, and agranular cingulate cortex. However, as already mentioned, these projections are differentially distributed across the motor cortex (see Rizzolatti *et al.*, 1998).

The strong and reciprocal connections with the parietal cortex are the major source of input to the motor cortex, and this is especially true for the parieto-dependent motor areas. Recent functional evidence indicates that, similar to the motor cortex, the posterior parietal cortex is also formed by a multiplicity of independent areas, each of which appears to deal with specific aspects of sensory information and with specific effectors (Fig. 26.3). Furthermore, these data show that the classical distinction between an inferior parietal lobule (IPL), related to both visual and somatosensory information, and a superior parietal lobule (SPL), exclusively related to the somatosensory domain, is incorrect. Instead, both the IPL and the SPL receive somatosensory and visual input. In general, IPL areas and the posterior areas of the SPL process either visual or somatosensory and visual information, whereas the rostral areas of the SPL appear to deal almost exclusively with somatosensory information (see Caminiti *et al.*, 1996; Rizzolatti *et al.*, 1997b; Wise *et al.*, 1997). Recent studies on the organization of the parietofrontal connections indicate that motor and

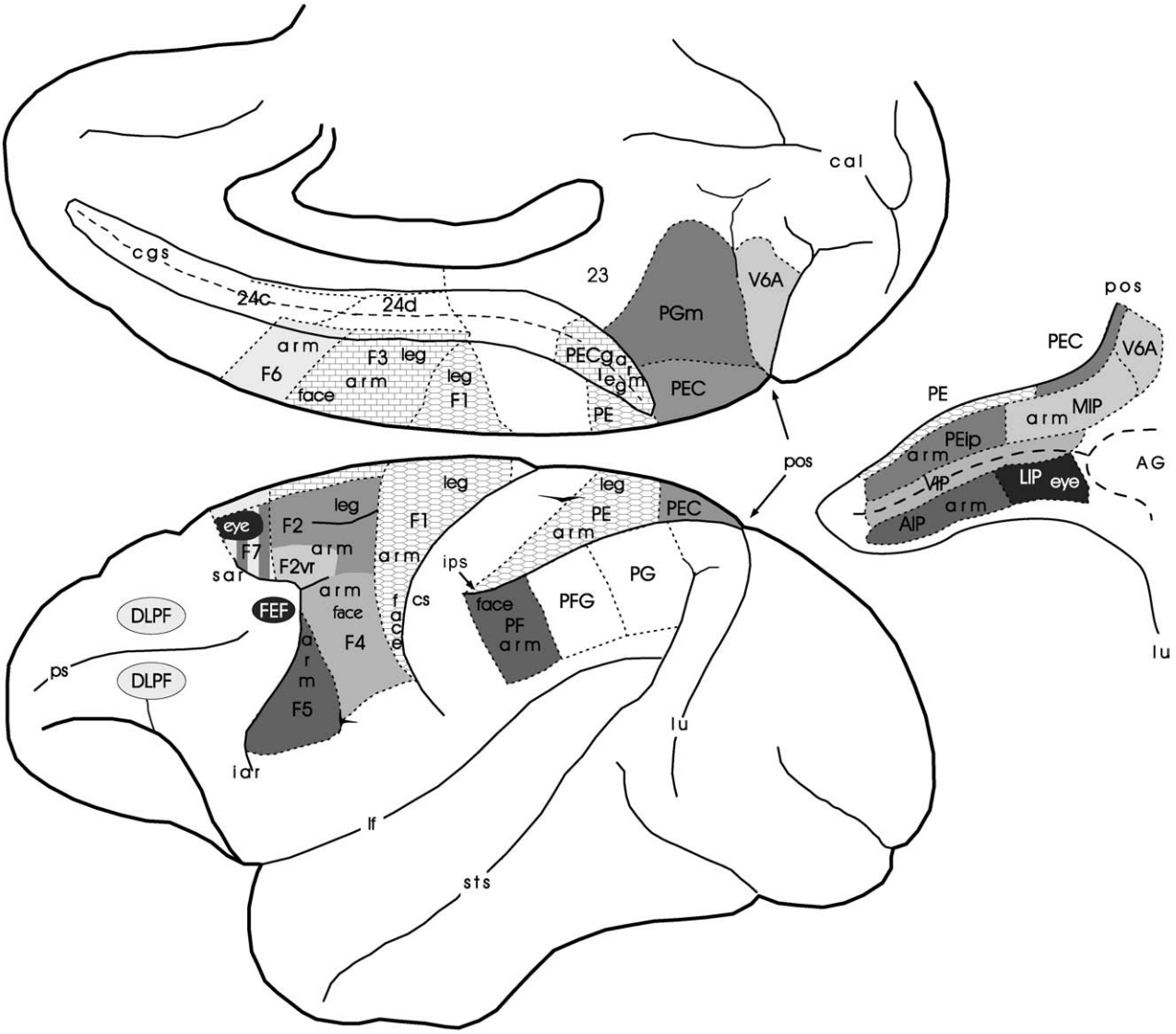

FIGURE 26.3 Mesial (top) and lateral (bottom) views of the macaque brain showing the cytoarchitectonic parcellation of the agranular frontal and posterior parietal cortex and the somatotopic representations of the body within each area. The motor areas are defined according to Matelli *et al.* (1985, 1991). The areas on the exposed surface of the parietal lobe are defined according to Pandya and Seltzer (1982), those within the intraparietal sulcus (ips) are defined according to physiological data (see text for further details) and are shown in an unfolded view of the sulcus in the right part of the figure. Frontal and parietal areas linked by predominant connections are depicted in identical gray tones or filling patterns. Abbreviations: AG, annectant gyrus; cal, calcarine fissure; cgs, cingulate sulcus; DLPF, dorsolateral prefrontal cortex; FEF, frontal eye field; lf, lateral fissure; lu, lunate sulcus; pos, parietooccipital sulcus; sts, superior temporal sulcus. Other abbreviations are as in Figure 26.2.

parietal areas are connected with each other in a very specific way (see Rizzolatti *et al.*, 1998). Each motor area is the target of a specific set of parietal areas. Typically, within such a set of parietal areas projecting to a given motor area, one area is the source of projections that are by far the strongest (predominant projections), whereas the other areas are the sources of moderate or weak projections (additional projections). Therefore, within the general framework of parieto-frontal connections, it is possible to identify a series of largely segregated anatomical circuits formed by parietal and motor areas linked by predominant connections. Functional evidence, when available, indicates that parietal and frontal areas forming each of these

circuits may share common functional properties. Therefore, the functional correlate of this anatomical organization is that each of these circuits appears to be dedicated to a particular aspect of sensory-motor transformation. The essence of this operation is the transformation of a description of the stimuli in sensory terms into their description in motor terms (Rizzolatti *et al.*, 1997b, 1998). It has been proposed that these parietofrontal circuits, and not the frontal motor areas in isolation, should be considered the functional units of the cortical motor system (Rizzolatti *et al.*, 1998).

Prefrontal projections to the motor cortex are primarily directed to F6 and F7 (Luppino *et al.*, 1993; Lu *et al.*, 1994; Luppino and Rizzolatti, 2000). However, the prefrontal input to F7 (except for the SEF) originates only from the dorsal part of the dorsolateral prefrontal cortex (DLPFd), whereas the input to F6 and the SEF originates from the dorsal and ventral parts of this prefrontal region. In addition, F6 and the SEF are also targets of strong afferents originating from the rostral cingulate cortex (area 24c). Our knowledge of the organization of the prefrontal and cingulate cortex is much less detailed than that of the parietal cortex. It is, however, widely accepted that these regions are not involved in the analysis of sensory stimuli but rather play a role in "higher order" functions such as working memory, temporal planning of actions, and motivation. Table 26.2 summarizes the sources of predominant and additional cortical afferents to each motor area. The connections among the various motor areas are not included.

From these anatomic considerations, the fact that parieto- and prefronto-dependent motor areas have a quite different functional role in motor control clearly emerges. Parieto-dependent areas, together with parietal areas, are involved in a parallel elaboration of sensory information for the transformation of it into potential motor actions. Prefronto-dependent areas, especially F6 and the SEF, appear to play a high hierarchical role in the control of body or eye movements. These areas convey inputs from the prefrontal and cingulate cortex to the parieto-dependent motor areas or to the FEF with an emphasis on motivation, long-term plans, and memories of past actions. On the basis of this information, the potential motor actions could either be implemented or remain as they are, that is that may be either cancelled or implemented later, when other contingencies allow it.

In the following sections the current knowledge of the functions of the various frontal motor areas and of

TABLE 26.2 Predominant and Additional Cortical Connections of the Motor Areas in the Macaque Monkey

Motor areas	Predominant connections	Additional connections	Proposed functional role
F1	PE	S1	Monitoring movement execution on the basis of somatosensory information
F2 dimple	PEC, PEip	CGp	Planning and controlling arm and leg movements on the basis of somatosensory information
F2vr	***MIP***	***V6A, PFG***	Planning and controlling arm trajectories on the basis of visual and somatosensory information
F3	PECg, 24d	PE, SII, S1, ***PFG***	Controlling postural adjustments that precede voluntary movements and, possibly, organizing motor sequences
F4	***VIP***	***PF,*** PEip, SII	Encoding peripersonal space and transforming object locations into appropriate movements toward them
F5ab	*AIP,* ***PF***	***PFG,*** SII	Transforming intrinsic object properties into appropriate hand movements
F5c	***PF***	*AIP,* SII	Representing action internally for action recognition and action imitation
F6	DLPF, 24c	***PFG,*** PG	Controlling sensorimotor transformations that are processed in the parieto-dependent motor areas; controlling visuomotor associations underlying the declarative phase of motor learning
F7	DLPF	***PGm, V6A,*** CGp	Coding object locations in space for orienting and coordinating arm-body movements
F7 (SEF)	FEF	DLPF, 24c, *LIP*	Organizing eye movements in an object-centered frame of reference; monitoring the consequences of saccadic activity

For abbreviations and nomenclature of parietal and cingulate areas see Figure 26.3; parietal areas processing only visual information are appear in italic; parietal areas processing both visual and somatosensory information are appear in bold italic.

the cortical circuits in which they are involved, will be presented in greater detail.

Area F1 (Area 4)

The precentral cortex, corresponding to F1, represents a nodal point of convergence of inputs from the other parieto-dependent motor areas. It is well accepted that area F1 plays a major role in the segmentation of actions, planned by other motor areas, into elementary movements and that it is virtually unique, among the motor areas, in controlling independent finger movements (see Porter and Lemon, 1993).

The classical studies of Woolsey *et al.* (1952) showed that this area can be roughly subdivided into three main somatotopic fields: a leg field located mesially and extending also on the dorsolateral convexity, an arm field in an intermediate position, and a face field, ventrolaterally toward the Sylvian fissure. Within each of these fields, proximal movements are represented more rostrally, and distal movements, more caudally (i.e., within the anterior bank of the central sulcus). The development of intracortical microstimulation (ICMS) or spike averaging techniques revealed more detailed information on the output organization of this area and, in particular, on the exact nature of the motor representation in this area. In their pioneering ICMS study, Asanuma *et al.* (1972) proposed an organization in terms of cortical columns, each of them related to a single muscle. However, according to the study of Kwan *et al.* (1978), in awake animals, movements in the arm field of F1 are represented in terms of joints, instead of muscles. These studies suggested the existence of a "core and surround" organization with a "core" representation of digit movements located mostly within the bank of the central sulcus and surrounding concentric bands representing wrist, elbow, and shoulder movements. More recent studies proposed an organization in terms of a "fractured" somatotopy, in which arm, hand, and digit movements are represented as overlapping neuronal populations. This overlap results partly from the convergence of outputs from a wide cortical territory onto the motor neuron pools that control muscles moving a given body part. These studies suggest, therefore, that in F1 there is a cortical representation of movements that lies beyond the simple muscle or joint level (Schieber and Hibbard, 1993).

Electrophysiological studies of the functional properties of F1 neurons showed that neurons in this area are strongly activated, almost exclusively, during movement execution and can be related to a number of dynamical or kinematic parameters of the movements, such as force, velocity, and movement direction (see Porter and Lemon, 1993). According to studies of the sensory properties of F1, this area can be subdivided into a rostral and a caudal sector (Lemon, 1981) on the basis of a differential distribution of neurons responding preferentially to tactile stimulation (located more caudally, mostly within the bank) or to proprioceptive stimulation (located more rostrally, on the cortical convexity). In line with this subdivision are data on a differential thalamic input to these two regions of F1 (Matelli *et al.*, 1989; Holsapple *et al.*, 1991). However, up to now, no description of a cytoarchitectonic counterpart of this possible subdivision of F1 has been provided in the macaque monkey.

Area F1 receives a primary parietal input from area PE (see, e.g. Matelli *et al.*, 1998). It is a classical notion that area PE (area 5) is a higher order somatosensory area, mostly devoted to the analysis of proprioceptive information. The most effective stimuli for many PE neurons are specific combinations of multiple joint positions or combinations of joint and skin stimuli (Sakata *et al.*, 1973; Mountcastle *et al.*, 1975). Recently, Lacquaniti *et al.* (1995) provided evidence that many neurons in area PE code the location of the arm in space in a body-centered coordinate system. The main role of the PE–F1 circuit could be to provide F1 with information on the location of body parts necessary for the control of limb movements.

Ventral Premotor Cortex

The inferior sector of Brodmann's area 6 is generally referred to as the ventral premotor cortex (PMv) and is made up of two distinct areas: F4 and F5 (Matelli *et al.*, 1985). Recent architectonic findings indicate that area F5 is not homogeneous but consists of two major sectors (Matelli *et al.*, 1996). One is located in the posterior bank of the inferior arcuate sulcus (F5ab); the other is located on the cortical convexity immediately adjacent to the arcuate sulcus (F5 of the cortical convexity, F5c). The F5ab sector corresponds to that part of area F5 from which corticospinal projections originate. Functional data confirmed this morphological subdivision.

Area F4

Microstimulation experiments showed that in F4 there is a representation of arm, neck, face, and mouth movements. Neurons in this area fire during reaching movements directed toward the body or away from it, others discharge during orofacial movements. Neurons related to distal movements are virtually absent (Gentilucci *et al.*, 1988). F4 neurons can be subdivided into two categories according to their responses to sensory stimuli: bimodal (visual and tactile) neurons (56%) and unimodal (mostly tactile) neurons (44%; Fogassi

et al., 1996). Unimodal and bimodal neurons have the same somatosensory characteristics. Their receptive fields (RFs) are rather large and predominantly located on the face, arm, and upper part of the body. The visual RFs are located in the peripersonal space, in register with the tactile fields. In a large majority of these neurons (70%), the position of the visual RF does not change when the gaze moves; that is, regardless of where the gaze is directed, the visual RF remains in the same location with respect to the body. Similarly, the visual RF remains anchored to the tactile RF, when the body part, on which the tactile RF is located, is moved. Thus, F4 neurons appear to code space in body-parts-centered coordinates (Graziano *et al.*, 1994; Fogassi *et al.*, 1996). This particular aspect of space coding is not based on a single reference point (head, arm, or body midline), but, rather, there is a multiplicity of reference points depending on the type of movement coded by a given set of neurons (Graziano *et al.*, 1997; Rizzolatti *et al.*, 1997a).

Parietal input to F4 originates almost exclusively from area VIP, located along the fundus of the intraparietal sulcus (Fig. 26.3; Luppino *et al.*, 1999). Area VIP is the target of various visual areas belonging to the "dorsal visual stream" (among them areas MST and MT), involved in the analysis of optic flow and in motion perception (see references in Rizzolatti *et al.*, 1998). In addition, VIP receives somatosensory information from areas PEc and PFG (Seltzer and Pandya, 1986). VIP neurons fall into two main categories: purely visual neurons and bimodal (visual and tactile) neurons (for references on VIP functional properties, see Colby, 1998). Bimodal neurons respond independently to visual and tactile stimuli. Their tactile RFs are located predominantly on the face, and their visual RFs are located in those parts of the field of vision that correspond to the tactile RFs, many of them limited to the peripersonal space. In about one third of visually responsive neurons, as in F4, the visual RF is coded in egocentric and not in retinal coordinates. On the basis of these data, it has been suggested that F4, together with VIP, is part of a parietofrontal circuit involved in encoding peripersonal space and in transforming object locations into appropriate movements toward them (Rizzolatti *et al.*, 1997b, 1998; Colby 1998).

Area F5ab

Area F5 is electrically excitable and contains a movement representation of the hand and the mouth. F5 neurons typically code goal-directed motor acts of the hand, the mouth, or both. Their firing is correlated with action execution and not with the individual movements forming it. According to the coded action, F5 hand neurons were subdivided into various classes. Neurons encountered more frequently are grasping, holding, tearing, and manipulating neurons. Most "grasping" neurons code specific types of hand prehension such as precision grip, whole hand prehension, and finger prehension (Rizzolatti *et al.*, 1988).

A considerable part of F5 neurons respond to visual stimuli. Most of the visually responsive neurons located in F5ab belong to a class of neurons referred to as "canonical" neurons. These neurons discharge to the presentation of three-dimensional objects, even when no immediate or subsequent action upon the object is allowed (Murata *et al.*, 1997). These responses are most likely the result of a "pragmatic" representation of the object in which the object's intrinsic properties (size, shape, and orientation) are coded for the selection of the most appropriate way to grasp it.

Area F5 receives predominant projections from two parietal areas: AIP and PF. Recent anatomical data, however, showed that the AIP projections are selectively directed to F5ab (Luppino *et al.*, 1999). Prefrontal afferents to F5 are very weak.

Area AIP occupies the rostral part of the lateral bank of the intraparietal sulcus (Fig. 26.3). AIP neurons were studied in monkeys trained to reach for and grasp objects of different size and shape, in dark or in light (Sakata *et al.*, 1995; Murata *et al.*, 2000). Most neurons discharge when grasping specific objects and may have visual responses selective for the type of object presented. AIP neurons were classified into three groups: "motor-dominant," "visual and motor," and "visual-dominant" neurons. Motor-dominant neurons are task-related and that fire equally well in dark or in light; visual and motor neurons are less active in dark than in light; and visual-dominant neurons fire only when the stimulus is visible, but not when the task is performed in the dark. Many visually responsive neurons also discharge when objects are simply fixated and no action upon them is required. In these neurons, the visual responses appear to represent specific intrinsic properties of the object. In most visual and motor neurons, the intrinsic characteristics of the object effective in triggering a neuron and the type of grip coded by that neuron matched, suggesting that these neurons correlate the intrinsic geometric properties of the object with the appropriate hand movement for grasping it. These data clearly show that there is a part of the dorsal visual pathways, in which AIP is involved, concerned with the aspect of form, orientation and/or size perception, relevant for the visual control of grasping movements.

On the basis of these data, it has been suggested that F5ab, together with AIP, is part of a parietofrontal circuit dedicated to visuomotor transformations for grasping (Jeannerod *et al.*, 1995).

Strong support for a crucial role of the F5ab-AIP circuit in visuomotor transformations for grasping was recently provided by studies in which the two areas were separately inactivated (Gallese *et al.*, 1994; Fogassi *et al.*, 2001). The independent inactivation of AIP and F5ab resulted in a disruption of the preshaping of the hand during grasping (i.e., a mismatch between the geometrical properties of the object to be grasped and the most appropriate position of the hand and fingers in order to accommodate this object). When the monkey eventually managed to grasp the objects, the grip was achieved only after a series of corrections based on the tactile exploration of the object. Therefore, a lesion of the AIP-F5ab circuit does not disrupt the ability to perform grasping movements, but only the capacity to transform the three-dimensional properties of the object into appropriate hand movements.

Area F5c

Neurons located in F5c are indistinguishable from F5ab neurons as far as their motor properties are concerned. As in F5ab, a considerable proportion of F5c neurons respond to visual stimuli. However, the visual properties of F5c neurons are markedly different from those in F5ab. Their main characteristic is that they discharge when the monkey observes another individual performing an action similar to that coded by the neuron. For example, a neuron activated by the actual performance of a grasping movement by the monkey also fires when the monkey observes the experimenter, or another monkey, grasping the object. Object presentation alone is not sufficient to activate them. Because of this correspondence between visual and motor properties, these neurons were referred to as mirror neurons (Gallese *et al.*, 1996; Rizzolatti *et al.*, 1997b).

The existence of these neurons suggests an important cognitive role for the motor cortex: that of representing actions internally. This internal representation, when evoked by an action made by others, as is the case in the previously mentioned experiments, could be involved in two related functions: action imitation and action recognition. This hypothesis is even more interesting if it is considered that, according to the classical literature, F5 should be the homologue of at least a part of, if not the entire, human Broca's region (for a review of the data and theoretical considerations, see Rizzolatti *et al.*, 1996a; Rizzolatti and Arbib, 1998). F5c receives predominant parietal projections preferentially from area PF. Although neurons with mirror characteristics appear to be present also in area PF (Fogassi *et al.*, 1998), our limited knowledge of the functional properties of this parietal area precludes, at the moment, any speculations about the possible functional role of this anatomical circuit.

Dorsal Premotor Cortex

Superior area 6, generally referred to as dorsal premotor cortex (PMd), is made up of two areas: F2 and F7 (Fig. 26.3). Although F2 appears to be cytoarchitectonically homogeneous, recent evidence (Fogassi *et al.*, 1999) suggests that it should be subdivided into two functional sectors: one located around the superior precentral dimple (F2 dimple, F2d) and the other occupying its ventrorostral part (F2vr). Support in favor of this subdivision has also been provided by anatomical data (Matelli *et al.*, 1998, see "Area F2"). Like F2, F7 is also made up of two distinct functional sectors: a dorsorostral and a ventrocaudal one. The dorsorostral sector corresponds to the supplementary eye field (Schlag and Schlag-Rey, 1987).

Area F2

Area F2 is electrically excitable and has a rough somatotopic organization with a leg and an arm representation located dorsal and ventral to the superior precentral dimple, respectively (Kurata, 1989; Dum and Strick, 1991; He *et al.*, 1993; Fogassi *et al.*, 1999). Functional studies of F2 were mostly focused on its motor properties, by employing visually instructed motor delay tasks (see Wise *et al.*, 1997). Typically, in these tasks, a motor response (very often an arm movement) is performed after a delay from the appearance of a visual stimulus instructing the monkey which particular movement to perform. Some F2 neurons discharge in association with movement onset (movement-related activity), others become active during the delay period when the monkey is waiting for the go signal (set-related activity), and others discharge at the appearance of the instruction stimulus (signal-related activity). The percentage of these "signal-related" neurons is higher in the rostral part of F2 than in its caudal part (dimple region; see Wise *et al.*, 1997). These data indicate that F2 is not simply involved in motor execution, but plays a role also in some aspects of motor preparation (see Wise *et al.*, 1997). There is little information on the responses of F2 neurons to sensory stimuli. Many F2 neurons respond to somatosensory stimuli and, in particular, to proprioceptive input. Recent evidence indicates that there is a differential distribution of sensory properties within F2. While in F2d, most neurons respond to proprioceptive stimuli; neurons in F2vr also respond to tactile and visual stimulation (Fogassi *et al.*, 1999). Furthermore, it has been reported that in F2vr, but not in F2d, information about the target location and the arm to be used can be integrated at the single neuron level to plan a forthcoming action (Hoshi and Tanji, 2000).

Hodological data showing that F2d and F2vr are involved in different parietofrontal circuits also

supports this functional segregation within F2. While F2d receives predominant projections from areas PEC and PEip, the primary parietal input to F2vr originates from area MIP and V6A (Matelli *et al.*, 1998). Furthermore, F2vr, but not F2d, is the target of a minor but consistent projection from the dorsal part of prefrontal area 46.

Our knowledge of the functional properties of area PEC is very limited. This area is richly connected with area PE (Pandya and Seltzer, 1982); therefore, it should be basically involved in the analysis of somatosensory stimuli for movement organization. Electrophysiological studies of neighboring regions, in which occasionally PEC neurons were recorded, confirm this conclusion (Galletti *et al.*, 1996).

Area PEip was defined as that part of the medial bank of the intraparietal sulcus (roughly its rostral half) that is the source of corticospinal projections (Matelli *et al.*, 1998). Functional studies showed that neurons in this region become active in association with arm movements (Kalaska *et al.*, 1990). Typically, the discharge is stronger when the arm is projected in a certain direction. The directional tuning is usually broad. Most PEip neurons respond to somatosensory stimuli (Mountcastle *et al.*, 1975; Iwamura and Tanaka, 1996). According to these data, F2d should be the target of higher order somatosensory information. Recent observations indicate that in a restricted region, most likely corresponding to the posterior part of area PEip, there are neurons with bimodal (tactile and visual) RFs (Iriki *et al.*, 1996). The functional properties of these neurons are, for many ways, similar to those of F4 neurons, but not to those of F2d; indeed, F4 is the target of additional projections from PEip. It is, therefore, possible that some kind of visual information also reaches F2d.

Even though PEip and PEC appear to be mostly involved in the somatosensory control of movements, both area MIP and area V6A use also visual information for the same purpose. Area MIP is located in the caudal part of the medial bank of the intraparietal sulcus (see Colby, 1998). Neurons in this area are strongly activated when the monkey reaches for a visual target. Many of them show responses to pure visual stimuli or to both visual and somatosensory stimuli (bimodal neurons). Area V6A is located in the dorsal part of the anterior bank of the parietooccipital sulcus (Galletti *et al.*, 1999). About half of the V6A neurons discharge in response to visual stimuli. The remainder discharges mostly in association with eye or arm movements. In contrast to what is observed in most visual areas, there is no magnification of the foveal representation in V6A.

In conclusion, the PEip/PEC-F2d circuit appears to be involved in planning and controlling arm (and leg) movements mostly on the basis of somatosensory information. In contrast, the MIP/V6A-F2vr circuit may use both somatosensory and visual information probably for the same purpose. Monitoring and controlling arm position during the transport phase of the hand toward the target could be one of the major functions of this circuit.

Area F7

As already mentioned, area F7 is also functionally not homogeneous. The dorsal part of this area contains the SEF, an oculomotor field that can be identified with intracortical microstimulation. Anatomically, the SEF is strongly connected with the FEF, but it is also the target of strong projections from both dorsal and ventral areas of the dorsolateral prefrontal cortex (DLPF; Huerta and Kaas, 1990; Luppino *et al.*, 1990). Furthermore, the SEF receives afferents from the rostral cingulate cortex (Huerta and Kaas, 1990; Luppino, *et al.*, 1990). These anatomical data suggest that the SEF could be involved in the control of eye movements at a higher hierarchical level than the FEF. In line with this hypothesis are functional data showing that SEF is involved in encoding saccades relative to an object-centered frame of reference (Olson and Gettner, 1995) or in monitoring the consequences of eye movements (Stuphorn *et al.*, 2000).

The remaining part of F7 is scarcely excitable and has been the target of only a few functional studies. Some F7 neurons show visual responses even when the stimulus is not instructing a subsequent movement (di Pellegrino and Wise, 1991). Others show visual responses when the location of the stimulus matches with the target of an arm movement (Vaadia *et al.*, 1986). F7 is the target of predominant projections from the DLPFd, mainly dorsal area 46 and area 8b. According to some authors (Wilson *et al.*, 1993), this prefrontal region should be mainly involved in the working memory of spatial positions. Minor inputs to F7 originate mainly from parietal area PGm, whose functional role is still largely unknown. Recent studies showed that PGm neurons may discharge during eye and/or arm movements (Ferraina *et al.*, 1997). On the basis of this information, it is possible to suggest that the DLPFd-F7 circuit could be involved, with the contribution of PGm, in coding object locations for orienting and coordinating arm–body movements.

Finally, ablation studies showed that monkeys, previously trained to make arbitrary goal-directed movements, following lesions of the postarcuate cortex, were no longer able to execute the task, although no obvious motor deficit was present. If one compares the location of the lesions reported in the literature (see references in Passingham, 1993), it emerges that F7, plus the rostralmost part of F2, were the only regions

damaged in all monkeys. Therefore, a further function of area F7, possibly with the contribution of F2vr, is to play a crucial role in conditional stimulus–response association tasks (see Passingham 1993).

Mesial Premotor Cortex

The mesial part of Brodmann's area 6 is occupied by two architectonic areas: F3, or SMA proper, and F6, or pre-SMA (Matelli *et al.,* 1991, Geyer *et al.,* 1999). Classically, this cortical sector was considered to be coextensive with the so-called supplementary motor area, defined by Woolsey using gross electrical stimulation (Fig. 26.2). It was widely accepted that the SMA collaborated with the primary motor cortex in movement execution, especially for proximal and axial movements. Later, experiments in monkeys and humans yielded conflicting results on the possible role of the SMA in motor control. Some data appeared to confirm an executive role of the SMA in motor control, while others favored what was called a "supramotor" role of the SMA, that is a role in those processes that precede the actual movement execution. The discovery that, in monkeys, mesial area 6 is composed of two distinct areas (Luppino *et al.,* 1991; Tanji 1994; Rizzolatti *et al.,* 1996c) was crucial for reconciling these apparently conflicting results.

Area F3 (SMA Proper)

Intracortical microstimulation studies showed that F3 is electrically excitable with low-intensity currents and contains a complete body movement representation (Luppino *et al.,* 1991). Evoked movements mainly involved proximal and axial muscles and, typically, a combination of different joints, even at the minimal effective current intensity. Distal movements, when evoked, were often observed in combination with the proximal ones. Single-unit recordings showed that many F3 neurons exhibit somatosensory responses. Most F3 neurons discharge in association with active movements, and their discharge onset is typically time-locked to the movement onset (movement-related activity). Some F3 neurons were found to fire exclusively in relation to specific sequences of movements (see Tanji and Shima, 1996).

Area F3 appears, therefore, in many ways functionally similar to F1. Some major differences, however, distinguish these two areas. First, in F1 proximal and distal movements are anatomically segregated, while they are mixed in F3 (Luppino *et al.,* 1991). Second, ICMS typically evokes single joint movements in F1, whereas movements involving two or more articulations are often observed in F3 (Luppino *et al.,* 1991). Finally, although still controversial (see, e.g., He *et al.,* 1995), in F3 proximal movements appear to be much more represented than are distal movements (Penfield and Welch 1951; Woolsey *et al.,* 1952; Luppino *et al.,* 1991; Maier *et al.,* 1997).

F3 is the target of predominant projections from the caudal and dorsal part of area 24 (area 24d) and from parietal area PECg, located in the caudalmost part of the cingulate sulcus (Luppino *et al.,* 1993). Area 24d is architectonically distinct from the rostral cingulate area 24c (Matelli *et al.,* 1991; Nimchinsky *et al.,* 1996) and roughly corresponds to what is also referred to as "caudal cingulate motor area" (Dum and Strick, 1993). This area is electrically excitable, contains a leg and an arm representation, and is the source of topographically organized projections to the spinal cord and to F1 (Luppino *et al.,* 1991, 1993; He *et al.,* 1995). Thus, area 24d can be considered as another motor area, functionally assimilable to the caudal group of the agranular frontal areas.

Area PECg was cytoarchitectonically defined by Pandya and Seltzer (1982). Anatomical data of the same authors showed that area PECg is connected with areas PE, PEC, and PGm. In the only one functional study of this area, Murray and Coulter (1981), claimed that this area contains a complete somatosensory map of the body. Because of this finding and its anatomical location, PECg was termed the supplementary sensory area.

Taken together, these data suggest that F3 (or possibly the PECg-F3 circuit) controls the motor activity in a global way. In particular, it has been proposed that F3 may use the knowledge of the actual limb position to prepare the posture necessary for forthcoming movements, thus playing a fundamental role in predictive postural adjustments (Massion, 1992). F3 also appears to contribute to the initial stages of learning of motor sequences that improve performance (Hikosaka *et al.,* 1999). According to others, F3 is involved in the execution of certain motor sequences (Tanji *et al.,* 1996).

Area F6 (Pre-SMA)

F6 is weakly excitable with intracortical microstimulation. Motor responses can be evoked from it only with rather high current intensities and, typically, they consist of slow and complex movements restricted to the arm (Luppino *et al.,* 1991). Visual responses are common in F6, while somatosensory responses are rare. When tested during active arm movements, F6 neurons show a long leading activity during preparation for movement, and some of them fire in relation to a redirection of an arm movement to a direction opposite to one previously rewarded (shift-

related activity; Matsuzaka and Tanji, 1996). Other experiments demonstrated that F6 neurons are excited or inhibited when objects, moved toward the animal, enter into its reaching distance and, therefore, appear to be modulated by the possibility of grasping an object (Rizzolatti *et al.*, 1990).

Finally, recent data showed that F6 plays a key role in the early stages of motor learning, precisely when the cognitive aspect of the procedure to be learned is acquired. This conclusion is based on the behavior of single neurons and on inactivation experiments showing that the number of errors for learning new sequences increases after muscimol injections into this area. In contrast, the performance of learned sequences is not affected by pre-SMA inactivation (see Hikosaka *et al.*, 1999).

The cortical connections of F6 are unique among the various motor areas in that only this area receives predominant projections from the dorsal and ventral parts of prefrontal area 46 and from the rostral cingulate area 24c (Luppino *et al.*, 1993; Lu *et al.*, 1994). F6, therefore, is a privileged site of convergence of information possibly related to the working memory of objects or space locations, to the temporal planning of actions, or to motivation that is, then, distributed to the other motor areas. These data suggest for F6 a double role in motor control. A first role is the control of the sensorimotor transformations that occur in the parieto-dependent motor areas. Normally, even when parietofrontal circuits are activated, the movement does not start. Only when external contingencies and motivational factors allow it, does F6 render the movement onset possible. A second possible role of F6 is more cognitive. It is in the control of visuomotor associations underlying the declarative phase of motor learning.

HUMAN MOTOR CORTEX

Comparative Architectonics of the Human and Monkey Motor Cortex

Cytoarchitectonically, area F1 is characterized by low cell density, poor lamination, the absence of layer IV, and a very prominent layer V with giant pyramidal cells arranged in multiple rows (Matelli *et al.*, 1991). On the mesial surface, the area next to F1 in the rostral direction is F3. As F1, area F3 is poorly laminated. One of its most important distinguishing feature is the increase in cellular density in the lower part of layer III and in layer Va. Layer Vb is pale as in F1. Giant pyramidal cells are absent in most of F3. The agranular area rostral to F3 is F6. Unlike areas F1 and F3, this area is clearly laminated and has a dark and very prominent layer V, well demarcated from the less dense layers III and VI. At the rostral border of F6, an incipient layer IV becomes recognizable. More recently, receptor autoradiographic data showed that clear-cut changes in the laminar binding patterns of glutamate (AMPA and kainate) and muscarinic cholinergic receptors closely match cytoarchitectonic borders in adjacent sections stained with the Nissl method (Matelli *et al.*, 1991; Geyer *et al.*, 1998). On the lateral convexity, area F2 is poorly laminated like areas F1 and F3, but unlike F1, it contains only few, scattered giant pyramidal cells especially in its caudal part. Lower layer III is characterized by a thin row of medium-sized pyramids. Layer V is slightly denser and darker than in F1, while the density of layers III and V is slightly lower than in area F3. Area F7 is clearly laminated and differs from F2 in two ways: the presence of a prominent layer V and the subdivision of layer VI into two sublayers. Layer VIa is pale, whereas layer VIb is dark and dense. The area rostral to F7 shows an incipient layer IV, and its laminar organization is more distinct than that of the agranular frontal cortex (Matelli *et al.*, 1991). Also the ventral part of area 6 consists of two areas: area F4 rostral to F1 and area F5 in the rostralmost part of ventral area 6. Area F5 has a common border with the prefrontal cortex. Although these areas have been identified on the basis of laminar differences in the distribution pattern of cytochrome-oxidase activity, preliminary cytoarchitectonic data confirm the histochemical parcellation. In area F4, the overall cell density is low, and pyramids increase in size from superficial to deep layer III. In layer V, large pyramidal cells are scattered especially in the dorsal part of area F4, near the spur of the arcuate sulcus. Area F5 is clearly laminated, and its cell density is higher than in F4. Single large pyramidal cells in layer V are present only in that part of area F5 that is buried in the posterior bank of the arcuate sulcus (F5ab). In contrast, a layer V devoid of large pyramids (Matelli *et al.*, 1996) characterizes the part of area F5 lying on the cortical convexity (F5c).

The cytoarchitectonic features and the topography of the human precentral motor cortex are very similar to those of the macaque. Also in humans, low cell density, poor lamination, the absence of layer IV, and Betz cells in layer V characterize the precentral motor cortex (Brodmann's area 4). Scattered or absent giant pyramidal cells and larger, more elongated, and more densely packed pyramids in lower layer III characterize Brodmann's area 6. Close to the midline, the rostral border of area 4 lies on the exposed cortical surface. More ventrolaterally, it recedes in the caudal direction and eventually disappears in the depth of the

central sulcus. The mesial part of area 4 occupies part of the paracentral lobule. Recently, human area 4 has been subdivided into a caudal (area 4 posterior or 4p) region and a rostral (area 4 anterior or 4a) region, based on differences in cytoarchitecture and neurotransmitter binding sites (Geyer *et al.*, 1996). The two areas form two parallel bands within area 4 running mediolaterally from the midline to the Sylvian fissure. Clear-cut changes in the laminar binding patterns, especially of muscarinic cholinergic (revealed with [^{3}H]oxotremorine-M) and serotoninergic (revealed with [^{3}H]ketanserine) binding sites, closely match corresponding cytoarchitectonic borders. Lower layer III pyramidal cells are small and loosely aggregated in area 4p, and larger and more densely packed in area 4a. Mean regional binding densities of many neurotransmitter binding sites tend to be higher in area 4p, whereas they are lower in area 4a. At present, it is unclear whether there is any homology between human areas 4a and 4p and the two functional or hodological subdivisions described in the macaque monkey (see "Area F1 (Area 4)"). Cytoarchitectonic similarities between humans and macaques are also obvious on the mesial cortical surface. Two recent comparative studies (Zilles *et al.*, 1995, 1996) found striking architectonic similarities between macaque areas F3 and F6 and the mesial parts of human areas 6aα and 6aβ (according to the nomenclature of the Vogts, 1919), respectively. Additional similarities have been found on a neurochemical basis (Zilles *et al.*, 1995, 1996; Geyer *et al.*, 1998). For example, [^{3}H]kainate binding sites are mainly concentrated in the deep layers in both areas, in macaques and humans. Binding density in area F3/mesial 6aα is higher than in the precentral motor cortex and higher than in the lateral premotor cortex in both species. [^{3}H]oxotremorine-M binding sites show a superficial and a deep cortical band of maximal binding densities in both species. There is a caudorostral increase in binding densities from the precentral motor cortex to area F6 in macaques and to mesial area 6aβ in humans. On this basis one may speculate that human mesial areas 6aα and 6aβ are possibly homologous to macaque areas F3 (SMA proper) and F6 (pre-SMA), respectively.

In humans, the border between the primary motor cortex and mesial area 6aα coincides approximately with the VCP line (vertical through the posterior commisure). The border between mesial area 6aα and mesial area 6aβ coincides approximately with the VCA line (vertical through the anterior commisure; Zilles *et al.*, 1996). The coincidence of the borders between the primary motor cortex/SMA proper and the SMA proper/pre-SMA with the VCP and VCA lines, respectively, has also been shown by Vorobiev *et al.* (1998). In the latter study, the human SMA proper has been further subdivided into a caudal (SMAc) and a rostral (SMAr) part. This subdivision of the human SMA proper may reflect different somatotopic representations or a more fine-grained functional differentiation (see "Mesial Premotor Cortex"). What is relevant in this study and in that of Geyer *et al.* (1996) is the greater fractionation of the human agranular cortex in comparison with that of the macaque. In particular, considering the cytoarchitectonic characteristics of SMAr and SMAc, it may be speculated that these two areas evolved from a common precursor, anatomically similar to the monkey F3, as a consequence of a process of differentiation of a single field into two fields. For a description of the adjoining areas of the cingulate cortex see Chapter 24.

On the cortical convexity of the macaque, a clear anatomical landmark—the arcuate sulcus—separates the agranular frontal from the granular prefrontal cortex. In the human brain, a comparable sulcus is not evident, but the spatial distribution of the agranular cortex (Brodmann's areas 4 and 6, plus dysgranular area 44; see "Ventral Premotor Cortex" for a further discussion on areas 44 and 45) is strikingly similar. In both species, the prefrontal cortex extends caudally in the middle of the dorsolateral convexity, as if pushing back the agranular cortex; conversely, it recedes rostrally in the dorsomedial and ventrolateral parts of the convexity. The prefrontal cortex is discussed in more detail in Chapter 25.

In a recent review article (Rizzolatti and Arbib, 1998), an attempt was made to define homologies between the human and macaque premotor cortex. It was proposed that the superior frontal and superior precentral sulcus (Fig. 26.4) represent the human homologue of the macaque superior arcuate sulcus (Fig. 26.4). Accordingly, the two areas that occupy the rostral part of the precentral gyrus and the caudal part of the superior frontal gyrus (superior part of area 6aα and area 6aβ according to Vogt and Vogt, 1919) could correspond to macaque areas F2 and F7, respectively. The inferior frontal sulcus and the ascending branch of the inferior precentral sulcus could correspond to the macaque inferior arcuate sulcus, while the descending branch of the inferior precentral sulcus could correspond to the inferior precentral dimple of the macaque monkey. Accordingly, the inferior part of area 6aα and area 44 should be homologous to macaque areas F4 and F5, respectively. An open issue is the macaque homologue of Brodmann's human area 45. Walker (1940) described an area, termed area 45, which lies in the rostral bank of the inferior arcuate sulcus of the monkey. Petrides and Pandya (1994) proposed that this area is the homologue of human

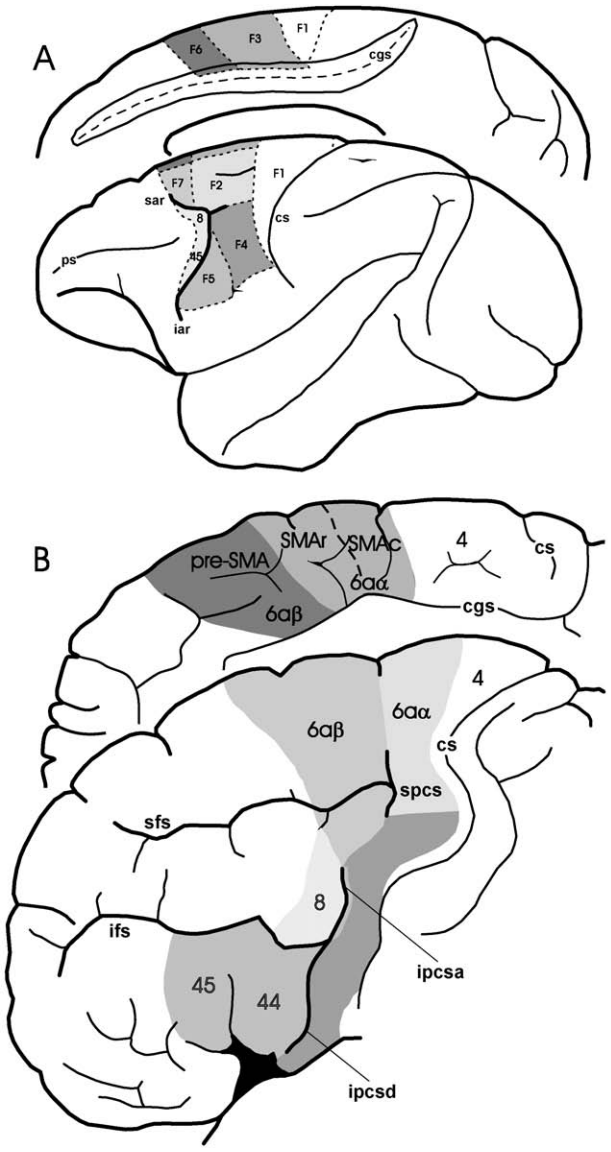

FIGURE 26.4 Proposed homologies between the monkey and human motor cortices. The monkey architectonic map **(A)** is according to Matelli *et al.* (1985, 1991). The human architectonic map **(B)** is according to Brodmann (1909); Brodmann's area 6 is further subdivided according to Vogt and Vogt (1919). Areas of the two species considered to be homologous are depicted in identical gray tones. The data are based on cytoarchitectonics, electrical stimulations, and sulcal ontogeny. The superior frontal sulcus (sfs) and the superior precentral sulcus (spcs) of the human brain are considered to correspond to the superior limb of the arcuate sulcus (sar) in the macaque. The inferior frontal sulcus (ifs) and the ascending branch of the inferior precentral sulcus (ipcsa) of the human brain are considered to correspond to the inferior limb of the arcuate sulcus (iar) in the macaque. The descending branch of the inferior precentral sulcus (ipcsd) is considered to correspond to the inferior precentral dimple (not labeled in A) in the macaque. For further details, see "Mesial Premotor Cortex." Abbreviations: cgs, cingulate sulcus; cs, central sulcus. Other abbreviations as in Figure 26.3.

area 45. However, available data suggest that, in the monkey, area 45 is mostly related to eye movements (Bruce *et al.*, 1985), while human area 45 is part of Broca's speech region. There are no reports in the literature that human area 45 might be involved in eye movements. The distinguishing cytoarchitectonic feature of human areas 44 and 45 is the presence of very large and darkly stained pyramidal neurons in layer III. As mentioned earlier, this is also a distinguishing feature of the motor areas rostral to the precentral motor cortex in both human and macaque. Area 44 is further characterized by the presence of a population of large pyramids in layer V and a barely recognizable dysgranular layer IV, which is invaded to different degrees by layer III and layer V pyramidal cells (Type 2 of general subdivision of the cerebral cortex of von Economo and Koskinas, 1925). Area 45 differs essentially from area 44 by an increase in the thickness of layer IV (Amunts *et al.*, 1999). A recent immunohistochemical study of the human inferior frontal gyrus (Hayes and Lewis, 1992) confirmed that the thickness and the cellular organization of layer IV is critical in differentiating area 44 from area 45. Therefore, if one considers the cytoarchitectonic similarities between human areas 44 and 45 and their similar age of myelinization onset (see Flechsig, 1898; Vogt and Vogt, 1919), an alternative interpretation would be that both areas evolved from the monkey area F5.

Taken together, modern architectonic studies of the human agranular frontal cortex reveal three main organizational principles: (1) the human motor cortex, as in monkeys, is formed by a mosaic of different architectonic areas; (2) in the human motor cortex, however, both the number of areas and the variability in their location and extent is larger than in the macaque; (3) in the human cortex, the spatial congruence between architectonic borders and macroscopic features (gyri, sulci) is lower than in the monkey. According to Rademacher *et al.* (1993), primary cortical areas bear a characteristic relationship to a set of sulci; therefore, their location can be predicted on the basis of sulcal patterns (class 2 variability). In contrast, it is impossible to predict with a high level of reliability the location of nonprimary cortical areas, on the basis of the sulcal pattern (class 1 variability). For an overview of the architecture of the cerebral cortex, see Chapter 27.

This spatial variability of most areal borders relative to surface landmarks is a crucial factor for the architectonic interpretation of activation foci in functional imaging studies. Classical maps, based on observations in single brains, cannot provide information on interindividual variability in the extent of cytoarchitectonic areas and their location relative to the sulcal pattern. The correlation between microstructure and

function of the agranular frontal cortex will became much more precise and valid when it will be possible to superimpose probability maps of cytoarchitectonically defined areas obtained from several brains, with activation foci obtained from functional imaging studies in the three-dimensional space of a common spatial reference system (e.g., the reference brain of a computerized atlas; Roland and Zilles, 1994).

Functional Organization of the Human Motor Cortex

Functional evidence, mostly from neuroimaging studies, indicates that the human motor cortex shares several general organizational principles with the monkey motor cortex. One important aspect is the existence of multiple representations of body movements in the human motor cortex. For example, Fink *et al.* (1997) observed that simple flexion and extension movements of the fingers induce several independent activations in the precentral motor cortex, the SMA proper, the dorsal premotor cortex, and the frontal operculum, as well as in the cingulate motor areas. Furthermore, this study showed that, in addition to the primary (S1) and secondary (SII) somatosensory areas, two further arm and finger representations are located in the superior and inferior parietal lobules. These observations fit well with the notion that multiple motor representations are also present in the posterior parietal cortex. Further evidence in favor of the existence of multiple representations of body movements in the motor and posterior parietal cortices comes from studies of motor imagery (see Jeannerod and Decety, 1995). A recent study, in which motor imagery was compared with motor execution, suggests that largely overlapping neural substrates, involving motor and parietal cortices, are involved in both aspects of motor control (Gerardin *et al.*, 2000). In this respect, one open question is the possible involvement of the precentral motor cortex in motor imagery. Several studies indicate that the precentral motor cortex is also activated during imagined movements, although to a lesser extent (Porro *et al.*, 1996; Roth *et al.*, 1996; Gerardin *et al.*, 2000).

The activation of several motor and parietal areas during motor execution and/or motor imagery is in line with the modern view, coming from monkey studies, that the basic elements of the cortical motor system are the parietofrontal circuits. Direct evidence supporting this concept also in humans comes from studies in which the issue of sensorimotor transformation for action has been specifically addressed, by using experimental paradigms similar to those used in monkey studies. Binkofski *et al.* (1999), asking subjects to manipulate complex nonrecognizable plastic objects, found activation in the ventral premotor cortex (probably Brodmann's area 44) and in a region in the intraparietal sulcus (most probably corresponding to the anterior parietal area AIP of the monkey). More recently, Bremmer *et al.* (2000), by presenting normal subjects with visual, tactile, and auditory stimuli, were able to identify an area in the depth of the intraparietal sulcus related to polymodal sensory stimulation. They suggested that this area is the human equivalent of monkey area VIP. A further activation focus was found in the dorsal part of the ventral premotor cortex, and this activation was suggested to reflect the connectivity between area VIP and area F4, as demonstrated in the monkey.

In the next sections, available functional evidence in favor of the proposed homologies between monkey and human motor areas will be elucidated in greater detail.

Precentral Motor Cortex (Area 4)

The most complete functional map of the human precentral cortex was provided in the 1930s by Penfield (see Penfield and Boldrey, 1937) who used surface electrodes to stimulate the cortex of epileptic patients during surgery. These studies gave a view of the general somatotopic organization of the human precentral motor cortex, essentially similar to what was proposed by Woolsey in the monkey. In this respect, it is important to note that surface electrical stimulation reveals mostly the origin of the spinal projection from the motor cortex that in the monkey is not restricted to area 4. Therefore, when considering that in humans the exposed convexity of the precentral gyrus is mostly occupied by area 6, it is reasonable to conclude that at least part of Penfield's homunculus belongs to premotor areas, functionally independent from area 4. Several positron emission tomography (PET) investigations confirmed the existence of a crude somatotopic organization of the human precentral motor cortex (see Grafton *et al.*, 2000). Two recent reports, taking advantage of the high spatial resolution functional magnetic resonance imaging (fMRI) technique, showed that, also in humans, multiple, partially overlapping sites of activation occur in a wide region of the precentral gyrus, in relation to wrist and single finger movements (Rao *et al.*, 1995; Sanes *et al.*, 1995). Such an organizational principle seems, therefore, to exists in both human and nonhuman primates.

In some studies, it has been found that regional cerebral blood flow (rCBF) changes in the human precentral motor cortex, as neuronal activity in the monkey area 4, is correlated with changes in the velocity

and force of the executed movements (Van Meter *et al.*, 1995; Dettmers *et al.*, 1996).

Finally, the study of Geyer *et al.* (1996) has shown that the proposed subdivision of area 4 into two areas (4a and 4p) may also have a functional counterpart. PET foci were correlated with the probability maps of areas 4a and 4p as obtained from the cytoarchitectonic analysis of postmortem brains. It was found that a roughness discrimination task activated area 4p significantly more than did a control condition of self-generated movements.

Ventral Premotor Cortex

Functional studies of this cortical region (ventral part of area 6aα, area 44, and, possibly, area 45) have been mostly devoted to investigations into the role of Broca's region in speech functions. Only recently, neuroimaging studies showed that the human ventral premotor cortex is also involved in the control of hand movements. These observations strongly support the proposed homology between Broca's region and monkey area F5.

Early studies of subjects performing grasp movements failed to identify activations in the ventral premotor cortex. Evidence in favor of the existence of a hand representation in this region can be found, however, in studies of learning finger movement sequences (Seitz and Roland 1992), of mental imagery of grasping (Decety *et al.*, 1994; Grafton *et al.*, 1996a), and of preparation of finger movements on the basis of a copied movement (Krams *et al.*, 1998). More direct evidence that the ventral premotor cortex contains a hand representation comes from a recent study of Binkofski *et al.* (1999). In this study, continuous manipulation of complex objects resulted in an activation of presumed area 44, while covertly naming manipulated objects resulted in an additional activation more rostrally in presumed area 45.

One very interesting result of this study was that object manipulation also activated a number of parietal areas, one of them located in the anterior part of the lateral bank of the intraparietal sulcus. It has been suggested that a parietofrontal circuit for manipulating objects also exists in humans and involves the homologues of area F5ab and area AIP of the monkey.

Several lines of experimental evidence indicate that an action recognition system (mirror system), described in monkey area F5c is also present in the human brain. First, experiments with transcranial magnetic stimulation (TMS) showed that, in normal subjects, the observation of hand actions produces a facilitation of the motor cortex, as shown by the increase of the amplitudes of the motor-evoked potentials in those hand muscles that are involved in the execution of the observed action (Fadiga *et al.*, 1995; Strafella and Paus, 2000). Second, electrophysiological studies showed that, when human subjects observe hand actions, there is a desynchronization of the motor cortex similar, although weaker, to that occurring during active movements (Hari *et al.*, 1998; Cochin *et al.*, 1999). Finally, brain imaging studies showed that observation of hand actions produces an activation of the ventral premotor cortex centered on the Broca's region (Rizzolatti *et al.*, 1996b; Grafton, *et al.*, 1996a; Decety *et al.*, 1997; Grezes *et al.*, 1998; Iacoboni *et al.*, 1999). The possibility that the activation of Broca's area during action observation is caused by internal verbalization rather than a mirror mechanism is ruled out by a recent study of Buccino *et al.* (2001). Taken together, these data suggest that in the human ventral premotor cortex (including Broca's region in a broad sense), as in monkey area F5, there is, in addition to the mouth representation, also a representation of hand movements. Thus, in the human brain, this cortical sector, in spite of its great development as a mouth motor field for speech, still maintains a role in hand motor control and in action recognition.

Dorsal Premotor Cortex

Electrophysiological, clinical, and neuroimaging evidence suggests that there are similarities between the human dorsal premotor cortex and its presumed homologues in the monkey. Stimulation studies showed that the electrically excitable cortex reaches beyond the anterior border of area 4 and extends approximately 2–3 centimeter rostral to the central sulcus (Uematsu *et al.*, 1992). This finding suggests that, as in the monkey, the caudal region of the human dorsal premotor cortex is the origin of a corticospinal projection.

Lesion studies pointed out an involvement of the dorsal premotor cortex in both preparation/execution of motor acts and motor learning. Unilateral damage of the dorsal premotor cortex causes an inability to perform arm or leg movements requiring temporal coordination of proximal muscles, whereas the performance of distal skilled movements was normal (Freund and Hummelsheim, 1985). PET data provide further evidence for an involvement of the dorsal premotor cortex in the motor control of arm and leg movements (Fink *et al.*, 1997). As far as arm movements are concerned, Colebatch *et al.* (1991) found an activation in the superior frontal gyrus, associated with the execution of simple movements involving proximal and distal joints. The mean rCBF increase associated with shoulder movements was significantly

higher than that associated with distal movements, suggesting that in this region, as in the monkey PMd, there is a wide representation of proximal movements. In agreement with these data are several neuroimaging reports showing that this cortical region was activated in tasks involving proximal and/or distal arm movements (Deiber *et al.*, 1991; Grafton *et al.*, 1992b, 1996b; Seitz *et al.*, 1997). As in the monkey, the human dorsal premotor cortex appears to be involved in movement preparation (Kawashima *et al.*, 1994) and in movement selection according to arbitrary rules. Learning complicated finger movement sequences (Seitz and Roland, 1992), acquiring new key press sequences on the basis of trial and error (Jenkins *et al.*, 1994), or performing reaching and pointing movements according to the internal representation of targets (Kawashima *et al.*, 1995) all produce activations in the superior frontal gyrus. Involvement of the human dorsal premotor cortex in movement selection according to arbitrary rules has recently been substantiated by two PET studies showing learning-related changes in this cortical region, as subjects learned to make an association between a cue and the direction of a movement (Deiber *et al.*, 1997) or when subjects had to select more complex movements, such as power grasp or precision grip, based on arbitrary cues (Grafton *et al.*, 1998). This particular role of the dorsal premotor cortex had already been identified in clinical studies showing that patients with lesions of this cortical region, but not patients with parietal or precentral motor cortex lesions, fail to associate hand movements in responses to arbitrary sensory cues (Halsband and Freund, 1990). A possible functional segregation within the dorsal premotor cortex has been proposed by Iacoboni *et al.* (1998). In a spatial compatibility task, these authors found an activation relatively rostral in the dorsal premotor cortex when, for both auditory and visual modalities, the incompatible condition was compared with the compatible one. In the same experiment, learning-related activation was observed in a relatively more caudal part of the dorsal premotor cortex. It was suggested that these two different parts of the human dorsal premotor cortex could correspond to the rostrocaudal subdivision into areas F7 and F2 of the monkey PMd.

Mesial Premotor Cortex

In humans, the possible role of the SMA in motor control has been a matter of debate for a long time. Electrical stimulation studies, clinical observations of deficits caused by vascular lesions or surgical ablations, recordings of the DC potential during the execution of motor tasks, and early functional imaging studies provided conflicting results (for a review of the literature, see Freund, 1996). On the one hand, the high electrical excitability of the SMA and its activation during the execution of simple aimless movements were taken as evidence in favor of an executive role in motor control. On the other hand, the presence of global akinesia or mutism in the absence of paralysis and the presence of slow negative shifts in the cortical DC potentials, long before the execution of motor tasks, as well as its activation when subjects were requested to rehearse a series of digit movements mentally, lead to the concept that the SMA is primarily involved in a so-called supramotor role in motor control. However, in all these studies no systematic attempt was made to identify anatomically the stimulated or damaged cortex, mainly because of the basic assumption that the SMA was a single functional entity. The discovery that the mesial premotor cortex in nonhuman primates is composed of two different anatomical and functional areas has been crucial for interpreting these apparently conflicting data in humans.

As mentioned in "Comparative Architectonics of the Human and Monkey Motor Cortex," recent cytoarchitectonic evidence has shown that two major architectonic areas form the mesial premotor cortex. The border between these two areas does not coincide with any macroscopical landmark but very closely corresponds to the VCA line. Using the cytoarchitectonic characteristics as a criterion, it was postulated that these two areas are the homologue of monkey areas F3 and F6 (Zilles *et al.*, 1996).

When data available in the literature are correlated with the location of the VCA line, it clearly emerges that the two areas forming mesial premotor cortex are also functionally distinct and that their roles in motor control are in many ways comparable with those proposed for monkey F3 (SMA proper) and F6 (pre-SMA). The results of electrical stimulation studies of mesial premotor cortex in humans seem, at first glance, not to be consistent with the proposed man–monkey homology because the stimulation of cortical sites on either side of the VCA line evokes relatively low threshold movements. However, by using chronically implanted subdural electrodes and a better stimulus control, it was also possible to demonstrate in humans a somatotopic organization of the SMA proper, comparable to that observed in monkeys (Luders *et al.*, 1987). In contrast, the electrical stimulation of a region spanning about 3 centimeters rostral to the region from which movements can be elicited more frequently (i.e., the SMA proper) produces an alteration of motor performance (e.g., speech arrest) or a block of the entire spectrum of motor

activities. Furthermore, the stimulation of this rostral region was also found to produce more complex responses such as the sensation of an "urge" to move the arm or the feeling of an impending movement (Fried, 1996). Such results led Fried to consider the caudal "motor excitable" zone to be comparable to the monkey SMA proper (F3) and the rostral "negative motor" or "motor arrest" zone to be comparable to the monkey pre-SMA (F6).

In a recent review of the neuroimaging literature, Picard and Strick (1996) analyzed increases in rCBF in the mesial frontal cortex in relation to a wide spectrum of motor behavior, from very simple tasks to much more complex tasks. Although the limit between simple and complex motor tasks is sometimes difficult to set, simple tasks activate, with few exceptions, sites caudal to the VCA line, whereas more complex tasks consistently activate sites rostral to it.

Simple motor tasks, such as the execution of aimless movements triggered by external stimuli produce activations only of the SMA proper (Colebatch, *et al.*, 1991; Grafton, *et al.*, 1992b, 1993; Matelli *et al.*, 1993). The same is also true for the execution of simple joystick movements in a fixed direction (Playford *et al.*, 1992). When, however, the performance of a given joystick movement requires a selection among various possibilities, the activation is located rostral to the VCA line, in the pre-SMA (Deiber *et al.*, 1991). This involvement of the pre-SMA in movement selection is also suggested by a study in which the SMA proper was activated when subjects had to move a finger in response to an instructing stimulus, while the pre-SMA was activated when subjects could freely choose a finger movement among various possibilities (Deiber *et al.*, 1996).

Another well-known role of human mesial premotor cortex is its involvement in the execution of motor sequences. Functional data indicate that the pre-SMA and SMA proper are differentially involved in the execution of this type of motor tasks. In particular, the SMA proper appears to play a role in the execution of well-learned, "automatic" motor sequences, whereas the pre-SMA seems to be crucial in the learning of new, "unfamiliar" sequences. This is the case in a study of Sergent *et al.* (1992) showing that the SMA proper is activated in professional pianists playing scales, whereas, in the same subjects, the pre-SMA is activated when playing an unfamiliar piece of music. Furthermore, functional experiments in which subjects were studied at different stages of learning motor sequences indicate a shift in the activation from the pre-SMA to the SMA proper, as the task is increasingly well practiced and eventually becomes automatic (Seitz and Roland, 1992; Grafton *et al.*, 1992a; Jenkins *et al.*, 1994; Schlaug *et al.*, 1994). Finally, data of Hikosaka *et al.* (1999) showed that the pre-SMA was involved in learning motor sequences by trial and error, while the execution of already learned sequences produced an activation only in the SMA proper. It is interesting to note that the same authors found similar results in inactivation experiments of monkey F6 and F3, thus further supporting the notion of a homology of these two mesial areas between humans and monkeys.

A further more general role of the pre-SMA in motor control, was suggested in a recent fMRI study by Petit *et al.* (1998) in which sustained activity in the pre-SMA was observed during the delay period of both spatial and face working memory tasks. The authors suggested that this activity may reflect a higher cognitive level than simple movement selection or preparation. This pre-SMA activity may be related to a state of preparedness for selecting a motor response, based on spatial and object information, held on-line. This proposed role of the human pre-SMA is very similar to that proposed for monkey F6 (see Rizzolatti *et al.*, 1996).

Finally, a set of experimental data concerns the role of the SMA proper in motor imagery. These data suggest a possible functional subdivision within the SMA proper that appears to fit well with the recently proposed cytoarchitectonic subdivision of the SMA proper into an SMAc and SMAr part (Vorobiev *et al.*, 1998). Although the physiological basis underlying motor imagery is still poorly understood, it has been suggested that this process may be functionally similar to motor preparation and that imagined movements may share common anatomical and functional substrates with actual movements (Jeannerod, 1994). Functional studies of the execution and imagination of arm movements showed two distinct activation foci, both located behind the VCA line: a more caudal one, related to motor execution and a more rostral one, related preferentially or exclusively to motor imagery (Tyszka *et al.*, 1994; Stephan *et al.*, 1995; Roth *et al.*, 1996). The location of the rostral and caudal activations appears to correspond very well to the SMAr and SMAc, respectively. Further evidence in favor a selective role of the SMAr in nonexecutive motor functions was also provided by Grafton *et al.* (1996a) and Rao *et al.* (1997). In the first study, subjects were tested while observing actions made by other individuals and while imagining themselves performing them. In both conditions, only the SMAr was activated. In the second study, subjects were instructed to perform tapping movements with their index finger, first synchronously with a tone given at constant intervals and, then, without the tone. The results showed an activation of the SMAr only in the latter

condition. These data suggest that the SMAc and SMAr are differentially involved in motor control with the SMAr being active in functions in which the representation of the movement plays a central role, irrespective of whether or not the movement is paced (Vorobiev *et al.*, 1998).

All together, these data indicate that, although the general organization of the mesial premotor cortex in humans and monkeys appears to be very similar, there is a greater degree of structural and functional fractionation in the mesial premotor cortex in humans than in monkeys.

CONCLUDING REMARKS

More than one century after Jackson's first proposal that the human cortical motor system is organized in a hierarchical way, the new empirical data still support this view. Even if our knowledge of the detailed organization of the motor cortical areas is still fragmentary, the identification of parietofrontal circuits as basic elements of the monkey cortical motor system suggests that, in addition to a hierarchical organization, there is also parallel information processing that relies on multiple neural circuits.

Over the last years, the investigation of the human cortical motor system has gained new insights into several aspects of the functional organization of motor control. The data reviewed in this chapter all seem to indicate that there are significant similarities in the basic organization of the motor cortex between humans and nonhuman primates. However, in humans, the correlation between functional data and anatomically defined cortical areas is flawed by our limited knowledge of the cortical connections and the structural organization of the motor cortex. Several cytoarchitectonists, among them the Vogts and their school (Ngowyang, 1934; Vogt and Vogt, 1919), von Economo and Koskinas and, in more recent years, Bailey and von Bonin, Sarkissov *et al.*, and Braak (see references in Braak, 1980) have proposed various subdivisions of the human frontal lobe that are indeed more congruent with our current view of the organization of the motor cortex than the Brodmann parcellation. However, this last map is still the most popular and is extensively used in neuroimaging studies. Thus, it will become extremely important to establish a reliable architectonic map of the human motor cortex in the near future, especially when considering the fact that many new histochemical and neurochemical techniques are now available. To this purpose, given the eminent role played by monkey studies for the investigation of human cortical functions, a special effort should be made to extend our knowledge of the comparative anatomy of the cortex of humans and nonhuman primates.

Acknowledgments

The authors thank Christine Opfermann-Rüngeler for excellent help with the artwork. This work has been supported by grants from MURST, CNR, and HFSP and from the Deutsche Forschungsgemeinschaft (SFB 194/A6), the European Commission (BioMed 2 and BioTech programs), and the Human Brain Project (funded jointly by the National Institute of Mental Health, National Institute of Neurological Disorders and Stroke, National Institute on Drug Abuse, and National Cancer Institute).

References

Amunts, K., Schleicher, A., Burgel, U., Mohlberg, H., Uylings, H.B., and Zilles, K. (1999). Broca's region revisited: Cytoarchitecture and intersubject variability. *J. Comp. Neurol.* **412,** 319–341.

Asanuma, H., and Rosén, I. (1972). Topographical organization of cortical efferent zones projecting to distal forelimb muscles in the monkey. *Exp. Brain Res.* **14,** 243–256.

Barbas, H., and Pandya, D.N. (1987). Architecture and frontal cortical connections of the premotor cortex (area 6) in the rhesus monkey. *J. Comp. Neurol.* **256,** 211–228.

Binkofski, F., Buccino, G., Posse, S., Seitz, R.J., Rizzolatti, G., and Freund, H.J. (1999). A fronto-parietal circuit for object manipulation in man: Evidence from an fMRI-study. *Eur. J. Neurosci.* **11,** 3276–3286.

Bonin, G. von., and Bailey, P. (1947). "The Neocortex of Macaca Mulatta." University of Illinois Press, Urbana.

Braak, H. (1980). "Architectonics of the Human Telencephalic Cortex." Springer, Berlin.

Bremmer, F., Schlack, A., Shah, N.J., Zafiris, O., Kubishick, M., Hofmann, K.-P., Zilles, K., and Fink, G.R. (2000). A polymodal intraparietal area for the encoding of motion: The human equivalent of monkey area VIP. *Soc. Neurosci. Abstr.* **26,** 249.6.

Brodmann, K. (1905). Beitraege zur histologischen Lokalisation der Grosshirnrinde. III. Mitteilung. Die Rindenfelder der niederen Affen. *J. Psychol. Neurol.* **4,** 177–266.

Brodmann, K. (1909). "Vergleichende Lokalisationslehre der Groshirnrinde." Barth, Leipzig (Reprinted 1925).

Bruce, C.J., Goldberg, M.E., Bushnell, C., and Stanton, G.B. (1985). Primate frontal eye fields. II. Physiological and anatomical correlates of electrically evoked movements. *J. Neurophysiol.* **54,** 714–734.

Buccino, G., Binkofski, F., Fink, G.R., Fadiga, L., Fogassi, L., Gallese, V., Seitz, R.J., Zilles, K., Rizzolatti, G., and Freund, H.-J. (2001). Action observation activates premotor and parietal areas in a somatotopic manner: An FMRI study. *Eur. J. Neurosci.* **13,** 400–404.

Caminiti, R., Ferraina, S., and Johnson, P.B. (1996). The sources of visual information to the primate frontal lobe: A novel role for the superior parietal lobule. *Cereb. Cortex* **6,** 319–328.

Campbell, A.W. (1905). "Histological Studies on the Localization of Cerebral Function." Cambridge University Press, New York.

Cochin, S., Barthelemy, C., Roux, S., and Maritneau, J. (1999). Observation and execution of movement: Similarities demonstrated by quantified electroencephalography. *Eur. J. Neurosci.* **11,** 1839–1842.

Colby, C.L. (1998). Action-oriented spatial reference frames in cortex. *Neuron* **20,** 15–24.

Colebatch, J.G., Deiber, M.-P., Passingham, R.E., Friston, K.J., and Frackowiak, R. S.J. (1991). Regional cerebral blood flow during voluntary arm and hand movements in human subjects. *J. Neurophysiol.* **65,** 1392–1401.

Decety, J., Grezes, J., Costes, N., Perani, D., Jeannerod, M., Procyk, E., Grassi, F., and Fazio, F. (1997). Brain activity during observation of actions—Influence of action content and subject's strategy. *Brain* **120,** 1763–1777.

Decety, J., Perani, D., Jeannerod, M., Bettinardi, V., Tadary, B., Woods, R., Mazziotta, J.C., and Fazio, F. (1994). Mapping motor representations with positron emission tomography. *Nature* **371,** 600–602.

Deiber, M.P., Ibanez, V., Sadato, N., and Hallett, M. (1996). Cerebral structures participating in motor preparation in humans: A positron emission tomography study. *J. Neurophysiol.* **75,** 233–247.

Deiber, M.-P., Passingham, R.E., Colebatch, J.G., Friston, K.J., Nixon, P.D., and Frackowiak, R.S.J. (1991). Cortical areas and the selection of movement: A study with positron emission tomography. *Exp. Brain Res.* **84,** 393–402.

Deiber, M.P., Wise, S.P., Honda, M., Catalan, M.J., Grafman, J., and Hallett, M. (1997). Frontal and parietal networks for conditional motor-learning: A positron emission tomography study. *J. Neurophysiol.* **78,** 977–991.

Dettmers, C., Connelly, A., Stephan, K.M., Turner, R., Friston, K.J., Frackowiak, R.S.J., and Gadian, D.G. (1996). Quantitative comparison of functional magnetic resonance imaging with positron emission tomography using a force-related paradigm. *NeuroImage* **4,** 201–209.

di Pellegrino, G., and Wise, S.P. (1991). A neurophysiological comparison of three distinct regions of the primate frontal lobe. *Brain* **114,** 951–978.

Dum, R.P., and Strick, P.L. (1991). The origin of corticospinal projections from the premotor areas in the frontal lobe. *J. Neurosci.* **11,** 667–689.

Dum, R.P., and Strick, P.L. (1993). Cingulate motor areas. In "Neurobiology of cingulate cortex and limbic thalamus" (B.A. Vogt , and M. Gabriel, eds.), pp. 415–441. Birkhaüuser, Boston.

Economo, C. von., and Koskinas, G.N. (1925). "Die Cytoarchitektonik der Hirnrinde des erwachsenen Menschen." Springer, Wien.

Fadiga, L., Fogassi, L., Pavesi, G., and Rizzolatti, G. (1995). Motor facilitation during action observation: A magnetic stimulation study. *J. Neurophysiol.* **73,** 2608–2611.

Ferraina, S., Johnson, P.B., Garasto, M.R., Battaglia-Mayer, A., Ercolani, L., Bianchi, L., Lacquaniti, F., and Caminiti, R. (1997). Combination of hand and gaze signals during reaching: Activity in parietal area 7m of the monkey. *J. Neurophysiol.* **77,** 1034–1038.

Fink, G.R., Frackowiak, R.S.J., Pietrzyk, U., and Passingham, R.E. (1997). Multiple nonprimary motor areas in the human cortex. *J. Neurophysiol.* **77,** 2164–2174.

Flechsig, P. (1898). Neue Untersuchungen uber die Markbildung in den menschlichen Grosshirnlappen. *Neurologie Centralbeit* **17,** 977–996.

Fogassi, L., Gallese, V., Buccino, G., Craighero, L., Fadiga, L., and Rizzolatti, G. (2001). Cortical mechanim for the visual guidance of hand grasping movements in the monkey. Areversible inactivation study. *Brain* **124,** 571–586.

Fogassi, L., Gallese, V., Fadiga, L., Luppino, G., Matelli, M., and Rizzolatti, G. (1996). Coding of peripersonal space in inferior premotor cortex (area F4). *J. Neurophysiol.* **76,** 141–157.

Fogassi, L., Gallese, V., Fadiga, L., and Rizzolatti, G. (1998). Neurons responding to the sight of goal-directed hand/arm actions in the parietal area PF (7b) of the macaque monkey. *Soc. Neurosci. Abstr.* **24,** 257.5.

Fogassi, L., Raos, V., Franchi, G., Gallese, V., Luppino, G., and Matelli, M. (1999). Visual responses in the dorsal premotor area F2 of the macaque monkey. *Exp. Brain Res.* **128,** 194–199.

Freund, H.-J. (1996). Historical overview. *In* "Supplementary Sensorimotor Area" (H. O. Luders, ed.), pp. 17–27. Lippincott-Raven, Philadelphia.

Freund, H.-J., and Hummelsheim, H. (1985). Lesions of premotor cortex in man. *Brain* **108,** 697–733.

Fried, I. (1996). Electrical stimulation of the supplementary sensorimotor area. *In* "Supplementary Sensorimotor Area" (H.O. Luders, ed.), pp. 177–185. Lippincott-Raven, Philadelphia.

Fulton, J.F. (1935). Definition of the motor and premotor areas. *Brain* **58,** 311–316.

Gallese, V., Fadiga, L., Fogassi, L., and Rizzolatti, G. (1996). Action recognition in the premotor cortex. *Brain* **119,** 593–609.

Gallese, V., Murata, A., Kaseda, M., Niki, N., and Sakata, H. (1994). Deficit of hand preshaping after muscimol injection in monkey parietal cortex. *Neuroreport* **5,** 1525–1529.

Galletti, C., Fattori, P., Battaglini, P.P., Shipp, S., and Zeki, S. (1996). Functional demarcation of a border between areas V6 abd V6A in the superior parietal gyrus of the macaque monkey. *Eur. J. Neurosci.* **8,** 30–52.

Galletti, C., Fattori, P., Kutz, D.F., and Gamberini, M. (1999). Brain location and visual topography of cortical area V6A in the macaque monkey. *Eur. J. Neurosci.* **11,** 575–582.

Gentilucci, M., Fogassi, L., Luppino, G., Matelli, M., Camarda, R., and Rizzolatti, G. (1988). Functional organization of inferior area 6 in the macaque monkey: I. Somatotopy and the control of proximal movements. *Exp. Brain Res.* **71,** 475–490.

Gerardin, E., Sirigu, A., Lehéricy, S., Poline, J.-B., Gaymard, B., Marsault, C., Agid, Y., and Le Bihan, D. (2000). Partially overlapping neural networks for real and imagined hand movements. *Cereb. Cortex* **10,** 1093–1104.

Geyer, S., Ledberg, A., Schleicher, A., Kinomura, S., Schormann, T., Burgel, U., Klingberg, T., Larsson, J., Zilles, K., and Roland, P.E. (1996). Two different areas within the primary motor cortex of man. *Nature* **382,** 805–807.

Geyer, S., Matelli, M., Luppino, G., Schleicher, A., Jansen, Y., PalomeroGallagher, N., and Zilles, K. (1998). Receptor autoradiographic mapping of the mesial motor and premotor cortex of the macaque monkey. *J. Comp. Neurol.* **397,** 231–250.

Grafton, S.T., Arbib, M.A., Fadiga, L., and Rizzolatti, G. (1996a). Localization of grasp representations in humans by positron emission tomography .2. Observation compared with imagination. *Exp. Brain Res.* **112,** 103–111.

Grafton, S.T., Fagg, A.H., Woods, R.P., and Arbib, M.A. (1996b). Functional anatomy of pointing and grasping in humans. *Cereb. Cortex* **6,** 226–237.

Grafton, S.T., Fagg, A.H., and Arbib, M.A. (1998). Dorsal premotor cortex and conditional movement selection: A PET functional mapping study. *J. Neurophysiol.* **79,** 1092–1097.

Grafton, S., Hari, R., and Salenius, S. (2000). The human motor system. *In* "Brain Mapping: The Systems" (A.W. Toga , and J.C. Mazziotta, eds.), pp. 331–363. Academic Press, San Diego.

Grafton, S.T., Mazziotta, J.C., Presty, S., Friston, K.J., Frackowiak, R.S.J., and Phelps, M.E. (1992a). Functional anatomy of human procedural learning determined regional cerebral blood flow and PET. *J. Neurosci.* **12,** 2542–2548.

Grafton, S.T., Mazziotta, J.C., Woods, R.P., and Phelps, M.E. (1992b). Human functional anatomy of visually guided finger movements. *Brain* **115,** 565–587.

Grafton, S.T., Woods, R.P., and Mazziotta, J.C. (1993). Within-arm somatotopy in human motor areas determined by positron emission tomography imaging of cerebral blood flow. *Exp. Brain Res.* **95,** 172–176.

Graziano, M.S.A., Hu, X.T., and Gross, C.G. (1997). Coding the locations of objects in the dark. *Science* **277,** 239–241.

Graziano, M.S.A., Yap, G.S., and Gross, C.G. (1994). Coding of visual space by premotor neurons. *Science* **266,** 1054–1057.

Grezes, J., Costes, N., and Decety, J. (1998). Top-down effect of strategy on the perception of human biological motion: a PET investigation. *Cogn. Neuropsychol.* **15,** 553–582.

Halsband, U., and Freund, H.-J. (1990). Premotor cortex and conditional motor learning in man. *Brain* **113,** 207–222.

Hari, R., Forss, N., Avikainen, S., Kirveskari, E., Salenius, S., and Rizzolatti, G. (1998). Activation of human primary motor cortex during action observation: A neuromagnetic study. *Proc. Natl. Acad. Sci. USA* **95,** 15061–15065.

Hayes, T.L., and Lewis, D.A. (1992). Nonphosphorilated neurofilament protein and calbindin immunoreactivity in layer III pyramidal neurons of human neocortex. *Cereb. Cortex* **2,** 56–57.

He, S.Q., Dum, R.P., and Strick, P.L. (1993). Topographic organization of corticospinal projections from the frontal lobe: Motor areas on the lateral surface of the hemisphere. *J. Neurosci.* **13,** 952–980.

He, S.Q., Dum, R.P., and Strick, P.L. (1995). Topographic organization of corticospinal projections from the frontal lobe: motor areas on the medial surface of the hemisphere. *J. Neurosci.* **15,** 3284–3306.

Hikosaka, O., Sakai, K., Nakahara, H., Lu, X., Miyachi, S., Nakamura, K., and Rand, M.K. (1999). Neural mechanisms for learning of sequential procedures. *In* "The New Cognitive Neurosciences" (M.S. Gazzaniga, eds.), pp. 553–572. MIT Press, Cambridge, Mass.

Holsapple, J.W., Preston, J.B., and Strick, P.L. (1991). The origin of thalamic inputs to the "hand" representation in the primary motor cortex. *J. Neurosci.* **11,** 2644–2654.

Hoshi, E., and Tanji, J. (2000). Integration of target and body-part information in the premotor cortex when planning action. *Nature* **408,** 466–470.

Huerta, M.F. , and Kaas, J.H. (1990). Supplementary eye field as defined by intracortical microstimulation: Connections in macaques. *J. Comp. Neurol.* **293,** 299–330.

Iacoboni, M., Woods, R.P., and Mazziotta, J.C. (1998). Bimodal (auditory and visual) left frontoparietal circuitry for sensorimotor integration and sensorimotor learning. *Brain* **121,** 2135–2143.

Iacoboni, M., Woods, R.P., Brass, M., Bekkering, H., Mazziotta, J.C., and Rizzolatti, G. (1999). Cortical mechanisms of human imitation. *Science* **286,** 2526–2528.

Iriki, A., Tanaka, M., and Iwamura, Y. (1996). Coding of modified body schema during tool use by macaque postcentral neurones. *Neuroreport* **7,** 2325–2330.

Iwamura, Y., and Tanaka, M. (1996). Representation of reaching and grasping in the monkey postcentral gyrus. *Neurosci. Lett.* **214,** 147–150.

Jackson, J.H. (1931). "Selected Writings of John Hughlings Jackson" (J. Tailor, ed.), Vol. 1. Hodder and Stoughton, London.

Jeannerod, M. (1994). The representing brain—neural correlates of motor intention and imagery. *Behav. Brain Sci.* **17,** 187–202.

Jeannerod, M., and Decety, J. (1995). Mental motor imagery: A window into the representational stages of action. *Curr. Opin. Neurobiol.* **5,** 727–732.

Jeannerod, M., Arbib, M. A., Rizzolatti, G., and Sakata, H. (1995). Grasping objects: The cortical mechanisms of visuomotor transformation. *Trends Neurosci.* **18,** 314–320.

Jenkins, I.H., Brooks, D.J., Nixon, P.D., Frackowiak, R.S.J., and Passingham, R.E. (1994). Motor sequence learning: a study with positron emission tomography. *J. Neurosci.* **14,** 3775–3790.

Kalaska, J.F., Cohen, D.A.D., Prud'homme, M., and Hyde, M.L. (1990). Parietal area 5 neuronal activity encodes movement kinematics, not movement dynamics. *Exp. Brain Res.* **80,** 351–364.

Kawashima, R., Roland, P.E., and Osullivan, B.T. (1994). Fields in human motor areas involved in preparation for reaching, actual reaching, and visuomotor learning: A positron emission tomography study. *J. Neurosci.* **14,** 3462–3474.

Kawashima, R., Roland, P.E., and Osullivan, B.T. (1995). Functional anatomy of reaching and visuomotor learning: A positron emission tomography study. *Cereb Cortex* **5,** 111–122.

Keizer, K., and Kuypers, H.G.J.M. (1989). Distribution of corticospinal neurons with collaterals to the lower brain stem reticular formation in monkey (*Macaca fascicularis*). *Exp. Brain Res.* **74,** 311–318.

Krams, M., Rushworth, M.F.S., Deiber, M.P., Frackowiak, R.S.J., and Passingham, R.E. (1998). The preparation, execution and suppression of copied movements in the human brain. *Exp. Brain Res.* **120,** 386–398.

Kurata, K. (1989). Distribution of neurons with set- and movement-related activity before hand and foot movements in the premotor cortex of rhesus monkey. *Exp. Brain Res.* **77,** 245–256.

Kwan, H.C., Mc Kay, W.A., Murphy, J.T., and Wong, Y.C. (1978). Spatial organization of precentral cortex in awake primates. II. Motor outputs. *J. Neurophysiol.* **41,** 1120–1131.

Lacquaniti, F., Guigon, E., Bianchi, L., Ferraina, S., and Caminiti, R. (1995). Representing spatial information for limb movement: Role of area 5 in the monkey. *Cereb. Cortex* **5,** 391–409.

Lashley, K.S. , and Clark, G. (1946). The cytoarchitecture of the cerebral cortex of Ateles: A critical examination of architectonic studies. *J. Comp. Neurol.* **85,** 223–305.

Lemon, R.N. (1981). Variety of functional organization within the monkey motor cortex. *J. Physiol.* **311,** 521–540.

Lorente de Nó, R. (1934). Studies on the structure of the cerebral cortex. *J. Psychol. Neurol.* **45,** 381–438.

Lu, M.T., Preston, J.B., and Strick, P.L. (1994). Interconnections between the prefrontal cortex and the premotor areas in the frontal lobe. *J. Comp. Neurol.* **341,** 375–392.

Luders, H., Lesser, R.P., Moris, H.H., Dinner, D.S., and Hahn, J. (1987). Negative motor responses elicited by stimulation of the human cortex. *Adv. Epileptol.* **16,** 229–231.

Luppino, G., and Rizzolatti, G. (2000). The organization of the frontal motor cortex. *News in Physiological Sciences* **15,** 219–224.

Luppino, G., Matelli, M., and Rizzolatti, G. (1990). Cortico-cortical connections of two electrophysiologically identified arm representations in the mesial agranular frontal cortex. *Exp. Brain Res.* **82,** 214–218.

Luppino, G., Matelli, M., Camarda, R., and Rizzolatti, G. (1993). Corticocortical connections of area F3 (SMA-Proper) and area F6 (Pre-SMA) in the macaque monkey. *J. Comp. Neurol.* **338,** 114–140.

Luppino, G., Matelli, M., Camarda, R., Gallese, V., and Rizzolatti, G. (1991). Multiple representations of body movements in mesial area 6 and the adjacent cingulate cortex: An intracortical microstimulation study. *J. Comp. Neurol.* **311,** 463–482.

Luppino, G., Murata, A., Govoni, P., and Matelli, M. (1999). Largely segregated parietofrontal connections linking rostral intraparietal cortex (areas AIP and VIP) and the ventral premotor cortex (areas F5 and F4). *Exp. Brain Res.* **128** (1–2), 181–187.

Maier, M.A., Davis, J.N., Armand, J., Kirkwood, P.A., Philbin, N., Ognjenovic, N., and Lemon, R.N. (1997). Comparison of corticomotoneuronal (CM) connections from macaque motor cortex and supplementary motor area. *Soc. Neurosci. Abstr.* **23,** 502.13.

Massion, J. (1992). Movement, posture and equilibrium: Interaction and coordination. *Progr. Neurobiol.* **38,** 35–56.

Matelli, M., Luppino, G., and Rizzolatti, G. (1985). Patterns of cytochrome oxidase activity in the frontal agranular cortex of macaque monkey. *Behav. Brain Res.* **18,** 125–137.

Matelli, M., Luppino, G., and Rizzolatti, G. (1991). Architecture of superior and mesial area 6 and of the adjacent cingulate cortex. *J. Comp. Neurol.* **311,** 445-462.

Matelli, M., Luppino, G., Fogassi, L., and Rizzolatti, G. (1989). Thalamic input to inferior area 6 and area 4 in the macaque monkey. *J. Comp. Neurol.* **280,** 468–488.

Matelli, M., Luppino, G., Govoni, P., and Geyer, S. (1996). Anatomical and functional subdivisions of inferior area 6 in macaque monkey. *Soc. Neurosci. Abstr.* **22,** 796.2.

Matelli, M., Govoni, P., Galletti, C., Kutz, D.F., and Luppino, G. (1998). Superior area 6 afferents from the superior parietal lobule in the macaque monkey. *J. Comp. Neurol.* **402,** 327–352.

Matelli, M., Rizzolatti, G., Bettinardi, V., Gilardi, M.C., Perani, D., Rizzo, G., and Fazio, F. (1993). Activation of precentral and mesial motor areas during the execution of elementary proximal and distal arm movements—A PET study. *Neuroreport* **4,** 1295–1298.

Matsuzaka, Y., and Tanji, J. (1996). Changing directions of forthcoming arm movements: neuronal activity in the presupplementary and supplementary motor area of monkey cerebral cortex. *J. Neurophysiol.* **76,** 2327–2342.

Mountcastle, V.B., Lynch, J.C.G.A., Sakata, H., and Acuna, C. (1975). Posterior parietal association cortex of the monkey: Command functions for operations within extrapersonal space. *J. Neurophysiol.* **38,** 871–908.

Murata, A., Fadiga, L., Fogassi, L., Gallese, V., Raos, V., and Rizzolatti, G. (1997). Object representation in the ventral premotor cortex (area F5) of the monkey. *J. Neurophysiol.* **78,** 2226-2230.

Murata, A., Gallese, V., Luppino, G., Kaseda, M., and Sakata, H. (2000). Selectivity for the shape, size, and orientation of objects for grasping in neurons of monkey parietal area AIP. *J. Neurophysiol.* **83,** 2580–2601.

Murray, E.A. , and Coulter, J.D. (1981). Supplementary sensory area. *In* "Cortical Sensory Organization, Vol 1: Multiple Somatic Areas" (C.N. Woolsey, eds.), Chapter 6, pp. 167–195. Humana Press, Clifton, N.J.

Ngowyang, G. (1934). "Die Cytoarchitektonic des menschlichen Stirnhirns. I. Teil. Cytoarchitektonische Felderung der Regio granularis und Regio dysgranularis. Monogr" 7. Nat. Res. Inst. Psycol. Acad. Sinica.

Nimchinsky, E.A., Hof, P.R., Young, W.G., and Morrison, J.H. (1996). Neurochemical, morphologic, and laminar characterization of cortical projection neurons in the cingulate motor areas of the macaque monkey. *J. Comp. Neurol.* **374,** 136–160.

Olson, C.R. , and Gettner, S.N. (1995). Object-centered direction selectivity in the macaque supplementary eye field. *Science* **269,** 985–988.

Pandya, D.N., and Seltzer, B. (1982). Intrinsic connections and architectonics of posterior parietal cortex in the rhesus monkey. *J. Comp. Neurol.* **204,** 196–210.

Passingham, R.E. (1993). "The Frontal Lobe and Voluntary Action." Oxford University Press, Oxford.

Paxinos, G., Huang, X.F., and Toga, A.W. (2000). "The Rhesus Monkey Brain in Stereotaxic Coordinates." Academic Press, San Diego.

Penfield, W., and Boldrey, E. (1937). Somatic and motor representation in the cerebral cortex of man as studied by electrical stimulation. *Brain* **60,** 389–443.

Penfield, W., and Welch, K. (1951). The supplementary motor area of the cerebral cortex. *Archiv. Neurol. Psychiatr.* **66,** 289–317.

Petit, L., Courtney, S.M., Ungerleider, L.G., and Haxby, J.V. (1998). Sustained activity in the medial wall during working memory delays. *J. Neurosci.* **18,** 9429–9437.

Petrides, M., and Pandya, D.N. (1994). Comparative architectonic analysis of the human and the macaque frontal cortex. *In* "Handbook of Neuropsychology" (F. Boller and J. Grafman, eds.), Vol. 9, pp. 17–58, Elsevier, Amsterdam.

Picard, N., and Strick, P.L. (1996). Motor areas of the medial wall: A review of their location and functional activation. *Cereb. Cortex* **6,** 342–353.

Playford, E.D., Jenkins, I.H., Passingham, R.E., Nutt, J., Frackowiak, R.S.J., and Brooks, D.J. (1992). Impaired medial frontal and putamen activation in Parkinson's disease: A positron emission tomography study. *Ann. Neurol.* **32,** 151–161.

Porro, C.A., Francescato, M.P., Cettolo, V., Diamond, M.E., Baraldi, P., Zuiani, C., Bazzocchi, M., and di Prampero, P.E. (1996). Primary motor and sensory cortex activation during motor performance and motor imagery: A functional magnetic resonance study. *J. Neurosci.* **16,** 7688–7698.

Porter, R., and Lemon, R. (1993). "Corticospinal Function and Voluntary Movement." Clarendon Press, Oxford.

Rademacher, J., Caviness, V.S., Steinmetz, H., and Galaburda, A.M. (1993). Topographical variation of the human primary cortices: implications for neuroimaging, brain mapping and neurobiology. *Cereb. Cortex* **3,** 313–329.

Rao, S.M., Binder, J.R., Hammeke, T.A., Bandettini, P.A., Bobholz, J.A., Frost, J.A., Myklebust, B.M., Jacobson, R.D., and Hyde, J.S. (1995). Somatotopic mapping of the human primary motor cortex with functional magnetic resonance imaging. *Neurology* **45,** 919–924.

Rao, S.M., Harrington, D.L., Haaland, K.Y., Bobholz, J.A., Cox, R.W., and Binder, J.R. (1997). Distributed neural systems underlying the timing of movements. *J. Neurosci.* **17,** 5528–5535.

Rizzolatti, G., and Arbib, M.A. (1998). Language within our grasp. *Trends Neurosci.* **21,** 188–194.

Rizzolatti, G., Camarda, R., Fogassi, M., Gentilucci, M., Luppino, G., and Matelli, M. (1988). Functional organization of inferior area 6 in the macaque monkey: II. Area F5 and the control of distal movements. *Exp. Brain Res.* **71,** 491–507.

Rizzolatti, G., Gentilucci, M., Camarda, R., Gallese, V., Luppino, G., and Matelli, M. (1990). Neurons related to reaching-grasping arm movements in the rostral part of area 6 (area 6ab). *Exp. Brain Res.* **82,** 337–350.

Rizzolatti, G., Fadiga, L., Gallese, V., and Fogassi, L. (1996a). Premotor cortex and the recognition of motor actions. *Cognitive Brain Res.* **3,** 131–141.

Rizzolatti, G., Fadiga, L., Fogassi, L., and Gallese, V. (1997a). The space around us. *Science* **277,** 190–191.

Rizzolatti, G., Fadiga, L., Matelli, M., Bettinardi, V., Paulesu, E., Perani, D., and Fazio, F. (1996b). Localization of grasp representations in humans by PET .1. Observation versus execution. *Exp. Brain Res.* **111,** 246–252.

Rizzolatti, G., Fogassi, L., and Gallese, V. (1997b). Parietal cortex: From sight to action. *Curr. Opin. Neurobiol.* **7,** 562–567.

Rizzolatti, G., Luppino, G., and Matelli, M. (1996c). The classic supplementary motor area is formed by two independent areas. *In* "Advances in Neurology, Vol. 70, Supplementary Sensorimotor Area" (H. O. Luders, eds.), pp. 45–56. Lippincott-Raven, Philadelphia.

Rizzolatti, G., Luppino, G., and Matelli, M. (1998). The organization of the cortical motor system: New concepts. *Electroencephalogr. Clin. Neurophysiol.* **106,** 283–296.

Roland, P.E., and Zilles, K. (1994). Brain-atlases—a new research tool. *Trends Neurosci.* **17,** 458–467.

Roth, R., Decety, J., Raybaudi, M., Massarelli, R., DelonMartin, C., Segebarth, C., Morand, S., Gemignani, A., Decorps, N., and Jeannerod, M. (1996). Possible involvement of primary motor

cortex in mentally simulated movement: A functional magnetic resonance imaging study. *Neuroreport* **7,** 1280–1284.

Sakata, H., Taira, M., Murata, A., and Mine, S. (1995). Neural mechanisms of visual guidance of hand action in the parietal cortex of the monkey. *Cereb. Cortex* **5,** 429–438.

Sakata, H., Takaoka, Y., Kawarasaki, A., and Shibutani, H. (1973). Somatosensory properties of neurons in the superior parietal cortex (area 5) of the rhesus monkey. *Brain Res.* **64,** 85–102.

Sanes, J.N., Donoghue, J.P., Thangaraj, V., Edelman, R.R., and Warach, S. (1995). Shared neural substrates controlling hand movements in human motor cortex. *Science* **268,** 1775–1777.

Schall, J.D., Morel, A., and Kaas, J.H. (1993). Topography of supplementary eye field afferents to frontal eye field in macaque—Implications for mapping between saccade coordinate systems. *Visual Neurosci.* **10,** 385–393.

Schieber, M.H., and Hibbard, L.S. (1993). How somatotopic is the motor cortex hand area? *Science* **261,** 489–492.

Schlag, J., and Schlag-Rey, M. (1987). Evidence for a supplementary eye field. *J. Neurophysiol.* **57,** 179–200.

Schlaug, G., Knorr, U., and Seitz, R. J. (1994). Inter-subject variability of cerebral activations in acquiring a motor skill—A study with positron emission tomography. *Exp. Brain Res.* **98,** 523–534.

Seitz, R.J., and Roland, P.E. (1992). Learning of sequential finger movements in man: A combined kinematic and positron emission tomography (PET) study. *Eur. J. Neurosci.* **4,** 154–165.

Seitz, R.J., Canavan, A.G.M., Yaguez, L., Herzog, H., Tellmann, L., Knorr, U., Huang, Y., and Homberg, V. (1997). Representations of graphomotor trajectories in human parietal cortex: Evidence for controlled processing and automatic performance. *Eur. J. Neurosci.* **9,** 378–389.

Seltzer, B., and Pandya, D.N. (1986). Posterior parietal projections to the intraparietal sulcus of the rhesus monkey. *Exp. Brain Res.* **62,** 459–469.

Sergent, J., Zuck, E., Terriah, S., and MacDonald, B. (1992). Distributed neural network underlying musical sight-reading and keyboard performance. *Science* **257,** 106–109.

Stephan, K.M., Fink, G.R., Passingham, R.E., Silbersweig, D., Ceballosbaumann, A.O., Frith, C.D., and Frackowiak, R.S.J. (1995). Functional anatomy of the mental representation of upper extremity movements in healthy subjects. *J. Neurophysiol.* **73,** 373–386.

Strafella, A.P., and Paus, T. (2000). Modulation of cortical excitability during action observation: A transcranial magnetic stimulation study. *NeuroReport* **11,** 2289–2292.

Stuphorn, V., Taylor, T.L., and Schall, J.D. (2000). Performance monitoring by supplementary eye field. *Nature* **408,** 857–860.

Tanji, J. (1994). The supplementary motor area in the cerebral cortex. *Neurosci. Res.* **19,** 251–268.

Tanji, J., and Shima, K. (1996). Supplementary motor cortex in organization of movement. *Eur. Neurol.* **36,** 13–19.

Tyszka, J.M., Grafton, S.T., Chew, W., Woods, R.P., and Colletti, P.M. (1994). Parceling of mesial frontal motor areas during ideation and movement using functional magnetic resonance imaging at 1.5 tesla. *Ann. Neurol.* **35,** 746–749.

Uematsu, S., Lesser, R., Fisher, R.S., Gordon, B., Hara, K., Krauss, G.L., Vining, E.P., and Webber, R.W. (1992). Motor and sensory cortex in humans: Topography studied with chronic subdural stimulation. *Neurosurgery* **31,** 59–71.

Vaadia, E., Benson, D.A., Hienz, R.D., and Goldstein, M.H. (1986). Unit study of monkey frontal cortex: Active localization of auditory and visual stimuli. *J. Neurophysiol.* **56,** 934–952.

Van Meter, J.W., Maisog, J.M., Zeffiro, T.A., Hallet, M., Herscovitch, P., and Rapaport, S.I. (1995). Parametric analysis of functional neuroimages: Application to a variable-rate motor task. *NeuroImage* **2,** 279–283.

Vogt, O., and Vogt, C. (1919). Ergebnisse unserer Hirnforschung. *J. Psychol. Neurol.* **25,** 277–462.

Vorobiev, V., Govoni, P., Rizzolatti, G., Matelli, M., and Luppino, G. (1998). Parcellation of human mesial area 6: Cytoarchitectonic evidence for three separate areas. *Eur. J. Neurosci.* **10,** 2199–2203.

Walker, E. (1940). A cytoarchitectural study of the prefrontal area of the macaque monkey. *J. Comp. Neurol.* **98,** 59–86.

Wilson, F.A., Scalaidhe, S.P., and Goldman Rakic, P.S. (1993). Dissociation of object and spatial processing domains in primate prefrontal cortex. *Science* **260,** 1955–1958.

Wise, S.P., Boussaoud, D., Johnson, P.B., and Caminiti, R. (1997). Premotor and parietal cortex: Corticocortical connectivity and combinatorial computations. *Annu. Rev. Neurosci.* **20,** 25–42.

Woolsey, C.N., Settlage, P.H., Meyer, D.R., Sencer, W., Pinto Hamuy, T., and Travis, A.M. (1952). Patterns of localization in precentral and "supplementary" motor areas and their relation to the concept of a premotor area. *Res. Publ. Assoc. Nerv. Ment. Dis.* **30,** 238–264.

Zilles, K., Schlaug, G., Matelli, M., Luppino, G., Schleicher, A., Qu, M.S., Dabringhaus, A., Seitz, R., and Roland, P.E. (1995). Mapping of human and macaque sensorimotor areas by integrating architectonic, transmitter receptor, MRI and PET data. *J. Anat.* **187,** 515–537.

Zilles, K., Schlaug, G., Geyer, S., Luppino, G., Matelli, M., Qu, M., Schleicher, A., and Schormann, T. (1996). Anatomy and transmitter receptors of the supplementary motor areas in the human and nonhuman primate brain. *In* "Advances in Neurology, Vol. 70: Supplementary Sensorimotor Area" (H.O. Luders, eds.), pp. 29–43. Lippincott-Raven, Philadelphia.

CHAPTER

27

Architecture of the Human Cerebral Cortex

Regional and Laminar Organization

KARL ZILLES

Institute of Medicine, Research Center Jülich, and
C. & O. Vogt-Institute of Brain Research, University of Düsseldorf
Düsseldorf, Germany

PRINCIPAL SUBDIVISIONS OF THE CEREBRAL CORTEX

The cerebral cortex of the human brain can be subdivided by microscopic anatomical ("architectonic") criteria into two major parts, *isocortex* and *allocortex* (Vogt, 1910). Despite regional variations, the largest part of the adult human isocortex is characterized by its six-layered structure visible in cell body-stained (e.g., Nissl-stained) sections.

Only two isocortical regions of the adult brain show a reduction or an increase in the number of cortical layers. Such notable exceptions are (1) the frontal agranular cortex, which does not contain a clearly visible inner granular layer (layer IV) in the adult brain and represents the anatomical correlate of the motor cortex (primary motor cortex, premotor cortex, supplementary and presupplementary motor cortices), and (2) the primary visual cortex, which displays a clearly visible subdivision of its layer IV into three sublayers (i.e., layers IVa, IVb, and IVc).

In contrast to the six-layered architecture of the isocortex, the laminar pattern of the allocortex shows a regionally highly variable appearance reaching from a hardly subdivisible single-cell band to a highly differentiated architecture with more than 10 layers (e.g., entorhinal area; Braak, 1972).

This principal cytoarchitectonic subdivision is paralleled by Brodmann's (1909) developmental classification of a *homogenetic* and *heterogenetic cortex*. The homogenetic cortex develops a six-layered structure during fetal stages, which is preserved in the adult isocortex with the previously mentioned exceptions of the primary visual cortex and agranular frontal (motor) cortex (see earlier). Therefore, the homogenetic cortex resembles the architectonicly defined isocortex. In cases of disturbed development of the cortex, the

normally occurring reduction of the motor cortex from the six-layered fetal pattern to the normal agranular five-layered cortical lamination around birth can fail as shown in children suffering from cerebral palsy (Amunts *et al.*, 1997b).

The isocortex contains *primary sensory areas* (primary somatosensory, auditory, or visual areas), which are main targets of unimodal sensory afferents originating in the ventroposterior nucleus of the thalamus, medial and lateral geniculate bodies, respectively. These primary areas project to a whole set of *higher order unimodal sensory areas* (secondary and tertiary sensory areas) in a hierarchical and parallel organization. The higher order unimodal sensory cortices border to *multimodal association areas*. Uni- and multimodal areas send projections to the motor cortex, which is again subdivided into a *primary motor area* and *nonprimary motor areas* (for a comprehensive description of the motor cortex, see Chapter 26).

The heterogenetic cortex never passes through a developmental stage with six layers nor does it show the six-layered architecture of the isocortex during adult stages. Thus, the heterogenetic cortex resembles the architectonically defined allocortex.

Finally, the allocortex precedes the isocortex during mammalian brain evolution. The isocortex has, therefore, been called *neocortex*. According to Filimonoff (1947) and Stephan (1975), the allocortex can be further subdivided into *paleocortex* and *archicortex*. The paleocortex comprises the olfactory bulb, retrobulbar (anterior olfactory nucleus), olfactory tubercle, septal (including diagonal band), and (pre)piriform regions, as well as a minor part of the amygdala. The archicortex includes the hippocampus (Ammon's horn, dentate gyrus, and subiculum), presubiculum, parasubiculum, entorhinal cortex, retrosplenial cortex, and a cortical band in the cingulate gyrus (Stephan, 1975).

A functional imaging study of the human cerebral cortex (Qureshy *et al.*, 2000) shows that the rostral parts of the allocortex mainly participate in olfactory functions *(rhinencephalon)*, whereas the more caudal and medial temporal parts are cortical portions of the *limbic system*.

Isocortex and allocortex show a stepwise transition of the architecture (histological structure) at their common border. This part of the isocortex, which forms a transition zone to the allocortex, is called *proisocortex* (Sanides, 1962; Vogt and Vogt, 1956), whereas the corresponding and adjoining part of the allocortex is called the *periallocortex* (Filimonoff, 1947). The two transition zones together are also termed *mesocortex* (Rose, 1927). According to Filimonoff (1947), the periallocortex is subdivided into *peripaleocortex* (claustral region) and *periarchicortex* (entorhinal, presubicular, retrosplenial, and parts of the cingulate gyrus).

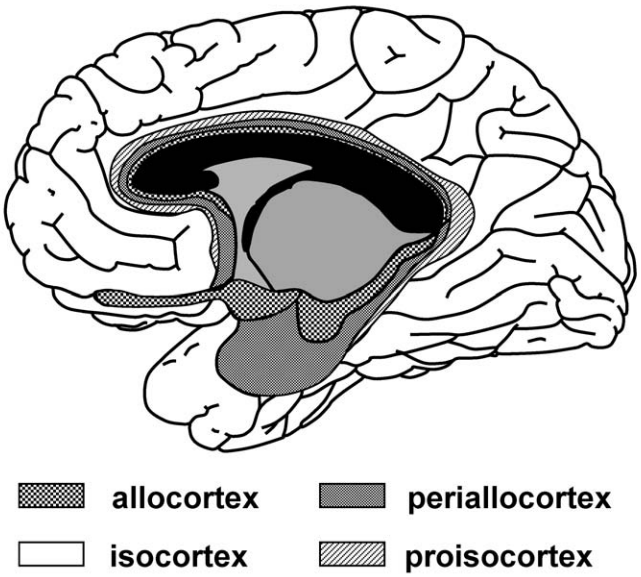

FIGURE 27.1 Medial aspect of the right hemisphere with the delineation of the principal subdivisions of the human cerebral cortex into isocortex, proisocortex, allocortex, and periallocortex. Modified after Stephan (1975).

Rose (1926) has proposed another system of subdividing the allocortex. According to this, the allocortex can be subdivided into *semicortex* (piriform and septal regions, amygdala, and olfactory tubercle), *schizocortex* (entorhinal and presubicular regions) and *holocortex* bistratificatus (retrobulbar and hippocampal regions).

Stephan (1975) has proposed a system based on his own extensive comparative neuroanatomical studies of insectivores and primates. This system is adopted here (Fig. 27.1) because it considers both the evolutionary history and the specificities of the human brain, and it does not refer to special histochemical methods. On a macroscopic level, the olfactory bulb, anterior perforate substance, paraterminal body, uncus, parts of the cingulate gyrus, lateral olfactory, semilunar, parahippocampal, and ambiens gyri contain allocortical regions. All other gyri of the human brain belong to the isocortex.

QUANTITATIVE ASPECTS OF THE CEREBRAL CORTEX

The *volume of the adult human cerebral cortex* varies between 197 and 331 cm^3 (right hemisphere: 264 ± 24 cm^3 (mean ± SD), left hemisphere 262 ± 24 cm^3; n = 43 females; age between 16 and 90 years; mean age 65 ± 2.7 years) and 242 and 358 cm^3 (right hemisphere: 292 ± 28 cm^3, left hemisphere: 291 ± 29 cm^3; n = 35 males; age between 32 and 91 years; mean age 64 ± 2.6 years) in one hemisphere (Zilles, 1972). Pakkenberg

and Gundersen (1997) reported 11–16% smaller volumes with 517 cm^3 and 440 cm^3 for both hemispheres in male and female brains, respectively. In both samples, males have a significantly larger (11–18%) cortical volume than females (Gundersen and Pakkenberg, 1997; Paul, 1971; Zilles, 1972). A similar relative gender difference of 11% is reported for the weight of male and female cerebral hemispheres in a sample of 196 male and 190 female brains (age between 70 and 79 years) (Skullerud, 1985). The larger cortical volumes in males may be explained by their larger overall brain size (Haug, 1984). Skullerud (1985) reported a 110 to 115 g smaller brain weight in women compared to men even after correction of body size using a body mass index. Both sexes show the same volumetric proportion (46%) of the cortex to the whole brain, and the same ratio (1.158 males and 1.152 females) between cortical to subcortical volumes (including amygdala, basal ganglia, and thalamus) of the prosencephalon (Zilles, 1972). A significant *hemispheric asymmetry* has been found in 109 brains of both sexes (Paul, 1971; Zilles, 1972). The cortical volume of the right hemisphere is larger than that of the left (Table 27.1). Structural hemispheric asymmetries are frequently reported (e.g., Galaburda *et al.*, 1978a,b; Galaburda and Geschwind, 1981; Geschwind and Levitsky, 1968) and have been correlated with their functional specialization (Broca, 1861; Geschwind, 1970; Zangwill, 1960). Anatomical observations describe asymmetries in the planum temporale, Sylvian fissure, inferior frontal gyrus, lateral ventricles, and temporooccipital region, all in favor of the left side. A further promising paradigm for studies of functional, structural, and developmental plasticity of right–left asymmetries is the human motor cortex, where correlations between macro- and microscopical features and functional features (motor skill, handedness) were demonstrated (Amunts *et al.*, 1996, 1997a, 1997c, 2000a). The only reported advantage of the right hemisphere is in the frontal lobe, which tends to be wider than that of the left (for review, cf. Galaburda and Geschwind, 1981). A slight right-over-left asymmetry in weight (mean 2.2 g) between both hemispheres has been described in 260 male and 207 female brains aged between 45 and 79 years (Skullerud, 1985). Thus, the wider right frontal lobe may contribute to the right-over-left asymmetry in cortical volume. Forty-two percent of the isocortical volume belongs to the frontal; 23%, to the temporal; 23%, to the parietal; and only 12%, to the occipital lobes (Pakkenberg and Gundersen, 1997).

The total *cortical surface* of both hemispheres varies between 1469 cm^2 (Blinkov and Glezer, 1968) and 2275 cm^2 (Elias and Schwartz, 1969). Pakkenberg and Gundersen (1997) reported 1900 ± 209 cm^2 for male and 1680 ± 235 cm^2 for male brains. In contrast to the cortical volumes, significant differences between the cortical surface of the right and left hemispheres have not been reported. Less than 1% of the surface is covered by paleocortex; 3.5%, by archicortex; and nearly 96%, by isocortex (Blinkov and Glezer, 1968; Stephan, 1975). Thirty-two percent of the isocortical surface belongs to the frontal; 30%, to the temporal; 23%, to the parietal; and only 15%, to the occipital lobes. As in the volumetric data (see earlier), the cortical surface data indicate a predominance of the frontal and temporal lobes, which contain beside motor and auditory cortices multimodal association areas and language-related regions.

The *depth of the human isocortex* varies between 1.5 and 5.0 mm (von Economo and Koskinas, 1925), depending on the cortical area studied (highest values in Brodmmann area 4, lowest in area 3) and position (lowest values on the sulcal floor, highest values on the gyral height). A comparison of the cortical thickness in different isocortical areas of the human brain (Table 27.2) illustrates both the variations in overall thickness and the laminar dimension. Pakkenberg and Gundersen (1997) reported a mean neocortical thickness of 2.72 ±

TABLE 27.1 Cortical Volumes in Human Male and Female Adult Brains (data from Paul, 1971 and Zilles, 1972)[a]

	Cortical volume (cm^3)	
	Male (N = 53)	Female (*N* = 56)
Right side	298.7 ± 4.2	267.2 ± 3.3
Left side	294.9 ± 4.1	263.8 ± 3.2
Right/left	3.8 ± 1.5	3.4 ± 1.7
	($p < .05$)	($p < .05$)

[a]Significance of hemispheric asymmetries is given in parentheses (the Wilcoxon matched-pair test).

TABLE 27.2 Thickness of Different Isocortical Areas and Layers in the Human Brain[a]

Layers	Area 4	Area 3	Area 41/42	Area 17	Area 18
I	200	220	260	246	272
II	100	280	280	89	92
III	1400	420	740	471	851
IV	—	280	450	653	148
V	900	220	530	218	279
VI	1250	400	640	278	395
I–VI	3850	1820	2900	1955	2037

[a]Thickness in micrometers. Data from von Economo and Koskinas (1925) and Zilles *et al.* (1986a).

0.24 mm in male and 2.61 ± 0.21 mm in female brains (significant gender difference).

According to the study of Pakkenberg and Gundersen (1997) using modern stereological methods the mean *total number of cortical neurons* in both hemispheres is $22.8 \times 10^9 \pm 3.9$ (mean ± SD) in male and $19.3 \times 10^9 \pm 3.3$ in female brains (49 left and 45 right hemispheres; age range 19–93 years). The gender difference of 15.5% is significant.

The *packing density of the cells* varies depending on the specific cortical area (Blinkov and Glezer, 1968; Haug, 1984). Pakkenberg and Gundersen (1997) reported a mean neuronal density of 44×106 per cm^3 with no significant difference between male and female brains. A two- to tenfold number of glial cells per neuron has been estimated depending on the cortical region (Blinkov and Glezer, 1968).

The midsagittal sections of the *corpus callosum* measures 6.2 ± 0.2 cm^2 in males and 6.3 ± 0.2 cm^2 in females (Zilles, 1972). While in agreement with the data of de Lacoste-Utamsing and Holloway (1982) and Witelson (1985), this difference is not significant, yet it seems remarkable that the commissural system in females reaches at least the same absolute size as in males, given that the female total cortical volume is significantly smaller. A significant correlation between the corpus callosum area and brain size has been shown (Zilles, 1972). This means a 10% larger commissural system in females, when scaled to cortical size, and indicates a gender difference in the structure of this system. On the basis of a relatively larger commissural system, it can be proposed that the female cortex shows a lesser degree of hemispheric lateralization (cf. also de Lacoste-Utamsing and Holloway, 1982).

All quantitative results mentioned in this section are highly variable between different individuals. Because these measures are correlated with total brain weight, changes in brain weight can influence cortical size. Some of the factors affecting total brain size have been reviewed (Haug, 1984). Secular acceleration (0.6 g/year), age, gender, and body size are among the most important. The volume of the cortex of a 75-year-old individual is about 4% smaller that that of a 25-year-old individual. The frontal cortex shows the largest age-dependent decrease (12%). However, these data and the frequently reported loss of cortical neurons with age must be critically reconsidered because secular acceleration may affect—at least partly—the lower cell counts in the older brains of cross-sectional studies. The age-dependent differential shrinkage during histological embedding (Haug, 1984) may also alter cell counts based on the measurement of cell numbers per volume cortical tissue.

One of the most prominent features of the human cortex is its distribution over a folded surface *(gyrification)*. Only one third of the human cortex is superficially exposed; two thirds are buried in the sulci (Elias and Schwartz, 1969; von Economo and Koskinas, 1925; Zilles *et al.*, 1988). The reasons for the gyrification of the brain are not completely understood. Because vertically oriented and side-by-side positioned cell columns represent the basic modular organization of the cerebral cortex, the cortical growth leads inevitably to a considerable enlargement of the cortical surface. A large unfolded cortical surface would require such an increase in volume of the skull, that a normal delivery would be impossible. Furthermore, the distance between cortical regions interconnected by projection fibers would increase to such a degree that information transmission between distant cortical regions would be delayed. Thus, gyrification is a solution for large brains to pack a maximal cortical surface into a minimal volume and to optimize the speed of neural transmission between neigboring cortical areas. Although all gyri and sulci are visible at birth, the depths of the sulci increase until two thirds of the cortical surface are hidden in the sulci after the 20th postnatal year (Armstrong *et al.*, 1995).

It has been demonstrated (Rakic *et al.*, 1991; Richman *et al.*, 1975) that the amount of gyrification depends on genetical and environmental constraints. Since Vogt (1910), Sanides (1962, 1972), and Welker and Campos (1963) have demonstrated that some of the sulci roughly demarcate cortical areas of different function and somatotopy, the sulcal and gyral pattern of the human cortex is both a sign of the functional, evolutionary, and individual development.

The human cortex shows the highest degree of folding, when compared with other primates (Zilles *et al.*, 1988). Moreover, the degree of folding varies over the rostrocaudal extension of the hemisphere. The highest values are found in the prefrontal and parietooccipitotemporal association cortex. The cortical regions where motor, premotor, and primary visual areas are located show the lowest degree of gyrification. The most significant increase in folding between human brains and those of nonhuman primates including gorilla, orangutan, and chimpanzee is visible in the prefrontal cortex (Zilles *et al.*, 1989). This underlines the advanced evolution of this part of the human cortex.

PALEOCORTEX

Olfactory Bulb

The olfactory bulb is not generally classified as a cortical area. Its laminar structure and comparative anatomical results, however, justify its identification as part of the paleocortex. The human olfactory bulb

shows the most extensive regression, both quantitatively and in its laminar pattern, when compared with other primates (Stephan, 1975). Nevertheless, the same laminar organization can be demonstrated in the human olfactory bulb as in most mammals, though it is less clearly visible.

The most important afferents come from the olfactory epithelium via the fila olfactoria of the first cranial nerve. In animal experiments, it has been shown that additional afferents originate in the diagonal band nuclei, the retrobulbar region, and the contralateral bulb and reach the olfactory bulb through the medial olfactory stria and the lateral olfactory tract. The lateral olfactory tract contains ipsilateral efferent fibers from the bulb to the retrobulbar and piriform region, olfactory tubercle, and amygdala (cortical amygdaloid nucleus).

Thus, the olfactory bulb is a cortical area for olfaction. The afferents from basal telencephalic regions modulate, via a complex intrabulbar system of interneurons, the information processing in the olfactory bulb. An accessory olfactory bulb, which is connected with the vomeronasal organ, cannot be found in the adult human brain, in contrast to other mammals (Stephan, 1975).

For a comprehensive description of the human olfactory system, see Chapter 32.

Retrobulbar Region (Anterior Olfactory Nucleus)

The retrobulbar region in the human brain has been demonstrated as an equivalent of a paleocortical region in other mammals (Stephan, 1975). The widely used term, anterior olfactory nucleus, is, therefore, misleading because the human retrobulbar region is a true cortical structure, despite its inconspicuous laminar pattern. Architectonic regression is a common aspect of the whole olfactory system in the human brain: A two-or three-layered structure recognizable in lower primates is not visible in the human brain (Fig. 27.2). Also, the delineation of several subareas that is possible in macrosmatic animals is hardly achievable in humans.

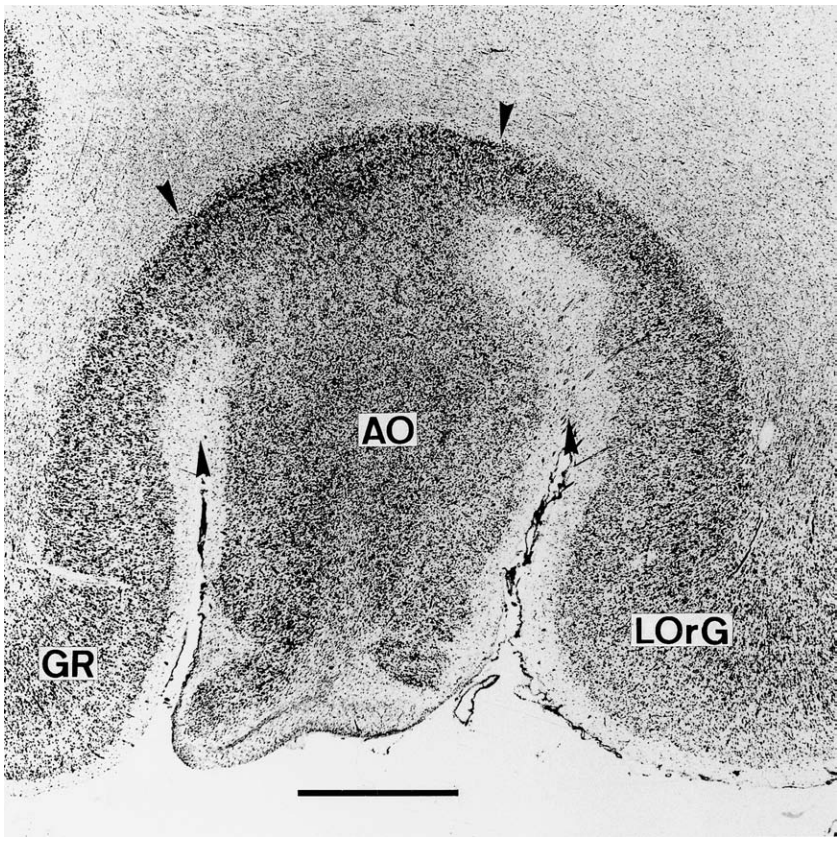

FIGURE 27.2 Coronal section through the human retrobulbar region (anterior olfactory nucleus, AO) at the basis of the telencephal. GR, gyrus rectus; LOrG, lateral orbital gyrus. Bar = 5 mm.

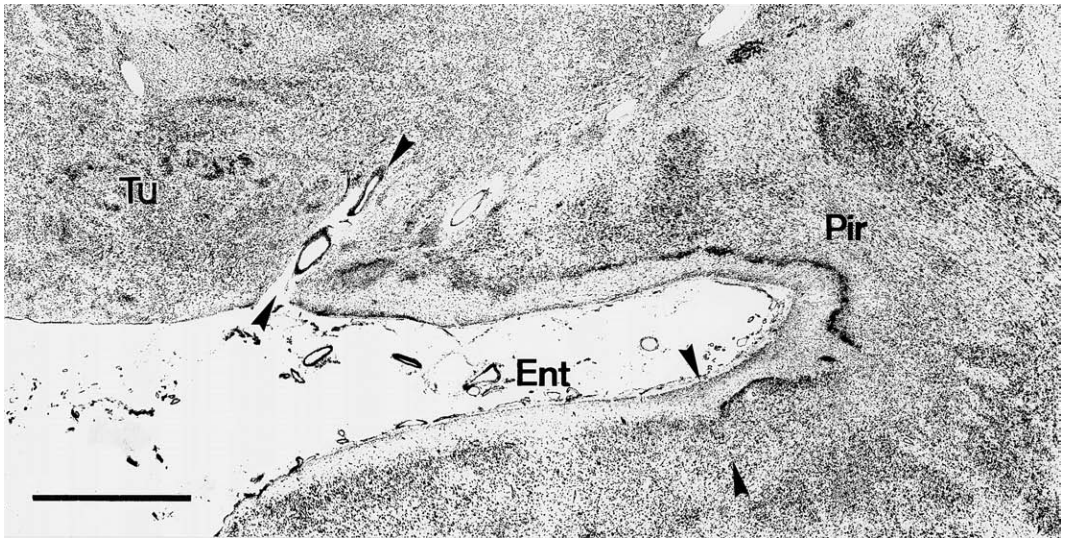

FIGURE 27.3 Coronal section through the human olfactory tubercle (Tu) and (pre-)piriform cortex (Pir). The entorhinal cortex (Ent) adjoins the piriform cortex. Bar = 2.5 mm.

The retrobulbar region is located in the caudal part of the olfactory bulb, at the place of fusion between the olfactory tract and the hemispheres, immediately rostral of the piriform cortex. It receives its main afferents from the ipsilateral olfactory bulb. At least in the rat, further afferents arrive from the piriform cortex, olfactory tubercle, and amygdala through the medial forebrain bundle and a rostrally directed system of associational fibers (Heimer, 1968, 1972). The projections from the retrobulbar region terminate, after coursing through the medial forebrain bundle, in the olfactory bulb of both sides and in the ipsilateral piriform cortex, olfactory tubercle, amygdala, mediodorsal thalamic, lateral habenular nuclei, and lateral hypothalamic and supraoptic areas (Ferrer, 1969; Lohmann and Lamers, 1967).

The retrobulbar region is an important station for processing olfactory information. A destruction of this region leads to anosmia or hyposmia and is mostly found in connection with impairment of the olfactory bulb. The retrobulbar region bilaterally modulates the information processing in the olfactory bulb.

Olfactory Tubercle

The olfactory tubercle is located immediately caudal to the retrobulbar region in the anterior perforate substance. This region is also heavily reduced in the human brain when compared with other primates (Stephan, 1975), but the homology with the same region in macrosmatic animals corroborates its classification as a paleocortical region. The three-laminar pattern of other mammals is completely obscured in the human brain. Islands of Calleja can be found within this region (Fig. 27.3). For further information about connectivity and function of the olfactory tubercle, see Chapter 32.

Piriform Cortex (Area 51 of Brodmann)

The human (pre)piriform cortex is located between the lateral olfactory tract and the temporal cortex (Brockhaus, 1940; Pigache, 1970; Rose, 1927; von Economo and Koskinas, 1925). According to Allison (1954), this region can be subdivided cytoarchitectonicly into a frontal and a temporal area. A three-layered structure is visible (Fig. 27.3) with a superficial molecular layer having only a few scattered neurons, a cell-dense second layer, and a less-dense third layer with polymorphic cells. The perikarya in the third layer are the largest. Along this layer a cell-free cleft (capsula extrema) is followed by the claustrum. The first layer contains the lateral olfactory tract in the frontal subregion of the piriform cortex.

The afferents to the piriform cortex originate in the olfactory bulb, retrobulbar region, olfactory tubercle, septal region, amygdala, orbitofrontal cortex, and contralateral piriform cortex. Commissural fibers are found in the anterior commissure. The efferent fibers from the piriform cortex reach all the areas that also have direct afferents from the olfactory bulb (Heimer, 1972; Price, 1973). Additionally, projections to the insular cortex, hippocampus, claustrum, and putamen have been described in many vertebrates (Allison,

1953; Druga, 1971; Hjorth-Simonsen, 1972), but it is not clear whether all these experimental results are also valid for the human brain.

The connectivity of the piriform cortex clearly indicates an olfactory function. Powell *et al.* (1965) emphasized the role of the piriform in sexual behavior because of the strong projections to the hypothalamus and because of behavioral experiments. For further information about connectivity and function of the olfactory tubercle, see Chapter 32.

Peripaleocortical Claustral Region (Area 16 of Brodmann)

Between the piriform cortex and the laterally adjoining isocortex, a transition zone can be demonstrated that has been called the peripaleocortical claustral region by Stephan (1975). This region is found in close topographical relation to the claustrum and constitutes the most rostral part of the insular cortex.

Brodmann (1905) has described four architectonicly different areas (areas 13–16) in the insular cortex with an increasing complexity in cytoarchitecture. These areas show a rostrocaudal sequence, with the most simply structured area rostrally (area 16). This area 16 has a position that compares well with the peripaleocortical claustral region and shows an agranular structure. Although Rose (1929) describes many more areas in the human insular cortex, he also delineates a rostral agranular area adjoining the piriform cortex. The most extensive architectonic study of the human insular cortex (Brockhaus, 1940) corroborates these earlier findings. The peripaleocortical claustral region is also comparable with the areas ID and TI of von Economo and Koskinas (1925). The laminar pattern of area 16 in humans shows a four-layered type (for further details see Stephan, 1975).

Connections of the peripaleocortical claustral region with the piriform cortex, amygdala, adjoining isocortex, claustrum, and contralateral area 16 have been described in primates (Allison, 1953; Astruc and Leichnetz, 1973; Nauta, 1961). The strong connections with the piriform cortex makes an olfactory function of the peripaleocortical insular cortex probable, but a definite statement for the human brain is presently not possible. For a comprehensive description of the amygdala, see Chapter 22.

ARCHICORTEX

The *archicortex* proper is formed by the hippocampus. The adjacent beltlike *periarchicortex* comprises the entorhinal, perirhinal, presubicular, parasubicular, retrosplenial, and the subgenual cortex as well as a part of the cingulate cortex. The periarchicortical areas are bordered by a proisocortical belt. Both regions represent together with the periarchi- and proisocortical belts of the orbitofrontal, insular, and temporopolar regions the paralimbic cortex *(mesocortex).* Thus, the forebrain contains a "hippocampocentric" (bordering the archicortex) and an "olfactocentric" (bordering the paleocortex) subdivision of the mesocortex (Mesulam and Mufson, 1985; see also "Insular Lobe"). The hippocampus can be subdivided into the retrocommissural hippocampus (Ammon's horn, dentate gyrus and subiculum), the supracommissural hippocampus (indusium griseum) and the precommissural hippocampus, which is located between the genu of the corpus callosum and the caudal end of the olfactory tract. The hippocampus, entorhinal area, presubiculum, and parasubiculum are represented pictorially and described comprehensively in Chapter 23.

Retrosplenial Region (Areas 26, 29, and 30 of Brodmann)

The retrosplenial region is located in the sulcus corporis callosi immediately behind the splenium of the corpus callosum. It is interposed between the presubiculum and the isocortical areas of the posterior cingulate gyrus. The retrosplenial region can be subdivided into a granular and an agranular part (Rose, 1928). The Brodmann classification (1909) gives three areas in the retrosplenial region: in the granular part (1) area 26 (ectosplenial cortex) and (2) area 29 (granular retrosplenial cortex), and in the agranular part (3) area 30 (agranular retrosplenial cortex). This has been confirmed by several histological studies (Armstrong *et al.,* 1986; Braak, 1979b; von Economo and Koskinas, 1925; Vogt *et al.,* 1995, 2001).

Although von Economo and Koskinas (1925) have subdivided the retrosplenial region into six different areas (LB_2, LD, LE_1, LE_2, LF_1, LF_2), a careful inspection of the figures shows that only LE_2, LE_1 and LD are comparable with the areas 26, 29, and 30 of Brodmann (1909; cf. also Stephan, 1975); LB_2, LF_1 and LF_2 belong to the supracommissural hippocampus. An architectural analysis of the whole posterior cingulate region shows an stepwise transition from a simple cortical structure to the elaborated isocortex, that is, from the supracommissural hippocampus over areas 26, 29, and 30 to the isocortical area 23 (Armstrong *et al.,* 1986, Vogt, 1985; Zilles *et al.,* 1986b). Each of the granular or agranular parts can further be subdivided according to Vogt (1993) and Vogt *et al.* (1995).

The ectosplenial area 26 has a primitive laminar pattern comprising a molecular layer, a cell-dense

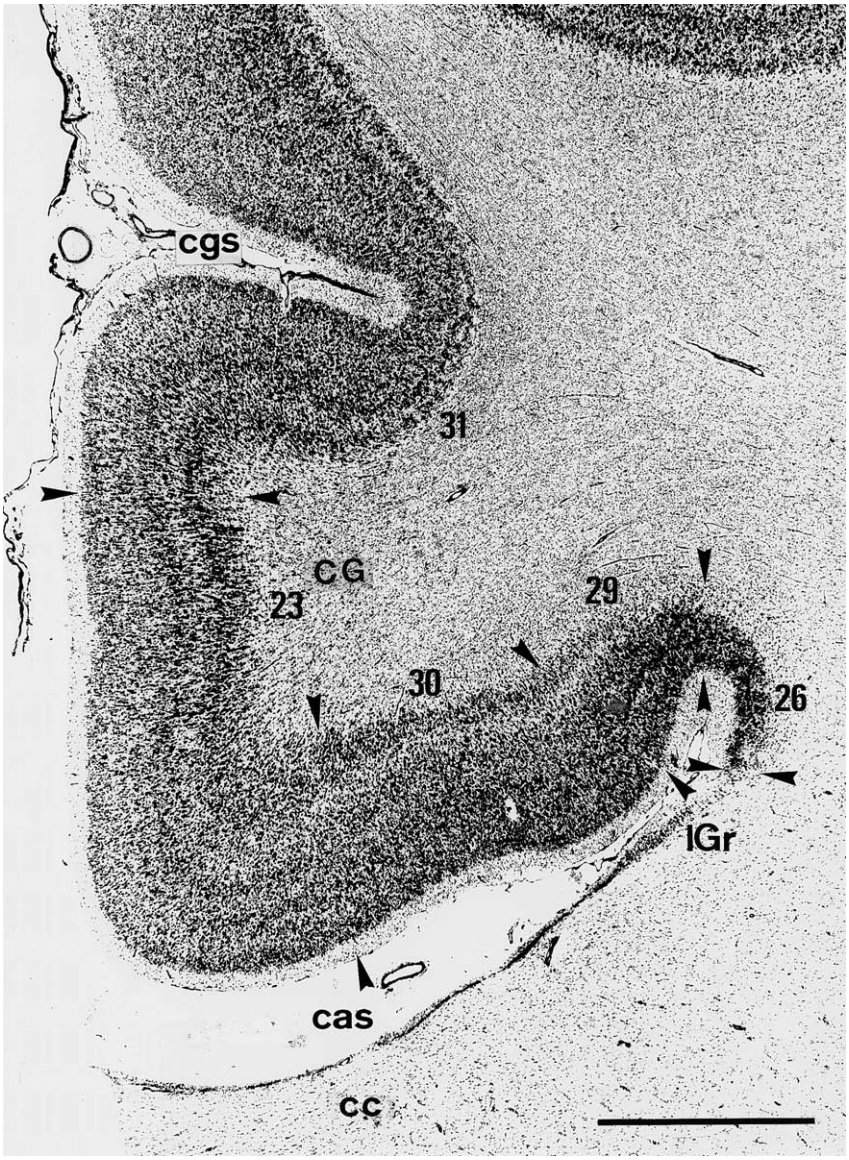

FIGURE 27.4 Coronal section through the posterior cingulate gyrus showing the transition from allo- to neocortex. Areas 26 and 29 belong to the allocortex, area 30 is part of the proisocortex and areas 23 and 31 are classified as neocortical regions. cas, sulcus of the corpus callosum; cc, corpus callosum; CG, cingulate gyrus; cgs, cingulate sulcus; IGr, indusium griseum. Bar = 3 mm.

external layer (small pyramidal cells), and an inner layer resembling the neuronal population of layer VI of the isocortex (Braak, 1979b; Vogt *et al.*, 2001). Area 29 shows a four-layered structure in Nissl-stained sections with a molecular layer, a cell-dense external pyramidal layer with small to medium-sized perikarya ("granular retrosplenial cortex"), an internal pyramidal layer with larger cells and a polymorphic layer (Fig. 27.4). Near the medial border of area 29, the laminar pattern changes. The external pyramidal layer differentiates into a cell-dense outer and a lighter inner layer (Vogt *et al.*, 2001). Area 30 shows a further progression of the laminar differentiation. Area 30 has an external pyramidal layer with a less obvious population of small ("granular") perikarya. Thus, this area has been classified as "agranular retrosplenial cortex." However, it shows also the first sign of an internal granular layer between the external and internal pyramidal layers ("dysgranular type"; Vogt *et al.*, 2001). This internal granular layer contains numerous small to medium-sized pyramidal cells and is, therefore, still different from the classical internal granular layer IV of the

isocortex (for further details, see Vogt *et al.*, 2001). Thus, area 30 can be classified as proisocortex. The adjoining area 23 has the typical isocortical structure with six layers.

The connectivity of the retrosplenial cortex further supports the principal subdivision into granular and agranular parts. In the rhesus monkey, the main cortical afferents to the granular retrosplenial areas 26/29 originate in the subiculum (Rosene and van Hoesen, 1977), whereas the agranular retrosplenial area 30 does not receive subicular axonal terminals. A main source for cortical afferents to area 30 is the extrastriate visual cortex, whereas these afferents are sparse in areas 26/29. The whole retrosplenial cortex receives afferents from area 24 and the anterior thalamic nuclei. Additionally, the intralaminar, laterodorsal, and lateroposterior thalamic nuclei (Baleydier and Mauguire, 1980; Vogt *et al.*, 1987), claustrum, diagonal band (Bigl *et al.*, 1982), locus coeruleus, raphe nuclei, and lateral hypothalamus project to this cortical region. The commissural connections are found in the corpus callosum. In the rhesus monkey, the efferent projections of the retrosplenial cortex terminate in the anterior thalamic nuclei, anterior cingulate cortex, and pons (van Hoesen *et al.*, 1993).

Periarchicortical Areas of the Cingulate Gyrus

This periarchicortical region accompanies the rostral part of the supracommissural and precommissural hippocampus.

Brodmann (1908, 1909), Vogt (1910), von Economo and Koskinas (1925), and Rose (1928) published different architectural subdivisions of the cingulate gyrus (Table 27.3). Brodmann (1908, 1909) includes in his regio cingularis the granular isocortical (Armstrong *et al.*, 1986; Zilles *et al.*, 1986b) areas 23 and 31 of the posterior cingulate gyrus, the agranular areas 24 and 32 of the anterior cingulate region, and the periarchicortical areas 25 and 33 (Fig. 27.5). The area 32 shows an isocortical structure, and area 24 represents the proisocortical part with a dorsal area medioradiata (MR) and a ventrally adjoining area infraradiata dorsalis (IRd) (for subdivisions of area 24, see Figure 27.5 and Chapter 26). According to Stephan (1975), the most rostral part of the periarchicortex is subdivided into an area infraradiata ventralis (area 33) adjoining the supracommissural hippocampus, and an area subgenualis (area 25) accompanying the precommissural hippocampus.

The common architectural feature of the anterior periarchicortical cingulate areas 25 and 33 is their reduced laminar differentiation, which includes the absence of the typical second layer (outer granular layer) of the isocortex. Thus, this region is of the transitional type between allo- and isocortex (Braak, 1980; Sanides, 1972; Yakovlev *et al.*, 1960).

Afferent fibers to area 25 of nonhuman primates have been demonstrated from the pole of the temporal lobe (Pandya and Kuypers, 1969) and from areas 7, 21 and 22 (Jones and Powell, 1970). Areas 25, 32, and 24 are interconnected by fibers running tangentially in the molecular layer (Gerebtzoff, 1939; Glees *et al.*, 1950). A further intracingulate connection exists between area 25 and the posterior cingulate cortex, including the retrosplenial region (Showers, 1959). Reciprocal connections have also been described between the prefrontal areas, the posterior cingulate cortex, and the posterior parietal gyri (Jones and Powell, 1970; Mesulam and Mufson, 1982; Mesulam *et al.*, 1977; Mufson and Mesulam, 1982; Nauta, 1964; Pandya *et al.*, 1971a, b, 1981; Petras, 1971; Vogt *et al.*, 1987).

Thalamic afferents in the monkey are differentially distributed over anterior and posterior cingulate areas. The anterior cingulate cortex receives afferents primarily from the paraventricular, reuniens, parafascicular,

TABLE 27.3 Comparison of the Various Architectural Parcellations of the Anterior Cingulate Cortex as Described by Various Authors

Brodmann (1908)	Vogt (1910)	von Econo and Koskinas (1925)	Rose (1928)	Stephan (1975)
32	3, 10, 11, 33–35	FCL, FDL, FEL, FHL	—	—
24	Subregio typica (17–24)	LA_2	Subregio infraradiata communis (IRBα-δ, IRCα-δ)	Area infraradiata dorsalis (Ird)
	Subregio medioradiata (25–32)	LA_1	Regio mediorata	Area mediorata (MR)
33	Subregio extrema (10, 15)	LA_3, LC_3	Subregio infraradiata ventralis (IRaα-δ)	Area infraradiata ventralis (Irv)
25	Areas 13, 14	FL, FM	Regio subgenualis (Sbga, Sbgp)	Area subgenualis (Sg)

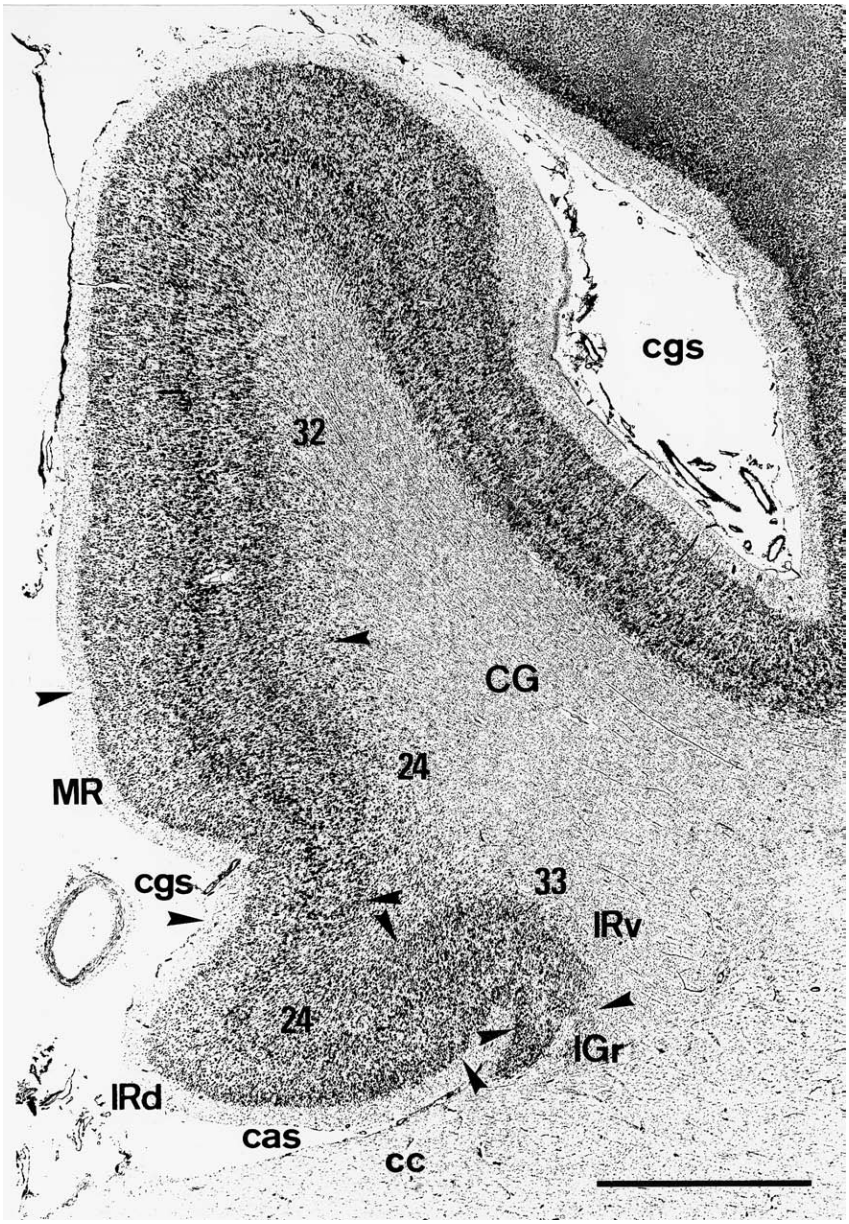

FIGURE 27.5 Horizontal section through the anterior cingulate and rostrally adjoining regions showing the transition from allo- to neocortex. The supracommissural hippocampus IGr (indusium griseum) is bordered by the periarchitectonical area 33 (IRv, area infraradiata ventralis). The adjacent area 24 can be subdivided into a proisocortical part (IRd, area infraradiata dorsalis) and an isocortical part (IMR, area mediorata). The isocortical area 32 follows rostrally. cas, sulcus of the corpus callosum; cc, corpus callosum; CG, cingulate gyrus; cgs, cingulate sulcus. Bar = 3 mm.

central superior lateral, central densocellular mediodorsal, and limitans nuclei. Further afferents to the cingulate cortex arrive from the substantia innominata, claustrum, raphe nuclei, and locus coeruleus (Vogt *et al.*, 1987). Furthermore, commissural fibers that interconnect the anterior cingulate cortex through the corpus callosum have been described (Locke and Yakovlev, 1965; Showers, 1959). Further afferents arrive from the septum and amygdala (Nauta, 1961). Efferent projections reach the amygdala, presubiculum, and retrosplenial and perirhinal cortex (Baleydier and Mauguire, 1980; Pandya *et al.*, 1981). For a comprehensive description of the cingulate region, see Chapter 24.

ISOCORTEX

Frontal Lobe

The isocortex of the frontal lobe can be subdivided cytoarchitectonicly into granular (with a clearly visible layer IV), dysgranular (with a weakly developed layer IV), and agranular (lacking layer IV) regions. The primary (Brodmann's area 4) and nonprimary (Brodmann's area 6) motor areas are agranular, Broca's speech region is dysgranular, the lateral prefrontal region is granular (except a dysgranular transitional region (Brodmann's area 8) between the motor and prefrontal cortex), and the medial prefrontal cortex (Brodmann's areas 24 and 32) is agranular. Broca's region can be further subdivided into anterior and posterior (i.e., Brodmann's areas 45 and 44; Figs. 27.8 and 27.35). The granular (lateral) prefrontal region can be further subdivided into a dorsolateral (Brodmann's areas 9, 10 and 46) and a ventroorbital part (Brodmann's areas 11, 12 and 47). The medial prefrontal cortex comprises the isocortical part of the anterior cingulate region. For a pictorial representation, see Figure 27.35. For comparison of different cytoarchitectonical terminologies in the frontal lobe, see Table 27.4.

A detailed architectonic study of the human frontal lobe has been published by Sanides (1962). This author delineates about 60 areas, which can be classified into cortical zones of different architecture (Fig. 27.6). His frontal motor zone (FmZ) resembles areas 4 and 6. The proisocortical zone (PrO) is an agranular cortex and corresponds to area 24. The dorsal and ventral paralimbic zones (PlZd, PlZv) are agranular to dysgranular regions and may be equivalents of area 32. The frontoopercular zone (FoZ) resembles areas 44, 45 and 47. The granular paraopercular zone (PoZ) corresponds to area 46; the paramotor zone (PmZ), to areas 9 and 8; the granular frontopolar zone (FpZ), to area 10; and the granular orbitomedian zone (OmZ), to areas 11–12.

Hopf (1956), Ngowyang (1934), Strasburger (1937), and Vogt (1910) have presented even more detailed cyto- and myeloarchitectonical studies of the human frontal lobe.

Prefrontal Region

The prefrontal cortex contains a larger granular (Fig. 27.7) and a smaller dysgranular part (Cavada and Goldman-Rakic, 1989a, b; Fuster, 1989; Goldman and Schwartz, 1982; Goldman-Rakic, 1984; McGuire *et al.*, 1991; Petrides and Pandya 1999; Preuss and Goldman-Rakic, 1990; Schwartz and Goldmann Rakic, 1988; Selemon and Goldman-Rakic, 1988; Walker, 1940). The inner granular layer in the prefrontal cortex is most obvious in its rostral part, whereas the more caudal part shows a transition to the dysgranular type (area 8) with a visible, but less remarkable inner granular layer. The granular part is unique in primates and reaches its largest expansion in humans (Preuss and Goldman-Rakic, 1991; Semendeferi *et al.*, 2001). For subdivisions of the prefrontal cortex of nonhuman primates see Paxinos *et al.* (2000).

A detailed study of the human prefrontal granular areas 9 and 46 (Rajkowska and Goldman-Rakic, 1995a, b) demonstrates cytoarchitectonic differences between both areas and the intersubject spatial variability of the areal borders. Area 9 extends along the middle third of the superior frontal gyrus and adjacent regions of the middle frontal gyrus. Area 46 is partially or completely surrounded by area 9 on the middle frontal gyrus. Rajkowska and Goldman-Rakic (1995b) clearly describe the lack of correlation between macroscopical landmarks (fundi of gyri, etc.) and areal borders and emphasize the considerable intersubject variability of the borders of these areas. Lamina IV is wider and contains more densely packed neuronal cell bodies in area 46 than in area 9; the sublamination of layers III and V is more differentiated in area 9 than in area 46. Area 46 is less myelinated than area 9.

The prefrontal cortex of primates receives major thalamic input from the mediodorsal nucleus, with the magnocellular part of this nucleus projecting to the ventroorbital, and the parvocellular part, to the dorsolateral prefrontal areas (Divac *et al.*, 1978; Fuster, 1989; Goldman, 1979, 1981; Kievit and Kuypers, 1977). Important cortical afferents to the prefrontal cortex in nonhuman primates arrive from various cortical areas of the same (ipsilateral associational) and of the opposite hemisphere (callosal connections) (Cavada and Goldman-Rakic, 1989b; Goldman and Nauta, 1977a, b; Jacobson and Trojanowski, 1977a, b; Künzle, 1978; Pandya *et al.*, 1971a, b; Preuss and Goldman-Rakic, 1989). The callosal connections are reciprocally organized (Goldman and Schwartz, 1982; McGuire *et al.*, 1991; Schwartz and Goldman-Rakic, 1988). Cortical afferents to the dorsolateral prefrontal cortex originate in the parietal (Petrides and Pandya, 1984; Cavada and Goldman-Rakic, 1989b) and premotor cortices (Barbas and Pandya, 1987; Lu *et al.*, 1994; Pandya and Yeterian, 1998). Contrastingly, the ventral prefrontal cortex receives its input from the temporal cortex (Bullier *et al.*, 1996; Pandya and Yeterian, 1998; Webster *et al.*, 1994). Ventral and dorsal parts of the prefrontal cortex are interconnected (Barbas, 1988; Pandya and Yeterian, 1998; Petrides and Pandya, 1999). The temporal pole and the anterior insula project to the ventroorbital part of the prefrontal cortex, which in turn is connected with the amygdala, basal forebrain,

TABLE 27.4 Comparison of Various Classification Schemes of the Human Cerebral Cortex[a]

Brodmann (1909)	Campbell (1905)	Smith (1907)	von Economo and Koskinas (1925)	Bailey and von Bonin (1951)	Sarkissov et al. (1955)
3, 1, 2	Postcentral Intermediate postcentral	Postcentralis, Postcentralis A Postcentralis B	P_A,P_B,P_C,P_D	Koniocortex Parakoniocortex	3, 1, 2
4	Precentral	Praecentralis A	F_A	Agranular gigantopyramidal	4
5	Intermediate postcentral and parietal	Postcentralis B	P_{A_2}	Parakoniocortex	—
6	Intermediate precentral	Praecentralis B	F_B	Agranular, dysgranular	6
7	Parietal	Parietalis superior A, Parietalis superior B	P_E	Homotypical	7, 7a
8	Frontal	Frontalis B, Frontalis superior anterior	F_C	Dysgranular	8
9	Frontal	Frontalis A, Frontalis B	F_D	Dysgranular	9
10	Prefrontal	Frontalis A, Frontalis B Frontalis C, Praefrontalis	F_E	Homotypical	10
11	Prefrontal	Praefrontalis	F_G,F_H	Homotypical, Juxtaallocortex	47 10
12	Prefrontal	Praefrontalis B	F_H	Homotypical	12
17	Visuosensory	Striata	O_C	Koniocortex	17
18	Visuopsychic	Parastriata, Peristriata, Temporalis occipitalis	O_B	Parakoniocortex	18
19	Temporal, Visuopsychic	Peristriata, Temporalis occipitalis	O_A	Homotypical	19
20	Temporal	Temporalis inferior	T_E	Homotypical	20
21	Temporal	Temporalis medius	T_E	Homotypical	21
22	Auditopsychic	Temporalis superior	T_A,T_B	Homotypical	22
23	Limbic C	Callosus A	L_C	Homotypical	23
24	Limbic A	Callosus B, Callosus C	L_{A_1},L_{A_2}	Mesocortex	24
25	Limbic B	Callosus D	F_L,F_M	Juxtaallocortex, Mesocortex	25 24
26	Limbic C	Parasplenialis	L_{E_2}	Allocortex	—
27	Limbic C	Subiculum (S), hippocampus (H)	H_D	Allocortex	—
28	Olfactory	Pyriformis	H_B,H_C	Allocortex	—
29	Limbic C	Parasplenialis	L_{E_1}	Allocortex	—
30	Limbic C	Parasplenialis	L_D	Homotypical	31
31	Limbic C	Callosus A	L_C	Homotypical	31
32	Frontal	Frontalis D	F_C,F_D,F_E,F_H	Juxtaallocortex	32
33	Limbic A	Callosus C	L_{A_3},L_{C_3}	Mesocortex	—
34	Olfactory	Pyriformis	H_A	Allocortex	—
35	Olfactory	Subiculum (S), hippocampus (H)	T_G,T_H	Juxtaallocortex	—
36	Temporal	Paradentatus	T_G;T_H	Juxtaallocortex	20
37	Temporal	Paratemporalis	P_H	Homotypical	37
38	Temporal	Temporalis polaris	T_G	Dysgranular	20/38, 21/38 22/38
39	Temporal	Parietalis inferior A, Parietalis inferior B, Parietalis occipitalis	P_G	Homotypical	39
40	Temporal	Parietalis inferior B and C,	P_F	Homotypical	40
41/42	Auditosensory	Temporalis superior	T_C,T_B	Koniocortex Parakoniocortex	—
43	Unlabeled area	Frontalis inferior, Postcentral A, Postcentral B	F_B,P_F	Dysgranular, Homotypical	43
44	Intermediate precentral	Frontalis inferior B,	F_{CBm}	Dysgranular	44
45	Intermediate precentral	Frontalis inferior	$F_{D\gamma}$	Homotypical	45
46	Frontal	Frontalis B, Frontalis inferior	F_D	Homotypical	46
47	Intermediate precentral	Orbitalis	F_F	Homotypical	47

[a]The classification schemes of various authors are compared with Brodmann's (1909) parcellation of the human cortex. Because the areal maps of the authors show incompletely matching patterns, often only parts of the areas are included in one Brodmann area.

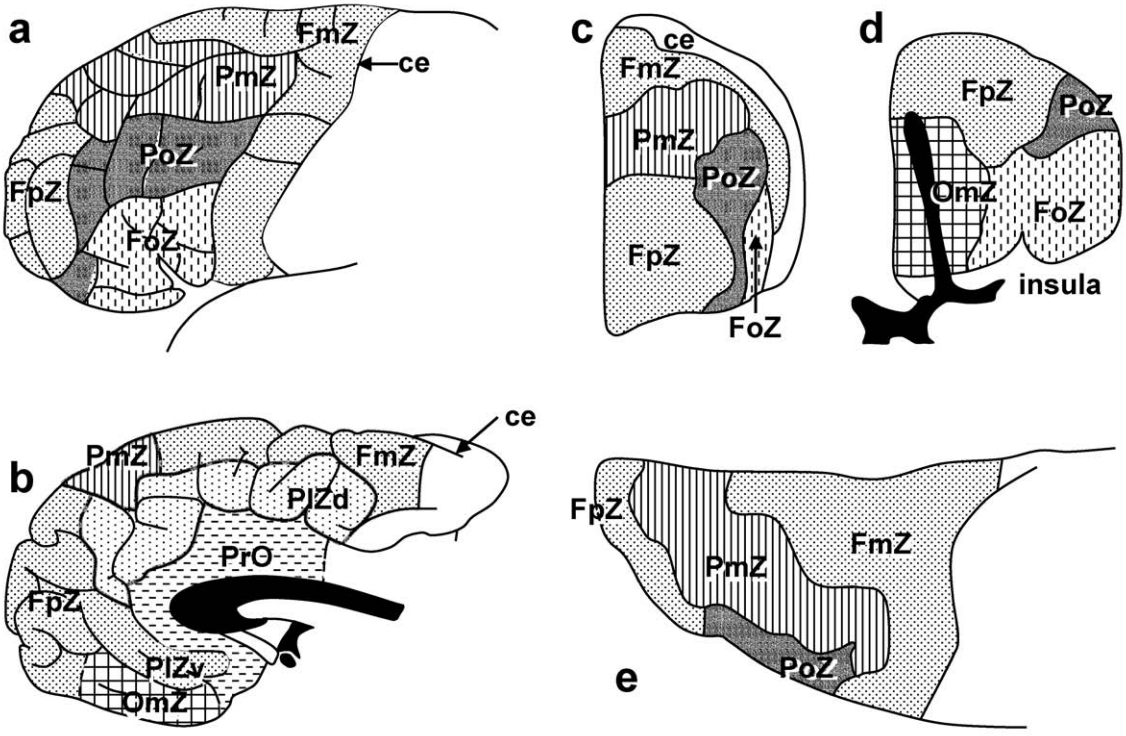

FIGURE 27.6 Areal map of the frontal lobe modified from Sanides (1962) in **(a)** lateral, **(b)** medial, **(c)** frontal polar, **(d)** basal, and **(e)** dorsal views. ce, central sulcus; FmZ, frontal motor zone; FoZ, frontoopercular zone; FpZ, frontopolar zone; OmZ, orbitomedian zone; PlZd, dorsal paralimbic zone; PlZv, ventral paralimbic zone; PmZ, paramotor zone; PoZ, paraopercular zone; PrO, proisocortex.

and magnocellular part of the mediodorsal thalamic nucleus (Barbas and DeOlmos, 1990; Goldman-Rakic and Porrino, 1985; Mesulam and Mufson, 1982, 1985; Pandya and Yeterian, 1985).

A major part of the prefrontal efferents projects to the striatum (Selemon and Goldman-Rakic, 1985). Further details on the connection can be found in Goldman and Nauta (1977a), Künzle (1975), and Johnson *et al.* (1968). Other efferents end in the dorsal thalamus (Goldman, 1979) and the superior colliculus (Goldman and Nauta, 1976). The dorsolateral prefrontal cortex is connected to the pulvinar, through which it can influence the cingulate and multi- as well as unimodal sensory areas (Goldman-Rakic and Porrino, 1985). Various other cortical and subcortical areas are further targets of the prefrontal efferent fibers (Selemon and Goldman-Rakic, 1988).

Studies in nonhuman primates (Goldman and Nauta, 1977b; Goldman-Rakic, 1984) have shown a remarkable columnar organization of the prefrontal cortex that is based on vertical units of neurons with special input–output relations and intrinsic synaptic connections. These columns are organized by alternating columns of ipsilateral and callosal corticocortical connections (Goldman and Schwartz, 1982). A two-dimensional reconstruction of the columns in the frontal section reveals a distribution in the form of stripes, which can bifurcate and show cross linkages and blind endings. The columns have a width of 300–700 μm and extend across all cortical layers. Since this structural pattern can be found in a variety of mammals (Goldman-Rakic, 1984) its existence in the human cortex is highly probable. The large increase in gyrification (Zilles *et al.*, 1989) and surface (Brodmann, 1912) of the human prefrontal cortex during evolution is, therefore, associated with an increasing number of cortical columns. While the interdigitating columnar pattern is shown for callosal and ipsilateral cortico-cortical systems, the same pattern has also been found for the cells constituting the efferent fibers for these connections (Schwartz and Goldman-Rakic, 1984). Thus, afferent terminals and efferent cell bodies of the same system are found in identical columns.

Since the corticocortical connections are only one part of the input and output of the prefrontal cortex, the corticostriatal and corticothalamic projections have been analyzed with respect to columnar organization. For both systems, a compartmentalization has been demonstrated. The corticothalamic neurons projecting to the mediodorsal nucleus form regularly spaced

FIGURE 27.7 Horizontal section through Brodmann's (1909) area 10, which belongs to the granular part of the prefrontal cortex. The Roman numerals indicate the six isocortical layers. Bar = 3 mm.

clusters in layer V of the prefrontal cortex. A further example of the modular organization in the primate prefrontal cortex is given by the efferents to the parahippocampal gyrus and the presubiculum (Goldman-Rakic, 1984).

The prefrontal cortex is a major anatomical substrate of various cognitive processes. The dorsolateral prefrontal cortex plays an important role in mnemonic encoding of visual space (Funahashi *et al.*, 1989). The columnar segregation of afferent systems may be the prerequisite for the various associative functions of this region. A great number of columns with different, well-segregated connections may allow for an even greater number of associative combinations by interaction between different columns. Destroying parts of the prefrontal lobe leads to disturbances of initiative and planning of activities, emotional status, social behavior, and memory functions (Milner and Petrides, 1984; Sawaguchi and Goldman-Rakic, 1991; Selemon and Goldman-Rakic, 1988). Destruction of the most rostrally and basally located areas leads to restlessness and hyperactivity (Jacobsen, 1935) and autonomic and emotional reactions (Kaada, 1960). Reduction of intellectual ability and ethical standards are immediately apparent phenomena after bilateral destructions of the human prefrontal cortex (Brodal, 1969). The orbitoprefrontal cortex is active during the processing of social behavior and the judging of the social consequences of actions (Fletcher *et al.*, 1995; Frith and Frith, 1999; Moll *et al.*, 2002). Additionally, visual object categorization is correlated with neural activity in the orbitoprefrontal cortex (Vogels *et al.*, 2002).

Atrophy of the frontal cortex is found in Pick's and Alzheimer's disease. Prefrontal leucotomy, a neurosurgical intervention introduced by Moniz (1936) has frequently been performed in the past in an attempt to cure symptoms of various mental disorders (schizophrenia, obsessions, etc.). Leucotomy has induced a controversal debate about the ethical problems involved with this procedure because, aside from influencing the symptoms of mental disorders, it severely changes personality.

More specific data about the function of granular prefrontal areas in the human brain is provided by imaging studies. A region comparable with the dorsal part of area 10 (Brodmann, 1909) shows the highest

metabolism and regional cerebral blood flow in conscious, wakeful subjects. These signs of activity ("hyperfrontality") disappear during sleep. Discrimination of tone sequences, mental calculation, and object categorization are associated with an increase of neuronal activity in this region. Working memory, learning, detection, association, discrimination, recognition, anticipatory tuning, and regulation of attention and abstraction are subserved by the granular prefrontal cortex. In summary, this part of the isocortex controls and regulates the operation of different sets of other cortical areas; that is, it is active whenever tasks require organization by the brain itself (for review, see Roland, 1993).

Recent functional imaging work shows a considerable segregation of the neural correlates of emotion, episodic memory retrieval, and working memory. The left dorsolateral areas seems to subserve monitoring operations during memory tasks, rostral and ventrolateral areas of both hemispheres are contributing to retrieval and cue-specific episodic memory retrieval operations, and the left ventroposterior as well as the bilateral dorsoposterior regions of the prefrontal cortex are subserving phonological and generic working memory operations, respectively (Cabeza *et al.*, 2002). The hippocampal and parahippocampal regions are active both during episodic memory retrieval and working memory. The medial prefrontal cortex plays a general role in emotion processes (for review, see Phan *et al.*, 2002).

Area 8 represents the dysgranular part of the prefrontal cortex. Sanides (1962) has delineated a paramotor zone PmZ (Fig. 27.6) which has a similar location but probably also includes parts of area 9. The FC area (Fig. 27.37) of von Economo and Koskinas (1925) seems to have a larger size than Brodmann's area 8. More recent functional observations have identified a frontal eye field in primates (Bruce and Goldberg, 1984), including humans (Roland, 1984), which is in good agreement with the ventrolateral part of area 8. Although earlier observations questioned the functional identification of area 8 as the frontal eye field, it has been demonstrated in a comparable region of nonhuman primates that this part of the dysgranular prefrontal cortex contains cells responsive to visual stimuli, which discharge before saccadic eye movements and in anticipation of saccadic behavior (Bruce and Goldberg, 1984). The saccadic direction is elicited in specific cell columns. Excitation in neighboring columns leads to different directions. As stated earlier, callosal and acallosal bands alternate (Goldman-Rakic, 1984), horizontal eye movements are controlled by acallosal columns, while vertical movements are controlled by callosal columns.

Clinical reports in humans suggest presaccadic activity in area 8 with metabolic activation during ocular fixation, pursuit eye movements, and various visual discrimination tasks (for review, see Roland, 1984). A dominance of the right frontal eye field is found when nonverbal signals are analyzed. For a comprehensive description of the prefrontal cortex, see Chapter 25.

Anterior Cingulate Region

Areas 24 and 32 constitute the proisocortical and isocortical parts of the anterior cingulate region. The agranular area 24 has been subdivided into several subareas in humans, monkeys, and rats (Matelli *et al.*, 1985, 1991; Vogt, 1993; Vogt *et al.*, 1995). Subarea 24d occupies the most caudal and dorsal part of human area 24. It is followed rostrally by subarea 24c′ at the level of the anterior commissure and by subarea 24c at the level anterior to the genu of the corpus callosum. Subareas 24d, c′, and c represent the dorsal subregion of area 24. Subareas 24b′ and b constitute the intermediate subregion, and subareas 24a′ plus 24a make up the ventral subregion (Vogt *et al.*, 1995), which is buried in the callosal sulcus (for figures and further details see Chapter 24). The anatomical correlate of the functionally defined human cingulate motor area (CMA; Paus *et al.*, 1993) comprises subarea 24d as caudal cingulate and subareas 24c′ and c as rostral cingulate motor areas (Roland and Zilles, 1996a; Zilles *et al.*, 1995, 1996). The motor function of the cingulate cortex has convincingly been demonstrated by microstimulation of the monkey cortex (Luppino *et al.*, 1991). It is presently not clear to what extent human area 32 or parts of it must also be interpreted as part of CMA.

CMA sends efferent fiber to the primary motor cortex (area 4) and the spinal cord (Luppino *et al.*, 1994). CMA appears to be activated during self-paced movements and controls the execution of motor responses (Naito *et al.*, 2000; Paus *et al.*, 1993). Vocalization and fear reactions also seems to be controlled by CMA. Ablation of areas 24 and 32 leads to increased tameness and reduction of social contacts in animals, together with a lowered performance in delayed alternation tasks (Divac, 1971; Glees *et al.*, 1950). For a comprehensive description of the cingulate region, see Chapter 24.

Broca's Speech Region

The caudal part of the left inferior frontal gyrus has been shown to represent the motor speech center (Broca, 1861; Penfield and Rasmussen, 1950; Roland, 1984) in 95% (Branche *et al.*, 1964) of right- and left-handers. A destruction of the dominant Broca area is accompanied in most cases by a loss of fluent speech, though language comprehension may not be affected.

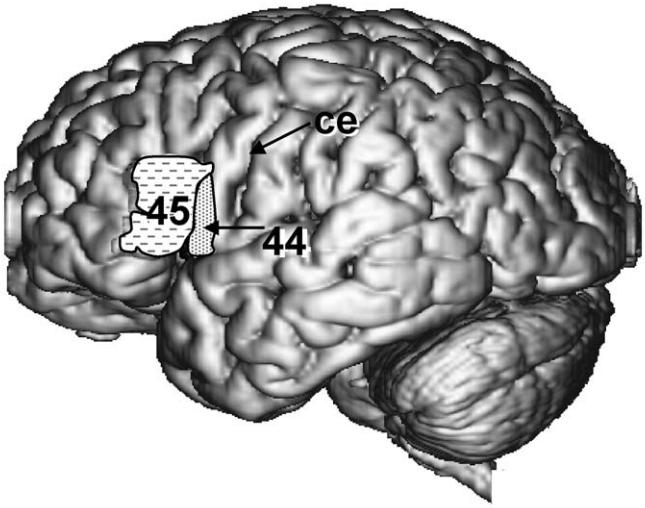

FIGURE 27.8 Areas 44 and 45 in a three-dimensional reconstructed human brain. The borders of both areas were determined using a quantitative cytoarchitectonic method (Schleicher *et al.*, 1999), which allows an observer-independent definition of the areal borders. ce, central sulcus.

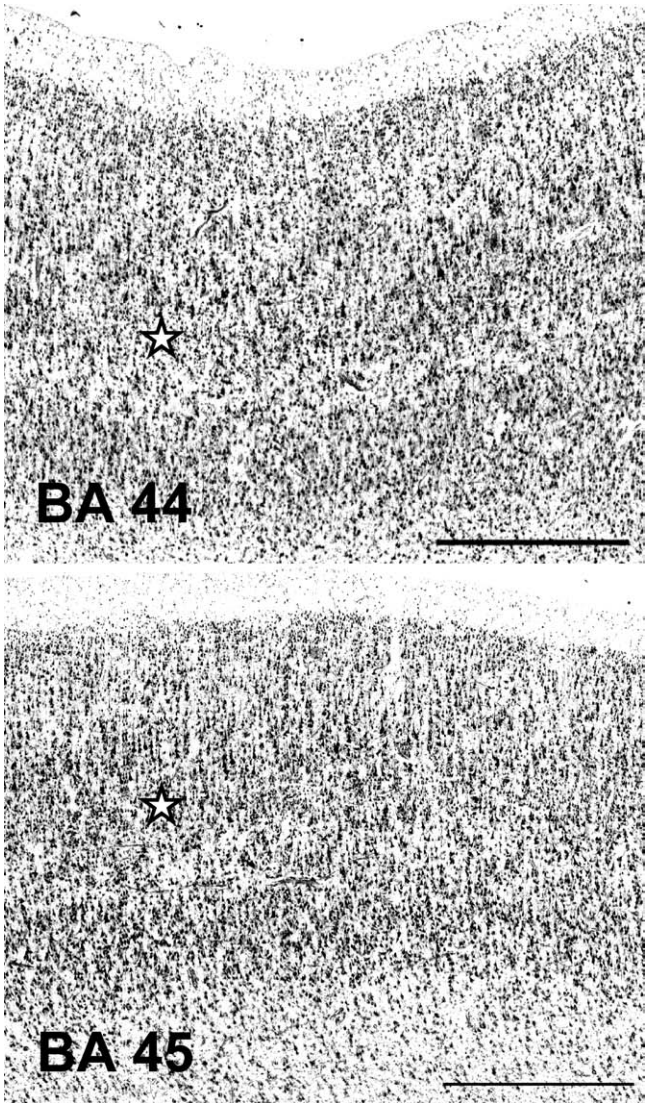

FIGURE 27.9 Cortical lamination in the dysgranular areas 44 and 45. The incipient layer IV is labeled by asterisks. Bar = 1 mm.

Detailed functions of Broca's region were examined by authors using different verbal tasks and functional imaging (Buckner *et al.*, 1996; Fox *et al.*, 1996; Frackowiak, 1994; Mazoyer *et al.*, 1993; Mazziotta and Mettner, 1988; Paulesu *et al.*, 1996; Petersen *et al.*, 1988, 1990; Petrides *et al.*, 1993; Zatorre *et al.*, 1996), and electrical stimulation (Penfield and Rasmussen, 1950; Ojeman, 1991). The homologous region in the right hemisphere is involved in prosodic aspects of speech (Botez and Wertheim, 1959) and the detection of syntactic errors (Bradvik *et al.*, 1991; Nichelli *et al.*, 1995).

Areas 44 and 45 (Fig. 27.8) are the cytoarchitectonic correlates of Broca's motor speech region (Amunts *et al.*, 1999; Brodmann 1909, 1914). Macroscopically, both areas are located bilaterally in the opercular (area 44) and triangular (area 45) region of the inferior frontal gyrus. Both areas reach the adjoining lower surface of the frontal operculum. An incipient inner granular layer (with an increasing granularity from caudal to rostral) is found in areas 44 and 45 (Amunts *et al.*, 1999; Brodmann, 1909; Sanides, 1962; Fig. 27.9). Layer IV of area 45 is still less clearly visible compared with the rostrally adjoining lateral prefrontal areas. Thus, the cortex of Broca's speech region can be classified as dysgranular (Amunts *et al.*, 1999). Further descriptions of cyto- and myeloarchitectonic aspects were published by Knauer (1909), von Economo and Koskinas (1925), Stengel (1930), Riegele (1931), Kononova (1949), Strasburger (1938), and Rabinowicz (1967). Considerable differences in the extent, location, and sizes of areas 44 and 45 are evident between the different maps, and the architectonic features were reported to be highly variable among subjects (Amunts *et al.*, 1999; Kononova, 1935). It is still a matter of discussion whether or not cytoarchitectonic features are associated with functional lateralization of speech (Galaburda, 1980; Hayes and Lewis, 1995, 1996; Scheibel *et al.*, 1985; Simonds and Scheibel, 1989). The functional segregation between areas 44 and 45 is presently not clear. In some neuroimaging studies, functional activation covered both areas (Demonet *et al.*, 1992; Hinke *et al.*, 1993; Hirano *et al.*, 1996; Mazoyer *et al.*, 1993), but in others activation was found to be restricted to area 44 or 45 or distributed over areas 44 and 6 (Fox *et al.*, 1996; Herholz *et al.*, 1996; Kim *et al.*, 1997; Paulesu *et al.*, 1996; Sergent *et al.*, 1992). These ambiguous results regard-

ing the precise anatomical location of neural activity may be caused not only by differences between the actual tasks in the different observations but also by differences in spatial resolution of the various functional imaging techniques. Furthermore, the warping of functional imaging data to anatomical atlases without architectonicly defined borders of cortical areas and without indications of the degree of intersubject variability of those borders may be a further confounding factor.

A series of studies report a possible architectonical homology (Petrides and Pandya, 1994; Rizzolatti *et al.*, 1996b, 1998) between Brodmann's areas 44/45 in the inferior frontal opercular part of the human brain (Brodmann, 1909; Amunts *et al.*, 1999) and the frontal premotor area F5 in monkeys (Matelli *et al.*, 1985, 1986, 1991). Area F5 contains mirror neurons (Di Pellegrino *et al.*, 1992; Rizzolatti *et al.*, 1996b), neurons that are active not only during grasping or tearing but also during the observation of another monkey performing the same action. Area F5 is, therefore, active during matching of observed and executed actions. Observation of actions and motor imagery tasks (Binkofski *et al.*, 2000; Grafton *et al.*, 1996; Iacoboni *et al.*, 1999; Krams *et al.*, 1998; Parsons and Fox, 1998; Rizzolatti *et al.*, 1996c) as well as imitation of target-directed actions are correlated with neuronal activity in the opercular part of the human inferior frontal gyrus (Koski *et al.*, 2002). Thus, functional similarities between the human opercular cortex of the inferior frontal gyrus and the monkey area F5 have been observed.

Recently, Amunts *et al.* (1999) published a quantitative cytoarchitectonic study that provides not only a three-dimensional representation of the microscopically defined borders of areas 44 and 45 but also population maps of these areas based on a sample of ten (five males and five females) human brains. The cytoarchitectonic borders of both areas did not consistently coincide with the sulcal pattern. Thus, macroscopical landmarks are not reliable indicators of cytoarchitectonic borders. Although the volume of area 44 varies considerably between subjects, the volume of area 44 was larger on the left than right side in all ten brains. All five male and three of the female brains had higher cell-packing densities on the left than on the right side (Amunts *et al.*, 1999). These morphological asymmetries of area 44 may represent a correlate of the functional lateralization of speech production (Galaburda, 1980). An ontogenetic study in six female and five male brains indicated a left-over-right asymmetry in the volume of area 45 in the male group (Uylings *et al.*, 1999). Further studies on a larger number of male and female subjects are needed to substantiate morphological asymmetries in Broca's region.

Major input to Broca's region arrives through corticocortical fibers of the arcuate fascicle, which originates in Wernicke's area of the temporal lobe. Efferents from areas 44 and 45 terminate in the face region of the primary motor cortex. Broca's region controls the complex motor pattern of neuronal assemblies in the face region of area 4, which in turn command the motor cranial nerve nuclei for the muscle activity during vocalization.

Primary Motor Cortex

Area 4 of Brodmann (1909) is the best candidate for the functionally defined primary motor cortex. Area 4 is agranular (Brodmann, 1903a; Marin-Padilla, 1970) and contains the giant Betz pyramidal cells (Fig. 27.10b). This cortical area is comparable to caudal parts of the precentral area of Campbell (1905; Fig. 27.33), caudal parts of the area precentralis A of Smith (1907; Fig. 27.34), area FAγ of von Economo and Koskinas (1925; Fig. 27.37), and the frontal ganglionic core of Braak (1980; Fig. 27.12; cf. Table 27.4).

Brodmann's (1903b) definition of the caudal border of area 4 (by the lack of an inner granular layer; see Fig. 27.10a) from the caudally adjoining area 3a (Fig. 27.11) in the fundus of the central sulcus has been widely accepted. The rostral border of area 4 was under dispute because here Brodmann's (1903b, 1909) parcellation is based exclusively on the presence of Betz cells in area 4 and their absence in area 6 (Fig. 27.10c). Most of the papers critically discussing Brodmann's delineation of the border between area 4 and area 6 are based exclusively on the drawing of his famous map (Brodmann, 1909). Here, area 4 seems to cover larger parts of the free surface of the precentral gyrus. One must understand, however, the limitations inherent in schematic representations and read the detailed description of area 4 in Brodmann's original paper (1903a; see also Zeki, 1979) for a discussion of the misuse of Brodmann's schematic drawing in other cortical regions. Area 4 is described in Brodmann's first article (1903a) as a wedge-shaped field that is very tiny on the laterobasal side and covers only the rostral wall of the central sulcus. That means that area 4 does not spread over the free cortical surface of the precentral gyrus to a considerable extent but is buried in the central sulcus. Also, the broad part of area 4 on the paracentral lobule of the medial hemispheric surface shows no major differences when compared with more recent observations (Geyer *et al.*, 1996, 2000c). Brodmann (1903a) described other characteristics of area 4 and the Betz cells (large cortical thickness, inconspicuous lamination pattern, low cell density, no clear boundary between layer VI and white matter, decreasing the size of the Betz cells along the mediolaterobasal extent).

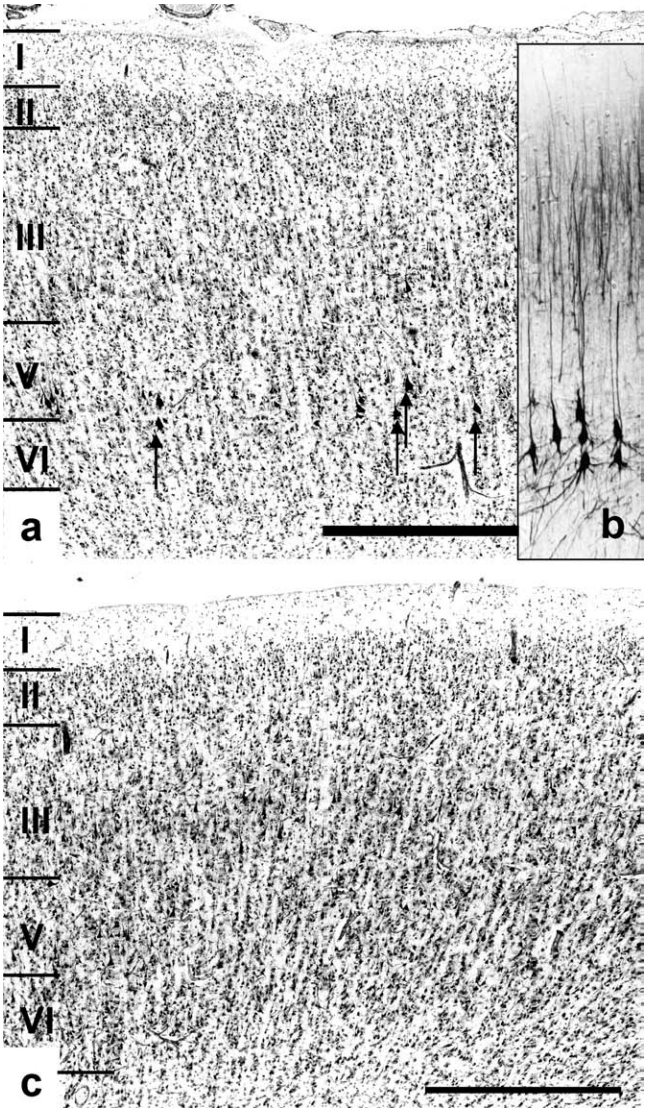

FIGURE 27.10 Cytoarchitecture of Brodmann's (1909) agranular areas 4 (a, b) and 6 (c). **(a)** Nissl-stained section of area 4. The arrows indicate several Betz-cells in layer V. **(b)** SMI-32-stained section of the macaque area 4 with prominently stained Betz cells. **(c)** Nissl-stained section of area 6. Bar = 1 mm.

Recently, Geyer *et al.* (1996) could demonstrate—by combining quantitative cytoarchitectonic mapping and transmitter receptor distributions with functional imaging data—the posterior and anterior borders of area 4, its intersubject variability and motor function, and a subdivision of area 4 into a rostral subarea 4a and a caudal subarea 4b.

Area 4 receives afferent fibers from both subcortical sources (caudal part of the ventrolateral and rostral part of the ventroposterolateral thalamic nuclei) and cortical sources (for details see Chapter 26). A major efferent pathway of area 4 is part of the pyramidal tract. However, area 4 is not the only cortical source of the pyramidal tract fibers. The nonprimary motor and the primary and secondary somatosensory cortices represent additional sources (Brodal, 1969; Kuypers, 1958; Minckler *et al.*, 1944). About 30% of pyramidal tract fibers originate from large, medium-sized, and small pyramidal cells in layer V of area 4. Whereas the volume of area 4 does not differ between the left and right side, the volume of this part of the pyramidal tract originating in area 4 is significantly larger in the left than right hemisphere (Rademacher *et al.*, 2001c). This left-over-right asymmetry of a part of the pyramidal tract may be related to the left-hemispheric dominance for handedness in more than 90% of the population. These axons terminate in motor nuclei of cranial nerves (corticonuclear tract), in pontine nuclei (corticopontine tract), on α-motoneurons, interneurons, and on γ-motoneurons of the spinal cord via interneurons (corticospinal tract). Area 4 controls the activity of both proximal and distal muscle groups, but only the motor activity of distal muscles is impaired after destruction of the lower corticospinal tract.

One of the most conspicuous aspects of organization in the primary motor cortex is its somatotopy. The studies of Penfield and Rasmussen (1950) have shown the representation of the various parts of the body in the motor cortex. The contralateral foot is found on the medial surface of the hemisphere followed by the leg and trunk around the upper margin of the hemisphere. A considerably large cortical area is covered by the hand representation in the upper half of area 4 on the lateral surface of the hemisphere. The site of the motor hand representation is visible in axial sections by a Ω-like protrusion of the precentral gyrus toward the central sulcus ("hand-knob") (Yousry *et al.*, 1997). The lower half of area 4 is occupied by the cortical representation of the face and especially the lips, tongue, pharynx, and larynx muscles.

The Betz cells differ from the other pyramidal cells of area 4 by their morphology (Scheibel and Scheibel, 1978). They show not only the major apical dendritic stem and typical basal dendrites but also the numerous additional dendrites originating from the whole circumference of their cell bodies (see also Fig. 27.10b).

Non-Primary Motor Cortex

Brodmann (1909) described the border between the primary motor cortex (area 4) and the rostrally adjoining nonprimary motor cortex, which is represented in his map by a single cortical field, his area 6. The distinction between these areas is based on the presence of Betz cells in layer V of area 4, cells that are not found in area 6 (Fig. 27.10c). However, this finding is a problematic criterion for the precise definition of the

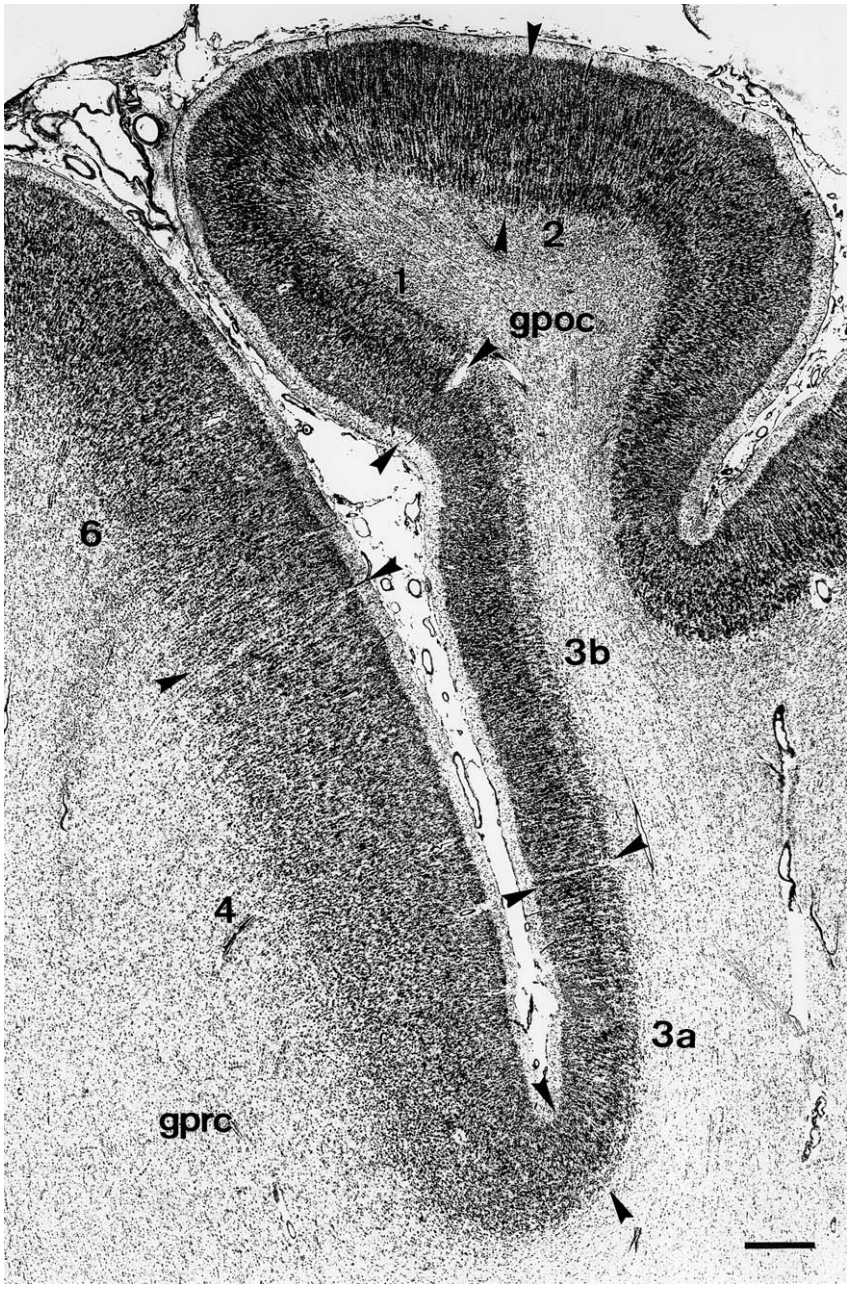

FIGURE 27.11 Horizontal, Nissl-stained section through the human precentral (gprc) and postcentral (gpoc) gyri with the agranular motor areas 4 and 6, the transition zone area 3a, and the granular somatosensory areas 3b, 1, and 2. Bar = 1 mm.

border between both areas. Wise (1985a, b) emphasized the difficulties of separating the Betz cell population from other pyramidal cells by using cell body size as the criterion. This is corroborated by Braak and Braak (1976), who used the histochemical method of lipofuscin staining ("pigmentoarchitectonics") to identify Betz cells. These cells show a vast agglomeration of lipofuscin granules in their perikarya not visible in other pyramidal cells of layer V. According to these results, the size distribution of Betz cell perikarya shows a wide overlap with that of large and medium-sized pyramidal cells. Therefore, the identification of the border between areas 4 and 6 is difficult when based exclusively on Nissl-stained sections and the criterion of cell size. Consequently, the true Betz cell area (frontal core in Fig. 27.12) delineated by Braak

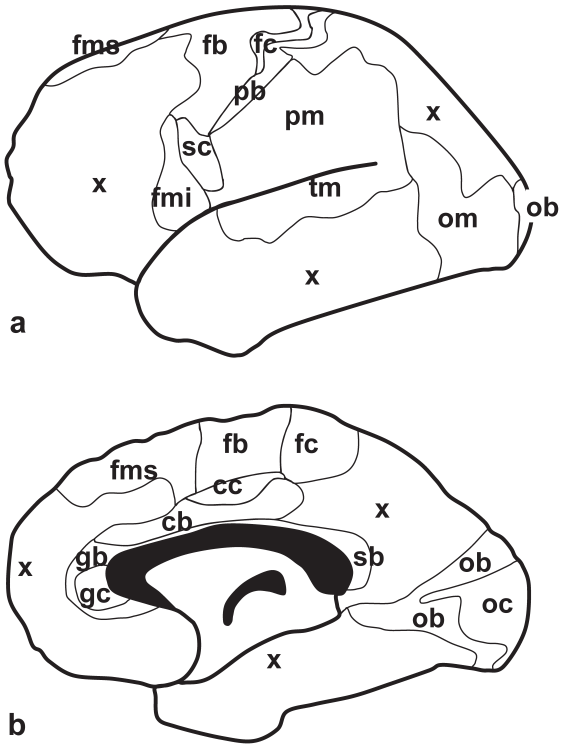

FIGURE 27.12 Cortical map based on pigmentoarchitectonic observations of Braak (1980) in **(a)** lateral and **(b)** medial views. cb, cingulate belt; cc, cingulate core; fb, frontal belt; fc, frontal core; fmi, frontal magnopyramidal region inferior part; fms, frontal magnopyramidal regions superior part; gb, genual belt; gc, genual core; ob, occipital belt; oc, occipital core; om, occipital magnopyramidal region; pb, parietal belt; pm, parietal magnopyramidal region; sb, splenial belt; sc, subcentral region; tm, temporal magnopyramidal region; x, cortical regions not parcellated.

(1979a, 1980) on the basis of pigmentoarchitectonical features is different from Brodmann's area 4 published in his famous map (Brodmann, 1909). The lateroventral part of the frontal core is completely buried in the central sulcus. According to the map in Figure 27.12, which is a simplified presentation of the detailed results of Braak's (1980) architectonic studies, Brodmann (1909) may have overestimated the extent of area 4. The area FAγ (see Fig. 27.37) of von Economo and Koskinas (1925) resembles more closely the frontal core area of Braak and area 4 as delineated by Geyer *et al.* (1996). Therefore, the architectonic delineation of the border between areas 4 and 6 needs further elaboration. The border between area 6 and the adjoining prefrontal areas is defined by the appearance of an inner granular layer (layer IV) in prefrontal areas, which is lacking in the nonprimary motor cortex. However, this criterion is not easy to recognize in Nissl-stained section.

The second feature of Brodmann's (1909) area 6, its appearance as a single cortical field, has been questioned by architectonic observations in human brains (Braak, 1976a, 1980; Sanides, 1962; Strasburger, 1937; Vogt, 1910). Comparative anatomical and functional studies substantiate the architectonical and functional segregation of area 6. Such observations in humans and nonhuman primates strongly support the concept of the nonprimary motor cortex as being composed of two major regions, the premotor and the supplementary motor cortex (for review, see Geyer *et al.*, 2000c and Chapter 26). This subdivision corresponds only partly with the frontal belt and cingulate core areas (Fig. 27.12), which have been delineated by Braak (1976a, 1979a, 1980). The premotor and supplementary cortices can be further subdivided by architectonic and functional criteria both in nonhuman primates and humans (Barbas and Pandya, 1987; Geyer *et al.*, 1998, 2000a, c; Luppino *et al.*, 1990, 1991, 1993, 1994, 1999; Matelli and Luppino, 1996; Matelli *et al.*, 1986, 1989, 1991, 1998; Paus *et al.*, 1993; Penfield and Welch, 1951; Picard and Strick, 1996; Rizzolatti *et al.*, 1988, 1990, 1996a–c, 1998; Roland and Zilles, 1996a; Roland *et al.*, 1980; Sanes *et al.*, 1995; Stephan *et al.*, 1995; Tanji, 1994; Tanji and Shima, 1994; Wiesendanger and Wiesendanger, 1984; Wiesendanger *et al.*, 1985; Wise, 1985a, b; Wise and Strick, 1984; Zilles *et al.*, 1995, 1996). A detailed description of the functional and connectional aspects of the complete motor cortex is given in Chapter 26.

Parietal Lobe

The human parietal cortex consists of the *postcentral* and *parietal regions* (Brodmann, 1909). The *postcentral region* comprises the postcentral gyrus, parts of the paracentral lobule mesially and parts of the operculum Rolandi ventrolaterally. The *parietal region* comprises the superior and inferior parietal lobules separated by the intraparietal sulcus, the most posterior part of the paracentral lobule, and the mesial extent of the superior lobule down to the subparietal sulcus and to the parietooccipital sulcus.

The cytoarchitectonic maps of Brodmann (1909) and von Economo and Koskinas (1925) still dominate the present concepts on the architectonic organization of the human parietal cortex (Fig. 27.13a–d). Brodmann's map strongly influenced the parcellation scheme of Sarkisov *et al.* (1949; Fig. 27.39), which differs only by minor details from his map. More recent architectonic studies (Bailey *et al.*, 1950; Pandya and Seltzer, 1982a, b; Eidelberg and Galaburda, 1984) further developed the Economo-Koskinas concept. However, all these maps do not reflect the high degree of functional segregation in the parietal cortex revealed by neuroimaging studies in the human brain (Bremmer *et al.*, 2001; Dong

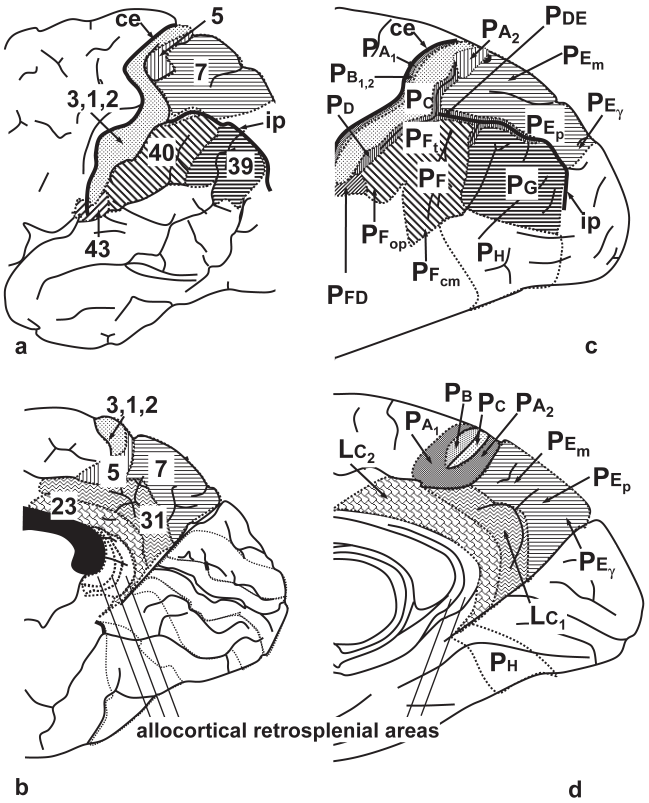

FIGURE 27.13 Cytoarchitectonic maps of human parietal areas. **(a)** lateral view and **(b)** medial view are modified after the map of Brodmann (1909); **(c)** lateral view and **(d)** medial view are modified after von Economo and Koskinas (1925). ce, central sulcus; ip, intraparietal sulcus; LC_1, area cingularis posterior dorsalis; LC_2, area cingularis posterior ventralis; PA_1, area postcentralis gigantopyramidalis sulcal part; PA_2, area postcentralis gigantopyramidalis (paracentral lobule); PB_1, area postcentralis oralis granulosa; PB_2, area postcentralis oralis simplex; PC, area postcentralis intermedia; PD, area postcentralis caudalis; PDE, transition zone between areas PE and PD; PEm, area parietalis superior magnocellularis; PE_p, area parietalis superior parvocellularis; PE_γ, area parietalis superior posterior gigantopyramidalis; PF, area supramarginalis; PF_{cm}, area supramarginalis magnocellularis columnata; PFD, transition zone between areas PF and PD; PF_{op}, area parietalis tenuicorticalis opercularis; PF_t, formatio supramarginalis tenuicorticalis; G, area angularis; PH, area parietalis basalis; PHO, area parietalis basalis limes occipitalis.

et al., 2000; Fink *et al.*, 2000a, b, 2001a, b; Grefkes *et al.*, 2002; Gurd *et al.*, 2002; Inoue *et al.*, 2001; Weiss *et al.*, 2000). Furthermore, numerous anatomical and functional (Bremmer *et al.*, 2000; Cavada, 2001; Colby and Duhamel, 1996; Galletti *et al.*, 1997; Luppino *et al.*, 1990, 1993, 1999; Matelli and Luppino, 2001; Matelli *et al.*, 1986, 1998; Rizzolatti *et al.*, 1997; Seltzer and Pandya, 1980) observations in the monkey also demonstrate a much higher degree of areal differentiation than that presented in Brodmann's (1909) maps of the human or monkey cortex. Thus, the parietal cortex is still an architectonicly insufficiently explored region of the human cerebral cortex. For a recent parcellation of the macaque parietal cortex, see Paxinos *et al.* (2000).

Postcentral Region

Brodmann (1909, 1910) divided the postcentral region into four architectonicly related areas, that is, areas 3, 1, and 2 (according to their anterior–posterior sequence; Fig. 27.13a, b), and area 43 on the operculum Rolandi, whereas von Economo and Koskinas (1925) defined six areas, that is, PA_1, PA_2, PB_1, PB_2, PC, PD (Fig. 27.13c, d) and one subarea Pcg (not shown). For a comparison of the different nomenclatural systems see Table 27.5.

The fundus of the central sulcus is a landmark of the architectonic border between the motor area 4 and the most rostral postcentral area 3a (Figs. 27.11 and 14a, b) in most human brains. In some cases, however, this border can encroach the posterior wall of the precentral gyrus or the anterior wall of the postcentral gyrus to variable distances. Furthermore, a small region displaying a mixture of the cytoarchitectonic characters of areas 4 and 3 can be found at the bottom of the central sulcus, the anterior part of the paracentral lobule, and the posterior part of the operculum Rolandi. This transitional region was identified by von Economo and Koskinas (1925) as their *area* PA_1 (Fig. 27.13c, d) and later called area 3a (for review, see Jones and Porter, 1980). The remaining and larger part of area 3 is the primary somatosensory area 3b (Fig. 27.11), which corresponds to von Economo's and Koskinas' *areas* PB_1 and PB_2. Area 3b has a conspicuous layer IV with small granular neurons invading layer III. Thus, area 3b is a typical koniocortex, that is, a heterotypical six-layered isocortex with a distinct and wide layer IV (Fig. 27.14b, c). This architectonical type is found in all primary sensory areas of the human brain. The subdivision of area 3b into PB_1 and PB_2 by von Economo and Koskinas was based on the stronger invasion of layer III of PB_1 by small granular cells compared to the reduced granularization of layer III in PB_2.

Area 3b is followed posteriorly by intermediate postcentral area 1 (Figs. 27.11 and 27.14c, d), which corresponds to von Economo's and Koskinas' *area* PC (Table 27.5). Area 1 reaches as a narrow strip (PC_γ of von Economo and Koskinas), the caudal part of the paracentral lobule on the mesial hemispheric surface and borders ventrolaterally to area 43. The cytoarchitecture of area 1 shows a homotypical six-layered isocortex with large pyramidal cells in deeper layer III and a less conspicious layer IV when compared with area 3b. Thus, area 1 fits into the general cytoarchitectonic feature of other unimodal sensory areas (e.g.,

TABLE 27.5 Comparison of Different Architectonic Parcellation Schemes of the Human Parietal Cortex

Brodmann (1909) cytoarchitecture	von Economo and Koskinas (1925) cytoarchitecture	Eidelberg and Galaburda (1984) myeloarchitecture	Vogt (1911) myeloarchitecture	Flechsig (1920) myelogenetic
1	P_C	—	70	2
2	P_D	—	71	—
	P_{DE}	—	(86?), (87?)	13
(3b)	P_{B_1}, P_{B_2}	—	69	2
(3a)	P_{A_1}	—	67	—
5	P_{A_2}	—	75	—
7	P_{E_m}, P_{E_p}, P_{E_γ}	PE	83, 85	16, 21
23	L_{C_2}	—	(76–82)	33
26	L_{F_1}	—	—	—
	L_{E_1}, L_{E_2}	—	(91–96)	6
	L_D	—	(91–96)	—
31	L_{C_1}	—	(76–82), 84	33
39	P_G	PG, PEG	90	34
40	P_F, P_{F_t}, $P_{F_{cm}}$	PF, PFG	88, (86?), 89	19
43	P_{FD}	—	72	—
Opercular	$P_{F_{op}}$	—	73, 74	—

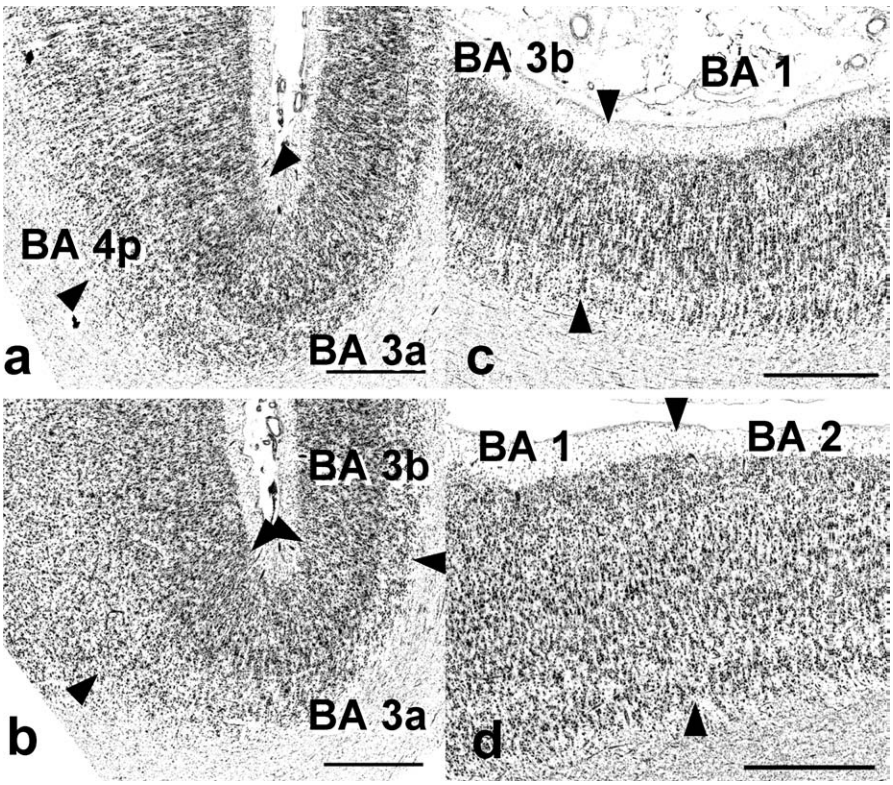

FIGURE 27.14 Cytoarchitecture of the areas 3a **(a, b),** 3b **(b, c),** 1 **(c, d),** and 2 **(d)** of the human postcentral gyrus. Bars = 1 mm.

area 18 or area 42 of the visual or auditory cortex, respectively). Subarea PC_γ differs from PC by its very large pyramidal cells in layer V and from area PA_2 by its better developed layer IV.

Area 1 is followed caudally by the postcentral area 2, which corresponds to von Economo's and Koskinas' *area* PD (Figs. 27.11 and 27.13c; Table 27.5). It is difficult to delineate area 2 from area 1 because both areas belong to the homotypical six-layered isocortex and contain large pyramidal cells in deeper layer III (Fig. 27.14d). Recently, this border between area 2 and 1 was demonstrated by using a quantitative cytoarchitectonic technique and receptor architectonic analysis (Geyer *et al.*, 1997, 1999, 2000b; Grefkes *et al.*, 2001). It was also demonstrated that area 2 is involved in somatosensory tasks of varying complexity (Bodegård *et al.*, 2000a, b; Naito *et al.*, 1999). Von Economo and Koskinas emphasized that PD can be differentiated from areas of the superior parietal lobule by numerous pyramidal-like cells in deeper layer VI of PD. In contrast to Brodmann (1909), but in accordance with von Economo and Koskinas (1925), it was demonstrated by Grefkes *et al.* (2001), that area 2 does not extend to the mesial hemispheric surface. Von Economo and Koskinas (1925) described a transition region between PD and PE, their area PDE. It continues on the upper and lower bank of the intraparietal sulcus (Figs. 27.11 and 27.13c). Thus, the intraparietal part of PDE can be compared with Brodmann's caudal part of area 2 in the intraparietal sulcus (Brodmann, 1909) and the "visuo-sensory band β" of Smith (1907). For a comprehensive description of the somatosensory system, see Chapter 28.

The subcentral area 43 (Brodmann, 1909) is located lateroventrally at the basis of the postcentral gyrus, approximately between the anterior and posterior subcentral sulci on the operculum Rolandi (Fig. 27.13a). It extends for a considerable distance along the depth of the Sylvian fissure. The most probable candidate for a comparable area in von Economo and Koskinas's map is their area PFD (Fig. 27.13c). Considering its location and extent, area 43 or parts of it may be candidates for the functionally defined second somatosensory cortex. Recently, Eickhoff *et al.* (2002) identified several cytoarchitectonic areas in the parietal operculum, which are not described in the classical cytoarchitectonic maps, but probably comprise the anatomical correlates of the functionally defined second somatosensory cortex SII and other functional areas (e.g., gustatory, vestibular; cf. Chapters 31 and 33).

The preparietal area 5 was classified by Brodmann (1909) as part of his parietal region, but von Economo and Koskinas (1925) identified their comparable area PA_2 as part of the postcentral region (Fig. 27.13). PA_2 shows extraordinarily huge pyramidal cells in layer V

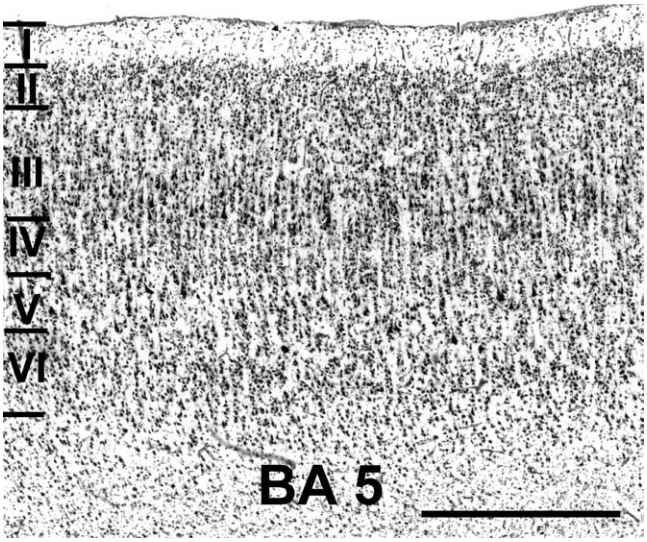

FIGURE 27.15 Cytoarchitecture of area 5 of the human parietal cortex. Bar = 1 mm.

(Fig. 27.15), which are comparable to the giant Betz cells of area 4. However, in sharp contrast to area 4, a conspicuous layer IV is visible in PA_2. Area 5 covers an area extending from the posterior part of the paracentral lobule to the rostral bank of the callosomarginal sulcus and continues laterally between the superior part of the postcentral sulcus and the anterior border of area 7.

Parietal Region

A complete architectonic map of the human parietal region compatible with the extensive regional segregation demonstrated by functional imaging is presently not available. Surprisingly, the practically forgotten myelo- and cytoarchitectonic studies by Vogt (1911), Gerhardt (1940), and Batsch (1956) indicate a much higher architectonic heterogeneity of the cortical organization than represented in the classical maps. Thus, we will briefly present here these forgotten maps, which may be of interest on the background of the high degree of functional segregation demonstrated by recent neuroimaging studies.

According to Brodmann (1908, 1909) and von Economo and Koskinas (1925), the parietal region comprises the four architectonical areas 5, 7, 39, and 40 (Fig. 27.13) or the eight areas PDE, PE_m, PE_p, PEγ, PF_t, PF_{op}, PF_{cm}, and PG, respectively. The major part of the basal parietal region PH of von Economo and Koskinas is located at the occipitotemporal transition zone, belongs to the visual cortex, and may include the functionally defined visual areas V4 and V5, among others. This area will be described later in "Temporal Lobe."

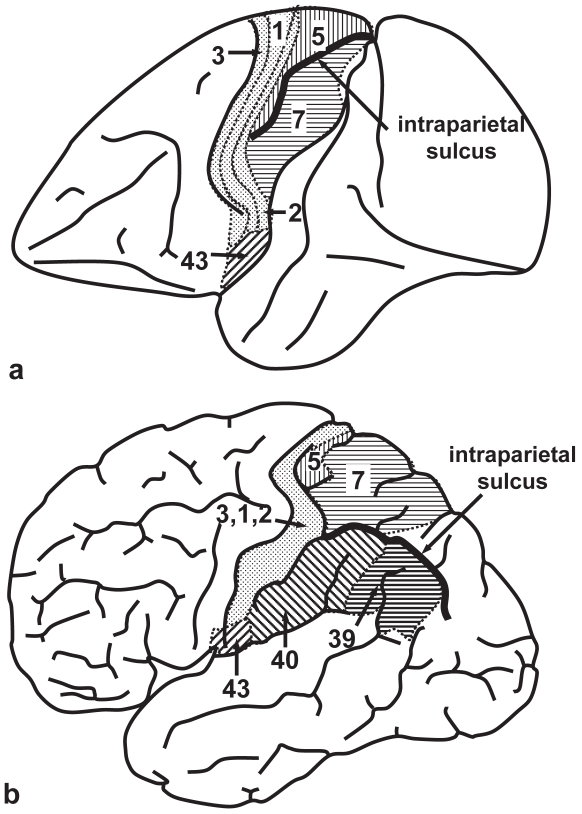

FIGURE 27.16 Areal pattern of the parietal cortex in the human **(a)** and macaque **(b)** brains after Brodmann (1909). According to these maps, the intraparietal sulcus has a different position relative to area 7 in the human compared to the macaque brain.

A major controversy concerning the architectonic organization arose from Brodmann's maps (Brodmann, 1909) of human and monkey parietal cortex (Fig. 27.16). Area 5 of monkeys covers the complete superior parietal lobule, and area 7 covers the complete inferior parietal lobule. In contrast, in the human cortex, areas 5 and 7 are found in the superior parietal lobule, whereas the inferior parietal lobule contains the "human-specific" areas 39 and 40. Vogt (1911) subdivided the superior lobule into areas 5a and 5b and the inferior lobule into areas 7a and 7b. Area 7a includes parts of Brodmann's areas 39 and 40; area 7b represents the most rostral part of area 40. Area 5 of Brodmann is a small part of the areas 5a and 5b of Vogt and Vogt (1926), which are covered almost completely by Brodmann's area 7.

Superior Parietal Lobule

The *superior parietal area 7* of Brodmann (1909) occupies most of the lateral superior parietal lobule and of the medial precuneus (Fig. 27.13a, b). A comparable location was described by von Economo and Koskinas (1925) for their PE areas (Fig. 27.13c, d; Table 27.5).

PE is characterized by a sharply delineated band of conspicuously low cell-packing density corresponding to deeper layer V (layer Vb), whereas the borders of this band are blurred in the inferior parietal areas 39 and 40. Further cytoarchitectonic criteria are provided by the generally smaller cells of inferior parietal lobule areas when compared with PE. PE was further subdivided into the anterior area PE_m, with a more pronounced magnocellular appearance compared to the posterior relatively smaller celled area PE_p. The border between PE_m and PE_p is marked approximately by the superior parietal sulcus. According to von Economo and Koskinas (1925), a transitional area PDE (or PED) is located between areas PD and PE. PDE extends into the intraparietal sulcus. A further subdivision was described in the most posterior part of PE_p, the gigantopyramidal area PE_γ. The larger part of this area is found on the anterior wall of the parieto-occipital sulcus. PE_γ is characterized by widely spaced, very large, but slim pyramidal cells in layers IIIc and V.

Inferior Parietal Lobule

The *angular area 39* corresponds broadly to the angular gyrus. Von Economo's and Koskinas' area PG is the equivalent to Brodmann's area 39 (Fig. 27.13; Table 27.5). PG is found posteriorly of the sulcus of Jensen, below the intraparietal sulcus, above area PH, and rostrally to the occipital cortex, which differs from PG by widely spaced larger pyramidal cells in lower layer IIIc, a conspicuously lighter and smaller layer V, and a more cell dense and smaller layer VI. The cytoarchitecture of PG takes an intermediate position between PE and PF. Layer III of PG is smaller than that of PE, layer V of PG appears lighter than its layer VI, and its overall cell size is smaller than in PE but larger than in PF.

The *supramarginal area 40* corresponds approximately to the supramarginal gyrus. Von Economo and Koskinas's area 40 is equivalent to area PF (Fig. 27.13; Table 27.5). PF occupies the rostral part of the inferior parietal lobule, is found on the posterior part of the operculum Rolandi and the operculum parietale, and reaches approximately to the sulcus Jensen. Von Economo and Koskinas (1925) did not describe sharp borders between PF and adjacent areas. The transitional areas PF_t, PF_{op}, and PF_{cm} are highly variable in their cytoarchitecture and size (for architectonic details of these transitional areas see Zilles and Palomero-Gallagher, 2001). The major part of PF is characterized by relatively small neurons in all layers, layers V and VI with a similar (low) cell density, wide layers II and IV, and a conspicuous, fine columnar arrangement of cells. In contrast to the occipital areas, PF shows relatively broad total cortical widths (2.5–3.6 mm). The

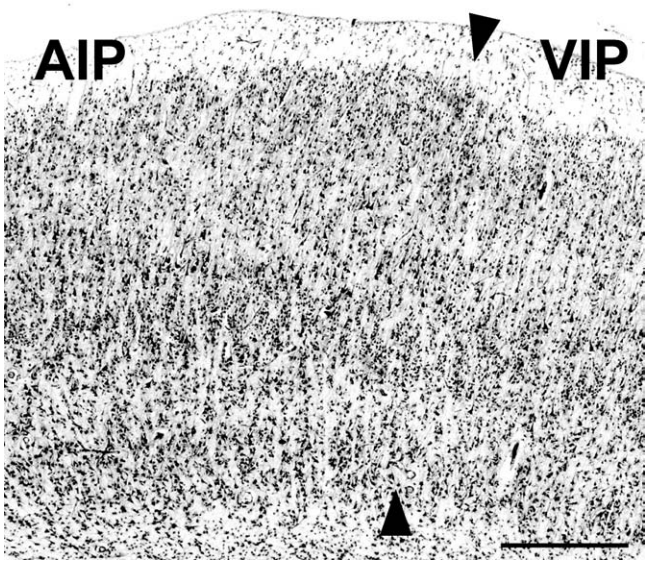

FIGURE 27.17 Cytoarchitecture of the intraparietal areas AIP and VIP of the human cerebral cortex. Bar = 1 mm.

delineation to the temporal areas is based on the higher cell density in layers V and VI of these areas in comparison to PF.

Neither Brodmann (1909) nor von Economo and Koskinas (1925) provided a distinct cytoarchitectonic parcellation of the cortex in the *intraparietal sulcus*. In monkeys, however, several areas—anterior intraparietal area (AIP; Sakata *et al.*, 1995, 1997), lateral intraparietal area (LIP; Andersen *et al.*, 1990b), medial intraparietal area (MIP; Colby *et al.*, 1988), posterior intraparietal area (PIP; Colby *et al.*, 1988), ventral intraparietal area (VIP; Colby *et al.*, 1993; Maunsell and van Essen, 1983; Ungerleider and Desimone, 1986); area PEip (Matelli and Luppino, 2001; Rizzolatti *et al.*, 1998), and area V6A (Galletti *et al.*, 1996, 1999)—were found in the intraparietal sulcus and at the junction with the parietooccipital sulcus, which have numerous connections with the frontal premotor and occipital cortices. Thus, it is highly probably that the human intraparietal sulcus can also be parcellated into equivalent cytoarchitectonic areas. Recently, Choi *et al.* (2002) delineated two areas that are the putative cytoarchitectonic correlates of the recently identified human AIP (Grefkes *et al.*, 2002) and VIP (Bremmer *et al.*, 2000) areas (Fig. 27.17).

Sufficiently precise data on the connectivity of the cytoarchitectonicly defined human parietal areas are presently not available. However, extensive studies on function and connectivity were reported in monkeys (Andersen *et al.*, 1990a, b; Blatt *et al.*, 1990; Cavada and Goldman-Rakic, 1989a, b, 1991, 1993; Cavada *et al.*, 2000; Colby and Duhamel, 1991; Colby and Goldberg, 1999; Colby *et al.*, 1988; Duhamel *et al.*, 1997; Galletti *et al.*, 1996, 1999; Hyvärinen, 1982a, b; Luppino *et al.*, 1999; Matelli *et al.*, 1998; Matelli and Luppino, 2001; Maunsell and van Essen, 1983; Mesulam *et al.*, 1977; Pandya and Seltzer, 1982a; Petrides and Pandya, 1984; Schmahmann and Pandya, 1990; Seltzer and Pandya, 1980, 1984, 1986; Sakata *et al.*, 1995, 1997; Yeterian and Pandya, 1985, 1993). The dorsal part of the premotor cortex receives afferents from the parietal area 7 (PEip and PEc; Rizzolatti *et al.*, 1998), MIP, area V6A, area 46, and the mesial posterior parietal cortex from the extrastriate visual cortex. The transformation of somatosensory and visual information for the control of hand movement toward the target and coding of object location in space for orienting and coordinated arm–body movements are possible function of these circuits (Matelli and Luppino, 2001). Further circuits are found between the ventral part of the premotor cortex and the parietal areas AIP, VIP, and von Economo's and Koskinas's (1925) area PF (area 40 of Brodmann, 1909). The VIP–premotor cortex circuit seems to encode peripersonal space according to a body part-centered frame of reference and transforms object locations into appropriate movements toward them (Matelli and Luppino, 2001). The AIP–premotor cortex circuit provides a representations of intrinsic object properties (size, shape, and orientation) for selection of the most appropriate way of grasping (Jeannerod *et al.*, 1995). The supplementary motor cortex SMA-proper and the presupplementary motor cortex pre-SMA are further targets of the areas PFG, PG, and PE of the superior and inferior parietal lobules. LIP, the frontal eye field (FEF), and the supplementary frontal eye field (SFEF) are interconnected. The LIP–FEF circuit uses eye position and retinotopic information for the transformation of the retinocentric into a craniocentric frame of reference (Matelli and Luppino, 2001).

Posterior parietal lesions in humans lead to apraxia and extinction (lesion of the left hemisphere) as well as neglect (lesions of the right hemisphere) (Balint, 1909; Denny-Brown *et al.*, 1952; Driver *et al.*, 2001; Fink *et al.*, 1997; 2000a, c, 2001b; Freund, 1987, 2001; Luria, 1959; Mesulam, 1999; Sirigu *et al.*, 1995; Tyler, 1968; Vallar, 1998, 2001). Lesions of the angular gyrus in the dominant hemisphere (areas PF and PG) lead to finger agnosia (inability to recognize, distinguish, and name one's fingers or those of other persons), pure agraphia, right–left disorientation, and dyscalculia (inability to recognize the value of a number). These symptoms have been summarized as Gerstmann's syndrome (Gerstmann, 1930).

The maintenance of a spatial reference system for goal-directed movements seems to be a major function

of the posterior parietal region. This function is a prerequisite for important human activities (i.e., tool use and conceptualization of actions). Recent functional imaging and other mapping studies (Bodegård *et al.*, 2000a, b; Bremmer *et al.*, 2001; Ehrsson *et al.*, 2000; Geyer *et al.*, 1996; Larsson *et al.*, 1999; Naito *et al.*, 1999, 2000; Roland and Zilles, 1994, 1996a, b, 1998; Zilles *et al.*, 1995, 1997) demonstrate that areas in the inferior parietal lobule and intraparietal sulcus were activated during imagining (Jeannerod, 2001) and executing (Binkofski *et al.*, 1999) grasping (Decety *et al.*, 1994; Grafton *et al.*, 1996), evaluation of the possible motor significance of sensory stimuli ("motor intention irrespectively of the likelihood of providing a response"; Toni *et al.*, 2001), perceptually based decisions and prospective action judgement (Parsons *et al.*, 1995), action observation (Buccino *et al.*, 2001), and visual presentation of graspable objects (Chao and Martin, 2000).

In a recent event-related fMRI study, the contribution of the parietal-temporal-premotor circuit to sensorimotor transformations was analyzed "where behavior is guided by rules rather than objects or places" (Passingham and Toni, 2001; Toni *et al.*, 2001; White and Wise, 1999). It could be shown, that (1) activation of the posterior parietal cortex can be correlated with motor intention, (2) the premotor cortex can be correlated with movement preparation, and (3) the posterior part of the superior temporal gyrus can be correlated with the extraction of contextual and intentional cues during goal-directed behavior. Finally, it has been shown that the superior posterior parietal cortex of the human brain is a multimodal region implicated in task switching, even when no visual or spatial component is part of the task (Gurd *et al.*, 2002).

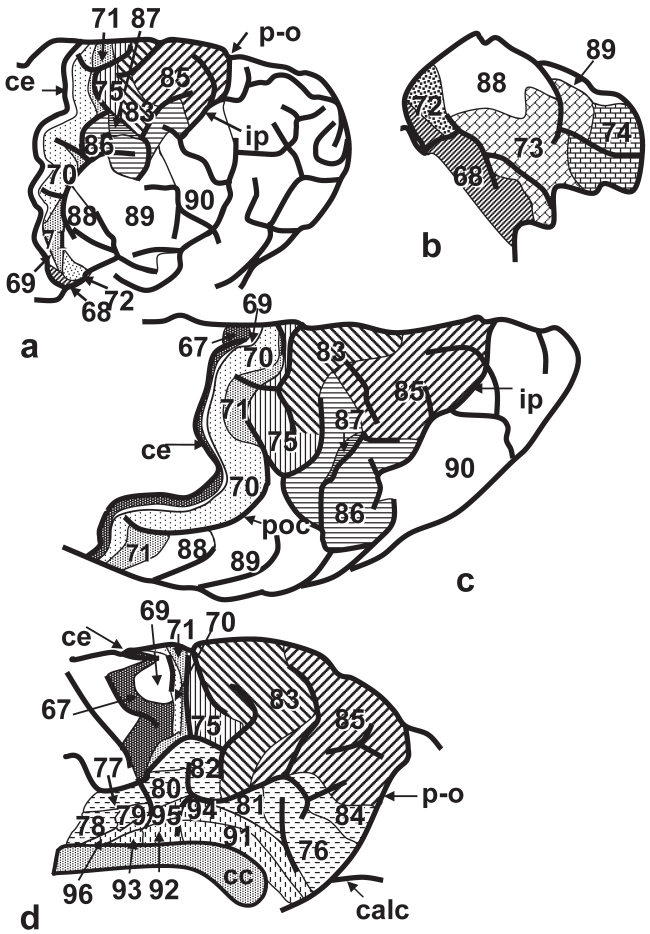

FIGURE 27.18 Myeloarchitectonic map of the human parietal cortex (modified after Vogt, 1911). **(a)** Lateral view, **(b)** surface of the parietal operculum, **(c)** dorsal view, and **(d)** mesial view. calc, calcarine sulcus; cc, corpus callosum; ce, central sulcus; ip, intraparietal sulcus; p-o, parieto-occipital sulcus; poc, postcentral sulcus. The Arabic numerals indicate the myeloarchitectonic areas, which are not identical the numerical scheme of Brodmann.

Forgotten Maps of the Human Parietal Cortex

Detailed cyto- (Gerhardt, 1940) and myeloarchitectonic (Vogt, 1911; Batsch, 1956) parcellations of the human parietal lobe are available. Vogt (1911) proposed a map of the human parietal cortex displaying 28 different myeloarchitectonic areas. However, these three studies of the Vogt School are practically forgotten. Here, a brief review of the detailed maps (Figs. 27.18–27.20) will be given (see Table 27.5 for comparison with other nomenclatures).

Major criteria in the myeloarchitectonic studies are interareal differences in the length, thickness, and spacing of the radial fiber bundles, the visibility or lack of the Kaes-Bechterew stripe (i.e., tangentially oriented myelinated nerve fibers in the most superficial part of layer III), the visibility or lack of the outer and inner Baillarger stripes (i.e., tangentially oriented myelinated nerve fibers in layer IV and deeper layer V, respectively), and the merging or separation of the outer and inner Baillarger stripes (Fig. 27.21).

The parcellation in the maps of Vogt (1911) and Batsch (1956) is quite comparable. Differences between both maps are only found when the sizes of equivalent areas are compared between the studies. This, however, is not surprising because the sizes of equivalent cortical areas in different brains show a considerable degree of intersubject variability (Amunts *et al.*, 1999, 2000b; Geyer *et al.*, 1996, 1999, 2000b; Grefkes *et al.*, 2001; Rademacher *et al.*, 2001b; Roland *et al.*, 1997; Zilles *et al.*, 1997). Thus, the two myeloarchitectonic studies provide a concordant map of the human parietal cortex. The myeloarchitectonic maps are further supported by

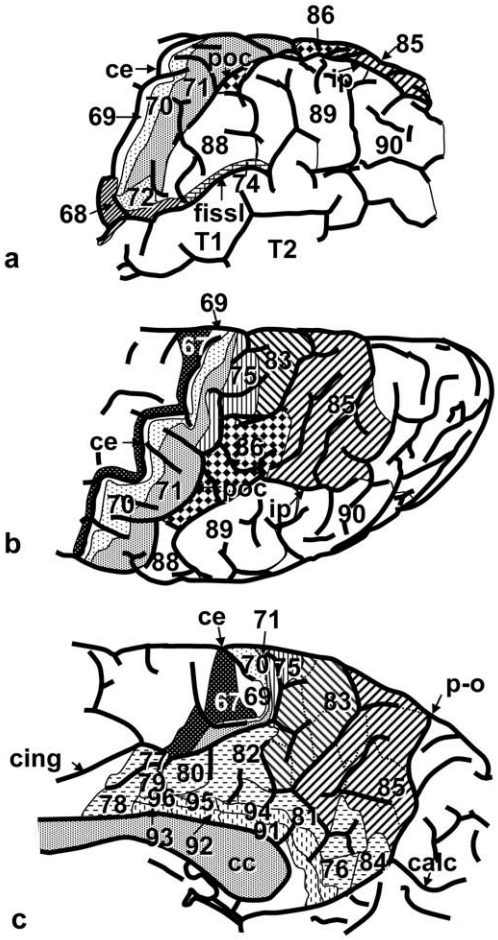

FIGURE 27.19 Cytoarchitectonic map of the human parietal cortex (modified after Gerhardt, 1940). **(a)** Lateral view, **(b)** dorsal view, and **(c)** mesial view. calc, calcarine sulcus; cc, corpus callosum; ce, central sulcus; fissl, lateral fissure; ip, intraparietal sulcus; p-o, parieto-occipital sulcus; poc, postcentral sulcus; T1, superior temporal gyrus; T2, inferior temporal gyrus. The Arabic numerals indicate the cytoarchitectonic areas of Gerhardt, which are not identical the numerical scheme of Brodmann but comparable to the myeloarchitectonic classification of Vogt as shown in Figure 27.18.

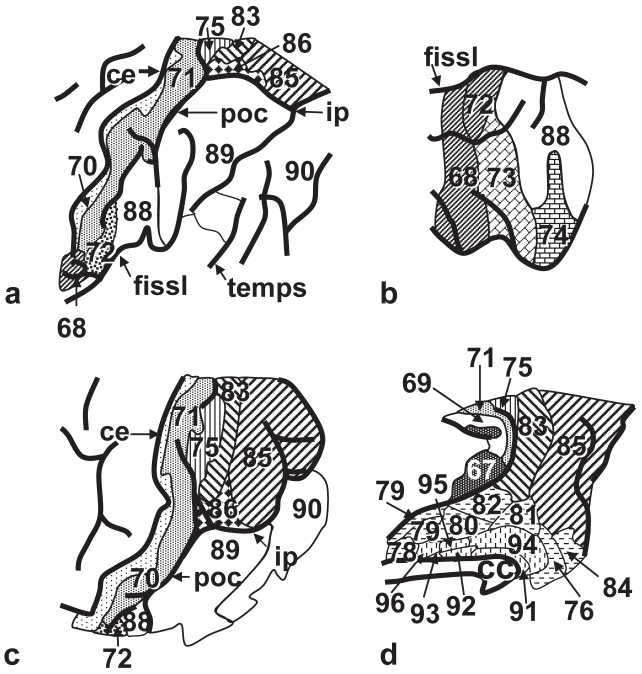

FIGURE 27.20 Myeloarchitectonic map of the human parietal cortex (modified after Batsch, 1956). **(a)** Lateral view, **(b)** surface of the parietal operculum, **(c)** dorsal view, and **(d)** mesial view. cc, corpus callosum; ce, central sulcus; fissl, lateral fissure; ip, intraparietal sulcus; poc, postcentral sulcus; temps, superior temporal sulcus. The Arabic numerals indicate the myeloarchitectonic areas of Batsch, which are not identical the numerical scheme of Brodmann but comparable with the myeloarchitectonic classification of Vogt as shown in Figure 27.18.

the cytoarchitectonic observations of Gerhardt (1940). This study provides an even more detailed map; however, the parcellation was based on only one hemisphere. Thus, not all of Gerhardt's subareas may be found in other brains. Only the major areas of this cytoarchitectonic map are reproduced here (Fig. 27.19) and show an areal pattern very similar to those observed by Vogt (1911) and Batsch (1956) in their myeloarchitectonic studies. These three studies indiate that the areal parcellations of Brodmann (1909) and von Economo and Koskinas (1925) do not give a sufficiently complete picture of the architectonical organization in the human parietal lobe.

Temporal Lobe

The temporal lobe consists of a large number of cortical areas differing in structure (isocortical to allocortical) and function (unimodal auditory, unimodal visual, multimodal association). The superior (transverse gyri, planum temporale) and dorsolateral (superior temporal gyrus) zone of the temporal lobe contains various isocortical areas, which are the structural correlates of the unimodal auditory cortex and the multimodal language area (i.e., the Wernicke region). The unimodal visual and multimodal isocortical areas of the inferior lateral and ventral zones of the temporal lobe—medial and inferior temporal gyri, fusiform (= lateral occipitotemporal) gyrus, rostral part of the lingual (= medial occipitotemporal) gyrus—are summed up here as the inferotemporal zone. This zone is followed most medially by allocortical regions, which comprise the multimodal medial zone of the temporal lobe. This latter zone consists of the periallocortical entorhinal, perirhinal, parasubicular, and presubicular areas as well as the allocortical regions of the hippocampus (dentate gyrus, Ammon's horn,

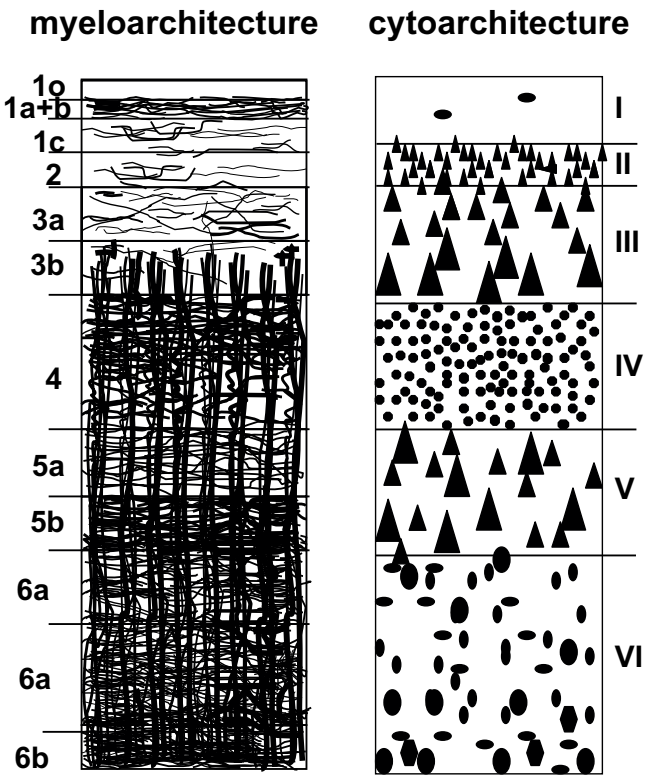

FIGURE 27.21 Schematic drawing of the myelo- and cytoarchitectonic lamination patterns in the human isocortex. Arabic numerals indicate the cortical layers in myelin-stained sections; Roman numerals indicate the cortical layers in cell body-stained sections. The myelinated fibers are running vertically or horizontally to the surface of the cerebral cortex. Only a few fibers are obliquely oriented. The vertical fiber bundles contain myelinated axons and are called radial fibers. This term may give rise for confusios because the same term is used for vertically oriented *glial* fibers in the fetal brain. The thickness, length, and packing density of the myelinated fiber bundles are important criteria for myeloarchitectonic parcellations. The horizontally oriented fiber bundels also contribute as important criteria to the myeloarchitectonic studies. The most superficial horizontal fiber bundel is the Exner-stripe in layer 1a+b, followed by the Kaes-Bechterew-stripe in layer 3a, the outer Baillarger-stripe in layer 4, and the inner Baillarger-stripe in layer 5b.

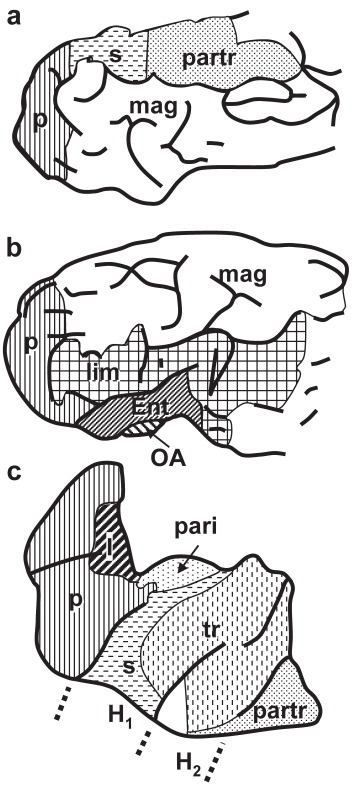

FIGURE 27.22 Areal map of the temporal lobe based on the myeloarchitectonic observations of Hopf (1954). **(a)** Lateral view, **(b)** basal view, **(c)** dorsal view. Ent, entorhinal area; H1, first transverse gyrus of Heschl; H2, second transverse gyrus of Heschl; I, insular region, lim, regio temporalis limitans; mag, regio temporalis magna; p, regio temporopolaris; pari, regio temporalis parainsularis; partr, regio temporalis paratransversa; s, regio temporalis separans; tr, regio temporalis transversa.

subiculum) and the small cortical part of the amygdala. The areas of this allocortical zone are described in detail in Chapters 22–24 and 32. The polar zone of the temporal lobe (Brodmann's area 38) consists of a multimodal region with a proisocortical architecture and was interpreted as part of the paralimbic belt by Mesulam (1998).

The most detailed anatomical studies of the human temporal isocortex are based on myeloarchitectonic observations (Hopf 1954, 1955, 1968). This author identified 7 regions, which were further subdivided into 20 subregions and 60 cortical areas. Figure 27.22 provides an overview of the different regions as described by Hopf (1954). A detailed comparison of the parcellation by Hopf (1954, 1955, 1968) with the cytoarchitectonic studies of Smith (1907), Brodmann (1909), and von Economo and Koskinas (1925), however, reveals considerable differences (cf Table 27.6). Braak's (1978) pigmentoarchitectonic observations (Fig. 27.23) are also at variance with all the other studies. Thus, it is presently not possible to provide a conforming and sufficiently detailed architectonic map of the temporal isocortex, that reconciles the different parcellation schemes.

Despite these controversies in detailed parcellation, a general pattern of the architectonic segregation of the temporal isocortex, which is based on the parcellation scheme of Brodmann (1909), can be described. The human temporal lobe comprises three main iso- or proisocortical regions: (1) a proisocortical polar (Brodmann's temporopolar area 38) together with a mediobasal (Brodmann's ectorhinal area 36 on the

TABLE 27.6 Comparison Between Different Areal Maps of the Temporal Lobe with the Myeloarchitectonic Map of Hopf (1954)[a]

Hopf (1954)	Smith (1907)	Brodmann (1909)	von Economo and Koskinas (1925)
Regio temporalis (= p)	Area temporopolaris (rostral part)	38	TG
Regio temporalis (= s)	Area temporalis superior	22, 41, 42	TA, TC, TB, TD
Regio parainsularis (=pa)	?	52	Medial parts of TB and TD
Regio temporalis transversa (=tr)	Area temporalis superior	41, 42	TC, TB
Regio temporalis paratransversa (= ptr)	Area temporalis superior	22	TA
Regio temporalis magna (= m)	Area temporalis media, Area temporalis inferior, Area paratemporalis	21 20 37	TE TE PH
Regio temporalis limitans (= l)	Area temporopolaris (posterior part), Area paradentata	35, 36 35, 36	TH, TF TH, TF

[a]See Fig. 27.22

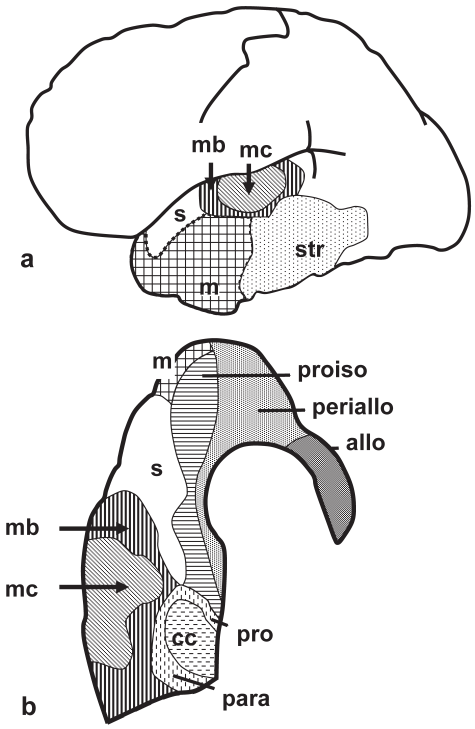

FIGURE 27.23 Areal map of the temporal lobe based on the pigmentoarchitectonical observations of Braak (1978). **(a)** Lateral view, **(b)** dorsal view. allo, allocortex; cc, koniocortial core area; m, area temporalis magna; mb, magnopyramidal temporal belt; mc, magnopyramidal temporal core; para, posterior part of the parakoniocortex; periallo, periallocortex; pro, prokoniocortex; proiso, proisocortex; s, area temporalis simplex; str, area temporalis stratiformis.

rostral prolongation of the lingual gyrus and adjacent parts of the parahippocampal gyrus) proisocortical region (p and lim in Fig. 27.22), which is very poor in myelinated fibers and is part of the paralimbic region of Pandya and Seltzer (1982b) and Mesulam (1998), (2) a large region on the middle temporal gyrus (Brodmann's middle temporal area 21) and inferior temporal and fusiform gyri (Brodmann's inferior temporal area 20 and occipitotemporal area 37), which is poor in myelinated fibers (mag in Fig. 27.22), and (3) an isocortical region on the superior and transverse temporal gyri and the planum temporale (Brodmann's area 42 and superior temporal area 22; s and partr in Fig. 27.22) surrounding rostrally, laterally and posteriorly the primary auditory area 41. These three areas are rich in myelinated fibers. According to Pandya and Seltzer's (1982b) studies in the rhesus monkey, the ptr region may project to the premotor cortex and the s and m regions to the prefrontal cortex. All these regions (ptr, s, m) project also to the paralimbic association cortex, parts of which are represented by the p region of Hopf (1954).

A small proisocortical region, immediately adjacent to the insular cortex, poor in myelinated fibers and of small cortical width (pari in Fig. 27.22), is architectonicly defined as Brodmann's parainsular area 52. This latter area is part of the temporal paralimbic cortex of Mesulam (1998) and of a proisocortical stripe (Fig. 27.23) described by Braak (1978).

Auditory Cortex

The human auditory cortex consists of various unimodal areas located on the dorsal surface of the temporal lobe and the superior temporal gyrus. A conspicious architectonic feature of the auditory cortex is its high content of myelinated fibers (Hopf, 1954, 1955, 1968) and the arrangement of neuronal perikarya in distinct vertical columns ("organ pipes" and "rain shower" formations of von Economo and Koskinas, 1925). The average column width and the interval between columns in all temporal auditory areas are

smaller in the right than in the left hemisphere (Seldon, 1981).

The principal structure of the connectivity of the auditory cortex supports the concept of three parallel streams of areas running in a rostrocaudal direction as proposed by Pandya (1995). The medial stream is represented by the parainsular cortex, the interposed (core) stream occupies the supratemporal plane, and the most lateral stream is located on the superior temporal gyrus. The areas of each stream have feedforward connections originating in layer III of one area and terminating in layer IV of the rostrally adjacent area. The feedback connections originate in the infragranular layers and terminate in layer I. The areas of the most medial and most lateral streams are connected with the prefrontal multimodal association areas and limbic areas. Additionally, the areas of the most lateral stream show a detailed connectivity according to their rostrocaudal sequence. The most rostral areas of this stream are connected with the orbital and medial prefrontal cortices; the intermediate group, with the lateral prefrontal areas; and the caudal group, with the caudal prefrontal cortex. The areas of the intermediate stream are preferentially related to the ventral nucleus of the medial geniculate body, whereas the areas of the medial and lateral streams are connected with the magnocellular and dorsal nuclei of the medial geniculate body, pulvinar, dorsomedial, and intralaminar thalamic nuclei.

Magnetic resonance imaging (Binder *et al.*, 1994; Schmid *et al.*, 1998; Strainer *et al.* 1997; Talavage *et al.*, 1999), magnetoencephalographic (Hari *et al.*, 1984; Langner *et al.*, 1997; Pantev *et al.*, 1995; Romani *et al.*, 1982), and electroencephalographic (Liegeois Chauvel *et al.*, 1991, 1994) studies have demonstrated auditory functions such as the response to pure tones and to acoustic frequency patterns that map onto the medial two thirds of the Heschl gyrus. A considerable function-depending plasticity of the representation in the auditory cortex was also demonstrated (Pantev *et al.*, 1998b; Rauschecker, 1999). In contrast to the established functional lateralization of language, asymmetries following acoustic stimulation are still a matter of discussion (Belin *et al.*, 1998; Lauter, 1992; Nicholls, 1998; Pantev *et al.*, 1998a; Poeppel *et al.*, 1996; Zouridakis *et al.*, 1998).

Primary auditory cortex (core region) The cytoarchitectonic areas 41 of Brodmann (1909) and TC of von Economo and Koskinas (1925) (Figs. 27.35 and 27.37) represent the putative cytoarchitectonic correlates of the human primary auditory cortex, which neurons are tuned to pure tones and pitch. Several studies demonstrated a tonotopic organization of the primary auditory cortex with responses to low-frequency stimuli originating more laterally and high-frequency stimuli originating more medially (Bilecen *et al.*, 1998; Hari *et al.*, 1984; Howard *et al.*, 1996; Lauter *et al.*, 1985; Pantev *et al.*, 1995; Reite *et al.*, 1994; Talavage *et al.*, 1997; Tiitinen *et al.*, 1993; Verkindt *et al.*, 1995; Yamamoto *et al.*, 1992). Area 41 has the typical koniocortical structure of primary sensory areas (i.e., a well-developed layer IV with densely packed small neurons, and a high cell density invading the supragranular layer III). Area 41 is located deep in the Sylvian fissure on the temporal transverse gyrus (Heschl) gyrus and is surrounded caudolaterally by the secondary auditory area 42, rostrally and laterally by areas 22 and 42, and medially by the area 52.

Rademacher *et al.* (1993) described two transverse gyri of Heschl separated by an intermediate transverse sulcus in 7 out of 20 hemispheres. In hemispheres with two transverse gyri, area 41 is located most frequently on the first transverse gyrus. Only in two of the seven cases with two transverse gyri does area 41 overflow across the intermediate sulcus and also cover the rostral part of the second transverse gyrus.

Braak's (1978) "granulous core field" (demonstrated by his pigment-staining technique) was identified as putative primary auditory cortex (Fig. 27.23) but covers only the rostral half of the first transverse gyrus of Heschl. Thus, his anatomical correlate of the primary auditory cortex seems to be smaller than shown in the classical maps of Brodmann (1909) and von Economo and Koskinas (1925). Galaburda and Sanides' (1980) temporal koniocortex (primary auditory cortex) shows also a much greater rostrocaudal extent compared with Braak's (1978) granulous core field. However, a considerable intersubject variability in size and shape of the transverse gyrus (gyri) must be considered (Leonard *et al.*, 1998; Penhune *et al.*, 1996; Steinmetz *et al.*, 1989; Thompson *et al.*, 1996). This makes a straightforward comparison between different maps difficult. Moreover, the maps of Brodmann (1909), von Economo and Koskinas (1925), and Braak (1978) do not allow—because of their schematic two-dimensional representation—a reliable spatial transformation into a common reference brain or stereotaxic system.

Recently, Morosan *et al.* (2001) and Rademacher *et al.* (2001a, b) published a cytoarchitectonic map of the primary auditory cortex. Because their maps are transformed into a three-dimensional reference system, the intersubject variability of this cortical area was defined by presenting probability maps, and the auditory function of the subareas could be corroborated using functional imaging (Johnsrude *et al.*, 2000). Most importantly, Morosan *et al.* (2001) and Rademacher *et al.* (2001a, b) demonstrated that the borders of the

cytoarchitectonicly defined primary auditory cortex cannot be assigned reliably to macroscopicly visible landmarks of the Heschl gyrus. Because this lack of coincidence between the borders of architectonic areas and macroscopic landmarks was found also in other cortical regions (Amunts *et al.*, 1999, 2000b; Geyer *et al.*, 1996, 1997, 1999, 2000b; Rademacher *et al.*, 1992; Roland and Zilles, 1996b, 1998; Zilles *et al.*, 1995, 1996, 1997), this finding seems to be a general caveat for any attempt to infer the position of cytoarchitectonic borders from macroscopic landmarks.

In contrast to Brodmann (1909), other authors identified two or more areas representing the primary auditory cortex (Economo and Koskinas, 1925; Galaburda and Sanides, 1980; Morosan *et al.* 2001; Rivier and Clarke, 1997; Sarkissov *et al.*, 1955). Morosan *et al.* (2001) subdivided their primary auditory area Te1 (equivalent to Brodmann's area 41) into the three subareas Te1.1 (caudomedial), Te1.0 (central), and Te1.2 (rostrolateral) (Fig. 27.24) using an observer-independent, quantitative cytoarchitectonic technique (Schleicher *et al.*, 1999). The functional meaning of this parcellation of the primary auditory cortex remains to be elucidated. The area Te1.0 shows the cytoarchitectonic features of the koniocortex (Fig. 27.25a), which is typical for primary sensory areas.

Secondary auditory cortex (belt region) Brodmann's (1909) area 42 (Fig. 27.35) and von Economo's and Koskinas's (1925) area TB (Fig. 27.37) are the putative architectonic correlates of the secondary auditory cortex. Area 42 is less granular (clearly visible but less densely populated and smaller layer IV; see Fig. 27.25b) when compared with area 41. In comparison to the adjoining area 22, area 42 is characterized by a higher cell density of layer II, a smaller layer IIIc, a more prominent layer IV, and a sharper layer VI/white matter boundary. Area 42 of Brodmann (1909) has correlates in the maps of Braak (1978) and Galaburda and Sanides (1980), which are named as pro- and parakoniocortical areas. Braak's (1978) pro- and parakoniocortical areas (putative secondary auditory cortex) surround completely the core field (putative primary auditory cortex). Area 42 (and area 22) represent phonological representations of words (Binder *et al.*, 1994; Howard *et al.*, 1992; Price and Giraud, 2001).

Stimulation by longer sound durations leads to an activation of a field in the most lateral part of the Heschl gyrus, which may correspond at least to parts of Brodmann's area 42 or the parakoniocortical field of Rivier and Clarke (1997). This field shows a mirror tonotopic organization (mediolateral low- to high-frequency gradient; Engelien *et al.*, 2002) compared with the primary auditory cortex (latero-medial low- to high-frequency gradient).

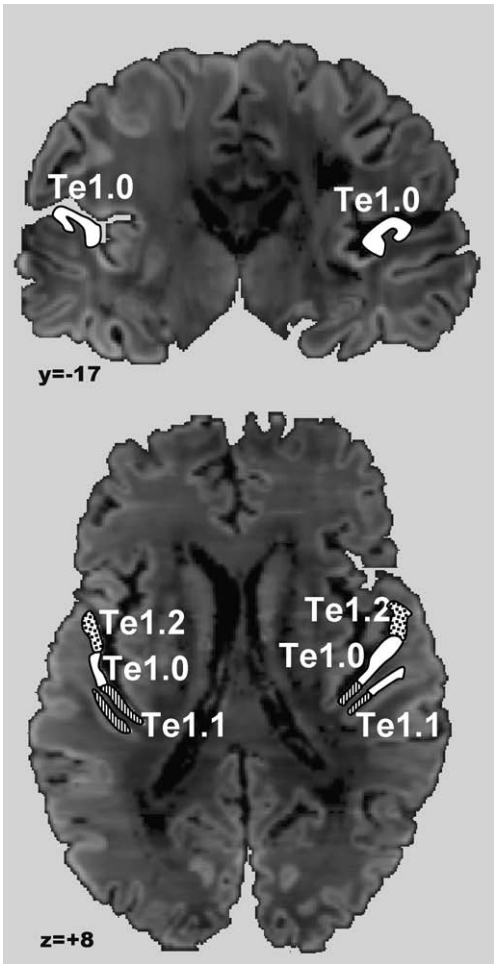

FIGURE 27.24 Areas Te1.2, Te1.0, and Te1.1 of the human primary auditory cortex Te1 on the Heschl gyrus in coronal *(upper part)* and horizontal *(lower part)* sections after spatial normalization to the corresponding postmortem magnetic resonance images (after Morosan *et al.*, 2001). Using the reference brain of the Human Brain Atlas (Roland and Zilles, 1996b, 1998) corresponding Talairach coordinates are calculated. The borders of the areas were identified (Morosan *et al.*, 2001) in cell body-stained sections using a quantitative cytoarchitectonic method (Schleicher *et al.*, 1999).

Further unimodal auditory areas The homotypic isocortical area 22 of Brodmann (1909) is found adjacent to the secondary auditory cortex (area 42) on the posterior two thirds of the superior temporal gyrus up to the beginning of the vertical branch of the lateral fissure. Most rostrally, area 22 is bordering the areas 41 and 52 (see Fig. 89 in Brodmann, 1909). The superior temporal gyrus processes phonologic word forms (Booth *et al.*, 2002). The neurons of the anterior and central parts of area 22 seem not to respond readily to

pure tones but are preferably responsive to specific phonetic parameters (Zatorre *et al.*, 1994) at a presemantic level because they are active both during exposition to meaningful words and to nonsense words (Creutzfeld *et al.*, 1989). Thus, the major part of this area is a higher order, but unimodal auditory cortex. Consequently, at least its rostral two thirds should not be lumped together with the posteriorly adjoining Wernicke region, which is a multimodal association cortex subserving complex language functions. In conclusion, at least the major part of area 22 constitutes together with the areas 41 and 42 the functionally defined human auditory cortex. This was already implicitly postulated by Brodmann (1909) on the basis of his microscopic observations. He stated that the cytoarchitecture of area 22 differs clearly from that of the isocortical areas 21 and 20 and the paralimbic (Mesulam, 1998) temporopolar area 38 and is more similar to that of the auditory areas 41 and 42.

Recent own quantitative cytoarchitectonic observations (Morosan *et al.*, unpublished) and studies of the regional distribution of transmitter receptors argue for further subdivisions of area 22. Area Te 3 (Fig. 27.25b) is found at the lateral border of the secondary auditory cortex. Te 3 is only a part of area 22, which seems to be a complex of several higher order auditory areas. This would correspond to the situation in the visual cortex provided by recent parcellations of Brodmann's area 19 into various functionally and architectonically definable higer order unimodal visual areas in the human brain (for review Zilles and Clarke, 1997). For a comprehensive description of the auditory system, see Chapter 34.

Wernicke Region

The free surface of the cortex on the superior temporal plane caudal to the first transverse gyrus and extending to the end of the lateral (Sylvian) fissure is defined as *planum temporale*. The left planum was found to be larger than its equivalent in the right hemisphere in most cases of a large human sample (Galaburda *et al.*, 1978a, b; Geschwind and Levitsky, 1968; Steinmetz *et al.*, 1989). Von Economo and Horn (1930) interpreted this gross anatomic asymmetry as a larger extent of the left auditory "association" cortex. Steinmetz *et al*. (1991) analyzed this asymmetry and its relation to handedness in 26 right and 26 left handers using magnetic resonance imaging. A correlation with handedness was found; a left-over-right asymmetry could be registered for the whole sample, but it was less strongly expressed in left handers compared with right handers. Thus, the overall left-over-right asymmetry has been interpreted as a morphological substrate for language lateralization.

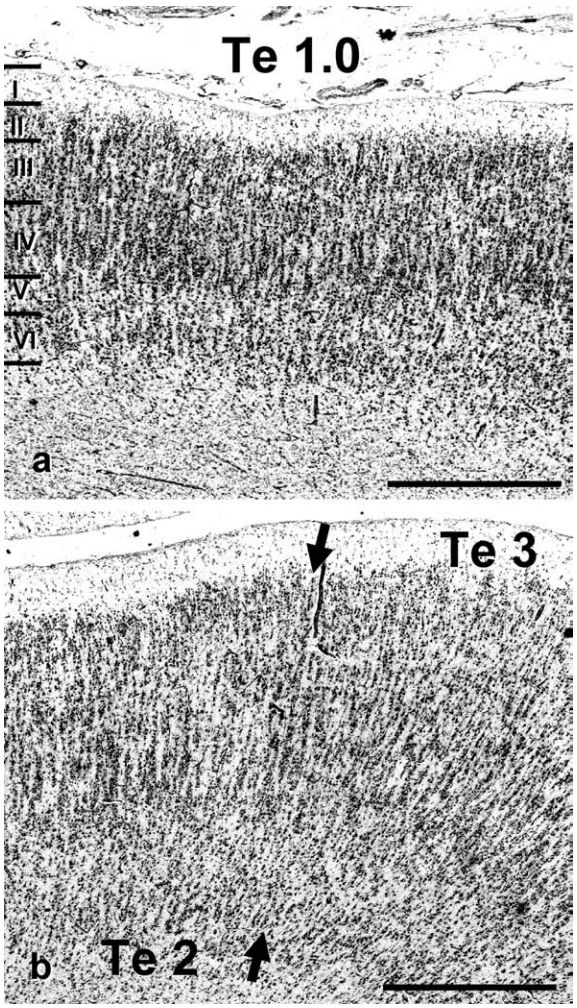

FIGURE 27.25 Cytoarchitecture of the primary auditory area Te 1.0 (a), secondary auditory area Te 2 (b), and surrounding unimodal sensory cortex Te 3 (b). This parcellation is based on a quantitative cytoarchitectonic study by Morosan *et al.* (2001). Bars = 1 mm.

The precise position of the architectonic borders of Wernicke's region (Wernicke, 1874), however, is presently not known. This multimodal language area covers at least the planum temporale of the superior temporal gyrus (Aboitiz and Garcia, 1997; Grabowski and Damasio, 2000). Thus, this area is commonly related to the most posterior part of area 22 (Brodmann, 1909), to area TA_1 of von Economo and Koskinas (1925), or to area Tpt (Galaburda and Sanides, 1980). Tpt (Fig. 27.26) includes posterior and lateral temporal regions in which lesions cause Wernicke's aphasia. Tpt was larger on the left side in all four cases measured (Galaburda *et al.*, 1978a) with relative differences between both sides showing an enormous variability between 14 and 626%.

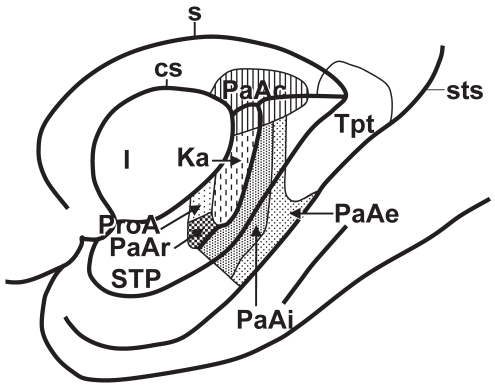

FIGURE 27.26 Areal map of the temporal lobe (lateral view, with a schematic opening of the insula) based on the cytoarchitectonic observations of Galaburda and Sanides (1980). cs, circular sulcus; I, insular cortex; Ka, koniocortex; PaAc, caudal parakoniocortex; PaAe, external parakoniocortex; PaAi, internal parakoniocortex; PaAr, rostral parakoniocortex; ProA, prokoniocortex; s, Sylvian fissure; STP, superior temporal plane; sts, superior temporal sulcus; Tpt, temporoparietal area.

Braak (1978) delineated magnopyramidal regions laterally adjoining the belt region of his auditory cortex (mb and mc in Figure 27.23). The most conspicuous indicators of this magnopyramidal temporal area are the large pyramidal cells in the lower part of layer III. Braak (1978) considers this field to represent the structural basis of the sensory speech region of Wernicke. The magnopyramidal area is surrounded by three isocortical areas on the rostromedial ("area temporalis simplex"; s in Figure 27.23), rostrolateral ("area temporalis magna"; m in Fig. 27.23), and posterolateral sides ("area temporalis stratiformis"; str in Fig. 27.23).

In contrast to area 42 (see previous discussion), the cortex resembling most probably the core of the Wernicke region has a rather cell-sparse layer II. The pyramidal cells of layers IIIc and V are of prominent size and density. The size of layer IIIc pyramidal cells seems to be increased compared with area 42. Layer IV is rather thin. The putative Wernicke region is separated from the neighboring area on the ventral wall of the superior temporal sulcus, which has a rather conspicuous cell layer II, a "cluster-like" arrangement of medium-sized IIIc pyramidal cells, a small layer IV, and rather cell-dense layers V and VI. Posteriorly, the here-described putative homologue of Wernicke's region borders the supramarginal cortex. The cytoarchitecture of this cortex is characterized by smaller and less densely packed pyramidal cells in layer IIIc, a small layer IV, and rather cell-dense layers V and VI.

The classical myeloarchitectonic maps (Beck, 1930; Hopf, 1954, 1955; Vogt and Vogt, 1919) indicate that a posterior part of Brodmann's area 22 may contribute to Wernicke's region. The putative myeloarchitectonic homologue of Wernicke's region is the area tpartr.p of Hopf (1954). This area is characterized by relatively densely packed myelinated fibers, the lack of the Kaes-Bechterew stripe (Fig. 27.21), and darkly stained outer and inner Baillarger stripes, which seem to merge to one broad stripe. In contrast, the auditory belt region has a lower fiber density than the Wernicke region, especially in layer III.

Inferotemporal Zone

The inferotemporal zone consists (in dorsoventromedial sequence) of the areas 21, 20, and 36 (Brodmann, 1909). Brodmann's area 37 is located as a transition region between the temporal, parietal, and occipital lobes (Fig. 27.35) and is included here as further part of the inferotemporal zone.

Parts of these four areas belong to the multimodal association cortices; other parts are members of the higher order unimodal visual and auditory cortices (Mesulam, 1998). Brodmann's middle temporal area 21, inferior temporal area 20, and occipitotemporal area 37 are characterized by the six-layered homotypical isocortex, whereas area 36 is found on the parahippocampal gyrus at the transition between the iso- and allocortex and shows some typical cytoarchitectonical modifications of the homotypical isocortex (see following discussion), which may justify the classification of at least parts of this area as proisocortex.

The cortex of areas 20 and 21 is very thick (3.0–3.8 mm according to von Economo and Koskinas, 1925), nearly as wide as the motor cortex. Layer III is relatively small, and its cell-packing density is very low. Layer IV is also very thin, and the cells are arranged in clearly visible vertical columns. In contrast to these more superficial layers, the deeper layers V and VI are very wide. Layer V contains conspiciously large pyramidal cells. Because areas 20 and 21 are difficult to separate by cytoarchitectonic criteria, von Economo and Koskinas (1925) classified both areas as one cortical region, their regio temporalis propria TE. The only criterion for a parcellation of this region into the subareas TE_1 and TE_2 seems to be the somewhat larger size of the pyramidal cells in layer III of TE_1 compared with TE_2. Equivalencies with the cortical terminologies of other authors are given in Tables 27.4 and 27.6.

Brodmann's ectorhinal area 36 (Fig. 27.35) is not only poor in myelinated fibers, but also shows a lower overall cell packing density compared with the adjacent isocortical area 20. The prominent appearance of large neurons in layers V and VI justifies the distinction of parts of area 36 as proisocortex from the other homotypical isocortical areas of the inferotemporal zone.

According to classical (von Economo and Koskinas, 1925) and more recent architectonic and functional imaging studies (for review Zilles and Clarke, 1997), Brodmann's area 37 is not a homogeneous cortical area. Some parts of area 37 are probably multimodal (Mesulam, 1998); others are higher order unimodal visual areas (e.g., V5/MT; see "Occipital Lobe"). It should be mentioned here that the fusiform gyrus, which contains parts of area 37 (and area 19), also displays orthographic representations of words (Fujimaki *et al.*, 1999; Nobre *et al.*, 1994; Petersen *et al.*, 1990). On the lateral cortical surface, area 37 covers the posterior parts of the middle and inferior temporal gyri and the anterior parts of the middle and inferior occipital gyri. The preoccipital incisure marks the center of area 37 at the border between the lateral and basal surface of the hemisphere. On the basomedial surface, area 37 covers the posterior part of the inferior temporal gyrus and reaches the lingual, fusiform, and parahippocampal gyri. Thus, area 37 is a region approximately comparable to the area paratemporalis of Smith (1907) (Fig. 27.34) and the area PH of von Economo and Koskinas (1925) (Fig. 27.37; Table 27.7). This area consists of small radial cell columns in layers III and IV, a narrow layer IV, and hardly delineable layers V and VI caused by relatively small cells in layer V and, thus, similar cell sizes in both layers. PH shows a sharp border between cortex and white matter. Von Economo and Koskinas (1925) emphasize that the cytoarchitecture of PH is not homogenous. It displays characteristics of the temporal, parietal, and occipital cortices depending on the region of interest within PH. Larger pyramidal cells are visible in the temporal and occipital parts of PH compared to the parietal part.

The isocortex on the medial temporal gyrus (approximately Brodmann's area 21) of the dominant hemisphere participates in short-term verbal memory (Ojemann *et al.*, 1987), verbal fluency and word generation (Petersen *et al.*, 1988; Frith *et al.*, 1991; Wise *et al.*, 1991), and tone and rhythm discrimination (parts of areas 21 and 22) as well as the ability to listen to stories (parts of areas 21 and 22) (Mazziotta *et al.*, 1982).

Parts of area 20 on the inferior temporal gyrus and at least the parts of area 37 on the fusiform gyrus belong to the "ventral stream" (Ungerleider and Mishkin, 1982; Mishkin *et al.*, 1983) of the visual cortex. Area 20 is active during imagery of route finding (Roland *et al.*, 1987). The parahippocampal gyrus (containing area 36), and the fusiform gyrus (containing parts of area 20) are found to be activated by attention to shape (Corbetta *et al.*, 1990).

In conclusion, the inferotemporal zone of the human cerebral cortex—as defined here—is a region where auditory, language, visual, and multimodal functions are represented (Nakamura *et al.*, 2000). This high degree of functional segregation supports the assumption of a parallel, much more differentiated architectonical segregation in this zone than presently shown by the available maps with only four areas (i.e., areas 20, 21, 36, and 37).

Occipital Lobe

The occipital lobe of the human brain contains most of its visual cortical areas, but visual areas are also found in the temporal and parietal lobe (see earlier discussion). These visual areas together constitute more than half of the human isocortex. This large size of the anatomical correlates reflects the importance of visual functions in the human brain.

A tripartition of the occipital lobe was proposed by Brodmann (1909) with area 17 as the primary visual cortex V1 and areas 18 and 19 as unimodal higher visual fields (Fig. 27.35). Comparable parcellations were

TABLE 27.7 Architectonic Subdivisions and Nomenclature of the Human Striate and Extrastriate Visual Cortex.

	Striate cortex	Extrastriate cortex	
Campbell (1905)	Visuo-sensory	Visuo-psychic	
Brodmann (1909)	Area 17	Area 18	Area 19
Smith (1907)	Area striata	Area parastriata	Area peristriata
Vogt and Vogt (1919)	Area 17	Area 18	Area 19 (19a, 19b)
Flechsig (1920)	Area 8	Area 23	Areas 15, 16, and 28
von Economo and Koskinas (1925)	OC	OB (OBγ; OBΩ)	OA (OA_1, OA_2, OA_m)
Filimonoff (1932–3)	Area 17	Area 18	Area 19
Bailey and von Bonin (1951)	Koniocortex	Parakoniocortex	
Sarkissov *et al.* (1955)	Area 17	Area 18	Area 19
Braak (1977–80)	Striate area	Parastriate area	Peristriate area

published by von Economo and Koskinas (1925; Fig. 27.37), Filimonoff (1932), and Sarkissov *et al.* (1949; Fig. 27.39). Von Economo's and Koskinas's area OC (Area striata) corresponds to Brodmann's area 17, their OB (Area parastriata) to area 18, and OA (Area peristriata) to area 19 (for further comparisons between the nomenclatures of different authors, see Table 27.7). Area 19 has been parcellated into numerous areas by Braak (1977) on the basis of pigmentoarchitectonic studies in the human brain. The borders of these areas exceed, however, the limits of the occipital lobe and extend into the parietal and temporal lobes (Fig. 27.27). Unfortunately, these areas cannot be directly compared with functional data because the schematic drawing of this areal pattern (Braak, 1977) cannot be warped to a stereotaxic system as used for anatomical identifications in functional imaging studies.

Brodmann's (1903b, 1909) architectonic and functional definition of area 17 is unanimously accepted. Also the location of a cytoarchitectonic area corresponding to area 18 of Brodmann (1909) could be corroborated in a recent quantitative cytoarchitectonic study (Amunts *et al.*, 2000b), which also provides an analysis of the intersubject variability of its borders. Brodmann's parcellation of the most rostral part of the visual cortex (his area 19), however, is not supported by axonal tracing and electrophysiological studies in nonhuman primates (for a recent map of the macaque occipital cortex, see Paxinos *et al.*, 2000) and does not match the results of functional imaging in the human brain (for review, see Zilles and Clarke, 1997). Therefore, it is not justified by our present knowledge to use the term "area 19" for a cortical region that is definitely not an architectonic and functionally homogeneous field. Brodmann's area 19 as well as adjacent cortical regions must be subdivided (Braak, 1980; Tootell *et al.*, 1998; van Essen, 1979; Zeki, 1969) into numerous visual areas differing in architecture and functional properties (e.g., retinotopy, direction and orientation selectivities, contrast sensitivity, motion and color preferences, and many more functional aspects; as an example of a proposed scheme, see Fig. 27.28).

Primary Visual Cortex

Area 17 of Brodmann (1903b, 1907, 1909, 1910, 1912) represents the primary visual cortex (Fig. 27.35). It extends from the occipital pole over the total length of the calcarine sulcus, and is the cortical representation of the entire contralateral visual hemifield plus a smaller part of the ipsilateral hemifield. The largest

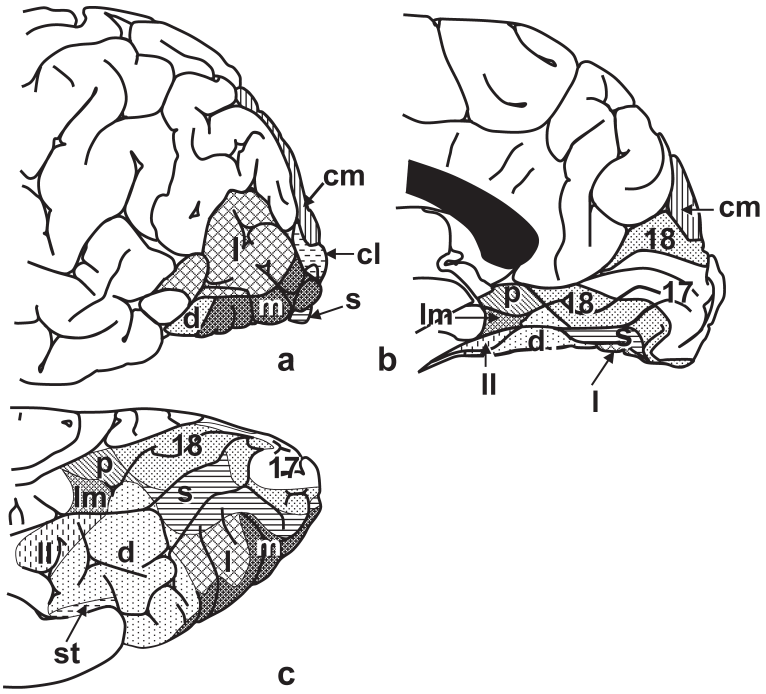

FIGURE 27.27 Areal map of the occipital lobe based on the pigmentoarchitectonical observations of Braak (1977). **(a)** Lateral, **(b)** medial, and **(c)** basal views. cm, Area peristriata cunealis medialis; cl, area peristriata cunealis lateralis; d, area peristriata densopyramidalis; l, area peristriata latopyramidalis; ll, area peristriata limitans lateralis; lm, area peristriata limitans medialis; m, area peristriata magnopyramidalis; p, area properistriata; s, area peristriata simplex; st, area peristriata stratiformis; 17, area 17; 18, area 18.

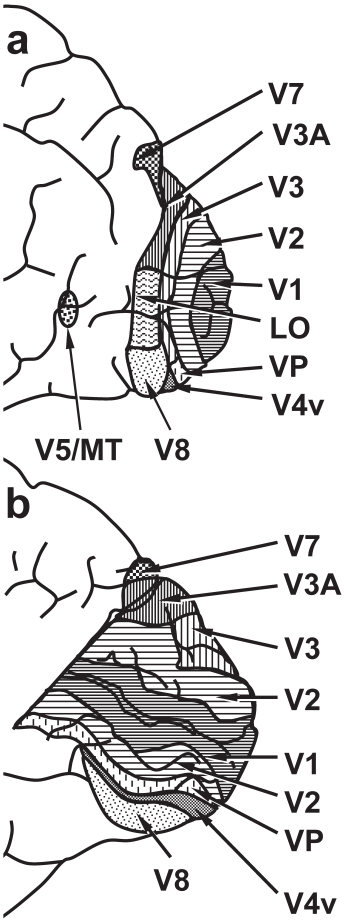

FIGURE 27.28 Areal map of the human visual cortex adopted from Tootell *et al*. (1998). **(a)** Lateral and **(b)** medial views.

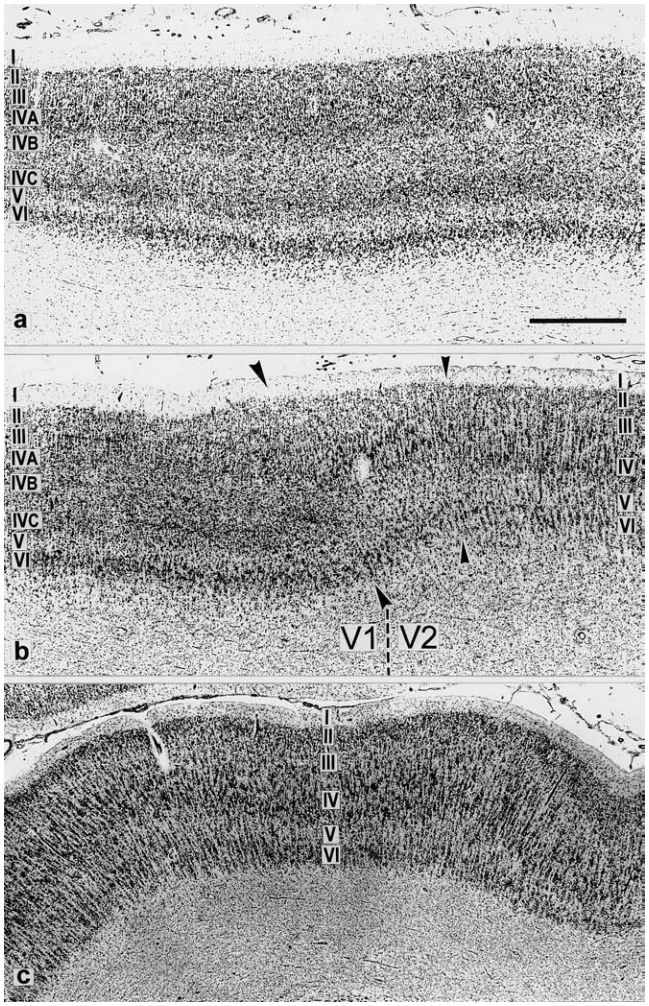

FIGURE 27.29 Cytoarchitecture of area 17 **(a, b),** 18 **(b)** and the most posterior part of area 19 **(c).** Roman numerals indicate the different layers. The large arrowheads in (b) mark the border between the areas 17 (V1) and 18 (V2). Immediately adjacent to the 17/18 border, the limes parastriatus gigantopyramidalis of von Economo and Koskinas (1925) is visible (small arrowheads). This part of area 18 contains very large pyramidal cells in the lower layer III. Bar = 1 mm.

portion of area 17 receives input from both eyes (binocular part) with the central part of the visual field at the occipital pole. The upper half of the visual field is represented in the lower wall of the calcarine sulcus and adjacent parts of the cortical surface, whereas the lower half is projected to the upper wall and adjacent parts of the cortical surface. Thus, the horizontal meridian is located in the fundus of the calcarine sulcus. The vertical meridian is located at the border between areas 17 and 18.

Area 17 shows the most differentiated laminar structure of all isocortical areas in the human brain (Fig. 27.29a, b). Human area 17 is characterized by a prominent, tripartite layer IV (sublayers IVA–C). Even these sublayers can be further subdivided. The parvocellular afferents from the lateral geniculate body reach their highest density in sublayer IVCβ (Braak, 1982). Layers III and V contain (beside the pyramidal cells) numerous small neurons, which leads to the visual impression of an extremely high "granularization" of the koniocortical area 17. Layer V is easily distinguishable from the dark layer VI. Further details of the highly differentiated laminar structure of human area 17, ultrastructure, ontogeny, and quantitative aspects have been described by E. Braak (1982), H. Braak (1976b, 1977), Brodmann (1903b), von Economo and Koskinas (1925), Filimonoff (1932), Garey (1984), Haug (1958), Horton and Hedley-White (1984), Preuss *et al*. (1999), Preus and Coleman (2002), and Zilles *et al*. (1986a). The high intersubject spatial variability of the borders of area 17 has been studied by Filimonoff (1932) and Amunts *et al*. (2000b; see Fig. 27.30). For comprehensive information about the visual system, see Chapter 35.

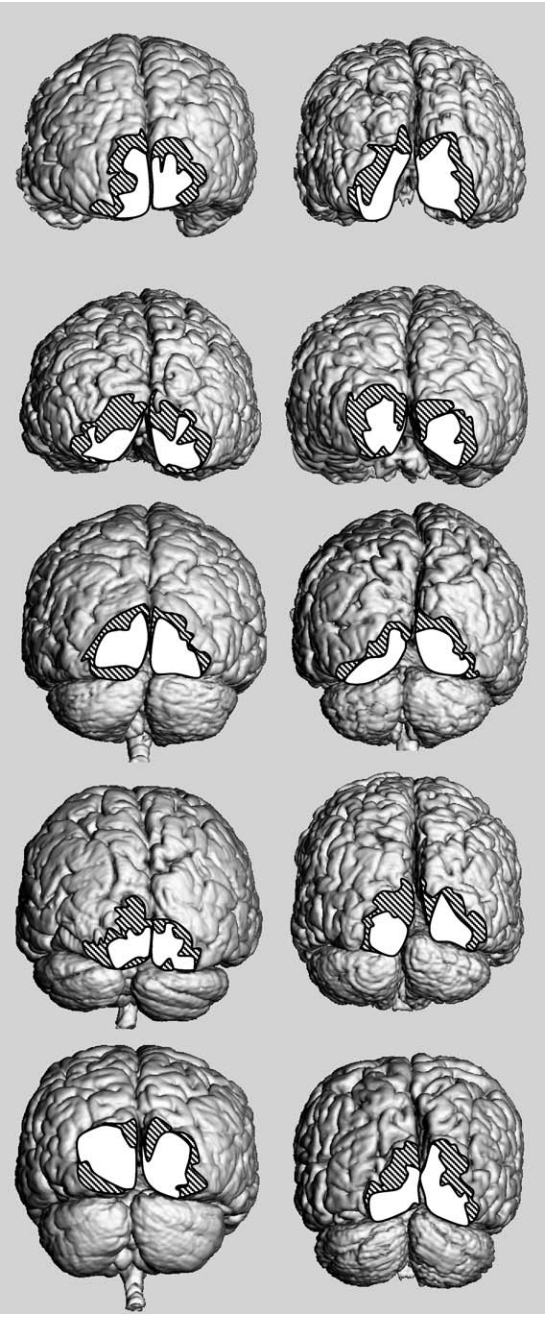

FIGURE 27.30 Intersubject variability of the primary visual cortex V1 (Brodmann's area 17) and the secondary visual area V2 (Brodmann's area 18) in ten human brains (modified from Amunts *et al.*, 2000b). V1, white area, V2, hatched area.

A comparison of area 17 with that of other nonhuman primates clearly demonstrates that the human primary visual cortex is architectonicly not the most evolved example within primates. The lamination pattern of layer IV, the major target of the retinal input via the lateral geniculate body, is much more differentiated in the prosimian *Tarsius* (Zilles *et al.*, 1982) and the areal proportions of area 17 on the total neocortex of this species exceeds that of humans by nine times (Stephan *et al.*, 1981). Also, all the other nonhuman primates have larger striate areas relative to the total neocortex. By controlling for body weight, however, Stephan (1969) showed that the human area 17 is enlarged by somewhat more than five times when compared with the prosimian *Lepilemur,* which has the smallest area in such allometric comparisons. A morphometric study in human, chimpanzee, gorilla, and orangutan (Zilles and Rehkämper, 1988) reveals no major differences in laminar pattern of the striate areas between us and our nearest relatives.

The neuropil volume of area 17, however, is much larger in the supragranular layers, in which a major part of intracortical processing takes place, in the human than in any other primate brain, including *Tarsius* (Zilles *et al.*, 1982). This dominance of the neuropil proportion in the supragranular layers is also found in extrastriate visual areas of the human brain. The human specific evolution of the primary visual cortex becomes even more evident when analyzing the termination of the magno- and parvocellular compartments of the geniculocortical input in specific layers of V1. Layer IVA of New World and Old World monkeys is characterized by a thin cytochrome oxidase-rich band in layer IVA, which is caused by parvocellular terminals (Wong-Riley, 1994). Humans and chimpanzees lack this band in layer IVA of V1 (Horton and Hedley-White, 1984; Preuss *et al.*, 1999). In contrast to nonhuman primates, human layer IVA shows a conspicuous immunoreactivity of antibodies against nonphosphorylated neurofilaments (NPNF) and an extracellular proteoglycan distributed in meshlike bands, as well as a dense irregular staining of calbindin (indicating most probably the presence of GABAergic inhibitory interneurons) in the territories between the meshlike bands of layer IVA (Hendry and Carder, 1993; Preuss and Coleman, 2002; Preuss *et al.*, 1999). Because the NPNF and the antibody-specific matrix proteoglycan are preferentially or exclusively expressed in the magnocellular pathway (Hof and Morrison, 1995; Preuss and Coleman, 2002; Preuss *et al.*, 1999), a considerable reorganization of the magno- and parvocellular pathways in human layer IVA occurs during the evolution of the human brain compared with monkeys and apes.

The border between areas 17 and 18 is very distinct, and its cyto- and myeloarchitecture displays some interesting specializations. A very myelin-dense layer (stripe of Gennari) occurs only in area 17 and stops abruptly at the border between area 17 and area 18 (Fig. 27.31a). At this site, layer IV of area 17 becomes

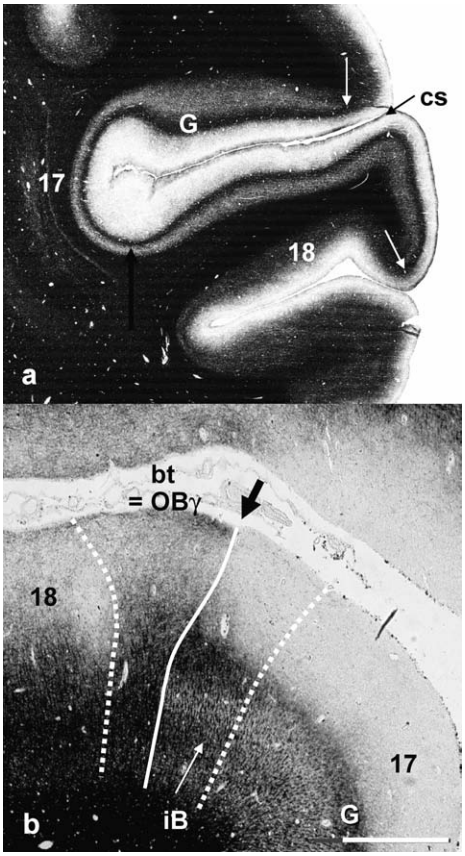

FIGURE 27.31 Myeloarchitecture of the human visual cortex at the border region between area 17 and area 18. The myeloarchitecture of area 17 is characterized by the prominent stripe of Gennari **(a). (b)** shows the various myeloarchitectonic changes at the border region. bt, border tuft; cs, calcarine sulcus; G, stripe of Gennari; iB, inner stripe of Baillarger; OBg, limes parastriatus gigantopyramidalis of von Economo and Koskinas (1925). The white arrows and the large black arrow indicate the border between area 17 and area 18. Bar = 1 mm.

considerably thinner, and the subdivision of layer IV into three sublayers A–C stops abruptly at the border to area 18 (Fig. 27.29b). A small zone with a very light layer V is found at the beginning of area 18. The neurons in this zone of area 18 are less densely packed than in the remaining part of this area. Layer IV is the broadest layer in area 17, but layer III is the most prominent layer in area 18. The packing density of cell bodies is generally higher in area 17 when compared with area 18. Thus, more space for dendrites, axons, and synapses is available in area 18 than in area 17. The border region between areas 17 and 18 is characterized myeloarchitectonicly by two small subareas (Lungwitz, 1937; Sanides and Vitzthum, 1965a, b)—one belongs to area 17 and the other to area 18. The "border tuft" subarea ("Grenzbüschel") of Sanides and Vitzthum (1965a, b) contains a distinct bundle of densely packed radial fibers (bt in Figure 27.31 b) and belongs to area 18. Very large pyramidal cells, "giant cells," are visible in layer III of this subarea. Thus, the border tuft subarea corresponds to area OBγ (Fig. 27.29b) as described by von Economo and Koskinas (1925), and adjoins a small subarea ("Randsaum") of Sanides and Vitzthum (1965a, b), which belongs to area 17. This subarea is characterized by the appearance of the inner Baillarger stripe (iB in Figure 27.31b), which is only found in this border zone, but not in the major part of area 17. The border region of area 17 with the conspicious inner stripe of Baillarger and the bt region of area 18 together are probably the architectonic correlates of the representation of the vertical meridian. This zone is the target of many callosal fibers and bridges equivalent points of the visual field on both sides of the vertical meridian in areas 17 and 18 (Clarke and Miklossy, 1990; Shoumura *et al.*, 1975; Van Essen and Zeki, 1978; Zeki, 1970; see also Chapter 35). Thus, the visualization of callosal axonal terminals provides useful landmarks for the delineation of extrastriate areas because callosal fibers are concentrated in border regions of many visual areas (Clarke and Miklossy, 1990; Van Essen *et al.*, 1982).

Layer IV of the primary visual cortex (V1) receives its major retinal input via the lateral geniculate body and the geniculocortical fibers (optic radiation). V1 projects (as shown in monkeys; e.g., Felleman and Van Essen, 1991; Van Essen *et al.*, 1986) to many extrastriate areas (V2, V3, V3A, V4, V5/MT, MST). The majority of projections terminate in V2, V3, and V5/MT. Layer V neurons of V1 give rise to connections projecting back through the superior colliculus and pulvinar to the parastriate belt (Trojanowski and Jacobson, 1976; for review, see Van Essen, 1979). Back projections from extrastriate visual areas to V1 establish together with the forward projections a complex system of reciprocal connectivity. Mostly reciprocal connections exist also between V1 and various subcortical regions (e.g., pulvinar, claustrum, amygdala, caudate nucleus, superior colliculus, pons, hypothalamus, and basal forebrain). Only a very small part of the afferents from the pulvinar projects to layers I and II of V1 (for review of the connectivity of the visual cortex in macaque monkeys, see Felleman and Van Essen, 1991).

Extrastriate Visual Cortex

The visual areas outside the striate area 17 (i.e., the extrastriate areas) have been subdivided by Brodmann (1905, 1909, 1910, 1912) into areas 18 and 19 (see Fig. 27.35). Many of the classical architectonical studies have proposed a comparable subdivision (cf. Tables 27.4 and 27.7), but more recent morphological and physiological observations have clearly demonstrated

a much higher number of cortical areas, particularly in the region of area 19 (see previous discussion). Thus, the frequently used and functionally based nomenclature of the visual areas (subdivisions into V1, V2, V3, etc.) is introduced here, whenever the comparability between functional and architectonic parcellations is demonstrated or highly probable.

Area V2 Area 18 of Brodmann (1909) is comparable with the functionally defined cortical field V2 (Fig. 27.28). It is a 10–3.4 cm wide cortical belt rostral to V1, and its surface is 1.7 times larger than that of V1 (Tootell and Taylor, 1995). The representation of the visual field in area 18 differs from that in area 17, where adjacent loci of the visual field are also located as neighboring sites in V1. In area 18, the horizontal meridian is located at the 18/19 border; this topological transformation leads to representation of the upper and lower quadrants of the visual field in separate, not adjacent, cortical places. Also, the normal point-to-point mapping of the visual field in the cortex is disrupted in area 18 (for review, Tootell *et al.*, 1998).

V2 shows a homotypical lamination pattern (six layers). Layer II and the upper part of layer III are difficult to separate in V2. The size of the pyramidal cells of lower layer III is increased compared with V1 (Clarke, 1994b). Very large cells in deep layer III are frequently found in the border region to V1 (Fig. 27.29b, c). The contrast in cell density between layers V and VI is not as distinct as in V1. Layer IV of V2 is slightly thinner than in V1, but it is thicker than in the other visual areas. The radial arrangement of cells in columns increases from V1 to V2 and from here to the other visual areas.

In contrast to the clear borderline between V1 and V2, the cytoarchitectonic border between V2 and the rostrodorsally adjoining area V3 is very difficult to detect by pure visual inspection of cell body-stained sections. Recently, this border could be reliably identified using a quantitative cytoarchitectonic technique, and the microstructural differences between V2 and V3 were statistically verified (Amunts *et al.*, 2000b). Staining of lipofuscin granules (pigmentoarchitectonic method) may also provide a reliable definition of this border as demonstrated by Braak (1977). According to the latter author, the border between area 18 and the peristriate region is defined by the unique appearance of pigmented "granule" cells in a small stripe in a position comparable with the central part of layer IV. This stripe is only visible in V2.

V2 is rostrolaterally bordered by VP in the inferior part of the occipital cortex (Fig. 27.28). VP shows a lighter myelin staining compared with V2 (Clarke, 1994b; Clarke and Miklossy, 1990; Zilles and Schleicher, 1993). A clearly visible inner Baillarger stripe is a further myeloarchitectonic sign of V2 (Clarke, 1994b). In flattened myelin-stained sections of human V2, alternating dense and light stripes are visible, and the respective stripes have a distance of 6–8 mm (Tootell and Taylor, 1995). These dark or light stripes in myelin-stained sections are not compatible in size and distance with the stripes and interstripes visible in cytochrome-oxidase (COX)-stained sections (Burkhalter and Bernardo, 1989; Hockfield *et al.*, 1990). The modular architecture of V2 visualized by the alternating pattern of COX-stripes and interstripes has also been found in nonhuman primates (DeYoe and Van Essen, 1985; Horton, 1984; Hubel and Livingston, 1987; Livingstone and Hubel, 1983; Tootell and Hamilton, 1989; Tootell *et al.*, 1993; Wong-Riley, 1994) where the COX-rich stripes are parvalbumin positive compartments (Blümcke and Celio, 1992). The thick COX-stripes of area V2 show a conspicuous immunoreactivity of the antibody Cat-301 against an extracellular matrix proteoglycan (Hendry *et al.*, 1984, 1988; Hockfield *et al.*, 1990). This proteoglycan is indicative of the magnocellular pathway of the human visual system. It is also present in the magnocellular layers of the lateral geniculate body, layer IVA of V1 (see earlier), and in area V5/MT (see later).

Area 18 receives massive input from area 17 and has reciprocal connections with many extrastriate areas. Layers III and IV of area 18 and other extrastriate areas receive also a major input from the pulvinar. The reciprocal connections from the extrastriate visual areas to the pulvinar originate in layer V (for review, see Felleman and Van Essen, 1991). Cells in layer VI of area 17, 18, and further extrastriate areas give rise to a pathway descending to the lateral geniculate body.

Over 70% of the cells in V2 of macaques are orientation selective, but only less than 15% are directionally selective, and only 8% have opponent color properties (Van Essen and Zeki, 1978; Zeki, 1978). It is difficult to get detailed information about the specific function of human V2 by older neuroimaging studies because the border between V1 and V2 as well as between V2 and V3 cannot be identified on the basis of macroscopic landmarks (Amunts *et al.*, 2000b). A reliable method, however, is now available, if the retinotopy is explored by functional imaging (Tootell *et al.*, 1998). Human V2 is activated during shape discrimination (Gulyás and Roland, 1994) by a task similar to illusory contour tasks, which reveal a V2 activation in monkeys (Peterhans and von der Heydt, 1989; von der Heydt and Peterhans, 1989). V2 and other extrastriate areas (not only V4, see following discussion) are activated by color discrimination tasks (Gulyás and Roland, 1991, 1994). V2 is also active during visual recall of real

objects (Le Bihan *et al.*, 1993). Thus, V2 is not just a region of simple perception, but it is also activated by complex perceptual, cognitive, and mnestic tasks (e.g., face and word processing; Halgren *et al.*, 1994).

Area V3 According to functional imaging studies (Sereno *et al.*, 1995; Tootell *et al.*, 1995a), area V3 is located dorsally and rostrally of V2 on the mesial and lateral surfaces of the occipital lobe, respectively (Fig. 27.28). The border between V3 and V2 represents the horizontal meridian. V3 contains the lower visual field (Tootell *et al.*, 1998).

Although it is problematic to compare the schematic drawings of classical cytoarchitectonic maps with functional imaging data, area V3 is best comparable by its location with the major part of the parvocellular posterior peristriate area O_{A_1} of von Economo and Koskinas (1925). O_{A_1} shows a very small layer I, layers II and III are difficult to separate, and layers III and V contain small pyramidal cells. Layer VI consists of particularly coarse cell columns. Nevertheless, the cyto- and myeloarchitectonic definition of the V2/V3 border by pure visual inspection is very difficult because of the high degree of microstructural similarity between both areas (Clarke, 1994b). Only recently using a quantitative cytoarchitectonic technique has this border been determined (Amunts *et al.*, 2000b).

Nearly all cells in extrastriate areas of monkeys are binocularly driven, and binocular depth cells are found in V2 and V3 (Poggio and Fischer, 1977). Most of the cells in monkey V3 are selective for orientation (Zeki, 1978). The role of human V3 in vision is not completely clear. Human V3 is less motion selective than V3 in macaques and V3A in humans (Tootell *et al.*, 1997). Dynamic form perception (Zeki and Shipp, 1988; Zeki, 1990a) and a high-contrast selectivity (Tootell *et al.*, 1995a) are functional characteristics of V3. This provides evidence for the classification of V3 as part of the magnocellular dorsal stream.

Area VP Human area VP is bordered posteriorly by V2 and dorsally by V3 on the lateral hemispheric surface, and medially by V2 on the mesial surface (Fig. 27.28). VP has been tentatively delineated by cyto- and myeloarchitectonic characteristics (Clarke and Miklossy, 1990; Zilles and Schleicher, 1993). It lacks large pyramidal neurons in both layers III and V, whereas adjacent V2 has large pyramids in layer III and adjacent area V4 in III and V. VP is lightly myelinated, and both striae of Baillarger are absent. VP differs also by its light COX staining from the adjacent, darkly stained areas V2 and V4 (Clarke, 1994a).

Human areas VP and V4 appear to be interconnected with the inferior part of medial pulvinar, while V5/MT is interconnected with the lateral pulvinar (see Table 6 in Zilles and Clarke, 1997).

Area V3A Human area V3A extends consistently below and above the lateral occipital sulcus (Tootell *et al.*, 1997) on the mesial and lateral hemispheric surface (Fig. 27.28). Its borders, however, as determined by retinotopic mapping show a considerable intersubject variability and cannot be reliably correlated with macroscopic landmarks. Sufficiently detailed architectonic descriptions of this area are presently not available.

Area V4 The cortex of the lingual and fusiform gyri seems to play an important role in color perception because lesions of this region cause achromatopsia (Damasio *et al.*, 1980; Meadows, 1974; Rizzo *et al.*, 1992; for review, see Zeki, 1990b), and functional imaging as well as electrophysiological observations demonstrate activation by color (Allison *et al.*, 1993; Corbetta *et al.*, 1991; Gulyás and Roland, 1991, 1994; Lueck *et al.*, 1989; Sakai *et al.*, 1995; Sereno *et al.*, 1995; Zeki *et al.*, 1991) and shape (Corbetta *et al.*, 1991). Thus, this region has been suggested to be the human correlate of the monkey V4, which is populated by color-, space- and shape-responsive neurons (Desimone and Schein, 1987; Desimone and Ungerleider, 1989; De Yoe *et al.*, 1994; Heywood *et al.*, 1992; Schiller and Lee, 1991; Van Essen and Zeki, 1978; Walsh *et al.*, 1993; Zeki, 1990b). Presently, however, it is controversly discussed whether this human V4 in the fusiform gyrus represents the equivalent of the monkey V4 (Heywood *et al.*, 1995; Meadows, 1974; Ungerleider and Haxby, 1994; Walsh *et al.*, 1993; Zeki, 1993).

This putative human V4 is located on the posterior part of the fusiform gyrus and abuts the rostral border of the putative human VP (Sereno *et al.*, 1995). The position and extent as well as the architecture of the area peristriata magnopyramidalis of Braak (1977) make this pigmentoarchitectonicly well-defined cortical region to an architectonic candidate for human V4. An area comparable to V4 has been called V8 by Tootell *et al.* (1998) (see also Fig. 27.28). V4 contains large pyramidal cells in layers III and V and shows a dark COX staining. Both criteria allow a delineation of this area from VP (Clarke, 1994a). The myelin density is well above average in human and monkey V4 (Zilles and Clarke, 1997).

A ventral area V4v—separable from V4—has been identified by using fMRI (Sereno *et al.*, 1995) and phase-encoded retinal stimulation. This area adjoins the ventral half of the anterior border of VP (Fig. 27.28). This border represents the vertical meridian, whereas the horizontal meridian is found at the anterior border

of V4v. Human V4v contains the upper visual field as in monkeys with a non–mirror image representation of the visual field. Architectonic descriptions of this area are presently not available.

Additional color foci were described on the human dorsolateral occipital cortex (Corbetta *et al.,* 1991). Colors as attributes of objects are also represented in a cortical region rostral to V4 (Martin *et al.,* 1995). A face and familiarity recognition area is identifiable medially of this region (Allison *et al.,* 1993, 1994; Clarke *et al.,* 1997; Nakamura *et al.,* 2000) in the posterior temporal part of the fusiform gyrus. This region is also activated by passive viewing of faces (Puce *et al.,* 1995) and by matching of unknown faces (Haxby *et al.,* 1994) in the right hemisphere, but is found more anterior and lateral in the left hemisphere. At least part of this left hemispheric region may be part of a cortical system representing working memory for faces (Haxby *et al.,* 1995).

Area V5/MT For the first time, area V5/MT was identified by functional and anatomical studies in the superior temporal sulcus of nonhuman primates (Albright, 1984; Allman and Kaas, 1971; Born and Tootell, 1992; Fiorani *et al.,* 1989; Maunsell and Van Essen, 1983, 1987; Van Essen *et al.,* 1981; Zeki, 1974, 1980).

PET and fMRI studies demonstrated a comparable area in the human brain activated by moving visual stimuli and during visual motion aftereffects (Cheng *et al.,* 1995; Corbetta *et al.,* 1990, 1991; Dupont *et al.,* 1994; Tootell *et al.,* 1995a, b; Watson *et al.,* 1993; Zeki *et al.,* 1991, 1993). This area is located close to the level of the AC–PC line and posterior to the contact of the ascending limb of the inferior temporal sulcus with the lateral occipital sulcus (Watson *et al.,* 1993). In parallel with monkey data, a retinotopic organization of human V5/MT was reported (Huk *et al.,* 2002). An even more characteristic feature of V5/MT in the monkey is the direction specificity (i.e., preference for one direction of moving visual stimuli; Zeki, 1974; Van Essen *et al.,* 1981). This property was recently demonstrated by functional imaging (Heeger *et al.,* 1999; Huk and Heeger, 2002) and focal electrical stimulation also for the human V5/MT area (Blanke *et al.,* 2002).

The putative architectonic correlate of human V5/MT is a relatively small, heavily myelinated area in the dorsal part of the ascending limb of the inferior temporal sulcus near the occipitotemporal junction on the lateral convexity (Clarke and Miklossy, 1990; DeYoe *et al.,* 1990; Tootell and Taylor, 1995). No comparable cortical area is delineated in the maps of Brodmann (1909) and Sarkissov *et al.* (1955). A small posterior part of Brodmann's area 37 (see "Temporal Lobe") and a small anterior part of his area 19 covers approximately cortical regions where V5/MT has been localized in functional imaging studies. Von Economo and Koskinas (1925) show a lateral area OAm (Fig. 27.37), which has a position approximately comparable with that of V5/MT, but the schematic presentation of their maps (and all classical architectonical maps) does not allow a direct comparison with functional imaging data. Flechsig's area 16 (subangular gyrus; Flechsig, 1920; Figure 27.36), however, was proposed to be a good candidate for V5/MT (Watson *et al.,* 1993), since it not only is found in a location (Clarke, 1994a; Tootell and Taylor, 1995) comparable to the functional imaging data but was also described as an early and heavily myelinating area during ontogeny (Flechsig, 1920). A destruction of this area leads to akinetopsia (i.e., visual motion blindness where a patient is not able to recognize moving stimuli in his visual field), although other functions of the visual system are completely intact (Mesulam, 1994; Zeki, 1991; Zihl *et al.,* 1991).

Although human V5/MT receives a major input from layer IVB of V1 and from V2 (for review, see Felleman and Van Essen, 1991), human V5/MT is activated by moving bar also in a completely hemianopic patient with a lesion in area V1 (Barbur *et al.,* 1993). The patient was consciously aware of the nature and direction of the stimulus. Thus, the input to V5/MT can bypass V1 and arrive directly from the lateral geniculate body (Benevento and Yoshida, 1981; Fries, 1981; Yukie and Iwai, 1981) and/or indirectly via the superior colliculus and the pulvinar (Benevento and Fallon, 1975; Keating, 1980; Pasik and Pasik, 1982; Standage and Benevento, 1983). Direct evidence for a component of directional motion discrimination bypassing human V1 comes from transcranial magnetic stimulation of V1 and V5/MT (Beckers and Zeki, 1995). The inactivation of V5/MT abolishes the motion perception and causes akinetopsia, whereas V1 inactivation had only marginal effects.

A further visual motion-selective area was also identified in the posterior parietal cortex using PET (Watson *et al.,* 1993) and fMRI (Tootell *et al.,* 1995a), which may be identical with the cytochrome oxidase-rich area PX described by Tootell and Taylor (1995) in macaque and human brains. Cytoarchitectonic descriptions of this area are lacking.

Medial superior temporal area MST There are functional imaging studies on the putative human homologue of the monkey area MST (Cheng *et al.,* 1995; Dupont *et al.,* 1994; Huk *et al.,* 2002). This putative human MST is located in the more anterior part of the lateral occipitotemporoparietal cortex anterior to human V5/MST in the inferior parietal lobule and on

the superior and middle temporal gyri. In contrast to V5/MT, this area does not show retinotopy but responded to peripheral stimuli in both the ipsilateral and contralateral hemifields, indicative of larger receptive fields (Cheng *et al.*, 1995; Huk *et al.*, 2002). Presently, architectonic observations of this area and further functionally identified visual areas are lacking. For a comprehensive description of the visual system, see Chapter 35.

Insular Lobe

The insular cortex of the adult brain is buried in the lateral fissure and covered by the frontal and parietal opercula as well as the temporal lobe. Its outer borders are demarcated by the circular sulcus of Reil with its superior limiting sulcus defining the border to the frontoparietal operculum and its inferior limiting sulcus indicating the border to the supratemporal plane. The inferior limiting sulcus has a lateral branch (i.e., the lateral limb of the inferior limiting sulcus), which represents approximately the border between the inferior proisocortical part of the insular cortex and its isocortical part (Fig. 27.32).

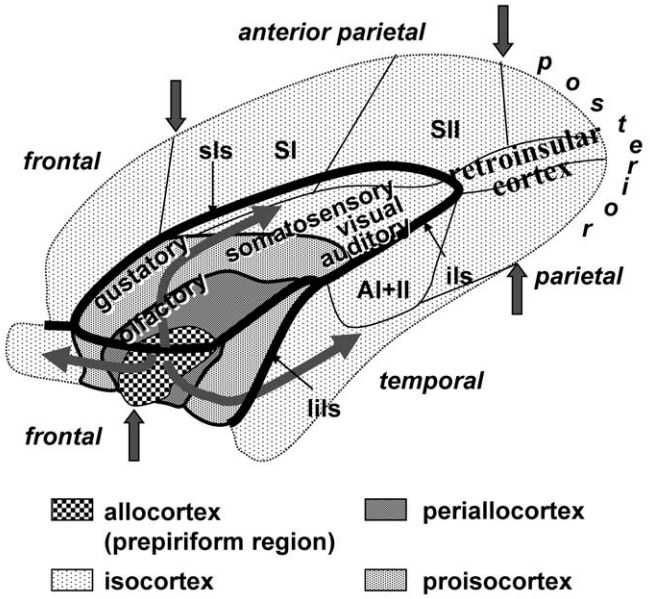

FIGURE 27.32 Schematic drawing after Mesulam and Mufson (1985) showing the principal organization of the insular cortex after opening the lateral fissure with the adjoining frontal parietal and temporal cortices. Auditory, gustatory, olfactory, somatosensory, and visual domains of the insular cortex are indicated. AI+II, primary and secondary auditory cortex; ils, inferior limiting sulcus (part of the circular sulcus of Reil); lils, lateral limb of the inferior limiting sulcus (part of the circular sulcus of Reil); sls, superior limiting sulcus (part of the circular sulcus of Reil); SI, primary somatosensory cortex; SII, secondary somatosensory cortex.

Mesulam and co-workers (for review see Mesulam and Mufson, 1985) demonstrated convincingly the radial organization of the insular cortex which surrounds the posterior part of the (pre)piriform cortex by three belt regions (Fig. 27.32). As discussed previously, the (pre)piriform cortex is part of the olfactory brain regions. The first belt consists of an agranular periallocortical region, the second belt of a dysgranular proisocortical region, and the outermost belt is true isocortex with clearly visible inner (layer IV) and outer (layer II) granular layers.

The *insular periallocortical belt* has (1) a superficial pyramidal cell layer that is a continuation of the pyramidal layer of the piriform cortex, and (2) an inner cell layer that is in continuation with the claustrum (Mesulam and Mufson, 1985). The granular layers II and IV are lacking. The agranular periallocortex of the insula shows no architectonicly detectable border to the adjacent agranular periallocortical regions of the orbitofrontal and temporopolar cortices.

The appearance of granular cells between the two cell layers of the periallocortical belt indicates the beginning of the *insular proisocortical belt*. The architecture of this cortical region is best classified by the term "dysgranular," indicating that its inner granular layer IV is not conspicous, but nevertheless detectable. Layers V and VI are also not as clearly demarcated from each other as in the true isocortex. The insular dysgranular proisocortex is also in continuation with the orbitofrontal and temporopolar proisocortical regions.

The *insular isocortical belt* is characterized by fully developed outer and inner granular layers (layers II and IV, respectively), a differentiation of layer III into sublayers and a clear demarcation of layer V from layer VI. The isocortical belt shows also the highest degree of myelination of all insular regions with a clearly visible outer stripe of Baillarger (Fig. 27.21).

Taking together the beltlike organization of periallocortical, proisocortical, and isocortical regions in the orbitofrontal, insular, and temporopolar cortex with the olfactory piriform region in the center, the insular cortex is a major part of the "olfactocentric component" (Mesulam and Mufson, 1985) of the paralimbic cortex. For the "hippocampocentric organization" (Mesulam and Mufson, 1985) of the paralimbic cortex (= mesocortex), see p. 135.

CORTICAL MAPS OF THE HUMAN BRAIN: PAST, PRESENT, FUTURE

A multitude of cyto- and myeloarchitectonic studies have been performed during the first half of the 20th century in different regions of the human cortex

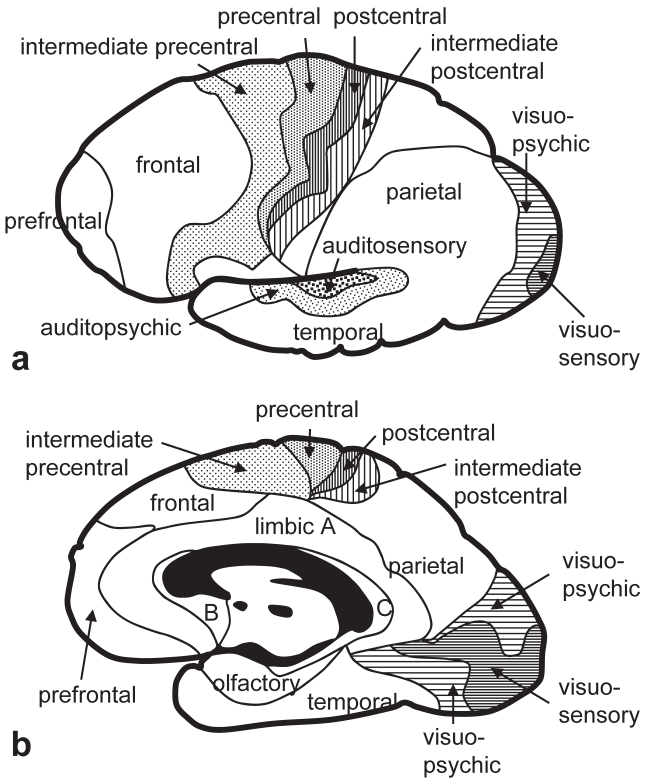

FIGURE 27.33 Areal map of the human cerebral cortex in **(a)** lateral and **(b)** medial views after Campbell (1905). For comparisons with other cortical maps, see Tables 27.4 and 27.7.

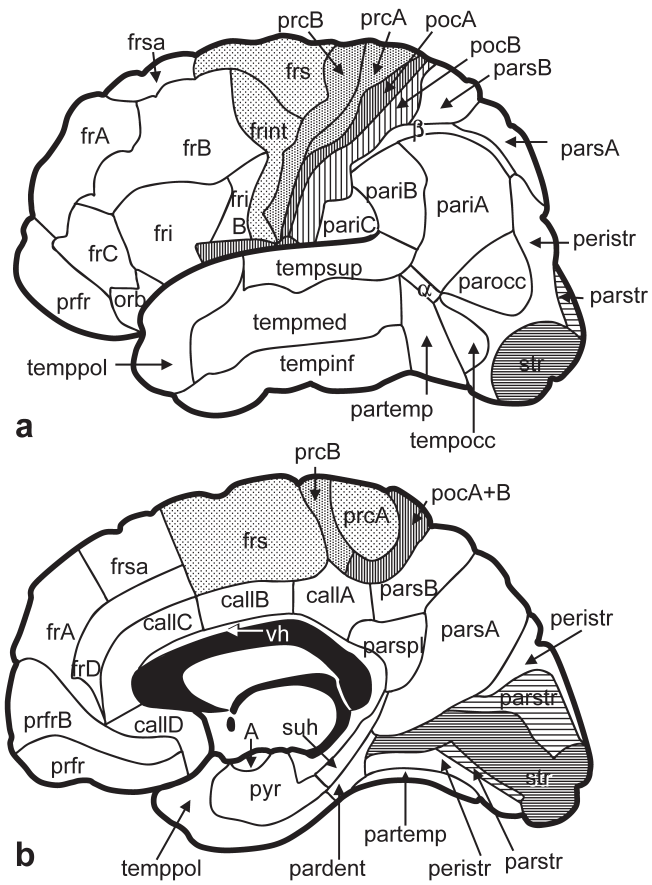

FIGURE 27.34 Areal map of the human cerebral cortex in **(a)** lateral and **(b)** medial views after Smith (1907). A, amygdala; α, visuoauditory band (probably area V5 of present functional nomenclature); β, visuo-sensory band; callA, area callosa A; callB, area callosa B; callC, area callosa C; callD, area callosa D; frA, area frontalis A; frB, area frontalis B; frC, area frontalis C; frD, area frontalis D; frs, area frontalis superior; frsa, area frontalis superior anterior; fri, area frontalis inferior; fri B, area frontalis inferior posterior; frint, area frontalis intermedia; orb, area orbitalis; pardent, area paradentata; pariA, area parietalis inferior A; pariB, area parietalis inferior B; pariC, area parasylvia; parsA, area parietalis superior posterior; parsB, area parietalis superior anterior; parspl, area parasplenialis; parstr, area parastriata; partemp, area paratemporalis; peristr, area peristriata; pocA, area postcentralis A; pocB, area postcentralis B; prcA, area praecentralis A; prcB, area praecentralis B; prfr, area praefrontalis; prfrB, area praefrontalis B; pyr, area pyriformis; str, area striata; suh, subiculum hippocampi; temppol, area temporopolaris; tempinf, area temporalis inferior; tempmed, area temporalis media; tempocc, area temporooccipitalis; tempsup, area temporalis superior; vh, vestigia hippocampi (hippocampus supracommissuralis). For comparisons with other cortical maps, see Tables 27.4, 27.6, and 27.7.

(Bailey and von Bonin, 1951; Batsch, 1956; Beck, 1928, 1930; Brockhaus, 1940; Brodmann, 1903a, b, 1905, 1908, 1909, 1910, 1912, 1914; Campbell, 1905; Filimonoff, 1932, 1947; Flechsig, 1920; Gerhardt, 1940; Hopf, 1954, 1955, 1956; Kreht, 1936; Lungwitz, 1937; Ngowyang, 1932, 1934; Riegele, 1931; Rose, 1926, 1927, 1928, 1929; Sarkissov *et al.*, 1955; Smith, 1907; Stengel, 1930; Strasburger, 1937, 1938; Vogt and Vogt, 1919, 1926, 1956; Vogt, 1910, 1911; von Economo and Horn, 1930; von Economo and Koskinas, 1925). The common goal of all these studies was the generation of a detailed and reliable map of the human cerebral cortex, which represents its regional inhomogeneity in cyto- and/or myeloarchitecture and its segregation into numerous structural–functional areas.

After more than 100 years of research, however, the architectonic parcellation of the human cerebral cortex is still not finished but is instead a work in progress. This conclusion is supported by a comparison between the classical maps—between the maps published by Bailey and von Bonin (1951), Brodmann (1909), Campbell (1905), Flechsig (1920), Sarkissov *et al.* (1955), Smith (1907), and von Economo and Koskinas (1925)—which shows a similar areal pattern only in some cortical regions, while the delineations differ markedly in other regions (Figs. 27.33–27.39). The reasons for this lack of agreement between the cortical maps of different observers are found in the morphological complexity

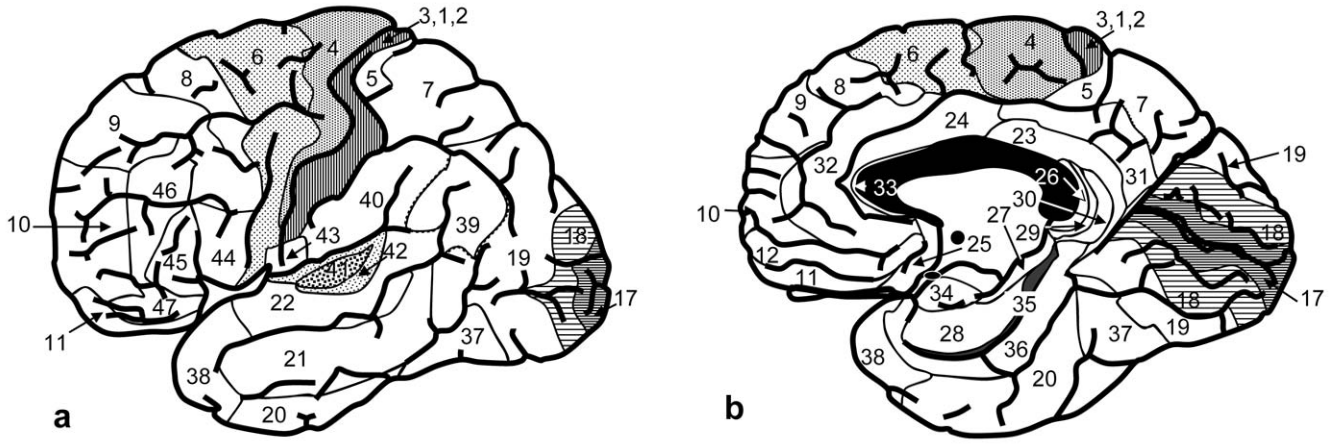

FIGURE 27.35 Areal map of the human cerebral cortex after Brodmann (1909, 1910, 1912, 1914). **(a)** Lateral and **(b)** medial views. 1, area postcentralis intermedia; 2, area postcentralis caudalis; 3, area postcentralis rostralis; 4, area gigantopyramidalis; 5, area praeparietalis; 6, area frontalis agranularis; 7, area parietalis superior; 8, area frontalis intermedia; 9, area frontalis granularis; 10, area frontopolaris; 11, area praefrontalis; 12, not explained by Brodmann; 17, area striata; 18, area occipitalis; 19, area praeoccipitalis; 20, area temporalis inferior; 21, area temporalis media; 22, area temporalis superior; 23, area cingularis posterior ventralis; 24, area cingularis anterior ventralis; 25, area subgenualis; 26, area ectosplenialis; 27, area praesubicularis; 28, area entorhinalis; 29, area retrolimbica (retrosplenialis) granularis; 30, area retrolimbica (retrosplenialis) agranularis; 31, area cingularis posterior dorsalis; 32, area cingularis anterior dorsalis; 33, area praegenualis; 34, area entorhinalis dorsalis; 35, area perirhinalis; 36, area ectorhinalis; 37, area occipitotemporalis; 38, area temporopolaris; 39, area angularis; 40, area supramarginalis; 41, area temporalis transversa medialis; 42, area temporalis transversa lateralis; 43, area subcentralis; 44, area opercularis; 45, area triangularis; 46, area frontalis media; 47, area orbitalis; 52, area parainsularis. For comparisons with other cortical maps, see Tables 27.3–27.7.

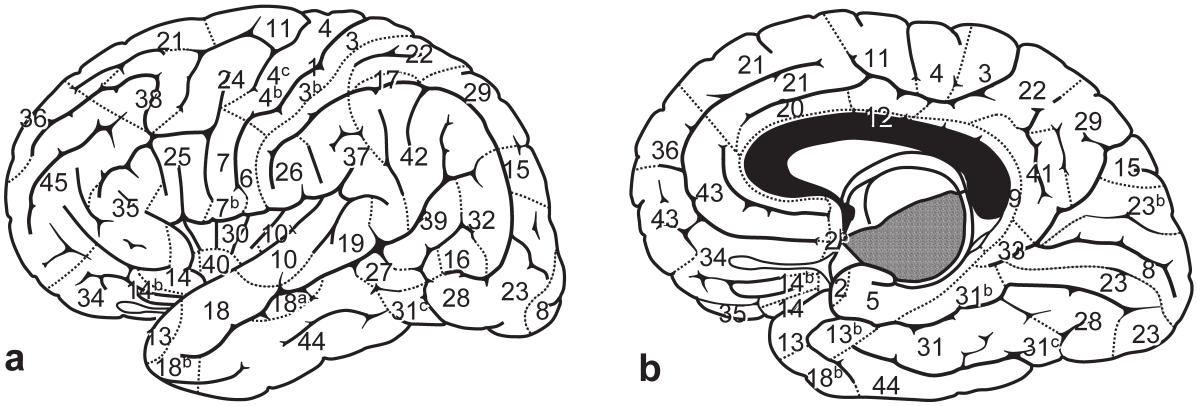

FIGURE 27.36 Areal map of the myelogenetic areas after Flechsig (1920) in the human cerebral cortex. **(a)** Lateral and **(b)** medial view. The numbers of the areas describe the sequence of myelination during fetal and early postnatal stages. The cortical regions with first signs of myelination before birth are Flechsig's primordial areas (areas 1–16), between birth and the end of the sixth postnatal week are his intermediate areas (17–28), and after the beginning of the second postnatal month are his terminal ("association") areas (29–45). For comparisons with other cortical maps, see Tables 27.5 and 27.7.

of the human cerebral cortex, the architectonic similarity of numerous isocortical areas particularly in the multimodal association regions, the interindividual variability of architectonic features (none of these maps is based on a larger sample or defines the range of variability between different individuals), the relatively simple methodical approach based on pure visual inspection of only Nissl- or myelin-stained sections, and the strong influence of the observer's criteria on delineations and definitions of areas. None of these objections denies that the classical maps, particularly Brodmann's map, represent pioneering work; however,

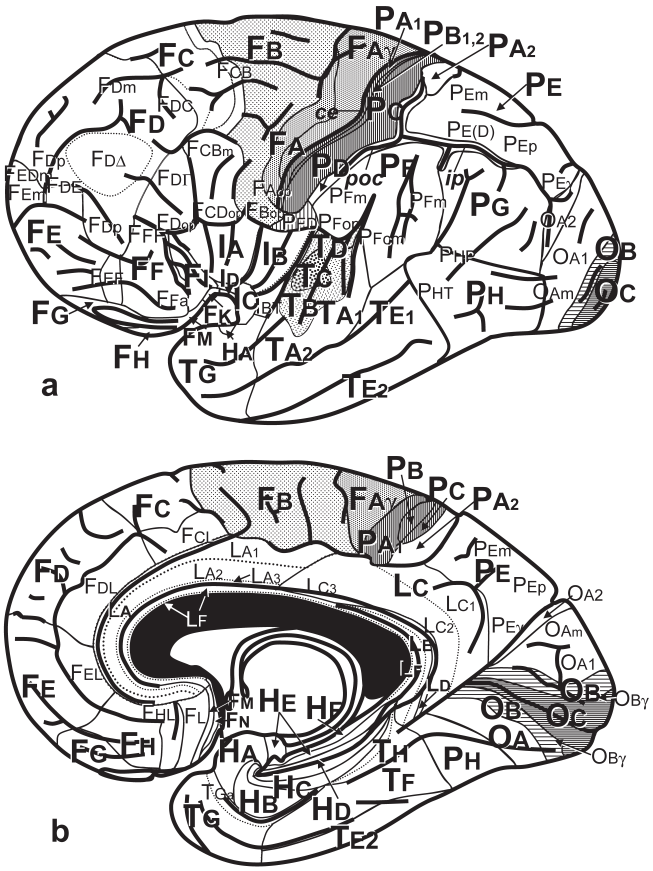

FIGURE 27.37 Areal map of the human cerebral cortex after von Economo and Koskinas (1925). **(a)** Lateral and **(b)** medial views. For comparisons with other cortical maps, see Tables 27.3–27.7.

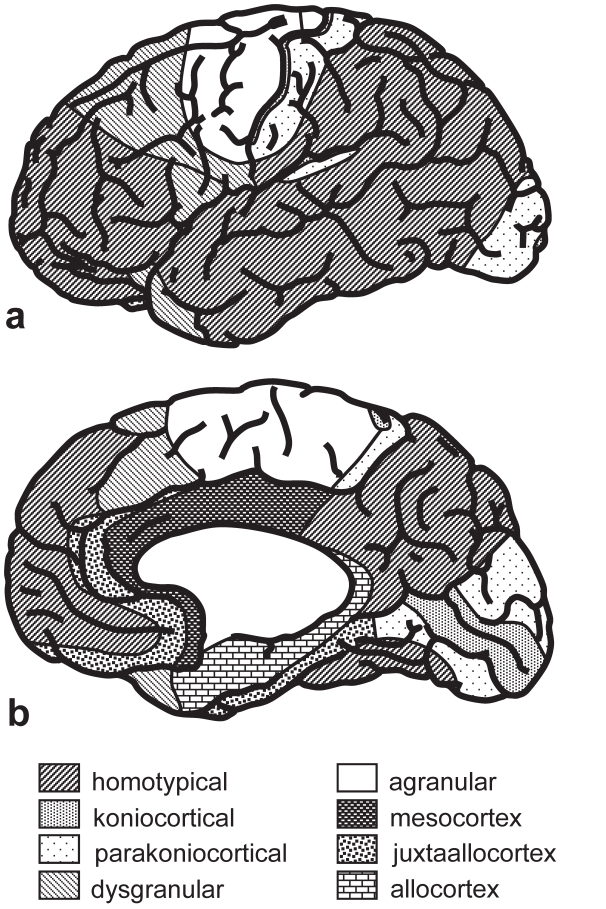

FIGURE 27.38 Areal map of the human cortex after Bailey and von Bonin (1951). **(a)** Lateral and **(b)** medial views. For comparisons with other cortical maps, see Tables 27.4 and 27.7.

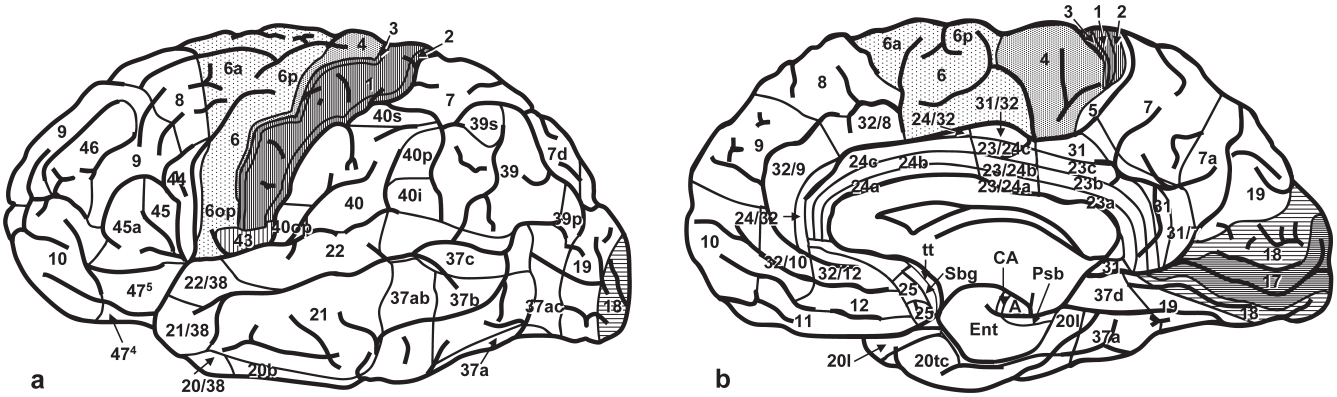

FIGURE 27.39 Areal map of the human cortex after Sarkissov *et al.* (1955). **(a)** Lateral and **(b)** medial views. The nomenclature follows Brodmann's scheme (see legend of Figure 27.35) and introduces self-explaining symbols for subparcellations and transition zones. A, amygdala; CA, Ammon's horn; Ent, entorhinal area; Psb, presubicular area; Sbg, subgenual area; tt, taenia tecta (precommissural hippocampus). For comparisons with other cortical maps, see Tables 27.4 and 27.7.

the previously listed problems can only be solved with the introduction of a novel approach to architectonics that uses various staining techniques as well as objective, observer-independent, and quantitative image analysis procedures and statistically testable criteria (Amunts and Zilles, 2001; Amunts *et al.*, 2002; Schleicher *et al.*, 1986, 1999; Zilles *et al.*, 1982, 1986a, b, 1995, 2002).

Furthermore, all the classical studies do not allow a direct comparison with three-dimensional datasets of functional imaging studies, which is a great obstacle for establishing architectonic/functional correlations. Therefore, an important aspect of present and future architectonic studies is the comparability of these microstructural data and areal borders with the results of functional imaging studies in the same spatial reference system (Amunts and Zilles, 2001; Amunts *et al.*, 1999, 2000b, 2002; Geyer *et al.*, 1996, 1999, 2000b; Grefkes *et al.*, 2001; Morosan *et al.*, 2001; Rademacher *et al.*, 1993, 2001a, b, c; Zilles *et al.*, 1997, 2001, 2002). Because the interindividual variability of the architectonic organization is a challenge for such correlations of structure and function, the novel concept of probability maps has been introduced (Roland and Zilles, 1994, 1996a, b, 1998; Roland *et al.*, 1997). Probabilistic brain mapping has meanwhile developed into a multisite international effort (Mazziotta *et al.*, 2001a, b).

Acknowledgments

This work was supported by grants of the Deutsche Forschungsgemeinschaft, the VW Stiftung, and the Human Brain Project/Neuroinformatics Research (funded by the National Institute of Biomedical Imaging and Bioengineering, the National Institute Neurological Disorders and Stroke, and the National Institute of Mental Health).

References

Aboitiz, F., and Garcia, R. (1997). The anatomy of language revisited. *Biol. Res.* **30,** 171–183.

Albright, T.D. (1984). Direction and orientation selectivity of neurons in visual area MT of the macaque. *J. Neurophysiol.* **52,** 1106–1130.

Allison, A.C. (1953). The morphology of the olfactory system in the vertebrates. *Bio. Rev. Cambridge Philos. Soc.* **28,** 195–244.

Allison, A.C. (1954). The secondary olfactory areas in the human brain. *J. Anat.* **88,** 481–488.

Allison, T., Begleiter, A., McCarthy, G., Roessler, E., Nobre, A.C., and Spencer, D.D. (1993). Electrophysiological studies of color processing in human visual cortex. *Electroencephalography Clin. Neurophysiol.* **88,** 343–355.

Allison, T., Ginter, H., McCarthy, G., Nobre, A.C., Puce, A., Luby, M., and Spencer, D.D. (1994). Face recognition in human extrastriate cortex. *J. Neurophysiol.* **71,** 821–825.

Allman, J.M., and Kaas, J.H. (1971). A representation of the visual field in the caudal third of the middle temporal gyrus of the owl monkey *(Aotus trivirgatus). Brain Res.* **31,** 85–105.

Amunts, K., and Zilles, K. (2001). Advances in cytoarchitectonic mapping of the human cerebral cortex. *In* "Neuroimaging Clinics of North America" (T. Naidich, T. Yousry, V. Mathews, eds.), Vol. 11, pp.151–169. W.B. Saunders Company, Philadelphia.

Amunts, K., Istomin, V., Schleicher, A., and Zilles, K. (1995). Postnatal development of the human primary motor cortex: A quantitative cytoarchitectonic analysis. *Anat. Embryol.* **192,** 557–571.

Amunts, K., Jäncke, L., Mohlberg, H., Steinmetz, H., and Zilles, K. (2000a). Interhemispheric asymmetry of the human motor cortex related to handedness and gender. *Neuropsychologia* **38,** 304–312.

Amunts, K., Malikovic, A., Mohlberg, H., Schormann, T., and Zilles, K. (2000b). Brodmann's areas 17 and 18 brought into stereotaxic space—Where and how variable? *NeuroImage* **11,** 66–84.

Amunts, K., Schlaug, G., Jäncke, L., Steinmetz, H., Schleicher, A., Dabringhaus, A., and Zilles, K. (1997a). Motor cortex and hand motor skills: Structural compliance in the human brain. *Human Brain Mapping* **5,** 206–215.

Amunts, K., Schlaug, G., Schleicher, A., Steinmetz, H., Dabringhaus, A., Roland, P.E., and Zilles, K. (1996). Asymmetry in the human motor cortex and handedness. *NeuroImage* **4,** 216–222.

Amunts, K., Schleicher, A., Bürgel, U., Mohlberg, H., Uylings, H.B.M., and Zilles, K. (1999). Broca's region revisited: Cytoarchitecture and intersubject variability. *J. Comp. Neurol.* **412,** 319–341.

Amunts, K., Schleicher, A., and Zilles, K. (1995). Persistence of layer IV in the primary motor cortex (area 4) of children with cerebral palsy. *J. Brain Res.* **38,** 247–260.

Amunts, K., Schleicher, A., and Zilles, K. (2002). Architectonic mapping of the human cerebral cortex. *In* "Cortical Areas: Unity and Diversity" (A. Schüz and R. Miller, eds.), pp. 29–52. Taylor & Francis, London, New York.

Amunts, K., Schmidt-Passos, F., Schleicher, A., and Zilles, K. (1997c). Postnatal development of interhemispheric asymmetry in the cytoarchitecture of human area 4. *Anat. Embryol.* **196,** 393–402.

Andersen, R.A., Asanuma, C., Essick, G., and Siegel, R.M. (1990a). Corticocortical connections of anatomically and physiologically defined subdivisions within the inferior parietal lobule. *J. Comp. Neurol.* **296,** 65–113.

Andersen, R.A., Bracewell, R.M., Barash, S., Gnadt, J.W., and Fogassi, L. (1990b). Eye position effects on visual, memory, and saccade-related activity in areas LIP and 7a of macaque. *J. Neurosci.* **10,** 1176–1196.

Armstrong, E., Zilles, K., Omran, H., and Schleicher, A. (1995). The ontogeny of human gyrification. *Cereb. Cortex* **5,** 56–63.

Armstrong, E., Zilles, K., Schlaug, G., and Schleicher, A. (1986). Comparative aspects of the primate posterior cingulate cortex. *J. Comp. Neurol.* **253,** 539–548.

Astruc, J., and Leichnetz, G.R. (1973). Fiber degeneration following lesions of the orbital cortex in *Macaca mulatta. Anat. Rec.* **175,** 266–267.

Bailey, P., and von Bonin, G. (1951). "The isocortex of Man." Univ. of Illinois Press, Urbana.

Baleydier, C., and Mauguire, F. (1980). The duality of the cingulate gyrus in monkey: Neuroanatomical study and functional hypothesis. *Brain* **103,** 525–554.

Balint, R. (1909). Seelenlähmung des "Schauens", optische Ataxie, räumliche Störung der Aufmerksamkeit. *Monatsschr. Psychiatr. Neurol.* **25,** 51–81.

Barbas, H. (1988). Anatomical organization of basoventral and mediodorsal visual recipient prefrontal region in the rhesus monkey. *J. Comp. Neurol.* **276,** 313–342.

Barbas, H., and DeOlmos, J. (1990). Projections from the amygdala to basoventral and mediodorsal prefrontal regions in the rhesus monkey. *J. Comp. Neurol.* **300,** 549–571.

Barbas, H., and Pandya, D.N. (1987). Architecture and frontal cortical connections of the premotor cortex (area 6) in the rhesus monkey. *J. Comp. Neurol.* **256,** 211–228.

Barbur, J., Watson, J., Frackowiak, R., and Zeki, S. (1993). Conscious visual perception without V1. *Brain* **116,** 1293–1302.

Batsch, E.-G. (1956). Die myeloarchitektonische Untergliederung des Isocortex parietalis beim Menschen. *J. Hirnforsch.* **2,** 225–258.

Beck, E.D. (1928). Die myeloarchitektonische Felderung des in der Sylvischen Furche gelegenen Teiles des menschlichen Schläfenlappens. *J. Psychol. Neurol.* **36,** 1–21.

Beck, E.D. (1930). Die Myeloarchitektonik der dorsalen Schläfenlappenrinde beim Menschen. *J. Psychol. Neurol.* **41,** 129–263.

Beckers, G., and Zeki, S. (1995). The consequences of inactivating areas V1 and V5 on visual motion perception. *Brain* **118,** 49–60.

Belin, P., Zilbovicius, M., Crozier, S., Thivard, L., Fontaine, A., Masure, M.C., and Samson, Y. (1998). Lateralization of speech and auditory temporal processing. *J. Cogn. Neurosci.* **10,** 536–540.

Benevento, L.A., and Fallon, J.H. (1975). The ascending projections of the superior colliculus in the rhesus monkey *(Macaca mulatta). J. Comp. Neurol.* 160, 339–362.

Benevento, L.A., and Yoshida, K. (1981). The afferent and efferent organization of the lateral geniculo-prestriate pathways in the macaque monkey. *J. Comp. Neurol.* **203,** 455–474.

Bigl, V., Woolf, N.J., and Butcher, L.L. (1982). Cholinergic projections from the basal forebrain to frontal, parietal, temporal, occipital and cingulate cortices: A combined fluorescent tracer and acetylcholinesterase analysis. *Brain Res. Bull.* **8,** 727–749.

Bilecen, D., Scheffler, K., Schmid, N., Tschopp, K., and Seelig, J. (1998). Tonotopic organization of the human auditory cortex as detected by BOLD-FMRI. *Hear. Res.* **126,** 19–27.

Binder, J.R., Rao, S.M., Hammeke, T.A., Yetkin, F.Z., Jesmanowicz, A., Bandettini, P.A., Wong, E.C., Estkowski, L.D., Goldstein, M.D., Haughton, V.M., and Hyde, J.S. (1994). Functional magnetic resonance imaging of human auditory cortex. *Ann. Neurol.* **35,** 662–672.

Binkofski, F., Amunts, K., Stephan, K.M., Posse, S., Schormann, T., Freund, H.-J., Zilles, K., and Seitz, R.J. (2000). Broca's region subserves imagery of motion: A combined cytoarchitectonic and fMRI study. *Human Brain Mapping* **11,** 273–285.

Binkofski, F., Buccino, G., Posse, S., Seitz, R.J., Rizzolatti, G., and Freund, H.J. (1999). A fronto-parietal circuit for object manipulation in man. *Eur. J. Neurosci.* **11,** 3276–3286.

Blanke, O., Landis, T., Safran, A.B., and Seeck, M. (2002). Direction-specific motion blindness induced by focal stimulation of human extrastriate cortex. *Eur. J. Neurosci.* **15,** 2043–2048.

Blatt, G.J., Andersen, R.A., and Stoner, G.R. (1990). Visual receptive field organization and cortico-cortical connections of the lateral intraparietal area (area LIP) in the macaque. *J. Comp. Neurol.* **299,** 421–455.

Blinkov, S.M., and Glezer, I. (1968). "Das Zentralnervensystem in Zahlen und Tabellen." Fischer, Jena.

Blümcke, I., and Celio, M.R. (1992). Parvalbumin and calbindin D-28k immunoreactivities coexist within cytochrome oxidase-rich compartments of squirrel monkey area 18. *Exp. Brain Res.* **92,** 39–45.

Bodegård, A., Geyer, S., Amunts, K., Naito, E., Zilles, K., and Roland, P.E. (2000a). Somatosensory areas in man activated by moving stimuli. Cytoarchitectonic mapping and PET. *NeuroReport* **11,** 187–191.

Bodegård, A., Ledberg, A., Geyer, S., Naito, E., Larsson, J., Zilles, K., and Roland, P. (2000b). Object shape differences reflected by somatosensory cortical activation. *J. Neuroscience* **20,** 1–5.

Booth, J.R., Burman, D.D., Meyer, J.R., Gitelman, D.R., Parrish, T.B., and Mesulam, M.M. (2002). Functional Anatomy of intra- and cross-modal lexical tasks. *NeuroImage* **16,** 7–22.

Born, R.T., and Tootell, R.B.H. (1992). Segregation of global and local motion processing in primate middle temporal visual area. *Nature* **357,** 497–499.

Botez, M.I., and Wertheim, N. (1959). Expressive aphasia and amusia following right frontal lesion in a right-handed man. *Brain* **82,** 186–202.

Braak, E. (1982). On the structure of the human striate area. *Adv. Anat. Embryol. Cell Biol.* **77,** 1–86.

Braak, H. (1972). Zur Prigmentarchitektonik der Grosshirnrinde des Menschen. I. Regio entorhinalis. *Z. Zellforsch. Mikrosk. Anat.* **127,** 407–438.

Braak, H. (1976a). A primitive gigantopyramidal field buried in the depth of the cingulate sulcus of the human brain. *Brain Res.* **109,** 219–223.

Braak, H. (1976b). On the striate area of the human isocortex. A Golgi and pigmentoarchitectonic study. *J. Comp. Neurol.* **166,** 341–364.

Braak, H. (1977). The pigment architecture of the human occipital lobe. *Anat. Embryol.* **150,** 229–250.

Braak, H. (1978). The pigment architecture of the human temporal lobe. *Anat. Embryol.* **154,** 213–240.

Braak, H. (1979a). The pigment architecture of the human frontal lobe. I. Precentral, subcentral and frontal region. *Anat. Embryol.* **157,** 36–68.

Braak, H. (1979b). Pigment architecture of the human telencephalic cortex. IV. Regio retrosplenialis. *Cell Tissue Res.* **204,** 431–440.

Braak, H. (1980). "Architectonics of the Human Telencephalic Cortex." Springer-Verlag, Berlin, New York.

Braak, H., and Braak, E. (1976). The pyramidal cells of Betz within the cingulate and precentral gigantopyramidal field in the human brain. A Golgi and pigmentarchitectonic study. *Cell Tissue Res.* **172,** 103–119.

Bradvik, B., Dravins, C., Holtas, C., Rosen, I., Ryding, E., and Ingvar, D.H. (1991). Disturbances of speech prosody following right hemisphere infarcts. *Acta Neurol. Scand.* **84,** 114–126.

Branche, C., Milner, B., and Rasmussen, T. (1964). Intracarotid sodium amytal for the lateralization of cerebral speech dominance. *J. Neurosurg.* **21,** 399–405.

Bremmer, F., Duhamel, J.R., Hamed, S.B., and Graf, W. (2000). Stages of self-motion processing in primate posterior parietal cortex. *Int. Rev. Neurobiol.* **44,** 173–198.

Bremmer, F., Schlack, A., Shah, N.J., Zafiris, O., Kubischik, M., Hoffmann, K.-P., Zilles, K., and Fink, G.R. (2001). Polymodal motion processing in posterior parietal and premotor cortex: A human fMRI study strongly implies equivalencies between humans and monkeys. *Neuron* **29,** 287–296.

Broca, M.P. (1861). Remarques sur le siége de la faculté du langage articulé, suivies d'une observation d'aphemie (Perte de la Parole). *Bulletins et Memoires de la Societe Anatomique de Paris* **36,** 330–357.

Brockhaus, H. (1940). Die Cyto- und Myeloarchitektonik des Cortex claustralis und des Claustrum beim Menschen. *J. Psychol. Neurol.* **49,** 249–348.

Brodal, A. (1969). "Neurological Anatomy in Relation to Clinical Medicine," 2nd ed. Oxford Univ. Press, London, New York.

Brodmann, K. (1903a). Beiträge zur histologischen Lokalisation der Grosshirnrinde. Erste Mitteilung: Die Regio Rolandica. *J. Psychol. Neurol.* **2,** 79–107.

Brodmann, K. (1903b). Beiträge zur histologischen Lokalisation der Grosshirnrinde. II. Der Calcarinustyp. *J. Psychol. Neurol.* **2,** 133–159.

Brodmann, K. (1905). Beiträge zur histologischen Lokalisation der Grosshirnrinde. III. Die Rindenfelder der niederen Affen. *J. Psychol. Neurol.* **4,** 177–226.

Brodmann, K. (1908). Beiträge zur histologischen Lokalisation der Grosshirnrinde. VI. Die Cortexgliederung des Menschen. *J. Psychol. Neurol.* **10,** 231–246.

Brodmann, K. (1909). "Vergleichende Lokalisationslehre der Grosshirnrinde." Barth, Leipzig.

Brodmann, K. (1910). Feinere Anatomie des Großhirns. *In* "Handbuch der Neurologie, Erster Band, Allgemeine Neurologie" (M. Lewandowsky, ed.), pp. 206–307. J. Springer, Berlin.

Brodmann, K. (1912). Neue Ergebnisse über die vergleichende histologische Lokalisation der Grosshirnrinde mit besonderer Berücksichtigung des Stirnhirns. *Anat. Anz.* **41,** 157–216.

Brodmann, K. (1914). Physiologie des Gehirns. *Neue Dtsch. Chir.* **11,** 85–426.

Bruce, C.J., and Goldberg, M.E. (1984). Physiology of the frontal eye fields. *Trends Neurosci.* **7,** 436–441.

Buccino, G., Binkofski, F., Fink, G.R., Fadiga, L., Fogassi, L., Gallese, V., Seitz, R.J., Zilles, K., Rizzolatti, G., and Freund, H.-J. (2001). Action observation activates premotor and parietal areas in a somatotopic manner: An fMRI study. *Eur. J. Neurosci.* **13,** 400–404.

Buckner, R.L., Corbetta, M., Schatz, J., Raichle, M.E., and Petersen, S.E. (1996). Preserved speech abilities and compensation following prefrontal damage. *Proc. Nat. Acad. Sci.* **93,** 1249–1253.

Bullier, J., Schall, J.D., and Morel, A. (1996). Functional streams in occipito-frontal connections in the monkey. *Behav. Brain Res.* **76,** 89–97.

Burkhalter, A., and Bernardo, K.L. (1989). Organization of cortico-cortical connections in human visual cortex. *Proc. Nat. Acad. Sci. USA* **86,** 1071–1075.

Cabeza, R., Dolcos, F., Graham, R., and Nyberg, L. (2002). Similarities and differences in the neural correlates of episodic memory retrieval and working memory. *NeuroImage* **16,** 317–330.

Campbell, A.W. (1905). "Histological Studies on the Localization of Cerebral Function." Cambridge Univ. Press, London, New York.

Cavada, C. (2001). The visual parietal areas in the macaque monkey. Current structural knowledge and ignorance. *NeuroImage* **14,** 21–26.

Cavada, C., and Goldman-Rakic, P.S. (1989a). Posterior parietal cortex in rhesus monkey. I. Parcellation of areas based on distinctive limbic and sensory corticocortical connections. *J. Comp. Neurol.* **287,** 393–421.

Cavada, C., and Goldman-Rakic, P.S. (1989b). Posterior parietal cortex in rhesus monkey. II. Evidence for segregated corticocortical networks linking sensory and limbic areas with the frontal lobe. *J. Comp. Neurol.* **287,** 422–445.

Cavada, C., and Goldman-Rakic, P.S. (1991). Topographic segregation of corticostriatal projections from posterior parietal subdivisions in the macaque monkey. *Neurosci.* **42,** 683–696.

Cavada, C., and Goldman-Rakic, P.S. (1993). Multiple visual areas in the posterior parietal cortex of primates. *Prog. Brain Res.* **95,** 123–137.

Cavada, C., Compañy, T., Tejedor, J., Cruz-Rizzolo, R.J., and Reinoso-Suárez, F. (2000). The anatomical connections of the macaque monkey orbitofrontal cortex. A review. *Cereb. Cortex* **10,** 220–242.

Chao, L.L., and Martin, A. (2000). Representation of manipulable man-made objects in the dorsal stream. *NeuroImage* **12,** 478–494.

Cheng, K., Fujita, H., Kanno, I., Miura, S., and Tanaka, K. (1995). Human cortical regions activated by wide-field visual motion: An $H_2{}^{15}O$ PET study. *J. Neurophysiol.* **74,** 413–427.

Choi, H.J., Amunts, K., Mohlberg, H., Fink, G.R., Schleicher, A., and Zilles, K. (2002). Cytoarchitectonic mapping of the anterior ventral bank of the intraparietal sulcus in humans. 8th International Conference on Functional Mapping of the Human Brain, Sendai. *NeuroImage* E.40401.01.

Clarke, S. (1994a). Modular organization of human extrastriate visual cortex: Evidence from cytochrome oxidase pattern in normal and macular degeneration cases. *Eur. J. Neurosci.* **6,** 725–736.

Clarke, S. (1994b). Association and intrinsic connections of human extrastriate visual cortex. *Proc. Roy. Soc. Lond. B* **257,** 87–92.

Clarke, S., and Miklossy, J. (1990). Occipital cortex in man: Organization of callosal connections, related myelo- and cyto-architecture, and putative boundaries of functional visual areas. *J. Comp. Neurol.* **298,** 188–214.

Clarke, S., Lindemann, A., Maeder, P., Borruat, F.-X., and Assal, G. (1997). Face recognition and postero-inferior hemispheric lesions. *Neuropsychologia* **35,** 1555–1563.

Colby, C.L., and Duhamel, J.-R. (1991). Heterogeneity of extrastriate visual areas and multiple parietal areas in the macaque monkey. *Neuropsychologia* **29,** 517–537.

Colby, C.L., and Goldberg, M.E. (1999). Space and attention in parietal cortex. *Annu. Rev. Neurosci.* **22,** 319–349.

Colby, C.L., Duhamel, J.-R., and Goldberg, M.E. (1993). Ventral intraparietal area of the macaque: Anatomic location and visual response properties. *J. Neurophysiol.* **69,** 902–914.

Colby, C.L., Gattass, R., Olson, C.R., and Gross, C.G. (1988). Topographical organization of cortical afferents to extrastriate visual area PO in the macaque: A dual tracer study. *J. Comp. Neurol.* **269,** 392–413.

Corbetta, M., Miezin, F.M., Dobmeyer, S., Shulman, G.L., and Petersen, S.E. (1990). Attentional modulation of neural processing of shape, color, and velocity in humans. *Science* **248,** 1556–1559.

Corbetta, M., Miezin, F.M., Dobmeyer, S., Shulman, G.L., and Petersen, S.E. (1991). Selective and divided attention during visual discrimination of shape, color and speed: Functional anatomy by positron emission tomography. *J. Neurosci.* **11,** 2383–2402.

Creutzfeld, O., Ojemann, G., and Lettich, E. (1989). Neuronal activity in the human lateral temporal lobe. I. Responses to speech. *Exp. Brain Res.* **77,** 451–475.

Damasio, A., Yamada, T., Damasio, H., Corbett, J., and McKee, J. (1980). Central achromatopsia: Behavioral, anatomical and physiological aspects. *Neurology* **30,** 1064–1071.

Decety, J., Perani, D., Jeannerod, M., Bettinardi, V., Tadary, B., Woods, R., Mazziotta, J.C., and Fazio, F. (1994). Mapping motor representations with PET. *Nature* **371,** 600–602.

de Lacoste-Utamsing, C., and Holloway, R.L. (1982). Sexual dimorphism in the human corpus callosum. *Science* **216,** 1431–1432.

Demonet, J.F., Chollet, F., Ramsay, S., Cardebat, D., Nespoulous, J.L., Wise, R., Rascol, A., and Frackowiak, R.S.J. (1992). The anatomy of phonological and semantic processing in normal subjects. *Brain* **115,** 1753–1768.

Denny-Brown, D., Meyer, J.S., and Horenstein, S. (1952). The significance of perceptual rivalry resulting from parietal lesions. *Brain* **75,** 433–471.

Desimone, R., and Schein, S.J. (1987). Visual properties of neurons in area V4 of the macaque: Sensitivity to stimulus form. *J. Neurophysiol.* **57,** 835–868.

Desimone, R., and Ungerleider, L.G. (1989). Neural mechanisms of visual processing in monkeys. *In* "Handbook of Neuropsychology," (F. Boller, and J. Grafman, eds.), Vol. 2. pp. 267–299. Elsevier, Amsterdam.

DeYoe, E.A., and Van Essen, D.C. (1985). Segregation of efferent connections and receptive field properties in visual area V2 of the macaque. *Nature* **317,** 58–61.

DeYoe, E.A., Felleman, D.J., Van Essen, D.C., and McClendon, E. (1994). Multiple processing streams in occipitotemporal visual cortex. *Nature* **371,** 151–154.

DeYoe, E.A., Hockfield, S., Garren, H., and Van Essen, D.C. (1990). Antibody labeling of functional subdivisions in visual cortex: CAT-301 immunoreactivity in striate and extrastriate cortex of the macaque monkey. *Vis. Neurosci.* **5,** 67–81.

Di Pellegrino, G., Fadiga, L., Fogassi, L., Gallese, V., and Rizzolatti, G. (1992). Understanding motor events: A neurophysiological study. *Exp. Brain Res.* **91,** 176–180.

Divac, I. (1971). Frontal lobe system and spatial reversal in the rat. *Neuropsychologica* **9,** 175–183.

Divac, I., Björklund, A., Lindvall, O., and Passingham, R.E. (1978). Converging projections from the mediodorsal thalamic nucleus and mesencephalic dopaminergic neurons to the neocortex in three species. *J. Comp. Neurol.* **180,** 59–72.

Dong, Y., Fukuyama, H., Honda, M., Okada, T., Hanakawa, T., Nakamura, K., Nagahama, Y., Nagamine, T., Konishi, J., and Shibasaki, H. (2000). Essential role of the right superior parietal cortex in Japanese kana mirror reading: An fMRI study. *Brain* **123,** 790–799.

Driver, J., Vuilleumier, P., Eimer, M., and Rees, G. (2001). Functional magnetic resonance imaging and evoked potential correlates of conscious and unconcious vision in parietal extinction patients. *NeuroImage* **14,** 68–75.

Druga, R. (1971). Projection of prepyriform cortex into claustrum. *Folia Morphol. (Prague)* **19,** 405–410.

Duhamel, J.-R., Bremmer, F., BenHamed, S., and Graf, W. (1997). Spatial invariance of visual receptive fields in parietal cortex neurons. *Nature* **389,** 845–848.

Dupont, P., Orban, G.A., De Bruyn, B., Verbruggen, A., and Mortelmans, L. (1994). Many areas in the human brain respond to visual motion. *J. Neurophysiol.* **72,** 1420–1424.

Ehrsson, H.H., Naito, E., Geyer, S., Amunts, K., Zilles, K., Forssberg, H., and Roland, P.E. (2000). Simultaneous movements of upper and lower limbs are coordinated by motor representations that are shared by both limbs: A PET study. *Eur. J. Neurosci.* **12,** 3385–3398.

Eickhoff, S., Geyer, S., Amunts, K., Mohlberg, H., and Zilles, K. (2002). Cytoarchitectonic analysis and stereotaxic map of the human secondary somatosensory cortex region. 8th International Conference on Functional Mapping of the Human Brain, Sendai. *NeuroImage* E.40401.01

Eidelberg, D., and Galaburda, A.M. (1984). Inferior parietal lobule. Divergent architectonic asymmetries in the human brain. *Arch. Neurol. (Chicago)* **41,** 843–852.

Elias, H., and Schwartz, D. (1969). Surface areas of the cerebral cortex of mammals determined by stereological methods. *Science* **166,** 1011–1013.

Engelien, A., Yang, Y., Engelien, W., Zonana, J., Stern, E., and Silbersweig, D.A. (2002). Physiological mapping of human auditory cortices with a silent event-related fMRI technique. *NeuroImage* **16,** 944–953.

Felleman, D.J., and Van Essen, D.C. (1991). Distributed hierarchical processing in the primate cerebral cortex. *Cereb. Cortex* **1,** 1–47.

Ferrer, N.G. (1969). Efferent projections of the anterior olfactory nucleus. *J. Comp. Neurol.* **137,** 309–319.

Filimonoff, I.N. (1932). Über die Variabilität der Großhirnrindenstruktur. Mitteilung II—Regio occipitalis beim erwachsenen Menschen. *J. Psychol. Neurol.* **44,** 2–96.

Filimonoff, I.N. (1947). A rational subdivision of the cerebral cortex. *Arch. Neurol. Psychiatry* **58,** 296–311.

Fink, G.R., Dolan, R.J., Halligan, P.W., Marshall, J.C., and Frith, C.D. (1997). Space-based and object-based visual attention: Shared and specific neural domains. *Brain* **120,** 2013–2028.

Fink, G.R., Driver, J., Rorden, C., Baldeweg, T., and Dolan, R.J. (2000c). Neural consequences of competing stimuli in both visual hemifields: A physiological basis for visual extinction. *Ann. Neurol.* **47,** 440–446.

Fink, G.R., Marshall, J.C., Gurd, J., Weiss, P.H., Zafiris, O., Shah, N.J., and Zilles, K. (2001a). Deriving numerosity and shape from identical visual displays. *NeuroImage* **13,** 46–55.

Fink, G.R., Marshall, J.C., Shah, N.J., Weiss, P.H., Halligan, P.W., Grosse-Ruyken, M., Ziemons, K., Zilles, K., and Freund, H.-J. (2000a). Line bisection judgements implicate right parietal cortex and cerebellum as assessed by fMRI. *Neurology* **54,** 1324–1331.

Fink, G.R., Marshall, J.C., Weiss, P.H., Shah, N.J., Toni, I., Halligan, P.W., and Zilles, K. (2000b). "Where" depends on "What": A differential functional anatomy for position discrimination in one- versus two-dimensions. *Neuropsychologia* **38,** 1741–1748.

Fink, G.R., Marshall, J.C., Weiss, P.H., and Zilles, K. (2001b). The neural basis of vertical and horizontal line bisection judgements: an fMRI study of normal volunteers. *NeuroImage* **14,** 59–67.

Fiorani, M., Jr., Gattas, R., Rosa, M.G.P., and Sousa, A.P.B. (1989). Visual area MT in the Cebus monkey: Location, visuotopic organization and variability. *J. Comp. Neurol.* **287,** 98–118.

Flechsig, P. (1920). "Anatomie des menschlichen Gehirns und Rückenmarks auf myelogenetischer Grundlage." Thieme, Leipzig.

Fletcher, P., Happé, F., Frith, U., Baker, S.C., Dolan, R.J., Frackowiak, R.S., and Frith, C.D. (1995). Other minds in the brain: A functional imaging study of "theory of mind" in story comprehension. *Cognition* **57,** 109–128.

Fox, P.T., Ingham, R.J., Ingham, J.C., Hirsch, T.B., Downs, J.H., Martin, C., Jerabek, P., Glass, T., and Lancaster, J.L. (1996). A PET study of the neural systems of stuttering. *Nature* **382,** 158–162.

Frackowiak, R.S.J. (1994). Functional mapping of verbal memory and language. *TINS* **17,** 109–115.

Freund, H.-J. (1987). Abnormalities of motor behavior after cortical lesions in humans. *In* "Handbook of Physiology, Section 1: The Nervous System, Vol. V: Higher Functions of the Brain, Part 2" (V.B. Mountcastle, section ed.; F. Plum, volume ed.), pp. 763–810. Williams and Wilkins, Baltimore.

Freund, H.-J. (2001). The parietal lobe as a sensorimotor interface: A perspective from clinical and neuroimaging data. *NeuroImage* **14,** 42–46.

Fries, W. (1981). The projection from the lateral geniculate nucleus to the prestriate cortex of the macaque monkey. *Proc. Roy. Soc. Lond. Ser. B* **213,** 73–80.

Frith, C.D., and Frith, U. (1999). Interacting minds—A biological basis. *Science* **286,** 1692–1695.

Frith, C.D., Friston, K., Liddle, P.F., and Frackowiak, R.S.J. (1991). PET study of word finding. *Neuropsychologia* **29,** 1–12.

Fujimaki, N., Miyauchi, S., Puetz, B., Sasaki, Y., Takino, R., Sakai, K., and Tamada, T. (1999). Functional magnetic resonance imaging of neural activity related to orthographic, phonological, and lexico-semantic judgments of visually presented characters and words. *Hum. Brain Mapping* **8,** 44–59.

Funahashi, S., Bruce, C.J., and Goldman-Rakic, P.S. (1989). Mnemonic coding of visual space in the monkey's dorsolateral prefrontal cortex. *J. Neurophysiol.* **61,** 331–349.

Fuster, J.M. (1989). "The Prefrontal Cortex," 2nd ed. Raven, New York.

Galaburda, A.M. (1980). La region de Broca: Observations anatomiques faites un siecle apres la mort de son decoveur. *Rev. Neurol. (Paris)* **136,** 609–616.

Galaburda, A. M., and Geschwind, N. (1981). Anatomical asymmetries in the adult and developing brain and their implications for function. *Adv. Pediatr.* **28,** 271–292.

Galaburda, A. M., and Sanides, F. (1980). Cytoarchitectonic organization of the human auditory cortex. *J. Comp. Neurol.* **190,** 597–610.

Galaburda, A. M., LeMay, M., Kemper, T.L., and Geschwind, N. (1978b). Right-left asymmetries in the brain. *Science* **199,** 852–856.

Galaburda, A. M., Sanides, F., and Geschwind, N. (1978a). Human brain: Cytoarchitectonic left-right asymmetries in the temporal speech region. *Arch. Neurol. (Chicago)* **35,** 812–817.

Galletti, C., Battaglini, P.P., and Fattori, P. (1997). The posterior parietal cortex in humans and monkeys. *News Physiol. Sci.* **12,** 166–171.

Galletti, C., Fattori, P., Battaglini, P.P., Shipp, S., and Zeki, S. (1996). Functional demarcation of a border between areas V6 and V6A in the superior parietal gyrus of the macaque monkey. *Eur. J. Neurosci.* **8,** 30–52.

Galletti, C., Fattori, P., Kutz, D.F., and Gamberini, M. (1999). Brain location and visual topography of cortical area V6A in the macaque monkey. *Eur. J. Neurosci.* **11,** 575–582.

Garey, L.J. (1984). Structural development of the visual system of man. *Hum. Neurobiol.* **3,** 75–80.

Gerebtzoff, M.A. (1939). Sur quelques voies d'association de l'écorce cérébrale (Recherches anatomo-expérimentales) *J. Belge Neurol. Psychiatr.* **39,** 205–221.

Gerhardt, E. (1940). Die Cytoarchitektonik des Isocortex parietalis beim Menschen. *J. Psychol. Neurol.* **49,** 367.

Gerstmann, J. (1930). Zur Symptomatologie der Hirnläsionen im Übergangsgebiet der unteren Parietal- und mittleren Occipitalwindung. *Nervenarzt* **3,** 691–695.

Geschwind, N. (1970). The organization of language and the brain. *Science* **170,** 940–944.

Geschwind, N., and Levitsky, W. (1968). Human brain: Left-right asymmetries in the temporal speech region. *Science* **161,** 186–187.

Geyer, S., Ledberg, A., Schleicher, A., Kinomura, S., Schormann, T., Bürgel, U., Klingberg, T., Larsson, J., Zilles, K. and Roland, P. E. (1996). Two different areas within the primary motor cortex of man. *Nature* **382,** 805–807.

Geyer, S., Matelli, M., Luppino, G., Schleicher, A., Jansen, Y., Palomero-Gallagher, N., and Zilles, K. (1998). Receptor autoradiographic mapping of the mesial motor and premotor cortex of the macaque monkey. *J. Comp. Neurol.* **397,** 231–250.

Geyer, S., Matelli, M., Luppino, G., and Zilles, K. (2000c). Functional neuroanatomy of the primate isocortical motor system. *Anat. Embryol.* **202,** 443–474.

Geyer, S., Schleicher, A., and Zilles, K. (1997). The somatosensory cortex of human: Cytoarchitecture and regional distributions of receptor-binding sites. *NeuroImage* **6,** 27–45.

Geyer, S., Schleicher, A., and Zilles, K. (1999). Areas 3a, 3b, and 1 of human primary somatosensory cortex: 1. Microstructural organization and interindividual variability. *NeuroImage* **10,** 63–83.

Geyer, S., Schormann, T., Mohlberg, H., and Zilles, K. (2000b). Areas 3a, 3b, and 1 of human primary somatosensory cortex. 2. Spatial normalization to standard anatomical space. *NeuroImage* **11,** 684–696.

Geyer, S., Zilles, K., Luppino, G., and Matelli, M. (2000a). Neurofilament protein distribution in the macaque monkey dorsolateral premotor cortex. *Eur. J. Neurosci.* **12,** 1554–1566.

Glees, P., Cole, J., Whitty, C.W.M., and Cairns, H. (1950). The effects of lesions in the cingulate gyrus and adjacent areas in monkeys. *J. Neurol. Neurosurg. Psychiatry* **13,** 178–190.

Goldman, P.S. (1979). Contralateral projections to the dorsal thalamus from frontal association cortex in the rhesus monkey. *Brain Res.* **166,** 166–171.

Goldman, P.S. (1981). Development and plasticity of primate frontal association cortex. *In* "The Organization of the Cerebral Cortex" (F.O. Schmitt, F.C. Worden, G. Adelman, and S.G. Dennis, eds.), pp. 69–97. MIT Press, Cambridge, MA.

Goldman, P.S., and Nauta, W.J.H. (1976). Autoradiographic demonstation of a projection from prefrontal association cortex to the superior colliculus in the rhesus monkey. *Brain Res.* **116,** 145–149.

Goldman, P.S., and Nauta, W.J.H. (1977a). An intricately patterned prefrontocaudate projection in the rhesus monkey. *J. Comp. Neurol.* **171,** 369–386.

Goldman, P.S., and Nauta, W.J.H. (1977b). Columnar distribution of corticocortical fibers in the frontal association, limbic and motor cortex of the developing rhesus monkey. *Brain Res.* **122,** 393–413.

Goldman, P.S., and Schwartz, M.L. (1982). Interdigitation of contralateral and ipsilateral columnar projections to frontal association cortex in primates. *Science* **216,** 755–757.

Goldman-Rakic, P.S. (1984). Modular organization of prefrontal cortex. *Trends Neurosci.* **7,** 419–424.

Goldman-Rakic, P.S., and Porrino, L.J. (1985). The primate mediodorsal (MD) nucleus and its projections to the frontal lobe. *J. Comp. Neurol.* **242,** 535–560.

Grabowski, T.J., and Damasio, A.R. (2000). Investigating language with functional neuroimaging. *In* "Brain Mapping—The Systems" (A.W. Toga, and J.C. Mazziotta, eds.), pp. 425–458. Academic Press, San Diego.

Grafton, S.T., Arbib, M.A., Fadiga, L., and Rizzolatti, G. (1996). Localization of grasp representations in humans by positron emission tomography. 2. Observation compared with imagination. *Exp. Brain Res.* **112,** 103–111.

Grefkes, C., Geyer, S., Schormann, T., Roland, P., and Zilles, K. (2001). Human somatosensory area. 2. Observer-independent cytoarchitectonic mapping, interindividual variability, and population map. *NeuroImage* **14,** 617–631.

Grefkes, C., Weiss, P.H., Zilles, K., and Fink, G.R. (2002). Crossmodal processing of object features in human anterior intraparietal cortex: An fMRI study strongly implies equivalencies between humans and monkey. *Neuron* **35,** 173–184.

Gulyás, B., and Roland, P.E. (1991). Cortical fields participating in form and colour discrimination in the human brain. *Neuroreport* **2,** 585–588.

Gulyás, B., and Roland, P.E. (1994). Processing and analysis of form, colour and binocular disparity in the human brain: Functional anatomy by positron emission tomography. *Eur. J. Neurosci.* **6,** 1811–1828.

Gurd, J.M., Amunts, K., Weiss, P.H., Zafiris, O., Zilles, K., Marshall, J.C., and Fink, G.R. (2002). Posterior parietal cortex is implicated in continuous switching between verbal fluency tasks: An fMRI study with clinical implications. *Brain* **125,** 1024–1038.

Halgren, E., Baudena, P., Heit, G., Clarke, M., and Marinkovic, K. (1994). Spatio-temporal stages in face and word processing. 1. Depth-recorded potentials in the human occipital and parietal lobes. *J. Physiol.* **88,** 1–50.

Hari, R., Hamalainen, M., Ilmoniemi, R., Kaukoranta, E., Reinikainen, K., Salminen, J., Alho, K., Naatanen, R., and Sams, M. (1984). Responses of the primary auditory cortex to pitch changes in a sequence of tone pips: neuromagnetic recordings in man. *Neurosci. Lett.* **50,** 127–132.

Haug, H. (1958). "Quantitative Untersuchungen an der Sehrinde." Thieme, Stuttgart.

Haug, H. (1984). Macroscopic and microscopic morphometry of the human brain and cortex. A survey in the light of new results. *In* "Pathology" (P.G. Pilleri and F. Tagliavini, eds.), vol. 1, pp. 123–149. Brain Anatomy Institute, Ostermundingen, Bern.

Haxby, J.V., Horwitz, B., Ungerleider, L.G., Maisog, J.M., Pietrini, P., and Grady, C.L. (1994). The functional organization of human extrastriate cortex: A PET-rCBF study of selective attention to faces and locations. *J. Neurosci.* **14,** 6336–6353.

Haxby, J.V., Ungerleider, L.G., Horwitz, B., Rapoport, S.I., and Grady, C.L. (1995). Hemispheric differences in neural systems for face working memory: A PET-rCBF study. *Human Brain Mapping* **3,** 68–82.

Hayes, T.L., and Lewis, D.A. (1995). Anatomical specialization of the anterior motor speech area: Hemispheric differences in magnopyramidal neurons. *Brain Language* **49,** 289–308.

Hayes, T.L., and Lewis, D.A. (1996). Magnopyramidal neurons in the anterior motor speech region. *Arch. Neurol.* **53,** 1277–1283.

Heeger, D.J., Boynton, G.M., Demb, J.B., Seidemann, E., and Newsome, W.T. (1999). Motion opponency in visual cortex. *J. Neurosci.* **19,** 7162–7174.

Heimer, L. (1968). Synaptic distribution of centripetal and centrifugal nerve fibers in the olfactory system of the rat. An experimental anatomical study. *J. Anat.* **103,** 413–432.

Heimer, L. (1972). The olfactory connections of the diencephalon in the rat. An experimental light- and electron-microscopic study with special emphasis on the problem of terminal degeneration. *Brain Behav. Evol.* **6,** 484–523.

Hendry, S.H.C., and Carder, R.K. (1993). Neurochemical compartmentation of monkey and human visual cortex: Similarities and variations in calbindin immunoreactivity across species. *Vis. Neurosci.* **10,** 1109–1120.

Hendry, S.H.C., Hockfield, S., Jones, E.G., and McKay, R. (1984). Monoclonal antibody that identifies subsets of neurones in the central visual system of monkey and cat. *Nature* **307,** 267–269.

Hendry, S.H.C., Jones, E.G., Hockfield, S., and McKay, R.D.G. (1988). Neuronal populations stained with the monoclonal antibody Cat-301 in the mammalian cerebral cortex and thalamus. *J. Neurosci.* **8,** 518–542.

Herholz, K., Thiel, A., Pietrzyk, U., von Stockhausen, H.M., Karbe, H., Kessler, J., Bruckbauer, T., Halber, M., and Heiss, W.D. (1996). Individual functional anatomy of verb generation. *NeuroImage* **3,** 185–194.

Heywood, C.A., Gadotti, A., and Cowey, A. (1992). Cortical area V4 and its role in the perception of color. *J. Neurosci.* **12,** 4056–1065.

Heywood, C.A., Gaffan, D., and Cowey, A. (1995). Cerebral achromatopsia in monkeys. *Eur. J. Neurosci.* **7,** 1064–1073.

Hinke, R.M., Hu, X., Stillman, A.E., Kin, S.G., Merkle, H., Salmi, R., and Ugurbil, K. (1993). Functional magnetic resonance imaging of Broca's area during internal speech. *Cognit. Neurosc. Neuropsych.* **4,** 675–678.

Hirano, S., Kojima, H., Naito, Y., Honjo, I., Kamoto, Y., Okazawa, H., Ishizu, K., Yonekura, Y., Nagahama, Y., Fukuyama, H., and Konishi, J. (1996). Cortical speech processing mechanisms while vocalizing visually presented language. *Neuroreport* **8,** 363–367.

Hjorth-Simonsen, A. (1972). Projection of the lateral part of the entorhinal area to the hippocampus and fascia dentata. *J. Comp. Neurol.* **146,** 219–231.

Hockfield, S., Tootell, R.B.H., and Zaremba, S. (1990). Molecular differences among neurons reveal an organization of human visual cortex. *Proc. Nat. Acad. Sci. USA* **87,** 3027–3031.

Hof, P.R., and Morrison, J.H. (1995). Neurofilament protein defines regional patterns of cortical organization in the macaque monkey visual system: A quantitative immunohistochemical analysis. *J. Comp. Neurol.* **352,** 161–186.

Hopf, A. (1954). Die Myeloarchitektonik des Isocortex temporalis beim Menschen. *J. Hirnforsch.* **1,** 208–279.

Hopf, A. (1955). Über die Verteilung myeloarchitektonischer Merkmale in der isokortikalen Schläfenlappenrinde beim Menschen. *J. Hirnforsch.* **2,** 36–54.

Hopf, A. (1956). Über die Verteilung myeloarchitektonischer Merkmale in der Stirnhirnrinde beim Menschen. *J. Hirnforsch.* **2,** 311–333.

Hopf, A. (1968). Photometric studies on the myeloarchitecture of the human temporal lobe. *J. Hirnforsch.* **10,** 285–297.

Horton, J.C. (1984). Cytochrome oxidase patches: A new cytoarchitonic feature of monkey cortex. *Phil. Trans. Roy. Soc. Lond. Biol.* **304,** 199–253.

Horton, J.C., and Hedley-White, E.T. (1984). Mapping of cytochrome oxidase patches and ocular dominance columns in human visual cortex. *Phil. Trans. Roy. Soc. Lond. Ser. B* **304,** 255–272.

Howard, M.A., Patterson, K., Wise, R., Brown, W.D., Friston, K., Weiller, C., and Frackowiak, R.S.J. (1992). The cortical localization of the lexicons: Positron emission tomography evidence. *Brain* **115,** 1769–1782.

Howard, M.A., Volkov, I.O., Abbas, P.J., Damasio, H., Ollendieck, M.C., and Granner, M.A. (1996). A chronic microelectrode investigation of the tonotopic organization of human auditory cortex. *Brain Res.* **724,** 260–264.

Hubel, D.H., and Livingstone, M.S. (1987). Segregation of form, color and stereopsis in primate area 18. *J. Neurosci.* **7,** 3378–3415.

Huk, A.C., and Heeger, D.J. (2002). Pattern-motion responses in human visual cortex. *Nat. Neurosci.* **5,** 72–75.

Huk, A.C., Dougherty, R.F., and Heeger, D.J. (2002). Retinotopy and functional subdivision of human areas MT and MST. *J. Neurosci.* **22,** 7195–7205.

Hyvärinen, J. (1982a). Posterior parietal lobe of the primate brain. *Physiol. Rev.* **62,** 1060–1129.

Hyvärinen, H. (1982b). "The Parietal Cortex of Monkey and Man." Springer-Verlag, Berlin, New York.

Iacoboni, M., Woods, R.P., Brass, M., Bekkering, H., Mazziotta, J.C., and Rizzolatti, G. (1999). Cortical mechanisms of human imitation. *Science* **286,** 2526–2528.

Inoue, K., Kawashima, R., Sugiura, M., Ogawa, A., Schormann, T., Zilles, K., and Fukuda, H. (2001). Activation in the ipsilateral posterior parietal cortex during a tool use: A PET study. *NeuroImage* **14,** 1469–1475.

Jacobsen, C.F. (1935). Functions of frontal association areas in primates. *Arch. Neurol. Psychiatry* **33,** 558–569.

Jacobson, S., and Trojanowski, J.Q. (1977a). Prefrontal granular cortex of the rhesus monkey. I. Intrahemispheric cortical afferents. *Brain Res.* **132,** 209–233.

Jacobson, S., and Trojanowski, J.Q. (1977b). Prefrontal granular cortex of the rhesus monkey. II. Interhemispheric cortical afferents. *Brain Res.* **132,** 235–246.

Jeannerod, M. (2001). Neural simulation of action: A unifying mechanism for motor cognition. *NeuroImage* **14,** 103–109.

Jeannerod, M., Arbib, M., Rizzolatti, G., and Sakata, H. (1995). Grasping objects: The cortical mechanisms of visuomotor transformation. *TINS* **18,** 314–320.

Johnson, T.N., Rosvold, H.E., and Mishkin, M. (1968). Projections from behaviorally-defined sectors of the prefrontal cortex to the basal ganglia, septum and diencephalon of the monkey. *Exp. Neurol.* **21,** 20–34.

Johnsrude, I.S., Morosan, P., Brett, M., Zilles, K., and Frackowiak, R.S.J. (2000). Functional specialization within three cytoarchitectonically defined primary auditory cortical areas in humans. *Soc. Neurosci. Abstr.* **26,** S1971.

Jones, E.G., and Porter, R. (1980). What is area 3a? *Brain Res. Rev.* **2,** 1–43.

Jones, E.G., and Powell, T.P.S. (1970). An anatomical study of converging sensory pathways within the cerebral cortex of the monkey, *Brain* **93,** 793–820.

Kaada, B. (1960). Cingulate, posterior orbital, anterior insular and temporal pole cortex. *In* "Handbook of Physiology" (J. Field, H.W. Magoun, and V.E. Hall, eds.), sect. 1, vol. II, pp. 1345–1372. Am. Physiol. Soc., Washington, DC.

Keating, E.G. (1980). Residual spatial vision in the monkey after removal of striate and preoccipital cortex. *Brain Res.* **187,** 271–290.

Kievit, J., and Kuypers, G.J.M. (1977). Organization of the thalamocortical connexions to the frontal lobe in the rhesus monkey. *Exp. Brain Res.* **29,** 299–322.

Kim, K.H.S., Relkin, N.R., Lee, K.-M., and Hirsch, J. (1997). Distinct cortical areas associated with native and second languages. *Nature* **388,** 171–174.

Knauer, A. (1909). Die Myeloarchitektonik der Brocaschen Region. *Neurol. Centralbl.* **28,** 1240–1243.

Kononova, E.P. (1935). Structural variability of the cortex cerebri. Inferior frontal gyrus in adults (Russian). *In* "Annals of the Brain Research Institute" (S.A. Sarkisov and I.N. Filimonov, eds.), Vol. I, pp. 49–118. State Press for Biological and Medical Literature, Moscow, Leningrad.

Kononova, E.P. (1949). The frontal lobe (Russian). *In* "The Cytoarchitecture of the Human Cortex Cerebri" (S.A. Sarkisov, I.N. Filimonov, and N.S. Preobrashenskaya, eds.), pp. 309–343. Medgiz, Moscow.

Koski, L., Wohlschläger, A., Bekkering, H., Woods, R.P., Dubeau, M.-C., Mazziotta, J.C., and Iacoboni, M. (2002). Modulation of motor and premotor activity during imitation of target-directed actions. *Cereb. Cortex* **14,** 847–855.

Krams, M., Rushworth, M.F.S., Deiber, M.-P., Frackowiak, R.S.J., and Passingham, R.E. (1998). The preparation, execution and suppression of copied movements in the human brain. *Exp. Brain Res.* **120,** 386–398.

Kreht, H. (1936). Cytoarchitektonik und motorisches Sprachenzentrum. *Z. Mikrosk. Anat. Forsch.* **39,** 351.

Künzle, H. (1975). Bilateral projections from precentral motor cortex to the putamen and other parts of the basal ganglia. An autoradiographic study in *Macaca fascicularis*. *Brain Res.* **88,** 195–209.

Künzle, H. (1978). An autoradiographic analysis of the efferent connections from premotor and adjacent prefrontal regions (areas 6 and 9) in *Macaca fascicularis*. *Brain Behav. Evol.* **15,** 185–234.

Kuypers, H.J.M. (1958). Cortico-bulbar connections to the pons and lower brain stem in man. *Brain* **81,** 364–388.

Langner, G., Sams, M., Heil, P., and Schulze, H. (1997). Frequency and periodicity are represented in orthogonal maps in the human auditory cortex: Evidence from magnetoencephalography. *J. Comp. Physiol. A.* **181,** 665–676.

Larsson, J., Amunts, K., Gulyás, B., Malikovic, A., Zilles, K., and Roland, P.E. (1999). Neuronal correlates of real and illusory contour perception: functional anatomy with PET. *Eur. J. Neurosci.* **11,** 4024–4036.

Lauter, J.L. (1992). Processing asymmetries for complex sounds: Comparisons between behavioral ear advantages and electrophysiological asymmetries based on quantitative electroencephalography. *Brain Cogn.* **19,** 1–20.

Lauter, J.L., Herscovitch, P., Formby, C., and Raichle, M.E. (1985). Tonotopic organization in human auditory cortex revealed by positron emission tomography. *Hear. Res.* **20,** 199–205.

Le Bihan, D., Turner, R., Zeffiro, T.A., Cuénod, C.A., Jezzard, P., and Bonnerot, V. (1993). Activation of human primary visual cortex during visual recall: A magnetic resonance imaging study. *Proc. Nat. Acad. Sci. USA* **90,** 11802–11805.

Leonard, C.M., Puranik, C., Kuldau, J.M., and Lombardino, L.J. (1998). Normal variation in the frequency and location of human auditory cortex landmarks. Heschl's gyrus: Where is it? *Cereb. Cortex* **8,** 397–406.

Liegeois Chauvel, C., Musolino, A., Badier, J.M., Marquis, P., and Chauvel, P. (1994). Evoked potentials recorded from the auditory cortex in man: Evaluation and topography of the middle latency components. *Electroencephalogr. Clin. Neurophysiol.* **92,** 204–214.

Liegeois Chauvel, C., Musolino, A., and Chauvel, P. (1991). Localization of the primary auditory area in man. *Brain* **114,** 139–151.

Livingstone, M.S., and Hubel, D.H. (1983). Specificity of cortico-cortical connections in monkey visual system. *Nature* **304,** 531–534.

Locke, S. and Yakovlev, P.I. (1965). Transcallosal connections of the cingulum of man. *Arch. Neurol. (Chicago)* **13,** 471–476.

Lohmann, A.H.M., and Lammers, J.J. (1967). On the structure and fibre connections of the olfactory centres in mammals. *Prog. Brain Res.* **23,** 65–82.

Lu, M.-T., Preston, J.R., and Strick, P.L. (1994). Interconnections between the prefrontal cortex and the premotor areas in the frontal lobe. *J. Comp. Neurol.* **341,** 375–392.

Lueck, C.J., Zeki, S., Friston, K.J., Dieber, M.P., Cope, P., Cunningham, V.J., Lammertsma, A.A., Kennard, C., and Frackowiak, R.S.J. (1989). The colour centre in the cerebral cortex of man. *Nature* **340,** 386–389.

Lungwitz, W. (1937). Zur myeloarchitektonischen Untergliederung der menschlichen Area praeoccipitalis (Area 19 Brodmann). *J. Psychol. Neurol.* **47,** 607–638.

Luppino, G., Matelli, M., Camarda, R.M., Gallese, V., and Rizzolatti, G. (1991). Multiple representations of body movements in mesial area 6 and the adjacent cingulate cortex: An intracortical microstimulation study in the macaque monkey. *J. Comp. Neurol.* **311,** 463–482.

Luppino, G., Matelli, M., Camarda, R., and Rizzolatti, G. (1993). Corticocortical connections of area F3 (SMA-proper) and area F6 (pre-SMA) in the macaque monkey. *J. Comp. Neurol.* **338,** 114–140.

Luppino, G., Matelli, M., Camarda, R., and Rizzolatti, G. (1994). Corticospinal projections from mesial frontal and cingulate areas in the monkey. *Neuroreport* **5,** 2545–2548.

Luppino, G., Matelli, M., and Rizzolatti, G. (1990). Cortico-cortical connections of two electrophysiologically identified arm representations in the mesial agranular frontal cortex. *Exp. Brain Res.* **82,** 214–218.

Luppino, G., Murata, A., Govoni, P., and Matelli, M. (1999). Largely segregated parietofrontal connections linking rostral intraparietal cortex (areas AIP and VIP) and the ventral premotor cortex (areas F5 and F4). *Exp. Brain. Res.* **128,** 181–187.

Luria, A.R. (1959). Disorders of "simultaneous perception" in a case of bilateral occipitoparietal brain injury. *Brain* **82,** 437–449.

Marin-Padilla, M. (1970). Prenatal and early postnatal ontogenesis of the human motor cortex: A Golgi study. I. The sequential development of the cortical layers. *Brain Res.* **23,** 167–183.

Martin, A., Haxby, J.V., Lalonde, F.M., Wiggs, C.L., and Ungerleider, L.G. (1995). Discrete cortical regions associated with knowledge of color and knowledge of action. *Science* **270,** 102–105.

Matelli, M., and Luppino, G. (1996). Thalamic input to mesial and superior area 6 in the macaque monkey. *J. Comp. Neurol.* **372,** 59–87.

Matelli, M., and Luppino, G. (2001). Parietofrontal circuits for action and space perception. *NeuroImage* **14,** 27–32.

Matelli, M., Covoni, P., Galletti, C., Kutz, D.F., and Luppino, G. (1998). Superior area 6 afferents from the superior parietal lobule in the macaque monkey. *J. Comp. Neurol.* **402,** 327–352.

Matelli, M., Camarda, R., Glickstein, M., and Rizzolatti, G. (1986). Afferent and efferent projections of the inferior area 6 in the macaque monkey. *J. Comp. Neurol.* **251,** 281–298.

Matelli, M., Luppino, G., Fogassi, L., and Rizzolatti, G. (1989). Thalamic input to inferior area 6 and area 4 in the macaque monkey. *J. Comp. Neurol.* **280,** 468–488.

Matelli, M., Luppino, G., and Rizzolatti, G. (1985). Patterns of cytochrome oxidase activity in the frontal agranular cortex of the macaque monkey. *Behav. Brain Res.* **18,** 125–136.

Matelli, M., Luppino, G., and Rizzolatti, G. (1991). Architecture of superior and mesial area 6 and the adjacent cingulate cortex in the macaque monkey. *J. Comp. Neurol.* **311,** 445–462.

Maunsell, J.H.R., and Van Essen, D.C. (1983). Functional properties of neurons in middle temporal visual area of the macaque monkey. I. Selectivity for stimulus direction, speed, and orientation. *J. Neurophysiol.* **49,** 1127–1147.

Maunsell, J.H.R., and Van Essen, D.C. (1987). Topographic organization of the middle temporal visual area in the macaque monkey. I. Representational biases and the relationship to callosal connections and myeloarchitectonic boundaries. *J. Comp. Neurol.* **266,** 535–555.

Mazoyer, B.M., Tzourio, N., Frak, V., Syrota, A., Murayama, N., Levrier, O., Salamon, G., Dehaene, S., Cohen, L., and Mehler, J. (1993). The cortical representation of speech. *J. Cogn. Neurosci.* **5,** 467–479.

Mazziotta, J.C., and Metter, E.J. (1988). Brain cerebral metabolic mapping of normal and abnormal language and its acquisition during development. *Res. Publ. Assoc. Res. Nerv. Ment. Dis.* **66,** 245–266.

Mazziotta, J.C., Phelps, M.E., Carson, R.E., and Kuhl, D.E. (1982). Tomographic mapping of human cerebral metabolism: Auditory stimulation. *Neurology* **32,** 921–937.

Mazziotta, J., Toga, A., Evans, A., Fox, P., Lancaster, J., Zilles, K., Woods, R., Paus, T., Simpson, G., Pike, B., Holmes, C., Collins, L., Thompson, P., MacDonald, D., Iacobini, M., Schormann, T., Amunts, K., Palomero-Gallagher, N., Geyer, S., Parsons, L., Narr, K., Kabani, N., Le Goualher, G., Boomsma, D., Cannon, T., Kawashima, R., and Mazoyer, B. (2001a). A probabilistic atlas and reference system for the human brain: International Consortium for Brain Mapping (ICBM). *Phil. Trans. Roy. Soc. Lond. Biol. Sci.* **356,** 1293–1322.

Mazziotta, J., Toga, A., Evans, A., Fox, P., Lancaster, J., Zilles, K., Woods, R., Paus, T., Simpson, G., Pike, B., Holmes, C., Collins, L., Thompson, P., MacDonald, D., Iacobini, M., Schormann, T., Amunts, K., Palomero-Gallagher, N., Geyer, S., Parsons, L., Narr, K., Kabani, N., Le Goualher, G., Boomsma, D., Cannon, T., Kawashima, R., and Mazoyer, B. (2001b). A four-dimensional probabilistic atlas of the human brain. *J. Am. Med. Inform. Assoc. JAMIA* **8,** 401–430.

McGuire, P.K., Bates, J.F., and Goldmann-Rakic, P.S. (1991). Interhemispheric integration. I. Symmetry and convergence of the corticocortical connections of the left and right principal sulcus (PS) and the left and right supplementary motor area (SMA) in the rhesus monkey. *Cereb. Cortex* **1,** 390–407.

Meadows, J.C. (1974). Disturbed perception of colours associated with localized cerebral lesions. *Brain* **97,** 615–632.

Mesulam, M.-M. (1994). Higher visual functions of the cerebral cortex and their disruption in clinical practice. *In* "Principles and Practice in Ophthalmology" (D.M. Albert and F.A. Jakobiec, eds.), pp. 2640–2653, Saunders, Philadelphia.

Mesulam, M.-M. (1998). From sensation to cognition. *Brain* **121,** 1013–1052.

Mesulam, M.-M. (1999). Spatial attention and neglect. Parietal, frontal and cingulated contributions to the mental representation and attentional targeting of salient extrapersonal events. *Phil. Trans. Roy. Soc. Lond. Ser. B Biol. Sci.* **354,** 1325–1346.

Mesulam, M.-M., and Mufson, E.J. (1982). Insula of the old world monkey. III. Efferent cortical output and comments of function. *J. Comp Neurol.* **212,** 38–52.

Mesulam, M.-M., and Mufson, E.J. (1985). The insula of Reil in man and monkey. Architectonics, connectivity, and function. *In* "Cerebral Cortex" (A. Peters and E.G. Jones, eds.), vol. 4, pp. 179–226. Plenum, New York.

Mesulam, M.-M., van Hoesen, G.W., Pandya, D.N., and Geschwind, N. (1977). Limbic and sensory connections of the inferior parietal lobe (area PG) in the rhesus monkey: A study with a new method for horseradish peroxidase histochemistry. *Brain Res.* **136,** 393–414.

Milner, B., and Petrides, M. (1984). Behavioural effects of frontal lobe lesions in man. *Trends Neurosci.* **7,** 403–407.

Minckler, J., Klemme, R.M., and Minckler, D. (1944). The course of efferent fibers from the human premotor cortex. *J. Comp. Neurol.* **81,** 259–277.

Miskin, M., Ungerleider, L.G., and Macko, K.A. (1983). Object and spatial vision: Two cortical pathways. *Trends Neurosci.* **6,** 414–417.

Moll, J., de Oliveira-Souza, R., Bramati, I.E., and Grafman, J. (2002). Functional networks in emotional moral and nonmoral social judgements. *NeuroImage* **16,** 696–703.

Moniz, E. (1936). "Tentatives operatoires dans le traitment de certaines psychoses." Masson, Paris.

Morosan, P., Rademacher, J., Schleicher, A., Amunts, K., Schormann, T., and Zilles, K. (2001). Human primary auditory cortex: Cytoarchitectonic subdivisions and mapping into a spatial reference system. *NeuroImage* **13,** 684–701.

Mufson, E.J., and Mesulam, M.M. (1982). Insula of the old world monkey. II. Afferent cortical input and comments on the claustrum. *J. Comp. Neurol.* **212,** 23–37.

Naito, E., Ehrsson, H.H., Geyer, S., Zilles, K., and Roland, P.E. (1999). Illusory arm movements activate cortical motor areas: A positron emission tomography study. *J. Neurosci.* **19,** 6134–6144.

Naito, E., Kinomura, S., Geyer, S., Kawashima, R., Roland, P.E., and Zilles, K. (2000). Fast reaction to different sensory modalities activate common fields in the motor areas, but the anterior cingulate cortex is involved in the speed of reaction. *J. Neurophysiol.* **83,** 1701–1709.

Nakamura, K., Kawashima, R., Sato, N., Nakamura, A., Sugiura, M., Kato, T., Hatano, K., Ito, K., Fukuda, H., Schormann, T., and Zilles, K. (2000). Functional delineation of the human occipito-temporal areas related to familiar scene processing. *Brain* **123,** 1903–1912.

Nauta, W.J.H. (1961). Fibre degeneration following lesions of the amygdaloid complex in the monkey. *J. Anat.* **95,** 515–531.

Nauta, W.J.H. (1964). Some efferent connections of the prefrontal cortex in monkey. *In* "The Frontal Granular Cortex and Behavior" (J.M. Warren and K. Akert, eds.), pp. 397–409. McGraw-Hill, New York.

Ngowyang, G. (1932). Die Zytoarchitektonik der Felder des Gyrus rectus. *J. Psychol. Neurol.* **44,** 475–493.

Ngowyang, G. (1934). Die Zytoarchitektonik des menschlichen Stirnhirns. *Natl. Res. Inst. Psychol. Sinica* **7,** 1.

Nichelli, P., Grafman, J., Pietrini, P., Clark, K., Lee, K.Y., and Miletich, R. (1995). Where the brain appreciates the moral of a story. *Neuroreport* **6,** 2309–2313.

Nicholls, M.E. (1998). Support for a structural model of aural asymmetries. *Cortex* **34,** 99–110.

Nobre, A.C., Allison, T., and McCarthy, G. (1994). Word recognition in the human inferior temporal lobe. *Nature* **372,** 260–263.

Ojeman, G.A. (1991). Cortical organization of language. *J. Neurosci.* **11,** 2281–2287.

Ojemann, G.A., Creutzfeld, O.D., and Lettich, E. (1987). Neuronal activity in human temporal cortex related to naming and short-term verbal memory. *In* "Fundamental Mechanisms of Human Brain Function" (J. Engel, Jr., G.A. Ojemann, H.O. Lüders, and P.D. Williamson, eds.), pp. 61–68. Raven Press, New York.

Pakkenberg, B., and Gundersen, H.J.G. (1997). Neocortical neuron number in humans: Effect of sex and age. *J. Comp. Neurol.* **384,** 312–320.

Pandya, D.N. (1995). Anatomy of the auditory cortex. *Rev. Neurol. (Paris)* **151,** 486–494.

Pandya, D.N., and Kuypers, H.G.J. M.(1969). Cortico-cortical connections in the rhesus monkey. *Brain Res.* **13,** 13–36.

Pandya, D.N., and Seltzer, B. (1982a). Intrinsic connections and architectonics of posterior parietal cortex in the rhesus monkey. *J. Comp. Neurol.* **204,** 196–210.

Pandya, D.N., and Seltzer, B. (1982b). Association areas of the cerebral cortex. *TINS* **5,** 386–390.

Pandya, D.N., and Yeterian, E. (1985). Architecture and connections of cortical association areas. *In* "Cerebral Cortex" (A. Peters and E.G. Jones, eds.), vol. 4 Association and Auditory Cortices, pp. 3–61. Plenum Press, New York.

Pandya, D.N., and Yeterian, E. (1998). Comparison of prefrontal architecture and connections. *In* "The Prefrontal Cortex" (A.C. Roberts, T.W. Robbins, and L. Weiskrantz, eds.), pp. 51–66. Oxford Univ. Press, Oxford.

Pandya, D.N., Dye, P., and Butters, N. (1971a). Efferent cortical projections of the prefrontal cortex of the rhesus monkey. *Brain Res.* **31,** 35–46.

Pandya, D.N., Karol, E.A., and Heilbronn, D. (1971b). The topographical distribution of interhemispheric projections in the corpus callosum of the rhesus monkey. *Brain Res.* **32,** 31–43.

Pandya, D N., van Hoesen, G.W., and Mesulam, M.M. (1981). Efferent connections of the cingulate gyrus in the rhesus monkey. *Exp. Brain Res.* **42,** 319–330.

Pantev, C., Bertrand, O., Eulitz, C., Verkindt, C., Hampson, S., Schuierer, G., and Elbert, T. (1995). Specific tonotopic organizations of different areas of the human auditory cortex revealed by simultaneous magnetic and electric recordings. *Electroencephalogr. Clin. Neurophysiol.* **94,** 26–40.

Pantev, C., Oostenveld, R., Engelien, A., Ross, B., Roberts, L.E., and Hoke, M. (1998b). Increased auditory cortical representation in musicians. *Nature* **392,** 811–814.

Pantev, C., Ross, B., Berg, P., Elbert, T., and Rockstroh, B. (1998a). Study of the human auditory cortices using a whole-head magnetometer: Left vs. right hemisphere and ipsilateral vs. contralateral stimulation. *Audiol. Neurootol.* **3,** 183–190.

Parsons, L.M., and Fox, P.T. (1998). The neural basis of implicit movements used in recognizing hand shape. *Cogn. Neuropsychol.* **15,** 583–615.

Parsons, L.M., Fox, P.T., Downs, J.H., Glass, T., Hirsch, T.B., Martin, C.C., Jerabek, P.A., and Lancaster, J.L. (1995). Use of implicit motor imagery for visual shape discrimination as revealed by PET. *Nature* **375,** 54–58.

Pasik, P., and Pasik, T. (1982). Visual functions in monkeys after total removal of visual cerebral cortex. *Contr. Sensory Physiol.* **7,** 147–200.

Passingham, R.E., and Toni, I. (2001). Contrasting the dorsal and ventral visual systems: Guidance of movement versus decision making. *NeuroImage* **14,** 125–131.

Paul, F. (1971). Biometrische Analyse der Volumina des Prosencephalon und der Grosshirnrinde von 31 menschlichen Gehirnen. *Z. Anat. Entwicklungsgesch.* **133,** 325–368.

Paulesu, E., Frith, U., Snowling, M., Gallagher, A., Morton, J., Frackowiak, R.S.J., and Frith, C.D. (1996). Is developmental dyslexia a disconnection syndrome? Evidence from PET scanning. *Brain* **119,** 143–157.

Paus, T., Petrides, M., Evans, A.C., and Meyer, E. (1993). Role of the human anterior cingulate cortex in the control of oculomotor, manual, and speech responses: A positron emission tomography study. *J. Neurophysiol.* **70,** 453–469.

Paxinos, G., Huang X.-F., and Toga, A.W. (2000). "The Rhesus Monkey Brain in Stereotaxic Coordinates." Academic Press, San Diego.

Penfield, W., and Rasmussen, T. (1950). "The Cerebral Cortex of Man." Macmillan, New York.

Penfield, W., and Welch, K. (1951). The supplementary motor area of the cerebral cortex. A clinical and experimental study. *Arch. Neurol. Psychiatry* **66,** 289–317.

Penhune, V.B., Zatorre, R.J., MacDonald, J.D., and Evans, A.C. (1996). Interhemispheric anatomical differences in human primary auditory cortex: Probabilistic mapping and volume measurement from magnetic resonance scans. *Cereb. Cortex* **6,** 661–672.

Peterhans, E., and von der Heydt, R. (1989). Mechanisms of contour perception in monkey visual cortex. II. Contours bridging gaps. *J. Neurosci.* **9,** 1749–1763.

Petersen, S.E., Fox, P.T., Posner, M.I., Mintum, M., and Raichle, M.E. (1988). Positron emission tomographic studies of the cortical anatomy of single-word processing. *Nature* **331,** 585–589.

Petersen, S.E., Fox, P.T., Snyder, A.Z., and Raichle, M.E. (1990). Activation of extrastriate and frontal cortical areas by visual words and word-like stimuli. *Science* **249,** 1041–1044.

Petras, J.M. (1971). Connections of the parietal lobe. *J. Psychiatr. Res.* **8,** 189–201.

Petrides, M., and Pandya, D. (1984). Projections to the frontal cortex from the posterior parietal region in the rhesus monkey. *J. Comp. Neurol.* **228,** 105–116.

Petrides, M., and Pandya, D. (1994). Comparative architectonic analysis of the human and the macaque frontal cortex. *In* "Handbook of Neuropsychology" (F. Boller and J. Grafman, eds.), pp. 17–58. Elsevier, Amsterdam.

Petrides, M., and Pandya, D. (1999). Dorsolateral prefrontal cortex: Comparative cytoarchitectonic analysis in the human and the macaque brain and corticocortical connection patterns. *Eur. J. Neurosci.* **11,** 1011–1036.

Petrides, M., Alivisatos, B., Meyer, E., and Evans, A.C. (1993). Functional activation of the human frontal cortex during the performance of verbal working memory tasks. *Proc. Nat. Acad. Sci.* **90,** 878–882.

Phan, K.L., Wager, T., Taylor, S.F., and Liberzon, I. (2002). Functional neuroanatomy of emotion: A meta-analysis of emotion activation studies in PET and fMRI. *NeuroImage* **16,** 331–348.

Picard, N., and Strick, P.L. (1996). Motor areas of the medial wall: A review of their location and functional activation. *Cereb. Cortex* **6,** 342–353.

Pigache, R.M. (1970). The anatomy of "Paleocortex." A critical review. *Ergeb. Anat. Entwicklungsgesch.* **43,** 1–62.

Poeppel, D., Yellin, E., Phillips, C., Roberts, T.P., Rowley, H.A., Wexler, K., and Marantz, A. (1996). Task-induced asymmetry of the auditory evoked M100 neuromagnetic field elicited by speech sounds. *Brain Res. Cogn. Brain Res.* **4,** 231–242.

Poggio, G.F., and Fischer, B. (1977). Binocular interaction and depth sensitivity in striate and prestriate cortex of behaving rhesus monkey. *J. Neurophysiol.* **40,** 1392–1405.

Powell, T.P.S., Cowan, W.M., and Raisman, G. (1965). The central olfactory connexions. *J. Anat.* **99,** 791–813.

Preuss, T.M., and Coleman, G.Q. (2002). Human-specific organization of primary visual cortex: Alternating compartments of dense Cat-301 and calbindin immunoreactivity in layer IVA. *Cereb. Cortex* **12,** 671–691.

Preuss, T.M., and Goldmann-Rakic, P.S. (1989). Connections of the ventral granular frontal cortex of macaques with perisylvian premotor and somatosensory areas: Anatomical evidence for somatic representation in primate frontal association cortex. *J. Comp. Neurol.* **282,** 293–316.

Preuss, T.M., and Goldmann-Rakic, P.S. (1990). Myelo- and cyto-architecture of the granular frontal cortex and surrounding regions in the strepsirhine primate Galago and the anthropoid primate *Macaca*. *J. Comp. Neurol.* **310,** 439–474.

Preuss, T.M., Qi, H., and Kaas, J.H. (1999). Distinctive compartmental organization of human primary visual cortex. *Proc. Nat. Acad. Sci. USA* **96,** 11601–11606.

Price, G., and Giraud, A.L. (2001). The constraints of functional neuroimaging places on classical models of auditory word processing. *J. Cogn. Neurosci.* **13,** 754–765.

Price, J.L. (1973). An autoradiographic study of complementary laminar patterns of termination of afferent fibers to the olfactory cortex. *J. Comp. Neurol.* **150,** 87–108.

Puce, A., Allison, T., Gore, J.C., and McCarthy, G. (1995). Face-sensitive regions in human extrastriate cortex studied by functional MRI. *J. Neurophysiol.* **74,** 1192–1199.

Qureshy, A., Kawashima, R., Imran, M.B., Sugiura, M., Goto, R., Okada, K., Inoue, K., Itoh, M., Schormann, T., Zilles, K., and Fukuda, H. (2000). Functional mapping of human brain in olfactory processing: A PET study. *J. Neurophysiol.* **84,** 1656–1666.

Rabinowicz, T. (1967). Quantitative appraisal of the cerebral cortex of the premature infant of 8 months. *In* "Regional Development of the Brain in Early Life" (A.A. Minkowsky, (eds.), pp. 92–118. Blackwell Sci Publ, Oxford.

Rademacher, J., Bürgel, U., Geyer, S., Schormann, T., Schleicher, A., Freund, H.-J., and Zilles, K. (2001c). Variability and asymmetry in the human precentral motor system. A cytoarchitectonic and myeloarchitectonic brain mapping study. *Brain* **124,** 2232–2258.

Rademacher, J., Caviness, V.S., Jr., Steinmetz, H., and Galaburda, A.M. (1993). Topographical variation of the human primary cortices: Implications for neuroimaging, brain mapping, and neurobiology. *Cerebr. Cortex* **3,** 313–329.

Rademacher, J., Galaburda, A.M., Kennedy, D.N., Filipek, P.A., and Caviness, V.S., Jr. (1992). Human cerebral cortex: Localization, parcellation and morphometry with magnetic resonance imaging. *J. Cogn. Neurosci.* **4,** 352–374.

Rademacher, J., Morosan, P., Schleicher, A., Freund, H.-J., and Zilles, K. (2001a). Human primary auditory cortex in women and men. *NeuroReport* **12,** 1561–1565.

Rademacher, J., Morosan, P., Schormann, T., Schleicher, A., Werner, C., Freund, H.-J., and Zilles, K. (2001b). Probabilistic mapping and volume measurement of human primary auditory cortex. *NeuroImage* **13,** 669–683.

Rajkowska, G., and P.S. Goldman-Rakic (1995a). Cytoarchitectonic definition of prefrontal areas in the normal human cortex. I. Remapping of areas 9 and 46 using quantitative criteria. *Cereb. Cortex* **5,** 307–322.

Rajkowska, G., and Goldman-Rakic, P.S. (1995b). Cytoarchitectonic definition of prefrontal areas in the normal human cortex. II. Variability in locations of areas 9 and 46 and relationship to the Talairach coordinate system. *Cerebral Cortex* **5,** 323–337.

Rakic, P., Suñer, I., and Williams, R.W. (1991). A novel cytoarchitectonic area induced experimentally within the primate visual-cortex. *Proc. Nat. Acad. Sci. USA* **88,** 2083–2087.

Rauschecker, J.P. (1999). Auditory cortical plasticity: A comparison with other sensory systems. *Trends Neurosci.* **22,** 74–80.

Reite, M., Adams, M., Simon, J., Teale, P., Sheeder, J., Richardson, D., and Grabbe, R. (1994). Auditory M100 component 1: Relationship to Heschl's gyri. *Brain Res. Cogn. Brain Res.* **2,** 13–20.

Richman, D.P., Stewart, R.M., Hutchinson, J.W., and Caviness, V.S. (1975). Mechanical model of brain convolutional development. *Science* **189,** 18–21.

Riegele, L. (1931). Die Cytoarchitektonik der Felder der Brocaschen Regionen. *J. Physiol. Neurol.* **42,** 496–514.

Rivier, F., and Clarke, S. (1997). Cytochrome oxidase, acetylcholinesterase, and NADPH-diaphorase staining in human supratemporal and insular cortex: Evidence for multiple auditory areas. *NeuroImage* **6,** 288–304.

Rizzo, M., Nawrot, M., Blake, R., and Damasio, A. (1992). A human visual disorder resembling area V4 dysfunction in the monkey. *Neurology* **42,** 1175–1180.

Rizzolatti, G., Camarda, R., Fogassi, L., Gentilucci, M., Luppino, G., and Matelli, M. (1988). Functional organization of inferior area 6 in the macaque monkey. II. Area F5 and the control of distal movements. *Exp. Brain Res.* **71,** 491–507.

Rizzolatti, G., Fadiga, L., Gallese, V., and Fogassi, L. (1996b). Premotor cortex and the recognition of motor actions. *Cogn. Brain Res.* **3,** 131–141.

Rizzolatti, G., Fadiga, L., Matelli, M., Bettinardi, V., Paulesu, E., Perani, D., and Fazio, F. (1996c). Localization of grasp representations in humans by PET. 1. Observation versus execution. *Exp. Brain Res.* **111,** 246–252.

Rizzolatti, G., Fogassi, L., and Gallese, V. (1997). Parietal cortex: From sight to action. *Curr. Opin. Neurobiol.* **7,** 562–567.

Rizzolatti, G., Gentilucci, M., Camarda, R.M., Gallese, V., Luppino, G., Matelli, M., and Fogassi, L. (1990). Neurons related to reaching-grasping arm movements in the rostral part of area 6 (area 6aβ). *Exp. Brain Res.* **82,** 337–350.

Rizzolatti, G., Luppino, G., and Matelli, M. (1996a). The classic supplementary motor area is formed by two independent areas. *In* "Supplementary Sensorimotor Area" (H.O. Lüders, eds.), pp. 45–56. Lippincott-Raven, Philadelphia.

Rizzolatti, G., Luppino, G., and Matelli, M. (1998). The organization of the cortical motor system: New concepts. *Electroencephalogr. Clin. Neurophysiol.* **106,** 283–296.

Roland, P. E. (1984). Metabolic measurement of the working frontal cortex in man. *Trends Neurosci.* **7,** 430–435.

Roland, P. E. (1993). "Brain Activation." Wiley-Liss, New York.

Roland, P.E., and Zilles, K. (1994). Brain atlases—A new research tool. *TINS* **17,** 458–467.

Roland, P.E., and Zilles, K. (1996a). Functions and structures of the motor cortices in humans. *Curr. Opin. Neurobiol.* **6,** 773–781.

Roland, P.E., and Zilles, K. (1996b). The developing European Computerized Human Brain Database for all imaging modalities. *NeuroImage* **4,** 39–47.

Roland, P.E., and Zilles, K. (1998). Structural divisions and functional fields in the human cerebral cortex. *Brain Res. Rev.* **26,** 87–105.

Roland, P.E., Eriksson, L., Stone-Elander, S., and Widén, L. (1987). Does mental activity change the oxidative metabolism of the brain. *J. Neurosci.* **7,** 2373–2389.

Roland, P.E., Geyer, S., Amunts, K., Schormann, T., Schleicher, A., Malikovic, A., and Zilles, K. (1997). Cytoarchitectural maps of the human brain in standard anatomical space. *Hum. Brain Mapp.* **5,** 222–227.

Roland, P.E., Larsen, B., Lassen, N.A., and Skinhoj, E. (1980). Supplementary motor area and other cortical areas in organization of voluntary movements in man. *J. Neurophysiol.* **43,** 118–136.

Romani, G.L., Williamson, S.J., and Kaufman, L. (1982). Tonotopic organization of the human auditory cortex. *Science* **216,** 1339–1340.

Rose, M. (1926). Über das histogenetische Prinzip der Einteilung der Grosshirnrinde. *J. Physiol. Neurol.* **32,** 97–160.

Rose, M. (1927). Die sog. Riechrinde beim Menschen und beim Affen. II. Teil des "Allocortex bei Tier und Mensch". *J. Psychol. Neurol.* **34,** 261–401.

Rose, M. (1928). Gyrus limbicus antior und Regio retrosplenialis (Cortex holorotoptychos quinquenstraficatus). Vergleichende Architektonik bei Tier und Mensch. *J. Psychol. Neurol.* **35,** 65–173.

Rose, M. (1929). Die Inselrinde des Menschen und der Tiere. *J. Psychol. Neurol.* **37,** 467–624.

Rosene, D.L. and van Hoesen, G.W.(1977). Hippocampal efferents reach widespread areas of cerebral cortex and amygdala in the rhesus monkey. *Science* **198,** 315–317.

Sakai, K., Watanabe, E., Onodera, Y., Uchida, I., Kato, H., Yamamoto, E, Koizumi, H., and Miyashita, Y. (1995). Functional mapping of the human color centre with echo-planar magnetic resonance imaging. *Proc. Roy. Soc. Lond. Ser. B Biol. Sci.* **261,** 89–98.

Sakata, H., Taira, M., Kusunoki, M., Murata, A., and Tanaka, Y. (1995). Neural mechanisms of visual guidance of hand action in the parietal cortex of the monkey. *Cereb. Cortex* **5,** 429–438.

Sakata, H., Taira, M., Kusunoki, M., Murata, A., and Tanaka, Y. (1997). The parietal association cortex in depth perception and visual control of hand action. *TINS* **20,** 350–357.

Sanes, J.N., Donoghue, J.P., Thangaraj, T., Edelman, R.R., and Warach, S. (1995). Shared neural substrates controlling hand movements in human motor cortex. *Science* **268,** 1775–1777.

Sanides, F. (1962). "Die Architektonik des menschlichen Stirnhirns." Springer Verlag, Berlin, New York.

Sanides, F. (1972). Representation in the cerebral cortex and its areal lamination patterns. *In* "The Structure and Function of Nervous Tissue" (G.H. Bourne, ed.), vol. 5, pp. 329–453. Academic Press, New York.

Sanides, F., and Vitzthum, H. (1965a). Die Grenzerscheinungen am Rande der menschlichen Sehrinde. *Dtsch. Z. Nervenheilkd.* **187,** 708–719.

Sanides, F., and Vitzhum, H.G. (1965b). Zur Architektonik der menschlichen Sehrinde und den Prinzipien ihrer Entwicklung. *Dt. Ztsch. Nervenheilk.* **187,** 680–707.

Sarkissov, S.A., Filimonoff, I.N., Kononowa, E,P., Preobrachenskaja, I.S., and Kukuew, L.A. (1955). "Atlas of the Cytoarchitectonics of the Human Cerebral Cortex." Medgiz. Moscow.

Sawaguchi, T., and Goldman-Rakic, P.S. (1991). D1 dopamine receptors in prefrontal cortex: Involvement in working memory. *Science* **251,** 947–950.

Scheibel, M.E. and Scheibel, A.B. (1978). The dendritic structure of the human Betz cell. *In* "Architectonics of the Cerebral Cortex" (A.A.B. Braxier and H. Pets, eds.), pp. 43–57. Raven Press, New York.

Scheibel, A.B., Paul, L.A., Fried, I., Forsythe, A.B., Tomiyasu, U., Wechsler, A., Kao, A., and Slotnick, J. (1985). Dendritic organization of the anterior speech area. *Exp. Neurol.* **87,** 109–117.

Schiller, P.H., and Lee, K. (1991). The role of the primate extrastriate area V4 in vision. *Science* **251,** 1251–1253.

Schleicher, A., Amunts, K., Geyer, S., Morosan, P., and Zilles, K. (1999). Observer-independent method for microstructural parcellation of cerebral cortex: A quantitative approach to cytoarchitectonics. *NeuroImage* **9,** 165–177.

Schleicher, A., Zilles, K., and Wree, A. (1986). A quantitative approach to cytoarchitectonics: Software and hardware aspects of a system for the evaluation and analysis of structural inhomogeneitis in nervous tissue. *J. Neurosci. Methods* **18,** 221–235.

Schmahmann, J.D., and Pandya, D.N. (1990). Anatomical investigations of projections from thalamus to posterior parietal cortex in the rhesus monkey: A WGA-HRP and fluorescent tracer study. *J. Comp. Neurol.* **295,** 299–326.

Schmid, N., Tschopp, K., Schillinger, C., Bilecen, D., Scheffler, K., and Seelig, J. (1998). Visualization of central auditory processes with functional magnetic resonance tomography. *Laryngorhinootologie* **77,** 328–331.

Schwartz, M.L., and Goldman-Rakic, P.S. (1984). Callosal and intrahemispheric connectivity of the prefrontal association cortex in rhesus monkey: Relation between intraparietal and principal sulcal cortex. *J. Comp. Neurol.* **226,** 403–420.

Schwartz, M.L., and Goldman-Rakic, P.S. (1988). Periodicity of GABA-containing cells in primate prefrontal cortex. *J. Neurosci.* **8,** 1962–1970.

Seldon, H.L. (1981). Structure of human auditory cortex. I. Cytoarchitectonics and dendritic distributions. *Brain Res.* **229,** 277–294.

Selemon, D.L., and Goldman-Rakic, P.S. (1985). Longitudinal topography and interdigitation of cortico-striatal projections in the rhesus monkey. *J. Neurosci.* **5,** 776–794.

Selemon, D.L., and Goldman-Rakic, P.S. (1988). Common cortical and subcortical target areas of the dorsolateral prefrontal and posterior parietal cortices in the rhesus monkey: Evidence for a distributed neural network subserving spatially guided behavior. *J. Neurosci.* **8,** 4049–4068.

Seltzer, B., and Pandya, D. N. (1980). Converging visual and somatic sensory cortical input to the intraparietal sulcus of the rhesus monkey. *Brain Res.* **192,** 339–351.

Seltzer, B., and Pandya, D.N. (1984). Further observations on parieto-temporal connections in the rhesus monkey. *Exp. Brain Res.* **55,** 301–312.

Seltzer, B., and Pandya, D.N. (1986). Posterior parietal projections to the intraparietal sulcus of the rhesus monkey. *Exp. Brain Res.* **62,** 459–469.

Semendeferi, K., Armstrong, E., Schleicher, A., Zilles, K., and van Hoesen, G.W. (2001). Prefrontal cortex in humans and apes: A comparative study of area 10. *Am. J. Phys. Anthropol.* **114,** 221–241.

Sereno, M.I., Dale, A.M., Reppas, J.B., Kwong, K.K., Belliveau, J.W., Brady, T.J., Rosen, B.R., and Tootell, R.B.H. (1995). Borders of multiple visual areas in humans revealed by functional magnetic resonance imaging. *Science* **268,** 889–893.

Sergent, J., Zuck, E., Levesque, M., and MacDonald, B. (1992). Positron emission tomography study of letter and object processing: Empirical findings and methodological considerations. *Cereb. Cortex* **2,** 68–80.

Shariff, G.A. (1953). Cell counts in the primate cerebral cortex. *J. Comp. Neurol.* **98,** 381–400.

Shoumura, K., Ando, T., and Kato, K. (1975). Structural organization of "callosal" Obg in human callosal agenesis. *Brain Res.* **93,** 241–252.

Showers, M.J.C. (1959). The cingulate gyrus: Additional motor area and cortical automatic regulator. *J. Comp. Neurol.* **112,** 231–301.

Simonds, R.J., and Scheibel, A.B. (1989). The postnatal development of the motor speech area: A preliminary study. *Brain and Language* **37,** 43–58.

Sirigu, A., Cohen, L., Duhamel, J.R., Pillon, B., Dubois, B., and Agid, Y. (1995). A selective impairment of hand posture for object utilization in apraxia. *Cortex* **31,** 41–55.

Skullerud, K. (1985). Variations in the size of the human brain. *Acta Neurol. Scand.* **71** (Suppl. 102), 1–94.

Smith, G.E. (1907). A new topographical survey of the human cerebral cortex, being an account of the distribution of the anatomically distinct cortical areas and their relationship to the cerebral sulci. *J. Anat.* **41,** 237–254.

Standage, G.P., and Benevento, L.A. (1983). The organization of connections between the pulvinar and visual area MT in the macaque monkey. *Brain Res.* **262,** 288–294.

Steinmetz, H., Rademacher, J., Huang, Y.X., Hefter, H., Zilles, K., Thron, A., and Freund, H.J. (1989). Cerebral asymmetry: MR planimetry of the human planum temporale. *J. Comput. Assist. Tomogr.* **13,** 996–1005.

Steinmetz, H., Volkmann, J., Jäncke, L., and Freund, H.-J. (1991). Anatomical left-right asymmetry of language-related temporal cortex is different in left- and right-handers. *Ann. Neurol.* **29,** 315–319.

Stengel, E. (1930). Morphologische und cytoarchitektonische Studien über den Bau der unteren Frontalwindung bei Normalen und Taubstummen. Ihre individuellen und Seitenunterschiede. *Z. Ges. Neur. Psychiat.* **130,** 630–677.

Stephan, H. (1969). Quantitative investigations on visual structures in primate brains. *Proc. Int. Congr. Primatol.,* 2nd, 1968, Vol. 3, pp. 34–42.

Stephan, H. (1975). Allocortex. *In* "Handbuch der mikroskopischen Anatomie des Menschen" (W. Bargmann, ed.), vol. 4, Part 9, pp. 1–998. Springer Verlag, Berlin, New York.

Stephan, H., Frahm, H., and Baron, G. (1981). New and revised data on volumes of brain structures in insectivores and primates. *Folia Primatol.* **35,** 1–29.

Stephan, K.M., Fink, G.R., Passingham, R.E., Silbersweig, D., Ceballos-Baumann, A.O., Frith, C.D., and Frackowiak, R.S.J. (1995). Functional anatomy of the mental representation of upper

extremity movements in healthy subjects. *J. Neurophysiol.* **73,** 373–386.

Strainer, J.C., Ulmer, J.L., Yetkin, F.Z., Haughton, V.M., Daniels, D.L., and Millen, S.J. (1997). Functional MR of the primary auditory cortex: an analysis of pure tone activation and tone discrimination. *Am. J. Neuroradiol.* **18,** 601–610.

Strasburger, E.H. (1937). Die myeloarchitektonische Gliederung des Stirnhirns beim Menschen und Schimpansen. *J. Psychol. Neurol.* **47,** 461 and 565.

Strasburger, E.H. (1938). Vergleichende myeloarchitektonische Studien an der erweiterten Brocaschen Region des Menschen. *J. Psychol. Neurol.* **48,** 477–511.

Talavage, T.M., Edmister, W.B., Ledden, P.J., and Weisskoff, R.M. (1999). Quantitative assessment of auditory cortex responses induced by imager acoustic noise. *Hum. Brain Mapp.* **7,** 79–88.

Talavage, T.M., Ledden, P.J., Sereno, M.I., Rosen, B.R., and Dale, A.M. (1997). Multiple phase-encoded tonotopic maps in human auditory cortex. *Neuroimage* **5,** 8.

Tanji, J. (1994). The supplementary motor area in the cerebral cortex. *Neurosci. Res.* **19,** 251–268.

Tanji, J., and Shima, K. (1994). Role for supplementary motor area cells in planning several movements ahead. *Nature* **371,** 413–416.

Thompson, P.M., Schwartz, C., Lin, R.T., Khan, A.A., and Toga, A.W. (1996). Three-dimensional statistical analysis of sulcal variability in the human brain. *J. Neurosci.* **16,** 4261–4274.

Tiitinen, H., Alho, K., Huotilainen, M., Ilmoniemi, R.J., Simola, J., and Naatanen, R. (1993). Tonotopic auditory cortex and the magnetoencephalographic (MEG) equivalent of the mismatch negativity. *Psychophysiology* **30,** 537–540.

Toni, I., Thoenissen, D., and Zilles, K. (2001). Movement preparation and motor intention. *NeuroImage* **14,** 110–117.

Tootell, R.B.H., and Hamilton, S.L. (1989). Functional anatomy of the second visual area (V2) in the macaque. *J. Neurosci.* **9,** 2620–2644.

Tootell, R.B.H., and Taylor, J.B. (1995). Anatomical evidence for MT and additional cortical visual areas in humans. *Cereb. Cortex* **5,** 39–55.

Tootell, R.B.H., Hadjikhani, N.K., Mendola, J.D., Marrett, S., and Dale, A.M. (1998). From retinotopy to recognition: fMRI in human visual cortex. *Trends Cogn. Sci.* **2,** 174–183.

Tootell, R.B.H., Mendola, J.D., Hadjikhani, N.K., Ledden, P.J., Liu, A.K., Reppas, J.B., Sereno, M.I., and Dale, A.M. (1997). Functional analysis of V3A and related areas in human visual cortex. *J. Neurosci.* **17,** 7060–7078.

Tootell, R.B.H., Reppas, J.B., Dale, A.M., Look, R.B., Sereno, M.I., Malach, R., Brady, T.J., and Rosen, B.R. (1995b). Visual motion aftereffect in human cortical area MT revealed by functional magnetic resonance imaging. *Nature* **375,** 139–141.

Tootell, R.B.H., Reppas, J.B., Kwong, K.K., Malach, R., Born, R., Brady, T.J., Rosen, B.R., and Belliveau, J.W. (1995a). Functional analysis of human MT and related visual cortical areas using magnetic resonance imaging. *J. Neurosci.* **15,** 3215–3230.

Trojanowski, J.Q., and Jacobson, S. (1976). Areal and laminar distribution of some pulvinar cortical efferents in rhesus monkey. *J. Comp. Neurol.* **169,** 371–392.

Tyler, H.R. (1968). Abnormalities of perception with defective eye movements (Balint's syndrome). *Cortex* **4,** 154–171.

Ungerleider, L.G., and Desimone, R. (1986). Cortical connections of visual area MT in the macaque. *J. Comp. Neurol.* **248,** 190–222.

Ungerleider, L.G., and Haxby, J.V. (1994). "What" and "where" in the human brain. *Curr. Opin. Neurobiol.* **4,** 157–165.

Ungerleider, L.G., and Mishkin, M. (1982). Two cortical visual systems. *In* "Analysis of Visual Behavior" (D.J. Ingle, M.A. Goodale, and R.J.W. Mansfield, eds.), pp. 549–586. MIT Press, Cambridge, MA.

Uylings, H.B.M., Malofeeva, L.I., Bogolepova. I.N., Amunts, and K., Zilles, K. (1999). Broca's language area from a neuroanatomical and developmental perspective. *In* "Neurocognition of Language" (C.M. Brown and P. Hagoort, eds.), pp. 319–336. Oxford University Press, Oxford.

Vallar, G. (1998). Spatial hemineglect in humans. *Trends Cogn. Sci.* **2,** 87–97.

Vallar, G. (2001). Extrapersonal visual unilateral spatial neglect and its neuroanatomy. *NeuroImage* **14,** 52–58.

Van Essen, D.C. (1979). Visual areas of the mammalian cerebral cortex. *Annu. Rev. Neurosci.* **2,** 227–263.

Van Essen, D.C., and Zeki, S. M. (1978). The topographic organization of rhesus monkey prestriate cortex. *J. Physiol. (London)* **277,** 193–226.

Van Essen, D.C., Maunsell, J.H.R., and Bixby, J.L. (1981). The middle temporal visual area in the macaque: Myeloarchitecture, connections, functional properties and topographic organization. *J. Comp. Neurol.* **199,** 293–326.

Van Hoesen, G.W., Morecraft, R.J., and Vogt, B.A. (1993). Connections of the monkey cingulate cortex. *In* "Neurobiology of Cingulate Cortex and Limbic Thalamus" (B.A. Vogt and M. Gabriel, eds.), pp. 249–284. Birkhäuser, Boston.

Van Essen, D.C., Newsome, W.T., and Bixby, J.L. (1982). The pattern of interhemispheric connections and its relationship to extrastriate visual areas in the macaque monkey. *J. Neurosci.* **2,** 265–283.

Van Essen, D.C., Newsome, W.T., Maunsell, J.H.R., and Bixby, J.L. (1986). The projections from striate cortex (V1) to areas V2 and V3 in the macaque monkey: Asymmetries, areal boundaries and patchy condensations. *J. Comp. Neurol.* **244,** 451–480.

Verkindt, C., Bertrand, O., Perrin, F., Echallier, J. F., and Pernier, J. (1995). Tonotopic organization of the human auditory cortex: N100 topography and multiple dipole model analysis. *Electroencephalogr. Clin. Neurophysiol.* **96,** 143–156.

Vogels, R., Sary, G., Dupont, P., and Orban, G.A. (2002). Human brain regions in volved in visual categorization. *NeuroImage* **16,** 401–414.

Vogt, B.A. (1985). Cingulate cortex. *In* "Cerebral Cortex" (A. Peters and E.G. Jones, eds.), vol. 4, pp. 89–149. Plenum Press, New York.

Vogt, B.A. (1993). Structural organization of cingulate cortex: Areas, neurons, and somatodendritic transmitter receptors. *In* "Neurobiology of Cingulate Cortex and Limbic Thalamus" (B.A. Vogt, and M. Gabriel, eds.), pp. 14–70. Birkhäuser, Boston.

Vogt, B.A., Nimchinsky, E.A., Vogt, L.J., and Hof, P.R. (1995). Human cingulate cortex: Surface features, flat maps, and cytoarchitecture. *J. Comp. Neurol.* 359, 490–506.

Vogt, B.A., Pandya, D.N., and Rosene, D.L. (1987). Cingulate cortex of the rhesus monkey. I. Cytoarchitecture and thalamic afferents. *J. Comp. Neurol.* **262,** 256–270.

Vogt, B.A., Vogt, L.J., Perl, D.P., and Hof, P.R. (2001). Cytology of human caudomedial cingulate, retrosplenial, and caudal parahippocampal cortices. *J. Comp. Neurol.* **438,** 353–376.

Vogt, C., and Vogt, O. (1919). Allgemeine Ergebnisse unserer Hirnforschung. *J. Psychol. Neurol.* **25,** 279–262.

Vogt, C., and Vogt, O. (1926). Die vergleichend-architektonische und die verlgeichend-reizphysiologische Felderung der Grosshirnrinde unter besonderer Berücksichtigung der menschlichen. *Naturwissenschaften* **14,** 1190-1194.

Vogt, C., and Vogt, O. (1956). Weitere Ausführungen zum Arbeitsprogramm des Hirnforschungsinstituts in Neustadt (Schwarzwald). *J. Hinforsch.* **2,** 403–427.

Vogt, O. (1910). Die myeloarchitektonische Felderung des menschlichen Stirnhirns. *J. Psychol. Neurol.* **15,** 221.

Vogt, O. (1911). Die Myeloarchitektonik des Isocortex parietalis. *J. Psychol. Neurol.* **18,** 379–390.

von der Heydt, R., and Peterhans, E. (1989). Mechanisms of contour perception in monkey visual cortex. I. Lines of pattern discontinuity. *J. Neurosci.* **9,** 1731–1748.

von Economo, C., and Horn, L. (1930). Über Windungsrelief, Massen und Rindenarchitektonik der Supratemporalfläche, ihre individuellen und Seitenunterschiede. *Z. Gesamt Neurol. Psychiatr.* **130,** 678–755.

von Economo, C., and Koskinas, G. N. (1925). "Die Cytoarchitektonik der Hirnrinde des erwachsenen Menschen." Springer-Verlag, Berlin.

Walker, A.E. (1940). A cytoarchitectural study of the prefrontal area of the macaque monkey. *J. Comp. Neurol.* **73,** 59–86.

Walsh, V., Carden, D., Butler, S.R., and Kulikowski, J.J. (1993). The effects of V4 lesions on the visual abilities of macaques: Hue discrimination and colour constancy. *Behav. Brain Res.* **53,** 51–62.

Watson, J.D., Myers, R., Frackowiak, R.S., Hajnal, J.V., Woods, R.P., Mazziotta, J.C., Shipp, S., and Zeki, S. (1993). Area V5 of the human brain: Evidence from a combined study using positron emission tomography and magnetic resonance imaging. *Cereb. Cortex* **3,** 79–94.

Webster, M.J., Bachevalier, J., and Ungerleider, L.G. (1994). Connections of the inferior temporal areas TEO and TE with parietal and frontal cortex in macaque monkeys. *Cereb. Cortex* **4,** 471–483.

Weiss, P.H., Marshall, J.C., Wunderlich, G., Tellmann, L., Halligan, P.W., Freund, H.-J., Zilles, K., and Fink, G.R. (2000). Neural consequences of acting in near versus far space: A physiological basis for clinical dissociations. *Brain* **123,** 2531–2541.

Welker, W.I., and Campos, G.B. (1963). Physiological significance of sulci in somatosensory cerebral cortex in mammals of the family Procyonidae. *J. Comp. Neurol.* **120,** 19–36.

Wernicke, C. (1874). "Der aphasische Symptomenkomplex." Springer Verlag, Berlin, Heidelberg, New York.

White, I.M., and Wise, P. (1999). Rule-dependent neuronal activity in the prefrontal cortex. *Exp. Brain Res.* **126,** 315–335.

Wiesendanger, M., and Wiesendanger, R. (1984). The supplementary motor area in the light of recent investigation. *Exp. Brain Res.* **9,** 382–392.

Wiesendanger, M., Hummelsheim, H., and Bianchetti, M. (1985). Sensory input to the motor fields of the agranualr frontal cortex: A comparison of the precentral, supplementary motor and premotor area. *Behav. Brain Res.* **18,** 89–94.

Wiesendanger, R., Wiesendanger, M., and Ruegg, D.G. (1979). An anatomical investigation of the corticopontine projection in the primate (*Macaca fascicularis* and *Saimiri sciureus*). II. The projection from frontal and parietal. *Neuroscience* **4,** 747–765.

Wise, R., Chollet, F., Hadar, U., Friston, K., Hoffner, E., and Frackowiak, R.S.J. (1991). Distribution of cortical neural networks involved in word comprehension and word retrieval. *Brain* **114,** 1803–1817.

Wise, S.P. (1985a). The primate premotor cortex fifty years after Fulton. *Behav. Brain Res.* **18,** 79–88.

Wise, S.P. (1985b). The primate premotor cortex: Past, present and preparatory. *Annu. Rev. Neurosci.* **8,** 1–19.

Wise, S.P., and Strick, P.L. (1984). Anatomical and physiological organization of the non-primary motor cortex. *Trends Neurosci.* **7,** 442–446.

Witelson, S.F. (1985). The brain connection: The corpus callosum is larger in left-handers. *Science* **229,** 665–668.

Wong-Riley, M.T.T. (1994). Primary visual cortex: Dynamic metabolic organization and plasticity revealed by cytochrome oxidase. *In* "Cerebral Cortex: Primary Visual Cortex in Primates" (A. Peters and K. Rockland, eds.), vol. 10, pp. 141–200. Plenum Press, New York.

Yakovlev, P.L., Locke, S., Koskoff, D.Y., and Patton, R.A. (1960). Limbic nuclei of thalamus and connections of limbic cortex. I. Organization of the projection of the anterior group of nuclei and of the midline nuclei of the thalamus to the anterior cingulate gyrus and hippocampal rudiment in the monkey. *Arch. Neurol. (Chicago)* **3,** 620–641.

Yamamoto, T., Uemura, T., and Llinas, R. (1992). Tonotopic organization of human auditory cortex revealed by multi-channel SQUID system. *Acta Otolaryngol. Stockh.* **112,** 201–204.

Yeterian, E.H., and Pandya, D.N. (1985). Corticothalamic connections of the posterior parietal cortex in the rhesus monkey. *J. Comp. Neurol.* **237,** 408–426.

Yeterian, E.H., and Pandya, D.N. (1993). Striatal connections of the parietal association cortices in rhesus monkey. *J. Comp. Neurol.* **332,** 175–197.

Yousry, T.A., Schmid, U.D., Alkadhi, H., Schmidt, D., Peraud, A., Buettner, A., and Winkler, P. (1997). Localization of the motor hand area to a knob on the precentral gyrus. A new landmark. *Brain* **120,** 141–157.

Yukie, M., and Iwai, E. (1981). Direct projection from the dorsal lateral geniculate nucleus to the prestriate cortex in macaque monkeys. *J. Comp. Neurol.* **201,** 81–97.

Zangwill, O.L. (1960). "Cerebral Dominance and its Relation to Psychological Function." Thomas, Springfield, Ill.

Zatorre, R.J., Evans, A.C., and Meyer, E. (1994). Neural mechanisms underlying melodic perception and memory for pitch. *J. Neurosci.* **14,** 1908–1919.

Zatorre, R.J., Meyer, E., Gjedde, A., and Evans, A.C. (1996). PET studies of phonetic processing of speech: Review, replication, and reanalysis. *Cereb. Cortex* **6,** 21–30.

Zeki, S.M. (1969). The secondary visual cortex of the monkey. *Brain Res.* **13,** 197–226.

Zeki, S.M. (1970). Interhemispheric connections of prestriate cortex in monkey. *Brain Res.* **19,** 63–75.

Zeki, S.M. (1974). Functional organization of a visual area in the posterior bank of the superior temporal sulcus of the rhesus monkey. *J. Physiol.* **236,** 549–573.

Zeki, S.M. (1978). Uniformity and diversity of structure and function in rhesus monkey prestriate visual cortex. *J. Physiol. (London)* **277,** 273–290.

Zeki, S.M. (1979). Zu Brodmann Area 18 and Area 19. *Exp. Brain Res.* **36,** 195–197.

Zeki, S.M. (1980). The response properties of cells in the middle temporal area (area MT) of owl monkey visual cortex. *Proc. Roy. Soc. Lond. Ser. B Biol. Sci.* **207,** 239–248.

Zeki, S.M. (1990a). Parallelism and functional specialization in human visual cortex. *Cold Spring Harb. Symp. Quant. Biol.* **55,** 651–661.

Zeki, S. (1990b). A century of cerebral achromatopsia. *Brain* **113,** 1721–1777.

Zeki, S.M. (1991). Cerebral akinetopsia (visual motion blindness). A review. *Brain* **114,** 811–824.

Zeki, S. (1993). "A Vision of the Brain." Blackwell, Oxford.

Zeki, S., and Shipp, S. (1988). The functional logic of cortical connections. *Nature* **335,** 311–317.

Zeki, S.M., Watson, J.D., and Frackowiak, R.S.J. (1993). Going beyond the information given: The relation of illusory visual motion to brain activity. *Proc. Roy. Soc. Lond. Ser. B Biol. Sci.* **252,** 215–222.

Zeki, S., Watson, J.D.G., Lueck, C.J., Friston, K.J., Kennard, C., and Frackowiak, R.S.J. (1991). A direct demonstration of functional specialization in human visual cortex. *J. Neurosci.* **11,** 641–649.

Zihl, J., von Cramon, D., Mai, N., and Schmid, C. (1991). Disturbance of movement vision after bilateral posterior brain damage. Further evidence and follow up observations. *Brain* **114,** 2235–2252.

Zilles, K. (1972). Biometrische Analyse der Frischvolumina verschiedener prosencephaler Hirnregionen von 78 menschlichen, adulten Gehirnen. *Gegenbaurs Morphol. Jahrb.* **118,** 234–273.

Zilles, K., and Clarke, S. (1997). Architecture, connectivity and transmitter receptors of human extrastriate visual cortex: Comparison with non-human primates. *In* "Cerebral Cortex, vol. 12, Extrastriate Cortex in Primates" (J.H. Kaas, K.S. Rockland, and A. Peters, eds.), pp. 673–742. Plenum Press, New York, London.

Zilles, K., and Palomero-Gallagher, N. (2001). Cyto-, myelo- and receptor architectonics of the human parietal cortex. *NeuroImage* **14,** 8–20.

Zilles, K., and Rehkämper, G. (1988). The brain, with special reference to the telencephalon. *In* "Orang-utan Biology" (J.H. Schwartz, ed.), pp. 157–176. Oxford Univ. Press, London, New York.

Zilles, K., and Schleicher, A. (1993). Cyto- and myeloarchitecture of human visual cortex and the periodical GABAA receptor distribution. *In* "Functional Organization of the Human Visual Cortex" (B. Gulyás, D. Ottoson, and P. Roland, eds.), pp. 111–121, Pergamon Press, Oxford.

Zilles, K., Armstrong, E., Moser, K.H., Schleicher A., and Stephan, H. (1989) Gyrification in the cerebral cortex of primates. *Brain Behav. Evolut.* **34,** 143–150.

Zilles, K., Armstrong, E., Schlaug, G., and Schleicher, A. (1986b). Quantitative cytoarchitectonics of the posterior cingulate cortex in primates. *J. Comp. Neurol.* **253,** 514–524.

Zilles, K., Armstrong, E., Schleicher, A., and Kretschmann, H.-J. (1988). The human pattern of gyrification in the cerebral cortex. *Anat. Emryol.* **179,** 173–179.

Zilles, K., Stephan, H., and Schleicher, A. (1982). Quantitative architectonics of the cerebral cortices of several prosimian species. *In* "Primate Brain Evolution: Methods and Concepts" (E. Armstrong and D. Falk, eds.), pp. 177–201. Plenum, New York.

Zilles, K., Werners, R., Büsching, U., and Schleicher, A. (1986a). Ontogenesis of the laminar structure in areas 17 and 18 of the human visual cortex. A quantitative study. *Anat. Embryol.* **174,** 339–353.

Zilles, K., Wree, A., Schleicher, A., and Divac, I. (1984). The molecular and binocular subfields of the rat's primary visual cortex. *J. Comp. Neurol.* **266,** 391–402.

Zilles, K., Schlaug, G., Geyer, S., Luppino, G., Matelli, M., Qü, M., Schleicher, A., and Schormann, T. (1996). Anatomy and transmitter receptors of the supplementary motor areas in the human and nonhuman primate brain. *In* "Supplementary Sensorimotor Area" (H.O. Lüders, ed.), Advances in Neurology, vol. 70, pp. 29–43, Lippincott-Raven, Philadelphia.

Zilles, K., Schlaug, G., Matelli, M., Luppino, G., Schleicher, A., Qü, M., Dabringhaus, A., Seitz, R., and Roland, P.E. (1995). Mapping of human and macaque sensorimotor areas by integrating architectonic, transmitter receptor, MRI and PET data. *J. Anat.* **187,** 515–537.

Zilles, K., Schleicher, A., Langemann, C., Amunts, K., Morosan, P., Palomero-Gallagher, N., Schormann, T., Mohlberg, H., Bürgel, U., Steinmetz, H., Schlaug, G., and Roland, P.E. (1997). Quantitative analysis of sulci in the human cerebral cortex: Development, regional heterogeneity, gender difference, asymmetry, intersubject variability and cortical architecture. *Human Brain Mapping* **5,** 218–221.

Zilles, K., Schleicher, A., Palomero-Gallagher, N., and Amunts, K. (2002). Quantitative analysis of cyto- and receptorarchitecture of the human brain. *In* "Brain Mapping: The Methods," 2nd ed. (A.W. Toga and J.C. Mazziotta, eds.), pp. 573–602. Academic Press, San Diego.

Zouridakis, G., Simos, P.G., and Papanicolaou, A.C. (1998). Multiple bilaterally asymmetric cortical sources account for the auditory N1m component. *Brain Topogr.* **10,** 183–189.

CHAPTER

28

Somatosensory System

JON H. KAAS
Department of Psychology, Vanderbilt University
Nashville, Tennessee, USA

This chapter outlines the organization of the somatosensory system of humans. The emphasis is on the components of this system that are important in identifying objects and features of surfaces by touch. Even though small shapes can be perceived with information solely from tactile receptors, most discriminations involve an active process of tactile exploration with multiple contacts on the skin and an integration of cutaneous and proprioceptive information as well as efferent control. Thus, this chapter concentrates on the pathways and neural centers for processing information from the low-threshold mechanoreceptors of the skin that provide information about touch, and the deeper receptors in joints and especially muscles that provide information about position. Conclusions are based on both studies in humans and studies in other primates, especially the frequently studied macaque monkeys. At least the early stages of processing are likely to be similar in humans and monkeys, but humans appear to have a more expanded cortical network for processing somatosensory information. The important subsystems dealing with afferents coding for pain and temperature are not covered here, but they are reviewed elsewhere (e.g., Chapter 30; Casey, 1999; Craig *et al.*, 1996; Berkley and Hubscher, 1995).

The basic parts and pathways of the somatosensory system of humans are diagrammed in Figure 28.1. In brief, peripheral nerve afferents related to receptors in the skin, muscles, and joints course centrally past their cell bodies in the dorsal root and cranial nerve ganglia to enter the spinal cord and brainstem. These afferents synapse on neurons in the dorsal horn of the spinal cord, or the equivalent in the brainstem, and send a collateral to the dorsal column-trigeminal nuclear

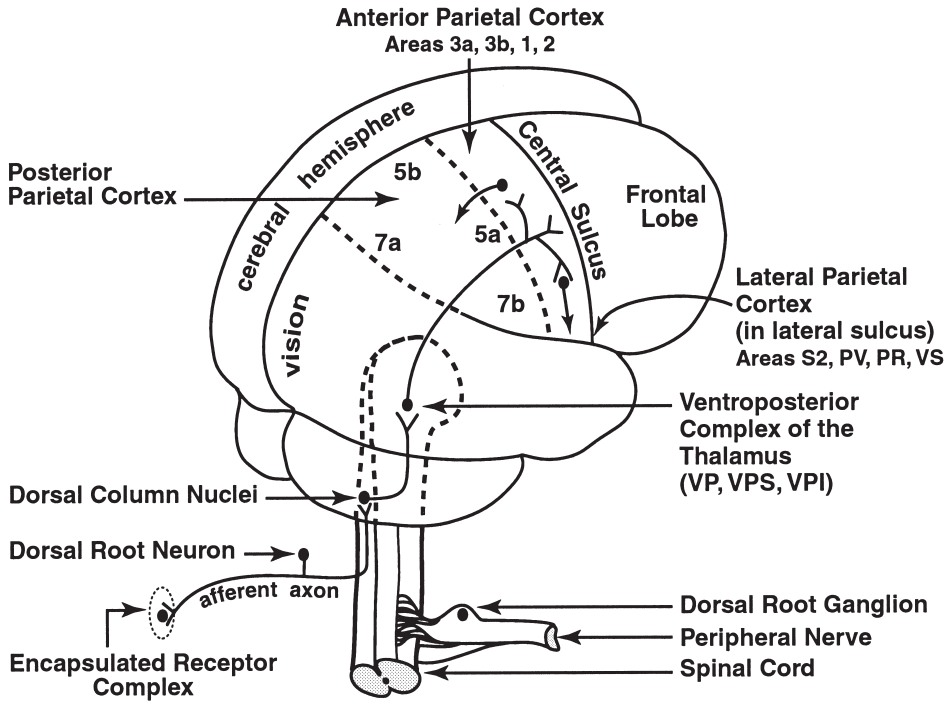

FIGURE 28.1 The basic components of the somatosensory system shown on a posterolateral view of a human brain. Receptors in the skin project to the dorsal column nuclei or the trigeminal nuclei to form the dorsal column trigeminal complex. The trigeminal complex in the brainstem provide second-order afferents, representing the face, that join those from the dorsal column nuclei, representing the body, to terminate in the contralateral ventrposterior complex of the thalamus. Third-order neurons in the thalamus project to anterior parietal cortex, where information is distributed to posterior and lateral parietal cortex.

complex. Most of the second-order neurons in this complex have axons that cross to the contralateral lower brainstem to form the medial lemniscus column of axons that ascend to the somatosensory thalamus. Second-order neurons representing the teeth and tongue project ipsilaterally to the thalamus, while other second-order neurons in the dorsal horn of the spinal cord and in the brainstem send axons to the contralateral side to form the anterolateral spinothalamic ascending pathway (Fig. 28.4). The low-threshold mechanoreceptor information from the skin and the information from muscle spindle receptors and joints course in the medial lemniscus to terminate in nuclei of the ventroposterior thalamic complex. The spinothalamic pathway carries information about pain, temperature, and touch to inferior and caudal parts of the ventroposterior complex.

The somatosensory thalamus has been subdivided in various ways (e.g., Chapter 20; Jones, 1985; Hirai and Jones, 1989; Mai *et al.*, 1997; Morel *et al.*, 1997). Because some of the earlier parcellations of thalamic nuclei were based solely on cytoarchitectonic and myeloarchitectonic criteria (e.g., Hässler, 1959) and because they do not reflect the many recent advances in understanding based on microelectrode recordings, studies of connections, and chemoarchitecture, we use more recently proposed subdivisions stemming from studies largely in monkeys (see Kaas and Pons, 1988, for review). Thus, the relay of afferents from the skin via the medial lemniscus is to the ventroposterior nucleus (VP), which has been traditionally subdivided into a ventroposterior medial subnucleus (VPM) representing the face and a ventroposterior lateral subnucleus (VPL) representing the body. The muscle spindle receptor inputs are relayed to a dorsal or superior part of the ventroposterior complex that is usually included in VPM and VPL. We distinguish this representation of deep receptors as the ventroposterior superior nucleus (VPS). The spinothalamic afferents terminate in a ventroposterior inferior nucleus (VPI). A caudal part of the VP complex that is often included in VPI or in the posterior group of nuclei has been recently distinguished as a distinct relay nucleus for pain and temperature, the ventromedial posterior nucleus (VMpo; Craig *et al.*, 1994; Blomquist *et al.*, 2000; Chapter 29). The somatosensory thalamus also includes nuclei without ascending somatosensory inputs. The anterior pulvinar (Pa) and the lateral posterior complex (LP)

receive inputs from somatosensory cortex and project back to somatosensory cortex.

The somatosensory cortex has also been variously subdivided into proposed subdivisions of functional significance. Most investigators recognize four subdivisions of the cortex of the postcentral gyrus—areas 3a, 3b, 1, and 2—stemming from the early architectonic studies of Brodmann (1909) and the Vogts (Vogt and Vogt, 1919, 1926). While all four areas were once considered parts of a single functional area, primary somatosensory cortex or S1, it has been clear for over 20 years that each constitutes a separate representation of the body, and that only area 3b corresponds to S1 of cats and rats (Kaas, 1983). Areas 3b and 1 contain parallel representations of cutaneous inputs, while areas 3a and 2 integrate cutaneous and deep receptor inputs. Yet, the term "S1" is commonly used to refer to all four areas in monkeys and humans. To avoid confusion, the architectonic terms for the four fields are used here. Thalamic projections to areas 3b and 1 are largely from VP, while VPS provides driving inputs to areas 3a and 2. VPI and Pa project widely to areas of somatosensory cortex, and LP projects to posterior parietal cortex. Areas 3b, l, and 2 form a hierarchial sequence of processing, while area 3a relates especially to motor cortex. All four areas project to somatosensory cortex of the lateral sulcus (lateral parietal cortex), especially the second somatosensory area, S2, and a more recently discovered parietal ventral somatosensory area, PV. These and other areas of the lateral sulcus relate to motor areas of cortex, and to perirhinal cortex to engage the hippocampus in a subsystem involved in object recognition and memory (Mishkin, 1979). Other connections of area 2 and subdivisions of lateral parietal cortex are with subdivisions of posterior parietal cortex that are involved with the early stages of motor guidance and control. Subdivisions of the posterior parietal cortex project to premotor and motor areas of the frontal lobe. Projections from the posterior parietal cortex also involve the medial limbic cortex of the parietal lobe in producing motivational and possibly emotional states. Aspects of this complex system are discussed in more detail later.

RECEPTOR TYPES AND AFFERENT PATHWAYS

In humans, the hand is the most important tactile organ for object identification (Darian-Smith, 1984). Receptors in the hand must convey information about texture and shape. This is done primarily from the fingerpads during active exploration; consequently, finger positions and temporal sequences are important. The glabrous (hairless) skin of the hand has the highest innervation density and tactile acuity of any body surface (Darian-Smith, 1984). Hairy skin is less important in object identification, and hairy skin is less sensitive to touch and vibration (Hamalainen and Jarvilehto, 1981). However, the hairs themselves provide an increased sensitivity to air movement and other stimuli that displace hairs (Hamalainen *et al.*, 1985).

Psychophysical, physiological, and anatomical studies on humans and other primates support the view that sensations of touch from the glabrous skin of the hand are almost completely mediated by four different types of myelinated, rapidly conducting mechanoreceptive afferents (Fig. 28.2). The afferent classes from the glabrous skin include two types of slowly adapting afferents and two types of rapidly adapting afferents. All of these types have been extensively studied physiologically in monkeys and related to receptor types. More recently, the response properties of these afferents have been characterized during recordings in humans, and sensations have been evoked by electrical stimulation in tactile discrimination. Muscle spindle receptors, perhaps aided by other deep receptors in joints and tendons and by one of the skin receptors noted earlier, play a significant role in the position sense of limbs and fingers. This sense is critical in the ability to recognize the form of objects. Afferents that are thin and slowly conducting relate to the sensations of cold, warm, pain, and crude touch. Other afferents may be related to the sensations of itch and tickle. This review concentrates on the afferents from the skin used in touch and the muscle spindle and skin receptors used in kinaesthesia (position sense). See Dykes (1983) and Willis and Coggeshall (1991) for further review.

Low-Threshold Mechanoreceptor Afferents from the Hand

Four types of low-threshold mechanoreceptors are found in the glabrous skin of primates, and afferents from these four types in the human have been studied electrophysiologically (Jarvilehto *et al.*, 1981; Johansson, 1976; 1978; Johansson and Vallbo, 1983; Johansson *et al.*, 1982a, b; Ochoa and Torebjork, 1983; Torebjork *et al.*, 1984; Vallbo, 1981; Vallbo *et al.*, 1984; Westling and Johansson, 1987). These results, together with psychophysical information on touch from humans, have led to a four-channel model of cutaneous mechanoreception (Bolanowski *et al.*, 1994, 1988). Tactile experience, according to the model, depends on various combinations of neural activity in the four channels, with particular channels providing the critical information for some sensations. Stimuli at threshold levels

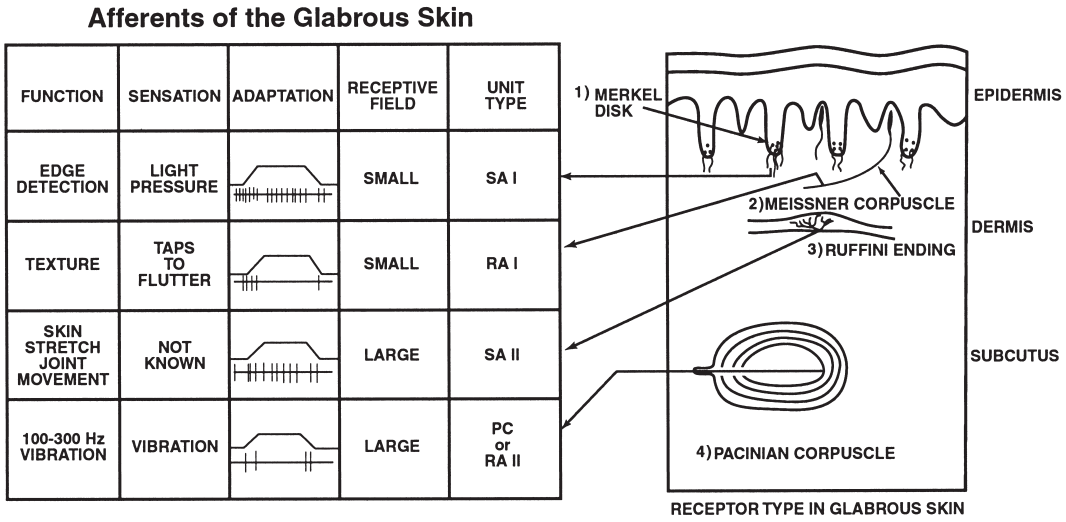

FIGURE 28.2 Receptor types (left) and afferent classes (right) of the glabrous skin of humans. four main classes of low-threshold, rapidly conducting afferents have been described as slowly adopting type I (SA I) and type II (SA II), rapidly adapting type I (RA I) and type II (RA II) or Pacinian corpuscle (PC). Each relates to a specialized receptor complex in the skin. Bsed on Johansson (1978), Johansson and Vallbo (1983), and Vallbo *et al.* (1984). The ramp in the adaptation column marks a short period of skin identation, and the vertical lines represent action potentials recorded during the indentation.

are signaled by the channel that is most sensitive to these stimuli, but suprathreshold sensations are typically the result of activity in two or more channels.

The SA-I Afferent or the Non-Pacinian III (NP III) Channel

In the superficial glabrous skin, the type I class of slowly adapting afferents (SA-I) are activated at receptor sites termed Merkel disks (see Darian-Smith, 1984). Each receptor site includes a specialized Merkel cell that is distinct from adjacent skin cells and a number of disklike nerve terminals originating from a myelinated (7–12 μm diameter) afferent fiber. SA-I receptors are densely distributed in the skin of the distal glabrous phalanges of the human hand, and they constitute about one fourth of the 17,000 tactile units of the hand (Johansson and Vallbo, 1979). Microelectrode recordings indicate that the SA-I afferents respond throughout a period of a skin indentation, even when the indentation is sustained for many seconds. Thus, they are slowly adapting to a maintained stimulus. Depending on the rate of the indentation, a large transient response also occurs during onset. The SA-I fibers have small, circumscribed receptive fields and seem especially responsive when the edge of an object indents skin within the receptive field. When stimulated by a train of electrical pulses, the single SA-I afferent signals the sensation of light, uniform pressure at a skin location corresponding to the receptive field. Single electrical impulses are not felt, and increases in stimulation frequency result in feelings of increased pressure. Thus, SA-I afferents are thought to be very important in mediating sensations of static pressure and providing information about the locations of edges and textures of held objects. SA-I afferents best preserve information about moving Braille-like dot patterns on the skin (Johnson and Lamb, 1981). After correlating human discrimination of skin indentation with the response profiles of skin afferents in monkeys, Srinivasan and LaMotte (1987) concluded that static discriminations of shape are based primarily on the spatial configuration of the active and the inactive SA afferents. In addition, under static conditions, the SA afferents provide most of the intensity information. Thus, form perception appears to be dominated by the SA-I system (Johnson and Hsiao, 1992).

The RA-I Afferent or the Non-Pacinian I (NPI) Channel

The predominant receptor afferent of the digit skin is the rapidly adapting RA-I fiber (Darian-Smith, 1984). Nearly half of the tactile afferents from the hand are of the RA-I type (Johansson and Vallbo, 1983). RA-I afferents innervate Meissner corpuscles, which are located in dermal papillae protruding into the epidermis. Meissner corpuscles are particularly dense in the glabrous skin of the distal phalanges; they are less

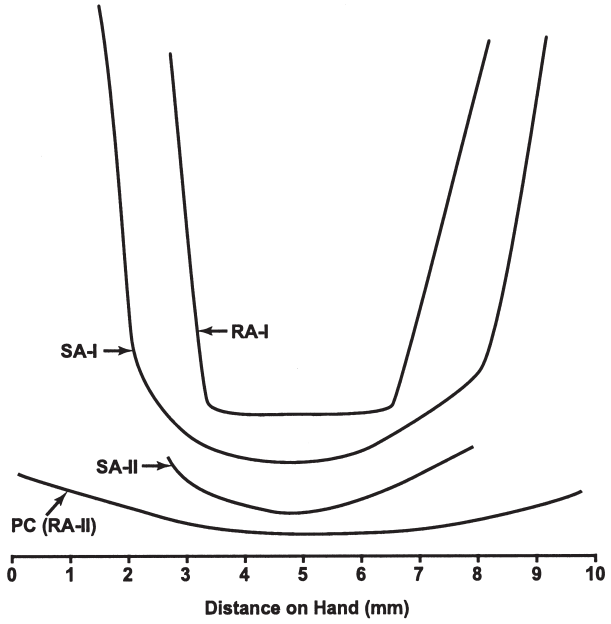

FIGURE 28.3 Changes in the sensitivity to tactile stimuli with distance across the receptive field for four classes of afferents from the glabrous skin of the human hand. Threshold levels on the vertical scale are arbitrary and do not indicate different thresholds. The rapidly adapting RA-I and the slowly adapting SA-I afferents have small receptive fields with sharp boundaries, while Pacinian (PC) or rapidly adapting RA-II and slowly adapting SA-II afferents have large receptive fields with poorly defined boundaries and a gradual change in sensitivity across the skin. Based on Johansson (1978).

common on the palm and are rare in hairy skin, being replaced by RA afferents related to hair shafts. The corpuscles consist of a core of nerve terminal disks and lamellae of Schwann cells surrounded by connective tissue extensions of the endoneural sheath. Meissner corpuscles are elongated (100 × 50 μm) perpendicular to the skin, and the outer collagen fibers of the corpuscles are linked with fibrils of adjacent epidermal cells, which allow skin deformations to stretch the corpuscle. Most corpuscles are innervated by two to six myelinated axons, and each axon innervates a tight group of corpuscles, providing a small receptive field of almost uniform sensitivity and sharp boundaries (Fig. 28.3). The RA-I afferents are thought to be responsible for the detection of movement between the skin and a surface, and for discrimination of surface texture (Johnson and Hsiao, 1992). They appear to detect microscopic slips between manipulated objects and skin to provide signals for grip control. RA-I afferents respond only to changes in skin indentation, and not to steady indentation (e.g., Srinivasan and LaMotte, 1982). Thus, RA-I afferents are capable of providing shape and intensity information during active touch (see LaMotte and Srinivasan, 1987). Single electrical impulses on RA-I afferents from the human hand often result in the detectable sensation of a light tap at a location corresponding to the receptive field. Low-frequency stimulation produces a sensation of a series of taps; at higher frequencies the taps merge into a fluttering sensation. No increase in the magnitude of the sensation follows increases in stimulation rate. These observations suggest that RA-I units are especially important in discriminations of textures moved across the skin, and of course in the sensation of flutter. Because RA-I afferents are frequently located near a joint on the back of the hand, and they respond to skin deformation during finger movements, they may also have a role in kinaesthesia (Edin and Abbs, 1991).

The SA-II Afferent or Non-Pacinian II (NP II) Channel

A second class of slowly adapting afferents, SA-II, terminate in encapsulated endings called Ruffini corpuscles (see Darian-Smith, 1984; Miller *et al.*, 1958), which are located somewhat deeper in the skin than the Merkel disks subserving SA-I afferents. Ruffini or Ruffini-like receptors are also found in deep tissues, including ligaments and tendons. Each Ruffini corpuscle contains an elongated (500–1000 μm × 200 μm) capsule of four to five layers of lamellar cells covered with a membrane, and a core of nerve fiber branches and longitudinally aligned collagen fibrils. Movement of the skin results in stretching of the corpuscle because the corpuscle is attached to surrounding tissue. Such stretching results in deformation and activation of the innervating axon. Each Ruffini corpuscle is innervated by one A-beta myelinated fiber, which may also innervate several other adjacent corpuscles. In the human hand, the SA-II class of afferents constitutes about one fifth of the tactile units (Johansson and Vallbo, 1979). SA-II fibers have large, poorly defined receptive fields (Fig. 28.3), often located near the nail bed or near skin folds on the digits or palm. These afferents are extremely sensitive to skin stretch, and often they are sensitive to direction of skin stretch. Normal movements of digits and limbs are very effective in activating these neurons. Electrical stimulation of single SA-II afferents may not be felt, or is reported as producing a buzzing sensation (Bolanowski *et al.*, 1994), so uncertainty remains about the role of SA-II afferents in tactile perception. However, there is psychophysical evidence that SA-II channels participate in the sense of touch (Bolanowski *et al.*, 1988). In addition, inputs from these skin stretch receptors may combine with sensory inputs from muscles and joints to provide limb and digit position and movement signals (e.g., McCloskey, 1978). These cutaneous mechanoreceptors

appear to contribute to a movement sense but not to an awareness of the static-position of a joint (see Clark *et al.*, 1986). Also, SA-II units are sensitive to skin shearing, and thus they might provide information about the weight of objects (McCloskey, 1974). Overall, SA-II afferents seem well suited for a role in motor guidance and control (Westling and Johansson, 1987).

The RA-II Afferent or Pacinian (P) Channel

The PC (Pacinian) or rapidly adapting RA-II afferents terminate in Pacinian corpuscles. These corpuscles are much less common than other receptor endings in the skin of the hand (10–15%), and they are also found in deeper tissues (see Darian-Smith, 1984; Johansson and Vallbo, 1979). Only about 200 corpuscles may be found in the human finger, where they are distributed within deeper skin, subcutaneous fat, and tendonous attachments of the ventral but not the dorsal finger. The PC corpuscles are large (0.3–1.5 mm $\times$ 0.2–0.7 mm) ovoids consisting of a central nerve fiber surrounded by an inner core of 60 or so layers of concentrically wrapped lamellar cells, a space filled with fluid, and an outer capsule of up to 30 less densely packed lamellae. The corpuscle acts as a mechanical filter, relaying high- frequency and attenuating low-frequency components of skin compression to the axon terminal. The PC afferents allow the detection of distant events via the transmission of high-frequency vibrations through objects and surfaces. PC afferents are extremely sensitive to transient indentations of the skin over large areas such as a complete digit and part of the palm. Thus, information is transmitted in the tissue to the region of the receptor. Sensitivity gradually decreases with distance from the receptor, and receptive field boundaries are not sharp (Fig. 28.3). PC units typically can be activated by gently blowing on the skin, and they respond to vibrations produced by tapping the table surface on which a skin surface rests. PC afferents, like RA-I fibers, respond to the indentation and release of the skin produced by a probe (Fig. 28.2), but fail to respond during steady indentation. The responses of Pacinian afferents follow the cycle of a sinusoidal vibratory stimulus. However, unlike RA-I afferents that respond with lowest thresholds in the 30–40 Hz range, PC afferents have lowest thresholds in the 250–350 Hz range. Thus, PC afferents appear to be the only afferents capable of subserving the sensation of high-frequency vibration. For most frequencies, PC and RA-I afferents both contribute to the perceived vibrotactile intensity (Hollins and Roy, 1996). Electrical stimulation of PC afferents in the human hand are not felt at low stimulation rates, but a sensation of vibration or tickle occurs at high stimulation rates. Often, the sensation is restricted to a part of the large, diffuse receptive field. PC afferents poorly resolve moving texture patterns (Johnson and Lamb, 1981), and they are apparently unimportant in object identification. Their major role, therefore, seems to be in detecting and roughly locating sudden skin deformations produced by ground and air vibrations, and by skin contacts.

Cutaneous Receptor Afferents of the Hairy Skin

As in the glabrous skin, the hairy skin has SA-I, SA-II, RA-I, and RA-II afferents. However, some modifications in the receptor mechanisms exist. First, Merkel cell disks of the SA-I receptor are often aggregated in small (0.25–0.5 μm) diameter touch domes that are slightly elevated from surrounding skin and can be visualized with a dissecting microscope. The Merkel touch spot or haarscheibe is innervated by a single, large (7–12 μm) myelinated fiber that branches to terminate in a number of disks associated with Merkel cells. Isolated Merkel cells are rare. Second, some RA-I and SA-I afferents relate to the shafts of hairs. The SA-I afferents seem to be activated by Merkel-type endings around hair follicles, and the RA-I afferents may have the equivalent of Meissner-type endings in glabrous skin. Third, the hairy skin does not have Pacinian corpuscles, but instead relies on a scattering of Pacinian corpuscles located in deep tissue around blood vessels and muscles (Bolanowski *et al.*, 1994). Thus, hairy skin is less sensitive to vibrations. Fourth, it is not yet clear how or if the SA-I afferents in hairy skin contribute to tactile sensation; in contrast, SA-II afferents may mediate sensations of pressure in hairy skin but not in glabrous skin (Bolanowski *et al.*, 1994). The hairy skin of humans also has C-mechanoreceptive afferents. The functional role of these afferents is uncertain, and they may not contribute to conscious percepts of touch (Vallbo *et al.*, 1999).

Deep Receptor Afferents

As noted earlier, SA-II type afferents associated with Ruffini-like endings are found not only in the skin, where they signal stretch, but also in deep tissues where they also signal stretch. The receptors are Ruffini corpuscles and Golgi tendon organs. SA-II afferents provide information about joint extension and tissue compression, but it is not clear that SA-II afferents have a role in the conscious awareness of joint position (Burgess *et al.*, 1982). Part of the evidence against a major role is that joint position sense survives joint removal and replacement (Cross and McCloskey, 1973). Nevertheless, there is psychophysical evidence

that joint afferents subserve joint position sense in fingers (Taylor and McCloskey, 1990).

Other important deep receptors are the muscle spindle receptors, which were once thought to participate only in reflexes via spinal cord pathways and motor control via a relay to the cerebellum. Muscle spindle afferents are now known to also relay to the cortex (Fig. 28.4), and to contribute to a sense of posture and movement (Burgess *et al.*, 1982; Clark *et al.*, 1986; Goodwin *et al.*, 1971; Jones, 1994; McCloskey, 1978). For static limb position, Clark *et al.* (1986), for example, argue that the nervous system computes joint angles and thus limb position from muscle spindle information about the lengths of the muscles that set the positions of joints.

Afferents Mediating Temperature and Pain

Other afferents in the skin and deeper tissues relate to the sensations of temperature, pain, itch, and crude touch. These include one or more types of specific nociceptors, afferents that respond to innocuous cooling, multimodal afferents responsive to heat, pinch, and cooling (HPC) and the wide-dynamic range (WDR) afferents (Chapter 30; Willis and Coggeshall, 1991). The specific nociceptors conduct in the A-delta range and mediate pricking pain, while the multimodal afferents conduct in the C range and mediate burning pain. Warm receptor afferents conduct in the C range while responding at body temperatures and higher, but not at noxious levels of heat.

Afferent Pathways

Afferents course from skin receptor and deep receptor locations to combine in nerve fascicles that join other fascicles to form the peripheral nerves. The peripheral nerves branch and segregate into dorsal sensory roots and ventral motor-sensory roots. The afferents that enter the dorsal roots terminate on neurons in the dorsal horn of the spinal cord or ascend to terminate on neurons in the dorsal column nuclear complex at the junction of the medulla and spinal cord (Figure 28.1; Chapter 7).

A number of investigators have attempted to determine the skin regions subserved by the nerves in each spinal root in humans and other mammals (see Chapter 30; Dykes and Terzis, 1981, for a review). Dissections have been used to reveal the gross patterns of these dermatomal distributions, but additional methods include using the zone of remaining sensibility after section of dorsal roots above and below the one studied, electrical recording or stimulation, interruptions of function produced by ruptured disks, and data from herpes zoster eruptions. For humans, the extensive dermatomal maps are those of Head (1920), based on skin regions affected by herpes zoster; Foerster (1933), from clinical cases where spinal roots were sectioned for the relief of pain; and Keegan (1943), from cases of local sensory loss subsequent to ruptures of intervertebral disks. Dykes and Terzis (1981) point out that these three maps of dermatomes differ considerably, and they suggest that none is accurate. However, the maps in humans, together with the results from other primates, allow several conclusions: (1) The field of each root is continuous, and tends to form a strip perpendicular to the spinal cord. (2) Adjacent dorsal root distributions overlap extensively. (3) There is little overlap at the ventral and dorsal body midlines. (4) There is considerable variability across individuals.

Within dorsal roots, studies in monkeys indicate that there is some crude organization of afferent fibers according to skin location, with distal receptive fields located caudal in the dorsal root, while fibers with proximal receptive fields tend to be rostral (Werner and Whitsel, 1967). These studies also indicate that ascending branches of axons entering the spinal cord in the dorsal columns (Fig. 28.4) tend to preserve their order of entry so that axons from lower spinal roots are medial to those from upper spinal roots (Whitsel *et al.*, 1972). In monkeys, inputs from muscle spindles branch and join the cuneate fasciculus for the upper limb, but terminate in the spinal cord for the lower limb.

Some afferent fibers with cell bodies in the dorsal root ganglia turn and enter the ventral root and then turn and retrace a path back to the dorsal root, as if correcting an error (see Willis, 1985; Chapter 8 for a review). These sensory fibers in the ventral root are largely unmyelinated axons, and many are nociceptors.

Terminations of Peripheral Nerve Afferents in the Spinal Cord and Brainstem

Afferent fibers entering the spinal cord either simply terminate on neurons in the dorsal horn of the spinal cord or also branch and send a collateral toward the brainstem to either terminate in the dorsal horn at higher levels or in the dorsal column-trigeminal nuclear complex of the lower brainstem. Figure 28.4 depicts sensory terminations in the spinal cord and relays to the medulla–spinal cord junction. Termination patterns of peripheral afferents have been investigated in monkeys and other mammals (see Chapter 8), and some rather consistent features can be assumed to apply to humans. Three general conclusions seem justified. First, the axons of specific types of afferents have characteristic termination patterns in the spinal

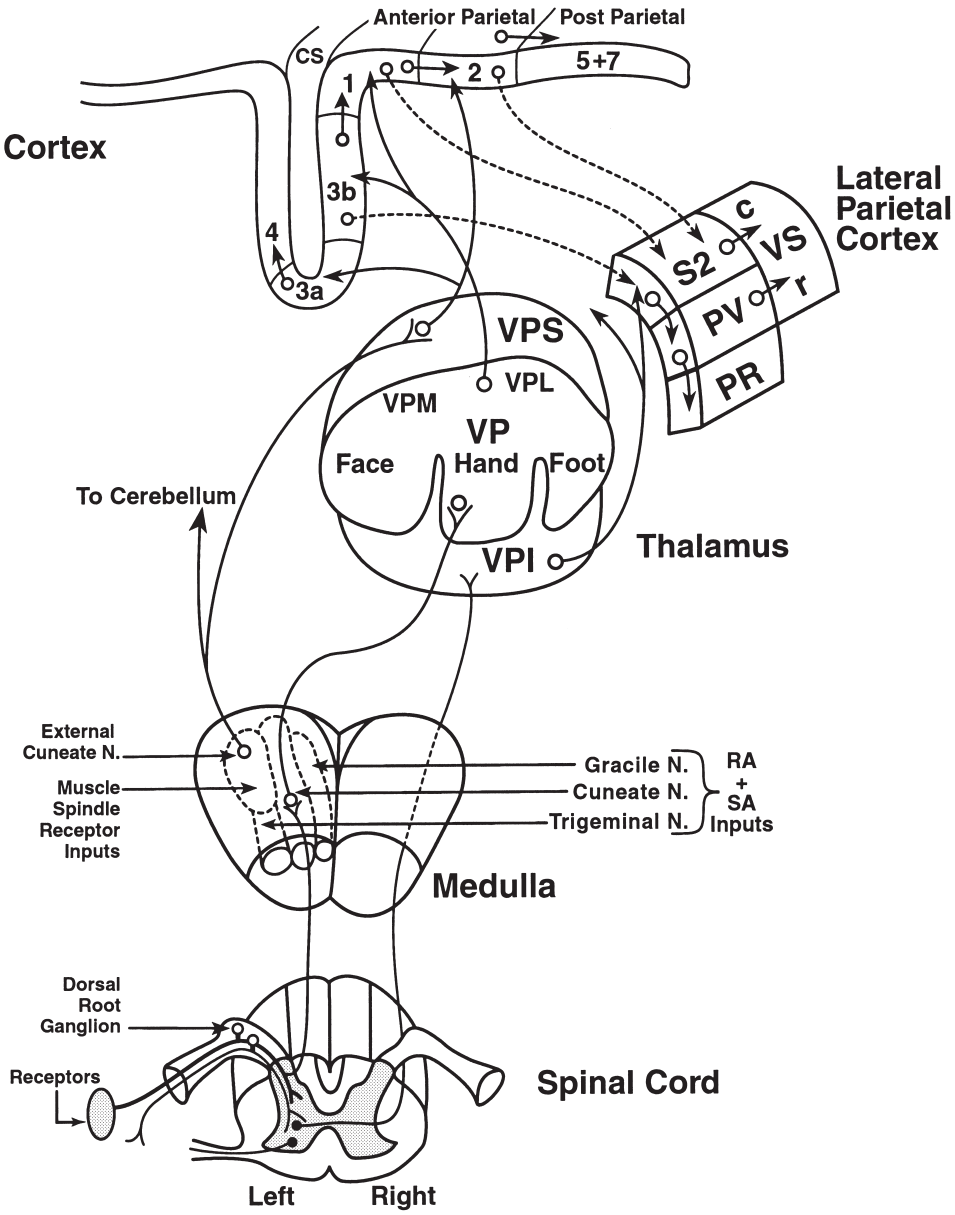

FIGURE 28.4 A more detailed overview of the basic components of the human somatosensory system. Inputs form the four main classes of cutaneous receptors (see Fig. 28.2) enter the spinal cord branch and terminate as neurons in the dorsal horn of the spinal cord and in the ipsilateral dorsal column nuclei of the lower brainstem. Muscle spindle afferents branch in a similar manner with the ascending branch covering the dorsal columns or more laterally to terminate in the gracile and cuneate subnuclei as well as the external cuneate nucleus. Other more slowly conducting afferents related to pain, touch, and temperature terminate on dorsal horn neurons that project contralaterally to form the spinothalamic pathway. Afferents from the face enter the brainstem to terminate in the main trigeminal nuclei for cutaneous and muscle spindle afferents and the spinal trigeminal nucleus for pain, temperature, and touch afferents. The gracile nucleus represents the hindlimb and lower body; the cuneate nucleus, the forelimb; and the principal trigeminal nucleus, the face for cutaneous inputs. These inputs activate second-order neurons that project to the contralateral thalamus by forming the medial lemniscus. Nuclei in the thalamus include the ventroposterior (VP) nucleus with ventroposterior medial (VPM) and ventroposterior lateral (VPL) subnuclei for the face and body representations, respectively. The foot, hand, and face are represented in a lateromedial sequence in VP. The ventroposterior superior (VPS) nucleus receives muscle spinal inputs (2nd or 3rd order), while the ventroposterior inferior nucleus receives spinothalamic axons. These nuclei project to subdividions of anterior parietal and lateral parietal cortex (see text). The second somatosensory area (S2), the parietal ventral area (PV), the parietal rostal area (PR) and caudal and rostral divisions of the ventral somatosensory (VS) complex are indicated. Brodmann's areas are numbered.

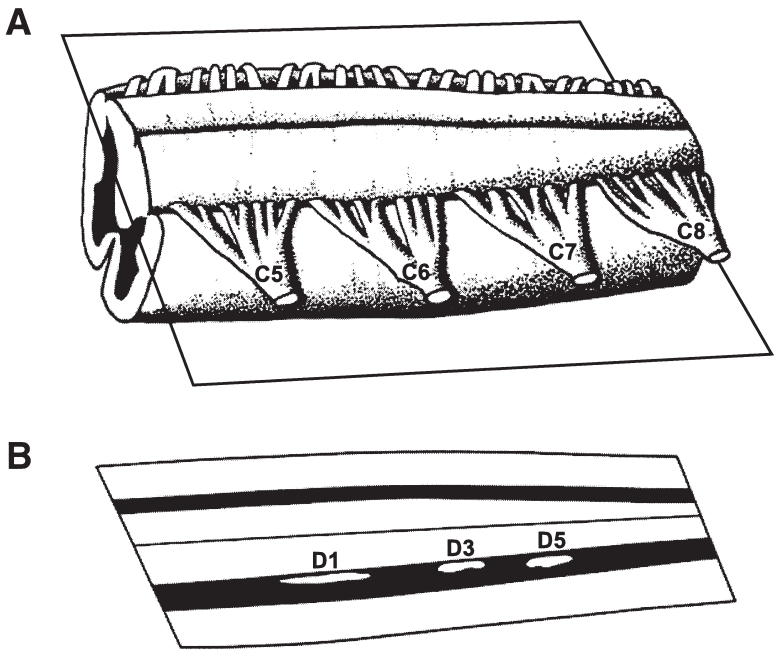

FIGURE 28.5 The rapidly conducting cutaneous afferents of peripheral nerves terminate in a somatotopic paterns in the dorsal horn of the spinal cord. In a macaque monkey, tracers were injected into the glabrus skin of digits 1, 3, and 5 (D1, D3, D5). Although afferents from each digit typically enter the spinal cord over more than one cervical dorsal root (C5, 6, 7, and 8), the inputs terminate in an orderly pattern. Inputs from D1, D3, and D5 terminate in a rostrocaudal pattern in the medial dorsal horn (white) with other digit inputs in between. The dorsal hand and palm are represented more laterally, and the forearm, in rostral and caudal bands. Based on Florence *et al.* (1988, 1989). The box in **(A)** indicates the plane illustrated in **(B).**

cord. Second, afferents from different skin regions terminate separately in the spinal cord to form a somatotopic map. Third, afferents ascending to the dorsal column nuclei terminate somatotopically.

The termination patterns of individual axons that have been physiologically identified and labeled with horseradish peroxidase are known from studies on cats (see Brown, 1981). All the four types of cutaneous afferents bifurcate as they enter the cord to send rostral and caudal branches that further branch to form a sagittally arranged series of terminal arbors. Individual RA-I collaterals form a separate arbor of about 500 μm in the sagittal plane and 50–300 μm in the transverse plane in layers III and IV. Collaterals of PC or RA-II axons terminate in several sagittally elongated arbors (400–750 μm) that extend vertically from layers III and IV to layers V and VI. SA-I axon collaterals give rise to spherical arbors (250–700 μm) that distribute in layers II, III, IV, and the dorsal margin of V. SA-II axon collaterals terminate over layers III, IV, V, and part of VI in rostrocaudally thin sheets (100–300 μm). While all types differ in the details of distribution, the results indicate that inputs from single receptive fields on the skin relate to rostrocaudal rows of cells in the dorsal horn. How axons from specific skin regions terminate in the spinal cord is known for a range of mammals, including monkeys. Similarities across species suggest that the termination pattern in humans is similar. Figure 28.5 shows that the terminations from the skin of the digits of the hand are arranged in a rostrocaudal row in the medial dorsal horn of the cervical spinal cord of macaque monkeys (see Florence *et al.*, 1988, 1989). More proximal parts of the limb are represented more laterally in the dorsal horn, and inputs from the foot demonstrate a similar orderly arrangement. As for the single axons, groups of axons from a limited skin region terminate in rostrocaudally elongated zones. Thus, body parts are represented in rostrocaudal slabs of cells. While different classes of afferents activate different groups of spinal cord cells, the single zones of label for each digit indicate that the dorsal horn cells activated from a given skin region are grouped together.

Ascending Spinal Cord Pathways

Traditionally, the ascending somatosensory pathways from the spinal cord include the dorsal column pathway and a ventrolateral pathway (Fig. 28.4). The dorsal column pathway comprises the axons of first-

order dorsal root ganglion neurons coursing ipsilaterally to the dorsal column nuclei. The ventrolateral pathway (see below) originates from second-order neurons of the dorsal horn, crosses to the opposite ventrolateral white matter of the spinal cord, and ascends to brainstem and thalamic targets, including the ventroposterior inferior nucleus of the thalamus. The ipsilateral dorsal column system was thought to deal with epicritic functions such as position sense and light touch, while the crossed spinothalamic system was thought to mediate protopathic sensibilities of crude touch, pain, and temperature. More recent research (see Chapter 8) has complicated this story by indicating that (1) second-order neurons also contribute to the ipsilateral dorsal columns; (2) additional ipsilateral pathways from second-order neurons exist, including a spinocervical system that is reduced in primates; (3) pathways from the upper and lower limbs differ; (4) crossed spinothalamic pathways vary in location; and (5) descending axons are mixed with ascending axons. Of course, these refinements are based on anatomical studies in nonhuman primates and other mammals, but findings are general enough that they are likely to apply to humans.

The Dorsal (Posterior) Column System

The extremely large dorsal column afferent pathway in humans occupies over a third of the spinal cord at high cervical levels (Wall, 1970). The two major divisions are the more medial gracile tract subserving the trunk and lower limb and the cuneate tract for the upper limb and associated trunk and neck. Inputs from the face and head via the trigeminal system form an analogous tract in the brainstem (see Chapter 29). The axons in the dorsal columns are largely myelinated dorsal root fibers that branch to ascend to the dorsal column nuclei, send descending collaterals for several segments in the dorsal columns, and emit a number of local collaterals to terminate on neurons in the dorsal horn. Other axons originate from spinal cord neurons and ascend over several segments to terminate in the spinal cord on local circuit neurons or on neurons that project to the brainstem. Some of these secondary sensory neurons project via the dorsal columns to the dorsal column nuclei. Thus, both first- and higher-order axons are found in the dorsal column pathway. A few descending fibers may also travel in the dorsal columns. Entering fibers from each dorsal root form a narrow layer at the lateral margin of fibers from lower levels, but some mixing of levels occurs as the axons ascend.

Most of what is known about the types of information conveyed by the dorsal columns comes from microelectrode recordings in monkeys (Whitsel *et al.*, 1969), although limited recordings in humans revealed nerve fibers activated by pressure and limb movement (Puletti and Blomquist, 1967). The gracile and cuneate tracts differ at high spinal cord levels in the classes of axons they contain. The gracile tract at lower levels contains a mixture of cutaneous afferents, largely rapidly adapting afferents (probably RA-I), and muscle afferents that leave to terminate in Clarke's nucleus, which projects in turn to the cerebellum and other structures via the dorsal spinocerebellar tract. At higher levels, the remaining axons that travel to nucleus gracilis are almost completely RA cutaneous afferents. The cuneate tract contains a mixture of RA cutaneous and muscle afferents, but the cutaneous inputs terminate in the cuneate nucleus, and the muscle afferents separate to innervate the external cuneate nucleus. Thus, lesions of the dorsal columns deactivate RA neurons, regardless of level, but muscle afferents from the lower body terminate on neurons that relay outside of the gracile tract. Presumably, the dorsal columns of monkeys and humans also contain SA-I, SA-II, and PC afferents, as in other mammals (see Willis and Coggeshall, 1978), but evidence is presently lacking. Lesions of the dorsal columns in humans have little effect on many simple tactile abilities, but major defects occur in the abilities to detect the speed and direction of moving stimuli and to identify figures drawn on the skin (Nathan *et al.*, 1986; see Mountcastle, 1975, and Wall and Noordenhos, 1977, for reveiws). These changes obviously can be attributed to the loss of inputs from RA cutaneous afferents. Other defects in the control of forelimb movements (Beck, 1976) may relate to disruption of muscle afferents. The sensory changes following dorsal column lesions in monkeys are similar, where they have been extensively studied (see Vierck and Cooper, 1998, for review).

The dorsal columns apparently carry all of the inputs from the upper body that activate anterior parietal cortex. After complete lesions of the dorsal columns at a high cervical level in monkeys, neurons throughout the forelimb and adjacent trunk representations in areas 3a, 3b, l, and 2 totally fail to respond to somatosensory stimuli (Jain *et al.*, 1997). Given the distribution of information from anterior parietal cortex to areas of posterior parietal and lateral parietal cortex (Fig. 28.4), the impact on somatosensory processing at the cortical level is major. However, the effects of dorsal column lesions on behavior has been difficult to study because the somatosensory system of adult primates has great plasticity, and the survival of only a few dorsal column axons can have great impact on cortical neurons (Jain *et al.*, 1997). As expected, humans (Nathan *et al.*, 1986) and monkeys (e.g., Vierck and Cooper, 1998) with dorsal column lesions are greatly impaired in somatosensory abilities and sensory

guidance of motor behavior, especially when lesions are cervical and affect forelimb and hand use rather than thoracic and affect leg and foot use. This may be partly because some of the relevant afferents from the leg travel outside the dorsal columns (see earlier discussion). The abilities that remain demonstrate the importance of the spinal cord connections and other ascending pathways, especially the spinothalamic pathway, although its mode of action in touch is uncertain.

Primary afferents from oral and facial structures travel in the trigeminal or fifth nerve and enter the brainstem to branch and terminate in the principal trigeminal nucleus and subdivisions of the spinal trigeminal complex (May and Porter, 1998; see Chapter 29). The axon branches terminating in the principal nucleus are largely of the low-threshold SA and RA classes, and they constitute the equivalent of the dorsal column pathway. Terminations in the subdivisions of the spinal trigeminal complex correspond to those from the body that terminate in the dorsal horn of the spinal cord.

Second-Order Axons of the Dorsolateral Spinal Cord (The Spinomedullothalamic System)

In monkeys, all the muscle afferents for the lower body apparently leave the gracile column and synapse on neurons that send axons in the dorsolateral (posterolateral) spinal cord to the dorsal column nuclear complex (Whitsel *et al.*, 1972). In humans, lesions of both the dorsal columns and the dorsolateral spinal cord result in severe defects in proprioception, but it is not certain that all proprioceptive axons from the lower limbs are in the dorsolateral pathway rather than the dorsal column pathway (Nathan *et al.*, 1986).

Many or all mammals have other inputs to the dorsolateral pathway, including a spinocervical pathway from second-order neurons in the dorsal horn that project ipsilaterally to the lateral cervical nucleus. A comparatively reduced lateral cervical nucleus has been described for humans (Truex *et al.*, 1970), but the types of inputs activating this nucleus are known only from studies on other mammals, especially cats (see Willis and Coggeshall, 1991, for review). Neurons projecting into the spinocervical tract have receptive fields on both the hairy and glabrous skin in monkeys (Bryan *et al.*, 1974). Peripheral inputs activating these neurons are cutaneous rapidly adapting afferents, and there is an apparent lack of slowly adapting cutaneous and deep receptor influences.

The Spinothalamic Pathways

Many second-order somatosensory neurons in the dorsal horn of the spinal cord have axons that cross in the spinal cord to ascend in the ventrolateral or dorsolateral white matter. Many axons in these pathways terminate before reaching the thalamus, but others branch to reach several thalamic nuclei. In Old World monkeys, a dorsolateral spinothalamic tract consists of locally crossing axons of lamina I cells of the dorsal horn, while the ventrolateral spinothalamic tract contains locally crossing axons of laminae I-X cells (Apkarian and Hodge, 1989a). In monkeys, spinothalamic tract neurons have been found to respond to tactile stimuli and movement of hairs, stimuli ranging from tactile to noxious (wide dynamic range neurons), noxious stimuli, and temperature (see Willis and Coggeshall, 1991; Craig *et al.*, 1999). In humans, some capacity for mechanoreceptive sensibility remains after large lesions of other ascending pathways, but electrical stimulation of the ventral quadrants of the spinal cord has produced sensations of only pain and temperature (Sweet *et al.*, 1950; Tasker *et al.*, 1976).

RELAY NUCLEI OF THE MEDULLA AND UPPER SPINAL CORD

Several groups of neurons in the spinal cord and medulla are important in relaying information to higher brain centers. These include the dorsal column nuclear complex, the dorsal nucleus of the spinal cord (Clarke's nucleus or column), and the lateral cervical nucleus. The trigeminal nuclear complex adds analogous pathways for information from the head.

Dorsal Column-Trigeminal Nuclear Complex

The dorsal column-trigeminal nuclear complex consists of groups of cells in the lower brainstem and upper spinal cord that receive inputs from ipsilateral low-threshold mechanoreceptors and project to the ventroposterior complex of the thalamus (Fig. 28.4). The part of the system originating in dorsal root ganglia and coursing in the dorsal columns terminates in the gracile nucleus for the lower body and the cuneate nucleus for the upper body. The trigeminal complex receives inputs from cutaneous mechanoreceptors in the face and mouth. The gracile, cuneate, and trigeminal "nuclei" form a somatotopic map from hindlimb to head in a mediolateral sequence in the lower medulla (Xu and Wall, 1996, 1999).

The gracile and cuneate nuclei are elongated in the rostrocaudal dimension (Fig. 28.4). The overall appearance of the nuclei in humans (see Chapter 10) is quite similar to that observed in macaque monkeys (Florence *et al.*, 1988, 1989). In both, the middle regions contain discrete clusters of neurons outlined by bands of myelinated fibers. Stains for the mitochondrial

enzyme cytochrome oxidase (CO) show that the cell clusters have more of the enzyme and, presumably, higher metabolic activity than the surrounding fiber regions. The details of the parcellation pattern of this nucleus in humans and monkeys are quite comparable (Florence *et al.*, 1989), suggesting the significance of the parcellation is the same. In monkeys, specific cell clusters in the central cuneate nucleus correspond to inputs from specific digits of the hand. Thus, the parcellation reflects the somatotopic organization of the nucleus. The rostral and caudal poles of the cuneate nucleus have more convergent terminations from afferents of the digits. Thus, the nucleus appears to segregate inputs into a discrete somatotopic map in the central part of the nucleus and into less precise maps in the rostral and the caudal poles of the nucleus in monkeys, and probably in humans, judging from the close match in appearance. There is evidence from studies in cats (Dykes, 1983) that RA-I and SA classes of cutaneous afferents activate neurons in the central zones of the dorsal column nuclei, while SA, joint, and muscle receptor afferents relate to the rostral parts of these nuclei, and Pacinian receptor afferents are concentrated caudally.

The projection neurons of the dorsal column nuclei send axons into the contralateral medial lemniscus, where they course to the ventroposterior complex (Rasmussen and Peyton, 1948). In humans, as in other mammals, some axons probably send collaterals to the inferior olive, which, in turn, projects to the cerebellum (see Schroeder and Jane, 1976; Molinari *et al.*, 1996). In monkeys and other mammals, the dorsal column nuclei, especially the rostral poles, receive inputs from the contralateral somatosensory and motor cortex (areas 4, 3a, 3b, l, and 2) that may modulate the relay of sensory information (e.g., Bentivoglio and Rustioni, 1986; Cheema *et al.*, 1985; Marino *et al.*, 1999, for a review).

The trigeminal complex includes the principal (Pr 5) or main sensory nucleus and the spinal trigeminal nucleus. The principal nucleus is thought to be analogous to the cuneate and gracile nuclei, and the three together form one or more systematic representations of cutaneous receptors of the body. The principal nucleus projects via the medial lemniscus to the medial subnucleus of the contralateral ventroposterior complex (VPM). The spinal trigeminal nucleus (Sp 5) is analogous to part of the dorsal horn of the spinal cord. As in the spinal cord, a marginal zone receives pain and temperature afferents (Craig *et al.*, 1999) and deeper neurons are activated by cutaneous and muscle receptors (e.g., Price *et al.*, 1976). Second-order neurons in the spinal trigeminal nucleus form a relay that joins the contralateral spinothalamic tract to terminate in the ventroposterior nuclear complex and the more medial thalamus (see Burton and Craig, 1979).

Lateral Cervical Nucleus, Nuclei X and Z, External Cuneate Nucleus, and Clarke's Column

Second- and third-order relay neurons are found in several structures (for the human brainstem, see Huang and Paxinos, 1995; Chapter 10) in addition to the dorsal column-trigeminal complex and the dorsal horn of the spinal cord.

Lateral Cervical Nucleus

A long column of neurons outside the gray matter proper of the dorsal horn of the spinal cord that extends from C4 to the caudal part of the medulla composes the lateral cervical nucleus. Rapidly adapting afferent fibers serving hairs and other tactile afferents enter the dorsal horn to relay on neurons forming the spinocervical tract in the dorsolateral white matter. These second-order neurons terminate on neurons in the ipsilateral lateral cervical nucleus. A subset of multimodal neurons with a convergence of nociceptive afferent inputs has been reported in the lateral cervical nucleus as well (see Boivie, 1978, for a review). The lateral cervical nucleus appears to relay touch, pressure, and vibration information, largely from the hairy skin, to the contralateral thalamus, inferior olive, and midbrain. In humans, the lateral cervical nucleus may be a rudimentary structure because it is only well defined in some individuals (Truex *et al.*, 1970). In such humans, the nucleus contains up to 4000 neurons, while nearly double that number may exist in cats (Boivie, 1983).

Nuclei X and Z

Other second-order axons of the dorsolateral fasciculus, possibly collaterals of spinocerebellar axons, terminate in two small medullary nuclei, termed X and Z by Pompeiano and Brodal (1957). Muscle spindle afferents for the hindlimb relay via the dorsolateral funiculus to nucleus Z, located just rostral to the gracile nucleus. Nucleus Z, which has been identified in the human brainstem (Sadjadpour and Brodal, 1968; see Chapter 10), projects to the contralateral ventroposterior complex in the thalamus. In monkeys, muscle spindle receptor afferents related to the forelimb relay over neurons projecting within the dorsal columns (Dreyer *et al.*, 1974). This probably also occurs in humans, since lesions of the dorsal columns impair motor control for the upper limbs (Nathan *et al.*, 1986). A separate nucleus X, not clearly present in humans, forms a second group of neurons receiving mostly

second-order muscle spindle afferents related to the lower limbs.

External Cuneate Nucleus

The muscle spindle afferents of the upper limbs and body course in the cuneate fasciculus to terminate in the external cuneate nucleus. Like nucleus X, the external cuneate nucleus relays to the contralateral ventroposterior complex of the thalamus, and to the cerebellum.

Clarke's Nucleus or Column

A long column of cells called Clarke's column is located just dorsolateral to the central canal in the medial part of the spinal cord of T1-L4 levels. Inputs are largely from muscle spindles. Clarke's column projects to nucleus Z and, via the dorsal spinocerebellar tract, to the cerebellum (for reviews, see Mann, 1973; Willis and Coggeshall, 1991; Chapter 11).

SOMATOSENSORY REGIONS OF THE MIDBRAIN

Studies in nonhuman mammals implicate several midbrain structures in somatosensory functions, but evidence for similar roles in humans is presently lacking. (1) Neurons in the external nucleus of the inferior colliculus respond to somatosensory stimuli and receive inputs from the dorsal column nuclei. The pericentral nucleus may have spinal cord inputs as well. Schroeder and Jane (1976) speculate that auditory and somatosensory systems interrelate in these structures in the detection of low-frequency vibratory stimuli. (2) The deeper layers of the superior colliculus contain neurons activated by somatosensory stimuli via inputs from the spinal trigeminal nucleus, the spinal cord, the lateral cervical nucleus, and the dorsal column nuclei (see Huerta and Harting, 1984, for a review). The somatosensory inputs form a representation that is matched in general spatial location with visual and auditory maps, and the presumed role of the matched maps is to function together in directing eye and head movements toward objects (sounds, touches, and images) of interest (see Meredith and Stein, 1985).

SOMATOSENSORY THALAMUS

Various proposals have been made for how to subdivide the human thalamus (see Chapter 20), but the thalamic structures related to somatosensory abilities have not been identified with complete certainty. In macaques and several families of New World monkeys, where considerable experimental evidence is available (see Kaas and Pons, 1988; Krubitzer and Kaas, 1992), we subdivided the somatosensory thalamus into a large ventroposterior nucleus, a ventroposterior superior nucleus (VPS), and a ventroposterior inferior nucleus (Fig. 28.4). The VP is the principal relay of information from rapidly adapting and slowly adapting cutaneous receptors to anterior parietal cortex, the VPS relays information from deep receptors in muscle and joints, while the significance of the VPI with spinothalamic inputs is less certain. Just caudal to VPI, a ventromedial posterior nucleus, VMpo appears to receive spinothalamic inputs mediating pain and temperature (Craig *et al.*, 1994). In addition, related nuclei of the posterior complex (Po) appear to have somatosensory functions. Other nuclei, notably the medial and anterior divisions of the pulvinar complex and the lateral posterior nucleus, are known to have connections with parietal cortex and thereby are implicated in somatosensory functions. However, these nuclei do not appear to have a role in relaying sensory information. The somatosensory nuclei are discussed and related to proposed subdivisions of the human thalamus later.

Ventroposterior Nucleus

The VP is a basic subdivision of the mammalian thalamus (Jones, 1985; Welker, 1974) that is characterized by (1) densely packed and darkly stained neurons; (2) a systematic representation of cutaneous receptors; (3) inputs from the dorsal column nuclei, the spinothalamic tract, and the trigeminal system; and (4) projections to "primary" somatosensory cortex. The nucleus has subnuclei of dense aggregates of neurons partially separated by cell-poor fiber bands, the most conspicuous of which is the arcuate lamina that separates the part of VP representing the face, the ventroposterior medial "nucleus" (VPM), from the portion representing the rest of the body, the ventroposterior lateral "nucleus" (VPL). Another notable fiber band separates the representations of the hand and foot in VPL.

In macaque monkeys, the dorsal boundaries of VP are not very distinct from the region we now identify as VPS (see Paxinos *et al.*, 2000). The VP of some investigators includes VPS, although this region has also been distinguished as the VP "shell." Another problem is that Olszewski's (1952) popular atlas of the thalamus of macaque monkeys includes additional parts of the thalamus related to motor cortex within an oral division of VPL (VPLo). This use of terminology is not consistent with that used in other mammals.

In the human thalamus, the region identified as the "ventrocaudalis group" or Vc (see Chapter 20)

corresponds closely to our VP in monkeys. Using the terminology of Hässler (1982), VPL is Vce (the external segment) and VPM is Vci (the internal segment of Vc). VP is composed of a range of neuron sizes that generally stain densely for Nissl substance. The dorsal border of the nucleus is described as indistinct, but medial borders with the anterior pulvinar and ventral borders with the VPI are distinct. Recent atlases of the human brain use the terms VPL and VPM (Mai *et al.*, 1997; Morel *et al.*, 1997).

The VP contains a single systematic representation of cutaneous receptors. Each location on the body surface activates a small volume of tissue or cluster of neurons in VP, and these clusters of neurons are arranged according to body part. The general form of the somatotopic organization in mammals has been reviewed by Welker (1974), and described in detail for squirrel monkeys by Kaas *et al.* 1984 (Fig. 28.6; see Rausell and Jones, 1991, for VPM of macaque monkeys). In all primates, including humans, we expect the tactile receptors of the tongue, teeth, and oral cavity to be represented medial to the lips and upper face for VPM. Because some of the inputs from the principal trigeminal nucleus are ipsilateral as well as contralateral, the ipsilateral and contralateral teeth and tongue are both represented in each VPM. More medially, a gustatory nucleus, the so-called VPM parvocellular part (VPMpc), is part of the system for taste (see Chapter 31). The medial portion of VPL contains a mediolateral sequential representation of the digits of the hand from thumb to little finger. The lateral portion of VPL is devoted to the foot, while dorsal portions of the nucleus relate to the proximal leg, the trunk, and the proximal arm in a lateromedial sequence. This arrangement, found in monkeys and in other mammals, is basically the order described for the human VP. Recordings and electrical stimulation with microelectrodes in VP of the human thalamus (Emmers and Tasker, 1975; Lenz *et al.*, 1988) indicate that the mouth and tongue relate to ventromedial portions of VPM, that the hand and foot are in ventrorostral VPL, and the back and neck are in dorsocaudal VPL. Furthermore, the fingers activate a large portion of medial VPL and the lips and tongue relate to a large part of VPM. Finally, often groups of neurons extending in the parasagittal plane are activated by the same restricted skin surface, indicating that lines of isorepresentation are largely in the parasagittal direction.

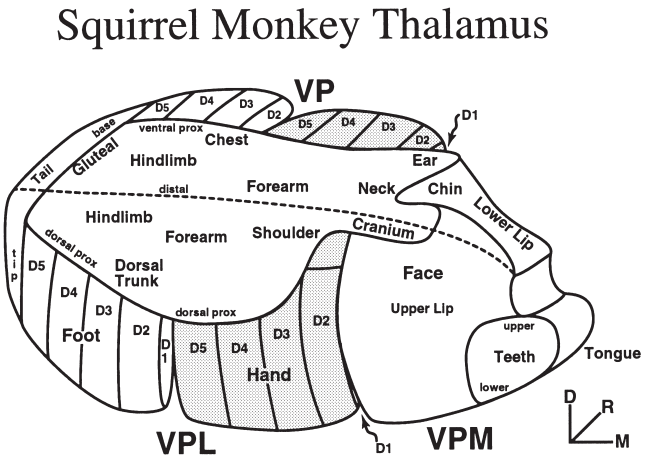

FIGURE 28.6 The somatotopic organization of the ventroposterior (VP) nucleus of squirrel monkeys. A similar organization, except for a lateral representation of the tail, exists in VP of humans (Lenz *et al.*, 1988). VP is subdivided into ventroposterior lateral (VPL) for the body and ventroposterior medial (VPM) for the face. VPL has further subnuclei for the hand and foot. Digits of the hand and foot are represented in mediolateral sequences with the tips ventral. Neurons in VP are activated by slowly and rapidly adapting afferents. Neurons activated by each class form small clusters with VP. Adapted from Kaas *et al.* (1984).

As in monkeys (e.g., Dykes *et al.*, 1981), most neurons in VP of humans are activated by RA-I or SA inputs, with local clusters of cells related to one or the other class of inputs (Lenz *et al.*, 1988). Thus, there is a double representation of the skin in VP, one for fragmented representation of RA-I afferents and one for SA afferents. The SA inputs could be SA-I or both SA-I and SA-II. There is little evidence for Pacinian (RA-II) inputs, but they may add to the complexity of the nucleus. A few neurons respond with an increasing frequency as light tactile stimuli become more intense and extend into the painful range (the wide-dynamic-range neurons); these neurons may have a role in pain perception (see Kenshalo *et al.*, 1980) or in signaling the intensity of stimuli. In humans, electrical stimulation of peripheral nerves results in evoked potentials in the contralateral VP with a latency of 14–17 ms (Celesia, 1979; Fukushima *et al.*, 1976). Electrical stimulation in sites in the nucleus or of input fibers in the medial lemniscus generally results in sharply localized sensations of numbness or tingling rather than light touch (Emmers and Tasker, 1975; Ervin and Mark, 1964; Tasker *et al.*, 1972; Davis *et al.*, 1996; Lenz *et al.*, 1998, 1988). Localized lesions of VP are followed by a persistent numbness in a restricted skin region corresponding to the body surface map in VP (Domino *et al.*, 1965; Garcin and LaPresle, 1960; Van Buren *et al.*, 1976).

The sources of ascending inputs to VP (Fig. 28.4) have been studied in many mammals, including macaque monkeys. The dense inputs are from the dorsal column nuclei via the medial lemniscus and the main sensory trigeminal nucleus via the trigeminal lemniscus. In humans, evoked potentials have been

recorded in VP after electrical stimulation of the dorsal columns (Gildenberg and Murthy, 1980). Less-dense, unevenly distributed inputs are from the spinothalamic tract and the lateral cervical nucleus (Berkley, 1980; Apkarian and Hodge, 1989b). In humans, degenerating spinothalamic terminations have been reported in VP after spinal cord damage (Mehler, 1966; see Bowsher, 1957, for a review of classical reports). The spinothalamic inputs appear to relate to small-cell regions of VP (possibly an extension of VPI) that project to superficial layers of areas 3b and 1 (Rausell and Jones, 1991). Thus, this relay likely has a modulatory role in somatosensory cortex.

The outputs of the ventroposterior nucleus have been studied extensively in primates and other mammals (see Kaas, 1983; Kaas and Pons, 1988; Darian-Smith *et al.*, 1990; Krubitzer and Kaas, 1992). In all mammals studied, VP projects to area 3b or its nonprimate homologue S1. In most mammals, other projections are to the second somatosensory area (S2) and possibly other fields, but in monkeys, and probably humans, projections to S2 are a trivial component of the output. In monkeys, VP also projects over thinner axons and in a less-dense manner to area 1, and, in macaque monkeys, a sparse input exists to part of area 2 related to the hand and even a specialized part of area 5 (Pons and Kaas, 1986). In humans, lesions of anterior parietal cortex including areas 3b and 1 cause retrograde degeneration and cell loss in VP (Van Buren and Borke, 1972), supporting the conclusion that the output patterns in humans and monkeys are similar. Furthermore, recordings from the surface of somatosensory cortex indicate that potentials evoked by median nerve stimulation are reduced or abolished by lesions of VP (Domino *et al.*, 1965).

Ventroposterior Superior Nucleus

There has been long-standing recognition that inputs from receptors in deep tissues are at least partially segregated from inputs from cutaneous receptors in the ventroposterior thalamus of primates (see Poggio and Mountcastle, 1963) and perhaps other mammals. The zone of activation by deep receptors is dorsal to that related to cutaneous receptors in monkeys, and the deep receptor zone is further distinguished by its pattern of cortical connections and architecture. We have termed the deep receptor zone the ventroposterior superior nucleus (VPS; see Kaas and Pons, 1988). Early investigators included the zone of activation by deep receptors in VP, and several recent researchers simply designate the deep receptor zone as the VP "shell." Others conclude that the deep receptor zone includes two nuclei, a VPS and a "ventroposterior oral" nucleus (see Dykes, 1983), but the evidence for such a subdivision in primates is inconclusive. Some term the VPS region VPO (see Chapter 20) as it is as much oral (anterior) as superior in some primates. Finally, the medial posterior nucleus of some investigators (see Krubitzer and Kaas, 1987, for a review) may be a nonprimate homologue of VPS.

In monkeys, VPS contains a representation of deep receptors, principally muscle spindle receptors (see Kaas and Pons, 1988; Wiesendanger and Miles, 1982). The representation parallels that in VP so that the face, hand, and foot activate the medial, middle, and lateral portions of VPS in sequence (Kaas *et al.*, 1984). The major input appears to be from the external cuneate nucleus (Boivie and Boman, 1981), and the output is largely or exclusively to area 3a and area 2. Many of the same neurons in VPS appear to project to both area 3a and area 2 via collaterals (Cusick *et al.*, 1985).

Evidence is less complete for VPS of humans. Deep receptors are represented in an orderly manner in part of the thalamus just rostrodorsal to the cutaneous representation in VP (Lenz *et al.*, 1990; Ohye *et al.*, 1993; Seike, 1993). The mediolateral progression in the representation corresponds to that in VPS with the jaw medial to fingers, followed by wrist, elbow, shoulder, and leg. VPS is probably within VP or a VL-VP "transition" zone identified as Vc.a.e. by Hässler (1959) and VPLa in more recent sudies (Hirai and Jones, 1989; Morel *et al.*, 1997).

Ventroposterior Inferior Nucleus

In all primates, including humans (e.g., Morel *et al.*, 1997), VPI is recognized as a narrow region just ventral to VP that is composed of small, pale-staining neurons. VPI is densely myelinated and reacts lightly for cytochrome oxidase. VPI extends dorsally into the cell-poor regions that separate face, hand, and foot subnuclei of VP (Krubitzer and Kaas, 1992). Because of this dorsal finger-like extension of parts of VPI, and its caudal extension into thalamic regions of similar appearance and perhaps function (see following discussion), some of the boundaries of VPI have been uncertain. As a result, the major inputs to VPI from the spinothalamic and caudal trigeminothalamic afferents have been variously described as including not only VPI but also VP as well as more caudal nuclei (see Apkarian and Hodge, 1989b). The inputs to VPI reveal a somatotopic pattern with the hindlimb inputs most lateral and the forelimb and face inputs more medial (Gingold *et al.*, 1991). Outputs to cortex also indicate this overall somatotopic pattern of organization (Cusick and Gould, 1990). Neurons in the VPI region of both monkeys (Apkarian and Shi, 1994) and

humans (Lenz *et al.*, 1993) are responsive to noxious stimulation. In monkeys, VPI projects densely to areas S2 and PV of lateral parietal cortex and less densely and more superficially to areas of anterior parietal cortex (Friedman and Murray, 1986; Cusick and Gould, 1990; Krubitzer and Kaas, 1992). Although VPI relays spinothalamic tract information, and VPI includes neurons responsive to noxious stimuli, it seems likely that the role of VPI projections to cortex are largely modulatory. They may have a role in experience-related plasticity of somatosensory cortex (see Kaas and Florence, 2000).

The Posterior Group and the Posterior Ventromedial Nucleus

A poorly defined group of nuclei with somatosensory, auditory, and multimodal functions, located just caudal to the ventroposterior complex, has been referred to as the posterior group or complex (Jones, 1985). The complex is commonly divided into separate limitans, suprageniculate, and posterior nuclei. The posterior "nucleus" is often subdivided into medial, lateral, and even intermediate nuclei. The medial posterior nucleus (Pom) is composed of small cells that seem to merge with caudal VPI. There is some evidence that neurons with large cutaneous receptive fields and multimodal responses in the lateral cervical nucleus relay to Pom (see Metherate *et al.*, 1987, for a review). Cortical projections of the posterior complex appear to be to cortex of the lateral fissure near S2.

Recently, a part of the posterior group has been distinguished in monkeys and humans as posterior ventromedial nucleus (Craig *et al.*, 1994; Davis *et al.*, 1999; Blomquist *et al.*, 2000). The nucleus receives somatotopically organized nociceptive and thermoreceptive inputs from layer I of the contralateral dorsal horn of the spinal cord via the spinothalamic tract. VMpo relays to part of lateral parietal cortex in the lateral fissure. This pathway appears to be important in mediating pain and temperature sensations (see Perl, 1998). VMpo projects to cortex in the lateral fissure in the region of the insula (Craig *et al.*, 1996).

Anterior Pulvinar, Medial Pulvinar, and Lateral Posterior Nucleus

Other thalamic structures without direct inputs from second-order somatic afferents can be considered part of the somatosensory system on the basis of connections with somatosensory cortex. These include the anterior (oral) pulvinar with widespread projections to anterior parietal cortex, posterior parietal cortex, and somatosensory cortex of the lateral fissure (Cusick and Gould, 1990; Krubitzer and Kaas, 1992); the medial pulvinar with connections with posterior parietal cortex and the temporal lobe (see Mesulam, 1981); and the lateral posterior nucleus with projections to posterior parietal cortex (see Kaas and Pons, 1988). In humans, degeneration has been noted in the anterior pulvinar after damage to parietal cortex of the lateral fissure, while LP degenerates after lesions of posterior parietal cortex (Van Buren and Borke, 1972). The roles of these nuclei in the processing of somatosensory information are unknown, but the lack of direct sensory input and the widespread cortical connections suggest modulatory and integrative functions.

ANTERIOR PARIETAL CORTEX

The anterior parietal cortex was first considered as several separate fields in early architectonic studies (e.g., Brodmann, 1909), then as a single primary somatosensory field or S-I on the basis of electrophysiological studies in monkeys (see Marshall *et al.*, 1937), and more recently as several fields again, as the validity of early subdivisions has been experimentally supported (see Kaas, 1983).

Early attempts to subdivide anterior parietal cortex resulted in the differing conclusions of Campbell (1905), Smith (1907), Brodmann (1909), Vogt and Vogt (1919), and von Economo and Koskinas (1925). The subdivisions made by Campbell and Smith fell into disuse, but the proposals of Brodmann, Vogt and Vogt, and von Economo are in use today (see Chapter 27). In brief, Brodmann distinguished a mediolateral strip of cortex in the caudal bank of the central (rolandic) fissure as area 3, an immediately superficial and caudal strip on the caudal lip of the sulcus as area 1, and a more caudal strip on the surface of the postcentral gyrus as area 2. Area 3 was described as a field with densely packed small granular cells in layer IV, as is characteristic of sensory fields, while area 1 and 2 had less dominant sensory features. Brodmann further described a "transitional" field in anterior (deep in the central fissure) area 3 with both prominent sensory (layer IV granule cells) and motor (layer V pyramidal cells) features. Vogt and Vogt (1919) added to this proposal by stressing the distinctiveness of anterior area 3, and subdivided area 3 into two fields, area 3a and area 3b (see Jones and Porter, 1980, for a review). These four architectonically defined subdivisions of postcentral somatosensory cortex are in common use today. However, some investigators use the terms of von Economo (1929) for these subdivisions.

Rather than number cortical fields, von Economo used two letters to denote fields, with the first letter

indicating the lobe of the brain for the field, and the second letter indicating the order in which fields were described in the lobe, typically starting with fields of obvious sensory nature. In general, Brodmann (1909) and von Economo (1929) divided the human brain in different ways, but the proposed subdivisions of anterior parietal cortex are quite similar, the agreement suggesting the validity of the divisions. Von Economo's most anterior field, deep in the central sulcus, is area PA, equivalent to area 3a. The adjacent field, area PB, was noted as sensory "koniocortex" as a result of the powder-like appearance of the small granule cells in layer IV of what clearly corresponds to area 3b. Area PC, characterized by a less distinct laminar structure, is equivalent to area 1. A more caudal strip of cortex with a more distinct layer IV and layer VI, is area PD, closely corresponding to area 2.

Anterior Parietal Cortex in Monkeys

Over the last few years, research on monkeys has greatly clarified the significance of the four architectonic strips. Conclusions based on an extensive number of anatomical and electrophysiological studies are briefly summarized next.

Area 3b

We have termed area 3b S-I proper because it appears to be the homologue of the primary somatosensory area, S-I, in nonprimates (Kaas, 1983). Area 3b contains a separate, complete map of the cutaneous receptors of the body. The representation proceeds from the foot in medial cortex to the face and tongue in lateral cortex, with the digits of the foot and hand pointing "rostrally" (or more precisely, deep in the central sulcus), and the pads of the palm and sole of the foot caudal in 3b near the area 1 border. Subdivisions of area 3b related to body parts can be seen as myelin-dense ovals separated by myelin-light septa (Jain *et al.,* 1998, 2001). The most conspicuous septum transects lateral area 3b where it separates the more medial hand representation from the more lateral face representation. In the hand representation, a narrow strip of cortex for each digit is bounded on each side by septa. The hand representation is bordered laterally by a caudorostral series of three myelin-dense ovals, first for the upper face, next for the upper lip, and then for the lower lip and chin. Next, a succession of four ovals represent the contralateral teeth, the contralateral tongue, the ipsilateral teeth, and the ipsilateral tongue. Except for the rostrolateral representation of ipsilateral tongue and teeth (also see Manger *et al.,* 1996), the area 3b representation, like other representations in anterior parietal cortex, is almost exclusively of the contralateral body surface. The septa-distinguishing body parts in area 3b usefully serve as an anatomical guide for other types of experiments. They have not been described in area 3b of humans, but they may be present.

The activation of area 3b neurons is from RA-I and SA (I and possibly II) afferents relayed from the ventroposterior nucleus. RA-I and SA inputs appear to be segregated into bands (columns) in layer IV (Sur *et al.,* 1984). Most of the large relay neurons in VP project to layer 4 of area 3b via thick rapidly conducting afferents. Smaller neurons in the septa of VP and in VPI project to the superficial layers (Rausell and Jones, 1991). Major outputs in area 3b are to area 1, area 2, and S2, and these fields provide feedback inputs. Area 3b is callosally interconnected with areas 3b, 1, and 2, and S2 of the opposite hemisphere. The callosal connections are unevenly distributed, with the large representation of the glabrous hand and foot having less dense connections (Killackey *et al.,* 1983). The excitatory receptive fields do not reflect the callosal connections, which may contribute to surround suppression or enhancement, but instead are confined to locations on the contralateral body surface. In monkeys, inactivation or lesions of area 3b or area 3b together with areas 1 and 2, result in impairments in all but the crudest of tactile discriminations involving texture and shape (Hikosaka *et al.,* 1985; Randolph and Semmes, 1974; Zanios *et al.,* 1997; Brochier *et al.,* 1999). Small objects are unrecognized by touch and are ignored, and coordination during grasping is impaired.

Area 1

Like area 3b, area 1 contains a systematic representation of the body surface. The representation parallels and also roughly mirrors that in area 3b. Thus, the foot, leg, trunk, forelimb, and face are represented in a mediolateral cortical sequence (as in area 3b), but the digit tips are represented caudally near the area 2 border rather than rostrally near the area 3b border. Most neurons in area 1 are rapidly adapting and respond as if they were related to RA-I cutaneous receptors. A small portion of neurons, perhaps 5%, respond as if activated by RA-II (Pacinian) afferents. Neurons in area 1 tend to have larger and more complex receptive fields (Iwamura *et al.,* 1993), including stronger suppressive or inhibitory surrounds, than area 3b neurons (Sur, 1980; Sur *et al.,* 1985). Some neurons code for the direction of movement on the skin (Hyvarinen and Poranen, 1978). The activity patterns of most area 1 neurons, but not area 3b neurons, are modified according to what motor behavior will follow the stimulus (Nelson, 1984). Area 1 receives strong activating inputs from both area 3b and the

ventroposterior nucleus. The VP inputs are partly from collaterals of neurons projecting to area 3b, and the terminations are largely of thinner axons than those of area 3b. Feedforward cortical outputs are predominantly to area 2 and S2, and feedback inputs are from these fields. Callosal connections are more evenly distributed than for area 3b, but connections in the hand, foot, and parts of the face regions remain sparse (Killackey *et al.*, 1983). The callosal connections largely modulate neurons with receptive fields on the contralateral body surface, but some neurons with ipsilateral or bilateral body midline receptive fields occur (Taoka *et al.*, 1998). In monkeys, lesions of area 1 impair discriminations of texture rather than shape (Carlson, 1981; Randolph and Semmes, 1974).

Area 2

Area 2 contains a complex representation of both cutaneous and noncutaneous receptors. Neurons appear to be influenced by cutaneous receptors, deep receptors, or both. The portions of area 2 related to the hand and face are most responsive to cutaneous stimulation. The representation is in parallel with those in areas 3b and 1 so that the foot, trunk, hand, and face form a mediolateral cortical sequence. A mirror reversal organization of that in area 1 is apparent for parts of area 2 near the area 1 border. However, the overall organization is more complex than in areas 3b and 1, and some body parts are represented more than once in area 2 (Pons *et al.*, 1985b). Receptive fields for neurons in area 2 are typically, but not always, larger than those for neurons in areas 3b and 1, and receptive field properties appear to be complex (Iwamura *et al.*, 1993). Many neurons are best activated by stimuli of certain shapes or directions of movement. The inputs from deep receptors are largely those related to muscle spindles, suggesting that area 2 combines information about limb and digit position with tactile information during active touch. The major thalamic input to area 2 is from VPS (Fig. 28.4), but a sparse input to the hand region of area 2 originates in VP. Major cortical inputs are from areas 1, 3b, and 3a. There also appear to be sparse inputs from the motor cortex and to S2. Callosal connections are fairly evenly distributed and include the hand representation (Killackey *et al.*, 1983). Neurons, however, have excitatory receptive fields mainly on the contralateral body. Lesions of area 2 in monkeys impair finger coordination (Hikosaka *et al.*, 1985) and discriminations of shape and size (Carlson, 1981).

Area 3a

Area 3a, in the depth of the central sulcus, forms the fourth systematic representation of the body in anterior parietal cortex. Area 3a is largely activated by muscle spindle and other deep receptors, but some cutaneous activation is also apparent, especially in the portion devoted to the hand. The representation parallels that in area 3b, but few details are known. Neurons in area 3a are responsive during movements and are influenced by behavioral intentions ("motor-set," see Nelson, 1984). The major input is from VPS and roughly half of the VPS relay neurons project to both area 3a and area 2, thus providing the same information. Area 3a projects to area 2, motor cortex, S2, and other fields (Huerta and Pons, 1990; Huffman and Krubitzer, 2001). Callosal connections are uneven, but the hand region has somewhat more dense callosal connections than the hand representation in area 3b.

Subcortical Projections

All four fields project to a number of subcortical fields including feedback to the thalamic relay nuclei, the basal ganglia, the anterior pulvinar, the pons, the dorsal column nuclei, and the spinal cord (see Kaas and Pons, 1988). These projections presumably function in modifying motor behavior and sensory afferent flow. The projections to the pons are to neurons that relay to the cerebellum (Vallbo *et al.*, 1999) where they may modify motor responses.

Anterior Parietal Cortex in Humans

Several types of evidence support the conclusion that the organization and functions of anterior parietal cortex in humans are similar to those in monkeys.

Architectonic Fields

As in monkeys, four architectonic fields can be identified in the anterior parietal cortex of humans—areas 3a, 3b, 1 and 2 (see Chapter 27). In early studies, the presumed boundaries of these fields varied somewhat, and other terminologies were sometimes used. Recently, a number of studies have reconsidered the issue of how anterior parietal cortex is divided into fields with the benefit of new chemoarchitectonic methods (Zilles, *et al.*, 1995; White *et al.*, 1997; Qi *et al.*, 1998). Area 3b is the most obvious field, and investigators closely agree on boundaries. Area 3a is also easily recognized as distinct from 3b and area 4 (motor cortex), although area 3a appears to have rostral and caudal subdivisions. The area 1 border with area 2 is also reasonably distinct, while the area 2 border with posterior parietal cortex (area 5) is the least obvious, as in monkeys. Detailed comparison of the architecture of these fields in monkeys (where somatotopy and connections have been studied), chimpanzees, and humans (Qi *et al.*, 1998) perhaps provide the most compelling evidence for functionally

significant boundaries. Overall, as in monkeys, areas 3a and 3b have chemoarchitectonic features that are characteristic of primary sensory areas, while areas 1, and 2 resemble secondary areas (see Eskenasy and Clarke, 2000), supporting the conclusion that areas 3b, 1, and 2 constitute a processing hierarchy in humans as in monkeys.

As in macaque monkeys, area 3a of humans occupies the depths of the central sulcus, where it extends somewhat from the posterior to the anterior bank. In area 3a, layers IV and VI are less pronounced than in area 3b, and layer V pyramidal cells are more obvious. Area 3b occupies roughly the middle half or more of the posterior bank of the central sulcus. The field appears on the surface as the central sulcus ends near the medial wall, and the field extends into the medial wall. Area 3b is easily distinguished over most of its extent by the dense packing of small cells in layer IV, and the relatively dense packing of cells in layer VI. The small cells have led to the terms "koniocellular cortex" and "parvicellular core" (see Chapter 27). Most investigators show area 3b as ending with the lateral extent of the central sulcus, but area 3b extends anteriorly past the end of the sulcus in monkeys, where it represents the mouth and tongue. However, these body parts may be represented more medially in humans (see following discussion). Area 1 occupies the anterior lip of the postcentral gyrus where it borders area 3b on the posterior bank of the central sulcus and extends over the anterior third of the postcentral gyrus. Layers IV and VI are less densely packed with cells in area 1 than in area 3b, so the overall appearance is of less conspicuous lamination. Area 1 would roughly correspond to the posterior half of the postcentral area of Campbell (1905), and the full extent (allowing for a protrusion onto the upper bank of the central sulcus that is not shown) of area 1 of Brodmann. Area 1 is unlikely to be as wide as area PC of von Economo and Koskinas (1925), area 1 of Sarkossov and co-workers (see Braak, 1980), or the medial half of the paragranulous belt of Braak (1980). Area 2 is characterized by a denser layer IV than is found in area 1. The caudal border is difficult to delimit in monkeys even with the aid of electrophysiological data, and the precise location of this border remains uncertain in humans. However, the expected width of area 2 would approximate that of area 1.

Maps in 3a, 3b, 1, and 2: Evidence from Scalp and Brain Surface Recordings

As part of efforts to localize abnormal tissue and for other clinical reasons, recordings have been made from the scalp, from the surface of anterior parietal cortex, and from depth probes in the cortex of 3b of patients. In addition, neuromagnetic recordings and scalp-evoked potentials have been recorded from healthy volunteers. Such recordings support the conclusion that separate representations with different functions exist in areas 3a, 3b, 1, and 2. The hand representation in area 3b appears to correspond to a bulge in the central sulcus (Sastre-Janer *et al.*, 1998).

1. Electrical stimulation of cutaneous afferents in the median nerve of the hand results in a focus of evoked potentials after 20–30 ms in area 3b of the caudal bank of the central sulcus and a second focus after 25–30 ms in area 1 of the dorsolateral surface of postcentral cortex (see Allison *et al.*, 1988; Ploner *et al.*, 2000). The two foci support the view that area 3b and area 1 have separate maps of the body surface. The area 1 potentials are caudal to the area 3b potentials, indicating parallel maps, although a slight medial shift of the area 1 focus suggests a small displacement of one map relative to the other. As in monkeys, activity was generated only from stimulating contralaterally.

2. Stimulation of muscle afferents from the human hand results in a focus of activity that is caudal to that for cutaneous afferents (Gandevia *et al.*, 1984). A reasonable interpretation of this result is that the muscle afferents activate area 2, which is caudal to the activity produced in areas 1 and 3b by cutaneous afferents. More recently, evoked potentials to joint movement in the fingers has been attributed to area 2 activation (Desmedt and Ozaki, 1991), suggesting that joint receptor afferents as well as muscle spindle afferents activate area 2.

3. Another focus of activity produced by deep receptor or muscle spindle afferents is deep to foci related to cutaneous stimulation. Using neuromagnetic recordings, Kaukoranta *et al.* (1986) found that mixed nerve stimulation resulted in a deeper focus of activity in the central sulcus than cutaneous nerve stimulation. The results were interpreted as evidence for muscle spindle receptor input to area 3a and cutaneous receptor input to area 3b. Similar results have been obtained with fMRI (Moore *et al.*, 2000; also see Mima *et al.*, 1996, 1997).

4. More recently, noninvasive imaging techniques have been used to explore the organization of anterior parietal cortex in awake humans. While positron emission tomography (PET) has been useful for gross localization of sites of induced activity (see Burton *et al.*, 1993, 1999), functional magnetic resonance imaging (fMRI) has provided more resolution. Most notably, vibratory and other stimuli applied to different finger tips provided evidence for separate representations in areas 3a, 3b, 1, and 2 (Francis *et al.*, 2000; Gelnar *et al.*, 1998; Lin *et al.*, 1996).

5. Recordings of scalp-recorded evoked potentials in humans also support the conclusion that the maps of receptor surfaces in anterior parietal cortex are organized much as they are in monkeys. Thus, electrical stimulation of the little finger activates cortex 1–2 cm medial to that activated by stimulating the thumb (see Hari and Kaukoranta, 1985), and activity evoked in cortex by tapping the tongue is lateral to that produced by tapping the finger (Ishiko *et al.*, 1980). Measurements of magnetic fields, thought to be generated in the depths of the central sulcus in area 3b, indicated that the thumb, index finger, and ankle are represented at successively more medial position (Okada *et al.*, 1984). These methods have now been used to show that the tongue, lower lip, upper lip, thumb through little finger, palm, forearm, elbow, upper arm, chest, thigh, ankle, and toes are represented in a lateromedial order (Nakamura *et al.*, 1998; Fig. 28.7).

6. Recently, functional magnetic resonance imaging has been used to demonstrate the representation of thumb to little finger in a lateromedial sequence in area 3b, area 1, and area 2 (Kurth *et al.*, 1998, 2000; Francis *et al.*, 2000), and show that the tongue, fingers, and toes are represented in a lateromedial sequence (Sakai *et al.*, 1995). Hoshiyama *et al.*, (1996) located the representation of the lower lip lateral (inferior) to that of the upper lip, as in monkeys (Jain *et al.*, 2001).

7. Finally, extensive observations on the somatotopy of postcentral cortex in humans come from recordings of evoked slow waves from the brain surface during neurosurgery (Woolsey *et al.*, 1979). In a sequence of recording sites along the posterior lip of the central sulcus, from near the medial wall to over two thirds of the distance to the lateral (Sylvian) sulcus, potentials were evoked from foot, leg, thigh, trunk, and hand. In individual patients, there was some notable variability in organization so that the leg representation extended from the medial wall onto the dorsolateral surface in some but not other cases. By electrically stimulating the dorsal nerve of the penis and recording evoked potentials from anterior parietal cortex of humans during surgery, Bradley *et al.* (1998) provided evidence that the penis is represented in cortex lateral to that of the foot (also see Rothemund *et al.*, 2002).

8. More details about the sequence of representation of body parts in postcentral cortex have been obtained by electrically stimulating the brain in patients. Using higher levels of stimulating current than used for motor cortex, Foerster (1931, 1936a) was able to produce a postcentral motor map that roughly matched the precentral motor map in the mediolateral cortical order of leg, hand, and face (Fig. 28.8). Penfield and Rasmussen (1950) also reported evoked movements for postcentral stimulation sites, with the postcentral

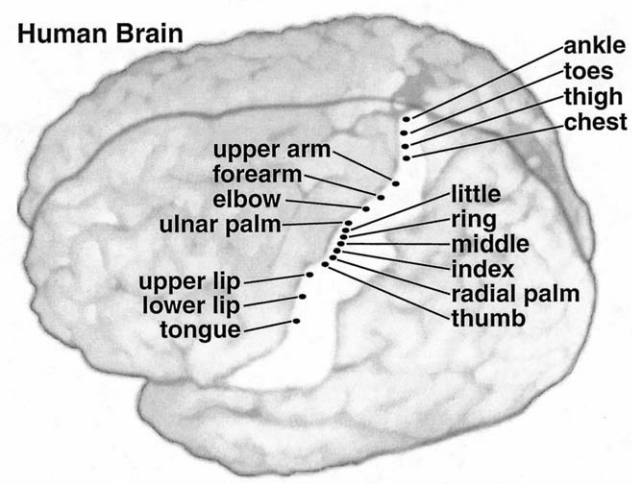

FIGURE 28.7 The organization of the anterior somatosensory cortex according to results obtained from the noninvasive recording of sensory-evoked magnetic fields (Nakamura *et al.* 1998). The center of activity for the different body parts are shown on the lip of the central sulcus, but the regions generating the magnetic fields were judged to be along the posterior bank o the central sulcus, most likely reflecting activity in area 3b and part of area 1. This map does not address the issue of separate representations, in each of area 3a, 3b, 1 and 2. In addition, center of activity for ankle and toes were likely generated from cortex on the melial wall.

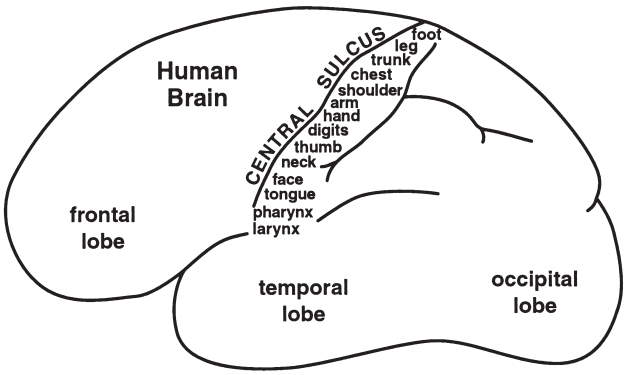

FIGURE 28.8 The order of representation in human postcentral cortex according to Foerster (1931). The summary was based on sensations reported when the surface of cortex was electrically stimulated. Most stimulation sites were in area 1 or area 2, as area 3b is largely in the central sulcus. No distinctions between the separate representations in areas 3a, 3b, 1, and 2 were made. Similar but more detailed maps were later produced by Penfield and Jasper (1954). Their maps placed the foot in the cortex of the medial wall and included the back of the head in center medial to the arm representation.

motor map roughly paralleling the precentral motor map in mediolateral organization. More precise information about the somatotopic organization of postcentral cortex has been obtained by noting where sensations are located during electrical stimulation of cortical sites. As one might expect, sensations evoked from stimulating the cortex match in somatotopic location the source of afferents related to the stimulation sites. Thus, stimulating cortex where evoked responses were obtained to ulnar nerve stimulation resulted in sensations largely confined to the ulnar hand (Jasper *et al.,* 1960). The extensive report of Penfield and Boldrey (1937) summarizes the results from stimulating precentral and postcentral cortex in 163 patients. Stimulation sites resulting in sensations were scattered over the precentral and postcentral gyri, and even a few more posterior or more anterior sites were effective. However, the vast majority of sites were along the posterior lip of the central sulcus and were probably evoking sensations by activating neurons in area 1 and perhaps even deeper to the electrode site in the superficial segment of area 3b. Surprisingly, the evoked sensations were not of light touch but were described as a localized numbness, tingling, or, infrequently, the feeling of movement. Sensations were evoked from the cortex extending from the medial wall, where the foot is represented, to the lateral fissure, where the mouth is represented. In general, the sensory order corresponds to the detailed maps compiled for monkeys (e.g., Nelson *et al.,* 1980). Cortex devoted to the foot and toes was most ventral on the medial wall. The back of the head and the neck were in medial cortex with the trunk representation, while the face was in lateral cortex separated from the head by the cortex devoted to the arm and hand. The digits were represented from little finger to thumb in a mediolateral sequence. As for the area 1 representation in macaque monkeys, the orbital skin and the nose were represented just lateral to the thumb in humans. In monkeys and humans, the tongue and mouth are most lateral in the responsive cortex. Thus, the mediolateral sequence of representation in the region of anterior area 1 appears to be quite similar in humans (Penfield and Boldrey, 1937; note more detail and some differences compared to summaries in Figs. 28.7 and 28.8) and monkeys (Nelson *et al.,* 1980). Little can be said about sequences of change in the rostrocaudal direction, however, because only microelectrode maps provide much detail about this direction in monkeys, and the surface stimulation and recordings in humans may involve amounts of tissue that are large relative to the narrow widths of the representations in areas 3b, 1, and 2.

9. Some aspects of somatosensory organization have long been known from the order of progressions of sensations or movements ("the Jacksonian march") during epileptic seizures. Because the seizure starts from a focus and spreads to more distant tissue, the order of sensations reflects the order of representation. Typical cases are described by Foerster (1936b) and Penfield and Jasper (1954). The orders of these sensory marches correspond to the evoked sensation map (Fig. 28.8). For example, a sensation of tingling or numbness in the thumb may be followed by tingling in the face, or a tingling that passes from thumb to fingers, to arm. Sensations are contralateral to the postcentral focus, and they seldom spread over many body parts (Mauguiere and Courjon, 1978).

Sensory and Perceptual Impairments Following Lesions

Damage to postcentral cortex, if extensive, causes severe and lasting impairments in pressure sensitivity, two-point discrimination, point localization, and discrimination of object shape, size, and texture (Corkin *et al.,* 1970; Head and Holmes, 1911; Roland, 1987a; Semmes *et al.,* 1960; Taylor and Jones, 1997). The spatial accuracy of motor movements is also impaired by the reduced sensory control (Aglioti *et al.,* 1996). However, the detection and crude localization of tactile stimuli remains intact. Roland (1987a) reported that lesions of the deep and anterior part of the hand region of postcentral cortex, presumably including much but not all of the area 3b representation and probably the area 1 representation, abolished the ability to discriminate edges from rounded surfaces, while lesions of the surface, apparently involving areas 1 and 2, left the ability to distinguish edges from rounded surfaces, but removed the ability to discriminate shapes and curvatures. This difference is similar to that reported for monkeys where lesions of areas 3b, 1, and 2 permanently abolished the ability to distinguish the speed of moving tactile stimuli (Zainos *et al.,* 1997) where lesions of area 1 impaired texture discriminations, while area 2 lesions altered discrimination of shape (Carlson, 1981; Randolph and Semmes, 1974; also see Lamotte and Mountcastle, 1979). Inactivations of the finger representations in area 2 of monkeys led to a major deficit in finger coordination while small food pieces were often ignored after contact with inactivation of area 3b (Hikosaka *et al.,* 1985). Remarkably, small lesions of part of the hand representation result in no obvious impairment in humans (Evans, 1935; Roland, 1987a, b). Roland (1987a) estimated that a notable impairment resulted only after lesions involving three fourths or more of the hand region of anterior parietal cortex. Furthermore, the larger the lesion of the region, the greater the impairment (Roland, 1987b). The preservation of abilities after

lesions to parts of somatotopically organized representations could be the result of cortical reorganizations that result in the recovery of lost parts of representations. Removing part of a representation or deactivating part of a representation in monkeys can be followed by cortical reorganization, even in adults, so that remaining cortex is activated by skin formerly related to the damaged area, and deactivated cortex becomes responsive to alternative inputs (see Kaas and Florence, 2000, for a review).

POSTERIOR PARIETAL CORTEX

The posterior parietal region is an arbitrary subdivision of the brain that includes most of the parietal lobe caudal to area 2 but excludes the cortex of the lateral (Sylvian) fissure and the supplementary sensory area of the medial wall. Current investigators commonly refer to the architectonic subdivisions of Brodmann (1909) or von Economo (1929), and both systems are in use. However, research on monkeys suggests that the proposed fields (areas 5a, 5b, 7a, and 7b or areas PD, PE, PF, and PG) have little validity other than denoting general regions of the lobe. Other subdivisions have been suggested by patterns of connections and the response characteristics of neuronal populations, but the organization of posterior parietal cortex is not well understood. Electrical stimulation in humans seldom produces any sensations or motor responses (Penfield and Rasmussen, 1950), although Foerster (1931, 1936a) was able to produce hand movements and leg movements on occasion with high levels of stimulating current. Posterior parietal cortex has been implicated in both somatosensory and visual functions as well as in premotor planning, but lesions do not produce simple sensory impairments. Rather, large lesions produce a variety of complex symptoms, many included within the general category of contralateral sensory neglect or inattention. In monkeys, impairments are basically the same regardless of the hemisphere of the lesion, but in humans, lesions of the right or "minor" hemisphere produce a much more profound defect. Major reviews of posterior parietal cortex organization and function in monkeys and humans include those of Mountcastle (1975), Lynch (1980), Hyvarinen (1982), Yin and Medjbeur (1988), Andersen *et al.* (1997), and Colby and Goldberg (1999). AAlso, see Chapter 26 for connections of subdivisions of posterior parietal cortex with motor areas of the frontal lobe.

Posterior Parietal Cortex in Monkeys

Since posterior parietal cortex in macaque monkeys may have many features or functional organization in common with posterior parietal cortex in humans, a brief review of current views of connections, neuron properties, and functional subdivisions in monkeys serves as a guide. As a point of caution, data in monkeys are still limited, and a consensus of opinions has not yet occurred.

One currently acceptable scheme for subdividing posterior parietal cortex in macaque monkeys is

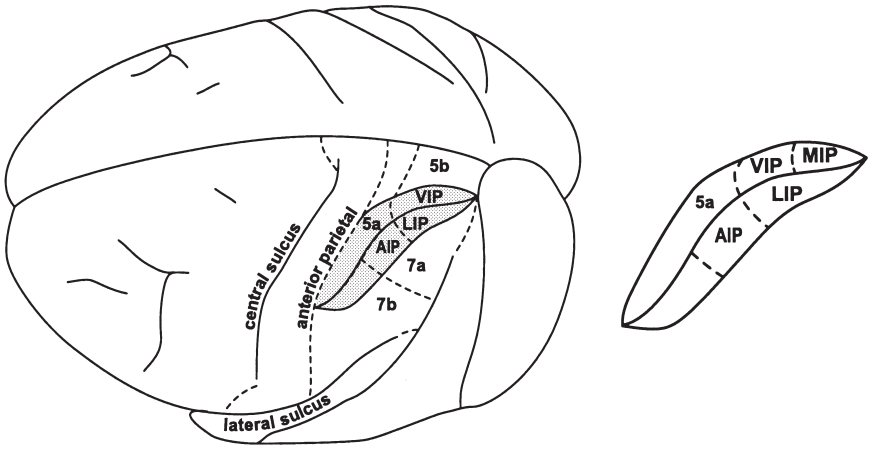

FIGURE 28.9 A dorsolateral view of the brain showing proposed subdivisions of posterior parietal cortex in macaque monkeys. Areas 5a, 5b, 7a, and 7b are traditional subdividions from Brodmann (1909) and Vogt and Vogt (1919). The ventral intraparietal region (VIP) and the lateral intraparietal region (LIP) are subdivisions that have been distinguished by visual and visuomotor connections (Anderson *et al.*, 1985; Maunsell and Van Essen, 1983). Other recently proposed fields include the medial (MIP) and the anterior (AIP) intraparietal region. The MIP region is also known as the parietal reach region (PRR).

shown in Figure 28.9 (also see Preuss and Goldman-Rakic, 1991; for an alternative proposal see Pandya and Seltzer, 1982; Seltzer and Pandya, 1980). The present proposal follows the traditional subdivision into areas 5a, 5b, 7a, and 7b introduced by Brodmann and the Vogts (Fig. 28.9), with the addition of the ventral intraparietal area (VIP) of Maunsell and Van Essen (1983) and the lateral intraparietal area (LIP) of Andersen *et al.* (1985). Both VIP and LIP overlap a region distinguished by Seltzer and Pandya as POa. Additional medial intraparietal (MIP), posterior intraparietal (PIP) and anterior intraparietal (AIP) areas have also been proposed. The most obvious flaw with the scheme summarized in Figure 28.9 is that considerable evidence suggests that anterior 7b is similar to area 5a in having predominantly somatosensory connections and functions, and that the distinction between 7b and 5a is poorly justified. Also, areas 5a, 5b, 7a, and 7b occupy large regions that are likely to be subdivided by future investigators (see Lewis and Van Essen, 2000a).

Area 5a

Area 5a is not uniform in histological structure, connections, and neuron types, but clear subdivisions have not yet been established. Subdivisions of anterior parietal cortex, especially area 2, provide direct somatosensory inputs from both deep and cutaneous receptors (Pons and Kaas, 1986). Major thalamic inputs are from the anterior pulvinar and the lateral posterior nucleus (see Yeterian and Pandya, 1985), nuclei without significant sensory inputs from the brainstem or spinal cord. However, a specialized portion of area 5 (Pons *et al.,* 1985a), receives some input from the ventroposterior nucleus (Pons and Kaas, 1986). Feedforward cortical projections are to area 7, S2, motor and premotor cortex, limbic cortex, and parts of the superior temporal gyrus; callosal connections are largely between matched regions of area 5 (see Hyvarinen, 1982). Subcortical projections include thalamic nuclei, the basal ganglia, the pontine nuclei, and the spinal cord through the pyramidal tract. Neuron properties include those related to both cutaneous and deep receptors and to passive and especially active limb movement (Iwamura and Tanaka, 1996). Receptive fields are generally much larger than those in areas 1 and 2. Specific combinations of positions in several joints may be the most effective stimulus for many neurons (Hyvarinen, 1982). Many neurons in area 5a respond to ipsilateral as well as contralateral stimulation, with receptive fields including the digits of both hands, and sometimes extending up onto the arm and even the trunk (Taoka *et al.,* 1998). Some neurons have both somatosensory and visual receptive fields (Iriki *et al.,* 1996), and visual stimuli may modulate proprioceptive activity. Thus, neurons in area 5a that were responsive to arm position when the arm was covered from view responded better to seeing the arm or even a fake arm in the correct position, but not better to a fake arm in the wrong position (Graziano *et al.,* 2000). Finally, ablation of cortex of the intraparietal sulcus including area 5a interferes with the ability to orient the hand correctly in grasping (Denny-Brown and Chambers, 1956). Overall, the results suggest that area 5a is involved in providing a mental model of what the body is doing, and thereby guiding relevant behavior such as reaching for objects.

Area 5b

Area 5b appears to be largely somatosensory in function, despite its position near the visual cortex. Major cortical inputs are from area 5a, while outputs include adjoining parietal cortex of the medial wall and parts of 7b as well as cortex caudal to S2 in the lateral fissure, and dorsal premotor cortex (Pandya and Seltzer, 1982; Marconi *et al.,* 2001).

Area 7b

Area 7b also appears to be involved in the higher-order processing of somatosensory information. Inputs to the anterior part include those from the anterior parietal cortex (Pons and Kaas, 1986). Thalamic connections include the ventral lateral nucleus and the anterior pulvinar. Cortical projections include premotor and prefrontal areas of the frontal lobe, more caudal regions in posterior parietal cortex, and the superior temporal sulcus (Cavada and Goldman-Rakic, 1989; Lewis and Van Essen, 2000a). Neurons respond to touching the skin, particularly on the head and face in anterior 7b and the hand and arm in posterior 7b (Krubitzer *et al.,* 1995; Leinonen, 1984).

Area 7a

Area 7a is related to visual and visuomotor activities. The visual functions are reflected in both connection patterns and neuron properties. Visual inputs include those from superior temporal cortex involved in processing visual motion information (see Maunsell and Van Essen, 1983). Other visual inputs are from adjacent dorsal portions of the prelunate gyrus (May and Andersen, 1986). Connections also include the cortex of the intraparietal sulcus, cortex of the medial wall, prefrontal cortex, multimodal and visual areas of the superior temporal sulcus, and cortex of the lateral sulcus (Cavada and Goldman-Rakic, 1989). Other connections are with the medial pulvinar. Several classes of visual and visuomotor neurons have been described (see Hyvarinen, 1982). Visual tracking

neurons respond during the visual pursuit of targets. Another class of neurons is activated during fixation on a moving or stationary visual target. Some neurons seem to be important to the visual guidance of reaching movements with the hand. Many neurons respond to visual stimuli, but these neurons respond poorly to visual stimuli when monkeys are not attending and visual responses are suppressed when gaze and attention is directed to the stimulus (Steinmetz *et al.,* 1994). The presence of neurons responding both to visual stimuli and to visuomotor and reaching behavior implicates areas 7a in guiding eye and hand movements.

LIP, VIP, PIP, and MIP

The cortex of the intraparietal sulcus has been subdivided into several proposed areas including the lateral intraparietal area (Andersen *et al.,* 1985), the ventral intraparietal area (Maunsell and Van Essen (1983), and sometimes the medial intraparietal area, and the posterior intraparietal area (Colby and Goldberg, 1999). Near the anterior end of the sulcus, the anterior intraparietal area has been distinguished (Preuss and Goldman-Rakic, 1991). There is evidence for functional and structural distinctions between these proposed fields, but even this number of proposed fields may not capture the architectonic complexity of the region (Lewis and Van Essen, 2000a). Seltzer and Pandya (1980) include VIP and LIP in their larger POa. LIP appears to be largely involved in attentional and oculomotor functions (Kusanoki *et al.,* 2000; Andersen *et al.,* 1997). Most neurons in LIP respond strongly before saccadic eye movements to targets in the neuron's movement field (Shandlen and Newsome, 1996), and to visual stimuli–evoking eye movements. With training with auditory signals for eye movement, some neurons come to respond to auditory signals (Grunewald *et al.,* 1999). LIP receives visual inputs from extrastriate visual areas (Blatt *et al.,* 1990), is interconnected with nearby posterior parietal fields, and projects to the frontal eye fields and the superior colliculus (Lewis and Van Essen, 2000b; May and Andersen, 1986). Eye movements can be induced by electrical stimulation of LIP (Thier and Andersen, 1998).

VIP has both visual and somatosensory functions. Most neurons respond to either visual stimuli or light touch (Duhamel *et al.,* 1998). The area seems to contain matched representations of the body surface and visual space. Small foveal visual receptive fields related to neurons with small tactile receptive fields on the muzzle and larger peripheral visual receptive fields were determined for neurons with larger receptive fields on the side of the head. VIP may have a crude somatotopic organization with nearly all of the area devoted to the head. Somatosensory inputs arise from areas 1 and 2, 5 and 7b, and S2 and nearby areas of the lateral sulcus (Lewis and Van Essen, 2000b). There also may be inputs from vestibular cortex and auditory areas. Visual inputs are from visual areas of the dorsal stream (especially the middle temporal visual area) and LIP. Outputs include projections to the frontal eye field and adjoining portions of the frontal lobe, as well as the ventral premotor area.

MIP occupies intraparietal cortex just medial and caudal to LIP. A proposed parietal reach region (PRR) overlaps MIP, but is larger. MIP is thought to function in the planning of reaching to targets with the arm (Snyder *et al.,* 2000). This cortex receives inputs from somatosensory and dorsal stream visual areas and projects especially to dorsal premotor cortex (Caminiti *et al.,* 1996).

AIP or the anterior intraparietal area may be included in area 5a or 7b of many reports. AIP occupies cortex on the anterior bank and borders of the intraparietal sulcus just anterior to LIP and VIP. AIP has somatosensory connections with S2 and adjoining areas, area 5 and area 7, as well as with VIP and LIP (Lewis and Van Essen, 2000b). A major target is an anterior division of ventral premotor cortex. Area AIP is thought to be important in the organization of grasping movements with the hand (Rizzolatti *et al.,* 1997). The term "PIP" is sometimes applied to the posterior portion of the intraparietal sulcus.

Posterior Parietal Lobe Function in Humans

Concepts of posterior parietal lobe function in humans are largely derived from the much discussed behavioral changes that typically follow large lesions (for reviews, see Critchley, 1949; Denney-Brown and Chambers, 1958; DeRenzi, 1982: Hyvarinen, 1982; Mesulam, 1981, 1983; see Chapter 27 for architecture). In brief, patients with posterior parietal lobe injury tend to neglect visual and tactile information coming from visual space or the body surface opposite the lesion (see Moscovitch and Behrman, 1994; Pouget and Driver, 2000). The defect is most severe after lesions of the right hemisphere that is nondominant for language. The defect may be profound, leading to bizarre symptoms, or it may be quite mild, resulting in little notable change in spontaneous behavior. Mild defects are typically revealed by bilateral stimulation. The expected result is that the ipsilateral stimulus is preferentially attended, either immediately or after a series of trials. In more dramatic cases, there is a denial of the existence of the contralateral (typically left) side of the body and of objects in the left side of the visual space. Patients may fail to shave or dress the neglected

side, and food on the contralateral side of the plate may be uneaten. The defect can be characterized as a change in attention, because it is clearly not a result of a sensory impairment. More specifically, a unique aspect of the impairment seems to be a difficulty in the ability to disengage attention from a current focus and move that attention to a new focus in the contralateral world (Posner *et al.*, 1984). Right-hemisphere damage produces a reluctance or inability to redirect attention from the right visual field to the left visual field, as well as a reluctance to shift attention within the left visual field (Baynes *et al.*, 1986). Other defects also occur (see Sirigu *et al.*, 1996).

1. Errors may exist in localizing objects so that accurate pointing does not occur. Right and left may be confused, and the patient may have difficulty in moving from place to place.
2. Eye movement patterns are altered, and a reduction in spontaneous eye movements and tracking movements may occur.
3. Errors in reaching into the contralateral hemifield are common. Targets may be missed by several inches. In addition, corrections of reach to displaced targets during reach are impaired during posterior parietal cortex inactivation with transcranial magnetic stimulation (Desmarget *et al.*, 1999).
4. Lesions of the right or minor hemisphere may produce a defect in drawing even simple objects such as a house and in constructing simple models. Furthermore, during constructional tasks, blood flow is increased in posterior parietal cortex (Roland *et al.*, 1980). Blood flow also increases in the superior parietal cortex and intraparietal sulcus of humans performing mental rotations of the hand (Bonda *et al.*, 1995, 1996).
5. Lesions, especially those involving the anterior half of posterior parietal cortex, may produce somatosensory deficits. Reported changes include impairment in length discrimination, weight judgment, shape discrimination, and limb position sense (see Hyvarinen, 1982).
6. Difficulties may exist in performing symbolic gestures and pantomimes. This is attributed to an inability to access or store representations of movements adequately.

Even though posterior parietal cortex is not uniform in function, much of the region appears to relate to premotor planning in relation to eye movements and reach. Clearly, the anterior part of posterior parietal cortex is more related to the somatosensory system, and the posterior part is more related to the visual system. The connections of posterior parietal cortex suggest that a motivational component depends on relationships with limbic cortex of the medial wall and perhaps the ventral temporal lobe (see Mesulam, 1981). Connections with the frontal lobe and connections with subcortical motor structures such as the superior colliculus and basal ganglia undoubtedly are important in initiating behavior. More specifically, Mountcastle (1975) hypothesized that posterior parietal cortex functions as a "command" center for movements in immediate extrapersonal space. Finally, the functional asymmetry of posterior parietal cortex in humans can be explained if the right hemisphere contains the neural substrate for attending to both sides of space, though predominantly contralateral space, while the left hemisphere is almost exclusively concerned with contralateral space (Mesulam, 1981). Thus, unilateral lesions of the left hemisphere are partially compensated by the functions of the right hemisphere, but the reverse does not hold. This difference may relate to the specialization of the left hemisphere for language.

SOMATOSENSORY CORTEX OF THE MEDIAL WALL: THE SUPPLEMENTARY SENSORY AREA AND CINGULATE CORTEX

The organization of the medial parietal cortex is not well understood. Penfield and Jasper (1954) postulated the existence of a supplementary sensory area, as an analogy to the supplementary motor area, on the medial wall of the cerebral hemisphere where electrical stimulation evoked sensations from the contralateral leg, arm, and face. Later, Woolsey *et al.* (1979) reported in a single patient that sensations were obtained from the arm or leg after electrical stimulation of sites on the medial wall. There have been only a few experimental studies in monkeys that relate to the existence or organization of a supplementary sensory area (see Murray and Coulter, 1982, for a review). In macaque monkeys, neurons on the medial wall respond to somatosensory stimuli, and there is some suggestion of anterior sites relating to the lower body and posterior sites relating to the upper body. These neurons have large receptive fields and appear to have inputs related to both skin and deep receptors. Major inputs are from dorsolateral posterior parietal cortex, especially the anterior half. Other connections of medial parietal cortex are with premotor and supplementary motor cortex and the lateral posterior nucleus of the thalamus. More recently, there is evidence for projections to the spinal cord and even sparse projections to primary motor cortex (see Wu *et al.*, 2000). The connections of posterior parietal cortex of the medial wall to

a presumptive supplementary motor area and adjoining sensory regions of cingulate cortex (see Mesulam, 1981; Chapter 26) may function to mediate motivational and attentional aspects to perception and behavioral plans (also see Chapter 24).

SOMATOSENSORY CORTEX OF THE LATERAL (SYLVIAN) SULCUS

Much of the cortex of the upper bank of the lateral sulcus and some of the cortex of the insula are somatosensory in function. Because of the general inaccessibility of this region in humans, there have been only a few attempts to reveal aspects of functional organization by stimulation or recording. However, there is clear evidence for the existence of several areas from fMRI. The lateral somatosensory cortex may be part of a critical corticolimbic pathway for touch (see Friedman *et al.*, 1986), as monkeys have severe deficits in tactile memory after combined removal of the amygdala and hippocampus (Murray and Mishkin, 1984a). The pathways for input to these limbic structures involve convergent inputs from areas 3a, 3b, 1, and 2 of the anterior parietal cortex and a relay from S2 over more rostral subdivisions of the somatosensory cortex in the lateral sulcus (Fig. 28.10). Because this lateral pathway is best understood in macaque monkeys, the organization of lateral somatosensory cortex in these primates is briefly reviewed next.

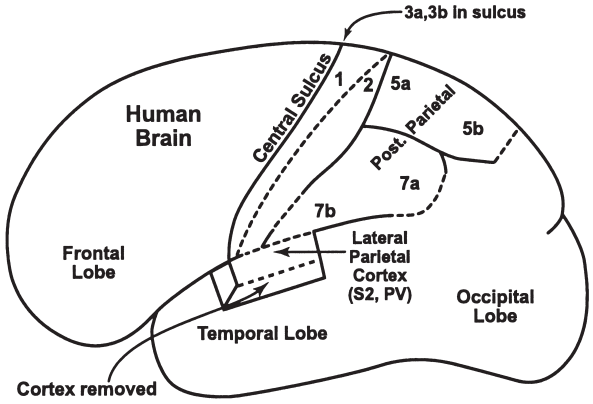

FIGURE 28.10 Posterior parietal and lateral cortex of humans The posterior parietal cortex has been variously subdivided by early investigators (for example, see Campbell, 1905; Smith, 1907; Brodmann, 1909; Economo and Koskinas, 1925; Vogt and Vogt, 1919, 1926). the subdivisions shown here reflect those of Vogt and Vogt, with the second somatosensory area (S2) and the parietal ventral area (PV) of the lateral sulcus added. Much of the region denoted here as 7b would be in Brodmann's area 40.

Organization of Cortex of the Lateral Sulcus in Monkeys

Much progress has been made in recent years in understanding the S2 functional organization of lateral somatosensory cortex in monkeys. One subdivision that has been repeatedly described is the second somatosensory area (S2), named because it was the second representation after S1 discovered in cats and later in other mammals. S2 appears to border the lateral extension of areas 3b and (or) areas 1 and 2 in monkeys, according to species (see Cusick *et al.*, 1989; Krubitzer and Kaas, 1990; Pons *et al.*, 1987; Krubitzer *et al.*, 1995; Burton *et al.*, 1995; Disbrow *et al.*, 2000). S2 forms a systematic representation of the contralateral body surface on the upper bank of the lateral sulcus with the face along the outer lip, the hand deeper in the sulcus, and the foot near the fundus. A parietal ventral area (PV) forms a second representation of the contralateral body surface just rostral to S2 (see Disbrow *et al.*, 2000, for review). S2 and PV adjoin along representations of the hand, and they form mirror-image representations of each other. PV and S2 are bordered in the fundus of the lateral sulcus by a ventral somatosensory area (VS), which extends somewhat onto the lower bank of the central sulcus and insula to border secondary auditory fields (Cusick *et al.*, 1989; Krubitzer *et al.*, 1995). More recent evidence suggests that VS actually includes separate rostral and caudal representations, one bordering PV and the other S2 (see Qi *et al.*, 2002). A caudomedial secondary auditory area (CM), that is very close and perhaps overlapping PV is responsive to both auditory and somatosensory stimuli (Schroeder *et al.*, 2000).

Cortex caudal to S2 includes part of 7b that extends into the lateral sulcus, and the retroinsular area (Ri). Neurons in both lateral 7b and Ri are responsive to cutaneous stimuli (Krubitzer *et al.*, 1995). Cortex caudal to VS on the lower bank of the lateral sulcus has neurons responsive to visual and somatosensory stimuli (Krubitzer *et al.*, 1995). Cortex rostral to PV receives inputs from PV and S2 and has been called the parietal rostral area (PR) (Krubitzer *et al.*, 1995; Krubitzer and Kaas, 1990). This somatosensory area may be part of the larger granular insular region described by Jones and Burton (1976).

S2 and PV receive feedforward inputs from all four areas of anterior parietal cortex (Burton *et al.*, 1995; Krubitzer and Kaas, 1990; Friedman *et al.*, 1986; Qi *et al.*, 2002), and removing these areas deactivates S2 and PV (Pons *et al.*, 1987; Burton *et al.*, 1990; Garraghty *et al.*, 1990). The inputs from the ventroposterior inferior nucleus do not seem to be capable of independently activating these neurons. Neurons in both S2 and PV respond to cutaneous stimulation within receptive

fields that are generally larger than those in area 3b or area 1. Inputs to S2 and PV from areas 3a and 2 undoubtedly provide some activation from deep receptors. Inputs from S2 and PV of the opposite hemisphere are particularly dense, and some bilateral receptive fields have been reported, although ipsilateral stimuli largely modulate activity based on contralateral receptive fields. Neurons in S2 may code for stimulus features such as roughness (Pruett *et al.*, 2000), but the response properties of PV and S2 neurons have not been extensively studied. Lesions of the PV-S2 region greatly impair the abilities of monkeys to make tactile discriminations and identifications (Murray and Mishkin, 1984b). Projections of PV and S2 include PR and perirhinal and entorhinal cortex (Friedman *et al.*, 1986). The processing series from anterior parietal to lateral parietal to perirhinal cortex and then to the hippocampus constitutes a proposed lateral hierarchy of areas involved in the recognition and memory of objects by touch (Mishkin, 1979; Murray and Mishkin, 1984a). The insula of lateral parietal cortex also contains a region of terminations of pain and temperature afferents from the VMpo nucleus of the thalamus (Craig *et al.*, 1994, 2000). The relationship of this termination zone to other fields of lateral parietal cortex is not yet clear. In addition, there is evidence of a thalamic relay of vestibular information to cortex of the insula (see Guldin *et al.*, 1992) called the parietoinsular vestibular cortex (PIVC). This vestibular region may overlap much of PV or Ri.

Lateral and Insular Parietal Cortex in Humans

There is increasing evidence that at least some of the cortex in the lateral fissure of humans is organized much as in monkeys. Most notably, a recent fMRI study using tactile stimuli applied to various body parts provided evidence for both S2 and PV, organized as mirror-reversal images of each other, both proceeding from face to forelimb to hindlimb from near the lip of the upper bank to the depths of the lateral fissure (Disbrow *et al.*, 2000; also see Burton *et al.*, 1993; Maeda *et al.*, 1999). Both S2 and PV demonstrate some increased activity with ipsilateral stimulation and more activity with bilateral stimulation (Disbrow *et al.*, 2001; Maldjian *et al.*, 1999). Much earlier Penfield and Rasmussen (1950) had electrically stimulated cortex in S2/PV region and produced sensations of numbness and tingling in contralateral skin locations, with sensations from the face, from the lip of the lateral fissure, and from the hand and leg from successively deeper locations on the upper bank. Recordings of evoked potentials with surface electrodes also support the view that the leg is represented deep to the hand and face in the fissure (Woolsey *et al.*, 1979). When subjects were instructed to attend to the roughness or duration of somatosensory stimuli, a greater increase in blood flow was found in the S2/PV region than in anterior parietal cortex (Burton *et al.*, 1999). As for monkeys, the lateral parietal and insular region in humans likely subserves tactile discriminations and recognition. Significantly more activity was found in the posteroventral insula in PET studies during tasks requiring tactual memories (Bundo *et al.*, 1996). While S2 and PV damage may not alter simple tactile abilities (see Roland, 1987a), disturbances in the ability to make tactile discriminations have been reported after lesions of the region (Caselli, 1993; also see Reed *et al.*, 1996, for a case of tactile agnosia after a lesion of the inferior parietal cortex). There is evidence for a relay of thalamic pain and temperature information to the insular region in humans (see Craig *et al.*, 1994).

SUMMARY

This chapter describes the organization of the parts of the somatosensory system thought to be concerned with object identification and tactile discriminations. The relevant sensory information depends on receptors in skin, muscles, and joints and is relayed over parallel afferent pathways to reach the ventroposterior complex of the thalamus. The ventroposterior complex includes a ventroposterior "proper" nucleus composed of ventroposterior lateral and ventroposterior medial subdivisions. The ventroposterior nucleus processes and relays information from rapidly and slowly adapting cutaneous receptors to area 3b of the cortex and information from rapidly adapting cutaneous receptors to area 1. Sparse projections exist to parts of area 2. The ventroposterior superior nucleus relays largely muscle spindle receptor information to areas 3a and 2. The ventroposterior inferior nucleus projects to the second somatosensory area (S2), but the significance of this projection is uncertain. The lateral posterior nucleus, the anterior pulvinar, and the medial pulvinar, without obvious sensory inputs, interconnect with subdivisions of somatosensory cortex, perhaps to modulate neural activity.

The somatosensory cortex includes anterior parietal cortex with four functional subdivisions (areas 3a, 3b, 1, and 2); posterior parietal cortex with at least five or six fields; the supplementary sensory area of the medial wall of the cerebral cortex; and the second somatosensory area and other fields in cortex of the upper bank and insula of the lateral fissure. Areas 3a, 3b, 1, and 2 all contain somatotopic representations of body receptors, with area 3b corresponding to the

primary field (S1) of nonprimates, though it is common and traditional to include all four fields of anterior parietal cortex in S-I. Basic processing of tactile information occurs in area 3b, higher-order processing of tactile information occurs in area 1, and tactile information is combined with limb and digit position information in area 2 for the recognition of shapes and objects during active touch. Muscle spindle receptor information in area 3a, combined with inputs from area 2, may relate to motor control mechanisms.

Information from anterior parietal cortex is relayed laterally to S2 and adjoining fields as part of a processing sequence related to object identification and memory, and to posterior parietal cortex for computations relating to intention, attention, motor behavior, and multimodal motor control. In particular, much of the posterior parietal cortex relates to the visual control of eye, hand, and arm movements via outputs to frontal cortex and to brainstem centers. Posterior parietal cortex is asymmetrical in humans, with the right (nondominant) hemisphere having a more dramatic role in mediating attention and motor behavior for the contralateral body and visual space. The significance of the supplementary sensory area is uncertain, but a role in motivation and other limbic cortex functions seems likely.

References

Aglioto, S., Beltramello, A., Bonazzi, A., and Corbetta, M. (1996). Thumb-pointing in human after damage to somatic sensory cortex. *Exp. Brain Res.* **109,** 92–100.

Allison, T., McCarthy, G., Wood, C.C., Parcey, T.M., Spenar, D.P., and Williamson, P.P. (1988). Human cortical potentials evoked by stimulation of median nerves. I. Cytoarchitectonic areas generating SI activity. *J. Neurophysiol.* **62,** 711–722.

Andersen, R.A., Asanuma, C., and Cowan, W.M. (1985). Callosal and prefrontal associational projecting cell populations of area 71 of the macaque monkey: A study using retrogradely transported fluorescent dyes. *J. Comp. Neurol.* **232,** 443–455.

Andersen, R.A., Snyder, L.H., Bradley, D.C., and Xing, J. (1997). Multimodal representation of space in the posterior parietal cortex and its use in planning movements. *Annu. Rev. Neurosci.* **20,** 303–330.

Apkarian, A.V., and Hodge, C.J. (1989a). Primate spinothalamic pathways. II. The cells of origin of the dorsolateral and ventral spinothalamic pathways. *J. Comp. Neurol.* **288,** 474–492.

Apkarian, A.V., and Hodge, C.V. (1989b). Primate spinothalamic pathways. III. Thalamic terminations of the dorsolateral and ventral spinothalamic pathways. *J. Comp. Neurol.* **288,** 493–511.

Apkarian, A.V., and Shi, T. (1994). Squirrel monkey lateral thalamus. I., Somatic nociresponsive neurons and their relation to spinothalamic terminals. *J. Neurosci.* **14,** 6779–6796.

Baynes, K., Holtzman, J.P., and Volpe, B.T. (1986). Components of visual attention: Alterations in response pattern to visual stimuli following parietal lobe infarction. *Brain* **109,** 99–114.

Beck, C.H. (1976). Dual dorsal columns: A review. *Can. J. Neurol. Sci.* **3,** 1–7.

Bentivoglio, M., and Rustioni, A. (1986). Corticospinal neurons with branching axons to the dorsal column nuclei in the monkey. *J. Comp. Neurol.* **25** (3), 260–276.

Berkley, K.J. (1980). Spatial relationships between the terminations of somatic sensory and motor pathways in the rostral brainstem of cats and monkeys. I. Ascending somatic sensory inputs to lateral diencephalon. *J. Comp. Neurol.* **193,** 283–317.

Berkley, K.J., and Hubscher, C.H. (1995). Are there separate central nervous system pathways for touch and pain? *Nature Med.* **1,** 766–773.

Blatt, G.J., Andersen, R.A., and Stoner, G.R. (1990). Visual receptive field organization and cortico-cortical connections of the lateral intraparietal area (Area LIP) in the Macaque. *J. Comp. Neurol.* **299,** 421–445.

Blomquist, A., Zhang, E.T., and Craig, A.D. (2000). Cytoarchitectonic and immunohistochemical characterization of a specific pain and temperature relay, the posterior portion of the ventral medial nucleus, in the human thalamus. *Brain* **123,** 601–619.

Boivie, J. (1978). Anatomical observations on the dorsal column nuclei, their thalamic projection and the cytoarchitecture of some somatosensory thalamic nuclei in the monkey. *J. Comp. Neurol.* **178,** 17–48.

Boivie, J. (1983). anatomic and physiologic features of the spinocervico-thalamic pathways. *In* "Somatosensory Integration in the thalamus" (G. Macchi, A. Rustioni, and R. Spreafico, eds.), pp. 63–106. Elsevier, Amsterdam.

Boivie, J., and Boman, K. (1981). Termination of a separate (proprioceptive?) cuneothalamic tract from external cuneate nucleus in money. *Brain Res.* **224,** 235–246.

Bolanowski, S.J., Gescheider, G.A., and Verrillo, R.T. (1994). Hairy skin: Psychophysical channels and their physiological substrates. *Somatosen. Motor. Res.* **11,** 1279–1290.

Bolanowski, S.J., Gescheider, G.A., Verrillo, R.T., and Checkosky, C.M. (1988). Four channels mediate the mechanical aspects of touch. *J. Acoust. Soc. Am.* **84,** 1680–1694.

Bonda, E., Frey, S., and Petrides, M. (1996b). Evidence for a dorsomedial parietal system involved in mental transformations of the body. *J. Neurophysiol.* **76,** 2042.

Bonda, E., Petrides, M., Frey, S., and Evans, A. (1995). Neural correlates of mental transformations of the body-in-space. *Proc. Nat. Acad. Sci.* USA. **92,** 11180.

Bonda, E., Petrides, M., and Evans, A. (1996a). Neural systems for tactual memories. *J. Neurophysiol.* **75,** 1730.

Bowsher, P. (1957). Termination of the central pain pathway in man: The conscious appreciation of pain. *Brain* **80,** 606–622.

Braak, H. (1980). Architectonics of the human telencephalic cortex. "Studies of Brain Function, vol. 4. Springer-Verlag, Berlin.

Bradley, W.E., Farrell, D.F., and Ojemann, G.A. (1998). Human cerebrocortical potentials evoked by stimulation of the dorsal nerve of the penis. *Somatosens. Mot. Res.* **15,** 118.

Brochier, T., Boudreau, M.J., Pare, M., and Smith, A.M. (1999). The effects of muscimal inactivation of small regions of motor and somatosensory cortex on independent finger movements and force control in the precision grip.

Brodmann, K. (1909). "Vergleichende Lokalisationslehre der Grosshirnrinde." Barth, Leipzig.

Brown, A.G. (1981). The primary afferent input: Some basic principles. In "Spinal Cord Sensation" (A.G. Brown and M. Rethelyi, eds), pp. 23–32. Scottish Academic Press, Edinburgh.

Bryan, R.N., Coulter, J.D., and Willis, W.D. (1974). Cells of origin of the spinocervical tract. *Exp. Brain Res.* **17,** 177–189.

Burgess, P.R. Wei, J.Y., Clark, F.J., and Simon, J. (1982). Signalling sensory receptors. *Annu. Rev. Neurosci.* **5,** 171–187.

Burton, H., and Craig, A.P., Jr. (1979). Distribution of trigeminothalamic projections cells in cat and monkey. *Brain Res.* **161,** 515–521.

Burton, H., Abend, N.S., MacLeod, A.M.K., Sinclair, R.J., Synder, A.Z., and Raichle, M.E. (1999). Tactile attention tasks enhance activation in somatosensory regions of parietal cortex: A positron emission tomography study. *Cereb. Cortex* **9,** 662–674.

Burton, H., Fabri, M., and Alloway, K. (1995). Cortical areas within the lateral sulcus connected to cutaneous representations in areas 3b and 1: A revised interpretation of the second somatosensory area in macaque monkeys. *J. Comp. Neurol* **355,** 539–562.

Burton, H., McLeod, A.M., Videen, T.D., and Raichle, M.E. (1997). Multiple foci in parietal and frontal cortex activated by rubbing embossed grating patterns across fingerpads: A positron emission tomography study in humans. *Cereb. Cortex* **7,** 3–17.

Burton, H., Sathian, K., and Dian-Hua, S. (1990). Altered responses to cutaneous stimuli in the second somatosensory cortex following lesions of the postcentral gyrus in infant and juvenile macaques. *J. Comp. Neurol.* **291,** 395–414.

Burton, H., Videen, T.O., and Raichle, M.E. (1993). Tactile-vibration-activated foci in insular and parietal-opercular cortex studied with positron emission tomography: Mapping the second somatosensory area in humans. *Somatosens. Mot. Res.* **10,** 297.

Caminiti, R., Ferraina, S., and Johnson, P.B. (1996). The sources of visual information to the primate frontal lobe: A novel for the superior parietal lobule. *Cereb. Cortex* **6,** 319–328.

Campbell, A.W. (1905). "Histological Studies on the Localization of Cerebral Function." Cambridge Univ. Press, London, New York.

Carlson, M. (1981). Characteristics of sensory deficits following lesions of Broadmann's areas 1 and 2 in the postcentral gyrus of *Macaca mulatta. Brain Res.* **204,** 424–430.

Caselli, R.J. (1993). Ventrolateral and dorsomedial somatosensory association cortex damage produces distinct somesthetic syndromes in humans. *Neurology* **43,** 762–771.

Casey, K.L. (1999). Forebrain mechanisms of nociception and pain: Analysis through imaging. *Proc. Nat. Acad. Sci. USA* **96,** 7668–7694.

Cavada, C., and Goldman-Rakic, P.S. (1989). Posterior parietal cortex in rhesus monkey. II. Evidence for segregated corticocortical networks linking sensory and limbic areas with the frontal lobe. *J. Comp. Neurol.* **187,** 411–445.

Celesia, G.G. (1979). Somatosensory evoked potentials recorded directly from human thalamus and Sm I cortical area. *Arch. Neurol. (Chicago)* **36,** 399–405.

Cheema, S., Rustioni, A., and Whitsel, B.L. (1985). Sensorimotor cortical projections to the primate cuneate nucleus. *J. Comp. Neurol.* **204,** 196–211.

Clark, F.J., Burgess, R.C., and Chapin, J.W. (1986). Proprioception with the proximal interphalangial joint of the index finger. *Brain* **109,** 1195–1208.

Colby, C.L., and Goldberg, M.E. (1999). Space and attention in parietal cortex. *Ann. Rev. Neurosci.* **22,** 319–349.

Colby, C.L., Duhamel, J.-R., and Goldberg, M.E. (1993). Ventral intraparietal area of the macaque: Anatomic location and visual response properties. *J. Neurophysiol.* **69,** 902–914.

Corkin, S., Milner, B., and Rasmussen, M. (1970). Somatosensory thresholds: Contrasting effects of postcentral gyrus and posterior parietal-lobe excisions. *Arch. Neurol (Chicago)* **23,** 41–58.

Craig, A.D., Bushnell, M.C., Zhang, E.T., and Blomquist, A. (1994). A thalamic nucleus specific for pain and temperature sensation. *Nature* **372,** 770–773.

Craig, A.D., Chen, K., Bandy, D., and Reiman, E.M. (2000). Thermosensory activation of insular cortex. *Nature Neurosci.* **3,** 184–190.

Craign, A.D., Reiman, E.M., Evans, A., and Bushnell, M.C. (1996). Functional imaging of an illusion of pain. *Nature* **384,** 258–260.

Craig, A.D., Zhang, E.T., and Blomquist, A. (1999). A distinct thermoreceptive subregion of lamina I in nucleus caudalis of the owl monkey. *J. Comp. Neurol.* **404,** 221–234.

Critchley, M. (1949). The phenomenon of tactile inattention with special reference in parietal lesions. *Brain* **72,** 538–561.

Cross, M.J., and McCloskey, D.I. (1973). Position sense following surgical removal of joints in man. *Brain Res.* 55443–55445.

Cusick, C.G., and Gould, H.J. (1990). Connections between area 3b of the somatosensory cortex and subdivisions of the ventroposterior nuclear complex and the anterior pulvinar nucleus in squirrrel monkeys. *J. Comp. Neurol.* **292,** 83–102.

Cusick, C.G., Steindler, D.A., and Kaas, J.H. (1985). Corticocortical and collateral thalamocortical connections of postcentral somatosensory cortical areas in squirrel monkeys: A double-labeling study with wheatgerm agglutinin (WGA) conjugated to horseradish peroxidase and radiolabeled WGA. *Somatosensory Res.* **3,** 1–31.

Cusick, C.G., Wall, J.T., Felleman, d.J., and Kaas, J.H. (1989). Somatotopic organization of the lateral sulcus of owl monkeys: Area 3b, S-II, and a ventral somatosensory area. *J. Comp. Neurol.* **282,** 169–190.

Darian-Smith, I. (1984). The sense of touch: Performance and peripheral neural processes. *In* "Handbook of Physiology," sect. 1, vol. III, pp. 739–788. Am. Physiol. Soc., Washington, DC.

Darian-Smith, C., Darian-Smith, I., and cheema, S.S. (1990). Thalamic projections to sensorimotor cortex on the macaque monkey: Use of multiple retrograde fluorescent tracers. *J. Comp. Neurol.* **299,** 17–46.

Davis, K.D., Kiss, Z.H.T., Tasker, R.R., and Dostrovsky, J.O. (1996). Thalamic stimulation-evoked sensations in chronic pain patients and in nonpain (movement disorder) patients. *J. Neurophysiol.* **75,** 1026–1037.

Davis, K.D., Lozano, R.M., Manduch, M., Tasker, R.R., Kiss, Z.H., and Dostrovsky, J.O. (1999). Thalamic relay site for cold perception in humans. *J. Neurophysiol.* **81,** 1970–1973.

Denny-Brown, D., and Chambers, R.A. (1956). The parietal lobe and behavior. *Res. Publ. Assoc. Res. Nerv. Ment. Dis.* **36,** 35–117.

Denny-Brown, D., and Chambers, R.a. (1958). The parietal lobe and behavior. *Res. Publ. Assoc. Res. Nerv. Ment. Dis.* **36,** 35–117.

DeRenzi, E. (1982). "Disorders of Space Exploration and Cognition." Wiley, New York.

Desmarget, M., Epstein, C.M., Turner, R.S., Prablans, C., Alexander, G.E., and Grafton, S.T. (1999). Role of the posterior parietal cortex in updating reaching movements to a visual target. *Nat. Neurosci.* **2,** 563–567.

Desmedt, J.E., and Ozaki, I. (1991). SEPs to finger joint input lack the N20–P20 response that is evoked by tactile inputs: Contrast between cortical generators in areas 3b and 2 in humans. *Electroceph. Clin. Neurophysiol.* **80,** 513–521.

Disbrow, E., Roberts, T., and Krubitzer, L. (2000). Somatotopic organization of cortical fields in the lateral sulcus of *Homo sapiens:* Evidence for SII and PV. *J. Comp. Neurol.* **418,** 1–21.

Disbrow, E., Roberts, T., Peoppel, D., and Krubitzer, L. (2001). Evidence for interhemispheric processing of inputs from the hands in the human second somatosensory and parietal ventral areas. *J. Neurophysiol.* **85,** 2236–2244.

Domino, E.F., Matsuoka, S., Waltz, J., and Copper, I.S. (1965). Effects of cryogenic thalamic lesions on the somesthetic evoked response in man. *Electroencephalogr. Clin. Neurophysiol.* **53,** 143–165.

Dreyer, D.A., Schneider, R.J., Metz, C.B., and Whitsel, B.L. (1974). Differential contributions of spinal pathways to body representation in postcentral gyrus of *Macaca mulatta. J. Neurophysiol.* **37,** 119–145.

Duhamel, J.-R., Colby, C.L., and Goldberg, M.E. (1998). Ventral intraparietal area of the macaque: Convergent visual and somatic response properties. *J. Neurophysiol.* **79** (1), 126–136.

Dykes, R.W. (1983). Parallel processing of somatosensory information: A theory. *Brain Res. Rev.* **6,** 47–115.

Dykes, R.W., and Terzis, J.K. (1981). Spinal nerve distributions in the upper limb: The organization of the dermatome and afferent myotome. *Philos. Trans. Roy. Soc. Lond. Ser. B.* **293,** 509–554.

Dykes, R.W., Sur, M., Merzenich, M.M., Kaas, J.H., and Nelson R.J. (1981). Regional segregation of neurons responding to quickly adapting, slowly adapting, deep and pacinian receptors within thalamic ventroposterior lateral and ventroposterior inferior nuclei in the squirrel monkey (*Saimiri sciureus*). *Neuroscience* **6,** 1687–1692.

Edin, B.B., and Abbs, J.H. (1991). Finger movement responses of cutaneous mechanoreceptors in the dorsal skin of the human hand. *J. Neurophysiol.* **65,** 657–670.

Emmers, R., and Tasker, R. R. (1975). "The Human somesthetic Thalamus." Raven Press, New York.

Ervin, F.R., and Mark, V.H. (1964). Studies of the human thalamus. IV. Evoked responses. *Ann. N.Y. Acad. Sci.* **112,** 81–92.

Eskenasy, A.C.E., and Clarke, S. (2000). Hierarchy. within human S1: Supporting data from cytochrome oxidase, acetylcholinesterase and NADPH-diaphorase staining patterns.

Evans, J.P. (1935). A study of the sensory defects resulting from excision of cerebral substance in humans. *Res. Publ. Assoc. Res. Nerv. Ment. Dis.* **15,** 331–366.

Florence, S.L., Wall, J.T., and Kaas, J.H. (1988). the somatotopic pattern of afferent projections from the digits to the spinal cord and cuneate nucleus in macaque monkeys. *Brain Res.* **452,** 388–392.

Florence, S.L., Wall, J.T., and Kaas, J.H. (1989). Somatotopic organization of inputs from the hand to the spinal grey and cuneate nucleus of monkeys with observations on the cuneate nucleus of humans. *J. Comp. Neurol.* **286,** 48–70.

Foerster, O. (1931). The cerebral cortex in man. *Lancet* **221,** 309–312.

Foerster, O. (1933). The dermatomes in man. *Brain* **56,** 1–39.

Foerster, O. (1936a). Motorische Felder und Bahnen. *In* "Handbuch der Neurologie" (O. Bumke and O. Foerster, eds.), vol. 6, pp. 1–357. Springer-Verlag, Berlin.

Foerster, O. (1936b). The motor cortex in man in the light of Hughlings Jackson's doctrines. *Brain* **59,** 135–159.

Francis, S.T., Kelly, E.F., Bowtell, R., Dunseath, W.J.R., folger, S.E., and Mcglone, F. (2000). fMRI of the responses to vibratory stimulation of digit tips. *NeuroImage* **11,** 188–202.

Friedman, D.P., and Murray, E.A. (1986) Thalamic connectivity of the second somatosensory area and neighboring somatosensory fields of the lateral sulcus of the macaque. *J. Comp. Neurol.* **252,** 348–373.

Friedman, D.P., Murray, E.A., ONeill, J.B., and Mishkin, M. (1986). Cortical connections of somatosensory fields of the lateral sulcus of macaques: Evidence for a corticolimbic pathway for touch. *J. Comp. Neurol.* **252,** 323–347.

Fukushima, T., Mayanagi, Y., and Bouchard, G. (1976). Thalamic evoked potentials to somatosensory stimulation in man. *Electroencephalogr. Clin. Neurophysiol.* **40,** 481–490.

Gandevia, S.C., Burke, D., and Mckeon, B.B. (1984). The projection of muscle afferents from the hand to cerebral cortex in man. *Brain* **107,** 1–13.

Garcin, R., and LaPresle, J. (1960). Deuxieme observation personnelle de syndrome sensitif de type thalamique et a topographie cherio-orale par lesion localisee du thalamus. *Rev. Neurol.* **103,** 474-481.

Garraghty, P.E., Pons, T.P., and Kaas, J.H. (1990). Ablations of areas 3b (S-I proper) and 3a of somatosensory cortex in marmosets deactivate the second and parietal ventral somatosensory area. *Somatosen Motor Res.* **7,** 125–135.

Gelnar, P.A., Krauss, R.B., Szeverenyi, N.M., and Apkarian, A.V. (1998). Fingertip representation in the human somatosensory cortex: An fMRI study. *NeuroImage* **7,** 261.

Gildenberg, P.L., and Murthy, K.S.K., (1980). Influence of dorsal column stimulation upon human thalamic somatosensory-evoked potentials. *Appl. Neurophysiol.* **43,** 8–17.

Gingold, S.I., Greenspan, J.D., and Apkarian, A.V. (1991). Anatomic evidence of nociceptive inputs to primary somatosensory cortex: Relationship between spinothalamic terminals and thalamocortical cells in squirrel monkeys. *J. Comp. Neurol.* **308,** 467–490.

Goodwin, G.J., McCloskey, D.I., and Matthews, P.B.C. (1971). The contribution of muscle afferents to Kinaesthesia shown by vibration inducing illusions of movement and by the effects of paralysing afferents. *Brain* **95,** 705–708.

Graziano, M.S., Cooke, D.F., and Taylor, C.S.R. (2000). Coding the location of the arm by sight. *Science* **290,** 1782–1786.

Grunewald, A., Lindin, J.R., and Andersen, R.A. (1999). Responses to auditory stimuli in macaque intraparietal area I. Effects of training. *J. Neurophysiol.* **82,** 330–342.

Guldin, W.O., Akbarian, S., and Grusser, O.J. (1992). Cortico-cortical connections of the primate vestibular cortex: A study in squirrel monkeys *(Saimiri Sciareus). J. Comp. Neurol.* **326,** 375–401.

Hamalainen, H., and Jarvilehto, T. (1981). Peripheral neural basis of tactile sensations in man. I. Effect of frequency and probe area on sensations elicited by single mechanical pulses on hair and glabrous skin of the hand. *Brain Res.* **219,** 1–12.

Hamalainen, H.A., Warren, S., and Gardner, E.P. (1985). Differential sensitivity to airpuffs on human hairy and glabrous skin. *Somatosensory Res.* **2,** 281–302.

Han, Z.S., Zhang, e.t., and Craig, A.D. (1998). Nociceptive and thermoreceptive lamina I neurons are anatomically distinct. *Nat. Neurosci.* **1,** 218–225.

Hari, R., and Kaukoranta, E. (1985). Neuromagnetic studies of somatosensory system: Principles and examples. *Prog. Neurobiol.* **24,** 233–256.

Hässler, R. (1959). Anatomy of the thalamus. *In* "Introduction to Stereotaxis with an Atlas of the Human Brain" (G. Schaltenbrand and P. Bailey, eds.), vol. I, pp. 230–290. Thieme, Stuttgart.

Hässler, R. (1982). Architectonic organization of the thalamic nuclei. *In* "Stereotaxy of he Human Brain" (G. Schaltenbrand and A.E. Walker, eds.), 2nd ed. Thieme, Stuttgart.

Head, H. (1920). "Studies in Neurology. H. Frowde, London.

Head, H., and Holmes, G. (1911). Sensory disturbances from cerebral lesions. *Brain* **34,** 102–254.

Hikosaka, O., Tanaka, M., Sokamoto, M., and Iwamura, Y. (1985). Deficits in manipulative behaviors induced by local injections of muscimol in the first somatosensory cortex of the conscious monkey. *Brain Res.* **325,** 375–380.

Hirai, T., and Jones, E.G. (1989). A new parcellation of the human thalamus on the basis of histochemical staining. *Brain Res. Rev.* **14,** 1–34.

Hollins, M., and Roy, E.A. (1996). Perceived intensity of vibrotactile stimuli: The role of mechanoreceptive channels. *Somatosen. Mot. Res.* **13,** 273–286.

Hoshiyama, M., Kakigi, R., Koyama, S., Kitamura, Y., Shimojo, M., and Watanabe, S. (1996). Somatosensory evoked magnetic field following stimulation of the lip in humans. *Electroenceph. Clin. Neurophysiol.* **100,** 96–104.

Huerta, M.F., and Harting, J.K. (1984). The mammalian superior colliculus: Studies of its morphology and connections. *In* "Comparative Neurology of the Optic Tectum" (H. Vanegas, ed.), pp. 687–783. Plenum, New York.

Huerta, M.F., and Pons, T.P. (1990). Primary motor cortex receives input from area 3a in macaques. *Brain Res.* **537,** 367–731.

Huffman, K.J., and Krubitzer, L. (2001). Area 3a: Topographic organization and cortical connections in marmoset monkeys. *Cereb Cortex* **11,** 849–867.

Hyvarinen, J. (1982). "The Parietal Cortex of Monkey and man.

Srpinger-Verlag, New York.
Hyvarinen, J., and Poranen, A. (1978). Movement-sensitive and direction and orientation-selective cutaneous receptive fields in the hand area of the post-central gyrus in monkeys. *J. Physiol. (London)* **283,** 523–537.
Iriki, A., Tanaka, M., and Iwamura, Y. (1996). Coding of modified body schema during tool use by macaque postcentral neurons. *Neuro. Report* **7,** 2325–2330.
Ishiko, N., Hanamori, T., and Murayama, N. (1980). Spatial distribution of somatosensory responses evoked by tapping the tongue and finger in man. *Electroencephalogr. Clin. Neurophysiol.* **50,** 1–10.
Iwamura, Y., and Tanaka M. (1996). Representation of reaching and grasping in monkey postcentral gyrus. *Neurosci Lett.* **214,** 147–150.
Iwamura, Y., Tanaka, M., Sakamoto, M., and Hikosaka, O. (1993). Rostrocaudal gradient in the neuronal receptive field complexity in the finger region of the alert monkey's postcentral gyrus. *Exp. Brain Res.* **92,** 360–368.
Jain, N., Catania, K.C., and Kaas, J.H. (1997). Deactivation and reactivation of somatosensory cortex after dorsal spinal cord injury. *Nature* **386,** 495–498.
Jain, N., Catania, K.C., and Kaas, J.H. (1998). A histologically visible representation of the fingers and palm in primate area 3b and its immuabillity following long term deafferentations. *Cereb. Cortex* **8,** 227–236.
Jain, N., Qi, H.X., Catania, K.C., and Kaas, J.H. (2001). Anatomical correlates of the face and oral cavity representations in somatosensory cortical area 3b of monkeys. *J. Comp. Neurol.* **429,** 455–468.
Jarvilehot, T., Hamalainen, H., and Soininen, K. (1981). Peripheral neural basis of tactile sensations in man. II. Characterustucs of human mechanoreceptors in the hairy skin and correlations of their activity with tacile sensations. *Brain Res.* **219,** 13–27.
Jasper, J., Lende, R., and Rasmussen, T. (1960). Evoked otentials from the exposed somatosensory cortex in man. *J. Nerv. Ment. Dis.* **130,** 526–537.
Johansson, R.S. (1976). Receptive sensitivity profile of mechanosensitive units innervating the glabrous skin of the human hand. *Brain Res.* **104,** 330–334.
Johansson, R.S. (1978). Tactile sensibility of the human hand: Receptive field characteristics of mechanoreceptive units in the glabrous skin. *J. Physiol. (London)* **281,** 101–123.
Johansson, R.S., and Vallbo, A.B. (1979). Tactile sensibility in the human hand: Relative and absolute densities of four types of mechanoreceptive units in glabrous skin. *J. Physiol. (London)* **286,** 283–300.
Johansson, R.S., and Vallbo, A.B. (1983). Tactile sensory coding in the glabrous skin of the human. *Trends neurosci.* **6,** 27–32.
Johansson, R.S., Landstrom, U., and Lundstrom, R. (1982b). Sensitivity to edges of mechanoreceptive afferent units innervating the glabrous skin of the human hand. *Brain Res.* **244,** 17–25.
Johnson, K.O., and Hsiao, S.S. (1992). Neural mechanisms of tactual form and texture perception. *Annu. Rev. Neurosci.* **15,** 227–250.
Johnson, K.O., and Lamb, G.D. (1981). Neural mechanisms of spatial tactile discrimination: Neural patterns evoked by braille-like dot patterns in the monkeys. *J. Physiol. (London)* **310,** 117–144.
Jones, E.G. (1985). "The Thalamus." Plenum, New York.
Jones, E.G., and Burton, H. (1976). Areal differences in the distribution of thalamic afferents in the insular, parietal and temporal regions of primates. *J. Comp. Neurol.* **168,** 197–248.
Jones, E.G., and Porter, R. (1980). What is the area 3a? *Brain Res. Rev.* **2,** 1–43.
Jones, L.A. (1994). Peripheral mechanisms of touch and proprioception. *Can. J. Physiol. Pharmacol.* **72,** 484–487.
Kaas, J.H. (1983). What, if anything, is S-I? The organization of the "first somatosensory area" of cortex. *Physiol. Rev.* **63,** 206–231.
Kaas, J.H., and Florence, S.L. (2000). Reorganization of sensory and motor systems in adult mammals after injury. *In* "The Mutable Brain" (J.H). Kaas, eds. pp. 165–242. Gorden and Breach Science Publishers, London.
Kaas, J.H., and Pons, T.P. (1988). The somatosensory system of primates. *In* "Comparative Primate Biology" (H.P. Steklis and J. Erwin, eds), vol. 4, pp. 421–468. Lis, New York.
Kaas, J.H., Nelson, R.J., Dykes, R.W., and Merzenich, M.M. (1984). The somatotopic organization of the ventroposterior thalamus of the squirrel money, *Samiri sciureus*. *J. Comp. Neurol.* **226,** 111–140.
Kaukoranta, E., Hamalianen, M., Sarvas, J., and Hari, R. (1986). Mixed and sensory nerve stimulations activate different cytoarchitectonic areas in the human primary somatosensory cortex S-I. *Exp. Brain Res.* **63,** 60–66.
Keegan, J.J. (1943). Dermatome hypalgesia associated with herniation of intervertebral disc. *Arch. Neurol. Psychiatry* **50,** 67–83.
Kenshalo, D.R. Jr., Giesler, G.J. Jr., Leonard, R.B., and Willis, W.P. (1980). Responses of neurons in primate ventral posterior lateral nucleus to noxious stimuli. *J. Neurophysiol.* **43,** 1594–1614.
Killackey, H.P., Gould, H.J., III, Cusick, C.G., Pons, T.P., and Kaas, J.H. (1983). The relation of corpus collasum connections to architectonic fields and body surface maps in sensorimotor cortex of New and Old World monkeys. *J. Comp. Neurol.* **219,** 384–419.
Krubitzer, L.A., and Kaas, J.H. (1987). Thalamic connection of three representations of the body surface in somatosensory cortex in grey squirrels. *J. Comp. Neurol.* **265,** 549–580.
Krubitzer, L.A., and Kaas, J.H. (1990). The organization and connections of somatosensory cortex in marmosets. *J. Neurosci.* **10,** 952–974.
Krubitzer, L.A., and Kaas, J.H. (1992). The somatosensory thalamus of monkeys: Cortical connections and a redefinition of nuclei in marmosets. *J. Comp. Neurol.* **319,** 1–18.
Krubitzer, L.A., Clarey, J., Tweedale, R., Elston, G., and Calford, M. (1995). A redefinition of somatosensory areas in the lateral sulcus of macaque monkeys. *J. Neurosci.* **15,** 3821–3839.
Kurth, R., Villringer, K., Curio, G., Wolf, K.J., Repenthin, J., Schwiemann, J., Deuchert, M., and Villringer, A. (2000). fMRI shows multiple somatotopic digit representation in human primary somatosensory cortex. *Neuroreport* **11,** 1487.
Kurth, R., Villringer, K., Mackert, B.M., Schwiemann, J., Braun J., Curio, G., Villringer, A., and Wolf, K.J. (1998). fMRI assessment of somatotopy in human Brodmann area 3b by electrical finger stimulation. *Neuroreport* **9,** 207.
Kusanoki, M., Gottlieb, J., and Goldberg, M.E. (2000). The lateral intraparietal area as a salience map: The representation of abrupt onset stimulus, motion, and task relevance. *Vis. Res.* **40,** 1459–1468.
LaMotte, R.H., and Mountcastle, V.B. (1979). Disorders in some stresses following lesions of parietal lobe. *J. Neurophysiol.* **42,** 400–419.
LaMotte, R.H., and Srinivasan, M.A. (1987). Tactile discrimination of shape: Responses of rapidly adapting mechanoreceptive afferents to a step stroked across the monkey fingerpad. *J. Neurosci.* **7,** 1672–1681.
Leinonen, L. (1984) Integration of somatosensory events in the posterior parietal cortex of the monkey. *In* "Somatosensory Mechanisms" (E. Eecles, O., Franzen, U., Lindblom, P., Ottoson, eds.), pp. 113–124. MacMillan Press, London.
Lenz, F.A., Dostrovsky, J.O., Tasker, R.R., Yamashiro, K., Kwan, H.C., and Murphy, J.T. (1988). Single-unit analysis of the human ventral thalamic nuclear group: Somatosensory responses. *J. Neurophysiol.* **59,** 299–316.

Lenz, F.A., Gracely, R.H., Baker, F.H., Richardson, R.T., and Dougherty, P.M. (1998). Reorganization of sensory modalities evoked by microstimulation in the region of the thalamic principal sensory nucleus in patients with pain due to nervous system injury. *J. Comp. Neurol.* **399,** 125–138.

Lenz, F.A., Kwan, H.C., Dostrovsky, J.O., Tasker, R.R., Murphy, J.T., and Lenz, Y.E. (1990. Single unit analysis of the human ventral thalamic nuclear group: Activity correlated with movement. *Brain* **113,** 1795–1821.

Lenz, F.A., Seike, M., Lin, Y.C., Baker, F.H., Rowland, L.H., Gracely, R.H., and Richardson, R.T. (1993). Neurons in the area of human thalamic nucleus ventralis caudalis respond to painful heat stimuli. *Brain Res.* **623,** 235–240.

Lewis, V.W., and Van Essen, D.C. (2000a). Mapping of architectonic subdivisions in the macaque monkey, with emphasis on parieto-occipital cortex. *J. Comp. Neurol.* **428,** 79–111.

Lewis, V.W., and Van Essen, D.C. (2000b). Corticocortical connections of visual, sensorimotor and multimodal processing areas in the parietal lobe of the macaque monkey. *J. Comp. Neurol.* **428,** 112–137.

Lin, W., Kupusamy, K., Haacke, E.M., and Buton, H. (1996). Functional MRI in human somatosensory cortex activated by touching textured surface. *J. Magn. Reson. Imaging* **6,** 565.

Lynch, J.L. (1980). The functional organization of posterior parietal association cortex. *Behav. Brain Sci.* **3,** 485–534.

Maeda, K., Kakigi, R., Hoshiyama, M., and Koyama, S. (1999). Topography of the second somatosensory cortex in humans: A magnetoencephalographic study. *Neuro. Report* **10,** 301–206.

Mai, J.K., Assheur, J., and Paxinos, G. (1997). "Atlas of the Human Brain." Academic Press, San Diego.

Maldjian, J.A., Gottschalk, A., Patel, R.S., Pincus, D., Detre, J.A., and Alsop, D.C. (1999). Mapping of secondary somatosensory cortex activation induced by vibrational stimulation: An fMRI study. *Brain Res.* **824,** 291.

Manger, P.R., Woods, T.M., and Jones, E.G. (1996). Representation of face and intraoral structures in area 3b of macaque monkey somatosensory cortex. *J. Comp. Neurol.* **371,** 513–521.

Mann, M.P. (1973). Clarke's column and the dorsal spinocerebellar tract: A review. *Brain Behav. Evol.* **7,** 34–83.

Marconi, B., Gonovesio, A., Ba Haglia-Mayer, A., Ferraina, S., Squatrito, S., Molinari, M., Lacyuaniti, F., and Caminiti, R. (2001). Eye-hand coordination during reaching. I. anatomicol relationships between parietal and frontal cortex. *Cerif. Cortex* **11,** 513–527.

Marino, J., Martinez, L., and Canedo, A. (1999). Sensorimotor integration at the dorsal column nuclei. *News Physiol. Sci.* **14,** 231–237.

Marshall, W., Woolsey, C.N., and Bard, P. (1937). Cortical representation of tactile sensibility as indicated by cortical potentials. *Science* **85,** 388–390.

Mauguiere, F., and Courjon, J. (1978). Somatosensory epilepsy: A review of 127 cases. *Brain* **101,** 307–332.

Maunsell, J.H.R., and Van Essen, D.C. (1983). the connections of the middle temporal visual area (MT) and heir relationship to a cortical hierarchy in the macaque monkeys. *J. Neurophysiol.* **3,** 2563–2586.

May, J.G., and "Andersen, R.A. (1986). Different patterns of corticopontine projections from separate cortical fields within the inferior parietal lobule and dorsal prelunate gyrus of the macaque. *Exp. Brain Res.* **63,** 265–278.

May, P.J., and Porter, J.D. (1998). The distribution of primary afferent terminals from the eyelids of macaque monkeys. *Exp. Brain Res.* **123,** 368–381.

McCloskey, P.I. (1974). Muscular and cutaneous mechanisms in the estimation of he weights of grasped objects. *neuropsychologia* **12,** 513–529.

McCloskey, P.I. (1978). Kinesthetic sensibility. *Physiol. Rev.* **58,** 763–820.

Mehler, W.R. (1966). The posterior thalamic region in man. *Confin. Neurol.* **27,** 18–29.

Meredith, M.A., and Stein, B.E. (1985). Descending efferents from the superior colliculus relay integrated multisensory information *Science* **6,** 657–659.

Mesulam, M.M. (1981). A cortical network for directed attention and unilateral neglect. *Ann. Neurol.* **10,** 309–325.

Mesulam, M.M. (1983). The functional anatomy and hemispheric specialization for directed attention. *Trends Neurosci.* **6,** 384–387.

Metherate, R.S., Da Costa, D.C., Herron, P., and Dykes, R.W. (1987). A thalamic terminus of the lateral cervical nucleus: The lateral division of the posterior nuclear group. *J. Neurophysiol.* **56,** 1498–1520.

Miller, M.R., Ralston, H.J., III, and Kasahara, M. (1958). The pattern of cutaneous innervation of the human hand. *Am. J. Anat.* **102,** 183–197.

Mima, T., Ikeda, A., Terada, K., Yazawa, S., Mikuni, M., Kunieda, T., Taki, W., Kimura, J., and Shibasaki, H. (1997). Modality-specific organization for cutaneous and proprioceptive sense in human primary sensory cortex studied by chronic epicortical recording. *Electroencephalogr. Clin. Neurophysiol.* **104,** 103.

Mima, T., Terada, K., Maekawa, M., Nagamine, T., Ikeda, A., and Shibasaki, H. (1996). Somatosensory evoked potentials following proprioceptive stimulation of fingers in man. *Exp. Brain Res.* **111,** 233.

Mishkin, M. (1979). Analogous neural models for tactual and visual learning. *Neurophychologia* **17,** 139–151.

Molinari, H.H., Schultze, K.E., and Strominger, N.L. (1996). Gracile, cuneate, and spinal trigeminal projections to inferior olive in rat and monkey. *J. Comp. Neurol.* **375,** 467–480.

Moore, C.I., Stern, C.E., Corkin, S., Fischl, B., Gray, A.C., Rosen, B.R., and Dale, A.M. (2000). Segregation of somatosensory activation in the human rolandic cortex using fMRI. *J. Neurophysiol.* **84,** 558.

Morel, A., Magnin, M., and Jeanmonod, P. (1997). Multiarchitectonic and stereotactic atlas of the human thalamus. *J. Comp. Neurol.* **387,** 588–630.

Moscovitch, M., and Behrmann, M. (1994). Coding of spatial information in the somatosensory system: Evidence from patients with neglect following parietal lobe damage. *J. Cog. Neurosci.* **66,** 151.

Mountcastle, V.B. (1975). The view from within: Pathways to the study of perception. *Johns Hopkins Med. J.* **136,** 109–131.

Murray, E.A., and Coulter, J.D. (1982). Supplementary sensory cortex: The medial parietal cortex in the monkey. *In* "Cortical Sensory Organization (N. Woolsey, ed.), vol. I, pp. 167–195. Humana Press, Clifton, NJ.

Murray, E.A., and Mishkin, M. (1984a). Severe tactual as well as visual memory deficits follow combined removal of the amygdala and hippocampus in monkeys. *J. Neurosci.* **4,** 2565–2580.

Murray, E.A., and Mishkin, M. (1984b). Relative contributions of S-II and area 5 to tactile discriminations in monkeys. *Behav. Brain Res.* **11,** 67–83.

Nakamura, A., Yamada, T., Goto, A., Kato, T., Ito, K., Abe, Y., Kachi, T., and Kakigi, R. (1998). Somatosensory homunculus as drawn by MEG. *NeuroImage* **7,** 377–386.

Nathan, P.W., Smith, M.C., and Cook, A.W. (1986). Sensory effects in man of lesions of the posterior columns and of some other afferent pathways. *Brain* **109,** 1003–1041.

Nelson, R.J. (1984). Responsiveness of monkey primary somatosensory cortical neurons to peripheral stimulation depends on "motor-set." *Brain Res.* **304,** 143–148.

Nelson, R.J., Sur, M., Felleman, D.J., and Kaas, J.H. (1980). The representations of the body surface in postcentral somatosensory cortex in *Macaca fascicularis*. *J. Comp. Neurol.* **192,** 611–643.

Ochoa, J.L., and Torebjork, H.E. (1983). Sensations evoked by intraneural microstimulation of single mechanoreceptor units innervating the human hand. *J. Physiol.* **342,** 633–653.

Ohye, C., Shihazaki, T., Hirai, T., Kawashima, Y., Hirato, M., and Matsumura, K. (1993). Tremor-mediated thalamic zone studied in humans and in monkeys. *Stereotact. Funct. Neurosurg.* **6,** 12–23.

Okada, Y.C., Tanenbaum, R., Williamson, S.J., and Kaufman, L. (1984). Somatotopic organization of the human somatosensory cortex revealed by neuromagnetic measurements. *Exp. Brain. Res.* **56,** 197–205.

Olszewski, J. (1952). "The thalamus of the *Macaca mulatta:* An Atlas for Use with the Stereotaxic Instrument." Karger, Basel.

Pandya, D.P., and Seltzer, B. (1982). Intrinsic connections and architectonics of posterior parietal cortex in the rhesus monkey. *J. Comp. Neurol.* **204,** 196–210.

Paxihos, G., and Huang, X.F. (1995). Atlas of the Human Brainstem." Academic Press, San Diego.

Paxinos, G., Huang, X.F., and Toya, A.W. (2000). "The Rhesus Monkey Brain. Academic Press, San Diego.

Penfield, W., and Boldrey, E. (1937). somatic motor and sensory representation in the cerebral cortex of man as studied by electrical stimulation. *Brain* **60,** 389–443.

Penfield, W., and Jasper, H.H. (1954). "Epilepsy and the Functional Anatomy of the Human Brain." Little, Brown, Boston, MA.

Penfield, W., and Rasmussen, T. (1950). "The Cerebral Cortex of Man." Macmillan, New York.

Perl, E.R. (1998). Getting a line on pain: Is it mediated by dedicated pathways? *Nat. Neurosci.* **1,** 177–178.

Ploner, M., Schmitz, F., Freund, H.V., and Schnitzler, A. (2000). Differential organization of touch and pain in human primary somatosensory cortex. *J. Neurophysiol.* **83,** 1770–1776.

Poggio, G.F., and Mountcastle, V.B. (1963). The functional properties of ventrobasal thalamic neurons studied in unanesthetized monkeys. *J. Neurophysiol.* **26,** 775–806.

Pompeiano, O., and Brodal, A. (1957). Spino-vestibular fibers in the cat. An experimental study. *J. Comp. Neurol.* **108,** 353–378.

Pons, T.P., and Kaas, J.H. (1986). Corticocortical connections of area 2, 1 and 5 of somatosensory cortex in macaque monkeys: A correlative anatomical and electrophysiological study. *J. Comp. Neurol.* **248,** 313–335.

Pons, T.P., Garraghty, P.E., Cusick, C.G., and Kaas, J.H. (1985b). The somatotopic organization of area 2 in macaque monkeys. *J. Comp. Neurol.* **241,** 445–466.

Pons, T.P., Garraghty, P.E., Friedman, D.P., and Mishkin, M. (1987). Physiological evidence for serial processing in somatosensory cortex. *Science* **237,** 417–420.

Posner, M.I., Walker, J.A., Friedrich, F.J., and Rafal, R.D. (1984). Effects of parietal injury on covert orienting of attention. *J. Neurosci.* **7,** 1863–1874.

Pouget, A., and Driver, V. (2000). Relating unilateral neglect to the neural coding of space. Curr. Opin. Neurobiol. **10,** 242–249.

Preuss, T.M., and Goldman-Rakic, P.S. (1991). Architectonics of the parietal and temporal association cortex in the strepsirhine primate *Galago* compared to the anthropoid primate *Macaca*. *J. Comp. Neurol.* **310,** 475–506.

Price, P.P., Dubner, R., and Ju, J.W. (1976). Trigeminothalamic neurons in nucleus caudalis responsive to tactile, thermal, and nociceptive stimulation of monkey's face. *J. Neurophysiol.* **39,** 936–953.

Pruett, J.R., Sinclair, R.J., and Burton, H. (2000). Response patterns in second somatosensory cortex (SII) of awake monkeys to passive applied tactile gratings. *J. Neurophysiol.* **84,** 780–797.

Puletti, F., and Blomquist, A.J. (1967). Single neuron activity in posterior columns of the human spinal cord. *J. Neurosurg.* **27,** 255–259.

Qi, H.-X., Jain, N., Preuss, T.M. and Kaas, J.K. (1998). Comparative architecture of areas 3a, 3b, and 1 of somatosensory cortex in chimpanzees, humans and macaque. *Soc. Neurosci. Abstrs.* **24,** 1125.

Qi, H.-X., Lyon, D.C., and Kaas, J.H. (2002). Corticol and thalamic connection of the parietal ventral somatosensory area in mamoset monkeys (*Callithrix jacchus*). *J. Comp. Neurol.* **443,** 168–182.

Randolph, M., and Semmes, J. (1974). Behavioral consequences of selective subtotal ablations in the postcentral gyrus of *Macaca mulatta*. *Brain Res.* **70,** 55–70.

Rausell, E, and Jones, E.G. (1991). Chemically distinct compartments of the thalamic VPM nucleus in monkeys relay principal and spinal trigeminal pathways to different layers of the somatosensory cortex. *J. Neurosci.* **11,** 226.

Reed, C.L., Caselli, R.J., and Farah, M.J. (1996) Tactile agnosia: Underlying impairment and implications for normal tactile object recognition. *Brain* **119,** 875–888.

Rizzolatti, G., Fogassi, L., and Gallese V. (1997). Parietal cortex: From sight to action. *Curr. Opin. Neurobiol,* **7,** 562–567.

Roland, P.E. (1987a). Somatosensory detection of microgeometry, macrogeometry and kinesthesia after localized lesions of the cerebral hemispheres in man. *Brain Res. Rev.* **12,** 43–94.

Roland, P.E. (1987(b). Somatosensory detection in patients with circumscribed lesions of the brain. *Exp. Brain Res.* **66,** 303–317.

Roland, P.E., Shinhj, E., Lassen, N.A., and Larsen, B. (1980). Different cortical areas in man in organization of voluntary movements in extrapersonal space. *J. Neurophysiol.* **43,** 137–150.

Rothemund, Y., Qi, H.-X., Collins, C.E., and Kaas, J.H. (2002). The genitals and gluteal skin are represented lateral to the foot in anterior parietal somatosensory cotex of macaque. *Somatosen. Mot. Res.* **19,** 302–315.

Sadjadpour, K., and Brodal, A. (1968). the vestibular nuclei in man. A morphological study in the light of experimental findigns in the cat. *J. Hirnforsch.* **10,** 299–323.

Sakai, K. Watanabe, E., Onodera, Y., Itagaki, H., Yamamoto, E., Koizumi, H., and Miyashita, Y. (1995). Functional mapping of the human somatosensory cortex with echo planar MRI. *Magn. Reson. Med.* **33,** 736–743.

Sastre-Janer, F.A., Regis, J., Belin, P., Mangin, J.F., Dormont, D., Masure, M.C., Remy, P., Frouin, V., and Samson, Y. (1998). Three-dimensional reconstruction of the human central sulcus reveals a morphological correlate of the hand area. *Cereb. cortex* **8,** 641.

Schroeder, C.E., Lindsley, R.W., Specht, C., Marcovici, A., Smiley, J.F., and Javitt, D.C. (2001). Somatosensory input to auditory association cortex in macaque monkey. *J. Neurophysiol.* **85,** in press.

Schroeder, D.M., and Jane, J.A. (1976). the intercollicular area of the inferior colliculus. *Brain Behav. Evol.* **13,** 125–141.

Seike, M. (1993). A study of the area of distribution of the deep sensory neurons of the human ventral thalamus. *Stereotact. Funct. Neurosurg.* **61,** 12–23.

Seltzer, B., and Pandya, D. (1980). Converging visual and somatic sensory cortical input to the intraparietal sulcus of the rhesus monkey. *Brain Res.* **192,** 339–351.

Semmes, J., Weinstein, S., Ghent, L., and Teuber, H.L. (1960). "Somatosensory Change after Penetrating Brain wounds in Man." Harvard Univ. Press, Cambridge Mas.

Shandlen, M.N., and Newsome, W.T. (1996). Motion perception: Seeing and deciding. *Proc. Nat Acad Sci.* **93,** 628–633.

Sirigu, A., Duhamel, J.R., Cohen, L., Pillon, B., Dubois, B., and Agid, Y. (1996). T6 mental representation of hand movements after parietal cortex damage. *Science* **273,** 1564–1568.

Smith, G.E. (1970). A new topographic survey of the cerebral cortex: Being an account of the distribution of the anatomically distinct cortical areas and their relationship to the cerebral sulci. *J. Anat.* **42,** 237–254.

Snyder, L.H., Batista, A.P., and Andersen, R.A. (2000). Intention-related activity in posterior parietal cortex: A review. V.s. Res. **40,** 1433–1441.

Srinivasan, M.A., and LaMote, R.H. (1987). Tactile discrimination of shape: Responses of slowly and rapidly adapting mechano-receptive afferents to a step indented into the monkey fingerpad. *J. Neurosci.* **7,** 1682–1697.

Steinmetz, M.A., Connor, C.E., Constantinidis, C., and McLaughlin, J.R. (1994). Covert attention suppresses neuronal responses in area 7a of the posterior parietal cortex. *J. Neurophysiol.* **72,** 1020–1023.

Sur, M. (1980). Receptive fields of neurons in areas 3b and 1 of somatosensory cortex in monkeys. *Brain Res.* **198,** 465–471.

Sur, M., Garraghty, P.E., and Bruce, C.J. (1985). Somatosensory cortex in macaque monkeys: Laminar differences in receptive field size in areas 3b and 1. *Brain Res.* **342,** 391–395.

Sur, M., Wall, J.T., and Kaas, J.H. (1984). Modular distribution of neurons with slowly adapting and rapidly adapting responses in area 3b of somatosensory cortex in monkeys. *J. Neurophysiol.* **51,** 724–744.

Sweet, W.N., White, J.C., Selveston, B., and Nilges, R.O. (1950). Sensory responses from anterior roots and from surface and interior of spinal cord in man. *Trans. Am. Neurol. Assso.* **75,** 165.

Taoka, M., Toda, T., and Iwamura, Y. (1998). Representation of the body midline trunk, bilateral arms, and shoulders in the monkey postcentral somatosensory cortex. *Exp. Brain Res.* **123,** 315–322.

Tasker, R.R., Organ, L.W., Rose, I.H., and Hawrylyshyn, P. (1976). Human spinothalamic tract—Stimulation mapping in the spinal cord and brain stem. *Adv. Pain Res. Ther.* **1,** 252–257.

Tasker, R.R., Richardson, P., Rewcastle, B., and Emmers, R. (1972). Anatomical correlation of detailed sensory mapping of the human thalamus. *Confin. neurol.* **34,** 184–196.

Taylor, L., and Jones, L. (1997). Effects of lesions invading the postcentral gyrus on somatosensory thresholds on the face. *Neuropsychologica* **7,** 953–961.

Thier, P., and Andersen, R.A. (1998). Electrical microstimulation distinguishes distinct saccade-related areas in the posterior parietal cortex. *J. Neurophysiol.* **80,** 1713–1735.

Torebjork, H.E., Ochoa, J.L., and Schady, W.J.L. (1984). Role of single mechanoreceptor units in tactile sensation. In "Somatosensory Mechanisms" (C. Von Euer, O. Franzen, U. Lindblom, and J.D. Ottoson, eds.), pp. 173–183. Macmillan, London.

Truex, R.C., Taylor, M.J., Smythe, M.Q., and Gildenberg, P.L. (1970). The lateral cervical nucleus of cat, dog, and man. *J. Comp. Neurol.* **139,** 93–98.

Vallbo, A.B. (1981). Sensations evoked from the glabrous skin of the human hand by electrical stimulation of unitary mechano-receptive afferents. *Brain Res.* **215,** 359–363.

Vallbo, A.B., Olsson, K.A., Westberg, K.G., and Clark, F.J. (1984). Microstimulation of single tactile afferents from the human hand. *Brain* **107,** 727–749.

Vallbo, K., Nicotra, G., Wiberg, M., and Bjaalie, J.G. (1999). Monkey somatosensory cerebrocerebellar pathways: Uneven densities of corticopontine neurons in different body representations of areas 3b, 1, and 2. *J. Comp. neurol.* **406,** 109–128.

Van Buren, J.M., and Borke, R.C. (1972). "Variations and Connections of the Human Thalamus," Vol. 1. Springer-Verlag, Berlin, New York.

Van Buren, J.M., Borke, R.C., and Modesti, L.M. (1976). Sensory and nonsensory portions of the nucleus "ventralis posterior" thalami of chimpanzee and man. *J. Neurosurg.* **45,** 37–48.

Vierck, C.J., and Cooper, B.Y. (1998). Cutaneous texture discrimination following transection of the dorsal spinal column in monkeys. *Somatosen. Mot. Res.* **15,** 309–315.

Vogt, C., and Vogt, O. (1919). Allgemeinere ergebnisse unsere hirnforschung. *J. Physiol. Neurol.* **25,** 279–462.

Vogt, C., and Vogt, O. (1926). Die vergleichend-arkitektonische und die vergleichend-reizphysiologische Felderung der Grosshirnrinde unter besonderer Berucksichtigung der Menchlichen, *Naturwissenchaften* **14,** 1191.

von Economo, C. (1929). "The Cytoarchitectonics of the Human Cortex." Oxford Univ. Press, London, New York.

von Economo, C., and Koskinas, G.N. (1925). "Die Cytoarchitectonik der Hirnrinde des erwachsenen Menschen." Springer-Verlag, Berlin.

Wall, P.D. (1970). The sensory and motor role of impulses travelling in the dorsal columns toward cerebral cortex. *Brain* **93,** 505–524.

Wall, P.D., and Noordenhos, W. (1977). Sensory functions which remain in man after complete transection of dorsal columns. *Brain* **100,** 641–653.

Welker, W.I. (1974). Principles of organization of the ventrobasal complex in mammals. *Brain Behav. Evol.* **7,** 253–336.

Werner, G., and Whitsel, B.L. (1967). The topology of dermatomal projection in the medial lemniscal system. *J. Physiol. (London)* **192,** 123–144.

Westling, G., and Johansson, R.S. (1987). Responses in glabrous skin mechanoreceptors during precision grip in humans. *Exp. Brain Res.* **66,** 128–140.

White, L.E., Andrews, T.J., Hulette, C., Richards, A., Groelle, M., Paydortor, J., and Purves, D. (1997). Structure of the human sensorimotor system. I. Morphology and cytoarchitecture of the central sulcus. *Cereb. Cortex* **7,** 18–30.

Whitsel, B.L., Petrucelli, L.M., Ha, H., and Dryer, D.A. (1972). The resorting of spinal afferents as antecedent to the body representation in the postcentral gyrus. *Brain Behav. Evol.* **5,** 303–342.

Whitsel, B.L., Petrucelli, L.M., and Sapiro, G. (1969). Modality representation in the lumbar and cervical fasciculus gracilis of squirrel monkeys. *Brain Res.* **15,** 67–78.

Wiesendanger, M., and Miles, T.S. (1982). Ascending pathway of low-threshold muscle afferents to the cerebral cortex and its possible role in motor control. *Physiol. Rev.* **62,** 1234–1270.

Wllis, W.D., Jr. (1985). "The Pain System." Karger, New York.

Wllis, W.D., and Coggeshall, R.E. (1991). "Sensory Mechanisms of the Spinal Cord," 2nd ed. Plenum Press, New York.

Woolsey, C.N., Erickson, T.C., and Gilson, W.E. (1979). Localization in somatic sensory and motor areas of human cerebrum as determined by direct recording of evoked potentials and elecrical stimulation. *J. Neurosurg.* **51,** 476–506.

Wu, C.W-H., Bichot, N.P., and Kaas, J.H. (2000). Converging evidence from microstimulation, architecture, and connections for multiple motor areas in the frontal and cingulate cortex of prosimian primates. *J. Comp. Neurol.* **423,** 140–177.

Xu, J., and Wall, J.T. (1996). Cutaneous representation of the hand and other body parts in the cuneate nucleus of a primate, and some relationships to previously described cortical representations. *Somatosen. Mot. Res.* **13,** 187–197.

Xu, J., and Wall, J.T. (1999). Functional organization of tactile inputs from the hand in the cuneate nucleus and its relationship to organization in the somatosensory cortex. *J. Comp. Neurol.* **411,** 369–389.

Yin, T., and Medjbeur, S. (1988). Cortical association areas and visual attention. *In* "Comparative Primate Biology" (H.P. Steklis and J. Erwin, eds.), vol. 4, pp. 393–419. Liss, New York.

Zainos, A., Merchant, H., Hernandez, A., Salinas, E., and Romo, R. (1997). Role of primary sensory cortex in categorization of tactile stimuli: Effects of lesions. *Exp. Brain Res.* **115,** 357–360.

Zilles, K., Schlaug, G., Matelli, M., Luppino, G., Schleincher, M., Qu, M., Dabringhaus, A., Seitz, R., and Roland, P.E. (1995). Mapping of human and macaque sensorimotor areas by integrating architectonic transmitter receptor, MRI and PET data. *J. Anat.* **187,** 515–537.

CHAPTER

29

Trigeminal Sensory System

PHIL M. E. WAITE and KEN W. S. ASHWELL
Department of Anatomy, School of Medical Science
The University of New South Wales
Sydney, Australia

Although generally considered part of the somatosensory system, the trigeminal sensory system has been assigned its own chapter for this second edition of the *Human Nervous System*. This chapter will address the unique anatomy of the pathway for facial sensations, involving the trigeminal ganglion and its associated nuclei within the brainstem. We will also comment on the innervation of specialized cranial structures such as the teeth, tongue, meninges, cornea, conjunctiva, and oral and nasal mucosa. Recent studies on the involvement of the trigeminal system in clinically relevant conditions such as toothache, headache, and trigeminal neuralgia are considered.

In outline, the trigeminal or fifth cranial nerve is a general sensory nerve carrying touch, temperature, nociception, and proprioception from the superficial and deep structures of the face. Trigeminal means literally "three twins" and refers to the three peripheral nerves that take origin together (i.e., are born) from each ganglion, the ophthalmic (V_1), maxillary (V_2), and mandibular (V_3) divisions. The central processes of the trigeminal ganglion cells form the trigeminal sensory root (or portio major), which enters the brainstem at midpontine level. Most fibers bifurcate to terminate in both the main sensory nucleus (Pr5, principal trigeminal nucleus) and the nuclei of the spinal trigeminal tract (Sp5, spinal trigeminal nuclei). A unique feature of the pathway is the location of proprioceptive neurons in the mesencephalic nucleus (Me5) in the brainstem, rather than in the trigeminal ganglion. From the trigeminal nuclei, second-order fibers concerned with sensation project via the dorsal and ventral trigeminothalamic tracts to several regions of the somatosensory thalamus, adjacent to projections from spinal inputs. Facial inputs then run parallel to the spinal thalamocortical projections to supply somatosensory regions of the cortex. The trigeminal motor nucleus and nerve, innervating the muscles of mastication, the mylohyoid

and anterior digastric, and the tensor tympani and tensor veli palatini muscles, will not be considered here. For the development of the receptors, trigeminal nerves and ganglion, see Chapter 4.

RECEPTORS AND THEIR INNERVATION

Receptors for the facial skin and scalp (reviewed Darian-Smith, 1973; Iggo, 1974) are similar to those in hairy skin of other body regions and are fully discussed in Chapter 28. For the glabrous skin of the lips, a comparative study reported a variety of encapsulated receptors, with the most complex structures seen in primates including man (Kadanoff *et al.*, 1980). Muscle spindles in facial and jaw muscles are similar in structure to those elsewhere in the body and are only discussed with reference to the location of their afferent somata and central connections. While innervation of the temporomandibular joint also corresponds to that for other synovial joints, it has attracted considerable recent clinical interest and so is briefly reviewed here.

Skin of the face is remarkable for its high tactile sensitivity, with pressure thresholds lower than any other body regions, in both men and women (Weinstein, 1968). The upper lip, nose, and tip of the tongue have the lowest detection thresholds reported (Rath and Essick, 1990). Regional differences in sensitivity to different stimuli have been reported, with the glabrous lip skin (vermilion) being especially sensitive to vibration and motion, compared with adjacent perioral hairy skin (Rath and Essick, 1990). For two-point discrimination, fingers have rather lower values (2.1 mm) than facial skin (3.3 mm, nose; 5–6 mm, upper perioral skin), although the tip of the tongue was lowest at 0.99 mm (McNutt, 1975; Rath and Essick, 1990).

Recordings from the human infraorbital nerve by microneurography, showed a high proportion of receptive fields at the angle of the mouth, indicating particularly dense innervation of perioral skin (Johansson *et al.*, 1988). Both slowly and rapidly adapting responses were recorded, similar to those reported for the hand (Vallbo *et al.*, 1979). Receptive fields for rapidly adapting units ranged from 2 to 118 mm^2 (median 17 mm^2) compared with 2 to 88 mm^2 (median 7 mm^2) for slowly adapting responses. Rapidly adapting thresholds were lower (median 0.5 mN) than for slowly adapting responses (cutaneous units, median 1 mN; mucosal, median 1.5 mN). A recent study on the tongue, also using microneurography to record from single nerve fibers, indicates that receptive fields (1–20 mm^2, mean 2.4 mm^2) and detection thresholds (0.03–2 mN, mean 0.15 mN) may be lower there than for any other body region (Trulsson and Essick, 1997).

Innervation of Specialized Cranial Structures: Teeth and Periodontal Ligament

Human permanent incisors and canines each receive about 360 myelinated fibers and some 1500–2000 unmyelinated afferents in adults (Johnsen and Johns, 1978). Small myelinated fibers include cholinergic afferents, while many unmyelinated fibers contain substance P and CGRP (Byers, 1984; Silverman and Kruger, 1987). Galanin-immunoreactive fibers have also been reported in several species including human (Wakisaka *et al.*, 1996). These fibers terminate mainly in free nerve endings, especially within the dental pulp (Fig. 29.1). Endings can extend for up to 200 μm into the dentinal tubules in both monkey and human teeth, particularly near the cusps of the crown (Byers and Dong, 1983; Frank, 1968). Besides these afferent fibers, unmyelinated sympathetic fibers supply blood vessels within the tooth pulp (Anneroth and Norberg, 1968). Although innervation is mainly ipsilateral, Byers and Dong (1983) used autoradiography to show that some contralateral innervation occurs in monkey mandibular incisors and canines. After tooth loss and reimplantation, reinnervation of human teeth can occur, although the number and caliber of regenerating fibers is reduced (Ohman, 1965).

Electrical, chemical, mechanical, and thermal stimuli can activate tooth receptors and usually give rise to the sensation of pain (reviewed Schults, 1992). Pain can be associated with dentinal, pulpal, gingival, or periodontal receptors, each with particular but overlapping characteristics (Sharav *et al.*, 1984). For dentinal receptors, pain is generally not spontaneous but evoked by heat, cold, and sweet stimuli. The transduction mechanism may involve odontoblasts, though this matter is not resolved. Dull ache is thought to arise from activity in unmyelinated axons, common within the tooth pulp. Pulpal pain is associated with inflammation, can be spontaneous, is generally poorly localized, and may outlast the stimulus (Hensel and Mann, 1956). The response of pulpal nerves to tooth injury and inflammation has been reviewed by Fristad (1997). In rodents, inflammation of the pulp and periodontium results in up-regulation of substance P and CGRP, as in other tissues.

Besides receptors within the tooth, the human periodontal ligament is rich in free nerve endings and a variety of coiled and Ruffini-type endings (Fig. 29.1; Maeda *et al.*, 1990; Lambrichts *et al.*, 1992). Fibers containing substance P have been demonstrated here and are likely to be associated with periodontal pain

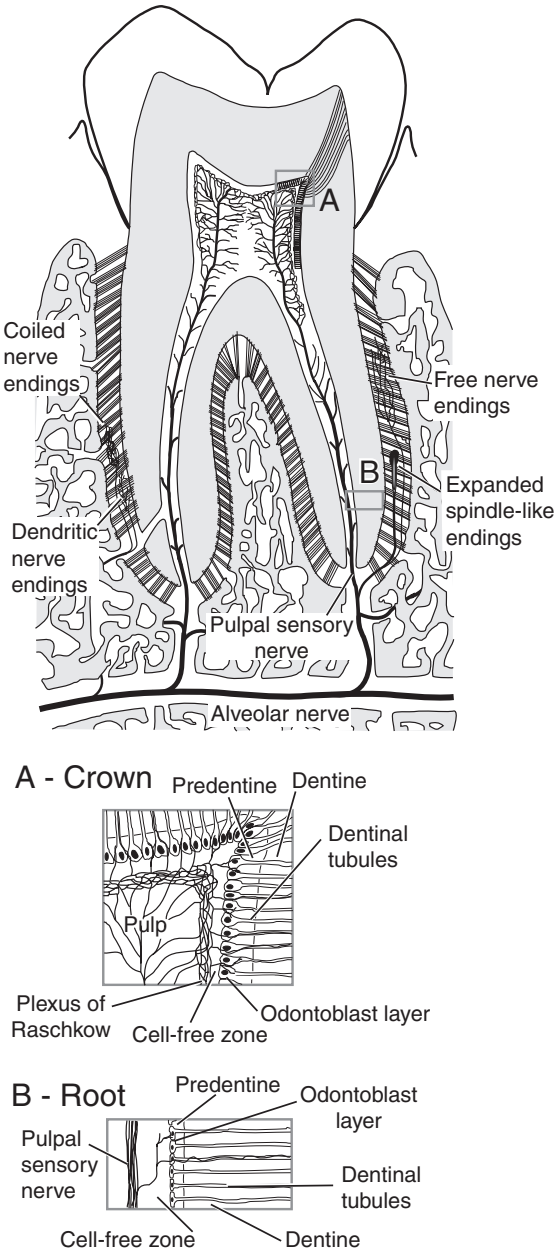

FIGURE 29.1 Diagram showing the distribution of nerve endings associated with the teeth. Free nerve endings are found within the pulp cavity and periodontium, and nerve fibers extend into the dentinal tubules. Coiled and expanded terminals also occur in the periodontium. (A) Details of pulpal and tubular innervation in the crown. (B) Innervation of dentinal tubules in the root.

(Fristad, 1997). Such pain is usually well localized and exacerbated by pressure.

In addition to nociceptors, microneurography of the inferior alveolar nerve in humans during applications of forces to the teeth has confirmed the presence of low-threshold, slowly adapting mechanoresponses from the periodontium (Trulsson and Johansson, 1996). These receptors encode food contact during biting and continuously discharge when food is held between the incisors. These response properties indicate that periodontal receptors are likely to contribute to the sensation of "dental touch" and the control of mastication, particularly on initial contact with food and its manipulation. Somata from periodontal afferents are found in both Me5 and the trigeminal ganglion (reviewed Capra and Dessem, 1992).

Temporomandibular Joint

The innervation of the temporomandibular joint (TMJ) has attracted interest in recent years, at least in part because of the involvement of the joint in a variety of painful conditions (see later). Immunostaining with neurospecific markers has shown that the human joint capsule and peripheral disc is richly innervated (Morani *et al.*, 1994). Most studies in humans have reported encapsulated receptors and free nerve endings in the joint capsule (Griffin and Harris, 1975; reviewed Zinny, 1988) and only free endings in the disc (Fig. 29.2A). However, Morani *et al.* (1994) found only free nerve endings in both locations. Reports on corpuscular endings in animals are also inconsistent with Ruffini-type and Paciniform endings described in cat and sheep, but only with free nerve endings in the mouse and rat (Dreessen *et al.*, 1990; Ichikawa *et al.*, 1990; Tahmasabi-Sarvestani *et al.*, 1996).

An interesting study on the fetal development of innervation in the human TMJ showed that nerves were present from around 9–10 weeks (Ramieri *et al.*, 1996). Innervation of the disc was particularly dense by 20 weeks and included encapsulated endings; however, this regressed during the third trimester. In adults, disc innervation was restricted to the periphery and only free nerve endings were present.

Oral Mucosa and Tongue

The oral mucosa in several primates, including humans, contains Merkel cells and free nerve endings (Fortman and Winkelmann, 1977; Luzardo-Baptista, 1973), although Ruffini endings were reportedly absent (Halata and Munger, 1983). In the human gingiva, fibers containing CGRP and substance P were seen in the lamina propria, as well as fibers containing NPY, tyrosine hydroxylase, and VIP in association with blood vessels (Luthman *et al.*, 1988). It was considered likely that the CGRP and Substance P fibers were sensory, probably associated with nociception.

In primate tongue, Meissner's corpuscles are found in the dermis close to the epidermal border, Ruffini-type endings occur in deeper dermal regions, and free

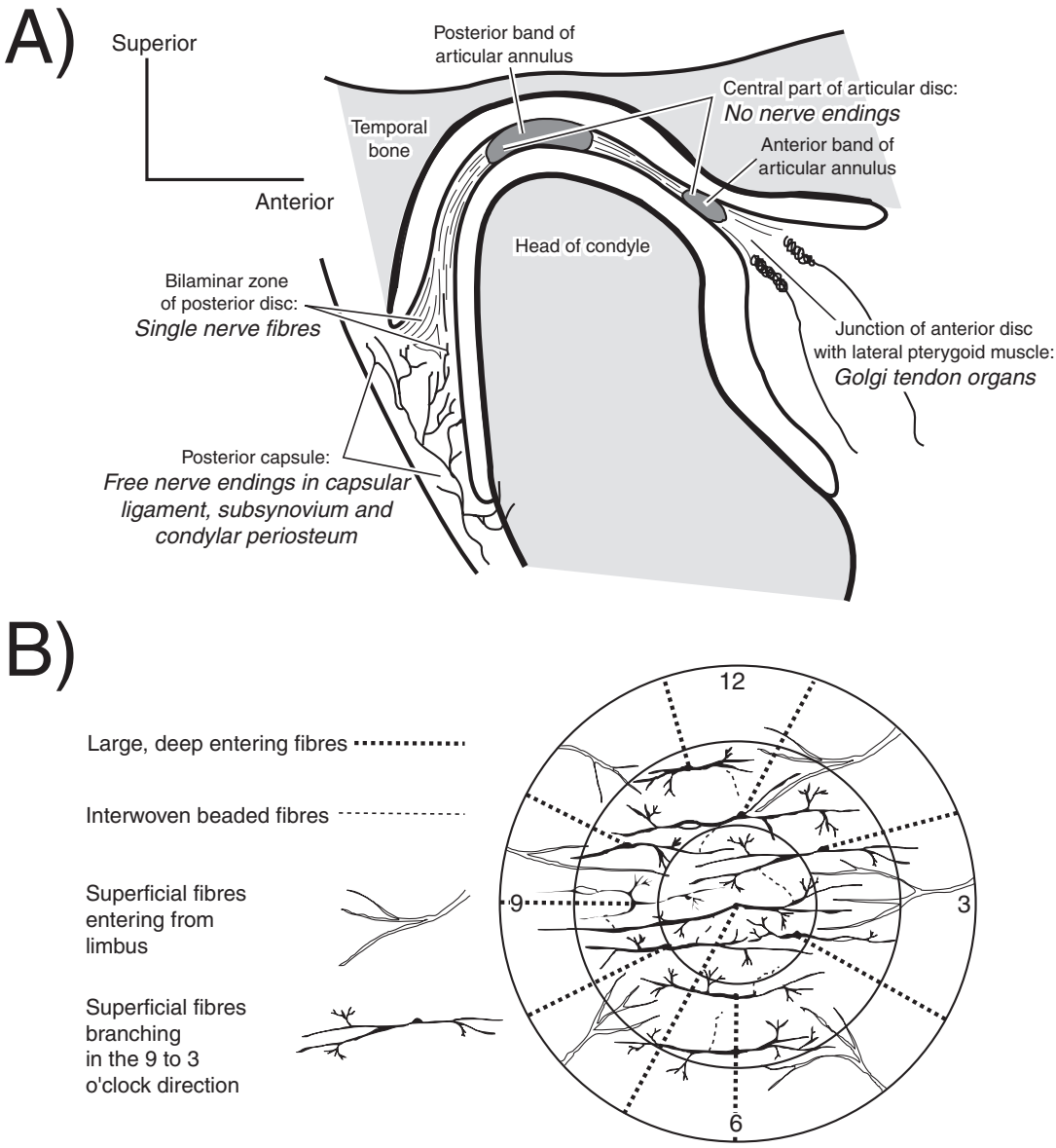

FIGURE 29.2 **(A)** Diagram showing a sagittal section through the temporomandibular joint. Encapsulated and free nerve endings are present in the posterior capsule and tendon of lateral pterygoid muscle. Free nerve endings are distributed to the periphery of the disc but are absent from the central region. **(B)** Diagram to show the distribution of nerves within the cornea. Fibers initially enter radially and then assume a predominantly temporonasal orientation within the stroma (from Figure 7, Müller *et al.*, 1997, Architecture of human corneal nerves. Invest. Ophthalmol. Vis. Sci. 38: 984–994, with permission from the copyright holder, the Association for Research in Vision and Ophthalmology, and the author).

nerve endings terminate within the epidermis (Zahm and Munger, 1985). Merkel cell complexes were not seen, confirming results from a previous study (Munger, 1973). Trigeminal afferents also innervate tongue papillae in primates and occasionally enter taste buds where they have been suggested to serve a trophic function (Zahm and Munger, 1985). Knock out studies in mice indicate that the development of gustatory and somatosensory afferents to the tongue require different trophic factors, namely BDNF for gustatory nerves and NT3 for trigeminal afferents (Nosrat, 1998).

The lingual nerve, a branch of the mandibular division, supplies tactile sensation for the anterior two-thirds of the tongue. A study of electrical activity recorded from the human lingual nerve showed some nerve fibers with low mechanical thresholds (mean force 0.15 mN) and small receptive fields (mean area 2.4 mm^2) considered to terminate near the tongue

surface (Trulsson and Essick, 1997). As noted earlier, these are lower than for any other site on the body. Both rapidly adapting responses and two types of slowly adapting units (SA I and SA II) were recorded, similar to those reported from the glabrous skin of the human hand. Generally, slowly adapting responses have been considered to be associated with Merkel cells (SA I) and Ruffini endings (SA II), so the lack of anatomically identified Merkel cells in the tongue requires reassessment. Besides these responses, lingual nerve responses to mechanical and thermal (cold) stimuli have been described (Kosar and Schwartz, 1990).

Two-point discrimination studies on the sides and tip of the tongue showed the tip had the lowest values (Ringel and Ewanowski, 1965; McNutt, 1975). However, there was an interesting difference in two point-discrimination values for the two sides in approximately half of the adults, which was not present in the children (McNutt, 1975). Either side could be more sensitive, with equal frequency. Because laterality differences were only noted in adults, they were attributed to central neural changes rather than peripheral mechanisms.

Cranial Vessels and Meninges

Major cranial blood vessels such as the middle cerebral and scalp arteries are richly innervated by trigeminal afferents, with fibers containing substance P found in the media and adventitia (Helme and Fletcher 1983; Chapter 37). A study of human temporal arteries showed both CGRP and substance P in nerve fibers in the adventitia and around the adventitia–media border (Jansen *et al.*, 1986). Two neuronal ganglia have been described on the human internal carotid artery (Suzuki and Hardebo, 1991). Although the majority of cells within these ganglia were considered to be parasympathetic, some contained CGRP and substance P, and it was suggesting a sensory function.

The dura of the anterior and middle cranial fossae receives trigeminal innervation. Animal studies have shown that the dural afferents contain substance P and CGRP (Andres *et al.*, 1987; Keller and Marfurt, 1991). Most end simply as free nerve endings within the connective tissue or adjacent blood vessels (rat, Knyihár-Csillik *et al.*, 1997). Release of peptides from these endings has been implicated in migraine (see later).

Cornea, Conjunctiva, and Nasal Mucosa

Human cornea and conjunctiva, like those of other mammals, are innervated by ophthalmic trigeminal afferents as well as sympathetic and parasympathetic efferents (Ruskell, 1985; Elsås *et al.*, 1994). Fibers containing CGRP, substance P, acetylcholine and catecholamines have all been confirmed in human cornea (Toivanen *et al.*, 1987; Ueda *et al.*, 1989; Uusitalo *et al.*, 1989). Radially oriented fiber bundles enter the cornea from the sclera and then travel, mainly with a temporonasal orientation (Fig. 29.2B), within the stroma (Müller *et al.*, 1997). Fibers penetrate Bowman's membrane and terminate between epithelial cells, mainly in the deeper layers (Müller *et al.*, 1996). Both myelinated Aδ and unmyelinated C fibers have been described in the peripheral cornea, although central cornea contains only unmyelinated fibers (Müller *et al.*, 1996). In the living human, cornea innervation can be studied with slit-scanning confocal microscopy (Auran *et al.*, 1995). This technique has been used to study regeneration of corneal innervation after operative procedures (Heinz *et al.*, 1996; Ritcher *et al.*, 1997).

The corneal innervation lacks any encapsulated receptors, being innervated by free nerve endings only (Weddell and Zander, 1950). Recordings in animals indicate that both mechanosensitive and thermosensitive afferents are present (Belmonte and Giraldez, 1981). The corneal responses are similar to those from Aδ and C skin afferents, except that mechanical thresholds are lower. In humans, most studies suggest that the only sensation evoked by corneal stimulation is pain (Beuerman and Tanelian, 1979). Lele and Weddell (1956) showed subjects could distinguish touch, cold, warmth and pain from the cornea; however, the stimulus used was air streams, and it is difficult to prevent the spread of air to adjacent conjunctiva or eyelids (Schults, 1992). The dense innervation of eyelid skin and eyelashes is well known, with Ruffini-type endings, lanceolate terminals, and Merkel cell complexes (monkey, Halata and Munger, 1980).

Trigeminal afferents also provide general somatic afferents to the nasal mucosa, again with free nerve endings only. Sensory fibers containing substance P and CGRP have been described in nasal epithelium (Hauser-Kronberger *et al.*, 1997). For the nasal vasculature, CGRP and neurokinin A fibers innervate arterial vessel walls, along with parasympathetic and sympathetic efferents (Baraniuk, 1992; Riederer *et al.*, 1995). Receptors for substance P (neurokinin 1) are present in human airway epithelium and submucosal glands (Shirasaki *et al.*, 1998), and substance P has been implicated in reflexes such as sneezing and allergic reactions (Nieber *et al.*, 1991; Baraniuk, 1992). Stimulation of nasal mucosa commonly results in a tingling sensation, which may outlast the duration of stimulation (Melzack and Eisenberg, 1968). Besides mechanical activation, many odorants stimulate trigeminal as well as olfactory afferents, although trigeminal thresholds

are generally higher (Doty, 1995). Such trigeminal sensations are described as irritant or pungent and have been shown to modify olfactory sensations.

TRIGEMINAL NERVES, GANGLION, AND ROOT

Peripheral Nerves

The three main trigeminal nerve divisions—ophthalmic, maxillary, and mandibular—together constitute the largest of the cranial nerves (reviewed Shankland, 2000). The mandibular division is the largest with some 78,000 myelinated fibers, compared with 50,000 fibers in the maxillary and only 26,000 in the ophthalmic divisions (Pennisi *et al.,* 1991). Myelinated fiber diameters range from 0.8 to 16 μm, with a similar bimodal distribution in each division (although the motor component of the mandibular division contains fibers with a larger diameter spectrum, 4–20 μm). Each division supplies a distinct dermatome on the head and face and the adjacent mucosal and meningeal tissues (Brodal, 1965; reviewed Usunoff *et al.*, 1997). Unlike spinal dermatomes, trigeminal nerve distributions show relatively little overlap. There is, however, considerable overlap with inputs from second and third cervical roots and vagal nerves (monkey, Denny-Brown and Yanagisawa, 1973). Communicating nerves between branches of the facial and trigeminal nerves are common. The best known of these is the chorda tympani, but others, such as the auriculotemporal, have been described (Namking *et al.*, 1994).

Fibres from the autonomic nervous system frequently join trigeminal nerves to reach peripheral tissues. Thus sympathetic fibers from the superior cervical ganglion travel with the external carotid artery then join the peripheral trigeminal nerves to reach sweat and mucosal glands in the facial skin and oral and nasal cavities. Sympathetic fibers also supply blood vessels in the connective tissue around the ganglion and nerves, as recently described by Smolier *et al.* (1998, 1999). Each trigeminal branch also receives parasympathetic fibers: the ophthalmic nerve from the ciliary ganglion, the maxillary from the pterygopalatine ganglion, the mandibular nerve from submandibular and otic ganglia. In addition, fibers from the facial nerve (chorda tympani) join the lingual nerve to provide the gustatory afferents for the anterior tongue.

Each trigeminal nerve branch exits the skull independently: the ophthalmic nerve through the superior orbital fissure, the maxillary nerve via the foramen rotundum and across the pterygopalatine fossa, and the mandibular nerve through the foramen ovale and the infratemporal fossa. Proprioceptive inputs from muscle spindles in the jaw muscles and some from the periodontal ligament travel with the motor nerve branch and have somata located in Me5 in the brainstem, rather than in the trigeminal ganglion. While the presence of muscle spindles is well established for jaw-closing muscles (temporalis, medial pterygoid, masseter; monkey, Kubota *et al.*, 1973; human, Voss, 1935; Freimann, 1954), their existence in jaw opening muscles (lateral pterygoid, digastric) was initially debated. They have been confirmed in the human lateral pterygoid (Gill, 1971; Rakhawy *et al.*, 1971) and the anterior belly of the digastic muscle in monkey and human (Voss, 1956). Recordings from mesencephalic tract axons in monkeys indicate that masseter muscle spindles are active during muscle contraction, rather than preceding it (therefore they are not gamma activated, Matsunami and Kubota, 1972). Animal studies indicate that other proprioceptive endings (e.g., Golgi tendon organs in jaw muscles and extraocular muscle spindles) have somata mainly in the ganglion; the location of any extraocular muscle proprioceptors in Me5 is controversial (reviewed Donaldson, 2000). For muscles of facial expression, propriceptive fibers may travel to the ganglion in the communicating nerves described between the facial and trigeminal paths (Namking *et al.*, 1994).

Trigeminal Ganglion

The trigeminal (semilunar, Gasserian ganglion) is crescent shaped and lies in Meckel's cave adjacent to the petrosal bone (Ferner, 1940). The gross morphology of the human ganglion in relation to the dura and the surrounding structures has been described in detail elsewhere (Soeira *et al.*, 1994; Kehrli *et al.*, 1997). In a study of ganglia from 64 subjects from 2 months to 81 years old, the mean neuronal count was 80,600 with no significant age or sex difference (Ball *et al.*, 1982). However, there was a marked variation in individual samples (range 20,000–157,000), which is surprising and worth investigation. Ganglion cells are pseudounipolar and invested by satellite cells, with some showing complex interdigitations with the neuronal membrane (Beaver *et al.*, 1965). There is an approximate somatotopy with ophthalmic somata lying anteromedially, mandibular cells posterolaterally, and maxillary in between (cat; Marfurt *et al.*, 1989).

As in the dorsal root ganglia, trigeminal ganglion cells can be classed as large, light (type A) cells and smaller, dark (type B) cells (Lieberman, 1976). On the

basis of ultrastructure, immunohistochemistry, and cytochemistry, Kai-Kai (1989) included a third group of small type C cells. A variety of peptides are known to be present in the ganglion, particularly in the smaller cells (see Chapter 30). For the human these include CGRP, substance P, somatostatin, galanin, and enkephalins (Del Fiacco and Quartu, 1994; Quartu and Del Fiacco, 1994; Quartu *et al.,* 1996). In the human ganglion, nearly half of the cells contain CGRP, with about 15% containing substance P, and some showing colocalization (Helme and Fletcher, 1983; Quartu *et al.,* 1992). Such cells are thought to be associated with nociceptive transmission (see later). CGRP fibers also form pericellular baskets around some ganglion cells, particularly in the fetal and newborn ganglion (Quartu *et al.,* 1992). In the rat, these fibers were shown to make synaptic contacts with trigeminal ganglion cells (Yamamoto and Kondo, 1989), but these were not seen in the monkey and are not known for humans. As in animals, discrete populations of human ganglion cells have been shown to express trkA, trkB, and trkC, receptors for the neurotrophins, often coexpressed on substance P and/or CGRP immunoreactive cells (Quartu *et al.,* 1996). The percentage of neurotrophin positive cells was lower in adults than in perinatal ganglia.

Besides the peptides, another transmitter for the trigeminal ganglion, like dorsal root ganglia, is likely to be glutamate. Wanaka *et al.* (1987) reported that about 45% of the rat trigeminal ganglion cells contain glutamate, particularly the larger cells. However, Kai-Kai and Howe (1991), also working in rat, found a lower percentage with glutamate (32%), predominantly localized in smaller cells, and this is in agreement with Cangro *et al.* (1985). Glutamatergic terminals are found throughout the trigeminal sensory complex (rat, Clements and Beitz, 1991) and there is evidence for involvement of glutamate in low-threshold mechanoresponses as well as in nociceptive responses from the tooth pulp and cornea (rat, Clements *et al.,* 1991; Bereiter and Bereiter, 1996). The percentage of glutamatergic cells in the human ganglion is unknown.

Kai-Kai and Keen (1985) confirmed the presence of serotonin in type B neurons, and mast cells in the rat trigeminal and spinal ganglia. The location of serotonin in afferent termination zones in the dorsal horn has led to its suggested role as a putative transmitter in primary afferents (Kai-Kai, 1989).

Trigeminal Root and Tract

Central processes of trigeminal ganglion cells travel posteriorly in the large sensory root (portio major, radix sensoria) to enter the brainstem at midpontine level. The smaller "motor" root (portio minor, radix motoria) arises as two or more rootlets, which join together and pass inferiorly to the sensory root and ganglion, to travel with the mandibular nerve. The total number of sensory root fibers has been estimated as 140,000 (Young, 1977) and 170,000 (Pennisi *et al.,* 1991), similar to the number of peripheral nerve fibers (154,000, Pennisi *et al.,* 1991) but considerably higher than the number of ganglion cells (80,000; Ball *et al.,* 1982). Whether this represents branching of fibers or errors in counting is not known; the puzzlingly large range of values reported for ganglion cells from different individuals has already been noted. Approximately 50% of the root fibers are unmyelinated (Young, 1977), less than the commonly quoted figure for dorsal roots (70–80%); possible reasons for this, such as the importance of discriminative sensations from the face, are discussed by Young (1977). Myelinated fibers are smaller (0.3–11 μm) than in the peripheral nerve (Kerr, 1967).

Within the sensory root, both electrophysiological recordings in monkeys and results of lesions in humans suggest that there is an approximate somatotopy, with each division maintaining individual, but overlapping, territories (Pelletier *et al.,* 1974). However there is no separation of modalities, with mechanical, thermal, and nociceptive afferents being intermingled. Similarly, in the motor root, responses from jaw muscle spindles are intermingled with motor fibers. Inputs are ipsilateral except for 2–3 mm of contralateral skin at the tip of the nose (Cushing, 1904).

From the root, most fibers pass caudally to form the spinal trigeminal tract in the dorsal and lateral brainstem. The spinal tract lies adjacent to the spinal trigeminal nucleus and extends from midpons to the second cervical level, where it becomes continuous with Lissauer's tract (Fig. 29.3). Some, but not all, root fibers bifurcate to give a short ascending branch to the principal sensory trigeminal nucleus, which they enter from the lateral, ventrolateral, and ventral aspects. Within the spinal tract there is an approximate topography, with ophthalmic fibers lying ventrally; maxillary, intermediate; and mandibular, dorsally (reviewed Capra and Dessem, 1992; Usunoff *et al.,* 1997) with all three divisions represented at all levels (Kerr, 1963).

Tract axons are relatively small, with 90% having a diameter of less than 4 μm in man (Sjoqvist, 1938). Comparison of rostral and caudal regions of the tract shows fewer myelinated fibers caudally (Usunoff *et al.,* 1997). Golgi impregnation in humans and animal studies in rat and cat (Cajal and Ramon, 1909; Hayashi, 1985 a, b; reviewed Capra and Dessem, 1992) show

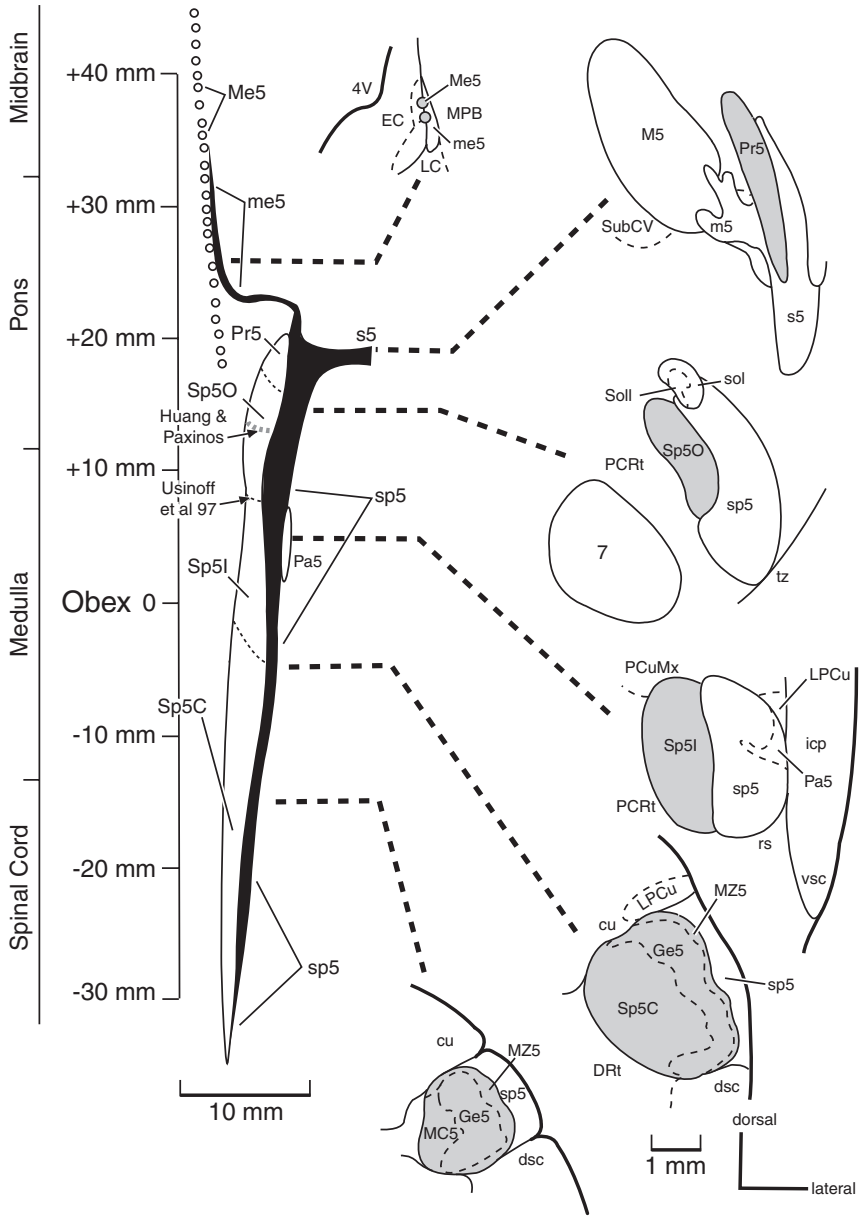

FIGURE 29.3 The left-hand side shows a diagrammatic representation of the brainstem trigeminal complex, drawn to scale from a dorsal view. The entering trigeminal root, s5, and tract Sp5 are shown in black. The mesencephalic (Me5), principal (Pr5), and spinal nuclei (Sp5I, SP50, Sp5C) are shown as well as the paratrigeminal nucleus (Pa5). Subnuclear borders are indicated; the border between Sp50 and Sp5I is shown at two locations, as described by Paxinos and Huang (1995) and Usunoff *et al.* (1997). The right-hand side of the figure shows the cross-sectional appearance of each of the nuclei (gray shading) and adjacent structures at the levels indicated, as taken from the atlas of Paxinos and Huang (1995, copyright Academic Press, reprinted with permission).

that individual axons in the tract give off a series of collateral branches that enter the nucleus at different levels. Collateral terminations in Sp5C show an arrangement that has been likened to an onion-skin, with midline and perioral face represented rostrally and more lateral facial skin represented caudally.

Mandibular and ophthalmic trigeminal primary afferents also cross the midline at caudal levels and project to the contralateral spinal nucleus caudalis (rat, Jacquin *et al.*, 1990; Marfurt and Rajchert, 1991; cat, Westrum and Henry, 1993), but this has not been confirmed in primates.

The trigeminal tract is joined by afferents from other nerves, such as the nervus intermedius, glossopharyngeal, vagal, and upper cervical nerves. Trigeminal afferents project to other brainstem regions, such as the nucleus of the solitary tract, and this has been confirmed in humans (Usunoff *et al.*, 1997). Projections to the solitary tract encompass both the rostral (gustatory) areas and caudal (cardiovascular, respiratory, and gastrointestinal) regions (rat, Marfurt and Rajchert, 1991). These inputs have been suggested to play a role in the integration of sensory activity from the mouth, pharynx, and oesophagus during mastication and swallowing.

Trigeminal afferents also project to the reticular formation, particularly alongside spinal nucleus interpolaris (reviewed Usunoff *et al.*, 1997). Direct projections to dorsal column nuclei have been reported, particularly to the cuneate nucleus and the external cuneate nucleus (monkey, Porter, 1986; Rhoton *et al.*, 1966). Such inputs have been suggested to be important in the integration of sensory inputs from neck muscles and cutaneous cranial afferents and for the coordination of head, neck, and eye movements (Porter, 1986). Finally, trigeminal projections to the paratrigeminal nucleus have been described in animals and it has been suggested that this nucleus plays a role in processing of nociceptive inputs (reviewed, Usunoff *et al.*, 1997). Trigeminal afferent inputs to regions such as the supratrigeminal nucleus and the motor trigeminal nucleus, as well as to vestibular nuclei, have been reported in animal studies but have not been substantiated in humans (reviewed by Usunoff *et al.*, 1997).

BRAINSTEM TRIGEMINAL SENSORY NUCLEI

The brainstem trigeminal sensory nuclei consist of the trigeminal sensory nuclear complex (the principal and spinal trigeminal nuclei), the mesencephalic nucleus, and a number of smaller collections of cells (paratrigeminal and peritrigeminal nuclei) thought to be predominantly sensory in function (see Chapter 10). These are all discussed later. Other trigeminal brainstem areas such as the motor trigeminal and intertrigeminal nuclei are associated with the motor control of jaw muscles (Lund and Olsson, 1983) and are not considered here. The supratrigeminal nucleus described in the mouse and cat is not seen in the human (Paxinos and Huang, 1995; Usunoff *et al.*, 1997), although Paxinos and Huang delineate a peritrigeminal zone around the motor nucleus.

Trigeminal Sensory Nuclear Complex, an Overview

The trigeminal nuclear complex is a long column of cells in the dorsolateral brainstem that extends from the rostral pons to the C_2 level, a distance of approximately 6 cm (Usunoff *et al.*, 1997). The complex is subdivided into four subnuclei (Fig. 29.3), the principal or main sensory trigeminal nucleus (Pr5), and three spinal trigeminal nuclei—oralis (Sp5O), interpolaris (Sp5I), and caudalis (Sp5C) (Olszewski, 1950; reviewed Capra and Dessem, 1992).

Animal studies using anatomical labeling (Marfurt, 1981; Shigenaga *et al.*, 1986), electrophysiological recordings (Eisenman *et al.*, 1963), and results of lesions in humans indicate a somatotopic organization throughout the complex, with the mandibular division lying dorsally; maxillary, centrally; and the ophthalmic, ventrally. Different facial regions are represented as long rostrocaudal columns of cells extending through the complex, with more midline regions (e.g., the nose) represented medially and more lateral skin represented laterally. However, particular facial regions have relative differences in central representation at the different levels, as noted later.

A major transmitter throughout the sensory complex is glutamate, with NMDA and non-NMDA receptors reported at all levels (rat, Petralia *et al.*, 1994; Tallaksen-Greene *et al.*, 1992). In addition, peptides such as substance P and CGRP are important transmitters, particularly for small diameter afferents, and may be colocalized with glutamate (Sessle, 2000). Ultrastructurally, a feature of synaptic organization at all trigeminal levels is the presence of synaptic glomeruli, in which a primary axon is surrounded by other terminals with axoaxonic synapses, with somewhat different structure at different levels (rat, Clements and Beitz, 1991).

Principal Sensory Trigeminal Nucleus

The principal sensory trigeminal nucleus is located in the lateral pontine tegmentum and extends for about 4 mm (from 17 to 20 mm rostral to the obex; Paxinos and Huang, 1995), approximately level with the motor trigeminal nucleus. In cross section, the nucleus is narrow and elongated dorsoventrally (Fig. 29.3). Most neurones are small and generally oval with some scattered medium-sized somata also present. Large neurones (more than 35 μm in diameter) are seen along the lateral border. Usunoff *et al.* (1997) describe a hint of dorsal and ventral subdivisions, with ventral cells somewhat larger and in clusters, while dorsal cells are smaller and more diffuse. However,

these subdivisions are less marked than in the cat (Shigenaga *et al.*, 1986b), and the dorsoventral subdivisions were not noted by Paxinos and Huang (1995). Ultrastructurally, Pr5 in both the rat and cat contains synaptic glomeruli (Gobel and Dubner, 1969; Gobel, 1971; Ide and Killackey, 1985).

Sections reacted for the enzyme acetylcholinesterase (AChE) show a striking organization of densely stained patches surrounded by paler regions. These patches are also seen with histochemical techniques for mitochondrial enzymes such as cytochrome oxidase (Goyal *et al.*, 1992). Animal studies indicate a similar parcellated organization. The patches of intense staining are particularly clear in rodents where they have a distinctive pattern and are known to be associated with the vibrissae (reviewed Waite and Tracey, 1995). However, they are also seen in the dorsal column nuclei in relation to the digits (Florence *et al.*, 1989). These patches have been considered to reflect regions of high innervation density (Goyal *et al.*, 1992). In rodents, similar patches also occur in spinal trigeminal nuclei Sp5I and Sp5C, but this has not been seen in primates (Noriega and Wall, 1991).

Animal studies have shown that cells in Pr5 are mechanoreceptive with low thresholds and small receptive fields (Jacquin *et al.*, 1988). Thus, Pr5 is thought to be analogous to the dorsal column nuclei in providing for discriminative tactile sensations for the face. It contains many projection cells, with its predominant projection being to the ventroposterior medial nucleus (VPM) of the thalamus. In the cat and rat, there is also a lesser projection to the posterior complex, Po (Jones, 1985) renamed as part of regio basalis (see Chapter 20), though this is unconfirmed in humans. In rodents, 60–70% of the projection cells in Pr5 contain glutamate (Magnusson *et al.*, 1987), though again this is not known for humans.

Pr5 also contains interneurones, many of which are immunoreactive for GABA (rat, Haring *et al.*, 1990). Somatostatin immunoreactive cells have also been described in the ferret (Boissonade *et al.*, 1993). In humans, somatostatin immunoreactive cells, fibers, and receptors are only seen in low levels in Pr5 (Bouras *et al.*, 1987; Carpentier *et al.*, 1996) and enkephalin-containing cells are present in the newborn (Yew *et al.*, 1991).

Spinal Trigeminal Nucleus Oralis

While all investigators agree that Sp5O extends caudally from Pr5 (level with the caudal pole of the motor trigeminal nucleus), its caudal boundary has been placed at different levels. Paxinos and Huang (1995) delineate an oblique caudal border level with the caudal pole of the facial motor nucleus (13 mm rostral to the obex), giving Sp5O a rostrocaudal extent of some 4 mm (Fig. 29.3). However, Usunoff *et al.* (1997) continue Sp5O to the level of the rostral pole of nucleus ambiguus (~7 mm rostral to the obex), a rostrocaudal distance of 10 mm. Sp5O is somewhat peanut-shaped in cross section. Usunoff *et al.* (1997) describe small (12–17 μm) oval cells and medium-sized oval, multipolar or fusiform cells (25–30 μm long and 10 μm or less wide).

AChE staining shows a few dark patches within the nucleus, especially within the central core (Paxinos and Huang, 1995). Studies in the rat, cat, and ferret have described subdivisions within the nucleus (e.g., dorsomedial and ventrolateral), but these were not noted by Usunoff *et al.* (1997) or Paxinos and Huang (1995). Many neurons in rodent Sp5O contain glutamate, likely to be the excitatory transmitter (Magnusson *et al.*, 1986). In the ferret, both somatostatin and enkephalin immunoreactive somata have been described (Boissonade *et al.*, 1993), and rodent Sp5O contains dispersed GABAergic cells (Haring *et al.*, 1990). Human Sp5O and Sp5I are high in receptors for somatostatin, although the functional significance of this in sensory processing is not yet clear (Carpentier *et al.*, 1996). Like Pr5, Sp5O contains synaptic glomeruli, often with glutamate immunoreactive profiles (rat, Clements and Beitz, 1991).

Sp5O has been shown to receive extensive intraoral projections (cat, Arvidsson and Gobel, 1981; Azerad *et al.*, 1982; rat, Marfurt and Turner, 1984; Takemura *et al.*, 1991) and this is consistent with loss of oral sensation after vascular lesions in humans (Graham *et al.*, 1988). Responses generally have very widespread receptive fields and can show modality convergence, for instance from both cutaneous and tooth receptors (rat, Jacquin and Rhoades, 1990). Indeed Sp5O has been implicated in intraoral pain, as discussed later. In the rat, Sp5O has extensive projections to the facial motor nuclei and spinal cord with less dense projections to the trigeminal motor nucleus, thalamus, and cerebellum (rat, Ruggiero *et al.*, 1981; Jacquin and Rhodes, 1990).

Spinal Trigeminal Nucleus Interpolaris

Located in the medulla, Sp5I extends between Sp5O and Sp5C. As noted earlier under Sp5O, there is some discrepancy about the rostral border of Sp5I; Paxinos and Huang (1995) delineate it as level with the caudal pole of the facial nucleus, whereas Usunoff *et al.* (1997) put the Sp5O/I border just rostral to nucleus ambiguus. Thus the rostrocaudal extent varies from 6 mm (Usunoff *et al.*, 1997) to about 13 mm (Paxinos and Huang, 1995).

With AChE staining, the nucleus stands out as an area of moderate to high reactivity. Usunoff *et al.* (1997)

describe a heterogeneous population of cells in human brain; many are small to medium-sized (15–20 μm) and oval or spindle-shaped. There are also some large scattered neurones (30–40 μm). Paxinos and Huang (1995) recognize a dorsomedial extension of Sp5I at caudal levels. Like Sp5O, the nucleus is crossed by prominent fiber bundles, for example from the glossopharyngeal nerve.

Sp5I has extensive inputs from intraoral structures, including tooth pulp, though these are generally less dense than for Sp5O (cat, Azerad *et al.,* 1982; rat, Marfurt and Turner, 1984; Takemura *et al.,* 1991). Cells responsive to both low-threshold mechanoceptors and nociceptors in the skin and periodontium have been described in rats (Jacquin *et al.,* 1989a). Glutamatergic and GABAergic neurones are present in the rat (Phelan and Falls, 1989; Usunoff *et al.,* 1997; Magnusson *et al.,* 1986, 1987; Haring *et al.,* 1990) as well as somatostatin and enkephalin neurones in ferrets (Boissonade *et al.,* 1993). In the rat, Petralia *et al.* (1994) described large multipolar neurons densely stained for NMDA R1 receptor.

Intracellular recording and staining has provided useful data on the detailed morphology of Sp5I cells in the rat. The responses and structure of projection cells (defined as cells that send axons outside the trigeminal complex), as well as "local circuit" neurons (with axons restricted to the trigeminal nucleus), were analyzed (Jacquin *et al.,* 1989a, b). The local circuit neurons often had widespread intranuclear axonal connections encompassing Pr5 and Sp5C, thus providing a mechanism for integration between subnuclei.

Sp5I projects to the thalamus, cerebellum, superior colliculus and spinal cord (rat, Kemplay and Webster, 1989; Huerta *et al.,* 1983; Jacquin *et al.,* 1989b; Phelan and Falls, 1991), with single cells often having very widespread connections (rat, Jacquin *et al.,* 1986; Patrick and Robinson, 1987; Bruce *et al.,* 1987; Phelan and Falls, 1991). In the rat, the thalamic projection is to both VPM and the medial part of Po (Chiaia *et al.,* 1991), with many of these projection cells containing glutamate (Magnusson *et al.,* 1987). The projection of Sp5I to the cerebellum has not been confirmed in the human (Usunoff *et al.,* 1997). Similarly, trigeminal inputs to the human superior colliculus have not been confirmed (for discussion see Chapter 28). Although localized receptive fields were noted for local circuit neurons, fields were generally widespread for projection cells, particularly those projecting to the thalamus (rat, Jacquin *et al.,* 1989b).

Spinal Trigeminal Nucleus Caudalis

The spinal trigeminal nucleus caudalis extends from the obex for approximately 15 mm to the C_2 level (Fig. 29.3), where it becomes continuous with the dorsal horn. Its similar laminar organization to the spinal dorsal horn (Chapter 7) has led to its alternative name, the medullary dorsal horn (Gobel *et al.,* 1981). Thus Sp5C contains a marginal zone (subnucleus zonalis, lamina 1), a substantia gelatinosa resembling Rexed's lamina 2, and a magnocellular layer, equivalent to nucleus proprius (lamina 3 and 4) of the dorsal horn (Fig. 29.3). In addition, some authors recognize a deeper zone corresponding to laminae 5 and 6.

The marginal zone in human tissue consists of a thin sheet of cells containing large multipolar neurones, some over 60 μm in diameter (Usunoff *et al.,* 1997) with small and medium-sized neurones also present. In rat, cat, and monkey, fusiform, pyramidal, and multipolar cells are described (Gobel, 1978; Zhang *et al.,* 1996; Yu *et al.,* 1999), with different functional properties for each (see later). Inputs to the marginal zone arise mainly from small-diameter myelinated fibers as well as unmyelinated afferents from all cranial tissues (reviewed Craig, 1996).

The human substantia gelatinosa was rather aptly described by Olszewski (1950) as horseshoe-shaped in cross section (Fig. 29.3) and consists of relatively densely packed small, oval, or fusiform cells (10–20 μm in diameter). This layer reacts strongly for AChE and is rich in neuropeptides such as substance P, CGRP, cholecystokinin, and somatostatin (Inagaki *et al.,* 1986; Clements and Beitz, 1987; Carpentier *et al.,* 1996). This region also contains the NGF receptor, trkA, which is especially dense in pre and perinatal human tissue, but is also present in adults (Quartu *et al.,* 1996). The region is rich in GABAergic somata and fibers (rat, Haring *et al.,* 1990; Ginestal and Matute, 1993). It receives predominantly small-diameter myelinated and unmyelinated afferents. Synaptic glomeruli, in which glutamatergic primary afferents are both pre- and postsynaptic to GABAergic terminals, have been described (rat, Clements and Beitz, 1987; cat, Iliakis *et al.,* 1996).

The magnocellular zone has medium-sized diameter (25 μm) oval or fusiform cells with scattered small and large neurones. In the rat, many cells here contain glutamate, and some of these project to VPM (Magnussen *et al.,* 1986, 1987). Synaptic glomeruli are present, often with scalloped glutamatergic profiles (Clements and Beitz, 1991). The magnocellular zone has a moderate level of AChE reactivity.

Low-threshold mechanical responses, high threshold nociceptive specific responses, thermosensitive specific (COLD) responses, HPC (heat, pinch, cold) cells, and wide dynamic range (WDR) neurones are all present in Sp5C (cat, Hu, 1990; monkey, Dostrovsky and Craig, 1996; reviewed Sessle, 2000). Low-threshold mechanical responses are found predominantly in the

magnocellular zone along with some thermal specific units (monkey, Price *et al.*, 1976). In contrast, the marginal zone contains nociceptive specific, COLD, HPC, and WDR responses (monkey, Price *et al.*, 1976; Bushell *et al.*, 1984; reviewed Sessle, 2000, and see later section on trigeminal nociception). Intracellular recordings from lamina 1 cells in cat spinal cord suggest that there is a structure/function correlation: fusiform and pyramidal cells correspond to nociceptive specific and COLD responses, respectively, whereas most multipolar cells showed HPC responsiveness (Han *et al.*, 1998). In monkey spinal cord, the fusiform and multipolar cells express the substance P receptor (neurokinin-1) supporting their role in nociception (Yu *et al.*, 1999). The role of trigeminal marginal zone neurons in nociception and thermal discrimination has been indicated by recordings in awake monkeys (Dubner *et al.*, 1981; Hayes *et al.*, 1981; Bushnell *et al.*, 1984). The responses of COLD cells depended on the behavioral significance of the stimuli, suggesting the involvement of these cells in sensory discrimination, rather than merely reflex activation.

Projections of Sp5C are extensive. Lamina 1 cells project to several thalamic regions including VPM, Po, and the midline and intralaminar nuclei (primate, Ganchrow, 1978; cat and monkey, Burton and Craig, 1979; cat, Shigenaga *et al.*, 1983; rat, Shigenaga *et al.*, 1979; Yoshida *et al.*, 1991; Iwata *et al.*, 1992; and see Chapter 30, Fig. 30.8B) as well as a new nucleus described by Blomqvist *et al.* (2000) as the posterior part of the ventral medial nucleus (VMpo, referred to as basalis nodalis in Chapter 20). Laminar 1 also gives both direct hypothalamic projections (rats, Malick and Burstein, 1998) and indirect projections through the parabrachial area (Slugg and Light, 1994; Jasmin *et al.*, 1997). The substantia gelatinosa projections are predominantly local, to the adjacent magnocellular zone and reticular formation (primate, Tiwari and King, 1974). The magnocellular zone projects to VPM, zona incerta, the facial nucleus, trigeminal motor nucleus, and adjacent reticular formation as well as ipsilateral spinal cord (Iwata *et al.*, 1992; Carpentier *et al.*, 1981). Magnocellular cells also project to more rostral trigeminal nuclei, Sp5O and Sp5I (primate, Tiwari and King, 1974; Price *et al.*, 1976; cat, Hu and Sessle, 1979; rat, Hallas and Jacquin, 1990). These intranuclear connections are likely to modulate activity in these rostral regions.

An interesting recent study has reported a discrete thermospecific region in lamina 1 in the owl monkey (Craig *et al.*, 1999). Cells here responded to cold stimuli (COLD cells) with small receptive fields on nasal and labial regions and had a pyramidal morphology similar to thermal cells in cats and rats. These cells project to the posterior ventromedial nucleus (VMpo), identified as a thermal and nociceptive region in monkey and human thalamus (Craig *et al.*, 1994, and referred to as basalis nodalis, in Chapter 20 and see later). This region of lamina 1 and the associated pathway was suggested to provide specialized thermosensitivity, likely to be relevant the nocturnal navigation and foraging behavior of the owl monkey Craig *et al.* (1999).

Mesencephalic trigeminal nucleus

The mesencephalic trigeminal nucleus comprises a band of scattered cells that extends from the level of rostral Pr5 through the pons and midbrain, a distance of some 22–24 mm (Olszewski and Baxter, 1954; Paxinos and Huang, 1995). The cells lie at the outer border of the periaqueductal gray in the midbrain and the central gray of the pons (Fig. 29.3). Me5 cells have a distinctive morphology, being mainly pseudounipolar with large, regular, oval or round somata, like that of other primary afferents. However, multipolar cells have also been seen in the human (Olszewski and Baxter, 1954) and identified in animal studies after peripheral labeling (reviewed Capra and Dessem, 1992). Cells of Me5 are the somata of proprioceptive afferents from the jaw muscles and periodontium.

Clustering of Me5 neurons with maculae adherens, gap junctions and electrotonic coupling between cells within a group have been described in the rat (Baker and Llinas, 1971; Liem *et al.*, 1991). Synapses on Me5 cells have been seen in rodents and cats, with a variety of transmitters identified including serotonin and dopamine (Liem *et al.*, 1992; reviewed Capra and Dessem, 1992), but the existence of synapses in humans is unconfirmed. Somatostatin positive fibers have been described around human Me5 cells (Bouras *et al.*, 1987). Besides these inputs, studies in rats show bilateral projections to Me5 from parvocellular reticular formation (Rokx *et al.*, 1988).

Me5 cells project to the motor trigeminal nucleus forming a monosynaptic reflex arc. In animals, Me5 also projects to the intertrigeminal and supratrigeminal nuclei probably involved in masticatory control (rat, Luo *et al.*, 1991) although, as noted previously, a human homologue of the supratrigeminal nucleus has not been confirmed. There are also projections to Pr5, which may provide a relay to the thalamus for proprioceptive sensation (Luo *et al.*, 1991, 1995) although direct projections to the ventral thalamus have been described (squirrel monkey, Pearson and Garfunkel, 1983). Thalamic projections were bilateral, but predominantly ipsilateral and may have included VPO (see later). Projections to other brainstem nuclei (the hypoglossal nucleus, nucleus of

the solitary tract, extraocular motor nuclei, and brainstem parvocellular reticular nucleus) as well as the cerebellum and spinal cord have been identified in animals (rat, Rokx *et al.*, 1986; Raappana and Arvidsson, 1993; cat, Matsushita *et al.*, 1982; Shigenaga *et al.*, 1989, 1990).

Other Sensory Trigeminal Nuclei

Besides the trigeminal sensory complex of four nuclei, the trigeminal sensory system also contains a group of cells within the spinal tract, at the level of caudal Sp5I and the Sp5I/C boundary (Fig. 29.3). There is considerable confusion about the nomenclature of this cell group (for discussion of this see Usunoff *et al.*, 1997). Originally described as interstitial cells by Cajal and Ramon (1909), this cell group was later considered part of the paratrigeminal nucleus of Chan-Palay (1978). Paxinos and Huang (1995) used the term "paratrigeminal" (Pa5), while Usunoff *et al.* (1997) reintroduced the use of "interstitial nucleus." In the human these cells are small and chromophobic (Usunoff *et al.*, 1997). Animal studies have shown that the interstitial/paratrigeminal nucleus receives a projection from the tooth pulp and cornea, with responses similar to those of the marginal zone of Sp5C (cat, Shigenaga *et al.*, 1986).

Other more scattered groups of cells, named by Paxinos and Huang (1995) as the peritrigeminal nucleus, lie lateral and ventral to the trigeminal tract at the level of Sp5I. The connections and functions of this group are unknown. A third group of large cells extends between the inferior cerebellar peduncle and the spinal and cuneate tracts, at the level of caudal Sp5I and rostral Sp5C (Fig. 29.3). This latter group of cells was named by Paxinos and Huang (1995) as the lateral pericuneate nucleus (LPCu). The cells are similar in appearance to those of the lateral cuneate nucleus and may well be related to cuneate inputs rather than the trigeminal system.

Brainstem Mechanisms in Trigeminal Nociception

Pain from the trigeminal distribution (including pain from the face, nasal sinuses, oral cavity and teeth, TMJ, and meninges) is one of the most common and distressing clinical symptoms known. In a study performed in the United States (Lipton *et al.*, 1993), it was found that 12% of adults had experienced toothache in the last six months, 5% had felt TMJ pain, while 1.4% had noticed face or cheek pain over the same period. Interestingly, there is a clear gender difference in some of these craniofacial pain syndromes, with women reporting a 28% higher incidence of pain from the TMJ than men.

Despite this major clinical significance, much of what we know about the nociceptive components of the trigeminal system is derived from animal studies, predominantly in rodents, although cat and primate studies have also contributed (see Chapters 12 and 30). Nevertheless, investigations in humans have usually been in agreement with animal-based findings, although some minor species differences in trigeminal nociceptive pathways cannot be excluded.

Nuclear Localization of Nociceptive Responses

Clinical findings involving transection of the trigeminal tract are consistent with findings in experimental animals indicating that Sp5C is the most important component of the trigeminal nuclear complex for perception of noxious stimuli applied to the craniofacial region (for review see Sessle, 2000). Cells in lamina 1 respond to noxious mechanical, thermal and chemical stimulation of structures such as the cornea, cerebral vasculature, oral and nasal mucosa, teeth, and TMJ. There is also evidence of the involvement of the trigeminal complex, in particular Sp5C, in the mediation of reflex responses to noxious craniofacial stimuli, such as changes in sweating, respiration, blood pressure, heart rate, and excitatory reflex effects in jaw-opening muscles and inhibitory effects in jaw-closing muscles. On the basis of c-fos immunoreactivity in the rat after noxious stimulation, Strassman and Vos (1993) have suggested the Sp5I/Sp5c border may be involved in these autonomic effects.

Besides the obvious involvement of Sp5C in trigeminal nociceptive activity, recordings from Sp5O and Sp5I indicate nociceptive responses are present in more rostral levels of the spinal trigeminal complex. Lesions or injections of analgesic chemicals into these rostral levels can also interfere with nociceptive behavior, particularly when the noxious stimulus is applied to intra- or perioral regions (Dallel *et al.*, 1998; Takemura *et al.*, 1993). Studies in awake monkeys indicate that Sp5O responses to dental stimulation are dependent on the behavioral state of the animal (Soja *et al.*, 1999). This indicates a role for the rostral, as well as caudal, spinal nuclei in trigeminal nociceptive mechanisms (Raboisson *et al.*, 1989; Panneton and Yavari, 1995). When the jaw-opening reflex is elicited by tooth pulp or perioral stimuli, lesion studies indicate that rostral subnuclei, such as Sp5O and Sp5I, are more crucial to the reflex than Sp5C (Dallel *et al.*, 1989; Hannam and Sessle, 1994). Involvement of rostral areas is also supported by clinical findings in patients with brainstem lesions in the caudal pons (Graham *et al.*, 1988).

It has recently been suggested, on the basis of the distinctive responses of Sp5O nociceptive neurons to noxious chemicals like formalin, that Sp5O is particularly important for processing information about short duration nociceptive stimuli, whereas Sp5C is more important for processing tonic nociceptive information (Raboisson *et al.*, 1995). Studies involving morphine administration in the superficial laminae of Sp5C indicate that these analgesics may exert their effect on Sp5O indirectly, by blocking C fiber inputs that relay in the Sp5C (Dallel *et al.*, 1998).

Nociceptive Transmitters, Response Characteristics, and Projections

As indicated previously, small-diameter afferents terminate mainly in the marginal zone and deep laminae (5 and 6) of Sp5C. These afferents contain neuropeptides and amino acids that have been implicated as excitatory neurotransmitters or neuromodulators (e.g., substance P, glutamate, nitric oxide) in central nociceptive transmission (see Sessle, 1996, 2000, for reviews). Antagonism of the substance P receptor mechanisms (NK1) blocks c-fos expression induced by noxious chemical stimulation of dural afferents (Shepheard *et al.*, 1995). In addition to substance P, studies indicate central involvement of excitatory amino acids in trigeminal nociception (Parada *et al.*, 1997). Jaw-muscle activity associated with TMJ nociception can be elicited by glutamate injection into the TMJ and blocked by glutamate receptor antagonists (Cairns *et al.*, 1998).

As noted earlier in "Spinal Trigeminal caudalis," responses to nociceptive input include nociceptive specific neurons, HPC cells and WDR neurons, all of which can be recorded from the marginal zone and deep laminae of Sp5C. The involvement of the marginal zone in nociception is supported by functional recordings as well as c-fos studies. However, comparable neurons have been reported to be present in rostral parts of the trigeminal spinal nucleus in both Sp5O and Sp5I (see Sessle, 2000, for review). Electrophysiological studies in all these regions often show a pattern of convergence of inputs from different regions, with cells responding to cutaneous nociceptive stimulation as well as stimulation of afferents supplying cranial blood vessels, dura, cornea, TMJ, or tooth pulp (Boissonade and Matthews, 1993; Meng *et al.*, 1997; also reviewed in Sessle, 2000).

There are substantial projections from the parts of the trigeminal nuclear complex involved in nociception to the thalamus (Craig and Dostrovsky, 1997; Sessle, 2000). There is also electrophysiological evidence for projections from nociceptive Sp5C neurons to the periaqueductal gray and parabrachial region (from which projections to the amygdala and hypothalamus follow), as well as direct projections to the hypothalamus (Malick and Burstein, 1998). These ascending non-thalamic projections are likely to be responsible for the affective aspects of nociception as seen clinically.

Modulation of Nociceptive Responses, Inflammation and Chronic Pain

As in the spinal cord (see Chapter 30), an important aspect of nociception is that the activity can be modulated by descending and afferent inhibitory mechanisms that are known to suppress pain in both humans and experimental animals. Projections from the nucleus raphe magnus, periaqueductal gray, sensorimotor cortex, pretectal area, and parabrachial area are capable of influencing nociceptive responses (for review see Sessle, 2000). Afferent induced modulation also appears to be an important mechanism in trigeminal nociception, studied, for instance, for responses from cat tooth pulp (reviewed Soja *et al.*, 1999). The responses of neurons to inputs evoked by deep and superficial noxious stimuli can be suppressed by low-threshold stimuli that excite large afferent fibers. Furthermore, noxious stimuli applied to other parts of the body may inhibit trigeminal responses to small fiber craniofacial nociceptive stimulation (i.e., "pain inhibits pain," Sessle, 2000).

There is also a large body of literature concerning the long-term effects of craniofacial injury and inflammation on nociception in the trigeminal complex. Deafferentation in the trigeminal system of experimental animals (e.g., by transection of the infraorbital nerve) is well known to lead to significant morphological, neurochemical, and physiological changes in the brainstem, thalamus, and somatosensory cortex (Woolsey, 1990; Weinberger, 1995). Endodontic removal of tooth pulps in adult animals also induces morphological and physiological changes in the trigeminal nuclear group, particularly in Sp5O and Sp5C (Hu and Sessle, 1989). The sensitivity of many nociceptive endings may increase after mild forms of injury, such as when the threshold of nociceptors is lowered as a result of repeated exposure to noxious stimuli—a phenomenon known as "peripheral sensitization" (see Levine and Taiwo, 1994, for review). Some of this sensitization may also be the result of central factors.

Relatively little attention has been given to models of chronic pain in the craniofacies. Chronic constrictive infraorbital nerve injury has been applied in a behavioral model of trigeminal neuropathic pain (Vos *et al.*, 1994) and has been shown to be associated with some of the features of neuropathic pain behavior, but

central effects of this model have not been fully investigated as yet. However, neuroplasticity of trigeminal nociceptive neurons has been found to be induced by dermal or deep tissue injection of mustard oil, which induces pain and other nociceptive behaviors in humans and experimental animals (see Sessle, 2000, for review). Accumulating evidence concerning the role of NMDA receptor mechanisms in these nociceptive processes has prompted the suggestion that NMDA antagonists may be beneficial in the treatment of chronic trigeminal injury and pain (Dubner and Basbaum, 1994).

The Trigeminovascular System: Implications for the Pathogenesis of Headache

The term "trigeminovascular system" refers to the cranial vessels and their trigeminal innervation, implying a functional network that may play an important role both in normal cerebrovascular function and in the aetiology of several types of headache. Sensory fibers innervating the pial and dural vessels of the anterior and middle cranial fossae arise from the trigeminal nerve, mostly within the ophthalmic division (Mayberg *et al.*, 1981; Liu-Chen *et al.*, 1984; Moskowitz *et al.*, 1983). On the other hand, the cell bodies of sensory afferents innervating the posterior cranial fossa and basilar arteries are located in the C1-C3 dorsal root ganglia (Keller *et al.*, 1985; Saito and Moskowitz, 1989). Electrical stimulation studies of the superior sagittal sinus have shown cells in Sp5C, the cervical dorsal horn, and in the dorsolateral spinal cord at the C2 level, which are responsive to dural stimulation and may be involved in vascular headache (Goadsby and Zagami, 1991; Angus-Leppan *et al.*, 1994). Convergence of inputs from facial skin and intracranial vessels could explain the pattern of referred pain seen in vascular headaches (Dostrovsky *et al.*, 1991).

For most of the 20th century, the prevailing theory of pathogenesis of migraine held that the pain was the result of abnormal dilation of intracranial dural and pial blood vessels. This dilation was believed to result in mechanical excitation of the sensory fibers associated with the vessel adventitia (Graham and Wolff, 1983). Recent studies have shown that vessel dilation does not always coincide with the onset of pain and that vessel constriction does not necessarily coincide with pain relief. Alternative theories have proposed a chemical mode of activation of meningeal perivascular sensory fibers, one that also implicates neurotransmitter release from the sensory fibers themselves in the pathogenesis of the condition (so-called neurogenic inflammation model of vascular headaches; Moskowitz, 1992).

It is now clear that meningeal blood vessels share some of the anatomical and physiological properties seen in other body tissues (e.g., joints) where pain commonly arises as a result of local sterile inflammatory processes. Importantly for the neurogenic inflammation model of vascular headaches, activation of trigeminovascular fibers can lead to release of vasoactive neuropeptides into the vessel wall (Goadsby *et al.*, 1988; Moskowitz *et al.*, 1989; Sicuteri *et al.*, 1990), thereby promoting neurogenic inflammation. Orthodromic and antidromic conduction along trigeminovascular fibers is believed to facilitate the spread of the inflammatory response to adjacent tissues, as well as to transmit the nociceptive information to Sp5C. Collaterals and higher order connections of these central fibers of the trigeminovascular system also terminate in centers associated with the generation of other symptoms of vascular headaches (e.g., nausea, emesis, autonomic activation, affective alterations; Allen and Pronych, 1997).

The triggering factor may involve temporary exposure to an unknown endogenous chemical agent that alters the sensitivity of trigeminovascular fibers to mechanical stimuli and leads to the sensation of head pain. Strassman and co-workers have shown that application of acidic and inflammatory agents to the dura causes sensitization of dural trigeminovascular fibers to mechanical stimuli that previously evoked minimal or no response (intracranial sensitization; Strassman *et al.*, 1996). This sensitization can also lead to enhanced responses of central neurons to stimuli applied at extracranial sites, thereby explaining the extracranial tenderness (mechanical and thermal allodynia) experienced by migraineurs in the absence of extracranial vascular pathology (Burstein *et al.*, 1998).

Agents that have been shown to be effective in the therapy of either migraines or cluster headaches (sumatriptan, ergotamine, somatostatin) may exert their influence by receptor-mediated effects on fibers of the trigeminovascular system. Both sumatriptan and dihydroergotamine have been shown to reduce the release of CGRP and inhibit increases in cranial blood flow resulting from trigeminal ganglion stimulation (Goadsby and Edvinsson, 1993). Somatostatin, which inhibits the effects of release of substance P from nerve terminals, is also effective in reducing the pain of cluster headaches (Sicuteri *et al.*, 1984). Similarly, repeated application of capsaicin to nasal mucosa leads to its desensitization, with a concomitant decrease in intensity and duration of cluster headaches. Experimental data support the idea that sumatriptan activates an inhibitory receptor resembling 5-HT1D on perivascular fibers and by so doing blocks

neuropeptide release and impulse conduction in the trigeminovascular system (Moskowitz, 1992).

Pathophysiology of Trigeminal Neuralgia

Recent work concerning the debilitating condition trigeminal neuralgia is worth commenting on here. Trigeminal neuralgia (TN) is characterized by severe unilateral paroxysmal pain of short duration and restricted to the trigeminal distribution (Türp and Gobetti, 2000). The symptoms are often triggered by nonnociceptive stimuli to the face (e.g., chewing or touching the face) applied to a trigger zone within the trigeminal distribution. The paroxysms last only seconds but may occur with varying frequency. Often there is a remission of weeks to months, but this only serves to heighten the patient's anxiety, sometimes to the point of suicide, as they wait for the next painful paroxysm (Choi and Fisher, 1994). TN has an increased prevalence among patients with multiple sclerosis, consistent with the presumed importance of demyelination in the pathophysiology.

The pathophysiology of TN remains controversial. One postulated cause is demyelination within the posterior trigeminal root entry zone and brainstem, leading to repetitive firing of the nerve and its central connection. A large proportion of patients with TN show evidence of external vascular compression (Hamlyn, 1997), with focal demyelination near the compression site.

Two physiological mechanisms have been postulated to explain how nerve compression may lead to painful paroxysms (Choi and Fisher, 1994). In the first, compression is believed to lead to selective demyelination of large sensory fibers with relative sparing of smaller nociceptive fibers. The segmental inhibitory effect of larger fibers is lost while transmission of painful impulses through the smaller undamaged nociceptive afferents continues uninhibited. In the other proposed mechanism, extra axon potentials are believed to be initiated at the site of injury. Such ectopic activity may arise by injury-induced repetitive firing of nociceptive afferents. Alternatively, ephaptic "cross-talk" between fiber classes has been proposed, with action potential currents in low-threshold afferents causing impulse generation in adjacent nociceptive fibers.

Studies of the ultrastructure of trigeminal roots removed during microvascular decompression surgery for TN have shown zones of de- and dysmyelination, juxtaposition of denuded axons, apparent axon loss and degeneration, and collagen deposition (Rappaport *et al.*, 1997). Those authors' observations of the proximity of denuded axons support the hypotheses of ectopic generation of impulses, ephaptic contacts, and crossed after-discharge. They have proposed that a small cluster of trigeminal ganglion cells (the ignition focus) develops autorhythmicity as a result of trigeminal root damage. Activity then spreads from this focus to other parts of the ganglion by release of neurotransmitter and potassium ions through the extracellular space (Rappaport and Devor, 1994). The effectiveness of phenytoin and carbamazepine in the treatment of TN is consistent with the importance of excitable membrane instability in the pathophysiology of the condition (Choi and Fisher, 1994).

The effectiveness of surgical microvascular decompression of the trigeminal root has long been taken as an indication of the importance of compressive nerve damage in the aetiology of TN. More recently, Tenser (1998) has questioned this presumption, pointing to the effectiveness of many other therapies for TN (e.g., glycerol or thermal rhizolysis, balloon compression, blunt trauma to the trigeminal root, alcohol injury, and radiation therapy), which probably produce controlled injury to the ganglion. Tenser maintains that similar effectiveness of a wide range of treatments for TN suggest that these therapies act through a common pathway (i.e., the induction of damage to trigeminal ganglion cells with alteration in ganglion cell transcription). He argues that altered ganglion cell function (as reflected in the high frequency of herpes simplex virus activation after these treatments), rather than reduction in ephaptic transmission or the elimination of ectopic signal generation, is responsible for bringing relief. Nevertheless, it remains to be explained how a general increase in ganglion cell transcription diminishes pain—an issue not adequately addressed by Tenser.

Correlation of with Clinical Features

Although much of the preceding discussion has been derived from studies in experimental animals, it is possible to correlate many of the results from animal studies with clinical experience. For example, many patients experiencing or anticipating craniofacial pain (e.g., dental patients) undergo or experience diverse effects including reflex changes in blood pressure, heart rate, respiration, and sweating, as well as coactivation of jaw-opening and -closing muscles. These phenomena have been shown in experimental animals to involve Sp5C. Effects on masticatory muscle tone may serve an adaptive function by "splinting" the TMJ, as often seen clinically after painful injury.

The poor localization of pain in most toothaches and headaches, and the common feature of pain referral in these conditions, probably reflects the extensive convergence of nociceptive afferents from diverse sources (tooth pulp, cranial vessels, and dura), as noted earlier

in findings from experimental animals (Sessle and Hu, 1991; Strassman *et al.*, 1994). Acute toothaches and headaches are often associated with intense pain and tenderness, often with radiation or referral to neighboring craniofacial regions. These aspects are considered to reflect convergence and peripheral sensitization phenomena (see Sessle, 2000, for review).

Studies of trigeminal nociception in experimental animals will continue to be an important area of research. Nevertheless, more correlation of findings from experimental animals with clinical experience is necessary to realize the full benefits of animal studies.

Trigeminothalamic Projections

As noted previously, there is an extensive thalamic projection from Pr5 to VPM. Both Sp5O and Sp5I also project to VPM, but to a lesser extent than Pr5, while Sp5I also gives projections to Po, at least in animal studies. For Sp5C, there are projections to VPM, Po, VMpo, and VPI as well as to the mediodorsal nucleus and the intralaminar nuclei. Some cells in the marginal zone also provide projections to VPI (Craig, 1996). There are also thalamic projections from Me5 in the squirrel monkey (Pearson and Garfunkel, 1983), possibly to a region anterior to VPM designated VPO by Percheron (Chapter 20) and VPS by Kaas and Pons (1988; Chapter 28). This region receives inputs from deep receptors (e.g. muscle spindles) mainly via the external cuneate nucleus and is topographically organized (Chapter 28).

Trigeminothalamic pathways have long been recognized for their ability to show species differences (Verhaart and Busch, 1960). Humans have both dorsal and ventral trigeminothalamic tracts (reviewed Usunoff *et al.*, 1997). The ventral pathway, also called the trigeminal lemniscus, arises from all levels of the trigeminal nuclear complex. Fibers run through the ventral pontine tegmentum and decussate to join the dorsomedial side of the contralateral medial lemniscus. They then travel with the medial lemniscus to terminate in various thalamic sites (see later). Lesions in the brainstem involving the trigeminal lemniscus lead to contralateral sensory loss of both touch and pain, supporting its crossed projection and its involvement in both low- and high-threshold responses (Kim, 1993).

The dorsal tract arises primarily from the dorsomedial (intraoral) part of Pr5 (cat, Azerad *et al.*, 1982; cat and monkey, Burton and Craig, 1979). Fibers pass dorsomedially in the dorsal pontine tegmentum, run ventral and lateral to the periaqueductal gray in the midbrain, and then pass laterally to enter the dorsomedial part of the ipsilateral VPM.

THALAMIC SITES FOR TRIGEMINAL SOMATIC SENSATIONS

Subdivisions of the thalamus are discussed by Percheron (Chapter 20) and the somatosensory thalamus is considered in detail by Kaas (Chapter 28). Rather than repeat this information, we consider here only those nuclei that are associated with cranial somatic sensations.

Brainstem trigeminal nuclei provide a major input to VPM, and also project to VPO and the midline and intralaminar nuclei. In addition, there are inputs to a region posterior and inferior to VPM and VPL, which Percheron (Chapter 20) has called regio basalis. This region includes, from medial to lateral, the suprageniculate, the Po and VMpo areas described by Blomqvist *et al.* (2000), and VPI. Regio basalis receives inputs from laminar 1 cells of Sp5C and the spinal cord (Hassler, 1959). For humans, information on trigeminal responses is available only for VPM, VMpo, and Po, and the following sections consider these. For trigeminal inputs to VPO and VPI, the only details available in the human, relate to somatotopy and are considered by Kaas in Chapter 28. Somatic inputs to the midline nuclei, such as the ventrocaudal part of the mediodorsal nucleus (MDvc), with its projections to the anterior cingulate cortex, are thought to be involved in the affective-motivational aspects of nociception (Rainville *et al.*, 1997; Craig, 1996; Peyron *et al.*, 2000). Responses in these areas show widespread receptive fields and modality convergence, which are not specific to facial sensations, and consequently are not considered further.

Ventroposterior Medial Nucleus

The (VPM) nucleus (also called Vci) lies medial to VPL and is separated from it by a narrow band of fibers sometimes referred to the arcuate lamina though is really only an accumulation of lemniscal fibers. VPM is characterized by relatively densely packed, small to medium-sized cells and shows a high level of parvalbumen immunoreactivity and, conversely, low calbindin levels (Morel *et al.*, 1997).

VPM is somatotopically organized, with the intraoral surface, including the tongue, lying medially. VPM is adjacent to, but excludes, the relatively parvocellular area (VPMpc), which receives gustatory inputs, also referred to as VMb or Varc. The most medial cells of VPM have ipsilateral intraoral receptive fields. This region receives input from dorsal (mandibular) Pr5 via the ipsilateral dorsal trigeminothalamic tract (Smith, 1975). The remainder of VPM receives contralateral inputs via the ventral trigeminothalamic tract, with

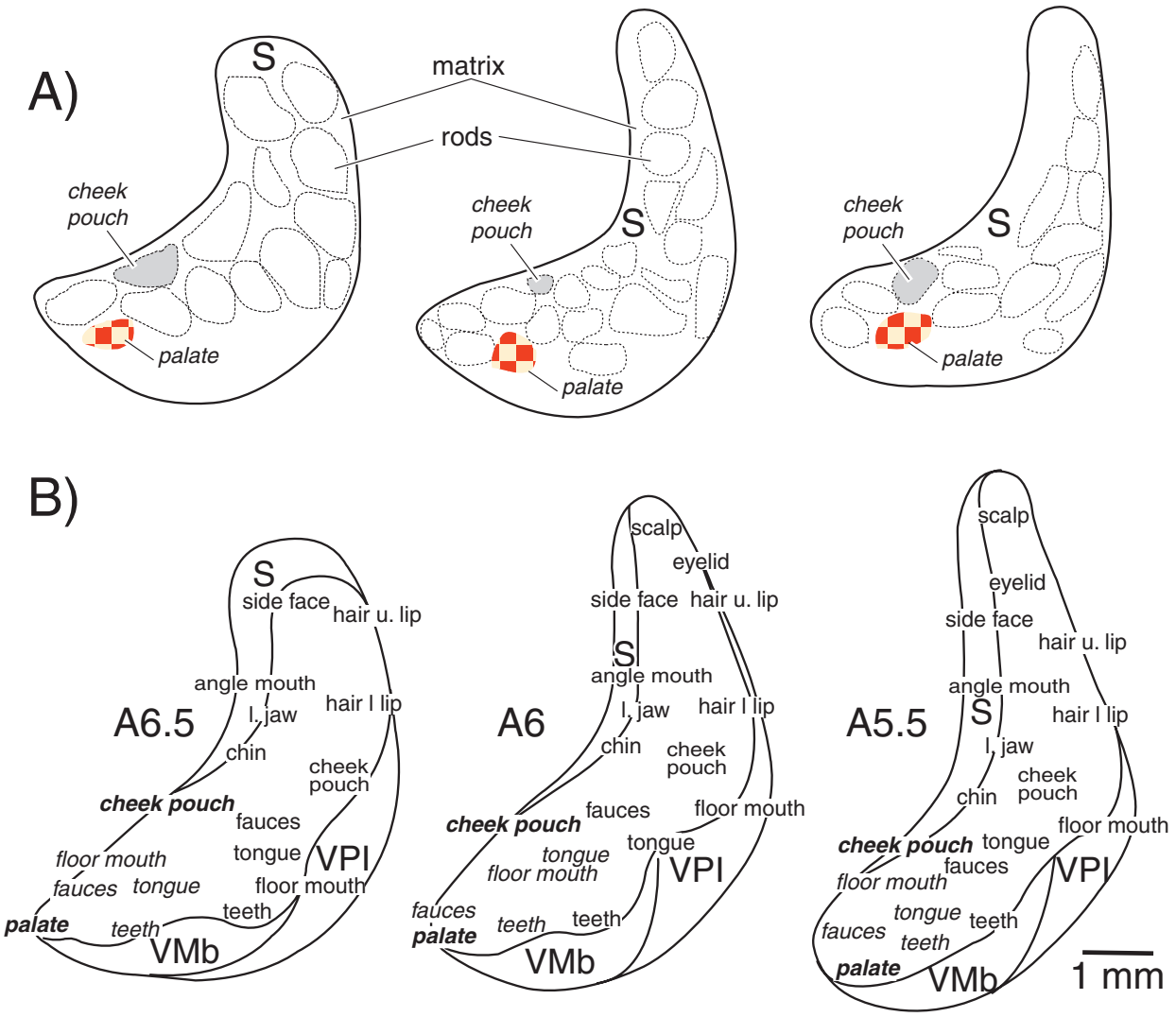

FIGURE 29.4 **(A)** Coronal cross sections through monkey VPM at three successive rostrocaudal levels (rostral to left) to show cytochrome oxidase (CO)-dense rods surrounded by a CO-pale matrix, S (after Fig. 4, Raussell and Jones 1991a, J. Neuroscience 11: 210–225, with permission, Copyright 1991, Society for Neuroscience). **(B)** Cross sections of VPM at similar levels to those shown in A with the peripheral receptive fields for cells at each site reconstructed from stereotaxic coordinates (Russell and Jones, 1991a, Fig 8, with permission, as in A). Receptive fields shown in italics are ipsilateral; those in roman type are contralateral. Some receptive fields such as the cheek pouch and palate (bold) can be localized to specific CO-rich rods (denoted in A) and identified at corresponding sites at each level. S indicates part of the small-celled matrix region; VPI, ventral posterior inferior nucleus; VMb, ventral medial basal nucleus receiving gustatory inputs.

intraoral and mandibular skin represented ventrally and ophthalmic regions dorsally (Fig. 29.4). Adjacent regions in VPL are responsive to finger and hand stimulation. The close proximity of these regions is indicated by the clinical finding that localized vascular lesions in this boundary region can lead to the cheiro-oral syndrome, in which there is a sensory disturbance of the contralateral face and hand (Fisher, 1982; Shintani *et al.*, 2000).

Raussel and Jones (1991a) described monkey VPM as consisting of cytochrome oxidase (CO)-rich rods surrounded by a CO pale matrix (see Fig. 29.4 and Table 29.1). The rods contain large and medium cells, which are parvalbumen positive, as well as smaller GABAergic cells. These areas also stain richly for AChE and tachykinin immunoreactive fibers (e.g., substance P, neurokinin A and B, Liu *et al.*, 1989). The rods extend as anterior–posterior columns within the nucleus, with all cells in a column having similar receptive fields. They receive their major input from Pr5 and project to cortical layer 4 of the primary somatosensory cortex (Raussel and Jones, 1991b). In contrast, the matrix lies around the rods and forms a shell at the edges of VPM, which can extend into adjacent nuclei (Jones, 1998). It contains small calbindin positive cells and some GABAergic neurones.

TABLE 29.1 Thalamic Sites concerned with Cranial Somatic and Gustatory Sensations

Nucleus	Parvalbumen	Calbindin	Substance P *(B)*	CGRP *(B)*	Input	Output	Functional Group
VPM Rods	+++ *(R)* (cells and fibers)	– *(R)*	+	?	Pr5 *(R)*	Primary SS cortex, areas 3b and 1 *(R)*	Touch, tactile discrimination GSA
VPM Matrix (VPc)	– *(R)*	+++ *(R)* (cells)			Sp5I + Sp5C *(R)*	Widespread, to superficial layers *(R)*	Modulatory, cortical excitation GSA
VPO (VPS) *K*	++ *(P)*	– *(P)*	?	?	? Me5 (DCN & ext. cuneate *(K)*	SS cortex areas 3a and 2 *(K)*	Kinaesthetic (muscles, tendons, joints) GSA
VPI (basalis lateralis) *P*	++ *(Mo)* + *(Mu)*	+++ *(Mo)* + *(Mu)*	+ (few patches)	+ (few patches)	Sp5C laminar I (+ spinal laminar I) *(D)* Sp5C Mg (+ spinal laminar V) *(D)*	Secondary SS *(D)* lat parietal cortex *(K)* Insular cortex *(J, P)*	Pain, ? modulatory, GSA
VMpo *B* (PVM) *P&H* (basalis nodalis) *P*	– *(B)*	+++ *(B)* (dense fibers)	+ (patches)	+ (between Sub P areas)	Sp5C laminar I (+ spinal laminar I) *D*	Insular cortex *(B)*	Pain and temperature GSA
Po *B* (basalis halo) *P*	?	+ (sparse) *(B)*	+ (few patches)	+++	Solitary nucleus *(B)* (+ spinal laminar I & V)	? Insular cortex	Enteroreception (glossopharyngeal, vagal and pelvic) GVA
VPMpc (VMb) *B* (Varc) *P*	+ *(Mo)* – *(P)*	+++ *(Mo)* +++ *(P)*	–	+	solitary nucleus *(N&P)*	Gustatory cortex Insula and operculum *(N&P)*	Taste SVA

GSA, general somatic afferent; GVA, general visceral afferent; SVA, special visceral afferent; DCN, dorsal column nuclei; SS, somatosensory cortex.

B, Blomqvist *et al.* 2000; *D,* Dostrovsky, 2000; *J,* Jones, 1985; *K,* Kass Chapter 28; *Mo,* Morel *et al.* 1997; *Mu,* Munkle *et al.* 2000; *P,* Percheron, Chapter 20; *P&H,* Paxinos and Huang, 1995; *R,* Rausell and Jones, 1991a.

P&N, Norgren and Pritchard, Chapter 31.

The predominant input to the matrix of VPM arises from Sp5C, mainly the deeper laminae. The calbindin positive matrix cells have widespread projections to superficial cortical layers.

Response properties of human VPM cells have been reported by a number of authors (Jasper and Bertrand, 1966; McComas *et al.*, 1970; Ohye *et al.*, 1972; Donaldson 1973; Lenz *et al.*, 1988). Most have reported low-threshold, mechanoreceptive responses to hair or skin stimulation. Besides cutaneous cells, responses to deep pressure and/or joint movement have been noted (Ohye *et al.*, 1972; Lenz *et al.*, 1988; Seike, 1993) though these may have been located in VPO (see Chapter 28, where it is referred to as VPS). In the rat, VPM receives inputs from the TMJ and jaw muscles and may be involved in proprioceptive sensations (Luo *et al.*, 1991; Ohya *et al.*, 1993) via Pr5 and Sp5I though this is not confirmed in humans.

All studies in humans agree that receptive fields are contralateral and generally small, similar in size to those on the fingers. There is a predominance of responses from the lips and perioral area (Donaldson, 1973; Lenz *et al.*, 1988). Many cells in VPM are activated by speech movements; for instance, cells with receptive fields on the lips may be activated when the subject makes the sound "p" (McClean *et al.*, 1990). Two-thirds of the responses are slowly adapting (Lenz *et al.*, 1988) and spontaneous activity, at up to 40–50 impulses/s, is present in some cells (Jasper and Bertrand, 1966). These results are similar to those in the alert monkey where Bushnell and Duncan (1987) found 90% of VPM cells had low-threshold cutaneous receptive fields, usually within one trigeminal division. Cells were activated by hair or skin stimulation, and both rapidly and slowly adapting responses were noted.

In most studies in primate VPM and VPL, responses to noxious stimulation have been rare or absent. In monkey VPM a small population of cells (10%) gave nociceptive, WDR responses (Bushnell and Duncan, 1987). Similarly, a study by Lenz *et al.* (1993a) in humans reported 6% of neurons in the ventrocaudal thalamus responded to noxious heat as well as innocuous thermal and mechanical stimuli, as for WDR responses. Moreover microstimulation of this region in humans evoked thermal and pain sensations (Lenz *et al.*, 1993b). Such sensations were more common (30% of sites) from the posteroinferior region, which may have corresponded to VPI, than from the "core" region (5%). An extensive study by Dostrovsky *et al.* (2000) found only 8% of sites evoked pain in normal subjects though this was markedly increased in patients with poststroke pain. Animal studies have also reported innocuous thermal responses in VPM to cooling of the tongue, but not other facial regions (monkey, Poulos and Benjamin, 1968). Cells were either cold-specific or responded to cooling and mechanical stimuli; no responses to warming were found. The paucity of thermal and nociceptive responses in VPM suggests that these modalities may activate additional thalamic sites and a major relay is probably the adjacent region VMpo (see later).

Ventromedial Nucleus, Posterior Part and Surrounding Po (Basalis Nodalis and Halo)

A relatively recently identified nucleus, thought to be a relay for pain and temperature sensations, has been described in monkey and human (Craig *et al.*, 1994; Blomqvist *et al.*, 2000). VMpo lies posterior and medial to VPM and VPL, ventral to the anterior pulvinar and center median nuclei and dorsal to the medial geniculate nucleus. It was designated the posterior ventromedial nucleus by Paxinos and Huang (1995), although Percheron (Chapter 20) considers it a discrete nucleus "Nodalis" within the regio basalis. VMpo contains small to medium-sized cells, loosely aggregated in clusters (Blomqvist *et al.*, 2000). In both monkey and human, it stains richly for calbindin with a dense plexus of immunopositive fibers (Craig *et al.*, 1994). Lamina 1 cells of Sp5C and the spinal dorsal horn have been shown to project to this region in monkeys (Craig *et al.*, 1994). Double labeling has been used to establish that the calbindin immunoreactivity in these terminals colocalized with anterogradely transported tracer from lamina 1 cells (Craig *et al.*, 1994). In human tissue, calbindin immunoreactive fibers of the spinal lemniscus form dense patches of terminals over VMpo neurons (Blomqvist *et al.*, 2000). Immunocytochemistry was used to show that fibers containing substance P or CGRP terminated in VMpo. Substance P staining frequently overlapped with that of calbindin, but was less dense, suggesting that substance P was present only in a subset of the calbindin-positive fibers. In contrast, CGRP immunoreactivity never overlapped with calbindin but lay between calbindin-rich areas.

Recordings from this region in monkeys show responses to innocuous thermal (cooling) or noxious stimuli. Cells had small receptive fields on the contralateral body surface, with clusters of adjacent cells sharing similar response properties (Craig *et al.*, 1994). Both recording experiments and tracing studies in monkeys indicate a topographic organization. Trigeminal inputs are represented anteromedially, posterior and ventromedial to VPM, whereas the limbs are represented more posterolaterally, posterior and ventromedial to VPL.

As in monkeys, recordings from this site in humans indicate that cold-specific (COLD) responses are present (Dostrovsky and Craig, 1996). Stimulation of this site in awake humans evoked cold sensations on localized parts of the contralateral body surface, including the face (Davis *et al.*, 1999). Moreover, imaging of the region shows activation with noxious and thermal stimuli (Craig *et al.*, 1996). Thus VMpo has been suggested to be a specific thalamic relay site for nociceptive and cold-specific responses from the whole body surface, with the possible exception of the tongue. Infarcts in this region are associated with analgesia and loss of thermal sensibility (Leijon *et al.*, 1989). VMpo projects to a localized region of the insula, which shows activation in PET studies with noxious or cooling stimuli (Craig *et al.*, 1996).

Blomqvist *et al.* (2000) have also identified a region around VMpo that they call Po, though this should not be confused with Po as described by Jones (1985). Percheron (Chapter 20) describes it as a "halo" around VMpo within the regio basalis (i.e., basalis halo, BH). Po (BH) is a curved region forming the anterior, lateral, and ventral aspects of VMpo. It contains patches of CGRP positive fibers known to be associated with visceral inputs (Blomqvist *et al.*, 2000; de Lacalle and Saper, 2000). Po (BH) has therefore been suggested to act a general visceral afferent for inputs from the glossopharyngeal, vagal and pelvic nerves (Blomqvist *et al.*, 2000).

Overview of Thalamic Relay Nuclei for Cranial Sensations

The sites associated with somatic and gustatory sensations in the human are summarized in Table 29.1. Staining for the Ca-binding proteins parvalbumen and calbinin has been included, although calretinin has been omitted as it is generally low or absent in these areas (Fortin *et al.*, 1998; Cicchetti *et al.*, 1998). In this schema, the rod component of VPM (and VPL, though not included here) forms the general somatic relay nuclei for tactile information, with its main output to area 3b the primary somatosensory cortex (Darian-Smith *et al.*, 1990; Chapter 28). In contrast, the matrix has more diffuse projections to superficial cortical layers and is suggested to have a modulatory role (Jones, 1998). VPO is likely to provide for proprioceptive sensation, although the extent of trigeminal involvement in this is unclear. VPMpc acts as a special visceral relay for taste, receiving inputs primarily from the nucleus of the solitary tract (Beckstead *et al.*, 1980; Chapter 31). Po (BH), with its dense plexus of CGRP fibers, may correspond to the relay for visceral afferents (glossopharyngeal, vagal, and pelvic inputs; Chapter 31), while VMpo, with its input of substance P positive fibers, comprises the relay for general somatic afferents for pain and temperature. VPI receives input from both superficial and deep laminae and, like the matrix of VPM and VPL, may have a more diffuse modulatory role (Chapter 28). VMpo, Po, and VPI have been considered part of the regio basalis by Percheron (Chapter 20).

CRANIAL SOMATOSENSORY CORTEX

As for the thalamus, we will not attempt to repeat here the organization and function of the whole somatosensory cortex and associated areas involved with somatosensory processing. These have been well covered in Chapter 28. Rather we focus on recent data addressing those aspects that are unique for cranial somatic sensations.

Organization of Orofacial Somatosensory Cortex

The overall organization of the primary somatosensory cortex, with face located laterally adjacent to the hand, has long been established. A recent report of the facial representation in owl and squirrel monkeys (Jain *et al.*, 2001) shows a remarkable pattern of myelin-dense patches within area 3b (Fig. 29.5). They are separated from each other by myelin-light septa, which mainly receive callosal inputs (Krubitzer and Kaas, 1990). Jain *et al.* (2001) used electrophysiological recordings to show that each patch represented a specific region: upper face, upper lip, chin and lower lip, contralateral teeth and tongue, and ipsilateral teeth and tongue. These representations extended in an orderly sequence from caudal to rostral in the cortex. In addition, within each patch, receptive fields were somatotopic; for example, for the upper face, the upper forehead was caudal to the lower forehead. Similar representations were also found in parallel strips of cortex medial and lateral to area 3b and were presumed to correspond to areas 3a and 1. A similar organization is found in the macaque monkey (Manger *et al.*, 1995, 1996), although macaques have a larger representation of the intraoral cheek pouches, likely to reflect their use of these for food storage.

Like other body regions (Woolsey *et al.*, 1979; Wood *et al.*, 1988), recordings of somatosensory-evoked potentials after stimulation of trigeminal nerves have been used to assess localization and topography of orofacial responses in humans (Stöhr and Petruch, 1979; Bennett and Jannetta, 1980; Findler and Feinsod,

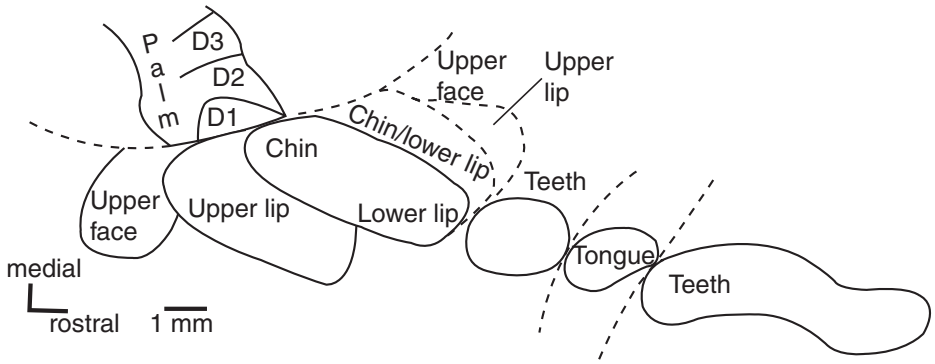

FIGURE 29.5 Trigeminal representation of the primary somatosensory cortex of the owl monkey. Myelin-rich regions in area 3b of the hand, face, and oral cavity representations are outlined (solid lines). Somatic positions for receptive fields for cells obtained from electrophysiological mapping experiments are superimposed for each region. Boundaries between regions, corresponding to myelin-light septa, are shown (dashed lines). Adapted from Figure 3, Jain *et al.* 2001, Anatomic correlates of the face and oral cavity representations in the somatosensory cortical area 3b of monkeys. *J. Comp. Neurol.* **429:** 455–468. Reprinted with permission of Wiley-Liss, Inc., a subsidiary of John Wiley and Sons, Inc.

1982; Badr *et al.*, 1983). Response latencies for somatosensory-evoked potentials from the orofacial region are generally shorter than for the hand region but otherwise show a similar series of waves (Ishiko *et al.*, 1980; Seyal and Browne, 1989). As found in animal studies, face representation is lateral to the hand, with an orderly progression of upper face, upper lip, lower lip, and tongue, from medial to lateral (Penfield and Rasmussen, 1950; McCarthy *et al.*, 1993). In contrast to most studies on the limbs, orofacial inputs have generally been found to give bilateral responses (Hashimoto, 1988).

Over the past decade or so, imaging techniques of positron emission tomography (PET; Fox *et al.*, 1987; Bittar *et al.*, 1999), magnetoencephalography (MEG; Nakamura *et al.*, 1988; Yang *et al.*, 1993; Hoshiyama *et al.*, 1996) and functional magnetic resonance imaging (fMRI; Sakai *et al.*, 1995; Moore *et al.*, 2000) have been used to address the organization of the human somatosensory cortex. These studies confirm the overall topography reported from somatosensory evoked potentials, with the orofacial representation lying lateral to that of the hand (see Chapter 28, Fig 28.7). As for evoked responses, PET has demonstrated the bilateral nature of the tongue representation (Pardo *et al.*, 1997).

Disbrow *et al.*, (2000) have recently used fMRI to show that besides SI, human cortex has both SII and parietal ventral (PV) representations within the lateral sulcus. Both regions are mirror-symmetrical and topographically organised with face most lateral on the lip of the upper bank of the lateral sulcus, similar to the macaque (Krubitzer *et al.*, 1995; Disbrow *et al.*, 2000; Chapter 28). They found that unlike areas 3b and 1, localized stimuli were less effective in SII and PV. Stimuli over larger skin areas and stimuli moving across the skin were particularly effective in SII and PV, suggesting, indirectly, that cells in these areas may have larger receptive fields. This was also supported by the finding that unilateral stimuli caused bilateral activation in both areas.

For intraoral representations, a recent PET study has considered the issue of somatosensory versus gustatory areas by using water as the stimulus (Zald and Pardo, 2000). Intraoral water caused activation of a large area of the pre- and post-central gyrus, insula, and operculum. Voluntary swallowing was used to eliminate areas thought to be associated with somatosensory and motor processing, as compared with gustation. Subtraction of activity associated with voluntary swallowing reduced activation in all these regions. Not surprisingly, the peak focus of somatosensory activation occurred in the post-central gyrus, in an area consistent with the representation of the tongue and oral cavity.

Orofacial Response Characteristics

Responses of cells in areas 3b, 1, and 2 in orofacial regions are similar to those from the limbs. Thus 3b gives primarily cutaneous responses with small receptive fields, while area 1 has larger, more complex responses and area 2 contains both cutaneous and deep receptors. These are discussed in Chapter 28. Nociceptive responses have also been reported in SI from trigeminal activation (Kenshalo and Isensee,

1983; Kenshalo *et al.*, 1988; Chudler *et al.*, 1990). Such responses are found within SI as well as in SII and adjacent regions (Dong *et al.*, 1989).

A series of experiments in awake macaque monkeys has provided the best information to date on responses of cells within orofacial regions of the primate SI cortex. Cells were located in areas 3b, 1, and 2. The most frequently recorded responses were from cells sensitive to stimulation of the lips, tongue and periodontium (Lin *et al.*, 1994a). Most cells were activated by low-threshold stimulation and gave rapidly adapting responses. Seventy-eight percent of the units responded to contralateral stimuli; the others being bilateral. The activity of many units was modified by a protrusion of the tongue, and in some cases activity could change significantly prior to the onset of EMG activity associated with the movement. However, biting movements did not change the firing pattern in most of the cells. Modification of somatosensory responses during facial movements would relate in part to movement-activated stimulation within the receptive field of the neuron. In addition, Lin *et al.* suggested that these sensory cells may provide an important input for controlling the movement or even initiating it. The role of these cells in regulating tongue movements was further supported by a study (Lin *et al.*, 1994b) in which monkeys were trained to protrude the tongue in different directions. Over half of the responses from areas 3b and 1 showed a difference in response in relation to the direction of tongue protrusion. Moreover it was shown that the response of cells to stimulation of their receptive fields on the lips or tongue were suppressed during a tongue protrusion movement. This suppression was not generalized across all the somatosensory cortex but rather was dependent on the location of a particular receptive field in relation to the movement being undertaken (Lin and Sessle, 1994). The importance of responses in SI for undertaking learned movements was shown by Lin *et al.* (1993) by cooling of SI during a tongue protrusion or biting task. During cooling, monkeys had difficulty in maintaining the steady tongue protrusive force during the holding period.

Plasticity of Trigeminal Responses

There is increasing evidence to support reorganization of somatosensory responses following deafferentation, for instance after nerve section or amputation. This is widely reported from animal studies (Wall, 1988; Garraghty *et al.*, 1994; Jain *et al.*, 1998; Waite, 2000) where representation of a body part adjacent to a denervated area expands into the deafferented representation. There is now considerable evidence that similar reorganization can occur in humans (Mogilner *et al.*, 1993; Ramachandran, 1993). Some of the most extensive changes involve cortical regions originally responsive to stimulation of the hand, becoming reorganized to respond to facial stimuli. For example, MEG imaging has shown an anatomical shift of the cortical area activated by facial stimuli after amputation (Elbert *et al.*, 1994). The facial area was shifted medially into the region normally associated with responses from the hand. Such changes may explain the finding that stimulation of the face evokes sensations on the "phantom" hand (Ramachandran *et al.*, 1992; Halligan *et al.*, 1993). Correspondingly, referral to the hand occurred after the removal of the maxillary and mandibular regions of the trigeminal ganglion (Clarke *et al.*, 1996). Some cortical reorganization occurs immediately after deafferentation, although it is clear that reorganization continues to become more extensive for years after the injury (Pons *et al.*, 1991).

The cortical reorganization reported in monkeys can extend for 10 to 14 mm (Pons *et al.*, 1991), well beyond the known overlap in thalamocortical projections (about 1.5 mm, Rausell and Jones, 1995). Similarly in humans shifts of approximately 2 cm have been demonstrated (Elbert *et al.*, 1994). One possible mechanism for such widespread remapping was suggested to involve changes in horizontal intracortical connections. However, Manger *et al.* (1997) showed that there were few such horizontal connections crossing the border between the hand and trigeminal areas in macaques. In contrast, the hand representation had extensive intracortical connections with lower jaw and neck regions innervated by C2 and C3 cervical nerves. These extended for some 3 mm and may, at least in part, explain the remapping after amputations or deafferentation. However, the limited extent of intracortical connections indicates that they are probably not sufficient to explain the total reorganization seen.

Another mechanism likely to contribute to the remapping that is seen at cortical level is the degree of subcortical change that can occur. Plasticity at both brainstem and thalamic levels have been documented in animal studies (reviewed Kaas *et al.*, 1999). For example, in the brainstem, trigeminal inputs grow into the cuneate nucleus after amputations or lesions of the dorsal columns (monkey, Jain *et al.*, 2000). There is now evidence for plasticity in the human thalamus, both immediately after a cold block of the receptive field of a neuron (Dostrovsky, 1999) and chronically after amputation (Kiss *et al.*, 1994). Similarly after spinal transections or surgery for chronic pain, expansions of border zone responses into anaesthetic areas were found (Lenz *et al.*, 1994). These changes suggest that

expansions from adjacent central representations can occur at any level of a sensory path. Thus besides cortical reorganization, changes in brainstem and thalamus may underlie trigeminal expansions into other central somatic territories. Similarly, limb inputs can invade trigeminal territories at all central levels after damage to trigeminal nerves or ganglion (rat, Waite, 2000; human, Clarke *et al.*, 1996).

References

Allen, G.V., and Pronych, S.P. (1997). Trigeminal autonomic pathways involved in nociception-induced reflex cardiovascular responses. *Brain Res.* **754,** 269–278.

Andres, K.H., von During, M., Muszynski, K., and Schmidt, R.F. (1987). Nerve fibers and their terminals of the dura mater encephali of the rat. *Anat. Embryol.* **175,** 289–301.

Angus-Leppan, H., Olausson, B., Boers, P., and Lambert, G.A. (1994). Convergence of afferents from superior sagittal sinus and tooth pulp on cells in the upper cervical spinal cord of the cat. *Neurosci. Lett.* **182,** 275–278.

Anneroth, G., and Norberg, K.A. (1968). Adrenergic vasoconstrictor innervation in the human dental pulp. *Acta Odontologica Scand.* **26,** 89–93.

Arvidsson, J., and Gobel, S. (1981). An HRP study of the central projections of primary trigeminal neurons which innervate tooth pulps in the cat. *Brain Res.* **210,** 1–16.

Azerad, J., Woda, A., and Albe-Fessard, D. (1982). Physiological properties of neurons in different parts of the cat trigeminal sensory complex. *Brain Res.* **246,** 7–21.

Badr, G.G., Hanner, P., and Edstrom, S. (1983). Cortical evoked potentials in response to trigeminal nerve stimulation in humans. *Clin. Electroencephalog.* **14,** 61–66.

Ball, M.J., Nuttall, K., and Warren, K.G. (1982). Neuronal and lymphocytic populations in human trigeminal ganglia: Implications for ageing and for latent virus. *Neuropathol. Appl. Neurobiol.* **8,** 177–187.

Baker, R., and Llinas, R. (1971). Electrotonic coupling between neurones in the rat mesencephalic nucleus. *J. Physiol.* **212,** 45–63.

Baraniuk, J.N. (1992). Sensory, parasympathetic, and sympathetic neural influences in the nasal mucosa. *J. Allergy Clin. Immunol.* **90,** 1045–1050.

Beaver, D.L., Moses, H.L., and Ganote, C.E. (1965). Electron microscopy of the trigeminal ganglion. II Autopsy study of the human ganglia. *Arch. Pathol.* **79,** 557–570.

Beckstead, R.M., Morse, J.R., and Norgren, R. (1980). The nucleus of the solitary tract in the monkey: Projections to the thalamus and brainstem nuclei. *J. Comp. Neurol.* **190,** 259–282.

Bennett, M.H., and Jannetta, P.J. (1980). Trigeminal evoked potentials in humans. *Electroencephalogr. Clin. Neurophysiol.* **48,** 517–526.

Bereiter, D.A., and Bereiter, D.F. (1996). *N*-methyl-*D*-aspartate and non-*N*-methyl-*D*-aspartate receptor antagonism reduces Fos-like immunoreactivity in central trigeminal neurons after corneal stimulation in the rat. *Neurosci.* **73,** 249–258.

Bittar, R.G., Olivier, A., Sadikot, A.F., Andermann, F., Comeau, R.M., Cyr, M., Peters, T.M., and Reutens, D.C. (1999). Localization of somatosensory function by using positron emission tomography scanning: A comparison with intraoperative cortical stimulation. *J. Neurosurg.* **90,** 478–483.

Blomqvist, A., Zhang, E-T., and Craig, A.D. (2000). Cytoarchitectonic and immunohistochemcial characterization of a specific pain and temperature relay, the posterior portion of the ventral medial nucleus, in the human thalamus. *Brain.* **123,** 601–619.

Boissonade F.M., and Matthews, B. (1993). Responses of trigeminal brainstem neurons and the digastric muscle to tooth pulp stimulation in awake cats. *J. Neurophysiol.* **69,** 174–186.

Boissonade, F.M., Sharkey, K.A., and Lucier, G.E. (1993). Trigeminal nuclear complex of the ferret: Anatomical and immunohistochemical studies. *J. Comp. Neurol.* **329,** 291–312.

Bouras, C., Magistretti, P.J., Morrison, J.H., and Constantinidis, J. (1987). An immunohistochemical study of pro-somatostatin-derived peptides in the human brain. *Neurosci.* **22,** 781–800.

Brodal, A. (1965) "The Cranial Nerves. Anatomy and Anatomico-Clinical Correlations," 2nd ed. Blackwell, Oxford.

Bruce, L.L., McHaffie, J.G., and Stein, B.E. (1987). The organization of trigeminotectal and trigeminothalamic neurons in rodents: A double labelling study with fluorescent dyes. *J. Comp. Neurol.* **262,** 315–330.

Burstein, R., Yamamura, H., Malick, A., and Strassman, A.M. (1998). Chemical stimulation of the intracranial dura induces enhanced responses to facial stimulation in brainstem trigeminal neurons. *J. Neurophysiol.* **79,** 964–982.

Burton, H., and Craig, A.D. (1979). Distribution of trigeminothalamic projection cells in cat and monkey. *Brain Res.* **161,** 515–521.

Bushnell, M.C., and Duncan, G.H. (1987). Mechanical response properties of ventroposterior medial thalamic neurons in the alert monkey. *Exp. Brain Res.* **67,** 603–614.

Bushnell, M.C., Duncan, G.H., Dubner, R., and He, L.F. (1984). Activity of trigeminothalamic neurons in medullary dorsal horn of awake monkeys trained in a thermal discrimination task. *J. Neurophysiol.* **52,** 170–187.

Byers, M.R. (1984). Dental sensory receptors. *Internat. Rev. Neurobiol.* **25,** 39–94.

Byers, M.R., and Dong, W.K. (1983). Autoradiographic location of sensory nerve endings in dentin of monkey teeth. *Anat. Rec.* **205,** 441–454.

Cairns, B.E., Sessle, B.J., and Hu J.W. (1998). Evidence that excitatory amino acid receptors with the temporomandibular joint region are involved in the reflex activation of the jaw muscles. *J. Neurosci.* **18,** 8056–8064.

Cajal, S., and Ramon, Y. (1909). Histologie du systeme nerveux de l'homme et des vertebres. Tome premier: generalities, moelle, ganglions rachidiens, bulbe et protubereance. Maloine, Paris (1972) Segunda reimpresion. Consejo Superior de Investigaciones Cientificas, Instituto Ramon y Cajal, Madrid.

Cangro, C.B., Sweetnam, P.M., Wrathall, J.R., Hasen, W.B., Curthoys, N.P., and Neale, J.H. (1985). Localization of elevated glutaminase immunoreactivity in small DRG neurones. *Brain Res.* **336,** 159–161.

Capra, N.F., and Dessem, D., (1992). Central connections of trigeminal primary afferent neurons: Topographical and functional considerations. *Crit. Rev. Oral Biol. Med.* **4,** 1–52.

Carpentier, V., Vaudry, H., Mallet, E., Laquerriere, A., Tayot, J., and Leroux, P. (1996). Anatomical distribution of somatostatin receptors in the brainstem of the human fetus. *Neurosci.* **73,** 865–879.

Chan-Palay, V. (1978). The paratrigeminal nucleus. I. Neurons and synaptic organization. *J. Neurocytol.* **7,** 405–418.

Chiaia, N.L., Rhoades, R.W., Bennett-Clark, C.A., Fish, S.E., and Killackey, H.P. (1991). Thalamic processing of vibrissal information in the rat. I. Afferent input to the medial ventral posterior and posterior nuclei. *J. Comp. Neurol.* **314,** 201–216.

Choi, C.H., and Fisher, W.S. III (1994). Microvascular decompression as a therapy for trigeminal neuralgia. *Microsurg.* **15,** 527–533.

Cicchetti, F., Lacroix, S., Beach, T.G., and Parent, A. (1998). Calretinin gene expression in the human thalamus. *Mol. Brain Res.* **54** 1–12.

Clarke, S., Regli, L., Janzer, R.C., Assal, G., and de Tribolet, N. (1996). Phantom face: Conscious correlate of neural reorganization after removal of primary sensory neurones. *NeuroReport*. **7,** 2853–2857.

Clements, J.R., and Beitz, A.J. (1987). A quantitative light microscopic analysis and ultrastructural description of cholecystokinin-like immunoreactivity in the spinal trigeminal nucleus of the rat. *Neurosci.***20**, 427–438.

Clements, J.R., and Beitz, A.J. (1991). An electron microscopic description of glutamate-like immunoreactive axon terminals in the rat principal sensory and spinal trigeminal nuclei. *J. Comp. Neurol*. 309, 271–280.

Clements, J.R., Magnusson, K.R., Hautman, J., and Beitz, A.J. (1991). Rat tooth pulp projections to spinal trigeminal sub-nucleus caudalis are glutamate-like immunoreactive. *J. Comp. Neurol.* **309,** 281–288.

Craig, A.D. (1996). An ascending general homeostatic afferent pathway originating in lamina I. *Prog. Brain Res.* **107,** 225–242.

Craig, A.D., and Dostrovsky J.O. (1997). Processing of nociceptive information at supraspinal levels. *In* "Anaesthesia: Biologic Foundations" (T.L. Yaksh, C Lynch III, W.M. Zapol, M. Maze, I.F. Biebuyck, and L.J. Saidman, eds.), pp. 625–642. Lippincott-Raven, Philadelphia.

Craig, A.D., Bushnell, M.C., Zhang, E.-T., and Blomqvist, A. (1994). A thalamic nucleus specific for pain and temperature sensation. *Nature.* **372,** 770–773.

Craig, A.D., Reiman, E.M., Evans, A., and Bushnell, M.C. (1996). Functional imaging of an illusion of pain. *Nature.* **384,** 258–260.

Craig, A.D., Zhang, E., and Blomqvist, A. (1999). A distinct thermoreceptive subregion of lamina I in nucleus caudalis of the owl monkey. *J. Comp. Neurol.* **404,** 221–234.

Curry, M.J. (1972). The exteroceptive properties of neurones in the somatic part of the posterior group (PO). *Brain Res.* **44,** 439–462.

Cushing, H. (1904). The sensory distribution of the fifth cranial nerve. *Bull. Johns Hopkins Hosp.* **15,** 213–232.

Dallel, R., Clavelou, P., and Woda, A. (1989). Effects of tractotomy on nociceptive reactions induced by tooth pulp stimulation in the rat. *Exp. Neurol.* **106,** 78–84.

Dallel, R., Dualé, C., and Molat, J-L. (1998). Morphine administration in the substantia gelatinosa of the spinal trigeminal nucleus caudalis inhibits nociceptive activities in the spinal trigeminal nucleus oralis. *J. Neurosci.* **18,** 3529–3536.

Darian-Smith, I. (1973). The trigeminal system. *In* "Somatosensory System, Handbook of Sensory Physiology" (A. Iggo, ed.), vol. II, pp. 271–314. Springer-Verlag, Berlin and New York.

Darian-Smith, C., Darian-Smith, I., and Cheema, S. S. (1990). Thalamic projections to sensorimotor cortex in the macaque monkey: Use of multiple retrograde fluorescent tracers. *J. Comp. Neurol*. **299,** 17–46.

Davis, K.D., Lozano, A.M., Manduch, M., Tasker, R.R., Kiss, Z.H.T., and Dostrovsky, J.O. (1999). Thalamic relay site for cold perception in humans. *J. Neurophysiol*. **81,** 1970–1973.

de Lacalle, S., and Saper, C.B. (2000). Calcitonin gene-related peptide-like immunoreactivity marks putative visceral sensory pathways in human brain. *Neurosci.* **100,** 115–130.

Del Fiacco, M., and Quartu, M. (1994). Somatostatin, galanin and peptide histidine isoleucine in the newborn and adult human trigeminal ganglion and spinal nucleus: Immunohistochemistry, neuronal morphometry and colocalization with substance P. *J. Chem. Neuroanat*. **7,** 171–184.

Denny-Brown, D., and Yanagisawa, N. (1973). The function of the descending root of the fifth nerve. *Brain.* **96,** 783–814.

Disbrow, E., Roberts, T., and Krubitzer, L. (2000). Somatotopic organization of cortical fields in the lateral sulcus of Homo *sapiens:* Evidence for SII and PV. *J. Comp. Neurol.* **418,** 1–21.

Donaldson, I.M.L. (1973). The properties of some human thalamic units. Some new observations and a critical review of the localization of thalamic nuclei. *Brain.* **96,** 419–440.

Donaldson, I.M.L. (2000). The functions of the proprioceptors of the eye muscles. *Phil. Trans. R. Soc. Lond. Ser. B* **355,** 1685–1754.

Dong, W.K., Salonen, L.D., Kawakami, Y., Shiwaku, T., Kaukoranta, E.M., and Martin, R.F. (1989), Nociceptive responses of trigeminal neurons in SII-7b cortex of awake monkeys. *Brain Res.* **484,** 314–324.

Dostrovsky, J.O. (1999). Immediate and long-term plasticity in human somatosensory thalamus and it's involvement in phantom limbs. *Pain Suppl.* **6,** S37–S43.

Dostrovsky, J. O. (2002). Role of thalamus in pain, *In* "Progress in Brain Research." (J. Sandkuhler, B Bromm, and G.F. Gebhart, eds.), pp. 245–257. Elsevier Science.

Dostrovsky, J.O., and Craig, A.D. (1996). Cooling-specific spinothalamic neurons in the monkey. *J. Neurophysiol*. **76,** 3656–3665.

Dostrovsky, J.O., Davis, K.D., and Kawakita, K. (1991). Central mechanisms of vascular headaches. *Canadian J. Physiol. Pharmacol.* **69,** 652–658.

Doty, R.L. (1995). Intranasal trigeminal chemoreception, *In* "Handbook of Olfaction and Gustation." (R.L. Doty, ed.), pp.821–833. Marcel Dekker, New York

Dreessen, D., Halata, Z., and Strasmann, T. (1990). Sensory innervation of the temporomandibular joint in the mouse. *Acta Anat.* **139,** 154–160.

Dubner, R., and Basbaum, A.J. (1994). Spinal dorsal horn plasticity following tissue or nerve injury. *In* "Textbook of Pain." (P.D. Wall and R. Melzack, eds.), pp. 225–241. Churchill-Livingstone, London.

Dubner, R., Hoffman, D.S., and Hayes, R.L. (1981). Neuronal activity in medullary dorsal horn of awake monkeys trained in thermal discrimination task. III. Task-related responses and their functional role. *J. Neurophysiol.* **46,** 444–464.

Dubner, R., Sessle, B.J., and Storey, A.T. (1978). "The Neural Basis of Oral and Facial Function." Plenum, New York.

Eisenman, J., Landgren, S., and Novin, D. (1963). Functional organization in the main sensory trigeminal nucleus and in the rostral subdivision of the nucleus of the spinal trigeminal tract in the cat. *Acta Physiol. Scand.* 59 [Suppl], **214,** 41–44.

Elbert, T., Flor, H., Birbaumer, N., Knecht, S., Hampson, S., Larbig, W., and Taub, E. (1994). Extensive reorganization of the somatosensory cortex in adult humans after nervous system injury. *NeuroReport* **5,** 2593–2597.

Elsås, T., Edvinsson, L., Sundler, F., and Uddman, R. (1994). Neuronal pathways to the rat conjunctiva revealed by retrograde tracing and immunochemistry. *Exp. Eye Res.* **58,** 117–126.

Ferner, H. (1940). Über den Bau des Ganglion semilunare (Gasseri) und der Trigeminuswurzel beim Menschen. *Zeitschr. Anat. Entw.gesch.* **110,** 391–404.

Findler, G., and Feinsod, M. (1982). Sensory evoked response to electrical stimulation of the trigeminal nerve in humans. *J. Neurosurg.* **56,** 545–549.

Fisher, C.M. (1982). Pure sensory stroke and allied conditions. *Stroke* **13,** 434–447.

Florence, S.L., Wall, J.T., and Kaas, J.H. (1989). Somatotopic organization of inputs from the hand to the spinal gray and cuneate nucleus of monkeys with observations on the cuneate nucleus of humans. *J. Comp. Neurol.* **286,** 48–70.

Fortin, M., Asselin, M-C., Gould, P.V., and Parent, A. (1998). Calretinin-immunoreactive neurons in the human thalamus. *Neurosci.* **84,** 537–548.

Fortman, G.J., and Winkelmann, R.K. (1977). The Merkel cell in oral human mucosa. *J. Dent. Res.* **56,** 1305–1312.

Fox, P.T., Burton, H., and Raichle, M.E. (1987). Mapping human somatosensory cortex with positron emission tomography. *J. Neurosurg.* **67,** 34–43.

Frank, R.M. (1968). "Dentine and Pulp: Their Structure and Functions" (N.B.B. Symons, ed.), pp. 115–145. Livingstone, London.

Freimann, R. (1954). Untersuchungen uber Zahl und Anordnung der Muskelspindeln in den Kaumuskeln des Menschen. *Anat. Anz.* **100,** 258–264.

Fristad, I. (1997). Dental innervation: functions and plasticity after peripheral injury. [Review] *Acta Odontologica Scand.* **55,** 236–254.

Ganchrow, D. (1978). Intratrigeminal and thalamic projections of nucleus caudalis in the squirrel monkey *(Saimiri sciureus):* A degeneration and autoradiographic study. *J. Comp. Neurol.* **178,** 281–312.

Garraghty, P.E., Hanes, D.P., Florence, S.L., and Kaas, J.H. (1994). Pattern of peripheral deafferentation predicts reorganizational limits in adult primate somatosensory cortex. *Somatosens. Motor Res.* **11,** 109–117.

Gill, H.I. (1971). Neuromuscular spindles in human lateral pterygoid muscles. *J. Anat.* **109,** 157–167.

Ginestal, E., and Matute, C. (1993). Gamma-aminobutyric acid-immunoreactive neurons in the rat trigeminal nuclei. *Histochem.* **99,** 49–55.

Goadsby, P.J., and Edvinsson, L. (1993). The trigeminovascular system and migraine: studies characterizing cerebrovascular and neuropeptide changes seen in humans and cats. *Ann. Neurol.* **33,** 48–56.

Goadsby, P.J., and Zagami, A.S. (1991). Stimulation of the superior sagittal sinus increases metabolic activity and blood flow in certain regions of the brainstem and upper cervical spinal cord of the cat. *Brain* **114,** 1001–1011.

Goadsby, P.J., Edvinsson, L., and Ekman, R. (1988). Release of vasoactive peptides in the extracerebral circulation of humans and the cat during activation of the trigeminovascular system. *Ann. Neurol.* **23,** 193–196.

Gobel, S. (1971). Structural organization in the main sensory trigeminal nucleus. *In* "Oral-Facial Sensory and Motor Mechanisms" (R. Dubner and Y. Kawamura, eds.), pp. 183–202. Appleton-Century-Crofts, New York.

Gobel, S. (1978). Golgi studies of the neurons in layer I of the dorsal horn of the medulla (trigeminal nucleus caudalis). *J. Comp. Neurol.* **180,** 375–394.

Gobel, S., and Dubner, R. (1969). Fine structural studies of the main sensory trigeminal nucleus in the cat and rat. *J. Comp. Neurol.* **137,** 459–493.

Gobel, S., Hockfield, S., and Ruda, M.A. (1981). Anatomical similarities between the medullary and spinal dorsal horns. *In* "Oral-Facial Sensory and Motor Functions" (Y. Kawamura and R. Dubner, eds.), pp. 211–223. Quintessence, Tokyo.

Goyal, R., Rasey, S.K., and Wall, J.T. (1992). Current hypotheses of structural pattern formation in the somatosensory system and their potential relevance to humans. *Brain Res.* **583,** 316–319.

Graham, J.R., and Wolff, H.G. (1938). Mechanism of migraine headache and action of ergotamine tartrate. *Arch. Neurol. Psychiat.* **39,** 737–763.

Graham, S.H., Sharp, F.R., and Dillon, W. (1988). Intraoral sensation in patients with brainstem lesions: Role of the rostral spinal trigeminal nuclei in pons. *Neurology.* **38,** 1529–1533.

Griffin, C.J., and Harris, R. (1975). Innervation of the temporomandibular joint. *Aust. Dental J.* **20,** 78–85.

Halata, Z., and Munger, B.L. (1983). The sensory innervation of primate facial skin. II. Vermilion border and mucosa of lip. *Brain Res. Rev.* **5,** 81–107.

Hallas, B.H., and Jacquin, M.F. (1990). Structure-function relationships in the rat brainstem subnucleus interpolaris. IX. Inputs from subnucleus caudalis. *J. Neurophysiol.* **64,** 28–45.

Halligan, P.W., Marshall, J.C., Wade, D.T., Davey, J., and Morrison, D. (1993). Thumb in cheek? Sensory reorganization and perceptual plasticity after limb amputation. *NeuroReport* **4,** 233–236.

Hamlyn, P.J. (1997). Neurovascular relationships in the posterior cranial fossa, with special reference to trigeminal neuralgia. 2. Neurovascular compression of the trigeminal nerve in cadaveric controls and patients with trigeminal neuralgia: Quantification and influence of method. *Clin. Anat.* **10,** 380–388.

Han, Z.-S., Zhang, E.-T., and Craig, A.D. (1998). Nociceptive and thermoreceptive lamina I neurons are anatomically distinct. *Nature Neurosci.* **1,** 218–225.

Hannam, A.G., and Sessle, B.J. (1994). Temporomandibular neurosensory and neuromuscular physiology. *In* "Temporomandibular joint and masticatory muscle disorders." (G.E. Zarb, G. Carlsson, B.J. Sessle, and N.D. Mohl, eds.), pp. 67–100. Munksgaard, Copenhagen.

Haring, J.H., Henderson, T.A., and Jacquin, M.F. (1990). Principalis- or parabrachial-projecting spinal trigeminal neurons do not stain for GABA or GAD. *Somatosens. Motor Res.* **7,** 391–397.

Hashimoto, I. (1988). Trigeminal evoked potentials following brief air puff: Enhanced signal-to-noise radio. *Ann. Neurol.* **23,** 332–338.

Hassler, R. (1959). Anatomy of the thalamus. *In* "Introduction to Stereotaxis with an Atlas of the Human Brain" (G. Schaltenbrand and P. Bailey, eds.), pp. 230–290. Thieme, Stuttgart.

Hauser-Kronberger, C., Hacker, G.W., Franz, P., Albegger, K., and Dietze, O. (1997). CGRP and substance P in intraepithelial neuronal structures of the human upper respiratory system. *Regulatory Peptides* **72,** 79–85.

Hayashi, H. (1985a). Morphology of central terminations of intra axonally stained, large, myelinated primary fibers from facial skin in the rat. *J. Comp. Neurol.* **237,** 195–215.

Hayashi, H. (1985b). Morphology of termination of small and large myelinated trigeminal primary afferent fibers in the cat. *J. Comp. Neurol.* **240,** 71–89.

Hayes, R.L., Dubner, R., and Hoffman, D.S. (1981). Neuronal activity in medullary dorsal horn of awake monkeys trained in a thermal discrimination task. II. Behavioural modulation of responses to thermal and mechanical stimuli. *J. Neurophysiol.* **46,** 428–443.

Heinz, P., Bodanowitz, S., Wiegand, W., and Kroll, P. (1996). In vivo observation of corneal regeneration after photorefredin keratectomy with confocal video microscopy. German *J. Ophthal.* **5,** 373–377.

Helme, R.D., and Fletcher, J.L. (1983). Substance P in the trigeminal system at postmortem: Evidence for a role in pain pathways in man. *Clin. Exp. Neurol.* **19,** 37–44.

Hensel, H., and Mann, G. (1956). Temperaturschmerz und Warmeleitung im menschlichen Zahn. *Stoma* **9,** 76–85.

Hoshiyama, M., Kakigi, R., Koyama, S., Kitamura, Y., Shimojo, M., and Watanabe, S. (1996). Somatosensory evoked magnetic fields following stimulation of the lip in humans. *Electroencephalogr. Clin. Neurophysiol.* **100,** 96–104.

Hu, J.W. (1990). Response properties of nociceptive and non-nociceptive neurons in the rat's trigeminal subnucleus caudalis (medullary dorsal horn) related to cutaneous and deep craniofacial afferent stimulation and modulation by diffuse noxious inhibitory controls. *Pain.* **41,** 331–345.

Hu, J.W., and Sessle, B.J. (1979). Trigeminal nociceptive and non-nociceptive neurons: brainstem intranuclear projections and modulation by orofacial, periaqueductal gray and nucleus raphe magnus stimuli. *Brain Res.* **170,** 547–555

Hu, J.W., and Sessle, B.J. (1989). Effects of tooth pulp deafferentation on nociceptive and non-nociceptive neurons of the feline trigeminal subnculeus caudalis (medullary dorsal horn). *J. Neurophysiol.* **61**, 1197–1206.

Huerta, M.F., Frankfurter, A., and Harting, J.K. (1983). Studies of the principal sensory and spinal trigeminal nuclei of the rat: Projections to the superior colliculus, inferior olive, and cerebellum. *J. Comp. Neurol.* **220,** 147–167.

Ichikawa, H., Matsuo, S., Wakisaka, S., and Akai, M. (1990). Fine structure of calcitonin gene related peptide immunoreactive nerve fibers in the rat temporomandibular joint. *Arch. Oral Biol.* **35,** 727–730.

Ide, L.S., and Killackey, H.P. (1985). Fine structural survey of the rat's brainstem sensory trigeminal complex. *J. Comp. Neurol.* **235,** 145–168.

Iggo, A. (1974). Cutaneous receptors. *In* "The Peripheral Nervous System" (J. Hubbard, ed.), pp. 347–404. Plenum, New York.

Iliakis, B., Anderson, N.L., Irish, P.S., Henry, M.A., and Westrum, L.E. (1996). Electron microscopy of immunoreactivity patterns for glutamate and □-aminobutyric acid in synaptic glomeruli of the feline spinal trigeminal nucleus (subnucleus caudalis). *J. Comp. Neurol.* **366,** 465–477.

Inagaki, S., Kito, S., Kubota, Y., Girgis, S., Hillyard, C.J., and Macintyre, I. (1986). Autroradiographic localization of calcitonin gene-related peptide binding sites in human and rat brains. *Brain Res.* **374,** 287–298.

Ishiko, N., Hanamori, T., and Murayama, N. (1980). Spatial distribution of somatosensory responses evoked by tapping the tongue and finger in man. *Electroencephalogr. Clin. Neurophysiol.* **50,** 1–10.

Iwata, K., Kenshalo, D.R., Dubner, R., and Nahin, R.L. (1992). Diencephalic projections from the superficial and deep laminae of the medullary dorsal horn in the rat. *J. Comp. Neurol.* **321,** 404–420.

Jacquin, M.F., and Rhoades, R.W. (1990). Cell structure and response properties in the trigeminal subnucleus oralis. *Somatosens. Motor Res.* **7,** 265–288.

Jacquin, M.F., Barcia, M., and Rhoades, R.W. (1989b). Structure-function relationship in rat brainstem subnucleus interpolaris: IV. Projection neurons. *J. Comp. Neurol.* **282,** 45–62.

Jacquin, M.F., Chiaia, N.L., and Rhoades, R.W. (1990). Trigeminal projections to the contralateral dorsal horn: Central extent, peripheral origins, and plasticity. *Somatosens. Motor Res.* **7,** 153–183.

Jacquin, M.F., Golden, J., and Panneton, W.M. (1988). Structure and function of barrel 'precursor' cells in trigeminal nucleus principalis. *Devel. Brain Res.* **43,** 309–314.

Jacquin, M.F., Golden, J., and Rhoades, R.W. (1989a). Structure-function relationship in rat brainstem subnucleus interpolaris: III. Local circuit neurons. *J. Comp. Neurol.* **282,** 24–44.

Jacquin, M.F., Mooney, R.D., and Rhoades, R.W. (1986). Morphology, response properties, and collateral projections of trigemino-thalamic neurons in brainstem subnucleus interpolaris of rat. *Exp. Brain Res.* **61,** 457–468.

Jain, N., Florence, S.L., and Kaas, J.H. (1998). Reorganization of somatosensory cortex after nerve and spinal cord injury. *News Physiol. Sci.* **13,** 143–149.

Jain, N., Florence, S.L., Qi, H-X., and Kaas, J.H. (2000). Growth of new brainstem connections in adult monkeys with massive sensory loss. *PNAS,* **97,** 5546–5550.

Jain, N., Qi, H.-X., Catania, K.C., and Kaas, J.H. (2001). Anatomic correlates of the face and oral cavity representations in the somatosensory cortical area 3b of monkeys. *J. Comp. Neurol.* **429,** 455–468.

Jansen, I., Uddman, R., Hocherman, M., Ekman, R., Jensen, K., Olesen, J., Stiernholm, P., and Edvinsson, L. (1986). Localization and effects of neuropeptide Y, vasoactive intestinal polypeptide, substance P, and calcitonin gene-related peptide in human temporal arteries. *Ann. Neurol.* **20,** 496–501.

Jasmin, L., Burkey, A.R., Card, J.P., and Basbaum, A.I. (1997). Transneuronal labeling of a nociceptive pathway, the spino-(trigemino-)parabrachio-amygdaloid, in the rat. *J. Neurosci.***17,** 3751–3765.

Jasper, H.H., and Bertrand, G. (1966). Thalamic units involved in somatic sensation and voluntary and involuntary movements in man. *In* "The Thalamus" (Purpura and Yahr, eds.), pp. 365–390. Columbia University Press, New York.

Johansson, R.S., Trulsson, M., Olsson, K.A., and Westberg, K.-G. (1988). Mechanoreceptor activity from the human face and oral mucosa. *Exp. Brain Res.* **72,** 204–208.

Johnsen, D.C., and Johns, S. (1978). Quantitation of nerve fibers in the primary and permanent canine and incisor teeth in man. *Arch. Oral Biol.* **23,** 825–830.

Jones, E.G. (1985). "The Thalamus." Plenum Press, New York.

Jones, E.G. (1998). Viewpoint: The core and matrix of thalamic organization. *Neurosci.* **85,** 331–345.

Kaas, J.H., and Pons, T.P. (1988). The somatosensory system of primates. *In* "Comparative Primate Biology" (H.P. Steklis and J. Erwin, eds.), vol. 4, pp. 421–468. Liss, New York.

Kaas, J.H., Florence, S.L., and Jain, N. (1999). Subcortical contributions to massive cortical reorganizations. *Neuron.* **22,** 657–660.

Kadanoff, D., Chouchkov, C., and Michailova, K. (1980). Evolution of encapsulated sensory nerve endings in the hairless part of the lips of mammals. *Z Mikrosk Anat. Forsch.* **94,** 943–951.

Kai-Kai, M.A. (1989). Cytochemistry of the trigeminal and dorsal root ganglia and spinal cord of the rat. *Comp. Biochem. Physiol.* **93A,** 183–193.

Kai-Kai, M.A., and Howe, R. (1991). Glutamate-immunoreactivity in the trigeminal and dorsal root ganglia, and intraspinal neurons and fibers in the dorsal horn of the rat. *Histochem. J.* **23,** 171–179.

Kai-Kai, M.A., and Keen, P.M. (1985). Localization of 5-hydroxytryptamine to neurones and endoneurial mast cells in sensory ganglia. *J. Neurocytol.* **14,** 63–78.

Kehrli, P., Maillot, C., and Wolff, M-J. (1997). Anatomy and embryology of the trigeminal nerve and its branches in the parasellar area. *Neurol. Res.* **19,** 57–65.

Keller, J.T., and Marfurt, C.F. (1991). Peptidergic and serotoninergic innervation of the rat dura mater. J. Comp. Neurol. 309, 515–534.

Keller, J.T., Saunders, M.C., Beduk, A., and Jollis, J.G. (1985). Innervation of the posterior fossa dura of the cat. *Brain Res. Bull.* **14,** 97–102.

Kemplay, S., and Webster, K.E. (1989). A quantitative study of the projections of the gracile, cuneate and trigeminal nuclei and of the medullary reticular formation to the thalamus in the rat. *Neurosci.* **32,** 153–167.

Kenshalo, D.R., and Isensee, O. (1983). Responses of primate SI cortical neurons to noxious stimuli. *J. Neurophysiol.* **50,** 1479–1496.

Kenshalo, D.R., Chudler, E.H. Anton, F., and Dubner, R. (1988). SI nociceptive neurons participate in the encoding process by which monkeys perceive the intensity of noxious thermal stimulation. *Brain Res.* **454,** 378–382.

Kerr, F.W.L. (1963). The divisional organization of afferent fibers of the trigeminal nerve. *Brain* **86,** 721–732.

Kerr, F.W.L. (1967). Correlated light and electron microscopic observations on the normal trigeminal ganglion and sensory root in man. *J. Neurosurg.* [suppl.]. **26,** 168–172.

Kim, J.S. (1993). Trigeminal sensory symptoms due to midbrain lesions. *Eur. Neurol.* **33,** 218–220.

Kiss, Z.H.T., Dostrovsky, J.O., and Tasker, R.R. (1994). Plasticity in human somatosensory thalamus as a result of deafferentation. *Stereotactic Funct. Neurosurg.* **62,** 153–163.

Knyihar-Csillick, E., Tatji, J., Samsam, M., Sary, G., Slezak, S., and Vecsei, L. (1997). Effect of serotonin agonist (Sumatriptan) on the peptidergic innervation of the rat cerebral dura mater and on the expression of *c-fos* in the caudal trigeminal nucleus in an experimental migraine model. *J. Neurosci. Res.* **48,** 449–464.

Kosar, E., and Schwartz, G.J. (1990). Effects of methanol on peripheral nerve and cortical unit responses to thermal stimulation of the oral cavity in the rat. *Brain Res.* **513,** 202–211.

Krubitzer, L.A., and Kaas, J.H. (1990). The organization and connections of somatosensory cortex in marmosets. *J. Neurosci.* **10,** 952–974.

Krubitzer, L.A., Clarey, J., Tweedale, R., Elston, G., and Calford, M. (1995). A redefinition of somatosensory areas in the lateral sulcus of macaque monkeys. *J. Neurosci.* **348,** 55–72.

Kubota, K., Masegi, T., and Osanai, K. (1973). Muscle spindle distribution in the masticatory muscle of the squirrel monkey (*Saimiri sciurea*). *Bull. Tokyo Med. Dent. Univ.* **20,** 275.

Lambrichts, I., Creemers, J., and van Steenberghe, D. (1992). Morphology of neural endings in the human periodontal ligament: An electron microscopic study. *J. Periodont. Res.* **27,** 191–196.

Leijon, G., Boivie, J., and Johansson, I. (1989). Central post-stroke pain—neurological symptoms and pain characteristics. *Pain.* **36,** 13–25.

Lele, P.P., and Weddell, G. (1956). The relationship between neurohistology and corneal sensibility. *Brain.* **79,** 119–154.

Lenz, F.A., Dostrovsky, J.O., Tasker, R.R., and Yamashiro, K. (1988). Single-unit analysis of the human ventral thalamic nuclear group: somatosensory responses. *J. Neurophysiol.* **59,** 299–316.

Lenz, F.A., Kwan, H.C., Martin, R., Tasker, R., Richardson, R.T., and Dostrovsky, J.O. (1994). Characteristics of somatotopic organization and spontaneous neuronal activity in the region of the thalamic principal sensory nucleus in patients with spinal cord transection. *J. Neurophysiol.* **72,** 1570–1587.

Lenz, F.A., Seike, M., Lin, Y.C., Baker, F.H., Rowland, L.H., Gracely, R.H., and Richardson, R.T. (1993a). Neurons in the area of human thalamic nucleus ventralis caudalis respond to painful heat stimuli. *Brain Res.* **623,** 235–240.

Lenz, F.A., Seike, M., Richardson, R.T., Lin, Y.C., Baker, F.H., Khoja, I., Jaeger, C.J., and Gracely, R.H. (1993b). Thermal and pain sensations evoked by microstimulation in the area of human ventrocaudal nucleus. *J. Neurophysiol.* **70,** 200–212.

Levine, J., and Taiwo, Y. (1994). Inflammatory pain. *In* "Textbook of Pain" (P.D. Wall and R. Melzack, eds.), 3rd ed., pp. 45–56. Churchill-Livingstone, London.

Lieberman, A.R. (1976). Sensory ganglia. *In* "The Peripheral Nerve" (Landan, ed.), pp. 188–278. Chapman and Hall, London.

Liem, R.S.B., Copray, J.C.V.M., and van Willigen, J.D. (1991). Ultrastructure of the rat mesencephalic trigeminal nucleus. *Acta Anat.* **140,** 112–119.

Liem, R.S.B., Copray, J.C.V.M., and van Willigen, J.D. (1992). Distribution of synaptic boutons in the trigeminal nucleus of the rat—a quantitative electron-microscopical study. *Acta Anat.* **143,** 74–78.

Lin, L.-D., Murray, G.M., and Sessle, B.J. (1993). The effect of bilateral cold block of the primate face primary somatosensory cortex on the performance of trained tongue-protrusion task and biting tasks. *J. Neurophysiol.* **70,** 985–996.

Lin, L.-D., Murray, G.M., and Sessle, B.J. (1994a). Functional properties of single neurons in the primate face primary somatosensory cortex. I. Relations with trained orofacial motor behaviors. *J. Neurophysiol.* **71,** 2377–2390.

Lin, L.-D., Murray, G.M., and Sessle, B.J. (1994b). Functional properties of single neurons in the primate face primary somatosensory cortex. II. Relations with different directions of trained tongue protrusion. *J. Neurophysiol.* **71,** 2391–2400.

Lipton, J.A., Ship, J.A., and Larach-Robinson, D. (1993). Estimated prevalence and distribution of reported orofacial pain in the United States. J. *Amer. Dental Assoc.* **124,** 115–121.

Liu, X.-B., Jones, E.G., Huntley, G.W., and Molinari, M. (1989). Tachykinin immunoreactivity in terminals of trigeminal afferent fibers in adult and fetal monkey thalamus. *Exp. Brain Res.* **78,** 479–488.

Liu-Chen, L.Y., Gillespie, S.A., Norregaard, T.V., and Moskowitz, M.A. (1984). Co-localization of retrogradely transported wheat germ agglutinin and the putative neurotransmitter substance P within trigeminal ganglion cells projecting to cat middle cerebral artery. *J. Comp. Neurol.* **225,** 187–192.

Lund, J.P., and Olsson, K.A. (1983). The importance of reflexes and their control during jaw movement. *TINS* **6,** 458–463.

Luo, P.F., Wang, B.R., Peng, Z.Z., and Li, J.S. (1991). Morphological characteristics and terminating patterns of masseteric neurons of the mesencephalic trigeminal nucleus in the rat: An intracellular horseradish peroxidase labelling study. *J. Comp. Neurol.* **303,** 286–299.

Luo, P.F., Wong, R., and Dessem, D. (1995). Ultrastructural basis for synaptic transmission between jaw-muscle spindle afferents and trigeminothalamic neurons in the rostral trigeminal sensory nuclei of the rat. *J. Comp. Neurol.* **363,** 109–128.

Luthman, J., Johansson, O., Ahlstrom, U., and Kvint, S. (1988). Immunohistochemical studies of the neurochemical markers, CGRP, enkephalin, galanin, □-MSH, NPY, PHI, proctolin, PTH, somatostatin, SP, VIP, tyrosine hydroxylase and neurofilament in nerves and cells of the human attached gingiva. *Arch. Oral Biol.* **33,** 149–158.

Luzardo-Baptista, M. (1973). Intraepithelia nerve fibers in the human oral mucosa. An electron microscopic study. *Oral Surg.* **35,** 372–376.

Maeda, T., Kannari, K., Sato, O., and Iwanaga, T. (1990). Nerve terminals in human periodontal ligament of as demonstrated by immunohistochemistry for neurofilament protein (NFP) and S-100 protein. *Arch. Histol. Cytol.* **53,** 259–265.

Magnusson, K.R., Clements, J.R., Larson, A.A., Madl, J.E., and Beitz, A.J. (1987). Localization of glutamate in trigeminothalamic projection neurons: A combined retrograde transport-immunohistochemical and immunoradiochemical study. *Somatosens Res.* **4,** 177–190.

Magnusson, K.R., Larson, A.A., Madl, J.E., Altschuler, R.A., and Beitz, A.J. (1986). Co-localization of fixative-modified glutamate and glutaminase in neurons of the spinal trigeminal nucleus of the rat: An immunohistochemical and immunoradiochemical analysis. *J. Comp. Neurol.* **247,** 477–490.

Malick, A., and Burstein, R. (1998). Cells of origin of the trigeminohypothalamic tract in the rat. *J. Comp. Neurol.* **400,** 125–144.

Manger, P.R., Woods, T.M., and Jones, E.G. (1995). Representation of the face and intra-oral structures in area 3b of squirrel monkey (*Saimiri sciureus*) somatosensory cortex, with special reference to the ipsilateral representation. *J. Comp. Neurol.* **363,** 597–607.

Manger, P.R., Woods, T.M., and Jones, E.G. (1996). Representation of face and intra-oral structures in area 3b of macaque monkey somatosensory cortex. *J. Comp. Neurol.* **371,** 513–521.

Manger, P.R., Woods, T.M., Munoz, A., and Jones, E.G. (1997). Hand/face border as a limiting boundary in the body representation in monkey somatosensory cortex. *J. Neurosci.* **17,** 6338–6351.

Marfurt, C.F. (1981). The somatotopical organization of the cat trigeminal ganglion as determined by the horseradish peroxidase technique. *Anat. Rec.* **201,** 105–118.

Marfurt, C.F., and Rajchert, D.M. (1991). Trigeminal primary afferent projections to "non-trigeminal" areas of the rat central nervous system. *J. Comp. Neurol.* **303,** 489–511.

Marfurt, C.F., and Turner, D.F. (1984). The central projections of tooth pulp afferent neurons in the rat as determined by the transganglionic transport of horseradish peroxidase. *J. Comp. Neurol.* **223**, 535–547.

Marfurt, C.F., Kingsley, R.E., and Echtenkamp, S.E. (1989). Sensory and sympathetic innervation of the mammalian cornea. A retrograde tracing study. *Invest. Ophthal. Visual Sci.* **30,** 461–472.

Matsunami, K., and Kubota, K. (1972). Muscle afferents of trigeminal mesencephalic tract nucleus and mastication in chronic monkeys. *Japanese J. Physiol.* **22,** 545–555.

Matsushita, M., Ikeda, M., and Okado, N. (1982). The cells of origin of the trigeminothalamic, trigeminospinal and trigeminocerebellar projections in the cat. *Neurosci.* **17,** 1439–1454.

Mayberg, M., Langer, R.S., Zervas, N.T., and Moskowitz, M.A. (1981). Perivascular meningeal projections from cat trigeminal ganglia: Possible pathway for vascular headaches in man. *Science* **213,** 228–230.

McCarthy, G., Allison, T., and Spencer, D.D. (1993). Localization of the face area of human sensorimotor cortex by intracranial recording of somatosensory evoked potentials. *J. Neurosurg.* **79,** 874–884.

McClean, M.D., Dostrovsky, J.O., Lee, L., and Tasker, R.R. (1990). Somatosensory neurons in human thalamus respond to speech-induced orofacial movements. *Brain Res.* **513,** 343–347.

McComas, A.J., Wilson, P., Martin-Rodriguez, J., Wallace, C., and Hankinson, J. (1970). Properties of somatosensory neurons in the human thalamus. *J. Neurology, Neurosurg. Psychiat.* **33,** 716.

McNutt, J.C. (1975). Asymmetry in two-point discrimination on the tongues of adults and children. *J. Commun. Disorders* **8,** 213–220.

Melzack, R., and Eisenberg, H. (1968). Sensory skin afterglows. *Science* **159,** 445–447.

Meng, I.D., Hu, J.W., Benetti, A.P., and Bereiter, D.A. (1997). Encoding of corneal input in two distinct regions of the spinal trigeminal nucleus in the rat: Cutaneous receptive field properties, responses to thermal and chemical stimulation, modulation by diffuse noxious inhibitory controls, and projections to the parabrachial area. *J. Neurophysiol.* **77,** 43–56.

Mogilner, A., Grossman, J.A.I., Ribary, U., Joliot, M., Volkmann, J., Rapaport, D., Beasley, R.W., and Llinas, R.R. (1993). Somatosensory cortical plasticity in adult humans revealed by magnetoencephalography. *Neurobiol.* **90,** 3593–3597.

Moore, C.L., Stern, C.E., Corkin, S., Fischl, B., Gray, A.C., Rosen, B.R., and Dale, A.M. (2000). Segregation of somatosensory activation in the human rolandic cortex using fMRI. *J. Neurophysiol.* **84,** 558–569.

Morani, V., Previgliano, V., Schierano, G.M., and Ramieri, G. (1994). Innervation of the human temporomandibular joint capsule and disc as revealed by immunohistochemistry for neurospecific markers. *J. Orofacial Pain.* **8,** 36–41.

Morel, A., Magnin, M., and Jeanmonod, D. (1997). Multiarchitectonic and stereotactic atlas of the human thalamus. *J. Comp. Neurol.* **387,** 588–630.

Moskowitz, M.A. (1992). Neurogenic versus vascular mechanisms of sumatriptan and ergot alkaloids in migraine. *TiPS* **13,** 307–311.

Moskowitz, M.A., Buzzi, M.G., Sakas, D.E., and Linnik, M.D. (1989). Pain mechanisms underlying vascular headaches. Progress Report 1989. *Revue Neurologique* **145,** 181–193.

Moskowitz, M.A., Liu-Chen, L.Y., Mayberg, M.R., Zervas, N.T., Han, D.H., and Brody, M.R. (1983). Cat pia-arachnoid contains immunoreactive substance P within neurons projecting from the fifth cranial nerve. *In* "Cerebrovascular Disease" (M. Reivich and H.I. Hurtig, eds.), pp. 363–371. Raven Press, New York.

Munger, B.L. (1973). Cytology and ultrastructure of sensory receptors in the adult and newborn primate tongue. *In* "Development of the Fetus and Infant, 4th Symposium on Oral Sensation and Perception" (J.F. Bosma, ed.), pp.75–95. DHEW Publication 73–540, Bethesda, USDHEW.

Nakamura, A., Yamada, T., Goto, A., Kato, T., Ito, K., Abe, Y., Kachi, T., and Kakigi, R. (1998). Somatosensory homonculus as drawn by MEG. *Neuroimage* **7,** 377–386.

Namking, M., Boonruangsri, P., Woraputtaporn, W., and Güldner, F.H. (1994). Communication between the facial and auriculotemporal nerves. *J. Anat.* **185,** 421–426.

Nieber, K., Baumgarten, C., Witzel, A., Rathsack, R., Oehme, P., Brunnee, T., Kleine-Tebbe, J., and Kunkel, G. (1991). The possible role of substance P in the allergic reaction, based on two different provocation models. *Internat. Arch. Allergy Appl. Immunol.* **94,** 334–338.

Noriega, A.L., and Wall, J.T. (1991). Parcellated organization in the trigeminal and dorsal column nuclei of primates. *Brain Res.* **565,** 188–194.

Nosrat, C.A. (1998). Neurotrophic factors in the tongue: Expression patterns, biological activity, relation to innervation and studies of neurotrophin knockout mice. *Ann. N.Y. Acad. Sci.* **855,** 28–49.

Ohman A. (1965). "Theoretical and Practical Clinical Aspects of Healing and Vitality Investigation in Traumatic Tooth Injuries," pp. 123–137. Arsbok, Goteborgs Tandlakare-Sallskaps.

Ohya, A., Tsuruoka, M., Imai, E., Fukunaga, H., Shinya A., Furuya, R., Kawawa, K., and Matsui, Y. (1993). Thalamic- and cerebellar-projecting interpolaris neuron responses to afferent inputs. *Brain Res Bull.* **32,** 615–621.

Ohye, C., Fukamachi, A., and Narabayashi, H. (1972). Spontaneous and evoked activity of sensory neurons and their organization in the human thalamus. *Z. Neurol.* **203,** 219–234.

Olszewski, J. (1950). On the anatomical and functional organization of the spinal trigeminal nucleus. *J. Comp. Neurol.* **92,** 401–413.

Olszewski, J., and Baxter, D. (1954). "Cytoarchitecture of the Human Brain Stem." Karger, Basel.

Panneton, W.M., and Yavari, P. (1995). A medullary dorsal horn relay for the cardiorespiratory responses evoked by stimulation of the nasal mucosa in the muskrat *Ondatra zibethicus:* Evidence for excitatory amino acid transmission. *Brain Res.* **691,** 37–45.

Parada, C.A., Luccarini, P., and Woda, A. (1997). Effect of an NMDA receptor antagonist on the wind-up of neurons in the trigeminal oralis subnucleus. *Brain Res.* **761,** 313–320.

Pardo, J.V., Wood, T.D., Costello, P.A., Pardo, P.J., and Lee, J.T. (1997). PET study of the localization and laterality of lingual somatosensory processing in humans. *Neurosci. Lett.* **234,** 23–26.

Patrick, G.W., and Robinson, M.A. (1987). Collateral projections from trigeminal sensory nuclei to ventrobasal thalamus and cerebellar cortex in rats. *J. Morphol.* **192,** 229–236.

Paxinos, G., and Huang, X.-F. (1995). "Atlas of the Human Brainstem." Academic Press, San Diego.

Pearson, J.C., and Garfunkel, D.A. (1983). Evidence for the thalamic projections from external cuneate nucleus, cell groups Z and X, and the mesencephalic nucleus of the trigeminal nerve in the squirrel monkey. *Neurosci. Lett.* **41,** 41–47.

Pelletier, V.A., Poulos, D.A., and Lende, R.A. (1974). Functional localization in the trigeminal root. *J. Neurosurg.* **40,** 504–513.

Penfield, W., and Rasmussen, T. (1950). "The Cerebral Cortex of Man. A Clinical Study of Localization and Function." Macmillan, New York.

Pennisi, E., Crucco, G., Manfredi, M., and Palladini, G. (1991). Histomeric study of myelinated fibers in the human trigeminal nerve. *J. Neurol. Sci.* **105,** 22–28.

Petralia, R.S., Yokotani, N., and Wenthold, R.J. (1994). Light and electron microscope distribution of the NMDA receptor subunit NMDARI in the rat nervous system using a selective anti-peptide antibody. *J. Neurosci.* **14,** 667–696.

Peyron, R., Laurent, B., and Garcia-Larrea, L. (2000). Functional imaging of brain responses to pain. A review and meta-analysis. *Neurophysiologie Clinique* **30,** 263–288.

Phelan, K.D., and Falls, W.M. (1989). An analysis of the cyto- and myeloarchitectonic organization of trigeminal nucleus interpolaris in the rat. *Somatosens. Motor Res.* **6,** 333–366.

Phelan, K.D., and Falls, W.M. (1991). A comparison of the distribution and morphology of thalamic, cerebellar and spinal projection neurons in rat trigeminal nucleus interpolaris. *Neurosci.* **40,** 497–511.

Pons, T.P., Garraghty, P.E., Ommaya, K., Kaas, J.H., Taub, E., and Mishkin, M. (1991). Massive cortical reorganization after sensory deafferentation in adult macaques. *Science* **252,** 1857–1860.

Porter, J. (1986). Brainstem terminations of extraocular muscle primary afferent neurons in the monkey. *J. Comp. Neurol.* **247,** 133–143.

Poulos, D.A., and Benjamin, R.M. (1968). Response of thalamic neurons to thermal stimulation of the tongue. *J. Neurophysiol.* **31,** 28–43.

Price, D.D., Dubner, R., and Hu, J.W. (1976). Trigeminothalamic neurons in nucleus caudalis responsive to tactile, thermal, and nociceptive stimulation of monkey's face. *J. Neurophysiol.* **39,** 936–953.

Quarto, M., and Del Fiacco, M. (1994). Enkephalins occur and colocalize with substance P in human trigeminal ganglion neurones. *NeuroReport.* **5,** 465–468.

Quartu, M., Diaz, G., Lai, M.L., and Del Fiacco, M. (1992). Immunohistochemical localization of putative peptide neurotransmitters in the human trigeminal sensory system. *Ann. N.Y. Acad. Sci.* **657,** 469–472.

Quartu, M., Setzu, M.D., and Del Fiacco, M. (1996). Trk-like immunoreactivity in the human trigeminal ganglion and subnucleus caudalis. *NeuroReport* **7,** 1013–1019.

Raappana, P., and Arvidsson, J. (1993). Location, morphology, and central projections of mesencephalic trigeminal neurons innervation rat masticatory muscles studied by axonal transport of choleragenoid-horseradish peroxidase. *J. Comp. Neurol.* **328,** 103–114.

Raboisson, P., Dallel, R., Clavelou, P., Sessle, B.J., and Woda, A. (1995). Effects of subcutaneous formalin on the activity of trigeminal brainstem nociceptive neurons in the rat. *J. Neurophysiol.* **73,** 496–505.

Raboisson, P., Dallel, R., and Woda, A. (1989). Responses of neurones in the ventrobasal complex of the thalamus to orofacial noxious stimulation after large trigeminal tractotomy. *Exp. Brain Res.* **77,** 569–576.

Rainville, P., Duncan, G.H., Price, D.D., Carrier, B., and Bushnell, M.C. (1997). Pain affect encoded in human anterior cingulate but not somatosensory cortex. *Science* **277,** 968–971.

Rakhawy, M.T., Shehata, S.H., and Badawy, Z.H. (1971). The proprioceptive innervation of the lateral pterygoid muscle in man and some other mammals. *Acta Anat.* **79,** 581–598.

Ramachandran, V.S. (1993). Behavioral and magnetoencephalographic correlates of plasticity in the adult human brain. *PNAS.* **90,** 10413–10420.

Ramachandran, V.S., Stewart, M., and Rogers-Ramachandran, D.C. (1992). Perceptual correlates of massive cortical reorganization. *NeuroReport* **3,** 583–586.

Ramieri, G., Bonardi, G., Morani, V., Panzica, G.C., Del Totto, F., Arisio, R., and Preti, G. (1996). Development of nerve fibers in the temporomandibular joint of the human fetus. *Anat. Embryol.* **194,** 57–64.

Rappaport, Z.H., and Devor, M. (1994). Trigeminal neuralgia: The role of self-sustaining discharge in the trigeminal ganglion. *Pain.* **56,** 127–138.

Rappaport, Z.H., Govrin-Lippmann, R., and Devor, M. (1997). An electron-microscopic analysis of biopsy samples of the trigeminal root taken during microvascular decompressive surgery. *Stereotact. Funct. Neurosurg.* **68,** 182–186.

Rath, E.M., and Essick, G.K. (1990). Perioral somesthetic sensibility: Do the skin of the lower face and the midface exhibit comparable sensibility? *J. Oral Maxillofacial Surg.* **48,** 1181–1190.

Rausell, E., and Jones, E.G. (1991a). Histochemical and immunocytochemical compartments of the thalamic VPM nucleus in monkeys and their relationship to the representational map. *J. Neurosci.* **11,** 210–225.

Rausell, E., and Jones, E.G. (1991b). Chemically distinct compartments of the thalamic VPM nucleus in monkeys relay principal and spinal trigeminal pathways to different layers of the somatosensory cortex. *J. Neurosci.* **11,** 226–237.

Rausell, E., and Jones, E.G. (1995). Extent of intracortical arborization of thalamocortical axons as a determinant of representational plasticity in monkey somatic sensory cortex. *J. Neurosci.* **15,** 4270–4288.

Rhoton, A.L., O'Leary, J.L., and Ferguson, J.P. (1966). The trigeminal, facial, vagal and glossopharyngeal nerves in the monkey. *Arch. Neurol.* **14,** 530–540.

Riederer, A., Knipping, S., Fischer, A., and Unger, J. (1995). Immunohistochemische untersuchungen zum vorkommen von calcitonin gene-related peptide (CGRP) in der nasenschleimhaut des menschen. *HNO* **43,** 724–727.

Ringel, R.L., and wanowski, S.J. (1965). Oral Perception: 1. Two-Point Discrimination. *J. Speech Hearing Res.* **8,** 289–298.

Rokx, J.T.M., Juch, P.J.W., Van and Willigen, J.D. (1986). Arrangement and connections of mesencephalic trigeminal neurons in the rat. *Acta Anat.* **127,** 7–15.

Rokx, J.T.M., Luiten, P.G.M., and Van Willigen, J.D. (1988). Afferent projections to the mesencephalic trigeminal nucleus in the rat. *Acta Anat.* **132,** 260-–264.

Ruggiero, D.A., Ross, C.A., and Reis, D.J. (1981). Projections from the spinal trigeminal nucleus to the entire length of the spinal cord in the rat. *Brain Res.* **225,** 225–233.

Ruskell, G.L. (1985). Innervation of the conjunctiva. *Trans. Ophthalmol. Soc. U.K.* **104,** 390–395.

Saito, K., and Moskowitz, M.A. (1989). Contributions from the upper cervical dorsal roots and trigeminal ganglia to the feline Circle of Willis. *Stroke* **20,** 524–526.

Sakai, K., Watanabe, E., Onodera, Y., Itagaki, H., Yamamoto, E., Koizumi, H., and Miyashita, Y. (1995). Functional mapping of the human somatosensory cortex with echo-planar MRI. *Magnet. Res. Med.* **33,** 736–743.

Schults, R.C. (1992). Nociceptive neural organization in the trigeminal nuclei. *In* "The Initial Processing of Pain and Its Descending Control: Spinal and Trigeminal Systems" (A.R. Light, R.C. Shults, and S.L. Jones, eds.), pp. 178–202. Karger, Basel.

Seike, M. (1993). A study of the area of distribution of the deep sensory neurons of the human ventral thalamus. *Stereotact. Funct. Neurosurg.* **61,** 12–23.

Sessle, B.J. (1996). Mechanisms of trigeminal and occipital pain. *Pain Rev.* **3,** 91–116.

Sessle, B.J. (2000). Acute and chronic craniofacial pain: Brainstem mechanisms of nociceptive transmission and neuroplasticity, and their clinical correlates. *Critical Rev. Oral Biol. Med.* **11,** 57–91.

Sessle, B.J., and Hu, J.W. (1991). Mechanisms of pain arising from articular tissues. *Canad. J. Physiol. Pharmacol.* **69,** 617–626.

Seyal, M., and Browne, J.K. (1989). Short latency somatosensory evoked potentials following mechanical taps to the face. Scalp recordings with a non-cephalic reference. *Electroencephalogr. Clin. Neurophysiol.* **74,** 271–276.

Shankland, W.E. (2000). The trigeminal nerve. Part 1: An over-view. *J. Craniomandib. Pract.* **18,** 238–248.

Sharav, Y., Leviner, E., Tzukert, A., and McGrath, P.A. (1984). The spatial distribution, intensity and unpleasantness of acute dental pain. *Pain.* **20,** 363–370.

Shepheard, S.L., Williamson, D.J., Williams, I., Hill, R.G., and Hargreaves, R.J. (1995). Comparison of the effects of sumatriptan and the NK1 antagonist CP-99,994 on plasma extravasation in dura mater and c-fos mRNA expression in trigeminal nucleus caudalis of rats. *Neuropharmacol.* **34,** 255–261.

Shigenaga, Y., Chen, L.C., Suemune, S., Nishimori, T., Nasution, I.D., Yoshida, A., Sato, H., Okamoto, T., Sera, M., and Hosoi, M. (1986a). Oral and facial representation within the medullary and upper cervical dorsal horns in the cat. *J. Comp. Neurol.* **243,** 388–408.

Shigenaga, Y., Doe, K., Suemune, S., Mitsuhiro, Y., Tsuru, K., Otani, K., Shirana, Y., Hosoi, M., Yoshida, A., and Kagawa, K. (1989). Physiological and morphological characteristics of periodontal mesencephalic trigeminal neurons in the cat—Intra-axonal staining with HRP. *Brain Res.* **505,** 91–110.

Shigenaga, Y., Mitsuhiro, Y., Shirana, Y., and Tsuru, H. (1990). Two types of jaw-muscle spindle afferents in the cat as demonstrated by intra-axonal staining with HRP. *Brain Res.* **514,** 219–237.

Shigenaga, Y., Nakatani, Z., Nishimori, T., Suemune, S., Kuroda, R., and Matano, S. (1983). The cells of origin of cat trigemino-thalamic projections: especially in the caudal medulla. *Brain Res.* **277,** 201–222.

Shigenaga, Y., Okamoto, T., Nishimori, T., Suemune, S., Nasution, Chen, I.C., Tsuru, K., Yoshida, A., Tabuchi, K., Hosoiu, M., and Tsuru, H. (1986b). Oral and facial representation in the trigeminal principal and rostral spinal nuclei of the cat. *J. Comp. Neurol.* **244,** 1–18.

Shigenaga, Y., Takabatake, M., Sugimoto, T., and Sakai, A. (1979). Neurons in marginal layer of trigeminal nucleus caudalis projecting to ventrobasal complex (VB) and posterior nuclear group (PO) demonstrated by retrograde labeling with horse-radish peroxidase. *Brain Res.* **166,** 391–396.

Shintani, S., Tsuruoka, S., and Shiigai, T. (2000). Pure sensory stroke caused by a cerebral hemorrhage: clinical-radiologic correlations in seven patients. *Amer. J. Neuroradiol.* **21,** 515–520.

Shirasaki, H., Asakura, K., Narita, S.-I., and Kataura, A. (1998). Expression of substance P (NK1) receptor mRNA in human nose. *Acta Otolaryngol.* **118,** 717–722.

Sicuteri, F., Fanciullacci, M., Nicolodi, M., Geppetti, P., Fusco, B.M., Marabini, S., Alessandri, M., and Campagnolo, V. (1990). Substance P theory: A unique focus on the painful and painless phenomena of cluster headache. *Headache* **30,** 69–79.

Sicuteri, F., Geppetti, P., Marabini, S., and Lembeck, F. (1984). Pain relief by somatostatin in attacks of cluster headaches. *Pain.* **18,** 359–365.

Silverman, J.D., and Kruger, L. (1987). An interpretation of dental innervation based upon the pattern of calcitonin gene-related peptide (CGRP)-immunoreactive thin sensory axons. *Somatosens. Res.* **5,** 157–175.

Sjoqvist, O. (1938). Studies on the pain conduction in the trigeminal nerve. A contribution to surgical treatment of facial pain. *Acta Psychiatr. Scand.* [Suppl] **17,** 1–139.

Slugg, R.M., and Light, A.R. (1994). Spinal cord and trigeminal projections to the pontine parabrachial region in the rat as demonstrated with *Phaseolus vulgaris* leucoagglutinin. *J. Comp. Neurol.* **339,** 49–61.

Smith, R.L. (1975). Axonal projections and connections of the principal sensory trigeminal nucleus in the monkey. *J. Comp. Neurol.* **163,** 347–376.

Smoliar, E., Smoliar, A., and Belkin,V.S. (1999). Innervation of human trigeminal nerve blood vessels. *Cells Tissues Organs.* **165,** 40–44.

Smoliar, E., Smoliar, A., Sorkin, L., and Belkin, V. (1998). Micro-circulatory bed of the human trigeminal nerve. *Anat. Rec.* **250,** 245–249.

Soeira, G., Abd El-Bary, T.H., Dujovny, M., Slavin, K.V., and Ausman, J.I. (1994). Microsurgical anatomy of the trigeminal nerve. *Neurol. Res.* **16,** 273–283.

Soja, P.J., Cairns, B.E., and Christensen, M.P. (1999). Transmission through ascending lumbar and trigeminal sensory pathways: Dependence on behavioural state. *In* "Handbook of Behavioural State Control: Cellular and Molecular Mechanisms" (R. Lydic and H.A. Baghdoyan, eds.), pp. 521–544. CRC Press, Boca Raton.

Stohr, M., and Petruch, F. (1979). Somatosensory evoked potentials following stimulation of the trigeminal nerve in man. *J. Neurol.* **220,** 95–98.

Strassman, A.M., and Vos, B.P. (1993). Somatotopic and laminar organization of fos-like immunoreactivity in the medullary and upper cervical dorsal horn induced by noxious facial stimulation in the rat. *J. Comp. Neurol.* **331,** 495–516.

Strassman, A.M., Potrebic, S., and Maciewicz, R.J. (1994). Anatomical properties of brainstem trigeminal neurons that respond to electrical stimulation of dural blood vessels. *J. Comp. Neurol.* **346,** 349–365.

Strassman, A.M., Raymond, S.A., and Burstein, R. (1996). Sensitization of meningeal sensory neurons and the origin of headaches. *Nature.* **384,** 560–564.

Suzuki, N., and Hardebo, J.E. (1991). Anatomical basis for a parasympathetic and sensory innervation of the intracranial segment of the internal carotid artery in man. Possible implication for vascular headache. *J. Neurol. Sci.* **104,** 19–31.

Tahmasebi-Sarvestani, A., Tedman, R.A., and Goss, A. (1996). Neural structures within the sheep temporomandibular joint. *J. Orofacial Pain* **10,** 217–31.

Takemura, M., Nagase, Y., Yoshida, A., Yasuda, K., Kitamura, S., Shigenaga, Y., and Matano, S. (1993). The central projections of the monkey tooth pulp afferent neurons. *Somatosens. Motor Res.* **10,** 217–227.

Takemura, M., Sugimoto, T., and Shigenaga,Y. (1991). Difference in central projection of primary afferent innervating facial and intraoral structures in the rat. *Exp. Neurol.* **111,** 324–331.

Tallaksen-Greene, S.J., Young, A.B., Penney, J.B., and Beitz, A.J. (1992). Excitatory amino acid binding sites in the trigeminal principal sensory and spinal trigeminal nuclei of the rat. *Neurosci. Lett.* **141,** 79–83.

Tenser, R.B. (1998). Trigeminal neuralgia. Mechanisms of treatment. *Neurol.* **51,** 17–19.

Tiwari, R.K., and King, R.B. (1994). Fiber projections from trigeminal nucleus caudalis in primate (squirrel monkey and baboon). *J. Comp. Neurol.* **158,** 191–206.

Toivanen, M., Tervo, T., Partanen, M., Vannas, A., and Hervonen A. (1987). Histochemical demonstration of adrenergic nerves in the stroma of human cornea. *Invest. Ophthal. Visual Sci.* **28,** 398–400.

Trulsson, M., and Essick, G.K. (1997). Low-threshold mechano-receptive afferents in the human lingual nerve. *J. Neurophysiol.* **77,** 737–748.

Trulsson, M., and Johansson, R.S. (1996). Encoding of tooth loads by human periodontal afferents and their role in jaw motor control. *Prog. Neurobiol.* **49,** 267–284.

Türp, J.C., and Gobetti, J.P. (2000). Trigeminal neuralgia—An update. *Compendium* **21,** 279–290.

Ueda, S., del Cerro, M., LoCascio, J.A., and Aquavella, J.V. (1989). Peptidergic and catecholaminergic fibers in the human corneal epithelium. An immunohistochemical and electron microscopic study. *Acta Ophthal.—Suppl.* **192,** 80–90.

Usunoff, K.G., Marani, E., and Schoen, J.H.R. (1997). The trigeminal system in man. *Adv. Anat. Embryol.* **136,** 1–118.

Uusitalo, H., Krootila, K., and Palkama, A. (1989). Calcitonin gene-related peptide (CGRP) immunoreactive sensory nerves in the human and guinea pig uvea and cornea. *Exp. Eye Res.* **48,** 467–475.

Vallbo, A.B., Hagbarth, K.-E., Torebjork, H.E., and Wallin, B.G. (1979). Somatosensory, proprioceptive and sympathetic activity in human peripheral nerves. *Physiol. Rev.* **59,** 919–957.

Verhaart, W.J.C., and Busch, H.F.M. (1960). Wallenberg's tract, the fasciculus tegmentalis dorsolateralis and Forel's fasciculi tegmentalis. *Acta Anat.* **40,** 41–58.

Vos, B.P., Strassman A.M., and Maciewicz R.J. (1994). Behavioural evidence of trigeminal neuropathic pain following chronic constriction injury to the rat's infraorbital nerve. *J. Neurosci.* **14,** 2708–2723.

Voss, H. (1935). Ein besonders reichliches vorkommen von muskelspindeln in der tiefen portion des m. masseter des menschen und der anthropoiden. *Anat. Anz.* **81,** 290–292.

Voss, H. (1956). Zahl und anordnung der muskelspindeln in der oberen zungenbeinmuskeln, im m. trapezius und m. latissimus dorsi. *Anat. anz.* **103,** 443–446.

Waite, P.M.E. (2000). Somatotopic organization in the barrel field after peripheral injury. *In* "Plasticity of Adult Barrel Cortex" (M. Kossut, ed.), pp. 151–174. FP Graham, Tennessee.

Waite, P.M.E., and Tracey, D.J. (1995). Trigeminal sensory system. *In* "The Rat Nervous System" (G. Paxinos, ed.), pp. 705–724.

Wakisaka, S., Itogowa, T., Youn, S.H., Kato, J., and Kurisu, K. (1996). Distribution and possible origin of galanin-like immunoreactive nerve fibers in the mammalian dental pulp. *Regulatory Peptides* **62,** 137–143.

Wall, J.T. (1988). Variable organization in cortical maps of the skin as an indication of the lifelong adaptive capacities of circuits in the mammalian brain. *TINS* **11,** 549–557.

Wanaka, A., Shiotani, Y., Kiyama, H., Matsuyama, T., Kamada, T., Shiosaka, S., and Tohyama, M. (1987). Glutamate-like immunoreactive structures in primary sensory neurons in the rat detected by a specific antiserum against glutamate. *Exp. Brain Res.* **65,** 691–694.

Weddell, G., and Zander, E. (1950). A critical evaluation of methods used to demonstrate tissue neural elements, illustrated by reference to the cornea. *J. Anat.* **84,** 168–195.

Weinberger, N.M. (1995). Dynamic regulation of receptive fields and maps in the adult sensory cortex. *Ann. Review Neurosci.* **18,** 129–158.

Weinstein, S. (1968). Intensive and extensive aspects of tactile sensitivity as a function of body part, sex and laterality. *In* "The Skin Senses" (D. Kenshalo, ed.), pp. 195–219. Springfield, IL, Thomas.

Westrum, L.E., and Henry, M.A. (1993). Unilateral retrogasserian rhizotomy causes colateral degeneration in spinal trigeminal nuclei of cats: an ultrastructural study. *Exp. Brain Res.* **93,** 28–36.

Wood, C.C., Spencer, D.D., Allison, T., McCarthy, G., Williamson, P.D., and Goff, W.R. (1988). Localization of human sensorimotor cortex during surgery by cortical surface recording of somatosensory evoked potentials. *J. Neurosurg.* **68,** 99–111.

Woolsey, T.A. (1990). Peripheral alteration and somatosensory development. *In* "Development of sensory systems in mammals" (J.R. Coleman, ed.), pp. 165–200. Wiley, New York.

Woolsey, C.N., Erickson, T.C., and Gilson, W.E. (1979). Localization in somatic sensory and motor areas of human cerebral cortex as determined by direct recording of evoked potentials and electrical stimulation. *J. Neurosurg.* **51,** 476–506.

Yamamoto, M., and Kondo, H. (1989). Calcitonin gene-related peptide (CGRP)-immunoreactive nerve varicosities in synaptic contact with sensory neurons in the trigeminal ganglion of rats. *Neurosci. Lett.* **104,** 253–257.

Yang, T.T., Gallen, C.C., Schwartz, B.J., and Bloom, F.E. (1993). Non-invasive somatosensory homunculus mapping in humans by using a large-array biomagnetometer. *Neurobiol.* **90,** 3098–3102.

Yew, D.T., Pang, K.M., and Mok, Y.C. (1991). Immunohistochemical and ultrastructural studies of the various nuclei of the trigeminal complex in the human newborn. *Neurosci.* **45,** 23–35.

Yoshida, A., Dostrovsky, J.O., Sessle, B.J., and Chiang, C.Y. (1991). Trigeminal projections to the nucleus submedius of the thalamus in the rat. *J. Comp. Neurol.* **307,** 609–625.

Young, R.F. (1977). Fiber Spectrum of the trigeminal sensory root of frog, cat and man determined by electronmicroscopy. *In* "Pain in the Trigeminal Region" (Anderson and Matthews, eds.), pp. 137–147. Elselvier/North-Holland Biomedical Press.

Yu, X.H., Zhang, E.-T., Craig, A.D., Shigemoto, R., Ribeiro-da-Silva, A., and De Koninck, Y. (1999). NK-1 receptor immunoreactivity in distinct morphological types of Lamina I neurons of the primate spinal cord. *J. Neurosci.* **19,** 3545–3555.

Zahm, D.S., and Munger, B.L. (1985). The innervation of the primate fungiform papilla—Development, distribution and changes following selective ablation. *Brain Res. Rev.* **9,** 147–186.

Zald, D.H., and Pardo, J.V. (2000). Cortical activation induced by intraoral stimulation with water in humans. *Chem. Senses.* **25,** 267–275.

Zhang, E.T., Han, Z.S., and Craig, A.D. (1996). Morphological classes of spinothalamic lamina I neurons in the cat. *J. Comp. Neurol.* **367,** 537–549.

Zimny, M.L. (1988). Mechanoreceptors in articular tissues. *Amer. J. Anat.* **182,** 16–32.

CHAPTER

30

Pain System

WILLIAM D. WILLIS, JR. and KARIN N. WESTLUND
Department of Anatomy and Neurosciences
University of Texas Medical Branch
Galveston, Texas, USA

The somatovisceral sensory system is responsible for signaling a variety of types of sensory information. Of particular interest in medicine is pain, since pain is the most common reason for a patient to confer with a physician. Pain signals are processed in humans and other mammals by the pain system (Willis, 1985), which is composed of primary afferent nociceptors, ascending spinal cord (and trigeminal) nociceptive pathways, descending modulatory pathways, and a number of brain structures that process information related to pain signals. There are a variety of reactions to painful stimuli (Hardy *et al.*, 1967), including not only sensory discrimination of pain but also motivational–affective responses to painful stimuli (Melzack and Casey, 1968; Price and Dubner, 1977), as well as somatic and autonomic reflexes, endocrine changes, and memories of pain. Transmission of pain signals to the brain also activates feedback circuits that can inhibit the effects of sensory input at the spinal cord or brain stem level or, alternatively, accentuate pain responses. The negative-feedback pathways are often referred to as the "endogenous analgesia system."

Evidence about the pain system has been reviewed previously, based on work utilizing a variety of laboratory mammals, especially rats (Willis, 1985; Besson and Chaouch, 1987; Willis *et al.*, 1995; Willis and Westlund, 1997; Millan, 1999; Willis and Coggeshall, 2003). This chapter emphasizes work concerning the pain system that is based primarily on experiments that used primates and on observations in human subjects. Although most of the studies described here refer to pathways that involve the spinal cord, there will be some reference to the comparable pain system that signals information conveyed by the trigeminal and other cranial nerves and their central connections (see also Chapters 28 and Chapter 29).

NOCICEPTORS

Cutaneous, Muscle, Joint, and Visceral Nociceptors

Painful stimuli are transduced by nociceptors, which are specialized peripheral nerve endings in the skin, muscle, joints, viscera, teeth and dura (Sherrington, 1906; Belmonte and Cervero, 1996; Kumazawa *et al.*,

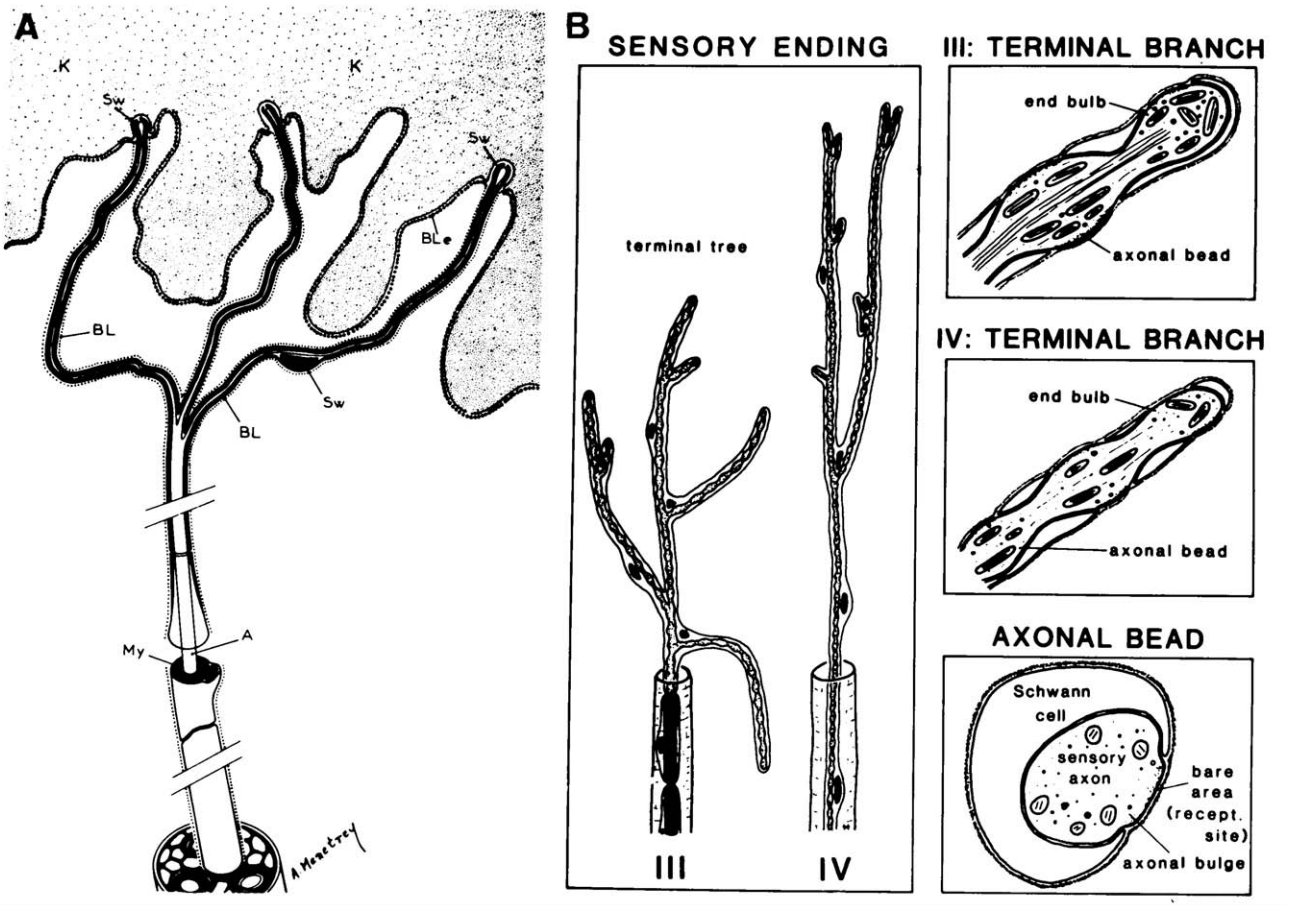

FIGURE 30.1 Structure of nociceptive terminals in the skin and the knee joint. In **A** are shown the terminals of an Aδ mechanical nociceptor in the skin of a cat. The reconstruction was based on electron microscopic observations. Note that the afferent fiber has several different endings that penetrate the basal lamina (BLe) and then extend into the epidermis. The myelin sheath (My) ends within the dermis. Most of the terminal membrane of the endings is covered by Schwann cell (Sw) processes. Other abbreviations: A, axon; K, keratinocytes. (From Perl, 1984.) In **B** are drawings of low- and high-magnification views of the endings of group III and IV joint afferents, as reconstructed from electron micrographs. The "free endings" are covered in large part by Schwann cell membrane. However, there are areas where the axonal membrane is exposed to the extracellular fluid. Such areas may be the sites of transduction or membrane regions that contain receptor molecules for bioactive substances. (From Schaible and Schmidt, 1996.)

1996). Nociceptors respond maximally to overtly damaging stimuli, although they generally also respond, but less vigorously, to stimuli that are merely threatening (Burgess and Perl, 1973). Axons that relay information about noxious input to the central nervous system (CNS) include small Aδ fibers, which are wrapped in a thin layer of myelin and which conduct at 4–35 m/s, and C fibers, which are very small, unmyelinated fibers with conduction velocities under 2.5 m/s (Boivie and Perl, 1975). In addition, more rapidly conducting nociceptive A fibers (up to 51 m/s) have been described in monkeys (Georgopoulos, 1976; Treede *et al.*, 1995).

Experiments on cats provide evidence that noxious cutaneous and joint stimuli are transduced by unencapsulated free nerve endings ensheathed by Schwann cells (Fig. 30.1) (Perl, 1984; Heppelmann *et al.*, 1990; Schaible and Schmidt, 1996). Areas of axon membrane bare of a Schwann cell covering may be sites of nociceptive transduction (Schaible and Schmidt, 1996) or the locations of surface membrane receptors for agents that modulate nociceptive transduction (Coggeshall and Carlton, 1997). Presumably, similar morphological arrangements would be found in human nociceptors.

The two main types of cutaneous nociceptors found in human skin are Aδ mechanical and C polymodal nociceptors, although other types of nociceptors have also been described (e.g., Davis *et al.*, 1993). Mechanical nociceptors respond to strong mechanical stimuli,

whereas several different types of noxious stimuli, such as noxious mechanical, thermal, and chemical stimuli, can activate polymodal receptors. Human nociceptors have been studied extensively in experiments utilizing the microneurography technique (Van Hees and Gybels, 1972; 1981; Torebjörk, 1974; Torebjörk and Hallin, 1974; Ochoa and Torebjörk, 1989; Torebjörk and Ochoa, 1990; Hallin *et al.*, 1981; Konietzny *et al.*, 1981; Adriaensen *et al.*, 1983; Bromm *et al.*, 1984; LaMotte *et al.*, 1992; Yarnitsky *et al.*, 1992; Koltzenburg and Handwerker, 1994; Schmetz *et al.*, 1994; Schmidt *et al.*, 1995; Treede *et al.*, 1998; Weidner *et al.*, 1999).

The sudden application of a painful stimulus, such as noxious heat, can elicit two distinct forms of pain in human skin: an initial sharp pain, followed by a burning pain. These sequential pain sensations are often termed "first" and "second" pain. Aδ nociceptors are responsible for first pain and C fibers for second pain (Lewis, 1942; Torebjörk and Hallin, 1973; Handwerker and Kobal, 1993; Treede *et al.*, 1995). Consistent with this, intraneural stimulation of Aδ nociceptors through a microneurography electrode evokes a sensation of stinging or sharp pain (Konietzny *et al.*, 1981; Schady *et al.*, 1983; Marchettini *et al.*, 1990), whereas stimulation of individual or small groups of C fibers evokes a sensation of burning or dull pain (Ochoa and Torebjörk, 1989; Torebjörk and Ochoa, 1990).

Pain arising from tissue that is deep to the skin is typically aching or cramping in quality (Lewis, 1942). For example, intraneural microstimulation experiments have shown that electrical or chemical stimulation of either group III or IV nociceptors in muscle nerves of human subjects causes a deep, aching, or cramping pain (Torebjörk *et al.*, 1984; Simone *et al.*, 1994; Marchettini *et al.*, 1996; Graven-Nielsen *et al.*, 1997a, b, 1998).

As in humans, the skin of monkeys is supplied by Aδ mechanical nociceptors and C polymodal nociceptors (Perl, 1968; Beitel and Dubner, 1976; Georgopoulos, 1976; Kumazawa and Perl, 1977; Meyer and Campbell, 1981; LaMotte *et al.*, 1982; 1983). Two different types of mechanoheat nociceptors with Aδ-size afferent fibers (types I and II) have been described in monkey skin (Treede *et al.*, 1995). Only the type II receptors have characteristics (strong heat responsiveness, sufficiently rapid conduction velocity) that can account for first pain.

C nociceptors in monkeys can generally be activated by mechanical, thermal, and chemical stimuli, leading to their designation as C polymodal nociceptors (Beitel and Dubner, 1976; Kumazawa and Perl, 1977). Similar receptors are found in humans (Torebjörk, 1974). However, mechanical and thermal stimuli are often the only noxious stimuli tested, in which case the fibers may be termed C mechanoheat receptors (LaMotte *et al.*, 1983; Treede *et al.*, 1990). C nociceptors that respond to noxious heat appear to end in both the epidermis and dermis of the skin of monkeys (Tillman *et al.*, 1995).

A large proportion of the cutaneous A and C nociceptors in monkeys are insensitive to mechanical stimulation when initially tested under normal conditions (Meyer *et al.*, 1991). These nociceptors, as well as many nociceptors that are initially sensitive to mechanical stimuli, have been shown to respond to chemical agents, including inflammatory mediators and capsaicin (Baumann *et al.*, 1991; Davis *et al.*, 1993). Such nociceptors often become sensitized to mechanical stimuli after tissue is damaged or becomes inflamed (Meyer and Campbell, 1981; LaMotte *et al.*, 1982; Thalhammer and LaMotte, 1982; Campbell and Meyer, 1983; Campbell *et al.*, 1988a; Davis *et al.*, 1993; Handwerker and Kobal, 1993; cf., Schmeltz *et al.*, 1994).

Most studies of nociceptors in tissues other than the skin have been performed on nonprimate laboratory animals. Free endings of finely myelinated and unmyelinated nociceptive afferents are located in the cornea (Belmonte and Gallar, 1996; see also Chapter 29), the fascia and the adventitia of blood vessels in muscle (Stacey, 1969; Mense, 1993, 1996), in joints (Fig. 30.1B) (Schaible and Grubb, 1993; Heppelmann *et al.*, 1996), dura (Messlinger, 1996; Hanesch, 1996), gastrointestinal tract (Gebhart, 1996), testis (Mizumura and Kumazawa, 1996), and many other organs (see reviews of the older literature by Willis, 1985, and Willis and Coggeshall, 2003).

Dorsal Root Ganglion Cells

Nociceptors, like other somatovisceral sensory receptors, have their cell bodies in dorsal root (or cranial nerve) ganglia (Willis and Coggeshall, 2003; see also Chapter 29). The cell body gives off a single process. At a short distance from the soma, this process divides into a peripheral and a central branch. The peripheral branch of each nociceptive dorsal root ganglion (DRG) cell follows the distribution of a peripheral nerve. The terminals of nociceptors innervate a target organ (Fig. 30.1). On the other hand, the central branch passes into the spinal cord and transmits sensory information from the target organ to the CNS. Most studies of DRG cells have been done on rodents.

DRG neurons may have large or small cell bodies ("large, light cells" and "small, dark cells"; reviewed in Willis and Coggeshall, 2003; see also Chapter 8). Large, light DRG cells give rise to myelinated axons, whereas small, dark DRG cells generally have unmyelinated axons.

Specific types of DRG cells can be labeled by antibodies against particular marker molecules. For example, large, light DRG cells are rich in neurofilaments, whereas small, dark DRG cells are poor in neurofilaments. Large, light DRG cells can be distinguished from small, dark ones by immunostaining the cells for neurofilament protein, using the RT97 antibody (Lawson and Waddell, 1991). DRG cells that can be immunostained for RT97 comprise about one-third of lumbar DRG cells (Bergman *et al.,* 1999; Perry and Lawson, 1998). Most lumbar dorsal root ganglion cells fail to immunostain for RT97 and are small, dark cells. Most of the latter are nociceptors.

Other markers include cell surface carbohydrates, which can be recognized by immunocytochemistry using monoclonal antibodies (Dodd and Jessell, 1985; Chou *et al.,* 1988; Alvarez *et al.,* 1989a, b). Antibodies against globoseries carbohydrates recognize DRG cells and primary afferents that project to laminae III and IV, whereas antibodies to lactoseries oligosaccarides recognize primary afferent neurons that terminate in laminae I and II.

Furthermore, primary afferent neurons that supply skin, muscle, or viscera have different phenotypes that can be distinguished based on their profiles of expression of different markers (Perry and Lawson, 1998). For example, an antibody for peanut agglutinin labels many more cutaneous and visceral afferents than muscle afferents, whereas the antibody 2C5 labels more cutaneous than muscle afferents, but very few visceral afferents. Antibodies to the antigens SSEA-3 and SSEA-4 label all sizes of somatic afferents but no visceral afferents.

Nociceptors are included in the subset of DRG neurons that have small, dark cell bodies (Lawson *et al.,* 1985, 1996, 1997) and therefore that do not immunostain for neurofilament protein (Lawson and Waddell, 1991). Small, dark DRG cells, most of which are nociceptors, can be further subdivided into peptidergic and nonpeptidergic primary afferent neurons. Small, dark peptidergic DRG cells contain substance P, calcitonin gene–related peptide (Lawson *et al.,* 1997), or other neuropeptides (Willis and Coggeshall, 2003). Two or more peptides may be co-localized in the same ganglion cell. The proportions of peptidergic DRG cells that contain a particular peptide may differ depending on the type of peripheral nerve. For example, calcitonin gene–related peptide is found in 50% of skin afferents, in 70% of muscle afferents, but in almost all visceral afferents. Similarly, substance P is found in 25% of skin afferents, in 50% of muscle afferents, but in more than 80% of visceral afferents. Somatostatin, on the other hand, is not found in visceral afferents, although it is present in a small number of somatic afferents. A large fraction of substance P–containing dorsal root ganglion cells have been shown to be nociceptors in electrophysiological experiments on guinea pigs (Lawson *et al.,* 1997).

Small, dark nonpeptidergic DRG cells usually have binding sites for the isolectin B4 (Wang *et al.,* 1994; Guo *et al.,* 1999). These small DRG cells presumably give rise to unmyelinated afferent fibers. This idea is reinforced by the observation that very few DRG cells that bind IB4 can be stained with RT97, a marker for myelinated primary afferent fibers (Lawson and Weddell, 1991).

Most IB4-positive DRG cells (85%) colocalize fluoride-resistant acid phosphatase and almost all of those that contain fluoride resistance acid phosphatase are IB4 positive (Wang *et al.,* 1994). Interestingly, human DRG cells appear to lack fluoride-resistant acid phosphatase (see Chapter 7). A clear distinction can generally be made between IB4-positive and peptidergic DRG cells (Guo *et al.,* 1999), although there is evidence for some overlap between IB4-positive and peptidergic DRG cells (Wang *et al.,* 1994). IB4-positive DRG cells usually contain $P2X_3$ purinoceptors, whereas peptidergic DRG cells generally do not. In fact, of DRG cells with $P2X_3$ receptors, more than 95% have IB4 binding sites (Bradbury *et al.,* 1998).

Additional chemical markers for nociceptors include a number of neurotransmitter receptor molecules. For example, glutamate has been identified by immunohistochemistry in primary afferent neurons, including rat dorsal root axons (Westlund *et al.,* 1989) and primate joint afferents (Westlund *et al.,* 1992b), as well as in DRG cells (Battaglia and Rustioni, 1988). Glutamate is believed to be a fast-acting central excitatory neurotransmitter substance that is released by many primary afferent nerve fibers, including nociceptors (De Biasi and Rustioni, 1988). Its central synaptic action is modulated by peptides, such as calcitonin gene–related peptide (CGRP) and substance P (Murase *et al.,* 1989; Dougherty and Willis, 1991). However, there also appears to be a role for glutamate released from the peripheral terminals of primary afferent nociceptors in the skin and in joints during sensory transduction as an initiating event in neurogenic inflammation (Ault and Hildebrand, 1993; Jackson *et al.,* 1995; Zhou *et al.,* 1996; Davidson *et al.,* 1997; Lawand *et al.,* 1997; 2000; Carlton and Coggeshall, 1999). This action depends on the presence of glutamate receptors on the peripheral nerve endings of primary afferent fibers (Carlton *et al.,* 1995, 2001b) and on other peripheral cell types.

Primary afferent terminals presumed to be nociceptors may also contain neuropeptide receptors, such as μ- and δ-opiate receptors (Coggeshall and Carlton,

1997; Coggeshall *et al.*, 1997; see Willis and Coggeshall, 2003), somatostatin receptors (Carlton *et al.*, 2001a), or substance P receptors (Carlton *et al.*, 1996). CGRP receptors are found on primary afferent endings in the dorsal horn and on DRG cells (Ye *et al.*, 1999), and so they may also be present on the peripheral terminals of nociceptors.

Other markers of nociceptors include vanilloid (VR-1) receptors, which are on the terminals of many unmyelinated and some finely myelinated nociceptors and respond to capsaicin, heat, or low pH (Holzer, 1991; Caterina *et al.*, 1997, 2000; Helliwell *et al.*, 1998; Tominaga *et al.*, 1998). By contrast, vanilloid-like-1 (VRL-1) receptors are on primary afferents with myelinated axons, have a high heat threshold, but do not respond to capsaicin or low pH (Caterina *et al.*, 1999). A very large fraction of DRG cells express these markers. For example, capsaicin sensitivity is observed in 88% of a sample of small- to medium-sized DRG cells in rats (Helliwell *et al.*, 1998). IB4 binds to 51% of rat DRG cells of all sizes (Wang *et al.*, 1994). Recently, mRNA for VR-1 has been shown to be widely distributed in the brains of both rats and humans, and so the role of these receptors in response to painful stimuli may be much more complex than previously thought (Mezey *et al.*, 2000).

Additional ligand-gated receptors that are found on the terminals of nociceptors include receptors for bradykinin, prostaglandin, serotonin, catecholamines, ATP, and histamine (Willis and Coggeshall, 2003). These contribute to the activation and/or sensitization of nociceptor endings, especially following tissue damage and inflammation. They are regarded as inflammatory mediators.

Additional molecules are beginning to be examined in studies of the mechanisms by which sensory transduction occurs in nociceptors. For example, a protein belonging to a family of non-voltage-gated sodium channels (DEG/ENaC) that has been characterized in *Caenorrhabditis elegans* has been proposed as the mechanical transducer in Aδ mechanical nociceptors (García-Añoveros *et al.*, 2001). The VR-1 and VRL-1 receptors are thought to transduce noxious heat signals, and VR-1 receptors are activated by lowered pH. However, pH changes during inflammation are also thought to be signaled by other acid-sensing (ASIC) channels (Habelt *et al.*, 2000; Immke and McCleskey., 2001).

Nociceptors are also influenced by the actions of growth factors. For example, peptidergic nociceptors, such as those containing substance P or CGRP, are regulated by nerve growth factor through an action on tyrosine kinase A (TrkA) receptors (McMahon *et al.*, 1994; Averill *et al.*, 1995). On the other hand, IB4-immunoreactive primary afferent neurons are regulated, at least in adult animals, by glial cell line–derived neurotrophic factor (GDNF) (Bennett *et al.*, 1996; Molliver *et al.*, 1997).

Nociceptive Input to Spinal Cord Dorsal Horn

In general, large primary afferent fibers enter the spinal cord medially in the dorsal roots, and many of these give rise to collaterals that ascend in the dorsal column (see Willis and Coggeshall, 2003). The small fibers enter more laterally and many end in the gray matter of the same or neighboring segments (Ranson and Billingsley, 1916). A similar arrangement is found in humans (Fig. 30.7B) (Sindou *et al.*, 1974, 1987; see also Chapter 8). However, it should be noted that peptidergic (CGRP and substance P containing) unmyelinated primary afferent axons can be found to ascend in the dorsal column to upper cervical levels and some appear to end in the dorsal column nuclei, at least in rats and cats (Patterson *et al.*, 1989, 1990; Tamatani *et al.*, 1989; Conti *et al.*, 1990; Fabri and Conti, 1990).

Nociceptive afferent fibers give rise to branches that may ascend or descend in Lissauer's tract before they send off collaterals that synapse in the gray matter of the spinal cord (Willis and Coggeshall, 2003). Lissauer's tract in monkeys is notable for its large content of unmyelinated axons, which are often arranged in bundles of 2,000 to 10,000 axons (Fig. 30.2) (Coggeshall *et al.*, 1981). Most of these unmyelinated axons in the primate Lissauer's tract are collaterals of primary afferent fibers, since 80% of them degenerate following transection of three successive dorsal roots (at, above, and below the particular segmental level that was examined). The majority of the unmyelinated primary afferent axons in Lissauer's tract of primates can be presumed to originate from nociceptors, but some must originate from other types of primary afferent neurons, and about 20% are probably the axons of interneurons.

Clinical Application

Lissauer's tract is important in pain transmission in humans, since surgical interruption of Lissauer's tract has been used successfully to improve the results of anterolateral cordotomy in relieving pain (Hyndman, 1942).

Rexed (1952) subdivided the gray matter of the spinal cord of cats into 10 laminae, based on its cytoarchitecture. A similar arrangement is also seen in the spinal cords of a variety of other animals and also in humans (for a detailed analysis of the cytoarchitecture and myeloarchitecture of the human spinal cord, see Chapter 7).

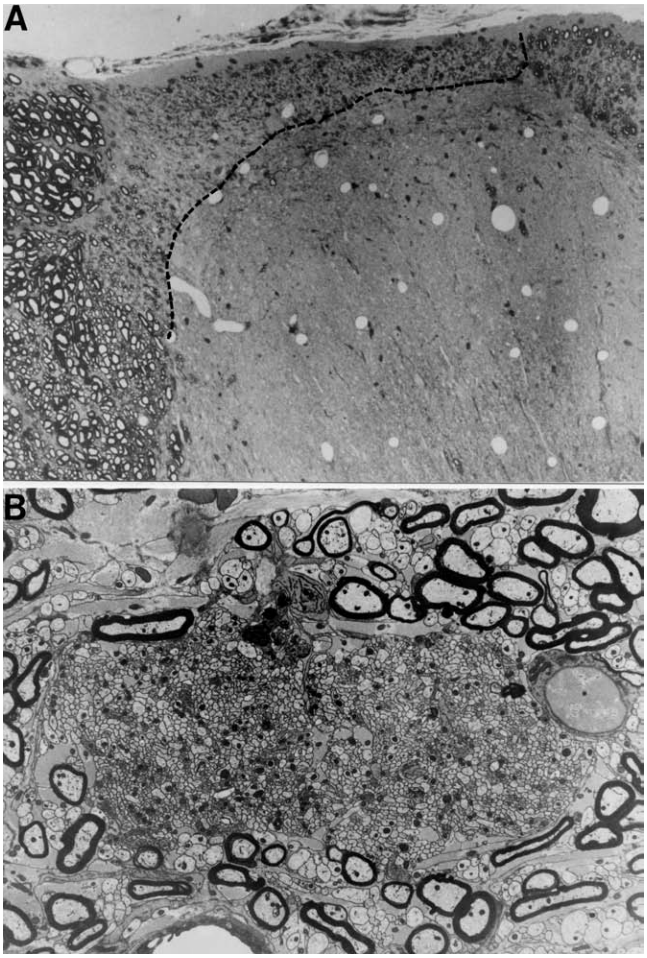

FIGURE 30.2 Unmyelinated axon bundles in monkey Lissauer tract. The light micrograph in **A** shows some of the dorsal white matter and the superficial dorsal horn in the S2 segment of a monkey spinal cord. The dashed line shows the boundary between Lissauer's tract and the dorsal horn. The dorsal column is to the left of the dorsal horn, and the dorsolateral fasciculus is to the right. The electron micrograph in **B** illustrates an axonal bundle in the medial part of Lissauer's tract in a monkey. The bundle contained 2038 unmyelinated axons. (From Coggeshall *et al.,* 1981.)

In cats and monkeys, cutaneous Aδ mechanical nociceptors have been shown by intracellular labeling of functionally identified axons to terminate chiefly in laminae I, V, and X (Fig. 30.3A, B) (Light and Perl, 1979). Most of the endings are ipsilateral, but some collaterals cross the midline to end in the gray matter on the contralateral side of the spinal cord (Fig. 30.3B). It is, of course, much more difficult to label C nociceptors by intracellular injection of a tracer into the axon. However, in guinea pigs, Sugiura *et al.* (1986, 1989) were able to inject *Phaseolus vulgaris* leucoagglutinin into cervical DRG cells belonging to cutaneous C polymodal nociceptors and to trace the axons into the spinal cord. Terminals were found in laminae I and II (Fig. 30.3C). Sugiura *et al.* (1989) also traced the axons of visceral C afferent fibers in guinea pigs in the same manner and found that these were distributed over more than five segments, in contrast to somatic afferents, which traveled only a short distance rostrocaudally from the dorsal root through which they entered the spinal cord. The terminals of visceral afferents were much more abundant than those of somatic afferents (cf. Fig. 30.3C, D). They were found not only in laminae I and II but also in laminae IV, V, and X (Fig. 30.3D), and some collaterals extended into the contralateral laminae V and X (Fig. 30.3D). In cats, anterograde labeling studies have demonstrated that fine muscle afferent fibers terminate in laminae I and V (Craig and Mense, 1983) and that joint afferent fibers end in laminae I, V–VII (Craig *et al.,* 1988). A similar distribution of primary afferent terminals would presumably be found in monkeys and humans, although this has not been demonstrated.

Typical of the superficial layers of the dorsal horn are large glomerular synaptic complexes, often referred to as scalloped primary afferent endings or "central terminals" (see reviews by Csillik and Knyihár-Csillik, 1986, and Willis and Coggeshall, 2003). There are several types of glomeruli. In monkeys, most of the glomeruli in lamina I are classified as large dense-core vesicle terminals, most in lamina II as dense sinusoid terminals, and most in lamina III as regular synaptic vesicle–containing terminals (Coimbra *et al.,* 1984; Csillik and Knyihár-Csillik *et al.,* 1986). All of these types of glomeruli degenerate following dorsal rhizotomy, indicating that they arise from primary afferent fibers (Csillik and Knyihár-Csillik *et al.,* 1986). Csillik and Knyihár-Csillik (1986) have proposed that the dense sinusoid terminals are supplied by unmyelinated fibers (see also Coimbra *et al.,* 1984) and that they are equivalent to the terminals in rodents that stain for fluoride-resistant acid phosphatase. Thus, these would be the endings of IB4-positive primary afferent neurons. The large dense-core vesicle glomeruli are thought to be the endings of peptidergic primary afferent neurons and the regular synaptic vesicle glomeruli are probably the endings of large, myelinated primary afferent fibers (Csillik and Knyihár-Csillik, 1986).

Evidence that large, dense core vesicles contain peptides comes from experiments that employ immunocytochemical staining at the ultrastructural level. For instance, electron microscopic studies of the superficial dorsal horn in monkeys show that many large, dense-cored vesicles contain substance P (Fig. 30.4A) or CGRP (Fig. 30.4B) (Csillik and Knyihár-Csillik, 1986; Carlton *et al.,* 1988; Hayes and Carlton, 1992; Alvarez *et al.,* 1993). In the human spinal cord, peptides

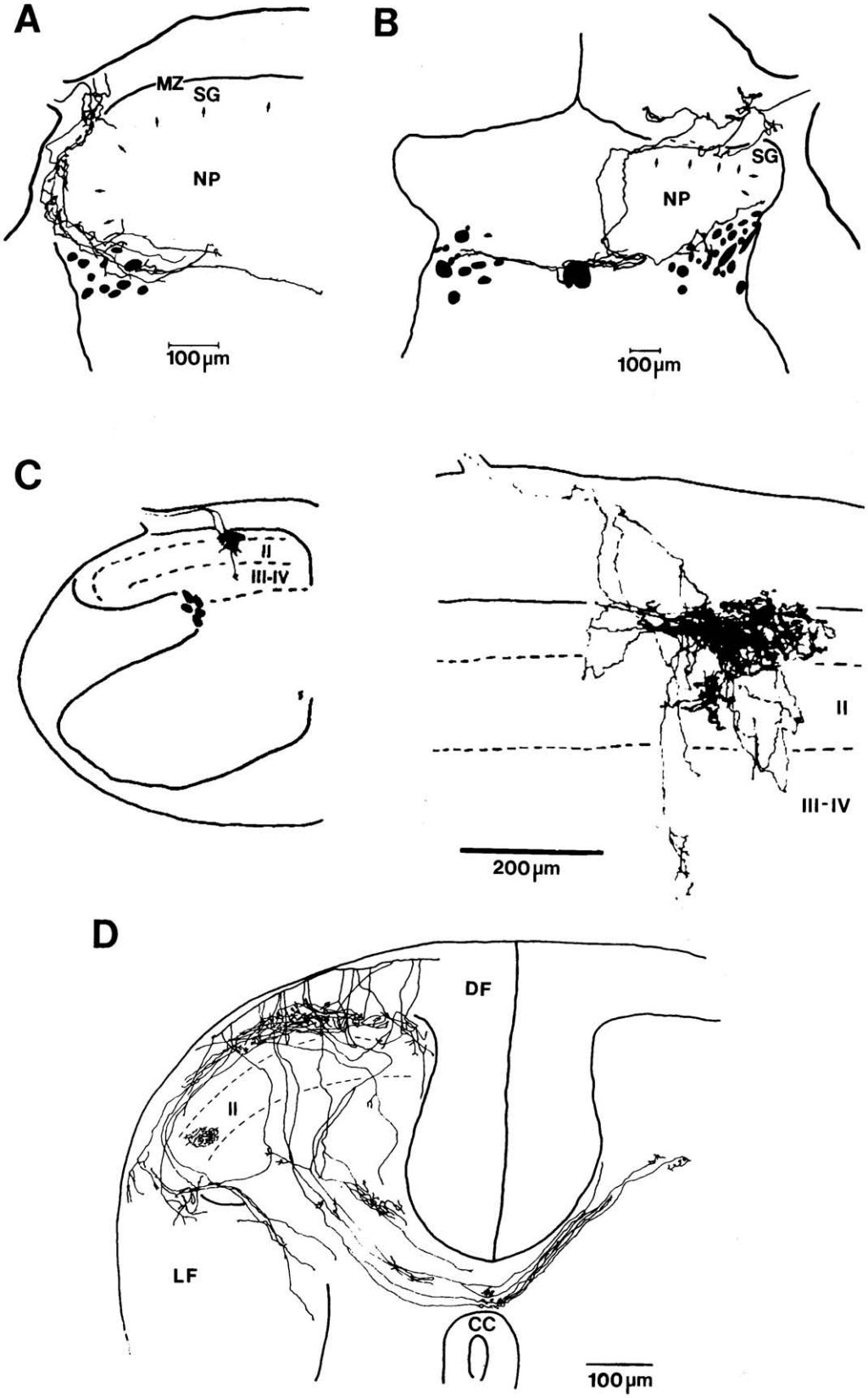

FIGURE 30.3 Projection of myelinated and unmyelinated primary afferent nociceptive axons into the spinal cord. The drawings in **A** and **B** show the distribution of the terminal branches of cutaneous Aδ mechanical nociceptors within the spinal cord of a cat **(A)** and a monkey **(B).** The axons were injected with horseradish peroxidase after the fibers were functionally identified. Laterally placed dark areas of the spinal cord represent bundles of longitudinally oriented myelinated axons. The shaded region at the midline in **B** is an area near the central canal in which some of the terminals could be found. The labeled afferent in **B** projected bilaterally. Abbreviations: MZ, marginal zone; NP, nucleus proprius; SG, substantia gelatinosa. (From Light and Perl, 1979.) The drawings in **C** show that the terminals of a somatic C-fiber in a guinea pig were chiefly in laminae I and II (with a slight extension into deeper layers). The axon was labeled anterogradely following injection of *Phaseolus vulgaris* leucoagglutinin into a dorsal root ganglion cell at an upper cervical level. The scale bar = 200 mm. (From Sugiura *et al.,* 1986). **D** illustrates the profuse spinal cord terminations of a visceral C-afferent fiber identified by stimulation of the celiac ganglion in a guinea pig. Abbreviations: CC, central canal; DF, dorsal funiculus; LF, lateral funiculus. (From Sugiura *et al.,* 1989.)

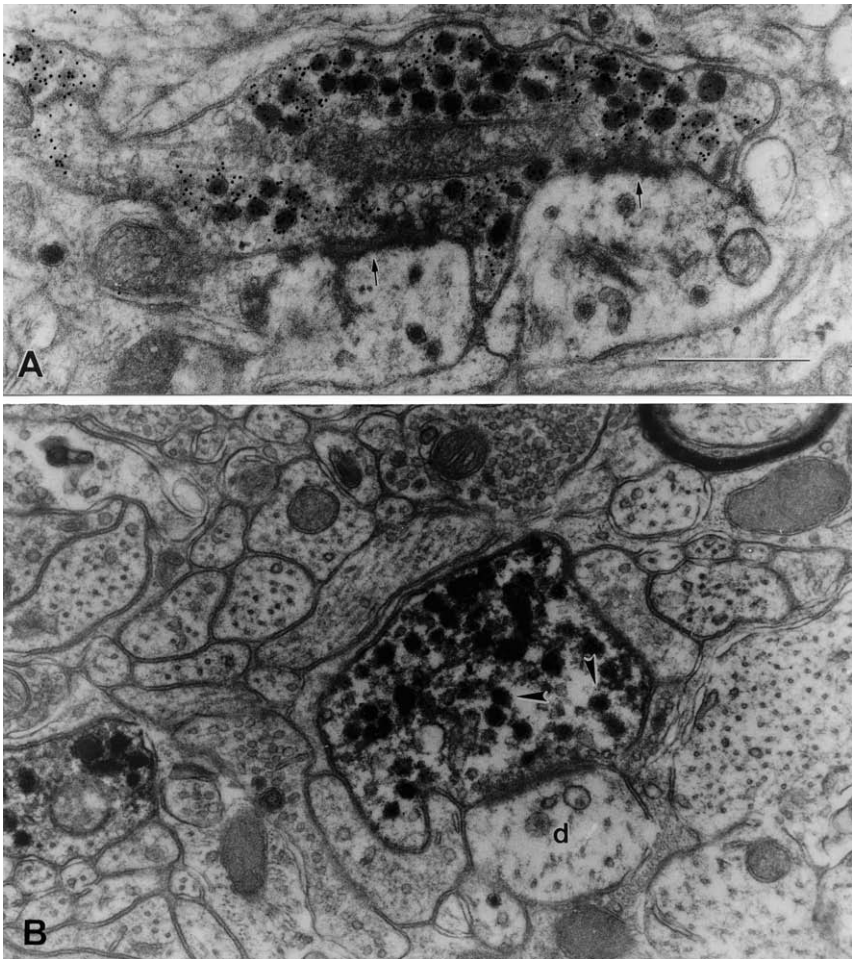

FIGURE 30.4 Peptide content of dense core vesicles in primary afferent synaptic terminals in the superficial dorsal horn of a monkey spinal cord. The electron micrograph in **A** illustrates a synaptic ending that was shown to be immunoreactive for substance P, using the immunogold staining technique. The gold particles are in close relationship to dense core vesicles. The arrows indicate synaptic contacts made by this ending on dendrites in the neuropil of the superficial dorsal horn. The scale is 1 μm. (From Alvarez *et al.,* 1993.) The electron micrograph in **B** shows an axodendritic synapse in the dorsal horn of a monkey. In this case the dense core vesicles in the terminal were stained for calcitonin gene–related peptide using the immunoperoxidase technique. (From Carlton *et al.,* 1988.)

that have been found in the superficial dorsal horn include CGRP (Fig. 30.5A, B) (Harmann *et al.,* 1988), bombesin, substance P, cholecystokinin, somatostatin, met-enkephalin, and vasoactive intestinal polypeptide (Fig. 30.5C) (Chung *et al.,* 1989; see also Chapter 7). The immunostaining of CGRP-containing terminals at the light microscopic level presumably reflects the distribution of primary afferent terminals, since CGRP staining in the dorsal horn is eliminated in rats following an extensive dorsal rhizotomy (Chung *et al.,* 1988). However, other peptides are often localized not only in primary afferent terminals but may also be contained in the terminals of pathways that descend from the brain or in the cell bodies or the processes of neurons intrinsic to the spinal cord.

The synapses made by primary afferent nociceptors in the spinal cord gray matter result in the activation of second-order postsynaptic neurons (reviewed in Willis and Coggeshall, 2003). Some of these neurons project to the brain and therefore convey nociceptive signals to higher levels of the nervous system (see **"Pain Transmission Neurons and Pathways"**). Other second-order neurons are excitatory or inhibitory interneurons. The excitatory interneurons may also activate projection neurons, or they may excite inhibitory interneurons or elicit reflex responses by exciting somatic

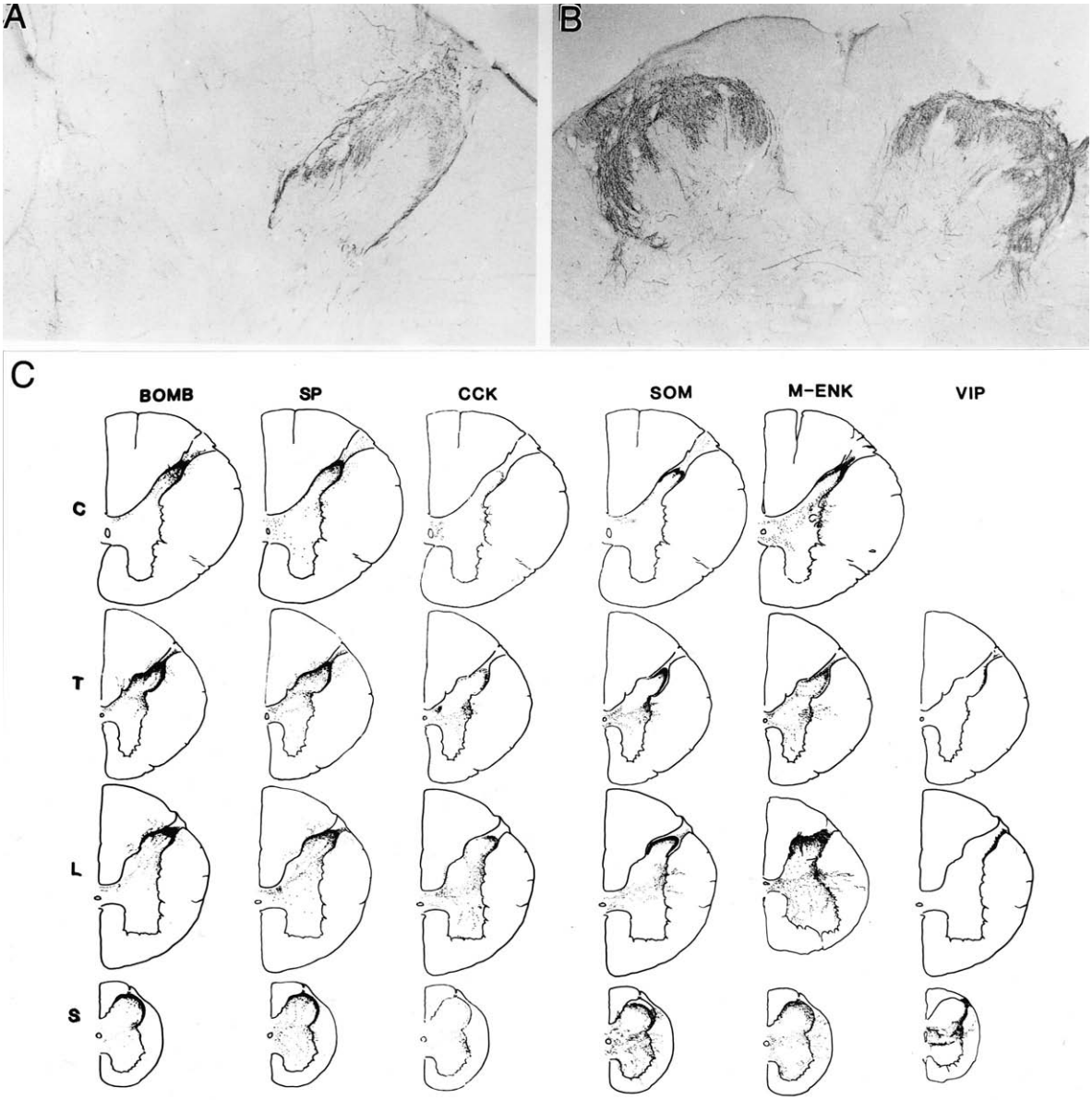

FIGURE 30.5 Peptides in the dorsal horn of the human spinal cord. **A** and **B** show the distribution of calcitonin gene-related peptide immunoreactivity in transverse sections of the lumbar and sacral dorsal horn of a human spinal cord. (From Harmann *et al.*, 1988.) **C** shows the distribution of several peptides (BOMB, bombesin; SP, substance P; CCK, cholecystokinin; SOM, somatostatin; M-ENK, met-enkephalin; VIP, vasoactive intestinal polypeptide) in drawings of transverse sections of the human cervical (C), thoracic (T), lumbar (L), and sacral (S) spinal cord. (From Chung *et al.*, 1989.)

or autonomic motor neurons. The projection neurons can activate not only brain mechanisms that lead to sensory experience and other pain responses, such as endocrine changes or memory, but also feedback systems that modulate nociceptive transmission in the spinal cord by way of descending projections. The circuits involved in such actions are complex and still incompletely known.

Inhibition of spinal nociceptive transmission following stimulation of the skin can occur through activation of segmental or supraspinal circuits or both. In the circuit proposed for the gate theory of pain by Melzack and Wall (1965), large, presumably mechanosensitive primary afferents activate inhibitory interneurons that in turn cause presynaptic inhibition of the actions of fine, nociceptive primary afferent fibers.

Thus, activation of large afferent fibers "closes the dorsal horn gate," reducing pain. Soon after the proposal of the gate theory, Wall and Sweet (1967) reported that pain can be diminished in human patients by stimulation of large primary afferent fibers in peripheral nerves. The anatomical substrate for this inhibitory interaction, which can reduce neurotransmitter release, is likely to be GABAergic interneurons in the superficial dorsal horn that are excited by synaptic release of glutamate from primary afferent terminals. These GABAergic interneurons in turn cause presynaptic inhibition by releasing GABA, which acts on $GABA_A$ receptors to depolarize the terminals of primary afferent fibers (Rudomin and Schmidt, 1999; Willis, 1999). GABAergic inhibition can also occur by means of a postsynaptic action of GABA on interneurons. Another mechanism of GABA action is the activation of $GABA_B$ receptors on primary afferent endings. Activation of $GABA_B$ receptors results in another form of presynaptic inhibition in which there is no primary afferent depolarization but rather a blockade of calcium channels and a reduction in transmitter release (see Willis and Coggeshall, 2003).

Evidence for the presence of GABAergic synapses on the synaptic endings of Aδ nociceptors is shown in Fig. 30.6A (Alvarez *et al.,* 1992). These synapses are presumably responsible for presynaptic inhibition of the actions of the Aδ axon endings on dorsal horn interneurons. In the same study, GABAergic inhibitory interneurons were also found to make synaptic connections with the dendrites of other spinal cord neurons. This is consistent with the well-known prominence of GABAergic postsynaptic inhibition in the dorsal horn (Willis and Coggeshall, 1991).

An effort has been made by several groups to determine if there are GABAergic terminals presynaptic to peptidergic synaptic endings, presumably of C fibers, in the superficial dorsal horn of monkeys. These synapses often contain both glutamate and peptides, such as substance P and/or CGRP (Hökfelt *et al.,* 1975; De Biasi and Rustioni, 1988; Hayes and Carlton, 1992). CGRP-labeled afferent fibers commonly synapse with GABAergic dendritic profiles (presumably of islet cells). However, the terminals of GABA-containing interneurons only occasionally make synaptic contacts back onto primary afferent endings, although they do form many synapses onto other dorsal horn neurons (Fig. 30.6B, C) (Hayes and Carlton, 1992).

Alvarez *et al.* (1993) were unable to demonstrate any GABAergic contacts onto the terminals of two intracellularly labeled C fibers in monkeys (including one that had been identified as a nociceptor prior to the injection of horseradish peroxidase into the axon). The C fiber endings contained CGRP, and so they were the endings of peptidergic primary afferent C fibers. However, Alvarez *et al.* (1993) frequently observed GABAergic endings that were presynaptic to nonpeptidergic glomerular terminals. It is conceivable that these were the endings of unmyelinated afferents that bind IB4. Interestingly, the densest staining for $GABA_A$ receptors in the dorsal horn is in the region of the densest terminations of IB4-labeled afferents (Alvarez *et al.,* 1996).

$GABA_A$ receptors might also be activated in a paracrine manner by volume conduction of GABA. However, no positive immunocytochemical evidence was found for the localization of $GABA_A$ receptors on glomerular primary afferent terminals at the light and ultrastructural levels, although this possibility could not be ruled out, especially since $GABA_A$ receptors were found on most of the DRG cells examined (Alvarez *et al.,* 1996).

Recently, it has been shown in rats that both Aδ and C primary afferent axons can be depolarized sufficiently following a strong noxious stimulus (capsaicin injection into the skin or adjuvant into a joint) to result in dorsal root reflex discharges. This action is mediated through glutamate receptors that are presumably on inhibitory interneurons and through $GABA_A$ receptors on the terminals of fine primary afferent fibers (Sluka *et al.,* 1993; Rees *et al.,* 1994; 1995; Lin *et al.,* 1999; 2000; see also Willis, 1999). Dorsal root reflexes are action potentials that originate near the primary afferent terminals in the spinal cord and then propagate antidromically out to the periphery. Dorsal root reflexes in nociceptors are thought to release neurotransmitters, such as glutamate, substance P, and CGRP, from their sensory nerve terminals in the periphery. These agents would then trigger neurogenic inflammation (Sluka *et al.,* 1994, 1995; Willis, 1999). For instance, released substance P would be expected to produce plasma extravasation and CGRP would result in vasodilation (Geppetti and Holzer, 1996).

The inhibitory circuit proposed in the gate theory is contained in the spinal cord dorsal horn, although inhibitory actions were suggested to be triggered or influenced by supraspinal loops (Melzack and Wall, 1965). On the other hand, the diffuse noxious inhibitory control (DNIC) system for inhibition of wide-dynamic-range neurons in the spinal cord by nociceptive afferent input from widespread regions of the body is dependent on a supraspinal loop. It has been proposed that DNIC is mediated through a descending pathway that originates from the subnucleus reticularis dorsalis of the medulla (LeBars *et al.,* 1979a, b; Villanueva and Le Bars, 1995). However, Almeida *et al.* (1996, 1999) disagree with this proposal, instead suggesting that the subnucleus reticularis dorsalis is pronociceptive. A

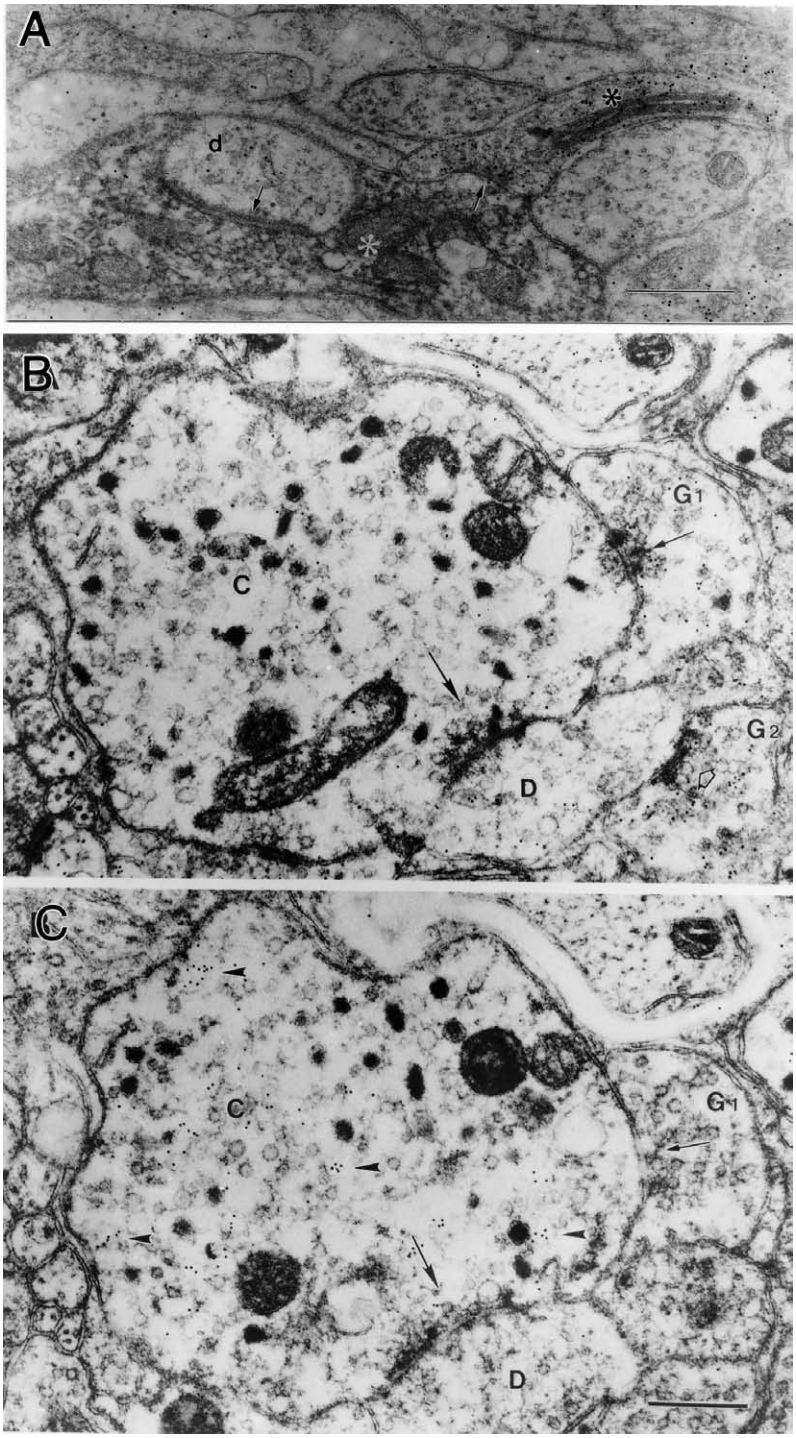

FIGURE 30.6 GABAergic synapses on the terminals of primary afferent axons in the dorsal horn. The electron micrograph in **A** is from a double labeling study. An Aδ mechanical nociceptor was identified and then injected with horseradish peroxidase. One of its terminals is indicated by the white asterisk. The section was also immunolabeled for GABA. The immunogold particles in the synaptic ending indicated by the black asterisk show that this ending was from a GABAergic inhibitory interneuron. The GABA-containing ending makes a symmetrical synapse with the nociceptor terminal. (From Alvarez *et al.,* 1992.) The electron micrographs in **B** and **C** are of serial sections of the terminal of a primary afferent axon in the dorsal horn of a monkey. The ending was labeled for calcitonin gene–related peptide (CGRP) by immunogold particles in **C.** In the adjacent section in **B,** a synapse formed by a GABAergic interneuron on the CGRP-containing terminal (G_1) is immunostained for GABA. The synapse is an asymmetrical one. Another GABAergic terminal (G_2) is seen to synapse with a dendrite (D). (From Hayes and Carlton, 1992.)

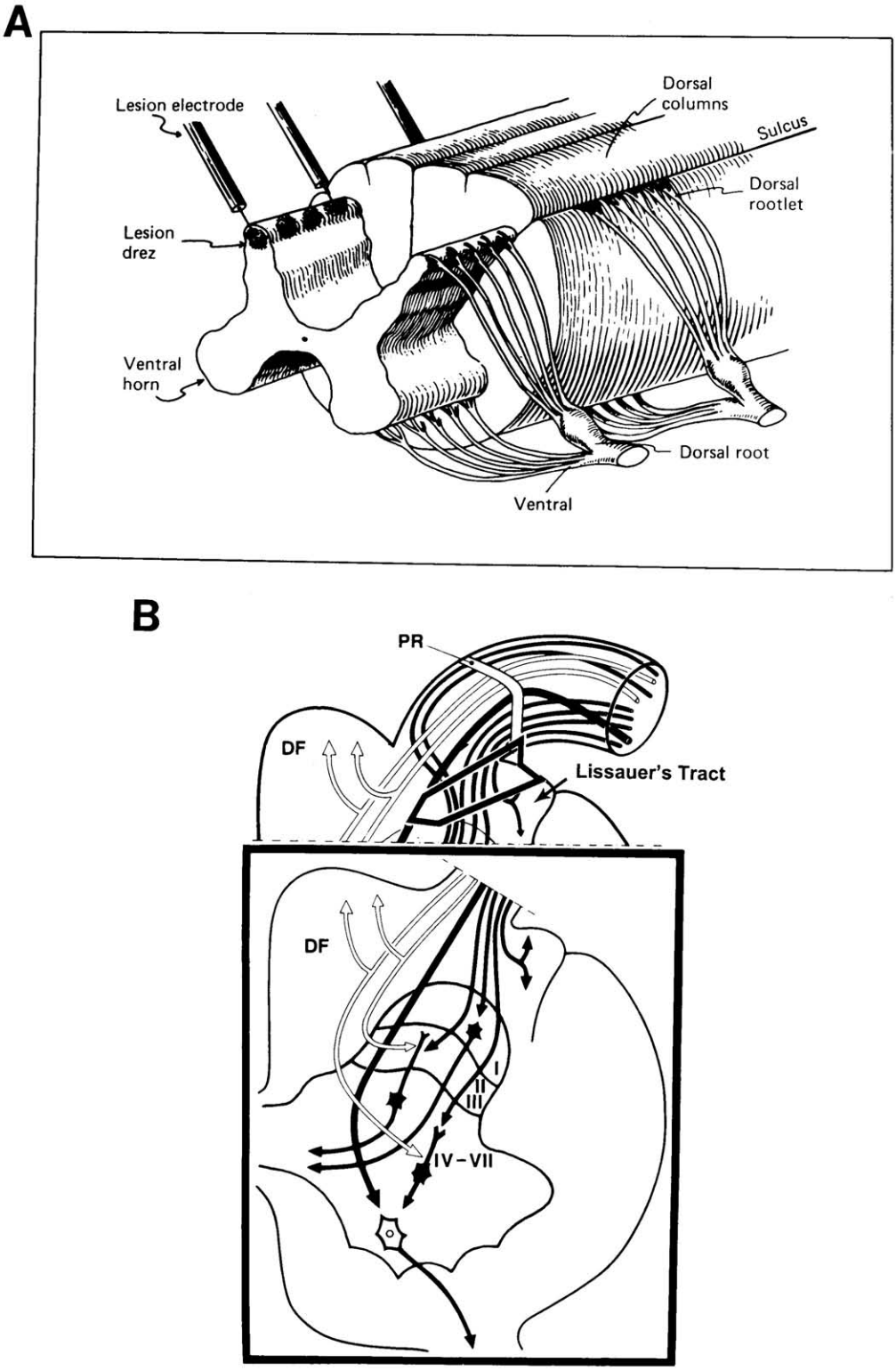

FIGURE 30.7 Dorsal root entry zone (drez) lesions. The drawing of the spinal cord in **A** shows the placement of dorsal root entry zone or "drez" lesions in the dorsal horn on one side of the spinal cord. (From Nashold and Ostdahl, 1979.) The drawing in **B** shows an alternative surgical approach in which a lesion interrupts fine nociceptive afferent fibers as they enter the spinal cord through the lateral aspect of each dorsal rootlet, travel in Lissauer's tract and penetrate into the dorsal horn. DF, dorsal funiculus. (From Jeanmonod and Sindou, 1991.)

number of investigations have shown that there is a functional DNIC system in monkeys (Villanueva *et al.*, 1990) and humans (Talbot *et al.*, 1987; Willer *et al.*, 1989; De Broucker *et al.*, 1990; Bouhassira *et al.*, 1993).

Experiments in which repetitive stimulation of peripheral nerves in monkeys at different intensities was used to determine the relative effectiveness of afferent volleys in large versus small afferent fibers in inhibiting the responses of spinothalamic tract neurons to C-fiber input showed that stimulation of fine afferents (presumably activating the DNIC mechanism) was much more effective than stimulation of large afferents (Chung *et al.*, 1984), suggesting that activation of the DNIC mechanism might be a more effective means for reducing pain than activation of the spinal cord gating mechanism.

Clinical Application

Chronic pain in humans is often associated with activity in primary afferent nociceptive neurons and the dorsal horn neurons on which the nociceptive afferents synapse. A surgical procedure that is sometimes used to relieve neuropathic pain due to avulsion of dorsal roots is the placement of a series of lesions in the "dorsal root entry zone" (drez lesions; Fig. 30.7A) (Nashold and Ostdahl, 1979; Nashold, 1984; Rawlings *et al.*, 1989; Campbell *et al.*, 1988b; Rath *et al.*, 1997). Similar lesions in monkeys destroy the region of Lissauer's tract and at least part of the dorsal horn (Singh *et al.*, 1989). Pain relief is presumably attributable to the loss of nociceptive afferent input to the dorsal horn, as well as to the destruction of many dorsal horn neurons. A different approach to drez lesions is the interruption of fine nociceptive afferents as they pass through the lateral part of the dorsal root and into Lissauer's tract (Fig. 30.7B) (Jeanmonod and Sindou, 1991). This procedure also seems to be effective for the management of neurogenic pain.

PAIN TRANSMISSION NEURONS AND PATHWAYS

A number of pathways that ascend from the spinal cord to the brain are activated by noxious stimuli. These have been reviewed previously (Willis, 1985; Willis and Westlund, 1997; Willis and Coggeshall, 2003; see also Chapters 8, 28, and 29). The emphasis here will be on the primate spinothalamic tract. The spinothalamic tract has long been regarded as the major pathway in humans that is responsible for evoking pain sensations. In addition, evidence for the recently described role of the dorsal column in conveying nociceptive signals from viscera will be described. Other pathways, such as the spinocervical, spinoreticular, spinomesencephalic, spinoparabrachial, spinohypothalamic, and spinolimbic tracts, will also be discussed briefly.

Spinothalamic Tract

Nociceptive neurons in the spinal cord include spinothalamic tract cells, most of which project directly to the contralateral thalamus. Early reports of the distribution of neurons that show chromatolysis in human patients following an anterolateral cordotomy (Foerster and Gagel, 1932; Kuru, 1949; Smith, 1976) do not permit a definitive determination of the locations of human spinothalamic tract cells, since chromatolysis would also be expected in the cells of origin of other tracts that ascend in the anterolateral spinal cord white matter (see Chapter 8). Another technique, such as retrograde labeling, is required, but this cannot be done in humans. However, retrograde labeling has been done in monkeys. It can be presumed that the organization of the spinothalamic tract is similar in humans and monkeys.

Spinothalamic tract neurons that are retrogradely labeled from the ventral posterior lateral (VPL) nucleus of the thalamus in monkeys are concentrated in lamina I and in the lateral half of the neck and base of the dorsal horn in laminae IV–VI (Fig. 30.8C, D) (Willis *et al.*, 2001; cf. Trevino and Carstens, 1975; Willis *et al.*, 1979; Hayes and Rustioni, 1980; Apkarian and Hodge, 1989a; Zhang and Craig, 1997). Other spinothalamic tract neurons are in the intermediate region and the ventral horn (laminae VII–X). Many of these send projections to the medial thalamus to end in the intralaminar complex, particularly in the central lateral nucleus (Willis *et al.*, 1979; Giesler *et al.*, 1981; Ammons *et al.*, 1985; Wang *et al.*, 1999). Other spinothalamic cells project to the ventral posterior inferior nucleus (Gingold *et al.*, 1991). (For a description of the thalamic nuclei receiving spinothalamic terminations, see Chapter 20.)

Lamina I spinothalamic tract cells have been suggested to project to a part of the posterior complex of the thalamus that was recently termed the posterior ventromedial (VMpo) nucleus by Craig *et al.* (1994) in monkeys and by Blomqvist *et al.* (2000) in humans and not to the VPL nucleus. This proposal has been critically reviewed (Willis *et al.*, 2002; see also the discussion of this nomenclature by Percheron in Chapter 20). The basis for part of the criticism was evidence from a recent retrograde tracing study (Willis *et al.*, 2001) and from antidromic mapping experiments (Zhang *et al.*, 2000a, b) showing that many primate lamina I spinothalamic tract cells do in fact project to the VPL nucleus (Fig. 30.8).

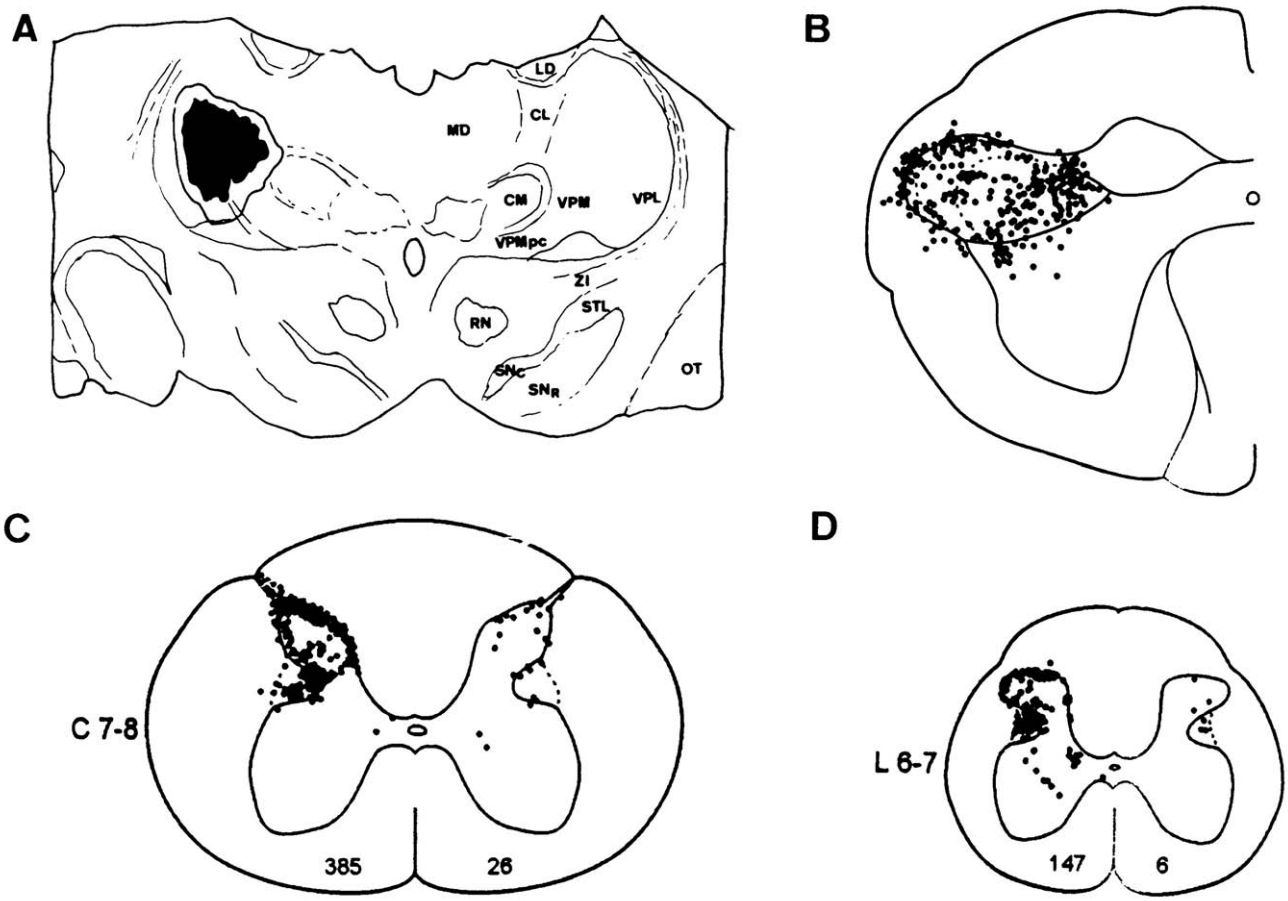

FIGURE 30.8 Projections from the marginal zone and deep dorsal horn of the spinal cord and medullary dorsal horn to the ventrobasal complex. The drawing in **A** shows the site of injection of a retrograde tracer, cholera toxin subunit B, into the ventral posterior lateral and ventral posterior medial nucleus of the thalamus in a monkey. The distribution of retrogradely labeled trigeminothalamic neurons in the spinal trigeminal nucleus, caudal part, is shown in **B** and labeled spinothalamic tract neurons in the cervical and lumbar segments of the spinal cord in **C** and **D**. (From Willis *et al.,* 2000.)

Most spinothalamic tract cells in lamina I of the monkey spinal cord are oriented rostrocaudally (Fig. 30.9A) (Zhang and Craig, 1997), whereas those in the neck of the dorsal horn are oriented in the transverse plane of the spinal cord (Fig. 30.9B–D) (Willis *et al.,* 1979; Apkarian and Hodge, 1989a; Carlton *et al.,* 1989; Westlund *et al.,* 1992a; cf. Chapter 7). These dendritic arrangements are presumably responsible for the finding that lamina I STT cells tend to have a more distinctly somatotopic organization than do STT cells in deeper layers of the dorsal horn (Willis *et al.,* 1974; see Willis and Coggeshall, 2003).

Functional studies have shown that a large fraction of primate spinothalamic tract cells are nociceptive, since they respond preferentially to noxious stimulation of skin, muscle, joints, and/or viscera (Willis *et al.,* 1974; Price *et al.,* 1978; Chung *et al.,* 1979; Foreman *et al.,* 1979; Kenshalo *et al.,* 1979; Milne *et al.,* 1981; Ferrington *et al.,* 1987; Ammons, 1989; Foreman, 1989; Dougherty *et al.,* 1992; Chandler *et al.,* 1998; Al-Chaer *et al.,* 1999). Spinothalamic tract cells are often classified according to their responses to graded intensities of cutaneous stimuli as low threshold (LT), wide dynamic range (WDR), and high threshold (HT; or nociceptive specific, NS) (Mendell, 1966; Chung *et al.,* 1979). The most effective stimuli for LT neurons are tactile ones, although these neurons may also respond to noxious stimuli. WDR neurons respond to some extent to innocuous cutaneous stimuli, but they are most powerfully activated by noxious stimuli. HT spinothalamic tract cells have no or only weak responses to tactile stimuli, and they respond chiefly or sometimes exclusively to noxious stimuli.

Cluster analysis has been utilized to provide an objective basis for classifying the responses of spinothalamic tract cells to mechanical stimulation of the

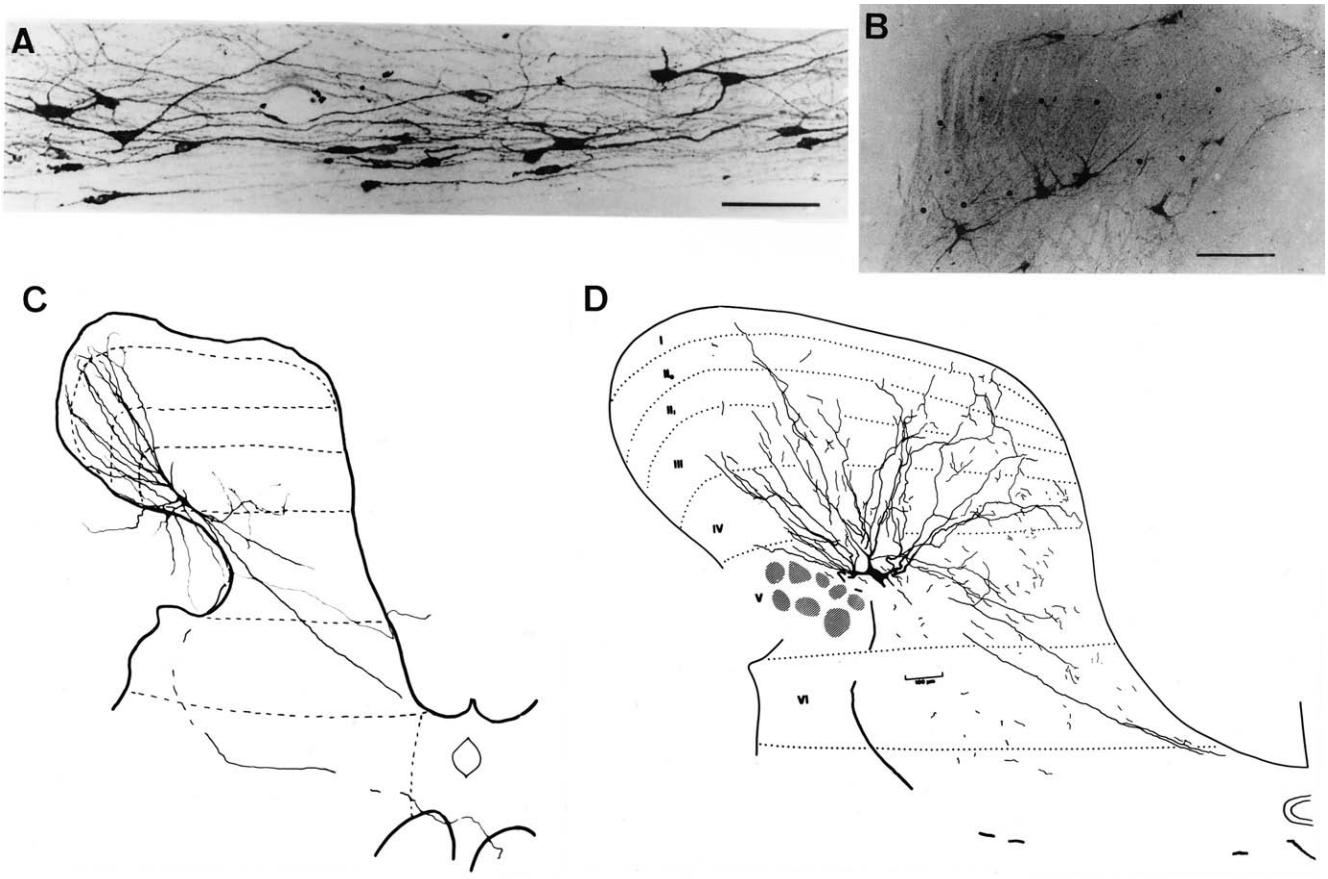

FIGURE 30.9 Cells of origin of the primate spinothalamic tract. In **A** is shown a horizontal section through lamina I of the spinal cord of a monkey. Numerous spinothalamic tract neurons were labeled retrogradely from the thalamus following an injection of cholera toxin subunit B. The scale is 100 µm. (From Zhang and Craig, 1997.) **B** shows a transverse section of a monkey spinal cord. Several retrogradely labeled spinothalamic tract cells are seen in lamina I, but their main dendritic trees are cut in cross-section because they are oriented at right angles to the section. Other labeled cells in the deep dorsal horn have elaborate dendritic trees in the plane of section. The retrograde label was wheat germ agglutinin conjugated to horseradish peroxidase. (From Apkarian and Hodge, 1989a.) The drawing in **C** is a reconstruction of a high-threshold spinothalamic tract cell that was injected intracellularly with horseradish peroxidase after its responses to cutaneous stimulation were recorded. (From Westlund *et al.,* 1992a.) The cell was contacted by both glutamate- and GABA-containing axonal endings. The drawing in **D** is of a similarly injected spinothalamic tract cell, but the response properties in this case were those of a wide dynamic range neuron. (From Carlton *et al.,* 1989.)

skin (Chung *et al.,* 1986b; Surmeier *et al.,* 1988; Owens *et al.,* 1992). One approach resulted in the identification in a large sample of spinothalamic tract cells of three clusters based on response profiles to graded intensities of mechanical stimulation. These clusters could be correlated with the LT, WDR, HT groups in the usual system of classification. Based on this analysis, most spinothalamic cells, whether in lamina I (69%) or V (59%), were judged to belong to the WDR class (Owens *et al.,* 1992). About 20% of the spinothalamic tract cells in lamina V were of the LT class. A substantial fraction of spinothalamic tract cells in either lamina I (29%) or V (22%) were HT cells.

The axons of most primate spinothalamic tract cells decussate near their cell bodies (Fig. 30.9C, D) and ascend to the brain in the contralateral anterolateral white matter. Spinothalamic axons can be seen in the monkey spinal cord following injection of wheat germ agglutinin–conjugated horseradish peroxidase into the thalamus (Stevens *et al.,* 1991), provided that axonal transport is blocked by ligation (Fig. 30.10A, upper panel) or by colchicine (Fig. 30.10A, lower two panels). In the thoracic spinal cord, axons of spinothalamic neurons that have a fine caliber are found in the middle of the lateral funiculus and even dorsal to the level of the dentate ligament, whereas axons with a

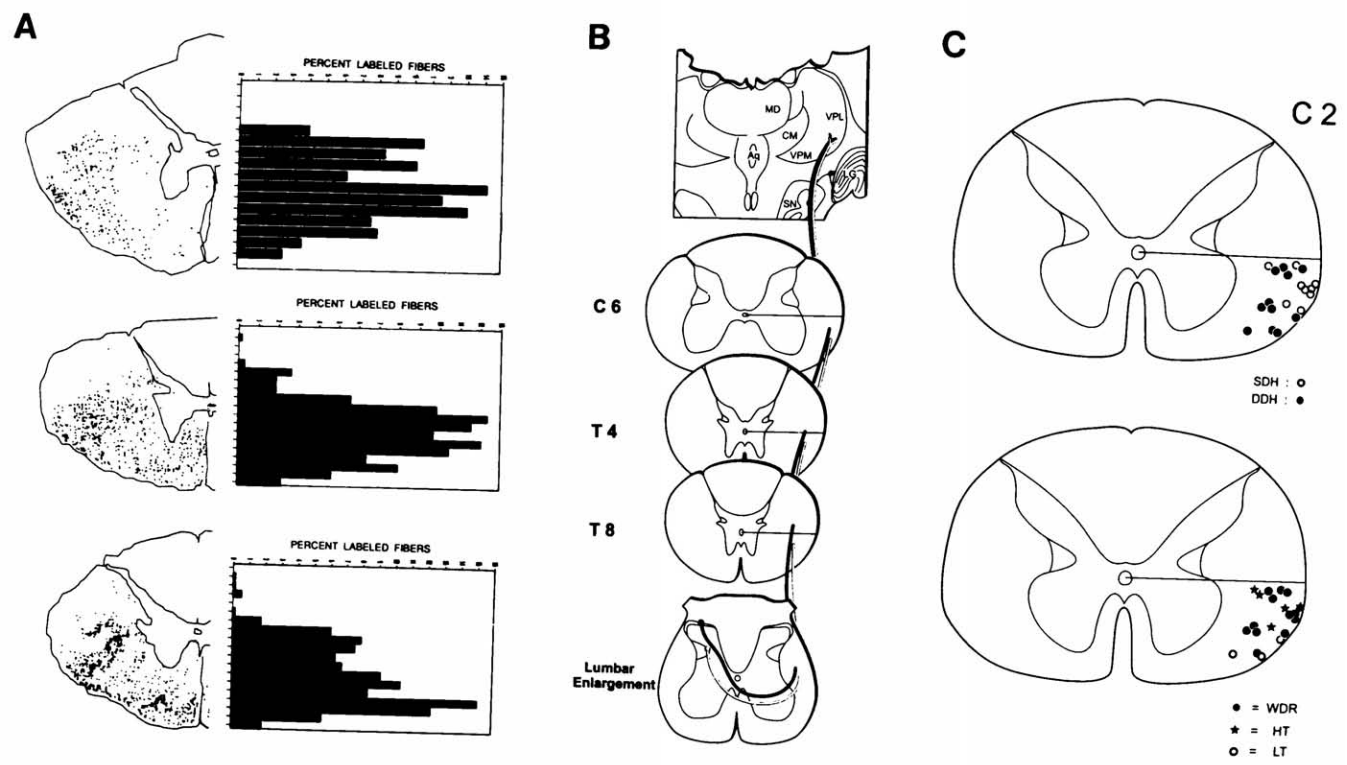

FIGURE 30.10 Location of spinothalamic tract axons in the lateral funiculus. The drawings in **A** are of transverse sections at the thoracic level of the spinal cord in three monkeys. The dots indicate the locations of individual axons that were retrogradely labeled from the thalamus. The histograms show the proportions of labeled STT axons at different dorsal-ventral levels of the cord. (From Stevens *et al.,* 1991.) The drawings in **B** are of sections of the spinal cord at different segmental levels, as well as of the posterior thalamus. The axons of spinothalamic tract cells of lamina I are represented by the black axon and those of spinothalamic tract cells in lamina V by the light axon. Both sets of axons belonged to neurons that could be activated antidromically by low current stimuli applied in the ventral posterior lateral (VPL) nucleus of the thalamus. (From Zhang *et al.,* 2000b.) The drawings of transverse sections of the C2 spinal cord in **C** show the locations of the axons of spinothalamic tract cells, as determined by antidromic mapping with low-current stimuli. The axons are identified in the top drawing by their origins from neurons in the superficial dorsal horn (SDH) or deep dorsal horn (DDH). The same axons are identified in the lower drawing by their response type as wide dynamic range (WDR), high threshold (HT), or low threshold (LT). (From Zhang *et al.,* 2000a.)

thicker diameter are seen ventrally in the lateral funiculus and also in the ventral funiculus (Stevens *et al.,* 1991). Antidromic microstimulation experiments show that, in the thoracic spinal cord, the axons of primate lamina I spinothalamic neurons are concentrated in the middle of the lateral funiculus in a region that extends dorsal to the level of the dentate ligament, whereas the axons of spinothalamic tract cells in the deep dorsal horn are located more ventrally, in the ventral part of the lateral funiculus (Fig. 30.10B) (Zhang *et al.,* 2000b; cf. Stevens *et al.,* 1991; Craig, 2000). However, axons that originate from lamina I spinothalamic cells of the lumbar enlargement shift ventrally as they ascend in the spinal cord. At the level of the upper cervical spinal cord, they become intermingled with the axons from spinothalamic cells in the deep dorsal horn of the lumbar enlargement (Fig. 30.10C) (Zhang *et al.,* 2000a).

Clinical Application

Anterolateral cordotomy is a surgical procedure that has been employed for many years to relieve pain, beginning with the pioneering operation by Spiller and Martin (1912) that was designed based on Spiller's observation that interruption of both anterolateral quadrants of the spinal cord by tuberculomas resulted in analgesia on both sides of the body (Spiller, 1905). At that time, it was already known that pain transmission depended on a pathway that ascended on the side opposite to that affected by a painful stimulus (Brown-Séquard, 1860; Gowers, 1878; Head and Thompson, 1906). Many neurosurgeons have since

performed anterolateral cordotomies with varying degrees of success (Foerster and Gagel, 1932; Hyndman and Van Epps, 1939; White *et al.*, 1950; White, 1963; see review in Gybels and Sweet, 1989). Percutaneous cordotomy is an improved approach in which a cordotomy is produced at a high cervical level without a laminectomy by making a lesion with a needle introduced into the anterolateral quadrant through the C1–C2 intervertebral foramen (Mullen *et al.*, 1963; Mullen, 1966; Rosomoff *et al.*, 1965, 1966). Cordotomies are no longer performed as frequently as in the past, in part because of the tendency for pain to recur even after an initially successful cordotomy and in part because of improvements in drug therapy for pain. Bilateral high cervical percutaneous cordotomies proved to be hazardous because of the complication of sleep-induced apnea following the interruption of descending pathways for respiratory control (Ischia *et al.*, 1984; see Gybels and Sweet, 1989). Attempts have also been made to interrupt the spinothalamic tract at medullary or midbrain levels, but such procedures have not been widely adapted (White, 1941; Walker, 1942a, b; Wycis and Spiegel, 1962).

Areas of analgesia associated with partial interruption of the anterolateral white matter on the two sides of the spinal cord at an upper thoracic segmental level in a human patient are shown in Figure 30.11A and B (Hydman and Van Epps, 1939). The lesion that was placed in the anterolateral white matter on the right side of the spinal cord was more extensive than that made on the left side of the cord (Fig. 30.11A). The lesion in the right anterolateral quadrant extended from just below the dentate ligament to the anterior funiculus. The analgesia on the left side included the left lower extremity and extended up the trunk as far rostrally as the T4 dermatome (Fig. 30.11B). The lesion on the left side of the spinal cord was restricted to an area near the dentate ligament. The corresponding analgesia was restricted to part of the right lower extremity. The explanation for the different distributions of the analgesia following these two anterolateral cordotomies is that the spinothalamic tract has a somatotopic organization in humans (Fig. 30.11C) (Hyndman and Van Epps, 1939; Walker, 1940; White *et al.*, 1956; see Gybels and Sweet, 1989). A similar somatotopic organization appears to be present in monkeys as well (Weaver and Walker, 1941; Yoss, 1953; Applebaum *et al.*, 1975). Presumably, the shift of the axons from spinothalamic tract cells in lamina I ventrally in the upper thoracic and cervical segments so that both sets of axons intermingle (Fig. 30.10B, C) permits a restricted anterolateral cordotomy to interrupt pain transmission more effectively (cf., Zhang *et al.*, 2000a, b). However, if pain transmission depended primarily on the set of axons from spinothalamic cells in lamina I, it would be difficult to explain why the anterolateral cordotomy illustrated in Figure 30.11 had to extend so far anteriorly to produce analgesia on the trunk. In fact, Gybels and Sweet (1989) stress that "total division of the spinothalamic tract by anterolateral cordotomy stops pain from cancer. This means that the section should include the medial and anterior portion of the anterior quadrant, extending 1–2 mm medial to the most medial fibers of the ventral root." This implies that the axons of spinothalamic cells of both the marginal zone and the deep dorsal horn contribute importantly to pain sensation (see also Mayer *et al.*, 1975; Ralston and Ralston, 1992). Anterolateral cordotomies in monkeys are also effective in reducing contralateral responses to noxious stimuli; as in humans, there is often substantial recovery with time (Yoss, 1953; Vierck and Luck, 1979; Greenspan *et al.*, 1986; Vierck *et al.*, 1990).

Additional evidence about the role of the anterolateral quadrant in pain comes from a case that was first reported by Noordenbos and Wall in 1976. A patient had been stabbed in the back, resulting in transection of all of the spinal cord except for one anterolateral quadrant (Fig. 30.12). The patient was examined initially and then reexamined a year later (Wall and Noordenbos, 1977). The findings in the physical examination of this patient provide positive evidence for the types of sensory experience that can be conveyed through one anterolateral quadrant. She could identify pain evoked by pinprick on the side contralateral to the intact anterolateral quadrant of the spinal cord but not on the ipsilateral side, although repeated pinpricks here could produce discomfort. Warm and cold stimuli were identified when applied to the side of the body contralateral but not ipsilateral to the side of the intact anterolateral quadrant, although application of heat to the ipsilateral side evoked an unpleasant burning sensation that continued after the stimulus was removed. Thus, axons ascending in the contralateral anterolateral quadrant are required for recognition of sharp pain and temperature sensations. However, an unpleasant, burning sensation can be conveyed by axons that ascend in the ipsilateral anterolateral quadrant.

Primate *(Macaca fascicularis)* spinothalamic neurons are believed to contain glutamate as a neurotransmitter (Westlund *et al.*, 1992a; cf. Magnusson *et al.*, 1987). Different populations of spinothalamic neurons in rats contain enkephalin, dynorphin, vasoactive intestinal polypeptide, cholecystokinin, bombesin, and/or galanin (Coffield and Miletic, 1987; Ju *et al.*, 1987; Leah *et al.*, 1988; Nahin, 1988). There is also indirect evidence that some spinothalamic cells may

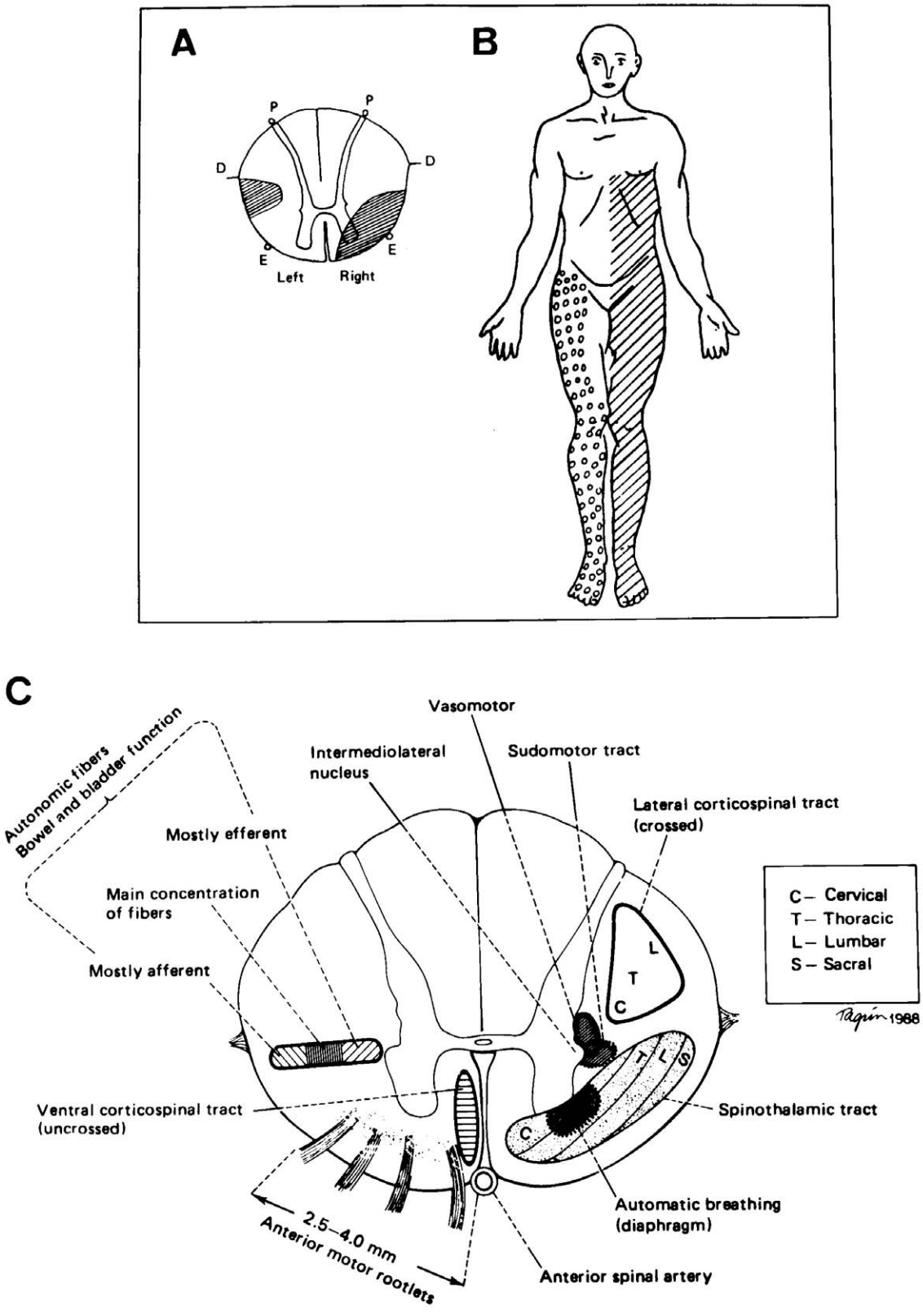

FIGURE 30.11 Differential anterolateral cordotomy in human patient based on somatotopic organization of the spinothalamic tract. **A** and **B** show the lesions made in the spinal cord to interrupt the spinothalamic tract and the distribution of the sensory changes that resulted from the cordotomy. The cancer patient had pain in the left hip and leg. There was radiographic evidence of metastases in the chest and in the fourth lumbar vertebra. After the anterolateral cordotomy shown in the illustration was performed, the patient was pain free at least until he was discharged from the hospital 4 weeks later. The drawing of the spinal cord shows how the cord was sectioned. The cross-hatched area on the diagram of the body indicates the distribution of complete loss of pain and temperature in this patient, and the open circles show where there was only a partial loss of these sensory modalities. Abbreviations: D, dentate ligament; E, exit line of anterior roots; P, entry line of posterior roots. (From Hyndman and Van Epps, 1939.) **C** shows a transverse section through the human upper thoracic spinal cord. A number of landmarks are shown. The location of the spinothalamic tract and its somatotopic organization are estimated based on a number of clinical reports. (From Gybels and Sweet, 1989.)

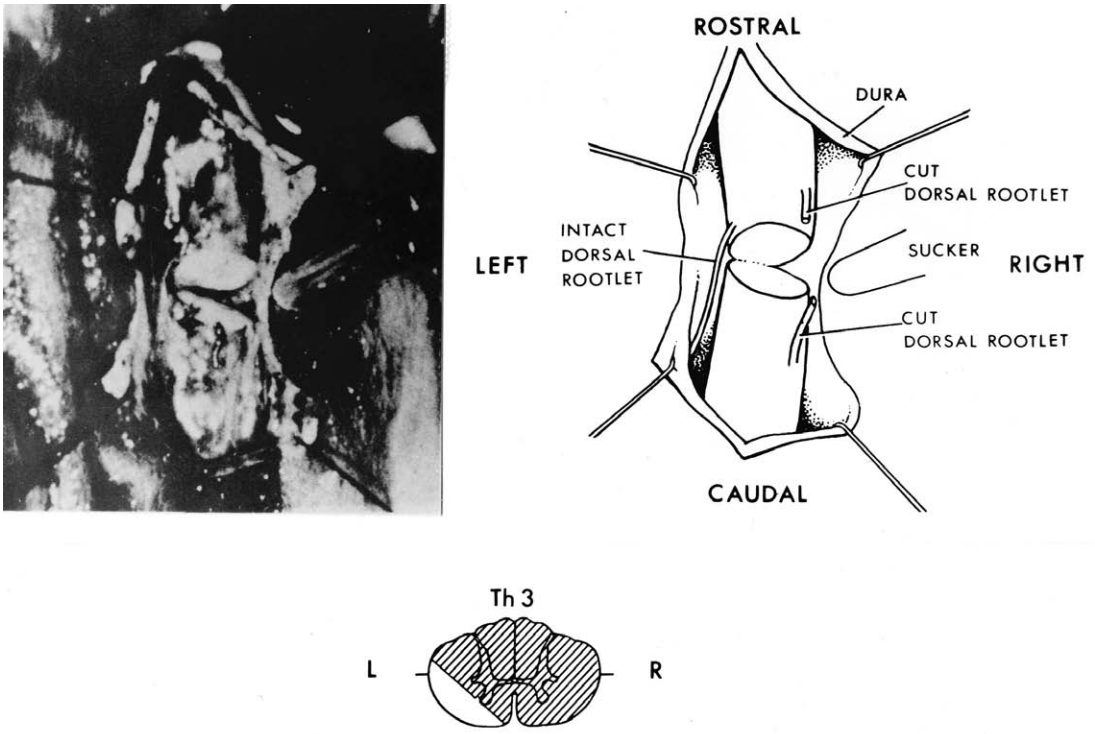

FIGURE 30.12 Interruption of all of the spinal cord except for one anterolateral quadrant in a patient following a stab wound in the back. The photograph shows the spinal cord after it was exposed by a T3–4 laminectomy. The drawing identifies the structures seen in the photograph, and the hatched area in the drawing of a transverse section of the cord is an estimate of the extent of the lesion. (From Noordenbos and Wall, 1976.)

contain substance P (Battaglia and Rustioni, 1992; Nishiyama *et al.*, 1995). Numerous terminals that label for glutamate contact primate spinothalamic cells (Westlund *et al.*, 1992a); other synaptic contacts contain GABA (Carlton *et al.*, 1992), noradrenergic markers (Westlund *et al.*, 1990), serotonin (C. C. LaMotte *et al.*, 1988), CGRP (Carlton *et al.*, 1990), or substance P (Carlton *et al.*, 1985).

Postsynaptic Dorsal Column Pathway

The dorsal column of mammals contains axons that ascend from spinal levels to synapse in the dorsal column nuclei (reviewed in Willis and Coggeshall, 2003). Many of these axons are collaterals of the central processes of DRG cells. However, others arise from projection neurons in the spinal cord gray matter. The latter are called postsynaptic dorsal column neurons. In monkeys, as in other mammals, most of the cells of origin of the postsynaptic dorsal column pathway are located in laminae III and IV of the dorsal horn, although some are near the central canal (Bennett *et al.*, 1983). In cats, postsynaptic dorsal column neurons respond to cutaneous stimuli, often including noxious stimuli (Uddenberg, 1968; Angaut-Petit, 1975; Jankowska *et al.*, 1979; Brown and Fyffe, 1981). However, interruption of the posterior column in humans does not prevent the perception of cutaneous pain (e.g., see Noordenbos and Wall, 1976; however, cf. Vierck *et al.*, 1971), and so these nociceptive projections are not necessary for this type of pain. Cutaneous pain presumably depends on information carried by the spinothalamic and associated tracts (see Al-Chaer *et al.*, 1996a; Palecek *et al.*, 2002).

Recently, a series of studies in rats and monkeys have shown that postsynaptic dorsal column neurons located in the vicinity of the central canal, where many visceral afferents have terminals (Fig. 30.3D) (Sugiura *et al.*, 1989), respond to noxious visceral stimuli (Al-Chaer *et al.*, 1996b, 1999). These postsynaptic dorsal column neurons are responsible for evoking visceral responses of neurons of the gracile nucleus. Evidence for this is that visceral nociceptive responses of gracile neurons are nearly eliminated either by a lesion of the dorsal column or by microdialysis administration of morphine or of a non-NMDA glutamate receptor antagonist into the sacral spinal cord to block synaptic transmission to postsynaptic dorsal column neurons

(Al-Chaer *et al.*, 1996b; Houghton *et al.*, 2001). These agents would not block conduction in primary afferent visceral nociceptors that might project directly to the dorsal column nuclei through the dorsal column, and so it was concluded that the visceral responses in the dorsal column nuclei depended primarily on information carried by the axons of postsynaptic dorsal column neurons. The responses of neurons of the cuneate nucleus to stimulation of cardiopulmonary afferents in monkeys are also dependent in part on activity transmitted in the dorsal column (Chandler *et al.*, 1998). Interruption of the dorsal column or placement of a lesion in the gracile nucleus profoundly reduces visceral responses of neurons in the ventral posterior lateral nucleus of the thalamus, suggesting that the thalamic responses depend largely on signals that are relayed by way of the dorsal column nuclei (Al-Chaer *et al.*, 1996a, 1997, 1998; Feng *et al.*, 1998). A lesion of the lateral column that would interrupt the spinothalamic tract has only a small effect on visceral nociceptive responses (Al-Chaer *et al.*, 1996a, 1998).

A lesion of the dorsal column in monkeys dramatically reduces the regional cerebral blood volume changes that are seen by functional magnetic resonance imaging in anesthetized animals (Willis *et al.*, 1999). This reduction persists for months after the surgery. Dorsal column lesions also reduce nociceptive behavioral responses in rats to visceral stimulation (Houghton *et al.*, 1997; Feng *et al.*, 1998; Palecek *et al.*, 2002).

An anterograde tracing study in rats has demonstrated the course of this pathway from lamina X both from sacral and from midthoracic levels of the spinal cord (Wang *et al.*, 1999). Axons from the sacral cord ascend near the midline to the gracile nucleus (Fig. 30.13D); those from the midthoracic cord ascend more laterally, near the dorsal intermediate septum, to the lateral gracile and medial cuneate nuclei.

Clinical Application

These observations in animal models of visceral nociception are consistent with clinical reports that neurosurgical interruption of the appropriate part of the posterior columns in human patients can relieve visceral pain, such as pelvic and epigastric cancer pain (Fig. 30.13A–C) (Gildenberg and Hirshberg, 1984; Hirshberg *et al.*, 1996; Nauta *et al.*, 1997; 2000; Becker *et al.*, 1999; Kim and Kwon, 2000). The clinical and research findings that visceral nociceptive input travels in the dorsal column midline may help explain why commissural myelotomies and upper cervical midline myelotomies can be highly effective in relieving pain from much more caudal parts of the body than might have been inferred from the locations of the surgical lesions (Armour, 1927; Putnam, 1934; Guillaume *et al.*, 1945; Wertheimer and Lecuire, 1953; Sourek, 1969; Hitchcock, 1970, 1974, 1977; Papo and Luongo, 1976; Schvarcz, 1976, 1978, 1984; King, 1977; see review by Gybels and Sweet, 1989). These procedures may have interrupted the visceral pain pathway that ascends in the posterior columns. Previously, the results were attributed to sectioning of a hypothetical pain pathway that was supposed to ascend in the central region of the spinal cord (however, see Karplus and Kreidl, 1914). An important issue with respect to midline myelotomy is that axons conveying nociceptive signals from the pelvis in rats, and presumably in humans as well, ascend near the midline of the dorsal columns (Wang *et al.*, 1999), and so a lesion near the midline can successfully relieve pelvic visceral pain (e.g., Fig. 30.13A, C). By contrast, nociceptive signals from abdominal or thoracic organs are carried by axons that ascend more laterally in the dorsal columns, and so the myelotomy must extend or enter more laterally on each side. For example, Figure 30.13B shows a lesion that was not optimally placed, at least on one side.

Spinocervical, Spinoreticular, and Spinomesecephalic Pathways

There are several other spinal cord projection systems that convey nociceptive information directly or indirectly to the brain stem and higher centers. These include the spinocervical, spinoreticular, and spinomesencephalic tracts.

The spinocervical tract originates from neurons that are located chiefly in the nucleus proprius of the dorsal horn (reviewed in Willis and Coggeshall, 2003). The tract ascends in the dorsal part of the ipsilateral lateral funiculus and synapses in the lateral cervical nucleus in the uppermost cervical segments. The lateral cervical nucleus is a distinctive nucleus just lateral to the dorsal horn in many species, including monkeys, but its presence in humans is controversial (however, see Truex *et al.*, 1970; see also Chapter 28). Axons from neurons in the lateral cervical nucleus decussate in the upper cervical spinal cord and then ascend to access the contralateral thalamus through the medial lemniscus. Nociceptive responses have been recorded from spinocervical tract neurons and neurons in the lateral cervical nucleus in monkeys (Downie *et al.*, 1988), as well as in cats (see Willis and Coggeshall, 2003). It is unclear if interruption of the nociceptive signals carried in the spinocervical tract has an influence on sensation or behavior. A lesion of the dorsal lateral funiculus in monkeys results in hyperresponsiveness of the animals to noxious stimuli (Vierck *et al.*, 1971), but this change presumably results from interruption of descending inhibitory pathways.

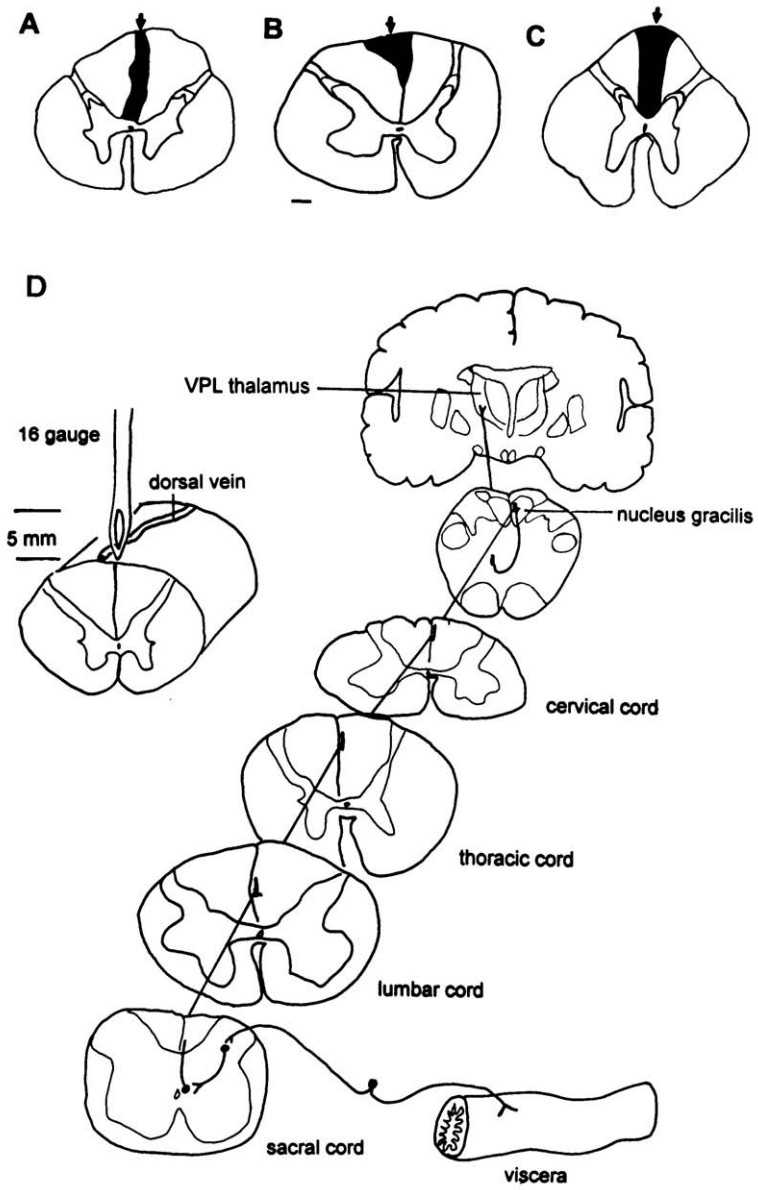

FIGURE 30.13 Interruption of the dorsal column to relieve visceral pain. The transverse sections of the spinal cord in **A–C** show the locations of midline myelotomies that were performed on three patients to relieve visceral pain. The lesion in **A** was from a successful case in which a lesion at T10 completely relieved pain due to colon cancer. The lesion shown in **B** was from a patient who had lung cancer. The lesion was made at T7, but it was not very effective, perhaps because it was not wide enough on one side to interrupt the axons of thoracic postsynaptic dorsal column neurons or because it was not placed sufficiently rostrally in the spinal cord. The lesion in **C** was in a patient whose pelvic cancer pain was successfully relieved for several years (From Willis and Westlund, 2000). **D** shows the posterior column visceral pain pathway as inferred from animal experiments. (From Willis and Westlund, 1997.)

The spinoreticular tract in monkeys arises mostly from neurons in the ventral part of the spinal cord gray matter, as shown by retrograde labeling (Kevetter *et al.*, 1982). Some spinoreticular neurons were found in laminae I, V, and X, but more than half were in laminae VII and VIII. The axons of many spinoreticular neurons decussate and ascend in the contralateral ventrolateral white matter. In monkeys, the spinoreticular tract has been shown to terminate in a number of reticular formation nuclei, including the nucleus medullae oblongatae centralis, lateral reticular nucleus, nucleus reticularis gigantocellularis, nucleus reticularis

pontis caudalis and oralis, nucleus paragigantocellularis dorsalis and lateralis, and nucleus subcoeruleus (Mehler *et al.*, 1960; see also Willis and Coggeshall, 2003). Some of these nuclei are involved in modulation of spinal cord nociceptive mechanisms (see below). Other reticular nuclei are interconnected with the cerebellum, regulate autonomic activity, participate in the control of states of consciousness, or conduct other functions of the reticular formation (Magoun, 1963). A spinoreticulothalamocortical pathway forms an indirect projection that allows painful input to influence the forebrain (however, cf. Blomqvist and Berkley, 1992). Particular functions presumably include attentional mechanisms and arousal.

The primate spinomesencephalic tract originates from the same regions of the spinal cord gray matter as the spinothalamic tract, i.e., mainly from laminae I and V, as well as from scattered neurons in other locations (Trevino, 1976; Willis *et al.*, 1979; Wiberg *et al.*, 1987). Given the similarity in location of spinothalamic and spinomesencephalic tract cells, it is not surprising that some neurons can be retrogradely labeled in monkeys from both the midbrain periaqueductal gray and the thalamus, indicating that some neurons project to both targets (Zhang *et al.*, 1990). Nociceptive responses have been recorded from neurons that project to the midbrain or to both the midbrain and the thalamus in monkeys (Yezierski *et al.*, 1987).

The spinomesencephalic tract projects to the nucleus cuneiformis of the midbrain reticular formation, the periaqueductal gray, the intercolliculus nucleus, the deep layers of the superior colliculus, the anterior and posterior pretectal nuclei, the nucleus of Darkschewitsch, the red nucleus, the Edinger–Westphal nucleus, and the interstitial nucleus of Cajal (see Fig. 12.10 in Chapter 12) (Mehler *et al.*, 1960; Wiberg *et al.*, 1987; Yezierski, 1988). The terminals of the spinomesencephalic tract have a caudal to rostral somatotopic organization (Wiberg *et al.*, 1987). The functions of many of these structures are probably unrelated to pain. However, the nucleus cuneiformis presumably contributes to attentional and alerting mechanisms, and the periaqueductal gray and the anterior pretectal nucleus are involved in the descending modulation of nociceptive transmission (see **"Descending Pain Modulatory Systems"**).

Clinical Application

Stimulation in the midbrain tegmentum in human patients can evoke paresthesias or pain on the contralateral side of the body, and stimulation in the periaqueductal gray can trigger emotional responses, such as an unpleasant feeling or even fear (Nashold *et al.*, 1969).

Spinoparabrachial, Spinohypothalamic, and Spinolimbic Pathways

Several projection systems that connect the spinal cord indirectly or directly with limbic system structures have been described during the past decade (see review by Burstein, 1996). These include spinoparabrachial, spinohypothalamic, and spinolimbic pathways.

The spinoparabrachial tract is sometimes lumped with the spinoreticular or spinomesencephalic tracts. However, it merits separate consideration, since many spinoparabrachial neurons in rats terminate in a part of the lateral parabrachial nuclear complex that projects to the amygdala (Bernard *et al.*, 1989; Bernard, 1999). This pathway and direct spinolimbic projections provide a special route for nociceptive information to access the limbic system (see review by Willis and Westlund, 1997). In addition, spinal connections to the parabrachial region, including the locus coeruleus and subcoeruleus, can activate catecholaminergic neurons that project caudally into the brain stem and spinal cord, providing a means for modulation of nociceptive transmission (see next section). The functions of spinoparabrachial tract neurons have not been investigated in monkeys, but many of these cells in cats are clearly nociceptive (Hylden *et al.*, 1986), as are neurons in the parabrachial region of rats that project to the amygdala (Bernard and Besson, 1990; Bernard *et al.*, 1994). Many parabrachial neurons respond to noxious visceral stimuli, as well as to noxious cutaneous stimuli (Bernard *et al.*, 1994). Buritova *et al.* (1998) have shown that the intraplantar injection of carrageenan into the paw in rats results in the expression of FOS protein in neurons in lamina I of the ipsilateral spinal cord dorsal horn (presumably including spinoparabrachial projection neurons) and in contralateral parabrachial subnuclei that project to the amygdala. Anterograde tracing studies have demonstrated projections of lamina I cells to the parabrachial region and locus coeruleus in monkeys (Craig, 1995; Bernard, 1999). En route through the brain stem reticular formation, the axons of these ascending tract cells contact catecholaminergic neurons throughout the medulla and pons (Westlund and Craig, 1996). In addition, parabrachial nuclei that receive spinal cord input through the spinoparabrachial pathway project to the hypothalamus, periaqueductal gray, nucleus raphe magnus, and ventrolateral medulla (Bernard, 1999).

A spinohypothalamic tract has recently been characterized functionally in monkeys (Zhang *et al.*, 1999). The spinohypothalamic neurons examined were all nociceptive, and most could also be activated antidromically from the thalamus, suggesting that at least some of these neurons project to both the hypothalamus

and the thalamus. Most of the work on the spinohypothalamic tract has been done in rats. Almost all (87%) of the spinohypothalamic neurons studied in rats, like those in monkeys (Zhang *et al.,* 1999), were nociceptive (Burstein *et al.,* 1991; Katter *et al.,* 1996). About 70% of the cells of origin of the rat spinohypothalamic tract are found contralaterally to the side of the spinal cord in which the axons ascend, and they are concentrated in the superficial and deep dorsal horn and around the central canal, although some are in the intermediate zone and ventral horn (Burstein *et al.,* 1990). The axons decussate, ascend through the brain stem, and pass ventral to the thalamus to enter the hypothalamus, where they terminate in a number of hypothalamic nuclei (Cliffer *et al.,* 1991). The axons of many of these neurons decussate a second time and then descend on the same side as the cell body to levels of the brain stem as far caudally as the medulla (Zhang *et al.,* 1995). Nociceptive neurons in this pathway could presumably affect autonomic and endocrine functions as part of the spectrum of reactions to painful stimuli.

Direct spinolimbic projections have also been described in rats (Cliffer *et al.,* 1991). These terminate in such structures as the central nucleus of the amygdala, septal nuclei, nucleus accumbens, bed nucleus of the stria terminalis, and even some areas of limbic cortex. Such pathways, along with the spinoparabrachioamygdalar pathway, could provide a means for nociceptive signals to influence parts of the brain that are likely to be involved in autonomic control, motivational–affective responses to pain, and learning and memory.

DESCENDING PAIN MODULATORY SYSTEMS

Nociceptive input is modulated at a variety of sites, but particularly in the dorsal horn of the spinal cord, by descending pathways that are parts of inhibitory and excitatory control systems. These pathways can profoundly influence the perception of pain. The concept that the brain can control sensory input was popularized in the 1950s by the discovery of the reticular formation by Moruzzi and Magoun (see Magoun, 1963). However, the notion that pain is subject to descending modulation came into focus only after the demonstration by Reynolds that abdominal surgery could be performed on awake rats during stimulation in the periaqueductal gray (Reynolds, 1969). Following this, a number of laboratories examined what came to be known as "stimulation-produced analgesia" and showed the relationship of this to opioid analgesia and "stress-induced analgesia" (see reviews by Willis, 1982; Besson and Chaouch, 1987).

The ability to inhibit nociceptive input to higher centers and thus to interfere with the perception of pain is likely to be accomplished through activation of complex supraspinal circuits. Descending inhibition of spinal nociceptive processes was initially proposed to occur through a periaqueductal gray relay to serotonergic neurons in the nucleus raphe magnus and the adjacent reticular formation (Liebeskind *et al.,* 1973; Oliveras *et al.,* 1974a, b, 1975, 1979; Proudfit and Anderson, 1975; Beall *et al.,* 1976; Willis *et al.,* 1977; Fields *et al.,* 1977; Basbaum *et al.,* 1978; Martin *et al.,* 1978; Basbaum and Fields, 1979; Chung *et al.,* 1983). However, subsequent findings suggest a more complicated circuitry that also involves descending catecholaminergic pathways (Yaksh, 1979; Hodge *et al.,* 1981; Budai *et al.,* 1998; Cui *et al.,* 1999), as well as descending opioidergic pathways (Budai and Fields, 1998). For reviews of many of the early studies, see Mayer and Price, 1976; Basbaum and Fields, 1978; Fields and Basbaum, 1978; Yaksh and Rudy, 1978; Willis, 1982; Besson and Chaouch, 1987; Fields and Besson, 1988; Willis and Coggeshall, 2003; see also Chapter 8. For evidence concerning the chemical anatomy of descending pathways in the human spinal cord, see Chapter 7.

There is an increasing appreciation that supraspinal circuitry is also responsible for descending modulation that results in enhancement or sensitization of the nociceptive responses of spinal cord dorsal horn neurons (see Haber *et al.,* 1980; Giesler *et al.,* 1981; Cervero and Wolstencroft, 1984; Urban *et al.,* 1996; Wei *et al.,* 1999). Whether this results from a decrease in descending inhibition or an enhancement of facilitatory mechanisms or both remains to be determined. For example, descending inhibitory influences on inhibitory interneurons in the dorsal horn could result in a decreased GABAergic and/or glycinergic tone. It has been proposed that the interactions between spinal and supraspinal circuits may be responsible for the decreased efficacy of morphine as tolerance develops (Heinricher *et al.,* 1994; Ossipov *et al.,* 1997).

Raphe Spinal and Reticulospinal Tracts

In primates, a large population of neurons with descending spinal projections has been identified in the raphe nuclei of the medulla and in the reticular formation of the midbrain, pons, and medulla (Kneisley *et al.,* 1978; Coulter *et al.,* 1979). Many raphe neurons have been shown to contain serotonin and are therefore the origin of descending serotonergic projections that can inhibit spinal nociceptive processing

(Bowker *et al.*, 1982a, b; see also Basbaum and Fields, 1978). However, other bulbospinal neurons do not contain serotonin, although they may contain any of several peptides (Bowker *et al.*, 1982b). Spinothalamic tract neurons in monkeys can be powerfully inhibited by stimulation in the nucleus raphe magnus or the adjacent medullary reticular formation (Beall *et al.*, 1976; Willis *et al.*, 1977; Gerhart *et al.*, 1981). However, only part of this inhibition appears to be mediated by serotonin (Yezierski *et al.*, 1982).

Nociceptive input may be relayed from the spinal cord to the reticular formation by ascending projections arising from laminae I and X (Craig, 1995; Wang *et al.*, 1999), as well as by spinoreticular projections from other parts of the spinal cord gray matter (Kevetter *et al.*, 1982). A direct spinal projection to the nucleus raphe magnus has recently been described to arise from the region around lamina X, the area from which the postsynaptic dorsal column visceral nociceptive pathway originates (Wang *et al.*, 1999; see above).

Serotonin is released in the spinal cord in animals following stimulation of either the nucleus raphe magnus (Sorkin *et al.*, 1990; 1993) or the periaqueductal gray (Cui *et al.*, 1999). Although serotonin has been identified as one of the major neurotransmitters involved in descending inhibitory mechanisms, it should be noted that serotonergic mechanisms in the spinal cord can exert either antinociceptive or pronociceptive actions through different serotonergic receptor subtypes (Alhaider *et al.*, 1991; Peng *et al.*, 1996a; Lin *et al.*, 1996a; Millan, 1997, 1999).

Clinical Application

It is known that spinal serotonin turnover is modified in chronic pain patients (Wolfe *et al.*, 1997; Weil-Fugazza, 1989; Von Knorring, 1989). Stimulation in the vicinity of the periaqueductal gray has been used to produce naloxone-reversible relief of pain in human patients (Hosobuchi *et al.*, 1977). When tolerance to such stimulation develops, the tolerance can be reversed by tryptophan administration, suggesting that serotonin release is involved in the analgesic action, as are opioids (Hosobuchi, 1978; Hosobuchi *et al.*, 1980).

Descending Catecholamine Projections

Descending noradrenergic input to the spinal cord provides an alternative mechanism for the inhibition of spinal nociceptive neurons. A large percentage of the spinally projecting neurons that have been identified in the locus coeruleus and the subcoeruleus in monkeys and rats are noradrenergic (Westlund and Coulter, 1980; Westlund *et al.*, 1983). Other catecholaminergic cell groups in the dorsolateral pons—the A5 cell group, the Kölliker–Fuse nucleus, and the parabrachial nuclei—also have projections to the spinal cord. There is no convincing evidence for descending noradrenergic input from medullary levels of the brain stem, although a small epinephrine-containing spinal projection from the ventrolateral medulla has been reported in primates (Carlton *et al.*, 1991). In monkeys and cats, the bilateral terminations of dorsal horn projections from the locus coeruleus and subcoeruleus region were found to be densest in nociceptive processing regions, including laminae I, II, V, and X, with the majority of the fibers ending contralaterally (Westlund and Coulter, 1980; Holstege and Kuypers, 1982). Noradrenergic terminals in the dorsal horn have been shown to contact identified spinothalamic neurons in laminae I and V (Westlund *et al.*, 1990).

Electrical stimulation of the dorsolateral pons produces analgesic effects (Segal and Sandberg, 1977; DeSalles *et al.*, 1985). Nociceptive responses are inhibited by norepinephrine acting on α_2 adrenoreceptors (Howe *et al.*, 1983). Iontophoretic release of norepinephrine in the dorsal horn inhibits nociceptive neurons, including primate spinothalamic neurons (Headley *et al.*, 1978; Fleetwood-Walker *et al.*, 1983; Willcockson *et al.*, 1984).

Periaqueductal Gray

The periaqueductal gray receives heavy innervation from ascending spinal pathways, including projections arising from laminae I and X (see section on the spinomesencephalic tract) (Craig, 1995, Wang *et al.*, 1999). However, no direct pathway from the periaqueductal gray to the spinal cord has been identified to account for the strong analgesia reported after stimulation of the periaqueductal gray. The periaqueductal gray, including its dorsolateral and ventrolateral regions, projects to brain stem regions containing epinephrine, norepinephrine, and serotonin cell groups with descending projections to the spinal cord in the rat (Cameron *et al.*, 1995). The ventrolateral periaqueductal gray projects preferentially to the nucleus raphe magnus (B3 serotonin group) and the dorsolateral region projects preferentially to the dorsolateral pons. The ventrolateral medulla, another site known to induce stimulation-produced analgesia, also receives projections from both of these regions of the periaqueductal gray. It has been shown that stimulation of the rostral part of the lateral paragigantocellular nucleus and the gigantocellular nucleus pars alpha produces analgesia in the rat through both serotonergic and noradrenergic mechanisms (Satoh *et al.*, 1983; Lovick, 1986). Since there are no noradrenergic spinal projections from this region, a complex circuitry

involving the noradrenergic dorsolateral pontine cells has been proposed (Holden and Proudfit, 1998).

Inhibition of primate spinothalamic cells is produced by stimulation of the midbrain periaqueductal gray (Hayes *et al.*, 1979; Gerhart *et al.*, 1984). Inhibition of nociceptive dorsal horn neurons following periaqueductal gray stimulation can be partially blocked by administration of antagonists of serotonin receptors (Yezierski *et al.*, 1982; Lin *et al.*, 1996a; Peng *et al.*, 1996a), of α_2 adrenoreceptors (Peng *et al.*, 1996b), or of inhibitory amino acid receptors (Lin *et al.*, 1994, 1996b). Electrical stimulation of the periaqueductal gray has been shown to cause the release of serotonin, norepinephrine, and glycine in the spinal cord (Sorkin *et al.*, 1990; Cui *et al.*, 1999). These same neurotransmitters can inhibit primate spinothalamic cells when released iontophoretically (Willcockson *et al.*, 1984; cf. Basbaum and Fields, 1979). Thus, it is likely that inhibition occurs following the release of serotonin and norepinephrine from the descending serotonergic and noradrenergic projections that were described above. Release of inhibitory amino acids may be either from the terminals of descending projections or from spinal cord interneurons that are activated by descending projections.

Thus, the brain stem circuitry involved in stimulation-produced analgesia involves not only the periaqueductal gray but also connections of the periaqueductal gray with the nucleus raphe magnus, the ventrolateral medulla, and the dorsolateral pons.

Anterior Pretectal Nucleus

Stimulation in the anterior pretectal nucleus produces antinociceptive actions, as detected by the tail flick, formalin, and paw pressure tests, by inhibition of nociceptive dorsal horn neurons (Rees and Roberts, 1993), including primate spinothalamic tract cells (Chen, 2000). The anterior pretectal nucleus has a minor direct input from laminae I and X of the spinal cord (Wiberg and Blomqvist, 1984; Craig, 1995; Wang *et al.*, 1999). Input from low-threshold afferent fibers to the anterior pretectal nucleus is relayed through the dorsal column nuclei (Rees and Roberts, 1989a, b). Activation of the latter pathway has been proposed as a mechanism that could explain the ability of dorsal column stimulation to inhibit pain in humans (Rees and Roberts, 1989b; cf. Shealy *et al.*, 1970; Gybels and Sweet, 1989). Projections from the anterior pretectal nucleus to the spinal cord have not been reported. Indications are that the antinociceptive actions following stimulation in the anterior pretectal nucleus are mediated through dorsolateral pontine noradrenergic descending pathways (Chen, 2000).

Thus, complex spinobulbospinal feedback loops are activated by nociceptive inputs that serve important functions associated with integration of sensory input relevant to the perception of pain. These pathways are likely to be part of an even more complex homeostatic control network involved in sensory, motor, and autonomic integration. Unfortunately, it is difficult to take practical advantage of these circuits for the purpose of producing pain relief by using electrical stimulation. For example, attempts to stimulate the nucleus raphe magnus or the dorsolateral pons in humans would probably be too dangerous.

Periventricular Gray and Ventrobasal Thalamus

Since stimulation in the periaqueductal gray has been shown to result in a powerful analgesic action in animals, comparable stimulation has been attempted in the periaqueductal gray of human pain patients. However, as mentioned earlier, this can produce emotional responses, such as fear, as well as eye movements. Richardson and Akil (1977a, b) and Hosobuchi *et al.* (1997) have reported pain relief in patients without these side effects following stimulation in the nearby periventricular gray matter (see review by Gybels and Sweet, 1989).

Stimulation in the ventrobasal complex of the thalamus has also been found to result in the inhibition of nociceptive dorsal horn neurons, including primate spinothalamic cells (Gerhart *et al.*, 1983; Dickenson, 1983). The inhibition has been attributed to the antidromic activation of collaterals of spinothalamic axons that terminate in the periaqueductal gray or nucleus raphe magnus (Gerhart *et al.*, 1983; Willis *et al.*, 1984; Tsubokawa *et al.*, 1985). Further evidence for this idea is that stimulation in the VPL nucleus of the monkey thalamus causes the release of serotonin in the spinal cord (Sorkin *et al.*, 1992). It has been found that stimulation in the VPL nucleus of the human thalamus can suppress acute pain induced experimentally (Gybels *et al.*, 1976).

Clinical Application

In general, nociceptive pain seems to respond better to stimulation in the periventricular gray matter, whereas neuropathic pain responds better to stimulation in the thalamic ventrobasal complex (Gybels and Sweet, 1989). Stimulation in both sites can be useful, especially if the pain is of both types. The duration of the analgesia that is produced often outlasts the period of stimulation by many hours (Hosobuchi *et al.*, 1977). This cannot be readily explained by the activation of brain stem neurons during the electrical

stimulation, since this activity in animal models does not greatly outlast the period of stimulation (Gybels and Sweet, 1989).

BRAIN STRUCTURES INVOLVED IN PAIN PERCEPTION AND INTEGRATION

While it is clear that the perception of pain in humans requires activity in higher centers of the brain, including parts of the thalamus and cerebral cortex, as well as in many subcortical structures, the precise regions of the brain that are involved are only now becoming clarified with the assistance of positron emission tomography (PET) and functional magnetic resonance imaging (fMRI; see also Chapter 28). Imaging studies have implicated the SI and SII somatosensory receiving areas of the cortex, as well as the anterior cingulate gyrus and the insula, as important structures for the higher processing of the pain that is evoked by acute noxious stimuli (Fig. 30.14, upper panels; Jones *et al.,* 1991; Talbot *et al.,* 1991; Casey *et al.,* 1994; Coghill *et al.,* 1994, 1999; Di Piero *et al.,* 1994; Andersson *et al.,* 1997; Rainville *et al.,* 1997; Silverman *et al.,* 1997; Davis *et al.,* 1998; Iadarola *et al.,* 1998; Bushnell *et al.,* 1999; Gelnar *et al.,* 1999; Tracey *et al.,* 2000; see also Treede *et al.,* 2000). Other areas that have been activated in at least some studies include the prefrontal, supplementary motor, and ventral premotor cortices, as well as the lentiform nucleus, cerebellum, thalamus, and several brain stem areas. Activation is generally contralateral in the SI cortex, but it is often bilateral in the SII, insula, and anterior cingulate cortices and in motor structures (Coghill *et al.,* 1999). The usual type of stimulus in these studies has been noxious heat, but in one investigation the noxious stimulus was intradermal injection of capsaicin (Iadarola *et al.,* 1998) and in another it was noxious visceral stimulation (Silverman *et al.,* 1997).

These studies support the view that the SI and SII cortices are involved in the sensory-discriminative aspects of pain, the anterior cingulate cortex in the affective component of pain, the insula in memory and learning of painful events, and parts of the motor system, such as the lentiform nucleus and cerebellum, in motor responses to painful stimuli. There is no longer any reason to adhere to the notion proposed by clinical investigators early in the 20th century that pain is perceived in the thalamus. This idea was based on evidence from patients with relatively focal lesions of the cerebral cortex that would not have affected other cortical regions involved in pain (Head and Holmes, 1911; Holmes, 1927). Hence, such lesions would have only partially interfered with pain reactions. Additional evidence came from studies in which the somatosensory cortex was stimulated electrically during surgery to remove epileptic foci (Penfield and Boldrey, 1937). Only rarely was a sensation of pain evoked. However, a sensation of pain was reported in those few cases. The current view is that painful stimuli activate multiple parallel circuits that process different aspects of the pain response (Coghill *et al.,* 1994, 1999).

Imaging studies of patients with chronic pain reveal that regional cerebral blood flow changes can occur in a different group of brain areas than those that are activated by acutely painful stimuli (Hseih *et al.,* 1994). For example, Kupers *et al.* (2000) recently reported a PET study of a patient who had chronic neuropathic pain in the right cheek following removal of an adenocarcinoma. Electrical stimulation of the left ventral posterior medial thalamic nucleus relieved the pain and also produced tingling and a sensation of warmth in the painful area (see **"Descending Pain Modulatory Systems"** above). For the PET study, the patient was imaged after the stimulation was turned off overnight, which was long enough for the pain to resume fully. After an imaging session while the patient was in pain, thalamic stimulation was initiated and the pain eliminated. Another imaging session was done during stimulation, and a third after stimulation was discontinued but while the pain was still absent. Figure 30.14 (A, lower row of panels) shows structures that had increased blood flow during chronic pain. These structures included the prefrontal cortex, the anterior insula, the hypothalamus, and the periaqueductal gray. No changes were seen in the SI or SII cortex or in the anterior cingulate gyrus. The regional blood flow produced by thalamic stimulation was also evaluated (Fig. 30.14, B in lower row of panels). Significant increases were seen in the amygdala, ventromedial frontal cortex, and anterior insula. Kupers *et al.* (2000) suggest that during the chronic pain state of this patient, the mechanisms responsible for sensory discrimination of pain did not play an important role. This is reasonable because the perception of stimulus localization or intensity would have no meaning in ongoing chronic neuropathic pain, which does not depend on peripheral stimulation. The activation of the ventromedial prefrontal cortex in this patient may have related to memory of the affective component of the pain (Rosen *et al.,* 1996). Kupers *et al.* (2000) propose that the increased blood flow in the hypothalamus and periaqueductal gray reflected activation of the descending analgesia system or of autonomic responses to the pain. Increases in blood flow in the

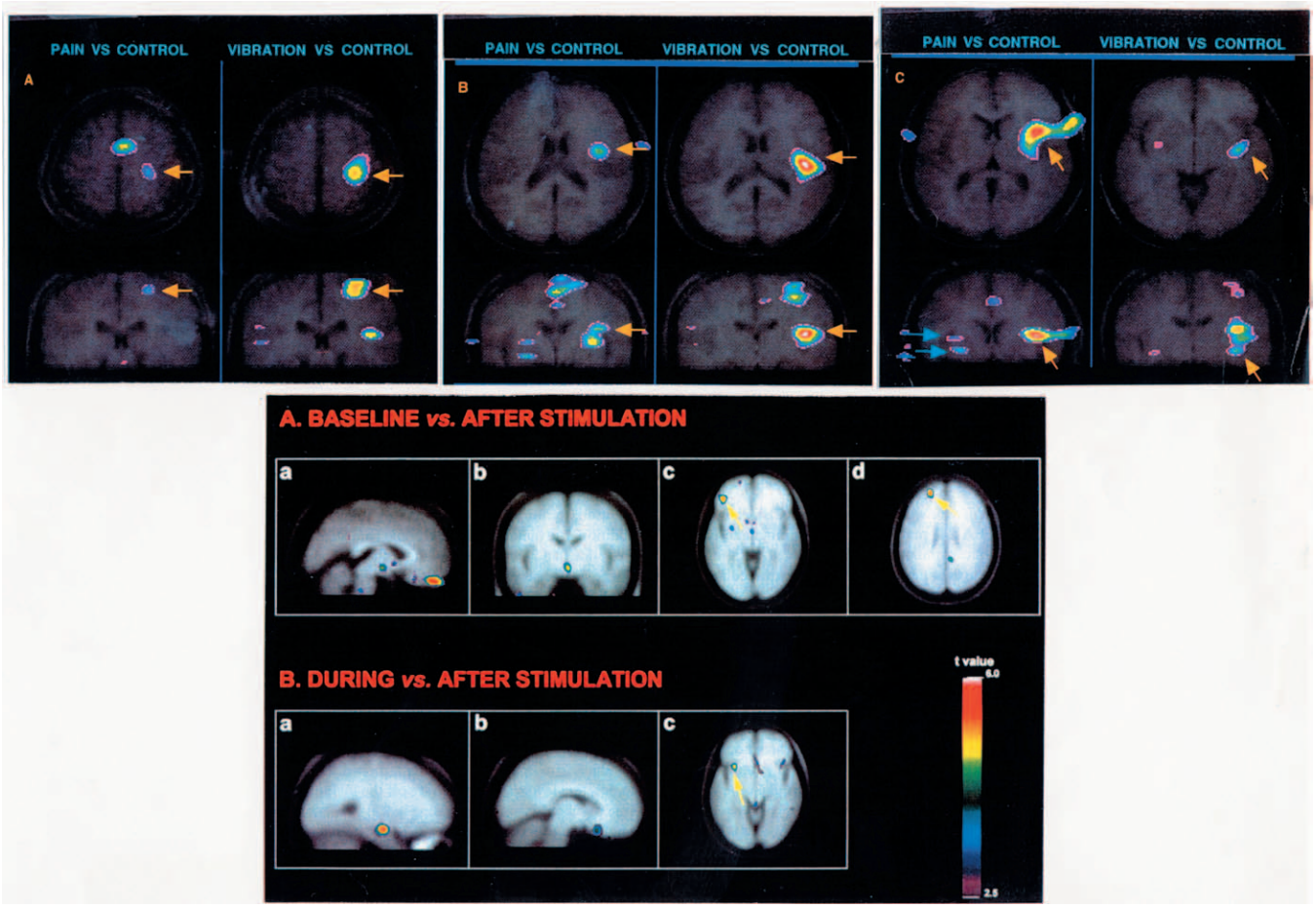

FIGURE 30.14 Imaging pain. **Upper panels.** Functional magnetic resonance images of areas of the human cerebral cortex that were activated during a painful stimulus in comparison to areas that were activated by a vibratory stimulus. The images in **A** show that both painful heat and vibrotactile stimuli activated the contralateral SI cortex *(arrows).* **B** shows that these same stimuli activated the contralateral SII cortex *(arrows)* and that the painful stimulus also activated the anterior cingulate gyrus. **C** shows that both stimuli activated the insula *(orange arrows).* Basal ganglia could also be involved following painful stimulation *(blue arrows.)* (From Coghill *et al.,* 1994.) **Lower panels.** Subtracted PET images of the brain of a patient who had chronic neuropathic pain in the cheek following removal of an adenocarcinoma. In **A** are shown the results of subtraction of images made of the regional blood flow observed in the chronic pain state during analgesic stimulation. Significant regional blood flow increases were seen in the orbitofrontal cortex (a), hypothalamus (b), inferior frontal gyrus (c), and superior frontal gyrus (d). In **B** are shown the results of subtraction of images made after analgesic stimulation was ended from the regional blood flow observed during thalamic stimulation. Stimulation in the ventral posterior medial thalamic nucleus activated the amygdala (a), ventromedial frontal cortex (b) and anterior insula (c). (From Kupers *et al.,* 2000.)

amygdala by thalamic stimulation may also have reflected the role of this structure in the descending analgesia system.

Thalamus

Most sensory input to the cerebral cortex, including that evoked by painful events, is first processed in the thalamus. The thalamus contains several nuclei that distribute sensory information to particular sensory receiving areas of the cerebral cortex by way of thalamocortical projections (Jones, 1985; see Chapter 28). Furthermore, the sensory regions of the cerebral cortex project in an orderly fashion back to the sensory nuclei of the thalamus through corticothalamic projections, and by this means the cerebral cortex regulates the flow of sensory input from the spinal cord and brain stem. Inhibitory interneurons in the thalamic reticular nucleus, as well as in the main relay nuclei at least in primates, play an important role in this

regulation of sensory transmission to the cerebral cortex (Jones, 1985, 1998).

The monkey and the human thalamus are organized in a similar fashion (Jones, 1985, 1997b, 1998; see also Chapter 20). Evidence about the areas of the thalamus that might be important for pain processing comes both from a knowledge of the parts of the thalamus that are connected with the cerebral cortical areas activated in monkeys and humans by painful stimuli and from parts of the thalamus that receive direct spinal projections. Some the pertinent regions in the monkey and the human posterior thalamus include the ventral posterior lateral (VPL) and ventral posterior medial (VPM) nuclei, the ventral posterior inferior (VPI) nucleus, the central lateral (CL) nucleus, and the medial part of the posterior complex (POm). The latter is dorsal to the magnocellular part of the medial geniculate (MGmc) nucleus and lateral to the suprageniculate (SG) nucleus (see discussion of the thalamic nuclei that receive spinothalamic input in Chapter 20).

Mehler (1962) described the terminations of spinal projections to the thalamus in a human subject by an anterograde degeneration study of a postmortem specimen from a patient who had had a bilateral anterolateral cordotomy for pain relief (Fig. 30.15B). Most of the terminals were in the VPL and CL nuclei (Fig. 30.15), but some were in the posterior complex. The endings in the VPL nucleus were in scattered patches (Fig. 30.15). Similar projections have been observed in monkeys following cordotomy (Mehler *et al.*, 1960).

The patches of STT terminals are in regions that correspond to the matrix areas of the VPL nucleus, which are rich in calbindin-immunoreactive neurons and presumably receive input from spinothalamic neurons (Jones and Hendry, 1989; Rausell *et al.*, 1992a; see also Jones, 1998). Further evidence for this comes from experiments in which cervical dorsal roots were sectioned chronically (3–20 years) and then immunostained for calcium-binding proteins after there was degeneration of parvalbumin-containing neurons in the dorsal column–medial lemniscus pathway. Figure 30.16A–C shows the area of the thalamus from which the dorsal column nuclear projection that represented the upper extremity was lost (Rausell *et al.*, 1992b; Jones and Pons, 1998). This area no longer stained for cytochrome oxidase (Fig. 30.16A), and staining for $GABA_A$ receptors (Fig. 30.16B) and for parvalbumin was markedly reduced (Fig. 30.16C) compared with that seen in normal animals. However, staining for calbindin was increased (Fig. 30.16D) compared to the normal brain (Fig. 30.16E). The animals appeared to have chronic central pain, which may have been related to a loss of GABAergic inhibition within the thalamus (cf. Ralston and Ralston, 1994) and an intact and even strengthened calbindin-staining nociceptive pathway.

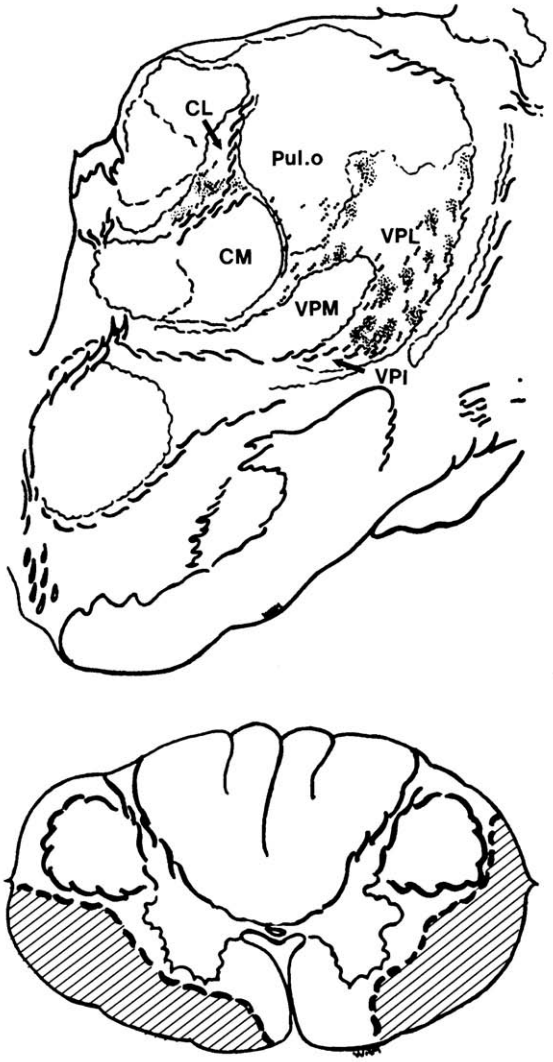

FIGURE 30.15 Terminations of the human spinothalamic tract in the thalamus. Anterograde degeneration of the spinothalamic tract was traced into the thalamus after a survival period of 12 days following a bilateral anterolateral cordotomy at a cervical level for the treatment of intractable pain. Results are shown for only one side, but the fiber degeneration was symmetrical. Terminals *(fine stipple)*, as well as fibers of passage *(large dots)*, are shown in several nuclei of the thalamus, including the ventral posterior lateral (VPL) and central lateral (CL) nuclei. The section of the spinal cord shows the extent of the anterolateral cordotomies. (From Mehler, 1962.)

Besides the VPL and CL nuclei, sites of termination of the STT include the densocellular and multiformis regions of the medial dorsal nucleus. However, Mehler regarded many of the cells in this part of the MD nucleus as belonging to the CL nucleus, although others have considered the cells in the densocellular

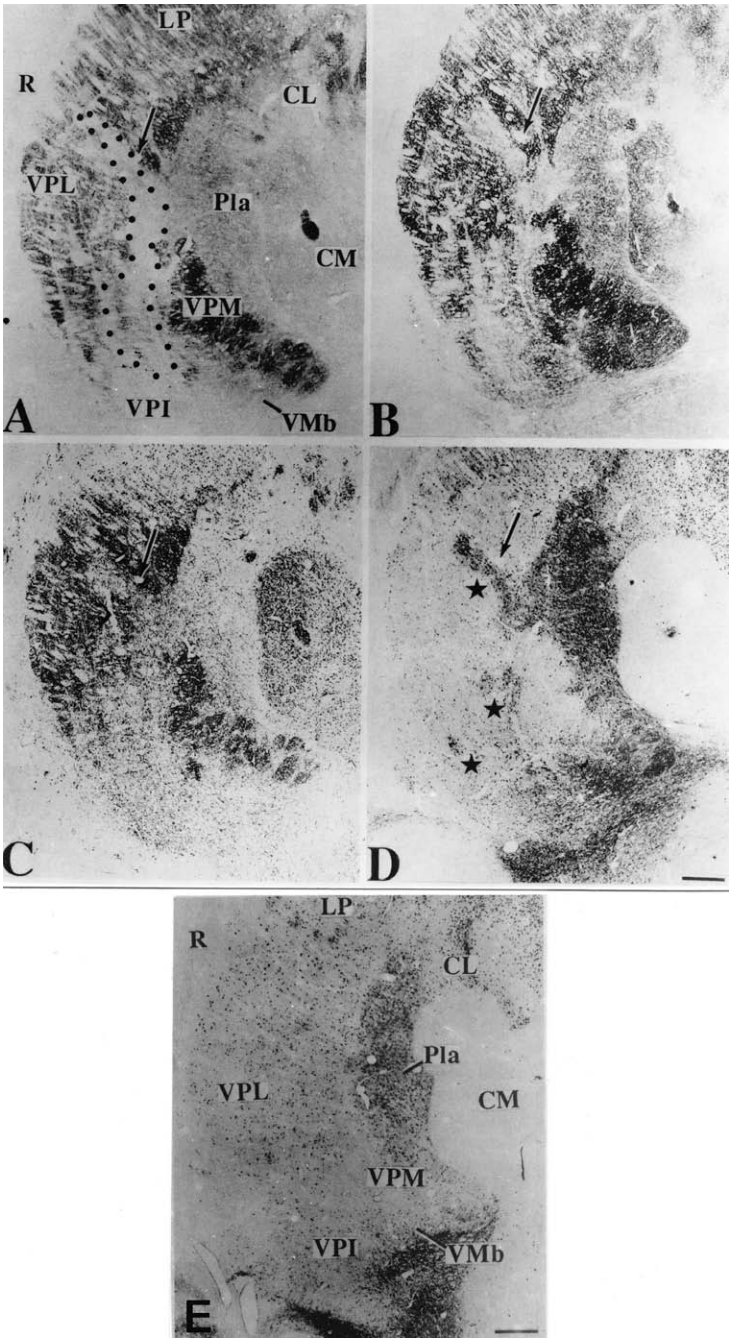

FIGURE 30.16 Loss of parvalbumin staining and increase in calbindin staining in a monkey after chronic multiple dorsal rhizotomies at a cervical level. In **A** is shown a frontal section stained for cytochrome oxidase. The section was taken through the posterior thalamus of a monkey. The monkey had had multiple cervical dorsal rhizotomies several years previously. Note the unstained area that corresponds to the expected region of termination of the part of the dorsal column–medial lemniscus pathway that represents the forelimb *(dotted zone in the VPL nucleus).* **B** and **C** show that there was decreased staining for $GABA_A$ receptors and for parvalbumin in the same area. However, **D** shows that staining for calbindin in this area was increased, as compared to the section in **E** from a normal animal. The arrows in **A–D** point to the same blood vessel. The asterisks in **D** indicate patches of enhanced calbindin staining in the affected area of the thalamus. The scale is 1 mm. Abbreviations for thalamic nuclei: CL, central lateral; CM, central median; LP, lateral posterior; Pla, anterior pulvinar; R, reticular; VMb, basal part of ventral medial; VPI, ventral posterior inferior; VPL, ventral posterior lateral; VPM, ventral posterior medial. (From Rausell *et al.*, 1992b.)

and multiformis subnuclei to be part of the MD nucleus proper (Apkarian and Hodge, 1989b). A number of morphological investigations on monkeys have demonstrated the projections to the posterior part of the VPL nucleus, CL, and the medial part of the posterior complex and have also included several other targets of the spinothalamic tract, such as the centralis medialis, the VPI nucleus, and what is now regarded as the anterior part of the VPL nucleus (Clark, 1936; Chang and Ruch, 1947; Bowsher, 1961; Boivie, 1979; Berkley, 1980; Mantyh, 1983; Apkarian and Hodge, 1989b; Gingold *et al.*, 1991; Stevens *et al.*, 1993). There may also be some spinothalamic terminations in the anterior pulvinar nucleus (Apkarian and Hodge, 1989b). Ralston and Ralston (1992) did not find a significant spinothalamic projection to the VPI nucleus, and they regard the main projections to the Po/SG region to originate from lamina I and those to the VPL and CL nucleus to come largely from the deep dorsal horn. However, the evidence shown in Fig. 30.8 indicates that both lamina I and lamina V spinothalamic cells project to the VPL nucleus (Willis *et al.*, 2000). For further discussion of the thalamic targets of the spinothalamic tract, see Chapter 20.

The VPL and VPM nuclei in monkeys contain nociceptive neurons that have properties suited for transmitting information to the SI and SII somatosensory cortex for sensory discrimination of pain signals (Perl and Whitlock, 1961; Gaze and Gordon, 1967; Pollin and Albe-Fessard, 1979; Kenshalo *et al.*, 1980; Casey and Morrow, 1983, 1987; Bushnell *et al.*, 1984, 1993; Chung *et al.*, 1986a; Bushnell and Duncan, 1987; Chandler *et al.*, 1992; Morrow and Casey, 1992; Duncan *et al.*, 1993; Apkarian and Shi, 1994; Brüggemann *et al.*, 1994; Al-Chaer *et al.*, 1998; see also review by Willis, 1997). For example, many of these nociceptive neurons have small contralateral receptive fields, they are somatotopically organized, they encode stimulus intensity, and they project to the SI cortex (as shown by antidromic activation experiments). Furthermore, a subpopulation of WDR neurons in the VPM nucleus can discriminate small changes in the intensity of noxious heat stimuli just as well as can an awake, behaving monkey (other WDR and HT neurons are not this responsive). The characteristics of these neurons in the VPL and VPM nuclei can be accounted for by input from spinothalamic and trigeminothalamic tract cells (cf. section on the *spinothalamic tract*; see also Price *et al.*, 1976; Hoffman *et al.*, 1981; Bushnell *et al.*, 1984; Dubner *et al.*, 1989; Kenshalo *et al.*, 1989; Maixner *et al.*, 1989). WDR neurons have also been recorded in the human thalamic principal somatic sensory nucleus (Lee *et al.*, 1999); however, in the absence of postmortem evidence, it is uncertain exactly in which nucleus the recordings were made (see discussion in Jones, 1998).

Nociceptive neurons have also been found in the VPI nucleus (Pollin and Albe-Fessard, 1979; Morrow and Casey, 1992; Apkarian and Shi, 1994). The receptive fields have a somatotopic organization, but they are larger than those of nociceptive neurons in the VPL nucleus, and the receptive fields of neurons in the ventral part of VPI may be complex or discontinuous. Many neurons in the VPI nucleus project to the SII cortex (Stevens *et al.*, 1993).

Neurons in the CL and other intralaminar nuclei in anesthetized animals are characterized by large, often bilateral receptive fields (Bushnell and Duncan, 1989). These neurons encode stimulus intensity. However, intensity coding is presumably important not only in sensory discrimination but also in affective responses, attentional mechanisms, and motor control (Coghill *et al.*, 1999). The responses of neurons in the CL nucleus can be accounted for by inputs from spinothalamic cells that project to the medial but not to the lateral thalamus (Giesler *et al.*, 1981; Ammons *et al.*, 1985). Some neurons of the CL nucleus project broadly to the cerebral cortex, including the SI cortex (Jones and Leavitt, 1974) and the SII cortex (Stevens *et al.*, 1993).

Craig *et al.* (1994) and Blomqvist *et al.* (2000) have proposed that there is a spinothalamic projection from lamina I to a region that is probably a part of the posterior complex, called by them the posterior part of the ventromedial thalamic nucleus (VMpo). They identified this area in both monkeys and humans. Craig *et al.* (1994) recorded thermoreceptive and nociceptive responses from neurons in this area. The significance of this nucleus is unclear (see Willis *et al.*, 2002). It was proposed that it may project to the insula. Burton and Jones (1976) used an anterograde tracing method to determine the cortical projection of neurons in the posterior thalamic region. They found that the medial part of the posterior complex projected to the retroinsular cortex, which is just posterior to SII.

Cerebral Cortex

As already discussed, imaging techniques have shown that the SI, SII, anterior cingulate, and insular cortex are generally activated following acutely painful stimulation of human volunteer subjects (Fig. 30.14, upper panels). The fact that multiple cortical areas are involved in the cerebral cortical response to pain explains why pain is not always reduced after brain injury (Head and Holmes, 1911; Holmes, 1927; Coghill *et al.*, 1994). However, it should be noted that there have been a number of reports of pain reduction

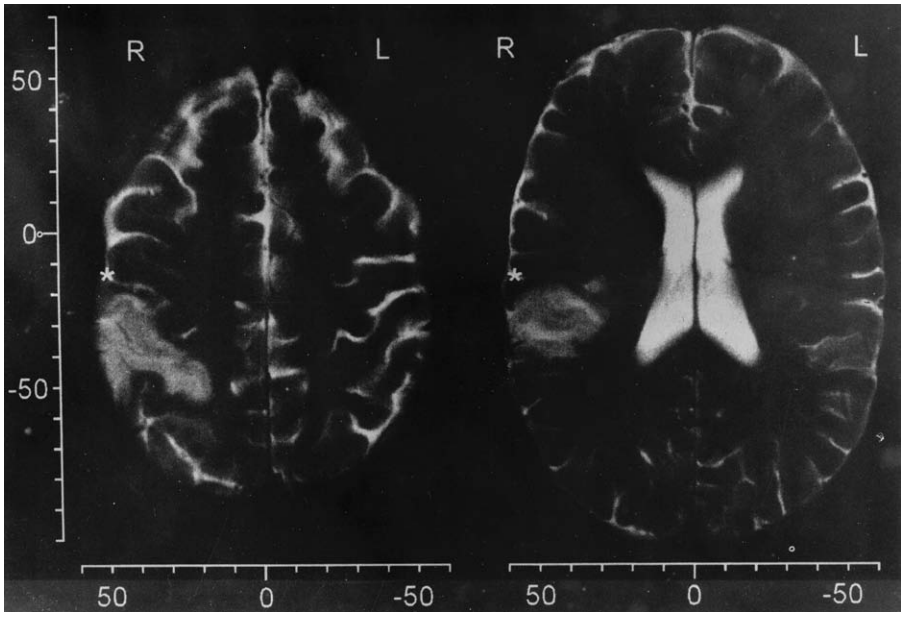

FIGURE 30.17 Images of the somatosensory cortex in a patient who had lost pain sensation in the hand without loss of the motivational–affective component of pain following a stroke that destroyed the hand area in the SI and SII somatosensory cortex. The functional magnetic resonance images were taken in transaxial planes 42 and 18 mm dorsal to the anteroposterior commissural line. The scales are in millimeters. The asterisks indicate the central sulcus. (From Ploner *et al.,* 1999a.)

following cortical damage (Russell, 1945; Marshall, 1951), and lesions of the somatosensory cerebral cortex in monkeys have been shown to reduce nociceptive behavioral responses (Peele, 1944; Brinkman *et al.*, 1985; Kenshalo *et al.,* 1989; see also reviews by Kenshalo and Willis, 1991; Treede *et al.,* 1999).

Clinical Application

Recently, a case was reported by Ploner *et al.* (1999a) of a patient who had a stroke that destroyed the hand area of the SI and SII cortices on one side of the brain (Fig. 30.17). The patient had a marked loss of sensory modalities that can be attributed to activity in the posterior column system (e.g., graphesthesia and stereognosis; see Nathan *et al.,* 1986). In addition, thermal sense was abolished, and the threshold for recognition of noxious thermal pulses applied by a laser was elevated. Suprathreshold heat stimulation was not recognized as painful and the source was poorly localized. For instance, noxious heat stimulation of the left hand of the patient produced an unpleasant feeling somewhere between the fingertips and shoulder. These findings were consistent with the interpretation that the SI and SII cortices are crucial for sensory discrimination of pain, but that other cortical areas (such as the anterior cingulate gyrus) mediate the aversive component of pain.

Imaging experiments support this interpretation. For example, hypnotic suggestion has been used to alter the perceived intensity of heat pain (Bushnell *et al.,* 1999). If attention is diverted from a painful stimulus, the degree of activation of the SI cortex is reduced. By contrast, if hypnosis is used to alter the unpleasantness of pain, activation of the anterior cingulate gyrus, but not the SI cortex, is altered (Rainville *et al.,* 1997). The particular region of SI cortex that is most closely associated with painful stimulation appears to be area 1. For example, painful stimuli produce more intense activation of area 1 than other areas of SI (Gelnar *et al.,* 1999).

The involvement of SI in acute responses to painful stimuli has been confirmed in human studies using magnetoencephalography (Arendt-Nielsen *et al.,* 1999; Ploner *et al.,* 1999b; Kanda *et al.,* 2000). This approach also confirmed the importance of area 1 in such responses (Ploner *et al.,* 2000).

Electrophysiological experiments have been done on monkeys to determine if nociceptive neurons can be found in the SI cortex (Kenshalo and Isensee, 1983; Kenshalo *et al.,* 1988; Chudler *et al.,* 1990; Kenshalo *et al.,* 2000). Both WDR and HT neurons have been identified in area 1 (Fig. 30.18). These cells are located in cortical layers III and IV among neurons that respond preferentially to tactile stimuli (Kenshalo *et al.,* 2000).

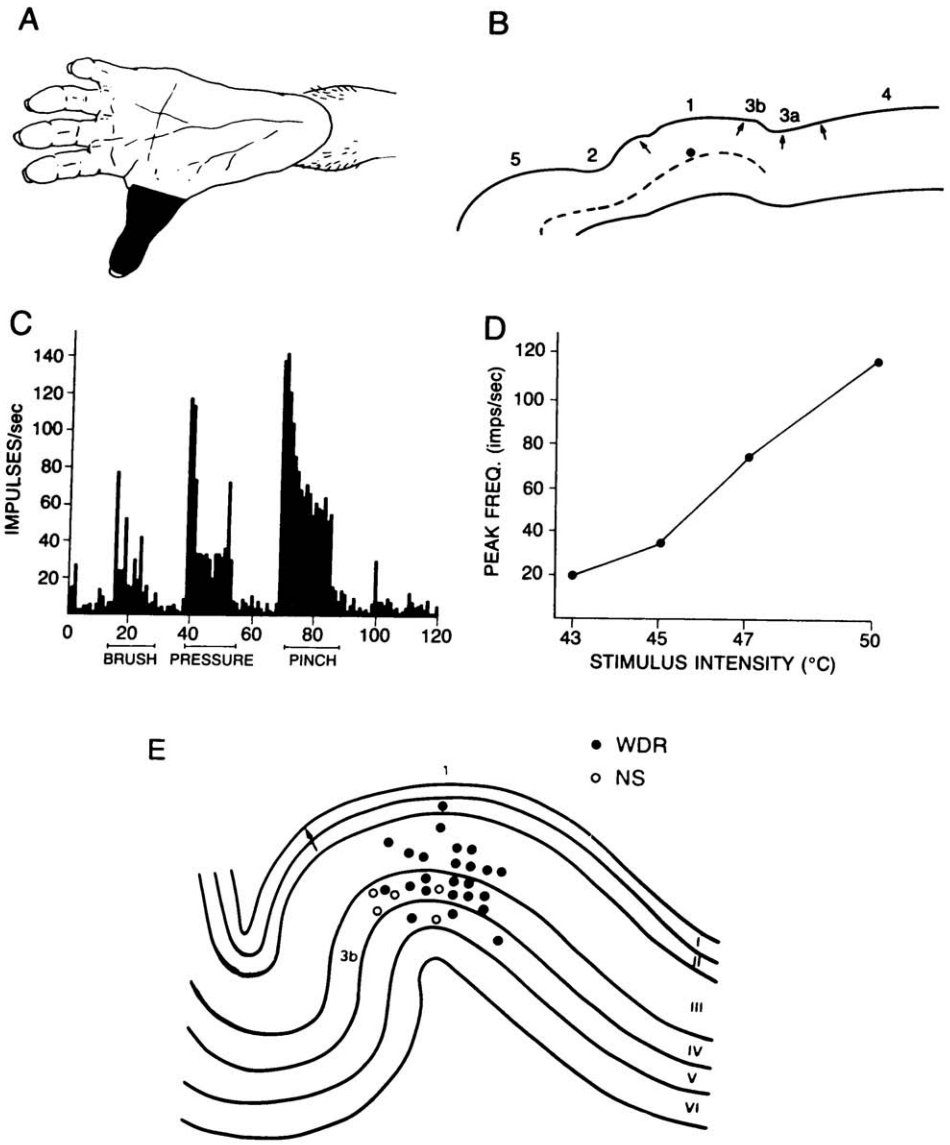

FIGURE 30.18 Nociceptive neurons in area 1 of the monkey SI somatosensory cortex. In **A** is the cutaneous receptive field of a wide dynamic range cortical neuron. Its location in area 1 is indicated in **B.** Responses to graded mechanical stimulation of the receptive field are seen in **C.** The curve in **D** shows the responses of the neuron to graded noxious heat stimuli. In **E** are plotted the locations of a population of wide dynamic range (WDR) and nociceptive-specific (NS) neurons in area 1. (From Kenshalo *et al.,* 2000.

The receptive fields are small and located contralaterally. The neurons respond in a graded manner to graded noxious heat stimuli, and they are also activated by intradermal injection of capsaicin. They do not respond to innocuous cooling or stimulation of deep tissue. Neurons in the SI cortex of monkeys have also been found that respond to visceral stimuli (Brüggemann *et al.,* 1997). Nociceptive cortical neurons in the face representation encode the intensity of noxious heat pulses applied to the face in awake, behaving monkeys (Kenshalo *et al.,* 1988; Chudler *et al.,* 1990). The responses of nociceptive neurons in the SI cortex can be accounted for by the response properties of nociceptive neurons in the VPL and VPM nuclei.

It is known that the VPL nucleus projects to all four areas of the SI cortex (including area 1) (e.g., Jones *et al.,* 1979; Friedman and Jones, 1981). However, the details of how areas of the VPL nucleus that are rich in particular calcium-binding proteins in the thalamus relate to the distribution of the terminals of nociceptive thalamic neurons in the SI cortex are still unclear. For example, neurons in the matrix area, which stain for calbindin and receive input from the STT, project preferentially to the superficial layers of the SI cortex

(see Jones, 1998); yet, as mentioned, the nociceptive neurons in area 1 of the SI cortex are located in layers 3 and 4 (Kenshalo *et al.*, 2000). Perhaps the calbindin-containing terminals end preferentially on the apical dendrites of the nociceptive neurons.

Nociceptive neurons have also been described in the anterior cingulate gyrus in rabbits (Vogt *et al.*, 1993). The receptive fields of these are large and unsuited to a role in stimulus localization. The responses resemble those of neurons in the intralaminar nuclei. In some cases, Vogt *et al*. (1993) were able to eliminate the nociceptive responses of anterior cingulate neurons by injecting lidocaine into the parafascicular nucleus.

SUMMARY AND CONCLUSIONS

Pain depends on sensory processing by the pain system. This includes (1) primary afferent nociceptors, which transduce noxious stimuli; (2) ascending nociceptive pathways, which transmit nociceptive information from the spinal cord (or brain stem) to higher centers; (3) descending modulatory pathways, which regulate pain signals; (4) forebrain structures, which process nociceptive information, leading to a variety of pain responses.

Nociceptors have small myelinated or unmyelinated axons and are found in most organs. They signal damage or potential damage. Nociceptors can respond to one or more types of noxious stimuli, and their activation may evoke a particular quality of pain, depending on the tissue innervated and the type of nociceptor. Many nociceptors are normally insensitive to mechanical stimuli but they may be sensitized by damage or inflammation, after which they may respond to very weak mechanical stimuli that now become painful. Primary afferent nociceptors in peripheral nerves originate from small DRG cells, which can be recognized by chemical markers, such as peptide content, VR-1 receptors, or IB4 binding sites. Many nociceptors release glutamate, as well as peptides, as neurotransmitters.

The central processes of nociceptive DRG cells enter the spinal cord through dorsal roots. The axons of cutaneous nociceptors travel only a short distance in Lissauer's tract; by contrast, those of visceral nociceptors may travel rostrocaudally as far as five segments. In primates, large bundles of unmyelinated afferents can be found within Lissauer's tract. Nociceptors often end in laminae I, II, V, and X, although particular types of nociceptors may have more restricted zones of termination. The synapses formed by nociceptors in the superficial dorsal horn are often glomerular endings. Some glomeruli probably belong to nociceptors with IB4 binding sites, whereas others are peptidergic. Nociceptor endings may receive synaptic contacts from GABAergic inhibitory interneurons; these connections are presumably responsible for presynaptic inhibition, such as that envisioned in the gate theory of pain. There are also inhibitory circuits (the so-called diffuse noxious inhibitory controls, DNICs) that depend on ascending input to the brain stem and a descending inhibitory pathway. The DNIC system seems to be more powerful than the gate mechanism.

There are a number of ascending pathways that transmit nociceptive information to the brain. These include the spinothalamic tract (STT), which has traditionally been regarded as the most important pain-signaling pathway. The cells of origin of this pathway are concentrated in laminae I and V of the dorsal horn, where many primary afferent nociceptors end. STT cells generally respond best to noxious stimuli. The axons of most STT cells cross at the segmental level and ascend to the thalamus in the anterolateral white matter. The axons of lamina I STT cells tend to be dorsal to those of lamina V STT cells until they reach the upper cervical spinal cord, where a ventral shift results in intermingling of axons of STT cells of both laminae. The STT has a somatotopic organization, which accounts for the distribution of the analgesia that results from anterolateral cordotomies for relief of pain in patients.

Recently, a visceral pain pathway has been described in the dorsal column. This is formed by the axons of postsynaptic dorsal column neurons, many of which are located in the vicinity of the central canal. The pathway is somatotopic, with the axons of neurons in the sacral cord ascending near the midline and those from the midthoracic cord near the dorsal intermediate septum. Higher levels of this pathway involve the dorsal column nuclei and the VPL thalamic nucleus. These observations in animal experiments help explain why midline myelotomies and commissural myelotomies in patients can relieve pelvic visceral pain even when performed at rostral levels of the spinal cord.

Other ascending nociceptive pathways include the spinocervical, spinoreticular, and spinomesecephalic pathways, as well as pathways that project to limbic structures, such as the spinoparabrachial, spinohypothalamic, and direct spinolimbic pathways.

The processing of pain signals is strongly affected by complex brain circuits that may either inhibit or facilitate nociception. Important modulatory pathways that originate in the brain stem and descend to the spinal cord include serotonergic neurons of the

medullary raphe and catecholaminergic neurons of the dorsolateral pons. Stimulation in the periventricular and periaqueductal gray or the ventrobasal thalamus in humans can be useful in producing pain relief in patients.

Imaging studies in humans have demonstrated that a number of cerebral cortical areas are activated by painful stimuli, including the SI and SII somatosensory areas, the anterior cingulate gyrus, and the insula. These different areas presumably contribute to different aspects of the reactions to painful stimuli. Evidence indicates that the SI and SII cortices are involved in sensory discrimination of pain. The anterior cingulate gyrus is likely to contribute to affective responses, and the insula may be involved in pain memories. Several motor system structures can also be activated; these may help with motor reactions to painful stimuli.

Activation of the cerebral cortex by painful stimuli engages the thalamus. The ventral posterior lateral and medial nuclei provide the main input to SI and SII. The ventral posterior inferior nucleus also projects to SII. These parts of the ventral posterior thalamus are presumably the main sources of input used for the sensory discrimination of pain by SI and SII. CL projects widely to the sensory motor cortex and may participate in arousal and attention. The large receptive fields of these neurons are not appropriate for spatial discrimination. It is unclear what the main sources of nociceptive inputs to the anterior cingulate gyrus and insula are.

Nociceptive neurons have been described in the SI cortex, in particular in area 1. This observation is consistent with the findings of imaging studies and also of magnetoencephalography in human subjects. Nociceptive neurons have also been found in the anterior cingulate cortex.

References

Adriaensen, H., Gybels, J., Handwerker, H.O., and Van Hees, J. (1983). Response properties of thin myelinated (A-δ) fibers in human skin nerves. *J. Neurophysiol.* **49,** 111–122.

Al-Chaer, E.D., Lawand, N.B., Westlund, K.N., and Willis, W.D. (1996a). Visceral nociceptive input into the ventral posterolateral nucleus of the thalamus: a new function for the dorsal column pathway. *J. Neurophysiol.* **76,** 2661–2674.

Al-Chaer, E.D., Lawand, N.B., Westlund, K.N., and Willis, W.D. (1996b). Pelvic visceral input into the nucleus gracilis is largely mediated by the postsynaptic dorsal column pathway. *J. Neurophysiol.* **76,** 2675–2690.

Al-Chaer, E.D., Westlund, K.N., and Willis, W.D. Nucleus gracilis: an integrator for visceral and somatic information. *J. Neurophysiol.* **78,** 521–527.

Al-Chaer, E.D., Feng, Y., and Willis, W.D. (1998). A role for the dorsal column in nociceptive visceral input into the thalamus of primates. *J. Neurophysiol.* **79,** 3143–3150.

Al-Chaer, E.D., Feng, Y., and Willis, W.D. (1999). Comparative study of viscerosomatic input onto postsynaptic dorsal column and spinothalamic tract neurons in the primate. *J. Neurophysiol.* **82,** 1876–1882.

Alhaider, A.A., Lei, S.Z., and Wilcox, G.L. Spinal 5-HT3 receptor-mediated antinociception: possible release of GABA. *J. Neurosci.* **11,** 1881–1888.

Almeida, A., Tjølsen, A., Lima, D., Coimbra, A., and Hole, K. (1996). The medullary dorsal reticular nucleus facilitates acute nociception in the rat. *Brain Res. Bull.* **39,** 7–15.

Almeida, A., Størkson, R., Lima, D., Hole, K., and Tjølsen, A. (1991). The medullary dorsal reticular nucleus facilitates pain behaviour induced by formalin in the rat. Eur. *J. Neurosci.* **11,** 110–122.

Alvarez, F.J., Rodrigo, J., Jessell, T.M., Dodd, J., and Priestley, J.V. (1989a). Morphology and distribution of primary afferent fibres expressing α-galactose extended oligosaccharides in the spinal cord and brainstem of the rat. Light microscopy. *J. Neurocytol.* **18,** 611–629.

Alvarez, F.J., Rodrigo, J., Jessell, T.M., Dodd, J., and Priestley, J.V. (1989b). Ultrastructure of primary afferent fibres and terminals expressing α-galactose extended oligosaccharides in the spinal cord and brainstem of the rat. *J. Neurocytol.* **18,** 631–645.

Alvarez, F.J., Kavookjian, A.M., and Light, A.R. (1992). Synaptic interactions between GABA-immunoreactive profiles and the terminals of functionally defined myelinated nociceptors in the monkey and cat spinal cord. *J. Neurosci.* **12,** 2901–2917.

Alvarez, F.J., Kavookjian, A.M., and Light, A.R. (1993). Ultrastructural morphology, synaptic relationships, and CGRP immunoreactivity of physiologically identified C-fiber terminals in the monkey spinal cord. *J. Comp. Neurol.* **329,** 472–490.

Alvarez, F.J., Taylor-Blake, B., Fyffe, R.E.W., De Blas, A.L., and Light, A.R. (1996). Distribution of immunoreactivity for the β_2 and β_3 subunits of the GABAA receptor in the mammalian spinal cord. *J. Comp. Neurol.* **365,** 392–412.

Ammons, W.S. (1989). Primate spinothalamic cell responses to ureteral occlusion. *Brain Res.* **496,** 124–130.

Ammons, W.S., Girardot, M.N., and Foreman, R.D. (1985). T_2-T_5 spinothalamic neurons projecting to medial thalamus with viscerosomatic input. *J. Neurophysiol.* **54,** 73–89.

Andersson, J.L.R., Lilja, A., Hartvig, P., Långström, B., Gordh, T., Handwerker, H., and Torebjörk, E. (1997). Somatotopic organization along the central sulcus, for pain localization in humans, as revealed by positron emission tomography. *Exp. Brain Res.* **117,** 192–199.

Angaut-Petit, D. (1975). The dorsal column system: II. Functional properties and bulbar relay of the postsynaptic fibres of the cat's fasciculus gracilis. *Exp. Brain Res.* **22,** 471–493.

Apkarian, A.V., and Hodge, C.J. (1989a). Primate spinothalamic pathways: I. A quantitative study of the cells of origin of the spinothalamic pathway. *J. Comp. Neurol.* **288,** 447–473.

Apkarian, A.V., and Hodge, C.J. (1989b). Primate spinothalamic pathways: III. Thalamic terminations of the dorsolateral and ventral spinothalamic pathways *J. Comp. Neurol.* **288,** 493–511.

Apkarian, A.V., and Shi, T. (1994). Squirrel monkey lateral thalamus. I. Somatic nociresponsive neurons and their relation to spinothalamic terminals. *J. Neurosci.* **14,** 6779–6795.

Applebaum, A.E., Beall, J.E., Foreman, R.D., and Willis, W.D. (1975). Organization and receptive fields of primate spinothalamic tract neurons. *J. Neurophysiol.* **38,** 572–586.

Arendt-Nielsen, L., Yamasaki, H., Nielsen, J., Naka, D., and Kakigi, R. (1999). Magnetoencephalographic responses to painful impact stimulation. *Brain Res.* **839,** 203–208.

Armour, D. (1927). Surgery of the spinal cord and its membranes. *Lancet* **1,** 691–697.

Ault, B., and Hildebrand, L.M. (1993). Activation of nociceptive reflexes by peripheral kainate receptors. *J. Pharmacol. Exp. Ther.* **265,** 927–932.

Averill, S., McMahon, S.B., Clary, D.O., Reichardt, L.F., and Priestley, J.V. (1995). Immunocytochemical localization of trkA receptors in chemically identified subgroups of adult rat sensory neurons. *Eur. J. Neurosci.* **7,** 1484–1494.

Basbaum, A.I., and Fields, H.L. (1978). Endogenous pain control mechanisms: review and hypothesis. *Ann. Neurol.* **4,** 451–462.

Basbaum, A.I., and Fields, H.L. (1979). The origin of descending pathways in the dorsolateral funiculus of the spinal cord of the cat and rat: further studies on the anatomy of pain modulation. *J. Comp. Neurol.* **187,** 513–532.

Basbaum, A.I., Clanton, C.H., and Fields, H.L. (1978). Three bulbospinal pathways from the rostral medulla of the cat: an autoradiographic study of pain modulating systems. *J. Comp. Neurol.* **178,** 209–224.

Battaglia, G., and Rustioni, A. (1988). Coexistence of glutamate and substance P in dorsal root ganglion neurons of the rat and monkey. *J. Comp. Neurol.* **277,** 302–312.

Battaglia, G., and Rustioni, A. (1992). Substance P innervation of the rat and cat thalamus. II. Cells of origin in the spinal cord. *J. Comp. Neurol.* **315,** 473–-486.

Baumann, T.K., Simone, D.A., Shain, C.N., and LaMotte, R.H. (1991). Neurogenic hyperalgesia: the search for the primary cutaneous afferent fibers that contribute to capsaicin-induced pain and hyperalgesia. *J. Neurophysiol.* **66,** 212–227.

Beall, J.E., Martin, R.F., Applebaum, A.E., and Willis, W.D. (1976). Inhibition of primate spinothalamic tract neurons by stimulation in the region of the nucleus raphe magnus. *Brain Res.* **114,** 328–333.

Becker, R., Sure, U., and Bertalanffy, H. (1999). Punctate midline myelotomy. A new approach in the management of visceral pain. *Acta Neurochir.* (Wien) **141,** 881–883.

Beitel, R.E., and Dubner, R. (1976). Response of unmyelinated (C) polymodal nociceptors to thermal stimuli applied to monkey's face. *J. Neurophysiol.* **39,** 1160–1175.

Belmonte, C., and Cervero, F. (eds.) (1996). "Neurobiology of Nociceptors." Oxford University Press, Oxford.

Belmonte, C., and Gallar, J. (1996). Corneal nociceptors. *In* "Neurobiology of Nociceptors" (C. Belmonte and F. Cervero, eds.), pp. 146–183. Oxford University Press.

Bennett, D.L.H., Averill, S., Clary, D.O., Priestley, J.V., and McMahon, S.B. (1996). Postnatal changes in the expression of the trkA high-affinity NGF receptor in primary sensory neurons. *Eur. J. Neurosci.* **8,** 2204–2208.

Bennett, G.J., Seltzer, Z., Lu, G.W., Nishikawa, N., and Dubner, R. (1983) The cells of origin of the dorsal column postsynaptic projection in the lumbosacral enlargements of cats and monkeys. *Somatosensory Res.* **1,** 131–149.

Bergman, E., Carlsson, K., Liljeborg, A., Manders, E., Hokfelt, T., and Ulfhake, B. (1999). Neuropeptides, nitric oxide synthase and GAP-43 in B4-binding and RT97 immunoreactive primary sensory neurons: normal distribution pattern and changes after peripheral nerve transection and aging. *Brain Res.* **832,** 63–83.

Berkley, K.J. (1980). Spatial relationships between the terminations of somatic sensory and motor pathways in the rostral brainstem of cats and monkeys. I. Ascending somatic sensory inputs to lateral diencephalon. *J. Comp. Neurol.* **193,** 283–317.

Bernard, J.F. (1999). La voie nociceptive spino-parabrachiale. *Doul et Anal.* **2,** 121–128.

Bernard, J.F., and Besson, J.M. (1990). The spino(trigemino)-pontoamygdaloid pathway: electrophysiological evidence for an involvement in pain processes. *J. Neurophysiol.* **63,** 473–490.

Bernard, J.F., Peschanski, M., and Besson, J.M. (1989). A possible spino (trigemino)-ponto-amygdaloid pathway for pain. *Neurosci. Lett.* **100,** 83–88.

Bernard, J.F., Huang, G.F., and Besson, J.M. (1994). The parabrachial area: electrophysiological evidence for an involvement in visceral nociceptive processes. *J. Neurophysiol.* **71,** 1646–1660.

Besson, J.M., and Chaouch, A. (1987). Peripheral and spinal mechanisms of nociception. *Physiol. Rev.* **67,** 67–186.

Blomqvist, A., and Berkley, K.J. (1992). A re-examination of the spino-reticulo-diencephalic pathway in the cat. *Brain Res.* **579,** 17–31.

Blomqvist, A., Zhang, E.T., and Craig, A.D. (2000). Cytoarchitectonic and immunohistochemical characterization of a specific pain and temperature relay, the posterior portion of the ventral medial nucleus, in the human thalamus. *Brain* **123,** 601–619.

Boivie, J. (1979). An anatomical reinvestigation of the termination of the spinothalamic tract in the monkey. *J. Comp. Neurol.* **186,** 343–370.

Boivie, J., and Perl, E.R. (1975). Neural substrates of somatic sensation. *In* "MTP International Review of Science, Physiology, Series 1, Vol. 3, Neurophysiology" (C.C. Hunt, ed.), pp. 303–411. University Park Press, Baltimore.

Bowker, R.M., Westlund, K.N., and Coulter, J.D. (1982a). Origins of serotonergic projections to the lumbar spinal cord in the monkey using a combined retrograde transport and immunocytochemical technique. *Brain Res. Bull.* **9,** 271–278.

Bowker, R.M., Westlund, K.N., Sullivan, M.C., Wilbur, J.F., and Coulter, J.D. (1982b). Transmitters of the raphe-spinal complex: immunocytochemical studies. *Peptides* **3,** 291–298.

Bowsher, D. (1961). The termination of secondary somatosensory neurons within the thalamus of Macaca mulatta: an experimental degeneration study. *J. Comp. Neurol.* **117,** 213–227.

Bradbury, E.J., Burnstock, G., and McMahon, S.B. (1998). The expression of P2X3 purinoreceptors in sensory neurons: effects of axotomy and glial-derived neurotropic factor. *Mol. Cell. Neurosci.* **12,** 256–268.

Brinkman, J., Colebatch, J.G., Porter, R., and York, D.H. (1985). Responses of precentral cells during cooling of post-central cortex in conscious monkeys. *J. Physiol.* **368,** 611–625.

Bromm, B., Jahnke, M.T., and Treede, R.D. (1984). Responses of human cutaneous afferents to CO_2 laser stimuli causing pain. *Exp. Brain Res.* **55,** 158–166.

Brown, A.G., and Fyffe, R.E.W. (1981). Form and function of dorsal horn neurones with axons ascending the dorsal columns in cat. *J. Physiol.* **321,** 31–47.

Brown-Séquard, C.E. (1860). "Course of Lectures on the Physiology and Pathology of the Central Nervous System." J.B. Lippincott, Philadelphia.

Brüggemann, J., Shi, T., and Apkarian, A.V. (1994). Squirrel monkey lateral thalamus. II. Viscerosomatic convergent representation of urinary bladder, colon, and esophagus. *J. Neurosci.* **14,** 6796–6814.

Brüggemann, J., Shi, T., and Apkarian, A.V. (1997). Viscero-somatic neurons in the primary somatosensory cortex (SI) of the squirrel monkey. *Brain Res.* **756,** 297–300.

Budai, D., and Fields, H.L. (1998). Endogenous opioid peptides acting at mu-opioid receptors in the dorsal horn contribute to midbrain modulation of spinal nociceptive neurons. *J. Neurophysiol.* **79,** 677–687.

Budai, D., Harasawa, I., and Fields, H.L. (1998). Midbrain periaqueductal gray (PAG) inhibits nociceptive inputs to sacral dorsal horn nociceptive neurons through alpha2-adrenergic receptors. *J. Neurophysiol.* **80,** 2244–2254.

Buhassira, D., Le Bars, D., Bolgert, F., Laplane, D., and Willer, J.C. (1993). Diffuse noxious inhibitory controls in humans: a neurophysiological investigation of a patient with a form of Brown-Sequard syndrome. *Ann. Neurol.* **34,** 536–543.

Burgess, P.R., and Perl, E.R. (1973). Cutaneous mechanoreceptors and nociceptors. *In* "Handbook of Sensory Physiology, Somatosensory System, Vol. II." (A. Iggo, ed.), pp. 29–78. Springer-Verlag, Heidelberg.

Buritova, J., Besson, J.M., and Bernard, J.F. (1998). Involvement of the spinoparabrachial pathway in inflammatory nociceptive processes: a c-fos protein study in the awake rat. *J. Comp. Neurol.* **397,** 10–28.

Burstein, R. (1996). Somatosensory and visceral input to the hypothalamus and limbic system. *In* "Prog. Brain Res.," Vol. 107 "G. Holstege, R. Bandler, and C.B. Saper, eds.), pp. 257–267. Elsevier, Amsterdam.

Burstein, R., Cliffer, K.D., and Giesler, G.J. (1990). Cells of origin of the spinohypothalamic tract in the rat. *J. Comp. Neurol.* **291,** 329–344.

Burstein, R., Dado, R.J., Cliffer, K.D., and Giesler, G.J. (1991). Physiological characterization of spinohypothalamic tract neurons in the lumbar enlargement of rats. *J. Neurophysiol.* **66,** 261–284.

Burton, H., and Jones, E.G. (1976). The posterior thalamic region and its cortical projection in new world and old world monkeys. *J. Comp. Neurol.* **168,** 249–302.

Bushnell, M.C., and Duncan, G.H. (1987). Mechanical response properties of ventroposterior medial thalamic neurons in the alert monkey. *Exp. Brain Res.* **67,** 603–614.

Bushnell, M.C., and Duncan, G.H. (1989). Sensory and affective aspects of pain perception: is medial thalamus restricted to emotional issues? *Exp. Brain Res.* **78,** 415–418.

Bushnell, M.C., Duncan, G.H., Dubner, R., and He, L.F. (1984). Activity of trigeminothalamic neurons in medullary dorsal horn of awake monkeys trained in a thermal discrimination task. *J. Neurophysiol.* **52,** 170–187.

Bushnell, M.C., Duncan, G.H., and Tremblay, N. (1993). Thalamic VPM nucleus in the behaving monkey. I. Multimodal and discriminative properties of thermosensitive neurons. *J. Neurophysiol.* **69,** 739–752.

Bushnell, M.C., Duncan, G.H., Hofbauer, R.K., Ha, B., Chen, J.I., and Carrier, B. (1999). Pain perception: is there a role for primary somatosensory cortex? *Proc. Natl. Acad. Sci. U.S.A.* **96,** 7705–7709.

Cameron, A.A., Khan, I.A., Westlund, K.N., and Willis, W.D. (1995). The efferent projections of the periaqueductal gray in the rat: a Phaseolus vulgaris leucoagglutinin study. II. Descending projections. *J. Comp. Neurol.* **351,** 585–601.

Campbell, J.N., and Meyer, R.A. (1983). Sensitization of unmyelinated nociceptive afferents in monkey varies with skin type. *J. Neurophysiol.* **49,** 98–110.

Campbell, J.N., Khan, A.A., Meyer, R.A., and Raja, S.N. (1988a). Responses to heat of C-fiber nociceptors in monkey are altered by injury in the receptive field but not by adjacent injury. *Pain* **32,** 327–332.

Campbell, J.N., Solomon, C.T., and James, C.S. (1988b). The Hopkins experience with lesions of the dorsal horn (Nashold's operation) for pain from avulsion of the brachial plexus. *Appl. Neurophysiol.* **51,** 170–174.

Carlton, S.M., and Coggeshall, R.E. (1999). Inflammation-induced changes in peripheral glutamate receptor populations. *Brain Res.* **820,** 63–70.

Carlton, S.M., LaMotte, C.C., Honda, C.N., Surmeier, D.J., DeLanerolle, N.C., and Willis, W.D. (1985). Ultrastructural analysis of substance P and other synaptic profiles innervating an identified spinothalamic tract neuron. *Neurosci. Abstr.* **11,** 578.

Carlton, S.M., McNeill, D.L., Chung, K., and Coggeshall, R.E. (1988). Organization of calcitonin gene-related peptide-immunoreactive terminals in the primate dorsal horn. *J. Comp. Neurol.* **276,** 527–536.

Carlton, S.M., LaMotte, C.C., Honda, C.N., Surmeier, D.J., Delanerolle, N., and Willis, W.D. (1989). Ultrastructural analysis of axosomatic contacts on functionally identified primate spinothalamic tract neurons. *J. Comp. Neurol.* **281,** 555–566.

Carlton, S.M., Westlund, K.N., Zhang, D., Sorkin, L.S., and Willis, W.D. (1990). Calcitonin gene-related peptide containing primary afferent fibers synapse on primate spinothalamic tract cells. *Neurosci. Lett.* **109,** 76–81.

Carlton, S.M., Honda, C.N., Willcockson, W.S., LaCramp, M., Zhang, D., Denoroy, L., Chung, J.M., and Willis, W.D. (1991). Descending adrenergic input to the primate spinal cord and its possible role in modulation of spinothalamic cells. *Brain Res.* **543,** 77–90.

Carlton, S.M., Westlund, K.N., Zhang, D., and Willis, W.D. (1992). GABA-immunoreactive terminals synapse on primate spinothalamic tract cells. *J. Comp. Neurol.* **322,** 528–537.

Carlton, S. M., Hargett, G. L., and Coggeshall, R. E. (1995). Localization and activation of glutamate receptors in unmyelinated axons of rat glabrous skin. *Neurosci. Lett.* **197,** 25–28.

Carlton, S. M., Zhou, S., and Coggeshall, R. E. (1996). Localization and activation of substance P receptors in unmyelinated axons of rat skin. *Brain Res.* **734,** 103–108.

Carlton, S.M., Du, J., Davidson, E., Zhou, S., and Coggeshall, R.E. (2001a). Somatostatin receptors on peripheral primary afferent terminals: inhibition of sensitized nociceptors. *Pain* **90,** 233–244.

Carlton, S.M., Hargett, G.L., and Coggeshall, R.E. (2001b). Localization of metabotropic glutamate receptors 2/3 on primary afferent axons in the rat. *Neuroscience* 105, 957–969.

Casey, K.L. (1996). Unit analysis of nociceptive mechanisms in the thalamus of the awake squirrel monkey. *J. Neurophysiol.* **29,** 727–750.

Casey, K.L., and Morrow, T.J. (1983). Ventral posterior thalamic neurons differentially responsive to noxious stimulation of the awake monkey. *Science* **221,** 675–677.

Casey, K.L., and Morrow, T.J. (1987). Nociceptive neurons in the ventral posterior thalamus of the awake squirrel monkey: observations on identification, modulation, and drug effects. *In* "Thalamus and Pain" (J.M. Besson, G. Guilbaud, and M. Peschanski, eds.), pp. 211–226. Elsevier, Amsterdam.

Casey, K.L., Minoshima, S., Berger, K.L., Koeppe, R.A., Morrow, T.J., and Frey, K.A. (1994). Positron emission tomographic analysis of cerebral structures activated specifically by repetitive noxious heat stimuli. *J. Neurophysiol.* **71,** 802–807.

Caterina, M.J., Schumacher, M.A., Tominaga, M., Rosen, T.A., Levine, J.D., and Julius, D. (1997). The capsaicin receptor: a heat-activated ion channel in the pain pathway. *Nature* **389,** 816–824.

Caterina, M.J., Rosen, T.S., Tominaga, M., Brake, A.J., and Julius, D. (1999). A capsaicin-receptor homologue with a high threshold for noxious heat. *Nature* **398,** 436–441.

Caterina, M.J., Leffler, A., Malmberg, A.B., Martin, W.J., Trafton, J., Petersen-Zeitz, K.R., Koltzenburg, M., Basbaum, A.I., and Julius, D. (2000). Impaired nociception and pain sensation in mice lacking the capsaicin receptor. *Science* **288,** 306–313.

Cervero, F., and Wolstencroft, J.H. (1984). A positive feedback loop between spinal cord nociceptive pathways and antinociceptive areas of the cat's brain stem. *Pain* **20,** 125–138.

Chandler, M.J., Hobbs, S.F., Fu, Q.G., Kenshalo, D.R., Blair, R.A., and Foreman, R.D. (1992). Responses of neurons in ventroposterolateral nucleus of primate thalamus to urinary bladder distension. *Brain Res.* **571,** 26–34.

Chandler, M.J., Zhang, J., and Foreman, R.D. (1998). Cardiopulmonary sympathetic input excites primate cuneothalamic neurons: comparison with spinothalamic tract neurons. *J. Neurophysiol.* **80,** 628–637.

Chang, H.T., and Ruch, T.C. (1947). Topographical distribution of spinothalamic fibres in the thalamus of the spider monkey. *J. Anat.* **81,** 155–164.

Chen, P.S. (2000). The role of anterior pretectal nucleus on descending inhibition of spinal cord dorsal horn cells in rats and identified spinothalamic cells in primates. Dissertation. University of Texas Medical Branch, Galveston, Texas.

Chou, D.K.H., Dodd, J., Jessell, T.M., Costello, C.E., and Jungalwala, F.B. (1988). Identification of a-galactose (a-fucose)-asialo-Gml glycolipid expressed by subsets of rat dorsal root ganglion neurons. *J. Biol. Chem.* **264,** 3409–3415.

Chudler, E.H., Anton, F., Dubner, R., and Kenshalo, D.R. (1990). Responses of nociceptive SI neurons in monkeys and pain sensation in humans elicited by noxious thermal stimulation: effect of interstimulus interval. *J. Neurophysiol.* **63,** 559–569.

Chung, J.M., Kenshalo, D.R., Gerhart, K.D., and Willis, W.D. (1979). Excitation of primate spinothalamic neurons by cutaneous C-fiber volleys. *J. Neurophysiol.* **42,** 1354–1369.

Chung, J.M., Kevetter, G.A., Yezierski, R.P., Haber, L.H., Martin, R.F., and Willis, W.D. (1983). Midbrain nuclei projecting to the medial medulla oblongata in the monkey. *J. Comp. Neurol.* **214,** 93–102.

Chung, J.M., Lee, K.H., Hori, Y., Endo, K., and Willis, W.D. (1984). Factors influencing peripheral nerve stimulation produced inhibition of primate spinothalamic tract cells. *Pain* **19,** 277–293.

Chung, J.M., Lee, K.H., Surmeier, D.J., Sorkin, L.S., Kim, J., and Willis, W.D. (1986a). Response characteristics of neurons in the ventral posterior lateral nucleus of the monkey thalamus. *J. Neurophysiol.* **56,** 370–390.

Chung, J.M., Surmeier, D.J., Lee, K.H., Sorkin, L.S., Honda, C.N., Tsong, Y., and Willis, W.D. (1986b). Classification of primate spinothalamic and somatosensory thalamic neurons based on cluster analysis. *J. Neurophysiol.* **56,** 308–327.

Chung, K., Briner, R.P., Carlton, S.M., and Westlund, K.N. (1989). Immunohistochemical localization of seven different peptides in the human spinal cord. *J. Comp. Neurol.* **280,** 158–170.

Chung, K., Lee, W.T., and Carlton, S.M. (1988). The effects of dorsal rhizotomy and spinal cord isolation on calcitonin gene-related peptide-labeled terminals in the rat lumbar dorsal horn. *Neurosci. Lett.* **90,** 27–32.

Clark, W.E. (1936). Le Gros. The termination of ascending tracts in the thalamus of the macaque monkey. *J. Anat.* **71,** 7–40.

Cliffer, K.D., Burstein, R., and Giesler, G.J. (1991). Distributions of spinothalamic, spinohypothalamic, and spinotelencephalic fibers revealed by anterograde transport of PHA-L in rats. *J. Neurosci.* **11,** 852–868.

Coffield, J.A., and Miletic, V. (1987). Immunoreactive enkephalin is contained within some trigeminal and spinal neurons projecting to the rat medial thalamus. *Brain Res.* **425,** 380–383.

Coggeshall, R.E., and Carlton, S.M. (1997). Receptor localization in the mammalian dorsal horn and primary afferent neurons. *Brain Res. Rev.* **24,** 28–66.

Coggeshall, R.E., Chung, K., Chung, J.M., and Langford, L.A. (1981). Primary afferent axons in the tract of Lissauer in the monkey. *J. Comp. Neurol.* **196,** 431–442.

Coggeshall, R.E., Zhou, S., and Carlton, S.M. (1997). Opioid receptors on peripheral sensory axons. *Brain Res.* **764,** 126–132.

Coghill, R.C., Talbot, J.D., Evans, A.C., Meyer, E., Gjedde, A., Bushnell, M.C., and Duncan, G.H. (1994). Distributed processing of pain and vibration by the human brain. *J. Neurosci.* **14,** 4095–4108.

Coghill, R.C., Sang, C.N., Maisog, J.M., and Iadarola, M.J. (1999). Pain intensity processing within the human brain: a bilateral distributed mechanism. *J. Neurophysiol.* **82,** 1934–1943.

Coimbra, A., Ribeiro-da-Silva, A., and Pignatelli, D. (1984). Effects of dorsal rhizotomy on the several types of primary afferent terminals in laminae I-III of the rat spinal cord. *Anat. Embryol.* **170,** 279–287.

Conti, F., De Biasi, S., Giuffrida, R., and Rustioni, A. (1990). Substance P-containing projections in the dorsal columns of rats and cats. *Neuroscience* **34,** 607–621.

Coulter, J.D., Bowker, R.M., Wise, S.P., Murray, E.A., Castiglioni, A.J., and Westlund, K.N. (1979). Cortical, tectal and medullary descending pathways to the cervical spinal cord. *In* "Reflex Control of Posture and Movement," Progress in Brain Research, Vol. 50 (R.Granit and O. Pompeiano, eds.), pp. 263–279. Elsevier, Amsterdam.

Craig, A.D. (1995). Distribution of brainstem projections from spinal lamina I neurons in the cat and the monkey. *J. Comp. Neurol.* **361,** 225–248.

Craig, A.D. (2000). Spinal location of ascending lamina I axons in the macaque monkey. *J. Pain* **1,** 33–45.

Craig, A.D., and Mense, S. (1983). The distribution of afferent fibers from the gastrocnemius-soleus muscle in the dorsal horn of the cat, as revealed by the transport of horseradish peroxidase. *Neurosci. Lett.* **41,** 233–238.

Craig, A.D., Heppelmann, B., and Schaible, H.G. (1988). The projection of the medial and posterior articular nerves of the cat's knee to the spinal cord. *J. Comp. Neurol.* **276,** 279–288.

Craig, A.D., Bushnell, M.C., Zhang, E.T., and Blomqvist, A. (1994). A thalamic nucleus specific for pain and temperature sensation. *Nature* **372,** 770–7733.

Csillik, B., and Knyihár-Csillik, E. (1986). *"The Protean Gate. Structure and Plasticity of the Primary Nociceptive Analyzer."* Akadémiai Kiadó, Budapest.

Cui, M., McAdoo, D.J., and Willis, W.D. (1999). Periaqueductal gray stimulation–induced inhibition of nociceptive dorsal horn neurons in rats is associated with the release of norepinephrine, serotonin and amino acids. *J. PET* **289,** 868–876.

Davidson, E.M., Coggeshall, R.E., and Carlton, S.M. (1997). Peripheral NMDA and non-NMDA glutamate receptors contribute to nociceptive behaviors in the rat formalin test. *Neuroreport* **8,** 941–946.

Davis, K.D., Kwan, C.L., Crawley, A.P., and Mikulis, D.J. (1998). Functional MRI study of thalamic and cortical activations evoked by cutaneous heat, cold, and tactile stimuli. *J. Neurophysiol.* **80,** 1533–1546.

Davis, K.D., Meyer, R.A., and Campbell, J.N. (1993). Chemosensitivity and sensitization of nociceptive afferents that innervate the hairy skin of monkey. *J. Neurophysiol.* **69,** 1071–1081.

De Biasi, S., and Rustioni, (1988). A. Glutamate and substance P coexist in primary afferent terminals in the superficial laminae of spinal cord. *Proc. Natl. Acad. Sci. U.S.A.* **85,** 7820–7824.

De Broucker, T., Cesaro, P., Willer, J.C., and Le Bars, D. (1990). Diffuse noxious inhibitory controls in man. Involvement of the spinoreticular tract. *Brain* **113,** 1223–1234.

DeSalles, A.A., Katayama, Y., Becker, D.P., and Hayes, R.L. (1985). Pain suppression induced by electrical stimulation of the pontine parabrachial region. Experimental study in cats. *J. Neurosurg.* **62,** 397–407.

Dickenson, A. (1983). The inhibitory effects of thalamic stimulation on the spinal transmission of nociceptive information in the rat. *Pain* **17,** 213–224.

Di Piero, V., Ferracuti, S., Sabatini, U., Pantano, P., Cruccu, G., and Lenzi, G.L. (1994). A cerebral blood flow study on tonic pain activation in man. *Pain* **56,** 167–173.

Dodd, J., and Jessell, T.M. (1985). Lactoseries carbohydrates specify subsets of dorsal root ganglion neurons projecting to the superficial dorsal horn of rat spinal cord. *J. Neurosci.* **5,** 3278–3294.

Dougherty, P.M., and Willis, W.D. (1991). Enhancement of spinothalamic neuron responses to chemical and mechanical stimuli following combined micro-iontophoretic application of N-methyl-D-aspartic acid and substance P. *Pain* **47,** 85–93.

Dougherty, P.M., Sluka, K.A., Sorkin, L.S., Westlund, K.N., and Willis, W.D. (1992). Neural changes in acute arthritis in monkeys. I. Parallel enhancement of responses of spinothalamic tract neurons to mechanical stimulation and excitatory amino acids. *Brain Res. Rev.* **17,** 1–13.

Downie, J.W., Ferrington, D.G., Sorkin, L.S., and Willis, W.D. (1988). The primate spinocervicothalamic pathway: responses of cells of the lateral cervical nucleus and spinocervical tract to innocuous and noxious stimuli. *J Neurophysiol.* **59,** 861–885.

Dubner, R., Kenshalo, D.R., Maixner, W., Bushnell, M.C., and Oliveras, J.L. (1989). The correlation of monkey medullary dorsal horn neuronal actvitiy and the perceived intensity of noxious heat stimuli. *J. Neurophysiol.* **62,** 450–457.

Duncan, G.H., Bushnell, M.C., Oliveras, J.L., Bastrash, N., and Tremblay, N. (1993). Thalamic VPM nucleus in the behaving monkey. III. Effects of reversible inactivation by lidocaine on thermal and mechanical discrimination. *J. Neurophysiol.* **70,** 2086–2096.

Fabri, M., and Conti, F. (1990). Calcitonin gene-related peptide-positive neurons and fibers in the cat dorsal column nuclei. *Neuroscience* **35,** 167–174.

Feng, Y., Cui, M., Al-Chaer, E.D., and Willis, W.D. (1998). Epigastric antinociception by cervical dorsal column lesions in rats. *Anesthesiology* **89,** 411–420.

Ferrington, D.G., Sorkin, L.S., and Willis, W.D. (1987). Responses of spinothalamic tract cells in the superficial dorsal horn of the primate lumbar spinal cord. *J. Physiol.* **388,** 681–703.

Fields, H.L., and Basbaum, A.I. (1978). Brainstem control of spinal pain-transmission neurons. *Annu. Rev. Physiol.* **40,** 217–248.

Fields, H.L., and Besson, J.M. (eds.) (1988). *"Pain Modulation."* Progress in Brain Research, Vol. 77. Elsevier, Amsterdam.

Fields, H.L., Basbaum, A.I., Clanton, C.H., and Anderson, S.D. (1977). Nucleus raphe magnus inhibition of spinal cord dorsal horn neurons. *Brain Res.* **126,** 441–453.

Fleetwood-Walker, S.M., Hope, P.J., Iggo, A., Mitchell, R., and Molony, V. (1983). The effects of iontophoretically applied noradrenaline on the cutaneous sensory responses of identified dorsal horn neurons in the cat. *J. Physiol.* (Lond) **342,** 63–64, 1983.

Foerster, O., and Gagel, O. (1932). Die Vorderseitenstrangdurchschneidung beim Menschen. Eine klinish-patho-physiologisch-anatomische Studie. *Z. Ges. Neurol. Psychiat.* **138,** 1–92.

Foreman, R.D. (1989). Organization of the spinothalamic tract as a relay for cardiopulmonary sympathetic afferent fiber activity. *In* "Progress in Sensory Physiology," Vol. 9 (D. Ottoson, ed.-in-chief), pp. 1–51. Springer-Verlag, Heidelberg.

Foreman, R.D., Schmidt, R.F., and Willis, W.D. (1979). Effects of mechanical and chemical stimulation of fine muscle afferents upon primate spinothalamic tract cells. *J. Physiol.* **286,** 215–231

Friedman, D.P., and Jones, E.G. (1981). Thalamic input to areas 3a and 2 in monkeys. *J. Neurophysiol.* **45,** 59–85.

García-Añoveros, J., Samad, T.A., Zuvela-Jelaska, L., Woolf, C.J., and Corey, D.P. (2001). Transport and localization of the DEG/EnaC ion channel BNaC1a to peripheral mechanosensory terminals of dorsal root ganglia neurons. *J. Neuroscience* **21,** 2678–2686.

Gaze, R.M., and Gordon, G. (1954). The representation of cutaneous sense in the thalamus of the cat and monkey. *Q. J. Exp. Physiol.* **39,** 279–304.

Gebhart, G.F. (1996). Visceral polymodal receptors. *In* "The Polymodal Receptor: A Gateway to Pathological Pain." Progress in Brain Res., Vol. 113 (T. Kumazawa, L. Kruger, and K. Mizumura, eds.), pp. 101–112. Elsevier, Amsterdam.

Gelnar, P.A., Krauss, B.R., Sheehe, P.R., Szeverenyi, N.M., and Apkarian, A.V. (1999). A comparative fMRI study of cortical representations for thermal painful, vibrotactile, and motor performance tasks. *NeuroImage* **10,** 460–482.

Georgopoulos, A.P. (1976). Functional properties of primary afferent units probably related to pain mechanisms in primate glabrous skin. *J. Neurophysiol.* **39,** 71–83.

Geppetti, P., and Holzer, P. (1996). (eds.). "Neurogenic Inflammation." CRC Press, Boca Raton.

Gerhart, K.D., Wilcox, T.K., Chung, J.M., and Willis, W.D. (1981). Inhibition of nociceptive and nonnociceptive responses of primate spinothalamic cells by stimulation in medial brain stem. *J. Neurophysiol.* **45,** 121–136.

Gerhart, K.D., Yezierski, R.P., Fang, Z.R., and Willis, W.D. (1983). Inhibition of primate spinothalamic tract neurons by stimulation in ventral posterior lateral (VPLc) thalamic nucleus: possible mechanisms. *J. Neurophysiol.* **49,** 406–423.

Gerhart, K.D., Yezierski, R.P., Wilcox, T.K., and Willis, W.D. (1984). Inhibition of primate spinothalamic tract neurons by stimulation in periaqueductal gray or adjacent midbrain reticular formation. *J. Neurophysiol.* **51,** 450–466.

Giesler, G.J., Yezierski, R.P., Gerhart, K.D., and Willis, W.D. (1981). Spinothalamic tract neurons that project to medial and/or lateral thalamic nuclei: evidence for a physiologically novel population of spinal cord neurons. *J. Neurophysiol.* **46,** 1285–1308.

Gildenberg, P.L., and Hirshberg, R.M. (1984). Limited myelotomy for the treatment of intractable cancer pain. *J. Neurol. Neurosurg. Psychiatry* **47,** 94–96.

Gingold, S.I., Greenspan, J.D., and Apkarian, A.V. (1991). Anatomic evidence of nociceptive inputs to primary somatosensory cortex: relationship between spinothalamic terminals and thalamocortcal cells in squirrel monkeys. *J. Comp. Neurol.* **308,** 467–490.

Gowers, W.R. (1878). A case of unilateral gunshot injury to the spinal cord. *Trans. Clin. Lond.* **11,** 24–32.

Graven-Nielsen, T., Arendt-Nielsen, L., Svensson, P., and Jensen, T.S. (1997a). Experimental muscle pain: A quantitative study of local and referred pain in humans following injection of hypertonic saline. *J. Musculoskel. Pain.* **5,** 49–69.

Graven-Nielsen, T., Arendt-Nielsen, L., Svensson, P., and Jensen, T.S. (1997b). Quantification of local and referred muscle pain in humans after sequential i.m. injections of hypertonic saline. *Pain* **69,** 111–117.

Graven-Nielsen, T., Fenger-Grøn, L.S., Svensson, P., Steengaard-Pedersen, K., Arendt-Nielsen, L., and Jensen, T.S. (1998). Quantification of deep and superficial sensibility in saline-pinduced muscle pain- a psychophysical study. *Somatosens. Motor Res.* **15,** 46–53.

Greenspan, J.D., Vierck, C.J., and Ritz, L.A. (1986). Sensitivity to painful and nonpainful electrocutaneous stimuli in monkeys: effects of anterolateral chordotomy. *J. Neurosci.* **6,** 380–390.

Guillaume, J., Mazars, G., and de Mouillac, V. (1945). La myélotomie commissurale. *La Presse Med.* **53,** 666–667.

Guo, A., Vulchanova, L., Wang, J., Li, X., and Elde, R. (1999). Immunocytochemical localization of the vanilloid receptor 1 (VR1): relationship to neuropeptides, the $P2X_3$ purinoceptor and IB4 binding sites. *Eur. J. Neurosci.* **11,** 946–958.

Gybels, J.M., and Sweet, W.H. (1989). "Neurosurgical Treatment of Persistent Pain." Pain and Headache, Vol. 11 (P.L. Gildenberg, ed.). Karger, Basel.

Gybels, J., Van Hees, J., and Peluso, F. (1976). Modulation of experimentally produced pain in man by electrical stimulation of some cortical, thalamic and basal ganglia structures. *Adv. Pain Res. Therap.* **1,** 475–478.

Habelt, C., Kessler, F., Distler, C., Kress, M., and Reeh, P.W. (2000). Interactions of inflammatory mediators and low pH not influenced by capsazepine in rat cutaneous nociceptors. *Neuroreport* **11,** 973–976.

Haber, L.H., Martin, R.F., Chung, J.M., and Willis, W.D. (1980). Inhibition and excitation of primate spinothalamic tract neurons by stimulation in region of nucleus reticularis gigantocellularis. *J. Neurophysiol.* **43,** 1578–1593.

Hallin, R.G., Torebjörk, H.E., and Wiesenfeld, Z. (1981). Nociceptors and warm receptors innervated by C fibres in human skin. *J. Neurol. Neurosurg. Psychiatry* **44,** 313–319.

Handwerker, H.O., and Kobal, G. (1993). Psychophysiology of experimentally induced pain. *Physiol. Rev.* **73,** 639–671.

Hanesch, U. (1996). Neuropeptides in dural fine sensory endings-involvement in neurogenic inflammation? *In* "The Polymodal Receptor: a Gateway to Pathological Pain." Progress in Brain Res., Vol. 113 (T. Kumazawa, L. Kruger, and K. Mizumura, eds.), pp. 299–317. Elsevier, Amsterdam.

Hardy, J.D., Wolff, H.G., and Goodell, H. (1967). "Pain Sensations and Reactions." Hafner Publishing, New York. Reprint of edition by Williams & Wilkins Co., 1952.

Harmann, P.A., Chung, K., Briner, R.P., Westlund, K.N., and Carlton, S.M. (1988). Calcitonin gene–related peptide (CGRP) in the human spinal cord: a light and electron microscopic analysis. *J. Comp. Neurol.* **269,** 371–380.

Hayes, E.S., and Carlton, S.M. (1992). Primary afferent interactions: analysis of calcitonin gene–related peptide-immunoreactive terminals in contact with unlabeled and GABA-immunoreactive profiles in the monkey dorsal horn. *Neuroscience* **47,** 873–896

Hayes, N.L., and Rustioni, A. (1980). Spinothalamic and spino-medullary neurons in macaques: a single and double retrograde tracer study. *Neuroscience* **5,** 861–874.

Hayes, R.L., Price, D.D., Ruda, M.A., and Dubner, R. (1979). Suppression of nociceptive responses in the primate by electrical stimulation of the brain or morphine administration: behavioral and electrophysiological comparisons. *Brain Res.* **167,** 417–421.

Head, H., and Holmes, G. (1911). Sensory disturbances from cerebral lesions. *Brain* **34,** 102–254.

Head, H., and Thompson, T. (1906). The grouping of afferent impulses within the spinal cord. *Brain* **29,** 537–741.

Headley, P.M., Duggan, A.W., and Griersmith, B.T. (1978). Selective reduction by noradrenaline and 5-hydroxytryptamine of nociceptive responses of cat dorsal horn neurons. *Brain Res.* **145,** 185–189.

Heinricher, M.M., Morgan, M., Tortorici, V., and Fields, H.L. (1994). Disinhibition of off-cells and antinociception produced by an opioid action within the rostral ventromedial medulla. *Neuroscience* **63,** 279–288.

Helliwell, R.J.A., McLatchie, L.M., Clarke, M., Winter, J., Bevan, S., and McIntyre, P. (1998). Capsaicin sensitivity is associated with the expression of the vanilloid (capsaicin) receptor (VR1) mRNA in adult rat sensory ganglia. *Neurosci. Lett.* **250,** 177–180.

Heppelmann, B., Messlinger, K., Neiss, W.F., and Schmidt, R.F. (1990). Ultrastructural three-dimensional reconstruction of group III and group IV sensory nerve endings ("free nerve endings") in the knee joint capsule of the cat: evidence for multiple receptive sites. *J. Comp. Neurol.* **292,** 103–116.

Hirshberg, R.M., Al-Chaer, E.D., Lawand, N.B., Westlund, K.N., and Willis, W.D. (1996). Is there a pathway in the posterior funiculus that signals visceral pain? *Pain* **67,** 291–305.

Hitchcock, E. (1970). Stereotactic cervical myelotomy. *J. Neurol. Neurosurg. Psychiatry* **33,** 224–230.

Hitchcock, E. (1974). Stereotactic myelotomy. *Proc. R. Soc. Med.* **67,** 771–772.

Hitchcock, E. (1997). Stereotactic spinal surgery. *Neurol. Surg.* **433,** 271–280.

Hodge, C.J., Apkarian, A.V., Stevens, R., Vogelsang, G., and Wisnicki, H.J. (1981). Locus coeruleus modulation of dorsal horn unit responses to cutaneous stimulation. *Brain Res.* **204,** 514–520.

Hoffman, D.S., Dubner, R., Hayes, R.L., and Medlin, T.P. (1981). Neuronal activity in medullary dorsal horn of awake monkeys trained in a thermal discrimination task. I. Responses to innocuous and noxious thermal stimuli. *J. Neurophysiol.* **46,** 409–427.

Hökfelt, T., Kellerth, J.O., Nilsson, G., and Pernow, B. (1975). Experimental immunohistochemical studies on the localization and distribution of substance P in cat primary sensory neurons. *Brain Res.* **100,** 235–252.

Holden, J.E., and Proudfit, H.K. (1999). Microinjection of morphine in the A7 catecholamine cell group produces opposing effects on nociception that are mediated by alpha1- and alpha2-adrenoceptors. *Neuroscience* **91,** 979–990.

Holmes, G. (1927). Disorders of sensation produced by cortical lesions. *Brain* **50,** 413–427.

Holstege, G., and Kuypers, H.G.J.M. (1982). The anatomy of brain stem pathways to the spinal cord in cat: a labeled amino acid tracing study. *Prog Brain Res* **57,** 145–147.

Holzer, P. (1991). Capsaicin: cellular targets, mechanisms of action, and selectivity for thin sensory neurons. *Pharmacol. Rev.* **43,** 143–201.

Hosobuchi, Y. (1978). Tryptophan reversal of tolerance to analgesia induced by central grey stimulation. *Lancet* **11,** 47.

Hosobuchi, Y., Adams, J.E., and Linchitz, R. (1997). Pain relief by electrical stimulation of the central gray matter in humans and its reversal by naloxone. *Science* **197,** 183–186.

Hosobuchi, Y., Lamb, S., and Bascom, D. (1980). Tryptophan loading may reverse tolerance to opiate analgesics in humans: a preliminary report. *Pain* **9,** 161–169.

Houghton, A.K., Kadura, S., and Westlund, K.N. (1997). Dorsal column lesions reverse the reduction of homecage activity in rats with pancreatitis. *Neuroreport* **8,** 3795–3800.

Houghton, A.K., Wang, C.-C., and Westlund, K.N. (2001). Do nociceptive signals from the pancreas travel in the dorsal column? *Pain* **89,** 207–220.

Howe, J.R., Wang, J.Y., and Yaksh, T.L. (1983). Selective antagonism of the antinociceptive effect of intrathecally applied alpha adrenergic agonists by intrathecal prazosin and intrathecal yohimbine. *J. PET* **224,** 552–558.

Hsieh, J.C., Belfrage, M., Stone-Elander, S., Hansson, P., and Ingvar, M. (1995). Central representation of chronic ongoing neuropathic pain studied by positron emission tomography. *Pain* **63,** 225–236.

Hylden, J.L.K., Hayashi, H., Dubner, R., and Bennett, G.J. (1986). Physiology and morphology of the lamina I spinomesencephalic projection. *J. Comp. Neurol.* **247,** 505–515.

Hyndman, O.R. (1942). Lissauer's tract section. A contribution to chordotomy for the relief of pain. *J. Int. Coll. Surgeons* **5,** 394–400.

Hyndman, O.R., and Van Epps, C. (1939). Possibility of differential section of the spinothalamic tract. *Arch. Surg.* **38,** 1036–1053.

Iadarola, M.J., Berman, K.F., Zeffiro, T.A., Byas-Smith, M.G., Gracely, R.H., Max M.B., and Bennett, G.J. (1998). Neural activation during acute capsaicin-evoked pain and allodynia assessed with PET. *Brain* **121,** 931–947.

Immke, D.C., and McCleskey, E.W. (2001). Lactate enhances the acid-sensing Na^+ channel on ischemia-sensing neurons. *Nature Neurosci.* **4,** 869–870.

Ischia, S., Luzzani, A., Ischia, A., and Maffezzoli, G. (1984). Bilateral percutaneous cervical cordotomy: immediate and long-term results in 36 patients with neoplastic disease. *J. Neurol. Neurosurg. Psychiatry* **47,** 141–147.

Jackson, D.L., Graff, C.B., Richardson, J.D., and Hargreaves, K.M. (1995). Glutamate participates in the peripheral modulation of thermal hyperalgesia in rats. *Eur. J. Pharmacol.* **284,** 321–325.

Jankowska, E., Rastad, J., and Zarzecki, P. (1979). Segmental and supraspinal input to cells of origin of nonprimary fibres in the feline dorsal columns. *J. Physiol.* **290,** 185–200.

Jeanmonod, D., and Sindou, M. (1991). Somtosensory function following dorsal root entry zone lesions in patients with neurogenic pain or spasticity. *J. Neurosurg.* **74,** 916–932.

Jones, A.K.P., Brown, W.D., Friston, K.J., Qi, L.Y., and Frackowiak, R.S.J. (1991). Cortical and subcortical localization of response to pain in man using positron emission tomography. *Proc. R. Soc. B* **244,** 39–44.

Jones, E.G. (1985). "The Thalamus." Plenum Press, New York.

Jones, E.G. (1997a). Thalamic organization and chemical anatomy. *In* "Thalamus, Vol. I, Organization and Function" (M. Steriade, E.G. Jones, and D.A. McCormick, eds.), pp. 31–174. Elsevier, Amsterdam.

Jones, E.G. (1997a). A description of the human thalamus. *In* "Thalamus, Vol. II, Experimental and Clinical Aspects" (M. Steriade, E.G. Jones, and D.A. McCormick, eds.), pp. 425–499. Elsevier, Amsterdam.

Jones, E.G. (1998). The thalamus of primates. *In* "Handbook of Chemical Neuroanatomy, Vol. 14, The Primate Nervous System, Part II" (F.E. Bloom, A. Björklund, and T. Hökfelt, eds.), pp. 1–298. Elsevier Science, Amsterdam.

Jones, E.G., and Hendry, S.H.C. (1989). Differential calcium binding protein immunoreactivity distinguishes classes of relay neurons in monkey thalamic nuclei. *Eur. J. Neurosci.* **1,** 222–246.

Jones, E.G., and Leavitt, R.Y. (1974). Retrograde axonal transport and the demonstration of non-specific projections to the cerebral cortex and striatum from thalamic intralaminar nuclei in the rat, cat and monkey. *J. Comp. Neurol.* **154,** 349–378.

Jones, E.G., and Pons, T.P. (1998). Thalamic and brainstem contributions to large-scale plasticity of primate somatosensory cortex. *Science* **282,** 1121–1125.

Jones, E.G., Wise, S.P., and Coulter, J.D. (1979). Differential thalamic relationbships of sensory-motor and parietal cortical fields in monkeys. *J. Comp. Neurol.* **183,** 833–882.

Ju, G., Melander, T., Ceccatelli, S., Hökfelt, T., and Frey, P. (1987). Immunohistochemical evidence for a spinothalamic pathway co-containing cholecystokinin- and galanin-like immunoreactivities in the rat. *Neuroscience* **20,** 439–456.

Kanda, M., Nagamine, T., Ikeda, A., Ohara, S., Kunieda, T., Fujiwara, N., Yazawa, S., Sawamoto, N., Matsumoto, R., Taki, W., and Shibasaki, H. (2000). Primary somatosensory cortex is actively involved in pain processing in human. *Brain Res.* **853,** 282–289.

Karplus, J.P., and Kreidl, A. (1914). Ein Beitrag zur Kenntnis der Schmerzleitung im Rückenmark. Pflügers *Arch. Physiol.* **158,** 275–287.

Katter, J.T., Dado, R.J., Kostarczyk, E., and Giesler, G.J. (1996). Spinothalamic and spinohypothalamic tract neurons in the sacral spinal cord of rats. II. Responses to cutaneous and visceral stimuli. *J. Neurophysiol.* **75,** 2606–2628.

Kenshalo, D.R., and Isensee, O. (1983). Responses of primate SI cortical neurons to noxious stimuli. *J. Neurophysiol.* **50,** 1479–1496.

Kenshalo, D.R., and Willis, W.D. (1991). The role of the cerebral cortex in pain sensation. *In* "The Cerebral Cortex, Vol. 9. Normal and Altered States of Function" (A. Peters and E. Jones, eds.), pp. 153–212. Plenum Press, New York.

Kenshalo, D.R., Leonard, R.B., Chung, J.M., and Willis, W.D. (1979). Responses of primate spinothalamic neurons to graded and to repeated noxious heat stimuli. *J. Neurophysiol.* **42,** 1370–1389.

Kenshalo, D.R., Giesler, G.J., Leonard, R.B., and Willis, W.D. (1980). Responses of neurons in the primate ventral posterior lateral nucleus to noxious stimuli. *J. Neurophysiol.* **43,** 1594–1614.

Kenshalo, D.R., Chudler, E.H., Anton, F., and Dubner, R. (1988). SI nociceptive neurons participate in the encoding process by which monkeys perceive the intensity of noxious thermal stimulation. *Brain Res.* **454,** 378–382.

Kenshalo, D.R., Anton, F., and Dubner, R. (1989). The detection and perceived intensity of noxious thermal stimuli in monkey and in human. *J. Neurophysiol.* **62,** 429–436.

Kenshalo, D.R., Iwata, K., Sholas, M., and Thomas, D.A. (2000). Response properties and organization of nociceptive neurons in area 1 of monkey primary somatosensory cortex. *J. Neurophysiol.* **84,** 719–729.

Kevetter, G.A., Haber, L.H., Yezierski, R.P., Chung J.M., Martin, R.F., and Willis, W.D. (1982). Cells of origin of the spinoreticular tract in the monkey. *J. Comp. Neurol.* **207,** 61–74.

Kim, Y.S., and Kwon, S.J. (2000). High thoracic midline dorsal column myelotomy for severe visceral pain due to advanced stomach cancer. *Neurosurgery* **46,** 85–90.

King, R.B. (1977). Anterior commissurotomy for intractable pain. *J. Neurosurg.* **47,** 7–11.

Kneisley, L.W., Biber, M.P., and LaVail, J.H. (1978). A study of the origin of brain stem projections to monkey spinal cord using the retrograde transport method. *Exp. Neurol.* **60,** 116–139.

Koltzenburg, M., and Handwerker, H.O. (1994). Differential ability of human cutaneous nociceptors to signal mechanical pain and to produce vasodilatation. *J. Neurosci.* **14,** 1756–1765.

Konietzny, F., Perl, E.R., Trevino, D., Light, A., and Hensel, H. (1981). Sensory experiences in man evoked by intraneural electrical stimulation of intact cutaneous afferent fibers. *Exp. Brain Res.* **42,** 219–222.

Kumazawa, T., and Perl, E.R. (1977). Primate cutaneous sensory units with unmyelinated (C) afferent fibers. *J. Neurophysiol.* **40,** 1325–1338.

Kumazawa, T., Kruger, L., and Mizumura, K. (eds.) (1996). "The Polymodal Receptor—*A Gateway to Pathological Pain*." Progress in Brain Research, Vol. 113. Elsevier, Amsterdam.

Kupers, R.C., Gybels, J.M., and Gjedde, (2000). A. Positron emission tomography study of a chronic pain patient successfully treated with somatosensory thalamic stimulation. *Pain* **87,** 295–302.

Kuru, M. (1949). "Sensory Paths in the Spinal Cord and Brain Stem of Man." Sogensya, Tokyo.

LaMotte, C.C., Carlton, S.M., Honda, C.N., Surmeier, D.J., and Willis, W.D. (1988). Innervation of identified primate spinothalamic tract neurons: ultrastructure of serotonergic and other synaptic profiles. *Neurosci. Abstr.* **14,** 852.

LaMotte, R.H., Thalhammer, J.G., Torebjörk, H.E., and Robinson, C.J. (1982). Peripheral neural mechanisms of cutaneous hyperalgesia following mild injury by heat. *J. Neurosci.* **2,** 765–781.

LaMotte, R.H., Thalhammer, J.G., and Robinson, C.J. (1983). Peripheral neural correlates of magnitude of cutaneous pain and hyperalgesia: a comparison of neural events in monkey with sensory judgments in human. *J. Neurophysiol.* **50,** 1–26.

LaMotte, R.H., Lundberg, L.E.R., and Torebjörk, H.E. (1992). Pain, hyperalgesia and activity in nociceptive C units in humans after intradermal injection of capsaicin. *J. Physiol.* **448,** 749–764.

Lawand, N.B., Willis, W.D., and Westlund, K.N. (1997). Excitatory amino acid receptor involvement in peripheral nociceptive transmission in rats. *Eur. J. Pharmacol.* **324,** 169–177.

Lewand, N.B. (2000). Glutamate receptors: a key role in peripheral nociceptive transduction. Dissertation, University of Texas Medical Research, Galveston.

Lawson, S.N. (1996). Peptides and cutaneous polymodal nociceptor neurones. *In* "The Polymodal Receptor: A Gateway to Pathological Pain." Progress in Brain Research, Vol. 113 (T. Kumazawa, L. Kruger, and K. Mizumura, eds.), pp. 369–385. Elsevier, Amsterdam.

Lawson, S.N., and Waddell, P.J. (1991). Soma neurofilament immunoreactivity is related to cell size and fibre conduction velocity in rat primary sensory neurons. *J. Physiol.* **435,** 41–63.

Lawson, S.N., Harper, E.I., Harper, A.A., Garson, J.A., Coakham, H.B., and Randle, B.J. (1985). Monoclonal antibody 2C5: a marker for a subpopulation of small neurones in rat dorsal root ganglia. *Neuroscience* **16,** 365–374.

Lawson, S.N., Crepps, B.A., and Perl, E.R. (1997). Relationship of substance P to afferent characteristics of dorsal root ganglion neurones in guinea-pig. *J. Physiol.* **505,** 177–191.

Leah, J., Menétrey, D., and De Pommery, J. (1988). Neuropeptides in long ascending spinal tract cells in the rat: evidence for parallel processing of ascending information. *Neuroscience* **24,** 195–207.

Le Bars, D., Dickenson, A.H., and Besson, J.M. (1979a). Diffuse noxious inhibitory controls (DNIC). I. Effects on dorsal horn convergent neurones in the rat. *Pain* **6,** 283–304.

Le Bars, D., Dickenson, A.H., and Besson, J.M. (1979b). Diffuse noxious inhibitory controls (DNIC). II: Lack of effect on non-convergent neurones, supraspinal involvement and theoretical implications. *Pain* **6,** 305–327.

Lee, J.I., Dougherty, P.M., Antezana, D., and Lenz, F.A. (1999). Responses of neurons in the region of human thalamic principal somatic sensory nucleus to mechanical and thermal stimuli graded into the painful range. *J. Comp. Neurol.* **410,** 541–555.

Lewis, T. (1942). "Pain." Macmillan, London.

Liebeskind, J.C., Guilbaud, G., Besson, J.M., and Oliveras, J.L. (1973). Analgesia from electrical stimulation of the periaqueductal gray matter in the cat: behavioral observations and inhibitory effects on spinal cord interneurons. *Brain Res.* **50,** 441–446.

Light, A.R., and Perl, E.R. (1979). Spinal termination of functionally identified primary afferent neurons with slowly conducting myelinated fibres. *J. Comp. Neurol.* **186,** 133–150.

Lin, Q., Peng, Y., and Willis, W.D. (1994). Glycine and $GABA_A$ antagonists reduce the inhibition of primate spinothalamic tract neurons produced by stimulation in periaqueductal gray. *Brain Res.* **654,** 286–302.

Lin, Q., Peng, Y.B., and Willis, W.D. (1996a). Antinociception and inhibition from the periaqueductal gray are mediated in part by spinal $5HT_{1A}$ receptors. *J. PET* **276,** 958–967.

Lin, Q., Peng, Y.B., and Willis, W.D. (1996b). Role of GABA receptor subtypes in inhibition of primate spinothalamic tract neurons: difference between spinal and periaqueductal gray inhibition. *J. Neurophysiol.* **75,** 109–123.

Lin, Q., Wu, J., and Willis, W.D. (1999). Dorsal root reflexes and cutaneous neurogenic inflammation after intradermal injection of capsaicin in rats. *J. Neurophysiol.* **82,** 2602–2611.

Lin, Q., Zou, X., and Willis, W.D. (2000). Small myelinated and unmyelinated primary afferents convey dorsal root reflexes following intradermal injection of capsaicin in rats. *J. Neurophysiol.* **84,** 2695–2698.

Lovick, T.A. (1986). Analgesia and cardiovascular changes evoked by stimulating neurons in the nucleus paragigantocellularis lateralis in the cat. *J. Physiol.* **389,** 23–35.

Magnusson, K.R., Clements, J.R., Larson, A.A., Madl, J.E., and Beitz, A.J. (1987). Localization of glutamate in trigeminothalamic projection neurons: a combined retrograde transport-immunohistochemical study. *Somatosens. Res.* **4,** 177–190.

Magoun, H.W. (1963). *"The Waking Brain,"* 2nd ed. Charles C Thomas, Springfield, IL.

Maixner, W., Dubner, R., Kenshalo, D.R., Bushnell, M.C., and Oliveras, J.L. (1989). Responses of monkey medullary dorsal horn neurons during the detection of noxious heat stimuli. *J. Neurophysiol.* **62,** 437–449.

Mantyh, P.W. (1983). The spinothalamic tract in the primate: A re-examination using wheatgerm agglutinin conjugated to horseradish peroxidase. *Neuroscience* **9,** 847–862.

Marchettini, P., Cline, M., and Ochoa, J.L.(1990). Innervation territories for touch and pain afferents of single fascicles of the human ulnar nerve. Mapping through intraneural microrecording and microstimulation. *Brain* **113,** 1491–1500.

Marchettini, P., Simone, D.A., Caputi, G., and Ochoa, J.L. (1996). Pain from excitation of identified muscle nociceptors in humans. *Brain Res.* **740,** 109–116.

Marshall, J. (1951). Sensory disturbances in cortical wounds with special refernce to pain. *J. Neurol. Neurosurg. Psychiatry* **14,** 187–204.

Martin, R.F., Jordan, L.M., and Willis, W.D. (1978). Differential projections of cat medullary raphe neurons demonstrated by retrograde labeling following spinal cord lesions. *J. Comp. Neurol.* **182,** 77–88.

Mayer, D.J., and Price, D.D. (1976). Central nervous system mechanisms of analgesia. *Pain* **2,** 379–404.

Mayer, D.J., Price, D.D., and Becker, D.P. (1975). Neurophysiological characterization of the anterolateral spinal cord neurons contributing to pain perception in man. *Pain* **1,** 51–58.

McMahon, S.B., Armanini, M.P., Ling, L.H., and Phillips, H.S. (1994). Expression and coexpression of Trk receptors in subpopulations of adult primary sensory neurons projecting to identified peripheral targets. *Neuron* **12,** 1161–1171.

Mehler, W.R. (1962). The anatomy of the so-called "pain tract" in man: an analysis of the course and distribution of the ascending fibers of the fasciculus anterolateralis. *In* "Basic Research in Paraplegia" (J.D. French and R.W. Porter, eds.),pp. 26–55. Charles C Thomas, Springfield, IL.

Mehler, W.R., Feferman, M.E., and Nauta, W.J.H. (1960). Ascending axon degeneration following anterolateral cordotomy. An experimental study in the monkey. *Brain* **83,** 718–751.

Melzack, R., and Casey, K.L. (1968). Sensory, motivational, and central control determinants of pain. A new conceptual model. *In* "The Skin Senses" (D.R. Kenshalo, ed.), pp. 423–439. Charles C Thomas, Springfield, IL.

Melzack, R., and Wall, P.D(1965). Pain mechanisms: a new theory. *Science* **150,** 971–979.

Mendell, L. (1966). Physiological properties of unmyelinated fiber projection to the spinal cord. *Exp. Neurol.* **16,** 316–332.

Mense, S. (1993). Nociception from skeletal muscle in relation to clinical muscle pain. *Pain* **54,** 241–289.

Mense, S. (1996). Nociceptors in skeletal muscle and their reaction to pathological tissue changes. *In* "Neurobiology of Nociceptors" (C. Belmonte and F. Cervero, eds.), pp. 184–201. Oxford Univ. Press, Oxford.

Messlinger, K. (1996). Functional morphology of nocicpetive and other fine sensory endings (free nerve endings) in different tissues. *In* "The Polymodal Receptor: A Gateway to Pathological Pain." Progress in Brain Research, Vol. 113 (T. Kumazawa, L. Kruger, and K. Mizumura, eds.), pp. 273–298. Elsevier, Amsterdam.

Meyer, R.A., and Campbell, J.N. (1981). Myelinated nociceptive afferents account for the hyperalgesia that follows a burn to the hand. *Science* **213,** 1527–1529.

Meyer, R.A., Davis, K.D., Cohen, R.H., Treede, R.D., and Campbell, J.N. (1991). Mechanically insensitive afferents (MIAs) in cutaneous nerves of monkey. *Brain Res.* **561,** 252–261.

Mezey, E., Toth, Z.E., Cortright, D.N., Arzubi,. M.K., Krause, J.E., Elde, R., Guo, A., Blumberg, P.M., and Szallasi, A. (2000). Distribution of mRNA for vanilloid receptor subtype 1 (VR1), and VR1-like immunoreactivity, in the central nervous system of the rat and human. *Proc. Natl. Acad. Sci. U.S.A.* **97,** 3655–3660.

Millan, M.J. (1997). The role of descending noradronergic and serotonergic pathways in the modulation of nociception: focus on receptor multiplicity. *In* "The Pharmacology of Pain. Handbook of Experimental Pharmacology," Vol. 130, (A. Dickenson and J.M. Besson, eds.), pp. 385–446. Springer-Verlag, Berlin.

Millan, M.J. (1999). The induction of pain: an integrative review. *In* "Progress in Neurobiology," Vol 57, pp. 1–164. Elsevier, Amsterdam.

Milne, R.J., Foreman, R.D., Giesler, G.J., and Willis, W.D. (1981). Convergence of cutaneous and pelvic visceral nociceptive inputs onto primate spinothalamic neurons. *Pain* **11,** 163–183.

Mizumura, K. and Kumazawa, (1996). T. Modulations of nociceptor responses by inflammatory mediators and second messengers implicated in their action—a study in canine testicular polymodal receptors. *In* "The Polymodal Receptor: A Gateway to Pathological Pain" (T. Kumazawa, L. Kruger, and K. Mizumura, eds.), pp. 115–141. Elsevier, Amsterdam.

Molliver, D.C., Wright, D.E., Leitner, M.L., Parsadanian, A.S., Doster, K., Wen, D., Yan, Q., and Snider, W.D. (1997). IB4-binding DRG neurons switch from NGF to GDNF dependence in early postnatal life. *Neuron* **19,** 849–861.

Morrow, T.J., and Casey, K.L. (1992). State-related modulation of thalamic somatosensory responses in the awake monkey. *J. Neurophysiol.* **67,** 305–317.

Mullan, S. (1966). Percuaneous cordotomy for pain. Surg. Clin. *N. Am.* **46,** 3–12.

Mullan, S., Harper, P.V., Hekmatpanah, J., Torres, H., and Dobbin, G. (1963). Percutaneous interruption of spinal-pain tracts by means of a strontium needle. *J. Neurosurg.* **20,** 931–939.

Murase, K., Ryu, P.D., and Randic, M. (1989). Excitatory and inhibitory amino acids and peptide-induced responses in acutely isolated rat spinal dorsal horn neurons. *Neurosci. Lett.* **103,** 56–63.

Nahin, R.L. (1988). Immunocytochemical identification of long ascending, peptidergic lumbar spinal neurons terminating in either the medial or lateral thalamus in the rat. *Brain Res.* **443,** 345–349.

Nashold, B.S. (1984). Current status of the DREZ operation: 1984. *Neurosurgery* **15,** 942–944.

Nashold, B.S., and Ostdahl, R.H. (1979). Dorsal root entry zone lesions for pain relief. *J. Neurosurg.* **51,** 59–69.

Nashold, B.S., Wilson, W.P., and Slaughter, D.G. (1969). Sensations evoked by stimulation in the midbrain of man. *J. Neurosurg.* **30,** 14–24.

Nathan, P.W., Smith, M.C., and Cook, A.W. (1986). Sensory effects in man of lesions of the posterior columns and of some other afferent pathways. *Brain* **109,** 1003–1041.

Nauta, H.J.W., Hewitt, E., Westlund, K.N., and Willis, W.D. (1997). Surgical interruption of a midline dorsal column visceral pain pathway: case report and review of the literature. *J. Neurosurg.* **86,** 538–542.

Nauta, H.J.W., Soukup, V.M., Fabian, R.H., Lin, J.T., Grady, J.J., Williams, C.G.A., Campbell, G.A., Westlund, K.N., and Willis, W.D. (2000). Punctate midline myelotomy for the relief of visceral cancer pain. *J. Neurosurg.* (Spine) **92,** 125–130.

Nishiyama, K., Kwak, S., Murayama, S., and Kanazawa, I. (1995). Substance P is a possible neurotransmitter in the rat spinothalamic tract. *Neurosci. Res.* **21,** 261–266.

Noordenbos, W., and Wall, P.D. (1976). Diverse sensory functions with an almost totally divided spinal cord. A case of spinal cord transection with preservation of part of one anterolateral quadrant. *Pain* **2,** 185–195.

Ochoa, J., and Torebjörk, E. (1989). Sensations evoked by intraneural microstimulation of C nociceptor fibres in human skin nerves. *J. Physiol.* **415,** 583–599.

Oliveras, J.L., Besson, J.M., Guilbaud, G., and Liebeskind, J.C. (1974a). Behavioral and electrophysiological evidence of pain inhibition from midbrain stimulation in the cat. *Exp. Brain Res.* **20,** 32–44.

Oliveras, J.L., Woda, A., Guilbaud, G., and Besson, J.M. (1974b). Inhibition of the jaw opening reflex by electrical stimulation of the periaqueductal gray matter in the awake, unrestrained cat. *Brain Res.* **72,** 328–331.

Oliveras, J.L., Redjemi, F., Guilbaud, G., and Besson, J.M. (1975). Analgesia induced by electrical stimulation of the inferior centralis nucleus of the raphe in the cat. *Pain* **1,** 139–145.

Oliveras, J.L., Guilbaud, G., and Besson, J.M. (1979). A map of serotoninergic structures involved in stimulation producing analgesia in unrestrained freely moving cats. *Brain Res.* **164,** 317–322.

Ossipov, M.H., Malan, T.P., Lai, J., and Porreca, F. (1997). Opioid pharmacology of acute and chronic pain. *In* "The Pharmacology of Pain. Handbook of Experimental Pharmacology," Vol. 130 (A.D. Dickenson and J.M. Besson, J.M. (eds.), pp. 305–334. Springer-Verlag, Berlin.

Owens, C.M., Zhang, D., and Willis, W.D. (1992). Changes in the response states of primate spinothalamic tract cells caused by mechanical damage of the skin or activation of descending controls. *J. Neurophysiol.* **67,** 1509–1527.

Palecek, J., Paleckova, V., and Willis, W.D. (2002). The role of pathways in the spinal cord lateral and dorsal funiculi in signaling nociceptive somatic and visceral stimuli in rats. *Pain* **96,** 297–307.

Papo, I., and Luongo, A. (1976). High cervical commissural myelotomy in the treatment of pain. J. Neurol. *Neurosurg. Psychiatry* **39,** 705–710.

Patterson, J.T., Head, P.A., McNeill, D.L., Chung, K., and Coggeshall, R.E. (1989). Ascending unmyelinated primary afferent fibers in the dorsal funiculus. *J. Comp. Neurol.* **290,** 384–390.

Patterson, J.T., Coggeshall, R.E., Lee, W.T., and Chung, K. (1990). Long ascending unmyelinated primary afferent axons in the rat dorsal column: immunohistochemical localizations. *Neurosci. Lett.* **108,** 6–10.

Peele, T.L. (1944). Acute and chronic parietal lobe ablations in monkeys. *J. Neurophysiol.* **7,** 269-286.

Penfield, W., and Boldrey, W. (1937). Somatic motor and sensory representation in the cerebral cortex of man as studied by electrical stimulation. *Brain* **60,** 389–443.

Peng, Y.B., Lin, Q., and Willis, W.D. (1996a). The role of 5-HT_3 receptors in periaqueductal gray-induced inhibition of nociceptive dorsal horn neurons in rats. *J. PET* **276,** 116–124.

Peng, Y.B., Lin, Q., and Willis, W.D. (1996b). Involvement of α_2-adrenoreceptors in the periaqueductal gray-induced inhibition of dorsal horn cell activity in rats. *J. PET* **278,** 125–135.

Perl, E.R. (1968). Myelinated afferent fibres innervating the primate skin and their response to noxious stimuli. *J. Physiol.* **197,** 593–615.

Perl, E.R. (1984). Characterization of nociceptors and their activation of neurons in the superficial dorsal horn: first steps for the sensation of pain. *In* "Advances in Pain Research and Therapy," Vol. 6 (L. Kruger and J. C. Liebekind, eds.), pp. 23551. Raven Press, New York.

Perl, E.R., and Whitlock, D.G. (1961). Somatic stimuli exciting spinothalamic projections to thalamic neurons in cat and money. *Exp. Neurol.* **3,** 256–296.

Perry, M.J., and Lawson, S.N. (1998). Differences in expression of oligosaccharides, neuropeptides, carbonic anhydrase and neurofilament in rat primary afferent neurons retrogradely labeled via skin, muscle or visceral nerves. *Neuroscience* **85,** 293–310.

Ploner, M., Freund, H.J., and Schnitzler, A. (1999a). Pain affect without pain sensation in a patient with a postcentral lesion. *Pain* **81,** 211–214.

Ploner, M., Schmitz, F., Freund, H.J., and Schnitzler, A. (1999b). Parallel activation of primary and secondary somatosensory cortices in human pain processing. *J. Neurophysiol.* **81,** 3100–3104.

Ploner, M., Schmitz, F., Freund, H.J., and Schnitzler, A. (2000). Differential organization of touch and pain in human primary somatosensory cortex. *J. Neurophysiol.* **83,** 1770–1776.

Pollin, B., and Albe-Fessard, D. (1979). Organzation of somatic thalamus in monkeys with and without section of dorsal spinal tracts. *Brain Res.* **173,** 431–449.

Price, D.D., and Dubner, R. (1977). Neurons that subserve the sensory-discriminative aspects of pain. *Pain* **3,** 307–338.

Price, D.D., Dubner, R., and Hu, J.W. (1976). Trigeminothalamic neurons in nucleus caudalis responsive to tactile, thermal, and nociceptive stimulation of monkey's face. *J. Neurophysiol.* **39,** 936–953.

Price, D.D., Hayes, R.L., Ruda, M.A., and Dubner, R. (1978). Spatial and temporal transformations of input to spinothalamic tract neurons and their relation to somatic sensations. *J. Neurophysiol.* **41,** 933–947.

Proudfit, H.K., and Anderson, E.G. (1975). Morphine analgesia: blockade by raphe magnus lesions. *Brain Res.* **98,** 612–618.

Putnam, T.J. (1934). Myelotomy of the commissure. *Arch. Neurol. Psychiatry* **32,** 1189–1193.

Rainville, P., Duncan, G.H., Price, D.D., Carrier, B., and Bushnell, M.C. (1997). Pain affect encoded in human anterior cingulate but not somatosensory cortex. *Science* **277,** 968–971.

Ralston, H.J., and Ralston, D.D. (1992). The primate dorsal spinothalamic tract: evidence for a specific termination in the posterior nuclei (Po/SG) of the thalamus. *Pain* **48,** 107–118.

Ralston, H.J., and Ralston, D.D. (1994). Medial lemniscal and spinal projections to the macaque thalamus: an electron microscopic study of differing GABAergic circuitry serving thalamic somatosensory mechanisms. *J. Neurosci.* **14,** 2485–2502.

Ranson, S.W., and Billingsley, P.R. (1916). The conduction of painful afferent impulses in the spinal nerves. *Amer. J. Anat.* **40,** 571–584.

Rasmussen, A.T., and Peyton, W.T. (1948). The course and termination of the medial lemniscus in man. *J. Comp. Neurol.* **88,** 411–424.

Rath, S.A., Seitz, K., Soliman, N., Kahamba, J.F., Antoniadis, G., and Richter H.P. (1997). DREZ coagulations for deafferentation pain related to spinal and peripheral nerve lesions: indication and results of 79 consecutive procedures. *Stereotact. Funct. Neurosurg.* **68,** 161–167.

Rausell, E., Bae, C.S., Vinuela, A., Huntley, G.W., and Jones, E.G. (1992a). Calbindin and parvalbumin cells in monkey VPL thalamic nucleus: distribution, laminar cortical projections, and relations to spinothalamic terminations. *J. Neurosci.* **12,** 4088–4111.

Rausell, E., Cusick, C.G., Taub, E., and Jones, E.G. (1992b). Chronic deafferentation in monkeys differentially affects nociceptive and nonnociceptive pathways distinguished by specific calcium-binding proteins and down-regulates γ-aminobutyric acid type A receptors at thalamic levels. *Proc. Natl. Acad. Sci. U.S.A.* **89,** 2571–2575.

Rawlings, C.E., El-Naggar, A.P., and Nashold, B.S. (1989). The DREZ procedure: an update on technique. *Br. J. Neurosurg.* **3,** 633–642.

Rees, H., and Roberts, M.H.T. (1989a). Activation of cells in the anterior pretectal nucleus by dorsal column stimulation in the rat. *J. Physiol.* **417,** 361–373.

Rees, H., and Roberts, M.H.T. (1989b). Antinociceptive effects of dorsal column stimulation in the rat: involvement of the anterior pretectal nucleus. *J. Physiol.* **417,** 375–388.

Rees, H., and Roberts, M.H.T. (1993). The anterior pretectal nucleus: a proposed role in sensory processing. *Pain* **53,** 121–135.

Rees, H., Sluka, K.A., Westlund, K.N., and Willis, W.D. (1994). Do dorsal root reflexes augment peripheral inflammation? *Neuroreport* **5,** 821–824.

Rees, H., Sluka, K.A., Westlund, K.N., and Willis, W.D. (1995).The role of glutamate and GABA receptors in the generation of dorsal root reflexes by acute arthritis in the anaesthetized rat. *J. Physiol.* **484,** 437–445.

Rexed, B. (1952). The cytoarchitectonic organization of the spinal cord in the cat. *J. Comp. Neurol.* **96,** 415–466.

Reynolds, D.V. (1969). Surgery in the rat during electrical analgesia induced by focal brain stimulation. *Science* **164,** 444-445.

Richardson, D.E., and Akil, H. (1977a). Pain reduction by electrical brain stimulation in man. I. Acute administration in periaqueductal and periventricular sites. *J. Neurosurg.* **47,** 178–183.

Richardson, D.E., and Akil, H. (1977b). Pain reduction by electrical brain stimulation in man. II. Chronic self-administration in the periventricular gray matter. *J. Neurosurg.* **47,** 184–194.

Rosen, S.D., Paulesu, E., Nihoyannopolulos, P, Tousoulis, D., Frackowiak, P., Frith, C.D., Jones, T., and Camici, P.G. (1996). Silent ischemia as a central problem: regional brain activation compared in silent and painful myocardial ischemia. *Ann. Intern. Med.* **124,** 939–949.

Rosomoff, H.L., Carroll, F., Brown, J., and Sheptak, P. (1965). Percutaneous radiofrequency cervical cordotomy: technique. *J. Neurosurg.* **23,** 639–644.

Rosomoff, H.L., Sheptak, P., and Carroll, F. (1966). Modern pain relief: percutaneous chordotomy. *JAMA* **196,** 108–112.

Rudomin, P., and Schmidt, R.F. (1999). Presynaptic inhibition in the vertebrate spinal cord revisited. *Exp. Brain Res.* **129,** 1–37.

Russell, W.R. (1945). Transient disturbances following gunshot wounds of the head. *Brain* **68,** 79–97.

Satoh, M.P., Oku, and Akaike, A. (1983). Analgesia produced by microinjection of L-glutamate into the rostral ventromedial bulbar nuclei of the rat and its inhibition by intrathecal alpha adrenergic blocking agents. *Brain Res.* **261,** 361–364.

Schady, W.J.L., Torebjörk, H.E., and Ochoa, J.L. (1983). Peripheral projections of nerve fibres in the human median nerve. *Brain Res.* **277,** 249–261.

Schaible, H.G., and Grubb, B.D. (1993). Afferent and spinal mechanisms of joint pain. *Pain* **55,** 5–54.

Schaible, H.G., and Schmidt, R.F. (1996). Neurobiology of articular nociceptors. *In* "Neurobiology of Nociceptors" (C. Belmonte and F. Cervero, eds.), pp. 202–219. Oxford University Press, Oxford.

Schmelz, M., Schmidt, R., Ringkamp, M., Handwerker, H.O., and Torebjörk, H.E. (1994). Sensitization of insensitive branches of C nociceptors in human skin. *J. Physiol.* **480,** 389–394.

Schmidt, R., Schmelz, M., Forster, C., Ringkamp, M., Torebjörk, E., and Handwerker, H. (1995). Novel classes of responsive and unresponsive C nociceptors in human skin. *J. Neurosci.* **15,** 333–341.

Schvarcz, J.R. (1978). Spinal cord stereotactic techniques re trigeminal nucleotomy and extralemniscal myelotomy. *Appl. Neurophysiol.* **41,** 99–112.

Schvarcz, J.R. (1976). Stereotactic extralemniscal myelotomy. *J. Neurol. Neurosurg. Psychiatry* **39,** 53–57.

Schvarcz, J.R. (1984). Stereotactic high cervical extralemniscal myelotomy for pelvic cancer pain. *Acta Neurochir. Suppl.* **33,** 431–435.

Segal, M., and Sandberg, D. (1977). Analgesia produced by electrical stimulation of catecholamine nuclei in the rat brain. *Brain Res.* **123,** 369–372.

Shealy, C.N., Mortimer, J.T., and Hagfors, N.R. (1970). Dorsal column electroanalgesia. *J. Neurosurg.* **32,** 560–564.

Sherrington, C.S. (1981). *"The Integrative Action of the Nervous System."* Yale University Press, New Haven, 1906; 2nd ed. 1947; Yale paperbound ed., 1981.

Silverman, D.H.S., Munakata, J.A., Ennes, H., Mandelkern, M.A., Hoh, C.K., and Mayer, E.A. (1997). Regional cerebral activity in normal and pathological perception of visceral pain. *Gastroenterology* **112,** 64–72.

Simone, D.A., Marchettini, P., Caputi, G., and Ochoa, J.L. (1994). Identification of muscle afferents subserving sensation of deep pain in humans. *J. Neurophysiol.* **72,** 883–889.

Sindou, M., Quoex, C., and Baleydier, C. (1974). Fiber organization at the posterior spinal cord-rootlet junction in man. *J. Comp. Neurol.* **153,** 15–26.

Sindou, M., Mifsud, J.J., Rosaiti, C., and Boisson, D. (1987). Microsurgical selective posterior rhizotomy in the dorsal root entry zone for treatment of limb spasticity. *Acta Neurochir.* **39,** 99–102.

Singh, J.P., Chandy, M.J., Joseph, T., and Chandi, S.M. (1989). Histopathological appraisal of carbon-dioxide laser dorsal root entry zone (DREZ) lesions in primates. *Br. J. Neurosurg.* **3,** 373–380.

Sluka, K.A., Willis, W.D., and Westlund, K.N. (1993). Joint inflammation and hyperalgesia are reduced by spinal bicuculline. *Neuroreport* **5,** 109–112.

Sluka, K.A., Willis, W.D., and Westlund, K.N. (1994). Central control of peripheral joint inflammation and heat hyperalgesia. *In* "Progress in Pain Research and Management," Proceedings of the7th World Congress on Pain (G.F. Gebhart, D.L. Hammond, and T. S. Jensen, eds.), pp. 359–371. IASP Press, Seattle.

Sluka K.A., Willis, W.D., and Westlund, K.N. (1995). The role of dorsal root reflexes in neurogenic inflammation. Pain *Forum* **4,** 141–149.

Smith, M.C. (1976). Retrograde cell changes in human spinal cord after anterolateral cordotomies. Location and identification after different periods of survival. *Adv. Pain Res. Ther.* **1,** 91–98.

Sorkin, L.S., McAdoo, D.J., and Willis, W.D. (1990). Release of serotonin following brainstem stimulation: correlation with inhibition of nociceptive dorsal horn neurons. *Serotonin and Pain, Excerpta Medica,* pp. 105–115 J.M. Besson (ed.). Elsevier, Amsterdam.

Sorkin, L.S., McAdoo, D.J., and Willis, W.D. (1992). Stimulation in the ventral posterior lateral nucleus of the primate thalamus leads to release of serotonin in the lumbar spinal cord. *Brain Res.* **581,** 307–310.

Sorkin, L.S., McAdoo, D.J., and Willis, W.D. (1993). Raphe magnus stimulation-induced antinociception in the cat is associated with release of amino acids as well as serotonin in the lumbar dorsal horn. *Brain Res.* **618,** 95–108.

Sourek, K. (1969). Commissural myelotomy. *J. Neurosurg.* **31,** 524–527.

Spiller, W.G. (1905). The occasional clinical resemblance between caries of the vertebrae and lumbothoracic syringomyelia, and the location within the spinal cord of the fibres for the sensations of pain and temperature. *Univ. Penn. Med. Bull.* **18,** 147–154.

Spiller, W.G., and Martin, E. (1912). The treatment of persistent pain of organic origin in the lower part of the body by division of the anterolateral column of the spinal cord. *J.A.M.A.* **58,** 1489–1490.

Stacey, M.J. (1969). Free nerve endings in skeletal muscle of the cat. *J. Anat.* **105,** 231–254.

Stevens, R.T., Apkarian, A.V., and Hodge, C.J. (1991). The location of spinothalamic axons within spinal cord white matter in cat and squirrel monkey. *Somatosens. Motor Res.* **8,** 97–102.

Stevens, R.T., London, S.M., and Apkarian, A.V. (1993). Spinothalamocortical projections to the secondary somatosensory cortex (SII) in squirrel monkey. *Brain Res.* **631,** 241–246.

Sugiura, Y., Lee, C.L., and Perl, E.R. (1986). Central projections of identified, unmyelinated (C) afferent fibers innervating mammalian skin. *Science* **234,** 358–361.

Sugiura, Y., Terui, N., and Hosoya, Y. (1989). Difference in distribution of central terminals between visceral and somatic unmyelinated (C) primary afferent fibers. *J. Neurophysiol.* **62,** 834–840.

Surmeier, D.J., Honda, C.N., and Willis, W.D. (1988). Natural groupings of primate spinothalamic neurons based upon cutaneous stimulation. Physiological and anatomical features. *J. Neurophysiol.* **59,** 833–860.

Talbot, J.D., Duncan, G.H., Bushnell, M.C., and Boyer, M. (1987). Diffuse noxious in inhibitory controls (DNICs): psychophysical evidence in man for intersegmental suppression of noxious heat perception by cold pressor pain. *Pain* **30,** 221–232.

Talbot, J.D., Marrett, S., Evans, A.C., Meyer, E., Bushnell, M.C., and Duncan, G.H. (1991). Multiple representations of pain in human cerebral cortex. *Science* **251,** 1355–1358.

Tamatani, M., Senba, E., and Tohyama, M. (1989). Calcitonin gene-related peptide- and substance P-containing primary afferent fibers in the dorsal column of the rat. *Brain Res.* **495,** 122–130.

Thalhamer, J.G., and LaMotte, R.H. (1982). Spatial properties of nociceptor sensitization following heat injury of the skin. *Brain Res.* **231,** 257–265.

Tillman, D.B., Treede, R.D., Meyer, R.A., and Campbell, J.N. (1995). Response of C fibre nociceptors in the anaesthetized monkey to heat stimuli: estimates of receptor depth and threshold. *J. Physiol.* **485,** 753–765.

Tominaga, M., Caterina, M.J., Malmberg, A.B., Rosen, T.A., Gilbert, H., Skinner, K., Raumann, B.E., Basbaum, A.I., and Julius, D. (1998). The cloned capsaicin receptor integrates multiple pain-producing stimuli. *Neuron* **21,** 531–543.

Torebjörk, H.E. (1974). Afferent C units responding to mechanical, thermal and chemical stimuli in human non-glabrous skin. *Acta Physiol. Scand.* **92,** 374–390.

Torebjörk, H.E., and Hallin, R.G. (1974). Identification of afferent C units in intact human skin nerves. *Brain Res.* **67,** 387–403.

Torebjörk, H.E., and Hallin, R.G. (1973). Perceptual changes accompanying controlled preferential blocking of A and C fibre responses in intact human skin nerves. *Exp. Brain Res.* **16,** 321–332.

Torebjörk, H.E., and Ochoa, J.L. (1990). New method to identify nociceptor units innervating glabrous skin of the human hand. *Exp. Brain Res.* **81,** 509–514.

Torebjörk, H.E., Ochoa, J.L., and Schady, W. (1984). Referred pain from intraneural stimulation of muscle fascicles in the median nerve. *Pain* **18,** 145–156.

Tracey, I., Becerra, L., Chang, I., Breiter, H., Jenkins, L., Borsook, D., and Gonzales, R.G. (2000). Noxious hot and cold stimulation produce common patterns of brain activation in humans: a functional magnetic resonance imaging study. *Neurosci. Lett.* **288,** 159–162.

Treede, R.D., Meyer, R.A., and Campbell, J.N. (1990). Comparison of heat and mechanical receptive fields of cutaneous C-fiber nociceptors in monkey. *J. Neurophysiol.* **64,** 1502–1513.

Treede, R.D., Meyer, R.A., Raja, S.N., and Campbell, J.N. (1995). Evidence for two different heat transduction mechanisms in

nociceptive primary afferents innervating monkey skin. *J. Physiol.* **483,** 747–758.

Treede, R.D., Meyer, R.A., and Campbell, J.N. (1998). Myelinated mechanically insensitive afferents from monkey hairy skin: heat-response properties. *J. Neurophysiol.* **80,** 1082–1093.

Treede, R.D., Kenshalo, D.R., Gracely, R.H., and Jones, A.K.P. (1999). The cortical representation of pain. *Pain* **79,** 105–111.

Treede, R.D., Apkarian, A.V., Bromm, B., Greenspan, J.D., and Lenz, F.A. (2000). Cortical representation of pain: functional characterization of nociceptive areas near the lateral sulcus. *Pain* **87,** 1134–119.

Trevino, D.L. (1976). The origin and projections of a spinal noicepetive and thermoreceptive pathway. *In* "Sensory Functions of the Skin in Primates, with Special Reference to Man" (Y. Zotterman, ed.), pp. 367–376. Pergamon Press, New York.

Trevino, D.L., and Carstens, E. (1975). Confirmation of the location of spinothalamic neurons in the cat and monkey by the retrograde transport of horseradish peroxidase. *Brain Res.* **98,** 177–182.

Truex, R.C., Taylor, M.J., Smythe, M.Q., and Gildenberg, P.L. (1965). The lateral cervical nucleus of cat, dog, and man. *J. Comp. Neurol.* **139,** 93–104.

Tsubokawa, T., Katayama, Y., Yamamoto, T., and Hirayama, T. (1985). Deafferentation pain and stimulation of the thalamic sensory relay nucleus: clinical and experimental study. *Appl. Neurophysiol.* **48,** 166–171.

Uddenberg, N. (1968). Functional organization of long, second-order afferents in the dorsal funiculus. *Exp. Brain Res.* **4,** 377–382.

Urban, M.O., Jiang, M.C, and Gebhart, G.F. (1996). Participation of central descending nociceptive facilitatory systems in secondary hyperalgesia produced by mustard oil. *Brain Res.* **37,** 83–91.

Van Hees, J., and Gybels, J. (1972). Pain related to single afferent *C* fibers from human skin. **48,** 397–400.

Van Hees, J., and Gybels, J. (1981). C nociceptor activity in human nerve during painful and non painful skin stimulation. *J. Neurol. Neurosurg. Psychiatry* **44,** 600–607.

Vierck, C.J., and Luck, M.M. (1979). Loss and recovery of reactivity to noxious stimuli in monkeys with primary spinothalamic cordotomies, followed by secondary and tertiary lesions of other cord sectors. *Brain* **102,** 233–248.

Vierck, C.J., Hamilton, D.M., and Thornby, J.I. (1971). Pain reactivity of monkeys after lesions to the dorsal and lateral columns of the spinal cord. *Exp. Brain Res.* **13,** 140–158.

Vierck, C.J., Greenspan, J.D., and Ritz, L.A. (1990). Long-term changes in purposive and reflexive responses to nociceptive stimulation following anterolateral chordotomy. *J. Neurosci.* **10,** 2077–2095.

Villanueva, L., and Le Bars, D. (1995). The activation of bulbo-spinal controls by peripheral nociceptive inputs: diffuse noxious inhibitory controls. *Biol. Res.* **28,** 113–125.

Villanueva, L., Cliffer, K.D., Sorkin, L.S., Le Bars, D., and Willis, W.D. (1990). Convergence of heterotopic nociceptive information onto neurons of the caudal medullary reticular formation in monkey (Macaca fascicularis). *J. Neurophysiol.* **63,** 1118–1127.

Vogt, B.A., Sikes, R.W., and Vogt, L.J. (1993). Anterior cingulate cortex and the medial pain system. *In* "Neurobiology of Cingulate Gyrus and Limbic Thalamus: a Comprehensive Handbook" (B.A. Vogt and M. Gabriel. eds.), pp. 313–344. Birkhäuser, Boston.

Von Knorring, L. (1989). Serotonin metabolites in the CSF of chronic pain patients. *In* "Serotonin and Pain" (J.M. Besson, ed.), pp. 85–303. Elsevier, Amsterdam.

Walker, A.E. (1940). The spinothalamic tract in man. *Arch. Neurol. Psychiatry* **43,** 284–298.

Walker, A.E. (1942a). Relief of pain by mesencephalic tractotomy. *Arch. Neurol. Psychiatry* **48,** 865–880.

Walker, A.E. (1942b). Somatotopic localization of spinothalamic and secondary trigeminal tracts in mesencephalon. *Arch. Neurol. Psychiatry* **48,** 884–889.

Wall, P.D., and Noordenbos, W. (1977). Sensory functions which remain in man after complete transection of dorsal columns. *Brain* **100,** 641–653.

Wall, P.D., and Sweet, W.H. (1967). Temporary abolition of pain in man. *Science* **155,** 108–109.

Wang, C.C., Willis, W.D., and Westlund, K.N. (1999). Ascending projections from the central, visceral processing region of the spinal cord: a PHA-L study in rats. *J. Comp. Neurol.* **415,** 341–367.

Wang, H., Rivero-Melián, C., Robertson, B., and Grant, G. (1994). Transganglionic transport and binding of the isolectin B4 from Griffonia simplicifolia I in rat primary sensory neurons. *Neuroscience* **62,** 539–551.

Weaver, T.A., and Walker, A.E. (1941). Topical arrangement within the spinothalamic tract of the monkey. *Arch. Neurol. Psychiatry* **46,** 877–883.

Wei, F., Dubner, R., and Ren, K. (1999). Nucleus reticularis gigantocellularis and nucleus raphe magnus in the brain stem exert opposite effects on behavioral hyperalgesia and spinal Fos protein expression after peripheral inflammation *Pain* **80,** 127–141.

Weidner, C., Schmelz, M., Schmdt, R., Hansson, B., Handwerker, H.O., and Torebjörk, H.E. (1999). Functional attributes discriminating mechano-insensitive and mechano-responsive C nociceptors in human skin. *J. Neurosci.* **19,** 10184–10190.

Weil-Fugazza, J. (1989). Control of metabolism and release of serotonin in pain and analgesia. *In* "Serotonin and Pain" (J.M. Besson, ed.), pp. 221–238. Elsevier, Amsterdam.

Wertheimer, P., and Lecuire, J. (1953). La myélotomie commissurale postérieure. A propos de 107 observations. *Acta Chir. Belgica* **52,** 568–574.

Westlund, K.N., and Coulter, J.D. (1980). Descending projection of the locus coeruleus and subcoeruleus/medial parabrachial nuclei in monkey; axonal transport studies and dopamine-β-hydroxylase immunocytochemistry. *Brain Res. Rev.* **2,** 235–264.

Westlund, K.N., and Craig, A.D. (1996). Association of spinal lamina I projections with brainstem catecholamine neurons in the monkey. *Exp. Brain Res.* **110,** 151–162.

Westlund, K.N., Bowker, R.M., Ziegler, M.G., and Coulter, J.D. (1983). Noradrenergic projections to the spinal cord of the rat. *Brain Res.* **263,** 15-31.

Westlund, K.N., McNeill, D.L., and Coggeshall, R.E. (1989). Glutamate immunoreactivity in rat dorsal root axons. *Neurosci. Lett.* **96,** 13–17.

Westlund, K.N., Carlton, S.M., Zhang, D., and Willis, W.D. (1990). Direct catecholaminergic innervation of primate spinothalamic tract neurons. *J. Comp. Neurol.* **299,** 178–186.

Westlund, K.N., Carlton, S.M., Zhang, D., and Willis, W.D. (1992a). Glutamate-immunoreactive terminals synapse on primate spinothalamic tract cells. *J. Comp. Neurol.* **322,** 519–527.

Westlund, K.N., Sun, Y.C., Sluka, K.A., Dougherty, P.M., Sorkin, L.S., and Willis, W.D. (1992b). Neural changes in acute arthritis in monkeys. II. Increased glutamate immunoreactivity in the medial articular nerve. *Brain Res. Rev.* **17,** 15–27.

White, J.C. (1941). Spinothalamic tractotomy in the medulla oblongata. *Arch. Surg.* **43,** 113–127.

White, J.C. (1963). Anterolateral cordotomy—its effectiveness in relieving pain of non-malignant disease. *Neurochirurgia* **6,** 83–102.

White, J.C., Sweet, W.H., Hawkins, R., and Nilges, R.G. (1950). Anterolateral cordotomy: results, complications and causes of failure. *Brain* **73,** 346–367.

White, J.C., Richardson, E.P., and Sweet, W.H. (1956). Upper thoracic cordotomy for relief of pain. Postmortem correlation of spinal incision with analgesic levels in 18 cases. *Ann. Surg.* **144,** 407–420.

Wiberg, M., and Blomqvist, A. (1984). The spinomesencephalic tract in the cat: its cells of origin and termination pattern as demonstrated by the intraaxonal transport method. *Brain Res.* **291,** 1–18.

Wiberg, M., Westman, J., and Blomqvist, A. (1987). Somatosensory projection to the mesencephalon: an anatomical study in the monkey. *J. Comp. Neurol.* **264,** 92–117.

Willcockson, W.S., Chung, J.M., Hori, Y., Lee, K.H., and Willis, W.D. (1984). Effects of iontophoretically released amino acids and amines on primate spinothalamic tract cells. *J. Neurosci.* **4,** 732–740.

Willer, J.C., De Broucker, T., and Le Bars, D. (1989). Encoding of nociceptive thermal stimuli by diffuse noxious inhibitory controls in humans. *J. Neurophysiol.* **62,** 1028–1038.

Willis, W.D. (1982). Control of nociceptive transmission in the spinal cord. *In* "Progress in Sensory Physiology," Vol.3 (D. Ottoson, ed.-in-chief). Springer-Verlag, Berlin.

Willis, W.D. (1985). "The Pain System. The Neural Basis of Nociceptive Transmission in the Mammalian Nervous System." Pain and Headache, Vol. 8 (P.L. Gildenberg, ed.). Karger, Basel.

Willis, W.D. (1997). Nociceptive functions of thalamic neurons. *In* "Thalamus, Vol. 2, Experimental and Clinical Aspects" (M. Steriade, E.G. Jones, and D.A. McCormick, eds.), pp. 373–424. Elsevier, Amsterdam.

Willis, W.D. (1999). Dorsal root potentials and dorsal root reflexes: a double-edged sword. *Exp. Brain Res.* **124,** 395–421.

Willis, W.D., and Coggeshall, R.E. (2003). "Sensory Mechanisms of the Spinal Cord," 3rd ed. Kluwer, New York.

Willis, W.D., and Westlund, K.N. (1997). Neuroanatomy of the pain system and of the pathways that modulate pain. *J. Clin. Neurophysiol.* **14,** 2–31.

Willis, W.D., and Westlund, K.N. (in press). The role of the dorsal column pathway in visceral nociception. Curr. Pain Headache Rep.

Willis, W.D., Trevino, D.L., Coulter, J.D., and Maunz, R.A. (1974). Responses of primate spinothalamic tract neurons to natural stimulation of hindlimb. *J. Neurophysiol.* **37,** 358–372.

Willis, W.D., Haber, L.H., and Martin, R.F. (1977). Inhibition of spinothalamic tract cells and interneurons by brain stem stimulation in the monkey. *J. Neurophysiol.* **40,** 968–981.

Willis, W.D., Kenshalo, D.R., and Leonard, R.B. (1979). The cells of origin of the primate spinothalamic tract. *J. Comp. Neurol.* **188,** 543–574.

Willis, W.D., Gerhart, K.D., Willcockson, W.S., Yezierski, R.P., Wilcox, T.K., and Cargill, C.L. (1984). Primate raphe-and reticulospinal neurons: effects of stimulation in periaqueductal gray or VPLc thalamic nucleus. *J. Neurophysiol.* **51,** 467–480.

Willis, W.D., Westlund, K.N., and Carlton, S.M. Pain. (1995). *In* "The Rat Nervous System," 2nd ed. (G. Paxinos, ed.), pp. 725–750. Academic Press, New York.

Willis, W.D., Al-Chaer, E.D., Quast, M.J., and Westlund, K.D. (1999). A visceral pain pathway in the dorsal column of the spinal cord. *Proc. Natl. Acad. Sci. U.S.A.* **96,** 7675–7679.

Willis, W.D., Zhang, X., Honda, C.N., and Giesler, G.J. (2001). Projections from the marginal zone and deep dorsal horn to the ventrobasal nuclei of the primate thalamus. *Pain* **92,** 267–276.

Willis, W.D., Zhang, X., Honda, C.N., and Giesler, G.J. (2002). A critical review of the role of the proposed VMpo nucleus in pain. *J. Pain* **3,** 79–94.

Wolfe, F., Russell, I.J., Vipraio, G., Ross, K., and Anderson, J. (1997). Serotonin levels, pain threshold, and fibromyalgia symptoms in the general population. *J. Rheumatol* **24,** 555.

Wycis, H.T., and Spiegel, E.A. (1962). Long-range results in the treatment of intractable pain by stereotaxic midbrain surgery. *J. Neurosurg.* **19,** 101–107.

Yaksh, T.L. (1979). Direct evidence that spinal serotonin and noradrenaline terminals mediate the spinal antinociceptive effects of morphine in the periaqueductal gray. *Brain Res.* **160,** 180–185.

Yaksh, T.L., and Rudy, T.A. (1978). Narcotic analgetics: CNS sites and mechanisms of action as revealed by intracerebral injection techniques. *Pain* **4,** 299–359.

Yarnitsky, D., Simone, D.A., Dotson, R.M., Cline, M.A., and Ochoa, J.L. (1992). Single C nociceptor responses and psychophysical parameters of evoked pain: effect of rate of rise of heat stimuli in humans. *J. Physiol.* **450,** 581–592.

Ye, Z., Wimalawansa, S.J., and Westlund, K.N. (1999). Receptor for calcitonin gene–related peptide: localization in the dorsal and ventral spinal cord. *Neuroscience* **92,** 1389–1397.

Yezierski, R.P. (1988). Spinomesencephalic tract: projections from the lumbosacral spinal cord of the rat, cat, and monkey. *J. Comp. Neurol.* **267,** 131–146.

Yezierski, R.P., Wilcox, T.K., and Willis, W.D. (1982). The effects of serotonin antagonists on the inhibition of primate spinothalamic tract cells produced by stimulation in nucleus raphe magnus or periaqueductal gray. *J. Pharmacol. Exp. Ther.* **220,** 266–277.

Yezierski, R.P., Sorkin, L.S., and Willis, W.D. (1987). Response properties of spinal neurons projecting to midbrain or midbrain-thalamus in the monkey. *Brain Res.* **437,** 165–170.

Yoss, R.E. (1953). Studies of the spinal cord. Part 3. Pathways for deep pain within the spinal cord and brain. *Neurology* **3,** 163–175.

Zhang, D., Carlton, S.M., Sorkin, L.S., and Willis, W.D. (1990). Collaterals of primate spinothalamic tract neurons to the periaqueductal gray. *J. Comp. Neurol.* **296,** 277–290.

Zhang, E.T., and Craig, A.D. (1997). Morphology and distribution of spinothalamic lamina I neurons in the monkey. *J. Neurosci.* **17,** 3274–3284.

Zhang, X., Kostarczyk, E., and Giesler, G.J. (1995). Spinohypothalamic tract neurons in the cervical enlargement of rats: descending axons in the ipsilateral brain. *J. Neurosci.* **15,** 8393–8407.

Zhang, X., Wenk, H.N., Gokin, A.P., Honda, C.N., and Giesler, G.J. (1999). Physiological studies of spinohypothalamic tract neurons in the lumbar enlargement of monkeys. *J. Neurophysiol.* **82,** 1054–1058.

Zhang, X., Honda, C.N., and Giesler, G.J. (2000a). Position of spinothalamic tract axons in upper cervical spinal cord of monkeys. *J. Neurophysiol.* **84,** 1180–1185.

Zhang, X., Wenk, H.N., Honda, C.N., and Giesler, G.J. (2000b). Locations of spinothalamic tract axons in cervical and thoracic spinal cord white matter in monkeys. *J. Neurophysiol.* **83,** 2869–2880.

Zhou, S., Bonasera, L., and Carlton, S.M. (1996). Peripheral administration of NMDA, AMPA or KA results in pain behaviors in rats. *Neuroreport* **7,** 895–900.

CHAPTER

31

Gustatory System

THOMAS C. PRITCHARD and RALPH NORGREN
Department of Neural and Behavioral Sciences
The Pennsylvania State University College of Medicine
Hershey, Pennsylvania, USA

The first edition of this chapter (Norgren, 1990) began with the following sentence: In humans, information about the central gustatory system is sparse at best, spread out, methodologically flawed, and inconsistent. A decade later, this statement remains substantially true despite the advent of new imaging techniques. Overall, the additional knowledge obtained from the modern imaging techniques has been vitiated by problems similar to those in the earlier literature. Thus, any discussion of the human central gustatory system must rely heavily on data from other primates, especially Old World monkeys (Pritchard, 1991). Even monkey experiments must be interpreted cautiously, however, because they remain relatively few in number and include very few species. Caution also is warranted because the central organization of intraoral sensory systems displays considerable variability across species (Bombardieri *et al.*, 1975; Jones *et al.*, 1986; Karamanlidis and Voogd, 1970).

The following description of the human gustatory system represents our best attempt to integrate the clinical and experimental literature. When the clinical reports contradict the experimental literature, we have weighed the likelihood of a species difference versus the possibility that the disagreement reflects differences in the quality of the data. In some instances, we gave more weight to the more rigorous studies; in other cases, the differences could not be reconciled. We deal primarily with the central organization of the gustatory system and emphasize its cortical organization, where most of the research over the last decade has been done. More detail about the peripheral anatomy of taste is available in the earlier version of this chapter (Norgren, 1990) and in Pritchard (1991). Functional issues such as transduction (Herness and Gilbertson, 1999), coding (Scott and Giza, 2000), and behavior (Kaplan *et al.*, 1995) are covered in recent review articles.

GUSTATORY APPARATUS AND PERIPHERAL INNERVATION

Oral Distribution of Taste Buds

Unlike its central ramifications, the human peripheral gustatory apparatus is both well described and similar to the general mammalian scheme. On the anterior tongue, taste buds occur in fungiform papillae. When present, there are from 1 to 36 taste buds per papilla, but perhaps as many as half the fungiform papillae have none (Arvidson and Freiberg, 1980). The density of taste buds on the anterior tongues

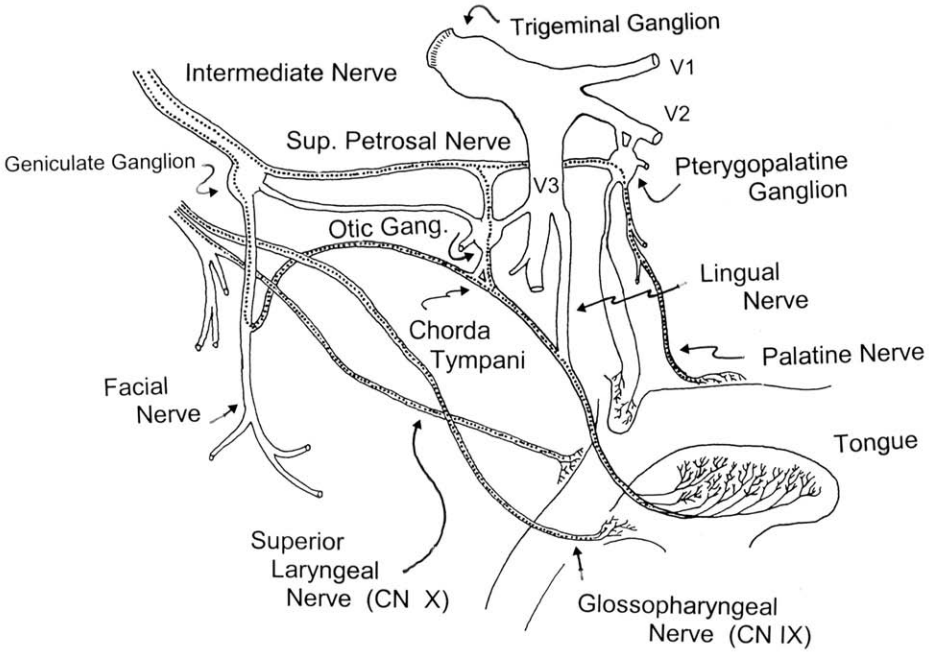

FIGURE 31.1 Diagram of taste pathways (dotted lines) from the anterior and posterior tongue, soft palate, pharynx, epiglottis, and upper esophagus. (Diagram adapted with permission from Oxford University Press.)

of adult cadavers varies by two orders of magnitude, and the differences are not attributable to age or race (see Miller, 1986, 1987). These differences in the number of taste buds per papilla are more than an anatomical curiosity. The number of fungiform papilla correlates positively with taste intensity, the inherited ability to taste bitterness, and the intensity of the "burn" produced by capsaicin, the active ingredient in chili peppers (Prutkin *et al.*, 2000).

As in other mammals, most taste buds are located in the trenches of the foliate papillae along the lateral edge of the tongue and the circumvallate papilla on the posterior third of the human tongue. In one study involving the foliate papillae of 115 cadavers, Mochizuki (1939) counted an average of 1279 taste buds per tongue, but the range varied by a factor of 22. Taste buds also are found on the soft palate, pharynx, epiglottis, and larynx of humans, but their numbers and exact distribution are subject to debate (Lalonde and Eglitis, 1961; Miller, 1977; Miller and Spangler, 1982; Wilson, 1905). Given the recent evidence from the anterior tongue, this debate may reflect methodological differences, age, or normal variation among humans. These extralingual gustatory receptors are histologically identical to those on the tongue, but are clustered in pseudostratified columnar or stratified squamous epithelium rather than in distinct papillae. Although a role in taste perception has not been ruled out (Miyaoka *et al.*, 1998; Stedman *et al.*, 1980), the extralingual taste buds most likely protect the airway from fluid aspiration.

Peripheral Innervation

By the end of the 19th century, the innervation of the lingual gustatory receptors was established to the satisfaction of most observers (Fig. 31.1). The chorda tympani branch of the facial nerve supplies both the taste buds in the fungiform papillae and a variable percentage of those in the foliates. The remaining buds in the foliates and all those in the circumvallate papillae receive axons via the lingual branch of the glossopharyngeal nerve. Although others came close earlier, Lussana (1869, 1872) first proposed this general arrangement based upon both clinical observations and experimental intervention in animals. The only other candidate proposed for conveying gustatory afferent activity was the trigeminal system. This assertion rested primarily upon clinical observations of ipsilateral loss of gustatory sensibility after intracranial section of the trigeminal roots, usually for relief of tic douloureux. Eventually, Lewis and Dandy (1930) demonstrated that, unless there was evidence of facial nerve damage, trigeminal root section alone did not interfere with taste. Based on their own surgical cases, Schwartz and Weddell (1938) suggested that, in a few

individuals, gustatory afferent axons innervating the anterior tongue passed through the greater superficial petrosal (GSP) branch of the facial nerve and the otic ganglion before rejoining the chorda tympani nerve.

Because of the lack of either human clinical or monkey experimental evidence, the innervation of the taste buds on the palate must be generalized from other species and cadaveric material. In rats, about 85% of the taste buds on the palate are innervated by the greater superficial petrosal nerve (Miller and Spangler, 1982). Based upon the pattern of nasopharyngeal innervation in human embryos described by Kanagasuntheram *et al.* (1969), Miller and Spangler (1982) suggested that the remaining buds are innervated by glossopharyngeal fibers traveling with the sympathetic plexus associated with the internal carotid artery. Another possibility for this residual palatal innervation is a tympanic branch of nerve IX that is diverted through the otic ganglion (Hamilton and Norgren, 1984). In humans, there are connections between the auricular branch of the vagus nerve (X), the tympanic branch of IX, and each of the petrosal nerves that could serve the gustatory receptors on the palate (Vidic and Young, 1969).

Based upon the electrophysiological literature and the similarity in laryngeal innervation between humans and other mammals, laryngeal gustatory sensation is carried by the superior laryngeal branch (SLN) of the vagus nerve (see Norgren, 1984, p. 1088, for a short review and Stedman *et al.*, 1980). The innervation of taste buds on adjoining surfaces, such as the epiglottis, uvula, and pharynx, might vary more among species. In addition to the anterior branches of the SLN, in human's gustatory afferent axons to these surfaces, particularly the pharynx, may travel in the tonsilar branch of IX.

The distribution of gustatory function among three cranial nerves confers at least two unusual properties upon the sense of taste. First, taste is difficult to eliminate. Very few individuals are ageusic, particularly permanently. In animals, experimental ageusia has yet to be reported. Second, taste is difficult to separate from intraoral somatosensory activity. In most nerves that contain gustatory afferent axons, the majority of sensory fibers respond to tactile or thermal stimuli. The chorda tympani nerve is the closest to a pure gustatory nerve, but even its taste fibers respond to thermal and perhaps tactile stimuli. In addition, central to the geniculate ganglion, chorda tympani axons join the intermediate nerve of Wrisberg, which has mixed chemical and somatosensory functions. These two properties of the peripheral gustatory apparatus—its resiliency and interdigitation with the somatosensory system—combine to make taste deficits resulting from central damage particularly difficult to evaluate.

THE CENTRAL NERVOUS SYSTEM

Medulla

Although the identities of the first-order gustatory nerves remained unsettled well into the 20th century, what was known in the late 1800s was sufficient to implicate the nucleus of the solitary tract (Sol) in taste function. Subsequent electrophysiological and anatomical studies conducted in a variety of species including the rat (Makous *et al.*, 1963), hamster (Travers and Smith, 1979), and monkey (Scott *et al.*, 1986a) have confirmed that early speculation. The organization of the Sol described later for the Old World monkey is similar to the other mammalian species and, by extension, is presumed to be the best approximation for humans.

Afferent Projections

The rostrocaudal organization of taste within the Sol of the monkey recapitulates the pattern of taste bud innervation within the oral cavity (Beckstead and Norgren, 1979). Axons of the intermediate nerve of Wrisberg (VII) that innervate taste buds on the anterior tongue and soft palate enter the lateral surface of the medulla, perforate the spinal tract of V, and terminate within the lateral aspect of the rostral Sol (Fig. 31.2A). Unlike the rat, in the monkey a small contingent of axons turns rostrally and ends in a narrow prefacial extension of the Sol (Beckstead and Norgren, 1979; Rhoton, 1968). The glossopharyngeal nerve enters the medulla caudally to VII and terminates within both lateral and medial divisions of the rostral Sol (Beckstead and Norgren, 1979; Satoda *et al.*, 1996; Fig. 31.2B). Although there is substantial overlap of the terminals of VII and IX in the lateral division of the Sol, the bulk of terminals from IX lie caudally to those of VII. Because IX contains both gustatory and somatosensory information, anatomical studies cannot rule out the possibility that the gustatory zone of Sol extends into the caudal half of the nucleus; if it did however, it would be a departure from the pattern seen in rodents (Travers and Norgren, 1995). Axons of the vagus nerve enter the medulla immediately caudal to the fibers of IX and terminate throughout the entire Sol. As Figure 31.2 shows, the terminal distributions of VII, IX, and X overlap considerably within the Sol, but in no place more than in the lateral division of the nucleus between the entry points for nerves VII and IX. After their entry into the Sol descending axons of

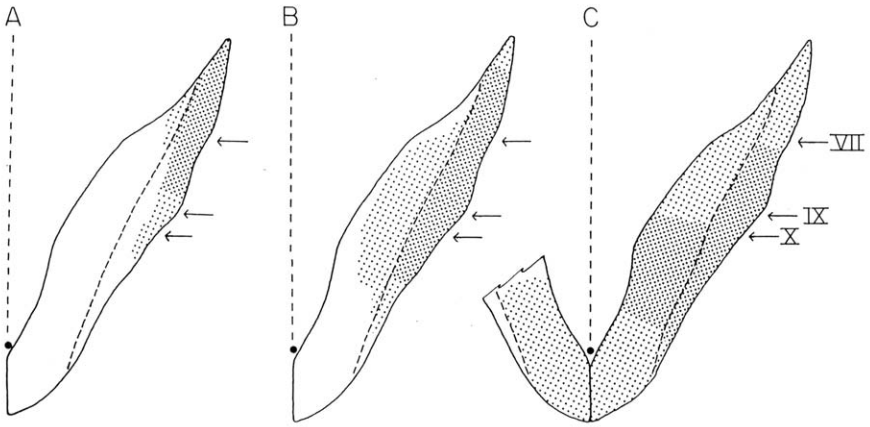

FIGURE 31.2 Terminal distributions of cranial nerves VII **(A),** IX **(B),** and X **(C)** within the Sol of the Old World monkey. Each panel shows an outline of the Sol as it appears in the horizontal plane. The vertical dotted line represents the midline, the obex is marked by a filled circle, and the level of entry of nerves VII, IX, and X into the nucleus is indicated by arrows. The medial and lateral subdivisions of the nucleus are separated from one another by a dotted line through the nucleus. Each panel is oriented with anterior to the top of the page and lateral to the right. The stippling represents the density of autoradiographic label within the Sol after injections of the respective ganglia for cranial nerves VII, IX, and X. Although there is some somatotopy within the Sol, the terminal areas of all three nerves show considerable overlap, especially within the rostral third of the nucleus. Of these three nerves, only the vagus projects to the contralateral side of the brain. (Diagram constructed with data originally summarized in Beckstead and Norgren (1979). Used with permission from Lippincott, Williams and Wilkins).

VII and IX follow an intranuclear path; vagal fibers, by comparison, descend within the solitary tract itself. In the human, it is possible that the solitary tract contains descending axons of nerves VII, IX, and X (Nageotte, 1906; Schwartz *et al.*, 1951).

In the monkey, the terminal distributions of nerves VII, IX, and X within the Sol suggest a division of the nucleus into rostral (gustatory) and caudal (visceral) segments. The Sol also has been divided into medial and lateral subdivisions in both humans (Olszewski and Baxter, 1954) and nonhuman primates (Beckstead and Norgren, 1979). In monkeys, the lateral subdivision is the terminal area of nerves VII and IX, while the vagus nerve projects mostly to the medial subdivision in the caudal half of the nucleus and the lateral subdivision in the rostral half (Beckstead and Norgren, 1979). The lateral and medial subdivisions in the monkey Sol appear to correspond, respectively, to the ventral and dorsal sensory nuclei of the vagus in human (Olszewski and Baxter, 1954). Cyto- and chemoarchitectural studies have shown that the Sol of the rat (Kalia and Sullivan, 1982), hamster (Whitehead, 1988), and cat (Loewy and Burton, 1978) can be divided into six to ten discrete subnuclei, which are relatively well-preserved across species. The human Sol has been divided into ten subnuclei, of which at least one, the interstitial nucleus, contains gustatory neurons (Tork *et al.*, 1990; Hyde and Miselis, 1992; McRitchie and Tork, 1993; see also Chapter 10).

In addition to the terminations in the Sol, cranial nerves VII, IX, and X contain axons that terminate elsewhere, primarily in the marginal subdivision of the caudal spinal trigeminal nucleus and in the dorsal horn as far caudally as the third cervical segment. Clinical evidence, with some experimental support (Nomura and Mizuno, 1984), has associated some of these projections with somatosensory innervation of the ear. Other clinical observations, together with anatomical and electrophysiological evidence from animals, suggest that these extrasolitary projections subserve somatosensory functions of the oral cavity (see Norgren, 1981 for discussion and references). Anatomic evidence indicates that the marginal zone of the caudal spinal trigeminal nucleus projects to the Sol, as well as to pontine and thalamic gustatory relays (Burton *et al.*, 1979; Fulwiler and Saper, 1984; Menetrey and Basbaum, 1987). Apparently these sensory areas have yet to be tested for gustatory responsiveness, but their anatomy suggests that, even if these neurons do not respond to pure gustatory stimuli, they might influence neurons that do.

Clinical Studies

Although the homology of the Sol between nonhuman primates and other animals is strong, few reports link the human Sol to either the animal literature or gustatory function. Lateral medullary strokes (Wallenberg syndrome) typically impair taste

perception, but have little localizing value. More precise localization has been obtained from anatomical studies that have traced terminal degeneration into the Sol after peripheral taste nerve damage. Of the human cases, by far the most informative was reported by Nageotte (1906). About a month prior to his death from stomach cancer, Nageotte's patient developed a right facial paralysis. Postmortem examination revealed that the paralysis resulted from "a metastatic nucleus as large as a grain of hempseed, situated in the aqueduct of Fallopius (facial canal) immediately *below* the geniculate ganglion" (Nageotte, 1906, p. 474, italics in original, parentheses added). Thorough postmortem histological analysis showed that the facial trunk and the axons of the chorda tympani nerve distal to the tumor were completely degenerated. Proximally, the geniculate ganglion, the extrapontine segment of the facial nerve, and the intermediate nerve all appeared intact. Within the brain, however, the radiations of the facial motor nerve were degenerated, as well as "all the fascicles of the intermediary nerve of Wrisberg" (p. 476). Because the tumor was distal to the geniculate ganglion, the degeneration observed by Nageotte in the intermediate nerve was of the transganglionic Wallerian variety that occurs when transected distal axons fail to regenerate (Csillik and Knyihar-Csillik, 1987; Whitehead *et al.*, 1995). The normal appearance of the intermediate nerve was caused by the intact greater superficial petrosal nerve, which was not damaged by the lesion.

According to Nageotte, degenerating fascicles entered the gustatory nucleus, a small, round nucleus "enclosed in a mantle of white matter" (1906, p. 477) and situated just dorsal to the spinal trigeminal nucleus. Nageotte traced degenerating axons both rostrally (1.5 mm) and caudally (4.5 mm) from their zone of entry to the Sol. Nageotte's description of the gustatory nucleus itself was based upon comparisons of the Marchi-stained sections with serial sections through three normal human brains. For present purposes, only a few additional points need to be summarized. First, the nucleus is continuous with what was then known as "the nucleus or *gelatinous substance of the solitary bundle*" (1906, p. 479, italics original). The nucleus of the gelatinous substance[1] corresponds to the nucleus ovalis of Olszewski and Baxter (1954) and the interstitial nucleus of the solitary tract in the present terminology (McRitchie and Tork, 1993). Paxinos *et al.* (1990) show serial sections of the intensely AChE-reactive interstitial nucleus of the solitary tract (see also McRitchie and Tork, 1993). Second, axons of the glossopharyngeal nerve reach the nucleus posterior to those of the intermediate nerve and both ascend and descend within the Sol. Finally, rostrally, just dorsal to the principal trigeminal nucleus, the nucleus expands to 0.8 mm in diameter, but contracts to only 0.1 mm in diameter at the level where axons of the intermediate nerve first approach it, only to expand again just rostral to the incoming fascicles of IX. Nageotte claimed that this enlargement of the Sol rostral to the entry of VII was observed previously by Wallenberg (1897a); it has since been described in the human (Pearson, 1947; McRitchie and Tork, 1993) and, by homology, in the Old World monkey (Beckstead and Norgren, 1979). Although the prefacial extension of the Sol does not exist in the rat (Rhoton, 1968; Kerr, 1962), its presence in the salamander (Herrick, 1914) suggests that it is not a recent evolutionary development.

Much of Nageotte's description can be confirmed from other examinations of the human Sol, but these studies lack the authority of Nageotte's case. They relied upon normal material, in which finely myelinated fiber tracts and preterminal ramifications are notoriously difficult to interpret, or when Marchi-stained material was available, the lesions involved several cranial nerves. Mellus (1902), using normal tissue, and Bruce (1898), using Marchi-stained material from a patient with complete destruction of the trigeminal and glossopharyngeal nerves, described nuclear areas associated with the human solitary tract that appear to be coextensive with the caudal half of Nageotte's gustatory nucleus. Unfortunately, both reports were not detailed enough to provide a confident verification of Nageotte's observations. Freeman (1927) provided a more detailed description of the entire Sol of a normal human fetal brain, including its rostral extension, but his interpretations relied too heavily upon previously published experimental material, including Nageotte's, to consider this report an independent confirmation. Olszewski and Baxter (1954) identified the prefacial extension of the Sol in normal material and renamed it nucleus ovalis. Schwartz *et al.* (1951) described the composition and course of the solitary tract based upon Marchi material from a patient who had the roots of cranial nerves V, VII, IX, X, and spinal nerves C1-C3 sectioned unilaterally to relieve intractable pain. Schwartz *et al.* (1951) confirmed Nageotte's description of the general organization of the Sol, but because of the number of degenerating nerves, they could not be specific about the contribution of each to the solitary tract or its nucleus.

The anatomical differences in the Sol between primate and nonprimate species should not overshadow

[1]Nageotte's use of the name gelatinous nucleus should not be confused with the modern term "nucleus gelatinosus," which describes a smaller nucleus located near the commissural Sol.

the significant similarities among these species. As discussed previously, the same three cranial nerves convey gustatory information to the Sol from the oral cavity. Within the Sol, electrophysiological data from nonhuman species, including the cat (Bernard and Nord, 1971), hamster (Travers, 1988), rat (Norgren, 1978), rabbit (Schwartzbaum and DiLorenzo, 1982), and monkey (Beckstead *et al.*, 1980; Scott *et al.*, 1986a) demonstrate that gustatory neurons are located within the rostral pole of the nucleus. In such a highly conserved system, the available clinical data suggest that the gustatory medullary relay in humans is located within the rostral pole of the Sol.

Gustatory/Trigeminal Overlap Within the Medulla

One possible difference between humans and other species in the organization of the Sol relates to potential contributions from primary trigeminal afferent axons. Both Astrom (1953) and Torvik (1956) recognized that trigeminal axons project to the lateral division of the Sol. In the rat, the rostral pole of the Sol actually abuts the spinal trigeminal nucleus, but trigeminal axons from the lingual nerve terminate more caudally within the terminal zone of the glossopharyngeal nerve (Hamilton and Norgren, 1984). In monkeys, axons from both the mandibular and ophthalmic divisions of the trigeminal nerve bypass the rostralmost aspect of the spinal trigeminal nucleus and terminate in the lateral Sol at glossopharyngeal levels. Based upon evidence from a case supplied by Wallenberg (1897b), Nageotte asserted that trigeminal axons terminate throughout the prefacial extension of the Sol, which places the human data at odds with the experimental evidence from other animals including primates. Nageotte's assertions, however, were not confirmed in other Marchi material from humans that involved trigeminal lesions (Schwartz *et al.*, 1951). Although this issue may seem esoteric, the organization of the remainder of the central gustatory system hinges upon it. The spatial proximity of trigeminal and chemosensory projections within the Sol raises the obvious possibility for gustatory/somatosensory integration, which has already been demonstrated in both single (Ogawa *et al.*, 1984; Travers and Norgren, 1995; Travers *et al.*, 1986) and multineuron (Halsell *et al.*, 1993) recording studies in the rat.

Pons

Afferent Projections

Chapter 10 provides detailed descriptions of the chemo- and cytoarchitecture of the pontine parabrachial (PB) nuclei. The afferent projections to the Sol in subprimate species were identified around the turn of the century, but its efferent projections were discovered only during the last 20 years. The early experiments used Marchi staining of degenerating myelinated axons to conclude that the efferent axons from the Sol of the guinea pig and rabbit ascended in the contralateral medial lemniscus and terminated in the ventrobasal thalamus (Allen, 1923; Gerebtzoff, 1939). In these studies, degeneration within the medial lemniscus and ventrobasal thalamus was probably caused by lesions of the Sol that encroached upon the dorsal column nuclei or internal arcuate fibers. Recent experiments using more sensitive and discrete neuroanatomical tract tracing techniques have shown that in both rat and cat, neurons in the rostral (gustatory) and caudal (visceral) regions of the Sol project to the PB (Loewy and Burton, 1978; Norgren and Leonard, 1973). Kinney (1978) employed the Fink-Heimer technique to trace degenerating axons in a single monkey from the rostral and intermediate Sol through the contralateral central tegmental tract to the rostral pole of the ventral posteromedial nucleus of the thalamus (VPMpc). Unfortunately, like the early degeneration studies in the guinea pig and rabbit (Allen, 1923; Gerebtzoff, 1939), the four large lesions (two dorsal pontine; two medullary) in Kinney's study almost certainly interrupted internal arcuate fibers crossing from the dorsal column nuclei to the contralateral medial lemniscus as well as crossing cerebellar and trigeminal pathways. Although the Fink-Heimer staining technique can identify both myelinated and unmyelinated degenerating axons, the survival time (14 days) in the Kinney study probably was too short to impregnate small caliber gustatory fibers.

Just as in the rabbit and guinea pig, the pathways identified by Kinney with the Fink-Heimer technique have not been confirmed with modern neuroanatomical tracing techniques. Beckstead *et al.* (1980), after making electrophysiologically-guided injections of tritiated amino acids at five different anterior–posterior levels of the Sol, concluded that projections from the rostral, primarily gustatory, part of the Sol ascend in the ipsilateral central tegmental tract, bypass the PB, and terminate within the caudal half of the parvicellular division of the ventroposteromedial nucleus (Fig. 31.3; Beckstead *et al.*, 1980). The PB of the monkey, by comparison, receives projections only from the caudal and commissural viscerosensory regions of the nucleus. These data were confirmed with injections of horseradish peroxidase into the thalamus that retrogradely labeled neurons within the rostrolateral Sol (Beckstead *et al.*, 1980; Pritchard *et al.*, 2000).

The anatomical data of Beckstead *et al.* (1980) are supported by other electrophysiological data that show gustatory information in the monkey ascends

FIGURE 31.3 Selected coronal sections through the brainstem and thalamus of a monkey, *Macaca fascicularis*, tracing the labeled axons and terminal fields that resulted from an injection of tritiated amino acid centered in the Sol, just rostral to the level at which axons of the intermediate nerve of Wrisberg reach the nucleus. Neurons at this location responded to sapid chemicals applied to the anterior tongue. Labeled fibers ascend ipsilaterally through the pontine (D) and midbrain tegmentum (C), and terminate in VPMpc (A and B). With an injection at this rostral level in the Sol, little label is evident in the pontine parabrachial nuclei (D). Injections more caudally in the Sol result in terminal label in both PB and VPMpc. Injections even further caudally in Sol, posterior to the level at which vagal axons reach the nucleus, result in terminal label in the PB, but not in the thalamus. Abbreviations: BC, brachium conjunctivum; BP, brachium pontis; cg, central gray; CL, nucleus centralis lateralis thalami; CM, central medial nucleus; CM-Pf, thalamic centromedian nucleus, thalamic parafascicular nucleus; FR, fasciculus retroflexus; H, H1, H2, fields H of Forel; HL, habenula lateralis; HM, habenula medialis; lc, locus coeruleus; LGN, lateral geniculate nucleus; MD, thalamic mediodorsal nucleus; MGN, medial geniculate nucleus; ML, medial lemniscus; MLF, medial longitudinal fasciculus; ntb, nucleus of the trapezoid body; OT, optic tract; Pf, parafascicular nucleus; pn, pontine nuclei; pp, peripeduncular nucleus; PP, pes pedunculi; rtp, nucleus reticularis tegmenti pontis; sc, superior colliculus; snc, substantia nigra, pars compacta; snr, substantia nigra, pars reticulata; so, superior olive; SPf, nucleus subparafascicularis thalami; stn, subthalamic nucleus; svn, superior vestibular nucleus; SVT, spinal trigeminal tract; TB, trapezoid body; VII, motor root of the facial nerve; VIm, abducens nucleus; Vp, principal sensory trigeminal nucleus; VPI, ventroposteroinferior nucleus; zi, zona incerta; III, oculomotor nerve. (Used with permission from John Wiley & Sons, Inc.).

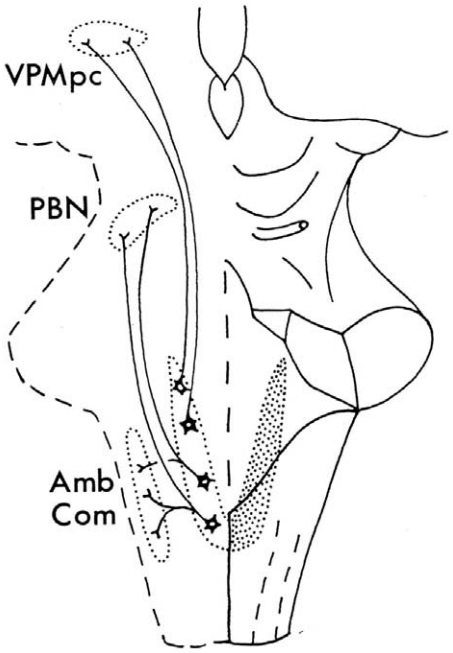

FIGURE 31.4 Dorsal view of the caudal brainstem and diencephalon of the Old World monkey showing the efferent projections of the Sol. The caudal part of the Sol that receives projections primarily from the vagus nerve projects to the PB. The efferent projections from neurons in the rostral primarily gustatory region of the Sol bypass the PB and project directly to VPMpc in the thalamus. (Used with permission from John Wiley & Sons, Inc.).

uncrossed from the tongue to the thalamus (see following discussion; Fig. 31.4). Assuming that the human nervous system resembles that of other primates more than it does other mammalian species, the best hypothesis is that most if not all axons of second-order gustatory neurons in the Sol ascend ipsilaterally within the central tegmental tract and terminate in the thalamic gustatory relay.

Efferent Projections

In the rat, the PB projects to the VPMpc as well as the ventral forebrain (central nucleus of the amygdala, bed nucleus of stria terminalis, lateral hypothalamus; Norgren and Leonard, 1973; Saper and Loewy, 1980). Although most of the projections to the ventral forebrain are presumed to be related to visceral sensation, some do convey gustatory information (Norgren, 1970, 1974, 1976; Azuma *et al.*, 1984; Schwartzbaum and Morse, 1978). The central pathways of the rodent gustatory system are described in more detail by Norgren (1995).

The efferent projections of the PB in monkey resemble those of the rat but are more consistent with those of a general visceral relay than a gustatory relay. Pritchard *et al.* (2000) used autoradiographic injections to demonstrate that the PB of the Old World monkey projects to the same ventral forebrain sites as in the rat, as well as restricted areas of the hypothalamus (dorsomedial, lateral, ventromedial) and the thalamus (VPMpc, VPM, central lateral, parafascicular/centromedian, reuniens). The projections of the PB to the extended amygdala and hypothalamus provide general visceral information entree to the entire limbic system. The projections to VPMpc are significant because they terminate in the rostral half of the nucleus that does not receive gustatory projections from the Sol (Beckstead *et al.*, 1980). Large injections of horseradish peroxidase into the caudal, gustatory half of VPMpc retrogradely labeled neurons within the rostral pole of the Sol, but not within the PB (Pritchard *et al.*, 2000). Thus, in monkeys, the PB does not appear to be an obligatory relay for ascending gustatory information as it is in rodents and lagomorphs (Norgren, 1984).

Gustatory Processing in the PB.

Numerous studies in rats (e.g., Hajnal *et al.*, 1998; Lundy and Norgren, 2001), rabbits (DiLorenzo and Schwartzbaum, 1982), and hamsters (Smith *et al.*, 1994), have recorded taste-responsive neurons within the PB. Although the PB has received much less scrutiny in the monkey than in these subprimate species, in more than a dozen preparations, we have never isolated a neuron in the monkey PB that responded to sapid stimulation of the anterior tongue (Pritchard *et al.*, 2000). In the same animals, electrically stimulating the glossopharyngeal and vagus nerves did elicit evoked potentials and drive some individual neurons and neuron clusters within the PB (Pritchard *et al.*, 2000). Could gustatory afferent activity from the anterior (facial) and posterior (glossopharyngeal) gustatory fields on the tongue ascend to the forebrain along separate brainstem pathways? Although possible, an Sol-PB-VPMpc route for taste responses of glossopharyngeal origin seems unlikely given that the PB projection to the thalamus terminates in the nongustatory part of VPMpc. Nevertheless, we cannot exclude the possibility that gustatory information passes through the PB on its way to the ventral forebrain. Taste-responsive neurons have been identified in the lateral hypothalamus (Aou *et al.*, 1984; Oomura *et al.*, 1991), in the substantia innominata (Nishijo *et al.*, 1986; Burton *et al.*, 1975), and throughout the amygdala (Karadi *et al.*, 1992; Scott *et al.*, 1993; Yan and Scott, 1996), but, as discussed below, the route by which taste information reaches these areas is uncertain.

Clinical Studies

Taste deficits may be among the presenting symptoms of pontine damage caused by hemorrhagic or embolic infarction (Goto *et al.*, 1983; Graham *et al.*, 1988; Nakajima *et al.*, 1983; Onoda and Ikeda, 1999) or multiple sclerosis (Combarros *et al.*, 2000; Uesaka *et al.*, 1998). These six reports describe eight patients whose pontine damage was accompanied by taste deficits. In each case, focal testing with sapid stimuli demonstrated either an ageusia or a hypogeusia on the side of the tongue ipsilateral to the pontine damage. The lesions varied considerably between patients, but in each case the damage within the pontine tegmentum included the central tegmental tract. In some but not all cases, the PB was damaged. Even a liberal reading of the published radiographs clearly shows that medial lemniscus was spared in most of the cases (e.g., Combarros *et al.*, 2000; Graham *et al.*, 1988; Uesaka *et al.*, 1998). Based upon the data from these eight patients, we believe that in humans, like the Old World monkey, the ascending gustatory projection from the Sol courses ipsilaterally though the pons. None of these studies provides a convincing demonstration for the PB being a taste relay.[2]

Thalamus

The only central taste relay that was known with certainty by 1940 was the Sol in the medulla. Gustatory cortex was assumed to reside near the olfactory areas in the temporal lobe, and a thalamic gustatory relay was presumed but not proven. After Le Gros Clark (1937) and Walker (1938) identified the thalamocortical projections of the somatosensory system in the monkey and Bornstein (1940a, b) published his influential reports on taste cortex in human, Blum *et al.* (1943) hypothesized that the thalamic gustatory relay would be located in VPMpc, which borders the medial aspect of the oral somatosensory nucleus, VPM. Blum *et al.* measured the rejection threshold for quinine hydrochloride in three rhesus monkeys before and after lesions were made in the vicinity of VPMpc. Two monkeys with incidental damage to VPMpc showed only a transient impairment in taste preference. A third monkey with severe damage to VPMpc showed a profound taste impairment that persisted for the duration of the experiment (57 days). Given the large size and poor placement of the lesions, these data were more suggestive than compelling, but at that time they were sufficient to establish VPMpc as the gustatory relay in the thalamus.

The thalamic gustatory nucleus, VPMpc, fills the wedge-shaped tip of the ventrobasal thalamus that lies immediately ventral to the centromedian/parafascicular nuclei. The dorsal, medial, and ventral boundaries of VPMpc are formed by the internal medullary lamina. By contrast, the anterior and posterior borders of VPMpc are vague but discernible as they blend with the cell-poor areas of the ventral lateral and posterior thalamic nuclei, respectively. The most difficult border to discern is the lateral border of VPMpc, which adjoins VPM. In Nissl stains, cell density is similar within VPM and VPMpc, but the median cell diameter is approximately 13% larger in VPM than VPMpc (20.3 μm vs. 18.0 μm; calculated from Van Buren and Borke, 1972). In myelin-stained material, VPMpc has a much paler, more gelatinous appearance than VPM whose fine myelinated fiber matrix gives it the appearance of felt. According to Jones and Hendry (1989), neurons in both VPM and VPMpc are immunoreactive for calbindin, but only VPM stains for parvalbumin. Jones *et al.* (1986) have shown that cytochrome oxidase (CO) preferentially stains VPM. In this latter study, the VPM/VPMpc boundary was defined by injecting the principal trigeminal nucleus with horseradish peroxidase. After the oral and perioral receptive fields of VPM were mapped, they plotted their electrophysiological data onto CO-stained charts of VPM/VPMpc, complete with the HRP-defined nuclear boundaries. In this manner, Jones *et al.* (1986) demonstrated that CO-staining defines VPM, but not its ventral neighbor, which they surmised was VPMpc. This ventral area did not receive ascending projections from the principal trigeminal nucleus and did not contain neurons responsive to somatosensory stimulation, but because gustatory stimuli were not included in their test battery, it was not possible to state with certainty whether this ventral area was VPMpc or the ventral posterior inferior nucleus. Staining for CO and the calcium-binding proteins calbindin and parvalbumin may provide a more decisive partition between VPM and VPMpc than traditional Nissl or myelin stains. Chapter 20 provides a comprehensive description of the entire thalamus, including VPMpc. Chapter 29 include a complete description of the connectivity and immunohistochemical properties of VPM.

Locating and describing the thalamic relay for taste has been easier than naming it. In the rhesus monkey

[2]Nine other reports were not considered because of inadequate documentation, usually in the method section, or their publication in a non-English language journal. Two of these reports described taste deficits in two patients with bilateral pontine damage. If we exclude those cases and accept at face value the results of the other seven reports, the data from six patients suggest that taste ascends ipsilaterally through the pons; the remaining two cases suggest a contralateral course for taste within the pons.

the crescent-shaped thalamic gustatory relay was originally called the arcuate or semilunar nucleus, but since Olszewski (1952) published his atlas of the rhesus monkey brain, this parvicellular region has been called VPMpc. In humans, the thalamic gustatory nucleus was called the nucleus ventrocaudalis parvocellularis internus (V.c.pc.i) by Hassler (1959), but Hirai and Jones (1989) suggested the name basal ventral medial nucleus (VMb). These differences in nomenclature and occasional shifts in nuclear boundaries typically reflect attempts to group different thalamic nuclei on the basis of cyto- or myeloarchitectural (Olszewski, 1952; Dewulf, 1971) or histochemical/immunocytochemical criteria (Hirai and Jones, 1989; Jones, 1990). A strictly functional term such as thalamic gustatory nucleus (Gus; Paxinos *et al.*, 2000), might resolve the nomenclature issue, but, in fact, it is a misnomer because this area also contains lingual thermal and tactile neurons, as well as neurons that respond to neither taste or somatosensory stimuli (Pritchard *et al.*, 1989). Based upon functional and hodological criteria, grouping the region containing gustatory neurons with the adjacent oral and facial somatosensory nucleus (VPM) appears to be the most logical solution. Accordingly, in this chapter we emphasize Olszewski's (1952) terminology for the thalamus, including VPMpc, for the thalamic gustatory relay.

In the years since Blum *et al.* (1943) first asserted that the gustatory relay for taste lies within VPMpc, numerous anatomical, electrophysiological, and clinical studies have reached the same conclusion. Anatomical studies have demonstrated that the thalamic gustatory relay occupies homologous structures in all mammals for which experimental data are available, including the *rat* (Karimnamazi and Travers, 1998; see Norgren, 1995 for a review), *rabbit* (Block and Schwartzbaum, 1983), *cat* (Ishiko *et al.*, 1967), *dog* (Ninomiya and Funakoshi, 1982), *hamster* (Halsell, 1992), and *monkey* (Beckstead *et al.*, 1980). Thus, it appears that the interspecies differences within the PB discussed earlier have little bearing on the locus of the gustatory area within the thalamus. As described previously, in nonhuman primates axons originating in the rostral, gustatory half of the Sol ascend ipsilaterally within the central tegmental tract and terminate within the caudal half of VPMpc (Beckstead *et al.*, 1980). The rostral half of VPMpc receives afferent projections from the PB (Pritchard *et al.*, 2000). This anatomical partition of VPMpc into rostral and caudal halves confirms electrophysiological data in the cat (Emmers, 1962) and squirrel monkey (Blomquist *et al.*, 1962) showing that electrical stimulation of the chorda tympani and glossopharyngeal nerves drives neurons in the posterior but not anterior half of the nucleus (see also Burton and Benjamin, 1971; Pritchard *et al.*, 2000). Given the role of the PB as a relay for ascending general visceral information, the anterior half of VPMpc and several nearby nuclei might serve as thalamic relays for general visceral information bound for the cerebral cortex (Cechetto and Saper, 1987; Craig *et al.*, 1994; Davis *et al.*, 1995; Saleh and Cechetto, 1993).

The most compelling evidence that VPMpc serves as the thalamic gustatory relay derives from electrophysiological studies. In both primate (Benjamin, 1963; Pritchard *et al.*, 1986, 1989; Reilly and Pritchard, 1995) and subprimate species (e.g., Scott and Erickson, 1971), gustatory neurons are located within VPMpc. When tested, the receptive fields for thalamic gustatory neurons in monkeys are on the ipsilateral side of the tongue (Pritchard *et al.*, 1989). Indeed, over the course of several hundred penetrations performed during the last two decades, we have never observed a taste response that originated from the contralateral side of the tongue. As in other species, gustatory neurons are not the sole tenants of VPMpc (Benjamin, 1963; Pritchard *et al.*, 1989). In addition to gustatory (36%) neurons, VPMpc contains tactile (11%) and thermal-responsive (<1%) neurons as well as other cells that are either unresponsive (18%) to the stimulus set or respond in anticipation of stimulus delivery (35%; Pritchard *et al.*, 1989). Gustatory neurons are located only within the medial half of VPMpc; the lateral half of the nucleus contains neurons responsive to oral somatosensory stimulation (Burton and Benjamin, 1971; Pritchard *et al.*, 1986). In three awake thalamotomy patients, Lenz *et al.* (1997) electrically stimulated the posterior thalamus in the vicinity of the ventroposterolateral nucleus, pars oralis and caudalis (VPLo, VPLc, respectively), and VPMpc. The patients reported tingling in various parts of the perioral cavity, and in several instances they described a sour taste and metallic sensation on the tongue as well as vinegar-like smells and nasal itching similar to that evoked by pepper. These sensations localized to the side of the tongue ipsilateral to the thalamic stimulation.

Despite the general agreement about the location of the thalamic taste relay in human and nonhuman primates, the laterality of the thalamic projection is disputed in the clinical literature. The earliest known study by Adler (1933; Walker, 1938, p. 61) describes a patient who, over a period of 2 years, lost taste function and tactile sensibility on the *contralateral* side of the face as a result of a glioblastoma that encroached upon VPMpc and the nucleus centromedianum. These findings are consistent with a report by Onoda and Ikeda (1999) who described a patient with a posterior thalamic infarction accompanied by a contralateral

hypogeusia. Taste thresholds within the chorda tympani and glossopharyngeal fields were tested with electrogustometry as well as with commercially available filter-paper disks impregnated with sucrose, sodium chloride (NaCl), tartaric acid, or quinine hydrochloride (QHCl; five concentrations each). During the electrogustometry testing there were no differences between the left and right sides of the tongue, but with the filter-disk method, the patient was unable to detect any of the four basic taste stimuli when they were applied to the contralateral side of the tongue (stimulus concentrations not reported). The conclusions of these two reports are contradicted by the data of Combarros *et al.* (1994), who describes a female patient with an ipsilateral taste deficit. This patient, diagnosed with multiple sclerosis, had demyelinating plaques in the medial part of the posterior thalamus and complained of numbness of the hand and corner of the mouth, both on the contralateral side. Her subjective reports of taste were normal, but, on testing, she was almost completely ageusic on the ipsilateral tongue. Despite perfect detection and identification when drops of 1.2*M* NaCl, 0.47*M* glucose, 0.17*M* tartaric acid, or 2.52 m*M* QHCl were applied to the contralateral side of the tongue, during ipsilateral testing, she detected only three of the eight stimuli, and for each of those, she misidentified the quality.

If the ascending taste pathway crosses, as the Adler (1933) and Onoda and Ikeda (1999) studies suggest, at what level does the crossing take place? As summarized in the previous section, the central gustatory pathways ascend ipsilaterally through the pons. After examining two patients with vascular lesions, Shikama *et al.* (1996) concluded that taste ascends ipsilaterally as far as the rostral midbrain. Crossing of the ascending taste pathway between the rostral midbrain and the posterior thalamus is possible but unlikely given the weight of evidence favoring an ipsilateral representation of taste within the cerebral cortex. Thus, the likelihood of a contralateral taste projection to the thalamus seems low, but until more cases are reported, this issue will not be resolved.

Cortex

Over the last decade, there has been more research on the cortical organization of taste than on all other levels of the gustatory neuraxis combined. Neuroanatomical and neurophysiological research in nonhuman primates has provided our first glimpse of taste processing in secondary and tertiary cortical areas. The last decade also witnessed the introduction of noninvasive imaging techniques such as functional magnetic resonance imaging (fMRI) and positron emission tomography (PET) to the field of gustation. Progress notwithstanding, significant questions remain, and just as a decade ago, the cortical organization of taste must be inferred by reconciling the experimental data derived from nonhuman primates with the clinical literature.

Clinical Studies

During the late 19th and early 20th centuries, seizure-induced auras originating in the uncus and hippocampus convinced the medical establishment that taste cortex was located near the olfactory areas within the temporal lobe. After Bornstein (1940a) reviewed the largely clinical literature that supported a temporal lobe localization for taste and found it wanting, he attempted to locate the primary gustatory cortex by testing the taste sensitivity of three head trauma patients. Based upon two experimental reports in rabbits (Gad, 1891; Schtscherbak, 1892) and a separate interpretation of data from dogs (Gorschkow, 1901) that buttressed his own clinical evaluations of his head trauma patients, Bornstein (1940b) localized gustatory cortex in humans to the base of the postcentral gyrus in Brodmann area 43. Bornstein's neurological and gustatory examinations were careful and well documented. He used graded concentrations of chemicals that humans categorize as sweet, salty, sour, and bitter, as well as thermal and tactile stimuli. In addition, Bornstein tested the tip, lateral edge, and base of the tongue independently on both sides. In each of the three cases, the lesion apparently included the base of the pre- and postcentral gyrus with varying involvement of the underlying operculum. Gustatory deficits were prominent in each case and were always more severe on the contralateral tongue. The publication of Bornstein's two reports not only effectively ended speculation about the role of the temporal lobe in taste perception but also placed taste cortex firmly in the parietal operculum.

Bornstein's (1940a, b) thorough testing methods and data presentation obscure problems inherent in those reports. For example, Bornstein (1940b, p. 144) identified gustatory cortex in his patients by projecting skull damage to the underlying cortex through a method he referred to as "neighboring signs and symptoms." Although brain injuries often result from insults to the overlying skull, this method is, at best, only an estimate of the locus of brain injury. Bornstein included taste dysfunction within the "parietal operculum syndrome," a constellation of symptoms observed in patients with damage to the foot of the postcentral gyrus. According to Bornstein, patients

with the "parietal operculum syndrome" demonstrate ageusia, furring of the contralateral tongue, hypesthesia, Broca's aphasia, or epileptic foci in the oral/perioral or digital region. Thus, he used the diagnosis of taste dysfunction to determine the locus of brain injury when a more prudent strategy would have been to make the anatomical determination independently. As a result, Bornstein gave little consideration to damage outside of Brodmann area 43, especially to cortical areas buried within the lateral sulcus.

Bornstein also demonstrated a strong bias toward the conventional contralateral sensory representation of the cerebral cortex that was already well established for the somatosensory system by the 1940s. In discussing one patient with temporal lobe damage and an ipsilateral taste loss, Bornstein (1940a) wrote, "Ipsilateral loss of taste can hardly be explained by a cortical lesion" (p. 723). Given this bias, it is not surprising that Bornstein never considered the possibility that furring of the tongue, which he observed in his patients and was more pronounced on the contralateral side, may have interfered with taste acuity. Perhaps for these reasons, Bornstein's observations are difficult to reconcile with subsequent studies that locate gustatory cortex within the anterior insula. Nevertheless, Bornstein is credited with making the first careful evaluation of gustatory deficits in humans with cortical damage.

More recently, Motta (1958, 1959) described gustatory deficits in patients who were decorticated, had brain tumors, or had suffered a cerebral vascular accident. Like Bornstein, Motta's tests were thorough, and his data address both the locus and laterality of gustatory cortex. Motta tested both the anterior and posterior tongue with concentration series of saccharin, NaCl, HCl, and QHCl. Patients with large temporal, occipital, or prefrontal lesions had normal taste function, whereas the ten patients with tumors in the parietal or rolandic region or with occlusions of the middle cerebral artery had moderate to severe gustatory deficits on the side of the tongue ipsilateral to the cortical defect. Patients whose taste deficits were caused by tumors in the parietal or rolandic area usually noticed improvement after removal of the tumor. Motta demonstrated with carotid angiograms that the initial taste deficits in these patients were likely caused by compression of the underlying insula and operculum. The patients described by Bornstein (1940b) also had space-occupying lesions (e.g., cysts, angiomas) capable of exerting pressure on the underlying brain, but it is not clear that he considered the possibility that the taste deficits he observed may have been caused by intracranial pressure transmitted to the underlying insular and opercular cortices.

Of the patients Motta tested, none reported a contralateral taste deficit, despite the fact that many had an accompanying contralateral hemiplegia. A thorough examination of three patients led Motta to conclude that gustatory deficits accompanied damage to the anterior insula. Two patients, who had hemiplegias caused by emboli lodged in the middle cerebral artery or the internal carotid artery, had normal taste perception and, as confirmed by carotid angiograms, normal circulation to the insula. The third patient, a gunshot victim, had a pellet of shot lodged in the middle cerebral artery immediately proximal to the anterior insula. Carotid angiography confirmed that the occlusion of the middle cerebral artery compromised both the insula and the precentral gyrus. This patient experienced a contralateral hemiplegia and an ipsilateral hypogeusia. Three other patients who had undergone decortication to manage intractable epilepsy were ageusic on the ipsilateral side of the tongue.

Other studies such as the classic research by Penfield and his colleagues on epileptic patients also suggests that the insula is involved in taste perception (Kahn *et al.*, 1969). Penfield and Jasper (1954) described a patient with an astrocytoma located in the insula who repeatedly experienced an unpleasant taste aura prior to the onset of a major seizure. According to the authors, "The patient has a sense of fear a few minutes before the bad taste sensation. [The patient was] unable to describe the taste (not salty, sour or bitter) which lasted about one minute" (p. 411). Occasionally the taste auras were triggered by the mere sight or the odor of food. One epileptic patient treated by Penfield and Faulk (1955) experienced taste auras that disappeared following surgical excision of the epileptic focus near the foot of the central sulcus. During a subsequent surgery to treat recurrent seizures, the taste auras could be evoked by electrical stimulation of the posterior insular cortex. In alert neurosurgical patients, Penfield and Faulk (1955) evoked distinct taste sensations by electrically stimulating the anterior insula. Because other visceral sensations from the epigastrium were evoked more often and from a more widespread area of the insula, Penfield's data were never considered definitive proof that taste cortex is located in the insula.

Additional support for an insular locus for taste cortex has been provided by Pritchard *et al.* (1999) who performed psychophysical testing on six patients with damage to the insula. In this report, four patients with damage to the rostrodorsal insula had significant deficits in taste intensity on the ipsilateral side of the tongue. No taste deficits were found in the other patients with damage to the ventral insula ($N = 1$) or the posterior insula ($N = 1$), patients in the head

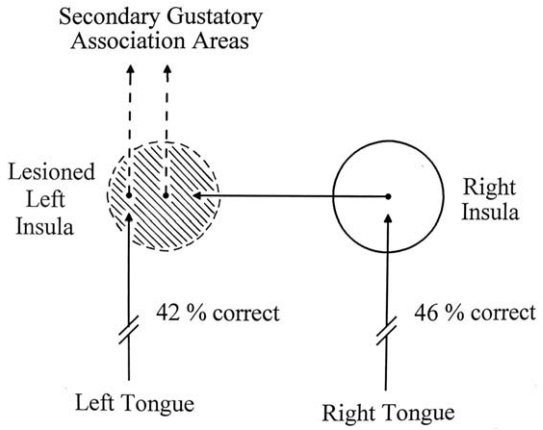

FIGURE 31.5 Taste quality identification following damage to the left insula. Subjects with left insular damage were impaired in taste quality identification for both sides of the tongue (42 and 46% correct), compared to subjects in the two control groups (62.5 and 69.3% correct). Left insular damage also impaired identification of taste quality for stimuli applied to the opposite (right) side of the tongue (46% correct). When sapid stimuli were applied to the left side of the tongue in patients with right insular damage, taste quality identification was comparable to the control subjects (63% correct). Damage to the left insula caused a bilateral impairment in taste quality identification, suggesting that the left hemisphere names taste quality for both sides of the tongue. (Used with permission from the American Psychological Association).

trauma group (N = 3), or the normal control subjects (N = 11). Damage to the left insula impaired taste *quality* identification on both sides of the tongue. These data suggest that taste quality recognition for both sides of the tongue takes place in the left hemisphere. Furthermore, these data suggest that taste information originating on the right side of the tongue reaches the language areas located in the left hemisphere by crossing in the vicinity of the insula (Fig. 31.5). Recent noninvasive imaging-based studies provide additional evidence for hemispheric specialization in the gustatory system (*vide infra*).

Two reports by Aglioti *et al.* (2000, 2001) addressed the issue of taste laterality in commissurotomy patients. The authors, after confirming that language was located in the left hemisphere of these right-handed subjects, applied sapid stimuli to either the left or right side of the tongue. The subjects were asked to point (with their right hand) to the name of the taste quality or an image representative of each taste quality (e.g., lemon = sour). One subject tested by Aglioti *et al.* (2001) had a complete section of the corpus callosum; in another subject the genu and rostrum of the corpus callosum was spared. If naming of taste quality takes place in the language areas of the left hemisphere, callosotomy patients should perform poorly on a tastes-naming task when the stimuli are applied to the right side of the tongue. As predicted, when sapid stimuli were applied to the right side of the tongue, the subjects correctly identified 56.3% of the tastants, compared to an 80.5% correct score when the tastants were applied to the left side of the tongue. Another subject, whose callosal section spared the splenium, also performed at an above chance level for sapid stimuli applied to the right side of the tongue. These data confirm a previous report from their laboratory that showed better than chance performance by a callosotomy patient who also had focal damage to the left orbital cortex and partial removal of the right frontal lobe (Aglioti *et al.*, 2000). Aglioti *et al.* (2000) also described a patient with congenital agenesis of the corpus callosum who was capable of almost perfect performance in a similar taste recognition task

The demonstration by Aglioti *et al.* (2000, 2001) that the left hemisphere of commissurized subjects has access to taste information originating from the right side of the tongue is both interesting and provocative. Before concluding that the taste pathway decussates during its ascent to cortex, however, several alternative explanations must be considered. First, Aglioti *et al.* (2000) note that the advantage for the left hemisphere decreased over trials in the verbal response sessions and suggested that this may have been caused by cross-cueing.[3] Second, the anterior commissure, which was not sectioned in these subjects, represents a potential conduit for taste information in the temporal lobe to cross from one hemisphere to the other (Small *et al.*, 1997a). Consistent with this view is the finding by Aglioti *et al.* (2001) that response latencies were longer when the right side of the tongue was stimulated. Third, Aglioti *et al.* (2001) speculated that interhemsipheric transfer of gustatory information may take place through the splenium of the corpus callosum. Although this is unlikely given the rostrocaudal correspondence between the corpus callosum and the cerebral hemispheres (Lomber *et al.*, 1994) and the fact that axons that originate in the parietal lobe form the splenium (Matsunami *et al.*, 1994), the interpretation of Aglioti *et al.* is supported by their data.

There are several reasons why it has been difficult to use the clinical literature to make a clear and compelling case for the location of gustatory cortex. First, patients with cortical injury often do not notice and thus do not report gustatory impairment. Second,

[3]In cross-cueing, the uninformed hemisphere guesses by pointing, speaking, and so on. When the informed hemisphere realizes that the answer was incorrect, an autonomic response is triggered and detected by the uninformed hemisphere, which then changes its answer.

confusion between taste and smell sensations by most patients (and some physicians) has interfered with the proper diagnosis of taste deficits. Third, when gustatory deficits are reported, they may not be observed in the clinic because of inadequate or superficial testing. Fourth, when taste deficits are reported and detected in the clinic, they typically are given less attention than the motor deficits caused by coincident damage to the perirolandic area. Fifth, this coincident damage makes identification of the core gustatory region impossible unless data are available from several similar cases.

Imaging Studies

A decade ago noninvasive imaging techniques such as computerized axial tomography (CT) and magnetic resonance imaging (MRI) scans were limited to diagnosis and localization of CNS damage. Both techniques facilitated correlation of the locus of CNS damage with gustatory deficits (e.g., Cascino and Karnes, 1990). The advent of other noninvasive imaging techniques such as fMRI, PET, and magnetoencephalography (MEG) has permitted observation of gustatory-evoked brain activity in awake, behaving human subjects. Few doubt that these techniques hold tremendous promise for gustatory research, but to date, they have raised more questions than they have answered. Small *et al.* (1999) used the Talairach coordinates of six published reports to calculate the common areas of taste-evoked activity in the cerebral cortex, as measured by PET (Frey and Petrides, 1999; Small *et al.*, 1997a, b; Kinomura *et al.*, 1994; Petrides *et al.*, 1996; Zald *et al.*, 1998). Their metaanalysis of these six studies showed increased activity in each of the regions of interest included in their analysis: the insula, the frontal and parietal opercula, and the orbitofrontal cortex, all of which have been implicated previously in taste processing by the clinical and experimental literature (Pritchard, 1991).

A closer look at the data from the individual studies shows tremendous variation within the insula and the operculum. Zald *et al.* (2002) reported that the PET activity evoked by quinine and sucrose was only marginally better than that seen during water trials. In other studies where significant responses were found in the insula, sapid stimulation of the tongue activated 15 different loci across 22 mm of the rostral insula (Zald *et al.*, 1998; Petrides *et al.*, 1996). In the dorsoventral plane, these 15 loci were scattered across 28 mm (Small *et al.*, 1997b; Petrides *et al.*, 1996). Twelve of these 15 taste-evoked loci were located in the right (nondominant) hemisphere.

Studies using fMRI and MEG also implicate the insula, the opercula, and the orbitofrontal cortex, but they introduce conflicting data as well. Barry *et al.* (2001) using fMRI reported that electric taste stimulation predominantly activates the dorsal insula in the right hemisphere. Small *et al.* (1999), in their review of the PET literature, also concluded that sapid stimulation of the tongue preferentially activates the right insula. But King *et al.* (1999), Faurion *et al.* (1999), and O'Doherty *et al.* (2001) using fMRI, and Kobayakawa *et al.* (1996, 1999) using MEG, reported that taste-evoked activity is represented bilaterally. Taste-evoked activity has been observed in the ventral insula, but there is disagreement about the laterality of the projection. Barry *et al.* (2001) using fMRI reported that taste stimulation activates the ventral insula primarily on the right (nondominant) side, while Del Parigi *et al.* (2002) found more PET activity in the left hemisphere of their right-handed subjects. Faurion *et al.* (1999), on the other hand, observed more fMRI activity in the dominant hemisphere of both right- and left-handed subjects. Laterality aside, there also is disagreement about the rostrocaudal location of primary taste cortex. King *et al.* (1999), O'Doherty *et al.* (2001), and Faurion *et al.* (1999) usually placed primary taste cortex in the rostral insula, while Francis *et al.* (1999) located it much further posteriorly, and Kobayakawa *et al.* (1999) placed it close to the caudal pole of the insula. Barry *et al.* (2001) reported significant taste-activated loci within the rostral half of the dorsal insula. Other studies have been unable to activate primary taste cortex (Small *et al.*, 1997a) or the thalamic taste relay (Barry *et al.*, 2001; King *et al.*, 1999). Similar problems attend the location of taste within orbitofrontal cortex (Small *et al.*, 1999; O'Doherty *et al.*, 2001).

The validity of these imaging techniques is unquestioned, but their application to the gustatory system may be more challenging than for other sensory systems. Noninvasive imaging techniques work best with robust systems that have large neurons concentrated in a moderately large area and, in the case of MEG, foci located close to the surface of the brain. Gustatory neurons, which account for at most 5–10% of the cells in the insula and the orbitofrontal cortex, are small, are diffusely distributed, and respond sluggishly to sapid stimulation of the tongue. Successful imaging of taste-related activity may require development of more powerful magnets and improved data analysis algorithms as well as more consistency in stimulus application and control conditions between studies. Until interstudy reliability improves, noninvasive imaging techniques are unsuitable for either confirming positive data obtained in the clinic/laboratory or for generating new findings.

Experimental Studies

Experimental attempts to locate gustatory cortex have been carried out in a variety of species (Old and

New World monkeys, cats, rabbits, hamsters, mice, and rats) using electrophysiological, anatomical, and lesion-behavioral techniques. Given the differences between lissencephalic and gyrencephalic species or even between gyrencephalic species (e.g. cats, monkeys), the most germane data must come from primates. The different techniques, each with its own strengths and weaknesses, provide a complex but still incomplete picture of how gustatory information is organized in the cerebral cortex.

Electrophysiological studies The earliest electrophysiological descriptions of gustatory cortex were obtained by mapping the evoked potentials produced by electrical stimulation of the chorda tympani nerve, lingual-tonsillar branch of the glossopharyngeal nerve, and the lingual branch of the trigeminal nerve (Benjamin and Burton, 1968; Benjamin *et al.*, 1968). This research conducted in New World monkeys showed that evoked potentials could be recorded from the insula and inner operculum after stimulation of either the ipsilateral chorda tympani or the glossopharyngeal nerve. Although stimulation of either nerve produced evoked potentials on the lateral convexity of both hemispheres, the ipsilateral responses had a shorter latency, had a larger magnitude, and were more widespread than the contralateral responses. The evoked responses within the chorda tympani and glossopharyngeal fields on the ipsilateral side overlapped each other and the rostral half of the lingual field. Benjamin and Burton concluded that the ipsilateral insula–operculum projection, unlike the field on the lateral convexity, was a "pure taste area uncontaminated by other lingual modalities" (p. 229). Ogawa *et al.* (1985), using similar techniques in the Old World monkey, recorded lingual as well as chorda tympani and glossopharyngeal evoked potentials both on the lateral convexity and in frontal opercular cortex.

Additional insight has been obtained by recording individual taste-responsive neurons located within the insula, inner operculum, and the lateral convexity of awake and anesthetized monkeys. In the first study of this kind, Sudakov *et al.* (1971) tested neurons in the insula and inner operculum of New World monkeys with gustatory, auditory, visual, and somatosensory stimuli. Almost 80% of the neurons isolated did not respond to these stimuli. Gustatory neurons, 3.2% (14 of 437) of the neurons tested, were located near the rostral pole of the insula, interspersed with tactile neurons whose receptive fields were located within the oral cavity. None of these neurons responded to both gustatory and tactile stimulation. Most of the neurons that responded to external somatosensory (8.8%; $N = 43$), auditory (10.7%; $N = 53$), and visual 0.4%; $N = 2$) stimulation were located further caudally in the insula. Within the frontal operculum, only 3.7% (19 of 509) of the driven neurons responded to gustatory stimulation.

Ogawa *et al.* (1989), using anesthetized monkeys, and Ito and Ogawa (1994), using awake, behaving monkeys, recorded from a more extensive area of the operculum. Both studies found taste-responsive neurons within the insula and Brodmann areas 3b, 1, and 2, but the distribution of taste neurons across these areas differed significantly. Ogawa *et al.* (1989) reported that the majority of gustatory neurons (13/25) were located within the granular insula adjacent to the crest of the superior circular sulcus (scir). Of the insular neurons that could be activated by sensory stimulation, 12.5% responded to sapid stimulation of the tongue; the remaining 91 neurons responded to mechanical stimulation of oral and perioral structures. Several of taste-responsive neurons also were driven by mechanical stimulation of the oral cavity. On the inner and outer opercula, taste stimulation was effective for only 3.1% (12 of 383) of the driven neurons. Ito and Ogawa (1994), by comparison, reported that most of the gustatory neurons were located within the dysgranular cortex of the inner operculum (Brodmann areas 1 and 2). It is noteworthy that the dysgranular part of the inner operculum does not receive a direct projection from the gustatory thalamus. In both studies the tactile neurons were broadly distributed across Brodmann areas 3, 1, 2, 4, 6, and SII. Ogawa *et al.* (1989) reported a concentration of tactile neurons around the inferior precentral sulcus, which Pritchard *et al.* (1986) showed receives a direct projection from VPMpc. Based upon the reports of Ogawa *et al.* (1989) and Ito and Ogawa (1994), somatosensory neurons vastly outnumber taste neurons within the insula and frontal operculum, but, more importantly, most of the neurons in these areas are unresponsive to the stimuli they tested.

Numerous electrophysiological reports, most within the last 10 years, have confirmed that gustatory neurons are located within the rostral pole of the insula and the inner operculum (Scott *et al.*, 1986b; Rolls and Baylis, 1994; Scott *et al.*, 1991). Although the actual size of the gustatory area differed slightly from experiment to experiment, in most reports it occupied approximately 50 mm^3 within the dorsal insula (Scott and Plata-Salaman, 1999). Unlike the previous reports by Ogawa *et al.* (1989) and Ito and Ogawa (1994), however, most of the taste-responsive neurons recorded by Rolls and Scott were located in the dysgranular insula (Fig. 31.6). Based on the data they collected from 12,659 neurons, Scott and Plata-Salaman (1999) report that taste-responsive neurons constitute only 6.5% of the neurons within the insula. Other neurons in the insula responded to mouth movements (23.8%), tactile

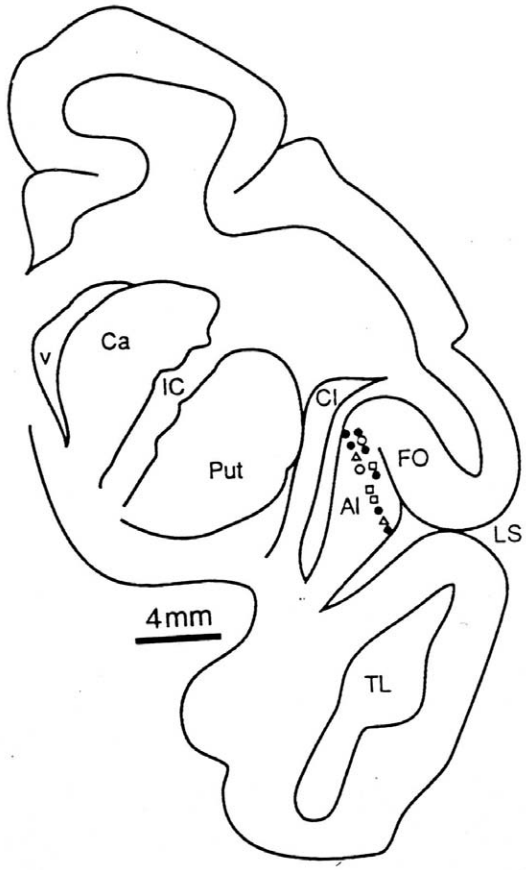

FIGURE 31.6 Chart of coronal section showing location of gustatory neurons recorded within the insula of an Old World monkey. Filled circles, glucose; squares, NaCl; triangles, HCl, open circles, QHCl. AI, anterior insula; Ca, caudate; Cl, claustrum; FO, frontal operculum; IC, internal capsule; LS, lateral sulcus; Put, putamen; TL, temporal lobe; v, lateral ventricle. (Adapted with permission from the American Physiological Society).

stimulation of the oral cavity (3.7%), approach of the stimulus delivery syringe (1.2%), or tongue extension (0.3%). The majority (64.6%) of the neurons they encountered did not respond to the stimulus battery employed in those experiments. Although multisensory convergence was not examined in most of these experiments, one study (Rolls and Baylis, 1994) reported that only 9 taste neurons from a sample of 2000 recorded from the insular-opercular and orbitofrontal cortices received convergent visual or olfactory information. In summary, gustatory neurons represent only a small fraction of the cells within the insular-opercular cortex, and unexpectedly, their spatial distribution covers a substantially larger area than the region that receives direct projections from the thalamic gustatory relay. As discussed later, local projections within the insula may account for the presence of taste neurons that lie within the insula but beyond the boundaries of primary taste cortex, as defined by anatomical tracing (Pritchard *et al.*, 1986).

Other gustatory neurons have been found throughout the posterior orbitofrontal cortex, but they are sparsely distributed and few in number (Rolls and Baylis, 1994; Rolls *et al.*, 1990, 1996). Estimates of the incidence of taste-responsive neurons within the OFC range from 1.6 to 7.3% ($\bar{X}$ = 3.8%; Thorpe *et al.*, 1983; Rolls *et al.*, 1990, 1996; Rolls and Baylis, 1994). These and other studies reported that some taste neurons receive convergent *visual* (0.8–32.4%; Rolls and Baylis, 1994; Critchley and Rolls, 1996), *olfactory* (Critchley and Rolls, 1996), *auditory* (1.4%; Thorpe *et al.*, 1983), or *somatosensory* (Critchley *et al.*, 1993) information. Still other neurons respond to the presentation of food (5.3%; Thorpe *et al.*, 1983) or the intraoral administration of fat (1.0%; Rolls *et al.*, 1999). Unlike gustatory neurons in the insula (Yaxley *et al.*, 1988) and inner operculum (Rolls *et al.*, 1989), the taste-evoked activity of OFC neurons can be modulated by the animal's level of hunger and satiety (Rolls *et al.*, 1989).

The studies by Rolls and colleagues have shown that taste-responsive neurons are scattered across the posterior OFC. Although the taste responsive neurons are located as far medially as the medial orbital sulcus and as far laterally as the precentral operculum (area PrCO), most of the cells are within Brodmann area 13, the lateral orbital cortex, and the agranular insular cortex that lies on the posterior orbital surface immediately rostral to primary taste cortex. The area of the caudolateral OFC designated by Rolls as secondary gustatory cortex (Rolls, 2000; Rolls *et al.*, 1990; Rolls and Baylis, 1994) lies along the lateral orbital surface, which has been designated as Brodmann area 12o (Carmichael and Price, 1994) and more recently as Brodmann area 47/12o (Paxinos *et al.*, 2000; Petrides and Pandya, 2001; Price, personal communication). The presence of multimodal neurons within the OFC has fueled speculation that flavor, the amalgam of taste, temperature, touch, and smell, first emerges here (Rolls and Baylis, 1994; Carmichael and Price, 1995a, 1996). Compared with gustatory neurons in the insula, operculum, thalamus, and medulla, those in the OFC are more narrowly tuned and have more complex response properties. It is clear that the OFC contains some higher order gustatory neurons; whether it should be considered secondary taste cortex is an issue discussed in the next section.

Anatomical studies Early anatomical experiments reported that neurons in VPMpc degenerate after combined, but not separate, lesions of the rostral insula and the lateral convexity (Roberts and Akert, 1963; Locke, 1967; Benjamin and Burton, 1968).

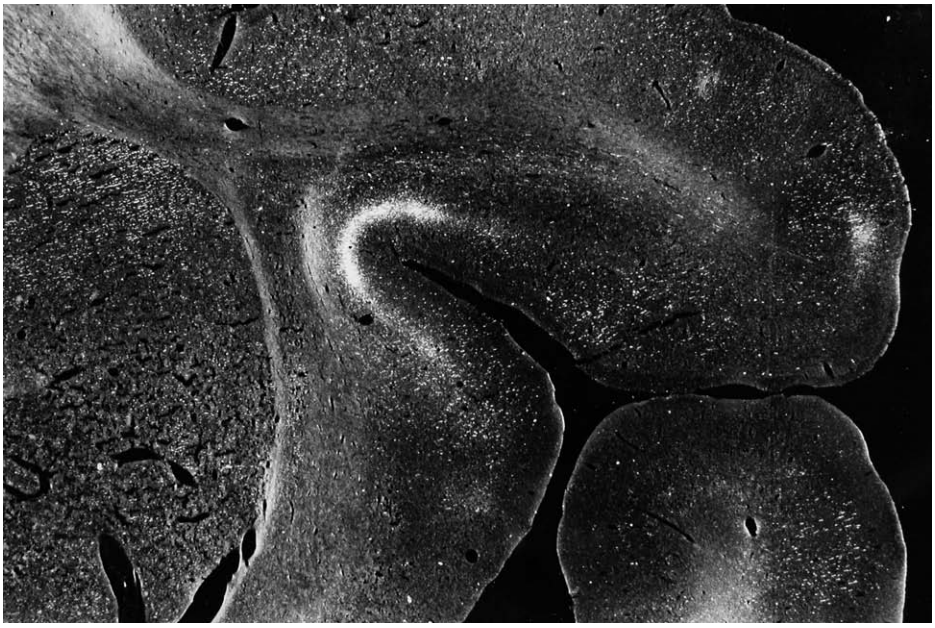

FIGURE 31.7 Darkfield photomicrograph of autoradiographic label in monkey cortex after an injection of tritiated amino acid into the VPMpc. The photomicrograph was taken at the same level as the chart in Figure 31.8B. (Adapted with permission from John Wiley and Sons, Inc.).

Because retrograde degeneration was observed only when both cortical projection areas were destroyed, Benjamin and Burton (1968) suggested that neurons in VPMpc have bifurcating axons that terminate in both cortical areas. Subsequently, the projections from the taste thalamus to the insula/inner operculum and lateral convexity were confirmed by injecting each cortical area with the retrograde tracer horseradish peroxidase (Pritchard *et al.*, 1986; Kusama *et al.*, 1985). Some doubt was cast upon the existence of a sustaining (bifurcating) pathway, however, when only single-labeled neurons were found in VPMpc after injections of the lateral convexity and the insula with two different fluorescent tracers (diamidino yellow and fast blue; Pritchard and Lu, unpublished observations). This issue deserves further investigation.

The clearest demonstrations of the location and extent of primary taste cortex in nonhuman primates derives from studies that have examined the efferent projections of the thalamic taste relay. Injections of anterograde tracers under electrophysiological guidance into VPMpc produced terminal label in two spatially separate cortical areas, the anterior insula/inner operculum and the outer operculum of the frontal lobe (Figs. 31.7 and 31.8; Pritchard *et al.*, 1986; Mesulam and Mufson, 1982; Carmichael and Price, 1995b). The larger of the two terminal distributions appeared as a continuum stretching from the dorsal aspect of the anterior insula around the scs and onto the adjacent inner operculum. The label was densest within the granular cortex (layers IIIb and IV) adjacent to the scs and gradually thinned out as it spread into dysgranular regions of the insula and the inner operculum. As such, the density of terminal label was proportional to the density of granule cells in cortical layers II and IV. The gustatory thalamus does not project to the agranular insula, which extends onto the orbital surface of the frontal cortex (Pritchard *et al.*, 1986; Carmichael and Price, 1995b), or include the lateral half of the inner operculum, as shown by Sanides (1968), Jones and Burton (1976) and Paxinos *et al.* (2000).

The smaller projection from VPMpc to the lateral convexity was located within Brodmann area 3b, immediately rostral to the oral and perioral somatosensory areas of S1 cortex (Figs. 31.7 and 31.8). In area 3b, the terminal label from the VPMpc injections was restricted to the deeper half of layers II, III, and IV, which fuse into a single stratum. In view of the miniscule number of taste cells and the relatively high percentage of tactile neurons located within the precentral extension of Brodmann area 3b, it is likely that this limited projection to this area reflects spread of the autoradiographic injection from VPMpc into the adjacent somatosensory relay, VPM.

In each of the electrophysiological studies cited in the previous section, it was assumed that the gustatory neurons recorded from the insula and operculum were located within primary taste cortex (Ogawa *et al.*, 1989;

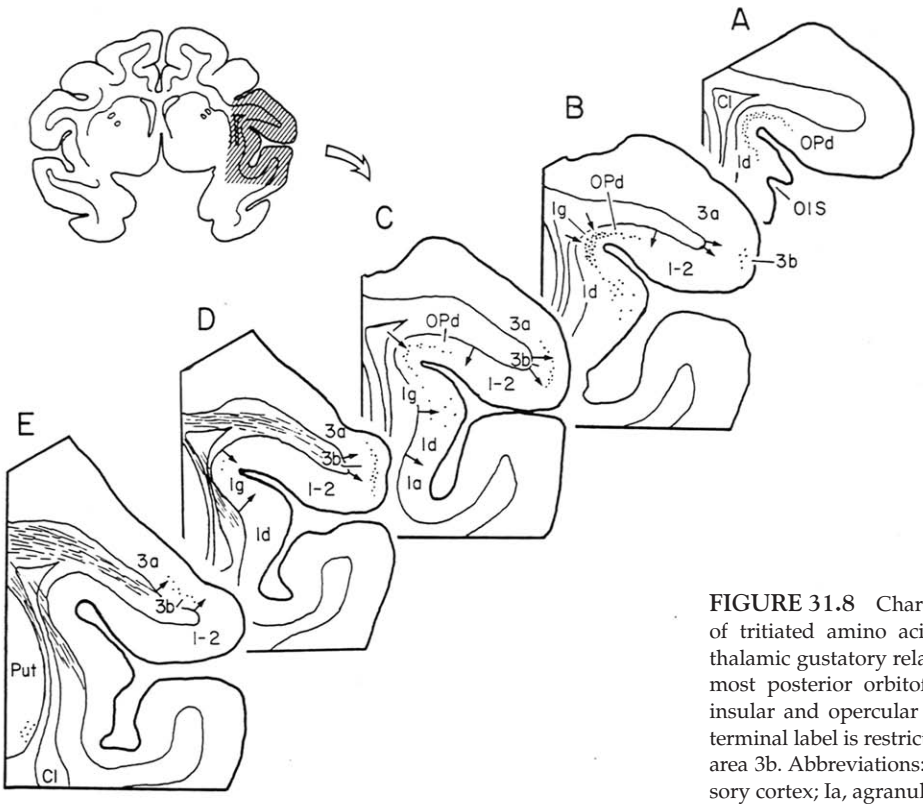

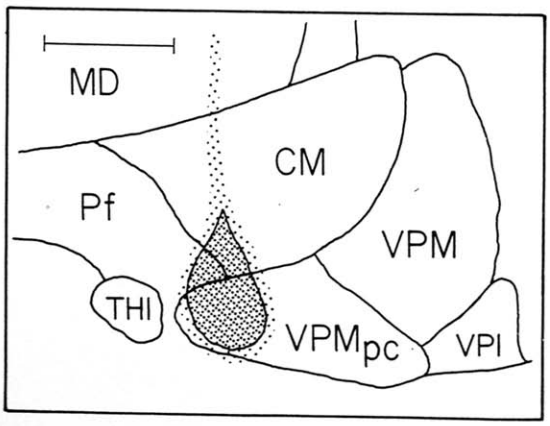

FIGURE 31.8 Charts of terminal label resulting from an injection of tritiated amino acid into the electrophysiologically identified thalamic gustatory relay, VPMpc. The buried field extends from the most posterior orbitofrontal cortex (A) caudally into the rostral insular and opercular cortices (B and C). In the precentral cortex, terminal label is restricted to the most rostral extension of Brodmann area 3b. Abbreviations: 3a, 3b, 1–2, areas of the primary somatosensory cortex; Ia, agranular insula; Id, dysgranular insula; Ig, granular insula; OIS, orbitoinsular sulcus; OPd, dysgranular operculum. (Used with permission from John Wiley and Sons, Inc.).

Ito and Ogawa, 1994; Scott *et al.*, 1986b; Yaxley *et al.*, 1988). Given this presumption, Rolls *et al.* (1990) asserted that the gustatory-responsive neurons within the caudolateral OFC constitute secondary taste cortex. The available electrophysiological and anatomical data suggest that these assertions about both primary and secondary gustatory cortex are, at best, only partly correct. The gustatory neurons recorded in these studies were scattered throughout the granular (Ig), dysgranular (Id), and agranular (Ia) subdivisions of the insula, and the dysgranular operculum (Plata-Salaman *et al.*, 1993). Although the Id receives the faintest projection from the gustatory thalamus, there is no direct projection to Ia or the dysgranular operculum (Pritchard *et al.*, 1986; Carmichael and Price, 1995b). Traditionally, the major determinant for designating an area of the cerebral cortex as primary sensory cortex has been whether that area receives a direct projection from one of the principal sensory relay nuclei in the thalamus. In addition, primary sensory areas within neocortex typically have a distinct granular appearance in layers II and IV, which Sanides (1968, 1970) has referred to as incipient koniocortex (area G). With these considerations in mind, only the Ig located at the insular/opercular junction of the frontal lobe should be considered

primary taste cortex (Pritchard *et al.*, 1986). Other anatomical evidence points to the ventral insula (areas Id and Ia) and the inner operculum (Brodmann areas 1 and 2), rather than the caudolateral OFC, as more likely candidates for secondary gustatory cortices.

If the dysgranular and agranular cortices within the rostral insula and operculum contain taste-responsive neurons but receive no direct projections from the gustatory thalamus, how does taste information reach those areas? Primary taste cortex (Ig) may account for the afferent taste projections to Id and Ia, but Ig has very few projections to the vast expanse of OFC that contains taste-responsive neurons (Rolls and Baylis, 1994; Thorpe *et al.*, 1983; Rolls *et al.*, 1996). The cortical taste areas more likely to project to the OFC are the Id and Ia. The Id receives direct afferent projections from Ig (Barbas, 1993; Mufson and Mesulam, 1982, Mesulam and Mufson, 1985) and the Ia receives projections from both Ig and Id (Barbas, 1993; Mesulam and Mufson, 1982; Carmichael and Price, 1995b; Morecraft *et al.*, 1992). According to Carmichael and Price (1994, 1995a, b), the caudolateral OFC (Brodmann area 47/12o) receives heavier projections from the Ia and Id than from the Ig (see also Mesulam and Mufson, 1982; Barbas, 1988; Morecraft *et al.*, 1992; Baylis *et al.*, 1995) (Fig. 31.9). Areas Ia and Id, but not Ig, also project to all of the other areas within the OFC where taste-responsive neurons have been found (Carmichael and Price, 1995b). For these reasons, Ia and Id are more likely candidates for secondary taste cortices. Anatomical investigations of the efferent projections of the insula suggest that taste-responsive neurons should be located within areas 13l, 13m, 13a, 13b, 47/12o, 14c, and 11l of the OFC (Carmichael and Price, 1995b). Based on the density and distribution of the insulo-orbitofrontal projections to the OFC, the highest concentration of chemosensory neurons are likely to be found in area 13l. To date, however, only a small fraction of the neurons within any part of the OFC appear to be taste-responsive (Rolls and Baylis, 1994), and an even smaller fraction respond to convergent visual, somatosensory, gustatory, and olfactory information (Rolls and Baylis, 1994). Both PET and fMRI studies have shown that gustatory stimuli activate parts of the OFC, but as in primary taste cortex, the papers often obtain different and sometimes contradictory results that are difficult to reconcile with the neurophysiological data collected in nonhuman primates (Zald *et al.*, 1998; O'Doherty *et al.*, 2001). The fact that aversive stimuli are more effective than positive stimuli and the tendency for these responses to be located in only a single hemisphere (typically the left) suggest that these OFC foci are processing the hedonic valence of the stimuli rather than their sensory characteristics. Because the OFC is the first synaptic level where gustatory, olfactory, and visual projections come into close proximity with one another, it is not surprising that even a small cohort of multimodal cells in the OFC has fueled speculation that this is the site where the perception of flavor first emerges.

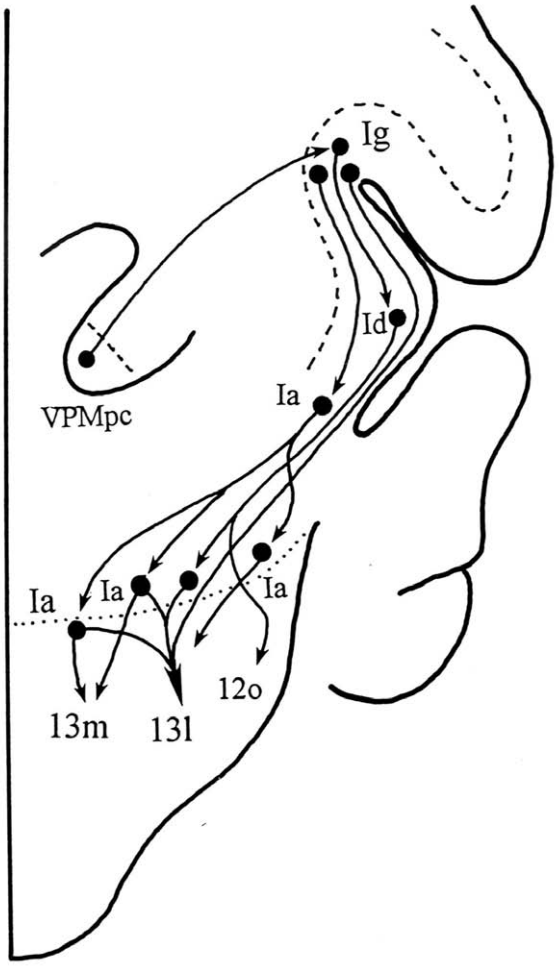

FIGURE 31.9 Thalamocortical and cortico-cortical gustatory projections of the macaque. The thalamic and insular gustatory relays are shown in the coronal plane appended to the ventral surface of the orbitofrontal cortex, oriented with its rostral pole downward. The dotted line indicates the posterior boundary of the orbitofrontal cortex. As shown in this schematic diagram, the orbitofrontal cortex receives more of its gustatory projections from the agranular insula than from either the dysgranular or granular insula. 12o, 13l, 13m, Brodmann areas; Ia, agranular insula; Id, dysgranular insula; Ig, granular insula.

FURTHER GUSTATORY PROCESSING

The ability of taste to provide both positive and negative reinforcement suggests that gustatory

afferent activity must gain access to the limbic system. In rodents and lagomorphs, gustatory information reaches the limbic system through the PB (Norgren, 1974, 1976), and, indeed, gustatory responsive neurons have been recorded in the hypothalamus (Norgren, 1970) and amygdala (Norgren, 1984; Schwartzbaum and Morse, 1978). Gustatory neurons represent only a small fraction of the neurons within the amygdala and the hypothalamus, and the majority of these cells also respond to other sensory modalities. In the monkey, gustatory neurons also are found within the hypothalamus (Nishijo *et al.*, 1986; Rolls *et al.*, 1986) and the amygdala (Scott *et al.*, 1993; Yan and Scott, 1996), but in each case, taste cells represent only a small fraction of

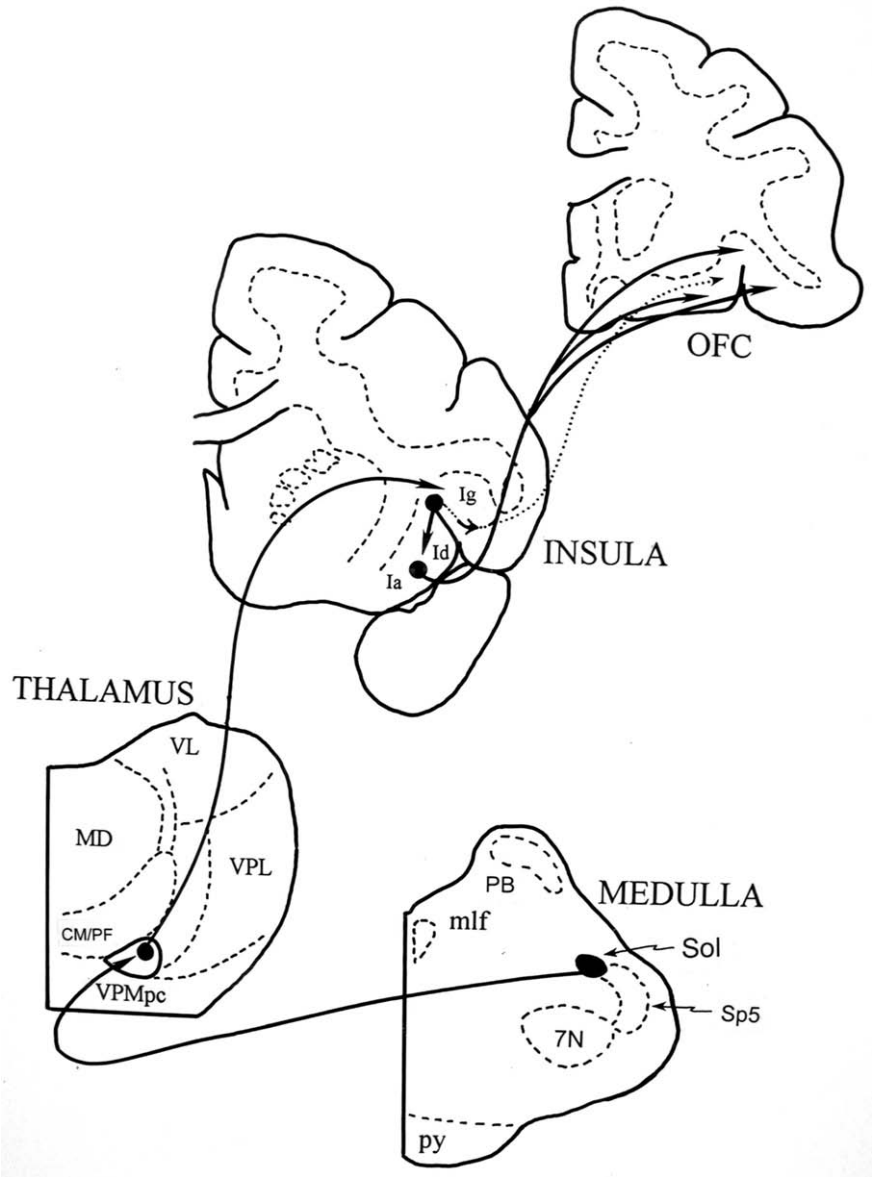

FIGURE 31.10 Central taste pathways of the Old World monkey. This schematic diagram shows the central taste pathways of the Old World monkey charted onto coronal sections of the rostral medulla, the posterior thalamus, the rostral insula, and the posterior OFC. As shown, second-order neurons in the Sol project to VPMpc. Third-order neurons in VPMpc project to the primary taste cortex, which is located in the granular insula (Ig) adjacent to the superior circular sulcus. Projections from the primary taste cortex ascend to the OFC directly and indirectly through the agranular (Ia) and dysgranular (Id) regions of the insula. 7N, facial nucleus; CM/PF, centromedian/parafascicular nuclei of the thalamus; Ia, agranular insula; Id, dysgranular insula; MD, medial dorsal nucleus of the thalamus; mlf, medial longitudinal fasciculus; py, pyramidal tract; Sp5, spinal trigeminal nucleus; VL, ventrolateral nucleus of the thalamus.

the neurons in the area. PET studies have shown that aversive concentrations of quinine and saline (but not sucrose) increase regional blood flow within the amygdala (Zald *et al.*, 1998, 2002), but this activity may have less to do with qualities of bitter and sour than the negative emotional valence of the stimuli (Aggleton, 1992). Following resection of the amygdala to treat pharmacologically intractble epilepsy, subjects report an increase in the intensity for QHCl (Small *et al.*, 2001a, b). If taste information is processed within the hypothalamus and amygdala, the route by which this information reaches these areas is unclear. The PB in primates projects to both the hypothalamus and the amygdala, but with no evidence to suggest that the PB is involved in gustatory function, another route to the ventral forebrain must be considered (Pritchard *et al.*, 1999). There are two possibilities. The thalamic gustatory relay in the cat projects to both the cerebral cortex and the lateral amygdala (Yasui *et al.*, 1987), but in rats and monkeys similar projections are either weak or absent (Aggleton *et al.*, 1980; Kosar *et al.*, 1986; Ottersen and Ben-Ari, 1978; Pritchard *et al.*, 1986; Turner and Herkenham, 1981). The orbitofrontal cortex and the insula both project to the amygdala, but there is no functional evidence that these projections convey gustatory afferent information (Aggleton *et al.*, 1980; McDonald, 1998; Turner *et al.*, 1980). This also applies to subcortical areas where taste-responsive neurons have been found such as the caudate, putamen, ventral striatum, and nucleus accumbens (Hollerman *et al.*, 1998; Tremblay *et al.*, 1998).

Given the logical relationship between taste, hedonic value, and reward expectation, it is not surprising that gustatory neurons have been found within the amygdala, the hypothalamus, and the striatum. Although the route by which taste information reaches the limbic system and striatum is uncertain, a more important issue is whether the minuscule number of taste neurons found in these areas can account for hedonic value and reward expectation.

SUMMARY

In this chapter, we relied heavily on experiments conducted in nonhuman primates and, where possible, reconciled these data with the few published clinical studies. Based upon this synthesis of the experimental and clinical literature, we concluded that all primary afferent gustatory neurons synapse in the rostral half of the nucleus of the solitary tract in the medulla. Unlike nonprimate species, neurons in the gustatory division of the nucleus of the solitary tract project to the thalamus rather than to the pons. The pontine gustatory relay found in rodents is either absent or attenuated in primates. Gustatory projections from the medulla, unlike most other sensory systems, are neither crossed nor lemniscal. They ascend primarily in the ipsilateral central tegmental tract and terminate in the most medial aspect of the ventral posterior nuclear complex, VPMpc. The thalamic gustatory relay projects primarily to the granular part of the rostral insula (primary taste cortex), which, in turn, projects to nearby dysgranular and agranular regions of the insula (secondary gustatory cortices). Subsequent projections across the orbitofrontal cortex may provide the anatomical substrate for integration of taste with visual, auditory, olfactory, somatosensory, and general visceral information.

In conclusion, a more complete view of the gustatory system in humans is available now than was available a decade ago when the first edition was published, but the picture remains incomplete. Most of the fundamental unanswered questions about the central organization of taste are likely to succumb to modern noninvasive imaging techniques. A decade from now, with the anatomical organization of taste reasonably complete, the emphasis in the field will likely shift to issues of function.

Acknowledgments

Our own research summarized here was supported by grants from the Public Health Service (NS20518 and DK59549, both TCP; DC00246 and MH43787, both RN), and the National Science Foundation (BNS9413025, TCP). During preparation of this review R.N. was supported by an NIMH Research Scientist Award (MH00653). Correspondence should be addressed to: Dr. T.C. Pritchard, Department of Neural and Behavioral Sciences, H181, The Pennsylvania State University College of Medicine, 500 University Drive, Hershey, PA 17033 (tcp1@psu.edu).

References

Adler, A. (1933). Zur topik des verlaufes der geschmackssinnsfasern und anderer afferenter bahnen im thalamus. *Z. Gesamte Neurol. Psychiatr.* **149,** 208–220.

Aggleton, J.P. (1992). The functional effects of amygdalar lesions in humans: A comparison with findings from monkeys. *In* "The Amygdala: Neurobiological Aspects of Emotion, Memory, and Mental Dysfunction" (J.P. Aggleton, ed.), pp. 485–503. Wiley-Liss, New York.

Aggleton, J.P., Burton, M.J., and Passingham, R.E. (1980). Cortical and subcortical afferents to the amygdala of the rhesus monkey (*Macaca Mulatta*). *Brain Res.* **190,** 347–368.

Aglioti, S., Tassinari, G., Corballis, M.C., and Berluchi, G. (2000). Incomplete gustatory lateralization as shown by analysis of taste discrimination after callosotomy. *J. Cognit. Neurosci.* **12,** 238–245.

Aglioti, S.M., Tassinari, G., Fabri, M., Del Pesce, M., Quattrini, A., Manzoni, T., and Berlucchi, G. (2001). Taste laterality in the brain. *Eur. J. Neurosci.* **13,** 195–200.

Allen, W.F. (1923). Origin and destination of the secondary visceral fibers in the guinea pig. *J. Comp. Neurol.* **35,** 275–310.

Aou, S., Oomura, Y., Lenard, L., Nishino, H., Inokuchi, A., Minami, T., and Misaki, Y. (1984). Behavioral significance of monkey hypothalamic glucose-sensitive neurons. *Brain Res.* **302,** 69–74.

Arvidson, K., and Freiberg, U. (1980). Human taste: Response and taste bud number in fungiform papillae. *Science* **209,** 807–808.

Astrom, K.E. (1953). On the central course of afferent fibers in the trigeminal, facial, glossopharyngeal, and vagal nerves and their nuclei in the mouse. *Acta Physiol. Scand. Suppl.* **106,** 209–320.

Azuma, S., Yamamoto, T., and Kawamura, Y. (1984). Studies on gustatory responses of amygdaloid neurons in rats. *Exp. Brain Res.* **56,** 12–22.

Barbas, H. (1988). Anatomic organization of basoventral and mediodorsal visual recipient prefrontal regions in the rhesus monkey. *J. Comp. Neurol.* **276,** 313–342.

Barbas, H. (1993). Organization of cortical afferent input to orbitofrontal areas in the rhesus monkey. *Neurosci.* **56,** 841–864.

Barry, M.A., Gatenby, J.C., Zeigler, J.D., and Gore, J.C. (2001). Hemispheric dominance of cortical activity evoked by focal electrogustatory stimuli. *Chem. Senses* **26,** 471–482.

Baylis, L.L., Rolls, E.T., and Baylis, G.C. (1995). Afferent connections of the caudolateral orbitofrontal cortex taste area of the primate. *Neurosci.* **64,** 801–812.

Beckstead, R.M., and Norgren, R. (1979). Central distribution of the trigeminal, facial, glossopharyngeal and vagus nerves in the monkey. *J. Comp. Neurol.* **184,** 455–472.

Beckstead, R.M., Morse, J.R., and Norgren, R. (1980). The nucleus of the solitary tract in the monkey: Projections to the thalamus and brain stem nuclei. *J. Comp. Neurol.* **190,** 259–282.

Benjamin, R.M. (1963). Absence of deficits in taste discrimination following cortical lesions as a function of the amount of preoperative practice. *J. Comp. Physiol. Psychol.* **52,** 255–258.

Benjamin, R.M., and Burton H. (1968). Projection of taste nerve afferents to anterior opercular-insular cortex in squirrel monkey (*Saimiri sciureus*). *Brain Res.* **7,** 221-231.

Benjamin, R.M., Emmers, R., and Blomquist, A.J. (1968). Projection of tongue nerve afferents to somatic sensory area I in squirrel monkey *(Saimiri sciureus). Brain Res.* **7,** 208–220.

Bernard, R.A., and Nord, S.G. (1971). A first-order synaptic relay for taste fibers in the pontine brain stem of the cat. *Brain Res.* **30,** 349–356.

Block, C.H., and Schwartzbaum, J.S. (1983). Ascending efferent projections of the gustatory parabrachial nuclei in the rabbit. *Brain Res.* **259,** 1–9.

Blomquist, A.J., Benjamin, R.M., and Emmers, R. (1962). Thalamic localization afferents from the tongue in squirrel monkey (*Saimiri sciureus*). *J. Comp. Neurol.* **118,** 77–87.

Blum, M., Walker, A.E., and Ruch, T.C. (1943). Localization of taste in the thalamus of *Macaca mulatta. Yale J. Biol. Med.* **16,** 175–191.

Bombardieri, R., Johnson, J., and Campas, G. (1975). Species differences in mechanosensory projections from the mouth to the ventrobasal thalamus. *J. Comp. Neurol.* **163,** 41–64.

Bornstein, W.S. (1940a). Cortical representation of taste in man and monkey. I. Functional and anatomical relations of taste, olfaction and somatic sensibility. *Yale J. Biol. Med.* **12,** 719–736.

Bornstein, W.S. (1940b). Cortical representation of taste in man and monkey. II. The localization of the cortical taste area in man, a method of measuring impairment of taste in man. *Yale J. Biol. Med.* **13,** 133–156.

Bruce, A. (1898). On the dorsal or so-called sensory nucleus of the glossopharyngeal nerve, and on the nuclei of origin of the trigeminal nerve. *Brain* **21,** 383–387.

Burton, H., and Benjamin, R.M. (1971). Central projections of the gustatory system. *In* "Handbook of Sensory Physiology. Chemical Senses. Taste." (L.M. Beidler, ed.), vol. 4, pt. 2, pp. 148–164. Springer-Verlag, Berlin.

Burton, H., Craig, A., and Poulos, D. (1979). Efferent projections from temperature sensitive recording loci within the marginal zone of the nucleus caudalis of the spinal trigeminal complex in the cat. *J. Comp. Neurol.* **183,** 753–778.

Burton, M.J., Mora, F., and Rolls, E.T. (1975). Visual and taste neurons in the lateral hypothalamus and substantia innominata: Modulation of responsiveness by hunger. *J. Physiol.* (Lond.) **252,** 51–51P.

Carmichael, S.T., and Price, J.L. (1994). Architectonic subdivision of the orbital and medial prefrontal cortex in the macaque monkey. *J. Comp. Neurol.* **346,** 366–402.

Carmichael, S.T., and Price, J.L. (1995a). Limbic connections of the orbital and medial prefrontal cortex in macaque monkeys. *J. Comp. Neurol.* **363,** 615–641.

Carmichael, S.T., and Price, J.L. (1995b). Sensory and premotor connections of the orbital and medial prefrontal cortex in macaque monkeys. *J. Comp. Neurol.* **363,** 642–664.

Carmichael, S.T., and Price, J.L. (1996). Connectional networks within the orbital and medial prefrontal cortex of macaque monkeys. *J. Comp. Neurol.* **371,** 179–207.

Cascino, G.D., and Karnes, W.E. (1990). Gustatory and second sensory seizures associated with lesions in the insular cortex seen on magnetic resonance imaging. *J. Epilepsy* **3,** 185–187.

Cechetto, D.F., and Saper, C.B. (1987). Evidence for a viscerotopic sensory representation in the cortex and thalamus in the rat. *J. Comp. Neurol.* **262,** 27–45.

Combarros, O., Miro, J., and Berciano, J. (1994). Ageusia associated with thalamic plaque in multiple sclerosis. *Eur. Neurol.* **34,** 344–346.

Combarros, O., Sanchez-Juan, P., Berchiano, J., and De Pablo, C. (2000). Hemiageusia from an ipsilateral multiple sclerosis plaque at the midpontine tegmentum. *J. Neurol. Neurosurg. Psychiat.* **68,** 796.

Craig, A.D., Bushnell, M.C., Zhang, E.-T., and Blomqvist, A. (1994). A thalamic nucleus specific for pain and temperature sensation. *Nature* **372,** 770–773.

Critchley, H.D., and Rolls, E.T. (1996). Hunger and satiety modify the responses of olfactory and visual neurons in the primate orbitofrontal cortex. *J. Neurophysiol.* **75,** 1673–1686.

Critchley, H.D., Rolls, E.T., and Wakeman, E.A. (1993). Orbitofrontal cortex responses to the texture, taste, smell, and sight of food. *Appetite* **21,** 170.

Csillik, B., and Knyihar-Csillik, E. (1987). Degeneration, transganglionic. *In* "Encyclopedia of Neuroscience." (G. Adelman, ed.), vol. 1, 306–307. Birkhauser, Basel.

Davis, K.D., Tasker, R.R., Kiss, Z.H.T., Hutchison, W.D., and Dostrovsky, J.L. (1995). Visceral pain evoked by thalamic microstimulation in humans. *Neuroreport* **6,** 369–374.

Del Parigi, A., Chen, K., Salbe, A.D., Gautier, J.-F., Ravussin, E., Reiman, E.M., and Tataranni, P.A. (2002). Tasting a liquid meal after a prolonged fast is associated with preferential activation of the left hemisphere. *Neuroreport* **13,** 1141–1145.

DeWulf, A. (1971). "Anatomy of the Normal Human Thalamus." Elsevier, New York.

DiLorenzo, P.M., and Schwartzbaum, J.S. (1982). Coding of gustatory information in the pontine parabrachial nuclei of the rabbit: Magnitude of neural response. *Brain Res.* **251,** 229–244.

Emmers, R. (1962). Localization of thalamic projection of afferents from the tongue in the cat. *Pflugers Arch.* **409,** 367–373.

Faurion, A., Cerf, B., Van De Moortele, P.-F., Lobel, E., MacLeod, P., and LeBihan, D. (1999). Human taste cortical areas studied with functional magnetic resonance imaging: Evidence of functional lateralization related to handedness. *Neurosci. Lett.* **277,** 189–192.

Francis, S., Rolls, E.T., Bowtell, R., McGlone, F., O'Doherty, J.O., Browning, A., Clare, S., and Smith, E. (1999). The representation of pleasant touch in the brain and its relationship with taste and olfactory areas. *NeuroReport* **10,** 453–459.

Freeman, W. (1927). The columnar arrangement of the primary afferent centers in the brain-stem of man. *J. Nerv. Ment. Dis.* **65,** 1–306.

Frey, S., and Petrides, M. (1999). Re-examination of the human taste region: A positron emission study. *Eur. J. Neurosci.* **11,** 2985–2988.

Fulwiler, C.E., and Saper, C.B. (1984). Subnuclear organization of the efferent connections of the parabrachial nucleus in the rat. *Brain Res. Rev.* **7,** 229–259.

Gad, J. (1891). Ueber Beziehungen des Grosshirns zum Fressakt beim Kaninchen. Du Bois Reymond's *Arch. Physiol.* 541–542. (Cited by Bornstein, 1940a.)

Gerebtzoff, M.A. (1939). Les voies centrales de la sensibilite et du gout et leurs terminaisons thalamiques. *Cellule* **48,** 91–146.

Gorschkow, Dr. (1901). Ueber Geschmacks- und Geruchszentren in der Hirnrinde. Inaug.—Diss. St. Petersburg [in Russian]. *Abst. Neurol. Zentralbl.* **20,** 1092–1093. (Cited by Bornstein, 1940a.)

Goto, N., Yamamoto, T., Kaneko, M., and Tomita, H. (1983). Primary pontine hemorrhage and gustatory disturbance: Clinicoanatomic study. *Stroke* **14,** 507–511.

Graham, S.H., Sharp, F.R., and Dillon, W. (1988). Intraoral sensation in patients with brainstem lesion: Role of the rostral spinal trigeminal nuclei in pons. *Neurol.* **38,** 1529–1533.

Hajnal, A., Takenochi, K., and Norgren, R. (1999). Effect of intraduodenal lipid on parabrachial gustatory coding in awake rats. *J. Neurosci.* **19,** 7182–7190.

Halsell, C.B. (1992). Organization of parabrachial nucleus efferents to the thalamus and amygdala in the golden hamster. *J. Comp. Neurol.* **317,** 57–78.

Halsell, C.B., Travers, J.B., and Travers, S.P. (1993). Gustatory and tactile stimulation of the posterior tongue activate overlapping but distinctive regions within the nucleus of the solitary tract. *Brain Res.* **632,** 161–173.

Hamilton, R.B., and Norgren, R. (1984). Central projections of gustatory nerves in the rat. *J. Comp. Neurol.* **222,** 560–577.

Hassler, R. (1959). Anatomy of the thalamus. *In* "Introduction to Stereotaxis with an Atlas of the Human Brain" (G. Schaltenbrand and P. Bailey, eds.), pp. 230–290. Thieme, Stuttgart.

Herness, M.S., and Gilbertson, T.A. (1999). Cellular mechanisms of taste transduction. *Ann. Rev. Physiol.* **61,** 873–900.

Herrick, C.J. (1914). The medulla of the larval *Amblystoma*. *J. Comp. Neurol.* **24,** 343–427.

Hirai, T., and Jones, E.G. (1989). A new parcellation of the human thalamus on the basis of histochemical staining. *Brain Res. Rev.* **14,** 1–34.

Hollerman, J.R., Tremblay, L., and Schultz, W. (1998). Influence of reward expectation on behavior-related neuronal activity in primate striatum. *J. Neurophysiol.* **80,** 947–963.

Hyde, T.M., and Miselis, R.R. (1992). Subnuclear organization of the human caudal nucleus of the solitary tract. *Brain Res. Bull.* **29,** 95–109.

Ishiko, N., Amatsu, M., and Sato, Y. (1967). Thalamic representation of taste qualities and temperature change in the cat. *In* "Olfaction and Taste, Vol. II." (T. Hayashi, ed.). Pergammon Press, New York.

Ito, S., and Ogawa, H. (1994). Neural activities in the frontal-opercular cortex of macaque monkeys during tasting and mastication. *Jap. J. Physiol.* **44,** 141–156.

Jones, E.G. (1990). Correlation and revised nomenclature of ventral nuclei in the thalamus of human and monkey. *Stereotact. Funct. Neurosurg.* **54+55,** 1–20.

Jones, E.G., and Burton, H. (1976). Areal differences in the laminar distribution of thalamic afferents in the cortical fields of the insular, parietal and temporal regions of primates. *J. Comp. Neurol.* **168,** 197–248.

Jones, E.G., and Hendry, S.H.C. (1989). Differential calcium binding protein immunoreactivity distinguishes classes of relay neurons in monkey thalamic nuclei. *Eur. J. Neurosci.* **1,** 222–246.

Jones, E.G., Schward, H.D., and Callahan, P.A., (1986). Extent of the ipsilateral representation in the ventral posterior medial nucleus of the monkey thalamus. *Exp. Brain Res.* **63,** 310–320.

Kahn, E.A., Crosby, E.C., Schneider, R.C., and Taren, J.A. (1969). "Correlative Neurosurgery." Charles C Thomas, Springfield, IL.

Kalia, M., and Sullivan, J.M. (1982). Brainstem projections of sensory and motor components of the vagus nerve of the rat. *J. Comp. Neurol.* **211,** 248–264.

Kanagasuntheram, R., Wong, W.C., and Chan, H.K. (1969). Some observations of the innervation of the human nasopharynx. *J. Anat.* **104,** 361–376.

Kaplan, J.M., Roitman, M.F., and Grill, H.J. (1995). Ingestive taste reactivity as licking behavior. *Neurosci. Biobehav. Rev.* **19,** 89–98.

Karadi, Z., Oomura, Y., Nishino, H., Scott, T.R., Lenard, L., and Auo, S. (1992). Responses of lateral hypothalamic glucose-sensitive and glucose-insensitive neurons to chemical stimuli in behaving rhesus monkeys. *J. Neurophysiol.* **67,** 389–400.

Karamanlidis, A.N., and Voogd, J. (1970). Trigemino-thalamic fibre connections in the goat: An experimental anatomical study. *Acta. Anat.* **75,** 596–622.

Karimnamazi, H., and Travers, J.B. (1998). Differential projections from gustatory responsive regions of the parabrachial nucleus to the medulla and forebrain. *Brain Res.* **813,** 283–302.

Kerr, F.W.L. (1962). Facial, vagal and glossopharyngeal nerves in the cat. *Arch. Neurol.* **6,** 264–281.

King, A., Menon, R.S., Hachinski, V., and Cechetto, D.F. (1999). Human forebrain activation by visceral stimuli. *J. Comp. Neurol.* **413,** 572–582.

Kinney, F.C. (1978). An experimental study of the central gustatory pathways in the monkey, *Macaca mulatta* and *cercopithecus aethiops*. *J. Hirnforsch.* **19,** 21–43.

Kinomura, S., Kawashima, R., Yamada, K., Ono, S., Itoh, M., Yoshioka, S., Yamaguchi, T., Matsui, H., Miyazawa, H., Itoh, H., Goto, R., Fujiwara, T., Satoh, K., and Fukuda, H. (1994). Functional anatomy of taste perception in the human brain studied with positron emission tomography. *Brain Res.* **659,** 263–266.

Kobayakawa, T., Endo, H., Ayabe-Kanamura, S., Kumagai, T., Yamauchi, Y., Kikuchi, Y., Takeda, T., Saito, S., and Ogawa, H. (1996). The primary gustatory area in human cerebral cortex studied by magnetoencephalography. *Neurosci. Lett.* **212,** 155–158.

Kobayakawa, T., Ogawa, H., Kaneda, H., Ayabe-Kanamura, S., Endo, H., and Saito, S. (1999). Spatio-temporal analysis of cortical activity evoked by gustatory stimulation in humans. *Chem. Senses* **24,** 201–209.

Kosar, E.M., Grill, H.J., and Norgren, R. (1986). Gustatory cortex in the rat. II. Thalamocortical connections. *Brain Res.* **379,** 342–352.

Kusama, T., Fujioka, M., Miyakawa, Y., and Fugii, M. (1985). Connections of the fronto-parietal operculum and the postcentral gyrus with the posterior ventral thalamic nucleus, especially its medial nucleus, in monkeys. *J. Hirnforsch.* **26,** 317–331.

Lalonde, E.R., and Eglitis, J.A. (1961). Number and distribution of taste buds on the epiglottis, pharynx, larynx, soft palate and uvula in a human newborn. *Anat. Rec.* **140,** 91–95.

Le Gros Clark, W.E. (1937). The connexions of the arcuate nucleus of the thalamus. *Proc. Roy. Soc. Lond.* **123,** 166–176.

Lenz, F.A., Gracely, R.H., Zirh, T.A., Leopold, D.A., Rowland, L.H., and Dougherty, P.M. (1997). Human thalamic nucleus mediating taste and multiple other sensations related to ingestive behavior. *J. Neurophysiol.* **77,** 3406–3409.

Lewis, D., and Dandy, W.E. (1930). The course of the nerve fibers transmitting sensation of taste. *Archiv. Surg.* **21,** 249–288.

Locke, S. (1967). Thalamic connections to insular and opercular cortex of monkey. *J. Comp. Neurol.* **129,** 219–240.

Loewy, A.D., and Burton, H. (1978). Nuclei of the solitary tract: Efferent projections to the lower brain stem and spinal cord of the cat. *J. Comp. Neurol.* **181,** 421–450.

Lomber, S.G., Payne, B.R., and Rosenquist, A.C. (1994). The spatial relationship between the cerebral cortex and fiber trajectory through the corpus callosum of the cat. *Behav. Brain Res.* **64,** 25–35.

Lundy, R.F., and Norgren, R. (2001). Pontine gustatory activity is altered by electrical stimulation in the central nucleus of the amygdala. *J. Neurophysiol.* **85,** 770–783.

Lussana (1869). Observations pathologiques sur les nerves due gout. *Arch. de physiol. norm. et path.* **2,** 20, 197. (Cited by Lewis and Dandy, 1930.)

Lussana (1872). Observations pathologiques sur les nerves due gout. *Arch. de physiol. norm. et path.* **4,** 150, 334. (Cited by Lewis and Dandy, 1930.)

Makous, W., Nord, S., Oakley, B., and Pfaffmann, C. (1963). The gustatory relay in the medulla. *In* "Olfaction and Taste" (Y. Zotterman, ed.), pp. 381–393. Pergammon Press, New York.

Matsunami, K., Kawashima, T., Ueki, S., Fujita, M., and Konishi, T. (1994). Topography of commissural fibers in the corpus callosum of the cat: A study using WGA-HRP method. *Neurosci. Res.* **20,** 137–148.

McDonald, A.J. (1998). Cortical pathways to the mammalian amygdala. *Prog. Neurobiol.* **55,** 257–332.

McRitchie, D.A., and Tork, I. (1993). The internal organization of the human solitary nucleus. *Brain Res. Bull.* **31,** 171–193.

Mellus, E.L. (1902). On a hitherto undescribed nucleus lateral to the fasciculus solitarius. *Am. J. Anat.* **2,** 361–364.

Menetrey, D., and Basbaum, A.I. (1987). Spinal and trigeminal projections to the nucleus of the solitary tract: A possible substrate for somatovisceral and viscerovisceral reflex activation. *J. Comp. Neurol.* **255,** 439–450.

Mesulam M.-M., and Mufson, E.J. (1982). Insula of the old world monkey. III. Efferent cortical input and comments on function. *J. Comp. Neurol.* **212,** 38–52.

Mesulam M.-M., and Mufson, E.J. (1985). The insula of Reil in man and monkey. *In* "Cerebral Cortex" (A. Peters and E.G. Jones, eds.), vol. 4, pp. 179–226.

Miller, I.J. (1977). Gustatory receptors of the palate. *In* "Food Intake and Chemical Senses" (Y. Katsuki, M. Sato, S. Takagi, and Y. Oomura, eds.), pp. 173–186. University of Tokyo Press, Tokyo.

Miller, I.J. (1986). Variation in human fungiform taste bud densities among regions and subjects. *Anat. Rec.* **216,** 474–482.

Miller, I.J. (1987). Human taste bud density across adult age groups. *J. Gerontol.* **43** (1), B26–B30.

Miller, I.J., Jr., and Spangler, K.M. (1982). Taste bud distribution and innervation on the palate of the rat. *Chem. Senses* **7,** 99–108.

Miyaoka, Y., Shingai, T., Yoshihiro, T., Nakamura, J.-I., and Yamada, Y. (1998). Responses of neurons in the parabrachial region of the rat to electrical stimulation of the superior laryngeal nerve and chemical stimulation of the larynx. *Brain Res. Bull.* **45,** 95–100.

Mochizuki, Y. (1939). Studies on the foliate papillae of Japanese. 2. The number of taste buds. *Okajimas Folia. Anat. Japan.* **18,** 355–369.

Morecraft, R.J., Geula, C., and Mesulam, M.-M. (1992). Cytoarchitecture and neural afferents of orbitofrontal cortex in the brain of the monkey. *J. Comp. Neurol.* **323,** 341–358.

Motta, G. (1958). "I fatttori centrali delle disgeusie." Tipografia Luigi Parma, Bologna.

Motta, G. (1959). I centri corticali del gusto. *Boll. Sci. Med.* **131,** 480–493.

Mufson, E.J., and Mesulam, M.-M. (1982). Insula of the Old World monkey. II. Afferent cortical input and comments on the claustrum. *J. Comp. Neurol.* **212,** 23–37.

Nageotte, J. (1906). The pars intermedia or nervus intermedius of Wrisberg, and the bulbo-pontine gustatory nucleus in man. *Rev. Neurol. Psychiatr.* **4,** 472–488.

Nakajima, Y., Utsumi, H., and Takahashi, H. (1983). Ipsilateral disturbance of taste due to pontine hemorrhage. *J. Neurol.* **229,** 133–136.

Ninomiya, Y., and Funakoshi, M. (1982). Relationship between spontaneous discharge rates and taste responses of the dog thalamic neurons. *Brain Res.* **242,** 67–76.

Nishijo, H., Ono, T., Nakamura, K., Kawabata, M., and Yamatani, K. (1986). Neuron activity in and adjacent to the dorsal amygdala of monkey during operant feeding behavior. *Brain Res. Bull.* **17,** 847–854.

Nomura, S., and Mizuno, N. (1984). Central distribution of primary afferent fibers in the Arnold's nerve (the auricular branch of the vagus nerve): A transganglionic HRP study in the cat. *Brain Res.* **292,** 199–205.

Norgren, R. (1970). Gustatory responses in the hypothalamus. *Brain Res.* **21,** 63–71.

Norgren, R. (1974). Gustatory afferents to ventral forebrain. *Brain Res.* **81,** 285–295.

Norgren, R. (1976). Taste pathways to hypothalamus and amygdala. *J. Comp. Neurol.* **166,** 17–30.

Norgren, R. (1978). Projections from the nucleus of the solitary tract in the rat. *Neurosci.* **3,** 207–218.

Norgren, R. (1981). The central organization of the gustatory and visceral afferent systems in the nucleus of the solitary tract. *In* "Brain Mechanisms of Sensation" (Y. Katsuki, R. Norgren and M. Sato, eds.). John Wiley and Sons, New York.

Norgren, R. (1984). Central neural mechanisms of taste. *In* "Handbook of Physiology—The Nervous System III, Sensory Processes." Darien-Smith, ed.; J. Brookhart and V. Mountcastle, section eds. American Physiological Society, Washington, DC.

Norgren, R. (1990). Gustatory system. *In* "The Human Nervous System" (G. Paxinos, ed.), pp. 845–861. Academic Press, San Diego.

Norgren, R. (1995). Gustatory system. *In* "The Rat Nervous System" (G. Paxinos, ed.). Academic Press, New York.

Norgren, R., and Leonard, C.M. (1973). Ascending central gustatory pathways. *J. Comp. Neurol.* **150,** 217–237.

O'Doherty, J., Rolls, E.T., Francis, S., Bowtell, R., and McGlone, F. (2001). Representation of pleasant and aversive taste in the human brain. *J. Neurophysiol.* **85:** 1315–1321.

Ogawa, H., Imoto, T., and Hayama, T. (1984). Responsiveness of solitario-parabrachial relay neurons to taste and mechanical stimulation applied to the oral cavity in rats. *Exp. Brain Res.* **54,** 349–358.

Ogawa, H., Ito, S.I., and Nomura, T. (1985). Two distinct projection areas from tongue nerves in the frontal operculum of macaque monkeys as revealed with evoked potential mapping. *Neurosci. Res.* **2,** 447–459.

Ogawa, H., Ito, S.I., and Nomura, T. (1989). Oral cavity representation at the frontal operculum of macaque monkeys. *Neurosci Res.* **6,** 283–298.

Olszewski, J. (1952). "The Thalamus of the *Macaca mulatta*. An Atlas for Use with the Stereotaxic Instrument." Karger, New York.

Olszewski, J., and Baxter, D. (1954). "Cytoarchitecture of the Human Brain Stem." J.B. Lippincott, Philadelphia.

Onoda, K., and Ikeda, M. (1999). Gustatory disturbance due to cerebrovascular disorder. *The Laryngoscope* **109,** 123–128.

Oomura, Y., Mishino, H., Karadi, Z., Aou, S., and Scott, T.R. (1991). Taste and olfactory modulation of feeding related neurons in behaving monkey. *Physiol. Behav.* **49,** 943–950.

Ottersen, O.P., and Ben-Ari, Y. (1978). Pontine mesencephalic afferents to the central nucleus of the amygdala of the rat. *Neurosci. Lett.* **8,** 329–334.

Paxinos, G., Huang, X.-F., and Toga, A.W. (2000). "The Rhesus Monkey Brain in Stereotaxic Coordinates." Academic Press, New York.

Paxinos, G., Tork, I., Halliday, G., and Mehler, W.R. (1990). Human homologs to brainstem nuclei identified in other animals as revealed by acetylcholinesterase activity. *In* "The Human Nervous System" (G. Paxinos, ed.), pp. 149–202. Academic Press, New York.

Pearson, A.A. (1947). The roots of the facial nerve in human embryos and fetuses. *J. Comp. Neurol.* **87,** 139–159.

Penfield, W., and Faulk, M.E. (1955). The insula. Further observations on its function. *Brain* **78,** 445–470.

Penfield, W., and Jasper, H. (1954). "Epilepsy and the Functional Anatomy of the Brain." Little, Brown, and Co., Boston.

Petrides, M., and Pandya, D.N. (2001). Comparative cytoarchitectonic analysis of the human and the macaque ventrolateral prefrontal cortex and corticocortical patterns in the monkey. *Eur. J. Neurosci.* **16,** 291–310.

Petrides, M., Alivisatos, B., Pandya, D., and Evans, A.C. (1996). Gustatory cortex: Comparative architectonic analysis in the human and the macaque brain and functional data. *NeuroImage* **3,** S344.

Plata-Salaman, C.R., Scott, T.R., and Smith-Swintosky, V.L. (1993). Gustatory neural coding in the monkey cortex: The quality of sweetness. *J. Neurophysiol.* **69,** 482–493.

Pritchard, T.C. (1991). The primate gustatory system. *In* "Smell and Taste in Health and Disease" (T.V. Getchell, R.L. Doty, L.M. Bartoshuk, and J.B. Snow, eds.). Raven Press, New York.

Pritchard, T.C., Hamilton, R., Morse, J., and Norgren, R. (1986). Projections from thalamic gustatory and lingual areas in the monkey, *Macaca fascicularis*. *J. Comp. Neurol.* **244,** 213–228.

Pritchard, T.C., Hamilton, R.B., and Norgren, R. (1989). Neural coding of gustatory information in the thalamus of *Macaca mulatta*. *J. Neurophysiol.* **61,** 1–14.

Pritchard, T.C., Hamilton, R.B., and Norgren, R. (2000). Projections of the parabrachial nucleus in the Old World monkey. *Exp. Neurol.* **165,** 101–117.

Pritchard, T.C., Macaluso, D.A., and Eslinger, P.J. (1999). Taste perception in patients with insular cortex lesions. *Behav. Neurosci.* **113,** 663–671.

Prutkin, J., Duffy, V.B., Etter, L., Fast, K., Gardner, E., Lucchina, L.A., Snyder, D.J., Tie, K., Weiffenbach, J., and Bartoshuk, L.M. (2000). Genetic variation and inferences about perceived taste intensity in mice and men. *Physiol. Behav.* **69,** 161–173.

Reilly, S., and Pritchard, T.C. (1995). The influence of thalamic lesions on taste preference behavior of Old World monkeys. *Exp. Neurol.* **135,** 56–66.

Rhoton, A.L., Jr. (1968). Afferent connections of the facial nerve. *J. Comp. Neurol.* **133,** 89–100.

Roberts, T. S., and Akert, K. (1963). Insular and opercular cortex and its thalamic projection in *Macaca mulatta*. Schweiz. *Arch. Neurol. Neurochir. Psychiatr.* **92,** 1–43.

Rolls, E.T. (2000). The orbitofrontal cortex and reward. *Cereb. Cortex* **10,** 284–294.

Rolls, E.T., and Baylis, L.L. (1994). Gustatory, olfactory, and visual convergence within the primate orbitofrontal cortex. *J. Neurosci.* **14,** 5437–5452.

Rolls, E.T., Critchley, H.D., Browning, A.S., Hernadi, I., and Lenard, L. (1999). Responses to the sensory properties of fat of neurons in the primate orbitofrontal cortex. *J. Neurosci.* **19,** 1532–1540.

Rolls, E.T., Critchley, H.D., Wakeman, E.A., and Mason, R. (1996). Responses of neurons in the primate taste cortex to the glutamate ion and to inosine 5′-monophosphate. *Physiol. Behav.* **59,** 991–1000.

Rolls, E.T., Murzi, E., Yaxley, S., Thorpe, S.J., and Simpson, S.J. (1986). Sensory-specific satiety: Food-specific reduction in responsiveness of ventral forebrain neurons after feeding in the monkey. *Brain Res.* **368,** 79–86.

Rolls, E.T., Sienkiewicz, Z.J., and Yaxley, S. (1989). Hunger modulates the responses to gustatory stimuli of single neurons in the caudolateral orbitofrontal cortex of the macaque monkey. *Eur. J. Neurosci.* **1,** 53–60.

Rolls, E.T., Yaxley, S., and Sienkiewicz, Z.J. (1990). Gustatory responses of single neurons in the caudolateral orbitofrontal cortex of the macaque monkey. *J. Neurophysiol.* **64,** 1055–1066.

Saleh, T.M., and Cechetto, D.F. (1993). Peptides in the parabrachial nucleus modulate visceral input to the thalamus. *Am. J. Physiol.* **262,** R668–R675.

Sanides, F. (1968). The architecture of the cortical taste nerve areas in squirrel monkey (Saimiri sciureus) and their relationships to insular, sensorimotor and prefrontal regions. *Brain Res.* **8,** 97–124.

Sanides, F. (1970). Functional architecture of motor and sensory cortices in primates in the light of a new concept of neocortex evolution. *In* "Advances in Primatology. The Primate Brain" (C. Noback and W. Montagna, eds.), vol. 1, pp. 137–208. Appleton, New York.

Saper, C.B., and Loewy, A.D. (1980). Efferent connections of the parabrachial nucleus in the rat. *Brain Res.* **197,** 291–317.

Satoda, T., Takahashi, O., Murakami, C., Uchida, T., and Mizuno, N. (1996). The sites of origin and termination of afferent and efferent components in the lingual and pharyngeal branches of the glossopharyngeal nerve in the Japanese monkey *(Macaca fuscata). Neurosci. Res.* **24,** 385–392.

Schtscherbak, A. (1892). Zur Frage uber die Lacalisation der Geschmackscentren in der Hindrinde. *Zentralbl. fur Physiol.* **5,** 289–298. (Cited by Bornstein, 1940a.)

Schwartz, H.G., and Weddell, G. (1938). Observations on the pathways transmitting the sensation of taste. *Brain* **61,** 99–115.

Schwartz, H.G., Roulac, G.E., Lam, R.L., and O'Learly, J.L. (1951). Organization of the fasciculus solitarius in man. *J. Comp. Neurol.* **94,** 221–239.

Schwartzbaum, J.S.,and DiLorenzo, P.M. (1982). Gustatory functions of the nucleus tractus solitarius in the rabbit. *Brain Res. Bull.* **81,** 285–292.

Schwartzbaum, J.S., and Morse, J.R. (1978). Taste responsivity of amygdaloid units in behaving rabbit: A methodological report. *Brain Res. Bull.* **3,** 131–141.

Scott, T.R., and Erickson, R.P. (1971). Synaptic processing of taste quality information in thalamus of the rat. *J. Neurophysiol.* **34,** 868–884.

Scott, T.R., and Giza, B.K. (2000). Issues of gustatory neural coding: Where they stand today. *Physiol. Behav.* **69,** 65–76.

Scott, T.R., and Plata-Salaman, C.R. (1999). Taste in the monkey cortex. *Physiol. Behav.* **67,** 489–511.

Scott, T.R., Karadi, Z., Oomura, Y., Nishino, H., Plata-Salaman, C.R., Lenard, L. et al. (1993). Gustatory neural coding in the amygdala of the alert Macaque monkey. *J. Neurophysiol.* **69,** 1810–1820.

Scott, T.R., Plata-Salaman, C.R., Smith, V.L., and Giza, B.K. (1991). Gustatory neural coding in the monkey cortex: Stimulus intensity. *J. Neurophysiol.* **65,** 76–86.

Scott, T.R., Yaxley, S., Sienkiewicz, Z.J., and Rolls, E.T. (1986a). Gustatory responses in the nucleus tractus solitarius of the alert cynomolgus monkey. *J. Neurophysiol.* **55,** 182–200.

Scott, T.R., Yaxley, S., Sienkiewicz, Z.J., and Rolls, E.T. (1986b). Gustatory responses in the frontal operculum of the alert cynomolgus monkey. *J. Neurophysiol.* **56,** 876–890.

Shikama, Y., Kato, T., Nagaoka, U., Hosoya, T., Katagiri, T., Yamaguchi, K., and Sasaki, H. (1996). Localization of the gustatory pathway in the human midbrain. *Neurosci. Lett.* **218,** 198–200.

Small, D.M., Jones-Gotman, M., Zatorre, R.J., Petrides, M., and Evans, A.C. (1997a). A role for the right anterior temporal lobe in taste quality recognition. *J. Neurosci.* **17,** 5136–5142.

Small, D.M., Jones-Gotman, M., Zatorre, R.J., Petrides, M., and Evans, A.C. (1997b). Flavor processing is more than the sum of its parts. *Neuroreport* **8,** 3913–3917.

Small, D.M., Zald, D.H., Jones-Gotman, M., Zatorre, R.J., Pardo, J.V., Frey, S., and Petrides, M. (1999). Human cortical gustatory areas: A review of functional neuroimaging data. *Neuroreport* **10,** 7–14.

Small, D.M., Zatorre, R.J., and Jones-Gotman, M. (2001a). Changes in taste intensity perception following anterior temporal lobe removal in humans. *Chem. Senses* **26,** 425–432.

Small, D.M., Zatorre, R.J., and Jones-Gotman, M. (2001b). Increased intensity perception of aversive taste following right anteromedial temporal lobe removal in humans. *Brain* **124,** 1566–1575.

Smith, D.V., Liu, H., and Vogt, M.B. (1994). Neural coding of aversive and appetitive gustatory stimuli: Interactions in the hamster brain stem *Physiol. Behav.* **56,** 1189–1196.

Stedman, H.M., Bradley, R.M., Mistretta, C.M., and Bradley, B.E. (1980). Chemosensitive responses from the cat epiglottis. *Chem. Senses* **5,** 223–245.

Sudakov, K., MacLean, P.D., Reeves, A., and Marino, R. (1971). Unit study of exteroceptive inputs to claustrocortex in awake, sitting, squirrel monkey. *Brain Res.* **28,** 19–34.

Thorpe, S.J., Rolls, E.T., and Maddison, S. (1983). The orbitofrontal cortex: Neuronal activity in the behaving monkey. *Exp. Brain Res.* **49,** 93–115.

Tork, I., McRitchie, D.A., Rikard-Bell, G.C., and Paxinos, G. (1990). Autonomic regulatory centers in the medulla oblongata. *In* "The Human Nervous System" (G. Paxinos, ed.), pp. 221–259. Academic Press, San Diego.

Torvik, A. (1956). Afferent connections to the sensory trigeminal nuclei, the nucleus of the solitary tract and adjacent structures: An experimental study in the rat. *J. Comp. Neurol.* **106,** 51–141.

Travers, J.B. (1988). Efferent projections from the anterior nucleus of the solitary tract of the hamster. *Brain Res.* **457,** 1–11.

Travers, J.B., and Smith, D.V. (1979). Gustatory sensitivities in neurons of the hamster nucleus tractus solitarius. *Sensory Processes* **3,** 1–26.

Travers, S.P., and Norgren, R. (1995). Organization of orosensory responses in the nucleus of the solitary tract of the rat. *J. Neurophysiol.* **73,** 2144–2162.

Travers, S.P., Pfaffmann, C., and Norgren, R. (1986). Convergence of lingual and palatal gustatory neural activity in the nucleus of the solitary tract. *Brain Res.* **365,** 305–320.

Tremblay, L., Hollerman, J.R., and Schultz, W. (1998). Modifications of reward expectation-related neuronal activity during learning in primate striatum. *J. Neurophysiol.* **80,** 964–977.

Turner, B., and Herkenham, M. (1981). An autoradiographic study of thalamo-amygdaloid connections in the rat. *Anat. Rec.* **199,** 260A.

Turner, B.H., Mishkin M., and Knapp, M. (1980). Organization of the amygdalopetal projections from modality-specific cortical association areas in the monkey. *J. Comp. Neurol.* **191,** 515–543.

Uesaka, Y., Nose, H., Ida, M., and Takagi, A. (1998). The pathway of gustatory fibers of the human ascends ipsilaterally in the pons. *Neurol.* **50,** 827–828.

Van Buren, J.M., and Borke, R.C. (1972). "Variation and Connections of the Human Thalamus. Vol. 1. The Nuclei and Cerebral Connections of the Human Thalamus." Springer-Verlag, New York.

Vidic, B., and Young, P.A. (1969). Gross and microscopic observations on the communicating branch of the facial nerve to the lesser petrosal nerve *Anat. Rec.* **158,** 257–262.

Walker, A.E. (1938). "The Primate Thalamus." Univ. Chicago Press, Chicago.

Wallenberg, A. (1897a). Das dorsale Gebeit der spinalen Trigeminuswurzel und seine Beziehungen zum solitaren Bundel beim Menchen. *Z. Nervenheilk* **11,** 391–405.

Wallenberg, A. (1897b). Die sekundare Bahn des sensiblen Trigeminus. *Anat. Anz.* **12,** 95–110.

Whitehead, M.C. (1988). Neuronal architecture of the nucleus of the solitary tract in the hamster. *J. Comp. Neurol.* **276,** 547–572.

Whitehead, M.C., McGlathery, S.T., and Manion, B.G. (1995). Transganglionic degeneration in the gustatory system consequent to chorda tympani damage. *Exp. Neurol.* **132,** 239–250.

Wilson, J.H. (1905). The structure and function of the taste-buds of the larynx. *Brain* **28,** 339–351.

Yan, J., and Scott, T.R. (1996). The effect of satiety on responses of gustatory neurons in the amygdala of alert cynomolgus macaques. *Brain Res.* **740,** 193–200.

Yasui, Y., Itoh, K., Sugimoto, T., Kaneko, T., and Mizuno, N. (1987). Thalamocortical and thalamo-amygdaloid projections from the parvicellular division of the posteromedial ventral nucleus in the cat. *J. Comp. Neurol.* **257,** 253–268.

Yaxley, S., Rolls, E.T., and Sienkiewicz, Z. (1988). The responsiveness of neurones in the insular gustatory cortex of the macaque monkey is independent of hunger. *Physiol Behav.* **42,** 223–229.

Zald, D.H., Hahen, M.C., and Pardo, J.V. (2002). Neural correlates of tasting concentrated quinine and sugar solutions. *J. Neurophysiol.* **87,** 1068–1075.

Zald, D.H., Lee, J.T., Fluegel, K.W., and Pardo, J.V. (1998). Aversive gustatory stimulation activates limbic circuits in humans. *Brain* **121,** 1143–1154.

CHAPTER

32

Olfaction

JOSEPH L. PRICE
Department of Anatomy and Neurobiology
Washington University School of Medicine
St. Louis, Missouri, USA

As with other sensory modalities, olfactory information must be transmitted from peripheral olfactory structures (the olfactory epithelium) to more central structures (the olfactory bulb and cortex), integrated to detect and discriminate specific stimuli, and then transferred to other parts of the brain in order to reach sensory consciousness and affect behavior. The olfactory system is different from the other sensory systems, however, in three fundamental ways.

First, the olfactory receptor neurons turn over throughout life and are replaced by mitotic division of the basal cells of the olfactory epithelium. Although other receptor-related cells also turn over, such as the taste buds, these are not true neurons that make synapses within the central nervous system. The olfactory receptors are the only neurons that are inserted in the surface epithelium of the body and are, therefore, directly exposed to the environment. It is likely that this makes them more vulnerable to insult and necessitates their regenerative capacity.

Second, olfaction is the only sensory modality that is directly connected into the cerebral hemisphere (in a sense, the telencephalon developed in relation to olfactory input). Possibly because of this phylogenetic relationship, olfactory sensory activity is transferred directly from the olfactory bulb to the olfactory cortex, without a thalamic relay. Although there is a subsequent projection from the olfactory cortex to the mediodorsal thalamic nucleus and from there to the posterior orbital/agranular insular cortex, this transthalamic pathway is less substantial (in terms of the number of neurons involved) than a direct, monosynaptic projection from the olfactory cortex to the same orbital/insular areas. The transthalamic projection is, therefore, not essential for relay of sensory information to the neocortex.

The third difference is that neural integration and analysis of olfactory stimuli may not involve a topographic organization beyond the olfactory bulb. Olfactory stimuli are not intrinsically ordered along spatial axes, like vision and somatic sensation, or along a frequency axis, like audition. Although an organization has been found in the projection from the olfactory epithelium to the olfactory bulb (e.g., Mombaerts *et al.*, 1996), there is little if any solid evidence for a topographic organization from the bulb to the olfactory cortex. Although it is possible that a more complex organization may eventually be discovered, on the present evidence it is more likely that spatiotemporal patterns across large regions of the

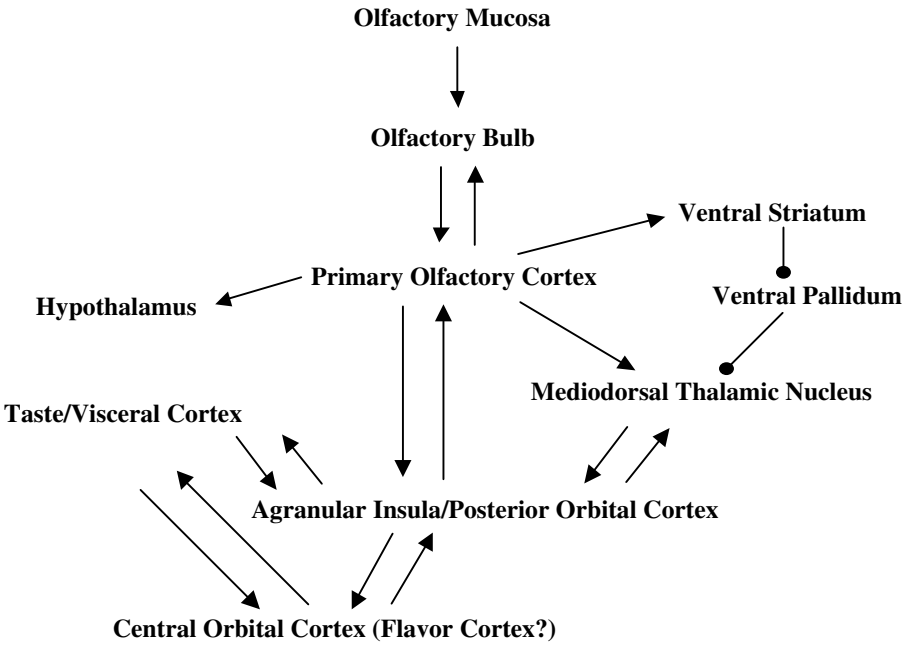

FIGURE 32.1 A schematic diagram of the major olfactory pathways that are discussed in this chapter.

olfactory cortex may be the critical factor in detecting and discriminating different odors.

This chapter will outline the human olfactory system, beginning with the peripheral receptor neurons in the nasal cavity and the first relay in the olfactory bulb (Fig. 32.1). The projections of the olfactory bulb to the primary olfactory cortical areas will be described in macaque monkeys, and the comparable olfactory areas in the human brain will be described. Finally, olfactory projections to the hypothalamus, thalamus, and frontal cortex will be discussed, based on experimental work in monkeys and on functional imaging studies in humans.

Humans are generally considered "microsmatic," with a relatively poorly developed olfactory system compared to that of "macrosmatic" mammals. Indeed, the structure and lamination of the olfactory bulb and primary olfactory cortex are not as well-defined in humans as in rodents and carnivores. Further, the olfactory structures certainly do not make up as large a fraction of the forebrain in humans as in rats and cats. However, almost all the major olfactory structures found in rats are also present in humans, and in absolute terms the human structures are far from rudimentary. For example, the volume of the olfactory bulb in a young adult human is reported to be 45–55 mm^3 (Bhatnager *et al.*, 1987), while it is only 15–20 mm^3 in rats (Hinds and McNelly, 1977). Similarly, the primary olfactory cortical areas such as the anterior olfactory nucleus, piriform cortex, and periamygdaloid cortex are readily recognizable around the junction of the frontal and temporal lobes of human brains.

The only major olfactory structures that may not be present in humans are the vomeronasal organ and the accessory olfactory bulb, which represent the peripheral receptors and first relay of the "accessory olfactory system" in other animals, including monkeys. The accessory olfactory system is anatomically and functionally distinct from the main olfactory system and has been implicated in perception of odors important for species-specific functions, including aspects of reproduction (Wysocki and Meredith, 1987). The vomeronasal organ has been reported to be present in human fetuses (Kreutzer and Jajek, 1980; Nakashima *et al.*, 1985), but reports of it in adult humans are sketchy (e.g., Zbar *et al.*, 2000). Further, an accessory olfactory bulb has not been recognized in humans (e.g., Meisami *et al.*, 1998). The major axonal target of the accessory olfactory bulb in rodents, the medial amygdaloid nucleus, is present in adult humans, but presumably has come to mediate nonolfactory functions.

OLFACTORY MUCOSA

Location

The peripheral olfactory receptor neurons in the human are situated within the olfactory epithelium, in the posterodorsal recess of the nasal cavity, 7 cm deep

to the nostril (e.g., see Jajek, 1983; Lovell *et al.*, 1982; Nakashima *et al.*, 1984). This specialized epithelium occupies an area of approximately 1 cm^2 (on each side) on the roof of the cavity (covering the cribiform plate), the adjacent nasal septum and superior turbinate. The remainder of the nasal cavity (60 cm^2 on a side) is occupied by a respiratory epithelium, which serves the major function of conditioning the air that passes through the nose. The inaccessibility of the olfactory epithelium serves an important role in protecting the receptor neurons, which are the only sensory neurons that are directly exposed to the external environment in the surface epithelium of the body.

Structure

The human olfactory epithelium is considerably thicker than the respiratory epithelium (70 versus 45 μm), and is generally described as containing bipolar receptor neurons, supporting or sustentacular cells, and basal cells. In addition, microvillar cells have been found near the surface, and Bowman's glands extend deep to the epithelium into the lamina propria. The epithelium is pseudostratified, and both the bipolar receptor cells and the sustentacular cells span the full thickness. Cilia or microvillae extend from the apical surface of the cells into a layer of mucus that covers the epithelium and separates it from the air of the nasal cavity.

The Bowman's glands are tubuloaveolar in nature, with ducts extending through the epithelium to the surface. In humans, they apparently secrete a serous fluid that contributes to the mucous layer overlying the epithelium (Jajek, 1983). Because of the number of these glands and their restricted distribution in the olfactory region, it has been suggested that the secretion of Bowman's glands may play a role in olfactory transduction, but this has not been well established.

The bipolar receptor neurons have a "dendrite" that extends to the surface of the epithelium and a thin (0.2–0.3 μm) axon that runs into the lamina propria. The axons then group together into small bundles or "fila" and run through the cribiform plate to the olfactory bulb. The cell bodies of the receptors occupy a broad band in the middle of the olfactory epithelium, deep to the nuclei of the supporting cells and superficial to the basal cells. Counts of the receptors in humans indicate that their density is about 30,000 per mm^2, or 6 million per nose (Moran *et al.*, 1982a). As in other mammals, the human receptor neurons and their processes show selective immunoreactivity for the olfactory marker protein (Nakashima *et al.*, 1985). Evidence from rats and other animals indicates that the transmitter used by the receptor neurons is glutamate (Berkowicz, *et al.*, 1994; Aroniadou-Anderjasska *et al.*, 1997).

Superficially, the receptor dendrite terminates in the knoblike olfactory vesicle, which protrudes above the surface of the epithelium. Ten to 30 nonmotile cilia arise from basal bodies in each olfactory vesicle and protrude into the mucous layer (Jajek, 1983). The cilia generally have the typical 9 pairs +2 microtubule structure, without dynein arms between the microtubule pairs. The ciliary membranes carry molecular odorant receptors, which mediate sensory transduction from odorant molecules to neural signals.

There are believed to be about 1000 odorant receptors, each of which binds a specific chemical moiety. The receptors are coded for by the largest known gene family in mammals (Buck and Axel, 1991; Glusman *et al.*, 2000). In humans, odorant receptor genes are distributed over at least 16 chromosomes, but as many as 72% of them are reported to have accumulated mutations that make them dysfunctional pseudogenes (Rouquier *et al.*, 1998). Studies in rodents have indicated that olfactory receptor neurons are organized into four zones within the olfactory epithelium, which express different groups of molecular odorant receptors (Ressler *et al.*, 1993; Vassar *et al.*, 1993; Mori *et al.*, 1999). Within each zone, neurons expressing specific odorant receptors are intermingled with neurons expressing other receptors.

The microvillar cells are flask-shaped cells in the superficial zone of the epithelium with a rapidly tapering neck that ends in a tuft of microvilli that extends out into the mucous layer (Jajek, 1983; Moran *et al.*, 1982b). Although the neuronal nature of these cells is not established, they have a thin, axon-like process that extends toward the deepest layer of the epithelium toward the olfactory bulb.

The supporting cells in the olfactory epithelium are columnar cells, with a microvillous border at their apex. Unlike similar cells in the adjacent respiratory epithelium, those in the olfactory epithelium do not show morphological specializations characteristic of mucous secretion. The function of the supporting cells is not clear, but several functions have been suggested, including secretion of a nonmucous substance, phagocytotic removal of substances from the mucous, or provision glia-like support for the receptor neurons (e.g., Jajek, 1983).

The basal cells are situated in the deepest zone of the olfactory epithelium. As in other vertebrates, the basal cells in humans are apparently stem cells, undergoing mitotic division and differentiation into receptor neurons lost to turnover or injury (Moran *et al.*, 1982a). Such replacement cannot keep up with degeneration over a human lifetime, however. In adults substantial

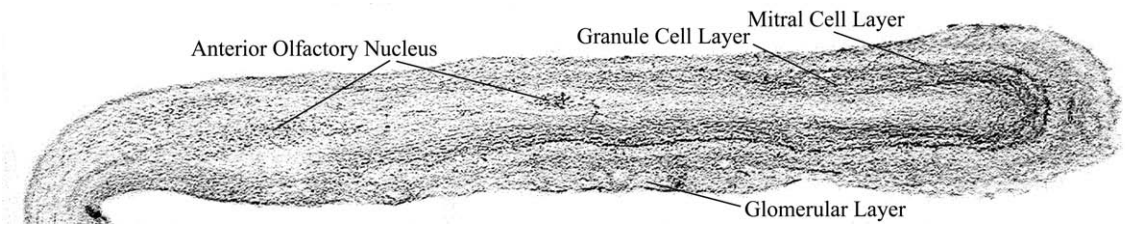

FIGURE 32.2 Photomicrograph of a sagittal section of the human olfactory bulb from a 61-year-old subject, stained with the Nissl method. The glomerular layer is relatively poorly formed, although the other layers are clear. Note the clusters of neurons that comprise the intrabulbar portion of the anterior olfactory nucleus.

areas of the olfactory epithelium are found to have degenerated or been replaced with respiratory epithelium (Nakashima, *et al.*, 1984, 1985; Morrison and Costanzo, 1992).

OLFACTORY BULB

In most primates, including humans, the olfactory bulb is pulled forward from its point of attachment to the cerebral hemisphere, remaining connected by a relatively long olfactory stalk or peduncle. The intrinsic structural features of the human olfactory bulb are similar to those in other species, but it is somewhat less sharply defined. As in all mammals, in humans the bulb has a concentric laminar structure with distinct neuronal somata and synaptic neuropil separated into layers (Fig. 32.2). Although our understanding of the synaptic organization of the olfactory bulb depends on observations made in rats and other animals (see Macrides *et al.*, 1985; Scott and Harrison, 1987; Mori *et al.*, 1999 for reviews), it is very likely that the human bulb has the same basic organization.

The olfactory nerve fibers ramify in the most superficial layer (olfactory nerve layer), after passing through the cribiform plate from the nasal cavity. Where the nerves first reach the olfactory bulb, rostrally and ventrally, the olfactory nerve layer is thick. It becomes progressively thinner in the more caudal and dorsal part of the bulb. Deep to the olfactory nerve layer, the fibers terminate in the characteristic glomerular formations both on the primary dendritic tufts of the "mitral" and "tufted" relay cells and on other cell types. In rats, the transmitter used at this synapse has been shown to be glutamate, which acts on both NMDA and non-NMDA receptors (Aroniadou-Anderjaska *et al.*, 1997).

In rodents, the organization of the olfactory epithelium into zones appears to be more or less preserved in the olfactory bulb, based on the distribution of zone-specific molecular markers (Mori *et al.*, 1999). Within each zone in the epithelium, axons from the several thousand receptor neurons that express a given molecular odorant receptor converge onto one or two glomeruli in the corresponding zone of the olfactory bulb (Vassar *et al.*, 1994; Ressler *et al.*, 1994). This suggests that the glomeruli are the unit structures for olfactory discrimination (e.g., Mori *et al.*, 1999). That is, the initial distinction between different odors is based on hard-wired connections between specific receptor neurons and specific glomeruli. Studies with 2-deoxygluclose as a functional imaging method have also shown that specific odorants activate a small, consistent portion of the olfactory bulb, again suggesting that initial olfactory discrimination depends on a spatial code in the olfactory bulb (e.g., Johnson and Leon, 2000; Xu *et al.*, 2000).

The synaptic neuropil of the glomeruli is outlined by somata of small "periglomerular cells." These interneurons send dendrites and axons into adjacent glomeruli and receive synapses from the olfactory nerves. Like the granule cells in the deeper part of the bulb, the periglomerular cell dendrites form "reciprocal" or bi-directional synapses with mitral and tufted dendrites. In humans as in other animals, most (at least) of the periglomerular cells are GABAergic and also contain one of the calcium-regulating proteins, parvalbumin or calbindin (Ohm *et al.*, 1990, 1991; Kosaka *et al.*, 1987). In addition, many are dopaminergic (Smith *et al.*, 1991). In rats it has been shown that GABA and dopamine colocalize within periglomerular cells (Kosaka *et al.*, 1985; Gall *et al.*, 1987). There are also a number of superficial "short axon cells" in the glomerular region.

Deep to the glomeruli is the external plexiform layer, with dendrites of mitral, tufted, and granule cells. The tufted cell somata are also scattered throughout this layer, but the mitral cell somata are located in a thin layer at the border between the external plexiform layer and the deeper granule cell layer. One or occasionally two "primary" dendrites of the mitral and tufted cells arise from the superficial aspect of the

somata and extend through the external plexiform layer to the glomeruli. Several "secondary" dendrites ramify in the external plexiform layer.

The small granule cells are by far the most numerous neuron type in the olfactory bulb, and the granule cell layer makes up approximately half of the volume of the bulb (Bhatnagar *et al.*, 1987). These interneurons lack an axon and instead send a superficial "dendritic" process into the external plexiform layer, where they form reciprocal synapses with mitral and tufted cell dendrites. Other dendrites ramify within the granule cell layer and are solely post-synaptic. There are also short axon cells in the granule cell layer, which synapse on the granule cells.

Studies in rats and other animals indicate that the mitral to granule cell component of the reciprocal synapse uses glutamate, acting on both NMDA and non-NMDA receptors (Chen *et al.*, 2000). The granule to mitral cell component of the synapse is GABAergic, acting on GABA-A receptors. The reciprocal synapses appear to allow for spatial and temporal modulation of activity in the relay cells, both on a local basis (at individual synapses) and on a more global level (through conduction along granule and mitral/tufted cell dendrites). It has been reported in nonhuman primates, including chimpanzees, that the somata and dendrites of many cells in the olfactory bulb may be ensheathed by compact myelin (Tigges and Tigges, 1980). Since many, at least, of these cells have presynaptic dendrites, it is possible that the myelin will affect conduction between different segments of the neuron.

In humans, approximately 8000 glomeruli and 40,000 mitral cells have been counted in young adults (Meisami *et al.*, 1998). There is a progressive decrease with age in the number and structural integrity of the glomeruli, and in the thickness of the glomerular/periglomerular layer (Bhatnagar *et al.*, 1987; Meisami *et al.*, 1998). In olfactory bulbs from very old individuals (>90 years old) less than 30% of the glomeruli and mitral cells were recognized. Together with the degeneration of the olfactory epithelium mentioned previously, this presumably is related to the decline in olfactory function with age (e.g., Murphy *et al.*, 2000).

PRIMARY OLFACTORY CORTEX

Cortical Structure and Projections of the Olfactory Bulb

The axons of mitral and tufted cells run through the granule cell layer and emerge from the caudolateral aspect of the olfactory bulb to form the lateral olfactory tract. This tract forms the bulk of the olfactory peduncle in humans and other primates. Although a "medial olfactory tract" has been described in the past, a large body of experimental studies in several mammalian species, including primates, has shown that all the axons from the olfactory bulb pass through the lateral olfactory tract. There is no medial olfactory tract in mammals. The lateral olfactory tract can be visualized readily in human brain sections stained for fibers or myelin. It runs just deep to the pial surface, from the olfactory peduncle onto the posterior ventral surface of the frontal lobe and then laterally around the junction between the frontal and temporal lobes (the limen insulae) and onto the anteromedial part of the temporal lobe. Most of the primary olfactory cortical areas have a relatively simple structure, with a broad plexiform layer composed of dendrites of neurons in deeper layers (I), a well-defined, compact layer of pyramidal-like cell somata (II) and a deeper layer(s) of pyramidal and nonpyramidal cells (III and higher).

The full efferent projection of the olfactory bulb can only be mapped with experimental methods, so the description of this projection is based on data from nonhuman primates (Heimer *et al.*, 1977; Turner *et al.*, 1978; Carmichael *et al.*, 1994; Fig. 32.3). As in lower animals, axons from the olfactory bulb in monkeys run caudally through the lateral olfactory tract and give off collaterals that extend medially, laterally, and deep to the tract to contact dendrites in the superficial part of layer I of the olfactory cortex. In addition, in primates a few axons from the olfactory bulb are found in and deep to layer II. In contrast to the olfactory bulb, there is very little evidence for a spatial organization that could support a spatial code in the olfactory cortex. That is, small areas of the olfactory bulb project to virtually the entire olfactory cortex, and small areas of the cortex receive fibers from virtually the entire olfactory bulb (e.g., Haberly and Price, 1977; Luskin and Price, 1982; Haberly 1985). There may be a more "fine-grain" organization within this (e.g., Ojima *et al.*, 1984), but it has not yet been recognized.

Anterior Olfactory Nucleus

The anterior olfactory (AO) nucleus is the most rostral of the tertiary olfactory structures (Figs. 32.3, 32.4, and 32.5). In primates, including humans, there is a "bulbar" part of this nucleus located in the rostral part of the olfactory peduncle, including several groups of pyramidal-like cells in the caudolateral part of the olfactory bulb. As in other olfactory cortical areas, axons of the mitral and tufted cells synapse on the distal segments of dendrites that extend into the plexiform layer around the neuron clusters. More

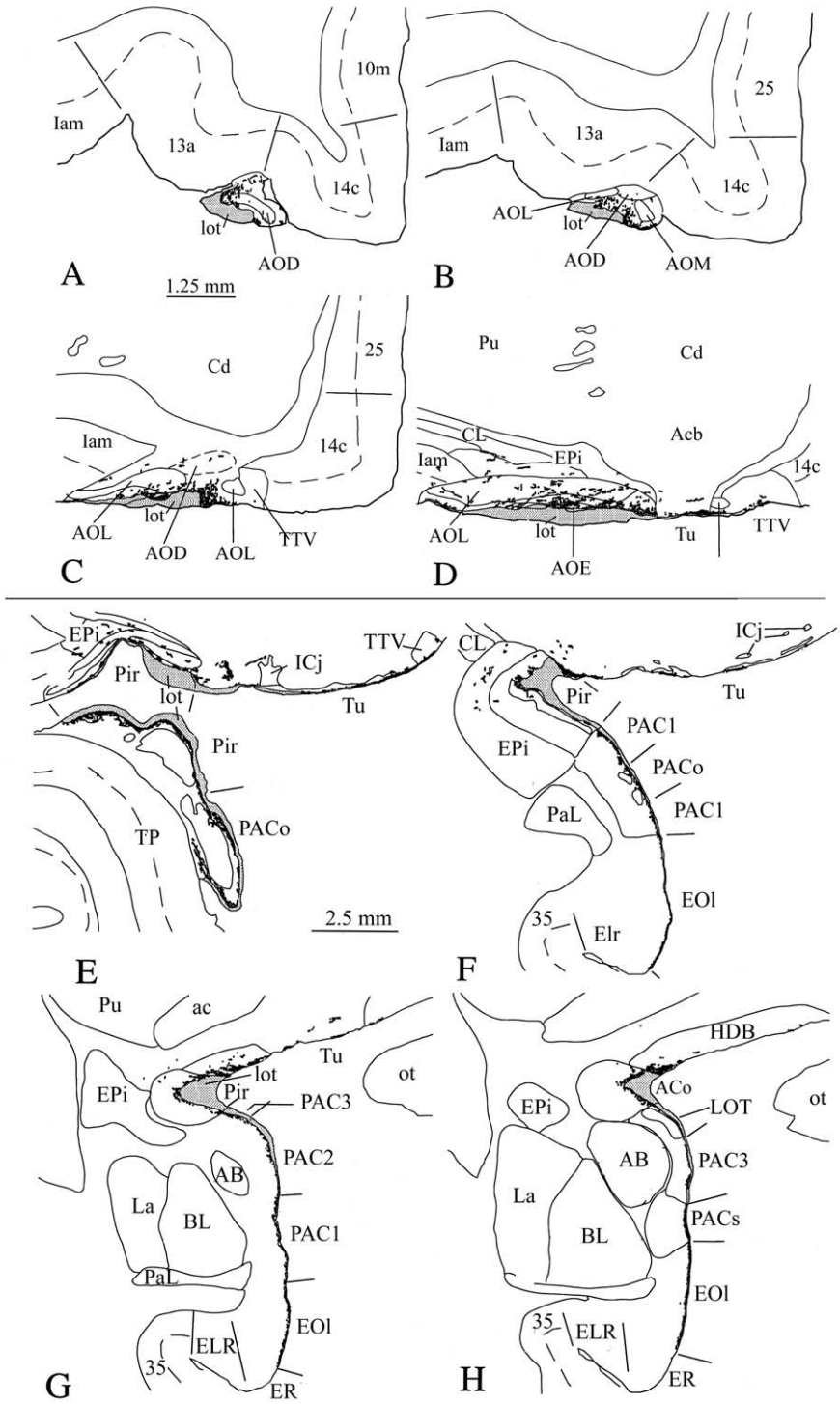

FIGURE 32.3 The distribution of fibers of the lateral olfactory tract in monkeys, that were labeled by an injection of the anterograde tracer biotinylated dextran amine into the olfactory bulb. The shaded area represents the lateral olfactory tract, which was heavily labeled. Dashes and dots represent labeled axons that extend from the tract into the primary olfactory cortex. Almost all of the fibers terminate in the most superficial layer of the olfactory cortex, just deep to the lateral olfactory tract or the pia. Taken from Carmichael *et al.* (1994). Note that the scale is different for the upper and lower parts of the figure.

FIGURE 32.4 Line drawings illustrating the location of the primary olfactory cortical areas in humans, on the ventral surface of the posterior frontal lobe and the anteromedial part of the temporal lobe.

caudal "medial" and "lateral" subdivisions of the AO are situated on either side of the lateral olfactory tract where it joins the orbital cortex, at the posterior end of the olfactory peduncle. In monkeys and other animals, "external" and "dorsal" subdivisions are also recognizable, but these are not readily distinguishable in humans.

Olfactory Tubercle

More caudally on the ventral surface of the frontal lobe, the lateral olfactory tract runs at the junction of the olfactory tubercle (Tu), medially, and the piriform cortex, dorsal and laterally (Figs. 32.3, 32.4, and 32.5). The olfactory tubercle is a prominent structure in rodents and carnivores with a well-developed laminar structure similar to that in other olfactory cortical areas. It is much less distinct in primates but still has a laminar arrangement of cell bodies and afferent fibers. In all mammals, collaterals of axons in the lateral olfactory tract leave the medial side of the tract and run through the superficial part of layer I of the olfactory tubercle to contact apical dendrites of cells with somata in layers II and III. Although this laminar structure is clearly cortical, other features of the olfactory tubercle resemble the underlying corpus striatum, and it has often been included with the nucleus accumbens in the "ventral striatum" (Chapter xx). For example, the tubercle has a high concentration of acetylcholinesterase (Hertz-Schuett and Mai, 1991), apparently related to intrinsic cholinergic neurons, and it receives a prominent dopaminergic input from the ventral midbrain. Its major output is to the "ventral pallidum," which is similar to and dorsally continuous with the globus pallidus.

The primary neurons of the olfactory tubercle closely resemble the "medium spiny" cells of other parts of the striatum in their dendritic structure and appearance. Between and deep to these cells are clusters of small neurons that constitute the islands of Calleja. In monkeys, ventral pallidal elements are distributed somewhat loosely within the deep part of the tubercle rostrally, although more distinct components of the ventral pallidum are found further caudally and dorsally. In humans, the olfactory tubercle is so poorly developed that it is difficult to delineate it precisely from the nucleus accumbens. The nucleus accumbens and, more caudally, the substantia innominata extend to the ventral surface in both monkeys and humans and occupy much of the area referred to as the olfactory tubercle in gross anatomical terms.

Piriform Cortex

The piriform cortex (Pir) is the largest and most distinctive olfactory cortical area. The area was previously referred to as the prepiriform or prepyriform cortex, apparently because it is partially situated

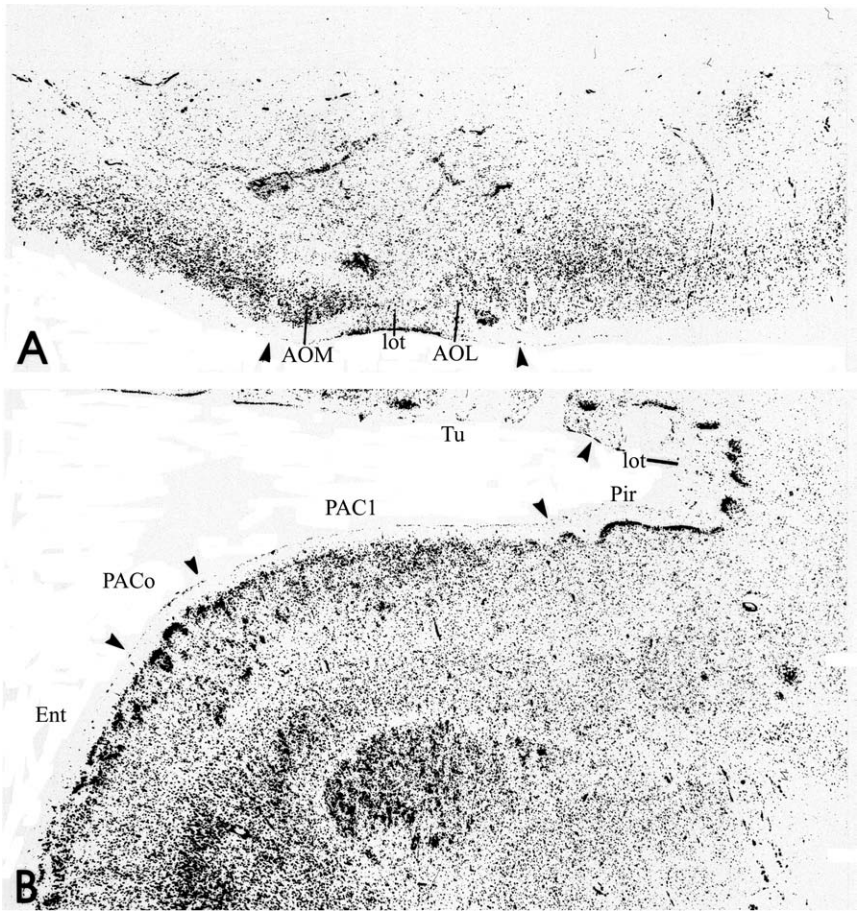

FIGURE 32.5 Photomicrographs of the human primary olfactory cortex. **(A)** The anterior olfactory nucleus, on the posterior orbital surface, just caudal to the point where the olfactory peduncle joins the frontal cortex. **(B)** The olfactory areas around the point of junction between frontal and temporal lobes. AOL and AOM; anterior olfactory subdivisions; Ent, entorhinal cortex; lot, lateral olfactory tract; PAC0 and PAC1, periamygdaloid subdivisions; Pir, piriform cortex; Tu, olfactory tubercle.

rostral to the "pyriform lobule" in carnivores. This designation is not descriptive in most animals, however, and the suffix "pre" has been dropped. In both monkeys and humans, the piriform cortex is situated deep and lateral to the lateral olfactory tract, from the caudolateral aspect of the frontal lobe, around the limen insulae, to the rostral dorsomedial aspect of the temporal lobe (Figs. 32.3 and 32.4). The piriform cortex is characterized by a densely packed layer II composed of moderately large pyramidal cell somata and a less dense layer III of slightly larger pyramidal cells and other neurons (Fig. 32.5). Layer II is found throughout the piriform cortex, but layer III is only well developed in the caudal part of the cortex. In monkeys, layer II is thick and prominent, but in humans layer II is relatively thin, and the boundaries of the cortex are not as distinct. Deep to the cortex, a ventral continuation of the claustrum forms the endopiriform nucleus. There is little data on this nucleus in primates, but in rodents it is closely interonnected with the overlying piriform cortex.

Axon collaterals leave the deep and lateral aspects of the lateral olfactory tract and terminate primarily on apical dendrites in the superficial part of layer I. In monkeys, although not in rodents or carnivores, a few fibers from the olfactory bulb also ramify in deeper layers. As discussed later, the piriform cortex gives rise to a substantial association fiber system that extends throughout all parts of the primary olfactory cortex.

Anterior Cortical Nucleus of the Amygdala and Periamygdaloid Cortex

Caudal and lateral to the piriform cortex, the axons from the olfactory bulb continue into several small areas on the medial surface of the amygdala (Figs. 32.3 and 32.4). The anterior cortical amygdaloid nucleus is

directly caudal to the piriform cortex and is characterized by a relatively loosely packed layer II and even more diffuse layer III. The periamygdaloid cortex is a larger area located ventrolateral to the piriform cortex. It is markedly heterogeneous and, in monkeys and humans, can be divided into five subdivisions—PAC_O, PAC_1, PAC_2, PAC_3, and PAC_S, based on architectonic differences (Price *et al.*, 1987; Amaral *et al.*, 1992; Carmichael *et al.*, 1994). All but the most caudal of these (PAC_S) receive input from the olfactory bulb in monkeys, although the layer of axons is thick only in PAC_O, and is quite thin in PAC_1, PAC_2, and PAC_3.

Rostral, "Olfactory" Entorhinal Cortex

In rodents and carnivores, a large fraction of the entorhinal cortex receives fibers directly from the olfactory bulb (e.g., Boeijinga and Van Groen, 1984; Price, 1973). In monkeys, however, olfactory bulb input is limited to a small "olfactory" zone at the rostral edge of the entorhinal cortex (Amaral *et al.*, 1987; Carmichael *et al.*, 1994; Figs. 32.3 and 32.4). Even in this region, the olfactory projection is relatively slight, both in density, and in the thickness of the superficial lamina in layer I in which the fibers end. EOl is characterized by a distinct but thin layer II, which is broken up into cell islands, as in other parts of the entorhinal cortex. The deeper layers are thicker and more complex than in other olfactory cortical areas, but less well developed than in other regions of the entorhinal cortex.

Accessory Olfactory Cortical Areas

Although humans lack an accessory olfactory bulb, the major target of the accessory olfactory tract in other animals, the medial amygdaloid nucleus, is present in humans. The medial nucleus is situated immediately caudal to the anterior cortical amygdaloid nucleus but has a slightly denser cellular layer II. In rodents, this nucleus has been shown to be involved in mating behavior and a variety of other related functions (Newman, 1999). Presumably, the medial amygdaloid nucleus may have similar functions in humans, but these may not be as strongly modulated by olfactory stimuli.

Centrifugal Projections to the Olfactory Bulb

All the olfactory cortical areas except the olfactory tubercle send fibers back to the olfactory bulb (Haberly, 1985; Price, 1987; Carmichael *et al.*, 1994). These fibers arise from cells in layers II and III of the cortex and end primarily in the granule cell layer of the olfactory bulb. The projection from the anterior olfactory nucleus and (in monkeys) the anterior part of the piriform cortex is bilateral, with fibers crossing in the anterior commissure. In addition, a thin "external" part of the anterior olfactory nucleus just deep to the most rostral part of the lateral olfactory tract projects solely or (in monkeys) primarily to the contralateral olfactory bulb.

There is also a substantial fiber projection from the nucleus of the diagonal band to the olfactory bulb (Mesulam *et al.*, 1983; Carmichael and Price, 1994). Although this fiber system is partially cholinergic, only about 10% of the cells stain for acetylcholinesterase (Mesulam *et al.*, 1983). In rats, other cells in the nucleus that project to the olfacotory bulb have been shown to be GABAergic (Zaborsky *et al.*, 1985).

Intracortical Associational Fiber System

Experimental studies in many mammals, including monkeys, have indicated that the "primary" olfactory cortex is organized in a very different way than other primary sensory cortices. In particular, there is an extensive system of intracortical connections with the primary olfactory cortex (e.g., Haberly, 1985; Price, 1973; Luskin and Price, 1983; Carmichael *et al.*, 1994; Johnson *et al.*, 2000). This system suggests that the olfactory cortex functions as a correlative region, comparable to a higher order "association" cortex in other sensory systems.

The greatest number of association fibers arises in the piriform cortex, but fibers originate in all of the olfactory cortical areas except the olfactory tubercle. The fibers are distributed throughout the olfactory cortex and to adjacent orbital and agranular insular areas. In rats, at least, individual neurons in the piriform cortex have axons that extend into all or most of these areas (Johnson *et al.*, 2000). Within the olfactory cortex itself, the association fibers terminate primarily in the deep part of layer I and in layer III. This laminar pattern of termination is complementary to the termination of the fibers from the olfactory bulb in the superficial part of layer I. In the tangential dimension of the cortex, there is a broad and relatively complex organization within the association fibers, which has been best defined in rats. Cortical regions near the lateral olfactory tract project to other parts of the olfactory cortex near the tract, while regions distant to the tract tend to project to regions at the edges of the olfactory cortex (Luskin and Price, 1983; Price, 1985; Carmichael *et al.*, 1994).

The association projections from the anterior olfactory nucleus and the anterior part of the piriform cortex also extend to the contralateral olfactory cortex, crossing in the anterior commissure (Luskin and Price, 1983; Carmichael and Price, 1994). The laminar and areal pattern of termination in the contralateral cortex are approximately the same as on the ipsilateral side.

Presumably, the association system interacts with the sensory activity being input to the cortex from the olfactory bulb to support olfactory discrimination. In contrast to the olfactory bulb, neither of these fiber systems has the sort of detailed topographic organization that would be expected if odors were represented in a spatial code. It is possible that cells related to different odors are dispersed in many parts of the cortex, and appropriate bulbar and association fibers synapse on them in a selective manner. It may be more likely, however, that olfactory discrimination depends on a system of spatiotemporal patterning across the cortex, in which adjustments in synaptic strength are built up from sensory experience.

OLFACTORY PROJECTIONS BEYOND THE PRIMARY OLFACTORY CORTEX

Olfactory information is transmitted from the primary olfactory cortex to several other parts of the forebrain, including the orbital cortex, amygdala, hippocampus, ventral striatum, hypothalamus and mediodorsal thalamus (Price, 1987; Russchen *et al.*, 1987; Carmichael *et al.*, 1994). Although these connections have been best studied in rodents, there is also some experimental data from monkeys, and functional imaging studies have recently provided data on humans (see following).

Projections to the Amygdala and Hippocampus

Both the amygdala and hippocampus have often been considered to be closely associated with olfaction, especially in lower animals. In primates, these limbic structures have become dominated by other sensory inputs, especially vision, but they still have direct olfactory connections. These arise primarily in the periamygdaloid cortex and the olfactory part of the entorhinal cortex, which project both to deep amygdaloid nuclei and to several parts of the hippocampus (Price, 1987; Jolkkonen *et al.*, 2001; Chapter 23).

Projections to the Hypothalamus

In rats, both electrophysiological recordings and axonal tracer experiments indicate that there are olfactory inputs to several parts of the hypothalamus (Price, 1985). The most direct projection arises from cells in the deepest layer of the piriform cortex and other olfactory cortical areas. Although the fibers run through the full rostrocaudal extent of the hypothalamus in the medial forebrain bundle, they terminate predominantly in the caudal half of the lateral hypothalamic area. Axons from the anterior cortical nucleus and medial nucleus of the amygdala end in more rostral and medial parts of the hypothalamus.

The olfactory inputs to the hypothalamus have not been as well defined in monkeys. Experiments with retrograde tracer injections in the lateral hypothalamus, however, label neurons in most of the olfactory cortical areas, as well as in related orbital/insular cortical areas (Öngür *et al.*, 1998). Electrophysiological responses to olfactory stimuli have also been recorded in the lateral hypothalamic area in monkeys (Tazawa *et al.*, 1987; Karadi *et al.*, 1989).

Olfactory Projections to the Striatum, Pallidum, and Thalamus

Along with the amygdala, the olfactory cortex projects to the ventral part of the striatum, including the accumbens nucleus and the olfactory tubercle. The olfactory projections are largely restricted to the olfactory tubercle and the caudal, ventrolateral part of the nucleus accumbens (Price, 1973; Luskin and Price, 1983; Fuller *et al.*, 1986; unpublished results in monkeys). These areas project out to the "ventral" pallidum, a continuation of the globus pallidus ventral to the anterior commissure. The major output of the ventral pallidum, in turn, is to the mediodorsal thalamic nucleus. As with the dorsal striato-pallidal-thalamic system, the inputs to the ventral striatum are glutamatergic, but the striatopallidal and pallidothalamic projections are GABAergic (Fuller *et al.*, 1986; Kuroda and Price, 1991).

As in other mammals, both electrophysiological recording and axonal tracing in monkeys also indicate excitatory olfactory input to the mediodorsal thalamic nucleus (MD) from the olfactory cortex (Yarita *et al.*, 1980; Russchen *et al.*, 1987). The neurons that project to MD are primarily located in the deep layers of the piriform cortex and other olfactory cortical areas. There are relatively small numbers of these neurons, and it appears that they may relay convergent activity from a relatively large portion of the olfactory cortex. Within MD in monkeys, fibers from small areas of the olfactory cortex or the amygdala end in small "patches," suggesting that inputs from restricted regions converge onto a few thalamic neurons (Russchen *et al.*, 1987; Ray and Price, 1993). Similarly, olfactory-responsive units are restricted to a relatively small region of the medial, magnocellular part of MD. Compared to the hypothalamus, the olfactory-related units in MD appear to be relatively broadly tuned and respond to many different odors (Yarita *et al.*, 1980).

In addition to MD, anatomical and electrophysiological studies in both rats and monkeys indicate that

there is an olfactory projection to the anteroventral portion of the submedial thalamic nucleus (SM; Price and Slotnick, 1983; Russchen *et al.*, 1987). SM is separated from MD only by the internal medullary lamina, and it may represent a portion of the same nucleus functionally. In rats, the projection to SM arises in a relatively restricted zone at the junction of the piriform cortex and olfactory tubercle (Price and Slotnick, 1983).

The portion of medial MD that receives olfactory input is reciprocally connected with several areas in the posterior orbital cortex and rostral agranular insular cortex (Russchen *et al.*, 1987). The cortical connections of SM are to a more restricted area near the junction of the olfactory peduncle and the frontal lobe (especially area 13a). It might be presumed, therefore, that MD would relay olfactory information to the orbital cortex. As discussed later, however, these same cortical areas receive more numerous, monosynaptic projections directly from the primary olfactory cortex. These corticocortical projections appear to be better suited to relay detailed sensory information. It is likely, therefore, that the transthalamic projection does not represent a sensory relay as such.

Olfactory Projections to Neocortical Areas

In the 1970s and 1980s, Takagi and his colleagues reported that odorant stimuli or electrical stimulation of the olfactory bulb could evoke neuronal responses in the orbital cortex (Tanabe *et al.*, 1975a, b; Yarita *et al.*, 1980; Takagi, 1986). Two areas, in the lateral and central parts of the posterior orbital cortex were identified. In the lateral area, the units were relatively specific, responding to only one or two odorants, whereas in the more central area units responded to several odorants. These studies suggested that the sensory information reached the orbital cortex from the primary olfactory cortex through the hypothalamus and thalamus. There is now clear anatomical evidence in monkeys and other animals, however, that the principal pathway is directly from the primary olfactory cortex to the orbital cortex.

Injections of anterograde axonal tracers in the piriform cortex of monkeys label axons in several areas of the agranular insula/posterior orbital cortex (areas Iam, Iapm, Iai, Ial, 13a, 13m, and 14c; Carmichael *et al.*, 1994; Fig. 32.6). All these cortical areas are agranular or dysgranular, and the areas nearest to the primary olfactory cortex have sometimes been referred to as the periallocortex. The projection is different from more usual sensory inputs to cortex that are relayed through the thalamus because the label is heaviest in layer I. Retrograde axonal tracer injections into the same agranular insula/posterior orbital areas label neurons in many parts of the primary olfactory cortex, including the anterior olfactory nucleus, piriform cortex, anterior cortical amygdaloid nucleus, periamygdaloid cortex, and olfactory part of the entorhinal cortex. The labeled cells are located in both layer II and layer III. Electrical stimulation of the olfactory bulb also evokes unit and field potential responses in most of the areas where there is anatomical evidence of olfactory input (Carmichael *et al.*, 1994).

The projections from the primary olfactory cortex are largely reciprocated by fibers from agranular insula/posterior orbital areas. Anterograde axonal tracer injections into several of the agranular insular areas label axons in the rostral parts of the primary olfactory cortex (Carmichael *et al.*, 1994). These include the olfactory tubercle, which is the only olfactory cortical area that does not project to the orbital cortex.

The agranular insula/orbital cortical areas that receive olfactory input interact with other areas on the orbital surface through corticocortical connections to integrate olfactory sensory information with other sensory modalities (Carmichael and Price, 1995, 1996). Taste information reaches the orbital cortex through the thalamic gustatory relay and the primary gustatory cortex (Chapter 31). The orbital cortex is the first place where olfactory and taste information converge, so it presumably underlies the sensation of flavor, which depends on both of the primary modalities. In addition, there are corticocortical somatosensory and visual inputs to the orbital cortex from the parietal and inferior temporal cortex. The somatosensory inputs appear to be related to the hand and mouth (Carmichael and Price, 1995). The corticocortical connections between orbital areas form an "orbital network" that appears to function in the integration and analysis of food-related sensory information (Carmichael and Price, 1996).

Recordings in the orbital cortex in monkeys show neuronal responses to food and food-related stimuli, including visual stimuli that are associated with food (Rolls, 2000). Importantly, the responses reflect the affective or reward significance of the stimuli as well as their sensory properties. For example, the neuronal response to a particular visual stimulus (e.g., a triangle) will change markedly if the association of the stimulus with a food reward changed. In addition, if the animal is feed to satiety with a food stimulus, the neuronal response to that food will decrease.

Imaging of Olfactory Sensory Activity in Humans

Several studies have used functional imaging methods to identify the human cortical areas activated by olfactory stimuli (see Zald and Pardo, 2000). Odorant-induced responses were first obtained in the

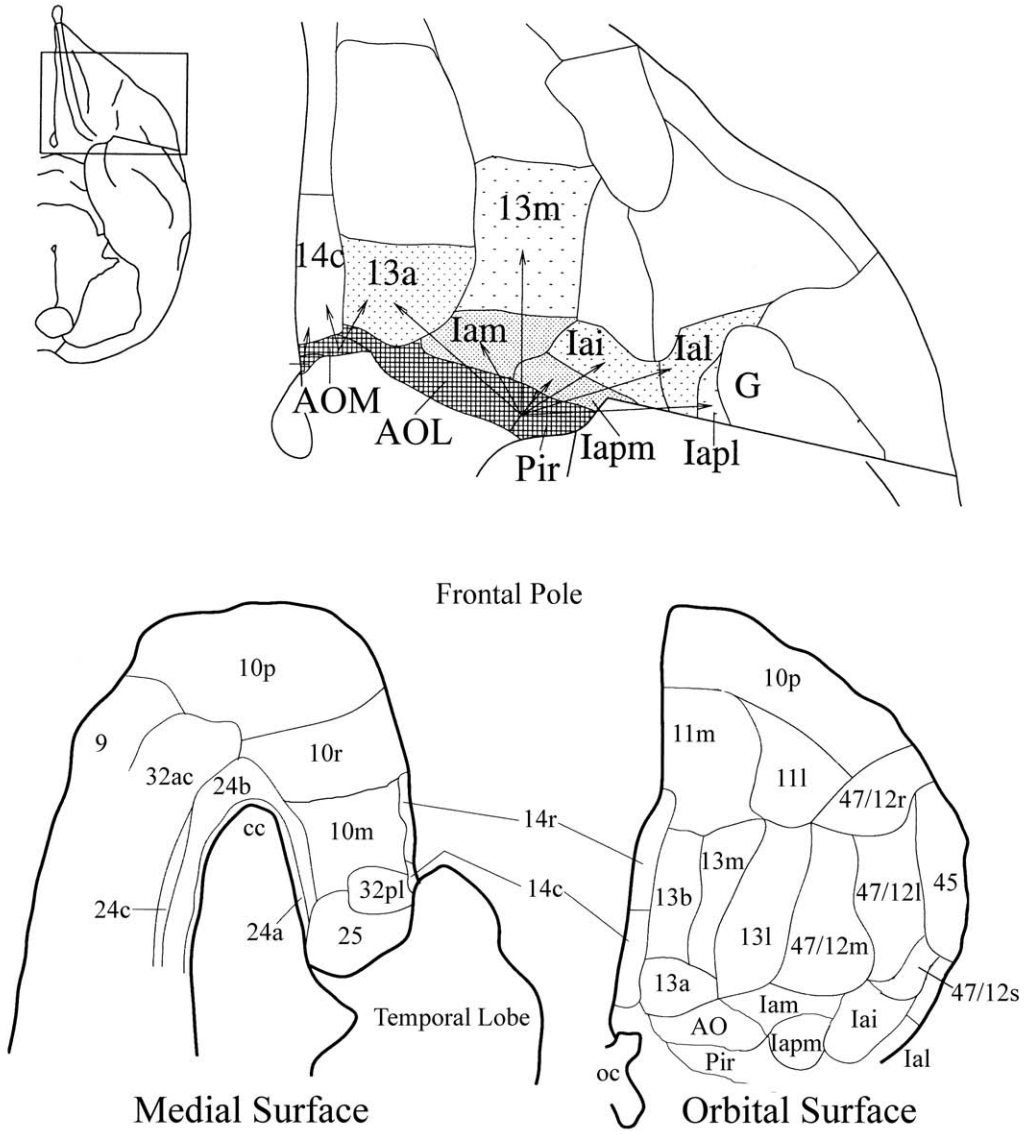

FIGURE 32.6 *Above:* A summary of the projections from the primary olfactory cortex to the agranular insula/posterior orbital cortex in monkeys. *Below:* A map of architectonic areas on the medial and orbital surface of frontal cortex in humans. The areas were delineated by applying the same criteria used to analyze the cortex in monkeys to analyze the human areas. Modified from Carmichael *et al.* (1994) and Öngür and Price (2000).

region of primary cortex by Zatorre *et al.* (1992) and have been confirmed by subsequent reports from the same research group (Small *et al.*, 1997; Dade *et al.*, 1998). Other studies have failed to find substantial activation of primary olfactory areas, however (e.g., Zald and Pardo, 1997; Yousem *et al.*, 1997; Sobel *et al.*, 1998). Several factors may explain the inconsistency. Technical factors such as the "susceptability" artifact related to nearby bone and air sinuses make it difficult to image this region with fMRI. Neuronal responses to odorants in the piriform cortex are also rapidly adapting and may be coded for by temporal or spatial patterns of activity instead of response amplitude. Further, sniff-related activity may mask odorant-related activity (Sobel *et al.*, 1998). When these are taken into account odorant-related activation can be visualized in the primary olfactory cortex (Sobel *et al.*, 2000).

Whether imaging studies did or did not detect activity in the primary olfactory cortex, olfactory-related activity has consistently been detected in the orbital cortex (e.g., Zatorre *et al.*, 1992; Small *et al.*, 1997; Zald and Pardo, 1997; Sobel *et al.*, 2000; Royet

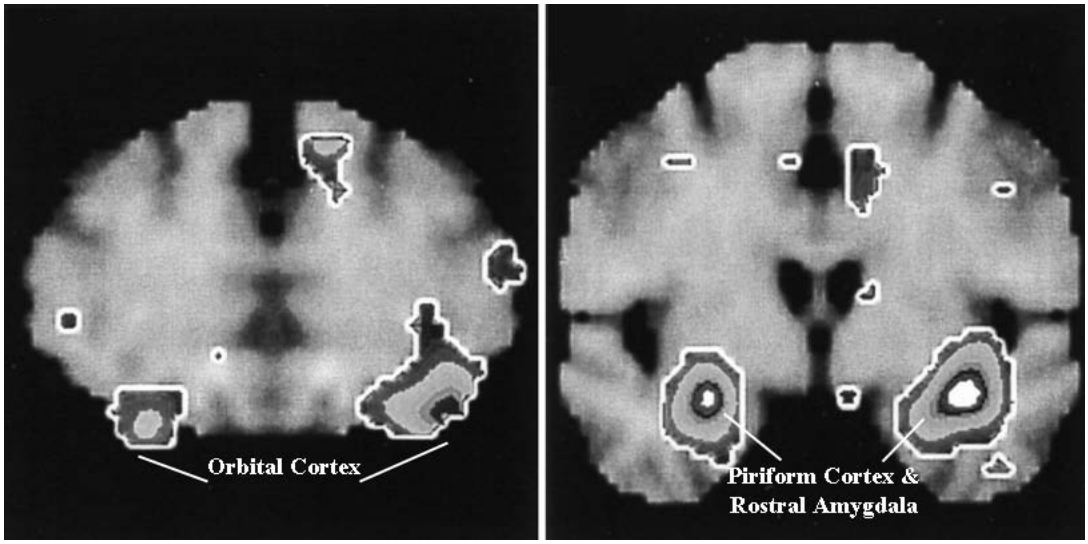

FIGURE 32.7 Cerebral activation (reflected as changes in regional cerebral blood flow) during exposure to aversive olfactory stimuli. On the left an area of activation is shown in the centrolateral orbital cortex, while on the right there is an area of activation in the region of the piriform cortex/anterior amygdala. Modified from Zald and Pardo (1997).

et al., 2001; Fig. 32.7). All these studies found an area of activation in the central orbital cortex, in some cases through the rostral to caudal extent (Sobel *et al.*, 2000). It is not yet possible to identify these areas in terms of the architectonic subdivisions of the orbital cortex, but they appear to correspond to the "orbital network" defined in monkeys (see previous discussion; Carmichael and Price, 1996). Zald and Pardo (1997) also identified an area in the lateral orbital/anterior insular cortex that was activated following stimulation with aversive odors; the region of the amygdala was also activated to the same odors.

The central orbital cortical region that responds to odorants also is activated by taste stimuli (Small *et al.*, 1999). This corresponds well with the anatomical evidence in monkeys that corticocortical interconnections within the orbital cortex relate olfactory and gustatory systems. The responses to simultaneous, matched taste and olfactory stimuli appear to be quantitatively different from both unimodal stimuli alone, suggesting that flavor is not a simple convergence of its component senses (Small *et al.*, 1997). As suggested by recordings in monkeys (see earlier discussion), the olfaction- and taste-related responses in the orbital cortex also depend on hedonic properties of the stimuli. For example, fMRI responses to food-related olfactory stimuli show specific decreases after feeding to satiety with that food (O'Doherty *et al.*, 2000). All together, the evidence indicates that the orbital cortex should be considered as part of a system for analysis of food and food-related stimuli, and more generally for the analysis of reward. It should not be considered as simply secondary olfaction cortex or secondary taste cortex.

References

Alheid, G.F., Heimer, L., and Switzer, R.C. (1990; update to 2002 chapter). Basal ganglia. *In* "The Human Nervous System" (G. Paxinos, ed.), pp. 483–582. Academic Press, San Diego.

Amaral, D.G., and Insausti, R. (1990; *update to 2002*). Hippocampal formation. *In* "The Human Nervous System" (G. Paxinos, ed.), pp. 711–755. Academic Press, San Diego.

Amaral, D.G., Insausti, R., and Cowan, W.M. (1987). The entorhinal cortex of the monkey. I. Cytoarchitectonic organization. *J. Comp. Neurol.* **264,** 326–355.

Amaral, D.G., Price, J.L., Pitkanen, A., and Carmichael, S.T. (1992). Anatomical organization of the primate amygdaloid complex. *In* "The Amygdala" (J.P. Aggleton, ed.), pp. 1–66. Wiley-Liss, New York.

Aroniadou-Anderjaska, V., Ennis, M., and Shipley, M.T. (1997). Glomerular synaptic responses to olfactory nerve input in rat olfactory bulb slices. *Neuroscience* **79,** 425–434.

Berkowicz, D.A, Trombley, P.Q., and Shepherd, G.M. (1994). Evidence for glutamate as the olfactory receptor cell neurotransmitter. *J. Neurophysiol.* **71,** 2557–2561.

Bhatnagar, K.P, Kennedy, R.C., Baron, G., and Greenberg, R.A. (1987). Number of mitral cells and the bulb volume in the aging human olfactory bulb: A quantitative morphological study. *Anat. Rec.* **218,** 73–87.

Boeijinga, P.H., and Van Groen, T. (1984). Inputs from the olfactory bulb and olfactory cortex to the entorhinal cortex in the cat. II. Physiological studies. *Exp. Brain Res.* **57,** 40–48.

Buck, L., and Axel, R. (1991). A novel multigene family may encode odorant receptors: A molecular basis for odor recognition. *Cell* **65,** 175–187.

Carmichael, S.T., and Price, J.L. (1996). Connectional networks within the orbital and medial prefrontal cortex of macaque monkeys. *J. Comp. Neurol.* **371,** 179–207.

Carmichael, S.T., Clugnet, M-F., and Price, J.L. (1994). Central olfactory connections in the macaque monkey. *J. Comp. Neurol.* **346,** 403–434.

Chen, W.R., Xiong, W., and Shepherd, G.M. (2000). Analysis of relations between NMDA receptors and GABA release at olfactory bulb reciprocal synapses. *Neuron* **25,** 625–633.

Dade, L.A., Jones-Gotman, M., Zatorre, R.J., and Evans, A.C. (1998). Human brain function during odor encoding and recognition. A PET activation study. *Ann. N.Y. Acad. Sci.* **855,** 572–574.

Fuller, T.A., Russchen, R.T., and Price, J.L. (1986). Sources of presumptive glutamergic/aspartergic afferents to the rat ventral striato-pallidal region. *J. Comp. Neurol.* **256,** 317–338.

Gall, C.M., Hendry, S.H., Seroogy, K.B., Jones, E.G., and Haycock, J.W. (1987). Evidence for coexistence of GABA and dopamine in neurons of the rat olfactory bulb. *J. Comp. Neurol.* **266,** 307–318.

Glusman, G., Bahar, A., Sharon, D., Pilpel, Y., White, J., and Lancet, D. (2000). The olfactory receptor gene superfamily: Data mining, classification, and nomenclature *Mamm. Genome* **11,** 1016–1023.

Haberly, L.B. (1985). Neuronal circuitry in olfactory cortex: Anatomy and functional implications. *Chem. Senses* **10,** 219–238.

Haberly, L.B., and Price, J.L. (1977). The axonal projection pattern of the mitral and tutfed cells of the olfactory bulb in the rat. *Brain Res.* **129,** 152–157.

Heimer, L., Van Hoesen, G.W., and Rosene, D.L. (1977). The olfactory pathwasys and the anterior perforated substance in the primate brain. *Int. J. Neurol.* **12,** 42–52.

Hertz-Schuett, C.G., and Mai, J.K. (1991). Cholinesterase-Aktivitaet im memschlichen Striatum unter besonderer Berueckssichtigung der Insulae terminals. *J. Hirnforsch.* **32,** 317–342.

Hinds, J.W., and McNelly, N.A. (1977). Aging of the rat olfactory bulb: Growth and atrophy of constituent layers and changes in size and number of mitral cells. *J. Comp. Neurol.* **72,** 345–367.

Jajek, B. (1983). Ultrastructure of human nasal mucosa. *Laryngoscope* **93,** 1576–1599.

Johnson, B.A., and Leon, M. (2000). Modular representations of odorants in the glomerular layer of the rat olfactory bulb and the effects of stimulus concentration. *J. Comp. Neurol.* **422,** 496–509.

Johnson, D.M., Illig, K.R., Behan, M., and Haberly, L.B. (2000). New features of connectivity in piriform cortex visualized by intracellular injection of pyramidal cells suggest that "primary" olfactory cortex functions like "association" cortex in other sensory systems. *J. Neurosci.* **20,** 6974–6982.

Jolkkonen, E., Miettinen, R., and Pitkanen, A. (2001) Projections from the amygdalo-piriform transition area to the amygdaloid complex: A PHA-l study in rat. *J. Comp. Neurol.* **432,** 440-465.

Karadi, Z., Oomura, Y., Nishino, H., and Aou, S. (1989). Olfactory coding in the monkey lateral hypothalamus: Behavioral and neurochemical properties of odor-responding neurons. *Physiol. Behav.* **45,** 1249–57

Kosaka, T., Hataguchi, Y., Hama, K., Nagatsu, I., and Wu, J.Y. (1985). Coexistence of immunoreactivities for glutamate decarboxylase and tyrosine hydroxylase in some neurons in the periglomerular region of the rat main olfactory bulb: Possible coexistence of gamma-aminobutyric acid (GABA) and dopamine. *Brain Res.* **343,** 166–171.

Kosaka, T., Kosaka, K., Heizmann, C.W., Nagatsu, I., Wu, J.Y., and Yanaihara, N., and Hama, K. (1987). An aspect of the organization of the GABAergic system in the rat main olfactory bulb: Laminar distribution of immunohistochemically defined subpopulations of GABAergic neurons. *Brain Res.* **411,** 373–378.

Kreutzer, E.W., and Jajek, B.W. (1980). The vomeronasal organ of Jacobson in the human embryo and fetus. *Otolarnyngol. Head Neck Surg.* **88,** 119–123.

Kuroda, M., and Price, J.L. (1991). Synaptic organization of projections from basal forebrain structures to the mediodorsal thalamic nucleus of the rat. *J. Comp. Neurol.* **303,** 513–533.

Lovell, M.A., Jajek, B.W., Moran, D.T., and Rowley, J.C. (1982). Biopsy of human olfactory mucosa: An instrument and a technique. *Arch. Otolaryngol. (Chicago)* **108,** 247–249.

Luskin, M.B., and Price, J.L. (1982). The distribution of axon collaterals from the olfactory bulb and the nucleus of the horizontal limb of the diagonal band to the olfactory cortex, demonstrated by double retrograde labeling techniques. *J. Comp. Neurol.* **209,** 249–263.

Luskin, M.B., and Price, J.L. (1983). The topographic organization of association fibers in the olfactory system in the rat, including centrifugal fibers to the olfactory bulb. *J. Comp. Neurol.* **216,** 264–291.

Macrides, F., Schonfeld, T.A., Marchand, J.E., and Clancy, A.N. (1985). Evidence for morphologically, neurochemically and functionally heterogeneous classes of mitral and tufted cells in the olfactory bulb. *Chem. Senses* **10,** 175–218.

Meisami, E., Mikhail, L., Baim, D., and Bhatnagar, K.P. (1998). Human olfactory bulb: Aging of glomeruli and mitral cells and a search for the accessory olfactory bulb. *Ann. N.Y. Acad Sci.* **855,** 708–715.

Mesulam, M.-M., Mufson, E.J., Levey, A.I., and Wainer, B.H. (1983). Cholinergic innervation of the cortex by the basal forebrain: Cytochemistry and cortical connections of the septal area, diagonal band nuclei, nucleus basalis *(Substantia innominata),* and hypothalamus in the rhesus monkey. *J. Comp. Neurol.* **214,** 170–197.

Moran, D.T., Rowley, J.C., III, and Jajek, B.W. (1982b). Electron microscopy of human olfactory epithelium reveals a new cell type: The microvillar cell. *Brain Res.* **253,** 39–46.

Moran, D.T., Rowley, J.C., III, Jajek, B.W., and Lowell, M.A. (1982a). The fine structure of the olfactory mucosa in man. *J. Neurocytol.* **11,** 721–746.

Mori, K., Nagao, H., and Yoshihara, Y. (1999). The olfactory bulb: Coding and processing of odor molecule information. *Science* **286,** 711–715.

Morrison, E.E., and Costanzo, R.M. (1992). Morphology of olfactory epithelium in humans and other vertebrates. *Microsc. Res. Tech.* **23,** 49–61.

Murphy, C., Morgan, C.D., Geisler, M.W., Wetter, S., Covington, J.W., Madowitz, M.D., Nordin, S., and Polich, J.M. (2000). Olfactory event-related potentials and aging: Normative data. *Int. J. Psychophysiol.* **36,** 133–145.

Nakashima, T., Kimmelman, C.P, and Snow, J.B., Jr. (1984). Structure of human fetal and adult olfactory neuroepithelium. *Arch. Otolaryngol. (Chicago)* **110,** 641–646.

Nakashima, T., Kimmelman, C.P., and Snow, J.B., Jr. (1985). Vomeronasal organs and nerves of Jacobson in the human fetus. *Acta Oto-laryngol.* **99,** 266–271.

O'Doherty, J., Rolls, E.T., Francis, S., Bowtell, R., McGlone, F., Kobal, G., Renner, B., and Ahne, G. (2000). Sensory-specific satiety-related olfactory activation of the human orbitofrontal cortex. *Neuroreport* **11,** 893–897.

Ohm, T.G., Muller, H., and Braak, E. (1991). Calbindin-D-28k-like immunoreactive structures in the olfactory bulb and anterior olfactory nucleus of the human adult: Distribution and cell typology—partial complementarity with parvalbumin. *Neurosci.* **42**(3), 823–840.

Ohm, T.G., Muller, H., Ulfig, N., and Braak, E. (1990). Glutamic-acid-decarboxylase-and parvalbumin-like-immunoreactive structures in the olfactory bulb of the human adult. *J. Comp. Neurol.* **291,** 1–8.

Ojima, H., Mori, K., and Kishi, K. (1984). The trajectory of mitral cell axons in the rabbit olfactory cortex revealed by intracellular HRP injection. *J. Comp. Neurol.* **230,** 77–87.

Öngür, D., and Price, J.L. (2000). The organization of networks within the orbital and medial prefrontal cortex of rats, monkeys and humans. *Cereb. Cortex* **10,** 206–219.

Öngür, D., An, Z., and Price, J.L. (1998). Prefrontal cortical projections to the hypothalamus in macaque monkeys. *J. Comp. Neurol.* **401,** 480–505.

Price, J.L. (1973). An autoradiographic study of complimentary laminar patterns of termination of afferent fibers to the olfactory cortex. *J. Comp. Neurol.* **150,** 87–108.

Price, J.L. (1987). The central olfactory and accessory olfactory systems. *In* "Neurobiology of Taste and Smell" (T.E. Finger and W.L. Silver, eds.), pp. 179–204. John Wiley and Sons, New York.

Price, J.L., and Slotnick, B.M. (1987). Dual olfactory representation in the rat thalamus: An anatomical and electrophysiological study. *J. Comp. Neurol.* **215,** 63–67.

Price, J.L., Russchen, F.T., and Amaral, D.G. (1987). The limbic region. II: The amygdaloid complex. *In* "Handbook of Chemical Neuroanatomy, Vol. 5: Integrated Systems of the CNS. Part I" (A. Bjorklund, T. Hokfelt, and L.W. Swanson, eds.), pp. 279–388. Elsevier Science, Amsterdam.

Ray, J.P., and Price, J.L. (1993). The organization of projections from the mediodorsal nucleus of the thalamus to orbital and medial prefrontal cortex in macaque monkeys. *J. Comp. Neurol.* **337,** 1–31.

Ressler, K.J., Sullivan, S.L., and Buck, L.B. (1993). A zonal organization of odorant receptor gene expression in the olfactory epithelium. *Cell* **73,** 597–609.

Ressler, K.J., Sullivan, S.L., and Buck, L.B. (1994). Information coding in the olfactory system: Evidence for a stereotyped and highly organized epitope map in the olfactory bulb. *Cell* **79,** 1245–1255.

Rouquier, S., Taviaux, S., Trask, B.J., Brand-Apron, V., van den Engh, G., Cemaille, J., and Giorgi, D. (1998). Distribution of olfactory receptor genes in the human genome. *Nat. Genet.* **18,** 243–250.

Royet, J.P., Hudry, J., Zald, D.H., Godinot, D., Gregoire, M.C., Lavenne, F., Costes, N., and Holley, A. (2001). Functional neuroanatomy of different olfactory judgments. *Neuroimage* **13,** 506–519.

Russchen, F.T., Amaral, D.G., and Price, J.L. (1987). The afferent input to the magnocellular division of the mediodorsal thalamic nucleus in the monkey, *Macaca fascicularis*. *J. Comp. Neurol.* **256,** 175–210.

Scott, J.W., and Harrison, T.A. (1987). The olfactory bulb: Anatomy and physiology. *In* "Neurobiology of Taste and Smell" (T.E. Finger and W.L. Silver, eds.) pp. 151–178. John Wiley and Sons, New York.

Small, D.M., Jones-Gotman, M., Zatorre, R.J., Petrides, M., and Evans, A.C. (1997). Flavor processing: more than the sum of its parts. *Neuroreport* **8,** 3913–3917.

Small, D.M., Zald, D.H., Jones-Gotman, M., Zatorre, R.J., Frey, S., and Petrides, M. (1999). Human cortical gustatory areas: A review of functional neuroimaging data. *Neuroreport* **10,** 7–14.

Smith, R.L., Baker, H., Kolstad, K., Spencer, D.D., and Greer, C.A. (1991). Localization of tyrosine hydroxylase and olfactory marker protein immunoreactivities in the human and macaque olfactory bulb. *Brain Res.* **548,** 140–148.

Sobel, N., Prabhakaran, V., Desmond, J.E., Glover, G.H., Goode, R.L., Sullivan, E.V., and Gabrieli, J.D.E. (1998). Sniffing and smelling: Separate subsystems in the human olfactory cortex. *Nature* **392,** 282–286.

Sobel, N., Prabhakaran, V., Zhao, Z., Desmond, J.E., Glover, G.H., Sullivan, E.V., and Gabrieli, J.D.E. (2000). Time course of odorant-induced activation in the human primary olfactory cortex. *J. Neurophysiol.* **83,** 537–551.

Takagi, S.F. (1986). Studies on the olfactory nervous system of the old world monkey. *Prog. Neurobiol.* **27,** 195–249.

Tanabe, T., Iino, M., and Takagi, S.F. (1975b). Discrimination of odors in the olfactory bulb, pyriform-amygdaloid areas, and orbitofrontal cortex of the monkey. *J. Neurophysiol.* **38,** 1284–1296.

Tanabe, T., Yarita, H., Iino, M., Ooshima, Y., and Takagi, S.F. (1975a). An olfactory projection area in orbitofrontal cortex of the monkey. *J. Neurophysiol.* **38,** 1269–1283.

Tazawa, Y., Onoda, N., and Takagi, S.F. (1987). Olfactory input to the lateral hypothalamus of the old world monkey. *Neurosci. Res.* **4,** 357–375.

Tigges, M., and Tigges, J. (1980). Distribution and morphology of myelinated perikarya and dendrites in the olfactory bulb of primates. *J. Neurocytol.* **9,** 825–834.

Turner, B.H., Gupta, K.C., and Mishkin, M. (1978). The location and cytoarchitecture of the projection areas of the olfactory bulb in *Macaca mulatta*. *J. Comp. Neurol.* **177,** 381–396.

Vassar, R., Chao, S.K., Sitcheran, R., Nunez, J.M., Vosshall, L.B., and Axel, R. (1994). Spatial segregation of odorant receptor expression in the mammalian olfactory epithelium. *Cell* **79,** 981–991.

Vassar, R., Ngai, J., and Axel, R. (1993). Spatial segregation of odorant receptor expression in the mammalian olfactory epithelium. *Cell* **74,** 309–318.

Wysocki, C., and Meredith, M. (1987). The vomeronasal system. *In* "Neurobiology of Taste and Smell" (T.E. Finger and W.L. Silver, eds.), pp. 125–150. John Wiley and Sons, New York.

Xu, F., Greer, C.A., and Shepherd, G.M. (2000). Odor maps in the olfactory bulb. *J. Comp. Neurol.* **422,** 489–495.

Yarita, H., Iino, M., Tanabe, T., Kogure, S., and Takagi, S.F. (1980). A transthalamic olfactory pathway to the orbitofrontal cortex in the monkey. *J. Neurophysiol.* **43,** 69–85.

Yousem, D.M., Williams, S.C., Howard, R.O., Andrew, C., Simmons, A., Allin, M., Geckle, R.J., Suskind, D., Bullmore, E.T., Brammer, M.J., and Doty, R.L. (1997). Functional MR imaging during odor stimulation: Preliminary data. *Radiology* **204,** 833–838.

Zaborsky, L., Carlsen, J., Brashear, H.R., and Heimer, L. (1985). Cholinergic and GABAergic afferents to the olfactory bulb in the rat with special emphasis on the projection neurons in the nucleus of the horizontal limb of the diagonal band. *J. Comp. Neurol.* **243,** 488–509.

Zald, D.H., and Pardo, J.V. (1997). Emotion, olfaction, and the human amygdala: Amygdala activation during aversive olfactory stimulation. *Proc. Nat. Acad. Sci.* **94,** 4119–4124.

Zald, D.H., and Pardo, J.V. (2000). Functional neuroimaging of the olfactory system in humans. *Int. J. Psychophysiol.* **36,** 165–181.

Zatorre, R.J., Jones-Gutman, M., Evans, A.C., and Meyer, E. (1992). Functional expression of a mammalian odorant receptor. *Science* **279,** 237–242.

Zbar, R.I., Zbar, L.I., Dudley, C., Trott, S.A., Rohrich, R.J., and Moss, R.L. (2000). A classification schema for the vomeronasal organ in humans. *Plast. Reconstr. Surg.* **105,** 1284–1288.

CHAPTER

33

Vestibular System

JEAN A. BÜTTNER-ENNEVER and NICOLAAS M. GERRITS

Institute of Anatomy, Ludwig-Maximilian University Munich
Munich, Germany, and
Department of Anatomy, Erasmus University
Rotterdam, The Netherlands

The vestibular complex is the collection of brainstem nuclei in receipt of primary afferents from the labyrinth of the inner ear *(see Koutcherov et al. Chapter 10)*. Long before axonal degeneration and tracer techniques were available, the different nuclei of the vestibular complex were outlined and described in great detail. These early observations started in human material. Later, after the introduction of Weigert's haematoxylin-method for impregnation of myelinated fibers, it became clear that a similar organization could be seen in all vertebrates (Straka *et al.*, 2001, 2002).

The first description of what in later years proved to be the vestibular nuclear complex comes from Clarke (1861), who distinguished on the basis of their fiber content a lateral area ("outer nucleus"), located within Stilling's (1843) juxtarestiform body, and a medial area ("inner nucleus"). Over the years, Clarke's outer nucleus became erroneously known as Meynert's (1871) "innere Abteilung des Kleinhirnstiels": loosely arranged (bundles of) fibers, considered an internal division of the restiform body. Giant cells in the rostral part of the juxtarestiform body were noted and described by Deiters (1865), whose name at present is still linked to this magnocellular nucleus. The caudal part of Clarke's outer nucleus contains characteristic rostrocaudally oriented fiber bundles, which were originally taken for descending acoustic root fibers. As a result of Roller's description (1882) of these fibers, this part of Clarke's outer nucleus was sometimes referred to as Roller's root or nucleus (Fuse, 1912), but more commonly as "spinale Acusticuswurzel" (Leidler, 1916). Its present name is spinal or descending vestibular nucleus and stems from the work of Ramón y Cajal (1896).

Bechterew (1885) traced the ascending branch of the vestibular nerve from the inner ear to a nucleus between the superior cerebellar peduncle and the dorsorostral aspect of Deiters' nucleus. This "angular" nucleus of Bechterew comprises the rostral pole of Clarke's inner nucleus; however, its caudal border has led to some dispute. According to Kohnstamm (1908),

Fuse (1912), and Van der Schueren (1914), the parvocellular region (known today as part of the medial vestibular nucleus), located medial to Von Monakow's (1890) acoustic striae in the lateral wall of the fourth ventricle, should be included in Bechterew's angular nucleus. The magnocellular portion of the medial nucleus, located lateral to the acoustic striae, contains a significant proportion of large cells and has often been included in Deiters' nucleus (Bechterew, 1887; Leidler, 1916; Ramón y Cajal, 1896). However, many authors recognized that this region's location outside the juxtarestiform body and its cytoarchitectonic features set it apart from the area with the giant Deiters' neurons (Fuse, 1912; Kohnstamm, 1908; Lewy, 1910; Sabin, 1897). It has become known under a variety of names, of which "magnocellular part of the medial vestibular nucleus" (Van der Schueren, 1914) seems the most appropriate.

The caudal extent of Clarke's inner nucleus retained for decades the name nucleus triangularis (Schwalbe, 1881). Although Ramón y Cajal (1909) refers to it as the dorsal or principal nucleus, it is known at present as the medial vestibular nucleus.

Since the turn of the century, the description and delimitation of the vestibular nuclei have not undergone significant changes. We still recognize the four "classical" components: the superior (Bechterew), lateral (Deiters), spinal or descending (Ramón y Cajal), and medial vestibular nucleus. Naturally, the elaboration of histological and axonal tracing techniques has provided more detailed understanding of the connections of the vestibular nuclei as well as the recognition of various subnuclei.

The subdivisions of the vestibular nuclei as used in this chapter largely correspond to those proposed by Brodal and Pompeiano (1957), Voogd (1964), and Gerrits *et al.* (1985b) for the cat; Van Rossum (1969) and Epema *et al*. (1988) for the rabbit; and Sadjadpour and Brodal (1968), Olszewski and Baxter (1982), and Suarez *et al*. (1997) for humans.

TOPOGRAPHY AND CYTOARCHITECTURE

Superior Vestibular Nucleus

The area with predominantly intermediate-sized cells, located dorsomedial to Deiters' nucleus, was first described by Bechterew (1885) and was subsequently referred to as the "angular nucleus of Bechterew" (Fuse, 1912; Jacobsohn, 1909). For unknown reasons Gray (1926) renamed it the superior vestibular nucleus (SuVe).

The SuVe is present in the lateral wall of the fourth ventricle (Fig. 33.1 and 33.4A, D; Paxinos and Huang, 1995, Figs. 29–36; Paxinos *et al.,* 2000, Figs. 98–107). Rostrally, at the level of the rostral pole of the principal sensory trigeminal nucleus, it flattens and is bordered by the parabrachial nuclei. At this level, SuVe is capped by the mesencephalic trigeminal tract (me5) and nucleus (Me5). Caudally SuVe tapers off and blends with group Y. Over most of its extent, SuVe is bordered dorsally by the superior cerebellar peduncle (scp). Laterally it is bordered by the juxtarestiform body, in which the giant Deiters' neurons are embedded. Sadjadpour and Brodal (1968) describe a ventral protrusion of the caudal part of SuVe into the lateral vestibular nucleus (LVe), but this view is not supported in the present study. Caudal to the facial nerve, SuVe is situated dorsal to the medial vestibular nucleus (MVe). It is difficult to distinguish SuVe from the parvocellular (MVpc) subdivision on cytoarchitectonic features alone.

The SuVe is characterized by the passage of a considerable number of fibers of presumably cerebellofugal nature. Corticovestibular fibers curve through the dorsal and lateral margin of SuVe and collect ventrally as bundles of the juxtarestiform body. Direct fastigiobulbar fibers form a rather compact bundle close to the ventricular surface and fan out ventrally through the rostral pole of MVpc. The most conspicious fiber system is present in the rostral part of the nucleus. Fibers with a presumed origin in ventral LVe, MVmc, and ventral SuVe suddenly change their course and run in the direction of the ventricle (Fig. 33.1A, planes 1, 2, 2B). They collect at the border between the reticular formation and the ventricular gray matter (Fig. 33.1A, planes1, 2; Fig. 33.2A) and join the medial longitudinal fascicle (mlf) in more rostral levels. These fibers were described by Winkler (1909) and Muskens (1913–14) as the "ascending tract of Deiters" (atd) see also introduction to this chapter).

Basically the topography of the human SuVe is not unlike the homologous structure in other mammals such as the rabbit (Epema *et al.,* 1988) and the cat (Brodal and Pompeiano, 1957; Gerrits *et al.,* 1985b). The largest difference is found in its rostral part. In most mammals, the initial segment of the superior cerebellar peduncle has a horizontal position, and SuVe envelops its lateral margin. In humans, the cerebellar peduncles are "pressed together" and leave no room for such lateral extension of SuVe.

The neurons of SuVe nucleus are small to medium sized (Fig. 33.3A), with cell size increasing from caudal to rostral (Suarez *et al.,* 1997). In primates, the medium-sized neurons form a central core with a small cells around the periphery, but the separation of the two

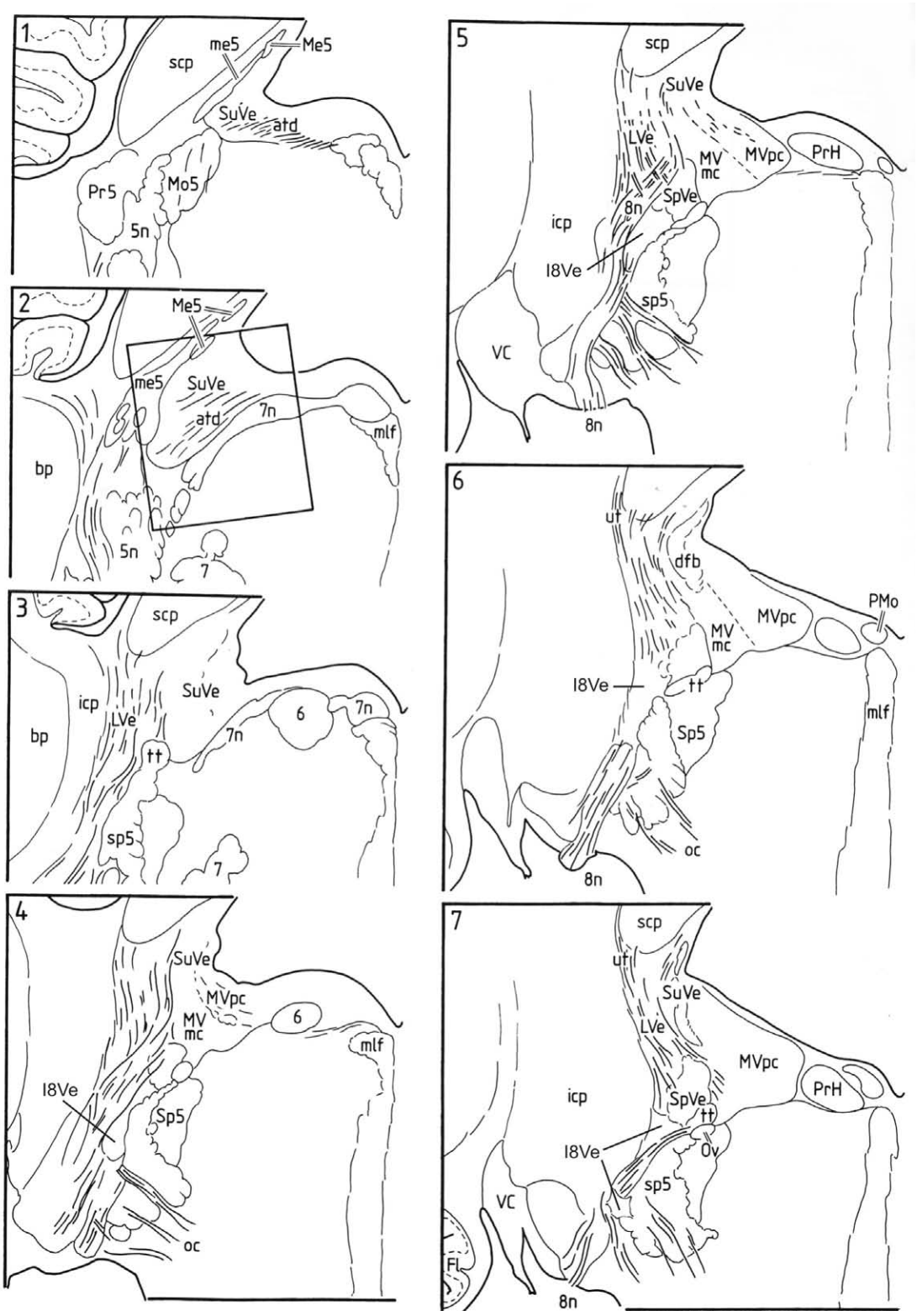

FIGURE 33.1 Drawings of equally spaced transverse levels (i.e., perpendicular to the long axis of the brainstem) through the left-sided human vestibular complex (interval 0.6 mm) based on 24-μm Klüver-Barrera stained frozen sections. The drawings are numbered in ascending order from rostral to caudal. Fibers running in the plane of sectioning are indicated with coarse lines, when cut across they are not indicated. The boxed area is illustrated in Figure 33.2. tt trigeminaothalamic (Wallenberg's) tract; Ov Nucleus ovalis; dfb direct fastigio-bulbar tract; ut uncinate tract. *Continued*

FIGURE 33.1 *Continued*

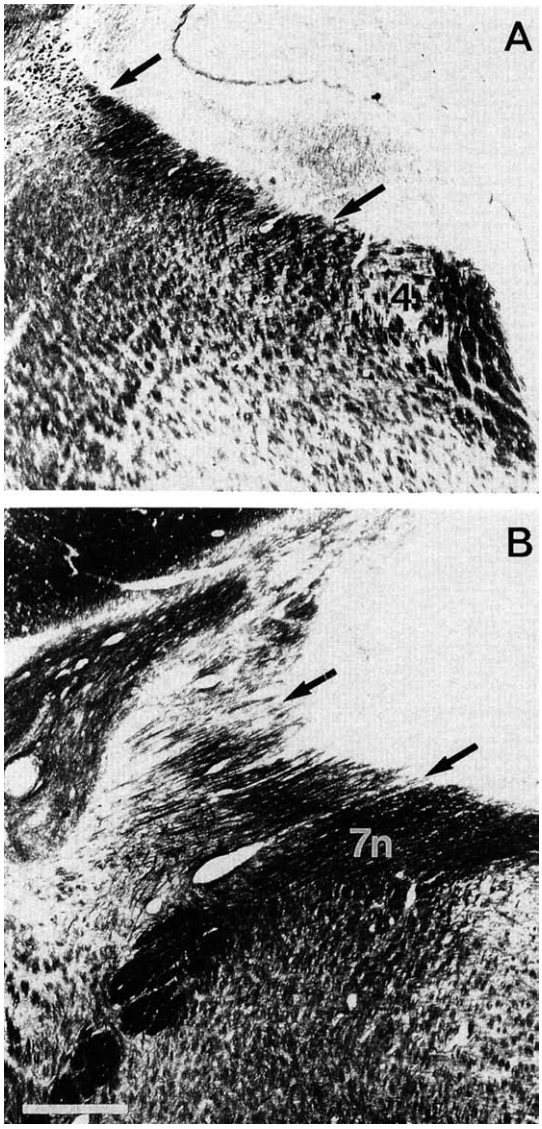

FIGURE 33.2 **(A)** Fibers of the ascending tract of Deiters at the border of the central gray matter and reticular formation (between arrows) directly lateral to the the mlf in which the trochlear nucleus (4) is embedded; section is approximately 1.5 mm rostral to Figure 33.2B. **(B)** Fibers of the atd (between arrows) running toward the ventricle through the rostral aspect of the superior vestibular nucleus. The position of the photograph indicated by the boxed area in Figure 33.1, plate 2. Scale bars in A and B = 1 mm.

types is less pronounced than that described in the rabbit (Epema *et al.*, 1988) and in the cat (Gacek, 1969). Some medium-sized neurons within the SuVe are glutamate decarboxylase (GAD) immunoreactive presumably representing the inhibitory secondary vestibulooculomotor neurons of the vertical system (Fig. 33.4B; Wentzel *et al.*, 1995; Holstein, 2000).

Group Y

Brodal and Pompeiano (1957) described in the cat small cells located dorsolateral to Deiters' nucleus, capping the restiform body, which they named group Y. But much earlier than this in his description of the human brainstem, Jacobsohn (1909) described the caudal part of group Y under the name "nucleus marginalis corporis restiformis" and indicated its apparent continuity in the lateral direction with Essick's (1907) corpus pontobulbare.

Neither Sadjadpour and Brodal (1968) nor Suarez *et al.* (1997) in their study of the human vestibular nuclei were able to distinguish a group Y. However, we have identified it in the human brains we analyzed and found that its position is almost identical to that in other mammals. Riding on the caudal slope of the inferior cerebellar peduncle (icp), it does not extend far rostrally since in humans, unlike most mammals, the icp surges upwards into the cerebellum the moment the cerebellum and brainstem touch each other (Fig. 33.1B, planes 9, 10,11; Fig. 33.4G; Paxinos and Huang, 1995, Figs. 27–30; Paxinos *et al.*, 2000; Figs. 107–110). Rostrodorsally, group Y is bordered by the fiber bundles in the ventral aspect of the floccular peduncle and abuts on the icp. At the medial side of the icp, it merges with the caudal part of SuVe. Caudally, the cells of group Y can be distinguished from the somewhat larger and more rounded neurons of the cochlear nuclei, and group Y is separated from the dorsal surface of the icp by the acoustic striae (das). Its cells spread medially over the dorsal surface of the spinal vestibular nucleus (SpVe) and MVc. It is possible that the neurons described by (Olszewski and Baxter, 1982) and Sadjadpour and Brodal (1968) as nucleus supravestibularis form the caudalmost part of group Y.

Group Y is well developed in most mammals. Mehler and Rubertone (1985) and Voogd *et al.* (1985) noted that the term "group Y" has been used to indicate two differing cell groups in both cat and monkey. They reserved the name group Y for the more ventrally lying compact group of small cells located in the floor of the lateral recess, continuous with the dorsolateral part of SuVe. The dorsal division is located within the floccular peduncle (pFl) and contains larger cells, some spindle-shaped (Figs. 33.3G; 33.4G). It is called the infracerebellar nucleus (Inf) by Gacek (1977), who demonstrated that group Y receives saccular afferents from the vestibular nerve, whereas Inf does not. Furthermore, only the Inf projects to the oculomotor nucleus (Sato and Kawasaki, 1987). Numerous medium-sized neurons within the Inf +Y group contain the calcium-binding protein calretinin (Fig. 33.4H), and medium-sized neurons can be seen in

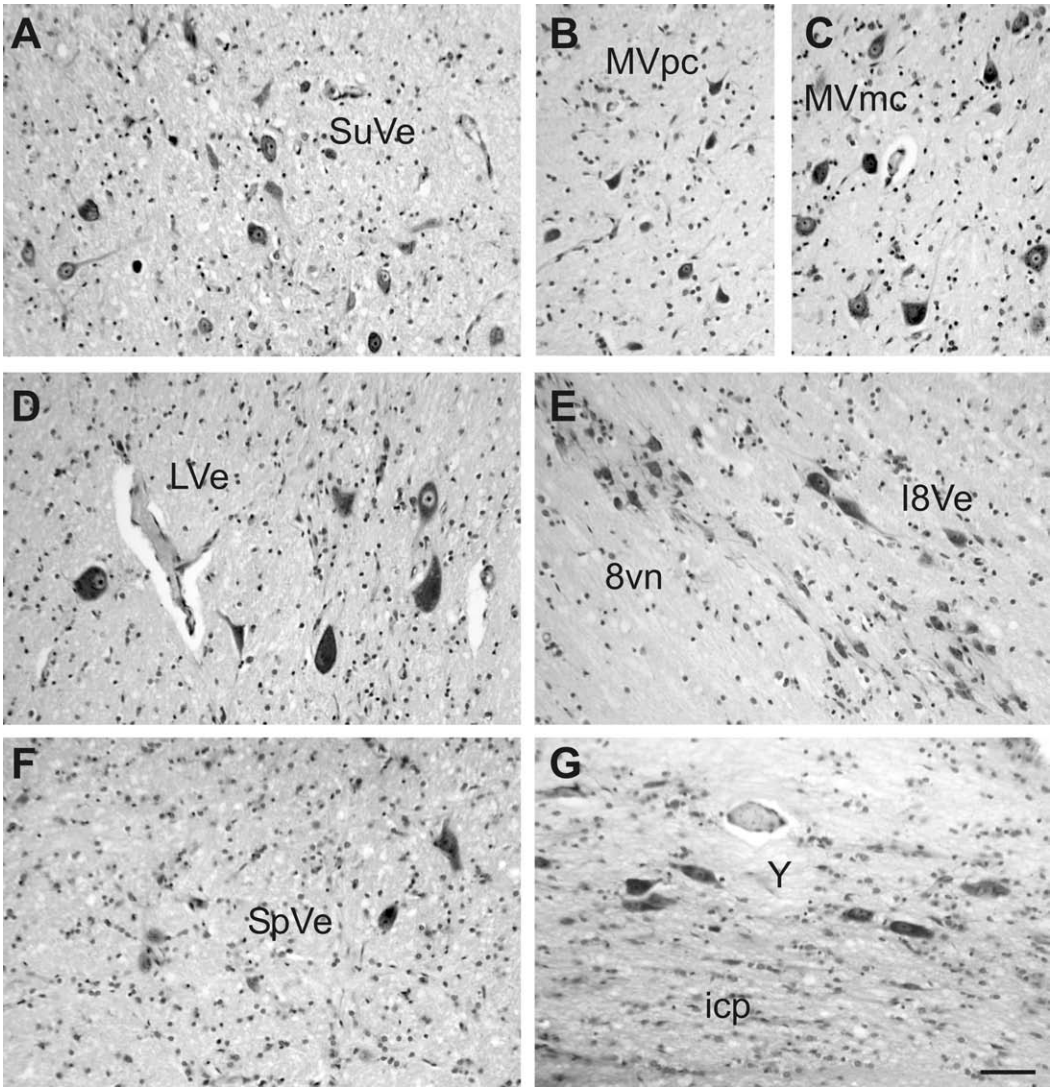

FIGURE 33.3 High-power photomicrographs of Nissl-stained human frontal sections to show the characteristics of the neurons within the vestibular nuclei. **(A)** Medium-sized neurons are within the superior vestibular nucleus (SuVe); **(B)** the medial vestibular nucleus is divided into a parvocellular part (MVpc), **(C)** a magnocellular part (MVmc) lies more ventrally and laterally; **(D)** the Deiter's cells in the lateral vestibular nucleus (LVe) represent the largest neurons within the vestibular nuclei; **(E)** the cells of the interstitial nucleus (I8Ve) are embedded as cell clusters in the vestibular nerve (8vn); **(F)** the neurons within the spinal vestibular nucleus (SpVe) are scattered between traversing fibers; **(G)** the neurons of the group Y abuts on the inferior cerebellar peduncle (icp) as thin layer. Calibration bar = 50 μm and applies for A–G.

Fig. 33.4I as GAD-immunoreactive, confirming the inhibitory GABAergic nature of some of these neurons (see "Oculomotor Nuclei Connections"; Kevetter, 1996; Partsalis and Highstein 1996).

Medial Vestibular Nucleus

The medial vestibular nucleus (MVe) is the largest within the vestibular complex and has the greatest number of neurons (Suarez *et al*., 1997). In their description of the vestibular complex in the rabbit, Epema *et al*. (1988) suggest that the MVe should be divided into three parts: a parvocellular (MVpc), a magnocellular (MVmc), and a caudal (MVc) section. In the present study, an attempt is made to apply this tripartition to the human brainstem. In rabbits and cats, the border between MVmc and MVpc is clearly emphasized by the acoustic striae (das), because the das traverse the vestibular complex as a rather compact

bundle. In humans, however, this border is less clear because the das are loosely arranged and have a relatively caudal position in the vestibular complex owing to the strong development of icp.

Parvocellular Medial Vestibular Nucleus

The MVpc commences at the caudal pole of SuVe and continues in a caudal direction along the ventrolateral wall of the fourth ventricle (Figs. 33.1; 33.4A, D; Paxinos and Huang, 1995; Figs. 30–33; Paxinos *et al.*, 2000, Figs. 98–110). Its rostral aspect is characterized by small bundles of cerebellofugal fibers, which have descended through SuVe. The neurons are smaller than those in MVmc (Fig. 33.3B, C) caudally, the size of its neurons increases although, until MVe abuts on the dorsal column nuclei, no obvious cytoarchitectonic border is present. The glossopharyngeal nerve (9n) is taken as a landmark for the (artificial) border between MVpc and MVc, where most fibers of the juxtarestiform body have converged into the descending bundles of spinal vestibular nucleus (Fig. 33.1, planes 1–8). Rostral to 9n MVpc is, on its lateral side, accompanied by MVmc. Ventrally MVpc is bordered by the facial nerve (7n) and caudally by the dorsal reticular formation. Caudomedially it abuts on the abducens nucleus (6N) and the rostral pole of the prepositus hypoglossal nucleus (PrH), and it contains the cell group described as "the marginal zone" ("Prepositus Hypoglossus Nucleus Connections," PrH).

Magnocellular Medial Vestibular Nucleus

The early students of the vestibular complex noted the presence of an area with large neurons (in addition to medium-sized and small ones) in the rostral part of Clarke's inner nucleus. This area lies ventromedially to the part of the juxtarestiform body that contains the giant Deiters' neurons and is separated from MVpc in the wall of the fourth ventricle by the fiber bundles of the acoustic striae (das). In humans, these parvocellular and magnocellular regions are not as clearly separated by the das fibers, and the area with large neurons is present over a larger dorsoventral extent along the medial margin of the juxtarestiform body (Fig. 33.1). The caudal border is at the level of the glossopharyngeal nerve (9n). The MVmc contains neurons of various diameters; the largest ones are similar to the large neurons between the fiber bundles of the spinal vestibular nucleus and differ clearly from the typical Deiters' neurons, which most frequently have an excentric nucleus (Fig. 33.3C, D, F). The MVmc provides the main output pathways of the nucleus, which project for example directly to the oculomotor neurons and form the second neuron of the VOR; for a review see (Büttner-Ennever (1992b).

All parts of MVe have a high level of acetylcholinesterase (AChE) activity in their neuropil, while this is absent in the lateral vestibular nucleus (Epema *et al.*, 1988; Paxinos and Huang, 1995; Figs. 28, 30, 32; Paxinos *et al.*, 2000, Figs. 101, 103, 105). The ventral part of MVe delineated by Paxinos and Watson (1986) in the rat corresponds well with MVmc in humans. In the rat, the AChE reactivity of MVmc is less than that of MVpc, but the AChE reactivity is still greater than in the nearly negative lateral vestibular nucleus. Choline acetyltransferase (Chat)-immunostained neurons of various sizes are present throughout the MVe being most numerous in the caudal part (Carpenter *et al.*, 1987b; Barmack, 2000). Strong cell body and neuropil labeling is seen with parvalbumin-antibodies in the MVe, whereas calretinin labels small neurons within the MVpc and scattered medium-sized or large neurons laterally (Fig. 33.4F; Kevetter, 1996). In the monkey, GABA-immunoreactive neurons were found in the MVpc and MVmc, some of which provide commissural inhibitory connections (Holstein, 2000; Holstein *et al.*, 1999).

Caudal Medial Vestibular Nucleus

To create a clear distinction between MVmc and MVpc in the rabbit, Epema *et al.* (1988) introduced the name "caudal medial nucleus" (MVc) for the part of MVe caudal to the facial genu. In humans, the point of transition is suggested more caudally at the level of the glossopharyngeal nerve (9n) (Fig. 33.1). The MVc contains small to medium-sized neurons, and the largest ones are located in the center of the nucleus. Caudally, MVc is accompanied at its lateral side by the spinal vestibular nucleus (SpVe) and its characteristic fiber bundles. Over most of its length, it is bordered ventrally by the solitary tract (sol) and its nucleus (SOL) (Fig. 33.1, planes 8–14). Caudally, SpVe and MVc diminish, and their place is taken by the rostral poles of the (internal) cuneate and gracile nuclei. The function of MVc is not known; it is not associated with the variety of vestibular-oculomotor–related activity found in the rostral third of the vestibular complex in behaving primates. It does receive otolith afferents (see later), and a small region in MVc, called nucleus parasolitarius, provides a GABAergic pathway to the inferior olive, which is its only source of otolith input (Barmack *et al.*, 1998).

Lateral Vestibular Nucleus

Deiters' (1865) description of the presence of giant neurons in the rostral part of the juxtarestiform body has resulted in almost as many interpretations of the

borders as there are students of the nucleus. In humans, LVe probably contains the largest neurons of the whole vestibular complex (Suarez *et al.*, 1997), but the difference in size between the Deiters' neurons and the largest neurons in neighboring structures (i.e., MVmc, SpVe, I8Ve) is smaller than, for instance, in cats and rabbits. In humans, the typical Deiters' neurons with their rather excentric nuclei (Fig. 33.3D) are confined to the rostral part of the juxtarestiform body, which is characterized by fibers running in small bundles in a dorsoventral (or vice versa) direction. This area abuts rostrally on the trigeminal nerve and its various nuclei and is easy to distinguish: the medially located SuVe, which does not contain large neurons at its most rostral levels; the MVmc, which has a much lower content of myelinated fibers, at its caudal levels; and the SpVe (ventral to LVe), which is characterized by longitudinally oriented fiber bundles. The largest neurons in MVmc and SpVe are rounder and smaller than those in LVe (Fig. 33.3C, F). Over most of its length, LVe is bordered ventrally not only by SpVe but also by the vestibular nerve and its interstitial nucleus (I8Ve, see "Interstitial Nucleus of the Vestibular Nerve"; Paxinos and Huang, 1995, Figs. 30–33; Paxinos *et al.*, 2000, Figs. 99–106).

The strong development of the human inferior cerebellar peduncle and brachium pontis (bp) relative to the homologous structures in other mammals leads to a "disturbance" of the topographic relations in the region of LVe and the entering root fibers. The LVe is "pushed" further medially than in most animals; consequently, the nucleus stretches over a larger dorsoventral extent along icp. Therefore some caution is required in the interpretation of the cytoarchitectonic data; since some of the neurons between the entering root fibers, as well as the unusual giant neurons in SpVE or MVmc, may turn out to be Deiters' neurons functionally.

The present description of the extent of LVe departs considerably from the studies of Sadjadpour and Brodal (1968), Olszewski and Baxter (1982), and Suarez *et al.* (1997) in humans; Brodal and Pompeiano (1957) in the cat, and Meessen and Olszewski (1949) in the rabbit because these authors did not recognize the differences between MVmc and LVe. The LVe receives very few primary afferent from the labyrinthine canals; the majority appear to arise from the sacculus (Imagawa *et al.*, 1998). It is has reciprocal connections with the cerebellum and is the source of the lateral vestibulospinal tract (Fig. 33.6; "Spinal Cord Connections"; Holstege, 1988). The LVe receives a strong supply from GABA-immunoreactive terminals, which in part arise from Purkinje cells of the cerebellum (Fig., 4E; Walberg and Jansen, 1961; Walberg *et al.*, 1990).

Interstitial Nucleus of the Vestibular Nerve

Ramón y Cajal (1896) described clusters of large neurons embedded in the vestibular nerve as its "noyau interstiel." Many of these neurons are very large, especially in humans (Figs. 33.3E and 33.4A) and suggest a relation with the Deiters' neurons in LVe (Fuse, 1912; Jacobsohn, 1909). To reach the vestibular complex, the vestibular nerve in humans passes between the dorsolateral aspect of the spinal trigeminal root (sp5) and the inferior cerebellar peduncle (icp). In doing so, most root fibers curve around a large area ventrolateral to LVe and to the rostral SpVe (Figs. 33.1 and 33.4). This area has no equivalent in rabbits and cats and contains some small, but mostly medium-sized and large, neurons, while some vestibular nerve fibers can be seen entering it. The absence of juxtarestiform fibers sets it clearly apart from LVe and SpVe. This area is considered as the main part of I8Ve, although the continuity with cell clusters in more distal parts of the vestibular nerve is difficult to establish. Neurons of the I8Ve are parvalbumin-immunoreactive (Fig. 33.4C). The vestibular nerve contains numerous parvalbumin-, calretinin-, and calbindin-positive fibers, which may be involved in different functions (Kevetter and Leonard, 1997).

On the basis of retrograde degeneration experiments in the cat, Brodal and Pompeiano (1957) reported that the connections of the neurons of the interstitial nucleus of the vestibular nerve (I8Ve) were similar to those of Deiters' neurons, based on retrograde degeneration experiments (Brodal and Pompeiano, 1958; Brodal and Torvik, 1957). However, retrograde transport of HRP has demonstrated that the connections of the two nuclei differ. There are descriptions of I8Ve commissural vestibular projections (Epema *et al.*, 1988; Pompeiano *et al.*, 1978), intrinsic vestibular (Epema *et al.*, 1988; Ladpli and Brodal, 1968), and cerebellar projections (Epema *et al.*, 1990; Kotchabhakdi and Walberg, 1978), in particular to the flocculus (Langer *et al.*, 1985a). More recent studies show that I8Ve receives afferents from canal afferents (Gacek, 1969), but no otolith inputs have been seen (Imagawa *et al.*, 1995, 1998).

Spinal Vestibular Nucleus

The spinal vestibular nucleus was referred to earlier as (the nucleus of) the spinal root of the vestibular nerve. In 1896 it was renamed the descending vestibular nucleus by Ramón y Cajal, but the earlier descriptions deserve credit for pointing at the charactistic feature of SpVe: its longitudinally oriented fiber bundles. Whereas the central and dorsal parts of the nucleus are

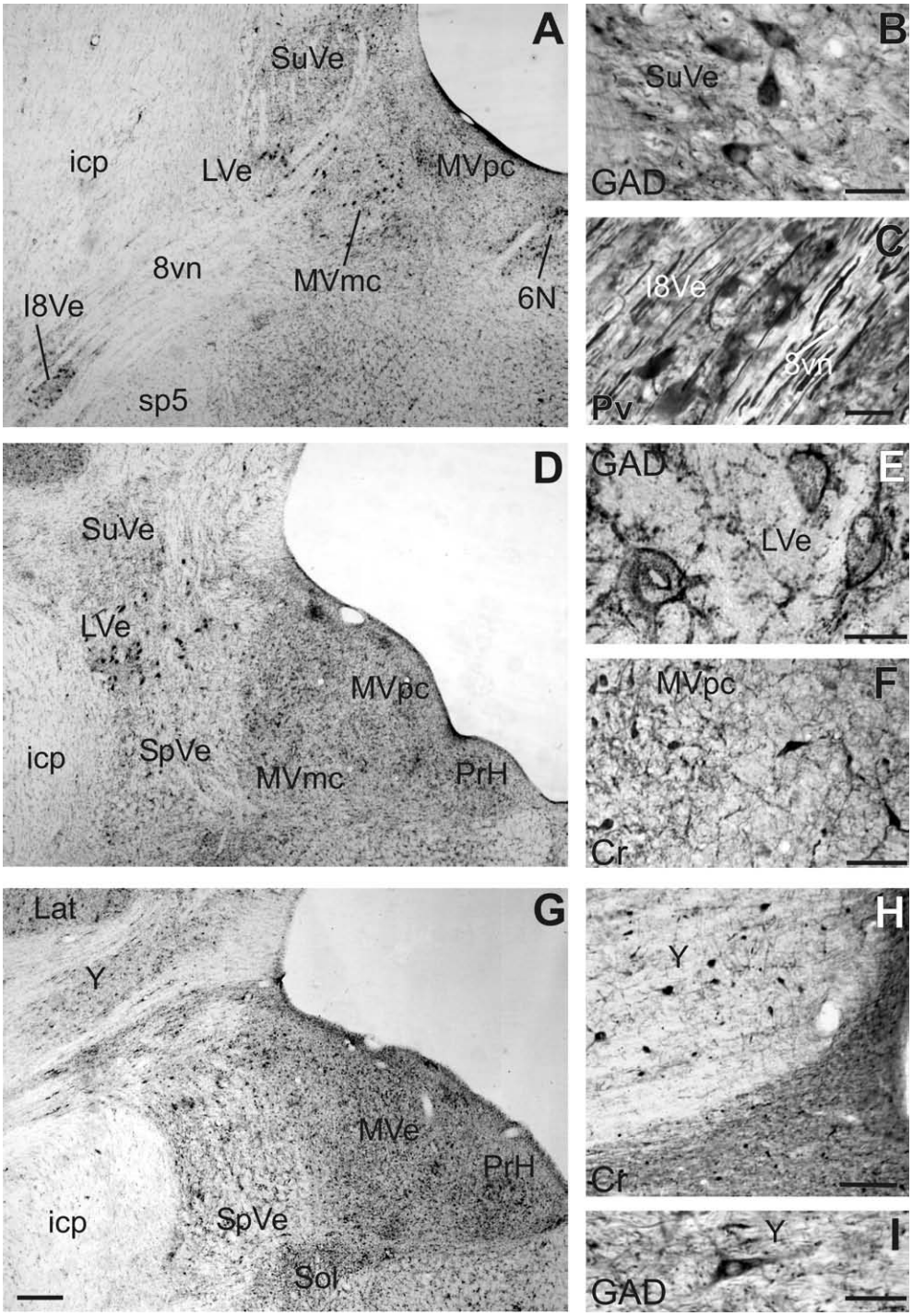

FIGURE 33.4 **(A, D, G)** Low-power microphotographs of frontal sections through the caudal brainstem of a macaque monkey to demonstrate the anatomical location of the vestibular nuclei. **(B, C, E, F, H, I)** High-power microphotographs to show histochemical properties of individual cells within the vestibular nuclei. **(B)** Medium-sized neurons within the superior vestibular nuclei (SuVe) are glutamate decarboxylase (GAD)-immunoreactive. **(C)** Many neurons of the interstitial nucleus of the vestibular nerve (I8Ve) contain parvalbumin (Pv) as most of the vestibular nerve (8vn) fibers. **(E)** The large Deiter's cells within the lateral vestibular nucleus (LVe) receive a very strong input from GAD-positive synaptic boutons. **(F)** Numerous small-sized neurons within the parvocellular medial vestibular nucleus (MVpc) are calretinin (Cr)-positive, medially bordered by a region containing scattered larger Cr-positve neurons; the dorsal part of group Y contain calretinin (H) and GAD (I). A, D, G calibration bar = 500 μm; B, C, E, I calibration bar = 50 μm; F, calibration bar = 100 μm; H, calibration bar = 200 μm.

rather "open," the organization of the fiber bundles becomes more compact toward its periphery. This nucleus has on average the smallest cells of the vestibular complex (Suarez *et al.*, 1997).

Over almost its entire length, SpVe is bordered laterally by the inferior cerebellar peduncle (Fig. 33.1B, planes 9–13; Paxinos and Huang, 1995; Figs. 21–31; Paxinos *et al.*, Figs. 101–118). A precise border between SpVe and icp is difficult to draw, because of the dense packing of the fiber bundles. Toward its caudal extreme, SpVe becomes separated from icp, first by group X and later by the external cuneate nucleus (ECu). The medial border of SpVe with MVc is sharp. The rostral pole of SpVe is easy to delineate from LVe because the fiber bundles of SpVe are longitudinally oriented, whereas LVe has transversely oriented fibers (Fig. 33.4D, G). The ventral border of SpVe is formed at rostral levels by the spinal trigeminal tract (sp5) and the trigeminothalamic fibers (tt) of Wallenberg's tract. Caudal from the level of the glossopharyngeal nerve (9n), SpVe is bordered ventrally by sp5, the solitary tract, and the solitary nucleus (Fig. 33.1, planes 9, 10; Fig. 33.4G). The nucleus ovalis (Ov) of Olzsewski and Baxter (1982), which is associated with SOL, is clearly visible at these levels. More caudally, where the Sp5 shifts lateralward, a loosely arranged cell group that may represent part of the repagulum cuneati of Braak (1971) lies between SpVe and the dorsal reticular formation (Fig. 33.1B, planes 11, 12). At the caudal tip of SpVe, olivocerebellar fibers (oc) enter through the gap between SOL and ECu.

The opinion that the fiber bundles in SpVe were composed of descending vestibular root fibers has never been rejected clearly, although Brodal and Pompeiano (1957) and Sadjadpour and Brodal (1968) suggest a contribution of cerebellofugal elements. Studies with anterograde axonal tracing in the rabbit in our laboratory have provided evidence that descending vestibular root fibers are almost exclusively present between the bundles. However, the bundles themselves are composed of fibers of the uncinate tract originating in the contralateral fastigial nucleus of the cerebellum, direct corticovestibular fibers from the flocculus and the uvula and nodulus of the caudal cerebellar vermis, and olivocerebellar climbing fibers (Gerrits, 1990, Fig. 5).

"Associated" Cell Groups

In their subdivision of the vestibular nuclei of the cat, Brodal and Pompeiano (1957) described a number of cell groups that do not receive afferents from the vestibular nerve (Walberg *et al.*, 1958; Brodal, 1984; Suarez *et al.*, 1997). For this reason alone, these cell groups should not be considered as part of the vestibular complex. To consider these cell groups as belonging to the vestibular nuclei on the basis of a spatial similarity rather than afferent inputs distorts the accepted definition of the vestibular nuclei (i.e., those in receipt of labyrinthine afferents; Brodal, 1974). Although Sadjadpour and Brodal (1968) described the groups F, G, and Z in the human brain, these groups could not be identified with certainty in the present study.

Group X of Brodal and Pompeiano (1957) is located between the ventrolateral caudal pole of SpVe and icp in the cat and the rabbit (Epema *et al.*, 1988). In humans, group X is located in the dorsolateral corner of SpVe, an area that contains only a few fiber bundles (Sadjadpour and Brodal, 1968; Suarez *et al.*, 1997; Paxinos and Huang, 1995, Figs. 25–27). As in the rabbit and the cat, the transition area between the rostral pole of the external cuneate nucleus (ECu) and SpVe contains neurons that are intermediate in size between those in the bordering nuclei and are considered here as group X (Fig. 33.1, planes 11,12). Although longitudinally oriented fiber bundles are present, a multitude of fibers in between give this area a fuzzy appearance.

CONNECTIONS

The vestibular nuclei are a sensorimotor complex that senses the movement and position of the head in space. Signals are generated in the labyrinth of the inner ear; the three canals responding to angular acceleration of the head, and the two otolith organs, the sacculus and the utricle responding to linear acceleration, including gravity. The information is conducted to the vestibular complex via the eighth cranial nerve and used to make compensatory eye and head movements as well as postural adjustments (Cohen, 1974). Hence, there are strong interconnections between the vestibular nuclei and the oculomotor system (see Chapter 16), to the spinal cord (see Chapter 8) and the cerebellum (see Chapter 11). There are several recent reviews of the afferent and efferent connections of the vestibular nuclei (Brodal, 1984; Carpenter, 1988; Highstein and McCrea, 1988; Cohen *et al.*, 1996; Voogd *et al.*, 1996; Büttner-Ennever, 1999, 2000; Graf *et al.*, 2002).

Vestibular Nerve Connections

Experimental studies in rabbits led to the recognition that the eighth cranial nerve is related to both the cochlea and the labyrinth (Forel, 1907; Onufrowicz, 1885). Bechterew (1887) showed in fetal human brain that the myelinization of the vestibular fibers in the

eighth nerve precedes that of the acoustic fibers. The individual character of both components was definitely proved by the experiments of Von Monakow (1890) who demonstrated the termination of the acoustic nerve in the acoustic tubercle, which in turn projects to the inferior colliculus by way of the acoustic striae.

The vestibular primary afferents are bipolar neurons with their cell bodies in the ganglion of Scarpa and utilize glutamate as a transmitter (Reichenberger *et al.*, 1997; Straka *et al.*, 1999). Golgi stains, and later tract tracing studies, have all demonstrated that the primary vestibular afferents enter the brainstem at the level of the Lve and divide into two branches, an ascending and a descending branch (Sato *et al.*, 1989; Hauglie-Hanssen, 1968; Lorente de Nó, 1933; Ramón y Cajal, 1909). The ascending branch passes through LVe to terminate in SuVe possibly continuing beyond into the cerebellar cortex), and the descending branch gives off terminal branches in SpVe and MVe.

The exact distribution of terminal branches in the vestibular complex has been controversial. Most of the early investigators assumed that the fibers distribute over the entire vestibular complex. Subsequent studies in the monkey, cat, and guinea pig (Stein and Carpenter, 1967; Carpenter *et al.*, 1972; Gacek, 1969; Kotchabachdi and Walberg, 1978; Korte, 1979; Gstoettner *et al.*, 1992) excluded only LVe from root input but included a hitherto unmentioned projection to the ventral group Y, as a recipient of sacculus afferents. For reviews, see Büttner-Ennever (1999, 2000), Brodal (1984), Carleton and Carpenter (1984), Carpenter *et al.* (1987a), Carpenter (1988), and Highstein and McCrea (1988).

In electron microscopic studies in the cat, Mugnaini *et al.* (1967) and Walberg and Mugnaini (1969) showed terminal degeneration in the central and ventral parts of their lateral vestibular nucleus, but these authors did not make a distinction into LVe and MVmc. Following injection of WGA-HRP into the vestibular ganglion of the rabbit-labeled fibers were found (in the light microscope) in LVe, although in low number as compared to Mvmc (Gerrits *et al.*, 1989). There are arguments to consider the LVe as one of the central cerebellar nuclei: the connections of LVe fit the monozonal, mononuclear organization proposed by Voogd (1964; Voogd and Bigare, 1980; Voogd *et al.*, 1996; see also Chapter 11): and LVe receives Purkinje cell axons from a single strip of cerebellar cortex (zone B) and shares a collateral climbing fiber innervation from the caudal dorsal accessory olive with this zone B (Groenewegen and Voogd, 1977).

Very little notice has been taken until recently of the differences in central projections of the canals compared to the otoliths (review: Büttner-Ennever, 1999). A differential termination of vestibular nerve axons from different canals and otoliths was proposed by Stein and Carpenter (1967), Gacek (1969), Carpenter *et al.* (1972), Carpenter and Cowie (1985a), Kevetter and Perachio (1986), and Maklad and Fritzsch (2002). The recent intraaxonal stains of identified canal primary afferents have shown that canal afferents terminate over most of the vestibular complex including MVe, SpVe, I8Ve, and SuVe, but excluding LVe and PrH (Sato *et al.*, 1989). In contrast, utricular afferents mainly target SpVe with some terminals also in MVe, LVe, SuVe, and the abducens nucleus (Imagawa *et al.*, 1995; Ishizuka *et al.*, 1980). Saccular afferents give off terminal branches mainly to LVe and SpVe; but up to now the intraaxonal labeling studies have not reported any saccular afferents to the ventral Y group, in contrast to the earlier tract-tracing experiments (Imagawa *et al.*, 1998). The otoliths also have direct projections to the cerebellum, which terminate mainly in the uvula, in contrast to the canals afferents that are associated primarily to the nodulus (Maklad and Fritzsch, 2003).

Following lesions close to the facial genu of the rabbit, Leidler (1916) observed degenerated fibers (bilaterally) in the vestibular nerve, which he interpreted as centrifugal. An efferent innervation of the labyrinthine sensory organs has been found in all vertebrates except the hagfish (review: Goldberg *et al.*, 2000). The cells of origin of the vestibular efferents, the so-called group e, are located directly lateral to the abducens nucleus and were also identified with retrograde tracers, histochemical and immunocytochemical methods (primates, Carpenter *et al.*, 1987a; Goldberg and Fernandez,1980; cat, Gacek *et al.*, 1965). The rat homologue has been termed the paragenual nucleus (Paxinos and Watson, 1986). Group e cells have long been known to use acetylcholine as a transmitter (Gacek and Lyon, 1974; Warr, 1975); more recent studies have also demonstrated the presence of the neuropeptide calcitonin gene-related peptide (Demêmes and Broca 1998; Tanaka *et al.*, 1988; Wackym *et al.*, 1991) and nitric oxide (Lysakowski and Singer, 2000).

Commissural Connections

Although all primary vestibular and cerebellar inputs to the vestibular nuclei are strictly ipsilateral, the vestibular nuclei of each side operate together owing to a massive commissural system (Büttner-Ennever, 1992b). Several studies have investigated its function in the control of sustained vestibular responses and vestibular compensation (Godaux and Cheron, 1993; Cartwright and Curthoys, 1996; Holler and Straka, 2001; Wearne *et al.*, 1997). The first mention of a vestibular commissure was by Ramón y Cajal

(1909) who erroneously took the vestibular efferent fibers described in the previous paragraph (his "faisceau vestibulaire croisé") for crossed vestibular root fibers. The presence of such fibers in the commissure was subsequently disproved in a number of studies using axonal degeneration techniques (Korte, 1979; Rasmussen, 1932; Stein and Carpenter, 1967; Walberg *et al.*, 1958).

Lesion studies (Carpenter, 1960; Ladpli and Brodal, 1968; Tarlov, 1969) and retrograde transport of HRP (Gacek, 1978; Ito *et al.*, 1985) have shown a large number of interconnections of SpVe, SuVe, and the ventral group Y with their contralateral homonyms (Fig. 33.10C). Other studies observed a much more divergent projection of individual vestibular nuclei to all vestibular nuclei on the contralateral side (Carleton and Carpenter, 1983; Carpenter and Cowie, 1985b; Pompeiano *et al.*, 1978; Carpenter 1988; Büttner-Ennever 1992b; Epema *et al.*, 1988). The neurons engaged in the commissural projection are distributed throughout the vestibular complex, with the exception of LVe and group X. The largest numbers of commissural connections arose from MVpc and MVc, the small-celled peripheral SuVe, and nucleus prepositus hypoglossi were also rich in commissural connections. A modest number was found in group Y, I8Ve and SpVe; very few were encountered in MVmc and the central, large-celled zone of SuVe. The commissural connections of nucleus prepositus hypoglossi arose from the principle cells (McCrea and Baker, 1985a). The crossing fibers from secondary vestibular neurons in MVe have an inhibitory effect on secondary vestibular neurons in the contralateral MVe, which is mediated by both GABA and glycinergic neruons (De Waele *et al.*, 1995; Holstein, 1999; Holstein *et al.*, 1999).

Investigations on the contribution of LVe fibers to the commissure have yielded ambiguous results. Some of the studies with lesions of LVe (Carpenter, 1960; Ladpli and Brodal, 1968; McMasters *et al.*, 1966) showed axonal degeneration in the contralateral LVe and SpVe. Later studies failed to demonstrate this connection in the rabbit (Epema *et al.*, 1988), the cat (Carleton and Carpenter, 1983; Carpenter and Cowie, 1985b; Gacek, 1978; Pompeiano *et al.*, 1978), and the monkey (Carleton and Carpenter, 1983; Carpenter, 1988).

Intrinsic Connections

The Golgi studies of Ramón y Cajal (1909) and Lorente de Nó (1933) suggested the presence of ipsilateral intrinsic vestibular connections, which were later experimentally verified (Ladpli and Brodal, 1968; Carleton and Carpenter, 1983; Carpenter and Cowie, 1985b; Epema *et al.*, 1988; Ito *et al.*, 1985; Rubertone *et al.*, 1983). In addition, observations on intracellularly stained vestibular neurons also support the earlier demonstration of intrinsic and commissural vestibular projections (Ishizuka *et al.*, 1980; McCrea *et al.*, 1980; Mitsacos *et al.*, 1983; Highstein and McCrea, 1988).

Epema *et al.* (1988) showed that within the vestibular complex of each side SuVe, Mve, and SpVe are reciprocally connected (Fig. 33.10D). However, the central SuVe and MVmc form a rostrocaudally oriented column of medium-sized and large neurons, which receives input from surrounding neurons but does not reciprocate this projection. Rather, it constitutes the origin of the main output pathways from the vestibular complex (Büttner-Ennever, 1992b). Efferents from ventral group Y terminate in SuVe, Mve, and SpVe. The infracerebellar nucleus and the interstitial nucleus of the vestibular nerve (I8Ve) supply fibers to MVe and SpVe. Studies using tract tracing combined with staining for nitric oxide NO-sensitive neurons revealed that the PrH receives projections from in the marginal zone and MVe, predominantly from the ipsilateral side, see following discussion (Moreno-Lopez *et al.*, 2001).

By comparing the commissural and intrinsic connections, Epema *et al.* (1988) concluded that quantitative differences in connectivity were present between a core region and the periphery. The core region (central SuVe, LVe, MVmc and rostral SpVe) receives predominantly intrinsic input from the peripherally located vestibular neurons but is itself only minimally involved in the commissural projection. This region is the origin of the major ascending and descending pathways leaving the vestibular nuclei (Büttner-Ennever, 1992b).

Oculomotor Nuclei Connections

Several parallel pathways, subserving compensatory and pursuit eye movements, run from the vestibular nuclei to the oculomotor nuclei, see also Figure 19.2 (Graf *et al.*, 2002). The best studied pathway is the three neuron arc involving the primary canal afferents projecting to the secondary vestibular neurons, which in turn send axons to the motoneurons in the abducens nucleus, the trochlear nucleus and the oculomotor nucleus, see Figures 33.5–33.9 (Epema, 1990; Carpenter and Cowie, 1985b; Gacek, 1977; Graybiel and Hartwieg, 1974; Tarlov, 1970). Most modern studies are consistent with the findings of careful intraaxonal staining reconstructions, which demonstrated that secondary vestibular neurons do not just excite or inhibit the motoneurons of one eye muscle but project to several pools of extraocular motoneurons (Fig. 33.6), and generate a particular *conjugate eye movement*, such as upward, downward, torsional, or horizontal movements. Many studies were used to compile the scheme

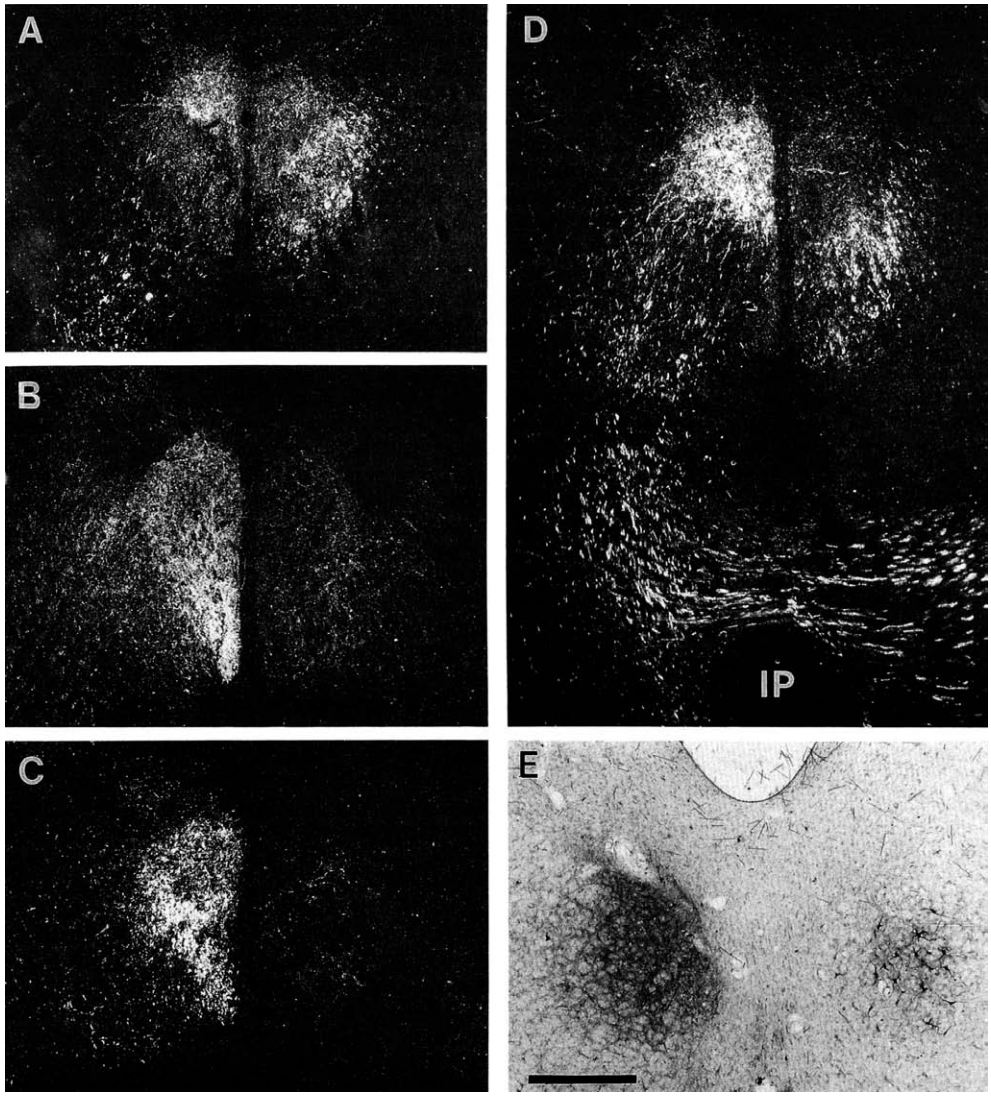

FIGURE 33.5 Distribution of terminal labeling in the oculomotor complex of the rabbit after injections of the anterograde tracer tritiated leucine into different regions of the vestibular complex. The results using this tracer are particularly valuable because, unlike others, it is not taken up by fibers of passage (all injection sites are shown on the right side of the illustrations). **(A)** Injection in SuVe: ipsilateral terminal labeling predominantly present in the medial and inferior rectus subdivisions. Contralateral terminal labeling mainly in the inferior oblique and superior rectus subdivisions. **(B)** Injection in MVc: mainly contralateral terminal labeling in the inferior oblique, and superior, medial and inferior rectus subdivisions, with an emphasis on the latter two. **(C)** Injection in SpVe: the labeling is similar to (B) MVc injections. **(D)** Injection in SuVe: labeled axons reach the ipsilateral medial and inferior rectus subdivisions through the mlf. The contralateral inferior oblique and superior rectus divisions are reached through the scp. Note the complementary pattern of labeling on the two sides, and the crossing of the scp fibers directly dorsal to the interpeduncular nucleus (IP). **(E)** Contralateral anterogradely labeled termination and ipsilateral retrogradely labeled neurons in the interstitial nucleus of Cajal following an injection of WGA-HRP involving MVc and the medial half of SpVe. All frames have the same magnification, scale bar = 200 μm.

of connections shown in Fig. 33.6 (Büttner-Ennever, 2000; Cohen, 1974; Graf *et al.*, 1983; Graf and Ezure 1986; Highstein, 1973; Hirai and Uchino, 1984; Isu *et al.*, 1988; Isu and Yokota, 1983; Ito *et al.*, 1973; McCrea *et al.*, 1980, 1987a, b; Mitsacos *et al.*, 1983; Ohgaki *et al.*, 1988; Precht, 1978, 1979). The secondary vestibular neurons have a dominant canal input and project to the motoneurons via the medial longitudinal fasciculus (mlf), or the superior cerebellar peduncle (scp) or crossing ventral tegmental tract (cvtt in Figs. 33.5D

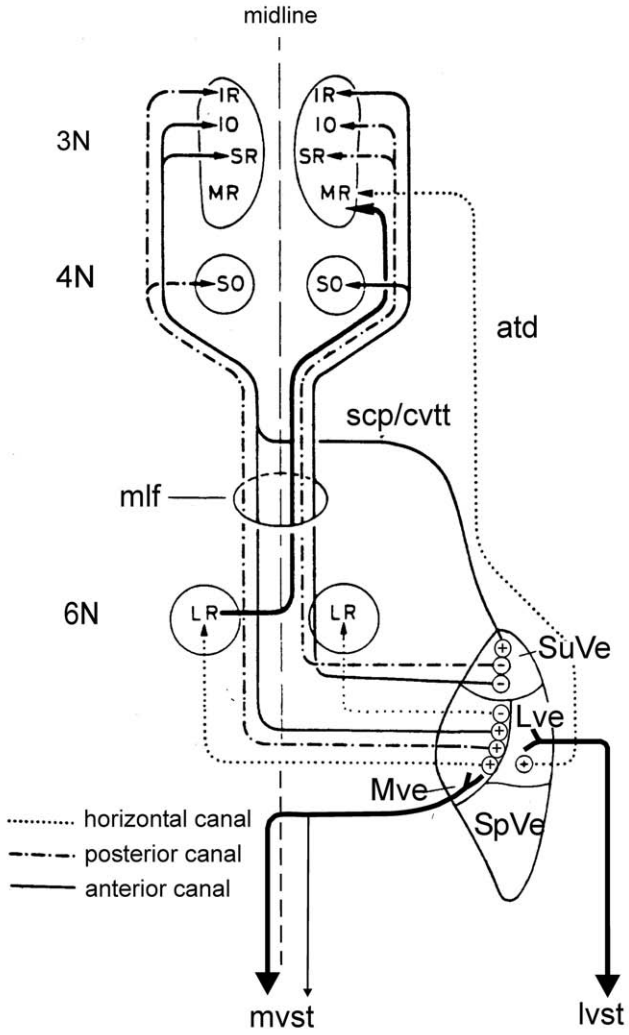

FIGURE 33.6 Direct pathways from secondary vestibular neurons to the oculomotor nuclei. The diagram indicates roughly the location of the cells of origin; it shows their dominant canal input, their excitatory or inhibitory character, and the extraocular motoneurons targeted to produce the compensatory eye movement after canal activation. The descending projections to the spinal cord are lvst and mvst.

and 33.6; Ghelarducci *et al.*, 1977; Carpenter and Cowie, 1985b; Sato *et al.*, 1984). Ipsilateral pathways are inhibitory and contralateral pathways excitatory; whereby the inhibitory transmitter for horizontal VOR is glycine that for the vertical VOR is GABA, and both use glutamate and/or aspartate as their excitatory transmitter (McElligott and Spencer, 2000; Spencer *et al.*, 1989, 2003). These second-order vestibular cells tend to lie in the central magnocellular regions of the vestibular complex in MVmc and the central SuVe (Büttner-Ennever, 2000).

Axons arising from the same region, MVmc and ventral LVe, project into the lateral mlf as the ascending tract of Deiters (Figs. 33.2 and 33.6). They terminate on ipsilateral medial rectus motoneurons in 3N and are modulated by both utricular inputs and the viewing distance of a visual target (Chen-Huang and McCrea, 1998; McCrea *et al.*, 1987b).

Many non–second order vestibular neurons also project to the oculomotor nuclei; they include those in the rostral MVpc and some inhibitory neurons in the marginal zone adjacent to PrH, which are particularly prominent in primates and may play a role in pursuit eye movements (Langer *et al.*, 1986; McFarland *et al.*, 1992). In addition, the dorsal division of the Y group, called the infracerebellar nucleus, has a strong monosynaptic connection to the trochlear and inferior rectus motoneurons, which may be inhibitory (Sato and Kawasaki, 1987). The function of Inf is considered to be related to motor learning or plasticity of the vertical vestibuloocular reflex and the generation of vertical smooth pursuit eye movements (Chubb and Fuchs, 1982; Partsalis and Highstein, 1996). A further non–second order vestibular group of neurons scattered over a large area of MVe and SpVe and possess bifurcating axons that project both to the oculomotor nuclei and to the spinal cord. They are called vestibulooculocollic neurons. Their axons travel caudally mainly in the contralateral mvst (Fig. 6; Minor *et al.*, 1990).

Interstitial Nucleus of Cajal Connections

In the older literature, specific connections between the vestibular nuclei and the interstitial nucleus of Cajal (InC; see Chapter 16) were rarely mentioned. Pompeiano and Walberg (1957) and Mabuchi and Kusama (1970) were the first to demonstrate, in degeneration studies, ipsilaterally descending fibers to a termination in MVe. Studies with retrograde transport of HRP have confirmed this projection (Fig. 33.5E; Carleton and Carpenter, 1983; Carpenter and Cowie, 1985b) and recent anterograde tracing in the squirrel monkey demonstrated fibers from the InC descending in the mlf and their terminations in the SuVe and MVe (Fig. 33.10E; Kokkoroyannis *et al.*, 1996). This projection may include neurons with downward on directions of the eyes that were identified in the InC of the cat and found to form a separate population from downward on direction neurons with commissural projections to the contralateral InC (Chimoto *et al.*, 1999). In turn, the vestibular nuclei send bilateral efferents to the InC. The degeneration that was observed in the InC following lesions of the mlf (Carpenter and Hanna, 1962; Carpenter and Strominger, 1965) was later attributed to an origin in the vestibular nuclei. The projection from SuVe is predominantly ipsilateral, that from MVe and SpVe is predominantly contralateral (Carleton and

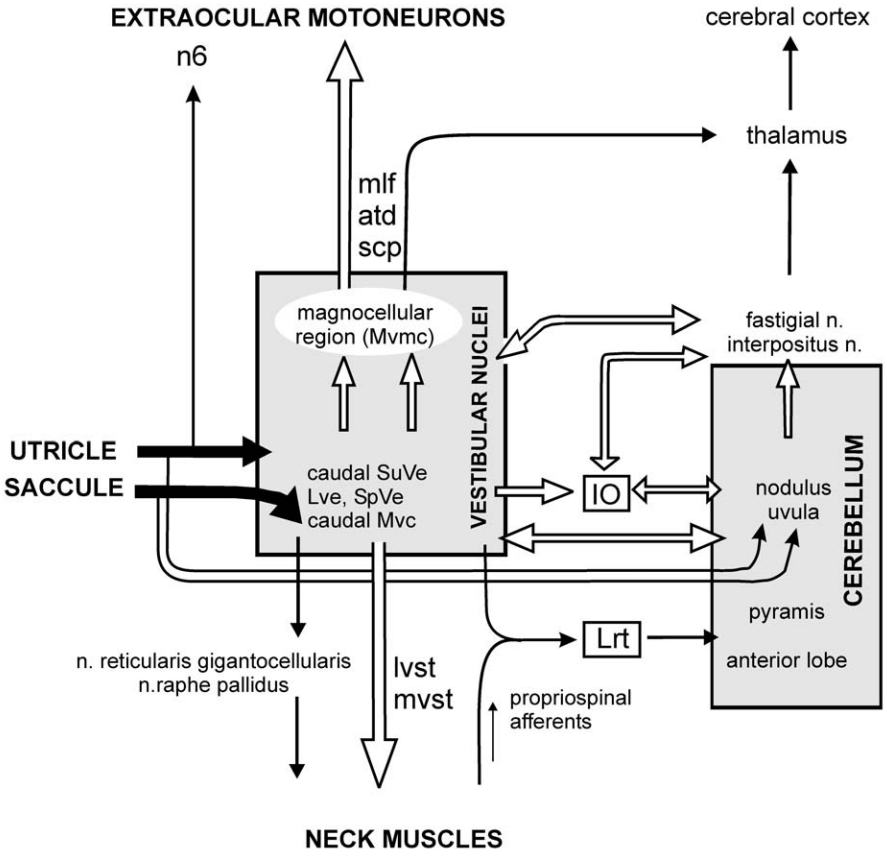

FIGURE 33.7 Summary of the structures and pathways carrying otolith signals. They are concentrated in the vestibular nuclei and cerebellum; they influence neck and postural muscles and probably the extraocular eye muscles.

Carpenter, 1983; Carpenter and Cowie, 1985b; Tarlov, 1969, 1970) (Fig. 33.10E). These projections may stem from collaterals of the secondary vestibular neurons mediating the vertical VOR (see "Oculomotor Nuclei Connections") as shown by intraaxonal HRP-injection studies in cat and monkey (Fig. 33.9, dashed arrows; McCrea *et al.*, 1987, a, b; Iwamoto *et al.*, 1990).

Nucleus Prepositus Connections

The nucleus prepositus hypoglossus (PrH) lies medial to the MVe (Fig. 33.4D, G) and is one site in the brain where there is an interaction between visual and vestibular systems. It is thought to contribute to the maintenance of eye position or gaze in the horizontal plane (Godaux *et al.*, 1993; Kaneko, 1997; McCrea, 1988). The major cytological features of the nucleus appear to be present in all species, including man. The reader is referred to the studies by Brodal and McCrea (Brodal 1983; McCrea 1988; McCrea and Baker, 1985a, b) for detailed reviews of the cytoarchitecture of the PrH in primates and cats, respectively. Three different types of soma-dendritic architecture were observed: (1) "multidendritic" cells in the caudomedial PrH; (2) small cells in the dorsolateral PrH; and (3) medium-sized "principal" cells in the rostral, central region of the PrH. Because afferents from the vestibular nerve do not terminate in the PrH, it is not included in the vestibular complex strictly speaking. However, with respect to its efferent connections, the PrH behaves like the vestibular nuclei (Belknap and McCrea, 1988; McCrea, 1988; McCrea and Baker, 1985a; McCrea *et al.*, 1979).

The PrH projects to almost all oculomotor structures see Figure 33.10: it projects to the abducens nucleus (Hikosaka and Igusa, 1980; Maciewicz *et al.*, 1977; Langer *et al.*, 1986), the oculomotor nucleus (Graybiel, 1977; Graybiel and Hartwieg, 1974; Hikosaka and Igusa, 1980; Steiger and Büttner-Ennever, 1979), the vestibulocerebellum (Epema *et al.*, 1990; Kotchabhakdi *et al.*, 1978; Thunnissen *et al.*, 1989; Langer *et al.*, 1985b) the pontomedullary reticular formation and the superior colliculus (Corvisier and Hardy, 1997). The PrH neurons that project to the ipsi- and contralateral

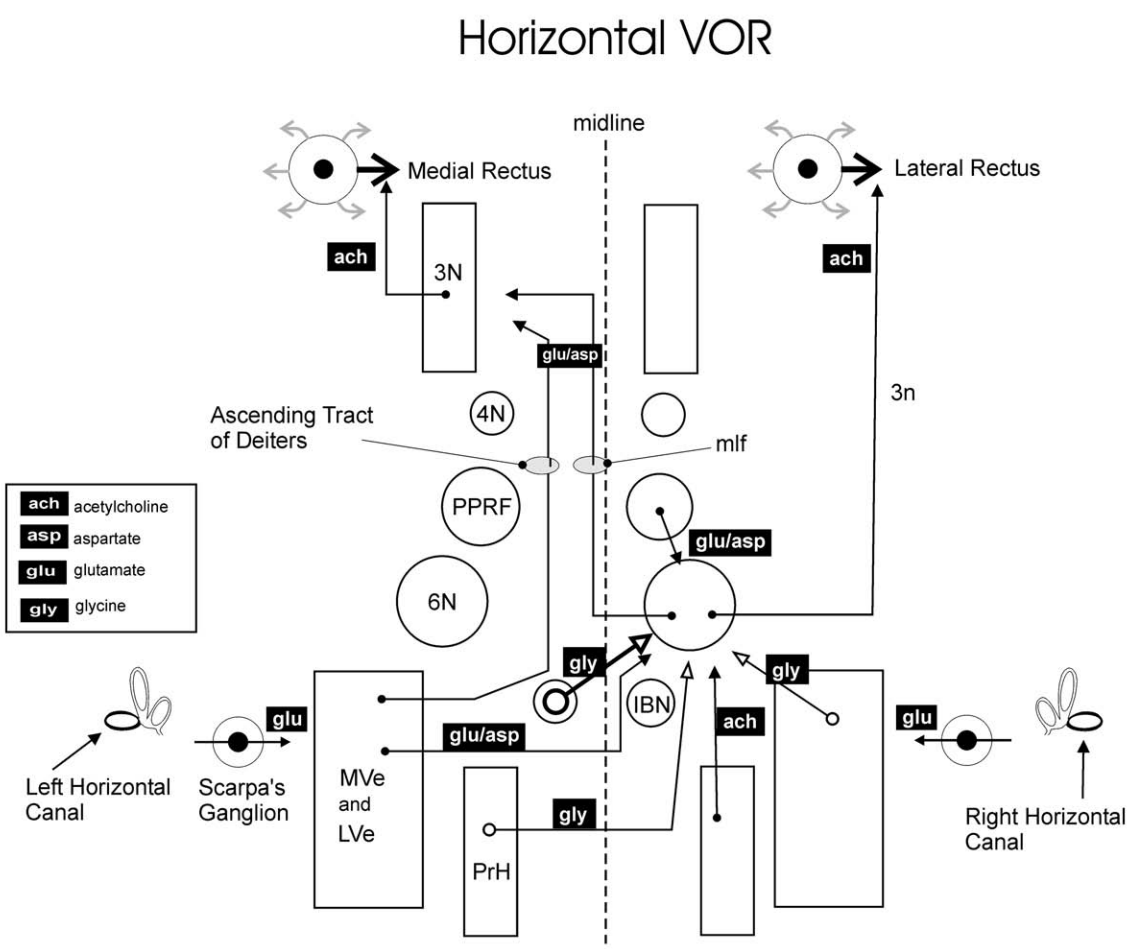

FIGURE 33.8 The principle pathways for the horizontal VOR and their major transmitters (modified from McElligott and Spencer, 2000). Open circles and arrows represent inhibitory paths, and closed circles and arrows, excitatory paths.

vestibular complex seem to be located peripherally in the caudal half of the nucleus (Epema *et al.*, 1988; McCrea *et al.*, 1979).

In primates, a subnucleus of the medial vestibular nucleus, the "marginal zone," forms the lateral border of the rostral half of PrH (Langer *et al.*, 1986). The marginal zone of the medial vestibular nucleus contains tightly packed, medium-sized neurons, most of which project either to the ipsilateral or to the contralateral abducens nucleus (Spencer *et al.*, 1989; Belknap and McCrea, 1988). In contrast to the PrH, the marginal zone is strongly parvalbumin immunoreactive, lacks calretinin, and contains GAD-immunoreactive neurons (McCrea and Horn, personal communication).

Nitric oxide (NO) is a diffusible gas, which was shown to act as an intercellular messenger participating in many functional roles (i.e., in ischemia, neurotoxicity, and neurodegenerative processes, and modulation of sensory function; Cudeiro and Rivadulla, 1999). It is converted from L-arginine to NO by the NADPH-dependent NO-synthase. The PrH of the cat and monkey exhibits a strong NO-synthase-immunoreactivity of neurons and the neuropil (monkey: Satoh *et al.*, 1995; Moreno-Lopez *et al.*, 2001). Interestingly, the marginal zone between the PrH and MVe contains numerous strongly NO-sensitive neurons but is devoid of NO-releasing (i.e., NO-synthase) neurons. This histochemical distinction between the PrH, and MVe was used to define the marginal zone in the cat anatomically for the first time (Moreno-Lopez *et al.*, 2001). The functional role of the NO system is not fully understood, but a pharmacological study in the alert cat demonstrated that the balanced production of NO by the PrH is neccessary for the correct performance of eye movements because unilateral injections of NO-synthase inhibitors into the PrH resulted in a severe long-lasting nystagmus (Moreno-Lopez *et al.*, 1996, 1998). The most important inputs arise from brainstem

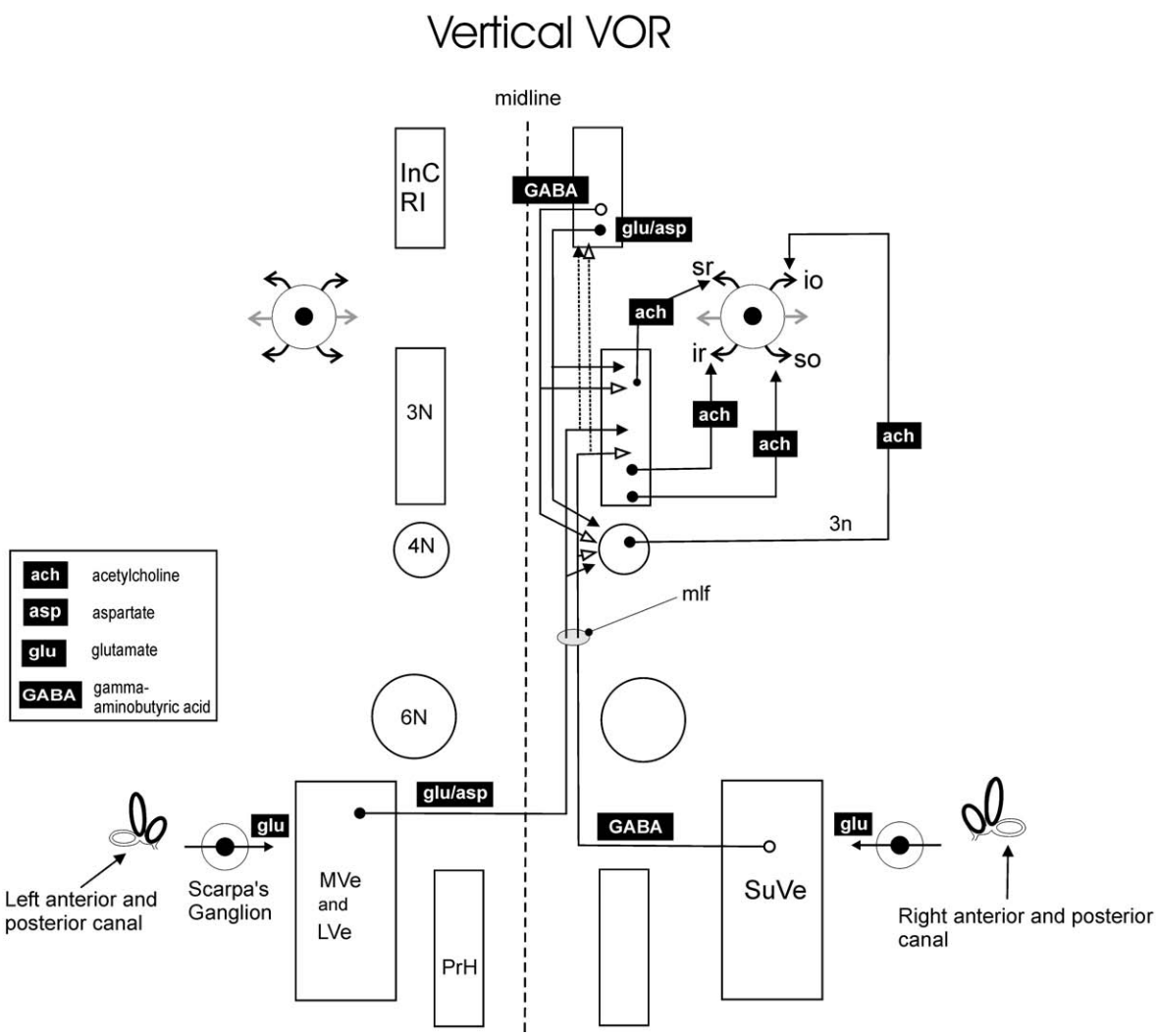

FIGURE 33.9 The principal pathways for the vertical VOR and their major transmitters (modified from McElligott and Spencer, 2000). Open circles and arrows represent inhibitory paths, and closed circles and arrows, excitatory paths.

areas (Belknap and McCrea, 1988): the perihypoglossal nuclei including the nucleus intercalatus and particularly the contralateral prepositus; the MVe and SpVe and a region of the ventrolateral vestibular complex, bilaterally (McCrea *et al.*, 1987a); the paramedian medullary reticular formation especially the regions contralateral to the PrH that contain inhibitory saccadic burst neurons including the ipsilateral paramedian pontine reticular formation (Büttner-Ennever and Henn, 1976; Gerrits and Voogd, 1986) and the vertical premotor cell groups of the mesencephalon (the ipsilateral rostral interstitial nucleus of the mlf, the interstitial nucleus of Cajal.); and the periextraocular motor nuclei and the surrounding regions including the vestibulocerebellum (Langer *et al.*, 1985a) and the fastigial nucleus (Noda *et al.*, 1990). In addition, the PrH receives visuomotor brainstem pathways from areas such as the ventral lateral geniculate nucleus (Belknap and McCrea, 1988) accessory nuclei of the optic tract (Cazin *et al.*, 1982; Graybiel, 1977; Büttner-Ennever *et al.*, 1996). The PrH of the human is displayed in Figures 25–30 (Paxinos and Huang, 1995); see Chapter 16 (Fig. 16.4L, M).

Cerebellar Connections

Vestibulocerebellar

The vestibular nuclei are the source of cerebellar mossy fibers transferring both canal and otolith information to the cerebellar cortex and deep nuclei, see Fig. 33.7 (for a reviews, see Chapter 11; Brodal, 1974; De Zeeuw *et al.*, 1997; Voogd *et al.*, 1996; Bower, 2002; Cohen *et al.*, 2002). The main recipients of the secondary mossy fibers afferents are the flocculus and the nodulus

(lobule 10), the ventral aspect of the uvula (lobule 9), and deep in the fissures of the lobules 1 and II of the anterior lobe. In a large number of experimental studies the origin of the projection has been reported to be in all vestibular nuclei, including group X and Y, but with the exception of LVe: specifically, the rat (Blanks *et al.*, 1983), the rabbit (Tan and Gerrits, 1992; Epema *et al.*, 1990; Magras and Voogd, 1985; Thunnissen *et al.*, 1989; Yamamoto, 1979), the cat (Brodal and Torvik, 1957; Carpenter, 1960; Kotchabhakdi and Walberg, 1978; Sato *et al.*, 1983), the bush-baby (Rubertone and Haines, 1981), and the macaque monkey (Brodal and Brodal, 1985; Langer *et al.*, 1985b). Different populations of neurons in the vestibular nuclei, which are not topographically separated, provide mossy fiber connections to individual lobules in each hemicerebellum (i.e., bilaterally).

Several transmitter specific pathways interconnect the vestibular system to the cerebellum (Barmack *et al.*, 1993): the vestibular nerve projects directly to the nodulus and uvula (but not the flocculus) through a glutaminergic primary afferents, the vestibular nuclei provide a cholinergic input from secondary vestibular neurons, the PrH relays its cholinergic efferents in the dorsal cap of the inferior olive which then projects via climbing fibers to the nodulus and uvula, and finally otolith signals from the vestibular complex are carried in a GABAergic pathway to the b-nucleus of the inferior olive and relayed, again by climbing fibers, to lobules 9 and 10 (Barmack, 1999). The zonal or modular organization of the climbing fiber inputs stands in sharp contrast to the more diffuse mossy fiber vestibular complex inputs (Voogd *et al.*, 1996).

Corticovestibular

The efferents of the cerebellum are arranged in a modular pattern (Chapter 11; Voogd *et al.*, 1996). The earliest observations of a corticovestibular projection from the anterior lobe (Ferrier and Turner, 1894; Klimoff, 1899; Probst, 1902; Hohman, 1929) were found to originate from a position directly lateral to the vermis and terminate in the ipsilateral LVe (Jansen and Brodal, 1940; Walberg and Jansen, 1961). Voogd (1964) demonstrated that the origin of the projection from the anterior lobe to LVe was a single strip of Purkinje cells, forming the B-zone of the cerebellar cortex. Retrograde transport of HRP showed that, in addition, Purkinje cells in the A2-zone project to MVmc (Voogd and Bigare, 1980).

In the caudal vermis, Purkinje cells projecting back to the vestibular complex were found in two longitudinal strips in lobules 8 (pyramis) and 9 (uvula) and through the mediolateral extent of the cortex of lobule 10 (flocculus) (Balaban, 1984; Epema *et al.*, 1985; Matsushita and Wang, 1986; Voogd and Bigare, 1980; Shojaku *et al.*, 1987). Terminal axons from nodulus Purkinje cells are found in the periphery of SuVe, and in MVe, SpVe and group X, while their presence in LVe is uncertain (Angaut and Brodal, 1967; Voogd and Bigare, 1980). The termination from lobules 8 and 9 has a similar distribution, although the medial Purkinje cells show a preference for MVe and those of the intermediate strip for SuVe (Voogd *et al.*, 1996; Wylie *et al.*, 1994).

The terminations from the flocculus efferents are distributed over the larger celled central and ventral parts of SuVe, the lateral half of MVe including the marginal zone, and group Y; few terminals are present in MVmc (Langer *et al.*, 1985a). Studies with retrograde transport of HRP following injections in the vestibular nuclei revealed in the flocculus a zonal arrangement of Purkinje cells. A central strip of Purkinje cells projecting to SuVe is flanked by strips projecting to MVe (Haines, 1977; Voogd and Bigare, 1980; Yamamoto and Shimoyama, 1977; Graf *et al.*, 2002). Current hypotheses consider these connections can be used to aid plasticity and "learning" in vestibulo-ocular functions (Hirata and Highstein, 2002).

Nucleovestibular

The caudal vermis projects not only back to the vestibular nuclei, but also to the fastigial nucleus, the most medial of the deep cerebellar nuclei. The projection arises from the most medial zone of Purkinje cells and is GABAergic. The early experiments of Ferrier and Turner (1894), Thomas (1897), Russel (1897), and Klimoff (1899) demonstrated the presence of direct and indirect fastigiofugal fibers in the rostral part of the juxtarestiform body. The direct fibers from the rostral part of the ipsilateral fastigial nucleus enter the vestibular complex close to the lateral wall of the fourth ventricle as the "direct fastigio-bulbar tract" (dfb, Fig. 33.1-6 and 8). Fibers from the caudal part of the contralateral fastigial nucleus cross in the cerebellum and curve around the dorsal and lateral side of the brachium conjunctivum as Russel's uncinate tract (ut, Fig. 33.1-7). The uncinate tract descends in the bundles of SpVe.

The fastigial fibers terminate in MVmc, SpVe, and the caudolateral MVc (Carpenter *et al.*, 1959; Noda *et al.*, 1990; Sugita and Noda, 1991). Voogd (1964) considered the labeling sometimes observed in LVe to result from transection of corticovestibular fibers. The autoradiographic tracing study of Batton *et al.* (1977), which has the advantage that label is not taken up by passing fibers, confirms Voogd's opinion. These pathways participate both in the control of vestibuloocular (caudal fastigial) and vestibulospinal (rostral fastigial) mechanisms (Büttner *et al.*, 1999).

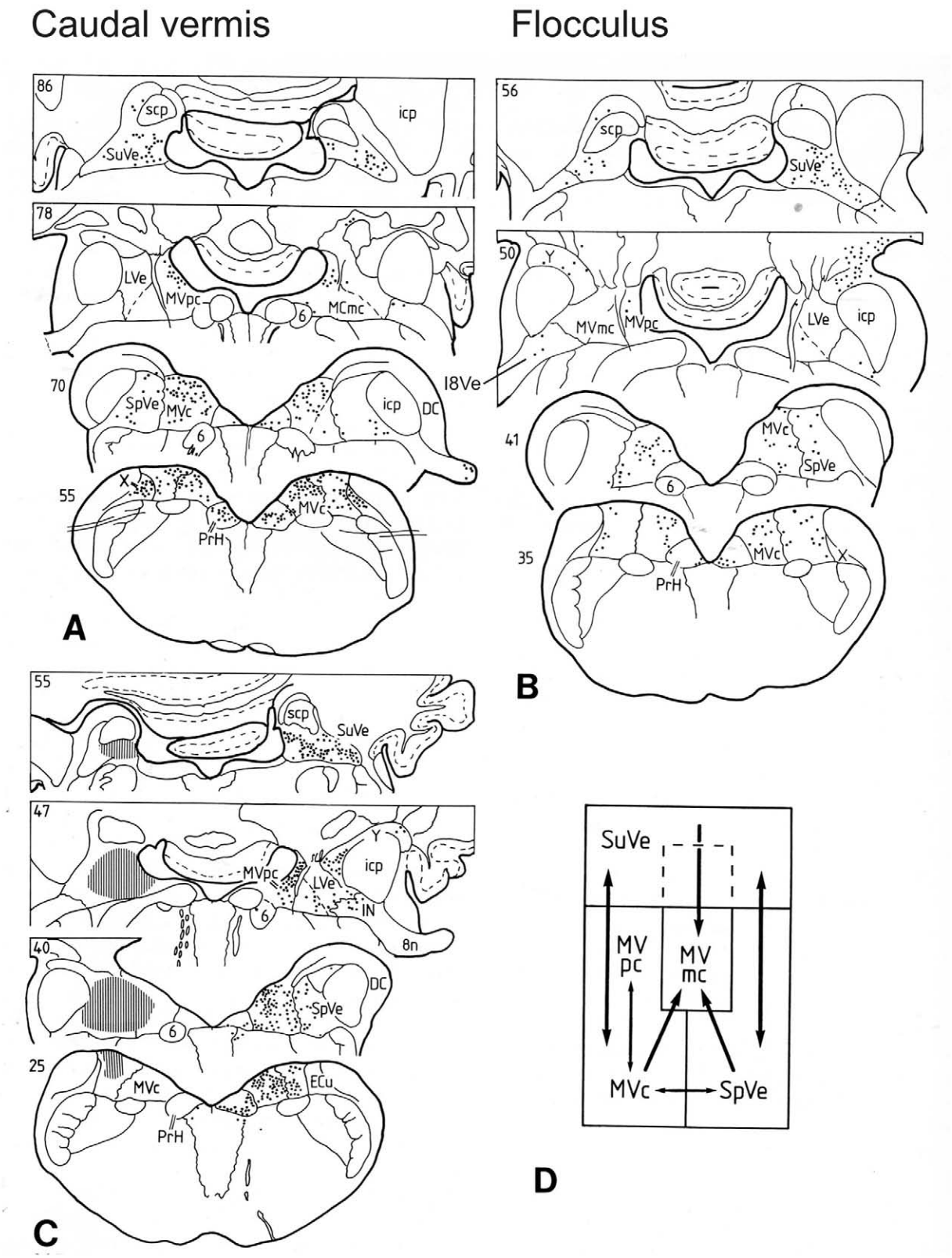

FIGURE 33.10 Distribution of efferent neurons in the rabbit vestibular complex, retrogradely filled by injections of horseradish peroxidase into **(A)** the caudal vermis; **(B)** the flocculus; **(C)** the contralateral vestibular complex. In each case,the injections are on the left side. From Epema *et al*. (1988). **(D)** The diagram shows how MVmc receives inputs from the surrounding nuclei by intrinsic connections: MVmc also provides a major output of the vestibular complex to the oculomotor nuclei (see text).

Inferior Olive Connections

Evidence for a vestibulo-olivary projection was first presented by Muskens (1934). Anterograde axonal tracing has corroborated this finding in different mammals (Martin *et al.*, 1975; Saint-Cyr and Courville, 1979; Swenson and Castro, 1983). One description of this projection is in the cat from Gerrits *et al.* (1985b), who confirmed a heavy projection from MVe and SpVe to subnucleus beta and the dorsomedial cell column. This region is referred to as the parasolitary nucleus by Barmack and colleagues (Barmack 1996; Barmack *et al.*, 1998) who showed that the connection was GABAergic and carried otolith signals to the inferior olive, which were relayed to the contralateral nodulus and uvula (Büttner-Ennever, 1999). The olivary subdivisions that do not receive a vestibular projection are the dorsal accessory olive, and perhaps the dorsal cap of Kooy whose cholinergic afferents arise from PrH (Barmack, 2000).

Olivovestibular connections have been convincingly demonstrated between the caudal part of the dorsal accessory olive and LVe containing Deiters' neurons (Groenewegen and Voogd, 1977; Gerrits 1990, Fig. 33.5C). Their results show a relatively large number of olivocerebellar fibers passing through the vestibular complex. These passing axons cast doubt on the results of Balaban (1984) who proposed climbing fiber collaterals terminated in different parts of the vestibular complex, based on retrograde transport of WGA-HRP.

Reticular and Paramedian Connections

Axonal tracing studies have demonstrated the sparse and diffuse nature of the reticulovestibular projections (degeneration techniques: Hoddevik *et al.*, 1975; Mehler, 1968; tritiated leucine: Büttner-Ennever and Henn, 1976; Gerrits and Voogd, 1986; retrograde transport of HRP: Carleton and Carpenter, 1983; Corvaja *et al.*, 1979; Pompeiano *et al.*, 1978; Kitama *et al.*, 1995). The intracellular staining of identified reticular formation neurons in PPRF showed that axonal branching of excitatory burst neurons reached PrH and medial MVe (Strassman *et al.*, 1986a), whereas from inhibitory burst neurons the terminals covered the magnocellular "output" region in the center of the vestibular complex (i.e., MVmc; Strassman *et al.*, 1986b). Other vertical premotor reticular areas in the mesencephalon also project to the vestibular nucleus but the exact topography of these projections is unclear.

Efferents of the vestibular complex to the reticular formation were described in early Golgi material (Lorente de Nó, 1933; Ramón y Cajal, 1909). More recent studies demonstrated the nonterminal nature of most vestibuloreticular fibers (Gerrits *et al.*, 1985a; Gerrits and Voogd, 1986). However one set of vestibular efferents that has recently been more clearly defined is that to the "cell groups of the paramedian tracts" (PMT cell groups; for reviews see Büttner-Ennever and Büttne, 1988; Büttner-Ennever, 1992a; Büttner-Ennever and Horn, 1996). These neurons lie in tight "nests" amongst the midline fiber bundles, just lateral to the raphe nuclei; they are seen in the pons and medulla in rat, cat, monkey, and man and project to the flocculus (Langer *et al.*, 1985b). They receive inputs from all oculomotor premotor nuclei including the secondary vestibular neurons (McCrea *et al.*, 1987a, b; see Chapter 16). However the projections are often described as innervating raphe nucle earlier, before the identity of the floccular-projecting PMT cell group were discovered.

Spinal Cord Connections

Vestibulospinal connections descend in two separate pathways: the ipsilateral lateral vestibulospinal tract (lvst) and the bilateral medial vestibulospinal tract (mvst) (Fig. 33.6; see Chapter 8; Pompeiano 1972; Matsushita and Li Wang 1986; Holstege, 1988). They carry canal and otolith signals to modulate spinal motoneuron activity (Isu *et al.*, 1988; Sato *et al.*, 1996, 1997; Shinoda *et al.*, 1994). Noradrenergic and cholinergic systems also have a modulatory effect on the vestibulospinal reflexes (Pompeiano, 2000).

The lvst was originally described in Golgi material (Held, 1893) although Deiters himself (1865) was already aware of the probability of spinal connections. It is the principal pathway through which gravito-inertial signals from the otoliths can regulate the body's extensor musculature (Pompeiano and Brodal, 1957a). It runs through the ventral reticular formation into the ventrolateral funiculus of the spinal cord, terminating in Rexed's laminae VII–IX (Holstege, 1988; Isu *et al.*, 1996). The pathway is somatotopically organized, with the dorsocaudal, a central, and a rostroventral (the equivalent of MVmc) subdivision, projecting respectively to the lumbosacral, the thoracic, and the cervical cord segments (Akaike, 1983). Neurons in SpVe and MVmc also contribute to the lvst (Fig. 33.11; Rapoport *et al.*, 1977). Three principal inputs drive the activity of lvst neurons and hence modulate vestibulospinal reflexes: the otolith input, the cerebellar vermis relayed via the fastigial nucleus, and ascending proprioceptive signals in spinovestibular pathways (Fig. 33.7; Büttner-Ennever, 1999; Pompeiano, 1972). The morphology of the lvst axons and their terminal fields has been elegantly demonstrated by intracellular recording and staining techniques (Boyle, 2000; Boyle *et al.*, 1996; Shinoda *et al.*, 1988).

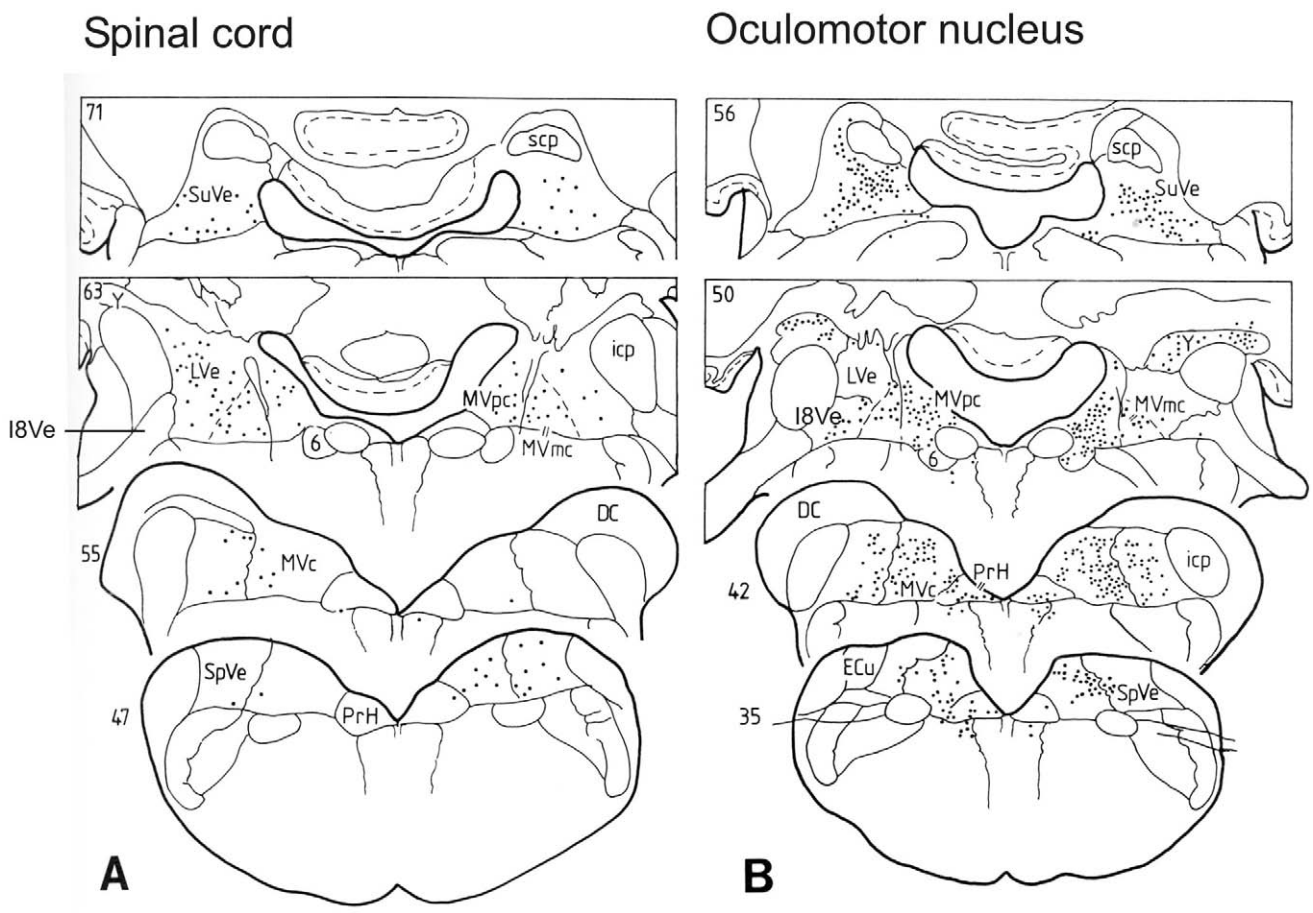

FIGURE 33.11 Distribution of efferent neurons in the vestibular complex of the rabbit projecting to the spinal cord and the oculomotor nucleus. Neurons are retrogradely labeled with horseradish peroxidase injections into **(A)** the left side of the spinal cord and **(B)** the left side of the oculomotor nucleus (Epema, 1990).

Vestibulospinal fibers descending bilaterally in the medial longitudinal fascicle (mlf) terminate in Rexed's laminae VII, VIII, and IX, mainly in the upper cervical cord (Shinoda *et al.*, 1992). Retrograde tracer studies and electrophysiological studies have shown that neurons in MVe mainly contribute to mvst, with a lesser contribution from SpVe and LVe (Huerta and Harting, 1982; Kuypers and Maisky, 1975; Minor *et al.*, 1990; Isu *et al.*, 1988), and some cells can be seen in SuVe in rabbit (Fig. 33.11; Epema, 1990). It was originally suggested that mvst inhibits neck and axial musculature but some excitatory axons have been reported in the tract (Akaike, 1983). Many of the contralaterally projecting mvst axons also have an ascending branch that terminates in the oculomotor nuclei and other regions of the brainstem such as the nucleus of Roller (Minor *et al.*, 1990).

Ascending proprioceptive influences are also intergrated into the activity of the vestibular complex (Pompeiano and Brodal, 1957b; Mehler and Rubertone, 1985; Pompeiano, 1972). The central cervical nucleus, at C1–C4, is an important relay for neck muscle afferents to the contralateral vestibular nuclei (Vincent and Rubertone, 1984).

Thalamocortical Connections

Vestibular fibers ascending into the thalamus have been described in the old degeneration studies by Van Gehuchten (1904), Whitaker and Alexander (1932), Hassler (1948), and Brodal and Pompeiano (1958). More convincing evidence was presented with anterograde axonal tracing in the studies by Lang *et al.* (1979), who used tritiated leucine autoradiography; Mehler and Voogd (1984) using WGA-HRP; and Shiroyama *et al.* with Phaseolus lectin (Lai *et al.*, 2000; Shiroyama *et al.*, 1995). The thalamic projections are bilateral and end in diffuse scattered patches in nucleus ventroposterior lateralis, pars oralis and to a lesser extent in ventroposterior inferior nucleus and ventroposterior centralis

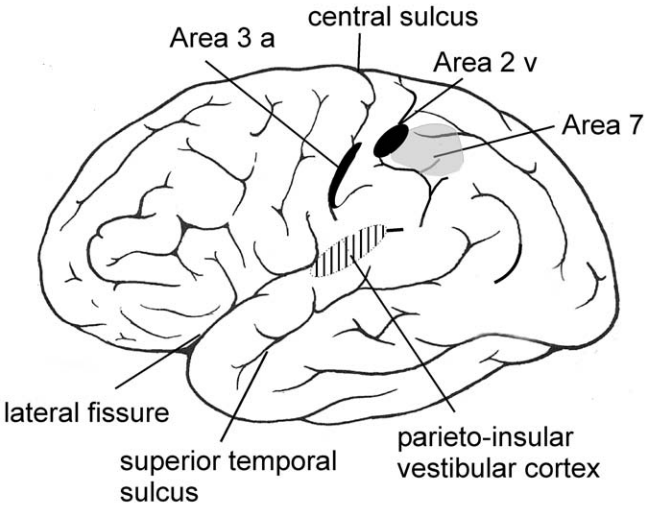

FIGURE 33.12 Homologous areas of vestibular cortex in human, based on results for monkey (Guldin and Grüsser, 1998) and for human (Foerster, 1936).

lateralis. An additional vestibulothalamostriatal pathway has been proposed in rat (Lai *et al.*, 2000). These studies confirm the observation of Kotchabhakdi *et al.* (1980) that MVc and the caudal part of SpVe project to the ventral posterolateral and ventrolateral thalamus, and SuVe and group Y project to the intralaminar region (see also Chapter 20). In turn, the regions of the thalamus targeted by the vestibular nuclei send efferents to vestibular cortical areas such as parietal area 2v, 7a and 7b, as well as to area 3a and the parietoinsular and retroinsular vestibular cortex (see Fig. 33.12) (Akbarian *et al.*, 1993; Brandt *et al.*, 1994; Büttner-Ennever, 2000; Friberg *et al.*, 1985; Guldin and Grüsser, 1998; Guldin *et al.*, 1992).

Descending pathways from the cerebral cortex to the vestibular nuclei have also been reported and may play a role in the suppression of reflex vestibular responses during voluntary movements (Akbarian *et al.*, 1994; Faugier-Grimaud and Ventre, 1989; Ventre and Faugier-Grimaud, 1988)

CONCLUSION

A clear cytoarchitectural pattern in the vestibular complex can be followed through vertebrate species (Straka *et al.*, 2002). However, experimental data on the afferent and efferent connections of the nuclei show that axon terminals do not respect these cytoarchitectural borders, perhaps with the exception of LVe. Primary afferents project throughout the majority of the vestibular complex, although it is only the rostral regions that are concerned with oculomotor "output" function. The central magnocellular regions of the vestibular complex are the source of the output projections; the parvocellular surrounds are engaged in either commissural, intrinsic, or cerebellar connections, and these comprise the majority of vestibular neurons. Caudal vestibular regions sustain otolith afferents that interact heavily with the cerebellum; and particularly saccular activity appears to be directed mainly toward spinal neural networks. Experiments on single unit recordings in head free behaving primates have shown that many new categories of neurons are discovered as soon as new techniques are established (McCrea *et al.*, 1999). Recent information on the transmitters used by the neurons, and their histochemical properties can be more easily related to the cytoarchitecture and functional subdivisions.

The interconnectivity of the vestibular complex with the cerebellum dominates the activity of the vestibular nuclei, a point that has been convincingly demonstrated, functionally and histochemically, by the series of experiments of Grüsser and colleagues, on mutant mice (Grüsser-Cornehls and Bäurle, 2001). Their work showed that the compensatory capacity of the vestibular complex, owing to the enhancement of intranuclear inhibitory circuits, is only evident when the overriding control from the Purkinje cells of the cerebellar cortex, or the cerebellar nuclei, is totally eliminated. In cases of cerebellar dysfunction, this can mean that the actual *destruction* of the remaining cerebellar cortex leads to a significant improvement in motor performance as a result of the release of adaptation mechanisms in vestibular circuitry. This has evident clinical consequences.

Acknowledgments

The authors thank Dr. Anja Horn and Rita Büttner for their assistance with the figures.They are indebted to Mrs. E.M. Rijpma, librarian at the Anatomical Laboratory in Leiden. Dr. E. Marani from the same institute is kindly thanked for giving permission to use the historical "Jelgersma collection" of human brain sections. The work was supported by the German Research Council SFB 624/B3.

References

Akaike, T. (1983). Neuronal organization of the vestibulospinal system in the cat. *Brain Res.* **259,** 217–227.

Akbarian, S., Grusser, O.J., and Guldin, W.O. (1993). Corticofugal projections to the vestibular nuclei in squirrel monkeys—Further evidence of multiple cortical vestibular fields, *J. Comp. Neurol.* **332,** 89–104.

Akbarian, S., Grusser, O.J., and Guldin, W.O. (1994). Corticofugal connections between the cerebral cortex and brainstem

vestibular nuclei in the macaque monkey. *J. Comp. Neurol.* **339,** 421–437.

Angaut, P., and Brodal, A. (1967). The projection of the "vestibulocerebellum" onto the vestibular nuclei in the cat. *Archs. Ital. Biol.* **105,** 441–479.

Baker, R., and Highstein, S.M. (1978). Vestibular projections to medial rectus subdivisions of oculomotor nucleus. *J. Neurophysiol.* **41,** 1629–1646.

Balaban, C.D. (1984). Olivo-vestibular and cerebello-vestibular connections in albino rabbits. *Neurosci.* **12,** 129–149.

Barmack, N.H. (1996). GABAergic pathways convey vestibular information to the beta nucleus and dorsomedial cell column of the inferior olive. *In* "New Directions in Vestibular Research" (S.M. Highstein, B. Cohen, and J.A. Büttner-Ennever, eds.), vol. 781, pp. 541–552. New York.

Barmack, N.H. (2000). Cholinergic pathways and functions related to the vestibulo-cerebellum. *In* "Neurochemistry of the Vestibular System" (A.J. Beitz and J.H. Anderson, eds.), pp. 269–285. CRC Press, Boca Raton, London, New York,Washington, DC.

Barmack, N.H., Baughman, R.W., Errico, P., and Shojaku, H. (1993). Vestibular primary afferent projection to the cerebellum of the rabbit. *J. Comp. Neurol.* **327,** 521–534.

Barmack, N.H., Fredette, B.J., and Mugnaini, E. (1998). Parasolitary nucleus: A source of GABAergic vestibular information to the inferior olive of rat and rabbit. *J. Comp. Neurol.* **392,** 352–372.

Batton III, R.R., Jayaraman, A., Ruggiero D., and Carpenter, M.B. (1977). Fastigial efferent projections in the monkey: An autoradiographic study. *J. Comp. Neurol.* **174,** 281–306.

Bechterew, W. von (1885). Ueber die innere Abtheilung des Strickkörpers und den achten Hirnnerven. *Neurol. Centralbl.* **7,** 145–147.

Bechterew, W. von (1887). Zur Frage ueber den Ursprung des Hörnerven und ueber die physiologische Bedeutung des N. vestibularis. *Neurol. Centralbl.* **6,** 193–198.

Belknap, D.B., and McCrea, R.A. (1988). Anatomical connections of the prepositus and abducens nuclei in the squirrel monkey. *J. Comp. Neurol.* **268,** 13–28.

Beusekom, G.T. van. (1955). *Fiber analysis of the anterior and lateral funiculi of the cord in the cat.* Thesis, Leiden, p. 143.

Blanks, R.H.I., Precht, W., and Torigoe, Y. (1983). Afferent projections to the cerebellar flocculus in the pigmented rat demonstrated by retrograde transport of horseradish peroxidase. *Exp. Brain Res.* **52,** 293–306.

Bower, J. (2002). The organisation of cerebellar circuitry revisited. *In* "The Cerebellum" (S. Highstein and W.T. Thatch, eds.), vol. 978, pp. 135–155. New York.

Boyle, R. (2000). Morphology of lumbar-projecting lateral vestibulospinal neurons in the brainstem and cervical spinal cord in the squirrel monkey. *Arch. Ital. Biol.* **138,** 107–122.

Boyle, R., Belton, T., and McCrea, R.A. (1996). Responses of identified vestibulospinal neurons to voluntary eye and head movements in the squirrel monkey. *In* "New Directions in Vestibular Research" (S.M. Highstein, B. Cohen, and J.A. Büttner-Ennever, eds.), vol. 781, pp. 244–264. New York.

Braak, H. (1971). Ueber die Kerngebiete des menschlichen Hirnstammes. IV. Der nucleus reticularis lateralis und seine Satelliten. *Zeitschr. f. Zellforschung* **122,** 145–159.

Brandt, T., Dieterich, M., and Danek, A. (1994). Vestibular cortex lesions affect the perception of verticality. *Ann. Neurol.* **35,** 403–412.

Brodal, A. (1974). Anatomy of the vestibular nuclei and their connections. *In* "Handbook of Sensory Physiology, Vol. VI, I: Vestibular System, Part 1: Basic Mechanisms" (H.H. Kornhuber, ed.), pp. 239–352. Springer, New York.

Brodal, A. (1983). The perihypoglossal nuclei in the macaque monkey and the chimpanzee. *J. Comp. Neurol.* **218,** 257-269.

Brodal, A. (1984). The vestibular nuclei in the macaque monkey. *J. Comp. Neurol.* **227,** 252–266.

Brodal, A., and Angaut, P. (1967). The termination of spinovestibular fibers in the cat. *Brain Res.* **5,** 494–500.

Brodal, A., and Brodal, P.(1985). Observations on the secondary vestibulocerebellar projections in the macaque monkey. *Exp. Brain Res.* **58,** 62–74.

Brodal, A., and Gogstad, A.C. (1957). Afferent connections of the paramedian reticular nucleus of the medulla oblongata in the cat. An experimental study. *Acta Anat. (Basel)* **30,** 133–151.

Brodal, A., and Pompeiano, O. (1957). The vestibular nuclei in the cat. *J. Anat. (London)* **91,** 438–454.

Brodal, A., and Pompeiano, O. (1958). The origin of ascending fibers of the medial longitudinal fasciculus from the vestibular nuclei. An experimental study in the cat. *Acta Morphol. neerl.-scand.* **1,** 306–328.

Brodal, A., and Torvik, A. (1957). Ueber den Ursprung der secundaren vestibulo-cerebellaren Fasern bei der Katze. Eine experimentell-anatomische Studie. *Arch. Psychiat. Nervenkr.* **195,** 550-567.

Büttner, U., Glasauer, S., Glonti, L., Kleine, J.F., and Siebold,C. (1999). *In* "Otolith Function in Spatial Orientation and Movement" (B. Cohen and B.J.M. Hess, eds.), vol. 871, pp. 81–93, New York.

Büttner-Ennever, J. A., (1992a). Paramedian tract cell groups: A review of connectivity and oculomotor function. *In* "Vestibular and Brain Stem Control of Eye, Head and Body Movements" (H. Shimazu and Y. Shinoda, eds.), pp. 323–330. Japan Scientific Societies Press, Karger, Tokyo, Basel.

Büttner-Ennever, J.A. (1992b). Patterns of connectivity in the vestibular nuclei. *Ann. N. Y. Acad. Sci.* **656,** 363-378.

Büttner-Ennever, J.A., (1999). A review of otolith pathways to brainstem and cerebellum. *In* "Otolith Function in Spatial Orientation and Movement" (B. Cohen and B.J.M. Hess, eds.) vol. 871, pp. 51–64. New York.

Büttner-Ennever, J.A. (2000). Overview of the vestibular system. *In* "Neurochemistry of the Vestibular System" (A.J. Beitz and J.H. Anderson, eds.) pp. 3–24, CRC Press, Boca Raton, London, New York, Washington, DC.

Büttner-Ennever, J.A., and Büttner, U. (1988). The reticular formation, *In* "Neuroanatomy of the oculomotor system" (J.A. Büttner-Ennever, ed.), *Rev. Oculomot. Res.* **2,** pp.119–176.

Büttner-Ennever, J.A., and Henn, V. (1976). An autoradiographic study of the pathways from the pontine reticular formation involved in horizontal eye movements. *Brain Res.* **108,** 155–164.

Büttner-Ennever, J.A., and Horn, A.K.E. (1996). Pathways from cell groups of the paramedian tracts to the floccular region. *In* "New directions in vestibular research" (S.M. Highstein, B. Cohen, and J.A. Büttner-Ennever, eds.), vol. 781, pp. 532–540. New York.

Büttner-Ennever, J.A., Cohen, B., Horn, A.K.E., and Reisine, H. (1996). Efferent pathways of the nucleus of the optic tract in monkey and their role in eye movements. *J. Comp. Neurol.* **373,** 90–107.

Carleton, S.C., and Carpenter, M.B. (1983). Afferent and efferent connections of the medial, inferior and lateral vestibular nuclei in the cat and monkey. *Brain Res.* **278,** 29–51.

Carleton, S.C., and Carpenter, M. B. (1984). Distribution of primary vesibular fibers in the brainstem and cerebellum of the monkey. *Brain Res.* **294,** 281–298.

Carpenter, M.B. (1960). Fiber projections from the descending and lateral vestibular nuclei in the cat. *Am. J. Anat.* **107,** 1–22.

Carpenter, M.B. (1988). Vestibular nulei: Afferent and efferent projections. *Prog. Brain Res.* **76,** 5–15.

Carpenter, M.B., and Cowie, R.J. (1985a). Transneuronal transport in the vestibular and auditory systems of the squirrel monkey and

the arctic ground squirrel. I. Vestibular system. *Brain Res.* **358,** 249–263.
Carpenter, M.B., and Cowie, R.J. (1985b). Connections and oculomotor projections of the superior vestibular nucleus and cell group 'Y'. *Brain Res.* **336,** 265–287.
Carpenter, M.B., and Hanna, G.R. (1962). Lesions of the medial longitudinal fasciculus in the cat. *Am. J. Anat.* **110,** 307–322.
Carpenter, M.B., and Strominger, N.L. (1965). The medial longitudinal fasciculus and disturbances of conjugate horizontal eye movements in the monkey. *J.Comp. Neurol.* **125,** 347–368.
Carpenter, M.B., Bard, D.S., and Alling, F.A. (1959). Anatomical connections between the fastigial nuclei, the labyrinth and the vestibular nuclei in the cat. *J. Comp. Neurol.* **111,** 1–25.
Carpenter, M.B., Chang, L., Pereira, A.B., Hersh, L.B., Bruce, G., and Wu, J.-Y. (1987a). Vestibular and cochlear efferent neurons in the monkey identified by immunocytochemical methods. *Brain Res.* **408,** 275–280.
Carpenter, M.B., Chang, L., Pereia, A.B., and Hersh, L.B. (1987b). Comparisons of the immunocytochemical localization of choline acetyltransferase in the vestibular nuclei of the monkey and rat, *Brain Res.* **418,** 403–408.
Carpenter, M.B., Stein, B.M., and Peter, P. (1972). Primary vestibulocerebellar fibers in the monkey. Distribution of fibers arising from distinctive cell groups of the vestibular ganglia. *Am. J. Anat.* **135,** 221–250.
Cartwright, A.D., and Curthoys, I.S. (1996). A neural network simulation of the vestibular system: Implications on the role of intervestibular nuclear coupling during vestibular compensation. *Biol Cybern.* **75,** 485–93.
Cazin, L., Magnin, M., and Lannou, J. (1982). Non-cerebellar visual afferents to the vestibular nuclei involving prepositus hypoglossal complex: An autoradiographic study in the rat. *Exp. Brain Res.* **48,** 309–313.
Chen-Huang, Ch., and McCrea, R.A. (1998). Viewing distance related sensory processing in the ascending tract of deiters vestibulo-ocular reflex pathway. *J. Vestib. Res.* **8,** 175–184.
Chimoto, S., Iwamoto, Y., and Yoshida, K. (1999). Projections and firing properties of down eye-movement neurons in the interstitial nucleus of Cajal in the cat. *J. Neurophysiol.* **81,** 1199–1211.
Chubb, M.C., and Fuchs, A.F. (1982). Contribution of y group of vestibular nuclei and dentate nucleus of cerebellum to generation of vertical smooth eye movements. *J. Neurophysiol.* **48,** 75–99.
Clarke, L. (1861). "Philosophical Transactions," p. 158. London.
Cohen, B. (1974). The vestibulo-ocular reflex arc. *In* "Handbook of Sensory Physiology" (H.H. Kornhuber, ed.), pp. 477–540. Springer, New York
Cohen, B., Highstein, S.M., and Büttner-Ennever, J.A. (1996). "New Directions in Vestibular Research" Ann. N.Y. Acad. Sci., New York.
Cohen, B., John, P., Yakushin, S., Buettner-Ennever, J.A., and Raphan, T. (2002). The nodulus and uvula: A source of cerebellar control of spatial orientation of the angular vestibulo-ocular reflex. *In* "The Cerebellum" (S. Highstein and W.T. Thatch, eds.), vol. 978, pp. 28–45.
Corvaja, N., Mergner, T., and Pompeiano, O. (1979). Organization of reticular projections to the vestibular nuclei in the cat. *Prog. Brain Res.* **50,** 631–644.
Corvisier, J., and Hardy, O. (1997). Topographical characteristics of preposito-collicular projections in the cat as revealed by Phaseolus vulgaris-leucoagglutinin technique. A possible organisation underlying temporal-to-spatial transformations. *Exp. Brain Res.* **114,** 461–471.
Cudeiro, J., and Rivadulla, C. (1999). Sight and insight—on the physiological role of nitric oxide in the visual system. *Trends Neurosci.* **22,** 109–116.
De Zeeuw, C.I., Strata, P., and Voogd, J. (1997). The cerebellum: From structure to control. *Prog. Brain Res.* **114,** 512–528.
Deiters, O. (1865). "Untersuchungen ueber Gehirn und Rueckenmark." Braunschweig.
Demêmes, D., and Broca, C. (1998). Calcitonin gene-related peptide immunoreactivity in the rat efferent vestibular system during development. *Brain Res. Dev. Brain Res.* **108,** 59–67.
De Waele, C., Muhlethaler, M., and Vidal, P.P. (1995). Neurochemistry of the central vestibular pathways. *Brain Res. Rev.* **20,** 24–46.
Epema, A.H. (1990). "Connections of the vestibular nuclei in the rabbit." Thesis, Rotterdam.
Epema, A.H., and Gerrits, N.M. (1990). Secondary vestibulocerebellar mossy fiber projections to the flocculus and uvulonodular lobule in the rabbit. A study using HRP and double fluorescent tracer techniques. *Exp. Brain Res.* **80,** 72–82.
Epema, A.H., Guldemond, J.M., and Voogd, J. (1985). Reciprocal connections between the caudal vermis and the vestibular nuclei in the rabbit. *Neurosci. Lett.* **57,** 273–278.
Epema, A.H., Gerrits, N.M., and Voogd, J. (1988). Commissural and intrinsic connections of the vestibular nuclei in the rabbit: A retrograde labeling study. *Exp. Brain Res.* **71,** 129–146.
Essick, C.R. (1907). The corpus ponto-bulbare—A hitherto undescribed nuclear mass in the human hindbrain. *Am. J. Anat.* **7,** 119–135.
Faugier-Grimaud, S., and Ventre, J. (1989). Anatomic connections of inferior parietal cortex (area 7) with subcortical structures related to vestibulo-ocular function in a monkey *(Macaca fascicularis). J. Comp. Neurol.* **280,** 1–14.
Ferrier, D., and Turner, W.A. (1894). A record of experiments illustrative of the symptomatology and degenerations following lesions of the cerebellum and its peduncles and related structures in monkeys. *Proc. Roy. Soc. Lond.* **54,** 476–478.
Forel, A. (1907). "Gesammelte hirnanatomische Abhandlungen." München.
Foerster, O. (1936). Sensible corticale Felder. *In* "Handbuch der Neurologie" (O. Bumke and O. Foerster, eds.), pp. 358–449. Springer-Verlag Berlin.
Friberg, L., Olsen, T.S., Roland, R.E., Paulson, O.B., and Lassen, N.A. (1985). Focal increase of blood flow in the cerebral cortex of man during vestibular stimulation. *Brain* **108,** 609–623.
Fuse, G. (1912). Die innere Abteilung des Kleinhirnstiels (Meynert I.A.K.) und der Deiterssche Kern. *Arb. Hirnanat. Inst. Zürich* **6,** 29–267.
Gacek, R.R. (1969). The course and central termination of first order neurons supplying vestibular endorgans in the cat. *Acta otolaryng. (Stockholm) Suppl.* **254,** 1–66.
Gacek, R.R. (1977). Location of brain stem neurons projecting to the oculomotor nucleus in the cat. *Exp. Neurol.* **57,** 725–749.
Gacek, R.R. (1978). Location of commissural neurons in the vestibular nuclei of the cat. *Exp. Neurol.* **59,** 479–491.
Gacek, R.R., and Lyon, M. (1974). The localization of vestibular efferent neurons in the kitten with horseradish peroxidase. *Acta Otolaryng.* **77,** 92–101.
Gacek, R.R., Nomura, Y., and Balogh, K. (1965). Acetylcholinesterase activity in the efferent fibers of the stato-acustic nerve. *Acta Otolaryng.* **59,** 541–553.
Gerrits, N.M. (1990). Vestibular nuclear complex. In "The Human Nervous System" (G. Paxinos ed.), pp. 863–888. Academic Press, San Diego.
Gerrits, N.M., and Voogd, J. (1986). The nucleus reticularis tegmenti pontis and the adjacent rostral paramedian reticular formation: Differential projections to the cerebellum and the caudal brain stem. *Exp. Brain Res.* **62,** 29–45.

Gerrits, N.M., Epema, A.H., Van Linge, A., and Dalm, E. (1989). The primary vestibulocerebellar projection in the rabbit: Absence of primary afferents in the flocculus. *Neurosci. Lett.* **105,** 27–33.

Gerrits, N.M., Voogd, J., and Magras, I.N. (1985a). Vestibular nuclear efferents to the nucleus raphe pontis, the nucleus reticularis tegmenti pontis and the nuclei pontis in the cat. *Neurosci. Lett.* **54,** 357–362.

Gerrits, N.M., Voogd, J., and Magras, I.N. (1985b). Vestibular afferents of the inferior olive and the vestibulo-olivo-cerebellar climbing fiber pathway to the flocculus in the cat. *Brain Res.* **332,** 325–336.

Ghelarducci, B., Highstein, S.M., and Ito, M. (1977). Origin of the preoculomotor projections through the brachium conjunctivum and their functional roles in the vestibulo-ocular reflex. *In* "Control of Gaze by Brain Stem Neurons" (R. Baker and A. Berthoz, eds.), pp. 167–175. Elsevier, Amsterdam.

Godaux, E., and Cheron, G. (1993). The role of the vestibular commissure in the gaze holding of the cat. *Neurosci. Lett.* **153,** 149–152.

Godaux, E., Mettens, P., and Cheron, G. (1993). Differential effect of injections of kainic acid into the prepositus and the vestibular nuclei of the cat. *J. Physiol.* **472,** 459–482.

Goldberg, J.M., and Fernandez, C. (1980). Efferent vestibular system in the squirrel monkey: Anatomical location and influence on afferent activity. *J. Neurophysiol.* **43,** 986–1025.

Goldberg, J.M., Brichta, A.M., and Wackym, P.A., (2000). Efferent vestibular system: anatomy, physiology, and neurochemistry. *In* "Neurochemistry of the Vestibular System" (A.J. Beitz and J.H. Anderson, eds.), pp. 61–94. CRC Press, Boca Raton, London, New York, Washington, DC.

Graf, W.M., and Ezure, K. (1986). Morphology of vertical canal related second order vestibular neurons in the cat. *Exp. Brain Res.* **63,** 35–48.

Graf, W., Gerrits, N., Yatim-Dhiba, N., and Ugolini, G. (2002). Mapping the oculomotor system: The power of transneuronal labelling with rabies virus. *Eur J Neurosci.* **15,** 1557–1562.

Graf, W.M., McCrea, R.A., and Baker, R. (1983). Morphology of posterior canal related secondary vestibular neurons in rabbit and cat. *Exp. Brain Res.* **52,** 125–138.

Gray, L.P. (1926). Some experimental evidence on the connections of the vestibular mechanism in the cat. *J. Comp. Neurol.* **41,** 319–364.

Graybiel, A.M. (1977). Organization of oculomotor pathways in the cat and rhesus monkey. *In* "Control of Gaze by Brainstem Neurons" (R. Baker and A. Bethoz, eds.), pp. 79–88. Elsevier, Amsterdam.

Graybiel, A.M., and Hartwieg, E.A. (1974). Some afferent connections of the oculomotor complex in the cat: An experimental study with tracer techniques. *Brain Res.* **81,** 543–551.

Groenewegen, H.J., and Voogd, J. (1977). The parasagittal zonation within the olivo-cerebellar projection. I. Climbing fiber distribution in the vermis of cat cerebellum. *J. Comp. Neurol.* **174,** 417–488.

Grüsser-Cornehls, U., and Bäurle, J. (2001). Mutant mice as a model for cerebellar ataxia. *Prog. Neurobiol.* **63,** 489–540.

Gstoettner, W., Burian, M., and Cartellieri, M. (1992). Central projections from singular parts of the vestibular labyrinth in the guinea pig. *Acta Oto-Laryngol.* **112,** 486–495.

Guldin, W., and Grüsser, O.J. (1998). Is there a vestibular cortex? *TINS* 254–259.

Guldin, W.O., Akbarian, S., and Grüsser, O.J. (1992). Cortico-cortical connections and cytoarchitectonics of the primate vestibular cortex: A study in squirrel monkeys (Saimiri sciureus). *J. Comp. Neurol.* **326,** 375–401.

Haines, D.E. (1977). Cerebellar corticonuclear and corticovestibular fibers of the flocculonodular lobe in a prosimian primate *(Galago senegalensis). J. Comp. Neurol.* **174,** 607–630.

Hassler, R. (1948). Forels Haubenfaszikel als vestibuläre Empfindungsbahn mit Bemerkungen über einige andere sekundäre Bahnen des Vestibularis und Trigeminus. *Arch. Psychiat. Nervenkr.* **180,** 23–53.

Hauglie-Hanssen, E. (1968). Intrinsic neuronal organization of the vestibular nuclear complex in the cat. A Golgi study. *Ergebn. Anat. Entwickl.-Gesch.* **40,** 1–105.

Held, H. (1893). Beiträge zur feineren Anatomie des Kleinhirns und des Hirnstammes. *Arch. Anat. Physiol. (Anat. Abt.)* 435–446.

Highstein, S.M. (1973). Organization of the vestibulo-oculomotor and trochlear reflex pathways in the rabbit. *Exp. Brain Res.* **17,** 285–300.

Highstein, S.M., and McCrea, R.A. (1988). The anatomy of the vestibular nuclei. *In* "Neuroanatomy of the Oculomotor System: Reviews of Oculomotor Research" (J.A. Büttner-Ennever, ed.), pp. 177–202. Elsevier, Amsterdam.

Hikosaka, O., and Igusa, Y. (1980). Axonal projections of prepositus hypoglossi and reticular neurons in the brain stem of the cat. *Exp. Brain Res.* **39,** 441–451.

Hirai, N., and Uchino, Y. (1984). Superior vestibular nucleus neurones related to the excitatory vestibulo-ocular reflex of anterior canal origin and their ascending course in the cat. *Neurosci. Res.* **1,** 73–79.

Hirata, Y., and Highstein, S. (2002). Plasticity of the VOR. A system identification approach to localizing the adaptive process. *In* "The Cerebellum" (S. Highstein and W.T. Thatch, eds.), vol. 978, pp. 480-495.

Hoddevik, G.H., Brodal, A., and Walberg, F. (1975). The reticulo-vestibular projection in the cat. An experimental study with silver impregnation methods. *Brain Res.* **94,** 383–399.

Hohman, L.B. (1929). The efferent connexions of the cerebellar cortex. Investigations based on experimental extirpation in the cat. *Assoc. Res. Nerv. Ment. Dis.* **6,** 445–460.

Holler, S., and Straka, H. (2001). Plane-specific brainstem commissural inhibition in frog second order semicircular canal neurons. *Exp. Brain Res.* **137,** 190–196.

Holstege, G. (1988). Brainstem-spinal cord projections in the cat, related to control of head and axial movements, *In* "Neuroanatomy of the Oculomotor System: Reviews of Oculomotor Research" (J.A. Büttner-Ennever, ed.), vol. 2, pp. 431–470. Elsevier, Amsterdam.

Holstein, G.R. (1999). Inhibitory amino acid transmitters in the vestibular nuclei. *In* "New Directions In Vestibular Research" (S.M. Highstein, B. Cohen, and J.A. Büttner-Ennever, eds.), vol. 781, pp. 162–143. New York.

Holstein, G.R., Martinelli, G.P., and Cohen, B. (1999). The ultrastructure of GABA-immunoreactive vestibular commissural neurons related to velocity storage in the monkey. *Neurosci.* **93,** 171–181.

Huerta, M.F., and Harting J.K. (1982). Tectal control of spinal cord activity: Neuroanatomical demonstration of pathways connecting the superior colliculus with the cervical spinal cord gray. *In* "Descending pathways to the Spinal Cord" (H.G.J.M. Kuypers and G.F. Martin, eds.), Prog. Brain Res. 57, 294-328.

Imagawa, M., Isu, N., Sasaki, M., Endo, K., Ikegami, H., and Uchino, Y. (1995). Axonal projections of utricular afferents to the vestibular nuclei and the abducens nucleus in cats. *Neurosci. Lett.* **186,** 87–90.

Imagawa, M., Graf, W.M., Sato, H., Suwa, H., Isu, N., Izumi, R., and Uchino, Y. (1998). Morphology of single afferents of the saccular macula in cats. *Neurosci. Lett.* **240,** 127–130.

Ishizuka, N., Mannen, H., Sasaki, S.-I., and Shimazu, H. (1980). Axonal branches and terminations in the cat abducens nucleus of

secondary vestibular neurons in the horizontal canal system. *Neurosci. Lett.* **16,** 143–148.

Isu, N., and Yokota, J. (1983). Morphophysiological study on the divergent projection of axon collaterals of medial vestibular nucleus neurons in the cat. *Exp. Brain Res.* **53,** 151–162.

Isu, N., Thomson, D.B., and Wilson, V.J. (1996). Vestibulospinal effects on neurons in different regions of the gray matter of the cat upper cervical cord. *J. Neurophysiol.* **76,** 2439–2446.

Isu, N., Uchino, Y., Nakashima, H., Satoh, S., Ichikawa, T., and Watanabe, S. (1988). Axonal trajectories of posterior canal-activated secondary vestibular neurons and their coactivation of extraocular and neck flexor motoneurons in the cat. *Exp. Brain Res.* **70,** 181–191.

Ito, J., Matsuoka, I., Sasa, M., and Takaori, S. (1985). Commissural and ipsilateral internuclear connection of vestibular nuclear complex of the cat. *Brain Res.* **341,** 73–81.

Ito, M., Nisimaru, N., and Yamamoto, M. (1973). The neuronal pathways relaying reflex inhibition from semicircular canals to extraocular muscles of rabbits. *Brain Res.* **55,** 189–193.

Iwamoto, Y., Kitama, T., and Yoshida, K. (1990). Vertical eye movement-related secondary vestibular neurons ascending in medial longitudinal fasciculus in cat I. Firing properties and projection pathways. *J. Neurophysiol.* **63,** 902–917.

Jacobsohn, L. (1909). Ueber die Kerne des menschlichen Hirnstammes (Medulla oblongata, Pons und Pedunculus cerebri). *Abh. K. Preuss. Akad. d. Wiss., Phys.-math. Klasse, Anhang. Abh. I.* 1–70 (mit XII Tafeln).

Jansen, J., and Brodal, A. (1940). Experimental studies on the intrinsic fibers of the cerebellum. II. The cortico-nuclear projection. *J. Comp. Neurol.* **73,** 267–321.

Kaneko, C.R. (1997). Eye movement deficits following ibotenic acid lesions of the nucleus prepositus hypoglossi in monkey. I. Saccades and fixation. *J. Neurophysiol.*

Kevetter, G.A. (1996). Pattern of selected calcium-binding proteins in the vestibular nuclear complex of two rodent species. *J. Comp. Neurol.* **365,** 575–584.

Kevetter, G.A., and Leonard, R.B. (1997). Use of calcium-binding proteins to map inputs in vestibular nuclei of the gerbil. *J. Comp. Neurol.* **386,** 317–327.

Kevetter, G.A., and Perachio A.A. (1986). Distribution of vestibular afferents that innervate the sacculus and posterior canal in the gerbil. *J. Comp. Neurol.* **254,** 410–424.

Kitama, T., Grantyn, A., and Berthoz, A. (1995). Orienting-related eye-neck neurons of the medial ponto-bulbar reticular formation do not participate in horizontal canal-dependent vestibular reflexes of alert cats. *Brain Res. Bull.* **38,** 337–347.

Klimoff, J. (1899). Ueber die Leitungsbahnen des Kleinhirns. *Arch. Anat. Physiol. Anat. Abt.* II–27.

Kohnstamm, O. (1908). Zentrale Verbindungen der Vestibulariskerne. *Zentralbl. f. Physiol.* **22,** 54–57.

Kokkoroyannis, T., Scudder, C.A., Balaban, C.D., and Highstein, S.M. (1996). Anatomy and physiology of the primate interstitial nucleus of Cajal I. Efferent projections. *J. Neurophysiol.* **75,** 725–739.

Korte, G.E. (1979). The brain stem projections of the vestibular nerve in the cat. *J. Comp. Neurol.* **184,** 279–292.

Kotchabhakdi, N., and Walberg, F. (1978). Cerebellar afferent projections from the vestibular nuclei in the cat: An experimental study with the method of retrorade axonal transport of horseradish peroxidase. *Exp. Brain Res.* **31,** 591–604.

Kotchabhakdi, N., Hoddevik, G.H., and Walberg, F. (1978). Cerebellar afferent projections from the perihypoglossal nuclei: An experimental study with the method of retrograde transport of horseradish peroxdase. *Exp. Brain Res.* **31,** 13–29.

Kotchabhakdi, N., Rinvik, E., Walberg, F., and Yingchareon, K. (1980). The vestibulothalamic projections in the cat studied by retrograde axonal transport of horseradish peroxidase. *Exp. Brain Res.* **40,** 405–418.

Kuypers, H.G.J.M., and Maiksy, V.A. (1975). Retrograde axonal transport of HRP from spinal cord to brain stem cell groups in the cat. *Neurosci. Lett.* **1,** 9–14.

Ladpli, R., and Brodal, A. (1968). Experimental studies of commissural and reticular formation projections from the vestibular nuclei in the cat. *Brain Res.* **8,** 65–96.

Lai, H., Tsumori, T., Shiroyama, T., Yokota, S., Nakano, K., and Yasui, Y. (2000). Morphological evidence for the vestibular-thalamo-striatal pathway via parafascicular nucleus in the rat. *Brain Res.* **872,** 208–214.

Lang, W., Büttner-Ennever, J.A., and Büttner, U. (1979). Vestibular projections to the monkey thalamus: An autoradiographic study. *Brain Res.* **177,** 3–17.

Langer, T.P., Fuchs, A.F., Chubb, M.C., Scudder, C.A., and Lisberger, S.G. (1985a). Floccular efferents in the rhesus macaque as revealed by autoradiography and horseradish peroxidase. *J. Comp. Neurol.* **235,** 26–37.

Langer, T.P., Fuchs, A.F., Scudder, C.A., and Chubb, M.C. (1985b). Afferents to the flocculus of the cerebellum in the rhesus macaque as revealed by retrograde transport of horseradish peroxidase. *J. Comp. Neurol.* **235,** 1–25.

Langer, T.P., Kaneko, C.R., Scudder, C.A., and Fuchs, A.F. (1986). Afferents to the abducens nucleus in the monkey and cat. *J. Comp. Neurol.* **245,** 379–400.

Leidler, R. (1916). Experimentelle Untersuchungen über das Endigungsgebiet des Nervus vestibularis. 2. Mitteilung. *Arb. Neurol. Inst. Wiener Univ.* **XXI,** 151–212.

Lewy, F.H. (1910). Der Deiterssche Kern und das Deiterospinale Bündel. *Arb. Hirnanat. Inst. Zürich* **4,** 227–244.

Lorente de Nó, R. (1933). Anatomy of the eighth nerve. The central projection of the nerve endings of the internal ear. *Laryngoscope (St. Louis)* **43,** 1–38.

Lysakowski, A., and Singer, M. (2000). Nitric oxide synthase localized in a subpopulation of vestibular efferents with NADPH diaphorase histochemistry and nitric oside synthase immunohistochemistry. *J. Comp. Neurol.* **427,** 508–521.

Mabuchi, M., and Kusama, T. (1970). Mesodiencephalic projections to the inferior olive and the vestibular and perihypoglossal nuclei. *Brain Res.* **17,** 133–136.

Maciewicz, R.J., Eagen K., Kaneko, C.R.S., and Highstein, S.M. (1977). Vestibular and medullary brain stem afferents to the abducens nucleus in the cat. *Brain Res.* **123,** 229–240.

Magras, I.N., and Voogd, J. (1985). Distribution of secondary vestibular fibers in the cerebellar cortex. An autoradiographic study in the cat. *Acta Anat. (Basel)* **123,** 51–57.

Maklad, A., and Fritzsch, B. (2002). The developmental segregation of posterior crista and saccular vestibular fibers in mice: A carbocyanine tracer study using confocal microscopy. *Brain Res. Dev. Brain Res.* **135,** 1–17.

Maklad, A., and Fritzsch, B. (2003). Partial segregation of posterior crista and saccular fibers to the nodulus and uvula of the cerebellum in mice, and its development. *Brain Res. Dev. Brain Res.* **140,** 223–236.

Martin, G.F., Dom, R., King, J.S., Robarts, M., and Watson, C.R.R. (1975). The inferior olive nucleus of the opossum *(Didelphis marsupialis virginiana):* Its organization and connections. *J. Comp. Neurol.* **160,** 507–533.

Matsushita, M., and Li Wang, C. (1986). Cerebellar corticovestibular projections from lobule IX to the descending vestibular nucleus in the cat. A retrograde wheat germ agglutinin-horseradish peroxidase study. *Neurosci. Lett.* **66,** 293–298.

Matsushita, M., Hosoya, Y., and Ikeda, M. (1979). Anatomical organization of the spinocerebellar system in the cat as studied

by retrograde transport of horseradish peroxidase. *J. Comp. Neurol.* **184,** 81–106.

McCrea, R.A. (1988). Neuroanatomy of the oculomotor system. The nucleus prepositus, *In* "Neuroanatomy of the Oculomotor System: Reviews of Oculomotor Research" (J.A. Büttner-Ennever, ed.), pp. 203–223. Elsevier, Amsterdam.

McCrea, R.A., and Baker, R. (1985a). Anatomical connections of the nucleus prepositus of the cat. *J. Comp. Neurol.* **237,** 377–407.

McCrea, R.A., and Baker, R. (1985b). Cytology and intrinsic organization of the perihypoglossal nuclei in the cat. *J. Comp. Neurol.* **237,** 360–376.

McCrea, R.A., Baker R., and Delgado-Garcia, J. (1979). Afferent and efferent organization of the prepositus hypoglossal nucleus. *Prog. Brain Res.* **50,** 653–665.

McCrea, R.A., Gdowski, G.T., Boyle, R., and Belton, T. (1999). Firing behavior of vestibular neurons during active and passive head movements: Vestibulo-spinal and other non-eye-movement related neurons. *J. Neurophysiol.* **82,** 416–428.

McCrea, R.A., Strassman, A., and Highstein, S.M. (1987a). Anatomical and physiological characteristics of vestibular neurons mediating the vertical vestibulo-ocular reflexes of the squirrel monkey. *J. Comp. Neurol.* **264,** 571–594.

McCrea, R.A., Strassman, E., May, E., and Highstein, S.M. (1987b). Anatomical and physiological characteristics of vestibular neurons mediating the horizontal vestibulo-ocular reflex of the squirrel monkey. *J. Comp. Neurol.* **264,** 547–570.

McCrea, R.A., Yoshida, K., Berthoz, A., and Baker, R. (1980). Eye movement related activity and morphology of second order vestibular neurons terminating in the cat abducens nucleus. *Exp. Brain Res.* **40,** 468–473.

McElligott, J., and Spencer, R. (2000). Neuropharmacological aspects of the vestibulo-ocular reflex. *In* "Neurochemistry of the Vestibular System" (A.J. Beitz and J.H. Anderson, eds.), pp. 199–222. CRC Press, Boca Raton, London, New York, Washington, DC.

McFarland, J.L., Fuchs, A.F., and Kaneko, C.R. (1992). The nucleus prepositus and nearby medial vestibular nucleus and the control of simian eye movements. *In* "Vestibular and Brain Stem Control of Eye, Head and Body Movements" (Y. Shinoda and H. Shimazu, eds.). Japan Scientific Societies Press, Tokyo.

McMasters, R.E., Weiss, A.H., and Carpenter, M.B. (1966). Vestibular projections to the nuclei of the extraocular muscles. Degeneration resulting from discrete partial lesions of the vestibular nuclei in the monkey. *Am. J. Anat.* **118,** 163–194.

Meessen, H., and Olszewski, J. (1949). "A Cytoarchitectonic Atlas of the Rhombencephalon of the Rabbit." Karger, Basel, New York.

Mehler, W.R. (1968). Reticulovestibular connections composed with spinovestibular connections in the cat. *Anat. Rec.* **160,** 485.

Mehler, W.R. (1969). Some neurological species differences—a posteriori. *Ann. N.Y. Acad. Sci.* **167,** 424–468.

Mehler, W.R., and Rubertone, J.A. (1985). Anatomy of the vestibular nucleus complex. *In* "The Rat Nervous System: Hindbrain and Spinal Cord" (G. Paxinos, ed.), vol 2, pp. 185–219. Academic Press, New York.

Mehler, W.R., and Voogd, J. (1984). Vestibulothalamic connections in the cat: A wheat germ aglutinin-horseradish peroxidase analysis. *Anat. Rec.* **208,** 116A.

Meynert, F. (1871). Vom Gehirne der Saugethiere."Stricker's Handbuch der Lehre von den Gewebe", vol 2. Leipzig.

Minor, L.B., McCrea, R.A., and Goldberg, J.M. (1990). Dual projections of secondary vestibular axons in the medial longitudinal fasciculus to extraocular motor nuclei and the spinal cord of the squirrel monkey. *Exp. Brain Res.* **83,** 9–21.

Mitsacos, A., Reisine, H., and Highstein, S.M. (1983). The superior vestibular nucleus: An intracellular HRP study in the cat. I Vestibuloocular neurons. *J. Comp. Neurol.* **215,** 78–91.

Moreno-Lopez, B., Escudero, M., Delgado-Garcia, J.M., and Estrada, C. (1996). Nitric oxide production by brain stem neurons is required for normal performance of eye movements in alert animals. *Neuron.* **17,** 739–745.

Moreno-Lopez, B., Escudero, M., De Vente, J., and Estrada, C. (2001). Morphological identification of nitric oxide sources and targets in the cat oculomotor system. *J. Comp. Neurol.* **435,** 311–324.

Moreno-Lopez, B., Estrada, C., and Escudero, M. (1998). Mechanisms of action and targets of nitric oxide in the oculomotor system. *J. Neurosci.* **18,** 10672–10679.

Mugnaini, E., Walberg, F., and Brodal, A. (1967). Mode of termiation of primary vestibular fibers in the lateral vestibular nucleus: An experimental electro microscopical study in the cat. *Exp. Brain Res.* **4,** 187–211.

Muskens, L.J.J. (1913–14). An anatomico-physiological study of the posterior longitudinal bundle in its relation to forced movements. *Brain* **36,** 352–426.

Muskens, L.J.J. (1934). Experimentelle und klinische Untersuchungen über die Verbindungen der unteren Olive und ihre Bedeutung für die Fallrichtung. *Arch. Psychiat. Nervenkr.* **102,** 558–613.

Noda, H., Sugita, S., and Ikeda, Y. (1990). Afferent and efferent connections of the oculomotor region of the fastigial nucleus in the macaque monkey. *J. Comp. Neurol.* **302,** 330–348.

Ohgaki, T., Curthoys, I.S., and Markham, C.H. (1988). Morphology of physiologically identified second-order vestibuar neurons in cat, with intracellularly injected HRP. *J. Comp. Neurol.* **276,** 387–411.

Olszewski, J., and Baxter, D. (1982). "Cytoarchitecture of the Human Brain Stem." 2nd ed., Karger, Basel, New York.

Onufrowicz, Br. (1885). Experimenteller Beitrag zur Kenntniss des Ursprungs des Nervus acusticus des Kaninchens. *Arch. f. Psychiat.* **16,** 711–742.

Partsalis, A.M., and Highstein, S.M. (1996). Role of the Y group of the vestibular nuclei in motor learning or plasticity of the vestibulo-ocular reflex in the squirrel monkey. *Ann. N.Y. Acad. Sci.* **781,** 513–524.

Paxinos, G., and Huang, X.-F. (1995). "Atlas of the Human Brainstem" (G. Paxinos and X.-F. Huang, eds.). Academic Press, San Diego.

Paxinos, G., and Watson, C. (1986). "The Rat Brain in Stereotaxic Coordinates." Academic Press, Sydney.

Paxinos, G., Huang, X.-F., and Toga, A.W. (2000). "The Rhesus Monkey Brain in Stereotaxic Coordinates" (G. Paxinos, X.-F. Huang, and A.W. Toga, eds.). Academic Press, San Diego.

Pompeiano, O., and Brodal, A. (1957a). The origin of vestibulospinal fibers in the cat. An experimental anatomical study, with comments on the descending medial longitudinal fasciculus. *Archs. Ital. Biol.* **95,** 166–195.

Pompeiano, O., and Brodal, A. (1957b). Spino-vestibular fibers in the cat. An experimental study. *J. Comp. Neurol.* **108,** 353–382.

Pompeiano, O., and Walberg, F. (1957). Descending connections to the vestibular nuclei. An experimental study in the cat. *J. Comp. Neurol.* **108,** 465–504.

Pompeiano, O. (1972). Spinovestibular relations: Anatomical and physiological aspects. *Prog. Brain Res.* **37,** 263–296.

Pompeiano, O. (2000). Control of vestibulo-spinal and vestibulo-ocular reflexes by noradrenergic and ACh systems. *In* "Neurochemistry of the Vestibular System" (A.J. Beitz and J.H. Anderson, eds.), pp. 223–267. CRC Press, Boca Raton, London, New York, Washington, DC.

Pompeiano, O., Mergner, T., and Corvaja, N. (1978). Commissural, perihypoglossal and reticular afferent projections to the vestibular nuclei in the cat. An experimental anatomical study

with the method of the retrograde transport of horseradish peroxidase. *Archs. Ital. Biol.* **116,** 130–172.
Precht, W. (1978). Neuronal operations in the vestibular system. "Studies in Brain Function," vol. 2, p. 223. Springer, Berlin, Heidelberg, New York.
Precht, W. (1979). Vestibular mechanisms. *Annu. Rev. Neurosci.* **2,** 265–289.
Probst, M. (1902). Zur Anatomie und Physiologie des Kleinhirns. *Arch. f. Psychiat.* **35,** 692–777.
Ramon y Cajal, S. (1896). "Beitrag zum Studium der Medulla Oblongata, des Kleinhirns und des Ursprungs der Gehirnnerven." Barth, Leipzig.
Ramón y Cajal, S. (1909). "Histologie du système nerveux de l'homme et des vertébrés." Maloine, Paris.
Rapoport, S., Susswein, A., Uchino, Y., and Wilson, V. J. (1977). Properties of vestibular neurones projecting to neck segments of the cat spinal cord. *J. Physiol. (Lond.)* **268,** 493–510.
Rasmussen, A.T. (1932). Secondary vestibular tracts in the cat. *J. Comp. Neurol.* **54,** 143–171.
Reichenberger, I., Straka, H., Ottersen, O. P., Streit, P., Gerrits, N. M., and Dieringer, N. (1997). Distribution of gaba, glycine, and glutamate immunoreactivities in the vestibular nuclear complex of the frog. *J. Comp. Neurol.* **377,** 149–164.
Roller, C.F.W. (1882). Die cerebralen und cerebellaren Verbindungen des 3–12. Hirnnervenpaares. Die spinalen Wurzeln der cerebralen Sinnesnerven. *Allg. Zeitschr. f. Psychiat.* **38,** 228–264.
Rubertone, J.A., and Haines, D.E. (1981). Secondary vestibulocerebellar projections to flocculonodular lobe in a Prosimian primate, Galago senegalensis. *J. Comp. Neurol.* **200,** 255–272.
Rubertone, J.A., and Haines, D.E. (1982). The vestibular complex in a prosimian primate (Galago senegalensis): Morphological and spinovestibular connections. *Brain Beh. Evol.* **20,** 129–155.
Rubertone, J.A., Mehler, W.R., and Cox, G.E. (1983). The intrinsic organization of the vestibular complex: Evidence for internuclear connectivity. *Brain Res.* **263,** 137–141.
Russel, J.S.R. (1897). The origin and destination of certain afferent and efferent tracts in the medulla oblongata. *Brain* **20,** 409–440.
Sabin, F.R. (1897). On the anatomical relations of the nuclei of reception of the cochlear and vestibular nerves. *Johns Hopkins Hosp. Bull.* **81,** 1–17.
Sadjadpour, K., and Brodal, A. (1968). The vestibular nuclei in man. A morphological study in the light of experimental findings in the cat. *J. f. Hirnforsch.* **10,** 299–323.
Saint-Cyr, J.A., and Courville, J. (1979). Projection from the vestibular nuclei to the inferior olive in the cat: An autoradiographic and horseradish peroxidase study. *Brain Res.* **165,** 189–200.
Sato, F., Sasaki, H., Ishizuka, N., Sasaki, S., and Mannen, H. (1989). Morphology of single primary vestibular afferents originating from the horizontal semicircular canal in the cat. *J. Comp. Neurol.* **290,** 423–439.
Sato, H., Endo, K., Ikegami, H., Imagawa, M., Sasaki, M., and Uchino, Y. (1996). Properties of utricular nerve-activated vestibulospinal neurons in cats. *Exp. Brain Res.* **112,** 197–202.
Sato, H., Imagawa, M., Isu, N., and Uchino, Y. (1997). Properties of saccular nerve-activated vestibulospinal neurons in cats. *Exp. Brain Res.* **116,** 381–388.
Sato, Y., and Kawasaki, T. (1987). Target neurons of floccular caudal zone inhibition in Y-group nucleus of vestibular nuclear complex. *J. Neurophysiol.* **57,** 460–480.
Sato, Y., Kawasaki, T., and Ikarashi, K. (1983). Afferent projections from the brainstem to the three floccular zones in cats. II. Mossy fiber projections. *Brain Res.* **272,** 37–48.
Sato, Y., Yamamoto, F., Shojaku, H., and Kawasaki, T. (1984). Neuronal pathway from floccular caudal zone contributing to vertical eye movements in cats—role of group y nucleus of vestibular nuclei, *Brain Res.* **294,** 375–380.
Satoh, K., Arai, R., Ikemoto, K., Narita, M., Nagai, T., Ohshima, H., and Kitahama, K. (1995). Distribution of nitric oxide synthase in the central nervous system of Macaca fuscata: Subcortical regions. *Neurosci.* **66,** 685-696.
Schwalbe, G. (1881). "Lehrbuch der Neurologie," Erlangen.
Shinoda, Y., Ohgaki, T., Futami, T., and Sugiuchi, Y. (1988). Vestibular projections to the spinal cord: The morpholgy of single vestibulospinal axons. *Prog. Brain Res.* **76,** 17–27.
Shinoda, Y., Ohgaki, T., Sugiuchi, Y., and Futami, T. (1992). Morphology of single medial vestibulospinal tract axons in the upper cervical spinal cord of the cat. *J. Comp. Neurol.* **316,** 151–172.
Shinoda, Y., Sugiuchi, Y., Futami, T., Ando, N., and Kawasaki, T. (1994). Input patterns and pathways from the six semicircular canals to motoneurons of neck muscles. 1. The multifidus muscle group. J. *Neurophysiol.* **72,** 2691–2702.
Shiroyama, T., Kayahara, T., Yasui, Y., Nomura, J., and Nakano, K. (1995). The vestibular nuclei of the rat project to the lateral part of the thalamic parafascicular nucleus (centromedian nucleus in primates). *Brain Res.* **704,** 130–134.
Shojaku, H., Sato, K., Ikarashi, K., and Kawasaki, K. (1987). Topographical distribution of Purkinje cells in the uvula and the nodulus projecting to the vestibular nuclei in cats. *Brain Res.* **416,** 100–112.
Snyder, R.L., Faull, R.L.M., and Mehler, W.R. (1978). A comparative study of the neurons of origin of spinocerebellar afferents in rat, cat and squirrel monkey based on the retrograde transport of horseradish peroxidase. *J. Comp. Neurol.* **181,** 833–852.
Spencer, R.F., Wang, S.F., and Baker, R. (2003). The pathways and functions of GABA in the oculomotor system. *Prog. Brain Res.* **90,** 307–331.
Spencer, R.F., Wenthold, R.J., and Baker, R. (1989). Evidence for glycine as an inhibitory neurotransmitter of vestibular, reticular, and prepositus hypoglossi neurons that project to the cat abducens nucleus. *J. Neurosci.* **9,** 2718–2736.
Steiger, H.J., and Büttner-Ennever, J.A. (1979). Oculomotor nucleus afferents in the monkey demonstrated with horseradish peroxidase. *Brain Res.* **160,** 1–15.
Stein, B.M., and Carpenter, M.B. (1967). Central projections of portions of the vestibular ganglia innervating specific part of the labyrinth in the rhesus monkey. *Am. J. Anat.* **120,** 281–318.
Stilling, B. (1843). "Ueber die Textur und Funktion der Medulla Oblongata," Erlangen.
Straka, H., Baker, R., and Gilland, E. (2001). Rhombomeric organiation of vestibular pathways in larval frogs. *J. Comp. Neurol.* **437,** 42–55.
Straka, H., Baker, R., and Gilland, E. (2002). The frog as a unique vertebrate model for studying the rhombomeric organization of functionally identified hindbrain neurons. *Brain Res. Bull.* **57,** 301–305.
Straka, H., Reichenberger, I., and Dieringer, N. (1999). Synaptic transmission by vestibular nerve afferent fibers. *In* "Neurochemistry of the Vestibular System" (A.J. Beitz and J.H. Anderson, eds.), pp. 47–60. CRC Press, Boca Raton, London, New York, Washington, DC.
Strassman, A., Highstein, S.M., and McCrea, R.A. (1986a). Anatomy and physiology of saccadic burst neurons in the alert squirrel monkey. I. Excitatory burst neurons. *J. Comp. Neurol.* **249,** 337–357.
Strassman, A., Highstein, S.M., and McCrea, R.A. (1986b). Anatomy and physiology of saccadic burst neurons in the alert squirrel monkey. II. Inhibitory burst neurons. *J. Comp. Neurol.* **249,** 358–380.

Suarez, C., Diaz, C., Tolivia, J., Alvarez, J. C., Gonzalez del Rey, C., and Navarro, A. (1997). Morphometric analysis of the human vestibular nuclei. *Anat. Rec.* **247,** 271–288.

Sugita, S., and Noda, H. (1991). Pathways and terminations of axons arising in the fastigial oculomotor region of macaque monkeys. *Neurosci. Res.* **10,** 118–136.

Swenson, R.S., and Castro, A.J. (1983). The afferent connections of the inferior olivary complex in rats: An anterograde study autoradiographic and axonal degeneration techniques. *Neurosci.* **8,** 259–275.

Tan, H., and Gerrits, N.M. (1992). Laterality in the vestibulocerebellar mossy fiber projection to flocculus and caudal vermis. A retrograde fluorescent double labeling study. Neurosci. **47,** 909–919.

Tanaka, M., Takeda, N., Senba, E., Tohyama, M., Kubo, T., and Matsunaga, T. (1988). Localization of calcitonin gene-related peptide in the vestibular end-organs in the rat: An immunohistochemical study. *Brain Res.* **447,** 175–177.

Tarlov, E. (1969). The rostral projections of the primate vestibular nuclei. An experimental study in macaque, baboon and chimpanzee. *J. Comp. Neurol.* **135,** 27–56.

Tarlov, E. (1970). Organization of vestibulo-oculomotor projections in the cat. *Brain Res.* **20,** 159–179.

Thomas, A. (1897). "Le cervelet." Paris.

Thunnissen, I.E., Epema, A.H., and Gerrits, N.M. (1989). The secondary vestibulocerebellar mossy fiber projection to the caudal vermis in the rabbit. *J. Comp. Neurol.* **290,** 262–277.

Van der Schueren, A. (1914). Etude anatomique du faisceau longitudinal postérieur. *Le Névraxe* **13,** 183–309.

Van Gehuchten, A. (1904). Connexions centrales du noyau de Deiters et des masses grises voisines. *Le Névraxe* **6,** 19–73.

Van Rossum, J. (1969). *Corticonuclear and corticovestibular projections of the cerebellum. An experimental investigation of the anterior lobe, the simple lobule and the caudal vermis in the rabbit.* Thesis, Van Gorcum, Assen.

Ventre, J., and Faugier-Grimaud, S. (1988). Projections of the temporo-parietal cortex on vestibular complex in the macaque monkey *(Macaca fascicularis). Exp. Brain Res.* **72,** 653–658.

Vincent, S.L., and Rubertone, J.A. (1984). The origin of the spinovestibular pathway: A horseradish peroxidase (HRP) study. *Anat. Rec.* **208,** 188A.

Von Monakow, C. (1883). Experimenteller Beitrag zur Kenntniss des Corpus restiforme, des 'äusseren Acusticuskerns' und deren Beziehung zum Rückenmark. *Arch. f. Psychiat.* **14,** 1–16.

Von Monakow, C. (1890). Striae acusticae und untere Schleife. *Arch. f. Psychiat.* **XXII,** 1–26.

Voogd, J. (1964). *The cerebellum of the cat. Structure and fiber connexions.* Thesis, Van Gorkum, Assen.

Voogd, J., and Bigare, F. (1980). Topographical distribution of olivary and cortico-nuclear fibers in the cerebellum: A review. *In* "The Inferior Olivary Nucleus. Anatomy and Physiology" (J. Courville, C. de Montigny, and Y. Lamarre, (eds.), pp. 207–234. Raven Press, New York.

Voogd, J., Gerrits, N.M., and Marani, E. (1985). Cerebellum. *In* "The Rat Nervous System, Vol. 2, Hindbrain and Spinal Cord" (G. Paxinos, ed.), pp.251–291. Academic Press, New York.

Voogd, J., Gerrits, N.M., and Ruigrok, T.J.H. (1996). Organization of the vestibulocerebellum. *In* "New Directions in Vestibular Research" (S.M. Highstein, B. Cohen, and J.A. Büttner-Ennever, eds.), vol. 781, pp. 553–579. Annals of the New York Academy of Sciences, New York.

Wackym, P. A., Popper, P., Ward, P. H., and Micevych, P. E. (1991). Cell and molecular anatomy of nicotine acetylcholine receptor subunits and calcitonin gene-related peptide in the rat vestibular system. *Otolaryngol. Head Neck Surg.* **105,** 493–510.

Walberg, F., and Jansen, J. (1961). Cerebellar corticovestibular fibers in the cat. *Exp. Neurol.* **3,** 32–53.

Walberg, F., and Mugnaini, E. (1969). Distinction of degenerating fibers and boutons of cerebellar and peripheral origin in Deiters' nucleus of the same animal. *Brain Res.* **14,** 67–75.

Walberg, F., Bowsher, D., and Brodal, A. (1958). The termination of primary vestibular fibers in the vestibular nuclei in the cat. An experimental study with silver methods. *J. Comp. Neurol.* **110,** 391–419.

Walberg, F., Ottersen, O. P., and Rinvik, E. (1990). GABA, glycine, aspartate, glutamate and taurine in the vestibular nuclei: An immunocytochemical investigation in the cat. *Exp. Brain Res.* **79,** 547–563.

Warr, W.B. (1975). Olivocochlear and vestibular efferent neurons of the feline brain stem: Their location, morphology and number determined by retrograde axonal transport and acetylcholinesterase histochemistry. *J. Comp. Neurol.* **161,** 159–182.

Wearne, S., Raphan, T., and Cohen, B. (1997). Contribution of vestibular commissural pathways to spatial orientation of the angular vestibuloocular reflex. *J. Neurophysiol.* **78,** 1193–1197.

Wentzel, P.R., Dezeeuw, C.I., Holstege, J.C., and Gerrits, N.M. (1995). Inhibitory synaptic inputs to the oculomotor nucleus from vestibulo-ocular-reflex-related nuclei in the rabbit. *Neurosci.* **65,** 161–174.

Whitaker, J.G., and Alexander, L. (1932). Die Verbindungen der Vestibulariskerne mit dem Mittel- und Zwischenhirn. *J. Psychol. Neurol.* **44,** 253–376.

Winkler, C. (1909). The central course of the nervus octavus and its influence on motility. *Verh. Kon. Acad. Wetensch.* **14,** 1–202.

Winkler, C., and Potter, A (1914). "An Anatomical Guide to Experimental Researches on the Cat's Brain. A Series of 35 Frontal Sections." W. Versluys, Amsterdam.

Wylie, D.R.W., De Zeeuw, C.I., Digiorgi, P.L., and Simpson, J.I. (1994). Projections of individual Purkinje cells of identified zones in the ventral nodulus to the vestibular and cerebellar nuclei in the rabbit. *J. Comp. Neurol.* **349,** 448–463.

Yamamoto, M. (1979). Topographical representation in rabbit cerebellar flocculus for various afferent inputs from the brainstem investigated by means of retrograde transport of horseradish peroxidase. *Neurosci. Lett.* **12,** 29–34.

Yamamoto, M., and Shimoyama, I. (1977). Differential localization of rabbit's flocculus Purkinje cells projecting to the medial and superior vestibular nuclei, investigated by means of the horseradish peroxidase retrograde transport method. *Neurosci. Lett.* **5,** 279–283.

CHAPTER

34

Auditory System

JEAN K. MOORE and FRED H. LINTHICUM, JR.
House Ear Institute
Los Angeles, California, USA

The purpose of this chapter is to review the structure of the human auditory system and to consider how its structural organization reflects its function. Although much of our understanding of the structure and function of the auditory system is based on the large body of work done in nonprimate mammals, this chapter emphasizes the specific organization of the human auditory system and cites, wherever possible, studies done in other species of primates. In general, the chapter focuses on the process of information transfer through progressively higher levels of the auditory system, beginning with the passage of mechanical impulses through the middle and inner ear, and continuing with the subsequent cellular and neural processes occurring at cochlear, brain stem, and forebrain levels. Evoked activity, functional imaging, and the effects of pathological conditions are considered from the standpoint of the insight they provide into normal auditory function.

An overview of the anatomy and dimensions of the human auditory system is provided by Figure 34.1. This diagram is a projection based on histological sections through the human brain stem and temporal lobe. The position and dimensions of the thalamus were recreated from human brain atlases (DeArmond *et al.*, 1989; Paxinos and Huang, 1995). As suggested by this diagram, the pattern of activity generated by sound stimuli in the cochlea is carried to the brain stem by the cochlear nerve. In the brain stem, the nerve terminates on neurons in the dorsal and ventral cochlear nuclei. Ascending pathways leave the cochlear nuclei in the dorsal, intermediate, and ventral acoustic striae and cross the midline as the trapezoid body. One ascending pathway provides information to the medial and lateral superior olivary nuclei, centers that reconstruct the spatial dimension of a sound stimulus. The surrounding periolivary cell groups receive ascending axons, but also receive descending projections and give rise to a feedback pathway to the inner ear (not shown). Other projections from the cochlear nuclei run directly to the upper brain stem, where they terminate mainly in the dorsal lemniscal nucleus and inferior colliculus. Both of these structures form commissures, namely, the dorsal commissure of the lateral lemniscus and the commissure of the inferior colliculus. Within the inferior colliculus, input from the lower brain stem auditory nuclei is synthesized to provide a

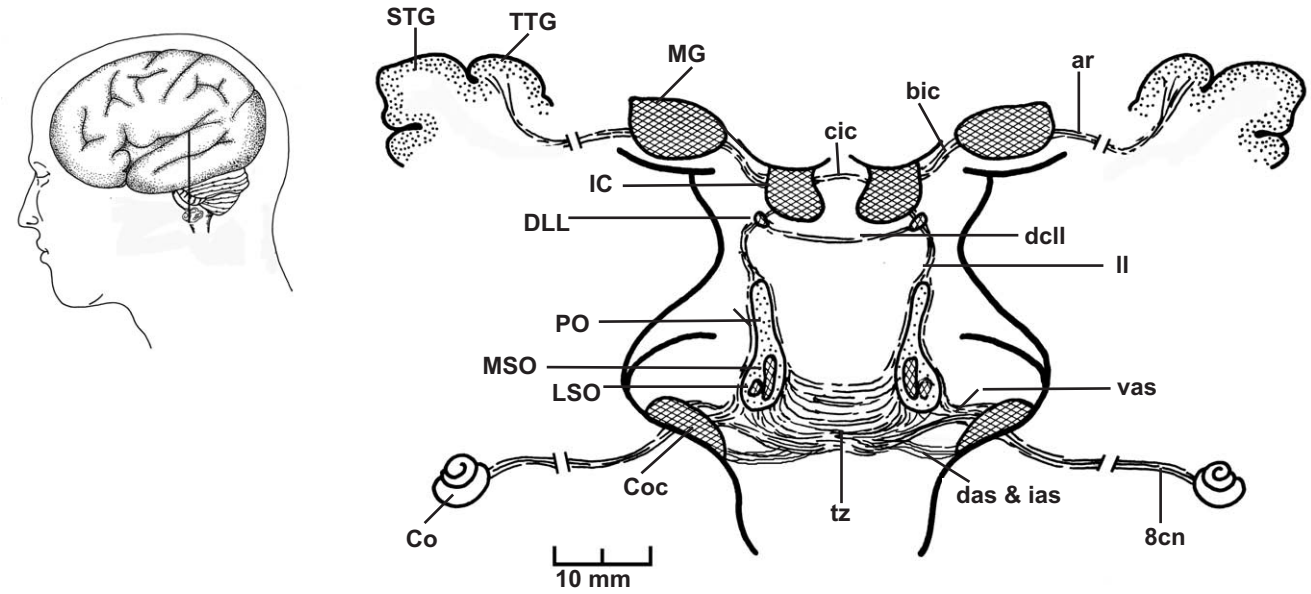

FIGURE 34.1 Diagramatic representation of the topography of the human auditory system in the plane shown in the inset figure. The diagram approximates the actual topography of the human auditory pathway, except that the full lengths of the cochlear nerve and auditory radiations are not represented. Nuclei are labeled on the left side and axonal pathways on the right side. bic, brachium of inferior colliculus; cic, commissure of inferior colliculus; Co, cochlea; Coc, cochlear nuclei; das, dorsal acoustic stria; dcll, dorsal commissure of lateral lemniscus; DLL, dorsal lemniscal nucleus; IC, inferior colliculas, ias, intermediate acoustic stria; ll, lateral lemniscus; LSO, lateral superior olivary nucleus; MG, medial geniculate; MSO, medial superior olivary nucleus; PO, periolivary nuclei; STG, superior temporal gyrus; TTG, transverse temporal gyrus; tz, trapezoid body; vas, ventral acoustic stria; 8cn, cochlear nerve.

cohesive representation of stimulus type and location. This synthesized auditory information is carried by the brachium of the inferior colliculus to the medial geniculate complex in the posterior thalamus. From the medial geniculate, information passes through the auditory radiations to reach the primary auditory cortex within the transverse temporal gyrus. Geniculate input is sparse outside of the primary auditory area, but transcortical pathways carry auditory information to higher levels of cortical processing in the superior temporal gyrus. Further projections to cortex outside of these classical auditory areas allow auditory information to play a role in the highest levels of cognition.

THE COCHLEA AND COCHLEAR NERVE

Middle Ear and Cochlea: Mechanical Transmission of Sound

Although the emphasis in this chapter is on neural mechanisms of information transfer, any description of the auditory system must begin with consideration of the structures of the external, middle, and inner ear that are involved in mechanical transmission of sound. These structures are depicted in a classic drawing by Brödel (1946) (Fig. 34.2). In this drawing, we see that the external ear consists of the auricle, or pinna, and the external auditory canal. The external canal ends at the tympanic membrane (ear drum), which separates it from the air-filled cavity of the middle ear. The middle and inner ears are housed within a portion of the temporal bone that is sometimes called the petrous ("stonelike") bone because of its density. The middle ear is ventilated by the eustachian tube, which passes to the nasopharynx, ending just above the soft palate. In sound transmission, pressure waves are collected by the auricle and passed through the external auditory canal, which slightly modifies the character of the waves (von Békésy, 1932). As pressure waves cause vibration of the tympanic membrane, its motion is transmitted across the middle ear by the chain of three ossicles (middle ear bones). The ossicles are named the malleus, incus and stapes because of their imagined resemblance to a hammer, anvil, and stirrup (Fig. 34.3A, B). Motion of the ossicles is modified by two small muscles that are attached to the wall of the middle ear. One of these, the stapedius muscle, is inserted into the stapes and contracts in response to

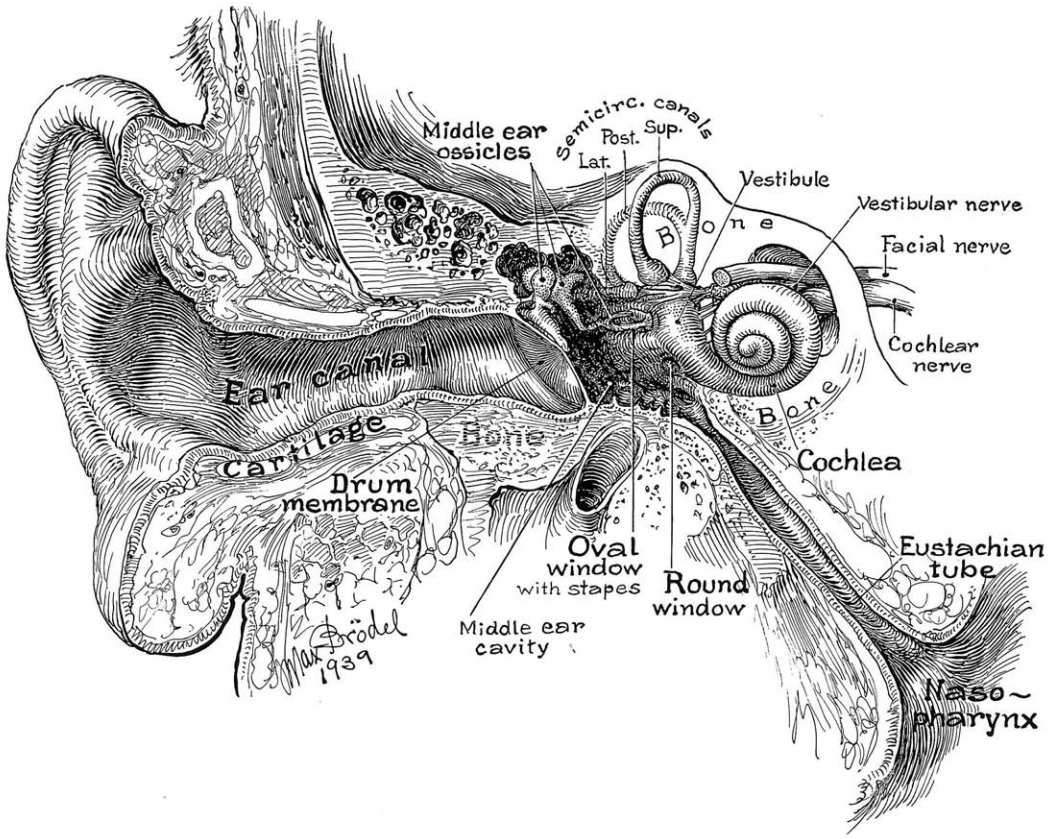

FIGURE 34.2 An artist's rendering of the structures of the human peripheral auditory system. Reprinted from M. Brödel, figure 1, "Three unpublished drawings of the anatomy of the human ear," 1946, with permission from W.B. Saunders Publishing Company.

sounds above 70 dB, the intensity of loud conversation. The other muscle, the tensor tympani, inserts into the malleus and contracts to louder sounds, especially impulse noises. By restricting ossicular motion, these muscles are believed to offer protection to the inner ear from damaging noise. In addition to ossicular transmission, sound is transmitted with a slight delay through the air of the middle ear to the round window membrane.

The auditory portion of the inner ear is a fluid-filled tube that is coiled two and a half times and named the cochlea because of its similarity to a snail. When seen in cross-section, it has a broad base, a pointed apex, and a central pillar called the modiolus (Fig. 34.4A). The cochlear lumen is divided into two compartments by a median partition. The fluid space on the apical side of the partition is known as the scala vestibuli, and that on the basal side is termed the scala tympani. The two perilymph compartments are, in fact, one space because they are continuous with each other at the extreme apical end of the cochlea, at a point called the helicotrema. Both compartments are filled with perilymph, a fluid that resembles extracellular fluid in being high in sodium and low in potassium. Ossicular motion is transmitted to the inner ear through the footplate of the stapes, which is held in place by the flexible annular ligament in the oval window of the cochlea. This aperture opens into the extreme basal end of the cochlea, near its junction with the vestibular organs. When acoustic stimuli impart oscillatory motion to the tympanic membrane and ossicles, the piston-like driving force of the stapes footplate creates waves in the fluid of the scala vestibuli. The confluence of the scalae at the helicotrema permits pressure exerted by movement of the stapes footplate to be relieved by a compensatory movement of the flexible round window membrane located at the basal end of the scala tympani. Congenital deformities that disrupt the integrity of the fluid channels, such as Mondini's deformity (Fig. 34.4B), can interfere with the normal hydrodynamic function of the cochlea.

The median partition of the cochlea extends from the shelf-like osseous spiral lamina medially to the spiral ligament on the lateral wall of the cochlea (Fig. 34.4C).

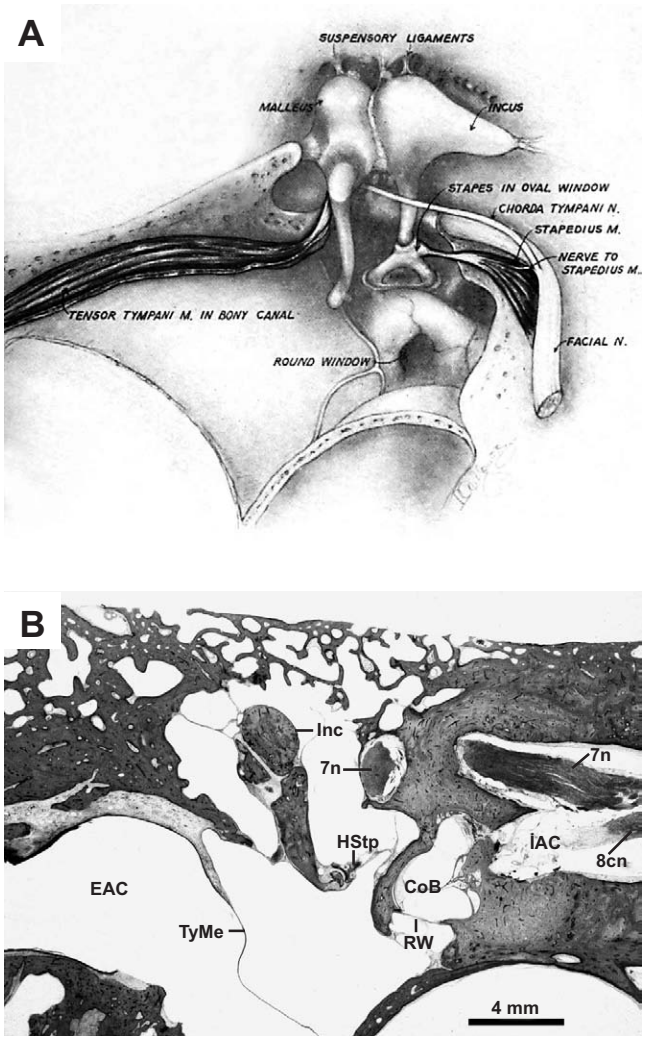

FIGURE 34.3 **(A)** Drawing of the human middle ear with the lateral wall and eardrum removed, illustrating the position of the ossicles and of the tensor tympani and stapedius muscles. Reprinted from *Archives of Otolaryngology* **86,** C.E. Blevins, figure 1, Innervation patterns of the human stapedius muscle, pp. 136–142, 1967, with permission from the Archives of Otolaryngology. Copyrighted 1967, American Medical Association. **(B)** In the human middle ear, the tympanic membrane (TyMe) separates the middle ear from the external auditory canal (EAC). The section passes through the incus (Inc) and a portion of the head of the stapes (HStp). The facial nerve (7n) can be seen on the medial wall of the middle ear and within the internal auditory canal (IAC). The cochlear branch of the eighth nerve (8cn) also passes through the internal auditory canal. Part of the wall of the basal turn of the cochlea (CoB) is formed by the membrane of the round window (RW). Celloidin section, hematoxylin–eosin stain.

A third fluid space, the scala media or cochlear duct, lies between the lateral end of the cochlear partition and the thin Reissner's membrane. This inner channel contains the sensory elements of the cochlea that make up the organ of Corti. The lateral wall of the cochlear duct is formed by the stria vascularis, a cellular layer on the surface of the spiral ligament. Through the action of the stria vascularis, the endolymphatic fluid of the scala media is held in a unique ionic composition of low sodium and high potassium. Maintenance of the ionic difference between perilymph and endolymph is a vital factor in cochlear function. Atrophy and degeneration of the stria (Fig. 34.4D) results in a loss of hearing across all frequencies that is proportional to the degree of loss of strial tissue (Pauler *et al.*, 1988).

The sensory organ of the cochlea, the organ of Corti, rests on an elastic portion of the cochlear partition, the basilar membrane. Oscillation of the stapes head produces an undulation, or rippling motion, along the basilar membrane. This motion was termed the traveling wave by von Békésy (1947). The basilar membrane varies in width along its length, being narrow at the base of the cochlea and wide at the apex. It also varies in stiffness, being stiffer at the base and more flaccid at the apex. As a result, the shape of the traveling wave varies from base to apex, with the short waves created by higher frequencies maximally displacing the narrower basal part of the membrane and the long waves generated by lower frequencies maximally displacing the broader apical segments. Approximately 10 octaves of sound, from 20 Hz to 20,000 Hz (20 kHz), are represented along the length of the basilar membrane. Because motion of the basilar membrane reflects the frequency–intensity pattern of the sound initiating the wave, distinct populations of cochlear hair cells in the organ of Corti will be set in motion by different sound stimuli. This differential displacement of the basilar membrane is the basis of tuning (frequency specificity) in auditory function.

Cochlear Hair Cells: Transduction and Amplification

Transduction, the conversion of mechanical energy to intracellular electrochemical events, occurs in the sensory cells of the organ of Corti. Views of the organ of Corti in a stained section (Fig. 34.5A) and a drawing (Fig. 34.5B) illustrate the single row of inner hair cells on the modiolar side of the cochlea and three rows of outer hair cells on the strial side. They also illustrate supporting cells and the triangular endolymph-filled space between the inner and outer hair cells, the tunnel of Corti. The name hair cell derives from the array of hairlike stereocilia on the free surface of these sensory cells. Electron microscopic images of the apical surface of human hair cells (Fig. 34.6A, B) demonstrate the different morphology of the stereociliary bundles on inner and outer hair cells. Stereocilia on inner hair cells are arranged in a shallow U curve, while those on outer hair cells have a more precise geometry, forming

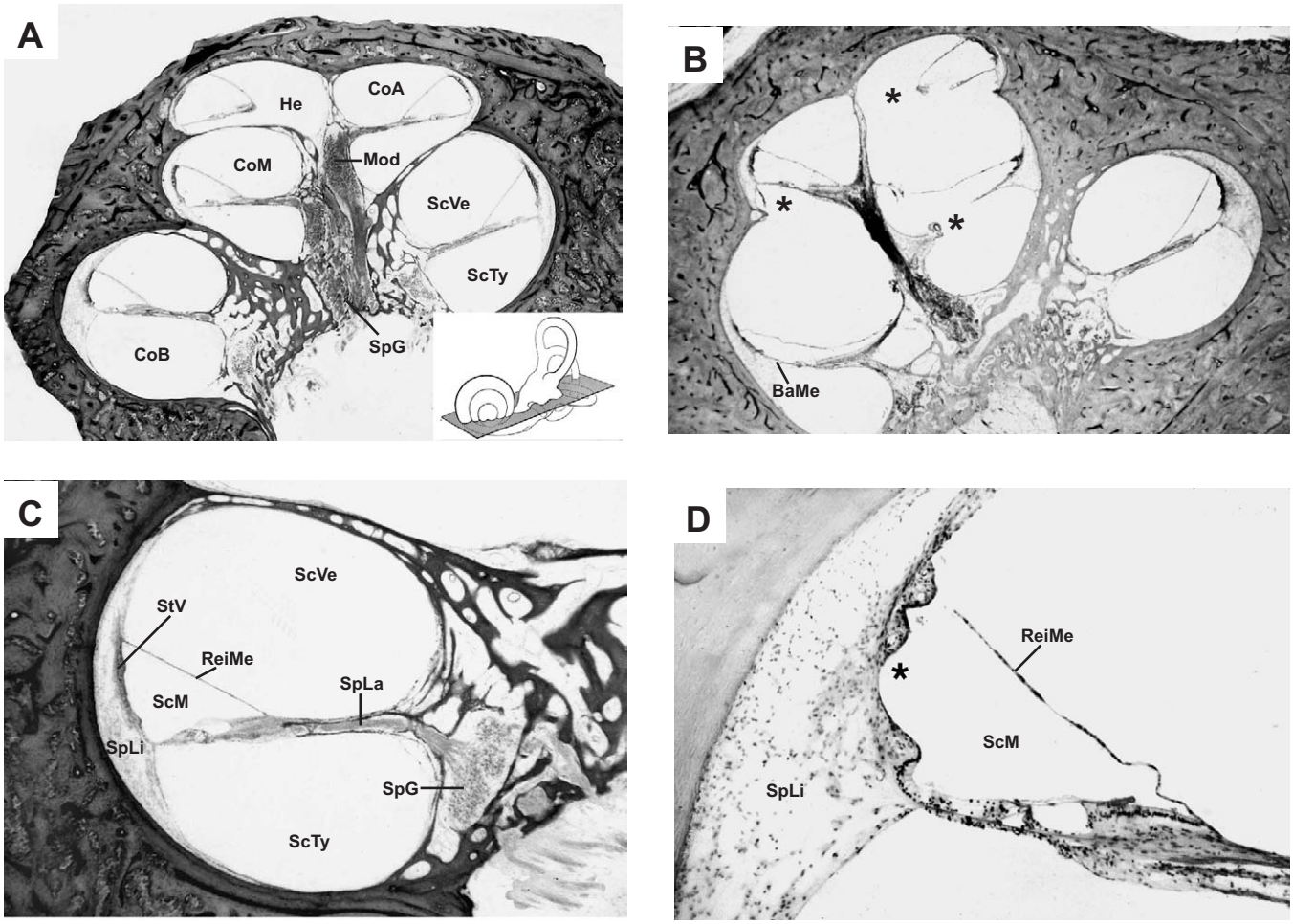

FIGURE 34.4 **(A)** A horizontal section through the human inner ear (plane shown in inset drawing) passes through the basal (CoB), middle (CoM) and apical (CoA) turns of the cochlea. The central pillar of the cochlea, the modiolus (Mod), contains the neurons of the spiral ganglion (SpG). Each turn of the cochlea is divided by a central partition into a scala tympani (ScTy) on the basal side and a scala vestibuli (ScVe) on the apical side. At the apex, the absence of this partition creates a confluence of the two scalae, the helicotrema (He). **(B)** In Mondini's deformity, a type of cochlear dysplasia, absence of the interscalar septum *(asterisks)* results in a confluence of the middle and apical turns. In addition, there is an abnormal basilar membrane (BaMe). **(C)** A single turn of the human cochlea is shown at higher magnification. A bony shelf, the spiral lamina (SpLa), divides the cochlea into two perilymph-containing compartments, the scala vestibuli (ScVe) and the scala tympani (ScTy). The lateral wall of the cochlea is formed by the spiral ligament (SpLi). On the surface of the spiral ligament is a densely cellular structure, the stria vascularis (StV). The thin Reissner's membrane (ReiMe) separates the scala vestibuli from the scala media (ScM). **(D)** Despite a normal-appearing organ of Corti, degeneration of the stria vascularis *(asterisk)* can cause hearing loss due to loss of normal electrolyte levels in the scala media. Celloidin sections, hematoxylin–eosin stain.

a V- or W-shaped bundle (Wright, 1981). On both types of hair cell, the rows of stereocilia are ordered in increasing height from inner to outer. A greater range from short to tall occurs in outer hair cells. In Figure 34.5A, as is usual after fixation and histological processing, the gelatinous tectorial membrane is not in contact with the hair cells. However, high-voltage electron microscopy on thick tissue sections (Takasaka *et al.*, 1983) has demonstrated that the tips of the tallest row of outer hair cell stereocilia are embedded in the underside of the tectorial membrane. Thus, the traveling wave displacement of the basilar membrane, with the organ of Corti on its surface, results in a shearing force exerted between the tallest row of stereocilia and the tectorial membrane.

Since only the tallest row of outer hair cell stereocilia is attached to the tectorial membrane, the shearing force might be expected to deflect only this

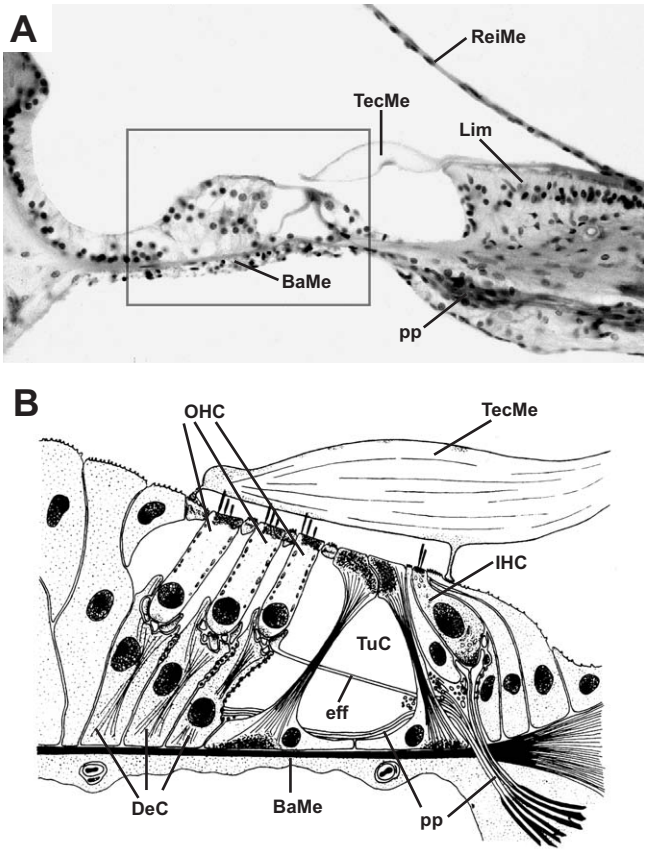

FIGURE 34.5 **(A)** Hair cells and other sensory structures are located in the organ of Corti *(boxed area)*. The gelatinous tectorial membrane (TecMe) is attached medially to a prominence, the limbus (Lim). Running medially from the organ of Corti are the peripheral processes of spiral ganglion cells (pp). Celloidin section, hematoxylin–eosin stain. **(B)** The organ of Corti rests on the basilar membrane (BaMe). Flask-shaped inner hair cells (IHC) are contacted by numerous peripheral processes of spiral ganglion neurons (pp). Outer hair cells (OHC) form three rows: they are more tubular in shape, and their bases are enclosed by Deiter's cells (DeC). A limited number of peripheral processes cross the tunnel of Corti (TuC) to contact outer hair cells. The longest stereocilia of outer hair cells are attached to the underside of the tectorial membrane. Adapted from A. Ryan and P. Dallos, figure 2–4, The physiology of the cochlea, pp. 15–31, in "Hearing Disorders", Ed., J. Northern, published by Allyn and Bacon, Boston, 1996, with permission.

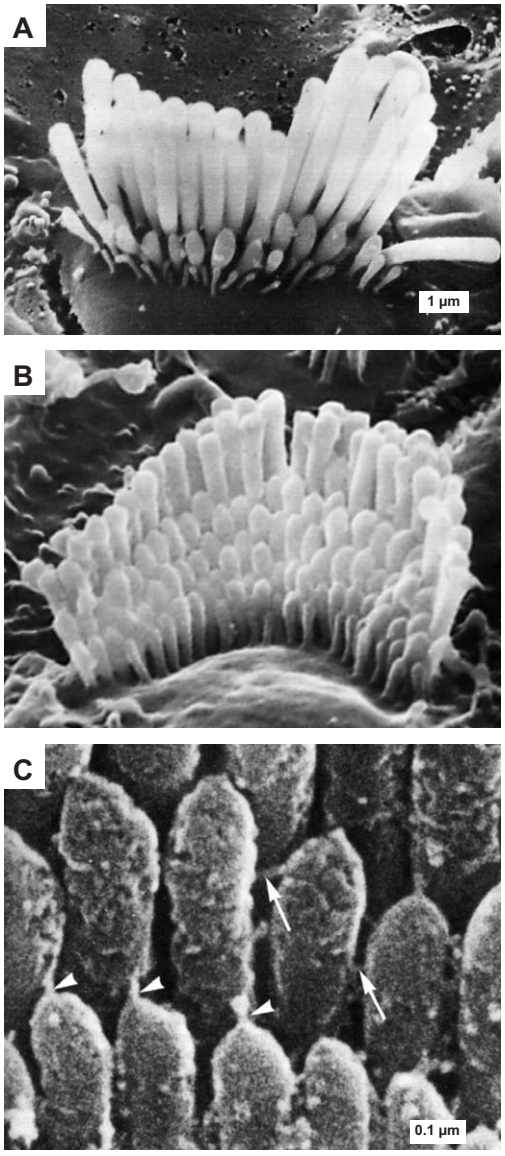

FIGURE 34.6 **(A)** Scanning electron micrographic image of the U-shaped array of stereocilia on the upper surface of a human inner hair cell. Marker bar applies to **A** and **B.** Reprinted from *Clinical Otolaryngology* **6,** A. Wright, figure 5, Scanning electron microscopy of the normal human cochlea, pp. 237–244, 1981, with permission from Black Scientific, U.K. **(B)** Scanning electron micrographic image of the V-shaped array of stereocilia on the apex of a human outer hair cell. Reprinted from *Clinical Otolaryngology* **6,** A. Wright, figure 6, Scanning electron microscopy of the normal human cochlea, pp. 237–244, 1981, with permission from Black Scientific, UK. **(C)** Scanning electron micrographic image of the stereocilia on the apical surface of a human hair cell. Stereocilia of the same row on each hair cell are joined by horizontally running links *(arrows)*. Each shorter stereocilium gives rise to a single vertically pointing link that runs upward to attach to the adjacent taller stereocilium *(arrowheads)*. Reprinted from *Journal of Laryngology and Otology* **99,** P.H. Rhys Evans, S.D. Comis, M.P. Osborne, J.O. Pickles, and J.R. Jeffries, figure 6, Cross-links between stereocilia in the human organ of Corti, pp. 11–19, 1985, with permission from the Royal Society of Medicine Press Limited, London.

row. In fact, this does not occur because of a network of fine filaments linking the stereocilia within each bundle. Side links join stereocilia in the same row, and tip links pass from the tips of stereocilia in the shorter rows to the next tallest row, both in animals (Pickles *et al.*, 1984) and in the human cochlea (Rhys Evans *et al.*, 1985) (Fig. 34.6C). These side-to-side and row-to-row connections form a regular lattice such that when the tallest row of stereocilia is displaced by the tectorial membrane the stereociliary bundle moves as a unit. In addition to their purely mechanical role in bundle

motion, stretching of stereociliary cross-links appears to activate ion channels in the stereociliary membrane (Hudspeth, 1989; Denk *et al.*, 1995). Deflection of the bundle toward tall stereocilia stretches tip links and opens the membrane channels, while deflection toward the shortest row relaxes the links and allows the ionic channels to close. Because hair cells and their stereocilia lie in high-potassium endolymph, it is possible that potassium ions enter through the membrane channels. One immediate result of inward ion flow is activation of contractile molecules within the stereocilia. Each stereocilium is filled with long actin filaments, organized into bundles and arrays by fimbrin (Flock *et al.*, 1981, 1982). The actin filaments extend through the rootlets of the stereocilia, anchoring them into the cuticular plate on the free surface of the hair cell. When traction on the fibrous links opens channels in the stereociliary membrane, the ionic influx activates these contractile molecules, stiffening the stereocilia.

A continuing question in cochlear function is the fact that the stereociliary bundles of inner hair cells do not seem to have a direct attachment to the tectorial membrane. It is possible that their stereocilia are deflected by viscous drag of the fluid in the subtectorial space. This difference may account for the fact that inner hair cell stereocilia are less anatomically specialized than those of outer hair cells. In addition, it appears that inner and outer hair cells have different roles in the transduction of activity within the cochlea. Inner hair cells provide direct input to virtually all of the axons in the cochlear nerve. However, their activity is modified by local amplification of the motion of the basilar membrane produced by outer hair cells. This role in amplification is related to an active contractile process located in their lateral cell wall. The contractile molecules in their cell membrane cause isolated outer hair cells to undergo rapid length changes when stimulated by an electric current (Brownell *et al.*, 1985; Kachar *et al.*, 1986; Ashmore, 1987), by a tone stimulus (Brundin *et al.*, 1989), or by deflection of the stereociliary bundle (Evans and Dallos, 1993). In an intact cochlea, the active shape changes occurring in populations of outer hair cells in response to stimulation by a tone (Brundin *et al.*, 1992) or electrical current (Mammo and Ashmore, 1993) are capable of displacing the basilar membrane. Observations in intact cochleas indicate that outer hair cell–related supporting cells (Dieter's and Hensen's cells) are also involved in the process of displacing the basilar membrane (Flock *et al.*, 1999). This localized amplification of basilar membrane motion can enhance the response of inner hair cells in a narrow frequency range, and is generally believed to be the basis of low threshold (sensitivity) in mammalian hearing.

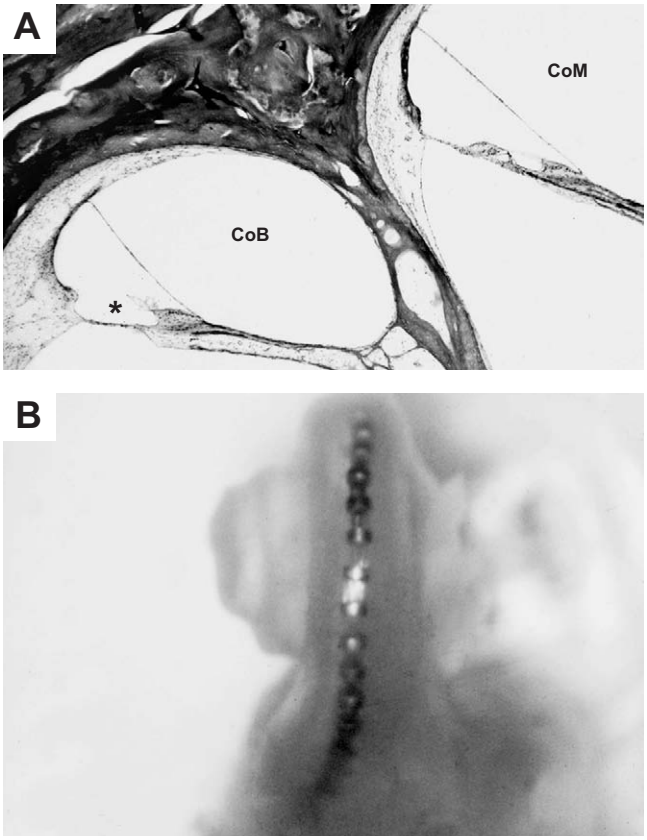

FIGURE 34.7 **(A)** Illustration of degeneration of the organ of Corti *(asterisk)* in the basal turn (CoB) of a human cochlea. The organ of Corti in the middle turn (CoM) is intact. Celloidin section, hematoxylin–eosin stain. **(B)** A multielectrode implant is shown in place in the basal turn of a skeletonized and cleared human cochlea.

Because hair cell transducer and amplification mechanisms are essential to the hearing process, it is not surprising that hair cell loss is the most common cochlear defect causing hearing loss. The base of the cochlea, where higher frequencies are transduced, is usually the most affected (Fig. 34.7A). In presbycusis, the hearing loss of the aged, the loss begins in midlife with degeneration of outer hair cells at the extreme basal end of the cochlea but does not seriously affect hearing until the upper range of speech frequencies, around 3000 Hz, is affected. Noise-induced hearing loss and severe blows to the head tend to affect the anterior basal turn of the cochlea, the region that processes 3000–4000 Hz (Linthicum, unpublished observations). The cause of the sensitivity of this specific area is unknown. Hearing loss due to inner hair cell absence is rare, but may occur as a congenital defect or as a result of advanced degeneration of the organ of Corti. In cases of hearing loss attributable to hair cell loss, some degree of hearing can be achieved by implantation of

a multiple-electrode stimulating device (Fig. 34.7B). Such a device bypasses cochlear hair cells and provides direct stimulation to the neural elements of the cochlea, the next step in the process of sound transmission.

Spiral Ganglion Cells and Cochlear Nerve: Neural Transmission

The transition from hair cell activity to neural activity occurs within the cochlea. Activation of the stereocilia creates changes in the intracellular potential that, in turn, lead to the release of a neurotransmitter from aggregations of synaptic vesicles located at the base of the hair cell. Opposite the cluster of synaptic vesicles, on the outer surface of the cell wall, are bulbous nerve terminals. Electron microscopy of human hair cells has demonstrated that from six to eight such terminals are present on the base of each inner hair cell, and a smaller number are located on each outer hair cell (Nadol, 1990). Each synaptic terminal continues into a short unmyelinated process, approximately 100 μm in length. The terminals, together with the short length of unmyelinated process beyond them, constitute the dendritic (information receiving) segment of cochlear nerve fibers. The unmyelinated processes pass through a series of small apertures in the osseous spiral lamina, the habenula perforata. At this point they become surrounded by a sheath of myelin created by Schwann cells (Spoendlin and Schrott, 1989) and thus become axons capable of rapid conduction. The entire cell process, including the unmyelinated tip and its myelinated continuation, is often referred to as a dendrite but is more correctly called the peripheral process of a spiral ganglion neuron because it includes both dendritic and axonal segments. In an osmicated cochlea (Fig. 34.8A), small bundles of peripheral processes can be seen passing from the organ of Corti toward the modiolus. As they leave the organ of Corti, these fascicles run between the two lamellae of bone that form the osseous spiral lamina (Fig. 34.8B).

The myelinated peripheral processes run along the spiral lamina, bend slightly downward as they enter the modiolus, and reach their cells of origin in the spiral ganglion (Fig. 34.8C). The spiral ganglion is so named because it spirals within Rosenthal's canal from the base of the modiolus to its midpoint. At the midpoint of the modiolus, the canal disappears and ganglion cells become a confluent mass. Because the ganglion reaches only halfway from the base of the cochlea to the apex, the peripheral processes contacting hair cells in the apical and upper middle turns of the cochlea extend down through the modiolus to reach the most apical ganglion cells. The number of human spiral ganglion cells varies with age from 36,000 in infants and 27,000 in the fourth decade, to only 18,000 in the elderly (Otte *et al.*, 1978). Human spiral ganglion cell bodies are unmyelinated, except for a few that become myelinated with age (Ota and Kimura, 1980).

Two types of neuron have been identified in the spiral ganglion of mammals (Kiang *et al.*, 1982) and humans (Spoendlin, 1985). A majority (90–95%) of the spiral ganglion neurons are type I cells, large round cells about 25–30 μm in diameter (Fig. 34.8D). Type I cells have peripheral processes contacting inner hair cells in a highly convergent manner in that each inner hair cell is contacted by terminals of peripheral processes of several type I ganglion cells. Thus, each inner hair cell drives a group of type I ganglion cells with its activity. In contrast, about 5–10% of the total number of cells in the spiral ganglion are type II cells, which are considerably smaller (15 μm in diameter; Fig. 34.8E) and generally located near the periphery of the ganglion. Their thin unmyelinated peripheral processes cross the tunnel of Corti (Fig. 34.5B) and branch to synapse with outer hair cells in a highly divergent manner, with one type II peripheral process contacting a number of outer hair cells. Because type II peripheral processes branch widely and overlap in their distribution, each outer hair cell is contacted by multiple terminals. The result of this differential innervation of inner and outer hair cells is that type I ganglion cells, relaying the activity of inner hair cells, constitute almost the entire volume and information content of the cochlear nerve. The contribution of outer hair cells to the pattern of activity in the nerve is mainly an indirect one, based on their ability to amplify the activity of subpopulations of inner hair cells.

Spiral ganglion cells of both types give rise to central processes that pass through the center of the modiolus and the cribriform area at its base to form the cochlear nerve. The central processes of ganglion cells innervated by apical hair cells are at the center of the nerve, and those representing the middle and basal segments of the cochlea are progressively more peripheral (Spoendlin and Schrott, 1989). The spiraling course of the cochlear nerve can be observed in the human nerve as it passes into the internal auditory canal within the temporal bone (Fig. 34.9A). Near the outlet from the internal auditory canal, the internal auditory meatus or porus acusticus, there is an abrupt change in the myelin sheath from one produced by Schwann cells to one produced by glial (oligodendroglial) cells of the central nervous system. It is the glial portion of the nerve that exits from the internal auditory canal and crosses the intradural space to reach the brain stem. Just medial to the cochlea in the internal auditory canal, the auditory nerve comes into contact with the

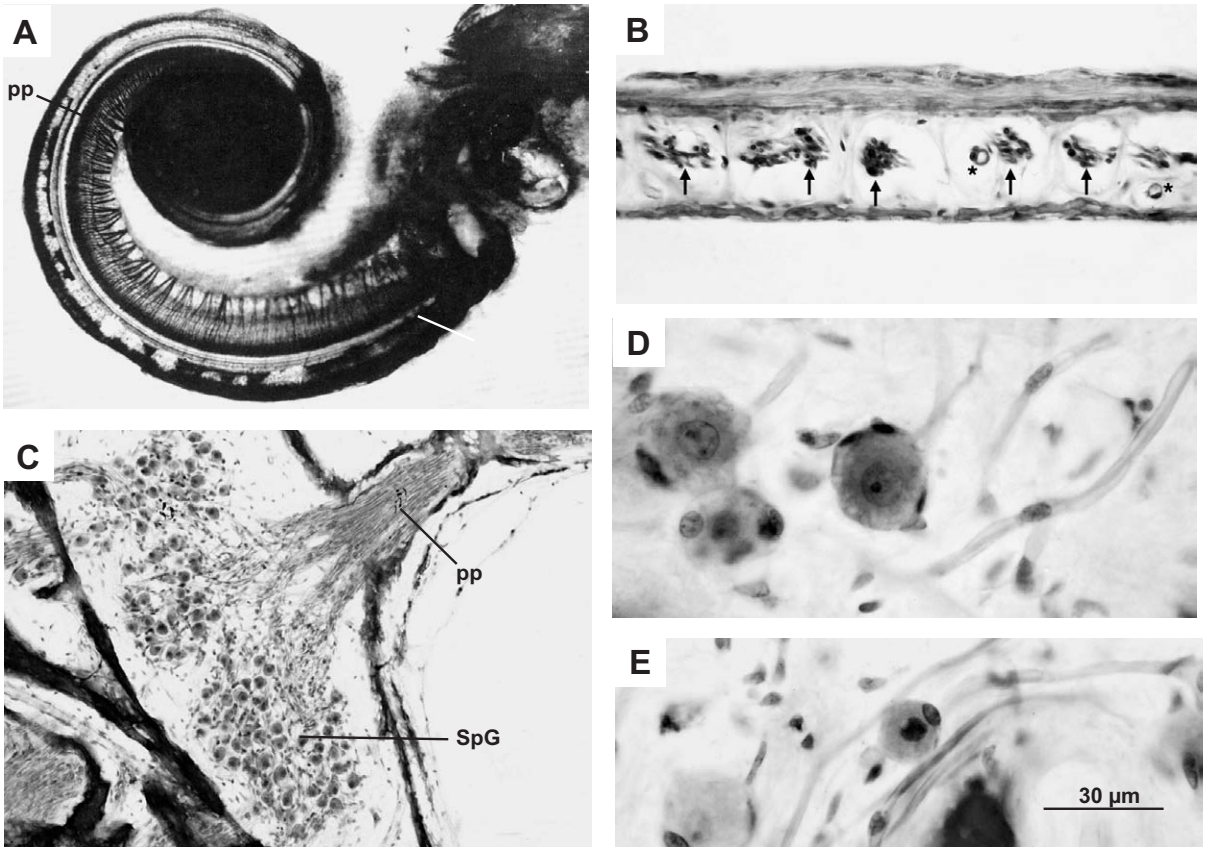

FIGURE 34.8 **(A)** A microdissected human temporal bone illustrates the coalescence of peripheral proceses (pp) of spiral ganglion neurons into fascicles. Reprinted from *Annals of Otology, Rhinology and Laryngology*, Suppl. **48,** L.G. Johnson, J.E. Hawkins, and F.H. Linthicum, Jr., figure 2, Cochlear and vestibular lesions in capsular otosclerosis as seen in microdissection, pp. 1–40, 1978, with permission from the Annals Publishing Company. **(B)** Fascicles of peripheral processes *(arrows)* run between the lamellae of bone that form the osseous spiral lamina. Capillaries are indicated by asterisks. Celloidin section, hematoxylin–eosin stain with osmium. **(C)** Peripheral processes (pp) in the osseous spiral lamina pass into the spiral ganglion (SpG) in Rosenthal's canal within the modiolus of a human cochlea. Celloidin section, hematoxylin–eosin stain. **(D)** Type I human spiral ganglion neurons. **(E)** Type II human spiral ganglion neuron. **D** and **E,** cellodin sections, hematoxylin–eosin stain with osmium.

nerve from the vestibular organs (Fig. 34.9B). Though there may be mingling of the fibers of the adjacent nerves, axons of the two nerves are generally distinguishable by their diameter (Natout *et al.*, 1987). Vestibular nerve axons are larger and more variable in size, with a majority of the fibers in the 7- to 15-µm size range. Cochlear nerve axons are smaller and more uniform, generally 3–5 µm in diameter.

Auditory Periphery: Generation of Evoked Activity

Because outer hair cell contraction can produce motion of the basilar membrane, it is thought to be responsible for otoacoustic emissions, which are audible sounds emitted by the ear (Kemp, 1978). The production of otoacoustic emissions is termed reverse transduction because it reverses the usual sequence of events during audition. Rhythmic contraction of outer hair cells, and possibly also their supporting cells, causes vibration of the basilar membrane. This, in turn, produces pressure waves in perilymph, motion of the ossicles, and oscillation of the tympanic membrane. Vibration of the tympanic membrane results in recordable sound waves being emitted from the ear. Otoacoustic emissions can be diminished or abolished by overexposure to substances, such as salicylates and quinine, which produce tinnitus and hearing loss in human subjects (Brownell, 1990). Microscopic examination of outer hair cells in guinea pigs exposed to salicylate reveals changes in the hair cell wall, including diliatation and vesiculation of subsurface cisternae

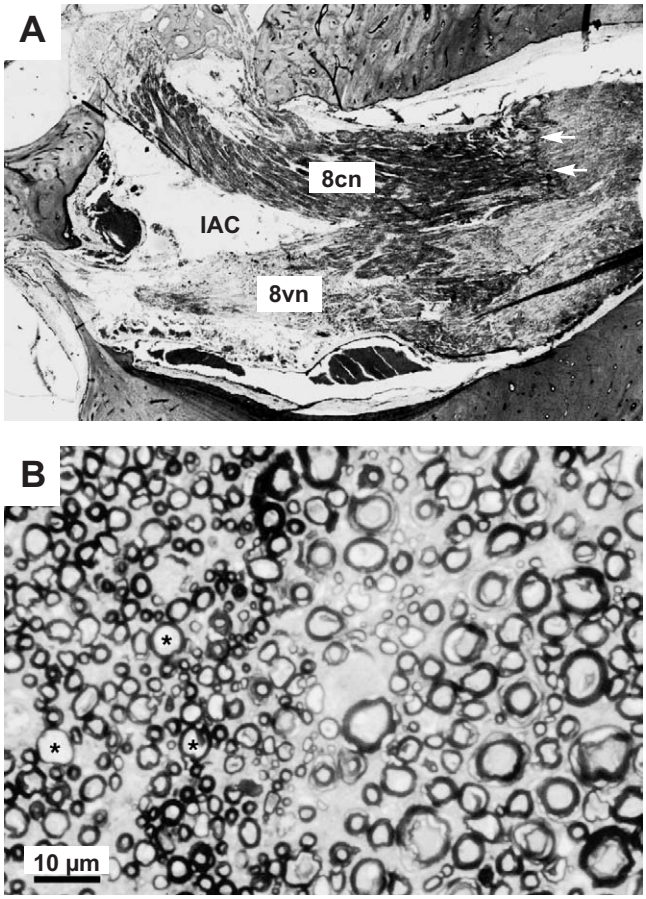

FIGURE 34.9 **(A)** Cochlear nerve (8cn) and vestibular nerve (8vn) in the internal auditory canal (IAC) of a human temporal bone. White arrows indicate the junction between Schwann cell and glial (oligodendrocyte) myelin on the cochlear nerve. Celloidin section, hematoxylin–eosin stain. **(B)** Higher power microphotograph of a cross-section through the human cochlear nerve *(left)* and vestibular nerve *(right)*. Axons in the cochlear nerve are smaller and more uniform in diameter than those in the vestibular nerve. Some larger vestibular axons *(asterisks)* are mingled with the cochlear axons. Plastic section, toluidin blue stain with osmium.

(Deiler *et al.*, 1991; Lue and Brownell, 1999). Similar changes are observed in guinea pig hair cells after treatment with quinine (Karlsson *et al.*, 1991). The pathological effects of these substances, and their interference with the lateral cell wall contractile mechanism, supports the idea that outer hair cell motion is a necessary part of the generation of otoacoustic emissions.

The activity of cochlear sensory cells and neurons also generates externally recordable bioelectric potentials. One of these early potentials, the cochlear microphonic, is a low-amplitude potential recorded from the external auditory canal or surface of the tympanic membrane during a sound stimulus. The cochlear microphonic disappears in guinea pigs whose hair cells have been destroyed by administration of the antibiotic kanamycin (Dallos and Cheatham, 1976). These experiments also demonstrated an imbalance in the contribution of inner and outer hair cells to the cochlear microphonic. On schedules of kanamycin administration that destroyed primarily inner hair cells, leaving an almost normal complement of outer hair cells, the cochlear microphonic was essentially normal. When outer hair cells were destroyed, the microphonic was only a small fraction of normal. Thus, the cochlear microphonic is believed to reflect hair cell activity, principally or exclusively that of outer hair cells, during the transduction process.

True neural activity is reflected in the auditory brain stem response (ABSR), an externally recordable series of small amplitude and short, latency wave-like potentials evoked by a transient stimulus, such as a click. Several studies in human subjects have shown that the earliest ABSR waves, waves I and II, are generated by the cochlear nerve. Intrasurgical recordings, made with a wire electrode placed directly on the auditory nerve and brain stem (Moller and Jannetta, 1982), concluded that the first two ABSR waves are generated prior to the entrance of the nerve into the brain stem. In animal studies, sectioning of the cochlear nerve at the internal acoustic meatus leaves wave I intact but abolishes all subsequent ABSR waves (Buchwald and Huang, 1975), indicating that wave I reflects activity in the most peripheral portion of the nerve fibers. A potential corresponding to wave II of the scalp-recorded ABSR can be recorded intrasurgically from the surface of the human cochlear nerve as it passes through the internal auditory meatus and crosses the intradural space (Martin *et al.*, 1995). In addition, a dipole localization study concluded that human wave II is generated as action potentials in the auditory nerve cross the conductivity boundary at the interface of the temporal bone and cerebrospinal fluid space (Scherg and von Cramon, 1985). Thus, both waves I and II of the human ABSR appear to be generated by activity in axons of the cochlear nerve.

The distinction between potentials generated by hair cells and neural potentials is supported by clinical observations in subjects with a condition known as auditory neuropathy. In these subjects, hearing thresholds measured by pure-tone audiometry are normal, but there is relatively poor speech perception (Starr *et al.*, 1991). Physiologically, normal cochlear microphonic potentials and otoacoustic emissions are present, implying that hair cell motility is intact. However, ABSR recordings are either highly distorted or completely absent in these subjects. Because a recordable potential requires synchronous activity in a population of axons, the loss of all waves of the ABSR in

these subjects suggests that transient stimuli do not produce synchronized firing in the cochlear nerve. The idea that absence of the ABSR represents a loss of neural synchrony is supported by the defects in myelination and neural conduction identified in some cases of this condition (Starr *et al.*, 1996).

THE BRAIN STEM AUDITORY SYSTEM

Cochlear Nuclei: Diversification of Cochlear Input

Activity generated in the cochlea is carried to the brain stem by the cochlear nerve. In man, as in other mammalian species, the cochlear nerve enters the ventral cochlear nucleus and forms a wedge-shaped nerve root tapering dorsally (Moore and Osen, 1979) (Fig. 34.10). The axons entering the nerve root are grouped into small fascicles that appear to have traveled together from their point of origin in the organ of Corti. Cochlear nerve axons bifurcate within the nerve root to form an ascending branch running toward the rostral end of the nucleus and a descending branch running caudally. The territory pierced by the ascending branches is termed the anteroventral cochlear nucleus, and the region innervated by the descending branches is the posteroventral cochlear nucleus. In most mammalian species, the nerve root forms a partition dividing the anteroventral and posteroventral divisions of the nucleus. In man, these two subdivisions are broadly confluent lateral to the nerve root, so that the division between the two regions is somewhat arbitrary. Though the greater part of the human ventral cochlear nucleus consists of cells lying among the ascending and descending cochlear nerve branches, there is a relatively large cap area that lies outside of the field of the primary fibers. The cap is saddle shaped, rising high above the ventral nucleus dorsally and extending down on both sides, with greater thickness on the lateral side of the nucleus. The cap area is traversed by very thin myelinated fibers that have been shown to be collaterals of the ascending and descending primary branches (Feldman and Harrison, 1969). At the surface of the nuclear complex, there is an amorphous zone of tissue that appears featureless in cell or myelin stains, but which is shown by immunostaining to be composed of massed astrocytic processes. This superficial glial layer, which is more prominent in the brain stems of humans and other higher primates than in nonprimate species, extends beyond the cochlear nuclei over the brain stem surface.

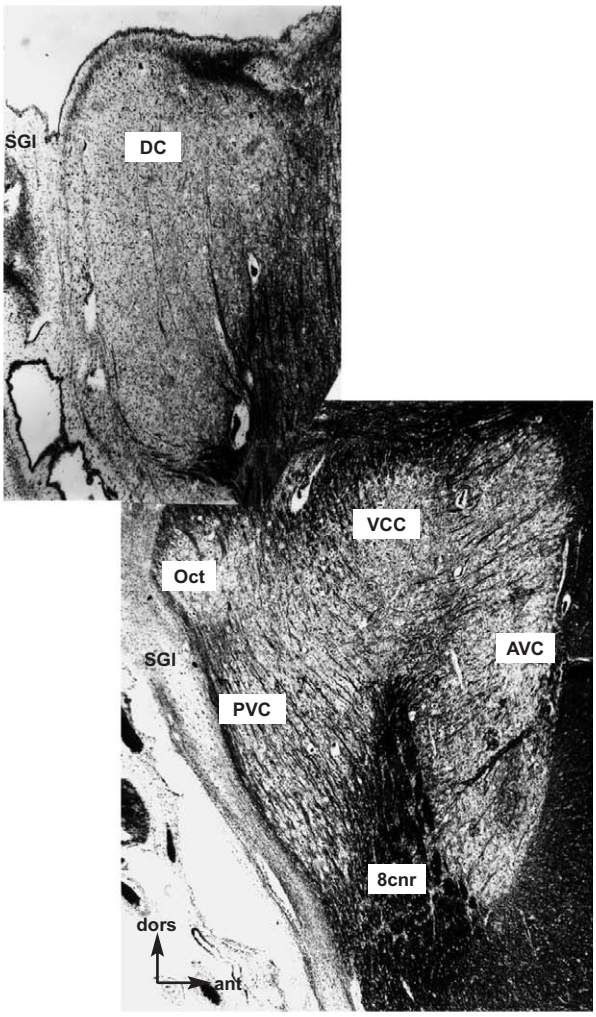

FIGURE 34.10 Collage of two myelin-stained sagittal sections through the human dorsal and ventral cochlear nuclei. Cochlear nerve fibers bifurcate in the cochlear nerve root (8cnr) in the center of the ventral cochlear nucleus. From the nerve root, ascending branches pass into the anteroventral nucleus (AVC). Descending branches of the nerve run through the posteroventral nucleus (PVC), including the octopus cell area (Oct), and continue into the dorsal cochlear nucleus (DC). Main-stem branches of the cochlear nerve do not enter the cap area (VCC) dorsal to the nerve root. Celloidin sections, Woelcke hematoxylin stain. A superficial glial zone (SGI) covers the surface of the nuclei.

A cochleotopic organization of the axons within the nerve has been demonstrated in squirrel monkeys with restricted cochlear lesions (Moskowitz and Liu, 1972). Axons of spiral ganglion cells innervating hair cells in the apex of the cochlea (activated by low tones) bifurcate in the ventral part of the nerve root, near the point of entry of the nerve. Axons of spiral ganglion cells innervating hair cells located at the base of the cochlea (activated by high tones) extend to the dorsal tip of the nerve root and bifurcate there. From the

nerve root, axons representing a point on the organ of Corti maintain their relative positions as they project through the cochlear nuclei as ascending and descending branches. Thus, in their course, each group of branches representing a point on the cochlea spreads to form a plane of fibers crossing the nuclei. Because the cochleotopic sequence of nerve distribution shown in the squirrel monkey is identical to that seen in other mammalian species, it is assumed that a similar organization exists in the human cochlear nerve.

The descending branches of the cochlear nerve run relatively straight caudally through the posteroventral nucleus until they reach its posterior tip, at which point they become distinctly convergent (Fig 34.10). From the posterior tip of the ventral nucleus, most of the descending branches continue into the dorsal nucleus. In most mammals, the descending cochlear branches entering the dorsal nucleus turn to run toward the surface of the nucleus, forming tonotopic planes orthogonal to the nuclear surface. In humans, however, the descending branches fan out across the width of the dorsal nucleus and run parallel to its surface. This change in direction is presumably related to altered cytoarchitecture in the human dorsal nucleus, changes that are discussed in the following sections. Ascending branches of the cochlear nerve do not, like the descending branches, converge in their course. Instead, the planes of axons retain the same spacing from their point of emergence from the nerve root, or may even diverge slightly. A regular laminar structure, with palisades of ascending branches alternating with tiers of cells, is characteristic of the entire anteroventral nucleus and is particularly clear at its rostral tip.

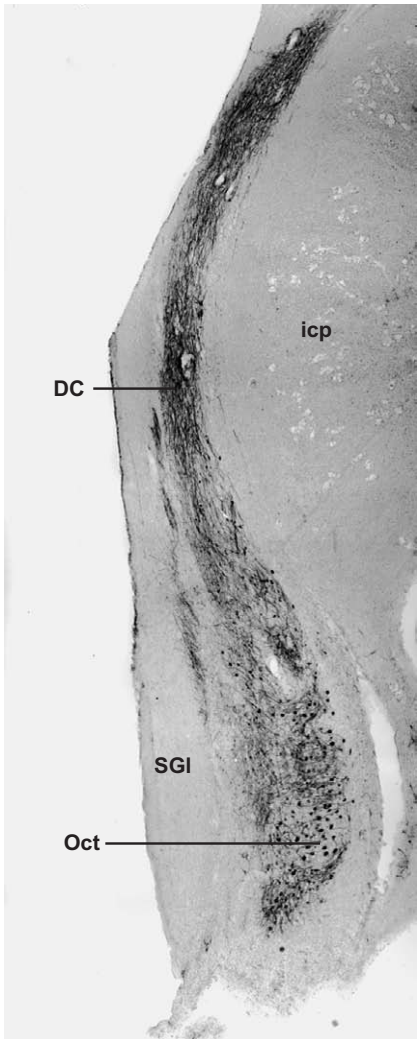

FIGURE 34.11 Transaxial section through a caudal level of the human cochlear nuclei. The dorsal cochlear nucleus (DC) is curved and flattened over the inferior cerebellar peduncle (icp). The posterior tip of the ventral nucleus consists of the octopus cell area (Oct). A superficial glial zone (SGl) covers the surface of the nuclei. Celloidin section, immunostained for MAP2 (microtubule-associated protein).

Projection Pathways

The cochlear nuclei are composed of a variety of neuronal types with distinctive patterns of dendritic branching. The cell types described in the human cochlear nuclei (Moore and Osen, 1979; Adams, 1986) are generally, but not always, similar to those of other mammalian species. An indication of this varied cellular morphology can be seen in transaxial sections immunostained for the neurofilaments in neuronal somata and dendrites. At the caudal end of cochlear nuclear complex, the elongated and flattened dorsal cochlear nucleus curves around the inferior cerebellar peduncle (Fig. 34.11). Ventrally, the most posterior tip of the ventral nucleus is seen as an oval region of larger cells, the octopus cell area (Fig. 12.8). Because the cochlear nerve terminates on a number of populations of neurons, the cochlear nuclei are a point of diversification where the single representation of cochlear activity carried in the nerve is transformed into multiple patterns traveling in parallel pathways up through the brain stem.

One projection pathway originates from the larger cells of the dorsal cochlear nucleus. These neurons are slender fusiform or bipolar cells with long polar dendrites extending parallel to the overlying surface (Fig. 34.12A, B). They were considered by Moore and Osen (1979) to be equivalent to fusiform cells of other species, despite their divergence from the characteristic mammalian morphology and orientation. Fusiform cells in most mammals are oriented radial to the nuclear surface and have two distinctive dendritic arbors extending from the cell soma, one toward the

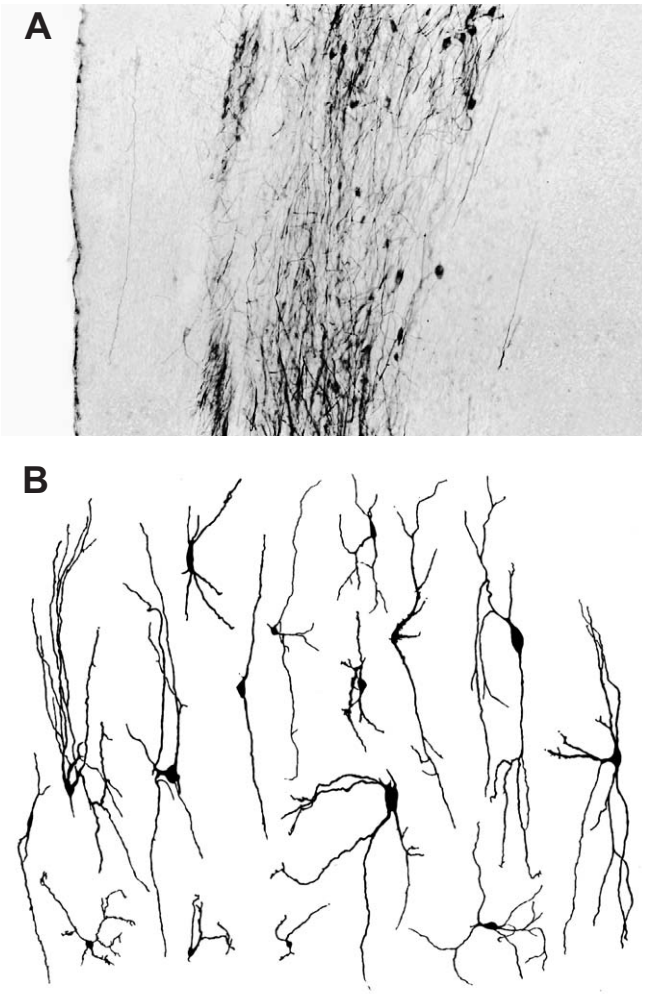

FIGURE 34.12 **(A)** Fusiform cells of the human dorsal cochlear nucleus are oriented along the long axis of the nucleus, parallel to the surface. Celloidin section, MAP2 immunostaining. **(B)** Drawing of Golgi impregnated fusiform cells in the human dorsal cochlear nucleus. Reprinted from *Archives of Otolaryngology, Head and Neck Surgery* **112,** J.C. Adams, figure 7, Neuronal morphology in the human cochlear nucleus, pp. 1253–1261, 1986, with permission from the American Medical Association.

surface of the nucleus and one into its central region. The chief basis for equating human dorsal nucleus neurons to fusiform cells in other mammals is the series of changes occurring in the dorsal nucleus in higher primates (Moore, 1980). Fusiform cells in prosimian primates and monkeys are peripherally located and orthogonally oriented, as in other mammals. In apes, however, with regression of the granule cell system (see discussion on intrinsic systems of cochlear nuclei), fusiform cells become progressively incorporated into the central part of the dorsal nucleus and come to lie horizontally within the field of cochlear nerve axons. This configuration is essentially identical to human dorsal nucleus cytoarchitecture. As in nonprimates, processed information leaves the primate and human dorsal nucleus through the dorsal acoustic stria, a band of thin myelinated axons running over the top of the inferior cerebellar peduncle (macaque, Strominger, 1973; chimpanzee, Strominger *et al.*, 1977; man, Moore and Osen, 1979).

A second brain stem pathway originates from a population of neurons located at the caudal end of the ventral nucleus, the octopus cells. The cells of this region were so named by Osen (1969) because of the emergence of several long thick dendrites from one side of the rounded cell soma, giving the cell a resemblance to an octopus (Fig. 34.13A, B). Because octopus cells are located at the point of maximal convergence of the descending branches of the cochlear nerve, their dendrites cross a large number of axons and receive a very wide spectrum of input from the cochlear nerve. This broad band input is reflected in their detection of coincident firing across groups of auditory nerve fibers and in their well-timed responses to periodic broad-band sounds such as clicks (Oertel *et al.*, 2000). In the macaque, chimpanzee, and man, as in nonprimate mammals, axons from the posterior tip of the ventral cochlear nucleus leave the nucleus in the intermediate acoustic stria, a band of thick beaded axons running deep to the dorsal stria over the top of the inferior cerebellar peduncle and into the brain stem (Strominger, 1973; Strominger *et al.*, 1977; Moore and Osen, 1979).

Farther rostral, at the level of cochlear nerve root, the ventral nucleus has a more compact, roughly triangular configuration (Figs. 34.14, 12.9). The central region of the ventral nucleus contains a heterogeneous population of neurons that vary in size and staining patterns. The name multipolar cell has been applied to all of these cell groups because of the multiple straight, relatively unbranched and appendage-free dendrites radiating from their somas (Fig. 34.15A, B). As a class, they are the most common cell type in the human cochlear nuclei. Many multipolar cell dendrites are oriented parallel to the tonotopic planes of the cochlear nerve and thus would receive relatively narrow band input from its axons. However, multipolar cells also give rise to dendrites that cross the tonotopic planes dorsoventrally. Numerous small bouton-type endings are formed by the cochlear nerve on the somata and extensive dendrites of multipolar cells (Tolbert and Morest, 1982). Efferent axons of neurons the central ventral nucleus leave the nucleus in the ventral acoustic stria and cross the midline in the trapezoid body (Strominger and Strominger 1971; Strominger *et al.*, 1977; Moore and Osen, 1979).

The anterior ventral nucleus contains a population of neurons that are distinguishable from multipolar

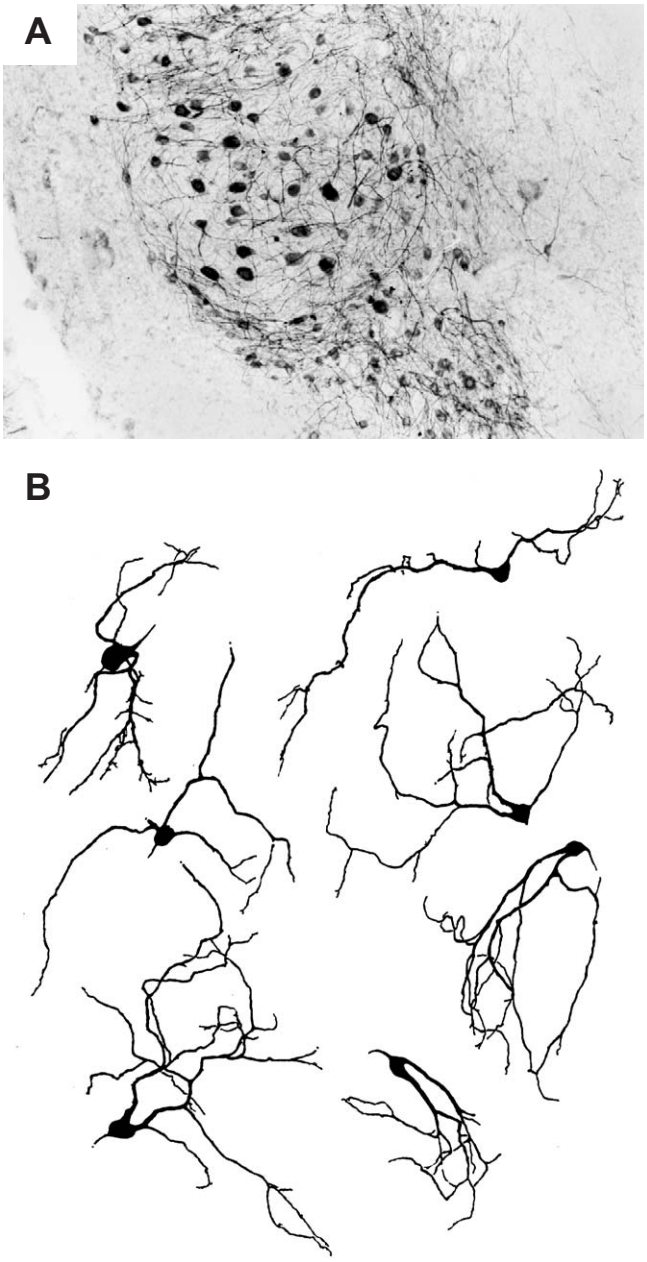

FIGURE 34.13 **(A)** Octopus cells of the human ventral cochlear nucleus are large ovoid neurons with thick radiating dendrites. Celloidin section, MAP2 immunostaining. **(B)** Drawing of Golgi-impregnated octopus cells in the human ventral cochlear nucleus. Reprinted from *Archives of Otolaryngology, Head and Neck Surgery* **112,** J.C. Adams, figure 5, Neuronal morphology in the human cochlear nucleus, pp. 1253–1261, 1986, with permission from the American Medical Association.

cells because of their rounded somata, short-stem dendrites, and tufted dendritic arbors (Fig. 34.16A, B). These neurons were given the name bushy cells by Brawer *et al.* (1972) because of their terminal dendritic tufts. They have been divided into two subtypes,

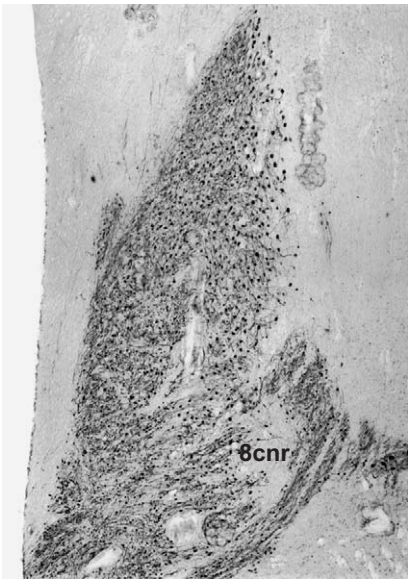

FIGURE 34.14 Transaxial section through the human ventral cochlear nucleus at the level of the cochlear nerve root (8cnr). Celloidin section, MAP2 immunostaining.

globular bushy cells and spherical bushy cells, both of which have been identified in the human ventral cochlear nucleus (Moore and Osen, 1979; Adams, 1986). Globular cells have somewhat longer, sparser dendrites and are most numerous close to and within the nerve root. Spherical cells have shorter, more distinctly tufted dendrites and are aligned in rows at the rostral pole of the nucleus. Both globular and spherical cells receive expanded bulb and calyceal-type endings that cover much of the cell soma and form multiple synaptic junctions (Cant and Morest, 1979; Ostapoff and Morest, 1991). Bushy cell innervation is thus quite different from the multiple small terminals contacting dendrites of octopus and multipolar cells. Because the somatic terminals arise from only a few cochlear nerve axons, bushy cells tend to reflect stimulus parameters very accurately in their firing pattern. Axons of both types of bushy cell leave the nucleus through the ventral acoustic stria and trapezoid body (Strominger and Strominger, 1971; Strominger *et al.*, 1977; Moore and Osen, 1979).

Intrinsic Systems

Not all cells in the cochlear nuclei are projection neurons forming ascending pathways. Some cell groups, particularly the smaller cells, appear to be intrinsic neurons with axons terminating entirely within the nuclei. Undoubtedly, much of the complexity and multiplicity in the transformation of auditory nerve input by cochlear nucleus neurons arises from the interaction of auditory nerve and intrinsic cochlear

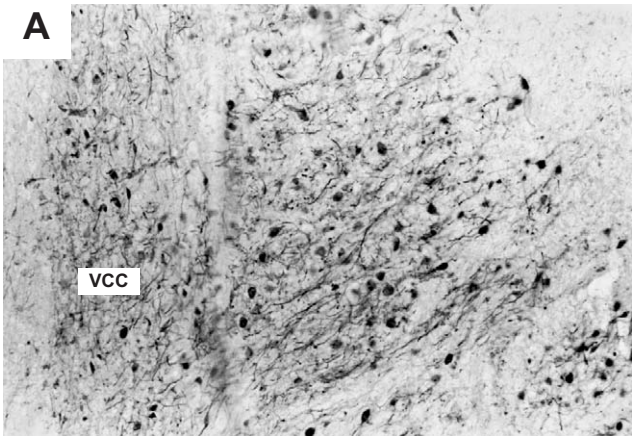

FIGURE 34.15 **(A)** Multipolar cells in the main portion of the human ventral cochlear nucleus have long dendrites that run parallel to the planes of entering cochlear nerve axons. In the cap area (VCC), dendrites are more randomly oriented. Celloidin section, MAP2 immunostaining. **(B)** Drawing of Golgi-impregnated multipolar cells in the human ventral cochlear nucleus. Reprinted from *Archives of Otolaryngology, Head and Neck Surgery* **112,** J.C. Adams, figure 3, Neuronal morphology in the human cochlear nucleus, pp. 1253–1261, 1986, with permission from the American Medical Association.

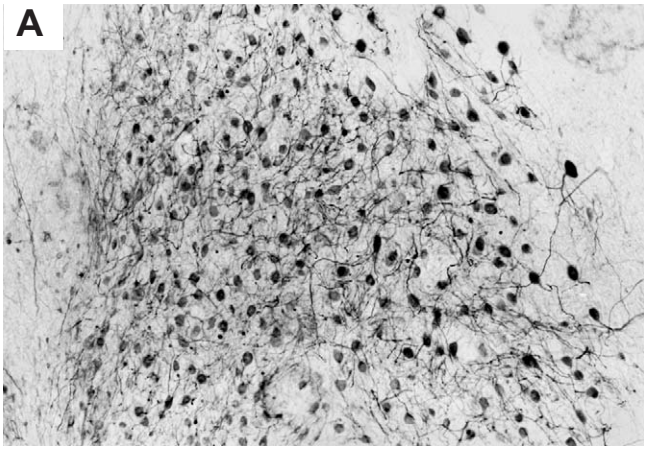

FIGURE 34.16 **(A)** In the human anteroventral cochlear nucleus, dendrites are shorter and have a more radial pattern than in the posterior region of the nucleus. Celloidin section, MAP2 immunostaining. **(B)** Drawing of Golgi impregnated spherical cells in the human ventral cochlear nucleus. Reprinted from *Archives of Otolaryngology, Head and Neck Surgery* **112,** J.C. Adams, figure 1, Neuronal morphology in the human cochlear nucleus, pp. 1253–1261, 1986, with permission from the American Medical Association.

activity. Many modulatory neurons have been identified by their content of the inhibitory amino acid neurotransmitters, γ-aminobutyric acid (GABA) and glycine. Studies of inhibitory neurons in the cochlear nuclei of the baboon (Moore *et al.*, 1996a) demonstrate the same four inhibitory systems as are seen in other mammals, namely, a granule–cartwheel cell system, a commissural projection, an association projection from the dorsal nucleus to the ventral nucleus, and a cap area. However, the anatomy of the human cochlear nuclei suggests that only the latter three modulatory systems are present in humans.

In regard to the granule cell system, the previous description of the human dorsal nucleus noted that its cytoarchitectural organization is different from that of most mammals. In nonprimates, the dorsal cochlear nucleus is covered by a thick molecular layer, formed by axons of cells in the superficial granular layer (Mugnaini *et al.*, 1980). The internal synaptic organization of the granule cell system is complex and very

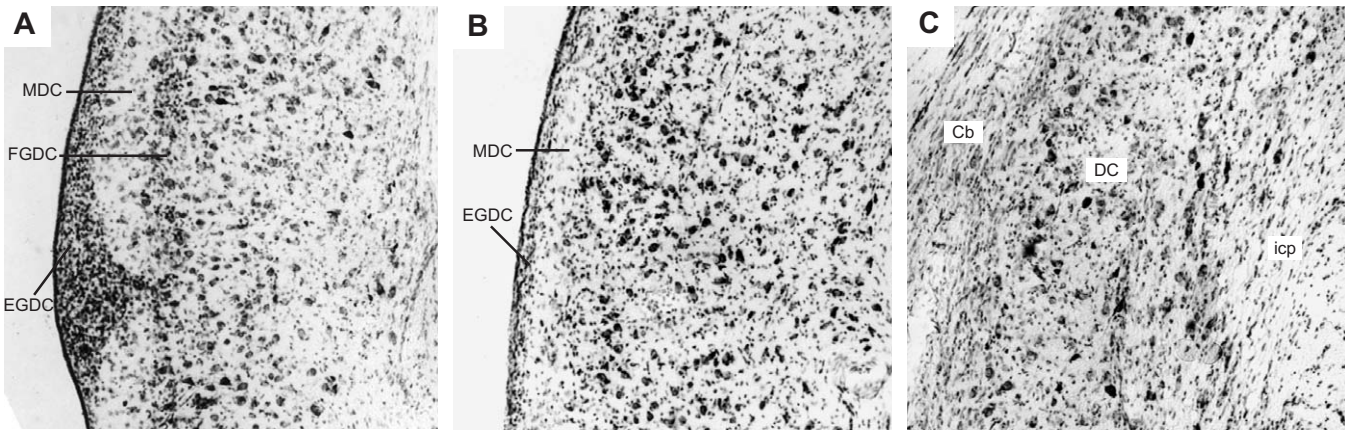

FIGURE 34.17 Progressive changes in the cytoarchitecture of the dorsal cochlear nucleus in primates. **(A)** In a prosimian, the loris, most granule cells are located on the surface of the nucleus in the external granular layer (EGDC). A smaller number of granule cells are present in the fusiform-granule cell layer (FGDC). Granule cell axons form a superficial molecular layer (MDC). **(B)** In a ceboid primate, the owl monkey, there is a thin external granular layer and a molecular layer. Fusiform cells are scattered through the body of the nucleus. **(C)** In the gibbon, with the disappearance of the granule cell layers, there is no evidence of lamination in the dorsal nucleus. Cb, cerebellum; icp, inferior cerebellar peduncle. Celloidin sections, Nissl stain. Adapted from *Journal of Comparative Neurology* **193,** J.K. Moore, 1980, figures 2, 3, and 4, The primate cochlear nuclei: loss of lamination as a phylogenetic process, pp. 609–629, 1980, with permission from Wiley-Liss, Inc., a subsidiary of John Wiley & Sons Inc., New York.

similar to that of the cerebellar cortex in that it includes several types of small inhibitory neuron, i.e., Golgi cells with strong glycine and GABA activity, small stellate cells with single GABA activity, and cartwheel cells with both glycine and GABA activity (Kolston *et al.*, 1992). In mammals, the granule cell system as a whole projects to the apical dendrites of dorsal nucleus fusiform cells and strongly modifies their activity. Across primates, however, there is a steady dissolution of this intrinsic inhibitory circuitry (Moore, 1980). In prosimian primates, the presence of an external granule cell layer indicates an incipient failure of inward migration and maturation of granule cells (Fig. 34.17A). The failure of migration is more pronounced in New and Old World monkeys, with the result that the granular layers are very reduced (Fig. 34.17B). In the baboon, GABA-glycine immunohistochemistry indicates that the number of granule cell–related inhibitory interneurons is reduced compared to nonprimate mammals. In apes (Fig. 34.17C) and humans, there are only vestigial clusters of granule cells near the surface of the dorsal and ventral nuclei. The reduction of this system in higher primates and its loss in the human cochlear nuclei must affect the information processing the human dorsal nucleus, but in a way that at present is difficult to assess.

In nonprimate mammals, large glycine-positive cells have been shown to project to the cochlear nuclei on the contralateral side of the brain stem (Wenthold, 1987), where their axons branch and distribute inhibitory terminals widely (Cant and Gaston, 1982). These anatomical findings agree with physiological evidence for inhibitory interactions between the cochlear nuclei. In an *in vitro* whole-brain study in guinea pigs, short-latency (3–9 ms) inhibitory potentials were recorded from most neurons after stimulation of the contralateral cochlear nerve (Babalian *et al.*, 1999). This widespread inhibition is presumably mediated by the glycinergic commissural axons. In the baboon, similar glycine-labeled neurons are found scattered throughout the central region of the ventral nucleus and occasionally in the overlying cap area (Fig. 34.18), and their thick glycine-positive axons leave the nuclei in the acoustic striae. In the human cochlear nuclei, giant cells are believed to be homologous to glycinergic commissural neurons in other species and, like those cells, should affect the balance of the level of activity in the cochlear nuclei on the two sides of the brain.

The human dorsal cochlear nucleus contains a number of small spindle-shaped neurons, less that 15 μm in diameter, oriented parallel to the nuclear surface (Fig. 34.13A). These small cells in man probably correspond to the glycine- and GABA-positive neurons in the central part of the dorsal nucleus of nonprimate mammals (Saint Marie *et al.*, 1991; Kolston *et al.*, 1992) and baboon (Moore *et al.*, 1995) (Fig. 34.18). They have been referred to as vertical cells, corn cells, or fan cells, and were designated tuberculoventral cells by Oertel

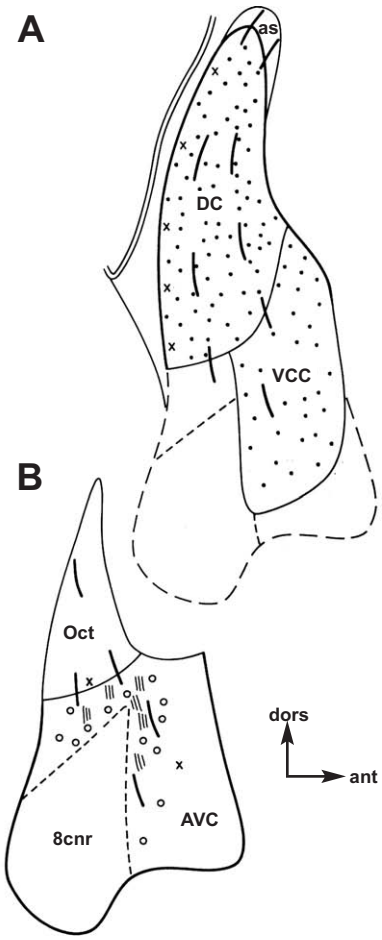

FIGURE 34.18 The distribution of GABA- and glycine-positive structures in the baboon cochlear nuclei is illustrated in schematic drawings of two sagittal sections. **(A)** In a more laterally located section, a few single-labeled GABA cells (**x**) are found around the margin of the dorsal nucleus. Neurons colocalizing GABA and glycine (✳) are numerous in the dorsal cochlear nucleus (DC) and the cap area (VCC). Solitary large-diameter glycine-positive commissural axons *(thick lines)* course obliquely upward toward the acoustic striae (as). **(B)** Large neurons in the central portion of the ventral cochlear nucleus (**o**) that are single labeled for glycine are the presumed origin of the commissural axons. Fascicles of double-labeled tuberculoventral axons *(thin lines)* run from the dorsal nucleus to the central portion of the ventral nucleus. Adapted from *Journal of Comparative Neurology* **369,** J.K. Moore, K.K. Osen, J. Storm-Mathisen, and O.P. Ottersen, figure 14, γ-aminobutyric acid and glycine in the baboon cochlear nuclei: an immunocytochemical colocalization study with reference to interspecies differences in inhibitory systems, pp. 497–519, 1996, with permission from Wiley-Liss, Inc., a subsidiary of John Wiley & Sons, Inc., New York.

and Wu (1989) because they form a very precise projection system from the dorsal nucleus (tuberculum acusticum) to the ventral nucleus. The projection is carried by small bundles of GABA- and glycine-positive axons passing into the central ventral nucleus, fascicles that are identical in size and location in the baboon to those observed in the cat and guinea pig. Tuberculoventral cells in the dorsal nucleus have been shown to project to bands of neurons in the ventral nucleus that are innervated by the same group of auditory nerve axons (Wickesberg and Oertel, 1988; Snyder and Leake, 1988). Thus, this system forms a frequency-specific feedback circuit to neurons in the ventral nucleus lying in the corresponding isofrequency plane.

As previously described, the cap area is a saddle-shaped region, extending over the top of the ventral nucleus and down its lateral and medial sides, and also abutting on the dorsal nucleus. In the baboon, as in mammals generally, the cap area is somewhat inconspicuous in normal histological sections but presents a uniformly dense distribution of labeled cells and synaptic terminals in GABA/glycine immunostaining (Fig. 34.18). These inhibitory terminals are not clustered into perisomatic arrays of the type that characterize the ventral nucleus but rather are more evenly scattered. This is in agreement with observations that many synaptic terminals in the cap area contain flattened or pleomorphic vesicles contacting dendritic shafts (Cant, 1993). At present, the only clue to the function of the cap area lies in its comparative anatomy. It is larger in carnivores than in rodents, is prominent in all primates, is strikingly large in the human cochlear nuclear complex, and constitutes a considerable fraction of the total volume of the cochlear nuclei in the porpoise (Osen and Jansen, 1965). Hypertrophy of the human cap area suggests an increasingly important role in information processing, but that role remains to be elucidated.

Superior Olivary Complex: Recreation of Auditory Space

Information processing in the auditory system differs in one respect from that in the visual or somatosensory systems in that locus of the stimulus is not directly coded in the peripheral receptor. Instead, the spatial dimension of sound stimuli must be recreated by the central auditory system. Behavioral studies in cats have implicated the superior olivary complex in this process. Cats with lesions above the level of the superior olivary complex, in the lateral lemniscus, inferior colliculus, medial geniculate body, or auditory cortex, are unable to locate a sound source in the spatial field contralateral to the lesion, whereas cats with lesions below the level of the olivary complex have more diffuse deficits (Casseday and Neff, 1975; Thompson and Masterton, 1978; Jenkins and Masterton,

1982). An analogous deficit has been observed in a human subject with an extensive midline pontine lesion that eliminated crossed input to the superior olivary complex on both sides (Griffiths *et al.*, 1997a). This patient had no difficulty in detecting frequency and amplitude modulation and no general deficit in detection of auditory temporal information, but was unable to determine by sound alone the location and direction of motion of objects in the environment, such as ringing telephones and passing trains. These human and animal studies suggest that the auditory spatial field is recreated in the brain stem by transformations occurring at the level of the superior olivary complex.

Medial and Lateral Olivary Nuclei

Ascending axons from the cochlear nuclei project to the superior olivary complex on both sides of the brain stem (Strominger, 1973; Strominger *et al.*, 1977). Cochlear nucleus axons innervate the lateral olivary nucleus on the same side of the brain stem, as well as the lateral neuropil of the medial olivary nucleus (Fig. 34.19). The axons then cross the midline in the trapezoid body and terminate on the medial neuropil of the contralateral medial nucleus. Because the configuration of the human medial and lateral olivary nuclei is similar to that of other primates (Figs. 10.10 and 10.11), their pattern of input is assumed to be similar. The projection to the medial and lateral olivary nuclei has been shown to be formed by axons of spherical bushy cells of the anteroventral cochlear nucleus (Warr, 1982; Smith *et al.*, 1993). Because spherical cells receive narrow band input and accurately preserve the pattern of activity in cochlear nerve axons, they are able to transmit precise information on stimulus parameters to the olivary nuclei.

The human medial olivary nucleus is a laminar structure, with long primary dendrites extending medially and laterally from a central column of cell bodies into the surrounding area of fine-fiber neuropil (Fig, 34.20A, B). As indicated in Figure 34.19, the laterally directed dendrites are innervated by the ipsilateral ventral cochlear nucleus and the medially directed dendrites by the nucleus on the contralateral side. The bilateral innervation of the medial nucleus allows its neurons to create a map of interaural time differences along the rostrocaudal axis of the nucleus (Yin and Chan, 1990). In both its input and its physiology, the medial nucleus is biased toward low-frequency information. Spherical cell axons representing the 1.2- to 5-kHz region of the ventral cochlear nucleus innervate most of the length of the medial nucleus (Warr, 1982). Physiologically, most medial nucleus neurons have best frequencies of less than 3–4 kHz (Galambos *et al.*, 1959; Goldberg and Brown, 1968; Guinan *et al.*, 1972).

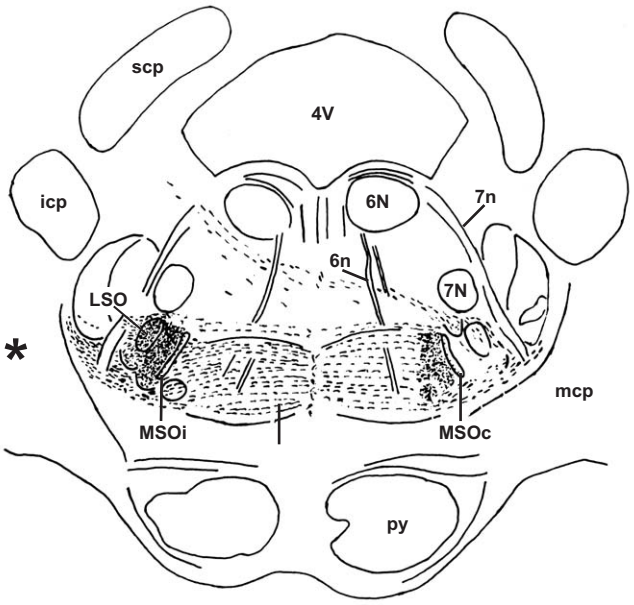

FIGURE 34.19 The pattern of projection by the cochlear nucleus axons into the superior olivary complex is shown by degenerating axons in the brain stem of the chimpanzee after a large lesion of the cochlear nuclei (lesion side indicated by asterisk). Axons run to the lateral olivary nucleus (LSO) ipsilaterally and to the neuropil on the facing side of the medial olivary nucleus, both ipsilaterally (MSOi) and contralaterally (MSOc). Icp, inferior cerebellar peduncle; py, pyramidal tract; scp, superior cerbellar peduncle; tz, trapezoid body; 4V, fourth ventricle; 6N, abducens nucleus, 6n, abducens nerve; 7N, facial nucleus; 7n, facial nerve. Adapted from *Journal of Comparative Neurology* **172,** N.L. Strominger, L.R. Nelson, and W.J. Dougherty, figure 4, Second order auditory pathways in the chmpanzee, pp. 349–365, 1977, with permission from Wiley-Liss Inc., a subsidiary of John Wiley & Sons, Inc., New York.

Because large head size increases the range of frequencies that can be utilized for interaural phase difference cues, our relatively large head size and low-frequency hearing range may account for the prominence of the human medial nucleus.

The human lateral olivary nucleus is a compact rounded nucleus (Fig. 34.20A, B), and thus differs from that of carnivores and rodents in which it is a prominent S- or U-shaped structure. As in other species, the human lateral nucleus is composed of neurons whose short dendrites are confined to the body of the nucleus. Recordings in the lateral olivary nucleus of the cat demonstrate an orderly representation of best frequencies, with low tones represented in the lateral limb of the nucleus and high tones in its medial limb (Guinan *et al.*, 1972). The best frequencies span the cat's entire auditory range, with much of the nucleus devoted to frequencies in the 10- to 40-kHz range. Because of its emphasis on higher frequencies, the lateral olivary

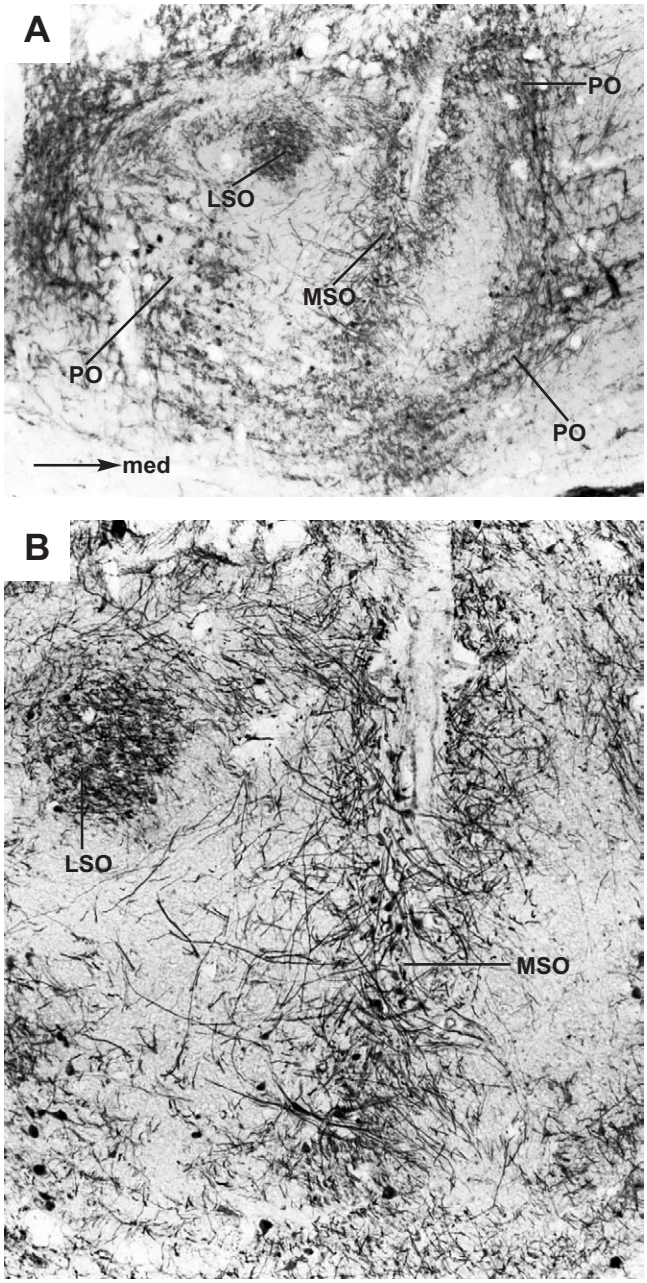

FIGURE 34.20 Morphology of the human superior olivary complex. **(A)** The lateral olivary nucleus (LSO) and medial olivary nucleus (MSO) are surrounded by a ring of periolivary neurons (PO). **(B)** In a higher power view of the same section, the cells of the medial olivary nucleus are seen to have elongated dendrites extending medially and laterally into the surrounding neuropil. Dendrites of neurons in the lateral olivary nucleus are short and confined to the body of the nucleus. Celloidin section, MAP2 immunostaining.

nucleus is extremely large in echolocating mammals with extended high-frequency hearing, such as bats and porpoises (Zvorykin, 1964; Irving and Harrison, 1967; Zook and Casseday, 1982). It is possible that the lateral olivary nucleus is small in humans because our range of usable frequencies is, by general mammalian standards, limited to low frequencies.

In most mammals, the superior olivary complex includes a prominent nucleus of the trapezoid body, a group of darkly staining oval cells lying among the fibers of the trapezoid body on the ventromedial aspect of the complex. The trapezoid nucleus is clearly identifiable in prosimian primates and monkeys, but is very indistinct in apes and is vestigial in the human olivary complex, consisting only of a few scattered, pale oval cells (Moore and Moore, 1971; Moore, 2000). The trapezoid nucleus of the cat has been shown to form a projection to the lateral olivary nucleus that is glycinergic and therefore inhibitory (Glendenning *et al.*, 1985; Bledsoe *et al.*, 1990), but the low-frequency end of the lateral nucleus receives less dense glycinergic input. It is possible that the human lateral olivary nucleus is equivalent to the low-frequency end of the mammalian lateral olivary nucleus and hence receives only a restricted inhibitory innervation. Little attention has been paid to the fact that the trapezoid nucleus also provides inhibitory input to medial nucleus neurons (Smith *et al.*, 1998). These findings suggest that the extreme reduction of the human nucleus of the trapezoid body affects the mechanism of information processing in both the medial and lateral olivary nuclei.

Periolivary Cell Groups

In the immunostained human olivary complex, the medial and lateral nuclei are seen to be surrounded by a capsule of dendrites of periolivary neurons (Fig. 34.20A). Periolivary cells, as their name implies, lie at the outer margin of the olivary complex, surrounding the main nuclei. In nonhuman species, periolivary cells are clustered into a number of distinct nuclei. In humans, they tend to be concentrated into medial, ventral, and lateral periolivary cell groups (Moore *et al.*, 1999) (Figs. 10.10–10.12). Human periolivary cells also form a rostral periolivary nucleus, a slender column of cells extending forward from the main part of the olivary complex through the pons (Figs. 34.1, 10.12–10.16). Along its length, ascending auditory axons lie ventral and lateral to the cell column. Periolivary neurons receive ascending input from multipolar cells of the ventral cochlear nucleus (Friauf and Ostwald, 1988; Thompson and Thompson, 1991), but their major connections are descending and will be discussed in "The Descending Auditory System".

Upper Brain Stem: Integration of Ascending Pathways

As ascending axons from the cochlear nuclei run past the olivary complex, they are joined by axons from the main olivary nuclei and periolivary cell groups. The total assembly of ascending axons constitutes the lateral lemniscus (Figs. 12.12–12.21). Anterograde projection studies in the monkey (Strominger and Strominger, 1971; Strominger, 1973) and the chimpanzee (Strominger *et al.*, 1977) demonstrate the primate pattern of termination of lemniscal axons in the nuclei of the lateral lemniscus and in the inferior colliculus (Fig. 34.21).

Lemniscal Nuclei

In most mammalian species, the lemniscus contains sizable ventral and intermediate lemniscal nuclei. These two nuclei are prominent in the cat (Moore, 1987) and are extremely large in mammals, such as the porpoise and bat that utilize ultrahigh frequencies (Zvorykin, 1964; Zook and Casseday, 1982; Covey and Casseday, 1991). However, they are indistinct in New World monkeys and difficult to define in apes (J. K. Moore, unpublished observations). In the human brain stem, sparse areas of neuropil in the lemniscus contain scattered cell clusters that appear to be vestiges of the ventral and intermediate nuclei (Figs. 12.17 and 12.18). The comparative development of the lower lemniscal nuclei across mammals suggests that their reduction in the human brain stem, like that of the lateral olivary nucleus, is related to our low-frequency range of hearing.

In contrast, the human dorsal lemniscal nucleus is a well-developed cell group, consisting of clusters of neurons lying in an island of neuropil in the upper lateral lemniscus (Geniec and Morest, 1971; Moore, 1987) (Figs. 34.22 and 10.18). Its axons form the dorsal commissure of the lateral lemniscus, a pathway that can be identified in human material stained for myelin (Moore, 1987) or immunostained for axonal neurofilaments (Moore *et al.*, 1997). Neurons of the dorsal lemniscal nucleus project to the inferior colliculus on the same side, and through the dorsal commissure to the dorsal lemniscal nucleus and inferior colliculus on the opposite side of the brain stem (Kudo, 1981). The dorsal nucleus has been shown to consist largely of neurons that are immunopositive for GABA (Adams and Mugnaini, 1984; Saint Marie *et al.*, 1997). Thus, its commissure forms a symmetrical and reciprocal inhibitory projection. Due to its inhibitory nature, the dorsal lemniscal nucleus is presumed to play a role in the balance of ipsilateral and contralateral activity in the inferior colliculus. Because afferent input to the dorsal nucleus comes mainly from the medial and lateral superior olivary nuclei (Glendenning *et al.*, 1981; Yang *et al.*, 1996), this balance may integrate activity reflecting the spatial location of sound stimuli.

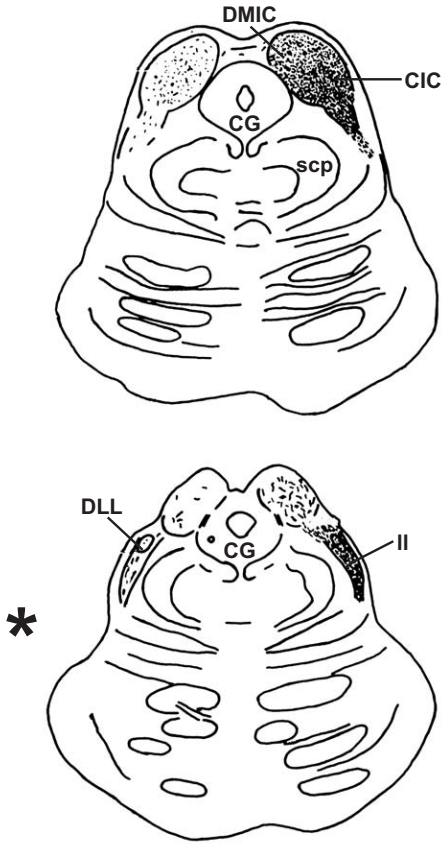

FIGURE 34.21 Projection pattern of the lateral lemniscus of the chimpanzee. After large lesions of the cochlear nuclei (lesion side indicated by asterisk), degenerating axons fill the contralateral lateral lemniscus (ll) and terminate heavily in the dorsal nucleus of the lateral lemniscus (DLL). Within the inferior colliculus contralateral to the lesion, there is dense terminal degeneration in the central nucleus (CIC) and somewhat less dense degeneration in the dorsomedial area (DMIC). Much lighter degeneration is seen in the side ipsilateral to the lesion. CG, central gray; scp, superior cerebellar peduncle. Adapted from *Journal of Comparative Neurology* **172,** N.L. Strominger, L.R. Nelson, and W.J. Dougherty, figure 3, Second order auditory pathways in the chmpanzee, pp. 349–365, 1977, with permission from Wiley-Liss Inc., a subsidiary of John Wiley & Sons, Inc., New York.

The Inferior Colliculus

The inferior colliculus consists of several subdivisions (Figs. 34.23A, 10.20, and 10.21), but the region of densest termination of lemniscal axons is the cup-shaped central nucleus. Retrograde labeling studies in nonprimate species (e.g., Adams, 1979; Brunso-Bechtold *et al.*, 1983) have demonstrated that the central nucleus

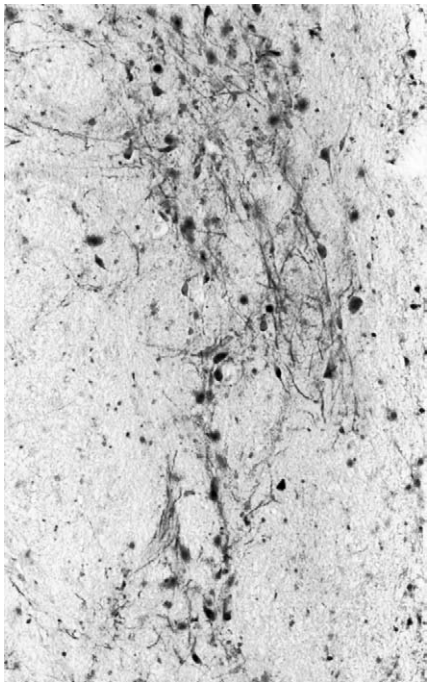

FIGURE 34.22 The human dorsal nucleus of the lateral lemniscus consists of patches of cells lying in an island of neuropil at the rostral end of the lateral lemniscus. Celloidin section, MAP2 immunostaining.

of the colliculus receives input from all of the lower brain stem auditory centers. A direct projection comes from the contralateral cochlear nuclei, originating in multipolar cells of the ventral cochlear nucleus and fusiform cells of the dorsal cochlear nucleus. The projection originating from the ipsilateral medial olivary nucleus is a major source of afferents to the low-frequency region of the central nucleus. Broader spectrum input comes from the lateral olivary nucleus on both sides of the brain stem. The periolivary projection arises mainly from the ipsilateral ventral periolivary region, but other periolivary cell groups on both sides of the brain stem also contribute. Finally, as just discussed, there is a projection from both the ipsilateral and contralateral dorsal lemniscal nuclei, with the contralateral projection coming though the dorsal commissure of the lateral lemniscus.

As axons enter the central nucleus, they form bands running from ventrolateral to dorsomedial. These axonal bands run parallel to cellular planes formed by neurons with flattened, disk-shaped dendritic fields (Fig. 34.23A). The laminar cytoarchitecture formed by alternating bands of axons and flattened cells characterizes the human central nucleus (Geniec and Morest, 1971) and that of the squirrel monkey (FitzPatrick, 1975), as well as most nonprimate mammals. Studies of evoked

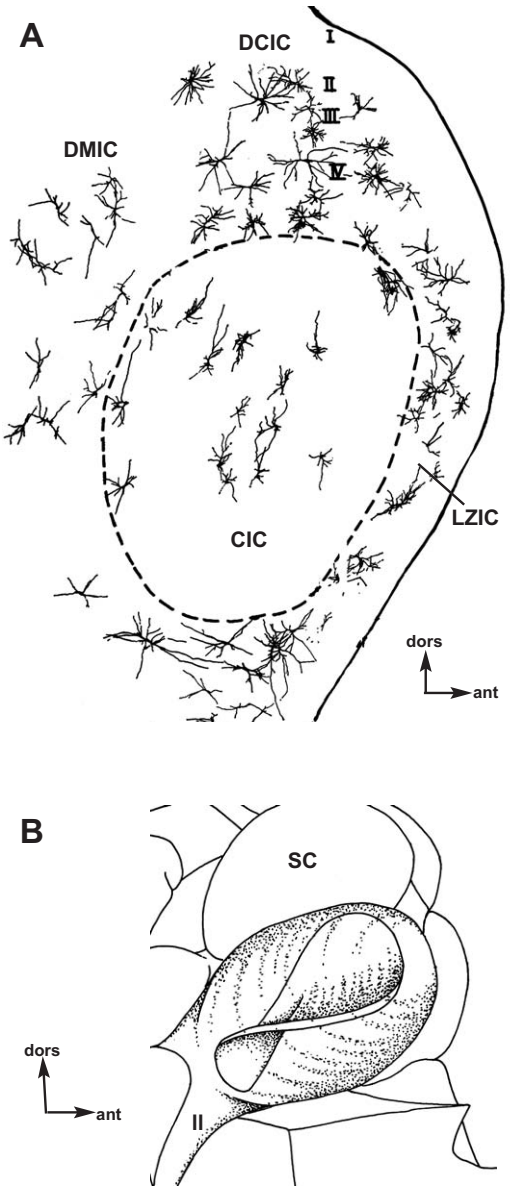

FIGURE 34.23 **(A)** Transaxial section through the human inferior colliculus. Golgi-impregnated neurons show distinct patterns in different subdivisions, i.e., the central nucleus (CIC), dorsomedial region (DMIC), dorsocaudal cortex (DCIC), and lateral zone (LZIC). Adapted from *Acta Otolaryngologica,* Suppl. **295,** P. Geniec and D.K. Morest, figure 7, The neuronal architecture of the human posterior colliculus. A study with the Golgi method, pp. 1–33, 1971, with permission from Taylor & Francis Inc., Philadelphia. **(B)** Orientation of a single isofrequency plane within the central nucleus of the inferior colliculus of the squirrel monkey. ll, lateral lemniscus; SC, superior colliculus. Adapted from *Journal of Comparative Neurology* **164,** K.A. Fitzpatrick, figure 10, Cellular architecture and topographic organization of the inferior colliculus of the squirrel monkey, pp. 185–208, 1975, with permission from Wiley-Liss, Inc., a subsidiary of John Wiley & Sons, Inc., New York.

activity and 2-deoxyglucose labeling in primates have shown that the laminae represent frequency-specific planes of the central nucleus (FitzPatrick, 1975; Webster *et al.*, 1984; Garey and Webster, 1989). The tonotopic planes are curved and tipped at about 20–30° from the horizontal (Fig. 34.23B), with a regular progression of best frequencies from low dorsally to high ventrally.

In addition to tonotopy, collicular processing includes information on the time parameters of neuronal activity and on the spatial localization of stimulus sources. Recordings in the cat show that neurons in the central nucleus respond to simulations of natural combinations of interaural time and intensity differences and to spectral cues indicating location of a sound source (Delgutte *et al.*, 1999). Most cells are sensitive to stimulus location along the horizontal azimuth, and about half of the neurons tested are sensitive to elevation. Overall, it seems safe to assume that multiple parameters of auditory stimuli, including frequency spectrum, loudness, time patterning, and spatial location, are correlated within the central nucleus to produce an integrated neural representation of the stimulus. Integrated information from the central nucleus is then passed on to the forebrain by axons running laterally across the nucleus to the lateral zone of the colliculus (Fig. 34.23A). Within the lateral zone, the axons coalesce to form the brachium of the inferior colliculus. Brachial axons then continue forward on the surface of the brain stem, lateral to the superior colliculus (Figs. 10.21 and 10.22).

The dorsomedial subdivision of the inferior colliculus (Fig. 34.23A) is distinguished from the central nucleus by the greater packing density of its cells and by its lack of laminar organization, both in humans (Geniec and Morest, 1971) and in squirrel monkeys (FitzPatrick, 1975). It receives somewhat lighter lemniscal input than the central nucleus and the terminals are diffusely distributed rather than forming bands. The dorsomedial area gives rise to the commissure of the inferior colliculus (Figs. 10.20 and 10.21), through which axons project to the opposite inferior colliculus and to the contralateral forebrain. The origin of the commissure is demonstrated by the increasing density of degenerating axons in primates with lesions invading the dorsomedial area (Moore *et al.*, 1977). In humans, the collicular commissure is a prominent structure that is clearly visible in myelin-stained material (Moore, 1987) and in material immunostained for axonal neurofilaments (Moore *et al.*, 1997).

Lemniscal input is very sparse into the pericentral zone of the colliculus, i.e., the portion of the colliculus outside of the central nucleus and dorsomedial region. The dorsal and caudal part of the pericentral zone is known as the dorsocaudal cortex (Figs. 10.19–10.21). Because this area is primarily a relay in the descending auditory pathway, it is discussed in "The Descending Auditory System". The rostral and ventral portion of the pericentral zone is termed the external cortex (Figs. 10.19–10.22). This region is also called the intercollicular area because it forms a bridge, anatomically and functionally, between the inferior and superior colliculi. Few or no lemniscal axons terminate in this area, but it receives auditory input from the central nucleus of the inferior colliculus and from both dorsal lemniscal nuclei (Coleman and Clerici, 1987; Olazábal and Moore, 1989). In addition, this area receives retinal input via the optic tract (Itaya and van Hoesen, 1982) and somatosensory input from the spinal trigeminal nucleus and the dorsal column nuclei (Wiberg *et al.*, 1987) (Fig. 34.24). Electrophysiological studies of the external cortex show that many cells are influenced by both auditory and somatosensory stimuli, and most have relatively nonspecific response fields, reflecting broad frequency ranges and large areas of the body (Aitkin *et al.*, 1981). The multisensory input and lack of precise tonotopic or somatotopic mapping within this region have led to the idea that it plays a role in spatial mapping of sound relative to body position. An organized map of auditory space has been demonstrated here (Binns *et al.*, 1992), and lesions in this area cause deficits in the ability to orient to sound (Thompson and Masterton, 1978). Neurons in the external cortex project to the deep layers of the superior colliculus (Edwards *et al.*, 1979; Olazábal and Moore, 1989), an area that projects in turn to the motor nuclei controlling head and eye turning. Thus, the external cortex of the inferior colliculus is the beginning of the process of integration of auditory input with visual and somatosensory information, leading to creation of a spatial map and, ultimately, direction of head and eye position by that map.

Brain Stem Topography: Generation of Evoked Potentials

As discussed in "The Cochlea: Generation of Evoked Activity," waves I and II of the auditory brain stem response are believed to be generated peripherally, by the auditory nerve. The subsequent waves III, IV, V, and VI are generated within the brain stem. The human brain stem auditory pathway is composed of essentially the same nuclear groups as that of other mammals, but because of the much larger size of the human brain stem, these auditory centers are spread across a considerably longer pathway. An estimate of the length of the human brain stem auditory pathway was obtained by computer reconstruction, based on

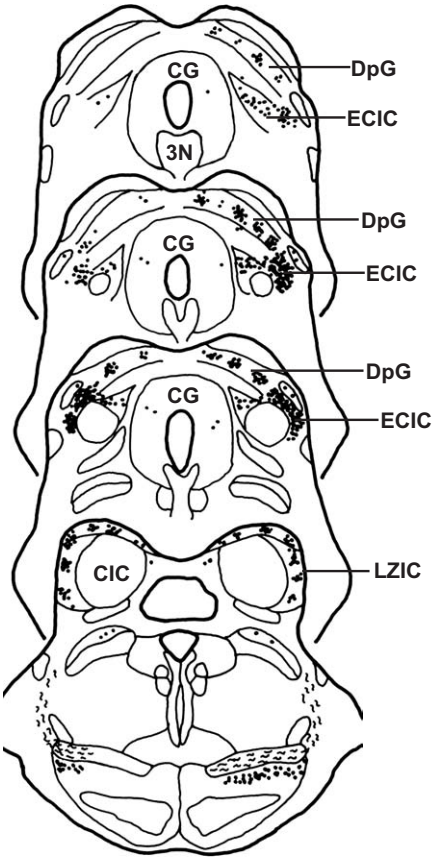

FIGURE 34.24 Projections into the tectum of the macaque monkey following injection of the dorsal column nuclei. Labeled terminals are absent from the central nucleus of the inferior colliculus (CIC), but are present in the lateral zone (LZIC), external cortex (ECIC) and deep gray layers of the superior colliculus (DpG). CG, central gray; 3N, oculomotor nuclei. Adapted from *Journal of Comparative Neurology* **264,** M. Wiberg, J. Westman, and A. Blomqvist, figure 10, Somatosensory projection to the mesencephalon: an anatomical study in the monkey, pp. 92–117, 1987, with permission from Wiley-Liss, Inc., a subsidiary of John Wiley & Sons, Inc., New York.

point-to-point measurements from digitized sections (Moore *et al*., 1996b). In humans, the distance that the axon of a neuron in the ventral cochlear nucleus travels to reach the ipsilateral medial superior olivary nucleus is approximately 10 mm (1 cm); to reach the contralateral medial superior olivary nucleus is 25 mm (2.5 cm); to reach the upper level of the contralateral lateral lemniscus is 40 mm (4 cm); and to reach the center of the contralateral inferior colliculus is 45 mm (4.5 cm). In the cat, by comparison, the total distance from the center of the cochlear nuclei to the center of the contralateral inferior colliculus is 18–20 mm.

Because of the differential length of the human and mammalian brain stem pathways, animal studies of ABSR wave generators have limited applicability. Instead, information has been gained from intrasurgical recordings made from the surface of the human brain stem. Electrodes placed over the cochlear nuclei record a wave, attributed to the firing of axons exiting the cochlear nuclear complex, that coincides with wave III of the scalp record (Moller and Janetta, 1982). In addition, human dipole studies concluded that wave III is generated by a volley of action potentials in axons emerging from the cochlear nuclei in the ventral acoustic stria (Scherg and von Cramon, 1985). Other evidence indicates that waves IV and V are generated further rostrally in the brain stem. When electrodes are placed on the pons during intrasurgical recording, potentials are recorded that correspond to scalp-recorded waves IV and V (Hashimoto *et al*., 1981; Moller and Jannetta, 1982). The same studies attribute the broad negative potential following the IV/V complex to depolarization of inferior colliculus neurons. In the computer reconstruction study that derived length of the human auditory pathway, that length was correlated with the latencies of waves IV and V to derive axonal conduction velocity (Moore *et al*., 1996b). The most reasonable conduction velocity, one closely matching that of the known conduction velocity of eighth nerve axons, was obtained by assuming that waves IV and V were generated at the level of the superior olivary complex contralateral to the stimulated ear, presumably by the bend in the axonal pathway occurring at that point.

The idea that waves IV and V are generated at the level of the superior olivary complex is supported by studies of the binaural interaction component of the auditory brain stem response. The binaural interaction component is obtained by subtracting the response to a binaural stimulus from the algebraic sum of the right and left ear monaural responses to the same stimulus. The reduction in total activity in the interaction component is presumed to reflect the fact that the binaural response involves convergence of activity from the right and left ears on some subset of brain stem auditory neurons. In recording responses to monaural and binaural clicks with a variety of interaural time and intensity differences, the binaural interaction component was localized to the pons (Polykov and Pratt, 1996). In further studies, six patients with small vascular lesions in the trapezoid body were shown to have absent or abnormal dipole orientation of the binaural interaction component occurring at the time of waves IV and V, whereas lesions in the rostral lateral lemniscus caused abnormalities in a dipole occurring later, at the time of wave VI (Pratt *et al*., 1998). These findings support the idea that waves IV and V are generated at the level of the superior olivary complex and wave VI higher in the brain stem.

THE FOREBRAIN AUDITORY SYSTEM

Auditory Thalamus: Information Relay

Auditory information reaching the forebrain originates primarily in the central nucleus of the inferior colliculus and is relayed through its brachium (Figs. 10.21–10.24). A similar pattern of degenerating axons is seen after lesions of the inferior colliculus in the loris, marmoset, squirrel monkey, macaque, and gibbon (Moore and Goldberg, 1966; Moore *et al.*, 1977) (Fig. 34.25). In all of these primate species, brachial axons distribute a small number of terminals to neurons in the adjacent parabrachial region and to cells interstitial to the brachium, but the majority of the axons continue forward on the surface of the brain stem. At the level of the superior colliculus, the medial geniculate forms a prominent tubercle on the surface of the midbrain. Further rostrally, the medial geniculate is bounded laterally, first by the inferior division of the pulvinar and then by the lateral geniculate nucleus (Figs. 10.23–10.25). Brachial axons bypass the caudal tip of the medial geniculate, but further rostrally they form a dense meshwork of pericellular terminals. In addition to the axons ascending in the brachium ipsilaterally, a number of fibers cross in the commissure of the inferior colliculus and ascend in the contralateral brachium to terminate in the medial geniculate on the opposite side. The contralateral projection is identical to that on the ipsilateral side but lighter and is heaviest if the lesion invades the dorsomedial division of the colliculus.

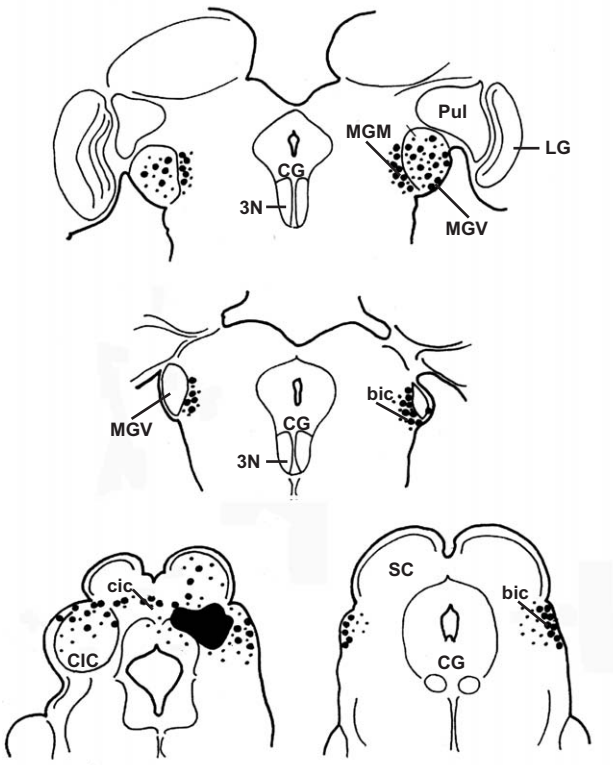

FIGURE 34.25 A lesion *(shaded black)* in the inferior colliculus in the squirrel monkey results in degenerating axons ascending in the brachium of the inferior colliculus (bic) bilaterally. Large dots represent degenerating axons and small dots indicate terminal degeneration. On the side ipsilateral to the lesion, degenerating axons bypass the caudal tip of the medial geniculate and end densely in its ventral division (MGV). More scattered fibers and terminals end in the medial division of the geniculate (MGM). The pattern of degeneration on the side contralateral to the lesion is similar but lighter. No degenerating axons are present within the pulvinar complex (Pul). CG, central gray; LG, lateral geniculate; SC, superior colliculus; 3N, oculomotor nucleus. Adapted from *Brain, Behavior and Evolution*, **14,** J.K. Moore, F. Karapas, and R.Y. Moore, figure 2, Projections of the inferior colliculus in insectivores and primates, pp. 301–327, 1977, with permission from S. Karger AG, Basel.

The cytoarchitecture of the medial geniculate has been described in lorisoid prosimians (Kanagasuntheram *et al.*, 1968), ceboid monkeys (FitzPatrich and Imig, 1978), cercopithecoid monkeys (Walker, 1937), apes (Walker and Fulton, 1938), and humans (Winer, 1984). Its largest subdivision, and the principal target of brachial axons, is the ventral nucleus, also known as the principal or parvocellular nucleus. This subdivision of the geniculate is a compact group of small to medium-sized ovoid neurons that are densely packed and aggregated in clusters. The ventral nucleus is very similar in apes and humans in absolute number of neurons (Armstrong, 1979), indicating that it is a stable and conservative part of the thalamus. In all primate species, there is some indication of an orientation of the cells in rows parallel to the entering brachial fibers. This tendency is most pronounced in the gibbon, in which infolding of the cell laminae gives the nucleus a distinctly convoluted appearance. In the human medial geniculate as well, a laminar cytoarchitecture is formed by planes of cells with bushy dendrites and fascicles of brachial axons running parallel to the dendritic planes (Winer, 1984). The dense input from the auditory brain stem to the ventral nucleus is reflected in the responses of these neurons to auditory stimuli. Electrophysiological studies in the squirrel monkey show responses to clicks, tone bursts, and noise bursts from almost all of the cells in the ventral nucleus (Symmes *et al.*, 1980). Though most neurons respond to species vocalizations, there is little selectivity to different calls.

Other subdivisions of the medial geniculate receive much less dense input from the brain stem. There is light terminal degeneration in the medial nucleus of the geniculate, also known as the magnocellular or

internal nucleus. In primates, as in other mammals, the medial nucleus of the geniculate lies medial and rostral to the ventral nucleus, but the nucleus is smaller in primates than in carnivores. Its cells are more dispersed than those in the ventral nucleus, and it exhibits the greatest range in cell size from large to small of any subdivision of the geniculate. A dorsal nucleus of the medial geniculate has also been described in monkeys and apes. Like the medial nucleus, it receives sparser input from the inferior brachium than does the ventral nucleus. In primates, no brachial axons have been traced into the pulvinar complex of the thalamus or into other thalamic areas surrounding the medial geniculate.

Auditory Cortex: Sequential Levels of Processing

Organization of Auditory Cortex

The classical area of human auditory cortex is located within the superior temporal lobe. This region is portrayed in the *Atlas of the Human Brain* (Mai *et al.*, 1997) in both diagrams (Figures 17–34) and photographs (Figures 53–65). A human brain from which the parietal lobe has been removed (Fig. 34.26A) allows a view of the superior temporal plane, i.e., the superior surface of the temporal lobe that is normally hidden within the lateral fissure. The transverse temporal gyrus (Heschl's gyrus) crosses the plane at an angle from caudomedial to rostrolateral. The transverse gyrus is often partially duplicated into a double, or occasionally triple, convexity (Leonard *et al.*, 1998). In this brain, the gyrus is bifid at its lateral end. A lateral view of the temporal lobe (Fig. 34.26B) illustrates the superior and middle temporal gyri, separated by the superior temporal sulcus. Though human auditory cortex has generally been considered to be limited to the superior temporal gyrus, functional studies reveal that auditory activation often extends into the middle temporal gyrus and into ventral portions of the parietal lobe.

The cytoarchitecture of human auditory cortex has been described by Brodmann (1908), von Economo (1929), and Galaburda and Sanides (1980). The primary auditory cortex (koniocortex or granular cortex) is identified as an area approximately 1 inch square on the medial end of the transverse temporal gyrus. It was designated area 41 by Brodmann, TC by von Economo, and KAm and KAlt (medial and lateral auditory koniocortex) by Galaburda and Sanides. In the latter classification, KAm is the most medial and the most granular area, while KAlt is located relatively more lateral and is less granular. As in all primary

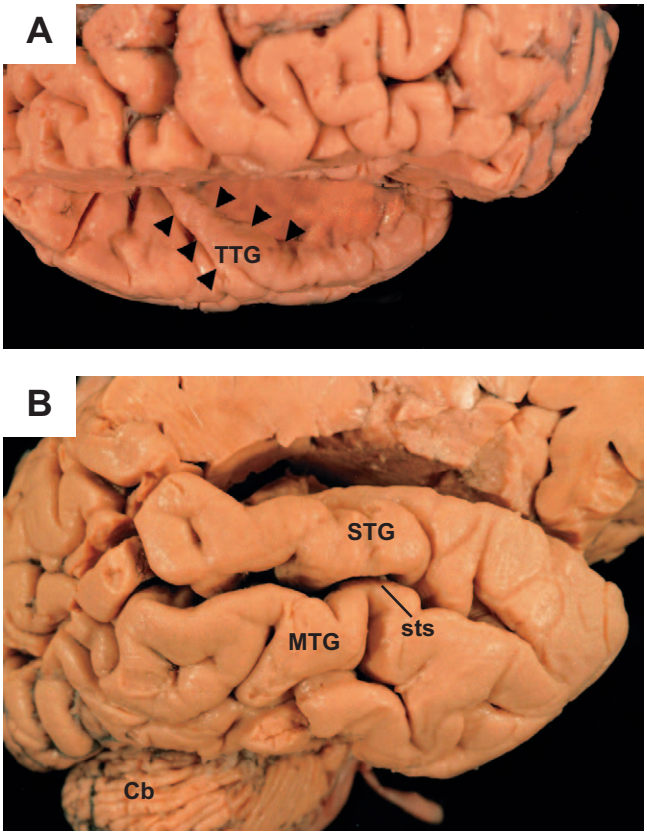

FIGURE 34.26 Photographs of the surface of the human temporal lobe. **(A)** Partial removal of the parietal operculum and frontal lobe provides a view of the superior temporal plane, including the transverse temporal gyrus (TTG, demarcated by arrowheads). **(B)** A side view of the temporal lobe illustrates the superior temporal gyrus (STG) and middle temporal gyrus (MTG), separated by the superior temporal sulcus (sts). Cb, cerebellum.

sensory areas, cell packing density is high in layers II-IV, while layers V and VI are thin and parvocellular. Layer IV is prominent, and the cells in layers II-IV form fine columns ("rain shower" formation) (Fig. 27.25a). There is considerable variability in size of the koniocortex, and its extent does not coincide with gyral and sulcal anatomy (Galaburda and Sanides, 1980; Rademacher *et al.*, 2001a). The absolute size of this area varies across individuals and between the right and left sides of the same individual, with areal values as high as 1840 mm^2 and as low as 860 mm^2 given by Galaburda and Sanides. A study comparing the size of auditory koniocortex in males and females found it to be consistently larger bilaterally in women (Rademacher *et al.*, 2001b).

Human auditory koniocortex (area 41/TC/KA) is homologous to the core area of auditory cortex identified in monkeys. The simian core area, usually called KA or A1, is located in the center of the superior

temporal plane (Merzenich and Brugge, 1973; Pandya and Sanides, 1973; Galaburda and Pandya, 1983; Luethke *et al.*, 1989). In addition to KA/A1, some studies identify primary areas termed R (rostral; Imig *et al.*, 1977; Morel *et al.*, 1993) and RT (rostrotemporal; Morel and Kaas, 1992; Hackett *et al.*, 1998a). The monkey core area can be identified by its high levels of acetylcholinesterase and cytochrome oxidase (Morel and Kaas, 1992; Morel *et al.*, 1993; Jones *et al.*, 1995; Hackett *et al.*, 1998a), features that also characterize human auditory koniocortex (Rivier and Clarke, 1997; Hackett *et al.*, 2001). The cellular density of layers III and IV in monkey core cortex, as well as its dense array of myelinated fibers, reflects the heavy input to the core area from the medial geniculate. In marmosets and monkeys, most neurons in the ventral division of the medial geniculate project to core cortex (Mensulam and Pandya, 1973; Burton and Jones, 1976; Aitkin *et al.*, 1988; Luethke *et al.*, 1989; Rauschecker *et al.*, 1997). The afferents from the ventral medial geniculate terminate in layers IV and lower III in regular patches of higher density label, separated by areas of less dense label (Pandya and Rosene, 1993; Hashikawa *et al.*, 1995). In contrast, the medial and dorsal divisions of the medial geniculate project to the core area diffusely, with axons from the medial nucleus becoming tangential fibers in layer I.

It seems likely that human primary auditory cortex also receives dense thalamic input, and that this input accounts for the cochleotopic organization shown in this area by functional imaging, including magnetoencephalography (Elberling *et al.*, 1982), positron emission tomography (Lauter *et al.*, 1985) and functional magnetic resonance imaging (Wessinger *et al.*, 1997). In the human transverse temporal gyrus, activation for high-frequency tones is located more posteriorly and medially than that for low-frequency tones (Fig. 34.27). This sequence of activation is often referred to as tonotopic, and many mapping studies have utilized pure tone stimuli. However, work with complex stimuli indicates that the organization in human cortex reflects, not stimulus frequency, but rather perceived pitch, including virtual pitch that is not actually present in the physical spectrum of the stimulus (Pantev *et al.*, 1989).

Human auditory koniocortex is surrounded rostrally, laterally and posteriorly by an area of parakoniocortex. This region covers the lateral portion of the transverse temporal gyrus, and extends anteriorly and posteriorly onto the superior temporal plane. In parakoniocortex, layer IV is thin and layers V and VI are somewhat thicker than in the koniocortex. Layer III is very well developed and is characterized by columns of small pyramidal cells ("organ-pipe" formation) (Fig. 27.25b).

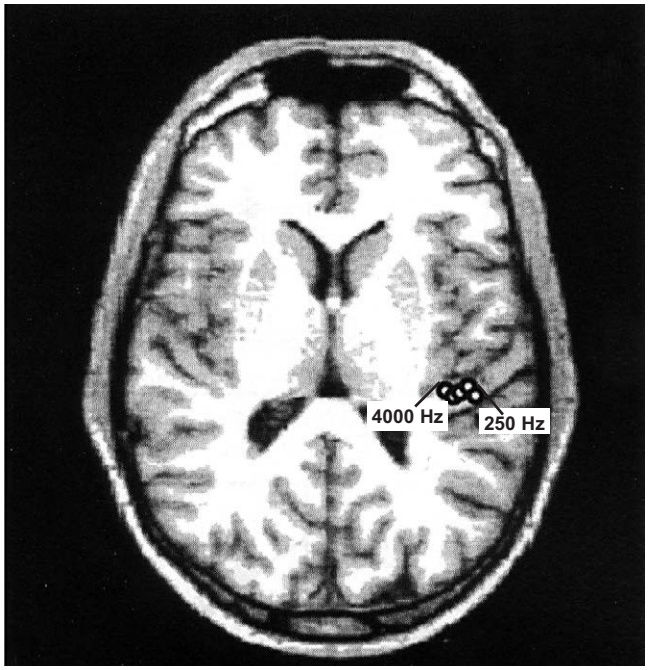

FIGURE 34.27 Tonotopic organization of human primary auditory cortex, as shown by magnetoencephalography. A view in the axial plane illustrates an area of demonstrated tonotopy at the medial end of the transverse temporal gyrus. Responses to high tones (4000 Hz) are represented medially and those to low tones (250 Hz) are located more laterally. Adapted from *Hearing Research* **101,** C. Pantev, L.E. Roberts, T. Elbert, B. Ross, and C. Wienbruch, figure 5, Tonotopic organization of the sources of human auditory steady-state responses, pp. 62–74, 1996, with permission from Elsevier Science, Oxford.

The parakoniocortex has been called area 42 by Brodmann and TB by von Economo. It was subdivided by Galaburda and Sanides into three regions: (1) a rostral area, PaAr (rostral auditory parakoniocortex) on the anterior aspect of the superior temporal plane; (2) a lateral area, PaAi (internal auditory parakoniocortex) that lies lateral to koniocortex and extends a short distance onto the superficial aspect of the superior temporal gyrus; and (3) a caudal area, PaAc (caudal auditory parakoniocortex) that covers the caudal portion of the superior temporal plane and extends around the insula to the parietal operculum (Fig. 27.26). The parakoniocortex is surrounded, in turn, by an extensive area of auditory cortex that covers the remainder of the superior temporal plane and the lateral surface of the superior temporal gyrus, with the exception of its rostral pole. This region was designated area 22 by Brodmann, TA by von Economo, and PaAe (external auditory parakoniocortex) by Galaburda and Sanides. Its cytoarchitecture is characterized by very well developed layers III and V, and by

column formation that extends from layer II through layer V.

Auditory cortical areas peripheral to the core cortex have also been identified in other species of primates. Anatomical and physiological studies define a belt area surrounding the core medially, rostrally, laterally and caudally (Pandya and Sanides, 1973; Imig *et al.*, 1977; Galaburda and Pandya, 1983; Morel and Kaas, 1992; Morel *et al.*, 1993; Hackett *et al.*, 1998a). The area rostral and lateral to the belt, on the anterior superior temporal plane and lateral surface of the superior temporal gyrus, has been called Ts2 and Ts3 (Pandya and Sanides, 1973) and more recently, parabelt (Morel *et al.*, 1993; Hackett *et al.*, 1998a). Both belt and parabelt cortex differ significantly from the core area in their pattern of thalamic input. Tracer injections into the macaque belt area label cells only in the medial and dorsal divisions of the medial geniculate (Rauschecker *et al.*, 1997). Thalamic input into the parabelt cortex also comes only from the dorsal and medial nuclei of the medial geniculate, and in addition, from the medial division of the pulvinar (Trojanowski and Jacobsen, 1975; Burton and Jones, 1976; Hackett *et al.*, 1998b; Fig. 34.45). Ablation of the core area of macaque auditory cortex eliminates responses to auditory stimuli in the adjacent belt region (Rauschecker *et al.*, 1997), which suggests that input from the medial and dorsal geniculate nuclei is not sufficient to support auditory processing in the absence of direct projections from the ventral medial geniculate. Instead, information processing in the secondary auditory cortical areas appears to depend on transcortical projections that pass successively from core to belt to parabelt cortex. Short association projections from the core to the belt have been demonstrated by older degeneration studies (Jones and Powell, 1970; Forbes and Moskowitz, 1977; Selzer and Pandya, 1978) and more recently by use of neuronal tracers (Fitzpatrick and Imig, 1980; Aitkin *et al.*, 1988: Luethke *et al.*, 1989; Morel and Kaas, 1992; Morel *et al.*, 1993). A second set of short association projections connects the belt to parabelt cortex (Morel and Kaas, 1992; Hackett *et al.*, 1998a).

Direct recordings of evoked activity support the idea that transcortical passage of information occurs also in human auditory cortex. Electrical stimulation of the transverse temporal gyrus results in short latency evoked potentials in the lateral superior temporal area, indicating transcortical passage of excitation (Liégeois-Chauvel *et al.*, 1994; Howard *et al.*, 2000). When the generation sites of evoked potentials were located by identification of the point of wave inversion (polarity reversal), the sources of the N/P 16 and N/P 30 potentials (waves following the stimulus by 16 and 30 msec) were located in the most medial part of the transverse temporal gyrus (Fig. 34.28). The generation site of the N/P 50 response was found more lateral in the transverse gyrus, and the N/P 60-75 was localized to the lateral end of the gyrus. The medial to lateral sequence of these evoked potentials may correspond to sequential activity in koniocortex, parakoniocortex and association cortex.

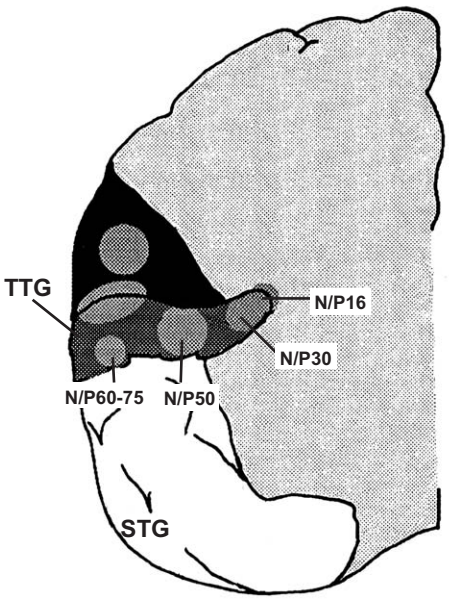

FIGURE 34.28 Diagrammatic representation of suface recordings made from human auditory cortex during surgery. Light circles indicate the polarity inversion sites of the earliest components of the auditory evoked response on the transverse temporal gyrus (TTG). N/P16, N/P30, N/P50, and N/P60-75 are potentials recorded subsequent to a transient stimulus. STG, superior temporal gyrus. Adapted from *EEG and Clinical Neurophysiology* **92,** C. Liegeois-Chauvel, A. Musolino, J.M. Badier, P. Marquis, and P. Chauvel, figure 8, Evoked potentials recorded from the auditory cortex in man, pp. 79–92, 1994, with permission from Elsevier Science, Oxford.

In addition to the connections from core to belt to parabelt within one hemisphere, monkey auditory cortex shows strong linkages between the two hemispheres. Lesions in the core, belt or parabelt result in degenerating axons and terminals in homologous areas in the contralateral hemisphere (Pandya and Sanides, 1973; Forbes and Moskowitz, 1977; Seltzer and Pandya, 1978; Aitkin *et al.*, 1988; Luethke *et al.*, 1989; Morel *et al.*, 1993; Pandya and Rosene, 1993; Hackett *et al.*, 1999). Callosal connections are largely between areas of like frequency, but may spread to adjoining fields. Like the thalamocortical projection, callosal axons end in spatially separated and irregular patches. Unlike thalamocortical axons, the commissural projection does not end primarily in layer IV. Instead it forms a double layer of terminals in layers V and II-III (Pandya and Rosene, 1993).

Functional Imaging of Auditory Cortex

The general function of auditory cortex can be deduced from cases of large lesions that destroy extensive areas of superior temporal cortex bilaterally. Subjects with such lesions suffer from cortical deafness (Hood *et al.,* 1994; Kaga *et al.,* 1997; Garde and Cowey, 2000), but they are not deaf in the same sense as persons who have disorders of the auditory periphery. Instead they retain normal peripheral hearing sensitivity, respond reflexively to sounds, detect and localize environmental sounds, judge loudness and pitch of tones, and can even discriminate monosyllables. Presumably processing of sound at a brain stem level allows this detection and identification of stimulus characteristics. However, these subjects suffer from auditory agnosia, in that they are unaware of the significance of auditory stimuli, including environmental sounds, speech and music. These findings suggest that the basic functional role of auditory cortex is to ascribe meaning to sounds that are processed at lower levels of the auditory system. It is difficult to obtain a more detailed view of the function of human auditory cortex from restricted cortical lesions because of problems in determining the exact extent and effect of the lesions. Alternatively, function of specific areas of human auditory cortex can be revealed by functional imaging, including, both PET and fMRI studies.

In imaging studies, simple auditory tasks, such as passive listening to white noise bursts, tones or CV (consonant-vowel) speech syllables, result in activation that is restricted to areas within the lateral fissure, on the superior temporal plane (Price *et al.,* 1992; Zatorre *et al.,* 1992, 1994; Binder *et al.,* 1994, 1997, 2000; Huckins *et al.,* 1998; Fig. 34.29A). The extent of the activation varies from subject to subject, and may spread anteriorly or posteriorly on the superior temporal plane, or occasionally onto the inferior surface of the parietal lobe. There is a tendency for activation to tones or syllables to spread further laterally than that from white noise bursts. The area of activation is generally within and around the transverse temporal gyrus, and probably includes the anatomically defined areas of koniocortex and parakoniocortex, but it is more variable in extent than the cytoarchitectural zones. With exposure of subjects to more complex stimuli, i.e., passive listening to tone patterns, single words, pseudowords or narrative text, activity is still present in the cortex of the superior temporal plane, but now foci of activation appear on the lateral aspect of the superior temporal gyrus, i.e., in area 22/TA/PaAe (Fig. 34.29B). Considerable intersubject variation is observed in the location of foci, but it is generally true that speech stimuli activate a more extensive region of the temporal lobe than does unmodulated noise. However, different speech stimuli (words, pseudowords, text) produce similar or identical activations. Overall, imaging of the response to auditory stimuli shows a spread of activity, beginning with activation by simple stimuli of a limited region of the superior temporal plane, and expanding with more complex stimuli to the surface of the superior temporal gyrus.

With higher level language processing, activation sometimes spreads ventrally into the superior temporal sulcus. The basis for this spread is likely to be projections from cortex of the superior temporal gyrus into the upper bank of the sulcus, as shown in monkeys (Seltzer and Pandya, 1978, 1994). The upper bank of the sulcus has been described as a voice-selective region because it shows greater neuronal activity when subjects listen to vocal sounds, either speech or nonspeech, rather than to nonvocal environmental sounds, scrambled voices, or amplitude-modulated noise (Mummery *et al.,* 1999; Binder *et al.,* 1994, 1997, 2000; Belin *et al.,* 2000). The posterior part of the superior temporal sulcus is more active during listening to sentences in a familiar language than to acoustically matched sentences in an unfamiliar language (Schlosser *et al.,* 1998; Fig. 34.29D). The posterior superior temporal sulcus has also been described as a face-selective area, showing activity when subjects view faces with moving eyes and mouth (Puce *et al.,* 1998). Finally, there is evidence suggesting that the sulcus is an integrative area for visual and auditory aspects of speech, in that activity spreads from visual cortex along the superior temporal sulcus during lip reading, i.e., perception of language from a moving face (Auer *et al.,* 2001).

The imaging studies note that activation is generally bilaterally equal, i.e., there is a similar amount of activity in the right and left hemispheres. However, with complex stimuli, particularly language, the question arises as to whether there is a right-left asymmetry in the response. Because handedness influences hemispheric lateralization, imaging studies of speech processing are normally restricted to neurologically normal right-handed persons. In right-handers, there is a tendency for greater activation of the left hemisphere during tasks that depend on word meaning, in that the total area of activity is greater on the left. The regions of asymmetry generally lie at the periphery of the active region. One such region is the cortex of the temporoparietal junction (Brodmann area 39), which may be equivalent to the area identified by Wernicke (1908) as a site where lesions can cause a sensory (receptive) aphasia. However, it is clear that this is not an area that processes speech in isolation, but rather a higher level of transcortical processing that begins in the primary auditory cortex. Left lateralization for speech characterizes both males and

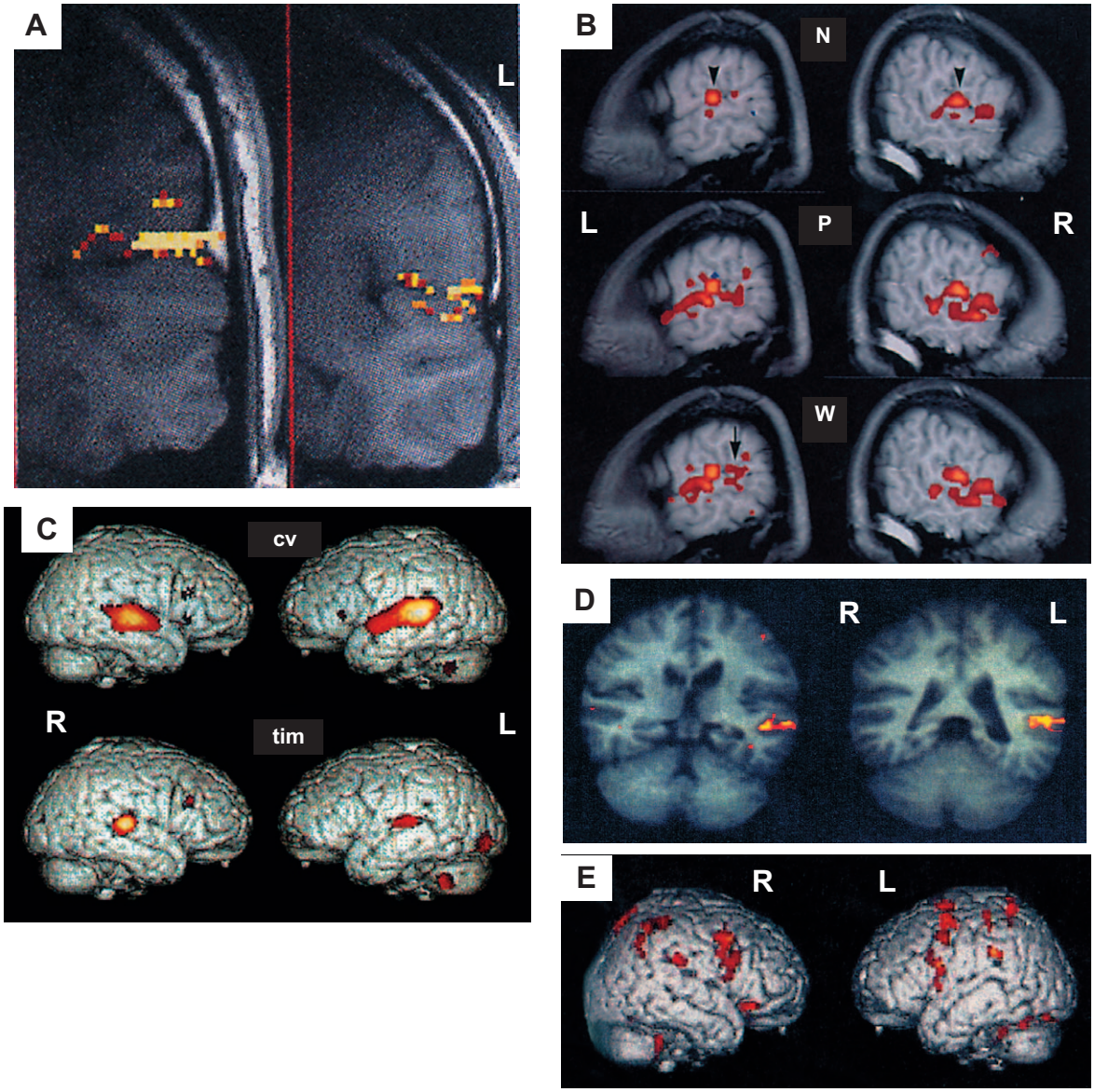

FIGURE 34.29 Functional imaging of human auditory cortex. R and L indicate right and left hemispheres. **(A)** Functional magnetic resonance imaging demonstrates activation of the superior temporal plane by consonant–vowel syllables. Adapted from *Journal of Speech, Language and Hearing Research* **41,** S.C. Huckins, C.W. Turner, K.A. Doherty, M.M. Fonte, and N.M. Szeverrenyi, figure 2, Functional magnetic resonance imaging measures of blood flow patterns in the human auditory cortex in response to sound, pp. 538–548, 1998, with permission of the American Speech–Language–Hearing Association and the first author. **(B)** Functional magnetic resonance imaging demonstrates that with noise stimuli (N), activation is confined to the superior aspect of the superior temporal gyrus bilaterally *(arrowheads).* With stimuli consisting of pseudowords (P) and words (W), activation spreads across the superior temporal gyrus and into the superior temporal sulcus. In the left hemisphere, there is activation in the region of the temporoparietal junction *(arrow).* Adapted from Annals of Neurology 35, J.R. Binder, S.M. Rao, T.A. Hammeke, F.Z. Yetkin, A. Jasmanowicz, P.A. Bandettini, E.C. Wong, L.D. Estkowski, M.D. Goldstein, V.M. Haughton, and J.S. Hyde, figure 4, Functional magnetic resonance imaging measures of blood flow patterns in the human auditory cortex in response to sound, pp. 662–672, 1994, with permission of Lippincott Williams & Wilkins, Philadelphia. **(C)** Positron emission tomography demonstrates activation of temporal and parietal cortex by CV consonants (cv) and musical timbre (tim). With syllable stimuli, activation is more extensive in the left temporal lobe. In the musical timbre task, activation is greater in the right temporal lobe. Adapted from *Neuropsychologia* **37,** K. Hugdahi, K. Bronnick, S. Kyllingbaek, I. Law, A. Gade, and O.B. Paulson, figure 2, Brain activation during dichotic presentations of consonant-vowel and music instrument stimuli: a ^{15}O-PET study, pp. 431–440, 1999, with permission of Elsevier Science, Oxford. **(D)** Functional magnetic resonance imaging demonstrates the area of activation of cortex of the superior temporal sulcus during listening to sentences in a familiar language, as compared to a nonfamiliar language. Adapted from *Brain Mapping* **6,** M.J. Schlosser, N. Aoyagi, R.K. Fulbright, J.C. Gore and G. McCarthy, figure 4, Functional MRI studies of auditory comprehension, pp. 1–13, 1998, with permission from Wiley-Liss, a subsidiary of John Wiley & Sons, Inc., New York. **(E)** Functional magnetic resonance imagning demonstrates activation of parietal lobe cortex bilaterally by simulated stimulus motion. Adapted from *Nature Neuroscience* **1,** T.D. Griffiths, G. Rees, A. Rees, G.G.R. Green, C. Witton, D. Rowe, C. Buchel, R. Turner, and S.J. Frackowiak, fitgure 3a, right patrietal cortex is involved in the perception of sound movement in humans, pp. 74–79, 1998, with permission from the Nature Publishing Group, New York, and the first author.

females (Frost *et al.*, 1999), but this left dominance is not absolute across subjects. In one fMRI study of a task dependent on word meaning, 94% of the right-handed subjects were left hemisphere dominant and 6% had bilaterally equal language representation (Springer *et al.*, 1999). Occasionally a reversed, or "mirror image", representation of language in the right hemisphere of a right-handed person is observed (Chee *et al.*, 1998). The functional significance of greater left hemisphere activity is implied by imaging studies of stroke patients after infarctions of the left posterior perisylvian area (Weiller *et al.*, 1995; Heiss *et al.*, 1997; Mummery *et al.*, 1999). Subjects who showed good recovery of speech perception had increasing activation of left temporal lobe cortex surrounding the infarct. Subjects with recruitment of additional cortex only in the right hemisphere showed single word comprehension, but continued impaired understanding of fluent speech. Like the results of the imaging studies of normal subjects, these findings suggest bilateral temporal lobe involvement in speech processing, with a final level of processing generally present (in right-handers) in the left hemisphere.

Some indications of an opposite asymmetry in processing musical stimuli come from cases of pathology. A patient with a right thalamic tumor experienced distorted perception of music but not of voices (Roeser and Daly, 1974). Cortical activity has been demonstrated in the right superior temporal lobe during musical hallucinations (Kasai *et al.*, 1999). A case of amusia, a form of auditory agnosia, was seen after an infarction involving the right insula (Griffiths *et al.*, 1997b). In this patient, a battery of tests confirmed a dissociated receptive musical deficit in the presence of normal appreciation of environmental sounds and speech. In imaging studies, listening to tone patterns or melodies causes foci of activity in the right temporal and parietal lobes (Roland *et al.*, 1981; Zattore *et al.*, 1994). However, the side of greatest activation can be influenced by the analysis strategy of the subject. Musically naive subjects show greater temporal and frontal lobe activity on the right side, whereas musically sophisticated subjects who visualize musical scores may have greater left-sided activity (Mazziota *et al.*, 1982). In discrimination of musical timbre (harpsichord/guitar/organ), the peak of activity in the superior temporal gyrus is larger on the right (Hugdahl *et al.*, 1999) (Fig. 34.29C), and right temporal lobe lesions create a significant deficit in timbre discrimination (Samson and Zatorre, 1994). However, different components of musical analysis do not always activate the same areas. One study has shown separate cortical areas for tasks involving attending to pitch, melodic interval, melodic contour, meter, and rhythm

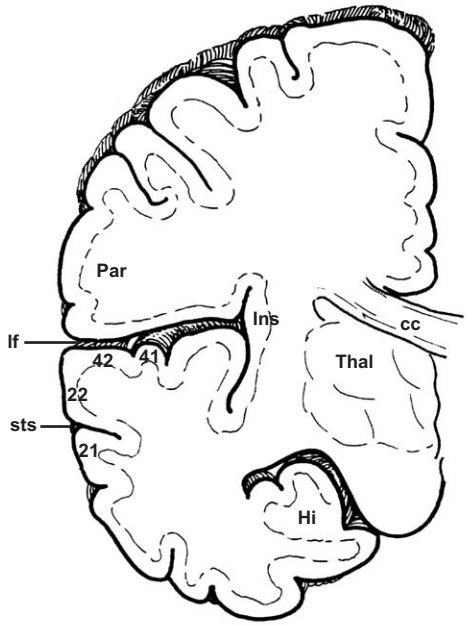

FIGURE 34.30 Cross section through one hemisphere of the human forebrain. The "what" pathway passes laterally and ventrally from area 41 across areas 42, 22, and 21. The "where" pathway passes medially and dorsally through the insula and into parietal cortex (Par). cc, corpus callosum; Hi, hippocampus; Ins, insula; lf, lateral fissure; sts, superior temporal sulcus; Thal, thalamus.

(Liégois-Chauvel *et al.*, 1998). In most of these tasks, there is greater right-sided activity, but melodic interval appears to be processed in the left hemisphere. Thus, analysis of music, like that of speech, is a complex process involving interaction of the two hemispheres, with some hemispheric specialization at the highest levels of analysis.

It is a commonly accepted view that auditory cortex is mainly confined to the temporal lobe, with activation spreading laterally and ventrally from the koniocortex. However, there is increasing evidence for a pathway responding to position and motion of auditory stimuli that extends medially and dorsally into the parietal lobe (Fig. 34.30). The idea of a "two stream" organization of sensory cortex originated in the visual system. In monkey and human visual cortex, information processing flows from the primary visual area in two broad functional streams (Goodale *et al.*, 1994). The ventral visual stream, known as the "what" pathway, leads to the inferior temporal region and is concerned with perceptual features of a visual stimulus. The dorsal stream, referred to as the "where" pathway, leads to the parietal region and is concerned with perception of an object's location and motion. A similar two-stream organization may exist in human auditory cortex. The right insula is activated by a moving sound image

(Griffiths *et al.*, 1994), and, conversely, a patient with a right hemisphere stroke causing atrophy of the right insula was unable to detect sound source movement by either phase or loudness cues (Griffiths *et al.*, 1996). Subjects listening to stimulus movement simulated by changes in binaural timing show maximal activity in the inferior parietal area, particularly on the right side (Griffiths *et al.*, 1998; Weeks *et al.*, 1999) (Fig. 34.29E). These findings suggest that there is transcortical passage of information from auditory koniocortex posteriorly and medially, across the insula and into the parietal lobe, during processing of information on sound source position and motion. They also suggest a dominant functional role of the right hemisphere in sound localization.

THE DESCENDING AUDITORY SYSTEM

Descending Projections from Cortex

The descending projections from auditory cortex to the thalamus are reciprocal, in the sense that cortical regions project back to the thalamic areas that are the source of their afferent input. Injection of neuronal tracers into the primary auditory cortex of the marmoset and macaque demonstrates a dense projection to the ventral medial geniculate and a much lighter projection to the medial and dorsal nuclei (Aitkin *et al.*, 1988; Pandya *et al.*, 1994). These descending projections originate mainly from pyramidal cells of layer VI, with some contributions from cells of layer V. In contrast, when tracer injections are made into the parabelt or into the cortex of the upper bank of the superior temporal sulcus, the descending axons end only in the medial and dorsal nuclei of the medial geniculate and in the medial pulvinar (Yeterian and Pandya, 1991; Pandya *et al.*, 1994; Hackett *et al.*, 1998b; Guteirrez *et al.*, 2000). Because there are few descending connections from the thalamus, these corticothalamic pathways form feedback loops that can allow reverberant activity of the thalamus and cortex.

Many of the axons descending from cortex bypass the thalamus and travel to the tectum, where they end in the inferior colliculus. Anterograde transport of tracers shows that the termination of these axonal projections is primarily in the caudal half of the pericentral colliculus, i.e., in the dorsocaudal cortex (squirrel monkey, FitzPatrick and Imig, 1978; marmoset, Luethke *et al.*, 1989). The dorsocaudal cortex is a multilayered structure, with neurons segregated into several layers and cells becoming progressively larger in the deeper layers. This cortical cytoarchitecture in monkey

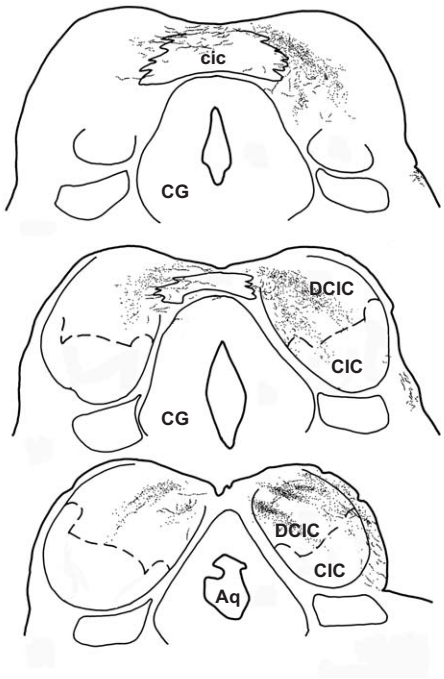

FIGURE 34.31 Following tracer injection into the auditory cortex of the marmoset, labeled bands of axons are present in the dorsocaudal cortex of the inferior colliculus (DCIC). Few degenerating axons enter the central nucleus of the inferior colliculus (CIC). Some degenerating axons cross in the commissure of the colliculus (cic) to end in the dorsocaudal cortex on the opposite side. Aq, aqueduct; CG, central gray. Adapted from *Journal of Comparative Neurology* **285,** L.E. Luethke, L.A. Krubitzer, and J.H. Kaas, figure 14, Connections of primary auditory cortex in the New World monkey, *Saguinus,* pp. 487–513, 1989, with permission from Wiley-Liss, a subsidiary of John Wiley & Sons, Inc., New York.

(FitzPatrick, 1975) and man (Geniec and Morest, 1971) is similar to that of nonprimate species. Within the dorsocaudal cortex, the descending cortical axons form bands oriented from dorsomedial to ventrolateral (Fig. 34.31). A smaller number of axons cross the midline in the commissure of the inferior colliculus and terminate in the dorsocaudal region of the colliculus on the opposite side. Because it is the primary target of corticofugal axons, the dorsocaudal cortex appears to be an important relay in the descending auditory pathway.

Descending Projections from Inferior Colliculus

Descending projections from the inferior colliculus originate predominantly from its dorsocaudal cortex (Moore and Goldberg, 1966). The descending axons run along the surface of the brain stem adjacent to the lateral lemniscus and terminate mainly in the region of the superior olivary complex. As in nonprimate

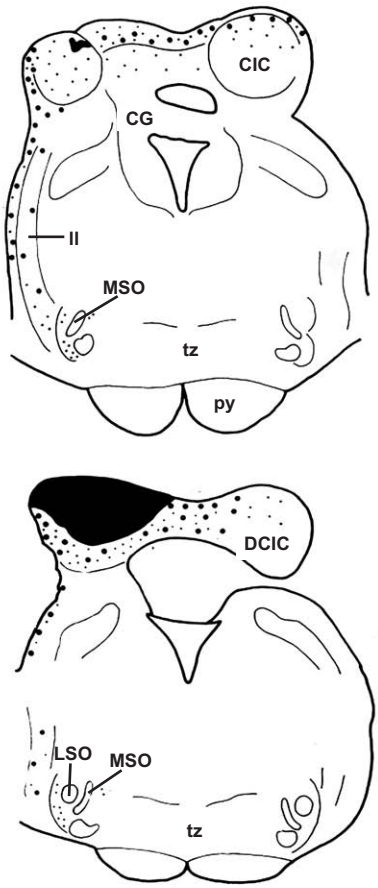

FIGURE 34.32 A lesion *(shaded black)* confined mainly to the dorsocaudal cortex of the inferior colliculus (DCIC) in the macaque results in degenerating axons *(large dots)* descending superficial to the lateral lemnisus (ll). Degenerating terminals (*small dots)* are present in the periolivary region (PO) of the superior olivary complex. Adapted from *Experimental Neurology* **14,** R.Y. Moore and J.M. Goldberg, figure 1, Projections of the inferior colliculus in the monkey, pp. 429–438, 1966, with permission of Harcourt Brace, a subsidiary of Academic Press.

mammals, terminals are found throughout the periolivary region, but not in relation to the medial and lateral olivary nuclei (Fig. 34.32). The density of terminals is greater ipsilaterally and is heaviest in the ventral periolivary cell groups.

Descending Projections from Periolivary Region

Descending projections from the superior olivary complex arise exclusively from periolivary cells. In nonprimate mammals, a sizable projection from periolivary cells terminates in the cochlear nuclei (Covey *et al.,* 1984; Spangler *et al.,* 1987). In the guinea pig, most of the descending axons have been shown to contain GABA or glycine, or to colocalize both inhibitory substances (Kolston *et al.,* 1992; Ostapoff *et al.,* 1997). The GABA- and glycine-immunostained axons run in the trapezoid body to the ventral cochlear nucleus, and many continue into the dorsal cochlear nucleus as the centrifugal bundle of Lorente de No. In the baboon, however, only scattered GABA- and glycine-immunoreactive axons are present in the trapezoid body and acoustic striae. In addition, the centrifugal bundle of Lorente de No cannot be identified in the human cochlear nuclear complex (Moore and Osen, 1979). Thus, the possibility must be considered that this part of the descending system is poorly developed in higher primates.

Periolivary neurons also form an efferent projection to the organ of Corti that is termed the olivocochlear pathway. Early demonstrations of olivocochlear neurons in mammals were done on the basis of their content of acetylcholinesterase (AChE), the degradative enzyme for acetylcholine (Brown and Howlett, 1972; Warr, 1975; Osen *et al.,* 1984). In the human brain stem, AChE-positive olivocochlear axons were traced dorsally from the human superior olivary complex and into the vestibular nerve (Moore and Osen, 1979). Antibodies to choline acetyltransferase (ChAT), the synthesizing enzyme of acetylcholine, have also been used to identify olivocochlear neurons in the periolivary region in the squirrel monkey (Thompson and Thompson, 1986), macaque (Carpenter *et al.,* 1987), and man (Moore *et al.,* 1999) (Fig. 34.33, ChAT).

In nonprimate mammals, two subdivisions of the olivocochlear system can be demonstrated by anterograde and retrograde transport of neuronal tracers (Warr and Guinan, 1979; Guinan *et al.,* 1983). In the lateral subdivision, axons of cells associated with the lateral olivary nucleus form synaptic terminals contacting afferent fibers from inner hair cells and, in some cases, inner hair cell somata. In the medial subdivision, axons of cells located throughout the periolivary region form synaptic terminals contacting outer hair cells and, occasionally, their afferent fibers. The two systems also differ in their chemical characteristics in that lateral olivocochlear neurons colocalize a variety of neuropeptides with the cholinergic enzymes. One of these peptides is calcitonin gene–related peptide (CGRP). In the human superior olivary complex, a cluster of mostly small oval cells that are both ChAT and CGRP positive is located adjacent to and surrounding the lateral olivary nucleus (Moore *et al.,* 1999) (Fig. 34.33, CGRP). It is likely these neurons are homologous to the mammalian lateral olivocochlear system. The remainder of the population, which is immunopositive only for ChAT, consists predominantly of larger multipolar cells distributed throughout the periolivary

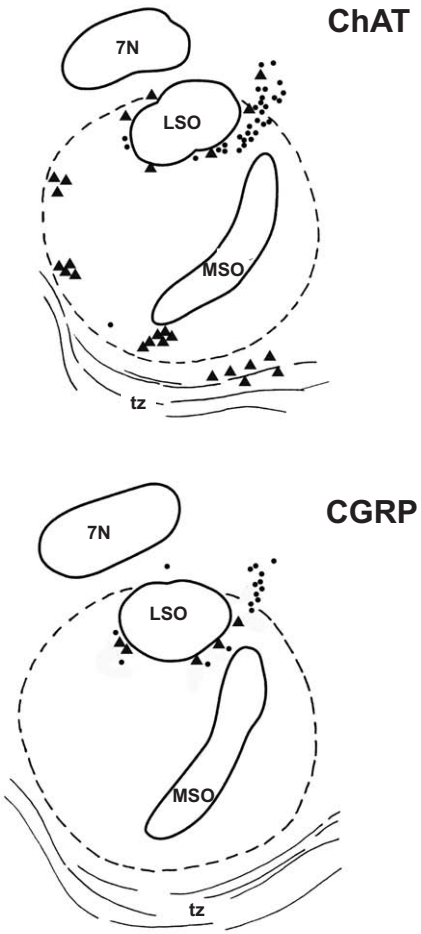

FIGURE 34.33 Distribution of immunoreactive neurons in the human superior olivary complex, including both large cells (▲) and small cells (✳). Immunostaining for choline acetyltransferase (ChAT) demonstrates the entire population of efferent neurons, including both the medial and lateral subsystems. Immunostaining for calcitonin gene–related peptide (CGRP) demonstrates only the lateral efferent neurons. LSO, lateral superior olivary nucleus; MSO, medial superior olivary nucleus; tz, trapezoid body; 7N, facial nucleus Adapted from *Audiology and Neuro-Otology* **4,** J.K. Moore, D.D. Simmons, and Y.-L. Guan, figure 5, The human olivocochlear system: organization and development, pp. 311–325, 1999, with permission from Karger AG, Basel.

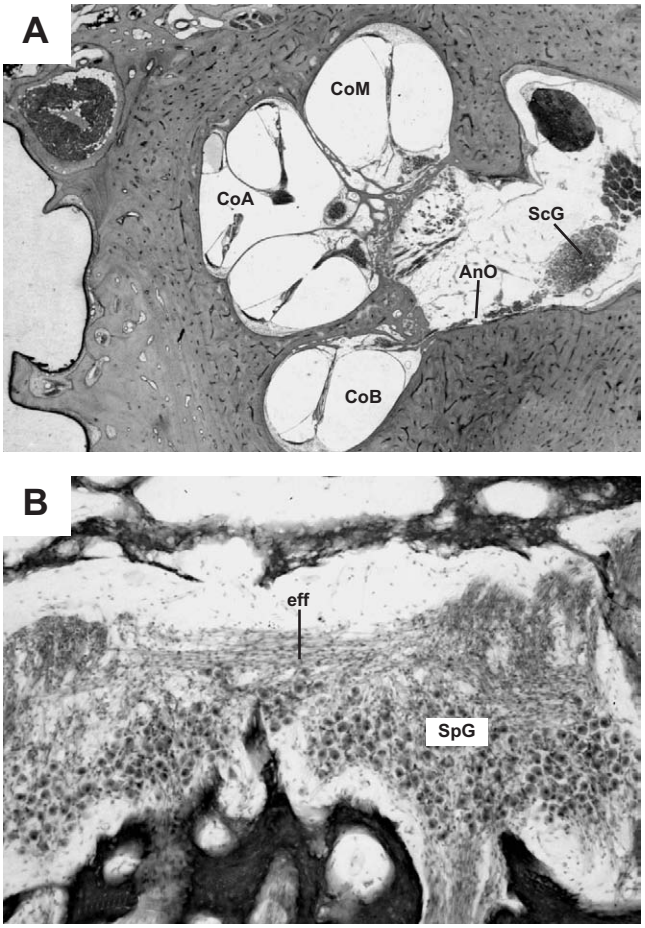

FIGURE 34.34 **(A)** Vertical section through the cochlea and internal auditory canal showing the vestibulocochlear anastomosis of Oört (AnO) passing from Scarpa's ganglion (ScG) of the inferior vestibular nerve into the basal turn of the cochlea (CoB). CoA, apical turn, CoM. middle turn. **(B)** A horizontal section through the cochlea illustrates the intraganglionic efferent bundle (eff) on the surface of the basal segment of the spiral ganglion (SpG). Celloidin sections, hematoxylin & eosin.

region (Fig. 34.33, ChAT). These cells are most heavily concentrated ventrally but are also scattered along the dorsal, medial, lateral, and rostral boundaries of the olivary complex. Because of their size and distribution, it seems likely that the cells are homologous to the medial olivocochlear system in nonprimate species.

Efferent Innervation of the Cochlea

Olivocochlear axons leave the brain stem in the vestibular nerve, traverse its inferior branch, and pass through the vestibulocochlear anastomosis or nerve of Oört (Oört, 1917) (Fig. 34.34A) to enter the basal turn of the cochlea. The bundle of efferent axons passes toward the apex of the cochlea in the lateral aspect of Rosenthal's canal. Early investigations demonstrated efferent axons and terminals within the human cochlea by their content of AChE (Schuknecht *et al.*, 1959; Ishi *et al.*, 1967). Some of the fibers, the thin axons of lateral efferent neurons, pass into the organ of Corti and run toward the apex of the cochlea as the inner spiral bundle. These efferent axons form synaptic terminals on the afferent axons of inner hair cells and, occasionally, on the inner hair cell bodies themselves.

Other efferent fibers, the thicker axons of the medial efferent neurons, traverse the tunnel of Corti as the tunnel-crossing fibers (Fig. 34.5B). They then form the outer spiral bundle whose fibers branch to synapse on the bases of outer hair cells. In the human cochlea, as in other mammalian species, efferent terminals are most numerous in relation to outer hair cells. In recent years, the efferent nature of axons in the inner spiral bundle, tunnel-crossing fibers, and terminals at the base of outer hair cells has been confirmed by immunostaining for ChAT (Schrott-Fischer *et al.*, 1994).

Because the principal neurotransmitter of the olivocochlear system is acetylcholine, its activity might be expected to affect the actin-based system of outer hair cell motility. In fact, experiments on outer hair cells isolated from guinea pig cochleas have shown that application of acetylcholine affects the electromotile responses of these cells (Slepecky *et al.*, 1988; Dallos *et al.*, 1997). The cells exposed to acetylcholine show increased motility, but the response occurs much more slowly than the rapid response to electrical and acoustic stimulation. In human subjects, stimulation of the olivocochlear pathway by acoustic input to the opposite ear causes suppression of spontaneous and evoked otoacoustic emissions (Mott *et al.*, 1989; Khalfa and Collet, 1996; Veuillet *et al.*, 1996; Hood *et al.*, 1996). This effect is believed to be due to the outer hair cell response to acetylcholine and to be mediated mainly by medial olivocochlear neurons.

Behavioral effects have also been demonstrated from activation of the olivocochlear system by contralateral ear stimulation. In functional studies of normal human subjects, these behavioral effects include enhancement of selective attention (Puel *et al.*, 988; Giard *et al.*, 1994; Scharf *et al.*, 1997) and improved processing of complex signals in noise (Giraud *et al.*, 1997). The idea that the behavioral changes are the results of olivocochlear system activity is supported by observations in subjects who have undergone vestibular neurectomy. These subjects, whose efferent pathway has been disrupted by severing the vestibular nerve, have no detectable change in hearing in quiet. In the presence of noise, however, there is increased subjective loudness and worsened intensity discrimination in the operated ear (Zeng *et al.*, 2000). It is true that the physiological and perceptual effects of efferent system activity have been demonstrated by artificial stimulation or disruption of the descending auditory system at a level only one neuron above the cochlea. Nonetheless, the continuity of the descending system from cortex to cochlea provides a potential route for the highest levels of auditory processing to bias the activity of the peripheral receptor.

References

Adams, J.C. (1979). Ascending projections to the inferior colliculus. *J. Comp. Neurol.* **183,** 519–538.

Adams, J.C. (1986). Neuronal morphology in the human cochlear nucleus. *Arch. Otol. Head Neck Surg.* **112,** 1253–1261.

Adams, J.C., and Mugnaini, E. (1984). Dorsal nucleus of the lateral lemniscus: A nucleus of GABAergic projection neurons. *Brain Res. Bull.* **13,** 585–590.

Aitkin, L.M., Kenyon, C.E., and Philpott, P. (1981). The representation of the auditory and somatosensory systems in the external nucleus of the cat inferior colliculus. *J. Comp. Neurol.* **196,** 25–40.

Aitkin, L.M., Kudo, M., and Irvine, D.R.F. (1988). Connections of the primary auditory cortex in the common marmoset, *Callithrix jaccus jacchus*. *J. Comp. Neurol.* **269,** 235–248.

Armstrong, E. (1979). A quantitative comparison of the hominoid thalamus; Specific sensory relay nuclei. *Am. J. Phys. Anthro.* **51,** 365–382.

Ashmore, J.K. (1987). A fast motile response in guinea-pig outer hair cells: The cellular basis of the cochlear amplifier. *J. Physiol.* **388,** 323–347.

Auer, E.T., Bernstein, L.E., and Singh,M. (2001). Comparing cortical activity during the perception of two forms of biological motion for language communication. *In* "Proceedings of AVSP 2001" (D. W. Massaro, J. Light, and K. Geraci, eds.), pp 40–44. Causal Productions, Australia.

Babalian, A.L., Ryugo, D.K., Vischer, M.W., and Rouiller, E.M. (1999). Inhibitory synaptic interactions between cochlear nuclei: Evidence from an *in vitro* whole brain study. *Neuroreport* **10,** 1913–1917.

Belin, P., Zatorre, R.J., Lafaille, P., Ahad, P., and Pike, B. (2000). Voice-selective areas in human auditory cortex. *Nature* **403,** 309–312.

Binder, J.R., Rao, S.M., Hammeke, T.A., Yetkin , F.Z., Jasmanowicz, A., Bandettini, P.A., Wong, E.C., Estkowski, I.D., Goldstein, M.D., Houghton, V.M., and Hyde, J.S. (1994). Functional magnetic resonance imaging of human auditory cortex. *Ann. Neurol.* **35,** 662–672.

Binder, J.R., Frost, J.A., Hammeke, T.A., Cox, R.W., Rao, S.M., and Prieto, T. (1997). Human brain language areas identified by functional magnetic resonance imaging. *J. Neurosci.* **17,** 353–362.

Binder, J.R., Frost, J.A., Hammeke, T.A., Bellgowan, P.S.F., Springer, J.A., Kaufman, J.N., and Possing, E.T. (2000). Human temporal lobe activation by speech and nonspeech sounds. *Cereb. Cortex* **10,** 512–528.

Binns, K.E., Grant, S., Withington, D.J., and Keating, M.J. (1992). A topographic representation of auditory space in the external nucleus of the inferior colliculus of the guinea pig. *Brain Res.* **589,** 321–242.

Bledsoe, S.C., Jr., Snead, C.R., Helfert, R.H., Prasad, V., Wenthold, R.J., and Altschuler, R. (1990). Immunocytochemical and lesion studies support the hypothesis that the projection from the medial nucleus of the trapezoid body to the lateral superior olive is glycinergic. *Brain Res.* **517,** 189–194.

Blevins, C. E. (1967). Innervation patterns of the human stapedius muscle. *Arch. Otolaryngol.* **86,** 136–142.

Brawer, J.R., Morest, D.K., and Kane, E.C. (1972). The neuronal architecture of the cochlear nucleus of the cat. *J. Comp. Neurol.* **155,** 251–300.

Brödel, M. (1946). "Three Unpublished Drawings of the Anatomy of the Human Ear." W. B. Saunders, Philadelphia.

Brodmann, K. (1908). Beitrage zur histologischen Lokalisation der Grosshirnrinde: VI Mitteilung: Die Cortexgliederung des Menschen. *J. Psych. Neurol.* **10,** 231–246.

Brown, J.C., and Howlett, B. (1972). The olivo-cochlear tract in the rat and its bearing on the homologies of some constitutent cell

groups of the mammalian superior olivary complex: A thiocholine study. *Acta Anat.* **83,** 505–526.
Brownell, W.E. (1990). Outer hair cell electromotility and otoacoustic emissions. *Ear Hear.* **11,** 82–92.
Brownell, W.E., Bader, C.R., Bertrand, D., and de Ribaupierre, Y. (1985). Evoked mechanical responses of isolated cochlear outer hair cells. *Science* **227,** 194–196.
Brundin, L., Flock, A., and Canlon, B. (1989). Sound-induced motility of isolated cochlear outer hair cells is frequency-specific. *Nature* **14,** 814–816.
Brundin, L., Flock, B., and Flock, A. (1992). Sound induced displacement response of the guinea pig hearing organ and its relation to the cochlear potentials. *Hear. Res.* **58,** 175–184.
Brunso-Bechtold, J., Thompson, G.C., and Masterton, R.B. (1981). Study of the organization of auditory afferents ascending to the central nucleus of the inferior colliculus in the cat. *J. Comp. Neurol.* **197,** 705–722.
Buchwald, J.S., and Huang, C.M. (1975). Far-field acoustic responses: Origins in the cat. *Science* **189,** 382–384.
Burton, H., and Jones, E.G (1976). The posterior thalamic region and its cortical projection in New World and Old World monkeys. *J. Comp. Neurol.* **168,** 249–301.
Cant, N.B. (1993) The synaptic organization of the ventral cochlear nucleus of the cat. *In* "The Mammalian Cochlear Nuclei: Organiation and Function" (M. A. Merchan, ed.), pp. 91–105. Plenum Press, New York.
Cant, N.B., and Gaston, K.C. (1982). Pathways connecting the right and left cochlear nuclei. *J. Comp. Neurol.* **212,** 313–326.
Cant, N.B., and Morest, D.K. (1979). The bushy cells in the anteroventral cochlear nucleus of the cat. A study with the electron microscope. *Neuroscience* **4,** 1925–1945.
Carpenter, M.B., Chang, L., Pereira, A.B., Hersh, L.B., Bruce, G., and Wu, J.-Y. (1987). Vestibular and cochlear efferent neurons in the monkey identified by immunocytochemical methods. *Brain Res.* **408,** 275–280.
Casseday, J.H., and Neff, W.D. (1975). Auditory localization: Role of auditory pathways in brain stem of the cat. *J. Neurophysiol.* **38,** 842–858.
Chee, M.W.L., Ruckner, R.L., and Savoy, R.L. (1998). Right hemisphere language in a neurologically normal dextral: An fMRI study. *Neuroreport* **9,** 3499–3502.
Coleman, J.R., and Clerici, W.J. (1987). Sources of projections to subdivisions of the inferior colliculus in the rat. *J. Comp. Neurol.* **262,** 215–226.
Covey, E., and Casseday, J.J. (1991). The monaural nuclei of the lateral lemniscus in an echolocating bat: Parallel pathways for analyzing temporal features of sound. *J. Neurosci.* **11,** 3456–3470.
Covey, E., Jones, D.R., and Casseday, J.H. (1984) Projections from the superior olivary complex to the cochlear nuclei in the tree shres. *J. Comp. Neurol.* **226,** 289–305.
Dallos, P., and Cheatham, M.A. (1976). Production of cochlear potentials by inner and outer hair cells. *J. Acoust. Soc. Am.* **60,** 510–512.
Dallos, P., He, D.Z., Lin, X., Sziklai, I., Mehta, S., and Evans, B.N. (1997). Acetylcholine, outer hair cell electromotility and the cochlear amplifier. *J. Neurosci.* **17,** 2212–2226.
DeArmond, S.J., Fusco, M.M., and Dewey, M.M. (1989). "Structure of the Human Brain. A Photgraphic Atlas." Oxford University Press, New York.
Deiler, R., Shehata-Dieler, W., and Brownell, W. (1991). Concomitant salicylate-induced alterations of outer hair cell subsurface cisternae and electromotility. *J. Neurocytol.* **20,** 637–653.
Delgutte, B., Joris, P.X., Litovsky, R.Y., and Yin, T.C. (1999). Receptive fields and binaural interactions for virtual-space stimuli in the cat inferior colliculus. *J. Neurophysiol.* **81,** 2833–2851.
Denk, W., Holt, J.R., Shepherd, G.M., and Corey, D.P. (1995). Calcium imaging of single stereocilia in hair cells: localization of transduction channels at both ends of tip links. *Neuron* **15,** 1311–1321.
Edwards. S.B., Ginsburgh, C.L., Henkel, C.K., and Stein, B.E. (1979). Sources of subcortical projections to the superior colliculus in the cat. *J. Comp. Neurol.* **184,** 309–330.
Elberling, C., Bak, C., Kofoed, B., Lebech, J., and Saermark, K. (1982). Auditory magnetic fields. Source localization and tonotopic organization in the right hemisphere of human brain. *Scand. Audiol.* **10,** 203–207.
Evans, B.N., and Dallos, P. (1993). Stereocilia displacement induced somatic motility of cochlear outer hair cells. *Prod. Natl. Acad. Sci. U.S.A.* **90,** 8347–8351.
Feldman, M., and Harrison, J.M. (1969). The acoustic nerve projecion to the ventral cochlear nucleus in the rat. *J. Comp. Neurol.* **137,** 267–292.
FitzPatrick, K.A. (1975). Cellular architecture and topographic organization of the inferior colliculus of the squirrel monkey. *J. Comp. Neurol.* **164,** 185–208.
FitzPatrick, K.A., and Imig, T.J. (1978). Projections of auditory cortex upon the thalamus and midbrain in the owl monkey. *J. Comp. Neurol.* **177,** 537–556.
FitzPatrick, K.A., and Imig, T.J. (1980). Auditory cortico-cortical connections in the owl monkey. *J. Comp. Neurol.* **192,** 589–610.
Flock, A., Cheung, H.C., Flock, B., and Utter, G. (1981). Three sets of actin filaments in sensory cells of the inner ear. Identification and functional orientation determined by gel electrophoresis, immunofluorescence and electron microscopy. *J. Neurocytol.* **10,** 133–147.
Flock, A., Bretscher, A., and Weber, K. (1982). Immunohistochemical localization of several cytoskeletal proteins in inner ear sensory and supporting cells. *Hear. Res.* **7,** 75–89.
Flock, A., Flock, B., Fridberger, A., Scarfone, E., and Ulfendahl, M. (1999). Supporting cells contribute to control of hearing sensitivity. *J. Neurosci.* **19,** 4498–4507.
Forbes, B.F., and Moskowitz, N. (1977). Cortico-cortical connections of the superior temporal gyrus in the squirrel monkey. *Brain Res.* **136,** 547–552.
Friauf, E., and Ostwald, J. (1988). Divergent projections of physiologically characterized rat ventral cochlear nucleus neurons as shown by intra-axonal injection of horseradish peroxidase. *Exp. Brain Res.* **73,** 263–284.
Frost, J.A., Binder, J.R., Springer, J.A., Hammeke, T.A., Belllrowan, P.S., Rao, S.M., and Cox, R.W. (1999). Language processing is strongly left lateralized in both sexes. Evidence from functional MRI. *Brain* **122,** 190–208.
Galaburda, A.M., and Pandya, D.N. (1983). The intrinsic architectonic and connectional organization of the superior temporal region of the rhesus monkey. *J. Comp. Neurol.* **221,** 169–184.
Galaburda, A., and Sanides, F. (1980). Cytoarchitectonic organization of the human auditory cortex. *J. Comp. Neurol.* **190,** 597–610.
Galambos, R., Schwartzkopff, J., and Rupert, A. (1959). Microelectrode study of superior olivary nuclei. *Am. J. Physiol.* **197,** 527–536.
Garde, M.M., and Cowey, A. (2000). "Deaf hearing": unacknowledged detection of auditory stimuli in a patient with cerebral deafness. *Cortex* **36,** 71–80.
Garey, L.J., and Webster, W.R. (1989). Functional morphology in the inferior colliculus of the marmoset. *Hear. Res.* **38,** 67–80.
Geniec, P., and Morest, D.K. (1971). The neuronal architecture of the human posterior collicuus. *Acta Oto-Laryngologica, Suppl* **295,** 1–33.
Giard, M.-H., Collet, L, Bouchet, P., and Pernier, J. (1994). Auditory selective attention in the human cochlea. *Brain Res.* **633,** 353–356.
Giraud, A., Garnier, S., Michel, C., Lina, G., Chays, A., and Chery-Croze, S. (1997). Auditory efferents involved in speech-in-noise intelligibility. *Neuroreport* **8,** 1779–1783.

Glendenning, K.K., Brunso-Bechtold, J.K., Thompson, G.C., and Masterton, R.B. (1981). Ascending auditory afferents to the nuclei of the lateral lemniscus. *J. Comp. Neurol.* **197,** 673–704.

Glendenning, K.K., Hutson, K.A., Nudo, R.J., and Masterton, R.B. (1985). Acoustic chiasm II: anatomical basis of binaurality in lateral superior olive of cat. *J. Comp. Neurol.* **232,** 261–285.

Goldberg, J.M., and Brown, P.B. (1968). Functional organization of the dog superior olivary complex: an anatomical and electrophysiological study. *J. Neurophysiol.* **31,** 639–656.

Goodale, M.A., Meenan, J.P., Bülthoff, H.H., Nicolle, D.A., Murphy, K.J., and Racicot, C.I. (1994). Separate neuronal pathways for the visual analysis of object shape in perception and prehension. *Curr. Biol.* **4,** 604–610.

Griffiths, T.D., Bench, C.J., and Frackowiak, R.S.J. (1994). Human cortical areas selectively activated by apparent sound movement. *Curr. Biol.* **4,** 892–895.

Griffiths, T.D., Rees, A., Witton, C., Shakir, R.A., Henning, G.B., and Green, G.G. (1996). Evidence for a sound movement area in the human cerebral cortex. *Nature* **3,** 425–427.

Griffiths, T.D., Bates, D., Rees, A., Witton, C., Gholkar, A., and Green, G.G.R. (1997a). Sound movement detection deficit due to a brainstem lesion. *J. Neurol. Neurosurg. Psychiatry* **62,** 522–526.

Griffiths, T.D., Rees, A., Witton, C., Cross, P.M., Shakir, R.A., and Green, G.G.R. (1997b). Spatial and temporal auditory processing deficits following right hemisphere infarction. A psychophysical study. *Brain* **120,** 785–794.

Griffiths, T.D., Rees, G., Rees, A., Green, G.G., Witton, C., Rowe, D., Buchel, C., Turner, R., and Frankowiak, R.S. (1998). Right parietal cortex is involved in the perception of sound movement in humans. *Nature Neurosci.* **1,** 74–79.

Guinan, J.J.Jr., Norris, B.E., and Guinan, S.S. (1972). Single auditory units in the superior olivary complex. II. Location of unit categories and tonotopic organization. *Int. J. Neurosci.* **4,** 147–166.

Guinan, J.J., Warr, W.B., and Norris, B.E. (1983). Differential olivocochlear projections from lateral versus medial zones of the superior olivary complex. *J. Comp. Neurol.* **221,** 358–370.

Gutierrez, C., Cola, M.G., Seltzer, B., and Cusick, C. (2000). Neurochemical and connectional organization of the dorsal pulvinar complex in monkeys. *J. Comp. Neurol.* **419,** 61–86.

Hackett, T.A, Stepniewska, I., and Kaas, J. H. (1998a). Subdivisions of auditory cortex and ipsilateral cortical connections of the parabelt auditory cortex in macaque monkeys. *J. Comp. Neurol.* **394,** 475–495

Hackett, T.A., Stepniewska, I., and Kaas, J.H. (1998b). Thalamocortical connections of the parabelt auditory cortex in macaque monkeys. *J. Comp. Neurol.* **400,** 271–286.

Hackett, T.A., Stepniewska, I., and Kaas, J.H. (1999). Callosal connections of the parabelt auditory cortex in macaque monkeys. *Eur. J. Neurosci.* **11,** 856–866.

Hackett, T.A., Preuss, T.M., and Kaas, J.H. (2001). Architectonic identification of the core region in auditory cortex of macaques, chimpanzees, and humans. *J. Comp. Neurol.* **441,** 197–222.

Hashikawa, T., Molinari, M., Rausell, E., and Jones, E. G. (1995). Patchy and laminar terminations of medial geniculate axons in monkey auditory cortex. *J. Comp. Neurol.* **362,** 195–208.

Hashimoto, I., Ishiyama, Y., Yoshimoto, T., and Nemoto, S. (1981). Brainstem auditory evoked potentials recorded directly from human brainstem and thalamus. *Brain* **104,** 841–859.

Heiss, W.-D., Karbe, H., Weber-Luxenburger, G., Herholz, K., Kessler, J., Pietrzyk, U., and Pawlik, G. (1997). Speech-induced cerebral metabolic activation reflects recovery from aphasia. *J. Neurol. Sci.* **145,** 213–217.

Hood, L.J., Berlin, C.I., and Allen, P. (1994). Cortical deafness: a longitudinal study. *J. Am. Acad. Audiol.* **5,** 330–342.

Hood, L.J., Berlin, C.I., Hurley, A., Cecola, R.P., and Bell, B.F. (1996). Contralateral suppression of transient-evoked otoacoustic emissions in humans: intensity effects. *Hear. Res.* **101,** 113–118.

Howard. M.A., Volkov. I.O., Mirsky, R., Garell, P.C., Noh, M.D., Granner, M., Damasio, H., Steinschneider, M., Reale, R.A., Hind, J.E., and Brugge, J.F. (2000). Auditory cortex on the human posterior superior temporal gyrus. *J. Comp. Neurol.* **416,** 79–92.

Huckins, S.C., Turner, C.W., Doherty, K.A., Fonte, M.M., and Szevernyi, H.M. (1998). Functional magnetic resonsnce imaging measures of blood flow patterns in the human auditory cortex in response to sound. *JSLHR* **41,** 538–548.

Hudspeth, A.J. (1989). Mechanoelectrical transduction by hair cells of the bullfrog's sacculus. *Prog. Brain Res.* **80,** 129–135.

Hugdahl, K., Bronnick, K., Kyllingsbaek, S., Law, I., Gade, A., and Paulson, O.B. (1999). Brain activation during dichotic presentations of consonant-vowel and musical instument stimuli: a 15O-PET study. *Neurophsychologica* **17,** 431–440.

Imig, T.J., Ruggero, M.A., Kitzes, L.M., Javel, E., and Brugge, J.F. (1977). Organization of auditory cortex in the owl monkey *(Aotus trivirgatus). J. Comp. Neurol.* **171,** 111–128.

Irving, R., and Harrison, J.M. (1967). The superior olivary complex and audition: a comparative study. *J. Comp. Neurol.* **130,** 77–86.

Ishi, T., Murakami, Y., and Balogh, K. (1967). Acetylcholinesterase activity in the efferent nerve fibers of the human inner ear. *Ann. Otol. Laryngol.* **76,** 115–123.

Itaya, S.K., and Van Hoesen, G.W. (1982). Retinal innervation of the inferior colliculus in rat and monkey. *Brain Res.* **233,** 45–52.

Jenkins, W.M., and Masterton, R.B. (1982). Sound localization: effects of unilateral lesions in central auditory system. *J. Neurophysiol.* **47,** 987–1016.

Johnsson, L.G., Hawkins, J.E., and Linthicum, F.H.Jr. (1978). Cochlear and vestibular lesions in capsular otosclerosis as seen in microdissection. *Ann. Otol. Rhinol. Laryngol., Suppl.* **48,** 1–40.

Jones, E.G., and Powell, T.P.S. (1970). An antomical study of converging sensory pathways within the cerebral cortex of the monkey. *Brain* **93,** 793–820.

Jones, E.G., Dell'anna, M.E, Molinari, M, Rausell, E., and Hashikawa, T. (1995). Subdivisions of macaque monkey auditory cortex revealed by calcium-binding protein immunoreactivity. *J. Comp. Neurol.* **362,** 153–170.

Kachar, B., Brownell, W.E., Altschuler, R.A., and Fex, J. (1986). Electro-kinetic shape changes of cochlear outer hair cells. *Nature* **322,** 365–368.

Kaga, K., Shindo, M., and Tanaka, Y. (1997). Central auditory information processing in patients with bilateral auditory cortex lesions. *Acta Otolaryngol., Suppl.* **532,** 77–82.

Kangasuntheram, R., Wong, W.C., and Krishnamurti, A. (1968). Nuclear configuration of the diencephalon in some lorisoids. *J. Comp. Neurol.* **133,** 241–268.

Karlsson, K.K., Flock, B., and Flock, A. (1991). Ultrastructural changes in the outer hair cells of the guinea pig cochlea after exposure to quinine. *Acta Otolaryngol.* **111,** 500–505.

Kasai, H., Asada, T., Yumoto, M., Jakeya, J., and Matsuda, H. (1999). Evidence for functional abnormality in the right auditory cortex during musical hallucinations. *Lancet* **354,** 1703–1705.

Kemp, D.T. (1978). Stimulated acoustic emissions from within the human auditory system. *J. Acoust. Soc. Am.* **64,** 1386–1391.

Khalfa, S., and Collet, L. (1996). Functional asymmetry of medial olivocochlear system in humans: towards a peripheral auditory lateralization. *Neuroreport* **7,** 993–996.

Kiang, N.Y., Rho, J.M., Northrop, C.C., Liberman, M.C., and Ryugo, D.K. (1982). Hair-cell innervation by spiral ganglion cells in adult cats. *Science* **217,** 175–177.

Kolston, J., Osen, K.K., Hackney, C.M., Ottersen, O.P., and Storm-Mathisen, J. (1992). An atlas of glycine- and GABA-like immunoreactivity and colocalization in the cochlear nuclear complex of the guinea pig. *Anat. Embryol.* **186,** 443–465.

Kudo, M. (1981). Projections of the nuclei of the lateral lemniscus in the cat: An autoradiographic study. *Brain Res.* **221,** 57–69.

Lauter, J.L., Herscovitch, P., Formby, C., and Raichle, M.E. (1985). Tonotopic organization in human auditory cortex revealed by positron emission tomography. *Hear. Res.* **20,** 199–205.

Leonard, C.M., Puranik, C., Kuldau, J.M., and Lombardino, L,J. (1998). Normal variation in the frequency and location of human auditory cortex landmarks. Heschl's gyrus: where is it? *Cereb. Cortex* **8,** 397–406.

Liégeois-Chauvel, A., Musolino, A., Badier, J. M., Marquis, P., and Chauvel, P. (1994). Evoked potentials recorded from the auditory cortex in man: Evaluation and topography of the middle latency components. *EEG Clin. Neurophysiol.* **92,** 204–214.

Liégeois-Chauvel, A., Peritz, I., Babaï, M., Laguitton, V., and Chauvel, P. (1998). Contribution of different cortical areas in the temporal lobes to music processing. *Brain* **121,** 1853–1867.

Lue, A. J.-C., and Brownell, W.E. (1999). Salicylate induced changes in outer hair cell lateral wall stiffness. *Hear. Res.* **135,** 163–168.

Luethke, L.E., Krubitzer, L.A., and Kaas, J.H. (1989). Connections of primary auditory cortex in the New World monkey, Saguinus. *J. Comp. Neurol.* **285,** 487–513.

Mai, J.K., Assheuer, J., and Paxinos, G. (1997). "Atlas of the Human Brain." Academic Press, San Diego.

Mammo, F., and Ashmore, J.F. (1993). Reverse transduction measured in the isolated cochlea by laser Michelson interferometry. *Nature* **365,** 838–841.

Martin, W.H., Pratt, H., and Schwegler, J.W. (1995). The origin of the human auditory brain stem response wave II. *EEG Clin. Electrophysiol.* **96,** 357–370.

Mazziotta, J.C., Phelps, M.E., Carson, R.E., and Kuhl, D.E. (1982). Tomographic mapping of human cerebral metabolism: auditory stimulation. *Neurology* **32,** 921–937.

Mensulam, M.-M., and Pandya, D.N. (1973). The projections of the medial geniculate complex within the sylvian fissure of the rhesus monkey. *Brain Res.* **60,** 315–333.

Merzenich, M.M., and Brugge, J.F. (1973). Representation of the cochlear partition on the superior temporal plane of the macaque monkey. *Brain Res.* **50,** 275–296.

Moller, A.R., and Jannetta, P.J. (1982). Auditory evoked potentials recorded intracranially from the brainstem in man. *Exp. Neurol.* **78,** 144–157.

Moore, J.K. (1980). The primate cochlear nuclei: loss of lamination as a phylogenetic process. *J. Comp. Neurol.* **193,** 609–629.

Moore, J.K. (1987). The human auditory brain stem. A comparative view. *Hear. Res.* **29,** 1–32.

Moore, J.K. (2000). Organization of the human superior olivary complex *Microsc. Res. Tech.* **51,** 403–412.

Moore, J.K., and Moore, R.Y. (1971). A comparative study of the superior olivary complex in the primate brain. *Folia Primat.* **16,** 35–51.

Moore, J.K., and Osen, K.K. (1979). The cochlear nuclei in man. *Am. J. Anat.* **154,** 393–418.

Moore, J.K., Karapas, F., and Moore, R.Y. (1977). Projections of the inferior colliculus in insectivores and primates. *Brain. Behav. Evol.* **14,** 301–327.

Moore, J.K., Osen, K.K., Storm-Mathisen, J., and Ottersen, O.P. (1996a). γ-Aminobutyric acid and glycine in the baboon cochlear nuclei: An immunocytochemical colocalization study with reference to interspecies differences in inhibitory systems. *J. Comp. Neurol.* **369,** 497–519.

Moore, J.K., Ponton, C.W., Eggermont, J.J., Wu, B.J.-C., and Huang, J.Q. (1996b). Perinatal maturation of the auditory brainstem response: Changes in path length and conduction velocity. *Ear Hear.* **17,** 411–418.

Moore, J.K., Guan, Y.-L., and Shi, S.-R. (1997). Axogenesis in the human fetal auditory system, demonstrated by neurofilament immunohistochemisty. *Anat. Embryol.* **195,** 15–30.

Moore, J.K., Simmons, D.D., and Guan, Y.-L. (1999). The human olivocochlear system: organization and development. *Audiol. Neuro-Otol.* **4,** 311–325.

Moore, R.Y., and Goldberg, J.M. (1966). Projections of the inferior colliculus in the monkey. *Exp. Neurol.* **14,** 429–438.

Morel, A., and Kaas, J.H. (1992). Subdivisions and connections of auditory cortex in owl monkeys. *J. Comp. Neurol.* **318,** 27–63

Morel, A., Garraghty, P.E., and Kaas, J.H. (1993). Tonotopic organization, architectonic fields, and connections of auditory cortex in macaque monkeys. *J. Comp. Neurol.* **335,** 437–459.

Moskowitz, N., and Liu, J.-C. (1972). Central projections of the spiral ganglion of the squirrel monkey. *J. Comp. Neurol.* **144,** 335–344.

Mott, J.B., Norton, S.J., Neely, S.T., and Warr, W.B. (1989). Changes in spontaneous otoacoustic emissions produced by acoustic stimulation of the contralateral ear. *Hear. Res.* **38,** 229–242.

Mugnaini, E., Warr, W.B., and Osen, K.K. (1980). Distribution and light microscopic features of granule cells in the cochlear nuclei of cat, rat and mouse. *J. Comp. Neurol.* **191,** 581–606.

Mummery, C.J., Ashburner, J., Scott, S.K., and Wise, R.J.S. (1999). Functional neuroimaging of speech perception in six normal and two aphasic subjects. *J. Acoust. Soc. Am.* **106,** 449–457.

Nadol, J.B. Jr. (1990). Synaptic morphology of inner and outer hair cells of the human organ of Corti. *J. Electron Microsc. Tech.* **15,** 187–196.

Natout, M.A., Terr, L.I., Linthicum, F.H., Jr., and House, W.F. (1987). Topography of vestibulocochlear nerve fibers in the posterior cranial fossa. *Laryngoscope* **97,** 954–958.

Oertel, D., and Wu, S.H. (1989). Morphology and physiology of cells in slice preparations of the dorsal cochlear nucleus of mice. *J. Comp. Neurol.* **283,** 228–247.

Oertel, D., Bal, R., Gardner, S.M., Smith, P.H., and Joris, P.X. (2000). Detection of synchrony in the activity of auditory nerve fibers by octopus cells of the mammalian cochlear nucleus. *Proc. Natl. Acad. Sci. U.S.A.* **97,** 11773–11779.

Olazábal, U.E., and Moore, J.K. (1989). Nigrotectal projection to the inferior colliculus: Horseradish peroxidase transport and tyrosine hydroxylase immunohistochemical studies in rats, cats, and bats. *J. Comp. Neurol.* **282,** 98–118.

Oört, H. (1918). über die Verästellung des Nervus octavus bei Säugetieren. *Anatom. Anzeig.* **51,** 272–280.

Osen, K.K., and Jansen, J. (1965). The cochlear nuclei in the common porpoise, Phocaena phocaena. *J. Comp. Neurol.* **125,** 223–257.

Osen, K.K., Mugnaini, E., Dahl, A.-L., and Christiansen, A.H. (1984). Histochemical localization of acetylcholinesterase in the cochlear and superior olivary nuclei: a reappraisal with emphasis on the cochlear granule cell system. *Arch. Ital. Biol.* **122,** 169–212.

Ostapoff, E.-M., and Morest, D.K. (1991). Synaptic organization of globular bushy cells in the ventral cochlear nucleus of the cat. *J. Comp. Neurol.* **314,** 598–613.

Ostapoff E.-M., Benson, C.G., and Saint Marie, R.L. (1997). GABA- and glycine-immunoreactive projections from the superior olivary complex to the cochlear nucleus in guinea pig. *J. Comp. Neurol.* **381,** 500–512.

Ota, C.Y., and Kimura, R.S. (1980). Ultrastructural study of the human spiral ganglion. *Acta Otolaryngol. (Stockh)* **89,** 53–62.

Otte, J., Schuknecht, H.F., and Kerr, A.F. (1978). Ganglion cell population in normal and pathological human cochlea. Implications for cochlear implantation. *Laryngoscope* **88,** 1231–1246.

Pandya, D.N., and Rosene, D.L. (1993). Laminar termination patterns of thalamic, callosal, and association afferents in the primary auditory area of the rhesus monkey. *Exp. Neurol.* **119,** 220–234.

Pandya, D.N, and Sanides, F. (1973). Architectonic parcellation of the temporal operculum in rhesus monkey and its projection pattern. *Z. Anat. Entwickl-Gesch.* **139,** 127–161.

Pandya, D.N., Rosene, D.L., and Doolittle, A.M. (1994). Cortocothalamic connections of auditory -related areas of the temporal lobe in the rhesus monkey. *J. Comp. Neurol.* **345,** 447–471

Pantev, C., Hoke, M., Lütkenhöner, and Lehnertz, K. (1989). Tonotopic organization of the auditory cortex: pitch versus frequency representation. *Science* **246,** 486–487.

Pauler, M., Schuknecht, H.F., and White, J.A. (1988). Atrophy of the stria vascularis as a cause of sensorineural hearing loss. *Laryngoscope* **98,** 754–759.

Paxinos, G., and Huang, X.-F. (1995). "Atlas of the Human Brainstem." Academic Press, San Diego.

Pickles, J.O., Comis, S.D., and Osborne, M.P. (1984). Cross-links between stereocilia in the guinea pig organ of Corti, and their possible relation to sensory transduction. *Hear. Res.* **15,** 103–112.

Polyakov, A., and Pratt, H. (1996). Evidence for spatio-topic organization of binaural processing in the human brainstem. *Hear. Res.* **94,** 107–115.

Pratt, H., Polyakov, A., Ahronson, V., Korczyn, A.D., Tadmor, R., Fullerton, B.C., Levine, R.A., and Furst, M. (1998). Effects of localized pontine lesions on auditory brain-stem evoked potential and binaural processing in humans. *EEG Clin. Neurophysiol.* **108,** 511–520.

Price, C., Wise, R., Ramsay, S., Friston, K., Howard, D., Patterson, K., and Frackowiak, R. (1992). Regional response differences within the human auditory cortex when listening to words. *Neurosci. Lett.* **146,** 179–182.

Puce, A., Allison, R., Bentin, S., Gore, J. C., and McCarthy, G. (1998). Temporal cortex activation in humans viewing eye and mouth movements. *J. Neurosci.* **18,** 2188–2199.

Puel, J.L., Bonfils, P., and Pujol, R. (1988). Selective attention modifies the active micromechanical properties of the cochlea. *Brain Res.* **447,** 380–383.

Rademacher, J., Morosan, P., Schlorman, T., Schleicher, A., Werner, C., Freund, H.J., and Zilles, K. (2001a). Probabilistic mapping and volume measurement of human primary auditory cortex. *Neuroimage* **13,** 669–683.

Rademacher, J., Morosan, P., Schleicher, A., Freund, H.J., and Zilles, K. (2001b). Human primary auditory cortex in women and men. *Neuroreport* **12,** 1561–1566.

Rauschecker, J.P., Tian, B., Pons, T., and Mishkin, M. (1997). Serial and parallel processing in rhesus monkey auditory cortex. *J. Comp. Neurol.* **382,** 89–103.

Rhys Evans, P.H., Comis, S.D., Osborne, M.P., Pickles, J.O., and Jeffries, J.R. (1985). Cross-links between stereocilia in the human organ of Corti. *J. Lanyngol. Otol.* **99,** 11–19.

Rivier, F., and Clarke, S. (1997). Cytochrome oxidase, acetylcholinesterase, and NADPH-diaphorase staining in human supratemporal and insular cortex: evidence for multiple auditory areas. *Neuroimage* **6,** 288–304.

Roeser, R.J. and Daly, D.D. (1974). Auditory cortex disconnection associated with thalamic tumor. A case report. *Neurology* **24,** 555–559.

Roland, P.E., Skinhoj, E., and Lassen, N.A. (1981). Focal activations of human cerebral cortex during auditory discrimination. *J. Neurophysiol.* **45,** 1139–1151.

Ryan, A., and Dallos, P. (1996). The physiology of the cochlea. *In* "Hearing Disorders" (J. Northern, ed.), 3rd ed., pp. 15–31. Allyn & Bacon, Boston.

Saint Marie, R.L., Benson, C.G., Ostapoff, E.M., and Morest, D.K. (1991). Glycine immunoreactive projections from the dorsal to the anteroventral cochlear nucleus. *Hear. Res.* **51,** 11–28.

Saint Marie, R.L., Shneiderman, A., and Stanforth, D.A. (1997). Patterns of γ-aminobutyric acid and glycine immunoreactivities reflect structural and functional differences of the cat lateral lemniscal nuclei. *J. Comp. Neurol.* **389,** 264–276.

Samson, S., and Zatorre, R.J. (1994). Contribution of the right temporal lobe to musical timbre discrimination. *Neuropsychologia* **12,** 231–240.

Scharf, B., Magnan, J., and Chays, A. (1997). On the role of the olivocochlear bundle in hearing: 16 case studies. *Hear. Res.* **103,** 101–122.

Scherg, M., and von Cramon, D. (1985). A new interpretation of the generators of BAEP waves I-V: results of spatio-temporal dipole modeling. *EEG Clin. Neurophysiol.* **62,** 290–299.

Schlosser, M., Aoyagi, N., Fulbright, R.K., Gore, J.C., and McCarthy, G. (1998). Functional MRI studies of auditory comprehension. *Brain Map.* **6,** 1–13.

Schrott-Fischer, A., Egg, G., Kong, W.-J., Renard, N., and Eybalin, M. (1994). Immunocytochemical detection of choline acetyltransferase in the human organ of Corti. *Hear. Res.* **78,** 149–157.

Schuknecht, H.F., Churchill, J.A., and Doran, R. (1959). The localization of acetylcholinesterase in the cochlea. *Arch. Otolaryngol.* **69,** 549–559.

Seltzer, B., and Pandya, D.N. (1978). Afferent cortical connections and architectonics of the superior temporal sulcus and surrounding cortex in the rhesus monkey. *Brain Res.* **149,** 1–24.

Seltzer, B., and Pandya, D.N. (1994). Parietal, temporal and occipital projections to cortex of the superior temporal sulcus in the rhesus monkey: a retrograde tracer study. *J. Comp. Neurol.* **343,** 445–463.

Slepecky, N., Ulfendahl, M., and Flock, A. (1988). Shortening and elongation of isolated outer hair cells in response to application of potassium gluconate, acetylcholine and cationized ferritin. *Hear. Res.* **34,** 119–126.

Smith, P.H., Joris, P.X., and Yin, T.C. (1993). Projections of physiologically characterized spherical bushy cell axons from the cochlear nucleus of the cat: evidence for delay lines to the medial superior olive. *J. Comp. Neurol.* **331,** 245–260.

Smith, P.H., Joris, P.X., and Yin, T.C. (1998). Anatomy and physiology of principal cells of the medial nucleus of the trapezoid body (MNTB) of the cat. *J. Neurophysiol.* **79,** 3127–3142.

Snyder, R.L., and Leake, P.A. (1988). Intrinsic connections within and between cochlear nucleus subdivisions in cat. *J. Comp. Neurol.* **278,** 208–225.

Spangler, K.M., Cant, N.B., Henkel, C.K., Farley, G.R., and Warr, W.B. (1987). Descending projections from the superior olivary complex to the cochlear nuclelus of the cat. *J. Comp. Neurol.* **259,** 452–465.

Spoendlin, H. (1985). Anatomy of cochlear innervation. *Am. J. Otolaryngol.* **6,** 453–467.

Spoendlin, H., and Schrott, A. (1989). Analysis of the human auditory nerve. *Hear. Res.* **143,** 25-38.

Springer, J.A., Binder, J.R., Hammeke, T.A., Swanson, S.J., Frost, J.A., Bellgowan, P.S.F., Brewer, C.C., Perry, H.M., Morris, G.L., and Mueller, W.M. (1999). Language dominance in neurologically normal and epilepsy subjects. A functional MRI study. *Brain* **122,** 2033–2045.

Starr, A., McPherson, D., Patterson, J., Don, M., Luxford, W., Shannon, R., Sininger, Y., Tonakawa, L., and Waring, M. (1991). Absence of both auditory evoked potentials and auditory percepts dependent on timing cues. *Brain* **114,** 1157–1180.

Starr, A., Picton, T.W., Sininger, Y., Hood, L.J., and Berlin, C.I. (1996). Auditory neuropathy. *Brain* **119,** 741–753.

Strominger, N.L. (1973). The origins, course and distribution of the dorsal and intermediate acoustic striae in the rhesus monkey. *J. Comp. Neurol.* **147,** 209–234.

Strominger, N.L., and Strominger, A.I. (1971). Ascending brain stem projections of the anteroventral cochlear nucleus in the rhesus monkey. *J. Comp. Neurol.* **143,** 217–242.

Strominger, N.L., Nelson, L.R., and Dougherty, W.J. (1977). Second order auditory pathways in the chimpanzee. *J. Comp. Neurol.* **15,** 349–365.

Symmes, A.N., Alexander, G.E., and Newman, J.D. (1980). Neural processing of vocalizations and artificial stimuli in the medial geniculate body. *Hear. Res.* **3,** 133–146.

Takasaka, T., Shirikawa, H., Hashimoto, S., Watanubi, K., and Kawamoto, K. (1983). High-voltage electron microscopic study of the inner ear. *Ann. Otol. Rhinol. Laryngol. 92, Suppl.* **102,** 1–12.

Thompson, A.M., and Thompson, G.C. (1991). Posteroventral cochlear nucleus projections to olivocochlear neurons. *J. Comp. Neurol.* **8,** 267–285.

Thompson, G.C., and Masterton, R.B. (1978). Brainstem auditory pathways involved in reflexive head orientation to sound. *J. Neurophysiol.* **541,** 1183–1202.

Thompson, G.C., and Thompson, A.M. (1986). Olivocochlear neurons in the squirrel monkey brainstem. *J. Comp. Neurol.* **254,** 246–258.

Tolbert, L.P., and Morest, D.K. (1982). The neuronal architecture of the anteroventral cochlear nucleus of the cat in the region of the cochlear nerve root: electron microscopy. *Neuroscience* **7,** 3053–3067.

Trojanowski, J.Q., and Jacobson, S. (1975). Areal and laminar distribution of some pulvinar cortical efferents in rhesus monkeys. *J. Comp. Neurol.* **169,** 371–392.

von Békésy, G. (1947). The variation of phase along the basilar membrane with sinusoidal vibrations. *J. Acoust. Soc. Am.* **19,** 452–460.

von Békésy, G. (1932). Zur Theorie des Hörens bei der Schallaufnahme durch Knockenleitung. *Ann. Phys.* **13,** 111–136.

von Economo, C. (1929). "The Cytoarchitectonics of the Human Cerebral Cortex." Oxford University Press, London.

Vueillet, E., Duverdy-Bertholon, F., and Collet, L. (1996). Effect of contralateral acoustic stimulation on the growth of click-evoked otoacoustic emissions in humans. *Hear. Res.* **93,** 128–135.

Walker, A.E. (1937). The projection of the medial geniculate body to the cerebral cortex in the macaque monkey. *J. Anat.* **17,** 319–331.

Walker, A.E., and Fulton, J.F. (1938). The thalamus of the chimpanzee. III. Metathalamus, normal structure and cortical connections. *Brain* **61,** 250–268.

Warr, W.B. (1975). Olivocochlear and vestibular efferent neurons of the feline brainstem: Their location, morphology and number determined by retrograde axonal transport and acetylcholinesterase histochemistry. *J. Comp. Neurol.* **161,** 159–182.

Warr, W.B. (1982). Parallel ascending pathways from the cochlear nucleus: Neuroanatomical evidence of functional specialization. *Contrib. Sens. Physiol.* **7,** 1–38.

Warr, W.B., and Guinan, J.J. (1979). Efferent innervation of the organ of Corti: Two separate systems. *Brain Res.* **173,** 152–155.

Webster, W.R., Servière, J., Crewther, D., and Crewther, S. (1984). Isofrequency 2-DG contours in the inferior colliculus of the awake monkey. *Exp. Brain Res.* **56,** 425–437.

Weeks, R.A., Aziz-Sultan, A., Bushara, K.O., Tian, B., Wessinger, C.M., Dang, N., Rauschecker, J.P., and Hallett, M. (1999). A PET study of human auditory spatial processing. *Neurosci. Lett.* **262,** 155–158.

Weiller, C., Isensee, C., Rijntjes, M., Huber, W., Müller, S., Bier, D., Dutschka, K., Woods, R.P., Noth, J.H., and Diener, H.C. (1995). Recovery from Wernicke's aphasia: a positron emission tomographic study. *Ann. Neurol.* **37,** 723–732.

Wenthold, R.J. (1987). Evidence for a glycinergic pathway connecting the two cochlear nuclei: An immunocytochemical and retrograde transport study. *Brain Res.* **380,** 7–18.

Wernicke, C. (1908). The symptom-complex of aphasia. *In* "Diseases of the Nervous System" (A. Church, ed.), pp. 621–700. Springer-Verlag, New York.

Wessinger, C.M., Buonocore, M.H., Kussmaul, C.L., and Mangun, R. (1997). Tonotopy in human auditory cortex examined with functional magnetic resonance imaging. *Hum. Brain Map.* **5,** 18–25.

Wiberg, M., Westman, J., and Blomqvist, A. (1987). Somatosensory projection to the mesencephalon: An anatomical study in the monkey. *J. Comp. Neurol.* **264,** 92–117.

Wickesberg, R.E., and Oertel, D. (1988). Tonotopic projection from the dorsal to the anteroventral cochlear nucleus of mice. *J. Comp. Neurol.* **268,** 389–399.

Winer, J.A. (1984). The human medial geniculate body. *Hear. Res.* **15,** 225–247.

Wright, A. (1981). Scanning electron microscopy of the normal human cochlea. *Clin. Otolaryngol.* **6,** 237–244.

Yang, L., Liu, Q., and Pollak, G.D. (1996). Afferent connections to the dorsal nucleus of the lateral lemniscus of the mustache bat: evidence for two functional subdivisions. *J. Comp. Neurol.* **373,** 575–592.

Yeterian, E.H., and Pandya, D.N. (1991). Corticothalamic connections of the superior temporal sulcus in rhesus monkeys. *Exp. Brain Res.* **83,** 268–284.

Yin, T.C.T., and Chan, J.C. (1990). Interaural time sensitivity in medial superior olive of cat. *J. Neurophysiol.* **645,** 465–488.

Zatorre, R.J, Evans, A.C., Meyer, E., and Gjedde, A. (1992). Lateralization of phonetic and pitch discrimination in speech processing. *Science* **256,** 846–849.

Zatorre, R.J., Evans, A.C., and Meyer, E. (1994). Neural mechanisms underlying melodic perception and memory for pitch. *J. Neurosci.* **14,** 1908–1919.

Zeng, F.-G., Martino, K.M., Linthicum, F.H., and Soli, S.D. (2000). Auditory perception in vestibular neurectomy subjects. *Hear. Res.* **142,** 102–112.

Zook, J.M., and Casseday, J.H. (1982). Cytoarchitecture of the auditory system in lower brainstem of the mustache bat, *Pteronotus parnellii*. *J. Comp. Neurol.* **207,** 1–13.

Zvorykin, V.P. (1964). Morphological substrate of ultrasonic and locational capacities in the dolphin. *Fed. Proc.* **23,** T647–T653.

CHAPTER

35

Visual System

RAINER GOEBEL,[1] LARS MUCKLI,[2] and DAE-SHIK KIM[3]

[1]*Department of Neurocognition, Faculty of Psychology, Universiteit Maastricht, Maastricht, The Netherlands*

[2]*Department of Neurophysiology, Max-Planck Institute of Brain Research, Frankfurt, Germany*

[3]*Center for Magnetic Resonance Research, University of Minnesota, Minneapolis, MN, USA*

In neuroscience we know more about vision than any other system. This knowledge is derived from a rich diversity of methodological approaches. The advanced state of the neuroscientific research of the visual system is important in itself but may also serve as a model system for understanding general principles about how the brain processes information. In the following, basic anatomical and functional properties of the visual nervous system will be described. First, the early stages of visual processing in the eye and the pathways from the retina to the visual cortex are presented. This is followed by a detailed description of the remarkable organization of primary visual cortex. Then the anatomical and functional properties of areas are described, which are located in extrastriate cortex, the visually responsive cortex outside the primary visual area. Finally, general theoretical approaches are discussed in an attempt to explain how the visual system integrates processing in various specialized areas so as to construct a vivid representation of the visual world.

CENTRAL VISUAL PATHWAY

Anatomy of the Central Visual Pathway

Eye

The structure of the eye (Fig. 35.1) serves various functions that contribute to the formation of a clear image on the retina. In many aspects the human eye can be compared to a camera (Wurtz and Kandel, 2000). However, the optical qualities of the eyes are surprisingly poor in comparison with those of a regular camera. If, for example, the retina were replaced by a color film, we would receive pictures of deficient quality. Nevertheless, the visual system of humans is the most sophisticated visual system in nature. Before we turn to the question of how the visual system generates its amazing precision, we take a quick look at the structure of the eye (Tripathi and Tripathi, 1984).

The human eye is an approximately spherical ball of 24 mm diameter, surrounded by white, tough fibrous tissue—the sclera. The anterior segment of this tissue, the cornea, is avascular, transparent, and more highly curved. In its way from the outside world to the retina, light passes through the conjunctiva—a delicate membrane covering the cornea—through the cornea, the anterior chamber (aqueous humor), the lens, and the vitreal chamber (vitreous humor) until it enters the ganglion cell layers of the retina. In this way light is refracted by a power of about 43 diopters (dpt) at the

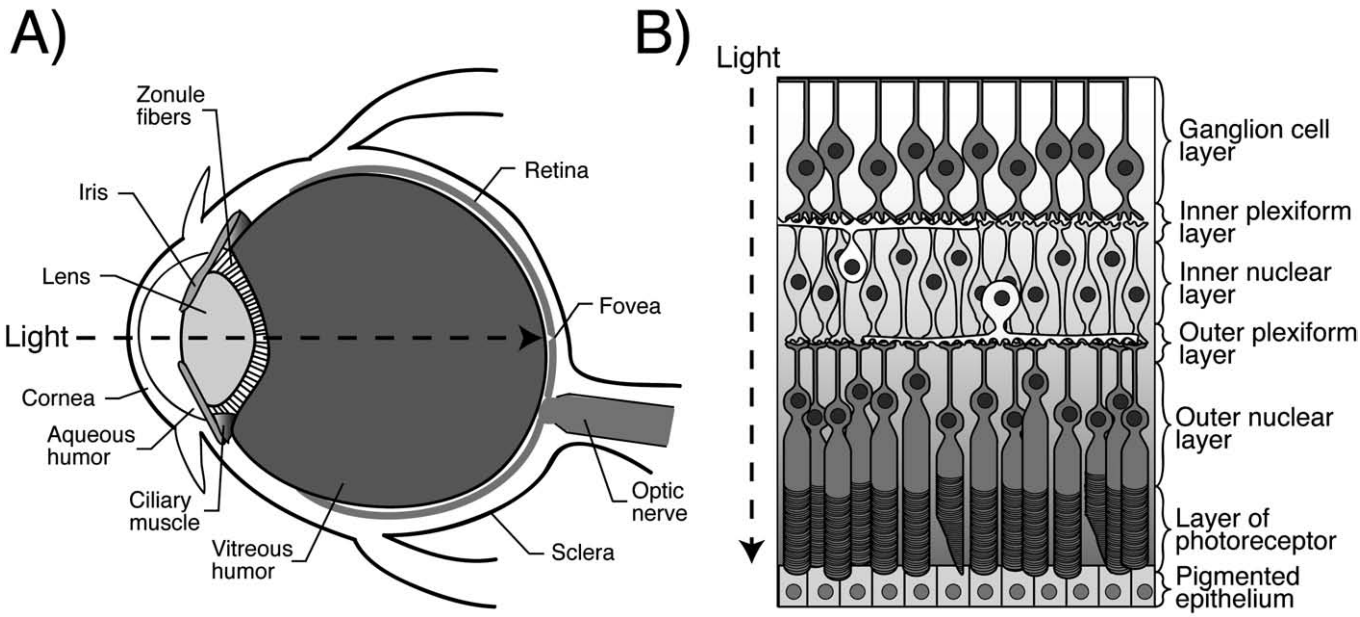

FIGURE 35.1 (A) The eye in cross section. (Adapted from Bear, Connor & Paradiso, 1996, p. 216). (B) The laminar structure of the retina, showing its five layers. Note that light must pass through these layers to reach the photoreceptors, which are situated at the back of the retina. (Adapted from Bear, Connor & Paradiso, 1996, p. 222).

cornea and about 20 dpt at the relaxed lens. Altogether 60 dpt refers to a focal point of 17 mm (1/60 m) after the lens.

The ***lens*** is an elastic body that is suspended by annular ligaments (zonule fibers), which originate in the ciliary muscle. The pressure of the inner eye tightens the lens through the annular ligaments. If the ciliary muscle, on which the annular ligaments are attached, contracts, the tension on the lens is relieved and the elastic lenses bend outward. A camera lens can be adjusted to focus on distant as well as on nearby objects by varying the distance between lens and projection plane. In the eyes, the refraction power is increased by flexion of the lenses. In the relaxed condition, the lenses are far-adjusted (10 m and above). In order to accommodate for nearby objects, the ciliary muscle is contracted so that the lenses can bend outward. Depending on the elasticity of the lenses, this can lead to a power of up to 8 dpt. The elasticity of the lens decreases with age, which leads to age-related farsightedness (presbyopia) (Bron *et al.*, 2000).

Farsightedness (hyperopia) also exists, independent of age, if the eyeball is too short and the refraction power is therefore not strong enough. In contrast, elongated eyeballs cause nearsightedness (myopia). At hyperopia the eyes try to compensate the missing refractory power by constant contraction of the ciliary muscle, but this compensation strategy becomes insufficient for near vision. In addition, ciliary muscle contraction leads automatically to an inward turning of the eyes, which is a useful mechanism for normal vision, allowing both eyes to fixate on an object even at close distances. In hyperopia, however, this mechanism misaligns the visual axes and leads to strabismus and double images. One strategy of the visual system to prevent double images is by constantly suppressing the information of one eye, which can eventually lead to amblyopia (Moore *et al.*, 1999; Sireteanu, 2000).

In front of the lens, there is another smooth muscle, the ***iris***, which has a function similar to that of the diaphragm of a camera in controlling the amount of light that enters the pupil. In this way the iris can quickly adjust to changing light intensities, the more effective but slower mechanism for light adaptation can be found in the section on Photoreceptors.

If the iris and the ciliary muscle are paralyzed, e.g., following application of atropine to the eyes, the iris will stay open and cause increased light irritability, and the ciliary muscle will remain relaxed, thus causing difficulties for near accommodation.

Retina

The main contribution of the eyes to vision is to project a picture from the external world onto the retina, upside down and focused, as in a camera. The retina's contribution, on the other hand, is much more complicated (Masland and Raviola, 2000). It transposes light into neuronal code (transduction) and processes

important features of the visual input (Meister and Berry, 1999). Right from the first synapse, the retina thereby feeds into parallel processing streams that are specialized for different visual features, such as contrasts, motion, or color, and that are kept in parallel for many processing steps until an undivided conscious percept is recovered somewhere in the neocortex (Wässle, 2002).

Some peculiarities of the retina are so distinct from other sensory organs that the retina is regarded as a peripheral part of the brain rather than a normal sensory organ. For one, the embryological development of the retina derives from a portion of the same neural ectoderm that gives rise to the rest of the brain (Graw, 1996). During the course of embryological development, the retina migrates to the periphery and then extends connecting links back to the rest of the brain. Moreover, the synaptic organization of the retina is similar to that of other regions of the brain.

The retina is structured into five layers named with reference to the center of the eyeball: outer nuclear layer, outer plexiform layer, inner nuclear layer, inner plexiform layer, and ganglion cell layer. Interestingly, light has to travel through all these layers until it reaches the photoreceptors—a fact that contributes to the relatively poor optical properties of the eyes mentioned earlier.

The fovea centralis—the region of best vision—is the only part of the retina at which the neuronal and vascular circuitry bends sideward, so that light reaches the photoreceptors directly. This part of the retina appears yellow—also referred to as yellow spot. Here single cones innervate distinct ganglion cells unlike in other regions of the retina where many photoreceptors converge to a few ganglion cells.

The retina itself is a thin layer about 2 mm thick and 270 mm wide. It contains about 120 million neurons. The pigmented epithelium at the outer end of the eyes (at the bottom of Fig. 35.1) assures that any remaining photons are absorbed if they have not been absorbed by the photoreceptors that are emedded in the epithelium.

Photoreceptors (Outer Nuclear Layer)

There are two main categories of photoreceptors in the outer nuclear layer: rods and cones (Schultze, 1866; Boycott and Wässle, 1999). The general structure of the 120 million rods and the 6 million cones is similar. They are composed of four parts: an outer segment containing the photosensitive substance (pigment), an inner segment, a cell body, and a synaptic terminal (pedicle). Human rods and cones are typical of a fairly general vertebrate pattern. Rods are more sensitive to dim light but not to color. Peripheral vision depends almost exclusively on rods, central vision on cones. At light intensities below the sensitivity of cones vision depends solely on rods (scotopic vision) and color processing is not possible. We become aware of our missing rod receptors in the fovea if we try to fixate a small light source, such as a star on a starry sky. Whenever we fixate that light source precisely it disappears and reappears only if we focus nearby (von Kries, 1896). Cones are less sensitive to dim light, but they are sensitive to color. In fact, there are three different kinds of cones in humans: S cones, which are maximally sensitive to short wavelength (420 nm, blue); M cones, sensitive to middle wavelength (531 nm; green); and L cones, sensitive to long wavelength (559 nm; red). Some birds and fishes have more then two cones; among mammals, only humans and some monkeys are trichromates (Jacobs, 1993, 2002; Wässle, 2002).

The wavelength to which the rods and cones are most sensitive depends on the absorption characteristics of the visual pigment it contains (rhodopsin; or one of three different cone opsins; Wurtz and Kandel, 2000). Visual pigment is a molecule found in the outer segment of photoreceptors, where thousands of lamellated membrane infoldings (cones) or free-floating membrane disks (rods) are tightly packed. Visual pigments consist of a large protein opsin and a small light-absorbing compound, retinal, which changes its configuration when activated by a specific wavelength of light and triggers a cascade of events that eventually lead to a hyperpolarization of the membrane potential. In darkness the concentration of the second-messenger molecule cGMP (cyclic guanosine 3′,5′-monophosphate) is high and opens cGMP-gated ion channels allowing a constant inward current that keeps the cell depolarized at –40 mV (dark current).

Light transduction leads to a reduction of cGMP and hence to hyperpolarization of the cell. Photoreceptors are sensitive to small changes in the illumination. Prolonged or slow changes of the illumination lead to light adaptation that is regulated by Ca^{2+} concentration changes. Dark-adapted rods are so light sensitive that they can detect a single photon. Upon the detection of a photon, the membrane potential hyperpolarizes, and increasing the release of glutamate at its synapses.

Until recently, it had been thought that the transformation of light to neuronal code is exclusively performed in rods and cones. Now, a retinal ganglion cell type has been found to contain a newly discovered light-responsive protein (melanopsin; Provencio *et al.*, 2000, 2002). These ganglion cells project primarily to the suprachiasmatic nucleus and are relevant for the control of the circadian clock (Hattar *et al.*, 2002).

Neuronal Processing (Inner to Outer Plexiform Layer)

The first neuronal computation that processes light information and extracts different features, which are

then processed in parallel (Stone, 1983) and projected from the retina toward the brain, is performed by four main cell types of neurons: ***horizontal cells***, ***bipolar cells***, ***amacrine cells***, and, finally, ***ganglion cells***. These cells collaborate on modulating the synapses between photoreceptors and bipolar cells, in the outer plexiform layer, and the synapses between bipolar cells and the ganglion cells, in the inner plexiform layer (cone pathway). It is the task of the bipolar cells to project the neural code forward to the ganglion cells. Horizontal cells have a modulatory influence at the photoreceptor synapse (outer plexiform layer). Amacrine cells have a modulatory influence at the ganglion cell synapse (inner plexiform layer). In the rod pathway there are A-II amacrine cells interposed between rod bipolar cells and ganglion cells (Kolb and Famiglietti, 1974). In this way, cells in the retina process the signals of one or many photoreceptors resulting in small or huge receptive fields. A receptive field corresponds to the region in space in which a light stimulus can induce a neuronal response, which can be either an enhancement (on cells) or a reduction (off cells) of activity.

Photopic Pathway The cone photoreceptors release the transmitter glutamate at their synaptic terminal, the cone pedicles, which inhibits off bipolar cells, and excites on bipolar and horizontal cells (Dogiel, 1891; Polyak, 1941; Boycott and Dowling, 1969; Kolb *et al.*, 1980; Boycott *et al.*, 1987). Horizontal cells, in turn, release the inhibitory transmitter γ-aminobutyric acid (GABA) at their termination zone, which is again at the cone pedicles. This synaptic arrangement has been named a triad (Missotten, 1965; Stell, 1965; Kolb, 1970; Boycott and Kolb, 1973). About 10 morphologically different types of bipolar cells project from the cone synapse to the inner plexiform layer (Boycott and Wässle, 1999). Four of them are off bipolar cell types; they respond more strongly if the stimulus is darker than the background, and six of them are on bipolar cell types, responding more strongly if the stimulus is brighter than the background. Two cone bipolar cell types, one on and one off bipolar, are especially sensitive to contrast information, another two are responsible for the red–green portion of light, and one is devoted to blue light (Dacey and Lee, 1994; Calkins *et al.*, 1998; Ghosh *et al.*, 1997). Furthermore, there are three cone bipolar cell types that specialize in detecting directional information, i.e., retinal drift or motion (Berry *et al.*, 1999). In the photopic pathway, cone bipolar cells synapse at dyads onto ganglion and amacrine cell dendrites.

Rod Pathway Rods are connected to rod bipolar cells (Boycott and Dowling, 1969; Kolb, 1970). These do not synapse directly onto ganglion cells but onto two kinds of amacrine cells, one of them being the all-amacrine cell (Wässle *et al.*, 1995). AII-amacrine cells make inhibitory synapses with off cone bipolar and off ganglion cells and contact on cone bipolar cells via large gap junctions. In this way, they are "through-conducting neurons" (Masland, 1986) that produce signals of opposite polarity in on and off ganglion cells.

Amacrine Cells Morphologically, there are 30–40 different types of these "axonless" amacrine cells (Masland and Raviola, 2000). Relatively little is known about the specific signal-processing properties of these different amacrine cells. One exception is the cholinergic starburst cell (Famiglietti, 1992), which has recently been shown to play an important role in the extraction of direction-selective information, which is fed forward to direction-selective ganglion cells. Direction-selective ganglion cells (Kuffler, 1953) respond to stimuli that are moving in one, but not in the opposite, direction. Yoshida *et al.* (2001) selectively eliminated the starburst amacrine cells in mice, which abolished direction selectivity in ganglion cells and the optokinetic eye reflex. This indicates that starburst cells are crucial for detecting the direction of movement in mice.

Ganglion Cells The retinal ganglion cells have their dendrites in the inner plexiform layer and their cell bodies in the ganglion cell layer. Retinal ganglion cells project their axons across the inner surface of the retina toward the optic disk, where the optic nerve is formed. The different response patterns of ganglion cells can be identified by microelectrode recordings (Kuffler, 1953). Ganglion cells either have on or off center response characteristics (see below; cf. Fig. 35.2B). Within each subgroup there are five to seven additional cell types. Their properties vary with respect to temporal dynamics (tonic or phasic), size of the receptive field, contrast sensitivity, and, as mentioned before, their capability to detect the direction of movement. Another ganglion cell type is devoted to the control of iris contraction (Berson *et al.*, 2002; Lucas *et al.*, 2001). Furthermore, there are ganglion cell types responding to red, green, or blue yellow light (color vision; Dacey, 1999).

The input from the photoreceptors (outer plexiform layer) to the ganglion cells arrives through bipolar and amacrine cells' synapses at the ganglion cells, dendrites in the inner plexiform layer. The inner plexiform layer is precisely organized into on and off layers, from which the respective on and off center ganglion cell dendrites originate.

Optic Nerve, Chiasm, Optic Tract

The axons of the retinal ganglion cells form the optic nerves, optic chiasm, and optic tracts. The optic nerves leave the retina at the optic disk and penetrate

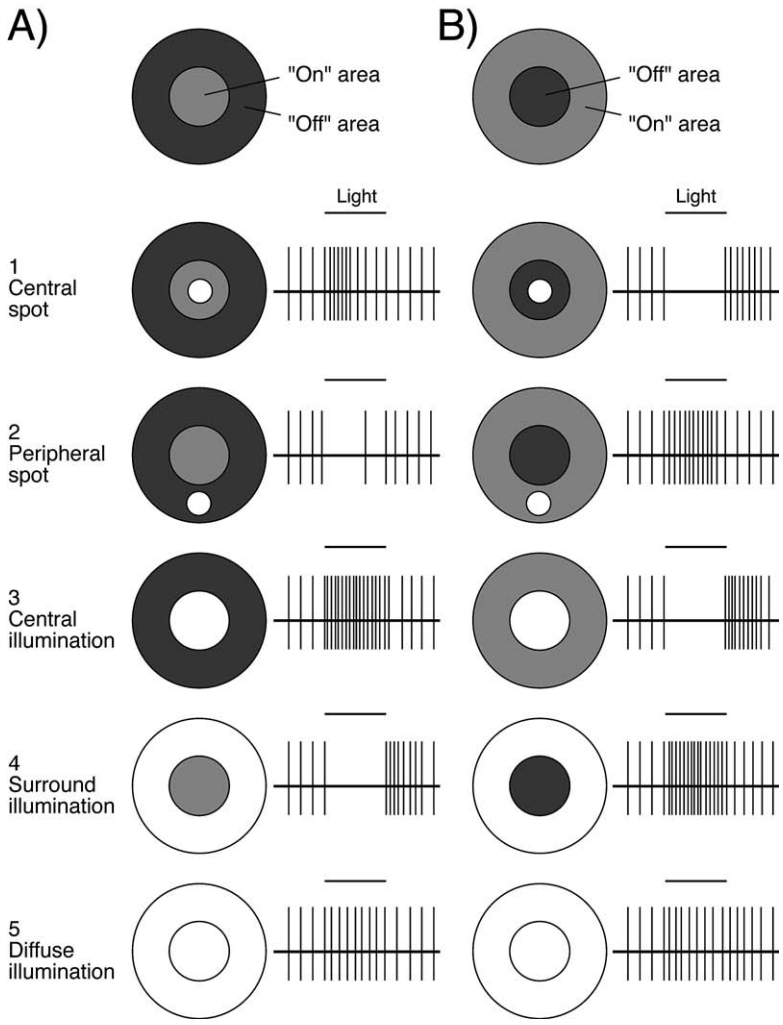

FIGURE 35.2 Retinal ganglion cells have circular receptive fields divided into a center and a surround. ON-center/OFF-surround cells are excited when illuminated in their center and inhibited when illuminated in their surround. OFF-center/ON-surround cells exhibit the opposite pattern. (A) ON-center cells respond maximally when (3) the center is illuminated and the surround is not and minimally in (4) the opposite illumination condition. Partial illumination of (1) center or (2) surround results in brief excitation and inhibition, respectively. Diffuse illumination (5) or darkness (not shown) results in a weak level of excitation because the center and surround tend to cancel each other's effects. (B) The activity of OFF-center cells is inhibited when (1, 3) their center is illuminated and excited when (2, 4) their surround is illuminated. As in the ON-center cells, opposing effects on center and surround caused by diffuse illumination (5) and darkness (not shown) produce weak levels of excitation. (Adapted from Kandel *et al.*, 1995, p. 418).

the lamina cribrosa. The area where the ganglion cell axons leave the retina does not have any photoreceptors; therefore, no visual information is detected in this region, which results in a blind spot in our visual field. This blind spot is easy to demonstrate; however, under normal circumstances the blind spot is not perceived but filled in. The optic nerve consists of about 1.5 million axons only. Most of them are 1 µm in diameter, about 10% of them are 2–10 µm, and all together a nerve fiber is 3–4 mm thick. Compared to the 120 million photoreceptors in the retina the signal has massively converged.

The neuronal circuitry in the retina has filtered and condensed the incoming information into 1 million specialized projections to the brain. About 5 cm after leaving the retina, the two optic nerves intermingle at the optic chiasm, where the containing axons are sorted into two optic tracts. In humans, about 50% of the axons cross the hemispheres. The distribution of fibers from one optic nerve into two optic tracts relates, in general, to the amount of binocularity. Thus, because in fish the eyes are placed far laterally, there is no overlap in the visual fields, and all the axons cross at the chiasm into the opposite optic tract. In animals in

which the eyes are set further forward, and thus the visual fields of the eyes overlap, the fibers cross only partially. This configuration is necessary to enable fusion of the corresponding retinal images. This principle was correctly deduced from optical considerations by Isaac Newton (Brewster, 1855), later by von Gudden (1874) and confirmed by von Monakow (1883). After crossing of the ganglion cells that originate in the nasal part of the retina, each optic tract contains always exclusively the information of the contralateral visual field. The nasal retinal ganglion cells process information from the lateral visual field. The retinal ganglion cells end mostly in the lateral geniculate nucleus (LGN) of the thalamus. In addition, right after the optic chiasm, there are a few other projections to midbrain structures (discussed below).

Lateral Geniculate Nucleus

In a cross section (Fig. 35.3) the lateral geniculate nucleus (LGN) appears somewhat like a bent knee, hence, the term geniculate, from the Latin for "knee." The LGN can be divided into six clearly visible layers, labeled 1–6 from ventral to dorsal. As mentioned above, 10% of the retinal ganglion cells are thicker in diameter. These belong to the heavily myelinated magnocellular system (M-type ganglion cells) and terminate in the lower layers 1 and 2 of the LGN. These layers consist of relatively large neurons and are called ***magnocellular layers***. Layers 3–6 contain small cells and are termed the ***parvocellular layers***, in which the P-type ganglion cells terminate. Crossed and uncrossed retinal fibers terminate in different laminae of the LGN; layers 1, 4, and 6 receive axons from the contralateral eye and 2, 3, and 5 from the ipsilateral eye. The cells of each layer constitute a ***retinotopic representation*** of the hemiretina that innervates it. The upper visual field projects inferior laterally in the LGN and the lower field superior medially (Connolly and Van Essen, 1984; Kaas *et al*., 1972; Malpeli and Baker, 1975). The maps of the six layers are precisely in register. The fovea projects to the posterior pole of the LGN and receives a disproportionately large representation (magnification factor).

Neurons in the magnocellular LGN (layers 1 and 2) are more sensitive to contrast, respond strongly to movement, but are insensitive to wavelength. In contrast, the majorities of parvocellular neurons respond weakly to movement but are color-opponent cells (concentric single opponent, concentric broadband opponent, and coextensive single opponent).

Optic Radiation

Four major projection streams project from the LGN to the visual cortex, two from the magnocellular layers of the LGN and two from the parvocellular layers. They form the optic radiation, which starts to bend slightly anteriorly and laterally before it swings posteriorly in the walls of the lateral ventricle to enter the white matter of the occipital pole. Their retinotopic structure is maintained throughout the projection from the LGN toward the visual cortex. Axons of the magnocellular layers synapse in layer IVCα, whereas parvocellular layers synapse in the neighboring but separate IVCβ.

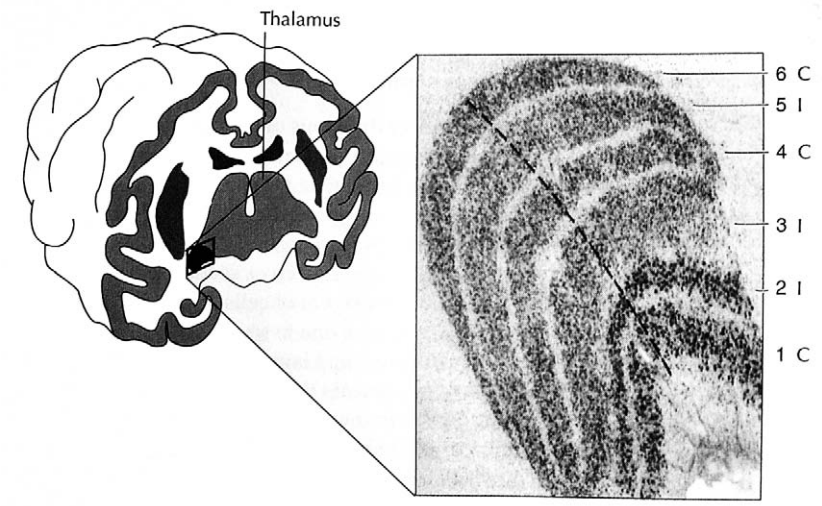

FIGURE 35.3 The lateral geniculate nucleus of the macaque monkey. The tissue has been stained to show cell bodies and reveals the LGN's six-layered organization, with the two ventral layers (magno-cellular layers) composed of larger cells than the other four layers (parvocellular layers). Each layer receives input exclusively from either the contralateral (C) or ipsilateral (I) eye. (Adapted from Bear, Connor & Paradiso, 1996, p. 249).

Retinotectal and Other Projections

The great majority—about 90%—of retinofugal projections terminate in the LGN (see above) Another eight different projection routes leave the retina to terminate in nuclei of the thalamus, the hypothalamus, or the brain stem.

Just below the optic chiasm is the termination region of the hypothalamus, the ***suprachiasmatic nucleus,*** which is important for the generation of the circadian rhythms (Moore, 1973).

Soon after, the optic chiasm projections branch off to ***pretectal*** nuclei (olivary nucleus) and to the ***superior colliculus***. The superficial layers of the colliculus receive input from the retina and V1; the deeper layers also receive inputs from other sensory systems. The major output of these laminae is to those deeper regions of the midbrain and the brain stem that are concerned with the generation of eye movements.

In addition, the pretectal nuclei and the ***ventral LGN*** control the pupillar contraction and also contribute to the control of eye movements. The ***accessory optic tract*** (dorsal, medial, and lateral accessory optic nucleus; Giolli, 1963) and the pretectal nuclei contribute to the detection of self-motion and the initiation of compensatory body movements (Weiskrantz, 1990). Among some smaller projection routes are those to the ***inferior pulvinar*** and the ventral LGN, and to the hypothalamus (suprachiasmatic nucleus).

Functional Aspects and Pathology of the Central Visual Pathway

Neural Processing in the Retina

As mentioned before, the eye is often compared to a camera and the retina to the film in the camera. However, the neuronal processing in the retina, is much more effective. It results in the output of 12–15 functionally distinct ganglion cell types, which can be regarded as 12–15 separate films that have been exposed with different temporal resolution, with different light sensitivity, and different spatial resolution, in addition to one separate film devoted to the recording of moving pictures. The massive parallel processing that is realized by the retina enables such an outstanding performance (Hubel and Wiesel, 1979).

An important feature of retinal ganglion cells is their divided antagonistic center-surround receptive field. The circular receptive fields have either an on center/off surround (often called on center) or an off center/on surround (off center). The antagonistic relationship of center and surround means that if the center and surround are illuminated simultaneously, the firing rate of the neuron will be relatively low (see Figs. 35.1 and 35.2). The same is true if both zones are not illuminated. The antagonistic nature of the receptive fields serves important functions for the visual system; it fosters ***contrast enhancement*** and contributes to ***lightness constancy***. In contrast enhancement, a darker area that is next to a lighter area appears to have an even darker band along the common boarder, whereas the lighter area appears to have an even lighter band along the common boarder (as can be illustrated by Mach bands). This process sharpens vision by exaggerating differences in lightness. The visual system is specialized to detect contours rather then absolute level of luminance. If the overall level of luminance increases, the center and the surround input of a ganglion cell is enhanced. Due to the antagonistic nature the net effect is constant firing across different intensities of illumination.

Visual Deficits Induced by Lesions to the Central Visual Pathway

The nature of the visual impairments seen after damage to different parts of the visual pathways reflects the anatomical relationships in the central visual pathway (Fig. 35.4). In the optic tract, the nasal half of each retina crosses over to the other side of the brain, whereas the fibers from the two temporal hemiretinas do not cross over. Each optic tract carries information from the ipsilateral temporal hemiretina and the contralateral nasal hemiretina, which means that each optic tract conveys the visual information of the contralateral visual field. Thus, damage to optic fibers anterior to the optic chiasm affects vision in one eye. Damage to the optic chiasm itself most often results in damage to its medial portions, causing bitemporal hemianopia.

PRIMARY VISUAL CORTEX

Anatomy and Lamination

The primary visual cortex is commonly known as area V1, or area 17 according to Brodmann (Brodmann, 1909), or area OC according to von Economo (Von Economo and Koskinas, 1925). The primary visual cortex is the first cortical area in which the visual data converge after their initial separate processing in the retina and subcortical nuclei, in particular LGN and superior colliculus. It is believed that the unity of the information needed for a complete reconstruction for the visual world is still preserved in this first processing stage of the cortical visual pathway. Beyond area V1, different features of the visual world are processed in separate cortical areas in a massively parallel manner

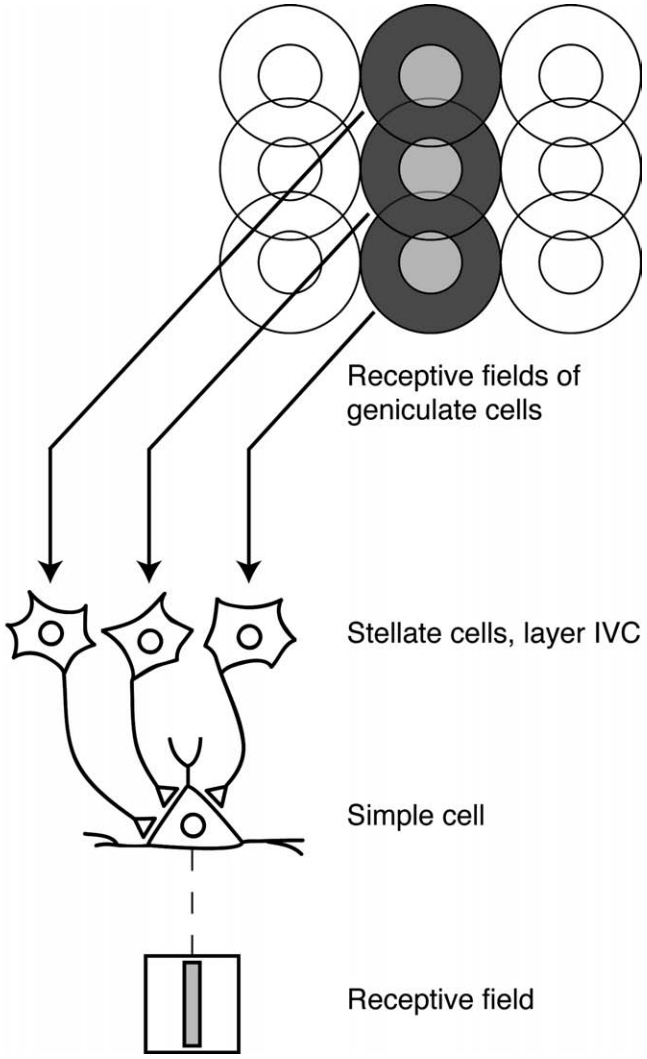

FIGURE 35.4 The mechanism by which the output of LGN cells with center-surround receptive fields is transformed into the elongated receptive fields of simple cortical cells is unknown. One hypothesis is that the simple cortical cell's receptive field is generated by the converging input of three or more ON-center LGN cells whose centers define its location and orientation. (Adapted from Kandel *et al.*, 1995, p. 435).

(Felleman and Van Essen, 1991; Ungerleider and Haxby, 1994). In other words, V1 might be assumed to be the gateway to the higher visual areas, and as such it has attracted a great deal of investigation in the past. While most of our knowledge about the structure and function of V1 originates from studies in nonhuman primates, in particular that of Old World monkeys (Felleman and Van Essen, 1991), the basic scaffold of the functional architecture in humans is generally assumed to be homologous to that of other primates.

In humans, much of area V1 lies on the medial surface of the respective hemispheres, surrounding the calcarine fissure in the occipital lobe (Bolton, 1900; Brodmann, 1909; Zilles, 1990). Rostrally and posterolaterally area V1 is bordered by the lunate and inferior occipital sulci, respectively. In adult macaque monkeys, 1 mm^3 of V1 tissue contains approximately 4700 neurons, 2900 microglia, 3400 oligodendrocytes, and 49,000 astrocytes (O'Kusky and Colonnier, 1982). The cell densities in human striate cortex might be considered to be around the same order of magnitude.

The primary visual cortex consists of a wide variety of cells (Lund, 1988; Peters and Jones, 1984). Traditionally, the cells in V1 have been classified into two morphologically and functionally distinct types: excitatory pyramidal and a wide variety of nonpyramidal cells (Peters and Jones, 1984). The axons of pyramidal cells provide the feedforward and feedback projects to the other cortical areas and subcortical structures, respectively (Lund, 1988; Rockland and Lund, 1983; Yoshitaka *et al.*, 1996). The axons of nonpyramidal cells are confined within the primary visual cortex (Callaway, 1998; Lund, 1988).

Around 80% of cells in the primary visual cortex are pyramidal (Callaway, 1998; Lund, 1988; Peters and Jones, 1984; Yoshitaka *et al.*, 1996). Their cell bodies are shaped like pyramids, and they have apical dendrites that extend toward the white matter. The dendrites are covered with numerous spines, thus identifying themselves as excitatory neurons. Most pyramidal cells can be found in the cortical layers II/III and V/VI (Callaway, 1998; Lund, 1988). Among the nonpyramidal cells, the stellate cells are the most ubiquitous ones. Stellate cells are generally smaller than pyramidal cells and their cell bodies are star shaped. Stellate cells are present in two variations: spiny and smooth (nonspiny). The spiny stellate cells are excitatory, whereas the smooth ones are inhibitory. Both the pyramidal and the spiny stellate neurons use mostly glutamate or aspartate as their neurotransmitter. The smooth, inhibitory stellate cells use mainly γ-aminobutyric acid (GABA) as their neurotransmitter (Fitzpatrick *et al.*, 1987).

Besides the pyramidal and the stellate cells, the primary visual cortex contains a large number of other, relatively low-density cells. While the exact number of different cell types in V1 will depend on the methodological criteria and taxonomical definitions applied, more than 40 types of cells have been identified based on cell morphology, dendritic arborization, physiology, and immunostainings (Lund, 1988; Peters and Jones, 1984). Some of the more prominent of these low-density cells are as follows:

1. *Inhibitory basket cells.* Basket cells have relatively large cell bodies with myelinated axonal branch extending laterally for a great distance; Their axonal

collaterals terminate on pyramidal cell bodies and dendrites in a manner resembling a basket.
2. *Chandelier cells* are inhibitory cells, with axons displaying characteristic branching into vertical sections.
3. *Inhibitory double-bouquet cells.* Double-bouquet cells have axon collaterals and dendrites extending vertically in a tight bundle.
4. *Neurogliaform cells.* These are inhibitory neurons resembling glial cells. Their axon and dendrites branch but mostly remain in the vicinity of the soma giving rise to a dense spherical region of fibers.
5. *Cajal–Retzius cells.* These inhibitory cells are one of the very few types found in layer I of the primary visual cortex. Cajal–Retzius cells are found predominantly in the neonatal brains. Although most Cajal–Retzius cells disappear during the postnatal development, some may survive into the adulthood.

Like other cortical areas, V1 consists of a laminated sheet of cells arranged in six main layers (most dorsal layer I through most ventral layer VI) with the full thickness from pia to the white matter of about 2 mm (O'Kusky and Colonnier, 1982). The laminated anatomical segregation and the unique pattern of connectivity between the laminae throughout V1 suggest a division of computational labor between the different laminae (Hubel and Wiesel, 1972; Lund, 1988; Rockland and Lund, 1983). Most commonly, the six layers of the primary visual cortex are subdivided into nine distinct layers of neurons: layers I, II, III, IVA, IVB, IVCα, IVCβ, V, and VI. There is a great variability of cell types, density, and pattern of connectivity from layer to layer.

Layer I is nearly devoid of neurons and is composed predominantly of dendritic and axonal connections (Lund and Wu, 1997). The apical dendrites from layers II–VB pyramidal cells form a dense network of synapses with axonal inputs from LGN, the pulvinar, feedback pathways from extrastriate areas, nonspecific thalamic nuclei, and other subcortical regions. Thus, while layer I contains few neurons, it is a networking layer that has a direct concerted effect on the firing properties of pyramidal cells in deeper layers.

Layers II/III (also called "supragranular" layers) consist of many somata and dendrites of excitatory pyramidal cells (Lund, 1988; Lund and Wu, 1997; Rockland and Lund, 1983). While layer II/III neurons receive only few thalamic inputs [with the exception of cells inside cytochrome oxidase (CO) blobs], they receive massive inputs from layer IVC neurons (directly from IVCβ and indirectly from IVCα through IVB). Layers II/III neurons are also connected through reciprocal projections with layer V neurons. Excitatory pyramidal cells in II/III project extensively to extrastriate cortical regions such as V2, V3, V4, and V5 (human homolog of primate MT). In addition, through a plexus of long-range horizontal connections, layer II/III excitatory pyramidal cells are interlinked with other pyramidal cells sharing similar receptive field properties (Lund, 1988; Malach *et al.*, 1993; Ts'o *et al.*, 1986). Such long-range horizontal connections can extend for up to several millimeters. About 20% cells in layers II/III are GABAergic and hence presumably inhibitory interneurons that do not project axons outside these layers. While their precise computational role remains elusive, it is generally believed that these interneurons perform dynamic gain control of cortical activity (Fitzpatrick *et al.*, 1987).

Layer IV (the "granular" layer) is divided into four horizontal sublayers: IVA, IVB, IVCα, and IVCβ. Layers IVCα and IVCβ are the major recipients of dorsal LGN (LGNd) innervation (Hubel and Wiesel, 1972; Lund, 1988). The LGNd magnocellular (M) and parvocellular (P) layers project to IVCα and the IVCβ, respectively [axons from interlaminar zones in LGNd (I) project to CO blobs neurons in II/III; see below]. Thus, the M and P streams remain segregated at this stage. Layer IVCα and IVCβ receive vertical inputs from layer VI neurons. Layer IVA shows up in the Nissl stain as a dark band of small granule-like cells. This and the lack of pyramidal cells differentiate this layer from layer IIIB. Layer IVB is a low-cell-density layer that contains a low-density arrangement of pyramidal cells. However, IVB plays a significant role in conveying the M-pathway information through two principal projections: (1) after receiving M-path way information from IVCα, IVB projects to CO blobs in II/III; and (2) layer IVB also provides direct projections to area V5 as well as the superior colliculus.

Layer V is subdivided into VA and VB (Lund, 1988; Lund and Yoshitaka, 1991; Rockland and Lund, 1983). Layer VA neurons do not project to IVB and only weakly innervate IVCβ. They innervate all other layers. VA neurons appear to project primarily to IIIB. Pyramidal neurons in VB send recurrent axons to layer IIIA. Meynert cells at the V/VI border and within layer VI project to both MT and SC. Layer V receives feedback projections from II/III neurons, and they provides strong feedback projections to layer VI neurons. Furthermore, layer V neurons provide corticofugal backprojections to subcortical nuclei such as superior colliculus (SC), pulvinar, and pons.

Layer VI neurons are known to send recurrent axons into IVCα and IVCβ (Lund, 1988). Other neurons (or possibly even the same ones) project axons back to the LGNd. While layer VI neurons receive most input

from layer V neurons, they also receive a direct input from the LGNd. Layer VI provide massive corticofugal projections to LGNd and claustrum.

Cytochrome oxidase (CO) blobs are regions of high staining for the metabolic enzyme cytochrome oxidase (Wong-Riley, 1989). CO blobs and the interleaved "interblob" regions form discrete organizing structures in cortical layers II/III and V/VI. Layer II/III neurons in the CO blob region receive direct input from the interlaminar cells of LGNd (I pathway), thus bypassing the vertical information processing in the primary visual cortex (Horton, 1984; Horton *et al.*, 1990). While the CO blobs have been speculated to be associated with information processing other than the parvo (P) and magno (M) pathways, their exact contribution for visual information processing remains elusive.

The overall flow of the information to and from the primary visual cortex provides the redistribution and recurrent projections of the M, P, and I visual information (Lund, 1988; Rockland and Lund, 1983). The M input from LGNd projects to IVCα and IVB, and then subsequently to V2, V3, V4, and V5. The P input to IVCβ from LGNd projects to the CO blob regions in II/III and then subsequently to the extrastriate areas. The CO interblob zones contain a mixture of M+P inputs conveyed through collective inputs from mid-IVC. Finally, the I path bypasses the aforementioned intracortical processing by providing direct inputs to the CO blob neurons. The recurrent projects are provided by II/III neurons that are projecting back to layers V and VI. Layer VI in its turn projects to layers IVCα and IVCβ, thus closing the computational loop.

Receptive Field Properties in V1

Given the complexity of the cell types and circuitry in V1, one might expect receptive field properties far beyond the simple center/surround types encountered in retina and LGN. In fact, it was found early on that the small spots of light that were found to be so effective in activating the LGN neurons were effective only in the layer IVC neurons, which receive direct inputs from LGN (Hubel and Wiesel, 1968; Kuffler, 1973). Neurons in most other layers responded vigorously only if the light stimulus provided linear properties, such as lines, slits, or bars (Hubel and Wiesel, 1968, 1977). Furthermore, V1 neurons were found to possess a preference with respect to the angle of those lines and bars with respect to their receptive fields (Hubel and Wiesel, 1974). Thus, we speak of "orientation selectivity" of V1 cells (Fig. 35.4). Orientation-selective cells in V1 are either of "simple" or "complex" type (Hubel and Wiesel, 1968). Simple cells respond best to a stationary light bar of certain orientation. To this end, their receptive field is subdivided into excitatory and inhibitory zones. If light falls on the excitatory zone, the spike rate increases, whereas light on inhibitory zone decreases the spike rate. The anatomical substrate of this orientation selectivity remains not completely understood. A parsimonious but increasingly accepted idea hypothesizes that this excitatory linear zone is made up of multiple, overlapping center/surround type of LGN inputs terminating within the same V1 cell's receptive field (Hubel and Wiesel, 1977). When first proposed by Hubel and Wiesel more than 40 years ago, this "feed-forward" model was met with skepticism, as it would require an exceedingly precise projection geometry of the thalamocortical projections. However, numerous correlation and pharmacological studies suggest the tentative validity of this simple model (Chapman *et al.*, 1991; Ferster, 1987; Reid and Alonso, 1995; Tanaka, 1983).

While the simple cells prefer stationary subdivision of their receptive fields into excitatory on and inhibitory off regions, respectively, the complex cells' response properties are invariant of the exact position of the light bars, as long as it has the correct orientation (Hubel and Wiesel, 1968, 1977). Complex cells also possess a larger receptive field than simple cells. A particularly effective stimulus for complex cells is a light bar of correct orientation moving across the receptive field. The anatomical correlate of complex cells remains elusive.

Despite an overwhelming number of experimental details, the overall function of the orientation selective simple and complex cells (and also that of more exotic hypercomplex and end stop cells) in V1 remains unknown. In fact, the overall function of V1 itself is still unknown. In any regard, it is surprising that the most favorite stimulus feature to activate V1 cells is that of line segments. Line segments can carry information about edges, or the contour of a perceived object, whereas they cannot code for a monotonous interior or background of an object.

Columnar Organization of Computational Modules in V1

It was found early on that the neurons in V1 are spatially organized according to their receptive field properties (Hubel and Wiesel, 1969). If one inserts a recording electrode vertically into the cortical plate, the measured receptive field properties of the neurons from pia to the white matter will be similar to each other. Thus, the primary visual cortex is parceled into narrow columns of cells sharing similar receptive field properties. Such clusters of isoreceptive field properties

are called "cortical columns" (Hubel and Wiesel, 1977). Cortical columns represent one of the most ubiquitous organizing principles of the cortical organization. Such columnar organization has been found across all cortical areas, ranging from somatosensory to auditory cortices.

In the primary visual cortex, the structure, layout, and function of the columnar layout have been particularly well studied using a variety of techniques in the past (Figs. 35.5 and 35.6). These include the single and multiunit recording techniques (Hubel and Wiesel, 1968), the 2-deoxyglucose technique (Hubel

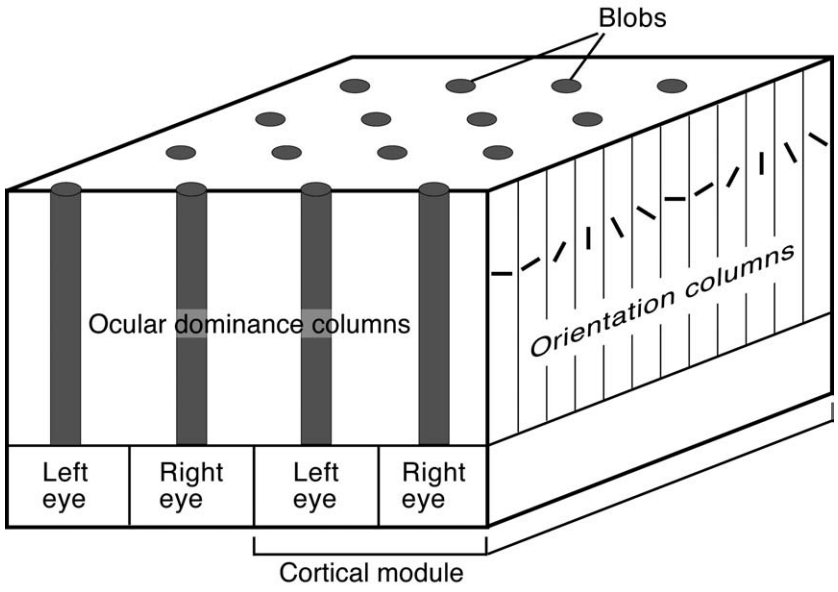

FIGURE 35.5 Schematic drawing of a cortical module. The primary visual cortex is organized into cortical modules, each consisting of a set of orientation columns crossed with ocular dominance columns. Within a cortical module, all cells have similar receptive fields (respond to the same small part of the visual field), but vary in terms of input source (left or right eye), orientation sensitivity, color sensitivity (Blobs), and size sensitivity (not shown). (Adapted from Bear, Connor & Paradiso, 1996).

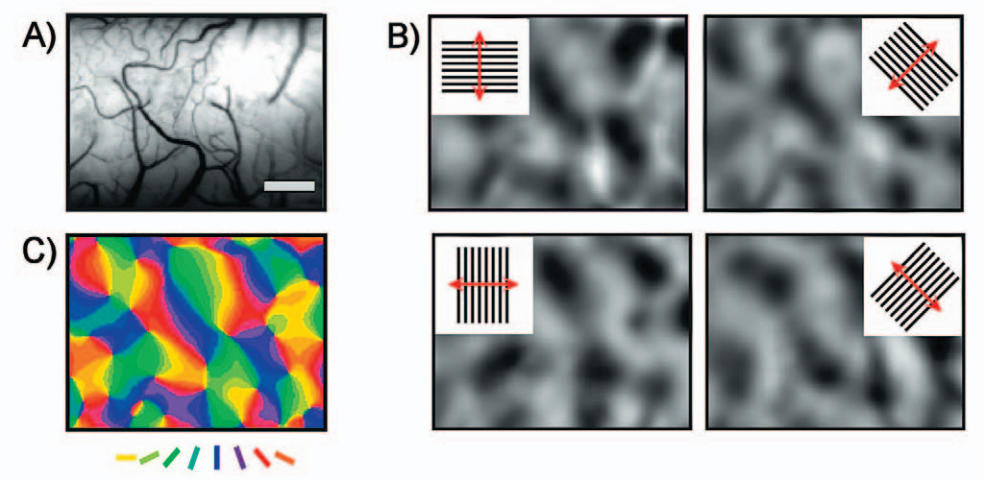

FIGURE 35.6 Details about the structure and function of cortical maps in the mammalian visual cortex have been revealed by the invasive technique of optical imaging of intrinsic signals (for details, see text). (A) Video image of exposed cat visual cortex (scale bar = 1mm). (B) Single condition maps obtained by stimulating the visual cortex with a large field of gratings. In each condition, gratings are presented in a different (fixed) orientation. To obtain strong responses, the gratings are moved forward and backward in directions orthogonal to the selected orientation. (C) Angle map obtained by integrating the results from the single condition maps. As indicated below the panel, colors code for the orientation yielding the maximal response at a given cortical patch.

et al., 1978), and the technique of optical imaging (using the intrinsic or voltage-sensitive dye signals) (Fig. 35.7) (Blasdel, 1992; Blasdel and Salama, 1986; Obermayer and Blasdel, 1993; Ts'o *et al.*, 1990). In particular, the recently developed "optical imaging of intrinsic signals" (Malonek and Grinvald, 1996; Ts'o *et al.*, 1990) provided a great deal of novel information about the details of the structure and function of the cortical maps in mammalian visual cortex. Optical imaging of intrinsic signals is based on the fact that following the onset of, for example, visual stimulation, cerebral metabolic rate of oxygen ($CMRO_2$) is increased rapidly without a commensurate elevation of cerebral blood flow (CBF) and cerebral blood volume (CBV), resulting in a net increase of deoxyhemoglobin around the microvasculature in active cortical regions. Utilizing the fact that gray matter tissues dominated by deoxyhemoglobin absorb relatively more light at near-infrared wavelength (605 ± 10 nm), one can discern the "active" areas of the cortex by shining a light on the exposed cortical surface (Malonek and Grinvald, 1996). The ability of optical imaging to resolve individual columns is assumed to be based on the facts that (1) individual neurons in mammalian cortex are never more than

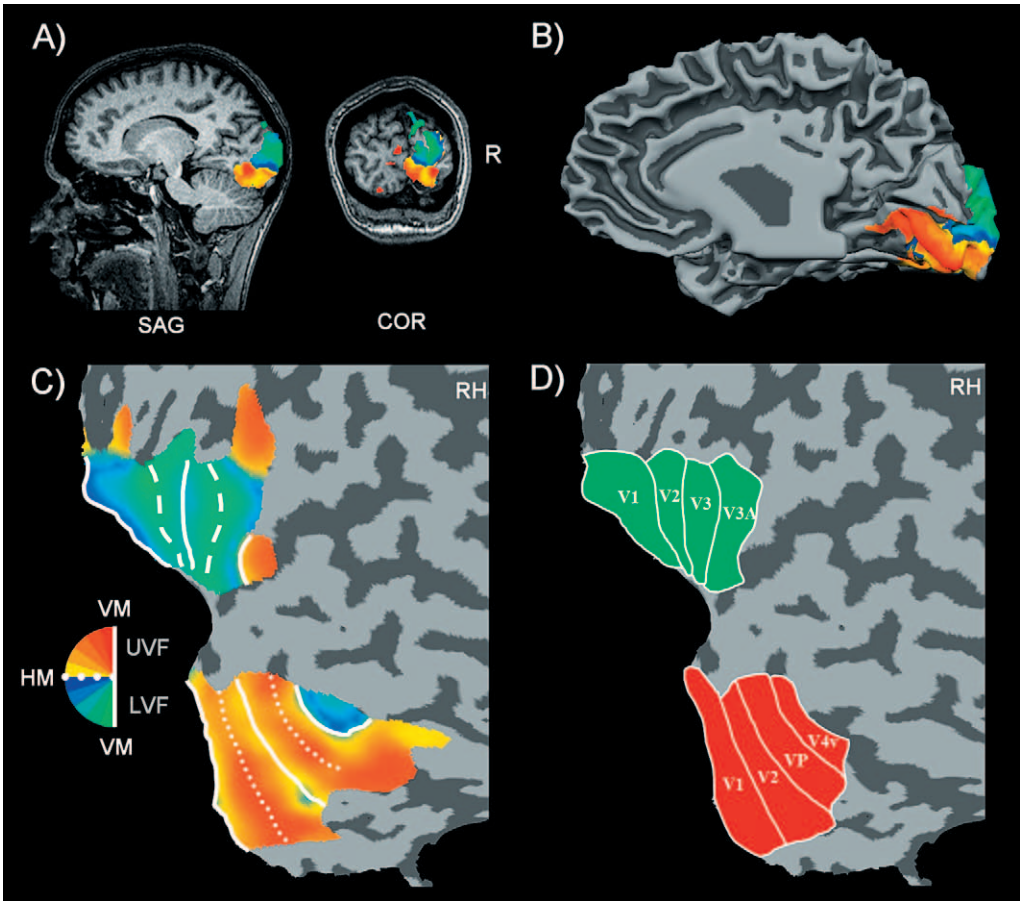

FIGURE 35.7 Details about the organization of human visual cortex have been revealed by the non-invasive technique of functional magnetic resonance imaging (fMRI). The figure shows a particular application of fMRI, the retinotopic mapping of early visual areas (for details, see text). (A) Result of a "polar mapping" experiment visualized on a sagittal and coronal anatomical slice. In a polar mapping experiment, a half-ray is slowly rotated around a central point, which the subject fixates. The ray, thus, stimulates different parts of the visual field at different moments in time (i.e. first the upper vertical meridian, then the left horizontal meridian, then the lower vertical meridian and so on). Different colors correspond to the position of the ray at which the maximal response within a cortical voxel is obtained (see legend in C). (B) The result of the same experiment visualized on a medial three-dimensional view of the right hemisphere of the scanned subject. (C) The same result visualized on a flattened representation of the right hemisphere. Note that such a "flat map" is ideally suited to visualize topologically organized information. (D) The "stripes" revealed on the flattened representation from the polar mapping experiment (see C) demarcate the borders of early visual areas (for details, see text).

20–30 μm away from a microcapillary (Pawlik *et al.*, 1981); and (2) mammalian neurons are spatially grouped according to their functional specificity (Hubel *et al.*, 1978). Good correlation between electrical activity and intrinsic signals has been observed (Crair *et al.*, 1998; Shmuel and Grinvald, 1996). However, this technique provides only very limited depth information, since only signals from the superficial 300–500 μm can be accessed. Furthermore, optical imaging is an invasive technique requiring a large craniotomy to allow for the light of specific wavelength to be illuminated on the cortical surface.

While invasive techniques such as optical imaging and single-unit recording have been used primarily to elucidate the layout of the cortical maps in mammalian brains other than humans (however, single/multiple techniques and optical imaging have been used to map the layout of the cortical maps in the human primary visual cortex during or before neurosurgical operations), there is no reason to believe that the human visual cortex will not follow this general scheme of the columnar parcellation of the brain. Indeed, recent advances in noninvasive functional magnetic resonance imaging (fMRI) based on blood oxygenation level dependent (BOLD) signals demonstrate the parsimonious validity of the columnar organization also in the human striate cortex (Cheng *et al.*, 2001; Dechent and Frahm, 2000; Goodyear and Menon, 2001).

Another important organizing principle in the primary visual cortex is that of maps (Swindale, 2001). This refers to the fact that as one moves tangentially from one cortical column to the next (with a step size of about 30–100 μm), there is a progressive change in the respective receptive field property (Hubel and Wiesel, 1968). Therefore, neighboring columns in V1 code for "neighboring" properties of the stimulus environment. The primary visual cortex contains therefore a topographic "map" of the respective stimulus parameter (Swindale, 2001). The most prominent of these cortical maps in V1 is the map of retinotopy. This map is based on topography-preserving projections from the retina to the LGN layers and from the LGN layers to area V1 (for details, see "Retinotopic Mapping of Early Visual Areas"). Besides the retinotopic map, the primary visual cortex contains a number of additional topographic maps (Bartfeld and Grinvald, 1992; Swindale, 2000). In the primary visual cortex of nonhuman primates, "columns" and "maps" have been reported for orientation, ocular dominance, direction, spatial frequency, and disparity. In humans, maps for retinotopy (Engel *et al.*, 1994; Sereno *et al.*, 1995) and ocular dominance (Cheng *et al.*, 2001; Goodyear and Menon, 2001) have been reported, and there is no reason to believe that the human primary visual cortex contains fewer cortical maps than that in primates or felines. The total number of cortical maps in the primary visual cortex is unknown, and likewise, it is not known whether there is a maximal number of cortical maps that can be represented in the primary visual cortex (Swindale, 2000). Theoretical considerations suggest this to be the case, as an ever increasing number of cortical maps should make it more and more difficult for the individual maps to maintain the topographic representation of their respective stimulus feature (Swindale, 2001; Swindale, 2000; Swindale *et al.*, 2000).

While each of the cortical maps displays a unique topological arrangement, recent studies using multielectrode and optical imaging techniques have uncovered a number of highly consistent geometrical features among multiple cortical maps (Bartfeld and Grinvald, 1992; Hubener *et al.*, 1997; Kim *et al.*, 1999; Swindale *et al.*, 2000).

The overall geometry of the maps tends to mirror the characteristic features of the respective receptive field property: binary properties, such as ocular dominance, are represented as an approximated binary map in the cortex (Hubel and Wiesel, 1969; Hubener *et al.*, 1997; Kim *et al.*, 1999). Isofunctional domains representing circular parameters, such as orientation, are arranged in a circular manner around particular foci in the cortex [termed "pinwheel centers" (Bonhoeffer and Grinvald, 1991)]. The complete sequence of the orientations appears only once around such foci, thereby giving rise to two types of pinwheel centers, distinguished by their chirality (Bonhoeffer and Grinvald, 1991). Finally, the direction of stimulus motion, which is invariant under 360° rotation, is represented continuously everywhere across the cortical surface, except around pinwheel centers. Here, only half of the full range of directions of motion can be represented, as the orientation is invariant under 180° rotation, resulting in "direction discontinuity lines," across which the preferred direction changes by 180° (Shmuel and Grinvald, 1996).

The layout of the multiple cortical maps are highly intercorrelated. A number of robust geometrical relationships among multiple maps tangential to the cortical plate have been described in mammalian visual cortices (Bartfeld and Grinvald, 1992; Hubener *et al.*, 1997; Kim *et al.*, 1999; Swindale *et al.*, 2000): (1) Orientation domains and ocular dominance borders tend to intersect at right angles. (2) Centers of pinwheel tend to coincide with the centers of ocular dominance columns and furthermore with CO blobs. This tendency is arguably stronger in macaques than in cats, where conflicting results exist. (3) Orientation singularities of opposite chiralities are connected always by an odd number of directional line discontinuities, where

the preferred direction of motion changes rapidly. (4) Isodirection domains tend to intersect ocular dominance borders at a right angle.

The tangential layouts of additional cortical maps (e.g., spatial frequency and disparity) and their geometrical relationships to the aforementioned columnar structures remain elusive (Issa *et al*., 2000; Shoham *et al*., 1997; Swindale, 2000). Notably, the functional architecture of the spatial frequency representation in the primary visual cortex has caused substantial controversy in recent years. Although some investigators argued that all spatial frequencies are represented continuously over the cortical surface (Tootell *et al*., 1981), recent evidence suggests that the primary visual cortex is rather parceled into two complementary domains—one for low spatial frequencies, and the other for high spatial frequencies (Shoham *et al*., 1997). The reason for this discrepancy remains unknown. Likewise, the origin and function of the geometrical relationships among multiple cortical maps remain—despite many speculations—elusive.

EXTRASTRIATE CORTEX

Anatomical and functional discoveries since the early 1970s in the monkey and human brain have caused a radical revision of theories of how the visual system is organized in the *extrastriate cortex*, the visually responsive cortex outside striate area 17 or V1. The most important of these discoveries is that many cortical regions outside primary visual cortex are specialized for the processing of specific aspects of vision, such as color, motion, and form. This specialization of function along relatively elementary dimensions was unexpected because that cortex was thought to be reserved for "associative" functions, including perception and object recognition. Instead of an expected large region of undifferentiated higher functioning, this *visual association cortex* [Brodmann areas (Bas) 18 and 19] consists of cytoarchitectonically distinct areas that subserve specific visual functions (Zeki, 1978; Zilles and Clarke, 1997; see chapter by Zilles, this volume). In addition, it is now known that the visual cortex extends into the temporal and parietal lobes (Felleman and Van Essen, 1991). Based mainly on vast anatomical data of monkey visual cortex (*Macaca mulatta*), the picture of a highly diverse yet hierarchically structured organization of the visual system has emerged (Felleman and Van Essen, 1991; DeYoe *et al*., 1994). Van Essen and colleagues identified 32 areas and 305 connections among these areas organized in a hierarchy of 10 cortical stages. Recently, our understanding of the functional organization of the human brain has greatly expanded due to the availability of functional neuroimaging techniques that allow direct noninvasive observation of brain activity. Results obtained with these techniques, most notably fMRI, suggest that the general organization of the extrastriate cortex is similar in monkey and man (Van Essen, 2002).

Occipital Visual Areas

The visual cortex in the occipital lobe outside V1 contains areas V2, V3, V3A, and V4v (Fig. 35.8). There are numerous additional areas located at the borders between the occipital lobe and the temporal and parietal lobes, including MT/V5, V3B/V7/KO, LOC, and V4/V8.

V2

Within area V2, subregions have been defined by the same method for cytochrome oxidase staining as described earlier for V1 (see "Anatomy and Lamination"). In the case of V2, the subareas are called *thin stripes*, *thick stripes*, and *interstripes*. Neurons originating in the blob areas of V1 project to the thin stripes of V2. Neurons within the thin stripes are wavelength sensitive, and many are also double opponent. They generally have larger receptive fields than the double-opponent cells of V1. Neurons in the thin-stripe regions of V2 project to V4. In addition, there are direct connections from the blob areas of V1 to V4.

Neurons in the interblob regions of V1 project to the interstripe regions of V2. Neurons within the interstripe regions have larger receptive fields but similar receptive field characteristics to those in the interblob V1 regions, i.e., the majority of cells are not wavelength but orientation selective. Neurons in the interstripe region of V2 project to V4. There are also direct connections from the interblob regions of V1 to V4.

Neurons in layer IVB of V1 project to the thick stripes of V2. As with the projections of the two parvocellular channels from V1, the most striking elaboration of this magnocellular projection is an increase in the size of receptive fields. The cells in the thick-stripe regions are orientation selective as well as direction selective, i.e., they fire when a stimulus moves in a particular direction. In addition, the cells are also sensitive to binocular disparity, which allows them to code depth information. From V2 there are projections to V3 and V5. There are also direct projections from layer IVB of V1 to these areas.

V3, VP, V3A

Area V3 receives input from layer IVB of V1 and from the thick stripes of V2. V3 represents the lower

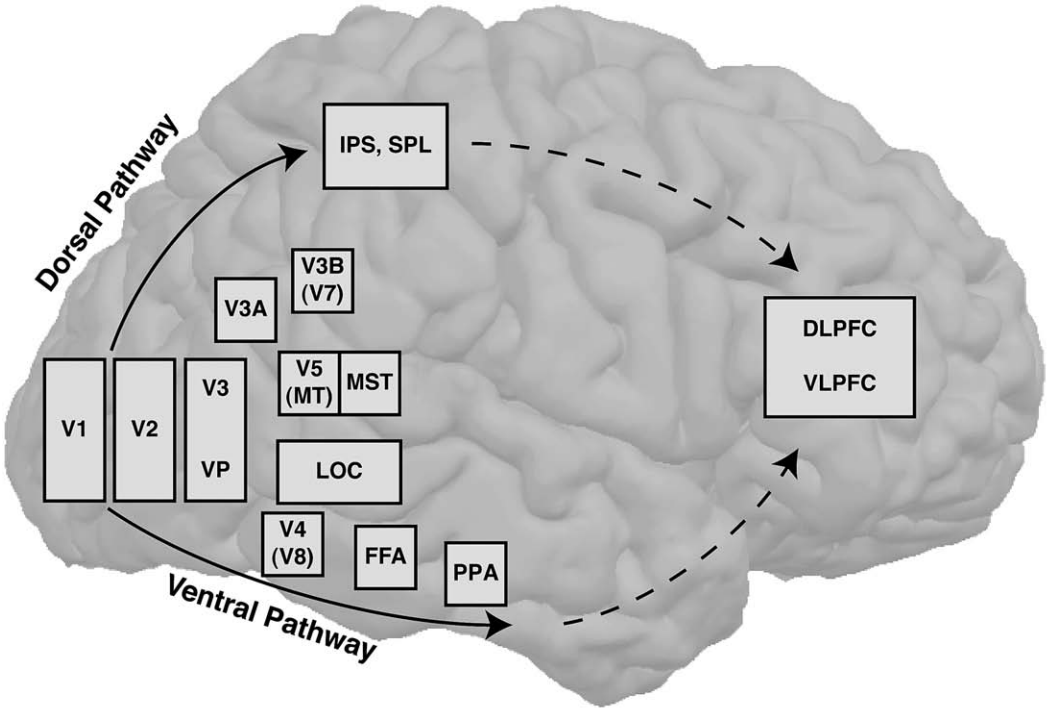

FIGURE 35.8 Prominent cortical visual areas as revealed by functional magnetic resonance imaging of the human visual cortex. As in monkey cortex, visual areas in the human brain are assumed to be organized in a dorsal (occipito-parietal) and ventral (occipito-temporal) pathway indicated by solid lines (for details, see text). Both pathways are assumed to extend into prefrontal cortex (dashed lines). Note that the two "pathways" consist not only of feedforward but also of massive feedback connections. MT, human homologue of monkey middle temporal area; MST, human homologue of monkey medial superior-temporal area; LOC, lateral occipital cortex; FFA, fusiform face area; PPA, parahippocampal place area; IPS, intra-parietal sulcus; SPL, superior parietal lobule; DLPFC, dorso-lateral prefrontal cortex; VLPFC, ventro-lateral prefrontal cortex.

visual field, and the majority of its neurons are orientation selective and exhibit high contrast selectivity. Many cells are both orientation and motion selective. Functional imaging has revealed that motion selectivity is stronger in adjacent area V3A than in V3 in humans while the opposite pattern has been observed for the homolog areas in the monkey (Tootell *et al.*, 1997). Area VP lies anterior to V2v representing the upper visual field. While areas V3 and VP have been considered to be separate areas (Burkhalter and Van Essen, 1986), it has recently been argued that VP is simply the ventral portion of V3 (Zeki, 2003).

V3B/V7/KO

Anterior to V3A, another area called KO has been described, which seems to be specialized for the processing of kinetic contours (Van Oostende *et al.*, 1997). Since this area appears to respond preferably to motion boundaries, it might play an important role for linking motion- and shape-related representations. However, a recent study, has shown that this area is active when subjects view simple shapes, whether derived by motion boundaries or other cues, such as luminance or color differences (Zeki *et al.*, 2003). The authors of this study further argue that area KO is not a new area but belongs to the "V3 family of areas." More specifically, they use the term V3B (following Smith *et al.*, 1998) to denote this area and specify its location in the lateral occipital cortex, posterior to V5 and in close proximity to the V3 complex. They also argue that V3B in each hemisphere represents both quadrants of the contralateral visual field. According to Tootell and colleagues, this region is also labeled as area V7.

V4

Area V4 contains many wavelength-selective cells. There are also cells whose receptive field properties correspond to a particular perceived *color*, i.e., these cells might mediate color constancy (Heywood and Cowey, 1987). In the human brain, a color-selective region has been located in the region of the lingual and posterior fusiform gyri (Lueck *et al.*, 1989; Hadjikhani *et al.*, 1998). Lesions in this region often cause *achromatopsia* (central color blindness; Meadows, 1974). This region is referred to as human V4 (McKeefry

and Zeki, 1997; Zeki *et al.*, 1998) or V8 (Hadjikhani *et al.*, 1998). As mentioned above, V4 receives input not only from the blob regions of V1 and the thin-stripe regions of V2 but also from the interblob regions of V1 and the interstripe regions of V2. These inputs to V4 suggest that this area is not involved only with color processing. Although the majority of cells in V4 are wavelength and some color selective, many are orientation selective and some are both color and orientation selective. It appears, therefore, that area V4 is involved in both color and form processing (see Cowey and Heywood, 1995, for a review).

MT/V5, MST, FST

In monkey cortex, the motion selective area MT (middle temporal area) is located in the middle temporal sulcus, close to the junction of the occipital, temporal, and parietal lobes (Van Essen *et al.*, 1981). As area V3, area MT receives direct input from layer IVB of V1 and from the thick stripes of V2, thus forming a second magnocellular channel. Its cells are responsive to the direction and speed of moving stimuli (Snowden *et al.*, 1992) and their inactivation causes deficiencies in motion direction discrimination. MT neurons have large receptive fields, which might provide a basis for determining whether a number of points (parts of an object) are moving together. Area MT is easily identified in histological sections because of its high myelination, and it is surrounded by several other specialized areas including MST (medial superior temporal area) and FST (fundus of the superior temporal area). These "satellites" of MT process higher order aspects of stimulus motion. The human visual cortex contains an area that is likely to correspond to monkey area MT and is located in the occipito temporo parietal pit. Bilateral lesions that include this area cause a severe impairment in detecting the movement of objects (cortical *akinetopsia*; see Zeki, 1991). Human imaging studies have shown that metabolism and blood flow in that region increase more in response to moving than to stationary stimuli, indicating preferential involvement of this area in the processing of motion information (e.g., Watson *et al.*, 1993; Tootell *et al.*, 1995; Goebel *et al.*, 1998). As functional imaging studies have not yet convincingly differentiated between the human homolog of area MT and its satellites, this motion selective region is often referred to as the *human motion complex* (hMT+) or V5.

Retinotopic-Mapping of Early Visual Areas

Using fMRI and appropriate visual stimuli, the described early visual areas can be charted in individual human brains (Sereno *et al.*, 1995). This is possible because the mapping from the retina to the primary visual cortex is topographical and because other early visual areas retain this retinal topography, but represent the visual field in either a mirrored or nonmirrored two-dimensional layout. In a topographical mapping, neighboring regions in one area (retina) project to neighboring regions in another area (primary visual cortex). Since this mapping is preserved also at the next cortical stages (V2, V3/VP, V3A, V4), neighboring positions in the visual field tend to be represented by groups of neurons that are adjacent but laterally displaced within the cortical gray matter of these areas. This transformation preserves the qualitative spatial relations of the retina but exhibits systematic distortions, i.e., there is much more cortical tissue devoted to foveal regions than peripheral regions of the visual field (cortical magnification). A successful delineation of the early visual areas with fMRI exploits the fact that successive visual areas alternate with a mirror or nonmirror representation of the visual field. Multiple horizontal and vertical meridian representations across the visual cortex, thus, indicate the transitions between early visual areas. With appropriate visual stimuli, fMRI studies have successfully been used to reveal multiple meridian representations arranged in approximately parallel bands along the flattened cortical surface (Sereno *et al.*, 1995). fMRI-based retinotopic mapping has quickly become an important tool to noninvasively define the borders of early visual areas (e.g., Tootell *et al.*, 1996, 1997; Goebel *et al.*, 1998, 2001; see Fig. 35.8).

In V1, the representation of the horizontal meridian is contained within the calcarine sulcus, such that the upper (dorsal) bank contains the lower visual field representation, and the lower (ventral) bank contains the upper visual field representation of the contralateral visual hemifield. The border between V1 and dorsal V2 (V2d) is identified by the first vertical meridian representation of the lower visual field. Similarly, the border between V1 and ventral V2 (V2v) is identified by the first vertical meridian representation of the upper visual field. Note that there are four spatially separated subparts of V2 (V2v and V2d in the left and right hemisphere), each representing one quadrant of the visual field (Fig. 35.8). In the dorsal part of the cuneus, the border between V2d and V3 is identified by the second horizontal meridian representation in each hemisphere. In a complementary fashion, the border between V2v and VP in the ventral cortex is identified by the second horizontal meridian representation in each hemisphere. V3 and VP in one hemisphere represent the contralateral visual hemifield and—combined across hemispheres—these areas provide a complete third representation of the visual field. The next retinotopically organized areas in the dorsal part are V3A and V7 (or V3B; see below), which, unlike V3,

contain a complete representation of the contralateral visual hemifield. The next retinotopically organized area in ventral visual cortex has been termed V4v, which is demarcated by another upper vertical meridian representation. The functional organization and naming convention in this region is currently debated (Hadjikhani *et al.*, 1998; Zeki, 2003). On the one hand, it has been suggested that there is one larger area, V4, consisting of a complete hemifield representation complementary to the representation in V3A in the dorsal cortex. On the other hand, an additional area beyond V4v has been suggested and termed "V8" containing an additional hemifield representation. Because of this debate, this region is at present often referred to as V4/V8.

In higher visual areas in the temporal and parietal lobes, it becomes increasingly difficult to show a retinotopic organization. One reason for this is that higher visual areas are much smaller than early visual areas, which makes it difficult to resolve the intra-areal layout with fMRI. Another reason might be that the spatial layout within these areas becomes less dominated by retinotopic but more complex organizational principles.

Two Main Cortical Pathways

Ungerleider and Mishkin (1982; Mishkin *et al.*, 1983) proposed that the extrastriate visual areas are organized into two hierarchically, functionally specialized, processing pathways (Fig. 35.9): an occipitotemporal pathway or "ventral stream" for object recognition and an occipitoparietal pathway or "dorsal stream" for spatial vision and visually guided actions. Areas along both pathways are organized hierarchically such that low-level inputs are transformed into more complex representations through successive stages of processing. The ventral stream or "what" system is supposed to perform a fine-grained analysis of the visual scene, including processing of color and shape (see "Ventral Visual Areas"). The dorsal stream or "where" system processes spatial characteristics of the visual scene (see "Parietal Visual Areas"). Emphasizing that the latter pathway is also involved in visuomotor transformations, Milner and Goodale (1995) proposed to distinguish between *vision for perception* (ventral pathway) and *vision for action* (dorsal pathway).

The two pathways have been originally described for nonhuman primates. They originate in areas V1 and V2 and extend into the temporal ("what" system) and parietal ("where" system) lobe, respectively. The ventral stream consists of the areas V1–V4, which belong to the occipital lobe, and the areas PIT (posterior IT) and AIT (anterior IT). This pathway is assumed to be mainly driven by the parvocellular system. The dorsal stream consists of the areas V1, V2, dorsal V3 (V3d) and MT/V5, MST, LIP, and VIP (lateral and ventral intraparietal area) and 7a. This pathway is assumed to be mainly driven by the magnocellular system.

With brain imaging techniques, the two major processing pathways have been convincingly demonstrated in the normal human brain (e.g., Haxby *et al.*, 1991), and several specialized areas have been identified on the basis of their stimulus preference profiles (see "Ventral Visual Areas").

Ventral Visual Areas

In the macaque monkey, cortex ventral to area MT and anterior to V4 is generally considered part of the ventral processing stream (see below). This region includes a cluster of inferotemporal areas that are implicated mainly in pattern recognition and form analysis (e.g., Tanaka, 1996, 2001). Electrophysiological studies in primates identified remarkable selectivities of IT cells for specified categories of complex stimuli such as faces or spatial layouts (Perrett *et al.*, 1982, 1985; Gross, 1992; Tanaka, 1996, 2001; Logothetis, 2000; Kreiman *et al.*, 2000). Another cluster of areas within the ventral superior temporal sulcus (ventral STS) includes polysensory regions and regions involved in both form and motion processing (Oram and Perrett, 1997). With human neuroimaging, specialized areas located in close proximity to area V4/V8 have been characterized, including the lateral occipital complex (LOC), the fusiform face area (FFA; Kanwisher *et al.*, 1997), the parahippocampal place area (PPA), and several overlapping regions sensitive to different object categories (e.g., Ishai *et al.*, 1999).

LOC

Several human imaging studies have shown that a region in the lateral occipital cortex extending anterior in the temporal cortex is involved in shape processing, responding strongly to images of objects but not to scrambled control stimuli. It has been further conjectured that this region, called LOC (lateral occipital complex; Malach *et al.*, 1995; Grill-Spector *et al.*, 2001; Malach *et al.*, 2002), represents perceived object shape (Kourtzi and Kanwisher, 2001). Studies using event-related potentials recorded from electrodes placed in the LOC region on the cortical surface of patients prior to surgery found object-specific waveforms that show stronger activation for a variety of objects (cars, flowers, hands, butterflies, and letters) than to scrambled control stimuli. In addition, lesion studies have revealed that damage to the fusiform and occipitotemporal junction results in a variety of recognition deficits. These findings suggest that LOC may

be necessary for object recognition containing most likely important midlevel representations of shape features. The LOC is largely nonretinotopic and is activated by both contralateral and ipsilateral visual fields. It contains at least two spatially segregated subdivisions, a dorsal caudal subdivision LO and a ventral anterior subdivision at the posterior aspect of the fusiform gyrus called pFs (postfusiform) or VOT (ventral occipitotemporal cortex; Malach *et al*., 2002; Grill-Spector, 2003). LO is situated posterior to MT in the lateral occipital sulcus and extends into the posterior inferior temporal sulcus. VOT/pFs is located bilaterally in the fusiform gyrus and occipito temporal sulcus (Grill-Spector, 2003; Malach *et al*., 2002). Each of these subdivisions contains a separate foveal representation. The fovea of LO is connected to the confluence of fovea of early visual areas, whereas pFs contains a separate foveal representation that is located on the lateral bank of the collateral sulcus extending into the fusiform gyrus. The anterior subregion of LOC has been shown to respond more invariantly to position, size, and small orientation changes than the posterior subregion (Grill-Spector *et al*., 2000). Anterior to LOC, several areas have been suggested as modules for representing and perceiving specific object categories, such as faces and places.

FFA

One of the most extensively studied areas in recent years is the fusiform face area (FFA). The FFA responds much more strongly to a wide variety of face stimuli (e.g., front view photographs of faces, line drawings of faces, cartoon faces, and upside-down faces) than to various nonface control stimuli (e.g., cars, scrambled faces, houses, hands). It has been proposed that the FFA is not specialized for face processing per se but is specialized for making any discriminations for which substantial *expertise* has been gained (Gauthier *et al*., 1999). Besides the FFA, there are other regions responding more to faces than to other object categories, which are located in a more posterior occipital region partially overlapping LO, and in a region near the posterior end of the superior temporal sulcus.

PPA

Another well-studied category-selective region of cortex is the parahippocampal place area (PPA; Epstein and Kanwisher, 1998) responding strongly to a wide variety of stimuli depicting places and/or scenes (e.g., outdoor and indoor scenes and houses) compared to various control stimuli (e.g., faces or scrambled scenes).

The description of areas FFA and PPA raises the question how many category-selective regions of cortex exist in the human visual system, and, more generally, how the ventral temporal cortex is organized. Hypotheses range from the assumption that there are a few specialized processing modules, i.e., for faces, places, letters, and human body parts (Puce *et al*., 1995, 1996; Kanwisher *et al*., 1997, 1999; Epstein and Kanwisher, 1998; Epstein *et al*., 1999; Polk *et al*., 2002; Downing *et al*., 2001) up to the proposal of widely distributed and overlapping cortical object representations (Ishai *et al*., 1999, 2000; Haxby *et al*., 2001). Effects of category-related expertise (Gauthier *et al*., 1999; Gauthier and Nelson, 2001) and, more recently, different category-related resolution needs (Levy *et al*., 2001; Hasson *et al*., 2002; Malach *et al*., 2002) have also been proposed to explain the topology of the human what pathway. Further insights into the question how objects are represented in ventral visual cortex might come from functional imaging studies investigating *within-category response*s, e.g., by comparing responses to single-object images, such as two different faces or two different houses (Kriegeskorte *et al*., 2003). It has also been proposed that the eccentricity gradient observed in early visual areas continues into the ventral visual cortex (Malach *et al*., 2002). For example, regions selective to faces (FFA) overlap with the representation of the fovea, whereas regions selective to houses (PPA) overlap with a peripheral visual representation located in the collateral sulcus. These findings suggest that the entire ventral visual cortex may be organized along an eccentricity axis (Fig. 35.10).

Parietal Visual Areas

Regions of the parietal cortex are thought to be involved fundamentally in spatial processing and the control of action. The parietal lobe also contains somatosensory regions, which are, not discussed here. In the monkey, the posterior parietal visual cortex includes several areas in and near the intraparietal sulcus (IPS), plus additional areas in more posterior regions. The most fine-grained parcellation of this region (Lewis and Van Essen, 2000) is based on immunohistochemical as well as cyto- and myeloarchitecture and includes seven distinct areas [7a, LIPd, LIPv (dorsal and ventral portion of lateral intraparietal), VIP (ventral intraparietal), MIP (medial intraparietal), MDP (mediodorsal parietal), and DP (dorsal parietal)] plus additional architectonic zones. Unfortunately, the terminology of parietal areas is somewhat confusing: area VIP of Ungerleider and Desimone (1986) corresponds to LIPv (ventral LIP) of Lewis and Van Essen (2000); areas LIP and VIP of Felleman and Van Essen (1991) correspond to LIPd (dorsal LIP) and LIPv/VIPl [ventral intraparietal (lateral)], respectively, of Lewis and Van Essen (2000). A second group of areas, near the posterior end of the intraparietal sulcus, includes areas MDP, MIP,

and DP, plus zone LOP (lateral occipitoparietal). Area MDP corresponds to V6A of Galletti *et al.* (1999). Zone LOP may correspond to the caudal subdivision of the IPS (cIPS or CIP; Taira *et al.*, 2000). Monkey neurophysiology has characterized many areas in the intraparietal sulcus that respond during specific visuomotor processes. These include areas specialized for saccades (LIP, Colby *et al.*, 1996), reaching (parietal reach region, PRR, which includes both area V6A and MIP; Galletti *et al.*, 1997; Snyder *et al.*, 1997), grasping [anterior intraparietal area (AIP), Taira *et al.*, 1990], processing of shape and orientation (cIPS, Sakata *et al.*, 1997), and movements towards and contact with the mouth and head (VIP, Colby *et al.*, 1993). These areas have been shown to code space in a variety of coordinate frames, including eye-centered (LIP), head-centered (VIP, V6), and body-centered (area 5, MIP) coordinates, and many are modulated by factors such as eye position.

In the human, the intraparietal sulcus separates the superior parietal lobe (BAs 5 and 7) and the inferior parietal lobe. The inferior parietal lobe contains BA 39, corresponding roughly to the angular gyrus, and BA 40, corresponding roughly to the supramarginal gyrus. Neuroimaging studies have revealed that human parietal cortex consists of numerous specialized subregions similar to those described for nonhuman primates (for a review, see Culham and Kanwisher, 2001). However, the detailed mapping of the human parietal cortex presents a challenge for current research because of the wide variety of tasks associated with the parietal lobe, including sensorimotor mapping, spatial visual attention, mental imagery, spatial working memory, and motion processing. This variety of functions is also evident from patients with lesions in the parietal lobe causing many cognitive deficits including attentional disorders, such as hemispatial *neglect* and *simultanagnosia*, spatial localization disorders, and sensorimotor coordination problems. There is increasing evidence that the activity in several parietal areas modulates activity in other visual areas within the occipital and temporal lobe. Since parietal activity may precede target stimuli in attention tasks and is often stronger than in earlier visual areas (e.g., Corbetta *et al.*, 2000), the parietal lobe is considered to be the source of attentional control signals (see next section).

Theoretical Perspectives and Outstanding Questions

The previous sections have described many specialized areas in the visual cortex devoted to specific aspects of vision. The functional properties of these areas have been revealed by numerous factors, including the physiological characteristics of single neurons, anatomical inputs and outputs, metabolic microarchitecture, effect of lesions, and an increasing number of noninvasive neuroimaging studies. Taken together, these findings are the reason why we know more details about the visual cortex than about any other cortical system. This advanced level of understanding brings with it profound problems that have yet to emerge in the study of other cortical areas. Knowing more details about a complex structure leads to a clearer view of the deeper questions. Two of the major questions arising are why these specialized areas exist and how the different aspects of the visual world processed in these separate areas of cortex are integrated into a unified representation of the world. At present, these questions cannot be answered satisfactorily, but the following sections present major theoretical perspectives on how the visual system as a whole processes information.

Bottom-up and Top-down Processing in the Visual Hierarchy

Felleman and Van Essen (1991) noted that the hierarchy of processing levels in the visual system consists not only of feedforward but also of massive feedback connections. The classical view of the visual system largely neglected these feedback connections and summarized its operation with a few general principles. First, processing as revealed by neuronal receptive fields is hierarchical, beginning with the simple and complex cells described by Hubel and Wiesel (1968; see "Receptive Field Properties in V1"). Neurons in higher cortical areas represent increasingly complex characteristics of images, objects, and categories (Maunsell and Newsome, 1987; Vogels and Orban, 1996). Higher neurons are also less dependent on coincidental spatial features, such as precise location, retinal size, viewpoint, lighting, and color. Another principle of the classical view is the presence of multiple areas belonging to parallel pathways, such as the dorsal and ventral streams (Ungerleider and Mishkin, 1982; Livingstone and Hubel, 1988; Goodale and Milner, 1992, see "Parietal Visual Areas"). Specialized areas and pathways are assumed to exist because of the need to solve difficult computational problems for different aspects of the visual world that require highly specialized neuronal organizations. Another principle of the classical view states that high-level processing such as learning (i.e., experience) and attention (i.e., context) occurs only in high cortical areas in the ventral and dorsal pathway (e.g., Bushnell *et al.*, 1981; Moran and Desimone, 1985; Malach *et al.*, 1995). Although it was known that feedback connections reach areas as low as V1 and even the LGN, their function was largely ignored.

Despite the fact that the precise functional roles and cognitive consequences of the feedback connections are still unknown, the feedback connections play a key role in recent theories of the visual system (e.g., Zeki, 1993; Tononi and Edelman, 1998; Singer, 1999; Hochstein and Ahissar, 2003) extending the classical view. These theories suggest a variety of functions for the recurrent connections between V1 and higher visual areas. Higher areas might send feedback signals to confirm the reliability of the information they receive from V1 or to modulate V1 activity on the basis of top-down knowledge, perceptual grouping, or attentional selection. Recent physiological and functional MRI studies have now confirmed strong top-down effects of learning and visual attention in V1 (e.g., Ahissar and Hochstein, 1997; Roelfsema *et al.*, 1998; Brefczynski and DeYoe, 1999; Somers *et al.*, 1999) and even in the LGN (O'Connor *et al.*, 2002). Multiple recordings of intracortical event-related potentials support the view that the observed modulations in early visual areas are indeed top-down effects by revealing that attentional modulation effects occur well after the initial transient response in V1 and that attentional effects in V4 and inferotemporal cortex precede those in V1 (Mehta *et al.*, 2000). Another important role that has been proposed for the recurrent connections is to integrate processing occurring in multiple specialized brain areas.

Unified Representations of the Visual World and the Binding Problem

According to the classical view focusing on feedforward processing, an integrated visual representation of the visual world should be accomplished by a master area on top of the hierarchy to which all of the specialized areas report. There are serious problems with this solution, however, both on conceptual and empirical grounds (e.g., Zeki, 1993; Singer, 1999; von der Malsburg, 1999). Conceptually, such a master map would presumably contain cells with highly specific receptive fields (conjunction units or "grandmother cells"; Barlow, 1995) that represent the culmination of the hierarchical integrative processes of the system. The conjunction neurons would respond only to specific combinations of features, such as shape, orientation, color, texture, motion, and position in space. Conceptually, it is difficult to imagine how there could be a sufficient number of conjunction neurons to represent uniquely all intra- and interareal feature constellations of real-world objects. In addition, it is hard to see how novel objects with entirely new relations among features could be represented in such a system. The master area hypothesis also has serious problems on empirical grounds. First, although there is good evidence of a hierarchical organization of the visual system, there is no anatomical evidence that the specialized visual areas all converge on one area (Felleman and Van Essen, 1992). The numerous forward and backward connections between areas at different stages of the hierarchy suggest that processing is not strictly hierarchical but highly interactive. Second, despite the fact that neurons have been found that respond selectively to hands or faces, these cells are not selective for a *specific* hand or face but are coarsely tuned to a broad spectrum of exemplars of the relevant category. Thus, it is more likely that individual objects are represented uniquely only by distributed representations or cell assemblies spread within and across numerous brain areas (Hebb, 1949).

The conceptual and empirical problems with the master area solution have stimulated alternative theories of integrative processing in which the massive feedback projections play an important role. In this view, reentrant connections from higher visual areas to V1 and V2 are assumed to provide the basis for integrating specialized processing occurring in higher visual areas (e.g., Zeki, 1993). Because V1 contains a high-resolution map of almost all relevant feature information and forms well-organized connections with retinotopic extrastriate areas, it could function as the central location to integrate perceptual information across multiple areas. This view puts the "master map" at the bottom instead at the top of the visual hierarchy. As an example, reentrant connections from V4 to V2 project not only back to the thin stripes and interstripes (V4's major input sources from V2), but also to the thick stripes of V2, which project to V3 and V5. This could represent a mechanism for integrating processing concerned with form and color—mediated by parvocellular channels—with the processing of form and motion mediated by magnocellular channels.

If this view of integrative processing is correct, the correlate of coherent percepts would be a distributed representation spread within and across many brain areas. Since in the real world many objects have to be represented at the same time, the question arises how such distributed representations could be tagged as related, i.e., how neurons could be linked together when participating in the representation of the same object and how they could be kept apart when participating in the representation of different objects. This problem of tagging belongingness is often referred to as the *binding problem*. The binding problem should be solved rather early in the visual hierarchy in order to assure that the responses of the neurons that constitute an assembly are processed and evaluated together at subsequent processing stages and are not confounded with other, unrelated responses. Several mechanisms to solve the binding problem have been proposed,

including suppression, enhancement, and temporal synchrony, which are assumed to occur during visual processes such as perceptual organization and selective visual attention. Suppression refers to the inhibition of unrelated responses excluding them from further processing. Enhancement refers to increasing the firing rates of the relevant neurons. Temporal synchrony refers to effects that increase the likelihood that relevant cells discharge in precise temporal synchrony. All three mechanisms enhance the relative impact of the selected responses and can therefore be used to tag them as related. There is empirical evidence that all three mechanisms play a crucial role in the selection and grouping of responses (e.g., Roelfsema *et al.*, 2002; Fries *et al.*, 2001). The temporal synchrony mechanism appears conceptually more flexible than the other mechanisms because it permits specification of relations independently of firing rate. This property is especially beneficial when multiple visual objects have to be represented simultaneously across potentially overlapping neuronal populations in early visual areas.

Visual Awareness

As outlined above, early visual areas play an essential role in recent theories of the visual system because they assume that V1 and V2 integrate the results of specialized processing occurring in higher visual areas (e.g., Zeki, 1993; Lamme and Roelfsema, 2000; Bullier, 2001). Because of the assumed essential role in integrative processing and feature binding, the question arises whether primary visual cortex contributes directly to conscious perception (Tong, 2003) despite the fact that V1 is located at the lowest level of the cortical visual hierarchy. Lesion studies indicate that V1 is necessary for normal visual function and awareness. Small lesions in V1 lead to scotomas or phenomenal blindness restricted to corresponding regions of the visual field as expected from the retinotopic organization of V1 (reviewed in Inouye, 2000). However, these findings do not answer the question whether V1 itself is important for visual awareness because the lesions disrupt the flow of information from V1 to higher visual areas. While proponents of the integrative role of primary visual cortex propose that V1 directly contributes to visual awareness (Zeki, 1993; Lamme and Roelfsema, 2000; Bullier, 2001), other researchers have proposed that only higher level extrastriate areas are directly involved in conscious perception (Crick and Koch, 1995; Rees *et al.*, 2002). In addition, they argue that only extrastriate areas that project directly to prefrontal cortex can directly contribute to consciousness, on the assumption that all conscious experiences must be reported and capable of directly generating a motor act. Because V1 lacks direct projections to prefrontal cortex, this theory assumes that V1 cannot directly contribute to visual awareness. More recent variants of this proposal assume that both frontal and parietal attention related areas are important for conscious perception, and that top-down signals from these areas to the extrastriate cortex might be important for selecting specific visual representations for awareness (Leopold and Logothetis, 1999). Proponents of the integrative role of V1 assume on the contrary that sustained activity between a given extrastriate area and V1 is necessary to maintain a visual representation in awareness. This means that V1, despite its lack of direct feedforward connections with the prefrontal cortex, can determine what extrastriate information reaches prefrontal areas by supporting or failing to support the information represented in intermediate extrastriate areas.

Evidence from neuroimaging studies indicate that V1 activity is tightly correlated with awareness under various conditions, such as binocular rivalry (Polonsky *et al.*, 2000; Tong and Engel, 2001) and near-threshold visual detection (Ress *et al.*, 2000). There are, however, other studies that show that V1 activity might be necessary but is not sufficient for perceptual awareness. For example, the responses of V1 neurons can follow flickering color gratings at temporal rates that are too fast to be received (Gur and Snodderly, 1997). According to current evidence from lesion studies, neither activity in V1 nor in higher visual areas is sufficient for awareness. A recent study of blindsight patients has shown that in the absence of V1 visual signals can still reach many extrastriate areas via subcortical projections but that activity in the extrastriate areas seems incapable of generating normal conscious experiences (Goebel *et al.*, 2001). It might be that the relationship between activity in certain visual areas and awareness is flexible and situation dependent rather than hard wired. Perhaps the information in V1 is necessary only for certain types of awareness, such as perception during focal attention or the perception of low-level features. Along these lines, a recent theory proposes that different areas contribute to visual awareness in two operational modes of the visual system, *vision at a glance* and *vision with scrutiny* (Hochstein and Ahissar, 2002). According to this theory, conscious perception begins at the top of the visual hierarchy, gradually returning downward as needed. The initial conscious percept, vision at a glance, matches a high-level, generalized, categorical scene interpretation. For later vision with scrutiny, *reverse hierarchy routines* focus attention to specific, active, low-level units, incorporating into conscious perception detailed information available from areas as low as V1.

Acknowledgments

This work was supported by the Human Frontiers Science Program (DSK, RG) and the Max Planck Society (LM). The authors are grateful to Bettina Sorger and Stefan Kiess for helpful comments on the manuscript, to Ralph Galluske for providing Fig. 35.6 and to Jens Schwarzbach for providing Fig. 35.7.

References

Ahissar, M., and Hochstein, S. (1997). Task difficulty and the specificity of perceptual learning. *Nature* **387,** 401–406.

Barlow (1995). The neuron doctrine in perception. *In* "The Cognitive Neurosciences" (M.S. Gazzaniga, ed.), pp. 415–434. MIT Press, Cambridge, MA.

Bartfeld, E., and Grinvald, A. (1992). Relationships between orientation preference pinwheels, cytochrome oxidase blobs, and ocular-dominance columns in primate striate cortex. *Proc. Natl. Acad. Sci. U.S.A.* **89,** 11905–11909.

Berry, M.J., Brivanlou, I.H., Jordan, T.A., and Meister, M. (1999). Anticipation of moving stimuli by the retina. *Nature* **398,** 334–338.

Berson, D.M., Dunn, F.A., and Takao, M. (2002). Phototransduction by retinal ganglion cells that set the circadian clock. *Science* **295,** 1070–1073.

Blasdel, G. G. (1992). Differential imaging of ocular dominance and orientation selectivity in monkey striate cortex. *J. Neurosci.* **12,** 3115–3138.

Blasdel, G. G., and Salama, G. (1986). Voltage-sensitive dyes reveal a modular organization in monkey striate cortex. *Nature* **321,** 579–585.

Bolton, J. S. (1900). The exact histological localisation of the visual area of the human cerebral cortex. *Philos Trans R. Soc. London Ser. B* **193,** 165–212.

Bonhoeffer, T., and Grinvald, A. (1991). Iso-orientation domains in cat visual cortex are arranged in pinwheel-like patterns. *Nature* **353,** 429–431.

Boycott, B.B., and Kolb, H. (1973). The horizontal cells of the rhesus monkey retina. *J. Comp. Neurol.* **148,** 115–139.

Boycott, B.B., and Wässle, H. (1999). Parallel processing in the mammalian retina: the Proctor Lecture. *Invest. Ophthalmol. Vis. Sci.* **40,** 1313–1327.

Boycott, B.B., Dowling, J.E., and Kolb, H. (1969). Organization of Primate Retina—Light Microscopy—A Second Type of Midget Bipolar Cell in Primate Retina. *Philos. Trans. R. Soc. Lond. B Biol. Sci.* **255,** 109–184.

Boycott, B.B., Hopkins, J.M., and Sperling, H.G. (1987). Cone connections of the horizontal cells of the rhesus monkey's retina. *Proc. R. Soc. Lond B Biol. Sci.* **229,** 345–379.

Brefczynski, J.A., and DeYoe, E.A. (1999). A physiological correlate of the "spotlight" of visual attention. *Nat. Neurosci.* **2,** 370–74.

Brewster, D. (1855). "Memories of the Life, Writings, and Discoveries of Sir Isaac Newton," Vol. 1. Thomas Constable and Co., Edinburgh.

Brodmann, K. (1909). "Vergleichende Lokalisationslehre der Grosshirnrinde," Johann Ambrosius Barth, Leipzip.

Bron, A.J., Vrensen, G.F., Koretz, J., Maraini, G., and Harding, J.J. (2000). The ageing lens. *Ophthalmologic,* **214,** 86–104.

Bullier, J. (2001). Integrated model of visual processing. *Brain Res. Rev.* **36,** 96–107.

Bushnell, M.C., Goldberg, M.E., and Robinson, D.L. (1981). Behavioral enhancement of visual responses in monkey cerebral cortex. I. Modulation in posterior parietal cortex related to selective visual attention. *J. Neurophysiol.* **46,** 755–772.

Calkins, D.J., Tsukamoto, Y., and Sterling, P. (1998). Microcircuitry and mosaic of a blue-yellow ganglion cell in the primate retina. *J. Neurosci.* **18,** 3373–3385.

Callaway, E. M. (1998). Local circuits in primary visual cortex of the macaque monkey. *Annu. Rev. Neurosci.* **21,** 47–74.

Chapman, B., Zahs, K. R., and Stryker, M. P. (1991). Relation of cortical cell orientation selectivity to alignment of receptive fields of the geniculocortical afferents that arborize within a single orientation column in ferret visual cortex. *J. Neurosci.* **11,** 1347–1358.

Cheng, K., Waggoner, R. A., and Tanaka, K. (2001). Human ocular dominance columns as revealed by high-field functional magnetic resonance imaging. *Neuron* **32,** 359–374.

Colby, C.L., Duhamel, J.R., and Goldberg, M. E. (1993). Ventral intraparietal area of the macaque: anatomic location and visual response properties. *J. Neurophysiol.* **6,** 902–914.

Colby, C.L., Duhamel, J.R., and Goldberg, M.E. (1996). Visual, presaccadic, and cognitive activation of single neurons in monkey lateral intraparietal area. *J. Neurophysiol.* **76,** 2841–2852.

Corbetta, M., Kincade, J.M., Ollinger, J.M., McAvoy, M.P., and Shulman, G.L. (2000). Voluntary orienting is dissociated from target detection in human posterior parietal cortex. *Nat. Neurosci.* **3,** 292–297.

Cowey, A., and Heywood, C.A. (1995). There's more to colour than meets the eye. *Behav. Brain Res.* **71,** 89–100.

Crair, M. C., Gillespie, D. C., and Stryker, M. P. (1998). The role of visual experience in the development of columns in cat visual cortex. *Science* **279,** 566–570.

Crick, F., and Koch, C. (1995). Are we aware of neural activity in primary visual cortex? *Nature* **375,** 121–123.

Culham, J.C., and Kanwisher, N.G. (2001). Neuroimaging of cognitive functions in human parietal cortex. *Curr. Opin. Neurobiol.* **11,** 157–163.

Dacey, D.M., and Lee, B.B. (1994). The 'blue-on' opponent pathway in primate retina originates from a distinct bistratified ganglion cell type. *Nature* **367,** 731–735.

Dechent, P., and Frahm, J. (2000). Direct mapping of ocular dominance columns in human primary visual cortex. *Neuroreport* **11,** 3247–3249.

DeYoe, E.A., Felleman, D.J., Van Essen, D.C., and McClendon, E. (1994). Multiple processing streams in occipito-temporal visual cortex. *Nature* **371,** 151–154.

Dogiel, A.S. (1891). Über die nervösen Elemente in der Retina des Menschen. *Arch. Mikrosk. Anat.* **38,** 317–344.

Downing, P.E., Jiang, Y., Shuman, M., and Kanwisher, N. (2001). A cortical area selective for visual processing of the human body. *Science* **293,** 2470–2473.

Engel, S. A., Rumelhart, D. E., Wandell, B. A., Lee, A. T., Glover, G. H., Chichilnisky, E. J., and Shadlen, M. N. (1994). fMRI of human visual cortex. *Nature* **369,** 525.

Epstein, R., and Kanwisher, N. (1998). A cortical representation of the local visual environment. *Nature* **392,** 598–601.

Epstein, R., Harris, A., Stanley, D., and Kanwisher, N. (1999). The parahippocampal place area: recognition, navigation, or encoding? *Neuron* **23,** 115–125.

Famiglietti, E.V. (1992). Dendritic co-stratification of ON and ON OFF directionally selective ganglion cells with starburst amacrine cells in rabbit retina. *J. Comp. Neurol.* **324,** 322–335.

Felleman, D. J., and Van Essen, D. C. (1991). Distributed hierarchical processing in the primate cerebral cortex. *Cereb. Cortex* **1,** 1–47.

Ferster, D. (1987). Origin of orientation selective EPSPs in simple cells of cat visual cortex. *J. Neurosci.* **7,** 1780–1791.

Fitzpatrick, D., Lund, J. S., Schmechel, D. E., and Towles, A. C. (1987). Distribution of GABAergic neurons and axon terminals in themacaque striate cortex. *J. Comp. Neurol. 264*.

Fries, P., Reynolds, J.H., Rorie, A.E., and Desimone, R. (2001). Modulation of oscillatory neuronal synchronization by selective visual attention. *Science* **291,** 1560–1563.

Galletti, C., Fattori, P., Kutz, D.F., and Battaglini, P.P. (1997). Arm movement-related neurons in the visual area V6A of the macaque superior parietal lobule. *Eur. J. Neurosci.* **9,** 410–413.

Galletti, C., Fattori, P., Gamberini, M., and Kutz, D.F. (1999). The cortical visual area V6: brain location and visual topography. *Eur. J. Neurosci.* **11,** 3922–3936.

Gauthier, I., and Nelson, C.A. (2001). The development of face expertise. *Curr. Opin. Neurobiol.* **11,** 219–224.

Gauthier, I., Tarr, M.J., Anderson, A.W., Skudlarski, P., and Gore, J.C. (1999). Activation of the middle fusiform "face area" increases with expertise in recognizing novel objects. *Nat. Neurosci.* **2,** 568–573.

Ghosh, K.K., Martin, P.R., and Grünert U (1997). Morphological analysis of the blue cone pathway in the retina of a new world monkey *Callithrix jacchus*. *J. Comp. Neurol*. 211–225.

Giolli R. A.(1963). An experimental study of the accessory optic system in the Cynomolgus monkey. *J. Comp. Neurol*. **121,** 89–108.

Goebel, R., Khorram-Sefat, D., Muckli, L., Hacker, H., and Singer, W. (1998). The constructive nature of vision: direct evidence from functional magnetic resonance imaging studies of apparent motion and motion imagery. *Eur. J. Neurosci.* **10,** 1563–1573.

Goebel, R., Muckli, L., Zanella, F.E., Singer, W., and Stoerig, P. (2001). Sustained extrastriate cortical activation without visual awareness revealed by fMRI studies of hemianopic patients. *Vis. Res.* **41,** 1459–1474.

Goodale, M.A., and Milner, A.D. (1992). Separate visual pathways for perception and action. *Trends Neurosci*. **15,** 20–25.

Goodyear, B. G., and Menon, R. S. (2001). Brief visual stimulation allows mapping of ocular dominance in visual cortex using fMRI. *Hum. Brain Mapping* **14,** 210–217.

Graw, J. (1996). Genetic aspects of embryonic eye development in vertebrates. *Dev. Genet*. **18,** 181–197.

Grill-Spector, K. (2003). The occipital lobe. *In* "Encyclopedia of the Neurological Sciences" (M. Aminoff and R. Daroff, eds.). Academic Press, San Diego.

Grill-Spector, K., Kushnir, T, Hendler, T., and Malach, R. (2000). The dynamics of object-selective activation correlate with recognition performance in humans. *Nat. Neurosci.* **3,** 837–843.

Grill-Spector, K., Kourtzi, Z., and Kanwisher, N. (2001). The lateral occipital complex and its role in object recognition. *Vis. Res*. **41,** 1409–1422.

Gross, C.G. (1992). Representation of visual stimuli in inferior temporal visual cortex. *Proc. R. Soc. Lond. [Biol.]* **335,** 3–10.

Gur, M., and Snodderly, D.M. (1997). A dissociation between brain activity and perception: chromaticity opponent cortical neurons signal chromatic flicker that is not perceived. *Vis. Res*. **37,** 377–382.

Hadjikhani, N., Liu, A.K., Dale, A.M., Cavanagh, P., and Tootell, R.B.H. (1998). Retinotopy and color sensitivity in human visual cortical area V8. *Nat. Neurosci.* **1,** 235–241.

Hasson, U., Levy, I., Behrmann, M., Hendler, T., and Malach, R. (2002). Eccentricity bias as an organizing principle for human high-order object areas. *Neuron* **34,** 479–490.

Hattar, S., Liao, H.W., Takao, M., Berson, D.M., and Yau, K.W. (2002). Melanopsin-containing retinal ganglion cells: architecture, projections, and intrinsic photosensitivity. *Science* **295,** 1065–1070.

Haxby, J.V., Grady, C.L., Horwitz, B., Ungerleider, L.G., Mishkin, M., Carson, R.E., Herscovitch, P., Schapiro, M.B., and Rapoport, S.I. (1991). Dissociation of object and spatial visual processing pathways in human extrastriate cortex. *Proc. Natl. Acad. Sci. U.S.A.* **88,** 1621–1625.

Haxby, J.V., Gobbini, M.I., Furey, M.L., Ishai, A., Schouten, J.L., and Pietrini, P. (2001). Distributed and overlapping representations of faces and objects in ventral temporal cortex. *Science* **293,** 2425–2430.

Hebb, D.O. (1949). "The Organization of Behavior." Wiley-Liss, New York.

Heywood, C.A., and Cowey, A. (1987). On the role of cortical area V4 in the discrimination of hue and pattern in macaque monkeys. *J. Neurosci.* **7,** 2601–2617.

Hochstein, S., and Ahissar, M. (2002). View from the top: hierarchies and reverse hierarchies in the visual system. *Neuron* **36,** 791–804.

Horton, J. C. (1984). Cytochrome oxidase patches: a new cytoarchitectonic feature of monkey visual cortex. *Philos. Trans. R. Soc. Lond. B Biol. Sci.* **304,** 199–253.

Horton, J. C., Dagi, L. R., McCrane, E. P., and de Monasterio, F. M. (1990). Arrangement of ocular dominance columns in human visual cortex. *Arch. Ophthalmol.* **108,** 1025–1031.

Hubel, D. H., and Wiesel, T. N. (1968). Receptive fields and functional architecture of monkey striate cortex. *J. Physiol.* **195,** 215–243.

Hubel, D. H., and Wiesel, T. N. (1969). Anatomical demonstration of columns in the monkey striate cortex. *Nature* **221,** 747–750.

Hubel, D. H., and Wiesel, T. N. (1972). Laminar and columnar distribution of geniculo-cortical fibers in the macaque monkey. *J. Comp. Neurol.* **146,** 421–450.

Hubel, D. H., and Wiesel, T. N. (1974). Sequence regularity and geometry of orientation columns in the monkey striate cortex. *J. Comp. Neurol.* **158,** 267–293.

Hubel, D. H., and Wiesel, T. N. (1977). Ferrier lecture. Functional architecture of macaque monkey visual cortex. *Proc. R. Soc. Lond. B Biol. Sci.* **198,** 1–59.

Hubel, D.H., and Wiesel, T.N. (1979). "The Brain: A Scientific American Book." WH Freeman, New York.

Hubel, D. H., Wiesel, T. N., and Stryker, M. P. (1978). Anatomical demonstration of orientation columns in macaque monkey. *J. Comp. Neurol.* **177,** 361–380.

Hubener, M., Shoham, D., Grinvald, A., and Bonhoeffer, T. (1997). Spatial relationships among three columnar systems in cat area 17. *J. Neurosci.* **17,** 9270–9284.

Inouye, T.(2000). Visual disturbances following gunshot wounds of the cortical visual area. *Brain* **123,** Suppl. 1–101.

Ishai, A., Ungerleider, L.G., Martin, A., Schouten, J.L., and Haxby, J.V. (1999). Distributed representation of objects in the human ventral visual pathway. *Proc. Natl. Acad. Sci. U.S.A.* **96,** 9379–9384.

Ishai, A., Ungerleider, L.G., and Haxby, J.V. (2000). Distributed neural systems for the generation of visual images. *Neuron* **28,** 979–990.

Issa, N. P., Trepel, C., and Stryker, M. P. (2000). Spatial frequency maps in cat visual cortex. *J. Neurosci.* **20,** 8504–8514.

Jacobs, G.H. (2002). Progress toward understanding the evolution of primate color vision. *Evol. Anthropol. Suppl* **1,** 132–135.

Jacobs, G.H. (1993). The distribution and nature of colour vision among the mammals. *Biol. Rev.* **68,** 413–471.

Kanwisher, N., McDermott, J., and Chun, M.M. (1997). The fusiform face area: a module in human extrastriate cortex specialized for face perception. *J. Neurosci.* **17,** 4302–4311.

Kanwisher, N., Stanley, D., and Harris, A. (1999). The fusiform face area is selective for faces not animals. *Neuroreport* **10,** 183–187.

Kim, D. S., Matsuda, Y., Ohki, K., Ajima, A., and Tanaka, S. (1999). Geometrical and topological relationships between multiple functional maps in cat primary visual cortex. *Neuroreport* **10,** 2515–2522.

Kolb, H. (1970). Organization of the outer plexiform layer of the primate retina: electron microscopy of Golgi-impregnated cells. Philos. *Trans. R. Soc. London Ser. B* **258,** 261–283.

Kolb, H., and Famiglietti, E.V. (1974). Rod and cone pathways in the inner plexiform layer of cat retina. *Science* **186,** 47–49.

Kolb, H., Mariani, A., and Gallego, A. (1980). A second type of horizontal cell in the monkey retina. *J. Comp Neurol.* **189,** 31–44.

Kourtzi, Z., and Kanwisher, N. (2001). Representation of perceived object shape by the human lateral occipital complex. *Science* **293,** 1506–1509.

Kreiman, G., Koch, C., and Fried, I. (2000). Category-specific visual responses of single neurons in the human medial temporal lobe. *Nat. Neurosci.* **3,** 946–953.

Kriegeskorte, N., Formisano, E., Sorger, B., van de Moortele, P.F., Adriany, G., Kim, D.S., and Goebel, R. (2003). Single-object-image response patterns in human inferotemporal cortex. *NeuroImage*, Suppl. (in press).

Kuffler, S.W. (1953). Discharge patterns and functional organization of mammalian retina. *J. Neurophysiol.* **16,** 37–68.

Kuffler, S. W. (1973). The single-cell approach in the visual system and the study of receptive fields. *Invest. Ophthalmol.* **12,** 794–813.

Lamme, V.A., and Roelfsema, P.R. (2000). The distinct modes of vision offered by feedforward and recurrent processing. *Trends Neurosci.* **23,** 571–579.

Leopold, D.A., and Logothetis, N.K. (1999). Multistable phenomena: changing views in perception. *Trends Cogn. Sci.* **3,** 254–264.

Levy, I., Hasson, U., Avidan, G., Hendler, T., and Malach, R. (2001). Center-periphery organization of human object areas. *Nat. Neurosci.* **4,** 533–539.

Lewis, J.W., and Vanesen, E.D. (2000). Mapping of architectonic subdivisions in the macaque monkey, with emphasis on parieto-occipital cortex. *J. Comp. Neurol.* **428,** 79–111.

Livingstone, M., and Hubel, D. (1988). Segregation of form, color, movement, and depth: anatomy, physiology, and perception. *Science* **240,** 740–749.

Logothetis, N.K. (2000). Object recognition: holistic representations in the monkey brain. *Spat. Vis.* **13,** 165–178.

Lucas, R.J., Douglas, R.H., and Foster, R.G. (2001). Characterization of an ocular photopigment capable of driving pupillary constriction in mice. *Nat. Neurosci.* **4,** 621–626.

Lueck, C.J., Zeki, S., Friston, K.J., Deiber, M.P., Cope, P., Cunningham, V.J., Lammertsma, A.A., Kennard, C., and Frackowiak, R.S. (1989). The colour centre in the cerebral cortex of man. *Nature* **340,** 386–389.

Lund, J. S. (1988). Anatomical organization of macaque striate visual cortex. *Annu. Rev. Neurosci.* **11,** 253–288.

Lund, J. S., and Wu, C. Q. (1997). Local circuit neurons of macaque monkey striate cortex: IV. Neurons of laminae 1-3A. *J. Comp. Neurol.* **384,** 109–126.

Lund, J. S., and Yoshitaka, T. (1991). Local circuit neurons of macaque monkey striate cortex: III. Neurons of laminae 4B, 5A, and 3B. *J. Comp. Neurol.* **311,** 234–258.

Malach, R. Y., Harel, A. H., and Grinvald, A. (1993). Novel aspects of columnar organzation are revealed by optical imaging and in vivo targeted biocytin injections in primate striate cortex. *Proc. Natl. Acad. Sci. U.S.A.* **9,** 10469–10473.

Malach, R., Reppas, J.B., Benson, R.R., Kwong, K.K., Jiang, H., Kennedy, W.A., Ledden, P.J., Brady, T.J., Rosen, B.R., and Tootell, R.B. (1995). Object-related activity revealed by functional magnetic resonance imaging in human occipital cortex. *Proc. Natl. Acad. Sci. U.S.A.* **92,** 8135–8139.

Malach, R., Levy, I., and Hasson, U. (2002). The topography of high-order human object areas. *Trends Cogn. Sci.* **6,** 176–184.

Malonek, D., and Grinvald, A. (1996). Interactions between electrical activity and cortical microcirculation revealed by imaging spectroscopy: implications for functional brain mapping. *Science* **272,** 551–554.

Masland, R.H., and Raviola, E. (2000). Confronting complexity: strategies for understanding the microcircuitry of the retina. *Annu. Rev. Neurosci.* **23,** 249–284.

Maunsell, J.H., and Newsome, W.T. (1987). Visual processing in monkey extrastriate cortex. *Annu. Rev. Neurosci.* **10,** 363–401.

McKeefry, D.J., and Zeki, S. (1997). The position and topography of the human colour centre as revealed by functional magnetic resonance imaging. *Brain* **120** (Pt 12), 2229–2242.

Meadows, J.C. (1974). Disturbed perception of colours associated with localized cerebral lesions. *Brain* **97,** 615–632.

Mehta, A.D., Ulbert, I., and Schroeder, C.E. (2000). Intermodal selective attention in monkeys. II: physiological mechanisms of modulation. *Cereb. Cortex* **10,** 359–370.

Meister, M., and Berry, M.J. (1999). The neural code of the retina. *Neuron* **22,** 435–450.

Milner, A.D., and Goodale, M.A. (1995). "The Visual Brain in Action." Oxford University Press, Oxford.

Mishkin, M., Ungerleider, L.G., and Macko, K.A. (1983). Object vision and spatial vision: two cortical pathways. *Trends Neurosci.* **6,** 414–417.

Missotten, L. (1965). "The Ultrastructure of the Human Retina." Arscia Uitgaven, Brussels.

Moore, B., Lyons, S.A., and Walline, J. (1999). A clinical review of hyperopia in young children. The Hyperopic Infants' Study Group, THIS Group. *J. Am. Optom. Assoc.* **70,** 215–224.

Moore, R. Y. (1973). Retinohypothalamic projection in mammals: a comparative study. *Brain Res.* **30,** 403–409.

Moran, J., and Desimone, R. (1985). Selective attention gates visual processing in the extrastriate cortex. *Science* **229,** 782–784.

Obermayer, K., and Blasdel, G. G. (1993). Geometry of orientation and ocular dominance columns in monkey striate cortex. *J. Neurosci.* **13,** 4114–4129.

O'Connor, D.H., Fukui, M.M., Pinsk, M.A., and Kastner, S. (2002). Attention modulates responses in the human lateral geniculate nucleus. *Nat. Neurosci.* **5,** 1203–1209.

O'Kusky, J., and Colonnier, M. (1982). A laminar analysis of the number of neurons, glia, and synapses in the visual cortex (area 17) of adult macaque monkeys. *J. Comp. Neurol.* **210,** 278–290.

Oram, M.W., and Perrett, D.I. (1996). Integration of form and motion in the anterior superior temporal polysensory area (STPa) of the macaque monkey. *J. Neurophysiol.* **76,** 109–129.

Pawlik, G., Rackle, A., and Bing, R. J. (1981). Quantitative capillary topography and blood flow in the cerebral cortex of cat: an in vivo microscopic study. *Brain Res.* **208,** 35–58.

Perrett, D.I., Rolls, E.T., and Caan, W. (1982). Visual neurones responsive to faces in the monkey temporal cortex. *Exp. Brain Res.* **47,** 329–342.

Perrett, D.I., Smith, P.A., Potter, D.D., Mistlin, A.J., Head, A.S., Milner, A.D., and Jeeves, M.A. (1985). Visual cells in the temporal cortex sensitive to face view and gaze direction. *Proc. R. Soc. Lond. B Biol. Sci.* **223,** 293–317.

Peters, A., and Jones, E. G. (1984). Classification of cortical neurons. *In* "Cerebral Cortex" (A. Peters and E.G. Jones, eds.), pp. 107–121. Plenum, New York.

Polk, T.A., Stallcup, M., Aguirre, G.K., Alsop, D.C., D'Esposito, M., Detre, J.A., and Farah, M.I. (2002). Neural specialization for letter recognition. *J. Cogn. Neurosci.* **15,** 145–159.

Polonsky, A., Blake, R., Braun, J., and Heeger, D.J. (2000). Neuronal activity in human primary visual cortex correlates with perception during binocular rivalry. *Nat. Neurosci.* **3,** 1153–1159.

Polyak, S. (1941). "The Retina." University of Chicago Press, Chicago.

Provencio, I., Rodriguez, I.R., Jiang, G., Hayes, W.P., Moreira, E.F., and Rollag, M.D. (2000). A novel human opsin in the inner retina. *J. Neurosci.* **20,** 600–605.

Provencio, I., Rollag, M.D., and Castrucci, A.M. (2002). Photoreceptive net in the mammalian retina. This mesh of cells may explain how some blind mice can still tell day from night. *Nature* **415,** 493.

Puce, A., Allison, T., Gore, J.C., and McCarthy, G. (1995). Face-sensitive regions in human extrastriate cortex studied by functional MRI. *J. Neurophysiol.* **74,** 1192–1199.

Puce, A., Allison, T., Asgari, M., Gore, J.C., and McCarthy, G. (1996). Differential sensitivity of human visual cortex to faces, letter-strings, and textures: a functional magnetic resonance imaging study. *J. Neurosci.* **16,** 5205–5215.

Rees, G., Kreiman, G., and Koch, C. (2002). Neural correlates of consciousness in humans. *Nat. Rev. Neurosci.* **3,** 261–270.

Reid, R. C., and Alonso, J. M. (1995). Specificity of monosynaptic connections from thalamus to visual cortex. *Nature* **378,** 281–284.

Ress, D., Backus, B.T., and Heeger, D.J. (2000). Activity in primary visual cortex predicts performance in a visual detection task. *Nat. Neurosci.* **3,** 940–945.

Rockland, K. S., and Lund, J. S. (1983). Intrinsic laminar lattice connections in primate visual cortex. *J. Comp. Neurol.* **216,** 303–318.

Roelfsema, P.R., Lamme, V.A., and Spekreijse, H. (1998). Object-based attention in the primary visual cortex of the macaque monkey. *Nature* **395,** 376–381.

Roelfsema, P.R., Lamme, V.A., Spekreijse, H., and Bosch, H. (2002). Figure-ground segregation in a recurrent network architecture. *J. Cogn. Neurosc.* **15,** 525–537.

Sakata, H., Taira, M., Kusunoki, M., Murata, A., and Tanaka, Y. (1997). The TINS Lecture. The parietal association cortex in depth perception and visual control of hand action. *Trends Neurosci.* **20,** 350–357.

Schultze, M. (1866). Zur Anatomie und Physiologie der Retina. *Arch. Mikrosk. Anat.* **2,** 175–286.

Sereno, M. I., Dale, A. M., Reppas, J. B., Kwong, K. K., Belliveau, J. W., Brady, T. J., Rosen, B. R., and Tootell, R. B. (1995). Borders of multiple visual areas in humans revealed by functional magnetic resonance imaging. *Science* **268,** 889–893.

Shmuel, A., and Grinvald, A. (1996). Functional organization for direction of motion and its relationship to orientation maps in cat area 18. *J. Neurosci.* **16,** 6945–6964.

Shoham, D., Hubener, M., Schulze, S., Grinvald, A., and Bonhoeffer, T. (1997). Spatio-temporal frequency domains and their relation to cytochrome oxidase staining in cat visual cortex. *Nature* **385,** 529–533.

Singer, W. (1999). Neuronal synchrony: a versatile code for the definition of relations? *Neuron* **24,** 49–65.

Sireteanu, R. (2000). The binocular visual system in amblyopia. *Strabismus* **8,** 39–51.

Smith, A.T., Greenlee, M.W., Singh, K.D., Kraemer, F.M., and Hennig, J. (1998). The processing of first- and second-order motion in human visual cortex assessed by functional magnetic resonance imaging (fMRI). *J. Neurosci.* **18,** 3816–3830.

Snowden, R.J., Treue, S., and Andersen, R.A. (1992). The response of neurons in areas V1 and MT of the alert rhesus monkey to moving random dot patterns. *Exp. Brain Res.* **88,** 389–400.

Snyder, L.H., Batista, A.P., and Andersen, R.A. (1997). Coding of intention in the posterior parietal cortex. *Nature* **386,** 167–170.

Somers, D.C., Dale, A.M., Seiffert, A.E., and Tootell, R.B. (1999). Functional MRI reveals spatially specific attentional modulation in human primary visual cortex. *Proc. Natl. Acad. Sci. U.S.A.* **96,** 1663–1668.

Stell, W.K. (1965). Correlation of retinal cytoarchitecture and ultrastructure in Golgi preparations. *Anat. Rec.* **153,** 389–397.

Stone, J. (1983). "Parallel Processing in the Visual System: The Classification of Retinal Ganglion Cells and Its Impact on the Neurobiology of Vision." Plenum Press, New York.

Swindale, N. (2001). Cortical cartography: what's in a map? *Curr. Biol.* **11,** R764–767.

Swindale, N.V. (2000). How many maps are there in visual cortex? *Cereb. Cortex* **10,** 633–643.

Swindale, N. V., Shoham, D., Grinvald, A., Bonhoeffer, T., and Hubener, M. (2000). Visual cortex maps are optimized for uniform coverage. *Nat. Neurosci.* **3,** 822–826.

Taira, M., Mine, S., Georgopoulos, A.P., Murata, A., and Sakata, H. (1990). Parietal cortex neurons of the monkey related to the visual guidance of hand movement. *Exp. Brain Res.* **83,** 29–36.

Taira, M., Tsutsui, K.I., Jiang, M., Yara, K., and Sakata, H. (2000). Parietal neurons represent surface orientation from the gradient of binocular disparity. *J. Neurophysiol.* **83,** 3140–3146.

Tanaka, K. (1983). Cross-correlation analysis of geniculostriate neuronal relationships in cats. *J. Neurophysiol.* **49,** 1303–1318.

Tanaka, K. (1996). Inferotemporal cortex and object vision. Ann. Rev. of Neurosci. **19,** 109–139.

Tanaka, K. (2001). Mechanisms of visual object recognition studied in monkeys. Spat. Vis. **13,** 147–163.

Tong, F. (2003). Primary visual cortex and visual awareness. *Nat. Rev. Neurosci.* **4,** 219–229.

Tong, F., and Engel, S.A. (2001). Interocular rivalry revealed in the human cortical blind-spot representation. *Nature* **411,** 195–199.

Tononi, G., and Edelman, G.M. (1998). Consciousness and complexity. *Science* **282,** 1846–1851.

Tootell, R.B., Silverman, M.S., and De Valois, R.L. (1981). Spatial frequency columns in primary visual cortex. *Science* **214,** 813–815.

Tootell, R.B., Reppas, J.B., Kwong, K.K., Malach, R., Born, R.T., Brady, T.J., Rosen, B.R., and Belliveau, J.W. (1995). Functional analysis of human MT and related visual cortical areas using magnetic resonance imaging. *J. Neurosci.* **15,** 3215–3230.

Tootell, R.B., Dale, A.M., Sereno, M.I., and Malach, R. (1996). New images from human visual cortex. *Trends Neurosci.* **19,** 481–489.

Tootell, R.B., Mendola, J.D., Hadjikhani, N.K., Ledden, P.J., Liu, A.K., Reppas, J.B., Sereno, M.I., and Dale, A.M. (1997). Functional analysis of V3A and related areas in human visual cortex. *J. Neurosci.* **17,** 7060–7078.

Tripathi, R.C., and Tripathi, B.J. (1984). Anatomy of the human eye, orbit and adnexa. *In* "The Eye" (E. Davson, ed.), pp. 1–268. Academic Press, Orlando.

Ts'o, D. Y., Gilbert, C. D., and Wiesel, T. N. (1986). Relationships between horizontal interactions and functional architecture in cat striate cortex as revealed by cross-correlation analysis. *J. Neurosci.* **6,** 1160–1170.

Ts'o, D. Y., Frostig, R. D., Lieke, E. E., and Grinvald, A. (1990). Functional organization of primate visual cortex revealed by high resolution optical imaging. *Science* **249,** 417–420.

Ungerleider, L.G., and Desimone, R. (1986) Cortical connections of visual area MT in the macaque. *J. Comp. Neurol.* **248,** 190–202.

Ungerleider, L.G., and Mishin, M. (1982). Two cortical visual systems. In: D.J. Ingle, *et al.* (eds)., pp. 549–586.

Ungerleider, L. G., and Haxby, J. V. (1994). "What" and "where" in the human brain. *Curr. Opin. Neurobiol.* **4,** 157–165.

Van, E.D., Maunsell, J.H., and Bixby, J.L. (1981). The middle temporal visual area in the macaque: myeloarchitecture, connections, functional properties and topographic organization. *J. Comp. Neurol.* **199,** 293–326.

Van Essen, D.C. (2002). Organization of visual areas in macaque and human cerebral cortex. *In* L. 6Chalupa and J.S. Werner (eds.), The Visual Neurosciences. MIT Press, Cambridge, MA.

Van Oostende, S., Sunaert, S., Van Hecke, P., Marchal, G., and Orban, G.A. (1997). The kinetic occipital (KO) region in man: an fMRI study. *Cereb. Cortex* **7,** 690–701.

Vogels, R., and Orban, G.A. (1996). Coding of stimulus invariances by inferior temporal neurons. *Prog. Brain Res.* **112,** 195–211.

von der Malsburg, C. (1999). The what and why of binding: the modeler's perspective. *Neuron* **24,** 95–25.

von Economo, C., and Koskinas, G. N. (1925). "Die Cytoarchitektonik der Hirnrinde des erwachsenen Menschen." Springer Verlag, Vienna.

von Gudden (1874). Über die Kreuzung von Fasern im Chiasma. Nervorum opticorum. *Arch. Ophtalmol. (Chicago)* **20,** 249.

von Kries, J. (1896). Über die Funktion der Netzhautstäbchen. *Z. Physiol. Psychol. Sinnesorgane* **9,** 81–123.

von Monakow, C. (1883). Experimentelle und pathologisch-anatomische Untersuchungen über die Beziehung der sogenannten Sehsphäre zu den infracorticalen Opticuscentren und zum N. opticus. *Arch. Psychiatr. Nervenkr.* **14,** 699–751

Wässle, H. (2002). Die Netzhaut, ein Gehirn im Auge. *In* "Jahrbuch 2001 der Deutschen Akademie der Naturforscher," pp. 493–506. Leopoldina, Halle/Saale.

Watson, J.D., Myers, R., Frackowiak, R.S., Hajnal, J.V., Woods, R.P., Mazziotta, J.C., Shipp, S., and Zeki, S. (1993). Area V5 of the human brain: evidence from a combined study using positron emission tomography and magnetic resonance imaging. *Cereb. Cortex* **3,** 79–94.

Weiskrantz (1990)

Wong-Riley, M. T. T. (1989). Cytochrome oxidase: an endogenous metabolic marker for neuronal activity. *Trends Neurosci.* **12,** 94–101.

Wurtz, R.H., and Kandel, E.R. (2000). Perception of motion, depth, and form. *In* "Principles of Neural Science" (E.R. Kandel, J.H. Schwartz, and T.M. Jessell, eds.), 4th ed. McGraw-Hill, New York.

Yoshida, K., Watanabe, D., Ishikane, H., Tachibana, M., Pastan, I., and Nakanishi, S. (2001). A key role of starburst amacrine cells in originating retinal directional selectivity and optokinetic eye movement. *Neuron* **30,** 771–780.

Yoshitaka, T., Blasdel, G. G., Levitt, J. B., and Lund, J. S. (1996). Relationship between pattern of intrinsic lateral connectivity, ocular dominance, and cytochrome oxidase-reactive regions in macaque monkey striate cortex. *Cereb. Cortex* **6,** 297–310.

Zeki, S.M. (1991). Cerebral akinetopsia (visual motion blindness). A review. *Brain* **114,** 811–824.

Zeki, S.M. (1978). Functional specialization in the visual cortex of the rhesus monkey. *Nature* **274,** 423–428.

Zeki, S.M. (2003). Improbable areas in the visual brain. *Trends Neurosci.* **26,** 23–26.

Zeki, S.M. (1993). "Vision of the Brain." Blackwell Scientific Publications, Cambridge, MA.

Zeki, S., McKeefry, D.J., Bartels, A., and Frackowiak, R.S. (1998). Has a new color area been discovered? *Nat. Neurosci.* **1,** 335–336.

Zeki, S.M., Perry, R.J., and Bartels, A. (2003). The processing of kinetic contours in the brain. *Cereb. Cortex* **13,** 189–202.

Zilles, K. (1990). Cortex. *In* "The Human Nervous System" (G. Paxinos, ed.), pp. 757–802. San Diego: Academic Press.

Zilles, K., and Clarke, S. (1997). *In* "Architecture, Connectivity, and Transmitter Receptors of Human Extrastriate Visual Cortex. Comparison with Non Human Primates" (K.S. Rockland, J.H. Kaas, and A. Peters, eds.), Vol. 12, pp. 673–742. Plenum, New York.

CHAPTER

36

Emotional Motor System

GERT G. HOLSTEGE, LEONORA J. MOUTON, and PETER O. GERRITS

Department of Anatomy and Embryology, Faculty of Medical Sciences
University of Groningen, Groningen, The Netherlands

For most clinical neurologists the motor system consists of the corticospinal or pyramidal tract, originating from the motor or premotor cortex and terminating in the brainstem and spinal cord. The reason is simple. Partial interruption of the pyramidal tract leads to inability to move particular parts of the body and complete unilateral interruption to hemiplegia.

However, many findings in mammals, including humans, point to the existence of a different motor system, called the "emotional motor system" (Holstege, 1992). An example are the patients with a central paresis of the lower face caused by an interruption of motor cortical fibers innervating the motoneurons of the face musculature. These patients are not able to use their oral muscles voluntarily on the contralateral side of the lesion (Fig. 36.1, left). Yet, when they enjoy a funny story or a joke, they suddenly smile and use these muscles on both sides of the face (Holstege, 2002; Fig. 36.1, right). Both, the somatic or voluntary (Fig. 36.2, left) and the emotional motor system (Fig. 36.2, right) make use of the same motoneurons and premotor interneurons. These inter- and motoneurons represent the basic motor system.

Although this chapter focuses on the emotional motor system, the basic and the somatic motor systems will be discussed shortly in order to point out the similarities and differences between the two systems.

BASIC MOTOR SYSTEM

Somatic and Autonomic Motoneurons

Movements are the result of contractions of striated and smooth muscles that are controlled by somatic and autonomic motoneurons, respectively. The motoneurons, in turn, are controlled by nearby or distant premotor interneurons.

Somatic motoneurons are located in various brainstem nuclei and in the ventral horn throughout the length of the spinal cord. They innervate striated muscles. In the spinal cord, motoneurons innervating distal limb muscles, such as those of the hand, arm,

FIGURE 36.1 A patient suffering from a lesion in the white matter nearby the the face area of the primary and premotor cortex. The patient is not able to show her teeth on the contralateral side of the lesion *(left)*, but on the same side she is able to smile *(right)*.

foot, and leg, are located in the lateral and dorsal parts of the ventral horn. Those innervating the most distal muscles, such as the digits, are found in the most dorsal parts (VanderHorst and Holstege, 1997b). On the other hand, motoneurons innervating the muscles between the trunk and limb and those innervating axial muscles lie ventrally and medially in the ventral horn, respectively.

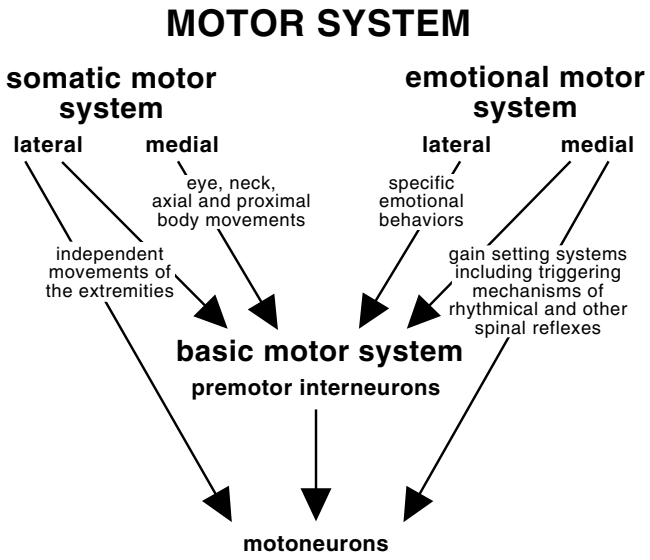

FIGURE 36.2 Scheme of the motor system consisting of a voluntary and an emotional motor component.

Autonomic (sympathetic and parasympathetic) motoneurons innervate glands and smooth muscles of viscera and blood vessels. There are preganglionic and postganglionic motoneurons, of which the preganglionics are located in the brainstem or spinal cord. Their axons run through a peripheral nerve and synapse on a postganglionic motoneuron in a peripheral ganglion. The sympathetic preganglionic motoneurons are active during basic survival behavior (fright, flight and fight), and are located in the intermediolateral cell column of the T1-L3 spinal segments. Each sympathetic preganglionic motoneuron controls about 30 postganglionic motoneurons.

The parasympathetic autonomic motoneurons, on the other hand, are especially active during rest and digest. They are located in the brainstem and in the intermediolateral cell column of the S2-S4 segments of the spinal cord. Each of these parasympathetic preganglionic motoneurons controls about two postganglionic motoneurons, located in so-called terminal ganglia in or close to the target organ.

Although the preganglionic and postganglionic sympathetic and parasympathetic motoneurons belong to the so-called autonomic system, they are not "autonomous" at all, but are under strong control of especially the emotional motor system.

Premotor Interneurons

Premotor interneurons project to somatic motoneurons or to preganglionic autonomic motoneurons. Premotor interneurons play a role not only in relatively simple motor activities such as reflexes but also in more complex motor activities. Many premotor interneurons lie in the intermediate zone near their target motoneurons, but in some cases they are located far from them (e.g., in respiration and micturition control systems).

Premotor interneurons projecting to distal muscle motoneurons innervating muscles of hip or shoulder, centrally; and those projecting to the trunk and axial motoneurons, medially in the intermediate zone (Fig. 36.3). The last projections are bilateral because of the bilateral function of the axial muscles. These interneuronal– motoneuronal projections belong to the so-called propriospinal pathways.

The motoneuronal cell groups (e.g., the motor trigeminal, facial, ambiguus, and the hypoglossal nuclei) in the caudal brainstem also receive many afferents from the premotor interneurons, the so-called propriobulbar pathways. These interneurons are located in the lateral tegmental field of the caudal pons and medulla oblongata as defined by Holstege *et. al.* (1977). The lateral tegmental field can be considered as the rostral extension of the intermediate zone of the spinal cord (Fig. 36.4).

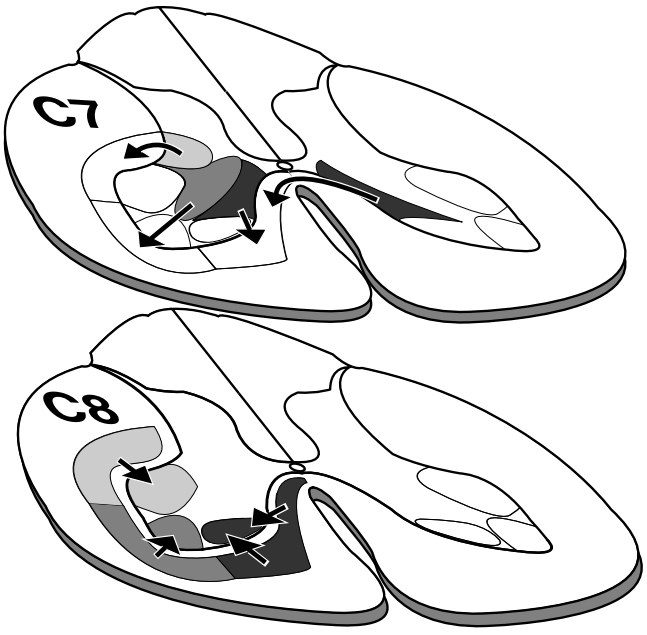

FIGURE 36.3 Schematic illustration of the projections from interneurons in the C7 intermediate zone (laminae V-VII) via the propriospinal pathways to the motoneurons at the C8 level.

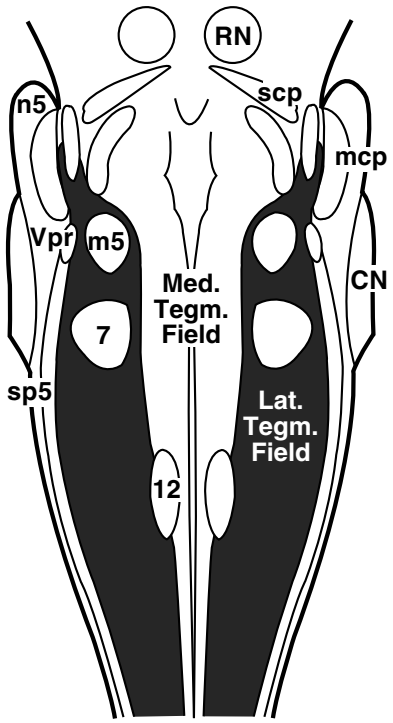

FIGURE 36.4 Schematic horizontal section through the brainstem. The lateral tegmental field is indicated in black.

Specific Premotor Interneuronal Systems Between Brainstem and Spinal Cord

Some premotor interneuronal projections to motoneurons are rather long. An example is the premotor projections to motoneurons involved in respiration. These motoneurons lie in the C4-C6 (phrenic nucleus motoneurons innervating the diaphragm) and the T1-L3 spinal cord (motoneurons innervating the intercostal and abdominal muscles). Their premotor interneurons are not located in the spinal cord because the respiratory afferents enter the central nervous system in the caudal. The inspiratory premotor interneurons innervating the phrenic and external intercostal motoneurons are located in the lateral solitary nucleus and rostral nucleus retroambiguus. The expiratory premotor interneurons innervating the abdominal and internal intercostal motoneurons are found in the caudal nucleus retroambiguus (Fig. 36.5). The abdominal muscles play an important role in postural control also, and the premotor interneurons for this function are located in the spinal cord near the abdominal motoneurons themselves. Another example of long basic system projections are the brainstem–spinal pathways involved in micturition (see "Pathways Involved in Micturition").

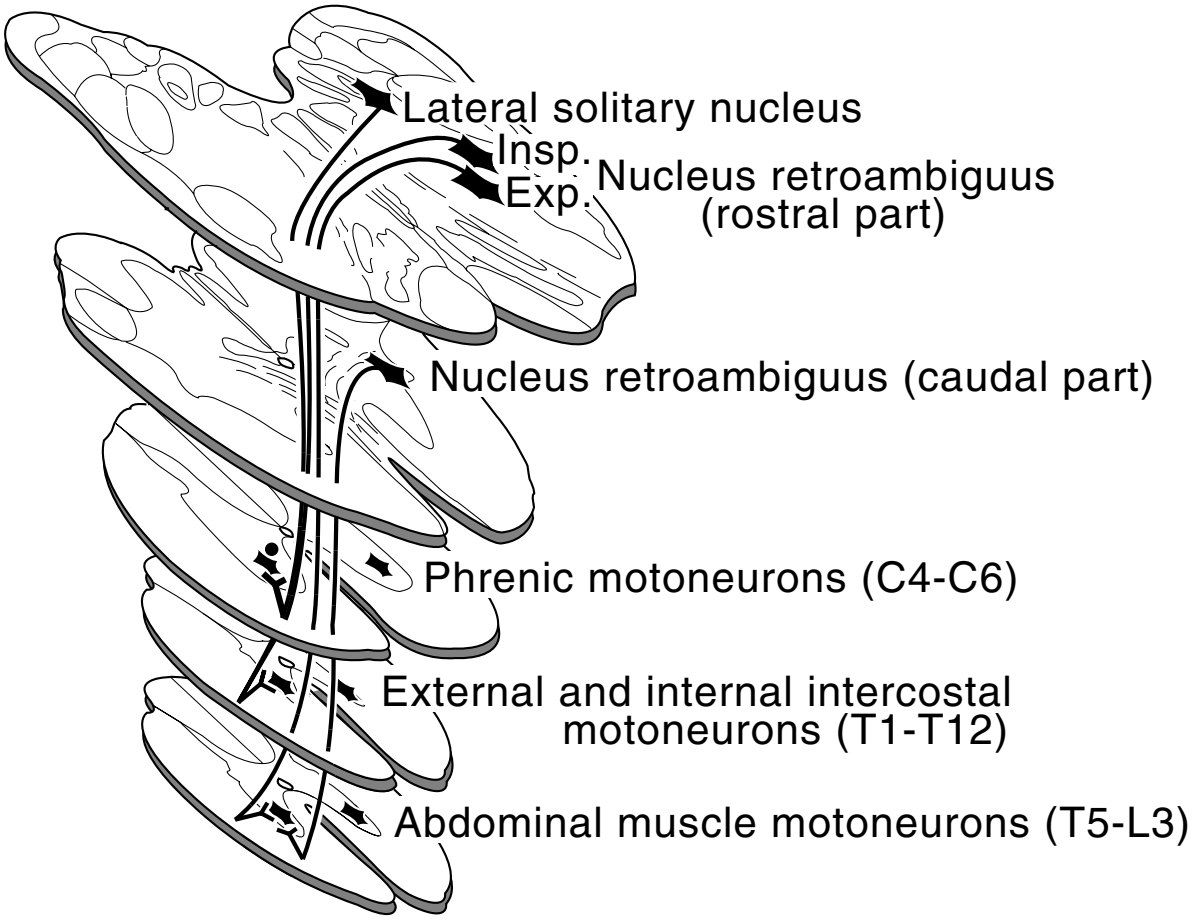

FIGURE 36.5 Schematic overview of the pathways controlling respiration and abdominal pressure. For the sake of clarity only the contralaterally descending pathways are indicated, although there exist to a limited extent some ipsilateral ones also.

SOMATIC MOTOR SYSTEM

The somatic motor system enables the individual to react voluntarily to events in its surrounding. As pointed out by Kuypers (1981), the somatic motor system consists of a medial and a lateral component controlling proximal and distal musculature, respectively.

Medial Component of the Somatic Motor System

The medial component represents a phylogenetically old supraspinal motor control system and is involved in maintenance of erect posture (antigravity movements), integration of body and limbs, synergy of the whole limb, and orientation of body and head. It controls the skeletal muscles of the neck, trunk, shoulders, and hip as well as the extrinsic eye muscles in the orbit.

Brainstem pathways belonging to the medial component of the somatic motor system are the interstitiospinal, vestibulospinal (Fig. 36.6, right), tectospinal, and reticulospinal tracts (Fig. 36.6, left). These pathways terminate mainly on premotor interneurons in the medial half of the ventral horn; in turn, the interneurons project to axial and proximal muscle motoneurons on both sides of the spinal cord.

There is also a corticospinal projection belonging to the medial component of the somatic motor system. It originates in the trunk, back, and neck representations of the primary motor and premotor cortex and descends bilaterally through the medial part of the ventral funiculus (Fig. 36.7, right). Similar to the brainstem–spinal fiber tracts, these corticospinal fibers terminate mainly on medially located premotor interneurons and not on motoneurons.

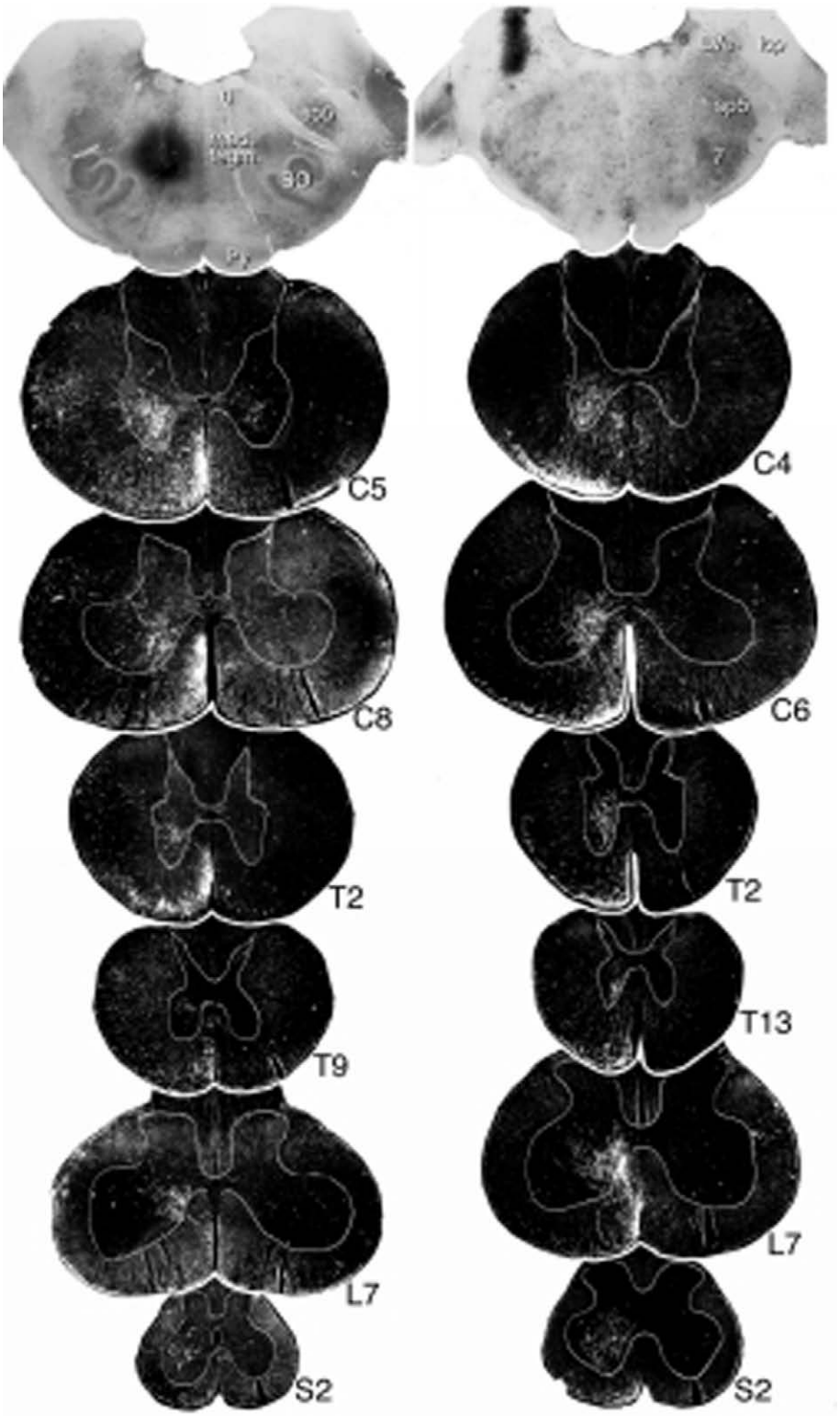

FIGURE 36.6 Brightfield photomicrographs of tritiated leucine injection sites in the medial reticular formation at the pontomedullary transition area *(left)* or in the vestibular complex *(right)*. Darkfield photomicrographs show the descending fibers and termination areas in the medial ventral horn in both cases.

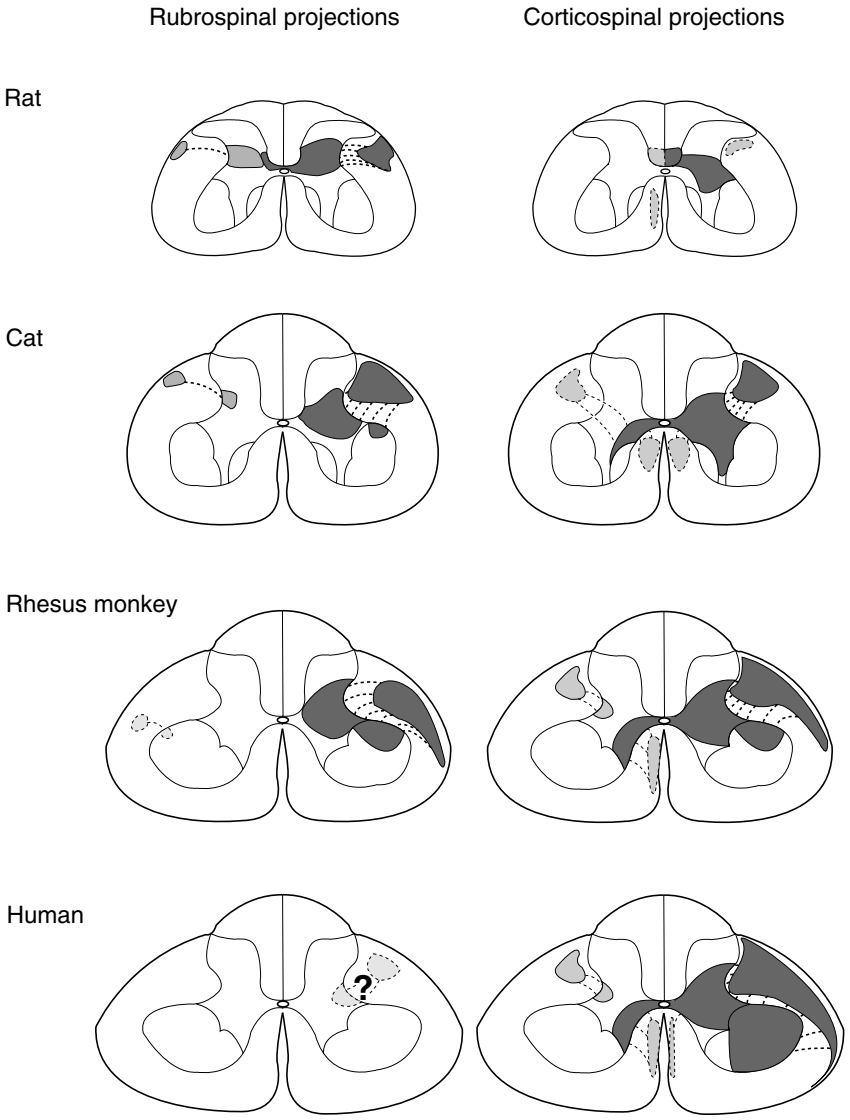

FIGURE 36.7 Schematic representation of the rubrospinal and corticospinal projections in rat, cat, rhesus monkey, and human at the level of C8. The gray areas in the white matter represent the descending pathways; those in the gray matter represent termination zones. Dark gray areas represent strong projections; lighter gray areas represent light projections.

Lateral Component of the Somatic Motor System

The lateral component of the somatic motor system controls the premotor interneurons and motoneurons of the distal muscles. This component consists of two pathways—the lateral corticospinal and the rubrospinal pathways. In humans, the lateral corticospinal pathway subserves the control of the independent movements of the extremities. It controls the motoneurons via direct projections as well as indirectly via strong projections to the laterally located premotor interneurons. The motoneurons innervating the muscles of the distal limbs receive the strongest direct projections from the motor cortex. This descending system enables humans to make most refined and extremely complex movements, such as independent finger movements and speech, the most complicated motor performance. In most mammals, both the lateral corticospinal and the rubrospinal pathways are important, but in humans the rubrospinal pathway seems to be irrelevant (Fig. 36.7).

The question is what drives the somatic motor system. The prefrontal cortex might play an essential role in deciding whether or not a motor activity is necessary to react to a certain situation. Since the

prefrontal cortex receives many afferents from limbic brain structures involved in emotional activity, one might argue that the somatic motor system is also a tool for the emotional brain to satisfy its needs.

EMOTIONAL MOTOR SYSTEM

Similar to the somatic motor system, the emotional motor system has a medial and a lateral component, each subserving different functions.

Medial Component of the Emotional Motor System

The medial component (Fig. 36.8) represents descending projections from the medial parts of the preoptic region, dorsal hypothalamus, and from the periaqueductal gray (PAG) to the caudal pontine and medullary ventromedial tegmental field. This region contains the caudal raphe magnus (RMg), pallidus (RPa), and obscurus nuclei (ROb), but the bulk of the neurons is located laterally adjoining the raphe nuclei. Neurons in the medullary ventromedial tegmental field give rise to descending pathways that terminate among almost all parts of the spinal gray matter, including the dorsal horn and the autonomic and somatic motoneuronal cell groups (Fig. 36.9, right). These projection systems are so diffuse that one particular ventromedial tegmental neuron sends axon collaterals to the caudal spinal trigeminal nucleus, to the cervical, and to the lumbosacral portions of the spinal cord (Martin *et. al.,* 1981; Hayes and Rustioni, 1981; Huisman *et. al.,* 1982; Lovick and Robinson, 1983). They do not produce specific movements, but act as "level setting" systems.

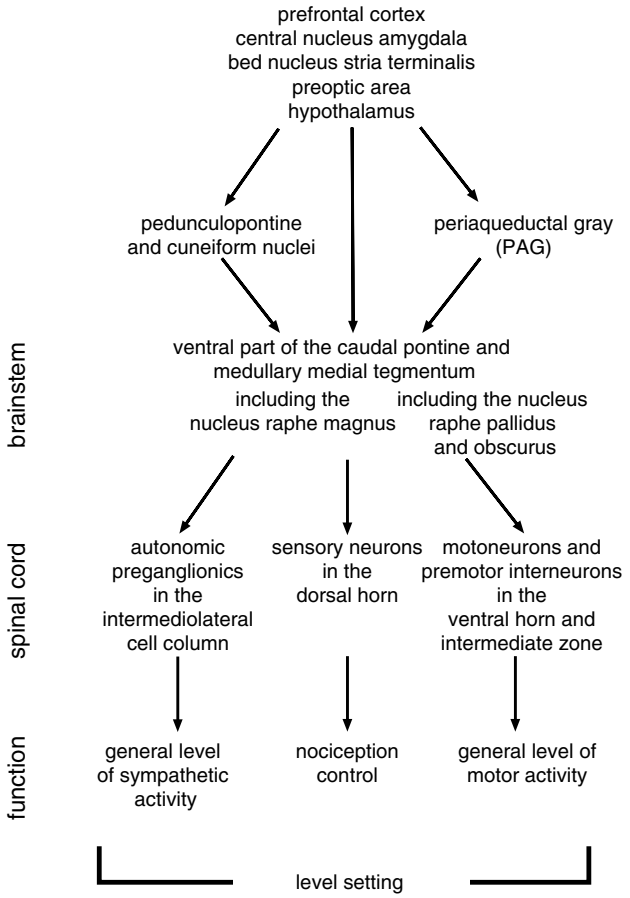

FIGURE 36.8 Schematic overview of the structures involved in the medial component of the emotional motor system.

Many different neurotransmitter substances exist in neurons in the medullary ventral tegmental field, of which serotonin (5HT) is the best known. Serotonin enhances the excitability of the motoneurons for inputs from other sources as the somatic motor system or the basic motor system (e.g., respiratory control systems). Several peptides are also present in the spinally projecting neurons in the ventromedial medulla and RPa and ROb. Many neurons contain substance P, thyrotropin-releasing hormone, somatostatin, and methionine- and leucine-enkephalin, and a few neurons contain vasoactive intestinal peptide and cholecystokinin. Most of these peptides coexist to a variable extent with serotonin in the same neuron. Most of the diffuse descending pathways to the spinal cord are not derived from serotonergic neurons. Possible neurotransmitter candidates for these pathways are acetylcholine and somatostatin and γ-aminobutyric acid (GABA). Even colocalization of serotonin and GABA in spinal cord-projecting neurons in the ventral medulla in the rat has been demonstrated. This means that some terminals taking part in this diffuse descending system may have inhibitory as well as facilitatory effects on the postsynaptic element (e.g., a motoneuron), although the majority is probably either facilitatory or inhibitory. Spinal motoneurons display a bistable behavior and can switch back and forth to a higher or lower excitable level. Bistable behavior disappears after spinal transection but reappears after subsequent intravenous injection of the serotonin precursor 5-hydroxytryptophan. Thus, intact descending pathways are essential for this bistable behavior of motoneurons, and serotonin is one of the neurotransmitters involved in switching to a higher level of excitation. GABA may possibly be involved in switching to a lower level of excitation (see Holstege, 1991, and Rekling *et. al.,* 2000, for reviews).

In summary, when the facilitory part of the diffuse system is active, less energy is needed by the somatic

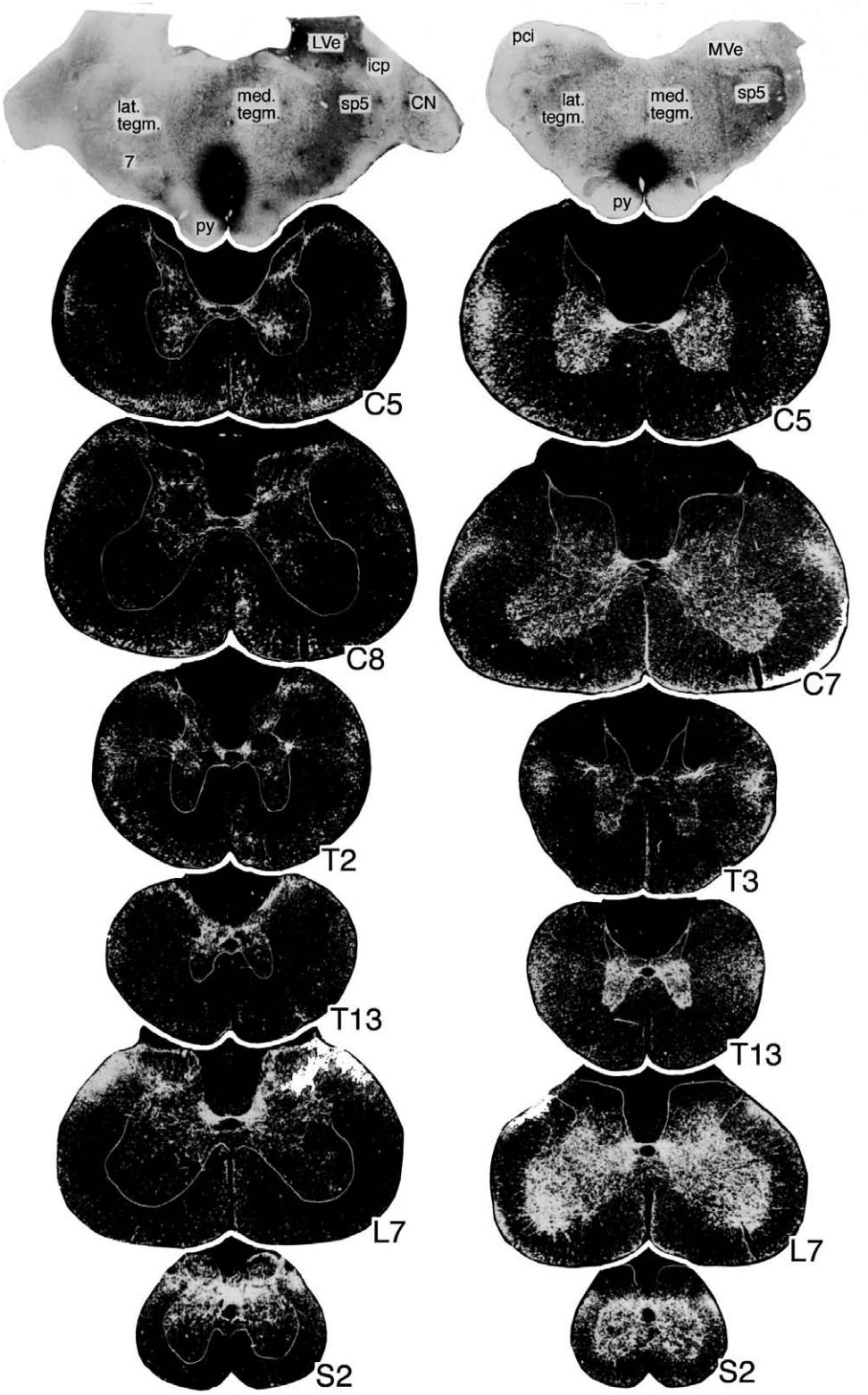

FIGURE 36.9 Brightfield photomicrographs of autoradiographs showing tritiated leucine injection sites in the ventral part of the medial tegmental field including the RMg *(left)* and Rpa *(right)*. Darkfield photomicrographs on the left show the distribution of the labeled fibers mainly to the dorsal horn (laminae I, the upper part of II and V), the intermediate zone, and the autonomic motoneuronal cell groups. On the right, the labeled fibers are distributed to the ventral horn (intermediate zone and autonomic and somatic motoneuronal cell groups).

motor system to "activate" specific premotor interneurons and motoneurons to produce a certain movement. Conversely, when the inhibitory part of the diffuse system is active, the somatic motor system needs more energy to produce the same effect. Possibly, the latter situation is predominant in patients suffering from depression causing the feeling that every movement requires "much more energy than normal."

The Medial Component and Nociception

The neurons in the ventromedial tegmentum have a great impact not only on the motor but also on the sensory system. The rostral medullary medial tegmentum including the RMg targets mainly laminae I and V neurons in the dorsal horn throughout the length of the spinal cord (Fig. 36.9, left). These pathways represent direct inhibitory connections with neurons in turn projecting to supraspinal levels (Antal *et. al.*, 1996; Light *et. al.*, 1986). Correspondingly, stimulation in the rostral ventromedial tegmentum produces an inhibition of the activity level of lamina I and V neurons, resulting in a strong inhibition of nociception (see Fields *et. al.*, 1991, for review).

Control of the Diffuse Pathways

Another question is which brain regions control the ventromedial medullary tegmentum, that gives rise to the diffusely projecting fiber systems? Perhaps the most important of these regions are the periaqueductal gray and the surrounding mesencephalic tegmentum (Fig. 36.10, left), but further rostrally the medial hypothalamus and medial preoptic region also project to the ventromedial tegmentum (Fig. 36.10, right). The caudal hypothalamus projects mainly to the caudal half of the ventromedial tegmentum including the RPa (i.e., to the "motor" part of the diffuse descending pathways), while more rostral regions of the medial hypothalamus and the preoptic region project to the RMg and adjacent regions, giving rise to diffuse projections to the dorsal horn (i.e., to the "somatosensory or nociceptive" part of the diffuse descending pathways; Holstege, 1987). Another projection originates from lateral limbic regions, such as the central nucleus of the amygdala, the lateral bed nucleus of the stria terminalis (Fig. 36.10, middle) and the lateral hypothalamus. Their main projections are to the lateral tegmental field of caudal pons and medulla, but there is a separate projection to the rostral (the somatosensory or nociceptive) part of the medullary medial tegmentum.

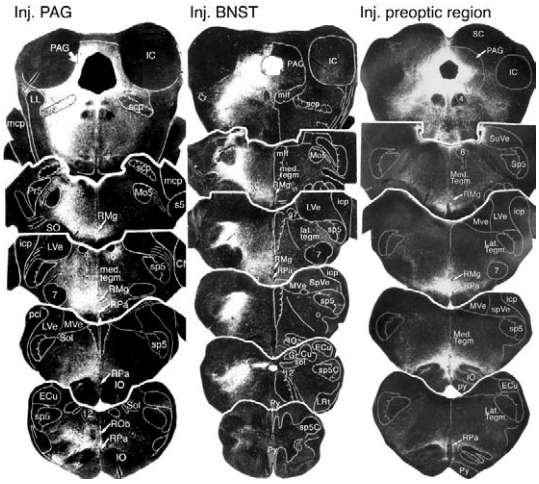

FIGURE 36.10 Three cases with injections in the periaqueductal gray (left), the bed nucleus of the stria terminalis (middle), and the preoptic region at the level of the anterior commissure (right). Note that in all three cases there is strong projection to the ventromedial tegmentum at the level of caudal pons and rostral medulla. In the PAG and BNST cases, these fibers come from lateral; the preoptic area sends its fibers to the ventromedial tegmentum via a medially descending fiber stream. Note also the differences with respect to the projections to the caudal ventromedial medullary tegmentum between the cases, and the strong projections to the lateral tegmentum in the BNST case.

In general terms, stimulation in the PAG in animals produces behavior associated with the direct survival, such as arousal, aggressive, or defensive behaviors accompanied by a strong inhibition of nociception. Because of this strong antinociceptive effect, in patients suffering from untreatable severe pains, neurosurgeons stimulated the PAG to see whether a similar antinociceptive effect could be achieved. However, at least in more caudal parts of the PAG, such stimulation resulted in fear and panic-like emotions such as anxiety, terror, and even feelings of imminent death.

Another well-known example in humans that arousal of the motor system coincides with inhibition of nociception has been described by doctors working in field hospitals in the First World War. In that war, soldiers were fighting in trenches against "the enemy" a few hundred yards away. There are several reports that soldiers had not felt that they were shot in the foot or leg. Their level setting system was functioning at a maximum, the motor system was maximally aroused, and nociception was maximally inhibited.

Lateral Component of the Emotional Motor System

The lateral component of the emotional motor system consists of pathways that subserve specific

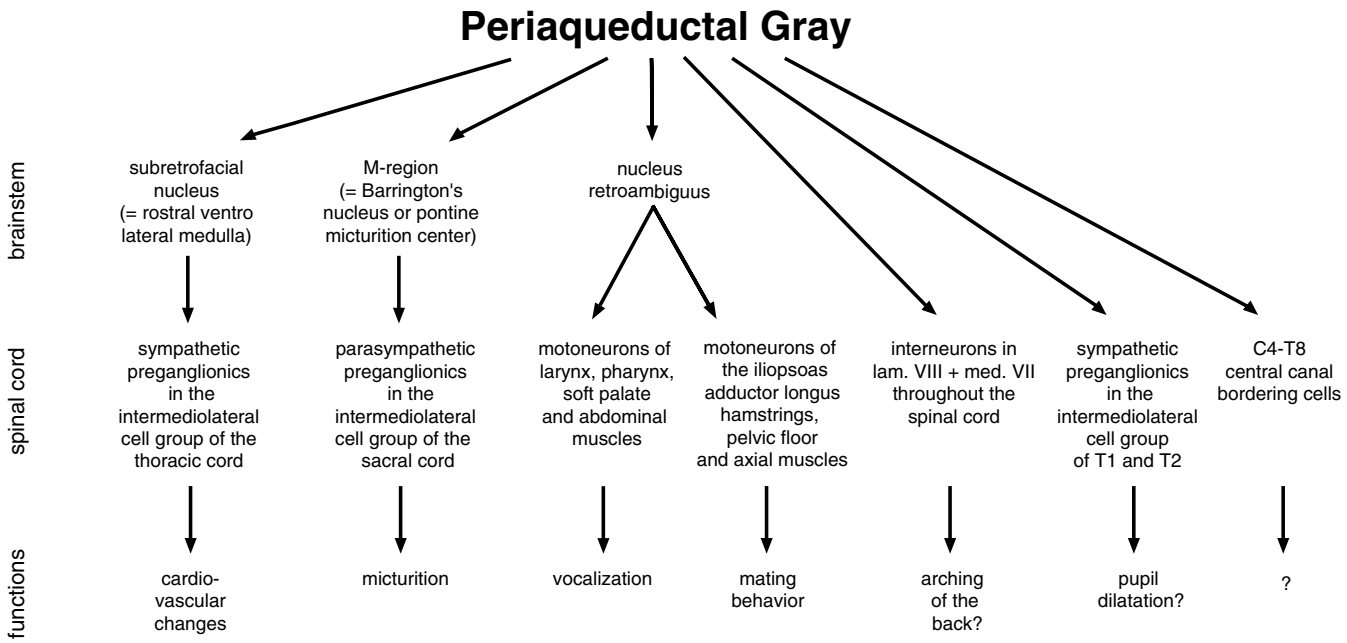

FIGURE 36.11 Schematic overview of some of the motor output systems of the PAG. All these motor systems are directly involved in basic survival behavior.

motor functions, in contrast to the unspecific diffuse pathways of the medial component. Examples of the specific functions are cardiovascular regulation, vocalization (= the production of sound), mating behavior, and micturition (Fig. 36.11). Pathways belonging to the lateral component originate in the PAG, lateral hypothalamus, central nucleus of the amygdala, and lateral part of the bed nucleus of the stria terminalis (Fig. 36.10, middle). The PAG sends projections to specific groups of interneurons in the caudal brainstem and spinal cord (Fig. 36.11), the lateral hypothalamus, central nucleus of the amygdala, and lateral part of the bed nucleus of the stria terminalis project to the lateral tegmentum (Figs. 36.4 and 36.10, middle), containing premotor interneurons to the somatic and preganglionic motoneurons in the caudal brainstem. An overview will be given of three projection systems, that for vocalization, mating behavior, and micturition.

Pathways Involved in Vocalization

Vocalization can be defined as the nonverbal production of sound and requires coordination between the activity of abdominal and expiratory intercostal muscles and muscles of the larynx, pharynx, and soft palate. Most animals use vocalization as an important tool for survival. Vocalization should not be confused with speech, the production of vowels and consonants in humans. Proper combination of vowels and consonants form words and sentences.

In animals as diverse as leopard frogs and chimpanzees, vocalization is brought about by different parts of the limbic system, but specifically by the PAG (see Holstege, 1989, for review). Stimulation in the caudal PAG results in vocalization, and bilateral PAG lesions completely abolish it, leading to mutism (Adametz and O'Leary, 1959). Also in humans a few clinical cases are known in which lesions in the PAG led to mutism (Botez and Barbeau, 1971; Esposito *et. al.*, 1999). The pathways involved originate in the PAG and descend to terminate in neurons in the nucleus retroambiguus (NRA) and on neurons in the adjoining caudal medullary lateral tegmental field. The latter neurons, in all likelihood, serve as a relay for the PAG to reach the motoneurons innervating lower mouth muscles and the muscles of the mouth opening and tongue. The NRA neurons project to the motoneurons in the nucleus ambiguus innervating pharynx and larynx, and to the motoneurons of the intercostal and abdominal muscles in the spinal cord.

In our concept, speech is the (pre-) motor cortex modulation of vocalization (Holstege and Ehling, 1996; Fig. 36.12). The cortical modulation is brought about by an enormous number of "memory" neurons in the premotor cortical regions that project to the motor cortex, which in turn has direct access to mouth, pharynx, and larynx muscle motoneurons. Only the human cortex contains such a large amount of motor memory (area of Broca), which makes humans the only species that is able to use speech for commu-

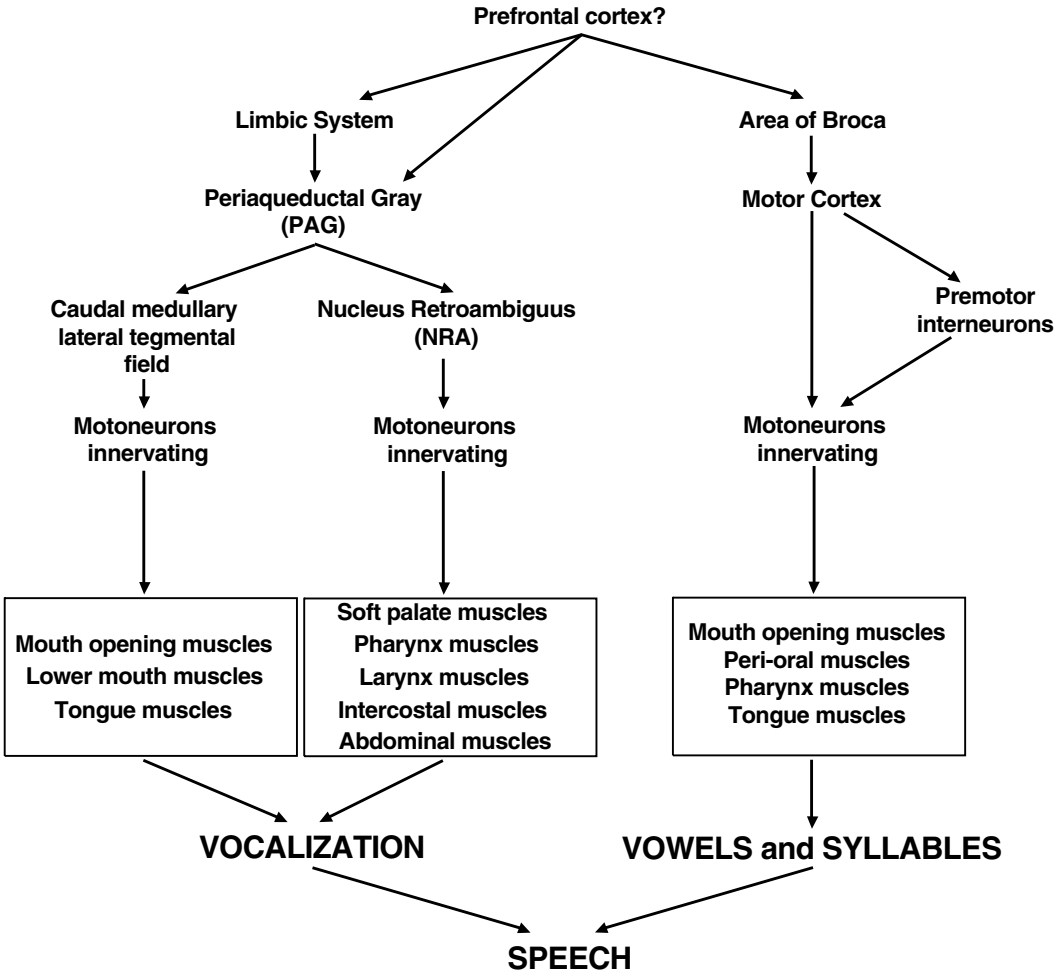

FIGURE 36.12 Schematic overview of the pathways possibly involved in the production of speech.

nication. Patients with damage of the area of Broca suffer from motor aphasia, but they still can vocalize (i.e., produce sounds) similar to animals. This is consistent with the concept that the motor output components of vocalization, possibly the PAG-NRA-motoneuronal pathways, are still intact in these patients.

Pathways Involved in Mating Behavior

Mating Behavior in Animals

The survival of the species depends on successful mating behavior. Although the behavioral aspects of mating are extensively studied, only little is known about the precise anatomical organization of the motor output systems of mating.

For example, in the rat, lesions in the preoptic region, lateral central tegmental field, or PAG cause problems with mating, but whether these regions have any connections with the motoneurons involved in mating behavior is not known. A first step in understanding this system are the studies in cat that show a direct pathway from the sacral cord to the PAG (Fig. 36.13), and from the PAG to the NRA in the caudal medulla. The NRA, in turn, projects to those motoneurons in the lumbosacral cord that produce the mating posture (Fig. 36.14). In normal estrous cats as well as in ovariectomized cats with subcutaneously administered estrogen, this hormone elicits so-called growth cones (Fig. 36.15) in the NRA fibers terminating on lumbar motoneurons. These growth cones produce an almost nine times increase of excitatory boutons with synapses on the dendrites of the lumbosacral mating motoneurons (VanderHorst and Holstege 1997; Fig. 36.16).

In male cats, the number of NRA terminals on "mating" motoneurons was about half of that found in estrous, which is still substantially more than in nonestrous females. Also the distribution pattern of

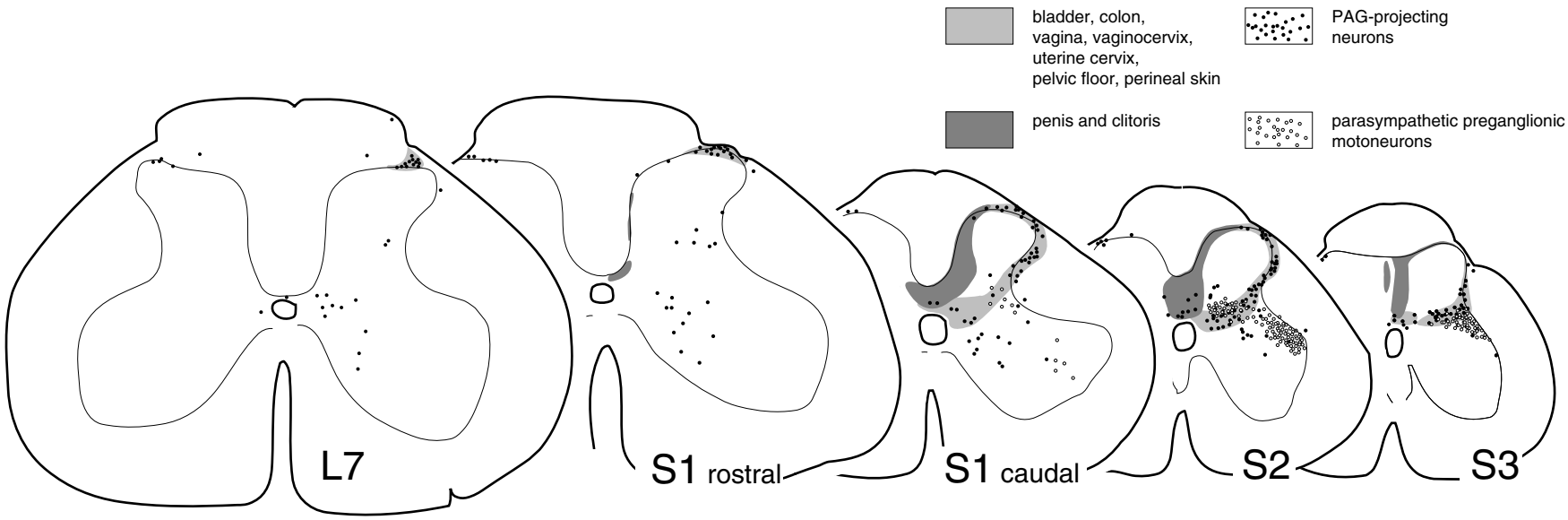

FIGURE 36.13 Schematic overview of where the urogenital afferent projections terminate in the sacral cord and where the neurons are located that project to the PAG.

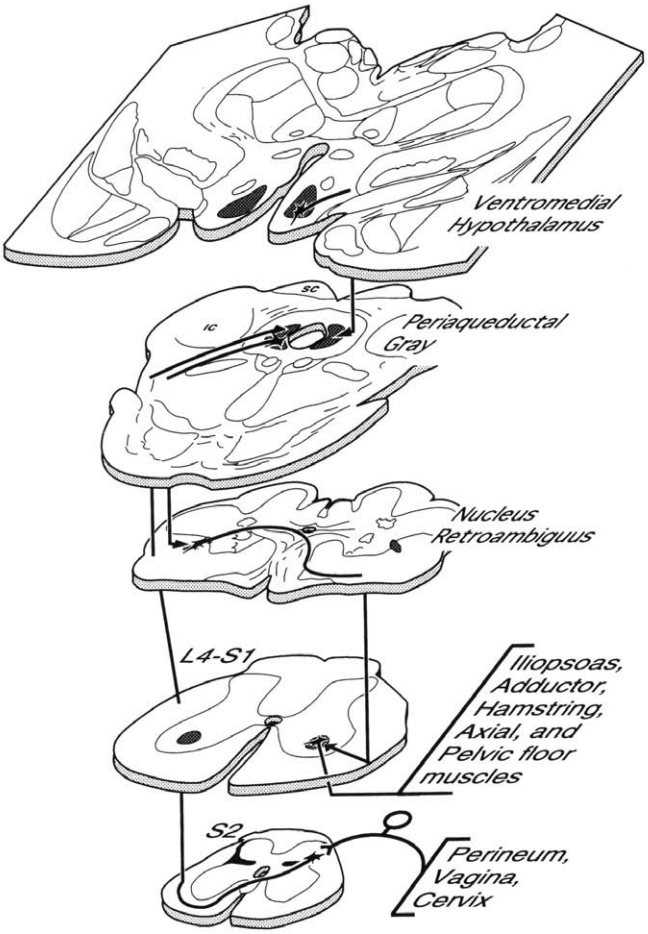

FIGURE 36.14 Schematic overview of the ascending and descending pathways that play a role in the mating reflex circuit in cats.

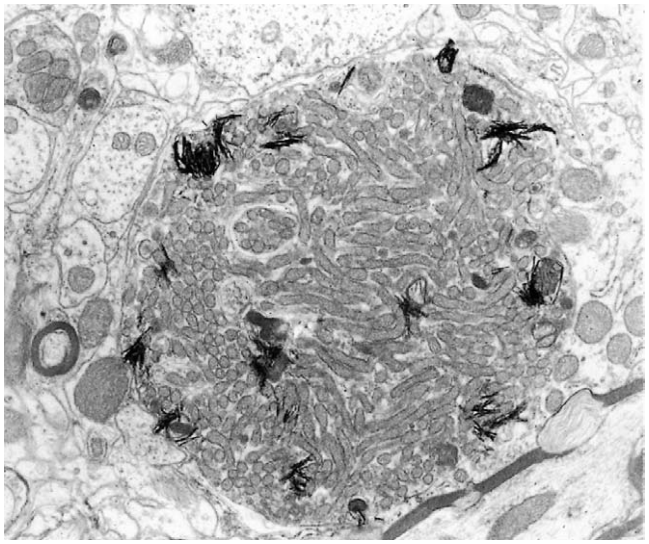

FIGURE 36.15 Electronmicrograph representing a labeled growth cone in the semimembranosus motoneuronal cell group in the sixth lumbar spinal segment of an estrous cat with an injection of wheatgerm agglutinin horseradish peroxidase (WGA-HRP) in the NRA. Note the tetramethylbenzidine (TMB) reaction products in mainly the peripheral parts of the cone.

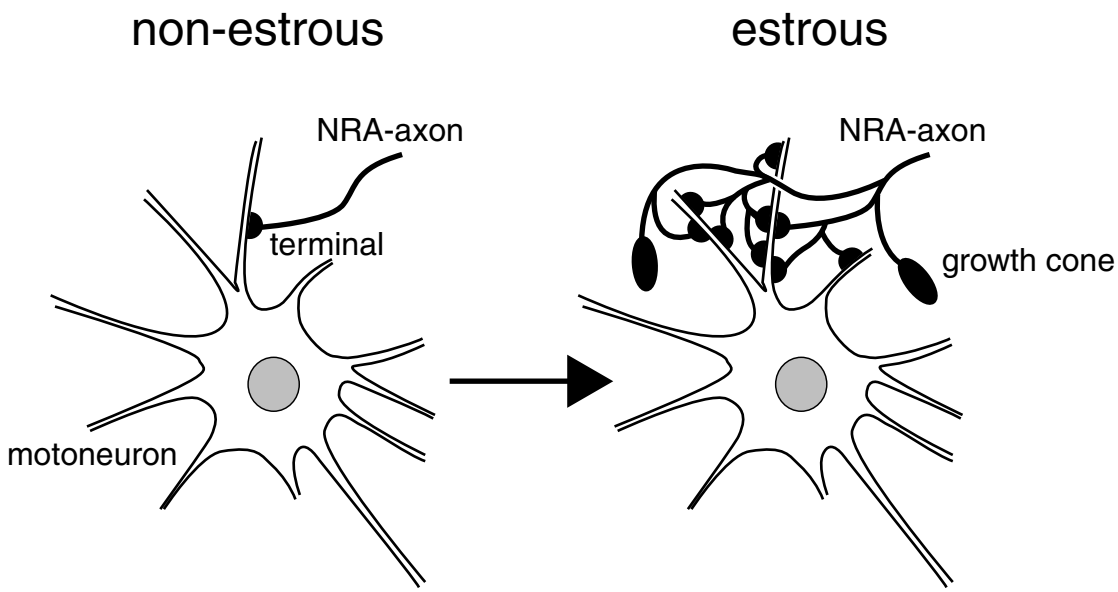

FIGURE 36.16 Schematic illiustration of the estrogen-induced axonal sprouting of NRA fibers to lumbosacral (semimembranosus) motoneurons.

the NRA terminals was slightly different in males than in females. Although further behavioral studies are needed to confirm this hypothesis, it seems likely that in cats the PAG-NRA-mating motoneuronal pathway generates the posture necessary for mating. Also in the female hamster, which shows a less complicated but very outspoken mating or lordosis posture, a similar PAG-NRA-axial muscle motoneuronal pathway seems to exist, possibly involved in lordosis (Gerrits and Holstege, 1999).

Mating Behavior in Humans

A largely unresolved matter is how mating is organized in humans. This species does not have a very distinct mating posture as in cat and hamster, but one might assume that also in humans the motor output related to mating depends on specific descending pathways. Although the techniques used in animals to investigate these pathways are not applicable to humans, modern neuroimaging techniques make it possible to reveal the human brain structures involved in mating and especially ejaculation and orgasm.

A Positron Emission Tomography (PET) study (Holstege *et. al.*, 2003a) was done in which male and female volunteers were asked to have an ejaculation or orgasm, brought about by manual stimulation of their female/male partner. The PET technique using radioactive water ($H_2{}^{15}O$) shows increases or decreases in blood flow in distinct parts of the brain, representing increases or decreases of activation of neurons in these areas. Although the resolution of PET is relatively limited, the results of the ejaculation/orgasm studies were remarkable. The strongest activation was in the so-called mesodiencephalic region, with structures such as the ventral tegmental area (VTA; known as the "reward" area), the subparafascicular nucleus, the ventromedial posterior thalamic nucleus, the intralaminar nuclei, and, especially in men, the lateral central tegmental field (Figs. 36.17 and 36.19). A similar region in the mesodiencephalic transition zone was activated during cocaine (Breiter *et. al.*, 1997) and especially heroin rush (Sell *et. al.*, 1999), suggesting that these experiences are similar to sexual orgasm. It might also explain why substances such as cocaine and heroin are so addictive.

Other findings in the ejaculation/orgasm studies are the increased activation of the lateral putamen (Fig. 36.18), certain parts of the prefrontal, temporal, parietal, and insular cortex and a very strong activation of the cerebellum (Fig. 36.19). In the study of men, strong activation was also found in the medial pontine tegmentum (Figs. 36.18 and 36.19). In correspondence with the findings in the cat in women increased activation was found in the PAG (Holstege *et. al.*, 2003b). Surprisingly, activation was not found in the hypothalamus or preoptic area in men or women (Fig. 36.18). One might speculate that these regions play a role in creating the conditions in which mating can take place (e.g., estrous versus nonestrous), but that they are not involved in the motor act itself.

An important decrease of activation was also found. The medial parts of the amygdalar regions (Fig. 36.20) were deactivated, not only during ejaculation or orgasm, but also during sexual stimulation and erection. A similar decrease of amygdalar activity was found during romantic love (Bartels and Zeki, 2000).

An active amygdala is crucial for individual survival by constantly monitoring environmental stimuli. In the case of possibly hazardous events, the amygdala elicits a fear response to protect the organism from harm. However, in the context of sexual behavior, such vigilance could easily block the sexual act, leading to unsuccessful reproduction. One might hypothesize that, in order to prevent such a disruption, brain structures involved in sexual behavior decrease vigilance by inhibiting amygdalar activity. Although deactivation of the amygdala may make the organism less concerned with potential danger, it enhances the odds

FIGURE 36.17 PET-scan results showing activations in the mesodiencephalic transition zone, comparing ejaculation with stimulation. In (a) increased activation is present in the area of the ventral tegmental area (vta), intralaminar and ventroposterior thalamic nuclei, sunparafascicular nucleus, and lateral part of the central tegmental field (lctf). The red lines on the glass brains (SPM's) indicate how the sections were made. The activations (ejaculation minus stimulation, $p < .01$, corrected for multiple comparisons) are superimposed on the average T1 weighted MRI of the subjects.

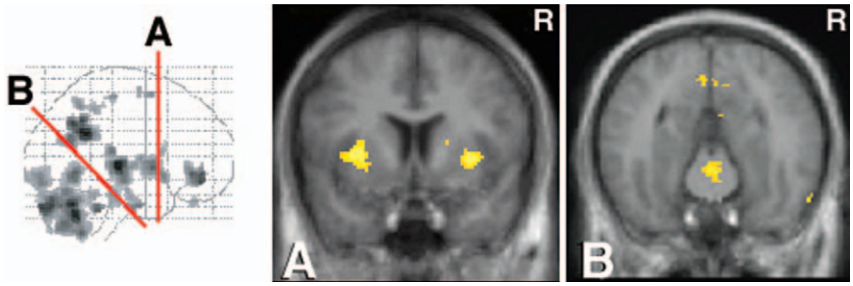

FIGURE 36.18 PET-scan results showing activations in ventrolateral putamen and adjoining parts of the claustrum and insula **(A)** and pontine medial tegmentum **(B)**, comparing ejaculation with stimulation. Note in A the absence of activity in the medial preoptic area, hypothalamus, and amygdala.

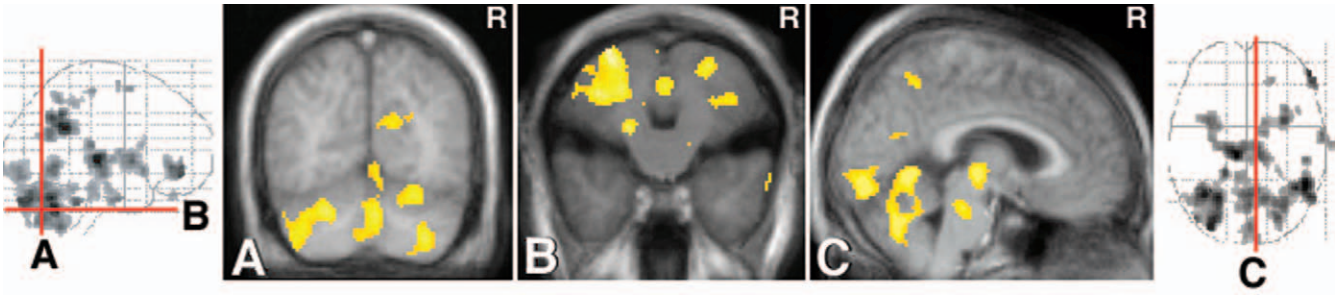

FIGURE 36.19 Frontal **(A),** horizontal **(B)** and sagittal sections show the strong activation in the cerebellum and area 18 of the cortex (A and C). Note in C also the activation in the mesodiencephalic region and the medial pontine tegmentum. The red lines on the glass brains (SPM's) indicate how the sections were made. The activations (ejaculation minus stimulation, p < .01, corrected for multiple comparisons) are superimposed on the average T1 weighted MRI of the subjects.

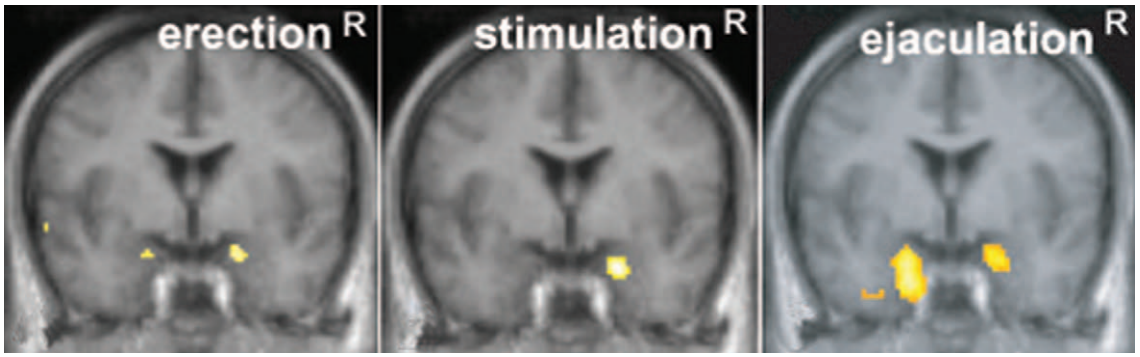

FIGURE 36.20 PET-scan results showing significant amygdala deactivations ($p < .001$, uncorrected; extent: 8 voxels), during erection *(left)*, during sexual stimulation *(middle)*, and during ejaculation *(right)*, all compared with a rest condition. The results were superimposed on the volunteers' averaged MRI. After small volume correction (height: $p < .05$), all amygdala deactivations survived multiple comparisons correction.

of species survival because reproduction is more likely to succeed.

Pathways Involved in Micturition

Micturition is the process of emptying the bladder when it is full. Because during micturition the individual is relatively vulnerable, it needs a "safe" surrounding. Thus, the micturition control centers in the central nervous system need information not only about bladder filling but also about the safety of the environment. They receive afferents concerning bladder filling via the lumbosacral cord and information concerning the safety of the individual from various limbic system regions.

Micturition itself is a coordinated action between the urinary bladder and the external urethral sphincter muscle, which takes part in the pelvic floor.

Pelvic Floor Motoneurons

The external urethral sphincter muscle and the external anal sphincter belong to the pelvic floor, all muscles of which are innervated by the pudendal nerve. In cat, dog, rhesus monkey, and humans, the motoneurons of the pelvic floor muscle are located in the so-called nucleus of Onuf, after Onufrowicz (1899). Onuf's nucleus is located on the ventrolateral border of the ventral horn in the sacral segments S1-S3. In the cat, the external urethral sphincter muscle motoneurons are located in the ventrolateral and the external anal sphincter motoneurons in the dorsomedial part.

Onuf nucleus motoneurons occupy a separate position between somatic and autonomic motoneurons. Arguments in favor of the Onuf motoneurons being somatic are that they (1) innervate striated muscles and (2) are under voluntary control. Arguments that favor Onuf's nucleus containing autonomic motoneurons are that (1) cytoarchitectonically they resemble autonomic motoneurons; (2) they have an intimate relationship with sacral parasympathetic motoneurons; (3) unlike all other somatic motoneurons, but similar to autonomic motoneurons, they receive direct hypothalamic afferents; (4) their neuropeptide and transmitter input resemble that of the sacral autonomic neurons; (5) together with the sacral autonomic (parasympathetic) motoneurons they are well preserved in the spinal cord of patients who have died from amyotrophic lateral sclerosis (ALS) and poliovirus infection, which explains why bladder and sphincter function remain intact until the last stages of ALS; and (6) they are affected in the Shy-Drager syndrome, which is characterized by loss of autonomic motoneurons. The conclusion must be that Onuf motoneurons represent a separate class of motoneurons (see Blok and Holstege, 1998 for review; see Chapter 6).

Bladder Motoneurons

The detrusor muscle of the bladder is a smooth muscle innervated by parasympathetic and sympathetic motoneurons. The parasympathetic postganglionic bladder motoneurons are located in the bladder wall. The parasympathetic preganglionic motoneurons lie in the intermediolateral cell column of the sacral spinal cord, and their axons reach the bladder via the pelvic nerve.

The sympathetic preganglionic motoneurons of the bladder are located in the intermediolateral cell group of the thoracolumbar cord (in the rat T11-L2). They send their axons to the sympathetic postganglionic cells in the sympathetic chain T12-L6, the inferior mesenteric ganglia and the major pelvic ganglia. Sympathetic postganglionic fibers run via the pelvic and hypogastric nerves to the bladder.

Micturition

More than 75 years ago, Barrington (1925) showed that normal micturition in adult cats depends on an intact spinal cord. He also showed that the dorsal tegmentum of the pons is crucial for the coordination of bladder contraction and sphincter relaxation during micturition. That is also the case in humans because patients with a transection of the spinal cord have great difficulty in emptying the bladder. When their detrusor muscle of the bladder contracts, the sphincter contracts also, which results in a so-called dyssynergic micturition.

Later physiological and anatomical work has demonstrated that the M-(medial)region or pontine micturition center or Barrington's nucleus has direct excitatory connections with the parasympathetic bladder motoneurons. Moreover, this same cell group, and possibly the same cells, has similar direct excitatory projections to the GABA-ergic and glycinergic neurons in the intermediomedial sacral cell group, which cells, in turn, inhibit the motoneurons in Onuf's nucleus. This way the pontine micturition center excites the bladder motoneurons leading to bladder contraction and at the same time inhibits the bladder sphincter allowing the urine to pass the urethra (Fig. 36.21).

As pointed out earlier, micturition is under strong emotional control, which explains why the afferent sources to the pontine micturition center originate from limbic regions (i.e., the PAG; Blok and Holstege, 1994; Taniguchi *et. al.*, 2002, and the preoptic region, Holstege, 1987). Neuroimaging studies in men and women (Blok *et. al.*, 1997, Blok and Holstege, 1998) suggest that the previously described system, based on cat experiments, is also present in humans (Fig. 36.22).

With respect to the basic scheme (Fig. 36.2), the descending projections from the pontine micturition center to the sacral cord belong to the basic motor system, and the afferent projections to the pontine micturition center belong to the lateral component of the emotional motor system.

Continence

During storage of urine, the detrusor muscle is relaxed and the external urethral sphincter muscle is activated. Because sympathetic fibers have an indirect inhibitory effect on the detrusor muscle and an excitatory effect on the smooth musculature of the urethra and base of the bladder, they are thought to promote continence during the storage phase. In fact, there exists a specific projection from the lateral pontine tegmentum, the so-called L= (lateral)-region, to Onuf's nucleus, which might also play a role in continence. This idea is corroborated by the finding that neuroimaging studies in men and women have revealed hyperactivity in the lateral pons when the

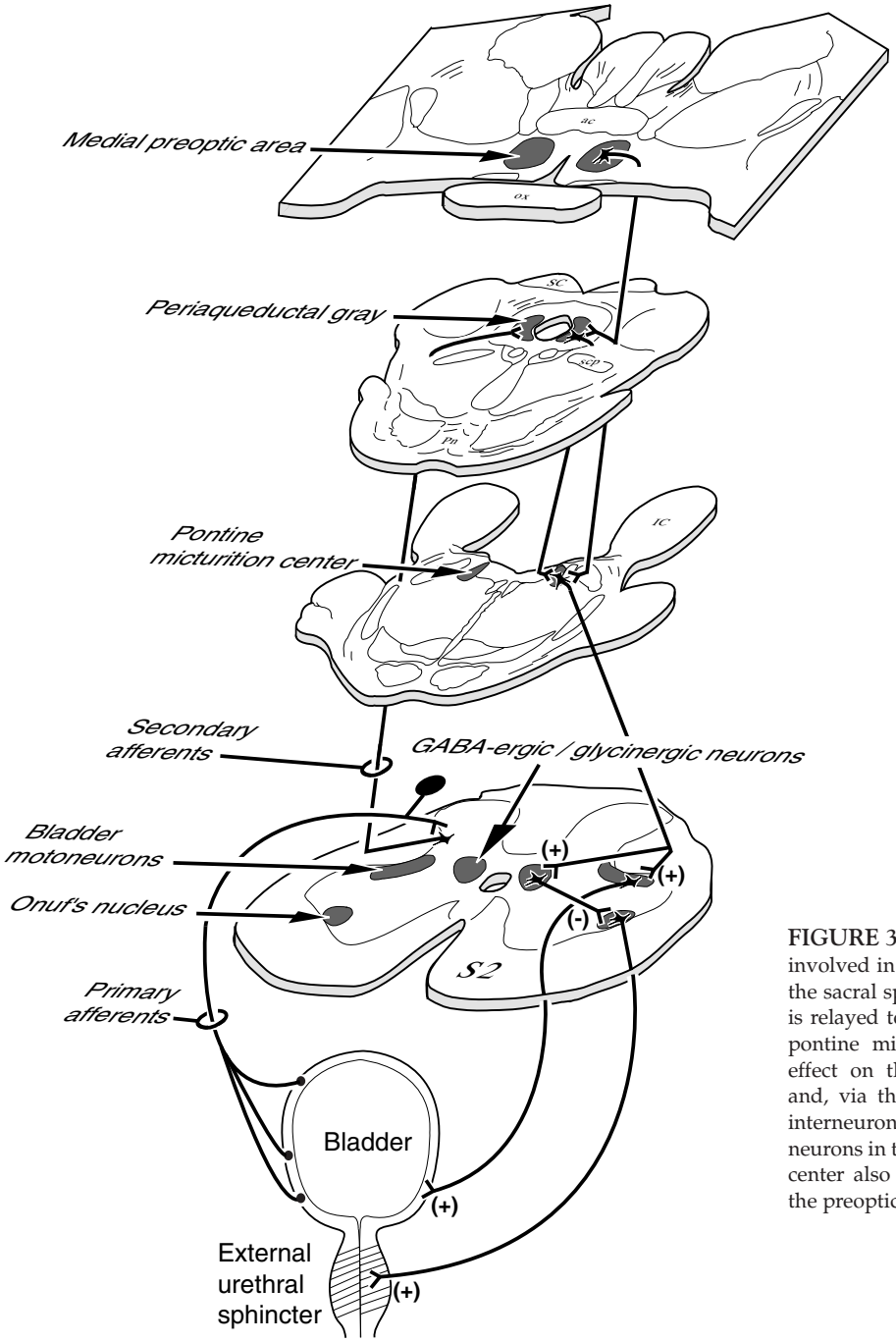

FIGURE 36.21 Schematic overview of the pathways involved in micturition control. Bladder afferents enter the sacral spinal cord, from where bladder information is relayed to the PAG. The PAG in turn projects to the pontine micturition center, which has an excitatory effect on the parasympathetic bladder motoneurons and, via the sacral GABA- and glycinergic premotor interneurons, an inhibitory effect on the sphincter motoneurons in the nucleus of Onuf. The pontine micturition center also receives specific afferent connections from the preoptic region.

volunteers involuntarily kept their pelvic floor strongly contracted for emotional reasons, (Blok and Holstege, 1997; Fig. 36.23).

The Emotional Motor System and the Cortex

Although the motor and premotor cortex with their descending projections are the best examples of the somatic motor system, it would be a misunderstanding that no part of the emotional motor system originates from the cortex. The prefrontal cortex contains many regions that have direct access to the PAG, caudal brainstem, and even spinal cord. Another cerebral cortex part that might play a role is the cingulate gyrus, which receives strong afferent connections from many parts of the limbic system, (Chapter 24). Its rostral part may play an important role in micturition control (Fig. 36.24), and its caudal part, in the emotional motor control of the face. Morecraft *et. al.* (2001) have demonstrated in monkey that the caudal cingulate gyrus, which they call the M4 (fourth motor) region, projects directly to motoneurons, especially those of the upper mouth muscles. Although this projection is

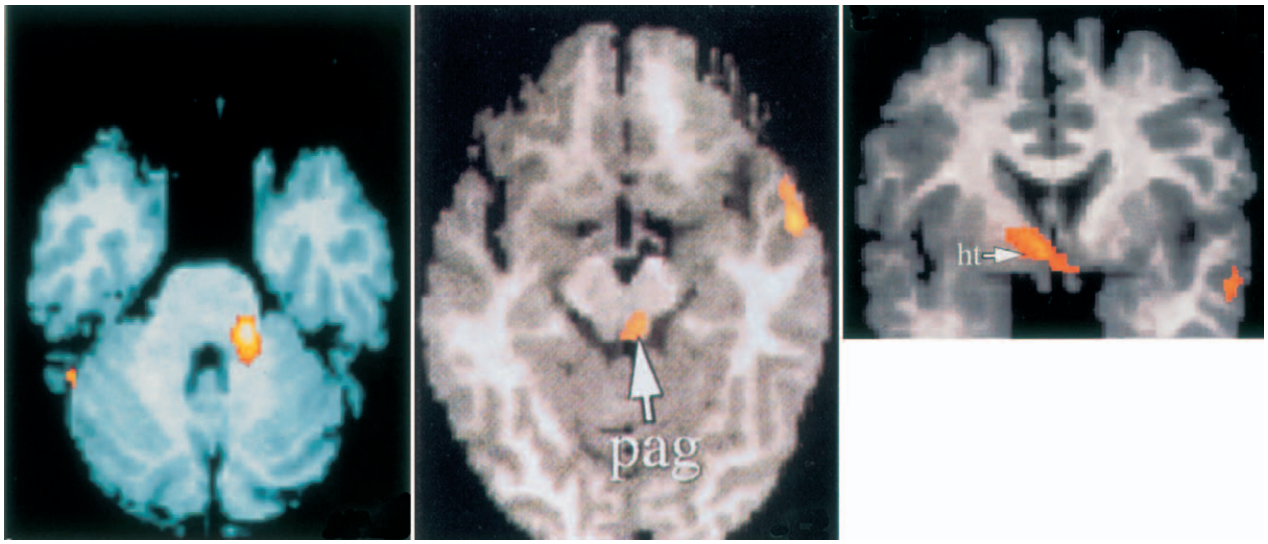

FIGURE 36.22 PET-scan results showing regions with significantly higher regional cerebral blood flow (rCBF; $p < .002$) comparing successful micturition with withholding of urine. Note the activation in the area of the pontine micturition center on the left, in the PAG in the middle, and in the hypothalamus on the right (see further Blok *et al.*, 1997).

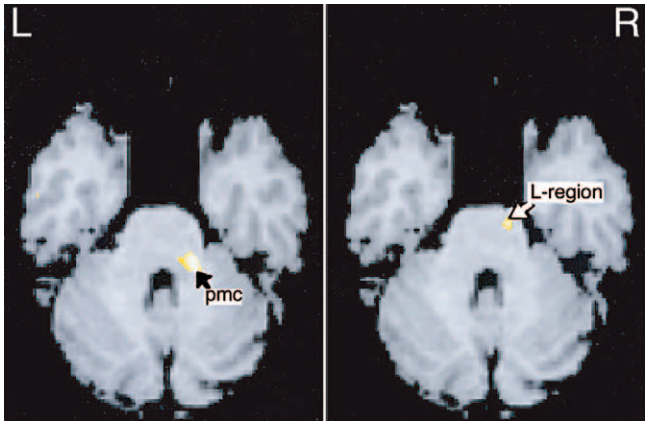

FIGURE 36.23 *Left:* PET-scan results showing significant differences in rCBF in the region of the pontine micturition center comparing successful micturition with withholding of urine. *Right:* Significant differences in rCBF in the region of the so-called L-region comparing unsuccessful micturition with with an empty bladder (uncorrected threshold of p < .002).

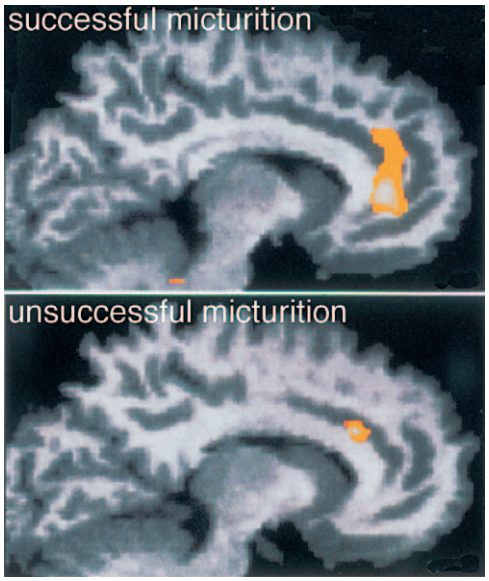

FIGURE 36.24 *Top:* PET-scan results showing significant differences in regional cerebral blood flow in the anterior cingulate gyrus, comparing sucessful micturition with voluntary withholding of urine. *Bottom:* PET-scan results comparing unsuccessful micturition with voluntary withholding of urine (uncorrected threshold $p < .001$). Note that a diiferent part of the cingulate gyrus is active during both activities.

much weaker than the projections originating in the motor and premotor cortex, it might play a role in the face movements of emotional expression (Fig. 36.1).

CONCLUDING REMARKS

The idea of the existence of an emotional motor system is primarily based on anatomical organization. The pathways of the somatic and emotional motor system are always separate until their termination on premotor interneurons or motoneurons. Also the function of the pathways is different. The emotional motor pathways play a role in basic survival behavior. The somatic or voluntary motor system, and especially its cortical parts, start operating only after a relatively long time of processing environmental data, combined with information from the extensive (visual, auditory, motor, sensory, and emotional) memory banks in the

various regions around the primary cortices. It is not so that the two components of the motor system exclude each other. Usually, they are active at the same time, and sometimes even within the framework of the same motor activity (e.g., human speech).

The behavioral differences between animals and humans are not located in the emotional, but in the somatic motor system, which, as pointed out earlier, is nothing more than a tool of the emotional or limbic system to fulfill its needs. In that respect, humans differ only slightly from other animals.

References

Adametz, J., and O'Leary, J.L. (1959). Experimental mutism resulting from periaqueductal lesions in cats. *Neurology* **9,** 636–642.

Antal, M., Petko, M., Polgar, E., Heizmann, C.W., and Storm-Mathisen, J. (1996). Direct evidence of an extensive GABAergic innervation of the spinal dorsal horn by fibres descending from the rostral ventromedial medulla. *Neurosci.* **73,** 509–518

Barrington, F.J.F. (1925). The effect of lesions of the hind- and mid-brain on micturition in the cat. *Quart. J. Exp. Physiol. Cogn. Med.* **15,** 81–102.

Bartels, A., and Zeki, S. (2000). The neural basis of romantic love. *Neuroreport* **11,** 3829–3834.

Blok, B.F.M., and Holstege, G. (1994). Direct projections from the periaqueductal gray to the pontine micturition center (M-region). An anterograde and retrograde tracing study in the cat. *Neurosci. Lett.* **166,** 93–96.

Blok, B.F.M., and Holstege, G. (1998). The central control of micturition in cats and humans. *Beh. Brain Res.* **92,** 119–125.

Blok, B.F.M., Willemsen, A.T.M., and Holstege, G. (1997). A PET study on the control of micturition and urine storage in humans. *Brain* **120,** 111–121.

Botez, M.I., and Barbeau, A. (1971). Role of subcortical structures and particularly of the thalamus, in the mechanisms of speech and language. *Int. J. Neurol.* **8,** 300-–320.

Breiter, H., et al. (1997). Acute effects of cocaine on human brain activity and emotion. *Neuron* **19,** 591–611.

Esposito, A., Demeurisse, G., Alberti, B., and Fabbro, F. (1999). Complete mutism after midbrain periaqueductal gray lesion. *Neuroreport* **10,** 681–685.

Fields, H.L., Heinricher, M.M., and Mason, P. (1991). Neurotransmitters in nociceptive modulatory circuits. *Annu. Rev. Neurosci.* **14,** 219–245.

Gerrits, P.O., and Holstege, G. (1999). Descending projections from the nucleus retroambiguus to the iliopsoas motoneuronal cell groups in the female golden hamster: Possible role in reproductive behavior. *J. Comp. Neurol.* **403,** 219–228.

Hayes, N.L., and Rustioni, A. (1981). Descending projections from brainstem and sensorimotor cortex to spinal enlargements in the cat. *Exp. Brain Res.* **41,** 89–107.

Holstege, G. (1987). Some anatomical observations on the projections from the hypothalamus to brainstem and spinal cord: An HRP and autoradiographic tracing study in the cat. *J. Comp. Neurol.* **260,** 98–126.

Holstege, G. (1989). An anatomical study of the final common pathway for vocalization in the cat. *J. Comp. Neurol.* **284,** 242–252.

Holstege, G. (1991). Descending motor pathways and the spinal motor system. Limbic and non-limbic components. *In* "Role of the Forebrain in Sensation and Behavior" (G. Holstege, ed.), vol. 87, pp. 307–421. Elsevier, Amsterdam.

Holstege, G. (1992). The emotional motor system. *Eur. J. Morph.* **30,** 67–81.

Holstege, G. (2002). Emotional innervation of facial musculature. *Mov. Disorders* 17 Suppl. 2:S12–16.

Holstege, G., and Ehling, T. (1996). Two motor systems involved in the production of speech. *In* "Vocal Fold Physiology; Controlling Complexity and Chaos" (P.J. Davis and N.H. Fletcher, ed.), pp. 153–169. Singular Publishing Group, San Diego, London.

Holstege, G., Georgiadis J. R., Paans A. M. J., Meiners L. C., van der Graaf, F.H.C.E., and Reinders, A.A.T.S. (2003a). Brain activation during human ejaculation. *J. Neurosci.,* in press.

Holstege, G., Georgiadis, J.R., Paans, A.M.J., Meiners, L.C., van der Graaf, F.H.C.E., and Reinders, A.A.T.S. (2003b). Brain activation during female sexual orgasm. *Soc. Neurosci. Abstr.* Volume 29 in press.

Holstege, G., Kuypers, H.G.J.M., and Dekker, J.J. (1977). The organization of the bulbar fibre connections to the trigeminal, facial and hypoglossal motor nuclei. II. An autoradiographic tracing study in cat. *Brain* **100,** 265–286.

Huisman, A.M., Kuypers, H.G.J.M., and Verburgh, C.A. (1982). Differences in collateralization of the descending spinal pathways from red nucleus and other brain stem cell groups in cat and monkey. *Progr. Brain Res.* **57,** 185–217.

Kuypers, H.G.J.M. (1981). Anatomy of the descending pathways. *In* "Handbook of Physiology, Section I, The Nervous System, Vol. II, Motor Systems" (R.E. Burke, ed.), pp.597–666. Washington American Physiological Society.

Light, A.R., Casale, E.J., and Menetrey, D.M. (1986). The effects of focal stimulation in nucleus raphe magnus and periaqueductal gray on intracellularly recorded neurons in spinal laminae I and II. *J. Neurophysiol.* **56,** 555–571.

Lovick, T.A., and Robinson, J.P. (1983). Bulbar raphe neurones with projections to the trigeminal nucleus caudalis and the lumbar cord in the rat: A fluorescence double-labelling study. *Exp. Brain Res.* **50,** 299–309.

Martin, G.F., Cabana, T., and Humbertson, A.O., Jr. (1981). Evidence for collateral innervation of the cervical and lumbar enlargements of the spinal cord by single reticular and raphe neurons. Studies using fluorescent markers in double-labelling experiments on the North American opossum. *Neurosci. Lett.* **24,** 1–6.

Morecraft, R.J., Louie, J.L., Herrick, J.L., and Stilwell-Morecraft, K.S. (2001). Cortical innervation of the facial nucleus in the non-human primate. A new interpretation of the effects of stroke and related subtotal brain trauma on the muscles of facial expression. *Brain* **124,** 176–208.

Onufrowicz, B. (1899). Notes on the arrangement and function of the cell groups in the sacral region of the spinal cord. *J. Nerv. Mental Dis.* **26,** 498–504.

Rekling, J.C., Funk, G.D., Bayliss, D.A., Dong, X.W., and Feldman, J.L. (2000). Synaptic control of motoneuronal excitability. *Physiol. Rev.* **80,** 767–852.

Sell, L.A., et al. (1999). Activation of reward circuitry in human opiate addicts. *Eur. J. Neurosci.* **11,** 1042–1048.

Taniguchi, N., Miyata, M., Yachiku, S., Kaneko, S., Yamaguchi, S., and Numata, A. (2002). A study of micturition inducing sites in the periaqueductal gray of the mesencephalon. *J. Urol.* **168,** 1626–1631.

VanderHorst, V.G.J.M., and Holstege, G. (1997a). Estrogen induces axonal outgrowth in the nucleus retroambiguus-lumbosacral motoneuronal pathway in the adult female cat. *J. Neurosci.* **17,** 1122–1136.

VanderHorst, V.G.J.M., and Holstege, G. (1997b). Organization of lumbosacral motoneuronal cell groups innervating hindlimb, pelvic floor and axial muscles in the cat. *J. Comp. Neurol.* **382,** 46–76.

CHAPTER

37

Cerebral Vascular System

OSCAR U. SCREMIN
Department of Veterans Affairs
Greater Los Angeles Healthcare System
Los Angeles, California, USA

Cerebral blood vessels were central to the ancient ideas of brain function embodied in the dogmas of antiquity. The rete mirabilis, an intricate system of branching arteries, usually intermingled with veins or sinuses, so delicate that in the words of Galen "no threads produced by the hand of man can compare with them in delicacy of composition or density of network" (Clarke and O'Malley, 1968) was one of the sites where in his conception the "vital spirits," in the blood transformed into the "animals spirits" which were the mediators of all movement and sensation. We recognize today that circulation of blood through the brain is needed for "all movement and sensation" not because it carries the "vital spirits" but the brain energy substrates instead. The "transformation" does not occur in the rete mirabilis, which exists in birds, cats, sheep, calf, and swine, although not in primates (Daniel *et al.*, 1953; Baker, 1982), but in the cerebral tissue itself. After all, brain function can proceed only for a few seconds after the flow of blood has been interrupted (Rossen *et al.*, 1943). The capillary network is that sector of the cerebral vasculature where those energy substrates are transferred and where blood flow materializes control of the neuronal microenvironment. The capillary network was only discovered in 1661 by Marcello Malpighi of Bologna (Young, 1929). It is interesting to note that the contemporary imaging techniques that have revolutionized the study of brain function are mostly based on blood flow–related variables. If Galen were to be resurrected almost two millenia later, although ignoring the details, he would not be a bit surprised.

The brain vascular system is both unique and heterogenous in terms of structure, microvascular organization, and function. Cerebral capillary abundance ranges from 260 mm/mm^3 (average of cerebrum white matter) to 2000 mm/mm^3 in the paraventricular and supraoptic nuclei of the hypothalamus (Zeman and Innes, 1963). In addition to these quantitative differences, which reflect variations in metabolic rate as well as the existence of specialized endocrine secretory mechanisms, there are also wide variations in capillary structure. Most vessels in the nervous system possess endothelial cell tight junctions that provide a seal and prevent or considerably hinder the passage of water-soluble molecules unless they interact with specialized

transport systems (Davson *et al.*, 1987). This phenomenon was first recognized in 1885 by Paul Ehrlich, who observed that coerulein sulphite, an acidic dye, stained all organs except the brain when injected systemically (Ehrlich, 1885). Capillaries in certain areas, however, are considerably more permeable and thus create microenvironments within brain tissue where many more blood constituents are accessible to nerve cells (Pardridge, 1988; Davson *et al.*, 1987; Gross *et al.*, 1986).

Another unique aspect of the brain circulation is the absence of a lymphatic system as known in most other organs. Although materials deposited in brain tissue or subarachnoid space can be recovered in the lymph nodes, this phenomenon is believed to be the result of transfer from cerebrospinal fluid to extracranial extracellular fluid through the cribriform plate and the spaces around the trunks of the emerging cranial and spinal nerves (Davson *et al.*, 1987).

In primates, as in all placental mammals, cerebral arteries and veins almost never run in pairs, even though they connect through a complex network of capillaries. In the brains of marsupials in contrast, arteries and veins meet at the surface of the brain, penetrate the brain tissue together, and remain paired throughout to the end of the terminal loop of capillaries (Wislocki and Campbell, 1937; Scharrer, 1962). Another important characteristic of the human cerebral vascular system, shared by most species, is the lack of direct communications between arteries and veins (arteriovenous anastomoses or A-V shunts).

For many years it was believed that the microvascular organization of the brain was dominated by terminal (nonanastomosing) arteries, an idea pioneered by Conheim who, based on the discrete distribution of infarcts after embolic occlusion of single vessels, coined the term "end arteries" (Conheim, 1872). It was not until the detailed anatomical work of Pfeiffer (1928) that the concept of brain blood vessels integrating into an almost uninterrupted vascular network was established. In addition, the existence of numerous interarterial and intervenous anastomoses create considerable redundancy and make it almost impossible to produce complete localized cessation of blood flow in the brain by selective occlusion of single blood vessels. However, occlusion of a single artery may produce a distinct area of necrosis when the perfusion pressure in its territory of distribution drops below the level required to maintain blood flow above a critical threshold of tissue viability. The existence of a continuous vascular network also explains the decrease of blood flow in areas surrounding an infarct, termed the "ischemic penumbra." and provides the basis for therapeutic interventions aimed at enhancing perfusion by collateral circulation in this zone.

ANATOMY OF CEREBRAL BLOOD VESSELS

Arteries

Extracranial Origins

Four arteries supply almost exclusively the brain: two internal carotids (ictd) and two vertebrals (vert). The contributions of blood flow to the brain of these systems in the adult human brain is approximately three fourths of the total for the carotids, and one fourth for the vertebrals (Scheel *et al.*, 2000). These vessels originate from branches stemming out of the aortic arch (ao). Phylogenetically, six branchial arches are recognized, of which in mammals the fourth gives origin to the aortic arch on the left and the subclavian artery (sbcl) on the right. The third branchial arch and the remnants of the primitive dorsal aorta originate the internal carotid, while the remnants of the primitive ventral aorta turn into the external carotid artery (ectd). A brachiocephalic trunk (bcph) originates from the convexity of the aorta and gives origin to the right subclavian and right common carotid artery (cctd). On the left side, the common carotid and subclavian arteries originate separately from the aorta, to the left of the brachiocephalic trunk origin. The vertebral arteries originate from the subclavians and run dorsally and medially to reach the transverse foramen of the sixth cervical vertebra (C6). They continue rostrally within the transverse canal, formed by the superposition of the transverse foraminae of the cervical vertebrae [Mai *et al.*, 1997, from here on referred to as "Atlas" (Coronal Section 9a)]. Inside the canal, the vertebral arteries give off radicular arteries that feed into the ventral and dorsal spinal arteries (Fig. 37.13) as well as numerous branches directed to the neck musculature. After it goes through the transverse foramen of the atlas, situated laterally to that of the axis, they turn anteromedially perforating the atlantooccipital membrane and dura (Atlas Coronal Section 10a and Sagittal Section 5p).

The forebrain (telencephalon and diencephalon) receives its arterial supply from the internal carotids, which divide intracranially into the anterior (acer) and middle (mcer) cerebral arteries (Atlas Coronal Section 8a; Fig. 37.1), and the anterior choroidal artery. The hindbrain (metencephalon and myelencephalon) as well as the mesencephalon receive their arterial supply from the vertebral arteries (Fig. 37.2; Atlas Coronal Section 10a), which join to form the basilar artery (Figs. 37.2 and 37.3; Atlas Coronal Section 9a). This vessel in turn divides into the two posterior cerebral arteries (Figs. 37.2 and 37.3; Atlas Horizontal Section 8p). The carotid and the vertebrobasilar system are precariously

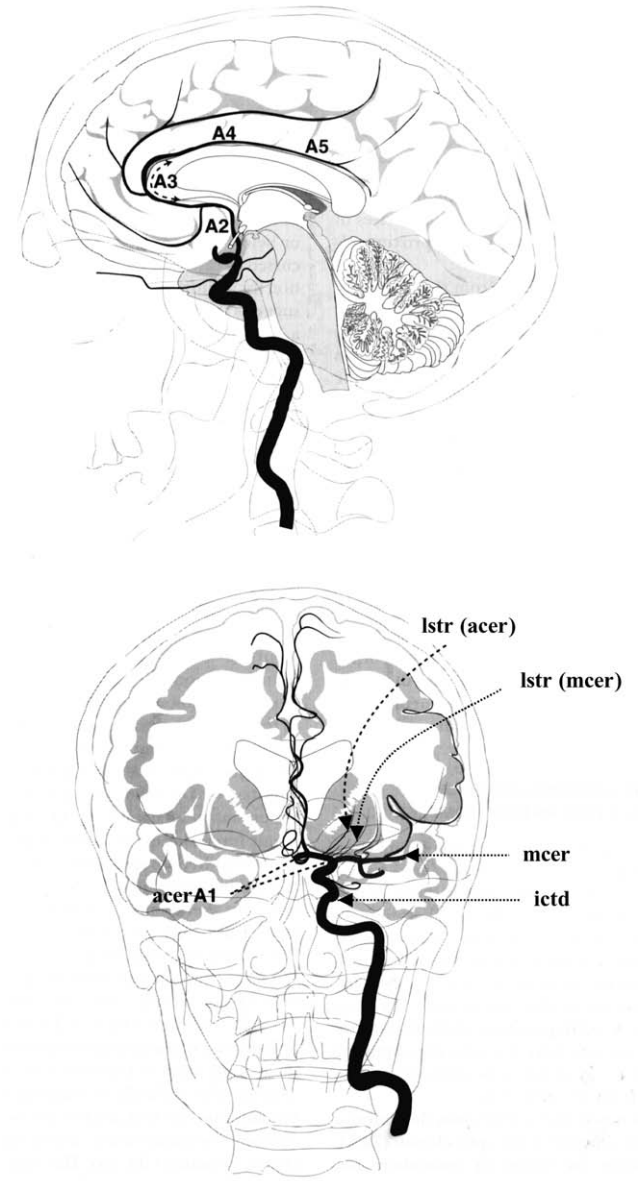

FIGURE 37.1 Segmental anatomy of the anterior cerebral artery in sagittal *(top)* and coronal *(bottom)* projections. The segments of this artery are defined thus: A1 from the internal carotid artery bifurcation to the anterior communicating, A2 to the junction of genu and rostrum of the corpus callosum, A3 around the genu, A4 to the plane of the coronal suture, and A5 from the coronal suture to the terminal branches. lstr, lenticulo striate arteries from anterior cerebral (acer) and middle cerebral (mcer); ictd, internal carotid artery. From Morris, P. (1997). *Practical Neuroangiography*. Williams & Wilkins, Baltimore, by permission of the author and publisher.

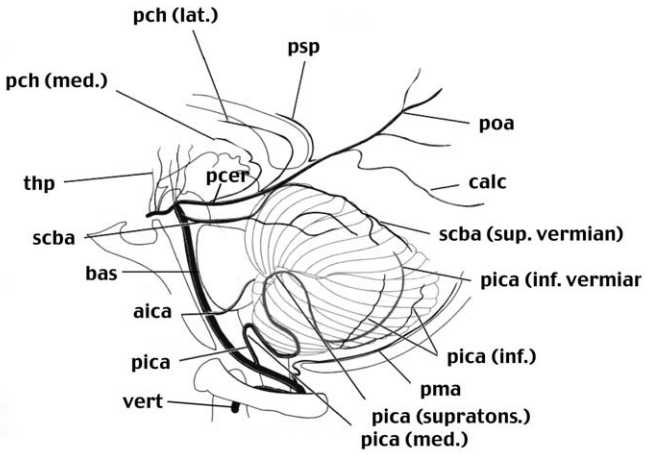

FIGURE 37.2 Projection on the sagittal plane of the posterior arterial circulation. vert, vertebral artery; pica, posterior inferior cerebellar, its medullary (med.), and supratonsilar (supratons.) segments, and its inferior hemispheric (inf.) and inferior vermian (inf. vermian) branches; bas, basilar; aica, anterior inferior cerebellar; scba, superior cerebellar with its superior vermian (sup. vermian) branch; pcer, posterior cerebral; thp, thalamo perforating; calc, calcarine; poa, parieto occipital; psp, perisplenial; pch (lat.), lateral posterior choroidal; pch (med.), medial posterior choroidal. From Morris, P. (1997). *Practical Neuroangiography*. Williams & Wilkins, Baltimore by permission of the author and publisher.

connected by a pair of posterior communicating arteries (pcoma) (Fig. 37.3; Atlas Horizontal Section 8p).

The Carotid System

The common carotid bifurcates into an external and an internal carotid at or slightly below the level of the hyoid bone, on the projection of the C3-C4 or C4-C5 vertebrae (Atlas Horizontal Section 16a). The internal carotid then courses in a cephalad direction, medial to the internal jugular vein, with the vagus nerve interposed between the two vessels (Atlas Horizontal Sections 13–15). The common carotid usually gives no branches proximal to its bifurcation, except for occasionally the superior thyroid or its laryngeal branch, the ascending pharyngeal, the inferior thyroid or, exceptionally, the vertebral artery.

The internal carotid artery lies first posterolaterally (Atlas Horizontal Sections 16a, 15p) and then medially (Atlas Horizontal Sections 13a, 14p) to the external carotid artery. It gives no significant branches on its cervical trajectory. In about 5–15% of subjects, tortuosity or kinking of this portion of the artery can be observed in angiograms (Osborn and Maack, 1980). In rare cases, this anomaly can induce occlusion of the vessel. Rarely this artery may be absent or hypoplastic. It enters the carotid canal at the base of the skull, just medial and rostral to the jugular foramen (Atlas Horizontal Section 11a). Inside the petrous bone it may give off two small branches—the vidian and the caroticotympanic arteries. Two intracavernous branches of the internal carotid artery deserve mention: the meningohypophyseal trunk, supplying the tentorium, the meninges, and the pituitary gland, and the artery of

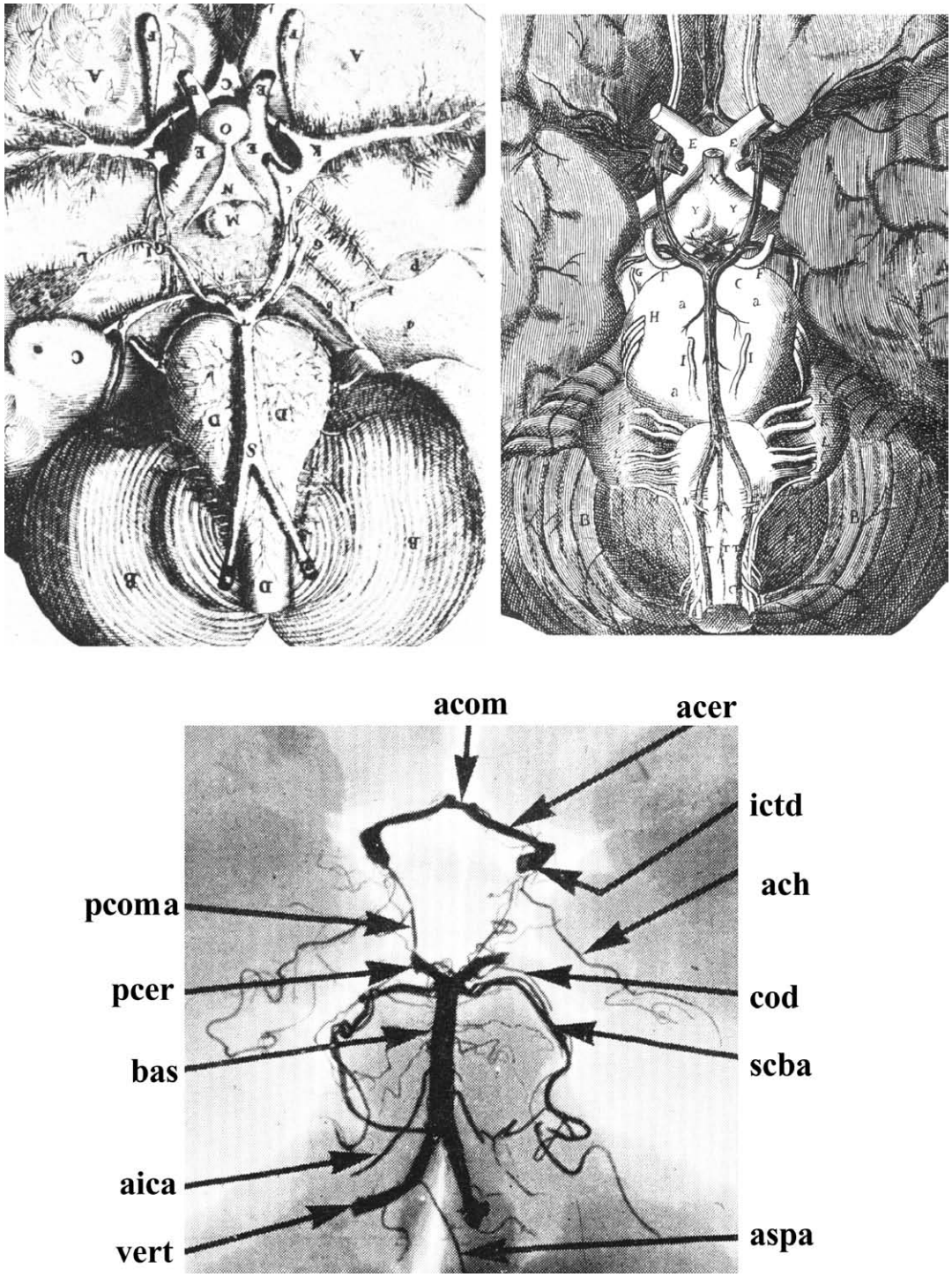

FIGURE 37.3 Classic illustrations of the arterial circle. *Top left:* The first published drawing by Guilio Casserio in Padova (1632). *Top right:* The second published drawing by Thomas Willis in London (1664). *Bottom:* An X-ray image obtained by Kaplan and Ford after injection of radioopaque material postmortem. acom, anterior communicating; acer, anterior cerebral; ictd, internal carotid; ach, anterior choroidal; cod, choroidal-diencephalic; scba, superior cerebellar; aspa, anterior spinal; vert, vertebral; aica, anterior inferior cerebellar; bas, basilar; pcer, posterior cerebral; pcoma, posterior communicating. From Casserio, G. (1632). *Tabulae Anatomicae xxiix.* Daniel Buiretius, Frankfurt, Willis, T. (1664). *Cerebri Anatome*. Martin & Allestry, London, and Kaplan and Ford (1966), and *The brain vascular system*, Elsevier, Amsterdam, by permission of the author.

the inferior cavernous sinus, which anastomoses with the external carotid artery territory via a branch traversing the foramen rotundum. It is noteworthy that the internal carotid artery lies inside a major sinus (cavernous), which drains blood from the orbit and nasal cavities. This arrangement creates the opportunity for heat exchange between the arterial input to the brain, bringing warm blood from the body core, and the cooler venous output from the nasal cavities, which are normally cooled by evaporation of water induced by the respiratory air stream. In animals with a carotid rete mirabilis, in which the exchange surface between arterial and venous components of this structure is quite extensive, this phenomenon affords protection of the brain from hyperthermia during exercise (Baker, 1982). Whether the same protective mechanism exists in humans, in which the rete is absent and the exchange surfaces are consequently limited, is a matter of controversy (Cabanac, 1986; Deklunder *et al.*, 1991).

After the internal carotid artery exits the cavernous sinus, it gives off the ophthalmic artery (oph), which provides the main arterial supply to the eye and the orbital contents. The oph anastomoses extensively with the territory of the external carotid artery and is a potential source of collateral circulation to the brain in cases of occlusion of the internal carotid artery below the origin of the oph. In fact, studies with transcranial Doppler sonography (TCD) indicate that when the internal carotid artery is occluded, the blood flow direction in the oph reverses (Rutgers *et al.*, 2000), providing the intracranial structures with blood from the external carotid artery. A recent evaluation using TCD and near infrared spectroscopy to measure regional cerebral oxygen saturation concluded that the external carotid artery contributes significantly to intracranial circulation in cases of severe internal carotid artery stenosis (Fearn *et al.*, 2000)

In the early stages of human development (35 day, 12–14 mm embryo), the internal carotid artery divides intracranially into four vessels: anterior, middle, and posterior cerebral (pcer), and anterior choroidal (ach) arteries (Kaplan and Ford, 1966) (Fig. 37.4). The posterior cerebral arteries anastomose caudally with the two terminal branches of the basilar artery, which supply the ventral mesencephalon, and continue beyond that point to supply the dorsal mesencephalon and caudal portion of the diencephalon. As the telencephalon develops, the posterior cerebral artery also supplies its caudal portion. Up until birth, the entire territory of the posterior cerebral artery appears to be supplied from the internal carotid artery. At later stages, however, the proximal portion of the artery (which is named posterior communicating artery in the adult) thins out, and the two terminal branches of the basilar (named the P1 or precommunicating segments of the posterior cerebral artery in the adult) take over the supply of the distal posterior cerebral artery (named the postcommunicating or P2 and P3 portions of the posterior cerebral artery). Thus in the most common adult configuration, the vertebrobasilar system supplies the mesencephalon and caudal forebrain via the posterior cerebral artery. In some cases, however, these brain areas are supplied by the internal carotid artery in the adult, when the fetal configuration persists, and the pcoma, P2, and P3 portions of the posterior cerebral artery appear as a single vessel of uniform size, while the posterior cerebral artery P1 segments become hypoplastic. This anomaly is called the "fetal" variant of the posterior cerebral artery (Padget, 1944).

Between the origin of the oph and the emergence of the pcoma, the internal carotid emits a number of small vessels that supply the anterior portion of the infundibulum, and the superior and inferior hypophyseal arteries that form an anastomotic circle with their symmetrical vessels to supply the infundibulum, pituitary stalk, and neurohypohysis (see Chapter 19). The hypophyseal arteries could also originate from the anterior portion of the pcoma.

The anterior cerebral artery is one of the terminal branches of the internal carotid artery. It courses rostromedially, dorsal to the optic nerve (Atlas Coronal Section 8a), to reach the interhemispheric fissure (Atlas Horizontal Section 8a, and Coronal Section 7a). At the midline, it anastomoses with its contralateral homonymous vessel through the anterior communicating artery (acom) (Fig. 37.3). Numerous variations in the shape and magnitude of this anastomosis have been described, including absence, duplication, and triplication of the acom. Along its precommunicating segment (A1), the anterior cerebral artery supplies perforator branches to the septal nuclei, the anterior portion of the hypothalamus, including the supraoptic nuclei, and the anterior portion of the striatum (lenticulostriate arteries, lstr) (Fig. 37.1). The recurrent artery of Heubner originates from the acer at or close to the anterior communicating artery, coursing caudally alongside the anterior cerebral artery. It provides a number of perforators just rostral to the similar branches of the middle cerebral artery, entering the lateral part of the anterior perforated substance. The terminal extra- and intraparenchymal arborizations of this vessel anastomose with branches of the middle cerebral artery and may provide collateral blood flow to the basal ganglia in cases of middle cerebral artery occlusion (Morris, 1997). Occasionally it also irrigates the orbital surface of the frontal lobe. This artery

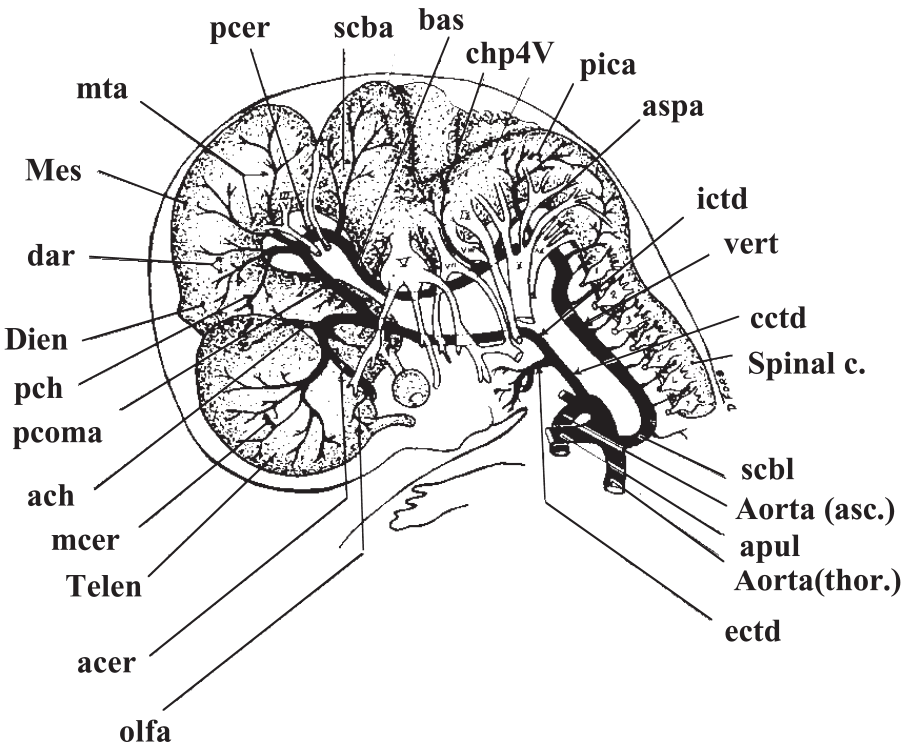

FIGURE 37.4 Continuity of the great anastomotic arch between common carotid and subclavian arteries is well established in the human embryo, shown in this semischematic representation at 35 days of age. Structures abbreviations: Telen, telencephalon; Mes, mesencephalon; chp4V, choroid plexus of fourth ventricle; Spinal c., cervical spinal cord. Arteries abbreviations: olfa, primitive olfactory; acer, anterior cerebral; mcer, middle cerebral; ach, anterior choroidal; pcoma, posterior communicating; pch, posterior choroidal; dar, diencephalic; mta, mesencephalic tectum arteries; pcer, posterior cerebral; scba, superior cerebellar; bas, basilar; pica, poterior inferior cerebellar; aspa, anterior spinal; ictd, internal carotid; cctd, common carotid; scbls, subclavian; Aorta (asc.), ascending aorta; apul, pulmonary; aorta (thor.), thoracic aorta; ectd, external carotid. From Kaplan and Ford (1966), *The brain vascular system,* Elsevier, Amsterdam, by permission of the author.

supplies the anterior limb of the internal capsule, the anterior putamen, and reaches the inferior portion of the caudate.

The anterior cerebral artery continues rostrodorsally, curves around the genu of the corpus callosum (Atlas Coronal Section 7a), and, as the pericallosal artery, supplies the medial aspect of the frontal lobe (Fig. 37.1) through the internal frontal branches (anterior, middle, and posterior) as well as the corpus callosum, its adjacent cortex, septum pellucidum, anterior pillars of the fornix, and the anterior commissure. Its largest branch, the callosomarginal artery, courses laterally into the cingulate sulcus. The terminal portion of the anterior cerebral artery branches anastomose with the cortical and perisplenial branches of the posterior cerebral artery. These channels may become important in cases of occlusion of the anterior cerebral artery, when some of its territory may become covered by the posterior cerebral artery and viceversa (Morris, 1997).

The medial aspects of both hemispheres could be irrigated from a single anterior cerebral artery, when a pericallosal artery provides branches to the contralateral side, or even more completely when an azygos (unpaired) anterior cerebral artery is present.

The middle cerebral artery is considered the continuation, or the main terminal branch, of the internal carotid. It is a vessel of paramount functional significance since in its territory are found the cortical representations of motor, somatosensory, language, and higher cognitive functions. It also provides irrigation to most of the striatum and long ascending and descending tracts. This artery originates from the internal carotid artery just lateral to the optic chiasm (Atlas Coronal Section 8a), and then it proceeds laterally, ventral to the olfactory trigone to enter the Sylvian fissure. Along the middle cerebral artery proximal trajectory, a variable number of perforators arise from its dorsal aspect and penetrate the base of the brain through the anterior perforated substance (Fig. 37.1). Two groups of these vessels are described as medial or lateral lenticulostriate arteries depending of whether they are situated medial or lateral to a parasagittal plane passing through the olfactory tract. These lenticulostriate arteries irrigate the lateral

portion of the rostral two thirds of the caudate nucleus and putamen. The anterior medial portion of these nuclei is irrigated by the lstr arteries from the anterior cerebral and recurrent artery of Heubner (Fig. 37.1).

The middle cerebral artery divides into its cortical branches generally at the level of the limen insulae, dorsal to the temporal pole (Atlas Coronal Section 8a). This division may take place, however, anywhere between 1 and 4 cm from its origin from the internal carotid artery, and this point may be different on each hemisphere of the same brain (Kaplan and Ford, 1966). The pattern of arborization of this artery on the cortical surface consists of a bifurcation (78% of hemispheres), trifurcation (12%), or division into multiple trunks (10%) (Gibo *et al.*, 1981). Although branching of the middle cerebral artery is variable, a description of the most commonly found named vessels is given, according to Morris (1997). The anterior temporal branch irrigates the temporal pole and a variable extent of the lateral temporal lobe. It originates as part of a trifurcation of the middle cerebral artery or in a common trunk with the orbitofrontal artery that distributes over the inferior and middle frontal gyri and the orbital surface of the frontal lobe. The prefrontal and precentral arteries cover two triangular-shaped areas of the frontal lobe with vertices toward the temporal pole, situated between the frontal pole and the precentral gyrus. The rolandic arteries supply the precentral and postcentral gyri. The angular artery runs caudally over the superior temporal gyrus and reaches the occipital lobe. Between this artery and the rolandic artery are several parietal branches.

The cortical branches of the middle cerebral artery anastomose with branches of the anterior cerebral artery and posterior cerebral artery (Fig. 37.5). The region over which these anastomosis occur has been diagramatically represented as a large diameter circle. This area is considered of clinical significance because it appears to be the site of "watershed" infarctions (Zülch, 1985).

The anterior choroidal artery (ach) branches out of the posterior wall of the internal carotid artery proximal to the origin of the middle cerebral artery and anterior cerebral artery, and distal to the posterior cerebral-internal carotid anastomosis (Fig. 37.3). The first branches from this vessel supply the amygdala and the rostral hippocampus. The anterior choroidal then continues caudally giving branches that irrigate the rest of the hippocampus, optic tract, the tail of the nucleus caudatus, medial pallidum, ventral thalamus, the posterior limb of the internal capsule, and lateral geniculate. The vessel then proceeds caudolaterally giving numerous branches to the choroid plexus of the temporal horn of the lateral ventricle. The anterior choroidal artery anastomoses with branches of the anterior cerebral artery, posterior cerebral artery, and middle cerebral artery. Occlusion of the anterior choroidal artery may be associated with contralateral hemiplegia (posterior limb of the internal capsule), hemianesthesia (thalamocortical tracts), hemianopsia (lateral geniculate), and memory loss (hippocampus) (Cooper, 1954).

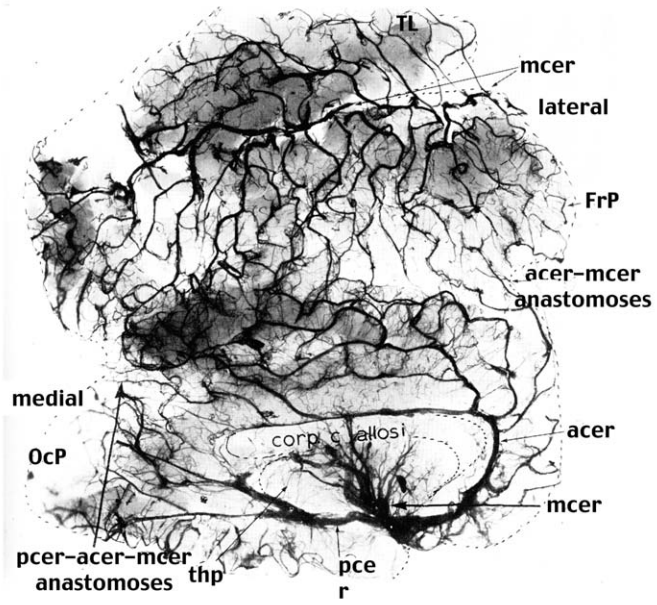

FIGURE 37.5 Postmortem angiogram in which the entire cerebral cortex has been flattened to show the multiple anastomoses between the territories of the anterior (acer), middle (mcer), and posterior (pcer) cerebral arteries. The thalamo-perforating branches (thp) are also shown. The corpus calllosum is outlined for reference. OcP, occipital pole; FrP, frontal pole; TL, temporal lobe. From Kaplan and Ford (1966), *The brain vascular system*, Elsevier, Amsterdam, by permission of the author.

Vertebrobasilar System

The vertebral arteries fuse to form the basilar artery (Fig. 37.3), which starts its course over the ventral portion of the medulla, usually at or a few millimeters below the inferior border of the clivus (Atlas Horizontal Section 10p). The anterior spinal artery (aspa) originates from both vertebral arteries, close to the point where they join, or occasionally from only one of them (Fig. 37.3). The remaining medial branches of the intracranial portion of the vertebral artery supply the anterior medulla and pyramids. The lateral branches of this portion include the posterior inferior cerebellar artery (pica) and branches to the inferior cerebellar peduncle, lateral medulla, and the inferior olive and associated structures (Fig. 37.2). The pica, which may alternatively originate from the basilar or from the extracranial

portion of the vertebral, irrigates the inferolateral cerebellar hemisphere (Fig. 37.2). The extent of the cerebellar distribution of the pica is variable and inversely related to the size of the territory covered by the anterior inferior cerebellar artery (aica), a branch of the basilar artery. Cases in which the pica originates from the internal carotid artery or branches of the external carotid artery have been described but are rare (Morris, 1997). On its course toward the cerebellum, the pica gives branches to the lower medulla and fourth ventricle. Proximal occlusion of the pica gives rise to the Wallenberg's syndrome, with homolateral cerebellar symptoms and trigeminal sensory deficits, and contralateral hemiplegia associated with deficits of pain and thermal sensations.

Blood flow in the basilar artery is laminar, as in practically all normal arteries in the body with the possible exception of the root of the aorta during the ejection phase (Fung, 1984). It is then conceivable that the streams of blood originating in both vertebral arteries may not mix along the course of the basilar. This phenomenon was first documented by McDonald using dye injections and direct observation of the exposed artery in rabbits (McDonald and Potter, 1951). It is also an observation of human intraarterial angiography (IAA) that in cases of low injection rates of contrast medium into the vertebral artery, a cerebellar artery or posterior cerebral artery contralateral to the site of injection may not fill simply because it is being perfused by nonopacified blood from the homolateral (noninjected) vertebral artery, and this should not be interpreted as a vessel occlusion (Morris, 1997). The same phenomenon has been demonstrated with selective saturation pulses on magnetic resonance angiography (MRA) (Smith and Bellon, 1995).

Numerous branches, called perforator arteries because they penetrate the substance of the brainstem, originate from the basilar artery along its course (Figs. 37.6 and 37.7). Median perforators (mper) originate from the posterior wall of the basilar and penetrate the pons and midbrain to irrigate structures adjacent to the midline, reaching the floor of the fourth ventricle. Branches destined to lateral structures, named circumflex (circ) or transverse, encircle the brainstem and penetrate its substance at variable distances from their origin. There are numerous anastomoses among the finer intraparenchymal branches of these vessels, although their distribution remains essentially unilateral.

The aica originates from the basilar as a single vessel or as several smaller twigs (Fig. 37.2). It courses caudolaterally and provides several perforators to

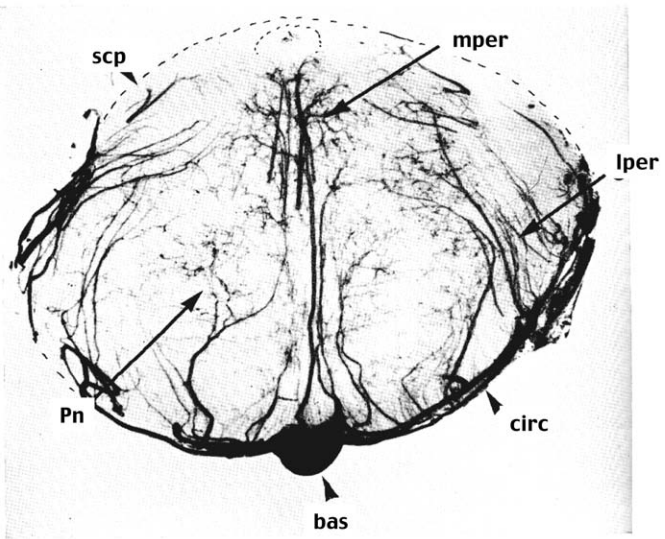

FIGURE 37.6 Angiography of the pons (rostral end) shown in a coronal section. Pn, pontine nucleus; scp, superior cerebellar peduncle. Arteries abbreviations: bas, basilar; mper, median perforators; lper, lateral perforators; circ, pontine circumflex. From Kaplan and Ford (1966), *The brain vascular system*, Elsevier, Amsterdam, by permission of the author.

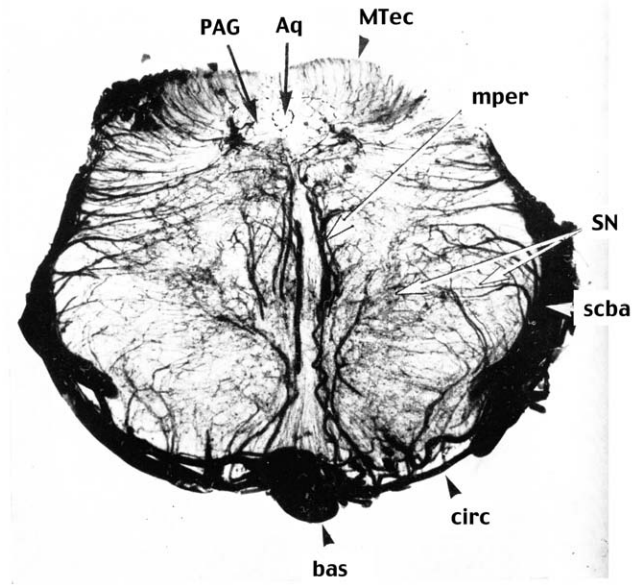

FIGURE 37.7 Angiography of the mesencephalon (caudal end) shown in a coronal section. PAG, periacqueductal gray; Aq, cerebral acqueduct; MTec, mesencephalic tectum; SN, substantia nigra. Arteries abbreviations: bas, basilar; mper, median perforators; scba, superior cerebellar; circ, mesencephalic circumflex. From Kaplan and Ford (1966), *The brain vascular system*, Elsevier, Amsterdam, by permission of the author.

the pons before it reaches the inferior surface of the cerebellar hemisphere (Fig. 37.8). Its area of distribution, as stated previously, depends on the size of the territory of the pica. Occasionally, when the pica is absent, the aica covers the territory of both arteries (aica–pica complex). These vessels contribute to the formation of the choroid plexus of the fourth ventricle. The labyrinthine artery, which arises commonly from the aica and occasionally from the basilar, accompanies the VII and VIII nerves into the internal acoustic meatus to reach the inner ear.

The superior cerebellar artery (scba) arises at or just caudal to the rostral division of the basilar into the two posterior cerebral arteries (Fig. 37.2). A large perforator arises from this artery at its origin or sometimes from the basilar, and a number of smaller perforators originate from the superior cerebellar artery and distribute to the pontine lateral tegmental region. There are usually three cerebellar branches of the scba: the medial, distributing mostly over the vermis, and the intermediate and lateral, over the cerebellar hemispheres (Fig. 37.8). There are numerous anastomoses on the surface of the cerebellum between branches of these vessels and those of the interfolial arteries that originate from them and course between the cerebellar folia (Fig. 37.8).

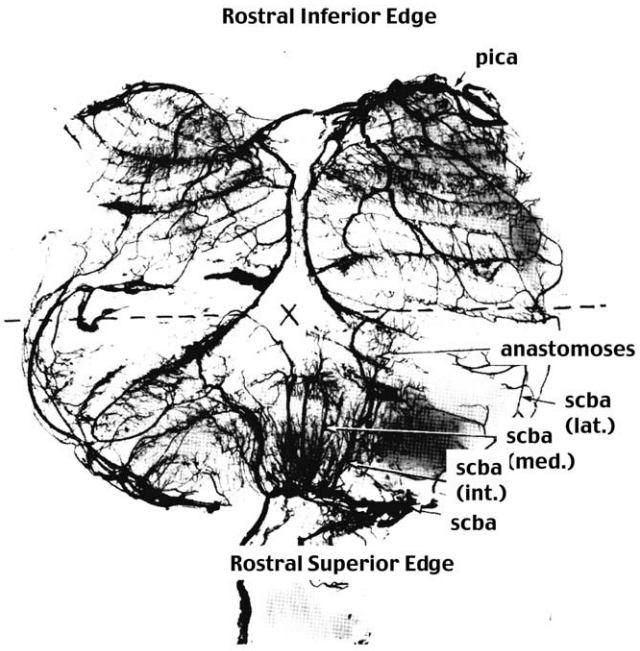

FIGURE 37.8 Postmortem angiogram in which the entire cerebellar cortex has been flattened to show the multiple anastomoses between the territories of the superior cerebellar (scba) and the posterior inferior cerebellar (pica) arteries. The lateral (lat.), intermediate (int.), and medial (med.) branches of the scba are shown. The rostral inferior edge of the cerebellum is at the top and the rostral superior edge at the bottom of the figure. The line labeled "X" represents the most caudal edge of the cerebellar cortex. From Kaplan and Ford (1966), *The brain vascular system*, Elsevier, Amsterdam, by permission of the author.

The basilar artery terminates dividing into two posterior cerebral arteries, which connect with the posterior communicating arteries (pcoma) (Fig. 37.3) and then curve around the midbrain. At this level, their position is usually superomedial to the tentorium (Atlas Coronal Section 10a), and they terminate in a number of cortical vessels over the calcarine fissure. In cases of supratentorial mass–occupying lesions or herniation of the temporal lobe, the brainstem may be compressed against the tentorium with the posterior cerebral artery or some of its branches becoming occluded or stretched resulting in severe ischemia and/or hemorrhage. Depending on the branching pattern of the posterior cerebral artery, the main trunk of the artery (in distal division patterns) or some of the branches (in the proximal division pattern) may be affected, with variable functional consequences (Ono *et al.*, 1984).

Three segments are commonly described in the posterior cerebral artery: P1 from its origin until the anastomosis with the posterior communicating, P2 from the end of P1 to the back of the midbrain, and P3 as the segment running through the lateral portion of the quadrigeminal cistern (Morris, 1997). A large number of perforating vessels arise from the P1 segment and are directed toward the peduncle and brainstem (peduncular perforating branches) and superiorly to irrigate the thalamus (thalamoperforator arteries), (see Chapter 20). Peduncular perforating branches also originate from the P2 segment. There are also circumflex branches that run parallel to the posterior cerebral artery before penetrating the thalamus or mesencephalon. The medial posterior choroidal artery (Fig. 37.2) originates from the P2 segment and courses around the brainstem giving off branches contributing to the irrigation of the midbrain, tectal plate, pineal gland, posterior thalamus, habenula, and medial geniculate body (Morris, 1997). It also supplies the homolateral choroid plexus of the third ventricle. Lateral to the medial posterior choroidal artery originate a number of lateral posterior choroidal arteries, up to nine per side. These vessels supply parts of the midbrain crus, the pineal body, splenium, posterior commissure, tail of the caudate nucleus, thalamus, and fornix. They enter the lateral ventricle where they supply the choroid plexus and then enter the foramen of Monro to anastomose with the medial posterior choroidal arteries (Morris, 1997).

The cortical branches of the posterior cerebral artery are the more distal to the origin of this artery and

distribute to the inferior and medial surface of the temporal lobe (anterior and posterior temporal branches) and to the medial aspect of the occipital lobe and posterior parietal lobe (calcarine and parietooccipital branches). Arteries at the edge of the posterior cerebral artery territory anastomose with the terminal arborizations of the middle cerebral and anterior cerebral arteries (Fig. 37.5). The overlapping of these territories is believed to establish efficient collateral circulation in cases of occlusion of the posterior cerebral artery, preventing extensive infarction and producing a spare of the macular territory (Strong and Elwyn, 1953).

The Arterial Circle

One of the notable characteristics of cerebrovascular anatomy is the abundance of anastomoses between large arteries, extracranially (angular to ophthalmic arteries) and intracranially (the arterial circle at the base of the brain) as well as between small arteries on the surface of the brain (the leptomeningeal plexus) (Fig. 37.9). Knowledge of these features dates back to Gabriel Fallopius (1523–1562) a disciple of Vesalius, who appears to be the first anatomist to mention the existence of an anastomotic circle of arteries at the base of the brain. The first illustration of this anatomical feature was provided by Guilio Casserio (1545–1605), one of William Harvey's professors at Padua (Fig. 37.3, top left) (Casserio, 1632). Interestingly enough this is an incomplete circle with one of the posterior communicating arteries either absent or considerably hypoplastic. Anomalies of this communicating vessel are known today to be present in approximately 40% of cases (Riggs and Rupp, 1963). Johan Vesling (1595–1649), from the School of Padua, and the Swiss anatomist Johan Wepfer (1620–1695) also described the arterial circle (Clarke and O'Malley, 1968). Thomas Willis, Sedleian Professor of Natural Philosophy at Oxford, was also aware of this feature and asked his friend Christopher Wren, the architect of Canterbury Cathedral, to illustrate the arterial circle which he did masterfully (Willis, 1664). The image is somewhat idealized (Fig. 37.3, top right) because all vessels appear symmetrical and with almost the same diameter, a condition that is indeed rare in the adult human brain. However, the name of Willis remains attached to this anatomical circle on account of his insight into its possible function. After observing autopsy material with a completely occluded carotid artery in patients with no symptoms, he reasoned that the circle served to provide collateral circulation from other supplying arteries. Willis also performed animal experiments such as the ligation of both carotid arteries in a dog. In the words of his assistant Richard Lower, "the animal was not altered … [such] that within a quarter of an hour after, he got loose and followed the doctor [Willis] into town, as he visited his patients" (Tower, 1991). However the success of this experiment probably related more to the notorious abundance of anastomoses among intra- and extracranial vessels in dogs (Sagawa and Guyton, 1961) and in particular to the existence of the anastomotic artery, a large vessel communicating the external carotid artery and the arterial circle in this animal.

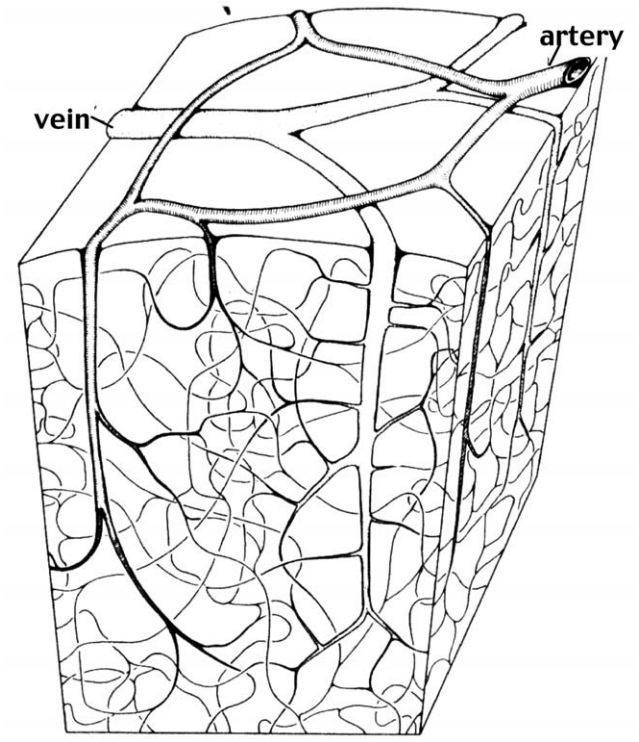

FIGURE 37.9 Schematic three-dimensional representation of the cerebral cortex vascular architecture. Arteries and veins run at a distance and connect at all levels through capillary loops inside the cortex. Small arterial circles join the cortical arteries and give origin to multiple perforators. From Scharrer, E. (1940). Arteries and veins in the mammalian brain. Anat. Rec. 78, 173–196. Reprinted by permission of Wiley-Liss, Inc., a subsidiary of John Wiley & Sons, Inc.

Understanding of the considerable amount of variability in the arterial circle composition was gained through exhaustive anatomical studies. The importance of these anomalies goes beyond the mere academic interest because they are very frequent (50–80% of cases depending on the authors), and they are associated with an increased risk of stroke (Hedera *et al.*, 1998; Schomer *et al.*, 1994). In 1947, Padget (1944) summarized the findings of a large number of anatomical specimens reported in the literature at the time. Starting with a "typical" circle with the anterior communicating as half to two thirds the size of the anterior cerebral, in turn half the size of the internal carotid, and the pcoma with half the size of the posterior cerebral, in turn

half the size of the basilar, agreement of the posterior portion of the circle (posterior communicating and posterior cerebral arteries) with this pattern was found in less than 50% of 1033 cases. The anterior portion of the circle (anterior cerebral and anterior communicating arteries) was considered to be more dependable than the posterior one as a source of collateral circulation, although no quantitative data was presented to support this statement.

Quantitative estimates of the prevalence of circle anomalies in 994 specimens (Riggs and Rupp, 1963) indicate that a complete "typical" circle is found in only 20% of cases. Anomalies included absence or hypoplasia of the anterior communicating artery (20%), posterior communicating arteries on one or both sides (38%), and proximal anterior cerebral artery (12%). The rest of the anomalies were represented by hypoplasia of the divisional branches of the basilar artery. When the latter were added to defects in the posterior communicating arteries, 48% of specimens had the carotids supplying all or a larger than expected portion of the hemispheres, with absent or limited capacity of the posterior circulation to compensate for deficits in carotid blood flow.

A serious limitation of the anatomical studies is that although they can identify cases of anatomical compromise of collateral circulation through the arterial circle when some of its component vessels are severely hypoplastic or absent, they cannot ascertain whether a vessel of "normal" caliber would be able to sustain a significant amount of additional blood flow to compensate for stenosis or occlusion of one or more of the circle-supplying vessels. The ability of the posterior communicating artery to supply collateral blood flow, for instance, has been found to depend not only on its diameter but also on the resistance of its afferent and efferent vessels (Hillen *et al.*, 1982). These variables in turn cannot be evaluated without blood flow and blood pressure data.

IAA and MRA can provide information on direction of flow in the component vessels of the circle in addition to the anatomical information (Hoksbergen *et al.*, 2000a). However, the transcranial color-coded duplex ultrasonography technique (TCCD) can provide currently the most accurate information regarding blood velocity (although not volumetric blood flow due to lack of vessel cross-sectional area information) in the blood vessels that supply the brain. Compression of one carotid artery in the neck in a subject with an anatomically complete circle, is associated with increased blood velocity in the contralateral precommunicating segment (A1) of the anterior cerebral artery, reversal of blood flow in the homolateral A1, and increased blood velocity in the homolateral precommunicating segment (P1) of the posterior cerebral artery (Hoksbergen *et al.*, 2000b). In a series of 76 subjects without cerebrovascular symptoms, Hoksbergen *et al.* found that only 29% of them responded with blood flow changes described previously as characteristic of a complete arterial circle, and 45% of the hemispheres examined had anomalies of the posterior part of the arterial circle that impaired collateral blood flow from the basilar to the internal carotid artery (Hoksbergen *et al.*, 2000b). Within the last group, they included cases in which posterior communicating artery blood velocity decreased (revealing an internal carotid origin of flow in the vessel) or failed to increase over 20% of baseline. Cross flow through the anterior part of the circle was not found in only 5% of the subjects. The higher prevalence of functional insufficiency in the posterior versus anterior communicating arteries is in general agreement with the anatomical information given earlier.

It is important to note that in the presence of an anatomically complete arterial circle, blood velocity in the homolateral middle cerebral artery decreased between 25% and 67% during brief unilateral carotid compression. In the hemispheres with nonfunctional pcoma, this range was 27–88% (Hoksbergen *et al.*, 1999). Thus it is obvious that even in the relatively small proportion of individuals with an anatomically "typical" arterial circle, this structure cannot provide complete compensation by collateral blood flow following sudden occlusion of one of the four vessels supplying the brain. In this context, it is important to note that failure of adequate collateral blood flow compensation during sudden unilateral internal carotid occlusion, defined as a decrease of middle cerebral artery blood velocity > 40%, has been reported to be followed by hemodynamic cerebral infarction if the occlusion becomes permanent (Sorteberg *et al.*, 1999).

The question of whether the vessels in the arterial circle are capable of remodeling over time after a permanent occlusion, or perhaps in response to slowly developing stenosis of one of its supplying arteries has been answered affirmatively by the work of Coyle and co-workers (Coyle and Panzenbeck, 1990), who showed hypertrophy of the posterior cerebral artery of rats following ligation of the common carotid artery. In humans it has been demonstrated that the vessels supplying a high flow arteriovenous malformation undergo a so-called angiomatous change, which is not considered to be part of the malformation but to represent adaptive remodeling owing to high flow conditions (Morris, 1997). The modest changes in collateral blood flow that take place in the arterial circle after occlusion of one of its afferent vessels may not be sufficient to generate remodeling in humans,

however. In an MRA study, Rutgers *et al.* (2000) have followed patients with uni- or bilateral occlusion of the internal carotid over 1.5 years and found no improvement in the patterns of collateral blood flow over time.

Microvascular Anatomy

The arteries on the surface of the human brain were described in the early work of Duret and Heubner (Duret, 1874; Heubner, 1874). The last author recognized the existence of numerous interarterial anastomoses between vessels of variable caliber. This arrangement is also found in other animals and has been described in great detail by several authors (Bar, 1980; Duvernoy *et al.*, 1981; Eecken, 1959; Mchedlishvili and Kuridze, 1984).

The diagram shown in Figure 37.9, which we owe to Scharrer (1940), illustrates the existence of a network of anastomosing pial arteries (the leptomeningeal plexus) from which penetrating vessels emerge at right angles, capillarize, and drain into collecting veins that course to the pial surface widely separated from the supplying arteries. The detailed anatomy of the intervening capillary plexus is extremely complex and highly dependent on the neuronal anatomy, to the extent that observation of the blood vessel network allows sometimes to recognize the underlying neuronal substrate. A striking example is observed in Figure 37.10, where the inferior olive and corticospinal tract precise structural limits can be followed in a specimen in which only the blood vessels have been made visible.

Detailed analysis of the intracortical vascular network reveals arterioles that traverse all cortical layers with minimal or no branching to reach the deeper layers and the subcortical white matter, where they give off capillaries that orient themselves in compliance with the general trajectories of nerve fibers (Fig. 37.11, A6). Other groups of arteries give branches to subcortical and cortical levels (Fig. 37.11, A5), all cortical levels (Fig. 37.11, A4), or restricted cortical layers (Fig. 37.11, A1-A3). In most areas of the cortex, many arteries converge over a single intracortical vein that are less numerous than arteries, and of a larger caliber, with their afferent vessels joining at right angles (Fig. 37.11, V4-V5).

Vascular Territories

A large number of descriptions of the territories covered by the various cerebral arteries are available in the literature (see review by van der Zwan *et al.*, 1992). Delineations of these territories are shown in the Atlas for horizontal and coronal brain sections. It is important to recognize that these limits are quite

FIGURE 37.10 Transverse section of medulla oblongata of a specimen injected with India ink/gelatin solution and cleared with the Spalteholtz technique. Contrast is provided by the microvascular density, which is much greater for gray than for white matter structures. IO, inferior olivary nucleus (a, medial; b, lateral; c, superficial); MAO, medial accessory olivary nucleus; DAO, dorsal accessory olivary nucleus; cs, corticospinal tract; ml, medial lemniscus; colv, central olivary vein; mper, medullary median perforator artery. Adapted from Duvernoy, H.M. (1978). *Human Brainstem Vessels.* Springer-Verlag, Berlin by permission of the author and publisher.

variable, on account of anatomical and hemodynamic factors. The line of separation between the territories of the anterior cerebral artery, middle cerebral artery, and posterior cerebral artery, for instance, depend on the hemodynamic conditions in each territory that determine the extent to which the three main supplying vessels contribute to their irrigation. Thus, proximal occlusion of the middle cerebral artery may induce the anterior cerebral artery and posterior cerebral artery territories to expand over that of the middle cerebral artery. Another condition of a shift in distribution of arterial supply may be found as described earlier with a high-flow arteriovenous malformation that would create a "sump" effect drawing blood from arteries of neighboring territories. A similar situation, generated by the increased collateral blood flow through the acer-mcer anastomoses, has been demonstrated in rats subjected to a middle cerebral artery occlusion (Coyle, 1984).

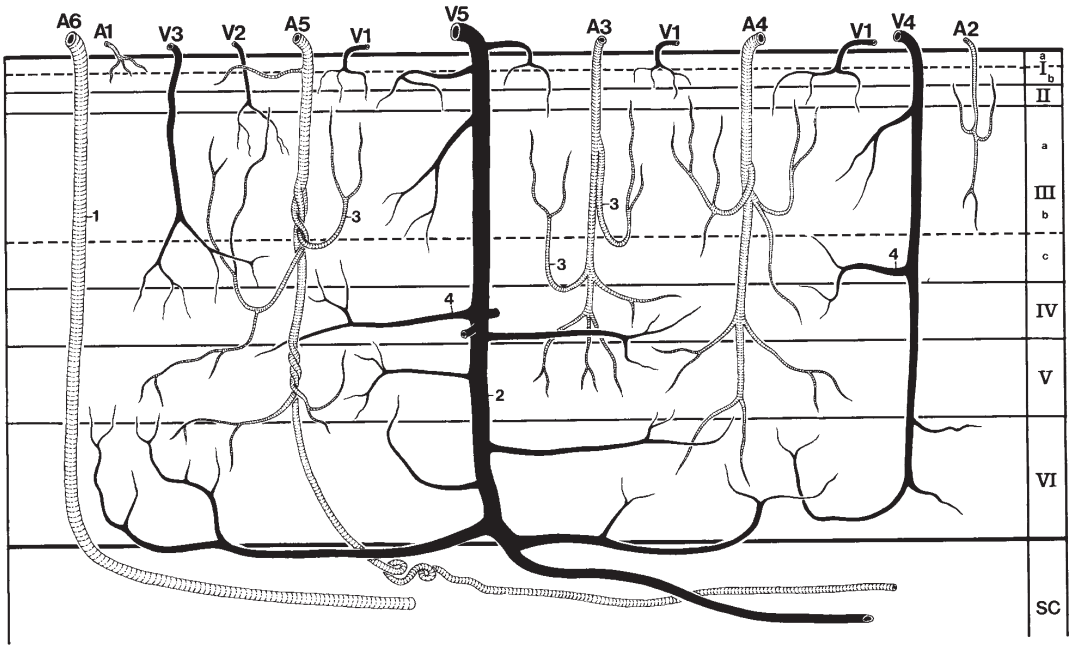

FIGURE 37.11 Schematic two-dimensional representation of the types of arteries and veins found in the human cerebral cortex. Arteries distribute to the superficial layers only (A1, A2), to layers I–V (A3), to all layers (A4, A5), or preferentially to the subjacent white matter (A6). This segmental arrangement creates the anatomical substrate for a differential control of blood flow to cortical layers. Veins (shown in solid black) are usually larger and receive afferent branches at right angles from circumscribed (V1–V3) or wide (V4, V5) distributions. I–VI, cortical layers; SC, subcortical white matter. From Duvernoy, H.M. (1999). *The Human Brain Surface, Three Dimensional Sectional Anatomy with MRI, and Blood Supply.* Springer, New York, by permission of the author and publisher.

Veins

The veins of the brain originate from an interconnecting network of superficial vessels that drain the capillary bed and usually run away from the arteries (Fig. 37.9), with the exception of marsupials and several other vertebrates in which veins and arteries run at close proximity in pairs (Wislocki and Campbell, 1937; Scharrer, 1940). These veins empty into sinuses, with walls formed by endothelium-lined recesses of the duramater, a meningeal layer with little compliance. This structural feature serves to make the volume of the cerebral venous compartment less dependent on variations in venous pressure than most other organs. These sinuses connect with the extracranial venous system of the head through "emissary" vessels. In humans, some of the more constant emissary veins can be found in the parietal (superior sagittal sinus) occipital (torcular), temporal (transverse sinus), and mastoid (transverse sinus) regions (Atlas Coronal Sections 11a, 12a). One of these emissaries, as detailed later, constitutes an important cranial venous outflow channel in most mammals, but the functional significance of emissary veins in humans remains a matter of debate (Deklunder *et al.*, 1991; Cabanac, 1986).

Two venous systems are usually considered (Strong and Elwyn, 1953): (1) an external or superficial system that drains the cerebral cortex and subcortical white matter into the superior sagittal, cavernous, petrosal, and transverse sinuses (Fig. 37.12A, B), and (2) the internal or ventricular system that drains the dorsal diencephalon, basal ganglia, and choroid plexuses into the great cerebral vein of Galen, which joins with the inferior sagittal sinus to form the straight sinus (Fig. 37.12C, D). The vein of Galen originates from the fusion of the two internal cerebral veins (icv; Atlas Coronal Section 11a), and it also receives additional tributaries including the basal vein (vein of Rosenthal), which drains extensive basal cortical areas, and the posterior callosal veins, which drain medial portions of the cortex (Fig. 37.12D). The internal cerebral veins are formed by the confluence of the posterior terminal vein, which runs between the dorsal thalamus and caudate, the anterior terminal vein, which drains the head of the caudate, and the septal and choroidal veins.

The superior sagittal and straight sinuses drain into two transverse sinuses at the torcular Herophilii (confluence of the sinuses) and from there blood flows

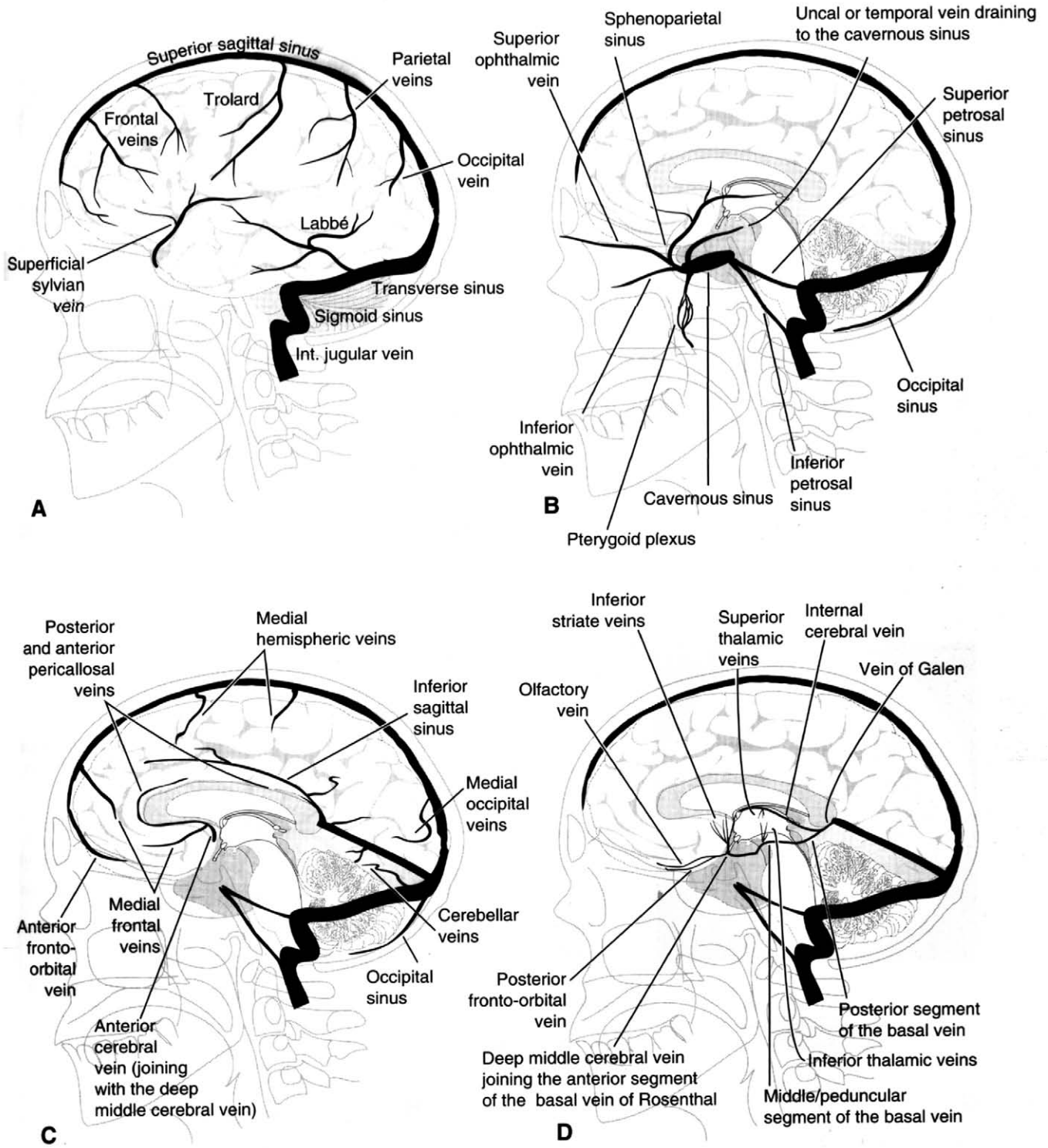

FIGURE 37.12 Anatomy of cerebral veins on a sagittal plane projection. **(A)** The superficial system is shown with the two main anastomotic channels, the veins of Labbé and Trolard and drainage toward the sagittal, transverse, and sigmoid sinuses into the internal jugular vein. **(B)** The anastomoses between the superior sagittal sinus, draining the superficial system, and the cavernous sinus through the superior and inferior petrosal sinuses are shown. The extracranial afferents to the cavernous sinus are also indicated. **(C)** Midline elements of the superficial venous system draining into the superior and inferior sagittal sinuses are shown. **(D)** Components of the deep cerebral venous system draining the diencephalon and striatum, as well as the basal vein carrying blood from the basal portion of the hemisphere into the vein of Galen are illustrated. From Morris, P. (1997). *Practical Neuroangiography*. Williams & Wilkins, Baltimore, by permission of the author and publisher.

down into the sigmoid sinus and into the internal jugular veins that exit the cranial cavity through the jugular foramen (Fig. 37.12). This is the main cerebral venous outflow in most primates including humans. In some primates (acrobatus pigmeus and rhesus), and most other mammals (with the notable exceptions of cats and pigs), the internal jugular veins share to a variable degree the venous outflow from the brain with the retroglenoid veins (also called temporal emissaries, dorsal cerebral, or superior cerebral veins; Padget, 1957), which are in essence extensions of the transverse sinuses that exit the cranial cavity through the postglenoid (also called spurious jugular) foraminae. Although blood from the internal jugular in humans and the retroglenoid vein in some well-studied experimental animals may be potentially contaminated by small amounts of blood from extracerebral territories, they constitute reliable sampling sources for the measurement of cerebral blood flow and cerebral uptake or release of gases and other molecules of interest (Kety and Schmidt, 1948; Nilsson and Siesjö, 1983; Scremin and Jenden, 1992).

The configuration of veins on the surface of the brain shows considerable variability. The general pattern observed includes 6 to 15 superior cerebral veins that collect blood from the medial and convex portions of the cortex and empty into the superior sagittal sinus (Atlas Coronal Sections 5–15). The inferior cerebral veins drain the lateral portion of the cortex and the base of the hemispheric surface into the middle cerebral vein, which runs into the Sylvian fissure to reach the cavernous (Atlas Coronal Sections 7a, 8a) or sphenoparietal sinuses. There is usually a large vein (vein of Trolard) that communicates the superior and inferior cerebral veins, establishing an anastomotic channel between the superior sagittal sinus and the middle cerebral vein and, hence, the cavernous sinus (Fig. 37.12A). Similarly, another anastomotic channel (vein of Labbé) communicates the middle cerebral vein with the transverse sinus (Fig. 37.12 A). The basal portion of the brain surface is drained by veins that empty into the transverse and superior petrosal sinuses (tentorial surface), cavernous and sphenoparietal sinuses (temporal surface), rostral portion of the superior and inferior sagittal sinuses (orbital portion), anterior cerebral vein (medial orbital cortex and hypothalamus), and the basal vein (Fig 12D), formed by the confluence of the anterior cerebral and inferior striate veins (medial portion of the temporal lobe and uncus).

The insula is drained by the deep cerebral vein, situated within the Sylvian fissure, and empties into the basal vein at the level of the anterior perforated substance (Fig. 37.12D). The ventral thalamus and hypothalamus are drained by vessels that end into the interpeduncular venous plexus and eventually into the cavernous sinus, sphenoparietal sinus, or basal vein.

The external and internal venous systems are widely interconnected through vessels running on the surface of the hemispheres, the most notable of which are the veins of Trolard and Labbé (Fig. 37.12A), providing communication between the dorsal, lateral, and basal dural sinuses, as well as through the depths of the brain through numerous collaterals joining the superior sagittal sinus and the internal cerebral vein (Fig. 37.12D) to the superficial and deep middle cerebral veins. This redundancy prevents interference with the cerebral circulation of lesions that occlude some of the important veins and sinuses of the brain, provided that the obstruction to blood flow develops gradually.

ANATOMY OF SPINAL CORD BLOOD VESSELS

Arteries

The spinal cord is supplied by three longitudinal anastomotic channels extending along its entire length: one anterior spinal artery (aspa), the largest and more important, found at the entrance of the ventral median fissure, and two posterior spinal arteries located just ventral to the entrance of the dorsal roots (Fig. 37.13). The anterior spinal artery connects rostrally with the two vertebral arteries at the level of the foramen magnum or occasionally at a lower point. The anterior and posterior spinal arteries are joined by transverse anastomoses that may take the form of a well-developed artery (transverse anastomotic circle) or an irregular anastomotic network.

The anterior and posterior spinal arteries are fed by anterior and posterior radicular arteries, respectively. There are 0–6 large (>0.2 mm in diameter) anterior radicular arteries in the cervical, 2–4 in the thoracic, and 1–2 in the lumbar region. Posterior radicular arteries are more numerous but of a smaller caliber. All roots not carrying a large radicular artery may have a small one (<0.2 mm in diameter) that supplies the root itself without reaching the anterior spinal artery (Turnbull, 1972). One anterior radicular artery, the artery of Adamkiewicz or anterior radicularis magna, is larger (1–1.3 mm) than the others (0.2–0.8 mm) and supplies the lumbar cord enlargement, entering most often on the left side with a root between T9 to T12 in 75% of the cases (Adamkiewicz, 1881, 1882; Lazorthes *et al.*, 1966). This vessel acquires importance in cases of obstruction of the aorta or aortic surgery requiring clamping of this artery. If an aortic occlusion or lesion

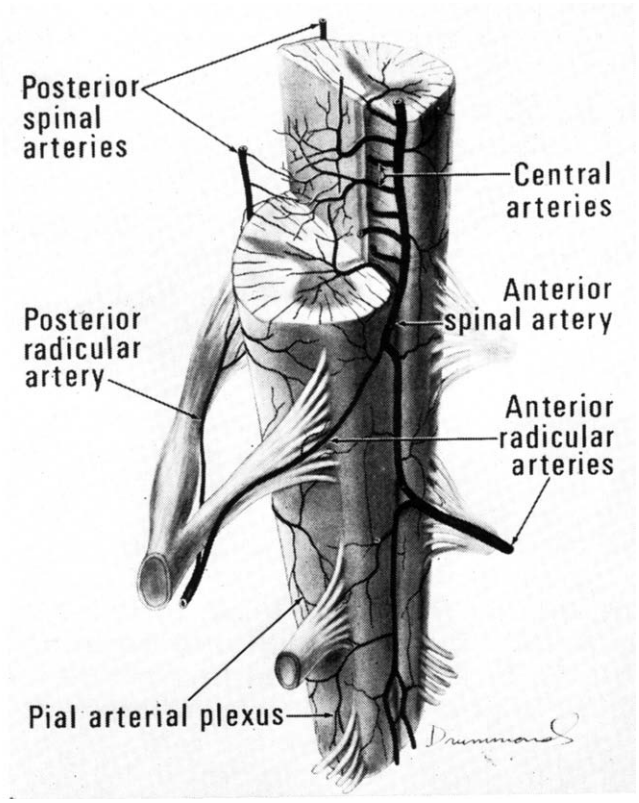

FIGURE 37.13 Arterial supply of the spinal cord. The single anterior spinal artery is shown receiving its supply from the anterior radicular arteries. Central arteries originate from the anterior spinal and distribute primarily to the ventral horns. An extensive pial plexus surrounds the cord and provides irrigation to the anterior and lateral columns. The dorsal horns and columns are supplied predominantly by the posterior spinal arteries. From Turnbull, I.M. (1971). Microvasculature of the Human Spinal Cord. *J Neurosurg* **35,** 141–147, by permission of the author and publisher.

is situated above the emergence of the anterior radicularis magna artery, blood supply of the lumbar cord may be severely compromised because collateral supply from caudal segments to the anterior spinal artery is often insufficient. The thoracic cord is particularly vulnerable to occlusion of a radicular artery leading to spinal cord ischemia because only a few, widely separated radicular arteries are found at this level.

The central (also named sulcal) arteries originate from the anterior spinal artery and run posteriorly to reach the anterior commissure after which they distribute unilaterally within the gray matter of the anterior (ventral) horns and the base of the posterior (dorsal) horns (Fig. 37.13). These vessels are part of the "centrifugal" arterial supply system. The "centripetal" system originates from the surface vessels that supply perforators that tend to converge toward the cord center.

Veins

The distribution and course of spinal veins resembles that of arteries, although they do not necessarily run in close proximity to each other. Radicular veins are more numerous and regular in distribution than their arterial counterparts described previously (Turnbull, 1972). They drain, depending on which level of the cord they are situated, into the vertebral, intercostal, lumbar, or sacral veins.

VASCULAR INNERVATION

Peripheral Autonomic Nerves

The parasympathetic outflow to the head and neck consists of preganglionic fibers from the nuclei of cranial nerves third, seventh, and ninth and postganglionic fibers from the ciliary (third), sphenopalatine (seventh), submaxillary (7th), carotid (7th), and otic (9th) ganglia, as well as from several other microscopic ganglia and scattered cells (Chorobski and Penfield, 1932; Suzuki *et al.*, 1990a, 1990b; Mitchell, 1953). All of these sources contribute nerve fibers to cerebral blood vessels or to the internal carotid plexus, a meshwork of nerve fibers that surrounds the internal carotid arteries.

The sympathetic supply to cerebral vessels originates in preganglionic fibers from neurons in the intermediolateral column of the eighth cervical and upper thoracic nerves and postganglionic fibers from the superior sympathetic ganglion emerging with its largest efferent branch, the carotid nerve which contributes to the carotid plexus (McNaughton, 1938; Falck *et al.*, 1968). Nerve fibers from the stellate ganglion can be traced to the vertebral and basilar arteries (Arbab *et al.*, 1988).

Histochemical studies have revealed that nerve fibers in cerebral blood vessels display immunoreactivity for ACh, and VIP, believed to originate from parasympathetic nerves (Hara *et al.*, 1989; Suzuki *et al.*, 1990b). Norepinephrine (NE), neuropeptide Y, (Edvinsson *et al.*, 1984) and in part 5-HT (Bonvento and Lacombe, 1993) containing fibers in cerebral blood vessels originate in sympathetic nerves.

Nerve fibers from the trigeminal nerve ophthalmic division have been known for a long time to contribute to the carotid plexus (Schumacher *et al.*, 1940; Ray and Wolff, 1940). Substance P and CGRP are found in these fibers (Norregaard and Moskowitz, 1985; Uddman *et al.*, 1985), as well as in those originating in the spinal cord (C2; Arbab *et al.*, 1986; Edvinsson *et al.*, 1989) and small ganglia within the carotid plexus (Suzuki *et al.*, 1989).

In vitro and *in vivo* studies indicate that acetylcholine (ACh), VIP, CGRP, and substance P induce vasodilatation and increase cerebral blood flow (CBF). NE and neuropeptide Y induce vasoconstriction while 5-HT induces vasoconstriction of large blood vessels and both vasodilatation or vasoconstriction in arterioles (Scremin, 1991, 1993; Tuor, 1993; Fahrenkrug, 1993a; Suzuki, 1993; Itakura and Okuno, 1993; Edvinsson *et al.*, 1993). This does not imply that those effects could physiologically be elicited by release from the peripheral innervation described earlier. In the case of the brain, at variance with most other tissues, neurotransmitter substances can originate in the parenchyma and reach blood vessels by diffusion to exert their effects. Furthermore, as reviewed below, many of the transmitters listed above are also found in nerve terminals from intracerebral pathways innervating blood vessels.

Central Pathways

It is believed that the adrenergic fibers making contact with intracerebral (as opposed to pial) microvessels originate in the locus coeruleous (Raichle *et al.*, 1975; Edvinsson *et al.*, 1973; Hartman *et al.*, 1972). Part of the 5-HT immunoreactive fibers found in cerebral blood vessels may originate from neurons in the raphe nucleus (Scheibel *et al.*, 1975; Edvinsson *et al.*, 1983; Bonvento *et al.*, 1990). Although there is morphological evidence for the existence of a central cholinergic innervation of cerebral vessels, its origin is still not clear. A number of stimulation and lesion experiments implicate the nucleus basalis as a source of at least some of the cholinergic innervation of cortical blood vessels. However, other forebrain, brainstem, and cortical sources cannot be discarded (Scremin *et al.*, 1980, 1983; Iadecola *et al.*, 1983; Biesold *et al.*, 1989; Scremin *et al.*, 1991; Dauphin *et al.*, 1991; Waite *et al.*, 1999).

MAPPING CEREBRAL FUNCTION WITH BLOOD FLOW

The existence of a correlation between functional activity of nervous tissue and blood flow had been already established at the beginning of last century by experiments showing an increase in temperature (a blood flow–dependent phenomenon) in the lateral geniculate body (Gerard, 1938) and occipital cortex (Schmidt and Hendrix, 1938) of experimental animals upon illumination of the eyes. An early description of enhancement of blood flow in the visual pathways by photic stimulation was provided by Kety and collaborators using tissue autoradiographic detection of a radioactive blood flow tracer gas (Kety *et al.*, 1955). This methodology was the basis for the development of noninvasive techniques (positron and single photon emission tomography, PET) currently used to image functionally induced changes in cerebral blood flow. In particular, $H_2{}^{15}O$ PET provides quantitative information on CBF (Phelps *et al.*, 1982) with a spatial resolution (full width at half maximum) of 3–4 mm. The short half life of ^{15}O (123 seconds) permits repetition of measurements at intervals of 10 minutes, thus allowing comparisons between different functional states in the same session.

One peculiar characteristic of functional hyperemia in the brain is that the increase in blood flow is in excess of the tissue metabolic requirements, resulting in an "overshoot" of tissue oxygen partial pressure, which translates in enhanced oxygen saturation of cerebral venous blood. The most widely used technique of functional magnetic resonance imaging (fMRI), blood oxygen level dependent (BOLD), detects this phenomenon by exploiting the difference in magnetic susceptibility between deoxygenated and oxygenated hemoglobin (Villringer and Dirnagl, 1995) and thus indicates the localization of the activated areas.

The techniques described here have advanced considerably the description of functional localization in the brain and can produce maps of neuronal activity derived from blood flow–related information. Because of their superior temporal resolution (20–120 seconds for $H_2{}^{15}O$ PET and approximately 2 seconds for BOLD fMRI; Villringer and Dirnagl, 1995), these techniques have largely replaced the estimation of brain glucose utilization by ^{18}F-2-deoxyglucose PET (temporal resolution 30–45 minutes), for functional brain mapping.

The Basic Mechanisms That Couple CBF and Function

The mechanisms that mediate the increase in blood flow associated with neuronal activity are still incompletely understood. It is generally assumed that blood flow is "coupled" to metabolism in the brain (i.e., blood flow changes presumably follow, and are a consequence of, the increase in metabolic activity). The ability of CO_2 to enhance CBF fueled the hypothesis that the metabolic production of this gas would provide an automatic mechanism of adjusting blood flow to metabolism. Many experimental facts challenge this interpretation. It has been shown, for instance, that during the initial phase of convulsive seizures CBF increases several fold, and simultaneous records of tissue pH not only fail to show an error signal

(acidification) but indicate tissue alkalosis instead, due to washout of CO_2 by enhanced circulatory convection (Astrup *et al.*, 1976).

Neuronal activity per se may not be enough to induce functional hyperemia. When spinal motoneurons are activated antidromically at rates of up to 100 Hz, no increase in local blood flow is observed in the ventral horn of the spinal cord, while a large increase in blood flow is found when the same population of cells are stimulated orthodromically (i.e., with intervention of a synapse) at a much lower rate (1 Hz) (Scremin and Decima, 1983). Thus, rather than a feedback mechanism based on a neuronal metabolic error signal, CBF may be controlled by a feedforward mechanism involving synaptically released neurotransmitters acting directly or indirectly on vascular smooth muscle. Such an "anticipatory," primarily vascular mechanism could explain why the increase in CBF observed in functional activation studies is often out of proportion (in excess) of the metabolic requirements, as described in the previous section. Such a mechanism would subserve many functions besides providing adequate supply of oxygen and glucose:

1. *Local temperature regulation.* Heat locally generated by enhanced metabolism in active brain areas needs to be cleared by circulatory convection requiring enhancement of blood flow to avoid a local elevation in temperature. This could maintain the local temperature of the functionally activated region invariant or even decrease it if the temperature of the incoming blood is lower than tissue temperature. Because cooling within a narrow range is associated with enhanced excitation, inhibition, and posttetanic potentiation (Koizumi *et al.*, 1954), an increase in blood flow could result in enhanced synaptic efficacy. Of course, too much brain cooling could be detrimental to neuronal function, and, in that case, an increase in local blood flow (assuming that the body core remains at a higher temperature than the brain) would warm up the area and enhance its function. In some exothermic animals, a mass of thermogenic tissue (brown fat) is juxtaposed to the arteries supplying the brain to warm up the incoming blood (Withers, 1992). The cerebrovascular system then becomes the brain's central heating device. In cold exposed humans, the rate of cooling of the head may be greater than that of the body core, and dangerously low brain temperatures of the centers recruited into function may be avoided, within limits, by functional hyperemia. A similar situation (lower brain than core temperature) may exist in anesthetized animals with open skulls, and this may turn a temperature-sensitive device into a blood flow probe, as in the experiments by Gerard cited.

2. *Termination of transmitter action.* Perfused blood vessels provide a "sink" for the effective dissipation by diffusion of neurotransmitter gradients, thus accelerating the termination of neurotransmitter action.

3. *Control of local PCO_2 and pH.* Given a stable metabolic CO_2 production and arterial PCO_2, local PCO_2 will be controlled by the level of blood flow. Enhanced perfusion in excess of that required to clear any excess production of CO_2 will decrease the local partial pressure of this gas, a phenomenon associated with an increase in synaptic efficacy (Esplin *et al.*, 1973). Thus, an increase in blood flow targeted to a brain region, by adjusting local conditions of the neuronal microenvironment that modulate synaptic transmission, may have an impact on its function beyond the supply of metabolic substrates.

4. *Vascular hydraulic skeleton.* When the brain is taken out of the skull, it collapses and deforms considerably because it lacks structural elements that could conserve its shape. Flotation in the cerebrospinal fluid and enclosure within an almost incompressible cavity contributes to minimizing gravitational effects on its shape *in situ.* However, variations in blood contents and pressure within the vasculature are known to alter the volume of the brain. For example, observation of the microvasculature of the cortex (see Figs. 37.9 and 37.11) indicates a well-oriented architecture with arterial vessels forming rings on the pial surface and a central vein with radiating branches. Expansion of this vascular structure by pressurization and enhanced blood contents in veins (attending effects of vasodilatation) could drag the neural elements attached to the blood vessels and induce changes in the subjacent neural architecture, such as variations in the size of the extracellular space. The functional effects of such mechanical phenomena secondary to a global or regional vasodilatation remain to be explored.

The concepts outlined here give support to the use of blood flow rather than glucose utilization for functional localization, as it may probe a wider spectrum of functions.

Mediators of CBF Control

The role of the synapse in the control of CBF introduced in the previous section suggests that understanding the mechanisms of neurovascular coupling requires knowledge of the effects of neurotransmitter/neuromodulators on CBF. One of the most outstanding examples is provided by acetylcholine. After pharmacologic inhibition of the enzymatic breakdown of ACh, the slope that defines the relationship of CBF to cerebral glucose utilization (CGU) is considerably increased

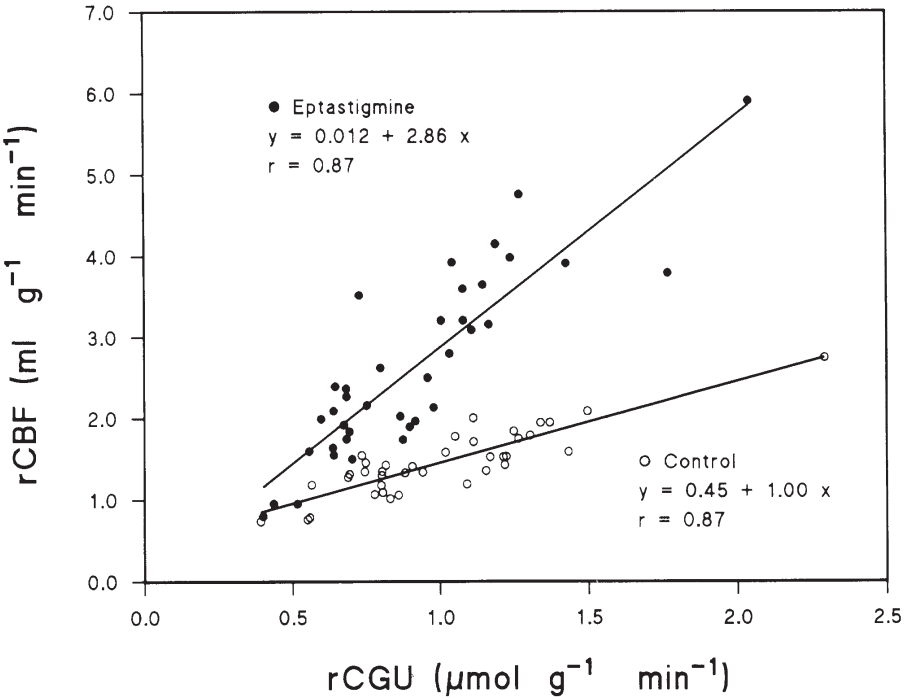

FIGURE 37.14 Scatter plots of paired values of regional cerebral blood flow (rCBF) on regional cerebral glucose utilization (rCGU) for a large number of brain regions in the rat. There is a tight coupling between metabolism and blood flow represented quantitatively by the regression of rCBF on rCGU. This relationship is not fixed however. The large increase in the slope of this relationship by enhancement of cholinergic transmission with the acetylcholinesterase inhibitor epatstigmine suggests a role of acetylcholine in neurovascular coupling. From Scremin, O.U., A.M. E. Scremin, D. Heuser, R. Hudgell, E. Romero, and B. Imbimbo (1993). Prolonged effects of cholinesterase inhibition with eptastigmine on the cerebral blood flow-metabolism ratio of normal rats. *J. Cereb. Blood Flow Metab.* **130,** 702–711, by permission of the authors and publisher

(Fig. 37.14) (Scremin *et al.*, 1993). Under such experimental conditions CBF of most regions increases without a change in glucose utilization. As a consequence, the oxygenation of hemoglobin in cerebral venous blood is enhanced (Scremin *et al.*, 1982), just as observed in the functional activation described previously. The opposite effect is observed with the cholinergic muscarinic blocker scopolamine that induces a decrease in the slope of the regression of CBF on CGU (Scremin and Jenden, 1996). These experiments suggest that ACh may be one of the neurotransmitters that mediate the anticipatory adjustments of CBF associated with synaptic activity inducing the local changes in the neuronal microenvironment discussed in the previous section.

A physiological role of ACh in CBF regulation has been suggested by the fact that the increase in CBF observed during spontaneous cortical arousal or somatosensory stimulation is markedly reduced by cholinergic blockade with atropine or scopolamine, and enhanced by inhibition of acetylcholinesterase with physostigmine (Scremin *et al.*, 1973; Pearce *et al.*, 1981; Tsukada *et al.*, 1997). Moreover, the increase in CBF induced by hypercapnia is enhanced by physostigmine and reduced by atropine or scopolamine (Rovere *et al.*, 1973; Kawamura *et al.*, 1975; Scremin *et al.*, 1978). Both cortical arousal and hypercapnia are known to enhance ACh release at the cerebral cortex (Metz, 1966; Hudson *et al.*, 1985), giving support to a cholinergic mechanism in the mediation of the cerebrovascular effects of both conditions.

ACh is probably one of many neurotransmitters/neuromodulators involved in the control of CBF, a system that might include considerable redundancy. A role has been proposed for NO, which may originate from endothelial cells, macrophages, neurons, or glia (Groves and Wang, 2000). Inhibitors of nitric oxide synthase (NOS), the enzyme that catalyzes the production of NO from arginine, have been reported to induce from 23% (Heinert *et al.*, 1998) to 70% (Harada *et al.*, 1997) inhibition of the hypercapnic hyperemia. The variation in this effect depends on the isoform of NOS predominantly inhibited, the magnitude of the hypercapnic stimulus, and the route of administration

of the inhibitor. Inhibition of the neuronal isoform of the enzyme (nNOS) by systemic rather than by local administration more readily blocks the hypercapnic hyperemia (Fabricius *et al.*, Wang *et al.*, 1995). However, in genetically altered mice lacking nNOS, the hypercapnic hyperemia is not affected (Irikura *et al.*, 1995). Moreover, while NOS inhibition has been shown to reduce the focal increase in CBF induced by somatosensory stimulation (Lindauer *et al.*, 1996), this response remains unaltered in mice lacking eNOS (Ayata *et al.*, 1996) or nNOS (Ma *et al.*, 1996). In these genetically altered animals, the ability of NOS inhibitors to modulate the CBF response to sensory stimulation or hypercapnia is lost. These facts point to the complexity of the role of NO in the control of CBF and to the ability of redundant systems to take over the role of NO when this agent is not present due to loss of synthesis from NOS.

In addition to ACh and NO, other neurotransmitters of widespread distribution within the central nervous system have the capacity to influence the cerebral circulation, and they could also be mediators of neurovascular coupling. Serotonin and phenylethylamine are known to constrict or dilate cerebral blood vessels, depending on the receptors involved and the physiological conditions (Cohen *et al.*, 1996; Scremin *et al.*, 1999; McCulloch and Harper, 1977), while CGRP, VIP, and substance P have been shown to induce vasodilatation (Rosenblum *et al.*, 1993; Juul *et al.*, 1994; Fahrenkrug, 1993b).

GLOBAL RESPONSES OF THE CEREBRAL CIRCULATION

Changes in Arterial Blood Pressure

One of the first observations of Kety and collaborators with the N_2O method of CBF measurement was that the CBF values of hypertensive patients were essentially similar to those of normal controls, in spite of a large difference in perfusion pressure (Kety *et al.*, 1948). This emphazises one of the fundamental characteristics of the cerebral circulation: stability in the face of variations in perfusion pressure. The phenomenon had already been studied by Fog (1937, 1939), who recorded the changes in diameter of pial vessels to oppose variations in arterial blood pressure. The dynamic characteristics of this phenomenon are important. A sudden, sustained rise in arterial blood pressure is followed by an increase in CBF, which over several minutes returns to the level prior to the hypertensive pulse. A similar time course is observed for the CBF and cerebrovascular resistance adjustments when arterial blood pressure is returned to normal (Yoshida *et al.*, 1966). The changes in cerebral vascular resistance that oppose the variations in perfusion pressure develop gradually and do not protect cerebral blood vessels from sudden increases or decreases in arterial pressure. The characteristic plots showing independence of CBF over a range of arterial blood pressure values (approximately between 50 and 150 mm Hg) are constructed by waiting until a new steady state of blood flow is established.

Blood Gases

Asphyxia, the combined occurrence of hypercapnia and hypoxia, was known to dilate cerebral blood vessels since the direct observations on pial blood vessels through skull windows by the dutch physician Franciscus Cornelius Donders published in 1850 (Purves, 1972). Although this phenomenon remained controversial for many years, the introduction of the nitrous oxide technique for the measurement of cerebral blood flow by Kety and Schmidt, and later direct measurements of global CBF from the internal carotid artery of humans with electromagnetic and ultrasound Doppler flow probes established quantitatively the cerebrovascular effects of changes in arterial PCO_2 and PO_2. Although hypercapnia and hypoxia interact in interesting ways, a rational description of their effects on the cerebral circulation is better approached separately.

Carbon Dioxide

The increase in CBF induced by hypercapnia is very rapid, with a time constant of about 20 s (Severinghaus and Lassen, 1967). The hypercapnic cerebral vasodilatation has been extensively studied in animals and humans, in spite of which its understanding remains incomplete. The simple idea of the effect being mediated by a decrease in tissue pH is contradicted by experiments showing blockade of the cerebrovascular action of CO_2 by lesions of the brainstem (Shalit *et al.*, 1967) or decerebration (Seylaz, 1968; Scremin *et al.*, 1978), as well as pharmacological interventions with cholinergic blockers (Rovere *et al.*, 1973; Scremin *et al.*, 1977; Kawamura *et al.*, 1975), and inhibitors of prostaglandin (Pickard and McKenzie, 1973) and NO synthesis (Iadecola, 1992). Blockade of 5-HT receptors or depletion of this transmitter enhance the cerebrovascular effect of CO_2 (Bonvento *et al.*, 1997; Kelly *et al.*, 1995). The magnitude of the CO_2 effect on cerebral blood flow is also dependent on the level and type of anesthesia (Scremin *et al.*, 1978). These facts point to the complex nature of the effect of hypercapnia on cerebral vessels.

Oxygen

The cerebrovascular effect of hypoxia exhibits a threshold around 50 mm Hg PaO_2, close to the point at which hypoxia induces loss of critical judgment (Siesjö, 1984). Below this level, CBF increases as arterial PO_2 decreases (Kogure *et al.*, 1970; Johannsson and Siesjo, 1975; Quint *et al.*, 1980). There is no effect of higher than normal arterial PO_2 except for extremely high levels with a decrease in CBF of 35% at 3.5 atmospheres (Lambertsen *et al.*, 1953).

References

Adamkiewicz, A. (1881). Die Blutgefässe des menschlichen Rückenmarkes. I. Die Gefässe der Rückenmarkssubstanz. *Akad. Wiss. (Heidelberg)* **84,** 469–502.

Adamkiewicz, A. (1882). Die Blutgefässe des menschlichen Rückenmarkes. II. Die Gefässe der Ruckenmarksoberfläche. *Akad. Wiss. (Heidelberg)* **85,** 101–130.

Arbab, M.A., Wiklund, L., Delgado, T., and Svendgaard, N.A. (1988). Stellate ganglion innervation of the vertebro-basilar arterial system demonstrated in the rat with anterograde and retrograde WGA-HRP tracing. *Brain Res.* **445,** 175–180.

Arbab, M.A., Wiklund, L., and Svendgaard, N.A. (1986). Origin and distribution of cerebral vascular innervation from superior cervical, trigeminal and spinal ganglia investigated with retrograde and anterograde WGA-HRP tracing in the rat. *Neurosci.* **19,** 695–708.

Astrup, J., Heuser, D., Lassen, N., Nilsson, B., Norberg, K., and Siesjö, B.K. (1976). Evidence against H+ and K+ as the main factors in the regulation of cerebral blood flow, epileptic discharges, acute hypoxemia, amphetamine intoxication, and hypoglycemia. A microelectrode study. *In* "Ionic Actions on Vascular Smooth Muscle" (E. Betz, ed.). Springer-Verlag, Berlin.

Ayata, C., Ma, J., Meng, W., Huang, P., and Moskowitz, M.A. (1996). L-NA-sensitive rCBF augmentation during vibrissal stimulation in type III nitric oxide synthase mutant mice. *J. Cereb. Blood Flow Metab.* **16,** 539–541.

Baker, M.A. (1982). Brain cooling in endotherms in heat and exercise. *Ann. Rev. Physiol.* **44,** 85–96.

Bar, T. (1980). The vascular system of the cerebral cortex. *Adv. Anat. Embryol. Cell Biol.* **59,** 1–62.

Biesold, D., Inanami, O., Sato, A., and Sato, Y. (1989). Stimulation of the nucleus basalis of Meynert increases cerebral cortical blood flow in rats. *Neurosci. Lett.* **98,** 39–44.

Bonvento, G., and Lacombe, P. (1993). Serotonin and the cerebral circulation. *In* "The Regulation of Cerebral Blood Flow" (John W. Phillis, ed.). CRC Press, Boca Raton, FL.

Bonvento, G., Borredon, J., Seylaz, J., and Lacombe, P. (1997). Cerebrovascular consequences of altering serotonergic transmission in conscious rat. *Brain Res.* **767,** 208–213.

Bonvento, G., Lacombe, P., MacKenzie, E.T., Rouquier, L., Scatton, B., and Seylaz, J. (1990). Differential effects of electrical stimulation of the dorsal raphe nucleus and of cervical sympathectomy on serotonin and noradrenaline concentrations in major cerebral arteries and pial vessels in the rat. *J. Cereb. Blood Flow Metab.* **10,** 123–126.

Cabanac, M. (1986). Keeping a cool head. *NIPS* **1,** 41–44.

Casserio, G. (1632). "Tabulae Anatomicae xxiix." Daniel Buiretius, Frankfurt.

Chorobski, J., and Penfield, W. (1932). Cerebral vasodilator nerves and their pathway from the medulla oblongata. *Arch. Neurol. Psychiatry* **28,** 1257–1289.

Clarke, E., and O'Malley, C.D. (1968). "The Human Brain and Spinal Cord—A Historical Essay Illustrated by Writings from Antiquity to the Twentieth Century." University of California Press, Berkeley, Los Angeles.

Cohen, Z., Bonvento, G., Lacombe, P., and Hamel, E. (1996). Serotonin in the regulation of brain microcirculation. *Progr. in Neurobiol.* **50,** 335–362.

Conheim, J. (1872). "Untersuchungen über die embolischen Prozesse." Hirschwald, Berlin.

Cooper, I.S. (1954). Surgical occlusion of the anterior choroidal artery in Parkinsonism. *Surg. Gynecol. Obstet.* **99,** 207–219.

Coyle, P. (1984). Diameter and length changes in cerebral collaterals after middle cerebral artery occlusion. *Anat. Rec.* **210,** 357–364.

Coyle, P., and Panzenbeck, M.J. (1990). Collateral development after carotid artery occlusion in Fischer 344 rats. *Stroke* **21,** 316–321.

Daniel, P.M., Dawes, J.D.K., and Prichard, M.M.L. (1953). Studies of the carotid rete and its associated arteries. *Philos. Trans. B* **237,** 173–215.

Dauphin, F., Lacombe, P., Sercombe, R., Hamel, E., and Seylaz, J. (1991). Hypercapnia and stimulation of the substantia innominata increase rat frontal cortical blood flow by different cholinergic mechanisms. *Brain Res.* **553,** 75–83.

Davson, H., Welch, K., and Segal, M.B. (1987). "Physiology and Pathophysiology of the Cerebrospinal Fluid." Churchill Livingstone, Edinburgh.

Deklunder, G., Dauzat, M., Lecroart, J.L., Hauser, J.J., and Houdas Y. (1991). Influence of ventilation of the face on thermoregulation in man during hyper- and hypothermia. *Eur. J. Appl. Phys.* **62,** 342–348.

Duret, H. (1874). Recherches anatomiques sur la circulation de l'encephale. *Arch. Phys. Norm. Path.* **2,** 60–91.

Duvernoy, H.M., Delon, S., and Vannson, J.L. (1981). Cortical blood vessels of the human brain. B*rain Res. Bull.* **7,** 519–579.

Edvinsson, L., Degueurce, A., Duverger, D., MacKenzie, E.T., and Scatton, B. (1983). Central serotonergic nerves project to the pial vessels of the brain. *Nature* **306,** 55–57.

Edvinsson, L., Emson, P., McCulloch, J., Tatemoto, K., and Uddman, R. (1984). Neuropeptide Y: Immunocytochemical localization to and effect upon feline pial arteries and veins in vitro and in situ. *Acta Physiol. Scand.* **122,** 155–163.

Edvinsson, L., Hara, H., and Uddman, R. (1989). Retrograde tracing of nerve fibers to the rat middle cerebral artery with true blue: Colocalization with different peptides. *J. Cereb. Blood Flow Metab.* **9,** 212–218.

Edvinsson, L., Lindvall, M., Nielsen, K.C., and Owman, C. (1973). Are brain vessels innervated also by central (non-sympathetic) adrenergic neurones? *Brain Res.* **63,** 496–499.

Edvinsson, L., MacKenzie, E.T., and McCulloch, J. (1993). "Cerebral Blood Flow and Metabolism." Raven Press, New York.

Eecken, H.M.V. (1959). "The Anastomoses between the Leptomeningeal Arteries of the Brain; Their Morphological, Pathological, and Clinical Significance." Charles C Thomas, Springfield, IL.

Ehrlich, P. (1885). "Das Sauerstoff-Bedürfniss des Organismus. Eine Farbenanalytische Studie." August Hirschwald, Berlin.

Esplin, D.W., Capek, R., and Esplin, B. (1973). An intracellular study of the actions of carbon dioxide on the spinal monosynaptic pathway. *Can. J. Physiol. Pharmacol.* **51,** 424–436.

Fabricius, M., Rubin, I., Bundgaard, M., and Lauritzen, M. (1996). NOS activity in brain and endothelium: Relation to hypercapnic rise of cerebral blood flow in rats. *Am. J. Physiol.* **271,** H2035–H2044.

Fahrenkrug, J. (1993a). Neural regulation of cerebral blood vessels: Vasoactive Intestinal Peptide (VIP). *In* "The Regulation of Cerebral Blood Flow" (John W. Phillis, ed.). CRC Press, Boca Raton, FL.

Fahrenkrug, J. (1993b). Transmitter role of vasoactive intestinal peptide. *Pharmacol. Toxicol.* **72,** 354–363.

Falck, B., Nielsen, K.C., and Owman, Ch. (1968). Adrenergic innervation of the pial circulation. *Scand. J. Clin. Lab. Invest. Suppl.* **102.**

Fearn, S.J., Picton, A.J., Mortimer, A.J., Parry, A.D., and McCollum, C.N. (2000). The contribution of the external carotid artery to cerebral perfusion in carotid disease. *J. Vascular Surg.* **31,** 989–993.

Fog, M. (1937). Cerebral circulation. The reaction of pial arteries to a fall in blood pressure. *Archs. Neurol. Psychiat. Chicago* **37,** 351–364.

Fog, M. (1939). Cerebral circulation: The reaction of pial arteries to increase in blood pressure. *Archs. Neurol. Psychiat. Chicago* **41,** 109–118.

Fung, Y.C. (1984). "Biodynamics." Springer-Verlag, New York.

Gerard, R.W. (1938). Brain metabolism and circulation. *Assoc. Res. Nerv. Ment. Dis. Proc.* **18,** 316–345.

Gibo, H., Carver, C.C., Rhoton, A.J., Lenkey, C., and Mitchell, R.J. (1981). Microsurgical anatomy of the middle cerebral artery. *J. Neurosurg.* **54,** 151–169.

Gross, P.M., N.M.Sposito, N.M., Pettersen, S.E., and Fenstermacher, J.D. (1986). Differences in function and structure of capillary endothelium in grey matter, white matter, and a cicumventricular organ of rat brain. *Blood Vessels* **23,** 261–270.

Groves, J.T., and Wan, C.C. (2000). Nitric oxide synthase: Models and mechanisms. *Curr. Opin. Chem. Biol.* **4,** 687–695.

Hara, H., Jansen, I., Ekman, R., Hamel, E., MacKenzie, E.T., Uddman, R., and Edvinsson, L. (1989). Acetylcholine and vasoactive intestinal peptide in cerebral blood vessels: Effect of extirpation of the spenopalatine ganglion. *J. Cereb. Blood Flow Metab.* **9,** 204–211.

Harada, M., Fuse, A., and Tanaka, Y. (1997). Measurement of nitric oxide in the rat cerebral cortex during hypercapnoea. *Neuroreport* **8,** 999–1002.

Hartman, B.K., Zide, D., and Udenfriend. S. (1972). The use of dopamine-hydroxylase as a marker for the central noradrenergic nervous system in rat brain. *Proc. Natl. Acad. Sci. USA* **69,** 2722–2726.

Hedera, P., Bujdakova, J., Traubner, P., and Pancak, J. (1998). Stroke risk factors and development of collateral flow in carotid occlusive disease. *Acta Neurol. Scand.* **98,** 182–186.

Heinert, G., Casadei, B., and Paterson, D.J. (1998). Hypercapnic cerebral blood flow in spontaneously hypertensive rats. *J. Hypertens.* **16,** 1491–1498.

Heubner, O. (1874). "Die luetische Erkrankung der Hirnarterien, nebst allgemeinen Erörterungen zur normalen und pathologischen Histologie der Arterien sowie zur Hirnzirkulation." Vogel, Leipzig .

Hillen, B., Gaasbeek, T., and Hoogstraten, H.W. (1982). A mathematical model of the flow in the posterior communicating arteries. *J. Biomech.* **15,** 441–448.

Hoksbergen, A.W., Fulesdi, B., Legemate, D.A., and Csiba, L. (2000a). Collateral configuration of the circle of Willis: Transcranial color-coded duplex ultrasonography and comparison with postmortem anatomy. *Stroke* **31,** 1346–1351.

Hoksbergen, A.W., Legemate, D.A., Ubbink, D.T., and Jacobs, M.J. (2000b). Collateral variations in circle of Willis in atherosclerotic population assessed by means of transcranial color-coded duplex ultrasonography. *Stroke* **31,** 1656–1660.

Hoksbergen, A.W., Legemate, D.A., Ubbink, D.T., de Vos, H.J., and Jacobs, N.J. (1999). Influence of the collateral function of the circle of Willis on hemispherical perfusion during carotid occlusion as assessed by transcranial colour-coded duplex ultrasonography. *Eur. J. Vasc. Endovasc. Surg.* **17,** 486–492.

Hudson, D.M., Jenden, D.J., Scremin, O.U., and Sonnenschein, R.R. (1985). Cortical acetylcholine efflux with hypercapnia and nociceptive stimulation. *Brain Res.* **338,** 267–272.

Iadecola, C. (1992). Does nitric oxide mediate the increases in cerebral blood flow elicited by hypercapnia? *Proc. Natl. Acad. Sci. USA* **89,** 3913–3916.

Iadecola, C., Mraovitch, S., Meeley, M.P., and Reis, D.J. (1983). Lesions of the basal forebrain in rat selectively impair the cortical vasodilation elicited from cerebellar fastigial nucleus. *Brain Res.* **279,** 41–52.

Irikura, K., Huang, P.L., Ma, J., Lee, W.S., Dalkara, T., Fishman, M.C., Dawson, T.M., Snyder, S.H., and Moskowitz, M.A. (1995). Cerebrovascular alterations in mice lacking neuronal nitric oxide synthase gene expression. *Proc. Natl. Acad. Sci. USA* **92,** 6823–6827.

Itakura, T., and Okuno, T. (1993). Tachykinins and cerebral blood flow. *In* "The Regulation of Cerebral Blood Flow" (John W. Phillis, ed.). CRC Press, Boca Raton, FL.

Johannsson, H., and Siesjo, B.K. (1975). Cerebral blood flow and oxygen consumption in the rat in hypoxic hypoxia. *Acta Physiol. Scand.* **93,** 269–276.

Juul, R., Aakhus, S., Bjornstad, K., Gisvold, S.E., Brubakk, A.O., and Edvinsso, L. (1994). Calcitonin gene-related peptide (human alpha-CGRP) counteracts vasoconstriction in human subarachnoid haemorrhage. *Neurosci. Lett.* **170,** 67–70.

Kaplan, H.A., and Ford, D.H. (1966). "The Brain Vascular System." Elsevier, Amsterdam.

Kawamura, Y., Meyer, J.S., Hiromoto, H., Aoyagi, M., Tagashira, Y., and Ott, E.O. (1975). Neurogenic control of cerebral blood flow in the baboon: Effects of the cholinergic inhibitory agent, atropine, on cerebral autoregulation and vasomotor reactivity to changes in $PaCO_2$. *J. Neurosurg.* **43,** 676–688.

Kelly, P.A., Ritchie, I.M., McBean, D.E., Sharkey, J., and Olverman, H.J. (1995). Enhanced cerebrovascular responsiveness to hypercapnia following depletion of central serotonergic terminals. *J. Cereb. Blood Flow Metab.* **15,** 706–713.

Kety, S.S., and Schmidt, C.F. (1948). The nitrous oxide method for the quantitative determination of cerebral blood flow in man: Theory, procedure and normal values. *J. Clin. Invest.* **27,** 476–483.

Kety, S.S., Hafkenschiel, W.A., Jeffers, W.A., Leopold, I.H., and Shenkin, H.A. (1948). The blood flow, vascular resistance, and oxygen consumption of the brain in essential hypertension. *J. Clin. Invest.* **27,** 511–514.

Kety, S.S., Landau, W.M., Jr.Freygang, W.H., Rowland, L.P., and Sokoloff. L. (1955). Estimation of regional circulation in the brain by the uptake of an inert gas. *Fed. Proc.* **14,** 85.

Kogure, K., Scheinberg, P., Reinmuth, O.M., Fujishima, M., and Busto, R. (1970). Mechanisms of cerebral vasodilatation in hypoxia. *J. Appl. Physiol.* **29,** 223–229.

Koizumi, K., Malcolm, J.L., and Brooks, C. (1954). Effect of temperature on facilitation and inhibition of reflex activity. *Am. J. Physiol.* **179,** 507–512.

Lambertsen,C.J., Kough, R.H., Cooper, D.Y., Emmel, H.H., Loeschcke, H.H., and Schmidt, C.F. (1953). Oxygen toxicity: Effects in man of oxygen inhalation at 1 and 3.5 atmospheres upon blood gas transport, cerebral circulation and cerebral metabolism. *J. Appl. Physiol.* **5,** 471–486.

Lazorthes, G., Gouazé, A., Gastide, G., Soutoul, J.H., Zadeh, O., and Santini, J.J. (1966). La vascularisation arteriélle de renflement lombaire; étude des variations et des suppléances. *Rev. Neurol. (Paris)* **114,** 109–122.

Lindauer, U., Megow, D., Schultze, J., Weber, J.R., and Dirnagl, U. (1996). Nitric oxide synthase inhibition does not affect somatosensory evoked potentials in the rat. *Neurosci. Lett.* **216,** 207–210.

Ma, J., Ayata, C., Huang, P.L., Fishman, M.C., and Moskowitz, M.A. (1996). Regional cerebral blood flow response to vibrissal stimulation in mice lacking type I NOS gene expression. *Am. J. Physiol.* **270,** H1085–H1090.

Mai, J.K., Assheuer J., and Paxinos, G. (1997). "Atlas of the Human Brain." Academic Press, San Diego.

McCulloch, J., and Harper, A.M. (1977). Phenylethylamine and cerebral blood flow. Possible involvement of phenylethylamine in migraine. *Neurology* **27,** 817–821.

McDonald, D.A., and Potter, J.M. (1951). The distribution of blood to the brain. *J. Physiol. Lond.* **114,** 356–371.

Mchedlishvili, G., and Kuridze, N. (1984). The modular organization of the pial arterial system in phylogeny. *J. Cereb. Blood Flow Metab.* **4,** 391–396.

McNaughton, F. (1938). The innervation of intracranial blood vessels and dural sinuses. *Res. Pubs. Ass. Res. Nerv. Ment. Dis.* **18,** 178–200.

Metz, B. (1966). Hypercapnia and acetylcholine release from the cerebral cortex and medulla. *J. Physiol.* **186,** 321–332.

Mitchell, G.A.G. (1953). "Anatomy of the Autonomic Nervous System." E & S Livingstone Ltd., Edinburgh.

Morris, P. (1997). "Practical Neuroangiography." Williams & Wilkins, Baltimore.

Nilsson, B., and Siesjö, B.K. (1983). A venous outflow method for measurement of rapid changes of the cerebral blood flow and oxygen consumption in the rat. *Stroke* **14,** 797–802.

Norregaard, T.V., and Moskowitz, M.A. (1985). Substance P and the sensory innervation of intracranial and extracranial feline cephalic arteries. Implications for vascular pain mechanisms in man. *Brain* **108** (Pt 2), 517–533.

Ono, M., Ono, M., Rhoton, A.J., and Barry, M. (1984). Microsurgical anatomy of the region of the tentorial incisura. *J. Neurosurg.* **60,** 365–399.

Osborn, A.G., and Maack, J.G. (1980). "Introduction to Cerebral Angiography." Harper & Row, Hagerstown.

Padget, D.H. (1944). The circle of Willis—Its embryology and anatomy. *In* "Intracranial arterial aneurisms" (W.E. Dandy, ed.). Comstock, Ithaca, NY.

Padget, D.H. (1957). The Development of the Cranial Venous System in Man from the Viewpoint of Comparative Anatomy. *Contr. Embryol. Carneg. Inst.* 79–140.

Pardridge, W.M. (1988). Recent advances in blood-brain barrier transport. *Ann. Rev. Pharmacol. Toxicol.* **28,** 25–39.

Pearce, W.J., Scremin, O.U., Sonnenschein, R.R., and Rubinstein, E.H. (1981). The electroencephalogram, blood flow, and oxygen uptake in rabbit cerebrum. *J. Cereb. Blood Flow Metab.* **1,** 419–428.

Pfeiffer, R.A. (1928). "Die Angioarchitektonik der Grosshirnrinde." Springer, Berlin.

Phelps, M.E., Mazziotta, J.C., and Huang, S.C. (1982). Study of cerebral function with positron computed tomography. *J. Cereb. Blood Flow Metab.* **2,** 113–162.

Pickard, J.D., and McKenzie, E.T. (1973). Inhibition of prostaglandin synthesis and the response of baboon cerebral circulation to carbon dioxide. *Nature (New Biol)* **245,** 187–188.

Purves, M.J. (1972). "The Physiology of the Cerebral Circulation." Cambridge University Press, Cambridge.

Quint, S.R., Scremin, O.U., Sonnenschein, R.R., and Rubinstein, E.H. (1980). Enhancement of the cerebrovascular effect of CO_2 by hypoxia. *Stroke* **11,** 286–289.

Raichle, M.E., Hartman, B.K., Eichling, J.O., and Sharpe, L.G. (1975). Central noradrenergic regulation of cerebral blood flow and vascular permeability. *Proc. Natl. Acad. Sci. USA* **72,** 3726–3730.

Ray, B.S., and Wolff, H.G. (1940). Experimental studies on headache. Pain sensitive structures in the head and their significance in headache. *Archs. Surg. Chicago* **41,** 813–856.

Riggs, H.E., and Rupp, C. (1963). Variation in form of the circle of Willis. *Arch. Neurol.* **8,** 24–30.

Rosenblum, W.I., Shimizu, T., and Nelson, G.H. (1993). Endothelium-dependent effects of substance P and calcitonin gene-related peptide on mouse pial arterioles. *Stroke* **24,** 1043–1047.

Rossen, R., Kabat, H., and Anderson, J.P. (1943). Acute arrest of cerebral circulation in man. *Arch. Neurol. Psychiatry* **50,** 510–528.

Rovere, A.A., Scremin, O.U., Beresi, M.R., Raynald, A.C., and Giardini, A. (1973). Cholinergic mechanism in the cerebrovascular action of carbon dioxide. *Stroke* **4,** 969–972.

Rutgers, D.R., Klijn, C.J., Kappelle, L.J., van Huffelen, A.C., and van der Grond, J. (2000). A longitudinal study of collateral flow patterns in the circle of Willis and the ophthalmic artery in patients with a symptomatic internal carotid artery occlusion. *Stroke* **31,** 1913–1920.

Sagawa, K., and Guyton, A.C. (1961). Pressure-flow relationships in isolated canine cerebral circulation. *Am. J. Physiol.* **200,** 711–714.

Scharrer, E. (1940). Arteries and veins in the mammalian brain. *Anat. Rec.* **78,** 173–196.

Scharrer, E. (1962). "Brain Function and the Evolution of Cerebral Vascularization." The American Museum of Natural History, New York.

Scheel, P., Ruge, C., Petruch, U.R., and Schoning, M. (2000). Color duplex measurement of cerebral blood flow volume in healthy adults. *Stroke* **31,** 147–150.

Scheibel, M.E., Tomiyasu, U., and Scheibel, A.B. (1975). Do raphe nuclei of the reticular formation have a neurosecretory or vascular sensor function? *Exp. Neurol.* **47,** 316–329.

Schmidt, C.F., and Hendrix, J.P. (1938). Action of chemical substances on cerebral blood vessels. *Assoc. Res. Nerv. Ment. Dis. Proc.* **18,** 229–276.

Schomer, D.F., Marks, M.P., Steinberg, G.K., Johnstone, I.M., Boothroyd, D.B., Ross, M.R., Pelc, N.J., and Enzmann, D.R. (1994). The anatomy of the posterior communicating artery as a risk factor for ischemic cerebral infarction. *N. Engl. J. Med.* **330,** 1565–1570.

Schumacher, G.A., Ray, B.S., and Wolff, H.G. (1940). Experimental studies on headache. Further analysis of histamine headache and its pain pathways. *Archs. Neurol. Psychiat. Chicago* **44,** 717.

Scremin, O.U. (1991). Pharmacological control of the cerebral circulation. *Annu. Rev. Pharmacol. Toxicol.* **31,** 229–251.

Scremin, O.U. (1993). Cholinergic control of Cerebral Blood Flow. *In* "The regulation of cerebral blood flow" (J. Phillis, ed.). CRC Press, Boca Raton, FL.

Scremin, O.U., and Decima, E.E. (1983). Control of blood flow in the cat spinal cord. *J. Neurosurg.* **58,** 742–748.

Scremin, O.U., and Jenden, D.J. (1992). Effects of hypoxia on choline exchange among organs. *J. Neurochem.* **59,** 906–914.

Scremin,O.U., and Jenden, D.J. (1996). Cholinergic control of cerebral blood flow in stroke, trauma and aging. *Life Sci.* **58,** 2011–2018.

Scremin, O.U., Holschneider, D.P., Chen, K., Li, M.G., and Shih, J.C. (1999). Cerebral cortical blood flow maps are reorganized in MAOB-deficient mice. *Brain Res.* **824,** 36–44.

Scremin, O.U., Rovere, A.A., Raynald, A.C., and Giardini, A. (1973). Cholinergic control of blood flow in the cerebral cortex of the rat. *Stroke* **4,** 232–239.

Scremin, O.U., Rubinstein, E.H., and Sonnenschein, R.R. (1977). Cholinergic modulation of the cerebrovascular response to CO_2 in the rabbit. *In* "Neurogenic Control of Brain Circulation" (C. Owman and L. Edvinsson, eds.). Pergamon Press, New York.

Scremin, O.U., Rubinstein, E.H., and Sonnenschein, R.R. (1978). Cerebrovascular CO_2 reactivity: Role of a cholinergic mechanism modulated by anesthesia. *Stroke* **9,** 160–165.

Scremin, O.U., Rubinstein, E.H., and Sonnenschein, R.R. (1980). Role of central pathways and cranial nerves in cerebral cholinergic vasodilatation. *In* "Advances in Physiological Sciences, Vol 9, Cardiovascular Physiology, Neural Control Mechanisms" (A.G.B. Kovach, P. Sandor, and M. Kollai, eds.. Pergamon Press, New York.

Scremin, O.U., Scremin, A.M.E., Heuser, D., Hudgell, R., Romero, E., and Imbimbo, B. (1993). Prolonged effects of cholinesterase inhibition with eptastigmine on the cerebral blood flow-metabolism ratio of normal rats. *J. Cereb. Blood Flow Metab.* **130,** 702–711.

Scremin, O.U., Sonnenschein, R.R., and Rubinstein, E.H. (1982). Cholinergic cerebral vasodilatation in the rabbit: Absence of concomitant metabolic activation. *J. Cereb. Blood Flow Metab.* **2,** 241–247.

Scremin, O.U., Sonnenschein, R.R., and Rubinstein, E.H. (1983). Cholinergic cerebral vasodilatation: Lack of involvement of cranial parasympathetic nerves. *J. Cereb. Blood Flow Metab.* **3,** 362–368.

Scremin, O.U., Torres, C.D., Scremin, A.M.E., O'Neal, M., Heuser, D., and Blisard, K.S. (1991). The role of the nucleus basalis in cholinergic control of cortical blood flow. *J. Neurosci. Res.* **28,** 382–390.

Severinghaus, J.W., and Lassen. N. (1967). Step hypocapnia to separate arterial from tissue PCO_2 in the regulation of cerebral blood flow. *Circ. Res.* **20,** 272–278.

Seylaz, J. (1968). Contribution a l'etude du mecanisme de la regulation du debit sanguine cerebrale. *Helv. Physiol. Acta* **26,** 33–61.

Shalit, M.N., Reinmuth, O.M., Shimoyo, S., and Scheimberg, P. (1967). Carbon dioxide and cerebral circulatory control. III. The effects of brain stem lesions. *Arch. Neurol.* **17,** 342–353.

Siesjö, B.K. (1984). Cerebral circulation and metabolism. *J. Neurosurg.* **60,** 883–908.

Smith, A.S., and Bellon, J.R. (1995). Parallel and spiral flow patterns of vertebral artery contributions to the basilar artery. *AJNR Am. J. Neuroradiol.* **16,** 1587–1591.

Sorteberg, W., Sorteberg, A., Lindegaard, K.F., Boysen, M., and Nornes, H. (1999). Transcranial Doppler ultrasonography-guided management of internal carotid artery closure. *Neurosurgery* **45,** 76–87.

Strong, O.S., and Elwyn, A. (1953). "Human Neuroanatomy." Williams and Wilkins, Baltimore.

Suzuki, Y. (1993). Calcitonin gene-related peptide (CGRP). *In* "The Regulation of Cerebral Blood Flow" (John W. Phillis, ed.). CRC Press, Boca Raton, FL.

Suzuki, N., Hardebo, J.E., Kahrstrom, J., and Owman, C. (1990b). Neuropetide Y co-exists with vasoactive intestinal polypetide and acetylcholine in parasympathetic cerebrovascular nerves originating in the sphenopalatine, otic , and internal carotid ganglia of the rat. *Neurosci.* **36,** 507–519.

Suzuki, N., Hardebo, J.E., and Owman, C. (1989). Trigeminal fibre collaterals storing substance P and calcitonin gene-related peptide associate with ganglion cells containing choline acetyltransferase and vasoactive intestinal polypeptide in the sphenopalatine ganglion of the rat: An axon reflex modulating parasympathetic ganglionic activity? *Neurosci.* **30** (3), 595–604.

Suzuki, N., Hardebo, J.E., and Owman, C. (1990a). Origin and pathways of choline acetyltransferase-positive parasympathetic nerve fibers to cerebral vessels in rats. *J. Cereb. Blood Flow Metab.* **10,** 399–408.

Tower, D.B. (1991). Cerebral circulation revisited: An historical essay. *Neurochem. Res.* **16,** 1085–1097.

Tsukada, H., Kakiuchi, T., Ando, I., and Ouchi, Y. (1997). Functional activation of cerebral blood flow abolished by scopolamine is reversed by cognitive enhancers associated with cholinesterase inhibition: A positron emission tomography study in unanesthetized monkeys. *J. Pharmacol. Exp. Ther.* **281,** 1408–1414.

Tuor, U.I. (1993). Neuropeptide Y and the cerebral circulation. *In* "The Regulation of Cerebral Blood Flow" (John W. Phillis, ed.). CRC Press, Boca Raton, FL.

Turnbull, I.M. (1972). Blood supply of the spinal cord: Normal and pathological considerations. *Clin. Neurosurg.* **20,** 56–84.

Uddman, R., Edvinsson, L., Ekman, R., Kingman, T., and McCulloch, J. (1985). Innervation of the feline cerebral vasculature by nerve fibers containing calcitonin gene-related peptide: Trigeminal origin and co-existence with substance P. *Neurosci. Lett.* **62,** 131–136.

van der Zwan, A., Hillen, B., Tulleken, C.A., Dujovny, M., and Dragovic, L. (1992). Variability of the territories of the major cerebral arteries. *J. Neurosurg.* **77,** 927–940.

Villringer, A., and Dirnagl, U. (1995). Coupling of brain activity and cerebral blood flow: Basis of functional neuroimaging. *Cerebrovasc. Brain Metabol. Rev.* **7,** 240–276.

Waite, J.J., Holschneider, D.P., and Scremin, O.U. (1999). Selective immunotoxin-induced cholinergic deafferentation alters blood flow distribution in the cerebral cortex. *Brain Res.* **818,** 1–11.

Wang, Q., Pelligrino, D.A., Baughman, V.L., Koenig, H.M., and Albrecht, R.F. (1995). The role of neuronal nitric oxide synthase in regulation of cerebral blood flow in normocapnia and hypercapnia in rats. *J. Cereb. Blood Flow Metab.* **15,** 774–748.

Willis, T. (1664). "Cerebri Anatome." Martin & Allestry, London.

Wislocki, G.B., and Campbell, A.C.P. (1937). The unusual manner of vascularization of the brain of the opossum *(Didelphys virginiana). Anat. Rec.* **67,** 177–191.

Withers, P.C. (1992). "Comparative Animal Physiology." Saunders College Publishing, Fort Worth, TX.

Yoshida, K., Meyer, J.S., Sakamoto, K., and Handa J. (1966). Autoregulation of cerebral blood flow. Electromagnetic flow measurements during acute hypertension in the monkey. *Circ. Res.* **19,** 726–738.

Young, J. (1929). Malpighi's "De Pulmonibus." *Proc. Roy. Soc. Med.* **23,** 1.

Zeman,W., and Innes, J.R.M. (1963). "Craigie's Neuroanatomy of the Rat." Academic Press, New York.

Zülch, K.J. (1985). "The cerebral infarct." Springer-Verlag, Berlin.

Index

B

C

D

E

F

M

N

R

S

T

W